Can. J. Chem. Downloaded from www.nrcresearchpress.com by 210.87.254.42 on 09/05/12
For personal use only.

Canadian Journal of Chemistry

Issued by THE NATIONAL RESEARCH COUNCIL OF CANADA

VOLUME 39 JANUARY 1961 NUMBER 1

GAS–LIQUID CHROMATOGRAPHY OF TERPENES

PART II. THE DEHYDRATION PRODUCTS OF α-TERPINEOL[1]

E. VON RUDLOFF

ABSTRACT

The complex mixture of terpenes obtained on dehydrating α-terpineol with aqueous oxalic acid was almost completely separated by gas–liquid chromatography (GLC), using rapeseed oil as a new liquid phase. Terpinolene, dipentene, α- and γ-terpinene, $\Delta^{2,4(8)}$-*p*-menthadiene, and 1,8-cineole were identified as the major reaction products; three minor and seven trace constituents were also detected. One of the minor components was *p*-cymene, one an oxide, and the third an unidentified hydrocarbon. The yield of these components after different reaction times was determined by GLC. The initial dehydration gives terpinolene and dipentene in the ratio of approximately 2:1. Terpinolene is isomerized to α- and γ-terpinene, $\Delta^{2,4(8)}$-*p*-menthadiene, and the unidentified hydrocarbon, but not to dipentene. 1,8-Cineole and the other oxide are formed in a reversible reaction. Dehydration of α-terpineol with several other acidic reagents yielded mixtures of products similar to that obtained with aqueous oxalic acid. With acetic acid or acetic anhydride, however, dipentene was formed preferentially and this reaction appears to proceed via the derived acetate.

INTRODUCTION

The first comprehensive study of the dehydration of α-terpineol (I) with acidic reagents was carried out by Wallach *et al.* (1, 2), who fractionated the steam-volatile reaction products by distillation and identified some of the constituents by conversion to known derivatives. In this manner terpinolene (II), dipentene (III), α-terpinene (IV), γ-terpinene (V), and 1,8-cineole (VI) were obtained by use of aqueous oxalic, sulphuric, or phosphoric acids. Mild conditions favored the formation of terpinolene, whereas longer reaction times gave higher yields of α-terpinene. In the reaction with fused potassium hydrogen sulphate only dipentene was identified. Reaction with acetic acid containing 2% sulphuric acid caused much resinification, whereas that with aqueous formic acid resulted in little dehydration. Flawitzky (3) found that when optically active α-terpineol was heated in a sealed tube with excess acetic anhydride, large amounts of limonene (optically active III) were formed. Baeyer (4) used the reaction with aqueous oxalic acid for the preparation of terpinolene (very short reaction time) and α-terpinene, but it is doubtful whether the pure hydrocarbons can be obtained in this manner (5). Using the same reaction for the preparation of α-terpinene, Alder and Rickert (6) reported the presence of an unidentified diene, which they thought to be possibly a seven-membered ring compound. O'Connor and Goldblatt (7), in a study of the spectral properties of terpene hydrocarbons, reported the preparation of α- and γ-terpinene and $\Delta^{2,4(8)}$-*p*-menthadiene (VII) and $\Delta^{3,8(9)}$-*p*-menthadiene (VIII) by dehydration of α-terpineol

[1]*Manuscript received August 24, 1960.*
Contribution from the National Research Council of Canada, Prairie Regional Laboratory, Saskatoon, Saskatchewan. Presented at the 43rd Annual Conference of the Chemical Institute of Canada, Ottawa, June 13–15, 1960.
Issued as N.R.C. No. 6037.

followed by high-efficiency fractional distillation of the reaction products, but did not give experimental details for these preparations. Terpinolene was obtained by Petrů (8) in the reaction between α-terpineol and phthalic anhydride, also using short reaction times.

The products obtained in the above reactions thus appear to be rather complex mixtures of *p*-menthadienes and 1,8-cineole and it is doubtful whether all constituents have been identified. The mixtures have a boiling range from about 173–183° C, and it is very difficult to obtain pure components by fractional distillation, even when high-efficiency columns are used. It is possible that azeotropes are formed (9), and in 1891 Wallach himself (10) wrote: "experience has shown that it is especially difficult to determine the presence of other terpenes (*p*-menthadienes) when these are admixed with α-terpinene". Obviously, different analytical techniques are required for the analysis of such mixtures and gas–liquid chromatography (GLC) appears to be the ideal tool at the present time.

GAS–LIQUID CHROMATOGRAPHIC SEPARATION

Previously (11), the mixture obtained in the reaction of α-terpineol with aqueous oxalic acid was used by the author as one of the test mixtures in a study of some of the general aspects of the separation of terpenoid compounds by means of GLC. Using 6-ft×1/4-in. diameter columns with Craig polyesters, polyethylene glycol, polyphenyl ether, or squalene as liquid phase, it was shown that the mixture was composed of at least seven compounds, but the degree of separation obtained with these columns was insufficient to allow quantitative calculations or qualitative separations for preparative purposes. The investigation was therefore continued in order to find conditions which would permit a satisfactory analysis of this mixture and thus facilitate the study of the dehydration reaction itself.

There are several ways by which the chromatographic separations can be improved (12). Increasing the column length is limited by the dimensions of the apparatus and eventually by excessive retention times. The use of thinner diameter columns and smaller samples (less than the 1 to 20 μl commonly used) may also lead to increased efficiency, but requires an exceedingly sensitive detector. A third means of improving the degree of separation is by selecting a more efficient liquid phase. Of the liquid phases used for the separation of terpene hydrocarbons as described in the literature of the past year (9, 13–16), none gave better results for the mixture under consideration than were already obtained previously. In Part I (11) it was shown that squalene was a useful liquid phase and a 12-ft column did indeed give almost complete separation. However, this material is subject to fairly rapid deterioration and cannot be used above 100–120° C for any length of time. It may be reasoned that aliphatic olefins of greater stability and larger molecular weight may give equal or better results. Such compounds are readily available in the form of the triglycerides of vegetable oils, with the added advantage that a wide choice in the degree of unsaturation is available. The additional polarity due to the ester groups would be favorable in this instance, since the polyester columns partially separated peak C into two components whilst the squalene column did not (11). Superior separations were, in fact, obtained when rapeseed or olive oil were used as liquid phase. Oils having a higher degree of unsaturation, e.g. linseed or sunflower seed oil, were not as efficient, a finding which indicates that triolein itself may be very suitable as liquid phase. Columns containing rapeseed or olive oil gave reproducible results during 2 to 3 months of continuous or intermittent use at 120° C or lower, provided they were kept under helium or nitrogen at all times.

A 13-ft rapeseed oil column at 90° C was found to give almost complete separation of

Can. J. Chem. Downloaded from www.nrcresearchpress.com by 210.87.254.42 on 09/05/12
For personal use only.

the components of the above mixture of terpenes with reasonable retention times. This allowed the near quantitative determination (±2 to 3%) of the nine components found to be present in the *p*-menthadiene range. Trace components (less than 0.5–1%) were also present in the camphene – *p*-menthene range (three peaks) and in the range between the *p*-menthadienes and unreacted α-terpineol (four peaks). This column, together with 12-ft polyester and polyethylene glycol and 6-ft polyphenyl ether columns, was used to determine the composition of the steam-volatile products obtained in the dehydration of α-terpineol.

EXPERIMENTAL

The gas-chromatographic equipment and procedures were those described previously (11). All columns were made up with the liquid phase on Chromosorb W (60–80 mesh) in the ratio of 1:6 (by weight). The retention times, measured from the time of injection to the initial emergence of a peak, of various terpenes on the columns used are shown in Table I. The percentage composition of a particular mixture was determined by the

TABLE I

Retention times* (in minutes) of terpenes on three GLC columns

Compound	Peak No.	13-ft rapeseed oil (90° C, 59 ml He/min)	6-ft polyester (APEG) + 6-ft polyethylene glycol (80° C, 46 ml He/min)	6-ft polyphenyl ether (120 ml He/min)	
				80° C	130° C
α-Pinene	—	43.5	8.6	3.9	—
Camphene	1	55.8	11.4	5.4	1.8
β-Pinene	—	58.1	15.1	6.3	—
Oxide 1	2	77.0	22.0	8.5	2.8
α-Terpinene	3	84.7	23.7	8.9	2.9
1,8-Cineole	4	92.4	31.0	12.7	3.6
Dipentene	5	96.5	27.0	10.4	3.1
p-Cymene	6	104.7	31.0	12.7	3.6
γ-Terpinene	7	109.6	36.2	14.4	4.2
Unidentified	8	134.8	41.7	17.0	4.7
Terpinolene	9	144.8	45.7	18.6	5.1
$\Delta^{2,4(8)}$-*p*-Menthadiene	10	154.7	47.0	18.8	5.1
Unidentified	11	—	—	—	10.4
Unidentified	12	—	—	—	12.2
Unidentified	13	—	—	—	14.2
α-Terpineol	14	—	—	—	16.1
Unidentified	15	—	—	—	18.5
α-Terpinyl acetate	16	—	—	—	30.6

*Measured from the time of injection to initial emergence of the peaks.

area under the curves. Test runs with a synthetic mixture of pure limonene, 1,8-cineole, and α-terpineol gave values within ±1.5% of the weight composition, provided the peaks did not tail. When tailing took place, as with α-terpineol on some columns, the calculated values were low by 2–3%. Duplicate runs on the same column agreed within 0.5%, but differed on different columns by as much as 3%. Preparative runs (10 to 50 mg) were carried out either on the analytical 1/4-in. diameter columns, or on a combination of a 3-ft×3/8-in. diameter silicone grease column used ahead of a 6-ft×1/4-in. polyphenyl ether column. Samples were collected with the detector current off (11), and the purity of the fractions collected was determined by injecting 1- to 3-μl aliquots into the analytical columns. At no time was there any evidence of decomposition or rearrangement of any of the components isolated. Individual components were identified by infrared and ultraviolet spectra, by retention times, and, where possible, by conversion

Can. J. Chem. Downloaded from www.nrcresearchpress.com by 210.87.254.42 on 09/05/12
For personal use only.

to known crystalline derivatives by standard techniques (5, 17) or as indicated. Melting points were determined on a Leitz hot-stage microscope. Infrared and ultraviolet spectra were recorded on Perkin–Elmer Model 21 infrared and Warren Electronic Inc. Spectracord spectrophotometers, respectively, using the film or potassium bromide disk method for the former instrument.

Commercial *dl*-α-terpineol was purified by fractional distillation through a Podbielniak 8-mm diameter spinning band column until GLC analysis showed less than 1% impurities to be present. Thus purified it had n_D^{20} 1.4829 (lit. (17) 1.4813, 1.4832) and gave the phenylurethane, m.p. 112–113° C (lit. (2, 5) m.p. 113° C), in good yield. α-Terpinyl acetate was prepared by refluxing α-terpineol with excess acetic anhydride in the presence of sodium acetate for 4 to 5 hours and was purified by fractional distillation; n_D^{20} 1.4666 (lit. (17) 1.4689).

Small-Scale Dehydration Experiments

α-Terpineol (1.0 g), oxalic acid (hydrate, 4.0 g), and water (5.0 ml) were placed in a 25-ml flask which had two necks with ground-glass joints. A small reflux condenser was attached to one of the joints whilst the other one was tightly stoppered. The mixture was brought to boil and refluxed for the required length of time. The reflux condenser was then changed to the horizontal position and the mixture was steam-distilled for 20 to 30 minutes. The distillate was collected in an ice-cooled flask and, after distillation was complete, the condenser was rinsed with a small amount of ether. The steam-volatile terpenes were recovered by extraction with small amounts of ether, the ethereal solution was washed with bicarbonate solution, then with water, and was dried over anhydrous sodium sulphate. The dried solution was quantitatively transferred to a weighed 25-ml flask having a long neck, and the ether was evaporated on a water bath at 80–90° C. In blank test runs with pure limonene the recovery was 94–98% with 3–5% ether remaining. Calculation of yields and percentage composition were, therefore, based on a 96% recovery. On this basis the yields were 98–100% of theory for reaction up to 8 hours. After that losses due to resinification became marked; for example, after 12 hours, the recovery was only 76% of theory.

In experiments using other dehydrating agents the same procedure was followed. The amounts of reagent used and reaction times are shown in Tables II and III.

Isolation and Identification of Individual Components

Terpinolene (Peak No. 9)

Oxalic acid (hydrate, 160 g) and water (200 ml) were brought to boil in a 500-ml flask which was equipped with a condenser, a dropping funnel, and an inlet tube. Steam was passed through the boiling solution and α-terpineol (40 g) was added dropwise (4), the steam distillate being collected in an ice-cooled flask. After the addition was complete, the mixture was steam-distilled for a further hour. The terpene mixture was recovered as described above. The crude product (38 g) was analyzed by GLC and then fractionally distilled through the spinning band column. The fractions collected were analyzed by GLC. The ninth (3.1 g), b.p. 92.5° at 41 mm Hg pressure, was found to contain better than 90% of peak 9 and had n_D^{20} 1.4914 (lit. (7) 1.4888). The infrared spectrum resembled that reported for terpinolene (7). The ultraviolet absorption was weak and devoid of any characteristic band due to conjugation. The fraction gave in good yield a crystalline bromide, m.p. 112–115° C, recrystallized from ether–methanol, m.p. 115.0–115.8° C (lit. (2) m.p. 116° C). Found: C, 26.48%; H, 3.68%; Br, 70.24%. Calculated for $C_{10}H_{16}Br_4$: C, 26.34%; H, 3.54%; Br, 70.12%. The derived tetrol was prepared as follows: terpinolene (126 mg) was added to an ice-cold solution of tertiary butanol (10 ml) and water (10 ml)

Can. J. Chem. Downloaded from www.nrcresearchpress.com by 210.87.254.42 on 09/05/12
For personal use only.

Can. J. Chem. Downloaded from www.nrcresearchpress.com by 210.87.254.42 on 09/05/12
For personal use only.

TABLE II

Yield of steam-volatile products in the reaction with α-terpineol (1.00 g)

Reagent	Reagent (ml)	Reaction time (hr)	Total yield (g)	Percentage of individual components in volatile product (Peak No.) 1	2	3	4	5	6	7	8	9	10	11	12	13	14	15	16
Sulphuric acid (33⅓%)	4	1	0.85	—	1.5	28.5	5	9	6	15	1	18.5	15	—	—	—	—	—	—
Phosphoric acid (20%)	4	1	0.96	—	3	7.5	3	7.5	2.5	6	—	11	1.5	2	1.5	4.5	49	—	—
Phosphoric acid (20%)	4	4	0.88	—	4.5	10	2	8	4	8	—	12.5	3	3.5	1.5	5	38	—	—
Acetone–H_2SO_4 (20%)	2+5	1	0.85	—	3	9	4	4	—	7.5	—	8.5	2.5	4	1	6	49.5	—	—
Ethanol–H_2SO_4 (98%)	4+1	1	0.43	16	1	27	3	5	5	13	1	8	6.5	3.5	—	3.5	4	—	—
$KHSO_4$, anh.	(2 g)	1	0.86	—	1	19	4	16	5.5	15.5	—	31	6	—	—	—	—	—	—
$KHSO_4$, anh. (pyro)	(3 g)	1	0.64	11	6	2	75	—	3	—	—	2	—	—	—	—	—	—	—
Phthalic anhydride	(2 g)	1	0.54	6.5	4.5	27	10	8.5	8	13	—	19	1	—	—	—	—	—	—
Acetic anhydride	5	16	1.02	—	1	3	1	32	1.5	3	—	6	—	—	—	—	3.5	—	50
Acetic acid (98%)	5	12	0.94	—	—	0.5	1.5	16	0.5	0.5	—	6	—	—	—	—	69.5	—	5
Acetic acid (50%)	5	2	0.95	—	—	0.5	1	5.5	—	0.5	—	6.5	—	—	0.5	1.5	84	—	—
Acetic acid (50%)	5	6	0.94	—	—	1.5	3	10.5	1	1.5	—	12	—	—	2	3	58.5	—	—
Acetic acid (50%)	5	18	0.75	—	3	10	9	15	4	11	—	29	3	1.5	1.5	2	8	—	—
Acetic acid + H_2SO_4 (5%)	5	2	0.21	18	5	2	37	1	0.5	0.5	—	1	—	—	—	—	—	32	1
Acetic acid + H_2SO_4 (5%)	5	3*	0.34	7.5	12.5	—	24	4	22	—	—	1	0.5	—	—	—	—	26	—
Formic acid (98%)	4	6	0.14	13	8	—	24	—	10	—	—	1.5	—	—	—	3	31.5	5	—

*At room temperature.

TABLE III

Yield of steam-volatile components in the reaction with α-terpinyl acetate (1.00 g)

Reagent	Reagent (ml)	Reaction time (hr)	Total yield (g)	Percentage of individual components in volatile product (Peak No.) 1	2	3	4	5	6	7	8	9	10	11	12	13	14	15	16
Acetic acid (98%)	5	18	0.56	—	—	1.5	0.5	46	—	2.5	—	21.5	—	—	—	—	4	—	29
Acetic acid + H_2SO_4 (5%)	5	3*	0.29	7	9	8	30	3	19	10	—	8	—	—	—	—	—	11	—
Acetic acid + H_2SO_4 (5%)	5	18*	0.18	12	6	2	27	2	18	4	0.5	5	—	—	—	—	—	20	—
Acetic anhydride	5	18	0.98	—	2	3	2	30	1	2.5	—	5	—	—	—	—	—	—	18
Acetic anhydride + H_2SO_4 (5%)	5	18	0.19	2.5	1	0.5	80	—	7	—	—	—	—	—	—	—	—	7.5	—

*At room temperature.

containing potassium hydroxide (0.1 g). To this was added with vigorous stirring and further cooling finely powdered potassium permanganate (0.4 g) in small aliquots. The initial permanganate color changed to black-purple, then to a dark green, and finally to a muddy brown. After complete addition and stirring for a further 10 minutes, the precipitated manganese dioxide was filtered off and the pH of the filtrate was brought to about 7 by leading in carbon dioxide. The solution was evaporated to dryness and extracted with ethanol:2-butanone (1:1 v/v). The mixture of solvents was evaporated and the residual material (192 mg) was taken up in a small volume of ethyl acetate or 2-butanone. The tetrol crystallized very slowly on keeping the solution at 0–2° C for several weeks. Recrystallization from these solvents was also very slow. Whilst the yield of crude tetrol was very good, that of crystalline material, m.p. 148–150° C (lit. (17) m.p. 149–150° C), was poor. Found: C, 58.71%; H, 9.78%. Calculated for $C_{10}H_{20}O_4$: C, 58.80%; H, 9.87%.

An aliquot of fraction 9 was purified by preparative GLC, 10 runs giving 100 mg of almost pure (99.2%) peak 9. It formed the terpinolene bromide in excellent yield and the derived tetrol more readily than the impure fraction.

Dipentene (Peak No. 5)

The first five fractions obtained in the above fractional distillation showed a high content of peak 5. These fractions were combined and redistilled to give a middle fraction containing about 80% of peak 5. This was further purified by preparative GLC, giving 98% pure peak 5. Its infrared spectrum corresponded to that of dipentene (7) and both the derived tetrabromide, m.p. 125.0–126.0° C (lit. (2, 17) m.p. 124–126° C) and tetrol, m.p. 191.5–192° C, were obtained in excellent yield. Found for the bromide: C, 26.52%; H, 3.67%; Br, 70.07% and for the tetrol: C, 58.66%; H, 9.84%.

α-Terpinene (Peak No. 3)

α-Terpineol (40 g) was refluxed with a mixture of oxalic acid (hydrate, 160 g) and water (200 ml) for 12 hours. The mixture was steam-distilled and the crude hydrocarbon mixture (29 g) recovered as above. Fractions 2 to 4 in the fractional distillation at 36 mm had a boiling point of 77–80° C and GLC analysis showed a high content of peak 3, with minor amounts of peaks 2, 4, 5, and 6 being present. Preparative GLC gave peak 3 in 95–96% purity, n_D^{20} 1.4792 (lit. (7) 1.4778). Its infrared and ultraviolet spectra corresponded to those of α-terpinene (7). No solid bromide was obtained nor did the permanganate oxidation give a derived tetrol. However, the acidified oxidation mixture on extraction with 2-butanone gave a good yield of α,δ-dihydroxy-α-methyl-δ-isopropyl adipic acid, m.p. 187–188° C (lit. (17, 18) m.p. 188–189° C). Found: C, 51.43%; H, 8.10%; neutral equivalent 115.5. Calculated for $C_{10}H_{18}O_6$: C, 51.27%; H, 7.75%; neutral equivalent 117.12. The compound melts with loss of water and forms the dilactone, m.p. 71–73° C, readily (18). The terpene gave the crystalline nitrosite, m.p. 155.5–156.5° C (lit. (2, 17) m.p. 155° C), in good yield.

γ-Terpinene (Peak No. 7)

Fractions 5 to 7 in the above fractional distillation had a boiling point of 80.5–84.5° C and showed a high content of peak 7. This was purified by GLC, when practically pure peak 7 was obtained; n_D^{20} 1.4748 (lit. (7) 1.4747). Its infrared spectrum was similar to that of γ-terpinene (7). The derived tetrol, m.p. 235–237° C (lit. (18) m.p. 237° C), was obtained in good yield. Found: C, 58.69%; H, 9.81%. This material also gave a crystalline nitrosochloride, m.p. 110–111° C, in fair yield.

$\Delta^{2,4(8)}$-p-Menthadiene (Peak No. 10)

The last two fractions in the above fractional distillation contained mainly peak 10

Can. J. Chem. Downloaded from www.nrcresearchpress.com by 210.87.254.42 on 09/05/12
For personal use only.

as well as some terpinolene (peak 9). Purification by GLC proved difficult, since these two peaks were not completely resolved. However, a small amount of peak 10, n_D^{20} 1.5030 (lit. (7) 1.5030), was obtained about 92–95% pure. The infrared and ultraviolet spectra (λ_{max} 243 mμ) corresponded to those of $\Delta^{2,4(8)}$-*p*-menthadiene (7). A nitrosite, m.p. 152–155° C, was obtained in poor yield. Pines and Eschinazi (19) report a melting point of 153–155° C for the β-nitrosite and melting points of 110°, 140–150° C for the α-nitrosite.

Oxides (Peaks Nos. 2 and 4) and p-Cymene (Peak 6)

An aliquot of the terpenoid mixture obtained in the preparation of terpinolene was oxidized exhaustively with cold, aqueous potassium permanganate. The unoxidized terpenes were recovered by extraction with ether. The dried ethereal solution was carefully evaporated and the residual material was analyzed by GLC. Peaks 2, 4, and 6 only were recorded, the major component being peak 4. The latter was isolated 95–96% pure by preparative GLC, and its infrared spectrum and retention times agreed with those of 1,8-cineole. This fraction formed the resorcinol adduct, m.p. 80–85° C (17), in fair yield. Peak 2 was not obtained pure in sufficient amount to allow positive identification. Its infrared spectrum resembled that of 1,8-cineole.

Peak 6 was also obtained only impure. However, its retention times and the ultraviolet spectrum were similar to those of *p*-cymene. Since only the other two oxides are the impurities present, there is little doubt that peak 6 corresponds to *p*-cymene.

Camphene (Peak No. 1)

The retention times of peak 1 on different columns agreed with those of camphene. α-Terpineol (40 g) was dissolved in 90% ethanol (160 ml) containing sulphuric acid (40 ml) and the mixture was refluxed for 1 hour. The steam-volatile terpenes (22 g) were recovered as before and fractionally distilled. The first fraction, b.p. 64–68° C at 20 mm pressure, contained about 80% of peak 1 and crystallized on seeding with camphene. The crystals were filtered off and recrystallized from ethanol–water, m.p. 47.5–49° C, undepressed in admixture with synthetic camphene.

Peak No. 8

This fraction was obtained only in very small amounts which were insufficient for characterization. Its spectral properties were similar to those of $\Delta^{3,8(9)}$-*p*-menthadiene (7).

RESULTS AND DISCUSSION

The amount of unreacted α-terpineol (I) and the percentage yield of the products formed in the reaction with aqueous oxalic acid after reaction times of 1/2 to 12 hours are shown in Figs. 1(*a*) and 1(*b*). Maximum yields of terpinolene (II), 1,8-cineole (VI), and oxide 1 were obtained within 1 to 3 hours and then diminished rapidly (Fig. 1(*a*)). The maximum yield of dipentene (III) was reached very quickly, decreasing only slowly after 4 to 6 hours. α-Terpinene (IV), γ-terpinene (V), $\Delta^{2,4(8)}$-*p*-menthadiene (VII), *p*-cymene, and peak 8 reached their maximum concentrations only after 8 hours, all but VII decreasing from then on. When pure II was treated under the same conditions for 6 hours, only IV, V, VII, and peak 8 were obtained (in approximately the same ratio); less than 1% of III was recorded. Thus, the four *p*-menthadienes, IV, V, VII, and peak 8, are clearly isomerization products of terpinolene. Pure limonene, under the same conditions, did not yield any isomerization or hydration products but resinified somewhat, explaining the loss of III as the reaction proceeds. Under similar conditions 1,8-cineole (VI) gave a product having the same chromatographic spectrum as was obtained for the reaction product obtained from α-terpineol (I) itself, 2–3% of I also being recorded. It

Can. J. Chem. Downloaded from www.nrcresearchpress.com by 210.87.254.42 on 09/05/12
For personal use only.

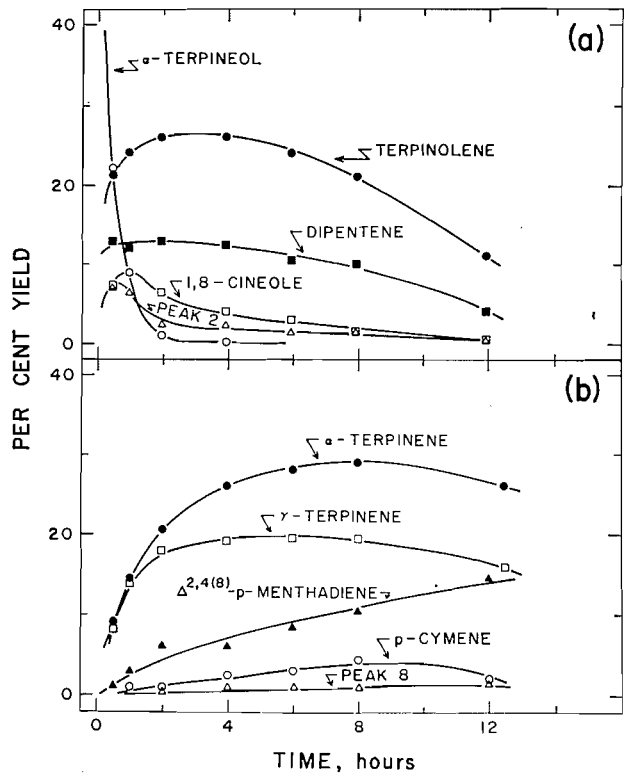


FIG. 1. Yields of individual components in the reaction of α-terpineol with aqueous oxalic acid: (*a*) initial products, (*b*) isomerization products.

can be concluded, therefore, that VI and I are in equilibrium with one another under these conditions. The similarity of the shape of the curves obtained for oxide 1 (peak 2) and VI (Fig. 1(*a*)) suggests that oxide 1 is formed in a similar reversible reaction. This could only be possible if this oxide is 2,8-cineole (dihydropinol), a finding which is further strengthened by the fact that its retention time is in good agreement with that expected for dihydropinol (as deduced from boiling points).

Thus, the reaction of α-terpineol with aqueous oxalic acid appears to proceed as follows:

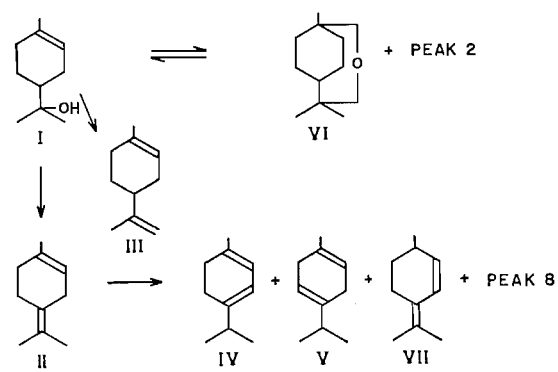


FIG. 2.

Can. J. Chem. Downloaded from www.nrcresearchpress.com by 210.87.254.42 on 09/05/12
For personal use only.

Semmler (20) has shown that alcoholic sulphuric acid isomerizes α-terpinene (IV) to V and II. Thus it is possible that these *p*-menthadienes are in a state of equilibrium under acid conditions. The above findings clearly show why it has been impossible to obtain II, IV, and V in a pure state when prepared under acidic reaction conditions.

The preferential formation of terpinolene (maximum yield about twice that of dipentene) is contrary to what would be expected from the postulate put forward by Brown *et al.* (21), according to which the exo-double bond should be formed in smaller amounts than the isopropenyl derivative. These authors quote Flawitzky (3) as having obtained limonene from I by dehydration with alcoholic sulphuric acid and use this as further evidence that tertiary alcohols of this type resist formation of an exo-double bond. Actually, Flawitzky used the alcoholic sulphuric acid to hydrate α-pinene (turpentine) to give I and the latter was then heated in a sealed tube with excess acetic anhydride to give appreciable amounts of limonene besides α-terpinyl acetate. As will be shown below, this reaction appears to be a deacetoxylation rather than a dehydration and proceeds via a different mechanism. Moreover, Brown *et al.* do not refer to the much more comprehensive studies of Wallach (1, 2), which clearly show that the exo-double bond, as in II, may be formed in substantial amounts in the acid-catalyzed dehydration. It is thus doubtful whether the olefin formation from compounds of the α-terpineol type can be included in the generalization put forward by Brown *et al.* Also, the isomerization of terpinolene does not proceed entirely according to this postulate, the exo-isomer VII being a major product besides the two endo-isomers IV and V. In a later communication, Brown (22) points out that their postulate has been misinterpreted by some workers by not considering the stability of the double bonds in cyclohexanes in conjunction with the corresponding cyclopentane derivatives. However, in the first paper, Brown *et al.* discuss the dehydration of α-terpineol and related compounds without any reference to the corresponding cyclopentanols. Recently (23), it has been shown that the whole question of the relative stabilities of methylene cycloalkanes and 1-methyl cycloalkenes is subject to some controversy.

In view of the above discrepancies, the work of Wallach and Flawitzky was repeated and the reaction with other acidic dehydrating agents was also investigated. The steam-volatile reaction products were analyzed by GLC as before and the results obtained are summarized in Table II. In the reaction with aqueous sulphuric and phosphoric acids, the reaction products had the same qualitative chromatographic spectra as that obtained with aqueous oxalic acid, confirming in essence Wallach's findings. When α-terpineol was dissolved in twice its volume of acetone and added dropwise to boiling aqueous sulphuric acid through which steam was passed (24), the steam-volatile product differed little from that obtained in the short-time reaction with aqueous oxalic acid, except that oxide 1 was produced in somewhat larger amounts and two additional peaks (11 and 13) became more prominent. Treatment with 90% ethanol – sulphuric acid (4:1 v/v) also gave a product of similar composition containing, however, a new major compound (peak 1) identified as camphene. Fused anhydrous potassium hydrogen sulphate also gave results similar to those obtained with aqueous oxalic acid, oxide formation being somewhat suppressed. This is contrary to the results Wallach obtained with "sharply dried" potassium hydrogen sulphate (2). Therefore, hydrogen sulphate was fused until fuming became extensive (pyrosulphate formation), and this was used in excess. Under these conditions I reacted to give a high yield of the oxides and camphene, but only traces of III. Thus, Wallach's findings could not be confirmed in this instance. That water is not responsible for any difference in the reaction follows from the results obtained with

Can. J. Chem. Downloaded from www.nrcresearchpress.com by 210.87.254.42 on 09/05/12
For personal use only.

phthalic anhydride. Here, anhydrous conditions again give a mixture similar to that obtained with aqueous acids.

The dehydration of α-terpineol with 50% aqueous acetic acid proceeds slowly (see Table II) and allows a better study of the early stages of the reaction. II and III are distinctly the first dehydration products and the yield of the former increases much faster than that of the latter as the reaction proceeds. Oxide formation and isomerization of II is slow, making the reaction well suited for the preparation of II and III, especially so since these two *p*-menthadienes can be separated by fractional distillation. The different results obtained with glacial acetic acid (or acetic anhydride) are noteworthy (see below).

Mosher (25) proposed for the acid-catalyzed isomerization of α-pinene (X) to the *p*-menthadienes rearrangement to the intermediate carbonium ion XI. Loss of a proton leads to terpinolene (II) and dipentene (III), and (via the carbonium ion XII) to α-terpinene (IV) and γ-terpinene (V) (Fig. 3). This mixture of *p*-menthadienes is very

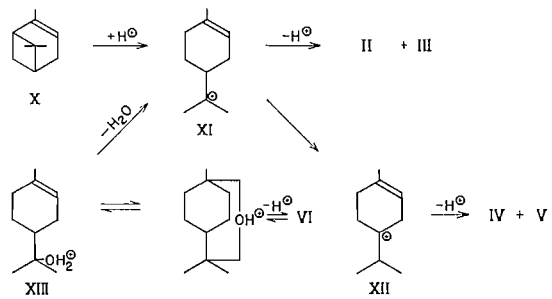


FIG. 3.

similar to that obtained in the acid-catalyzed dehydration of α-terpineol. Thus, it is likely that α-terpineol, in the protonated form (XIII), loses the elements of water to give the same intermediate carbonium ion XI. The present findings that terpinolene isomerizes readily to IV, V, and VII, but not to III, suggest that the ion XI rearranges rapidly and irreversibly to ion XII. The formation of VII, however, demands the presence of another intermediate ion. Cyclization of the protonated alcohol (XIII) and loss of a proton would lead to 1,8-cineole (VI) in a reversible reaction.

Refluxing I with excess acetic anhydride for 16 hours gave a yield of 50% α-terpinyl acetate, 32% III, and small amounts of *p*-menthadienes and oxides (see Table II), confirming, in essence, the findings of Flawitzky (3). The reaction with glacial acetic acid is similar, though the amount of α-terpineol which had reacted after 12 hours was only 30%. Since, in this reaction, I may be converted to the acetate first and this, on loss of the elements of acetic acid, could give III as the main elimination product, α-terpinyl acetate was treated in the same manner. Appreciable amounts of III, and smaller amounts of the other *p*-menthadienes, were formed (see Table III). Thus, it is possible that the preferential formation of III is due to deacetoxylation of the acetate rather than the dehydration of the parent alcohol.

Recently, Roček (26) has studied the kinetics of the dehydration of 1-methyl cyclohexanol as well as the deacetoxylation of the derived acetate, using acetic acid containing small amounts of sulphuric acid at room temperature. From the data obtained Roček concluded that both the dehydration and the deacetoxylation proceeds via the same intermediate carbonium ion and the rate-controlling step is given as the elimination of

Can. J. Chem. Downloaded from www.nrcresearchpress.com by 210.87.254.42 on 09/05/12
For personal use only.

water from the protonated alcohol, or of acetic acid from the protonated ester. In the reaction of α-terpineol and its acetate with this reagent at room temperature or under reflux, appreciable amounts of camphene and the oxides, but only small amounts of the *p*-menthadienes, were obtained (see Tables II and III). The yield of steam-volatile products dropped markedly and a new peak (No. 15) in the α-terpineol range was recorded. Thus, with this reagent a third type of reaction was encountered in which the normal dehydration (or deacetoxylation) products did not survive the reaction, if these were formed at all. Similar results were also obtained when formic acid was used as dehydrating agent (Table II). Since this was no longer a normal dehydration reaction, it was not further investigated.

The presence of small amounts of *p*-cymene (peak No. 6) in most reaction products deserves some comment. Its formation in the acid-catalyzed dehydration of α-terpineol was already suspected by Wallach and Kerkhoff (2). Since the reaction conditions are not conducive to dehydrogenation, disproportionation of one or more of the *p*-menthadienes to *p*-cymene and *p*-menthenes may take place. This would account for the presence of the trace components in the *p*-menthene range.

CONCLUSIONS

The dehydration of α-terpineol with acidic reagents can occur in two different ways: (*a*) With aqueous acids, anhydrous potassium hydrogen sulphate, or phthalic anhydride, terpinolene is the major reaction product in the early stages of the reaction. About half as much dipentene and smaller amounts of 1,8-cineole and a second oxide, possibly 2,8-cineole, are also formed. As the reaction proceeds, terpinolene isomerizes to give mainly α-terpinene, somewhat less γ-terpinene and $\Delta^{2,4(8)}$-*p*-menthadiene, and a small amount of an unidentified terpene. Drastic conditions, or long reaction times, tend to cause resinification. The oxides are in equilibrium with α-terpineol and give the same reaction products on prolonged treatment. (*b*) With acetate-forming reagents, dipentene is formed preferentially. Apparently the acetate is an intermediate and subsequent loss of the elements of acetic acid favors the production of this *p*-menthadiene.

The present findings show that by proper choice of conditions the preferential formation of terpinolene, dipentene, α- and γ-terpinene, or $\Delta^{2,4(8)}$-*p*-menthadiene can be achieved. However, it is impossible to synthesize by this means any one of these *p*-menthadienes without concomitant formation of smaller amounts of several isomers. Only in very favorable instances can such mixtures be separated completely by fractional distillation. If very pure specimens of these *p*-menthadienes are required other sources must be sought, or the products obtained in the above reactions can be fractionated on a 0.01- to 0.1-g scale by preparative gas–liquid chromatography.

ACKNOWLEDGMENTS

The author wishes to thank Mr. M. Granat for technical assistance, Miss I. M. Gaffney for recording the infrared spectra, and Mr. M. Mazurek for the microanalyses.

REFERENCES

1. O. Wallach. Ann. **239**, 20 (1887).
2. O. Wallach and F. Kerkhoff. Ann. **275**, 103 (1893).
3. F. Flawitzky. Ber. **20**, 1956 (1887).
4. A. Baeyer. Ber. **27**, 436 (1894).
5. J. L. Simonsen. The terpenes. Vol. I. Cambridge University Press. 1947. pp. 166, 175.
6. K. Alder and H. F. Rickert. Ber. **70**, 1364 (1937).
7. R. T. O'Connor and L. A. Goldblatt. Anal. Chem. **26**, 1726 (1954).

Can. J. Chem. Downloaded from www.nrcresearchpress.com by 210.87.254.42 on 09/05/12
For personal use only.

8. F. PETRŮ. Chem. listy, **43**, 75 (1949); cf. Chem. Abstr. **45**, 537*i* (1951).
9. W. J. ZUBYK and A. Z. CONNER. Anal. Chem. **32**, 912 (1960).
10. O. WALLACH. Ber. **24**, 3984 (1891).
11. E. VON RUDLOFF. Can. J. Chem. **38**, 631 (1960).
12. A. I. M. KEULEMANS. Gas chromatography. Reinhold Publishing Corp., New York. 1957.
13. G. P. CARTONI and A. LIBERTI. J. Chromatog. **3**, 121 (1960).
14. V. LUKÉS, R. KOMERS, and V. HEROUT. J. Chromatog. **3**, 303 (1960).
15. R. A. BERNHARD. J. Chromatog. **3**, 471 (1960).
16. D. M. SMITH, J. C. BARTLET, and L. LEVI. Anal. Chem. **32**, 568 (1960).
17. E. GUENTHER and D. ALTHAUSEN. The essential oils. Vol. II. D. Van Nostrand Co. Inc., New York. 1949.
18. O. WALLACH. Ann. **362**, 296 (1908).
19. H. PINES and H. E. ESCHINAZI. J. Am. Chem. Soc. **77**, 6314 (1955).
20. F. W. SEMMLER. Ber. **42**, 962 (1909).
21. H. C. BROWN, J. H. BREWSTER, and H. SHECHTER. J. Am. Chem. Soc. **76**, 467 (1954).
22. H. C. BROWN. J. Org. Chem. **22**, 439 (1957).
23. A. C. COPE, D. AMBROS, E. CIGANEK, C. F. HOWELL, and Z. JACURA. J. Am. Chem. Soc. **82**, 1750 (1960).
24. H. RUPE and P. SCHLOCHOFF. Ber. **38**, 1719 (1905).
25. W. A. MOSHER J. Am. Chem. Soc. **67**, 2127 (1949).
26. J. ROČEK. Collection Czechoslov. Chem. Communs. **25**, 375 (1960).

Can. J. Chem. Downloaded from www.nrcresearchpress.com by 210.87.254.42 on 09/05/12
For personal use only.

Can. J. Chem. Downloaded from www.nrcresearchpress.com by 210.87.254.105 on 09/05/12
For personal use only.

HYDROGEN ATOM ABSTRACTION BY ETHYL-d_5 RADICALS. PART II[1]

P. J. BODDY[2] AND E. W. R. STEACIE

ABSTRACT

Further experiments are reported on the hydrogen atom abstraction reactions of deuterated ethyl radicals produced by the photolysis of 3-pentanone-d_{10}.

The compounds studied include hydrogen, *n*-hexane, and cyclohexane. The activation energies for hydrogen atom abstraction relative to ethyl-d_5 recombination are respectively 11.3±0.5, 10.1±0.5, and 10.4±0.5 kcal/mole.

INTRODUCTION

Recently experimental data were reported for hydrogen atom abstraction from a series of typical alkanes by ethyl-d_5 radicals (1). This paper represents a continuation of that work in an effort to provide further points of comparison with the much investigated methyl radical reactions (2). The apparently arbitrary choice of compounds was dictated largely by what was possible analytically by conventional distillation and mass spectrometric techniques.

The photolysis of diethyl ketone is understood in some detail (3, 4). The mechanism is assumed to be similar for the deuterated species and is as follows (rate constants, of course, may be different):

$$(C_2D_5)_2CO \xrightarrow{h\nu} 2C_2D_5\cdot + CO \qquad [1]$$

$$2C_2D_5\cdot \rightarrow C_4D_{10} \qquad [2]$$

$$2C_2D_5\cdot \rightarrow C_2D_6 + C_2D_4 \qquad [3]$$

$$C_2D_5\cdot + (C_2D_5)_2CO \rightarrow C_2D_6 + C_2D_5COC_2D_4\cdot \qquad [4]$$

$$C_2D_5\cdot + C_2D_5COC_2D_4\cdot \rightarrow C_2D_5COC_4D_9 \qquad [5]$$

$$2C_2D_5COC_2D_4\cdot \rightarrow (C_2D_5COC_2D_4\cdot)_2 \qquad [6]$$

$$C_2D_5COC_2D_4\cdot \rightarrow C_2D_5\cdot + CO + C_2D_4 \qquad [7]$$

$$C_2D_5\cdot + RH \rightarrow C_2D_5H + R\cdot \qquad [8]$$

It can be shown that

$$\frac{k_8}{k_2^{1/2}} = \frac{R_{C_2D_5H}}{R_{C_4D_{10}}^{1/2}[RH]}$$

and

$$\frac{k_8}{k_4} = \frac{[\text{ketone}]}{[RH]} \cdot \frac{R_{C_2D_5H}}{R_{C_2D_6}},$$

where $R_{C_2D_5H}$ and $R_{C_2D_6}$ are the rates of formation of ethane-d_5 and ethane-d_6 from reactions [8] and [4]. Hence, the activation energy and frequency factor of reaction [8] may be determined relative to reactions [2] or [4] both of which are quantitatively understood (5, 1, 6, 7).

[1]*Manuscript received September 12, 1960.*
Contribution from the Division of Pure Chemistry, National Research Council, Ottawa, Canada.
Issued as N.R.C. No. 6039.

[2]*N.R.C. Postdoctorate Fellow 1957–59 now at Bell Telephone Laboratories, Murray Hill, New Jersey, U.S.A.*

Difficulty arises due to the fact that the diethyl ketone is not completely deuterated. The sample used by us contained only a small percentage of the d_9-ketone, and the necessary corrections to the data, which have previously been described in detail (1), were made accordingly.

Another complication is due to the occurrence of reaction [7], which becomes considerable above 200° C. This may lead to errors in the estimation of C_2D_6 from reaction [4] since it is assumed that all of the C_2D_4 arises from reaction [3] and that this is equal to the C_2D_6 from the same source. In the absence of quantitative knowledge of reaction [7], it is difficult to estimate the magnitude of the error involved. In the present work only the hydrogen experiments extended much above this temperature and since the data gave a linear Arrhenius plot throughout the whole range, it is concluded that the error is not large in this case.

Some experiments were attempted with methane and benzene. With these compounds, as in the corresponding methyl radical reactions (2), the rate constants for hydrogen atom abstraction appear to be relatively small. This necessitates working at high RH: ketone ratios and elevated temperatures. Under these conditions reaction [7] becomes much more significant and the experiments were unsuccessful.

EXPERIMENTAL

The apparatus and experimental methods have been described previously (1).

n-Butane-d_{10} was collected as the fraction between −165° C and −125° C and its identity was checked by mass spectrometry. A correction was made for the *n*-butane-d_9 content which was found to be a constant fraction.

MATERIALS

The purity of the 3-pentanone-d_{10} was discussed previously (1).

n-Hexane and cyclohexane were Phillips Research Grade materials. They were degassed and stored under vacuum in blackened bulbs behind mercury cutoffs. Purities were in excess of 99.5%.

Hydrogen was purified before each experiment by passage through a heated palladium thimble.

RESULTS

The experimental data for the three compounds are presented in Tables I–III. The calculated values of $\log_{10}(k_8/k_4)$ are plotted in Fig. 1 as a function of $1/T$. The familiar departure from linearity at low temperatures (1, 4, 7) is apparent. The slopes and intercepts were calculated by the least squares method. Points lying on the dashed portion of the curves (lowest temperatures) were not included in the analysis. The results are summarized below. The values for $E_4-\frac{1}{2}E_2$ and $\log_{10}(A_4/A_2^{1/2})$ were determined previously (1) (the units throughout are molecules/ml, and seconds):

$$E_4-\tfrac{1}{2}E_2 = 9.0\pm0.5 \text{ kcal/mole},$$

$$\log_{10}\frac{A_4}{A_2^{1/2}} = \bar{8}.36\pm0.20.$$

Can. J. Chem. Downloaded from www.nrcresearchpress.com by 210.87.254.105 on 09/05/12
For personal use only.

Can. J. Chem. Downloaded from www.nrcresearchpress.com by 210.87.254.105 on 09/05/12
For personal use only.

TABLE I

Ethyl-d_5 with hydrogen

Ketone	Hydrogen	Temp.,	Time,	$R_{C_2D_5H}$	$R_{C_2D_6}$	$R_{C_2D_4}$	$R_{C_2D_3H}$	$R_{C_4D_{10}}$	$2+\log\frac{k_8}{k_4}$	$13+\log\frac{k_4}{k_2^{\frac{1}{2}}}$	$15+\log\frac{k_8}{k_2^{\frac{3}{2}}}$
molecules/ml $\times 10^{-17}$		°K	sec	molecules/ml sec $\times 10^{-12}$							
9.66	8.89	375	3600	0.108	0.906	0.528	0.020	5.30	1.25	0.24	1.51
13.02	8.23	391	4740	0.132	1.29	0.600	0.071	6.24	1.27	0.29	1.55
7.23	7.23	501	3660	1.78	4.05	—	—	3.37	1.64	1.45	3.09
5.42	5.82	481	2760	1.18	3.10	0.105	0.0216	3.64	1.55	1.42	2.97
4.83	5.25	469.5	3600	0.772	2.21	0.145	0.019	3.76	1.53	1.29	2.82
12.72	5.07	448	3180	0.732	4.77	0.510	0.0595	7.70	1.51	1.05	2.56
7.48	6.92	432.5	3840	0.524	2.27	0.423	0.0313	6.63	1.45	0.92	2.37
4.15	3.92	419	4740	0.0929	0.556	0.139	0.0171	2.51	1.24	1.80	2.05
8.38	9.36	392	3600	0.186	1.32	0.649	0.0328	7.95	1.33	0.35	1.68
7.10	6.33	374	3780	0.089	1.12	0.694	0.030	6.58	0.98	0.41	1.40
7.19	5.15	356	3600	0.0543	1.05	0.736	0.0348	6.72	0.51	0.14	0.82
6.33	4.06	595	3655	4.40	12.6	1.01	0.224	2.16	1.70	2.12	3.81
5.76	3.84	553	3600	2.39	7.62	0.218	0.115	2.05	1.62	1.95	3.57
5.06	9.19	515	4640	2.59	3.94	0.096	0.0553	3.03	1.56	1.61	3.18

Can. J. Chem. Downloaded from www.nrcresearchpress.com by 210.87.254.105 on 09/05/12
For personal use only.

TABLE II

Ethyl-d_5 with *n*-hexane

Ketone	*n*-Hexane	Temp.,	Time,	$R_{C_2D_5H}$	$R_{C_2D_6}$	$R_{C_2D_4}$	$R_{C_2D_3H}$	$R_{C_4D_{10}}$	$1+\log\frac{k_8}{k_4}$	$13+\log\frac{k_4}{k_2^{\frac{1}{2}}}$	$14+\log\frac{k_8}{k_2^{\frac{1}{2}}}$
molecules/ml $\times 10^{-17}$		°K	sec	molecules/ml sec $\times 10^{-12}$							
3.11	4.89	497.5	3600	1.66	2.05	0.185	0.0034	2.53	0.73	1.58	2.31
3.77	4.32	525	3640	2.77	4.07	0.070	0.056	3.91	0.74	1.72	2.48
4.63	4.51	467	3816	1.07	2.35	0.379	0.044	4.73	0.70	1.28	1.99
3.89	4.82	447	4500	0.594	1.20	0.344	0.0042	3.82	0.70	1.06	1.76
4.60	4.31	428	5540	0.367	1.13	0.421	0.015	4.90	0.67	0.847	1.53
4.37	6.14	404	4330	0.261	0.814	0.433	0.017	3.69	0.62	0.660	1.28
5.12	6.44	388.3	3825	0.186	0.825	0.497	0.017	4.37	0.55	0.393	1.05
5.23	5.77	360	3665	0.073	0.616	0.475	0.017	5.22	0.45	0.039	0.518

TABLE III

Ethyl-d_5 with cyclohexane

Ketone	Cyclohexane	Temp.,	Time,	$R_{C_2D_5H}$	$R_{C_2D_6}$	$R_{C_2D_4}$	$R_{C_2D_3H}$	$R_{C_4D_{10}}$	$1+\log\frac{k_4}{k_8}$	$13+\log\frac{k_4}{k_2^{\frac{1}{2}}}$	$14+\log\frac{k_8}{k_2^{\frac{1}{2}}}$
molecules/ml $\times 10^{-17}$		°K	sec	molecules/ml sec $\times 10^{-12}$							
4.36	4.32	521	3635	2.86	3.70	0.375	—	1.89	0.91	1.75	2.66
5.29	2.99	484	4040	1.22	2.94	0.426	0.022	2.72	0.88	1.46	2.34
6.11	8.39	403	3640	0.588	1.41	0.725	0.012	6.10	0.73	0.67	1.40
7.60	7.47	380	4000	0.225	1.12	0.703	—	7.51	0.60	0.33	0.93
10.0	13.6	371.5	3670	0.126	0.292	0.113	0.007	1.16	0.67	0.21	0.89
8.80	21.6	395	3600	0.334	0.342	0.093	0.005	0.954	0.72	0.46	1.18
6.55	14.7	450	3600	0.701	0.563	0.028	0.002	0.399	0.75	1.11	1.86
5.26	11.5	496	3600	0.946	0.650	0.001	0.005	0.131	0.81	1.53	2.34
5.67	12.8	477	4100	0.874	0.647	—	—	0.192	0.76	1.42	2.18
5.90	11.7	566	7933	1.53	0.975	0.079	0.025	0.044	0.90	1.88	2.78

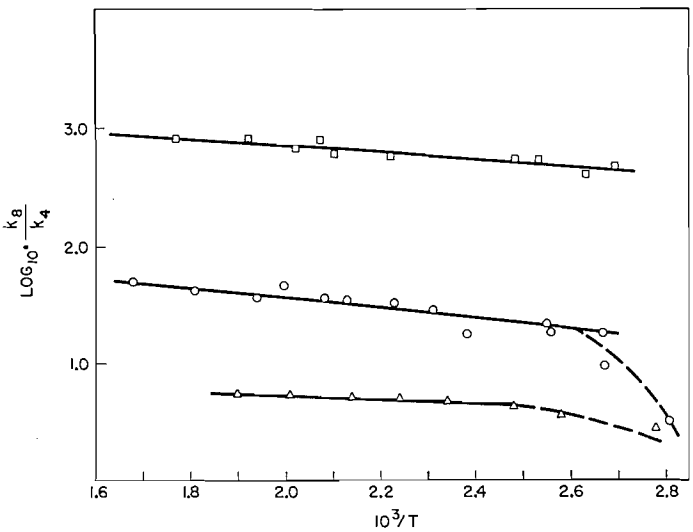


FIG. 1. $\log_{10}(k_8/k_4)$ as a function of $1/T$. Curves displaced up by number of units in parentheses. ○ H_2 (+2), △ n-C_6H_{14} (+1), □ cyclo-C_6H_{12} (+3).

For hydrogen

$$E_{8a}-E_4 = 2.3\pm0.2 \text{ kcal/mole},$$

$$\log_{10}\frac{A_{8a}}{A_4} = 0.56\pm0.086;$$

whence

$$E_{8a}-\tfrac{1}{2}E_2 = 11.3\pm0.5 \text{ kcal/mole},$$

$$\log_{10}\frac{A_{8a}}{A_2^{1/2}} = \bar{8}.92\pm0.2.$$

For n-hexane

$$E_{8b}-E_4 = 1.06\pm0.1 \text{ kcal/mole},$$

$$\log_{10}\frac{A_{8b}}{A_4} = 0.19\pm0.055;$$

therefore

$$E_{8b}-\tfrac{1}{2}E_2 = 10.1\pm0.5 \text{ kcal/mole},$$

$$\log_{10}\frac{A_{8b}}{A_2^{1/2}} = \bar{8}.55\pm0.2.$$

For cyclohexane

$$E_{8c}-E_4 = 1.4\pm0.14 \text{ kcal/mole},$$

$$\log_{10}\frac{A_{8c}}{A_4} = 0.47\pm0.07;$$

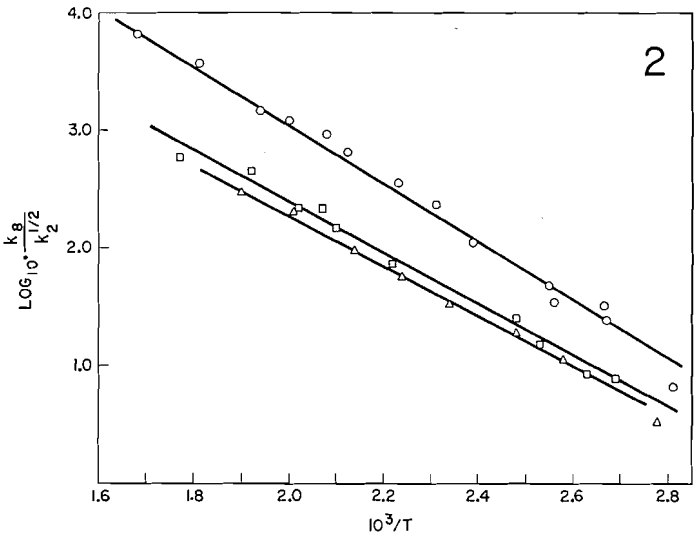
Can. J. Chem. Downloaded from www.nrcresearchpress.com by 210.87.254.105 on 09/05/12
For personal use only.

therefore

$$E_{8c}-\tfrac{1}{2}E_2 = 10.4\pm0.5 \text{ kcal/mole},$$

$$\log_{10}\frac{A_{8c}}{A_2^{1/2}} = \bar{8}.83\pm0.2.$$

Plots of $\log_{10}(k_8/k_2^{1/2})$ as a function of $1/T$ (Fig. 2) yield results agreeing with those above within the quoted error.



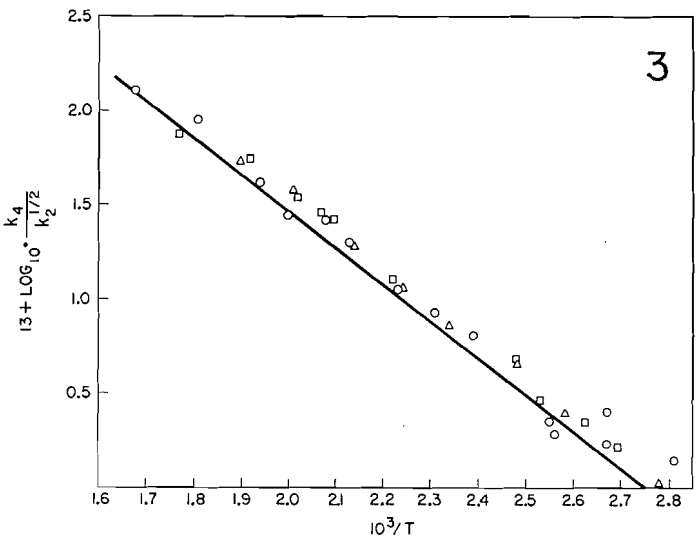


FIG. 2. $\text{Log}_{10}(k_8/k_2^{1/2})$ as a function of $1/T$. Key as in Fig. 1. Hydrogen curve displaced up by 2 units.
FIG. 3. $\text{Log}_{10}(k_4/k_2^{1/2})$ as a function of $1/T$. Key as in Fig. 1.

In Fig. 3 the data for abstraction from the ketone during these experiments are plotted. The solid line is the result of experiments on the ketone alone (1). There is a tendency

Can. J. Chem. Downloaded from www.nrcresearchpress.com by 210.87.254.105 on 09/05/12
For personal use only.

for the points to lie above the line by about 15% in $k_4/k_2^{1/2}$, but the slopes are not in disagreement and it appears there are no serious errors involved either in the chemical analyses or the methods used to compute the data.

DISCUSSION

The reaction between ethyl-d_0 radicals and molecular deuterium has been studied (8) and it was tentatively suggested that the activation energy for abstraction of a hydrogen atom from molecular hydrogen was 11.5±1 kcal/mole, in very good agreement with the value reported above.

If we write

$$C_2H_5 + D_2 \rightarrow C_2H_5D + D \qquad [8a]$$

$$2C_2H_5 \rightarrow C_4H_{10} \qquad [2a]$$

and

$$C_2D_5 + H_2 \rightarrow C_2D_5H + H \qquad [8]$$

$$2C_2D_5 \rightarrow C_4D_{10} \qquad [2]$$

$k_{8a}/k_{2a}^{1/2}$ may be calculated to be 1.0×10^{-13} at 182° C (4, 7). $k_8/k_2^{1/2}$ is 3.4×10^{-13} at the same temperature.

The ratio of these figures is quite close to that for the corresponding methyl radical reactions ($CD_3 + H_2$, $CH_3 + D_2$), which is 5.3 (9). The ratio is even closer to that for the reactions

$$\frac{CH_3+H_2}{CH_3+D_2} = 3.6 \qquad \text{at } 182° \text{ C} \qquad [9]$$

$$\frac{CD_3+H_2}{CD_3+D_2} = 3.7$$

and suggests that possibly ethyl-d_0 and ethyl-d_5 are more similar than the corresponding pair methyl-d_0 and methyl-d_3.

It is interesting to observe that, as compared with methyl, ethyl radicals seem to react relatively faster with hydrogen than with hydrocarbons at 182° C. Some rate constants (expressed in the same way as above) are:

$CH_3 + H_2$	12.6×10^{-13} (9)	$C_2D_5 + H_2$	4.3×10^{-13}
+ neo-C_5H_{12}	6.3 (2)	+ neo-C_5H_{12}	0.45 (1)
+ iso-C_4H_{10}	42 (2)	+ iso-C_4H_{10}	6.1 (1)

The reason for this is not understood.

The rate constant $(k_8/k_2^{1/2})_{182°C}$ for *n*-hexane is 5.7×10^{-13} (ml/molecule sec)$^{1/2}$. Correcting for the presence of the six primary hydrogen atoms (2) using the neopentane data (1), the rate constant per secondary hydrogen atom becomes 0.68×10^{-13}, in excellent agreement with the figure 0.70×10^{-13} obtained for *n*-butane (1). This may be compared with the figure for the reaction of ethyl-d_0 radicals with *n*-heptane (10), where $(k_8/k_2^{1/2})_{182°C}$ (our notation) is 10.7×10^{-13}: after correcting for the primary hydrogens using the ethyl-d_5 data, which should be approximately correct (the correction is very small in any case), the rate constant per secondary hydrogen atom becomes 1.05×10^{-13}. Thus, it appears that ethyl-d_0 is about 50% more reactive than ethyl-d_5. It is rather perplexing

Can. J. Chem. Downloaded from www.nrcresearchpress.com by 210.87.254.105 on 09/05/12
For personal use only.

that an effect similar in magnitude but in the opposite direction is observed for the reaction of methyl-d_0 and -d_3 with H_2 and D_2 (9). A difference has been observed in the reaction of methyl radicals (-d_3 and -d_0) with neopentane amounting to about 15% and in the same direction that we observe, i.e., methyl-d_0 more reactive (11).

The rate constant for cyclohexane at 182° C is 7.2×10^{-13} (ml/molecule sec)$^{1/2}$ corresponding to a value of 0.6×10^{-13} per hydrogen atom. This agrees with the methyl radical results where cyclohexane was found to give a value typical of a secondary paraffinic hydrogen atom (2).

The authors wish to thank Mrs. R. H. Riem, who carried out the mass spectrometric analyses.

REFERENCES

1. P. J. Boddy and E. W. R. Steacie. Can. J. Chem. **38**, 1576 (1960).
2. A. F. Trotman-Dickenson and E. W. R. Steacie. J. Chem. Phys. **19**, 329 (1951); A. F. Trotman-Dickenson. Gas phase kinetics. Butterworth Scientific Publications, London. 1955. pp. 196–207.
3. L. M. Dorfman and Z. D. Sheldon. J. Chem. Phys. **17**, 511 (1949).
4. K. O. Kutschke, M. H. J. Wijnen, and E. W. R. Steacie. J. Am. Chem. Soc. **74**, 714 (1952).
5. A. Shepp and K. O. Kutschke. J. Chem. Phys. **26**, 1020 (1957).
6. M. H. J. Wijnen and E. W. R. Steacie. Can. J. Chem. **29**, 1902 (1951).
7. D. G. L. James and E. W. R. Steacie. Proc. Roy. Soc. (London), A, **245**, 470 (1958).
8. M. H. J. Wijnen and E. W. R. Steacie. J. Chem. Phys. **20**, 205 (1952).
9. T. G. Majury and E. W. R. Steacie. Discussions Faraday Soc. **14**, 45 (1953).
10. D. G. L. James and E. W. R. Steacie. Proc. Roy. Soc. (London), A, **244**, 289 (1958).
11. A. F. Trotman-Dickenson, J. R. Birchard, and E. W. R. Steacie. J. Chem. Phys. **19**, 163 (1951).

Can. J. Chem. Downloaded from www.nrcresearchpress.com by 210.87.254.105 on 09/05/12
For personal use only.

Can. J. Chem. Downloaded from www.nrcresearchpress.com by 210.87.254.6 on 09/05/12
For personal use only.

DEUTERATED ORGANIC COMPOUNDS

XXII. SYNTHESIS OF SOME DEUTERATED BENZENE DERIVATIVES[1]

R. N. RENAUD, D. KOVACHIC,[2] AND L. C. LEITCH

ABSTRACT

The deamination of certain aromatic amines in deuterohypophosphorous acid with sodium or isoamyl nitrite has been used to label aromatic compounds in a specific position with deuterium. Aniline 2,3-d_2 was synthesized by this method.

Exchange with deuterium sulphate has been extended to the deuteration of nitrotoluenes, bromotoluenes, and polychlorobenzenes.

Previous communications in this series (1, 2, 3) have dealt very largely with the synthesis of deuterated aliphatic compounds. Aromatic compounds were investigated only incidentally and then interest was centered on introducing deuterium into the side chain rather than into the nucleus. In this paper the deuteration of aromatic compounds will be formally discussed.

The total replacement of hydrogen by deuterium in the aromatic series is in general effected more readily than in aliphatic compounds. Some years ago one of us (4) showed that benzene-d_6 could be conveniently prepared by exchange with deuterium oxide at 100° C in the presence of platinum black. Others (5, 6, 7) have since reported that benzene derivatives such as benzoic acid or aniline and polynuclear hydrocarbons can be deuterated as well. In contrast, alkanes undergo exchange under these conditions only when deuterium gas is also present.

The exchange with deuterium oxide catalyzed by platinum black yields compounds completely deuterated in the ring. The method is therefore inapplicable for the preparation of compounds containing deuterium in specific positions. Several methods of obtaining such compounds have, however, been investigated in the past.

In early attempts to prepare deuterated benzenes, calcium salts of aromatic acids were decarboxylated in the presence of calcium deuteroxide. Morita and Titani (8) prepared benzene-d_1 by this method from anhydrous calcium benzoate. Later, Redlich and Stricks (9) obtained benzene-1,2-d_2 from calcium phthalate and Weldon and Wilson (10) synthesized benzene-1,3,5-d_3 from the calcium salt of mesitylene carboxylic acid. Finally, Erlenmeyer carried the method to its logical conclusion by preparing benzene-d_6 from calcium mellitate (11). The reaction was later reinvestigated by Best and Wilson (12), who showed that the isotopic purity of the products was low due to exchange under the drastic conditions employed.

Another method of obtaining deuterated benzenes is the hydrolysis of Grignard reagents with deuterium oxide or deuterium chloride. However, only one atom of deuterium can usually be introduced in this way. Redlich and Stricks (13) had prepared benzene-1,2-d_2 from 1,2-diiodobenzene in this manner but later work by Best and Wilson (12) showed the dimagnesium reagent from 1,4-dibromobenzene exchanged with ether presumably by a free radical mechanism to give benzene-1,4-d_2 of low isotopic purity. They circumvented this difficulty by introducing the deuterium in two stages, i.e. by two separate Grignard preparations and hydrolyses. In any event the application of Grignard

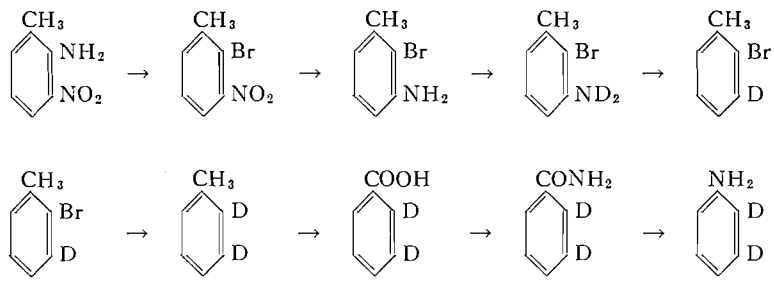
[1]*Manuscript received August 19, 1960.*
Contribution from the Division of Pure Chemistry, National Research Council, Ottawa, Canada. Presented at the 43rd Conference of the Chemical Institute of Canada, Ottawa, June, 1960.
Issued as N.R.C. No. 6046.
[2]*Terminated May, 1959.*

reagents to the problem of deuteration is severely restricted by the incompatibility of organometallic halides with several other functional groups such as nitro, carboxyl, amino, etc. Nevertheless, the Grignard synthesis is probably the best method of preparing benzene-d_1, the three deuterated toluenes, and perhaps other deuterated alkyl benzenes.

Deamination is a well-known method of replacing an amino group by hydrogen (14). It is usually carried out by heating the diazonium salt of the amine in ethanol. The mechanism of this reaction has recently been shown by deTar and Turetzky (15) to be a free radical process. It is not attractive for replacing an amino group by deuterium because ethyl alcohol labelled with deuterium on the methylene group is required. In the present work deamination in isopropyl alcohol was investigated since isopropyl-2-*d* alcohol, $CH_3CD(OH)CH_3$, is easily prepared from acetone and lithium aluminum deuteride. However, the yields obtained in the decomposition of the diazonium fluoborate in isopropyl alcohol were very poor and the method was abandoned in favor of deamination in hypophosphorous acid.

In conventional deamination with hypophosphorous acid (16) the amine is first diazotized in hydrochloric or sulphuric acid and the solution of the diazonium salt is treated with an excess of 50% hypophosphorous acid. Since preparation of diazonium salts in deuterium oxide as solvent is prohibitive on economic grounds, it was decided to deaminate some representative amines directly in 50% hypophosphorous acid solutions by addition of sodium nitrite. It was felt hypophosphorous acid would be strong enough to allow diazotization to take place. This was indeed found to be the case. Bromobenzene was obtained in 70% yield from 2-bromoaniline. A search of the literature revealed only one case of diazotization in H_3PO_2, Henry and Finnegan (17) having deaminated 5-aminotetrazole in 5% hypophosphorous acid. In the present work 2-bromo-3-methylaniline, 1-naphthylamine, and pentachloroaniline were similarly deaminated in 50% hypophosphorous acid.

The replacement of NH_2 by deuterium by the above method was an important step in a synthesis of aniline-2,3-d_2 which was required in connection with some work in N.M.R. spectroscopy (18). The most feasible route to this compound appeared to be the sequence of reactions shown below:



The preparation of the starting compound, 3-nitro-2-aminotoluene, has been reported in *Organic syntheses* (19). The amino group was replaced by bromine by a Sandmeyer reaction. The nitro group was successfully reduced to amino without simultaneous loss of bromine by reduction with activated iron powder in dioxane as described by Hazlett and Dornfeld (20). Deamination in hypophosphorous acid containing a low concentration of deuterium has been shown to be subject to a high deuterium isotope effect in favor of hydrogen (21). This meant that rigorous exclusion of exchangeable hydrogen was absolutely

Can. J. Chem. Downloaded from www.nrcresearchpress.com by 210.87.254.6 on 09/05/12
For personal use only.

Can. J. Chem. Downloaded from www.nrcresearchpress.com by 210.87.254.6 on 09/05/12
For personal use only.

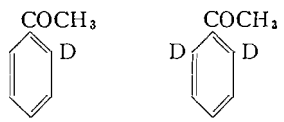
necessary to obtain a high concentration of deuterium in the product. Consequently, hypophosphorous acid was exchanged with deuterium oxide as described by Hammond and Grundemeier (22) until the hydrogen atom signal in the N.M.R. spectrum was absent. Similarly the hydrogen in the amino group of the amine was replaced by deuterium by several exchanges in slightly alkaline deuterium oxide. The 2-bromotoluene-3*d* isolated in 50% yield was 96 mole% C_7H_6BrD. The second deuterium atom was introduced via a Grignard synthesis. The deuterium content of the toluene-2,3-d_2 was 83 mole %. It was oxidized to benzoic-2,3-d_2 acid in aqueous alkaline permanganate without loss of deuterium. Aniline-2,3-d_2 was obtained from the acid via the acid chloride and the amide by the Hofmann degradation.

The benzene-1,2-d_2 prepared from the deuterated aniline by deamination analyzed 82.1% $C_6H_4D_2$ and 17.1% C_6H_5D. The slightly low content of deuterium may be due to a small loss of deuterium by exchange in each of the two reactions involving introduction of deuterium. In any event the compound was pure enough isotopically for the purpose. Deamination by means of deuterohypophosphorous acid thus offers a convenient means of replacing an amino group by deuterium in an aromatic compound. Another recent example of its use is the deamination of vicinal xylidine to 1,3-xylene-2-*d* by Fraser (23).

Yet another method of deuterating aromatic compounds is the action of deuterium chloride in the presence of anhydrous aluminum chloride. Klit and Langseth prepared benzene-d_6 by this method (24). The reaction is essentially an exchange catalyzed by the Lewis acid $DAlCl_4$. It probably cannot be used for deuterating in a specific position.

Important confirmation of an earlier prediction by Ingold, Raison, and Wilson (25) was obtained in 1936 when these authors observed a reasonably rapid exchange between benzene and 50 mole % deuterium sulphate in deuterium oxide at room temperature without any appreciable sulphonation. Several years later in continuation of their brilliant work on the spectroscopic investigation of the structure of benzene, Ingold, Wilson, and co-workers turned again to the exchange method to prepare benzene-d_6 and 1,4-dibromobenzene-d_4 (12). In deuterating bromobenzene by this method they were unable to avoid undue sulphonation. Apparently in this case the rates of sulphonation and exchange are very similar. A third deuterobenzene, the 1,3,5-d_3 isomer was prepared from aniline, in which exchange occurs under comparatively milder conditions than in benzene. It is sufficient to heat the hydrochloride in deuterium oxide for a day to establish equilibrium. Deuterium enters the ortho and para positions. After several such exchanges the deuterium in the amino group was washed out with ordinary water and the amine was deaminated to benzene-1,3,5-d_3. Since the paper by Best and Wilson (12) no appreciable use has been made of this reaction to deuterate aromatic compounds.

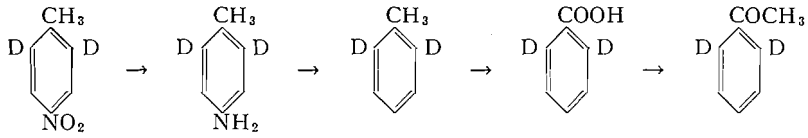
One of the aims of the present work was to extend the exchange method to a variety of substituted benzenes in order to obtain compounds of interest for infrared measurements. Two of these were acetophenone-2-*d* and acetophenone-2,6-d_2. The synthesis of 2-deuteroacetophenone was straightforward. It started with 2-bromotoluene, which was



converted to toluene-2-*d* by the Grignard reaction discussed above. The toluene-2-*d* was oxidized to benzoic-2-*d* acid without loss of the deuterium label by alkaline permanganate.

The deuterium was determined by combustion and estimation of the deuterium content of the water by infrared analysis. Acetophenone was prepared from benzoyl-2-*d* chloride and dimethyl cadmium as described by Cason (26).

For the synthesis of acetophenone-2,6-d_2 4-nitrotoluene was found to be a satisfactory starting material.



With 95% deuterium sulphate at 95° C, 4-nitrotoluene underwent exchange in the 2- and 6-positions without much sulphonation. After two exchanges the compound gave no signal in the N.M.R. corresponding to the 2,6-hydrogen atoms. The signal for the 3,5-hydrogen atoms occurs at lower field. The deuteronitrotoluene was reduced with tin and hydrochloric acid; deamination and oxidation took place with complete retention of the deuterium label. The other steps were the same as for the monodeutero compound. It is noteworthy that exchange occurs at the positions predicted by the orienting effects of the methyl and nitro substituents. It is also striking that exchange proceeds so smoothly when it is considered that toluene and nitrobenzene cannot be exchanged without considerable loss due to sulphonation. It has been found that 2- and 3-nitrotoluenes exchange readily with 95% D_2SO_4 to give 2-nitrotoluene-d_4 and 3-nitrotoluene-d_4. In these cases no selective deuteration occurs; all positions are affected by the substituents.

The bromotoluenes were next investigated. 4-Bromotoluene exchanged its ring protons readily in 95% D_2SO_4 at 80° C after 3 hours. Under these conditions 2-bromotoluene was sulphonated even at room temperature. However, 90% D_2SO_4 at room temperature brought about considerable exchange and little sulphonation in 24 hours. After three equilibrations with this acid the ring proton signals in the N.M.R. spectrum were no longer visible. 3-Bromotoluene sulphonated readily in 95% D_2SO_4 at room temperature. Exchanges with 80, 85, and 90% D_2SO_4 at room temperature were carried out without achieving any exchange. No change was apparent in the N.M.R. spectrum of the products.

In connection with a joint project with Lecomte (27) the synthesis of several polychlorodeuterobenzenes by exchange was investigated. 1,4-Dichlorobenzene was readily exchanged in 88 mole % D_2SO_4 as had been reported earlier by Best and Wilson (12) for the dibromo derivative. The more highly chlorinated benzenes such as the 1,3,5-trichloro, the 1,2,4,5-tetrachloro, and the pentachloro were expected to exchange under more drastic conditions due to the deactivating influence of the chlorine atoms. 1,3,5-Trichlorobenzene underwent exchange at 100° C but a temperature of 150° C was required to bring about exchange in the tetra- and penta-chlorobenzenes. Loss due to simultaneous sulphonation was, however, appreciable.

It appears that deuteration of ring protons follows the course to be expected from a consideration of the orienting effects of the substituents. The feasibility of exchange in any given case depends, however, upon the relative rates of sulphonation and exchange.

EXPERIMENTAL

Deamination of p-Nitrobenzenediazonium Fluoborate in Isopropyl Alcohol

p-Nitrobenzenediazonium fluoborate (4.0 g) prepared from *p*-nitroaniline as described by Starkey (28) was added to a suspension of 4.0 g of powdered anhydrous sodium acetate

Can. J. Chem. Downloaded from www.nrcresearchpress.com by 210.87.254.6 on 09/05/12
For personal use only.

in 10 ml of isopropyl alcohol. Rapid evolution of nitrogen took place and the reaction mixture turned very dark. After the mixture had been standing for an hour the alcohol was removed under vacuum and the residue was taken up in pentane. The pentane solution was then washed with water and dried over a pellet of alkali. The residue which remained after the pentane was distilled off was transferred to a Späth bulb and distilled. Yield of nitrobenzene, 0.5 g (35%).

Deamination of 2-Bromoaniline in Hypophosphorous Acid

2-Bromoaniline (6.88 g, 0.04 mole) was treated, while being stirred, in a 100-ml three-necked round-bottomed flask with 25 ml of 50% hypophosphorous acid. The solution was heated to boiling and then cooled to −5° C. Sodium nitrite (3.0 g) was added in portions to the cold solution. Nitrogen was evolved after each addition of nitrite. The reaction mixture was stirred at 0° C for 3 hours and then poured on ice in a flask equipped for steam distillation. The distillate was taken up in ether, and the solution was dried over a pellet of alkali and then freed of solvent. The residue was purified by distillation on the vacuum line. Yield, 4.8 g (78%); $n_D^{24.5}$, 1.5521.

2-Amino-3-nitrotoluene

This compound was prepared as described in reference 19 in 53% yield.

2-Bromo-3-nitrotoluene

2-Amino-3-nitrotoluene (50 g, 0.3 mole) was dissolved in 160–175 ml of 48% hydrobromic acid heated on a hot plate. The solution was cooled to room temperature while 300 ml of water was slowly added. The solution was diazotized at −12° C with 30 g of sodium nitrite dissolved in 40 ml of water and filtered. The filtrate was added in portions to a solution of cuprous bromide prepared from 60 g of copper sulphate, 24 g of copper turnings, 400 ml of water, and a solution of 60 g of potassium bromide in 270 ml of 48% hydrobromic acid. The mixture was heated for ½ hour on the steam bath and then distilled in steam. Yield, 57 g (81%).

2-Bromo-3-aminotoluene

Activated iron was prepared by mixing 240 g of iron powder and 82 ml of 48% hydrobromic acid as described in reference 20. The mixture was evaporated nearly to dryness in a vacuum evaporator at 60° C. At this stage the mass of activated iron had broken up into small balls which were removed and pulverized in a mortar. Residual moisture was removed on the vacuum line but without further shaking on a water bath at 100° C.

The reduction was carried out using 20 g of 2-bromo-3-aminotoluene as described in the reference cited above except that dioxane was used instead of benzene. The reaction mixture from the reduction was steam-distilled to remove all the dioxane after addition of 80 ml of hydrobromic acid to convert the amine to the hydrobromide. The residue was basified with 35 g of sodium hydroxide in 70 ml of water and steam distillation continued to obtain the amine. The bromotoluidine was taken up in ether in the usual way. The yield of amine recovered from a distillation in a Späth bulb at 60° C under vacuum was 65–70%; n_D^{23}, 1.6034; n_D^{20}, 1.6050.

2-Bromo-3-amino-d_2-toluene

The amine (20.5 g, 0.11 mole) was stirred vigorously at 80° C for 8 hours with 25 ml of deuterium oxide containing one pellet of alkali. The exchanged amine was separated from the water in a separatory funnel and returned to the original flask for a second exchange. Two more exchanges were considered sufficient to replace all the amino hydrogen by deuterium. There was practically no loss during these operations.

Can. J. Chem. Downloaded from www.nrcresearchpress.com by 210.87.254.6 on 09/05/12
For personal use only.

Deuterohypophosphorous Acid

Hypophosphorous acid was exchanged 10 times with deuterium oxide as described in reference 22 until the deuterium content as judged from the deuterium content of a sample of benzene-*d*, prepared by deamination of aniline-ND_2, was 95.91%.

2-Bromotoluene-3-d

To 20 g of 2-bromo-3-amino-d_2-toluene in a 250-ml round-bottomed flask with a side arm for a separatory funnel was added, while being cooled in ice water, 58 ml of 50% deuterohypophosphorous acid – deuterium oxide and finally 30 ml of additional deuterium oxide. To the mixture was added, very slowly, a solution of 8.0 g of sodium nitrite in 8 ml of deuterium oxide; during the addition, the temperature was still kept around 0° C, the mixture was stirred, and the rate of nitrogen evolution was observed. The reaction mixture was protected from moisture and kept in the refrigerator overnight. In the morning all the volatile material was distilled on the vacuum line into a Stock trap. The distillate was extracted with ether and the bromotoluene recovered in the vacuum line by distillation. Yield, 10 g (55%). Mass analysis: 93.9% C_7H_6DBr.

In a second run from 17.6 g of amine-d_2 there was obtained 9.4 g of 2-bromotoluene-3-d_1, n_D^{23} 1.5539. The boiling point was 181° C. Yield, 59%. 2-Bromotoluene has n_D^{23} 1.5540, b.p. 181° C. Mass analysis: 95.98% C_7H_6DBr, 4.0% C_7H_7Br.

Toluene-2,3-d_2

Magnesium (0.9 g) was placed in a 100-ml two-necked round-bottomed flask equipped with a separatory funnel and a reflux condenser. The apparatus was connected to a vacuum line flamed and pumped for 1 hour to remove traces of moisture. Dry air (freed of CO_2 by Ascarite) was introduced at the end. A few milliliters of ether dried over sodium wire was added to the magnesium followed by 5.7 g of 2-bromotoluene-3-*d* dissolved in 20 ml of anhydrous ether. Reaction started almost at once. After the solution was stirred for about 3 hours the ether was removed under reduced pressure. The residue was cooled in a bath of ice water and deuterium oxide (7.0 ml) was added dropwise. The toluene that was formed and ether were distilled into a Stock trap. The toluene was taken up in more ether, water was separated, and the ether solution was dried. The ether was removed on the vacuum line keeping the solution at −26° C. It was condensed in a trap cooled in dry ice and acetone at −78° C. During this operation the stopcocks are set so that a little ether distills slowly but continuously from the solution. When the pressure in the system has fallen to 1 mm the residue is virtually free of ether. Yield, 2.3 g (74%). Mass analysis:

	I	II
$C_7H_6D_2$	82.7%	80.1%
C_7H_7D	16.5%	17.8%
C_7H_8	0.6%	1.2%

Benzoic-2,3-d_2 Acid

Toluene-2,3-d_2 (4.5 g, 0.05 mole) and 400 ml of water were heated to boiling under a reflux condenser. Potassium permanganate (15.6 g, 0.1 mole) was added in portions over a period of 4 hours. After being heated under reflux for a further period of 4 hours the reaction mixture was filtered. The filtrate and washings were concentrated under reduced pressure to a volume of 50 ml. The solution was then acidified with concentrated hydrochloric acid (3.2 ml) and the white precipitate of benzoic-2,3-d_2 acid was filtered off and washed once with a little cold water. Yield, 4.3 g (73%); m.p. 123.4° C.

Can. J. Chem. Downloaded from www.nrcresearchpress.com by 210.87.254.6 on 09/05/12
For personal use only.

The use of a copper flask as described by Bigelow (29) did not lead to higher yields in test experiments.

Benzoyl-2,3-d_2 Chloride

Benzoic-2,3-d_2 acid (3.8 g, 0.03 mole) was heated under reflux with 4.6 g freshly distilled thionyl chloride for 2 hours. Hydrogen chloride and excess thionyl chloride were pumped off on the vacuum line and the residue was distilled into a Stock trap. Yield, 4.0 g (92%).

Benzamide-2,3-d_2

Benzoyl-2,3-d_2 chloride (4.0 g) was added slowly to 17.0 ml of concentrated ammonium hydroxide while the mixture was being stirred, and cooled in an ice bath. The solid was filtered and washed with cold water. Recrystallization from 17 ml of hot water gave 2.8 g of benzamide-2,3-d_2 (81%), m.p. 127–129° C.

Aniline-2,3-d_2

A solution of 4.2 g of potassium hydroxide in 50 ml of water in a 400-ml beaker was cooled to 0° C in an ice bath. Bromine (4.5 g) was added in one portion and the mixture was stirred until all the bromine had dissolved. Another solution of 6.0 g of potassium hydroxide in 10 ml of water was prepared. Finely powdered benzamide-2,3-d_2 (2.8 g, 0.02 mole) was added all at once to the potassium hypobromite, with vigorous stirring; at the same time there was added the concentrated solution of alkali prepared above. After 5 minutes all the solid had dissolved. The reaction mixture was transferred to a flask set for steam distillation and heated on the steam bath for 2 minutes. The oil which collected on the top was distilled over in a current of steam. The aniline-2,3-d_2 was taken up in ether, dried over alkali, filtered, and freed of solvent. The residue was distilled slowly into a trap in the vacuum line. Yield, 1.8 g (83%); n_D^{20}, 1.5844.

The deuterium content of the aniline was determined by deaminating it to benzene-1,2-d_2. The mass analysis of the latter was 82.1% $C_6H_4D_2$, 17.1% C_6H_5D, and 0.8% C_6H_6.

Deuterium Sulphate

Deuterium sulphate for exchange reactions was prepared by the modification described below of the procedure of Best and Wilson (12).

To a condenser with ground-glass joints set for downward distillation were connected a 1-liter Claisen flask and a receiver with a side arm to which was attached a drying tube filled with glass wool and phosphorus pentoxide. The other end of the drying tube was connected by means of rubber tubing to a filter flask with a controllable leak. No lubricant was used on any of the joints but they were covered with paraffin wax on the outside.

Stabilized sulphur trioxide (300 ml) purchased from Allied Chemical of Canada, Montreal, Quebec, under the name of "Sulfan B" was poured into the distilling flask and 100 g of 99.7% deuterium oxide was weighed into the tared receiver cooled in crushed ice. When the distilling flask was gently heated and slight suction from a glass aspirator pump was applied, sulphur trioxide distilled slowly into the water.

At the end of the distillation an aliquot of deuterium sulphate was removed and analyzed by titration against $N/10$ alkali. The concentration of deuterium sulphate was then adjusted as required by addition of the appropriate amount of deuterium oxide.

4-Nitrotoluene-2,6-d_2

A solution of 7.0 g (0.06 mole) of 4-nitrotoluene in 25 g of 94.81% deuterium sulphate was heated at 90° C for 24 hours. The reaction mixture was cooled, and poured onto

Can. J. Chem. Downloaded from www.nrcresearchpress.com by 210.87.254.6 on 09/05/12
For personal use only.

cracked ice. The oil was extracted with ether. The ether solution was washed with water, dried over calcium chloride, and freed of solvent. The exchanged 4-nitrotoluene (5.6 g) was equilibrated twice more with fresh quantities of deuterium sulphate.

The course of the exchange was followed by examining the N.M.R. spectrum of the compound. The normal compound shows two doublets spaced 25 c.p.s. apart and 200 c.p.s. lower than the methyl signal. In the exchanged compound the doublet at higher field and therefore corresponding to the 2,6-hydrogen atoms disappeared. The spectrum was essentially unchanged after the third exchange.

4-Nitrobenzoic-2,6-d_2 Acid

4-Nitrotoluene-2,6-d_2 (19.0 g, 0.015 mole) was oxidized with potassium permanganate as described by Bigelow (29) in a Pyrex rather than a copper flask. The yield of 4-nitrobenzoic-2,6-d_2 acid was 17.2 g (78%).

4-Aminobenzoic-2,6-d_2 Acid

The 4-nitro acid was reduced with tin and hydrochloric acid as described by Vogel (30). The yield was 71% of product, m.p. 186–186.5° C.

Benzoic-2,6-d_2 Acid

The amino acid was diazotized and deaminated as described by Kornblum (16). The yield from 10 g of amino acid was 4.9 g (55%), m.p. 121.5–122.0° C. Analysis by combustion gave a deuterium content of 1.96 atoms. All the reactions were therefore carried out without any appreciable loss of deuterium.

Benzoyl-2,6-d_2 Chloride

The chloride was prepared from thionyl chloride as described above for benzoic-2,3-d_2 acid.

Acetophenone-2,6-d_2

The acid chloride was converted into acetophenone exactly as described by Cason (26). The yield was 78% of product, n_D^{25} 1.5296, m.p. 17.5° C. For normal acetophenone, n_D^{25} is 1.5307.

3-Nitrotoluene-d_4

3-Nitrotoluene (6.0 g) was heated with 25 g of 97.3% deuterium sulphate for 24 hours at 75–80° C. The product was worked up as already described for the 4-nitro isomer. Recovery was 91%. Loss due to simultaneous sulphonation is therefore slight. After three exchanges there was no signal observed in the N.M.R. spectrum where the ring hydrogens occur in the light compound.

2-Nitrotoluene-d_4

Nuclear proton exchange was carried out under the same conditions as for the other two isomers. The N.M.R. spectrum indicated that exchange occurred in all positions as expected though more slowly than in the other isomers.

4-Bromotoluene-d_4

A mixture of 7.0 g of 4-bromotoluene (.04 mole) and 25 ml of 95.7% deuterium sulphate was stirred for 24 hours at room temperature. The exchanged 4-bromotoluene was isolated from the reaction mixture as described above. After two more exchanges the ring proton signals in the N.M.R. spectrum had disappeared while the signals due to the protons in the methyl group had their original intensity. All ring protons therefore exchange under these conditions. At 80° C the 4-bromotoluene was almost completely sulphonated after only 3 hours.

Can. J. Chem. Downloaded from www.nrcresearchpress.com by 210.87.254.6 on 09/05/12
For personal use only.

Non-exchange of 3-Bromotoluene

In 95.5% deuterium sulphate 3-bromotoluene is almost completely sulphonated after 3 hours at room temperature. Deuterium sulphate diluted with deuterium oxide to 80% acid did not sulphonate 3-bromotoluene at room temperature after 60 hours stirring but there was no change in the N.M.R. spectrum. Evidently no exchange had occurred. At room temperature 85% deuterium sulphate gave about 20% sulphonated product but again there was no evidence of exchange in the recovered 3-bromotoluene. In 90% deuterium sulphate at room temperature the amount of sulphonated product increased but there was still no evidence of exchange as judged from the N.M.R. spectrum. Apparently the rate of sulphonation in 3-bromotoluene is much more rapid than that of exchange.

2-Bromotoluene-d_4

The optimum condition for exchange was to stir 2-bromotoluene at room temperature with 90% deuterium sulphate for 24 hours. More concentrated acid or higher temperature both led to extensive sulphonation. After three exchanges the signal for the ring protons had completely disappeared from the N.M.R. spectrum while the methyl proton signal retained its original intensity.

Non-exchange in 1,2-Dimethyl-4-nitrobenzene

In 97% deuterium sulphate the compound gave only tar. In a second attempt to bring about proton exchange the compound was stirred at room temperature in 85% deuterium sulphate. At this concentration of acid there was 40% loss due to sulphonation but no change in the N.M.R. spectrum of the recovered nitro compound.

2-Chloronitrobenzene-3,5-d_2

2-Chloronitrobenzene (5.5 g) was heated at 70° C in 30 g of 95% deuterium sulphate for 30 hours. The product was isolated in the usual manner. There was hardly any loss due to sulphonation. After a second exchange the N.M.R. spectrum of the compound was measured. Some of the signals for the ring protons were considerably reduced. From a consideration of the orienting effects of the chlorine and nitro groups it would appear that deuteration occurred in the 3- and 5-positions.

p-Dichlorobenzene-d_4

p-Dichlorobenzene (5.0 g) was heated with 45 g of 95% deuterium sulphate at 105° C with stirring for 6 hours. The cold reaction mixture was poured onto cracked ice and the 1,4-dichlorobenzene was filtered off and washed with water. The product obtained after two more exchanges was recrystallized from ethyl alcohol. Yield, 2.5 g (50%); m.p. 54.5° C. The N.M.R. spectrum measured in cyclohexane gave no signal for benzene ring protons.

1,3,5-Trichlorobenzene-d_3

The conditions were essentially those employed to exchange the dichlorobenzene. Two exchanges were sufficient to cause the disappearance of the ring proton signal in the N.M.R. spectrum. The loss due to simultaneous sulphonation was again 50%.

1,2,4,5-Tetrachlorobenzene-d_2

1,2,4,5-Tetrachlorobenzene (5.0 g) and 45 g of 97% deuterium sulphate were heated for 12 hours in a sealed tube at 150° C. The exchanged product was isolated as described for 1,4-dichlorobenzene-d_4 above. After three exchanges 3.2 g of the tetrachloro compound were recovered. It was recrystallized from benzene, m.p. 141.5–142° C. The signal due to the ring protons in the N.M.R. spectrum had completely disappeared.

Can. J. Chem. Downloaded from www.nrcresearchpress.com by 210.87.254.6 on 09/05/12
For personal use only.

Pentachlorobenzene

Pentachloronitrobenzene was reduced to pentachloroaniline in dioxane solution with activated iron and water as described above. An excellent yield of pentachloroaniline, m.p. 243–244° C, was obtained.

Pentachloroaniline was deaminated in 50% hypophosphorous acid in the presence of dioxane using isoamyl nitrite as the source of nitrous acid. One gram of the amine was dissolved in 15 ml of dioxane and 15 ml of 50% hypophosphorous acid. The stirred suspension was treated with 2 ml of isoamyl nitrite at room temperature. Nitrogen was slowly evolved for about 2 hours. The reaction mixture was poured into water and the solid filtered off. Recrystallization from ethyl alcohol gave 0.3 g of pentachlorobenzene, m.p. 84° C. The product was also purified by sublimation *in vacuo* from a bath at 70° C.

Pentachlorobenzene-d

The exchange was carried out with 97% deuterium sulphate as described for tetrachlorobenzene. Evidence of exchange having taken place was obtained from both N.M.R. and infrared spectra. The treatment with acid seemed to remove a small amount of impurity as the melting point of the exchanged product was raised to 86.5° C.

The compound was also prepared by deamination of pentachloroaniline in 50% deuterohypophosphorous acid but the pentachlorobenzene-*d* contained some of the normal compound (which probably arose from H in the amino group) and had to be enriched in deuterium by exchange with deuterium sulphate just the same.

ACKNOWLEDGMENTS

The authors wish to thank Mrs. R. H. Riem for several mass analyses, Mrs. M. A. Mackenzie for an analysis by combustion, and Mr. J. R. Nicholson for some N.M.R. spectra.

Thanks are also due to the Olin-Mathieson Chemical Corporation, Baltimore, Maryland, for the gift of a sample of pentachloronitrobenzene.

REFERENCES

1. M. E. Isabelle and L. C. Leitch. Can. J. Chem. **36**, 440 (1958).
2. A. T. Morse, T. F. Massiah, and L. C. Leitch. Can. J. Chem. **37**, 1 (1959).
3. A. T. Morse and L. C. Leitch. J. Org. Chem. **23**, 990 (1958).
4. L. C. Leitch. Can. J. Chem. **32**, 813 (1954).
5. W. G. Brown and J. L. Garnet. J. Am. Chem. Soc. **80**, 5272 (1958).
6. A. T. Morse. Unpublished work.
7. L. Pichat. Unpublished work.
8. N. Morita and T. Titani. Bull. Chem. Soc. Japan, **10**, 557 (1935).
9. O. Redlich and W. Stricks. Monatsh. Chem. **67**, 213 (1936); **68**, 374 (1937).
10. L. H. P. Weldon and C. L. Wilson. J. Chem. Soc. 244 (1946).
11. H. Erlenmeyer and H. Lobeck. Helv. Chim. Acta, **18**, 1464.
12. A. P. Best and C. L. Wilson. J. Chem. Soc. 235 (1946).
13. O. Redlich and W. Stricks. Monatsh. Chem. **68**, 47 (1936).
14. N. Kornblum. *In* Org. Reactions. Vol. II. Chap. 7, p. 262.
15. D. F. deTar and M. N. Turetzky. J. Am. Chem. Soc. **77**, 1746 (1955).
16. N. Kornblum. *In* Org. Syntheses Coll. Vol. III. p. 295.
17. R. A. Henry and W. G. Finnegan. J. Am. Chem. Soc. **76**, 290 (1954).
18. W. G. Schneider. Unpublished work.
19. J. C. Howard. Org. Syntheses, **35**, 3 (1955).
20. S. E. Hazlet and C. A. Dornfeld. J. Am. Chem. Soc. **66**, 1781 (1944).
21. E. R. Alexander and R. E. Burge. J. Am. Chem. Soc. **72**, 3100 (1950).
22. G. S. Hammond and W. Grundemeier. J. Am. Chem. Soc. **77**, 2445 (1955).
23. R. Fraser. Can. J. Chem. **38**, 2226 (1960).
24. A. Klit and A. Langseth. Z. physik. Chem. (Leipzig), A, **176**, 65 (1936).
25. C. K. Ingold, C. G. Raison, and C. L. Wilson. Nature, **134**, 734 (1934).
26 J. Cason. J. Am. Chem. Soc. **68**, 2078 (1946).
27. S. Saeki and L. C. Leitch. Compt. rend. **249**, 2307 (1959).
28. E. B. Starkey. *In* Org. Syntheses Coll. Vol. II. p. 225. 1944.
29. L. A. Bigelow. J. Am. Chem. Soc. **41**, 1559 (1919).
30. A. I. Vogel. Practical organic chemistry. 3rd ed. Longmans Green. 1956. Chap. IV, p. 562.

Can. J. Chem. Downloaded from www.nrcresearchpress.com by 210.87.254.6 on 09/05/12
For personal use only.

Can. J. Chem. Downloaded from www.nrcresearchpress.com by 210.87.254.105 on 09/05/12
For personal use only.

THE DONOR CHARACTERISTICS OF THE CARBONYL GROUP

II. THE EFFECT OF ANGULAR VARIATIONS AT THE CARBONYL GROUP[1]

DENYS COOK

ABSTRACT

The effect of variations in the angle X—C—X′ (in a typical carbonyl compound XX′C=O) on the carbonyl stretching frequency ($\nu_{C=O}$) is examined in the light of recently published empirical relations between $\nu_{C=O}$ and the ionization potential.

INTRODUCTION

In a recent paper dealing with the donor characteristics of the carbonyl group (1) empirical relationships were demonstrated between the carbonyl stretching frequency ($\nu_{C=O}$) and the ionization potential (IP). Two classes of compounds were noted: those having no group conjugated with the carbonyl group (A), and those with a group capable of such conjugation (B). The parameters of those molecules were expressed, respectively, by the equations

$$\nu_{C=O} = 49.35\ IP + 1249, \qquad [1a]$$

$$\nu_{C=O} = 29.20\ IP + 1409. \qquad [1b]$$

The variation of these parameters within each class was interpreted in terms of inductive and resonance effects due to the different groups attached to the carbonyl group.

The variation of IP with the carbonyl force constant $k_{C=O}$ was considered many years ago by Walsh (2). He pointed out the relationship between IP, $k_{C=O}$, and C=O bond length and a parameter defining the percentage of polarity of the C=O bond. Since that time many more IP's have been accurately measured though the number of determinations of force constants of C=O bonds is still relatively small.

Previously (1) no allowance was made for the effect of variations in angle XCX′ (α) (in the compound ) on $\nu_{C=O}$. This will now be considered.

VARIATION OF $\nu_{C=O}$ WITH α

The fact that $\nu_{C=O}$ increases on decreasing the size of a cycloalkanone ring has been known for some time (3). The phenomenon is not restricted to simple cyclic ketones, for similar compounds with heteroatoms in the ring show the same effect.

Figure 1 shows a graph of $\nu_{C=O}$ and α for a wide variety of cyclic carbonyl compounds, the data and source being listed in Table I. Points lying on the same curve in Fig. 1 are for compounds containing the same functional group, with different ring sizes depending on the number of —CH_2— groups contained therein. These lines do not have quite the same slope but get steeper from the bottom line to the top in a fairly smooth manner.

[1]*Manuscript received April 4, 1960.*
Contribution No. 27 from the Exploratory Research Laboratory, Dow Chemical of Canada, Limited, Sarnia, Ontario, Canada.

TABLE I

Compound	α(degrees)[a]	$\nu_{C=O}$(cm^{-1})	Solvent
1. δ-Valerolactone	120	1748[d]	CCl_4
2. γ-Butyrolactone	108	1783[d]	CCl_4
3. β-Propiolactone	94[b]	1841[d]	CCl_4
4. 5,6-Dihydro-α-pyrone	120	1743[e]	CCl_4
5. $\Delta^{\alpha\beta}$ Butenolide	108	1785[e]	CCl_4
6. 2-Tetralone	120	1717[f]	(Raman)
7. 2-Indanone	108	1751[f]	(Raman)
8. Cyclohexanone	117[c]	1716[g]	CCl_4
9. Cyclopentanone	108	1751[h]	CCl_4
10. Cyclobutanone	94	1784[i]	?
11. 1-Tetralone	120	1695[h]	CCl_4
12. 1-Indanone	108	1723[j]	CCl_4
13. Cyclohexenone	120	1686[k]	CCl_4
14. Cyclopentenone	108	1716[l]	?
15. 2-Piperidone	120	1671[h]	CCl_4
16. 2-Pyrrolidone	108	1700[h]	CCl_4

[a]Structural investigations have been made on only a few of the compounds in this table. For those without reference, reasonable estimates of α have been made depending on the size of the ring, and on the known structure of similar compounds. This results in 120° for six-membered rings, 108° for five-membered rings, and 94° for four-membered rings. Minor discrepancies in these angles will slightly affect the slope of the lines in Fig. 1, but will not alter the conclusions.

[b]J. Bregman and S. H. Bauer. J. Am. Chem. Soc. **77**, 1955 (1955).

[c]C. Romers. Rec. trav. chim. **75**, 956 (1956).

[d]S. Searles, M. Tamres, and G. M. Barrow. J. Am. Chem. Soc. **75**, 71 (1953).

[e]R. N. Jones, C. L. Angell, T. Ito, and R. J. D. Smith. Can. J. Chem. **37**, 2007 (1959).

[f]D. Biquard. Bull. soc. chim. France, **8**, 55 (1941).

[g]See reference 1.

[h]Measured in this laboratory.

[i]See reference 3. It is assumed that this band is for the pure liquid as these authors do not mention any solvent.

[j]W. M. Schubert and W. A. Sweeney. J. Am. Chem. Soc. **77**, 4172 (1955).

[k]From the files of the Spectroscopy Laboratory, Dow Chemical Company, Midland, Michigan, U.S.A.

[l]R. N. Jones and C. Sandorfy. Chemical applications of spectroscopy. *In* Techniques of organic chemistry. Vol. IX. Interscience Publishers, Inc., New York. 1956. p. 484.

They all intersect fairly closely at one point, and a general equation has been developed which fits these lines quite closely. It has the form

$$[2] \qquad \nu_{C=O}^{120} = \frac{96(\nu_{C=O}-1439)}{(216-\alpha)}+1439$$

where α is in degrees and ν is in reciprocal centimeters. This equation then represents the variation of $\nu_{C=O}$ with α and should be valid whatever the nature of the group attached to the carbonyl group, for example $-CH_2-$, $-O-$, $-\overset{|}{N}-$, $-CH=CH-$, etc. These groups, because of differences in inductive capacity, or ability to conjugate with the carbonyl group alter the vertical displacement in Fig. 1.

An equation similar to [2] was recently derived by Halford (4), who showed how the secular determinant could be solved to define the dependence of $\nu_{C=O}$ on α. Over the range $\alpha = 80°$ to $\alpha = 130°$ the relation was virtually linear and was described by the equation

$$[3] \qquad \nu_{C=O} = 1278 + 68k_{C=O} - 2.2\alpha$$

Can. J. Chem. Downloaded from www.nrcresearchpress.com by 210.87.254.105 on 09/05/12
For personal use only.

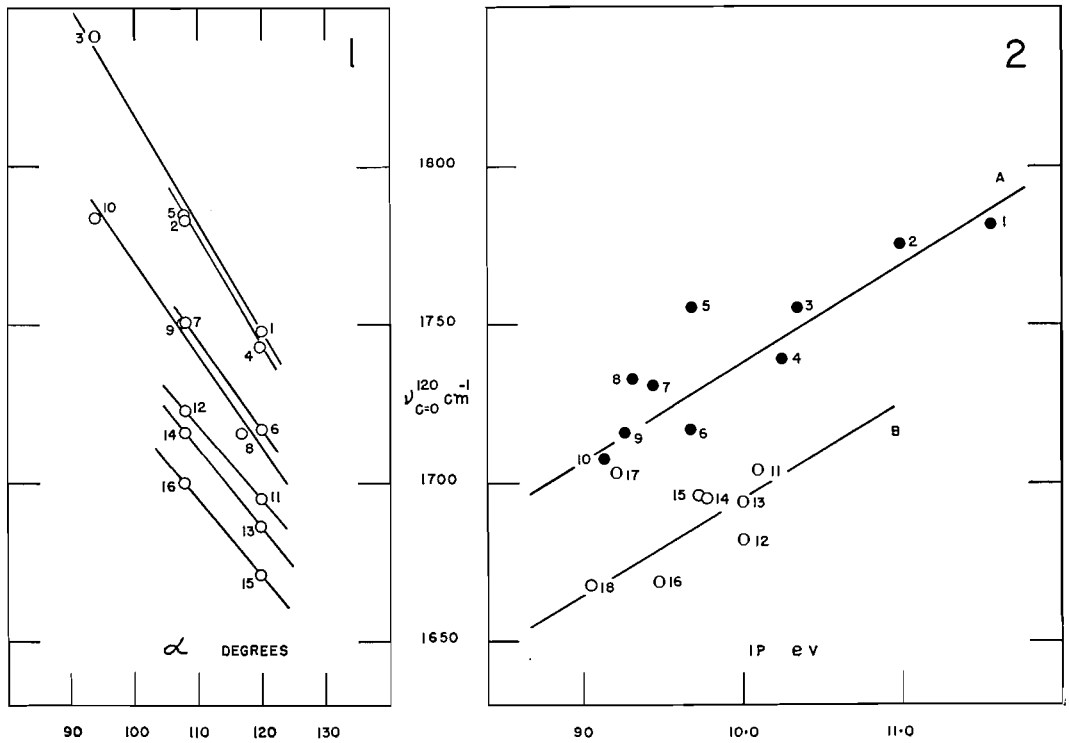


FIG. 1. Variation of $\nu^{120}_{C=O}$ with α for compounds listed in Table I.
FIG. 2. Variation of $\nu^{120}_{C=O}$ with IP for compounds listed in Table II.

where $k_{C=O}$ is the force constant of the carbonyl group in practical units. This equation rests on the assumptions that the masses X and X′ and the force constants of the C—X′ bonds are fixed.

The effect of altering α then seems to have a large effect on the value of $\nu_{C=O}$, but as Halford's results also show, little effect on $k_{C=O}$. What is applicable to ring compounds as just described should apply with no loss of validity to non-cyclic carbonyl compounds. In such compounds where $\alpha \neq 120°$ because of the dependence of $\nu_{C=O}$ on α, $\nu_{C=O}$ may be altered even though $k_{C=O}$ and therefore the IP and the carbon–oxygen bond distance do not alter greatly. Such alteration in $\nu_{C=O}$ would obscure the relationship between $\nu_{C=O}$ and IP as shown in reference 1. It is interesting therefore to adjust, by means of equation [2] the value of $\nu_{C=O}$ to what it would be if α were 120°. Such adjusted values are listed under the heading $\nu^{120}_{C=O}$ in Table II for many compounds where α is accurately known. The adjusted values are shown plotted against IP in Fig. 2.*

**Aldehydes have been excluded from this correlation. When the mass of a group attached to the carbonyl group is less than about 15 Halford (4) has shown that $\nu_{C=O}$ then becomes mass dependent and the phase relationships of vibrations of the carbonyl group may be altered. Aldehydes, therefore, represent an extreme case, where atypical carbonyl values may be expected. For the same reason formamides and formates have been excluded. The well-known anomaly of formates having lower frequencies than acetates, when the reverse would be expected, exemplifies this point.*

Can. J. Chem. Downloaded from www.nrcresearchpress.com by 210.87.254.105 on 09/05/12
For personal use only.

TABLE II

Compound	$\nu_{C=O}$(cm^{-1})	α(degrees)[a]	$\nu_{C=O}^{120}$(eq. 2)	IP(ev)
(A) Unconjugated molecules				
1. $COCl_2$	1813[b]	111[f]	1781	11.57[u]
2. $CHCl_2COCl$	1810[b]	110[g]	1775	11.00[v]
3. CH_3COOH	1768[b]	116[h]	1755	10.35[t]
4. CH_3COOCH_3	1751[b]	116[i]	1739	10.26[t]
5. β-Propiolactone	1841[c]	94[j]	1755	9.70[t]
6. CH_3COCH_3	1717[b]	120[k]	1717	9.69[t]
7. $CH_3COC_2H_5$	1722[b]	123[l]	1731	9.54[t]
8. $C_2H_5COC_2H_5$	1724[d]	123[l]	1733	9.32[t]
9. Cyclopentanone	1751[d]	(108)[m]	1716	9.27[t]
10. Cyclohexanone	1716[b]	117[n]	1708	9.14[t]
(B) Conjugated molecules				
11. CH_2CHCHO	1704[b]	(120)[o]	1704	10.10[t]
12. $CH_3CONHCH_3$	1700[b]	113[p]	1682	10.01[w]
13. CH_3COSH	1721[d]	110[q]	1694	10.01[t]
14. CH_3CONH_2	1714[b]	113[p]	1695	9.78[w]
15. $CH_3CHCHCHO$	1696[b]	(120)[o]	1696	9.73[t]
16. Tropone	1647[e]	129[r]	1669	9.48[w]
17. $CH_3COCOCH_3$	1717[b]	115[s]	1703	9.21[t]
18. $(CH_3)_2CCHCOCH_3$	1697[b]	(108)[m]	1668	9.05[t]

[a]It is preferable to use values of α from structural studies in the gas phase, i.e. electron diffraction or microwave techniques. The angles in crystals may conceivably be constrained due to lattice forces.
[b]See reference 1.
[c]See Table I, reference *d*.
[d]Measured in this laboratory.
[e]See reference 10.
[f]G. W. Robinson. J. Chem. Phys. **21**, 1741 (1953).
[g]See S. Mizushima *et al.* Spectrochim. Acta, **13**, 161 (1958).
[h]R. E. Jones and D. H. Templeton. Acta Cryst. **11**, 484 (1958).
[i]J. M. O'Gorman, W. Shand, and V. Schomaker. J. Am. Chem. Soc. **72**, 4222 (1950).
[j]See Table I, reference *b*.
[k]P. W. Allen, H. J. M. Bowen, L. E. Sutton, and O. Bastiansen. Trans. Faraday Soc. **48**, 951 (1952).
[l]C. Romers and J. E. G. Creutzberg. Rec. trav. chim. **75**, 331 (1956).
[m]Assumed, see text.
[n]See Table I, reference *c*.
[o]H. Mackle and L. E. Sutton. Trans. Faraday Soc. **47**, 691 (1951).
[p]M. Kimura and M. Aoki. Bull. Chem. Soc. Japan, **26**, 429 (1952).
[q]W. Gordy. J. Chem. Phys. **14**, 560 (1946).
[r]K. Kimura. Bull. Chem. Soc. Japan, **31**, 1051 (1958).
[s]J. E. LuValle and V. Schomaker. J. Am. Chem. Soc. **61**, 3520 (1939).
[t]K. Watanabe. J. Chem. Phys. **26**, 542 (1957), and private communication. IP under this reference are photo-ionization data. All others are electron impact data, and have been arbitrarily reduced by 0.2 ev.
[u]J. D. Morrison and A. J. C. Nicholson. J. Chem. Phys. **20**, 1021 (1952).
[v]W. C. Steele. Private communication.
[w]K. Higasi, I. Omura, and H. Baba. Nature, **178**, 652 (1956).

DISCUSSION

With a few exceptions the points in Fig. 2 define two straight lines separated by more than the experimental error. The upper line, curve A, is for non-conjugated compounds, the lower, curve B, for compounds with a conjugated carbonyl group. This behavior was noted in reference 1 but by taking into account angular variations the significant difference emerges that the lines in Fig. 2 are nearly parallel, being defined by the equations (derived by the method of least squares):

$$\nu_{C=O}^{120} = 30.57\ \text{IP} + 1432,$$

$$\nu_{C=O}^{120} = 30.07\ \text{IP} + 1394.$$

Can. J. Chem. Downloaded from www.nrcresearchpress.com by 210.87.254.105 on 09/05/12
For personal use only.

Adjusting these equations so that they have the same slope leads to

$$[4a] \qquad \nu^{120}_{C=O} = 30.50\ IP + 1433,$$

$$[4b] \qquad \nu^{120}_{C=O} = 30.50\ IP + 1390.$$

In the previous treatment (1) curves A and B converged at low $\nu_{C=O}$ values. The present case seems to be more satisfactory since it means that conjugation has approximately the same effect on the carbonyl frequency in all cases. The difference between the two lines at constant IP is about 43 cm^{-1}. This is a little larger than the difference in $\nu_{C=O}$ between non-conjugated and conjugated compounds, i.e. ~35 cm^{-1} (5), but a simple explanation is possible.

Consider the compounds in Table III, differing only in having a single or a double bond

TABLE III[a]

Compound	$\nu_{C=O}$	IP	$\Delta\nu_{C=O}$	ΔIP
$CH_3COCH_2CH_3$	1722	9.54	33	−0.17
$CH_3COCHCH_2$	1689	9.71		
$HCOCH_2CH_3$	1738	9.86	34	−0.24
$HCOCHCH_2$	1704	10.10		
$HOOCCH_2CH_3$	1758	10.27	37	−0.43
$HOOCCHCH_2$	1721	10.70		
$HCOCH_2CH_2CH_3$	1729	9.81	33	+0.08
$HCOCHCHCH_3$	1696	9.73		
		Average	34	−0.19

[a]Data from reference 1.

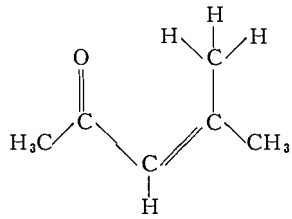
in the α position to the carbonyl group. The change from non-conjugated to conjugated compound decreases $\nu_{C=O}$ by 34 cm^{-1} but the IP increases by 0.19 ev. From equation [4] 0.19 ev corresponds to 6 cm^{-1}. The 35 cm^{-1} difference is therefore made up of two quantities of opposite sign, of approximate magnitudes 43 cm^{-1} and 6 cm^{-1}.

The conjugated molecules that have been considered here all have atomic skeletons that are planar so that there is no steric resistance to conjugation which would obscure the relation between IP and $\nu_{C=O}$. One compound which illustrates this point is benzophenone. By analogy with the known structure of substituted benzophenones, for example, 4,4′-dichlorobenzophenone (6) and 4,4′-dimethoxybenzophenone (7), in which the phenyl rings are about 38° out of the $\rangle C{=}O$ plane, there will be inhibited conjugation between the C=O group and the ring. For benzophenone $\nu_{C=O}$ = 1668 cm^{-1}. Assuming α = 125°, then $\nu^{120}_{C=O}$ = 1681 cm^{-1}. The IP is 9.00 ev and according to the equations [4*a*] and [4*b*] would require $\nu^{120}_{C=O}$ to be 1665 and 1708 cm^{-1} respectively. The actual value of $\nu^{120}_{C=O}$ lies in between these two values but nearer the conjugated value (curve B).

Two further molecules can be considered in detail, since they exemplify the arguments put forward here. The first is mesityl oxide, which when previously considered (1) did not lie on the appropriate curve B for a conjugated ketone, but was very close to curve A for non-conjugated compounds. Steric strain due to bulky methyl groups was invoked to account for the non-coplanarity of the double bonds and the consequent belief that

Can. J. Chem. Downloaded from www.nrcresearchpress.com by 210.87.254.105 on 09/05/12
For personal use only.

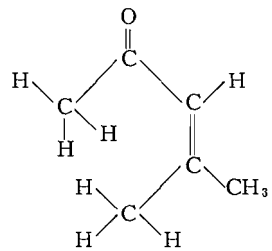
the compound was properly placed on curve A. A more plausible explanation is now possible. The suggested model is planar and in the cis configuration I. This is in keeping with enhanced intensity of the C=C vibration at 1624 cm^{-1} (8) and dipole moment studies (9). The interference between the methyl group and the carbonyl oxygen is relieved



I

by decreasing (α) thus bending the carbonyl oxygen away from the methyl group. From a study of molecular models (Stuart-Briegleb) a decrease in α of about 12° would give ample clearance. Applying equation [2] again, $\Delta\nu$ would be 31 cm^{-1}. The effect of the change in angle then is to increase $\nu_{C=O}$ by 31 cm^{-1}. $\nu^{120}_{C=O}$ is therefore 1668 cm^{-1} and taking IP = 9.05 ev Fig. 2 shows that the point lies very close to curve B for conjugated molecules.

It is interesting to apply similar reasoning to the trans structure II. In this case the



II

interference is between the methyl groups. To relieve this situation α would have to increase and the value of $\nu_{C=O}$ would be lower than that corresponding to α = 120. In applying the correction therefore $\nu^{120}_{C=O}$ would be greater than 1697 cm^{-1}, and the point for mesityl oxide would be further from the curve than before.

The second molecule is tropone. Its carbonyl frequency is 1642 cm^{-1} (10). This value must be adjusted since it is for the pure liquid, which is well known to be invariably lower than that for a dilute solution in an inert solvent like CCl_4. The gas phase value is 1652 cm^{-1} (11). If a value of $\nu_{C=O}$ = 1647 cm^{-1} is assumed then $\nu^{120}_{C=O}$ now comes to 1669 cm^{-1}. Figure 2 shows how much more closely tropone approaches curve B than the unadjusted value.

The origin of the angle-dependent frequency shift has been made clear in some recent work by Overend and Scherer (12). After calculating the force constants of C=O bonds in carbonyl halides the surprising result was established that $k_{C=O}$ for COF_2 was little different from that of $COCl_2$, 12.85 and 12.61 md/Å respectively, while there was a difference of 101 cm^{-1} in $\nu_{C=O}$. On calculation of the relative displacement of the atoms in the normal vibrations of the carbonyl halides these authors found that as the C=O

Can. J. Chem. Downloaded from www.nrcresearchpress.com by 210.87.254.105 on 09/05/12
For personal use only.

bond stretched the carbon atom moved back into the two fluorine atoms. The C—F bonds were therefore compressed and the FCF angle increased. For COF_2 where k_{C-F} = 4.5 md/Å the resistance to these motions results in the greater frequency for COF_2 compared with $COCl_2$, where k_{C-Cl} = 2.0 md/Å.

Carbon–carbon single bonds have force constants of the order of 4 md/Å, quite comparable to the C—F bond. The C—O force constant is of similar magnitude. Consequently in the compounds discussed in this paper there will be an appreciable effect similar to that in the carbonyl halides. Moreover, it will be obvious that as the angle XCX′ decreases this effect will get larger since the movement of the C atom during a carbonyl stretching vibration will be more nearly along the line of the C—X atom.

A similar conclusion was reached by Bratŏz and Besaïnou (13). These authors started with a frequency value for an isolated carbonyl group then added increments depending on the type of group attached to the C=O group. The largest contributions arose from mechanical interaction between the carbon or oxygen atom next to the carbonyl group. This was shown to get larger as α became smaller, as has been shown above too.

No three-membered cyclic saturated ketone is known, unfortunately, so that it has not been possible to see, whether there is any point at which equation [2] breaks down. It has been shown that for propiolactone, the smallest ring compound for which both the IP and $\nu_{C=O}$ are known, a great improvement is achieved by use of equation [2] but that it is far from being a good correlation.* While no direct test of a three-membered cyclic ketone is possible due to lack of data, some approximations can be calculated for a substituted cyclopropenone recently synthesized. This is 2,3-diphenylcyclopropenone whose carbonyl frequency is 1852 cm^{-1} (14). Allowing about 40 cm^{-1} for the effect of conjugation and unsaturation the hypothetical cyclopropanone might have a frequency of 1892 cm^{-1}. Assuming α = 60°, $\nu^{120}_{C=O}$ is 1718 cm^{-1} in quite good agreement with saturated aliphatic ketones.

CONCLUSIONS

The present work goes some way toward an understanding of the large variations in carbonyl frequencies. From the results presented, however, it is apparent that there remain some unsatisfactory anomalies. Until, however, accurate force constants for a large number of molecules have been worked out, involving prodigious labor, methods such as the present one offer some hope of reducing the problem.

ACKNOWLEDGMENTS

I am grateful to Dr. J. Overend and Dr. J. R. Scherer for allowing me to see their paper before publication.

REFERENCES

1. D. Cook. J. Am. Chem. Soc. **80**, 49 (1958).
2. A. D. Walsh. Trans. Faraday Soc. **43**, 158 (1947).
3. S. L. Fries and P. E. Frankenberg. J. Am. Chem. Soc. **74**, 2679 (1952).
4. J. O. Halford. J. Chem. Phys. **24**, 830 (1956).
5. W. Brugel. Einführung in die Ultrarotspektroscopie. Steinkopf, Darmstadt. 1957. p. 325.
6. J. Toussaint. Bull. Soc. Sci. Liege, **17**, 10 (1948).
7. I. L. Karle, H. Hauptman, J. Karle, and A. B. Wing. Acta Cryst. **10**, 481 (1957).

**It is assumed that the IP is a measure of the energy required to remove an electron from one of the carbonyl oxygen lone pair orbitals.*

Can. J. Chem. Downloaded from www.nrcresearchpress.com by 210.87.254.105 on 09/05/12
For personal use only.

8. R. MECKE and K. NOACK. Spectrochim. Acta, **12**, 391 (1958).
9. J. B. BENTLEY, K. B. EVERARD, R. J. B. MARSDEN, and L. E. SUTTON. J. Chem. Soc. 3957 (1949).
10. W. VON E. DOERING and F. L. DETERT. J. Am. Chem. Soc. **73**, 876 (1951).
11. J. KINUMAKI, K. AIDA, and Y. IKEGAMI. Sci. Repts. Research Insts., Tohoku Univ. Ser. A, **8**, 263 (1956). Chem. Abstr. **51**, 2400 (1959).
12. J. OVEREND and J. R. SCHERER. J. Chem. Phys. **32**, 1296 (1960).
13. S. BRATOŽ and S. BESNAINOU. J. chim. phys. **56**, 555 (1959).
14. R. BRESLAU, R. HAYNIE, and J. MURVA. J. Am. Chem. Soc. **81**, 247 (1959).

Can. J. Chem. Downloaded from www.nrcresearchpress.com by 210.87.254.105 on 09/05/12
For personal use only.

Can. J. Chem. Downloaded from www.nrcresearchpress.com by 210.87.254.40 on 09/05/12
For personal use only.

A PROTON MAGNETIC RESONANCE INVESTIGATION OF ROTATIONAL ISOMERISM IN 1,1,2,2-TETRACHLORO-1-FLUOROETHANE[1]

R. J. ABRAHAM[2] AND H. J. BERNSTEIN

ABSTRACT

The doublet separation in the proton resonance spectrum of the liquid was measured from −53 to 100° C. From the variation of the separation with temperature approximate values of the trans and gauche HF coupling constants were obtained. The values of $\Delta H \approx 400$ cal/mole and $\Delta S \approx 0$ are also consistent with the data.

Nuclear magnetic resonance has been used with some success in the investigation of problems concerned with rotation about single bonds (1, 2, 3). Data from other techniques, such as vibrational spectroscopic, for information regarding ΔH, the enthalpy difference of the rotamers, and the assumption that the entropy difference is negligible, has usually gone into the derivation of the coupling constants.

The purpose of this work was to investigate the simplest possible proton magnetic resonance spectrum, the spacing of which depends on the relative concentrations of the rotational isomers. $CFCl_2 \cdot CHCl_2$* is admirably suited for this since the proton magnetic resonance is a simple doublet. The doublet separation was measured with a Varian spectrometer at a radio frequency of 40 Mc/s as accurately as possible (to ±0.02 cycle/second) by the wiggle beat (4) method in a temperature-controlled (±1°) cell which has been previously described (5). The results are shown in Fig. 1 and Table I.

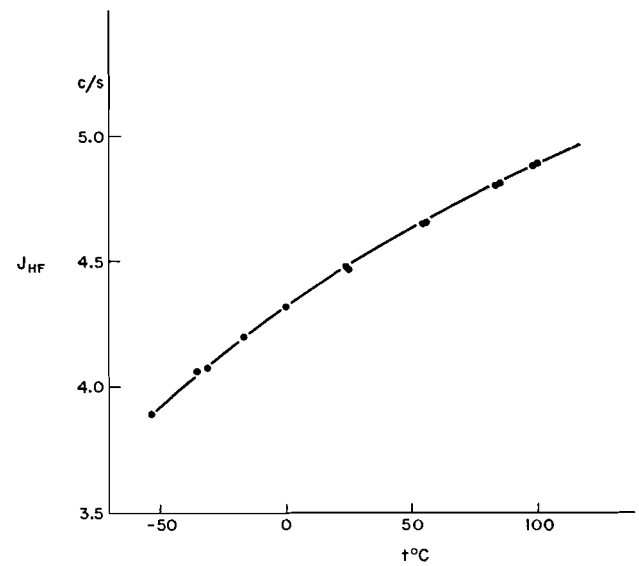


FIG. 1.

[1]*Manuscript received August 31, 1960.*
Contribution from the Division of Pure Chemistry, National Research Council, Ottawa, Canada.
Issued as N.R.C. No. 6060.
[2]*N.R.C. Postdoctorate Fellow 1957–59. Present address: Basic Physics Division, N.P.L. Teddington, Middlesex, England.*
**We are indebted to R. Kagarise for supplying this compound.*

TABLE I

t, °C	J_{obs}	J_{calc}	Obs.−calc.
−53	3.89	3.88	0.01
−35	4.06	4.05	0.01
−31	4.07_5	4.08	−0.005
−16.5	4.20	4.20	0.00
0	4.32	4.30	0.02
24	4.48	4.48	0.00
25	4.47	4.49	−0.02
54.4	4.65	4.66	−0.01
55.2	4.65_5	4.66	−0.005
83.2	4.80	4.80	0.00
85.0	4.81	4.82	−0.01
98	4.89	4.89	−0.01
99.7	4.89	4.89	0.00

The molecule $CFCl_2 \cdot CHCl_2$ exists in three conformations, one in which H and F are trans oriented and a pair of mirror image gauche forms. If we denote the fraction of the trans form as p, that of each gauche form is $(1-p)/2$, and the total fraction of molecules in the gauche form is $1-p$, at any temperature

$$[1] \qquad \frac{p}{1-p} = \tfrac{1}{2}e^{-\Delta F/RT} = \tfrac{1}{2}e^{\Delta S/R} \cdot e^{-\Delta H/RT}$$

where the factor $\frac{1}{2}$ takes into account the two mirror image magnetically equivalent gauche forms. The observed spacing (i.e. coupling constant J in cycles/second) for this compound depends on the number average of the coupling constants in the trans (J_T) and gauche (J_G) forms (6) and is given by

$$[2] \qquad J = pJ_T + (1-p)J_G.$$

Eliminating p from [1] and [2] gives

$$J = J_T - \frac{J_T - J_G}{1 + \frac{1}{2}e^{\Delta S/R} \cdot e^{-\Delta H/RT}}.$$

In principle it is possible to evaluate the four unknowns in this equation (J_T, J_G, ΔS, ΔH). However, very much greater accuracy than ± 0.02 cycle/second in a measurement of J is required. A least squares solution attempt on the data of Table I turned out to be rather complicated due to the presence of the exponential function and did not give an acceptable result.* Various graphical methods were employed consisting chiefly of solving for J_T and J_G for different assumed values of ΔS and ΔH. It turns out that the following values of the parameters are consistent with the data of Table I:

$$J_G = 1.03 \text{ cycles/second},$$
$$J_T = 18.08 \text{ cycles/second},$$
$$\Delta S = 0,$$
$$\Delta H = 400 \text{ cal/mole}.$$

The values of J, calculated with the above, give the column of calculated J values in

**Because of the small available experimental range, the curve in Fig. 1 can be described within the experimental error by a three-parameter function. For this reason the least squares solution to determine all four parameters is not significant and when carried out leads to physically unacceptable results.*

Can. J. Chem. Downloaded from www.nrcresearchpress.com by 210.87.254.40 on 09/05/12
For personal use only.

Table I. The value of $\Delta S = 0$ is not inconsistent with the very small entropy difference in the gas phase (7) for the rotamers of 1,2-dichloroethane. The fact that ΔH is positive shows that the gauche isomer is more stable than the trans isomer. This information and the value of $\Delta H = 400$ cal/mole are in agreement with the infrared studies on this molecule (8).

The values found for the coupling constants, entropy difference, and enthalpy difference are considered reliable to about 10%. Very much higher accuracy in the measurement of J, or a very much extended temperature range, would be required to improve on these numbers. There is no doubt, however, that J_T is considerably larger than J_G. This is analogous to the situation in substituted ethylenes (9) where the trans HF coupling constant is larger than the cis. Also, it is interesting to note that for the HH coupling constants in substituted ethanes (3), $J_T \gg J_G$. Presumably the same reasons (10) are valid for HF coupling constants that are invoked to explain the higher trans HH coupling constant.

REFERENCES

1. J. J. Drysdale and W. D. Phillips. J. Am. Chem. Soc. **79**, 319 (1957).
2. J. N. Shoolery and B. Crawford. J. Mol. Spectroscopy, **1**, 270 (1957).
3. N. Sheppard and J. J. Turner. Proc. Roy. Soc. (London), A, **252**, 506 (1959).
4. R. E. Glick and A. A. Bothner-By. J. Chem. Phys. **25**, 362 (1956); C. A. Reilly. J. Chem. Phys. **25**, 604 (1956).
5. W. G. Schneider, H. J. Bernstein, and J. A. Pople. J. Chem. Phys. **28**, 601 (1958).
6. J. A. Pople, W. G. Schneider, and H. J. Bernstein. High resolution nuclear magnetic resonance. McGraw-Hill Book Co., New York. 1959. p. 381.
7. S. Mizushima. Internal rotation. Academic Press, New York. 1954. p. 51.
8. R. E. Kagarise. J. Chem. Phys. **29**, 680 (1958).
9. H. M. McConnell, A. D. McLean, and C. A. Reilly. J. Chem. Phys. **23**, 1152 (1955).
10. M. Karplus. J. Chem. Phys. **30**, 11 (1959).

Can. J. Chem. Downloaded from www.nrcresearchpress.com by 210.87.254.40 on 09/05/12
For personal use only.

Can. J. Chem. Downloaded from www.nrcresearchpress.com by 210.87.254.5 on 09/05/12
For personal use only.

AN INFRARED STUDY OF THE ADSORPTION OF BUTENES ON SURFACES OF POROUS VYCOR GLASS[1]

L. H. LITTLE,[2] H. E. KLAUSER,[3] AND C. H. AMBERG

ABSTRACT

The adsorption and reactions of the four butenes on porous Vycor glass at room temperature have been studied by infrared spectroscopy. Initial adsorption was rapid and was found to perturb the surface hydroxyl groups of the glass. In the case of the *n*-butenes rapid isomerization took place at room temperature. In addition to this the adsorbate spectra showed the occurrence of a slower reaction which led to an increase in saturated C—H groupings. C_8 and higher compounds were shown to have formed; on outgassing at room temperature small amounts of cracking products were collected. The polymerization of isobutene was particularly rapid. Experiments at low coverage ($\theta \sim 0.001$–0.002) gave identical initial spectra for the *n*-butenes. These were discussed in terms of possible models for butene adsorption. A reduction in the alumina and zirconia content of the glass by acid leaching resulted in decreased rates of isomerization and polymerization, suggesting that one or both of these oxides are at least partially responsible for the activity of the glass. A pure silica aerogel was almost completely inactive. Quantitative measurements of the spectra of several monoolefins in solution were made for comparison with the surface species, in particular with respect to their molar intensities of absorption.

INTRODUCTION

The adsorption of olefins on catalytically active surfaces is a prerequisite to subsequent isomerization, polymerization, and cracking reactions (1). For instance, in a recent publication MacIver, Zabor, and Emmett (2) discussed the chemisorption, followed by cracking and polymerization, of 1-butene and 1-octene on silica–alumina cracking catalysts; their data were consistent with the formation of carbonium ion intermediates. Few other studies of the adsorption of butenes or higher olefins on similar surfaces have appeared in the literature, probably because of the complexity of the resulting systems.

It was the object of the present investigation to study the adsorption of butenes on porous Vycor glass by infrared spectroscopy. The adsorbent was suitable owing to its high transmission in the region of 3.4 μ, where the bands due to C—H stretching modes in hydrocarbons occur. Moreover, it had a high surface area, so that even at low fractional coverages, sufficiently large quantities of adsorbed material remained in the sample to ensure good infrared sensitivity. An extensive review of infrared spectra of adsorbed molecules was given by Eischens and Pliskin (3).

EXPERIMENTAL

The samples of porous Vycor glass (Corning Glass, No. 7930) were generally in the form of plates 1 mm thick, 2 cm wide, and 5 cm long; 2-mm and 0.1-mm plates were used in some instances. They were cleaned by heating to 400° C in oxygen, cooled, weighed, and then transferred to the combined infrared and adsorption cell.

One of these cells consisted of a silica test tube of 1.5 mm wall thickness, 15 cm length, and 2.4 cm diameter. It was mounted in a vertical position with the infrared light beam passing through its walls. An infrared gas cell of 10-cm path length and fitted with sodium chloride windows was attached at the upper end of the silica tube through a

Manuscript received August 10, 1960.
Contribution from the Division of Applied Chemistry, National Research Council, Ottawa, Canada.
Presented at the 43rd Canadian Chemical Conference of the C.I.C., Ottawa, June 13–15, 1960.
Issued as N.R.C. No. 6064.
[2]*National Research Council Postdoctorate Fellow 1958–1960.*
[3]*National Research Council Postdoctorate Fellow 1957–1959. Present address: I.B.M. Corp., Endicott, N.Y.*

ground-glass joint. When required, this cell could be placed in the light beam. The whole assembly could be connected to a vacuum and gas-handling system. Another type of cell of 10-cm path length and 4 cm in diameter was wound with a heater along about 5 cm of its central section. Sodium chloride windows were attached at the ends by means of silicone resin (Dow Corning, No. 996); temperatures of at least 150° C could thus be tolerated at the windows. A flattened glass tube with just enough clearance for 2-mm Vycor plates was mounted to the cell in a vertical position. At its upper end there was provided a short piece of glass rod led horizontally into the cell through a ground-glass joint. Sample plates were suspended from it on a spun-glass thread; by rotating the rod they could be wound up and out of the infrared beam for the determination of vapor-phase spectra. A sketch of this cell is shown in Fig. 1.

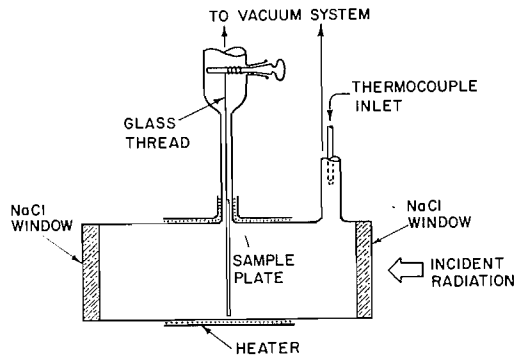


FIG. 1. Sketch of cell showing windlass arrangement for sample plate.

Samples were outgassed at 300° and cooled to room temperature, after which the background spectrum was recorded. The silica test tube transmitted in the same spectral region as the Vycor plates and thus did not interfere. After admission of gas to the sample the spectrum composed of background, adsorbate, and gas phase was recorded, as well as that of the gas phase alone. The latter was necessary to correct the adsorbate spectrum, where indicated, and was also useful for purposes of identifying reaction products. With the silica cell, corrections were usually not more than 10% of the absorption of the surface species; at low coverage they were completely negligible. All experiments were performed at room temperature.

The spectra were recorded on a Perkin–Elmer Model 21 spectrophotometer fitted with either a sodium chloride or a calcium fluoride prism, or alternately on a Beckman IR4 spectrophotometer with a lithium fluoride prism. All spectra reproduced in the diagrams are tracings from experimental records, while all data in the tables under the heading "Adsorbate" refer to the surface phase only. The time shown for each spectrum refers to time after gas admission.

The following spectral parameters were measured or computed for absorption bands of surface species: frequency ν cm^{-1}; optical density $D = \log_{10} J_0/J$, where J_0/J is the ratio of incident to transmitted radiant energy at a given frequency; extinction coefficient $\epsilon = D/cl$ mole^{-1} liter cm^{-1}, where c is the concentration of adsorbate in terms of moles of butene per liter of sample (external dimensions) and l is the total path length through the sample in centimeters; integral band intensity $I = \int D\, d\nu$ cm^{-1} and molar intensity $\bar{I} = I/cl$ mole^{-1} liter cm^{-2}. As long as c refers to actual butenes adsorbed on the glass

Can. J. Chem. Downloaded from www.nrcresearchpress.com by 210.87.254.5 on 09/05/12
For personal use only.

surface, $\bar{I}$ represents the true value for butenes and is, within the experimental limits, an absolute intensity. However, when part or all of the butenes have polymerized, then $\bar{I}$ is a composite of all species present, expressed in molar concentrations of C_4. We have used these values for comparisons with pure butenes, or higher monoolefins similarly expressed in terms of C_4 concentrations (see Appendix).

Errors in the determination of $\bar{I}$ were $\pm 15\%$ at the worst, but usually somewhat better. Apart from errors inherent in the integrating procedure (Simpson's rule), the chief contributing factor was the uncertainty involved in constructing the background spectrum. This spectrum was subject to small changes from that originally measured on the pure adsorbent; these were due to (*a*) perturbation of the adsorbent by the adsorbate and (*b*) the occasional removal of the cell from the spectrometer and subsequent repositioning. Consistency between the three different prisms was about $\pm 5\%$. Errors in the volume adsorbed were usually less than $\pm 2\%$.

Neither extinction coefficients nor intensities were corrected for finite spectrometer resolving power, because of the overlapping nature of the bands. Bands above 3000 cm^{-1} were resolved graphically from the group of bands below for the purpose of determining their relative intensity. The errors involved, depending somewhat on the separation and intensities of the bands, were usually of the order of $\pm 10\%$, but in some cases higher.

The frequencies, indicated vertically in the figures, have uncertainties of ± 10 cm^{-1} for sodium chloride and ± 3 cm^{-1} for lithium fluoride optics. Spectral slit widths were, respectively, 18 cm^{-1} and 6 cm^{-1}. For some bands extinction coefficients were added in parentheses in the diagrams.

Supplementary analyses were undertaken by means of mass spectrometry and gas–liquid chromatography. Vapor-phase and weakly sorbed materials were collected by condensation into a liquid nitrogen trap. More severe stages of outgassing involved the additional use of a vacuum pump for periods of up to 20 hours and finally the application of heat to the sample.

A modified Vycor adsorbent was prepared by leaching the glass for 6 hours in boiling concentrated nitric acid and by carefully washing it. Spectrographic analyses showed that, of the chief constituents other than silica, boron had remained unchanged, while aluminum and zirconium, both present in approximately equal amounts, had decreased to about one-half their former value. Subsequent quantitative analysis showed B_2O_3 to have remained constant at 2.1% while R_2O_3 had decreased from 0.89% to 0.36%. The B.E.T. surface areas, determined with nitrogen at $-195°$ C, had changed from 165 m^2/g to 148 m^2/g.

The silica aerogel (Cab-O-Sil, Godfrey L. Cabot, Inc.) used had a surface area of 166 m^2/g. An infrared transparent plate was prepared from it by pressing at 40 tons/in^2.

The preparation of a sample of Vycor glass with black nickel oxide dispersed in its pores has been previously described (4).

RESULTS AND DISCUSSION

(i) Adsorption of n-Butenes on Porous Vycor Glass at $\theta \sim 0.1$

Rapid adsorption of *n*-butenes at an initial pressure of about 2 cm Hg occurred on a Vycor sample in the first 15- to 20-minute period; this was followed by a much slower uptake. Coverage in this series of experiments was of the order of 0.1 monolayer (see Section (*ii*)). In the early stages, adsorption of a predominant fraction of the surface molecules was of a physical nature (including interactions due to hydrogen bonding). This was inferred from the similarity between the initial spectra and the corresponding

Can. J. Chem. Downloaded from www.nrcresearchpress.com by 210.87.254.5 on 09/05/12
For personal use only.

spectra in carbon tetrachloride solution (Fig. 8). For example, the characteristic absorption bands associated with olefinic C—H stretching vibrations were clearly discernible in either case (1-butene: 3080 cm^{-1}, Fig. 2(*a*); 2-butenes: 3020 cm^{-1}, Figs. 2(*b*) and 2(*c*)). Moreover, the ratios of olefinic to total C—H band intensities (Table I) were approximately the same as the corresponding ones in carbon tetrachloride solution (Table VI). In addition to this the adsorbed molecules perturbed the surface hydroxyl groups of the glass with the result that the ν_{OH} band was broadened and displaced to lower frequencies; these changes are generally caused by hydrogen bonding (5) and may be attributable to the formation of such bonds involving surface hydroxyls and the

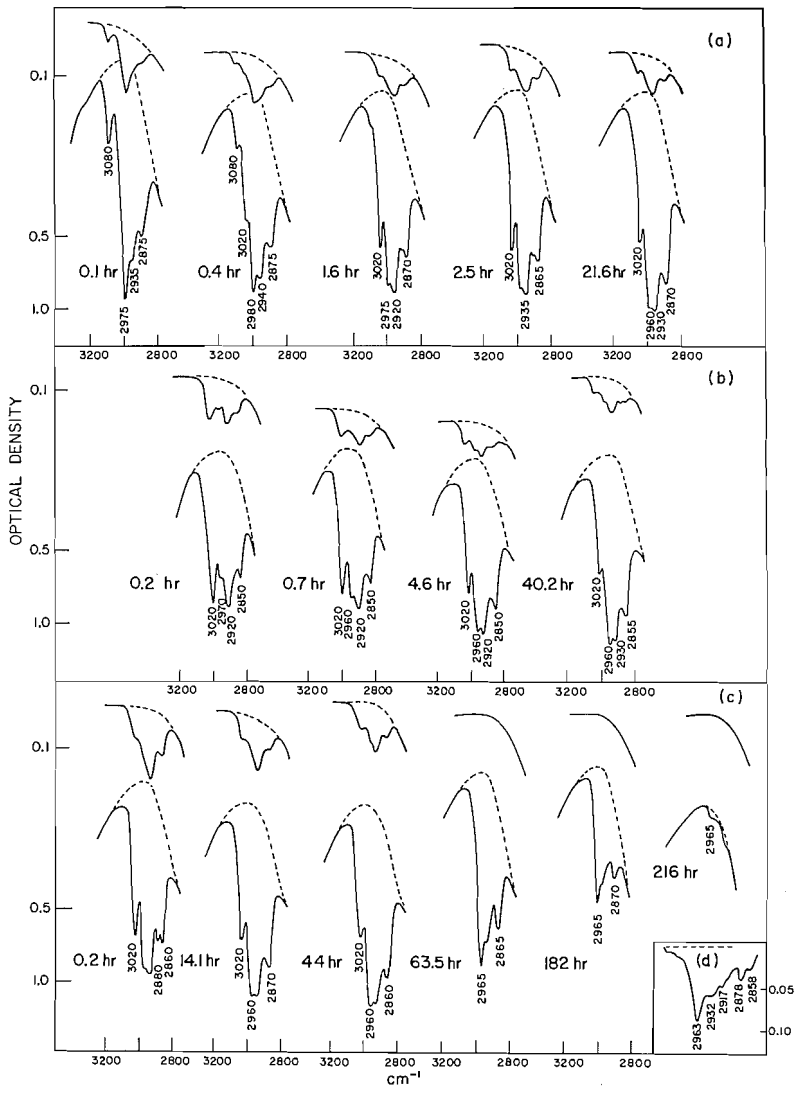


FIG. 2. Adsorption of *n*-butenes on porous Vycor glass at $\theta \sim 0.1$: (*a*) 1-butene, (*b*) *cis*-2-butene, (*c*) *trans*-2-butene; the last three spectra represent successive stages of outgassing. The upper spectrum in all cases is that of the vapor phase. (*d*) Polymeric residue from *trans*-2-butene at higher resolution; calculated spectrum of surface phase only. Optics: NaCl for (*a*), (*b*), and (*c*); LiF for (*d*).

Can. J. Chem. Downloaded from www.nrcresearchpress.com by 210.87.254.5 on 09/05/12
For personal use only.

TABLE I

Adsorption of *n*-butenes on porous Vycor glass at $\theta \sim 0.1$

		Adsorbate							
		Total (as butenes)			Olefinic-bands		Gas		
Compound	Time, hours	Conc., moles $l.^{-1}$	I, cm^{-1}	$\bar{I}$, $mole^{-1}$ $l.\ cm^{-2}$	ν,* cm^{-1}	Intensity % of total	I, cm^{-1}	Pressure, cm Hg	Outgassing procedure
1-Butene	0.1	0.22						2.88	
	0.2		123	5400	3080 3020	7 4	112		
	0.6		132	~5800	3080 3020	4.5 5	111		
	10.3		162	~5700	3020	8.5	95	2.70	
	11.3		88		3020	5	10		Condensed 5 minutes
	13.9		52		3020	3.5	0		Condensed 2 hours
	39.5		46		3020	2.5	0		Heated to 100° for 12 minutes
	112		21		3020	0	0		Heated to 120° for 45 minutes
	128		5.5		3020	0	0		Heated to 160° for 1 hour
cis-2-Butene	0.1	0.18						1.50	
	0.2		94	5200	3020	29	12		
	0.7		96	5300	3020	24	10.5		
	4.6		121	~5500	3020	15	9		
	16.0		133	~6600	3020	8	8		
	16.4		123	~5600	3020	8.5	8		
	40.2		151	6900	3020	5	7.5		
	41.7	0.21						0.96	
trans-2-Butene	0.2	0.19	95	5000	3020	16	16	1.72	
	0.8		100	5200	3020	14	16		
	14.1		132		3020	7	10.5		
	20.9		138		3020	8.5	12.5		
	21.1		131		3020	7.5			
	43		157		3020	7	10		
	44	0.22	158	~7300	3020	6.5		1.14	
	63.5		73		3020	2	0		Condensed 6.5 hours
	182		37		3020	0	0		Heated to 100° for 3.5 hours
	216		2		3020	0	0		Heated to 155° for 6.5 hours

*Exact frequencies given in Fig. 2.

π-electrons of the adsorbed olefin (6). In the early stages of an experiment 70% of the adsorbed phase could be condensed into a liquid nitrogen trap within ~5 minutes; the condensate consisted of butenes only. By further outgassing it was possible to restore the surface hydroxyl band almost to its original shape.

Isomerization

Rapid double-bond isomerization of the *n*-butenes occurred on adsorption at room temperature. This is readily demonstrated by both the adsorbate and gas-phase spectra (Fig. 2). For instance, in the case of 1-butene (Fig. 2(*a*)), the band at 3080 cm^{-1} due to the asymmetric stretching mode of the $=CH_2$ group progressively decreased in intensity, while the =CH— band of the 2-butenes at 3020 cm^{-1} became stronger. At the same time the ratio of the olefinic to total C—H band intensity increased from the initial 8–10% of 1-butene to 14.5% (estimated from Table I and confirmed by subsequent runs), i.e. it approached the higher values of a predominantly cis–trans mixture (Table VI).

Two hours after admission of any one of the *n*-butenes the contour of the spectra of

Can. J. Chem. Downloaded from www.nrcresearchpress.com by 210.87.254.5 on 09/05/12
For personal use only.

the gas phase in contact with the surface showed these to consist largely of *trans*-2-butene by comparison with the spectra of the pure gases in Fig. 8. GLC analyses gave percentages of 3.5, 71.5, and 25.0 respectively for 1-butene, *trans*- and *cis*-2-butene both for the residual gas phase and for material removed from the sample by outgassing. The corresponding equilibrium values at 25° C calculated from the data of Rossini (7) are 2.42, 74.24, and 23.34%.

Polymerization and Cracking

After the isomerization process had reached equilibrium, the contour of the bands changed with further standing. The olefinic C—H band at 3020 cm^{-1} decreased, while the band at 2965 cm^{-1} due to saturated C—H groupings, increased in intensity. These results were consistent with a process of polymerization occurring on the surface, i.e. with a decrease in the number of double bonds per total number of bonds in the molecule. The process continued with standing and after 40 hours the intensity of the band at 3020 cm^{-1} had decreased from between 10 and 20% of the total to only 5% (for typical results, see *cis*-2-butene in Table I). This is approximately the value found for 2-octene in carbon tetrachloride solution (Table VI).

When the system was evacuated, unsaturated material, which was found to contain largely butenes, was removed and the intensity of the 3020 cm^{-1} band decreased to about 2–3% of the total intensity. This would indicate that the remaining material was composed of C_8 and possibly larger molecules. Along with the butenes, monoolefins with the following composition were identified in the condensate: C_3, C_5, C_6, C_7, C_8, and C_9.

In a further series of tests, the adsorbate was taken up in pentane, the resulting solution concentrated and analyzed by GLC on an Apiezon column. Various available pure monoolefins showed good linear correlation on a logarithmic elution time versus boiling point plot. On this basis a complex mixture of some 12 constituents boiling between 80° and 210° (C_6 to C_{12} region) was eluted.

By increasing the severity of outgassing after the condensation of what were largely butenes, the material removed from the surface contained a greater proportion of cracked and polymerized products. Intensity measurements of the residual adsorbate after outgassing for 1 hour at 50–150° C showed that 80–90% of the surface C—H groups had been removed. No bands due to unsaturated species were detectable. The bands at 2965, 2930, and 2870 cm^{-1} due to saturated C—H vibrations suggested a preponderance of methyl over methylene groups, i.e. branched rather than linear polymers. The ratio of the heights of these bands did not appear to change with outgassing (see Section (*vi*)).

(ii) Low-coverage Adsorption of n-Butenes, $\theta \sim 0.001$–0.002

In the spectra described above, the strong bands due to physically adsorbed material in the early stages of the adsorption process would almost certainly mask any bands due to a possible chemisorbed butene species and thus preclude its identification. After polymerization has set in, the intense bands of the polymeric surface species are again liable to interfere. It was thought that optimum conditions might be attained by working at low initial pressures. Small doses of butene were therefore admitted so that within 1–2 minutes the pressure had dropped to below 0.01 mm Hg. The initial measurements were made within 5–15 minutes after gas admission. Using the nitrogen area of 165 m^2/g and a molecular area for butenes of 31 $Å^2$ we estimate a coverage of 0.001–0.002 of a monolayer in these experiments (Fig. 3, Table II). Similarly, the coverage in the experiments described in the previous section was in the region of $\theta = 0.1$.

Can. J. Chem. Downloaded from www.nrcresearchpress.com by 210.87.254.5 on 09/05/12
For personal use only.

TABLE II

Adsorption of butenes on porous Vycor glass at $\theta \sim 0.001$–0.002

		Adsorbate*				
		Total (as butenes)			Olefinic bands	
Compound	Time, hours	Conc., moles $l.^{-1}$	I, cm^{-1}	$\bar{I}$, $mole^{-1}\,l.\,cm^{-2}$	ν,† cm^{-1}	Intensity % of total
1-Butene	0.3	1.7×10^{-3}	5	4500	3020	12.5
	1.3		4.5	4200	3020	11
	23.5		5	4500	3020	10.5
	50.5		4.5	4200	3020	11.5
	143.5		5.5	4900	3020	4
cis-2-Butene	0.1	2.3×10^{-3}	3.5	2500	3020	11.5
	3		4	3000	3020	14
	23.9		4	3000	3020	12
	112.8		5	3500	3020	8
	162		5.5	3800	3020	2
trans-2-Butene	0.2	2.4×10^{-3}	5.5	3800	3020	12.5
	4.8		4.5	3200	3020	11
	22.2		5	3600	3020	9.5
	29.5		5.5	3800	3020	7.5
	53.8		5.5	3800	3020	5.5
	120		6	4300	3020	1.5
Isobutene	0.1	2.8×10^{-3}	8.5	5000	—	0
	16.5		11	6400	—	0
	117		9.5	5500	—	0

*Gas phase not observable. †Exact frequencies given in Fig. 3.

Because of the small amount of adsorbed material it was necessary to record the spectra through six plates, each 1 mm thick, in order to obtain bands of measurable intensity. The absorption and reflection from six plates of Vycor glass was itself appreciable in the spectral region being studied. Moreover, the spectrum of the samples was steeply sloping such as to make observation of weak bands superimposed upon this background very difficult. This was corrected by placing a similar but evacuated cell containing six 1-mm Vycor plates in the reference beam. Spectra were then recorded relative to this compensating cell. Figure 3(*a*) demonstrates the effect, and clearly emphasizes the necessity, of compensating for glass absorption in this case.

Within 5 minutes after admitting the *n*-butenes to the samples the spectra showed that the surface species were identical for the three *n*-butenes; presumably rapid isomerization had occurred on the surface. The band at 3020 cm^{-1} characteristic of the =CH— group was found in all three cases, i.e. it had replaced the $=CH_2$ band at 3080 cm^{-1} in the case of the 1-butene. Possible models for this surface species will be discussed below. The spectra for *cis*-2-butene are not reproduced in Fig. 3, since they differ in no way from the other two.

The molar intensities of absorption were well below the values for adsorbed butenes at the higher coverage of $\theta \sim 0.1$. It is interesting to note, though, that the fractional intensity of the band at 3020 cm^{-1} had remained in the same range as that found for $\theta \sim 0.1$ after the attainment of isomerization equilibrium.

The slow increase in total band intensity noticeable after a period of several days (Table II) was indicative of slow polymerization. The increase was particularly marked in the2965 cm^{-1} band; it was matched by an equally slow decrease of the 3020 cm^{-1} band. Furthermore the contours of the final spectra closely resembled those of the polymerized species found at $\theta \sim 0.1$ (Fig. 2).

Can. J. Chem. Downloaded from www.nrcresearchpress.com by 210.87.254.5 on 09/05/12
For personal use only.

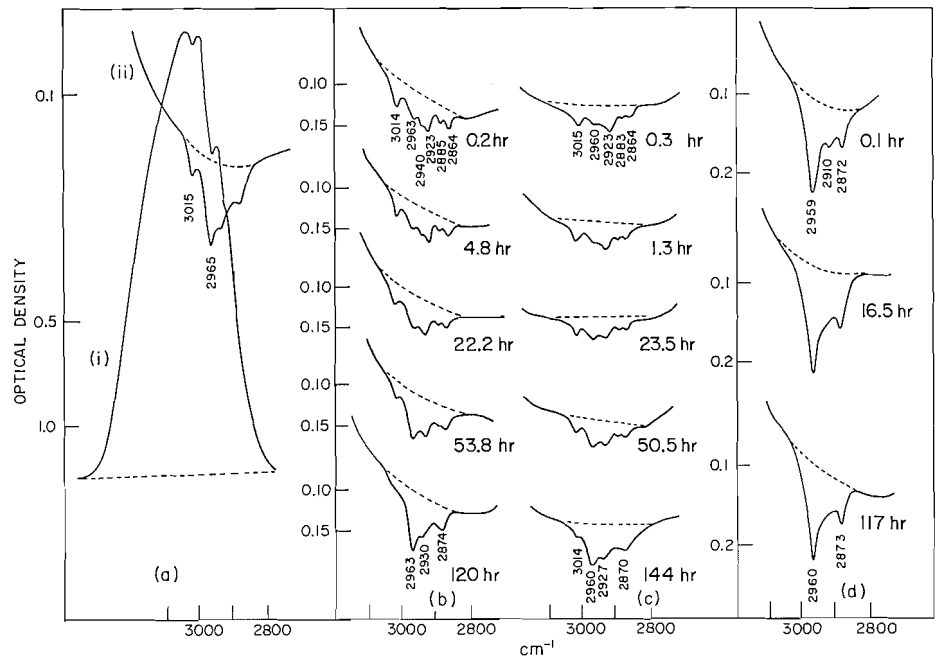


FIG. 3. Adsorption of butenes on porous Vycor glass at $\theta \sim 0.001$–0.002: (*a*) spectrum (i) before and (ii) after compensating for background absorption, (*b*) *trans*-2-butene, (*c*) 1-butene, (*d*) isobutene. Optics: LiF.

(iii) Adsorption of Isobutene on Porous Vycor Glass

When sufficient isobutene for 0.03 monolayer coverage was admitted to the Vycor sample, adsorption was very rapid. Within 5 minutes the entire dose had adsorbed and no gas spectrum was detectable. The following observations confirm the view that a very fast polymerization process had occurred.

The spectrum of the surface species (Fig. 4) showed very intense absorption bands

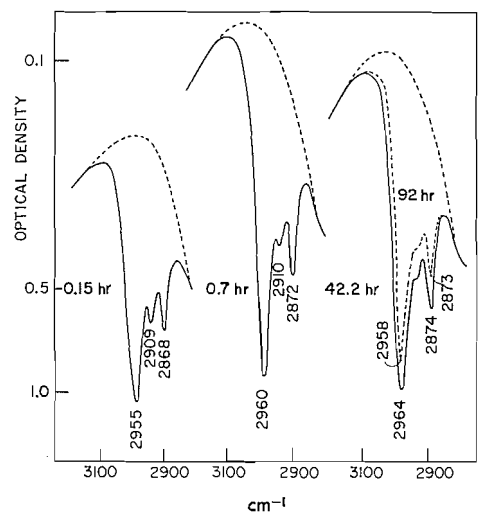


FIG. 4. Adsorption of isobutene on porous Vycor glass at $\theta \sim 0.03$. The broken line (92 hours) shows spectrum after outgassing. Optics: LiF.

Can. J. Chem. Downloaded from www.nrcresearchpress.com by 210.87.254.5 on 09/05/12
For personal use only.

of saturated hydrocarbon groups only. The frequencies and relative intensities of the bands at 2960 and 2870 cm^{-1} in the isobutene spectrum were the same as those in the spectrum of polymerized *n*-butenes (Fig. 2); in the former case the band at 3020 cm^{-1} due to unsaturated material was absent and the band at 2910 cm^{-1} was somewhat less resolved from that at 2960 cm^{-1}. The intensity of the 2910 cm^{-1} band in the isobutene spectrum decreased on standing, while the total intensity remained relatively unchanged.

On outgassing through a liquid nitrogen trap the intensity of the surface bands at 2960, 2910, and 2870 cm^{-1} decreased slightly, while their relative heights did not change. The gases thus condensed were shown to contain cracked and polymerized products similar to those found for the *n*-butenes.

The results of experiments at low coverage ($\theta = 0.002$) follow the same pattern as was found for the *n*-butenes. There was a significant decrease in molar intensity in going from $\theta = 0.03$ to 0.002 (Tables III and II), but the contours of the spectra were

TABLE III

Adsorption of isobutene on porous Vycor glass at $\theta \sim 0.03$

	Adsorbate				
	Total (as butene)*			Gas	
Time, hours	Conc., moles $l.^{-1}$	I, cm^{-1}	$\bar{I}$, $mole^{-1}$ l. cm^{-2}	I, cm^{-1}	Pressure, cm Hg
0.1	0.068				0.07
0.15		70	10000	0	0.00
0.2		65	9200	0	
0.4		54	7600	0	
0.7		54	7600	0	
1.1		62	8900	0	
42.2		70	9300	0	
42.2		67	8900	0	
43.6		75	10000	0	
43.9	0.073				
92†		52		0	

*Olefinic bands not observable. †Sample outgassed for 30 hours.

identical (Figs. 4 and 3). The intensity of the 2910 cm^{-1} band again decreased. Eischens and Pliskin have assigned this band to tertiary C—H groups in surface molecules (3).

(iv) Adsorption of Butenes on Porous Glass Leached with Nitric Acid

Eight minutes after admitting 1-butene to a sample of the acid-leached glass to attain a coverage of $\theta \sim 0.1$, the spectrum (Fig. 5) was very similar to that of 1-butene in carbon tetrachloride solution (Fig. 8); the molar intensity of the surface material (Table IV) was in the same range as on the original glass (Table I), both being considerably less than the value in solution. Adsorption was rapid during the first 20 minutes, after which it slowed down markedly. In this respect adsorption proceeded likewise in a manner similar to that on unleached specimens. In contrast to this, however, the time to reach isomerization equilibrium had increased from approximately 1 to 50 hours. Appreciable isomerization had occurred already after 6 hours, the surface spectrum having changed to resemble that of *trans*-2-butene in solution (Fig. 8). Isomerization was similarly indicated by the gas-phase spectrum. After 4 days relatively little polymerization had occurred. This can be seen in Table IV, for instance, by the high fractional intensity of the 3020 cm^{-1} band. After the butenes had been removed by condensation,

Can. J. Chem. Downloaded from www.nrcresearchpress.com by 210.87.254.5 on 09/05/12
For personal use only.

TABLE IV

Adsorption of butenes on acid-leached Vycor glass at $\theta \sim 0.1$; also 1-butene at $\theta \sim 0.01$

		Adsorbate							
		Total (as butenes)			Olefinic bands		Gas		
Compound	Time, hours	Conc., moles $l.^{-1}$	I, cm^{-1}	$\bar{I}$, $mole^{-1}$ l. cm^{-2}	ν,* cm^{-1}	Intensity % of total	I, cm^{-1}	Pressure, cm Hg	Outgassing procedure
1-Butene	0.1	0.17						2.22	
	0.15		97	5500	3080	7	16.5		
	0.3		87	5000	3080 3020	7.5 1.5	16.5		
	6.4		92	5250	3080 3020	3 13	14		
	16.9		81	4600	3080 3020	0.5 22	16		
	51.3	0.18	110	5900	3080 3020	0.5 14.5	14		
	89	0.19	113	5850	3020	14	13		
	91	0.19						2.07	
	93		15.5		3020	13.5	0		Condensed 10 minutes
	117		6		3020	5	0		Condensed 6 hours
	141		4.5		3020	4.5	0		Condensed 7 hours
1-Butene	0.05	0.011						0.07	
	0.1		7	4900	3080 3020	1.5 10	0		
	0.3		8	4800	3080 3020	1 12.5	0	0.00	
	0.5	0.018							
	0.7		8	4200	3020	15	0		
	2.1		8.5	4500	3020	15.5	0		
	5.2		9.5	5000	3020	13	0		
	21		9.5	5000	3020	13	0		
cis-2-Butene	0.3	0.20						2.00	
	0.35		81	3900	3020	23.5	15		
	0.9		84	4150	3020	22.5	15		
trans-2-Butene	0.25	0.18						2.12	
	0.3		89	4700	3020	15	18.5		
	0.6		80	4300	3020	15.5	18.5		
Isobutene	0.1	0.19						1.71	
	0.2		110	5650	3077	5	8		
	0.8	0.23						1.32	

*Frequencies exact for isobutene only; all others given in Figs. 5–7.

weak bands remained, the contours of which (Fig. 5) were similar to those of the polymerized material remaining on unleached samples under comparable conditions (Fig. 2). The band intensities were, however, one order of magnitude less.

In a second experiment with 1-butene the effect of reducing the coverage to $\theta \sim 0.01$ was examined (Table IV, Fig. 6). The outstanding feature of the results was the shortening of the period within which the 3080 cm^{-1} band was replaced by that at 3020 cm^{-1}. While formerly the 3080 cm^{-1} band was still recognizable after 2 days, it had now completely disappeared after 40 minutes.

The adsorption of *trans*- and *cis*-2-butene was studied at $\theta \sim 0.1$ (Table IV); spectra (Fig. 7) were recorded at 20 and 40 minutes after gas admission, when isomerization was negligible. The molar intensities were again considerably less than the corresponding values in solution (Fig. 8). However, both ratios of olefinic to total C—H band intensities agreed remarkably well with the solution values.

Can. J. Chem. Downloaded from www.nrcresearchpress.com by 210.87.254.5 on 09/05/12
For personal use only.

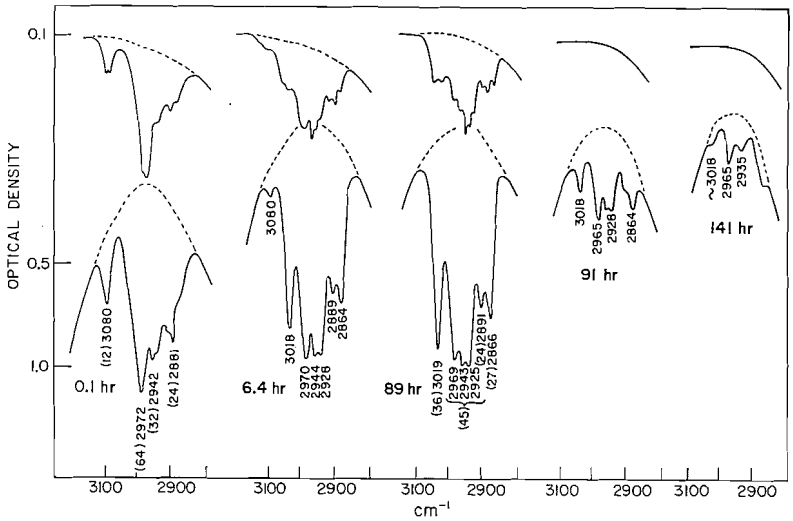


FIG. 5. Adsorption of 1-butene on acid-leached Vycor glass at $\theta \sim 0.1$. The upper spectra are those of the vapor phase. The last two spectra represent successive stages of outgassing. Optics: LiF.

Isobutene (Table IV) reacted far more rapidly than the *n*-butenes on the leached sample; as a result of this the gas uptake at a comparable initial pressure was greater. The fractional intensity of the 3080 cm^{-1} band even at 12 minutes after gas admission was about one-half the value in carbon tetrachloride solution (Table VI). It may be presumed from this that again considerable polymerization had taken place, although the rate of disappearance of the 3080 cm^{-1} band was far slower than with the unleached glass.

(v) Adsorption Sites. Structure of Adsorbed Butenes

The 10% decrease in surface area which occurred during leaching could not by itself

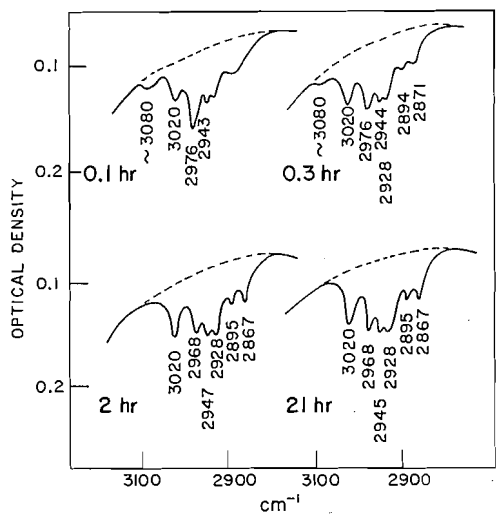


FIG. 6. Adsorption of 1-butene on acid-leached Vycor glass at $\theta \sim 0.01$. Optics: LiF.

Can. J. Chem. Downloaded from www.nrcresearchpress.com by 210.87.254.5 on 09/05/12
For personal use only.

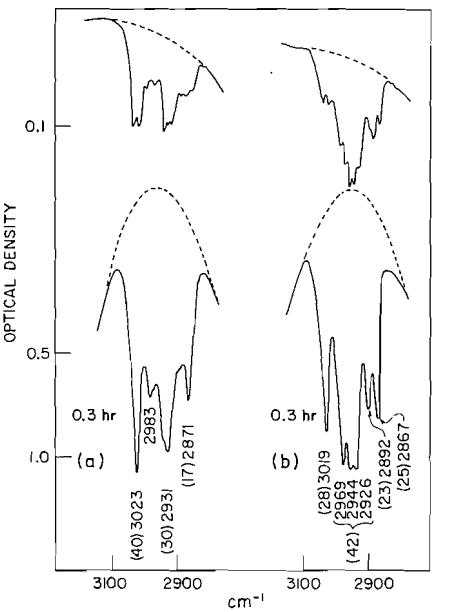


FIG. 7. Initial spectra of (*a*) *cis*- and (*b*) *trans*-2-butene on acid-leached Vycor glass at $\theta \sim 0.1$. The upper spectra are those of the vapor phase. Optics: LiF.

account for the marked decrease observed in the isomerization and polymerization rates.

In an effort to characterize more closely the source of these changes in activity, we attempted to observe the effect on the ν_{OH} band of the surface hydroxyl groups by the nitric acid leaching. This was not feasible with samples 1 mm thick, because they absorb completely all radiation between 3800 cm^{-1} and 3400 cm^{-1}. However, 0.1-mm samples transmit throughout this region and permit a complete study of the ν_{OH} band.

No significant change in the optical density and half-width of the ν_{OH} band after acid treatment was found.

Previous workers with Vycor glass (8) and similar materials (9) have discussed a second type of surface site, apart from the silanol group. This was tentatively ascribed to the Si–O–Si grouping or, more specifically, silicon atoms in the surface.

From the evidence presented in our case it is almost certain that the alumina (and probably also the zirconia) was involved in the adsorption and reaction of the butenes. If our examination of the change in the hydroxyl structure with leaching was sufficiently sensitive, then this would exclude a predominant role being played by surface hydroxyls in the activity changes discussed in the previous section. The metal or oxide sites would themselves form the adsorption centers or, possibly, act as proton acceptors for carbonium ions formed on neighboring surface hydroxyls. Removal of the centers would then result in decreased reaction rates at a given butene coverage. An extreme sample of this would be represented by the results of some experiments which we have conducted with a pure silica aerogel (Cab–O–Sil). The surface area of the silica was comparable to that of the Vycor glass. It had no R_2O_3 content, but an appreciable concentration of free surface hydroxyls. After standing in contact with butene for about 1 month, isomerization was barely perceptible; no polymeric species were detected.

Can. J. Chem. Downloaded from www.nrcresearchpress.com by 210.87.254.5 on 09/05/12
For personal use only.

Can. J. Chem. Downloaded from www.nrcresearchpress.com by 210.87.254.5 on 09/05/12
For personal use only.

On the other hand, the spectroscopic evidence regarding the ν_{OH} band is by no means unambiguous and the following picture would be equally consistent with the changes observed after leaching. If we accept a carbonium ion mechanism to be operative in the reactions (1), then adsorption on a surface hydroxyl (Si–OH or Al–OH) is a plausible first step towards subsequent proton transfer and carbonium ion formation. Of interest in this connection are the recent data of Scholze (10), who found that the content of free hydroxyls in alkali silicate glasses increased with Al_2O_3 content, although B_2O_3 showed the same effect to a high degree. However, our present data do not permit us to distinguish between these various possibilities.

It is instructive to estimate the concentration of "active sites" relative to initial butene coverage in the various experiments described. Such estimates must remain approximate inasmuch as we are ignorant not only of the exact nature of the sites, but also of their energy distributions. We shall confine ourselves therefore to estimating R_2O_3 concentrations in the surface.

Taking the R_2O_3 content (see Experimental Section) to be equally divided between alumina and zirconia, we arrive at a total (Al + Zr) concentration of 0.18 gram-atom/liter of Vycor. The density of the glass is 1.45 g/cc.* For a homogeneous dispersion of R_2O_3 we estimate about 15% or 0.027 gram-atom/liter to reside on the surface. This is by analogy with the silica surface-to-bulk ratio arrived at under the assumption of a 10 Å^2 area for repeat units of silica in the surface. After leaching, 40% of the original R_2O_3 remained in the glass, corresponding to a maximum of 0.011 gram-atom/liter in the surface, but probably very much less.

1-Butene is the most suitable of the *n*-butenes with which to follow the process of isomerization. Not only is almost all of it converted, but it is clearly recognizable down to low concentrations in butene mixtures, owing to the well-resolved band at 3080 cm^{-1}. In Table V we have grouped together data for the adsorption of 1-butene in the order

TABLE V

Correlation of 1-butene to (Al + Zr) ratio with activity and initial molar intensity

Mole ratio, 1-butene:(Al+Zr)	Glass	$\sim\theta$	3080 cm^{-1} band disappeared at $\sim$ hours	$\bar{I}_{initial}$, mole^{-1} l. cm^{-2}
15	Leached	0.1	50	5500
8	Original	0.1	1	5400
1	Leached	0.01	0.7	4900
0.06	Original	0.001	<0.1	3000–5000*

*Estimated from the identical spectra arising from *n*-butenes at low coverage.

of decreasing ratios of initial adsorbate to "active sites". These follow the same trend as the time it takes for isomerization to come to equilibrium. This correlation supports the view that the removal of R_2O_3 is the primary cause of the deactivation of the glass.

As a possible alternative to leaching out "active sites" we attempted to block them. (*a*) Unsupported nickel oxide is considered to be inactive as a butene isomerization catalyst below 400° (11). We found that when 1-butene was adsorbed on Vycor impregnated with ~2% nickel oxide, neither the isomerization nor the polymerization rates were significantly affected and the system behaved in every respect like that shown in

*Corning Glass, Specifications.

Can. J. Chem. Downloaded from www.nrcresearchpress.com by 210.87.254.5 on 09/05/12
For personal use only.

Fig. 2. Although this result is inconclusive, it throws additional light on the work of one of us (L.H.L.): Ethylene, which did not polymerize on Vycor alone, did so when nickel oxide was present, giving rise to a *trans*-2-butene spectrum (4). On continued standing, the butene polymerized further. We are now able to infer that it was the Vycor support rather than the nickel oxide which had catalyzed subsequent C_4 polymerization. (*b*) We performed a series of experiments involving several successive cycles of adsorption and partial desorption. This was done by admitting either a fresh dose of pure butene for each cycle, or else by readmitting the previously isomerized mixture. In no case were we able to detect inhibition of isomerization or polymerization activity due to polymer build-up on the surface. Since in all experiments the initial ratio of butene:(Al + Zr) was of the order of 10, our results tend to support the mechanism which involves the enhancement of surface hydroxyls by the R_2O_3 constituents. In other words the estimated ratio of 10 must be several times too small and far more extensive polymer coverage would be required for deactivation.

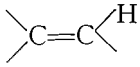
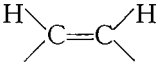
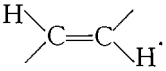
The last column in Table V shows the initial molar intensities for 1-butene. There is an apparent decrease with preponderance of "active sites" per mole of adsorbed butene, i.e. when the spectrum originates from an increasingly large fraction of strongly sorbed molecules in the adsorbed layer. This is in line with the lower values generally found in our case in the surface phase when compared with values in a solvent medium, but should nevertheless be regarded with caution because of the large probable error.

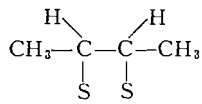
In this connection it is interesting to note that if the spectra in Fig. 3 ($\theta \sim 0.001$) are indeed those of predominantly *trans*-2-butene as was suggested by their contours, then the fractional intensities of the 3020 cm^{-1} band (Table II) are 30% lower than would be expected from the values in solution (Table VI). Barring the early onset of polymerization, which we consider unlikely, this indicates that the perturbation of the molecule by the surface was intensified about the double bond. Conversely, the agreement between the values in Table IV (leached glass, $\theta \sim 0.1$) and those in Table VI could be explained by the fact that the relevant surface spectra were chiefly determined by the large proportion of weakly sorbed butenes in the surface layer.

Within our limits of accuracy, extinction coefficients experienced the same fractional decrease from solution to surface as did the molar intensities, i.e. we could not observe any significant changes in band shape (compare corresponding numbers in parentheses in Figs. 5, 7, and 8). In most cases frequencies were not significantly different within the limits of error, although for *trans*-2-butene we have observed an apparently real shift in the olefinic stretching band from 3021 cm^{-1} in solution to 3019 and 3015 cm^{-1} at high and low surface coverages respectively. Small shifts of this type are commonly encountered in condensations from gaseous to liquid-type phases, as can be seen in Fig. 8, where the decrease from gas to solution for the butenes was in the range 7–9 cm^{-1}.

All the available evidence cited so far, as well as the probable short life of reaction intermediates (2), favors some type of physical adsorption to have been responsible for the observed spectra. However, we cannot entirely exclude the possibility that the spectra are those of a chemisorbed butene species, if not composites of both types. As discussed in Section (*ii*), the low-coverage spectra are the most suitable for examining this question. From these we may draw certain conclusions as to the possible structure of a spectrally predominant species.

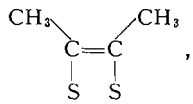
(*a*) Since a band appeared at 3020 cm^{-1}, the species must contain one or more of the

groups  ,  , or  . This would exclude adsorption by such mechanisms as



(I)

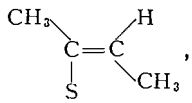
or



(II)

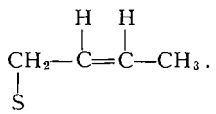
where S indicates a surface site.

(*b*) The 10–12% intensity ratio of the 3020 cm^{-1} band would make a polymeric species unlikely (see Table VI). It would probably also exclude a structure such as



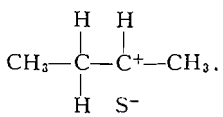
(III)

where only one H-atom is associated with the olefinic carbons (see 2-methyl-2-butene, Table VI). However, a species formed by the dissociation of hydrogen from an α-methyl group would be consistent with the observed spectra



(IV)

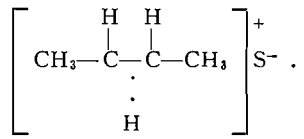
(*c*) The carbonium ion frequently postulated as the intermediate species in double-bond isomerization and polymerization reactions may be considered as existing in two stable forms (1). One of these is the σ-complex (12)



(V)

Only bands in the region of saturated C—H absorption might be expected from such a structure, i.e. it would not be consistent with the spectra in Fig. 3. However, evidence given below in connection with (VI) would suggest retention of some double-bond character in (V) as well. Exclusion of any species does not, of course, rule out participation in the processes under discussion, unobservable though it may be by spectroscopic means. The second form is the π-complex (12)

Can. J. Chem. Downloaded from www.nrcresearchpress.com by 210.87.254.5 on 09/05/12
For personal use only.



(VI)

Recently Powell and Sheppard (13) have determined the infrared spectra of a number of platinum and palladium complexes with ethylene. In their case weak bands in the C—H stretching region and frequencies similar to those of gaseous ethylene were observed. Earlier Chatt and Duncanson (14) had found that the olefinic character in the spectra of a number of metal–olefin π-complexes had been essentially preserved. We quote this work to show that a relatively stable π-complex with the surface might still be expected to give rise to absorption above 3000 cm^{-1} and would be compatible with the spectra in Fig. 3. A weaker type of interaction with surface hydroxyls, which also involves the π-electrons of the olefinic double bond and which can be regarded as hydrogen bonding, we have already discussed in Section (*i*). Presumably this latter type of bond would represent the first stage in carbonium ion formation.

(vi) Band Assignments for Adsorbed Species

In the past, bands at 2965 cm^{-1} and 2870 cm^{-1} have been assigned to vibrations of methyl groups and bands at 2930 cm^{-1} and 2850 cm^{-1} to vibrations of methylene groups for spectra of adsorbed molecules (3, 4), although Eischens and Pliskin (3) have commented on the uncertainties in making such assignments. They are made by analogy with spectra of normal liquid hydrocarbons (15) and are probably correct for large adsorbed molecules. On the other hand, for such molecules as *trans*-2-butene, the occurrence of bands at 2930 and 2850 cm^{-1} clearly cannot indicate the presence of methylene groups. The multiplicity of bands in the spectra of small unsaturated molecules arises *inter alia* from overtones of C—H deformation vibrations.

A further difficulty arises from the fact that large regions of the spectrum may be obscured by intense absorption bands of the adsorbent. Thus confirmation of a likely structure by observing bands in other spectral regions may not be possible, and structural conclusions have to depend on observations of a limited number of bands.

For assigning structures to adsorbed molecules we have confined ourselves to comparing the spectra with analogous ones in solution. The only exception to this has been the assignment of bands occurring at wave numbers higher than 3000 cm^{-1} to unsaturated groupings. This was substantiated by quantitative intensity measurements as well as by GC and mass spectrometric analyses after desorption of the materials responsible for those bands.

APPENDIX

As indicated in the preceding sections, spectral determinations of pure olefins have been made for purposes of comparison with surface species (Table VI, Figs. 8 and 9).

Butene solutions were analyzed by mass spectrometry immediately after the recording of a spectrum. Following this, the spectrum was re-recorded to check for possible evaporation losses.

All butenes used were Phillips Research Grade. Of the higher olefins, all were Phillips Research Grade, except for 2-octene and 2,4,4-trimethyl-2-pentene which were Phillips

Can. J. Chem. Downloaded from www.nrcresearchpress.com by 210.87.254.5 on 09/05/12
For personal use only.

TABLE VI

C—H stretching modes of olefins in carbon tetrachloride solution

Compound	Conc., moles l.$^{-1}$	Total bands $\bar{I}$ (real), mole^{-1} l. cm^{-2}	Total bands $\bar{I}$ (as C_4)	Olefinic bands ν, cm^{-1}	Olefinic bands Intensity % of total
1-Butene	1.00	7350	7350	3085	9.5
cis-2-Butene	0.97	6850	6850	3026	22
trans-2-Butene	1.16	6750	6750	3021	16
Isobutene	1.97	6350	6350	3080	12.5
2-Methyl-1-butene	0.54	9550	7650	3069	6.5
2-Methyl-2-butene	0.69	10500	8400	3027	5.0
Cyclopentene	0.58	10500	8400	3056	9.0
1-Hexene	0.36	13700	9150	3076	4.5
				~3020	~0.5
Tetramethylethylene	0.52	14200	9500	—	0.0
1-Octene	0.66	20300	10200	3082	3.0
				~3020	~1.5
2-Octene	0.27	19600	9800	3015	4.5
2,4,4-Trimethyl-2-pentene	0.37	19000	9500	~3020	~1.5

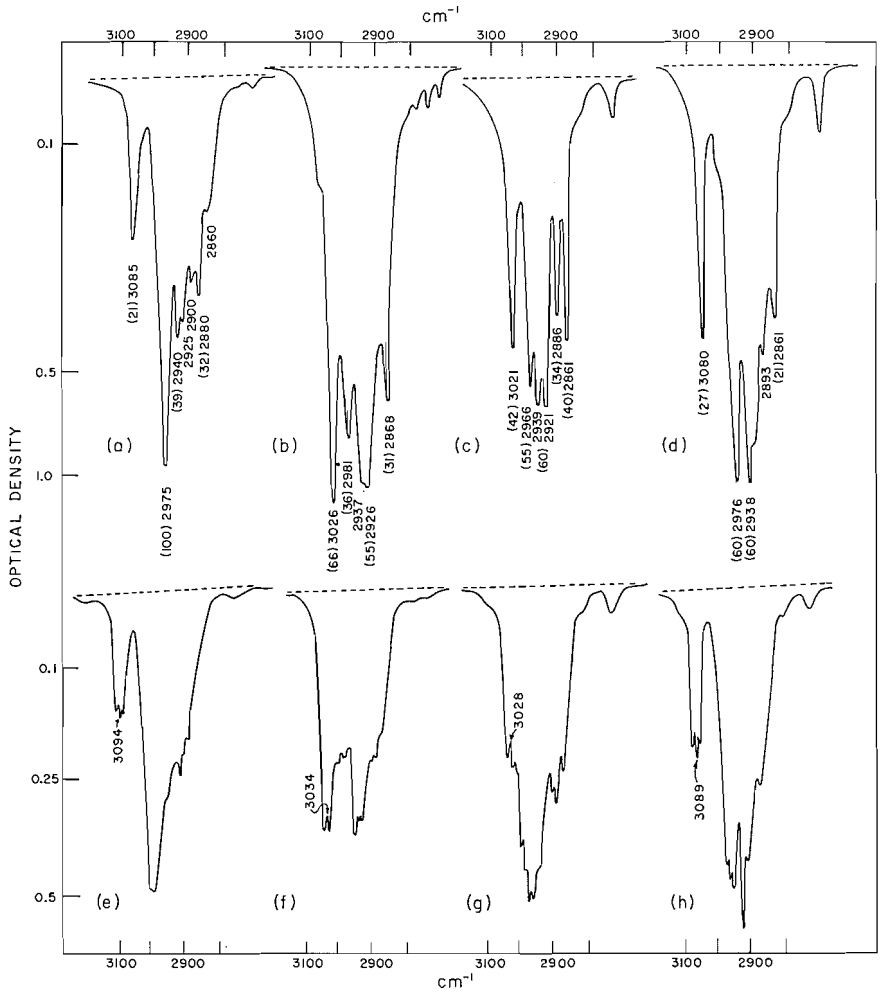


FIG. 8. Spectra of (*a*) 1-butene, (*b*) *cis*-2-butene, (*c*) *trans*-2-butene, and (*d*) isobutene in carbon tetrachloride solution. The corresponding vapor spectra (*e*)–(*h*) are shown in the same order; pressure, 2.1 cm Hg; path length, 5 cm. Optics: LiF.

Can. J. Chem. Downloaded from www.nrcresearchpress.com by 210.87.254.5 on 09/05/12
For personal use only.

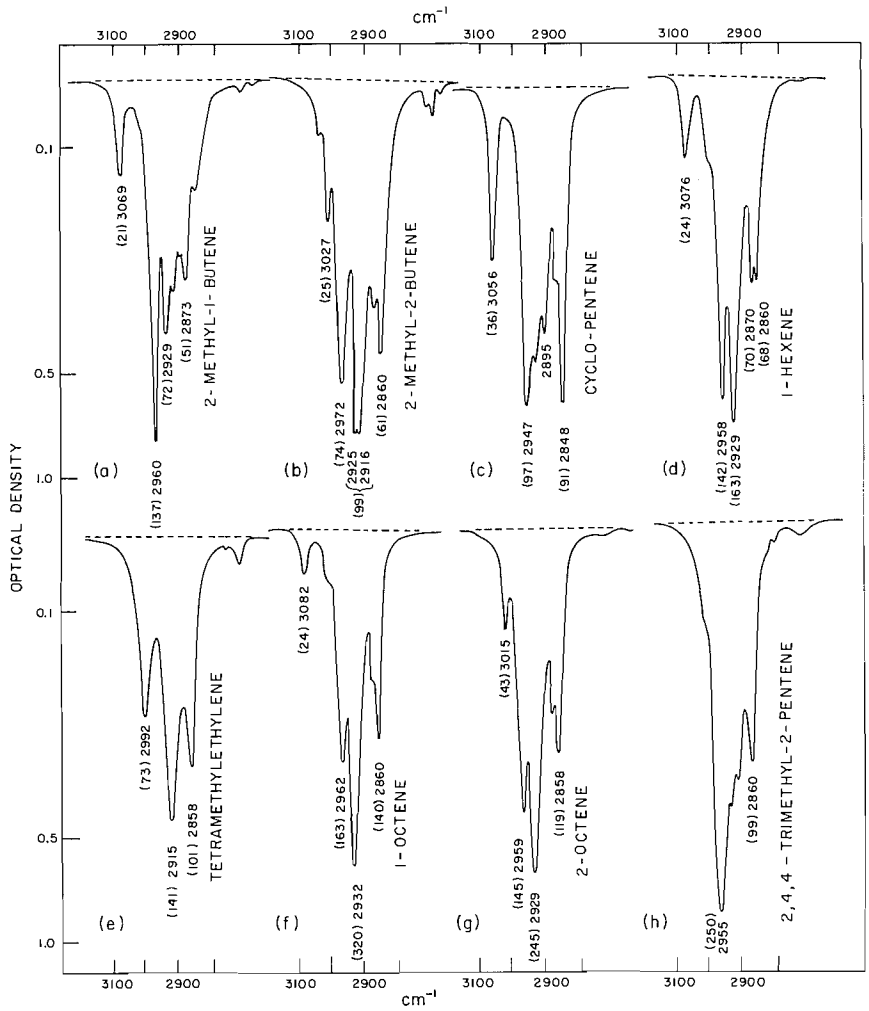


FIG. 9. Spectra of C_5–C_8 monoolefins in carbon tetrachloride solution. Optics: LiF.

Technical grade (95 mole% minimum). Their purity was checked by mass spectra; these were in good agreement with API values. A small trace of hexene was found in the 2-methyl-1-butene. Tetramethylethylene was a NBS high-purity sample.

ACKNOWLEDGMENTS

The authors wish to express their gratitude to Dr. R. J. Cvetanović for suggesting this topic and for his constant and helpful interest in its progress. They wish to thank the following persons for assistance: Dr. A. Tickner and Mr. R. L. Sander for mass spectrometric analyses, Mr. M. Bednas for several of the gas chromatographic analyses, and Mr. D. Kulawic for the determination of B.E.T. surface areas. They are indebted to Dr. M. E. Nordberg of Corning Glass for the gift of a number of thin Vycor plates and also for an interesting discussion.

REFERENCES

1. F. E. CONDON. *In* Catalysis. *Edited by* P. H. Emmett. Vol. 6. Reinhold, New York. 1958. p. 43.
2. D. S. MACIVER, R. C. ZABOR, and P. H. EMMETT. J. Phys. Chem. **63**, 484 (1959).

Can. J. Chem. Downloaded from www.nrcresearchpress.com by 210.87.254.5 on 09/05/12
For personal use only.

3. R. P. EISCHENS and W. A. PLISKIN. Advances in Catalysis, **10**, 1 (1958).
4. L. H. LITTLE. J. Phys. Chem. **63**, 1616 (1959).
5. See, for instance, review by N. Sheppard. *In* Hydrogen bonding. *Edited by* D. Hadži. Pergamon Press, London, 1959. p. 85.
6. A. TERENIN and V. FILIMONOV. *In* Hydrogen bonding. *Edited by* D. Hadži. Pergamon Press, London, 1959. p. 545
7. F. D. ROSSINI. Selected values of physical and thermodynamic properties of hydrocarbons. Carnegie Press, Pittsburgh. 1953.
8. M. FOLMAN and D. J. C. YATES. Proc. Roy. Soc. (London), A, **246**, 32 (1958); J. Phys. Chem. **63**, 183 (1959).
9. A. N. SIDOROV. J. Phys. Chem. (U.S.S.R.) **30**, 995 (1956).
10. H. SCHOLZE. Glastech. Ber. **32**, 142 (1959).
11. R. J. CVETANOVIĆ and N. F. FOSTER. Discussions Faraday Soc. No. 28, 201 (1959).
12. H. C. BROWN and J. D. BRADY. J. Am. Chem. Soc. **74**, 3570 (1952).
13. D. B. POWELL and N. SHEPPARD. Spectrochim. Acta, **13**, 69 (1958).
14. J. CHATT and L. A. DUNCANSON. J. Chem. Soc. 2939 (1953).
15. L. J. BELLAMY. The infrared spectra of complex molecules. John Wiley & Sons, New York. 1954.

Can. J. Chem. Downloaded from www.nrcresearchpress.com by 210.87.254.5 on 09/05/12
For personal use only.

Can. J. Chem. Downloaded from www.nrcresearchpress.com by 210.87.254.105 on 09/05/12
For personal use only.

OXIDATION OF WHEAT STARCH WITH ALKALINE HYPOCHLORITE[1]

A. A. EISENBRAUN[2] AND C. B. PURVES

ABSTRACT

The starch was oxidized with 5.5 base molar equivalents of 0.43 *M* calcium hypochlorite kept near pH 12 and 20°. The rate of oxidation was consistent with the occurrence of two first-order reactions differing in rate by a factor of 10, the more rapid of which consumed about 4 moles of hypochlorite for each $C_6H_{10}O_5$ unit actually oxidized. Oxalic acid (0.21 mole) and perhaps carbonic acid (⩾0.17 mole) were formed directly, but it was necessary to hydrolyze the product in order to liberate D-glucose (0.4 mole), glyoxylic acid (0.03 mole), D-erythronic acid (0.11 mole), mesotartaric acid (0.02 mole), D-tartaric acid (0.02 mole), L-tartaric acid (0.01 mole), D-glucuronic acid (0.004 mole), and probably tartronic acid (⩾0.03 mole).

The oxidation of various species of starch with alkaline hypochlorite, a process of industrial as well as academic interest, has been studied for many years. Reviews (1, 2) of the subject show that most of the early interest was attracted to the changes produced by various amounts of oxidant in such properties as viscosity and copper-reducing power, ease of retrogradation, and the adsorption of dyes. Degradation products were isolated and identified in only a very few instances. McKillican and Purves (3) more recently obtained evidence that hypochlorous acid near pH 4 oxidized wheat starch in the second and sixth positions of the glucose residues to yield in part 2-keto and uronic acid derivatives. Whistler and his collaborators (4, 5), employing corn amylose and amylopectin with hypochlorite kept at 25° and at various pH values between 3 and 13, dialyzed the products and showed that both the dialyzable and the non-dialyzable portions yielded D-glucose, glyoxylic acid, D-erythronic acid, and D-erythronolactone after hydrolysis with acid. Oxidations near pH 7 produced the maximum amount (about 0.3 mole) of glyoxylic acid. The present research provided additional information about the course of the reaction at pH 12 and 20°.

Preliminary experiments, employing 0.12 *M* and 0.06 *M* calcium hypochlorite with mole ratios per $C_6H_{10}O_5$ unit of 1:1 or 1:0.5, confirmed the observation (5) that such oxidations were exceedingly slow. Sodium hypochlorite yielded solutions from which it was more difficult to isolate the organic products. The use of a greater excess (mole ratio, 5.5:1) of a more concentrated (0.43 *M*) hypochlorite increased the speed of the oxidation to a convenient value, and had the additional advantage that the rate constant for the disappearance of hypochlorite would tend to follow the first-order kinetic equation. A semilogarithmic plot of the data (Fig. 1, plot A) became linear after about 76 hours and could be represented by the equation $\log 0.24/(0.24-b) = 2.2\times10^{-3}T$, where b was the concentration of hypochlorite consumed at time T, the units being moles, liters, and hours. Substitution of values of T between zero and 76 hours then yielded values of b from which, by difference from the observed values, the corresponding data b_1 for the initial, fast reaction could be calculated. These data (plot B) also fitted a first-order equation, $\log 0.19/(0.19-b_1) = 2.2\pm0.1\times10^{-2}\ T$.

The above calculations suggested that the oxidation of starch with hypochlorite at pH 12 consisted of a relatively rapid reaction consuming 2.34 moles of hypochlorite

[1]*Manuscript received September 19, 1960.*
Contribution from the Division of Industrial and Cellulose Chemistry, McGill University, and the Division of Wood Chemistry, Pulp and Paper Research Institute of Canada, Montreal, Que. Abstracted from a Ph.D. thesis submitted to the University in April 1959 by A.A.E.
[2]*Present address: Research Department, Allied Chemical Corporation, Nitrogen Division, Hopewell, Va., U.S.A.*

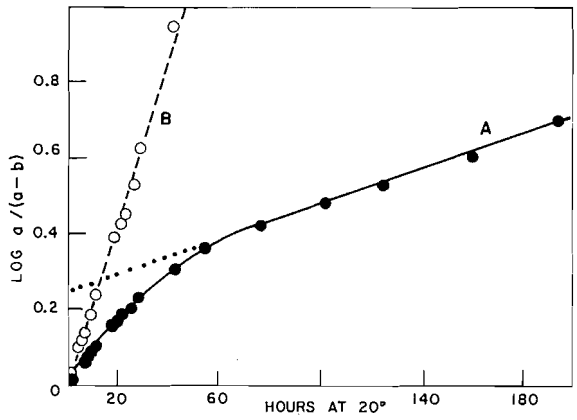


FIG. 1. Rate of oxidation of 0.183 base molar starch solution at pH 12 and 20° with 1.33 volumes of 0.756 *M* calcium hypochlorite. Ordinates, logarithm of initial to remaining concentration of hypochlorite. Plot A (full line), observed data; plot B, (broken line) calculated for initial rapid reaction.

per anhydroglucose unit, and a second reaction proceeding at about one-tenth the speed. Although at pH 12 aqueous calcium hypochlorite was in equilibrium with about 0.5% of undissociated hypochlorous acid (5), the two reaction rates could not be attributed to the independent action of these two species of oxidant, because any disequilibrium between them would be redressed almost instantaneously. The assumption that the anhydroglucose units of starch underwent a rapid initial oxidation followed by a much slower secondary oxidation seemed more plausible, but failed to explain why about two-fifths of these units remained unoxidized at the end of the initial reaction (see below). The three-fifths that reacted therefore reduced an average of about 4 moles of hypochlorite per glucose residue, or enough to oxidize the whole of this portion to the level of oxalic and erythronic acids. A more detailed kinetic study of this oxidation, employing different concentrations and mole ratios of hypochlorite, would be desirable.

The conditions noted in Fig. 1 were used in subsequent oxidations, but when 3.0 moles of calcium hypochlorite per anhydroglucose unit had been utilized acetone was added to convert the excess hypochlorite to chloroform. The liquors from the oxidation contained no organic substances of interest, and the crude insoluble products, ranging in weight from 143 to 225% of the original starch, contained 20 to 31.3% of calcium. An attempt to remove this calcium as the oxalate yielded the information that much was already present in that form, and another attempt at removal as the alcohol-soluble chloride showed that most of the organic acids liberated were also soluble in 70 to 90% ethanol at −10°.

Better results were obtained by adjusting an aqueous suspension of the calcium salts to pH 7 with dilute hydrochloric acid, removing those that failed to dissolve (fraction I, 37.5% by weight of the starch), and diluting the liquor with ethanol. In this way, any calcium hydroxide was eliminated as the soluble chloride, and the remaining calcium salts of the sugar acids were precipitated (fraction II, 87%). Calculations from the extensive analytical data showed that the free sugar acids from fraction I amounted to 22.5% of the starch, and those from fraction II to 62.5%; a further 3.7% was recovered as carbon dioxide present as calcium carbonate in the two fractions, but some or all of this amount might have been acquired adventitiously. Although hydrolyzates of the two fractions gave no chromatographic evidence of pentose sugars, the original sugar

Can. J. Chem. Downloaded from www.nrcresearchpress.com by 210.87.254.105 on 09/05/12
For personal use only.

acids yielded 0.73% and 2.34%, respectively, of furfural. These amounts were therefore attributed to the presence of 3.5% and 11.9% of uronic anhydride (6). After inorganic carbon dioxide had been removed, the conventional uronic anhydride determination gave the values 6.9% and 17.4%, respectively. These values were rejected as being too high, because Daniels (7) recently showed that only a small proportion of the "uronic anhydride" carbon dioxide yielded by a hypochlorite oxycellulose-6-C^{14} originated from position 6, and that the determination could not be interpreted in such cases.

Preliminary experiments on the hydrolysis of the major fraction II with boiling *N* sulphuric acid showed that its copper-reducing power as glucose, originally 2.8%, increased to a nearly constant value of 46.4% within 3 hours; the carbon dioxide evolved in the same time corresponded to the destruction of 13% of "uronic anhydride". The latter observation suggested that the low final reduction reflected the presence of non-reducing constituents rather than that of acid-resistant aldobiuronic acids. After inorganic ions had been removed, the hydrolyzate was chromatographed with *n*-butanol – formic acid – water both on paper and on a cellulose column. The major fractions yielded four acidic compounds, of which three had the flow rates of glyoxylic, erythronic, and optically active tartaric acid. The column when subsequently eluted with water yielded 46% of a partly crystalline syrup consisting almost entirely of glucose, which was thoroughly identified. Even when the glucose was removed by a prior fermentation with yeast, the acidic products could not be obtained in a crystalline condition.

Khym and Doherty (8), however, separated glucuronic and galacturonic acids by adsorption on a column of anion-exchange resin followed by elution with 0.15 *M* acetic acid, the order of elution depending on the relative dissociation constants of the acids and the eluent. After preliminary experiments, the hydrolyzed acids from fraction II, freed from calcium and sulphate ions, were adsorbed on the anion-exchange resin, which failed to absorb the glucose. The column was then eluted exhaustively and in succession with 2 *N* acetic acid, *N* formic acid, and 0.5 *N* trifluoroacetic acid, the effluent being collected in 20-ml or 25-ml volumes which were examined by paper chromatography (Table I).

Although erythronic acid and erythronolactone were removed simultaneously from the column by 2 *N* acetic acid, they had different R_F values when chromatographed on paper; both were isolated as the crystalline lactone. Glucuronic acid, however, chromatographed on paper as a single chemical individual. As expected, crystalline glyoxylic acid, mesotartaric acid, and DL-tartaric acid were recovered in the order of their dissociation constants, reported as $10^4 K = 4.74$, 6.3, and 9.7, respectively (9, 10, 11). DL- and D-Tartaric acids had the same dissociation constant, and were therefore isolated from the ion-exchange column together; they were subsequently separated by fractional crystallization from water, in which the latter was about seven times more soluble than the former (12). Both were obtained with their correct melting points, the first being optically inactive and the second having its correct specific rotation of $-14°$ in water (*c*, 5.5%). The racemic acid was probably not an artifact, because an authentic sample of L-tartaric acid underwent no change in rotation when kept for 3 days in water buffered to pH 12 (as in the oxidation of the starch), or when boiled for 2.5 hours in *N* sulphuric acid (as in the hydrolysis of the oxidized starch). Prolonged attempts to isolate tartronic acid in the crystalline form, or as a crystalline derivative, failed.

The water-insoluble calcium salts comprising fraction I of the oxidized starch were next examined. Extraction with aqueous acetic acid left a residue of crude calcium oxalate. After calcium and a small amount of chloride ions had been removed from the

Can. J. Chem. Downloaded from www.nrcresearchpress.com by 210.87.254.105 on 09/05/12
For personal use only.

TABLE I

Column chromatography of hydrolyzed fraction II[a]

Eluent fraction	R_F on paper[b]	Weight, g	Substance	Eluent fraction	R_F on paper[b]	Weight, g	Substance
Column eluent 2 *N* acetic acid				Column eluent *N* formic acid			
60–98	.04–.09[c,e]	—	Glucose	1850–2175	.00[e] .05–.07[e] .38–.45[e]	0.47	—
151–225	.12–.17[e]	0.33	—				
226–340	.12–.17[g]	0.85	—				
341–375	.12–.15[f] .72–.74[f]	0.43	—	2176–2375	.01–.03[e] .05–.31[g]	1.58	Mesotartaric
376–509	.23–.28[g] .40–.45[g] .58–.61[e]	4.83	Erythronic acid and lactone[d]	2376–2465	.00[e]	0.18	—
				2466–2650	.10–.28[g]	1.27	DL-Tartaric D-Tartaric
510–525	.01–.13[f] .23–.28[e] .40–.45[f]	0.04	—				
				2651–3125	.00[e] .02–.04[e]	.35	—
526–880	.01–.13[f] .14–.17[e]	0.78	—				
881–1150	.04–.07[f]	0.34	Glucuronic	Column eluent 0.5 *N* trifluoroacetic acid			
1151–1300	.64–.74[e]	0.09		3516–3594	.00–.22[g] .32–.39[g] .52–.61[f] .81–.85[e]	1.16	Oxalic Tartronic
1301–1620	.07–.11[e] .66–.74[g]	1.00	Glyoxylic				
1621–1849		0.11	—	Total		12.3 g	

[a]From 50 g of fraction II after deashing. Column of Dowex 1-X-4 resin (acetate form).
[b]*n*-Butanol – formic acid – water eluent and bromphenol blue spray.
[c]*o*-Aminodiphenyl spray.
[d]Acid R_F, 0.23–0.28; lactone R_F, 0.40–0.45.
[e]Faint spot.
[f]Medium-sized spot.
[g]Large intense spot.

extract, evaporation left 13.6% of fraction I as a colorless glass containing the free sugar acids. Hydrolysis of the acids followed by paper chromatography revealed the presence of glucose and glyoxylic acid, together with non-reducing compounds with R_F values close to those of mesotartaric, L-tartaric, D-erythronic, and tartronic acids and of D-erythronolactone. The crude mixture amounted to only 5.1% of the starch, and was not separated quantitatively.

In Fig. 2, the total molar yield of each product was given the first time the substance was recorded; these yields were minimum estimates, with the exception of those for carbonic and tartronic acids, whose authenticity was doubtful. Together with the carbonic acid lost by decarboxylation during hydrolysis, they accounted for between 70 and 80% of the hypochlorite used in the oxidation. Only oxalic acid, and perhaps carbonic acid, occurred as such among the original, unhydrolyzed products, about 80% of which dialyzed through cellophane in aqueous solution and were therefore of no great molecular size. Nevertheless, paper chromatograms failed to reveal erythronic acid and lactone, glyoxylic, tartronic, and the tartaric acids in circumstances where their mobilities would have rendered them readily detectable. Since any ester groups would not have survived the alkalinity of the oxidation, the conclusion seemed inevitable that the acids remained attached to adjacent units of the oxystarch structure by glucosidic or acetal bonds until liberated by acid hydrolysis. Any speculation concerning the course of the oxidation had to take account of this circumstance.

Can. J. Chem. Downloaded from www.nrcresearchpress.com by 210.87.254.105 on 09/05/12
For personal use only.

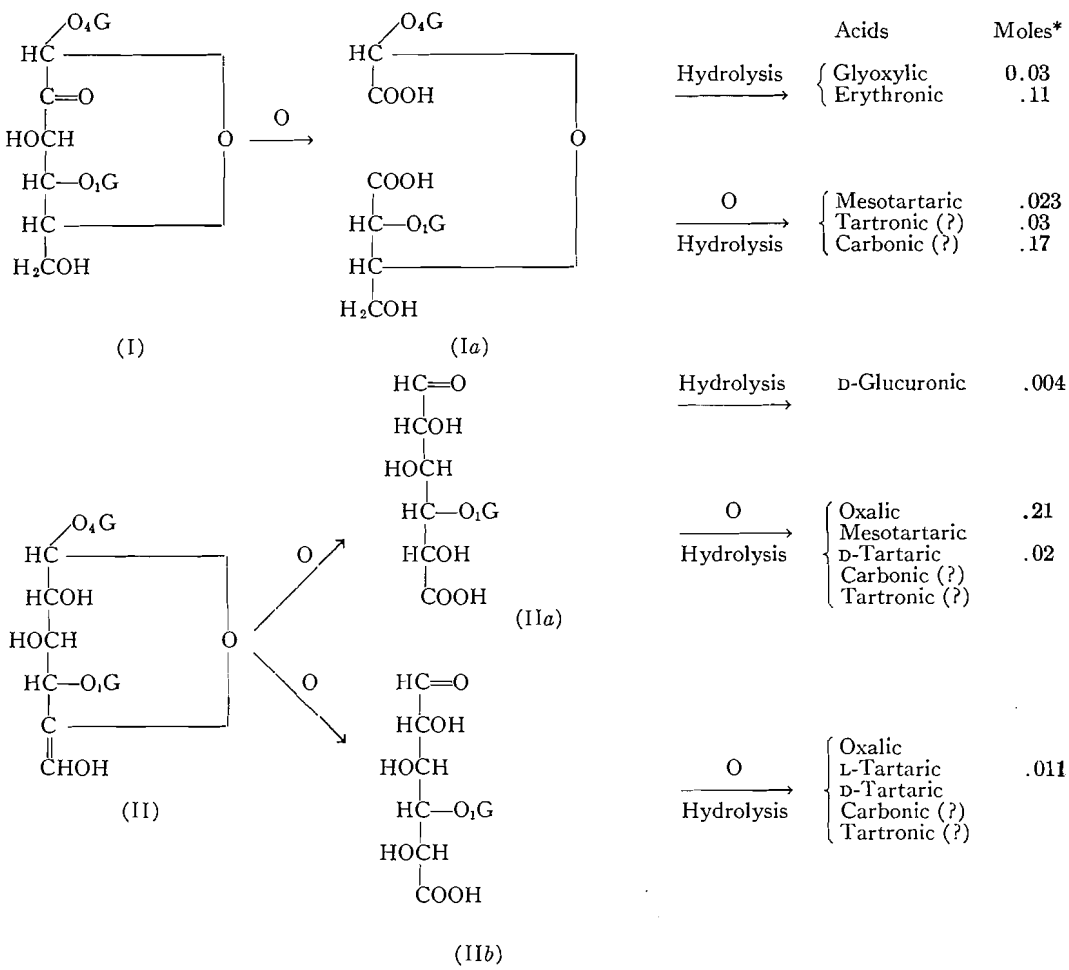


FIG. 2. Identified end products and postulated intermediates in oxidation of starch with calcium hypochlorite at pH 12. Adjacent anhydroglucose units, linked through fourth and first positions, denoted as $_4$G and $_1$G, respectively.

The relatively large yields of D-erythronic acid and lactone were readily explained by oxidation of an anhydroglucose unit in starch to the 2-keto structure I, followed by oxidative cleavage between the second and third positions to I*a*, as Whistler and his collaborators (4, 5) had already supposed. Further oxidation of I*a* would readily yield the precursors of mesotartaric and of tartronic acid. The other probable site of initial oxidation was the primary or sixth position of the anhydroglucose unit. It appeared necessary to assume that the enolic form of the 6-aldehyde structure II had at least a transitory existence, and yielded on further oxidation not only the D-glucuronic moiety II*a* but also the L-iduronic derivative II*b*, although only the former was isolated. Farley and Hixon (13) also isolated a small amount of glucuronic acid from a starch oxidized with 4 equivalents of bromine in neutral solution. By analogy with the easy cleavage of methyl-α-D-galactopyranuronoside and of pectic acid to free galacturonic acid by alkaline hypochlorite (14), the present oxidation at position 6 would lead to the collapse

**Per anhydroglucose unit in starch.*

Can. J. Chem. Downloaded from www.nrcresearchpress.com by 210.87.254.105 on 09/05/12
For personal use only.

of the glycosidic linkage at position 1, as shown in structures II*a* and II*b*. Further oxidation in the 2,3-positions would yield more mesotartaric acid from II*a*, but L-tartaric acid from II*b*, the other product in each case probably being oxalic acid. If oxidation occurred in the 1,2- and 5,6-positions, the product in both cases would be D-tartaric acid and carbonic acid.

Höning and Ruziczka (15), who oxidized starch with barium hypobromite in 0.02 *N* barium hydroxide, found maltobionic, and perhaps gluconic acid, among the products. These two substances were not detected on the present occasion. Neither were saccharinic acids, which might have been formed by the action of alkali on reducing structures such as I and II (16). D-Glucaric acid (saccharic acid) was not found, although mucic acid was prominent among the oxidation products of pectic acid (14); there was no evidence of 5-carbon acids such as arabonic and trihydroxyglutaric. At least some of these negative results might have arisen from the limitations of the experimental methods used.

EXPERIMENTAL

Materials and Analytical Methods

Unless stated otherwise, all liquors were concentrated in a rotary evaporator at little more than room temperature, and analyses quoted were the mean of concordant duplicate or triplicate determinations. Specific rotations referred to the *D*-line of sodium and to 20°.

The commercial, unbleached wheat starch was simultaneously freed from fat and ash, and converted to the thin-boiling state, by being steeped for 5 days in changes of 97% acetic acid at room temperature (17). Periodate oxystarch, when reoxidized with bromine (18) and hydrolyzed, yielded brucine D-erythronate from which a solution of the free acid was prepared via the barium salt. Provided the brucine and barium salts were carefully purified, the D-erythronolactone crystallized when the solution was evaporated and the last traces of moisture were removed by distillation with toluene. Recrystallization from ethyl acetate yielded material with the correct (19) melting point, 102°, and specific rotation, −72.8°. This lactone, and also crystalline glyoxylic acid (20), were synthesized for reference purposes.

Solutions of reagent grade calcium hypochlorite were filtered through sintered glass and were standardized iodometrically or by the arsenite method. A blank, determined as 0.118 *M* by both methods, remained unchanged in titer for at least 44 hours at 20°, and conversion to chlorate was therefore negligible (5). The calcium content of the oxystarch was determined either as carbonate by incineration to constant weight at 475° to 525°, or as sulphate by incineration at 900° after treatment with sulphuric acid; precipitation as the oxalate and titration of the latter with 0.1 *N* potassium permanganate in dilute sulphuric acid (21) was also used. To determine inorganic chloride, an aqueous solution or suspension of the sample was acidified with pure, 6% nitric acid and was titrated potentiometrically with 0.1 *N* silver nitrate to an end point at 275 millivolts (22). Inorganic carbonate was estimated by decomposing a 1- to 2-g sample with 12% hydrochloric acid at 70° in an uronic acid apparatus (23) and weighing the carbon dioxide evolved; uronic anhydride carbon dioxide was then determined separately by boiling a similar still residue under reflux for 3 and 5 hours and extrapolating the data to zero time. Somogyi's method (24) was used to determine copper-reducing power, the reagents being standardized with pure glucose.

Salts were usually converted to the free acids by passing the aqueous solution through a column of the cation-exchange resin, "Amberlite IR-120", which was subsequently

Can. J. Chem. Downloaded from www.nrcresearchpress.com by 210.87.254.105 on 09/05/12
For personal use only.

eluted with water until the effluent became neutral. Aliquots of the effluents could then be examined by descending paper chromatography, the eluent being the organic phase of a water – *n*-butanol – 85% formic acid mixture (385:500:115) equilibrated by boiling under reflux for 1 hour (25). Since bromphenol blue in 95% ethanol (26) was almost always the spray, the chromatograms first had to be dried *in vacuo* at 110° for 8 hours to eliminate the last traces of formic acid. The other acids then gave well-defined yellow spots on a blue background. An acidic solution of *o*-aminodiphenyl (27) gave brown, purple, and yellow spots with glucose, D-glucuronic acid and its lactone, and with glyoxylic acid, respectively, while a spray of alkaline hydroxylamine followed by ferric chloride in 1% hydrochloric acid (28) gave clear brown spots with lactones.

Rate of Oxidation (Fig. 1)

The starch, 2.50 g with 10.7% moisture (13.7 mmoles), was dispersed in 12.5 ml of water and the mixture was gelatinized by the addition of 37.5 ml of boiling water. After immersion in a boiling water bath for 10 minutes, the solution was cooled to room temperature (20°), and mixed with 125 ml of water containing 75.6 mmoles of calcium hypochlorite and 1 g of powdered calcium hydroxide. The flask used was protected from light, the mixture was mechanically stirred, and the hydrogen ion concentration was kept at all times within the limits pH 12.1 to 11.6 by the addition of two 1-g portions of calcium hydroxide. Aliquots were removed at intervals and the amount of residual hypochlorite was determined iodometrically.

Larger-Scale Oxidation

A 225-g sample of the starch (7.2% moisture) was dissolved in 5 liters of water in the way described, and was oxidized with 10 liters of calcium hypochlorite kept near 20°. The concentrations of the starch per $C_6H_{10}O_5$ unit and of hypochlorite were 86 mmoles and 443 mmoles per liter, respectively. A total of 210 g of powdered calcium hydroxide was added during the oxidation to maintain the alkalinity between pH 11.8 and 12.1. After 2.98 moles of hypochlorite per anhydrohexose unit had been consumed, the reaction was stopped by the addition of 500 ml of acetone. The mixture was filtered and the insoluble material was repulped in 1000 ml of water.

The combined liquors were neutralized with carbon dioxide, the precipitated calcium carbonate was discarded, and the concentrated mother liquor was diluted with much ethanol. Crystalline calcium acetate monohydrate (from the acetone), contaminated with the chloride and carbonate, separated, but no salt derived from the oxidized starch could be found.

A slurry of the above, insoluble calcium salts in 2000 ml of fresh water was then neutralized to pH 7.0 by adding 300 ml of concentrated hydrochloric acid, neutralization being considered complete after the pH remained unchanged for 24 hours. The insoluble residue was recovered, slurried with 1000 ml of water in a Waring Blendor to reduce the particle size, extracted twice more with a total of 1100 ml of water, and dried in the air. Yield of fraction I, 78.2 g or 37.5% by weight of starch. All the neutral filtrates and washings from fraction I were combined, concentrated to 700 ml, and diluted with 2 volumes of ethanol to precipitate the water-soluble calcium salts of the oxystarch. This precipitation was repeated twice more to remove calcium chloride, and the product was dried in the air. All alcoholic liquors were combined, concentrated, and again diluted with ethanol to recover another 14 g of calcium salts. These salts were combined with the main crop to give 181.7 g (87%) of fraction II.

Found for fraction I: ash at 1200° (CaO), 32.4; Cl, 0.23; moisture, 8.1; furfural, 0.73;

Can. J. Chem. Downloaded from www.nrcresearchpress.com by 210.87.254.105 on 09/05/12
For personal use only.

uronic anhydride, 6.9; inorganic CO_2, 5.5%. Samples, 0.139 g, 0.204 g, and 0.200 g, reduced 9.7 ml, 14.2 ml, and 14.1 ml, respectively, of acid potassium permanganate, the corresponding oxidation equivalent being 51.3, 51.3, and 51.9% of calcium oxalate monohydrate. When corrected for calcium chloride, calcium carbonate, and moisture, the calcium content of the product was 22.9%, giving a yield of 60.1% of fraction I (22.5% of the starch) as sugar acids of average equivalent weight 68.3.

Found for fraction II: ash (as $CaSO_4$), 37.3; Cl, 1.45; moisture, 11.9; furfural, 2.34; uronic anhydride, 17.3; inorganic CO_2, 1.84%. Correction for calcium carbonate, calcium chloride, and moisture gave Ca, 10.4% for the salts of the sugar acids, whose equivalent weight was 173 and whose yield was 73.6% of fraction II or 64% of the starch.

A solution of fraction II (2 g) in 15 ml of water was freed of cations and the effluent was diluted to 100 ml. One 20-ml aliquot of this acidic effluent, corresponding to 0.4 g of fraction II, yielded 0.282 g, or 70.5%, of sugar acids when dried *in vacuo* to constant weight. Two other aliquots were mixed with 0.1 *N* sodium hydroxide and were back-titrated after 16 hours to a phenolphthalein end point with 0.1 *N* hydrochloric acid; the aliquots neutralized 4.46, 4.52 milliequivalents per gram. Since 1 g of fraction II originally contained 0.41 milliequivalent of chloride, the value for the sugar acids was 4.08, corresponding to a neutralization equivalent of 705/4.08 or 173. Both this value and the yield were in good agreement with those calculated from the analytical data.

A 1.32-g sample of fraction II was freed from cations and the solution was dialyzed through collodion against two 4-liter volumes of 0.01 *N* hydrochloric acid for 36 hours, then against the same volumes of distilled water to remove the hydrochloric acid. Evaporation of the residual liquor yielded 0.153 g or 11.6% of non-dialyzable material, corresponding to 16% of the free sugar acids.

Products from Hydrolysis of Fraction II

A solution of fraction II, 0.598 g, in 20 ml of *N* sulphuric acid was boiled under reflux, aliquots being periodically removed and neutralized with sodium hydroxide. After 0, 0.25, 0.5, 1.0, 2.0, 3.0, 4.0, 5.0, 6.6, and 8.6 hours the copper reduction as glucose (24) was 2.8, 11.0, 17.8, 26.0, 33.5, 35.9, 37.0, 38.7, 41.2, and 42%, respectively. Hydrolysis for 2.5 hours was judged sufficient in the subsequent work. A mixture of fraction II, 1.02 g, and 60 ml of *N* sulphuric acid, contained in the uronic acid apparatus (22), was freed from inorganic carbon dioxide by the passage of nitrogen for 1 hour, and was then boiled under reflux for 2.5 hours. Found: uronic anhydride, 9.4%, corresponding to the decomposition during hydrolysis of 13.1% of carboxyl groups in the sugar acids.

An aqueous solution of the fraction II from an earlier oxidation, 2 g, was decationized, evaporated almost to dryness, and redissolved in 40 ml of *N* sulphuric acid. After hydrolysis as just described, sulphate ion was precipitated by the exact amount of aqueous barium hydroxide, and the filtrate on evaporation yielded 1.86 g of a syrup. This syrup, 1.58 g, was chromatographed on a cellulose column. All acidic material was removed by the passage of 5500 ml of the butanol – formic acid – water mixture, and then the glucose was eluted with 5000 ml of water. Evaporation of the aqueous effluents left 0.675 g of a syrup (43% of the calcium-free material) which partly crystallized when stored *in vacuo* over solid sodium hydroxide. The phenylosazone (29) decomposed at 198–199°, or in the proper range for the glucose derivative. The corresponding osotriazole (30) had the melting point 195.5°, not depressed by admixture with authentic glucose phenylosotriazole, m.p. 195°.

Fifty grams of fraction II, suspended in water and mixed with 70 g of "Amberlite

Can. J. Chem. Downloaded from www.nrcresearchpress.com by 210.87.254.105 on 09/05/12
For personal use only.

Can. J. Chem. Downloaded from www.nrcresearchpress.com by 210.87.254.105 on 09/05/12
For personal use only.

IR-120", was put on the top of a column of the same resin and eluted with water. Evaporation of the effluent left 51 g of calcium-free, acidic syrup which was hydrolyzed, the hydrolyzate then being freed from sulphate ion by the addition of the exact amount of aqueous barium hydroxide. The filtrate and washings were concentrated to 1500 ml and passed through a 25 cm×3.5 cm column containing "Dowex 1-X-4" anion-exchange resin (free base) at a rate of 17 ml per minute. Paper chromatography of the effluent revealed no evidence of any sugar save glucose, and epimerization to other sugars had not occurred during the 90-minute exposure to the strongly basic resin (31). The resin with its adsorbed sugar acids, but no more than traces of glucose, was transferred without delay to the top of a 100×5.6 cm column containing the same resin in its acetate form. Elution of the column at once began with 2 *N* acetic acid at a flow rate of 1.5 ml to 3 ml per minute, and the effluent was collected in 25-ml or 20-ml fractions. Every 20th or 30th fraction was evaporated to 0.3 ml, and chromatographed on paper. When nothing more was extracted by the acetic acid, the eluent was changed to *N* formic acid, which was later replaced by 0.5 *N* trifluoroacetic acid, the total volume of effluents being more than 60 liters. Fractions shown by paper chromatography to contain the same compound or compounds were combined and concentrated to syrups. Of these syrups, those derived from the following sets of fractions (Table I) were examined.

Fractions 226–340

The corresponding syrup, 0.85 g, yielded several spots, revealed by the bromphenol blue spray, when chromatographed on paper for several days. When a solution was titrated with alkali to pH 7, the behavior was that of a lactone. Several attempts to obtain a crystalline acid or calcium salt from the syrup failed.

D-*Erythronolactone*

Fractions 376–510 yielded 4.83 g of a syrup which crystallized when nucleated with 2 mg of pure D-erythronolactone; 1.2 g of crystals melting at 85–95° separated. Recrystallization yielded 1 g of material whose neutralization equivalent, 117.4, melting point, 101–103°, and specific rotation, −72.9° (*c*, 4.57, water) agreed with accepted values (19, 32). A mixed melting point with an authentic sample was undepressed and the infrared spectra of both samples were identical.

D-*Glucuronic Acid*

The syrup, 0.322 g, from fractions 924–1105 was adsorbed on a microcolumn of "Dowex 1-X-4" anion-exchange resin (free base form), which was quickly eluted with water to remove any cations. Elution with 2 *N* acetic acid began immediately, and evaporation of the first 85 ml yielded 0.249 g of a syrup. Nucleation of this syrup with 0.3 mg of D-glucuronic acid caused the crystallization of 0.106 g of the crude material, which was isolated by pressing the partly crystalline mass between pads of filter paper. The material recovered from the paper was heated to convert it to the lactone, but the product could not be crystallized. The glucuronic acid, after recrystallization from aqueous ethanol, melted correctly at 154–155° and had the correct (33) equilibrium specific rotation in water, +35.6° (*c*, 2). The infrared spectrum was identical with that of pure D-glucuronic acid prepared from the crystalline lactone.

Glyoxylic Acid

Fractions 1301–1500 yielded 0.917 g of a syrup which when chromatographed on paper gave a yellow spot, R_F 0.61–0.70, with the *o*-aminodiphenyl spray, and a spot of R_F 0.66–0.74, with bromphenol blue. The behavior of authentic glyoxylic acid was

identical. The syrup gave 59% of the theoretical yield of yellow, crystalline, glyoxylic acid 2,4-dinitrophenylhydrazone melting with decomposition at 189–191°, in agreement with the recorded (4) value. Found: N, 22.1. Calc. for $C_8H_6N_4O_6$: N, 22.1%.

Mesotartaric Acid

The syrup, 1.226 g, from fractions 2176–2300 partly crystallized when nucleated with 0.3 mg of mesotartaric acid, and its R_F value, 0.61–0.70, when chromatographed on paper was identical with that observed for an authentic L-tartaric acid. Some of this syrup, 0.41 g, was neutralized to pH 8 with 0.345 *N* barium hydroxide, and 0.40 g of a crystalline barium salt separated. Found (after purification): Ba, 63.1%. Calc. for $BaC_4H_4O_6.H_2O$: Ba, 65.1; for $BaC_4H_4O_6.2H_2O$: Ba, 61.1%.

A portion, 0.206 g, of the above salt when deionized gave 0.100 g of the crystalline free acid which melted at 130–137°. These crystals were neutralized to pH 3.5 with 0.25 *N* potassium hydroxide; dilution of the liquor with 2 volumes of ethanol and the addition of 0.3 mg of monopotassium mesotartrate caused the crystallization of that substance. Yield, 0.082 g after purification by extraction with ethanol. Found: ash as carbonate, 36.5%. Calc. for $KC_4H_5O_6$: K_2CO_3, 36.7%. Upon recovery from this salt, the colorless crystals of the free acid were optically inactive and had the melting point, 139–140°, reported for pure mesotartaric acid (34).

DL- *and* D-*Tartaric Acid*

Fractions 2466–2600 yielded a mixture, of which 0.612 g crystallized and 0.48 g remained as syrup. After recrystallization from acetone, the crystals melted at 203–204° and their neutralization equivalent of 76.1 was close to that, 75, calculated for a tartaric acid. A 0.315-g sample of these crystals yielded 0.298 g of the white monopotassium salt which was then twice recrystallized from water. Found: ash as carbonate, 36.7%. Calc. for $KC_4H_5O_6$: K_2CO_3, 36.7%.

A part of this salt, 0.14 g, yielded 0.11 g of crystalline free acid melting with decomf position at 204° after recrystallization from tetrahydrofurane. The melting point o, DL-tartaric acid was 204–206° (35). As expected, the crystals were optically inactive and yielded a precipitate when an aqueous solution was diluted with a saturated aqueous solution of calcium sulphate. This test distinguished the racemic from the optically active forms of tartaric acid (36). The paper chromatographic flow rate of an aqueous solution of the crystals (Table I) was identical with that of authentic DL-tartaric acid, which was a streak of R_F 0.32–0.62 with reference to L-tartaric acid as standard.

Most of the syrup from the original crystallization, 0.41 g, was freed of any contaminating cations, and was converted as above to the monopotassium salt, a solution of which in 66% ethanol was seeded with a trace of monopotassium D-tartrate. The crystals which separated after 24 hours near 0°, 0.30 g, were washed in ethanol and twice recrystallized from hot water. Yield 0.29 g. Found: ash as carbonate, 36.9%. Calc. for $KC_4H_5O_6$: K_2CO_3, 36.7%. When a solution of this purified salt was freed from cations, the acidic effluent crystallized solidly; melting point, 168–170°, and specific rotation in water $-14.0\pm0.6°$ (*c*, 5.5). The melting point reported (35) for D-tartaric acid was 170°, and the specific rotation for *c*, 5.5, was calculated from Landolt's formula (37) as −14.3°. When chromatographed on paper, the flow rate of an aqueous solution of the crystals was identical with that of authentic L-tartaric acid.

Can. J. Chem. Downloaded from www.nrcresearchpress.com by 210.87.254.105 on 09/05/12
For personal use only.

Can. J. Chem. Downloaded from www.nrcresearchpress.com by 210.87.254.105 on 09/05/12
For personal use only.

Fractions 3516–3553

These fractions were evaporated to 15 ml, diluted with water, and evaporated several times to expel most of the trifluoroacetic acid. Continuous extraction of the final aqueous residue for a total of 17 hours with ether yielded 1.16 g of syrup, the first portion of which, 0.93 g, partly crystallized during isolation. An aqueous solution of these crystals, 0.21 g, was decolorized with absorbent carbon and was then evaporated over solid sodium hydroxide at 30-mm pressure. A control experiment showed that oxalic acid dihydrate was stable under these conditions, but became anhydrous when drying agents more powerful than sodium hydroxide were used. The residual, transparent crystals after recrystallization from hot water had the melting point, 100–101°, of oxalic acid dihydrate. A mixed melting point with an authentic sample was not depressed. A 16-mg sample reduced 9.74 ml of 0.026 *N* potassium permanganate, the value calculated for oxalic acid dihydrate being 9.73 ml.

The ether extract from which the oxalic acid had originally crystallized yielded 0.71 g of a syrup, 0.2 g of which was freed of any cations. When the concentrated, acidic effluent was neutralized with 0.044 *M* calcium hydroxide about 15 mg of calcium oxalate separated and was removed. Dilution of the concentrated filtrate with 2 volumes of ethanol precipitated 0.155 g of a calcium salt (A) and evaporation of the mother liquor yielded a further 0.087 g (B). Calcium salts (A) and (B) were separately freed from calcium ions and the acidic effluents were chromatographed on paper. At low concentrations the R_F values for authentic tartronic acid, acids A and B, were 0.30–0.34, 0.27–0.31, and 0.32–0.34, respectively; at higher concentrations the values were 0.30–0.47, 0.40–0.48, and 0.40–0.47. The similar variations in R_F with concentration made it probable, but failed to prove, that acids A and B consisted of tartronic acid. Acid A was adsorbed on a micro "Dowex-1-X-4" anion-exchange column, which was then eluted with *N* acetic acid before the product was recovered in 25% aqueous formic acid. The syrup from the effluent, however, failed to crystallize, either as such or when converted to the neutral potassium or calcium salts. Control experiments with authentic, crystalline tartronic acid showed that it was eluted readily from the above resin with formic acid, and readily yielded a crystalline potassium salt and a precipitate of calcium salt.

Examination of Fraction I

Five grams of the original, water-insoluble calcium salts was mechanically agitated for several hours in an excess of aqueous 5% acetic acid. The undissolved portion was re-extracted in the same way, was washed with water, and was dried. Yield 3.1 g or 62%. Found: ash as sulphate, 77.9%; or Ca, 22.9%. Calc. for $CaC_2O_4.H_2O$: Ca, 27.4%. A solution of this product in 40 ml of 20% hydrochloric acid was continuously extracted with ether for 14 hours, and evaporation of the extracts yielded 2.15 g of crude oxalic acid. Recrystallization from a little hot water left 2.08 g of the pure substance with the correct permanganate equivalent. The yield corresponded to 48.2% of calcium oxalate monohydrate in fraction I.

An acetic acid extract from another 5 g of fraction I was freed by an ion-exchange resin from calcium ions, and then from chloride ions by shaking with a slight excess of silver carbonate, the final filtrate being concentrated to dryness. A brittle glass remained; weight 0.67 g (5.1% of the starch) of which 69% passed through a cellophane membrane when dialyzed against water. A part of this glass was hydrolyzed and the sulphuric acid was precipitated as the barium salt. The filtrate when chromatographed on paper

yielded spots with R_F values corresponding to the substances noted in Table I, those for D-glucose, D-erythronic acid, and D-tartaric acid being most intense.

ACKNOWLEDGMENTS

The authors thank K. M. Gaver and the Ogilvie Flour Mills Company Limited for a gift of the purified wheat starch used. One of them (A.A.E.) also thanks the Gottesman Foundation of New York for the Fellowship held during the research. Analyses for inorganic carbonate, uronic acid, and pentosan were carried out in the Analytical Department of the Institute under the supervision of Mr. J. E. Tasman.

REFERENCES

1. J. A. RADLEY (*Editor*). Starch and its derivatives. 2nd ed. Chapman & Hall, Ltd., London. 1943. Chap. III. p. 180.
2. R. W. KERR (*Editor*). Chemistry and industry of starch. Academic Press, Inc., New York. 1950. Chap. X, XI. pp. 183, 307.
3. M. E. MCKILLICAN and C. B. PURVES. Can. J. Chem. **32**, 312 (1954).
4. R. L. WHISTLER, E. G. LINK, and S. KAZENIAC. J. Am. Chem. Soc. **78**, 4704 (1956).
5. R. L. WHISTLER and R. SCHWEIGER. J. Am. Chem. Soc. **79**, 6460 (1957).
6. F. W. NORRIS and C. E. RESCH. Biochem. J. **29**, 1590 (1935).
7. J. W. DANIEL. Tappi, **42**, 534 (1959).
8. J. X. KHYM and D. G. DOHERTY. J. Am. Chem. Soc. **74**, 3199 (1952).
9. W. OSTWALD. Z. physik. Chem. **3**, 188 (1889).
10. B. HOLMBERG. J. prakt. Chem. **84** (2), 166 (1911).
11. W. OSTWALD. Z. physik. Chem. **3**, 372 (1889).
12. E. LEIDIE. Z. anal. Chem. **22**, 269 (1883).
13. F. F. FARLEY and R. M. HIXON. Ind. Eng. Chem. **34**, 677 (1942).
14. R. H. ZIENIUS and C. B. PURVES. Tappi, **43**, 27 (1960).
15. M. HÖNING and W. RUZICZKA. Biochem. Z. **218**, 397 (1930).
16. G. MACHEL and G. N. RICHARDS. J. Chem. Soc. 4500 (1957).
17. A. C. ELLINGTON and C. B. PURVES. Can. J. Chem. **31**, 801 (1953).
18. G. JAYME and S. MARIS. Ber. **77**, 383 (1944).
19. F. W. JENSEN and F. W. UPSON. J. Am. Chem. Soc. **47**, 3019 (1925).
20. A. A. EISENBRAUN and C. B. PURVES. Can. J. Chem. **38**, 622 (1960).
21. I. M. KOLTHOFF and E. B. SANDELL. Textbook of quantitative inorganic analysis. 3rd ed. McMillan Publishing Corp., New York. 1952.
22. C. R. N. STROUTS, J. H. GILFILLAN, and H. N. WILSON. Analytical chemistry. Oxford University Press. 1955. p. 522.
23. B. L. BROWNING. Tappi, **32**, 119 (1949).
24. M. SOMOGYI. J. Biol. Chem. **195**, 19 (1952).
25. R. A. EDINGTON and E. PERCIVAL. J. Chem. Soc. 3554 (1955).
26. B. S. LUH and H. J. PHAFF. Arch. Biochem. Biophys. **51**, 103 (1954).
27. T. E. TIMELL, C. P. J. GLAUDEMANS, and A. L. CURRIE. Anal. Chem. **28**, 1916 (1956).
28. M. GEE and R. M. MCCARTHY. Anal. Chem. **29**, 257 (1957).
29. N. TAKETONI and K. MIURA. J. Soc. Chem. Ind., Japan, **32**, 776 (1929); Chem. Zentr. **100**, II, 2553 (1929).
30. R. M. HANN and C. S. HUDSON. J. Am. Chem. Soc. **66**, 735 (1944).
31. E. PACSU and L. REBENFELD. J. Am. Chem. Soc. **75**, 4370 (1953).
32. J. W. E. GLATTFELD and L. R. FOBRICH. J. Am. Chem. Soc. **56**, 1209 (1934).
33. W. F. GOEBEL and F. H. BABERS. J. Biol. Chem. **100**, 573 (1933).
34. P. WALDEN. Ber. **29**, 1702 (1896).
35. C. A. BISCHOFF and P. WALDEN. Ber. **22**, 1812 (1889).
36. F. K. BEILSTEIN. Handbuch der organischen Chemie. Vol. III. p. 524.
37. H. LANDOLT. Ber. **6**, 1075 (1873).

Can. J. Chem. Downloaded from www.nrcresearchpress.com by 210.87.254.105 on 09/05/12
For personal use only.

Can. J. Chem. Downloaded from www.nrcresearchpress.com by 210.87.254.5 on 09/05/12
For personal use only.

PHOTOOXIDATION OF AZOMETHANE

IV. THE ROLE OF FORMALDEHYDE[1]

M. SHAHIN[2] AND K. O. KUTSCHKE

ABSTRACT

The photooxidation of azomethane has been reinvestigated over a range of conversion extending to at least 7% at relatively high oxygen pressure and at 162° C. Kinetic and tracer (added $C^{13}H_2O$) studies support the view that the formaldehyde formed in the reaction can act as a source of the oxides of carbon. These were found to be enriched in C^{13} in the tracer work.

INTRODUCTION

One of the puzzling features of the mechanism of the photooxidation of azomethane (1) has been the nature of the product responsible for the self-inhibition (2, 3) of the reaction. Formaldehyde, nitrous oxide, and "excess nitrogen" (3) are produced at rates which decrease with the time of exposure. These products are thought (1, 3) to arise via the reactions

$$R + CH_3N_2CH_3 \rightarrow RH + CH_2{-}N_2CH_3, \quad [1]$$

$$CH_3N_2CH_2 + O_2 \rightarrow N_2O + CH_2O + CH_3, \quad [2]$$

$$\rightarrow N_2 + CH_2O + CH_3O, \quad [3]$$

where R is some radical in the system and [2] and [3] are written as over-all processes which might occur in stages. Provided methyl and methoxyl, or radical products of their reaction with oxygen, can function as R in [1], the elements of a chain reaction are present in the mechanism as appears to be required by the data (3).

It was recognized (2, 3) that when this chain was inhibited by some product, the inhibition mechanism must involve the production of carbon monoxide and, probably, of carbon dioxide. The mechanism suggested was a competition for the radicals R by the inhibiting substance, here designated by R'H.

$$R + R'H \rightarrow RH + R' \quad [4]$$

$$R' + O_2 \rightarrow CO + \text{other products} \quad [5]$$

$$\rightarrow CO_2 + \text{other products} \quad [6]$$

It is postulated that the "other products" do not propagate chains to any extent. Initially it was suggested that formaldehyde should be identified as R'H (2). While this suggestion led to a satisfactory qualitative explanation of the phenomenon, it was not compatible with later (3) quantitative data. Therefore another mechanism, which identified R'H with performic acid, was advanced.

The purpose of the present work was to obtain data confirming, or otherwise, the hypothesis that formaldehyde could not function as R'H. In addition to a purely kinetic approach, experiments were done in which formaldehyde-C^{13} was added to the reaction system. From a kinetic point of view the concentration of formaldehyde found at the end of an experiment, including that formed in the reaction, is indicative of whether or not formaldehyde was consumed in the reaction. If such consumption did indeed

[1]*Manuscript received August 2, 1960.*
Contribution from the Division of Pure Chemistry, National Research Council, Ottawa, Canada.
Issued as N.R.C. No. 6062.
[2]*National Research Council Postdoctorate Fellow 1958–60.*

occur, and if the mechanism of the consumption involves the inhibition mechanism [4], [5], and [6], the oxides of carbon found should be enriched in C^{13}.

EXPERIMENTAL

Apparatus

The vacuum apparatus, thermostatted air oven, and optical arrangements were essentially those used in an earlier investigation (3) with only minor modifications. The volume of the 5-cm diameter reaction cell was 180 cc, that of the complete reaction system, including the stirrer, 256 cc. All connecting tubing through which formaldehyde was required to pass could be heated to 140° C to prevent polymerization of that substance.

Materials

Azomethane (Merck of Canada, Montreal) was purified in the vacuum system in the usual manner (1, 2, 3). Gas chromatographic separation and estimation along with mass spectrometric identification of impurities revealed the presence in this sample of trimethyl hydrazine (<2%), methyl chloride (<0.1%), and methanol (<0.1%). The latter impurity was particularly objectionable in the experiments done at low conversions and, for these, it was removed by gas chromatography.

Oxygen was prepared by heating potassium permanganate and was separated from condensable impurities by passage through a trap at −196° C.

Formaldehyde-C^{13} (C^{13}/C^{12} = 20.4%) was obtained as required by heating a sample of enriched α-polyoxymethylene supplied by Dr. L. C. Leitch of these laboratories.

The trisodium salt of chromatropic acid (4,5-dihydroxy-2,7-naphthalene disulphonic acid, trisodium salt) used in the analysis of formaldehyde was prepared by titration of an aqueous solution (15%) of chromatropic acid disodium salt (Eastman Kodak) with a solution of sodium hydroxide (3%) to pH 7 as measured on a pH-meter. The salt was purified by fractional precipitation (3) and the beige-colored crystals were kept in dark bottles.

Procedure

Aside from minor details most operations in an experiment were done as described previously (3).

For the experiments with added formaldehyde-C^{13}, several break-seal bulbs, whose volumes were known, were filled from a manifold at one time using the filling technique developed earlier (3). The formaldehyde content of one bulb was determined and that of each of the others was calculated from the known volumes. Mixtures of azomethane, formaldehyde, and oxygen were prepared in the reaction system as described before (3).

Analysis of Products

After an exposure the products were condensed at −196° C in a U tube and the noncondensable gases (O_2, N_2, CO) were collected and analyzed over a hot mixture of copper and cupric oxide (1). Carbon dioxide and nitrous oxide were separated from a Le Roy still (4) at −160° C and analyzed by mass spectrometry. Small quantities of formaldehyde, methyl chloride (present as an impurity), and azomethane always appeared in this fraction and prevented accurate estimation of the major components. Some uncertainty is also introduced into the C^{13}/C^{12} ratio of the carbon dioxide because of the effects of these impurities.

Can. J. Chem. Downloaded from www.nrcresearchpress.com by 210.87.254.5 on 09/05/12
For personal use only.

Formaldehyde was separated from the remaining liquid products by a single passage through a Le Roy still held at −130° C and condensed onto a frozen solution of the trisodium salt of chromatropic acid held at −196° C. All connecting tubing accessible to the formaldehyde vapor was held at 140° C. Procedures developed earlier (3) were followed in detail for the remaining steps in this modification of the chromatropic acid method (5). The liquid products were collected and analyzed for methanol by gas chromatography in a column developed by Blake and Kutschke (6) (25% dinonyl phthalate and 5% glycerol on Fischer Columpak; 29° C; H_2 flow rate, 45 cc/min). Peak areas were compared with those of standard samples.

RESULTS

Table I gives the data from several experiments at 162° C. The conditions were maintained as closely as possible to the earlier work (3). Oxygen concentration was sufficiently high to suppress completely the formation of methane and ethane. The trend of the

TABLE I

Yields of products in the photooxidation
(p_{azo} = 57 mm, p_{O_2} = 7 mm at 0° C; reaction temperature, 162° C;
$I_a = 4.0 \times 10^{-13}$ quanta/cc sec)

Time, minutes	μmoles					
	N_2	CO	CO_2	N_2O	CH_2O	CH_3OH
1	—	—	—	—	—	0.8
2.5	—	—	—	—	—	1.4
4	—	—	—	—	—	2.2
5	5.0	1.33	0.7	2.1	2.8	4.0
5	5.2	1.15	—	—	2.4	—
15	12.7	5.10	1.6	4.4	3.9	12.5
15	13.5	5.04	—	—	4.2	12.4
25	21.7	8.90	2.2	5.0	5.3	22.4
35	30.4	12.2	3.7	7.5	4.9	33.4
45	42.1	17.5	4.9	7.0	5.7	41.9
45	39.7	17.0	4.5	6.8	—	42.3
55	46.8	20.8	5.2	7.7	5.8	48.8
20	14.17	Oxygen absent				
40	28.50	Oxygen absent				

yields with time is shown in Fig. 1 in which quantum yields of a product, defined as the ratio of the amount of a product formed per unit time to that of nitrogen formed in the absence of oxygen with otherwise identical conditions, are plotted as a function of conversion. The latter corresponds to D_1 of reference 2 and is calculated with the assumptions that (*a*) each molecule of azomethane which disappears gives rise to a molecule of nitrogen or of nitrous oxide, and that (*b*) the stirring was completely efficient. Aside from that of methanol and formaldehyde the general forms of the curves in Fig. 1 agree with those obtained earlier (2, 3).

Results from experiments with added formaldehyde-C^{13} are given in Table II. The amount of formaldehyde added corresponded to a concentration about twice as great as that found after long experiments without added formaldehyde. Figure 2 shows that the concentration of formaldehyde rapidly adjusts to that same, approximately steady,

Can. J. Chem. Downloaded from www.nrcresearchpress.com by 210.87.254.5 on 09/05/12
For personal use only.

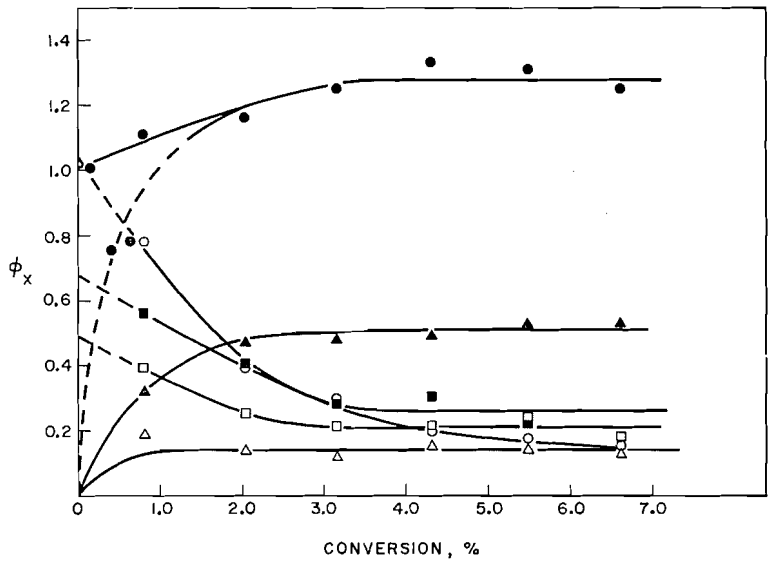


FIG. 1. Quantum yields as a function of conversion at 162° C: ● methanol, ○ formaldehyde, ■ nitrous oxide, □ secondary nitrogen, ▲ carbon monoxide, △ carbon dioxide.

TABLE II

Yields of products in the photooxidation
(Presence of 9.7 μmoles of formaldehyde-C^{13})

Time, minutes	μmoles			$100C^{13}/C^{12}$	
	N_2	CO	CH_2O	CO	CO_2
1	—	0.9	6.2	12	19
2	2.4	1.4	6.4	16	14
5	5.2	3.2	5.9	13	10
15	10.2	6.9	5.4	12	—
20	14.2	7.9	6.0	13	14

NOTE: Conditions as in Table 1.

concentration and thereafter remains unchanged. The yields of carbon monoxide obtained from experiments of low conversion were much greater in the presence of added formaldehyde than in its absence. This is shown in Fig. 3 as a plot of the absolute amounts of carbon monoxide formed at various times for the two sets of conditions. The slope of the curve (Fig. 3, open circles) obtained in the presence of formaldehyde becomes constant at about the degree of conversion at which the formaldehyde concentration reaches its approximately steady value (Fig. 2).

The last two columns of Table II present the data on the isotopic composition of the oxides of carbon found. There is little doubt that these compounds are enriched in C^{13}. Mixtures of formaldehyde-C^{13} and carbon monoxide were carried through the procedure of an experiment in the absence of ultraviolet illumination. On analysis no detectable enrichment was observed in the carbon monoxide.

Can. J. Chem. Downloaded from www.nrcresearchpress.com by 210.87.254.5 on 09/05/12
For personal use only.

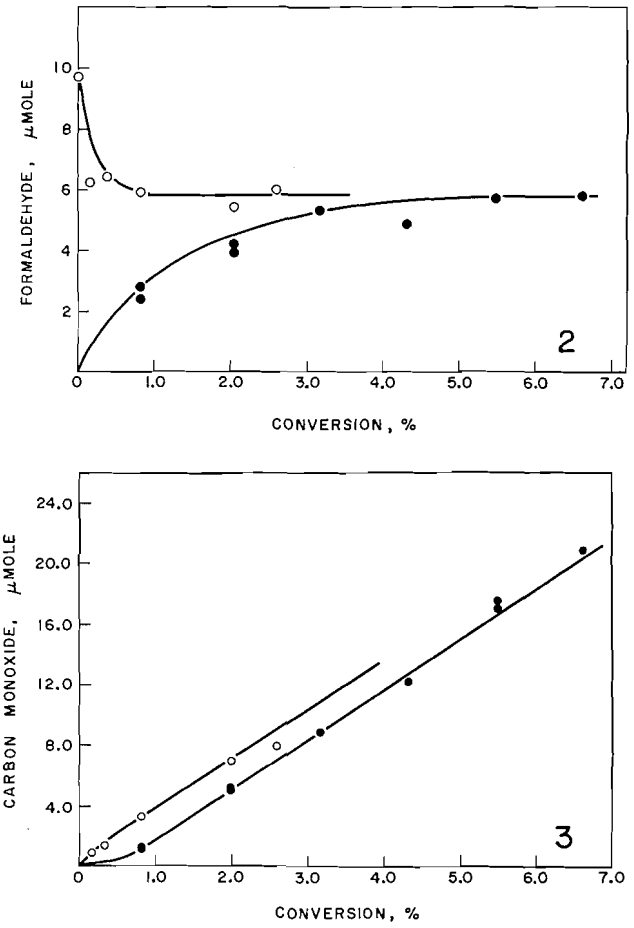


FIG. 2. Variation of the yield of formaldehyde with conversion: ● normal photooxidation, ○ 9.8 μmoles formaldehyde-C^{13} added initially.

FIG. 3. Variation of the yield of carbon monoxide with conversion: ● normal photooxidation, ○ 9.8 μmoles formaldehyde-C^{13} added initially.

DISCUSSION

This report is concerned only with the reaction at 162° C with conditions used in earlier investigations (1, 2, 3) and is confined largely to the discussion of the likelihood that formaldehyde can inhibit the reaction under these conditions. Moreover, the discussion is limited to the region of conversion greater than about 1%. At lower conversions, reproducible data are very difficult to obtain.

In an earlier communication (3) several arguments were offered to refute the hypothesis that formaldehyde could participate in the inhibition mechanism. These were of two types: kinetic, which discussed the shape of the yield vs. time curves, and isotopic, which involved the results of a photooxidation experiment done in the presence of formaldehyde enriched in oxygen-18.

In considering the kinetic arguments it must be borne in mind that, to a precision of about 10–15%, good agreement between this and the earlier study is found in the

Can. J. Chem. Downloaded from www.nrcresearchpress.com by 210.87.254.5 on 09/05/12
For personal use only.

Can. J. Chem. Downloaded from www.nrcresearchpress.com by 210.87.254.5 on 09/05/12
For personal use only.

yield vs. time curves of many of the products. This agreement is excellent in the curves for total nitrogen, carbon monoxide, nitrous oxide and, with somewhat less precision, for secondary nitrogen and carbon dioxide. Analogous curves for formaldehyde and methanol yields differ significantly.

The present data indicate quite definitely that formaldehyde concentration does indeed approach a stationary value with time. The earlier data, covering a somewhat smaller range of conversion, did not exhibit such a limit although the existence of such a limit is not incompatible with those data. For some reason as yet unknown the limiting concentration, or possible limiting concentration in the case of the earlier work, found in the two sets of data differ by a factor of about two as does the time (or conversion) required to attain that limit. The excellent agreement between the yields of other products, especially those of carbon monoxide, indicate that the two sets of data were taken under very similar conditions. The only possible explanations involve either an unknown systematic error in one or the other analytical techniques (which were virtually identical) or a difference in surface characteristics causing this specific effect. At present no choice is possible between these alternatives.

More extensive data are presented here concerning the effect of added formaldehyde on the yields of some products. In particular, Fig. 2 shows that formaldehyde is not inert in the system as was required by the mechanism suggested earlier (3).

That the consumption of formaldehyde is accompanied by the production of carbon monoxide is indicated by the enhanced rate of production of that product when excess formaldehyde is present initially (Fig. 3). After formaldehyde has been depleted to approximately its stationary value (i.e. about 0.5% conversion, Fig. 2), the yield–time curve for the formation of carbon monoxide is not inconsistent with a rate of production similar to that found in the absence of added formaldehyde (Fig. 3).

The C^{13} experiments (Table II) also indicate that carbon monoxide can be formed in this system from a formaldehyde intermediate. In addition it is clear that carbon dioxide also can arise from the same intermediate (values of the absolute yield of nitrous oxide and of carbon dioxide were not measured in these experiments). While these conclusions disagree with those reached on the basis of the O^{18} work reported earlier (3) the relative insensitivity of the present technique to errors caused by possible exchange over the hot copper oxide suggest that they are the more reliable. The value of the C^{13}/C^{12} ratio found in the oxides of carbon are lower than that of the added formaldehyde. This implies that some compound, presumably formaldehyde, which is produced in the system also acts as a precursor to the oxides of carbon.

It may be concluded from the present data that formaldehyde is not inert in this photooxidation system and that the oxides of carbon can be formed from the reactions of this compound.

If equations [5] and [6] represent the major sources of the oxides of carbon, then $R_{CO}/R_{CO_2} = k_5/k_6$. The data from 15 minutes to 55 minutes yield a value $k_5/k_6 = 3.7 \pm 0.1$, a value which is somewhat lower than that ($\sim$5) which can be deduced from similar data in the earlier work (3). A detailed mechanism has been suggested (7) for these reactions which involves the formation of HCO_3 radicals followed by isomerization to O=COOH and decomposition either to carbon monoxide and HO_2 radical or to carbon dioxide and an hydroxyl radical.

If, in addition to the assumption above, it is also valid to assume (*a*) that nitrous oxide and secondary nitrogen arise only from [2] and [3], and (*b*) that [2] and [3] represent the sole fates of $CH_2N_2CH_3$ radicals formed in [1], and [5] and [6] the sole fates of formyl

radicals formed in [4], then it follows that $(R_{CO}+R_{CO_2})[A]/\{(R_{N_2})_{secondary}+R_{N_2O}\}[F] = k_1/k_4$. Calculations based on the data of Table I give $k_1/k_4 = 212\pm10$ with no obvious trend with conversion. If A_1/A_4 is taken as unity approximately, this calculation indicates that $E_1 = E_4 = 4$–5 kcal/mole. Since it has not been established that the radical R in [1] and [4] is a single species (probably OH, HO_2, CH_3O, and CH_3O_2 enter into these reactions at various rates), the value calculated cannot be ascribed to a single reaction. However, it might be noted that the difference obtained is relatively large compared with the difference E_1-E_4 when R is a methyl radical. This latter difference has been reported as 2.2 kcal/mole (8).

Brief mention should be made at this point of the shape of the curve of the quantum yield of methanol as a function of conversion (Fig. 1). Analytical uncertainties are rather large in the low-conversion region and rigorous attention had to be paid to the purity of the reactants. The combination of these two factors renders the determination of quantum yields in this region highly imprecise. On the basis of the present data it is impossible to decide whether Φ_{CH_3OH} approaches unity or zero at these conversions (Fig. 1). While of obviously considerable significance, possible explanations of either extrapolation are closely associated with the mechanism of formation of methyl hydroperoxide recently found to be a product in this system (9). Detailed consideration of these points will be presented at a later time.

ACKNOWLEDGMENTS

The authors wish to thank Dr. E. W. R. Steacie for his interest and advice during the course of this work. They are also indebted to Mrs. R. H. Riem for the mass spectrometric analyses.

REFERENCES

1. G. R. Hoey and K. O. Kutschke. Can. J. Chem. **33**, 496 (1955).
2. R. L. Strong and K. O. Kutschke. Can. J. Chem. **37**, 1456 (1959).
3. F. Wenger and K. O. Kutschke. Can. J. Chem. **37**, 1546 (1959).
4. D. J. Le Roy. Can. J. Research, B, **28**, 492 (1950).
5. C. E. Bricker and W. A. Vail. Ind. Eng. Chem., Anal. Ed. **17**, 400 (1945).
6. A. R. Blake and K. O. Kutschke. Can. J. Chem. In press.
7. A. M. Mazkovich and L. F. Filippova. Zhur. Fiz. Khim. **31**, 2649 (1957).
8. S. Toby and K. O. Kutschke. Can. J. Chem. **37**, 672 (1959).
9. M. Shahin and K. O. Kutschke. J. Phys. Chem. In press.

Can. J. Chem. Downloaded from www.nrcresearchpress.com by 210.87.254.5 on 09/05/12
For personal use only.

Can. J. Chem. Downloaded from www.nrcresearchpress.com by 210.87.254.40 on 09/05/12
For personal use only.

THE PREPARATION AND SOME PROPERTIES OF GERMANIUM DIFLUORIDE[1]

NEIL BARTLETT AND K. C. YU

ABSTRACT

Germanium difluoride can be prepared by the reduction of germanium tetrafluoride with germanium metal. It is a white solid, m.p. 110°, and is orthorhombic, $a = 8.30$, $b = 5.17$, $c = 4.67$ Å. It possesses strong reducing properties.

INTRODUCTION

Evidence for the existence of germanium difluoride was noted by Winkler (1), who heated potassium fluorogermanate in a stream of hydrogen and obtained a dark-colored mass, an aqueous extract of which yielded germanous sulphide with hydrogen sulphide. The only other description of a difluoride of germanium is that given by Dennis and Laubengayer (2) and it is their findings which are widely quoted. They characterized the fluoride as a white, sublimable, hygroscopic solid which disproportionated on heating. An aqueous solution of it possessed the reducing properties of divalent germanium but the identity of the solid was not established by analysis.

We have prepared material similar to the latter and have proved it to be germanium difluoride. Some of the physical and chemical properties of the compound have also been examined.

DISCUSSION AND RESULTS

Dennis and Laubengayer prepared the difluoride by passing the gaseous tetrafluoride, produced by the pyrolysis of barium hexafluorogermanate, over powdered germanium, above 100°. We repeated this procedure and undoubtedly germanium difluoride was formed, but on no occasion was a sufficiently large or pure sample secured for analysis. The difluoride prepared in this way could not be transferred by distillation nor by pouring of the melt, without extensive interaction with the glass and disproportionation. These difficulties were associated with the presence of impurities, including water and hydrogen fluoride, as was manifest from the etching of the glass apparatus and may account for the delay in substantiating the earlier reports of the difluoride.

When germanium tetrafluoride was used which had been prepared by the direct fluorination of germanium metal, under strictly anhydrous conditions, the reduction proceeded smoothly and extensively in the temperature range 150–300° and in this way gram samples of the compound could be prepared and transferred without decomposition.

The stoichiometry, GeF_2, was established by germanium and fluorine analysis and the divalency was confirmed by iodine titration.

The white solid, m.p. 110°, distills without decomposition *in vacuo* at temperatures slightly above the fusion point. At higher temperatures disproportionation begins, as indicated by the appearance of an orange-red solid together with the concurrent evolution of germanium tetrafluoride. With some samples the temperature of decomposition was above 160° but since the decomposition is evidently catalyzed by impurities it is possible that more thermally stable material than this can be made. As the temperature is raised the orange-red product becomes red-brown and finally black, the last being associated

[1]*Manuscript received August 18, 1960.*
Contribution from the Department of Chemistry, University of British Columbia, Vancouver, British Columbia.

with the presence of germanium metal. This behavior resembles that of germanium dichloride and it is probable that the orange-red intermediate is a polymeric subfluoride $(GeF)_x$, since a similar material $(GeCl)_x$ has been reported as arising from the thermal decomposition of the dichloride (3, 4).

In ordinary moist air the difluoride deliquesces and on prolonged exposure orange germanous hydroxide separates. A mild exothermic hydrolysis occurs with water and the hydroxide precipitates. The fluoride is, however, totally soluble in 48% hydrofluoric acid and this solution has reducing properties, silver being deposited in the cold from a silver nitrate solution. The fluoride also dissolves in ethanol and forms an etherate with diethyl ether, but is insoluble in carbon tetrachloride.

The reducing properties expected to be associated with divalent germanium have been illustrated in several reactions.

Selenium tetrafluoride is reduced to selenium by the difluoride, which is oxidized to the tetrafluoride. The germanium tetrafluoride combines with excess selenium tetrafluoride to give the crystalline solid, fluoroselenonium hexafluorogermanate. The sequence of reactions is

$$2GeF_2 + SeF_4 = 2GeF_4 + Se,$$
$$GeF_4 + 2SeF_4 = (SeF_4)_2GeF_4.$$

The latter material, which will be an acid in the solvent selenium tetrafluoride, is isostructural with the acids $(SeF_4)_2PtF_4$ and $(SeF_4)_2PdF_4$, prepared recently in this laboratory. Details of these and other fluoroselenonium compounds will be given in a forthcoming communication.

The α form of sulphur trioxide is reduced explosively by the difluoride, when the mixture is warmed, the reaction probably being

$$GeF_2 + SO_3 = GeOF_2 + SO_2.$$

Liquid chlorine combines rapidly with the difluoride to produce a mixture containing germanium tetrafluoride, germanium tetrachloride, and chlorofluorides of germanium. The failure to prepare pure germanium dichlorodifluoride is in agreement with the observation of Booth and Morris (5) that this compound changes to a mixture of the tetrafluoride and the tetrachloride. The reaction sequence is probably

$$GeF_2 + Cl_2 = GeF_2Cl_2,$$
$$3GeF_2Cl_2 = 2GeF_3Cl + GeCl_4,$$
$$4GeF_3Cl = 3GeF_4 + GeCl_4.$$

Iodine in ether solution reacts with the difluoride to give germanium tetraiodide,

$$2GeF_2 + 2I_2 = GeF_4 + GeI_4.$$

It would appear that germanium difluoride will be a useful reducing agent for the preparation of lower fluorides of the transition metals and certain aspects of this work are in hand.

Germanium difluoride, like its congeners arsenic trifluoride and selenium tetrafluoride, possesses a nonbonding valence electron pair. The steric effect of the nonbonding electron pair is evident in the molecular structure of both arsenic trifluoride (6) and selenium tetrafluoride (7). A similar steric influence is evidently responsible for the absence in the difluoride of the hexagonal (low quartz) and tetragonal (rutile) arrangements found (8, 9) in the two forms of germanium dioxide. These require, respectively, regular tetrahedral and octahedral co-ordination of the germanium atom. The X-ray powder pattern

Can. J. Chem. Downloaded from www.nrcresearchpress.com by 210.87.254.40 on 09/05/12
For personal use only.

of the difluoride was indexed on the basis of an orthorhombic unit cell $a = 8.30$, $b = 5.17$, $c = 4.67$ Å. As there are no systematic absences of general *hkl* reflections the cell must be primitive. A density measurement shows that it contains four molecules.

In view of the low melting point and the volatility of the compound it is probable that a pseudotetrahedral co-ordination of the germanium atom with three fluorine atoms and a nonbonding electron pair would be more likely than an approximate hexaco-ordination. A pseudotetrahedral arrangement would result in a selenium dioxide type of structure (10) with the pseudo tetrahedron sharing fluorine atoms to form chains. It is perhaps not without significance that the cell dimensions $a = 8.35$, $c = 5.05$ Å (10) of the tetragonal unit cell of selenium dioxide are very similar to two of the dimensions of the germanium difluoride unit cell.

EXPERIMENTAL

Apparatus and Techniques

Pyrex glass apparatus was used in the various experiments and when silica was incorporated it was joined to the glass by graded seals.

Progressive hydrolysis of the fluorides and etching of the apparatus was avoided by rigidly excluding water. All glassware was heated strongly under vacuum with a luminous flame and in those experiments conducted at atmospheric pressure, ingress of moisture was prevented by using U traps immersed in liquid oxygen.

The Preparation of Germanium Tetrafluoride

The tetrafluoride was made by the fluorination of germanium metal (arsenic content 0.05 p.p.m., as supplied by Johnson, Matthey & Co. Ltd.) contained in a shallow bed in a 12-mm clear silica tube joined to a train of collecting traps, each one of which was provided with a break seal. Fluorine, diluted with nitrogen, was passed and the combustion of the germanium, which burned with a blue-green flame, was initiated with the heat from a small flame.

Apart from germanium tetrafluoride, silicon tetrafluoride was also formed, the latter arising from interaction of fluorine with the container and both products were collected at liquid oxygen temperature. By allowing the traps to warm to about $-90°$, most of the silicon fluoride was removed in the nitrogen stream used to purge the apparatus of fluorine. Each trap was sealed under vacuum, after recooling to liquid oxygen temperature, and was kept at $-180°$ until required.

The Reduction of Germanium Tetrafluoride

The most satisfactory preparation of the difluoride used lump germanium metal of the same quality as that employed above. The pieces of metal were approximately 4–5 mm in diameter and were arranged along the bottom of a 12-mm glass tube, at each end of which was joined a pair of traps. A side arm, provided with a break seal to collect the product, was situated beyond the metal and the reduction was carried out with the tetrafluoride streaming over the metal towards the side arm. In this way the product collected in the neighborhood of the side arm and was readily melted into it.

Germanium tetrafluoride, from the storage break-seal bottles, was transferred under vacuum into the appropriate set of traps, whence it was slowly passed to the second set beyond the germanium metal and the collecting side arm. With the tetrafluoride passing in this direction, reduction was affected by heating the metal with a very small flame, to maintain the temperature in the range 150–300°. The difluoride collected on the cooler glass as a colorless liquid which rapidly crystallized. Unchanged tetrafluoride condensed

Can. J. Chem. Downloaded from www.nrcresearchpress.com by 210.87.254.40 on 09/05/12
For personal use only.

in the second set of traps, cooled in liquid nitrogen. When this transference was complete, the germanium was cooled and the tetrafluoride retransferred to the first set of traps, prior to continuation of the reduction of the gas. Since the reduction took place slowly, 10 or more passings of the tetrafluoride over the metal were usually necessary to make a 1- to 2-g sample.

Attempts to improve the speed and efficiency of the reduction were abandoned when it was found that finely powdered germanium metal transferred in the gas streams and contaminated the product, which disproportionated to or was reduced to an orange product, in the presence of the metal.

When germanium tetrafluoride was used, as prepared by the pyrolysis at 600–700°, of barium hexafluogermanate contained in a silica bulb joined to an apparatus similar to that described above, the germanium metal became inactive after the formation of only small quantities of difluoride. These samples disproportionated at lower temperatures than the more pure material and the evidence of etching indicated that hydrogen fluoride, presumably arising from impure barium fluorogermanate, was responsible for this behavior. Drying of the barium salt at 200° *in vacuo* did not overcome these difficulties.

The difluoride melted at 110° and could be distilled *in vacuo* at 130°. Disproportionation, indicated by gas evolution and the appearance of a solid orange phase, began in some samples above 160°, the color of the product changing to orange-red to red-brown to black, as the temperature rose to 200°. The decomposition temperature was, however, markedly dependent upon the purity of the material and one sample showed only slight decomposition at 180°.

Analysis: A 2-g sample of the fluoride was dissolved in a mixture of ammonium hydroxide and hydrogen peroxide, the solution being subsequently boiled to destroy excess of the latter. Aliquots were taken for fluorine and germanium estimation. Fluorine was determined as lead chlorofluoride in the fluosilicic acid, hydrofluoric acid distillate produced by distilling the solution with sulphuric acid at 132–138°. The purity of the lead chlorofluoride was checked by determination of chlorine as silver chloride. Germanium was estimated as magnesium orthogermanate (11). Found: Ge, 65.6; F, 34.8%. GeF_2 requires: Ge, 65.6; F, 34.4%. A second sample was dissolved in dilute sulphuric acid and was titrated against $N/10$ iodine solution. One mole required 1.92 equivalents of iodine.

X-Ray powder photograph.—A 0.5-mm Pyrex capillary was charged with the finely powdered difluoride, the dry-box technique being employed. Photographs were taken using a 14.32-cm camera and Cu-K_α radiation in conjunction with a nickel filter. See Table I for the X-ray data.

Behavior with Miscellaneous Solvents

Water.—The difluoride was instantly hydrolized in a mild exothermic reaction. The initial yellow precipitate of germanous hydroxide rapidly turned orange. The filtrate decolorized permanganate and precipitated silver from a nitrate solution.

48% Hydrofluoric acid.—The fluoride was completely soluble in the acid and the solution possessed the reducing properties of the aqueous extract.

Ethanol.—The fluoride dissolved readily in the anhydrous solvent.

Diethyl ether.—The fluoride dissolved in dry ether but a white solid crystallized slowly from this solution. Evaporation of the ether *in vacuo* led to the breakdown of this solid, leaving what appeared to be germanium difluoride. The etherate was not investigated further.

Carbon tetrachloride.—A small particle of the difluoride remained undissolved by approximately 20 cc of the tetrachloride.

Can. J. Chem. Downloaded from www.nrcresearchpress.com by 210.87.254.40 on 09/05/12
For personal use only.

TABLE I

Calculated and observed X-ray data for GeF_2

hkl	$1/d^2$ Calc.	$1/d^2$ Obs.	Relative intensities, I	hkl	$1/d^2$ Calc.	$1/d^2$ Obs.	Relative intensities, I	hkl	$1/d^2$ Calc.	$1/d^2$ Obs.	Relative intensities, I
101	.0519	.0524	w	205	.5123	.5136	vvw	502	.9943	.9922	vw
011	.0602	.0604	m	313	.5132			243	1.0115	1.0117	mw
110	.0832	.0832	vs	006	.5220	.5232	vvw	118	1.0112		
102	.0955	.0956	s	025	.5453	.5457	vw	512	1.0400	1.0402	w
111	.0977	.0975	m	230	.5611	.5618	w	326	1.0422		
012	.1037	.1035	s	106	.5594			503	1.0668	1.0663	w
112	.1412	.1418	w	224	.5646	.5659	w	341	1.0827	1.0815	w
200	.1498	.1499	m	322	.5778	.5785	mw	236	1.0838		
103	.1680	.1692	vw	400	.5992	.5995	vw	335	1.1108		
013	.1762	.1765	vw	314	.6147	.6157	mw	028	1.1108	1.1111	vw
020	.1828	.1834	w	232	.6191	.6183	mw	513	1.1125		
210	.1955	.1966	vw	034	.6433	.6442	vvw	342	1.1262	1.1255	vvw
202	.2078	.2076	vw	134	.6808	.6812	vvw	416	1.1669	1.1648	vw
004	.2320	.2333	w	007	.7105	.7093	w	009	1.1745	1.1769	vw
212	.2535	.2543	s	216	.7175	.7177	w	218	1.1775		
104	.2694	.2714	vvw	040	.7312	.7304	vvw	514	1.2140	1.2132	vw
122	.2782	.2787	ms	403	.7297			228	1.2606	1.2603	vw
114	.3151	.3162	ms	126	.7422	.7420	vw	146	1.2906	1.2890	vw
213	.3260	.3245	vvw	041	.7457	.7460	vw	250	1.2912		
220	.3326	.3337	m	315	.7452			407	1.3097	1.3092	vw
300	.3370	.3398	vvw	331	.7628	.7653	vvw	530	1.3476	1.3466	vvw
123	.3508	.3519	vw	420	.7820	.7827	vw	515	1.3445		
310	.3827	.3834	ms	404	.8312	.8297	w	435	1.3749	1.3730	vw
302	.3950	.3955	m	043	.8617	.8589	vw	0010	1.4500	1.4498	vw
024	.4148	.4160	ms	306	.8590			328	1.4482		
031	.4267	.4272	vvw	240	.8810	.8805	vw	620	1.5310	1.5296	vw
130	.4496	.4498	w	217	.9308	.9306	vw	444	1.5624	1.5630	vvw
223	.4631	.4634	vvw	044	.9632	.9633	vvw	604	1.5802	1.5776	vw
032	.4693	.4718	w	334	.9803	.9807	w				

vs > s > ms > m > mw > w > vw > vvw

The Determination of the Density of the Solid

A 2-ml-capacity density bottle, provided with a ground-glass cap, was loaded in a dry box. All weighings were made with the bottle and its contents at 23°. Carbon tetrachloride was employed as the displacement fluid. $d_{23°} = 3.7$ g/cc.

With four molecules per unit cell ($a = 5.17$, $b = 4.67$, $c = 8.30$ Å), $d_{calc} = 3.66$ g/cc.

The Reaction of Germanium Difluoride with Selenium Tetrafluoride

Selenium tetrafluoride prepared as described by Aynsley, Peacock, and Robinson (12) was transferred by vacuum distillation to a bulb at −180°, situated beneath an upturned break-seal bottle containing a sample of the difluoride. This sample was melted down on to the excess of selenium tetrafluoride. The difluoride dissolved in the selenium fluoride when the mixture was warmed to 20°. Green colloidal selenium was produced almost immediately and this rapidly transformed to red selenium. As the reaction proceeded a white solid also crystallized from the solution. When the reaction was judged to be complete the excess of selenium tetrafluoride was removed by vacuum distillation and a residue of red selenium and a white solid remained. The latter sublimed at ca. 100° (1 atm).

An X-ray powder photograph of the residual mixture was taken, in the manner described.

Can. J. Chem. Downloaded from www.nrcresearchpress.com by 210.87.254.40 on 09/05/12
For personal use only.

The Preparation of $(SeF_4)_2GeF_4$

An excess of germanium tetrafluoride was mixed with selenium tetrafluoride at atmospheric pressure. A white solid formed immediately. The excess of germanium tetrafluoride was removed under vacuum at 0°. This solid sublimed at ca. 100° (1 atm). An X-ray powder photograph of the solid was taken and the pattern was found to conform with the major pattern of the residue from the selenium tetrafluoride – germanium difluoride reaction.

Analysis: A weighed sample was dissolved in sodium carbonate solution and aliquots were analyzed for selenium, which was determined as the element by reduction with sulphurous acid in strong hydrochloric acid solution, and fluorine which was determined as previously described. Found: Se, 34.4; F, 51.0%. $(SeF_4)_2GeF_4$ requires: Se, 34.5; F, 49.7%.

Germanium Difluoride with α-Sulphur Trioxide

Liquid sulphur trioxide was prepared by the distillation of 60% oleum with phosphorus pentoxide, followed by a second distillation from phosphorus pentoxide. The apparatus used for this preparation was rigorously dried and ingress of moisture was prevented by three U traps, in series, at −180°. A sample of the trioxide was distilled under vacuum into a break-seal bottle cooled in ice.

A break-seal bottle (cooled in ice) containing a sample of germanium difluoride was opened and sulphur trioxide was distilled into it, under vacuum. The apparatus was opened to the air via a series of U traps immersed in liquid oxygen and the mixture was allowed to warm to room temperature. The difluoride did not dissolve noticeably in the liquid trioxide up to 25° and when the mixture was warmed there was an explosion which destroyed the containing bottle.

Germanium Difluoride with Chlorine

Chlorine was melted on to a 0.5-g sample of the difluoride. The immediate and vigorous reaction, which followed, was moderated by cooling with liquid oxygen. On completion of the reaction, excess chlorine was removed from the mixture under vacuum at −78° and a colorless liquid remained. A gas, which condensed to a white solid was removed with the chlorine. This solid resembled germanium tetrafluoride.

The colorless liquid which had a vapor pressure of 20 cm at 24° transferred rapidly and completely in a vacuum, at room temperature. Anal. Found: mol. wt., 197. Calc.: mol. wt. GeF_2Cl_2, 181.6; mol. wt. $GeFCl_3$, 198.1; $GeCl_4$, 214.6.

Infrared spectra of successive fractions of the vapor showed a strong absorption band at 740 cm^{-1}, indicative of Ge—F stretching. There was no band at 800 cm^{-1}, which is the location for a strong germanium tetrafluoride absorption band (13). A small peak at 1050 cm^{-1} showed silicon tetrafluoride (arising from fluoride attack on the glass apparatus) to be present in low concentration.

A gravimetric analysis for chlorine as silver chloride was made on the least volatile fraction of the liquid. Found: Cl, 60.8%. Calc. for $GeCl_4$: Cl, 66.4%; for $GeFCl_3$: Cl, 53.7%. Although both GeF_2Cl_2, b.p. −2.8° (5), and $GeFCl_3$, b.p. 37.5° (5), are probably present, it is not possible at this time to say which of the chlorofluorides predominates in the mixture with germanium tetrachloride.

Germanium Difluoride with Iodine

A solution of iodine in ether was added to a suspension of germanium difluoride in ether, until the iodine color persisted. Evaporation of the ether under vacuum left an

Can. J. Chem. Downloaded from www.nrcresearchpress.com by 210.87.254.40 on 09/05/12
For personal use only.

orange residue. This was washed with a small quantity of ether and was dried in a vacuum. It was identified as germanium tetraiodide, m.p. 146°, literature value 146° (14).

ACKNOWLEDGMENTS

The authors wish to thank the National Research Council of Canada and the President's Research Fund, The University of British Columbia, for financial support.

REFERENCES

1. C. WINKLER. J. prakt. Chem. **36**(2), 193 (1887).
2. L. M. DENNIS and A. W. LAUBENGAYER. Z. physik. Chem. (Leipzig), **130**, 530 (1927).
3. R. SCHWARTZ and E. BARONETZKY. Z. anorg. Chem. **275**, 1 (1954).
4. C. W MOULTON and J. G. MILLER. J. Am. Chem. Soc. **78**, 2702 (1956).
5. H. S. BOOTH and W. C. MORRIS. J. Am. Chem. Soc. **58**, 90 (1936).
6. P. KISLIUK and S. GESCHWIND. J. Chem. Phys. **21**, 828 (1953).
7. R. E. DODD, H. L. ROBERTS, and L. A. WOODWARD. Trans. Faraday Soc. **52**, 1052 (1956).
8. W. ZACHARIASSEN. Z. Krist. **67**, 226 (1928).
9. V. M. GOLDSCHMIDT. Z. physik. Chem. (Frankfurt), **17**, 172 (1932).
10. J. D. MCCULLOUGH. J. Am. Chem. Soc. **59**, 790 (1937).
11. SCOTT'S STANDARD METHODS OF CHEMICAL ANALYSIS. Vol. I. D. Van Nostrand and Co., Inc., New York. 1939. p. 430.
12. E. E. AYNSLEY, R. D. PEACOCK, and P. L. ROBINSON. J. Chem. Soc. 1231 (1952).
13. P. J. H. WOLTZ and A. H. NIELSON. J. Chem. Phys. **20**, 307 (1952).
14. A. W. LAUBENGAYER and P. L. BRANDT. J. Am. Chem. Soc. **54**, 621 (1932).

Can. J. Chem. Downloaded from www.nrcresearchpress.com by 210.87.254.40 on 09/05/12
For personal use only.

Can. J. Chem. Downloaded from www.nrcresearchpress.com by 210.87.254.6 on 09/05/12
For personal use only.

THE DECOMPOSITION OF METHANE IN THE NEGATIVE GLOW[1]

A. W. TICKNER

ABSTRACT

The decomposition of methane was studied in the negative glow of a d-c. discharge at pressures of 0.30 and 0.050 mm. The discharge tube was cooled by liquid or solid nitrogen.

The main products were ethane, ethylene, and acetylene in addition to hydrogen and a nonvolatile product which appeared mainly on the cathode as a solid having the formula $(CH)_n$. Smaller amounts of propane, propene, propyne, butane, butene, butadiene, and pentene were also found. Lowering the temperature of the discharge tube from −196° to −210° C greatly increased the amount of ethylene recovered.

The solid product is apparently transported to the cathode in the form of ions and may result from ionic polymerization of the acetylene. Acetylene is the volatile product formed closest to the cathode which suggests that it may also be formed by ionic processes. The formation of the remaining products is consistent with an excitation mechanism in which the C_2 products are formed first and the higher hydrocarbons are formed from them.

INTRODUCTION

The decomposition of methane in the glow discharge has been studied for many years; the early work is summarized in reference 1. More recently, Yeddanapalli (2) studied the decomposition of methane in a d-c. glow discharge using a discharge tube cooled in liquid air. He worked at pressures of a few millimeters and found that the products consisted of ethane, ethylene, and acetylene as well as hydrogen and a nonvolatile product having the formula $(CH_2)_n$. Wiener and Burton (3), using a d-c. glow discharge at atmospheric pressure, showed that under conditions of high conversion and relatively high temperature the only significant products were acetylene, hydrogen, and carbon. McCarthy (4) found that, in addition to acetylene, ethylene and ethane were obtained as products when the gas from a microwave discharge in methane was allowed to impinge directly on a wall cooled by liquid nitrogen.

The low-pressure d-c. glow discharge is suitable for investigations of this type because it permits studying the decomposition in a number of different discharge regions for which the electrical processes are reasonably well understood (5, 6). In addition, the vapor pressures of methane and its decomposition products are such that most of the products can be removed rapidly from the reaction by freezing them out on the discharge tube wall. There is thus the possibility of obtaining direct information about the primary products of the decomposition. This approach was used by Yeddanapalli (2), whose work, however, had two main weaknesses: (*a*) at the temperature of liquid air the vapor pressure of ethylene is sufficiently high that much of it would have remained in the gas phase, and (*b*) his method of analysis was such that the products were determined as acetylene and ethylene with the remainder assumed to be ethane. Any higher hydrocarbons which might have been formed would thus not have been detected.

The negative glow was chosen as a suitable region with which to begin a study of the decomposition of methane in the electric discharge. It was known to be a region of great chemical activity which could be to a considerable degree operated independently of other discharge regions. The experiments reported here were intended primarily to clarify the work of Yeddanapalli and to serve as a basis for a more detailed study of the discharge decomposition. In order to recover the first products more completely, temperatures lower than those in the earlier work have been used. The use of a direct pumping system

[1]*Manuscript received August 17, 1960.*
Contribution from the Division of Applied Chemistry, National Research Council, Ottawa, Canada. Issued as N.R.C. No. 6063.

instead of the circulating system previously employed (2) enabled the experiments to be carried out at constant pressure and reduced the residence time in the discharge zone.

EXPERIMENTAL

The experiments were carried out in the apparatus shown diagrammatically in Fig. 1. It consisted of a jacketed discharge tube with a fixed cathode and an anode which could be moved by a rack and gear as shown. The discharge tube diameter of 3.4 cm was

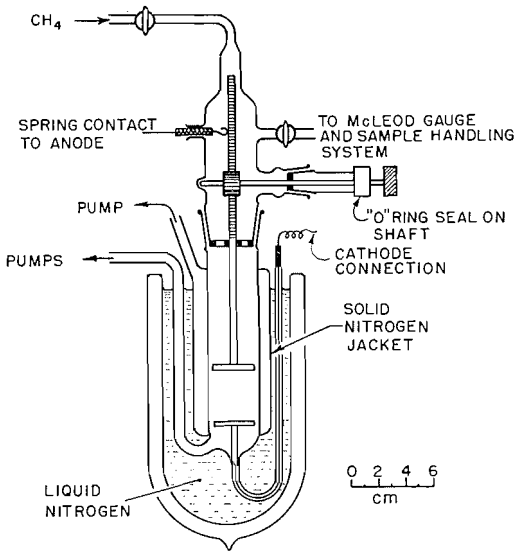


FIG. 1. Discharge tube.

chosen as a reasonable compromise between the requirements for efficient trapping of products (small diameter) and ideal glow discharge conditions (large diameter). The electrodes were 3.0 cm in diameter and were made of stainless steel. A mercury diffusion pump with a pumping speed of 10 liters per second and a forepump allowed the system to be evacuated to pressures of less than 10^{-5} mm of mercury. The residence time in the discharge zone with the electrodes placed to include the entire negative glow was 0.05 second for a discharge pressure of 0.3 mm and 0.5 second for a discharge pressure of 0.05 mm. Pressures were measured by a small McLeod gauge.

A variable voltage d-c. power supply having a ripple of less than 0.1 volt supplied power to the discharge through a 10,000-ohm series resistor. The discharge current was controlled manually.

The discharge tube was cooled by filling the jacket with liquid nitrogen and pumping on it until the nitrogen solidified. By controlling the pumping speed it was possible to maintain a constant pressure over the nitrogen in the jacket and thus to maintain a constant discharge tube wall temperature for a period of about 15 minutes. Temperatures down to $-220°$ C could be obtained in this way. The temperature of the discharge tube wall was determined by measuring the vapor pressure of methane corresponding to a given jacket pressure and comparing this with the vapor pressure of methane as given by Ziegler (7).

The methane used was Matheson C.P. grade; it was purified by fractional distillation

Can. J. Chem. Downloaded from www.nrcresearchpress.com by 210.87.254.6 on 09/05/12
For personal use only.

Can. J. Chem. Downloaded from www.nrcresearchpress.com by 210.87.254.6 on 09/05/12
For personal use only.

before admitting it to the storage reservoir. Its flow rate was controlled by a needle valve and it was admitted through a trap maintained at either the temperature of liquid nitrogen or the triple point of nitrogen depending upon the methane pressure being used. When necessary a correction was made for the small amount of ethane which was found to be present in blank runs.

The lengths of the negative glow and cathode dark space were determined by measuring the voltage drop across the discharge for various electrode spacings at constant discharge current (5). For the purpose of this work the length of the cathode dark space was taken as equal to the electrode spacing at which the voltage began to rise steeply when the anode was being moved towards the cathode. The anode end of the negative glow was taken as equal to the electrode spacing at which the voltage began to increase when the anode was being moved away from the cathode.

The experiments were performed by cooling the discharge tube to the required temperature, establishing the methane flow, and operating the discharge for a suitable period which in practice varied from 3 to 12 minutes. After the discharge was turned off, the discharge tube was pumped briefly to a low pressure, isolated, and warmed to room temperature. The volatile products were then transferred to a gas burette for measurement and analyzed on a mass spectrometer. The carbon content of the nonvolatile discharge product was determined by oxidizing it *in situ* with an oxygen discharge and measuring the carbon dioxide produced. The method has been described previously (8).

RESULTS

Preliminary experiments demonstrated that the amount of ethylene recovered at about 1% methane decomposition increased nearly 10-fold when the discharge tube temperature was lowered from that of liquid nitrogen (−196° C) to the triple point of nitrogen (−210° C). The amount of ethane recovered also increased by about one-third and some of the higher products, especially propene and butene, decreased in amount. Extrapolation of the existing vapor pressure data for ethylene and ethane (7) indicates that their vapor pressures are less than 10^{-6} mm at −210° C. Thus, the recovery of these products should be practically quantitative at this temperature, assuming equilibrium at the wall.

In several experiments at approximately 2% methane decomposition the gas downstream from the discharge was sampled and analyzed on a mass spectrometer. In each case the amount of hydrogen found agreed, within the accuracy of the analysis, with that calculated on the basis of the products formed.

The variation of the products with discharge current was studied in a series of experiments at a pressure of 0.30 mm, which is the vapor pressure of methane at −210° C. The electrode spacing used was 3.0 cm, equal to the length of the negative glow at this pressure. The results are shown in Fig. 2. The amount of methane decomposed was calculated from the composition of the products; the percentage decomposition was 0.5% for a current of 1 ma. Values shown for the nonvolatile product give its carbon content in gram-atoms. In these experiments the voltage drop across the discharge increased from 330 volts for a current of 1 ma to 390 volts for a current of 4.5 ma.

A pressure of 0.05 mm was chosen as a convenient one for most of the experiments. The choice of a lower pressure made control of the wall temperature less critical and reduced the number of collisions undergone by product molecules in diffusing to the cold wall. In addition, the increased lengths of the cathode dark space and the negative

Can. J. Chem. Downloaded from www.nrcresearchpress.com by 210.87.254.6 on 09/05/12
For personal use only.

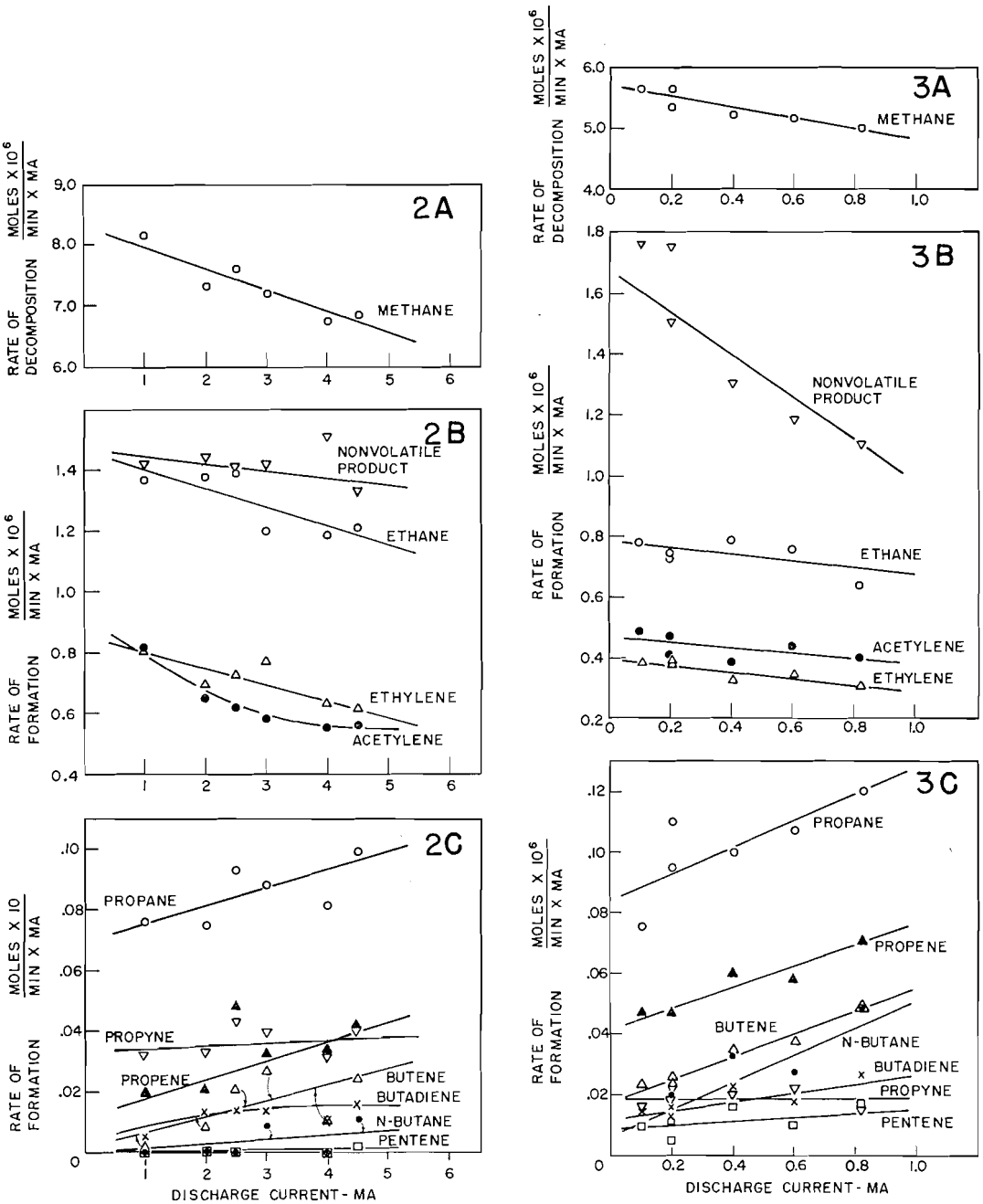


FIG. 2. Effect of discharge current on the decomposition of methane in the negative glow at −210° C. Methane pressure, 0.30 mm. Electrode spacing, 3.0 cm.

FIG. 3. Effect of discharge current on the decomposition of methane in the negative glow at 0.050-mm pressure. Electrode spacing, 10 cm. Temperature, −213° C.

glow made it easier to detect any variation in the products along the discharge. A wall temperature of about −213° C was used in experiments at this pressure.

The effect of discharge current on the rates of formation of the products at a pressure of 0.050 mm is shown in Fig. 3. An electrode spacing of 10 cm was used, corresponding to the length of the negative glow at this pressure. A discharge current of 0.10 ma corresponded to 0.6% decomposition of the methane. The discharge voltage increased from 385 volts for a current of 0.10 ma to 750 volts for a current of 0.82 ma.

Hydrogen was the only product whose effect on the reaction could be conveniently tested. Figure 4 gives the results of a series of experiments in which hydrogen was added to the methane to give mixtures having total hydrogen contents of up to 20 mole%. The hydrogen formed in the decomposition was taken into account in calculating the compositions of the mixtures.

The distribution of products along the negative glow was studied in another series of experiments in which the electrode spacing was varied. The results are shown in Fig. 5. As the anode was moved towards the cathode the negative glow was eliminated progressively from the anode end. This appeared to have little effect on the operation of the discharge until the edge of the cathode dark space was reached at an electrode spacing of about 1.8 cm. In order to make the experiments comparable over as wide a range as possible a discharge current of 0.50 ma was chosen; lower currents could not be maintained at the smallest electrode spacings used.

The nonvolatile product which formed in the discharge experiments was visible only as a solid deposit on the cathode. This deposit appeared to be a continuous film and interference colors showed it to be of uniform thickness over the area of the electrode covered. In one of the experiments at a pressure of 0.05 mm a flat Pyrex disk having a diameter of 4 mm and a thickness of 0.025 mm was placed on the surface of the cathode. Although a uniform and readily visible deposit was formed on the cathode all around the disk, and extending up to the edge of it, no deposit was visible on the disk itself. It appeared therefore that the deposit was formed only on that part of the cathode which was bombarded by incoming ions.

In order to obtain enough of the cathode deposit for a chemical analysis, several experiments were carried out in which the discharge was operated for periods of about 30 minutes at currents of 7 or 8 ma. The upper electrode was made the cathode in these experiments to facilitate the removal of the deposit. Two samples of about 2 mg each, obtained at the temperature of liquid nitrogen, gave analyses corresponding to $C_{1.00}H_{1.01}$ and $C_{1.00}H_{1.02}$. In another experiment the liquid nitrogen level was maintained about 1 cm below the cathode in order to reduce the possibility that a deposit of frozen product gases was contributing to the formation of the solid. Analysis of this sample gave a composition represented by $C_{1.00}H_{0.75}$. A further sample of the cathode deposit, prepared by operating the discharge at room temperature, was found to have the composition given by $C_{1.00}H_{0.70}$. Although the removal of the solid from the cathode was not quantitative the amount recovered accounted in every case for more than half the nonvolatile product calculated to be formed on the basis of the results in Fig. 2. It seems probable therefore that the cathode deposit accounts for nearly all of the nonvolatile product. The only evidence of any other accumulation of a nonvolatile product was the appearance of interference colors on the anode during these experiments. This may have indicated the formation there of much smaller quantities of another solid product.

It was not possible to determine from the mass spectra whether the product which appeared at $m/e = 42$ was propene or cyclopropane. This product was separated from the others by gas chromatography and shown to be propene.

Can. J. Chem. Downloaded from www.nrcresearchpress.com by 210.87.254.6 on 09/05/12
For personal use only.

Can. J. Chem. Downloaded from www.nrcresearchpress.com by 210.87.254.6 on 09/05/12
For personal use only.

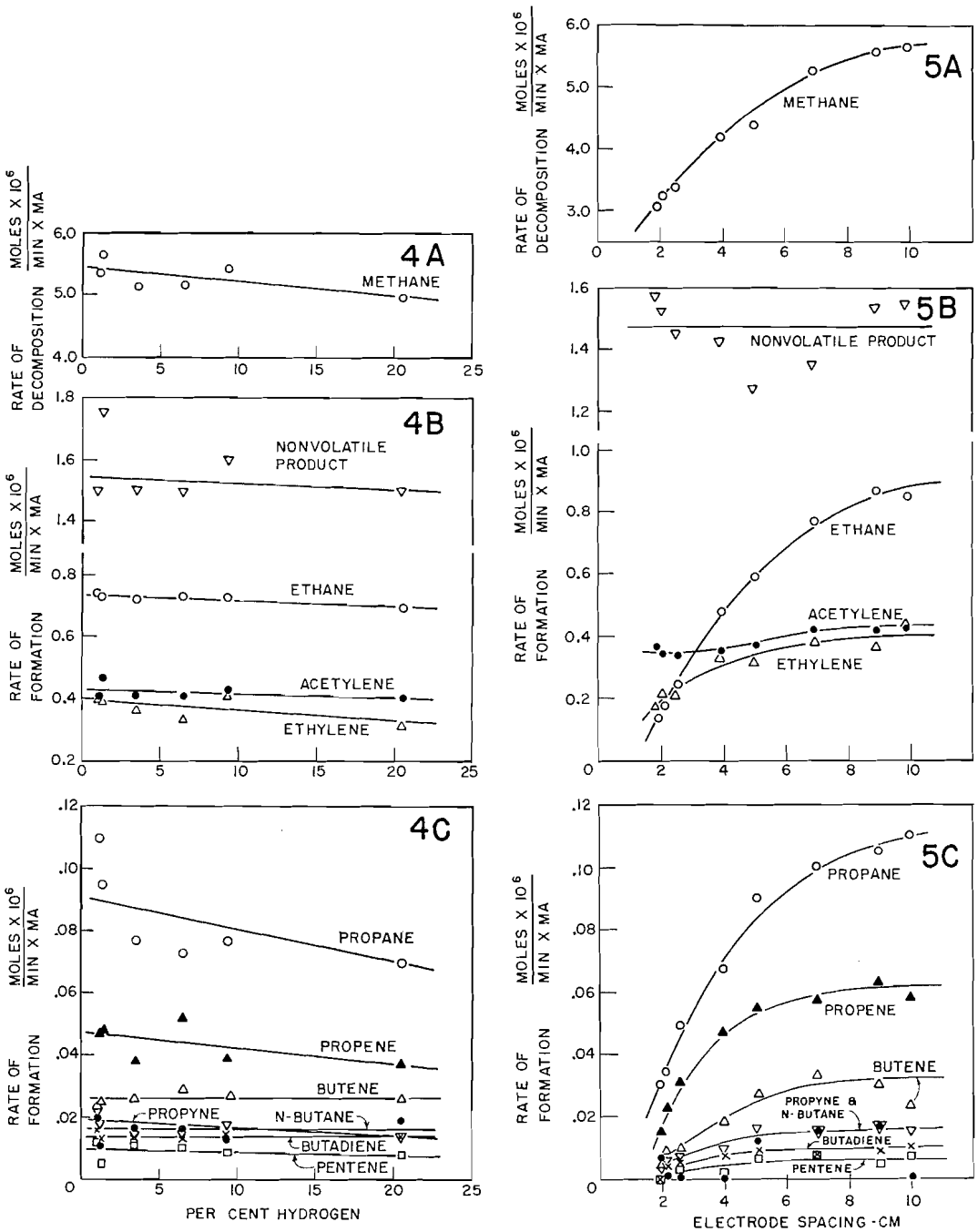


FIG. 4. Effect of hydrogen on the decomposition of methane in the negative glow. Total pressure, 0.050 mm. Current, 0.20 ma. Electrode spacing, 10 cm. Temperature, −213° C.

FIG. 5. Effect of electrode spacing on the decomposition of methane. Pressure, 0.050 mm. Current, 0.50 ma. Temperature, −213° C.

Can. J. Chem. Downloaded from www.nrcresearchpress.com by 210.87.254.6 on 09/05/12
For personal use only.

DISCUSSION

The products obtained in this work were considerably more complex than those obtained by Yeddanapalli (2). This was due mainly to the improved analytical technique used. In addition, the increased recovery of ethylene at wall temperatures of $-210°$ C or lower indicates that the yield of ethylene found by Yeddanapalli was too low because much of it would not have been removed from the reaction at the temperature of liquid air. Instead of a polymer having the formula $(CH_2)_n$ as indicated by Yeddanapalli's results, the nonvolatile product was found to consist mostly of a solid of formula $(CH)_n$ which appeared on the cathode.

Yeddanapalli's conclusion that the rate of decomposition in the negative glow is proportional to the current and independent of the pressure holds only approximately for these experiments which extend into the abnormal discharge region. The electron efficiency in this work is defined as the number of methane molecules decomposed per electron charge carried by the current. In the experiments at 0.30-mm pressure (Fig. 2), for which the discharge is nearly normal, the electron efficiency decreases from 12.8 at 1.0 ma to 10.7 at 4.5 ma. At 0.050 mm where the discharge is more abnormal the electron efficiency decreases from 9.0 at 0.10 ma to 8.0 at 0.82 ma. These values are to be compared with the average value of 10 obtained by Yeddanapalli (2) at pressures ranging from 2 to 9 mm and discharge currents between 10 and 30 ma. It is evident that the electron efficiency for the negative glow plus the cathode dark space is approximately 10 over a fairly wide range of discharge conditions.

The products found in these experiments are very similar to those found by Manton and Tickner (9) in their study of the decomposition of methane by a beam of electrons. Since it is known that the electrons in the negative regions of a d-c. glow discharge possess beam properties and have energies similar to those used in the electron beam experiments, this suggests that the products of the negative glow are formed by a mechanism similar to the one which they proposed. The higher electron efficiencies obtained in the glow are accounted for by the many secondary electrons which acquire energy in the electric field, lose it in exciting gas molecules, and subsequently recombine with ions without contributing to the discharge current.

The work of Manton and Tickner indicated that the products were due mainly to excitation rather than to ionization and provided some evidence that the higher products were formed by the reaction of some species, such as excited methylene radicals, with the lower hydrocarbon products. The results obtained here are consistent with this mechanism. In the experiments at both 0.30 mm (Fig. 2) and 0.050 mm (Fig. 3) the yields of the C_2 products fall off with increasing current while the yields of the higher hydrocarbons increase. Also, lowering the discharge tube temperature from $-196°$ C to $-210°$ C while greatly increasing the recovery of ethylene resulted in a decrease in the amounts of propene and butene. Thus, there seems to be definite evidence that the higher hydrocarbons are formed at the expense of the C_2 products.

It has been suggested (10) that the addition of excited methylene to a double bond often results in the formation of an energy-rich cyclic compound which may then rearrange to an olefin. Since no cyclopropane is found among the discharge products there is no evidence of this kind that excited methylene is the active species.

The addition of hydrogen to the methane in concentrations up to 20 mole% appears to have little effect on the products. The small lowering of all yields as the concentration of hydrogen is increased is consistent with the explanation put forward by Yeddanapalli that hydrogen behaves as a diluent, absorbing some of the electrical energy. Since some

Can. J. Chem. Downloaded from www.nrcresearchpress.com by 210.87.254.6 on 09/05/12
For personal use only.

decomposition of the hydrogen into atoms would be expected, it seems probable that under our conditions of fast trapping the reactions of hydrogen atoms do not play an important part. It is possible, however, that the number of hydrogen atoms generated from the added hydrogen is small compared with the number formed in the methane decomposition and that for this reason the effect of the added hydrogen is not appreciable.

The results obtained by varying the distance between the electrodes (Fig. 5) indicate that the products are not formed uniformly throughout the negative glow. While it is possible that moving the anode into the glow may alter the mechanism it seems to be accepted (5) that the operation of a discharge is disturbed to a relatively small extent until the anode reaches the cathode edge of the glow. Judging by the observed current–voltage relationship this seems to hold true for these experiments. Thus, there appears to be good evidence that most of the acetylene, and possibly part of the ethylene, are formed either at the edge of the negative glow nearest the cathode or, perhaps, in the cathode dark space. The other products appear to be formed in the body of the glow although the results in Fig. 5 may indicate that the distribution is not the same for all of them.

It seems likely that the variation in the relative amounts of the various products along the glow is related to the variation in the electron energy distribution. At the cathode edge of the glow a relatively large number of electrons have sufficient energy to ionize but their number falls off rapidly with increasing distance from the cathode. In the interior of the glow, electrons of much lower energy predominate (5, 6). The fact that most of the acetylene is apparently formed in a region in which there are relatively large numbers of high-energy electrons appears to indicate that it depends on ionization for its formation. This would not be inconsistent with the findings of Manton and Tickner (9) because acetylene constituted a relatively small part of the total product on which their conclusions were based. The remaining products are formed in the interior of the glow where excitation processes are more important. Thus, with the possible exception of acetylene, the mechanism put forward by Manton and Tickner seems to offer a reasonable explanation of the products of the negative glow.

The conclusion that acetylene was the product formed nearest the cathode takes on interesting implications when related to the formation of the solid product. At the low temperatures and low currents used in these experiments a solid product having exactly the formula $(CH)_n$ formed in visible quantities only on the cathode. Since no deposit formed on an insulator covering part of the cathode surface it seems likely that the solid layer was formed by the incoming ions. This conclusion is consistent with the observation that the rate of formation of the nonvolatile product was affected little by changes in wall temperature, pressure, or electrode spacing as shown in Figs. 2 to 5. Experiments in which the cathode was kept above the liquid nitrogen level or in which the discharge was operated at room temperature indicate that the deposit did not originate in a layer of acetylene frozen out on the cathode surface. Instead, these experiments provide some evidence that at higher temperatures the cathode deposit loses hydrogen under ion bombardment. These considerations lead to the conclusion that the solid product on the cathode is an acetylene polymer similar to the cuprene formed in the high-energy irradiation of acetylene (11, 12). There is a considerable amount of evidence that the cuprene formed in these irradiation studies depends on ionization for its formation (12, 13, 14). It seems possible therefore that in the glow discharge acetylene formed near the cathode becomes ionized, either directly or by charge exchange, and then polymerizes in a series of ion–molecule reactions while on its way to the cathode.

The appearance of traces of an involatile product on the anode may indicate that small amounts of a polymer are also formed by another mechanism.

ACKNOWLEDGMENTS

The author wishes to express his appreciation to Mr. R. L. Sander, who performed the mass spectrometric analyses, and to Mr. J. R. H. Seguin, who analyzed the solid product appearing on the cathode.

REFERENCES

1. C. L. THOMAS, G. EGLOFF, and J. C. MORRELL. Chem. Revs. **28**, 1 (1941).
2. L. M. YEDDANAPALLI. J. Chem. Phys. **10**, 249 (1942).
3. H. WIENER and M. BURTON. J. Am. Chem. Soc. **75**, 5815 (1953).
4. R. L. MCCARTHY. J. Chem. Phys. **22**, 1360 (1954).
5. G. FRANCIS. Handbuch der Physik. Vol. XXII. The glow discharge at low pressure. *Edited by* S. Flügge. Springer, Berlin. 1956. p. 53.
6. A. VON ENGEL. Ionized gases. Oxford University Press, London. 1955. Chap. 8, Glow discharge.
7. W. T. ZIEGLER. Natl. Bur. Standards (U.S.) Tech. Note, No. 4. 1959.
8. A. W. TICKNER. Can. J. Chem. **36**, 718 (1958).
9. J. E. MANTON and A. W. TICKNER. Can. J. Chem. **38**, 858 (1960).
10. H. M. FREY and G. B. KISTIAKOWSKY. J. Am. Chem. Soc. **79**, 6373 (1957). H. M. FREY. Proc. Roy. Soc. A, **250**, 409 (1959); A, **251**, 575 (1959).
11. E. COLLINSON and A. J. SWALLOW. Chem. Revs. **56**, 471 (1956).
12. L. M. DORFMAN and F. J. SHIPKO. J. Am. Chem. Soc. **77**, 4723 (1955). L. M. DORFMAN and A. C. WAHL. Radiation Research, **10**, 680 (1959).
13. P. S. RUDOLF and C. E. MELTON. J. Phys. Chem. **63**, 916 (1959).
14. R. BARKER, W. H. HAMILL, and R. R. WILLIAMS. J. Phys. Chem. **63**, 825 (1959).

Can. J. Chem. Downloaded from www.nrcresearchpress.com by 210.87.254.6 on 09/05/12
For personal use only.

Can. J. Chem. Downloaded from www.nrcresearchpress.com by 210.87.254.6 on 09/05/12
For personal use only.

OXIDATION OF MANGANATE BY HYPOCHLORITE[1]

M. W. Lister and Y. Yoshino[2]

ABSTRACT

The oxidation of potassium manganate to potassium permanganate by potassium hypochlorite has been examined. The rate of the reaction is proportional to the square of the manganate concentration and the first power of the hypochlorite, and it is inversely proportional to the permanganate concentration and to the square of the hydroxide ion concentration. It seems probable that the reaction involves the intermediate formation of hypomanganate ions from a relatively fast disproportionation of manganate, followed by a slower oxidation by hypochlorite. The following mechanism is tentatively proposed:

$$MnO_4^{--} + H_2O \rightleftharpoons HMnO_4^- + OH^-$$

$$2HMnO_4^- \rightleftharpoons H_2MnO_4^- + MnO_4^-$$

$$H_2MnO_4^- + OCl^- \rightarrow MnO_4^- + Cl^- + H_2O.$$

Data on the over-all rate and effective activation energy (19.6 kcal/g-molecule) are given; but at present it is not possible to separate all the rate constants and equilibrium constants.

The present writers have examined in a recent paper (1) the mechanism of the oxidation of manganate by periodate ions. It was found that this reaction goes chiefly through the intermediate formation of hypomanganate ions, arising from the equilibrium

$$2MnO_4^{--} \rightleftharpoons MnO_4^{-3} + MnO_4^-.$$

The hypomanganate ions are then oxidized in a bimolecular reaction with periodate. The reaction of manganate with hypochlorite ions is at first sight a similar reaction. This reaction also takes place in alkaline solution, the over-all change being

$$2K_2MnO_4 + KOCl + H_2O \rightarrow 2KMnO_4 + KCl + 2KOH.$$

As with periodate, the hypochlorite ion changes by two oxidation steps, while the manganate ion changes by one; so a reaction in at least two steps, or else a termolecular reaction, seemed probable. With periodate ions a termolecular reaction is largely avoided by the two-stage reaction involving hypomanganate ions. The evidence which will be given below shows that a very similar mechanism operates with hypochlorite ions.

EXPERIMENTAL METHOD

Mixtures of potassium manganate, potassium hypochlorite, and potassium hydroxide of various concentrations were made up in aqueous solution. They were kept in a thermostat controlled to 0.1° C, and samples were taken at intervals for analysis. The reaction was followed by measuring the optical density of the solutions, mostly at 610 mμ, on a Beckmann DU spectrophotometer. This wave length is at the absorption maximum for manganate ions; the extinction coefficients used were the same as in the earlier paper (1). It was assumed that all the manganese was present either as manganate or permanganate ions. This was confirmed in several ways. Firstly the solutions showed no signs of precipitated manganese dioxide, which is the most probable alternative form for the manganese. Secondly, the total oxidizing normality of the solution (measured by adding potassium iodide and sulphuric acid, and titrating with sodium thiosulphate) was found not to change during a run. Thirdly, measurements were also made at 550 mμ, where the

[1]*Manuscript received August 25, 1960.*
Contribution from the Department of Chemistry, University of Toronto, Toronto, Ontario.
[2]*College of General Education, University of Tokyo, Tokyo, Japan.*

permanganate ion has an absorption maximum; the concentrations of manganate and of permanganate, calculated from the measurements at the two wave lengths, were in good agreement.

Potassium manganate was made as described by Carrington and Symonds (2). Potassium hypochlorite was made by the usual method of passing chlorine into cold potassium hydroxide solution; hence the reaction mixtures always contained potassium chloride.

The initial concentrations in various runs are given in Table I. In most of these runs

TABLE I

Initial concentrations

Run	Temp., °C	$[K_2MnO_4]$, $\times 10^{-4}$ M	[KOCl], $\times 10^{-4}$ M	[KOH], M	$[KMnO_4]$, $\times 10^{-4}$ M	Slope, $\times 10^2$
1	35.0	3.08	100	0.094	0	6.8
2	"	4.16	100	0.106	0	6.9
3	"	2.16	100	0.099	0	7.5
4	"	3.13	100	0.049	0	29.8
5	"	3.09	10	0.049	0	3.7
6	"	3.11	20	0.103	0	1.47
7	45.0	3.08	100	0.096	0	22.0
8	25.0	3.14	100	0.106	0	2.25
9	35.0	3.15	200	0.106	0	11.9
10	"	3.19	10	0.102	0	0.70
11	"	3.19	50	0.102	0	3.5
12	"	3.15	100	0.204	0	1.97
13	"	3.15	100	0.029	0	58
14	"	2.75	100	0.098	0	5.4
15	"	3.21	100	0.100	3.00	9.1
16	"	3.03	100	0.098	1.03	7.7
17	"	3.14	100	0.0995	2.06	8.35
18	"	3.35	100	0.0995	4.12	8.9
19	"	3.21	100	0.099	3.00	9.5
20	"	3.04	100	0.030	0	63

the potassium hypochlorite was in sufficient excess so that it remained effectively constant throughout the run. The ionic strength was regulated at an initial value of 0.2 by addition of potassium nitrate. The ionic strength changed by an insignificant amount during any run.

RESULTS

The concentrations of manganate ions at various times were calculated for all runs. These concentrations will be presented in terms of the equation that they were found to fit, as described below. At first the usual equations for a monomolecular or a bimolecular mechanism were tried, but the results did not fit these simple equations. The rate of reaction was rapid at first, but slowed up very markedly with time; in fact in some runs the rate was not far from being proportional to the fourth power of the manganate concentration. This slowing up cannot be attributed to reversibility of the reaction, as the relevant standard electrode potentials (3) are

$$MnO_4^{--} \rightarrow MnO_4^{-} + e^{-}, \qquad E_0 = -0.564 \text{ volt};$$

$$Cl^{-} + 2\,OH^{-} \rightarrow OCl^{-} + H_2O + 2e^{-}, \qquad E_0 = -0.89 \text{ volt}.$$

Hence at equilibrium, for the conditions used, virtually all the manganese would be present as permanganate ions.

It was found, however, that the following mechanism gave an equation which fitted

Can. J. Chem. Downloaded from www.nrcresearchpress.com by 210.87.254.6 on 09/05/12
For personal use only.

the experimental results:

$$2MnO_4^{--} \rightleftharpoons MnO_4^{-3} + MnO_4^{-}, \quad \text{(i)}$$

$$MnO_4^{-3} + OCl^- + H_2O \rightarrow MnO_4^- + Cl^- + 2OH^-. \quad \text{(ii)}$$

The initial equilibrium in reaction (i) is assumed to be fast relative to reaction (ii), which determines the rate. If k_2 is the rate constant of the second reaction, then

$$\frac{d[MnO_4^{--}]}{dt} = -2k_2[MnO_4^{-3}] \,.\, [OCl^-]$$

as two manganate ions react to give one hypomanganate ion. If K is the equilibrium constant of reaction (i), and if the concentration of hypomanganate ion at any time is very small, then

$$[MnO_4^{-3}] = \frac{K.\,[MnO_4^{--}]^2}{[MnO_4^{-2}]_0 - [MnO_4^{-2}] + [MnO_4^-]_0}$$

where the subscript "0" indicates the initial concentration. If we substitute this in the rate equation, and allow for the fact that the potassium hypochlorite is also used up, integration of the rate equation gives

(A) $2K.k_2[OCl^-]_0(1-b/2)t = (1+w)(a-1) - [(1+wb/2)/(1-b/2)] \ln [a(1-b/2+b/2a)]$

where $a = [MnO_4^{--}]_0/[MnO_4^{--}]$,

$b = [MnO_4^{--}]_0/[OCl^-]_0$,

and $w = [MnO_4^-]_0/[MnO_4^{--}]_0$.

In most runs the initial hypochlorite concentration was so large that b can be taken to be negligibly small; equation (A) then reduces to

(B) $$2K.k_2[OCl^-]_0 t = (1+w)(a-1) - \ln a.$$

Equation (B) is accurate to within 1% for all runs except 5, 6, and 10, which were done with low hypochlorite ion concentrations, and even here the error in the calculated rate constants by using equation (B) would be about 5%. Equation (A) was used for these runs.

If this theory of the reaction mechanism is correct, then a plot of $[(1+w)(a-1)-\ln a]$ against time should be linear. These plots are shown in the figures, and do in fact give straight lines for all runs. Data for a typical run are:

Run 1; $w = 0$

Time, minutes	$[MnO_4^{--}]$, $\times 10^{-4}$ M	$[a-1-\ln a]$	Time, minutes	$[MnO_4^{--}]$, $\times 10^{-4}$ M	$[a-1-\ln a]$
0	3.08	0	26	1.84	0.159
1	2.92	0.002	34	1.72	0.208
2½	2.74	0.007	43	1.61	0.264
4	2.62	0.014	57	1.45	0.371
6	2.45	0.028	70	1.34	0.466
9	2.32	0.044	90	1.22	0.598
13	2.19	0.066	110	1.12	0.738
18	2.03	0.105	131	1.04	0.876

Can. J. Chem. Downloaded from www.nrcresearchpress.com by 210.87.254.6 on 09/05/12
For personal use only.

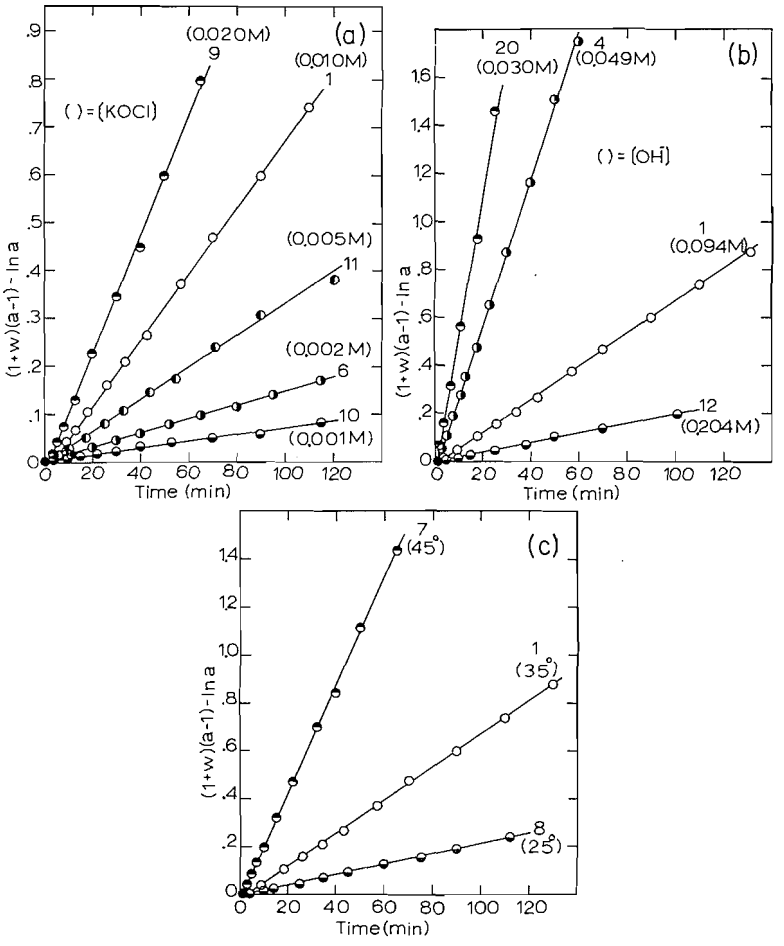


FIG. 1. Results showing agreement of experiment with equation (B). (*a*) Effect of hypochlorite concentration. (*b*) Effect of hydroxide concentration. (*c*) Effect of temperature.

In many runs there is a slight deviation from a straight line initially. This is partly due to the assumption that initially $[MnO_4^-]$ is zero, while in practice reaction (i) would inevitably provide a small quantity of permanganate. Once the reaction has started, errors due to this approximation will rapidly become negligible. However, this effect is in general not large enough to account for the observed deviation, which is presumably due to a trace of permanganate present as an impurity in the potassium manganate. Apart from the points obtained during the first few minutes of any run, the experimental points, plotted according to equation (B), always fell on a straight line.

A further argument in favor of the above mechanism is that addition of potassium permanganate does in fact slow down the reaction. This was found in runs 15, 16, 17, 18, and 19; and in addition, as will be seen later, the amount of the slowing down is close to that calculated from the proposed mechanism, so that equation (B) is still obeyed.

Equation (B) requires that $[(1+w)(a-1)-\ln a]$ plotted against time should give a straight line of slope $2k_2K.[OCl^-]_0$. The observed values of these slopes are given in

Can. J. Chem. Downloaded from www.nrcresearchpress.com by 210.87.254.6 on 09/05/12
For personal use only.

the last column of Table I, under the heading "Slope", and in what follows when a "slope" is mentioned it is this slope that is meant. It can be seen from Table I that the slope is proportional to $[OCl^-]_0$, as required. For instance the following runs were done at 35° C in approximately 0.1 *M* potassium hydroxide:

Run	Slope, $\times 10^{-3}$	$[OCl^-]_0$, $\times 10^{-4}$ *M*	Slope/$[OCl^-]_0$, $\times 10^{-1}$
1	6.8	100	6.8
2	6.9	100	6.9
3	7.5	100	7.5
6	1.47	20	7.35
9	11.9	200	5.95
10	0.70	10	7.0
11	3.5	50	7.0

It is also apparent that the rate is affected by the hydroxide ion concentration, and in fact it is approximately inversely proportional to the square of this concentration. Hence the quantity, slope.$[OH^-]^2/[OCl^-]_0$, should be constant, and this is seen to be at least approximately so for the following runs, all at 35° C:

Run	$[OH^-]$, *M*	Slope. $[OH^-]^2/[OCl^-]_0$, $\times 10^{-3}$	Run	$[OH^-]$, *M*	Slope. $[OH^-]^2/[OCl^-]_0$, $\times 10^{-3}$
1	0.094	6.0	12	0.024	8.2
2	0.106	7.75	13	0.029	4.9
3	0.099	7.35	14	0.098	5.2
4	0.049	7.2	15	0.100	9.1
5	0.049	8.9	16	0.103	8.2
6	0.103	7.8	17	0.0995	8.3
9	0.106	6.7	18	0.0995	8.8
10	0.102	7.3	19	0.099	9.3
11	0.102	7.3	20	0.030	5.7

There is some scatter in the results, with a slight decrease in the quantity, slope.$[OH^-]^2/[OCl^-]_0$, at low hydroxide ion concentrations. However, the general trend is clear; the average value of slope.$[OH^-]^2/[OCl^-]_0$ at 35° C is 7.45×10^{-3}. It will be seen that runs 15–19 with added potassium permanganate fall into line. The explanation of these results in terms of mechanism will be considered below, after noting the effect of temperature.

The runs at different temperatures give:

Run	Temp., °C	Slope.$[OH^-]^2/[OCl^-]_0$, $\times 10^{-3}$
8	25	2.53
Mean	35	7.45
7	45	20.3

These give a good straight line for the plot of log(slope.$[OH^-]^2/[OCl^-]_0$) against $1/T$, corresponding to an activation energy of 19.6 kcal/g-molecule.

Returning to a general consideration of the mechanism, the first point to note is that in the present reaction it is the second stage that is the slower, while in the oxidation by periodate it is the first stage; at least this is true for concentrations in the region of 10^{-4}

Can. J. Chem. Downloaded from www.nrcresearchpress.com by 210.87.254.6 on 09/05/12
For personal use only.

to 10^{-3} M such as were used in these experiments. This is in agreement with the activation energies for it was found (1) that the activation energy of reaction (i) is 13.9 kcal/g-molecule, while the effective activation energy for the oxidation by potassium hypochlorite is 19.6 kcal/g-molecule. This, of course, is not a simple activation energy, since equation (B) shows that

$$\text{slope} \cdot [OH^-]^2/[OCl^-]_0 = 2K \cdot k_2[OH^-]^2$$

so that the 19.6 kcal/g-molecule should contain the heat of reaction (i) plus the activation energy of reaction (ii). Carrington and Symonds (2) give ΔH for reaction (i) as 5.5 kcal, which makes the activation energy for reaction (ii) only 14.1 kcal. However, these conclusions ignore the question of the effect of potassium hydroxide, which must now be considered.

Higher concentrations of potassium hydroxide retard the reaction. It is not at present possible to explain this in terms of mechanism with any certainty, since more than one mechanism could give the observed fact that the rate is inversely proportional to the square of the potassium hydroxide concentration. Presumably this dependence means that hydrolyzed species, such as hypochlorous acid or $HMnO_4^{-2}$ ions, are reacting in the rate-determining step; and that two hydrogen ions have combined with the hypomanganate or hypochlorite ions. These two hydrogen ions could go one each on the hypomanganate and hypochlorite ions, in which case the reaction would be

$$HOCl + HMnO_4^{-2} \rightarrow MnO_4^- + Cl^- + H_2O. \quad \text{(iii)}$$

Alternatively both hydrogen ions might be attached to the hypomanganate ion, when the reaction would be

$$OCl^- + H_2MnO_4^- \rightarrow MnO_4^- + Cl^- + H_2O. \quad \text{(iv)}$$

The hydrolysis constant of hypochlorite ions is 5.5×10^{-7} at 35° C (4). The hydrolysis constant of hypomanganate ions is unknown, but they are probably more easily hydrolyzed than manganate ions. It was found in the study of the reaction between manganate and periodate ions that the results could be explained if the second ionization constant of manganic acid is about 7×10^{-11}. Therefore it is probable that hypomanganate ions are more easily hydrolyzed than hypochlorite ions, and this would on the whole make reaction (iv) a little more probable. It is possible to suggest simple mechanisms for both reactions (iii) and (iv), in terms of either electron or hydrogen atom transfer, so that on this score there is nothing to choose between them.

REFERENCES

1. M. W. Lister and Y. Yoshino. Can. J. Chem. **38**, 2342 (1960).
2. A. Carrington and M. C. R. Symonds. J. Chem. Soc. 3373 (1956).
3. W. M. Latimer. Oxidation potentials. 2nd ed. Prentice-Hall Inc., New York. pp. 55, 239.
4. M. W. Lister. Can. J. Chem. **30**, 879 (1952).

Can. J. Chem. Downloaded from www.nrcresearchpress.com by 210.87.254.6 on 09/05/12
For personal use only.

Can. J. Chem. Downloaded from www.nrcresearchpress.com by 210.87.254.42 on 09/05/12
For personal use only.

FREE RADICALS BY MASS SPECTROMETRY

XXII. PRIMARY DECOMPOSITION STEPS IN THE MERCURY-PHOTOSENSITIZED DECOMPOSITION OF METHANOL AND DIMETHYL ETHER[1]

R. F. POTTIE,[2] A. G. HARRISON,[3] AND F. P. LOSSING

ABSTRACT

The Hg $^3P_1$ photosensitized decomposition of methanol at low pressures proceeds mainly by a dissociation into CH_3O radicals and H atoms. No formation of CH_2OH radicals is observed. A subsidiary reaction to form CH_3 and OH may also be a primary step. Formation of CH_2OH radicals at higher pressures is attributed to an abstraction reaction of CH_3O with CH_3OH.

Two primary modes of dissociation are found to occur for dimethyl ether:

$$Hg\ ^3P_1 + CH_3OCH_3 \rightarrow CH_3OCH_2 + H + Hg\ ^1S_0,$$
$$\rightarrow CH_3O + CH_3 + Hg\ ^1S_0.$$

The relative probabilities of occurrence at low pressures are ~45% and ~50%, respectively. The possibility that the second reaction proceeds by formation of an excited molecule is discussed.

INTRODUCTION

The mercury-photosensitized decomposition of methanol has been examined in some detail by Phibbs and Darwent (1) over a pressure range from 30 to 100 mm Hg and from 25° C to 500° C. They found the products of the reaction below 400° to be almost entirely hydrogen and ethylene glycol, and concluded that the primary step was

$$Hg\ ^3P_1 + CH_3OH \rightarrow CH_2OH + H + Hg\ ^1S_0. \quad [1]$$

From experiments with CH_3OD, they concluded that the alternative primary reaction to form CH_3O did not occur,

$$Hg\ ^3P_1 + CH_3OH \rightarrow CH_3O + H + Hg\ ^1S_0. \quad [2]$$

At temperatures above 400° C CH_2O and CO were formed in addition, evidently by dissociation of the radical formed in the primary step.

The direct photolysis of methanol was recently investigated by Porter and Noyes (2) using λ 1800–2000. They found that two primary steps occurred:

$$CH_3OH + h\nu \rightarrow CH_2O + H_2, \quad [3]$$

$$CH_3OH + h\nu \rightarrow CH_3O + H. \quad [4]$$

Since it had been shown that CH_3O radicals abstract H atoms rapidly (3), they pointed out that formation of CH_3O radicals by [4] would be followed by an abstraction reaction,

$$CH_3O + CH_3OH \rightarrow CH_3OH + CH_2OH, \quad [5]$$

in which CH_2OH radicals would be produced. Using CD_3OH they found no formation of D_2 except at high conversions, and concluded that the evidence against a split into $CH_2OH + H$ in the direct photolysis was fairly strong.

It appeared, therefore, that a re-examination of the mercury-photosensitized reaction of methanol at low pressures under conditions where the occurrence of reaction [5] would be negligibly slow might provide further evidence as to the relative probabilities of the primary reactions [1] and [2].

[1]*Manuscript received September 16, 1960.*
Contribution from the Division of Pure Chemistry, National Research Council, Ottawa, Canada.
Issued as N.R.C. No. 6061.
[2]*National Research Council Postdoctorate Fellow 1958–60.*
[3]*National Research Council Postdoctorate Fellow 1957–59.*

The mercury-photosensitized decomposition of dimethyl ether has been examined by Marcus, Darwent, and Steacie (4), who found the main products at 25° C to be hydrogen and 1,2-dimethoxyethane, corresponding to the primary decomposition step,

$$Hg\ ^3P_1 + CH_3OCH_3 \rightarrow CH_3OCH_2 + H + Hg\ ^1S_0. \quad [6]$$

Subsequent reactions were

$$H + CH_3OCH_3 \rightarrow CH_3OCH_2 + H_2, \quad [7]$$

$$2CH_3OCH_2 \rightarrow (CH_3OCH_2)_2. \quad [8]$$

At 265° C products corresponding to the decomposition of the CH_3OCH_2 radical were found,

$$CH_3OCH_2 \rightarrow CH_3 + CH_2O. \quad [9]$$

They found no evidence for the formation of excited molecules in this reaction, and no evidence for a primary rupture of the C—O bond,

$$Hg\ ^3P_1 + CH_3OCH_3 \rightarrow CH_3O + CH_3 + Hg\ ^1S_0. \quad [10]$$

EXPERIMENTAL

The mercury-photosensitized reactions were examined using a fast-flow system coupled to a mass spectrometer, the apparatus and method of operation being the same as that employed earlier (5, 6). In this apparatus the reactant and mercury vapor at partial pressures of a few microns are carried in a stream of helium at 8 mm pressure through a tubular reactor which is strongly illuminated by a low-pressure lamp of high intensity. The reactor is maintained at 55° C. The residence time in the illuminated zone is about 0.001 second. Directly following the illuminated zone the reaction stream passes over a small orifice through which a portion flows directly into the ionization chamber of a mass spectrometer. The bulk of the stream passes into a fast-pumping system. As discussed earlier (6), the reaction conditions resemble those of flash photolysis, in as much as radical–radical reactions are greatly favored over radical–substrate reactions.

The sample of CD_3OH was obtained from Merck and Co., Montreal. The isotopic purity was greater than 99%.

RESULTS AND DISCUSSION

Methanol

In preliminary experiments on methanol, it was found that although products such as CH_2O, CO, CH_4, H_2, and methyl radicals could be easily detected, no increase in the 31 peak attributable to the CH_3O or CH_2OH radicals could be found. It was concluded therefore that the sensitivity of the mass spectrometer to radicals of this type was quite low, and that a distinction between reactions [1] and [2] could not be made by identifying by mass the radicals produced in the decomposition of CD_3OH:

$$Hg\ ^3P_1 + CD_3OH \rightarrow CD_2OH + D + Hg\ ^1S_0, \quad [1a]$$

$$\rightarrow CD_3O + H + Hg\ ^1S_0. \quad [2a]$$

An alternative means for identifying the radicals, which had earlier been found useful (7), was employed. The addition of a small partial pressure of $Hg(CH_3)_2$ to the reaction stream resulted, by the mercury-photosensitized decomposition of the dimethyl mercury, in the production of methyl radicals. The combination of these with radicals formed in the primary decomposition of the compound under examination then resulted in the formation of identifiable stable products. In the case of methanol it was advantageous

Can. J. Chem. Downloaded from www.nrcresearchpress.com by 210.87.254.42 on 09/05/12
For personal use only.

to employ CD_3OH instead of CH_3OH, and to add CD_3 radicals by the use of $Hg(CD_3)_2$. Assuming that both primary steps [1*a*] and [2*a*] were occurring, the two combination reactions of CD_3 radicals would be

$$CD_3 + CD_2OH \rightarrow CD_3CD_2OH \text{ (parent mass 51)}, \quad [11]$$

$$CD_3 + CD_3O \rightarrow CD_3OCD_3 \text{ (parent mass 52)}. \quad [12]$$

Since ethanol and dimethyl ether have large parent peaks, the identification of the combination product by mass number was quite straightforward. As shown in Fig. 1,

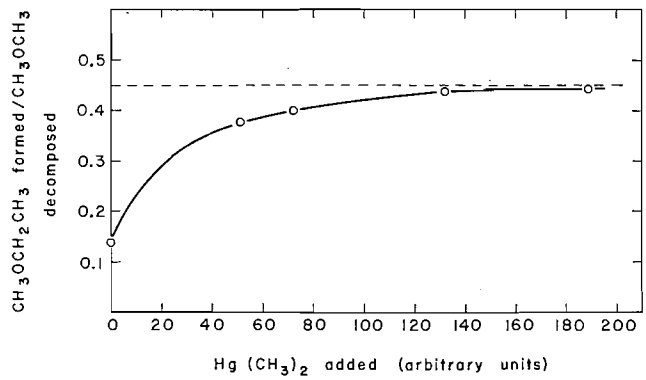


FIG. 1. Yield of $CH_3OCH_2CH_3$ formed by reaction of the CH_3OCH_2 radicals produced in primary decomposition of dimethyl ether with excess CH_3 radicals from added $Hg(CH_3)_2$.

only CD_3OCD_3 was produced in this experiment. (Additional confirmation for the identity of CD_3OCD_3 is provided by the ratio of peaks at mass 50 and 52 (2.00), which was the same as the corresponding ratio for mass 45/46 in CH_3OCH_3 (2.09).) After correction of the mass 51 peak height in the spectrum in Table I, the net CD_3CD_2OH peak is less than 1% of the CD_3OCD_3 peak. Since the parent peak sensitivity for dimethyl ether is about three times that for ethanol, it is evident that an upper limit for CD_3CD_2OH formation is 3% of the CD_3OCD_3 formation. Assuming that the rates of the combination reactions [11] and [12] are not greatly different, as seems reasonable, it seems clear that under the present experimental conditions the fraction of the primary reaction leading to the formation of CH_2OH radicals is less than 3%, and that the predominating mode of dissociation is to CH_3O and H. This is in agreement with the direct photolytic result of Porter and Noyes (2).

It is probable that the apparent contradiction between the present work and that of Phibbs and Darwent (1) concerning CH_2OH formation arises from the fact that the present work was carried out at very low partial pressures of methanol. This difference in conditions could affect the result in two ways. The first is the possibility that CH_3O formation results from dissociation of an excited molecule produced in a primary step,

$$Hg\ ^3P_1 + CH_3OH \rightarrow CH_3OH^* + Hg\ ^1S_0, \quad [13]$$

which is deactivated at high pressures, while CH_2OH results from direct removal of a H-atom by the excited mercury atom. This explanation is quite unsatisfactory, however. If one accepts the present result that reaction [1] has a cross section less than 3% of that for reaction [2], this explanation would require the quantum yield of H_2 (or other products) at high pressures to be less than 0.03. Since Phibbs and Darwent found the quantum yield of H_2 to be 0.43 under their conditions, this possibility can be ruled

Can. J. Chem. Downloaded from www.nrcresearchpress.com by 210.87.254.42 on 09/05/12
For personal use only.

out. To be consistent with this observation it would be necessary to postulate two excited states, one leading to the other by collision. Following reaction [13] one would require

$$CH_3OH^* \rightarrow CH_3O + H, \quad [14]$$

$$CH_3OH^* + M \rightarrow CH_3OH^{**} + M, \quad [15]$$

$$CH_3OH^{**} \rightarrow CH_2OH + H. \quad [16]$$

It seems more probable, however, that the apparent discrepancy arises from the rapid conversion of CH_3O into CH_2OH by reaction [5] as pointed out by Porter and Noyes (2). This reaction is exothermic by 7–8 kcal/mole (8), and at the pressures employed by Phibbs and Darwent it is quite possible that it would be much faster than the alternative reactions of CH_3O:

$$2CH_3O \rightarrow CH_3OOCH_3, \quad [17]$$

$$2CH_3O \rightarrow CH_2O + CH_3OH. \quad [18]$$

Reaction [17] appears in any case to be quite slow. No formation of dimethyl peroxide was observed by Wijnen (3) in the photolysis of methyl acetate. In an earlier paper of this series (6) the amount of dimethyl peroxide formed by [17] was found to be negligibly small under conditions favorable for its occurrence. In the present work it was not found in the experiments on CH_3OH and CH_3OCH_3, although CH_3O radicals were evidently present in good yields. A failure to detect dimethyl peroxide, as in Phibbs and Darwent's work, provides therefore no evidence for the absence of CH_3O. An analysis of the products from methanol photodecomposition is given in Table II. The reason

TABLE I

Combination products in the photosensitized decomposition of CD_3OH in presence of CD_3 radicals

m/e	Observed spectrum	^{13}C isotope correction	Net spectrum of products	Parent species
52	1.00	—	1.00	CD_3OCD_3
51	0.05	0.044	<0.01	CD_3CD_2OH
50	2.00	—	2.00	—

TABLE II

Mercury-photosensitized decomposition of CH_3OH at 55° C in 8 mm helium

Species		Partial pressure (μ)	
CH_3OH		Lamp off	5.01
		Lamp on	4.65
		Decomposed	0.36
CH_3OCH_3			0.008
CH_2O			0.150
CO			0.081
C_2H_6			0.010
CH_4			0.019
CH_3			0.028
H_2O			0.065
O balance	87%	Total CH_3	0.075
C balance	85%	Total OH	0.065

Can. J. Chem. Downloaded from www.nrcresearchpress.com by 210.87.254.42 on 09/05/12
For personal use only.

for the low carbon and oxygen material balances is not apparent, since there was no visible formation of polymeric deposits in the reactor. The presence of C_2H_6, CH_4, and CH_3, which cannot be derived from a primary split giving CH_3O, and the formation of H_2O which is evidently derived from OH radical, suggest the occurrence of a second primary decomposition,

$$Hg\ ^3P_1 + CH_3OH \rightarrow CH_3 + OH + Hg\ ^1S_0. \qquad [19]$$

The sum of products derived from CH_3, $2(C_2H_6) + (CH_4) + (CH_3OCH_3)$, is equal to 0.075 μ, in fair agreement with the yield of H_2O, which is 0.065 μ. Reaction [19] would therefore account for about 18% of the methanol decomposed. The possibility cannot be entirely ruled out that these products result in part from an atomic cracking reaction,

$$H + CH_3O \rightarrow CH_3OH^* \rightarrow CH_3 + OH. \qquad [20]$$

Dimethyl Ether

Although the present results confirm the occurrence of reaction [6] as an important primary mode of dissociation of dimethyl ether, they provide strong evidence that a primary dissociation by a C—O split, reaction [10], is equally important at low pressures. An analysis of the products of the mercury-photosensitized reaction at 55° C in the presence of 8 mm of helium is given in Table III. The combination products $(CH_3OCH_3)_2$,

TABLE III

Mercury-photosensitized decomposition of CH_3OCH_3 at 55° C in 8 mm helium

Species		Partial pressure (μ)	
CH_3OCH_3		Lamp off	10.84
		Lamp on	10.35
		Decomposed	0.49
$(CH_3OCH_2)_2$			0.025
$CH_3OCH_2OCH_3$			0.016
$CH_3OCH_2CH_3$			0.070
CH_3OH			0.094
CH_2O			0.144
CO			0.076
C_2H_6			0.057
CH_4			0.057
CH_3			0.086
O balance	95.1%		
C balance	94.8%		

$CH_3OCH_2OCH_3$, and $CH_3OCH_2CH_3$ were identified by comparison of the spectra with those of pure samples of these compounds examined in separate experiments. These three products were evidently formed from CH_3OCH_2 radicals by the combination reactions:

$$2CH_3OCH_2 \rightarrow (CH_3OCH_2)_2, \qquad [21]$$

$$CH_3OCH_2 + OCH_3 \rightarrow CH_3OCH_2OCH_3, \qquad [22]$$

$$CH_3OCH_2 + CH_3 \rightarrow CH_3OCH_2CH_3. \qquad [23]$$

Taken together the quantities of these three products correspond to 0.136 μ of CH_3OCH_2 radical, that is, 27.8% of the dimethyl ether decomposed. Since some CH_3OCH_2 radicals may decompose (see below), this figure is evidently a lower limit for their formation.

A more reliable estimate for the relative probability of reaction [6] was obtained by

Can. J. Chem. Downloaded from www.nrcresearchpress.com by 210.87.254.42 on 09/05/12
For personal use only.

measuring the yield of $CH_3OCH_2CH_3$ in the presence of methyl radicals added to the reaction stream. It can be seen from Fig. 1 that this yield reached a limiting value of 0.45 in the presence of a large excess of methyl radicals. An almost identical limit was obtained for the yield of $CH_3OCH_2CD_3$ when CD_3 radicals were added (Fig. 2). This limit must correspond quite closely to the relative probability of reaction [6].

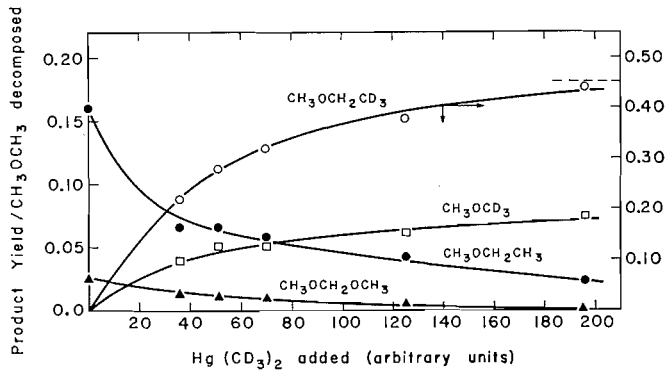


FIG. 2. Yields of products formed by radical interaction in the dimethyl ether decomposition in the presence of added CD_3 radicals.

The difference between the yield of 0.45 and the yield of 0.28 as a lower limit obtained from the data in Table III must represent CH_3OCH_2 radicals which are formed, but which, in the absence of excess CH_3 radicals, do not appear as dimeric products. Since the radical appears to be thermally stable at 55° C (4) it must disappear mainly by reaction with an excited mercury atom,

$$Hg^* + CH_3OCH_2 \rightarrow CH_3 + CH_2O + Hg. \quad [24]$$

The extent of this reaction is equivalent to 0.49 (0.45−0.28) = 0.084 μ of CH_3OCH_2 radical.

From the data in Table III the relative probability of the primary reaction [10] can be estimated in two ways: from products derived from CH_3, and from products derived from CH_3O.

(*a*) Reactions removing CH_3 radicals would be reaction [23], and the following:

$$2CH_3 \rightarrow C_2H_6, \quad [25]$$

$$CH_3 + OCH_3 \rightarrow CH_4 + CH_2O. \quad [26]$$

The total amount of products derived from CH_3 is then, from Table III,

$$(CH_3OCH_2CH_3) + 2(C_2H_6) + (CH_4) + (CH_3) = 0.327\ \mu.$$

To obtain the amount of CH_3 formed in reaction [10] one must subtract 0.084 μ of CH_3 produced by [24]. On this basis the relative probability of reaction [10] is 0.243 μ/0.49 μ = 0.49_6.

(*b*) Reactions removing CH_3O radicals would be [18], [22], [26], and the following:

$$Hg^* + CH_3O \rightarrow CH_2O + H + Hg, \quad [27]$$

$$H + CH_3O \rightarrow CH_2O + H_2. \quad [28]$$

The CO found was most probably formed from CH_2O by reaction with an excited

Can. J. Chem. Downloaded from www.nrcresearchpress.com by 210.87.254.42 on 09/05/12
For personal use only.

mercury atom, since this reaction has a large relative cross section (9). The quantity of products derived from CH_3O is therefore

$$(CH_3OCH_2OCH_3) + (CH_3OH) + (CH_2O) + (CO) - (CH_2O \text{ from } [24]) = 0.246\ \mu.$$

This corresponds to a relative probability of 0.50_2 for the primary reaction [10], in good agreement with the value obtained from the yield of methyl. Although these two estimates for reaction [10] are independent of one another, their close agreement arises from the near equality of the carbon and oxygen balances given in Table III.

These estimates should be regarded as only approximate, since some re-formation of dimethyl ether may occur by the following reactions:

$$CH_3OCH_2 + CH_3O \rightarrow CH_3OCH_3 + CH_2O, \quad [29]$$

$$CH_3OCH_2 + H \rightarrow CH_3OCH_3, \quad [30]$$

$$CH_3O + CH_3 \rightarrow CH_3OCH_3. \quad [31]$$

In the experiment in which a large excess of CD_3 radicals was added, the yield of CH_3OCD_3 amounted to only about 7% of the dimethyl ether decomposed, as shown in Fig. 2. When no methyl radicals were added as for the data in Table III, the extent of reaction [31] would be considerably less, certainly not more than 2–3%. Since the concentrations of CH_3OCH_2, CH_3O, and H were of the same order or less than CH_3, interference by reactions [29] and [30] would also be small. Moreover it should be noted that the same limit for CH_3OCH_2 production was reached by CH_3 addition and by CD_3 addition, even though in the latter experiment reaction [31] would not interfere with the measurement of the amount of CH_3OCH_3 decomposed. This also indicates that the limits of 0.45 and 0.50 for reactions [6] and [10] are not seriously in error as a result of interference by back reactions.

Some question may be raised as to whether some or all of the CH_3O formation observed at these low pressures results from an atomic cracking reaction rather than from a primary dissociation. The following series of reactions could be proposed to explain the formation of CH_3O at low pressures and its absence under the higher pressure conditions of Marcus, Darwent, and Steacie (4):

$$CH_3OCH_2 + H \rightarrow CH_3OCH_3^*, \quad [32]$$

$$CH_3OCH_3^* \rightarrow CH_3O + CH_3, \quad [33]$$

$$CH_3OCH_3^* + M \rightarrow CH_3OCH_3 + M. \quad [34]$$

The results given in Figs. 1 and 2 show, however, that this series of reactions does not play a significant role under the present conditions. As shown in Fig. 1, the addition of an excess of CH_3 radicals, which would suppress reaction [32], gives an upper limit of 0.45 for the relative probability of reaction [6], and not nearly unity as would be the case if reaction [6] were the only primary mode of decomposition. The yield of $CH_2OCH_2CD_3$ in Fig. 2 confirms this observation. Moreover, the yield of CH_3OCD_3 (Fig. 2) does not pass through a maximum and then decrease with increasing CD_3 addition as would be expected if reactions [32] and [33] were important under these conditions. It seems quite clear from these results that at low pressures CH_3O is formed in a primary decomposition step with a probability of about 0.50. The non-occurrence of this mode of dissociation at pressures in the 28- to 500-mm region (4) suggests that it may go by formation of an excited molecule,

$$Hg\ ^3P_1 + CH_3OCH_3 \rightarrow CH_3OCH_3^* + Hg\ ^1S_0, \quad [35]$$

followed by the dissociation and deactivation reactions [33] and [34]. Since the 8 mm

Can. J. Chem. Downloaded from www.nrcresearchpress.com by 210.87.254.42 on 09/05/12
For personal use only.

of helium used in the present experiments would be completely ineffective in quenching excited molecules, the effective pressure is that of the ether itself, i.e. about 0.010 mm, and deactivation would be quite slow. Even in the experiments in which methyl radicals were added, the total partial pressure effective for deactivation was still well below 0.05 mm.

REFERENCES

1. M. K. PHIBBS and B. DE B. DARWENT. J. Chem. Phys. **18**, 495 (1950).
2. R. P. PORTER and W. A. NOYES. J. Am. Chem. Soc. **81**, 2307 (1959).
3. M. H. J. WIJNEN. J. Chem. Phys. **27**, 710 (1957); **28**, 271 (1958).
4. R. A. MARCUS, B. DE B. DARWENT, and E. W. R. STEACIE. J. Chem. Phys. **16**, 987 (1948).
5. F. P. LOSSING, D. G. H. MARSDEN, and J. B. FARMER. Can. J. Chem. **34**, 701 (1956).
6. P. KEBARLE and F. P. LOSSING. Can. J. Chem. **37**, 389 (1959).
7. J. COLLIN and F. P. LOSSING. Can. J. Chem. **35**, 778 (1957).
8. P. GRAY and A. WILLIAMS. Chem. Revs. **59**, 240 (1959).
9. A. G. HARRISON and F. P. LOSSING. Can. J. Chem. **38**, 544 (1960).

Can. J. Chem. Downloaded from www.nrcresearchpress.com by 210.87.254.42 on 09/05/12
For personal use only.

Can. J. Chem. Downloaded from www.nrcresearchpress.com by 210.87.254.5 on 09/05/12
For personal use only.

EXCEPTIONS TO HUDSON'S RULES OF ISOROTATION

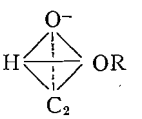
THE NUCLEAR MAGNETIC RESONANCE SPECTRA OF ANOMERIC PYRIMIDINE 2-DEOXY-D-RIBONUCLEOSIDES[1]

R. U. LEMIEUX AND M. HOFFER

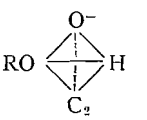
ABSTRACT

Nuclear magnetic resonance spectroscopy and optical rotatory dispersion measurements were used to correlate the configurations of anomeric pairs for the 1-(2-deoxy-D-ribofuranosyl) derivatives of 5-methyl- and 5-fluoro-uracil. The optical rotations of the anomers were found opposite to those expected on the basis of Hudson's rules of isorotation.

Hudson's rules of isorotation in their earliest form (1) in effect stated that for D-glycosides the more dextrorotatory (or less levorotatory) anomer is to be named α-D-. As evidence for the absolute configurations of glycopyranosides accumulated, it became evident that the rules correlate rotation and anomeric configuration (2). It has consequently become a widespread practice to assign absolute anomeric configurations on the basis of Hudson's rules and the assumption that the absolute configurations are those which follow.



α-D or β-L



β-D or α-L

The purpose of this communication is to report that the rules of isorotation are violated in every respect in the case of certain 2-deoxy-D-ribonucleosides. Thus, although the rules are well tested and are undoubtedly of value in assigning anomeric configurations to *O*-glycopyranosyl compounds, reserve is indicated in their application to the kinds of glycosides for which there exists no compelling empirical evidence (3).

Hoffer, Duschinsky, Fox, and Young (4) recently have reported syntheses of the anomeric pairs for the pyrimidine 2-deoxy-D-ribonucleosides I and II, and III and IV (see Fig. 3). The optical rotations for these compounds measured with the *D-line of sodium* are presented in Table I.

On the basis of the anomeric configurations assigned to the compounds in Table I, *except* for the anomers V and VI and the anomers I and II the rotations for these compounds when measured in dimethylformamide are opposite to those required by Hudson's rules. The assignments of configuration are those made by Hoffer and co-workers (4) on the basis of the fact that all the natural 2-deoxyribonucleosides possess the β-D-configuration (5) and the assumption that the anomers obtained in the greater yield, in their syntheses (4) from crystalline 3,5-di-*O*-*p*-toluyl-2-deoxy-D-ribofuranosyl chloride, are configurationally related.

Application of Hudson's rules to isomeric glycosyl compounds of course requires that the compounds differ only in the configuration of the anomeric center. Hoffer (6) has shown, in this respect, that methylation of compounds V and VI introduces a methyl

[1]*Manuscript received September 1, 1960.*
Contribution from the Department of Chemistry, University of Ottawa (R.U.L.), Ottawa, Ontario, and Hoffmann-LaRoche, Inc. (M.H.).

TABLE I

Optical rotations of pyrimidine 2-deoxy-D-ribonucleosides

Compound	$[\alpha]_D$	Solvent (c, 2)
1. 1-(2-Deoxy-α-D-ribofuranosyl)-5-methyluracil (I)	+7.2°	Water
	+13	*N* Sodium hydroxide
	+46.6	Dimethylformamide
2. 1-(2-Deoxy-β-D-ribofuranosyl)-5-methyluracil (II) (thymidine)	+20	Water
	+32.8*	*N* Sodium hydroxide
	+15.1	Dimethylformamide
3. 1-(2-Deoxy-α-D-ribofuranosyl)-5-fluorouracil (III)	−21	Water
	+20.5	Dimethylformide
4. 1-(2-Deoxy-β-D-ribofuranosyl)-5-fluorouracil (IV)	+37	Water
	+48.6	Dimethylformamide
5. 3,5-Di-*O*-*p*-toluyl I (V)	−14.5	Pyridine
	−20.4	Dimethylformamide
6. 3,5-Di-*O*-*p*-toluyl II (VI)	−50	Pyridine
	−36.5	Dimethylformamide
7. 3,5-Di-*O*-*p*-toluyl III (VII)	−72.5	Pyridine
	−69.2	Dimethylformamide
8. 3,5-Di-*O*-*p*-toluyl IV (VIII)	−17	Pyridine
	−4	Dimethylformamide

*P. A. Levene and E. S. London. J. Biol. Chem. **83**, 793 (1929); see also X. Schindler. Helv. Chim. Acta, **32**, 979 (1949).

group in each case at position-3 of the pyrimidine ring. Thus, in view of the synthesis of V and VI from pure 3,5-di-*O*-*p*-toluyl-2-deoxy-D-ribofuranosyl chloride (4), there can be no doubt that I and II are truly anomeric. The ultraviolet absorption spectral data obtained with solutions of III and IV as well as I and II at varying pH also provided evidence for the anomeric relationship between the fluorides III and IV (6). As will be seen below, the nuclear magnetic resonance spectra and optical rotatory dispersion curves for these compounds confirm these conclusions.

Lemieux, Kullnig, Bernstein, and Schneider (7) have shown that the anomeric configurations of aldosides in principle often can be determined by proton magnetic resonance spectroscopy. The application usually requires detection of the fine structure for the signal of the anomeric hydrogen and a knowledge of the conformation of the compound. It is clear, however, that unless changes in the aglycon of a glycoside change the conformation of the sugar residue, then the fine structure of the signals for the protons of the sugar residue should not be altered appreciably. Also, the chemical shifts can be expected to be relatively constant. Certainly, when the fine structure and chemical shifts are substantially the same for the protons in the sugar portions of two glycosides differing only in the aglycon, the two compounds must possess the same anomeric configurations. Thus, proton magnetic resonance spectroscopy should be useful for classifying anomeric compounds even in the absence of a knowledge of their configurations.

The proton magnetic resonance spectra for the nucleosides listed in Table I are given in Figs. 1 and 2. The signals in the spectra can be readily assigned to the hydrogens in the compounds on the basis of the experience with related compounds (7, 8) but these assignments are not needed for the present purpose of grouping the compounds into two series of configurationally related substances—a feat which is not possible on the basis of optical rotations measured at the *D*-line of sodium only. However, as seen in Fig. 3, the optical rotatory dispersion curves for compounds I to IV clearly indicate the configurational relationships at the anomeric centers for these compounds. That is, it must

Can. J. Chem. Downloaded from www.nrcresearchpress.com by 210.87.254.5 on 09/05/12
For personal use only.

Can. J. Chem. Downloaded from www.nrcresearchpress.com by 210.87.254.5 on 09/05/12
For personal use only.

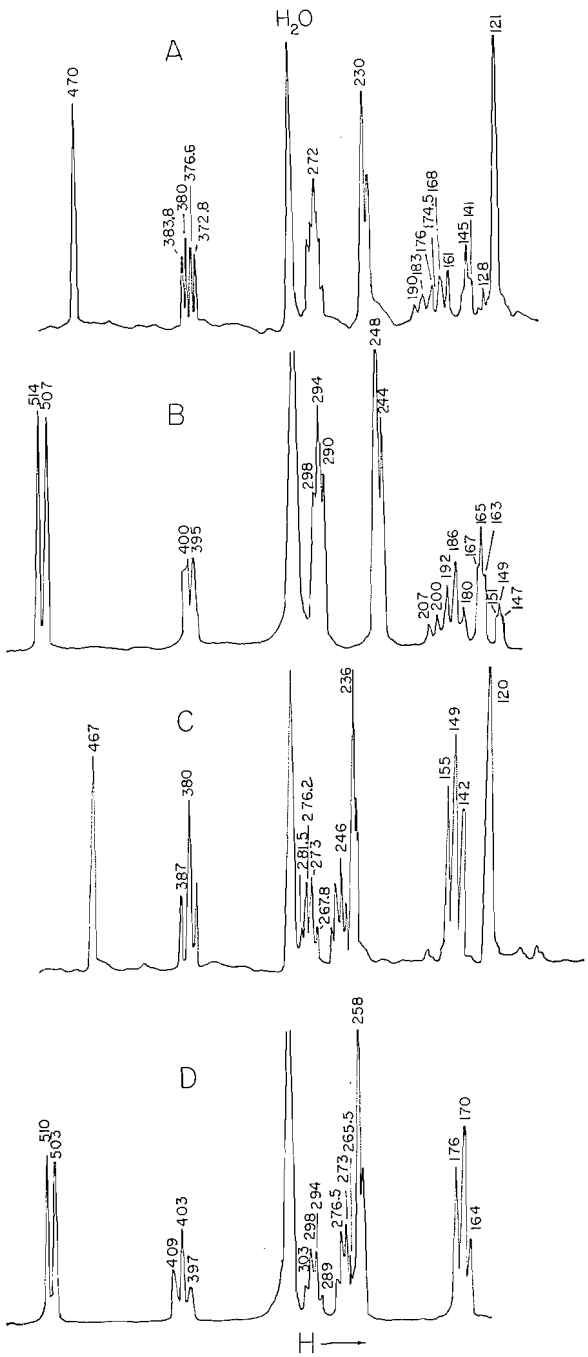


FIG. 1. The nuclear magnetic resonance spectra of anomeric glycofuranosides measured in deuterium oxide with a high-resolution Varian spectrometer operating at 60 Mc/sec. The positions of the signals are from tetramethylsilane used as an external standard.

(A) 1-(2-Deoxy-α-D-ribofuranosyl)-5-methyluracil (I).
(B) 1-(2-Deoxy-α-D-ribofuranosyl)-5-fluorouracil (II).
(C) 1-(2-Deoxy-β-D-ribofuranosyl)-5-methyluracil (III).
(D) 1-(2-Deoxy-β-D-ribofuranosyl)-5-fluorouracil (IV).

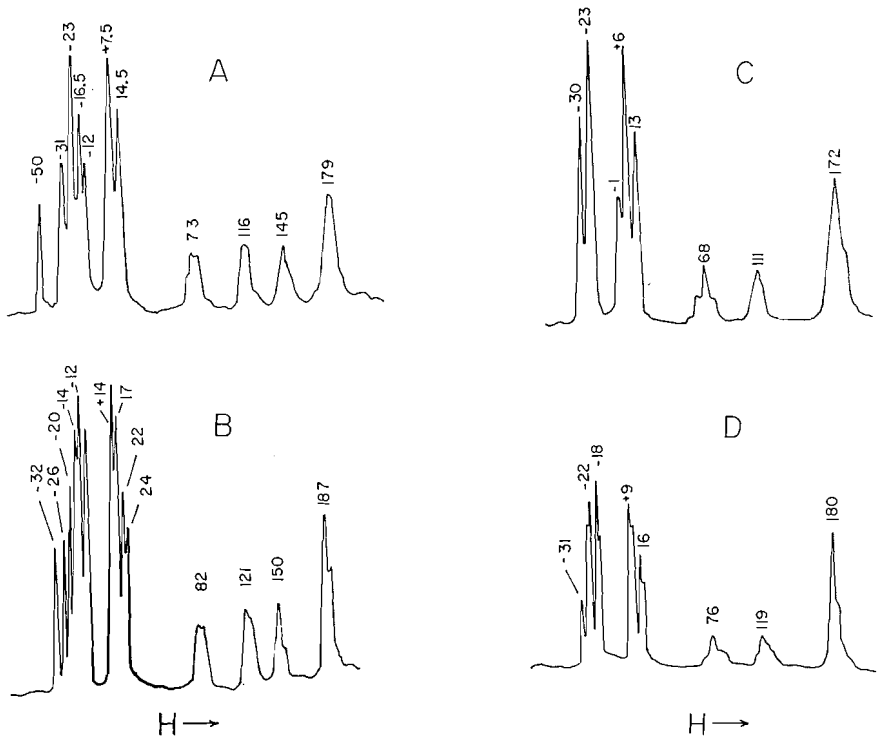


FIG. 2. The nuclear magnetic resonance spectra of anomeric glycofuranosides measured in dimethyl sulphoxide with a high-resolution Varian spectrometer operating at 60 Mc/sec. The positions of the signals are from chloroform used as an external standard. The signals at higher field were obscured by those of the solvent.

(A) 1-(Di-*O*-*p*-toluyl-2-deoxy-α-D-ribofuranosyl)-5-methyluracil (V).
(B) 1-(Di-*O*-*p*-toluyl-2-deoxy-α-D-ribofuranosyl)-5-fluorouracil (VII).
(C) 1-(Di-*O*-*p*-toluyl-2-deoxy-β-D-ribofuranosyl)-5-methyluracil (VI).
(D) 1-(Di-*O*-*p*-toluyl-2-deoxy-β-D-ribofuranosyl)-5-fluorouracil (VIII).

be expected (9) that for such closely related substances, the two compounds whose specific rotations follow similar trends with decreasing wavelength are configurationally related. These results show clearly that the anomalous rotations (from the viewpoint of Hudson's rules and the assigned configurations (4)) obtained with the *D*-line of sodium are not the result of a fortuitous crossing-over of the rotatory dispersion curves but, instead, that the anomalous rotations are a characteristic of the compounds at all the wavelengths used.

Thus, the nuclear magnetic resonance spectra and optical rotatory dispersion curves leave no doubt as to which of the compounds (I to IV) are configurationally related. The conclusion that the rotations of these compounds do not agree with predictions based on Hudson's rules of course requires unequivocal proof of the absolute configuration of at least one of the compounds. Michelson and Todd (5) have established the configuration of thymidine (I). As indicated above synthetic evidence already exists for the configurations and structures depicted in Fig. 3 for compounds II, III, and IV. It was also found possible to deduce the configurations and conformations of thymidine (I) and its anomer (II) from their nuclear magnetic spectra and the range of coupling constants calculated by Karplus (10) for two protons on neighboring saturated carbons. A detailed consideration of these matters is reserved for a separate report (11).

Can. J. Chem. Downloaded from www.nrcresearchpress.com by 210.87.254.5 on 09/05/12
For personal use only.

Can. J. Chem. Downloaded from www.nrcresearchpress.com by 210.87.254.5 on 09/05/12
For personal use only.

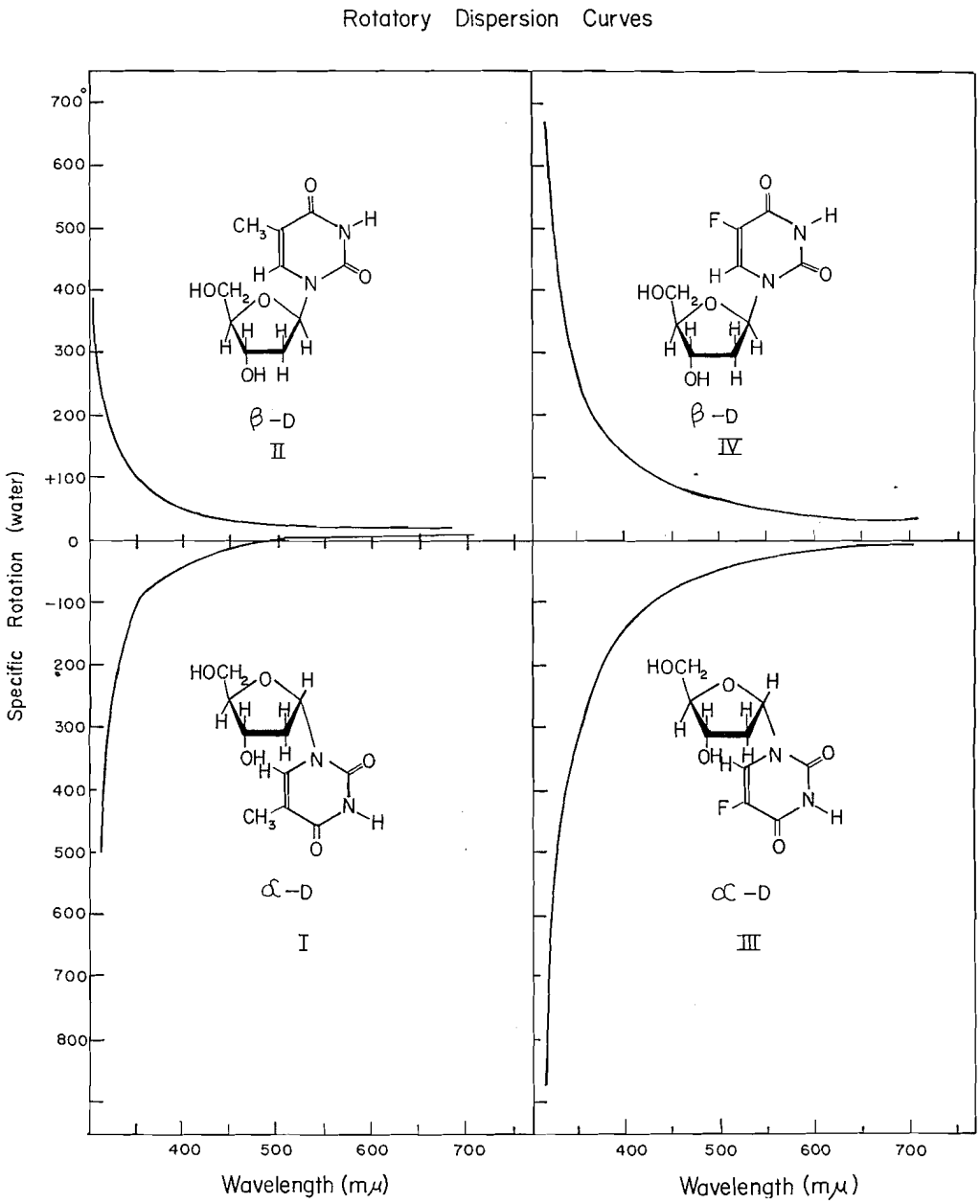


FIG. 3. Optical rotatory dispersion curves of the indicated compounds measured, using about 0.75% solutions in water, at 24–25°.

Fox (12) has already anticipated the failure of Hudson's rules of isorotation in the series of pyrimidine nucleosides. Evidence has been obtained (13) that the rotations of 2-deoxyglucopyranosides and 2-deoxyribopyranosides follow Hudson's rules. Indications that this may not have been the case was suggested by the rotations observed (14) for 2-deoxy-D-glucose tetraacetates. The so-called α-D- ($[\alpha]_D$ +12.3° (ethanol)) and β-D-compounds ($[\alpha]_D^{20}$ +30° (ethanol)) were found (13) to be both impure preparations of 2-deoxy-β-D-glucopyranose tetraacetate.

In conclusion, the configurations of thymidine (I) and its α-anomer (II) are opposite to those which would have been anticipated on the basis of Hudson's rules of isorotation and the rotations measured either in water or aqueous sodium hydroxide. The rotations of the compounds are, however, in accordance with Hudson's rules when measured in dimethylformamide as are the rotations of their di-*O*-toluyl derivatives V and VI, respectively, when measured either in pyridine or dimethylformamide. The substitution of the methyl group in the thymine residue by fluorine atom results in compounds, III and IV, whose rotations are opposite to those expected from Hudson's isorotation rules when measured either in water or dimethylformamide. Also, the rotations of the di-*O*-toluyl derivatives of III and IV (VII and VIII, respectively) are not in agreement with Hudson's rules when measured either in pyridine or dimethylformamide. Thus, it is evident that the precise meaning of the α- and β-designations which are used to describe carbohydrate structures needs revision. The convention, as was seen above, used in carbohydrate nomenclature which employs two different designations to represent each of the two absolute configurations for anomeric centers is unique in the field of organic chemistry. It seems reasonable in view of the above described exceptions to Hudson's rules of isorotation that serious consideration be given to a substitution of these rules of nomenclature by rules that are more compatible with the more widely accepted procedures for naming such structures.

ACKNOWLEDGMENTS

The authors are grateful to Mrs. A. Westland for technical assistance and the National Research Council of Canada for financial assistance in the operation and maintenance of the nuclear magnetic resonance spectrometer. Mr. J. A. Findlay, University of New Brunswick, made the optical rotatory dispersion measurements.

REFERENCES

1. C. S. HUDSON. J. Am. Chem. Soc. **31**, 66 (1909).
2. C. S. HUDSON. Advances in Carbohydrate Chem. **3**, 1 (1948).
3. R. U. LEMIEUX and J. P. BARRETTE. J. Am. Chem. Soc. **80**, 2243 (1958).
4. M. HOFFER, R. DUSCHINSKY, J. J. FOX, and N. YOUNG. J. Am. Chem. Soc. **81**, 4112 (1959).
5. A. M. MICHELSON and A. R. TODD. J. Chem. Soc. 816 (1955).
6. M. HOFFER. Private communication.
7. R. U. LEMIEUX, R. K. KULLNIG, H. J. BERNSTEIN, and W. G. SCHNEIDER. J. Am. Chem. Soc. **80**, 6098 (1958).
8. C. D. JARDETZKY. J. Am. Chem. Soc. **82**, 229 (1960).
9. C. DJERASSI. Optical rotatory dispersion, applications to organic chemistry. McGraw-Hill Book Co. Inc., New York. 1960.
10. M. KARPLUS. J. Chem. Phys. **30**, 11 (1959).
11. R. U. LEMIEUX. Can. J. Chem. **39**, 116 (1961).
12. J. J. FOX. Advances in Carbohydrate Chem. **14**, 340 (1959).
13. R. U. LEMIEUX, S. LEVINE, and M. A. SAEED. In preparation.
14. W. G. OVEREND, M. STACEY, and J. STANEK. J. Chem. Soc. 2841 (1949).

Can. J. Chem. Downloaded from www.nrcresearchpress.com by 210.87.254.5 on 09/05/12
For personal use only.

Can. J. Chem. Downloaded from www.nrcresearchpress.com by 210.87.254.105 on 09/05/12
For personal use only.

THE CONFIGURATION AND CONFORMATION OF THYMIDINE[1]

R. U. LEMIEUX

ABSTRACT

The nuclear magnetic resonance spectrum for the anomer of the naturally occurring deoxyribonucleoside thymidine allowed a conclusion as to its anomeric configuration through an interpretation of the fine structure observed in the signals for the H_1', H_2', and H_2'' atoms. Thus, indirect evidence for the configuration of thymidine was obtained. The nuclear magnetic resonance spectrum of thymidine suggests that the compound possesses considerable conformational purity when dissolved in water since an interpretation of the spectrum leads to the assignment of the plausible conformation wherein all of the large substituents on the furanose ring are in partially staggered orientations with the neighboring atoms.

The anomeric configuration of thymidine has been established beyond any reasonable doubt by Michelson and Todd (1). A purpose of this communication is to show that it is possible to arrive at the same conclusion by a consideration of the nuclear magnetic resonance spectra for thymidine and its α-anomer (2, 3). More important, the results of the present investigation allow conclusions as to the conformation of thymidine in aqueous solution.

It was not possible to establish the configuration of thymidine directly from its N.M.R. spectrum (see Fig. 1) since there proved to be little, if any, chemical shift between the 2-hydrogens (H_2' and H_2''). For this reason, the signal of the 1-hydrogen (H_1') was found to be in the form of a triplet, the spacing (7.0 ± 0.2 c.p.s.) of which reflects the

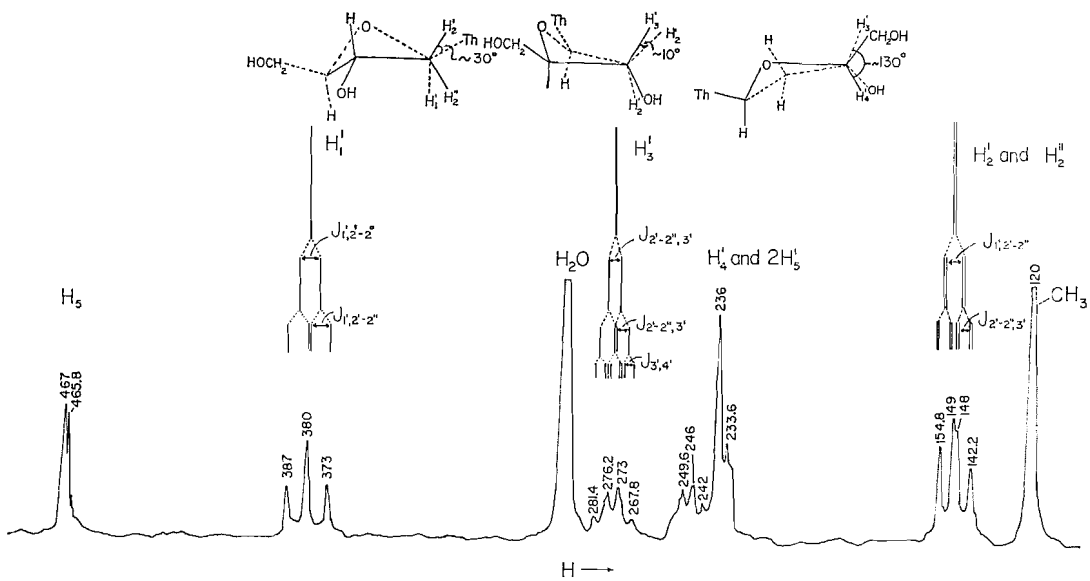


FIG. 1. The experimental and calculated nuclear magnetic resonance spectra of thymidine. The spectrum was measured using a 20% solution in deuterium oxide at 25° with a high-resolution spectrometer operating at 60 Mc/sec. The positions of the signals are from tetramethylsilane used as an external standard. The projection formulas represent the conformation for thymidine suggested by the spectrum. The projections are those obtained by viewing the molecular model first along the C_2 to C_1 bond with C_2 in front, secondly along the C_3 to C_2 bond with C_3 in front, and thirdly along the C_4 to C_3 bond with C_4 in front.

[1]*Manuscript received September 1, 1960.*
Contribution from the Department of Chemistry, University of Ottawa, Ottawa, Canada.

average of the coupling with H_2' and H_2'' (4). The magnitude of the coupling requires that H_1' be coupled strongly ($J > 5$ c.p.s.) with H_2', since the coupling of H_1' with H_2'' should not be greater than 9. In view of the dependency of the coupling between neighboring hydrogens on their spatial arrangement relative to the bridging carbons (5, 6) and the fact that H_1' is coupled to an extent of less than 3 c.p.s. with H_2' in pyrimidine ribonucleosides (7), it is apparent that the pyrimidine deoxyribonucleosides and the pyrimidine ribonucleosides possess *different* conformations for the furanoside rings.

The N.M.R. spectrum for the anomer of thymidine (Fig. 2) which was recently

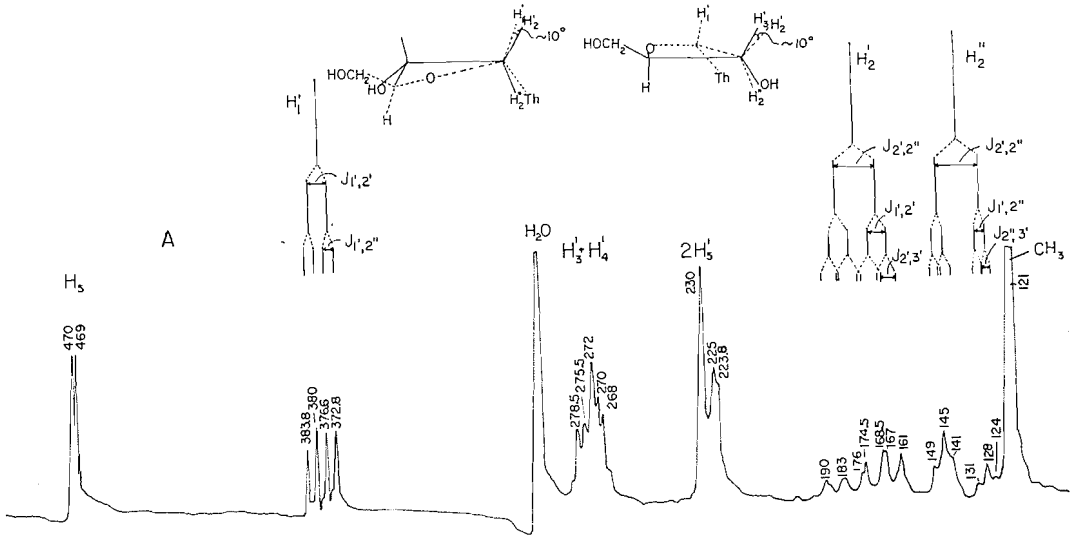


FIG. 2. The experimental and calculated nuclear magnetic resonance spectra of the α-anomer of thymidine. The spectrum was measured using a 20% solution in deuterium oxide at 25° with a high-resolution spectrometer operating at 60 Mc/sec. The positions of the signals are from tetramethylsilane used as an external standard. The projection formulas are to be interpreted as is indicated in Fig. 1 for the β-anomer and represent the conformation for the compound suggested by the spectrum.

synthesized by Hoffer and co-workers (3) provides evidence for its configuration and, consequently, an indirect proof for the configuration of thymidine. Also, the spectrum for thymidine (Fig. 1) allows a conclusion as to the conformation of the compound. The procedure used is based on two assumptions which must be recognized. First of all, the procedure requires the assumption that the compounds are conformationally pure under the conditions that their spectra were measured, namely, in a 20% solution in deuterium oxide at 25°. Secondly, it must be assumed that the variation in the coupling between neighboring hydrogens calculated by Karplus (6) exists for the type of structure under consideration with sufficient precision to warrant their application in this manner. It is noteworthy in this respect that the application does not require a high degree of precision. Consequently, it is felt unlikely that variations (in coupling versus projected angle) from the expected values should arise which would be sufficiently great as to be misleading. In view of these assumptions, the main justification for the approach, at this stage of the development of the nuclear magnetic resonance spectroscopy of carbohydrate structures, is the results obtained. Certainly, as will be seen in the interpretations that follow, wherever it was possible to anticipate a result the approach based on nuclear magnetic

Can. J. Chem. Downloaded from www.nrcresearchpress.com by 210.87.254.105 on 09/05/12
For personal use only.

Can. J. Chem. Downloaded from www.nrcresearchpress.com by 210.87.254.105 on 09/05/12
For personal use only.

resonance spectroscopy provided a confirmation of the expectation. Also, the conformation arrived at for thymidine is intrinsically attractive from the point of view of nonbonded interactions.

The signals for the 2-hydrogens of the anomer of thymidine (see Fig. 2) are chemically shifted by 37 c.p.s. and these (average) are shifted about 222 and 120 c.p.s. from the signals for H_1' and H_3'. Under these circumstances, the fine structures observed for signals of the H_1', H_2', and H_2'' atoms can be analyzed simply on the basis of first-order perturbation theory (8). The spacing of the quartet observed for the H_1' atom requires this proton to be coupled with the H_2' and H_2'' atoms by amounts of 7.2 ± 0.2 c.p.s. and 3.8 ± 0.2 c.p.s. The signal for one of the 2-hydrogens appears as two triplets separated by 17 c.p.s. This separation infers that the carbon valence angle for the 2-hydrogens is about 107° (9). The spacing for both these triplets is 4.0 ± 0.2 c.p.s. Therefore, the particular 2-hydrogen which is weakly coupled with H_1' is coupled to nearly the same extent with H_3'. The signal for the 2-hydrogen which occurs at lower field is *roughly* in the form of a broad quintet. This must be the 2-hydrogen which is strongly coupled, $J = 7.2\pm0.2$ c.p.s., with H_1'. The spacing of the quintet requires this 2-hydrogen also to be strongly coupled, $J = 7\pm0.5$ c.p.s., with H_3'. The knowledge of these coupling constants and the configuration of 2-deoxy-D-ribose together with the values calculated by Karplus (6, 7) for the dihedral angles the neighboring protons can be expected to define in order to provide the coupling observed allows the following deduction of the conformation of the synthetic anomer of thymidine. Precise atomic models of the conformational type described by Barton (10) were employed as a basis for these deductions.

For the H_3' atom to be coupled 4.0 ± 0.2 c.p.s. with a 2-hydrogen, it must define a dihedral angle of either 45 to 50° or 125 to 130° with the 2-hydrogen. If H_3' projected between H_2' and H_2'', then it would define dihedral angles of 45 to 50° and 70 to 75° with the 2-hydrogens. This situation would result in coupling constants of 3.6 ± 0.4 and 0.6 ± 0.4 c.p.s. and, therefore, can be eliminated as a possibility. If H_3' should be sufficiently axially oriented to define a dihedral angle of 45 to 50° with H_2' and if the compound possessed the β-D-configuration (1,3-*trans*-configuration) (2) then H_1' would necessarily project between the hydrogens at position 2 and define dihedral angles in the range 10 to 30° with H_2'' and, consequently, 90 to 110° with H_2'. Thus, H_1' would be coupled to the extents of 6 to 7.6 and -0.4 to 0.8 c.p.s. with the hydrogens at the 2-position, coupling constants which are not in agreement with those observed (7.2 ± 0.2 and 3.8 ± 0.2 c.p.s.). Consequently, the possibility that the compound exists in both this configuration and conformation can also be eliminated. In view of the fact that the configuration of a 2-deoxy-D-ribofuranoside does not allow a dihedral angle of 125–130° to be defined by H_3' and H_2', only one conformation remains possible on the assumption that the compound possesses the β-D-configuration; namely, the conformation which would have H_3' and H_2'' define a dihedral angle of 125–130°. In this conformation, H_1' would necessarily project between H_2' and H_2''. As was seen above for a similar situation, the coupling constants observed for H_1' and H_2' and for H_1' and H_2'' cannot be accounted for in this event. *Therefore, the anomer of thymidine cannot possess the* β-D-*configuration.* That the compound indeed possesses the α-D-configuration is supported not only by the fact that an interpretation of its spectrum is possible on the basis of this configuration but also by the fact that the interpretation places the compound in a favorable conformation.

As was seen above, the coupling constants observed for H_1' with the 2-hydrogens cannot be accounted for should H_1' project between H_2' and H_2''. Therefore, since the

anomer of thymidine has the α-D-configuration, should H_3' define the rather unlikely dihedral angle of 45 to 50° with H_2', H_1' would define a dihedral angle of 10 to 30° with H_2' and 130 to 150° with H_2''. On this basis the coupling constants for H_2' and H_2'' with H_3' would be 5.8 to 7.6 and 4.4 to 6.8 c.p.s., respectively. Although these coupling constants are reasonably close to those observed, the conformation they would imply is much less attractive than that which would have H_3' define a dihedral angle of only 5 to 10° with H_2' and, therefore, a dihedral angle of 125 to 130° with H_2''. On this basis, the coupling constants for H_3' with H_2' and H_2'' would be expected to be in the ranges 7.6 to 8.2 and 3.2 to 4.0 c.p.s., respectively, as compared with the observed values of 7 ± 0.5 and 4.0 ± 0.2 c.p.s. It would follow that H_1' would be similarly oriented relative to H_2' and H_2'', a condition which would meet the observed coupling constants of 7.2 ± 0.2 and 3.8 ± 0.2 found for H_1'. Therefore, the conformation of the anomer of thymidine (1-(2-deoxy-α-D-ribofuranosyl)-5-methyluracil) must be that represented in Fig. 2 in which none of the substituents about the furanoside ring are eclipsed with their neighbors. Jardetzky (7) has commented on this type of conformation in relation to the conformations of ribonucleosides. It is seen that H_2' and H_2'' are in "equatorial" and "axial" orientations, respectively. Therefore, it would be expected (5) that the signal for H_2' would be at lower field than that for H_2'', as is in fact the case. The first-approximation, theoretical spectrum for the compound is shown in Fig. 2. The resemblance of this spectrum to that actually determined should be noted.

The N.M.R. spectrum (see Fig. 1) of the natural 2-deoxyribonucleoside, thymidine, sheds considerable light on the conformation of this important biochemical. The average coupling of H_1' with the 2-hydrogens, 7.0 ± 0.2 c.p.s., requires that H_1' define dihedral angles of about 150° and 30° with H_2' and H_2'', respectively. The structure of the signal for H_2' and H_2'' requires that the average of the coupling constants of these protons with H_3' is about 5.8 c.p.s. The structure of the signal for H_3' supports this contention.

The signal in the form of a rough quartet at about 274.5 c.p.s. can be assigned to H_3'. The assignment can be made first of all on the basis that the spacing between the first and second lines of 5.2 c.p.s. is in close agreement with the coupling constant, 5.8 c.p.s., observed for the average of the coupling of the two hydrogens at the 2-position with H_3'. Secondly, the structure for the signal for the two hydrogens at position 5 at 236 c.p.s. clearly indicates that the signal for these hydrogens is not greatly chemically shifted from the signal for H_4'. However, the signal for H_3' cannot be a simple quartet but must be an octet in view of the coupling of H_3' with H_2', H_2'', and H_4'. As is indicated in Fig. 1, the structure of the signal can be reasonably accounted for as resulting from coupling interactions of 5.8 c.p.s. with each of the hydrogens at the 2-position and 3.2 c.p.s. with H_4'. On this basis, the conformation for thymidine which is best accommodated by the results is that depicted in Fig. 1. The geometrical and spectral features for thymidine and its α-anomer are summarized in Table I. The conformation implied by the spectrum for thymidine clearly possesses a favorable disposition of the groups about the furanoside ring. It is noteworthy that thymidine possesses a conformation for the furanoside ring which closely approximates the C_s conformation for cyclopentane (11) while the conformation of the α-anomer is closer to the so-called C_2 conformation for cyclopentane. It is also of interest to note that the substitution of H_2'' by a hydroxyl group to form a ribonucleoside would require a near eclipsing of the hydroxyl with the 3-hydroxyl. Consequently, it is not surprising that, as seen above, the conformation of the furanoside ring of thymidine is different to that of pyrimidine ribonucleosides. The general features of the N.M.R. spectrum of thymidine requires that it possess considerable conformational

Can. J. Chem. Downloaded from www.nrcresearchpress.com by 210.87.254.105 on 09/05/12
For personal use only.

TABLE I

Conformational and N.M.R. spectral features for thymidine and its α-anomer

Neighboring atoms	Projected angle	Spin–spin coupling constant, c.p.s.	
		Expected (6,7)	Found
1. Thymidine			
H_1', H_2''	30°	6.0	
H_1', H_2'	150°	6.5	
		6.3 (average)	7.0
H_2', H_3'	10°	7.5	
H_2'', H_3'	130°	3.5	
		5.5 (average)	5.8
H_3', H_4'	130°	3.5	3.2
2. α-Thymidine			
H_1', H_2''	130°	3.5	3.8
H_1', H_2'	10°	7.5	7.2
H_2', H_3'	10°	7.5	7.0
H_2'', H_3'	130°	3.5	4.0

purity, a matter which is noteworthy in view of the role of deoxynucleosides as building units of the templates of living processes.

In conclusion, it is of interest to note that the present results provide further evidence of the fact that nuclear magnetic resonance spectroscopy can be an important tool for elucidation of the detailed structure of biochemicals in aqueous solution.

ACKNOWLEDGMENTS

The author gratefully thanks the Hoffmann–LaRoche Co., Inc., for their generous gift of the compounds used in this work, financial support from the National Research Council of Canada, the technical assistance provided by Mrs. A. Westland, and valuable discussions with Drs. F. A. L. Anet and R. R. Fraser.

REFERENCES

1. A. M. Michelson and A. R. Todd. J. Chem. Soc. 816 (1955).
2. M. Hoffer, R. Duschinsky, J. J. Fox, and N. Young. J. Am. Chem. Soc. **81**, 4112 (1959).
3. R. U. Lemieux and M. Hoffer. Can. J. Chem. **39**, 110 (1961).
4. R. E. Richards and T. Schaefer. Mol. Phys. **1**, 331 (1958).
5. R. U. Lemieux, R. K. Kullnig, H. J. Bernstein, and W. G. Schneider. J. Am. Chem. Soc. **80**, 6098 (1958).
6. M. Karplus. J. Chem. Phys. **30**, 11 (1959).
7. C. D. Jardetzky. J. Am. Chem. Soc. **82**, 229 (1960).
8. R. U. Lemieux, R. K. Kullnig, and R. Y. Moir. J. Am. Chem. Soc. **80**, 2237 (1958).
9. H. S. Gutowsky, M. Karplus, and D. M. Grant. J. Chem. Phys. **31**, 1278 (1959).
10. D. H. R. Barton. Chem. & Ind. (London), 1136 (1956).
11. J. E. Kilpatrick, K. S. Pitzer, and R. Spitzer. J. Am. Chem. Soc. **69**, 2483 (1947).

Can. J. Chem. Downloaded from www.nrcresearchpress.com by 210.87.254.105 on 09/05/12
For personal use only.

Can. J. Chem. Downloaded from www.nrcresearchpress.com by 210.87.254.105 on 09/05/12
For personal use only.

CHEMICAL EFFECTS OF THE (n,γ) ACTIVATION OF BROMINE IN THE ALKYL BROMIDES: THE HALOMETHANES[1]

W. E. HARRIS[2]

ABSTRACT

Techniques for studying the chemical effects accompanying the neutron irradiation of the halomethanes with a neutron flux of only 10^8 neutrons per square centimeter per second are described. Results are presented from the irradiation of mixtures of bromine with the four bromomethanes and carbon tetrachloride. The formation of organic products which occur as the result of "hot", "hot-spot diffusive", and "thermal" reactions are discussed. The amounts of products resulting from these three types of reactions are estimated. Observations with respect to the formation of bromoethanes are also discussed.

INTRODUCTION

When a sample containing bromine atoms is irradiated with thermal neutrons, the bromine isotopes of masses 79 and 81 are converted to radioactive bromine of masses 80 and 82 by the (n,γ) nuclear reaction. In this transformation, the nucleus emits from two to six gamma rays in cascade. The resulting recoil momentum gives the radiobromine sufficient energy to dissociate it from the parent molecule and bring about chemical reactions with the other molecules present.

If an organic bromide is irradiated some of the radioactive bromine is converted to an inorganic form (1) and some is retained in various organic forms. The predominant organic product is usually the parent molecule in which radiobromine has been substituted for the inactive bromine, but in addition, a wide variety of new organic compounds are formed. Conversely, it has been found that when a mixture of bromine and pentane (2) or carbon tetrachloride (3) are irradiated, some of the radiobromine is converted to an organic form by recoil labelling and some remains as inorganic bromine. Thus, when a mixture of bromine and an alkyl bromide is irradiated, the bromine atoms in the organic radiobromine compounds originate from both the alkyl bromide and the bromine. Thus it appears that the initial chemical form of the bromine is of secondary importance. Reviews of the many papers in this field have been published by Willard (4, 5).

Many studies (5) have been made with the haloalkanes to determine the fraction of radiohalogen appearing in organic combination, called the organic yield, under a variety of conditions. Experiments have also determined the nature of the new organic products. The organic yield of the irradiated sample has been classically determined by extraction with an aqueous solution of reducing agent and carrier salt and counting the radioactivity of the organic and aqueous layers separately. The organic compounds have frequently been determined by addition of carriers to the extracted organic phase followed by a fractional distillation to separate the components. Evans and Willard (6) have shown that gas chromatography can be applied to the direct separation of the organic products with or without the addition of carriers.

The present work describes the results of neutron irradiation of a wide range of bromomethane–bromine mixtures. The organic yields were determined by a new technique involving reaction of the inorganic radiobromine in the gas phase with solid potassium ferrocyanide (7), and the organic products were separated by gas chromatography.

[1]*Manuscript received September 8, 1960.*
Contribution from the Research Chemistry Branch, Chemistry and Metallurgy Division, Atomic Energy of Canada, Chalk River, Ontario.
Issued as A.E.C.L. No. 1140.
[2]*Present address: Department of Chemistry, University of Alberta, Edmonton, Alberta.*

EXPERIMENTAL

Sample Preparation

In order to attain the high purity required (8, 9) for a study of hot-atom reactions, samples were purified by gas chromatography prior to irradiation. About 0.5-ml samples of reagent grade bromoalkanes were purified with a column 2.5 meters long and 2.2 cm i.d. which contained a packing of Dow-Corning high-vacuum silicone grease on firebrick. The effluent was monitored with a thermal detector which was bypassed in favor of a condenser when the desired material was eluting from the column. A central fraction was condensed and collected in the irradiation vessel which consisted of a 0.5-ml bulb blown at the end of 4-mm soft-glass tubing. The samples were cooled with liquid air, evacuated, sealed, and immediately wrapped with black electrical pressure-sensitive tape to exclude light. When desired, a measured volume of either liquid bromine or its saturated vapor was transferred to the irradiation vessel prior to the collection of the bromoalkane.

Because of the low boiling point (3.6°) of bromomethane, samples of it required special handling. Before addition to the gas chromatographic column a sample was frozen in an ampoule with liquid air. This was opened and put into a chamber at the inlet to the column where the sample evaporated into the eluent gas stream. The condenser at the outlet of the column was cooled by a stream of air precooled with liquid nitrogen. The bromomethane was collected in ampoules cooled with Dry Ice.

Irradiation

The samples were irradiated at ambient temperature, about 25°, for 10 to 50 hours in a special facility (7) on the external face of the shielding of the Chalk River NRX reactor. The neutron flux of this position was slightly over 10^8 neutrons per square centimeter per second and a measurement of the gamma flux with a portable survey meter gave a maximum reading of 11 roentgens per hour. Thus the total gamma-ray dosage was considerably less than the value of 2×10^4 roentgens which has been shown to be the threshold value for gamma-ray effects (10).

Analysis for Radioactive Organic Products

The organic products of the reactions were separated by a programed temperature gas chromatography column, 2.5 meters long and 5 mm i.d., packed with Dow-Corning silicone grease on a crushed firebrick support. Helium was used as the eluent gas at 50 ml per minute. The irradiated sample was introduced into the column by first freezing it in liquid nitrogen, opening the ampoule, and immediately putting it into a small chamber at the entrance to the column. The column and accessories were arranged so that the sample came in contact with only the glass parts of the equipment. The amount of radioactivity associated with the samples was too low for convenient use of a recorder along with a radioactivity detector which monitored the continuous flow from the chromatographic column (6, 11). A method was therefore developed for concentrating the radiobromine in the effluent in a number of fractions through the use of a series of charcoal tubes put at the outlet of the chromatographic column. The charcoal tubes were cooled by a stream of air through a loose-fitting air condenser. To ensure retention of the low-boiling bromoalkanes with the continued flow of eluent gas, those tubes used to collect extremely volatile substances such as bromomethane were cooled with air which had passed through a coil immersed in liquid nitrogen. In the usual analysis a fraction was collected each minute and the radioactivity was determined by inserting the tube in a well attached to a thallium-activated sodium iodide scintillation crystal.

Can. J. Chem. Downloaded from www.nrcresearchpress.com by 210.87.254.105 on 09/05/12
For personal use only.

When the radioactivity of each sample was plotted as a function of time of elution, chromatograms such as in Fig. 1 were obtained. The identity of the activity associated

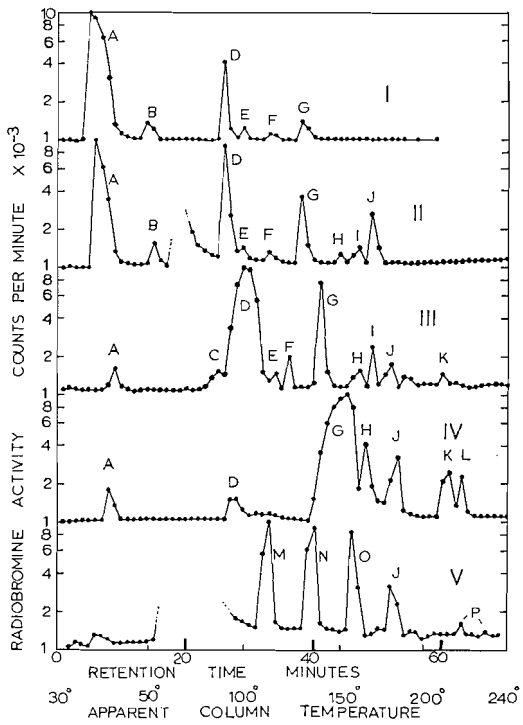


FIG. 1. Examples of chromatograms obtained from neutron-irradiated halomethanes: (I) pure monobromomethane; (II) monobromomethane with about 6 mole% bromine; (III) pure dibromomethane, (IV) pure tribromomethane; (V) tetrachloromethane with about 70 mole% bromine.

The peak assignments are as follows: (A) monobromomethane; (B) monobromoethane; (C) unidentified, probably unsaturated dibromoethane; (D) dibromomethane; (E) 1,1-dibromoethane; (F) 1,2-dibromoethane; (G) tribromomethane; (H) 1,1,1-tribromoethane; (I) 1,1,2-tribromoethane; (J) tetrabromomethane; (K) 1,1,1,2-tetrabromoethane; (L) 1,1,2,2-tetrabromoethane; (M) monobromotrichloromethane; (N) dibromodichloromethane; (O) tribromomonochloromethane; (P) bromochloroethanes.

In (II) and (V) the discontinuous portion of the curves are for bromine elution.

with the various peaks was inferred in most instances by running macro amounts of known alkyl bromides through the column under the same conditions but using a thermal detector. In other cases, such as for the polybromoethanes, samples were not available and the identities of these have been presumed from boiling-point characteristics and position on the chromatogram (12).

It has been shown (13, 14) that similar results with respect to organic retention and organic products are obtained for both bromine 80 and 82. Therefore in these studies no attempt was made to distinguish between the radioactivity resulting from these two isotopes. In addition, since most of the organic radiobromine activity associated with a sample was determined during an interval of only a few minutes, corrections to a standard time to allow for decay generally amounted to less than 0.2% and were therefore negligible. With an irradiation of normally about 20 hours followed by analysis within a few hours the radioactivity in terms of counts per minute would be divided roughly equally beteeen the two isotopes.

Can. J. Chem. Downloaded from www.nrcresearchpress.com by 210.87.254.105 on 09/05/12
For personal use only.

Analysis for Organic Yield

Organic-yield measurements were made from separate irradiations using the absorption technique previously described (7) with an absorption tube as shown in Fig. 2. The

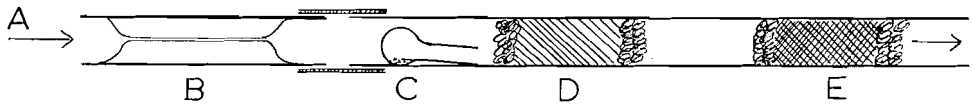


FIG. 2. Apparatus for organic-yield measurements. (A) Air 15 lb/in². (B) Thermometer capillary allowing about 50 to 100 ml/min air flow. (C) Irradiation vial with sample. (D) Potassium ferrocyanide, 50–100 mesh. (E) Charcoal about 100 mesh, cooled with Dry Ice while air was flowing.

inorganic bromine was retained by the potassium ferrocyanide and the organic compounds were retained by the charcoal. The organic retention was determined by cutting the tube and measuring the radioactivity associated with each part.

EXPERIMENTAL RESULTS

Organic Yield

Although they were not of primary interest, organic-yield measurements were made to enable one to make calculations of the distribution of the total radiobromine among the various organic products. In Fig. 3 are shown the organic-yield results obtained

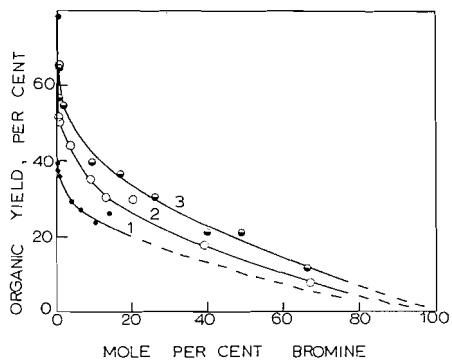


FIG. 3. Organic yield as a function of mole% of bromine: (1) ● monobromomethane; (2) ○ dibromomethane; (3) ◒ tribromomethane.

with the bromomethanes. These data indicate that the organic yield for pure bromomethanes was much higher than for pure monobromoethane or monobromopropane (8, 15). The organic yield for tribromomethane was comparable to that found previously (16). It is evident from these curves that sensitivity to the scavenging action of small amounts of bromine decreases in the order mono-, di-, and tri-bromomethane.

Distribution of Organic Products

Typical chromatograms obtained by the charcoal absorption tube technique for irradiated mono-, di-, and tri-bromomethanes and for a carbon tetrachloride–bromine mixture are shown in Fig. 1. It should be noted that the chromatographic peaks for the parent materials were not so sharp as the other peaks because samples of about 100 to 200 mg of the irradiated bromoalkane were used. This amount of sample caused flooding of the column. In the interests of uniformity, in Fig. 1, the original experimental results were recalculated to a background activity of about 1000 c.p.m. and to a highest peak of 10,000 c.p.m.

Can. J. Chem. Downloaded from www.nrcresearchpress.com by 210.87.254.105 on 09/05/12
For personal use only.

Detailed experimental results from irradiated bromomethanes are shown in Tables I and II. A considerable variety of organic products were obtained in each case. The number of products was not so numerous as was found for irradiated bromopropane (6) because, in the former case, the parent molecules contained only one carbon atom. Since the molecular weight of the largest molecules likely to have been formed in the irradiations would be low, the data of Tables I and II include results for all of the probable organic reaction products formed in appreciable amounts.

TABLE I

Neutron irradiation of monobromomethane – bromine mixtures

Retention time, minutes*	Assignment	Mole% bromine: 0	0.066	1.96	5.94	11.9	40.8	72.7	84.6
		Percentage of total radiobromine activity							
8	Bromomethane	64.0	34.1	17.8	13.8	11.4	4.5	1.7	0.9
14	Bromoethane	1.7	1.8	0.7	0.5	0.3	0	0	0
27	Dibromomethane	8.6	12.1	8.3	7.7	6.8	4.1	1.9	1.1
29	1,1-Dibromoethane	0.6	0.9	0.6	0.3	0.1	0.05	0.01	0
33	1,2-Dibromoethane	0.5	0.4	0.2	0.3	0.1	0.05	0.01	0
38	Tribromomethane	2.5	3.2	2.9	2.5	2.4	1.7	0.9	0.5
44	1,1,1-Tribromoethane	0	0.2	0.3	0	0	0.01	0	0
46	1,1,2-Tribromoethane	0.3	0.8	0.7	0.3	0.3	0.06	0.01	0
48	Tetrabromomethane	0.2	0.2	1.5	1.4	1.9	1.5	0.9	0.5
57	1,1,1,2-Tetrabromoethane	0	0.1	0.2	0.2	0.3	0.05	0	0
	Inorganic (HBr, Br_2)†	21.5	46	67	73	76	88	95	97

*Using programed temperature chromatography with the temperature program indicated in Fig. 1.
†Estimated from the data of Fig. 3.

TABLE II

Neutron irradiation of di- or tri-bromomethane – bromine mixtures

Retention time, minutes*	Assignment	Compound irradiated: CH_2Br_2	CH_2Br_2	CH_2Br_2	CH_2Br_2	$CHBr_3$	$CHBr_3$	$CHBr_3$	$CHBr_3$
		Mole% bromine: 0	2.0	16.0	68.9	0	2.0	18.4	66.1
		Percentage of total radiobromine activity							
8	Bromomethane	1.0	0.9	0.4	0.02	1.0	0.4	0.1	0.01
14	Bromoethane	0.1	0	0	0	0	0	0	0
25	Unidentified	0.5	0	0	0	0	0	0	0
27	Dibromomethane	45.1	28.0	15.8	3.2	1.3	0.8	0.4	0.06
29	1,1-Dibromoethane	0.4	0.2	0.1	0	0.2	0.1	0.03	0
33	1,2-Dibromoethane	1.9	1.4	0.3	0	0.3	0.1	0.03	0.01
38	Tribromomethane	11.6	9.1	6.6	1.9	47.7	31.3	18.1	5.5
44	1,1,1-Tribromoethane	0.8	0	0	0.01	5.1	2.3	0.7	0.01
46	1,1,2-Tribromoethane	1.9	1.7	0.5	0.01	0	0.1	0	0
48	Tetrabromomethane	1.0	3.7	3.9	1.7	4.6	13.6	12.5	5.5
58	1,1,1,2-Tetrabromoethane	0.7	1.5	0.6	0.03	2.9	2.8	1.3	0.09
60	1,1,2,2-Tetrabromoethane	0.4	0.7	0.3	0.02	1.7	1.9	0.8	0.04
70	Pentabromoethane	0	0	0	0	0.06	0.4	0.3	0.01
	Inorganic (HBr, Br_2)†	34.6	53	72	93	35	46	66	89

*Using programed temperature chromatography with the temperature program indicated in Fig. 1.
†Estimated from the data of Fig. 3.

Some experiments involving irradiation of solid tetrabromomethane indicated that radioactive tetrabromomethane was the only organic product formed. Hexabromoethane, whose presence might be expected, was not detectable to the extent of even a trace. In

Can. J. Chem. Downloaded from www.nrcresearchpress.com by 210.87.254.105 on 09/05/12
For personal use only.

contrast, carbon tetrachloride when irradiated in the presence of bromine produced bromochloroethanes to a little less than 1% in addition to all the possible bromochloromethanes (Table III). This aspect of the study was not pursued.

TABLE III

Neutron irradiation of carbon tetrachloride – bromine mixtures

Retention time, minutes*	Radiobromine product assignment	Mole% bromine		
		19	38	70
		Percentage of total radiobromine activity		
33	Monobromotrichloromethane	7.2	5.0	1.7
40	Dibromodichloromethane	5.8	4.8	1.7
46	Tribromomonochloromethane	2.2	2.3	1.2
52	Tetrabromomethane	0.2	0.2	0.3
63, 67	Haloethanes ($C_2Cl_xBr_{6-x}$)	0.6	0.2	0.04
	Inorganic (HBr, Br_2)†	84	88	95

*Using programed temperature chromatography with the temperature program indicated in Fig. 1.
†Estimated from data of reference 3.

DISCUSSION

It is noteworthy that the total yields of the bromoethanes from the mono-, di-, and tri-bromomethanes without bromine were 3.1, 6.2, and 10.3%. These results are reasonable when interpreted in light of the processes leading to the formation of the various products which have been described (4, 5, 8) in terms of a random fragmentation model. In this model the recoiling radiobromine atom and the atoms with which it collides are limited to a "hot spot". When the radiobromine has lost its excess energy it will be in this hot spot of a few hundred cubic Angstroms (17). In this thermalization region, there is a high local concentration of free radicals or ions formed by disruptive collisions during the thermalization of the bromine atom. The bromine atom may combine with one of these fragments during or after thermalization or it may diffuse into the surrounding medium before reaction. The above yields of bromoethanes therefore seem reasonable when it is realized that thermalization would occur in a smaller volume with the tribromomethane than with the monobromomethane. There would be a more efficient transfer of energy between the hot radiobromine atom and a highly brominated substrate due to there being a higher "concentration" of atoms of equivalent atomic mass. This more efficient confinement by tribromomethane would give a higher local concentration of the reactive fragments in the thermalization region than would monobromomethane. The higher concentration of reactive fragments would produce the larger proportions of bromoethanes observed since the formation of a bromoethane molecule requires that there be a collision between two one-carbon fragments.

To explain some of the chemical effects of nuclear transformations nine possible elementary reactions involving radiobromine have been discussed (8). On the basis of scavenger effects, the reactions have generally been described as either "hot" or "thermal" by Willard (4, 5). Those reactions involving a thermalized radiobromine atom after it has had an opportunity of undergoing thermal collisions are termed diffusive or thermal and the other reactions are termed hot. If a small amount of bromine scavenger is added to the irradiated substance, the radiobromine will probably exchange with the inactive bromine before it has opportunity to diffuse into the surrounding medium and react to give an organic product. Thus the products of thermal reactions are normally considered

Can. J. Chem. Downloaded from www.nrcresearchpress.com by 210.87.254.105 on 09/05/12
For personal use only.

to be those that are readily scavenged. For instance, the percentage of radioactive monobromomethane was decreased from about 64% to 21% in going from 0% to 1 mole% bromine in monobromomethane irradiations. This dramatic decrease must be ascribed almost wholly to the elimination of thermal reactions. The reactions taking place in the radiobromine recoil zone or "hot spot" are relatively insensitive to the presence of scavenger and therefore are generally classed as hot. Hence products formed by these two kinds of reactions are distinguishable by how they are affected by the addition of scavenger.

In Tables I and II are shown data relating to the effect of the addition of bromine scavenger on the amounts of the various products formed. Detailed examination of these data shows that the irradiation products were formed by three classes of reactions instead of the two referred to above. Again, a thermal reaction, i.e. one that was eliminated by a small amount of bromine scavenger, was observed and this type of reaction appeared to be largely confined to the formation of the parent compound. Of the remaining products one group, formed by hot reactions, was insensitive to bromine concentration. In addition, there was a group of products which were gradually suppressed by very high bromine concentration. It is suggested that this last group be termed "hot-spot diffusive".

The hot reactions as considered here may roughly correspond to the "primary recombination" reaction discussed by Noyes (18) in connection with pairs of reactive fragments produced from a molecule. In a similar way, there is possible parallelism between hot-spot diffusive reactions and Noyes' "secondary recombination" reaction. In this connection, it should be pointed out that the hot reactions as discussed here are defined very broadly to include some reactions which are not conventionally thought of as being hot. Thus, the hot reactions of the present system could include, in addition to primary recombination in a "cage", the reactions involving hot replacement of a bromine atom by an energetic radiobromide atom and also reactions involving neutron activation of bromine in an alkyl bromide which fails to rupture the parent carbon–bromine bond. Evidence of the failure of the carbon–bromine bond to rupture in some cases has already been cited (19).

The amount of radioactive parent formed by thermal reactions was estimated from the decrease brought about by the addition of 1 to 2% of bromine to the pure bromomethane. To make a tentative assignment of the amounts of the organic radiobromide products formed by the hot and hot-spot diffusive reactions the data of Table I and II were corrected for the simple dilution effect of increasing amounts of bromine in the bromomethane–bromine mixtures. The formation of an organic radiobromine product in a system containing a hot radiobromine atom in an environment of bromomethane and bromine molecules would depend upon the chance that the atom would encounter a carbon-containing molecule or fragment. Therefore, it was most reasonable to normalize the data by multiplying the observed percentages of the total radiobromine in the various organic molecules by (100/mole% of bromomethane in the mixture). The organic products were divided into groups and, when the normalized data for the groups of products were plotted against the mole per cent of the bromine, in the manner shown in Fig. 4, sets of straight lines were obtained.[3] It can be seen that the results for one group of products were essentially independent of the amount of bromine in the mixture

[3]*An alternative set of graphs analogous to those of Fig. 4 were drawn involving atom per cent bromine and involving a normalization on the basis of the number of bromine atoms in the alkyl bromide. The use of those graphs led to virtually the same conclusions as those given in the text. For the reason given, it seemed best to normalize the organic radioactivity in terms of the carbon atoms present in the system.*

Can. J. Chem. Downloaded from www.nrcresearchpress.com by 210.87.254.105 on 09/05/12
For personal use only.

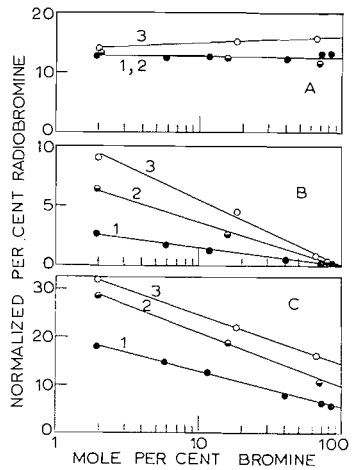


FIG. 4. Normalized organic radiobromine activity as a function of mole% of bromine in bromine–bromomethane mixtures.

(A) Curves for the group of products more highly brominated than the parent: (1) ● di-, tri-, and tetra-bromomethane from monobromomethane as parent; (2) ◒ tri- and tetra-bromomethane from dibromomethane as parent; (3) ○ tetrabromomethane from tribromomethane as parent.

(B) Curves for the group of products consisting of all others than (A) above or the parent: (1) ● from monobromomethane; (2) ◒ from dibromomethane; (3) ○ from tribromomethane.

(C) Curves for the parent: (1) ● monobromomethane; (2) ◒ dibromomethane; (3) ○ tribromomethane.

in the range from 100 to about 1 or 2 mole%. This group consisted of bromomethanes with more bromine than the parent molecule irradiated. Thus, for example, with irradiated dibromomethane this group consisted of tri- and tetra-bromomethane. A second group of products fell on a straight line which extrapolated to zero at the limit of 100 mole% bromine. This group comprised all of the other non-parent organic products. For example, with irradiated dibromomethane these consisted of monobromomethane and all of the bromoethanes. The parent materials formed a third set of straight lines which showed dependence on bromomethane concentration but extrapolated to a finite value at 100 mole% bromine.

The formation of a bromoethane molecule from bromomethane almost certainly must involve a collision of two one-carbon fragments. This implies a diffusive step following the formation of the appropriate one-carbon radicals or ions at the site of thermalization of the radiobromine atom. Since bromine would be an active competitor in reactions involving these fragments, its addition to the system would be expected to decrease the chance of reaction between two one-carbon fragments. Hence, the bromoethanes should be formed nearly exclusively in the hot-spot or thermalization zone. In order for the reaction to be significantly scavenged the concentration of scavenger would have to be comparable to the concentration of the reacting fragments in the reaction zone. The mole per cent of reactive fragments in the hot spot would be expected to be high and hence the bromine concentration must also be high to bring about a significant decrease in the extent of reaction leading to the formation of bromoethanes. It can be seen from Fig. 4B and Tables I and II that, although at 50 mole% bromine the fraction of these products was notably reduced, they could be considered to be completely scavenged only when the mole per cent of bromine approaches 100. Thus, these are hot-spot diffusive products. The chance of two fragments from bromomethane molecules colliding outside of the hot spot would be remote and hence the formation of bromoethanes by thermal

Can. J. Chem. Downloaded from www.nrcresearchpress.com by 210.87.254.105 on 09/05/12
For personal use only.

Can. J. Chem. Downloaded from www.nrcresearchpress.com by 210.87.254.105 on 09/05/12
For personal use only.

reactions does not occur to an appreciable extent. The observation that traces of bromine had little effect on the proportions of those products bears out the contention that they were not formed outide the thermalization region. In this connection, it is noteworthy that the formation of bromoethanes from monobromomethane was even enhanced by a trace of bromine since 4.2% of bromoethanes was obtained with 0.066 mole% bromine while 3.1% was obtained when no bromine was present. This increase may have been due to an efficient scavenging of the hydrogen atoms or ions formed during thermalization. If hydrogen atoms or ions were scavenged more readily than the other fragments, there could be an increased formation of products resulting from recombinations of the remaining fragments, providing, of course, that the bromine concentrations were not too high. The hot-spot diffusive products discussed above appear to include the bromomethanes with less bromine that the parent molecule. Such products must be formed from an extensively fragmented bromomethane and radiobromine. For instance, to obtain radioactive monobromomethane from irradiated tribromomethane at least two and probably three carbon–bromine bonds must have been broken. It is not unreasonable to suppose that the one-carbon fragment and the radiobromine would have to diffuse together to form the product.

The products which persisted (Fig. 4A) in spite of large amounts of bromine must have been formed by hot processes (8) involving direct reaction of the recoiling radiobromine and a molecule or fragment in its environment. The extent of formation of products from this type of reaction should be independent of the concentration of the bromine scavenger after allowance is made for the dilution effect of the increasing amounts of bromine. It appears from these data that the hot products include all the bromomethanes with more bromine than the parent.

The lines in Fig. 4C suggest that in the presence of bromine the parent was formed by both hot and hot-spot diffusive reactions. It is proposed that the values obtained by extrapolation to 100 mole% of bromine are measures of the parent radiobromine-containing molecules formed by hot reactions. Similarly, radioactive parent formed in excess of this extrapolated value in the presence of a trace of bromine are measures of that formed by hot-spot diffusive recombination of radiobromine with an appropriate radical, ion, or molecule. As pointed out earlier, an estimate of the parent formed by thermal reactions was obtained from the effect of a small amount of bromine. It would thus appear that radioactive parent was formed by all three modes of reaction.

In Table IV are shown estimates made on the basis of the preceding discussion of the

TABLE IV

Estimated amounts of products formed by hot, thermal, and hot-spot diffusive reactions

	Percentage of total radiobromine activity				
	Parent			Non-parent organic	
Material irradiated	Hot	Hot-spot diffusive	Thermal	Hot	Hot-spot diffusive
CH_3Br	5.4	16	41	13*	2.5†
CH_2Br_2	9.4	21	15	13‡	6§
$CHBr_3$	14.3	20	5 to 10	14‖	9¶

*Di-, tri-, and tetra-bromomethanes.
†All bromoethanes.
‡Tri- and tetra-bromomethanes.
§Monobromomethane and bromoethanes.
‖Tetrabromomethane.
¶Mono- and di-bromomethane and bromoethanes.

distribution, according to the three types of reactions, of the products which made up the 78%, 65%, and 65% organic yield observed for mono-, di-, and tri-bromomethane (Tables I and II). It is interesting that the amount of parent formed by hot reactions was approximately in the ratio of 1 to 2 to 3 for mono-, di-, and tri-bromomethane. It would suggest that the chance of forming radioactive parent molecules by the types of hot reactions previously mentioned was directly proportional to the number of bromine atoms in the molecule.

ACKNOWLEDGMENTS

The author makes grateful acknowledgment to Dr. W. H. McFadden, who collaborated in the development of the experimental techniques and preliminary measurements and who reviewed part of the manuscript. Helpful discussions with Drs. G. R. Freeman, W. J. Wallace, F. W. Birss, and R. H. Betts are also acknowledged.

REFERENCES

1. L. Szilard and T. A. Chalmers. Nature, **134**, 462 (1934).
2. L. Friedman and W. F. Libby. J. Chem. Phys. **17**, 647 (1949).
3. J. F. Hornig and J. E. Willard. J. Am. Chem. Soc. **75**, 461 (1953).
4. J. E. Willard. Ann. Rev. Nuclear Sci. **3**, 193 (1953).
5. J. E. Willard. Ann. Rev. Phys. Chem. **6**, 141 (1955).
6. J. B. Evans and J. E. Willard. J. Am. Chem. Soc. **78**, 2908 (1956).
7. W. E. Harris, W. H. McFadden, and W. G. McIntosh. J. Phys. Chem. **63**, 1784 (1959).
8. S. Goldhaber and J. E. Willard. J. Am. Chem. Soc. **74**, 318 (1952).
9. J. C. W. Chien and J. E. Willard. J. Am. Chem. Soc. **75**, 6160 (1953).
10. J. C. W. Chien and J. E. Willard. J. Am. Chem. Soc. **77**, 3441 (1955).
11. R. Wolfgang and F. S. Rowland. Anal. Chem. **30**, 903 (1958).
12. W. H. McFadden. Anal. Chem. **30**, 479 (1958).
13. R. H. Schuler and C. E. McCauley. J. Am. Chem. Soc. **79**, 821 (1957).
14. G. Levy and J. E. Willard. J. Am. Chem. Soc. **78**, 2351 (1956).
15. M. Milman and P. F. D. Shaw. J. Chem. Soc. 1303 (1957).
16. J. C. W. Chien and J. E. Willard. J. Am. Chem. Soc. **76**, 4735 (1954); **79**, 4872 (1957).
17. M. S. Fox and W. F. Libby. J. Chem. Phys. **20**, 487 (1952).
18. R. M. Noyes. J. Am. Chem. Soc. **77**, 2042 (1955).
19. S. H. Chiang and J. E. Willard. J. Am. Chem. Soc. **74**, 6213 (1952).

Can. J. Chem. Downloaded from www.nrcresearchpress.com by 210.87.254.105 on 09/05/12
For personal use only.

Can. J. Chem. Downloaded from www.nrcresearchpress.com by 210.87.254.40 on 09/05/12
For personal use only.

PERFLUOROALKYL DERIVATIVES OF TIN

II. DIMETHYLTRIFLUOROMETHYLTIN CHLORIDE[1,2]

R. D. CHAMBERS, H. C. CLARK, AND C. J. WILLIS

ABSTRACT

A methyl group is cleaved by chlorine in preference to trifluoromethyl from trimethyltrifluoromethyltin and dimethyltrifluoromethyltin chloride; the significance of this is discussed in terms of the electronegativity of the trifluoromethyl group. The influence of trifluoromethyl on the acceptor properties of the tin atom in dimethyltrifluoromethyltin chloride has been illustrated by means of conductivity measurements. Nuclear magnetic resonance measurements of trimethyltrifluoromethyltin and dimethyltrifluoromethyltin chloride are also reported.

INTRODUCTION

Perfluoroalkyl derivatives of tin have been prepared recently by the reaction of hexamethylditin with perfluoroiodoalkanes (1, 2, 3),

$$Me_3Sn{-}SnMe_3 + R_FI \rightarrow Me_3SnR_F + Me_3SnI.$$

The reaction has since been shown to be applicable to other compounds containing metal–metal, or metalloid–metalloid, bonds and has led to the synthesis of new perfluoroalkyl compounds of arsenic (4) and phosphorus (5). Tin is the most electropositive element for which a stable trifluoromethyl derivative has been prepared, and the resultant compound has been shown to have interesting properties (1, 11). Because of this, and also because of the valuable synthetic properties of alkyltin halides, we have studied further the halogenation of trimethyltrifluoromethyltin.

EXPERIMENTAL

Preparation of Trimethyltrifluoromethyltin

Trimethyltrifluoromethyltin was prepared by irradiating, with ultraviolet light, a mixture of hexamethylditin and excess trifluoroiodomethane contained in a Carius tube. The details of this preparation have been described (1, 3).

Chlorination of Trimethyltrifluoromethyltin

Chlorine (2.68 g, 38 mmoles) was condensed into a Carius tube which contained a solution of trimethyltrifluoromethyltin (9.5 g, 41 mmoles) in chloroform (15 ml). The tube was sealed under vacuum and transferred to a cooling bath at −46°; the bath was allowed to warm to room temperature and after 2 days the reaction mixture had become colorless. Volatile material was removed under vacuum and, apart from chloroform, it consisted essentially of methyl chloride, together with small amounts of chlorotrifluoromethane and fluoroform. A white solid remained from which dimethyltrifluoromethyltin chloride (8 g, 77% yield), m.p. 46–47°, was sublimed *in vacuo* at 60–70°.

Chlorination of Dimethyltrifluoromethyltin Chloride

Chlorine (0.75 g, 10.6 mmoles) was condensed into a Carius tube which contained a solution of dimethyltrifluoromethyltin chloride (2.55 g, 10.1 mmoles) in carbon tetrachloride (15 ml). The color due to the chlorine did not appear to have diminished after 10 days and therefore the tube was warmed to 60° for 48 hours, during which time the

[1]*Manuscript received September 2, 1960.*
Contribution from the Chemistry Department, University of British Columbia, Vancouver 8, B.C.
[2]*Part I. H. C. Clark and C. J. Willis. J. Am. Chem. Soc.* **82**, *1888 (1960).*

mixture had become colorless. The volatile material was distilled into a vacuum system and then fractionated. A fraction condensing at −195° (0.10 g) was shown by infrared examination to consist of chlorotrifluoromethane together with a small amount of fluoroform; the fraction condensing at −132° (0.44 g) consisted mainly of methyl chloride and a small amount of some unidentified material. A white solid (1 g) remained in the Carius tube; the solid was triturated with carbon tetrachloride and the mixture filtered. The filtrate was evaporated, leaving a solid (0.6 g) which melted at 103°. Dimethyltin dichloride melts at 106°; a mixed melting point gave no depression. The insoluble residue did not melt below 200°; it contained no chlorine and analyzed: C, 9.51; H, 1.57; F, 37.54. The infrared spectrum (Nujol mull) showed strong bands at 1150 and 1080 cm^{-1}, which are characteristic of C—F stretching modes for trifluoromethyl attached to tin (trimethyltrifluoromethyltin and dimethyltrifluoromethyltin chloride give almost identical absorption in this region (1)). A band at 800 (m) was present, which is characteristic of a tin–methyl rocking mode (1). Thus, from the analysis and infrared spectrum, the residue appears to contain methyl, trifluoromethyl, and fluoride in the ratio 1:1:2.

Conductometric Measurements

Measurements were carried out using a standard a-c. bridge. The cell used was fitted with a stopper to prevent evaporation of the solutions; and the cell constant was found to be 0.2958 by using a standard aqueous solution of potassium chloride, made up by weight.

Titration of Dimethyltrifluoromethyltin Chloride in Nitrobenzene with Pyridine

Nitrobenzene was purified by several distillations, and "Analar" grade pyridine was used. Additions of liquid to the cell were made by means of a weight pipette which incorporated a "Teflon" stopcock.

A solution of dimethyltrifluoromethyltin chloride (0.344 g) in nitrobenzene (60 g) was added to the cell. For the initial measurements a solution of pyridine (8 g) in nitrobenzene (50 g) was added from the weight pipette. Pure pyridine was used for the later measurements.

The titration of trimethyltin chloride (0.27 g) in nitrobenzene (59.63 g) was carried out in the same manner.

Dissociation Constant of Dimethyltrifluoromethyltin Chloride in Absolute Ethanol

Kraus and Callis (6) found that trimethyltin chloride behaved as a weak electrolyte in ethanol and that a dissociation constant could be determined. We have carried out the same procedure for dimethyltrifluoromethyltin chloride. The specific conductance of a solution of dimethyltrifluoromethyltin chloride in absolute ethanol was measured at various concentrations up to 1.50×10^{-2} moles per liter, and a graph was drawn of specific conductance as abscissa against the reciprocal of equivalent conductance as ordinate. If the "law of mass-action" can be applied, then the slope of the graph represents $(1/K_{diss}\Lambda_0^2)$ and the intercept with the ordinate represents $(1/\Lambda_0)$. The graph was a straight line up to a concentration of 0.59×10^{-2} mole per liter (showing that the "law of mass-action" can be applied in this case) with a slope 2.016×10^{5} and intercept with the ordinate 0.14, giving $K_{diss} = 9.73\times10^{-5}$ moles per liter at 25° (Table II).

Proton and Fluorine Resonance Spectra

The measurements were made at a fixed frequency of 40 Mc/sec on a Varian Model V-4300B high-resolution N.M.R. spectrometer. An internal standard (benzene) was used for the proton resonance, using carbon tetrachloride as solvent, and an external standard

Can. J. Chem. Downloaded from www.nrcresearchpress.com by 210.87.254.40 on 09/05/12
For personal use only.

TABLE I

Proton resonance spectra*			Fluorine resonance spectra†	
Compound	Shift	Increment	Compound	Shift
Me_4Sn	286	—	Me_3SnCF_3	1165
Me_3SnCl	266	20	Me_2CF_3SnCl	1128
Me_3SnBr	264	22		
Me_2SnCl_2	251	35		
Me_3SnCF_3	279	7		
Me_2CF_3SnCl	264	22		

*Chemical shift (in cycles per second) from the resonance of benzene (internal standard).
†Chemical shift (in cycles per second) from the resonance of trifluoroacetic acid (external standard).

TABLE II

Dimethyltrifluoromethyltin chloride in absolute ethanol at 25°

Conc. $\times 10^4$, equiv. per liter	Specific conductance, l. $\times 10^7$	Equivalent conductance
0.3615	2.16	5.98
0.9757	4.47	4.58
1.712	6.19	3.62
3.672	10.53	2.87
4.647	12.03	2.70
18.12	26.60	1.47
19.92	28.13	1.41
37.76	40.00	1.06
59.69	51.30	0.859
79.29	66.58	0.840
13.01	80.00	0.615
150.7	88.94	0.590

(trifluoroacetic acid) was used for the fluorine resonance. The sample concentration used was 10–15%, and 2–5% benzene. A "side-banding" technique was used for these determinations.

DISCUSSION

The reaction of trimethyltrifluoromethyltin with an equimolar quantity of chlorine has previously been studied (1); a methyl group was easily removed at room temperature giving methyl chloride and dimethyltrifluoromethyltin chloride. This reaction has now been carried out in chloroform solution and improved yields have been obtained. Further chlorination of dimethyltrifluoromethyltin chloride in carbon tetrachloride, with an equimolar quantity of chlorine, was considerably more difficult and required heating to 60° for 2 days to complete the reaction. A complex mixture of volatile products was obtained which could not be completely separated by fractionation and was investigated spectroscopically. The two isolated fractions were methyl chloride, containing a small amount of some unidentified material, and trifluorochloromethane. Traces of fluoroform were also detected. The ratio of the weights of these two fractions, taken in conjunction with their infrared spectra, showed that the ratio of methyl chloride to trifluorochloromethane in the products was approximately 8:1.

The solid residue was separated by extraction with carbon tetrachloride into dimethyltin dichloride and a white intractable solid which was shown by analysis and its infrared spectrum to contain methyl, trifluoromethyl, and fluoride in the ratio, 1:1:2. It is clear,

Can. J. Chem. Downloaded from www.nrcresearchpress.com by 210.87.254.40 on 09/05/12
For personal use only.

then, that preferential removal of a methyl group occurred, followed by rearrangement of the products. The formation of fluorides most likely takes place through the elimination of difluorocarbene from trifluoromethyl. The difluorocarbene eliminated might interact with some of the compounds present and greatly increase the complexity of the reaction mixture. Decomposition of trimethyltrifluoromethyltin and dimethyltrifluoromethyltin chloride has already been shown to occur in this way. A similar reaction of dimethyltrifluoromethyltin chloride with two equivalents of chlorine gave an equally complex mixture and no trifluoromethyltin trichloride could be isolated. The failure to isolate this compound may be due to its low thermal stability, which would be in accord with the much lower stability of dimethyltrifluoromethyltin chloride as compared with trimethyltrifluoromethyltin.

Thus, the tendency for a methyl group to be eliminated in preference to trifluoromethyl, at least in the first two stages of chlorination, has been illustrated. It has been shown by other workers (7) that the cleavage of organotin compounds by electrophilic reagents follows the empirical rule that the most electronegative group is preferentially eliminated and, on this basis, the cleavage of methyl in preference to trifluoromethyl is surprising. It has been shown (8) that the perfluorovinyl group is very easily cleaved by electrophilic reagents, and that it falls into the cleavage series of $CF_2{=}CF$, $C_6H_5 > CH_3 > CF_3$. It has been postulated (9) that such cleavage series may be explained in terms of electrophilic attack on the carbon atom with the highest electron density, and other workers (10) have suggested that, because of the inductive effect of the fluorine atoms, the carbon atom of the trifluoromethyl group is more electron deficient than the carbon atoms of the methyl groups in trimethyltrifluoromethyltin. This view does not take into account the ability of the trifluoromethyl group to behave as a separate electronegative entity, as illustrated by the removal of a trifluoromethyl group from trimethyltrifluoromethyltin by boron trifluoride (11). These compounds react under anhydrous conditions, in an inert solvent, with transfer of a trifluoromethyl anion to the boron trifluoride forming the very stable $[BF_3CF_3]^-$ ion. There is clearly a considerable difference in the behavior of the two electrophilic reagents, chlorine and boron trifluoride.

Lagowski (12) has concluded on the basis of thermochemical and infrared data that the value of the effective electronegativity of the trifluoromethyl group lies between those of fluorine and chlorine. Although other factors must also be involved, it is interesting then to note the similar behavior of the trifluoromethyl group and halogens in organotin compounds, with respect to cleavage reactions.

$$Me_3SnCF_3 + HCl\ (or\ Cl_2) \rightarrow Me_2CF_3SnCl + CH_4\ (or\ CH_3Cl)$$
$$Me_3SnCl + HCl\ (or\ Cl_2) \rightarrow Me_2SnCl_2 + CH_4\ (or\ CH_3Cl)$$
$$Me_3SnCF_3 + NaOH\ aq. \rightarrow Me_3SnOH + CF_3H$$
$$Me_3SnCl + NaOH\ aq. \rightarrow Me_3SnOH + HCl$$

It appears that as a result of its high electronegativity the trifluoromethyl group in trimethyltrifluoromethyltin is attached to the tin atom by a highly polarized bond, and, as such, differs from other organic groups which have been attached to a tin atom and placed in the cleavage series. The importance of this polarity in determining the properties of certain organotin compounds has recently been considered by Seyferth and Kahlen (13), who have discussed the properties of trimethyltin cyanide in terms of the highly polarized tin–carbon bond of the cyanide group.

In the cleavage of trimethyltrifluoromethyltin by electrophilic reagents, the relative

Can. J. Chem. Downloaded from www.nrcresearchpress.com by 210.87.254.40 on 09/05/12
For personal use only.

Can. J. Chem. Downloaded from www.nrcresearchpress.com by 210.87.254.40 on 09/05/12
For personal use only.

tin–carbon bond energies resulting from the polarized nature of the tin–trifluoromethyl bond may then be the controlling factors. Cleavage of a methyl in preference to a trifluoromethyl group on reaction with chlorine under non-polar conditions may result from the presence of this highly polarized bond which, by its influence on the tin–carbon bond energies, may make this elimination energetically favorable.

Trimethyltin chloride will react with pyridine and ammonia to form stable 1:1 co-ordination compounds, whereas dimethyltin dichloride adds on two donor molecules (14). It was our aim to prepare similar complex compounds using dimethyltrifluoromethyltin chloride, establish their constitution, and hence compare trifluoromethyl and chlorine with respect to their influence on the acceptor properties of an adjoining tin atom. We were not able to isolate complex salts, since direct reaction with pyridine gave a solid which did not contain trifluoromethyl. It was therefore necessary to use conductometric measurements in order to illustrate the acceptor properties of the tin atom in dimethyltrifluoromethyltin chloride.

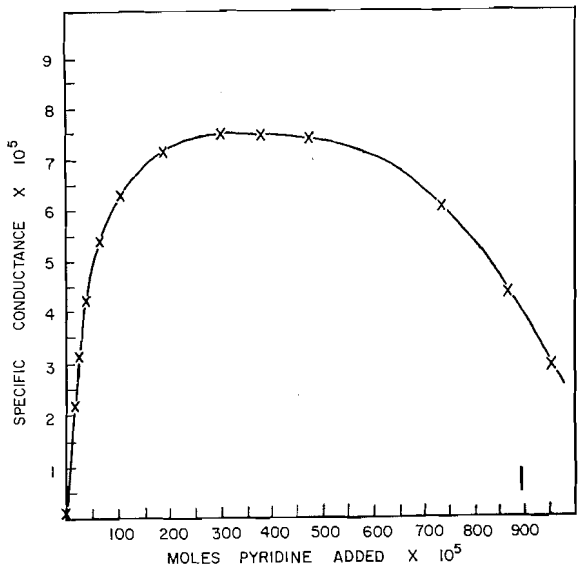
It has been shown (15) that trimethyltin chloride is non-conducting in non-donor solvents and that addition of pyridine to a solution of trimethyltin chloride in nitrobenzene is accompanied by a rise in conductivity of the solution. Trimethyltrifluoromethyltin was found to be non-conducting in nitrobenzene and no significant rise in conductivity was observed with the addition of pyridine, indicating that there was little or no tendency to form a co-ordination compound which could yield ionic species. We have also compared the changes in conductivity of equimolar solutions of trimethyltin chloride and dimethyltrifluoromethyltin chloride in nitrobenzene (2.7×10^{2} moles of chloride per liter) with the addition of pyridine. Dimethyltrifluoromethyltin chloride was non-conducting in nitrobenzene but the conductivity rose very sharply with the addition of pyridine (Fig. 1) in an analogous manner to trimethyltin chloride (Fig. 2). The specific conductance of a 0.015 *M* solution of dimethyltrifluoromethyltin chloride in ethanol, which is a solvent of lower dielectric constant than nitrobenzene, was found to be 88.94×10^{-7} ohm^{-1} cm^{-1}. Thus, conducting species are formed, presumably due to co-ordination of pyridine to the tin atom in dimethyltrifluoromethyltin chloride. The resulting co-ordination complex appears to be a much stronger electrolyte than the corresponding complex between trimethyltin chloride and pyridine, since the conductivity of the dimethyltrifluoromethyltin chloride solution rises much more quickly than that of trimethyltin chloride (compare Fig. 1 and Fig. 2) for equivalent amounts of pyridine added during the first part of the experiment. The maximum values of specific conductance reached were 7.54×10^{-5} ohm^{-1} cm^{-1} for dimethyltrifluoromethyltin chloride, and 11.25×10^{-6} ohm^{-1} cm^{-1} for trimethyltin chloride.

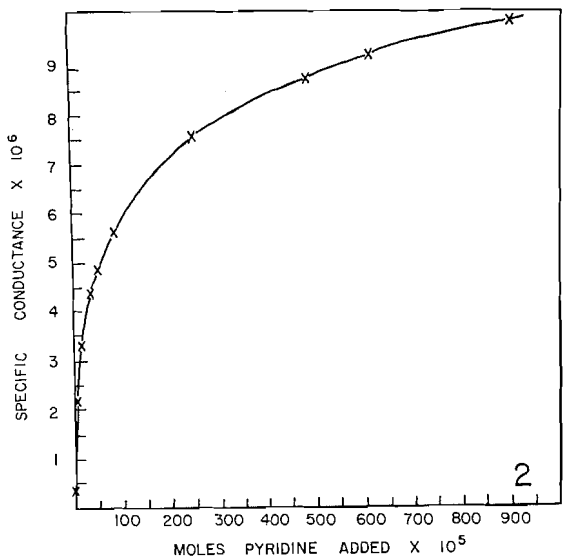
A dissociation constant for the reaction

$$Me_2CF_3SnCl + EtOH \rightleftharpoons Me_2CF_3\overset{+}{S}nEtOH + Cl^-$$

was determined by the method used by Kraus and Callis (6) and found to be 9.7×10^{-5} moles per liter at 25° C (cf. 3.5×10^{-5} moles per liter at 25° C for trimethyltin chloride). The strong inductive effect of the trifluoromethyl group probably increases the acceptor properties of the tin atom, thus increasing the ionization of any co-ordination complex.

During the titration of dimethyltrifluoromethyltin chloride, after a concentration of 7.42×10^{-2} moles of pyridine per liter had been reached (Fig. 1) a further reaction occurred. The conductivity of the solution decreased and this was accompanied by the appearance of a precipitate in the cell; analysis and the infrared spectrum showed that this compound did not contain trifluoromethyl, and that it was identical with the uncharacterized





FIGS. 1 and 2.

compound obtained by direct reaction of pyridine and dimethyltrifluoromethyltin chloride. The nature of this secondary reaction was not investigated further.

We have attempted to extend the anionic transfer reaction with boron trifluoride, by adding trimethyltrifluoromethyltin to other acceptor molecules where the formation of complex ions is possible.

Preliminary experiments (16) have shown that compounds of the type $Me_3Sn[MCl_3X]$ (where M = Al or Ga, and X = halogen) can be prepared. However, reaction between aluminum trichloride or gallium trichloride and trimethyltrifluoromethyltin did not yield complex compounds of the form $Me_3Sn[MCl_3CF_3]$, (M = Al or Ga). Further

Can. J. Chem. Downloaded from www.nrcresearchpress.com by 210.87.254.40 on 09/05/12
For personal use only.

investigation of complex compounds involving trimethyltin and dimethyltin cations is proceeding.

Thus the reactions of trimethyltrifluoromethyltin with chlorine and with boron trifluoride demonstrate the "halogen-like" character of the trifluoromethyl group. The foregoing results show, however, that this analogy has several limitations, particularly under conditions where reaction with the trifluoromethyl groups leads to its decomposition.

Brown and Webster (17) have determined the changes in chemical shift in the proton resonance of a series of methyltin chlorides [Me_xSnCl_{4-x}] and have observed approximately equal increments for each methyl group replaced by chlorine, from tetramethyltin to methyltin trichloride. We have also observed this effect and have determined the proton and fluorine chemical shifts in trimethyltrifluoromethyltin and dimethyltrifluoromethyltin chloride. These results are shown in Table I and, since all shifts are to low field, an increase of shift corresponds to a decrease in the shielding. The increment of shift from tetramethyltin caused by the introduction of trifluoromethyl is not of the same order as the increment due to introduction of a halogen atom. This, however, cannot be taken as a comparison of the chemical similarity of trifluoromethyl and halogens since chemical shift appears to depend on so many factors other than electronegativity (18).

ACKNOWLEDGMENTS

The authors wish to thank Dr. D. E. McGreer for the N.M.R. measurements. We express our appreciation of the financial support of the U.S. Office of Naval Research.

REFERENCES

1. H. C. Clark and C. J. Willis. J. Am. Chem. Soc. **82**, 1888 (1960).
2. H. D. Kaesz, J. R. Phillips, and F. G. A. Stone. Chem. & Ind. (London), 1409 (1959).
3. R. D. Chambers, H. C. Clark, and C. J. Willis. Chem. & Ind. (London), 76 (1960).
4. W. R. Cullen. Can. J. Chem. **38**, 439 (1960).
5. M. A. A. Beg and H. C. Clark. Unpublished results.
6. C. A. Kraus and C. F. Callis. J. Am. Chem. Soc. **45**, 2624 (1923).
7. S. D. Rosenberg, E. Debreczeni, and E. L. Weinberg. J. Am. Chem. Soc. **81**, 973 (1959) and references therein.
8. H. D. Kaesz, S. L. Stafford, and F. G. A. Stone. Abstracts, 137th National Meeting, American Chemical Society, Cleveland. April, 1960. 38M.
9. J. G. Noltes and G. J. M. Van der Kerk. Functionally substituted organotin compounds. Tin Research Council, England. p. 60.
10. H. D. Kaesz, S. L. Stafford, and F. G. A. Stone. J. Am. Chem. Soc. **81**, 6336 (1959).
11. R. D. Chambers, H. C. Clark, and C. J. Willis. Proc. Chem. Soc. 114 (1960). J. Am. Chem. Soc. **82**, 5298 (1960).
12. J. J. Lagowski. Quart. Revs. (London), **13**, 236 (1959).
13. D. Seyferth and N. Kahlen. J. Org. Chem. **25**, 809 (1960).
14. C. A. Kraus and W. N. Greer. J. Am. Chem. Soc. **45**, 3078 (1923).
15. C. A. Kraus and W. N. Greer. J. Am. Chem. Soc. **45**, 2946 (1923).
16. R. D. Chambers, H. C. Clark, and C. J. Willis. Unpublished results.
17. M. P. Brown and D. E. Webster. Technical Report Contract No. Nonr-1866(13), Chemistry Branch, U.S. Office of Naval Research. August, 1959.
18. A. D. Buckingham, T. Schaefer, and W. G. Schneider. J. Chem. Phys. **32**, 1227 (1960).

Can. J. Chem. Downloaded from www.nrcresearchpress.com by 210.87.254.40 on 09/05/12
For personal use only.

Can. J. Chem. Downloaded from www.nrcresearchpress.com by 210.87.254.6 on 09/05/12
For personal use only.

COCATALYSIS IN FRIEDEL–CRAFTS REACTIONS

IV. BORON FLUORIDE – METHANOL[1]

JOAN M. CLAYTON[2] AND A. M. EASTHAM

ABSTRACT

The kinetics of the isomerization of *cis*- and *trans*-2-butenes, catalyzed by methanol and boron fluoride mixtures, have been studied. The rate was found to be proportional to the concentrations of the boron fluoride – methanol complex and of free boron fluoride but independent of the butene concentration.

In previous papers (1, 2) we have reported the results of some experiments on the isomerization of *cis*- and *trans*-2-butenes in ethylene dichloride solution, using boron fluoride – water mixtures as catalyst. In order to interpret the results of those experiments it was necessary to estimate the position of the equilibrium between the mono- and di-hydrates of boron fluoride,

$$(BF_3.H_2O)^2 = (BF_3)(BF_3.2H_2O),$$

and this was done from measurements of the vapor pressure of boron fluoride over solutions of water in ethylene dichloride. From the resulting values for the concentrations of the hydrates it was concluded that the rate expression for the conversion of one butene isomer into the other was

$$d(\text{isomer}_B)/dt = k(BF_3)(BF_3.H_2O)(\text{isomer}_A).$$

The equilibrium constant obtained for the monohydrate–dihydrate reaction was at best an approximate one for, as its measurement was dependent upon small differences between large numbers, a considerable error was possible. With the catalyst system boron fluoride – methanol, however, this uncertainty can be largely avoided because the dialcoholate is very much less stable than the monoalcoholate and one may therefore assume that the concentration of the latter is approximately that of the added alcohol. Furthermore, the rates are much slower, and hence more easily measured, than those with water as cocatalyst, the catalyst mixtures are completely soluble over a wide range of concentrations, and the higher vapor pressure of the methanol permits more accurate dispensing of the cocatalyst. The present paper reports the results of some studies of the isomerization of the 2-butenes by boron fluoride – methanol mixtures.

EXPERIMENTAL

Materials were prepared and handled essentially as previously described. Methanol was dried with magnesium methoxide and measured as the vapor at pressures well below the saturation vapor pressure at room temperature.

Rates were measured in a reaction flask equipped with a manometer and having a total free space of about 215 ml. Ethylene dichloride (35 ml) was used as solvent and the temperature was controlled at 20° C by water circulating around the flask. Samples were removed as previously described and analyzed either by infrared spectroscopy or by gas chromatography. Isomerization of the trans isomer was followed by the appearance

[1]*Manuscript received July 14, 1960.*
Contribution from the Division of Applied Chemistry, National Research Council, Ottawa, Canada.
Issued as N.R.C. No. 6056.
[2]*National Research Council Postdoctorate Fellow.*

of the cis peak in the infrared spectrum while that of the cis isomer was followed by the appearance of the trans peak in the chromatogram of a column prepared from 30 g silver nitrate dissolved in 30 ml glycerine, supported on 58 g Celite and packed into 16 feet of stainless steel tubing. The chromatographic method is suitable for mixtures containing up to about 75% of the trans isomer and is more accurate than the spectrographic method because it is not affected by traces of solvent. At low cis concentrations, however, the peaks for the two isomers overlap in the chromatogram and the infrared method gives the better results if a correction is made for the small absorption due to residual solvent.

The vapor pressure of boron fluoride over solutions of methanol in ethylene dichloride is shown in Fig. 1 and indicates clearly the essentially quantitative formation of the

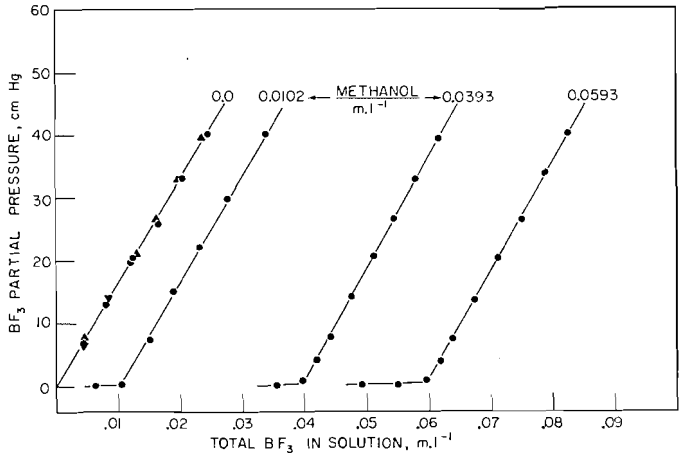


FIG. 1. The vapor pressure of boron fluoride over solutions of methanol in ethylene dichloride.

1:1 complex at all boron fluoride concentrations in excess of the methanol (compare the corresponding data for water (2)).

In this paper most concentrations have been expressed as moles per liter, calculated from the number of moles of reactant introduced into the reaction vessel divided by the volume of solvent. Concentrations expressed in this way give a reasonably accurate statement of the amount of dissolved material when the vapor pressure of the reactant is low, e.g. the methanol – boron fluoride complex, and are also quite accurate for the butenes since about 95% of the added olefin is in solution under the conditions of these experiments. In the case of boron fluoride, however, since about 80% of the free reagent is in the gas phase, the following terms, all based on the volume of solvent, have been used to define the concentrations:

$(BF_3)_{total}$ = the total BF_3 added to the system whether complexed, dissolved, or in the gas phase.

$(BF_3)_{free}$ = all uncomplexed BF_3 whether dissolved or in the gas phase.

$(BF_3)_{solution}$ = that part of the free BF_3 (about 20%) which is in solution.

RESULTS

In Fig. 2, the initial rates of isomerization of *trans*-2-butene are shown for a series of experiments in which the methanol concentration was varied at constant concentrations

Can. J. Chem. Downloaded from www.nrcresearchpress.com by 210.87.254.6 on 09/05/12
For personal use only.

of butene and of total boron fluoride (1.0 mole $l.^{-1}$ and 6.0×10^{-3} moles $l.^{-1}$ respectively). It is evident that the variation in rate is essentially similar in type to that observed for cocatalysis by water (1), but the rates are much slower. Because of differences in temperature, in the free space of the reaction vessel, and perhaps in the kinetics, the relative rates for the two cocatalysts cannot be estimated accurately but for the conditions of this particular set of experiments, water appears to be about 50 times as effective as methanol.

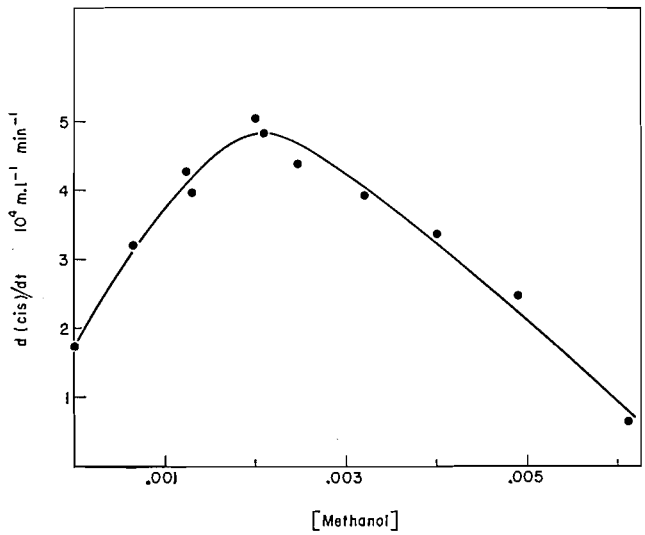


FIG. 2. The rate of isomerization of *trans*-2-butene at constant total boron fluoride concentration and varying methanol concentration.

The kinetics were examined in more detail by varying each of the three reactants in turn. For the experiments shown in Fig. 3(*a*) the initial *trans*-butene and methanol concentrations were fixed at 1.0 mole $l.^{-1}$ and 2.1×10^{-3} moles $l.^{-1}$, respectively, and the boron fluoride concentration was varied. For the experiments of Fig. 3(*b*) the *trans*-butene concentration was again 1.0 mole $l.^{-1}$ but the methanol concentration was varied and the boron fluoride adjusted to produce a constant 1.0×10^{-2} moles $l.^{-1}$ excess over the methanol. The dependence of the rate upon the concentrations of both free boron fluoride and the methanol – boron fluoride complex appears to be of the first order.

The dependence of the rate upon butene concentration is rather more difficult to determine, especially in the conversion of the trans to the cis isomer. In the previous work with water as cocatalyst, the limited evidence available suggested a first-order dependence on butene but the present results show clearly an order approaching zero (Table I). Furthermore the initial rates are almost identical when either isomer is used as starting material, indicating that the equilibrium is not determined primarily in the rate-controlling step. There is some indication in the experiments with *trans*-butene that the rates may not be entirely independent of the butene concentration but as the divergence is greatest where the experimental error is greatest we are inclined to believe that the data for the cis isomer are the more reliable.

The rate constants in the above table must be regarded as peculiar to the present

Can. J. Chem. Downloaded from www.nrcresearchpress.com by 210.87.254.6 on 09/05/12
For personal use only.

Can. J. Chem. Downloaded from www.nrcresearchpress.com by 210.87.254.6 on 09/05/12
For personal use only.

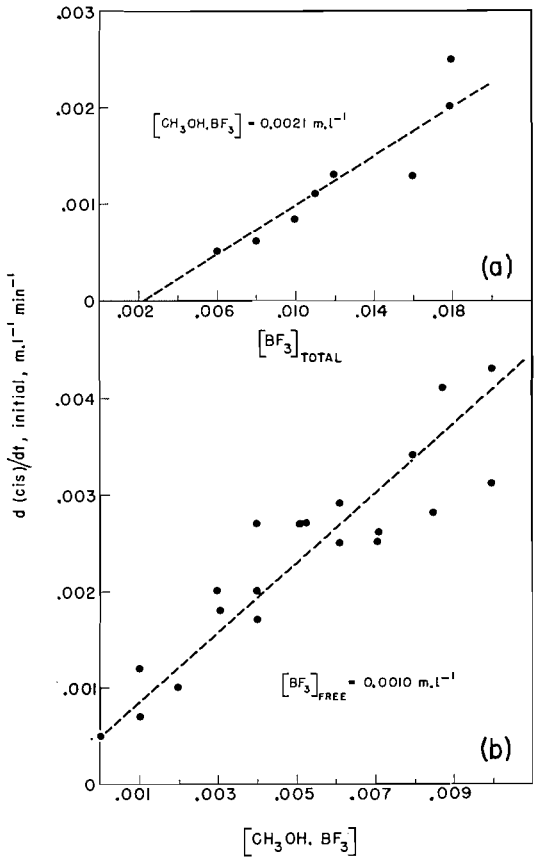


FIG. 3. The rate of isomerization of *trans*-2-butene: (*a*) at constant concentration of $CH_3OH \cdot BF_3$; (*b*) at constant concentration of free boron fluoride.

TABLE I

Initial butene, moles l.$^{-1}$	k_{obs}	$k_{initial}$	Initial butene, moles l.$^{-1}$	k_{obs}	$k_{initial}$
cis, 2.0	.0030	.0026	trans, 2.75	.0033	.0027
1.0	.0020	.0020	2.0	.0032	.0024
0.50	.0023	.0023	1.5	.0028	.0025
0.25	.0021	.0022	1.0	.0017	.0018
0.125	.0021	.0019	0.5	(.0010)	(.0010)
	Average .0023 moles l.$^{-1}$ min^{-1}			Average .0024 moles l.$^{-1}$ min^{-1}	

apparatus where about 80% of the free boron fluoride is in the gas phase. For purposes of comparison with other work, the value of k' in the expression

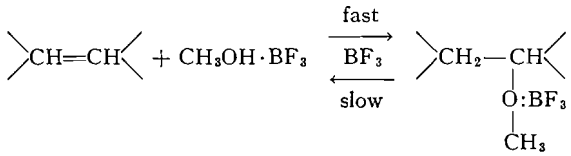
$$dx/dt = k'(CH_3OH \cdot BF_3)(BF_3)_{solution}$$

may be assigned the value 4.0×10^2 l. mole^{-1} min^{-1}.

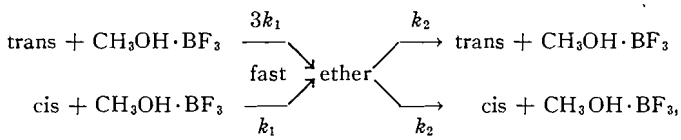
Polymerization of the butene becomes important at high reactant concentrations and can be observed by the falling vapor pressure of the solutions. A few data gathered

throughout the course of this work suggest that the rate of polymerization is strongly dependent upon the concentrations of butene and of the methanol – boron fluoride complex but seemingly less dependent upon the concentration of free boron fluoride. The present evidence does not suggest that isomerization and polymerization are the parallel reactions one would expect if both were to occur through a common intermediate (e.g. a carbonium ion). This aspect of the problem is now under investigation.

The zero-order dependence of the isomerization upon butene concentration suggests either that butene reacts rapidly with catalyst to form a relatively stable intermediate, or else that the rate is controlled by some slow step not involving butene as for example a reaction between the two catalyst components. The only obvious stable intermediate would be the ether resulting from addition of methanol to the olefin (2-methoxy-butane), and indeed a reaction of the form



could account completely for all of the kinetic data reported here. If one assumes that equilibrium is determined entirely in the addition of the boron fluoride – methanol complex to the olefin and not in the regeneration of the olefin, that the equilibrium mixture contains only the cis and trans isomers in a 1:3 ratio, that steady-state conditions apply to the unreacted boron fluoride – methanol complex, and that all reactions are



catalyzed by free boron fluoride, then the following integrated rate expressions are obtained for the reactions:

$$\text{trans} \rightarrow \text{cis} \qquad k_{obs}t = \frac{3a}{8} \ln \frac{a}{a-4x} - \frac{x}{2},$$

$$\text{cis} \rightarrow \text{trans} \qquad k_{obs}t = \frac{3a}{8} \ln \frac{3a}{3a-4x} + \frac{x}{2}.$$

In these expressions a is the initial concentration of one isomer, x the concentration of the other formed in time t, and $k_{obs} = k_2\,(CH_3OH \cdot BF_3)_{initial}(BF_3)_{free}$. The values of k_{obs} obtained from these expressions hold very well over one or two half-lives of the reactions and agree reasonably well with the values obtained from initial rates (Table I).

However, although a treatment of this kind seems to account for these data, more recent experiments in this laboratory indicate that the isomerization cannot occur in this way. The addition and elimination of methanol do indeed occur under boron fluoride catalysis, but the rates seem to be too slow to explain the isomerization. It is possible that some other intermediate less stable than the ether is involved but it is difficult to conceive of one which would not be in equilibrium with free butene.

Can. J. Chem. Downloaded from www.nrcresearchpress.com by 210.87.254.6 on 09/05/12
For personal use only.

If the reaction does not involve a stable intermediate then presumably some reaction of the catalyst system, as, for example,

$$CH_3OH \cdot BF_3 + BF_3 \rightleftarrows CH_3O(BF_3)_2^- + H^+,$$

must be rate controlling. A reaction of this kind would explain the need for free boron fluoride in the isomerization but we have been reluctant to postulate intermediates in which two boron fluoride molecules are attached to one oxygen atom because of the absence of any independent evidence for them. Their existence as transitory species is not, however, impossible. One of the difficulties with this approach is that it suggests the direct protonation of olefins to form carbonium ions and there is a growing body of evidence which suggests that, because of the high reactivity of such ions, their formation is not readily reversible (3) and hence cannot account for the rapid isomerization. A loosely bound proton–olefin complex such as a π-complex would, on the other hand, be reversible but probably would not disturb the olefin structure sufficiently to produce isomerization.

REFERENCES

1. A. M. EASTHAM. J. Am. Chem. Soc. **78**, 6040 (1956).
2. J. M. CLAYTON and A. M. EASTHAM. J. Am. Chem. Soc. **79**, 5368 (1957).
3. S. J. TAUBER and A. M. EASTHAM. J. Am. Chem. Soc. **82**, 4888 (1960).

Can. J. Chem. Downloaded from www.nrcresearchpress.com by 210.87.254.6 on 09/05/12
For personal use only.

Can. J. Chem. Downloaded from www.nrcresearchpress.com by 210.87.254.105 on 09/05/12
For personal use only.

CONTRIBUTION À L'ÉTUDE DE LA RÉACTION DE VON RICHTER

I. SUR L'IDENTIFICATION DE QUELQUES PRODUITS ACIDES[1]

E. CULLEN[2] ET PH. L'ÉCUYER

RÉSUMÉ

La réaction de von Richter avec le *p*-chloronitrobenzène fournit, outre l'acide *m*-chlorobenzoïque attendu, un mélange de produits dont le 4,4′-dichloro-2,2′-dicarbamylazobenzène, le 3,8-dichloro-6-cétoquinazolo[1,2,2′,3′]indazol et l'acide 4,4′-dichloroazoxybenzène-2,2′-dicarboxylique. Ce dernier se transforme en la lactone de l'acide 5-chloro-2-[5-chloro-3-oxyindazyl-(2)]-benzoïque par sublimation.

Avec le nitrobenzène, outre l'acide benzoïque, seul le 6-cétoquinazolo[1,2,2′,3′]indazol a été isolé.

Dans le but de déterminer la position des substituants dans les dérivés du nitrobenzène, von Richter (1, 2, 3) a fait réagir les dérivés nitrés du nitrobenzène avec le cyanure de potassium en solution alcoolique. Comme il obtenait des acides carboxyliques et que la réaction était invariablement accompagnée de la perte d'un groupe nitré, il supposa que le groupement nitrile substituait le groupe nitré et se transformait en groupement carboxylique. Toutefois, à la suite d'études de structures exécutées concurremment par Griess (4) et Korner (5), von Richter (6) dut admettre que le groupement nitrile se fixe en ortho de la fonction éliminée au lieu de déplacer directement le groupe nitré, ce qui a depuis été vérifié par Holleman (7) et tout récemment par Bunnett, Cormack et McKay (8). La transformation du *p*-bromonitrobenzène en acide *m*-bromobenzoïque peut servir d'exemple de cette réaction.

Sauf le travail de Holleman, la réaction est demeurée dans l'oubli jusqu'en 1950 alors que Bunnett et des collaborateurs (8, 9, 10) entreprirent d'en étudier la portée et le mécanisme. En plus de confirmer les résultats déjà obtenus par von Richter, ces chercheurs ont étendu le champ des observations antérieures. Ils ont, en particulier, montré qu'il est préférable de faire bouillir les réactifs dans l'alcool aqueux plutôt que de chauffer en tube scellé à 150°; car une température élevée favorise l'hydrolyse du cyanure (9, 11).

Cette réaction fournit, en plus de l'acide attendu, des produits neutres (insolubles en milieu alcalin) et des produits acides (insolubles en milieu neutre ou acide), dont les uns ou les autres prédominent suivant la nature des substituants dans le cycle du benzène (10).

I. RÉACTION AVEC LE *p*-CHLORONITROBENZÈNE (Tableau I)

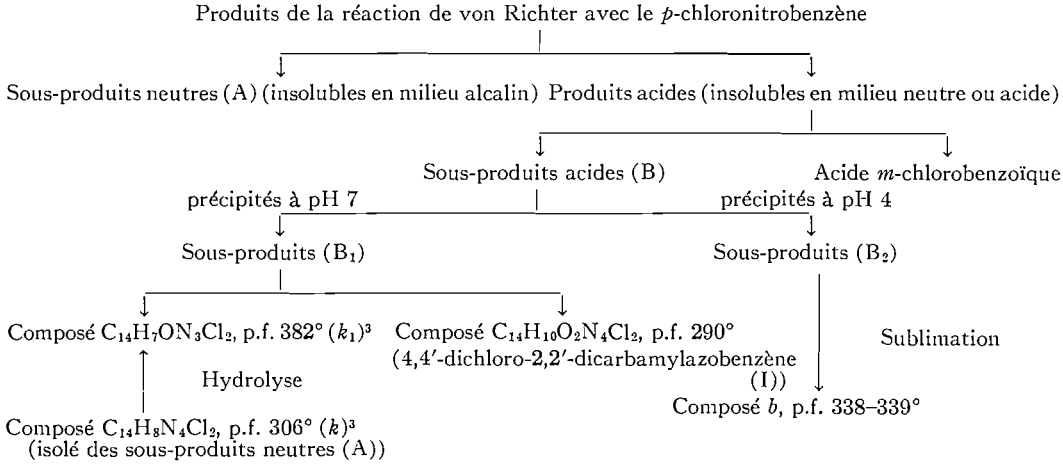
Suivant les indications de Bunnett (9), nous avons isolé, à partir du *p*-chloronitrobenzène, 10% de produits neutres (A), 37% d'acide *m*-chlorobenzoïque et 12% d'autres produits acides (B). Nous avons réussi à obtenir proportionnellement plus d'acide *m*-chlorobenzoïque et de produits B en modifiant la façon de les isoler.

Une fois les produits A essorés, le filtrat est acidifié et les produits acides sont isolés et extraits à la ligroïne dans un Soxhlet. Seul l'acide *m*-chlorobenzoïque se dissout. Les produits B constituent le résidu. Ils peuvent être dissous dans de la soude diluée contenant un peu d'éthanol et séparés en deux groupes de composés: les premiers (B_1) précipitent à pH 7 et les seconds (B_2), à pH 4. Le même résultat est atteint, si les substances B_1

[1]*Manuscrit reçu le 21 septembre 1960.*
Contribution du Département de Chimie, Faculté des Sciences, Université Laval, Québec, Qué.
[2]*Bénéficiaire de bourses d'études accordées par le Conseil national de Recherches du Canada, les firmes C.I.L. et Shell Oil et l'Office de Recherches scientifiques de la Province de Québec.*

TABLEAU I

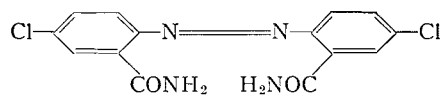
Produits de la réaction de von Richter avec le *p*-chloronitrobenzène



sont d'abord précipités dans le filtrat à pH 7, et ensuite les composés B_2 à pH 4. L'acide *m*-chlorobenzoïque est alors obtenu de ces derniers par extraction à la ligroïne.

Nature des produits B_1 et B_2

Du mélange de produits B_1 nous avons isolé deux substances. La première, $C_{14}H_7ON_3Cl_2$, fond à 382°. D'après un point de fusion mixte et les spectres infrarouges, elle s'est avérée identique à un composé (k_1) obtenu par l'hydrolyse d'une substance (*k*), p.f. 306°, qui appartient au groupe des produits neutres (A) de la réaction.[3] La seconde fond à 290° et a pour formule empirique $C_{14}H_{10}O_2N_4Cl_2$. Elle possède une fonction azoïque et un groupe amide. Nous sommes d'avis qu'elle est le 4,4′-dichloro-2,2′-dicarbamylazobenzène (I). Bunnett et Rauhut (12) ont récemment isolé une substance analogue, le 4,4′-diméthoxy-2,2′-dicarbamylazoxybenzène, à partir du *p*-nitroanisole.



(I)

Après avoir extrait l'acide *m*-chlorobenzoïque, nous avons sublimé, sous 12 mm de pression, le résidu des produits acides (B_2). Le sublimé, recueilli entre 180 et 350°, se dissout dans le β-éthoxyéthanol bouillant et fournit par cristallisation une substance (*b*) de point de fusion de 338–339°. Nous avons tenté de séparer le sublimé par sublimation fractionnée. Trois fractions ont été recueillies entre 180 et 210°, 210 et 290° et 290 et 350°. La troisième fraction contient la substance (*b*), qui est évidemment un produit de transformation, puisqu'elle n'est plus soluble dans la soude diluée. Quant aux fractions 1 et 2, il a été impossible de les purifier.

Identification du composé b (Tableau II)

D'après son analyse élémentaire, le composé *b*, p.f. 338–339°, possède la formule brute $C_{14}H_6O_2N_2Cl_2$. Il est insoluble dans les solvants organiques usuels ainsi que dans les

[3]*La description de ces deux substances, k et k_1, et de leurs analogues k′ et k_1′, paraîtra bientôt dans ce journal.*

Can. J. Chem. Downloaded from www.nrcresearchpress.com by 210.87.254.105 on 09/05/12
For personal use only.

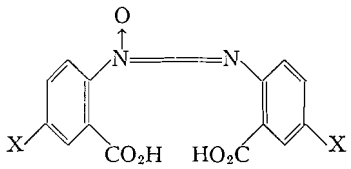
TABLEAU II

Réactions qui ont conduit à l'identification du composé *b*

Acide 4,4′-dichloroazoxybenzène-2,2′-dicarboxylique (II) (un des sous-produits acides B_2)	Acide azoxybenzène-2,2′-dicarbozylique (III)
↓ Sublimation	↓ Sublimation
Composé *b*, $C_{14}H_6O_2N_2Cl_2$, p.f. 338–339° ou lactone de l'acide 5-chloro-2-[5-chloro-3-oxy-indazyl-(2)]-benzoïque (IX)	Composé *b*′, $C_{14}H_8O_2N_2$, p.f. 292° ou lactone de l'acide 2-[3-oxyindazyl-(2)]-benzoïque (VIII)
↓ NaOH alcoolique	↓ NaOH alcoolique
Composé b_1, $C_{14}H_8O_3N_2Cl_2$ ou acide 5-chloro-2-[5-chloro-3-oxy-indazyl-(2)-]-benzoïque (VII)	Composé b_1′, $C_{14}H_{10}O_3N_2$ ou acide 2-[3-oxyindazyl-(2)]-benzoïque (VI)
HNO_3 ↓ [O]	HNO_3 ↓ [O]
Composé b_2, $C_{14}H_8O_4N_2Cl_2$, noircit vers 278–280° et fond à 308–310° ou acide 4,4′-dichloroazobenzène-2,2′-dicarboxylique (V)	Composé b_2′ $C_{14}H_{10}O_4N_2$, p.f. 237° ou acide azobenzène-2,2′-dicarboxylique (IV) (14)
↓ Chaleur	↓ Chaleur
Composé *b*	Composé *b*′

alcalis et les acides dilués, mais soluble dans la potasse alcoolique et l'acide sulfurique concentré dans lequel il précipite par addition d'eau.

Nous nous sommes rendus compte que cette substance résulte d'une transformation de l'acide 4,4′-dichloroazoxybenzène-2,2′-dicarboxylique (II) qui se produit au cours de sa sublimation. Désirant vérifier comment cet acide se comporte, lorsqu'il est soumis aux conditions de la réaction de von Richter,[4] nous l'avons synthétisé suivant la méthode utilisée (13) pour préparer l'acide non-chloré III correspondant. Nous avons constaté que, lorsqu'il est sublimé, il se transforme en la substance *b*, comme le révèlant un point de fusion mixte et les spectres infrarouges (Fig. 1).



(II) X = Cl
(III) X = H

Au cours de cette transformation, l'acide perd une molécule d'eau et une molécule d'oxygène (équation 1, X = Cl).

$$C_{14}H_8O_5N_2X_2 \rightarrow C_{14}H_6O_2N_2X_2 + H_2O + O_2 \qquad [1]$$

X = H ou Cl

Les bandes dues à l'absorption des groupes carboxyliques à 3050–2550, à 1420 et 1300 cm^{-1} dans le spectre infrarouge de l'acide n'apparaissent pas dans celui du composé *b*, qui toutefois montre, à 1700 cm^{-1}, la bande due à la présence du groupe carbonyle.

[4]*Il ne change pas.*

Can. J. Chem. Downloaded from www.nrcresearchpress.com by 210.87.254.105 on 09/05/12
For personal use only.

Can. J. Chem. Downloaded from www.nrcresearchpress.com by 210.87.254.105 on 09/05/12
For personal use only.

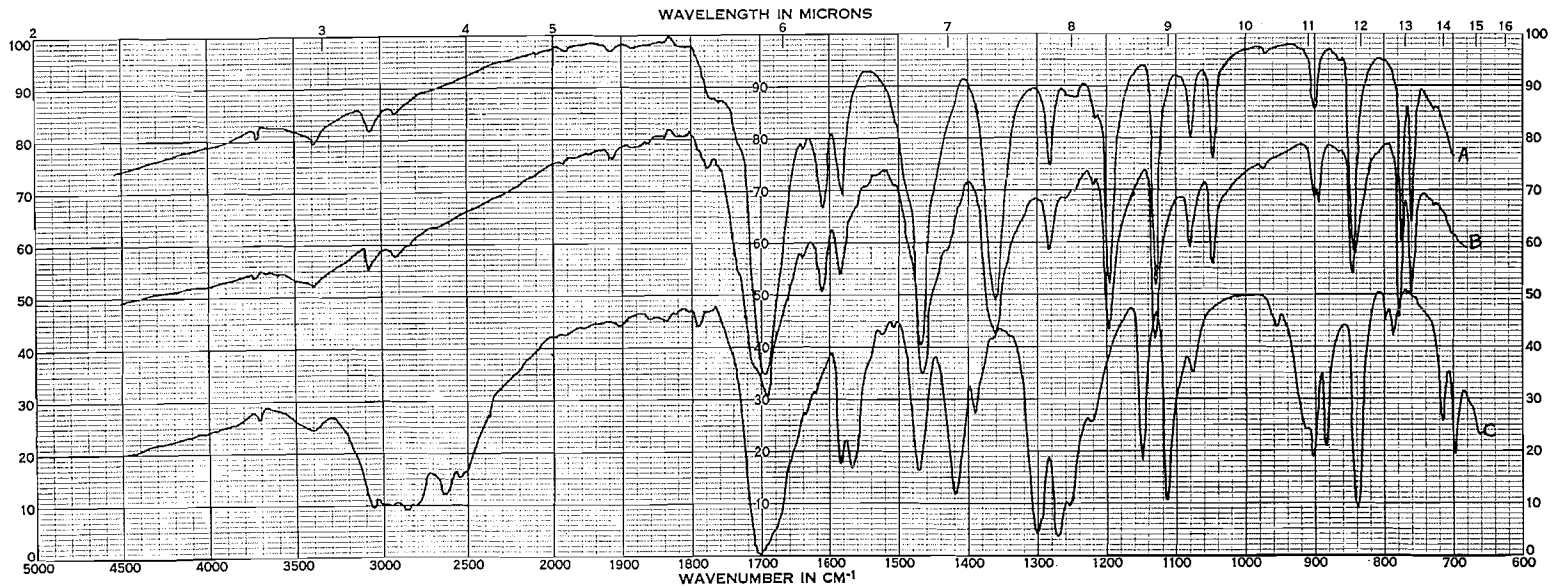


FIG. 1. Spectres infrarouges. (A) Lactone de l'acide 5-chloro-2-[5-chloro-3-oxy-indazyl-(2)]-benzoïque obtenue par sublimation de l'acide 4,4′-dichloroazoxybenzène-2,2′-dicarboxylique. (B) Lactone de l'acide 5-chloro-2-[5-chloro-3-oxy-indazyl-(2)]-benzoïque obtenue par sublimation des produits B_2 provenant de la réaction de von Richter avec le *p*-chloronitrobenzène. (C) Acide 4,4′-dichloroazoxybenzène-2,2′-dicarbonylique.

Can. J. Chem. Downloaded from www.nrcresearchpress.com by 210.87.254.105 on 09/05/12
For personal use only.

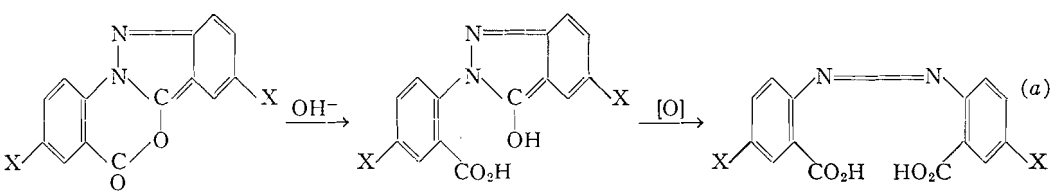
La substance *b* ne possède pas de fonction azoïque, azoxyque, nitrée, amine tertiaire ou amide secondaire. Elle donne le test des 1,2-dicétones, mais n'est pas oxydée par un mélange de peroxyde d'hydrogène et d'acide perchlorique et ne se condense pas avec l'*o*-phénylènediamine. Elle n'est réduite ni par l'étain ou le fer en milieu acide, ni par l'hydrogène et le palladium à la pression atmosphérique.

Par ébullition dans la soude alcoolique, le composé *b* se transforme en une substance blanche (b_1) qui est très soluble dans la soude diluée. Le spectre infrarouge de cette dernière présente les caractéristiques des dimères des acides carboxyliques (bande d'absorption due au groupement carbonyle à 1728 cm^{-1} et, dans la région de 3100–2400 cm^{-1}, une série de bandes attribuables aux groupes hydroxyles fortement associés par ponts hydrogène).

L'analyse centésimale et le poids moléculaire du produit de saponification b_1 correspondent à la formule brute $C_{14}H_8O_3N_2Cl_2$. Celle-ci ne diffère de celle de la substance *b* que par les éléments d'une molécule d'eau en plus. La substance b_1 est oxydée par l'acide nitrique en un produit jaune-orangé, $C_{14}H_8O_4N_2Cl_2$ (b_2), qui noircit vers 278–281° et fond à 308–310°. Sous l'action de la chaleur, elle perd une molécule d'eau et redonne la substance *b*. À ce stade-ci du travail, nous avons poursuivi cette étude de structure en utilisant l'acide azoxybenzène-2,2′-dicarboxylique (III) correspondant.

Cet acide non-chloré, $C_{14}H_{10}O_5N_2$, tel que prévu, se transforme facilement par sublimation (équation 1, X = H) en la substance $C_{14}H_8O_2N_2$ (b'), p.f. 292°, qui est l'analogue du composé *b*. Saponifiée par la soude alcoolique, la substance b' donne un composé blanc, $C_{14}H_{10}O_3N_2$ (b_1'), analogue au composé b_1. L'oxydation du composé b_1' à l'acide nitrique donne un produit orangé, $C_{14}H_{10}O_4N_2$ (b_2'), de point de fusion de 237°, analogue à la substance b_2 et identique à l'acide azobenzène-2,2′-dicarboxylique (IV) (14).

Carré (15, 16) a synthétisé ce dernier acide en oxydant l'acide 2-[3-oxy-indazyl-(2)]-benzoïque (VI), obtenu par la saponification de la lactone correspondante (VIII) (*a*). Or toutes les propriétés de la substance b' montrent qu'elle est identique à la lactone VIII (17). Par analogie, nous pouvons conclure que le composé *b* est la lactone de l'acide 5-chloro-2-[5-chloro-3-oxy-indazyl-(2)]-benzoïque (IX).



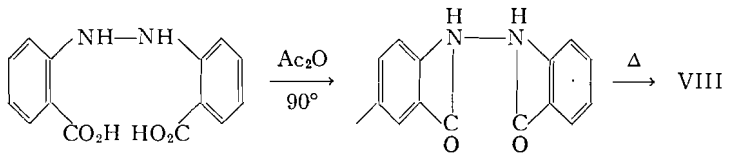
(VIII) X = H
(IX) X = Cl

(VI) X = H
(VII) X = Cl

(IV) X = H
(V) X = Cl

D'ailleurs, le produit b_1, qui provient de la saponification de la substance *b*, doit nécessairement être l'acide 5-chloro-2-[5-chloro-3-oxy-indazyl-(2)]-benzoïque (VII); car, le composé jaune-orangé (b_2) qu'il donne, lorsqu'il est oxydé par l'acide nitrique, est l'acide 4,4′-dichloroazobenzène-2,2′-dicarboxylique (V) de point de fusion de 308–310°. En effet, un point de fusion mixte et les spectres infrarouges ont montré que ce dernier acide est identique à l'acide que nous avons obtenu par synthèse, en réduisant l'acide 2-nitro-5-chlorobenzoïque par le zinc et la soude en l'acide 4,4′-dichlorohydrazobenzène-2,2′-dicarboxylique et oxydant celui-ci par l'acide nitrique.

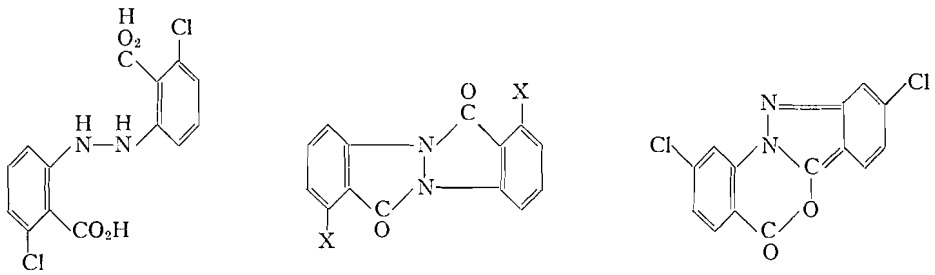
Diverses opinions ont été émises concernant la structure de composés du genre de la lactone VIII. Celle-ci peut être obtenue par la déshydratation de l'acide hydrazobenzène-2,2′-dicarboxylique (X). D'après Heller (18), cette réaction se ferait par l'intermédiaire du bisanthranile (XI) (*b*).



(*b*)

(X) (XI)

Reich et Merki (19) ont, par ailleurs, transformé le 2-nitro-6-chlorobenzaldéhyde en l'acide 3,3′-dichlorohydrazobenzène-2,2′-dicarboxylique (XII) et, celui-ci en une substance de point de fusion de 347–348°, insoluble dans les acides et les bases, à laquelle ils attribuent la structure dilactame XIII.



(XII) (XIII) X = Cl (XIV) X = H (XV)

D'autre part, par déshydratation de l'acide 5,5′-dichlorohydrazobenzène-2,2′-dicarboxylique, Heller (18) a obtenu un isomère de la substance XIII, fondant à 335°, et lui attribue la structure XV.

Enfin, à la suite d'une étude des spectres infrarouges du bisanthranile XI de Heller et de la lactone VIII, Mosby (20) prétend qu'il faudrait attribuer au bisanthranile la structure lactone VIII et à la supposée lactone VIII, la structure dilactame XIV.

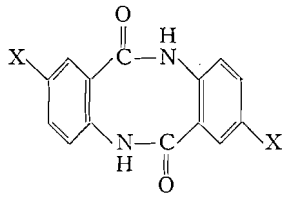
Nous sommes d'avis que la saponification des substances *b* et *b′* en acides 2-[3-oxy-indazyl-(2)]-benzoïques VII et VI justifie une structure lactone, mais non dilactame. En effet, l'obtention de ces acides VI et VII par la saponification des dilactames XIV et XIII ne pourrait s'expliquer que par une transformation facile des acides hydrazobenzène-2,2′-dicarboxyliques en acides 2-[3-oxy-indazyl-(2)]-benzoïques. Dans ce cas cette transformation devrait alors se produire en premier lieu au moment de la cyclisation au lieu de la transformation en dilactame.

Au cours de cette étude, nous avons voulu synthétiser la 2,9-dichlorophénomazine XVI. Selon Cooper et Partridge (21), l'anthranilate de méthyle se condense en présence de sodium métallique et de benzonitrile pour donner la phénomazine (XVII) et un peu de 4-hydroxy-2-phénylquinazoline (XVIII).

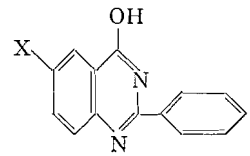
Le 5-chloroanthranilate de méthyle peut être préparé en chlorurant l'anthranilate de méthyle (22) ou en estérifiant l'acide 5-chloroanthranilique (23). Nous l'avons obtenu

Can. J. Chem. Downloaded from www.nrcresearchpress.com by 210.87.254.105 on 09/05/12
For personal use only.

en réduisant le 2-nitro-5-chlorobenzoate de méthyle par le fer activé. Le 5-chloro-anthranilate de méthyle se condense dans le xylène en présence de benzonitrile et de sodium métallique; mais nous n'avons isolé que de la 6-chloro-2-phényl-4-hydroxyquinazoline (XIX).



(XVI) X = Cl
(XVII) X = H



(XVIII) X = H
(XIX) X = Cl

II. Réaction avec le nitrobenzène

La réaction de von Richter avec le nitrobenzène a fourni de l'acide benzoïque et une substance, $C_{14}H_9ON_3$, fondant à 334–336°. D'après un point de fusion mixte et les spectres infrarouges, elle s'est avérée identique à un composé (k_1') obtenu par l'hydrolyse d'une substance (k'), p.f. 222–223°, qui est un produit neutre de la réaction.[3]

Partie expérimentale[5]

I. Réaction avec le *p*-chloronitrobenzène

En ce qui concerne la réaction proprement dite, le mode opératoire suivi est, à peu de variantes près, celui de Bunnett et ses collaborateurs (9). Une solution comprenant 1 partie de *p*-chloronitrobenzène et 4 parties de cyanure de potassium dans 10 parties (en volume) d'éthanol à 50% est bouillie à reflux pendant 48 heures. Le produit de la réaction est ensuite étendu à cinq fois son volume avec de l'eau et filtré. (Avant de filtrer, le mélange peut être soumis à une distillation à la vapeur d'eau. Celle-ci permet de récupérer environ 1% de la quantité initiale de *p*-chloronitrobenzène, qui est rapidement entraînée par la vapeur, et d'améliorer de 10% le rendement en acide *m*-chlorobenzoïque.) On obtient ainsi un solide neutre A jaune-verdâtre et un filtrat A.

(1) Isolement de l'acide m-chlorobenzoïque

L'acide *m*-chlorobenzoïque peut être extrait du filtrat A selon la méthode de Bunnett (8) ou suivant la modification suivante. Le filtrat A est acidifié à pH 4 et maintenu à 5° pendant au moins 12 heures. Les acides précipités sont alors filtrés et lavés à l'eau. Le filtrat et les eaux de lavage sont extraits au chloroforme et les extraits chloroformés épuisés à la soude 5%. La solution alcaline est chauffée pour en chasser les traces de chloroforme, puis est refroidie et acidifiée. Les acides ainsi précipités sont essorés, ajoutés aux acides déjà isolés, séchés sous pression réduite et extraits à la ligroïne (Eb = 65–110°) dans un Soxhlet. Seul l'acide *m*-chlorobenzoïque est extrait. L'extrait est ensuite évaporé à siccité. Le résidu, cristallisé dans le même solvant, fournit l'acide *m*-chlorobenzoïque (rendement 46% de la théorie) de point de fusion de 155–157°.

[5]*Les points de fusion (p.f.) ont été pris en tubes capillaires et ne sont pas corrigés. Les spectres infrarouges ont été déterminés au moyen d'un spectromètre Beckman IR4; les solides étaient mélangés à du bromure de potassium et pressés; seules les bandes servant à l'identification des composés sont indiquées; les valeurs en cm^{-1} correspondent au maximum d'absorption, sauf celles qui correspondent aux groupes hydroxyles des acides carboxyliques et qui montrent la région entière de l'absorption. Les microanalyses ont été effectuées par M. W. Manser, Zürich, Suisse.*

Can. J. Chem. Downloaded from www.nrcresearchpress.com by 210.87.254.105 on 09/05/12
For personal use only.

(2) Isolement et identification d'autres produits

Du filtrat A, en plus de l'acide *m*-chlorobenzoïque, on peut isoler des produits (B) qui précipitent à différents pH.

(a) À pH 7

En ajoutant lentement au filtrat A, refroidi dans un bain glacé, de l'acide chlorhydrique 6 *N* jusqu'à ce que le pH devienne 5, puis la quantité de carbonate de sodium nécessaire pour le ramener à 7, des produits (B_1) (10 à 15% du poids de *m*-chloronitrobenzène de départ) précipitent et sont filtrés.

4,4'-Dichloro-2,2'-dicarbamylazobenzène (I) et 3,8-dichloro-6-cétoquinazolo[1,2,2',3']indazol (k_1).— Les produits B_1 (5.56 g), sublimés, sous 12 mm de mercure entre 180 et 350°, donnent un sublimé jaune-orangé (1.5 g). Lorsque celui-ci est sublimé de nouveau sous pression réduite, on recueille deux portions, l'une (0.386 g) au-dessous, et l'autre (0.919 g) au-dessus de 200°. Cette dernière peut être séparée en deux autres fractions par une troisième sublimation. Le composé qui constitue la première fraction est recueilli au-dessous de 220° et fond à 290°. D'après son analyse élémentaire et ses propriétés, il serait le 4,4'-dichloro-2,2'-dicarbamylazobenzène (I). Calculé pour $C_{14}H_{10}O_3N_2Cl_2$: C, 49.87%; H, 2.99%; N, 16.62%. Trouvé: C, 50.09%; H, 2.64%; N, 16.85%. Le produit de la deuxième fraction, recueilli entre 250 et 350°, cristallise dans la N,N-diméthylformamide en aiguilles de couleur jaune pâle et de point de fusion de 382°. Un point de fusion mixte de cette substance et du composé k_1 (le produit d'hydrolyse d'une substance *k* qui appartient aux produits neutres (A) de la réaction) n'est pas abaissé et les spectres infrarouges des deux sont identiques. Cette substance est le 3,8-dichloro-6-céto-quinazolo[1,2,2',3'] indazol.

(b) À pH 4

En portant à 4 le pH du filtrat obtenu en (*a*) et en procédant de la façon qui est décrite précédemment pour l'extraction de l'acide *m*-chlorobenzoïque à la ligroïne, d'autres produits acides (B_2) ont été isolés. Le résidu de l'extraction à la ligroïne (Eb = 65–110°) constitue ces produits.

Lactone de l'acide 5-chloro-2-[5-chloro-3-oxy-indazyl-(2)]-benzoïque (IX) (b).—Tout comme les produits B_1, les produits B_2 (18–20% du poids de *p*-chloronitrobenzène de départ) n'ont pu être séparés que par sublimation. Trois températures ont été arbitrairement choisies pour recueillir trois fractions: (i) au-dessous de 200°, (ii) entre 210 et 240° et (iii) au-dessus de 250°. Il a été impossible de purifier les deux premières substances, soit par cristallisation, soit par sublimation. Le premier composé (i) fond à 205–210°. Calculé pour $C_{14}H_8O_7N_4Cl_2$: C, 39.54%; H, 4.27%; N, 13.18%. Trouvé: C, 39.70%; H, 4.15%; N, 13.03%. Le second fond à 280–290°. Calculé pour $C_{15}H_9O_3N_3Cl_2$: C, 51.45%; H, 2.59%; N, 12.00%. Trouvé: C, 51.88%; H, 2.53%; N, 11.60%. Quant à la troisième substance (iii), elle est la plus abondante des trois et correspond à la lactone de l'acide 5-chloro-2-[5-chloro-3-oxy-indazyl-(2)]-benzoïque. Elle cristallise dans le β-éthoxyéthanol ou la 3-pentanone en paillettes lustrées de point de fusion 338–339°. Calculé pour $C_{14}H_6O_2N_2Cl_2$: C, 55.11%; H, 1.98%; N, 9,18%. Trouvé: C, 55.02%; H, 2.14%; N, 9.32%. L'acide 4,4'-dichloroazoxybenzène-2,2'-dicarboxylique (0.100 g), dont la synthèse apparaît plus loin, se sublime sous 12 mm de mercure, entre 250 et 350°, pour donner la lactone de l'acide 5-chloro-2-[5-chloro-3-oxy-indazyl-(2)]-benzoïque (0.053 g) qui, après cristallisation dans le β-éthoxyéthanol, fond à 338°. Un point de fusion mixte d'un mélange de ce composé et de la substance (iii), décrite précédemment, n'est pas abaissé et les spectres infrarouges des deux sont identiques (Fig. 1). Calculé

Can. J. Chem. Downloaded from www.nrcresearchpress.com by 210.87.254.105 on 09/05/12
For personal use only.

pour $C_{14}H_6O_2N_2Cl_2$: C, 55.11%; H, 1.98%; O, 10.42%; N, 9.18%; Cl, 23.24%. Trouvé: C, 54.70%; H, 2.32%; O, 10.42%; N, 9.18%; Cl, 22.96%. Les essais de synthèse de l'acide 4,4′-dichloroazoxybenzène-2,2′-dicarboxylique à partir de l'acide 5-chloro-2-nitrobenzoïque (4.0 g) selon la méthode utilisée pour la préparation de l'acide 4,4′-diméthoxyazoxybenzène-2,2′-dicarboxylique (12) ou pour celle de l'acide azoxybenzène-2,2′-dicarboxylique (24) n'ont pas permis d'obtenir l'acide à l'état pur par la cristallisation des produits engendrés. Toutefois, en sublimant ces derniers sous 12 mm de mercure, on recueille, au-dessous de 200°, de l'acide 5-chloroanthranilique (p.f. 213–214°), et, entre 210 et 350°, un sublimé qui cristallise dans le β-éthoxyéthanol en paillettes lustrées de couleur jaune pâle et de point de fusion de 338–339°. Ce dernier est la lactone de l'acide 5-chloro-2-[5-chloro-3-oxy-indazyl-(2)]-benzoïque (*b*) identique à la substance (iii). Calculé pour $C_{14}H_6O_2N_2Cl_2$: N, 9.18%. Trouvé: N, 9.11%.

Acide 5-chloro-2-[5-chloro-3-oxy-indazyl-(2)]-benzoïque (VII) (b_1).—De la lactone de l'acide 5-chloro-2-[5-chloro-3-oxy-indazyl-(2)]-benzoïque (*b*) (0.030 g), dissoute dans 3 ml de soude 5 *N* et 3 ml d'éthanol, est chauffée à reflux pendant 2 heures. On dilue ensuite par l'eau à 25 ml et acidifie par l'acide chlorhydrique. L'acide 5-chloro-2-[5-chloro-3-oxy-indazyl-(2)]-benzoïque précipite. Il cristallise dans l'acide acétique à 80% en lamelles blanches. Spectre infrarouge: —OH(—COOH), 2400–3400 cm^{-1}; =CO acide, 1730 cm^{-1}. Chauffé au-dessus de 100°, il redonne lentement la lactone de départ. Calculé pour $C_{14}H_8O_3N_2Cl_2$: C, 52.03%; H, 2.49%; N, 8.67%. Trouvé: C, 52.18%; H, 2.37%; N, 8.81%.

Acide 4,4′-dichloroazoxybenzène-2,2′-dicarboxylique (II).—Un mélange d'acide 2-nitro-5-chlorobenzoïque (5.0 g), d'hydroxyde de potassium (5.0 g) et d'éthanol (20 ml) est chauffé au bain-marie durant 2 heures et ensuite évaporé à siccité. Le résidu est dilué par l'eau, refroidi par addition de glace et acidifié par l'acide chlorhydrique. L'acide précipité est agité pendant environ 15 minutes avec 300 ml d'eau de baryte. On filtre, fait barboter un courant d'anhydride carbonique dans le filtrat pour précipiter l'excès de baryte et filtre de nouveau. En acidifiant le filtrat, l'acide 4,4′-dichloroazoxybenzène-2,2′-dicarboxylique (1.62 g, 36% de la théorie) précipite. Il cristallise dans l'acide acétique en courtes aiguilles de point de fusion de 272° (avec décomposition). Calculé pour $C_{14}H_8O_5N_2Cl_2$: C, 47.36%; H, 2.27%; N, 7.88%; Cl, 19.96%. Trouvé: C, 47.31%; H, 2.21%; N, 7.67%; Cl, 19.88%.

Acide 4,4′-dichloroazobenzène-2,2′-dicarboxylique (V) (b_2).—À une solution de 0.21 g de l'acide 5-chloro-2-[5-chloro-3-oxy-indazyl-(2)]-benzoïque dans 30 ml de soude à 2%, on ajoute 30 ml d'acide nitrique concentré et chauffe au bain-marie pendant 2 heures. Après un repos de quelques minutes à la température ambiante, on filtre, lave à l'eau et sèche le précipité qui s'est formé. L'acide 4,4′-dichloroazobenzène-2,2′-dicarboxylique cristallise dans l'éthanol en fines aiguilles jaunes qui noircissent vers 278–280° et fondent à 308–310°. Calculé pour $C_{14}H_8O_4N_2Cl_2$: C, 49.57%; H, 2.38%; N, 8.26%. Trouvé: C, 49.46%; H, 2.59%; N, 8.55%. Un point de fusion mixte de cette substance et de l'acide obtenu par synthèse de la façon décrite ci-après n'est pas abaissé. Les spectres infrarouges de l'acide provenant des deux sources différentes sont de plus identiques.

On dissout 4.65 g d'acide 2-nitro-5-chlorobenzoïque dans 30 ml d'éthanol, ajoute à cette solution 6 ml de soude à 50% et chauffe au bain-marie. Sous agitation mécanique, on introduit ensuite peu à peu du zinc en poudre jusqu'à ce que la solution de rouge sombre passe au rouge pâle (environ 2 heures). Après un repos de quelques minutes, le mélange est filtré et le précipité d'oxyde de zinc ainsi que l'excès de zinc est lavé par de

Can. J. Chem. Downloaded from www.nrcresearchpress.com by 210.87.254.105 on 09/05/12
For personal use only.

Can. J. Chem. Downloaded from www.nrcresearchpress.com by 210.87.254.105 on 09/05/12
For personal use only.

l'éthanol bouillant. Le filtrat est réuni à l'éthanol de lavage, dilué par un égal volume d'eau et acidifié par de l'acide chlorhydrique concentré. Le précipité jaune pâle, qui se forme, est essoré, lavé à l'eau et séché. On dissout ensuite ce solide (1.15 g) dans 280 ml d'acide acétique bouillant, ajoute 15 ml d'acide nitrique concentré à la solution et la fait bouillir à reflux pendant quelques minutes. À la température ambiante l'acide 4,4′-dichloroazobenzène-2,2′-dicarboxylique cristallise en aiguilles jaune-orangé. Après deux cristallisations dans l'acide acétique, il noircit vers 278–280° et fond à 308–310°. Calculé pour $C_{14}H_8O_4N_2Cl_2$: C, 49.57%; H, 2.38%; N, 8.26%. Trouvé: C, 49.31%; H, 2.51%; N, 8.42%.

4-Hydroxy-6-chloro-2-phénylquinazoline (XIX).—Le 5-chloro-2-nitrobenzoate de méthyle (12) est réduit en 5-chloroanthranilate de méthyle par le fer activé dans le benzène humide selon la méthode générale de Hazlet et Dornfeld (25) avec un rendement de 91%. On introduit ensuite, sous agitation mécanique, 5.0 g de 5-chloroanthranilate de méthyle et 4.2 g de benzonitrile dans un ballon muni d'un réfrigérant et contenant 1.2 g de sodium pulvérisé dans 125 ml de xylène anhydre. Une réaction exothermique s'amorce immédiatement. Une fois celle-ci atténuée (environ une demi-heure), on chauffe à reflux pendant 2 heures et on extrait ensuite à la soude 5 *N* le produit de la réaction. En acidifiant la solution alcaline, on obtient la 4-hydroxy-6-chloro-2-phénylquinazoline qui cristallise dans le xylène contenant un peu d'éthanol. Son point de fusion est de 292° et le rendement de 1.97 g (27% de la théorie). Calculé pour $C_{14}H_9ON_2Cl$: C, 65.41%; H, 3.54%; N, 10.94%. Trouvé: C, 65.00%; H, 3.53%; N, 10.90%.

Lactone de l'acide 2-[3-oxy-indazyl-(2)]-benzoïque (VIII) (b′).—L'acide azoxybenzène-2,2′-dicarboxylique se transforme par sublimation en la lactone de l'acide indazylbenzoïque. Sous 12 mm de mercure, lorsque la température du bain atteint 160°, l'acide ramollit, se gonfle et se solidifie de nouveau vers 200°. Il faut alors discontinuer l'opération et pulvériser la masse avant de continuer. Au-dessus de 280°, la sublimation se fait assez rapidement. À partir de 2.0 g de l'acide, on obtient 0.71 g de la lactone de l'acide 2-[3-oxy-indazyl-(2)]-benzoïque. Elle cristallise dans la 3-pentanone ou le β-éthoxy-éthanol en paillettes lustrées de couleur jaune pâle et fond à 292° (p.f. lit. 294° (16)). Calculé pour $C_{14}H_8O_2N_2$: C, 71.18%; H, 3.14%; N, 11.86%. Trouvé: C, 71.02%; H, 3.42%; N, 11.76%.

Acide 2-[3-oxy-indazyl-(2)]-benzoïque (VI) et acide azobenzène-2,2′-dicarboxylique (IV) (b_1′).—L'acide 2-[3-oxy-indazyl-(2)]-benzoïque est obtenu en faisant bouillir à reflux une suspension de 0.5 g de la lactone de l'acide 2-[3-oxy-indazyl-(2)]-benzoïque (obtenu précédemment par sublimation) dans 30 ml de soude 5 *N* et 30 ml d'éthanol. L'acide isolé (0.49 g) cristallise dans l'eau en lamelles blanches et fond à environ 285° après ramollissement vers 230° (p.f. lit. 230° (16)). De l'acide 2-[3-oxy-indazyl-(2)]-benzoïque (0.4 g) dissous dans la soude à 2% (40 ml) est oxydé par l'acide nitrique concentré (40 ml), comme il est décrit précédemment pour l'acide 4,4′-dichloroazobenzène-2,2′-dicarboxylique. L'acide azobenzène-2,2′-dicarboxylique obtenu cristallise dans l'eau et fond à 237° avec décomposition.

II. Réaction avec le nitrobenzène

Un mélange de 20.0 g de nitrobenzène, de 60.0 g de cyanure de potassium et de 200 ml de glycol à 90% est bouilli à reflux pendant 3 heures et abandonné à la température ambiante pendant 15 heures. En diluant avec de l'eau à environ 3000 ml, tout comme

dans le cas de la réaction avec le *p*-chloronitrobenzène, on obtient un solide neutre A′ jaune-verdâtre et un filtrat A′.

L'acide benzoïque (20% de la théorie) est extrait du filtrat A′ en procédant exactement tel que décrit précédemment pour l'acide *m*-chlorobenzoïque. Le résidu de l'extraction à la ligroïne (Eb = 65–110°) contient le produit acide B′.

Isolement et identification du produit acide B′

Le solide B′, obtenu précédemment après l'extraction de l'acide benzoïque à la ligroïne, ne se sublime qu'au-delà de 250°, sous 12 mm de mercure. Le sublimé ne correspond pas à la lactone de l'acide 2-[3-oxy-indazyl-(2)]-benzoïque, mais bien au 6-cétoquinazolo-[1,2,2′,3′]-indazol.[3] En effet, cristallisé dans l'acide acétique, il fond à 334–336°. Un point de fusion mixte de cette substance et du composé k_1' (le produit d'hydrolyse d'une substance k', un produit neutre de la réaction) n'est pas abaissé. Calculé pour $C_{14}H_9ON_3$: C, 71.48%; H, 3.85%; N, 17.86%. Trouvé: C, 71.39%; H, 4.14%; N, 17.78%.

REMERCIEMENTS

Nous remercions le Conseil national de Recherches du Canada, les firmes C.I.L. et Shell Oil, ainsi que l'Office de Recherches scientifiques de la Province de Québec pour des bourses d'études accordées à l'un de nous (E. C.).

BIBLIOGRAPHIE

1. V. von Richter. Ber. **4**, 21 (1871).
2. V. von Richter. Ber. **4**, 459 (1874).
3. V. von Richter. Ber. **7**, 1145 (1874).
4. P. Griess. Ber. **5**, 192 (1872).
5. W. Korner. Gazz. chim. ital. 306 (1874).
6. V. von Richter. Ber. **8**, 1418 (1875).
7. A. F. Holleman. Rec. trav. chim. **24**, 194 (1905).
8. J. F. Bunnett, J. F. Cormack et F. C. McKay. J. Org. Chem. **15**, 481 (1950).
9. J. F. Bunnett, M. M. Rauhut, D. Kutson et G. E. Bussell. J. Am. Chem. Soc. **76**, 5755 (1954).
10. J. F. Bunnett et M. M. Rauhut. J. Org. Chem. **21**, 934 (1956).
11. B. Migrdichian. The chemistry of cyanogen compounds. Reinhold Publishing Corp., New York. 1947. p. 38.
12. M. M. Rauhut et J. F. Bunnett. J. Org. Chem. **21**, 939 (1956).
13. P. Griess. Ber. **7**, 1609 (1874).
14. P. Freundler. Bull. soc. chim. France, **32** (3), 449 (1904).
15. P. Carré. Bull. soc. chim. France, **33** (3), 1161 (1905).
16. P. Carré. Bull. soc. chim. France, **35** (3), 1275 (1906).
17. P. Freundler. Bull. soc. chim. France, **31** (3), 862 (1904).
18. G. Heller. Ber. **49**, 523 (1916).
19. S. Reich et W. Merki. Bull. soc. chim. France, **21** (4), 8 (1917).
20. W. L. Mosby. Chem. & Ind. (London), 17 (1957).
21. F. C. Cooper et M. W. Partridge. J. Chem. Soc. 3429 (1954).
22. M. M. Endicott, B. W. Alden et M. L. Sherrill. J. Am. Chem. Soc. **68**, 1303 (1946).
23. P. Freundler. Bull. soc. chim. France, **9** (4), 605 (1911).
24. H. W. Galbraith, E. F. Degering et E. F. Hitch. J. Am. Chem. Soc. **73**, 1323 (1951).
25. S. E. Hazlet et C. A. Dornfeld. J. Am. Chem. Soc. **66**, 1781 (1944).

Can. J. Chem. Downloaded from www.nrcresearchpress.com by 210.87.254.105 on 09/05/12
For personal use only.

Can. J. Chem. Downloaded from www.nrcresearchpress.com by 210.87.254.40 on 09/05/12
For personal use only.

CONTRIBUTION À L'ÉTUDE DE LA RÉACTION DE VON RICHTER

II. SUR L'IDENTIFICATION DE PRODUITS NEUTRES[1]

E. CULLEN[2] ET PH. L'ÉCUYER

RÉSUMÉ

La réaction de von Richter fournit, en plus de produits acides, des composés neutres. Avec le *p*-chloronitrobenzène, elle donne le 3,8-dichloro-6-iminoquinazolo[1,2,2′,3′]indazol et le 4,4′-dichloro-2-carbamylazoxybenzène, et avec le nitrobenzène, le 6-iminoquinazolo[1,2,2′,3′]-indazol.

La réaction de von Richter fournit, outre l'acide attendu, des produits neutres et des produits acides. Nous avons décrit précédemment (1) deux de ces derniers formés par la réduction du groupement nitré. Dans le présent mémoire nous décrivons trois produits neutres. Deux proviennent de la réaction avec le *p*-chloronitrobenzène et l'autre, de la réaction avec le nitrobenzène. En extrayant à la butanone les produits bruts neutres (A), essorés après la réaction avec le *p*-chloronitrobenzène, nous avons isolé trois substances, *k*, *m* et *n* (cette dernière en traces seulement), fondant respectivement à 306, 422 et 228–229°. L'extraction du filtrat (A) fournit même des traces d'un quatrième composé de point de fusion 164°.

La substance *k* est insoluble dans les bases et les acides dilués, mais se dissout dans l'acide sulfurique concentré. Elle est presque insoluble dans l'éther et peu soluble dans les autres solvants organiques usuels. En solution dans l'éthanol ou la butanone elle exhibe une forte fluorescence jaune-verdâtre. Son analyse élémentaire et la détermination de son poids moléculaire ont permis de déduire la formule empirique $C_{14}H_8N_4Cl_2$. Elle forme un chlorhydrate, $C_{14}H_8N_4Cl_2 \cdot HCl$, qui fond avec décomposition à 300–310°, et un dérivé acétylé, $C_{16}H_{10}ON_4Cl_2 \cdot \frac{1}{2}(CH_3CO)_2O$, de point de fusion de 260–261°.

Cette substance *k* est hydrolysée par l'acide chlorhydrique concentré en solution acétique et saponifiée par les bases inorganiques dans le glycol en libérant de l'ammoniac. Son produit d'hydrolyse (k_1) est insoluble dans les bases et les acides dilués, presque insoluble dans les solvants organiques, mais soluble à chaud dans les acides concentrés et la potasse alcoolique. Une fois sublimé, il fond à 378–380°. Son analyse centésimale correspond à la formule brute $C_{14}H_7ON_3Cl_2$. Il forme un sel de potassium $C_{14}H_6N_3Cl_2OK \cdot 2H_2O$, fondant à 420–422° (cristallisé dans l'eau), ou $C_{14}H_6N_3Cl_2OK \cdot H_2O$, de point de fusion 410° (cristallisé dans l'isopropanol), un sel de baryum, $(C_{14}H_6N_3Cl_2O)_2Ba \cdot 4H_2O$, et un éther méthylique, $C_{14}H_6N_3Cl_2OCH_3$, de point de fusion de 278–279°, mais pas de dérivé acétylé.

Les deux composés, *k* et k_1, donnent les tests des amines secondaires et des amides secondaires. Que le produit d'hydrolyse k_1 possède une fonction amide secondaire semble de plus confirmé par le fait qu'il forme une N-nitrozolactame dont l'hydrolyse donne le composé $C_{14}H_8O_3N_4Cl_2$ de point de fusion de 418–420°.

Le spectre infrarouge de la substance *k* indique une fonction imine (absorption à 3325 et 1650 cm^{-1}) et celui de la substance k_1, une fonction carbonyle (absorption à 1670 cm^{-1}), mais aucune vibration définie attribuable au groupe hydroxyle dans la région de 3500 cm^{-1}. Il est évident que c'est la fonction imine de la substance *k* qui est acétylée;

[1]*Manuscrit reçu le 21 septembre 1960.*
Contribution du Département de Chimie, Faculté des Sciences, Université Laval, Québec, Qué.
[2]*Bénéficiaire de bourses d'études accordées par le Conseil national de Recherches du Canada, les firmes C.I.L. et Shell Oil et l'Office de Recherches scientifiques de la Province de Québec.*

car, après l'élimination de cette fonction par hydrolyse, l'acétylation n'est plus possible.

La substance *k* n'est pas réduite par le fer activé, l'hydrogène en présence de palladium, ou l'hydrure de lithium et d'aluminium. Le composé *k* ou son dérivé acétylé est décomposé par l'acide chromique ou le permanganate neutre ou alcalin; mais il fournit, tout comme son produit d'hydrolyse k_1, des composés définis, lorsqu' ils sont traités par le peroxyde d'hydrogène à 95% et l'acide perchlorique en milieu acétique. Dans le premier cas, la substance obtenue fond à 252–254° et a la formule brute $C_{14}H_8O_2N_4Cl_2$. Dans le second, le composé formé, de point de fusion de 266°, a la formule empirique $C_{14}H_7O_3N_3Cl_2$.

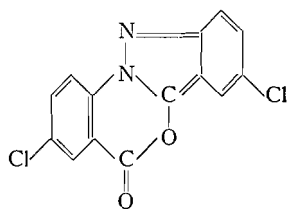
Ces deux produits d'oxydation, qui possèdent deux atomes d'oxygène de plus que les composés de départ, libèrent de l'iode dans une solution d'iodure de potassium à 10%. Ils se comportent comme des oxydes d'amines et seraient formés par l'oxydation de deux atomes d'azote tertiaire, laissant intactes la fonction amidine de la substance *k* et la fonction amide du composé k_1; car, ils peuvent encore réagir avec les nitrites.

Par analogie avec la lactone de l'acide 5-chloro-2-[5-chloro-3-oxy-indazyl-(2)]-benzoïque (I) (1), nous suggérons la structure II pour la substance *k*, et la formule III pour son produit d'hydrolyse k_1.

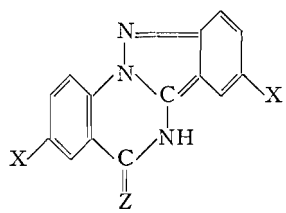
Nous avons aussi isolé parmi les produits neutres de la réaction de von Richter avec le nitrobenzène une substance *k'*, $C_{14}H_{10}N_4$, de point de fusion de 222–223°, analogue à la substance *k*. Par hydrolyse elle fournit un composé k_1', $C_{14}H_9ON_3$, analogue au composé k_1.

Ces deux substances, *k'* et k_1', sont relativement plus solubles dans les solvants organiques que leurs analogues chlorés, mais elles possèdent les mêmes propriétés chimiques et caractéristiques physiques. Ainsi, leurs solutions alcooliques montrent une forte fluorescence en lumière ultraviolette et les vibrations imine et carbonyle, qui apparaissent respectivement dans le spectre infrarouge des substances *k* et k_1, se retrouvent aussi dans celui des composés *k'* et k_1'. Nous suggérons les structures respectives IV et V pour ces substances *k'* et k_1'.

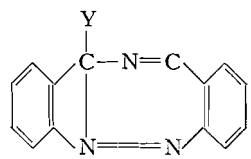
La substance *k'* semble identique à celle que Pinnow et Müller (2) ont isolée parmi les produits de la réduction de l'*o*-nitrobenzonitrile et qui, d'après eux, serait la diphénylaminopyrodiazoline (VI). Les deux ont le même point de fusion, donnent le même chlorhydrate, le même dérivé acétylé, le même dérivé benzoylé et le même produit d'hydrolyse (VII, d'après Pinnow et Müller).



(I)



(II) X = Cl; Z = NH
(III) X = Cl; Z = O
(IV) X = H; Z = NH
(V) X = H; Z = O

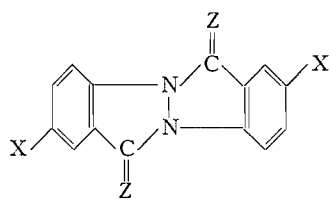


(VI) Y = NH_2
(VII) Y = OH

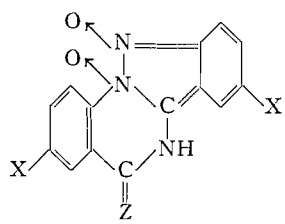
À notre avis, les structures VI et VII proposées par Pinnow et Müller sont inacceptables; les tests indiquent la présence d'une fonction amidine, mais non celle d'une fonction amine primaire dans la molécule de la substance *k'*. D'ailleurs, les spectres infrarouges des substances *k* et *k'* excluent la présence d'une fonction amine primaire et

Can. J. Chem. Downloaded from www.nrcresearchpress.com by 210.87.254.40 on 09/05/12
For personal use only.

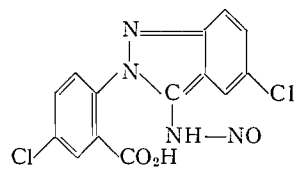
ceux de leurs produits d'hydrolyse, k_1 et k_1', celle d'un groupe hydroxyle. Il semble aussi impossible d'attribuer la structure VIII à la substance k; car, si celle-ci possédait cette formule, elle aurait donné la dilactame correspondante IX, au lieu de la lactame que nous avons obtenue par hydrolyse. Nous proposons donc respectivement pour la substance k' et son produit d'hydrolyse k_1' les structures IV et V qui rendent bien compte de leurs spectres infrarouges et de leurs propriétés chimiques.



(VIII) X = Cl; Z = NH
(IX) X = Cl; Z = O



(X) X = Cl; Z = NH
(XI) X = Cl; Z = O



(XII)

Les substances k et k' seraient donc le 3,8-dichloro-6-iminoquinazolo[1,2,2',3']indazol (II) et le 6-iminoquinazolo[1,2,2',3']indazol (IV), et leurs produits d'hydrolyse, k_1 et k_1', le 3,8-dichloro-6-cétoquinazolo[1,2,2',3']indazol (III), et le 6-cétoquinazolo[1,2,2',3']-indazol (V).

Ajoutons que le comportement des deux substances, k et k', vis-à-vis de l'oxydation et de la réduction ressemble à celui de l'indazol lui-même (3). C'est d'ailleurs aussi fort probablement à la présence du squelette de l'indazole qu'il faut attribuer la formation d'un produit rouge sous l'action de l'acide nitrique sur le composé d'hydrolyse k_1 (réaction de Knorr (4)). De plus, il est connu que la 2,4-dicétotétrahydroquinazoline se forme facilement par chauffage de l'acide *o*-uraminobenzoïque dans la soude concentrée (5), qu'elle se sublime à haute température et forme des sels de sodium hydratés tout comme le composé k_1.

Les structures X et XI semblent acceptables pour les produits d'oxydation, $C_{14}H_8O_2N_4Cl_2$ et $C_{14}H_7O_3N_3Cl_2$, de la substance k et de son produit d'hydrolyse k_1.

La substance $C_{14}H_8O_3N_4Cl_2$, qui est obtenue par nitrosation du produit d'hydrolyse k_1, pourrait avoir la structure XII, ce qui expliquerait sa solubilité dans la soude et ses caractéristiques d'amine secondaire. Son spectre infrarouge présente une forte vibration carbonyle à 1700 cm^{-1}, alors que la large bande entre 3200 et 2700 cm^{-1} du spectre du composé k_1 est absente. Ceci laisse entendre que l'hydrogène de la fonction amine est vraiment substitué.

Enfin, l'allure identique de la courbe d'absorption de la substance k' et de celle de la lactone de l'acide 5-chloro-2-[5-chloro-3-oxy-indazyl-(2)]-benzoïque (I) dans l'ultraviolet est conforme à la structure IV.

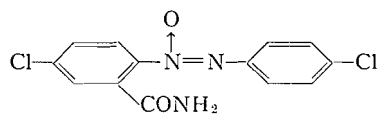
Il ne fait aucun doute que l'intermédiaire de la substance k est un produit de réduction du *p*-chloronitrobenzène, puisqu'une substance identique au produit non-chloré k' a été isolé par Pinnow et Müller (2) par réduction de l'*o*-nitrobenzonitrile. Toutefois, il est très peu probable que le nitrile soit un intermédiaire de la réaction de von Richter; car, après avoir fait bouillir pendant 20 heures une solution alcoolique de 2-nitro-5-chlorobenzonitrile dans les conditions de la réaction, nous n'avons pas obtenu le 3,8-dichloro-6-iminoquinazolo[1,2,2',3']indazol (II).

Can. J. Chem. Downloaded from www.nrcresearchpress.com by 210.87.254.40 on 09/05/12
For personal use only.

Can. J. Chem. Downloaded from www.nrcresearchpress.com by 210.87.254.40 on 09/05/12
For personal use only.

Nous avons alors voulu vérifier si la substance *k'* pouvait être produite par la transformation du 2,2'-dicyanohydrazobenzène; il est, en effet, connu que l'acide hydrazobenzène-2,2'-dicarboxylique peut être transformé en la lactone de l'acide 2-[3-oxyindazyl-(2)]-benzoïque (6). En conséquence, nous avons traité le 2,2'-dicyanoazoxybenzène dans les conditions de la réaction de von Richter, et nous avons obtenu, probablement par l'intermédiaire du composé hydrazoïque, le 6-iminoquinazolo[1,2,2',3']-indazol (IV), comme l'ont confirmé un point de fusion mixte et les spectres infrarouges.

Le composé *n*, p.f. 228–229°, a la formule brute $C_{13}H_9O_2N_3Cl_2$. Il est insoluble dans les acides et les alcalis dilués et très peu soluble dans l'éther. Il donne le test du groupe azoxyque et celui des amides. Son spectre infrarouge ne montre aucune vibration nitrile, mais des bandes d'absorption correspondant à la déformation de valence d'une fonction amide secondaire. D'autre part, la seule bande d'absorption de son spectre ultraviolet indiquerait la fonction azoxyque (7). Ces données font croire que la substance *n* est le 4,4'-dichloro-2-carbamylazoxybenzène (XIII).



(XIII)

PARTIE EXPÉRIMENTALE[3]

Trois substances, *k*, *m* et *n*, peuvent être isolées du mélange de produits neutres (A) qui sont essorés une fois la réaction de von Richter avec le *p*-chloronitrobenzène terminée (1).

$(C_{30}H_{20}O_2N_{10}Cl_4)_n$ *(m)*

Le résidu (environ 2%), obtenu après l'extraction du solide neutre (A) à la butanone dans un Soxhlet, cristallise dans la N,N-diméthylformamide en aiguilles jaunes de point de fusion de 422–423°. Calculé pour $(C_{30}H_{20}O_2N_{10}Cl_4)_n$: C, 51.65%; H, 2.90%; N, 20.17%; Cl, 20.02%. Trouvé: C, 51.45%; H, 2.84%; N, 19.79%; Cl, 20.00%. Spectre ultraviolet: max $\lambda m\mu$ 234 (ϵ 38,800); $\lambda m\mu$ 245 (ϵ 38,200); $\lambda m\mu$ 315 (ϵ 11,560); $\lambda m\mu$ 420 (ϵ 4,400). Les valeurs de ϵ sont calculées pour $n = 1$.

3,8-Dichloro-6-iminoquinazolo[1,2,2',3']indazol (k) (II)

L'extrait du solide (A) à la butanone est d'abord refroidi à 0°, puis porté à environ 50° et filtré, pour éliminer les dernières traces de la substance *m*. En refroidissant le filtrat, le 3,8-dichloro-6-iminoquinazolo[1,2,2',3']indazol (environ 60–70% du solide (A)) cristallise sous forme de lamelles lustrées et transparentes de couleur jaune-verdâtre. Après deux cristallisations dans la butanone la substance fond à 306°. Calculé pour $C_{14}H_8N_4Cl_2$: C, 55.46%; H, 2.66%; N, 18.48%. Trouvé: C, 55.27%; H, 2.42%; N, 18.32%. Dans l'isopropanol elle cristallise en longues aiguilles transparentes, p.f. 307°, qui contiennent une demi-molécule de solvant de cristallisation. Calculé pour $C_{14}H_8N_4Cl_2 \cdot \frac{1}{2}C_3H_8O$: C, 55.86%; H, 3.63%; N, 16.82%; Cl, 21.28%; O, 2.40%. Trouvé: C, 55.46%; H, 3.48%; N, 16.90%; Cl, 20.82%; O, 2.36%. Spectre infrarouge: 1650, 3325 (=NH), 3150 cm^{-1} (—NH— associé).

[3]*Les points de fusion (p.f.) ont été pris en tubes capillaires et ne sont pas corrigés. Les spectres ultraviolets ont été déterminés au moyen d'un spectromètre Beckman DU, en solution dans l'éthanol, et les spectres infrarouges, à l'aide d'un spectromètre Beckman IR-4; les solides étaient mélangés à du bromure de potassium et pressés; seules les bandes servant à l'identification des composés sont indiquées; les valeurs en cm^{-1} correspondent au maximum d'absorption, sauf celles qui correspondent au groupe* =CO—NH— *des amides secondaires qui montrent la région entière de l'absorption. Les microanalyses ont été effectuées par M. W. Manser, Zürich, Suisse.*

Can. J. Chem. Downloaded from www.nrcresearchpress.com by 210.87.254.40 on 09/05/12
For personal use only.

La solution éthérée de l'indazol II traitée à l'acide chlorhydrique gazeux forme facilement un chlorhydrate blanc, qui jaunit rapidement et fond avec décomposition entre 300 et 310°. Calculé pour $C_{14}H_8N_4Cl_2 \cdot HCl$: Cl, 30.77%. Trouvé: Cl, 29.50%. Spectre infrarouge: 1662 (NH·HCl), 2440 à 3050 cm^{-1} (déplacement et élargissement) (8).

Le dérivé acétylé de l'indazol II est obtenu en faisant bouillir 50 mg de l'indazol dans 25 ml d'acide acétique, 0.5 ml de pyridine et 1 ml d'anhydride acétique et en cristallisant le produit dans l'acide acétique et ensuite le xylène. Il contient une demi-molécule d'anhydride acétique de cristallisation et fond à 260–261°. Calculé pour $C_{16}H_{10}ON_4Cl_2 \cdot \frac{1}{2}C_4H_6O_3$: C, 54.57%; H, 3.30%; N, 14.14%. Trouvé: C, 54.99%; H, 3.07%; N, 14.28%.

3,8-Dichloro-6-cétoquinazolo[1,2,2′,3′]indazol (k_1) (III)

On chauffe à reflux 0.522 g de 3,8-dichloro-6-iminoquinazolo[1,2,2′,3′]indazol et 1 g d'hydroxyde de potassium dans 20 ml de glycol. Durant l'ébullition il se dégage de l'ammoniac. La solution prend d'abord une teinte rouge et tourne rapidement au jaune-vert pâle. La réaction terminée, on refroidit la solution, la dilue par l'eau à environ 100 ml, l'acidifie à l'acide acétique ou chlorhydrique et l'abandonne à la température ambiante pendant 12 heures. On filtre ensuite le solide, le lave abondamment à l'eau et le sèche sous-vide. Le 3, 8-dichloro-6-cétoquinazolo[1,2,2′,3′]indazol (0.434 g) cristallise dans la N,N-diméthylformamide et fournit 0.315 g d'aiguilles jaunes de point de fusion de 382° qui contiennent une demi-molécule de solvant de cristallisation. Calculé pour $C_{14}H_7ON_3Cl_2 \cdot \frac{1}{2}HCON(CH_3)_2$: C, 54.81%; H, 2.82%; N, 14.43%; Cl, 20.88%. Trouvé: C, 55.13%; H, 2.79%; N, 13.99%; Cl, 21.10%.

Lorsqu'on purifie le produit brut par sublimation, on obtient, sous 12 mm de mercure entre 250 et 350°, un sublimé jaune pâle fondant à 378–380°. Calculé pour $C_{14}H_7ON_3Cl_2$: C, 55.28%; H, 2.32%; O, 5.26%; N, 13.82%; Cl, 23.32%. Trouvé: C, 55.18%; H, 2.28%; O, 5.60%; N, 13.85%; Cl, 23.22%. Spectre infrarouge: 1670 (=CO), 2400–3200 cm^{-1} (=CO—NH— associé).

Le sel de potassium s'obtient lorsqu'on fait bouillir du 3,8-dichloro-6-cétoquinazolo-[1,2,2′,3′]indazol (100 mg) dans la potasse à 10% (15 ml). Après une demi-heure d'ébullition, on ajoute prudemment la quantité d'eau chaude requise pour rendre la solution limpide et on la laisse refroidir à la température ambiante. Le sel cristallise en fines aiguilles de point de fusion de 420–422° avec deux molécules d'eau. Calculé pour $C_{14}H_6ON_3Cl_2K \cdot 2H_2O$: C, 44.57%; H, 2.67%; N, 11.14%; Cl, 18.80%. Trouvé: C, 43.92%; H, 2.51%; N, 10.71%; Cl, 18.95%. Dans l'isopropanol ou la N,N-diméthylformamide le sel de potassium cristallise en aiguilles jaune pâle de point de fusion 410°. Calculé pour $C_{14}H_6ON_3Cl_2K \cdot H_2O$: C, 46.67%; H, 2.24%; N, 11.66%. Trouvé: C, 46.89%; H, 2.53%; N, 11.47%.

Le sel de baryum s'obtient en additionnant de l'eau de baryte à une solution de sel de potassium. Le sel de baryum précipite. Il est filtré, lavé à l'eau et séché. Il noircit vers 340°, mais ne fond pas au-dessous de 500°. Calculé pour $Ba(C_{14}H_6ON_3Cl_2)_2 \cdot 4H_2O$: C, 41.22%; H, 2.47%; N, 10.30%. Trouvé: C, 40.91%; H, 2.30%; N, 10.03%.

Ether méthylique du 3,8-dichloro-6-cétoquinazolo[1,2,2′,3′]indazol

Le 3,8-dichloro-6-cétoquinazolo[1,2,2′,3′]indazol (50 mg) est bouilli à reflux pendant une demi-heure dans 50 ml de potasse à 10%. Le sel de potassium précipite à la température ambiante. Il est dissous par addition d'eau et, sous agitation, est traité par un excès de sulfate de méthyle (1 ml). Un solide jaune pâle précipite presque immédiatement. Après un séjour de 6 heures à la température ambiante, il est essoré, lavé, séché et cristallisé successivement dans l'acide acétique et le xylène. L'éther méthylique du 3,8-dichloro-6-cétoquinazolo[1,2,2′,3′]indazol apparaît sous la forme d'aiguilles microscopiques de

point de fusion de 278–279°. Calculé pour $C_{15}H_9ON_3Cl_2$: C, 56.62%; H, 2.85%; N, 13.20%. Trouvé: C, 57.02%; H, 2.94%; N, 13.05%.

5-Chloro-3-nitrosamino-2-[4-chloro-2-carboxyphényl-(2)]indazol (XII)

Le 3,8-dichloro-6-cétoquinazolo[1,2,2′,3′]indazol (0.140 g) est dissous dans l'acide sulfurique à 70% (en volume) et la solution, sous agitation, est refroidie à 5°. À la suspension du sulfate, on ajoute goutte à goutte, tout en maintenant la solution à 10°, 2 ml d'une solution de nitrite de sodium à 20%. On laisse séjourner le mélange dans le bain glacé durant 2 heures, on décompose ensuite l'excès de nitrite par addition d'urée et dilue finalement le tout par l'eau à 50 ml. On essore, lave et sèche le précipité (0.146 g). Cristallisé successivement dans la N,N-diméthylformamide et l'acide acétique, le 5-chloro-3-nitrosamino-2-[4-chloro-2-carboxyphényl-(2)]indazol forme des aiguilles jaunes de point de fusion de 418–420°. Calculé pour $C_{14}H_8O_3N_4Cl_2$: C, 47.88%; H, 2.30%; N, 15.96%. Trouvé: C, 48.18%; H, 1.97%; N, 15.81%. Spectre infrarouge: 1680 cm^{-1} (—COOH).

3,8-Dichloro-6-imino-11,12-dioxoquinazolo[1,2,2′,3′]indazol (X)

On dissout 0.536 g de 3,8-dichloro-6-iminoquinazolo[1,2,2′,3′]indazol dans 60 ml d'acide acétique glacial, et, tout en maintenant la température de la solution au-dessous de 20°, on ajoute 1.5 ml d'acide perchlorique à 60% et ensuite 1.5 ml de peroxyde d'hydrogène à 95%. On chauffe à reflux jusqu'à ce que soit disparue la coloration rouge qui apparaît au début de l'ébullition, ce qui exige environ une demi-heure. La solution est alors refroidie, diluée par l'eau à environ 175 ml et alcalinisée par la soude diluée. Le 3,8-dichloro-6-imino-11,12-dioxoquinazolo[1,2,2′,3′]indazol (0.134 g) jaune pâle précipite dès que le pH atteint la valeur de 3 à 4. Recristallisé deux fois dans le xylène, il se présente sous forme d'aiguilles crèmes de point de fusion de 252–254°. Calculé pour $C_{14}H_8O_2N_4Cl_2$: C, 50.14%; H, 2.40%; N, 16.72%. Trouvé: C, 50.16%; H, 2.45%; N, 16.44%.

3,8-Dichloro-6-céto-11,12-dioxoquinazolo[1,2,2′,3′]indazol (XI)

À une suspension de 0.310 g de 3,8-dichloro-6-cétoquinazolo[1,2,2′,3′]indazol dans 75 ml d'acide acétique, on ajoute à la température ambiante 1.5 ml d'acide perchlorique et 1.5 ml de peroxyde d'hydrogène à 95%. Après $1\frac{1}{2}$ heure d'ébullition à reflux, la solution est refroidie et diluée par l'eau. La solution colloïdale, qui apparaît d'abord, se coagule après quelque temps en un solide jaune (0.110 g). Celui-ci est essoré et sublimé entre 150 et 250° sous 12 mm de mercure. On recueille le 3,8-dichloro-6-céto-11,12-dioxoquinazolo[1,2,2′,3′]indazol qui fond à 250–252°, puis se solidifie et fond de nouveau à 266°. Calculé pour $C_{14}H_7O_3N_3Cl_2$: C, 49.87%; H, 2.39%; N, 12.46%. Trouvé: C, 49.97%; H, 2.42%; N, 12.29%.

4,4′-Dichloro-2-carbamylazoxybenzène (XIII)

En évaporant à siccité les filtrats provenant de la cristallisation du 3,8-dichloro-6-iminoquinazolo[1,2,2′,3′]indazol, la substance *k* décrite précédemment, et en cristallisant le résidu successivement dans divers solvants tels que l'acide acétique, l'éthanol et le 2-chloroéthanol, on parvient à isoler une troisième substance (*n*). Pour obtenir le 4,4′-dichloro-2-carbamylazoxybenzène à l'état pur, il faut le traiter à chaud par la soude alcoolique diluée, l'essorer, le laver à l'eau et le recristalliser dans l'acide acétique dans lequel il forme des aiguilles crèmes fondant à 228–229°. Calculé pour $C_{13}H_9O_2Cl_2$: C, 50.34%; H, 2.92%; N, 13.55%. Trouvé: C, 50.33%; H, 2.87%; N, 13.56%. Spectre ultraviolet: max $\lambda m\mu$ 335 (ϵ 20,800). Spectre infrarouge: 1680 (=CO), 3150 et 3400 cm^{-1} (—$CONH_2$).

Can. J. Chem. Downloaded from www.nrcresearchpress.com by 210.87.254.40 on 09/05/12
For personal use only.

6-Iminoquinazolo[1,2,2′,3′]indazol (k′) (IV)

Le solide (A′), qui est obtenu à la suite de la réaction de von Richter avec le nitrobenzène (20 g) dans le glycol à 90% (200 ml) (1), cristallise dans l'éthanol en aiguilles (1.3 g) lustrées et transparentes de couleur jaune-verdâtre et de point de fusion de 222–223°. Toutefois, la plupart du temps, pour réussir à le purifier, il faut d'abord l'extraire à la butanone, évaporer l'extrait à siccité et cristalliser le résidu dans le même solvant. Calculé pour $C_{14}H_{10}N_4$: C, 71.77%; H, 4.30%; N, 23.92%. Trouvé: C, 71.72%; H, 4.41%; N, 23.78%. Spectre infrarouge: 1670 et 3310 (=NH), 3120 cm^{-1} (—NH—). Spectre ultraviolet: max $\lambda m\mu$ 236 (ϵ 56,800); $\lambda m\mu$ 300 (ϵ 18,800); $\lambda m\mu$ 375 (ϵ 9,500).

Le chlorhydrate du 6-iminoquinazolo[1,2,2′,3′]indazol s'obtient en dissolvant l'indazol IV dans l'acide chlorhydrique concentré à 60°. En laissant refroidir la solution à la température ambiante, le chlorhydrate cristallise. Il forme des cristaux jaunes de point de fusion de 279–280° (lit. 277° (2)).

Une solution de 2,2′-dicyanoazoxybenzène (1.0 g) et de cyanure de potassium (30.0 g) dans le glycol à 90% (100 ml) est bouillie à reflux pendant 3 heures, refroidie et diluée par l'eau (500 ml). Le précipité jaune-verdâtre (0.051 g), qui apparaît, est filtré, lavé, séché et extrait à la butanone. L'extrait est evaporé à siccité. Le résidu, cristallisé deux fois dans l'éthanol (noir animal), fournit des lamelles lustrées et transparentes de point de fusion de 221–222°. Un point de fusion mixte de cette substance et du 6-iminoquinazolo-[1,2,2′,3′]indazol obtenu précédemment n'est pas abaissé et les spectres infrarouges des deux composés sont identiques.

6-Cétoquinazolo[1,2,2′,3′]indazol (k_1′) (V)

Le 6-iminoquinazolo[1,2,2′,3′]indazol (0.500 g) est traité par l'hydroxyde de potassium dans le glycol (10 ml), comme il est décrit précédemment pour le 3,8-dichloro-6-céto-quinazolo[1,2,2′,3′]indazol. Le produit obtenu fournit par sublimation, à environ 280° sous 12 mm de mercure, un sublimé de 6-cétoquinazolo[1,2,2′,3′]indazol. Il cristallise dans l'acide acétique en aiguilles jaunes de point de fusion de 334–336°. Calculé pour $C_{14}H_9ON_3$: C, 71.48%; H, 3.85%; N, 17.86%. Trouvé: C, 71.55%; H, 3.85%; N, 17.94%. Spectre infrarouge: 1680 (=CO), 2500–3200 cm^{-1} (=C—NH— associé).

REMERCIEMENTS

Nous remercions le Conseil national de Recherches du Canada, les firmes C.I.L. et Shell Oil et l'Office de Recherches scientifiques de la Province de Québec pour des bourses d'études accordées à l'un de nous (E.C.).

BIBLIOGRAPHIE

1. E. Cullen et Ph. L'Écuyer. Can. J. Chem. **39**, 144 (1961).
2. J. Pinnow et E. Müller. Ber. **28**, 149 (1895).
3. P. Schad. Ber. **26**, 216 (1893).
4. L. Knorr. Ber. **26**, 100 (1893).
5. M. T. Bogert et G. Scatchard. J. Am. Chem. Soc. **41**, 2052 (1919).
6. P. Carré. Bull. soc. chim. France, **35** (3), 1275 (1906).
7. G. Costa. Gazz. chim. ital. **85**, 548 (1955).
8. J. C. Grivas et A. Taurins. Can. J. Chem. **37**, 60 (1959).

Can. J. Chem. Downloaded from www.nrcresearchpress.com by 210.87.254.40 on 09/05/12
For personal use only.

Can. J. Chem. Downloaded from www.nrcresearchpress.com by 210.87.254.42 on 09/05/12
For personal use only.

THE KINETICS AND MECHANISM OF THE Cu^{++}-CATALYZED REDUCTION OF Cr^{VI} BY HYDROGEN IN AQUEOUS SOLUTIONS[1]

E. A. Hahn and E. Peters

ABSTRACT

The kinetics of the Cu^{++}-catalyzed reduction of Cr^{VI} by H_2 in aqueous perchlorate solutions have been investigated between 160° and 200° C. The mechanism proposed to account for the kinetics gives rise to a rate law of the form

$$\frac{-d[H_2]}{dt} = \frac{k_1[Cu^{++}][H_2]\{(k_2/k_{-1})[Cu^{++}]+(k_3/k_{-1})[Cr^{VI}]\}}{[H^+]+(k_2/k_{-1})[Cu^{++}]+(k_3/k_{-1})[Cr^{VI}]},$$

where

$$k_1 = 5.3\times10^{10}\exp(-25{,}800/RT) \text{ liter mole}^{-1}\text{ sec}^{-1},$$
$$k_2/k_{-1} = 2.5\pm0.7 \quad \text{and} \quad (k_3/k_{-1}) = 48\pm10.$$

As a consequence of these studies an important anomaly between the previously published rate law for dichromate reduction and a more recent kinetic study of the cupric-perchlorate-catalyzed hydrogen–oxygen recombination has been resolved.

INTRODUCTION

The reduction of dichromate by hydrogen in aqueous cupric perchlorate solutions has been described previously by Peters and Halpern (1), who observed simple second-order kinetics in the temperature range 80° to 140° C, the reaction being zero-order in dichromate, first-order in hydrogen, and first-order in cupric perchlorate. It was noted that perchloric acid additions above .025 M retarded the rate slightly, and subsequent studies (2) showed that this acid effect, at concentrations up to 1.00 M $HClO_4$, could be incorporated into the rate law to yield the expression

$$[1] \qquad \frac{-3d[Cr_2O_7^{=}]}{dt} = \frac{-d[H_2]}{dt} = \frac{k_1[H_2][Cu^{++}]^2}{[Cu^{++}]+(k_{-1}/k_2)[H^+]},$$

where k_1, k_{-1}, and k_2 are rate constants applicable to the slow steps of the following reaction sequence:

$$Cu^{++} + H_2 \underset{k_{-1}}{\overset{k_1}{\rightleftharpoons}} CuH^+ + H^+, \qquad [2a]$$

$$CuH^+ + Cu^{++} \xrightarrow{k_2} 2Cu^+ + H^+, \qquad [2b]$$

$$2Cu^+ + Cr_2O_7^{=} \xrightarrow{\text{fast}} 2Cu^{++} + \text{products}. \qquad [2c]$$

The rate law predicts a simple second-order reaction at low H^+ concentrations, as previously observed, and a more complex reaction approaching second-order dependence in copper at high acidities, which was later verified (2). Subsequently, it was observed that the initial reduction kinetics for copper precipitation from perchlorate solutions by hydrogen (3) followed the same law at temperatures up to 160° C. In this case a disproportionation process replaces step [2c] above, i.e.

$$2Cu^+ \xrightarrow{\text{fast}} Cu^{++} + Cu^0. \qquad [2d]$$

The object of the present investigation was to determine the effect of higher temperatures on the dichromate reaction, which had not been studied above 140° C, in order

[1]*Manuscript received September 8, 1960.*
Contribution from the Department of Mining and Metallurgy, University of British Columbia, Vancouver, British Columbia.

to learn more about the reaction mechanism and in particular the rate constants k_{-1} and k_2. Because of the very strong temperature effect, which doubled the reaction rate for approximately every 10° C increase in temperature, the cupric perchlorate concentrations were lowered substantially, while the initial dichromate levels were raised from those used in previous investigations in order to obtain reaction times long enough for good rate measurements.

EXPERIMENTAL

The experiments were conducted in the 1-gallon titanium-lined autoclave described in connection with earlier investigations (1, 2, 3, 4, 5), using a similar procedure. Silicon carbide, about 240 mesh, was packed between the titanium liner and the stainless steel autoclave to provide a heat transfer medium, to replace water which had been used previously, but which was unsatisfactory at higher temperatures. Glass wool was packed above the silicon carbide powder to prevent contamination of the solution. By this arrangement the temperature was controlled to within ±0.3° C with a Leeds and Northrup Micromax controller–recorder.

The exit tube from the sampling valve consisted of 3 feet of titanium tubing in the form of a coil which was water-cooled to eliminate flashing of the samples when they were drawn from the autoclave at temperatures up to 200° C.

All chemicals used were of reagent grade, supplied by Baker and Adamson Limited. Stock solutions were prepared with distilled water. Cupric perchlorate was prepared from perchloric acid and cupric oxide. Commercial hydrogen gas, supplied in cylinders by Canadian Liquid Air Company, was used without further purification.

Two and one-half liters of solution of the desired composition were placed in the titanium liner of the autoclave, which was then sealed, flushed with nitrogen, and heated to the desired temperature. Experiments were performed at temperatures of 160°, 180°, and 200° C. Hydrogen was introduced after the autoclave had been maintained at the reaction temperature for an appreciable amount of time. Samples of the solution were withdrawn at intervals both before and after the addition of hydrogen, and analyzed to determine the course of the reaction. Dichromate determinations were made spectrophotometrically at the 350 mμ absorption peak, using a Beckman DU spectrophotometer. Copper was determined electrolytically, and free acid was titrated with sodium tetraborate solutions.

RESULTS AND DISCUSSION

Early in this investigation it was observed that the plots depicting the reduction of dichromate by hydrogen in the presence of cupric perchlorate were not straight lines, as found at lower temperatures, lower dichromate levels, and higher copper concentrations, by previous investigators (1, 2). Typical rate plots, shown in Fig. 1, indicate that the rate is dichromate dependent, and the extent of this dependence increases as the acidity is increased.

Rate measurements were made from these plots by measuring slopes at various dichromate levels.*

On the assumption that the kinetics of this reaction obeyed a rate law that bears some

**To make rate measurements, the best smooth curve was drawn through the points with a flexible curved ruler, and tangents were drawn by the mirror-image method. The measurements have a maximum precision near the mid-point of the curve of about ±5%, with the precision falling off at both ends, because of the scatter of experimental points.*

Can. J. Chem. Downloaded from www.nrcresearchpress.com by 210.87.254.42 on 09/05/12
For personal use only.

relation to equation 1, in spite of the partial dichromate dependence, the effect of varying the hydrogen ion concentration was studied. The reduction plots of one set of these experiments are presented in Fig. 1, and the inverse rates of these plots measured at several dichromate levels are shown in Fig. 2. The latter plots are seen to be straight lines, indicating that an inverse dependence of the rate on hydrogen ion concentration exists at all dichromate levels. In the same plot, the dichromate dependence appears to vanish at low hydrogen ion concentration.

A mechanism has been proposed that will account for all of these observations and involves a simple modification of mechanism [2]. The steps are:

$$Cu^{++} + H_2 \underset{k_{-1}}{\overset{k_1}{\rightleftharpoons}} CuH^+ + H^+, \qquad [3a]$$

$$CuH^+ + Cu^{++} \xrightarrow{k_2} 2Cu^+ + H^+, \qquad [3b]$$

$$CuH^+ + Cr^{VI} \xrightarrow{k_3} \text{intermediates} \xrightarrow{\text{fast}} Cu^{++} + \text{products}, \qquad [3c]$$

$$2Cu^+ + Cr^{VI} \xrightarrow{\text{fast}} 2Cu^{++} + \text{products}. \qquad [3d]$$

When this mechanism is subjected to the steady-state treatment in CuH^+, the following rate law is obtained:

$$[4] \qquad \frac{-3d[Cr_2O_7^{=}]}{dt} = \frac{-d[H_2]}{dt} = \frac{k_1[Cu^{++}][H_2]\{(k_2/k_{-1})[Cu^{++}]+(k_3/k_{-1})[Cr^{VI}]\}}{[H^+]+(k_2/k_{-1})[Cu^{++}]+(k_3/k_{-1})[Cr^{VI}]}.$$

The above expression can be inverted to give the function in H^+ that is plotted in Fig. 2. The intercept on this plot is seen to be

$$[5] \qquad I = \frac{1}{k_1[Cu^{++}][H_2]},$$

while the slope can be expressed as

$$[6] \qquad S = \frac{1}{k_1[Cu^{++}][H_2]\{(k_2/k_{-1})[Cu^{++}]+(k_3/k_{-1})[Cr^{VI}]\}}.$$

From equation 6, it is apparent that the reciprocals of the slopes in Fig. 2 should be linear in Cr^{VI}. This is demonstrated in Fig. 3, where the inverse slopes of the lines in Fig. 2, $1/S$, are plotted against Cr^{VI} for the three different temperatures. The equation representing these lines is obtained by inverting equation 6, i.e.,

$$[7] \qquad \frac{1}{S} = k_1[Cu^{++}][H_2]\{(k_2/k_{-1})[Cu^{++}]+(k_3/k_{-1})[Cr^{VI}]\}.$$

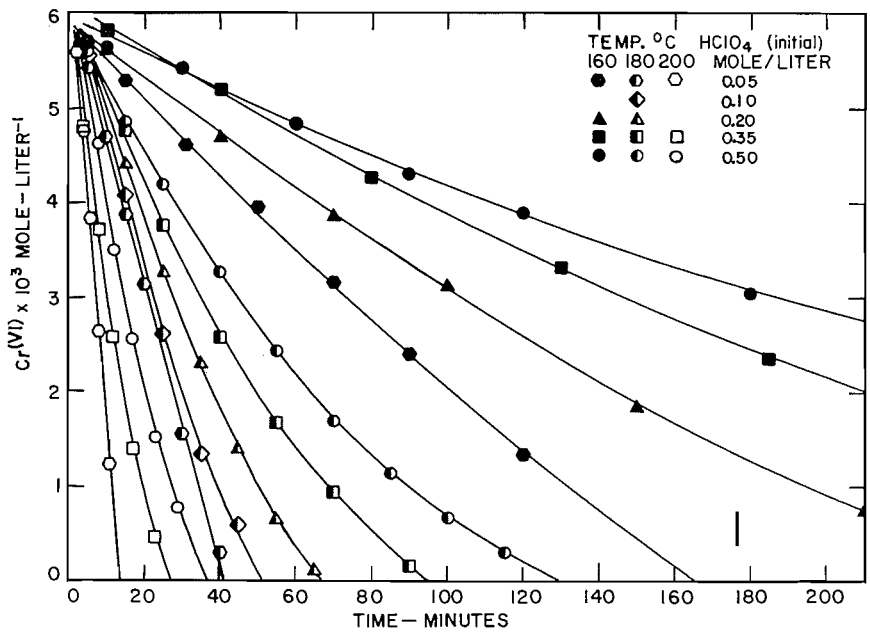
Thus it can be seen that the slopes of Fig. 3 represent the value of $k_1[Cu^{++}][H_2](k_3/k_{-1})$ and the intercepts represent the value $k_1[Cu^{++}][H_2](k_2/k_{-1})[Cu^{++}]$.

A further simplification can be obtained by dividing equation 7 through by $k_1[Cu^{++}][H_2]$ which is the value of the reaction rate extrapolated to zero hydrogen ion concentration, that is, the inverse intercept of Fig. 2, expressed by equation 5. The resulting expression is given by

$$[8] \qquad \frac{I}{S} = \frac{k_2}{k_{-1}}[Cu^{++}]+\frac{k_3}{k_{-1}}[Cr^{VI}].$$

Can. J. Chem. Downloaded from www.nrcresearchpress.com by 210.87.254.42 on 09/05/12
For personal use only.

Can. J. Chem. Downloaded from www.nrcresearchpress.com by 210.87.254.42 on 09/05/12
For personal use only.



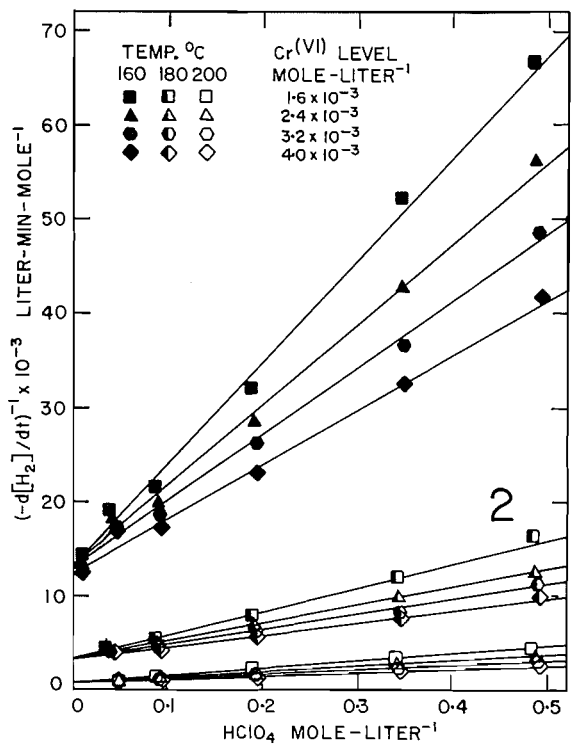


FIG. 1. Typical rate plots of the dichromate reduction by hydrogen: 10 atm H_2, 0.02 M $Cu(ClO_4)_2$.
FIG. 2. Dependence of 1/rate on H^+ concentration: 10 atm H_2, 0.02 M $Cu(ClO_4)_2$.

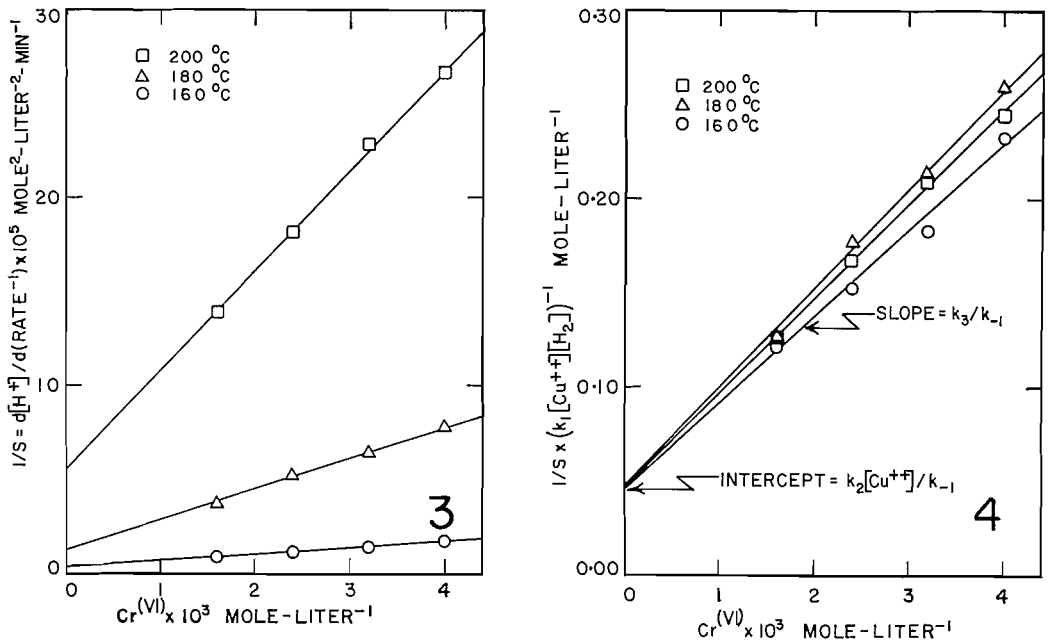


FIG. 3. Dependence of the function $d[H^+]/d(\text{rate}^{-1})$ on the dichromate level in solution.
FIG. 4. Dependence of the function $(d[H^+])/\{k_1[Cu^{++}][H_2]\times d(\text{rate}^{-1})\}$ on the dichromate level.

A plot of I/S vs. Cr^{VI} is given in Fig. 4, for the three temperatures that were studied. It can be seen that fairly straight lines are obtained and that the temperature dependence that appears so pronounced in Fig. 3 virtually disappears in Fig. 4. It can, therefore, be concluded that only k_1 is particularly temperature dependent and that k_2/k_{-1} and k_3/k_{-1} are relatively insensitive to temperatures in this region. Values of k_2/k_{-1} and k_3/k_{-1} that are obtained from the slopes and intercepts of Fig. 4 are listed in Table I, together with values of k_1 obtained from intercepts of Fig. 2.

TABLE I

Rate constants at various temperatures

Temperature, °C	k_1,* l. mole^{-1} sec^{-1}	k_2/k_{-1}	k_3/k_{-1}
110	9.5×10^{-5}†	3.85‡	—
160	$5.4\times10^{-3}\pm15\%$	$2.7\pm30\%$	$42\pm20\%$
180	$1.8\times10^{-2}\pm15\%$	$2.3\pm30\%$	$54\pm20\%$
200	$5.7\times10^{-2}\pm15\%$	$2.6\pm30\%$	$49\pm20\%$

*Obtained from intercepts in Fig. 2, using Cu^{++} = .02 mole/liter and new H_2 solubility data (6).
†Values at 110° C were obtained from reference 2.
‡Value of k_2/k_{-1} at 110° C is the reciprocal of the value for k_{-1}/k_2 (= 0.26) given in reference 2.

The temperature dependence of k_1 is depicted by means of an Arrhenius plot in Fig. 5. The activation energy of 25.8 kcal, obtained from the slope of this plot, is in excellent agreement with the value (26.6 kcal), obtained earlier (5). The rate constant k_1 is thus given by

[9] $$k_1 = 5.3\times10^{10}\exp(-25{,}800/RT) \text{ liter mole}^{-1}\text{ sec}^{-1}.$$

Can. J. Chem. Downloaded from www.nrcresearchpress.com by 210.87.254.42 on 09/05/12
For personal use only.

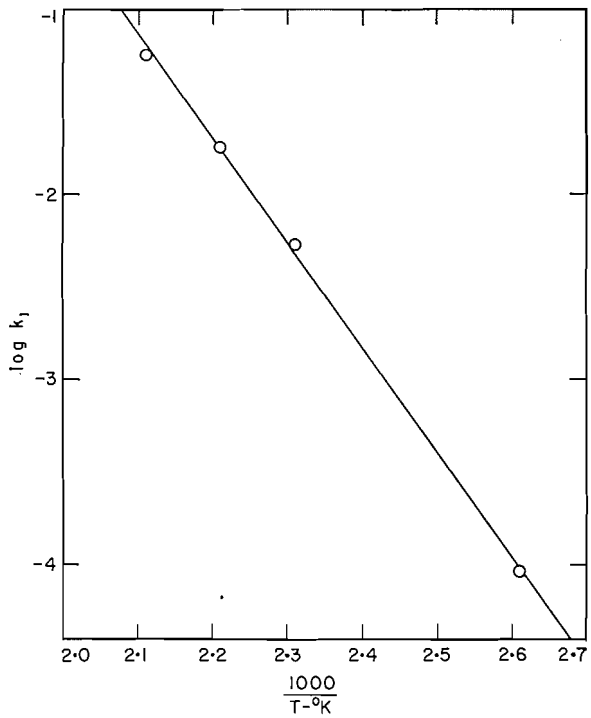


FIG. 5. Arrhenius plot of k_1: 0.02 M $Cu(ClO_4)_2$, 10 atm H_2.

The plots shown in Figs. 1–4 inclusive indicate that the data are consistent with the proposed mechanism [3], and the resulting rate law [4]. The data can be treated another way, by inverting equation 4 to obtain

$$[10] \qquad \frac{1}{R} = \frac{[H^+]}{R_0\{(k_2/k_{-1})[Cu^{++}]+(k_3/k_{-1})[Cr^{VI}]\}}+\frac{1}{R_0}$$

where R is the measured rate $= (-d[H_2])/dt$ and R_0 is the value of $k_1[Cu^{++}][H_2]$. Rearranging the above we obtain

$$[11] \qquad \frac{R[H^+]}{R_0-R} = \frac{k_2}{k_{-1}}[Cu^{++}]+\frac{k_3}{k_{-1}}[Cr^{VI}]$$

and a linear plot would be expected if the function $(R[H^+])/(R_0-R)$ were plotted against Cr^{VI}. The results of this type of a plot, using three of the 180° C experiments, are depicted in Fig. 6. There is a significant departure from linearity in both directions at higher Cr^{VI} levels. However, the rate measurements in this region are erratic because they are near the beginning of a run. The best results are obtained on this form of plot when using the highest acid experiments, since in this case the rate difference, R_0-R, is the largest value obtainable.

The significance of this reaction is that a process that is first-order in Cr^{VI} is competing with a forward reaction involving Cu^{++} and a back reaction involving H^+. The effects of these three species are interrelated through the three terms in the denominator of equation 4, and the dependence of the forward reaction on $[H^+]$, $[Cu^{++}]$, or $[Cr^{VI}]$ is a function of the relative values of these three terms. At low values of $[H^+]$ the equation

Can. J. Chem. Downloaded from www.nrcresearchpress.com by 210.87.254.42 on 09/05/12
For personal use only.

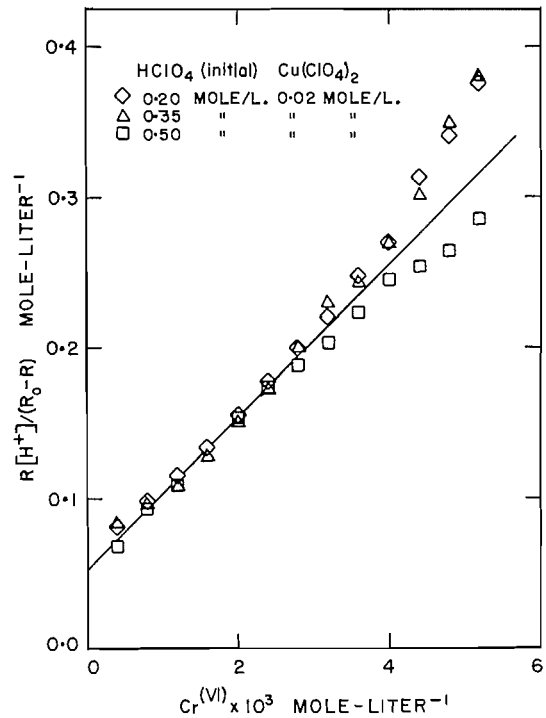


FIG. 6. Dependence of the function (rate$\times$[H$^+$])(k_1[Cu^{++}][H$_2$]$-$rate)$^{-1}$ on the dichromate level: 180° C.

reduces to a second-order reaction that is first-order in each of Cu^{++} and H$_2$. At high H$^+$ concentrations the reaction may be second-order in Cu^{++} and zero-order in Cr^{VI}, or first order in each of Cu^{++} and Cr^{VI}, depending on their relative concentrations.

Of interest here is a related reaction involving the recombination of hydrogen and oxygen in nuclear reactors, which is catalyzed by Cu^{++} ions. This reaction was studied in sulphate and in perchlorate solutions at temperatures in the 200° to 300° C range by McDuffie and co-workers (7). McDuffie found that at 250° C and in solutions containing up to .05 mole/liter free perchloric acid, the reaction was first-order in Cu^{++} and independent of acidity. He observed that this was inconsistent with the rate law expressed by equation 1 unless the value for k_{-1}/k_2 was far smaller than 0.26 as predicted by Peters and Halpern (1), because the value of [Cu^{++}] in McDuffie's work was very small, of the order of 0.002 mole/liter.

However, if oxygen, like Cr^{VI}, directly attacks the CuH$^+$ complex, the rate expression describing the oxygen–hydrogen recombination kinetics would resemble equation 4, with O$_2$ replacing Cr^{VI}. This mechanism would be written as follows:

$$Cu^{++} + H_2 \underset{k_{-1}}{\overset{k_1}{\rightleftharpoons}} CuH^+ + H^+, \qquad [12a]$$

$$CuH^+ + Cu^{++} \xrightarrow{k_2} 2Cu^+ + H^+, \qquad [12b]$$

$$CuH^+ + O_2 \xrightarrow{k_3'} \text{intermediates} \xrightarrow{\text{fast}} Cu^{++} + \text{products}, \qquad [12c]$$

$$2Cu^+ + O_2 \xrightarrow{\text{fast}} 2Cu^{++} + \text{products}. \qquad [12d]$$

Can. J. Chem. Downloaded from www.nrcresearchpress.com by 210.87.254.42 on 09/05/12
For personal use only.

The rate expression for this mechanism, obtained via the steady-state approximation in CuH^+, is

$$[13] \qquad \frac{-2d[O_2]}{dt} = \frac{-d[H_2]}{dt} = \frac{k_1[Cu^{++}][H_2]\{(k_2/k_{-1})[Cu^{++}]+(k_3'/k_{-1})[O_2]\}}{[H^+]+(k_2/k_{-1})[Cu^{++}]+(k_3'/k_{-1})[O_2]}.$$

The conditions under which McDuffie *et al.* examined the kinetics in perchlorate solutions were 250° C, .002 mole/liter Cu^{++}, up to .05 mole/liter H^+, and initial oxygen partial pressures of the order of 400 p.s.i. At this pressure, the application of known oxygen solubility data (8) yields a concentration of .076 mole/liter O_2.

Assuming the value of k_2/k_{-1} to be unchanged from the 200° C value of 2.6 the second term of the denominator of equation 13, $(k_2/k_{-1})[Cu^{++}]$, would have a value of .0052. The first denominator term $[H^+]$ would be .05 and, since McDuffie did not observe an acid dependence, this term must be small compared with the third term, $(k_3'/k_{-1})[O_2]$. This last term must have a value of at least 0.5 for the acid effect to be less than 10%. At .076 mole/liter O_2, this places the value of k_3'/k_{-1} at greater than 6.6. Such a large value is entirely reasonable in view of the large values of k_3/k_{-1} observed in the 160° to 200° C range in the present work when the oxidant is Cr^{VI} instead of O_2, even though there is no reason to assume that k_3' and k_3 must be equal.

A relatively surprising result of this study is that there is no significant temperature dependence of the rate constant ratios k_2/k_{-1} and k_3/k_{-1}. These ratios have not been determined with sufficient precision for accurate analysis, but it is clear that the activation energies of the three competing reactions involving the decomposition of CuH^+ do not differ by more than about 1.5 kcal/mole. This is not sufficient to account for the relatively large value of the rate constant ratio k_3/k_{-1}, which at a value of 48 would require an activation energy difference of 3.4 kcal in favor of the Cr^{VI} reaction, although it can account for the value of k_2/k_{-1}, which at 2.6 would require an activation energy difference of only 800 calories. It is therefore likely that activation entropy differences must be called upon to account completely for the differences in the rates by which CuH^+ is attacked by different oxidants.

CONCLUSIONS

The kinetics of dichromate reduction by hydrogen in aqueous cupric perchlorate solutions are more complex than previously noted (2) in that they show some dichromate dependence at low Cu^{++} and high Cr^{VI} levels. A mechanism involving the direct attack of the CuH^+ intermediate by both Cu^{++} and Cr^{VI}, followed by fast conversion of resulting intermediates to the stable final species, has been shown to be consistent with these results. The same form of attack of CuH^+ by O_2 in the hydrogen – oxygen recombination studies by McDuffie *et al.* (7) could account for the kinetics obtained by these workers who observed no acid dependence at 250° C in the cupric perchlorate system, such as would be expected if mechanism [2] is applied, where CuH^+ is attacked only by H^+ and Cu^{++}.

ACKNOWLEDGMENTS

This work was supported by a grant from the National Research Council of Canada, and in part by a Fellowship awarded to one of the authors (E. A. H.) from the Consolidated Mining and Smelting Company of Canada Limited, Trail, B.C.

Can. J. Chem. Downloaded from www.nrcresearchpress.com by 210.87.254.42 on 09/05/12
For personal use only.

REFERENCES

1. E. PETERS and J. HALPERN. J. Phys. Chem. **59**, 793 (1955).
2. J. HALPERN, E. R. MACGREGOR, and E. PETERS. J. Phys. Chem. **60**, 1455 (1956).
3. E. R. MACGREGOR and J. HALPERN. Trans. AIME, **212**, 244 (1958).
4. E. PETERS and J. HALPERN. Can. J. Chem. **33**, 356 (1955).
5. R. G. DAKERS and J. HALPERN. Can. J. Chem. **32**, 969 (1954).
6. R. T. MCANDREW and E. PETERS. To be published.
7. H. F. MCDUFFIE *et al.* J. Phys. Chem. **62**, 1030 (1958).
8. H. A. PRAY, C. E. SCHWEICHERT, and B. H. MINNICH. Ind. Eng. Chem. **44**, 1146 (1952).

Can. J. Chem. Downloaded from www.nrcresearchpress.com by 210.87.254.42 on 09/05/12
For personal use only.

Can. J. Chem. Downloaded from www.nrcresearchpress.com by 210.87.254.42 on 09/05/12
For personal use only.

THE INFRARED AND THE NEAR-ULTRAVIOLET ABSORPTION SPECTRA OF POLYPHENYL DERIVATIVES OF THE ELEMENTS OF GROUPS IV*b* AND V*b*[1]

C. N. R. Rao,[2] J. Ramachandran,[3] and A. Balasubramanian

ABSTRACT

The near-ultraviolet absorption spectra of polyphenyl derivatives of the IV*b* and V*b* elements have been studied in detail. In the case of the triphenyl derivatives of the V*b* elements, the unshared *p*-electrons on the central atoms interact strongly with the π-orbitals of the benzene rings. When the central atoms do not possess unshared electrons as in the case of the derivatives of the IV*b* and the pentavalent V*b* elements, there appears to be no such resonance interaction. The Hammett reactivity constants of the para- and meta-trityl, triphenylsilyl, and triphenylgermanyl groups are estimated to be close to zero. However, the reactivity constant of the triphenylsilyl group in the para position of phenol is estimated to be about 0.30. The infrared spectra of the phenyl derivatives of the IV*b* and V*b* elements show smooth trends due to mass effects of the central atoms, in the C=C skeletal, C—H out-of-plane, and other vibrations. The absorption frequencies which are assigned to the phosphorus–phenyl and silicon–phenyl bonds in the literature do not appear to be unique for these linkages.

INTRODUCTION

The preliminary results on the infrared and the near-ultraviolet absorption spectra of some polyphenyl derivatives of the IV*b* and V*b* elements have been published earlier by Rao *et al.* (1). In this communication, the spectroscopy of these systems has been reported and discussed in detail. In the case of the V*b* elements, the spectra of derivatives in which the central atoms possess and do not possess unshared *p*-electrons (i.e. derivatives of the atoms in their "trivalent" and "pentavalent" states respectively) have been studied. The ultraviolet and the infrared spectra of substituted tetraphenylmethane, tetraphenylsilicane, and tetraphenylgermanium have also been investigated in order to be able to estimate the reactivity and resonance parameters of these groups.

EXPERIMENTAL

All the polyphenyl derivatives of the IV*b* and V*b* elements (mentioned in Table I) were commercially available and they were further purified before use. The trityl, triphenylsilyl, and triphenylgermanyl benzene derivatives with functional groups were prepared by the methods reported by Benkeser *et al.* (2, 3, 4).

The ultraviolet absorption spectra were recorded using a Cary Model 11 recording spectrophotometer and a Hilger spectrophotometer, H700. All the solvents were fractionated before use.

The infrared spectra were recorded using a Baird-Atomic spectrometer (Model KM 1) and a Perkin–Elmer (Model 21) spectrometer, both with NaCl optics. The samples were prepared as mulls in Nujol or as solutions in chloroform. The relative intensities of the peaks have been recorded as follows: S, strong; M, medium; and W, weak. The carbonyl frequencies reported in Table III are correct to within 5 cm^{-1}.

[1]*Manuscript received April 11, 1960.*
Contribution from the Department of Inorganic and Physical Chemistry, Indian Institute of Science, Bangalore-12, India.
[2]*To whom all the correspondence should be addressed, at the Department of Inorganic and Physical Chemistry, Indian Institute of Science, Bangalore-12, India.*
[3]*Hormone Research Laboratory, University of California, Berkeley 4, California, U.S.A.*

Can. J. Chem. Downloaded from www.nrcresearchpress.com by 210.87.254.42 on 09/05/12
For personal use only.

RESULTS AND DISCUSSION

All the triphenyl derivatives of the V*b* elements show fairly strong bands in their ultraviolet spectra (Table I). Triphenylamine exhibits two bands at 228 and 297 mμ. By analogy with the assignments in aniline,* the lower wavelength band is probably the

TABLE I

The near-ultraviolet absorption spectra of polyphenyl derivatives of elements of groups IV*b* and V*b**

Compound	λ_{max}, mμ	Compound	λ_{max}, mμ	log ϵ_{max}	Compound	λ_{max}, mμ
$CH(C_6H_5)_3$	250, 256, 263, 270	$N(C_6H_5)_3$	228, 297	3.87, 4.41	$P(C_6H_5)_4Br$	257†, 263, 269, 277
$C(C_6H_5)_4$	253†, 262, 272	$P(C_6H_5)_3$	260	4.06	$As(C_6H_5)_4Cl$	256†, 260, 266, 273
$Si(C_6H_5)_4$	254, 260, 265, 271	$As(C_6H_5)_3$	248	4.12	$Sb(C_6H_5)_4Br$	252, 258, 263, 270
$Sn(C_6H_5)_4$	251, 258, 264, 269	$Sb(C_6H_5)_3$	255	4.09	$Sb(C_6H_5)_3Cl_2$	253, 258, 263, 270
$Pb(C_6H_5)_4$	250, 257, 263, 268†	$Bi(C_6H_5)_3$	253†, 281.5	3.63	$Bi(C_6H_5)_3Cl_2$	— — — —

*All the spectra in 95% ethanol. †Shoulder.

so-called "primary" benzenoid band or the *E*-band. The longer wavelength band at 297 mμ is the "secondary" band or the *B*-band. The other triphenyl derivatives of the V*b* elements (with the exception of triphenylbismuthine) show only one band in the near-ultraviolet region, which may be *tentatively* assigned to the *B*-band.†

The *B*-band of benzene ($\pi \rightarrow \pi^*$ transition around 260 mμ) shows vibrational fine structure. The absence of the vibrational structure in the *B*-bands of the triphenyl derivatives of the V*b* elements is probably due to the interaction of the non-bonded *p*-electrons on the central atoms with the π-orbitals of the benzene rings. Of course, one would imagine that the electrons are delocalized over the entire molecule (6). Further, there is a progressive increase in the *B*-band wavelength with the increase in the number of phenyl groups around the central atom. The *B*-bands of aniline, diphenylamine, and triphenylamine are found at 280, 285, and 297 mμ respectively. The phosphorus, arsenic, and antimony derivatives also show similar variations of the *B*-band. As Robertson and Matsen (5) have pointed out, the dissimilarity between the spectra of compounds $(C_6H_5)_2X$ and $(C_6H_5)XH$ is a measure of the resonance interaction of the phenyl groups and the central atom. In general, the results of the present investigation and the interpretations offered are in agreement with the earlier work (6, 7, 8).

Among the triphenyl derivatives of the V*b* elements, triphenylamine exhibits the *B*-band at the largest wavelength with the maximum intensity. This is understandable since nitrogen, being a first row element, will have greater tendency for double-bond formation. There is a marked decrease in the *B*-band wavelength and intensity, in the case of triphenylphosphine and a further decrease in triphenylarsine. In phosphorus, the 3*d*-shell is vacant, while in arsenic it is completely filled. While going from triphenylarsine to triphenylstibine and triphenylbismuthine, there is a progressive increase in the *B*-band wavelength (248, 256, and 280 mμ respectively). This is possibly due to the predominating influence of the decreasing ionization potential (9) of the central atom. Apparently, the similarity of the electronic structures of the inner shells in arsenic, antimony, and bismuth (all the three with filled *d*-shells) is responsible for exhibiting such a marked effect of the decreasing ionization potential on the absorption spectra. The importance of the

Aniline exhibits bands at 230 and 280 mμ. These have been labelled as "primary" and "secondary" bands by Doub and Vandenbelt (J. Am. Chem. Soc.* **69, *2714 (1947)); as E and B bands by Gillam and Stern (In Electronic absorption spectroscopy. Edward Arnold Ltd., London. 1957. p. 140).*

†Jaffe (6) makes a similar assignment. The discussion of the results will not be affected by any possible change in the assignment.

ionization potentials in determining bathochromic shifts has been pointed out earlier (10, 11). Triphenylbismuthine exhibits another band at 250 mμ which may represent the dissociation process.

The polyphenyl derivatives of the V*b* elements in their pentavalent state, in contrast to the triphenyl derivatives, show vibrational structure in their *B*-bands (Table I) similar to benzene itself. In Fig. 1, the spectra of triphenylstibine and triphenylstibonium-

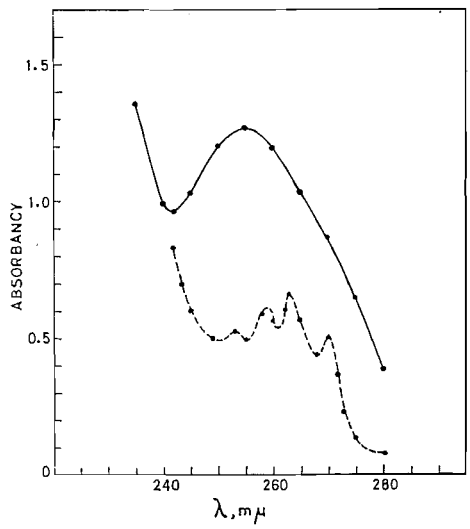


FIG. 1. Near-ultraviolet absorption spectra of triphenylstibine (——) and triphenylstiboniumdichloride (– – –) in ethanol.

dichloride are reproduced for purposes of comparison. The presence of the vibrational structure in the *B*-bands of these derivatives of V*b* elements indicate negligible or no resonance interaction of the central atoms with the π-orbitals of the benzene rings. This is understandable since the central atoms do not possess any unshared electrons. Further, *B*-band positions of these derivatives show little variation with the number of phenyl groups attached to the central atom, and the intensity seems to be directly proportional to the number of phenyl groups. The results with these derivatives agree well with the earlier work on similar systems (7, 8, 12) and the explanations offered are similar to those of Jaffe (6).

The ultraviolet spectra of the polyphenyl derivatives of the IV*b* elements (Table I) are very similar to the spectra of the derivatives of the V*b* elements in their pentavalent state. Here also, the *B*-bands show vibrational structure. The *B*-band position does not depend on the number of phenyl groups and the intensity contribution by a phenyl group is constant and additive. The results on the IV*b* derivatives reported here are similar to those of Milazzo (13) and Bowden and Braude (7) on derivatives of the type $C_6H_5MR_3$ (R = alkyl group).

Among the IV*b* derivatives, the silicon derivative seems to show a slightly larger bathochromic shift. Similarly, the phosphorus derivative seems to show a larger bathochromic shift among the V*b* pentavalent derivatives. These observations may possibly be taken as evidence for the "expansion of the valence shells" in these two second row elements. The formation of π-bonds by the second row elements, using 3*d* orbitals

Can. J. Chem. Downloaded from www.nrcresearchpress.com by 210.87.254.42 on 09/05/12
For personal use only.

appears to be quite general (14). Recently, reviews giving experimental evidence for d_π-orbitals in silicon (15) and phosphorus (16) have been published. The inductive effects of phosphorus and silicon will also be considerably different from those of the corresponding first row elements. But, it is more likely that resonance or π-orbital interaction is responsible for the bathochromic shifts in these phosphorus and silicon derivatives rather than inductive effects.

The ultraviolet spectrum of pentaphenylphosphorus is supposed to be very close to that of triphenylphosphine.* However, the ultraviolet spectrum of pentaphenylantimony shows vibrational fine structure. It is not possible, therefore, to explain Van Wazer's observation in a simple fashion. The possibility of some type of steric crowding in the case of pentaphenylphosphorus cannot be excluded. Such steric crowding will be less significant in the antimony derivative by virtue of the larger atomic volume of antimony compared with phosphorus.

The solvent effects on the ultraviolet spectra of some of the derivatives of the IV*b* and V*b* elements were studied. The spectra of tetraphenylmethane and tetraphenylphosphoniumbromide did not show any change with the solvents. The triphenyl derivatives of the V*b* elements showed very small solvent blue-shifts in polar solvents, although there is no possibility of $n \rightarrow \pi^*$ transitions (17) in these molecules.

All the ortho-, meta-, and para-substituted trityl, triphenylsilyl, and triphenylgermanyl benzene derivatives show vibrational structure in their *B*-bands. The absorption maxima of some of the derivatives are summarized in Table II. The para-carbonyl derivatives show fairly well-defined peaks due to the *E*-bands (at wavelengths lower than their *B*-bands), while the meta-carbonyl derivatives show only the vibrational structure of the *B*-bands (see Fig. 2). The *E*-band wavelengths in the para-carbonyl derivatives vary in the order, trityl > triphenylsilyl > triphenylgermanyl. These differences are, however, very small in magnitude. In any case, it appears fairly certain that all the

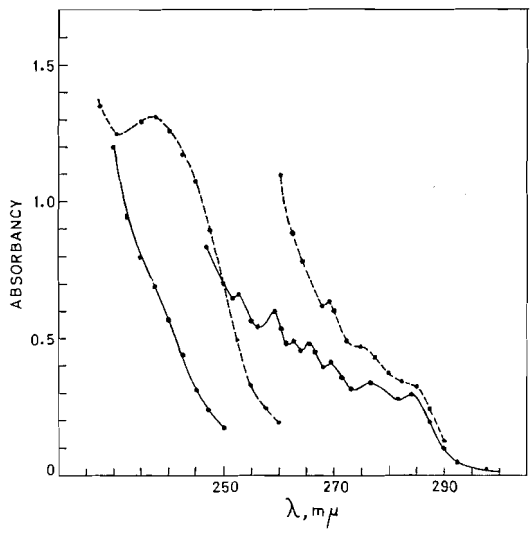


FIG. 2. Near-ultraviolet absorption spectra of *para*-triphenylgermanyl (– – –) and *meta*-triphenylgermanyl (——) benzoic acids.

*J. R. Van Wazer. Personal communication.

Can. J. Chem. Downloaded from www.nrcresearchpress.com by 210.87.254.42 on 09/05/12
For personal use only.

Can. J. Chem. Downloaded from www.nrcresearchpress.com by 210.87.254.42 on 09/05/12
For personal use only.

TABLE II

The near-ultraviolet absorption spectra of some *para*- and *meta*-substituted trityl-, triphenylsilyl-, and triphenylgermanyl-benzenes*

Trityl		Triphenylsilyl		Triphenylgermanyl	
R	λ_{max}, mμ	R	λ_{max}, mμ	R	λ_{max}, mμ
p-OH	265, 274, 281, 287	*p*-OH	237,† 260, 265, 275, 283	—	—
m-OH	265, 274, 280, 285	*m*-OH	260, 265, 272, 285	—	—
p-COOMe	250 (266, 272, 284)†	*p*-$CONH_2$	240 (261, 272)†	*p*-$CONH_2$	238 (261, 274, 284)†
m-COOMe	264, 272, 281, 285	*m*-$CONH_2$	254, 260, 265, 272, 280‡	—	—
p-COOH	243 (266, 272, 284)†	*p*-COOH	240 (260, 272)†	*p*-COOH	238 (264, 269, 276, 284)†
m-COOH	263, 272, 280, 285‡	*m*-COOH	254, 262, 265, 272, 285‡	*m*-COOH	252, 258, 265, 276, 284‡

*All the spectra in 95% ethanol.
†Not very well defined.
‡All the maxima in the vibrational fine structure are not included.

three groups do not interact strongly with the benzene nucleus in these derivatives. The resonance parameters, σ_R (18), for the three groups in these systems are estimated to be less than 0.10 by employing the λ_{max}–σ_R correlations of Rao (19, 20). This is in agreement with the Hammett reactivity constants, σ, proposed for the meta- and para-trityl (3), triphenylsilyl, and triphenylgermanyl (4) groups by Benkeser *et al.*

Benkeser *et al.* (4) have pointed out that silicon and germanium atoms are capable of valence shell expansion when conjugated with strong electron-donating groups like in phenols and anilines. The *B*-bands of *m*- and *p*-trityl phenols are similar to those of *m*- and *p*-triphenylsilyl phenols (Table II). However, in *p*-triphenylsilylphenol an additional band is observed at 237 mμ which may be the displaced *E*-band. The *E*-band of phenol itself is found to be at about 210 mμ. The bathochromic shift observed in the *E*-band of *p*-triphenylsilylphenol may then be interpreted as due to the resonance interaction of the *p*-triphenylsilyl group (20). If the assignment of the 237 mμ band as the *E*-band is correct, the Hammett σ-value of the *p*-triphenylsilyl group may be estimated employing the correlation of the *E*-band absorption maxima with the σ-constants of substituents proposed by Rao (20). The Hammett σ-value* thus estimated is about 0.30 ± 0.10. This is in agreement with the σ^--value of 0.31 proposed by Benkeser *et al.* (4).

The carbonyl stretching frequencies in some of the meta- and para-trityl, triphenylsilyl, and triphenylgermanyl derivatives are shown in Table III. It is seen that the carbonyl

TABLE III

Infrared carbonyl stretching frequencies in some *p*- and *m*-substituted trityl-, triphenylsilyl-, and triphenylgermanyl-benzenes*

Substituents	$\nu_{C=O}$, cm^{-1}	Substituents	$\nu_{C=O}$, cm^{-1}
$C(C_6H_5)_3$, *p*-$COOCH_3$	1724	$Si(C_6H_5)_3$, *p*-COOH	1704
$C(C_6H_5)_3$, *m*-$COOCH_3$	1723	$Si(C_6H_5)_3$, *m*-COOH	1702
H, $COOCH_3$	1723	$Ge(C_6H_5)_3$, *p*-COOH	1703
$C(C_6H_5)_3$, *p*-COOH	1702	$Ge(C_6H_5)_3$, *m*-COOH	1701
$C(C_6H_5)_3$, *m*-COOH	1703	H, COOH	1704

*In chloroform solution.

stretching frequencies in these compounds do not vary considerably from those in the unsubstituted compounds. It has been shown (21, 22) that the carbonyl frequencies in *m*- and *p*-substituted benzene derivatives may be directly correlated with the reactivity constants of the substituents. The data in Table III therefore suggest that the Hammett σ-values for the meta- and para-trityl, triphenylsilyl, and triphenylgermanyl groups are close to zero. This is in agreement with the conclusions drawn earlier from the ultraviolet absorption spectra and the kinetic data of Benkeser *et al.* (3, 4).

The major frequencies in the infrared spectra of the polyphenyl derivatives of IV*b* and V*b* elements are summarized in Table IV. The C=C skeletal vibration around 1580 cm^{-1}, some of the C—H in-plane deformation vibrations and ring vibrations, and the C—H out-of-plane deformation vibration around 740 cm^{-1} show nice trends due to mass effects of the central atoms. Similar mass effects have been observed in the spectra of metal alkyls (23). Typical plots of the change in frequency, $\Delta\nu$ (compared with the

**This should be denoted by the symbol, σ^-, according to the recently accepted symbols for substituent constants, since this value of the parameter is only for phenols.*

Can. J. Chem. Downloaded from www.nrcresearchpress.com by 210.87.254.42 on 09/05/12
For personal use only.

Can. J. Chem. Downloaded from www.nrcresearchpress.com by 210.87.254.42 on 09/05/12
For personal use only.

TABLE IV

Infrared spectra of the polyphenyl derivatives of the elements of groups IV*b* and V*b*

Compound	C=C skeletal	C—H in-plane deformations and other ring vibrations					C—H out-of-plane deformation	
$N(C_6H_5)_3$	1594 S	—	1176 M	1156 W	1079 M	1030 W	1002 W	752 S	696 S
$P(C_6H_5)_3$	1587 W	1439 S	1179 W	1156 W	1070 W	1028 M	996 W	752 S	697 S
$As(C_6H_5)_3$	1580 W	1437 M	1183 W	1156 W	1070 M	1026 M	1000 M	736 S	696 S
$Sb(C_6H_5)_3$	1575 W	1429 M	1183 W	1156 W	1066 S	1020 S	1000 M	730 S	697 S
$Bi(C_6H_5)_3$	1570 W	1429 W	1178 W	1155 W	1058 M	1016 M	998 M	726 S	696 S
$P(C_6H_5)_4Br$	1594 M	—	—	1111 S	1096 S	—	1000 M	764 S	692 S
$As(C_6H_5)_4Cl$	—	—	—	1084 M	1069 S	—	1000 W	750 S	690 S
$Sb(C_6H_5)_4Br$	1550 W	—	—	1070 W	1054 S	—	998 M	740 S	690 S
$Bi(C_6H_5)_3Cl_2$	1536 M	—	—	—	1036 S	—	—	729 S	—
$C(C_6H_5)_4$	1572 W	—	1185 M	—	1084 S	1038 M	1005 W	752 S	702 S
$Sn(C_6H_5)_4$	1552 M	1433 S	1176 W	1152 W	1075 S	1028 W	1000 M	733 S	700 S
$Pb(C_6H_5)_4$	1545 M	1434 S	1173 W	1153 W	1064 M	1021 M	999 M	729 S	698 S

first compound of the series) against the atomic weight, A_M, of the central atom are shown in Fig. 3. The mass effects seem to be more prominent in the derivatives of the

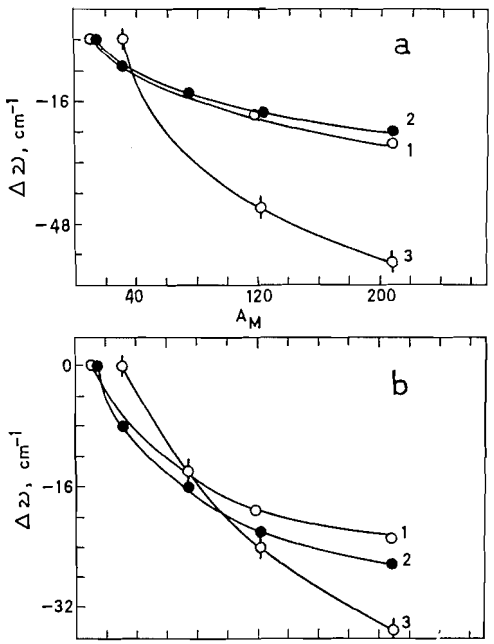


FIG. 3. Plots of $\Delta\nu$ versus the atomic weight of the central atom in (1) tetraphenyl derivatives of IV*b* elements, (2) triphenyl derivatives of V*b* elements, (3) polyphenyl derivatives of V*b* elements in pentavalent state. (*a*) C=C skeletal vibration (1536–1594 cm^{-1}) and (*b*) C—H out-of-plane deformation (726–764 cm^{-1}).

V*b* elements in their pentavalent state than in their trivalent state. Apparently, the resonance interaction involving the unshared electrons in the triphenyl derivatives is responsible for such a behavior.

The splitting reported earlier (1) in the C—H out-of-plane vibrations have been found to be mere solid state anomalies, since the splittings are not noticed in solution spectra. Daasch and Smith (24) have observed bands of moderate intensity in the regions 1450–1435 cm^{-1} and 1005–995 cm^{-1}, in compounds containing the phosphorus–phenyl linkages. Although the latter band has been suspected to arise from some activated ring vibration, the former band around 1440 cm^{-1} was suggested to be characteristic of the phosphorus–phenyl linkage (25). On the basis of literature data, Bellamy (25) has suggested that bands around 1429 and 1130–1090 cm^{-1} are characteristic of the silicon–phenyl linkage. A survey of the data in Table IV shows that bands are observed in all the above-mentioned regions in the spectra of several polyphenyl derivatives. It is therefore suggested that they may all be due to some activated ring vibrations. In the case of triphenylamine, however, definite assignment of the C—N linkage to the strong band at 1337 cm^{-1} is possible.

ACKNOWLEDGMENTS

The authors are indebted to the authorities of the Purdue University and the University of California for facilities of the spectroscopy laboratories. They are thankful to Prof.

Can. J. Chem. Downloaded from www.nrcresearchpress.com by 210.87.254.42 on 09/05/12
For personal use only.

M. R. A. Rao for his keen interest and to Prof. R. A. Benkeser for kindly providing them with some of the compounds used in this study.

REFERENCES

1. C. N. R. Rao, J. Ramachandran, M. S. C. Iah, S. Somasekhara, and T. V. Rajkumar. Nature, **183**, 1475 (1959).
2. R. A. Benkeser and R. B. Gosnell. J. Am. Chem. Soc. **78**, 4914 (1956).
3. R. A. Benkeser and R. B. Gosnell. J. Org. Chem. **22**, 327 (1957).
4. R. A. Benkeser, C. E. DeBoer, R. E. Robinson, and D. M. Sauve. J. Am. Chem. Soc. **78**, 682 (1956).
5. W. W. Robertson and F. A. Matsen. J. Am. Chem. Soc. **72**, 5250 (1950).
6. H. H. Jaffe. J. Chem. Phys. **22**, 1430 (1954).
7. K. Bowden and E. A. Braude. J. Chem. Soc. 1068 (1952).
8. H. H. Jaffe and L. D. Freedman. J. Am. Chem. Soc. **74**, 1069 (1952).
9. C. E. Moore. Atomic energy levels. Vol. III. Natl. Bur. Standards (U.S.), Circ. No. 467. 1958.
10. A. L. Sklar. J. Chem. Phys. **7**, 984 (1939).
11. F. A. Matsen *et al.* J. Am. Chem. Soc. **72**, 5243, 5248, 5252 (1950).
12. F. G. Mann, I. T. Millar, and B. B. Smith. J. Chem. Soc. 1130 (1953).
13. G. Milazzo. Gazz. chim. ital. **71**, 73 (1941).
14. L. Pauling. J. Phys. Chem. **56**, 361 (1952).
15. F. G. A. Stone and D. Seyferth. J. Inorg. & Nuclear Chem. **1**, 112 (1955).
16. J. R. Van Wazer. Phosphorus and its compounds. Vol. I. Interscience Publishers Inc., New York. 1958.
17. J. W. Sidman. Chem. Revs. **58**, 689 (1958).
18. R. W. Taft, Jr. *In* Steric effects in organic chemistry. *Edited by* M. S. Newman. John Wiley & Sons, Inc., New York. 1956. Chap. 13.
19. C. N. R. Rao. Chem. & Ind. (London), 1239 (1957).
20. C. N. R. Rao. J. Sci. Ind. Research. (India), **17B**, 56 (1958).
21. C. N. R. Rao and G. B. Silverman. Current Sci. (India), **26**, 375 (1957).
22. H. W. Thompson, R. W. Needham, and D. Jameson. Spectrochim. Acta, **9**, 208 (1957).
23. C. W. Young, J. S. Koehler, and D. S. McKinney. J. Am. Chem. Soc. **69**, 1410 (1947).
24. L. W. Daasch and D. C. Smith. Anal. Chem. **23**, 853 (1951).
25. L. J. Bellamy. The infrared spectra of complex molecules. 2nd ed. John Wiley & Sons, Inc., New York. 1958.

Can. J. Chem. Downloaded from www.nrcresearchpress.com by 210.87.254.42 on 09/05/12
For personal use only.

Can. J. Chem. Downloaded from www.nrcresearchpress.com by 210.87.254.6 on 09/05/12
For personal use only.

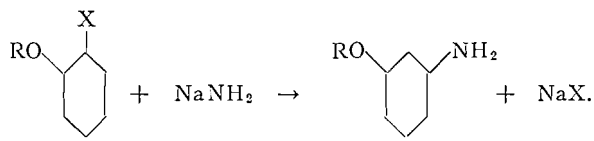
HYDROGEN ISOTOPE EFFECT IN THE AMINATION OF CHLOROBENZENE BY SODAMIDE[1]

G. E. Dunn, Peter J. Krueger,[2] and Walter Rodewald

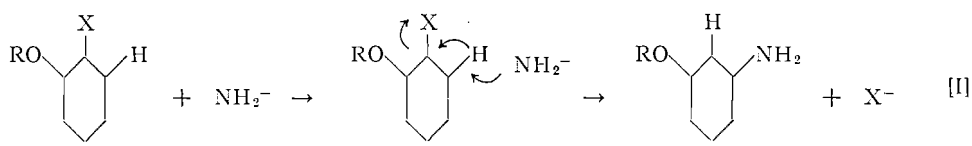
ABSTRACT

Mixtures of chlorobenzene and chlorobenzene-2-^{2}H have been subjected to partial amination by sodamide in liquid ammonia and both the unreacted starting material and the product aniline have been analyzed for deuterium. Deuterium in the aniline is distributed approximately equally between the ortho and meta positions. The results give strong support to the mechanism proposed by Roberts and co-workers in which the slow step is the formation of an intermediate, such as benzyne, which is symmetrical with respect to carbon atoms 1 and 2.

The amination of aromatic halides by alkali metal amides in liquid ammonia was discovered in 1936 by Bergstrom and co-workers (1), who were able to convert chloro-, bromo-, and iodo-benzene into aniline and a mixture of by-products containing diphenylamine, triphenylamine, and *p*-aminobiphenyl. Fluorobenzene did not react. In 1945 Gilman and Avakian reported that a number of ortho-halogenated ethers on treatment by Bergstrom's procedure gave meta-aminoethers (2) as illustrated by the equation



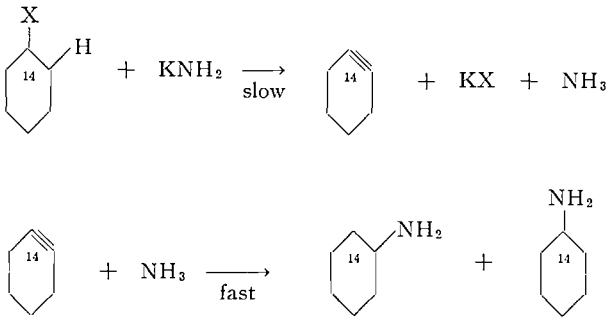
Bunnett and Zahler reviewed the reaction in 1951 (3) by which time aminations with rearrangement under the Bergstrom conditions had been observed with halogen substituents located ortho and para to ether, sulphide, sulphone, and trifluoromethyl groups. It had also been demonstrated, largely by Benkeser and co-workers (4), that the entering amide displaces a hydrogen atom ortho to the halogen atom. Bunnett and Zahler proposed a mechanism for the rearrangement in which attack by amide ion on carbon atom 2 of a halobenzene forces the migration of a hydride ion from carbon 2 to carbon 1 and the displacement of a halide ion by this hydride ion. The sequence of reactions in equation I below illustrates this mechanism.



[I]

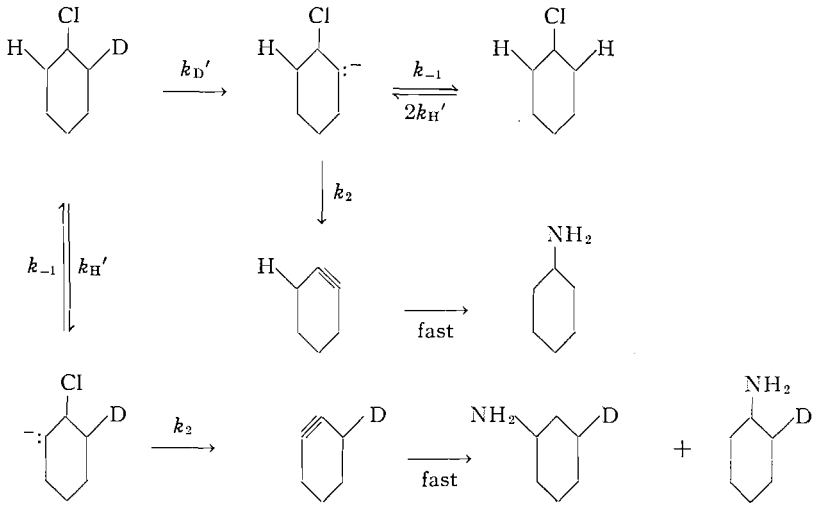
In 1953 Roberts and co-workers (5) showed that rearrangement occurs even in unsubstituted halobenzenes by demonstrating that chlorobenzene-1-^{14}C with potassium amide in liquid ammonia gives aniline-1-^{14}C and aniline-2-^{14}C in almost equal amounts. The near equality of rearranged and unrearranged product suggested the participation of an intermediate symmetrical with respect to carbons 1 and 2. They considered the most likely intermediate to be benzyne, which would enter into the mechanism as shown in sequence II.

[1]*Manuscript received July 11, 1960.*
Contribution from the Chemistry Department of the University of Manitoba, Winnipeg, Manitoba.
[2]*Holder of a National Research Council bursary, 1955–56.*



[II]

The existence of a symmetrical intermediate was further indicated when Roberts and co-workers (6) reported in 1956 that chlorobenzene-1-^{14}C, bromobenzene-1-^{14}C, and iodobenzene-1-^{14}C with potassium amide all give aniline-1-^{14}C and aniline-2-^{14}C in approximately equal quantities. They also studied the reaction of ortho-deuterated fluoro-, chloro-, and bromo-benzene by aminating mixtures of deuterated and undeuterated halobenzenes and comparing the percentage of deuterium before reaction with that after partial reaction. In deuterated bromobenzene the percentage of deuterium increased with the percentage of reaction indicating that the undeuterated material reacts faster, and the isotope effect, $i = k_H/k_D$, was found to be about 5.5. Fluorobenzene-2-^{2}H was found to exchange deuterium with the solvent very rapidly. Dilute solutions of chlorobenzene-2-^{2}H in chlorobenzene showed a small increase in deuterium content after partial reaction while concentrated solutions showed a decrease. This was taken to mean that chlorobenzene-2-^{2}H exchanges deuterium with the solvent at a rate comparable with the amination. On the basis of these and other observations the mechanism III was postulated for the amination and exchange of chlorobenzene-2-^{2}H.



[III]

Before the appearance of Roberts' second paper the authors had performed some experiments intended to distinguish between mechanisms I and II by finding out whether or not deuterium is lost from the aromatic ring when chlorobenzene-2-^{2}H is aminated by sodamide in liquid ammonia. Mechanism I predicts that chlorobenzene-2-^{2}H should

Can. J. Chem. Downloaded from www.nrcresearchpress.com by 210.87.254.6 on 09/05/12
For personal use only.

give aniline-^{2}H with the same total deuterium content, while mechanism II predicts aniline-^{2}H with a smaller deuterium content than the starting material. The results of these preliminary experiments are shown in Table I.

TABLE I

Atom per cent deuterium in the labelled positions of reactants and products

Experiment	Chlorobenzene-2-^{2}H		Aniline-^{2}H		2,4,6-Tribromoaniline†
	Initial*	Final*	Initial*	Final*	
1. Aniline recovered by acid extraction	—	—	84.7±2.0‡	81.9±0.3‡	—
2. Aniline recovered by distillation	—	—	84.7±2.0‡	83.6±1.2‡	—
3. Chlorobenzene and 1.7 moles sodamide	64.3±1.9	—	—	35.4±0.1	—
4. Chlorobenzene and 1.7 moles sodamide	64.3±1.9	—	—	30.8±1.2	17.3
5. Chlorobenzene and 1.7 moles sodamide	64.3±1.9	—	—	30.4±0.1	16.3
6. Chlorobenzene and 0.5 mole sodamide	44.1±1.5	44.1±1.8	—	—	—

*Mean of three analyses ±maximum deviation.
†One analysis.
‡This material is probably a mixture of 2-, 2,4-, and 2,4,6-deuterated aniline but the analyses are calculated on the assumption that it is aniline-^{2}H.

Experiments 1 and 2, Table I, were intended to find out whether or not ring-deuterated aniline exchanges hydrogen isotopes with the reaction mixture or during recovery and purification. In experiment 1 a sample of aniline partially deuterated in the ortho and para positions was treated with sodamide in liquid ammonia and recovered by Bergstrom's method (1) which involves extraction of aniline from the reaction mixture with aqueous hydrochloric acid. It is seen that some deuterium was lost by this procedure. In experiment 2 the use of acid was avoided by extracting the reaction mixture with ether and recovering aniline by fractional distillation. The recovery of aniline was reduced by almost half but Table I shows that the loss of deuterium by this method was negligible.

A mixture of chlorobenzene and chlorobenzene-2-^{2}H was then treated with 1.7 times the equivalent quantity of sodamide in liquid ammonia and the aniline was recovered. Experiments 3, 4, and 5, Table I, show that the aniline produced contained about half the deuterium originally present in the starting material. This aniline was then brominated and the 2,4,6-tribromoaniline produced was analyzed for deuterium. Experiments 4 and 5, Table I, show that almost half the deuterium in the aniline was displaced by bromine so that a little more than half the deuterated aniline must have had its deuterium in the meta position.

These results were taken to favor mechanism II since it predicts a loss of deuterium and the formation of equal quantities of ortho- and meta-deuterated aniline. However, if the reaction did take place by mechanism II, the fact that half the deuterium was lost would lead to the surprising conclusion that protium and deuterium are lost at equal rates. A further test of this point was made by reacting a mixture of chlorobenzene and chlorobenzene-2-^{2}H with half the equivalent quantity of sodamide and recovering the unreacted chlorobenzene. The data from experiment 6, Table I, show that there was no change in the deuterium content of the chlorobenzene, which seemed to confirm that protium and deuterium react at equal rates.

With the appearance of the second paper by Roberts and co-workers (6) it was evident

Can. J. Chem. Downloaded from www.nrcresearchpress.com by 210.87.254.6 on 09/05/12
For personal use only.

Can. J. Chem. Downloaded from www.nrcresearchpress.com by 210.87.254.6 on 09/05/12
For personal use only.

that our results could be accounted for by mechanism III in a very particular combination of circumstances. As the reaction proceeds, the usual isotope effect tends to increase the deuterium in the unreacted chlorobenzene and the product aniline, but exchange would tend to decrease it, so that a suitable combination of rate of amination, rate of exchange, initial concentration of deuterium, and percentage of reaction could result in a 50% loss of deuterium and no change in the deuterium content of the chlorobenzene. Since Roberts and co-workers did not measure the deuterium in their aniline and we did not measure the deuterium in our unreacted chlorobenzene it was not possible to determine whether or not the combination of factors necessary to fit our data to mechanism III actually existed. Since the fit of Roberts' own data to mechanism III was far from precise, it seemed worth while to repeat and extend our experiments to include in one set of reactions all the measurements necessary for a test of the mechanism.

EXPERIMENTAL

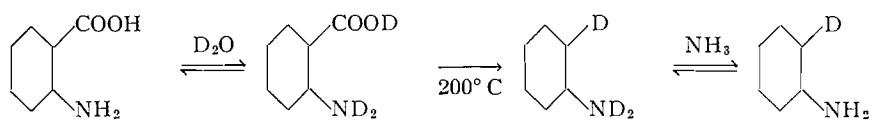
Chlorobenzene-2-^2H

Grignard reagent was prepared from 194 g of Eastman Kodak white label *o*-chloroiodobenzene (0.814 mole) in a flame-dried flask under an atmosphere of dry nitrogen. Acid titration of the solution indicated 90–97% yields. In the preliminary experiments the Grignard was decomposed by adding 1.63 g of deuterium oxide* (0.814 mole) very slowly with vigorous stirring. Gilman's color test I (7) was negative at the end of the addition. The solution was then washed with water and dried over anhydrous potassium carbonate. The product was recovered from the ether layer by fractionation through a 10-cm Vigreaux column. Yields ranged from 45% to 65%, b.p. 128–132° C at 742 mm, $n_D^{21.8} = 1.5261$. Deuterium analyses averaged about 80% chlorobenzene-2-^2H.

Since Roberts and co-workers reported the preparation of pure chlorobenzene-2-^2H (without stating the method of analysis) by decomposing *o*-chlorophenylmagnesium iodide with deuteroacetic acid, this method was tried. To the Grignard reagent prepared as described above was added 112.4 g (1.84 mole) of deuteroacetic acid slowly with vigorous stirring. At the end of the addition Gilman's color test I was negative (7). Water was added to dissolve the magnesium salts and the ether layer was separated. The ethereal solution was washed with sodium hydroxide to remove excess acetic acid, dried over anhydrous calcium sulphate, and distilled through an approximately 20-plate column. The yield of chlorobenzene was 49.6 g (53.8%), b.p. 130.0–130.5° C at 745 mm, $n_D^{25} = 1.5209$. This material analyzed 81.6% chlorobenzene-2-^2H. Two samples of deuteroacetic acid were used with identical results; one sample was prepared by hydrolyzing freshly distilled acetic anhydride with deuterium oxide, the other was obtained from Merck and was certified by the supplier to contain more than 98% deuteroacetic acid.

Deuterated Aniline

The preparation of aniline-2-^2H was attempted by the decarboxylation of deuterated anthranilic acid as shown in the following sequence of reactions.



Decarboxylation of aromatic acids with calcium deuteroxide at 500° C has been shown

**Obtained from the Commercial Products Division of Atomic Energy of Canada Ltd., and reported by the supplier to contain 99.83 atom% deuterium.*

to give a mixture of isomerically deuterated products (8), but it was thought that the mild conditions possible in the decarboxylation of anthranilic acid might permit success.

Thirty grams of anthranilic acid (0.219 mole) was dissolved in 70 ml of dioxane in a distilling flask and 6.6 g of deuterium oxide (0.330 mole) was added. After the solution had stood for 160 hours at room temperature the solvents were removed under vacuum. A condenser and receiver were attached to the distilling flask and the latter was heated in an oil bath at 200–210° C until no more aniline distilled over. This crude aniline was redistilled to give 16.2 g of product (85% yield), b.p. 179–183° C at 742 mm, $n_D^{21.8}$ = 1.5826. Deuterium analyses of the aniline obtained from two runs, A and B, gave the atom per cent deuterium in product A = 21.2±0.5% and in product B = 12.0±0.1%. (These analyses would correspond to an aniline-$^2H_3$ content of 49.4±1.2% in A and 27.9±0.2% in B.) In order to remove deuterium from the amino group of the aniline, it was twice dissolved in about 500 ml of liquid ammonia and allowed to stand until the ammonia had evaporated. Distillation gave aniline, b.p. 60–65° C at 2.5 mm, $n_D^{21.8}$ = 1.5834, in which the intensity of the NH stretching overtone at 1498 mμ matched that of ordinary aniline.* Analysis showed 12.1±0.3 at.% deuterium in A and 6.66±0.02 at.% in B. (This would correspond to an aniline-2-^2H content of 84.7±2.0% in A and 46.6±0.1% in B.)

These results show that the deuterated aniline obtained by decarboxylating partially deuterated anthranilic acid has a little more than half its deuterium in the ring instead of one-third as predicted for a statistical distribution, or less than one-third as would be expected if there were a normal isotope effect in the decarboxylation. This requires that the decarboxylation take place by a mechanism such that either deuterium migrates in preference to protium or deuterium enters more than one position in the ring. The latter possibility seems much the more likely, especially in view of the observation (8) that this actually happens with simple aromatic acids on decarboxylation with $Ca(OD)_2$. In order to find out how general the redistribution of deuterium is, some of the aniline from run B was converted to 2,4,6-tribromoaniline as described below. This tribromoaniline contained no deuterium so the most likely hypothesis is that decarboxylation gives a mixture of aniline-2-^2H, aniline-2,4-$^2H_2$, and aniline-2,4,6-$^2H_3$.

2,4,6-Tribromoaniline

To determine the fraction of deuterium in the meta position of the deuterated aniline obtained by decarboxylation or by amination the sample in question was brominated and the 2,4,6-tribromoaniline was analyzed for deuterium. This method has been used previously by Lauer and Errede (9). About 1.0–1.5 g of deuterated aniline was dissolved in 20 ml of water. The solution was cooled in ice and a solution of bromine in ethanol (25% by weight) was added from a burette until the first appearance of a permanent yellow tinge. The precipitate was filtered, washed with water, dissolved in alcohol, and reprecipitated by the addition of water. The material obtained in this way melted sharply at 118° C (uncorr.) and was analyzed for deuterium as described below.

Amination of Chlorobenzene-2-^2H

In the preliminary experiments the procedure of Bergstrom was used. Sodamide was prepared by the method of Vaughan, Vogt, and Nieuwland (10) from 5.2 g of sodium (0.226 g-atom) in about 600 ml of liquid ammonia. When the blue color of the metal solution had turned to the grey of sodamide, 15 g of chlorobenzene-2-^2H (0.133 mole)

**Spectral measurements were made on a Beckman spectrophotometer model DK-1.*

Can. J. Chem. Downloaded from www.nrcresearchpress.com by 210.87.254.6 on 09/05/12
For personal use only.

Can. J. Chem. Downloaded from www.nrcresearchpress.com by 210.87.254.6 on 09/05/12
For personal use only.

was added dropwise over a period of 20 minutes. After another 40 minutes, 11 g of ammonium chloride (0.202 mole) was added and the solvent was allowed to evaporate overnight. Ether was added to the residue and refluxed to drive off residual ammonia. The ether-insoluble salt was dissolved in water and the aniline was extracted from the aqueous layer with ether. The ether solution was dried over anhydrous potassium carbonate, and the aniline was recovered by repeated fractionations through a 10-cm Vigreaux column at 60–65° C at 20 mm. Purity of the aniline was checked by comparison of the intensity of the 1498 mμ peak with that of pure aniline. Yields of pure product averaged about 25% by this method of recovery. Bergstrom's method of acid extraction gave yields of 40% but could not be used because of the danger of exchange between the acid and ring hydrogen. Deuterium analyses on the product were carried out as described below.

In later experiments, where it was desired to isolate unreacted chlorobenzene as well as aniline, Roberts' procedure was used. The chlorobenzene-2-^{2}H in 150 ml of liquid ammonia was added to the sodamide solution over a period of 1 minute. Three minutes after the addition was complete the reaction was stopped by the addition of 20 g of ammonium nitrate (0.250 mole) dissolved in 100 ml of liquid ammonia. Anhydrous ether, 150 ml, was added to the reaction mixture and the ammonia was allowed to evaporate overnight. Then 200 ml of water was added and stirred for 10 minutes. The ether layer was separated and washed with water. The aqueous layer and washings were boiled to remove excess ammonia and ether, then analyzed for chloride by the Volhard method. The ethereal solution was dried over anhydrous calcium sulphate, then distilled. Fractionation through a 13-cm Vigreaux column gave aniline, b.p. 55–65° C at 4–5 mm, $n_D^{25} = 1.5836$, and chlorobenzene, b.p. 130.0–130.5° C at 754 mm, $n_D^{25} = 1.5207$. The initial separation of aniline and chlorobenzene was most convenient at reduced pressure but the final purification of chlorobenzene was done at atmospheric pressure in a 20-plate column. Each substance was shown to be free of the other by its infrared spectrum. Each was analyzed for deuterium as described below.

Deuterated Aniline under Amination Conditions

In order to determine whether or not aniline loses deuterium after it is produced in the reaction or during recovery, the first amination procedure was repeated exactly except that the deuterated aniline obtained from the decarboxylation of anthranilic acid was used instead of chlorobenzene. The results are shown as experiments 1 and 2, Table I.

Deuterium Analyses

The samples were burned in a standard macrocombustion apparatus using a Vycor tube and a plug of silver wire to trap halogens. The water of combustion was collected in a Dry Ice trap and treated with clean copper wire to remove halogens, or barium carbonate, to remove soluble oxides of nitrogen. It was then purified by the method of Keston, Rittenberg, and Schoenheimer (11) except that calcium oxide and potassium permanganate were used instead of potassium hydroxide and chromium trioxide. The density of the water of combustion was determined by the gradient density tube method described by Anfinsen (12). This gives the weight per cent, w, of deuterium oxide in the water of combustion. From this the atom per cent deuterium in the labelled positions of the molecule was calculated by the equation

$$\text{atom per cent deuterium in } n' \text{ positions} = (n/n') \cdot 900w/(1000-w),$$

where n' = number of labelled positions in the molecule and n = total number of hydrogen atoms in the unlabelled molecule.

In the case of chlorobenzene, combustion analyses were supplemented by spectrophotometric analyses using a Perkin–Elmer model 21 spectrophotometer. Measurements were made at 10.115 μ with slit width 160 μ and at 10.555 μ with slit width 248 μ. These correspond to spectral slit widths of 0.020 μ and 0.028 μ respectively. All measurements were made by the base-line technique in 0.025-mm cells. Mixtures of chlorobenzene and the 81.6% chlorobenzene-2-^{2}H described above gave linear Beer's law plots which were used to analyze the chlorobenzene obtained from the amination reactions. Table II shows the data for standard mixtures and Table III shows those for reaction products.

TABLE II

Infrared analyses of known mixtures of chlorobenzene and chlorobenzene-2-^{2}H

Mole % chlorobenzene-2-^{2}H	Wavelength	I_0†	I‡	log I_0/I
81.6±1.9*	10.115	82.1	45.5	0.256
	10.555	84.2	61.3	0.140
69.5±1.6	10.115	82.5	49.7	0.220
	10.555	84.0	63.7	0.120
55.3±1.3	10.115	82.6	56.0	0.169
	10.555	83.8	68.4	0.0881
41.8±1.0	10.115	82.5	62.0	0.125
	10.555	83.4	72.7	0.0597
27.8±0.6	10.115	82.3	69.0	0.0766
	10.555	83.2	77.0	0.0336
16.4±0.4	10.115	82.7	74.9	0.0430
	10.555	83.5	81.3	0.0116

*Determined by combustion.
†% Transmission at the base line.
‡% Transmission at the peak.

TABLE III

Infrared analyses of chlorobenzene – chlorobenzene-2-^{2}H mixtures obtained from amination reactions

Run	Wavelength	I_0*	I†	log I_0/I	Mole % o-DC_6H_4Cl‡	Average mole % o-DC_6H_4Cl
1	10.115	82.4	64.5	0.106	35.8	
	10.555	83.8	75.0	0.0481	34.3	35.0±0.8
2	10.115	83.7	62.0	0.130	42.7	
	10.555	83.8	72.9	0.0605	40.0	41.3±1.4
3	10.115	82.9	67.1	0.0919	28.5	
	10.555	83.5	76.0	0.0405	29.5	29.0±0.5
4	10.115	82.4	70.8	0.0660	23.5	
	10.555	83.3	78.6	0.0252	21.8	22.7±0.9

*% Transmission at the base line.
†% Transmission at the peak.
‡Calculated from log I_0/I and the data of Table II.

RESULTS AND DISCUSSION

Roberts and co-workers (6) derived a kinetic expression from mechanism III to account for the change in deuterium content of chlorobenzene during amination. It will be necessary to reproduce their derivation in order to extend it to cover the deuterium content of the aniline produced in the reaction.

Can. J. Chem. Downloaded from www.nrcresearchpress.com by 210.87.254.6 on 09/05/12
For personal use only.

If k_2 is large compared with k_H' and k_D', as seems likely, the rate of disappearance of deuterated chlorobenzene, D, is given by the expression

$$\frac{-d[D]}{dt} = (k_H'+k_D')[D][NH_2^-]-k_{-1}[\text{anion B}].$$

Application of the steady-state approximation to anion B gives

$$[\text{anion B}] = \frac{k_H'}{k_{-1}+k_2}[D][NH_2^-],$$

which converts the preceding expression to

$$\frac{-d[D]}{dt} = (k_H'+k_D')[D][NH_2^-]-\frac{k_{-1}k_H'}{k_{-1}+k_2}[D][NH_2^-].$$

By a similar process the rate of disappearance of chlorobenzene, H, is found to be

$$\frac{-d[H]}{dt} = 2k_H'[H][NH_2^-]-\frac{k_{-1}}{k_{-1}+k_2}(2k_H'[H][NH_2^-]+k_D'[D][NH_2^-]).$$

Letting the isotope effect, $k_H'/k_D' = i$, and the fraction of anion returning to starting material, $k_{-1}/(k_{-1}+k_2) = F$, division of one rate expression by the other gives

$$\frac{d[D]}{d[H]} = \frac{[i(1-F)+1][D]}{2i(1-F)[H]-F[D]}.$$

Integration of this expression yields

$$[1] \qquad \ln[D]\Bigg]_{[D]_0}^{[D]_t} + \frac{1+i-iF}{1-i+iF}\ln\left[(-1+i-iF)\frac{[H]}{[D]}-F\right]\Bigg]_{\frac{[H]_0}{[D]_0}}^{\frac{[H]_t}{[D]_t}} = 0.$$

Roberts' equation [1] can be more conveniently applied by setting the fraction of chlorobenzene deuterated at time $t = d$, and the fraction of starting material which has reacted at time $t = P$. Equation [1] then becomes

$$[2] \qquad \log\frac{d}{d_0}(1-P) = \frac{i(1-F)+1}{i(1-F)-1}\log\frac{(1/d)-1-[F/\{i(1-F)-1\}]}{(1/d_0)-1-[F/\{i(1-F)-1\}]}.$$

Equation [1] or [2] concerns only the change in concentration of deuterium in unreacted chlorobenzene. In order to calculate the aniline composition predicted by mechanism III it is necessary to extend the kinetic treatment as follows. Let A_D and A_H represent deuterated and undeuterated aniline, respectively,

$$\frac{d[A_D]}{dt} = k_2[B],$$

$$\frac{-d[D]}{dt} = (k_H'+k_D')[D][NH_2^-]-k_{-1}[B].$$

Can. J. Chem. Downloaded from www.nrcresearchpress.com by 210.87.254.6 on 09/05/12
For personal use only.

Dividing one rate by the other gives

$$\frac{-d[A_D]}{d[D]} = \frac{k_2[B]}{(k_H' + k_D')[D][NH_2^-] - k_{-1}[B]}.$$

Substituting the steady-state expression for B and introducing i and F, where appropriate, gives

$$\frac{-d[A_D]}{d[D]} = \frac{i(1-F)}{i(1-F)+1}.$$

Integrating with the condition that $[A_D] = 0$ when $[D] = [D]_0$ gives

$$[A_D] = \frac{i(1-F)}{i(1-F)+1}([D]_0 - [D]).$$

If it is assumed that $([A_D]+[A_H])/([D]_0+[H]_0) = P$ and that $([D]+[H])/([D]_0+[H]_0) = 1-P$ the above expression becomes

$$\frac{[A_D]}{[A_D]+[A_H]} = \frac{1}{P}\frac{i(1-F)}{i(1-F)+1}\frac{[D]_0}{[D]_0+[H]_0} - (1-P)\frac{[D]}{[D]+[H]}.$$

This expression is simplified by letting the fraction of aniline which is deuterated $= a$, and the fraction of chlorobenzene which is deuterated $= d$, which gives

[3] $$a = \frac{i(1-F)}{i(1-F)+1}\frac{d_0 - d(1-P)}{P}.$$

Equations [2] and [3] were used to calculate a and d according to mechanism III and the results are compared with the experimental results in Table IV. The F values shown in Table IV were calculated from equation [2] using Roberts' value of $i = 5.7$. The constancy of F through four different runs is strong support for the Roberts' mechanism of concurrent amination and exchange. The average value of 0.864 ± 0.020 is much more precise than the 0.56 ± 0.20 reported by Roberts and co-workers (6). The different magnitudes of F in the two investigations may be due to some difference in experimental conditions, such as the fact that potassium amide was used in one case and sodamide in the other, or it may be the result of a difference in the method of analyzing chlorobenzene for deuterium. A spectrophotometric method was used in both cases and the standard sample on which all the analyses rest was prepared in the same way in both investigations. In our case the standard sample analyzed 81.6% chlorobenzene-2-^{2}H by combustion, while in Roberts' case the standard sample was reported to be 100% chlorobenzene-2-^{2}H without mention of the method of analysis. If the two standard samples are assumed to be both about 80% deuterated then the two ranges of F values overlap, although the precision of the set by Roberts and co-workers is not improved.

The a values in Table IV were calculated from equation [3] using $i = 5.7$ and the calculated values of F. Comparison of the calculated and observed values of a shows that the former is lower by about 10% in each case. Although the a values calculated for Roberts' mechanism are low, they parallel the observed values so closely as to leave little room for doubt that the mechanism is essentially correct.

The 10% discrepancy is probably due largely to the method of determining P by measuring the moles of chloride ion produced. Bergstrom and co-workers (1) showed

Can. J. Chem. Downloaded from www.nrcresearchpress.com by 210.87.254.6 on 09/05/12
For personal use only.

Can. J. Chem. Downloaded from www.nrcresearchpress.com by 210.87.254.6 on 09/05/12
For personal use only.

TABLE IV

Amination of mixtures of chlorobenzene and chlorobenzene-2-^{2}H

Run	d_0*†	d*‡	P*§	F_{calc}‖	a_{calc}¶**	a_{obs}* **
1	0.407±.003	0.350±.008	0.452±.006	0.844±.011	—	—††
2	0.816±.019	0.414±.014	0.718±.006	0.870±.005	0.416±.004	0.441±.000
3	0.594±.014	0.290±.005	0.819±.012	0.868±.001	0.283±.004	0.326±.005
4	0.396±.009	0.227±.009	0.783±.007	0.874±.005	0.185±.001	0.204±.003

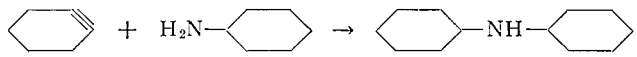
*Each datum is the mean of three analyses ± the maximum deviation from the mean.
†d_0 = mole fraction chlorobenzene-2-^{2}H at zero time.
‡d = mole fraction chlorobenzene-2-^{2}H at time t.
§P = mole fraction starting material converted to chloride ion at time t.
‖The maximum value was calculated from equation [2] using the minimum value of d and the maximum values of d_0 and P; the reverse combination gave the minimum value.
¶The maximum value was calculated from equation [3] using the minimum value of d and the maximum values of d_0, P, and F.
**a = mole fraction aniline-^{2}H at time t.
††Not enough product for analysis.

that the aniline produced by amination of chlorobenzene is always accompanied by by-products, among which they identified diphenylamine, triphenylamine, and *p*-aminobiphenyl. They suggested that these are formed from aniline as illustrated in the following equations:

$$C_6H_5NH_2 + NaNH_2 \rightleftarrows C_6H_5NHNa + NH_3,$$

$$C_6H_5NHNa + C_6H_5Cl \rightarrow (C_6H_5)_2NH + NaCl.$$

It is seen that these side reactions produce chloride ion while consuming both chlorobenzene and aniline in a manner not included in the Roberts' mechanism. Since the side reactions should consume ring-deuterated and undeuterated reactants at equal specific rates, they will not alter the mole fraction of deuterated chlorobenzene, d, or aniline, a, but they will make the apparent percentage of reaction, $100P$, too large. Insertion of the experimental values of a, d, d_0, and $i = 5.7$ into equations [2] and [3] give calculated P values of 0.646, 0.647, and 0.648 in runs 2, 3, and 4, Table IV, respectively. While the precision of the calculated P values among runs is probably largely fortuitous, they show that a reasonable amount of side reaction of the type proposed by Bergstrom could account for the low calculated a values. A more attractive mechanism for the formation of by-products within the Roberts' mechanism would be the following:



but the effect on a would be the same as that suggested for the Bergstrom mechanism.

In summary, our data and the predictions of Roberts' mechanism of concurrent amination and exchange are in excellent agreement on the deuterium content of partially reacted chlorobenzene, on the ortho-to-meta ratio of the deuterated aniline produced, and in reasonable agreement on the total deuterium content of the aniline. There can be little doubt that the mechanism is essentially correct.

A referee has pointed out that the excess of aniline-3-^{2}H over aniline-2-^{2}H (56% and 54% of the former in experiments 4 and 5, Table I) suggests a secondary isotope effect on the rates of addition of ammonia to benzyne-2-^{2}H. Roberts and co-workers (13) have observed that inductive electron withdrawal by the substituent in a 2-substituted benzyne favors the formation of 3-substituted addition products. This would indicate that deuterium has a $-I$ effect, as has been suggested by Shiner on other grounds (14). The agreement of our data with Shiner's prediction is interesting, but we doubt whether the accuracy of the analysis warrants a definite conclusion.

ACKNOWLEDGMENTS

The authors wish to thank Dr. H. R. Coish for suggestions regarding the mathematical derivations, Miss A. Hetherington and Dr. B. L. Funt for assistance with the Bendix G-15 computer, and the National Research Council of Canada for a grant in aid of this research.

REFERENCES

1. F. W. Bergstrom, R. E. Wright, C. Chandler, and W. A. Gilkey. J. Org. Chem. **1**, 170 (1936). R. E. Wright and F. W. Bergstrom. J. Org. Chem. **1**, 179 (1936).
2. H. Gilman and S. Avakian. J. Am. Chem. Soc. **67**, 349 (1945).
3. J. F. Bunnett and R. E. Zahler. Chem. Revs. **49**, 382 (1951).

Can. J. Chem. Downloaded from www.nrcresearchpress.com by 210.87.254.6 on 09/05/12
For personal use only.

4. R. A. BENKESER and W. E. BUTING. J. Am. Chem. Soc. **74**, 3011 (1952). R. A. BENKESER and G. SCHROLE. J. Am. Chem. Soc. **75**, 3196 (1953). R. A. BENKESER and R. G. SEVERSON. J. Am. Chem. Soc. **71**, 3838 (1949).
5. J. D. ROBERTS, H. E. SIMMONS, JR., L. A. CARLSMITH, and C. W. VAUGHAN. J. Am. Chem. Soc. **75**, 3290 (1953).
6. J. D. ROBERTS, D. A. SEMENOW, H. E. SIMMONS, JR., and L. A. CARLSMITH. J. Am. Chem. Soc. **78**, 601 (1956).
7. H. GILMAN and F. SCHULZE. J. Am. Chem. Soc. **47**, 2002 (1925).
8. L. H. P. WELDON and C. L. WILSON. J. Chem. Soc. 244 (1946).
9. W. M. LAUER and L. A. ERREDE. J. Am. Chem. Soc. **76**, 5162 (1954).
10. T. H. VAUGHAN, R. R. VOGT, and J. A. NIEUWLAND. J. Am. Chem. Soc. **56**, 2120 (1934).
11. A. S. KESTON, D. RITTENBERG, and R. SCHOENHEIMER. J. Biol. Chem. **122**, 227 (1937).
12. C. ANFINSEN. *In* Preparation and measurement of isotopic tracers. D. W. Wilson, A. O. C. Nier, and S. S. Reimann. Ann Arbor, Mich. 1946. pp. 61–65.
13. J. D. ROBERTS, C. W. VAUGHAN, L. A. CARLSMITH, and D. A. SEMENOW. J. Am. Chem. Soc. **78**, 611 (1956).
14. V. J. SHINER, JR. J. Am. Chem. Soc. **82**, 2655 (1960).

Can. J. Chem. Downloaded from www.nrcresearchpress.com by 210.87.254.6 on 09/05/12
For personal use only.

Can. J. Chem. Downloaded from www.nrcresearchpress.com by 210.87.254.5 on 09/05/12
For personal use only.

THE STRUCTURE OF THE "GUM ASAFOETIDA" POLYSACCHARIDE[1]

J. K. N. JONES AND G. H. S. THOMAS[2]

ABSTRACT

The polysaccharide from gum asafoetida contains D-galactose, L-arabinose, L-rhamnose, 4-*O*-methyl-D-glucuronic acid, and D-glucuronic acid. It is a highly branched polymer which contains a backbone of D-galactopyranose residues which are very probably mainly 1,3-β-linked.

The side chains consist of residues of L-arabinofuranose, D-galactopyranose, D-glucuronic acid, and its 4-*O*-methyl ether.

INTRODUCTION

Oleogum resins such as asafoetida (1), frankincense (2), and myrrh (3) consist in the main of a mixture of polysaccharide and aromatic substances. The impure carbohydrate portion remains when the crude gum is extracted with a solvent such as methanol. It may be purified by pouring its clarified aqueous solution into alcohol. Application of the above procedure to gum asafoetida gave the neutral salt (equiv. wt. 1500) of the polysaccharide as a white powder, readily soluble in cold water to form a conducting solution, which possessed a negative optical rotation (−48°). All attempts to fractionate it were unsuccessful and it was concluded that the polysaccharide was homogeneous. Acidic hydrolysis yielded a mixture of sugars which were characterized as D-galactose, L-arabinose, L-rhamnose, and D-glucuronic acid together with its 4-*O*-methyl derivative and were present in the approximate proportions 5:3:trace:1. Somewhat different figures (14.2%, 26.5%, 1.7%, 17.1% respectively) were obtained by Bézanger-Beauquesne and Chosson (4).

When the polysaccharide was partially broken down by acid, small amounts of two neutral disaccharides and larger amounts of two aldobiouronic acids were isolated. The neutral oligosaccharides were not obtained crystalline; they yielded D-galactose only on hydrolysis and were tentatively characterized by their rates of movement on chromatograms and by the infrared absorption spectra of their acetates (5) as 6-*O*-β-D-galactopyranosyl-D-galactose (6) and the 3-*O*-β-D-galactopyranosyl-D-galactose. Both the acidic disaccharides give D-galactose on hydrolysis, that which moved faster on the chromatogram also yielded 4-*O*-methyl-D-glucuronic acid, which was characterized as the amide of 4-*O*-methyl methyl-α-D-glucuronoside (7). The slower-moving aldobiouronic acid yielded D-glucuronic acid on hydrolysis. Both, after methylation, reduction with lithium aluminum hydride, and further methylation, followed by hydrolysis, gave 2,3,4,6-tetra-*O*-methyl-D-glucose and 2,3,4-tri-*O*-methyl-D-galactose and were therefore identified because of their low positive rotations as 6-*O*-(β-D-glucopyranosyluronic acid)-D-galactose (8) and as 6-*O*-(4-*O*-methyl-β-D-glucopyranosyluronic acid)-D-galactose (9). When the acidic, ash-free, polysaccharide was dissolved in water and the solution heated autohydrolysis occurred with the liberation of L-arabinose and L-rhamnose together with traces of D-galactose and oligosaccharides, leaving a degraded gum which contained D-galactose, D-glucuronic acid, and its 4-*O*-methyl derivatives, and traces (ca. 5%) of L-arabinose. Hydrolysis of the gum with 0.1 *N* hydrochloric acid at 100° for 17 hours

[1]*Manuscript received September 2, 1960.*
Contribution from the Department of Chemistry, Queen's University, Kingston, Ontario, Canada. An abstract of this paper was given at the Atlantic City meeting of the American Chemical Society, September, 1959.
[2]*Present address: Department of Chemistry, Ohio State University, Columbus, Ohio, U.S.A.*

Can. J. Chem. Downloaded from www.nrcresearchpress.com by 210.87.254.5 on 09/05/12
For personal use only.

failed to remove all the L-arabinose residues. The degraded gum at this stage contained a galactose-to-arabinose ratio of approximately 15 to 1. It is possible therefore that some of the pentose residues were in the pyranose form.

Methylation experiments showed that both the original polysaccharide and the degraded polysaccharide were of the branched chain type. The methylated sugars isolated were identified as 2,3,5-tri-*O*-methyl-L-arabinose, 2,3,4,6-tetra-, 2,4,6-tri-, 2,4-di-, and 2-*O*-methyl-D-galactose and 2,3,4-tri-*O*-methyl-D-glucuronic acid. The 2-*O*-methyl-D-galactose derivative was not encountered in the products of hydrolysis of the degraded gum. An L-rhamnose derivative and an L-arabinose (?) derivative remain to be identified in the products of hydrolysis of the undegraded gum. The amounts of sugars were determined by the hypoiodite method of Hirst, Hough, and Jones (10) and were found to be present in the following approximate molecular proportions in the methylated original polysaccharide: 2,3,5-tri-*O*-methyl-L-arabinose plus 2,3,4,6-tetra-*O*-methyl-D-galactose (end groups), (3 + tr. parts); dimethyl-L-arabinose (?) (small); 2,4,6-tri- (2 parts), 2,4-di- (2 parts), and 2-mono-*O*-methyl-D-galactose (1 part); and 2,3,4-tri-*O*-methyl-D-glucuronic acid (1 part). The methylated degraded gum gave the neutral sugars 2,3,5-tri-*O*-methyl-L-arabinose; 2,3,4,6-tetra-*O*-methyl-, 2,4,6-tri-*O*-methyl-, 2,4-di-*O*-methyl-D-galactose; and 2,3,4-tri-*O*-methyl-D-glucuronic acid in the approximate proportion of 1:2:9:6:5. An aqueous solution of the gum was oxidized with sodium metaperiodate solution (cf. 10*a*) and yielded 0.11 mole of formic acid with the consumption of 0.65 mole of metaperiodate per sugar residue (calc. as $C_6H_{10}O_5$) in 30 hours. These figures show that for every sugar oxidized with the formation of formic acid, four other sugars were oxidized and that, in all, approximately half the sugar residues in the polysaccharide were destroyed by the reagent. This supposition is in fair agreement with the methylation results.

Some overoxidation of the polysaccharide would occur because of the presence of end groups of D-glucuronic acid but it is believed that this would not be great because (ca. 75% of) the D-glucuronic acid residues were substituted at C_4 by methoxyl groups which would prevent the formation of an easily overoxidized intermediate. It is assumed that formyl ester production was small.

The degraded gum consumed 0.83 mole of periodate with the production of 0.26 mole of formic acid (per $C_6H_{10}O_5$). Therefore, apparently approximately 75% of the polysaccharide was oxidized and a little over a quarter of the sugar residues were present as end groups which would yield formic acid. These results are not in good agreement with those obtained by the methylation procedure, which indicates that 33% of the polysaccharide should be oxidized and that approximately 20% of the sugars contain hydroxyl groups on each of three contiguous carbon atoms. The reason for the discrepancy is not clear but it may be due to an excess of consumption of metaperiodate at the reducing end of the polysaccharide or to "overoxidation".

The gum was degraded by first oxidizing it with sodium metaperiodate to a polyaldehyde as described above which was reduced with sodium borohydride to the polyalcohol. The product was then degraded by the action of cold dilute acid (Smith *et al.* (11), cf. 11*a*, 11*b*). The degraded polysaccharide was isolated when its solution was poured into ethanol. This material gave galactose and arabinose (ca. 5:1) only on complete hydrolysis. It had a slightly branched structure since on further periodate oxidation it yielded a small amount of formic (0.18 mole per $C_6H_{10}O_5$) and consumed some metaperiodate (0.34 mole per $C_6H_{10}O_5$). The alcohol-soluble fraction contained glycerol, ethylene glycol, and glycosides of arabinose and galactose which yielded these sugars on

acidic hydrolysis. The degraded gum when subjected to further degradation in similar fashion gave a galactan ($[\alpha]_D$ +31°) which was oxidized to a small extent by periodate (0.21 mole consumed per $C_6H_{10}O_5$) and produced traces (0.08 mole per $C_6H_{10}O_5$) of formic acid only on oxidation with metaperiodate.

These results indicate that the polysaccharide consisted of a main chain of mainly 1,3-linked-β-D-galactopyranose residues to which are attached D-galactopyranose, L-arabinofuranose, and L-arabinopyranose (?) residues. The mode of linkage of the last sugar was not identified. To the side chains are attached residues of D-glucuronic acid, its 4-*O*-methyl ether, L-rhamnose, and D-galactose (all in the pyranose form). It is not possible to give an unambiguous structure for gum asafoetida at this stage. The polysaccharide has a much smaller percentage of uronic acid residues than has that from frankincense (2) or that from myrrh (3).

EXPERIMENTAL

Paper chromatography was performed by the descending method on Whatman No. 1 paper. Small-scale qualitative separations were carried out by the method of Hirst, Hough, and Jones (12) on Whatman No. 3MM paper. Larger-scale separations were carried out by partition chromatography on cellulose columns using the method of Hough, Jones, and Wadman (13). Chromatographic separations were also conducted on charcoal columns (14) which consisted of a mixture (1:1 w/w) of activated charcoal (Darco C-60) and "Celite". Charcoal columns were eluted with water and/or ethanol.

The following solvent systems were used to separate the neutral sugars by paper chromatography (all v/v):

(A) butan-1-ol, ethanol, water (3:1:1);
(B) butan-1-ol, pyridine, water (10:3:3);
(C) benzene, ethanol, water (169:15:47).

Acidic solvents were used to separate uronic acids and their derivatives.

(D) ethyl acetate, acetic acid, water (9:2:2);
(E) ethyl acetate, acetic acid, formic acid, water (18:3:1:4).

The sugars were detected on paper chromatograms either by spraying them with a 1% solution of *p*-anisidine hydrochloride (15) in butan-1-ol followed by heating the chromatogram, or the chromatogram was sprayed with a 1% solution of silver nitrate in acetone followed by 2% ethanolic sodium hydroxide. The rates of movement of sugars are quoted relative to a standard sugar, e.g. R_{Rh} and R_G (relative to rhamnose, and 2,3,4,6-tetra-*O*-methyl-D-glucose). Paper electrophoresis was carried out in a borate buffer at pH 10 (16). Solutions were concentrated under reduced pressure at ca. 40° C or lower. Optical rotations were measured in water and at 26°±2° (unless otherwise stated).

Extraction of the Gum

The crude material consisted of the oleogum resin admixed with sand, bark, and organic debris. This material (707 g) was exhaustively extracted with hot methanol until a sample of the methanol extract gave no turbidity when poured into water. The residue was collected by centrifugation and extracted with water. The brownish-green extracts were concentrated to a volume of 150 ml and poured into ethanol (2 l.) to which hydrochloric acid (5 ml:10 *N*) had been added. The precipitate was collected (centrifuge), redissolved in ice-cold water (150 ml), and the precipitation procedure repeated twice more. The solid resulting was well washed with ethanol to remove hydrochloric acid, then with ether and was dried under reduced pressure. Yield, 120 g (17%).

Can. J. Chem. Downloaded from www.nrcresearchpress.com by 210.87.254.5 on 09/05/12
For personal use only.

Attempted Fractionation of the Polysaccharide

The polysaccharide (20 g) was dissolved in water (1 liter) and ethanol (500-ml portions) was added with vigorous stirring. The polysaccharide was collected by centrifugation after each addition of ethanol. Four main fractions were obtained. Each fraction had $[\alpha]_D$ $-48°\pm2°$; equiv. wt., 1490 ± 10; and OMe, 1.6%. Each fraction gave on hydrolysis sugars which moved on paper chromatograms, at the rate of L-arabinose, D-galactose, and L-rhamnose plus 4-*O*-methyl-D-glucuronic acid.

Use of "Cetavlon" (17)

The polysaccharide (1 g) was dissolved in water (10 ml) and aqueous "Cetavlon" (20% w/v) was added until precipitation was complete. The precipitate was collected, dissolved in a minimum volume of aqueous sodium chloride (10% w/v), and the solution was poured into ethanol. The precipitate was dissolved in water and dialyzed against tap water until the solution was free from chloride (2 days). The dialyzate was concentrated and poured into two volumes of ethanol. The precipitate was collected, washed with ethanol and ether, and dried. Yield, 0.87 g.

The fraction which was not precipitated by "Cetavlon" was recovered when the solution was concentrated and poured into ethanol. The solid was dissolved in water, the solution dialyzed and recovered as described above. The product weighed 0.04 g. Both fractions had $[\alpha]_D$ $-48°\pm2°$ (*c*, 1.0) and equiv. wt. 1500 ± 10.

Preparation of Gum Acetate

The polysaccharide (5 g) was added, in small portions, to *N*,*N*-dimethylformamide (100 ml) at 30° C. After stirring for 1 hour the suspension had dissolved. Pyridine (90 ml) was then added portionwise during 30 minutes followed by acetic anhydride (32 ml) which was added in four equal portions during 4 hours. The solution was stirred for a further 5 hours at 32° C and then left at 20° C overnight. The solution was then poured with vigorous stirring into cold hydrochloric acid (1 liter; 2%) plus chopped ice (50 g). The precipitated cream-colored product was collected by filtration, washed well with hydrochloric acid (0.5%), and then with water (250 ml, ×5). The product (8 g) had $[\alpha]_D$ $-52°$ (*c*, 2.0 in $CHCl_3$). Found: $-COCH_3$, 42%.

The fractionation of this product by the method of Goodban and Owens (18) was attempted and yielded fractions with $[\alpha]_D$ $-46°\pm2°$ (*c*, 2.0 in $CHCl_3$) and $-COCH_3$, 41 ± 1%. No fractionation had been achieved.

Autohydrolysis of the Gum Polysaccharide

The gum (15 g) was obtained in an ash-free form by passing its aqueous solution through columns of ion-exchange material (Amberlite IR-120 and IR-4B). The acidic eluate was concentrated to a small volume and was precipitated by adding its solution to three volumes of ethanol. The precipitate was dissolved in water (750 ml) and the resulting viscous brown solution was heated under reflux on a steam bath.

At intervals samples were withdrawn and were analyzed chromatographically. The darkness of the solution prevented polarimetric observation being taken. L-Arabinose was the first reducing sugar to appear in the autohydrolyzate and no other sugar was detected until after 26 hours, when traces of D-galactose and L-rhamnose were liberated. The solution was then concentrated to a small volume (30 ml) and poured into ethanol with vigorous stirring. The precipitated degraded product was collected, washed with ethanol and acetone, and dried (yield 11 g, 73%). The supernatant solution from the precipitation was concentrated to a syrup which was dissolved in hot methanol and the

Can. J. Chem. Downloaded from www.nrcresearchpress.com by 210.87.254.5 on 09/05/12
For personal use only.

solution was filtered first through charcoal and then through celite. Concentration of this filtrate gave crystalline L-arabinose of melting point 160° C and $[\alpha]_D$ +105°.

Further Hydrolyses of the Degraded Polysaccharide

The degraded polysaccharide (5 g) was dissolved in formic acid solution (1%; 500 ml) and the solution was boiled under reflux for 10 hours. The solution was then evaporated to a syrup which was boiled with water and the solution was again evaporated to hydrolyze formyl esters. This process was repeated several times. Finally the residue was dissolved in water (50 ml) and the solution was poured into ethanol (2 l.) and the precipitate was collected. This product was washed well with ethanol and dried. It had $[\alpha]_D$ +2° (*c*, 1.0). The supernatant was concentrated to a syrup and examined chromatographically. It contained sugars which moved at the rate of galactose, arabinose, and rhamnose (solvent A and B) plus two neutral oligosaccharides and an aldobiouronic acid (solvent E).

The syrup was fractionated on a cellulose column (4×30 cm) using solvent D as the mobile phase and yielded fraction I: L-rhamnose, $[\alpha]_D$ +9° (*c*, 1.0), m.p. 91° C, identical with an authentic sample; fraction II: L-arabinose, $[\alpha]_D$ +100° (*c*, 1.0), m.p. 160° C, not depressed on admixture with an authentic sample; fraction III: D-galactose, $[\alpha]_D$ +81° (*c*, 1.0), m.p. 119° C, indistinguishable from an authentic specimen; fraction IV: had $R_{galactose}$ 0.61 and behaved like an aldobiouronic acid. It had $[\alpha]_D$ +1° (*c*, 1.0) and equiv. wt. 364 and after hydrolysis with 2 *N* sulphuric acid, yielded sugars which moved at the rates of 4-*O*-methyl-D-glucuronic acid and D-galactose. Fraction V was a neutral oligosaccharide which on hydrolysis with 2 *N* sulphuric acid yielded D-galactose only. Fraction VI was also a neutral oligosaccharide which on hydrolysis with 2 *N* sulphuric acid gave D-galactose only.

Characterization of Fractions V and VI

Their rates of movement on chromatograms indicated that both these substances were D-galactose-containing disaccharides. Their rates of movement on paper chromatograms in solvents A, B, D, and E and a comparison of their infrared spectra indicated that they were 3- and 6-*O*-β-D-galactopyranosyl-D-galactose. The corresponding acetates (amorphous) were prepared on the microscale by the method of White *et al.* (5) and their infrared absorption spectra were compared with authentic specimens and found to be identical. Neither disaccharide was obtained crystalline.

Large-scale Preparation of Aldobiouronic Acids

Insufficient quantity of fraction IV was available for characterization and a further quantity was prepared. The original polysaccharide (15 g) was dissolved in water (200 ml) and deionized by passing its solution down columns of ion-exchange resin (Amberlite IR-120).

The eluate was concentrated to a small volume (25 ml) and poured into ethanol (2 liters). The precipitate was collected (centrifuge), and washed with ethanol and acetone, and dried. The dried acidic polymer (8 g) was dissolved in sulphuric acid (800 ml, 2 *N*) and the solution was heated under reflux for 8 hours. Test experiments on small quantities of material had indicated that these conditions gave maximum yields of aldobiouronic acids. The solution was cooled, neutralized ($BaCO_3$), filtered and the filtrate was concentrated to a small volume and poured into ethanol (five volumes). The barium salts were collected, washed with alcohol, and dried. The ethanol solution on concentration gave a syrup which contained D-galactose, L-arabinose, and L-rhamnose.

Can. J. Chem. Downloaded from www.nrcresearchpress.com by 210.87.254.5 on 09/05/12
For personal use only.

Can. J. Chem. Downloaded from www.nrcresearchpress.com by 210.87.254.5 on 09/05/12
For personal use only.

The barium salts were dissolved in water, deionized (Amberlite IR-120 resin) and the solution was concentrated. The mixture of monosaccharides and oligosaccharides was separated on a squat charcoal – celite column by the method of Hough *et al.* (19). Elution with water removed the monosaccharides and elution with up to 30% aqueous ethanol displaced two aldobiouronic acids which were not separated from one another. Separation of these was achieved on sheets of Whatman 3MM paper using solvent E for development. The faster-moving component was identical with fraction IV (above) and was identified as 6-*O*-(4-*O*-methyl-D-glucopyranosyl uronic acid)-D-galactose. The slower-moving component was the corresponding unmethylated aldobiouronic acid.

Proof of Structure of the Aldobiouronic Acids

The acid (fraction IV, 200 mg) was dissolved in water (3 ml) and methylated with dimethyl sulphate (1.5 ml) and sodium hydroxide (30%; 3 ml) in the usual way. The partially methylated acid was isolated and methylated with Purdie's reagent (20). The resultant methylated ester glycoside (180 g) was dissolved in tetrahydrofuran (50 ml) and reduced by the dropwise addition with stirring of a solution of lithium aluminum hydride (600 ml) in tetrahydrofuran (25 ml).

After 24 hours, excess of lithium aluminum hydride was destroyed by the cautious addition first of ethyl acetate and then of water. The slurry was filtered and the filtrate was evaporated to a small volume which was continuously extracted with chloroform. Complete methylation of the disaccharide was achieved, by the gradual addition during 3 hours of dimethyl sulphate (3 ml) to a stirred solution of the syrup in tetrahydrofuran (15 ml) containing pulverized sodium hydroxide (26 g).

After 16 hours water was added to dissolve the solids and the mixture was heated to 80° to decompose dimethyl sulphate. The solution was neutralized, concentrated, and the residual solution exhaustively extracted with chloroform. Concentration of the extracts yielded the methylated neutral disaccharide (138 mg). Found: OMe, 54.2%. Calc. for $C_{20}H_{38}O_{11}$: OMe, 54.8%.

The methylated disaccharide (135 gm) was hydrolyzed by boiling its solution in formic acid (50%, 25 ml) for 6 hours, and after evaporation of the formic acid, with boiling hydrochloric acid (*N*; 25 ml), for 4 hours.

The hydrolyzate was neutralized (Ag_2CO_3), filtered, and the filtrate was evaporated to a syrup. Paper chromatography of the syrup indicated the presence of three sugars, the two major components were tentatively identified as 2,3,4,6-tetra-*O*-methyl-D-glucose and 2,3,4-tri-*O*-methyl-D-galactose. A third trace component of R_G 0.84 (solvent A) was not identified. The sugars were separated on 3MM paper and the two major fractions were identified in the usual way. The fast-moving component had $[\alpha]_D$ +80° (*c*, 1.0) and gave a crystalline *N*-phenylglycosylamine derivative on boiling its solution in ethanol with aniline. The product had a melting point of 116–117° C and $[\alpha]_D$ +205° (*c*, 1.0 in acetone). Its melting point was not depressed on admixture with authentic 2,3,4,6-tetra-*O*-methyl *N*-phenyl-D-glucosylamine.

The slow-moving syrup (R_G, 0.69 in solvent A) had $[\alpha]_D$ +96° (*c*, 1.0). On heating it in ethanol solution with aniline characteristic rhombic crystals of 2,3,4-tri-*O*-methyl-*N*-phenyl-D-galactosylamine were produced, $[\alpha]_D$ −50° → +46° (*c*, 1.0 in methanol), m.p. 169° C not depressed on admixture with an authentic specimen.

The second aldobiouronic acid contained no methoxyl residue and on hydrolysis with sulphuric acid (2 *N*) it yielded D-galactose, D-glucuronic acid, and D-glucurone (chromatographic evidence). It was methylated and then reduced with lithium aluminum

hydride as described above. The product was remethylated then hydrolyzed and yielded 2,3,4,6-tetra-*O*-methyl-D-glucose and 2,3,4-tri-*O*-methyl-D-galactose characterized as described above.

Quantitative Determination of Component Sugars Present in the Polysaccharide

The ash-free gum (40 g) was dissolved in *N* sulphuric acid (10 ml) and the solution was boiled under reflux for 10 hours. The solution was cooled, ribose (10 mg) was added, and the solution was then neutralized ($BaCO_3$) and filtered. The filtrate was concentrated to a syrup and the sugars were separated on Whatman 3MM paper. The position and quantity of sugars were determined by the method of Hirst, Hough, and Jones (10). Found: arabinose, 33%; rhamnose, 2%. Galactose was not determined.

Periodate Oxidation of the Undegraded Polysaccharide

The polysaccharide (100 mg) was dissolved in water (20 ml) and titrated to neutrality with sodium hydroxide (0.01 *N*) using screened methyl red as indicator. Sodium metaperiodate solution (5 ml; 0.3 *M*) was added and the solution was made up to 100 ml. A blank solution was prepared similarly. Oxidation was allowed to proceed in the dark at 20°. The periodate uptake was determined by the method of Willard and Greathouse (20) but using phosphate in place of borate and the formic acid production by the method of Halsall, Hirst, and Jones (21). Found: moles of metaperiodate consumed and moles of formic acid produced per $C_6H_{10}O_5$: 0.22, 0.08 (1 hour); 0.32, 0.08 (3 hours); 0.36, 0.10 (6 hours); 0.48, 0.11 (11 hours); 0.57, 0.11 (23 hours); 0.65, 0.11 (36 hours). Acidic hydrolysis of the periodate-oxidized polysaccharide yielded galactose only.

Periodate Oxidation of the Degraded Polysaccharide

The degraded polysaccharide (100 mg) was oxidized with sodium metaperiodate solution as described above. Found: (moles of metaperiodate consumed and moles of formic acid produced for $C_6H_{10}O_5$): 0.37, 0.15 (1 hour); 0.45, 0.15 (3 hours); 0.57, 0.15 (6 hours); 0.63, 0.16 (11 hours); 0.73, 0.19 (23 hours); 0.83, 0.26 (30 hours).

When the periodate-oxidized polysaccharide was recovered and hydrolyzed with dilute sulphuric acid galactose was the only sugar which could be detected chromatographically.

Periodate Oxidation and Degradation of the Gum. Stage I

The gum (16.2 g) was dissolved in water (100 ml) and oxidized with sodium metaperiodate (25 g) in water (150 ml) during 72 hours at 20° C with stirring. The solution was diluted with methanol (500 ml) and the precipitated salts were removed by filtration. The filtrate was evaporated to a small volume and sodium borohydride (6 g) in water (100 ml) was added to the solution. Sulphuric acid (2 *N*; 100 ml) was added and the mixture was left at 20° C for 18 hours. The solution was neutralized ($BaCO_3$), filtered, and the filtrate deionized with Amberlite resin 1R-120 (H). The filtrate was concentrated to 25 ml under reduced pressure and poured into ethanol. The precipitate was collected, dried, and weighed; yield, 4.5 g. This product (equiv. wt., 4300) was insoluble in water after it was dried. It contained galactose and arabinose in the approximate ratio of 5 to 1 (chromatographic evidence) and traces of acid. The alcoholic filtrate on concentration yielded a syrup (8 g) which contained glycerol, glycol, and glycosides, which on hydrolysis yielded galactose and arabinose in the approximate ratio of 1 to 1 (chromatographic evidence).

Periodate Oxidation of the Periodate-degraded Polysaccharide

The sample (20 mg) was oxidized in a volume of 100 ml by the addition of sodium

Can. J. Chem. Downloaded from www.nrcresearchpress.com by 210.87.254.5 on 09/05/12
For personal use only.

metaperiodate solution (0.1 *M*, 5 ml) and water at 4° C in the dark. At intervals samples were withdrawn and the metaperiodate uptake and formic acid production were measured. Found: moles of metaperiodate consumed and moles of formic acid produced per 162 g polysaccharide: 0.27, 0.10 (4 hours); 0.3, 0.14 (6 hours); 0.36, 0.18 (24 hours); 0.40, 0.15 (48 hours); 0.42, 0.15 (72 hours); 0.44, 0.18 (96 hours).

Periodate Oxidation of the Gum. Stage II

The periodate-oxidized and periodate-degraded gum (3.5 g) was shaken with a solution of sodium metaperiodate (3 g) in water (50 ml) for 6 days at 20° C. The oxidized product was isolated from the clear solution as described above; the substance was reduced with a solution of sodium borohydride (3 g) in water (100 ml). After 24 hours, the solution was acidified with sulphuric acid (2 *N*, 100 ml) and kept at 20° C for a further 24 hours. The solution was then neutralized ($BaCO_3$), filtered, and the filtrate was deionized (Amberlite ion exchange resin, IR 120-H). The twice-degraded neutral polysaccharide (2 g) was isolated as described above. This material on hydrolysis yielded galactose only (chromatographic evidence) and had $[\alpha]_D$ $+31°\pm5°$ (*c*, 1.0). The alcohol-soluble material contained glycerol, glycol, and small quantities of galactose-containing glycosides.

Periodate Oxidation of the Gum. Stage III

The degraded gum (20 mg) was oxidized at a concentration of 20% with aqueous sodium metaperiodate (0.1 *M*, 5 ml) at 4° C in the dark. Found: moles of periodate consumed and moles of formic acid produced per $C_6H_{10}O_5$: 0.17, 0.08 (4 hours); 0.17, 0.08 (14 hours); 0.21, 0.08 (24 hours); 0.23, 0.10 (48 hours); 0.27, 0.12 (72 hours); 0.32, 0.11 (96 hours). Extrapolation to zero time gave an uptake of 0.21 mole of metaperiodate and a formation of 0.08 of formic acid per $C_6H_{10}O_5$.

Methylation of the Undegraded Polysaccharide

The acetylated polysaccharide (11 g) was dissolved in acetone (200 ml) and methylated with dimethyl sulphate and sodium hydroxide in the usual way. The product was dissolved in a mixture of methanol and methyl iodide and the solution was boiled under reflux; silver oxide was added portionwise to the solution. At the completion of the experiment (24 hours) the product was isolated in the usual way. Methylation was completed when the product was dissolved in dry tetrahydrofuran (200 ml), admixed with powdered sodium hydroxide (40 g), and dimethyl sulphate (13.5 ml) added with stirring at 20° C during 24 hours. The product (6 g) was isolated from the aqueous solution by extraction with chloroform, after the solution had been diluted with water, neutralized with dilute sulphuric acid, and dialyzed against tap water to remove salts, and concentrated. The methylated product had $[\alpha]_D$ $-76°$ (*c*, 1.0 in $CHCl_3$). Found: OMe, 40.5%. The product was fractionated by extracting it with mixtures of chloroform – light petroleum (b.p. 60–80° C). Two major products were isolated: (1) $[\alpha]_D$ $-75°$; OMe, 42%; and (2) $[\alpha]_D$ $-76°$ (*c*, 1.0 in $CHCl_3$); OMe, 42%. The fractions (1 g and 5 g, respectively) were combined and hydrolyzed as described below.

Hydrolysis of Methylated Gum

The methylated polysaccharide (5 g) was dissolved in formic acid (50%, 400 ml) and the solution was heated under reflux until the optical rotation reached a constant value (+35°). The solvent was removed and the syrupy residue was boiled with water and the solution concentrated. This process was repeated once more. The residue was dissolved in dilute sulphuric acid (2 *N*, 100 ml) and the solution was heated at 100° for 4 hours.

Can. J. Chem. Downloaded from www.nrcresearchpress.com by 210.87.254.5 on 09/05/12
For personal use only.

The cooled solution was then neutralized ($BaCO_3$), filtered, and the filtrate was concentrated to a syrup. The product was dissolved in water and the solution passed down columns of Amberlite ion exchange resins, IR-120 and IR-4B, and the effluent was concentrated to a syrup (4.28 g) which contained neutral sugars only. The acidic sugars (0.64 g) were recovered when the basic resin (IR-4B) was washed with 30% formic acid and the effluent was concentrated.

A quantitative determination of the sugars present in this mixture was made by the method of Hirst, Hough, Jones (10). Found: end group (3 parts); tri-*O*-methyl hexose (2 parts); di-*O*-methyl hexose (2 parts); mono-*O*-methyl hexose (1 part); and methylated uronic acid (end group) (1 part).

Characterization of the Methylated Neutral Sugars

The syrup (4.28 g) was separated on a cellulose column (50×4 cm) using light petroleum (b.p. 100–120° C):butan-1-ol (7:3) as the mobile phase. Six fractions were obtained: Fraction I had $[\alpha]_D$ −30° and OMe 47.2% and consisted chromatographically of one component only. A portion (100 mg) of the syrup was oxidized with bromine water in the usual way and the resulting lactone was dissolved in methanolic ammonia to yield crystalline 2,3,5-tri-*O*-methyl-L-arabonamide, m.p. and mixed m.p. 134° C, $[\alpha]_D$ −15° (*c*, 1.0). Fraction II was chromatographically pure and had $[\alpha]_D$ +108° and moved at the same rate as 2,3,4,6-tetra-*O*-methyl-D-galactose in solvent A, B, and C. Found: OMe, 51.9. Calc. for $C_{10}H_{20}O_6$: OMe, 52.5%. A portion of the syrup was boiled with ethanolic aniline and yielded 2,3,4,6-tetra-*O*-methyl-*N*-phenyl-D-galactosylamine, m.p. 192° C, not depressed on admixture with an authentic specimen, $[\alpha]_D$ 40° (in acetone, equilibrium value). Fraction III was a mixture and was not characterized. Fraction IV moved chromatographically at the same rate as 2,4,6-tri-*O*-methyl-D-galactose and had OMe, 41.6% (calc. for $C_9H_{18}O_6$: OMe, 41.9%) and $[\alpha]_D$ 87°. The derived crystalline *N*-phenylglycosylamine derivative was identified as 2,4,6-tri-*O*-methyl-*N*-phenyl-D-galactosylamine, of m.p. 176°, not depressed by an authentic specimen. The infrared spectra of the derivative and of an authentic specimen were identical. Fraction V crystallized. It behaved chromatographically like 2,4-di-*O*-methyl-D-galactose in solvents A, B, and C. It had m.p. 102° C, not depressed on admixture with an authentic specimen and $[\alpha]_D$ +130° → 86° (constant 2 hours) (*c*, 1.0). The derived *N*-phenyl-D-galactosylamine had m.p. 215° C and was indistinguishable from an authentic specimen. Fraction VI was a syrup and had the properties of a mono-*O*-methyl hexose. (Found: OMe, 15.8%. Calc. for $C_7H_{14}O_6$: OMe, 16%). When nucleated with 2-*O*-methyl-D-galactose the syrup crystallized. The product had m.p. 148° C, not depressed on admixture with an authentic specimen and $[\alpha]_D$ +60° → 89° (2 hours constant) (*c*, 1.0). The derived *N*-phenyl-D-galactosylamine had m.p. 163° C and this product was indistinguishable from an authentic specimen.

Characterization of the Acidic Fraction

This syrupy material moved as one component (R_G 0.84) on a chromatogram (solvent E) and had $[\alpha]_D$ +40° (*c*, 1.0). Further hydrolysis with hot dilute acid did not liberate any neutral sugars. The syrup (250 mg) was dissolved in methanolic hydrogen chloride (2%; 20 ml) and boiled under reflux for 8 hours. The solution was then non-reducing to Fehling's solution. The solution was neutralized (Ag_2CO_3), filtered, and the filtrate was concentrated to a syrup. This was dissolved in dry tetrahydrofuran and the solution was added dropwise to a solution of lithium aluminum hydride (0.1 g) in tetrahydrofuran. After 24 hours the reduced product was isolated in the usual way and hydrolyzed with hot

Can. J. Chem. Downloaded from www.nrcresearchpress.com by 210.87.254.5 on 09/05/12
For personal use only.

(92° C) dilute hydrochloric acid (2 *N*, 10 ml) for 6 hours. The resultant sugar had R_G 0.85 (solvent A) and was indistinguishable from 2,3,4-tri-*O*-methyl-D-glucose, $[\alpha]_D$ 65° (*c*, 1.0) (Found: OMe, 41.5%. Calc. for $C_9H_{18}O_6$: OMe, 41.9%). When the sugar was dissolved in ethanol containing aniline and the mixture heated under reflux for 5 hours 2,3,4-tri-*O*-methyl-*N*-phenyl-D-glucosylamine, m.p. and mixed m.p. 145° C, was produced.

Methylation of the Degraded Polysaccharide

The polysaccharide (5 g) was acetylated using the conditions described above for the acetylation of the original polysaccharide. The acetylated product (7 g) was methylated with sodium hydroxide and dimethyl sulphate in the usual manner and the methylated product was isolated. This material still contained hydroxyl groups (infrared spectrum) and methylation was therefore completed by the method of Kuhn *et al.* (22). The product (3 g) had OMe, 42.5%, and its infrared spectrum showed a trace of hydroxyl band.

Fractionation.—The acidic methylated degraded gum was treated with diazomethane and the neutral product was extracted with chloroform – light petroleum mixture (b.p. 100–120° C) of increasing chloroform concentration. Two main fractions were obtained which had $[\alpha]_D$ −50°±1° (*c*, 1.0, acetone); OMe, 44%; and equiv. wt., 940.

Hydrolysis of the Methylated Degraded Gum

The methylated degraded gum (2.9 g) was hydrolyzed with hot 50% aqueous formic acid as described for the hydrolysis of the original methylated polysaccharide. The sugars (2.9 g) were separated into neutral (2.2 g) and acidic (0.61 g) fractions on ion-exchange columns. A quantitative analysis of the mixture by the method of Hirst, Hough, and Jones (10) and by weighing the fractions eluted from the cellulose chromatographic columns (see below) gave an approximate ratio of end group:tri-*O*-methyl-hexose:di-*O*-methyl-hexose of 1:2:1(for fuller details see theoretical section).

Fractionation of Neutral Sugars

The neutral sugars (2.2 g) were fractionated on a cellulose column by the method of Hough, Jones, and Wadman (23). Six fractions were obtained. Fraction I (120 mg) had $[\alpha]_D$ −30° (*c*, 1.0) and was chromatographically identical in solvents A, B, and C with 2,3,5-tri-*O*-methyl-L-arabinose. Demethylation of a portion of the product with aqueous hydrobromic acid indicated the presence of arabinose only. A sample of the sugar was oxidized to the acid, the derived amide had a melting point of 134° C, $[\alpha]_D$ −15° (*c*, 1.0) and was indistinguishable from 2,3,5-tri-*O*-methyl-L-arabonamide. Fraction II (180 mg) was chromatographically pure and identical with 2,3,4,6-tetra-*O*-methyl-D-galactose. It had R_G 0.88 (solvent A) $[\alpha]_D$ +82° (*c*, 1.0) and the derived 2,3,4,6-tetra-*O*-methyl-*N*-phenyl-D-galactosylamine had a melting point of 190–191° C, not depressed on admixture with an authentic specimen, and $[\alpha]_D$ +40° (*c*, 1.0 in acetone; equilibrium value). Fraction III (130 mg) was a mixture of 2,3,4,6-tetra-*O*-methyl-D-galactose (30 mg) and an unknown sugar (100 mg). Fraction IV (500 mg) was chromatographically pure and was identified as 2,4,6-tri-*O*-methyl-D-galactose with R_G 0.71 (solvent A), and $[\alpha]_D$ +87° (*c*, 1.0). The *N*-phenylglycosylamine derivative had a melting point of 171° C and $[\alpha]_D$ 40° (*c*, 1.0, acetone) and was indistinguishable by infrared spectroscopy from an authentic specimen. Fraction V (700 mg) was a mixture of 2,4,6-tri-*O*-methyl-D-galactose and of the 2,4-di-*O*-methyl derivative. Fraction VI (570 mg) had $[\alpha]_D$ +80° and crystallized. It was recrystallized from acetone and was identified as 2,4-di-*O*-methyl-D-galactose, m.p. 102° C, $[\alpha]_D$ +86° (*c*, 1.0), which was further characterized as the aniline derivative of melting point 215° C.

Can. J. Chem. Downloaded from www.nrcresearchpress.com by 210.87.254.5 on 09/05/12
For personal use only.

Characterization of the Acidic Fraction

The acidic fraction (0.61) moved as one material on the chromatogram and had $[\alpha]_D$ +40° (*c*, 1.0). It was not affected by hot dilute hydrochloric acid and therefore did not contain any oligosaccharide derivatives. It was converted by boiling its solution in methanolic hydrogen chloride to the corresponding ester $\alpha+\beta$-glycoside. When this syrupy ester was dissolved in methanol and the solution was saturated with ammonia, the crystalline amides were produced. Recrystallization from ethanol–ether yielded pure 2,3,4-tri-*O*-methyl methyl α-D-glucuronamide, which had a melting point of 183° C and $[\alpha]_D$ +138° (*c*, 1.0) (7).

ACKNOWLEDGMENTS

The authors thank Queen's University and National Research Council of Canada for financial assistance (NRC-T39) which made this work possible.

REFERENCES

1. G. E. TREASE. Textbook of pharmacognosy. Bailiere, Tindall, and Cox, London. 1949. p. 447.
2. J. K. N. JONES and J. R. NUNN. J. Am. Chem. Soc. **77**, 5745 (1955).
3. J. K. N. JONES and J. R. NUNN. J. Chem. Soc. 3001 (1954).
4. L. BÉZANGER-BEAUQUESNE and J. CHOSSON. Ann. pharm. franç. **16**, 665 (1958).
5. J. W. WHITE, C. R. EDDY, J. PETTY, and N. HOBAN. Anal. Chem. **30**, 506 (1958).
6. D. H. BALL and J. K. N. JONES. J. Chem. Soc. 905 (1958).
7. F. SMITH. J. Chem. Soc. 2646 (1951).
8. S. W. CHALLINOR, W. N. HAWORTH, and E. L. HIRST. J. Chem. Soc. 258 (1931).
9. J. I. CUNNEEN and F. SMITH. J. Chem. Soc. 1141 (1948).
10. E. L. HIRST, L. HOUGH, and J. K. N. JONES. J. Chem. Soc. 928 (1949).
10.(*a*) J. J. CONNELL, R. M. HAINSWORTH, E. L. HIRST, and J. K. N. JONES. J. Chem. Soc. 1696 (1950).
11. I. J. GOLDSTEIN, G. W. HAY, B. A. LEWIS, and F. SMITH. Abstracts of Papers, 135th Meeting of the American Chemical Society, Boston, Mass. 1959. 3D.
11.(*a*) T. DILLON, D. F. O'CEALLACHAN, F. DONNACHADHA, and P. O'COLLA. Proc. Roy. Irish Acad. B, **55**, 331 (1953).
(*b*) E. L. HIRST, J. K. N. JONES, and A. J. ROUDIER. J. Chem. Soc. 1779 (1948).
12. E. L. HIRST, L. HOUGH, and J. K. N. JONES. J. Chem. Soc. 928 (1949).
13. L. HOUGH, J. K. N. JONES, and W. H. WADMAN. J. Chem. Soc. 2511 (1949).
14. R. L. WHISTLER and D. F. DURSO. J. Am. Chem. Soc. **72**, 677 (1950).
15. L. HOUGH, J. K. N. JONES, and W. H. WADMAN. J. Chem. Soc. 1702 (1950).
16. A. B. FOSTER. Advances in Carbohydrate Chem. **12**, 81 (1957).
17. B. C. BERA, A. B. FOSTER, and M. STACEY. J. Chem. Soc. 3788 (1955).
18. A. E. GOODBAN and H. S. OWENS. J. Polymer Sci. **23**, 825 (1957).
19. P. A. ANDREWS, L. HOUGH, and D. B. POWELL. Chem. & Ind. (London), 658 (1956).
20. H. H. WILLARD and L. H. GREATHOUSE. J. Am. Chem. Soc. **60**, 2869 (1938).
21. T. G. HALSALL, E. L. HIRST, and J. K. N. JONES. J. Chem. Soc. 1399, 1427 (1947).
22. R. KUHN, H. TRISCHMAN, and I. LÖW. Angew. Chem. **67**, 32 (1955).

Can. J. Chem. Downloaded from www.nrcresearchpress.com by 210.87.254.5 on 09/05/12
For personal use only.

Can. J. Chem. Downloaded from www.nrcresearchpress.com by 210.87.254.5 on 09/05/12
For personal use only.

SHEAR DEPENDENCE IN THE VISCOMETRY OF HIGH POLYMER SOLUTIONS

A NEW VARIABLE-SHEAR CAPILLARY VISCOMETER[1]

L. H. CRAGG[2] AND H. VAN OENE[2]

ABSTRACT

The principles of capillary viscometry are reviewed, and design criteria for capillary viscometers to be used with non-Newtonian liquids are discussed. A description is given of a new type of variable-shear capillary viscometer—a modification of the Ubbelohde suspended-level viscometer—designed for measurements in the low-shear range. The instrument is rugged, convenient, and precise, and makes possible measurements at free fall over a 10-fold range of shear stress (or shear rate), a range that can easily be extended by use of two or more suitably modified instruments or by the application of external pressure. Experimental evidence is presented to show that proper choice of the dimensions of the instrument eliminates or minimizes most of the "effects" that limit the precision of measurements of relative viscosity (and related functions) of high polymer solutions in the range of low shear stresses.

A. INTRODUCTION

For many years now the measurement of viscosity has been a powerful and much-used procedure in the study of high polymer systems and particularly of polymers in dilute solutions. In most of these studies, capillary viscometers have been used, because they are relatively inexpensive and convenient. Many different types of capillary viscometers have been designed to meet special needs. One particularly convenient viscometer (1), a modification of the Ubbelohde instrument (2), makes possible dilution in the viscometer itself and so greatly facilitates obtaining the data necessary for the determination of intrinsic viscosities (limiting viscosity numbers).

The ordinary capillary viscometers (Ostwald, Cannon-Fenske, Ubbelohde, etc.), when used as they were meant to be used, provide measurements all made at the same (or very nearly the same) driving pressure. They were not designed for use with non-Newtonian liquids, with which measurements should be made at a number of different driving pressures. Until fairly recently this seldom mattered. Now, however, there is more and more interest in polymers whose solutions are non-Newtonian liquids. For these, the familiar instruments and the time-honored procedures are not satisfactory and, unless suitably modified, may yield completely spurious results.

Several capillary viscometers that have been designed for use with non-Newtonian systems have been described (3, 4, 5, 6, 7). These give good results at relatively large shear stresses, say in the range 5–20 dynes/cm^2. But most of them are not satisfactory for use at low stresses and hence cannot provide the data for a reliable extrapolation to zero shear stress. This is a serious inadequacy, for it is generally accepted that, in the study of polymers whose dilute solutions are non-Newtonian (polymers of very high molecular weight or with very stiff molecules), the quantity of greatest interest is the intrinsic viscosity at zero shear stress, a quantity that must be determined by extrapolation of data obtained at low shear stresses. That there is need for a rethinking of designs and procedures is evidenced by the fact that careful measurements with different variable-shear capillary viscometers have given results in the low-shear region that are

[1]*Manuscript received August 24, 1960.*
Contribution from the Department of Chemistry, McMaster University, Hamilton, Ontario, based on a thesis submitted by H. van Oene in October, 1958, in partial fulfillment of the degree M.Sc., and presented in part at 42nd Annual Conference of the Chemical Institute of Canada, Halifax, May 1959.
[2]*Present address: Department of Chemistry, University of Alberta, Edmonton, Alberta.*

at variance both with theory and with other experiments. Theory (8, 9) required a quadratic dependence on the shear stress to account for the fact that the viscosity of a liquid does not depend on the direction of the flow, that is, on the sign of the shear stress; and results obtained with Couette-type viscometers, which are intrinsically much better suited to shear-dependence studies, did in fact show this quadratic dependence (10), rather than a linear or exponential dependence indicated by results obtained with capillary viscometers (11, 12).

Since, in our judgment, existing variable-shear viscometers were either unsuited to, or inconvenient for, making precise, reliable measurements in the desirable range of low shear stresses, we have carefully reviewed the theoretical and experimental basis of capillary viscometry with a view to designing a suitable variable-shear capillary viscometer. As a result, we have developed a viscometer that has proved its worth during 3 years of use.

In this paper, we describe the new viscometer and discuss briefly the considerations which governed its design.

B. DESIGNING THE VISCOMETER

I. The Requirements

Ideally the viscometer should meet the following requirements:

(*a*) It should be rugged and compact.

(*b*) It should be simple and convenient to use. For example, it should not readily "clog"; it should be easy to load; it should permit dilution of the polymer solution in the instrument itself; and the flow times should not be excessively long.

(*c*) It should yield precise data. The flow times should not be too short, and the driving pressure should be reproducible and steady.

(*d*) It should make possible measurements at a number of different shear stresses in the low-stress range.

(*e*) Its dimensions should be such that the kinetic energy effect, the drainage effect, and the effects of surface tension will be negligible at all shear stresses (or at least can be readily corrected for).

II. The Poiseuille Equation and its Application

In designing an instrument to meet the requirements listed above, it is necessary to consider the Poiseuille equation (the basis of capillary viscometry) and reasons for deviations from it, and, in particular, the effects on these deviations of changes in concentration and in the shear stress.

The familiar form of the Poiseuille equation is

$$\eta = \frac{\pi R^4 p}{8VL} \cdot t \qquad [1]$$

where R is the radius of the capillary and L is its length (cm), V is the volume (cm^3) of liquid flowing through the capillary in time t (sec), and p is the driving pressure (dynes/cm^2). In a viscometer in which the liquid flows under its own head, $\bar{h}$ (cm), the driving pressure is related to the head by the equation $p = \bar{h}gd$, where d is the density of the liquid. Then

$$\eta = \frac{\pi R^4 \bar{h} g d}{8VL} \cdot t. \qquad [2]$$

Can. J. Chem. Downloaded from www.nrcresearchpress.com by 210.87.254.5 on 09/05/12
For personal use only.

In deriving this equation, certain assumptions are made.

(*a*) The flow is laminar.

(*b*) There is no slip at the wall of the capillary, that is, the velocity of flow at the wall is zero. (For stresses less than 10^2 dynes/cm^2 this assumption seems to be valid (39).)

(*c*) The liquid is incompressible.

(*d*) All the energy applied to the liquid is used to overcome viscous resistance and is dissipated as heat (none, for example, being used to start the liquid flowing (no "yield value"), or to overcome effects due to surface tension, or to impart kinetic energy to the liquid).

This last assumption is never strictly valid. There is always a "kinetic energy effect" more or less large. When allowance is made for this, the Poiseuille equation becomes

$$\eta = \frac{\pi R^4 \bar{h} g d}{8VL} \cdot t - \frac{mV}{8\pi L} d \cdot \frac{1}{t} \qquad [3]$$

where m is a semiempirical constant whose value depends on the shape of the capillary ends and on the velocity of flow (13, 14, 15). Because of this uncertainty in the value of m, the kinetic energy correction must be determined by calibration or, much better, made negligible by appropriate choice of the dimensional parameters. (It may easily be shown that the kinetic energy correction, expressed as a percentage correction, is proportional to R^4, $\bar{h}$, and $1/L^2$). If, then, the viscometer is appropriately designed, the simple Poiseuille equation [2] may be used in calculations.

In polymer-solution studies, the quantity desired is the viscosity ratio η/η_0 (the ratio of the solution viscosity to the solvent viscosity) rather than the viscosity of the solution. The assumption is usually made that $\eta/\eta_0 = t/t_0$. This assumption really involves four assumptions:

(*a*) that Poiseuille's equation [1] applies to both solution and solvent;

(*b*) that the kinetic energy correction is negligible;

(*c*) that the density ratio d/d_0 differs negligibly from unity; and

(*d*) that the quantity

$$\frac{\pi R^4 \bar{h} g}{8VL},$$

collectively called the apparatus constant A, is really a constant, R, $\bar{h}$, V, and L having the same value for different pure liquids and solutions.

The first of these assumptions is valid for Newtonian liquids; but if the solution is non-Newtonian, the equation applies only under conditions such that the deviations from Newtonian behavior are slight (16, 17).

The second assumption we have already discussed.

The error involved in making the third assumption can be calculated (18) or can be determined by density measurements (19).

But what of the fourth assumption, that the parameters R, $\bar{h}$, V, and L in the apparatus constant are truly constant? Let us consider each of these parameters in turn.

The Radius of the Capillary, R

The radius of the capillary may be altered in changing from solvent to solution if polymer is absorbed on the capillary wall. The effective radius R^* then would be

$$R^* = R - a$$

Can. J. Chem. Downloaded from www.nrcresearchpress.com by 210.87.254.5 on 09/05/12
For personal use only.

where a is the thickness of the absorbed layer.[3] Öhrn (22) has obtained evidence of such a reduction in radius. It leads to an apparent viscosity ratio, η_r^*, that is greater than the true ratio, η_r. According to Öhrn

$$\eta_r = \eta_r^*\left(1-\frac{4a}{R}\right).$$

From this it follows that

$$[4] \qquad \frac{\eta_r-1}{c} = \frac{\eta_r^*-1}{c} - \frac{4a}{R}\cdot\frac{\eta_r^*}{c}$$

and that the "absorption" error, expressed as a percentage of the true reduced viscosity, amounts to

$$\frac{4a}{R}\cdot\frac{\eta_r^*}{(\eta_r^*-1)}\cdot 100.$$

Even at $\eta_r = 1.2$, the error in $(\eta_{sp})/c$ is still 1.2% assuming that the thickness of the absorbed layer is 1250 Å (which is about what Öhrn found it to be) and that the radius of the capillary is 0.0250 cm. Since the error in $(\eta_{sp})/c$ is larger the lower the concentration of the solution, the slope of the $(\eta_{sp})/c$ versus c line will be greater when corrected values of $(\eta_{sp})/c$ are plotted than when uncorrected values are plotted.[4] Hence the true value of $[\eta]$ will be smaller than that obtained if corrections are not made. This suggests that in the determination of $[\eta]$ by extrapolation, greater weight should be given to the points at higher concentrations than to those where η_r approaches 1.2. It is, however, worth mentioning that if the desorption of the polymer layer is slow (24), the error due to absorption will be smaller if the measurements are made with progressively more dilute solutions (as they are when dilution is made in the bulb of the viscometer) and if the flow time of solvent is measured after rather than before the flow times of the solutions are measured.

The Hydrostatic Head, $\bar{h}$

In any capillary viscometer, the hydrostatic head decreases during flow. Therefore a mean head must be used in calculations. What this mean head is depends upon the shape of the efflux bulb, and on whether the liquid flows out of the capillary into the air as in the Ubbelohde suspended-level viscometer or into another vessel, as in an Ostwald-type viscometer. In a Ubbelohde viscometer[5] in which the efflux bulb is spherical and in which there is negligible kinetic energy effect, the true mean head $\bar{h}$ for discharge into air is given by the expression (26)

$$[5] \qquad \bar{h} = \frac{4/3R_b}{2c-(c^2-1)\ln\frac{c+1}{c-1}}$$

[3]*Actually an apparent reduction in radius of this form may be due in part or whole to other effects such as the "size effect" encountered with suspensions of rigid particles (20) and the hydrodynamic repulsion by the wall which increases with the velocity of flow (21). Regardless of the cause, the observed apparent reduction in radius is of the order of magnitude of a particle radius.*

[4]*It may be shown (23) that the error in the slope, expressed as a percentage error, is equal to*

$$\frac{400a/R}{k'[\eta]^2c^2}.$$

For example, with our polystyrene fraction T_5, for which $[\eta] = 9.32$ dl/g and $k' = 0.31$ the percentage error would be 1.87% at a concentration, c, of 0.063 g per 100 ml (at which $\eta_r = 1.6$) and 7.2% at a concentration of 0.032 g per 100 ml (at which $\eta_r = 1.3$). To keep this error reasonably small, the measurements should be made at concentrations such that η_r is not less than about 1.5 (or else an absorption correction should be made).

[5]*The calculation of the mean head in an Ostwald-type viscometer is more complicated. It is discussed in a recent paper by Overbeek (25).*

Can. J. Chem. Downloaded from www.nrcresearchpress.com by 210.87.254.5 on 09/05/12
For personal use only.

where R_b is the radius of the bulb and $c = h_m/R_b$ and h_m is the algebraic mean of the initial and final heads (provided that the fiducial marks are equidistant from the spherical bulb). After expansion of the logarithmic term this reduces to

$$\bar{h} = \frac{h_m}{1\ 0.200\ \frac{1}{c^2}\ 0.086\ \frac{1}{c^4}} \qquad [6a]$$

or, for all practicable heads,

$$\bar{h} = h_m. \qquad [6b]$$

Expression [5] is not strictly valid for non-Newtonian liquids (27). Nevertheless, the deviation from it is negligibly small, much smaller, say, than the error due to kinetic energy effect, even in a well-designed viscometer.

There is, however, an effect on the hydrostatic head which may not be negligible, namely, that due to *surface tension*. With organic solvents and their solutions the effect is very small in the usual capillary viscometers ($h \sim 10$ cm); but in viscometers with very low heads ($h < 3$ cm), and with the smaller bulb that must be used at these low heads to give a convenient flow time, the effect becomes very significant. Indeed with water and with aqueous solutions, it can amount to 30% or more of the mean head. Accordingly, a variable-shear viscometer for use at low shear stress should be so designed that surface tension effects are effectively eliminated or, failing that, can be corrected for with as little inconvenience as possible.

In various viscometers that have been designed for use at low shears, attempts have been made to eliminate the surface tension effect by having the effect of surface tension at the advancing meniscus exactly offset that at the receding (or falling) meniscus (see, for example, Sprokel's design for an Ostwald viscometer (28), Golub's work with a simple U-tube viscometer (11), and Signer and Berneis' work with an inclined capillary (5)). In all of these, however, one meniscus is advancing onto a dry surface and the other is receding from a wet surface. This gives rise to a hysteresis effect which manifests itself as an apparent yield value (29). This effect is the more serious the lower the hydrostatic head. In other words, it is most serious just where reliable data are most desired.

The viscometer in which the surface tension can best be coped with is the Ubbelohde, or suspended-level, viscometer. In this there is only one moving meniscus—the falling one. The other one is kept stationary and given a fixed radius of curvature, at the suspended level. The radius of curvature of the inverted surface can be selected so that surface tension exerts a downward pull at the suspended level that exactly counterbalances the upward pull at the falling meniscus. The required radius of curvature is calculated from the relation

$$R_0 = \frac{2\gamma}{d} \cdot \frac{1}{\langle h_\gamma \rangle} \qquad [7]$$

where γ is the surface tension and $\langle h_\gamma \rangle$ is the "volume average" capillary rise in the bulb and the tubing between the fiducial marks. Values of the quantity $\langle h_\gamma \rangle$ can be calculated (30, 13, 31) from the expression

$$\langle h_\gamma \rangle = \frac{\sum \langle h_1 \rangle_\gamma \Delta V_1}{\sum \Delta V_1} \qquad [8]$$

where $\Sigma \Delta V_1$ is the total volume of the bulb, including the volume of tubing between the marks.

Can. J. Chem. Downloaded from www.nrcresearchpress.com by 210.87.254.5 on 09/05/12
For personal use only.

Contrary to Ubbelohde's claim, a value of R_0 calculated for a given liquid does not apply for every other liquid; it applies only when that liquid, or another liquid for which the ratio γ/d has the same value, is used in the viscometer. Fortunately many of the common organic solvents do have nearly the same surface tension – density ratio, namely, about 30 dynes cm^2 g^{-1} (see Table I). Fortunately, too, a dilute polymer solution

TABLE I

Surface tension–density ratios (25° C)
(Data obtained from (32) and (33))

Solvent	γ, dynes/cm	d, g/cm^3	γ/d, dynes cm^2/g
Toluene	27.20	0.862	31.5
Benzene	27.47	0.874	31.4
Cyclohexane*	23.82	0.769	31.0
Methyl ethyl ketone	24.0	0.799	30.0
Acetone†	23.32	0.791	29.5
Carbon tetrachloride	26.15	1.58	16.5
Water	72.0	0.997	72.2

*At 30° C. †At 20° C.

in an organic solvent has very nearly the same value of the γ/d ratio as the solvent itself. So a viscometer designed for use with one organic solvent and its solutions is suitable for use with most others. It is *not*, however, suitable for use with water, for which $\gamma/d = 72.2$ dynes cm^2 g^{-1}, or for aqueous solutions.

The Efflux Volume, V

The actual volume of the efflux bulb does not necessarily equal the efflux volume V, the volume of liquid that passes through the capillary in flow. The true efflux volume will be the volume of the bulb (the volume between the fiducial marks) less the volume V_d of liquid left adhering to the walls. This volume, the *drainage correction* in the efflux volume, varies directly as the viscosity of the liquid and inversely as its flow time. It is, therefore, independent of the liquid *provided that the liquid flows under its own head* (34). Hence a drainage correction in the viscosity ratio (and derived functions) is not necessary if all measurements are made at free fall; it is necessary, however, if external pressures are used to vary the shear stress (27).

The Capillary Length, L

The effective length of the capillary L is not identical with the actual length of the capillary L_0, but is greater than it by the quantity nR, where R is the radius of the capillary and n is a parameter whose value is about 0.566. When a capillary of length L is divided into two sections, as in our viscometer, the end correction would be doubled, becoming $2nR$. The value of n may vary slightly with driving pressure, but in any event the end correction may be made negligible by making L large enough. (For viscoelastic liquids there is another "end correction" related to the "recoverable shear", S_R (35). Taking this into account, the total end correction in our viscometer amounts to $2(n+S_R/2)R$, where $S_R = 0$ for Newtonian liquids, $S_R \sim 1$ for most polymer solutions, and $S_R \sim 10$–100 for highly viscoelastic liquids such as molten polyethylene and aluminum soap solutions.)

III. The Design

The viscometer, Fig. 1, was designed taking all these factors into consideration. Some features of it need comment.

Can. J. Chem. Downloaded from www.nrcresearchpress.com by 210.87.254.5 on 09/05/12
For personal use only.

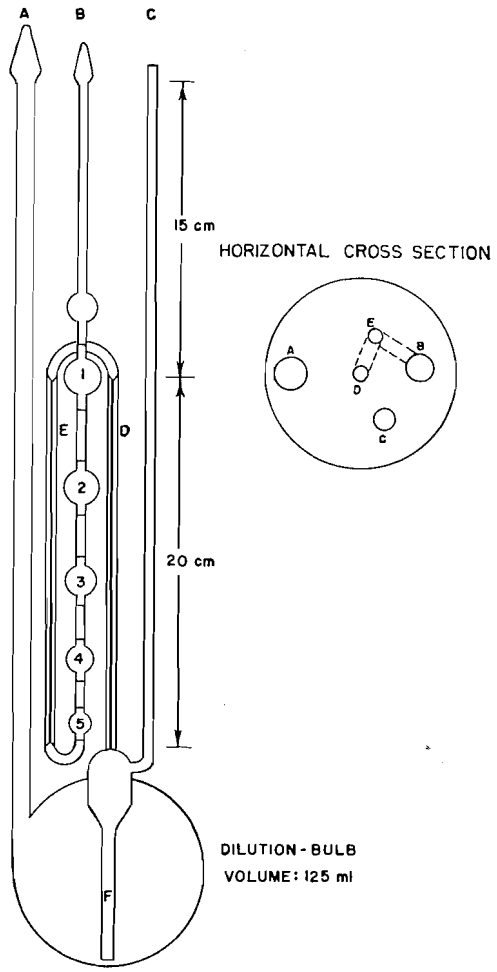


FIG. 1. Modified Ubbelohde variable-shear viscometer: (A) filling tube, O.D. 1 cm; (B) bulb system; (C) air inlet tube, O.D. 0.6 cm; (F) O.D. 0.6 cm, I.D. 0.4 cm (F almost touches the bottom of dilution bulb).

(*a*) The viscometer is provided with five efflux bulbs, each with its own pair of fiducial marks. With these can be achieved five different accurately reproducible mean heads, corresponding to shear stresses varying over a 10-fold range. Since the heads are built into the instrument, drainage corrections are unnecessary (so long as external pressure is not applied)

(*b*) The viscometer is of the Ubbelohde type, to facilitate elimination or correction of surface tension effects. The radius of curvature of the hemispherical suspended level is such that there is no surface tension effect at the lowest head when toluene is the solvent. (This means an overcorrection for the other bulbs, but the resulting negative corrections are very small in the next higher head and small even at the highest head. The *relative* error is always negligible with toluene as solvent and indeed with the other organic solvents of Table I for which $\gamma/d \approx 30$.)

(*c*) The viscometer is modified so that dilution of the solution can be accomplished without removing the solution from the instrument. This is possible because the position

Can. J. Chem. Downloaded from www.nrcresearchpress.com by 210.87.254.5 on 09/05/12
For personal use only.

of the second meniscus is independent of the volume of liquid in the viscometer. Incidentally, this feature of the Ubbelohde also eliminates loading errors.

(*d*) Precision-bore capillary tubing is used, and with no bends in it, to ensure that liquid flow in the capillary will be truly laminar (at the driving pressures used).

(*e*) A lowest head of about 2 cm is achieved, in conjunction with the long length of capillary required to minimize the end effect and kinetic energy effect, by dividing the length of capillary tube into two lengths joined by a wider-bore U tube. With the two lengths of capillary disposed vertically, the whole instrument is compact and rugged.

IV. Dimensions of the Viscometer

The radius R and the length L of capillary tubing, the volumes of the bulbs, and the heights of the bulbs above the suspended level (which of course govern the heads) were chosen after balancing all relevant factors (see Table II). Two viscometers were designed

TABLE II

Considerations affecting the choice of dimensional parameters R, L, V, and h

Shear stress, dynes/cm²	Proportional to	R,	L^{-1},		h
Flow time, t	Proportional to	R^{-4},	L,	V,	h^{-1}
Kinetic energy effect (%)	Proportional to	R^{4},	L^{-2}		
Surface tension effect (%) (if not compensated for)	Proportional to			$V_b^{-1/3}$*,	h^{-1}
End effect (%)	Proportional to	R,	L^{-1}		
Absorption effect (%)	Proportional to	R^{-1}			

*For spherical bulbs of dry volume V_b.

to provide two different, and overlapping, shear-stress ranges.

The specifications for the two viscometers are listed in Tables III and IV. (The viscometers themselves, as fabricated by the master glassblower of Canadian Laboratory Supplies, Montreal, conformed very closely to these specifications.)

C. EVALUATION OF THE VISCOMETER

I. Experimental Tests

A simple and direct test is to compare measured flow-time ratios with kinematic viscosity ratios, for two different liquids. The Poiseuille equation [3] may be written in the form

$$[9] \qquad \nu = \frac{\pi R^4 \bar{h} g}{8VL} \cdot t - \frac{mV}{8\pi L} \frac{1}{t} = At - B\frac{1}{t}$$

where ν is the kinematic viscosity η/d. If the kinetic energy term is negligible, this reduces to

$$[10] \qquad \nu = \frac{\pi R^4 \bar{h} g}{8VL} \cdot t = At.$$

If A is constant, the ratio of flow time for two different liquids should be the ratio of their kinematic viscosities. Furthermore, if the two liquids are Newtonian, this ratio should be the same at all shear stresses.

Such a comparison was made for several pairs of liquids in two viscometers, IIA-1 and IIB-1, made to the specifications of Tables III and IV, respectively. The results of one comparison, using benzene[6] and toluene,[6] are given in Table V.

[6]*The solvents used in the experiments discussed in this paper were carefully purified in the manner already described (36).*

Can. J. Chem. Downloaded from www.nrcresearchpress.com by 210.87.254.5 on 09/05/12
For personal use only.

Can. J. Chem. Downloaded from www.nrcresearchpress.com by 210.87.254.5 on 09/05/12
For personal use only.

TABLE III

Specifications for viscometer IIA (organic solvents)
(Shear stress range, 0.5–4 dynes/cm²)

Radius, R, of capillary	0.025 cm (precision bore)				
Length, L, of capillary (2×25.0 cm)	50.0 cm				
Radius of curvature, R_0, of hemisphere	0.33 cm				
Bulbs (spherical)	1	2	3	4	5
Head h_m (cm)	20	15	10	5	2
Volume V (cm³)	1.50	1.12	0.75	0.40	0.30
Flow time (sec) for benzene	171	170	171	183	345
Kinetic energy correction (%)	0.11	0.08	0.06	0.03	0.01

TABLE IV

Specifications for viscometer IIB (organic solvents)
(Shear stress range, 1.5–11 dynes/cm²)

Radius, R, of capillary	0.025 cm (precision bore)				
Length, L, of capillary (2×15)	30.0 cm				
Radius of curvature, R_0, of hemisphere	0.413 cm				
Bulbs (spherical)	1	2	3	4	5
Head h_m (cm)	30	20	15	9	4
Volume V (cm³)	3.0	2.0	1.5	0.9	0.4
Flow time (sec) for benzene	137	137	137	137	137
Kinetic energy correction (%)	0.47	0.31	0.24	0.14	0.06

TABLE V

Comparison of flow-time ratios and kinematic viscosity ratios for benzene and toluene at 20° C

Benzene	γ/d = 31.4 dynes cm²/g		ν_B = 0.738 (c.s.t.)			ν_B/ν_T = 1.092
Toluene	γ/d = 31.5 dynes cm²/g		ν_T = 0.676 (c.s.t.)			
			Viscometer IIA			
Bulb	1	2	3	4	5	
t_B (sec)	147.99	148.27	147.20	161.48	294.78	
t_T (sec)	135.44	135.78	134.43	147.72	269.78	
t_B/t_T	1.093	1.092	1.095	1.093	1.093	Av. 1.093
			Viscometer IIB			
Bulb	1	2	3	4	5	
t_B	134.36	133.78	137.07	134.63	142.70	
t_T	123.08	122.44	125.48	123.16	130.87	
t_B/t_T	1.092	1.093	1.092	1.093	1.090	Av. 1.092

The constancy of the flow-time ratios, and the agreement with the kinematic viscosity ratio, indicate that both kinetic energy and surface tension effects are minor.

That the surface tension effect on t_r is negligible is indicated by the fact that the ratio has the same value at very low heads (bulb 5) as at heads 10 times greater (bulb 1).

This constancy, however, is not proof that the surface tension effect on h, and therefore on t, is negligible.

It may be shown that (with negligible kinetic energy effect)

$$\nu_r = t_r\left[1-\frac{1}{\bar{h}}(\langle h_\gamma\rangle_1-\langle h_\gamma\rangle_2) - \frac{1}{\bar{h}^2}(\langle h_\gamma\rangle_1\langle h_\gamma\rangle_2-\langle h_\gamma\rangle_2^2)\right]$$

where $\bar{h}$ is the mean head, $\langle h_\gamma\rangle_1$ is the correction in the head due to surface tension of liquid 1, and $\langle h_\gamma\rangle_2$ is the correction in the head due to surface tension of liquid 2. Since $\langle h_\gamma\rangle$ depends on γ/d, the surface tension – density ratio, it follows that (except for

hysteresis effects which are eliminated in an Ubbelohde-type viscometer) the surface tension effect in the *ratio* of the kinematic viscosities will be nil if the two liquids have the identical γ/d ratios, and will be negligible except when γ/d ratios differ appreciably.

This means that the effect of surface tension in t_r or η_r (or other relative functions like $(\eta_{sp})/c$ or $[\eta]$ can be neglected with most organic solvents and their solutions even when there is an appreciable surface tension effect in h. It does *not* mean, however, that *all* surface tension effects can be neglected. There can be a very significant effect on the shear stress. With non-Newtonian liquids, for example, the shear stress τ (or the shear rate D) is a very significant variable. It is calculated from the mean head $\bar{h}$. But a calculation of the mean head in flow from measured values of h_{initial} and h_{final} using equation [5] (or its simplified forms [6*a*] or [6*b*]) does not take into account the capillary rise in the bulb and, hence, yields a mean head which is in error (the relative error being greater the smaller $\bar{h}$ is). At low heads the percentage error in $\bar{h}$, and therefore in τ or D, can be very large. On the other hand, with a viscometer such as ours, the $\bar{h}$'s whose direct measurement would lead to greatest error, the small heads, can be determined indirectly. Since

$$\bar{h} = \frac{\eta}{d}\frac{8VL}{\pi R^4 g}\cdot\frac{1}{t},$$

measurements at the large values of $\bar{h}$ (when surface tension effects are negligible) with a liquid of known η/d, give a measure of $8L/g\pi R^4$ which, combined with measurements of V and t at the low heads, make it possible to calculate $\bar{h}$.

That the kinetic energy effects are small in these viscometers is also indicated by the constancy of the flow-time ratios. The kinetic energy effect on $t_{\text{benzene}}/t_{\text{toluene}}$ should be *relatively* larger in bulb 1 than in bulbs 5 or 4; but within the limits of error no difference in the ratio, as measured with bulb 1 and with bulbs 5 or 4, is detectable. But this is not surprising. If the percentage kinetic energy effect is small in a flow time, and we designed the viscometer to make it so, it will be much smaller still in a flow-time ratio. In other words, the test is not a very sensitive one.

A second and more sensitive test of the extent to which unwanted effects have been reduced involves the determination of the constants A and B in the modified viscosity equation [9]. These can be evaluated, as suggested by Higgins (37), from a plot of ν/t versus $1/t^2$; A is then the intercept and B is the slope constant. For this evaluation, we measured the flow times of benzene at 20° and 40° and toluene at 20°, 40°, and 60° C and we obtained the corresponding kinematic viscosities from Timmermans (32). Values of A and B obtained from the plots are given in Table VI.

TABLE VI

Calibration constants for the two viscometers

	IIA			IIB		
Bulb	$A\times10^{-5}$	$B\times10^{-2}$	% Kinetic energy correction*	$A\times10^{-5}$	$B\times10^{-2}$	% Kinetic energy correction*
1	5.02	0.621	.31	5.55	1.196	.66
2	5.01	0.516	.26	5.56	0.929	.52
3	5.02	0.101	.05	5.42	0.752	.41
4	4.50	0.094	.04	5.50	0.520	.29
5	2.50	0.093	.02	5.14	0.066	.03

*Calculated for a liquid for which $\nu = 10^{-2}$ stokes.

Can. J. Chem. Downloaded from www.nrcresearchpress.com by 210.87.254.5 on 09/05/12
For personal use only.

From the values of A and B, the percentage kinetic energy correction in the flow time, AB/ν^2, can be readily calculated. In Table VI are listed the corrections for benzene at 20° C. Considering the difficulty of fabricating an instrument like this exactly to specifications, these agree remarkably well with those calculated in Tables III and IV.

From our value of A and B and our measured values of t, we calculated kinematic viscosities of toluene at 20°, 40°, and 60°. These are given in Table VII.

TABLE VII

Kinematic viscosities of toluene at 20°, 40°, and 60° C (calculated as At and as $At-B/t$ (in c.s.t.))

	20° C		40° C		60° C	
Bulb	$\nu = At$	$\nu = At-B/t$	$\nu = At$	$\nu = At-B/t$	$\nu = At$	$\nu = At-B/t$
			Viscometer II-A-1			
1	.681	.676	.553	.547	.465	.459
2	.680	.676	.552	.548	.464	.458
3	.689	.675	.549	.546	.463	.458
4	.677	.676	.546	.546	.460	.459
5	.673	.673	.540	.540	.455	.455
			Viscometer II-B-1			
1	.648	.674	.557	.545	.469	.454
2	.681	.674	.553	.544	.465	.454
3	.680	.674	.550	.543	.463	.454
4	.677	.673	.546	.541	.460	.454
5	.673	.673	.544	.543	.454	.454
Average		.674		.544		.456

From these data it is clear that the kinetic energy corrections are small but still significant, in the kinematic viscosities. In a flow-time ratio they would be very small. Even in a specific viscosity η_{sp} or intrinsic viscosity $[\eta]$ the corrections would, in the usual range $\eta_r = 1.1$–1.9, always be less than 1% and in the lower three bulbs less than 0.1%.

The kinematic viscosities measured at widely different heads are identical within experimental error. This fact is not, in itself, proof that the surface tension effects have been eliminated in these viscometers, for the apparatus constant A for each bulb was obtained by calibration. It is possible, however, to calculate from the calibration values of A the effective mean hydrostatic head corresponding to each bulb. If the surface tension effect has been eliminated, these effective mean heads should be the same as the mean heads calculated from measured initial and final heads ($\bar{h} = h_m$). The appropriate measurements and calculations were made, and the results for viscometer II-A-1 are assembled in Table VIII.

TABLE VIII

Comparison of mean heads calculated from apparatus constant A and from measured heads

Bulb	$\bar{h}_{calib}$ (cm)	h_m (cm)
	Viscometer II-A-1	
1	20.57	20.53
2	15.47	15.52
3	10.43	10.38
4	5.23	5.17
5	2.16	2.17

Can. J. Chem. Downloaded from www.nrcresearchpress.com by 210.87.254.5 on 09/05/12
For personal use only.

The agreement between the measured mean head h_m and the calculated mean head $\bar{h}_{calib}$ is convincing evidence that the effect of surface tension on the mean head has been eliminated.

In summary, these and other similar calibration data show that the viscometers do indeed measure viscosities precisely, and over a wide range of shear stresses.

The measurements so far discussed have been made with pure solvents. Over the past 3 years, these, and other viscometers made to the same design, have been used in several different investigations, and all have proved to be very satisfactory both in routine measurements and for research purposes. They are easy to use and to clean and they are capable of giving precise data even at shear rates as low as 40 sec^{-1}.

The data obtained in these investigations will be given and discussed elsewhere. Here, it is probably sufficient to provide one example. Measurements were made with solutions, in toluene, of a polystyrene of very high molecular weight. For preparation of the solutions and purification of the solvent, see reference 36. The measurements were made at different concentrations to permit extrapolation to zero concentration at all the shear stresses obtainable at free fall in the two viscometers II-A-1 and II-B-1. The measured flow times for the solutions, which were markedly non-Newtonian, were used to calculate relative flow times (t/t_0) and from these relative viscosities (at the maximum shear stress τ_R, at the wall) were calculated according to the equation (38)

$$(\eta_r)_{\tau_R} = t_r[4/(3+d \log q_R/d \log \tau_R)].$$

From $(\eta_r)_{\tau_R}$ the corresponding values of reduced specific viscosity $(\eta_{sp}/c)_{\tau_R}$ were calculated and used to obtain the intrinsic viscosity at constant shear stress $[\eta]_{\tau_R}$. A typical plot of $(\eta_{sp}/c)_{\tau_R}$ vs. c and of $[\eta]_{\tau_R}$ vs. τ_R is given in Figs. 2 and 3.

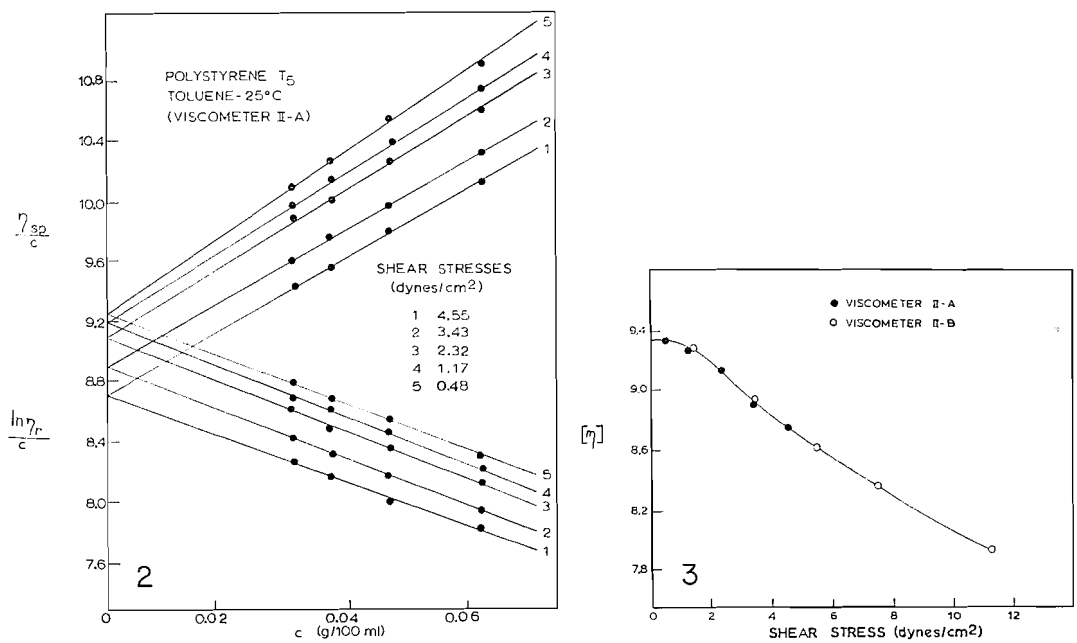


FIG. 2. A typical set of data obtained in the new variable-shear viscometer (reduced viscosities and inherent viscosities at five different shear stresses).

FIG. 3. Variation of intrinsic viscosity with shear stress for a polystyrene fraction of very high molecular weight, T_5. (Note the overlapping of the data obtained in the two different viscometers.)

Can. J. Chem. Downloaded from www.nrcresearchpress.com by 210.87.254.5 on 09/05/12
For personal use only.

The points obtained with the two viscometers fall satisfactorily on the same curve. The curve exhibits the expected levelling off at low shear stresses, a feature that makes extrapolation to zero stress simple and safe.

It is worth stressing that this levelling off can be, and probably has been in some other investigations, obscured by effects of hysteresis and surface tension already mentioned. For example, even though surface tension effects may almost cancel out in η_r (and, therefore, in η_{sp}/c) they can still be significant in the shear stress τ (or the shear rate D), and being greater the lower the shear stress, they can be the cause of a spurious upcurve at very low shear stresses.

Our experience with these viscometers convinces us that they should be very useful both for determining whether or not a polymer–solvent system is non-Newtonian and for making measurements with it if it is. Further, the instruments are suitable both for making the low-shear measurements necessary for a reliable extrapolation to zero shear and for making determinations of viscosity functions at some arbitrary shear rate or shear stress.

ACKNOWLEDGMENTS

Financial support from the Defence Research Board of Canada is gratefully acknowledged.

REFERENCES

1. A. W. Craig and D. A. Henderson. J. Polymer Sci. **19**, 215 (1956).
2. L. Ubbelohde. J. Inst. Petrol. Technologists, **23**, 427 (1937).
3. A. Peterlin and M. Copick. Bull. sci., Conseil acad. RPF Yougoslavie, **3**, 41 (1956).
4. P. J. Flory and T. G. Fox, Jr. J. Am. Chem. Soc. **73**, 1904 (1951).
5. R. Signer and K. Berneis. Makromol. Chem. **8**, 268 (1952).
6. E. Wada. J. Sci. Research Inst. (Tokyo), **47**, 47, 159 (1953).
7. J. Hermans, Jr. Ph.D. Thesis, Leiden. 1958.
8. W. Kuhn and H. Kuhn. Helv. Chim. Acta, **28**, 1533 (1945).
9. R. Cerf. J. phys. radium, **19**, 127 (1958).
10. H. Eisenberg. J. Polymer Sci. **25**, 257 (1957).
11. M. A. Golub. Can. J. Chem. **35**, 381 (1957).
12. S. Claesson. Kolloid Chem. Makromol. Naturstoffe, **18**, 155 (1958).
13. J. F. Swindells, R. C. Hardy, and R. L. Cottington. J. Research Natl. Bur. Standards, **52**, 105 (1954).
14. P. Tuomikoski. Ann. Acad. Sci. Fennicae, Ser. A. I. No. 189 (1955).
15. S. Peter and E. Wagner. Z. physik. Chem. **17**, 184 (1958).
16. F. Schultz-Grunow and H. Weymann. Kolloid-Z. **131**, 61 (1953).
17. L. Prandtl and Fr. Vandrey. Z. angew. Math. Mech. **30**, 169 (1950).
18. C. T. Tanford. J. Phys. Chem. **59**, 798 (1955).
19. L. H. Cragg and J. E. Simpkins. Can. J. Research, B, **27**, 961 (1949).
20. A. D. Maude. Brit. J. Appl. Phys. **10**, 371 (1959).
21. F. Schultz-Grunow. Rheol. Acta, **1**, 289 (1958).
22. O. E. Öhrn. Arkiv Kemi, **12**, 397 (1958).
23. M. Takeda and R. Endo. J. Phys. Chem. **60**, 1202 (1956).
24. H. W. Zweegman and J. J. Hermans. Koninkl. Ned. Akad. Wetenschap., Proc. Ser. B, **62**, 102 (1959).
25. R. H. Ottewill and J. Th. G. Overbeek. Koninkl. Ned. Akad. Wetenschap., Proc. Ser. B, **62**, 236 (1959).
26. G. Barr. A monograph of viscometry. Humphrey Milford, New York. 1931.
27. C. A. I. Tuijnman. Ph.D. Thesis, Leiden. 1956.
28. G. J. M. Sprokel. Ph.D. Thesis, Utrecht. 1952.
29. D. T. F. Pals and J. J. Hermans. Rec. trav. chim. **71**, 433 (1952).
30. G. Barr. Proc. Phys. Soc. London, B, **58**, 575 (1946).
31. H. van Oene. M.Sc. Thesis, McMaster University. 1958.
32. J. Timmermans. Physico chemical constants of pure organic compounds. Elsevier Publishing Co., New York. 1950.
33. A. Weissberger and E. S. Proskauer; J. A. Riddick and E. E. Toops, Jr. *In* Technique of organic chemistry. Vol. VII. 2nd ed. Interscience Publishers Inc., New York. 1956.
34. C. A. I. Tuijnman and J. J. Hermans. J. Polymer Sci. **25**, 385 (1957).
35. W. Philippoff and F. H. Gaskins. Trans. Rheol. Soc. **2**, 263 (1958).
36. L. J. Sharman, R. H. Sones, and L. H. Cragg. J. Appl. Phys. **24**, 703 (1953).
37. W. F. Higgins. Collected Researches of Natl. Phys. Lab. (Teddington, Eng.), **9**, 1 (1914).
38. A. B. Bestul and H. V. Belcher. J. Colloid Sci. **5**, 303 (1950).
39. B. A. Toms. J. Colloid Sci. **4**, 511 (1949).

Can. J. Chem. Downloaded from www.nrcresearchpress.com by 210.87.254.5 on 09/05/12
For personal use only.

Can. J. Chem. Downloaded from www.nrcresearchpress.com by 210.87.254.6 on 09/05/12
For personal use only.

THE ANALYSIS OF NUCLEAR MAGNETIC RESONANCE SPECTRA

V. THE ANALYSIS OF DECEPTIVELY SIMPLE SPECTRA[1]

R. J. ABRAHAM[2] AND H. J. BERNSTEIN

ABSTRACT

The analyses of the ABX, A_2X_2, and $ABXY$ types of spectra are discussed in detail under the conditions for which the observed spectra give less than the theoretical number of transitions. These conditions for which an observed spectrum is deceptively simple are derived from the general analyses, and experimental examples of such spectra are given.

The complete analyses of the more simple types of nuclear magnetic resonance spectra have been presented in the preceding papers of this series (1, 2, 3, 4). From these and other papers (8) it is seen that the problem of the analysis of any N.M.R. spectrum for which explicit energies and intensities can be formulated reduces to the problem of assigning the experimentally observed transitions. In some cases it is found that considerably fewer transitions are observed than one would expect from the theoretical spectra. This is due to the fact that some of the theoretical transitions nearly coalesce and others are very weak. In principle, higher resolution might reveal more lines but in practice many such spectra are encountered in which it is not possible to resolve the overlapping lines with presently available N.M.R. spectrometers. In these cases there may be more than one assignment and interpretation of the spectrum. In this paper some of the general analyses will be considered in detail for those cases for which this deceptively simple type of spectrum is obtained. In these cases it is found that the separation of the lines in each group of the spectrum becomes equal to the average of two or more of the coupling constants involved and explicit values for each of the coupling constants cannot be obtained from such spectra. The simplest system for which this type of spectrum can be obtained is the ABX system. This system will now be considered in some detail, as the behavior of the spectrum for more complex systems is very similar, although the calculations become more laborious.

The ABX System

The general ABX analysis has already been given by Bernstein, Pople, and Schneider (1). It is convenient to use the nomenclature of reference 1 with the additional definitions

$$L = \tfrac{1}{2}(J_{AX}-J_{BX}), \qquad \delta = \sigma_B-\sigma_A, \qquad [1]$$
$$N = \tfrac{1}{2}(J_{AX}+J_{BX}).$$

Parameters D and ϕ are then defined from

$$D_\pm \cos 2\phi_\pm = \tfrac{1}{2}\eta H_0\delta \pm (L/2), \qquad [1a]$$
$$D_\pm \sin 2\phi_\pm = \tfrac{1}{2}J_{AB}.$$

The transition energies and intensities for this system are given in terms of these quantities in Table I. This system in the general case gives the 12 transitions shown in Fig. 1(*a*)

[1]*Manuscript received September 1, 1960.*
Contribution from the Division of Pure Chemistry, National Research Council, Ottawa, Canada.
Issued as N.R.C. No. 6095.
[2]*N.R.C. Postdoctorate Fellow 1957–59.*

TABLE I

Energies and intensities for ABX

Transition	Origin	Energy	Relative intensity
1	B	$\frac{1}{2}\eta H_0(2-\sigma_A-\sigma_B)-\frac{1}{2}N-\frac{1}{2}J_{AB}-D_-$	$1-\sin 2\phi_-$
2	B	$\frac{1}{2}\eta H_0(2-\sigma_A-\sigma_B)+\frac{1}{2}N-\frac{1}{2}J_{AB}-D_+$	$1-\sin 2\phi_+$
3	B	$\frac{1}{2}\eta H_0(2-\sigma_A-\sigma_B)-\frac{1}{2}N+\frac{1}{2}J_{AB}-D_-$	$1+\sin 2\phi_-$
4	B	$\frac{1}{2}\eta H_0(2-\sigma_A-\sigma_B)+\frac{1}{2}N+\frac{1}{2}J_{AB}-D_+$	$1+\sin 2\phi_+$
5	A	$\frac{1}{2}\eta H_0(2-\sigma_A-\sigma_B)-\frac{1}{2}N-\frac{1}{2}J_{AB}+D_-$	$1+\sin 2\phi_-$
6	A	$\frac{1}{2}\eta H_0(2-\sigma_A-\sigma_B)+\frac{1}{2}N-\frac{1}{2}J_{AB}+D_+$	$1+\sin 2\phi_+$
7	A	$\frac{1}{2}\eta H_0(2-\sigma_A-\sigma_B)-\frac{1}{2}N+\frac{1}{2}J_{AB}+D_-$	$1-\sin 2\phi_-$
8	A	$\frac{1}{2}\eta H_0(2-\sigma_A-\sigma_B)+\frac{1}{2}N+\frac{1}{2}J_{AB}+D_+$	$1-\sin 2\phi_+$
9	X	$\eta H_0(1-\sigma_X)-N$	1
10	X	$\eta H_0(1-\sigma_X)+D_+-D_-$	$\cos^2(\phi_+-\phi_-)$
11	X	$\eta H_0(1-\sigma_X)-D_++D_-$	$\cos^2(\phi_+-\phi_-)$
12	X	$\eta H_0(1-\sigma_X)+N$	1
13	Comb.	$\eta H_0(1+\sigma_X)$	0
14	Comb.	$\eta H_0(1-\sigma_X)-D_+-D_-$	$\sin^2(\phi_+-\phi_-)$
15	Comb.	$\eta H_0(1-\sigma_X)+D_++D_-$	$\sin^2(\phi_+-\phi_-)$

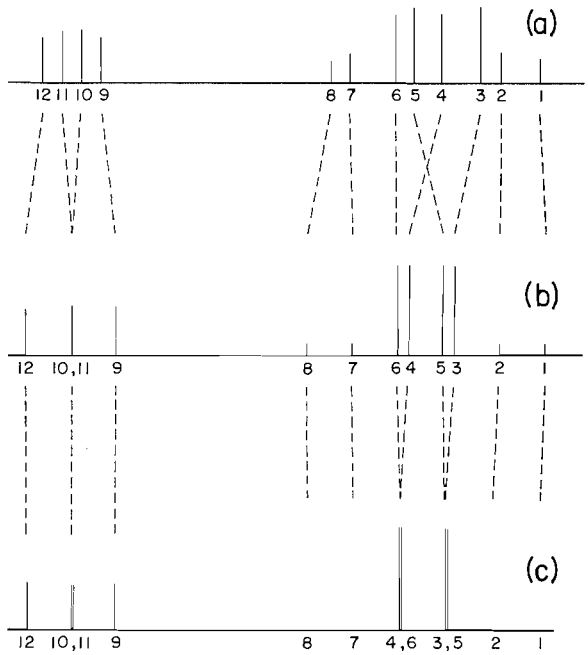


FIG. 1. Typical spectra of the ABX system when (*a*) δ_{AB} is large compared to J_{AB}, (*b*) δ_{AB} or $L = 0$, (*c*) $\delta_{AB} = 0$ and $L/J_{AB} \to 0$.

(ignoring the weak combination lines which are rarely observed). However, the number of observable transitions can be reduced in certain cases, down to a minimum of five lines (e.g. Fig. 1(*c*)). The conditions necessary for the 12-line spectrum to simplify to the 5-line one can be found from Table I. First consider the spectrum when the chemical shift difference between nuclei A and B (i.e. δ) equals zero. In this case from eqs. [1*a*]

$$D_+ = D_- = \tfrac{1}{2}\{J_{AB}{}^2+L^2\}^{\frac{1}{2}}$$

and

$$\sin 2\phi_\pm = \frac{J_{AB}}{2D_+} = \frac{J_{AB}}{2D_-} = \frac{J_{AB}}{2D}\,.$$

Can. J. Chem. Downloaded from www.nrcresearchpress.com by 210.87.254.6 on 09/05/12
For personal use only.

The X spectrum is now a triplet, transitions 10 and 11 having coalesced, but the AB portion will still be an 8-line spectrum (see Fig. 1(b)); thus the complete spectrum has 11 lines and the assignment is straightforward. A similar spectrum is obtained for the case when $L = 0$. However, by inspection of Table I, it can be seen that if $\delta = 0$, and also L is small compared with J_{AB}, i.e. $2D \rightarrow J_{AB}$ and $\sin 2\phi_{\pm} \rightarrow 1$, then the intensities of transitions 1, 2, 7, and 8 will approach zero and the strong transitions 3 and 5, and 4 and 6 will coalesce (see Fig. 1(c)). The X spectrum remains a triplet, thus the total spectrum will now consist of only five lines. Also the separation between transitions (3, 5) and (4, 6) and between transitions 9, (10, 11), and 12 is constant and equal to N, i.e. $\frac{1}{2}(J_{AX}+J_{BX})$.

The conditions necessary for the 12-line spectrum to degenerate to a simple 5-line spectrum can now be derived directly from Table I. For this to occur, the separations between lines 3 and 5, 4 and 6, and 10 and 11 must all be less than the half-height width of the component lines ($\Delta\nu_{\frac{1}{2}}$), and the intensities of lines 1, 2, 7, and 8 must all be less than a given fraction (i) of the total intensity. These two sets of conditions are covered by the limits

[2] $$(\eta H_0\delta+L)^2/2J_{AB} < \Delta\nu_{\frac{1}{2}}$$

and

[3] $$\frac{1}{2}\left(\frac{\eta H_0\delta+L}{J_{AB}}\right)^2 < i$$

where here $\eta H_0\delta$ and L refer to the absolute magnitudes of these quantities. If J_{AB} is less than $\Delta\nu_{\frac{1}{2}}/i$, eq. [3] is the more general case, if J_{AB} is greater than $\Delta\nu_{\frac{1}{2}}/i$, eq. [2] must be used. The quantities $\Delta\nu_{\frac{1}{2}}$ and i will be determined by the spectrometer used. For the Varian spectrometer operating at a radio frequency of 60 Mc/sec, the line width ($\Delta\nu_{\frac{1}{2}}$) is about 0.3 c.p.s. and the sensitivity is such that a small peak of 1/50th of the intensity of a neighboring strong line can be observed. If the strong peak is taken as one of the AB lines, then $i \approx 2/50$. Thus eq. [3] is used for J_{AB} less than 8 c.p.s., eq. [2] for J_{AB} greater than 8 c.p.s. However, for values of J_{AB} which are usually encountered (between 5 and 15 c.p.s.) the error involved in using eq. [2] only is not appreciable in view of the uncertainty in the measurement of i.

In any ABX system, when eq. [2] holds, the normal 12-line pattern degenerates to a simple 5-line spectrum in which the separation of the lines in the AB and X groups is equal to N i.e. the average of the two coupling constants J_{AX} and J_{BX}. The converse of this statement is equally important. This states that if an ABX system gives rise to a simple 5-line spectrum then the only constants that can be derived from the analysis of such a spectrum are the average values of J_{AX} and J_{BX}. It has been assumed previously (5) that if such a spectrum was obtained from an ABX system, then $J_{AX} = J_{BX}$ and $\delta = 0$. We see, however, that this is only one set of values which interprets the spectrum and in general only $J_{AX}/2$ and J_{BX} can be evaluated from the spacings.

The conditions for obtaining a 5-line spectrum in the 3-spin system ABX can be derived in an alternative manner. Consider the ABX system when L and δ are small compared to J_{AB}. In this case, the parameters $D_{\pm}$ in eq. [1a] can be written by neglecting higher powers of $(\eta H_0\delta\pm L)/J_{AB}$. This gives

$$D_{\pm} = \tfrac{1}{2}J_{AB}+\tfrac{1}{4}(\eta H_0\delta\pm L)^2/J_{AB}$$

and

$$\sin 2\phi_{\pm} = 1-\frac{1}{2}\left(\frac{\eta H_0\delta\pm L}{J_{AB}}\right)^2.$$

Can. J. Chem. Downloaded from www.nrcresearchpress.com by 210.87.254.6 on 09/05/12
For personal use only.

The energies and intensities in Table I can now be given directly in terms of $\eta H_0\delta$, L, and J_{AB} (Table II). The conditions necessary for the ABX system to give the 5-line

TABLE II

Energies and intensities for ABX when L and δ are small compared to J_{AB}

Transition	Origin	Energy	Relative intensity
1	B	$\frac{1}{2}\eta H_0(2-\sigma_A-\sigma_B)-J_{AB}-(N/2)-\frac{1}{4}(\eta H_0\delta-L)^2/J_{AB}$	$\frac{1}{2}\left(\frac{\eta H_0\delta-L}{J_{AB}}\right)^2$
2	B	$\frac{1}{2}\eta H_0(2-\sigma_A-\sigma_B)-J_{AB}+(N/2)-\frac{1}{4}(\eta H_0\delta+L)^2/J_{AB}$	$\frac{1}{2}\left(\frac{\eta H_0\delta+L}{J_{AB}}\right)^2$
3	B	$\frac{1}{2}\eta H_0(2-\sigma_A-\sigma_B)-(N/2)-\frac{1}{4}(\eta H_0\delta-L)^2/J_{AB}$	2
4	B	$\frac{1}{2}\eta H_0(2-\sigma_A-\sigma_B)+(N/2)-\frac{1}{4}(\eta H_0\delta+L)^2/J_{AB}$	2
5	A	$\frac{1}{2}\eta H_0(2-\sigma_A-\sigma_B)-(N/2)+\frac{1}{4}(\eta H_0\delta-L)^2/J_{AB}$	2
6	A	$\frac{1}{2}\eta H_0(2-\sigma_A-\sigma_B)+(N/2)+\frac{1}{4}(\eta H_0\delta+L)^2/J_{AB}$	2
7	A	$\frac{1}{2}\eta H_0(2-\sigma_A-\sigma_B)+J_{AB}-(N/2)+\frac{1}{4}(\eta H_0\delta-L)^2/J_{AB}$	$\frac{1}{2}\left(\frac{\eta H_0\delta-L}{J_{AB}}\right)^2$
8	A	$\frac{1}{2}\eta H_0(2-\sigma_A-\sigma_B)+J_{AB}+(N/2)+\frac{1}{4}(\eta H_0\delta+L)^2/J_{AB}$	$\frac{1}{2}\left(\frac{\eta H_0\delta+L}{J_{AB}}\right)^2$
9	X	$\eta H_0(1-\sigma_X)-N$	1
10	X	$\eta H_0(1-\sigma_X)+\eta H_0\delta.L/J_{AB}$	1
11	X	$\eta H_0(1-\sigma_X)-\eta H_0\delta.L/J_{AB}$	1
12	X	$\eta H_0(1-\sigma_X)+N$	1

spectrum (eqs. [2] and [3]) are given by inspection of Table II. This table is of further use in the analysis of spectra in which transitions 4 and 6 may be resolved and some of the weaker lines can be observed (e.g. Fig. 1(b)), but in which L and δ are still small compared to J_{AB}.

The results obtained in this analysis may be conveniently expressed in terms of a correlation diagram. Figure 1 shows (a) a typical 12-line ABX pattern, (b) the 11-line spectrum obtained when δ or $L = 0$, and (c) the unresolved 5-line spectrum obtained when δ and L are small compared to J_{AB}.

The different types of ABX spectrum mentioned above can sometimes be obtained for the same compound, merely by altering the relative chemical shift δ by dissolving the compound in various solvents. Figure 2 shows the observed and calculated spectra for the ABX system of the ring protons of 2-furfurol in three different environments, i.e. for three different values of δ. Analysis of the spectrum 2c gives the following values for the coupling constants: $J_{AB} = 3.16$ c.p.s., $J_{AX} = 1.89$ c.p.s., and $J_{BX} = 0.91$ c.p.s. where A, B, and X represent protons 4, 3, and 5 respectively. In 2(a) $\delta \rightarrow 0$ thus the spectrum is the simple 5-line spectrum since eq. [2] is valid. In 2(b) $\delta = 1.83$ c.p.s. ($\sigma_B > \sigma_A$). This value is such that eq. [1] no longer holds, i.e. the spectrum is not a simple one, but L and δ are still small compared to J_{AB} thus the analysis of Table II can still be used and is in fact the most convenient method of analyzing the spectrum. In 2(c) $\delta = 4.13$ c.p.s. and thus the spectrum is the full 12-line pattern. The dotted lines are drawn between corresponding transitions. It can be seen that all the B transitions (1.2.3.4) move together as do all the A lines (5.6.7.8). The actual values of the ring coupling constants used in the calculations were obtained from the analysis of the spectrum of Fig. 2(c).

The spectrum of the ring protons of liquid furfurol at 40 Mc/sec has the simple 5-line pattern (5) and was interpreted previously (5) on the basis of L and $\delta = 0$. The value of δ for liquid furfurol at 60 Mc/sec = 1.83 c.p.s. (Fig. 2(b)). Thus the value of δ at

Can. J. Chem. Downloaded from www.nrcresearchpress.com by 210.87.254.6 on 09/05/12
For personal use only.

Can. J. Chem. Downloaded from www.nrcresearchpress.com by 210.87.254.6 on 09/05/12
For personal use only.

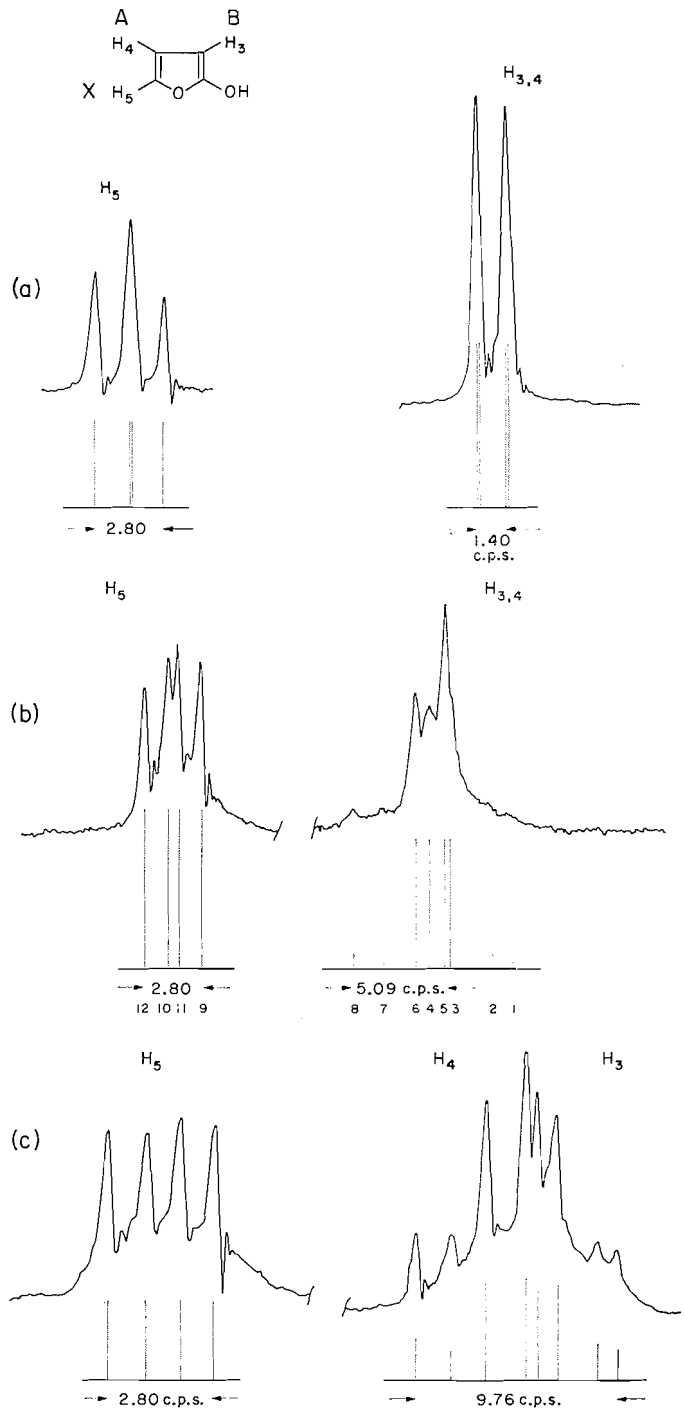


FIG. 2. Observed and calculated spectra of the ring protons of 2-furfurol at 60 Mc/sec: (*a*) in a 25% solution in benzene, (*b*) in the pure liquid, (*c*) in a 50% solution in dioxane.

40 Mc/sec = 1.21 c.p.s. Using this value and the values given above for the coupling constants, the left-hand side of eq. [2] becomes 0.40 c.p.s. Since this was about the limit of resolution of the instrument when the spectrum was obtained, it is understandable that the simple spectrum was observed. A further example of an ABX system giving the 5-line spectrum is the ring spectrum of 2,6-dichloro-3-fluorobenzotrifluoride (6) in which the spacing in the triplet and doublet is 6.2 c.p.s. (6). From the above consideration $J_{\mathrm{HF_{ortho}}}+J_{\mathrm{HF_{meta}}} = 12.4$ c.p.s. Since the 5-line spectrum was obtained, eq. [2] gives

$$\frac{(J_{\mathrm{HF_{ortho}}} - J_{\mathrm{HF_{meta}}})^2}{2J_{AB}} < 0.3.$$

Assuming the spectrometer used was comparable to the Varian high-resolution instrument, and since J_{AB} is the spin coupling between adjacent protons in a benzene ring (ca. 8 c.p.s.), $J_{\mathrm{HF_{ortho}}}-J_{\mathrm{HF_{meta}}} \leqslant 2.2$, so that $J_{\mathrm{HF_{ortho}}} < 7.3$ and $J_{\mathrm{HF_{meta}}} > 5.1$ is the maximum information obtainable about the coupling constants from this spectrum. This example demonstrates that a 5-line spectrum can be obtained from a system in which the values of J_{AX} and J_{BX} are comparable to the value of J_{AB}.

Richards and Schaeffer also found very similar behavior in the spectra of some trisubstituted benzenes (7). In this case, ABC-type systems in which $\delta_B \approx \delta_C$ were found to give spectra which approximate to the AB_2 type, i.e. the spectrum has 5 lines characteristic of the AB_2 pattern, not the many transitions obtained in the general ABC case. This is analogous behavior to the case considered above, which is essentially an ABX system giving an A_2X spectrum. Richards and Schaeffer used, in the analyses of these ABB' systems, pseudosymmetric wave functions i.e. the wave functions for the AB_2 case were used and then two values of J_{AB} and J_{AB}' were introduced. This is an approximation and not a strictly rigorous treatment as some matrix elements were neglected. However, it is difficult to give a rigorous analysis in this case as the general ABC calculation does not give explicit values of the energies and intensities. The consequence of using pseudosymmetric wave functions in the ABX case is that only an 8-line spectrum (if the combination line is neglected) is obtained, 4 X lines and 4 AB lines. The weak transitions seen in the spectrum of Fig. 2(b), however, are to this approximation of zero intensity.

An equation analogous to eq. [2] can be written for these ABC systems, i.e. when

$$[4] \qquad \frac{\{\delta_{BC}+\frac{1}{2}(J_{AB}-J_{AC})\}^2}{2J_{BC}} < \Delta\nu_{\frac{1}{2}}$$

the ABC system may be expected to give a spectrum of the AB_2 type in which only the average of the coupling constants J_{AB} and J_{AC}, and the chemical shifts σ_B and σ_C, will be given explicitly. However, this equation has not been verified theoretically, though the experimental results of Richards and Schaeffer are not inconsistent with this statement.

The A_2X_2 Spectrum

The complete analysis for this system has already been given (2, 8) and is in a convenient form for the analysis of all possible types of spectra. Thus there is little value in formulating the complete energy level table under the conditions for which simple

Can. J. Chem. Downloaded from www.nrcresearchpress.com by 210.87.254.6 on 09/05/12
For personal use only.

spectra are obtained. However, the simple A_2X_2 spectrum of two triplet groups which is obtained under certain conditions has been widely misinterpreted and thus the conditions for the formation of this simple spectrum will be considered in detail.

The nomenclature of reference 2 will be used.

The A_2X_2 spectrum consists of two triplet groups when the separation between lines 10 and 11, and 6 and 7 is less than $\Delta\nu_{\frac{1}{2}}$ and the intensities of lines 5, 8, 9, and 12 are less than i. These conditions are covered by the equations

[5] $$(L^2/2M) < \Delta\delta_{\frac{1}{2}}$$

and

[6] $$(L^2/4M^2) < i$$

where

$$L = J-J',$$

$$M = J_A-J_X.$$

In this case the separation between the lines in each triplet group will be equal to $N/2$ i.e. $\frac{1}{2}(J+J')$.

As in the ABX case, eqs. [5] and [6] overlap, and again only eq. [5] will be considered.

As an example of the use of eq. [5], consider the spectrum of furan. This consists of two simple triplet groups and it has been widely interpreted (9, 10, 5, 6) as meaning that $J_{23}(J)$ and $J_{24}(J')$ are both equal to the line separation in the triplet groups, namely 1.3 c.p.s. (see Fig. 3 for the numbering of the protons). This is a possible interpretation

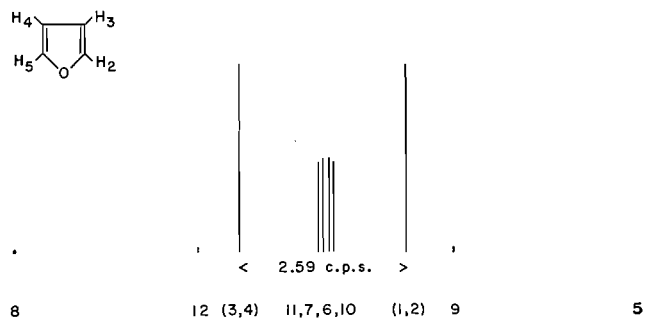


FIG. 3. The calculated spectrum of one of the triplet groups in furan.

of this spectrum. However, a more plausible interpretation can be obtained by considering the variation of coupling constants in the furan ring with substitution. It has been shown (11) that for a number of substituted furans the coupling constants are relatively insensitive to substitution and have the mean values $J_{23}(J) = 1.80$ c.p.s., $J_{24}(J') = 0.80$ c.p.s., $J_{25}(J_X) = 1.55$ c.p.s., and $J_{34}(J_A) = 3.53$ c.p.s. Using these values, eq. [5] holds and thus these coupling constants should explain the observed spectrum. In Fig. 3 the spectrum of furan, calculated with the above values of the coupling constants, is shown.

Can. J. Chem. Downloaded from www.nrcresearchpress.com by 210.87.254.6 on 09/05/12
For personal use only.

Can. J. Chem. Downloaded from www.nrcresearchpress.com by 210.87.254.6 on 09/05/12
For personal use only.

It is immediately apparent why the spectrum is observed as a simple triplet. The transitions labelled 5, 9, 8, and 12 are too weak to be observed and the spacings in the 11, 7, 6, 10 group are too small to be resolved. Strong support for this interpretation is the fact that the value of $J+J'$ obtained experimentally from the furan spectrum (2.6 c.p.s.) agrees exactly with the value obtained independently from the spectra of the substituted furans.

Similar types of simple spectra, which give, however, more information about the coupling constants involved, are the proton resonance spectra of the compounds $CF_2X—CH_2X$ where X is chlorine or bromine (12). These spectra have again essentially the triplet pattern but in these cases the center line is a doublet with a very small spacing. In these compounds J_{FF} is so much larger than J_{HH} that J_{HH} can be neglected and in this case the splitting of the central peak is equal to $L^2/2J_{FF}$. Once again, only the average value of $J+J'$ can be found explicitly from the observed spectrum, but if J_{FF} can be estimated e.g. by analogy with similar compounds, L can be calculated and thus both J and J' can be found. In the bromo compound the splitting of the central peak is well resolved (0.6 c.p.s.) but in the chloro compound the splitting (0.25 c.p.s.) can only be estimated by an analysis of the beats. Note that in this case eq. [5] holds (i.e. with a resolution of 0.3 c.p.s. only the main triplet structure would be observed) even though L has the quite large value of 10 c.p.s.* Using the formula given above gives the same results as Shoolery and Crawford for the chloro and iodo compounds, thus proving the validity of the approximation involved in neglecting J_{HH}, but the value for L obtained for the bromo compound is 14.5 c.p.s. Thus $J_T = 20$, and $J_C = 6$ c.p.s. respectively. The slight difference from the reported values is due to an arithmetical error (12). Here we have preferred $J_T > J_C$ in keeping with our unpublished results on the relative sizes of J_T and J_C in 1,1,2,2-tetrachloro-1-fluoroethane.†

The ABXY Spectrum

The ABX analysis considered earlier shows that a simple spectrum is obtained when J_{AB} is large compared to δ_{AB} and $J_{AX}-J_{BX}$. The same general statement is true for the A_2X_2 system remembering that in this case due to the symmetry of the system, the actual functions involved in the analysis are sums and differences of the coupling constants. By analogy, an $ABXY$ system will be expected to give a simple spectrum when J_{AB} and J_{XY} are large compared to δ_{AB}, δ_{XY} and terms like $J_{AX}-J_{BX}$.

The quantitative expression of this statement will now be derived. The transition energies and intensities for the $ABXY$ system cannot be derived explicitly in the general case as this involves solving a 4×4 determinant. However, in the case considered here, this 4×4 determinant can be solved explicitly and thus the energies and intensities can be written down completely.

This calculation follows the procedure laid down in reference 1. The basic functions, diagonal elements, and off-diagonal elements needed are given in Table III. Some off-diagonal elements, e.g. $\mathfrak{H}_{24}$ are not given as they are not involved in the calculation. These basic functions do not mix when (*a*) there is a difference in the total spin quantum number (this separation is shown by the full lines) and (*b*) there is an energy difference of the form $\delta_A-\delta_X$ (this is shown by the dotted lines in Table III).

**L is defined in reference 12 as $\frac{1}{2}(J+J')$ thus it has one-half the value of L used here.*

†Given at the Symposium on Molecular Spectra, Columbus, Ohio, June 1959.

TABLE III

Basic functions and matrix elements for $ABXY$

	$ABXY$	F	Diagonal	Matrix elements* $\frac{1}{4}J_{AB}$	$\frac{1}{4}J_{AX}$	$\frac{1}{4}J_{AY}$	$\frac{1}{4}J_{BX}$	$\frac{1}{4}J_{BY}$	$\frac{1}{4}J_{XY}$
1	$\alpha\alpha\alpha\alpha$	2	$(\nu_0/2)(H_A+H_B+H_X+H_Y)$	+	+	+	+	+	+
2	$\alpha\alpha\alpha\beta$	1	$(\nu_0/2)(H_A+H_B+H_X+H_Y)$	+	+	−	+	−	−
3	$\alpha\alpha\beta\alpha$	1	$(\nu_0/2)(H_A+H_B-H_X+H_Y)$	+	−	+	−	+	−
4	$\alpha\beta\alpha\alpha$	1	$(\nu_0/2)(H_A-H_B+H_X+H_Y)$	−	+	+	−	−	+
5	$\beta\alpha\alpha\alpha$	1	$(\nu_0/2)(-H_A+H_B+H_X+H_Y)$	−	−	−	+	+	+
6	$\alpha\alpha\beta\beta$	0	$(\nu_0/2)(H_A+H_B-H_X-H_Y)$	+	−	−	−	−	+
7	$\alpha\beta\alpha\beta$	0	$(\nu_0/2)(H_A-H_B+H_X-H_Y)$	−	+	−	−	+	−
8	$\alpha\beta\beta\alpha$	0	$(\nu_0/2)(H_A-H_B-H_X+H_Y)$	−	−	+	+	−	−
9	$\beta\alpha\alpha\beta$	0	$(\nu_0/2)(-H_A+H_B+H_X-H_Y)$	−	−	+	+	−	−
10	$\beta\alpha\beta\alpha$	0	$(\nu_0/2)(-H_A+H_B-H_X+H_Y)$	−	+	−	−	+	−
11	$\beta\beta\alpha\alpha$	0	$(\nu_0/2)(-H_A-H_B+H_X+H_Y)$	+	−	−	−	−	+
12	$\alpha\beta\beta\beta$	−1	$(\nu_0/2)(H_A-H_B-H_X-H_Y)$	−	−	−	+	+	+
13	$\beta\alpha\beta\beta$	−1	$(\nu_0/2)(-H_A+H_B-H_X-H_Y)$	−	+	+	−	−	+
14	$\beta\beta\alpha\beta$	−1	$(\nu_0/2)(-H_A-H_B+H_X-H_Y)$	+	−	+	−	+	−
15	$\beta\beta\beta\alpha$	−1	$(\nu_0/2)(-H_A-H_B-H_X+H_Y)$	+	+	−	+	−	−
16	$\beta\beta\beta\beta$	−2	$(\nu_0/2)(-H_A-H_B-H_X-H_Y)$	+	+	+	+	+	+

Off-diagonal matrix elements

$\mathcal{H}_{2,3} = \frac{1}{2}J_{XY}$, $\mathcal{H}_{4,5} = \frac{1}{2}J_{AB}$

$\mathcal{H}_{7,8} = \frac{1}{2}J_{XY}$, $\mathcal{H}_{7,9} = \frac{1}{2}J_{AB}$, $\mathcal{H}_{7,10} = 0$

$\mathcal{H}_{8,9} = 0$, $\mathcal{H}_{8,10} = \frac{1}{2}J_{AB}$

$\mathcal{H}_{9,10} = \frac{1}{2}J_{XY}$

$\mathcal{H}_{12,13} = \frac{1}{2}J_{AB}$, $\mathcal{H}_{14,15} = \frac{1}{2}J_{XY}$

*The + and − signs represent +1 and −1 respectively.

Thus to determine the energies and wave functions in this case four 2×2 determinants and one 4×4 determinant have to be solved.

The former can be solved explicitly. It is convenient to define the following constants.

$$L = \tfrac{1}{2}(J_{AX}-J_{AY}) \qquad R = \tfrac{1}{2}(J_{BX}+J_{BY})$$
$$T = \tfrac{1}{2}(J_{BX}-J_{BY}) \qquad M = \tfrac{1}{2}(J_{AB}-J_{XY})$$
$$N = \tfrac{1}{2}(J_{AX}+J_{AY}) \qquad K = \tfrac{1}{2}(J_{AB}+J_{XY})$$
$$\delta_{AB} = \nu_0(H_A-H_B) \qquad \delta_{XY} = \nu_0(H_X-H_Y)$$

and

$$C_\pm \cos 2\phi_\pm = \tfrac{1}{2}\delta_{XY} \pm \tfrac{1}{2}(L+T)$$
$$C_\pm \sin 2\phi_\pm = \tfrac{1}{2}J_{XY}$$
$$D_\pm \cos 2\phi_\pm = \tfrac{1}{2}\delta_{AB} \pm \tfrac{1}{2}(N-R)$$
$$D_\pm \sin 2\phi_\pm = \tfrac{1}{2}J_{AB}$$

The energy levels and wave functions for all the states except 7, 8, 9, and 10 can now be given in terms of these quantities (Table IV). These have been derived for the

Can. J. Chem. Downloaded from www.nrcresearchpress.com by 210.87.254.6 on 09/05/12
For personal use only.

TABLE IV

Explicit energies and wave functions for $ABXY$

	Energy	Wave function*
1	$(\nu_0/2)(H_A+H_B+H_X+H_Y)+\frac{1}{2}(K+N+R)$	(1)
2′	$(\nu_0/2)(H_A+H_B)+\frac{1}{2}M+C+$	$\cos\theta_+(2)+\sin\theta_+(3)$
3′	$(\nu_0/2)(H_A+H_B)+\frac{1}{2}M-C+$	$-\sin\theta_+(2)+\cos\theta_+(3)$
4′	$(\nu_0/2)(H_X+H_Y)-\frac{1}{2}M+D+$	$\cos\phi_+(4)+\sin\phi_+(5)$
5′	$(\nu_0/2)(H_X+H_Y)-\frac{1}{2}M-D+$	$-\sin\phi_+(4)+\cos\phi_+(5)$
6′	$(\nu_0/2)(H_A+H_B-H_X-H_Y)+\frac{1}{2}(K-N-R)$	(6)
7′	$K/2$	$(\frac{1}{2}+p)(7)+(\frac{1}{2}+q)(8)+(\frac{1}{2}-q)(9)+(\frac{1}{2}-p)(10)$
8′	$-\frac{1}{2}K+M$	$(-\frac{1}{2}-q)(7)+(\frac{1}{2}+p)(8)+(-\frac{1}{2}+p)(9)+(\frac{1}{2}-q)(10)$
9′	$-\frac{1}{2}K-M$	$(-\frac{1}{2}+q)(7)+(-\frac{1}{2}+p)(8)+(\frac{1}{2}+p)(9)+(\frac{1}{2}+q)(10)$
10′	$-3/2K$	$(\frac{1}{2}-p)(7)+(-\frac{1}{2}+q)(8)+(-\frac{1}{2}-q)(9)+(\frac{1}{2}+p)(10)$
11	$(\nu_0/2)(-H_A-H_B+H_X+H_Y)+\frac{1}{2}(K-N-R)$	(11)
12′	$(\nu_0/2)(-H_X-H_Y)-\frac{1}{2}M+D_-$	$\cos\phi_-(12)+\sin\phi_-(13)$
13′	$(\nu_0/2)(-H_X-H_Y)-\frac{1}{2}M-D_-$	$-\sin\phi_-(12)+\cos\phi_-(13)$
14′	$(\nu_0/2)(-H_A-H_B)+\frac{1}{2}M+C_-$	$\cos\theta_-(14)+\sin\theta_-(15)$
15′	$(\nu_0/2)(-H_A-H_B)+\frac{1}{2}M-C_-$	$-\sin\theta_-(14)+\cos\theta_-(15)$
16	$(\nu_0/2)(-H_A-H_B-H_X-H_Y)+\frac{1}{2}(K+N+R)$	(16)
	$p=\frac{\Delta}{8}\left(\frac{1}{J_{AB}}+\frac{1}{J_{XY}}\right)$	$q=\frac{\Delta}{8}\left(\frac{1}{J_{AB}}-\frac{1}{J_{XY}}\right)$

*The numbers in parentheses refer to the spin functions given in Table III.

general $ABXY$ system. However, in order to solve the 4×4 secular determinant (eq. [7]), the case for which L, T, δ_{AB}, and δ_{XY} are small compared to J_{XY} and J_{AB}, must be considered.

$$[7]\qquad \begin{vmatrix} \frac{1}{2}(\delta_{AB}+\delta_{XY}-K+L-T)-E & \frac{1}{2}J_{XY} & \frac{1}{2}J_{AB} & 0 \\ \frac{1}{2}J_{XY} & \frac{1}{2}(\delta_{AB}-\delta_{XY}-K-L+T)-E & 0 & \frac{1}{2}J_{AB} \\ \frac{1}{2}J_{AB} & 0 & \frac{1}{2}(-\delta_{AB}+\delta_{XY}-K-L+T)-E & \frac{1}{2}J_{XY} \\ 0 & \frac{1}{2}J_{AB} & \frac{1}{2}J_{XY} & \frac{1}{2}(-\delta_{AB}-\delta_{XY}-K+L-T)-E \end{vmatrix} = 0$$

The difference of two small quantities, i.e. $\delta_{AB}-\delta_{XY}$ and $L-T$ in eq. [7], will be neglected. Thus, defining

$$F = -K-2E \qquad \text{and} \qquad \Delta = \delta_{AB}+\delta_{XY}$$

eq. [7] becomes

$$[8]\qquad \begin{vmatrix} \Delta+F & J_{XY} & J_{AB} & 0 \\ J_{XY} & F & 0 & J_{AB} \\ J_{AB} & 0 & F & J_{XY} \\ 0 & J_{AB} & J_{XY} & -\Delta+F \end{vmatrix} = 0$$

Expanding this determinant and reuniting in terms of M and K gives

$$F^4-4F^2[K^2+M^2+(\Delta^2/4)]+16M^2K^2 = 0.$$

Neglecting $(\Delta/2)^2$ with respect to $K^2 + M^2$ gives the roots

$$F = \pm 2K; \qquad \pm 2M$$

and thus the energies of the states 7′, 8′, 9′, and 10′.

Can. J. Chem. Downloaded from www.nrcresearchpress.com by 210.87.254.6 on 09/05/12
For personal use only.

Can. J. Chem. Downloaded from www.nrcresearchpress.com by 210.87.254.6 on 09/05/12
For personal use only.

The wave functions for these states are given by introducing these energy values successively in eq. [8] and solving the four simultaneous equations obtained using the normalizing condition for the coefficients of the basic functions, neglecting Δ^2 when it occurs. The complete wave functions and energies are given in Table IV. As we have included now (for states 7′, 8′, 9′, and 10′) the condition of L, T, δ_{AB}, and δ_{XY} being small compared to J_{AB} and J_{XY}, we will consider how the energies and intensities of the remaining states change when this condition holds before giving the transition energies and intensities. When this condition holds,

$$C_{\pm} = \tfrac{1}{2}J_{XY}\{1+\tfrac{1}{2}(\alpha_{\pm}/J_{XY})^2\},$$
$$D_{\pm} = \tfrac{1}{2}J_{AB}\{1+\tfrac{1}{2}(\beta_{\pm}/J_{AB})^2\},$$

and

$$(\cos\theta_{\pm}-\sin\theta_{\pm})^2 = \tfrac{1}{2}(\alpha_{\pm}/J_{XY})^2,$$
$$(\cos\phi_{\pm}-\sin\phi_{\pm})^2 = \tfrac{1}{2}(\beta_{\pm}/J_{AB})^2,$$
$$(\cos\theta_{\pm}+\sin\theta_{\pm})^2 = (\cos\phi_{\pm}+\sin\phi_{\pm})^2 = 2,$$

where

$$\alpha_{\pm} = \delta_{XY}\pm(L+T),$$
$$\beta_{\pm} = \delta_{AB}\pm(N-R).$$

The transition energies and intensities can be derived simply from Table IV. Including in these expressions the above equations gives the transition energies and relative intensities explicitly for the $ABXY$ system in the case considered. These are shown in Table V.

Table V is in the same form as Table II for the ABX case and the type of spectrum obtained when Table V is valid (the AB part is shown in Fig. 4(b)) is very similar in form to the AB part of the spectrum of Fig. 2(b). The spectrum of Fig. 4(b) approximates to that of a simple triplet group (Fig. 4(c)) and the conditions under which this simple spectrum is obtained can be derived in exactly the same manner as in the ABX case. The conditions under which an $ABXY$ system will give a simple spectrum of two triplet groups are

[9] $$\{\delta_{XY}+(L+T)\}^2/2J_{XY} < \Delta\nu_{\frac{1}{2}},$$

[10] $$\{\delta_{AB}+(N-R)\}^2/2J_{AB} < \Delta\nu_{\frac{1}{2}},$$

and

[11] $$\tfrac{1}{2}\{(\delta_{XY}+L+T)/J_{XY}\}^2 < i,$$
$$\tfrac{1}{2}\{(\delta_{AB}+N-R)/J_{AB}\}^2 < i,$$
$$\tfrac{1}{2}\{(\delta_{AB}+\delta_{XY})/2J_{AB}\}^2 < i,$$
$$\tfrac{1}{2}\{(\delta_{AB}+\delta_{XY})/2J_{XY}\}^2 < i,$$

and when these conditions hold, the spacing in the triplet groups is equal to $\frac{1}{2}(N+R)$.

These results may also be conveniently expressed in the form of a correlation diagram (Fig. 4). This gives the AB part of an $ABXY$ spectrum (the XY half will be very similar), and in this case, as the general $ABXY$ spectrum cannot be given explicitly, Fig. 4(a) gives the AB spectrum in the first-order approximation when δ_{AB} and δ_{XY} are large compared to the coupling constants. In Fig. 4(b), the spectrum is given when Table V

TABLE V

Energies and intensities for $ABXY$

		Energy	Relative intensity
A Transitions			
(*a*)	$5' \rightarrow 1$	$(\nu_0/2)(H_A+H_B)+J_{AB}+\frac{1}{2}(N+R)+\frac{1}{4}\beta_+^2/J_{AB}$	$\frac{1}{2}(\beta_+/J_{AB})^2$
(*b*)	$9' \rightarrow 2'$	" $+J_{AB}$ $+\frac{1}{4}\alpha_+^2/J_{XY}$	$\frac{1}{2}(\Delta/2J_{AB})^2$
(*c*)	$10' \rightarrow 3'$	" $+J_{AB}$ $-\frac{1}{4}\alpha_+^2/J_{XY}$	$\frac{1}{2}(\Delta/2J_{AB})^2$
(*d*)	$11 \rightarrow 4'$	" $+\frac{1}{2}(N+R)+\frac{1}{4}\beta_+^2/J_{AB}$	2
(*e*)	$13' \rightarrow 6$	" $+J_{AB}-\frac{1}{2}(N+R)+\frac{1}{4}\beta_-^2/J_{AB}$	$\frac{1}{2}(\beta_-/J_{AB})^2$
(*f*)	$14' \rightarrow 7'$	" $-\frac{1}{4}\alpha_-^2/J_{XY}$	$2+\alpha_-/2J_{XY}^2(\Delta-\alpha_-)$
(*g*)	$15' \rightarrow 8'$	" $+\frac{1}{4}\alpha_-^2/J_{XY}$	$2+\alpha_-/2J_{XY}^2(\Delta-\alpha_-)$
(*h*)	$16 \rightarrow 12'$	" $-\frac{1}{2}(N+R)+\frac{1}{4}\beta_-^2/J_{AB}$	2
B Transitions			
(*a*)	$4' \rightarrow 1$	$(\nu_0/2)(H_A+H_B)$ $+\frac{1}{2}(N+R)-\frac{1}{4}\beta_+^2/J_{AB}$	2
(*b*)	$7' \rightarrow 2'$	" $+\frac{1}{4}\alpha_+^2/J_{XY}$	$2+\alpha_+/2J_{XY}^2(\Delta-\alpha_+)$
(*c*)	$8' \rightarrow 3'$	" $-\frac{1}{4}\alpha_+^2/J_{XY}$	$2+\alpha_+/2J_{XY}^2(\Delta-\alpha_+)$
(*d*)	$11 \rightarrow 5'$	" $-J_{AB}+\frac{1}{2}(N+R)-\frac{1}{4}\beta_+^2/J_{AB}$	$\frac{1}{2}(\beta_+/J_{AB})^2$
(*e*)	$12' \rightarrow 6$	" $-\frac{1}{2}(N+R)-\frac{1}{4}\beta_-^2/J_{AB}$	2
(*f*)	$14' \rightarrow 9'$	" $-J_{AB}$ $-\frac{1}{4}\alpha_-^2/J_{XY}$	$\frac{1}{2}(\Delta/2J_{AB})^2$
(*g*)	$15' \rightarrow 10'$	" $-J_{AB}$ $+\frac{1}{4}\alpha_-^2/J_{XY}$	$\frac{1}{2}(\Delta/2J_{AB})^2$
(*h*)	$16 \rightarrow 13'$	" $-J_{AB}-\frac{1}{2}(N+R)-\frac{1}{4}\beta_-^2/J_{AB}$	$\frac{1}{2}(\beta_-/J_{AB})^2$
X Transitions			
(*a*)	$3' \rightarrow 1$	$(\nu_0/2)(H_X+H_Y)+J_{XY}+\frac{1}{2}(N+R)+\frac{1}{4}\alpha_+^2/J_{XY}$	$\frac{1}{2}(\alpha_+/J_{XY})^2$
(*b*)	$6 \rightarrow 2'$	" $+\frac{1}{2}(N+R)+\frac{1}{4}\alpha_+^2/J_{XY}$	2
(*c*)	$8' \rightarrow 4'$	" $+J_{XY}$ $+\frac{1}{4}\beta_+^2/J_{AB}$	$\frac{1}{2}(\Delta/2J_{XY})^2$
(*d*)	$10' \rightarrow 5'$	" $+J_{XY}$ $-\frac{1}{4}\beta_+^2/J_{AB}$	$\frac{1}{2}(\Delta/2J_{XY})^2$
(*e*)	$12' \rightarrow 7'$	" $-\frac{1}{4}\beta_-^2/J_{AB}$	$2+\beta_-/2J_{AB}^2(\Delta-\beta_-)$
(*f*)	$13' \rightarrow 9'$	" $+\frac{1}{4}\beta_-^2/J_{AB}$	$2+\beta_-/2J_{AB}^2(\Delta-\beta_-)$
(*g*)	$15' \rightarrow 11$	" $+J_{XY}-\frac{1}{2}(N+R)+\frac{1}{4}\alpha_-^2/J_{XY}$	$\frac{1}{2}(\alpha_-/J_{XY})^2$
(*h*)	$16 \rightarrow 14'$	" $-\frac{1}{2}(N+R)+\frac{1}{4}\alpha_-^2/J_{XY}$	2
Y Transitions			
(*a*)	$2' \rightarrow 1$	$(\nu_0/2)(H_X+H_Y)$ $+\frac{1}{2}(N+R)-\frac{1}{4}\alpha_+^2/J_{XY}$	2
(*b*)	$6 \rightarrow 3'$	" $-J_{XY}+\frac{1}{2}(N+R)-\frac{1}{4}\alpha_+^2/J_{XY}$	$\frac{1}{2}(\alpha_+/J_{XY})^2$
(*c*)	$7' \rightarrow 4'$	" $+\frac{1}{4}\beta_+^2/J_{AB}$	$2+\beta_+/2J_{AB}^2(\Delta-\beta_+)$
(*d*)	$9' \rightarrow 5'$	" $-\frac{1}{4}\beta_+^2/J_{AB}$	$2+\beta_+/2J_{AB}^2(\Delta-\beta_+)$
(*e*)	$12' \rightarrow 8'$	" $-J_{XY}$ $-\frac{1}{4}\beta_-^2/J_{AB}$	$\frac{1}{2}(\Delta/2J_{XY})^2$
(*f*)	$13' \rightarrow 10'$	" $-J_{XY}$ $+\frac{1}{4}\beta_-^2/J_{AB}$	$\frac{1}{2}(\Delta/2J_{XY})^2$
(*g*)	$14' \rightarrow 11$	" $-\frac{1}{2}(N+R)-\frac{1}{4}\alpha_-^2/J_{XY}$	2
(*h*)	$16 \rightarrow 15'$	" $-J_{XY}-\frac{1}{2}(N+R)-\frac{1}{4}\alpha_-^2/J_{XY}$	$\frac{1}{2}(\alpha_-/J_{XY})^2$

is valid, i.e. L, T, δ_{AB}, and δ_{XY} are small compared to J_{AB} and J_{XY}, but eqs. [9], [10], and [11] do not hold, and in Fig. 4(*c*) is shown the simple 3-line spectrum obtained when eqs. [9], [10], and [11] are valid. The actual values of the coupling constants J_{AB}, J_{XY}, J_{AX}, J_{AY}, J_{BX}, and J_{BY} used in Fig. 4 were 10, 12, 9.5, 8.5, 9.5, and 4.5 c.p.s., respectively, and the chemical shift values are $\delta_{AB} = 48$ c.p.s. in Fig. 4(*a*) (δ_{XY} is not involved in this case), $\delta_{AB} = 3$ c.p.s., and $\delta_{XY} = 4$ c.p.s. in Fig. 4(*b*), and $\delta_{AB} = \delta_{XY} = 0$ c.p.s. in Fig. 4(*c*).

The calculations in this section have given the quantitative condition necessary in order that the $ABXY$ system will give a simple spectrum, and it is seen that the assumption made in the beginning of this section, i.e. that the simple spectrum is obtained when J_{AB} and J_{XY} are large compared to terms like δ_{AB}, δ_{XY}, and $J_{AX}-J_{BX}$, which was obtained merely by inspection of the results for the ABX and A_2X_2 systems, is valid. In the next section, the results for the three systems considered are compared in order to obtain the general condition necessary for these simple spectra to be obtained.

The General Case

The conditions under which the ABX, A_2X_2, and $ABXY$ systems give these deceptively

Can. J. Chem. Downloaded from www.nrcresearchpress.com by 210.87.254.6 on 09/05/12
For personal use only.

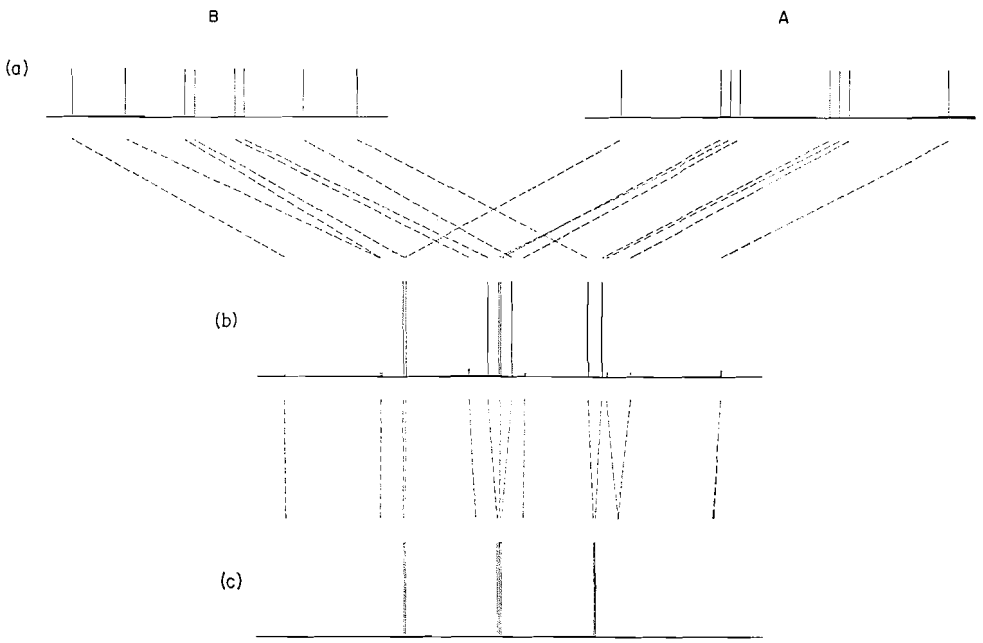


FIG. 4. Typical spectra of the AB part of the $ABXY$ system when (*a*) δ_{AB} and δ_{XY} are large compared to J_{AB} and J_{XY}; (*b*) J_{AB} and J_{XY} are large compared to δ_{AB}, δ_{XY}, L, and T; (*c*) equations [7] and [8] are valid.

simple spectra (eqs. [2], [5], [9], and [10]), can be compared most easily by rewriting these equations in terms of the actual coupling constants involved. These equations become

$$[2a] \qquad \{\delta_{AB}+\tfrac{1}{2}(J_{AX}-J_{BX})\}^2/2J_{AB} < \Delta\nu_{\frac{1}{2}},$$

$$[5a] \qquad (J-J')^2/2(J_A-J_X) < \Delta\nu_{\frac{1}{2}},$$

$$[9a] \qquad \{\delta_{XY}+\tfrac{1}{2}(J_{AX}-J_{AY}+J_{BX}-J_{BY})\}^2/2J_{XY} < \Delta\nu_{\frac{1}{2}},$$

$$[10a] \qquad \{\delta_{AB}+\tfrac{1}{2}(J_{AX}-J_{BX}+J_{AY}-J_{BY})\}^2/2J_{AB} < \Delta\nu_{\frac{1}{2}}.$$

It can be seen that eqs. [2*a*] and [10*a*] are equivalent, but the latter has extra terms involving the new nucleus Y which are of the same form as those involving X in eq. [2*a*]. This result shows that any general condition valid for the $ABXY$ case will also be valid for the ABX case merely by removing the terms in Y and also it indicates that one explicit condition for the $ABXYZ\ldots$ system to give a simple spectrum will be

$$[12] \qquad \{\delta_{AB}+\tfrac{1}{2}(J_{AX}-J_{BX}+J_{AY}-J_{BY}+J_{AZ}-J_{BZ}+\ldots)\}^2/J_{AB} < \Delta\nu_{\frac{1}{2}}.$$

The conditions necessary for the general system $ABC\ldots XYZ\ldots$ to give a simple spectrum cannot, however, be derived explicitly, but from the form of the equations above, the nature of these conditions may be given in a qualitative fashion, as follows. The system $ABC\ldots XYZ\ldots$ will be expected to give a simple spectrum when the terms of the type J_{AB}, J_{XY} are large compared to the chemical shift differences δ_{AB}, δ_{XY} plus terms of the form $J_{AX}-J_{AY}$, etc. and in this case the spectrum will be a simple first-order A_mX_n spectrum in which the separation of the lines in each group of the spectrum is given by the average of the coupling constants J_{AX}, J_{AY}, etc.

Can. J. Chem. Downloaded from www.nrcresearchpress.com by 210.87.254.6 on 09/05/12
For personal use only.

Can. J. Chem. Downloaded from www.nrcresearchpress.com by 210.87.254.6 on 09/05/12
For personal use only.

spacing of 0.64 c.p.s.* The observed proton spectrum of this compound is given in Fig. 5 and the triplet spacing of 0.55 c.p.s. agrees excellently with the predicted value.

The above result for benzene-d_1 may be extended to almost any monodeutero-substituted compound as in these compounds the proton–deuterium coupling constants will be much less that the proton–proton coupling constants. Thus in these compounds the general statement above will apply and therefore monodeuterium substitution in a molecule containing more than two hydrogen atoms will generally only give the average of all the proton–deuterium couplings which are present in the molecule.

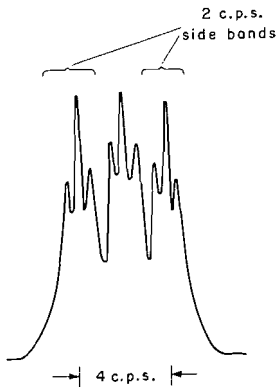


FIG. 5. The proton spectrum of liquid benzene-d_1 at 60 Mc/sec with a 2 c.p.s. side band.

REFERENCES

1. H. J. BERNSTEIN, J. A. POPLE, and W. G. SCHNEIDER. Can. J. Chem. **35**, 65 (1957).
2. J. A. POPLE, W. G. SCHNEIDER, and H. J. BERNSTEIN. Can. J. Chem. **35**, 1060 (1957).
3. W. G. SCHNEIDER, H. J. BERNSTEIN, and J. A. POPLE. Can. J. Chem. **35**, 1487 (1957).
4. R. J. ABRAHAM, J. A. POPLE, and H. J. BERNSTEIN. Can. J. Chem. **36**, 1302 (1958).
5. R. J. ABRAHAM and H. J. BERNSTEIN. Can. J. Chem. **37**, 1056 (1959).
6. H. S. GUTOWSKY, C. H. HOLM, A. SAIKA, and G. A. WILLIAMS. J. Am. Chem. Soc. **79**, 4596 (1957).
7. R. E. RICHARDS and T. SCHAEFFER. Mol. Phys. **1**, 331 (1958).
8. H. M. MCCONNELL, A. D. MCLEAN, and C. A. REILLY. J. Chem. Phys. **23**, 1152 (1955).
9. E. J. COREY, G. SLOMP, SUKH DEV, S. TOKINOGA, and E. R. GLAZIER. J. Am. Chem. Soc. **80**, 1204 (1958).
10. J. B. LEANE and R. E. RICHARDS. Trans. Faraday Soc. **55**, 518 (1955).
11. R. J. ABRAHAM and H. J. BERNSTEIN. In press.
12. J. N. SHOOLERY and B. CRAWFORD, JR. J. Mol. Spectroscopy, **1**, 270 (1957).
13. T. SCHAEFFER. Can. J. Chem. **37**, 882 (1957).
14. T. SCHAEFFER and W. G. SCHNEIDER. Can. J. Chem. **37**, 2078 (1959).
15. E. B. BAKER. J. Chem. Phys. **23**, 984 (1955).
16. H. S. GUTOWSKY, L. H. MEYER, and D. W. MCCALL. J. Chem. Phys. **23**, 982 (1955).
17. D. ROUX. Helv. Phys. Acta, **31**, 511 (1958).
18. J. A. POPLE, W. G. SCHNEIDER, and H. J. BERNSTEIN. High-resolution nuclear magnetic resonance. McGraw-Hill Book Co., New York. 1959. p. 193.

**The proton–proton spin coupling constants have been divided by $U_H I_D / U_D I_H$ to obtain the corresponding deuterium–proton spin coupling constants. U_H is the magnetic moment and I_H is the spin of the proton and U_D and I_D the corresponding quantities for the deuteron.*

Can. J. Chem. Downloaded from www.nrcresearchpress.com by 210.87.254.6 on 09/05/12
For personal use only.

Can. J. Chem. Downloaded from www.nrcresearchpress.com by 210.87.254.5 on 09/05/12
For personal use only.

THE PREPARATION, PAPER CHROMATOGRAPHY, AND COLOR REACTIONS OF SEVERAL 5,6-DIHYDROXYINDOLES AND 5,6-DIACETOXYINDOLES[1]

R. A. HEACOCK, M. E. MAHON, AND B. D. SCOTT

ABSTRACT

The paper chromatographic behavior of several 5,6-dihydroxyindoles has been studied. The colors given by nine dihydroxyindoles with 16 chromogenic reagents are reported. The R_f values of this group of compounds on Whatman No. 1 paper with 2% acetic acid in water or *n*-butanol/acetic acid/water (6:1:2) as running solvents have been determined. The 5,6-dihydroxyindoles can be chromatographed satisfactorily using Zaffaroni-type systems (i.e. formamide-treated paper and non-polar running solvents). Satisfactory R_f values can also be obtained for the 5,6-diacetoxyindoles on formamide-treated paper using a suitable non-polar mobile phase. The preparations of several new 5,6-dihydroxyindoles and 5,6-diacetoxyindoles are described and improved procedures for the syntheses of some known members of these groups are reported.

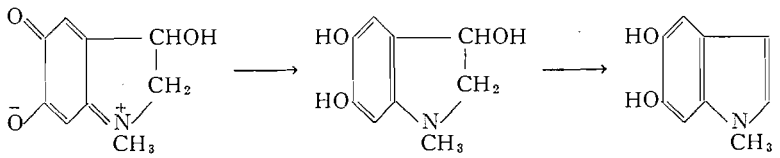
The importance of the 5,6-dihydroxindoles as intermediates in the production of the dark pigments known as melanins, in plants and animals, has been recognized for some time (for references see reviews by Lerner (1), Mason (2), and Thomas (3)), but it is only in relatively recent years that many of these highly reactive compounds have been obtained in pure crystalline form (see (3) and (4) for references). Although there has been a considerable volume of work carried out on the chromatography of the indoles in the past decade, there have been relatively few studies reported of the paper chromatographic behavior of the 5,6-dihydroxyindoles and their derivatives. In a study of the urine melanogens observed in cases of malignant melanoma of the liver, Leonhardi reported the R_f values of some 5,6-dihydroxyindole derivatives (e.g. *O*-acetyl, *O*-methyl, *O*-sulphatoxy, etc.) in several different solvent systems. These compounds were employed as models for the urinary melanogens which were considered by Leonhardi to be 5,6-dihydroxyindole derivatives (5). During an investigation into the metabolism of β-(3,4-dihydroxyphenyl)-alanine in albino rats Pellerin and D'Iorio obtained a product with a R_f of 0.85 in a *n*-butanol/acetic acid/water system which they suggested was possibly 5,6-dihydroxyindole (6).

One of the main difficulties encountered in carrying out paper chromatographic studies with the 5,6-dihydroxyindoles is the ease with which they undergo destructive oxidation to melanitic pigments, especially under alkaline conditions; consequently basic solvent systems, including the isopropanol/aqueous ammonia systems widely favored for indole chromatography, are quite useless with this group of indole derivatives. In an investigation of the reduction of adrenochrome with various reducing agents, carried out in these laboratories (7, 8, 9), we have made extensive use of paper chromatographic procedures in the examination of the reaction products. Many of the products encountered in this program were either 5,6-dihydroxyindoles or their derivatives, and one of the most satisfactory systems for the study of these reaction mixtures was found to be 2% acetic acid in water using chromatographic paper that had been extensively prewashed with the running solvent, prior to use. The possible use of *n*-butanol/acetic acid/water (6:1:2) as the running solvent was also considered but it gave somewhat less satisfactory results than 2% acetic acid. In parallel studies on the relatively unstable aminochromes derived

[1]*Manuscript received August 8, 1960.*
Contribution from the Psychiatric Research Unit, University Hospital, Saskatoon, Saskatchewan. This investigation was supported by grants from the Government of Saskatchewan, the Department of National Health and Welfare (Ottawa), and the Rockefeller Foundation.

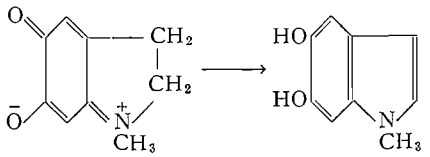
from "DOPA", dopamine and noradrenaline, Bouchilloux and Kodja utilized paper chromatographic and paper electrophoretic procedures to investigate both the spontaneous transformations these compounds undergo in aqueous solution and their behavior with reducing agents, using distilled water and *n*-butanol/acetic acid/water as running solvents (10, 11, 12). These authors stress the need to work with well-washed paper to ensure that all traces of sulphites, which can form addition compounds with the 5,6-dihydroxyindoles and the aminochromes have been removed from the chromatographic paper before use.

5,6-Dihydroxyindoles can arise from the aminochromes in at least two ways. If the aminochrome is of the type with a 3-hydroxyl group, reduction leads initially to the formation of an unstable leuco compound, which immediately loses water to form the 5,6-dihydroxyindole (e.g. adrenochrome (I) would be initially reduced to "leuco-adrenochrome" (II) which apparently only has a transient existence and loses water forming 5,6-dihydroxy-*N*-methylindole (III) (see (4) for references)). However, the aminochromes



I II III

with no 3-hydroxyl substituent undergo an internal oxidation–reduction reaction with considerable ease resulting in the formation of a 5,6-dihydroxyindole. This reaction is catalyzed by OH^- and Zn^{++} ions, but will also occur spontaneously even in the solid state (e.g. epinochrome (IV) readily rearranges to 5,6-dihydroxy-*N*-methylindole (III)). (See (4) for references.)



IV III

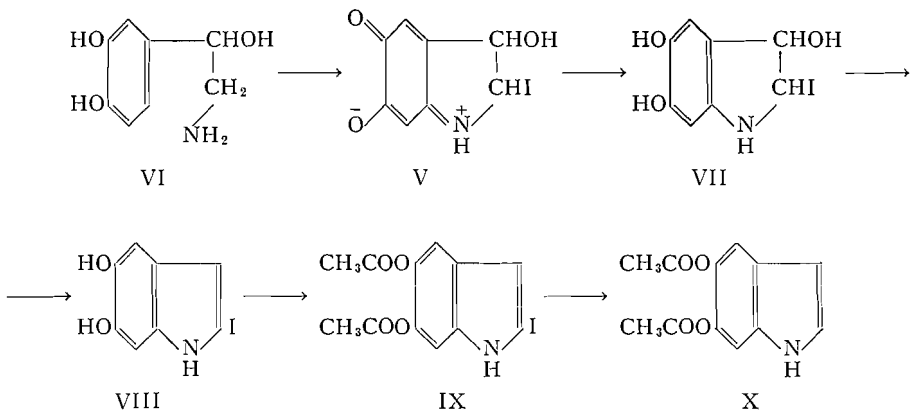
The 5,6-dihydroxyindoles used in this investigation were, with the exception of 5,6-dihydroxyindole itself (which was prepared by the method of Beer *et al.* (13)), prepared by the reduction of the corresponding aminochrome. 5,6-Dihydroxy-*N*-methylindole had previously been obtained in about 30% yield from either the hydrogenation of, or the sodium hydrosulphite reduction of, adrenochrome, adrenolutin being obtained as a by-product in each case (14). It was observed, as a result of a preliminary paper chromatographic examination of the reduction mixtures obtained from adrenochrome with a variety of reducing agents, that sodium hydrosulphite always gave the sodium bisulphite addition compound of adrenochrome and smaller amounts of a second water-soluble indole as well as 5,6-dihydroxy-*N*-methylindole (8). However, chromatograms of the zinc and 2% acetic acid, hydrogen sulphide, or sodium borohydride reduction products of adrenochrome showed 5,6-dihydroxy-*N*-methylindole as a very intense spot and only one other relatively weak spot due to an unidentified by-product in each case (8). Contamination of the product with sulphur was a serious disadvantage which was encountered during the use of hydrogen sulphide as the reducing agent for a preparative procedure,

Can. J. Chem. Downloaded from www.nrcresearchpress.com by 210.87.254.5 on 09/05/12
For personal use only.

Can. J. Chem. Downloaded from www.nrcresearchpress.com by 210.87.254.5 on 09/05/12
For personal use only.

but either zinc and 2% acetic acid or sodium borohydride have proved very satisfactory for the preparation of 5,6-dihydroxy-*N*-methylindole and yields of up to ca. 70% have been obtained from adrenochrome. Attempts to prepare crystalline *N*-ethyl-5,6-dihydroxyindole or 5,6-dihydroxy-*N*-isopropylindole by adaptation of the procedures used for the preparation of 5,6-dihydroxy-*N*-methylindole have, as yet, been unsuccessful, the products being obtained as colorless gums. However, crystalline diacetyl derivatives have been prepared from both the dihydroxy compounds. Ethereal solutions of *N*-ethyl-5,6-dihydroxyindole and 5,6-dihydroxy-*N*-isopropylindole (suitable for examination of their paper chromatographic behavior) can be obtained easily by ether extraction of the products obtained from the reduction of *N*-ethylnoradrenochrome and *N*-isopropylnoradrenochrome respectively. (The reduction can be conveniently carried out with zinc and 2% acetic acid, sodium borohydride, or sodium hydrosulphite.) A simple method has been developed for the preparation of the diacetyl derivatives of 5,6-dihydroxy-*N*-methylindole, *N*-ethyl-5,6-dihydroxyindole, and 5,6-dihydroxy-*N*-isopropylindole, directly from the corresponding catecholamine. The catecholamine is oxidized with silver oxide; the resulting aminochrome solution reduced with zinc and dilute acetic acid (or sodium borohydride) and the crude *N*-alkyl-5,6-dihydroxyindole solution acetylated directly with acetic anhydride in aqueous alkali.

The preparation of 2-iodonoradrenochrome (V) by the oxidation of noradrenaline (VI) with potassium iodate had been reported by Bu'Lock and Harley-Mason but only a relatively low yield of crystalline product was obtained after discarding much tarry material (15). In view of the success of the dilute solution technique, first described by Sobotka and Austin for the preparation of 2-iodoadrenochrome (16) and subsequently used for the preparation of the *N*-ethyl and *N*-isopropyl analogues (17), an attempt was made to prepare 2-iodonoradrenochrome (V) this way. Although a deep-violet solution was obtained, no precipitation of the desired aminochrome occurred, even on standing at 0° for 24 hours, presumably due to its higher water solubility. However, the deep-violet color of the solution was rapidly discharged by the addition of excess ascorbic acid and



VI V VII

VIII IX X

5,6-dihydroxy-2-iodoindole (VIII) could be extracted from the reaction mixture with ether; VIII had presumably arisen from the spontaneous dehydration of the initial "leuco" derivative, 2,3-dihydro-3,5,6-trihydroxy-2-iodoindole (VII). In fact, there are several other water-soluble indoles produced in this reaction; this will be discussed in more detail in a later publication (18). 5,6-Diacetoxy-2-iodoindole (IX) could be obtained

from the dihydroxy compound (VIII) by acetylation with acetic anhydride and pyridine. 5,6-Diacetoxyindole (X) was obtained by the deiodination of 5,6-diacetoxy-2-iodoindole with zinc and acetic acid using the procedure described by Bu'Lock and Harley-Mason for the deiodination of several 5,6-di- and 3,5,6-triacetoxyiodoindoles (15). 5,6-Dihydroxy-2-iodo-*N*-methylindole was obtained in crystalline form from 2-iodoadrenochrome by reduction with sodium hydrosulphite (cf. 19) (acetylation with acetic anhydride in pyridine readily gave 5,6-diacetoxy-2-iodo-*N*-methylindole (19)). Reduction of the *N*-ethyl and *N*-isopropyl analogues with sodium hydrosulphite gave *N*-ethyl-5,6-dihydroxy-2-iodoindole and 5,6-dihydroxy-2-iodo-*N*-isopropylindole, respectively; as yet, both of these substances have only been obtained as amorphous solids, but their crystalline diacetyl derivatives have been described (17).

The 5,6-dihydroxyindoles can be very easily detected by color reactions; these highly reactive compounds possess the indole ring system and consequently give colors with the conventional indole reagents such as Ehrlich's reagent, cinnamaldehyde, *p*-dimethylaminocinnamaldehyde, the Hopkins-Cole reagent, and terephthalaldehyde. They also contain phenolic hydroxyl groups and give colored products with many phenol-detecting reagents such as diazotized *p*-nitroaniline, Gibb's reagent, ferric chloride, and Folin and Ciocalteu's reagent. The 5,6-dihydroxyindoles are also catechol derivatives and have strong reducing properties and will reduce such reagents as ammoniacal silver nitrate and ferric chloride/potassium ferricyanide; the 5,6-dihdroxyindoles undergo air oxidation with extreme ease, under alkaline conditions, and spraying with dilute aqueous alkali or even exposing the papers to ammonia fumes converts the compound into a dark insoluble melanin-like pigment. The colors obtained with several chromogenic reagents are given in Table I. In the 5,6-diacetoxyindoles the catechol function is blocked and consequently these compounds are not so readily oxidized as the free hydroxy compounds, nevertheless, they do give colors with most of the usual indole and phenol reagents. The results obtained with several chromogenic reagents are given in Table III.

In view of the success attending the use of 2% acetic acid in water, on acid-washed paper, as a medium for preliminary paper chromatographic studies of the crude reaction mixtures, containing several 5,6-dihydroxyindoles and their derivatives, obtained by reduction of the aminochromes (cf. 7, 8, 9, 19), the R_f values of several standard 5,6-dihydroxyindoles on acid-washed Whatman No. 1 paper, using 2% acetic acid as running solvent, were determined both by the descending and circular techniques (the results are given in Table II). It will be seen that, in general, the R_f values obtained by the circular procedure are somewhat higher than those obtained by the descending method. *n*-Butanol /acetic acid/water solvent mixtures have also been employed for paper chromatographic investigations in this field (7, 10, 11, 12) and consequently the R_f values of several 5,6-dihydroxyindoles were determined in *n*-butanol/acetic acid/water (6:1:2). The results are given in Table II.

Acetic acid (2%) cannot be used satisfactorily as a running solvent for the paper chromatography of the 5,6-diacetoxyindoles owing to their low water solubility; *n*-butanol /acetic acid/water systems are of little value either since the diacetoxy compounds run almost to the solvent front in this solvent. A method for studying the paper chromatographic behavior of steroids was introduced about 10 years ago (20, 21) which used a highly polar stationary phase (e.g. paper treated with formamide or propylene glycol) and a non-polar mobile phase (e.g. cyclohexane, benzene, chloroform, etc.); this type of system has subsequently been widely used for the chromatographic separation of the ergot alkaloids (22, 23, 24). This technique has now been extended successfully to include

Can. J. Chem. Downloaded from www.nrcresearchpress.com by 210.87.254.5 on 09/05/12
For personal use only.

Can. J. Chem. Downloaded from www.nrcresearchpress.com by 210.87.254.5 on 09/05/12
For personal use only.

the 5,6-diacetoxyindoles which can be easily separated on formamide-treated paper (the "pH" of the formamide was adjusted to 5 by the cautious addition of 98% formic acid prior to impregnation of the paper) using non-polar running solvents, such as: light petroleum, cyclohexane, benzene/light petroleum (1:9), carbon tetrachloride, etc. Benzene gave satisfactory R_f's with the 5,6-diacetoxyindoles not alkylated on the nitrogen atom; however, the *N*-alkyl derivatives ran almost to the solvent front. The results obtained are given in Table V. It was possible to utilize this general procedure for a study of the paper chromatography of the 5,6-dihydroxyindoles, although it was necessary to use a slightly more polar mobile phase: i.e. benzene/chloroform (1:1), chloroform, benzene/ethyl acetate (3:1), chloroform/ethyl acetate (4:1), and dichloromethane. With these solvent systems satisfactory R_f values could be obtained for all the dihydroxy compounds studied; the results obtained are given in Table IV. The "pH" of the formamide was adjusted to 5, prior to impregnation of the paper, in all cases, since air oxidation of the 5,6-dihydroxyindoles was slower, under weakly acid, than neutral or alkaline conditions. Some experiments were carried out with the "pH" of the formamide adjusted to 7 or 9 before treatment of the paper, but in both cases, particularly the latter, considerable dark streaking behind the 5,6-dihydroxyindole spots was observed, presumably due to melanin formation. Changing the "pH" of the stationary phase also alters the R_f's of the compounds but only relatively few runs were carried out and will not be reported here. Throughout these investigations involving the use of formamide-treated paper it was desirable to saturate the mobile phase with formamide; however, with the chlorinated solvents, particularly dichloromethane it was found that it was better, in practice, to add slightly less than the amount of formamide required to saturate the solvent so as to ensure that the formamide remains in solution during the running of the chromatograms. If the solvents become cloudy due to separation of free formamide, inconsistent and unsatisfactory results are obtained. Gröger used the formamide/dichloromethane system to separate the Clavin group of ergot alkaloids and stressed that the mobile phase must not be allowed to become cloudy during the development of the chromatograms (25). During the course of these investigations the authors became aware of a paper by Prochazka *et al.* on the paper chromatography of indoles in general and the R_f's of several indoles on formamide-treated paper with cyclohexane, benzene, and chloroform as the mobile phases were reported (26); however, no 5,6-dihydroxyindoles or 5,6-diacetoxyindoles were included in the group of substances studied.

EXPERIMENTAL

Chemical

(I) *5,6-Dihydroxyindoles*

(*A*) *5,6-Dihydroxyindole*

5,6-Dihydroxyindole was prepared by the method of Beer, Clarke, Khorana, and Robertson (13).

(*B*) *5,6-Dihydroxy-N-methylindole*

(i) *From adrenochrome.*—(*a*) A solution of adrenochrome (1.0 g) in water (100 ml) was added slowly, with stirring, to a solution of sodium borohydride (0.3 g) in water (25 ml); the red color of the adrenochrome solution was instantly discharged and a pale yellow solution obtained. After decomposition of excess reducing agent by the cautious dropwise addition of 2 *N* sulphuric acid, the reaction mixture was extracted with peroxide-free ether (4×100 ml). The combined, dried (Na_2SO_4) extracts were concentrated to small

bulk, under nitrogen, below 30°; dry benzene (100 ml) was added and the remaining ether distilled off. (It was found that if the original ethereal solution was evaporated to dryness, the residue would not completely redissolve in benzene.) The product was adsorbed on a silica gel* column (10×2.4 cm); elution of the column with benzene (150 ml) and benzene /ethyl acetate (95:5) (300 ml) gave white solids (the solvent having been removed *in vacuo*, under nitrogen, below 30°), which on recrystallization from light petroleum (b.p. 100–120°) gave 5,6-dihydroxy-*N*-methylindole (0.68 g) as colorless needles (m.p. 134–135°). (Found: C, 66.14; H, 5.58. $C_9H_9NO_2$ requires C, 66.25; H, 5.56%.) The melting point of this substance is quoted in the literature as 136° (14) and 133° (27).† (*b*) Zinc dust (40.0 g) was added, with vigorous stirring, to a solution of adrenochrome (1.0 g) in 2% acetic acid (200 ml). The red color of the solution was rapidly discharged and stirring was maintained for a further 4 to 5 minutes. The reaction mixture was filtered (suction) and both the residue and filtrate repeatedly extracted with peroxide-free ether. The combined, dried (Na_2SO_4) ethereal extracts were concentrated and the product worked up and purified chromatographically as described above (see Subsection i(*a*) above). 5,6-Dihydroxy-*N*-methylindole (0.35 g) was obtained in colorless needles (m.p. 133–134°).

(ii) *From adrenaline.*—Silver oxide (10 g) was added to a well-stirred solution of adrenaline bitartrate (2.5 g) in water (50 ml). The reaction mixture was vigorously stirred, with external cooling, for a further 3 minutes after which time the resulting deep-red suspension was filtered (with suction) through a Dowex-1(Cl^-) resin bed (3.5×1.5 cm‡) directly into a vigorously stirred solution of sodium borohydride (0.6 g) in water (25 ml). (It was necessary to add a few drops of peroxide-free ether from time to time to control the vigorous frothing that occurred.) Sulphuric acid (2 *N*) was added dropwise to decompose the excess sodium borohydride and the solution was immediately extracted with peroxide-free ether (4×125 ml). The combined, dried (Na_2SO_4) extracts were concentrated and the products were worked up and purified chromatographically, as described in Subsection i(*a*) above, to give 5,6-dihydroxy-*N*-methylindole in colorless needles (0.37 g), m.p. 133–134°.

(*C*) *N-Ethyl-5,6-dihydroxyindole*

N-Ethyl-5,6-dihydroxyindole was prepared in solution in peroxide-free ether. As yet, *N*-ethyl-5,6-dihydroxyindole has only been obtained as a yellow gum, however, a crystalline diacetyl derivative has been prepared (see Section II(*C*)). Sodium hydrosulphite (50 mg) was added to a solution of *N*-ethylnoradrenochrome (20 mg, prepared by the method of Heacock and Scott (17)) in water (10 ml); the red color of the solution was rapidly discharged and the reaction mixture extracted with peroxide-free ether (2×4 ml). The dried (Na_2SO_4) ethereal extract containing the *N*-ethyl-5,6-dihydroxyindole (concentration, ca. 1 mg/ml) was used directly for the chromatographic studies.

(*D*) *5,6-Dihydroxy-N-isopropylindole*

5,6-Dihydroxy-*N*-isopropylindole was prepared in solution in peroxide-free ether (at a concentration of ca. 1 mg/ml) from *N*-isopropylnoradrenochrome (17) in an analogous manner to the method described above for the preparation of the *N*-ethyl derivative. As in the case of the *N*-ethyl analogue, 5,6-dihydroxy-*N*-isopropylindole has, as yet, only

**In this and subsequent experiments described in this paper the chromatographic silica gel used was obtained from L. Light & Co. (200/300 mesh size).*

†In this case the substance was prepared by the rearrangement of epinochrome.

‡The resin (200/400 mesh size) was purified by extensive washing with: (a) 2 N hydrochloric acid and (b) water until neutral to litmus. This procedure was used for the preparation of the resin beds described throughout this paper.

Can. J. Chem. Downloaded from www.nrcresearchpress.com by 210.87.254.5 on 09/05/12
For personal use only.

been obtained as a yellow gum, but a crystalline diacetyl derivative has been prepared (see Section II(*D*)).

(*E*) *5,6-Dihydroxy-2-iodoindole*

Potassium iodate (3.2 g) was added to a solution of noradrenaline hydrochloride (2.0 g) in water (1600 ml) and the reaction mixture was stirred at room temperature for 2 hours. An excess of solid ascorbic acid was added (until the deep-violet color of the solution was discharged) and the reaction mixture extracted with peroxide-free ether (5×200 ml). Dry benzene (250 ml) was added to the dried (Na_2SO_4) ethereal extract and the ether was removed *in vacuo*, under nitrogen (bath temperature below 30°); the final traces of ether were removed by the addition of further small quantities of dry benzene and removal of them *in vacuo*. (If the ether extract was concentrated to dryness without the prior addition of benzene, the dark residue obtained was only partially soluble in benzene.) The crude product (obtained in solution in benzene by the method described above) gave 5,6-dihydroxy-2-iodoindole (1.1 g), m.p. 108–108.5° (with decomposition), in pale yellow needles after chromatographic purification on a silica gel column (7×2.4 cm) (adsorption from benzene – light petroleum (b.p. 80–100°) (1:1) and elution with this solvent and benzene). (Found: C, 35.05; H, 2.21; I, 45.93. $C_8H_6NO_2I$ requires C, 34.94; H, 2.20; I, 46.14%.) This product was relatively unstable and decomposed to a black vitreous substance on standing 4 weeks at room temperature.

(*F*) *5,6-Dihydroxy-2-iodo-N-methylindole*

5,6-Dihydroxy-2-iodo-*N*-methylindole was prepared in the manner described by Heacock and Scott (19).

(*G*) *N-Ethyl-5,6-dihydroxy-2-iodoindole*

N-Ethyl-5,6-dihydroxy-2-iodoindole was prepared in solution in peroxide-free ether; although, as yet, *N*-ethyl-5,6-dihydroxy-2-iodoindole has only been obtained as a brownish-yellow amorphous solid, a crystalline diacetyl derivative has been described (17). Sodium hydrosulphite (60 mg) was added to a stirred suspension of *N*-ethyl-2-iodonoradrenochrome (30 mg, prepared by the method of Heacock and Scott (17)) in water (10 ml). After being stirred for ca. 2 minutes the cloudy yellow suspension was filtered from residual solid material and the filtrate was extracted with peroxide-free ether (4×4 ml). The dried (Na_2SO_4) ethereal extract containing the *N*-ethyl-5,6-dihydroxy-2-iodoindole (concentration, ca. 1 mg/ml) was used directly for the chromatographic studies.

(*H*) *5,6-Dihydroxy-2-iodo-N-isopropylindole*

5,6-Dihydroxy-2-iodo-*N*-isopropylindole was prepared in peroxide-free ether solution (from 2-iodo-*N*-isopropylnoradrenochrome (17)) at a concentration of ca. 1 mg/ml in an analogous manner to that described above for the *N*-ethyl derivative. As yet, 5,6-dihydroxy-2-iodo-*N*-isopropylindole has only been obtained as a greenish-brown amorphous solid but a crystalline diacetyl derivative has been described (17).

(*I*) *2-Bromo-5,6-dihydroxy-N-methylindole*

2-Bromo-5,6-dihydroxy-*N*-methylindole was prepared by the method described by Harley-Mason (14).

(II) *5,6-Diacetoxyindoles*

(*A*) *5,6-Diacetoxyindole*

Zinc powder (6.0 g) was added portionwise, during a period of 15 minutes, to a solution of 5,6-diacetoxy-2-iodoindole (0.9 g, prepared by the method described below (Section II

Can. J. Chem. Downloaded from www.nrcresearchpress.com by 210.87.254.5 on 09/05/12
For personal use only.

(*E*)) in glacial acetic acid (12 ml). The reaction mixture was filtered and the residual zinc was washed with glacial acetic acid (3×5 ml); the combined filtrate and washings were poured into ice water. The aqueous reaction mixture was extracted with peroxide-free ether (5×150 ml) and the ethereal extract washed free of acetic acid with saturated aqueous sodium bicarbonate. Concentration (*in vacuo*), of the dried (Na_2SO_4) ethereal extract, gave a red-brown gum, which by chromatographic purification on a short silica gel column using benzene as eluent and recrystallization from light petroleum (b.p. 80–100°) gave 5,6-diacetoxyindole in colorless needles (0.1 g), m.p. 139–140°. (Found: C, 61.77; H, 4.71. $C_{12}H_{11}NO_4$ requires C, 61.80; H, 4.75%.) Beer *et al.* (13), who prepared this compound by a different route report a melting point of 130–133°.

(*B*) *5,6-Diacetoxy-N-methylindole*

(i) Adrenaline (1.6 g) was suspended in water (50 ml) and concentrated hydrochloric acid was added dropwise until a clear solution was obtained. Silver oxide (8 g) was added to the stirred solution, and the stirring continued for a further 3 minutes. The reaction mixture was filtered (with suction) through a Dowex-1 (Cl^-) resin bed (1.5×2.5 cm) directly into a stirred solution of sodium borohydride (0.6 g) in water (25 ml). (The addition of a few drops of peroxide-free ether was necessary at this stage to control the vigorous frothing that occurred.) The excess reducing agent was decomposed by the addition of glacial acetic acid (3 ml). A rapid stream of nitrogen was passed through the stirred solution, cooled to ca. 10–15°, and 40% aqueous sodium hydroxide (10 ml) was added, followed directly by acetic anhydride (5 ml). After being stirred at room temperature for 30 minutes (the cooling bath was removed after 5 minutes), the reaction mixture was extracted with peroxide-free ether (5×100 ml). The combined ethereal extracts were washed with 5% aqueous sodium bicarbonate (2×100 ml) and water (100 ml), dried (Na_2SO_4), and concentrated to dryness (*in vacuo*, below 40°). The product, a greenish-brown gum, was dissolved in benzene – light petroleum (b.p. 80–100°) (1:1) and adsorbed on a silica gel column (12.5×2.4 cm). Elution of the column with the same solvent (100 ml) gave a small quantity of a pale-yellow gum which was discarded; further elution with benzene (400 ml) gave a white solid which on recrystallization from light petroleum (b.p. 80–100°) gave 5,6-diacetoxy-*N*-methylindole (0.69 g), m.p. 109–110°. (Found: C, 63.10; H, 5.24; N, 5.56. $C_{13}H_{13}NO_4$ requires C, 63.15; H, 5.30; N, 5.66%.) This melting point is somewhat higher than those previously quoted in the literature: 101–102° (27), 101° (28), and 104–105° (14). (The product obtained above did not depress the melting point of a sample prepared by direct acetylation of crystalline 5,6-dihydroxy-*N*-methylindole with acetic anhydride in pyridine.)

(ii) Adrenaline (1.6 g) was suspended in water (40 ml) and concentrated hydrochloric acid added dropwise until a clear solution was obtained. Silver oxide (8.0 g) was added to the stirred solution and the stirring continued for 3 minutes and the reaction mixture was filtered through a Dowex-1 (Cl^-) resin bed (1.5×2.5 cm). Glacial acetic acid (2 ml) was added to the vigorously stirred filtrate followed by zinc powder (40.0 g), which caused a rapid discharge of the red color. The product was filtered; the zinc residue was washed with acetone (3×5 ml), and the washings were added to the filtrate. The solution of crude 5,6-dihydroxy-*N*-methylindole so obtained was acetylated directly and the products worked up and purified chromatographically by the methods described above (Subsection *B*(i)) giving 5,6-diacetoxy-*N*-methylindole (0.42 g), m.p. 109.5–110.5°.

(*C*) *5,6-Diacetoxy-N-ethylindole*

N-Ethylnoradrenaline (1.6 g) was suspended in water (40 ml) and concentrated

Can. J. Chem. Downloaded from www.nrcresearchpress.com by 210.87.254.5 on 09/05/12
For personal use only.

Can. J. Chem. Downloaded from www.nrcresearchpress.com by 210.87.254.5 on 09/05/12
For personal use only.

hydrochloric acid was added dropwise until a clear solution was obtained; silver oxide (8.0 g) was added to the stirred solution and stirring continued for 3 minutes; the product was filtered through a Dowex-1 (Cl^-) resin bed (1.5×2.5 cm) and glacial acetic acid (2 ml), followed by zinc powder (40 g), added to the stirred filtrate. The reaction mixture was filtered; the residual zinc was washed with acetone (3×5 ml); and the washings were added to the filtrate. A rapid stream of nitrogen was passed through the stirred filtrate, cooled to ca. 10–15°, and 40% sodium hydroxide (10 ml) was added, followed directly by acetic anhydride (5 ml). After stirring at room temperature for 30 minutes (the cooling bath was removed after about 5 minutes), the reaction mixture was extracted with peroxide-free ether (5×100 ml). The combined ethereal extracts were washed with 5% aqueous sodium bicarbonate (2×100 ml) and water (100 ml). Concentration, *in vacuo*, below 40°, of the dried (Na_2SO_4) extract, afforded a greenish-brown gum which was dissolved in benzene – light petroleum (b.p. 80–100°) (1:1) and adsorbed on a silica gel column (12.5×2.4 cm). Elution of the column with this solvent (100 ml) gave a trace of gum which was rejected; further elution with benzene (500 ml) gave a white crystalline solid which yielded 5,6-diacetoxy-*N*-ethylindole (0.5 g), m.p. 107–108.5°, on recrystallization from light petroleum (b.p. 80–100°). (Found: C, 64.52; H, 5.78; N, 5.14. $C_{14}H_{15}NO_4$ requires C, 64.37; H, 5.79; N, 5.36%.)

(*D*) *5,6-Diacetoxy-N-isopropylindole*

(i) Silver oxide (16 g) was added to a solution of *N*-isopropylnoradrenaline hydrochloride (4 g) in water (80 ml) and the suspension vigorously stirred for 2 to 3 minutes. The reaction mixture was filtered through a Dowex-1 (Cl^-) resin bed (2.5×1.5 cm) directly into a cooled stirred solution of sodium borohydride (0.75 g) in water (20 ml). (Excessive foaming at this stage was controlled by the addition of small quantities of peroxide-free ether.) The reaction mixture was acidified with glacial acetic acid (3 ml), and a rapid stream of nitrogen passed through the solution, cooled to ca. 10–15°. Aqueous sodium hydroxide (40%, 20 ml) was added, followed directly by acetic anhydride (10 ml). After being stirred at room temperature for 30 minutes (the cooling bath was removed after 5 minutes), the reaction mixture was extracted with peroxide-free ether (5×100 ml); the combined ethereal extracts were washed with 5% aqueous sodium bicarbonate (2×50 ml) and water (100 ml), dried (Na_2SO_4), and concentrated to dryness *in vacuo*, below 40°. The product was dissolved in benzene – light petroleum (b.p. 80–100°) (1:1) and adsorbed on a silica gel column (12.5×2.4 cm). Elution of the column with this solvent (150 ml) gave only traces of gums which were rejected, further elution with benzene (450 ml) gave a white solid, which on recrystallization from benzene – light petroleum (b.p. 80–100°), gave 5,6-diacetoxy-*N*-isopropylindole as colorless prisms (0.5 g), m.p. 90.5–91°. (Found: C, 65.60; H, 6.15; N, 4.94. $C_{15}H_{17}NO_4$ requires C, 65.43; H, 6.23; N, 5.09%.)

(ii) A solution of *N*-isopropylnoradrenochrome (from 2 g of *N*-isopropylnoradrenaline sulphate) in water (40 ml) prepared by the method described above was acidified with glacial acetic acid (5 ml) and reduced with zinc powder (40 g). The reaction product was acetylated directly with acetic anhydride (5 ml) in the presence of 40% aqueous sodium hydroxide (10 ml) by the method previously described. The product was extracted and purified chromatographically by the above method and 5,6-diacetoxy-*N*-isopropylnoradrenochrome was obtained in colorless elongated prisms (0.75 g), m.p. 89.5–90.5°.

(*E*) *5,6-Diacetoxy-2-iodoindole*

An ethereal solution of crude 5,6-dihydroxy-2-iodoindole was prepared by the method

described in Section I(*E*). A mixture of acetic anhydride (15 ml) and dry* pyridine (15 ml) was added and the ether removed *in vacuo*, under nitrogen (bath temperature below 40°). The residual acetylation mixture was allowed to stand overnight at room temperature, after which time it was poured, with stirring, into an ice-water mixture. A brown oil separated, which did not solidify. The product was extracted with peroxide-free ether (5×150 ml) and the ethereal extract washed free of acetic acid with saturated aqueous sodium bicarbonate. Concentration of the dried (Na_2SO_4) ethereal extract gave a brownish residue which was dissolved in a mixture of benzene and light petroleum (b.p. 80–100°) (1:1) and purified chromatographically on a short silica gel column, the same solvent being used for elution. 5,6-Diacetoxy-2-iodoindole (1.1 g), m.p. 125–126.5°, was obtained in fluffy white needles. (Found: C, 40.02; H, 2.77; I, 35.30. $C_{12}H_{10}NO_4I$ requires C, 40.15; H, 2.81; I, 35.35%.)

(*F*) *5,6-Diacetoxy-N-methyl-2-iodoindole*

5,6-Diacetoxy-*N*-methyl-2-iodoindole was prepared by the method of Heacock and Scott (19).

(*G*) *5,6-Diacetoxy-N-ethyl-2-iodoindole*

5,6-Diacetoxy-*N*-ethyl-2-iodoindole was prepared in the manner described by Heacock and Scott (17).

(*H*) *5,6-Diacetoxy-2-iodo-N-isopropylindole*

5,6-Diacetoxy-2-iodo-*N*-isopropylindole was prepared in the manner described by Heacock and Scott (17).

Chromogenic Reagents

(*a*) *Ehrlich's reagent.*—*p*-Dimethylaminobenzaldehyde (1 g) was dissolved in a mixture of concentrated hydrochloric acid (30 ml) and ethanol (30 ml) and the solution was diluted to 100 ml with water.

(*b*) *Cinnamaldehyde solution* (cf. Sen and Leopold (29)).—Cinnamaldehyde (5 ml) was dissolved in a mixture of ethanol (95 ml) and concentrated hydrochloric acid (5 ml).

(*c*) *p-Dimethylaminocinnamaldehyde solution* (cf. Harley-Mason and Archer (30)).—*p*-Dimethylaminocinnamaldehyde (2 g) was dissolved in 6 *N* hydrochloric acid (100 ml) and ethanol (100 ml). The stock solution (10 ml) was diluted with ethanol (40 ml) prior to use.

(*d*) *Hopkins-Cole reagent* (cf. Benedict (31)).—A saturated aqueous solution of oxalic acid (250 ml) was added slowly to a cooled suspension of magnesium filings (10 g) in sufficient water to just cover the metal. After addition of the acid the flask was vigorously shaken for a few minutes and the solution filtered. The filtrate was stabilized by the addition of a little glacial acetic acid and diluted to 1000 ml with water.

(*e*) *Acidic oxidizing reagent* (cf. Jepson (32), p. 125).—Freshly prepared saturated potassium persulphate solution (1 ml†) was mixed with concentrated hydrochloric acid (10 ml) and acetone (40 ml), and the solution used immediately.

(*f*) *Salkowski reagent* (cf. Sen and Leopold (29)).—Ferric chloride (0.5 *M*, 2 ml) was added to 5% perchloric acid (100 ml).

(*g*) *Terephthalaldehyde solution* (cf. Curzon and Giltrow (33)).—Terephthalaldehyde (0.2 g) was dissolved in a mixture of acetone (90 ml) and acetic acid (10 ml). After being

**Distilled from phosphorus pentoxide.*

†This quantity of potassium persulphate solution is greater than that used by Jepson and gives more intense colors in the cases studied. The use of the stronger reagent was suggested to the authors by Dr. F. Wightman of Carleton University, Ottawa.

Can. J. Chem. Downloaded from www.nrcresearchpress.com by 210.87.254.5 on 09/05/12
For personal use only.

Can. J. Chem. Downloaded from www.nrcresearchpress.com by 210.87.254.5 on 09/05/12
For personal use only.

sprayed with this solution the chromatograms were sprayed with 2% concentrated hydrochloric acid in acetone.

(*h*) *Nitrose reagent* (cf. Jepson (32), p. 127).—Sodium nitrite (1 ml of a 5% aqueous solution) was added to a solution of concentrated nitric acid (5 ml) in acetone (45 ml) and the mixture was used directly.

(*i*) *Formaldehyde/hydrochloric acid* (cf. Prochazka *et al.* (26)).—Aqueous formaldehyde solution (10 ml of a 30 to 40% solution) was mixed with concentrated hydrochloric acid (10 ml) and water (20 ml). In order to develop the colors, the chromatograms were warmed to 90–95° after spraying.

(*j*) *Xanthydrol reagent* (cf. Dickmann and Crockett (34)).—Xanthydrol (0.2 g) was dissolved in ethanol (90 ml) and concentrated hydrochloric acid (10 ml).

(*k*) *Gibb's reagent.*—*N*-2,6-Trichloro-*p*-quinoneimine (2 g) was dissolved in ethanol (100 ml).

(*l*) *Diazotized p-nitroaniline* (cf. Bray *et al.* (35)).—A *p*-nitroaniline solution (25 ml) of a 0.3% solution in 8% (w/v) hydrochloric acid was diazotized with sodium nitrite solution (1.5 ml of a 5% solution) immediately prior to use. (The second spraying with aqueous alkali was omitted.)

(*m*) *Folin and Ciocalteu's reagent.*—This solution was available commercially (B. D. H.) and was diluted with two volumes of water prior to use.

(*n*) *Sodium molybdate/hydrochloric acid* (cf. Coulson and Evans (36)).—Sodium molybdate solution (10%, 20 ml) was diluted with 0.5 *N* hydrochloric acid (10 ml).

(*o*) *Ferric chloride/potassium ferricyanide reagent* (as described by Heacock *et al.* (37)).—Ferric chloride (3%, 5 ml) and potassium ferricyanide (3%, 5 ml) were mixed immediately prior to use and the solution was diluted to 100 ml with water. In order to prevent discoloration of the papers after spraying with this reagent, they were subsequently washed with (*a*) water, (*b*) 2 *N* hydrochloric acid, and (*c*) water.

(*p*) *Ferric chloride solution.*—Ferric chloride (3 g) was dissolved in water (100 ml) containing a few drops of hydrochloric acid.

(*q*) *Ammoniacal silver nitrate.*—Ammonia solution (5 *N*) was added dropwise to 0.1 *N* aqueous silver nitrate, until the precipitate which initially formed just redissolved.

Chromatographic Procedure (5,6-Dihydroxyindoles)

(*A*) *Descending*

1. Paper.—Whatman No. 1 paper was washed with 2% acetic acid for 48 hours and dried prior to use.

2. Solvents.—S_1, 2% acetic acid in water; S_2, *n*-butanol:glacial acetic acid:water (6:1:2).

3. Detection.—All the chromogenic reagents mentioned above give colors with the 5,6-dihydroxyindoles (see Table I). Satisfactory color intensities were obtained with spots derived from 10 to 25 μg of the compounds. The unhalogenated 5,6-dihydroxyindoles also show a definite light blue to mauve fluorescence in ultraviolet light.

(*B*) *Circular*

1. Paper.—(*a*) Whatman No. 1 paper, slotted disks (diameter = 26.5 cm*); (*b*) disks (diameter = 26.5 cm) of Whatman 3MM paper were dipped into a 30% solution of reagent grade formamide ("pH" = 5)† in acetone, removed, blotted dry, and allowed to dry in air for 20 minutes.

**As supplied by the Shandon Scientific Company Ltd.*
†The "pH" of the formamide was adjusted to 5 by the careful dropwise addition of 98% formic acid.

TAI

Color reactions
of some 5,6-dihydroxyindoles

5,6-Dihydroxyindole derivative	Code name	R_1	R_2	Ehr.	Cin.	DMCA	H.C.†	TPA†
5,6-Dihydroxyindole	DHI	H	H	BV → GyG	OrB → RBr	GyG → BG	P	OG
5,6-Dihydroxy-*N*-methylindole	DHMI	CH_3	H	BV	OrBr → VBr	BG → B	PV	OG
N-Ethyl-5,6-dihydroxyindole	DHEI	C_2H_5	H	BV	OrBr → VBr	BG → B	PV	OG
5,6-Dihydroxy-*N*-isopropylindole	DHPrI	*i*-C_3H_7	H	BV → V	OrBr → VBr	BG → BGy	PV	GyV
5,6-Dihydroxy-2-iodoindole	IodoDHI	H	I	BV → GyG	RP → Br	B → BG	Gy → GyP	Br → GyBr
5,6-Dihydroxy-2-iodo-*N*-methylindole	IodoDHMI	CH_3	I	BV	RP → VBr	BG → B	V	GyV
N-Ethyl-5,6-dihydroxy-2-iodoindole	IodoDHEI	C_2H_5	I	BV	RP → VBr	BG → B	GyV	GyV
5,6-Dihydroxy-2-iodo-*N*-isopropylindole	IodoDHPrI	*i*-C_3H_7	I	BV	RP → GyP	BG → BV	GyV	GyV
2-Bromo-5,6-dihydroxy-*N*-methylindole	BromoDHMI	CH_3	Br	BV	RP → VBr	BG → BGy	GyV	Gy

*Initial colors and colors after 24 hours (if significantly different) are given.
†These colors develop slowly.
‡First change occurs rapidly; final change occurs overnight. The initial color changes observed with this reagent are confusing and its use is not recommended.
REAGENTS: Ehr. = Ehrlich's reagent; Cin. = cinnamaldehyde; DMCA = *p*-Dimethylaminocinnamaldehyde; H.C. = Hopkins–Cole reagent; TPA = terephthalaldehyde; FHCl = Formaldehyde/hydrochloric acid reagent; Ac.ox. = Acidic oxidizing reagent; Sal. = Salkowski reagent; nitrose = nitrose reagent; DPNA = Diazotized *p*-nitroaniline; Gib. = Gibb's reagent;

2. Solvents.—S_1, 2% acetic acid in water; S_3, chloroform* (10 ml) and benzene† (10 ml) containing 0.1 ml formamide; S_4, chloroform* containing 1.4% formamide; S_5, ethyl acetate* (5 ml) and benzene† (15 ml) saturated with formamide: a small quantity of formamide was added to this mixture; the mixture was well shaken, allowed to stand and the clear supernatant layer was decanted and used; S_6, ethyl acetate* (4 ml) and chloroform* (16 ml) containing 0.2 ml formamide; S_7, dichloromethane* containing 1.4% formamide.

3. Apparatus.—A modified form of the Kawerau circular chromatography apparatus‡ was used. The glass capillary solvent feed supplied with the apparatus was unsatisfactory and was replaced by a cotton yarn wick (1/8 in.). The solvent was contained in a 6-cm petri dish.

4. Detection.—(*a*) Any of the chromogenic reagents described in the previous section could be used to detect the spots when the runs were carried out with 2% acetic acid on untreated paper. (*b*) With the runs on formamide-treated paper, either fluorescence in ultraviolet light or the colors given with Ehrlich's reagent were used to locate the spots.

Chromatographic Procedure (5,6-Diacetoxyindoles)

Circular

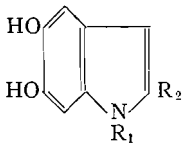
1. Paper.—Formamide-treated paper was prepared as described in the previous section.

2. Solvents.—S_8, light petroleum (B.D.H. A.R. grade, b.p. 60–80°); S_9, cyclohexane,* S_{10}, benzene† (1 ml) mixed with light petroleum (B.D.H. A.R. grade, b.p. 60–80°) (9 ml); S_{11}, benzene† (In each of the above cases a small quantity of formamide was added to the

**Reagent grade.*
†*Dried over sodium.*
‡*As supplied by the Shandon Scientific Company Ltd.*

Can. J. Chem. Downloaded from www.nrcresearchpress.com by 210.87.254.5 on 09/05/12
For personal use only.

LE I



	Colors* with chromogenic reagents									
FHCl	Ac.ox.	Sal.	Nitrose	DPNA	Gib.	F. and C.	S.M.	Fe	AmAg	Xan.
G → BGy	Y → VBr	Gy	P → Br → Gy‡	M → VBr	Br	Gy → BGy	GyG	Gy	Bl	G → GyG
YG → BGy	Br → GyBr	Y → Gy	OG → GyBr → YBr‡	M → VBr	Br	Gy → BGy	GyG	Bl	DBr	Gy
YG → BGy	Br → GyBr	Y → YBr	OG → GyBr → YBr‡	M → VBr	Br	Gy → BGy	GyG	Bl	DBr	GyV → Gy
Y → Gy	Br → GyBr	Or → GyBr	OG → Y → YBr‡	RB → Br	Br	Gy → BGy	BGy → GyG	Bl	DBr	GyV → Gy
OG → B	Y → Gy	YBr → Gy	B → GyY → GyBr‡	M → VBr	Br	Gy → BGy	BBl	Gy	Bl	GyV
OG → B	Y → GyBr	Y → GyBr	B → GyG → GyBr‡	GyM → Br	GyBr → Br	Gy → BGy	GyG	Gy	Br	BG → YG
OG → B	Y → GyBr	Y → YBr	Br → YBr	GyM → Br	GyV → Br	Gy → BGy	GyG	Gy	Br	B → YG
BG → Gy	Y → Br	Gy → Br	Br → YBr	GyM → Br	GyV → Br	Gy → BGy	Gy → Br	Gy	Br	B
G → B	Y → GyY	YGy → GyP	GyP → DBr	GyM → VBr	GyBr → Br	Gy → BGy	BGy → GyG	Gy	DBr	Gy → OG

F. and C. = Folin and Ciocalteu's reagent; S.M. = sodium molybdate/hydrochloric acid reagent; Fe = ferric chloride; AmAg = ammoniacal silver nitrate; Xan. = xanthydrol reagent.

COLORS: B = blue; BV = blue-violet; BG = blue-green; BGy = blue-grey; V = violet; VBr = violet-brown; GyV = grey-violet; PV = pink-violet; M = magenta; GyM = grey-magenta; P = pink; OrP = orange-pink; RP = red-pink; GyP = grey-pink; PBr = pink-brown; Br = Brown; DBr = dark brown; OrBr = orange-brown; Or = orange; YBr = yellow-brown; GyBr = grey-brown; BlBr = black-brown; Y = yellow; GyY = grey-yellow; YG = yellow-green; G = green; OG = olive green; GyG = grey-green; Gy = grey; Bl = Black; BBl = blue-black.

TABLE II

The R_f values of some 5,6-dihydroxyindoles on Whatman No. 1 paper

	Average R_f† in solvent:		
Substance*	S_1‡	S_1§	S_2
DHI‖	40	56	64
DHMI‖	46	58	76
DHEI	53	65	81
DHPrI	58	71	84
IodoDHI‖	21	36	77
IodoDHMI‖	20	29	83
IodoDHEI	25	38	84
IodoDHPrI	27	40	87
BromoDHMI	23	—	79

*Code names as defined in Table I.

†$R_f \times 100$.

‡Descending.

§Circular.

‖The R_f's of DHI, DHMI, iodoDHI, and iodoDHMI have been reported as 65, 79, 83, 89 on unwashed paper with *n*-butanol/acetic acid/water (78:5:17) as running solvent (11, 12).

solvent; the mixture was well shaken, allowed to stand and the clear supernatant layer decanted and used.); S_{12}, carbon tetrachloride* saturated with formamide. (A few drops of formamide were added to the carbon tetrachloride; the mixture shaken, allowed to stand and the clear lower layer separated and used directly.)

3. Detection.—The 5,6-diacetoxyindoles give colors with all the usual indole reagents

**Reagent grade.*

Can. J. Chem. Downloaded from www.nrcresearchpress.com by 210.87.254.5 on 09/05/12
For personal use only.

Can. J. Chem. Downloaded from www.nrcresearchpress.com by 210.87.254.5 on 09/05/12
For personal use only.

TAB

The color reactions of some 5,6-diacetoxyindoles

5,6-Diacetoxyindole derivative	Code name	R_1	R_2	Ehr.	Cin.	DMCA
5,6-Diacetoxyindole	DAI	H	H	PV → BGy	OrP → Br	B → BG
5,6-Diacetoxy-*N*-methylindole	DAMI	CH_3	H	PV → BV	OrP → Br	BG → GyG
5,6-Diacetoxy-*N*-ethylindole	DAEI	C_2H_5	H	PV → BV	OrP → Br	BG
5,6-Diacetoxy-*N*-isopropylindole	DAPrI	*i*-C_3H_7	H	PV → BV	OrP → Br	BG
5,6-Diacetoxy-2-iodoindole	IodoDAI	H	I	PV	P → BV → Y§	B → BG‡
5,6-Diacetoxy-2-iodo-*N*-methylindole	IodoDAMI	CH_3	I	PV	P → BV → Y§	BG → GyB‡
5,6-Diacetoxy-*N*-ethyl-2-iodoindole	IodoDAEI	C_2H_5	I	PV	P → BV → Y§	B → BG‡
5,6-Diacetoxy-2-iodo-*N*-isopropylindole	IodoDAPrI	*i*-C_3H_7	I	PV	P → BV → Y§	B → BG‡

*Initial colors and colors after 24 hours (if significantly different are given).
†The abbreviations for the chromogenic reagents and colors produced are the same as those used in Table I.
‡Initial colors slow to develop.

TABLE IV

The R_f values of some 5,6-dihydroxyindoles on formamide-treated paper

	Average R_f† in solvent:				
Substance*	S_3	S_4	S_5	S_6	S_7
DHI	0	0	11	11	09
DHMI	11	23	39	49	46
DHEI	19	35	52	62	61
DHPrI	29	48	64	72	72
IodoDHI	07	09	39	35	27
IodoDHMI	37	49	71	70	78
IodoDHEI	51	64	81	81	86
IodoDHPrI	66	77	88	88	93

*Code names as defined in Table I.
†$R_f \times 100$.

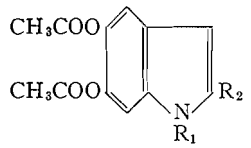
TABLE V

The R_f values of some 5,6-diacetoxyindoles on formamide-treated paper

	Average R_f† in solvent:				
Substance*	S_8	S_9	S_{10}	S_{11}	S_{12}
DAI	0	0	04	60	13
DAMI	24	24	40	s.f.	77
DAEI	39	41	56	s.f.	87
DAPrI	53	57	70	s.f.	92
IodoDAI	07	09	15	79	48
IodoDAMI	47	52	63	s.f.	90
IodoDAEI	61	66	74	s.f.	93
IodoDAPrI	74	78	84	s.f.	95

*Code names as defined in Table III.
†$R_f \times 100$.
NOTE: s.f. = the R_f was very high; the substance was virtually on the solvent front.

LE III



	Colors* with chromogenic reagents†						
TPA	FHCl	Ac. ox.	Sal.‡	Nitrose	DPNA	Gib.	Xan.
OrP → P	PV → Br	Br	Or → Gy	V → PBr	RP → Br	PBr → VBr	Pr → Gy
P	PV → V	VBr	P → VBr	V → PBr	RP → Br	PBr → GyBr	V → GyV
P	PV → V	VBr	P → VBr	V → PBr	RP → Br	PBr → GyBr	V → GyV
P	PV → V	GyV	OrP → VBr	V → PBr	RP → Br	PBr → GyBr	V → GyV
P → OrP	PV → Br	VBr	GyP → GyV	PBr	V → PBr	VBr → Br	PV → GyV
P	PV → PBr	BGy	PV → GyV	GyV → PBr	V → PBr	PBr → Br	V → Gy‖
P	PV	BGy	PV → GyV	GyV → PBr	GyV → PBr	PBr → Br	V → Gy‖
P	P	Y	PV → VBr	Y → YBr	OrP → YBr	PBr → Br	V → Gy‖

§First change occurs rapidly; final change occurs overnight.
‖Color fades after 48 hours.

and the colors obtained with several reagents are given in Table III. For the purposes of R_f determination with the systems illustrated above, Ehrlich's reagent was employed to locate the zones.

ACKNOWLEDGMENTS

The authors wish to express their thanks to Dr. Leo Vining of the National Research Council (Prairie Regional Laboratory) for several useful discussions and to the Winthrop Laboratories of Canada Ltd. and the Wyeth laboratories for generous gifts of chemicals.

REFERENCES

1. A. B. LERNER. Advances in Enzymol. **14**, 75 (1953).
2. H. S. MASON. Advances in Enzymol. **16**, 163 (1955).
3. M. THOMAS. *In* Modern methods of plant analysis. Vol. IV. *Edited by* K. PAECH and M. V. TRACEY. Springer-Verlag, Berlin. 1955. p. 668.
4. R. A. HEACOCK. Chem. Revs. **59**, 181 (1959).
5. G. LEONHARDI. Naturwissenschaften, **41**, 141 (1954).
6. J. PELLERIN and A. D'IORIO. Can. J. Biochem. and Physiol. **33**, 1055 (1955).
7. R. A. HEACOCK and B. D. LAIDLAW. Nature, **182**, 526 (1958).
8. R. A. HEACOCK and B. D. LAIDLAW. Chem. & Ind. (London), 1510 (1958).
9. R. A. HEACOCK and B. D. SCOTT. Can. J. Biochem. and Physiol. **37**, 1087 (1959).
10. S. BOUCHILLOUX and A. KODJA. Compt. rend. **247**, 2484 (1958).
11. S. BOUCHILLOUX. Compt. rend. soc. biol. **153**, 1818 (1959).
12. S. BOUCHILLOUX and A. KODJA. Bull. soc. chim. biol. **42**, 65 (1960).
13. R. J. S. BEER, K. CLARKE, H. G. KHORANA, and A. ROBERTSON. J. Chem. Soc. 2223 (1948).
14. J. HARLEY-MASON. J. Chem. Soc. 1276 (1950).
15. J. BU'LOCK and J. HARLEY-MASON. J. Chem. Soc. 712 (1951).
16. H. SOBOTKA and J. AUSTIN. J. Am. Chem. Soc. **73**, 3077 (1951).
17. R. A. HEACOCK and B. D. SCOTT. Can. J. Chem. **38**, 516 (1960).
18. R. A. HEACOCK and B. D. SCOTT. In preparation.
19. R. A. HEACOCK and B. D. SCOTT. Can. J. Chem. **38**, 508 (1960).
20. A. ZAFFARONI, R. B. BURTON, and E. H. KEUTMAN. Science, **111**, 6 (1950).
21. R. B. BURTON, A. ZAFFARONI, and E. H. KEUTMAN. J. Biol. Chem. **188**, 763 (1951).
22. K. MACEK, A. CERNY, and M. SEMONSKY. Pharmazie, **9**, 388 (1954).
23. K. MACEK, J. HACAPERKOVA, and B. KAKAC. Pharmazie, **11**, 533 (1956).
24. R. J. BLOCK, E. L. DURRUM, and G. ZWEIG. A manual of paper chromatography and paper electrophoresis. 2nd ed. Academic Press Inc., New York. 1958. p. 359.

Can. J. Chem. Downloaded from www.nrcresearchpress.com by 210.87.254.5 on 09/05/12
For personal use only.

25. D. GRÖGER. Arch. Pharm. **292**, 649 (1959).
26. Z. PROCHAZKA, V. SANDA, and K. MACEK. Collection Czechoslov. Chem. Communs. **24**, 2928 (1959).
27. J. AUSTIN, J. D. CHANLEY, and H. SOBOTKA. J. Am. Chem. Soc. **73**, 2395, 5299 (1951).
28. F. BERGEL and A. L. MORRISON. J. Chem. Soc. 48 (1943).
29. S. P. SEN and A. C. LEOPOLD. Physiol. Plantarum, **7**, 98 (1954).
30. J. HARLEY-MASON and A. A. P. G. ARCHER. Biochem. J. **69**, 60P (1958).
31. S. R. BENEDICT. J. Biol. Chem. **6**, 51 (1909).
32. J. B. JEPSON. *In* Chromatographic techniques—clinical and biochemical applications. *Edited by* I. Smith. William Heinemann Medical Books Ltd., London. 1958.
33. G. CURZON and J. GILTROW. Nature, **173**, 314 (1954).
34. S. R. DICKMANN and A. L. CROCKETT. J. Biol. Chem. **220**, 957 (1956).
35. H. G. BRAY, W. V. THORPE, and K. WHITE. Biochem. J. **46**, 271 (1950).
36. C. B. COULSON and W. C. EVANS. J. Chromatog. **1**, 374 (1958).
37. R. A. HEACOCK, C. NERENBERG, and A. N. PAYZA. Can. J. Chem. **36**, 853 (1958).

Can. J. Chem. Downloaded from www.nrcresearchpress.com by 210.87.254.5 on 09/05/12
For personal use only.

Can. J. Chem. Downloaded from www.nrcresearchpress.com by 210.87.254.6 on 09/05/12
For personal use only.

CHARACTERISTIC VIBRATIONS OF THE SULPHURYL GROUP[1]

E. A. ROBINSON

ABSTRACT

A compilation of the S—O symmetric and asymmetric stretching frequencies is given for a large number of compounds containing an —SO_2— group. It is shown that a linear relationship between $\nu_{SO_2(sym)}$ and $\nu_{SO_2(asym)}$ is valid for a large number of sulphuryl and polysulphuryl compounds and that the actual frequencies depend in a systematic manner on the electronegativities of the attached groups. These relationships have proved very useful in assigning and in some cases reassigning the S—O bands in the infrared and Raman spectra of a number of sulphuryl compounds. It is pointed out that there is a relationship between the SO_2 frequencies of some sulphonic acids and their acid strengths.

The calculation of values for group electronegativities from the vibration frequencies of the P═O and SO_2 groups is discussed.

For a variety of organic compounds including sulphones, sulphonyl chlorides, covalent sulphates, sulphonamides, sulphonic acid esters, and sulphonates, the sulphur–oxygen symmetrical and antisymmetrical stretching frequencies obtained from infrared and Raman spectra have been characterized. A compilation of these frequencies has been given by Bellamy (1).

In 1957 Bellamy and Williams (2) pointed out that any change in the symmetric frequency, $\nu_{SO_2(sym)}$, is accompanied by a proportional change in the asymmetric frequency, $\nu_{SO_2(asym)}$. They plotted $\nu_{SO_2(sym)}$ against $\nu_{SO_2(asym)}$ for 29 compounds taken from the work of Haszeldine and Kidd (3, 4), Barnard, Fabian, and Koch (5), and of Baxter, Cymerman-Craig, and Willis (6) and obtained a good straight line. They pointed out that since the —SO_2— stretching frequencies are essentially free from mass and coupling effects such a correlation is expected and that the exact positions of $\nu_{SO_2(sym)}$ and $\nu_{SO_2(asym)}$ depend on the nature of the substituents attached to the sulphuryl group. It is expected that the more electronegative the groups that are attached the stronger the S═O bonds will be and hence the higher the vibrational frequencies.

In recent years symmetric and asymmetric vibrations for sulphuryl groups in a large number of compounds including several inorganic compounds have been reported. Data for different compounds are reported in Table I and are plotted in Fig. 1. It is clear that the symmetrical and asymmetrical S—O vibrations for compounds of the type X_2SO_2, $XYSO_2$, (including $X(OH)SO_2$), for ions such as XSO_3^- and SO_4^{--} (although strictly speaking the S—O vibrations in these cases should not be described in this manner), and for more complex compounds containing —SO_2— as part of a ring or chain, all fit the linear relationship of Bellamy and Williams (2) reasonably well.

When the —SO_2— group is bonded to two alkyl groups $\nu_{SO_2(sym)}$ comes in the narrow range 1136 to 1145 cm^{-1}, whereas for two aryl groups, or for one alkyl group and one aryl group this frequency is in the range 1150 to 1160 cm^{-1}. In all cases $\nu_{SO_2(asym)}$ is in the range 1312 to 1334 cm^{-1}. When an alkyl or an aryl group is replaced by the more electronegative —NH_2 group (e.g. in the sulphonamides), a slight shift of $\nu_{SO_2(sym)}$ and a corresponding shift of $\nu_{SO_2(asym)}$ to higher frequencies is noted; $\nu_{SO_2(sym)}$ is in the range 1152 to 1169 cm^{-1} and $\nu_{SO_2(asym)}$ in the range 1336 to 1358 cm^{-1}. Similarly on replacing the —NH_2 group by oxygen (e.g. in the sulphonic acid esters), further shifts of the S—O bands to yet higher frequencies are observed. In general, replacement of groups attached

[1]*Manuscript received September 15, 1960.*
Contribution from the Department of Chemistry, McMaster University, Hamilton, Ontario.

Can. J. Chem. Downloaded from www.nrcresearchpress.com by 210.87.254.6 on 09/05/12
For personal use only.

TABLE I

Symmetric and asymmetric vibration frequencies of the —SO_2— group*†

	SO_2(sym)	SO_2(asym)	
Sulphones $RR'SO_2$			
1. Methyl ethyl sulphone	1145	1330	(24)
2. Dibutyl sulphone	1139	1330	(23)
3. Methyl propyl sulphone	1139	1299–1316	(19)
4. Diphenyl sulphone	1158	1319	(20, 24)
5. Phenyl benzyl sulphone	1155	1325	(24)
6. Phenyl methyl sulphone	1160	1334	(5)
7. Dibenzyl sulphone	1155	1325	(24)
8. Phenyl vinyl sulphone	1153	1324	(19)
9. Methyl vinyl sulphone	1139	1312	(19)
10. Methyl allyl sulphone	1136	1307	(19)
11. Phenyl allyl sulphone	1150	1325	(24)
12. β-Chlorethyl phenyl sulphone	1156	1330	(19)
13. Cyclohexyl methyl sulphone	1144	1321	(5)
14. Dicyclohexyl sulphone	1130	1312	(5)
Thiolsulphonates $RSO_2.SR$			
15. $CF_3.SO_2.S.CF_3$	1235	1422	(20)
16. Phenyl thiolsulphonate	1144	1331	(20)
17. *p*-Cyanophenyl thiolsulphonate	1154	1342	(20)
18. p-$C_6H_4.CO.NH_2.SO_2.S.R$	1154	1342	(20)
19. p-$C_6H_4.C(OEt)$=$NH.HCl.SO_2.S.R$	1154	1341	(20)
Esters of sulphonic acids $RSO_2.OR'$			
20. Phenyl *p*-toluene sulphonate	1170	1375	(22)
21. 2,4-Dinitrophenyl *p*-toluene sulphonate	1175	1355	(22)
22. Phenoxyethyl *p*-toluene sulphonate	1168	1350	(22)
23. Methyl *p*-toluene sulphonate	1185	1375	(24)
24. *n*-Butyl *p*-toluene sulphonate	1185	1370	(24)
25. Methyl methane sulphonate	1171	1358	(33)
26. Ethyl methane sulphonate	1172	1352	(33)
27. Methyl ethane sulphonate	1165	1356	(33)
28. Ethyl ethane sulphonate	1170	1355	(33)
Sulphonamides $R.SO_2.NH_2$			
29. Benzene sulphonamide	1167	1358	(24)
30. *o*-Toluene sulphonamide	1162	1346	(24)
31. *p*-toluene sulphonamide	1167	1358	(24)
32. Sulphanilimide	1152	1337	(22)
33. Methane sulphonamide	1169	1336	(22)
Covalent sulphates $(RO)_2SO_2$			
34. Dimethyl sulphate	1193	1412	(17, 24)
35. Diethyl sulphate	1187	1415	(17, 24)
Sulphonyl chlorides RSO_2Cl			
36. Methane sulphonyl chloride	1175	1370	(4, 7, 33)
37. Benzene sulphonyl chloride	1185	1390	(24)
38. *o*-Toluene sulphonyl chloride	1183	1382	(4)
39. *m*-Toluene sulphonyl chloride	1169	1384	(4)
40. *p*-Toluene sulphonyl chloride	1172	1379	(4)
41. *p*-Chlorphenyl sulphonyl chloride	1183	1404	(4)
42. CF_3SO_2Cl	1239	1439	(3)
43. CCl_3SO_2Cl	1183	1404	(3)
44. Methoxy sulphuryl chloride	1191	1404	(33)
Sulphonyl fluorides RSO_2F			
45. Methane sulphonyl fluoride	1210	1401	(7)
46. Benzene sulphonyl fluoride	1205	1420	(7)
47. *o*-Toluene sulphonyl fluoride	1209	1402	(7)
48. *m*-Toluene sulphonyl fluoride	1203	1405	(7)
49. *p*-Toluene sulphonyl fluoride	1205	1412	(7)
50. CF_3SO_2F	1239	1463	(4)
Acids XSO_3H			
51. *p*-Toluene sulphonic acid	1170	—	(22)
52. Benzene sulphonic acid	1182	—	(22)
53. Ethane sulphonic acid	1171	—	(22)
54. Methane sulphonic acid	1174	1354	(27)
55. Sulphuric acid	1195	1368	(10, 12)
56. Fluorsulphuric acid	1230	1445	(10, 12)
57. Chlorsulphuric acid	1209	1408	(10, 12)
Inorganic sulphuryl compounds			
58. Sulphuryl fluoride	1269	1501	(33)
59. Sulphuryl chloride	1182	1414	(25)
60. Sulphamide	1163	1350	(26)
61. FSO_3F	1248	1501	(29)
62. $MeSO_3F$	1235	1465	(30)
63. $S_2O_6F_2$	1246	1495	(30)

Can. J. Chem. Downloaded from www.nrcresearchpress.com by 210.87.254.6 on 09/05/12
For personal use only.

TABLE I (*Concluded*)

Symmetric and asymmetric vibration frequencies of the —SO_2— group*†

	SO_2(sym)	SO_2(asym)	
Polysulphuryl compounds			
64. Methane sulphonic anhydride	1197	1355	(39)
65. $S_2O_5F_2$	1255	1490	(12)
66. $S_2O_5Cl_2$	1209	1444	(12, 18)
67. $S_2O_5(OH)_2$ (disulphuric acid)	1220	1440	(12)‡
68. $FS_2O_5.OH$	1240	1450	(12)‡
69. $ClS_2O_5.OH$	1225	1452	(12)‡
70. $S_3O_8F_2$	1260	1510	(12)
	1210	1485	
71. $S_3O_8Cl_2$	1220	1480	(12)
	1205	1447	
Ring compounds			
72. $(SO_2.N)_3^{3-}$, sulphimide	1216	1390	(26)
73. $(SO_3)_3$, trimeric sulphur trioxide	1270	1515	(37, 13)
74. Sultone I	1164	1348, 1384	(21)§
75. Sultone II	1164	1372, 1384	(21)§
76. Sultone III	1173	1364	(21)§
77. Sultone IV	1171	1368	(21)§
78. Sultone V	1169	1363	(21)§
79. $(CH_2)_4SO_2$	1224	1412	(12)
80. 1:2 $(CH_3)_2(CH)_2(CH_2)_2.SO_2$	1228	1424	(12)

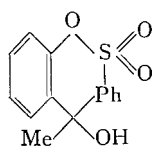
	SO_2(sym)	SO_2(asym)	
Ions			
81. $NH_2.SO_3^-$	1059	1202	(26)
82. $N(SO_3)_2^{3-}$	1064	1175	(26, 35)
83. $HN(SO_3)_2^{2-}$	1082	1218	(26)
84. $CF_3.SO_3^-$	1030	1176, 1274	(4)‖
	1025–1042	1266–1279	(4)¶
85. FSO_3^-	1080	1228	(12)**
86. $ClSO_3^-$	1054	1209	(12)††
87. $CH_3.SO_3^-$	1056–1075	1157–1177	(32)
88. $CH_3O.SO_3^-$	1063	1221	(32)
89. HSO_4^-	1040	1200	(12)
90. $EtSO_3^-$	1053	1176	(4)
91. $Pr.SO_3^-$	1048	1182	(4)
92. $Bu.SO_3^-$	1044	1176	(4)‡‡
93. $C_5H_{11}.SO_3^-$ Na salts	1044	1172	(4)
94. $CH_2(SO_3)_2^{3-}$	1042	1183	(4)
95. $HS_2O_7^-$	1077	1237	(4)
96. SO_4^{--}	986	1090	(42)
97. SO_2	1150	1334	(25)

*Most of the measurements refer to pure liquids or solutions. Momose *et al.* (39) have shown that in the solid state ν_{as} in many sulphones is about 20 cm^{-1} below the value in chloroform solutions while ν_s remains unchanged.

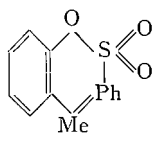
†See also the collected data of Momose *et al.* (39) for other phenyl sulphonyl derivatives and the work of Hersjarvi and Tommila (40) on sulphonyl halides and esters of sulphonic acids.

‡Taken from measurements on dilute solution of SO_3, in H_2SO_4, $HFSO_3$, and $HClSO_3$, respectively (13).

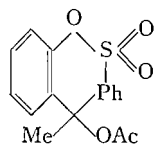
§



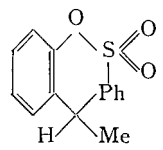
(I)



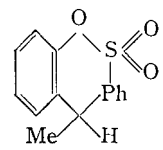
(II)



(III)



(IV)



(V)

‖Aqueous acid (see text).

¶Salts.

**Raman c.f. 1080, 1287 from I. R. (35).

††From spectrum of Na_2SO_4 in $HClSO_3$ and NaCl in $HClSO_3$.

‡‡Sodium salts.

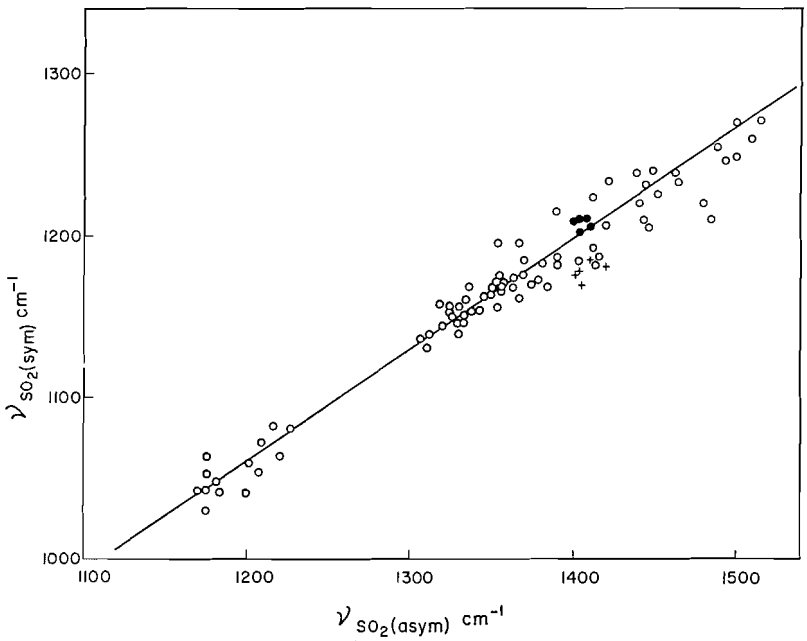


FIG. 1. Correlation of symmetric and asymmetric S—O stretching frequencies.

to the sulphuryl group by groups having a greater effective electronegativity leads to a shift in the S—O stretch to higher frequency (Table II).

The shift of the SO_2 stretching frequencies to higher values as the electronegativities of the attached groups increase indicates increasing strength of the S=O bonds which

TABLE II

Extended correlation table for S—O symmetric and asymmetric vibrations

		S—O	
Grouping	Type of compound	Symmetric	Asymmetric
C—SO_2—C	Sulphone (alkyl)	1136–1145	1307–1330
	Sulphone (alkyl–aryl)	1150–1160	1325–1334
	Sulphone (aryl)		
C—SO_2—N	Sulphonamide	1152–1169	1336–1358
C—SO_2—O	Sulphonic acid and esters	1165–1185	1350–1375
C—SO_2—F	Sulphonyl fluoride	1203–1210	1401–1412
C—SO_2—S	Thiosulphonates	1144–1154	1331–1342
C—SO_2—Cl	Sulphonyl chloride	1169–1185	1364–1390
N—SO_2—N	e.g. Sulphamide	1163	1350
O—SO_2—O	Covalent sulphates	1187–1195	1390–1415
O—SO_2—F	e.g. FSO_3F, HSO_3F, $S_2O_5F_2$, $S_3O_8F_2$	1230–1260	1445–1510
O—SO_2—Cl	$HClSO_3$, $S_2O_5Cl_2$, $S_3O_8Cl_2$	1205–1225	1408–1452
	Ions e.g. HSO_4^-, FSO_3^-, $MeSO_3^-$	1026–1080	1175–1221

Can. J. Chem. Downloaded from www.nrcresearchpress.com by 210.87.254.6 on 09/05/12
For personal use only.

Can. J. Chem. Downloaded from www.nrcresearchpress.com by 210.87.254.6 on 09/05/12
For personal use only.

may be reasonably attributed at least partly to increased double-bond character. The more electronegative are the groups X and Y in $XYSO_2$ the less important are contributions from structures such as $XYS^{+}\!\!<\!\!\begin{matrix}O^{-}\\O\end{matrix}$ compared with the double-bonded structure $XYS\!\!<\!\!\begin{matrix}O\\O\end{matrix}$.

An example of how the above correlation of $\nu_{SO_2(sym)}$ with $\nu_{SO_2(asym)}$ and of both of these frequencies with the effect of the attached groups may be used is afforded by the sulphonyl fluorides. Bands at 1177, 1180, 1178, 1169, and 1184 cm^{-1}, respectively, for methane, benzene, *o*-toluene, *m*-toluene, and *p*-toluene sulphonyl fluorides, have been assigned previously to the symmetrical stretch by Ham and Hambly (7). We suggest, however, that bands at 1210, 1205, 1209, 1203, and 1205 cm^{-1}, respectively, assigned by the above workers to a vibration of the SO_2F group should be reassigned to the S—O symmetrical stretch. This vibration has a frequency in the range 1170 to 1180 cm^{-1} in the corresponding chlorides and it is reasonable to expect a shift from this value to a higher value on substituting fluorine for chlorine, e.g. on passing from SO_2Cl_2 to SO_2F_2 the S—O symmetrical stretch shifts from 1180 to 1269 cm^{-1}. Moreover the reassigned frequencies fit the straight line rather better (points indicated ● on Fig. 1) than the original assignments (indicated by + on Fig. 1).

Figure 1 also shows that for anions, XSO_3^-, the S—O bands come at much lower frequencies than for any neutral molecule. This is consistent with the smaller double-bond character of the S—O bonds in these species. The effect of the X substituent, although much reduced, is also apparent in these anions, e.g. $\nu_{SO_2(sym)}$ for FSO_3^- is at 1080 cm^{-1} while this vibration has the frequency 1054 cm^{-1} for $ClSO_3^-$ and 1040 cm^{-1} for HSO_4^-. The straight-line relationship between the two S—O frequencies is not so good for some of these anions possibly due to inaccuracies in the frequencies resulting from the difficulty of resolving bands in some of the spectra.

Another example of the use of the above correlation in structure determination is afforded by the observation of two bands assigned to the S—O stretches, at 1030 and 1240 cm^{-1} in the spectrum of *p*-toluenesulphonic acid monohydrate. It is immediately clear from Fig. 1 that these bands are characteristic of the *p*-toluene sulphonate ion and not the parent acid so that the compound is actually the salt $H_3O^+ \cdot CH_3 \cdot C_6H_4 \cdot SO_3^-$. Again Haszeldine and Kidd (4) report the S—O bands for CF_3SO_3H at 1030 and 1176 cm^{-1} but from Fig. 1 it seems that they should be assigned not to the acid but to its anion $CF_3 \cdot SO_3^-$.

The $—SO_2—$ group frequencies in the molecule XSO_3H can be related to its strength as an acid. A similar correlation of the —OH stretching frequency in carboxylic acids with their strengths has been pointed out by Goulden (8) and the change in the carbonyl stretching frequency has been used similarly (9). The frequencies of the $—SO_2—$ symmetrical stretch in the sulphonic acids appears to increase with increasing acid strength as is shown in Table III. Disulphuric acid, $H_2S_2O_7$, is a moderately weak acid of the sulphuric acid system (10). Fluorsulphuric and chlorsulphuric acids are very weak acids in sulphuric acid (11) while *p*-toluene sulphonic and benzene sulphonic acids behave as weak bases of the sulphuric acid system (12) and are presumably therefore weaker acids than sulphuric acid. Comparison of CF_3SO_2Cl ($\nu_{SO_2(sym)}$ = 1239, $\nu_{SO_2(asym)}$ = 1439 cm^{-1}) with SO_2Cl_2 ($\nu_{SO_2(sym)}$ = 1182, $\nu_{SO_2(asym)}$ = 1414 cm^{-1}) would suggest that the SO_2 frequencies in CF_3SO_3H would be higher than in $ClSO_3H$ and it might be predicted therefore that CF_3SO_3H would be a stronger acid than $ClSO_3H$. Unfortunately the

TABLE III

Correlation of $\nu_{SO_2(sym)}$ with the acid dissociation constants of sulphonic acids in sulphuric acid

	SO_2(sym) (cm^{-1})	K_a, moles kg^{-1} (25° C)
Disulphuric acid	1240	0.014
Fluorsulphuric acid	1230	0.002
Chlorsulphuric acid	1209	0.001
Sulphuric acid	1195	—
Benzenesulphonic acid	1182	Base
p-Toluenesulphonic acid	1170	Base

ionization of CF_3SO_3H in sulphuric acid has not been studied. It can also be predicted from a comparison of the SO_2 frequencies of CF_3SO_2F at 1239 and 1463 cm^{-1} and those of FSO_2F (1269 cm^{-1}, 1501 cm^{-1}) that CF_3SO_3H would be a weaker acid than FSO_3H. Thus the following is probably the order of the strengths of these sulphonic acids,

$$H_2S_2O_7 > FSO_3H > CF_3SO_3H > ClSO_3H > H_2SO_4 > MeSO_3H.$$

A similar effect of electronegative substituents on the characteristic frequency of a group has been observed in other cases, e.g. for phosphoryl compounds (13) and for carbonyl compounds (14), and attempts have been made to devise quantitative relationships between the vibrational frequency of a group and the effective electronegativities of the attached substituents.

Bell and co-workers assumed that the P=O frequency in phosphoryl compounds is directly related to the sum of the effective electronegativities of the groups X, Y, Z, in the molecule (XYZ)P=O ($\Sigma\psi = \psi_X+\psi_Y+\psi_Z$). By assuming the Pauling values (4.0, 3.0, and 2.8) for the electronegativities of fluorine, chlorine, and bromine, respectively, they were able to obtain a correlation between the Raman shifts of the P=O group and the sum of the electronegativities of the halogens attached to it. The weakness of the method is that it assumes that the effect of the halogen is to be entirely attributed to its changing the effective electronegativity of the phosphorus atom and ignores any possible effects due to double-bond formation with the halogen which may be particularly important for fluorine. Generally the P—F bond distance is found to be considerably less than the sum of the covalent radii (41), and this has been attributed (15) to partial double-bond formation between fluorine and phosphorus. We find that if we consider first only the phosphoryl compounds not containing fluorine and correlate the P=O stretching frequency (Table IV) with the sum of the Pauling electronegativities in these compounds (Fig. 2), then a good straight line can be drawn which has a different slope

TABLE IV

Values of the P—O stretching frequency in phosphoryl halides (XYZ). P=O*

X	Y	Z	$\Sigma\psi$†	$\nu_{P=O}$ (cm^{-1})	X	Y	Z	$\Sigma\psi$†	$\nu_{P=O}$ (cm^{-1})
Cl	Cl	Cl	19.0	1290	F	F	Cl	10.2	1358
Cl	Cl	Br	8.8	1285	F	F	Br	10.0	1360, 1340 } 1350
Cl	Br	Br	8.6	1275	F	Cl	Cl	9.6	1331
Br	Br	Br	8.4	1261	F	Br	Br	9.2	1303
F	F	F	10.8	1395	F	Cl	Br	9.4	1319

*Taken from Bell and co-workers (13).
†Sum of effective electronegativities ($\Sigma\psi = \psi_X+\psi_Y+\psi_Z$).

Can. J. Chem. Downloaded from www.nrcresearchpress.com by 210.87.254.6 on 09/05/12
For personal use only.

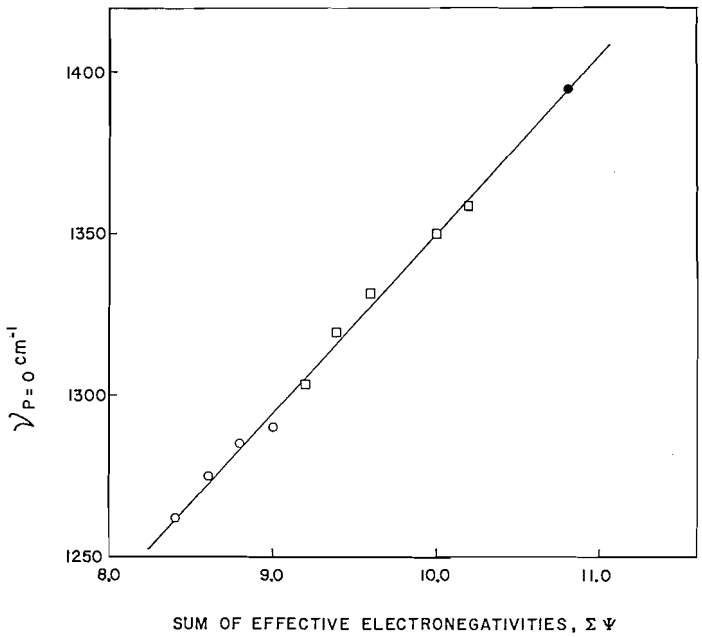


FIG. 2. Correlation of P—O stretching frequency with $\Sigma\psi$. ○ chloro, bromo, and chloro–bromo compounds; ● POF_3; □ chloro–fluoro and bromo–fluoro compounds and POFClBr.

from the line proposed by Bell and co-workers (13). The correlation is probably justified for chloro and bromo phosphorus compounds, since the phosphorus halogen bond lengths are nearer to the sum of the covalent radii (41), indicating that the bonds are probably near to single. On the basis of the new straight line we find that a value of 3.6 is required for the effective electronegativity of fluorine in order for the P=O frequency in POF_3 to fall on the straight line (Fig. 2). This can be attributed to the fact that double bonding between fluorine and phosphorus reduces the extent of P—O double bonding and thus apparently reduces the effective electronegativity of fluorine. The value 3.6 seems to be appropriate for all phosphoryl compounds since if we use this value for fluorine and the Pauling values for chlorine and bromine, then the present straight line is also found to hold for all mixed halogen–fluorine phosphoryl compounds (Fig. 2).

It is clear from the above discussion that evaluation of electronegativities for groups is complicated by the probable occurrence of double bonding. Nevertheless the order of electronegativities of groups can probably be established from the spectra. For phosphoryl compounds the order

$$F > CF_3 > OAr \simeq OR > CN > Cl > Br > SR > Ar > R \simeq NH_2$$

is obtained.

The multiplicity of P—F bonds implied by the low apparent electronegativity of fluorine and the short bond lengths is consistent with the P—F symmetrical stretching frequency in fluorphosphorus compounds. For the PF_6^- ion the P—F distance is apparently single (1.73 Å) and the P—F stretching frequency is at 741 cm^{-1} whereas in other P—F compounds where the P—F distance is abnormally short this particular vibration is at a much higher frequency (820 to 940 cm^{-1}), implying a strengthening of the bond. In PF_6^- the outer shell contains six electron pairs and P—F double-bond

Can. J. Chem. Downloaded from www.nrcresearchpress.com by 210.87.254.6 on 09/05/12
For personal use only.

formation presumably cannot occur whereas in the other compounds considered the valency shell contains less than six electron pairs making partial double-bond formation very probable (16). A similar effect has been recognized (15), in the case of bonds of fluorine with silicon. For example, in SiF_4 the Si—F bond length is 1.54 Å and the Si—F stretching frequency is at 800 cm^{-1} while in SiF_6^{--} the bond length is 1.71 Å and the stretching frequency is at 656 cm^{-1}.

In view of the obvious defects in the calculations of effective electronegativities by the method of Bell and co-workers and because few reference compounds are available no attempt has been made to evaluate the electronegativities of groups attached to the SO_2 group in sulphuryl compounds. However, the order of electronegativities is probably

$$F > OF > CF_3 > OR \simeq OH > Cl \simeq CCl_3 > SR \simeq NH_2 > Ar > R,$$

which is very similar to the order found for these groups attached to the phosphoryl group.

Recently Lagowski (38) using the S—O frequencies for the compounds SO_2F_2, SO_2Cl_2, CF_3SO_2F, and CF_3SO_2Cl has deduced that the effective electronegativity of the CF_3 group is between those of fluorine and chlorine and the effect of substituted alkyl and aryl substituents on ν_s and ν_{as} has been discussed by Momose *et al.* (39).

Difficulties with regard to S—F double bonding are to be expected. Thus in SF_6 where no double bonding between sulphur and fluorine is expected the S—F stretching frequency is at 775 cm^{-1}, but in most other fluorosulphur compounds this vibration has a higher frequency in the range 820 to 850 cm^{-1} which could be attributed to partial double-bond character of the S—F bonds.

ACKNOWLEDGMENTS

The author wishes to thank Dr. R. J. Gillespie for useful comments on and discussion of the manuscript and the National Research Council of Canada and the Ontario Research Foundation for financial support.

REFERENCES

1. L. J. Bellamy. The infrared spectra of complex molecules. 2nd ed. Methuen, London. 1958. p. 350.
2. L. J. Bellamy and R. L. Williams. J. Chem. Soc. 863 (1957).
3. R. N. Haszeldine and J. M. Kidd. J. Chem. Soc. 4229 (1954).
4. R. N. Haszeldine and J. M. Kidd. J. Chem. Soc. 2901 (1955).
5. D. Barnard, J. M. Fabian, and H. P. Koch. J. Chem. Soc. 2442 (1949).
6. J. N. Baxter, J. Cymerman-Craig, and J. B. Willis. J. Chem. Soc. 669 (1955).
7. N. S. Ham and A. N. Hambly. Australian J. Chem. **6**, 33, 135 (1953).
8. J. D. S. Goulden. Spectrochim. Acta, **6**, 129 (1954).
9. R. H. Gillette. J. Am. Chem. Soc. **58**, 1143 (1936).
10. R. J. Gillespie. J. Chem. Soc. 2493 (1950).
11. J. Barr, R. J. Gillespie, and E. A. Robinson. Unpublished.
12. R. J. Gillespie and E. A. Robinson. Unpublished.
13. J. V. Bell, J. Heisler, H. Tannebaum, and J. Goldeson. J. Am. Chem. Soc. **76**, 5185 (1954).
14. R. E. Kagarise. J. Am. Chem. Soc. **77**, 1377 (1955).
15. L. Pauling. The nature of the chemical bond. 2nd ed. Oxford University Press. 1940.
16. R. J. Gillespie. J. Am. Chem. Soc. To be published.
17. H. G. Houlton and H. V. Tartar. J. Am. Chem. Soc. **60**, 544 (1938).
18. H. Gerding and A. C. Linden. Rec. trav. chim. **61**, 735 (1942).
19. C. C. Price and H. Mosita. J. Am. Chem. Soc. **75**, 4747, 4750 (1953).
20. J. Cymerman and J. B. Willis. J. Chem. Soc. 1332 (1956).
21. E. Philbin, E. R. Stuart, R. F. Timoney, and T. S. Wheeler. J. Chem. Soc. 4414 (1956).
22. R. S. Tipson. J. Am. Chem. Soc. **74**, 1354 (1952).
23. M. T. Rodgers, G. M. Barrow, and F. G. Bordwell. J. Am. Chem. Soc. **78**, 1790 (1956).
24. K. Schreiber. Anal. Chem. **21**, 1168 (1949).
25. J. Cabannes and A. Rousset. Ann. phys. **19**, 229 (1933).
26. H. J. Hofmann and K. R. Andress. Naturwiss. **41**, 94 (1954).

Can. J. Chem. Downloaded from www.nrcresearchpress.com by 210.87.254.6 on 09/05/12
For personal use only.

27. A. SIMON and H. KRIESGSMANN. Z. physik. Chem. **204**, 369 (1955).
28. H. GERDING and H. W. MAARSON. Rec. trav. Chim. **77**, 374 (1958).
29. F. B. DUDLEY, G. H. CADY, and D. F. EGGERS. J. Am. Chem. Soc. **78**, 290 (1956).
30. J. E. ROBERTS and G. H. CADY. J. Am. Chem. Soc. **81**, 4166 (1959).
31. H. C. CLARKE and H. J. EMELEUS. J. Chem. Soc. 190 (1958).
32. A. SIMON, H. KRIEGSMANN, and H. DUTZ. Chem. Ber. **89**, 2390 (1956).
33. A. SIMON and H. KRIEGSMANN. Chem. Ber. **89**, 2378, 2384, 1883 (1956).
34. H. SIEBERT. Z. anorg. Chem. **292**, 167 (1957).
35. H. SIEBERT. Z. anorg. Chem. **289**, 14 (1957).
36. H. GERDING. J. Chem. Phys. **45**, 55 (1948).
37. H. GERDING and W. J. NIJVELD. Rec. trav. Chim. **59**, 1206 (1940).
38. J. J. LAGOWSKI. Quart. Revs. (London), **13**, 233 (1959).
39. T. MOMOSE, Y. VEDA, and T. SHOJI. Pharm. Bull. (Tokyo), **6**, 415 (1958).
40. P. HERSJARVI and E. TOMMILA. Ann Acad. Sci. Fennicae, Ser. A, II. No. 78 (1957).
41. INTERATOMIC DISTANCES. *Edited by* L. E. SUTTON. Chemical Society Special Publ. No. 11. 1958.
42. J. H. HIBBEN. The Raman effect and its chemical applications. Reinhold Publishing Corp., New York. 1939. p. 397.

Can. J. Chem. Downloaded from www.nrcresearchpress.com by 210.87.254.6 on 09/05/12
For personal use only.

Can. J. Chem. Downloaded from www.nrcresearchpress.com by 210.87.254.5 on 09/05/12
For personal use only.

NOTES

STUDIES ON THE CRYSTALS SEPARATING FROM AQUEOUS LITHIUM NITRATE SOLUTION

G. ARAVAMUDAN* AND S. RAMASESHAN

Systematic studies (1, 2, 3, 4) on lithium nitrate–water systems have established the existence of $LiNO_3.3H_2O$. In fact Campbell and Bailey (3*c*) have not only isolated this salt but have succeeded in recording its X-ray powder diagram. During the course of some investigations on $LiNO_3$–H_2O systems in this Institute (5) very good single crystals of $LiNO_3.3H_2O$ were obtained. This note reports the determination of its space group as well as some morphological studies of anhydrous $LiNO_3$ crystals separating from aqueous solution at various temperatures.

When an aqueous $LiNO_3$ solution corresponding to the composition of the trihydrate (56.11% $LiNO_3$ by weight) is cooled to $-5°$ C spontaneous crystallization occurs with the deposition of a mass of $LiNO_3.3H_2O$ crystals. If one of these tiny crystals is used to inoculate a more dilute solution (50% $LiNO_3$) and the temperature maintained constant (say at 25° C), extremely well defined euhedral crystals, sometimes as large as 6 cm × 2 cm × 1.5 cm, could be grown during the course of 2 days.

The crystals appeared to belong to the orthorhombic system and the peculiar distribution of the faces suggested a hemimorphic form lacking a center of symmetry (point group *mm*2). The *a* and *b* faces were well developed while the *c* face (perpendicular to the axis of elongation) could be recognized only in rare cases. Two prominent faces which made respectively 28° and 46° with the *b* face were later identified as the (110) and (120) planes. These angles were measured with a contact goniometer because of the inherent difficulty of mounting these excessively hygroscopic, low-melting crystals on a two-circle goniometer.

Using a few flawless crystals the density was determined by the flotation method (bromoform + xylene mixture) to be 1.55.

Rotation and Weissenberg photographs about the *c* axis were taken with a single crystal enclosed in a Lindemann glass tube. The crystal belongs to the orthorhombic symmetry with unit cell dimensions $a = 6.82$ Å, $b = 12.78$ Å, and $c = 6.05$ Å. The observed density gave four molecules in the unit cell.

From *hk*0, *hk*1, and *hk*2 Weissenberg photographs it was found that the constraining condition for the appearance of *hkl* reflections was $h+k = 2n$, while that for the *h*0*l* reflections was ($h = 2n$), $l = 2n$. All the other reflections like *hk*0, 0*kl*, *h*00, 0*k*0, and 00*l* were also governed by these two conditions. The only space groups consistent with these conditions are (6):

centrosymmetric space group — $Cmcm$—D_{2h}^{17} (No. 63)

or

non-centrosymmetric space groups — $Cmc2$—C_{2v}^{16} (No. 40)

$Cmc2_1$—C_{2v}^{12} (No. 36).

**Present address: Department of Chemistry, Indian Institute of Technology, Madras, S. India.*

If any weight could be given to the cursory morphological examination mentioned earlier, the crystal should belong to one of the latter two non-centrosymmetric space groups. The crystal structure analysis of this substance is in progress.

A powder photograph of $LiNO_3.3H_2O$ was taken using a 9-cm Unicam powder camera. Since the specimen diameter was nearly 0.6 mm, high resolution could not be attained. Table I gives an approximate visual estimate of the intensity of each line, its spacing,

TABLE I

Powder data of $LiNO_3.3H_2O$

No.	Intensity	*d*, observed	Index	*d*, calculated	*d*, Campbell and Bailey
1	VW	6.40	020	6.395	6.13
2	W	6.01	110	6.015	
3	S	4.31	021	4.358	4.20
			111	4.268	
4	W	3.40	200	3.410	3.47
5	VW	3.10	040	3.198	
			131	3.102	
6	VS	3.01	002	3.025	2.99
			220	3.007	
7	W	2.85	041	2.838	2.79
8	M	2.70	020	2.734	
			112	2.702	2.68
			221	2.693	
9	S	2.34	150	2.392	
			240	2.332	2.37
			132	2.320	
10	S	2.13	222	2.133	2.13
			060	2.130	
11	VW	2.05	061	2.010	2.02
			330	2.005	
12	VW	1.88	331	1.904	1.90
			152	1.878	
13	M	1.80	212	1.800	1.80

its index, and spacing computed from the Weissenberg data as also the values reported by Campbell and Bailey. The present measurements are accurate to 1% only.

The work of Campbell and his co-workers has definitely disproved the existence of lithium nitrate hemihydrate ($LiNO_3.\frac{1}{2}H_2O$) which Donnan and Burt (1) reported. According to these authors the anhydrous salt separating at higher temperatures (70 to 90° C) had a different crystal form from the "hemihydrate" crystals which they claimed were formed in their experiments at about 40° C. However, this suggested that the morphological study of crystals grown from concentrated aqueous solution by evaporation or by cooling at various temperatures from 0° C to 90° C would be of interest. These crystals were most carefully examined optically and goniometrically. A simple plastic attachment was made to the Unicam two-circle goniometer to completely prevent moist air from coming in contact with the hygroscopic crystals. Although the measurement of the angles were necessarily inaccurate (due to the intervening thin plastic cover) there was no doubt from the stereographic projections that all the crystals obtained were definitely the anhydrous rhombohedral $LiNO_3$. The crystals, however,

Can. J. Chem. Downloaded from www.nrcresearchpress.com by 210.87.254.5 on 09/05/12
For personal use only.

exhibited a profusion of faces and forms, the most prominent being $c(0001)$, $m(10\bar{1}0)$, $r(10\bar{1}1)$, $0(02\bar{2}1)$, $e(01\bar{1}2)$, and $v(21\bar{3}1)$. Measurement of the rhombohedral angle gave a value 72° 30′ well in agreement with that computed from X-ray data (7) (72° 42′) for anhydrous $LiNO_3$.

It is perhaps worth while mentioning that it was impossible to separate out the trihydrate crystals from concentrated solutions of lithium nitrate even at temperatures as low as 0° C. Neither do these crystals form on the slow removal of water from saturated solution above −5° C. This is due to the strong tendency of $LiNO_3.3H_2O$ to supercool and it is precisely for this reason that seeding of the solution has to be resorted to for preparing the trihydrate crystals at ambient temperature (25° C).

The authors wish to thank Professor K. R. Krishnaswamy and Professor R. S. Krishnan for their kind interest in this work.

1. F. G. Donnan and B. C. Burt. J. Chem. Soc. **83**, 335 (1903).
2. A. Massink. Z. physik. Chem. **92**, 351 (1918).
3(*a*). A. N. Campbell. J. Am. Chem. Soc. **64**, 2680 (1942).
3(*b*). A. N. Campbell and E. M. Kartzmark. Can. J. Chem. **34**, 1404 (1956).
3(*c*). A. N. Campbell and R. N. Bailey. Can. J. Chem. **36**, 518 (1958).
4. G. Aravamudan. Current Sci. (India), **26**, 49 (1957).
5. G. Aravamudan. Ph.D. Thesis, Mysore University, India. 1958.
6. International Tables for X-Ray Crystallography. Vol. 1. Kynoch Press, Birmingham.
7. W. H. Zachariasen. *In* R. W. G. Wyckoff. Crystal structures. Vol. 1. Interscience, New York.

Received October 3, 1960.
Indian Institute of Science,
Bangalore 12,
South India.

THE FLUORINE MAGNETIC RESONANCE IN THE IONS $[BF_4]^-$ AND $[BF_3CF_3]^-$

R. D. Chambers, H. C. Clark, L. W. Reeves, and C. J. Willis

Three of the authors have recently reported the new $[BF_3—CF_3]^-$ anion (1), the first compound with a perfluoroalkyl–boron bond. The present note presents the nuclear magnetic resonance data at 40 Mc for this ion and the $[BF_4]^-$ ion in aqueous solution. The resonance signals were referred to an external capillary containing CF_3COOH. No corrections for diamagnetic susceptibility differences in a cylindrical tube have been employed because the magnitude of the chemical shifts observed is so large (2, 3).

At the left of the figure are shown F^{19} magnetic resonance spectra of the CF_3 region of the $[CF_3BF_3]^-$ ion (I) and the peak due to trifluoroacetic acid (II). Peak III, which is shifted +77.3 p.p.m. to high field, is the F^{19} resonance of the BF_3 region of the ion. The correspondence of these chemical shifts to the boron–fluorine and the carbon–fluorine electronegativity differences and the equal intensity is satisfactory proof of the formulation of the ion (4, 5). At the right of the figure the spectrum of the $[BF_4]^-$ ion is shown from a concentrated aqueous solution of the sodium salt. Chemical shifts are indicated above the respective spectrum.

The spectra all show a quartette with some underlying structure which is not resolved.

Can. J. Chem. Downloaded from www.nrcresearchpress.com by 210.87.254.5 on 09/05/12
For personal use only.

exhibited a profusion of faces and forms, the most prominent being $c(0001)$, $m(10\bar{1}0)$, $r(10\bar{1}1)$, $0(02\bar{2}1)$, $e(01\bar{1}2)$, and $v(21\bar{3}1)$. Measurement of the rhombohedral angle gave a value 72° 30′ well in agreement with that computed from X-ray data (7) (72° 42′) for anhydrous $LiNO_3$.

It is perhaps worth while mentioning that it was impossible to separate out the trihydrate crystals from concentrated solutions of lithium nitrate even at temperatures as low as 0° C. Neither do these crystals form on the slow removal of water from saturated solution above −5° C. This is due to the strong tendency of $LiNO_3.3H_2O$ to supercool and it is precisely for this reason that seeding of the solution has to be resorted to for preparing the trihydrate crystals at ambient temperature (25° C).

The authors wish to thank Professor K. R. Krishnaswamy and Professor R. S. Krishnan for their kind interest in this work.

1. F. G. Donnan and B. C. Burt. J. Chem. Soc. **83**, 335 (1903).
2. A. Massink. Z. physik. Chem. **92**, 351 (1918).
3(*a*). A. N. Campbell. J. Am. Chem. Soc. **64**, 2680 (1942).
3(*b*). A. N. Campbell and E. M. Kartzmark. Can. J. Chem. **34**, 1404 (1956).
3(*c*). A. N. Campbell and R. N. Bailey. Can. J. Chem. **36**, 518 (1958).
4. G. Aravamudan. Current Sci. (India), **26**, 49 (1957).
5. G. Aravamudan. Ph.D. Thesis, Mysore University, India. 1958.
6. International Tables for X-Ray Crystallography. Vol. 1. Kynoch Press, Birmingham.
7. W. H. Zachariasen. *In* R. W. G. Wyckoff. Crystal structures. Vol. 1. Interscience, New York.

Received October 3, 1960.
Indian Institute of Science,
Bangalore 12,
South India.

Can. J. Chem. Downloaded from www.nrcresearchpress.com by 210.87.254.105 on 09/05/12
For personal use only.

THE FLUORINE MAGNETIC RESONANCE IN THE IONS $[BF_4]^-$ AND $[BF_3CF_3]^-$

R. D. Chambers, H. C. Clark, L. W. Reeves, and C. J. Willis

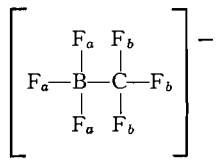
Three of the authors have recently reported the new $[BF_3—CF_3]^-$ anion (1), the first compound with a perfluoroalkyl–boron bond. The present note presents the nuclear magnetic resonance data at 40 Mc for this ion and the $[BF_4]^-$ ion in aqueous solution. The resonance signals were referred to an external capillary containing CF_3COOH. No corrections for diamagnetic susceptibility differences in a cylindrical tube have been employed because the magnitude of the chemical shifts observed is so large (2, 3).

At the left of the figure are shown F^{19} magnetic resonance spectra of the CF_3 region of the $[CF_3BF_3]^-$ ion (I) and the peak due to trifluoroacetic acid (II). Peak III, which is shifted +77.3 p.p.m. to high field, is the F^{19} resonance of the BF_3 region of the ion. The correspondence of these chemical shifts to the boron–fluorine and the carbon–fluorine electronegativity differences and the equal intensity is satisfactory proof of the formulation of the ion (4, 5). At the right of the figure the spectrum of the $[BF_4]^-$ ion is shown from a concentrated aqueous solution of the sodium salt. Chemical shifts are indicated above the respective spectrum.

The spectra all show a quartette with some underlying structure which is not resolved.

This quartette arises from indirect spin–spin interaction between the 81.2% abundant B^{11} isotope and F^{19}. It is to be noted that the individual multiplets are much narrower in the $[BF_4]^-$ ion because the tetrahedral symmetry minimizes the electric field gradients at the boron nucleus (6, 7, 8).

The spectrum of the $[BF_3—CF_3]^-$ ion should reflect the following coupling constants $J_{B^{11}-F_a{}^{19}}$, $J_{B^{11}-F_b{}^{19}}$, and $J_{F_a{}^{19}-F_b{}^{19}}$ from



The values obtained are $J_{B^{11}-F_b{}^{19}} = 34$ c.p.s., $J_{B^{11}-F_a{}^{19}} = 39.0$ c.p.s., and $J_{F_a{}^{19}-F_b{}^{19}}$ is not resolved. The value of $J_{B^{11}-F_a{}^{19}}$ is similar to that observed in BF_3 (6). In the $[BF_4]^-$ ion $J_{B^{11}-F^{19}}$ is only 4.8 c.p.s.

The spectrum for the $[BF_4]^-$ shows that no other species such as $[BF_3(OH)]^-$ is present in any appreciable amount, in agreement with the observations of Wamser (9) that the degree of hydrolysis of $[BF_4]^-$ in concentrated solutions is very small. It has already been found that the $[CF_3BF_3]^-$ ion is not appreciably hydrolyzed in aqueous solution (1) and the simple N.M.R. spectrum found is therefore to be expected, in the absence of species such as $[CF_3BF_2OH]^-$.

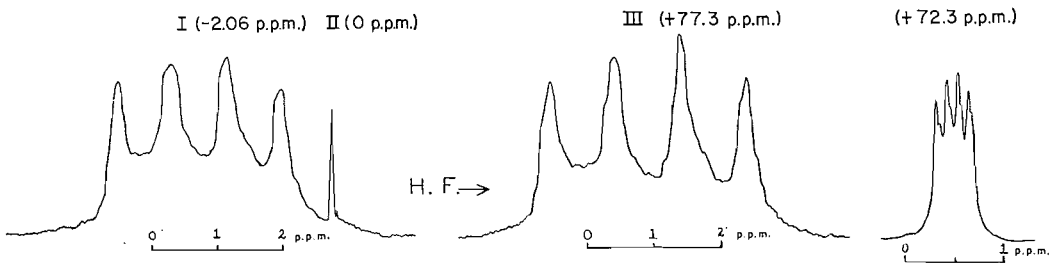


FIG. 1.

The authors appreciate the financial support of the Office of Naval Research, and Research Corporation.

1. R. D. CHAMBERS, H. C. CLARK, and C. J. WILLIS. Proc. Chem. Soc. 114 (1960). J. Am. Chem. Soc. **82**, 5298 (1960).
2. L. W. REEVES and W. G. SCHNEIDER. Can. J. Chem. **35**, 251 (1957).
3. H. S. GUTOWSKY and C. J. HOFFMAN. J. Chem. Phys. **19**, 1259 (1951). Phys. Rev. **80**, 110 (1950).
4. L. H. MEYER, A. SAIKA, and H. S. GUTOWSKY. J. Am. Chem. Soc. **75**, 4567 (1953).
5. A. SAIKA and C. P. SLICHTER. J. Chem. Phys. **22**, 26 (1954).
6. J. A. POPLE, W. G. SCHNEIDER, and H. J. BERNSTEIN. High resolution nuclear magnetic resonance. McGraw-Hill Book Co., Inc., New York. 1959. pp. 317–345.
7. J. KELLY, J. D. RAY, and R. A. OGG. Phys. Rev. **54**, 767 (1954).
8. R. A. OGG and J. D. RAY. Discussions Faraday Soc. **19**, 239 (1955).
9. C. A. WAMSER. J. Am. Chem. Soc. **70**, 1209 (1948).

RECEIVED AUGUST 29, 1960.
DEPARTMENT OF CHEMISTRY,
UNIVERSITY OF BRITISH COLUMBIA,
VANCOUVER, BRITISH COLUMBIA.

Can. J. Chem. Downloaded from www.nrcresearchpress.com by 210.87.254.105 on 09/05/12
For personal use only.

REARRANGEMENT IN THE REACTION BETWEEN THIONYL CHLORIDE AND 3-METHYL-2-BUTANOL

C. C. Lee and A. J. Finlayson

Nucleophilic displacements which occur with retention of configuration have been designated S_Ni reactions (1). The most extensively studied reaction of this type is that between thionyl chloride and secondary alcohols. Recent work in this field has led to the conclusion that S_Ni reactions possess considerable ionic characteristics, with carbonium ions or ion-pairs suggested as intermediates (2–5). Rearrangements typical of intermediate carbonium ions have been observed by Cram (2) for the reaction of thionyl chloride with the stereoisomers of 3-phenyl-2-butanol, 2-phenyl-3-pentanol, and 3-phenyl-2-pentanol. The present communication reports the formation of a rearranged product from the reaction between thionyl chloride and 3-methyl-2-butanol.

3-Methyl-2-butanol was added dropwise, with stirring, to a 100% excess of purified thionyl chloride at −35° C. Stirring was continued for 2 hours at −35° C. The hydrogen chloride produced was pumped off at about 25 mm pressure. The reaction mixture was then allowed to stand at room temperature for 1.5 hours before the excess thionyl chloride was distilled at 29–31° C at 25–30 mm. The resulting chlorosulphite was decomposed by heating at 40–50° C for 1.5 hours. Evolution of sulphur dioxide was noted during the decomposition. On raising the temperature, the crude product distilled. The distillate was washed with water and with dilute sodium carbonate solution until the washing remained basic. The washed product was dissolved in ether and dried over phosphorus pentoxide. After removal of the solvent, the residue was distilled to give about 20% yields of alkyl chloride, b.p. 84–85° C (lit. (6*a*) for *t*-amyl chloride, b.p. 86° C), which gave an immediate precipitate with alcoholic silver nitrate at room temperature. The infrared absorption spectrum of this product showed all the absorption peaks as known *t*-amyl chloride together with an extra, weak and broad band in the 1725 to 1750 cm^{-1} region. These results appear to indicate that the reaction product may be *t*-amyl chloride contaminated with a small amount of unknown impurity.

To confirm the identity of the reaction product as chiefly *t*-amyl chloride, it was converted to the Grignard reagent followed by reaction with carbon dioxide to give dimethylethylacetic acid (7, 8) with an over-all yield of 35%. The low yield was to be expected since it is difficult to prepare Grignard reagents from *t*-alkyl halides. The dimethylethylacetic acid was identified by conversion to the *p*-phenylphenacyl ester, which melted alone and on admixture with an authentic sample at 84° C (lit. (6*b*) m.p. 86.5° C). Considering these results, it is reasonable to conclude that *t*-amyl chloride was obtained from the reaction of thionyl chloride with 3-methyl-2-butanol. A 1,2-hydride shift must have occurred in the reaction. A similar type of 1,2-shift has been noted in the reaction of thionyl chloride with 2-butanol-1-C^{14}, resulting in the formation of some 2-butyl-4-C^{14} chloride.* The rearrangement in the labelled 2-butyl system was found to occur during the S_Ni reaction itself and did not arise during the process of purification or degradation. With these findings in mind, it appears safe to conclude that the *t*-amyl chloride obtained in the present study actually resulted from rearrangement during the reaction between thionyl chloride and 3-methyl-2-butanol. Rearrangements resulting from 1,2-shifts in the 3-methyl-2-butyl system have also been noted in carbonium ion-type reactions

* *Unpublished work of C. C. Lee and D. G. Lee.*

Can. J. Chem. Downloaded from www.nrcresearchpress.com by 210.87.254.5 on 09/05/12
For personal use only.

(9, 10). The present finding, therefore, supports the suggestion that reactions of thionyl chloride with secondary alcohols involve ionic intermediates.

The financial support given by the National Research Council of Canada is gratefully acknowledged.

1. W. A. COWDREY, E. D. HUGHES, C. K. INGOLD, S. MASTERMAN, and A. D. SCOTT. J. Chem. Soc. 1267 (1937).
2. D. J. CRAM. J. Am. Chem. Soc. **75**, 332 (1953).
3. E. S. LEWIS and C. E. BOOZER. J. Am. Chem. Soc. **74**, 308 (1952).
4. C. E. BOOZER and E. S. LEWIS. J. Am. Chem. Soc. **75**, 3182 (1953).
5. S. H. SHARMAN, F. F. CASERIO, R. F. NYSTROM, J. C. LEAK, and W. G. YOUNG. J. Am. Chem. Soc. **80**, 5965 (1958).
6.(*a*) I. HEILBRON and H. M. BUNBURY. Dictionary of organic compounds. Vol. I. Eyre & Spottiswoode, London. 1953. p. 152. (*b*) I. HEILBRON and H. M. BUNBURY. Dictionary of organic compounds. Vol. II. Eyre & Spottiswoode, London. 1953. p. 288.
7. B. B. CORSON, J. S. THOMAS, and D. D. WAUGH. J. Am. Chem. Soc. **51**, 1950 (1929).
8. S. V. PUNTAMBECKER and E. A. ZOELLNER. Org. Syntheses, **8**, 104 (1928).
9. A. J. FINLAYSON and C. C. LEE. Can. J. Chem. **37**, 940 (1959).
10. A. J. FINLAYSON and C. C. LEE. Can. J. Chem. **38**, 787 (1960).

RECEIVED AUGUST 25, 1960.
DEPARTMENT OF CHEMISTRY,
UNIVERSITY OF SASKATCHEWAN,
SASKATOON, SASKATCHEWAN.

SYNTHESIS OF α-POLYOXYMETHYLENE-C^{13} AND α-POLYOXYMETHYLENE-O^{18}*

R. N. RENAUD AND L. C. LEITCH

Several methods of preparing formaldehyde labelled with C^{14} have been proposed (3). In all these syntheses the aldehyde is obtained as an aqueous solution. An earlier paper on the synthesis of deuterated formaldehyde by one of us (1) indicated the difficulty of obtaining polymeric formaldehyde from such solutions. Nevertheless, according to Jones and Skraba (2), evaporation of an aqueous solution obtained by hydrolysis of chloromethyl-C^{14} acetate leaves a residue of dry formaldehyde-C^{14} polymer. In our experience only traces of polymer were ever obtained under these conditions. Consequently, polyoxymethylene-C^{13} was prepared from chloromethyl-C^{13} acetate by a modification of the procedure employed in making deuterated polymeric formaldehyde. When a solution of chloromethyl-C^{13} acetate in benzene is heated with the calculated amount of water the ester is slowly hydrolyzed to formaldehyde-C^{13}, which is deposited as α-polyoxymethylene of melting point 168–170° C on the wall of the condenser in 77% yield.

The chloromethyl-C^{13} acetate was prepared by chlorinating methyl-C^{13} acetate by means of sulphuryl chloride and a trace of peroxide instead of elemental chlorine as described by Jones and Skraba (2). In this way formation of the dichloroester is almost entirely suppressed. The methyl-C^{13} acetate was prepared by heating methyl-C^{13} iodide and silver acetate in a sealed tube.

Polyoxymethylene labelled with O^{18} was prepared by heating the normal compound with water containing approximately 20% excess O^{18} and a trace of sulphuric acid. The product isolated from the reaction analyzed 9% CH_2O^{18}. Hydrolysis of chloromethyl acetate with H_2O^{18} gave polyoxymethylene, which contained only 2.7% CH_2O^{18}.

**Issued as N.R.C. No. 6047.*

Can. J. Chem. Downloaded from www.nrcresearchpress.com by 210.87.254.5 on 09/05/12
For personal use only.

(9, 10). The present finding, therefore, supports the suggestion that reactions of thionyl chloride with secondary alcohols involve ionic intermediates.

The financial support given by the National Research Council of Canada is gratefully acknowledged.

1. W. A. COWDREY, E. D. HUGHES, C. K. INGOLD, S. MASTERMAN, and A. D. SCOTT. J. Chem. Soc. 1267 (1937).
2. D. J. CRAM. J. Am. Chem. Soc. **75**, 332 (1953).
3. E. S. LEWIS and C. E. BOOZER. J. Am. Chem. Soc. **74**, 308 (1952).
4. C. E. BOOZER and E. S. LEWIS. J. Am. Chem. Soc. **75**, 3182 (1953).
5. S. H. SHARMAN, F. F. CASERIO, R. F. NYSTROM, J. C. LEAK, and W. G. YOUNG. J. Am. Chem. Soc. **80**, 5965 (1958).
6.(*a*) I. HEILBRON and H. M. BUNBURY. Dictionary of organic compounds. Vol. I. Eyre & Spottiswoode, London. 1953. p. 152. (*b*) I. HEILBRON and H. M. BUNBURY. Dictionary of organic compounds. Vol. II. Eyre & Spottiswoode, London. 1953. p. 288.
7. B. B. CORSON, J. S. THOMAS, and D. D. WAUGH. J. Am. Chem. Soc. **51**, 1950 (1929).
8. S. V. PUNTAMBECKER and E. A. ZOELLNER. Org. Syntheses, **8**, 104 (1928).
9. A. J. FINLAYSON and C. C. LEE. Can. J. Chem. **37**, 940 (1959).
10. A. J. FINLAYSON and C. C. LEE. Can. J. Chem. **38**, 787 (1960).

RECEIVED AUGUST 25, 1960.
DEPARTMENT OF CHEMISTRY,
UNIVERSITY OF SASKATCHEWAN,
SASKATOON, SASKATCHEWAN.

SYNTHESIS OF α-POLYOXYMETHYLENE-C^{13} AND α-POLYOXYMETHYLENE-O^{18}*

R. N. RENAUD AND L. C. LEITCH

Several methods of preparing formaldehyde labelled with C^{14} have been proposed (3). In all these syntheses the aldehyde is obtained as an aqueous solution. An earlier paper on the synthesis of deuterated formaldehyde by one of us (1) indicated the difficulty of obtaining polymeric formaldehyde from such solutions. Nevertheless, according to Jones and Skraba (2), evaporation of an aqueous solution obtained by hydrolysis of chloromethyl-C^{14} acetate leaves a residue of dry formaldehyde-C^{14} polymer. In our experience only traces of polymer were ever obtained under these conditions. Consequently, polyoxymethylene-C^{13} was prepared from chloromethyl-C^{13} acetate by a modification of the procedure employed in making deuterated polymeric formaldehyde. When a solution of chloromethyl-C^{13} acetate in benzene is heated with the calculated amount of water the ester is slowly hydrolyzed to formaldehyde-C^{13}, which is deposited as α-polyoxymethylene of melting point 168–170° C on the wall of the condenser in 77% yield.

The chloromethyl-C^{13} acetate was prepared by chlorinating methyl-C^{13} acetate by means of sulphuryl chloride and a trace of peroxide instead of elemental chlorine as described by Jones and Skraba (2). In this way formation of the dichloroester is almost entirely suppressed. The methyl-C^{13} acetate was prepared by heating methyl-C^{13} iodide and silver acetate in a sealed tube.

Polyoxymethylene labelled with O^{18} was prepared by heating the normal compound with water containing approximately 20% excess O^{18} and a trace of sulphuric acid. The product isolated from the reaction analyzed 9% CH_2O^{18}. Hydrolysis of chloromethyl acetate with H_2O^{18} gave polyoxymethylene, which contained only 2.7% CH_2O^{18}.

**Issued as N.R.C. No. 6047.*

Can. J. Chem. Downloaded from www.nrcresearchpress.com by 210.87.254.105 on 09/05/12
For personal use only.

Can. J. Chem. Downloaded from www.nrcresearchpress.com by 210.87.254.105 on 09/05/12
For personal use only.

EXPERIMENTAL

Methyl-C^{13} Acetate

Silver acetate (21.0 g, 0.125 mole) was placed in a high-pressure glass tube which was constricted near the top to facilitate sealing later and attached to the vacuum line. The salt was dried at 80° for 4 hours by continuous pumping. Methyl-C^{13} iodide (14.3 g, 0.1 mole) containing 24% excess C^{13} was distilled into the tube of silver acetate, which was then sealed off at the constriction. The tube was heated in a rocking furnace for 24 hours at 90–100° C. It was then cooled in dry ice, opened, and attached to the vacuum line. Volatile products were distilled from the silver iodide into another trap on the vacuum line. Yield, 7.6 g (theoretical amount). Fractional distillation in a small column packed with glass helices gave 6.4 g of methyl-C^{13} acetate, b.p. 56.2–56.4° C. Yield, 84%.

Chloromethyl-C^{13} Acetate

Methyl-C^{13} acetate (6.4 g, 0.08 mole) and 0.15 g of dibenzoyl peroxide were placed in a small flask with a side arm carrying a separatory funnel. The neck of the flask was surmounted by a condenser and a spiral trap cooled to −78° in dry ice and acetone. A drying tube filled with Drierite was attached to the open end of the trap. Freshly distilled sulphuryl chloride (13 g, 0.1 mole) was added very slowly to the methyl-C^{13} acetate, which was heated just below its boiling point. The progress of the reaction was followed by observing the volume of liquid in the trap. It took 2 days to complete the reaction. When the reaction mixture is heated too rapidly free chlorine begins to appear in the trap. The rate of the reaction is considerably reduced by traces of methyl iodide, which acts as a peroxide inhibitor.

The reaction mixture was placed on the vacuum line, freed of dissolved hydrogen chloride and sulphur dioxide, and distilled into another trap on the line. The distillate obtained was fractionated in a column packed with glass helices to give 5.2 g of product, b.p. 114° C (70% of the theoretical amount).

Polyoxymethylene-C^{13}

Chloromethyl-C^{13} acetate (5.2 g, 0.05 mole) in 10 ml of benzene was added all at once to a mixture of 20 ml of benzene, 0.9 ml of water, and one drop of concentrated sulphuric acid in a 50-ml three-necked round-bottomed flask equipped with a thermometer, an inlet tube for passing in nitrogen, a stirring bar, and a reflux condenser. A Stock trap cooled to −78° in dry ice and acetone was connected to the condenser. The reaction mixture was gradually heated to 65–70° C while a slow current of nitrogen was passed through it. Rapid stirring is required to keep the water suspended in the benzene. After 7 hours' heating and stirring, white polymeric material began to appear on the wall of the condenser. After another 8 hours the flask was removed from the condenser and replaced by a plug. Liquid in the condenser was pumped away and the hard white solid scraped off. It was washed with a little absolute ether and dried. Yield, 0.3 g. By replacing the flask with the reaction mixture and resuming heating and stirring for another 10 hours, more polymer was obtained. The total yield of product isolated was finally 1.1 g (77% of the theoretical). This product melted at 169–171° C and analyzed 24% excess C^{13} by mass spectrometry. There was 1% of an unknown impurity of mass 61.

Polyoxymethylene-O^{18}

A mixture of 0.5 g of polyoxymethylene, 20 ml of benzene, 5.5 ml of water containing 20% excess O^{18}, and a drop of concentrated sulphuric acid was heated for 24 hours in a sealed tube at 80° C. The contents of the tube were then transferred to the apparatus

used to prepare the C^{13}-labelled compound and heated as described in that preparation. A small amount of polymer, m.p. 145–150° C, which contained 9.5% CH_2O^{18} was isolated.

Hydrolysis of chloromethyl acetate with H_2O^{18} and a trace of sulphuric acid under the conditions used to prepare polyoxymethylene-C^{13} gave a polymer which contained only 2.73% CH_2O^{18}. This is what would have been expected from our knowledge of the hydrolysis of esters in H_2O^{18}. The presence of the small amount of CH_2O^{18} is due to exchange.

ACKNOWLEDGMENT

We wish to thank Mrs. R. H. Riem for several mass spectrometric analyses of the polyoxymethylene.

1. R. A. BANNARD, A. T. MORSE, and L. C. LEITCH. Can. J. Chem. **31**, 351 (1953).
2. A. R. JONES and W. J. SKRABA. J. Am. Chem. Soc. **74**, 2437 (1952).
3. A. MURRAY, III and D. L. WILLIAMS. Organic synthesis with isotopes. Interscience Publishers, New York. 1958. Part I, Chap. 6, p. 607.

RECEIVED AUGUST 19, 1960.
DIVISION OF PURE CHEMISTRY,
NATIONAL RESEARCH COUNCIL,
OTTAWA, CANADA.

Can. J. Chem. Downloaded from www.nrcresearchpress.com by 210.87.254.105 on 09/05/12
For personal use only.

Can. J. Chem. Downloaded from www.nrcresearchpress.com by 210.87.254.40 on 09/05/12
For personal use only.

Canadian Journal of Chemistry

Issued by THE NATIONAL RESEARCH COUNCIL OF CANADA

VOLUME 39 FEBRUARY 1961 NUMBER 2

INFLUENCE OF pH AND TEMPERATURE ON MYOSIN INACTIVATION[1]

GÉRARD E. PELLETIER[2] AND LUDOVIC OUELLET[3]

ABSTRACT

The inactivation of myosin adenosine triphosphatase activity was studied in 0.6 *M* potassium chloride solution at pH ranging from 7.0 to 10.6 and for 5° C to 40° C. The inactivation is a first-order process with respect to time and 0.6th order with respect to the concentration of protein. The rate of inactivation is independent of the pH for pH 7.0 to pH 8.5 at 35° C and increases rapidly with pH at higher pH. At 12° C, close to pH 10.4, the rate is inversely proportional to the 4.5th power of the hydrogen ion concentration. The energies of activation are 56 kcal mole^{-1} at pH 8.0 and 58 kcal mole^{-1} at pH 10.5. A discussion of the data stresses the importance of structural changes and indicates a possible role for the electrostatic charge in the inactivation process.

INTRODUCTION

The enzymatic activity of myosin, a muscular protein and an adenosine triphosphatase, increases with pH up to pH 9.3 at 25° C (1). The rapid decrease in activity at a higher pH was attributed by Blum (2) to enzyme inactivation. A maximum in enzymatic activity is not obtained. This work on myosin inactivation was necessitated to define the region of pH in which the kinetics of the adenosine triphosphatase activity of protein could be studied at different temperatures.

In a previous preliminary study (3), the inactivation was shown to be a first-order process with a high energy of activation. Adenosine triphosphate (ATP) decreases the rate of inactivation at pH 7.0. Mommaerts and Green (4) have reported on the stability of myosin on storage and noted that the myosin solutions are more stable at higher protein concentrations. The influence of calcium ions was also indicated. Poglasov and his collaborators (5) have suggested that heat denaturation occurs along with a decrease in the number of free sulphydryl groups. Yasui and his group (6, 7) have found that the rate of inactivation is pH independent from pH 5.7 to pH 8.9 and that the energy of activation is 57 kcal mole^{-1}. Protection by pyrophosphate was also reported by these authors.

EXPERIMENTAL

Reagents

Rabbit muscle myosin of the Weber-Edsall type (8) was used throughout these experiments. Protein concentrations were determined by a micro-Kjehldahl nitrogen determination method (9). The myosin had on the average a specific activity of 5.1×10^{-6} moles of ATP hydrolyzed per second per gram of protein, in 0.6 *M* potassium chloride,

[1]*Manuscript received October 24, 1960.*
Contribution from the Department of Chemistry, University of Ottawa, Ottawa, Ontario. Part of the work was done at l'Université Laval, Quebec, Que.
[2]*Present address: Research Department, Imperial Oil Ltd., Sarnia, Ontario.*
[3]*Present address: Département de Chimie, Université Laval, Quebec, Que.*

0.01 *M* calcium chloride, and 0.1 *M* THAM, at pH 7.5, at 25° C. Myosin preparations were stored in 0.6 *M* potassium chloride at 4° C and their activity was checked periodically.

The disodium salt of adenosine triphosphate (Pabst Laboratories, Milwaukee, Wisconsin) was used throughout these experiments.

Potassium chloride, sodium chloride, calcium chloride, trichloroacetic acid, potassium carbonate (anhydrous), and potassium bicarbonate were certified reagents. Tris(hydroxymethyl)aminomethane (THAM) was a purified reagent. Glycine and acetic acid were of the reagent grade. All solutions were made in glass-distilled water.

All reactions were carried out in buffered solutions containing 0.6 mole per liter of potassium chloride and 0.1 mole per liter of a suitable buffer. For pH values ranging from 7.5 to 9.0, a solution of THAM (pK_a 8.5 at 25° C) and acetic acid was used as buffer. Glycine (pK_a 10.3 at 0° C) – sodium hydroxide was used at higher pH's. These buffers were adjusted to the required pH at each temperature by addition of concentrated solutions of acetic acid or sodium hydroxide, pH values being read off a Beckman pH meter, model GS, equipped with shielded exterior electrodes (Beckman No. 1440). No salt-effect correction was applied.

Procedure

Activity Determination

The activity of the enzyme was determined by allowing a solution of myosin to catalyze the hydrolysis of ATP in the presence of 0.012 *M* calcium ions, the number of moles of inorganic phosphate produced per liter per second at pH 8.5 and 12° C taken as a measure of the enzyme activity. A 5-ml sample of a myosin solution whose activity was to be measured was pipetted into 20 ml of a THAM buffer containing 0.012 mole per liter of calcium chloride, incubated in a constant-temperature bath at 12° C and adjusted at pH 8.5. The resultant concentrations were such that the concentration of ATP was much greater than K_m, the Michaelis constant. The hydrolysis reaction was followed by pipetting at measured intervals of time 5-ml samples of the reaction mixture into 3 ml of a 20% solution of trichloroacetic acid, filtering the precipitated myosin, and determining phosphate concentrations in the filtrate by the Fiske and SubbaRow method (10) using a Beckman DU spectrophotometer. A plot of phosphate concentration against time gave a straight line, the slope of which was proportional to the activity of the enzyme.

Inactivation Rates

The inactivation of myosin was studied by incubating a solution of the enzyme in a buffer at the required temperature and pH and following its activity as a function of time. A flask containing 95 ml of a buffer, THAM or glycine, was placed in a constant-temperature bath and the pH of the solution was adjusted to the required value. Five milliliters of a stock solution of myosin was added and the resulting mixture thoroughly mixed by swirling of the flask. At measured intervals of time 5-ml samples were withdrawn and pipetted into a flask containing 20 ml of a THAM buffer at pH 8.5 and 12° C, and containing 0.012 mole of calcium chloride per liter.

The activity of each sample was then measured as described previously by reaction with ATP. Results presented later in the investigation show that under these conditions of pH and temperature no appreciable inactivation occurs. The above THAM buffer therefore served the dual purpose of stopping the inactivation rate and acting as a medium for activity determinations.

Can. J. Chem. Downloaded from www.nrcresearchpress.com by 210.87.254.40 on 09/05/12
For personal use only.

The logarithms of the myosin activity were then plotted against the time that the enzyme was exposed under the conditions of pH and temperature studied and the half-life was determined from these graphs. The inactivation rate constant (k_D) was calculated from the half-life of the enzyme.

RESULTS AND DISCUSSION

Order of the Reaction

As suggested by Letort (11) a distinction should be made for complex reactions between the order with respect to time and that with respect to concentration. This can readily be accomplished experimentally by applying van't Hoff's differential method to data for a single-rate determination to obtain the order with respect to time, and by applying the same method to the initial conditions of rate and concentration for a series of individual reactions to obtain the order with respect to concentration.

Figure 1 represents typical results obtained when the percentage of the initial myosin

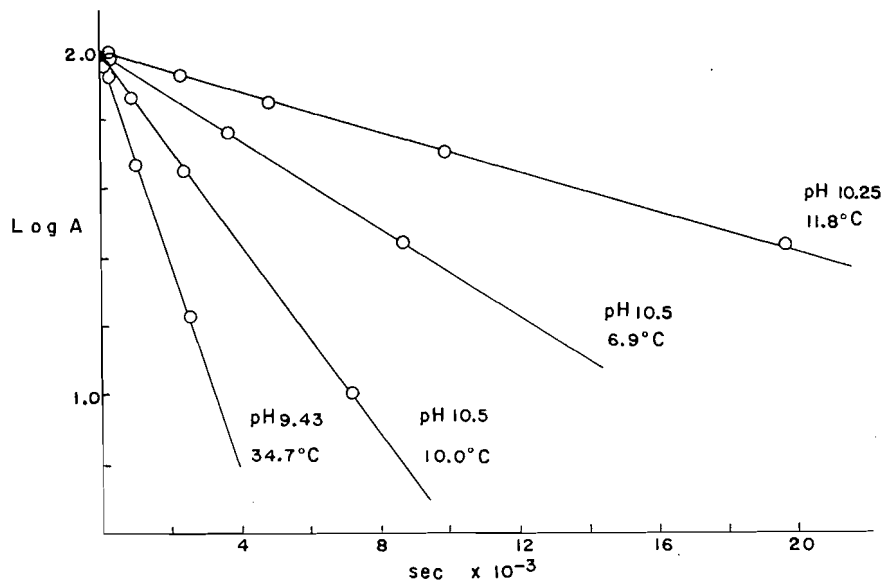


FIG. 1. Logarithms of the activity of myosin, in percentage of initial activity, as a function of time under different conditions.

activity, which is proportional to the percentage of the initial myosin concentration, was plotted against the time that the myosin was exposed to the indicated conditions of temperature and pH, at a protein concentration of 0.6 gram per liter. The straight lines obtained indicate adherence to first-order kinetics with respect to time. In some cases (e.g. curve *b*) reactions were followed to over 90% completion without departure from linearity in the log activity versus time plot. In similar experiments Yasui *et al.* (6, 7) have observed a drift towards second-order kinetics as the reaction proceeds. This difference in behavior could be attributed to slightly different myosin preparations or to the fact that Yasui *et al.* used a THAM–maleate buffer whereas we used a THAM–acetate buffer.

The order with respect to concentration is, however, more complex. Figure 2 shows the results obtained when the logarithms of the initial inactivation rates were plotted

Can. J. Chem. Downloaded from www.nrcresearchpress.com by 210.87.254.40 on 09/05/12
For personal use only.

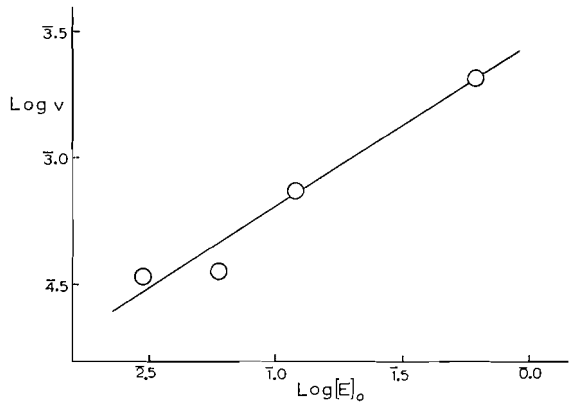


FIG. 2. Determination of the order of the inactivation reaction of myosin with respect to concentration; V is in arbitrary units and $[E]_0$, the initial concentration of myosin is in grams per liter.

against the logarithms of the initial concentrations for a series of inactivation reaction at pH 10.5 and 12.6° C over a 20-fold range of enzyme concentrations extending from 0.03 gram per liter to 0.6 gram per liter. The slope of the curve obtained is less than unity, giving a fractional order with respect to concentration, of about 0.6 to 0.7. Although most investigations on protein denaturation include only the order with respect to time, which is usually one, departure from first-order kinetics with respect to concentration (and even with respect to time) is not unfamiliar. Orders of less than one with respect to concentration have been reported in particular for the denaturation of tobacco mosaic virus (12) and potato β-amylase (13). Protection by a substance present in the protein preparation could explain the above behavior. Such a scheme has been proposed by Lauffer to explain his results on tobacco mosaic virus (12).

Influence of Calcium Chloride

In the presence of 0.005 M calcium chloride at 11.8° C at pH 10.5 the half-life of myosin was found to be 2.7×10^3 sec while it is 1.2×10^3 sec at the same protein concentration (0.6 gram per liter) under identical conditions in the absence of added calcium chloride. This would suggest an interaction between calcium ions and an area of the protein sensitive to inactivation.

Influence of pH

In common with other denaturation processes the rate of inactivation of myosin was found to be markedly dependent on the hydrogen ion concentration. Figure 3 shows the dependence of the logarithm of the first-order inactivation constant k_D of myosin on the pH of the solution at 34.7° C at a protein concentration of 0.6 gram per liter. As previously shown by Yasui (6, 7) the inactivation rate is practically independent of pH from pH 7.5 to pH 8.5. Above pH 8.5, however, the inactivation rate increases sharply with pH. Points on the curve between pH 9.2 and pH 9.64 give a straight line of slope 1.35. Above pH 10, myosin is inactivated so rapidly that rates are difficult to measure at 35° C. Accordingly, above this pH, inactivation was studied at a lower temperature. Figure 4 shows the results obtained at 11.8° C from pH 10.25 to pH 10.62. The slope of the curve obtained has a value of approximately 4.5.

Can. J. Chem. Downloaded from www.nrcresearchpress.com by 210.87.254.40 on 09/05/12
For personal use only.

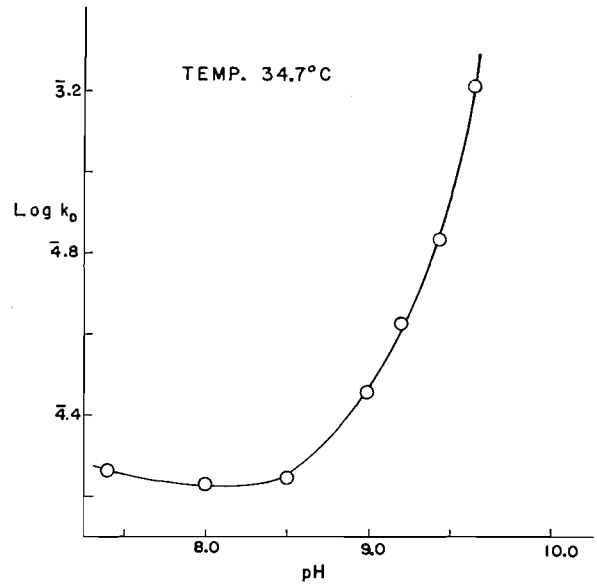


FIG. 3. Variation of the inactivation constant k_D (in sec^{-1}) as a function of pH at 34.7° C.

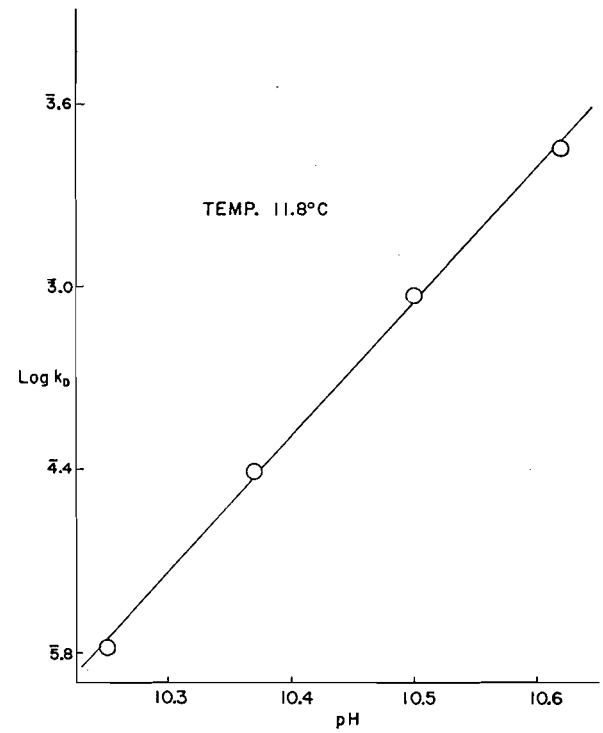


FIG. 4. Variation of k_D (in sec^{-1}) as a function of pH at 11.8° C at high pH.

Can. J. Chem. Downloaded from www.nrcresearchpress.com by 210.87.254.40 on 09/05/12
For personal use only.

Influence of Temperature

The variation of the rate of inactivation of myosin with temperature follows the usual Arrhenius law. Figure 5 gives the usual plot of log k_D versus $1/T$. The energy of

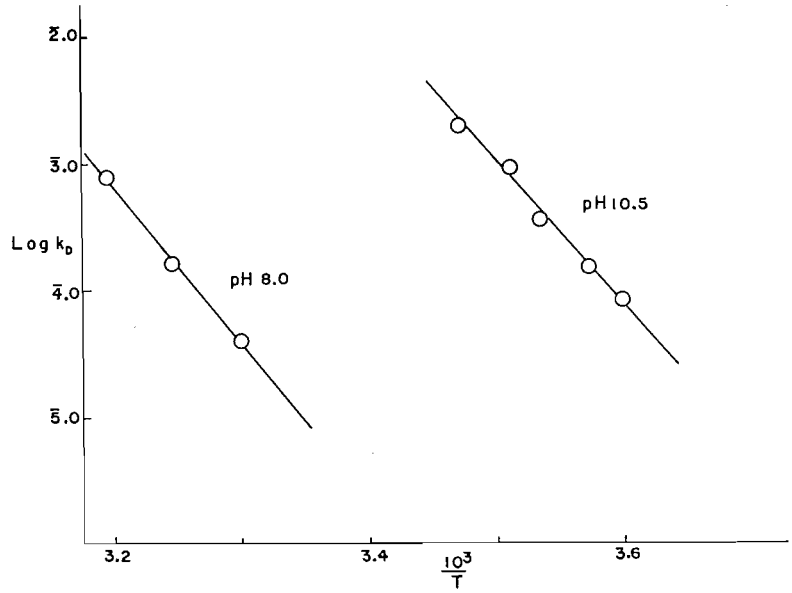


FIG. 5. Influence of temperature on the inactivation rate of myosin.

activation is 56 kcal mole^{-1} at pH 8.0 and 58 kcal mole^{-1} at pH 10.5. The data at pH 8.0 were obtained from 30 to 40° C and those at 10.5 from 5 to 15° C. Using the well-known Eyring's relation, the entropies of activation are calculated to be 107 cal deg^{-1} mole^{-1} at pH 8.0 and 137 cal deg^{-1} mole^{-1} at pH 10.5. These large energies and entropies of activation are normal for enzyme inactivation and protein denaturation. For myosin, Yasui *et al.* (7) have reported an energy of activation of 57 kcal mole^{-1} at pH 7.5, a value in line with ours.

The discussion of the effects of hydrogen ion concentration and temperature should refer to the classical work of Levy and Benaglia (14). The basic hypothesis is made that the protein exists in different ionic states, dependent on the pH, and that each species has a different inactivation rate constant.

The fact that the order increases monotonously at almost five with respect to hydroxyl ion concentration would indicate that the lowest pK of ionization is larger than 10. The fractional order would suggest that a plot of $1/k_D[H^+]^4$ vs. $[H^+]$ might yield the ionization constant. However, pH measurements are not accurate enough to justify such operations.

The energy of activation of 56 kcal mole^{-1} comes within 10 kcal of the accepted value (67 kcal) for the S—S bond (15). Although the idea of the breaking of a single bond to form the active complex is attractive, it is difficult to imagine that the breaking of a cystine bridge should involve such a large entropy change in the activated state. The breaking of several low-energy bonds, possibly accompanied by dehydration, might correspond to the structural changes usually mentioned in connection with this phenomenon. It would require, for example, the breaking of a large number of hydrogen bonds to lower the energy of activation to a reasonable value. These could be expressed as a

Can. J. Chem. Downloaded from www.nrcresearchpress.com by 210.87.254.40 on 09/05/12
For personal use only.

series of equilibrium constants and would participate in the thermodynamics of formation of the activated complex as long as the concentration of the species is small compared with the total concentration of the enzyme. We believe that such structural changes are important in the case of myosin. This could be accompanied by considerable dehydration as advanced by Klotz (16).

At higher pH, the dependence of the rate on hydrogen ion concentration forces us to consider the proton dissociation. As the proteinic groups ionizing in alkaline solutions (SH, OH, phenol, NH_3^+) have heats of ionization from 6 to 13 kcal mole^{-1} (17), four to five of these could explain a major part if not all of the energy of activation of 58 kcal mole^{-1}.

A group with a pK of ionization higher than 10 has a standard free energy of ionization larger than 13 kcal mole^{-1}. This value, combined with the above heats of ionization, leads to a negative entropy of ionization, which is in line with the reported values (18, 19).

If the reference state for myosin is taken as the five times ionized species, rather than the non-ionized species, the energy of activation is drastically reduced but the entropy of activation is increased. A plausible interpretation would then involve structural changes possibly similar to those postulated at lower pH. Structural changes possibly pertaining to inactivation at high pH have been described by Blum (2).

It is also possible that the ionization of specific groups is less important than the charge on the enzyme. A comparison between the curve in Fig. 3 and the curve representing the charge on the protein as a function of pH, as published by Mihalyi (20), has led to the relation plotted in Fig. 6. The rather good straight line obtained when

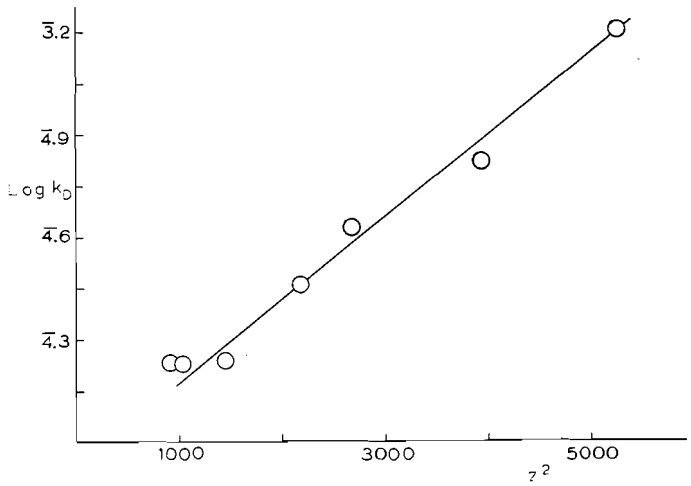


FIG. 6. Plot of log k_D as a function of the square of the charge on myosin, Z^2; k_D at 34.7° C (Fig. 4), Z is read off a figure representing titration data obtained by Mihalyi (20) at 38° C.

the logarithm of k_D is plotted against the square of the charge would indicate that the stability of the protein far from its isoionic point depends on its charge. Of course, the energy of activation should then be calculated for conditions involving the same charge on the protein molecule. With the present data, this is not possible.

CONCLUSION

As with all protein denaturation processes, the inactivation of myosin is complex and it is difficult to suggest a simple mechanism that would account for all the experimental

Can. J. Chem. Downloaded from www.nrcresearchpress.com by 210.87.254.40 on 09/05/12
For personal use only.

data. The order of the reaction with respect to concentration can be readily explained on the basis of protection but temperature and hydrogen ion concentration effects cannot be rationalized by a simple explanation. At low pH's where the rate is pH independent, it seems that structural changes and (or) dehydration are the main factors. At high pH's, however, dissociation most certainly occurs on inactivation. Dissociation in this region can account for the high energies of activation observed but cannot explain the high entropies of activation obtained. In fact, dissociation would most probably increase to a considerable extent the already high entropy terms. Considerable structural changes and (or) extensive dehydration of the protein would therefore seem to be required to account for the data. If the active center is a small area, the considerable amount of structural changes or the large amount of dehydration necessary to account for the thermodynamic values obtained suggest that the process measured in these experiments is not merely the inactivation of the active center but the denaturation of the protein as a whole, leading to a loss of enzymatic activity. The influence of pH could also be interpreted as a purely electrostatic effect.

With regards to the investigation on the influence of hydrogen ion concentration the following practical remarks can be made on the stability of myosin ATPase at high pH's. The data show that at pH 10.5 the half-life of myosin is approximately 42,000 seconds at 0° C, 8000 at 5° C, and 2000 seconds at 10° C. At pH 10.7 the pH dependence is such that these figures must be divided by a factor of 8. As a normal kinetic run for the measurement of the rate of hydrolysis of ATP takes about 200 seconds, data obtained above pH 10.7 would not be reliable except in the vicinity of 0° C. At pH 10.5, the upper limit of temperature would be 5° C, while that at pH 10.3, 10° C would be a maximum value. Above these limits, any decrease in activity could be attributed to enzyme inactivation unless there is a definite protection by the substrate.

REFERENCES

1. W. F. H. M. Mommaerts and K. Seraidarian. J. Gen. Physiol. **30**, 401 (1947).
2. J. J. Blum. Arch. Biochem. Biophys. **43**, 176 (1953).
3. L. Ouellet, K. J. Laidler, and M. F. Morales. Arch. Biochem. Biophys. **39**, 37 (1952).
4. W. F. H. M. Mommaerts and I. Green. J. Biol. Chem. **208**, 833 (1954).
5. B. F. Poglasov, V. Biluski, and A. A. Baew. Biokhimiya, **23**, 269 (1958).
6. T. Yasui, T. Fukazawa, Y. Hashimoto, and A. T. Sasaki. J. Biochem., (Tokyo), **45**, 717 (1958).
7. T. Yasui, Y. Hashimoto, and Y. Tonomura. Arch. Biochem. Biophys. **87**, 55 (1960).
8. J. Botts and M. F. Morales. J. Cellular Comp. Physiol. **37**, 27 (1951).
9. W. F. Hillebrand, G. E. F. Lundell, H. A. Bright, and J. I. Hoffman. Applied inorganic analysis. John Wiley & Sons, Inc., New York. 1953.
10. C. H. Fiske and J. SubbaRow. J. Biol. Chem. **81**, 629 (1929).
11. M. Letort. Bull. soc. chim. France, **9**, 1 (1942).
12. M. A. Lauffer and W. C. Price. J. Biol. Chem. **133**, 1 (1940).
13. S. Nakayama and Y. Kono. J. Biochem., (Tokyo), **44**, 25 (1957).
14. M. Levy and E. Benaglia. J. Biol. Chem. **186**, 829 (1950).
15. T. L. Cottrell. The strength of chemical bonds. Butterworth Scientific Publications, London. 1954. p. 445.
16. I. M. Klotz and H. G. Gurme. J. Am. Chem. Soc. **70**, 939 (1948).
17. E. J. Cohn and J. T. Edsall. Proteins, amino acids, and peptides. Reinhold Publishing Corp., New York. 1943. p. 445.
18. H. M. Papée, W F. Canady, T. W. Zawidzki, and K. J. Laidler. Trans. Faraday Soc. **55**, 1734 (1959).
19. R. A. Alberty. *In* The proteins. Vol. I. *Edited by* H. Neurath and K. Bailey. Academic Press Inc., New York. 1953. p. 472.
20. E. Mihalyi. Enzymologia, **14**, 224 (1950).

Can. J. Chem. Downloaded from www.nrcresearchpress.com by 210.87.254.40 on 09/05/12
For personal use only.

Can. J. Chem. Downloaded from www.nrcresearchpress.com by 210.87.254.5 on 09/05/12
For personal use only.

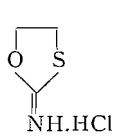
THE REARRANGEMENT OF 2-IMINO-1,3-OXATHIANE[1]

MARCEL MENARD, AVERIL M. WRIGLEY, AND FRANCIS L. CHUBB

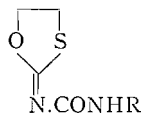
ABSTRACT

2-Imino-1,3-oxathiolane, in the free state, evolves cyanic acid spontaneously and gives rise to ethylene sulphide. This rearrangement is characteristic of all substituted 2-imino-1,3-oxathiolanes. It has now been found that rearrangement of the next higher homologue, 2-imino-1,3-oxathiane, does not give the anticipated trimethylene sulphide but only tris-3-mercaptopropyl cyanurate. The mechanism of this rearrangement is discussed.

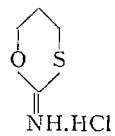
Wagner-Jauregg and Haring (1) have reported the synthesis and reactions of a series of 2-imino-1,3-oxathiolane hydrochlorides (I) and N-carbamyl-2-imino-1,3-oxathiolanes (II). Several of the last-mentioned compounds possessed hypoglycemic activity. They also prepared 2-imino-1,3-oxathiane (III) by the action of thiocyanic acid on trimethylene oxide. The work herein reported, which describes the preparation of some new derivatives of III, was undertaken in the hope of obtaining some new hypoglycemic compounds.



(I)

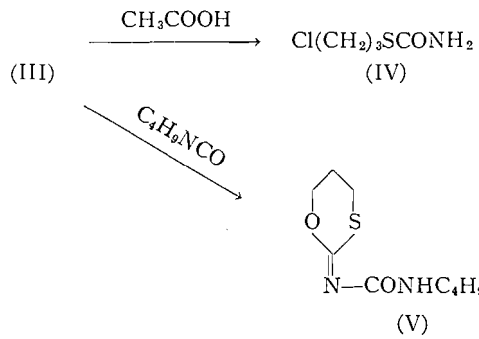


(II)



(III)

3-Hydroxypropyl thiocyanate was obtained in 55% yield from the corresponding chloroalcohol. Cyclization with hydrogen chloride in ether solution at 0° afforded a good yield of a water-soluble hydrochloride which was found to be identical with the 2-imino-1,3-oxathiane (III) described by Wagner-Jauregg and Haring. On standing, or upon heating for a few minutes with glacial acetic acid, III was transformed into a water-insoluble chlorine-containing compound. This rearrangement is similar to that of I which is rapidly converted to 2-chloroethylthiol carbamate in boiling acetic acid. The infrared spectrum and analytical data showed that this compound was the analogous 3-chloropropylthiol carbamate (IV). IV was also obtained by the action of hydrogen chloride on 3-hydroxypropyl thiocyanate at room temperature. The reaction of *n*-butyl isocyanate with III in aqueous dioxane yielded the expected N-(butylcarbamyl)-2-imino-1,3-oxathiane (V).

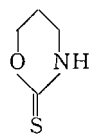


(V)

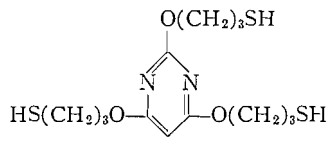
[1]*Manuscript received October 4, 1960.*
Contribution from the Department of Organic Chemical Research, Frank W. Horner Limited, Montreal, Que.

The reaction of III with potassium cyanate afforded none of the expected N-carbamyl derivative, analogous to II, but a crystalline compound having the same empirical formula as the free 2-imino-1,3-oxathiane. It was found that the compound was also obtained by the action of 1 mole of carbonate or hydroxide on III, which suggested that it was a rearrangement product. Infrared data showed the presence of the —SH, —C=N—, and —C—O—C— groups in the molecule. Of the possible rearrangement products tetrahydro-1,3-oxazine-2-thione (VI) seemed the most probable, since rearrangement of III to VI could be expected to take place through ring opening and recyclization (2). But synthesis of VI by two unequivocal methods (3, 4) gave a compound different from the rearrangement product. Acid or basic hydrolysis of the rearrangement product yielded cyanuric acid and in the case of acid hydrolysis, an elastic sulphur-containing polymer. An elastic polymer was again obtained when the rearrangement product was oxidized with hydrogen peroxide, indicating that more than one thiol group may have been present in the molecule.

Finally attempted desulphurization with lead nitrate was unsuccessful, but desulphurization with Raney nickel yielded a solid melting at 30–33°, which was shown to be tris-*n*-propyl cyanurate. This established the structure of the rearrangement product as tris-mercaptopropyl cyanurate (VII).



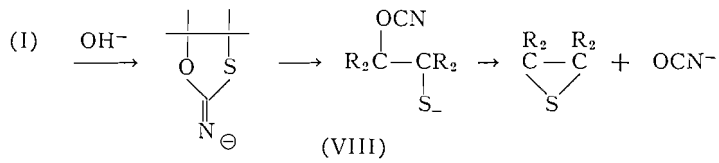
(VI)



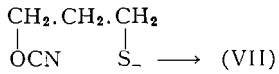
(VII)

That 2-imino-1,3-oxathiolanes are intermediates in the conversion of ethylene oxides to episulphides has been shown by Van Tamelen (5) and Price and Kirk (6). The mechanism of the conversion of 2-imino-1,3-oxathiolanes to episulphides as proposed by Van Tamelen is shown below. The abnormal behavior of 2-imino-1,3-oxathiane, compared with the corresponding oxathiolanes, can be easily understood in terms of this mechanism. Once the ring has opened to form the mercaptoalkyl cyanate (VIII) two reactions are possible. Alkyl cyanates are unstable substances which normally trimerize to cyanurates. However, another competing reaction is the backside attack of the sulphur atom on the adjacent carbon to form an episulphide. In the case of the mercaptoethyl cyanate the trans conformation of the intermediate is energetically favored and steric conditions for the S_N2 displacement of the cyanate ion by sulphur are favorable. Hence formation of the episulphide is expected to predominate. This is in accord with the results of Van Tamelen (5) and Price and Kirk (6), who have isolated good yields of episulphides by the treatment of 2-imino-1,3-oxathiolanes with base. In the case of the mercaptopropyl intermediate (IX) the steric requirements for the formation of the four-membered sulphide ring are not so easily fulfilled as is shown by the slow rate of formation of trimethylene oxides as compared with ethylene oxides (7). The trimerization reaction might be expected to be faster in this case, and this is confirmed by formation of VII from III in 80% yield.

Can. J. Chem. Downloaded from www.nrcresearchpress.com by 210.87.254.5 on 09/05/12
For personal use only.



(VIII)



(IX)

EXPERIMENTAL

Melting points are uncorrected. Microanalyses were performed by E. Thommen, Thannerstrasse 45, Basel, Switzerland.

3-Hydroxypropyl Thiocyanate

To a boiling solution of 130 g (1.3 moles) of potassium thiocyanate in 340 ml of 95% ethanol, 94.5 g (1 mole) of 3-chloropropanol was slowly added. After the mixture was stirred and refluxed for 4 hours it was allowed to stand overnight. Following the evaporation of about 250 ml of ethanol on the steam cone 500 ml of water was added and the solution was extracted with 3×150 ml ether. The combined organic layers were washed with water, dried, and concentrated. Distillation of the residue yielded 64.5 g (55%) of 3-hydroxypropyl thiocyanate, boiling at 140–150° under a pressure of 25 mm. No analysis is reported for this compound since it is unstable like the corresponding 2-hydroxyethyl thiocyanate (6).

2-Imino-1,3-oxathiane Hydrochloride

An excess of dry hydrogen chloride was passed through a solution of 41 g of 3-hydroxypropyl thiocyanate in 200 ml of anhydrous ether at 0° in an ice bath. After standing for 1 hour the crystalline hydrochloride was filtered and washed with ether. A yield of 47 g (87%), m.p. 88° (lit. m.p. 81.5–83°), was obtained.

3-Chloropropylthiol Carbamate

(a) From 3-hydroxypropyl thiocyanate.—An excess of dry hydrogen chloride was passed through 21 g of 3-hydroxypropyl thiocyanate at room temperature. The solid was broken up, suspended in ether, and treated again with dry hydrogen chloride. Filtration of the solid and recrystallization from water gave 19.2 g (70%) of colorless plates melting at 101–102°. Anal. Calculated for C_4H_8ONSCl: C, 31.27; H, 5.25; N, 9.12%. Found: C, 31.63; H, 5.26; N, 9.07, 9.27%. Infrared spectrum: maxima at 3580, 3475 cm^{-1} (N—H), and 1700, 1590 cm^{-1} (amide I and II).

(b) From 2-imino-1,3-oxathiane hydrochloride.—A mixture of 5 g of 2-imino-1,3-oxathiane hydrochloride and 25 ml of glacial acetic acid was stirred and heated on the steam bath for 1 hour. Water was added to the cooled solution and the crystalline thiolcarbamate was filtered and recrystallized from water to give 2.9 g (58%) of colorless plates melting at 101–102°, not depressed on admixture with a sample prepared according to (*a*).

N-(Butylcarbamyl)-2-imino-1,3-oxathiane

2-Imino-1,3-oxathiane hydrochloride (2 g) and butyl isocyanate (1.3 g) were slurried in 10 ml of dioxane. Anhydrous sodium carbonate (1 g) was added and the mixture was

Can. J. Chem. Downloaded from www.nrcresearchpress.com by 210.87.254.5 on 09/05/12
For personal use only.

stirred and heated to 60° but with no reaction. After the addition of 10 ml of water, heat was evolved and an oil separated. Stirring was continued for 15 minutes, a further 20 ml of water was added, and the mixture was extracted with ether (3×10 ml). The combined organic layers were washed with water, dried, and concentrated. Repeated recrystallization of the residue from ethyl acetate – petroleum ether gave 1.7 g (60%) of a white powder melting at 91–92°. Anal. Calculated for $C_9H_{16}O_2N_2S$: C, 49.59; H, 7.46; N, 12.95%. Found: C, 49.96; H, 7.56; N, 13.80%.

Tris-3-mercaptopropyl Cyanurate

An aqueous solution of 1 equivalent of either potassium cyanate, potassium acetate, or sodium carbonate was added all at once to a freshly prepared solution of 1 equivalent of 2-imino-1,3-oxathiane hydrochloride in water. An exothermic reaction took place and a white precipitate soon appeared. After standing for 1 hour the solid was filtered and recrystallized from 95% ethanol to give a 75% yield of colorless needles melting at 97°. A slow titration of 2-imino-1,3-oxathiane hydrochloride in the cold with 1 *N* sodium hydroxide yielded the same compound. Anal. Calculated for $C_{12}H_{21}O_3N_3S_3$: C, 41.00; H, 6.02; N, 11.95%. Found: C, 40.93; H, 5.96; N, 11.90, 12.06%. Infrared spectrum: maxima at 2550 cm^{-1} (SH), 1580 (—C=N—), and 1145 cm^{-1} (—C—O—C—).

Hydrolysis of tris-3-Mercaptopropyl Cyanurate

(a) Alkaline.—The mercaptopropyl cyanurate (0.5 g) was refluxed for 2 hours with 20 ml of a 20% sodium hydroxide solution. On cooling a colorless solid was obtained which was filtered, washed with dilute hydrochloric acid, and recrystallized from water to give 0.15 g of cyanuric acid.

(b) Acidic.—The cyanurate (0.5 g) was refluxed for 2 hours with 20 ml of a 30% sulphuric acid solution. On cooling, colorless needles of cyanuric acid were obtained. A sulphur-containing polymer was formed on the wall of the condenser.

Desulphurization of tris-Mercaptopropyl Cyanurate

A mixture of 2 g of tris-mercaptopropyl cyanurate, 100 ml of 95% ethanol, and 15 g of Raney nickel was stirred and refluxed for 2 hours. Filtration of the catalyst, removal of the solvent, and distillation of the residue furnished 0.2 g (13%) of a colorless liquid, $b.p._{10}$ 180°, which solidified in ice to give colorless crystals melting at 30–33°. A mixed melting point determination and a comparison of infrared spectra have shown this compound to be identical with tris-*n*-propyl cyanurate (8).

Tetrahydro-1,3-oxazine-2-thione

(*a*) Carbon disulphide (20 ml) was added in small portions to a solution of 24.2 g of propanolamine in 50 ml of methanol cooled in an ice bath. With the temperature kept at 0°, a methanolic solution of iodine (15%) was added slowly from a burette until a faint permanent yellow color was obtained. The white solid, which had precipitated, was filtered, washed several times with methanol, and slurried in 150 ml of water. The slurry was then gradually heated to boiling over a period of 1 hour. The resulting solution was acidified with dilute sulphuric acid, cooled, filtered to remove suspended sulphur, saturated with sodium chloride, and extracted many times with small portions of ethyl acetate. Concentration of the ethyl acetate solution yielded 5 g (13%) of a white powder, m.p. 125–126°. Recrystallization of this solid from ethanol afforded 3.2 g of colorless needles melting at 125–126°. Anal. Calculated for C_4H_7ONS: C, 41.00; H, 6.02; N, 11.96; S, 27.37%. Found: C, 41.18; H, 6.07; N, 11.72; S, 27.00%.

(*b*) A solution of 12.3 g of propanolamine and 11 g of potassium hydroxide in 100 ml of

Can. J. Chem. Downloaded from www.nrcresearchpress.com by 210.87.254.5 on 09/05/12
For personal use only.

water, kept at 0° in an ice bath, was stirred vigorously for 5 minutes with a solution of 13 g of carbon disulphide in 80 ml of dioxane; 5.5 g of potassium hydroxide in 100 ml of water was added followed by a solution of 55 g of lead nitrate in 300 ml of water. The suspension was stirred at 60° for ½ hour and the precipitated lead sulphide was filtered and washed with hot water. Concentration of the filtrates under reduced pressure left a dark residue which was extracted twice with 350 ml of boiling benzene. Evaporation of the benzene extracts afforded 13.2 g (70%) of crude product which, upon recrystallization from ethanol, yielded 11 g of colorless needles melting at 125–126° and giving no melting point depression with a sample prepared according to (*a*).

REFERENCES

1. T. WAGNER-JAUREGG and M. HARING. Helv. Chim. Acta, **41**, 377 (1598).
2. P. G. SERGEEV and B. S. KOLYCHEV. J. Gen. Chem. (U.S.S.R.) (Eng. Transl.) **7**, 1390 (1937); Chem. Abstr. **32**, 2534.
3. A. A. ROSEN. J. Am. Chem. Soc. **74**, 2994 (1952).
4. M. G. ETTLINGER. J. Am. Chem. Soc. **72**, 4792 (1950).
5. E. E. VAN TAMELEN. J. Am. Chem. Soc. **73**, 3444 (1951).
6. C. C. PRICE and P. F. KIRK. J. Am. Chem. Soc. **75**, 2396 (1953).
7. G. M. BENNETT. Trans. Faraday Soc. **37**, 794 (1941).
8. M. SPIELMAN, W. CLOSE, and I. WILK. J. Am. Chem. Soc. **73**, 1775 (1951).

Can. J. Chem. Downloaded from www.nrcresearchpress.com by 210.87.254.5 on 09/05/12
For personal use only.

Can. J. Chem. Downloaded from www.nrcresearchpress.com by 210.87.254.6 on 09/05/12
For personal use only.

THE OXIDATION OF DI-*tertiary*-BUTYL PEROXIDE[1]

A. R. BLAKE[2] AND K. O. KUTSCHKE

ABSTRACT

The oxidation of di-*t*-butyl peroxide has been investigated in a static system at low conversion at 124° C with sufficient oxygen present to suppress completely the formation of methane and ethane. The decomposition of the *t*-butoxy radical is unaffected by the presence of oxygen. A major product of the oxidation is formaldehyde whose yield rapidly approaches a stationary value. It is postulated that the major source of formaldehyde is the decomposition of methyl peroxy radicals, which may also abstract hydrogen from formaldehyde to form methyl hydroperoxide, and that this competition leads to the stationary concentration of formaldehyde actually observed. Methyl hydroperoxide was demonstrated to be unstable in the system and the predominant decomposition product was methanol, a compound also found in high yields in the oxidation. Experiments with added formaldehyde-C^{13} showed that formaldehyde can be converted to carbon monoxide in the system and indicated that formaldehyde was a likely precursor to the carbon monoxide found in the oxidation.

INTRODUCTION

The pyrolysis of di-*t*-butyl peroxide (DTBP) provides a particularly convenient source of methyl radicals because of the high activation energy (1) required for the abstraction of hydrogen from that compound. Raley *et al.* (2) used this method to study the oxidation of methyl radicals but their reactions were carried to large conversions. The experiments reported by Bose (3) were also done at high conversion. The present study was undertaken to extend this work to lower (<5%) conversions and to investigate the effect of conversion on the rates of production of the major products. The role of formaldehyde as a hydrogen donor in the photooxidation of azomethane has been investigated previously in this laboratory (4, 5, 6). Experiments are reported in which formaldehyde-C^{13} was added to the reactants in the present system to investigate this point further.

EXPERIMENTAL

Most of the apparatus was the same as that described in a previous communication (1). A reaction was started by expanding a mixture of oxygen and DTBP from a preheater held at 80° C, where pressures could be measured on a quartz spiral gauge, to the Pyrex reaction vessel (volume, 550 ml) the temperature of which could be held to within 0.1° C.

Analyses were made for carbon monoxide, acetone, methanol, and formaldehyde; the yields of methane and ethane were vanishingly small. Formaldehyde, oxygen, and carbon monoxide were separated from the liquid products (acetone, methanol, and unreacted DTBP) by passage through a trap held at −130° C. Formaldehyde was condensed in a second trap at −196° C and the permanent gases were transferred to a tube containing a mixture of copper and cupric oxide where the carbon monoxide was oxidized at 270° C. The liquid products were analyzed by gas chromatography on a 10-ft column containing 25% dinonyl phthalate and 5% glycerol on Fisher Columpak (30–60 mesh). With a hydrogen flow rate of 45 ml/minute at 29° C appearance times of 28, 56, 77, and 121 minutes were observed for acetone, methanol, *t*-butanol (present as an impurity), and DTBP, respectively.

[1]*Manuscript received September 26, 1960.*
Contribution from the Division of Pure Chemistry, National Research Council, Ottawa, Canada.
Issued as N.R.C. No. 6097.
[2]*National Research Council Postdoctorate Fellow 1957-59. Present address: The Chemistry Department, the University of Bristol, Bristol, England.*

Considerable difficulty has been encountered in the past in the analysis of small amounts (less than 10 μmoles) of formaldehyde in the presence of large amounts (several hundred micromoles) of unchanged reactant. The analytical procedure used for this analysis will, therefore, be reported in some detail. Part of the analytical system is shown in Fig. 1.

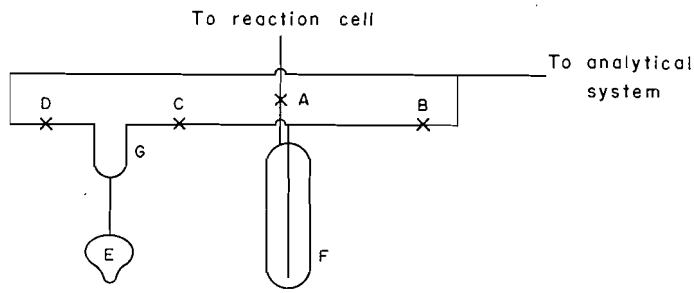


FIG. 1. Part of the apparatus used for the separation of formaldehyde. A, metal valve; B, C, and D, mercury cutoffs.

To stop a reaction, valve A (Hoke type 413 situated within the thermostat) was opened with B closed and D and C open. Liquid products were collected in trap F at $-130°$ C and formaldehyde was collected in the U-tube G at $-196°$ C. The permanent gases were transferred to the rest of the analytical system at this time. Liquid products were removed from F with C and D closed. All of the apparatus between A, B, and D was then heated to 150° C to volatilize any polymerized formaldehyde and the monomeric material was collected in bulb E at $-196°$ C which had been charged previously with 7.5 ml concentrated H_2SO_4 and 2 ml of chromotropic acid solution (7) (0.6 g disodium salt of chromotropic acid in 25 ml water). Bulb E was sealed off, heated for 30 minutes, and the colored solution which resulted diluted to 50 ml. The optical density of the solution at 570 mμ was measured and the formaldehyde yield estimated by comparison with a calibration curve.

DTBP was purified as described previously (1); a residual of about 0.1% *t*-butanol could not be removed. Oxygen was prepared by heating potassium permanganate *in vacuo*. Formaldehyde was obtained by heating α-polyoxymethylene containing 20.6% C^{13}; the polymer was provided by Dr. L. C. Leitch of these laboratories. A sample of methyl hydroperoxide was also supplied by Dr. Leitch.

RESULTS

Products of the oxidation of DTBP at 124° C are shown in Table I. Traces of isobutylene oxide were also formed and the presence of this compound hampered the mass spectrometric estimation of carbon dioxide since a cracking pattern for the former was not available. Consequently data for the yields of carbon dioxide are not recorded.

The formation of acetone was virtually unaffected by the addition of oxygen. Rate constants, k_1, for the pyrolysis of DTBP calculated from the acetone formed in the experiments in Table I are in excellent agreement with the value 0.105×10^{-4} sec^{-1} which had been obtained at the same temperature in the absence of oxygen (1).

The variation of the yields of the various products with time of reaction are shown in Fig. 2. The high yields of formaldehyde relative to those of methanol in the early stages

Can. J. Chem. Downloaded from www.nrcresearchpress.com by 210.87.254.6 on 09/05/12
For personal use only.

TABLE I

Products of the oxidation at 124° C
(Reaction volume = 550 ml)

Time (sec)	DTBP (10^{-6} mole/ml)	O_2	$(CH_3)_2CO$	CH_2O (10^{-6} mole)	CH_3OH	CO	k_1* (10^{-5} sec^{-1})	Con.† (%)	C‡ Balance	H§
1000	0.352	0.538	4.7	1.5	0.41	0.41	1.21	1.2	0.56	0.63
2000	0.354	0.525	8.0	5.1	1.49	0.81	1.04	2.1	0.93	0.66
2500	0.363	0.522	—	7.2	—	—	—	—	—	—
3000	0.354	0.502	12.7	7.9	1.89	1.34	1.09	3.3	0.94	0.66
4000	0.356	0.525	17.0	10.0	3.18	2.00	1.09	4.4	0.92	0.63
4000	0.356	0.522	15.6	—	3.37	—	0.99	5.0	—	—
5000	0.363	0.492	21.1	—	4.27	2.93	1.06	5.3	—	—
6000	0.354	0.522	25.2	11.7	6.66	3.37	1.08	6.5	0.90	0.64
7000	0.355	0.522	—	13.9	—	4.24	—	—	—	—
7500	0.355	0.518	31.8	—	10.1	—	1.09	8.2	—	—
50000‖	0.352	0.513	134	(16)	55.6	37.7	0.69	34.5	(0.91)	(0.66)

*k_1 = $[(CH_3)_2CO]/2[DTBP]t$.
†Conversion (%) = $100([(CH_3)_2CO]/2[DTBP])$.
‡Carbon balance = $([CH_2O]+[CH_3OH]+1.25[CO])/[(CH_3)_2CO]$.
§Hydrogen balance = $(2[CH_2O]+4[CH_3OH])/3[(CH_3)_2CO]$.
‖Values in parentheses calculated from an assumed carbon balance of 0.91.

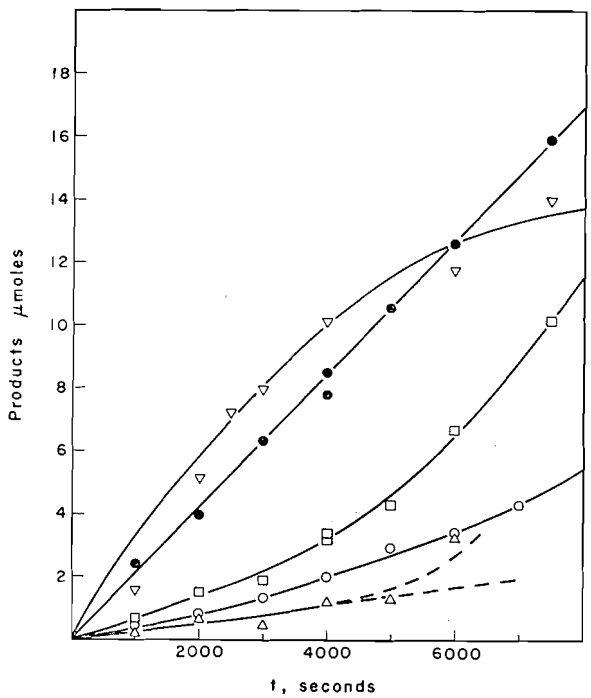


FIG. 2. Yields of products at various times: ● 1/2 acetone; ▽ formaldehyde; □ methanol; ○ carbon monoxide; △ methanol – carbon monoxide – carbon dioxide.

of the reaction are particularly striking; after 1000 seconds of reaction, $[CH_2O]/[CH_3OH] = 4$. As the reaction proceeds this ratio decreases markedly because of an increase in the rate of formation of methanol and a decrease in that of formaldehyde. It is evident that the yield of the latter approaches a stationary value at about 15 μmoles, which corresponds to 2.7×10^{-8} mole/ml. This point is emphasized by the single experiment at 34% conversion; if a carbon balance of 0.91 is assumed for that experiment, the formaldehyde yield corresponds to 3×10^{-8} mole/ml. In agreement with the data of Raley *et al.* (2),

Can. J. Chem. Downloaded from www.nrcresearchpress.com by 210.87.254.6 on 09/05/12
For personal use only.

the present results indicate that methanol and carbon monoxide are indeed the major products found in this system at high conversions.

Material balances based on acetone are also given in Table I. For the calculation of the carbon balance it was assumed that $CO_2/CO = 0.25$ as has been obtained recently in the photooxidation of azomethane (6). Uncertainties in this assumption will have only a small effect on the carbon balance. From the balances shown in Table I it would appear that all the major carbon-containing compounds were determined and that the only product likely to have been missed was, as indicated by the low hydrogen balance, water. No attempt was made to measure this product.

The addition of formaldehyde-C^{13} to the system caused a marked increase in the rate of formation of carbon monoxide in the early stages of the reaction. The enhanced rate was independent of time over the region studied and its value is similar to that approached by the rate of formation of carbon monoxide in the absence of added formaldehyde, Fig. 3. Mass spectrometric analysis of the carbon dioxide recovered from the copper/cupric oxide after oxidation of the carbon monoxide indicated enrichment in C^{13} (Table II).

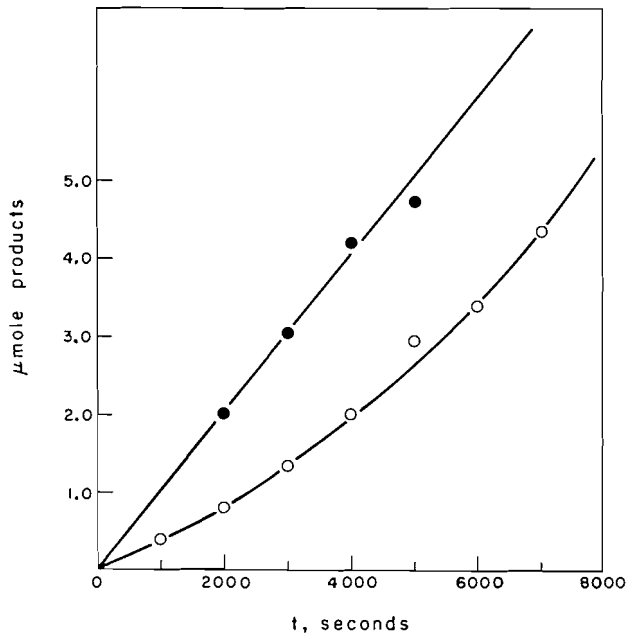


FIG. 3. Yields of carbon monoxide in the oxidation: ○ formaldehyde absent; ● 15 μmoles formaldehyde-C^{13} added.

TABLE II

Carbon monoxide yield in presence of 15 μmoles enriched CH_2O*

Time (sec)	Total CO (μmoles)	$C^{13}O/C^{12}O$	CO† (%)
2000	2.0	0.152	74
3000	3.0	—	—
4000	4.2	0.148	72
5000	4.7	0.132	64

*C^{13}/C^{12} in formaldehyde = 20.6%.
†Carbon monoxide derived from added formaldehyde-C^{13}.

Can. J. Chem. Downloaded from www.nrcresearchpress.com by 210.87.254.6 on 09/05/12
For personal use only.

Can. J. Chem. Downloaded from www.nrcresearchpress.com by 210.87.254.6 on 09/05/12
For personal use only.

DISCUSSION

The agreement between the rate constant for DTBP calculated from the rate of acetone formation in the presence of oxygen (Table I) and the known rate constant at the same temperature is strong evidence that the rate of formation of methyl radicals by [1] and [2] is unaffected by the presence of oxygen. Raley *et al.* came to the same conclusion (2).

$$(CH_3)_3COOC(CH_3)_3 \rightarrow 2(CH_3)_3CO \quad [1]$$

$$(CH_3)_3CO \rightarrow CH_3 + CH_3COCH_3 \quad [2]$$

The experiment of shortest duration in Table I indicates an enhanced rate of formation of acetone ($k_1 = 0.120 \times 10^{-4}$ sec^{-1}) at this conversion. This in turn suggests the possibility of radical attack on the peroxide followed by decomposition of the resulting free radical to *t*-butoxy radical and isobutylene oxide giving the elements of a chain reaction. Much more data is required at very low conversion before any definite conclusion can be drawn in this respect.

The material balances shown in Table I suggest that no important product containing carbon has been omitted in the analytical scheme. Carbon dioxide was not determined quantitatively but was identified by mass spectrometry and a rough estimate of its yield on this basis agreed with the ratio $CO/CO_2 \sim 4$ used in computing the material balance. The latter ratio was found in a recent reinvestigation of the photooxidation of azomethane (6), where it was proposed that these two products arise by a mechanism identical with that to be suggested below. The hydrogen balance indicates that relatively large quantities of hydrogen are unaccounted for; a relatively large yield of water, which was not estimated, could account for the decrement. Little can be said in this regard until reliable techniques are devised for the recovery of water from the system and for the determination of that compound in the mixture of liquid products.

It is important to note the trend with time (or conversion) of the yields of the various products. At very low conversions it would appear that formaldehyde is the only product; the hydrogen balance suggests that water is also formed in good yield. As formaldehyde builds up in the system carbon monoxide and methanol begin to appear. Even after 1000 seconds of reaction (about 1% conversion based on acetone formed) the ratio formaldehyde/methanol is as great as four. Thus one of the mechanisms suggested by Bell *et al.* (8) for the oxidation of methyl radicals, viz.,

$$CH_3 + O_2 \rightarrow CH_3O_2$$

$$2CH_3O_2 \rightarrow 2CH_3O + O_2$$

$$2CH_3O \rightarrow CH_3OH + CH_2O$$

cannot operate in the present system since it requires that the ratio formaldehyde/methanol be no greater than unity. If abstraction reactions of methoxy radicals leading to methanol are considered, the ratio is expected to be even less.

The association of methyl radicals with oxygen has been demonstrated to require a third body (9, 10, 11), and some evidence has been presented (10) which suggests that there are two modes of dissociation of the methyl peroxy radical formed initially.

$$CH_3 + O_2 \rightarrow CH_3O_2^* \quad [3]$$

$$CH_3O_2^* \rightarrow CH_3 + O_2 \quad [4]$$

$$CH_3O_2^* \rightarrow CH_2O + OH \quad [5]$$

$$CH_3O_2^* + M \rightarrow CH_3O_2 + M \quad [6]$$

Considering the relatively low total pressure used in these experiments it is not unreasonable to suggest that the present conditions would tend to favor [4] and [5] at the expense of [6]. This is especially so if it could be demonstrated that DTBP were not an efficient third body, M.

For these reasons it is proposed that reactions [1] to [5] describe the main features of the reaction in its early stages. Presumably the fate of hydroxyl radicals is reaction with DTBP to form water. The radical $CH_2(CH_3)_2COOC(CH_3)_3$ formed by that abstraction might decompose to isobutylene oxide and a *t*-butoxy radical so that, taken with [2], [3], and [5], the elements of a chain are present. It was pointed out above that the presence of a short chain in this region of conversion is not incompatible with the acetone yield observed.

As the reaction proceeds and formaldehyde accumulates in the system, reactions of methyl peroxy radicals with this substance become possible.

$$CH_3O_2^* + CH_2O \rightarrow CH_3O_2H + HCO \quad [7]$$

$$HCO + O_2 \rightarrow CO + HO_2 \quad [8]$$

$$\rightarrow CO_2 + OH \quad [9]$$

Reaction [7] inhibits the possible chain and its operation over a range of conversion will lead to the observed steady state in formaldehyde concentration and the formation of new products, methyl hydroperoxide and the oxides of carbon.

The former product has not been observed in the present system. However, it was demonstrated that a synthetic sample of methyl hydroperoxide (30 μmoles) introduced into the reaction vessel for 2000 seconds at 124° C was recorded by the analytical method as methanol along with small quantities of formaldehyde. Even when the sample was taken from the reaction cell to the mass spectrometer without an intervening chromatographic separation, no peak at *m/e* 48, which was prominent from the original material, was observed. It is not clear whether the decomposition was homogeneous, was catalyzed by the metal and glass surfaces, or was induced by mercury vapor. The observation is similar to that made by Cvetanović *et al.* (12, 13), who observed that ethyl hydroperoxide, after being mixed with liquid mercury, was converted, almost quantitatively, to ethanol, with only small amounts of acetaldehyde being formed. It is not in harmony with the observations of Hanst and Calvert (14), who found methyl hydroperoxide to be stable up to 200° C in their system.

Therefore it is proposed that reaction [7] is an important fate of the methyl peroxy radical formed in [6]. This should not be taken to imply that the radical must in all systems be in a vibrationally excited form, as the asterisk indicates, in order to undergo reaction [7]. As discussed above, however, it is felt that, in this system, a large fraction of these radicals are indeed in a high vibrational level.

The experiments with added formaldehyde-C^{13} were devised to test the suggestion that formaldehyde could act as the precursor to carbon monoxide in this system. Since the amount of formaldehyde added approximated closely to the steady-state concentration of that product, it was expected that the rate of formation of carbon monoxide should also be nearly that corresponding to the later stages of the reaction in the absence of added formaldehyde. The yields of carbon monoxide shown in Table II and Fig. 3 are fully in agreement with that prediction. The isotopic composition of the carbon monoxide (Table II) also shows that formaldehyde is an efficient source of carbon monoxide in this system. A similar conclusion was reached by an application of the same technique to the photooxidation of azomethane (6).

Can. J. Chem. Downloaded from www.nrcresearchpress.com by 210.87.254.6 on 09/05/12
For personal use only.

One further point should be mentioned. The mechanism proposed, if complete, requires that $[CH_3O_2H(=CH_3OH)]-[CO]-[CO_2]$ vanish for all conditions. Figure 2 shows that the data are not quite in agreement with this prediction since the function shows a slow but steady rise with conversion. This can be explained if it is assumed that, as it becomes more concentrated in the system, acetone can compete with formaldehyde in a reaction analogous to [7]. The data for the experiment of greatest duration also suggest that acetone is not completely inert in the system as indicated by the very low value of k_1 calculated from the acetone yield. Depletion of DTBP at this long time is not sufficient to account for the low yield of acetone in this experiment.

ACKNOWLEDGMENTS

The authors wish to thank Dr. E. W. R. Steacie for his continued interest in this work, Dr. M. Shahin for many helpful discussions, and Mrs. R. H. Riem for the mass spectrometric analyses.

REFERENCES

1. A. R. Blake and K. O. Kutschke. Can. J. Chem. **37**, 1462 (1959).
2. J. H. Raley, L. M. Porter, F. F. Rust, and W. E. Vaughan. J. Am. Chem. Soc. **73**, 15 (1951).
3. A. N. Bose. Trans. Faraday Soc. **55**, 778 (1959).
4. R. L. Strong and K. O. Kutschke. Can. J. Chem. **37**, 1456 (1959).
5. F. Wenger and K. O. Kutschke. Can. J. Chem. **37**, 1546 (1959).
6. M. Shahin and K. O. Kutschke. Can. J. Chem. **39**, 73 (1961).
7. C. E. Bricker and H. R. Johnson. Ind. Eng. Chem., Anal. Ed. **17**, 400 (1945).
8. E. R. Bell, J. H. Raley, F. F. Rust, F. H. Seubold, and W. E. Vaughan. Discussions Faraday Soc. **10**, 242 (1950).
9. D. E. Hoare and A. D. Walsh. Trans. Faraday Soc. **53**, 1102 (1957).
10. M. I. Christie. Proc. Roy. Soc. (London), A, **244**, 411 (1958).
11. W. C. Sleppy and J. G. Calvert. J. Am. Chem. Soc. **81**, 769 (1959).
12. R. J. Cvetanović and A. B. Callear. Private communication.
13. R. J. Cvetanović and A. H. Turner. Private communication.
14. P. L. Hanst and J. G. Calvert. J. Phys. Chem. **63**, 71 (1959).

Can. J. Chem. Downloaded from www.nrcresearchpress.com by 210.87.254.6 on 09/05/12
For personal use only.

Can. J. Chem. Downloaded from www.nrcresearchpress.com by 210.87.254.42 on 09/05/12
For personal use only.

RATES OF DECARBOXYLATION OF SUBSTITUTED ANTHRANILIC ACIDS IN NITROBENZENE SOLUTION[1]

G. E. Dunn and Russell Prysiazniuk

ABSTRACT

The synthesis of a series of meta- and para-substituted anthranilic acids is reported with their rates of decarboxylation in nitrobenzene solution at 210.5° C. The reaction is second order with respect to anthranilic acid. The rate is increased by electron-releasing substituents and decreased by deuterium in the functional groups. The relative rates are interpreted by means of the Hammett equation and its extensions and it is concluded that the rate-determining step involves attack by proton from one anthranilic acid molecule on carbon 1 of a second molecule.

Previous investigations of anthranilic acid decarboxylation have shown that the reaction is first order in boiling aqueous solution but catalyzed by mineral acids (1, 2). The aqueous-acid-catalyzed reaction was considered to involve attack by a proton from the mineral acid on carbon 1 of the aromatic ring (2) and therefore to belong to the class of S_E2 aromatic displacement reactions (3). Decarboxylation in the melt, however, must involve shift of a proton to the ring from one of the functional groups of anthranilic acid itself. Several possibilities for such a proton transfer are available: it may occur in the neutral acid or the zwitterion, it may involve the carboxyl group or the amino group, and it may be intermolecular or intramolecular. The present investigation is an attempt to decide among these various possibilities.

In order to determine whether the reaction is intermolecular or intramolecular it is desirable to know the order of the reaction. In the melt the reaction has been reported to be first order (2, 4) but this is not very informative since the composition of the reaction mixture changes during the decarboxylation from pure anthranilic acid to pure aniline. Since aniline could serve as proton donor it might take over the role of a second molecule of anthranilic acid in an intermolecular reaction. An aprotic solvent would be preferable and it must be a high-boiling one since the temperature required for thermal decarboxylation is around 200° C. We have had some success with 1-methylnaphthalene as solvent but nitrobenzene proved to be more satisfactory since it is a better solvent for acids. In both these solvents the reaction is second order with respect to anthranilic acid and the reaction is therefore probably intermolecular.

In an intermolecular reaction there are several possibilities for the rate-determining step. It may involve (*a*) hydrogen–oxygen bond breaking, (*b*) hydrogen–nitrogen bond breaking, (*c*) hydrogen–carbon bond making, or (*d*) carbon–carbon bond breaking. Stevens, Pepper, and Lounsbury have eliminated possibility (*d*) by showing that there is no carbon isotope effect in the decarboxylation of anthranilic acid either in aqueous solution or in the melt (2). The three remaining possibilities may be distinguished by the site of the rate-determining step: in (*a*) it is the carboxyl group, in (*b*) it is the amino group, and in (*c*) it is carbon 1 of the ring. We have attempted to decide among the possibilities by application of the Hammett equation to the rates of decarboxylation of substituted anthranilic acids.

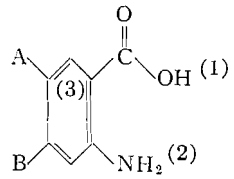
[1]*Manuscript received September 26, 1960.*
Contribution from the Chemistry Department of the University of Manitoba, Winnipeg, Manitoba. Presented in part, at the 42nd annual conference of the Canadian Institute of Chemistry, Halifax, May 1, 1959.

Hammett has shown (5) that the effect of substituents on the reactivity of a side chain in *m*- and *p*-substituted benzene derivatives can be expressed by the equation

$$\log k/k_0 = \rho\sigma$$

where k and k_0 are the rates or equilibrium constants for the reactions of the substituted and unsubstituted derivatives, respectively, ρ is a constant characteristic of the reaction, and σ is a constant characteristic of the substituent. The treatment has been extended by Brown and co-workers (6) to cover electrophilic aromatic substitution, in which the reaction site is on the ring instead of the side chain, by means of a new set of constants, σ^+. In a molecule where there are two or more possible reaction sites a substituent which is meta to one site may be para to the other so that its influence on the reactivity of the molecule will be different depending on the location of the reaction site. Jaffe has shown (7, 8) that in favorable circumstances this difference can be used to determine the location of the reaction site.

In anthranilic acid the three likely reaction sites may be numbered as shown below.



The influence of a substituent at A or B on reactivity at sites 1, 2, and 3 will be given by equations 1, 2, and 3, respectively,

[1] site 1: $\log k/k_0 = \rho_1\sigma_1$

[2] site 2: $\log k/k_0 = \rho_2\sigma_2$

[3] site 3: $\log k/k_0 = \rho_3\sigma_3$

where σ_1 is Hammett's σ for carboxylic acid reactions, σ_2 is Hammett's σ for amines and phenols, and σ_3 is Brown's σ^+. Of course, any two or all three reaction sites may be involved in the rate-determining step and the most general case is represented by equation 4,

[4] all sites: $\log k/k_0 = \rho_1\sigma_1+\rho_2\sigma_2+\rho_3\sigma_3$.

The nature of the reaction site may then be determined by finding which of equations 1–4 best fits the rates of decarboxylation of a series of substituted anthranilic acids. It should be noted that σ_1 differs most from σ_2 for substituents capable of strong mesomeric electron withdrawal while σ_1 differs most from σ_3 for substituents capable of strong mesomeric electron release. Therefore, substituents of both these types should be included in the series.

EXPERIMENTAL

Nitrobenzene and 1-methylnaphthalene were commercial products. They were fractionated through a 14-in. Vigreaux column, collecting the fractions boiling at 210–210.5° C at 745 mm and 240–241° C at 744 mm, respectively, and stored over anhydrous sodium sulphate and sodium wire, respectively. Anthranilic, 5-chloroanthranilic, N-methylanthranilic, N-phenylanthranilic, and *p*-aminobenzoic acids were commercial products recrystallized to constant melting point. The remaining acids were synthesized as de-

Can. J. Chem. Downloaded from www.nrcresearchpress.com by 210.87.254.42 on 09/05/12
For personal use only.

Can. J. Chem. Downloaded from www.nrcresearchpress.com by 210.87.254.42 on 09/05/12
For personal use only.

scribed below. Melting points were determined with a Hershberg melting point apparatus (9) using Anschütz thermometers calibrated against a U.S. Bureau of Standards platinum resistance thermometer.

4-Bromoanthranilic Acid

o-Acetotoluidide was prepared by the method of Berkenheim and Livshits (10). *o*-Toluidine, 100 ml (0.93 mole), was refluxed with 102 ml of acetic anhydride (1.00 mole) in 200 ml of benzene for 1 hour. The benzene was distilled off and the residue was poured over ice. The crude product was recrystallized from benzene and 106 g of *o*-acetotoluidide (70% yield), m.p. 110–111° C, was obtained.

o-Acetotoluidide was brominated by an adaptation of the method of Wheeler (11). Thirty grams of *o*-acetotoluidide (0.20 mole) in 300 ml of glacial acetic acid at 15–16° C was treated with 10.5 ml of bromine (0.20 mole). After 1 hour the solution was poured into cold water and the hydrobromide was collected.

The salt was decomposed by boiling in 1 liter of water for 1 hour. The hot filtrate yielded most of the product and repeated extraction of the residue yielded the balance. Thirty-seven grams (84% yield) of 2-methyl-5-bromoacetanilide, m.p. 158–159° C, was obtained.

This material was oxidized by the method of Justoni, Ternizzi, and Pirola (12). Seven grams of 2-methyl-5-bromoacetanilide (0.030 mole) was suspended in 3.5 liters of water at 85° C and 10 g of magnesium sulphate and 15 g of potassium permanganate were added. The solution was allowed to remain at 80° C overnight. After being cooled, the manganese dioxide was filtered out and the product was precipitated by acidification with hydrochloric acid. Recrystallization from hot water gave 5.5 g 4-bromoacetoanthranilic acid (65% yield), m.p. 214–215° C. Hydrolysis of this acetyl derivative was accomplished by boiling 5.5 g (0.022 mole) with 50 ml of 1:1 sulphuric acid for 1 hour. Diluting and neutralizing the solution gave 4 g of 4-bromoanthranilic acid, m.p. 217–218° C, after two recrystallizations from dilute ethanol.

5-Bromoanthranilic Acid

This compound was prepared by brominating anthranilic acid by Wheeler's method (11) as described above for *o*-acetotoluidide. A 65% yield of 5-bromoanthranilic acid, m.p. 215–217° C, was obtained after two recrystallizations from dilute ethanol.

4-Nitroanthranilic Acid

This compound was prepared by the method of Hillers, Lokenbacks, and Majs (13). Sixty grams of *o*-acetotoluidide dissolved in 400 ml of concentrated sulphuric acid was nitrated for 4 hours at −5° C with 40 ml of concentrated nitric acid in 120 ml of concentrated sulphuric acid. The acid solution when poured over ice yielded 35 g (45%) of 2-methyl-5-nitroacetanilide, m.p. 135–140° C. Several crystallizations from hot water raised the melting point to 149–150° C. The purified product was oxidized by treating 10 g (0.051 mole) in 3 liters of water at 95° C with 25 g of potassium permanganate and 12 g magnesium sulphate and allowing the solution to stand at about 90° C overnight. Seven grams of the corresponding acid was obtained (61% yield) with a melting point of 215–216° C after recrystallization from water. Heating 10 g (0.044 mole) of this material in 30 ml of alcohol and 120 ml of concentrated hydrochloric acid for 2 hours gave 7.5 g (90% yield) of 4-nitroanthranilic acid. After several recrystallizations from water it melted at 262–264° C with decomposition. 4-Nitroanthranilic acid with identical properties was also prepared from 2-methyl-5-nitroaniline as described below for 5-nitroanthranilic acid.

Can. J. Chem. Downloaded from www.nrcresearchpress.com by 210.87.254.42 on 09/05/12
For personal use only.

5-Nitroanthranilic Acid

This compound was prepared by a modification of the method of Iguchi (14). Fifty grams of 2-methyl-4-nitroaniline (0.33 mole) was acetylated by refluxing with 138 g of acetic anhydride (1.35 mole) for 2 hours. Excess acetic anhydride was destroyed by boiling the solution with water whereupon 44 g (70% yield) of 2-methyl-4-nitroacetanilide, m.p. 198–200° C, precipitated. This was oxidized and hydrolyzed as described under 4-nitroanthranilic acid, to give 5-nitroanthranilic acid, m.p. 268–269° C with decomposition.

4-Chloroanthranilic Acid

A modification of the method of Cohn (15) was used. 2-Methyl-5-chloroaniline was acetylated by dissolving 2.5 g (0.18 mole) in 100 ml of boiling glacial acetic acid, adding 75 ml of acetic anhydride (0.67 mole), and refluxing for 15 minutes. A yield of 27 g (91%) of 2-methyl-5-chloroacetanilide, m.p. 131–132° C, was obtained on diluting the solution with water. This was oxidized and hydrolyzed as described above to give 4-chloroanthranilic acid, m.p. 234–235° C, after recrystallization from dilute alcohol.

5-Methylanthranilic Acid

m-Toluic acid was nitrated by the method of Giacolone and Russo (16). Twenty grams of potassium nitrate (0.20 mole) in 120 ml of concentrated sulphuric acid was added cautiously to 20 g of *m*-toluic acid dissolved in 120 ml of concentrated sulphuric acid at 0° C. The mixture was poured on ice and a mixture of 2-nitro-3-methylbenzoic acid and 2-nitro-5-methylbenzoic acid precipitated. The latter was extracted from the mixture with hot water, yielding 13 g (36%) of 2-nitro-5-methylbenzoic acid, m.p. 131–132° C. This nitro acid was reduced by the method of Wheeler and Hoffman (17). Four grams (0.022 mole) was dissolved in 100 ml of concentrated ammonium hydroxide and 50 g of ferrous sulphate heptahydrate (0.17 mole) in 200 ml of water was added. The solution was brought to a boil and after it was cooled the inorganic salts were filtered out. Acidification and cooling the solution yielded 3 g of 5-methylanthranilic acid (90% yield). It melted at 175–177° C after recrystallization from dilute alcohol.

4-Aminoanthranilic Acid

This compound was prepared by reduction of 4-nitroanthranilic acid by the method of Wheeler and Hoffman (17) described above. It gave a 40% yield of 4-aminoanthranilic acid, m.p. 134–136° C, after recrystallization from dilute alcohol.

N-Acetylanthranilic Acid

This compound, m.p. 184–185° C, was prepared in 80% yield by acetylation of anthranilic acid in boiling acetic anhydride.

Anthranilic Acid-$^2H_3$

Anthranilic acid, 23 g, was exchanged four times with heavy water by dissolving it in 54 ml of purified dioxane and 5 g of deuterium oxide. The solvents were removed under reduced pressure and the acid was dried at 85° C in a vacuum oven at 15-mm pressure. This material analyzed 78.5±.08 at. % anthranilic acid-$^2H_3$ by the method previously described (18).

Rate Measurements

The rates of decarboxylation were measured by absorption of the evolved carbon dioxide on ascarite which was weighed at regular intervals. The apparatus is shown in Fig. 1. The thermostat was a 1-liter two-necked flask heated by an electric mantle. In

this flask diphenyl ether was refluxed so that the vapors bathed the reaction vessel (*a*) which was a 25-ml test-tube-shaped vessel made from a 34/45 standard taper male joint. A gas inlet tube (*b*) extended to the bottom of the reaction vessel and a stream of dry carbon-dioxide-free nitrogen passing through this tube swept the evolved carbon dioxide through a condenser (*c*), an *n*-butyl phthalate bubbler (*d*), a sulphuric acid bubbler (*e*), a U tube of anhydrous calcium sulphate (*f*), into the ascarite weighing bottle (*h*) which was protected from the atmosphere by a tube (*i*) containing calcium sulphate and ascarite. A second ascarite weighing bottle could be interchanged with (*h*) by means of the three-way stopcock (*g*).

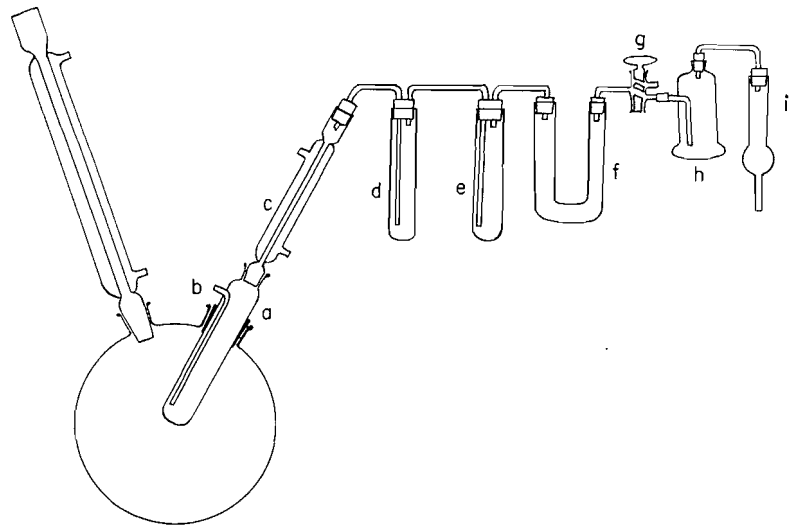


FIG. 1. Apparatus for decarboxylation.

About 10 ml of nitrobenzene was placed in the reaction vessel and the nitrogen flow was adjusted to a suitable rate. Since diphenyl ether has a higher boiling point (259° C) than nitrobenzene (210.5° C) or 1-methylnaphthalene (242° C) the solvent boiled gently in the reaction vessel. Attempts to operate at thermostat temperatures below the boiling point of the solvent gave poor temperature control because the sweeping nitrogen cools the solvent and fluctuations in its rate of flow cause temperature fluctuations and difficulty in reproducing temperatures between runs. An iron–constantan thermocouple introduced into the reaction vessel through the condenser showed that temperature variations during a run in refluxing solvent did not exceed 0.2° C. Temperature variation between runs varied as much as 0.5° C because of different solute concentrations and the high boiling-point-elevation constant of nitrobenzene. When the system had come to equilibrium a pellet of about 0.4 g of the acid to be decarboxylated was dropped into the reaction vessel. The refluxing solvent dissolved it quickly and the evolved carbon dioxide was weighed in the ascarite weighing bottles at intervals.

Rate constants were calculated from the slopes of plots of $1/(a-x)$ against time, where $a-x$ = initial moles of anthranilic acid less moles of carbon dioxide at time t all divided by the volume of the solution corrected to 210.5° C by means of the coefficient of cubic expansion of nitrobenzene. Data from a typical run are shown in Fig. 2. Rate constants for the various anthranilic acids in nitrobenzene are shown in Table I and

Can. J. Chem. Downloaded from www.nrcresearchpress.com by 210.87.254.42 on 09/05/12
For personal use only.

those for the three acids which could be dissolved in 1-methylnaphthalene are shown in Table II. The rates for 4-aminoanthranilic acid were so large that enough points for a plot could not be obtained so the rate was calculated from the observed half lives in seven runs. The variation of the observed half lives for this acid and anthranilic acid itself confirm the second order shown in Fig. 2.

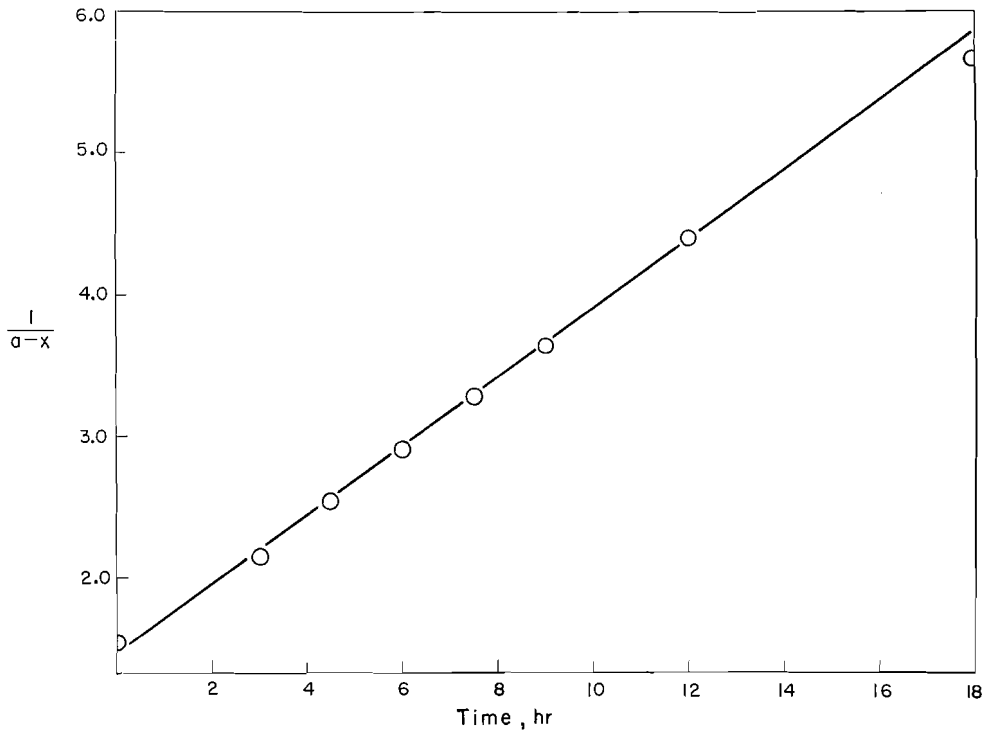


FIG. 2. Anthranilic acid in nitrobenzene at 210.5° C.

In order to obtain the rate constant for pure anthranilic acid-$^2H_3$ from the apparent constant for partly deuterated anthranilic acid the following calculations were made:

$$\frac{d[CO_2]}{dt} = k'([A_H]+[A_D])^2$$

where A_H = anthranilic acid, A_D = anthranilic acid-$^2H_3$, and k' is the apparent rate constant for partially deuterated acid. The apparent rate can also be written

$$\frac{d[CO_2]}{dt} = k_H[A_H]^2+k_H[A_H][A_D]+k_D[A_H][A_D]+k_D[A_D]^2$$

so that

$$k'([A_H]+[A_D])^2 = ([A_H]+[A_D])(k_H[A_H]+k_D[A_D])$$

and

$$k'([A_H]+[A_D]) = k_H[A_H]+k_D[A_D].$$

Substituting $k_H = (6.17\pm.17)\times10^{-5}$, $k' = (3.14\pm.22)\times10^{-5}$, $[A_H] = 0.215\pm.001$, and $[A_D] = 0.785\pm.001$ gives $k_D = (2.32\pm.34)\times10^{-5}$. This makes the isotope effect, $k_H/k_D = 2.66\pm.46$.

Can. J. Chem. Downloaded from www.nrcresearchpress.com by 210.87.254.42 on 09/05/12
For personal use only.

TABLE I

Rates of decarboxylation in nitrobenzene at 210.5° C

Acid	Concentration, moles/liter	Half life, hours	$k\times10^5$, moles/l. sec	$k\times10^5$, mean
Anthranilic	0.542	8.2	6.12	6.17±0.17
	0.322	—	5.90	
	0.647	6.7	6.41	
	0.332	12.6	6.25	
	0.441	—	6.15	
5-Chloroanthranilic	0.362		1.87	1.92±0.13
	0.358		1.80	
	0.483		2.10	
4-Chloroanthranilic	0.324		3.05	3.18±0.10
	0.360		3.30	
	0.320		3.20	
4-Bromoanthranilic	0.239		2.78	2.66±0.12
	0.307		2.54	
5-Bromoanthranilic	0.133		2.45	2.37±0.08
	0.123		2.30	
5-Methylanthranilic	0.212		9.35	9.61±0.18
	0.171		9.70	
	0.365		9.80	
4-Nitroanthranilic	0.399		0.180	0.175±0.013
	0.348		0.167	
	0.228		0.192	
	0.364		0.153	
5-Nitroanthranilic	0.181		0.500	0.527±0.027
	0.208		0.555	
4-Aminoanthranilic	0.112	0.11	310	300±28
	0.093	0.12	300	
	0.084	0.17	290	
	0.064	0.19	270	
	0.059	0.18	310	
	0.051	0.22	320	
	0.044	0.28	280	
N-Methylanthranilic	0.465		43	43
N-Acetylanthranilic	0.159		0.61	0.61
N-Phenylanthranilic	0.255	14	6.88	6.69±0.19
	0.133	28	6.50	
Anthranilic-$^2H_3$ (78.5%)	0.423		3.20	3.14±0.22
	0.395		2.81	
	0.565		3.40	
p-Aminobenzoic	0.418	16	1.25	1.32±0.07
	0.265	24	1.39	

TABLE II

Rates of decarboxylation in 1-methylnaphthalene at 242° C

Acid	Concentration, moles/liter	Half life, hours	$k\times10^4$, moles/l. sec	$k\times10^4$, mean
Anthranilic	0.514	3.6	1.52	1.58±0.05
	0.556	3.3	1.58	
	0.597	3.0	1.57	
	0.171	9.2	1.65	
4-Chloroanthranilic	0.380		1.14	1.17±0.03
	0.169		1.20	
5-Chloroanthranilic	0.440		0.76	0.74±0.02
	0.485		0.72	

Can. J. Chem. Downloaded from www.nrcresearchpress.com by 210.87.254.42 on 09/05/12
For personal use only.

Can. J. Chem. Downloaded from www.nrcresearchpress.com by 210.87.254.42 on 09/05/12
For personal use only.

DISCUSSION

The data of Fig. 2 and Tables I, II, and III show that the decarboxylation of anthranilic acids is second order with respect to the acid in both nitrobenzene and 1-methylnapththalene. The second-order kinetics shows that there are two molecules of anthranilic acid in the transition state or some step preceding it and so suggests that the proton transfer is intermolecular. It is possible that anthranilic acid forms a dimer in solution and that proton transfer could be intramolecular within this dimer, although extensive dimerization in boiling nitrobenzene seems unlikely.

Rates were measured in boiling solutions so that rates in the two solvents are not directly comparable. In 1-methylnaphthalene at 242° C the rate is about 2.5 times that in nitrobenzene at 210° C so that rates in the two solvents at the same temperature can not be very different. Since nitrobenzene is a considerably more polar solvent than 1-methylnaphthalene (ϵ_{25} = 35 and 2.7 respectively) the small difference in rates suggests that the polarity of the transition state is not greatly different from that of the reactant.

Anthranilic acid is seen to decarboxylate 2 to 3 times faster than functionally deuterated anthranilic acid so that proton transfer must be involved in the rate-determining step or some step preceding it. It is obvious from Table I that electron-releasing groups accelerate the decarboxylation and this must account for the fact that anthranilic and *p*-aminobenzoic acids decarboxylate while benzoic acid does not. The increased rates with N-methyl- and N-phenyl-anthranilic acids and the decreased rate with N-acetylanthranilic acids are in agreement with this interpretation of the role of the *o*-amino group. These observations show that decarboxylation must take place from the neutral acid rather than the zwitterion since protonation of the amino group would destroy its electron-releasing properties. If reaction takes place from the neutral molecule, proton donation must come from the carboxyl group and electron-releasing substituents should hinder, not help, the donation. This rules out site 1 as the only reaction center but leaves the possibility that more than one site is involved in the transition state, with the substituent effect at site 1 outweighed by that at the others.

In Figs. 3, 4, and 5 the data of Table I are plotted according to equations 1, 2, and 3, respectively. It is seen that the fit to a single straight line is not good in any of the three. Table III shows the results of a standard statistical analysis (19), of the fit of the data to a linear equation $Y = a+bX$, where $Y = \log k/k_0$, $X = \sigma$, $b = \rho$, s_E is the standard error in the estimate of Y, s_b is the standard error in b, r is the linear correlation coefficient in equations 1–3 or the multiple correlation coefficient in equation 4, and F is the variance ratio (19). Comparison of columns b and s_b show that equations 1 and 3 fit the data much better than 2 and 4. Column F makes the comparison quantitative, and shows (19) b ($= \rho$) different from zero at the 99% confidence level for equations 1 and 3, at the 95% confidence level for equation 2, and at no significant level for equation 4. Evidently site 1 or site 3 is of predominant importance in the transition state and the negative sign of ρ requires that it be site 3, as has been indicated previously. Jaffe has shown (8) that in order to distinguish between one site or two by means of substituent effects it is necessary that the σ's for the substituents referred to the two sites have a correlation coefficient less than 0.9. The substituents used in the present investigation have the following correlation coefficients: $r_{12} = 0.817, r_{23} = 0.702, r_{13} = 0.974$. Evidently the Jaffe treatment of our data can rule out participation by site 2 in the transition state, but not joint participation by sites 1 and 3. The conclusion is, then, that site 3 is of predominant importance in the transition state with less important contributions from site 1.

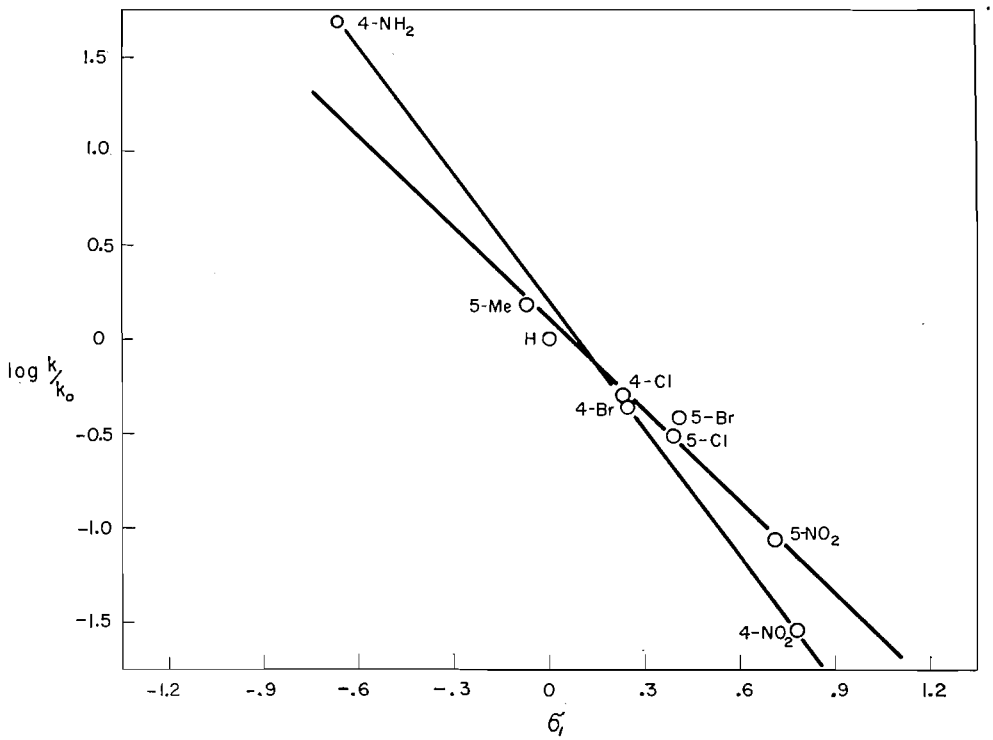


FIG. 3. Equations 1, 5, and 6.

TABLE III

Relationship between rates and substituents constants

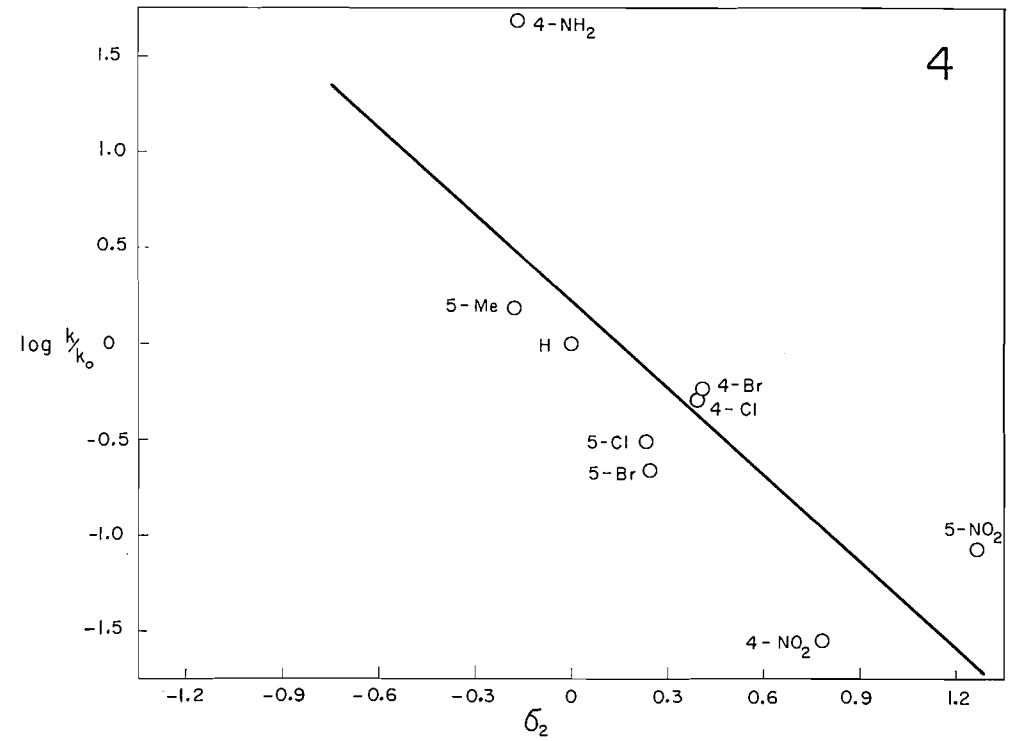
Equation	a	b	s_b	s_E	r	F
1	0.191	−2.04	0.134	0.163	0.985	23.9
2	0.221	−1.50	0.488	0.628	0.759	9.5
3	−0.070	−1.45	0.109	0.189	0.985	23.7
4	0.023	−1.45 (b_1)	1.166	0.177	0.988	1.6
		−0.08 (b_2)	0.353			
		−0.48 (b_3)	0.672			
5	0.195	−2.26	0.035	0.036	0.999	1500
6	0.110	−1.60	0.143	0.079	0.986	141

Although the data do not fit any of the four equations well, it is remarkable that in Fig. 1 the points for 4-substituents fall on one line and those for 5-substituents fall on another. The line for 4-substituents is represented by equation 5 and that for 5-substituents by equation 6 in Table III and it is seen that the fit to the separate equations is much better than to any one of the preceding four equations. It will be noted that ρ_4 (b, equation 5, Table III) is numerically larger than ρ_5 (b, equation 6, Table III) which suggests that in anthranilic acid decarboxylation the electron density at the reaction site is more sensitive to resonance effects from substituents than it is in ionization of benzoic acid, the standard reaction from which Hammett's σ's are determined. This agrees with site 3 as the principal reaction center since site 1 is equivalent to that in the standard reaction.

Similar splits between meta and para substituent effects are well known in the reactions

Can. J. Chem. Downloaded from www.nrcresearchpress.com by 210.87.254.42 on 09/05/12
For personal use only.

Can. J. Chem. Downloaded from www.nrcresearchpress.com by 210.87.254.42 on 09/05/12
For personal use only.



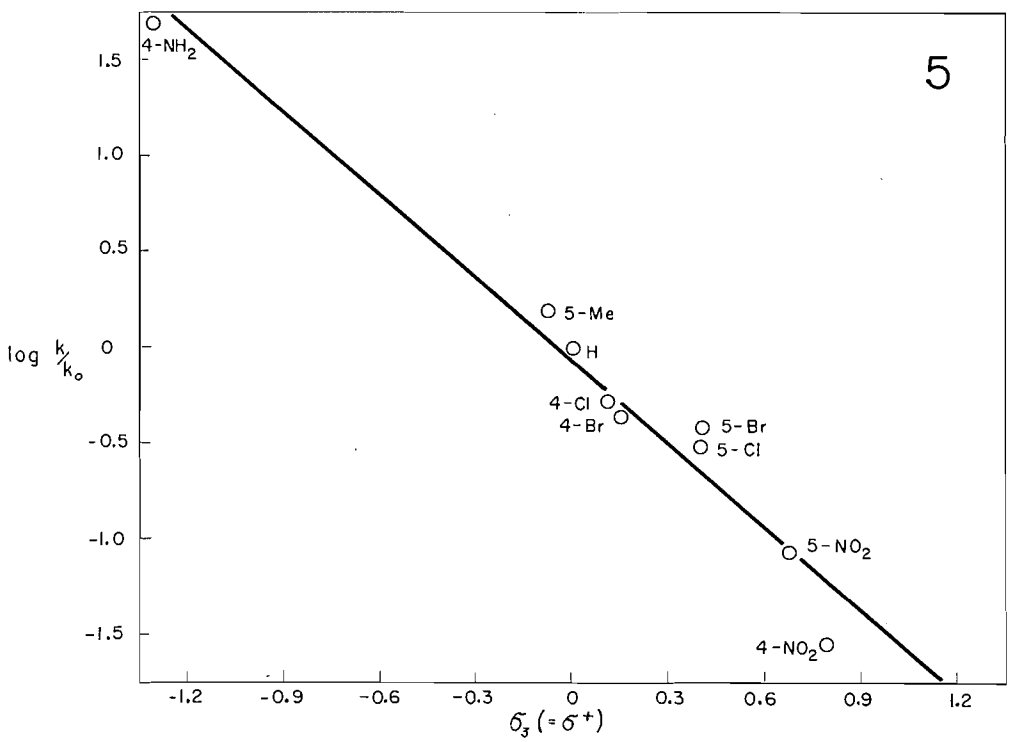
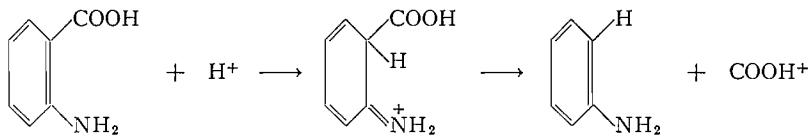


FIG. 4. Equation 2.
FIG. 5. Equation 3.

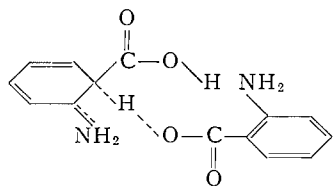
of amines and phenols on the one hand and in substitution reactions on aromatic and benzyl compounds on the other. The former case led Hammett to assign separate $+\sigma$'s for the reactions of amines and phenols (5), but new $-\sigma$'s were not necessary since mesomeric increase of electron density on amines and phenols is limited by the lack of low-energy orbitals on oxygen and nitrogen to receive it. In aromatic and benzyl substitutions, on the other hand, the increased efficiency of substituents with $-\sigma$'s led Brown to the establishment of separate values, $-\sigma^+$, for these cases. Thus far, $+\sigma^+$'s have not been found to be significantly different from Hammett's $+\sigma$'s, presumably because in the transition states of such reactions the reaction center bears a large positive charge and so is incapable of mesomeric electron release.

In anthranilic acid decarboxylation para substituents seem to be more effective for *both* electron release and electron attraction than in the standard reaction, which would require that the reaction center in the transition state of decarboxylation be capable of either accepting or releasing electrons. This would be the case at site 3 only if the ring carbon still has a π electron available for conjugation; that is, if either the new bond or the old is weak. By analogy with the accepted mechanism of aromatic substitution, an intermediate may be postulated in decarboxylation, as shown below.



In the usual aromatic substitution reactions the large magnitude of ρ and the absence of a hydrogen isotope effect show that the transition state resembles the intermediate, but in decarboxylation the preceding arguments suggest that the transition state must be closer to reactant or product than is the case in the usual aromatic substitutions. Stevens' observation (2) that there is no carbon isotope effect in the decarboxylation shows that the transition state can not lie between intermediate and product.

The deuterium isotope effect in decarboxylation shows that a proton is involved in the reaction site but its small magnitude, $k_H/k_D = 2$–3 suggests that the O—H bond is weakened but not broken in the transition state. This is consistent, too, with the small importance of acid strength on the rate as indicated by the negative value of ρ. The small magnitude of ρ compared to that in most aromatic substitutions (6) confirms that charge at the reaction site is small (20), as does the small solvent effect mentioned previously. Taken together these considerations indicate a transition state something like that represented by the formula



in which the O—H bond is weakened but not yet broken and the C—H bond is only partially formed. The role of the left-hand amino group in stabilizing the transition state is obvious and the proximity of the right-hand amino group to the leaving carboxyl group

Can. J. Chem. Downloaded from www.nrcresearchpress.com by 210.87.254.42 on 09/05/12
For personal use only.

suggests that the transfer of a proton to the ring may be accompanied or immediately followed by transfer of a second proton from the departing carbon dioxide molecule to the right-hand amino group. The previously noted unimportance of the amino group in the rate-determining step requires that this second proton transfer have a low activation energy, as is usually observed for proton transfer O to N. The right-hand molecule, in catalyzing the decarboxylation, would be converted from a neutral molecule to a zwitterion, like the bifunctional catalysts described by Swain (21). Such a bifunctional catalysis should provide a relatively low-energy route for proton transfer in a solvent of low dielectric constant, especially since the zwitterion could revert to neutral molecule intramolecularly. This interpretation agrees with the observation that *p*-aminobenzoic acid decarboxylates at only one-fifth the rate of anthranilic acid.

In summary, then, we conclude that decarboxylation takes place in the neutral molecule, not the zwitterion, that proton transfer is intermolecular, that the rate-determining step involves proton attack on the ring carbon, and that in the transition state the carbon–hydrogen bond is just beginning to be formed. It is possible that catalysis by the second anthranilic acid molecule is bifunctional in character.

ACKNOWLEDGMENT

The authors are grateful to the National Research Council of Canada for a grant-in-aid of this research.

REFERENCES

1. L. McMaster and R. L. Shriner. J. Am. Chem. Soc. **45**, 751 (1923).
2. W. H. Stevens, J. M. Pepper, and M. Lounsbury. Can. J. Chem. **30**, 529 (1952).
3. B. R. Brown. Quart. Revs. (London), **5**, 131 (1951).
4. B. Pawlewski. Ber. **37**, 592 (1904).
5. L. P. Hammett. Physical organic chemistry. McGraw-Hill, New York. 1940.
6. H. C. Brown and Y. Okamoto. J. Am. Chem. Soc. **80**, 4979 (1958).
7. H. H. Jaffe. Chem. Revs. **53**, 191 (1953).
8. H. H. Jaffe. J. Am. Chem. Soc. **76**, 4261 (1954).
9. E. B. Hershberg. Ind. Eng. Chem., Anal. Ed. **8**, 312 (1936).
10. A. M. Berkenheim and R. S. Livshits. J. Gen. Chem. (U.S.S.R.) **6**, 1025 (1936); Chem. Abstr. **31**, 1778 (1937).
11. H. L. Wheeler. J. Am. Chem. Soc. **31**, 566 (1909).
12. R. Justoni, M. Ternizzi, and C. Pirola. Farm. Sci. e tec. **3**, 509 (1948); Chem. Abstr. **43**, 2189 (1949).
13. S. Hillers, A. Lokenbacks, and L. Majs. Latvijas PSR Zinātņu Akad. **3**, 7 (1950); Chem. Abstr. **48**, 9964 (1954).
14. S. Iguchi. J. Pharm. Soc. Japan, **72**, 122 (1952); Chem. Abstr. **46**, 11187 (1952).
15. H. Cohn. Monatsh. Chem. **22**, 485.
16. A. Giacolone and F. Russo. Gazz. chim. ital. **65**, 840 (1935).
17. H. L. Wheeler and C. Hoffman. Am. Chem. J. 44, 113 (1910).
18. G. E. Dunn, P. Krueger, and W. Rodewald. Can. J. Chem. **39**, 180 (1961).
19. B. Ostle. Statistics in research. Iowa State College Press, Ames, Iowa. 1954. Chaps. 6–8.
20. C. G. Swain and W. Langsdorf. J. Am. Chem. Soc. **73**, 2813 (1951).
21. C. G. Swain and J. F. Brown. J. Am. Chem. Soc. **74**, 2534, 2538 (1952).

Can. J. Chem. Downloaded from www.nrcresearchpress.com by 210.87.254.42 on 09/05/12
For personal use only.

Can. J. Chem. Downloaded from www.nrcresearchpress.com by 210.87.254.42 on 09/05/12
For personal use only.

CHALKOGENIDES OF THE TRANSITION ELEMENTS

II. EXISTENCE OF THE π PHASE IN THE M_9S_8 SECTION OF THE SYSTEM Fe–Co–Ni–S[1,2]

OSVALD KNOP AND MOHAMMAD ANWAR IBRAHIM

ABSTRACT

The face-centered cubic phase π(Fe,Co,Ni,S) has been shown to exist, at room temperature, within wide composition limits in or close to the M_9S_8 section of the quaternary system Fe–Co–Ni–S. The M:S ratio of the binary phase π(Co,S) is 9:8 with very narrow homogeneity ranges on both sides of Co_9S_8, but in π(Fe,Co,Ni,S) the ratio is somewhat higher and appears to increase with decreasing cobalt content. Stoichiometric Co_9S_8 probably contains a small number of vacancies in both sublattices. It is quite likely that the sulphur sublattice is nearly fully occupied and that departures from stoichiometry are caused by the varying degree of occupancy of the metal sublattice.

The crystal structure, which was proposed for Co_9S_8 and for the mineral pentlandite by Lindqvist *et al.*, has been confirmed for these two substances and for π(Fe,Co,Ni,S) in general by X-ray and neutron powder diffraction. The present evidence does not support the crystal structure suggested for natural pentlandite by Eliseev; Eliseev's model does not, in fact, account for the diffraction data of any of the substances examined in this work.

Replacement of cobalt in π(Co,S) by iron or nickel or both results in an expansion of the unit cell, the maximum increase in $a(\pi)$ amounting to about 3%. Cobalt in π(Co,S) cannot be replaced completely by iron or by nickel in samples prepared by dry synthesis, but if the substitution is simultaneous, the π structure will be preserved over a considerable range of compositions even on total replacement. The stability limits of π(Fe,Ni,S) have been found somewhat wider than those stated by Lundqvist.

In π phases with the compositions Co_8MS_8 the metal atoms can conceivably be present in ordered sublattices. This possibility was explored by neutron diffraction in slowly cooled Co_8NiS_8. Unlike in spinels, where nickel shows a strong preference for octahedral co-ordination, the cobalt and nickel atoms were found to be distributed at random.

INTRODUCTION

Nature of the π Phase

The first definite evidence for the existence of phases containing less than 50 at.% sulphur in the system cobalt–sulphur was presented in 1908 by Friedrich (1), who investigated the system by thermal analysis. He concluded that three such phases existed in the system and ascribed them the formulae Co_4S_3, Co_5S_4, and Co_6S_5, the latter two, however, only tentatively. The first of these sulphides was investigated by X-ray diffraction by Cagliotti and Roberti (2). They found that the sulphide had face-centered cubic symmetry and that its powder pattern resembled that of the mineral bornite. Since the formula of bornite was then thought to be Cu_3FeS_3, Cagliotti and Roberti concluded by analogy that Co_4S_3 was the stoichiometric composition of the phase.

Hülsmann and Weibke (3) reinvestigated the system in 1936. They confirmed the existence of the face-centered cubic sulphide but found by microscopic examination that a sulphide of the gross composition Co_4S_3 was not homogeneous. They considered the formula Co_6S_5 to be more consistent with the experimental facts.

A detailed study of this phase was undertaken in 1936 by Lindqvist, Lundqvist, and Westgren (4, abbreviated in the following to LLW). The space group of the sulphide was shown to be O_h^5—$Fm3m$, and from its experimental density it was inferred that there were four Co_9S_8 formula units per unit cell. The 36 cobalt atoms were distributed over two sets of equivalent lattice sites, one containing 32, and the other 4, atoms. Similarly the 32 sulphur atoms were split up into a set of 8 and a set of 24 atoms. The agreement between the calculated and the visually estimated powder-pattern intensities

[1]*Manuscript received August 15, 1960.*
Contribution from the Department of Chemical Engineering, Nova Scotia Technical College, Halifax, N.S., with financial assistance from the National Research Council of Canada.
[2]*Part I of this series appeared in Can. J. Chem.* **34**, *1142 (1956).*

Can. J. Chem. Downloaded from www.nrcresearchpress.com by 210.87.254.42 on 09/05/12
For personal use only.

was satisfactory. The correctness of the proposed formula Co_9S_8 was thus supported by a crystal-structure argument.

The crystal structure of the mineral pentlandite was discussed in the same paper. Although pentlandite is one of the most important nickel minerals, its formula remained uncertain for a long time. Alsén (5) proposed for it a crystal structure based on the space group O_h^5—*Fm3m*, taking the number of atoms per unit cell as 64. This would correspond with the LLW structure of Co_9S_8 containing only the 32 metal atoms, so that the corresponding formula would be (Fe,Ni)S. The agreement between the calculated and observed intensities was rather good, but there were certain discrepancies. These Alsén attributed to slight errors in his choice of the atomic parameters, which, incidentally, were the same as those proposed later by LLW for Co_9S_8. However, LLW considered pentlandite to be isostructural with Co_9S_8, so that the incomplete agreement between Alsén's calculated and observed intensities was, in their view, due to an incorrect formula, i.e., to the additional four metal atoms per unit cell of pentlandite. The formula of the mineral would then be $(Fe,Ni)_9S_8$, in complete analogy with Co_9S_8. The LLW structure proposed for these two substances was later incorporated as the structure type $D8_9$ in the *Strukturbericht* (7).

LLW prepared two artificial pentlandites, $Fe_{4.5}Ni_{4.5}S_8$ and $Fe_6Ni_3S_8$. The powder patterns of these two samples contained the lines of the Co_9S_8 pattern and, in addition, faint lines of a pyrrhotite phase. No explanation was advanced for the presence of the pyrrhotite lines.

The investigation of the system Co–S was repeated by a number of workers, all of whom presented evidence in support of the existence of a cubic phase at or near Co_9S_8. Lundqvist and Westgren (8) did not observe any changes in the lattice constant of Co_9S_8 on annealing and quenching from 200, 500, 650, and 800° C, regardless of whether cobalt or CoS was also present. They concluded that Co_9S_8 in their experiments had a sharp, constant composition. In an investigation of the $CoS_{1.05}$–$Fe_{12}S_{13}$ section of the system Co–Fe–S, Curlook and Pidgeon (9) prepared a number of Co–S samples with compositions in the vicinity of Co_9S_8. They reported that the sample containing 32 wt.% sulphur was essentially cubic but small amounts of a hexagonal phase were detected by X-ray spectrometer analysis. From this and from the previous finding (4) that a sample with 31.6 wt.% sulphur had contained free cobalt, they concluded that the composition of the cubic sulphide would be better expressed by the formula $Co_{15}S_{13}$.

Rosenqvist (10) measured the sulphur pressures and the H_2S/H_2 equilibria in the systems Co–S, Fe–S, and Ni–S between 400 and 1200° C. He confirmed that the phase Co_9S_8 was stable up to about 835° C and that it had only a very narrow homogeneity range. He also suggested that Co_9S_8 and pentlandite, being isostructural, were stabilized primarily by the electron/atom ratio. Stubbles (11) reinvestigated the stoichiometry of the sulphide between 585 and 800° C by the same method. He came to the conclusion that, while at higher temperatures there was a homogeneity range representable by the formula $Co_{9+x}S_8$ with x between -0.013 and $+0.031$, the limiting composition of the phase in equilibrium with cobalt remained slightly higher in cobalt than the stoichiometric as the temperature was decreased, though the limiting sulphur content was probably still above 47.05 at.% sulphur. The limiting composition of the phase saturated with sulphur could not be determined from Stubbles's data, as it was not possible to predict the trend of his sulphur-pressure curves for temperatures below 585° C.

Lundqvist (12) later extended his structural investigations to the system Fe–Ni–S. The expected narrowness of the homogeneity range of $(Fe,Ni)_9S_8$ with respect to the

M:S ratio seemed to be confirmed by the fact that he did not observe any variation in the lattice constant with the sulphur content of the samples. Varying the Ni:Fe ratio did affect the lattice constant, however, and from this variation Lundqvist established the stability limits of the synthetic pentlandite phase below 200° C as 0.42±2 and 0.58±2 Fe/(Fe+Ni). The sulphur content of the phase was stated to be invariably 47.0 at.% sulphur, irrespective of the total sulphur content of the samples or of the quenching temperature.

Lundqvist referred to the synthetic pentlandite phase as the π phase. Since the letter π has not been used to designate any other well-defined type of alloy phases and no confusion is likely to arise, it is proposed that the term π phase be reserved for phases of the $D8_9$ type regardless of their stoichiometry. The introduction of this notation in preference to definite formulae seems desirable, as there are indications (see above) that the formula M_9S_8 may not be a correct representation of the composition of the two π phases, π(Co,S) and π(Fe,Ni,S). Furthermore, phases of this type have recently been claimed to exist in systems other than Co–S and Fe–Ni–S (13, 14), so that compounds of this and of related types may be more numerous than hitherto supposed.

Literature references to the composition and properties of natural pentlandite are numerous and often contradictory. Since a structural investigation of the mineral will be the subject of another paper in this series (15) a review of the pertinent facts will be found there.

Crystal Structures Proposed for the π Phase

The crystal structures proposed for Co_9S_8 and for pentlandite by LLW are identical except for the nature of the metal atoms. The space group is O_h^5—$Fm3m$, with four formula units M_9S_8 per unit cell. The atoms are distributed over the lattice sites as follows (6):

32 M in 32(f): xxx etc. ($x_M = 1/8$),
4 M in 4(b): 1/2 1/2 1/2 etc.,
24 S in 24(e): $x00$ etc. ($x_S = 1/4$),
8 S in 8(c): 1/4 1/4 1/4 etc.

The 32 metal atoms occupy expanded tetrahedral interstices in a face-centered cubic lattice of sulphur atoms, while the remaining 4 atoms are in octahedrally co-ordinated positions. The sulphur atoms in 24(e) have the co-ordination number five, and those in 8(c) are four-co-ordinated. The metal atoms, which in Co_9S_8 are simply cobalt atoms with either four or six nearest sulphur neighbors, are in pentlandite distributed statistically over the two sets of sites.

With the above choice of x_M and x_S the co-ordination tetrahedra and octahedra of the metal atoms are regular. Their edge length is $a\sqrt{2}/4$, and the M–S distances are $a\sqrt{3}/8$ and $a/4$, respectively. The co-ordination tetrahedra of the 8 sulphur atoms are identical with those of the metal atoms. The metal atoms surrounding the five-co-ordinated sulphur are at the corners of a square pyramid with a base edge of $a/4$ and a height of $3a/8$. The distance of the sulphur atom from the apex is $a/4$, the other four metal atoms being equidistant and at $a\sqrt{3}/8$.

Eliseev (16) suggested in a recent study of the composition and crystal structure of natural pentlandite that the structure of the mineral differed from the LLW structure by the positions of the octahedrally co-ordinated metal atoms. From his drawing of the proposed structure it appears that he placed the four metal atoms in 4(a):000 etc. Since the LLW structure can be thought of as a regular array of antifluorite-type unit cells

Can. J. Chem. Downloaded from www.nrcresearchpress.com by 210.87.254.42 on 09/05/12
For personal use only.

alternating with face-centered unit cubes containing a single metal atom in the center, Eliseev's structure would differ from this arrangement by concentrating all the metal atoms in the antifluorite-type cells, leaving the alternate cubes empty (Fig. 1).

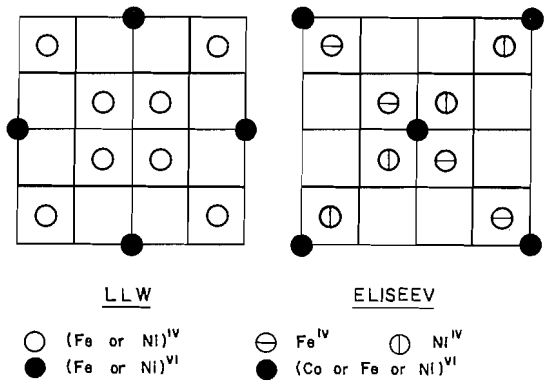


FIG. 1. Schematic representation of the differences between the two crystal structures proposed for pentlandite. The unit-cell contents between $z = -1/4$ and $1/4$ are projected on the 001 plane. The origin of Eliseev's structure is shifted by 1/4, 1/4, 1/4 to match the LLW structure. Sulphur atoms, which would appear at the intersections of the 1/4-co-ordinates, are omitted.

The iron and nickel atoms occupying $32(f)$ in Eliseev's structure were assumed to be present in the ratio 1:1 and completely ordered. Excess iron, or nickel, or cobalt sometimes present in small amounts in natural pentlandite would be located in $4(a)$, thereby balancing the over-all composition. The ordered arrangement of the metal atoms would be expected to lower the observable symmetry of the unit cell, as there is no 16-fold position in O_h^5—$Fm3m$ and the only 8-fold position has been utilized by the sulphur atoms. Eliseev believed to have evidence in support of his modified pentlandite structure in the doubling of certain lines in the powder photographs of the mineral and in the broadening of many "single" lines, as, for instance, 440. He stated that the doublets were often strong and that they all could be indexed on the basis of the same unit cell. The doubling was observed not only in powder but also in rotation photographs. The splitting of the pentlandite lines was said to be similar to that observed by Micheev (17) with mineral diarsenides of iron and nickel. Micheev had shown that the line splitting was due to a lowering of the crystal symmetry with a simultaneous preservation of the general character of the structure.

The M_9S_8 Section of the System Fe–Co–Ni–S

The composition triangle of this section is defined by the three compositions Fe_9S_8, Co_9S_8, and Ni_9S_8. Of these only Co_9S_8 can be obtained readily as a homogeneous phase by dry synthesis from the elements.

Ni_9S_8 has been reported by Peyronel and Pacilli (18) to consist, below 400° C, of a mixture of millerite and a phase of unknown structure with an approximate formula Ni_7S_6 (N). N gave the poorest diffraction lines of all the Ni–S phases studied by these authors. Its powder pattern, which was obtained with unfiltered FeK radiation in a 57.3-mm camera, contained a large number of lines and differed from that of π(Co,S). From this it was concluded that N had a low symmetry.* Presumably the same phase was

**The statement attributed in reference 19 to Peyronel and Pacilli that N possessed a monoclinic symmetry does not appear in reference 18. It is probably due to a translator's error in the abstract of reference 18 in Chem. Zbl. 1943 I, 1457, which Lundqvist used instead of the original paper not available to him at the time.*

Can. J. Chem. Downloaded from www.nrcresearchpress.com by 210.87.254.42 on 09/05/12
For personal use only.

observed later by Lundqvist (19, 12), though he never succeeded in obtaining it in the pure state. These observations are in agreement with our own experience with this phase and with the analogous phase in the system Ni–Se (20). Lundqvist also stated that almost all the strongest lines of N were close to, and possibly split up from, the strongest lines of the π-phase pattern, and he advanced the suggestion that N may have a degenerate π structure. On the other hand, Sokolova (21), who reinvestigated the Ni–S system between 30 and 50 at.% sulphur by a number of methods, denied the existence of Ni_7S_6, but reported a homogeneous phase with a composition Ni_9S_8. She claimed to have shown by X-ray diffraction that a sample of the appropriate composition consisted, on annealing at 200° C (and presumably also at 380° C), of the pure phase. She also obtained a local minimum in the electrical conductivity vs. composition curve close to Ni_9S_8.* The available evidence concerning the identity and formula of the intermediate phase is thus quite conflicting. One cannot, of course, exclude the possibility of existence of more than one low-temperature phase between Ni_3S_2 and NiS, nor can much reliance be placed in the above interpretations of diffraction patterns of inferior quality. Leaving aside the exact nature of this phase, we shall refer to it in the following simply as N.

No iron sulphide higher in iron than FeS has ever been mentioned to exist in preparations obtained by dry synthesis or by degradation of higher iron sulphides. However, a cubic sulphide was reported quite recently (14) to form on the surface of mild steel exposed to wet hydrogen sulphide. The sulphide was first noticed as a corrosion product of steel in the sour crude wells of Kansas and was given the name kansite. Its X-ray powder pattern was reported to be compatible with a face-centered cubic lattice with $a = 10.1 \pm 0.05$ Å. On this and some analytical evidence it was suggested that the sulphide had the formula Fe_9S_8 and that it was isostructural with Co_9S_8.

Although a number of studies of the three ternary systems, Fe–Ni–S, Fe–Co–S, and Co–Ni–S, are available (22, 23, 24, 12, 25, 26, 27, 9, 28), structural data concerning the M_9S_8 sections are scanty. Curlook and Pidgeon (9) reported the existence of a cubic phase in alloys containing 0–32 wt.% $Fe_{12}S_{13}$ in the section $CoS_{1.05}$–$Fe_{12}S_{13}$. The phase was detected by powder photography in alloys containing up to 30 wt. % and in polished sections of alloys containing up to 32 wt.% $Fe_{12}S_{13}$. Its lattice parameter was stated to increase by only 0.008 Å over the composition range 0–30 wt.% $Fe_{12}S_{13}$, which was taken as an indication that the cubic phase contained very little iron.

The only ternary system investigated in detail by X-ray diffraction was Fe–Ni–S (12). Lundqvist established the saturation limits of the homogeneous π phase in the $(Fe,Ni)_9S_8$ section (see above) as well as the nature of the phases coexisting with π in the adjacent phase spaces below 200° C. This and other available evidence points to the existence of a ternary π phase over a considerable region of the M_9S_8 plane.

Purpose of this Investigation

The state of our knowledge of the π phase that can be obtained by collating the available data may be summarized as follows.

A ternary π phase exists in the system Fe–Co–Ni–S over an appreciable composition range. Arguments based on the crystal structure proposed for Co_9S_8 by LLW lead to the formula $(Fe,Co,Ni)_9S_8$, but there is evidence that the metal content of the phase

**The experimental evidence presented in Sokolova's paper in support of the formula Ni_9S_8 is not entirely convincing. There are no details of the X-ray investigation, and nothing is said about the diffraction pattern of the phase. The position of the conductivity vs. composition minimum seems to favor the formula Ni_7S_6 at least as well as Ni_9S_8, as far as can be judged from Fig. 3 of the original paper. The constitution diagram of Fig. 1 of her paper does not obey the phase rule along the line e–s–t–d.*

Can. J. Chem. Downloaded from www.nrcresearchpress.com by 210.87.254.42 on 09/05/12
For personal use only.

may be higher than would correspond to an M:S ratio of 9/8. The homogeneity range with respect to the sulphur content of the phase is probably narrow. Since Co_9S_8 and natural pentlandite, $(Fe,Ni)_9S_8$, had been reported by LLW to be isostructural, Rosenqvist proposed that the π phase is stabilized by the electron/atom ratio, the electron stabilization being similar to that encountered in the Hume–Rothery and related phases. On the other hand, Eliseev suggested that the LLW structure for Co_9S_8, though similar, does not apply to natural pentlandite and that the correct structure of the mineral is a modified version of the LLW structure. His argument was based on the observation, which he claimed to have made, that the diffraction symmetry of pentlandite was lower than that of Co_9S_8.

Since Co_9S_8 and natural pentlandite are the only two substances listed in the *Strukturbericht* and elsewhere as belonging to the $D8_9$ type, Eliseev's statement is of sufficient importance to merit a re-examination of the structural evidence, and this was one of the aims of this study. A number of comments apropos of the two postulated structures can, however, be made immediately. When examining the evidence presented in support of the modified structure, attention should be drawn to the fact that Eliseev seems to have used unfiltered FeK radiation and a powder camera of 66-mm diameter. The reproduction of a powder photograph of pentlandite on page 57 of Eliseev's paper, intended to demonstrate the line splitting, is hardly of a quality suitable for examining the nature of the reported doublets. Since LLW found their focusing-camera photographs of Co_9S_8 and natural pentlandite to be identical (except for a lineshift due to different values of a), evidence for the correctness of Eliseev's pentlandite structure would also be evidence against the LLW structure proposed for the cobalt sulphide. Interchanging the occupancy of 4(a) and 4(b) would produce observable changes in the line intensities for the two substances, but this point is not discussed in Eliseev's paper at all. The atomic arrangement in Eliseev's structure is not very probable on entropy grounds, and there are certain symmetry arguments against symmetry degeneration brought about by the ordering. It is not known if Eliseev's modification would apply to synthetic pentlandite. There may be significant differences between the natural and the synthetic material whose possible existence must be kept in mind.

Regardless of which of the two structures is correct in any given case, there exists a possibility of ordering of the metal atoms in homogeneous π phases containing two kind of metal atoms in the ratio 1:8. That such preferential arrangement is likely to be expected with certain elements is well known from the crystallography of spinel-type compounds. No π phase of such composition had been reported in the literature prior to this work (cf. 29). If ordered homogeneous π phases of compositions Co_8FeS_8 and Co_8NiS_8 can be obtained, the ordering would be difficult to detect because of the close similarity of the X-ray atomic scattering amplitudes of the three metals and the unfavorable ratio of the two metals in such phases. The segregation of the iron or nickel metals into octahedral sites could, however, be demonstrated by neutron diffraction.

Rosenqvist's suggestion that the π phase may be 3d-electron stabilized is worth while examining. The phase has a certain amount of metallic character, but the reported existence of Fe_9S_8 (14) and the possibly close relationship of π and N (19, 12) throw some doubt on such stabilization. A preliminary to a more detailed study of this point would be the knowledge of the limits of existence of the π phase at room temperature in the M_9S_8 section of the Fe–Co–Ni–S system. To obtain this information by X-ray techniques is the main purpose of this work. The stoichiometry of the π phase and the correctness of representing its composition by the formula M_9S_8 will also be examined.

Can. J. Chem. Downloaded from www.nrcresearchpress.com by 210.87.254.42 on 09/05/12
For personal use only.

Can. J. Chem. Downloaded from www.nrcresearchpress.com by 210.87.254.42 on 09/05/12
For personal use only.

EXPERIMENTAL

Materials

Sulphur, Sublimed Merck, USP, was distilled four times *in vacuo* and kept in tightly closed containers. Carbonyl iron powder, G. A. and F. Grade L, of average particle size 20 microns was used throughout. The supplied analysis of the powder was 99.6–99.9% Fe, 0.01–0.06% C, 0.10–0.30% O, 0–0.005% N. The powder was reduced with purified hydrogen before use. Spectrographic analysis of the reduced powder gave 0.03% Ni; cobalt was not detected.

The bulk of the nickel used in the investigation consisted of carbonyl nickel shot kindly donated by the International Nickel Company of Canada, Limited. The supplied analysis read 99.9% Ni, 0.008% Cu, 0.025% Fe, 0.04% C, 0.01% S. The shot was cleaned in acid immediately before use and was in most cases degassed by heating *in vacuo*. Since it was impractical to use the shot where small amounts of nickel were required, a quantity of nickel powder was obtained by reduction of nickel oxide with purified hydrogen. The oxide was prepared by calcining nickelous nitrate hexahydrate low in cobalt (Baker and Adamson Reagent Special). The supplied lot analysis of the nitrate, expressed as maximum limits of impurities, was as follows: insoluble, 0.005%; 0.002% SO_4; 0.001% Fe; 0.002% Co; 0.005% Cu; 0.005% Pb; 0.001% Cl; 0.05% NH_3; alkalies and earths, 0.10%; total impurities, 0.17%. Spectrographic analysis of the metal powder gave 0.002% Fe and 0.002% Co.

Nickel shot caused difficulties in the quartz glass reaction tubes during the initial heating. As the nickel beads grew in size, owing to the formation of the less dense sulphide, the tubes cracked on a number of occasions. In addition, the pellets were too large for convenient handling when filling the reaction tubes. A large amount of Ni_3S_2 was therefore prepared separately and crushed to 100 mesh for use instead of the shot.

Purified cobalt powder low in nickel (Fisher Scientific No. C-363) was reduced with hydrogen before use. Spectrographic analysis of the reduced powder, which was carried out only after most of the samples had been prepared, revealed the presence of 0.3% iron and 0.4% nickel. The purity was thus much inferior to what had been expected, so that the iron and nickel contents of the cobalt powder must be taken into account when stating the compositions of the samples. However, the Fe:Ni ratio was sufficiently close to one for all the sample compositions to be shifted by small amounts in the same direction, namely almost parallel with the constant-ratio line Co_9S_8–$Fe_{4.5}Ni_{4.5}S_8$ of the composition triangle. The shift would be largest for Co_9S_8 and it would decrease in proportion to the cobalt content of the samples. Samples with no cobalt would not be affected, while the true composition of No. 1 (see Table I) would be $Fe_{0.027}Co_{8.937}Ni_{0.036}S_8$ rather than Co_9S_8. The deviation from the intended composition is quite small and one finds that the change in a produced by the impurities can be expected to affect only the fourth decimal (see Results and Discussion). Since the accuracy of the lattice constant of Co_9S_8 is of some importance, especially in view of the discrepancies in the reported values, four additional samples (Nos. 46, 47, 48, 49) were prepared from Johnson Matthey spectrographic-purity cobalt sponge. The sponge was freshly reduced before use. A small variation in the sulphur content was introduced to establish if there was any change in a arising from the possible existence of a narrow homogeneity range. However, the a values of these samples were all within the error limits of the value 9.929 ± 2 Å obtained for No. 1. The lattice constant of π(Co,S) is thus indeed quite insensitive to the presence of small amounts of iron and nickel, so that the lattice constants obtained with samples

TABLE I

Compositions and properties of $Fe_xCo_yNi_zS_8$ alloys

No.	$Fe_xCo_yNi_zS_8$ x	y	z	No. of annealings	Phases present*	$a(\pi)$, Å†	d,‡ g/cm³
1	—	9	—	1	π	9.929±2	5.233±9
2	4.5	—	4.5	2	$\pi+P+T$?	10.115 2	4.944 40
5	—	8	1	2	π	9.946 1	5.226 9
6	3	3	3	2	$\pi+P$?	10.016 1	
10	1	8	—	2	$\pi+T$	9.943 2	5.205 1
11	4.186	—	4.814	2	$\pi+P+T$?	10.105 2	
12	1	1	7	2	$\pi+$?	10.050 2	
13	—	2.25	6.75	2	$\pi+$?	10.008 2	
14	—	4.5	4.5	2	$\pi+$?	10.004 2	
15	5.571	—	3.429	2	$\pi+T$	10.154 1	
16	3.286	—	5.714	3	$\pi+P$	10.097 2	
17	3.857	1.286	2.857	2	$\pi+T+P$?	10.058 2	
18	4	1	4	2	$\pi+P$	10.069 1	
19	3	1	5	2	$\pi+P$	10.062 2	
20	2	1	6	3	$\pi+P$	10.061 2	
21	2.25	—	6.75	2	$\pi+$?	10.086 2	
22	6.75	—	2.25	2	$\pi+T$	10.211 2	
23	5	1	3	2	$\pi+T+P$?	10.102 2	
24	6	1	2	2	$\pi+T$	10.119 2	
25	5.4	1.8	1.8	2	$\pi+T+P$?	10.081 2	
26	1	—	8	3	$\pi+$?	10.090 5	
27	—	1	8	2	?	—	
28	1.8	1.8	5.4	2	$\pi+$?	10.041 1	
29	—	—	9	1	N+NiS	—	
30	1.667	1	6.333	2	$\pi+$?	10.057 3	
31	7.2	—	1.8	2	$\pi+T+\gamma$?	10.210 2	
32	8	—	1	2	$\pi+T$	10.22§	
33	7	1	1	2	$\pi+T$	10.087 3	
34	4.091	2.4545	2.4545	2	$\pi+T$	10.044 2	
35	1.286	3.857	3.857	2	π	10.000 1	
36		Ni_7S_6		2	N	—	
37	—	6.75	2.25	2	π	9.963 1	
38	—	5.625	3.375	2	π	9.984 1	
39	1	5	3	2	π	9.982 1	
40	1.8	5.4	1.8	2	$\pi+P$	9.974 2	
41	3.857	3.857	1.286	2	$\pi+T$	10.023 2	
42	4.5	4.5	—	2	$\pi+T$	9.975 2	
43	3.375	5.625	—	2	$\pi+T$	9.977 2	
44	2.25	6.75	—	2	$\pi+T$	9.960 1	
45¶	—	1.8	7.2	2	?	—	
46¶	—	9	—	1	π	9.9279 5	5.295±9
47¶	$Co_{15}S_{13} = Co_{9.230}S_8$			1	π	9.9283 9	5.324 9
48¶	$Co_{9.412}S_8$			1	π	9.9287 9	5.350 23
49¶	$Co_{8.889}S_8$			1	π	9.9256 10	5.319 7
50	2.4545	2.4545	4.091	2	$\pi+M$??	10.022 2	
51	5	3	1	2	$\pi+T+\gamma$?	10.030 2	
52	3	5	1	2	$\pi+T$	9.990 2	
Neutron	—	9	—	1	π	9.9286 20	
Neutron	—	8	1	1	π	9.9426 27	

*P, pyrrhotite; T, troilite; M, millerite; γ, face-centered (Fe,Ni); N, "Ni_7S_6". †The uncertainty in a refers to the last decimal figure. ‡Average of three determinations. §Estimated from graph. ¶Prepared from spectrographic-purity cobalt.

prepared with the impure cobalt powder remained unaffected within the accuracy limits of this work.

The lattice constants of the reduced iron, cobalt, and nickel powders were 2.8659±5 Å; 2.506 and 4.078 Å; and 3.5237±1 Å, respectively. The lattice constants of Ni_3S_2 were 5.743 and 7.154 Å, c/a = 1.246. All these values were in good agreement with the literature values (30, 31).

Can. J. Chem. Downloaded from www.nrcresearchpress.com by 210.87.254.42 on 09/05/12
For personal use only.

Preparation of Samples

In order to keep the number of samples at a minimum the sample compositions were chosen in such a way that they would fall on constant-percentage or constant-ratio lines of the composition triangle Fe_9S_8–Co_9S_8–Ni_9S_8 (Fig. 2 and Table I). The total

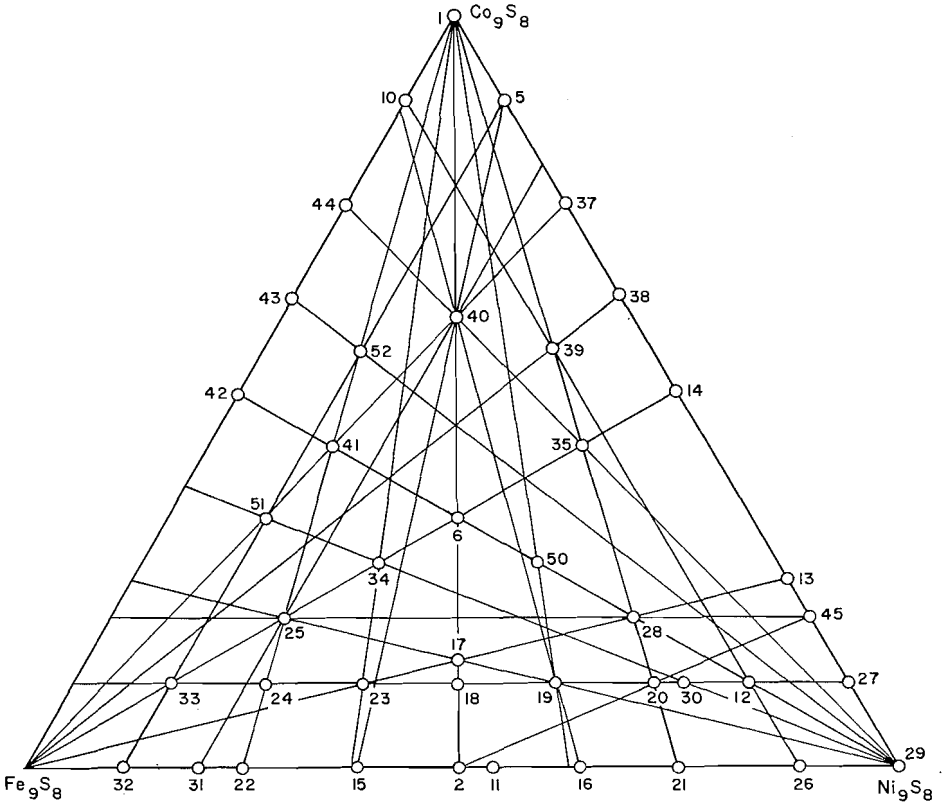


FIG. 2. Compositions of the synthetic samples.

amount of each sample was not less than 10 grams. Carefully weighed quantities of the elements were transferred quantitatively into clean degassed tubes of transparent silica. The tubes were evacuated to 10^{-5}–10^{-6} mm Hg, sealed off, and transferred into a deep horizontal tubular furnace with a steep temperature gradient and the hot zone at about 700° C. The strongly exothermic reaction between the fine metal powders and the free sulphur required extra care and some skill in initiating the reaction (29). When all the sulphur had reacted the tube was pushed completely into the hot zone and left there for about half an hour to ensure complete conversion of the metal, as otherwise the malleable metal particles would cause difficulties in subsequent handling. On cooling the tube was opened carefully, the sample removed, inspected for glass chips, and crushed to pass 100 mesh. The thoroughly mixed powder was again transferred into a transparent silica tube, which was then evacuated, sealed, and transferred into a vertical tubular furnace for homogenization. This procedure was repeated to ensure equalization of composition both by mechanical mixing and by diffusion.

Can. J. Chem. Downloaded from www.nrcresearchpress.com by 210.87.254.42 on 09/05/12
For personal use only.

Can. J. Chem. Downloaded from www.nrcresearchpress.com by 210.87.254.42 on 09/05/12
For personal use only.

The progress of homogenization was determined from powder photographs and from the internal consistency of the lattice constants. Wherever necessary a third homogenization was carried out. The samples were kept at the annealing temperature, which was usually in the vicinity of 800° C, up to 120 hours (29). Absence of reliable information on the phase equilibria in the system Fe–Co–Ni–S made the choice of the upper temperature limit for subsolidus annealing uncertain. It seems that the solidus must be somewhere in the vicinity of 820° C for most compositions of interest.

The strong shrinkage on homogenization indicated good consolidation of the initially loose powder. The sintered ingots were so compact that they had to be crushed in a hardened-steel mortar before grinding. The shrinkage was particularly appreciable for samples low in cobalt.*

The annealed samples were allowed to cool slowly in the furnace at a cooling rate of not less than 70° C/hour. The silica glass in contact with samples rich in cobalt devitrified to a white milky surface layer. The thickness of the layer varied with the length of contact and with the maximum temperature to which the tube had been exposed. The powder photographs of the devitrified product showed it to be ordinary crystalline quartz. Only in a few instances, where the samples were kept at temperatures over 810° C for long periods of time, was there a slight blue or purplish coloration of the silica in contact with the sulphide.

The color of the sintered powders varied from grey to pale yellow, depending on the composition. Samples rich in iron tended to be grey, those rich in nickel were pale yellow. Massive cobalt-rich alloys were greyish-white. All the alloys were brittle.

X-Ray Diffraction Technique

Powder diffraction photographs of the samples were taken in Straumanis-type cameras of 114.6- and 57.3-mm diameter. Filtered and unfiltered FeK and CrK radiations were employed throughout except for the nickel samples, where CuK radiation was used. The following wavelengths were used in the calculations: CrK_{α_1}, 2.28962 Å; CrK_{α_2}, 2.29352 Å; FeK_{α_1}, 1.93597 Å; FeK_{α_2}, 1.93991 Å; CuK_{α_1}, 1.54050 Å; CuK_{α_2}, 1.54434 Å. Care was taken to avoid disproportionation in the preparation of the fiber-mounted specimens. Nelson–Riley extrapolation was used in the lattice-constant determinations, utilizing reflections with θ at least 30° and fitting the straight lines by least squares.

Although some samples gave very good patterns with sharp lines even at high Bragg angles, the quality of most of the high-angle lines was only fair. The diffuseness of these lines could not be improved appreciably by annealing the 325-mesh powders below 400° C for 2 or 3 days. The improvement was not great enough to warrant the time and effort spent in the long annealing process. Samples near the Ni_9S_8 corner were the most troublesome (Nos. 12, 13, 26, 27, 29, 45). Their photographs contained many fine and diffuse interfering lines which made accurate measurement impossible.† Almost equally troublesome were the compositions near Fe_9S_8, the only difference being that the interfering lines were fewer (Nos. 32, 33, 42). The lines of the π phase in some of these photographs were, however, still distinguishable and could be measured. Thus for composition Nos. 13, 26, 32, 33, and 42 the lattice constants of the equilibrium π phase

**It is not certain whether the strong shrinkage of the samples low in cobalt, or with no cobalt at all, was caused by higher surface mobilities of iron and nickel atoms or by solidus temperatures lower than in the system* Co–S. *In the latter case the annealing temperature might have been above the solidus and the consolidation could have been aided by small amounts of a liquid phase.*

†The same difficulty was encountered by Lundqvist (19) in his study of the system Ni–S, *and in our laboratory with nickel selenides of similar compositions.*

could still be evaluated. The values of a obtained from these films were, of course, of lower accuracy, although a check using a $\sin^2\theta(844)$ vs. a graph showed that the discrepancies were not serious.

Either FeK or CrK radiation was used, except for Nos. 13, 27, 29, and 36, where photographs were taken with both radiations. The CrK photographs were obtained to increase the resolution, which was inadequate with FeK radiation.

Diffraction lines not belonging to the π-phase pattern were frequently present in the photographs. Except for the above samples the foreign lines did not interfere with the measurement of the π-phase lines.

The relative intensities were obtained by planimetering the diffraction peaks on diffractometer charts taken with filtered FeK radiation.

Neutron-Diffraction Study

The lead-crystal neutron spectrometer installed at the NRU reactor of the Atomic Energy of Canada, Ltd., in Chalk River was used to obtain the neutron powder diffraction patterns of Co_9S_8 and Co_8NiS_8. These samples were prepared in sufficiently large quantities especially for this purpose.* Co_9S_8 was kept at 750° C for 6 days and then cooled in the furnace which was controlled to give an average cooling rate of 38°/hour. The Co_8NiS_8 sample was kept at 810° C for 4 days. It was then brought to 445° C at an average rate of 2°/hour. Below this temperature it was allowed to cool at the natural cooling rate of the furnace.

The 200-mesh powders were sandwiched between two pieces of aluminum foil 0.005 in. thick in a circular aluminum specimen holder of 4-in. diameter. The thickness of the powder sandwich was 1/8 inch. Transmission half-angling scans were made in 1/4° (2θ) steps. The neutron beam of an effective wavelength of 1.910 Å was contaminated by about 8% of second-order neutrons of 0.955 Å wavelength. The amount of interference due to the second-order reflections was determined by making each run twice, once with a Norton No. 0′ blank disk and then with a Norton No. 3 samarium oxide disk, which reduced the second-order intensities to about one-third. Even so, however, the composite effect of the background and of the reduced second-order peaks did not permit evaluation of the intensities of weak first-order reflections.

The integrated intensities were obtained by planimetering the diffraction maxima.

Density Measurement

Densities of the samples were determined with pyknometers of 25- and 50-ml capacity using degassed paraffin oil (Stanolax) as displacement liquid. About 4 g of 100- or 200-mesh powder was placed in the dry, weighed pyknometer. The pyknometer was transferred to a vacuum desiccator, evacuated, and filled with the degassed oil without breaking the vacuum. The filled pyknometers were brought to 25±0.02° C before inserting the stoppers. Three separate determinations were made for each powder filling.

The average of four calibration runs with C.P. KCl was 1.9826±14 g/cm³, which is only 0.08% lower than the usually quoted density, 1.984 g/cm³, and 0.2% lower than the value of 1.9867 g/cm³ based on $a(25°\text{ C}) = 6.2929$ Å (32) and $N = 6.0235\times10^{23}$.

**The cobalt used was 99.55% electrolytic cobalt donated by the International Nickel Company of Canada, Ltd.; it contained 0.4% nickel. Correction for the nickel content was made when preparing Co_8NiS_8. The small discrepancies in $a(\pi)$ of the neutron-diffraction specimens in Table I are probably due to the varying impurity content of the cobalt metal.*

Can. J. Chem. Downloaded from www.nrcresearchpress.com by 210.87.254.42 on 09/05/12
For personal use only.

Can. J. Chem. Downloaded from www.nrcresearchpress.com by 210.87.254.42 on 09/05/12
For personal use only.

RESULTS AND DISCUSSION

The Lattice Constants and Existence Limits of π(Fe,Co,Ni,S) *in the* M_9S_8 *Section*

The results of the lattice-constant determinations are listed together with the sample compositions and densities in Table I.

Figure 3 shows the variation of $a(\pi)$ with composition as well as the limits within

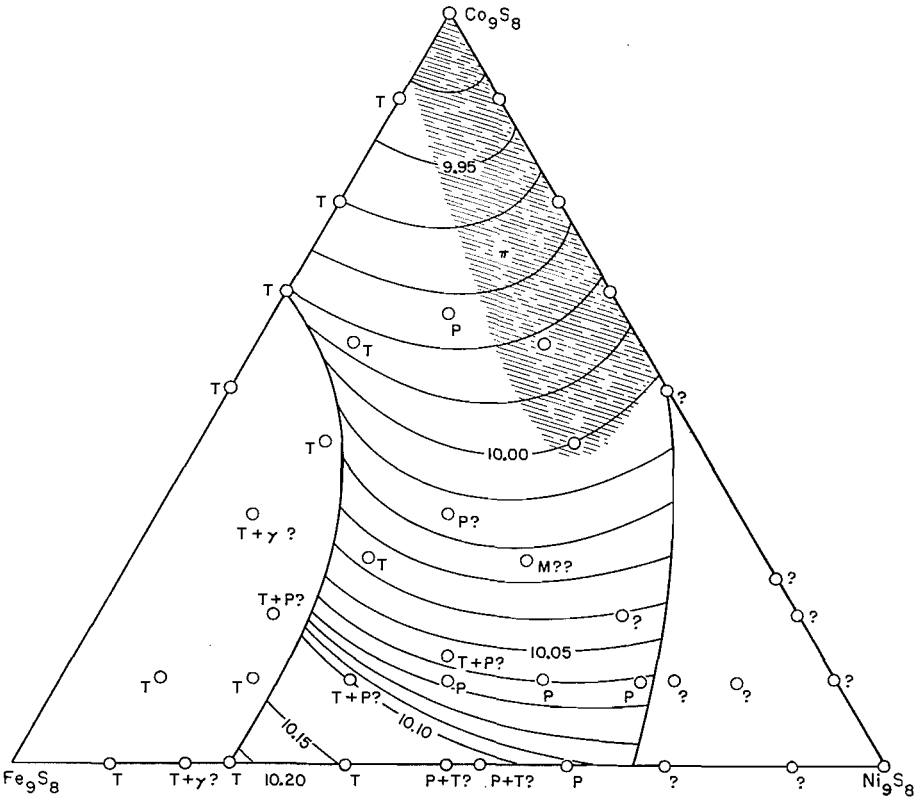


FIG. 3. Limits of existence of π in the M_9S_8 section. Shaded area: pure π. Area within curved boundaries: quasihomogeneous π field. For abbreviations, see text.

which π(Fe,Co,Ni,S) occurs in the M_9S_8 section of the quaternary system at room temperature. Only the samples within the shaded area gave diffraction patterns of the π phase free from foreign lines. All the other samples contained admixtures of other phases in varying amounts. The phase boundaries of the homogeneous π field were estimated from the variation of $a(\pi)$ along the constant-percentage and constant-ratio lines. It is evident that the M_9S_8 plane cuts through the π space of the Fe–Co–Ni–S composition tetrahedron at most only in the region indicated by the shaded area.* Outside this region lines of troilite (T), pyrrhotite (P), and millerite (M) began to appear in the diffraction patterns. This would indicate that the thin π-space slab drops below the M_9S_8 plane towards the Fe–Co–Ni side of the tetrahedron. Assuming that the samples were reasonably near their equilibrium states, the saturated π phases must have con-

**The reliability of the boundary determination depends, of course, on the sensitivity of detection of the admixed phases by powder photography. No effort was made to ascertain the sensitivity limits, but it is estimated that admixture of as little as 1–2 mole% of γ and 5 mole% or less of the other phases can be detected.*

Can. J. Chem. Downloaded from www.nrcresearchpress.com by 210.87.254.42 on 09/05/12
For personal use only.

tained less sulphur than would correspond to the formula $(Fe,Co,Ni)_9S_8$. This finding is in agreement with the presence of faint P lines in the powder patterns of the two artificial pentlandites prepared by LLW, $Fe_{4.5}Ni_{4.5}S_8$ and $Fe_6Ni_3S_8$ (cf. Introduction).

To judge by the relative intensities of the foreign lines the M_9S_8 plane must be quite close to the sulphur-saturation boundary surface of the π space. Furthermore, the thickness of the π slab cannot be appreciable (4, 12, 11). The tentative isoparametric contour lines in the quasihomogeneous π field refer, except for the shaded area, to sulphur-saturated π in equilibrium with the admixed phases rather than to homogeneous π of compositions identical with the gross sample compositions. They must, however, very nearly coincide with the appropriate contour lines in the boundary surface of the π space, the displacement caused by the projection of the two-phase tie lines being quite small.

The saturation limits of $\pi(Fe,Ni,S)$ were estimated from the discontinuities in the $a(\pi)$ vs. composition curves as $Fe_{6.8}Ni_{2.2}S_8$ and $Fe_{2.6}Ni_{6.4}S_8$, the lattice constants of the saturated phases being 10.210 ± 3 Å and 10.087 ± 5 Å, respectively. The homogeneity region of $\pi(Fe,Ni,S)$ at room temperature is thus wider than stated by Lundqvist, whose values would correspond to the formulae $Fe_{5.22\pm18}Ni_{3.78\pm18}S_8$ and $Fe_{3.78\pm18}Ni_{5.22\pm18}S_8$. Lundqvist's lattice constants for these limiting compositions were 10.195 and 10.095 Å,* respectively, the former value having probably been arrived at from $a(\pi)$ in $Fe_6Ni_3S_8$ (4).†

Immediately outside the boundaries of the quasihomogeneous π region of the M_9S_8 section there are three-phase sections through the adjacent room-temperature phase spaces. On the iron side the coexisting phases are γ-Fe, T, and π of equilibrium composition. On the nickel side π coexists with M and N. Since the sulphur-saturation boundary of the π space clears the M_9S_8 plane on approaching the Fe_9S_8–Ni_9S_8 base line, small amounts of the *B8* phase (P) will coexist with π in samples outside the shaded (homogeneous) area. P will also appear in small amounts as a third phase with π and T, and with π and M, respectively, outside the boundaries of the quasihomogeneous region.

Except very near the iron and nickel corners of the composition triangle of Fig. 3 the amounts of phases admixed with π were small. The relative weakness of the foreign lines in the π diffraction pattern did not permit an evaluation of the composition dependence of the unit-cell dimensions of the P phase, although the positions of the 100, 101, and 102 lines of the P pattern in samples within the quasihomogeneous π region seemed to vary somewhat with composition. In fact, the faintness of the strongest foreign lines in some films made it difficult to distinguish between the T and P phases. Thus there is some uncertainty as to whether the second phase in sample Nos. 15, 23, 34, and 52 was T or P. A further factor complicating the identification is our lack of knowledge concerning the stability and metastability of the nickel-saturated troilite.

In the nickel corner the circumstances are even less favorable for an adequate phase analysis. The phases in equilibrium are π, M, and N (or, more correctly, $\pi+P+M$, $\pi+M$, and $\pi+N+M$). According to reference 12 M seems to have little ability to substitute iron for nickel, and one would think that the millerite pattern would be easily recognizable in the photographs. However, as Lundqvist (19) observed in the system Ni–S for compositions near N, the diffraction patterns were rather indistinct and difficult to measure with confidence. The composite patterns of samples in the

**The values 10.175 and 10.075 of reference 12, though quoted in Ångström units, were really in kX, as were all the lattice constants in references 4, 8, 9, 12, and probably also in reference 2.*

†The value of 9.91 Å originally quoted for this composition in reference 4 was a misprint. It was corrected o 10.175 in reference 12 (cf. preceding footnote).

nickel corner thus hardly encourage attempts to clarify the phase relationships further than indicated in Fig. 3. This matter may be resolved later, when more information is available on the pertinent portion of the system Ni–S.

The agreement between the present values of $a(\pi)$ and those reported previously for π(Co,S) and $Fe_{4.5}Ni_{4.5}S_8$ is quite good, provided that the latter are converted to Ångström units wherever this seems warranted (cf. footnotes 4 and 5 of Table I). For π(Co,S) the available values are 9.924±7 Å (3), 9.927 Å (4, 8), 9.924±6 Å (9), and 9.93 Å (2). These values compare favorably with our values 9.929±2 Å for No. 1 and 9.9279±5 Å for No. 46. For $Fe_{4.5}Ni_{4.5}S_8$ (No. 2) the present value of 10.115±2 Å agrees well with the value reported in reference 4, 10.11 Å.

Only after the experimental work on this paper had been terminated the results of Stubbles' redetermination of a for π(Co,S) came to our attention (11). The powder photographs of his carefully equilibrated specimens were taken with filtered CoK radiation in a 19-cm Bradley-Jay type camera. The reported lattice constants of his two quenched samples, $Co_{9.032}S_8$ (S_{F5}) and $Co_{8.989}S_8$ (S_{F8}), were 9.9282±4 Å and 9.9264±4 Å, respectively. Both values fit well into our series of four samples prepared from spectrographic-purity cobalt (Nos. 48, 47, 46, and 49), although the uncertainty in our values is higher. Stubbles regarded the slight difference in a as significant and indicative of a narrow homogeneity range of the phase. This point will be considered in the next section.

Substitution of cobalt by iron or nickel in π(Co,S) causes an expansion of the unit cell. This is true for iron and nickel separately as well as for simultaneous substitution at different Fe:Ni ratios. Iron is capable of replacing cobalt to the extent of about 37.5% and with a corresponding increase in a of 0.049 Å. The variation of a with the iron content is, within the limits of our accuracy, practically linear. The nickel substitution in π(Co,S) does not cause a second phase to appear up to about 50%, the corresponding lattice expansion amounting to 0.076 Å. The variation of a is almost linear.

Although homogeneous π(Co,Fe,S) and π(Co,Ni,S) are confined to the above limits, cobalt in π(Co,S) can be replaced completely and the π phase preserved if Fe and Ni are introduced simultaneously. For the Fe:Ni ratio equal to unity the lattice constant increases on complete replacement by 0.188 Å, i.e., less than 2%. For Fe:Ni ratios greater than 1, a increases to its limiting value, 10.210±3 Å, whereas for smaller ratios it decreases to the limit of 10.087±5 Å. The saturation limit on the nickel side cannot be determined accurately since the a vs. composition curve flattens out. The relationship between a and the Fe:Ni ratio, which is of some importance for the mineralogy of natural pentlandite, will be dealt with more fully in reference 15.

The existence of π(Fe,Co,Ni,S) within wide Fe:Co:Ni limits on both sides of the Co_9S_8–$Fe_{4.5}Ni_{4.5}S_8$ in or near the M_9S_8 plane satisfies the phenomenological requirement of an essentially constant 3d-electron content per unit cell which underlies Rosenqvist's suggestion that the π phase might be electron-stabilized. In fact, the boundaries of the quasihomogeneous π field coincide roughly with the 6.5 and the 7.5 3d-electron-per-atom contour lines of the M_9S_8 section. Whether or not it is meaningful to speak of such stabilization can be shown only by demonstrating that a homogeneous π(Fe,S) or a homogeneous π(Ni,S) or both exist. If satisfactory evidence of the existence of such phases is obtained, the above suggestion cannot hold, and in any case the requirement of a constant 3d-electron concentration per unit cell ought to be reformulated in more fundamental terms.

Though the relationship between natural pentlandite and the synthetic π(Fe,Co,Ni,S) phase will be discussed more fully in reference 15, it is of interest to note that the formula

Can. J. Chem. Downloaded from www.nrcresearchpress.com by 210.87.254.42 on 09/05/12
For personal use only.

$Fe_4^{IV}Ni_4^{IV}(Co,Ni,Fe)_{0-1}^{VI}S_8$, proposed for the mineral by Eliseev, has been invalidated by the recent discovery of natural pentlandites containing up to 70% Co/(Fe+Co+Ni) (33).

Crystal Structure and Composition of π(Fe,Co,Ni,S)

Intensities of the powder diffraction lines of Co_9S_8 were calculated for FeK radiation using both the LLW model and the structure proposed by Eliseev for natural pentlandite. The parameter of the cobalt atom was taken as 1/8 and that of sulphur as 1/4. Neutral atomic form factors (34) were used in the calculation. For comparison, the form factors of Co^{2+} (estimated) and S^{2-} were also used up to 222. The slightly different I_{calc} values based on the ionic form factors are listed in Table II in parentheses. Temperature and absorption factors were not included in the calculations. The calculated values were compared with integrated intensities obtained by planimetering the diffractometer peaks of Co_9S_8 (average of four samples, Nos. 846, 847, 848, and 849), $Fe_{4.5}Ni_{4.5}S_8$ (No. 2), and Sudbury pentlandite (SI AU).

As may be seen in Table II, the agreement between I_{obs} (Co_9S_8) and the intensities calculated for the LLW structure is, on the whole, good. It is even slightly improved by using the ionic form factors for the first few reflections. The adopted parameters

TABLE II

Observed and calculated X-ray powder intensities for Co_9S_8, $Fe_{4.5}Ni_{4.5}S_8$ (No. 2), and Sudbury pentlandite (SI AU)

	I_{calc}, FeK		I_{obs}, FeK		
hkl	LLW	Eliseev	Co_9S_8	No. 2	SI AU
111	39 (36)	172 (156)	33	27	45
200	6	6	6	5	5
220	5	5	7	9	5
311	93 (90)	21	89	75	82
222	21 (22)	21 (22)	31	31	31
400	6	6	5	6	4
331	9	40	15	15	21
420	2	2	3	5	—
422	2	2	1	4	3
511;333	29	7	33	29	29
440	100	100	100	100	100
531	6	28	5	6	<1
600;442	<2	<2	3	—	3
620	1	1	<1	1	—
533	10	2	12	11	15
622	8	8	11	7	9
444	1	1	2	—	4
711;551	4	16	4	1	5
640	<1	<1	—	—	—
642	1	1	<2	—	3
731;553	21	4	20	23	18
800	21	21	19	20	22
733	2	7	5	3	7
820;644	1	1	<2	—	—
822;660	<1	<1	—	—	—
751;555	16	3	21	26	23
662	6	6	9	12	11
840	3	3	3	—	—
911;753	6	22	6	8	6
842	1	1	—	—	—
664	<1	<1	—	—	—
931	18	4	19	16	28
844	138	138	122	123	120
933;771;755	9	29	14	8	10
10.00;860	5 (14)	5 (34)			

Can. J. Chem. Downloaded from www.nrcresearchpress.com by 210.87.254.42 on 09/05/12
For personal use only.

must thus be very nearly correct. A small adjustment might result in further improvement, but the powder intensities were not considered sufficiently reliable to warrant such treatment.* In view of the relatively high proportion of multiple reflections no attempt has been made to calculate the customary reliability index. The interatomic distances calculated from the above parameters are Co^{IV}–S, 2.150 Å, and Co^{VI}–S, 2.482 Å.

Since the atomic form factors of iron and nickel are very similar to the form factor of cobalt, $Fe_{4.5}Ni_{4.5}S_8$ should yield, according to LLW, the same diffraction intensities as Co_9S_8, and this should also be true of natural pentlandite. That this is indeed the case may be seen in the table, but it is possible that the small discrepancies are not entirely accidental.

I_{calc} values for Eliseev's structure model for pentlandite also are shown in Table II. The interchange of the four metal atoms in 4(*b*) of the LLW structure with 4(*a*) of Eliseev's structure affects only those reflections for which all three indices are odd. Inspection of the table shows that Eliseev's model does not apply to any of the three substances examined. The essential correctness of the LLW structure of π is thus substantiated.

The homogeneity range of π(Co,S) is difficult to establish with confidence. Stubbles' equilibrium data (11) leave no doubt about its narrowness at temperatures above 600° C. At room temperature its width can be expected to be even less. An estimate has been attempted by plotting Stubbles' and our own $a(\pi)$ values for samples on both sides of Co_9S_8 against at.% sulphur (Fig. 4). The consistency of the two sets of points is

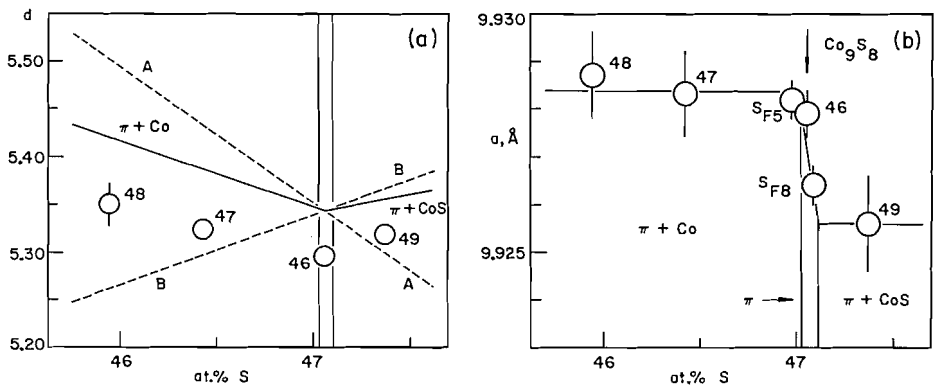


FIG. 4. (*a*) Densities of Co–S samples in the vicinity of Co_9S_8: A, density of π(Co,S) assuming full occupancy of the S sites; B, density of π(Co,S) assuming full occupancy of the Co sites. (*b*) Variation of $a(\pi)$ with composition in the vicinity of Co_9S_8. Vertical lines indicate precision of individual determinations.

surprisingly good. The homogeneity boundaries would appear to be at ca. 47.04 ($Co_{9.006}S_8$) and 47.11 at.% sulphur ($Co_{8.987}S_8$). These limits are wider than the equilibrium data would suggest (cf. Introduction), but considering the uncertainties in drawing the lines of Fig. 4, the agreement must be viewed as reasonable.

The lattice constant of π(Co,S) saturated with sulphur is estimated to be 9.9256±10 Å and that of the cobalt-saturated phase, 9.9284±10 Å. This corresponds to a decrease of *a* by about 0.003 Å for an increase of 0.07 at.% sulphur.

**Geller (35) obtained recently a value of 0.126 for x_{Co} from limited single-crystal data for Co_9S_8, while x_S did not yield to refinement. Since $x_{Co} \neq 1/8$ necessitates a distortion of the co-ordination polyhedra, a full-scale three-dimensional refinement of the structure would be desirable.*

Can. J. Chem. Downloaded from www.nrcresearchpress.com by 210.87.254.42 on 09/05/12
For personal use only.

The measured densities (Table I and Fig. 4) are too few to be of any value for an estimate of the width of the homogeneity region. They are all consistently lower, by roughly the same amount, than the densities calculated from the X-ray density of Co_9S_8 for mixtures of Co_9S_8+Co and Co_9S_8+CoS. As can be seen from the graph, taking into account the width of the homogeneity region would make relatively little difference to the positions of the lines calculated for the mixtures, regardless of whether full occupancy of the available sulphur sites or that of the cobalt sites required by the LLW model is postulated for the structure of nonstoichiometric π(Co,S). The discrepancy between the densities can be explained by assuming that stoichiometric Co_9S_8 is intrinsically defective and that 0.86% atoms of each kind are missing. This amounts to 0.310 cobalt vacancies and 0.275 sulphur vacancies per unit cell, the corresponding formula of the stoichiometric phase being $Co_{8.924}S_{7.932}$.

The existence of Schottky defects in stoichiometric binary oxides and chalkogenides has been demonstrated a number of times. Among the classical examples is stoichiometric CrS, which was shown to contain about 8% vacancies in each sublattice (36), and stoichiometric δ-TiO, in which the concentration of vacancy pairs is even higher, amounting to about 15% (37). Intrinsically defective phases of this type are usually 1:1 compounds but in principle there is no reason why a phase whose ideal composition is well defined by its crystal symmetry could not behave in a similar manner.

The assumption of vacancies in the sulphur sublattice is not consistent with the very low mobility of sulphur in Co_9S_8. Stubbles determined the self-diffusion coefficient of sulphur in π(Co,S) of varying stoichiometry at 800° C and found that the anion mobility was extremely low even along grain boundaries. From this he concluded that the sulphur sublattice contained few imperfections. The mobility of cobalt, on the other hand, is quite high; the self-diffusion coefficient of cobalt in Co_9S_8 at 800° C is about 10^4 larger than the self-diffusion coefficient of Fe in Fe_3O_4 at the same temperature. This Stubbles attributed to the possibility of migration of the cobalt atoms between unoccupied octahedral sites in the structure. In stoichiometric Co_9S_8 this diffusion mechanism would presuppose an intrinsically disordered occupancy of the cobalt sublattice with some cobalt atoms in octahedral sites other than 4(*b*). These would also be the sites occupied by the excess cobalt atoms in phases with nonstoichiometric compositions $Co_{9+x}S_8$, and the same diffusion mechanism would operate. In $Co_{9-x}S_8$ there is the additional possibility of migration between 4(*b*) and the other octahedral positions. According to this model the general formula of π(Co,S) would be $Co_{9\pm x}S_{8-y}$, where $y \ll x$. Since $|x|_{max}$ reported in reference 11 was 0.031, the above value of $y = 0.068$ estimated from density data for stoichiometric Co_9S_8, is certainly not of the right order of magnitude. On the other hand, the reliability of even very careful density determinations on powders is admittedly somewhat open to question, and the true densities may be higher than stated in Table I (the uncertainty quoted there refers to precision, not accuracy).

As for the high self-diffusion mobility of cobalt, vacancies in the cobalt sublattice of stoichiometric Co_9S_8 would facilitate migration of the metal atoms and satisfy the condition of intrinsic disorder equally well as the displaced atoms postulated by Stubbles. Since tetrahedral as well as octahedral sites would be unoccupied, the differences in the potential (and activation) energies associated with the different types of sites (and jumps) would have to be considered when proposing a self-diffusion mechanism on the assumption of a structure deficient in both sublattices. It is, of course, possible for the structure of stoichiometric Co_9S_8 to conform with the formula $Co_{9(1-\delta)}S_{8(1-\delta)}$ and yet contain some of the cobalt atoms in interstitial, octahedrally co-ordinated positions,

Can. J. Chem. Downloaded from www.nrcresearchpress.com by 210.87.254.42 on 09/05/12
For personal use only.

though it cannot be determined from the densities whether this is the case. The X-ray diffraction intensities are too insensitive to be of use for small values of δ.

Evidence presented in the preceding section shows that in π(Fe,Co,Ni,S) the M:S ratio was not exactly 9:8 but higher. Of the several possibilities to account for the excess metal the most likely one seems the arrangement proposed by Stubbles for $Co_{9+z}S_8$, though not necessarily with the sulphur sites fully occupied. The correctness of this contention cannot, however, be supported from density measurements, as the observed densities do not refer to homogeneous π but to π-containing admixtures of other phases. Densities and relative amounts of the admixed phases have not been determined, since the gross compositions of the samples were restricted to the M_9S_8 section.

Neutron-Diffraction Study of Co_8NiS_8 *and the Possibility of Existence of an Ordered* π *Phase*

It seemed worth while to investigate whether in the stoichiometrically favorable samples Co_8FeS_8 and Co_8NiS_8 the Fe and Ni atoms would segregate into the octahedral sites with cobalt remaining in the tetrahedral positions. Since nickel appeared to enter the π structure more readily than iron, Co_8NiS_8 rather than Co_8FeS_8 was the composition selected for a neutron-diffraction study.

The coherent neutron scattering amplitudes of iron, cobalt, and nickel are, in 10^{-12} cm, 0.96, 0.28, and 1.03 respectively (38). The appreciable difference between the scattering amplitudes of iron and nickel on the one hand and that of cobalt on the other makes it possible to distinguish between the two extreme cases of distribution of metal atoms, i.e., between the completely random arrangement and complete segregation.

All the neutron-diffraction maxima appearing in the experimentally accessible angular region 7.5–40.5° (θ) in the powder patterns of slowly cooled Co_9S_8 and Co_8NiS_8 were accounted for on the basis of the chemical unit cell of π. The relative diffraction intensities of the more prominent maxima are listed in Table III. These figures provide, at the

TABLE III

Neutron diffraction intensities of Co_9S_8 and Co_8NiS_8

			$I(Co_8NiS_8)$					
	$I(Co_9S_8)$		Random		Ordered		I_{obs}	
hkl	LLW	E	LLW	E	LLW	E	Co_9S_8	Co_8NiS_8
111	5	24	7	31	<1	43	3	7
311	21	5	27	6	37	<1	25	29
222	27	27	19	19	7	7	31	20
331	3	13	4	17	<1	24	6	6
511;333	14	3	17	4	23	<1	16	20
440	100	100	100	100	100	100	100	100
531	4	17	5	22	<1	31	4	4

			Intensity ratio $I(Co_8NiS_8)/I(Co_9S_8)$				
	Structure factor*		LLW		E		
hkl	LLW	E	Random	Ordered	Random	Ordered	Observed
111	$-4f_{Ni}+11.3f_{Co}$	$4f_{Ni}+11.3f_{Co}$	1.66	0.22	1.66	2.90	(2.3)†
311	$-4f_{Ni}-11.3f_{Co}$	$4f_{Ni}-11.3f_{Co}$	1.66	2.90	1.66	0.22	1.65
222	$4f_{Ni}-32f_S$		0.93	0.44	0.93	0.44	0.92
331	$-4f_{Ni}+11.3f_{Co}$	$4f_{Ni}+11.3f_{Co}$	1.66	0.22	1.66	2.90	1.67
420	$4f_{Ni}$		1.65	13.55	1.65	13.55	1.7
422	$4f_{Ni}$		1.65	13.55	1.65	13.55	(3.2)†
511;333	$-4f_{Ni}-11.3f_{Co}$	$4f_{Ni}-11.3f_{Co}$	1.66	2.90	1.66	0.22	1.55
440	$4f_{Ni}+32f_{Co}+32f_S$		1.31	1.63	1.31	1.63	1.3

*For completely ordered Co_8NiS_8; f_{Co}, 0.28; f_{NI}, 1.03; f_S, 0.31; f_{mixed}, 0.36.
†Value uncertain.

Can. J. Chem. Downloaded from www.nrcresearchpress.com by 210.87.254.42 on 09/05/12
For personal use only.

same time, information concerning the degree of order in Co_8NiS_8 and a correctness test for the two proposed structure models of the phase. From the intensity values normalized to I_{440} (upper half of Table III) one finds that a comparison of I_{obs} and I_{calc} of Co_9S_8 favors the LLW model. This provides an independent confirmation of a similar conclusion based on the X-ray diffraction data. For Co_8NiS_8 the best agreement is obtained for the random LLW structure.

Since interference from the second-order maxima could not be eliminated completely even with a samarium oxide filter, it may be argued that the agreement between I_{obs} and I_{calc} is to some extent fortuitous. This objection is removed if one considers that the integrated diffraction maxima from atomic planes of Co_9S_8 and Co_8NiS_8 with identical indices are of the same order of magnitude. Consequently in the ratios $I(Co_8NiS_8)/I(Co_9S_8)$ the effect of the second-order maxima will be very substantially reduced and the comparison will be more accurate and reliable, provided only that the diffraction peaks are reasonably strong. This is indeed the case (lower half of Table III). Comparison of the observed intensity ratios with those calculated for four different models confirms the conclusion made in the preceding paragraph, but unfortunately the uniqueness of choice between the LLW and Eliseev's models with statistical distribution is reduced. There is, however, no doubt that the Co_8NiS_8 sample had a randomized structure.

That ordered Co_8MS_8 phases of this type exist has been shown in cases with M other than nickel (39). The failure of Co_8NiS_8 to form an ordered phase must then be due to the lack of preference of nickel for octahedral co-ordination, though the ordered phase $Co_8^{IV}Ni^{VI}S_8$ might still be obtainable by even longer annealing at a more favorable (as yet unknown) temperature. In this respect Co_8NiS_8 differs from the oxidic spinels, in which divalent nickel has been shown to favor octahedral positions (cf., for instance, references 40, 41, and 42). The metal distribution in the somewhat related sulphocobaltite $NiCo_2S_4$ (43) is not yet known, but for the corresponding cobaltites McClure (41) has predicted that $FeCo_2O_4$ and Co_3O_4 should be normal spinels, whereas $NiCo_2O_4$ should be of the inverse type.

We have not been able to corroborate Eliseev's contention that the O_h^5—$Fm3m$ symmetry is lowered in natural pentlandite by an ordering of the iron and nickel atoms in $32(f)$, but the possibility of such an arrangement cannot be ruled out, since the symmetry degeneration caused by the ordering may be virtually undetectable (see 15 for a more detailed discussion).

Some idea of the tendency of nickel and iron to form ordered sublattices in $4(b)$ might be obtained from a comparison of the self-diffusion coefficients of nickel and iron in Co_8NiS_8 and Co_8FeS_8 (or its nearest homogeneous equivalent) with those of cobalt in Co_9S_8 over a range of temperatures. A similar investigation of the variation of the mobility of cobalt with composition along the line Co_9S_8–$Fe_{4.5}Ni_{4.5}S_8$ might also be useful as an extension of Stubbles' work.

Further Observations

Our diffraction data are not adequate to demonstrate the exact shape of the cobalt and sulphur co-ordination polyhedra in the π structure. Before the parameters x_{Co} and x_S are known with sufficient accuracy, reliable values for the interatomic distances in π(Co,S) cannot be obtained, nor can conclusions be made from the co-ordination stereochemistry of the atoms about their orbital configurations.

In π(Fe,Co,Ni,S) there is an additional complication arising from the possibility of existence of ordered sublattices at certain compositions. For example, in Co_8NiS_8 with the cobalt and nickel atoms distributed statistically over the tetrahedral and octahedral sites, x_{Co} and x_{Ni} might have somewhat different values, so that only average values of

Can. J. Chem. Downloaded from www.nrcresearchpress.com by 210.87.254.42 on 09/05/12
For personal use only.

the M–S distances could be obtained from $a(\pi)$. The same holds a fortiori for compositions that preclude ordered arrangements.

As for the increase of $a(\pi)$ on replacing cobalt in Co_9S_8 severally by iron and nickel, one would not expect to find that both kinds of atoms expand the lattice. Lotgering (43) reported a similar situation for the spinel-type cobaltites $Fe_{0.99}Co_{2.01}S_4$, Co_3O_4, and $NiCo_2O_4$, whose lattice parameters were 8.254, 8.092, and 8.121 Å, respectively. He did not succeed in preparing the sulphocobaltite $FeCo_2S_4$, but the lattice constants of Co_3S_4 and $NiCo_2S_4$, 9.416 and 9.392 Å, respectively, show the reverse trend on going from cobalt to nickel. The interatomic distances "M^{2+}–X" in the chalkogenides of the 3d-series do show a minimum at cobalt for octahedrally co-ordinated M (44), but with a ratio of 8:1 of tetrahedral to octahedral sites in π attempts to rationalize the situation seem, in the absence of more detailed information on the distribution of the metal atoms in the nonionic Co_8FeS_8 and in the sulphospinels, premature. The increasing departure of π(Co,S) from the stoichiometric formula on progressive replacement of the cobalt with iron and nickel, and the possibility of some of the metal atoms being accommodated interstitially, may be partly responsible for the variation of $a(\pi)$ with composition and should be considered in addition to the effect of the interatomic distances.

ACKNOWLEDGMENTS

The authors would like to express their gratitude to the following persons and agencies: Colombo Plan Administration, Ottawa, for a scholarship awarded to one of them (M.A.I.); Nova Scotia Research Foundation for providing the salary of a student assistant for two summers; Mr. Muntaz Ali and Miss Judith Osyany for assistance with the experimental work; Dr. L. Castelliz for evaluation of a number of X-ray diffraction photographs; Dr. B. N. Brockhouse, Atomic Energy of Canada Ltd., Chalk River, Ontario, for permission to use his neutron spectrometer; Dr. J. R. Stubbles, Department of Metallurgy, University of Manchester, for loan of his unpublished Ph.D. Thesis; and Mr. S. Bender, Application Laboratory, Philips Electronic Instruments, Mount Vernon, N.Y., for obtaining some of the diffractometer charts.

REFERENCES

1. K. Friedrich. Metallurgie, **5**, 212 (1908).
2. V. Cagliotti and G. Roberti. Gazz. chim. ital. **62**, 19 (1932).
3. O. Hülsmann and F. Weibke. Z. anorg. Chem. **227**, 113 (1936).
4. M. Lindqvist, D. Lundqvist, and A. Westgren. Svensk Kem. Tidskr. **48**, 156 (1936).
5. N. Alsén. Geol. Fören. i Stockholm Förh. **47**, 54 (1925).
6. International Tables for X-Ray Crystallography. Vol. 1. The Kynoch Press, Birmingham. 1952.
7. Strukturbericht, **4**, 26 (1936). Akademische Verlagsgesellschaft, Leipzig. 1938.
8. D. Lundqvist and A. Westgren. Z. anorg. Chem. **239**, 85 (1938).
9. W. Curlook and L. M. Pidgeon. Trans. Can. Inst. Mining Met. **56**, 143 (1953).
10. T. Rosenqvist. J. Iron Steel Inst. (London), **176**, 37 (1954).
11. J. R. Stubbles. Ph.D. Thesis, Imperial College, University of London. 1957.
12. D. Lundqvist. Arkiv Kemi, Mineral. Geol. A, **24**, No. 22 (1947).
13. F. Bøhm, F. Grønvold, H. Haraldsen, and H. Prydz. Acta Chem. Scand. **9**, 1510 (1955).
14. F. H. Meyer, O. L. Riggs, R. L. McGlasson, and J. D. Sudbury. Corrosion, **14**, 69 (1958).
15. O. Knop and M. A. Ibrahim. In preparation.
16. E. N. Eliseev. Zapiski Všesojuz. Mineral. Obščestva, **84**, 54 (1955).
17. V. I. Micheev. Sb. statej "Kristallografija". Trudy Fedorovskoj naučnoj sessii 1951 g. Moskva. 1952. p. 75.
18. G. Peyronel and E. Pacilli. Atti Accad. Italia, Rend. classe sci. fis. mat. nat. **3** (7), 278 (1941).
19. D. Lundqvist. Arkiv Kemi, Mineral. Geol. A, **24**, No. 21 (1947).
20. O. Knop and H. Haraldsen. To be published.
21. M. A. Sokolova and V. G. Kuznec. Doklady Akad. Nauk S.S.S.R. **106**, 286 (1956).
22. W. Guertler and H. Schack. Metall u. Erz, **20**, 361, 426 (1923).
23. G. G. Urazov and N. A. Filin. Metallurg, **13**, No. 2–3, 3 (1938).

Can. J. Chem. Downloaded from www.nrcresearchpress.com by 210.87.254.42 on 09/05/12
For personal use only.

24. R. SCHENCK and P. VON DER FORST. Z. anorg. Chem. **249**, 76 (1942).
25. R. VOGEL and R. AU. Z. Metallk. **40**, 290 (1949).
26. P. ASANTI and E. J. KOHLMEYER. Z. anorg. Chem. **265**, 90 (1951).
27. R. VOGEL and G. F. HILLNER. Arch. Eisenhüttenw. **24**, 133 (1953).
28. I. KUSHIMA and N. ASANO. Nippon Kôgyô Kwaishi, **69**, 297 (1953); Chem. Abstr. **48**, 11900 (1954).
29. M. A. IBRAHIM. M.E. Thesis. Nova Scotia Technical College, Halifax, N.S., September 1958.
30. M. HANSEN and K. ANDERKO. Constitution of binary alloys. 2nd ed. McGraw-Hill, New York. 1958. pp. 1266–1267.
31. A. WESTGREN. Z. anorg. Chem. **239**, 82 (1938); cf. Structure Repts. **11**, 299 (1947–48).
32. P. G. HAMBLING. Acta Cryst. **6**, 98 (1953).
33. O. KOUVO, M. HUHMA, and Y. VUORELAINEN. Am. Mineralogist, 44, 897 (1959).
34. INTERNATIONALE TABELLEN ZUR BESTIMMUNG VON KRISTALLSTRUKTUREN. Bd. 2. Gebr. Borntraeger, Berlin. 1935.
35. S. GELLER. Private communication. 1959.
36. H. HARALDSEN. Z. anorg. Chem. **234**, 372 (1937).
37. P. EHRLICH. Z. Elektrochem. **45**, 362 (1939).
38. G. E. BACON. Neutron diffraction. Oxford University Press, Oxford. 1955.
39. O. KNOP. Occurrence of the π phase among chalkogenides. Paper No. 5.30. 5th Intern. Congr. of the Intern. Union Cryst., Cambridge, August, 1960.
40. F. C. ROMEIJN. Philips Research Repts. **8**, 304 (1953).
41. D. S. MCCLURE. Phys. and Chem. Solids, **3**, 311 (1957).
42. J. D. DUNITZ and L. E. ORGEL. Phys. and Chem. Solids, **3**, 20, 318 (1957).
43. F. K. LOTGERING. Philips Research Repts. **11**, 337 (1956).
44. N. S. HUSH. Discussions Faraday Soc. No. 26, 149 (1958).

Can. J. Chem. Downloaded from www.nrcresearchpress.com by 210.87.254.42 on 09/05/12
For personal use only.

Can. J. Chem. Downloaded from www.nrcresearchpress.com by 210.87.254.6 on 09/05/12
For personal use only.

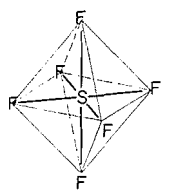
BOND LENGTHS AND BOND ANGLES IN OCTAHEDRAL, TRIGONAL-BIPYRAMIDAL, AND RELATED MOLECULES OF THE NON-TRANSITION ELEMENTS[1]

R. J. GILLESPIE

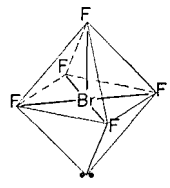
ABSTRACT

The stereochemistry of molecules in which there are five or six pairs of electrons in the valency shell of a central atom is discussed in terms of the repulsions that exist between pairs of electrons in the valency shell as a consequence of the operation of the Pauli exclusion principle. An explanation is given for the difference in lengths of the axial and equatorial bonds in molecules such as PCl_5 and ClF_3 whose structures are based on the trigonal-bipyramidal arrangement of five valency-shell electron pairs. The fact that in molecules with a central atom with a valency shell of six electron pairs, one of which is a lone pair and which have the structure of a square pyramid, the central atom always lies below rather than in, or above, the base of the square pyramid, is also accounted for.

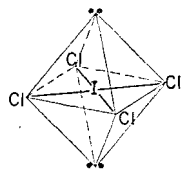
The stereochemistry of an atom in a molecule is determined by the total number of electron pairs, including both lone pairs and bonding pairs, in its valency shell (1). The operation of the Pauli exclusion principle which keeps electrons of the same spin as far apart as possible determines the arrangement of these electron pairs and this in turn determines the stereochemistry (2, 3). For non-transition elements, five and six pairs of valency-shell electrons adopt the trigonal-bipyramidal and octahedral arrangements respectively (1, 3). If we denote a central atom by A, a ligand by X, and an unshared pair of electrons by E then AX_6 molecules are octahedral (e.g., SF_6(I)), AX_5E molecules are square pyramidal (e.g., BrF_5(II)), AX_4E_2 molecules are square planar (e.g., ICl_4^-(III)), AX_5 molecules are trigonal-bipyramidal (e.g., PCl_5(IV)), AX_4E molecules have the structure of $TeCl_4$(V), and AX_3E_2 molecules are T-shaped (e.g., ClF_3(VI)). In these molecules the bond angles are only equal to the "ideal" values of 120° and 90°



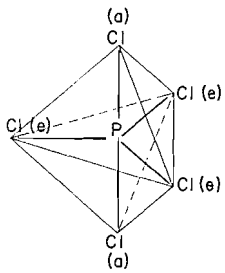
(I)



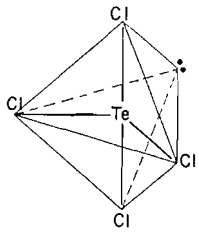
(II)



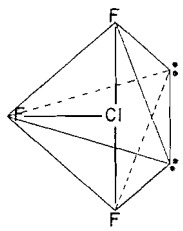
(III)



(IV)



(V)



(VI)

[1]*Manuscript received September 12, 1960.*
Contribution from the Department of Chemistry, McMaster University, Hamilton, Ontario.

and the covalent radius of the central atom is only the same for all the bonds if all the electron pairs are strictly equivalent to each other. In many of these molecules the valency-shell electron pairs are not all equivalent even when all the ligands are the same and therefore deviations of the bond angles from the ideal values and differences in bond lengths are to be expected. These deviations from ideal structures which have been briefly considered in a previous publication (3) are discussed in detail in this paper.

AX_5, AX_4E, AND AX_3E_2 MOLECULES

Bond Lengths

It is a special feature of the trigonal-bipyramidal arrangement of five electron pairs that the positions occupied by the electron pairs are not all equivalent to each other in contrast to the completely equivalent positions of all the electron pairs in the tetrahedral, octahedral, and square antiprism arrangements of four, six, and eight electron pairs respectively. In the trigonal bipyramid the two axial positions are not equivalent to the three equatorial positions (*a* and *e*, respectively, in IV). An electron pair in an *a* position has three nearest neighbors at an angle of 90° and one further away at 180° while an electron pair in an *e* position has two nearest neighbors at an angle of 90° and two further away at 120°.

The Pauli repulsion forces which determine the arrangement of the electron pairs are of such a nature that they are very small when the orbitals of the two electron pairs do not overlap to an appreciable extent but they increase very considerably as the interelectron distance is reduced and the orbitals begin to overlap appreciably, i.e., they may be approximately represented as a function of some large inverse power of the distance (3). Thus, when considering the resultant magnitude of the repulsions between sets of electron pairs the repulsions between nearest neighbors are much more important than those between electron pairs that are further apart, and, to a first approximation, all repulsions except those between nearest neighbors may be neglected. In the trigonal-bipyramidal arrangement of five electron pairs the two axial pairs each have three equatorial pairs at an angle of 90° as nearest neighbors while the equatorial pairs each have only two axial pairs at 90° as nearest neighbors. Hence the total repulsion exerted on the axial pairs is greater than that exerted on the equatorial pairs. This means that a trigonal-bipyramidal arrangement with the electron pairs all at the same distance from the nucleus will not be the true equilibrium arrangement but the distances of the electron pairs from the nucleus will adjust themselves so as to equalize the repulsions between any pair of electrons. Evidently this will result in the axial electron pairs being at a greater distance from the nucleus than the equatorial pairs. Therefore the lengths of bonds to identical ligands in the axial and equatorial positions will not be the same (as is necessarily the case for bonds to four, six, and eight identical ligands in the tetrahedral, octahedral, and square antiprism arrangements, respectively), but the axial bonds will be longer than the equatorial bonds. More generally, to take account of cases where the ligands are not all identical, we can say that the covalent radius of the central atom will be greater in the axial than in the equatorial direction.

When one or more of the electron pairs is a lone pair another factor must be considered. Bonding pairs which are under the influence of two nuclei occupy more restricted "thinner" orbitals than lone pairs which are under the influence of only one nucleus and occupy less restricted "fatter" orbitals (3). These larger lone-pair orbitals overlap more than the smaller bonding orbitals and consequently lone-pair electrons repel other lone-pair or bonding electrons more strongly than bonding electrons repel each other.

Can. J. Chem. Downloaded from www.nrcresearchpress.com by 210.87.254.6 on 09/05/12
For personal use only.

Thus in AX_4E and AX_3E_2 molecules where there are one or two lone pairs in equatorial positions the greater repulsions exerted by the lone pairs will reinforce the difference in the lengths of axial and equatorial bonds discussed above.

Covalent radii for phosphorus, tin, selenium, tellurium, chlorine, bromine, and iodine in AX_5, AX_4E, and AX_3E_2 molecules have been calculated from the experimental bond distances by subtracting the covalent radii (4) of the ligand atoms and the values are given in Table I. It may be seen that for all 13 molecules whose bond lengths have been

TABLE I

Equatorial and axial radii of 10-electron valency-shell central atoms in AX_5, AX_4E, and AX_3E_2 molecules

Molecule	r_{eq}(Å)	r_{ax}(Å)	Reference
	AX_5		
PCl_5	1.05	1.20	5
PCl_2F_3	0.95	1.06	5
$SbCl_5$	1.32	1.44	5
	AX_4E		
$(C_6H_5)_2SeBr_2$	1.14	1.36	5
$(C_6H_5)_2SeCl_2$	1.14	1.31	5
$(CH_3.C_6H_4)_2SeCl_2$	1.17	1.40	5
$(CH_3.C_6H_4)_2SeBr_2$	1.17	1.40	5
$(CH_3)_2TeCl_2$	1.33	1.52	6
$(C_6H_5)_2TeBr_2$	1.37	1.54	7
$IO_2F_2^-$	1.27	1.36	5
	AX_3E_2		
ClF_3	0.94	1.04	5
$C_6H_5ICl_2$	1.23	1.46	5
BrF_3	1.08	1.18	8, 9

determined with sufficient accuracy the axial radius of the central atom is greater than its equatorial radius by 0.1 to 0.2 Å.

The five electron pairs are of course not strictly localized at the corners of the trigonal bipyramid. These are simply the positions at which they are most probably to be found and they may be regarded as effectively occupying all the space in the valency shell, each pair occupying an orbital which is directed towards one of the corners of the trigonal bipyramid; these are essentially the sp^3d orbitals of valence-bond theory. Just as the five positions for the electron pairs are not equivalent to each other so the five sp^3d orbitals are similarly not equivalent. It has been shown by making certain assumptions concerning the effective atomic numbers of the atoms involved that maximum overlap of an orbital of the ligand atom with an equatorial orbital of the central atom occurs at a slightly smaller internuclear distance than for an axial orbital (10) and therefore the axial bonds are expected to be slightly longer than the equatorial bonds. This is an alternative explanation to that given above but it involves some arbitrary assumptions and is in a sense less fundamental. Although the hybrid orbitals that it uses are a convenient way of describing the electron arrangement this arrangement is essentially determined by the operation of the Pauli exclusion principle. McCullough and Marsh (11) have suggested that s orbitals of the next highest quantum shell (e.g. 6s rather than 5s for tellurium) contribute to the hybrid orbitals involved in the axial bonds. Such orbitals may indeed make a small contribution to the actual bonding orbitals but this is not a satisfactory *explanation* of the anomalous length of the axial bonds but only a convenient approximate *description* of the bond orbitals.

Can. J. Chem. Downloaded from www.nrcresearchpress.com by 210.87.254.6 on 09/05/12
For personal use only.

The difference in bond lengths in ClF_3 has been attributed to double bonding between the equatorial fluorine atom and the chlorine, but no explanation was given for why double bonding occurs with the equatorial and not the axial fluorine atoms (12). Moreover, such a special explanation is not necessary in view of the fact that this molecule has a five electron pair valency shell in which we have seen that axial single bonds will be longer than equatorial single bonds to the same ligands.

Bond Angles

For AX_5 molecules with five identical ligands or with three identical equatorial and two identical axial ligands, as in PF_3Cl_2, all the bond angles would be expected, and are found, to be equal to either 90° or 120°. In all other cases where there are two or more different ligands small deviations from the 90° and 120° bond angles would be expected, but no bond angles have been determined for such molecules.

For AX_4E molecules the extra repulsion exerted by the lone pair would be expected, in addition to lengthening the axial bonds as explained above, to decrease the angles between all the bonds. It may be seen from Table II that the angle between equatorial

TABLE II

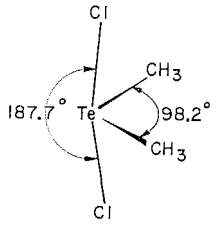
Bond angles in AX_4E and AX_3E_2 molecules

	Bond angle		Reference
	AX_4E molecules		
	e–e	*a–a*	
Ph_2SeBr_2	110°	180°	5
Ph_2SeCl_2	—	180	5
$(p.CH_3.C_6H_4)_2SeBr_2$	108	183	5
$(p.CH_3.C_6H_4)_2SeCl_2$	106.5	182	5
$(CH_3)_2TeCl_2$	98.2	172.3	6
$(C_6H_5)_2TeBr_2$	96.3	182	7
$IO_2F_2^-$	100	180	5
	AX_3E_2 molecules		
ClF_3	87.5°		5
BrF_3	86.2		8
$C_6H_5ICl_2$	86		5

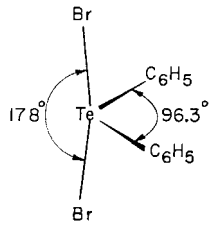
bonds is in every case reduced to a value considerably less than 120°. The angle between the two axial bonds differs only slightly from the value of 180°. It has been pointed out previously (13) that for second and subsequent row elements repulsions between valency-shell electron pairs do not become of appreciable magnitude until they make angles of approximately 90° with each other at the nucleus. It is reasonable then that the greatest distortion should occur in the angle between the equatorial bonds which is 120° in the ideal case as the repulsion between these electron pairs is small. The axial bond electrons make an ideal angle of 90° with the equatorial bond electrons, and any reduction in the angle between the axial bonds necessitates a simultaneous reduction in the angle that they make with the equatorial bonds. Such a decrease in this angle will be strongly opposed by the strong electron-pair repulsions which come into play at an angle of approximately 90°. In the case of $(CH_3)_2TeCl_2$ (VIII) the Cl—Te—Cl angle is slightly less than 180°, i.e., the Te—Cl bonds are bent slightly towards the Te—C bonds and away from the lone pair, as would be expected. In all other cases where a deviation from the ideal angle of 180° has been recorded the angle between the axial bond is slightly greater than 180°, i.e., the axial bonds are bent slightly away from the equatorial

Can. J. Chem. Downloaded from www.nrcresearchpress.com by 210.87.254.6 on 09/05/12
For personal use only.

bonds and towards the lone pair, e.g., $(C_6H_5)_2TeBr_2$ (VIII). This is not in accordance with the prediction made above but it may be noted that in all these cases the equatorial



(VII)



(VIII)

ligands are phenyl, or substituted phenyl, groups and there may be additional repulsions between the bulky phenyl groups and the axial ligands and, moreover, the lone pair on the central atom might be expected to be conjugated with, and partially delocalized into, the aromatic rings which will reduce its repulsive effect on the bond electron pairs. The increased electron density in such partial double bonds between the tellurium and the benzene rings would increase the repulsions between these bonds and the axial bonds and this would also tend to decrease the angle between the axial bonds.

For AX_3E_2 molecules the extra repulsions exerted by the two lone pairs in the equatorial positions cause the axial bonds to lengthen as discussed above and the angles between the axial and equatorial bonds to be slightly smaller than 90° as shown by the examples in Table II.

AX_6, AX_5E, AND AX_4E_2 MOLECULES

In octahedral AX_6 molecules all the bonds to identical ligands will be the same length, i.e., the radius of the central atom will be the same in all directions. For AX_5E molecules which have a square pyramidal shape the extra repulsion exerted by the lone pair would be expected to cause the neighboring four bonds, i.e., those at the base of the square pyramid to be slightly longer than the fifth bond to the apex. Experimental evidence on molecules of this type is scanty (5). The four square-planar bonds are longer than the single bond to the apex in $SbCl_5^{2-}$ but they appear to be shorter in SbF_5^{2-}. The extra repulsion exerted by the lone pair would also be expected to decrease the angles between the bonds to slightly less than 90° giving a molecule in which the central atom is slightly below the base of the square pyramid. It has been recently pointed out by Grednic and Scavnicar (14) that this type of structure is observed in the following substances which all contain five-co-ordinated tervalent antimony with a square pyramidal configuration: K_2SbF_5, $KSbF_4$, $FeSb_2S_4$, $HgSb_4F_8$, $PbAgSbS_3$, Sb_2S_3. The same structure is also found for BrF_5 (15). In each case the central atom is found to be 0.1–0.3 Å below the base of the square pyramid. No example is known where the central atom in an AX_5E molecule is either in, or above, the base of the square pyramid formed by the five ligands.

Molecules of the type AX_4E_2 (e.g., ICl_4^- and BrF_4^-) are expected, and are found, to be square planar with equal bond angles and bond lengths (5, 16).

REFERENCES

1. R. J. Gillespie and R. S. Nyholm. Quart. Revs. **11**, 339 (1957).
2. P. G. Dickens and J. W. Linnett. Quart. Revs. **11**, 291 (1957).
3. R. J. Gillespie. Can. J. Chem. **38**, 818 (1960).

Can. J. Chem. Downloaded from www.nrcresearchpress.com by 210.87.254.6 on 09/05/12
For personal use only.

4. L. PAULING. Nature of the chemical bond. 3rd ed. Cornell University Press. 1960. p. 224.
5. INTERATOMIC DISTANCES. Chemical Society, London. 1958.
6. G. D. CHRISTOFFERSON, R. A. SPARKS, and J. D. MCCULLOUGH. Acta Cryst. **11**, 782 (1958).
7. G. D. CHRISTOFFERSON and J. D. MCCULLOUGH. Acta Cryst. **11**, 249 (1958).
8. D. W. MAGNUSSON. J. Chem. Phys. **27**, 223 (1957).
9. R. D. BURBANK and F. N. BENSEY. J. Chem. Phys. **27**, 983 (1957).
10. D. P. CRAIG, R. S. NYHOLM, A. MACCOLL, L. E. ORGEL, and L. E. SUTTON. J. Chem. Soc. 332 (1954).
11. J. D. MCCULLOUGH and R. E. MARSH. Acta Cryst. **3**, 41 (1950).
12. R. D. BURBANK and F. N. BENSEY. J. Chem. Phys. **21**, 602 (1953).
13. R. J. GILLESPIE. J. Am. Chem. Soc. In press.
14. D. GREDNIC and S. SCAVNICAR. Proc. Chem. Soc. 147 (1960).
15. R. D. BURBANK and F. N. BENSEY. J. Chem. Phys. **27**, 983 (1957).
16. W. G. SLY and R. E. MARSH. Acta Cryst. **10**, 378 (1957).

Can. J. Chem. Downloaded from www.nrcresearchpress.com by 210.87.254.6 on 09/05/12
For personal use only.

Can. J. Chem. Downloaded from www.nrcresearchpress.com by 210.87.254.105 on 09/05/12
For personal use only.

π-BONDING IN INORGANIC COMPOUNDS

II. THE TRANSMISSION OF ELECTRONIC EFFECTS THROUGH SQUARE-PLANAR COMPLEXES[1, 2]

A. D. WESTLAND AND L. WESTLAND

ABSTRACT

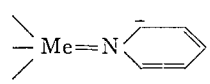
Measurement of the transmission of electronic effects through square-planar complexes of platinum has provided evidence of double bonding to halogen and nitro ligands. The nuclear magnetic resonance chemical shift of the β-protons in pyridine ligands serves as an indicator of electron drift in the complexes. Justification is thus provided for the assumed mechanism of the trans effect involving π-bonding. The observations are in accord with the assumption that the increase in trans-directing powers with atomic number of the halogen is due to an increasing tendency to accept *d*-electrons from the central atom.

Chatt, Duncanson, and Venanzi have sought to explain the trans-directing power of certain ligands in substitution reactions involving complex compounds by making use of a model involving the donation of *d*-electrons (1). Their explanation rests upon an examination of N—H stretching frequencies of amines situated trans to various ligands. It was argued that since the frequencies showed no correlation with trans-directing power the effect could not be due to a weakening of the metal – amine bond as a result of the inductive influence of ligands at the antipode of the molecule. These experiments were actually inconclusive, however, for if the trans effect operates as postulated by Grinberg (2) it does not depend simply upon the strength of the bond to the group being replaced but rather upon its strength *relative* to that of a similar bond in the cis direction. In a subsequent publication (3), Chatt and co-workers examined the infrared spectra of some complexes having cis configuration, as well as others having trans configuration, but this time they found no need to postulate the existence of π-bonds in their compounds.

A number of authors have questioned the generality of the theory of π-bonding (4, 5, 6). In fact it appears that the only evidence cited in support of the theory which is not circumstantial in character is that of Reeves (7), who found by means of a broad-line N.M.R. investigation of dichlorodiethylene-μ,μ'-dichlorodiplatinum(II) that the ethylene ligand is not free to rotate. Thus π-bonding to olefins seems clearly established. The present authors, in seeking evidence of such bonding to the *d*-orbitals of halogen atoms have examined the electron drift in the cis and trans forms of square-planar complexes of platinum(II) and a description of this investigation follows.

DISCUSSION AND RESULTS

The stability of complexes containing pyridine, α,α'-dipyridyl, *o*-phenanthroline, etc. may be variously accounted for as being due to (i) the mesomeric effect involving a partial double bond from the central atom to the nitrogen atom:



or (ii) an unusually large interaction energy resulting from a high polarization. Condition (i) would give rise to a π-electron drift toward the ligand as well as a σ-electron drift

[1]*Manuscript received May 30, 1960.*
Contribution from the Department of Chemistry, University of Ottawa, Ottawa, Ontario.
[2]*Part I: Can. J. Chem.* **38**, *1300 (1960).*

away, whereas condition (ii) would involve only a drift away from the ligand. It therefore seemed promising to examine the high-resolution N.M.R. spectra of complexes containing pyridine.

If the bonding in *trans*-dipyridinedichloroplatinum(II) and *trans*-dipyridinedichloropalladium(II) is solely of σ-type, the stronger bonding of the former compound should stem from a greater polarization of the ligands. A comparison of the spectra of these two compounds failed to detect any significant difference in chemical shifts, however (see Table I). It is assumed that the chemical shift of the β-proton in pyridine com-

TABLE I

Chemical shifts of the pyridine β-hydrogen atoms in metal complexes (Values are given in cycles per second at 60 megacycles with respect to 0.6 mole% uncomplexed pyridine in dimethylsulphoxide)

Compound	I cis form	II trans form	Difference (II − I)
[Pt $py_2(NH_3)_2$]Cl_2	−14.1	−24.6	−10.5
[Pt py_2Cl_2]	−3.4	−6.5	−3.1
[Pt py_2Br_2]	−5.9	−3.6	+2.3
[Pt py_2I_2]	−4.2	−0.7	+3.5
[Pt $py_2(NO_2)_2$]	−8.0	−16.0	−8.0
[Pd py_2Cl_2]		−6.3	
[Pd py_2Br_2]		−5.8	
[Pd py_2I_2]		−4.8	

plexes relative to uncomplexed pyridine is a measure of the net inductive effect to which the ligand is subject.* If, on the other hand, the greater stability of the platinum compound is due at least in part to stronger double bonding, the π-electron drift would tend to compensate for the change in σ-bond polarity. The result is thus suggestive of π-bonding.

The examination of N.M.R. spectra of dipyridine – platinum complexes in cis and trans configurations revealed direct evidence that ligands which possess vacant *d*-type orbitals do indeed draw electrons away from the central atom as well as form a σ-bond with it. This supports the theory of Chatt, Duncanson, and Venanzi (1) that a large trans effect is due to π-bonding of the ligand responsible, with a consequent diminution of the *d*-orbital electron density on the opposite side of the molecule.

Figure 2 illustrates the conceived nature of the electron drift. Solid lines to the ligands represent σ-bonds and dotted lines represent π-bonds. It will be noted that if the acido group, X, forms π-bonds, the *d*-electrons of the platinum atom are subjected to a "pull" from all four directions. This condition would lead to bonding of various strengths and bond orders. This is indicated qualitatively in the figure by the relative densities of the dots. The distinction between cis and trans configurations can be rationalized following Chatt, Duncanson, and Venanzi. Two ligands trans to each other along the *x*-axis must both draw their *d*-electrons from the d_{xy} and d_{xz} orbitals. If a group be in the cis position, it draws its electrons from the d_{xy} and the d_{yz} orbitals. Because there is a competition for the *d*-electrons, a strongly bonding ligand in the *x*-direction will weaken the π-bond to a ligand in trans position more than that to one in the cis position. The groups X,

**The β-proton is the best choice for comparison because its chemical shift should be relatively independent of changes in the resonance of the ring due to complexing and it should be less subject to field effects than the α-shift. The spectra revealed very little or no changes in resonance in all the complexes studied in any case. A comparison of typical spectra is shown in Fig. 1.*

Can. J. Chem. Downloaded from www.nrcresearchpress.com by 210.87.254.105 on 09/05/12
For personal use only.

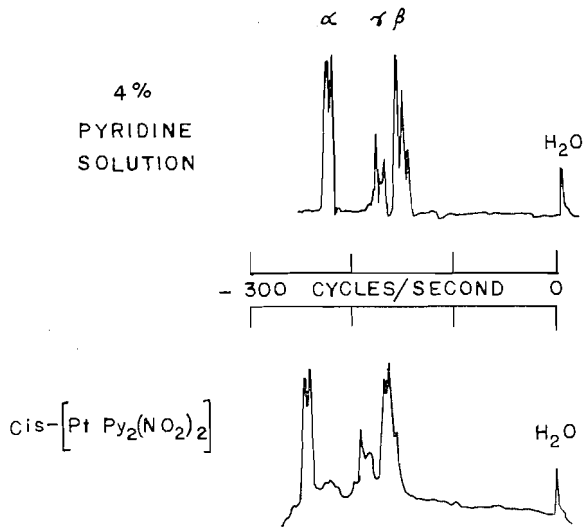


FIG. 1. Comparison of the spectra of free and complexed pyridine in dimethylsulphoxide solution.

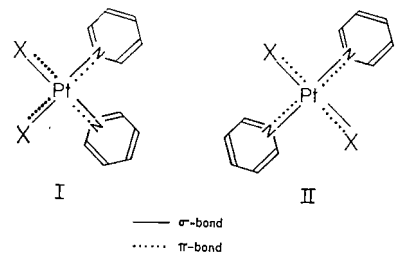


FIG. 2. Relative strengths of the π-bonds in *cis*- and *trans*-[Pt py_2X_2].

in Fig. 2, are considered more strongly π-bonding than pyridine. Thus we have shown the π-bonds to pyridine as being weaker in I than in II. It must be remembered that the σ-bonds will likewise differ somewhat in strength in the two configurations respectively. Therefore, in interpreting the nuclear magnetic resonance spectra of these complexes, account must be taken of inductive effects due to both *d*-acceptor character and electronegativity differences.

The chemical shift of the β-protons in a series of corresponding cis and trans isomers relative to that in uncomplexed pyridine and the differences between these values are given in Table I. The compounds are listed downwards in order of increasing trans-directing power of the "X" ligands (1). The difference column shows a gradual increase from a negative value at [Pt $py_2(NH_3)_2]Cl_2$ to the most positive value at [Pt py_2I_2] but there is a reversal in trend at [Pt $py_2(NO_2)_2$]. These results cannot be explained on the basis of the electron-donating power of the ligands alone. In what follows, the correctness of the π-bonding theory will be assumed and the chemical shifts rationalized accordingly.

Consider the compound [Pt $py_2(NH_3)_2]Cl_2$ in which there is little or no π-bonding to the NH_3 groups. The relatively large electron-donor character of ammonia will give rise to a smaller shift to lower magnetic field strength when ammonia is trans to pyridine, i.e. in the cis isomer, than would be the case when the other pyridine is in the trans

Can. J. Chem. Downloaded from www.nrcresearchpress.com by 210.87.254.105 on 09/05/12
For personal use only.

position assuming that operation of inductive effects through a straight angle is more pronounced than that through a right angle. Moreover, the diamagnetic effect of "ring current" in rotating pyridine rings would also have the effect of shifting the resonance in the cis compound to higher field relative to the trans compound. The negative entry in the difference column of the table is therefore plausible. The difference value for [Pt py_2Cl_2] is still negative even though in this case the chlorine atom has a stronger trans influence than pyridine. The inductive effect through the σ-bonds therefore still predominates over any electron drift in the opposite direction due to π-bonding.

As the trans influence of the various halogens increases with atomic number, the effect of π-bonding appears in the chemical shifts of the cis isomers becoming greater than those of the trans forms. If it were not for the decreasing electronegativity of the halogen atoms, as is evidenced by the decreasing shifts down the series of trans isomers, we might have obtained an even more pronounced trend among the difference values. Thus the near constancy of the chemical shifts in the cis halo compounds indicates an approximate compensation of the increasing double-bond character and decreasing electronegativity in this configuration.

The nitro group has a large trans-directing power but in the isomers of [Pt $py_2(NO_2)_2$] it provides chemical shifts giving a large negative difference value, viz. −8.0. This is not really anomalous when one reasons as follows. The nitro group is negative and the nitrogen atom is almost as strongly electronegative as chlorine. Neglecting *d*-electron drift for the moment, we should expect the chemical shift of *trans*-[Pt $py_2(NO_2)_2$] to be slightly more positive than −6.5, the value for *trans*-[Pt py_2Cl_2]. The value is actually −16.0, however, which is plausible if one considers the influence of π-bonding and mesomerism of the nitro group. The nitrogen atom is much smaller than chlorine so that it would be expected to exert a greater inductive effect through the σ-bonds, in fact about as much as in [Pt $py_2(NH_3)_2$]Cl_2 which provides a difference value of ca. −10.5. The difference value for the nitro compound is less than this which is qualitatively what is expected from the influence of π-bonding.

Because the differences in chemical shift are very small it might be argued that they are caused by field or solvent influences. Thus the trend in the different values among the various halogen complexes, which is due principally to the trend among the trans-isomers, might be ascribed to an increasing field effect with increase in atomic number of the halogen atoms. However, the chemical shift along the analogous series of trans-complexes of palladium exhibits only a slight trend to higher field strength. Since the palladium analogues have nearly the same molecular dimensions as the platinum compounds, the difference in behavior must be due to a difference in the character of the metal atoms.

The same experiment shows that the trend in chemical shift of the platinum compounds is not due simply to a direct solvent interaction with the ring protons. Nevertheless, because of the highly polar nature of the solvents which it was found necessary to use, the question of solvent influence is nevertheless a serious one.* In order to investigate the influence of the solvent, the following control experiment was carried out.

Trans-pyridinetri-*n*-propylphosphinedihaloplatinum compounds were found to be soluble in solvents of low polarity as well as in dimethylsulphoxide and they should be closely analogous to *trans*-dipyridine complexes. Chemical shifts relative to that of the chloro compound in carbon tetrachloride are given in Table II for three compounds in

**The authors are indebted to the referee for emphasizing this point.*

Can. J. Chem. Downloaded from www.nrcresearchpress.com by 210.87.254.105 on 09/05/12
For personal use only.

TABLE II

Influence of solvent on the chemical shift
(Values are expressed in cycles per second with respect to [Pt py(PPr_3)Cl_2] in CCl_4)

	Solvent					
Compound	CCl_4	Difference	$(CH_3)_2SO$	Difference	$(CH_3)_2CO$	Difference
[Pt py(PPr_3)Cl_2]	0.0	2.3	+13.2	1.9	+53.6	2.4
[Pt py(PPr_3)Br_2]	+2.3	0.0	+15.1	0.4	+56.0	0.0
[Pt py(PPr_3)I_2]	+2.3		+15.5		+56.0	

each of three solvents. Although there is a large solvent effect, the difference columns show that it is essentially the same for all three compounds. We assume that the dipyridine compounds are not more affected by field and solvent influences.

EXPERIMENTAL

The nuclear magnetic resonance spectra were obtained with a Varian Associates 60 megacycle spectrometer, Model V 4302, adjusted for high resolution. Spectra were calibrated with respect to an external water standard (1% protons in D_2O) by means of a Hewlett – Packard side-band oscillator, which, in turn, was calibrated with a Hewlett – Packard electronic counter. The temperature of the resonant system was constant to $\pm 0.5°$ C. Each of the values of chemical shift reported is the mean of 8 to 14 determinations on a single sample and was calculated simply on the basis of the positions of the sharpest peaks in the β-proton resonance. This procedure appeared to be justified for there were no apparent differences in coupling among the several spectra obtained. The chemical shifts of the dipyridine complexes are expressed relative to 0.6 mole% pyridine in dimethylsulphoxide. Bulk diamagnetic susceptibility corrections were carried out following the method of Pople, Schneider, and Bernstein (8).

Because of the low solubilities of the dipyridine salts, 0.3 mole% solutions were used for N.M.R. examinations. The chloride salts were dissolved in D_2O and the remaining compounds in dimethylsulphoxide. Ten per cent (w/v) solutions of the tri-*n*-propylphosphine complexes in dimethylsulphoxide, acetone, and carbon tetrachloride were employed for the investigation of solvent effect. The chemical shifts were corrected for bulk diamagnetic susceptibility of the media.

Debye – Scherrer diffraction patterns showed that all of the compounds could be recrystallized unchanged from their respective solvents.

Preparations

Trans-dipyridinedihalopalladium, *cis*- and *trans*-dipyridinedichloroplatinum, *cis*- and *trans*-dipyridinediammineplatinum monohydrate, and *cis*- and *trans*-dipyridinedinitroplatinum were prepared by existing procedures (9, 10, 11, 12). Carbon, hydrogen, platinum, and palladium analyses agreed well with the calculated compositions.

Cis-dipyridinedibromoplatinum

Finely powdered *cis*-dipyridinedichloroplatinum (200 mg) was suspended in a gently boiling solution containing 10 ml water, 15 ml acetone, and 2 g KBr. After 60 minutes the solid was separated by filtration and washed successively with hot water and methanol. The yellow color of the product was slightly more intense than that of the chloro analogue. The X-ray diffraction pattern revealed a homogeneous product

Can. J. Chem. Downloaded from www.nrcresearchpress.com by 210.87.254.105 on 09/05/12
For personal use only.

having a crystal lattice isomorphous with, but slightly larger than, that of the chloro compound. Anal. Calc. for [Pt py_2Br_2]: C, 23.6; H, 1.96; Pt, 38.1. Found: C, 23.7; H, 1.96; Pt, 38.6.

Trans-dipyridinedibromoplatinum

The preparation was similar to that described for the cis compound starting, however, with *trans*-dipyridinedichloroplatinum. The color of the product was slightly deeper than that of the cis analogue. The X-ray diffraction pattern showed the product to be homogeneous and isomorphous with, but distinct from the starting material. Anal. Calc.: *vide supra*. Found: C, 23.9; H, 2.11; Pt, 38.6.

Cis-dipyridinediiodoplatinum

This was prepared in a manner similar to that of the bromo compound except that the product was easily soluble in the reaction mixture and had to be isolated by evaporation. The product consisted of well-formed orange crystallites which were more readily dissolved by organic solvents than the other halogen analogues. Anal. Calc. for [Pt py_2I_2]: C, 19.9; H, 1.66; Pt, 32.2. Found: C. 20.3; H, 1.70; Pt, 32.3.

Trans-dipyridinediiodoplatinum

Starting from *trans*-dipyridinedichloroplatinum, the same procedure was used as in the case of the cis compound except that 100 ml instead of 15 ml of acetone were used in preparing the reaction solvent. The product was again orange in color and well crystallized. Anal. Calc.: *vide supra*. Found: C, 19.7; H, 1.73; Pt, 31.4.

Trans-pyridinetri-n-propylphosphinedichloroplatinum

This was prepared by a procedure analogous to that used by Chatt (13) to prepare *trans-p*-toluidine-tri-*n*-propylphosphinedichloroplatinum except that pyridine was used in place of *p*-toluidine. The product recrystallized from ethanol was bright yellow. Anal. Calc. for [Pt $(C_3H_7)_3P$ py Cl_2]: C, 33.3; H, 5.18; Pt, 38.6. Found: C, 33.7; H, 5.28; Pt, 38.9.

Trans-pyridinetri-n-propylphosphinedibromoplatinum

The method of preparation was the same as that used for the chloro analogue except that dibromobis-(tri-*n*-propylphosphine)-μ,μ'-dibromodiplatinum was used. This latter compound was prepared as described by Chatt (14). The product was golden yellow in color. Anal. Calc. for [$Pt(C_3H_7)_3P$ py Br_2]: C, 28.3; H, 4.41; Pt, 32.8. Found: C, 28.0; H, 4.34; Pt, 29.6.

Trans-pyridinetri-n-propylphosphinediiodoplatinum

This also was prepared in a similar manner using diiodobis-(tri-*n*-propylphosphine)-μ,μ'-diiododiplatinum (14). The product was yellow-orange. Anal. Calc. for [$Pt(C_3H_7)_3$-Ppy I_2]: C, 24.4; H, 3.81; Pt, 28.3. Found: C, 24.5; H, 3.78; Pt, 28.8.

ACKNOWLEDGMENTS

The authors wish to thank Drs. F. A. L. Anet and R. R. Fraser for helpful discussions and Miss E. Busk for technical assistance. The financial support of the National Research Council is gratefully acknowledged.

REFERENCES

1. J. CHATT, L. A. DUNCANSON, and L. M. VENANZI. J. Chem. Soc. 4456 (1955).
2. A. A. GRINBERG. Ann. inst. platine (U.S.S.R.) **10**, 58 (1932).
3. J. CHATT, L. A. DUNCANSON, B. L. SHAW, and L. M. VENANZI. Discussions Faraday Soc. **26**, 131 (1958).

Can. J. Chem. Downloaded from www.nrcresearchpress.com by 210.87.254.105 on 09/05/12
For personal use only.

4. R. N. KELLER and R. W. PARRY. *In* Chemistry of coordination compounds. *Edited by* J. C. Bailar. Reinhold, New York. 1956. p. 190.
5. R. J. P. WILLIAMS. Proc. Chem. Soc. 20 (1960).
6. A. D. WESTLAND. Can. J. Chem. **38**, 1300 (1960).
7. L. W. REEVES. Can. J. Chem. **38**, 736 (1960).
8. J. A. POPLE, W. G. SCHNEIDER, and H. J. BERNSTEIN. High-resolution nuclear magnetic resonance. McGraw-Hill, New York. 1959. p. 80.
9. A. COSSA. Atti R. Accad. dei Lincei Roma, **5**, I, 245 (1896); Gmelins Handbuch der anorganischen Chemie. System Nr. 65. 8 Auflage. Verlag Chemie, Berlin. p. 396.
10. S. M. JÖRGENSEN. J. prakt. Chem. **33**, 489 (1886).
11. H. D. K. DREW, F. W. PINKARD, W. WARDLAW, and E. G. COX. J. Chem. Soc. 1004 (1932).
12. S. G. HEDIN. Acta Univ. Lundensis, **22**, 1 (1886); Gmelins Handbuch der anorganischen Chemie. System Nr. 68D. 8 Auflage. Verlag Chemie, Berlin. p. 283.
13. J. CHATT. J. Chem. Soc. 2301 (1950).
14. J. CHATT. J. Chem. Soc. 652 (1951).

Can. J. Chem. Downloaded from www.nrcresearchpress.com by 210.87.254.105 on 09/05/12
For personal use only.

Can. J. Chem. Downloaded from www.nrcresearchpress.com by 210.87.254.42 on 09/05/12
For personal use only.

SOME PROPERTIES OF PURE POLYOXYETHYLENEGLYCOL ETHERS IN SOLUTION[1]

A. F. Sirianni and B. A. Gingras

ABSTRACT

Solution properties of a series of hexaoxyethyleneglycol ethers having 8 to 16 carbon atoms in a paraffin chain along with a number of diethers were assessed in ethanol at 48 and 60° C. The molecular weights at infinite dilution indicated that the compounds are unassociated. Solvation effects were observed for the monoethers having 14 or more carbon atoms in the hydrophobic portion of the molecule, but were absent for those molecules containing 12 carbon atoms or less. The apparent micellar weights suggested that association did not proceed beyond a dimer for most of the hexaoxyethyleneglycol compounds. The diethers obeyed Raoult's law up to the critical micelle concentration while different apparent association patterns were observed beyond this concentration.

INTRODUCTION

The molecular weight, critical micelle concentration (cmc) and apparent association patterns of surface-active materials in solution have been determined by means of vapor pressure depression using various means for its measurement. Data have been obtained in this way by McBain *et al.* (1) using thermistors and aqueous solutions of alkyl – aryl sulphonates, by Kitahara (2) on dodecyl-ammonium-benzoate, -caprylate, and -butyrate in cyclohexane and by Debye (3) with a series of α-glycerides in a variety of nonaqueous solvents.

Additional information concerning the micellar weight and critical micelle concentration of nonionic detergents, based on ethylene oxide, has been obtained from light scattering measurements in aqueous (4) and in benzene solutions (5). Recently, ultracentrifugal measurements on aqueous systems have been employed (6). Large differences between weight-average (Mw) and number-average (Mn) molecular weight exist. Debye (7) pointed out that small amounts of impurities enhance light scattering leading to anomalous micellar sizes. Low molecular weight impurities decrease the number-average molecular weight, thus widening the gap between these two methods of measurement. Becher *et al.* (8) presented some evidence that nonequilibrium solutions containing an appreciable concentration of micelles may be present below the critical micelle concentration.

The present investigation was undertaken in an effort to assess the colligative properties of some pure nonionic detergents by vapor pressure depression measurements, utilizing the difference in vapor pressure between pure solvent and solutions for a series of chemically well-defined polyoxyethyleneglycol ethers. Their physical properties and method of preparations were given by Gingras and Bayley (9, 10). The compounds examined were mono- and di-ethers of hexaoxyethyleneglycol, covering a molecular weight range from 390 to 730. Some other pure compounds of different ethylene oxide content were also studied. A list of the various compounds is given below:

I. Monoethers containing six ethylene oxide units:

$$R—O—(CH_2CH_2O)_6H;\quad R = n\text{-}C_8H_{17},\ n\text{-}C_{12}H_{25},\ n\text{-}C_{14}H_{29},\ n\text{-}C_{16}H_{33}.$$

II. Monoether containing seven ethylene oxide units:

$$p\text{-iso-}C_8H_{17}—C_6H_4—O(CH_2CH_2O)_7H.$$

[1]*Manuscript received October 4, 1960.*
Contribution from the Division of Applied Chemistry, National Research Council, Ottawa, Canada. Issued as N.R.C. No. 6115.

III. Diethers containing six ethylene oxide units:

$$R—O(CH_2CH_2O)_6R \qquad R = n\text{-}C_{12}H_{25} \text{ and } n\text{-}C_{18}H_{33}.$$

IV. Diether containing two ethylene oxide units:

$$n\text{-}C_{18}H_{37}O(CH_2CH_2O)_2C_{18}H_{37}.$$

V. Diether derivative of *n*-butane:

$$p\text{-iso-}C_8H_{17}—C_6H_4—O(CH_2)_4O—C_6H_4—C_8H_{17}\text{-}p\text{-iso}.$$

The preparation and physical properties of the latter two substances, which have not been reported before, are described in the experimental part.

The diethers are not soluble in water. Monoethers become less hydrophilic with increase in the number of carbon atoms in the paraffin chain, with decreasing ethylene oxide content and with increased temperature. In order to compare the behavior of the mono- with the di-ethers it was found desirable to carry out the measurements in an hydroxylated dissociating solvent of reasonably high dielectric constant. Ethanol was used for this purpose. It has been reported that in the case of some ionic detergents, micelles form in alcohol with the same value of the cmc as in water (11). This is not the case with the nonionic detergents since they lack the electrical forces necessary to impede aggregation (12) and the cmc is expected to be solvent dependent.

While most of the vapor pressure measurements were made on alcohol solutions at 48° C a few determinations have been made at 60° C and some measurements were conducted in water and in benzene at other temperatures in order to extend the data and compare them with other published results.

EXPERIMENTAL

The experimental technique and the apparatus used to carry out the differential vapor pressure measurements have been described in detail elsewhere (13). About 0.3 to 6 mg of material is weighed from the bulk sample into 4-mm i.d. pyrex tube previously fire-polished and steamed to remove any possible extraneous soluble impurities. The sample is washed to the bottom of the cell with about 0.4 to 0.6 ml of a solution of distilled alcohol and benzene. After evaporation of the solvents, the glass tube is sealed on the apparatus and evacuated to a pressure of about 10^{-5} mm Hg. Care is taken, however, to maintain the viscous liquids at 0° C with an ice-water bath to prevent loss of solute by evaporation during the evacuation process. Solutions of different concentrations are made by adding various amounts of alcohol, usually between the limits of 20 to 90 mg. With several weighed portions of solute it is possible to cover a reasonably wide range of concentrations. The system is arranged in such a manner that the solvent can be recycled after each determination. Solutions reach equilibrium within several hours after each filling. Readings of the vapor pressure depressions are taken at intervals of 1 to 2 hours. The null point of the apparatus is measured at the end of each determination.

Preparation of 1,4-Bis(p-isooctylphenoxy) Butane (V)

p-Isooctylphenol (1,1,3,3-tetramethylbutyl phenol) (41.2 g, 0.2 mole) was added to a solution of sodium (2.3 g, 0.1 g-atom) in MeOH (150 ml). When the solution was completed, 1,4-dibromobutane (21.6 g, 0.1 mole) was added and the resulting mixture was refluxed for 3 hours, after which it was neutral to litmus paper. The solid that crystallized on cooling was collected by filtration and was recrystallized from a mixture of MeOH–*n*-hexane, 1:1. The product obtained had m.p. 100° C, yield 30 g, 74%. Calculated for $C_{32}H_{50}O_2$, M.W. 466: C, 82.4; H, 10.7%. Found: C, 82.29; H, 10.62%.

Can. J. Chem. Downloaded from www.nrcresearchpress.com by 210.87.254.42 on 09/05/12
For personal use only.

Can. J. Chem. Downloaded from www.nrcresearchpress.com by 210.87.254.42 on 09/05/12
For personal use only.

Preparation of Di-(n-octadecyl) Ethyleneglycol Ether

Potassium (7.8 g, 0.2 g-atom) was added to diethyleneglycol (10.6 g, 0.1 mole) at 60° C, in an atmosphere of nitrogen. *n*-Hexane (ca. 50 ml) was added to keep the mixture in suspension for better stirring. After 0.5 hour, all the potassium had reacted and octadecyl chloride (57.8 g, 0.2 mole) was added slowly. The temperature was kept at 60° C and the slurry was stirred for 2 days. Then the mixture was heated to 180° C for 1 hour while a heavy precipitate was formed. After cooling, acetone (200 ml) was added and the precipitate, collected by filtration, was washed with water to remove the potassium chloride, and dried. The product was crystallized from benzene and recrystallized from ethanol; m.p. 90° C, 24 g, 40%. Calculated for $C_{40}H_{82}O_3$, M.W. 610: C, 78.6; H, 13.45%. Found: C, 78.88; H, 13.51%.

RESULTS AND DISCUSSION

The variation of the apparent molecular weight with solute concentration for a number of hexaoxyethyleneglycols having a terminal hydroxyl group etherified with a hydrocarbon chain of 8 to 16 carbon atoms, is shown in Fig. 1. The molecular weights at finite concentrations were calculated by means of Raoult's law. Curves 1, 2, 3, and 4 represent the data obtained for the monoethers (I). Curve 5 was obtained with heptaoxyethyleneglycol mono-*p*-isooctylphenyl ether (II).

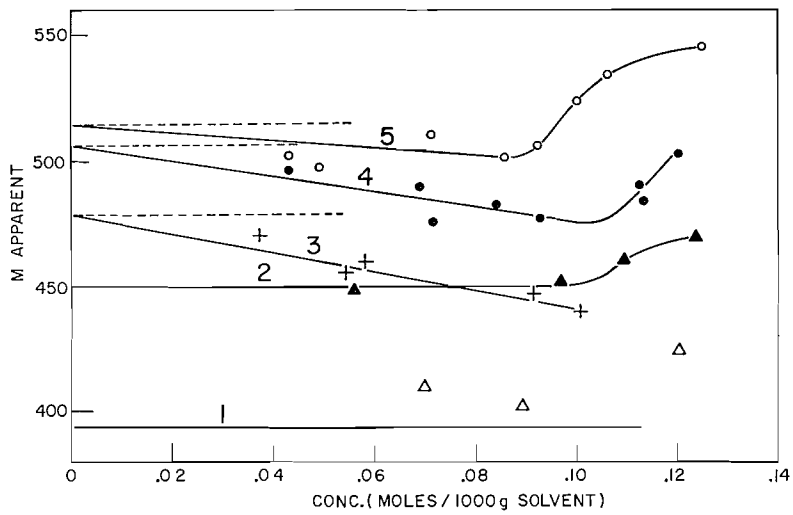


FIG. 1. Apparent molecular weight versus solute concentration for a series of hexaoxyethyleneglycol monoethers in alcohol at 48° C.

Curve 1, type I $C_8H_{17}(E.O)_6H$; heavy line drawn independent of concentration denotes the theoretical molecular weight of the compound.
Curve 2, type I $C_{12}H_{25}O(E.O)_6H$.
Curve 3, type I $C_{14}H_{29}O(E.O)_6H$. The broken line corresponds to the theoretical molecular weight of the compounds.
Curve 4, type I $C_{16}H_{33}O(E.O)_6H$.
Curve 5, type II *p*-iso-$C_8H_{17}C_6H_4O(E.O)_7H$.

The apparent molecular weight of the monoether (I, R = $C_{16}H_{33}$, curve 4) decreases with increasing concentration up to about 0.1 molal followed by a rapid increase at higher concentrations. The monoether (I, R = $C_{14}H_{29}$, curve 3) behaves in a similar way over the concentration range studied. The solutions of ether (I, R = $C_{12}H_{25}$, curve 2) behaves in an ideal fashion up to the cmc with evidence of solute association beyond 0.1 molal.

The observed molecular weights for the ether (I, R = C_8H_{17}, curve 1) are about 3–5% higher than the theoretical value, below 0.1 molal which should be well below the cmc. The concentration at which the solute associates is similar for all of the compounds of the type I. Compound II (curve 5) behaves similarly to compound (I) having the same number of carbon atoms in the hydrocarbon chain. The cmc is somewhat lower however, and the apparent molecular weight rises more steeply with increased concentration.

While the reason for the unusual change in solution properties in going from C_{12} to C_{14} and C_{16} compounds of type I, is not too clear, it may be related to the influence of the free primary hydroxyl groups and the length of the hydrocarbon adduct.

The behavior is similar to that of a typical polymeric system when a "good" solvent is employed. The monoether II, which possesses a short hydrocarbon chain, is probably reasonably well balanced in its solvophilic – solvophobic properties, and a smaller amount of solute – solvent interaction occurs. No interaction was observed with a hydrocarbon chain of 12 carbon atoms or less. Solvation of the lyophilic portion of the molecule could cause the observed effect provided the degree of solvation increased with effective increase in the concentration of the lyophobic part of the solute molecule. The slopes of the curves for the monoethers containing 14 and 16 carbon atoms in the chain may not be drawn sufficiently steeply. Owing to the difficulty of obtaining reliable data at the very low concentrations these have been extrapolated to the theoretical value at zero concentration. Actually in this regard the solution may be ideal and a point of inflection reached when the concentration of hydrocarbon is sufficient to increase the solvation of the nonhydrocarbon portion of the solute molecule.

The apparent molecular weight appears to decrease in a rather orderly fashion with solute concentration. The effect was sufficiently pronounced that curve 2 actually crossed curve 3 at a concentration of about 0.75 molal. An error of the order of 8% at 0.1 molal would be required to account for this effect and this is 4 times the error of reproducibility of individual determinations.

It is interesting to note that anomalies have also been observed with surface tension measurements of aqueous solutions of similar homologous series of polyoxyethyleneglycol ethers (14). Lange (14) observed that surface tension lowering increases regularly for a C_{12} monoether, but the sharp bend at the cmc disappeared for the C_{14} surfactant. The curves relating surface tension with solute concentration for the two compounds crossed.

The anomalous behavior of the monoethers was not found with diethers having hydrocarbon chains of similar lengths. Raoult's law was closely followed up to cmc, association of solute then occurred, particularly for the systems of low oxygen content. These results are recorded graphically by Fig. 2. The solid lines represent the theoretical molecular weight of the compounds below the cmc. Curves 1 and 2 represent the behavior of the diether (V) at 48 and 60° C respectively. In this case the hydrophilic oxygens are spaced 4 carbon atoms apart and an enormous change in cmc occurred with increased temperature. After the early stages of association, the apparent molecular weight increases virtually linearly with concentration. Although not shown in the graph, this system was followed up to about 0.5 molal. Owing to the increasing magnitude of the association factors with concentration, it is suggested that micelles of higher order than dimers are being formed. As the temperature was raised to 60° C the cmc appeared to be appreciably higher. Higher concentrations gave vapor pressure depressions beyond the calibrated range of the instrument.

Curve 3 was obtained with a sample of pure di-(*n*-octadecyl) ethyleneglycol ether

Can. J. Chem. Downloaded from www.nrcresearchpress.com by 210.87.254.42 on 09/05/12
For personal use only.

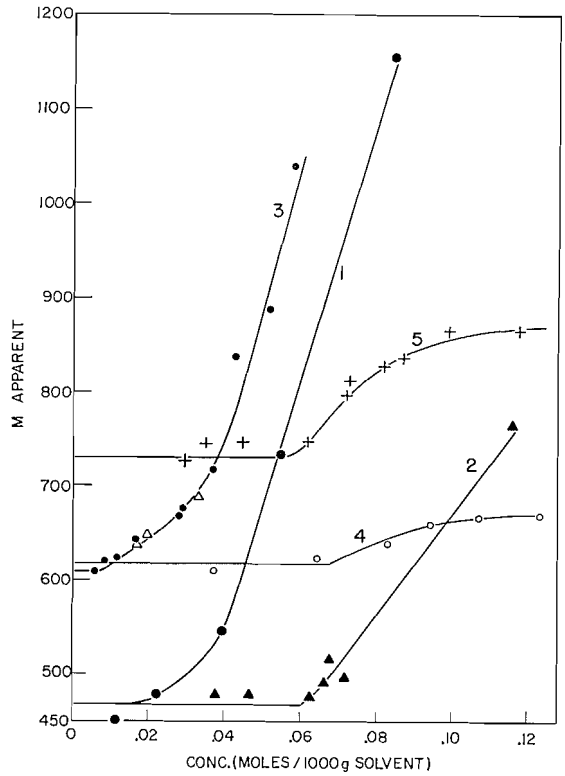


FIG. 2. Apparent molecular weight versus solute concentration for a series of diethers at 48° C. The heavy lines drawn independent of concentration correspond to the theoretical molecular weight of the compounds.

Curve 1, type V *p*-iso-$C_8H_{17}C_6H_4O(CH_2)_4OC_6H_4.C_8H_{17}$-*p*-iso.
Curve 2, same compound at 60° C.
Curve 3, type IV $C_{18}H_{37}O(CH_2CH_2O)_2C_{18}H_{37}$. Filled triangles at 60° C.
Curve 4, type III $C_{12}H_{25}O(CH_2CH_2O)_6C_{12}H_{25}$.
Curve 5, type III $C_{16}H_{33}O(CH_2CH_2O)_6C_{16}H_{33}$.

(IV). Measurements were carried out at 48° C (filled circles) and a few more at 60° C (triangles). The cmc is low and little affected by temperature. The apparent molecular weight rises almost linearly with concentration.

Curves 4 and 5 illustrate the behavior of the diethers (III, R = *n*-$C_{12}H_{25}$ and *n*-$C_{16}H_{33}$). In sharp contrast to the behavior of the corresponding monoethers, these compounds obeyed Raoult's law up to the cmc. In both cases, the apparent molecular weight reaches an almost constant value after the initial stages of association suggesting that aggregation does not proceed beyond an equilibrium mixture of monomers and dimers. A similar phenomenon has been observed for trichloroacetanilide in benzene by Davis and Thomas (15). A particular association pattern was not ascribed for their system beyond the dimerization stage.

The apparent association factors, f, described as the ratio of observed, M_a, to theoretical molecular weight, M_0, are obviously of the same order of magnitude for both diethers at 0.115 molal. The percentage association is higher with the C_{16} compound by approximately a factor of 4, however.

Table I contains a summary of the results illustrated by Figs. 1 and 2.

Can. J. Chem. Downloaded from www.nrcresearchpress.com by 210.87.254.42 on 09/05/12
For personal use only.

TABLE I

Summary of results indicated from vapor pressure measurements on solutions of pure nonionic substances in alcohol

Compound	M_0	cmc: M_a vs. N plot	cmc: N_a vs. N plot	Type of association
Type I				
n-$C_8H_{17}O(E.O)_6H$	394	0.09 0.12	—	—
n-$C_{12}H_{25}O(E.O)_6H$	450	0.10	—	Limited, monomers and dimers indicated
n-$C_{14}H_{29}O(E.O)_6H$	478	—	—	Solvation effects
n-$C_{16}H_{33}O(E.O)_6H$	506	0.10	—	Solvation effects and probable association
Type II				
p-iso-$C_8H_{17}C_6H_4O(E.O)_7H$	514	0.09	0.088	Limited, monomers and dimers
Type III				
n-$C_{12}H_{25}O(E.O)_6C_{12}H_{25}$	618	0.07	0.071	Limited, monomers and dimers
n-$C_{16}H_{33}O(E.O)_6C_{16}H_{33}$	730	0.059	0.054	Limited, monomers and dimers
Type IV				
n-$C_{18}H_{37}O(CH_2CH_2O)_2C_{18}H_{37}$	610	0.008 at 48° C	0.01	Continuous above cmc, monomers, dimers, and probably polymers of higher order
Type V				
p-iso-$C_8H_{17}C_6H_4O(CH_2)_4O$-$C_6H_4C_8H_{17}$-$p$-iso	466	0.034 at 48° C 0.062 at 60° C	−0.033 —	Continuous above cmc, monomers, dimers, and polymers of higher order

Since a large number of experimental points would be necessary to trace accurately the position of the cmc from the M_a vs. N graphs at the incipient state of micellization, a closer approximation may be made by the following relation due to Kitahara (2):

$$N_a = N[(f-1)/f],$$

N_a = associated solute molality,

N = total solute molality,

f = association factor = M_a/M_0.

Values for N_a are calculated at finite concentration and plotted as a function of N. A straight line joining these points when extrapolated to $N_a = 0$, gives an average value for the cmc in molality units. These values and those obtained from the M_a vs. N plots are summarized in Table I.

The fraction of the monomer associated is calculated according to the following relation, without making any assumption as to the degree of aggregation.

$$X = (M_a - M_0)/M_a \qquad \text{(cf. Davy and Sidgwick (16)).}$$

The total mean molal concentration of all species

$$= \bar{N} = N(M_0/M_a) \qquad \text{(cf. Davies and Thomas (15)).}$$

The weight of the micelle Mm is obtained from the following relation, which assumes that a certain number of molecules remain in solution as monomers and the remainder associate to form larger aggregates:

$$Mm = \left(\frac{1}{x}\right)M_a - \left(\frac{1-x}{x}\right)M_0.$$

Can. J. Chem. Downloaded from www.nrcresearchpress.com by 210.87.254.42 on 09/05/12
For personal use only.

Can. J. Chem. Downloaded from www.nrcresearchpress.com by 210.87.254.42 on 09/05/12
For personal use only.

Our experimental results, which were obtained with rigorously dry pure solvent necessary to establish vapor pressure equilibrium quickly, indicate that aggregation occurs in alcohol. The behavior of systems containing six ethylene oxide units suggests that the micellar solution is composed of an equilibrium mixture of monomer and dimer at 48° C and that, in fact, the micelles present have an aggregation number of two. Continuous association occurs for diethyleneglycol octadecyl diether (IV) after the cmc is reached. The cmc, however, increases very little with rising temperature. In comparison, the aromatic diether (V) is quite temperature sensitive, since an appreciable rise in cmc occurred on increasing the temperature from 48° to 60° C.

The general behavior of the hexaoxyethyleneglycol ethers indicates that alcohol is a good solvent for these systems. The solvophilic – solvophobic balance of these compounds appears to inhibit the formation of large clusters of monomers. The results reported by Becher (5) from light-scattering measurements of benzene solutions of pure $C_{12}H_{25}O(CH_2CH_2O)_2H$ and $C_{13}H_{27}O(CH_2CH_2O)_6H$ indicated that benzene is a better solvent for the 2-ethylene oxide compound than for the 6-ethylene oxide monoether since a smaller micellar weight was obtained. Alcohol works in the reverse fashion, probably due to the inversion of the portion of the molecule responsible for the screening effect in going from an hydroxylated to a hydrocarbon solvent.

A few determinations in benzene at 30° C with the monoethers (I, R = *n*-$C_{12}H_{25}$, and *n*-$C_{14}H_{29}$) indicated that the apparent molecular weights were virtually independent of concentration from about 0.013 to 0.07 molal within ±2% in all cases. The association factors of the order 1.22 for I(C_{12}) and 1.14 for I(C_{14}) suggests that the systems consisted of monomers and dimers only. The cmc, which occurred at 0.0045 and 0.005 moles/1000 grams of solvent for I(C_{12}) and I(C_{14}) respectively, is in reasonably good agreement with other published results (5). The micellar weights obtained from light scattering at 25° C by Becher (5) with hexaoxyethylene *n*-tridecanol are about a factor of 50 higher than those found here from vapor pressure lowering measurements at 30° C. This ratio is unexpectedly high for these compounds, which differ only by plus or minus one carbon atom in the hydrophobic portion of the molecule, and the C_{13} compound used by Becher. However, large differences in micellar weights obtained by light-scattering and vapor pressure measurements have been noted with α-glycerides by Debye (3). Such differences may be due to heterogeneity of sizes or more likely to the kinetic mobility of a portion of the molecules forming the clusters, which may be sufficient to allow them to act as independent units in the vapor pressure lowering without affecting the amounts of scattered light.

A sample of pure *n*-decyl hexaoxyethyleneglycol monoether was examined in water in the vicinity of the cloud point (9). The solutions were made up at concentrations above the expected cmc. Ultracentrifugal measurements on a variety of commercial nonionic detergents showed that micellar weights should not vary with concentration (6). The results given in Table II suggest, however, that the micellar weight does increase

TABLE II

Behavior of $C_{10}H_{21}O(CH_2CH_2O)_6H$ in water

Temp. (° C)	Molal conc. (*N*)	App. M_a	Micellar mol. wt. (*Mm*)	Aggregate number (*n*)
50	0.0399	4615	5,000	12
56	0.0399	5270	5,650	13.4
63	0.0493	9600	10,000	24

with rising temperature in aqueous solutions, and this is in qualitative agreement with previous work (17).

The behavior of these compounds and a number of commercial nonionic detergents is now being examined in other solvents.

ACKNOWLEDGMENT

The authors wish to thank Dr. I. E. Puddington for his interest and for the many stimulating discussions concerning this work.

REFERENCES

1. H. Huff, J. W. McBain, and A. P. Brady. J. Phys. & Colloid Chem. **55**, 311 (1951).
2. A. Kitahara. Bull. Chem. Soc. Japan, **31**, 288 (1958).
3. P. Debye and H. Coll. Technical Report No. 2, Contract Nunr-401 (17), Task No. 051-360. Office of Naval Research. 1959.
4. L. M. Kushner and W. O. Hubbard. J. Phys. Chem. **58**, 1163 (1954).
5. P. Becher. J. Phys. Chem. **64**, 1221 (1960).
6. C. W. Dwiggins, Jr., R. J. Bolen, and H. H. Dunning. J. Phys. Chem. **64**, 1175 (1960).
7. P. Debye and W. Prins. J. Colloid Sci. **13**, 86 (1958).
8. P. Becher and N. K. Clifton. J. Colloid Sci. **14**, 519 (1959).
9. B. A. Gingras and C. H. Bayley. Can. J. Chem. **35**, 599 (1957).
10. B. A. Gingras and C. H. Bayley. Can. J. Chem. **36**, 1320 (1958).
11. N. Sata and H. Sasaki. Kolloid-Z. **152**, 76 (1957).
12. C. R. Bury and J. Browning. Trans. Faraday Soc. **49**, 209 (1953).
13. A. F. Sirianni and I. E. Puddington. Can. J. Chem. **33**, 755 (1955).
14. H. Lange. Kolloid-Z. **163**, 9 (1959).
15. M. Davis and D. K. Thomas. J. Phys. Chem. **60**, 763 (1956).
16. L. G. Davy and N. V. Sidgwick. J. Chem. Soc. 281 (1933).
17. K. Nakagawa, H. Inoue, K. Tori, and K. Kuriyama. Nippon Kagaku Zasshi, **79**, 1194 (1958).

Can. J. Chem. Downloaded from www.nrcresearchpress.com by 210.87.254.42 on 09/05/12
For personal use only.

Can. J. Chem. Downloaded from www.nrcresearchpress.com by 210.87.254.42 on 09/05/12
For personal use only.

ORGANOGERMANIUM COMPOUNDS

PART I. THE INTERACTION OF HEXAMETHYLDIGERMOXANE AND TRIMETHYLMETHOXYGERMANE WITH BORON TRIFLUORIDE[1]

J. E. GRIFFITHS[2] AND M. ONYSZCHUK

ABSTRACT

Boron trifluoride does not form a stable adduct with hexamethyldigermoxane. Instead, cleavage of the Ge—O—Ge linkage occurs with quantitative formation of trimethylfluorogermane and boron trioxide. Trimethylmethoxygermane and boron trifluoride form a 1:1 addition compound which sublimes without decomposition. Dative d_π–p_π bonding, if present in the Ge—O linkage of trimethylmethoxygermane, does not appear to affect appreciably the electron-donor activity of the oxygen atom toward boron trifluoride. The preparation and some properties of CH_3GeH_2Br, CH_3GeHCl_2, $(CH_3)_3GeCl$, $(CH_3)_3GeF$, $[(CH_3)_3Ge]_2O$, and $(CH_3)_3GeOCH_3$ are described.

Boron trifluoride and organic ethers form 1:1 adducts of the type, R_2O,BF_3, which are so stable that they can be distilled without decomposition (1). Methyldisiloxanes, on the other hand, do not give stable addition compounds with boron trifluoride (2). Instead, cleavage of the Si—O—Si linkage occurs at −78° in two stages:

$$(CH_3SiH_2)_2O + BF_3 = CH_3SiH_2OBF_2 + CH_3SiH_2F,$$

$$3CH_3SiH_2OBF_2 = 3CH_3SiH_2F + BF_3 + B_2O_3,$$

and the methylsiloxyboron difluoride formed in the first step is too unstable to be isolated. The experiments described in this paper were made to examine the interaction of boron trifluoride with the Ge—O—Ge and Ge—O—C linkages in hexamethyldigermoxane and trimethylmethoxygermane respectively.

Preparation of Germyl Ethers

Hexamethyldigermoxane, a new compound, was prepared in 61% yield by the interaction of gaseous trimethylchlorogermane with dry silver carbonate:

$$2(CH_3)_3GeCl + Ag_2CO_3 \rightarrow [(CH_3)_3Ge]_2O + CO_2 + 2AgCl.$$

The same compound was probably obtained in the hydrolysis of trimethylbromogermane (3) and trimethylchlorogermane (4), but it was not identified in these reactions. Hexaethyldigermoxane, the only simple digermoxane reported previously, has been prepared in 97% yield by hydrolysis of triethylbromogermane with aqueous potassium hydroxide (5).

By reaction with anhydrous sodium methoxide, trimethylbromogermane was converted into trimethylmethoxygermane in 98% yield, according to the reaction:

$$(CH_3)_3GeBr + NaOCH_3 \rightarrow (CH_3)_3GeOCH_3 + NaBr.$$

Trimethylmethoxygermane had been obtained previously in 56% yield by the reaction of impure trimethyliodogermane with sodium methoxide in methanol (6).

We tried to prepare a partially methylated digermoxane, such as 1,1′-dimethyldigermoxane, $(CH_3GeH_2)_2O$, by the interaction of a methylhalogenogermane with silver carbonate. While preparing methylchlorogermane, CH_3GeH_2Cl, by the interaction of

[1]*Manuscript received October 13, 1960.*
Contribution from the Inorganic Chemistry Laboratory, McGill University, Montreal 2, Quebec, with financial assistance from the National Research Council of Canada. Presented at the 42nd Annual Conference of the Chemical Institute of Canada, Halifax, N.S., May 25–27, 1959.
[2]*Holder of N.R.C. Studentships, 1956–58. Present address: Bell Telephone Laboratories, Inc., Murray Hill, New Jersey.*

methylgermane with hydrogen chloride in the presence of aluminum trichloride, we found that methyldichlorogermane, CH_3GeHCl_2, was formed instead. Using hydrogen bromide and aluminum tribromide, however, methylgermane was converted in 53% yield into methylbromogermane, CH_3GeH_2Br. This new compound did not react with dry silver carbonate to give the expected 1,1′-dimethyldigermoxane; carbon dioxide, and an unidentified, non-volatile, transparent, viscous liquid were obtained instead. Evidently an initial reaction producing the digermoxane was followed by a rapid change of the digermoxane into complex methylgermoxane polymers.

An attempt to prepare the mixed ether methylmethoxygermane, $CH_3GeH_2OCH_3$, was equally unsuccessful. The reaction at $-80°$ of methylbromogermane with sodium methylate produced a volatile substance which was mainly methylmethoxygermane, and which decomposed slowly into methanol and an unidentified white, non-volatile solid. The latter was probably a polymer of the type $(CH_3GeH)_x$ formed by decomposition of methylmethoxygermane, as represented by:

$$xCH_3GeH_2OCH_3 \rightarrow xCH_3OH + (CH_3GeH)_x.$$

The amount of methanol recovered was roughly in agreement with this reaction.

The conclusion that germyl ethers with Ge—H bonds are unstable is also supported by the observation that digermoxane, $(GeH_3)_2O$, cannot be obtained either by hydrolysis of chlorogermane (7) or by reaction of chlorogermane with silver carbonate (8). Moreover, the anticipated 1,1′-di-*n*-butyldigermoxane was not formed by hydrolysis of *n*-butylchlorogermane (9). The apparent instability of such germyl ethers is in marked contrast with the stable silyl ethers containing Si—H bonds (10, 11).

Reaction of Trimethylmethoxygermane with Boron Trifluoride

Trimethylmethoxygermane and boron trifluoride formed a white solid 1:1 adduct which melted in the range 41 to 46°, and which sublimed at 25° without decomposition. It formed a transparent jelly when heated at 235° for 16 hours.

The formation of this adduct shows that the electron-donor activity of the oxygen atom is not appreciably less in germyl ethers than it is in alkyl ethers. This result is surprising, since one might expect that the electron-donor power would be reduced by d_π–p_π dative bonding from oxygen to germanium, similar to that in the Si—O bond (10). This so-called back co-ordination of electrons from oxygen to silicon in disiloxane and the methyldisiloxanes accounts for the unexpectedly large Si—O—Si bond angle, and also for the apparent lack of donor activity in these compounds (10). Theoretical considerations indicate that the amount of d_π–p_π bonding should be approximately independent of the size of the atom having the *d*-orbitals (12). Since silicon and germanium have similar covalent radii, 1.17 and 1.22 Å respectively (13), the extent of π-bonding to germanium and silicon should be roughly the same. Some experimental data on the dissociation constants of para-substituted benzoic acids with general formula p-$R_3M \cdot C_6H_4 \cdot CO_2H$, where M = C, Si, Ge, and Sn, and R = CH_3 and C_2H_5, provide strong evidence that dative π-bonding occurs between the benzene ring and Si, Ge, or Sn, approximately to the same degree in all three cases (14). Moreover, Hammett sigma values for the *meta*- and *para*-triphenylsilyl and -triphenylgermyl groups also show that the amount of partial double bonding between the benzene ring and silicon or germanium is almost identical (15). On the other hand, measurements of hydrogen bonding in triphenylhydroxyl compounds of the type $(C_6H_5)_3MOH$, where M = C, Si, Ge, Sn, and Pb, indicate that π-bonding from oxygen to M atoms is strong in $(C_6H_5)_3SiOH$, weaker in $(C_6H_5)_3GeOH$, and negligible in the other three compounds (16). Our results indicate

Can. J. Chem. Downloaded from www.nrcresearchpress.com by 210.87.254.42 on 09/05/12
For personal use only.

that dative d_π–p_π bonding, if it occurs in the Ge—O bond of trimethylmethoxygermane, does not appreciably alter the electron-donor activity of the oxygen atom toward boron trifluoride, since trimethylmethoxygermane and boron trifluoride form a stable 1:1 adduct.

Reaction of Hexamethyldigermoxane with Boron Trifluoride

Hexamethyldigermoxane and boron trifluoride did not yield a stable 1:1 adduct, but cleavage of Ge—O bonds occurred at 25° with quantitative formation of trimethylfluorogermane and boron trioxide, as given by the stoichiometric equation:

$$3[(CH_3)_3Ge]_2O + 2BF_3 = 6(CH_3)_3GeF + B_2O_3.$$

This reaction provides a new and more convenient method for the preparation of trimethylfluorogermane, previously obtained in 71% yield from the reaction of tetramethylgermane with liquid hydrogen fluoride in copper apparatus (17).

While the 1:1 adduct could not be isolated and there was no dissociation into original reactants, the possibility of its formation at low temperatures could not be excluded, since its decomposition at −80° made it impossible to detect and identify the adduct. The mechanism of this decomposition, as outlined below, might involve four-center cyclic transition states of the type proposed for the analogous interaction of boron trichloride and tribromide with alkyl ethers (18) and disiloxanes (19) respectively.

$$(CH_3)_3Ge\cdots O(F)\cdots BF_2\text{—}Ge(CH_3)_3 \longrightarrow (CH_3)_3GeF + (CH_3)_3GeOBF_2,$$

$$(CH_3)_3Ge\cdots O(F)\cdots BF \longrightarrow (CH_3)_3GeF + BOF,$$

$$3BOF \longrightarrow B_2O_3 + BF_3.$$

Although trimethylgermoxyboron difluoride and boron oxyfluoride could not be isolated, they were identified with the white solid which decomposed slowly at 20° into boron trifluoride, boron trioxide, and additional trimethylfluorogermane. Boron oxyfluoride exists below −140° as a cyclic trimer called trifluoroboroxine and decomposes rapidly at higher temperatures into boron trifluoride and boron trioxide (20). The yields of trimethylfluorogermane and boron trioxide for the over-all decomposition were quantitatively in agreement with the stoichiometric equation.

The failure of hexamethyldigermoxane to form a stable adduct with boron trifluoride does not necessarily imply a lack of electron-donor activity at the oxygen atom in the Ge—O—Ge linkage, since bond cleavage concealed possible adduct formation. This is in sharp contrast with the trimethylmethoxygermane – boron trifluoride system in which the absence of bond cleavage apparently allowed the isolation of the 1:1 adduct. Since bond polarities and inductive and steric effects determine the stabilities of co-ordination compounds of boron trifluoride (1), it is necessary to obtain information about their relative importance in germyl ether – boron trifluoride adducts. Experiments planned to give this information are now in progress and the results will be reported later.

EXPERIMENTAL

Apparatus

A Pyrex glass high-vacuum apparatus of the conventional type was used to manipulate volatile substances. Ground-glass joints and stopcocks were lubricated with Apiezon N grease. Vapor pressures were measured with a null-point glass spoon gauge. Molecular

Can. J. Chem. Downloaded from www.nrcresearchpress.com by 210.87.254.42 on 09/05/12
For personal use only.

weights (M) were obtained by the direct weight method. The Stock magnetic plunger apparatus was used for the determination of melting points (21). Temperatures below $-20°$ were measured with calibrated copper – constantan thermocouples in conjunction with a sensitive potentiometer. A column of the type described by Le Roy (22) was used for fractional distillations and condensations in the range -196 to $-20°$.

Materials

Methylgermane was obtained from reaction of methyl iodide with germylsodium as described by Teal and Kraus (23). Found: M, 90.5, v.p. 24.5 mm at $-99.7°$, yield, 51%. Calc. for CH_3GeH_3: M, 90.6. Although methylgermane had been characterized previously by its boiling point, melting point, and analysis (23), its vapor pressure – temperature relationship has not yet been reported. We found that vapor pressures, listed in Table I, of a tensiometrically pure sample are expressed in the range -114 to $-43°$ by the equation $\log_{10} p(\text{mm}) = 6.266-(850/T)$, which gives an extrapolated boiling point of $-22.2\pm0.5°$ (lit. (23), $-23.0°$), a heat of vaporization of 3965 cal mole^{-1}, and a Trouton constant of 15.9. The melting point was $-153.7\pm0.3°$ (lit. (23), $-158.0°$).

Tetramethylgermane was prepared by reaction of dimethylzinc with germanium tetrachloride (24). Found: M, 132.4, v.p. 139.1 mm at 0°, yield, 67%. Calc. for $Ge(CH_3)_4$: M, 132.6, v.p. 139.3 mm at 0°.

Trimethylbromogermane was obtained by reaction of bromine with tetramethylgermane (25). Found: M, 198.0, yield, 95%, v.p. 5.6 mm at 0°. Calc. for $(CH_3)_3GeBr$: M, 197.5, v.p. 5.6 mm at 0°.

Commercial boron trifluoride was used only after it had been distilled and its vapor pressure and molecular weight had been checked.

Preparation of Methylbromogermane

Methylgermane (3.08 mmole) and hydrogen bromide (3.08 mmole) were condensed in a vessel the walls of which had first been coated with anhydrous aluminum tribromide. After the mixture was heated at 100° for 4 hours, the hydrogen formed in the reaction was pumped away through a trap held at $-196°$, which retained condensable gases. Unreacted methylgermane and hydrogen bromide were removed together by three distillations at $-96°$, leaving tensiometrically pure methylbromogermane. Found: Br, 47.0%; M, 169.7, v.p. 26.8 mm at 0°, yield, 53%. Calc. for CH_3GeH_2Br: Br, 47.11%; M, 169.6.

Methylbromogermane had vapor pressures (0 to 60°) given by the equation $\log_{10} p(\text{mm}) = 7.800-(1740/T)$, which gives an extrapolated boiling point of $80.5\pm0.5°$, a latent heat of vaporization of 7960 cal mole^{-1}, and a Trouton constant of 22.5. A list of the measured vapor pressures is given in Table II. The melting point was $-89.2\pm0.2°$.

Preparation of Methyldichlorogermane

A bulb (5 l.) previously coated with anhydrous aluminum trichloride was charged with methylgermane (1.46 mmole) and hydrogen chloride (1.12 mmole) and heated for 4 hours at 100°. Hydrogen was pumped off. Unreacted methylgermane and hydrogen chloride were removed by distillation in the range -130 to $-92°$. Methyldichlorogermane was separated from the residue by several distillations at $-45.2°$. Found: Cl, 43.1%; M, 160.3, v.p. 25.8 mm at 20°. Calc. for CH_3GeHCl_2: Cl, 43.41%; M, 159.6. Vapor pressures of methyldichlorogermane, which are listed in Table III, obey the equation $\log_{10} p(\text{mm}) = 7.551-(1800/T)$, giving an extrapolated boiling point of $112.2\pm0.5°$, a latent heat of vaporization of 8250 cal mole^{-1}, and a Trouton constant of 21.4. The melting point was found to be $-63.1\pm0.1°$.

Can. J. Chem. Downloaded from www.nrcresearchpress.com by 210.87.254.42 on 09/05/12
For personal use only.

Reaction of Methylbromogermane with Silver Carbonate

Methylbromogermane (1.42 mmole) was slowly passed through a glass wool – silver carbonate (2.0 g) plug which turned black during the process. Hydrogen (0.3 mmole) was pumped away through a trap cooled with liquid air which retained condensable vapors. These were distilled at −96° to separate carbon dioxide (2.15 mmole. Found: M, 47.5. Calc. for CO_2: M, 44.0) from the residue. Redistillation of the residue at −45.2° gave a distillate which was mainly unreacted methylbromogermane (0.14 mmole. Found: M, 155.5. Calc. for CH_3GeH_2Br: M, 169.5) and a residue which was a clear viscous liquid with undetectable vapor pressure at room temperature. It was not identified.

Reaction of Methylbromogermane with Sodium Methylate

Methylbromogermane (1.94 mmole) and dry sodium methylate kept at −80° for 30 minutes gave on distillation at −80° a fraction (1.83 mmole. Found: M, 107.4) which was probably methylmethoxygermane (Calc.: M, 120.6) contaminated with methanol (Calc.: M, 32.0). Redistillation of this fraction at −65° and again at 20° yielded only methanol (1.63 mmole. Found: M, 38.1. Calc. for CH_3OH: M, 32.0) and an unidentified, non-volatile white solid residue.

Preparation of Trimethylchlorogermane

Tetramethylgermane (2.27 mmole) and hydrogen chloride (2.15 mmole) were condensed in a reaction bulb which had previously been charged with aluminum trichloride. The mixture was warmed to room temperature and, after 1 hour, methane was pumped off. Condensable vapors were separated into three fractions by distillation through a series of traps held at −80, −130, and −196°. Hydrogen chloride (0.66 mmole) was condensed in the trap maintained at −196°, while tetramethylgermane (0.14 mmole) collected in the trap held at −130°. The fraction retained at −80° was trimethylchlorogermane. Found: M, 153.1, yield 33%. Calc. for $(CH_3)_3GeCl$: M, 153.1.

Vapor pressures of trimethylchlorogermane (0 to 68°) are expressed by the equation $\log_{10} p(\text{mm}) = 7.665-(1795/T)$, which gives an extrapolated boiling point of 102.0±0.5°, a latent heat of vaporization of 8210 cal mole^{-1}, and a Trouton constant of 21.9. Vapor pressures are listed in Table IV. Rochow (4) reported the boiling points of dimethyldichlorogermane and trimethylchlorogermane as 124° and 115° respectively. Since he obtained trimethylchlorogermane by distillation from a mixture rich in dimethyldichlorogermane, his trimethylchlorogermane fraction was probably contaminated with a small amount of the dichloro compound resulting in a higher boiling point than we obtained by extrapolation of vapor pressure data.

Reaction of Trimethylchlorogermane with Silver Carbonate

Silver carbonate (1 g) and trimethylchlorogermane (1.17 mmole) were kept together for 3 hours at room temperature with frequent shaking. Distillation at −80° yielded a distillate of carbon dioxide (0.86 mmole. Found: M, 44.6. Calc. for CO_2: M, 44.0) and a residue of impure hexamethyldigermoxane. Unreacted trimethylchlorogermane was separated from hexamethyldigermoxane by several distillations at −22.9° leaving a residue of tensiometrically pure hexamethyldigermoxane. Found: M, 250, v.p. 5.7 mm at 18.2°, yield, 60.5%. Calc. for $[(CH_3)_3Ge]_2O$: M, 251.2. Vapor pressure measurements in the range of 18.2 to 72.4°, listed in Table V, determine the equation $\log_{10} p(\text{mm}) = 8.580-(2290/T)$, which indicates an extrapolated boiling point of 129°, a latent heat of vaporization of 10,540 cal mole^{-1}, and a Trouton constant of 26.0. The compound melted sharply at −61.1±0.1°.

Can. J. Chem. Downloaded from www.nrcresearchpress.com by 210.87.254.42 on 09/05/12
For personal use only.

Can. J. Chem. Downloaded from www.nrcresearchpress.com by 210.87.254.42 on 09/05/12
For personal use only.

TABLE I

Vapor pressures of methylgermane

t, °C	−114.4	−99.7	−90.0	−85.3	−73.0	−65.0	−61.7	−50.6	−46.2	−43.0
p_{mm} (obs.)	9.1	24.5	44.6	56.0	102.8	153.5	173.0	282.7	334.5	376.3
p_{mm} (calc.)	8.2	23.6	42.6	56.0	106.1	154.1	176.4	282.8	335.0	376.8

TABLE II

Vapor pressures of methylbromogermane

t, °C	0.0	9.5	23.4	30.3	32.0	36.9	38.9	42.2	48.0	53.6	57.6	60.0
p_{mm} (obs.)	26.8	44.2	85.4	116.0	125.8	156.0	169.5	189.8	241.8	306.0	347.7	378.0
p_{mm} (calc.)	26.9	44.7	86.0	115.7	126.0	155.1	170.0	191.7	241.0	305.1	348.0	380.2

TABLE III

Vapor pressures of methyldichlorogermane

t, °C	7.9	13.9	20.0	24.7	32.8	34.0	36.0	40.0	43.6	46.2	50.0	60.3	69.9	73.0	67.2	58.0	39.3	23.4
p_{mm} (obs.)	13.0	18.4	25.4	32.3	47.1	49.2	53.3	63.1	74.0	82.0	95.5	141.1	200.8	223.6	186.8	131.8	63.2	30.3
p_{mm} (calc.)	14.1	19.1	26.0	32.2	47.0	49.1	53.9	63.5	74.3	82.7	95.6	141.6	200.5	225.1	186.0	131.8	63.0	30.7

TABLE IV

Vapor pressures of trimethylchlorogermane

t, °C	0.0	9.5	19.0	26.8	29.9	35.1	43.5	52.6	56.5	62.0	65.4	68.4
p_{mm} (obs.)	12.8	20.8	34.2	49.9	55.6	70.1	101.1	143.6	166.9	205.7	232.5	260.0
p_{mm} (calc.)	12.5	21.1	34.1	48.6	55.6	70.3	100.8	143.0	167.9	206.1	233.5	260.0

Can. J. Chem. Downloaded from www.nrcresearchpress.com by 210.87.254.42 on 09/05/12
For personal use only.

TABLE V

Vapor pressures of hexamethyldigermoxane

t, °C	18.2	21.5	25.2	30.2	36.6	42.0	49.1	53.3	56.0	60.2	63.5	66.8	67.5	70.0	72.4
p_{mm} (obs.)	5.2	6.0	8.2	11.2	16.2	21.5	31.6	39.7	45.4	53.7	65.0	71.6	78.8	83.0	92.5
p_{mm} (calc.)	5.3	6.7	8.2	10.7	16.2	21.8	31.6	39.3	44.3	53.5	64.0	73.0	76.0	85.2	93.5

TABLE VI

Vapor pressures of trimethylmethoxygermane

t, °C	0.0	14.4	16.0	20.0	24.6	26.9	29.4	31.9	36.9	40.9	44.9	49.4	54.7	57.6	60.2	61.9
p_{mm} (obs.)	18.0	42.6	47.5	56.2	70.6	77.5	86.0	95.9	117.8	137.7	161.2	190.5	232.0	258.6	282.6	301.0
p_{mm} (calc.)	21.0	43.8	47.0	56.5	69.5	77.7	86.0	95.3	117.3	139.0	161.7	191.1	231.0	258.0	282.6	300.0

TABLE VII

Vapor pressures of liquid trimethylfluorogermane

t, °C	12.7	22.2	33.0	36.2	42.0	44.6	46.8	48.9	51.9	60.2	68.9	71.9
p_{mm} (obs.)	52.7	83.5	130.9	149.7	190.9	210.8	230.5	251.0	280.0	378.9	503.2	553.7
p_{mm} (calc.)	53.5	83.7	133.9	150.1	189.1	211.0	230.9	253.9	279.0	375.5	507.0	556.0

TABLE VIII

Sublimation pressures of trimethylfluorogermane

t, °C	−23.0	−16.0	−7.9	−5.0	−3.4	−2.0	−0.1	0.7	1.5	2.0	2.9	3.9	4.5	6.9	9.0
p_{mm} (obs.)	5.0	8.2	15.2	18.3	20.0	22.3	24.7	26.1	27.5	28.0	29.6	32.0	33.7	38.0	43.5
p_{mm} (calc.)	5.1	8.3	14.7	18.2	20.1	21.7	25.0	26.1	27.4	27.9	30.2	32.7	33.6	38.7	43.8

Reaction of Trimethylbromogermane with Sodium Methylate

Trimethylbromogermane (8.05 mmole) was condensed on excess sodium methylate which had first been dried at 90° for 5 hours in vacuum. After the reaction mixture had been kept at −22.9° for 90 minutes, volatile products were distilled out and treated with freshly cut sodium to remove methanol impurities. Trimethylmethoxygermane was then distilled through a trap maintained at −45.2° to remove any hexamethyldigermane formed during the treatment with sodium. Found: M, 147.0, yield, 98%. Calc. for $(CH_3)_3GeOCH_3$: M, 148.6. Vapor pressures, measured in the range 0 to 61.9° and listed in Table VI, obey the equation $\log_{10} p(\text{mm}) = 7.531-(1695/T)$, which gives an extrapolated boiling point of 91.1±0.5°, a latent heat of vaporization of 7750 cal mole^{-1}, and a Trouton constant of 21.2. The melting point was −102.2±0.3°. The boiling point determined here from vapor pressure data is 4.1° higher than that previously reported for a sample obtained by distillation of trimethylmethoxygermane from a methanolic solution (6). Since it is difficult to remove the last traces of methanol from trimethylmethoxygermane by vacuum distillation, 91.1° appears to be a more reliable value for the boiling point.

Reaction of Hexamethyldigermoxane with Boron Trifluoride

Hexamethyldigermoxane (0.672 mmole) and boron trifluoride (0.448 mmole) in a 3:2 mole ratio were maintained at −80° for 12 hours. Only three-quarters of the boron trifluoride was consumed at this temperature. The product was a white solid. On warming to 20°, consumption of boron trifluoride was complete and, after 4 hours, the white solid decomposed into a volatile substance and an involatile white solid. The volatile fraction was pure trimethylfluorogermane (1.31 mmole. Found: M, 136.4, v.p. 83.5 mm at 22.2°. Calc. for $(CH_3)_3GeF$: M, 136.6). The involatile residue of boron trioxide was titrated, in the presence of mannitol, with sodium hydroxide to the phenolphthalein end point. Calculations based on the stoichiometric equation, $3[(CH_3)_3Ge]_2O + 2BF_3 = 6(CH_3)_3GeF + B_2O_3$, indicated that boron trioxide and trimethylfluorogermane were formed in 97.5 and 97.6% yield, respectively, thus proving the composition of hexamethyldigermoxane.

Vapor pressures of liquid trimethylfluorogermane in the range 12.7 to 71.9°, listed in Table VII, are expressed by the equation $\log_{10} p(\text{mm}) = 7.655-(1695/T)$, which gives an extrapolated boiling point of 81.1±0.5°, a latent heat of vaporization of 7750 cal mole^{-1}, and a Trouton constant of 21.8. A boiling point of 77–78° at 755 mm had previously been reported for this compound (17). Sublimation pressures of trimethylfluorogermane in the range −23 to 9°, given in Table VIII, are expressed by the equation $\log_{10} p(\text{mm}) = 9.028-(2083/T)$, which indicates a latent heat of vaporization of 9550 cal mole^{-1}. The latent heat of fusion was 1800 cal mole^{-1} and the melting point was 1.9±0.4°.

Reaction of Trimethylmethoxygermane with Boron Trifluoride

Trimethylmethoxygermane (0.307 mmole) and boron trifluoride (0.307 mmole) gave a white solid when left overnight at room temperature. This adduct was sublimed at 25° without decomposition. Saturation vapor pressures in the range 16.5 to 33.0°, listed in Table IX, are expressed by the equation $\log_{10} p(\text{mm}) = 10.790-(3105/T)$. At about 41° large positive deviations from the sublimation pressure equation began to occur. On cooling to less than 41°, sublimation pressures again followed the sublimation pressure plot. The adduct melted in the range 41 to 46°.

Can. J. Chem. Downloaded from www.nrcresearchpress.com by 210.87.254.42 on 09/05/12
For personal use only.

TABLE IX

Sublimation pressures of $(CH_3)_3GeOCH_3 \cdot BF_3$

	t, °C			
	16.5	16.9	28.9	33.0
p_{mm} (obs.)	1.04	1.25	3.25	4.34
p_{mm} (calc.)	1.20	1.23	3.24	4.57

ACKNOWLEDGMENTS

We are grateful to the National Research Council for its financial assistance.

REFERENCES

1. N. N. GREENWOOD and R. L. MARTIN. Quart. Revs. (London), **8**, 1 (1954).
2. H. J. EMELÉUS and M. ONYSZCHUK. J. Chem. Soc. 604 (1958).
3. L. M. DENNIS and W. I. PATNODE. J. Am. Chem. Soc. **52**, 2779 (1930).
4. E. G. ROCHOW. J. Am. Chem. Soc. **70**, 436 (1948).
5. C. A. KRAUS and E. A. FLOOD. J. Am. Chem. Soc. **54**, 1622 (1932).
6. R. WEST, H. R. HUNT, and R. O. WIPPLE. J. Am. Chem. Soc. **76**, 310 (1954).
7. L. M. DENNIS and P. R. JUDY. J. Am. Chem. Soc. **51**, 2321 (1929).
8. J. E. GRIFFITHS. Ph.D. Thesis, McGill University, Montreal, Que. 1958.
9. H. H. ANDERSON. J. Am. Chem. Soc. **82**, 3016 (1960).
10. A. G. MACDIARMID. Quart. Revs. (London), **10**, 208 (1956).
11. H. J. EMELÉUS, M. ONYSZCHUK, and W. KUCHEN. Z. anorg. u. allgem. Chem. **283**, 74 (1956).
12. D. P. CRAIG, A. MACCOLL, R. S. NYHOLM, L. E. ORGEL, and L. E. SUTTON. J. Chem. Soc. 332 (1954).
13. L. PAULING. The nature of the chemical bond. 3rd ed. Cornell University Press, Ithaca. 1960. p. 246.
14. J. CHATT and A. A. WILLIAMS. J. Chem. Soc. 4403 (1954).
15. R. A. BENKESER, C. E. DEBOER, R. E. ROBINSON, and D. M. SAUVE. J. Am. Chem. Soc. **78**, 682 (1956).
16. R. WEST and R. H. BANEY. J. Phys. Chem. **64**, 822 (1960).
17. B. M. GLADSHTEIN, V. V. RODE, and L. Z. SOBOROVSKII. J. Gen. Chem. (U.S.S.R.) **29**, 2155 (1959).
18. W. GERRARD and M. F. LAPPERT. J. Chem. Soc. 2545 (1951).
19. C. EABORN. Organosilicon compounds. Butterworth Scientific Publications, London. 1960. p. 265.
20. H. D. FISHER and I. SHAPIRO. Abstracts of the 138th Meeting of the American Chemical Society. Division of Inorganic Chemistry. 1960. p. 39N.
21. A. STOCK. Hydrides of boron and silicon. Cornell University Press, Ithaca, N.Y. 1933. p. 184.
22. D. J. LE ROY. Can. J. Research, B, **28**, 492 (1950).
23. G. K. TEAL and C. A. KRAUS. J. Am. Chem. Soc. **72**, 4706 (1950).
24. J. W. LENGEL and V. H. DIBELER. J. Am. Chem. Soc. **74**, 2683 (1952).
25. M. P. BROWN and G. W. A. FOWLES. J. Chem. Soc. 2811 (1958).

Can. J. Chem. Downloaded from www.nrcresearchpress.com by 210.87.254.42 on 09/05/12
For personal use only.

Can. J. Chem. Downloaded from www.nrcresearchpress.com by 210.87.254.6 on 09/05/12
For personal use only.

A KINETIC ISOTOPE EFFECT STUDY OF THE TSCHUGAEFF REACTION[1]

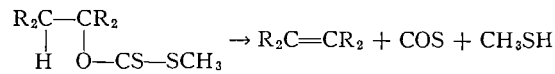
RICHARD F. W. BADER[2] AND A. N. BOURNS

ABSTRACT

Three different kinetic isotope effects have been measured in the thermal decomposition of S-methyl-*trans*-2-methyl-1-indanyl xanthate: the S^{32}/S^{34} effect for the thio-ether sulphur atom, the S^{32}/S^{34} effect for the thion sulphur, and the C^{12}/C^{13} effect for the carbonyl carbon. The results of these measurements provide strong support for a two-step mechanism, in which the rate-determining step is the removal through a cyclic transition state of the cis beta hydrogen atom by the thion sulphur atom.

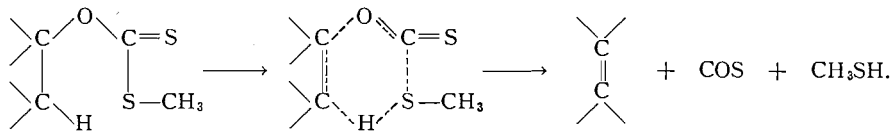
INTRODUCTION

The pyrolytic decomposition of a xanthate ester to yield an alkene, carbonyl sulphide, and a mercaptan



is named the Tschugaeff reaction in honor of its discoverer (1). It belongs to that class of reactions known as pyrolytic cis eliminations, a class which also includes the thermal decomposition of such compounds as esters, amine oxides, and organic chlorides. The steric course of the reaction was first established by Hückel, Tappe, and Legutke (2), who, from a study of the products obtained from the thermal decomposition of the xanthates derived from *l*-menthol, *d*-neomenthol, and the isomeric decalols, discovered the then surprising fact that a cis beta hydrogen is preferentially removed in the elimination process. Subsequent studies by Cram (3), Alexander and Mudrak (4, 5, 6), Barton (7), and Bordwell and Landis (8) have provided ample confirmation of the steric course of the reaction. Recently, DePuy and King (9) have summarized this and other work on the Tschugaeff reaction in a review dealing with pyrolytic cis elimination processes.

As with other cis eliminations, the Tschugaeff reaction is found to be unimolecular and to possess a negative entropy of activation (10, 11). These observations, including the cis behavior, are accommodated by mechanisms which involve a cyclic transition state, such as were first postulated by Hückel *et al.* (2) and by Stevens and Richmond (12). The mechanisms proposed by these two groups of investigators, however, differed in the assignment of the sulphur atom, which was considered to play the role of the nucleophilic agent in the hydrogen abstraction. Hückel *et al.* assigned this role to the thio-ether sulphur atom and pictured the reaction as a one-step process proceeding through a six-membered cyclic transition state as follows:

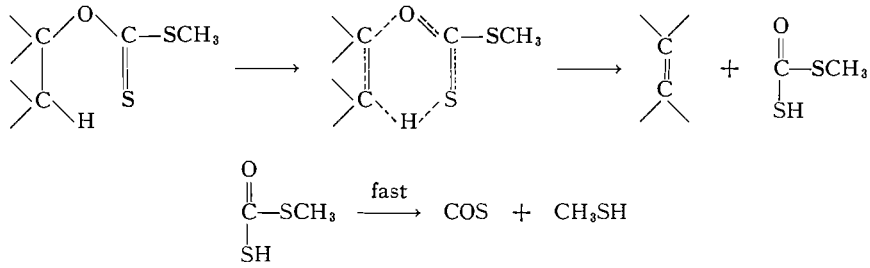


MECHANISM I

This mechanism for xanthate decomposition, which in subsequent discussion will be referred to as mechanism I, has been cited by Barton (7), Ingold (13), and Bartlett (14).

[1]*Manuscript received November 4, 1960.*
Contribution from the Burke Chemical Laboratories, Department of Chemistry, McMaster University, Hamilton, Ontario. Presented at the XIVth International Congress of Pure and Applied Chemistry, Zürich, 1955.
[2]*Present address: Department of Chemistry, University of Ottawa, Ottawa, Ontario.*

In contrast to Hückel's proposal, Stevens and Richmond (12) cast the thion sulphur atom in the role of hydrogen abstractor. This choice also provides for the formation of a six-membered cyclic transition state. The decomposition of this transition state, however, does not lead directly to all of the observed products. Rather, it results in the initial formation of the alkene and an unstable xanthic acid, the latter being expected to dissociate in a subsequent fast step to carbonyl sulphide and mercaptan.



MECHANISM II

Cram (3) also favored this mechanism, which shall be termed mechanism II, on the grounds that resonance structures for the xanthate grouping place more negative charge on the thion than on the thio-ether sulphur atom. He further maintained that the ester group would present steric problems not to be encountered with the thion sulphur atom. Alexander and Mudrak (4) held essentially similar views. The two possible mechanisms thus exhibit a fundamental difference not only in the functions assigned to the sulphur atoms but also in the manner in which the activated complexes revert to products.[3]

Classical methods, such as steric and kinetic studies have led to a general formulation of the reaction mechanism, but they afford no obvious method for differentiating between the two mechanisms, I and II. There is, however, a more subtle method of gaining an insight into the properties of a transition state molecule. This method is dependent upon the measurement of kinetic isotope effects. The object of this paper is to decide between the two proposed mechanisms for the Tschugaeff reaction by offering evidence obtained from such measurements.

Two isotopic species will exhibit a difference in their relative rates of reaction whenever their bonding energy undergoes a change in or before that step of the reaction which determines the over-all rate. Since the changes in bonding predicted for the thion and thio-ether sulphur atoms are very different in the two mechanisms, a knowledge of the isotopic fractionation incurred by these atoms will permit the assigning of definite roles to each in the rate-determining step. In addition, the mechanisms involve quite different bonding changes for the carbonyl (xanthate) carbon atom, and, therefore, information regarding its isotopic fractionation should also prove helpful in distinguishing between the two possibilities.

It is possible to make predictions concerning the magnitude of the isotope effects to be expected for each mechanism by use of the familiar Bigeleisen equation which relates the kinetic isotope effect to isotopic mass and vibrational frequencies (17):

[3]*Tarbell and Harnish (15) have proposed a mechanism based on an initial isomerization of the xanthate ester to a dithiolcarbonate. This mechanism, aside from being difficult to reconcile with the known steric results for the Tschugaeff reaction, may be completely discounted by the observations of Salomaa (16) that the dithiolcarbonates are much more stable than the corresponding xanthate esters.*

Can. J. Chem. Downloaded from www.nrcresearchpress.com by 210.87.254.6 on 09/05/12
For personal use only.

$$k_1/k_2 = (m_2^{\ddagger}/m_1^{\ddagger})^{\frac{1}{2}}\left[1+\sum_{i}^{3n-6} G(u_i)\Delta u_i+\sum_{i}^{3n'-6} G(u_i^{\ddagger})\Delta u_i^{\ddagger}\right]$$

where k is the rate constant, $m^{\ddagger}$ is the effective mass of the transition state in the direction of the reaction co-ordinate, $G(u_i)$ is a free energy function defined by Bigeleisen and Mayer (18), $3n-6$ is the number of vibrational modes of the molecule, and Δu_i is equal to $(\nu_1-\nu_2)h/kT$. The subscripts 1 and 2 refer to light and heavy isotopic molecules, respectively.

A common procedure used in calculating, from vibrational frequency data, the free energy (square bracket) term of this equation for a bond-rupture process, is to assume a model for the transition state in which the bond in question is completely broken and the vibrational frequencies of all other bonds are unchanged (19). On this basis, if the reaction is one involving the rupture of a single bond associated with the isotopic atom, the summation for the transition state is zero and that of the initial state may be readily calculated from the vibrational stretching frequency of the isotopic bond. For a reaction in which the main covalency change involving the isotopic atom is the conversion of a double to a single bond, the initial state and transition state summations may be evaluated from a knowledge of the double and single bond vibrational stretching frequencies, respectively. This method of approximation is crude, but it can be justified on the basis that the calculations are readily made, and what is of greater importance, the results in general have been found to give surprisingly good agreement with experimental data (19).

By application of this method and by reference to known examples, the following predictions have been made concerning the direction and magnitude of the isotope effects to be expected for each mechanism of xanthate decomposition.[4] Since a compound of natural isotopic abundance was used in the experimental study, these predictions refer to S^{32}/S^{34} and C^{12}/C^{13} rate ratios.

A. Thio-ether Sulphur

Mechanism I.—The bond between the thio-ether sulphur atom and the carbonyl carbon atom is broken in the rate-determining step. Using the Slater theorem (19, 20) for the evaluation of the effective mass term and a vibrational stretching frequency of 650 cm^{-1} (21) for the C—S bond, an isotope effect $(k_{32}/k_{34}-1)$ of 1.2% is calculated for reaction at 78° C.

Mechanism II.—The bond between the thio-ether sulphur atom and the carbon atom undergoes no significant change in the rate-determining step. A zero isotope effect, therefore, would be predicted, or, if there is some C—S bond weakening in the transition state leading to the xanthic acid, an effect of a few tenths of one per cent at the most.

B. Thion Sulphur

Mechanism I.—The carbon–sulphur double bond is not appreciably altered in the rate-determining step, with the result that the isotope effect should be small or zero.

Mechanism II.—The carbon–sulphur double bond becomes a carbon–sulphur single bond. Using C—S (single bond) as a model for the transition state, and vibrational stretching frequencies of 1150 cm^{-1} and 650 cm^{-1} (21) for double and single bonds of

[4]*In addition, a number of fairly detailed calculations were performed to give more substance to the predicted isotope effects. These calculations involved the determination of the normal frequencies and their isotopic shifts for simplified models which approximated the xanthate portion of the molecule for the initial state and the two possible transition states. The isotope effects were then calculated from the frequencies and the effective masses thus obtained by substitution in the Bigeleisen equation. This more refined treatment gives results which are in close agreement with those obtained by the more approximate method.*

Can. J. Chem. Downloaded from www.nrcresearchpress.com by 210.87.254.6 on 09/05/12
For personal use only.

sulphur to carbon, respectively, one obtains a free energy term of 1.007 at 78° C. The effective mass term, however, will be very small since the rate-determining step does not lead to a separation of the sulphur atom, but only to a lengthening of its bond to carbon. The isotope effect for the thion sulphur atom would be expected to be between 0.7 and 1.0%.

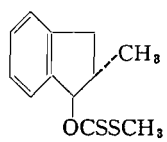
C. Carbonyl Carbon

Mechanism I.—A carbon–sulphur single bond is broken in the rate-determining step. Treatment of the reaction as simply the dissociation of a C—S diatomic molecule into its constituent atoms leads to the prediction of a carbon-13 isotope effect of 3 to 4% at 78° C. That the isotope effects found in the somewhat analogous reaction of decarboxylation fall within this range (19) lends support to this prediction.

Mechanism II.—In the rate-determining step no bond involving isotopic carbon is completely broken, but rather a carbon–sulphur double bond becomes a single bond and a carbon – oxygen single bond becomes a double bond. If these two processes occur to about the same extent in the transition state, the free energy summations for the initial and transition state terms might be expected to effectively cancel each other. Since there is no separation of atoms, the effective mass term should also be small. The net result then will be a very small or zero isotope effect for the carbonyl carbon.

RESULTS AND DISCUSSION

The compound employed in this investigation was S-methyl-*trans*-2-methyl-1-indanyl xanthate (I), the pyrolytic decomposition of which had been previously investigated by Alexander *et al.* (6). This compound was chosen for the following reasons: it possesses but one hydrogen atom on a beta carbon; the configuration is such that cis elimination only can occur; it is a solid readily purified by recrystallization; its decomposition proceeds with better than 80% yield of the gaseous products.



I

The observed isotope effects for each of the two sulphur atoms and for the carbonyl carbon are given in Table I, together with a summary of the effects predicted for the two mechanisms.

It is seen from Table I that the experimental results are incompatible with the predictions of mechanism I. The absence of any isotope effect whatsoever for the xanthate carbon atom and a very small one for the thio-ether sulphur atom proves conclusively that the bond between these two atoms is not severed in the rate-determining step, as would be required by this mechanism. Furthermore, mechanism I allows for only a very small isotope effect for the thion sulphur atom, and can in no manner account for the 9/10% actually observed. The experimental results are, however, in excellent agreement with the predictions of mechanism II. The zero isotope effect for the xanthate carbon is entirely compatible with this mechanism in which there is concurrent partial π bond formation and rupture in the transition state of the rate-determining step. The 9/10% isotope effect for the thion sulphur atom is also in accord with mechanism II. Though this is a relatively small effect, it does show that the bonding of this atom is altered

Can. J. Chem. Downloaded from www.nrcresearchpress.com by 210.87.254.6 on 09/05/12
For personal use only.

TABLE I

Sulphur and carbon isotope effects in the decomposition of S-methyl-*trans*-2-methyl-1-indanyl xanthate

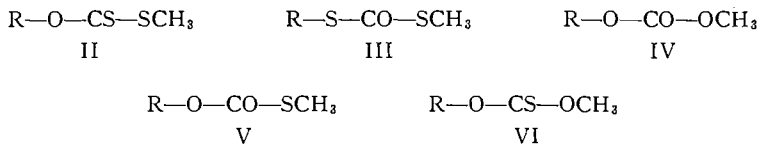
	% isotope effect, $100(k^L/k^H-1)$		
	Thio-ether sulphur S^{32}/S^{34}	Thion sulphur S^{32}/S^{34}	Carbonyl carbon C^{12}/C^{13}
Experimental			
I	0.14	0.84	0.00
II	0.28	1.03	0.00
III	—	1.01	—
IV	0.28	0.62	0.13
V	0.18	0.83	0.00
VI	0.19	0.85	0.12
Average[a]	0.21±0.07	0.86±0.16	0.04±0.06
Predicted			
Mechanism I	~1.2	~0.0	3.0–4.0
Mechanism II	~0.0	0.7–1.0	~0.0

[a]Precision expressed as 95% confidence limit.

significantly in the rate-determining step. The 2/10% isotope effect observed for the thio-ether sulphur atom is explicable only if it is assumed to be undergoing no significant change in bond energy or type in the rate-determining step. This is the case in mechanism II.

From this comparison it is concluded that a mechanism is operative in the Tschugaeff reaction which follows the major steps outlined for mechanism II, i.e., the reaction proceeds via a two-step mechanism wherein the thion sulphur atom abstracts the cis beta hydrogen atom resulting in the formation of an unstable xanthic acid intermediate. This is analogous to the mechanism which is currently accepted for the thermal decomposition of carboxylic acid esters (9).

The absence of an isotope effect for the carbonyl carbon atom provides a further insight into the more detailed aspects of the reaction. O'Connor and Nace (11), in order to account for the decreased thermal stability of cholesteryl xanthates with increased electronegativity of R— in the xanthate group, —O—C(=S)—SR, had pictured the oxygen atom as forming a π-bond with the carbonyl carbon atom during the rate-determining step. The more electronegative the xanthate group, the larger the induced positive charge on the carbon atom and hence the greater the driving force due to the partial π bond formation. Some recent work by Salomaa (16) has demonstrated the importance of this particular driving force in pyrolytic ester decompositions. He investigated the thermal properties of compounds of types II to VI:



which are respectively, the xanthate ester, the dithiolcarbonate, the carbonate ester, the thio ester, and the thio carbonate ester. Compounds of types II and VI possess the

Can. J. Chem. Downloaded from www.nrcresearchpress.com by 210.87.254.6 on 09/05/12
For personal use only.

system —O—C=S, which is capable of providing driving force (···O···C···S···) for the reaction and only these compounds are found to be thermally unstable. Compounds of the types III, IV, and V contain the ester grouping —S—C=O or —O—C=O, and their reaction, therefore, must give rise to a transition state in which there has been either an increase in the bonding of the carbonyl carbon to sulphur at the expense of its bonding to oxygen, which would be energetically unfavorable, or a change in bonding from one oxygen atom to another, which would involve only a very small free energy change. Salomaa found that these compounds remain unchanged on distillation, which is in accord with these considerations.

The absence of an isotope effect for the carbonyl carbon shows clearly that this partial π-bond driving force is indeed present. A calculation has shown that if there were no concurrent π bond formation of the oxygen with the carbonyl carbon, the isotope effect for this carbon atom would be of the order of 1%. A lower value can only arise as a consequence of participation of oxygen in π bond formation; and the fact that the observed isotope effect in the present study is zero, within the limits of measurement, strongly suggest that the two bond changes involving carbon are nearly balanced. In other reaction systems this need not be the case, and it should be possible to relate the change in the observed isotope effect with a change in driving force as, for example, the ester grouping is made more electronegative.

EXPERIMENTAL

The synthetic work entailed the preparation of the ketone 2-methyl-1-indanone, which under proper conditions could be hydrogenated to yield only the trans form of the alcohol, 2-methyl-1-indanol. The 2-methyl-1-indanone was prepared according to the procedure given by Alexander and Mudrak (6) and also by an alternative method reported by Fuson and Burckhalter (22). Of the two synthetic procedures, the latter method was found to give the purer product and the higher over-all yield, namely 50%, as compared to 30%. The procedure of Alexander and Mudrak (6) was used for the stereospecific hydrogenation over copper chromite of the ketone to *trans*-2-methyl-1-indanol, as was also his method for the conversion of the alcohol to the xanthate ester. The carbon disulphide employed in the synthesis contained carbon and sulphur of natural isotopic abundance. S^{34} is found in natural sulphur to the extent of 4.2% and C^{13} occurs naturally to the extent of 0.7%. Both of these abundances are quite sufficient for precise mass spectrometric analysis.

Since it was necessary to measure the isotopic fractionation of the thion and thio-ether sulphur atoms and also of the carbonyl carbon atom, a method for their quantitative separation and recovery was required. The products of the decomposition of the xanthate ester (I) are 2-methyl-1-indene, methyl mercaptan, and carbonyl sulphide. The alkene is a high-boiling compound and remains in the reaction flask. Carbonyl sulphide and methyl mercaptan are both gases at room temperature and may be rapidly removed from the reaction mixture with a stream of inert gas. The thio-ether sulphur atom is found in the methyl mercaptan, and the thion sulphur and the carbonyl carbon atoms in the carbonyl sulphide.

The separation of the two gaseous products (and thus of the two forms of sulphur) was based on the fact that carbonyl sulphide is unaffected by cold, fuming nitric acid (23), whereas methyl mercaptan is very rapidly oxidized to non-volatile methanesulphonic acid.

Can. J. Chem. Downloaded from www.nrcresearchpress.com by 210.87.254.6 on 09/05/12
For personal use only.

The gaseous product consisting of methyl mercaptan and carbonyl sulphide was swept into the fuming nitric acid trap, A, in Fig. 1, by a stream of purified nitrogen gas. After

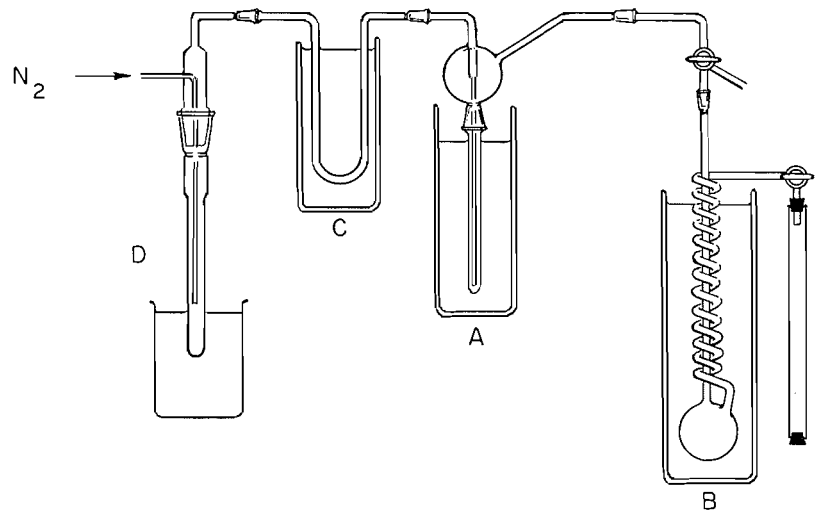


FIG. 1. Apparatus for total decompositions.

the completion of the experiment the tube and bubbler of trap A were sealed in a Carius tube and heated for 24 hours in a furnace maintained at 260 to 270° C. This treatment oxidized all of the methanesulphonic acid to sulphate ion, carbon dioxide, and water. The sulphate ion was then precipitated as barium sulphate according to the procedure outlined by Kolthoff and Sandell (24), after the excess nitrate ion was first removed by three successive evaporations in the presence of hydrochloride acid. The carbonyl sulphide was swept unreacted through the fuming nitric acid and collected in trap B, which was immersed in liquid air and contained lead hydroxide and excess base. Subsequent warming of the closed, isolated trap converted the carbonyl sulphide into lead sulphide and lead carbonate. The latter was decomposed by the addition of acetic acid and the evolved carbon dioxide precipitated as barium carbonate according to the procedure outlined by Calvin *et al.* (25). The thio-ether and thion sulphur atoms of the xanthate ester were thus recovered as barium sulphate and lead sulphide, respectively, while the barium carbonate contained the carbonyl carbon.

The quantitativeness of the separation of the two gaseous compounds and of the recovery of the three resulting products was established using pure samples of methyl mercaptan and carbonyl sulphide. In the experiments using carbonyl sulphide alone, no sulphur in any form was detected in the fuming nitric acid trap, and recovery of sulphur as lead sulphide was better than 98%. With synthetic mixtures of the two gases, yields of lead sulphide ranged from 96 to 101%, of barium sulphate 96 to 103%, and of barium carbonate 100 to 102%.

In the final stages of the procedure the three solid products, barium sulphate, lead sulphide, and barium carbonate, were converted to gaseous products suitable for mass spectrometer analysis, namely, sulphur dioxide and carbon dioxide. The barium sulphate was reduced to hydrogen sulphide by treatment with a solution containing hydriodic acid, concentrated hydrochloric acid, and hypophosphorous acid. The hydrogen sulphide was precipitated as cadmium sulphide and then converted to silver sulphide. This silver

Can. J. Chem. Downloaded from www.nrcresearchpress.com by 210.87.254.6 on 09/05/12
For personal use only.

sulphide, as well as the lead sulphide formed from carbonyl sulphide, was burned in a stream of purified oxygen to sulphur dioxide, which was purified and collected using high-vacuum techniques. These procedures for the conversion of metal sulphates and sulphides to sulphur dioxide have been previously described by Thode and his co-workers (26) and have been shown to involve no significant isotopic fractionation. Barium carbonate was treated with concentrated sulphuric acid in a high-vacuum system and the resulting carbon dioxide purified and collected. Yields of purified carbon dioxide were shown to be better than 98%.

An isotope effect is conveniently determined by intercomparison of the isotopic ratio for the atom in question in the original reactant and in the product formed from some small measured extent of reaction. In the present investigation the isotopic ratios in the reactant were determined by allowing the reaction of a sample of the xanthate to proceed to completion, separating the products, converting them to sulphur dioxide and carbon dioxide, and analyzing the gases mass spectrometrically. These ratios were then combined with corresponding ratios obtained for the products of a partial reaction and the isotope effects were calculated using an expression derived by Stevens and Attree (27) which takes into account the extent of reaction.

Total Decompositions

The total decompositions were carried out in the manner described below, employing the apparatus shown in Fig. 1. On the day previous to which an experiment was performed, the xanthate ester was repeatedly recrystallized until it exhibited a constant melting point. The material was then stored overnight in a vacuum desiccator containing phosphorus pentoxide. A small portion of the xanthate ester, in the neighborhood of 1 millimole, was accurately weighed and placed in the decomposition tube D. Before traps A and B, charged as previously described, were attached to the line, tubes D and C were flushed for 1 hour with purified nitrogen gas. A dry ice – acetone bath was placed around trap C, an ice-water bath around trap A, and a liquid-air bath around trap B. Without interruption of the nitrogen gas flow an oil bath, heated to a temperature of 103° C, was placed around tube D at such a height that the liquid level of the bath was slightly higher than that of the solid inside tube D. The temperature of the bath was maintained at approximately 100° C, resulting in the rapid melting of the xanthate and in the evolution of gaseous products. The methyl mercaptan condensed in the U tube C, where it was visible as a clear, colorless liquid. At no time did any of the 2-methyl-1-indene distill into tube C. One-half hour after the initial application of heat, the dry ice – acetone bath was slowly lowered from around trap C; and when a total of $1\frac{1}{2}$ hours had elasped, the heating was discontinued. The nitrogen sweep was continued for $\frac{1}{2}$ hour more, after which time traps A and B were removed from the line and their contents treated as previously described.

The work of Alexander and Mudrak (6) had indicated that the pyrolysis of S-methyl-*trans*-2-methyl-1-indanyl xanthate produced approximately 80% of the theoretical amount of gaseous products, a figure arrived at by measuring the volume of the evolved carbonyl sulphide and methyl mercaptan. Trial runs using the procedure outlined above gave results slightly higher than those reported by Alexander and Mudrak. Table III lists the results of three such runs. The percentage yield of the methyl mercaptan is expressed in terms of the recovered barium sulphate, and the carbonyl sulphide is similarly expressed in terms of the recovered lead sulphide and barium carbonate.

Although the yields of products are less than quantitative, the isotopic ratios obtained for thio-ether sulphur and for carbonyl carbon should not differ significantly from the

Can. J. Chem. Downloaded from www.nrcresearchpress.com by 210.87.254.6 on 09/05/12
For personal use only.

TABLE II

Percentage yields of methyl mercaptan and carbonyl sulphide obtained from thermal decompositions of S-methyl-*trans*-2-methyl-1-indanyl xanthate

Xanthate ester (mmoles)	% yield		
	PbS	$BaCO_3$	$BaSO_4$
1.01	85.6	91.4	83.5
1.15	85.5	89.4	91.6
0.974	86.2	88.5	92.4

TABLE III

Experimental data for the total and partial decompositions of S-methyl-*trans*-2-methyl-1-indanyl xanthate

Expt. No.	Temp. (°C)	% yield			Isotopic abundance ratios		
		$BaSO_4$	PbS	$BaCO_3$	Thio-ether S S^{32}/S^{34}	Thion S S^{32}/S^{34}	Carbonyl C C^{12}/C^{13}
TD-I	100	77.6	81.0	84.2	22.28	22.20	93.63
PD-I	77	4.4	3.7	4.1	22.31	22.38	93.63
TD-II	100	83.3	83.5	82.6	22.27	22.18	93.72
PD-II	79	7.8	7.9	8.3	22.33	22.40	93.72
TD-III	100	—	88.0	83.0	—	22.20	—
PD-III	76	—	4.8	—	—	22.42	—
TD-IV	100	67.6	87.8	90.8	22.30	22.22	93.78
PD-IV	80	6.9	9.4	9.9	22.36	22.35	93.90
TD-V	100	86.7	86.7	93.4	22.31	22.23	94.25
PD-V	75	6.5	5.7	6.6	22.35	22.41	94.25
TD-VI	100	91.5	88.0	94.3	22.31	22.28	94.34
PD-VI	81	11.2	10.6	11.4	22.35	22.46	94.43

ratios in the original reactant, since these atoms undergo little or no isotopic fractionation in the pyrolytic reaction. The thion sulphur atom is, however, isotopically fractionated, and the failure to achieve complete conversion to carbonyl sulphide in the "total" decompositions might conceivably give a product whose S^{32}/S^{34} ratio is slightly higher than that in the original reactant. This would mean that the true isotope for this atom would be somewhat higher than that obtained by the intercomparison of ratios for the partial and "total" reaction products. In this event, mechanism II would be even more strongly indicated.

Partial Decompositions

Since the partial decompositions required only short heating periods, varying from 2 to 3 minutes, there was a possibility that some of the carbonyl sulphide and methyl mercaptan would remain dissolved in the unchanged reactant and the 2-methyl-1-indene. To circumvent this difficulty, the partial decompositions were performed in an evacuated system and the products collected in a liquid-air trap, thus insuring the complete and rapid removal of the gaseous products from the melt. A pair of total and partial decompositions were always carried out on the same day.

The apparatus employed for the partial decompositions is shown in Fig. 2. A weighed amount of the xanthate ester, of the order of 20 mmoles, was placed in the bulb of flask E, which was attached to a U tube F, provided with two stopcocks. The other arm of the U tube was connected to a high-vacuum system. Stopcocks S_5 and S_6 were both opened and the system was evacuated to a pressure of 10^{-5} mm of mercury or less. Tube F was then immersed in a liquid-air bath, stopcock S_6 was closed, and an oil bath

Can. J. Chem. Downloaded from www.nrcresearchpress.com by 210.87.254.6 on 09/05/12
For personal use only.

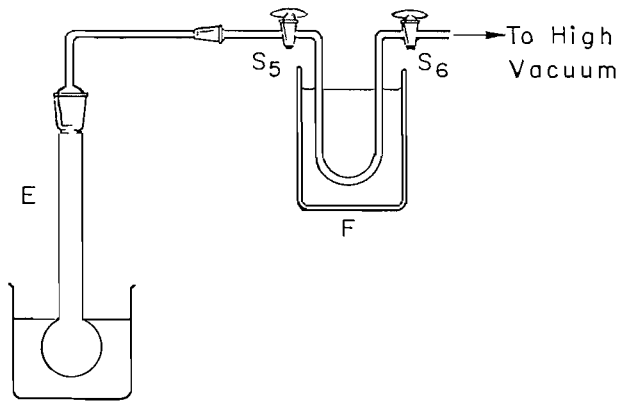


FIG. 2. Apparatus for partial decompositions.

at 70° C was raised to cover the bulb of tube E.[5] The solid in tube E melted rapidly and the temperature was then quickly raised to the desired value of 75 to 80° C. The reaction was allowed to proceed to only a small extent, usually 3 to 10% of completion. The oil bath was removed and the contents of the bulb were allowed to cool. Stopcock S_5 was then closed, tube F detached from E and the vacuum line, and, while still immersed in liquid air, connected to traps A and B. (Tube F has thus replaced D and C in Fig. 1.) With stopcocks S_5 and S_6 closed, a dry ice – acetone slurry was substituted for the liquid-air bath. Stopcock S_5 was then slowly opened to admit a stream of purified nitrogen gas. When the pressure within the tube had reached atmospheric, stopcock S_6 was opened and the nitrogen gas allowed to flow through the remainder of the apparatus. Tube F was kept immersed in the dry ice – acetone bath for $\frac{1}{2}$ hour, after which time the slurry was removed and the flushing with nitrogen continued for another $1\frac{1}{2}$ hours. The line was then dismantled and the contents of traps A and B were treated as previously described.

Mass Spectrometry

The relative abundances of the sulphur and carbon isotopes were measured using a 180°, directional focusing mass spectrometer of the Nier type equipped with an automatic recorder. The S^{32}/S^{34} ratios were obtained from the mass 64/mass 66 ion current ratios after applying a suitable correction for the contribution to mass 66 of the molecular species $S^{32}O^{16}O^{18}$ (28). Similarly, the C^{12}/C^{13} ratios were obtained from 44/45 ion current ratios with a correction being made for the contribution of $C^{12}O^{16}O^{17}$ to mass 45 (29). All of the mass spectrometer ratios reported have a precision of 0.1% or better.

The experimental data pertaining to the total decompositions (TD) and the partial decompositions (PD) are listed in Table III.

ACKNOWLEDGMENTS

Grateful acknowledgment is made to the National Research Council for financial support of this work and to the Ontario Research Foundation for the award of a fellowship to R. F. W. B. We are indebted also to Dr. W. H. Fleming for performing the mass spectrometric analyses.

[5]*By first melting the xanthate ester at a temperature lower than that actually employed for the decompositions, it was possible to obtain a homogeneous reaction at the higher temperature while incurring only a minor amount of decomposition during the melting process.*

Can. J. Chem. Downloaded from www.nrcresearchpress.com by 210.87.254.6 on 09/05/12
For personal use only.

REFERENCES

1. L. TSCHUGAEFF. Ber. **32**, 3332 (1899).
2. W. HÜCKEL, W. TAPPE, and G. LEGUTKE. Ann. **543**, 191 (1940).
3. D. J. CRAM. J. Am. Chem. Soc. **71**, 3883 (1949).
4. E. R. ALEXANDER and A. MUDRAK. J. Am. Chem. Soc. **72**, 1810 (1950).
5. E. R. ALEXANDER and A. MUDRAK. J. Am. Chem. Soc. **72**, 3194 (1950).
6. E. R. ALEXANDER and A. MUDRAK. J. Am. Chem. Soc. **73**, 59 (1951).
7. D. H. R. BARTON. J. Chem. Soc. 2174 (1949).
8. F. G. BORDWELL and P. S. LANDIS. J. Am. Chem. Soc. **80**, 6379, 6383 (1958).
9. C. H. DE PUY and R. W. KING. Chem. Revs. **60**, 431 (1960).
10. G. L. O'CONNOR and H. R. NACE. J. Am. Chem. Soc. **74**, 5454 (1952).
11. G. L. O'CONNOR and H. R. NACE. J. Am. Chem. Soc. **75**, 2118 (1953).
12. P. G. STEVENS and J. H. RICHMOND. J. Am. Chem. Soc. **63**, 3132 (1941).
13. C. K. INGOLD. Structure and mechanism in organic chemistry. Cornell University Press, Ithaca, N.Y. 1953. p. 471.
14. P. D. BARTLETT. *In* Organic chemistry, an advanced treatise. Vol. 3. H. Gilman (*Editor-in-Chief*). John Wiley & Sons, Inc., New York. 1953. p. 53.
15. D. S. TARBELL and D. P. HARNISH. Chem. Revs. **49**, 60 (1951).
16. E. SALOMAA. Ann. Acad. Sci. Fennicae, Ser. A, II, No. 94, 1 (1959).
17. J. BIGELEISEN. J. Chem. Phys. **17**, 675 (1949).
18. J. BIGELEISEN and M. G. MAYER. J. Chem. Phys. **15**, 261 (1947).
19. J. BIGELEISEN. J. Phys. Chem. **56**, 823 (1952).
20. N. B. SLATER. Proc. Roy. Soc. (London), A, **194**, 112 (1948).
21. L. J. BELLAMY. Infra-red spectra of complex molecules. 2nd ed. Methuen and Co., London. 1958.
22. J. H. BURCKHALTER and R. C. FUSON. J. Am. Chem. Soc. **70**, 4184 (1948).
23. J. W. MELLER. A comprehensive treatise on inorganic and theoretical chemistry. Vol. 5. Longmans, Green and Co., London. 1924. p. 976.
24. I. M. KOLTHOFF and E. B. SANDELL. Text-book of quantitative inorganic analysis. 3rd ed. Macmillan Co., New York. 1952. p. 330.
25. M. CALVIN, C. HEIDELBERGER, J. C. REID, B. M. TOLBERT, and P. F. YANKWICH. Isotopic carbon. John Wiley & Sons, Inc., New York. 1949. p. 83.
26. H. G. THODE, J. MONSTER, and H. B. DUNFORD. Bull. Am. Assoc. Petrol. Geologists, **42**, 2619 (1958).
27. W. H. STEVENS and R. W. ATTREE. Can. J. Research, B, **27**, 807 (1949).
28. H. G. THODE, J. MACNAMARA, and W. H. FLEMING. Geochim. et Cosmochim. Acta, **3**, 235 (1953).
29. J. B. STOTHERS and A. N. BOURNS. Can. J. Chem. **38**, 923 (1960).

Can. J. Chem. Downloaded from www.nrcresearchpress.com by 210.87.254.6 on 09/05/12
For personal use only.

Can. J. Chem. Downloaded from www.nrcresearchpress.com by 210.87.254.42 on 09/05/12
For personal use only.

PHASE TRANSITIONS IN SOME ANHYDROUS POTASSIUM SOAPS[1]

R. F. GRANT[2] AND B. A. DUNELL

ABSTRACT

The proton magnetic resonance absorption of the anhydrous potassium soaps of palmitic, myristic, lauric, and capric acids has been studied. Pronounced changes in the proton magnetic resonance line widths correspond to known phase transitions in these soaps.

INTRODUCTION

The anhydrous potassium soaps of long-chain fatty acids pass through several reversible phase transitions before melting (1, 2). Since the nature of some of these transitions is not well understood, their investigation by the broad-line nuclear magnetic resonance (n.m.r.) technique was undertaken. In a previous study, the proton magnetic resonance absorption in anhydrous potassium stearate was discussed in some detail and two phase transitions were identified (3). The work reported here is the continuation of this earlier investigation to the proton magnetic resonance absorption in the anhydrous potassium soaps of palmitic, myristic, lauric, and capric acids.

METHOD AND RESULTS

These soaps were made from Eastman Kodak white label grade acids which had been purified by a low-temperature crystallization technique (4). The method used in preparing the potassium soap sample (3) and the details of the nuclear magnetic resonance spectrometer (5) have been previously described. The variation of the proton magnetic resonance line width of potassium palmitate, C_{16}, myristate, C_{14}, laurate, C_{12}, and potassium caprate, C_{10}, is shown in Fig. 1. The line width is taken as the separation in gauss of the points of maximum and minimum slope of the proton magnetic resonance absorption line.

With the exception of potassium caprate, all the potassium soaps investigated show a relatively small change in line width between $-180°$ C and 20° C. They all exhibit a comparatively abrupt change in line width over a short temperature range, which falls between 50° C and 75° C. The line widths decrease somewhat gradually again as the temperature is raised above this range, and the line-width-vs.-temperature curve levels off above 130° C in the case of potassium laurate and caprate. Finally, at higher temperatures there is an abrupt change where the line width decreases from a value between 3 and 5 gauss, to a value which seems to be governed by the inhomogeneity of the magnetic field over the sample.

DISCUSSION

In potassium stearate it has been shown that molecular motion is probably confined to torsional oscillation of small amplitude at temperatures below about 20° C (3). However, this motion about the longitudinal axes of the paraffin chains increases considerably as the temperature is raised through the crystal-structure transition which is known to occur at some temperature between 50° C and 80° C in most potassium soaps (6). At temperatures above the crystal-structure transition the oscillation or twisting of the

[1]*Manuscript received November 10, 1960.*
Contribution from the Department of Chemistry, University of British Columbia, Vancouver 8, B.C.
[2]*Holder of National Research Council Studentships. Present address: British Columbia Research Council, Vancouver 8, B.C.*

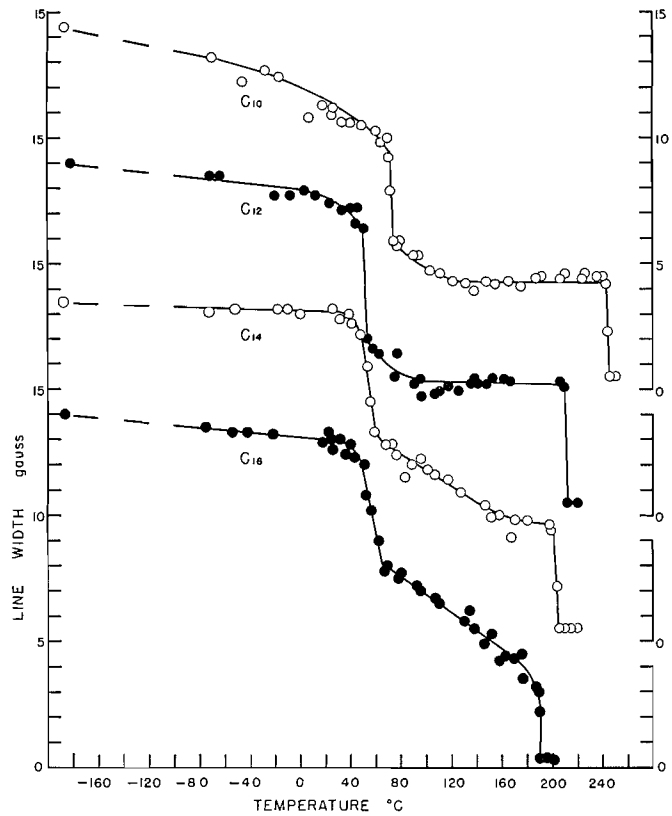


FIG. 1. Line width versus temperature for potassium caprate (C_{10}), potassium laurate (C_{12}), potassium myristate (C_{14}), and potassium palmitate (C_{16}).

paraffin chains appears to increase in violence until abruptly, at a higher temperature phase transition, motion of the paraffin chains is unrestricted except for the probable constraint that the polar chain ends remain in lattice array. These changes in motion are indicated by changes in line width and second moment, the final phase transition being indicated by the abrupt narrowing of the line to the limits of the spectrometer resolution (3). The line-width changes of the potassium soaps studied here parallel those changes observed in potassium stearate, and it is assumed that the same sequence of molecular motion occurs in each of these soaps.

The temperatures of the crystal-phase transitions in the potassium soaps from the stearate to caprate are given in Table I. For the n.m.r. case, these temperatures are those

TABLE I

Crystal transition temperature in potassium soaps

Soap	Hot stage (6)	Method and temperature (°C)	
		Calorimetric	n.m.r.
Stearate, C_{18}	78	57 (2)	62 (3)
Palmitate, C_{16}	68	60 (1)	66*
Myristate, C_{14}	61	60 (2)	60*
Laurate, C_{12}	54	53 (2)	53*
Caprate, C_{10}	76	—	74*

*This work.

Can. J. Chem. Downloaded from www.nrcresearchpress.com by 210.87.254.42 on 09/05/12
For personal use only.

at which the abrupt line narrowing is completed, and it can be seen that the n.m.r. transition temperatures agree reasonably well with the crystal transition temperatures obtained by calorimetric (2) and X-ray (6) methods. The only significant disagreement is for potassium stearate between the microscopic study and the other two methods.

The temperature at which the n.m.r. line becomes very narrow is given for each potassium soap in Table II, and is compared with the temperature of the nearest significant transition found calorimetrically (2) and with transition temperatures found by

TABLE II

A mesomorphic transition temperature in potassium soaps

		Method and temperature (°C)	
Soap	n.m.r.	Calorimetric	Other
Stearate, C_{18}	171 (3)	170(2)	162,† 165†,‡
Palmitate, C_{16}	190*	176(2), 174(1)	173,§ 174‡,‖
Myristate, C_{14}	204*	197(2)	
Laurate, C_{12}	212*	218(2)	
Caprate, C_{10}	246*		

*This work.
†Dilatometric (1, 8, 9).
‡Light transmission (10).
§Hot-stage microscopy (1).
‖X-Ray diffraction (11).

other methods. The agreement is not close, particularly for potassium palmitate. The abrupt narrowing of the line width to less than half a gauss suggests that this transition is similar in nature to the supercurd-to-subwaxy transition in sodium soaps (3). In the sodium soaps, however, the supercurd-to-subwaxy transition temperatures are almost independent of chain length and show no trend to higher or lower values with changing length of chain (7), whereas this transition temperature increases gradually with decreasing chain length in the potassium soaps. It is probably reasonable to attribute this rise in transition temperature to increased effectiveness of the polar ends of the molecules in maintaining a firm lattice as the ratio of polar ends to CH_2 groups increases with decreasing size of hydrocarbon chain. The levelling off of line width with increasing temperature at temperatures below the transition indicates that a limiting extent of motion is reached in the shorter-chain soaps (C_{14} and shorter) at temperatures appreciably below the temperature which allows very extensive motion of the hydrocarbon chains. As one goes from C_{18} to C_{10} the temperature of levelling off is lower and the maximum amount of motion is less (as indicated by greater line width), both phenomena indicating the increasing effectiveness of the polar end groups in binding the lattice more tightly as the hydrocarbon chain gets shorter.

At temperatures below the crystal transition temperature, on the other hand, the shorter hydrocarbon chains can move, within the limits to which any motion is possible, more freely than the longer chains. Such behavior is indicated by the greater decrease in line width of the shorter-chain soaps as the crystal transition temperature is approached from below, and is consistent with the view of low-temperature molecular motion in these salts suggested in an earlier paper (3). The hydrocarbon chains are believed to be capable of torsional oscillation of amplitude increasing from the fixed polar ends to the terminal CH_3 group. The constraints on the motion of the hydrocarbon chain alone are smaller for the shorter chains.

Although clear indication of phase transitions at temperatures falling between the crystal transition temperature and 170° C have been obtained from calorimetric and

Can. J. Chem. Downloaded from www.nrcresearchpress.com by 210.87.254.42 on 09/05/12
For personal use only.

microscopic studies of potassium soaps (1, 2), no corresponding n.m.r. transitions have been observed. Such behavior is consistent with the fact that the n.m.r. line is narrowed by reorientations which are of low frequency compared with frequencies required to produce a thermodynamic effect. The fact that n.m.r. and thermal transitions do not necessarily coincide at one temperature was discussed by Gutowsky and Pake (12), and in the light of their discussion it is suggested that the transitions occurring between approximately 90° and 160° C are non-co-operative. A dilatometric anomaly has been reported for potassium palmitate at 130° C (1). It is, however, only a "small inflection" in the specific-volume-vs.-temperature curve, a fact which would not contradict the interpretation given here for the n.m.r. results.

ACKNOWLEDGMENTS

We thank the National Research Council for a studentship awarded to one of us (R.F.G.) and for a grant-in-aid of the research.

REFERENCES

1. R. D. VOLD and M. J. VOLD. J. Phys. Chem. **49**, 32 (1945).
2. G. B. RAVICH and N. A. NECHITAYLO. Doklady Akad. Nauk S.S.S.R. **83**, 117 (1952).
3. R. F. GRANT and B. A. DUNELL. Can. J. Chem. **38**, 1951 (1960).
4. J. B. BROWN and D. K. KOLB. Progress in the chemistry of fats and other lipids. Vol. 3. Pergamon, London. 1955. p. 58.
5. R. F. GRANT and B. A. DUNELL. Can. J. Chem. **38**, 359 (1960).
6. T. R. LOMER. Acta Cryst. **5**, 11 (1952).
7. R. D. VOLD. J. Am. Chem. Soc. **63**, 2915 (1941).
8. M. J. VOLD, M. MACOMBER, and R. D. VOLD. J. Am. Chem. Soc. **63**, 166 (1941).
9. D. P. BENTON, P. G. HOWE, R. FARNAND, and I. E. PUDDINGTON. Can. J. Chem. **33**, 1798 (1955).
10. D. P. BENTON, P. G. HOWE, and I. E. PUDDINGTON. Can. J. Chem. **33**, 1384 (1955).
11. O. E. A. BOLDUAN, J. W. McBAIN, and S. Ross. J. Phys. Chem. **47**, 528 (1943).
12. H. S. GUTOWSKY and G. E. PAKE. J. Chem. Phys. **18**, 162 (1950).

Can. J. Chem. Downloaded from www.nrcresearchpress.com by 210.87.254.42 on 09/05/12
For personal use only.

Can. J. Chem. Downloaded from www.nrcresearchpress.com by 210.87.254.40 on 09/05/12
For personal use only.

ORGANIC DEUTERIUM COMPOUNDS

XXIII. SYNTHESIS OF DEUTERATED OLEFINS[1]

D. KOVACHIC[2] AND L. C. LEITCH

ABSTRACT

The synthesis of some deuterated ethylenes, propylenes, butenes, and pentenes is described. Homolytic addition of hydrogen bromide and deuterium bromide to allene and some deutero-allenes was investigated and found to give 2-bromopropylene and deutero-2-bromopropylenes rather than the 3-bromo isomers. The preparation of 3-bromopentadeuteropropene by the allylic bromination of hexadeuteropropene is described. Bromotrichloromethane and 1,3-butadiene gave, under homolytic conditions, *trans*-5,5,5-trichloro-1-bromo-2-pentene, which was debrominated to a mixture of 5,5,5-trichloropentenes. The latter was then dechlorinated to 1-pentene, which contained some 2-pentenes. Hexadeuterobutadiene reacted similarly to give the corresponding deuterated compounds.

Two previous communications in this series dealt with the synthesis of deuterated alkanes (1) and diolefins (2). This paper describes the synthesis of several deuterated olefins embracing compounds from C_2 to C_5. Some of these are now reported for the first time while others have been obtained by a shorter route or in higher isotopic purity than previously.

Synthetic methods have been reported for four of the six possible deuterated ethylenes. Tetradeuteroethylene was prepared by partial reduction of dideuteroacetylene over palladium (3) or by the debromination of 1,2-dibromotetradeuteroethane (4, 5). *cis*- and *trans*-Dideuteroethylene were obtained by the reduction of dideuteroacetylene with zinc and hydrochloric acid (6) and chromous chloride respectively (7). 1,1-Dideuteroethylene was formed in 37% yield during the electrolysis of α-deuterated propionic acid (8). A mixture of all three mono-, di-, and tri-deuteroethylenes was obtained when ethylene was exchanged with deuterium oxide at 150° over a nickel catalyst (9). Finally an outline showing the preparation of several deuteroethylenes from acetylene or dideuteroacetylene and deuterium bromide has appeared in a review by de Hemptinne (10).

Three of the possible deuteroethylenes have now been prepared more conveniently and in better yield by the sequence shown below:

$$CH_2{=}CHCl \xrightarrow[h\nu]{DBr} CH_2BrCHDCl \xrightarrow{Zn} CH_2{=}CHD$$

$$CH_2{=}CDCl \xrightarrow[h\nu]{DBr} CH_2BrCD_2Cl \xrightarrow{Zn} CH_2{=}CD_2$$

$$CH_2{=}CDBr \xrightarrow[h\nu]{HBr} CD_2BrCHDCl \xrightarrow{Zn} CD_2{=}CHD$$

The vinyl bromide deuterated on the carbon atom bearing the chlorine was reported by us in a previous paper (11). Trideuterovinyl bromide was obtained by treating 1,2-dibromotetradeuteroethane with alkali.

Only a few deuterated propenes have been reported up to now. In the course of their studies on the mechanism of electrolysis of fatty acids, Schanzer and Clusius (12) reported

[1]*Manuscript received August 19, 1960.*
Contribution from the Division of Pure Chemistry, National Research Council, Ottawa, Canada. Presented at the 136th meeting of the American Chemical Society, Atlantic City, N.J., September 1959.
Issued as N.R.C. No. 6135.
[2]*Present address: Production and Marketing Branch, Department of Agriculture, Ottawa, Canada.*

the formation of 2-deutero-1-propene from the deuterated isobutyric acid $(CH_3)_2CDCO_2D$, 3,3,3-trideutero-1-propene from butyric acid labelled on the terminal carbon atom, $CD_3CH_2CH_2COOH$, and 1,1-dideutero-1-propene from butyric acid labelled in the α-methylene group, $CH_3CH_2CD_2CO_2H$. *cis*-1-Deutero-1-propene was obtained by the reduction of 1-deutero-1-propyne (6). 3-Deuteropropene was prepared by the dechlorination of 3-chloropropene with zinc and acetic deuteroacid (13). According to McNesby, 3,3,3-trideuteropropene is formed in significant amount in the reaction between trideuteromethyl radicals and 1-butene at 325° (14).

Investigation of the addition of hydrogen and deuterium bromides to allene and tetradeuteroallene opened a route to a large number of deuteropropenes. Addition was found to take place in accordance with Markovnikov's rule to give mainly 2-bromopropene even under homolytic conditions, viz. in the presence of dibenzoyl peroxide or under ultraviolet illumination. Only very small amounts of the isomeric 3-bromopropene were found in the products. This result is unexpected in view of Haszeldine's (15) observation that trifluoromethyl iodide adds to allene homolytically to give $CF_3CI{=}CH_2$. However, theoretical considerations indicate 2-bromopropene may be expected since its formation involves the intermediate $\dot{C}H_2CBr{=}CH_2$ radical, which would be more stable than the alternative $CH_2Br\dot{C}{=}CH_2$ radical required for the formation of 3-bromopropene. While this result disrupted a projected route to deuterated allylbromide, it opened the way to the wide diversity of deuterated propenes shown in Table I. The

TABLE I

Deuterated propenes obtainable from C_3H_4, C_3D_4, and sym-$C_3H_2D_2$

Olefin	Halide added	Addition product	Debromination product
$CH_2{=}C{=}CH_2$	DBr	$CH_2DCBr{=}CH_2$	—
$CH_2DCBr{=}CH_2$	DBr	$CH_2DCDBrCH_2Br$	$CH_2DCD{=}CH_2$
$CH_2DCBr{=}CH_2$	HBr	$CH_2DCHBrCH_2Br$	$CH_2DCH{=}CH_2$
$CD_2{=}C{=}CD_2$	HBr	$CD_2HCBr{=}CD_2$	—
$CD_2HCBr{=}CD_2$	HBr	$CD_2HCHBrCD_2Br$	$CD_2HCH{=}CD_2$
$CD_2HCBr{=}CD_2$	DBr	$CD_2HCDBrCD_2Br$	$CD_2HCD{=}CD_2$
$CD_2{=}C{=}CD_2$	DBr	$CD_3CBr{=}CD_2$	—
$CD_3CBr{=}CD_2$	DBr	$CD_3CDBrCD_2Br$	$CD_3CD{=}CD_2$
$CD_3CBr{=}CD_2$	HBr	$CD_3CHBrCD_2Br$	$CD_3CH{=}CD_2$
$CHD{=}C{=}CHD$	HBr	$CH_2DCBr{=}CHD$	—
$CH_2DCBr{=}CHD$	HBr	$CH_2DCHBrCHDBr$	$CH_2DCH{=}CHD$
$CH_2DCBr{=}CHD$	DBr	$CH_2DCDBrCHDBr$	$CH_2DCD{=}CHD$
$CHD{=}C{=}CHD$	DBr	$CHD_2CBr{=}CHD$	—
$CHD_2CBr{=}CHD$	DBr	$CHD_2CDBrCHDBr$	$CHD_2CD{=}CHD$
$CHD_2CBr{=}CHD$	HBr	$CHD_2CHBrCHDBr$	$CHD_2CH{=}CHD$

synthesis of these compounds was vastly facilitated by the discovery of a method of preparing 1,3-dideuteroallene and tetradeuteroallene in one step which was reported recently by one of us (2).

The only deuterated butene reported is a trideuterobutene which is formed by terminal addition of CD_3 radicals to 1-butene (14). Hexadeutero-2-butene was prepared in the present work from hexadeuterobutadiene by addition of deuterium iodide followed by deiodination of the iodobutene with zinc dust and deuterium oxide. 4,4,4-Trideutero-1-butene, $CD_3CH_2CH{=}CH_2$, was prepared by addition of bromotrichloromethane to allyl chloride as described by Kharasch (16, 17) followed by dehalogenation of the bromochlorobutane formed by treatment with zinc dust and deuterium oxide. Synthesis

Can. J. Chem. Downloaded from www.nrcresearchpress.com by 210.87.254.40 on 09/05/12
For personal use only.

of the inversely deuterated 1-butene, $CH_3CD_2CD{=}CD_2$, by this route involved first the preparation of deuterated allyl bromide. Unsuccessful attempts to add deuterium bromide to allene were delineated above. Consequently, other routes to this intermediate were investigated.

In one of the earliest reports of allylic bromination, a dibromopropylene was obtained from propylene and N-bromoacetamide (18). Several attempts were made in the present work to brominate propylene to 3-bromopropene by means of N-bromosuccinimide. However, as no conditions could be found which gave a yield higher than 10%, this approach was abandoned.

An alternative method is the vapor-phase halogenation of propylene. Whereas there are several references to patents on this reaction very few papers have appeared on the subject. Actually the only reference to bromination is in a paper by Groll and Hearne (19), who reported the preparation of 3-bromopropene in 65% yields or more, based on bromine, by employing a high ratio of propylene to bromine. Yields based on propene consumed are, however, only 25–30%. Nevertheless this appeared to be the most practical way of preparing deuterated allyl bromide. 1,1,2,3,3-Pentadeutero-1-butene was synthesized from deuterated allyl bromide and methyl magnesium bromide.

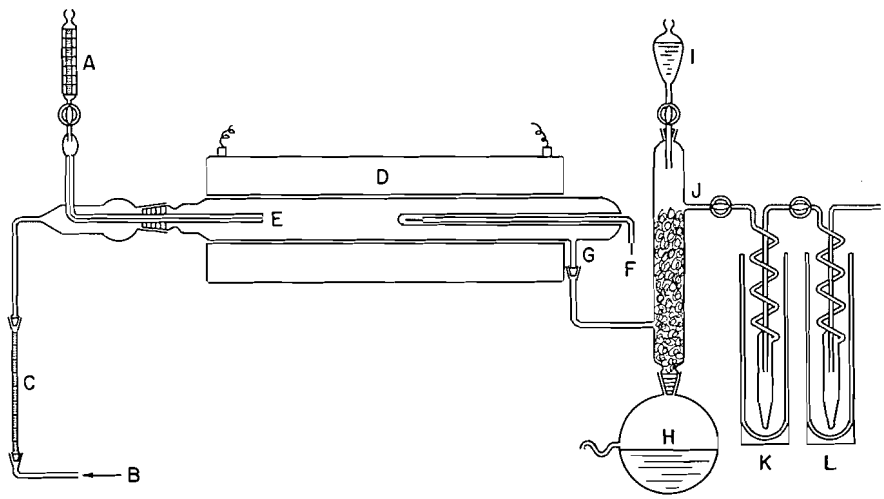


FIG. 1. Apparatus for preparation of 3-bromo-pentadeuteropropene.

Of the possible deuterated pentenes only 1,1,1,3-tetradeutero-2-pentene, $CD_3CH{=}CDCH_2CH_3$, has been reported (20). The facile preparation of hexadeuterobutadiene from hexachlorobutadiene (2) makes it an attractive starting material for the synthesis of several deuteropentenes. One of these, C_5D_{10}, gives on reduction completely deuterated *n*-pentane, which is a useful solvent for N.M.R. investigations.

According to Kharasch (17), the homolytic addition of bromotrichloromethane to butadiene produces a mixture of bromotrichloropentenes, presumably $CCl_3CH_2CHBrCH{=}CH_2$ and $CCl_3CH_2CH{=}CHCH_2Br$, which are reported to boil about 10° apart. In the present work the main product isolated was a compound, b.p. 88 to 90° under 6 mm. Its index of refraction was identical with that of one of the isomers reported by Kharasch. Attempts to oxidize the pentene to a trichloroacid with permanganate gave an inseparable mixture of acids. A capillary film of the compound gave the infrared spectrum shown in Fig. 2*a*. Absorption is consistent with a *trans*-ethylenic compound. The strong band

Can. J. Chem. Downloaded from www.nrcresearchpress.com by 210.87.254.40 on 09/05/12
For personal use only.

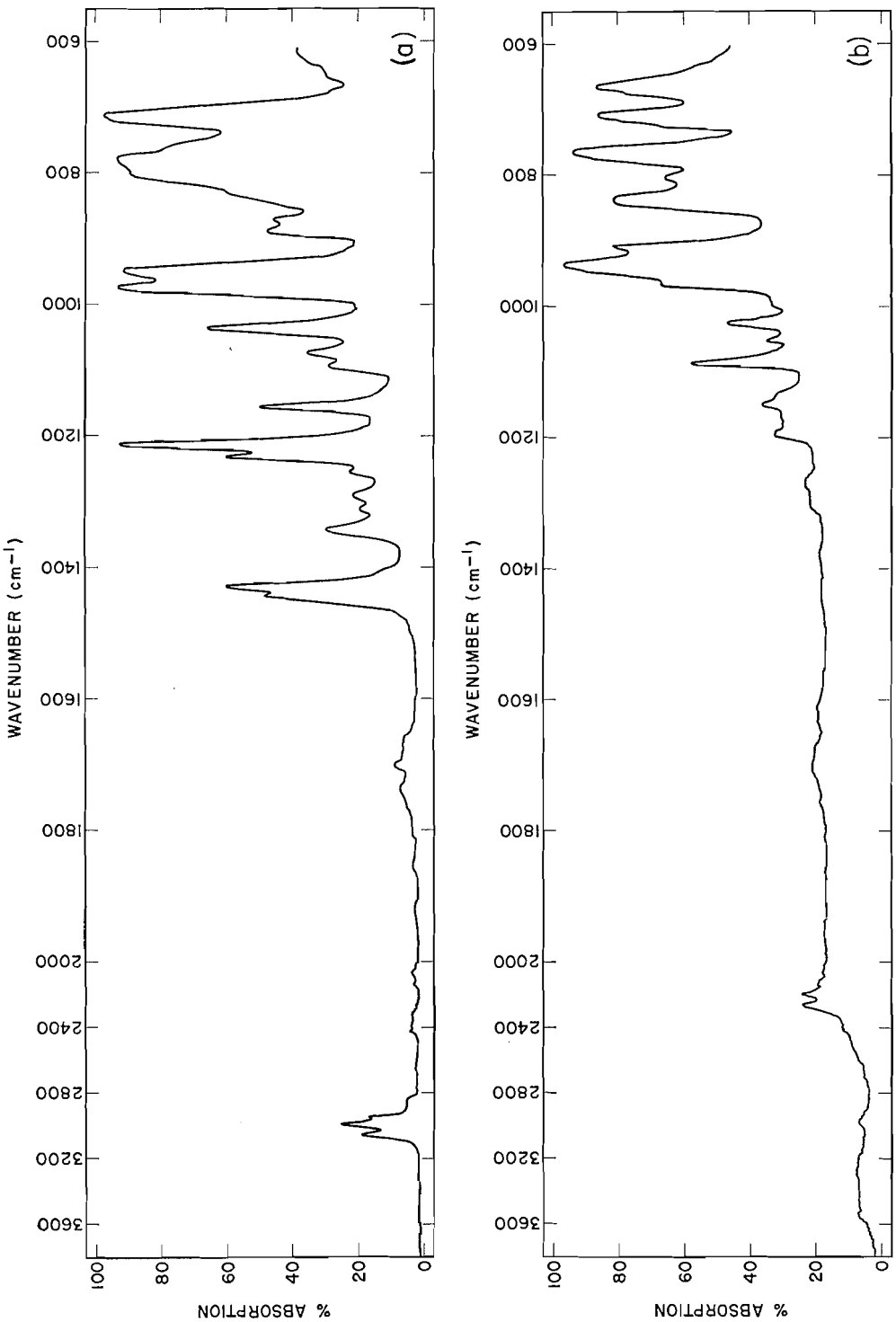


FIG. 2.

Can. J. Chem. Downloaded from www.nrcresearchpress.com by 210.87.254.40 on 09/05/12
For personal use only.

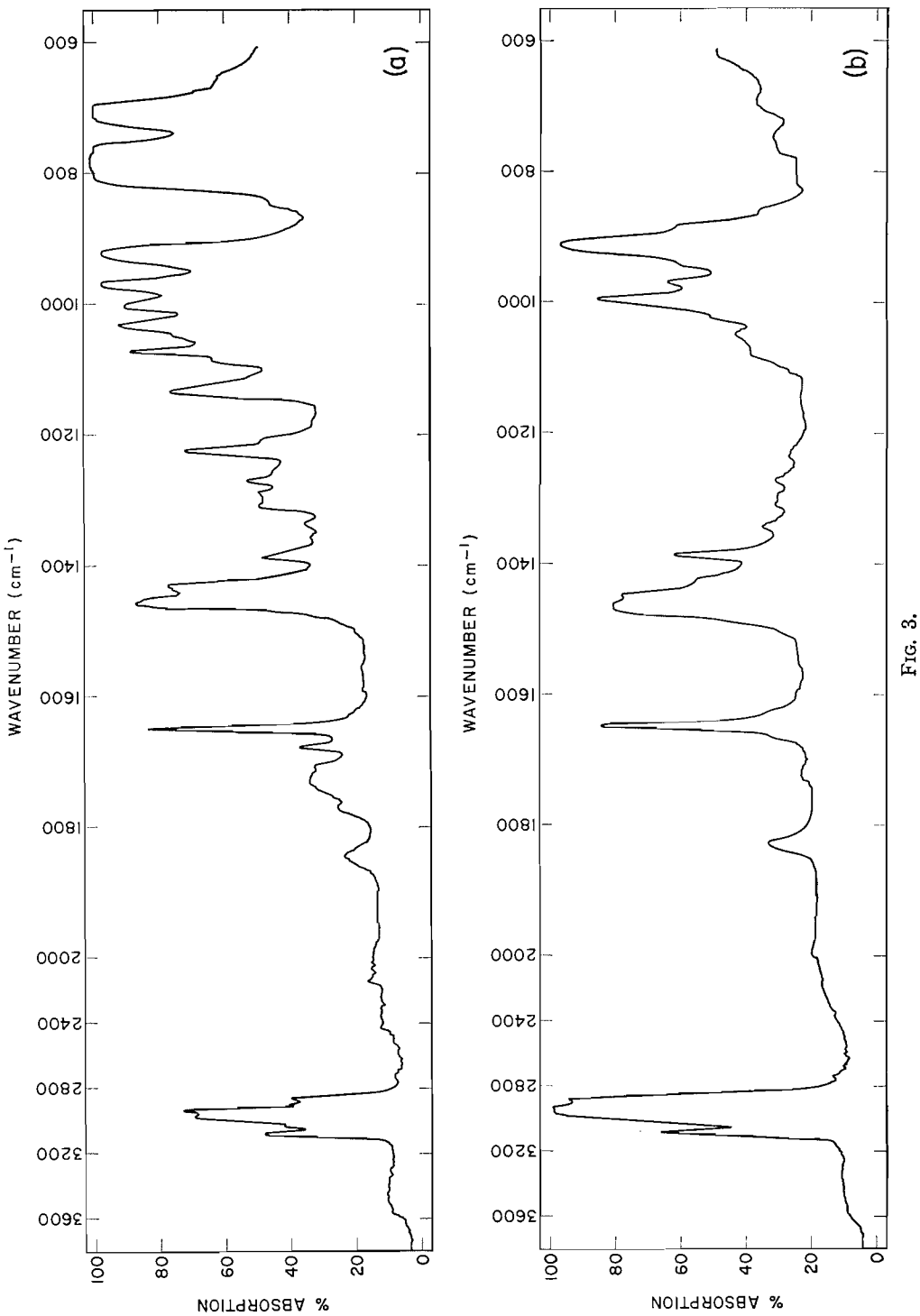


FIG. 3.

Can. J. Chem. Downloaded from www.nrcresearchpress.com by 210.87.254.40 on 09/05/12
For personal use only.

at 967 cm^{-1} usually assigned to the C—H out-of-plane bending vibration of the *trans*-ethylenic structure is present. On the other hand the band in the 1640 cm^{-1} region due to C=C stretching in vinyl compounds is absent. Furthermore, there are no bands in the 995–985 cm^{-1} and 910–905 cm^{-1} regions characteristic of C—H out-of-plane bending vibrations in vinyl compounds. The compound is therefore *trans*-5,5,5-trichloro-1-bromo-2-pentene. The two bands at 765 cm^{-1} and 700 cm^{-1} are attributed to the C—Cl vibration in the trichloromethyl group. The strong band at 1205 cm^{-1} could not be positively identified. From a comparison with the spectrum of the deuterated chlorobromopentene (Fig. 2*b*) prepared in the same manner from hexadeuterobutadiene it was possible to assign several bands of medium to low intensity to —C—C— skeletal vibrations. Absorption at 937, 1025, 1065, 1083, and 1140 cm^{-1} is probably of this type.

Owing to the enhanced activity of the bromine atom in the allylic position it was found possible to dehalogenate the halide selectively to a trichloropentene. Oxidation of the latter gave formic acid and a trichlorobutyric acid identical with 4,4,4-trichlorobutyric acid prepared by Bruson (21) by a different method. Apparently the trichloropentene was predominantly the 1-isomer, $CCl_3CH_2CH_2CH{=}CH_2$. An examination of the infrared spectrum of the compound confirmed this structure (Fig. 3*a*). A band of medium intensity now appears at 1650 cm^{-1} and two other strong bands characteristic of a vinyl grouping appear at 990 and 910 cm^{-1}. However, the band at 967 cm^{-1} attributed to *trans*-ethylenic compounds persists. The compound therefore contains some of the 2-pentene. It seems that an allylic rearrangement of the bromine atom has taken place during the dehalogenation.

Complete dehalogenation of the compound gave an olefin whose infrared spectrum indicated it was a mixture of the 1- and 2-pentenes (Fig. 3*b*). From the intensity of the bands in the 1640 cm^{-1} and 1000–900 cm^{-1} regions it appears to contain mainly 1-pentene. The presence of a slight peak at 967 cm^{-1} indicates the presence also of the 2-isomer.

By dehalogenating in the appropriate medium it is obviously possible to prepare pentenes deuterated only in the methyl group or only in the rest of the chain, namely $CD_3CH_2CH_2CH{=}CH_2$ or $CH_3CD_2CD_2CD{=}CD_2$. From earlier unpublished studies in this laboratory on catalytic reduction with deuterium it should be possible to reduce these compounds to labelled pentanes without concomitant exchange.

EXPERIMENTAL

Hydrogen Bromide

The apparatus consisted of a magnetic stirring bar in a 250-ml round-bottomed flask equipped with a separatory funnel and reflux condenser to which were connected a U tube containing moist phosphorus and a spiral trap of 25-ml capacity cooled to −78° in dry ice and acetone. A drying tube filled with Drierite was attached to the outlet of the spiral trap. Hydrogen bromide was generated by adding 10.0 ml (31.2 g) of bromine dropwise over a period of 2 hours to a stirred, boiling suspension of 7.0 g of red phosphorus and 6.0 ml of water in 150 ml of carbon tetrachloride. The yield of anhydrous hydrogen bromide was 16.0 ml (34.0 g), i.e. nearly quantitative.

Deuterium Bromide

To ensure a product of high deuterium content it is essential to employ dry carbon tetrachloride and dry bromine. The phosphorus must also be freed of traces of phosphoric acid by stirring it with 10% aqueous sodium hydroxide, filtering the suspension, and drying the product in a vacuum desiccator. The yield of deuterium bromide was quantitative.

Can. J. Chem. Downloaded from www.nrcresearchpress.com by 210.87.254.40 on 09/05/12
For personal use only.

Hydrogen (or Deuterium) Iodide

In this case water (6.0 ml) or deuterium oxide was added dropwise to a suspension of 7 g of phosphorus in a solution of 50 g of iodine in 150 ml of carbon tetrachloride.

1-Bromo-2-chloro-2-deuteroethane, $CH_2BrCHDCl$

The addition of deuterium bromide to vinyl chloride was carried out in a 500-ml round-bottomed quartz flask connected by a "cold finger" condenser to a vacuum line fitted with the necessary stopcocks and traps. After the apparatus was evacuated, vinyl chloride (5.5 ml) was condensed from a cylinder into a graduated tube and distilled into the quartz flask by placing chips of dry ice in the condenser. While the quartz flask was irradiated with light from a Hanovia lamp, deuterium bromide from another trap was distilled in small fractions into the quartz flask where it reacted rapidly to form the bromochloroethane. When addition was complete as indicated by the manometer, the excess deuterium bromide was distilled off into the exhaust trap and the product purified by distillation in a Vigreux column. The yield of pure bromochloroethane, b.p. 105–105.5°, n_D^{20} 1.4896 was 14.5 g (90% of the theoretical amount).

1-Bromo-2-chloro-2,2-dideuteroethane, CH_2BrCD_2Cl

Deuterium bromide (6.0 ml; 18.0 g) reacted in the same manner with 1-chloro-1-deuteroethene (11.0 g) prepared as described in reference 11. The yield of product, b.p. 105°, n_D^{25} 1.4862 was 13.7 ml (22.7 g, 72% of the theoretical amount).

Trideuterovinyl Bromide, $CD_2{=}CDBr$

To 17.0 g of pulverized potassium hydroxide in a 250-ml round-bottomed flask equipped with a heating mantle, a separatory funnel, and an air-cooled condenser leading to a spiral trap cooled in dry ice and acetone, there was added 27.0 g of 1,2-dibromo-tetradeuteroethane dropwise during heating of the alkali. Reaction was immediate. Trideuterovinyl bromide in the apparatus at the end of the reaction was swept into the spiral trap by a current of nitrogen. The yield of product was 6.3 ml (11.3 g) measured at −78° (73% of the theoretical amount).

1,2-Dibromo-1,1,2-trideuteroethane, $CD_2BrCHDBr$

The addition of hydrogen bromide to the vinyl bromide was carried out as already described above. The yield of product, n_D^{21} 1.5370, from 11.3 ml of trideuterovinyl bromide and 8.2 g of hydrogen bromide was 8.1 ml (17.9 g) i.e. nearly quantitative. For normal 1,2-dibromoethane, n_D^{20} is 1.5380.

Monodeuteroethylene

The dehalogenation of 1-bromo-2-chloro-2-deuteroethane was carried out as described previously with zinc dust in dioxane (4). The yield of monodeuteroethylene was nearly quantitative. Mass analysis, 96.0% C_2H_3D.

1,1-Dideuteroethylene

1-Bromo-2-chloro-2,2-dideuteroethane was dehalogenated as reported previously (4) in nearly quantitative yield. Mass analysis, 97.4 mole% C_2H_2D.

Trideuteroethylene

1,2-Dibromo-1,1,2-trideuteroethane was dehalogenated as reported previously (4) in nearly quantitative yield. Mass analysis, 70% C_2D_3H, 11.8% $C_2H_2D_2$, 9.4% C_2H_3D.

The low deuterium content was due to the presence of CH_2BrCD_2Br in the dibromoethane employed to prepare the vinyl compound.

Can. J. Chem. Downloaded from www.nrcresearchpress.com by 210.87.254.40 on 09/05/12
For personal use only.

Propadiene-1,3

1,2-Dibromo-2-propene was debrominated with zinc dust in ethanol as described in reference 4.

Tetradeutero-1,3-propadiene

Hexachloropropene was dehalogenated with zinc dust in dioxane – deuterium oxide as described in reference 2.

Addition of Hydrogen Bromide to Propadiene

The preparation of 2-bromopropene and 1,2-dibromopropane to be described is typical of all the addition reactions carried out in this work between hydrogen or deuterium bromide and propadiene or deuteropropadiene. To facilitate manipulation all transfers of gases were made in an evacuated system.

Propadiene (7.0 g; 0.18 mole) was condensed from a gas holder or distilled from a trap into a 500-ml round-bottomed quartz flask attached to the end of the vacuum line by means of a cold finger condenser. The flask was immersed in a bath of dry ice and acetone at −78°. On irradiation of the flask with ultraviolet light at room temperature, reaction with hydrogen bromide was rapid as indicated by the rise in the manometer.

The product was placed in a separatory funnel immersed in ice-cold water and washed with aqueous sodium bicarbonate. Distillation in a Vigreux column gave mainly 2-bromopropene, b.p. 47.5–48.5°. Yield: 10.5 g (50%). The temperature then rose rapidly to the boiling point of 1,2-dibromopropane. The amount of 3-bromopropene formed was apparently very small.

Addition of two moles of hydrogen bromide in this manner gave nearly quantitative yields of 1,2-dibromopropane.

By varying the order of addition of hydrogen and deuterium bromide the deuterated 2-bromopropenes and 1,2-dibromopropanes shown in Table I were readily obtained. The series of compounds obtainable from 1,3-dideuteropropadiene, CHD=C=CHD, also shown in the table was not actually prepared in this work but the same procedure obviously applies.

Debromination of the 1,2-Dibromopropanes

The deuterated propylenes I to VII in Table I were prepared by dehalogenation of the halides with zinc dust in ethanol essentially as described in reference 4.

The purity of the compounds was determined by mass analysis and found to be of the order of 97%.

1-Iodo-4-deutero-2-butene, $CH_2ICH{=}CHCH_2D$

This halide was prepared by the addition of deuterium iodide to butadiene in the apparatus used to prepare the deuterated bromopropenes. Butadiene (21.0 ml; 12.6 g; 0.23 mole) was condensed from a cylinder attached to the vacuum line into a graduated trap to measure its volume at −25°, and distilled from there into a 500-ml round-bottomed flask connected at the end of the line by a cold finger condenser. To the frozen butadiene was added 0.5 to 0.75 ml of deuterium iodide condensed in a trap on the line. When the mixture melted rapid reaction occurred. The butadiene was frozen again and more deuterium iodide was introduced until a total of 12 ml had been added. When the temperature of the mixture rose much above −78° some iodine was liberated. The iodobutene was distilled into a trap from the reaction flask. The yield was 28.0 g (75%). Owing to the intense lachrymatory action of the compound the index of refraction was not determined.

Can. J. Chem. Downloaded from www.nrcresearchpress.com by 210.87.254.40 on 09/05/12
For personal use only.

1,4-Dideutero-2-butene, $CH_2DCH{=}CHCH_2D$

In a 250-ml three-necked round-bottomed flask fitted with a separatory funnel, thermometer, and reflux condenser to which was connected a spiral trap cooled to −78° in dry ice and acetone, 28 g of 1-iodo-2-deutero-2-butene was added slowly to a stirred suspension of 20.0 g of zinc dust in a boiling solution of 5.5 g of deuterium oxide in 150 ml of anhydrous dioxane. The yield of liquid butene in the trap amounted to 5.4 g measured at −78° (60% of the theoretical). Mass analysis gave ambiguous results but by analogy with the analyses of octadeuterobutene given below the deuterium content of the butene was about 97%.

Dechlorination of 1,4-dichloro-2-butene regenerates butadiene instead of giving 2-butene. It is therefore impossible to prepare dideuterobutene by this method.

1-Iodo-heptadeutero-2-butene, $CD_2ICD{=}CDCD_3$

This compound was prepared by addition of deuterium iodide to hexadeuterobutadiene as described above. The hexadeuterobutadiene was prepared from hexachlorobutadiene as described in reference 2. From 9.2 ml of the liquid diene and 5.0 ml of liquid deuterium iodide there was obtained 8.6 g (48%) of iodobutene, n_D^{22} 1.5239.

By addition of hydrogen iodide to hexadeuterobutadiene, 1-iodo-1,1,2,3,4,4-hexadeutero-2-butene would result.

Octadeutero-2-butene

1-Iodo-2-heptadeuterobutene was deiodinated as described above with zinc dust and deuterium oxide. Yield: 55%. Mass analysis: 73 mole% C_4D_8 and 26% C_4D_7H or 97 atom%.

Deiodination with zinc dust in water would of course lead to $CD_2HCD{=}CDCD_3$.

4,4,4-Trideutero-1-butene, $CD_3CH_2CH{=}CH_2$

This deuterobutene was prepared by the dehalogenation of 1,1,1,4-tetrachloro-3-bromobutane. The latter was synthesized from allyl chloride and bromotrichloromethane by the method of Kharasch, Reinmuth, and Urry (16).

To a mixture of 20 g of zinc dust, 40 ml of anhydrous dioxane and 5.0 ml of deuterium oxide in a 100-ml round-bottomed flask fitted with a reflux condenser to which was attached a trap cooled to −78° in dry ice and acetone, there was added with stirring and heating 5.0 ml (9.0 g) of 1,1,1,4-tetrachloro-3-bromobutane. After 5 hours' heating under reflux, 3.2 ml (90%) of butene had condensed in the trap. The vapor pressure of several fractions collected at −30° was constant.

3-Bromopropene, $CH_2BrCH{=}CH_2$, *and 3-Bromopentadeuteropropene*, $CD_2BrCD{=}CD_2$

(a) By Bromination of Propylene with N-Bromosuccinimide

In a pressure bottle ordinarily used for low-pressure hydrogenations 150 ml of methylene chloride, 17.4 g (0.1 mole) of N-bromosuccinimide, and 2.0 g of dibenzoylperoxide were heated under three atmospheres of propylene. The bottle was wrapped in glass heating tape and heated to 90°. After 3 hours' heating and shaking the reaction mixture was worked up. Methylene chloride was distilled off in a Vigreux column and the residue fractionated on the vacuum line; the index of refraction of the residue, n_D^{25} 1.4360, was only slightly higher than that of pure methylene chloride (lit. n_D^{20} 1.4320).

When carbon tetrachloride was used instead of methylene chloride propylene reacted preferentially with it under the influence of peroxide to give what appeared to be the tetrachlorobutane, $CCl_3CH_2CHClCH_3$. From the excess CCl_4 removed by distillation a small amount of the isothiourea picrate of 3-bromopropene, m.p. 153° (lit. 155°), was

Can. J. Chem. Downloaded from www.nrcresearchpress.com by 210.87.254.40 on 09/05/12
For personal use only.

obtained by means of thiourea and picric acid. The yield was, however, very low. In any event the use of carbon tetrachloride as a solvent is not practical because it boils very close to 3-bromopropene.

An experiment was carried out with propylene, peroxide, and N-bromosuccinimide in a sealed tube heated to 100° C. After 3 hours' heating the solid had melted and turned dark. A product was isolated which had b.p. 131°, n_D^{25} 1.5160, the physical constants of 1,2-dibromoethane. At this stage further experiments with N-bromosuccinimide were abandoned.

(b) By Bromination of Propylene at 350°

The bromination of propene and hexadeuteropropene was carried out in the apparatus illustrated in Fig. 1. The reactor was made from a piece of glass tubing about 1 m long and 2.5 mm in diameter. Hexadeuteropropene was introduced at B from a gasholder and metered in the flowmeter C. Bromine was added at a constant rate from funnel A through a needle valve and capillary E. J was a scrubbing tower 12 in. high and 1 in. in diameter filled with glass beads. Water was added through funnel I to wash the effluent gases free of deuterium bromide. The washings were collected with a portion of the product in H. Unreacted deuteropropene, which was always used in excess to reduce additive bromination, was condensed along with the deutero-3-bromopropene in the spiral traps K and L, which were cooled in dry ice and acetone to −78°.

At the start of a run the furnace D was heated to 350–375°, the temperature being measured by means of the thermocouple F inserted in the well. Hexadeuteropropene (9.0 l.) and bromine (10.0 ml; 0.19 mole) were added at such a rate that a run was completed in $1\frac{1}{4}$ to $1\frac{1}{2}$ hours. The actual rate was determined by making several trial runs with ordinary propene. The apparatus was flushed with nitrogen at the end. The dark oily liquid in H was drawn off through the capillary and fractionated on the vacuum line. About 1.5 ml of deuterated-3-bromopropene were distilled off leaving a residue of undetermined composition which was probably a mixture of polybrominated compounds. Unreacted deuteropropene was redistilled at −40°, from the traps K and L back into the gas holder to be reused. Residual deuterated 3-bromopropene in traps K and L was combined with the product recovered from the oil and fractionated on the vacuum line. The yield of 3-bromopentadeuteropropene was generally 8.5 to 10.0 g per run. The product from several runs was combined and fractionated in a column with a whirling band. The fraction, b.p. 66.5°, was collected. An infrared spectrum of this material measured in the vapor phase showed only traces of absorption in the C—H stretching region of the spectrum.

Although the yield was only 25–30% per run and the synthesis has disadvantages from other points of view, it appears to be the only practical way to obtain deuterated 3-bromopropene at present.

1,1,2,3,3-Pentadeutero-1-butene, $CD_2{=}CDCD_2CH_3$

Methylmagnesium bromide was prepared in the usual manner from 1.2 g of magnesium turnings and 7.1 g of methyl iodide in 25 ml of *n*-dibutyl ether. After attaching a spiral trap cooled to −78° in dry ice and acetone to the reflux condenser, 3-bromopentadeuteropropene (6.0 g; 0.05 mole) was added slowly to the Grignard reagent. Residual butene in the apparatus at the end was flushed out by a slow stream of nitrogen. The deuterated butene was freed of traces of ether by distillation on the vacuum line from a bath at −30°. The yield was 1.5 ml (50% of the theoretical). Mass analysis, 84 mole% $C_4D_5H_3$ and 12.8 mole% $C_4D_4H_4$ or 90.4 atom%.

Can. J. Chem. Downloaded from www.nrcresearchpress.com by 210.87.254.40 on 09/05/12
For personal use only.

Can. J. Chem. Downloaded from www.nrcresearchpress.com by 210.87.254.40 on 09/05/12
For personal use only.

5,5,5-Trichloro-1-bromo-2-pentene, $CCl_3CH_2CH{=}CHCH_2Br$

Redistilled bromotrichloromethane (150 ml) was placed in a 500-ml quartz flask attached through a cold finger condenser to the vacuum line. The system was evacuated and butadiene from a cylinder was condensed in a trap on the line until the volume of liquid was 30 ml. When dry ice was placed in the finger of the condenser the butadiene distilled into the bromotrichloromethane. The quartz flask was irradiated with ultraviolet light for 5 to 6 hours. Excess halomethane was distilled off into a trap on the vacuum line. The residue was distilled under reduced pressure through a Vigreux column at a reflux ratio of 10:1. After a small fraction (4.0 ml) was collected at 84–97° at 8 mm pressure, the product came over at 97–98° at 8 mm. Yield: 89.5 g, n_D^{26} 1.5320, n_D^{20} 1.5351. Kharasch (16) gives n_D^{20} 1.5349 for a fraction, b.p. 84° at 1.5 mm.

The absorption bands in the infrared spectrum of the compound confirm the structure of a trans-substituted olefin (Fig. 2*a*). It would seem that only very small amounts, if any, of the isomeric halopentene are formed by 1,2-addition.

5,5,5-Trichloro-1-pentene, $CH_2{=}CHCH_2CH_2CCl_3$

The selective dehalogenation of the bromotrichloropentene was carried out by adding zinc dust in portions to a stirred solution of the halide (23.5 g; 0.15 mole) in 25 ml of methanol kept at room temperature by immersion in a water bath. After 4 hours' stirring the reaction mixture was filtered with suction from excess zinc and the filtrate was poured into water. Acetic acid was added to dissolve basic zinc salts and the oil was taken up in ether. After the solution was dried over potassium carbonate, the ether was distilled off. The residue was distilled under reduced pressure in a Vigreux column at a reflux ratio of 10 to 1. After collecting the main faction at 64–65° at 40 mm the boiling point rose rapidly to 100°, and then to the boiling point of bromotrichloropentene. The yield of product was 6.1 g (60% based on the recovered halide), n_D^{28} 1.4648. Anal: Calc. for $C_5H_7Cl_3$: Cl, 61.38%. Found: Cl, 61.10%.

A second run starting with 65 g of bromotrichloropentene gave 17.0 g of product, b.p. 78–80° at 90 mm, n_D^{27} 1.4650.

The infrared absorption spectrum of the compound indicates it is predominantly trichloro-1-pentene (Fig. 3*a*).

4,4,4-Trichlorobutyric Acid, $CCl_3CH_2CH_2COOH$

The trichloropentene (3.7 g) was added to a stirred solution of 5% aqueous potassium permanganate. Further amounts of permanganate solution were added until no further decolorization took place; a total of 250 ml of oxidizing agent was required. The manganese dioxide was filtered off and the filtrate was evaporated to dryness. The residue was acidified with 6 *N* H_2SO_4 and extracted several times with ether. Distillation of the ether left a residue which was dried by pumping off volatile material into a trap on the vacuum line. With aqueous silver nitrate the material in the trap gave a thick white precipitate which rapidly decomposed to metallic silver. This behavior is characteristic of silver formate; indeed sodium formate gave the same unstable precipitate with silver nitrate. Since formic acid is only produced in the oxidation of olefins of the type $R{-}CH{=}CH_2$, a strong presumption exists that there is a terminal double bond in the trichloropentene.

The residue obtained after pumping off the formic acid was recrystallized from pentene after decolorizing the solution with Norite. On cooling, white crystals separated which melted at 49–50°. Recrystallization from water gave an acid, m.p. 53–54°; 0.686 g of this product required 3.3 ml of *N*/10 alkali for neutralization. Neutralization equivalent:

208. The calculated neutralization equivalent for $C_4H_5O_2Cl_3$, H_2O is 209.5. Bruson (21) reported that 4,4,4-trichlorobutyric acid prepared from acrylonitrile melts at 55°. The second oxidation product of trichloropentene is therefore 4,4,4-trichlorobutyric acid. The trichloropentene must evidently be very largely the 1-butene. Since the yields on oxidation are far from quantitative one cannot say with certainty there is none of the 2-isomer.

1-Pentene

trans-5,5,5-Trichloro-1-bromo-2-pentene (6.0 g; 0.025 mole) was added dropwise to a stirred suspension of zinc dust (10.0 g) in acetic acid (30 ml) in a flask attached to a vacuum line through a reflux condenser. Evolved gas was collected in a trap cooled with dry ice and acetone to −78° C. The halide reacted vigorously; stirring was continued for an hour after addition of the halide had been completed. The liquid in the trap was fractionated on the vacuum line and yielded 1.6 ml (65%, measured at 0°) of liquid which was predominantly 1-pentene but also contained some of the 2-isomer.

5,5,5-Trichloro-1-bromo-hexadeutero-2-pentene, $CCl_3CD_2CD{=}CDCD_2Br$

Hexadeuterobutadiene was prepared from hexachlorobutadiene as described in reference 2. From 7.9 g of butadiene, 30.7 g (93%) of addition product, n_D^{20} 1.5330, were obtained.

Decadeutero-1-pentene

The halide was dehalogenated as described for the normal compound using a solution of 6.6 g of deuterium oxide in 35 ml of anhydrous dioxane (previously distilled over sodium) instead of acetic acid. The yields were similar. An N.M.R. spectrum showed no signals for hydrogen. The compound is therefore useful as a solvent for substances to be examined by N.M.R.

From the dioxane solution there was obtained in addition to the deuteropentene a small amount (0.1 ml) of by-product with a vapor pressure of only 3 mm at room temperature and an index of refraction 1.4470. This is thought to be a decadiene produced by doubling of the C_5 chain.

ACKNOWLEDGMENTS

We wish to thank Dr. J. E. Francis for preparing monodeuteroethylene and Dr. F. P. Lossing for a number of mass analyses.

REFERENCES

1. M. E. Leblanc, A. T. Morse, and L. C. Leitch. Can. J. Chem. **34**, 354 (1956).
2. A. T. Morse and L. C. Leitch. J. Org. Chem. **23**, 990 (1958).
3. J. C. Boursnell, G. E. Francis, and C. Dornwall. Biochem. J. **40**, 743 (1946).
4. L. C. Leitch and A. T. Morse. Can. J. Chem. **30**, 924 (1952).
5. C. L. Wilson and A. W. Wylie. J. Chem. Soc. 596 (1941).
6. B. S. Rabinovitch and F. S. Looney. J. Am. Chem. Soc. **75**, 2652 (1953).
7. W. I. Patterson and V. du Vigneaud. J. Biol. Chem. **123**, 329 (1938).
8. A. Kruis and W Schanzer. Z. physik. Chem. A, **191**, 301 (1942).
9. G. Joris, H. S. Taylor, and J. C. Jungers. J. Am. Chem. Soc. **60**, 1982 (1938).
10. M. de Hemptinne. *In* Les isotopes; rapports et discussions. *Edited by* R. Stoops. Brussels. 1948. p. 263.
11. J. E. Francis and L. C. Leitch. Can. J. Chem. **35**, 500 (1957).
12. W. Schanzer and K. Clusius. Z. physik. Chem. A, **190**, 243 (1941).
13. C. D. Hurd and J. L. Azorlosa. J. Am. Chem. Soc. **73**, 33 (1951).
14. J. R. McNesby. J. Chem. Educ. **34**, 130 (1957).
15. R. N. Haszeldine and B. R. Steele. J. Chem. Soc. 2040 (1954).
16. M. S. Kharasch, O Reinmuth, and W. H. Urry. J. Am. Chem. Soc. **69**, 1106 (1947).
17. M. S. Kharasch. U.S. Patent No. 2,468,208 (August 26, 1949).
18. A. Wohl and K. Jaschinowski. Ber. **54**, 481 (1921).
19. H. P. A. Groll and G. Hearne. Ind. Eng. Chem. **31**, 1531 (1939).
20. C. E. Boozer and E. S. Lewis. J. Am. Chem. Soc. **76**, 794 (1954).
21. H. A. Bruson, W. Niederhauser, T. Reiner, and W. F. Hester. J. Am. Chem. Soc. **67**, 601 (1945).

Can. J. Chem. Downloaded from www.nrcresearchpress.com by 210.87.254.40 on 09/05/12
For personal use only.

Can. J. Chem. Downloaded from www.nrcresearchpress.com by 210.87.254.6 on 09/05/12
For personal use only.

A WATER-SOLUBLE GALACTOMANNAN FROM COCONUT (COCOS NUCIFERA)

PART I. METHYLATION STUDIES[1]

C. V. N. Rao, D. Choudhury, and P. Bagchi

ABSTRACT

A water-soluble polysaccharide isolated from the kernel of coconut (*Cocos nucifera*) had $[\alpha]_D$ −85° and contained D-galactose (1 mole) and D-mannose (2 moles). Methylation and hydrolysis yielded 2,3,4,6-tetra-*O*-methyl-D-mannose (0.51 mole); 2,3,4,6-tetra-*O*-methyl-D-galactose (0.5 mole); 2,3,6-tri-*O*-methyl-D-mannose (5.52 moles); 2,3,6-tri-*O*-methyl-D-galactose (1.51 moles); and a di-*O*-methyl-D-galactose (1 mole). These data agree with those of periodate oxidation. The structural significance of these results is discussed.

The kernel of coconut (*Cocos nucifera*), a tree which is generally found in coastal regions of India and south-east Asia is a popular food. The kernel is soft when the fruit is young and becomes hard when old. Although much work has been done on the oil (1) extracted from the kernel, copra (2), the liquid (3) within the shell, and other parts of the fruit such as the coir (4) etc., the polysaccharide in the kernel does not appear to have been investigated.

This paper deals with the studies on the polysaccharide precipitated from the aqueous extract of the kernel with ethanol. Hydrolysis of the polysaccharide $[\alpha]_D^{29}$ −85° (in 4% sodium hydroxide solution) gave D-galactose and D-mannose in the proportion 1:2 as revealed by chromatographic analysis (5). Traces of arabinose were also formed. Purification of the polysaccharide via the copper complex (6) removed the arabinose-containing impurities as well as traces of uronides, and hydrolysis showed that the galactose: mannose ratio was the same as before.

The galactomannan was methylated first by methyl sulphate and sodium hydroxide and then by Purdie's method. The resulting methylated galactomannan, which showed no hydroxyl band at 3500–3600 cm^{-1} in I.R. spectrum, was light yellow in color and had $[\alpha]_D^{25}$ +25° in chloroform. After methanolysis of the methylated polysaccharide and hydrolysis of the methyl glycosides the mixture of methylated sugars was resolved on a cellulose column (7) using butanone–water azeotrope (8) as eluant.

From the results of the column chromatography the mixture was found to consist of 2,3,4,6-tetra-*O*-methyl-D-mannose (0.51 mole), 2,3,4,6-tetra-*O*-methyl-D-galactose (0.5 mole), 2,3,6-tri-*O*-methyl-D-mannose (5.52 moles), 2,3,6-tri-*O*-methyl-D-galactose (1.51 moles), and a di-*O*-methyl-galactose (1 mole). The proportions of the above sugars were determined in a separate experiment using alkaline hypoiodite method (9). It will be evident from the above results that the proportion of tetra-:tri-:di-*O*-methyl sugars is as 1:7:1 indicating that the polysaccharide possesses a highly branched structure and that the average repeating unit consists of about 9 hexose residues.

The two tetra-*O*-methyl sugars were separated on filter papers. The 2,3,4,6-tetra-*O*-methyl-D-mannose obtained as sirup after elution and evaporation, having $[\alpha]_D^{30}$ +3° in water, was characterized as *N*-phenyl-2,3,4,6-tetra-*O*-methyl-D-mannosylamine, m.p. and mixed m.p. 142°, $[\alpha]_D^{30}$ −8°. The 2,3,4,6-tetra-*O*-methyl-D-galactose ($[\alpha]_D^{30}$ +110°

[1]*Manuscript received September 29, 1960.*
Contribution from the Department of Macromolecules, Indian Association for the Cultivation of Science, Calcutta 32, India.

in water) was characterized as its anilide, m.p. and mixed m.p. 187–188°, $[\alpha]_D^{31}$ −40° in acetone.

The 2,3,6-tri-*O*-methyl-D-mannose obtained as a sirup ($[\alpha]_D^{30}$ −9° in water) was characterized through its crystalline 1,4-di-*p*-nitrobenzoate whereas the 2,3,6-tri-*O*-methyl-D-galactose having specific rotation +89° (in water) was identified as the corresponding gamma lactone.

The dimethyl sugar fraction on demethylation was found to contain only galactose and was chromatographically homogeneous. No anilide could be prepared and its $R_{rhamnose}$ value (10) in paper chromatography differed from those of the known isomers. From these results it is tentatively assumed that the dimethyl sugar is 3,6-di-*O*-methyl galactose.

The identification of the hydrolysis products of the methylated polysaccharide enables the general structural features of the polysaccharide to be deduced. The demonstration of the presence of the 2,3,4,6-tetra-*O*-methyl derivatives of D-galactose and D-mannose shows that the terminal non-reducing ends in the polysaccharide consist of pyranose units of D-galactose and D-mannose in equal proportions.

The characterization of the 2,3,6-tri-*O*-methyl derivatives of the D-galactose and D-mannose indicates that the components arise from 1 → 4 linked residues of D-galactose and D-mannose of the pyranose type.

The unidentified di-*O*-methyl derivative of D-galactose shows that the branching in the molecule occurs at certain of the units of D-galactose in the main chain. If the methylated galactose derivative is 3,6-di-*O*-methyl-D-galactose then branching could occur at either C_2 or C_4. The ratio of the number of non-reducing terminal groups to branching units is about 1:1 as required by theory.

The methylation data indicating a ratio of terminal to non-terminal units of 1:8 is supported by the finding that during periodate oxidation 1 molar proportion of formic acid is liberated for every 8 hexose units and that the periodate consumption is 1.03 moles per hexose unit. The periodate-oxidized polysaccharide, on reduction and hydrolysis gave glycerol, erythritol, threitol, and D-galactose in a molar ratio of 1:6.8:1.9:0.9. These compounds were characterized as crystalline derivatives and the amounts obtained were in reasonable agreement with the amounts of *O*-methyl ethers arising from the same structural units. Thus the glycerol represented non-reducing terminal units (1.01 moles from methylation); threitol arose from 1 → 4 linked D-galactose units (1.51 moles by methylation); erythritol came from 1 → 4 linked D-mannose units (5.52 moles by methylation); and D-galactose must have represented branch points (1.0 mole by methylation). Demonstration of the presence of D-galactose in the hydrolysis product of periodate-oxidized galactomannan definitely shows that the branch units are not linked through C_6 of galactose moiety. The implication of this fact is that the di-*O*-methyl sugar mentioned previously is in all probability 3,6-di-*O*-methyl-D-galactose. More definite evidence in favor of its structure will be supplied in a subsequent communication.

The polysaccharide, whose methylated derivative has a moleculer weight of 1.25×10^5, as determined by light scattering, appears to be linked largely by β-linkage since the polysaccharide displays a negative specific rotation.

The constitutional studies of the galactomannans have shown that all of them possess a 1 → 4 linked D-mannopyranose backbone and to C_6 of certain of these mannose units are attached side chains terminated by D-galactose units (10*a*). The galactomannan from coconut kernel differs from these in having 1 → 4 linked D-galactose units and with branches being located on D-galactose rather than D-mannose residues.

Can. J. Chem. Downloaded from www.nrcresearchpress.com by 210.87.254.6 on 09/05/12
For personal use only.

Can. J. Chem. Downloaded from www.nrcresearchpress.com by 210.87.254.6 on 09/05/12
For personal use only.

EXPERIMENTAL

Methods

The following solvents were used for partition chromatography:

(A) ethyl acetate:pyridine:water (8:2:1),
(B) *n*-butanol:acetic acid:water (4:1:5), upper layer,
(C) *n*-butanol:pyridine:benzene:water (5:3:1:3), upper layer,
(D) *n*-butanol:ethanol:water (40:11:19),
(E) butanone–water azeotrope,
(F) *n*-butanol:ethanol:water (4:1:5), upper layer.

Spray reagents were:

(*a*) saturated solution of aniline oxalate (11),
(*b*) aniline phthalate in *n*-butanol saturated with water,
(*c*) 3% solution of *p*-anisidine hydrochloride in *n*-butanol, and
(*d*) ammoniacal silver nitrate.

Unless otherwise stated all evaporations were carried out *in vacuo* at 30–40°. All the optical rotations given are at equilibrium.

Isolation and Purification of the Polysaccharide

The kernel of the green coconut obtained from the market was peeled. The outer hard brown layer, which was found to contain large amounts of lignin, was carefully removed. The white kernel was sliced and macerated in a high speed "Kenmix 55" blender for 5 minutes in ethanol. The resulting mass was kept under ethanol for 2 hours, filtered, and freed from alcohol by squeezing. This was dried over a water bath at 60°. The material gave a positive test for the presence of nitrogen. The oil in the material was removed by Soxhlet extraction for 24 hours with a mixture of benzene and ethanol (2:1). The dried material gave a negative test for nitrogen.

The crude material (100 g) was soaked with 2 liters of water in a round-bottomed flask for 2 hours. The flask was then heated on a water bath for 5 hours at 90° with stirring. The slurry obtained was kept overnight and squeezed through fine cloth. The extraction was repeated for the second time, but heated for 2 hours only. The combined extracts were passed through Sharples super centrifuge (at a speed of 25,000 to 30,000 r.p.m.) for clarification. It was then acidified to pH 4 to 5 with acetic acid and added to twice its volume of 95% ethanol dropwise, when the polysaccharide precipitated in the form of long fibers. The polysaccharide was separated by filtration of the mixture through a fine cloth and was kept overnight under absolute alcohol. It was triturated four times with absolute alcohol, washed with ether, and finally dried *in vacuo* at 40°. The yield was 7 g; ash 0.35%, lignin (12, p. 369 (after Klason's method)) 0.7%, pentosan (12, p. 381 (A. W. Schorger's method)) 1.68%, uronic acid (12, p. 391 (uronic acid estimation)) 2.14%, methoxyl 0.46%; $[\alpha]_D^{29}$ −85° in 4% sodium hydroxide solution (*c*, 1); intrinsic viscosity, 1.13 (dl/g) in 4% sodium hydroxide solution. D-Galactose, D-mannose, and traces of L-arabinose were detected by paper chromatography using solvents A, B, and C, after hydrolysis. The amounts of D-galactose and D-mannose were determined by separating the hydrolyzate on a paper chromatogram, using solvent A, followed by elution in the usual way and estimation by the periodate method (5). The ratio of D-galactose to D-mannose was found to be 1:2, L-arabinose being present in insignificant amount.

The crude polysaccharide was purified by complexing with Fehling's solution (6).

The polysaccharide (10 g) was dissolved in 4% sodium hydroxide (500 ml) in an atmosphere of nitrogen and freshly prepared Fehling's solution (250 ml) was added. The

precipitate was removed by centrifuging, washed with water, and stirred with 0.5 *N* hydrochloric acid (700 ml) at 0° for 4 hours. The resulting solution was poured into ethanol (1400 ml) and the precipitate was washed with 0.1 *N* hydrochloric acid in a mixture of acetone and water (6:4). The material was finally dried after washing with methanol. The copper complex purification step was repeated once again. Yield 6 g; $[\alpha]_D^{29}$ −89° 4% sodium hydroxide solution. Hydrolysis of the polysaccharide as before gave a mixture of D-galactose (1 part) and D-mannose (2 parts). L-Arabinose and uronic acid were not present.

Hydrolysis and Identification of D-*Galactose and* D-*Mannose*

The polysaccharide (2 g) was kept with 72% sulphuric acid (13, 14), (25°) overnight and made up to a normal solution with respect to sulphuric acid by cautious dilution (to avoid reprecipitation) with water. The solution was heated for 10 hours in boiling water bath, when the hydrolysis, which was followed iodometrically (15), was found to be complete.

The solution was neutralized with barium carbonate, filtered, and passed through Amberlite IR-120 (H)* and Amberlite IR-45 (OH).* After concentration the sirup containing 200 mg of the hydrolyzate was spread on Whatman No. 3 MM filter paper over a length of 12 cm. The mixture was separated by solvent A. The strips corresponding to D-galactose and D-mannose were eluted with water (20 ml). The eluents were evaporated to yield sirups.

D-Galactose $[\alpha]_D^{30}$ +80° in water (*c*, 1),
D-mannose $[\alpha]_D^{30}$ +14° in water (*c*, 1).

The D-galactose and D-mannose components were each treated with *p*-nitroaniline in acidified methanol (16). The galactose components afforded *N*-*p*-nitrophenyl-D-galactosylamine, m.p. and mixed m.p. 217–218°, $[\alpha]_D^{29}$ −247° in dry pyridine (*c*, 0.5), lit. −248° (16), and D-mannose component gave *N*-*p*-nitrophenyl-D-mannosylamine, m.p. and mixed m.p. 217–218°, $[\alpha]_D^{29}$ −326° in dry pyridine (*c*, 1), lit. −325° (16).

Methylation of Galactomannan

The galactomannan (5 g) was methylated according to the method adopted by Adams (17). The product (2.75 g) was treated with silver oxide and methyl iodide in the usual manner to give the methylated polysaccharide (2.24 g), $[\alpha]_D^{29}$ +25° in chloroform (*c*, 1). (Anal. Calc. for $C_9H_{16}O_5$: OCH_3, 44.7. Found: OCH_3, 43.7.) The methylated polysaccharide showed no hydroxyl absorption band in the infrared. Intrinsic viscosity 0.36 (dl/g) in chloroform.

The molecular weight of the methylated galactomannan was determined by the light-scattering method using a Brice-phoenix photometer (Model OM 1000 A) using semi-octagonal cells. The concentration used was over a range of $(1–4)\times10^{-3}$ g/ml. The molecular weight was found to be 1.25×10^5 calculated by the dissymmetry method (18).

Methanolysis and Hydrolysis of the Methylated Galactomannan

A solution of methylated galactomannan (0.5 g) in 5% methanolic hydrogen chloride (40 ml) was refluxed till the rotation reached a constant value (16 hours). The solution was evaporated to a sirup under reduced pressure, *N* hydrochloric acid (40 ml) was added, and the mixture was refluxed for 14 hours when the rotation reached a constant value. The solution was cooled, neutralized with silver carbonate, and filtered. The resulting solution was deionized by passage through Amberlite IR-120 (H) and Amberlite IR-45 (OH). The solution was evaporated to a thin sirup.

**A product of Rohm and Hass Company, Pennsylvania, U.S.A.*

Can. J. Chem. Downloaded from www.nrcresearchpress.com by 210.87.254.6 on 09/05/12
For personal use only.

Upon paper chromatographic analysis of the mixture using solvent D and a saturated solution of aniline oxalate in water as spray reagent the following spots were identified:

Spot No.	R_G	
1	.96	2,3,4,6-tetra-*O*-methyl-D-mannose,
2	.91	2,3,4,6-tetra-*O*-methyl-D-galactose,
3	.82	2,3,6-tri-*O*-methyl-D-mannose,
4	.74	2,3,6-tri-*O*-methyl-D-galactose,
5	.53	di-*O*-methyl-D-galactose.

(R_G values are with reference to 2,3,4,6-tetra-*O*-methyl-D-glucose.)

Separation of Mixture of Methylated Sugars by Column Chromatography

The mixture of methylated sugars (ca. 300 mg) was separated on a cellulose column (7) using solvent E (8). The results are given below.

TABLE I

Tube No.	Yield (mg)	Methoxyl (%)	Components
14 and 15	31.2	52.5	2,3,4,6-Tetra-*O*-methyl-D-mannose and 2,3,4,6-tetra-*O*-methyl-D-galactose
16	69.2	41.2	2,3,6-Tri-*O*-methyl-D-mannose
17	80.7	41.6	2,3,6-Tri-*O*-methyl-D-mannose and 2,3,6-tri-*O*-methyl-D-galactose
18 and 19	35.1	41.9	2,3,6-Tri-*O*-methyl-D-galactose
21 and 24	30.1	29.7	Di-*O*-methyl-D-galactose

Identification of 2,3,4,6-Tetra-O-methyl-D-mannose and 2,3,4,6-Tetra-O-methyl-D-galactose

A part of the sirup (5 mg) obtained from test tubes 14 and 15 was demethylated (19) by heating with 48% hydrobromic acid. The resulting sirup obtained after the usual treatment, on paper chromatographic analysis using solvent A, gave spots corresponding to those for D-mannose and D-galactose along with spots for partially methylated sugars. The mixture of sugars, when examined chromatographically using solvent E, gave spots having R_F values corresponding to those of 2,3,4,6-tetra-*O*-methyl-D-mannose and 2,3,4,6-tetra-*O*-methyl-D-galactose. The remaining sirup was separated on Whatman No. 3 MM paper using solvent E. The zones corresponding to the two tetramethyl sugars were eluted and evaporated.

The 2,3,4,6-tetra-*O*-methyl-D-mannose component, having $[\alpha]_D^{30}$ +3° in water (*c*, 0.5), lit. +1.2° (20), +2.4° (21) was characterized by converting it to the anilide, m.p. and mixed m.p. 143–144°, lit. 142–143° (22), 144–145° (23); $[\alpha]_D^{30}$ −38° in acetone (*c*, 0.5), lit. −38.9° (22). The 2,3,4,6-tetra-*O*-methyl-D-galactose, obtained as a sirup having $[\alpha]_D^{30}$ +110° in water (*c*, 0.5), lit. +109.5° (24), was converted into *N*-phenyl-2,3,4,6-tetra-*O*-methyl-D-galactosylamine in the usual way, m.p. and mixed m.p. 187–189°, lit. 186–188° (25), 188–190° (26), 192° (27); $[\alpha]_D^{31}$ +40° in acetone (*c*, 0.5), lit. +39° (26), +40.7° (27).

Identification of 2,3,6-Tri-O-methyl-D-mannose

The 2,3,6-tri-*O*-methyl-D-mannose component (69.2 mg) from test tube 16, which was chromatographically pure, had $[\alpha]_D^{30}$ −9° in water (*c*, 1), lit. −13° (28), −10° (29). It afforded 2,3,6-tri-*O*-methyl-D-mannose-1,4-di-*p*-nitrobenzoate (30), m.p. and mixed m.p. 189–190°, lit. −191° (28); $[\alpha]_D^{30}$ −35° in chloroform (*c*, 1), lit. −33° (30).

Identification of 2,3,6-Tri-O-methyl-D-galactose

The 2,3,6-tri-*O*-methyl-D-galactose component from test tubes 18 and 19, which was

Can. J. Chem. Downloaded from www.nrcresearchpress.com by 210.87.254.6 on 09/05/12
For personal use only.

found to be chromatographically pure, having $[\alpha]_D^{30}$ +89° in water (*c*, 1), lit. +87° (31), +78° (32), +80° (33), was obtained as sirup. It was converted to 2,3,6-tri-*O*-methyl-D-galactonolactone, m.p. and mixed m.p. 97–98°, lit. 99° (31), 101° (35), 97–98° (34); $[\alpha]_D^{30}$ −28° in water (*c*, 1), lit. −28° (31), −21.3° (34).

*Examination of the Mixture of 2,3,6-Tri-O-methyl-*D*-mannose and 2,3,6-Tri-O-methyl-*D*-galactose*

The sirup obtained from test tube 17 (80.7 mg) on demethylation in the above manner gave D-galactose and D-mannose together with partially methylated sugars when examined chromatographically using solvent A. On paper chromatographic separation of the same sirup using solvent E, two spots were detected corresponding to 2,3,6-tri-*O*-methyl-D mannose and 2,3,6-tri-*O*-methyl-D-galactose.

Identification of Di-O-methyl-sugar

The sirup (30.1 mg) obtained from test tubes 21–24, having specific rotation −55° in water (*c*, 1) was chromatographically homogeneous and gave on demethylation in the usual way, only D-galactose. No anilide could be prepared. R_{rhamnose} value (10) (1.30) in solvent D does not correspond to any known di-*O*-methyl-D-galactose (2,4; 2,6; 3,4; 4,6).

Quantitative Estimation of Methyl Sugars

A small quantity of the mixture of methylated sugars (ca. 10 mg) was separated by paper chromatography using solvent E. The zones corresponding to each methyl sugar were eluted and estimated by alkaline hypoiodite method (9). The molar ratio of various methyl sugars determined in duplicate experiments were as follows:

2,3,4,6-tetra-*O*-methyl-D-mannose : 2,3,4,6-tetra-*O*-methyl-D-galactose : 2,3,6-tri-*O*-methyl-D-mannose : 2,3,6-tri-*O*-methyl-D-galactose : di-*O*-methyl galactose is as 0.51:0.5:5.52:1.51:1.

Periodate Oxidation

The polysaccharide (94.8 mg) was treated with 0.1 *N* sodium metaperiodate (100 ml) and the reaction was carried out in dark at 25°. The liberated formic acid and the periodate consumed in the reaction were estimated in the usual way (36). After 37 hours the liberation of formic acid became constant, corresponding to 7.86 hexose residues per 1 mole of formic acid and after 44 hours the periodate uptake became constant corresponding to 1.03 moles of periodate per hexose residue.

Reduction of the Periodate-Oxidized Galactomannan

The periodate-oxidized galactomannan was neutralized with barium hydroxide and filtered and to the clean solution (150 ml) sodium borohydride (200 mg) was added. The reduction was allowed to proceed for $3\frac{1}{2}$ hours at room temperature. The resulting solution was treated in the usual way and the sirup obtained was examined chromatographically using solvent F and spray reagent D. Four spots corresponding to erythritol, threitol, glycerol, and D-galactose were detected.

The above mixture was separated on Whatman No. 3 MM filter paper using solvent F. The zones corresponding to glycerol, erythritol, threitol, and galactose were eluted separately and evaporated to sirups. Glycerol and erythritol were characterized through their crystalline tri- and tetra-tosyl derivatives respectively. Tri-*O*-tosyl-glycerol, m.p. and mixed m.p. 102–104°, lit. 103–104° (37). Tetra-*O*-tosyl-erythritol, m.p. and mixed m.p. 164–165°, lit. 165–166° (37). Threitol was characterized as dibenzylidine threitol, m.p. 219–221°, lit. 221–223° (38). The galactose was identified by observing its optical rotation $[\alpha]_D^{30}$ +80.0° in water (*c*, 0.5).

Can. J. Chem. Downloaded from www.nrcresearchpress.com by 210.87.254.6 on 09/05/12
For personal use only.

Quantitative Estimation of D-*Galactose and Polyhydric Alcohols*

The mixture was separated quantitatively by paper chromatography. D-Galactose was estimated by phenol – sulphuric acid method (39) and the polyhydric alcohols by oxidation with periodate followed by the determination of formaldehyde with chromotroptic acid (40). The ratio of the components of the hydrolyzate is glycerol (1 mole), galactose (0.9 mole), erythritol (6.8 moles), threitol (1.9 moles).

REFERENCES

1. E. JANTZEN and H. WITGERT. Fette u. Seifen, **46**, 563 (1939); Chem. Abstr. **34**, 3115 (1940).
2. ISAO UMEDA and MINERU HATANO. J. Agr. Chem. Soc. Japan, **23**, 856 (1949); Chem. Abstr. **44**, 5035 (1950).
3. M. V. L. RAO, N. SUBRAMANIAN, and M. SRINIVASAN. J. Sci. Ind. Research (India), **15C**, 39 (1956).
4. S. R. K. MENON. J. Textile Inst. **27**, T 229 (1936).
5. E. L. HIRST and J. K. N. JONES. J. Chem. Soc. 1659 (1949).
6. S. K. CHANDA, E. L. HIRST, J. K. N. JONES, and E. G. V. PERCIVAL. J. Chem. Soc. 1289 (1950).
7. L. HOUGH, J. K. N. JONES, and W. H. WADMAN. J. Chem. Soc. 2511 (1949).
8. L. BOGGS, L.S. CUENDET, I. EHRENTHAL, R. KOCH, and F. SMITH. Nature, **166**, 520 (1950).
9. E. L. HIRST, L. HOUGH, and J. K. N. JONES. J. Chem. Soc. 928 (1949).
10. P. ANDREWS, L. HOUGH, and J. K. N. JONES. J. Chem. Soc. 806 (1954).

10*a*. F. SMITH and R. MONTGOMERY. The chemistry of plant gums and mucilages. Reinhold Publishing Corpn., New York. 1959. p. 336.

11. R. H. HORROCKS and G. B. MANNING. Lancet, **256**, 1042 (1949).
12. CHARLES DOREE. The methods of cellulose chemistry. 2nd ed. Chapman and Hall Ltd., London. 1947.
13. E. HAGGLAND and C. L. BRATT. Svensk Kem. Tidskr. **48**, 125 (1936).
14. J. K. HAMILTON and E. V. PARTLOW. J. Am. Chem. Soc. **80**, 4880 (1958).
15. F. L. BAKER and H. F. E. HALTON. Biochem. J. **14**, 754 (1920).
16. F. WEYGAND, W. PERKOW, and P. KUHNER. Chem. Ber. **84**, 594 (1951).
17. G. A. ADAMS. Can. J. Chem. **36**, 755 (1958).
18. P. DEBYE. J. Phys. Chem. **51**, 18 (1947).
19. L. HOUGH, J. K. N. JONES, and W. H. WADMAN. J. Chem. Soc. 1702 (1950).
20. J. C. IRVINE and A. M. MOODIE. J. Chem. Soc. **87**, 1462 (1905).
21. R. D. GREEN and W. L. LEWIS. Science, **64**, 206 (1926); J. Am. Chem. Soc. **50**, 2813 (1928).
22. J. C. IRVINE and D. MCNICOLL. J. Chem. Soc. **97**, 1449 (1910).
23. W. N. HAWORTH, R. L. HEATH, and S. PEAT. J. Chem. Soc. 833 (1941).
24. J. C. IRVINE and A. CAMERON. J. Chem. Soc. **85**, 1071 (1904).
25. R. JOHNSTON and E. G. V. PERCIVAL. J. Chem. Soc. 1994 (1950).
26. P. ANDREWS, L. HOUGH, and J. K. N. JONES. J. Am. Chem. Soc. **74**, 4029 (1952).
27. W. N. HAWORTH and G. C. LEITCH. J. Chem. Soc. **113**, 188 (1918).
28. N. PRENTICE, L. S. CUENDET, W. F. GEDDES, and F. SMITH. J. Am. Chem. Soc. **81**, 684 (1959).
29. E. L. HIRST and J. K. N. JONES. J. Chem. Soc. 1278 (1948).
30. P. A. REBERS and F. SMITH. J. Am. Chem. Soc. **76**, 6097 (1954).
31. W. N. HAWORTH, H. RAISTRICK, and M. STACEY. Biochem. J. (London), **31**, 640 (1937).
32. S. MURAKAMI. Acta Phytochim. (Japan), **11**, 201 (1940); Chem. Abstr. **35**, 1384 (1941).
33. J. J. CONNEL, R. M. HAINSWORTH, E. L. HIRST, and J. K. N. JONES. J. Chem. Soc. 1696 (1950).
34. E. PACSU, S. M. TRISTER, and J. W. GREEN. J. Am. Chem. Soc. 2444 (1939).
35. W. N. HAWORTH, E. L. HIRST, and M. STACEY. J. Chem. Soc. 2481 (1932).
36. P. FLEURY and J. LANGE. J. pharm. chim. **17**(8), 107 (1933).
37. J. K. HAMILTON and F. SMITH. J. Am. Chem. Soc. **78**, 5907 (1956).
38. H. J. LUCAS and W. BAUMGARTEN. J. Am. Chem. Soc. **63**, 1653 (1941).
39. M. DUBOIS, K. A. GILLES, J. K. HAMILTON, P. A. REBERS, and F. SMITH. Anal. Chem. **28**, 350 (1956).
40. M. LAMBERT and A. C. NEISH. Can. J. Research, B, **28**, 83 (1950).

Can. J. Chem. Downloaded from www.nrcresearchpress.com by 210.87.254.6 on 09/05/12
For personal use only.

Can. J. Chem. Downloaded from www.nrcresearchpress.com by 210.87.254.42 on 09/05/12
For personal use only.

CONTRIBUTION À L'ÉTUDE DE LA RÉACTION DE VON RICHTER

III. SUR LA RÉACTION AVEC DIVERS NITRONAPHTALÈNES[1]

E. CULLEN[2] ET PH. L'ÉCUYER

RÉSUMÉ

Dans la réaction de von Richter avec les dérivés du naphtalène, le rendement des acides naphtoïques formés est nettement inférieur à celui des acides benzoïques obtenus dans la série du benzène. Par contre, des aminoamides se trouvent parmi les produits de la réaction et, lorsque celle-ci est exécutée dans des conditions bien définies avec le 1-nitronaphtalène ou le 1-chloro-4-nitronaphtalène, deux substances, $C_{22}H_{16}O_3N_4$ et $C_{22}H_{14}O_3N_4Cl_2$, peuvent être isolées. Ces dernières pourraient être des intermédiaires de la réaction, puisqu'elles se transforment respectivement en acides 2-naphtoïque et 4-chloro-2-naphtoïque, lorsqu'elles sont traitées selon les conditions de la réaction de von Richter.

Au cours de travaux précédents (1, 2) nous avons établi la structure de quelques composés neutres et acides qui sont isolés parmi les produits de la réaction de von Richter avec le nitrobenzène ou le *p*-chloronitrobenzène. Lorsque cette réaction est exécutée à partir de dérivés nitrés du naphtalène, l'acide naphtoïque qui se forme est difficile à purifier directement (3). Nous y sommes aisément parvenus, en extrayant au benzène les produits acides dans un Soxhlet, en évaporant l'extrait à siccité et en cristallisant ensuite l'acide dans le xylène.

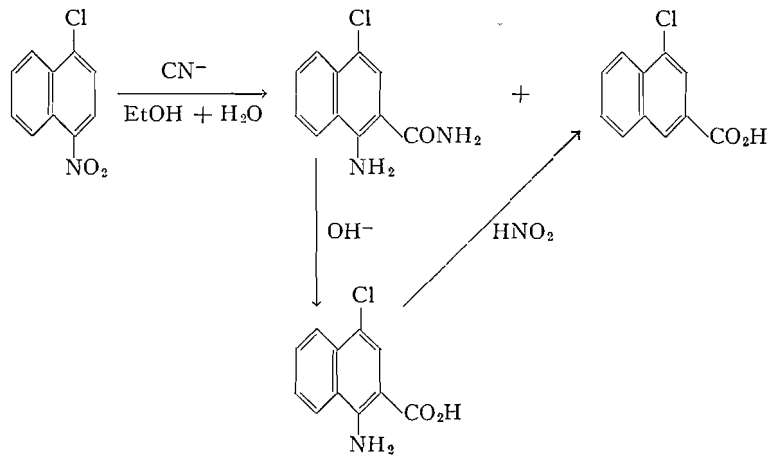
En variant les conditions expérimentales de la réaction avec le 1-chloro- ou le 1-bromo-4-nitronaphtalène, nous avons vérifié que les meilleurs résultats s'obtiennent dans l'alcool à 75 au lieu de 48% et avec le cyanure de sodium plutôt qu'avec le cyanure de potassium (Tableau I). La réaction est plus rapide avec les nitronaphtalènes qu'avec les nitrobenzènes.

Après la réaction avec le 1-chloro-4-nitronaphtalène, outre l'acide 4-chloro-2-naphtoïque de p.f. 241° (4), nous avons recueilli une substance fondant à 235–236°, qui, d'après son analyse élémentaire et son poids moléculaire, possède la formule empirique $C_{11}H_9ON_2Cl$. Cette substance traitée à l'ébullition par la potasse dans le glycol dégage de l'ammoniac et forme un sel. L'acide $C_{11}H_8O_2NCl$, qui en est obtenu par neutralisation de ce sel, cristallise dans le xylène et fond à 252°. Cet acide contient une fonction amine primaire qui peut être éliminée par diazotation pour donner naissance à l'acide 4-chloro-2-naphtoïque. La substance de p.f. 235–236° est donc la 4-chloro-1-amino-2-naphtamide (*a*).

Nous avons obtenu de la même façon, à partir du 1-bromo-4-nitronaphtalène, la 4-bromo-1-amino-2-naphtamide de p.f. 226°, et l'acide 4-bromo-2-naphtoïque fondant à 245–246°.

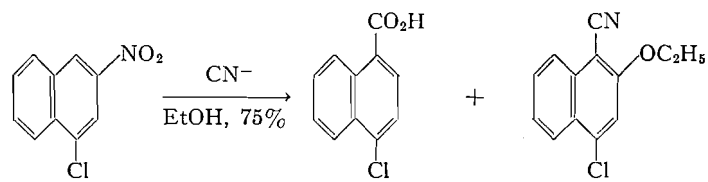
Avec le 1-nitronaphtalène nous avons isolé l'acide 2-naphtoïque et une amide de formule brute $C_{11}H_{10}ON_2$, fondant à 192–193°. Celle-ci est la 1-amino-2-naphtamide, puisque par hydrolyse nous en avons obtenu l'acide 1-amino-2-naphtoïque de p.f. 202–205° (5). Avec le 5-bromo-1-nitronaphtalène nous avons recueilli un peu d'acide 5-bromo-2-naphtoïque de p.f. 249–250° (6), et une amide, $C_{11}H_9ON_2Br$, de p.f. 246°, qui ne peut être que la 1-amino-5-bromo-2-naphtamide.

[1]*Manuscrit reçu le 11 octobre 1960.*
Contribution du Département de Chimie, Faculté des Sciences, Université Laval, Québec, Qué.
[2]*Bénéficiaire de bourses d'études accordées par le Conseil national de Recherches du Canada, les firmes C.I.L. et Shell Oil et l'Office de Recherches scientifiques de la Province de Québec.*



(*a*)

Après la réaction avec le 1-chloro-3-nitronaphtalène, nous n'avons pas décelé la présence d'acide 1-chloro-2-naphtoïque dans le mélange de produits obtenus. Nous n'avons recueilli qu'un peu d'acide 4-chloro-1-naphtoïque et une substance, $C_{13}H_{10}ONCl$, fondant à 103–104° (33% de la théorie). Ce composé doit être le 2-éthoxy-4-chloro-1-naphtonitrile (*b*); car il est reconnu que, au cours de la réduction de dérivés nitrés du benzène en milieu alcoolique, le groupement alcoxyle peut occasionnellement (7) substituer un groupe nitré. D'autre part, le groupe nitrile doit entrer en position 4 du 1-chloro-3-nitronaphtalène plutôt qu'au sommet 2, parce que la localisation de la double liaison aux positions 2,3 exige 15 kcal/mole de plus qu'en 1,2 (8) et que l'acide 1-chloro-2-naphtoïque ne se forme pas au cours de la réaction.



(*b*)

La réaction du 1-chloro- ou du 1-bromo-2-nitronaphtalène avec les cyanures alcalins dans l'éthanol aqueux n'a fourni que 14% de produits acides et aucun produit neutre. Même après avoir été bouilli à reflux pendant 48 heures, 50% du matériel de départ n'a pas encore réagi. Quant au produit acide obtenu, il s'agit du 2-nitronaphtol.

Durant l'ébullition à reflux d'une solution de 1-chloro-4-nitronaphtalène et de cyanure de potassium dans l'éthanol à 48%, il se forme un précipité verdâtre (*r*) (environ 10% du produit de départ). Celui-ci n'apparaît pas lorsque la réaction est exécutée dans l'alcool à 75%, et le rendement de l'acide 4-chloro-2-naphtoïque est alors deux fois plus élevé (Tableau I).

Une substance non-chlorée analogue (*r'*) prend aussi naissance, lorsqu'une solution de 1-nitronaphtalène et de cyanure de potassium dans l'éthanol à 75% est gardée pendant un mois à une température variant de 5 à 25°. Il semble que l'emploi d'éthanol dont la concentration est supérieure à 50% ou une élévation de la température de réaction favorise la transformation de ces substances et empêche de les isoler.

Can. J. Chem. Downloaded from www.nrcresearchpress.com by 210.87.254.42 on 09/05/12
For personal use only.

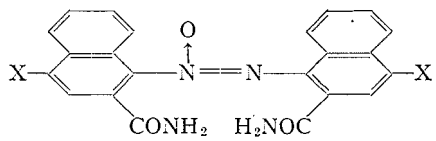
TABLEAU I

Réaction de 1-halo-4-nitronaphtalènes avec le cyanure de potassium ou de sodium dans divers solvants

4-Nitronaphtalène	Solvant	Cyanure	Temps (heures)	Produits %		
					Acides	
				Neutres	Bruts	4-Halo-2-naphtoïque
1-Chloro-	Éthanol 48%	KCN	48	50	31	3.5
"	Éthanol 48%	KCN	2	50	34	3.5
"	Éthanol 99%	KCN	4	—	9	Traces
"	Éthanol 75%	KCN	4	66	35	6.0
"	Éthanol 75%	NaCN	4	64	42	7.6
"	Éthanol 48%	NaCN	4	—	31	5.7
"	Glycol 70%	KCN	5	—	20	Traces
"	Glycol 90%	KCN	4	—	50	0.0
"	Dioxane 50%	KCN	4	—	31	4.0
1-Bromo-	Éthanol 48%	KCN	4	63	26	3.4
"	Éthanol 75%	KCN	4	—	33	5.0
"	Éthanol 75%	NaCN	4	73	27	7.0

Ces composés *r* et *r'* sont insolubles dans les bases et les acides dilués, presque insolubles dans les solvants organiques usuels, mais solubles à chaud dans la potassse alcoolique. En solution dans l'acide sulfurique concentré ils donnent une forte coloration bleue. L'analyse centésimale du premier (*r*), p.f. 308°, correspond à la formule empirique $C_{22}H_{14}O_3N_4Cl_2$; celle du second (*r'*), p.f. 266°, à la formule brute $C_{22}H_{16}O_3N_4$.

Le spectre infrarouge de la substance *r* suggère qu'elle possède une fonction amide primaire (bandes d'absorption à 3410, 3220 et 1655 cm^{-1}). Ces substances pourraient être respectivement le 4,4'-dichloro-2,2'-dicarbamylazoxynaphtalène (I) et le 2,2'-dicarbamylazoxynaphtalène (II). Elles sont probablement des intermédiaires de la réaction. En effet, en solution dans le glycol, elles sont saponifiées par l'hydroxyde de potassium en dégageant de l'ammoniac, et se transforment respectivement en l'acide 4-chloro-2-naphtoïque et l'acide 2-naphtoïque. Nous tentons présentement d'éclaircir ce point.



I X = Cl
II X = H

DISCUSSION DES RÉSULTATS

De tous les dérivés nitrés du naphtalène qui ont été essayés, le 2-nitronaphtalène est celui qui, dans les conditions de la réaction de von Richter, donne le plus fort pourcentage d'acide, soit 14% (3) et, dans ce cas, seul l'acide 1-naphtoïque est obtenu. Il y a deux positions ortho libres auxquelles l'ion cyanure peut se fixer, mais la localisation d'une double liaison en position 2,3 du naphtalène exige 15 kcal/mole de plus qu'en 1,2 (8).

Pour le 1-nitro- et le 2-nitro-naphtalène, on peut présumer que la réactivité ne dépend que de la polarisabilité du sommet attaqué. Avec le 1-nitronaphtalène, l'activation par le groupe nitré est utilisée, en partie du moins, pour neutraliser le supplément d'énergie de polarisation que requiert le sommet 2 par rapport au sommet 1, soit environ 3 kcal/mole (9). L'effet ortho, dû au voisinage de l'hydrogène péri et du groupement nitré,

Can. J. Chem. Downloaded from www.nrcresearchpress.com by 210.87.254.42 on 09/05/12
For personal use only.

empêche, sans doute par défaut de coplanéité, la transmission totale des effets électroniques du noyau vers la position 2 (10).

Il est à noter que, grâce à l'activation d'un atome d'halogène en position para du groupe nitré, le rendement de l'acide naphtoïque augmente considérablement. Il est de 8% dans le cas de l'acide 4-chloro-2-nitronaphtoïque obtenu à partir du 4-chloro-1-nitronaphtalène, alors qu'il n'est que de 1% pour l'acide 5-bromo-2-naphtoïque produit par le 5-bromo-1-nitronaphtalène dans lequel l'effet de l'atome de brome ne peut se faire sentir en position 2.

La réaction avec le 2-nitro-1-chloronaphtalène confirme la résistance du sommet 3 à l'attaque des réactifs et il est à propos de faire ici un rapprochement avec le 2-naphtol. On sait, en effet, que les réactions de ce dernier (par exemple, le couplage avec les diazoïques) intéressent toujours le sommet 1 et non la position 3 et que, parallèlement au cas précédent, l'occupation de la position 1 conduit, s'il y a réaction, à l'élimination du groupe substituant à ce sommet.

Enfin, en ce qui concerne la réaction avec le 1-chloro-3-nitronaphtalène, on constate une désactivation importante par l'atome de chlore, son effet électromère neutralisant celui du groupe nitré. Pour les mêmes raisons que précédemment, il faut rejeter la possibilité que l'ion cyanure se fixe en position 2 et, par conséquent, que se forment le 1-chloro-3-éthoxy-2-naphtonitrile et l'acide 1-chloro-2-naphtoïque.

Dans les réactions avec les nitronaphtalènes, les faibles rendements en acides naphtoïques ne semblent pas attribuables à la difficulté que l'ion cyanure éprouve à se fixer au noyau du naphtalène, mais plutôt à une modification des étapes subséquentes. En effet, nous avons observé que même si l'on abaisse le pH de la solution en y faisant passer un courant d'anhydride carbonique durant la réaction du 1-chloro-4-nitronaphtalène, le groupe nitrile se fixe quand même; mais, alors que le rendement de la 4-chloro-1-amino-2-naphtamide s'accroît du double (14%), celui de l'acide naphtoïque devient nul.

PARTIE EXPÉRIMENTALE[3]

Le 1-chloro- et le 1-bromo-4-nitronaphtalène, le 1-chloro- et le 1-bromo-2-nitronaphtalène ainsi que le 2-chloro-1-nitronaphtalène ont été préparés selon Hodgson et Walker (11). Ces composés cristallisent beaucoup mieux dans la ligroine (Eb = 65–110°) que dans l'éthanol tel que suggéré.

Le 1,8-dinitro-4-chloronaphtalène a été préparé selon Bassilios (12), le 1-nitro-5-bromonaphtalène selon McLeish et Campbell (13), le 1-chloro-3-nitronaphtalène, selon Hodgson et Elliott (14), la 8-nitro-1-naphtylamine selon Hodgson et Davey (15), la 1-nitro-2-naphtylamine selon Saunders et Hamilton (16), la 4- et la 2-nitro-1-naphtylamine selon Hodgson et Walker (17), le 1-nitronaphtalène selon Berkebile et Fries (18) et, finalement, le 2-nitronaphtalène par désamination de la 2-nitro-1-naphtylamine d'après la méthode générale de Hodgson et Walker (11).

Avec le 1-chloro-4-nitronaphtalène

Un mélange de 1-chloro-4-nitronaphtalène (2.0 g), de cyanure de sodium (8.0 g) et d'éthanol à 75% (100 ml) est chauffé à reflux durant 4 heures et ensuite versé dans 300 ml d'eau. On essore la suspension et recueille 0.98 g d'un produit neutre brun-verdâtre et

[3]*Les points de fusion (p.f.) ont été pris en tubes capillaires et ne sont pas corrigés. Les spectres infrarouges ont été déterminés au moyen d'un spectromètre Beckman IR-4; le solide était mélangé à du bromure de potassium et pressé; seules les bandes servant à l'identification du composé sont indiquées; les valeurs en cm^{-1} correspondent au maximum d'absorption. Les microanalyses ont été effectuées par M. W. Manser, Zürich, Suisse.*

Can. J. Chem. Downloaded from www.nrcresearchpress.com by 210.87.254.42 on 09/05/12
For personal use only.

un filtrat. En épuisant le filtrat à l'éther, on peut obtenir une quantité additionnelle (0.30 g) du produit neutre, ce qui donne en tout 1.28 g.

Acide 4-chloro-2-naphtoïque

Le filtrat est d'abord chauffé pour en chasser les dernières traces d'éther, puis refroidi et acidifié par addition d'acide chlorhydrique. Les acides précipités (0.837 g) sont essorés et extraits au benzène dans un Soxhlet. L'extrait est traité avec un peu de noir animal, filtré et évaporé à siccité. Le résidu, cristallisé dans le xylène, fournit 0.152 g (7.6% de la théorie) d'acide 4-chloro-2-naphtoïque de p.f. 241°. Recristallisé dans l'acide acétique et ensuite le xylène, l'acide fond à 244° (p.f. lit. 241° (14)).

4-Chloro-1-amino-2-naphtamide

Le produit neutre (1.28 g) est extrait au benzène dans un Soxhlet et l'extrait évaporé à siccité. Cristallisé successivement dans le xylène et l'acide acétique à 95% (noir animal), le résidu donne la 4-chloro-1-amino-2-naphtamide (0.12 g) sous forme d'aiguilles crèmes de p.f. 235–236°. Recristallisée dans le xylène, elle fond à 236–237°. Calculé pour $C_{11}H_9ON_2Cl$: C, 60.32%; H, 4.32%; N, 12.67%. Trouvé: C, 59.87%; H, 4.11%; N, 12.70%.

Acide 4-chloro-1-amino-2-naphtoïque

De la 4-chloro-1-amino-2-naphtamide (0.227 g) et de l'hydroxyde de potassium (1.0 g) sont dissous dans le glycol (20 ml) et chauffés à reflux pendant $2\frac{1}{2}$ heures. La solution jaune pâle est ensuite refroidie, diluée par l'eau et acidifiée. L'acide 4-chloro-1-amino-2-naphtoïque filtré et séché cristallise dans le xylène en aiguilles crèmes de p.f. 250°. Calculé pour $C_{11}H_8O_2NCl$: C, 59.60%; H, 3.64%; N, 6.32%. Trouvé: C, 59.45%; H, 3.60%; N, 6.12%.

Cet acide (0.290 g) donne, par désamination suivant la méthode générale de Hodgson (11), l'acide 4-chloro-2-naphtoïque (0.113 g) qui cristallise dans le xylène en aiguilles de p.f. 242°. Le point de fusion mixte de cet acide et de l'acide isolé après la réaction de von Richter avec le 1-chloro-4-nitronaphtalène n'est pas abaissé et les spectres infrarouges des deux échantillons sont superposables.

Composé $C_{22}H_{14}O_3N_4Cl_2$ (r)

Lorsque la réaction de von Richter avec le 1-chloro-4-nitronaphtalène (2.0 g) est effectuée dans l'alcool à 48 au lieu de 75%, il se forme durant l'ébullition à reflux un précipité vert (*r*) (0.20 g) qui est recueilli en filtrant à chaud. Le filtrat, traité comme précédemment, donne 5% de 4-chloro-1-amino-2-naphtamide mais seulement 3% d'acide 4-chloro-2-naphtoïque.

Le produit vert (*r*) est insoluble dans les bases et les acides dilués et la plupart des solvants organiques. Il cristallise dans un mélange de N,N-diméthylformamide et de xylène (4:1) (noir animal) en minuscules aiguilles jaune-verdâtre de p.f. 308°. Calculé pour $C_{22}H_{14}O_3N_4Cl_2$: C, 58.29%; H, 3.11%; N, 12.36%. Trouvé: C, 58.34%; H, 3.19%; N, 12.33%. Les résultats de cette analyse correspondent exactement à la formule du 4,4′-dichloro-2,2′-dicarbamylazoxynaphtalène, mais les tests ne confirment ni la présence du groupe azoïque, ni celle du groupement azoxyque. Spectre infrarouge: 1655, 3220 et 3410 cm^{-1} (—$CONH_2$).

Ce composé (0.50 g) en solution dans le glycol est saponifié par l'hydroxyde de potassium (1.5 g) en faisant bouillir à reflux pendant 3 heures. Le dégagement d'ammoniac terminé, le produit de la réaction est refroidi et acidifié et l'acide (0.20 g) essoré. Celui-ci cristallise dans le xylène (noir animal) en aiguilles crèmes fondant à 241°. Un point de fusion mixte de cet acide avec l'acide 4-chloro-2-naphtoïque authentique n'est pas abaissé. Les spectres infrarouges des deux sont identiques.

Can. J. Chem. Downloaded from www.nrcresearchpress.com by 210.87.254.42 on 09/05/12
For personal use only.

Can. J. Chem. Downloaded from www.nrcresearchpress.com by 210.87.254.42 on 09/05/12
For personal use only.

Avec le 1-bromo-4-nitronaphtalène ou le 5-bromo-1-nitronaphtalène

En opérant dans l'alcool à 75%, comme il est décrit précédemment pour le 1-chloro-4-nitronaphtalène, on obtient avec le 1-bromo-4-nitronaphtalène un acide A et une amide B, et avec le 5-bromo-1-nitronaphtalène, un acide 1A et une amide 1B.

Acide 4-bromo-2-naphtoïque

L'acide A est extrait au benzène dans un Soxhlet, l'extrait évaporé à siccité et le résidu sublimé à 250° sous 12 mm de mercure. L'acide 4-bromo-2-naphtoïque (0.142 g) (7.1% de la théorie) ainsi obtenu, cristallise dans le benzène en aiguilles crèmes de p.f. 245–246°. Calculé pour $C_{11}H_7O_2Br$: C, 52.62%; H, 2.81%; Br, 31.83%. Trouvé: C, 52.74%; H, 2.81%; Br, 30.95%.

4-Bromo-1-amino-2-naphtamide

L'amide B (1.20 g) est extraite au xylène dans un Soxhlet, l'extrait évaporé à siccité et le résidu cristallisé successivement dans l'acide acétique et le toluène. La 4-bromo-1-amino-2-naphtamide (environ 6% de la théorie) cristallise en aiguilles de p.f. 226°. Calculé pour $C_{11}H_9ON_2Br$: C, 49.80%; H, 3.40%; N, 10.60%. Trouvé: C, 49.67%; H, 3.55%; N, 10.48%.

Acide 5-bromo-2-naphtoïque

L'acide 1A est extrait au tétrachlorure de carbone dans un Soxhlet et l'extrait évaporé à siccité. Le résidu cristallisé dans le toluène (noir animal) fournit l'acide 5-bromo-2-naphtoïque en aiguilles jaunes pâles, de p.f. 249–250° (p.f. lit. 248–250° (10)).

1-Amino-5-bromo-2-naphtamide

L'amide 1B est extraite au xylène dans un Soxhlet et l'extrait est traité au noir animal, concentré et refroidi. La 1-amino-5-bromo-2-naphtamide précipitée, est filtrée et cristallisée dans l'acide acétique. On en obtient 0.234 g (7.0% de la théorie) sous forme d'aillures jaunes pâles de p.f. 246°. Calculé pour $C_{11}H_9ON_2Br$: C, 49.80%; H, 3.40%; N, 10.60%. Trouvé: C, 49.92%; H, 3.49%; N, 11.55%.

Avec le 1-chloro-3-nitronaphtalène

La réaction est effectuée comme précédemment dans 20 ml d'éthanol à 75% à partir de 0.512 g de 1-chloro-3-nitronaphtalène et 2.0 g de cyanure de sodium. La solution est ensuite diluée par l'eau à 100 ml. Il précipite alors un produit neutre jaune-orangé qui est essoré (0.44 g). Le filtrat est acidifié et fournit 0.050 g d'acide.

2-Éthoxy-4-chloro-1-naphtonitrile

Le produit neutre se sublime entre 90 et 200° sous 12 mm de mercure. Le sublimé cristallise dans l'éthanol en aiguilles de couleur jaune-orangé de p.f. 103–104°. C'est le 2-éthoxy-4-chloro-1-naphtonitrile (0.103 g; 18% de la théorie). Calculé pour $C_{13}H_{10}ONCl$: C, 67.39%; H, 4.35%; N, 6.05%. Trouvé: C, 67.30%; H, 4.50%; N, 6.12%.

Acide 4-chloro-1-naphtoïque

Le produit acide est sublimé sous 12 mm de mercure entre 120 et 160°. On recueille l'acide 1-chloro-4-naphtoïque qui, cristallisé dans l'acide acétique, puis dans le benzène, fond à 224° (p.f. lit. 223–224° (19)).

Avec le 1-nitronaphtalène

Après avoir fait bouillir à reflux une solution de 1-nitronaphtalène (5.0 g) et de cyanure de sodium (15 g) dans de l'éthanol à 50% (200 ml), on obtient, en extrayant à l'éther

le mélange de la réaction dans un extracteur liquide – liquide, une amide dans la phase éthérée et un produit acide dans la phase aqueuse. En acidifiant cette dernière, la majeure partie des acides (2.05 g) précipite. Une quantité supplémentaire d'acide (0.167 g) peut être obtenue en procédant comme il a déjà été décrit précédemment pour la réaction avec le *p*-chloronitrobenzène (1).

Acide 2-naphtoïque

Le produit acide (2.24 g) est extrait à la ligroïne (Eb = 65–110°) et l'extrait bouilli avec un peu de noir animal, filtré et concentré. L'acide 2-naphtoïque (0.108 g) cristallise en aiguilles de p.f. 184–185° (p.f. lit. 185° (20)).

1-Amino-2-naphtamide

L'extrait éthéré est évaporé au bain-marie et le résidu dilué par l'eau et acidifié par l'acide acétique. Le précipité est essoré, séché, extrait au benzène et traité au noir animal. Après deux cristallisations dans le benzène, la 1-amino-2-naphtamide (0.124 g; 2.3% de la théorie) apparaît sous forme d'aiguilles lustrées de teinte jaune pâle, fondant à 193–194°. Calculé pour $C_{11}H_{10}ON_2$: C, 70.96%; H, 5.41%; N, 15.05%. Trouvé: C, 71.08%; H, 5.29%; N, 14.96%.

Acide 1-amino-2-naphtoïque

La 1-amino-2-naphtamide (0.097 g) est hydrolysée par l'hydroxyde de potassium (0.50 g) dans le glycol (5 ml) en acide 1-amino-2-naphtoïque qui cristallise dans l'acide acétique en aiguilles crèmes de p.f. 205° (p.f. lit. 202–205° (5)).

Composé $C_{22}H_{16}O_3N_4$ (r')

Lorsqu'une solution de 1-nitronaphtalène (10.0 g) et de cyanure de potassium dans l'éthanol à 75% (100 ml) séjourne alternativement à la température ambiante pendant 24 heures et au réfrigérateur à 5° pendant une semaine durant une période d'un mois, il se forme un solide qui cristallise dans un mélange de N,N-diméthylformamide et de xylène (3:1) en aiguilles jaune-verdâtre de p.f. 266°. Calculé pour $C_{22}H_{16}O_3N_4$: C, 68.74%; H, 4.20%; N, 14.58%. Trouvé: C, 68.88%; H, 4.24%; N, 14.61%. Les résultats de l'analyse centésimale correspondant à la formule du 2,2'-dicarbamylazoxynaphtalène; mais ni la présence du groupe azoïque, ni celle du groupement azoxyque, n'a pu être vérifiée.

Cette substance saponifié par l'hydroxyde de potassium dans le glycol perd de l'ammoniac et donne l'acide 2-naphtoïque dont le point de fusion (185°), après deux cristallisations dans la ligroïne (Eb = 65–110°), n'est pas abaissé lorsque l'acide est mélangé à un échantillon d'acide 2-naphtoïque authentique.

Avec le 2-nitro-1-bromonaphtalène ou le 2-nitro-1-chloronaphtalène

2-Nitro-1-naphtol

Le produit qui est obtenu en faisant bouillir (24 heures) du 2-nitro-1-bromonaphtalène (4.7 g) et du cyanure de sodium (15 g) dans l'éthanol à 50% est versé dans 500 ml d'eau. Le solide est essoré et cristallisé dans le 1,1-diméthyléthanol; c'est du 2-nitro-1-bromonaphtalène (60%) qui n'a pas réagi. En acidifiant le filtrat, le 2-nitro-1-naphtol est isolé. Cristallisé successivement dans la ligroïne (Eb = 65–110°) et l'alcool, il forme des lamelles jaunes de p.f. 129° (p.f. lit. 128° (21)). Calculé pour $C_{10}H_7O_3N$: C, 63.49%; H, 3.73%; N, 7.41%. Trouvé: C, 63.64%; H, 3.89%; N, 7.58%.

Le 2-nitro-1-chloronaphtalène fournit aussi le même naphtol.

Can. J. Chem. Downloaded from www.nrcresearchpress.com by 210.87.254.42 on 09/05/12
For personal use only.

Avec le chloro-4-nitronaphtalène dans une atmosphère d'anhydride carbonique

La réaction de von Richter avec le 1-chloro-4-nitronaphtalène (1.0 g) en solution dans l'alcool à 75% (50 ml) dont le pH est maintenu constant par un courant d'anhydride carbonique, ne donne pas de produit acide. Quant au produit neutre, sublimé entre 150 et 250° sous 12 mm de mercure, il donne 0.15 g d'une substance jaune, qui cristallise dans le xylène en aiguilles de p.f. 235° et est identique à la 4-chloro-1-amino-2-naphtamide, comme le montre le point de fusion mixte avec un échantillon de l'amide authentique.

REMERCIEMENTS

Nous remercions le Conseil national de Recherches du Canada, les firmes C.I.L. et Shell Oil et l'Office de Recherches scientifiques de la Province de Québec pour des bourses d'études accordées à l'un de nous (EC).

BIBLIOGRAPHIE

1. E. Cullen et Ph. L'Écuyer. Can. J. Chem. **39**, 144 (1961).
2. E. Cullen et Ph. L'Écuyer. Can. J. Chem. **39**, 155 (1961).
3. J. F. Bunnett et M. M. Rauhut. J. Org. Chem. **21**, 934 (1956).
4. B. E. Cross et H. P. K. Drew. J. Chem. Soc. 1532 (1949).
5. P. Friedlaender et S. Littner. Ber. **48**, 331 (1915).
6. F. C. Whitmore et A. L. Fox. J. Am. Chem. Soc. **51**, 3363 (1929).
7. P. T. Izzo. J. Org. Chem. **24**, 2026 (1959).
8. R. D. Brown. Australian J. Sci. Research, Ser. A, **2**, 564 (1949); J. Chem. Soc. 3249 (1950).
9. F. L. J. Sixma. Rev. trav. chim. **68**, 915 (1949).
10. E. Berliner, M. J. Quinn et P. J. Edgerton. J. Am. Chem. Soc. **72**, 5305 (1950).
11. H. H. Hodgson et J. J. Walker. J. Chem. Soc. 1620 (1933).
12. H. F. Bassilios. Bull. soc. chim. France, 1022 (1952).
13. M. McLeish et N. Campbell. J. Chem. Soc. 1103 (1937).
14. H. H. Hodgson et R. L. Elliott. J. Chem. Soc. 1850 (1935).
15. H. H. Hodgson et W. Davey. J. Chem. Soc. 348 (1939).
16. C. R. Saunders et C. S. Hamilton. J. Am. Chem. Soc. **54**, 636 (1932).
17. H. H. Hodgson et J. J. Walker. J. Chem. Soc. 1205 (1933).
18. J. M. Berkebile et A. H. Fries. J. Chem. Educ. **25**, 617 (1948).
19. T. L. Jacobs, S. Winstein, J. W. Ralls et J. H. Robson. J. Org. Chem. **11**, 27 (1946).
20. C. G. Derick et O. Kamn. J. Am. Chem. Soc. **38**, 400 (1916).
21. C. Liebermann. Ann. **183**, 246 (1876).

Can. J. Chem. Downloaded from www.nrcresearchpress.com by 210.87.254.42 on 09/05/12
For personal use only.

Can. J. Chem. Downloaded from www.nrcresearchpress.com by 210.87.254.105 on 09/05/12
For personal use only.

NOTES

IMPROVEMENTS IN THE ACIDOLYSIS PROCEDURE FOR LIGNIN ISOLATION AND IN THE PROCEDURE FOR THE ANALYSIS OF LIGNIN OXIDATION PRODUCTS

J. M. Pepper and M. Siddiqueullah*

Improvements in the Acidolysis Procedure for Lignin Isolation

The acidolysis of wood meal, whereby an only moderately modified lignin fraction may be obtained in good yields in a short time, has proved of value in lignin research (1, 2). Recently some modifications have resulted in a simpler extraction procedure with resultant improved yields of lignin. Previously, after the initial acid-catalyzed dissolution of lignin into the dioxane–water (9:1) solvent medium, the procedure was to neutralize the acid with sodium bicarbonate, and then to obtain the lignin by first concentrating this solution and then precipitating the concentrate together with the bicarbonate sludge into a 1% sodium sulphate solution. Subsequent extensive washings, with water, of the precipitated lignin, gave rise to stable suspensions which would not clear even on prolonged centrifugation. Since large volumes of water were required to remove all the inorganic contaminants, an appreciable amount of lignin was lost in the discarded washings.

It has now been observed that the lignin may be recovered without the use of either sodium bicarbonate or sodium sulphate. After acidolysis, the acidic extract was concentrated under reduced pressure and the lignin in the concentrate was precipitated into a large excess of vigorously stirred water. The lignin settled readily in a coagulated state leaving a clear mother liquor. In subsequent water washing of the recovered lignin there was little tendency for a colloidal suspension to be formed. Indeed with fewer ions to be removed less washing was required.

No significant difference could be detected in the analyses of lignin samples isolated from the same pre-extracted aspen wood meal under conditions of 0.2 *N* initial hydrogen chloride concentration and 0.5-hour extraction time, but using the two methods of purification. The color, infrared absorption spectra, methoxyl content, and percentage phenolic aldehydes obtained by alkaline nitrobenzene oxidation were very similar. This modified technique has been used successfully for the isolation of a lignin fraction from several woody plants and cereal straws.

Modifications in the Analytical Procedure for the Alkaline Nitrobenzene Oxidation Products of Lignin

The widely adopted procedure of Stone and Blundell (3) for the quantitative estimation of the phenolic aldehydes, vanillin, syringaldehyde, and *p*-hydroxybenzaldehyde resulting from the alkaline nitrobenzene oxidation of lignin has certain limitations. The oxidation mixture is not homogeneous and the presence of small oily droplets of nitrobenzene and its reduction products makes it difficult to pipette accurately the small aliquot sample of the aqueous phase that is required for spotting on the chromatographic paper. To overcome this difficulty, as well as to eliminate the step involving acidification of the paper using boiling acetic acid, it has been found preferable to use the following modification. The alkaline reaction products were extracted continuously with ether to

**Colombo Plan Fellow in Canada, 1957–1960.*

remove excess nitrobenzene and its reduction products, then acidified, and further extracted with ether to remove the required lignin oxidation products. Solvent exchange with ethanol gave an alcoholic solution from which an aliquot was readily taken for the subsequent chromatographic separations.

In the original publication (3) no mention was made of the need for proper equilibration of the chromatographic paper prior to use. Experience has shown that for best results this is an important consideration. It is recommended that all papers be equilibrated over water in a closed vessel, preferably for at least 2 days, and that during the charging of the samples much care be exercised to maintain this equilibrium.

1. J. M. PEPPER, P. E. T. BAYLIS, and E. ADLER. Can. J. Chem. **37**, 1241 (1959).
2. E. ADLER, J. M. PEPPER, and E. ERIKSOO. Ind. Eng. Chem. **49**, 1391 (1957).
3. J. E. STONE and N. J. BLUNDELL. Anal. Chem. **23**, 771 (1951).

RECEIVED OCTOBER 31, 1960.
DEPARTMENT OF CHEMISTRY,
UNIVERSITY OF SASKATCHEWAN,
SASKATOON, SASKATCHEWAN.

Can. J. Chem. Downloaded from www.nrcresearchpress.com by 210.87.254.105 on 09/05/12
For personal use only.

Can. J. Chem. Downloaded from www.nrcresearchpress.com by 210.87.254.42 on 09/05/12
For personal use only.

Canadian Journal of Chemistry

Issued by THE NATIONAL RESEARCH COUNCIL OF CANADA

VOLUME 39 MARCH 1961 NUMBER 3

EXCHANGE REACTIONS BETWEEN ZINC AND ITS IONS[1]

J. E. SANDOR[2]

ABSTRACT

The exchange reaction between zinc metal and zinc ions in solution has been studied by means of radioactive zinc-65. Polycrystalline zinc and bicrystals of zinc were used under conditions where the radioactive material was incorporated either in the solid or the liquid phase. Strain-free clean surfaces were obtained and autoradiographs taken.

The results of the experiments using bicrystals were interpreted on the basis that a local cell action sets up an electrochemical potential between liquid and solid at the beginning of the reaction. Exchange was found to take place in both directions, but the reaction did not follow a simple logarithmic law.

INTRODUCTION

The extensive use of radioisotopes has made possible the study of many exchange reactions. In 1915, Hevesy (1) showed that in the system $Pb^{++}/Pb(NO_3)_2$ a deep exchange takes place in a very short period of time, i.e. more than one monolayer exchanges, and this was found later to happen in other metals, too. Various mechanisms have been suggested for such exchange reactions, but no conclusive explanation has yet been put forward. In the general case one expects more or less rapid exchange in the surface layer, followed by slow penetration to the interior of the metal at a speed controlled by the diffusion coefficient and orientation of the crystals.

The heterogeneous exchange reaction between zinc and its ions has been studied by Rollin (2) in zinc dust, by Gaudin and Vincent (3), Haenney and Mivelaz (4), Matsura (5), and King and Evans (6), in both zinc dust and zinc foil; and Bushmanov and Vozdvizhenky (7) in zinc single crystals. There are considerable variations in the results obtained by the different authors in this field, due to the fact that some factors, such as surface preparation, oxidation, corrosion, are not always fully considered.

In this investigation, zinc metal was dipped in different solutions of zinc salt to show that the exchange reaction $Zn^0_{metal} \rightleftarrows Zn^{++}_{sol}$ takes place in both directions. This was done by labeling either the metal or the zinc solution with radioactive zinc-65, and following the change in activity for different times of immersion. The influence of oxide or hydroxide on the exchange was also investigated. Finally, the exchange reaction between zinc bicrystals and carrier-free solutions of Zn^{65} was studied.

The following factors were considered of importance in this study: (1) preparing undistorted zinc surfaces; (2) working in an oxygen-free atmosphere; (3) minimizing of corrosion and adsorption. It is known that zinc is a soft metal, easily worked, and that the depth of distorted metal after mechanical polishing may commonly extend to at

[1]*Manuscript received May 13, 1960.*
Contribution from the Mineral Sciences Division, Mines Branch, Department of Mines and Technical Surveys, Ottawa, Canada.
[2]*National Research Council Postdoctorate Fellow, Mineral Sciences Division, Mines Branch, Department of Mines and Technical Surveys, Ottawa, Canada; now with Semiconductor Products Department, General Electric Co., Syracuse, N.Y.*

least 20 times the penetration of the deepest scratch (8). For silver, Tingley, Henderson, and Coffin (9) have shown definitely that the exchange reaction is notably different with different surface preparation techniques.

Zinc is a chemically reactive metal, easily oxidized, and considerable corrosion can take place in solution in the presence of oxygen as a result of electrochemical action.

EXPERIMENTAL DETAILS

Materials

Zinc metal.—Zinc metal, 99.999% purity, was cast in an argon atmosphere in rods of 1.56-cm diameter. Disks of 0.62-cm thickness and 1.56-cm diameter were cut by means of a lathe, annealed 12 hours at 350° C and mounted in Lucite in such a way that only one face was used in the experiments.

Active metal.—From the same 99.999% Zn rods as before, a number of disks of 1.56-cm diameter were cold-rolled to 0.78-mm thickness, cut in strips of 2.5-cm length, annealed for 24 hours at 350° C, and sent to Chalk River, Ont., for irradiation. The specific activity after irradiation was 5.1 mc/g. These samples were checked for purity with a 100-channel pulse height analyzer, to see if there was any unwanted activity not resulting from Zn^{65}.

Carrier-free zinc.—Carrier-free zinc was used in some experiments. Obtained from Nuclear Science and Engineering Corporation (Pittsburgh), it had an activity of 0.8 mc and a specific concentration of 1.1 mc/ml.

Preparation of Samples

The polycrystalline samples were mechanically polished with emery papers, and on microcloth laps using Al_2O_3 suspensions. They were finally etched with a cold solution of equal parts of HNO_3, C_2H_5OH, and H_2O_2. When the underlying structure of the zinc became visible under a microscope and no twins appeared (10), it was considered that an undistorted surface was obtained.

To avoid oxidation of the samples after etching and rinsing, the samples were immediately immersed in the exchange solution. Solutions of active and inactive deaerated $Zn(NO_3)_2$ were used. The molarities were 10^{-1} and 10^{-2} and the pH varied between 5.2 and 6.2. The active solutions had a specific activity of 0.4 mc/g. The solutions were thoroughly deaerated.

After polishing the polycrystalline metal samples, they were introduced into a dry box, in which the etching and exchange were carried out in an inert atmosphere of argon. The apparatus was set up so that the exchange process of six samples could be observed simultaneously in the same solution. This solution was kept in a thermostat at $25° \pm 0.5°$ C. The periods of immersion were varied between 1 hour and 1 week.

Bicrystals were grown from seeds provided by Dr. F. Weinberg; the bicrystals were annealed, strongly etched to remove the worked and recrystallized material, and, finally electropolished by using an orthophosphoric acid – ethanol solution (1:1). Carrier-free deaerated zinc solutions of pH 6 were used. Argon was bubbled continuously and the samples were immersed for short periods of time, ranging from a few seconds to a few minutes. The samples were then rinsed with water, washed with alcohol, and dried, and an autoradiograph was taken with No-Screen X-ray film. Different exposure times—depending on the activity of the samples—were tried, ranging from 8 to 64 hours.

For the purpose of studying the influence of oxidation on the exchange, one sample was pretreated for 24 hours in an air-free 10^{-2} *M* $Zn(NO_3)_2$ solution; this led to formation of a $Zn(OH)_2$ film. Then half of the sample was etched and the other half was left with

Can. J. Chem. Downloaded from www.nrcresearchpress.com by 210.87.254.42 on 09/05/12
For personal use only.

the hydroxide. Again, care was taken, during the rinsing of the samples, to avoid activities resulting from contamination only and not from exchange itself.

Some 99.999% Zn irradiated samples were immersed for short periods in a glass immersion cell, which had argon bubbling continuously through the solutions. The volume of solution was 100 ml, and fresh portions were used for each immersion period. Aliquots were taken out and counted for 30 minutes in a well-type scintillation counter.

To ensure radiochemical purity, solution samples were checked for possible contamination with the gamma-ray spectrometer. Samples had to be rinsed carefully, in order to remove all traces of the etching solution prior to the exchange experiment.

Activity measurements.—The activity measurements were done with a 3-in. well-type NaI(Tl) scintillation counter, mounted on a 6655 RCA photomultiplier. For measuring the metal activity, the samples were mounted in 1-in. diameter Lucite mounts which fitted exactly the well of the counter.

RESULTS

1. *Active Solution – Inactive Metal*

It has been shown by MacKay (11), and others, that any homogeneous exchange reaction can be described by the following type of equation:

$$[1] \qquad -\log(1-F) = kt,$$

where F is the fraction exchanged, k is a constant, and t is the exchange time. For a heterogeneous reaction, this type of equation holds only as long as the reacting mixture remains chemically unchanged, and if the isotopic distribution is uniform in each phase during the course of the reaction.

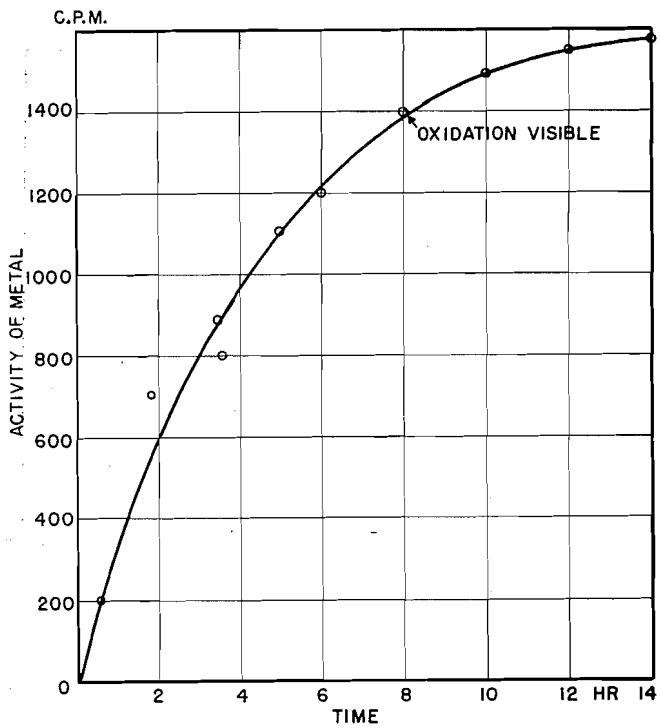


FIG. 1. Exchange between inactive metal and active 10^{-1} M $Zn(NO_3)_2$ solution.

Can. J. Chem. Downloaded from www.nrcresearchpress.com by 210.87.254.42 on 09/05/12
For personal use only.

The results of the experiments done so far indicate that the activity increase (or exchanged fraction) varies exponentially with time (Figs. 1 and 2), but not in accordance

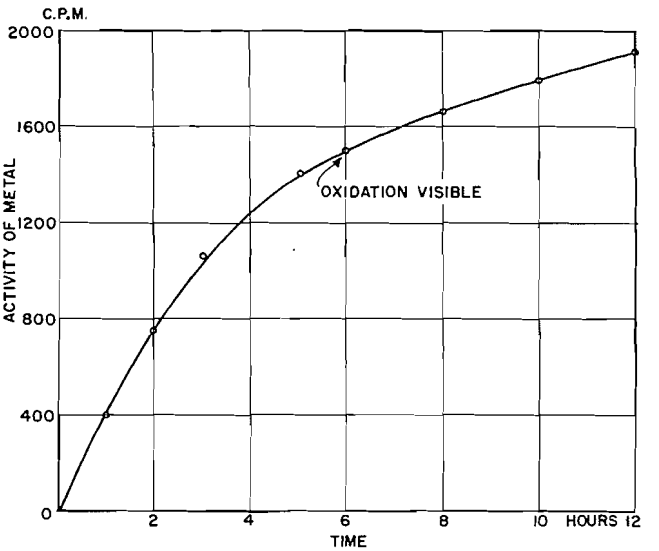


FIG. 2. Exchange between inactive metal and active 10^{-2} M $Zn(NO_3)_2$ solution.

with equation [1]. In Figs. 3 and 4 the logarithm of the exchanged fraction F is plotted as a function of time of immersion and it is seen that the slope is not constant.* At the

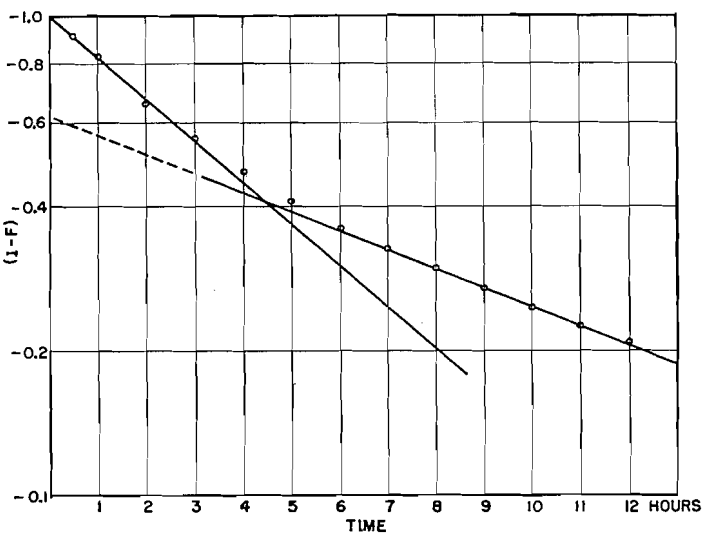


FIG. 3. Fraction exchanged as function of time. Plotted from results of Fig. 1.

same time it was observed that some visible film, presumably $Zn(OH)_2$, was formed during the second stage of the reaction marked in Figs. 1 and 2. The onset of this film

*$F = A_t/A_\infty$, *where* A_t *is activity of sample at time* t *and* A_∞ *is activity when apparent equilibrium is approached.*

Can. J. Chem. Downloaded from www.nrcresearchpress.com by 210.87.254.42 on 09/05/12
For personal use only.

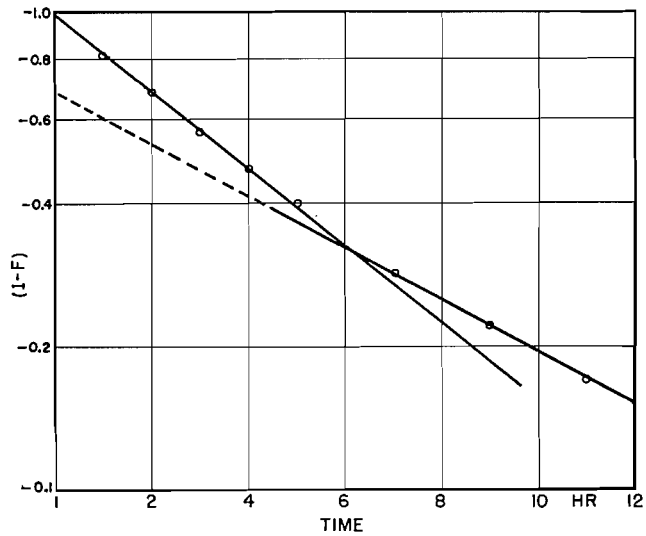


FIG. 4. Fraction exchanged as function of time. Plotted from results of Fig. 2.

formation can not be accurately determined. It was found that apparent exchange equilibrium was approached after 48 hours. Experiments with one week of immersion showed considerable scatter of results.

2. Active Metal – Inactive Solution

When the metal was immersed in acidulated water at pH 4.8, continuous dissolution was observed. No continuous increase in activity took place at pH 5.2 and 6.2; the aliquots taken had an activity slightly higher than the background. The same happened when a sample was pretreated for 24 hours in 10^{-2} *M* $Zn(NO_3)_2$ solution. When the exchange was done for 1 to 6 seconds, wide scattering was obtained giving unreliable results.

During the last set of experiments, when the exchange time was 1 to 6 minutes, it was found that a rapid exchange takes place: in 6 minutes, 20 apparent layers of atoms took part in the exchange. The samples were etched before each immersion. The curve presented in Fig. 5 was obtained when the samples were etched only at the beginning. No difference was observed between tests at pH 5.2 and tests at pH 6.2.

3. Bicrystal Experiments

The autoradiographs of three bicrystal samples shown in Fig. 6 showed a preferential exchange in one of their crystal faces. At the same time it was observed that the difference in activity acquired by each crystal soon disappeared and that after 30 seconds an even distribution of activity was obtained. (Figure 6*a* corresponds to 10-second, 6*b* to 20-second, and 6*c* to 30-second immersion.)

Preferential exchange was shown also by a bicrystal that was markedly twinned (Fig. 7). A sample pretreated for 24 hours and half-etched showed much higher activity in the oxide layer than in the etched layer, but in this latter area a clear difference could be seen in comparing the exchange between each grain (Fig. 8). Other autoradiographs showed that there is a difference in activity between worked and unworked areas, as had been reported for silver and other metals (9).

Can. J. Chem. Downloaded from www.nrcresearchpress.com by 210.87.254.42 on 09/05/12
For personal use only.

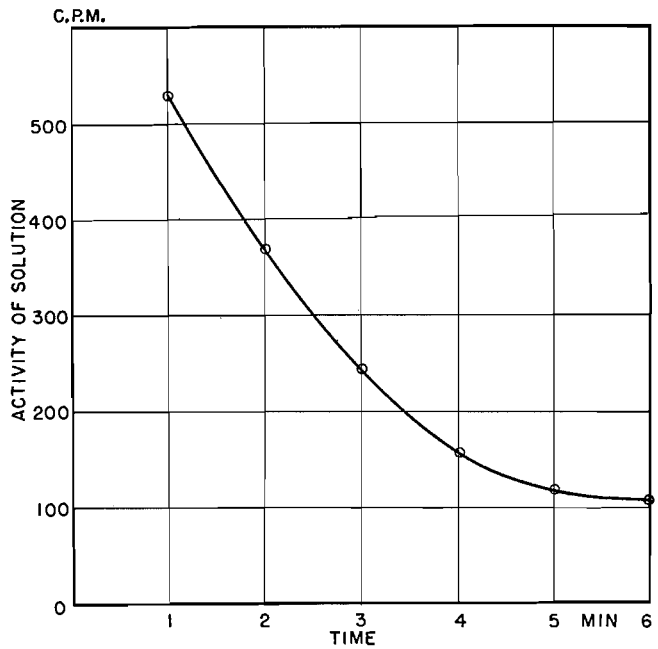


FIG. 5. Exchange between active metal and inactive $Zn(NO_3)_2$ solution.

DISCUSSION AND CONCLUSIONS

Heterogeneous exchange between atoms from a work-free zinc surface and atoms from a zinc solution was observed under conditions that minimized adsorption, corrosion, and oxidation. It could not be fully ascertained that an oxide-free surface was obtained, even if the immersion followed immediately after the etching or if the work was done under argon. (The etchants used are generally oxidizing agents.) It was observed that hydroxide formation took place even in the absence of O_2.

According to the definition of an exchange reaction (12), for a given system the rate of the reaction is independent of the nature of the compound tagged by the indicator; so, if $A^* \xrightarrow{k_1} B$ and $B^* \xrightarrow{k_2} A$; then $k_1 = k_2$. The results of these experiments show that an exchange takes place with deaerated 10^{-1} or 10^{-2} M $Zn(NO_3)_2$ solution at pH 5.2 or 6.2 in both directions. It could not be proved that $k_1 = k_2$, because in these experiments the rate of transfer of active zinc of one phase to the other is measured and not the exchange rate alone.

It has also been seen that the results of the $Zn^*_{sol} \rightarrow Zn_{metal}$ reactions do not fit a simple equation of the form $-\log(1-F) = kt$, because the reaction is controlled by either a recrystallization or a self-diffusion process. It would fit an exponential function of two terms, as Matsura (5) found, of the general form:

$$[2] \qquad F = 1-[A_r \exp(-k_r t)+A_s \exp(-k_s t)],$$

where F = fraction exchanged, A_r, A_s, k_r, k_s = constants.

It is concluded, from the experimental results available so far, that the exchange of zinc cannot be presented simply as a diffusion process or a recrystallization-controlled process, in spite of the fact that fast exchange has been obtained in the $Zn^*_{metal} \rightarrow Zn_{sol}$ reaction. More information is needed about the adsorption properties of zinc ions on

Can. J. Chem. Downloaded from www.nrcresearchpress.com by 210.87.254.42 on 09/05/12
For personal use only.

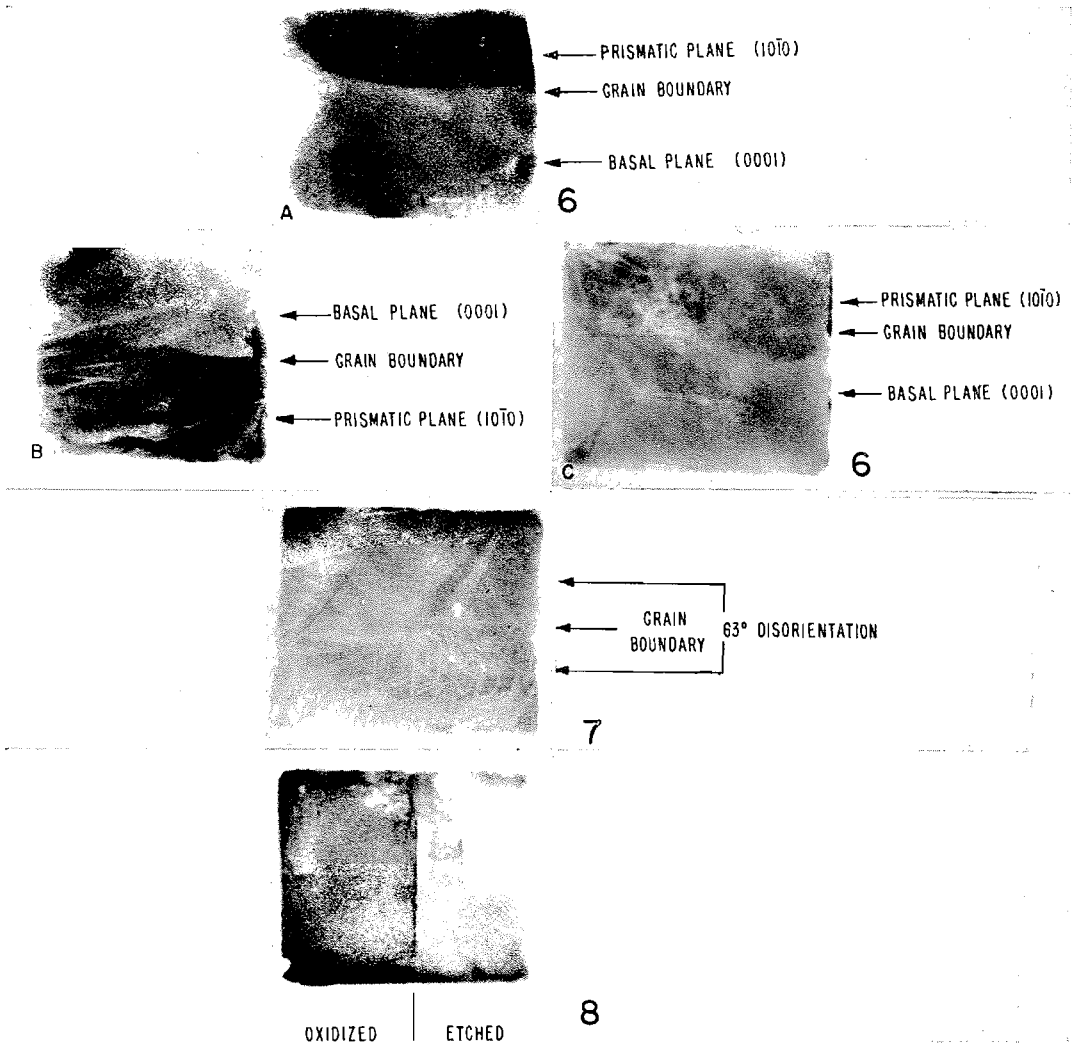


FIG. 6. Autoradiographs of zinc bicrystals.
FIG. 7. Autoradiograph of twinned zinc bicrystal.
FIG. 8. Autoradiograph of a preferentially oxidized zinc bicrystal.

Can. J. Chem. Downloaded from www.nrcresearchpress.com by 210.87.254.42 on 09/05/12
For personal use only.

zinc metal. Some work has been done by Matsura with zinc dust, but he did not take into consideration either the surface oxidation or the preparation of the samples.

In the present work a deep exchange has been found between the active metal and the inactive solution in a relatively short period of time. The same effect has been found in silver (13) and it has been explained as caused by a disordered layer of atoms close to the surface giving rise to a very fast diffusion process near the surface of the solid. The surface reaction is not a simple one. In addition to exchange with surface atoms, there always takes place an exchange resulting from local cell action, as postulated by Hevesy (1). It is the author's suggestion that the rapid exchange noticed at the beginning of the experiments is due mainly to this type of mechanism, i.e., one crystal face behaves as an anodic area and the other as a cathodic.

It has been known for some time that the different crystallographic faces of a metal have different electrochemical and physical properties, and hence different electrode potentials, dissolution and oxidation rates, and adsorption. Preferential adsorption may take place, but is relatively unimportant here, since the solutions were very dilute and the immersion periods were very short.

The experiment performed with a half-oxidized and half-etched sample showed that the oxide layer picked up much more activity than did the etched one. This would indicate that the preferential exchange could be caused by preferential oxidation (possibly by the same electrochemical corrosion mechanism as mentioned before). The fact that the activities were soon evened out in the samples indicated that a very small "exchange current" flowed between the two "electrodes". In support of this idea, the recent work of Bushmanov and Vozdvizhenky (7) shows that different crystal faces of zinc single crystals that are connected together act as a galvanocouple. They also found that the different faces exchange at different rates. Alternatively the difference in exchange and adsorption can be ascribed to the difference in surface free energy associated with the different atom densities along the lattice planes involved.

It should be pointed out that in the carrier-free solutions the concentration of the tracer is so low that the products formed may not be the same as those formed at ordinary concentrations, because of rate effects, equilibrium shifts, etc. In some respects this is an advantage, because with so low a concentration no spurious precipitations can happen, since the solubility product cannot be exceeded.

While there is strong evidence that an exchange reaction is involved as a first step in the pickup of activity, this reaction is likely accompanied by other processes, e.g. corrosion and oxidation.

There are considerable variations in the exchange processes described in the literature, mainly because of difficulties in obtaining reproducible, clean metallic surfaces that correspond in composition and structure to the bulk of the metal. It is believed that the surfaces used in this work were of a cleanness comparable with or better than those used in published experiments, but the difference in surface conditions obtained make direct comparisons of results difficult. Even in the case where an oxide-free surface is obtained it is always covered by a thin layer of gases and vapors. Holm and Meissner (14) in their work on platinum had to heat platinum wires for hours at 1100° C in a perpetually evacuated glass vessel, the walls of which were cooled with liquid hydrogen, to obtain a thoroughly degassed surface.

Another problem that has to be solved is to obtain an exact knowledge of the "true" area of the sample, as compared with the geometric area, because in exchange experiments the results are generally expressed in "number of exchanged atom layers". Several methods

Can. J. Chem. Downloaded from www.nrcresearchpress.com by 210.87.254.42 on 09/05/12
For personal use only.

are available to determine the surface roughness of metals and some general information is available about the average height of the "hills" and "valleys" in a metallic surface (15); this magnitude is of the following order:

in steel, lapped or polished	—	2 to 25×10^{-6} cm,
die-cast	—	40 to 400×10^{-6} cm,
ground	—	50 to 250×10^{-6} cm,
turned, shaped	—	300 to 600×10^{-6} cm.

There are no similar figures for zinc, but since it is a very soft metal and flows very easily during the polishing operations, comparable figures may differ from those for steel by as much as a factor of 10.

The results can be summarized as follows:

1. The zinc exchange reaction takes place with work-free surfaces in deaerated 10^{-1} and 10^{-2} M $Zn(NO_3)_2$ solutions at pH 5.2. to 6.2 and it takes place in both directions.

2. The reaction $Zn^{++}{}_{sol} \rightarrow Zn^{0}{}_{metal}$ can be described by a relation of the form

$$F = 1-[A_r \exp(-k_r t)+A_s \exp(-k_s t)],$$

rather than by a single exponential function.

3. Fast exchange has been found in the reaction $Zn^{0}{}_{metal} \rightarrow Zn^{++}{}_{sol}$, indicating that adsorption was low compared with exchange under the conditions of the experiments.

4. ZnO and $Zn(OH)_2$ are formed in the metallic samples, preventing the exchange from continuing. $Zn(OH)_2$ is formed even in the absence of air.

5. Preferential exchange on certain crystal faces has been found to take place in zinc bicrystals.

6. It is suggested that the deep-exchange mechanism involved in the short periods is a local cell action, one crystal behaving as an anode and the other as a cathode.

ACKNOWLEDGMENTS

The author wishes to express his appreciation to Dr. G. G. Eichholz for his help during all this work, to Dr. F. Weinberg and Mr. I. I. Tingley for many helpful discussions, to J. R. Barkley for some experimental help, and to many members of the Physics and Radiotracer Section of the Mineral Sciences Division, Mines Branch, for their advice and assistance. This work was done during the tenure of a National Research Council of Canada postdoctorate fellowship at the Mines Branch of the Department of Mines and Technical Surveys, Ottawa. This paper is published by permission of the Director of the Mines Branch, Department of Mines and Technical Surveys.

REFERENCES

1. G. v. Hevesy. Physik. Z. **16**, 52 (1915).
2. B. V. Rollin. J. Am. Chem. Soc. **62**, 86 (1940).
3. A. M. Gaudin and K. Vincent. Trans. Am. Inst. Mining Met. Engrs. **169**, 340 (1946).
4. C. Haenney and P. Mivelaz. Helv. Chim. Acta, **31**, 633 (1948).
5. Niro Matsura. Sci. Papers Coll. Gen. Educ., Univ. Tokyo, **5**, 97 (1955).
6. C. V. King and S. Evans. J. Phys. Chem. **63**, 1816 (1959).
7. B. N. Bushmanov and G. S. Vozdvizhenky. Doklady Akad. Nauk S.S.S.R. **114**, 1046 (1957).
8. G. L. Kehl. The principles of metallographic laboratory practice. McGraw-Hill Book Company, New York. 1943.
9. I. I. Tingley, I. H. S. Henderson, and C. C. Coffin. Can. J. Chem. **34**, 14 (1956).
10. F. Weinberg. Private communication. Mines Branch, Ottawa. 1959.
11. H. MacKay. Nature, **142**, 997 (1938).
12. M. Haissinsky. J. chim. phys. **47**, 957 (1950).
13. J. E. Sandor. Exchange reactions between silver and its ions. Mines Branch Research Report R 62. Department of Mines and Technical Surveys, Ottawa. 1960.
14. R. Holm and W. Meissner. Z. Physik, **74**, 715 (1932).
15. J. J. Bikerman. Surface chemistry. Academic Press, New York. 1958.

Can. J. Chem. Downloaded from www.nrcresearchpress.com by 210.87.254.42 on 09/05/12
For personal use only.

Can. J. Chem. Downloaded from www.nrcresearchpress.com by 210.87.254.42 on 09/05/12
For personal use only.

PROTONATION OF THE AMIDE GROUP

II. DICYCLOHEXYLUREA-O^{18} [1]

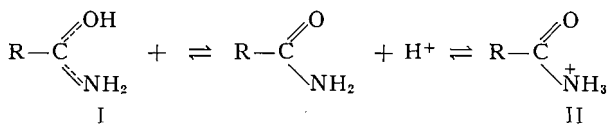
ROSS STEWART AND L. J. MUENSTER

ABSTRACT

Dicyclohexylurea-O^{18} containing 78% oxygen-18 has been prepared. The amide I and II bands in this molecule are located at 1611 and 1575 cm^{-1} respectively compared to 1628 and 1575 cm^{-1} in ordinary dicyclohexylurea (KBr disk). Thus the amide I band (carbonyl stretching) undergoes the expected shift to lower frequency on isotopic substitution. The *p*-toluenesulphonate salt of dicyclohexylurea has been prepared and been found to have a band at 1669 cm^{-1} commonly attributed to carbonyl stretching in amide salts. This band, however, undergoes no isotopic shift and is clearly not due to a carbonyl stretching motion. This result casts doubt on the infrared evidence supporting N-protonation of amides.

INTRODUCTION

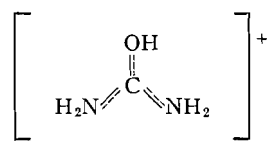
In the previous paper in this series the evidence both for N-protonation and for O-protonation of amides was reviewed (1). In that paper we reported the basicity of a series of benzamides and pointed out that this evidence lent some support to the charge-localized structure II (N-protonated form) for the amide conjugate acid rather than the resonance-stabilized structure I (O-protonated form).



I II

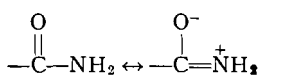
This situation is in contrast to that of the carboxyl group where the resonance-stabilized form appears almost certainly to be the more stable (2).

The principal evidence favoring O-protonation is provided by N.M.R. spectroscopy (2*a*, 2*b*). The principal evidence favoring N-protonation is provided by infrared spectroscopy, viz., the observed shift of the carbonyl stretching band to higher frequencies when amides are converted to their salts (3, 4, 5, 6). Thus the carbonyl stretching frequency in propionamide at 1660 cm^{-1} is replaced by a band at 1710 cm^{-1} in the hydrobromide (6). Urea, more than ordinary amides, would be expected to undergo O-protonation because of the very favorable resonance possibilities in the conjugate acid, III. Urea salts, however, in particular the well-known urea nitrate, are reported to



III

have infrared spectra which include a carbonyl stretching band (3, 4). This band is at higher frequency in agreement with the idea that N-protonation would produce more double bond character in the carbonyl group by eliminating resonance of the following type.



[1]*Manuscript received October 6, 1960.*
Contribution from the Department of Chemistry, University of British Columbia, Vancouver, B.C.

Can. J. Chem. Downloaded from www.nrcresearchpress.com by 210.87.254.42 on 09/05/12
For personal use only.

This evidence in favor of N-protonation is difficult to controvert if it can be proved that the bands in question are, in fact, due to carbonyl stretching motions. The purpose of this research was to check the identity of this band in an amide salt by the use of oxygen-18. Halmann and Pinchas have studied the infrared spectra of benzophenone labelled with oxygen-18 (76%) in the carbonyl group (7). They found the only significant difference in the spectra of benzophenone and benzophenone-O^{18} was in the carbonyl stretching region; benzophenone absorbs at 1664 cm^{-1}, benzophenone-O^{18} at 1635 cm^{-1} in carbon tetrachloride. This shift of 29 cm^{-1} to shorter frequency on isotopic substitution is similar to that observed by Braude and Turner (8) for the shift (30 cm^{-1}) of the carbonyl band in cinnamyl *p*-nitrobenzoate on isotopic substitution. More recently Pinchas, Samuel, and Weiss-Broday have prepared benzamide-O^{18} and have made a thorough study of its infrared spectrum (9). They found that the carbonyl band, amide I, shifts by 24 cm^{-1} (in carbon tetrachloride), the N—H bonding, amide II, by 10 cm^{-1} (in chloroform).

We attempted to prepare urea labelled in the carbonyl group but had little success with controlled hydration of cyanamide using stoichiometric amounts of water. We have turned therefore, to dicyclohexylurea, which can be readily prepared by the hydration of dicyclohexylcarbodiimide. This proved to be a very satisfactory alternative.

Dicyclohexylurea-O^{18} was prepared from dicyclohexylcarbodiimide according to the following equations.

$$C_6H_{11}N{=}C{=}NC_6H_{11} + D_2O^{18} \rightarrow C_6H_{11}NDC(=O^{18})NDC_6H_{11} \xrightarrow{EtOH} C_6H_{11}NHC(=O^{18})NHC_6H_{11}$$

The para toluenesulphonate salt can have either structure IV or V.

$$C_6H_{11}NHC(=O)NHC_6H_{11} + C_7H_8SO_3H \rightleftharpoons \left[C_6H_{11}NH{=}C(OH){-}NHC_6H_{11}\right]^+ C_7H_8SO_3^-$$

IV

$$C_6H_{11}\overset{+}{N}H_2C(=O)NHC_6H_{11} \quad C_7H_8SO_3^-$$

V

EXPERIMENTAL

Apparatus and Reagents

Infrared spectra were recorded with a Perkin–Elmer Model 21 instrument equipped with sodium chloride optics using potassium bromide pellets. Since it is known that the latter can sometimes give spurious results (10) the spectra of dicyclohexylurea-O^{16} and -O^{18} and their *p*-toluenesulphonate salts were also recorded in Nujol mulls. The spectra were virtually identical in the two media. The mass spectrometric work was done on a Metropolitan-Vickers mass spectrometer, type 45/1.

The D_2O^{18} (91% O^{18}, 1.1% O^{17}) was obtained from The Weizmann Institute of Science, Israel.

N,N'-Dicyclohexylurea-O^{18}

To 15 ml of dioxane (purified and dried with sodium metal) contained in a 50-ml beaker was added 2.34 g (0.0114 mole) of dicyclohexylcarbodiimide. The beaker was placed in an ice-water bath and 0.25 g (0.0114 mole) of D_2O^{18} was pipetted into the solution. Dry hydrochloric acid gas was bubbled through the mixture via a capillary

for $1\frac{1}{2}$ minutes. The resulting white precipitate was filtered at the pump, washed with a little dioxane, and dried in a vacuum desiccator. The crude product weighed 1.66 g or 64% of the theoretical yield.

To obtain a deuterium-free sample, 300 mg of the crude product was dissolved in 5 ml of boiling absolute ethanol. On cooling of the solution to room temperature, colorless, broad needles separated out which melted at 237–238° (uncorr.).

The percentage of O^{18} contained in the compound was determined according to the method by Rittenberg and Ponticorvo (11). The oxygen-18 content of the carbon dioxide was measured by scanning the masses from 44 to 48. The average value obtained from five determinations was 78.3% O^{18}, though the precision was rather low (standard deviation of the mean: ±2.3%).

N,N'-Dicyclohexylurea-O^{18} p-Toluenesulphonate

N,N'-Dicyclohexylurea-O^{18} (0.50 g, 0.0021 mole) and *p*-toluenesulphonic acid (0.38 g, 0.0021 mole) were added to 2 ml of dry dioxane and refluxed for 10 minutes. On cooling to room temperature colorless, small needles separated out. After several recrystallizations from thiophene-free dry benzene 0.33 g (39% of the theory) of the *p*-toluenesulphonate was obtained which melted at 154–155° (corr.). Calc. for $C_{20}H_{32}N_2SO_3O^{18}$: C, 60.24; H, 8.10; N, 7.03; O, 16.56; S, 8.04. Found: C, 60.33; H, 8.02; N, 6.91; O, 16.23; S, 8.02.

When this salt was crystallized from absolute ethanol it reverted to dicyclohexylurea with no loss of isotopic oxygen. This was shown to be so by a comparison of infrared spectra.

Urea p-Toluenesulphonate

Urea (3.0 g, 0.05 mole), *p*-toluenesulphonic acid (10.7 g, 0.06 mole), and 100 ml of dry dioxane were heated to boiling. The voluminous white precipitate which formed was filtered and washed with ice-cold water and ether. After one recrystallization from water the yield was 8.9 g (77%). During three subsequent recrystallizations from water the melting point remained constant at 181–183° (corr.). Calc. for $C_8H_{12}N_2O_4S$: C, 41.37; H, 5.21; N, 12.05; S, 13.80%. Found: C, 41.36; H, 5.14; N, 12.02; S, 13.61%.

The melting point of this compound is near that reported for the covalent compound, *p*-toluenesulphonylurea (m.p., 191–2° (12)) and its resistance to hydrolysis during crystallization from water is also compatible with the latter structure. The analytical data together with the following facts show the compound to be the salt: (*a*) titration with standard base gives the correct neutral equivalent, (*b*) passage of a solution of the compound through a strongly acid cation-exchange column (Nalco HCR-W) produces *p*-toluenesulphuric acid.

RESULTS AND DISCUSSION

The infrared spectra of dicyclohexylurea, dicyclohexylurea-*d*-O^{18}, and dicyclohexylurea-O^{18} are shown in Fig. 1. The spectra of the *p*-toluenesulphonates of dicyclohexylurea and dicyclohexylurea-O^{18} are shown in Fig. 2.

Dicyclohexylurea

The infrared spectrum of this compound (Fig. 1) is similar to those of other substituted ureas and to that of urea itself (13, 14, 15, 16). The amide I band (carbonyl stretching) is at 1628 cm^{-1} and the amide II band (17, 18) is at 1575 cm^{-1}. In addition a third band is present in dicyclohexylurea at 1539 cm^{-1} which is also present (1550 cm^{-1}) in monocyclohexylurea (14). The "amide band" locations are listed in Table I.

Can. J. Chem. Downloaded from www.nrcresearchpress.com by 210.87.254.42 on 09/05/12
For personal use only.

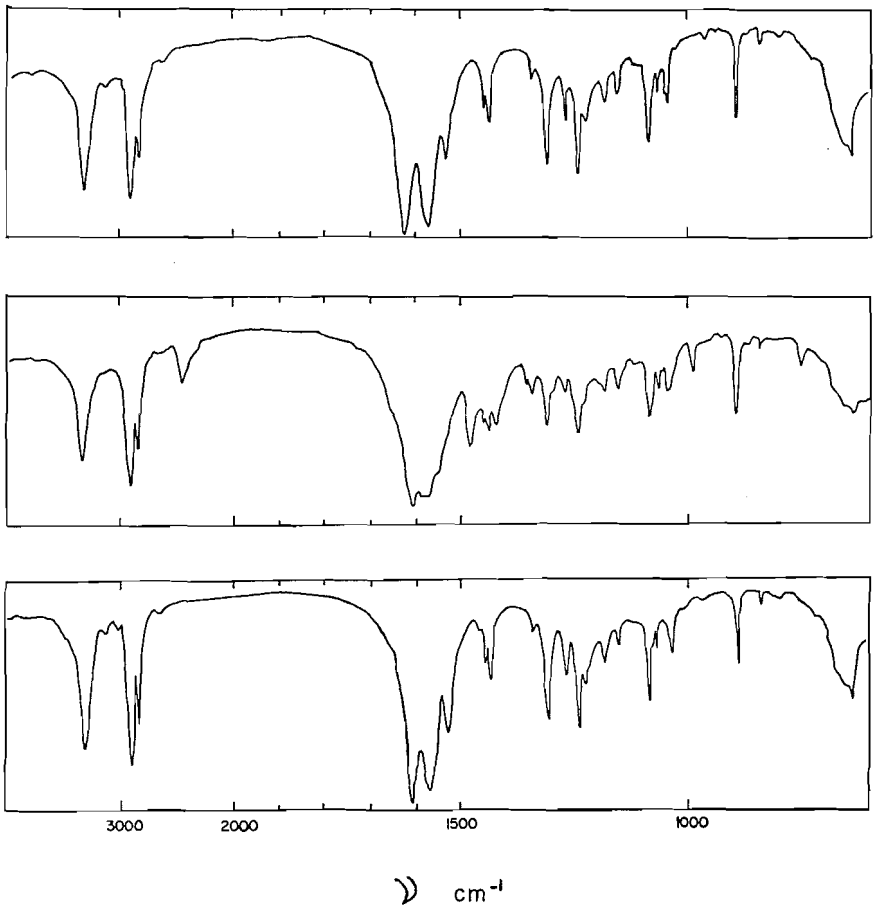


FIG. 1. The infrared spectra of dicyclohexylurea (upper), dicyclohexylurea-*d*-O^{18} (middle), and dicyclohexylurea-O^{18} (lower).

TABLE I

"Amide bands",* cm^{-1}

	I	II	(†)
Dicyclohexylurea	1628	1575	1539
Dicyclohexylurea-O^{18}	1611		
Dicyclohexylurea-O^{18}	1611	1575	1533
Dicyclohexylurea *p*-toluenesulphonate	1669	1620	
Dicyclohexylurea-O^{18} *p*-toluenesulphonate	1668	1618	

*The first two bands in both the amides and amide salts are designated here as amide I and II bands.
†*The third band in this region.*

Dicyclohexylurea-d-O^{18}

The percentage deuterium in this compound is unknown. However, the considerably greater intensity of the N—H stretching band at 3343 cm^{-1} than the N—D stretching band at about 2480 cm^{-1} indicates that there is probably more protium than deuterium present. The amide II band at 1575 cm^{-1} is broadened and five new peaks at 2480, 1480, 1425, 988, and 795 cm^{-1} appear in the spectrum of the partly deuterated compound.

Can. J. Chem. Downloaded from www.nrcresearchpress.com by 210.87.254.42 on 09/05/12
For personal use only.

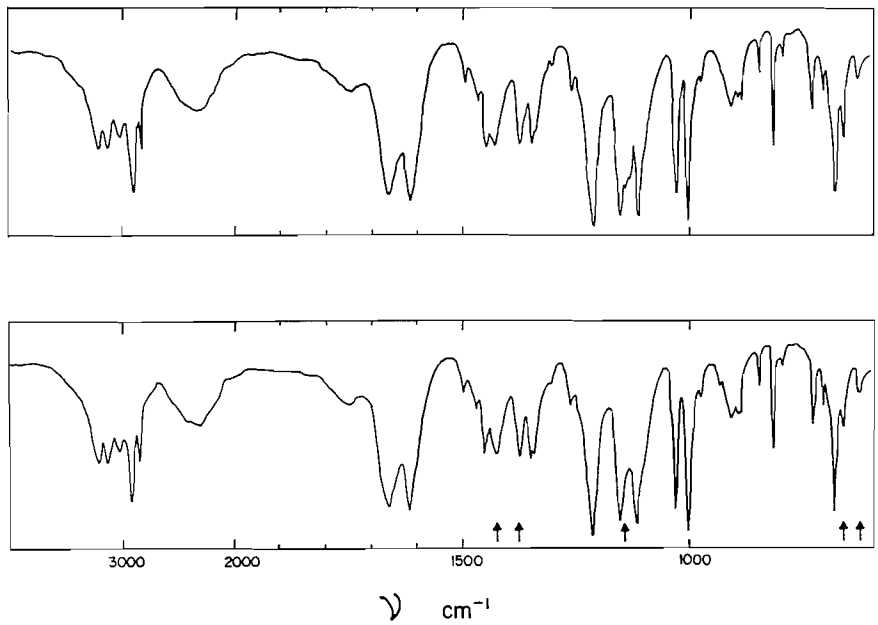


FIG. 2. The infrared spectra of dicyclohexylurea *p*-toluenesulphonate (upper) and dicyclohexylurea-O^{18} *p*-toluenesulphonate (lower).

Dicyclohexylurea-O^{18}

The principal feature of interest in this system is the shift of the amide I band on isotopic substitution. This band, which is generally attributed to carbonyl stretching, shows the isotopic shift to lower frequency expected for such a band. The shift of 17 cm^{-1} (1628 to 1611 cm^{-1} in KBr) is smaller than the corresponding shift observed for benzophenone (29 cm^{-1} in CCl_4) (7), and for benzamide (24 cm^{-1} in CCl_4) (9). (The magnitude of the isotopic shift appears to depend on the medium since Pinchas *et al.* (9) observed that it was considerably less in chloroform than in carbon tetrachloride.) The smaller shift in the present case may be due to a contribution from the C—N stretching vibration to the amide I band as suggested by Myazawa *et al.* (18). (See, however, ref. 9.)

The amide II band at 1575 cm^{-1} undergoes no isotopic shift at all. The third band in this region, the one at 1539 cm^{-1} in ordinary dicyclohexylurea undergoes a small isotopic shift and appears at 1533 cm^{-1} in the oxygen-18 compound. Table II lists the bands in the amide which undergo oxygen isotopic shifts of 3 cm^{-1} or more.

TABLE II

Isotopic shifts,* cm^{-1}

Dicyclohexylurea	1628	1539	1160	1047	643
Dicyclohexylurea-O^{18}	1611	1532	1157	1038	640
Dicyclohexylurea *p*-toluenesulphonate	1437	1378	1135	666	635
Dicyclohexylurea-O^{18} *p*-toluenesulphonate	1427	1375	1129	661	629

*3 cm^{-1} or more.

Dicyclohexylurea p-Toluenesulphonate

Above 1600 cm^{-1} the spectrum of this compound resembles that of urea nitrate. The N—H stretching bands are broadened and shifted to lower frequency in both compounds

Can. J. Chem. Downloaded from www.nrcresearchpress.com by 210.87.254.42 on 09/05/12
For personal use only.

resulting in a set of moderately sharp bands above 3000 cm^{-1} and a very broad absorption in the 2400–2600 cm^{-1} region. These changes in the N—H absorption and the absence of an O—H stretching band contributed to the rejection by Davies and Hopkins (3) and Spinner (4) of the idea of O-protonation in urea nitrate.

In the carbonyl stretching region between 1600 and 1700 cm^{-1} there are two bands in both urea nitrate and dicyclohexylurea *p*-toluenesulphonate. These are located at 1705 and 1675 cm^{-1} in the former (Davies and Hopkins (3) report 1708 and 1670 cm^{-1}) and at 1669 and 1620 cm^{-1} in the latter. The 1670 band in urea nitrate has been assigned by Davies and Hopkins to carbonyl absorption and the shift from 1610 cm^{-1} in urea attributed to the increase in carbonyl bond order as a result of N-protonation (3). Other investigators have assigned carbonyl stretching in urea to the band in the 1680 cm^{-1} region (15, 16). If one of these bands in the spectrum of the salt of dicyclohexylurea is in fact due to carbonyl stretching an isotopic shift should be observed in the oxygen-18 compound.

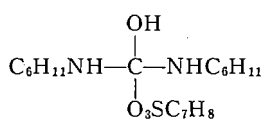
Dicyclohexylurea-O^{18} p-Toluenesulphonate

Figure 2 shows the spectrum of this compound and Table II lists those peaks which undergo an isotopic shift of 3 cm^{-1} or more. The largest of these is the shift of the 1437 peak which moves 10 cm^{-1} to lower frequency. Particularly significant is the fact that the peak at 1669 cm^{-1} is in virtually the same place in the oxygen-18 compound. An average of several runs gave the peak locations as 1669 and 1668 cm^{-1} in the isotopically unsubstituted and substituted compounds respectively. One can therefore conclude that this band in dicyclohexylurea *p*-toluenesulphonate is not, in fact, caused by a carbonyl stretching motion and its location at higher frequency than the amide I band in dicyclohexylurea *does not* constitute support for the idea of N-protonation of amides.

The infrared evidence, in fact, supports the idea of O-protonation of urea-type compounds. (It is true that an O—H stretching band cannot be detected in the infrared (14) but this band may be shifted and masked by the broad N—H absorption. Furthermore, hydrogen stretching bands are sometimes of very low intensity in organic cations (19).) The isotopic shift in dicyclohexylurea *p*-toluenesulphonate (Table II) from 1437 cm^{-1} to 1427 cm^{-1} probably corresponds to O—H bending (20) and the isotopic shift from 1135 cm^{-1} to 1129 cm^{-1} can also be explained on the basis of O-protonation since C—OH stretching vibrations are usually found in this region. The first band in the carbonyl region of the urea and dicyclohexylurea *p*-toluenesulphonates may be due to N—H bending increased in frequency by strong inner hydrogen bonding with the tosylate oxygen atoms. (We are grateful to Dr. S. Pinchas for drawing our attention to some of these points.)

Ionic Character

We have considered the possibility that the *p*-toluenesulphonate of dicyclohexylurea might be a covalent compound of some such structure as the following.



Although this is unlikely in view of the high stability of the *p*-toluenesulphonate ion we attempted to prepare other salts of this compound. Our attempts to prepare the perchlorate, hydrochloride, and nitrate were unsuccessful, however.

Can. J. Chem. Downloaded from www.nrcresearchpress.com by 210.87.254.42 on 09/05/12
For personal use only.

We turned then to a comparison of the infrared spectra of other *p*-toluenesulphonates, both covalent and ionic, with that of the compound in question. Table III lists the

TABLE III

p-Toluenesulphonate infrared bands below 1200 cm^{-1}

Dicyclohexylurea compound (cm^{-1})	Sodium salt (cm^{-1})	Potassium salt (cm^{-1})	Ammonium salt (cm^{-1})	Methyl ester (cm^{-1})	Urea compound (cm^{-1})
1218	1222				1201
	1188	1185–1205	1155–1200	1190	
1156	1179			1179	1153
1118	1130	1127	1127		1129
				1095	
1031	1045	1038	1036		1038
1007	1014	1013	1011	1020	1013
				990	
888					871
849	854	846	845		
					818
817	816	813	815	817	814
				765	
730					
710	711	709	708	705	710
683	688	687	686	687	690
	678				
				662	

principal absorption bands below 1200 cm^{-1} of the following *p*-toluenesulphonates:

(*a*) the dicyclohexylurea compound,
(*b*) the sodium, potassium, and ammonium salts (ionic),
(*c*) the methyl ester (covalent).

A comparison of the absorption bands shows a very close correspondence between the bands in the ionic sulphonates (except for the band at 1156 cm^{-1}) and those in the dicyclohexylurea compound whereas the bands in the covalent methyl ester are missing in the latter. We conclude that dicyclohexylurea *p*-toluenesulphonate is an ionic compound.

The similarity between dicyclohexylurea *p*-toluenesulphonate and urea nitrate can be seen by a comparison of the infrared spectra of these compounds and those of other salts of urea. We have prepared the *p*-toluenesulphonates and perchlorates of urea and it can be seen from the absorption data in Table IV that the peaks of these compounds

TABLE IV

Infrared bands in urea and its compounds in the range, 1500–2500 cm^{-1}

Urea	Urea nitrate	Urea *p*-toluenesulphonate	Urea perchlorate*
1680	1705	1709	1700
1615	1675	1670	1650
	1570	1564	1558

*Hygroscopic, poor spectrum.

in the carbonyl stretching region correspond closely to those of the well-studied salt, urea nitrate, indicating that the character (presumably ionic) of these two compounds is the same. If one then examines the spectrum of one of these, urea *p*-toluenesulphonate,

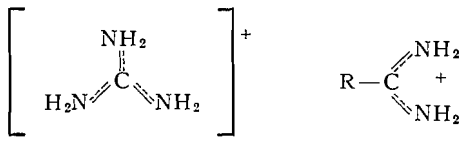
Can. J. Chem. Downloaded from www.nrcresearchpress.com by 210.87.254.42 on 09/05/12
For personal use only.

in the region below 1250 cm^{-1} where the tosylate group absorption occurs, one can see (Table III) that the peaks correspond fairly closely to those of dicyclohexylurea *p*-toluenesulphonate and sodium, potassium, and ammonium *p*-toluenesulphonates.

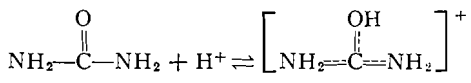
Thus both urea nitrate and dicyclohexylurea *p*-toluenesulphonate appear to be ionic compounds. Both show an amide I band at higher frequency than in the neutral compounds. This evidence does not support N-protonation, however, since this band, at least in the one case, does not correspond to carbonyl stretching. One cannot, of course, conclude that the band assigned to carbonyl stretching in the salts of ordinary amides is misassigned but the present work shows that caution should be used in making the assignment. We intend to conduct a similar investigation to the present one using ordinary amides.

Amidine Protonation

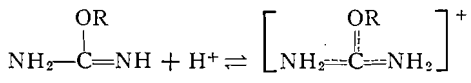
It should be made clear that the uncertainty with regard to the structure of the amide cation does not apply to the guanidinium ion, or amidinium ions in general, where the following resonance-stabilized structures are unquestionably the stable ones.



It seems clear, however, that the high basicity of amidines is due as much to decreased resonance in the neutral molecules (compared to urea and ordinary amides) as it is to increased resonance in the ions. Indeed, the fact that O-alkyl ureas are about 10^{10} times as basic as urea (21, 22) must be attributed almost entirely to the difference in resonance energies of the neutral molecules VI and VIII, since it is highly improbable that ions VII and IX have very different resonance energies. (The equilibrium between N- and O-protonated forms of urea does not affect this argument.)



VI VII



VIII IX

ACKNOWLEDGMENT

We thank Dr. D. C. Frost for the mass spectrometric analysis and the National Research Council for its financial support. The helpful comments of Drs. S. Pinchas and D. Samuels are gratefully acknowledged.

REFERENCES

1. J. T. EDWARD, H. S. CHANG, K. YATES, and R. STEWART. Can. J. Chem. **38**, 1518 (1960).
2. R. STEWART and K. YATES. J. Am. Chem. Soc. **82**, 4059 (1960).
2*a*. A. BERGER, A. LOEWENSTEIN, and S. MEIBOOM. J. Am. Chem. Soc. **81**, 62 (1959).

Can. J. Chem. Downloaded from www.nrcresearchpress.com by 210.87.254.42 on 09/05/12
For personal use only.

2*b*. G. FRAENKEL and C. FRANCONI. J. Am. Chem. Soc. **82**, 4478 (1960).
3. M. DAVIES and L. HOPKINS. Trans. Faraday Soc. **53**, 1563 (1957).
4. E. SPINNER. Spectrochim. Acta, **2**, 95 (1959).
5. E. H. WHITE. J. Am. Chem. Soc. **77**, 6215 (1955).
6. K. YATES. Ph.D. Thesis. University of British Columbia, Vancouver, B.C. 1959.
7. M. HALMANN and S. PINCHAS. J. Chem. Soc. 1703 (1958).
8. E. A. BRAUDE and D. W. TURNER. Chem. & Ind. (London), 1223 (1955).
9. S. PINCHAS, D. SAMUEL, and M. WEISS-BRODAY. Personal communication.
10. C. C. WATSON. Chem. & Ind. (London), 964 (1960) and references therein.
11. D. RITTENBERG and L. PONTICORVO. Intern. J. Appl. Radiation and Isotopes, **1**, 208 (1956).
12. F. KURZEN and J. R. POWELL. J. Chem. Soc. 1497 (1955).
13. P. A. BOIVIN, W. BRIDGEO, and J. L. BOIVIN. Can. J. Chem. **32**, 242 (1954).
14. J. L. BOIVIN and P. A. BOIVIN. Can. J. Chem. **32**, 561 (1954).
15. J. E. STEWART. J. Chem. Phys. **26**, 248 (1957).
16. R. B. PENLAND, S. MIZUSHIMA, C. CURRAN, and J. V. QUAGLIANO. J. Am. Chem. Soc. **79**, 1575 (1957).
17. R. N. JONES and C. SANDORFY. *In* Technique of organic chemistry. Vol. IX. *Edited by* A. Weissberger. Interscience Publishers, New York. 1956. p. 521.
18. T. MIYAZAWA, T. SHIMANOUCHI, and S. MIZUSHIMA. J. Chem. Phys. **24**, 408 (1956).
19. R. STEWART, M. MOCEK, and R. B. MOODIE. To be published.
20. R. N. JONES and C. SANDORFY. *In* Technique of organic chemistry. Vol. IX. *Edited by* A. Weissberger. Interscience Publishers, New York. 1956. pp. 431–434.
21. M. ZIEF and J. T. EDSALL. J. Am. Chem. Soc. **59**, 2245 (1937).
22. C. R. NOLLER. Chemistry of organic compounds. 2nd ed. W. B. Saunders Co., Philadelphia. 1957. p. 319.

Can. J. Chem. Downloaded from www.nrcresearchpress.com by 210.87.254.42 on 09/05/12
For personal use only.

Can. J. Chem. Downloaded from www.nrcresearchpress.com by 210.87.254.105 on 09/05/12
For personal use only.

STEROIDS

V. PYRIDINIUM BETAINES OF 2-α-BROMOCHOLESTAN-3-ONE[1,2]

G. FRANGATOS[3] AND A. TAURINS

ABSTRACT

2-α-Bromocholestan-3-one reacts with pyridine, and 3- and 4-methylpyridines to give the 1-[2-(3-oxocholestanyl)]pyridinium bromides which, on dehydrobromination with bases, form the betaines of 1-[2-(3-oxocholestanyl)]pyridinium hydroxides.

DISCUSSION

The treatment of α-bromo ketones with pyridine and its homologues leads to the elimination of hydrogen bromide from the α-bromo ketone and to the formation of a double bond in α,β-position to the carbonyl group. On several occasions it has been observed that intermediate adducts are formed in the reaction of steroidal α-bromo ketones and pyridine bases. In some instances differences in opinion exist regarding the structure of the intermediates. Thus two entirely different structural formulae II and III have been proposed by Ruzicka (1), and Inhoffen (2), respectively, for the product of the reaction between 2-α-bromocholestan-3-one (I) (3) and pyridine.

In an attempt to establish which of the structures was correct, the present work was undertaken. If the formula set forth by Ruzicka is correct, then elimination of a molecule of hydrogen bromide from II (a pyridinium bromide) should result in the formation of a pyridinium enol betaine (IV) (4,5). Elimination of hydrogen bromide from III (a hydrobromide of a 4-substituted pyridine), on the other hand, should produce a 4-substituted pyridine base. With this in mind, hydrogen bromide was eliminated from the reaction product of pyridine and 2-α-bromocholestan-3-one (I), and isolation of the reaction product attempted. When a solution of the product in chloroform was treated with solid anhydrous potassium carbonate, a deep-red oil was isolated which resisted all attempts of crystallization and exhibited a pronounced tendency to form thin films. It was sensitive to heat and decomposed gradually on exposure to light. Elementary analysis indicated the presence of nitrogen but not of bromine. Upon treatment with hydrogen bromide, the product afforded the starting material. When an aqueous solution of perchloric acid was added to the oil, the corresponding colorless perchlorate was formed readily.

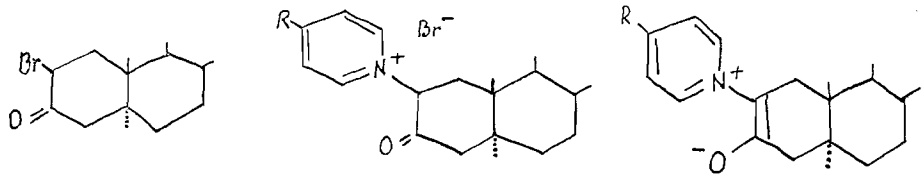
These experimental facts supported the assumption that the reaction product of pyridine and the bromo ketone (I) was the pyridinium salt (II) which formed the betaine of 1-[2-(3-hydroxy-2-cholestanyl)]pyridinium hydroxide (IV) upon elimination of a molecule of hydrogen bromide.

In other attempts to obtain the betaine (IV), the pyridinium bromide (II) was suspended in water or ethanol and treated with aqueous solutions of inorganic bases. Piperidine, morpholine, and guanidine carbonate reacted similarly, and in all cases hydrogen bromide was eliminated. However, the betaine (IV) was always obtained as an amorphous material. Finally, the betaine of 1-[2-(3-hydroxy-2-cholestanyl)] pyridinium hydroxide (IV) was obtained in crystalline form, when the dehydrobromination of the

[1]*Manuscript received October 28, 1960.*
Contribution from the Department of Chemistry, McGill University, Montreal, Quebec, with financial assistance from the National Research Council, Ottawa, Canada.
[2]*Steroids. IV. T. H. Waid and A. Taurins. Can. J. Chem. 38, 1983 (1960).*
[3]*Holder of a Canadian Industries (1954) Limited Fellowship, 1954–55, and of a National Research Council Studentship, 1955–1956.*

pyridinium bromide (II) was carried out in the three-component system ethanol – water – dimethylamine. The ultraviolet spectrum of the betaine showed three absorption maxima at 245, 304, and 430 mμ. The similarity in pattern of the spectrum of IV and of the betaines obtained from methylpyridines and 2-bromo-1,3-indandione by Frangatos and Taurins (5) provided further proof that IV was a typical pyridinium betaine.

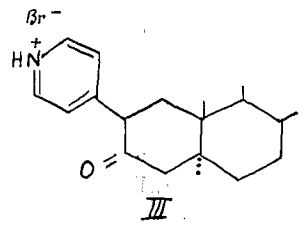
On the basis of the assumptions made by Inhoffen (2), the addition product of pyridine and 2-α-bromocholestan-3-one (I) should be a 4-substituted pyridine hydrobromide. If this is correct, then 4-methylpyridine should not react with the bromo ketone (I). It was found, however, that the reaction of 4-methylpyridine with I proceeded smoothly to give the salt, 1-[2-(3-oxocholestanyl)]4-methylpyridinium bromide (V). The dehydrobromination of V was achieved in chloroform solution using anhydrous potassium carbonate. The product, the betaine of 1-[2-(3-hydroxy-2-cholestanyl)]4-methylpyridinium hydroxide (VI), was an amorphous, dark-red solid. In sunlight, it gradually decomposed, and on



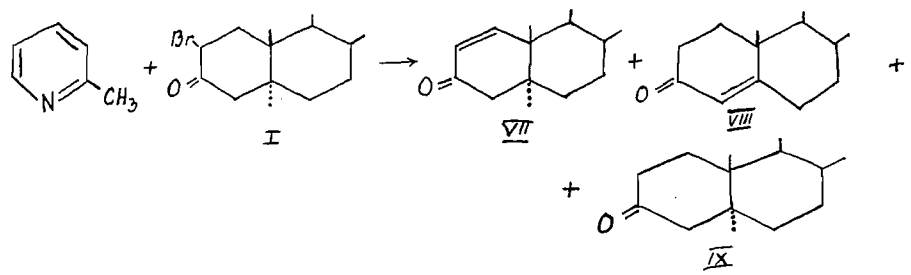
I

II : R = H
V : R = CH_3

IV : R = H
VI : R = CH_3



III



I

VII

VIII

IX

treatment with acids, colorless solids, the pyridinium salts, were formed. Elementary analysis and the ultraviolet absorption spectrum of VI were in agreement with the assignment of a betaine structure to this compound. 3-Methylpyridine reacted similarly and the betaine of 1-[2-(3-hydroxy-2-cholestanyl)]3-methylpyridinium hydroxide was obtained as a dark-red powder which could not be crystallized.

The reaction of the bromo ketone (I) with 2-methylpyridine did not afford the corresponding pyridinium bromide. Instead 2-methylpyridine hydrobromide was isolated from

Can. J. Chem. Downloaded from www.nrcresearchpress.com by 210.87.254.105 on 09/05/12
For personal use only.

the reaction mixture indicating that dehydrobromination of the bromo ketone (I) had occurred. Dehydrobromination could proceed directly or through the formation of the intermediate salt, 1-[2-(3-oxocholestanyl)]2-methylpyridinium bromide. However, by analogy with the reactions of pyridine, and 3- and 4-methylpyridines and the bromo ketone (I), the formation of the salt would seem improbable since it would interfere with the elimination of hydrogen bromide. This assumption was confirmed experimentally by taking samples from the reaction mixture at different times, and treating them with alkali. No change in color was observed. If 1-[2-(3-oxocholestanyl)]2-methylpyridinium bromide had been present in the reaction mixture, it should have undergone a dehydrobromination and formed the corresponding betaine. This process would have been accompanied by a change in color. It was presumed that dehydrobromination of the bromo ketone (I) yielded a mixture of compounds (VII, VIII, IX), similar to those isolated by Jacobsen (6) from the reaction of I with 2,4,6-trimethylpyridine.

EXPERIMENTAL

The melting points below 225° were determined in a Thiele–Dennis melting-point tube containing sulphuric acid. Those above 225° were determined in a melting-point block constructed according to the specifications of Fieser (7). All melting points are uncorrected. Pyridine and methylpyridines were dried and purified. The analyses were carried out by Schwarzkopf in Woodside, N.Y. The ultraviolet absorption spectra were measured by means of a Beckman recording spectrophotometer Model DK1.

1-[2-(3-Oxocholestanyl)]pyridinium Bromide (II)

A solution of 2-α-bromocholestan-3-one (I) (7 g, 0.015 mole) in pyridine (34 ml) was heated, in a nitrogen atmosphere, to the reflux temperature. After 10 minutes, a solid material separated rapidly. When the reaction mixture had been refluxed for 2 hours, it was allowed to cool to room temperature. The solid material was filtered off, washed thoroughly with three 25-ml portions of petroleum ether (b.p. 60–90°), and dried. Recrystallization from ethanol provided 1-[2-(3-oxocholestanyl)]pyridinium bromide (II) (6.2 g), m.p. 310° (decomposed); lit. (1) m.p. 310° (decomp.); λ_{max}^{EtOH} 261 mμ (log ε 3.5).

1-[2-(3-Hydroxy-2-cholestanyl)]pyridinium Hydroxide, Betaine (IV)

1-[2-(3-Oxocholestanyl)]pyridinium bromide (II) (0.54 g, 0.001 mole) was suspended in alcohol (3 ml), and stirred in a nitrogen atmosphere at the reflux temperature, while a 25% aqueous solution of dimethylamine was added dropwise. Gradually the solid material passed into solution. The addition of dimethylamine was continued until the yellow solution had become turbid. As the reaction mixture cooled very slowly to room temperature, fine yellow needles separated from the solution. Recrystallization from alcohol and aqueous 25% dimethylamine in a nitrogen atmosphere gave the betaine of 1-[2-(3-hydroxy-2-cholestanyl)] pyridinium hydroxide (IV) (0.029 g), m.p. 169° (decomp.); λ_{max}^{EtOH} 245, 304, 430 mμ (log ε 3.8, 3.0, 3.7). An analytical sample was dried *in vacuo* over phosphorus pentoxide at 34° for 72 hours in the dark. Anal. Calcd. for $C_{32}H_{49}NO$: N, 3.02. Found: N, 3.19%.

1-[2-(3-Oxocholestanyl)]4-methylpyridinium Bromide (V)

A solution of 2-α-bromocholestan-3-one (I) (4.65 g, 0.01 mole) in 4-methylpyridine (15 ml) was refluxed for 4 hours; the reaction mixture was allowed to cool to room temperature. The solid precipitate was collected, washed with petroleum ether, and dried. Recrystallization from hot acetic acid gave 1-[2-(3-oxocholestanyl)]4-methylpyridinium

Can. J. Chem. Downloaded from www.nrcresearchpress.com by 210.87.254.105 on 09/05/12
For personal use only.

bromide (V) (3.7 g) in shining colorless prisms, m.p. 316° (decomp.); λ_{max}^{EtOH} 225, 257.5 mμ (log ε 4.0, 3.6). Anal. Calcd. for $C_{33}H_{52}BrNO$: C, 70.95; H, 9.36; N, 2.5. Found: C, 71.35; H, 9.57; N, 2.75%.

1-[2-(3-Hydroxy-2-cholestanyl)]4-methylpyridinium Hydroxide, Betaine (VI)

The pyridinium bromide (V) (0.28 g, 0.005 mole) was added to a stirred suspension of anhydrous potassium carbonate (1 g) in chloroform (10 ml). The mixture became orange immediately, and deepened in color as the reaction proceeded. The reaction mixture was refluxed gently for 5 minutes in a nitrogen stream. Then it was cooled to 0°, filtered, and washed with two 5-ml portions of chloroform. The washings and filtrate were combined and evaporated to dryness. The residue was dried *in vacuo* at 34° for 72 hours, and in this way the betaine (VI) (0.19 g) was obtained. The substance softened above 100° but had an indefinite melting point. λ_{max}^{EtOH} 248, 308, 431 mμ. Anal. Calcd. for $C_{33}H_{51}NO$: N, 2.93. Found: N, 2.92%.

1-[2-(3-Oxocholestanyl)]3-methylpyridinium Bromide

This substance was prepared in a manner analogous to that used for the preparation of compounds (II) and (IV). Colorless plates (from a 2:3 acetic acid – water mixture), m.p. 314° (decomp.).

1-[2-(3-Hydroxy-2-cholestanyl)]3-methylpyridinium Hydroxide, Betaine

This betaine was obtained in a manner analogous to that employed for the preparation of compounds (IV) and (VI). Yellow needles (from chloroform); the substance softened at 128°, but did not melt at a definite temperature. λ_{max}^{EtOH} 255, 314, 432 mμ (log ε 3.2, 3.2, 3.0). Anal. Calcd. for $C_{33}H_{51}NO$: N, 2.93; Found: N, 2.74%.

Reaction of 2-α-Bromocholestan-3-one (I) with 2-Methylpyridine

A mixture of 2-methylpyridine (10 ml) and I (2.33 g, 0.005 mole) was refluxed, in a nitrogen atmosphere, for 5 hours. No precipitate was formed at any time during the reflux period. Several samples were taken by means of a micropipette at different times; no pronounced change in color was observed when those samples were added to dilute alkaline solutions. The excess 2-methylpyridine was removed from the reaction mixture in a stream of nitrogen under reduced pressure. A white substance, sublimed from the residue at 125–130° under 2 mm pressure, was characterized as 2-methylpyridine hydrobromide.

REFERENCES

1. L. RUZICKA, P. A. PLATTNER, and R. AESCHBACHER. Helv. Chim. Acta, **21**, 866 (1938).
2. H. H. INHOFFEN, G. ZUHLSDORFF, and HUANG-MINLON. Ber. deut. chem. Ges. **73**, 451 (1940).
3. A. BUTENANDT and A. WOLFF. Ber. deut. chem. Ges. **68**, 2091 (1935).
4. F. KRÖHNKE. Ber. deut. chem. Ges. **68**, 1177 (1935).
5. G. FRANGATOS and A. TAURINS. Can. J. Chem. **37**, 835 (1959).
6. R. P. JACOBSEN. J. Am. Chem. Soc. **62**, 1620 (1940).
7. L. F. FIESER. Experiments in organic chemistry. 2nd ed. D. C. Heath & Co., New York. 1941. p. 329.

Can. J. Chem. Downloaded from www.nrcresearchpress.com by 210.87.254.105 on 09/05/12
For personal use only.

Can. J. Chem. Downloaded from www.nrcresearchpress.com by 210.87.254.40 on 09/05/12
For personal use only.

INFRARED SPECTRA – STRUCTURE CORRELATIONS OF N-SUBSTITUTED TRIFLUOROACETAMIDINES[1]

JOHN C. GRIVAS[2] AND ALFRED TAURINS

ABSTRACT

A correlation between the infrared spectra and the structure of some N-mono- and N-disubstituted trifluoroacetamidines is presented. It was found that there was a considerable similarity between the infrared spectra of trifluoroacetamidines and those of the corresponding trichloroacetamidines. Additional information of the existence of these amidines in the imino form, CF_3—C(=NH)NHR, was provided by the infrared study of N,N-dideuterioamidines.

INTRODUCTION

In a previous communication (1) the evidence for the existence of N-alkyl- and N-aryltrichloroacetamidines in the form I was presented.

(I) $CCl_3C(=NH)NHR$ (R = alkyl, aryl)

Prevoršek (2) in a study of the infrared spectra of N-substituted benzamidines (II*a* and II*b*) concluded that when R′ was an alkyl group (ethyl) the benzamidines existed in the form II*a*, but when R′ was an aryl group (phenyl) the amidine had the structure II*b*.

$C_6H_5C(=NH)NHR'$ (II*a*) $\qquad$ $C_6H_5C(NH_2)=NR'$ (II*b*)

The infrared spectrum of alkyl-substituted amidines II*a* showed a very strong "amidine II" band at 1560 cm^{-1} which was displaced in solution. In the spectra of deuterated amidines (II*a*) this band was not present but a new band appeared at 1400 cm^{-1}. There was no "amidine II" band for the aryl-substituted benzamidines (II*b*) between 1580–1500 cm^{-1} since such displacement of the band observed did not occur on deuteration and was not also sensitive to the breaking of hydrogen bonds on dilution. Therefore the structure II*b* of aryl-substituted benzamidines was accepted. Prevoršek (2) also found that the observed $\nu_{sym}(NH)$ vibrations were in good agreement with those calculated by the Bellamy equation (3):

$$\nu_{sym}(NH) = 345.5 + 0.876\nu_{asym}.$$

EXPERIMENTAL

The trifluoroacetamidines used in this infrared study were prepared by known methods (4) or by procedures outlined in the previous paper (6). The deuterioamidines were synthesized from nitriles and N,N-deuterioamines according to the following reaction scheme:

$$R{-}C{\equiv}N + R'ND_2 \rightarrow R{-}C(=ND){-}NDR'.$$

(R = Cl_3C—, F_3C—)
(R′ = CH_3, C_6H_5)

[1]*Manuscript received November 10, 1960.*
Contribution from the Department of Chemistry, McGill University, Montreal, Quebec, with financial assistance from the National Research Council of Canada, Ottawa.
[2]*Holder of the National Research Council Studentship, 1954–1958, and 1958–1959.*

The infrared spectra were recorded on a Perkin–Elmer Model 21 spectrometer equipped with a sodium chloride prism. The solid substances were investigated in potassium bromide pellets or in Nujol mulls. Liquid substances were examined in a thin layer between two sodium chloride plates. Amidines were also studied by infrared in tetrachloroethylene solutions (10 mg in 1 ml of the solvent), and sodium chloride cells 1 mm thick were used.

N-Methyl-α,α,α-trifluoroacetamidine-d_2

Trifluoroacetonitrile (0.04 mole) was condensed in a Pyrex tube (20×700 mm) previously flushed with nitrogen. The lower part of the tube, 30 cm in length, was immersed in a dry ice – acetone mixture. Methylamine-d_2 (2 ml) was then allowed to condense through a long glass tube leading to about 5 cm above the bottom of the Pyrex tube. The top of the last tube was closed with a well-fitting rubber stopper carrying two short tubes, 4 and 0.5 mm in diameter. The two tubes allowed the slow circulation of dry nitrogen through the upper part of the Pyrex tube during the whole operation, thus preventing the condensation of atmospheric moisture in the reaction mixture. Finally the stream of nitrogen was stopped, and the tube was quickly sealed and left at room temperature for 4 hours. The mixture was then transferred quickly to a semimicro distillation apparatus and distilled at reduced pressure in a nitrogen atmosphere to give a colorless amidine, b.p. 39–40°/15 mm (yield 80%).

N-Methyl-α,α,α-trichloroacetamidine-d_2

For the synthesis of this compound the same method was used. Equimolar amounts of trichloroacetonitrile and methylamine-d_2 were allowed to react in a sealed tube and were then distilled at reduced pressure in nitrogen atmosphere. B.p. 50–52°/15 mm.

N-Phenyl-α,α,α-trichloroacetamidine-d_2

Aniline-d_2 (1 g) and an excess of trichloroacetonitrile were mixed and left in a tightly closed sublimation apparatus at room temperature for 5 days. The excess of the nitrile was then eliminated in vacuum and the remainder sublimed at 1 mm pressure. The first portion was discarded and the sublimation continued until pure amidine-d_2, was collected. All the operations were conducted in a dry nitrogen atmosphere.

RESULTS AND DISCUSSION

Table I summarizes the positions of absorption maxima (cm^{-1}) in the infrared spectra of N-substituted trifluoroacetamidines. As was expected, the infrared spectra of these compounds showed a considerable similarity to those of the corresponding N-substituted trichloroacetamidines, except the bands produced by C—F and C—Cl respectively.

I. Region 4000–1800 cm^{-1}

The spectra of trifluoroacetamidine, CF_3—C(=NH)NH_2 (III), and trichloroacetamidine, CCl_3—C(=NH)NH_2 (IV) showed three absorption peaks in dilute tetrachloroethylene solutions. These peaks corresponded to the asymmetric and symmetric stretching vibrations of the primary amino group ($\nu(NH_2)$) and the stretching vibration of the imino group (ν(=N—H)). They were in agreement with the spectrum of perfluorobutyramidine, C_2F_7C(=NH)NH_2 (5).

This proves that the $\nu(NH_2)_{sym}$ and ν(=NH) absorption bands do not overlap in the spectrogram and this circumstance may be used in deciding which of the two tautomeric forms of the N-substituted trifluoroacetamidines is present.

Assuming that the validity of the Bellamy equation holds in N-substituted trifluoroacetamidines having the structure (V*b*), the difference, $\Delta\nu = \nu_{sym\ calc} - \nu_{sym\ obs}$, was calculated. Although these values were obtained using a NaCl prism possessing a low

Can. J. Chem. Downloaded from www.nrcresearchpress.com by 210.87.254.40 on 09/05/12
For personal use only.

Can. J. Chem. Downloaded from www.nrcresearchpress.com by 210.87.254.40 on 09/05/12
For personal use only.

TABLE I

Positions of absorption maxima (cm^{-1}) in the infrared spectra of N-substituted trifluoroacetamidines

No.	Trifluoro-acetamidine	State[1]	ν(N—H)	ν(=N—H)	Hydrogen-bonded ν(N—H)	ν(C=N)	δ(NH) "amidine II"	$\nu(C_{ar}—N)$	$\nu(C_{alk}—N)$
1	N-Methyl-	L	3515m		3350sh, 3300sh, 3220s	1655vs	1555m		
		Sol	3515m	3380w	None	1660vs	1530m		
2	N-Ethyl-	L	3475s		3250vs,[2] 3090vs	1645vs	1545s		
		Sol	3475s	3355m	None	1655vs	1530m		
3	N-*n*-Butyl-	L		3300s[2]	3500w, 3100m	1650vs	1455s		
		Sol	3460m	3340w	None	1653vs	1527m		
4	N-Benzyl	S	3485m		3300m, 3260m, 3150s[2]	1650vs	absent[4]		
		Sol (1.3 *M*)	3475m	3340	3270s, 3200s	1650vs	1530s		
		Sol	3465m	3360	None	1655vs	1517s		
5	N-Phenyl-	S	3465s		3270s, 3140s[2]	1670vs	1607vs		
		Sol	3535s	3425m	None	1690vs	1582vs[5]	1410vs	
6	N,N-Dimethyl-	L		3375m[3]	3330sh	1615vs			1090vs
		Sol		3355m	None	1620vs			1090vs
7	N,N-Diethyl-	L		3365s[3]	3360sh	1625vs			1070vs
		Sol		3375m	None	1625vs			1070vs

[1]S = solid, L = liquid, Sol = solution.
[2]Broad band with inflections.
[3]Sharp bands.
[4]The "amidine II" bands disappear in the solid state.
[5]Together with the C=C aromatic mode.

$CF_3—C(=NH)—NH_2$	$CCl_3—C(=NH)—NH_2$	Assignment
3580 s	3530 s	$\nu(NH_2)_{asym}$
3480 w	3425 m	$\nu(NH_2)_{sym}$
3410 m	3370 m	$\nu(=N—H)$
3290 m, 3120 s	3350 w, 3150 s	Hydrogen-bonded N—H groups

resolving power in the high-frequency region and so cannot be considered very accurate, they were in the range of 17–35 cm^{-1}, much larger than the standard deviation of 4.8 cm^{-1} reported for 64 primary amines examined. Such evidence favored the structure (V*a*) for both the N-alkyl and N-aryl series of trifluoroacetamidines, although the value of the deviation decreased in passing from the first to the second series. N-substituted trichloroacetamidines behaved in a similar way.

$CF_3—C(=NH)—NH—R$ (V*a*) $\qquad$ $CF_3—C(NH_2)=N—R$ (V*b*)

N-substituted trifluoroacetamidines, $CF_3—C(=NH)NHR$, showed strong association in the liquid and solid phase except the N-dialkyl compounds, which presented only one inflection on the sharp $\nu(=NH)$ band in the condensed phase. Thus, in the spectra of the solid and liquid amidines, more than two bands were found, and in some cases it was difficult to distinguish between the free and bonded NH stretching frequencies. Dilution in tetrachloroethylene resulted in two sharp peaks only. For example, four strong bands were present in the spectrum of N-benzyl-α,α,α-trifluoroacetamidine and were still persistent near 3475, 3340, 3270, and 3200 cm^{-1} at 1.3 *M* concentration in tetrachloroethylene. Upon further dilution they were replaced by a sharp band, $\nu(\rangle NH)$, of medium intensity at 3465 cm^{-1} and a weak one, $\nu(=NH)$, at 3360 cm^{-1}.

In N-monosubstituted amidines (V*a*) there are two hydrogen atoms which might be involved in hydrogen bonding. Theoretical considerations demonstrate that amino hydrogen bears a partial positive charge owing to resonance and is more acidic than the imino hydrogen (=N—H).

II. Region 1800–1000 cm^{-1}

(a) The $\nu(C=N)$ Absorption

This easily recognizable frequency appeared as a very strong band at 1615–1690 cm^{-1} in all the spectra examined. Upon dilution it was slightly displaced to the higher frequencies as was expected for a $\nu(C=N)$ vibration. The $\nu(C=N)$ absorption bands in the N-aryl-, N-alkyl-, and N-dialkyl-trifluoroacetamidines followed exactly the same pattern as those of the trichloroamidines (1) and provided evidence for the existence of the N-substituted trihaloacetamidines in the imino form (V*a*).

A comparison of the $\nu(C=N)$ vibration of the following amidines in dilute tetrachloroethylene solutions showed the occurrence of this mode at the same frequency:

Can. J. Chem. Downloaded from www.nrcresearchpress.com by 210.87.254.40 on 09/05/12
For personal use only.

$Cl_3C—\underset{\underset{NH}{\|}}{C}—NH_2$: 1670 cm^{-1}; $Cl_3C—\underset{\underset{NH}{\|}}{C}—NHAr$: 1667–1672 cm^{-1};

$F_3C—\underset{\underset{NH}{\|}}{C}—NH_2$: 1690 cm^{-1}; $F_3C—\underset{\underset{NH}{\|}}{C}—NHAr$: 1690 cm^{-1}.

This behavior may not be a pure coincidence but may indicate that the presence of the aryl groups does not influence the resonance within the amidine system, whereas substitution by one or two alkyl radicals in the amino group does increase the contribution of the ionic structures of the resonance hybrid. This results in the progressive displacement of the C=N stretching vibration towards the lower frequencies which has its lowest value in the case of N-dialkyl-substituted amidines.

(*b*) *The "Amidine II" Band, δ(N—H)*

This infrared absorption appeared as a medium to strong band in the spectra of four N-alkyltrifluoroacetamidines (see Table I). It was absent from the spectra of the N-dialkyl compounds and was displaced to the higher frequencies (10–20 cm^{-1}) when association occurred. Nevertheless, it was not found in the spectrum of the solid N-benzyl-α,α,α-trifluoroacetamidine but appeared as usual (at 1530–1517 cm^{-1}) when solutions of this substance were studied. The δ(N—H) band was also identified when the spectrum of the melted N-benzyl-α,α,α-trifluoroacetamidine was taken but vanished when the melt was left to resolidify, this being done several times with the same result. Since the melting point of the compound was low (51°), decomposition by heating was not likely to occur and the spectrum of the solidified melt was exactly the same as that of the original substance in Nujol mull or in potassium bromide pellet. This behavior, which presents an example unique in the literature, could only be attributed to changes in the crystal lattice.

A strong absorption band with two well-separated peaks at 1607 and 1582 cm^{-1} appeared in the spectrum of the solid N-phenyl-α,α,α-trifluoroacetamidine but was replaced by only one very strong band at 1582 cm^{-1} upon dilution. The 1607 cm^{-1} band was taken as evidence for the "amidine II" vibration which had been displaced and therefore coincided with the aromatic ring absorption.

The assignment of the "amidine II" band to the 1570–1590 cm^{-1} absorption in N-aryl-trifluoro- and -trichloro-acetamidines was supported by the study of the infrared spectrum of the deuterated N-phenyl-α,α,α-trichloroacetamidine, $Cl_3C—C(=ND)NHC_6H_5$. The 1580 cm^{-1} band of the ordinary N-phenyl-α,α,α-trichloroacetamidine could not be observed in the deuterated analogue. A similar phenomenon was also noted with the deuterated N-methyl-α,α,α-trifluoro- and N-methyl-α,α,α-trichloro-acetamidine. In this case, changes in the infrared spectra occurred in the low-frequency region, indicating that coupled (mixed) rather than pure vibrations were present in this type of molecule.

(*c*) *The ν(C—N) Frequencies*

The very strong absorption bands of the F_3C-group varying in number from two to five even for the simplest molecules occurred in the same region (1100 to 1250 cm^{-1}) as the ν(C—N) vibrations and produced complicated infrared spectra. However, the $\nu(C_{ar}—N)$ frequency could be related to a very strong absorption at 1407 cm^{-1} in the N-phenyl-α,α,α-trifluoroacetamidine. This was clearly understood, since it was the only strong band between 1125 and 1480 cm^{-1}, and it was not present in the spectrum of trifluoroacetamidine and did not change on deuteration. The existence of a strong

Can. J. Chem. Downloaded from www.nrcresearchpress.com by 210.87.254.40 on 09/05/12
For personal use only.

absorption near 1080 cm^{-1} in the spectra of N-dialkyl amidines could be attributed to a $\nu(C_{alk}—N)$ mode in these N-dialkyl compounds, since this band was absent in the case of the N-monoalkyl compounds.

REFERENCES

1. J. C. GRIVAS and A. TAURINS. Can. J. Chem. **37**, 795 (1959).
2. D. PREVORŠEK. J. chim. phys. **55**, 840 (1958).
3. L. J. BELLAMY and R. L. WILLIAMS. Spectrochim. Acta, **9**, 341 (1957).
4. W. L. REILLY and H. C. BROWN. J. Am. Chem. Soc. **78**, 6032 (1956).
5. D. HUSTED. U.S. Patent No. 2,676,985 (April 27, 1954); Chem. Abstr. **49**, 5511 (1955).
6. J. C. GRIVAS and A. TAURINS. In press.

Can. J. Chem. Downloaded from www.nrcresearchpress.com by 210.87.254.40 on 09/05/12
For personal use only.

Can. J. Chem. Downloaded from www.nrcresearchpress.com by 210.87.254.6 on 09/05/12
For personal use only.

THE REACTION OF ALKYL IODIDES WITH IODO-ARSINES IN THE PRESENCE OF MERCURY[1]

M. M. Baig and W. R. Cullen

ABSTRACT

The reaction of alkyl iodides with iodo-arsines in the presence of mercury generally gives arsonium derivatives of triiodomercury (II). Thus tetramethylarsonium triiodomercury (II) is obtained from the reactions of methyl iodide with the compounds $(CH_3)_{3-n}AsI_n$ (n = 1, 2, 3). Phenyl-iodo-arsines give the new compounds $C_6H_5AsR_3HgI_3$ and $(C_6H_5)_2AsR_2HgI_3$ (R = CH_3 or C_2H_5) from similar reactions. However, the reaction of iododimethylarsine with ethyl iodide gives the 1:1 arsine complex $(CH_3)_2AsC_2H_5.HgI_2$. The compounds $(C_2H_5)_4AsI$ and $(C_2H_5)_4AsHgI_3$ were reinvestigated, and used to prepare the compound $((C_2H_5)_4As)_2HgI_4$.

DISCUSSION AND RESULTS

The reaction of alkyl- and aryl- iodo-arsines with perfluoroalkyl iodides in the presence of excess mercury has been found to yield alkyl- or aryl- perfluoroalkyl-arsines (1, 2). In the present investigation the reactions of alkyl iodides with iodo-arsines in the presence of mercury have been studied. Apart from one reaction, the main products are compounds which in the past have been named as arsonium derivatives of triiodomercury (II) (3, 4). Similar derivatives are known for other elements which form -onium compounds and there is good evidence that some of these mercuri-iodides are ionic in solution and that one of the ions is HgI_3^- (4, 5). However, solid state structural studies are clearly necessary.

The reactions involving alkyl iodides, mercury, and iodo-arsines, which were investigated, are shown in Table I and the new compounds prepared in this way are listed in Table II.

TABLE I

Reactants	Time of reaction	Products	Yields*
$AsI_3+Hg+CH_3I$	10 days	$(CH_3)_4AsHgI_3$	32%
$MeAsI_2+Hg+CH_3I$	10 days	$(CH_3)_4AsHgI_3$	98%
$Me_2AsI+Hg+CH_3I$	5 days	$(CH_3)_4AsHgI_3$	87%
$C_6H_5AsI_2+Hg+CH_3I$	18 days	$C_6H_5As(CH_3)_3HgI_3$ and CH_3HgI	44% 38 g
$C_6H_5AsI_2+Hg+C_2H_5I$	18 days	$C_6H_5As(C_2H_5)_3HgI_3$ and C_2H_5HgI	33% 14 g
$(C_6H_5)_2AsI+Hg+CH_3I$	21 days	$(C_6H_5)_2As(CH_3)_2HgI_3$	91%
$(C_6H_5)_2AsI+Hg+C_2H_5I$	21 days	$(C_6H_5)_2As(C_2H_5)_2HgI_3$ and C_2H_5HgI	>90%† 4 g
$(CH_3)_2AsI+Hg+C_2H_5I$	5 days	$(CH_3)_2AsC_2H_5.HgI_2$	37%

*Yields are based on the iodo-arsine added (ca. 10 g).
†Estimated because of difficulty in separating the two compounds.

Like the other arsonium mercuri-iodides the new compounds are low-melting yellow solids, easily soluble in hot acetone and alcohol. The reaction between ethyl iodide, mercury, and iododimethylarsine, however, gives as a main product the 1:1 complex of mercuric iodide and ethyldimethylarsine. The molecular weight of this substance in camphor indicates that it is predominantly in the form of a monomer instead of the

[1]*Manuscript received November 16, 1960.*
Contribution from the Chemistry Department, University of British Columbia, Vancouver, B.C.

TABLE II

Compound	m.p.	Analysis									
		Found %					Calculated %				
		C	H	Hg	I	Mol. wt.	C	H	Hg	I	Mol. wt.
$C_6H_5As(CH_3)_3HgI_3$	128°	12.9	1.80	24.4	48.0	822	13.7	1.80	25.8	48.8	779
$C_6H_5As(C_2H_5)_3HgI_3$	129°	17.8	2.44	24.1	46.7	847	17.5	2.44	24.5	46.4	821
$(C_6H_5)_2As(CH_3)_2HgI_3$	131°	19.9	1.60	23.6	45.4	814	19.9	1.90	23.9	45.3	841
$(C_6H_5)_2As(C_2H_5)_2HgI_3$	86°	22.3	3.03	23.3	44.0	918	22.1	2.30	23.2	43.8	869
$(CH_3)_2AsC_2H_5.HgI_2$	111°	8.15	1.94	34.1	43.0	615	8.15	1.87	34.1	43.2	589

expected halogen-bridged dimer (6), and consequently could contain 3-co-ordinate mercury. A similar situation is found in certain 1:1 tertiary phosphine mercuric iodide complexes (7). The arsine complex seems to decompose slowly and cannot be repurified by fractional crystallization. The alkyl-mercury iodides isolated from the reactions involving aryl-iodo-arsines are probably produced by the side reaction

$$RI + Hg \rightarrow RHgI.$$

Such reactions are well known for alkyl iodides and would be catalyzed by any free iodine present in the iodo-arsines (8).

The rate of reaction of alkyl iodides with the aryl-iodo-arsines in the presence of mercury seems to be slower when there are two iodine atoms on the arsenic. Similar behavior is found when these arsines are reacted in the same way with trifluoroiodomethane (2). The reaction of methyl iodide with arsenic triiodide and mercury is slower than with the substituted iodo-arsines, though it appears that methyl iodide reacts more easily in such reactions than does trifluoroiodomethane (1, 2). The latter compound does not react with arsenic triiodide and mercury (9). Antimony triiodide also reacts with methyl iodide in the presence of mercury but not with trifluoroiodomethane (10).

The most probable mechanism for the formation of the arsonium mercuri-iodides appears to be firstly, the formation of an arsine mercuric iodide complex (most likely 1:1), followed by the addition of alkyl iodide to give the final product: for example

$$(CH_3)_2AsI + Hg + CH_3I \rightarrow (CH_3)_3As.HgI_2,$$
$$(CH_3)_3As.HgI_2 + CH_3I \rightarrow (CH_3)_4AsHgI_3.$$

This route is supported by the isolation in one instance of the 1:1 arsine mercuric iodide complex, by the result that 2:1 arsine mercuric iodide complexes add on alkyl halides to give arsonium derivatives of tetraiodomercury (II) (7), and by the result that only aryl- and alkyl-perfluoroalkyl-arsines are isolated when perfluoroalkyl iodides are used in similar reactions (1, 2). Unfortunately the reactions so far studied give little indication as to which of the many possible mechanisms is the operative one in the formation of the perfluoroalkyl-arsine or the arsine mercuric iodide complex.

Two other arsonium mercuri-iodides have been studied in the present investigation, these are tetraethylarsonium triiodomercury (II) and bis(tetraethylarsonium) tetraiodomercury (II). The latter, a new compound, is a pale yellow crystalline substance, m.p. 238°. The triiodomercury (II) derivative is the usual low-melting yellow solid (m.p. 117°). Their preparation and relationship can be shown as follows.

$$(C_2H_5)_4AsI + HgI_2 \text{ (excess)} \xrightarrow[EtOH]{\text{cold}} (C_2H_5)_4AsHgI_3$$

$$(C_2H_5)_4AsI \text{ (excess)} \downarrow \text{EtOH, hot}$$

$$(C_2H_5)_4AsI \text{ (excess)} + HgI_2 \xrightarrow[EtOH]{\text{hot}} ((C_2H_5)_4As)_2HgI_4$$

Can. J. Chem. Downloaded from www.nrcresearchpress.com by 210.87.254.6 on 09/05/12
For personal use only.

The anomalously low melting point of tetraethylarsonium iodide (160° (decomp.) (11)) is now found to be incorrect. The compound prepared and characterized in this investigation decomposed at 307°, a more reasonable figure in view of the value of 326° (decomp.) for tetramethylarsonium iodide (12). The low melting points of other tetraalkylarsonium compounds are probably also incorrect.

The infrared spectra of these arsonium derivatives have been measured. These are in the main complex and further work is in progress in an attempt to correlate these spectra with those of other arsenic compounds.

EXPERIMENTAL

Preparation of the Arsonium Derivatives of Triiodomercury (II)

The alkyl- and aryl- iodo-arsines were prepared as previously described (1, 2), the arsenic triiodide was prepared using the procedure in *Inorganic syntheses* (13).

The reactions shown in Table I were carried out at room temperature in sealed tubes (250-ml capacity) in the absence of air and light. The reaction mixtures were shaken continuously to ensure the exposure of a clean mercury surface to the solution of the iodo-arsine in the alkyl iodide. A large excess of mercury (ca. 200 g) and alkyl iodide (ca. 60 g) was used: the amount of iodo-arsine was 10 g. The reaction mixture was worked up by extracting the contents of the tubes with acetone and separating the soluble components by fractional crystallization from this solvent. Final purification was achieved by repeated crystallization from alcohol. The by-products of alkyl-mercury halides produced in the reactions of the aryl-iodo-arsines were identified in each case by analysis. Anal.: Methylmercury iodide: found: C, 3.52; H, 0.93; Hg, 57.9; I, 36.8%; mol. wt. 319; m.p. 147°. CH_3HgI requires: C, 3.50; H, 0.87; Hg, 58.6; I, 37.0%; mol. wt. 343; m.p. 152° (8). Ethylmercury iodide: found: C, 6.83; H, 1.41; Hg, 55.5; I, 35.7%; mol. wt. 340; m.p. 187°. C_2H_5HgI requires: C, 6.72; H, 1.40; Hg, 56.3; I, 35.6%; mol. wt. 357; m.p. 186° (8).

In the reaction producing dimethyldiphenylarsonium triiodomercury (II) a small fraction was isolated which contained an impurity melting at 122°. Infrared spectra and X-ray powder photographs were used in order to establish the impurity as methylmercury iodide or the complex $(C_6H_5)_2AsCH_3.HgI_2$ which was prepared for the purpose of comparison (m.p.: found, 117°; lit. value, 116° (14)). However, no definite conclusions could be reached from either the spectra or the powder photographs. The tetramethylarsonium compound was identified by its melting point, found: m.p. 189°; lit. value, 185° (11), and by the identity of its infrared spectrum with that of a sample produced from tetramethylarsonium iodide and mercuric iodide (11).

No unchanged iodo-arsine was recovered from these reactions.

Reaction of Iododimethylarsine with Ethyl Iodide in the Presence of Mercury

The iodo-arsine (7.1 g), ethyl iodide (50 g), and mercury (200 g) in a sealed tube (250 ml) which was not evacuated, were shaken at room temperature for 5 days. The contents of the tube were extracted with acetone. The solution was diluted by an equal volume of alcohol and a yellow precipitate appeared. This was soluble on warming, and on cooling 6 g of the mercuric iodide complex of ethyldimethylarsine were obtained (see Table II for analysis results). The complex was recrystallized from the mixed solvent, m.p. 111°. On the addition of more ethanol to the combined mother liquors a pale red liquid separated which was insoluble in boiling ethanol but crystallized on standing to

Can. J. Chem. Downloaded from www.nrcresearchpress.com by 210.87.254.6 on 09/05/12
For personal use only.

pale yellow needles. This solid phase seemed to contain more than one compound and was not further characterized.

The arsine mercuric iodide complex was unstable as after 2 months the melting point changed from 111° to 100–110° and repurification could not be achieved by fractional crystallization. One of the larger fractions, m.p. 105–108°, analyzed as follows: found: Hg, 30.9; I, 41.1%. Calc. for $C_4H_{11}AsHgI_2$: Hg, 34.1; I, 43.2%.

Preparation of Tetraethylarsonium Iodide

Triethylarsine was prepared by a Grignard reaction using arsenic trichloride and ethyl bromide: the product distilled at 138–139° in a nitrogen atmosphere (15). When excess ethyl iodide was added to the arsine at room temperature a colorless solution was obtained which slowly deposited a white solid. After 2 days the solid was filtered off and purified by dissolving it in ethanol and reprecipitating by adding a large volume of ether. The product was identified as tetraethylarsonium iodide. Anal.: found: C, 30.3; H, 6.44; I, 39.3%. $C_8H_{20}AsI$ requires: C, 30.2; H, 6.39; I, 39.9%. The compound decomposed at 307° without melting (lit. value, 160° (decomp.) (11)).

Preparation of Tetraethylarsonium Triiodomercury (II) and Bis(tetraethylarsonium) Tetraiodomercury (II)

When a solution of tetraethylarsonium iodide in ethanol was added to a stirred solution of excess mercuric iodide in ethanol at room temperature, a yellow precipitate was obtained. This solid was washed with ethanol and was identified as tetraethylarsonium triiodomercury (II). Anal.: found: C, 12.4; H, 2.78; Hg, 25.8; I, 48.9%; mol. wt. 731; m.p. 117°. $C_8H_{20}AsHgI_3$ requires: C, 12.4; H, 2.59; Hg, 26.0; I, 49.3%; mol. wt. 773; m.p. 112° (11). When hot arsonium iodide and excess mercuric iodide solutions were mixed a yellow precipitate was obtained, m.p. 87–90°, containing two phases which could not be separated by fractional crystallization. However, the infrared spectrum of this mixture indicated that it was mainly the arsonium triiodomercury (II) derivative. When a hot solution of excess tetraethylarsonium iodide in ethanol was added to a hot solution of mercuric iodide in ethanol, a pale yellow precipitate was obtained. This was filtered, washed with alcohol, recrystallized, and identified as bis(tetraethylarsonium) tetraiodomercury (II). Anal.: found: C, 18.0; H, 3.66; Hg, 18.2; I, 46.2%; m.p. 238°. Calc. for $C_{16}H_{40}AsHgI_4$: C, 17.5; H, 3.66; Hg, 18.4; I, 46.4%. The same compound was produced when a solution of tetraethylarsonium triiodomercury (II) (0.5 g) in a minimum volume of hot ethanol was added to a solution of excess tetraethylarsonium iodide (1 g) in hot ethanol (5 ml). The bis(tetraethylarsonium) tetraiodomercury (II) which was precipitated was identified by its melting point of 236–238° and by its infrared absorption spectrum.

ACKNOWLEDGMENTS

The authors wish to acknowledge financial assistance from the National Research Council. One of us (M.M.B.) expresses thanks for a scholarship received under the auspices of the Colombo Plan. Microanalyses were carried out by Dr. Alfred Bernhardt.

REFERENCES

1. W. R. CULLEN. Can. J. Chem. **38**, 439 (1960).
2. W. R. CULLEN. Can. J. Chem. **38**, 445 (1960).
3. W. J. JONES, W. J. C. DYKE, G. DAVIES, D. C. GRIFFITHS, and J. H. E. WEBB. J. Chem. Soc. 2284 (1932).

Can. J. Chem. Downloaded from www.nrcresearchpress.com by 210.87.254.6 on 09/05/12
For personal use only.

4. N. V. SIDGWICK. The chemical elements and their compounds. Oxford University Press, London. 1950.
5. H. J. CAVELL and S. SUGDEN. J. Chem. Soc. 2572 (1930).
6. R. C. EVANS, F. G. MANN, H. S. PEISER, and P. PURDIE. J. Chem. Soc. 1209 (1940).
7. R. C. CASS, G. E. COATES, and R. G. HAYTER. J. Chem. Soc. 4007 (1955).
8. E. KRAUSE and A. VON GROSSE. Die Chemie der Metal-organischen Verbindungen. Borntraeger, Berlin. 1937.
9. W. R. CULLEN. To be published.
10. M. M. BAIG and W. R. CULLEN. To be published.
11. E. MANNHEIM. Ann. **341**, 182 (1905).
12. W. STEINKOPF and G. SCHWENN. Ber. **54**, 1437 (1921).
13. W. C. FERNELIUS. Inorganic syntheses. Vol. I. McGraw-Hill Book Co. Inc., New York. 1946.
14. J. J. ANDERSON and G. J. BURROWS. J. Proc. Roy. Soc. N.S. Wales, **70**, 63 (1936).
15. W. J. C. DYKE and W. J. JONES. J. Chem. Soc. 2426 (1930).

Can. J. Chem. Downloaded from www.nrcresearchpress.com by 210.87.254.6 on 09/05/12
For personal use only.

Can. J. Chem. Downloaded from www.nrcresearchpress.com by 210.87.254.40 on 09/05/12
For personal use only.

THE COMPLEX DIELECTRIC CONSTANT AT LOW MICROWAVE FREQUENCIES OF ETHYL CHLORIDE ADSORBED ON POROUS VYCOR GLASS[1]

J. D. McCowan[2] and R. McIntosh

ABSTRACT

The complex dielectric constant of the system Vycor glass – ethyl chloride has been measured at three temperatures in the range +11° C to −33° C and in the frequency range between 500 Mc sec^{-1} and 4000 Mc sec^{-1} by the use of a coaxial line. The real and imaginary parts of the dielectric constant of the adsorbate have also been evaluated. Appreciable loss in the adsorbed matter is found for small quantities adsorbed, and loss is again detected at the highest frequencies and lowest temperatures for the matter held in multilayers or condensed in capillaries. The frequency range and accuracy of measurement were not sufficient to classify the type of loss curve, but other evidence suggests that the loss for the first quantities adsorbed will turn out to be that for rotational oscillators. In general earlier observations of this system are confirmed and extended.

INTRODUCTION

In a series of papers from this and other laboratories, the apparent dielectric constants have been reported of polar and non-polar substances adsorbed on porous adsorbents. There is agreement among several of the investigators (1, 2, 3, 4, 5, 6, 7) that there are at least two linear sections of the primary data of either dielectric constant or capacitance change as a function of quantity adsorbed. Channen and McIntosh (5) have stressed the need to understand the experimental observation that the second linear region has a lower slope than the first, even for non-polar butane. As this is found only with porous adsorbents, Petrie and McIntosh (7) suggested that the internal field in which the matter is located changes suddenly at some critical quantity of adsorbate, and that this change is due to the location of the molecules in relation to the internal structure of the solid. In the case of polar adsorbates it is possible that explanations in terms of the value of the orientational polarization might be possible. Thus, molecules adsorbed initially with large apparent polarization, might, in the later stages of adsorption, be followed by molecules which are rotational oscillators with a lesser average dipole moment in the field. Although such concepts are unable to provide an explanation of the behavior of normal butane, nevertheless, since it is possible that adsorbates show specific differences of properties, any evidence concerning the dipolar character of adsorbates would be of value. To this end techniques have been developed to permit examination of adsorbates from 20° C to −183° C over a frequency range 3000 cycles sec^{-1} to 4 Mc sec^{-1} and from 10° C to −40° C in the frequency range 500 Mc sec^{-1} to 4000 Mc sec^{-1}. A description of the devices used for the high frequency experiments and the results found for ethyl chloride on porous Vycor glass are given in this paper. The reproducibility of results has proved excellent although the variation from one frequency to another has caused disappointment, and seems to be due to the coaxial line itself. Before describing the experimental assembly and reporting the results, it is useful to state what experimental findings can be (at least qualitatively) interpreted in elucidating the nature of the adsorbed phase.

[1]*Manuscript received October 24, 1960.*
Contribution from the Department of Chemistry based upon a thesis submitted by J. D. McCowan as partial fulfillment of the requirements for the Ph.D. degree.
[2]*Graduate Student and holder of National Research Council Studentship 1958–59. University of Toronto Open Fellowship 1959–60. Present address: Christ's College, Cambridge, England.*

(1) A negative temperature coefficient of dielectric constant, from experience gained with bulk matter, signifies an assembly of molecules free to align themselves in the field, or of dipolar molecules with several possible orientations relative to the field, as discussed by Frohlich (8). Such systems, if of normal liquid density, would be expected to possess a fairly large value of the dielectric constant, approximately that of the liquid state.

(2) Alternatively, experiment might reveal a negligible temperature coefficient of the dielectric constant of the adsorbate. This as Kurbatov (9), and Benson, Channen, and McIntosh (10) have stated, suggests that the adsorbate consists of an assembly of rotational oscillators. For these the orientational polarization, and hence the dielectric constant of the assembly, might be small.

(3) If the adsorbate exists in thick liquid-like layers, dispersion might be expected in the frequency and temperature ranges normal to the liquid state.

(4) Lastly, in the first adsorbed layer, dispersion of rotational oscillators, which would presumably be the nature of the adsorbed molecules, might not be found until very high frequencies. An estimate of the frequency was attempted by Benson, Channen, and McIntosh (10) for a simple molecule like hydrogen chloride adsorbed on a sodium chloride surface. The frequency at which dispersion occurs would depend, of course, upon the molecular structure of the adsorbate and the surface.

In the results given below, the real and imaginary parts of the dielectric constant of the total system, and of the adsorbate, are given. The tedious calculations necessary to obtain the adsorbate properties were based upon the extended Böttcher treatment which has been discussed in earlier papers (5, 7), and allowance had to be made for the lossy character of the substrate itself. The omission of the values of the real part of the dielectric constant for the total system and the fact that the properties of the adsorbate were not computed by Waldman (11) has much reduced the significance of that work. The findings of the present investigation may be briefly summarized as follows:

1. The measurement of the real and imaginary parts of the dielectric of both the adsorbent and a polar adsorbate has been successfully achieved over a temperature range $+11°$ to $-33°$ C and a frequency range 500 Mc sec^{-1} to 4000 Mc sec^{-1} by means of a coaxial line system. The reproducibility of any given measurement was finally established as better than $\pm 0.2\%$ over the 40 degree temperature range studied, but random variations with frequency amounted to $\pm 2\%$. This variation appears to be inherent in the line used, not in the method employed, nor in the procedures of amplification.

2. The existence of losses in the adsorbed dielectric has been established for the first time in this temperature range. Moreover, the losses of the adsorbate alone have been evaluated, and, as might be anticipated from the knowledge that the measurable loss of the total dielectric is caused by a comparatively small amount of adsorbate, the loss in the adsorbate is substantial.

3. The pronounced losses are found for the adsorbate in equilibrium with low relative pressures, and little loss is to be observed for the adsorbate in the multilayer or capillary condensed material, although a slight loss is observed at the lowest temperature and highest frequencies.

4. The existence of loss permits the occurrence of a positive temperature coefficient of the real part of the dielectric constant. Earlier work with the same adsorbent–adsorbate system (7) has shown a negligible temperature coefficient of the dielectric constant when measuring frequencies that were too low to create losses were employed. Since a

Can. J. Chem. Downloaded from www.nrcresearchpress.com by 210.87.254.40 on 09/05/12
For personal use only.

negligible temperature coefficient suggests rotational oscillators, the loss detected appears to be for an oscillatory or resonant type of motion.

5. No evidence of hysteresis in the dielectric constant was obtained, as found by Thorp (12) for several systems, and more recently by Fiat (13). The lack of hysteresis confirms the statement by Petrie and McIntosh (7) published without supporting evidence. A graph of their results, which were obtained with greater precision than the present data, is included below.

EXPERIMENTAL

The equipment used for the preparation of the materials and to obtain adsorption data was relatively simple and described in detail elsewhere (14, 15, 16). Hoke type 413 metal valves were used throughout the measuring system to ensure that no mercury or stopcock grease could distill into the cell.

Small equilibrium pressures were measured by condensing the gas from a large known volume to a small volume in which the pressure was measured. From a knowledge of all the volumes in the system, equilibrium pressures and amount adsorbed were calculated.

The dielectric measurements were carried out by setting up a standing electromagnetic wave for which the node positions and voltage standing wave ratio were dependent on the complex dielectric constant of the adsorbate–adsorbent system.

The cell is shown in Fig. 1. The two coaxial cylinders which channel the microwave were of 0.007-inch wall German silver tubing. Their dimensions, and those of the tapers leading to the UG30C/U adapter, were chosen to present an impedance of 50.0 ohms to the microwave. The adapter formed a vacuum seal and, together with the gasketed plate behind the shorting plate, permitted evacuation of the sample chamber and the admission of known quantities of gas. The evacuation and admission were accomplished through a copper tube leading to the small chamber behind the short and through a pinhole in the outer conductor.

Around this whole structure, a brass cylinder was attached which could be sealed by a gasket at its open end. The Genitron 21, used to control the temperature of the sample, was circulated through this chamber. Details of the temperature control may be found elsewhere (17).

Temperature was measured by calibrated copper–constantan thermocouples inserted in the wells shown in the diagram. They showed a temperature gradient of 0.3° C and fluctuation of ± 0.2 C° for a temperature of $+11$° C and a gradient of 1.5 C° and long term fluctuations of ± 1 C° at -33° C.

The porous Vycor glass, brand number 7930, was ground to make a sliding fit with both conductors. In the final assembly, care was taken to have it adjacent to the short. Both ends were planar and orthogonal to the axis.

Preparation of the Vycor involved gentle heating, first in a succession of 30% nitric acid solutions and then in distilled-water baths. It was then sealed in the final assembly and the water pumped off gently over 2 days. The glass was then heated to 65° C and pumping continued for 1 day more. An ultimate vacuum of 10^{-6} mm Hg was obtained.

Three signal generators, covering a range from 200 to 4000 Mc sec^{-1}, could be connected, in turn, to two General Radio LBA slotted lines in series. Connections between a generator and the first line, called the reference line, and between the reference line and the second or signal line, were made by RG21/U attenuating cable. This reduced reflection into the generator. The signal line was attached directly to the cell. In this slotted line, the standing wave pattern was studied by means of a travelling carriage

Can. J. Chem. Downloaded from www.nrcresearchpress.com by 210.87.254.40 on 09/05/12
For personal use only.

Can. J. Chem. Downloaded from www.nrcresearchpress.com by 210.87.254.40 on 09/05/12
For personal use only.

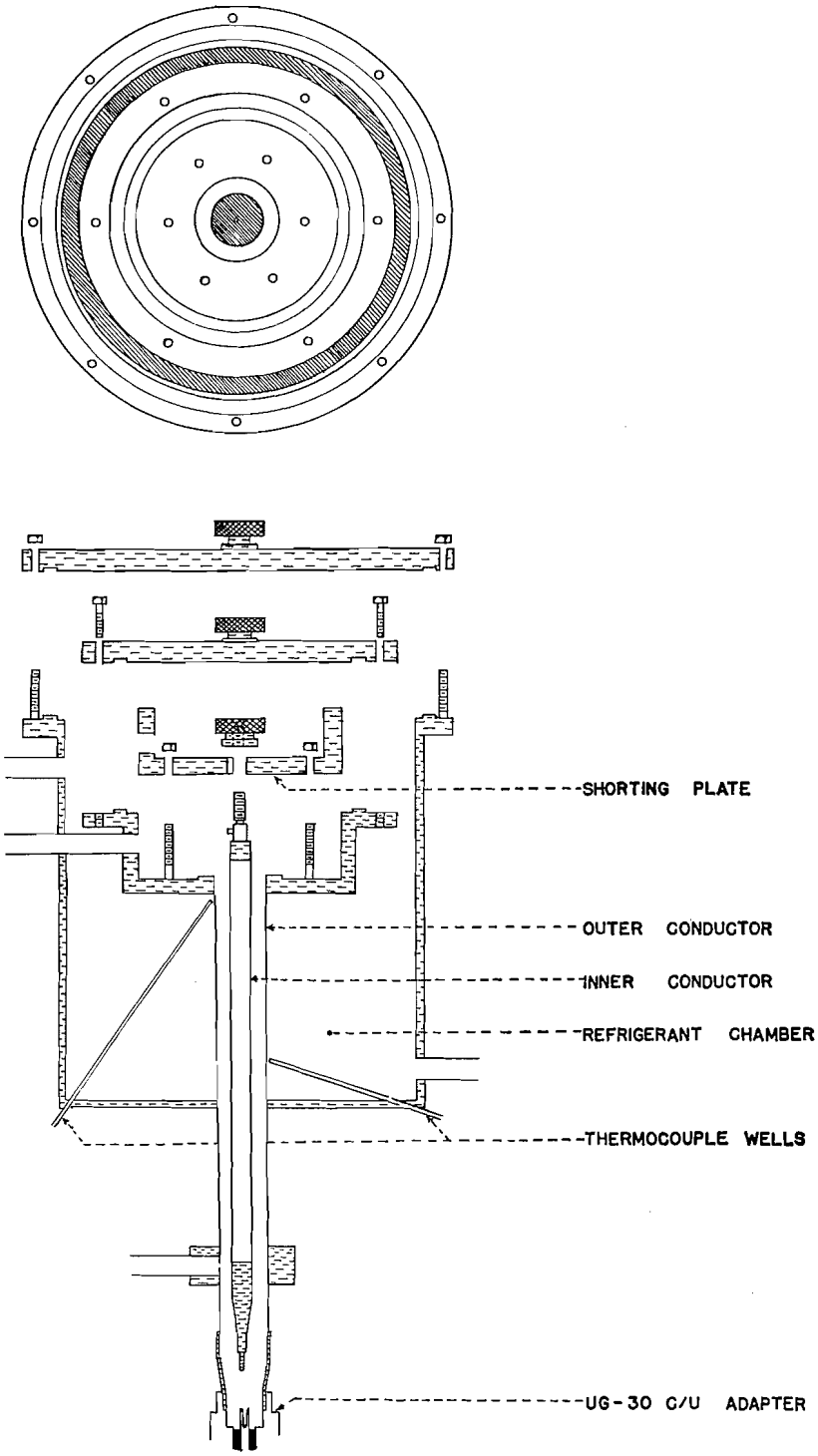


FIG. 1. Side cross-sectional and end views of coaxial cell assembly.

containing a probe and a 1N21B crystal diode. The output of this diode showed no detectable departure from square law response in the voltage range studied. The carriage was moved by the rotation of a threaded bar running the length of the slotted section. Motion of the carriage could be estimated to 0.002 cm.

The line nearer the signal source was not fitted with the worm drive device and was used to produce a reference voltage.

The d-c. outputs of the crystal diodes were fed into two identical d-c. amplifiers each with amplifications of 10^2, 3×10^2, and 10^3. The amplifiers were of a negative feedback type employing the action of a light beam reflected from a galvanometer on two photocells in series. Separate power supplies must be used for the two amplifiers. Oscillations in the output occur if several resistors are not kept within fairly narrow tolerances (15).

Precautions were taken to ensure that ground potential was the same throughout the d-c. system. Small contact potentials were eliminated from input switches by the use of Leeds and Northrup type 31-3 switches but it was found impossible to eliminate them from the spring type General Radio connectors of the slotted lines.

The output of the reference amplifier was applied to the input of a General Radio decade voltage divider. The divided output was fed, through a switch, to one terminal of a galvanometer. The output of the signal amplifier was applied to the other terminal. For a null reading of the galvanometer, the voltage divider box read the exact ratio of the signal amplifier output to the reference amplifier output. A block diagram is shown in Fig. 2. The signal was measured as a ratio, rather than in absolute terms, to eliminate

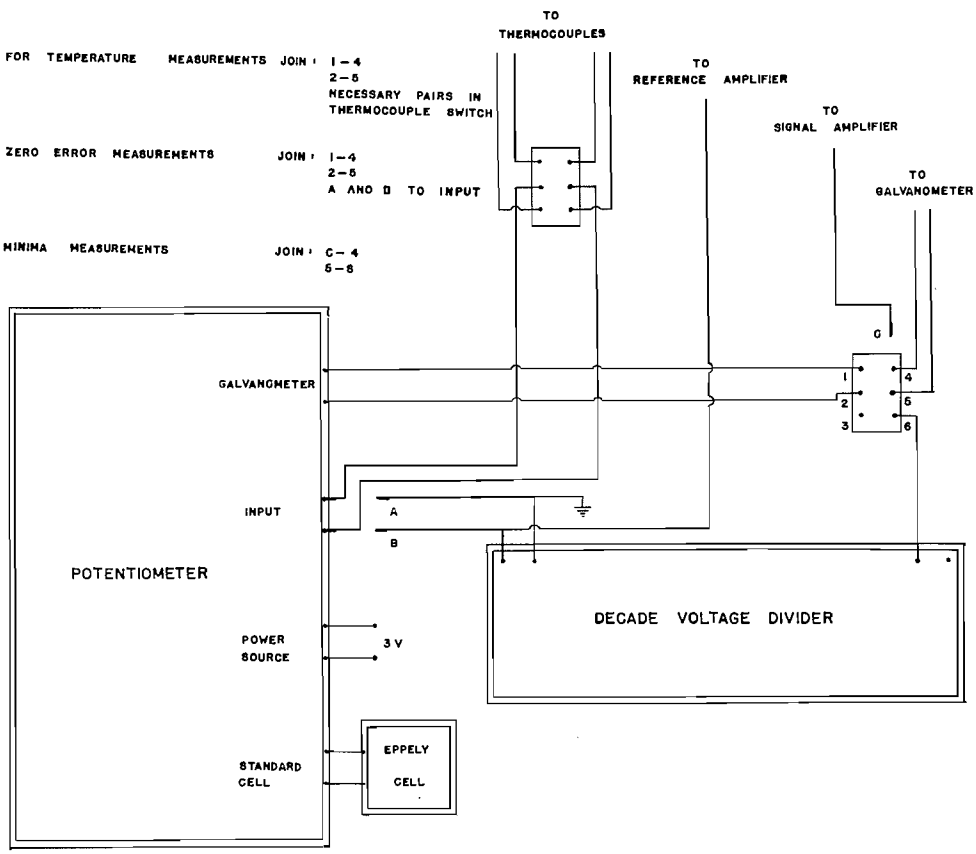


FIG. 2. Block diagram showing all external d-c. circuits.

Can. J. Chem. Downloaded from www.nrcresearchpress.com by 210.87.254.40 on 09/05/12
For personal use only.

the effects of both the short and comparatively long term variations in the source voltage from the signal generator.

In practice, this ratio, K, differed from the ratio of the crystal voltages, k, by about 1% due to the zero errors arising from the spring contacts. These small voltages of less than 3 microvolts were measured for every minimum as was the total output of the reference amplifier, V. If x and y are the residual voltages of the signal and reference amplifiers respectively for no microwave signal, then

$$k = \frac{A_s S + x}{A_r R + y}$$

and

$$K = \frac{S}{R} = \frac{A_r}{A_s}\left[k + \frac{ky}{V-y} - \frac{x}{V-y}\right]$$

where A_s and A_r are the amplifications, and S and R the magnitudes of the crystal voltages for the signal and reference lines respectively.

The probe carriage had a range of travel of about 45 cm and, for each determination, the two minima furthest apart within this range were studied. Voltage readings were recorded every 0.025 cm or, in the case of broad minima, every 0.050 or 0.100 cm, in the region of the minimum. Care was taken to extend these readings beyond the points of twice minimal voltage.

CALCULATIONS

Von Hippel (18) shows that

$$\frac{\tanh \gamma_2 d}{\gamma_2 d} = \frac{-j\lambda_1}{2\pi d} \frac{\frac{E_{min}}{E_{max}} - j \tan \frac{2\pi X_0}{\lambda_1}}{1 - j \frac{E_{min}}{E_{max}} \tan \frac{2\pi X_0}{\lambda_1}} \equiv Ce^{j\zeta}$$

where γ_2 is the propagation factor of medium 2, the adsorbate–adsorbent system; d is the sample length; λ_1 is the wavelength of the radiation in the slotted section; E_{min}/E_{max} is the inverse voltage–standing wave ratio; and X_0 is the position of the first minimum from the surface of the sample. X is defined as positive in the direction of the incident wave and has its origin at the interface of the sample. The short, then, occurs at $x = d$.

If $\gamma_2 d = Te^{j\tau}$, then, once C and ζ are known, T and τ can be evaluated either by charts (19, 20, 21) as was done in the present work or by a series approximation of the function $\tanh Te^{j\tau}/Te^{j\tau}$. Hence

$$\frac{\epsilon^*}{\epsilon_s} = \frac{\gamma_2^2}{\gamma_s^2} = \frac{\lambda_1^2}{(2\pi d)^2} (T_e{}^{j\tau})^2.$$

ϵ^* is the complex dielectric constant of medium 2, and ϵ_s is the dielectric constant of free space.

An examination of the above formulae shows that, depending entirely on the magnitudes of the primary data, great variations in the accuracy of the calculated values can occur. This fact has its source in two stages of the calculation.

One is the nature of equation for $Ce^{j\zeta}$. It will be seen that, if X_0 is very small or very near $-(\lambda_1/2)$, the term $\tan(2\pi X_0/\lambda_1)$, cannot be evaluated with great accuracy, even although the precision and accuracy of the primary data remain unchanged. Similarly,

Can. J. Chem. Downloaded from www.nrcresearchpress.com by 210.87.254.40 on 09/05/12
For personal use only.

Can. J. Chem. Downloaded from www.nrcresearchpress.com by 210.87.254.40 on 09/05/12
For personal use only.

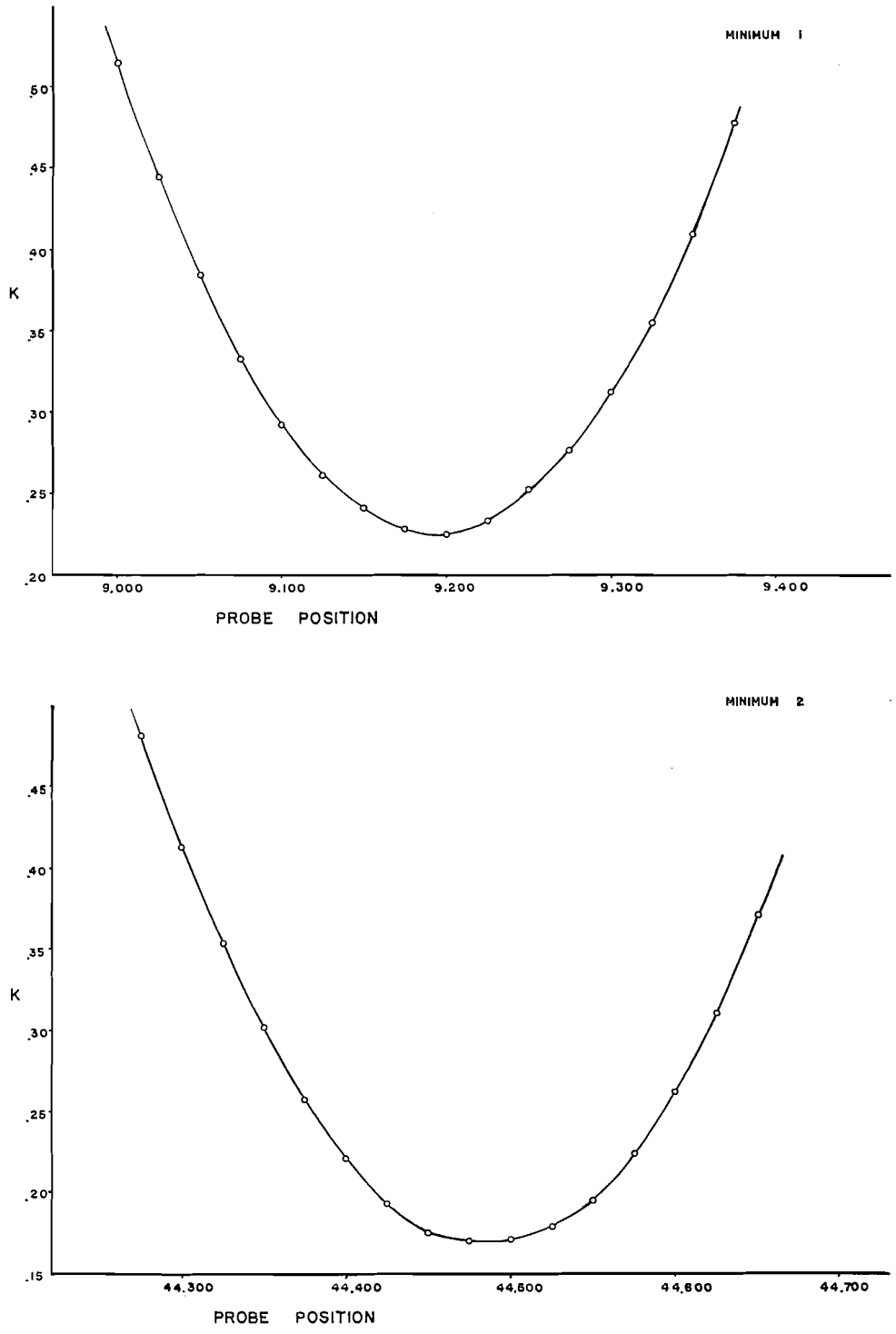


FIG. 3. Plots of K against probe position for measurements of 1280 Mc sec^{-1}, 339.8 cc of ethyl chloride adsorbed, and $-33.2°$ C.

when X_0 is approximately equal to $-(\lambda_1/4)$, $\tan 2\pi X_0/\lambda_1$ varies very rapidly with X_0 and the accuracy of Ce^{jr} becomes much less than that of the primary data.

It is the nature of these measurements that, as ϵ' increases, all else remaining equal, X_0 decreases from $-\lambda_1/2$ to 0 in cycles. Hence it was inevitable in the course of these measurements that, for a fixed sample length, certain regions of interest were not capable of accurate analysis. This was true, for example, at 1600 megacycles for comparatively low dielectric values and at 1280 megacycles for comparatively high dielectric values, despite the fine primary data, an example of which is shown in Fig. 3.

The other source of variation in the magnitude of the error is the $T-\tau$ chart. In each $T-\tau$ chart are areas of curvature and skew which make linear interpolation between the plotted lines very approximate. Other areas are nearly Cartesian in their regularity and can be read to four significant figures with ease. It is suggested that the programing of a computer to solve equation for γ_2 by a series approximation would be an improvement.

Care was taken to apply corrections to ΔX for attenuation in the line and its fittings (22), for asymmetry (22), and for deviations of the wave form, at low standing wave ratios, from the assumed form (18, 19, 20, 23) by which E_{min}/E_{max} was evaluated from the width of the curve at twice minimal voltage.

RESULTS

For small admission of gas, a fixed amount of gas was put in the cell system and the temperature varied. For large admissions, the temperature was kept constant while known amounts of gas were admitted to the system. This procedure was adopted in the multilayer since it was one of the purposes of this research to determine if hysteresis existed in the dielectric data corresponding to the hysteresis in the adsorption data. The latter method proved very satisfactory, although slightly slower, and is recommended. Isotherms for the three temperatures studied are shown in Fig. 4.

For each isotherm, dielectric constants were obtained at from six to nine chosen frequencies for eight or nine adsorptions. A disappointing error between frequencies was observed, which hindered accurate assessment of the dependence of ϵ' or ϵ'' on frequency.

For glass alone, no variations of ϵ' or ϵ'' with temperature could be observed. Average values of the dielectric constants, with their average deviations, are shown in Table I.

TABLE I

Dielectric constants of Vycor glass. Average, for each frequency, of data obtained at three temperatures at which isotherms were studied

Frequency (Mc sec^{-1})	ϵ' ± av. dev.	ϵ'' ± av. dev.
530	3.304 ± .015	.0674 ± .0032
640	3.246 ± .006	.0739 ± .0017
820	3.113 ± .006	.0797 ± .0040
1020	3.116 ± .003	.0859 ± .0024
1280	3.120 ± .015	.0720 ± .0044
1600	2.935 ± .004	.0890 ± .0032
2000	3.000 ± .008	.0763 ± .0020
2550	3.071 ± .002	.0853 ± .0084
3200	3.186 ± .021	.0956 ± .0060

Can. J. Chem. Downloaded from www.nrcresearchpress.com by 210.87.254.40 on 09/05/12
For personal use only.

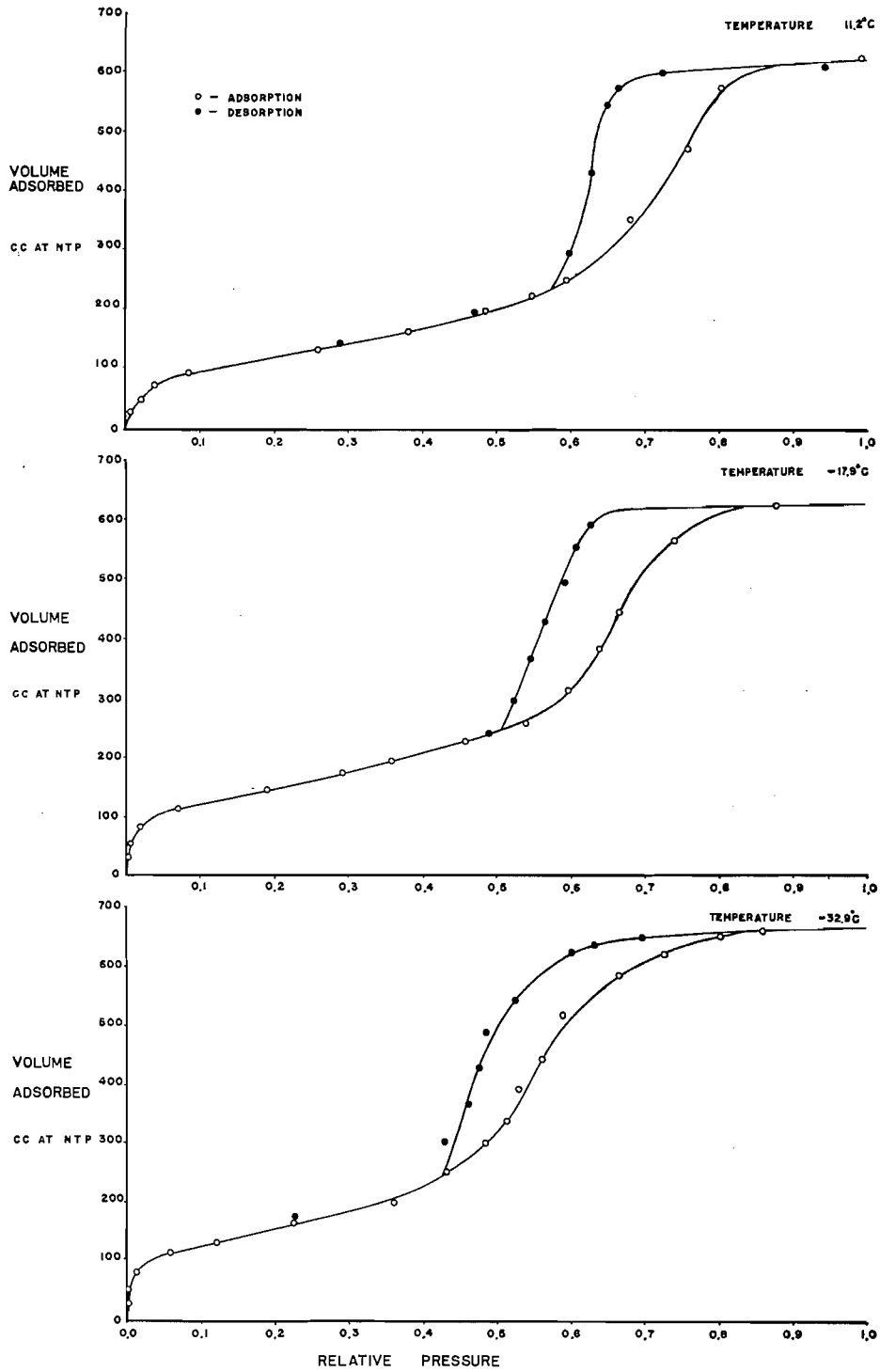


FIG. 4. The variation of volume adsorbed with relative pressure for the three temperatures studied.

Can. J. Chem. Downloaded from www.nrcresearchpress.com by 210.87.254.40 on 09/05/12
For personal use only.

Plots of ϵ' and ϵ'' against volume adsorbed were made. Examples are shown in Figs. 5 and 6. It will be seen that the plots of ϵ' against volume adsorbed consist of two linear portions. The second section, beginning between 100 and 150 cc adsorbed, always has a lower slope than the first. This is in agreement with results obtained by McIntosh, Rideal, and Snelgrove (3) and Petrie and McIntosh (7).

Straight lines are fitted to the data by the least-squares method, different lines being fitted above and below 125 cc. Since the values of ϵ_0' for glass were the means of three determinations, the additional constraint was put on the first section that it pass through this point. The values of the slopes, calculated by this method are shown in Table II.

TABLE II

Slopes of plots of ϵ' against volume adsorbed

Temperature (°C)	Frequency (Mc sec^{-1})						
	530	640	1020	1280	1600	2000	3200
+11.2	.00464	.00445	.00541	.00437	.00552	.00420	.00426
−17.9	.00464	.00408	.00482	.00414	.00480	.00392	.00368
−32.9	.00438	.00386	.00469	.00394	.00446	.00357	.00329

Values of the dielectric constant of the adsorbed phase were calculated using the extension of Böttcher's treatment (3, 5). This was done for two representative points in each straight line portion. (See below.)

In calculating the adsorbate dielectric constant, the volume fraction of pore space was taken as 0.370 (24). The density of the ethyl chloride was taken to be that of the liquid at the appropriate temperature (25). Calculated values are shown in Table III.

Since the expressions arising in the extended Böttcher treatment are complicated when both the solid adsorbent and adsorbate exhibit loss, a statement concerning the method of solution and the necessary equations will be given.

The usual expression of the extended treatment, when the dielectric constant of the gas phase is taken as 1.0, is

$$[1] \qquad \frac{\epsilon+2}{3}-\frac{3\epsilon}{2\epsilon+1}\,\delta_3=\frac{\epsilon_0-1}{4\pi C_1}+\frac{\epsilon-\epsilon_0}{4\pi C_2};$$

ϵ is the dielectric constant of the composite system, ϵ_0 of the porous glass, δ_3 the volume fraction of free space, C_1 and C_2 the volume average polarizability of the glass and adsorbate, respectively. It must be remembered in the general case that ϵ, ϵ_0, C_1, and C_2 are complex quantities. On making these terms complex and equating real and imaginary quantities, one obtains

$$[2] \qquad \frac{\epsilon'+2}{3}-3\delta_3\left[\frac{2(\epsilon')^2+\epsilon'+2\epsilon''^2}{(2\epsilon'+1)^2+(2\epsilon'')^2}\right]=\frac{\epsilon_0'C_1'-C_1'+\epsilon_0''C_1''}{4\pi(C_1'^2+C_1''^2)}+\frac{(\epsilon_1'-\epsilon_0')C_2'+(\epsilon''-\epsilon_0'')C_2''}{4\pi(C_2'^2+C_2''^2)}$$

$$[3] \qquad -\frac{\epsilon''}{3}+3\delta_3\left[\frac{\epsilon''}{(2\epsilon'+1)^2+(2\epsilon'')^2}\right]=\frac{C_1''(\epsilon_0'-1)-C_1'\epsilon_0''}{4\pi(C_1'^2+C_1''^2)}+\frac{(\epsilon'-\epsilon_0')C_2''+(\epsilon_0''-\epsilon'')C_2'}{4\pi(C_2'^2+C_2''^2)}.$$

Calling the left-hand sides of equations [2] and [3] L_1 and L_2, respectively, and the first term of the right-hand side of each of equations [2] and [3], A_1 and A_2, respectively, it

Can. J. Chem. Downloaded from www.nrcresearchpress.com by 210.87.254.40 on 09/05/12
For personal use only.

follows that

$$[4] \qquad \frac{L_1-A_1}{L_2-A_2} = \frac{C_2'(\epsilon'-\epsilon_0')+C_2''(\epsilon''-\epsilon_0'')}{C_2''(\epsilon'-\epsilon_0')+C_2'(\epsilon_0''-\epsilon'')}$$

and therefore that

$$[5] \qquad C_2'' = \frac{(\epsilon_0''-\epsilon'')(L_1-A_1)-(\epsilon'-\epsilon_0')(L_2-A_2)}{(\epsilon''-\epsilon_0'')(L_2-A_2)-(\epsilon'-\epsilon_0')(L_1-A_1)}\, C_2' = XC_2'.$$

TABLE III

Dielectric constants of adsorbed phase

Temp. (°C)	Frequency (Mc sec^{-1})						
	530	640	1020	1280	1600	2000	3200
40 cc adsorbed ϵ_2'							
11.2	10.22	9.68	12.29	9.45	12.50	8.99	8.93
−17.9	10.09	9.28	11.26	9.24	11.23	8.67	8.06
−32.9	9.76	8.77	11.18	8.89	10.22	8.19	7.16
40 cc adsorbed ϵ_2''							
11.2	1.20	.56	.51	.88	1.10	1.06	.89
−17.9	1.71	1.42	1.68	1.77	2.35	2.13	1.93
−32.9	2.56	2.04	2.27	2.62	3.67	3.05	2.42
100 cc adsorbed ϵ_2'							
11.2	10.31	9.66	12.31	9.49	12.55	9.03	8.96
−17.9	10.28	9.41	11.33	9.39	11.49	8.83	8.20
−32.9	10.17	9.02	11.27	9.24	10.91	8.53	7.43
100 cc adsorbed ϵ_2''							
11.2	.53	.24	.22	.62	.68	.89	.65
−17.9	.78	.76	1.36	1.21	1.46	1.71	1.50
−32.9	1.41	1.23	2.00	1.77	2.29	2.45	1.87
250 cc adsorbed ϵ_2'							
11.2	5.63			5.83		6.59	5.86
−17.9	5.62			5.85		6.57	5.85
−32.9	5.62			5.84		6.55	5.81
250 cc adsorbed ϵ_2''							
11.2	.10			.14		.33	.24
−17.9	.17			.30		.57	.43
−32.9	.29			.39		.70	.68
500 cc adsorbed ϵ_2'							
11.2	5.63			5.86		6.60	5.86
−17.9	5.63			5.80		6.59	5.86
−32.9	5.62			5.85		6.58	5.85
500 cc adsorbed ϵ_2''							
11.2	.08			.13		.26	.24
−17.9	.13			.21		.34	.28
−32.9	.23			.24		.49	.41

Substitution in [2] for C_2'' yields

$$L_1 = A_1+\frac{1}{4\pi C_2'}\,\frac{(\epsilon'-\epsilon_0')+(\epsilon''-\epsilon_0'')X}{1+X^2}.$$

A plot of L_1 versus the coefficient of $1/(4\pi C_2')$ gives the value of C_2', C_2'' follows from equation [5]. Once these two quantities are known the values of ϵ_2' and ϵ_2'' may be obtained by equating the real and imaginary parts of the equation

$$[6] \qquad \frac{4}{3}\,\pi(C_2'-jC_2'') = \frac{\epsilon_2'-1-j\epsilon_2''}{\epsilon_2'+2-j\epsilon_2''}$$

and solving for ϵ_2' and ϵ_2''.

Can. J. Chem. Downloaded from www.nrcresearchpress.com by 210.87.254.40 on 09/05/12
For personal use only.

Can. J. Chem. Downloaded from www.nrcresearchpress.com by 210.87.254.40 on 09/05/12
For personal use only.

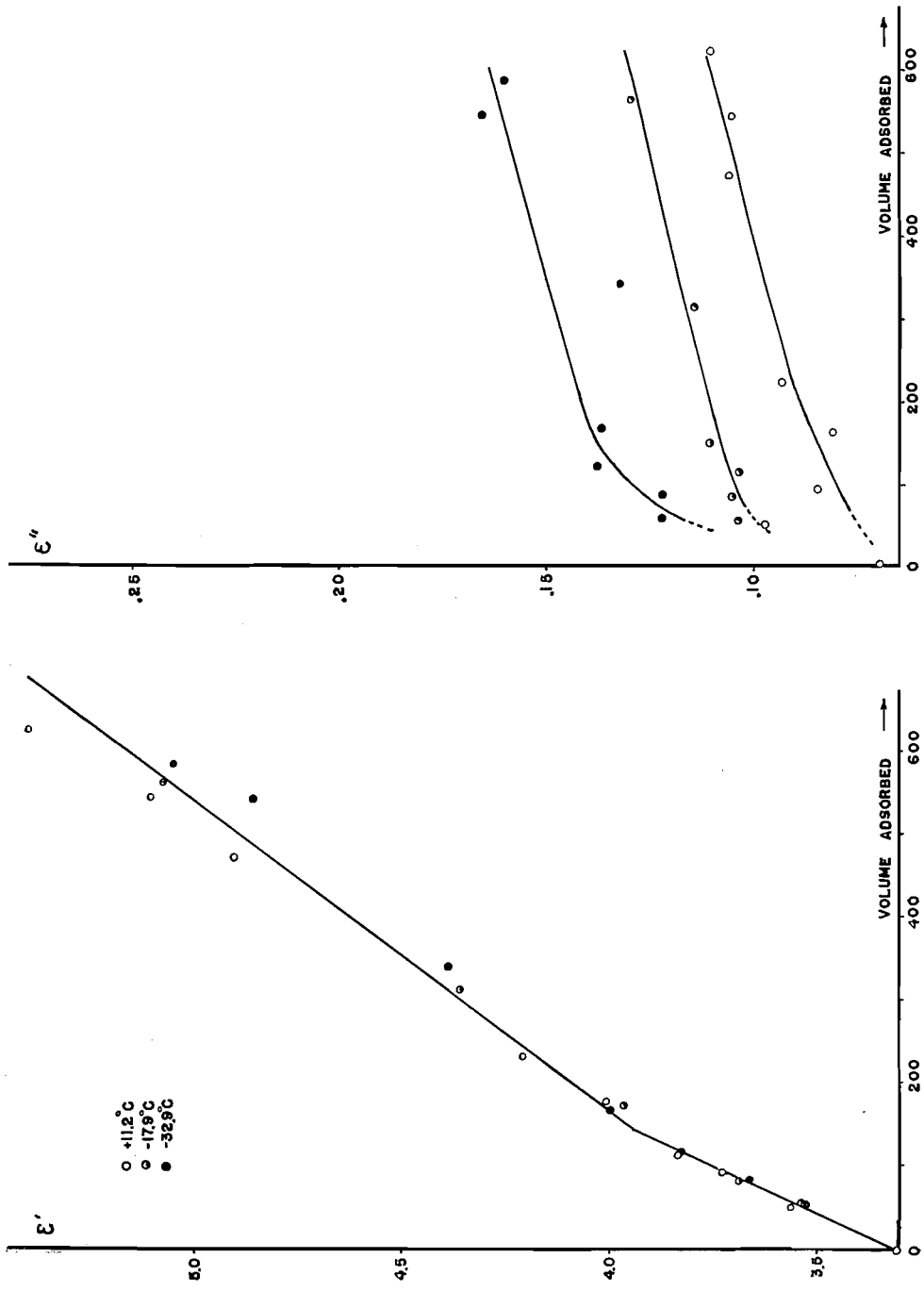


FIG. 5a.

Can. J. Chem. Downloaded from www.nrcresearchpress.com by 210.87.254.40 on 09/05/12
For personal use only.

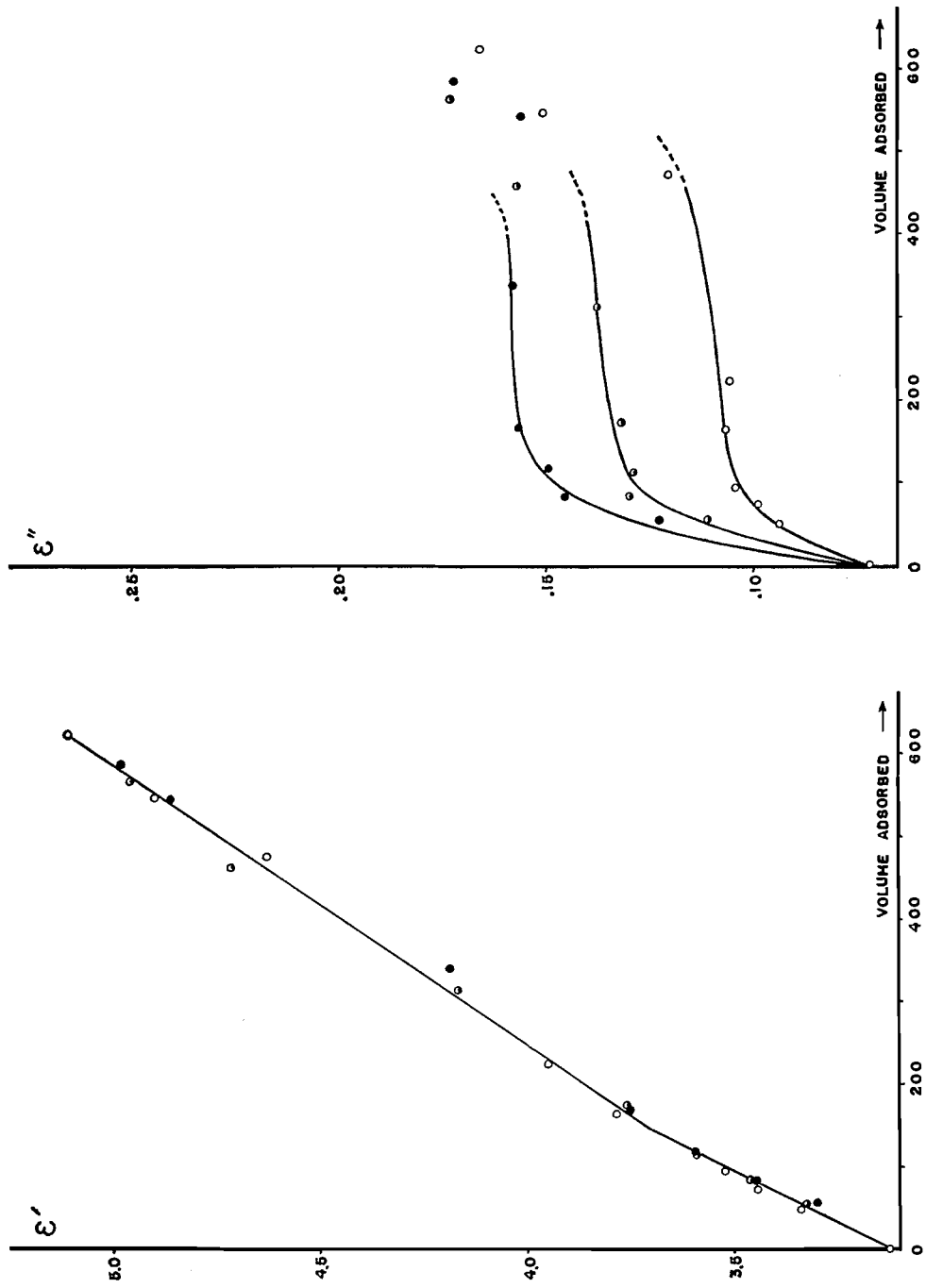


FIG. 5. Variation of dielectric constant with volume adsorbed at (*a*) 530 Mc sec^{-1}, (*b*) 1280 Mc sec^{-1} for 10.241 g of Vycor glass.

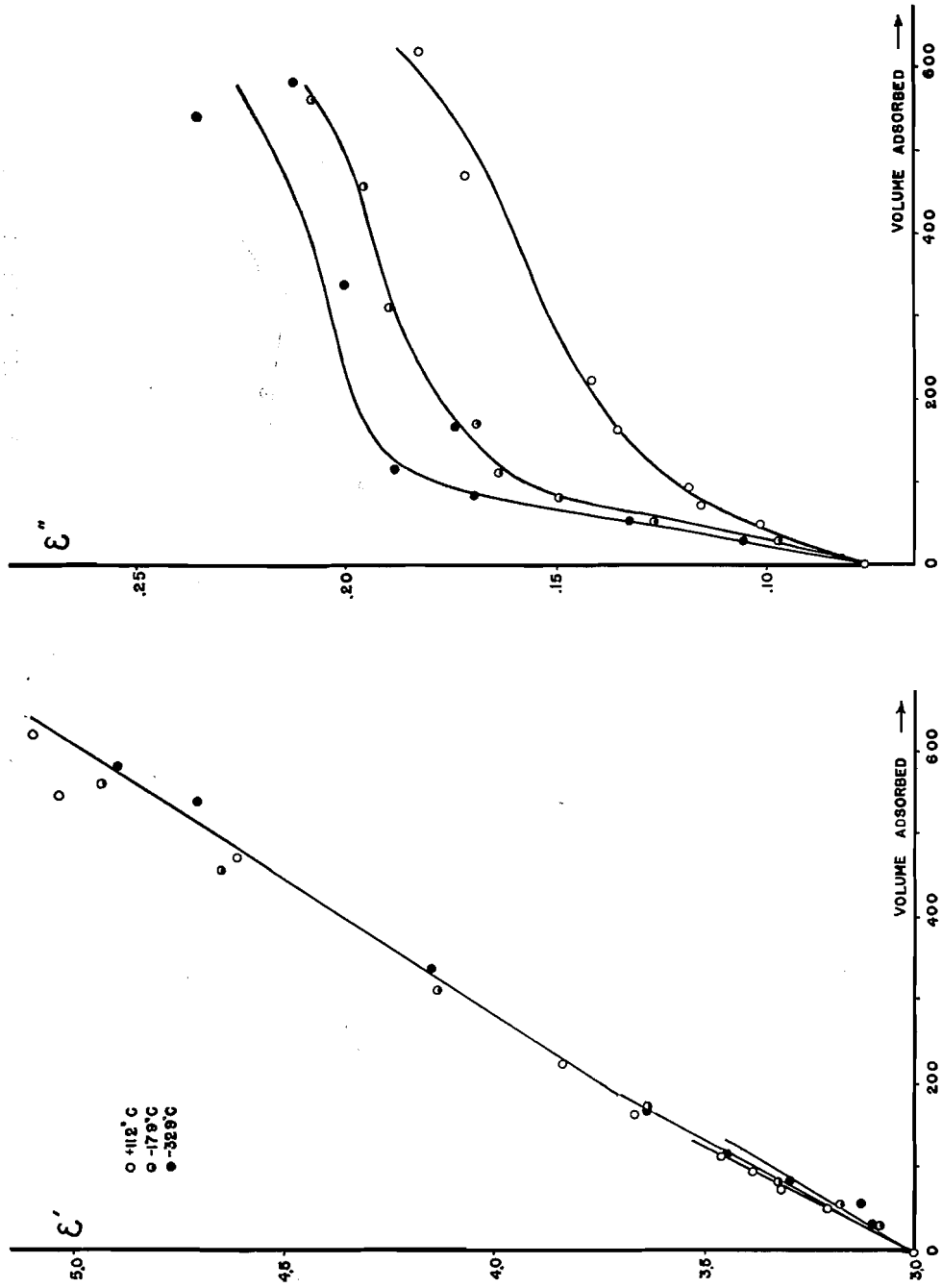


FIG. 6a.

Can. J. Chem. Downloaded from www.nrcresearchpress.com by 210.87.254.40 on 09/05/12
For personal use only.

Can. J. Chem. Downloaded from www.nrcresearchpress.com by 210.87.254.40 on 09/05/12
For personal use only.

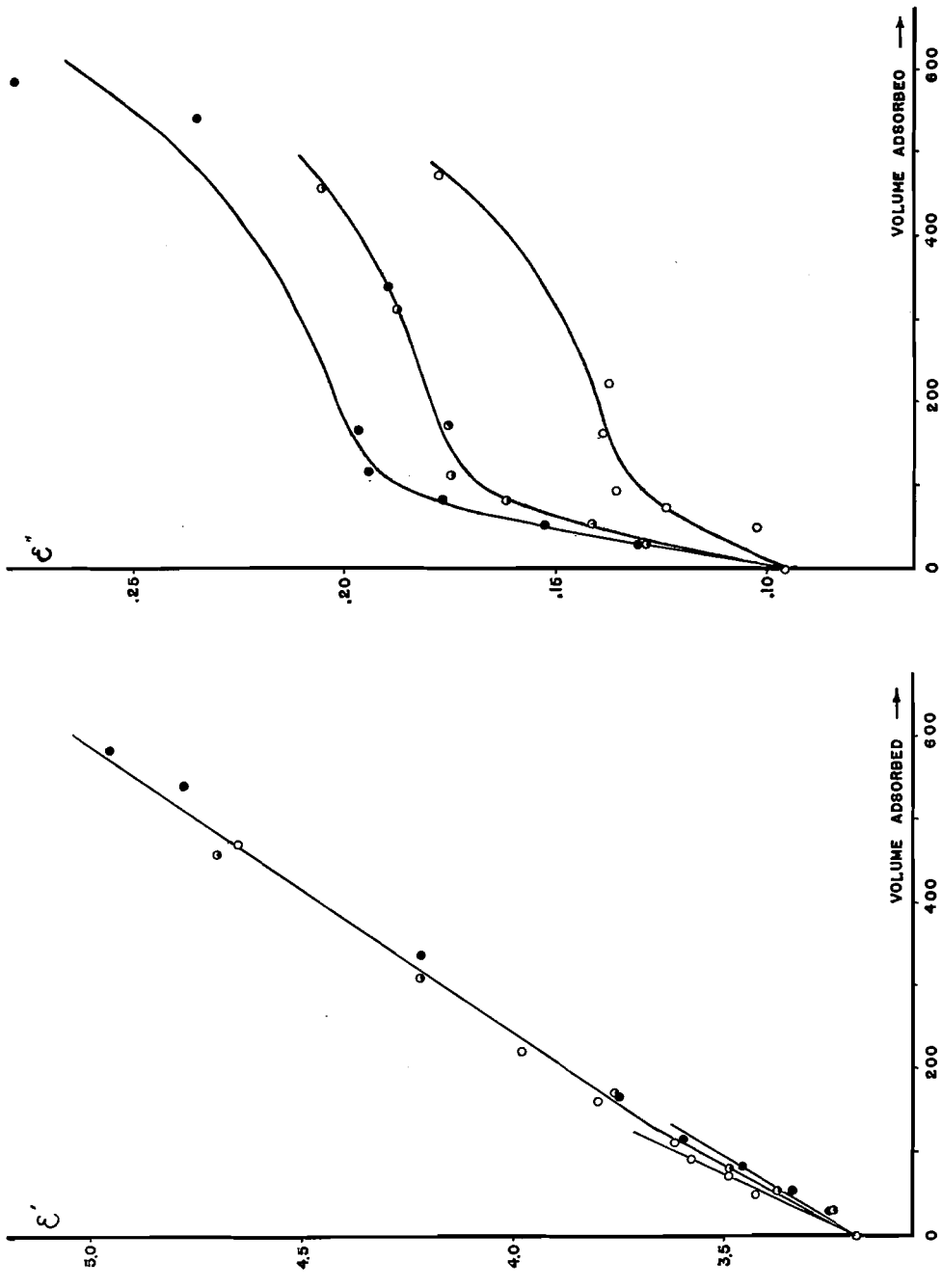


FIG. 6. Variation of dielectric constant with volume adsorbed at (*a*) 2000 Mc sec^{-1}, (*b*) 3200 Mc sec^{-1} for 10.241 g of Vycor glass.

Can. J. Chem. Downloaded from www.nrcresearchpress.com by 210.87.254.40 on 09/05/12
For personal use only.

DISCUSSION

In spite of the scatter of results as a function of frequency, the reality of certain findings appears definite. Thus, for quantities of gas adsorbed below about 140 cc, a slight positive temperature coefficient of ϵ_2' and large values of ϵ_2'' are found. These facts are sufficient to establish the existence of dispersion in the adsorbate for coverages which suggest the formation and the filling of the first layer. Since, as was suggested in the introduction, a zero or negligible temperature coefficient implies rotational oscillators it is not improbable that when the loss curve is adequately established, it will turn out to have a form associated with resonance absorption.

The values of ϵ_2'' are much higher for 40 cc adsorbed than for 100 cc adsorbed although ϵ'' for the total system is higher at 100 cc. This indicates that the new material in the adsorbed phase contributes less to the loss. The same observation is even more marked for higher adsorptions.

The absolute values of ϵ_2' and ϵ_2'' are, of course, subject to the uncertainties which have been pointed out in earlier papers (5).

In the present instance the value of ϵ_2' is quite close to that of bulk liquid for adsorption below 140 cc, and this must mean that the amplitude of the oscillations of the adsorbed molecules is large. This, in turn, implies that the frequency of rotational oscillations need not be very great. Assuming, then, that the adsorbed molecules do behave as rotational oscillators and that the evidence of a loss maximum at a frequency in the order of a few thousand megacycles per second may be accepted, the two findings are not mutually inconsistent. Where estimates have been attempted to ascertain the natural frequency of such a mode of motion for an adsorbed molecule (10), a much simpler molecule and surface were assumed, and the frequency was much higher than observed here.

According to Figs. 5 and 6 the value of ϵ' of the total system and that of ϵ'' change in a different manner with volume adsorbed once about 140 cc of gas has been adsorbed. The anomaly of low values of ϵ_2' which results from these primary data even when there is no evidence of dispersion has already been emphasized in earlier publications (5). As the calculated value of ϵ_2' is appreciably greater than could be accounted for by distortion polarization alone, a situation which is not found in the case of normal butane, it is again possible that rotational oscillations of smaller amplitude than for the first adsorbed matter could account for the result. In the present instance, however, the variation of ϵ_2'' with amount adsorbed is much less than for the initially adsorbed matter. Moreover, the effect of temperature on the loss, as the plots of ϵ'' show, is much less than for the first section of the data. The matter does not behave, however, as bulk liquid, since the temperature coefficient of ϵ_2' is negligible. Moreover, the beginning of absorption in the multilayer region is evident only at the highest frequencies used and for the highest adsorptions where the material might be expected to approximate most closely to the liquid structure. Calculations for the absorption peak for liquid ethyl chloride (26) based on the equation of Debye (27) and Powles (28) show that the peak for the liquid should occur between 7000 and 10,000 Mc sec^{-1} at $-30°$ C. Between 140 and 400 cc adsorbed, there is little evidence of loss. It would seem, then, that the adsorbate, particularly at the beginning of the multilayer region, does not have liquid properties. It is thus shown that the lower absolute value of ϵ_2' is not wholly caused by whatever factor brings about the low value of dielectric constant in butane.

Although it is true that absolute values of ϵ_2' differ to some extent from values reported by Petrie, Channen, and McIntosh (16) for rutile as the substrate, and by Petrie and

McIntosh (7) for powdered Vycor glass and silica gel as the adsorbent, the general measure of agreement is good. All work has shown higher dielectric constants for the first matter adsorbed than for the second on porous adsorbents, and the temperature coefficients are small or zero, except for the situation described here of a positive temperature coefficient in a region where dispersion is clearly apparent.

Comment upon the existence of hysteresis in the dielectric curves as claimed by Thorp (12) and more recently by Fiat (13) is difficult. No evidence in support of their claims appears in this work or in that done by Petrie (see Fig. 7). Thorp's claim to relate

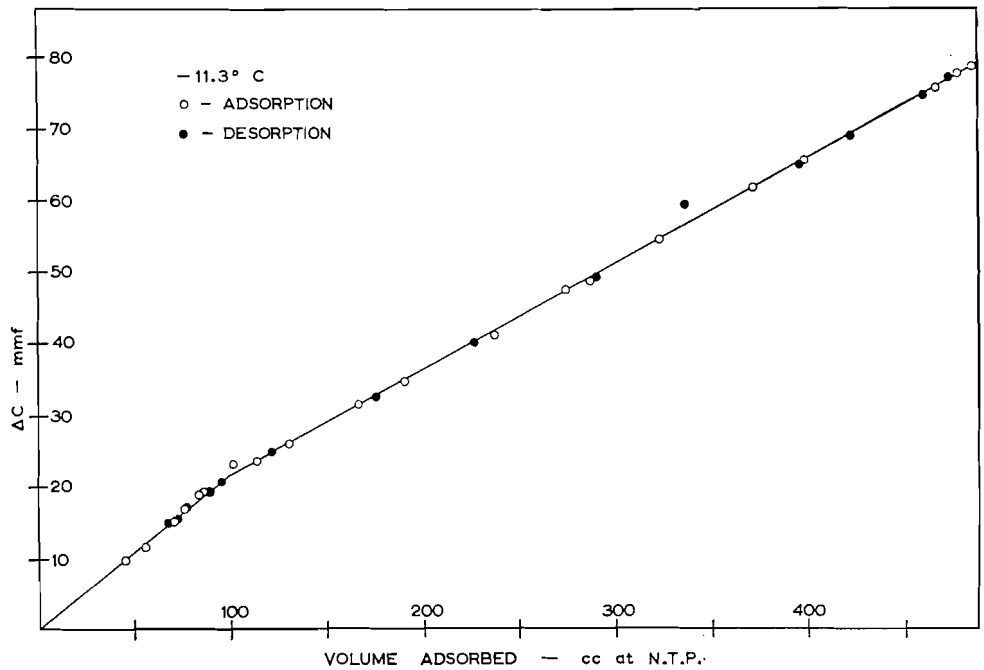


FIG. 7. Variation of capacity with volume adsorbed at −11.3° C, 3.70 Mc sec^{-1}, and 7.053 g of Vycor glass granules.

the variations of type of hysteresis to pore-size distribution appears unwarranted in view of the doubt that pore-size distributions may be assessed even qualitatively from the shape of isotherms and the Kelvin theory (29). On the other hand, gel systems like Vycor glass, activated carbon, etc. are known to shrink and swell due to the presence of adsorbate (24, 30, 31), and such movement may cause changes of packing in powders. Additionally, very long time lags occur before the establishment of apparent equilibrium, and possibly these are involved. In any event, some difference of experimental procedure of the several investigators seems to be the cause of the discordant results, because the gel systems employed appear very similar in terms of the type of adsorption isotherm which they exhibit.

ACKNOWLEDGMENTS

Grateful acknowledgment is made to the National Research Council and to the Advisory Committee on Research of the University of Toronto for financial support

Can. J. Chem. Downloaded from www.nrcresearchpress.com by 210.87.254.40 on 09/05/12
For personal use only.

of this work. It is also a pleasure to acknowledge once again our indebtedness to Professor J. M. Anderson of the Department of Physics for his aid in connection with the amplifiers and his advice on all aspects of the electrical measurements.

REFERENCES

1. R. L. McIntosh, H. S. Johnson, N. Hollies, and L. McLeod. Can. J. Research, B, **25**, 566 (1947).
2. I. Higuti. Sci. Repts., Tohoku Univ. **33**, 99, 174, 231 (1949).
3. R. McIntosh, E. K. Rideal, and J. A. Snelgrove. Proc. Roy. Soc. (London), A, **208**, 292 (1951).
4. S. Kurosaki. J. Phys. Chem. **58**, 320 (1954).
5. E. W. Channen and R. L. McIntosh. Can. J. Chem. **33**, 172 (1955).
6. M. H. Waldman, J. A. Snelgrove, and R. L. McIntosh. Can. J. Chem. **33**, 268 (1955).
7. S. E. Petrie and R. L. McIntosh. Can. J. Chem. **35**, 183 (1957).
8. H. Frohlich. Theory of dielectrics. Oxford. 1949.
9. L. N. Kurbatov. J. Phys. Chem. (U.S.S.R.) **24**, 899 (1950).
10. G. C. Benson, E. W. Channen, and R. L. McIntosh. J. Colloid Sci. **11**, 593 (1956).
11. M. H. Waldman. J. phys., radium, **17**, 426 (1956).
12. J. M. Thorp. Trans. Faraday Soc. **55**, 442 (1958).
13. Fiat. Private communication. 1960.
14. S. E. Petrie. Ph.D. Thesis, University of Toronto, Toronto, Ont. 1957.
15. J. D. McCowan. Ph.D. Thesis, University of Toronto, Toronto, Ont. 1960.
16. S. E. Petrie, R. McIntosh, and E. W. Channen. Can. J. Chem. **35**, 1534 (1957).
17. M. H. Waldman and R. McIntosh. Can. J. Chem. **33**, 268 (1955).
18. A. R. von Hippel. Dielectrics and waves. Wiley, New York. 1954.
19. S. Roberts and A. von Hippel. Phys. Rev. **57**, 1056 (1940).
20. S. Roberts and A. von Hippel. J. Appl. Phys. **17**, 610 (1946).
21. A. R. von Hippel. Dielectric materials and applications. Wiley, New York. 1954.
22. E. M. Purcell. Techniques of microwave measurements. *Edited by* C. G. Montgomery. New York. 1947.
23. A. von Hippel, D. G. Jelatis, and W. B. Westphal. The measurement of dielectric constant and loss with standing waves in coaxial wave guides. Massachusetts Institute of Technology, Cambridge, Mass. 1943.
24. C. H. Amberg and R. McIntosh. Can. J. Chem. **30**, 1012 (1952).
25. J. D. Nickerson and R. McIntosh. Can. J. Chem. **35**, 1325 (1957).
26. I. D. Chapman. Private communication.
27. P. Debye. Polar molecules. Chemical Catalogue, New York. 1929.
28. J. G. Powles. J. Chem. Phys. **21**, 633 (1953).
29. H. W. Quinn and R. McIntosh. Proceedings of Second International Congress of Surface Activity. Butterworth Scientific Publications. 1957.
30. R. S. Haines and R. McIntosh. J. Chem. Phys. **15**, 28 (1947).
31. E. A. Flood and R. D. Heyding. Can. J. Chem. **32**, 660 (1954).

Can. J. Chem. Downloaded from www.nrcresearchpress.com by 210.87.254.40 on 09/05/12
For personal use only.

Can. J. Chem. Downloaded from www.nrcresearchpress.com by 210.87.254.40 on 09/05/12
For personal use only.

THE ALUMINUM REDUCTION OF MAGNESIUM OXIDE

I. THE VAPOR PRESSURE OF MAGNESIUM OVER THE SYSTEM Al–MgO[1]

K. GRJOTHEIM, O. HERSTAD, AND J. M. TOGURI

ABSTRACT

The equilibrium vapor pressure of magnesium over the reaction between magnesium oxide and aluminum was measured by means of the transportation method. In the temperature range 850–1150° C the results can be expressed by the equation $\log P_{\text{mm of Hg}} = -9617/T + 8.93$. From X-ray diffraction analysis this reaction proceeds according to the equilibrium

$$4MgO(s)+2Al(l) = MgAl_2O_4(s)+3Mg(g).$$

INTRODUCTION

Very little information exists in the literature on the reaction between solid magnesium oxide and metallic aluminum. On the assumption that this reaction proceeds according to equation [I],

$$3MgO + 2Al = Al_2O_3 + 3Mg, \qquad [I]$$

Treadwell (1) has calculated the equilibrium vapor pressure of magnesium over this reaction. His calculations showed that at 1470° C the equilibrium pressure of magnesium is 7.6 mm of Hg.

Later Beljajew (2) has reported that the equilibrium pressure of magnesium over reaction [I] is 1 atm at 1300° C.

From the available thermodynamic data (3) the present authors have calculated the pressure of magnesium over reaction [I] to be 98 mm of Hg at 1300° C.

Since this discrepancy exists, it was the purpose of the present investigation to examine the reaction between solid magnesium oxide and metallic aluminum. The logical approach to the study of reactions of this type, involving components in the vapor, is the measurement of the equilibrium vapor pressure associated with the reaction, and to identify the end products of the reaction in order to establish the reaction scheme.

EXPERIMENTAL

The experimental method adopted to measure the equilibrium vapor pressure of magnesium was the transportation method, since the expected vapor pressure range was 10^{-2}–10^{2} mm of Hg over the desired temperature range. This method of measuring vapor pressure has proved to be successful for a number of similar reactions (4, 5). It is a dynamic method, in which the magnesium vapor in equilibrium with the solid components is carried away by a stream of inert gas flowing at a constant velocity. The amount of magnesium vapor transported is determined by condensing the vapor in a suitable condenser. The vapor pressure is then proportional to the mass of entrained vapor divided by the total volume of gas leaving the equilibration zone.

The important feature of the transportation method is the geometry of the apparatus. It must be designed to insure saturation of the carrier gas over a range of flow rates where the diffusion errors are negligible, and where the measured pressure is independent of flow rate.

[1]*Manuscript received October 3, 1960.*
Contribution from the Institute of Inorganic Chemistry, The Technical University of Norway, Trondheim, Norway.

Can. J. Chem. Downloaded from www.nrcresearchpress.com by 210.87.254.40 on 09/05/12
For personal use only.

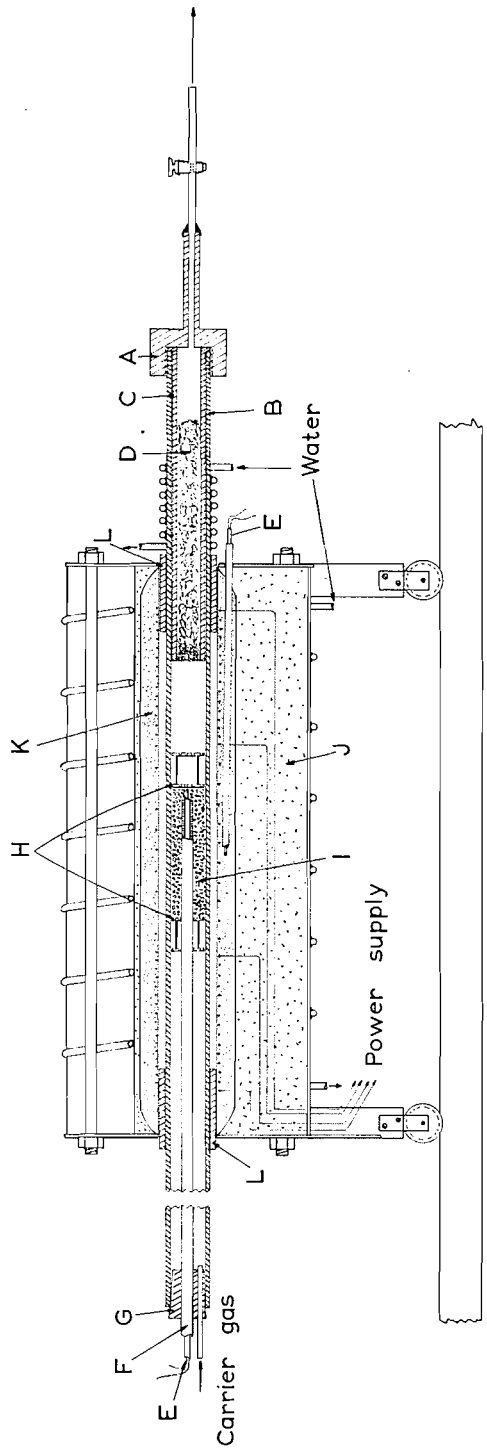


FIG. 1. Diagram of furnace showing position of sample.

A. Muffle
B. Retort tube
C. Condenser
D. Steel wool
E. Thermocouple (Pt-Pt 10% Rh)
F. Protecting tube for thermocouple
G. Rubber stopper
H. Perforated spacers
I. Reaction material
J. Silica gel (insulating material)
K. Heating element
L. Pythagoras tube

The furnace utilized for this purpose is shown in Fig. 1. It is a Kanthal A wire-wound electrical furnace similar to that described in detail by Motzfeldt (6). With this furnace an uniform temperature zone was obtained readily to within ±1.5° C, along the middle 15 cm of the furnace for temperatures of 800–1200° C.

An inconel tube (76% Ni, 15% Cr, and 9% Fe) of 3.2-cm I.D. was used as the reaction tube, since it was found to be chemically inert against the reactants and products of the reaction concerned, below 1150° C.

The charge is placed between two inconel perforated spacers, as shown in Fig. 1. These spacers not only keep the charge in place but also aid in packing the charge together, thus contributing towards the saturation of the carrier gas.

A steel condenser filled with washed steel wool is placed near the outlet of the reaction tube. This serves to condense and collect completely the evolved magnesium gas.

The carrier gas utilized throughout this investigation was S-argon gas obtained from Norsk Hydro, the analysis given was 99.94%. The impurities CO_2 and H_2O were removed by passing the argon through an Ascarite and a Dehydrite tower respectively. The hydrogen was obtained from Norsk Surstof og Vandstoffabrik A/S (99.7%) and was similarly purified.

The gas flow rate was measured using a calibrated rotameter and the total volume was determined by means of a calibrated gas meter.

A Pt–Pt 10% Rh thermocouple was placed into the charge, as shown in Fig. 1, to measure the temperature in conjunction with a precision Tinsley potentiometer with a mirror Lange-galvanometer.

PREPARATION OF CHARGE

The magnesium oxide and aluminum powder used throughout this investigation was obtained from Merck, Germany. The magnesium oxide was of pro analysis grade and the analysis of the aluminum was 99.9%.

Before use, the MgO was dried at 1000° C for 12 hours. The MgO and aluminum was then mixed and ground in a ball mill. The powdered mixture was pressed into briquettes at 500 kg/cm². The size of the briquettes were 2.0 cm in diameter by 1.5 cm in height.

These briquettes were broken into pieces of approximately 5 mm and packed into the reaction tube. Approximately 120 g of charge was used. The reactants prepared in this manner gave rise to a large sample surface area to reaction tube volume ratio and thus a condition which is favorable for insuring saturation of the carrier gas.

The experiment was started by moving the furnace, which is 100° C higher than the required temperature, along the reaction tube to a position such that the sample was located in the uniform temperature zone. During this period a stream of argon was passed from the opposite end until the required temperature was obtained, a period of approximately 5 to 10 minutes. When the temperature was reached the flow of argon was reversed and zero time was observed.

RESULTS AND DISCUSSION

(A) Effect of Flow Rate on the Apparent Vapor Pressure

A number of experiments were carried out to determine the effect of the flow rate of the carrier gas on the measured vapor pressure. In Fig. 2 results are shown for such experiments carried out at 998° C. In the case of argon as the carrier gas, the flow rate

Can. J. Chem. Downloaded from www.nrcresearchpress.com by 210.87.254.40 on 09/05/12
For personal use only.

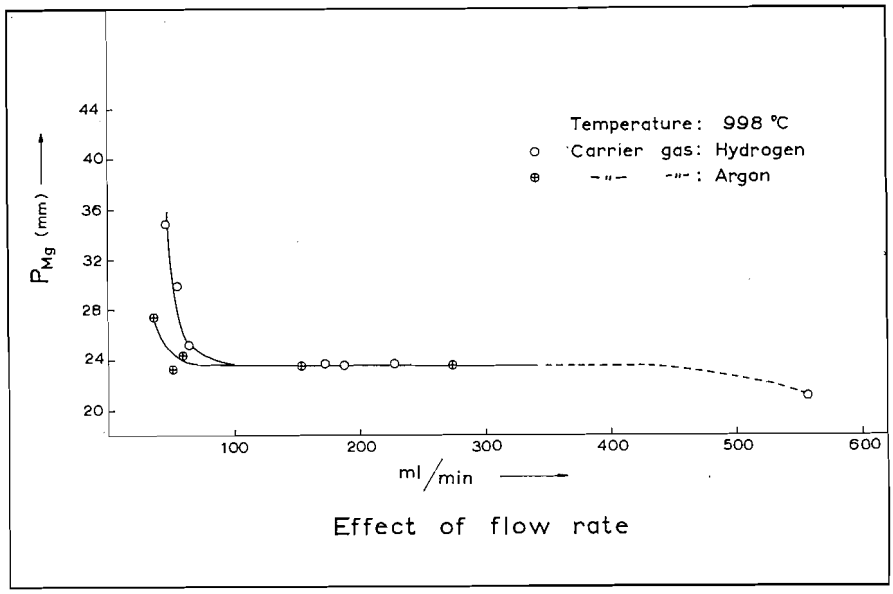


FIG. 2. Effect of flow rate using hydrogen and argon as carrier gas.

was varied from 37 to 274 ml/minute. For flow rates exceeding 100 ml/minute, there appears a plateau where the vapor pressure is independent of the flow rate. At lower flow rates, the resulting pressure, that is the mass of magnesium collected per unit volume, is much higher. This indicates that in addition to the equilibrium concentration of the vapor in the carrier gas, there is movement of vapor due to thermal diffusion and self-diffusion. This feature has been analyzed by Lepore and Van Wazer (7).

The existence of a relatively large region where the pressure is independent of the flow rate insured saturation of the carrier gas as well as a satisfactory design of the apparatus.

(B) Effect of Carrier Gas on the Vapor Pressure

To insure that the pressure measurements were independent of the nature of the carrier gas, hydrogen was also utilized as the entrainment gas. The results are shown in Fig. 2, at a temperature of 998° C. The flow rate was varied from 43 to 557 ml/minute. In the range from 100–350 ml/minute the vapor pressure is independent of the flow rate and is identical to that observed with argon. However, as expected the pressure increases very rapidly at low flow rates. At 43 ml/minute a 50% increase in pressure was observed.

These experiments showed that the measured pressure is independent of the nature of the carrier gas in the region of the plateau.

(C) Vapor Pressure Measurements over the Reaction

Measurements of the equilibrium vapor pressures of magnesium were carried out over the temperature range 870 to 1141° C. The results are shown in Fig. 3 and tabulated in Table I.

Can. J. Chem. Downloaded from www.nrcresearchpress.com by 210.87.254.40 on 09/05/12
For personal use only.

TABLE I

Experimental vapor pressure of magnesium

Temp. (° C)	Pressure (mm of Hg)
870	3.55
921	7.56
959	13.3
998	23.6
1072	56.0
1106	89.0
1115	100.1
1117	102.5
1141	143.2

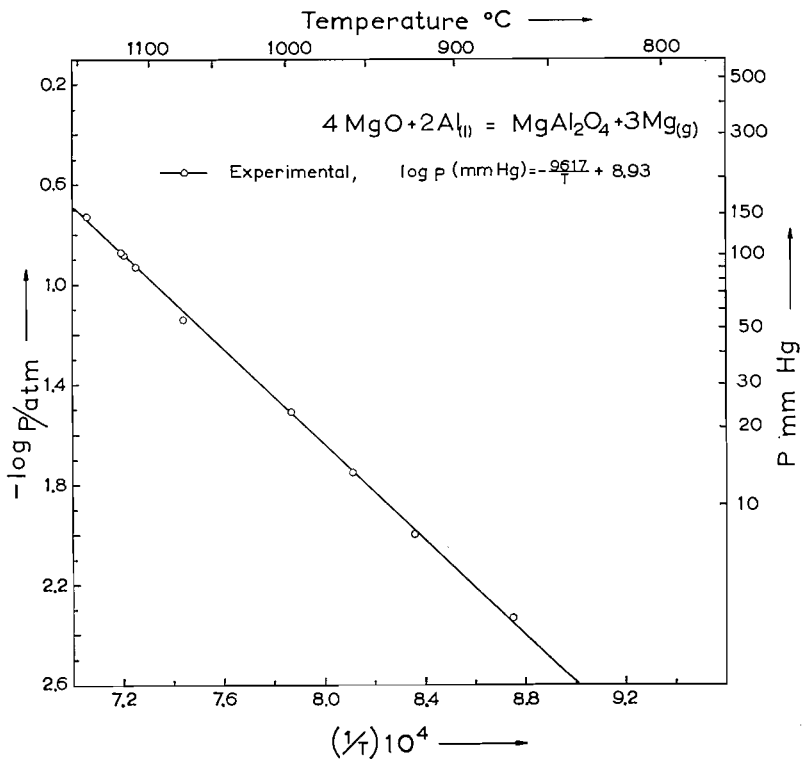


FIG. 3. Log P_{atm} of Mg versus $1/T°$ K.

In the temperature range investigated the data may be represented as a straight line and fitted to the equation,

$$\log P_{\text{mm of Hg}} = -(9617/T)+8.93,$$

where P is pressure in mm of Hg and T the absolute temperature.

(D) Analysis of the Reaction Product

The observed vapor pressure of magnesium in this investigation is in the same order of magnitude as that given by Beljajew (2) for reaction [I]. However, because the

Can. J. Chem. Downloaded from www.nrcresearchpress.com by 210.87.254.40 on 09/05/12
For personal use only.

measured and calculated vapor pressure is so vastly different for this reaction, the reaction product was determined by X-ray diffraction analysis.

It was found that the product is not Al_2O_3 but consisted of the spinel $MgAl_2O_4$ as shown in Fig. 4, and as compared to the ASTM Index (8). When the unreacted MgO and Al were removed by washing the reaction product in 0.5 *M* HCl acid, the resulting X-ray analysis showed only the spinel $MgAl_2O_4$. Chemical analysis of the product also confirmed the formation of the spinel.

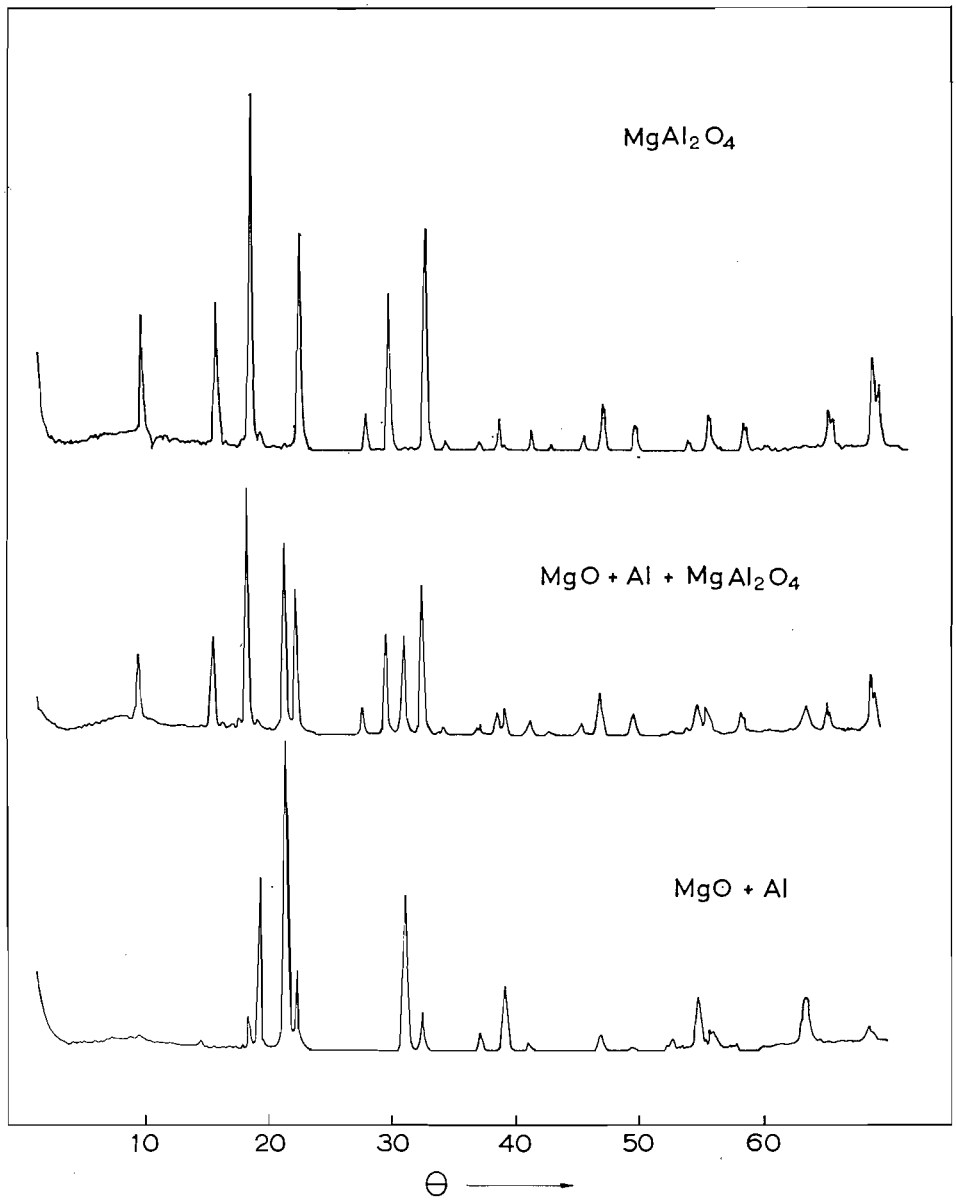


FIG. 4. X-Ray diffraction patterns obtained on using Cu target and Ni filter. The bottom shows the diffraction pattern of the reactants, the middle the residue. The top figure shows the pattern obtained after washing the residue with 0.5 *M* HCl acid, and indicates only $MgAl_2O_4$.

Can. J. Chem. Downloaded from www.nrcresearchpress.com by 210.87.254.40 on 09/05/12
For personal use only.

The reaction can therefore be represented by the equation

$$4MgO(s)+2Al(l) = MgAl_2O_4(s)+3Mg(g). \quad [II]$$

Upon altering the ratio of MgO/Al from 2/1 to 3/2 the measured vapor pressures were found to be identical.

(E) Thermodynamic Considerations

In the reaction concerned, aluminum appears as a liquid, and thus some solution of magnesium would be expected. For this reason the unreacted aluminum balls were collected from the reaction products and analyzed. In a few experiments small beads of aluminum were placed between the charge and condenser, in the uniform temperature zone, and these were also analyzed. The results at four temperatures are shown in Table II.

TABLE II

Analysis of magnesium in aluminum

Temp. (° C)	Mole% of Mg in aluminum	Activity of magnesium	
		From analysis of aluminum	From pressure measurements
870	3.7±5%	0.037	0.048
921	5.9±5%	0.059	0.056
959	6.0±5%	0.060	0.066
998	10.4±5%	0.104	0.079

Assuming ideality, the activity of magnesium has been calculated from the analysis. This is found to be in good agreement with the activity derived from the measured pressure, as shown in Table II.

Thus it was assumed that within the limits of the error of the analysis, aluminum formed an ideal solution with magnesium at the temperature at which the investigation was carried out.

In order to derive the thermodynamic functions of the spinel $MgAl_2O_4$, the equilibrium constant of the reaction was calculated for each temperature investigated, on the assumption that aluminum formed an ideal solution with magnesium. The phase diagram for the system MgO–$MgAl_2O_4$ (9) shows no solid solubility thus the activity of the oxides are assumed to equal unity. A "Σ-plot" has been carried out using the specific heat functions recommended by Kelley (10). The derived functions are shown in Table III for the over-all reaction.

TABLE III

Thermodynamic functions for the reaction $4MgO(s) + 2Al(l) = MgAl_2O_4(s)+3Mg(g)$ where $a_{Al} = 1$ (in the temperature range 932–1423° K)

$$\Delta C_p = -3.01-0.56\times10^{-3}T-3.86\times10^{5}T^{-2}$$
$$\Delta H^0_T = 137{,}400-3.01T-0.28\times10^{-3}T^2+3.86\times10^{5}T^{-1}$$
$$\Delta G^0_T = 137{,}400+6.93T\log T+0.28\times10^{-3}T^2+1.93\times10^{5}T^{-1}-109.74T$$
$$\Delta H^0_{1280°K} = 133{,}400 \text{ cal}$$
$$\Delta G^0_{1280°K} = 25{,}100 \text{ cal}$$
$$\Delta S^0_{1280°K} = 84.61 \text{ e.u.}$$

NOTE: It must be emphasized that these functions are also subjected to the inaccuracies of the C_p values obtained from the literature.

Can. J. Chem. Downloaded from www.nrcresearchpress.com by 210.87.254.40 on 09/05/12
For personal use only.

Combining the experimental data with the data on MgO and Al_2O_3 given by Kubaschewski and Evans (3), one obtains for reaction [III]

$$MgO + Al_2O_3 = MgAl_2O_4 \qquad [III]$$

the following data, $\Delta H^0_{298° K} = +1.1$ kcal, $\Delta G^0_{298° K} = -1.9$ kcal, and $\Delta S^0_{298° K} = 10.1$ e.u. The positive heat and the unreasonable large value of the entropy can be accounted for by the assumptions made with respect to the solubility of MgO in $MgAl_2O_4$ and the ideality of the Al–Mg system as well as the uncertainty of the existing literature data which is accumulated in the above type of calculation.

CONCLUSIONS

The reaction between solid magnesium oxide and metallic aluminum was found to proceed according to the equation

$$4MgO(s) + 2Al(l) = MgAl_2O_4(s) + 3Mg(g).$$

The solid reaction product is the spinel $MgAl_2O_4$ and not Al_2O_3 as reported by previous investigators.

The equilibrium pressure of magnesium over this reaction, in the temperature range 850–1150° C, can be represented by the equation,

$$\log P_{\text{mm of Hg}} = -(9617/T) + 8.93$$

as determined by means of the transportation method.

ACKNOWLEDGMENTS

This investigation, one of the series on the reduction of magnesium compounds, has been carried out under a research grant from ELEKTROKEMISKS FORSKNINGSFOND, for which the authors are grateful. One of the authors (J.M.T.) is indebted to the National Research Council of Canada for financial support in a form of a Postdoctorate Overseas Fellowship.

REFERENCES

1. W. D. TREADWELL. Helv. Chim. Acta, **19**, 126 (1936).
2. A. I. BELJAJEW. Metallurgie des Aluminiums. Vol. II. VEB Verlag Technik, Berlin. 1956. p. 281.
3. O. KUBASCHEWSKI and E. EVANS. Metallurgical thermochemistry. Pergamon Press Ltd., London. 1958.
4. L. M. PIDGEON and J. A. KING. Discussions Faraday Soc. 4, 197 (1948).
5. T. ROSENQVIST and B. ELLINGSAETER. J. Metals, **212**, 1111 (1956).
6. K. MOTZFELDT. Physico-chemical measurements at high temperature. Butterworths Scientific Pub., London. 1959. p. 51.
7. J. V. LEPORE and J. R. VAN WAZER. U. S. Atomic Energy Commission, MDDC 1188. 1948.
8. ASTM X-RAY POWDER DATA. File 5-0672.
9. E. LEVIN, H. MCMURDIE, and F. HALL. Phase diagram for ceramists. Am. Ceram. Soc. 1956.
10. K. K. KELLEY. U.S. Bureau of Mines Bulletin 584. 1960.

Can. J. Chem. Downloaded from www.nrcresearchpress.com by 210.87.254.40 on 09/05/12
For personal use only.

Can. J. Chem. Downloaded from www.nrcresearchpress.com by 210.87.254.6 on 09/05/12
For personal use only.

THE CRYSTAL SPECTRUM OF PERYLENE[1]

ROBIN M. HOCHSTRASSER

ABSTRACT

The electronic absorption spectrum of crystalline perylene has been examined in the spectral region 3000–4700 Å. The lowest energy electronic state of perylene has a large oscillator strength and the crystal spectrum deviates considerably from that calculated from a weak coupling (Davydov) model.

The sublimation flakes were examined at room temperature and at the temperature of boiling nitrogen. The lowest energy crystal state was polarized along the crystallographic a-axis (B_u) and the factor group splitting of lowest vibrational envelope of the electronic band was 800 cm^{-1}. The whole spectrum was more intense along the a- than along the b-axis of the crystal. These results are consistent with the notion that the crystal spectrum is derived from dipole-induced dipole interactions between molecular B_{2u} levels of perylene and neighboring unexcited molecules. This assignment of the lowest excited level of perylene is in agreement with theory.

The molecular vibrational structure is severely altered in the crystal and the observed crystal shift is much smaller than that predicted by the Davydov theory.

INTRODUCTION

It is now well established that the Davydov theory of the energy states of molecular crystals (1) can predict to a fair degree of accuracy the main features of the electronic absorption spectra of crystals. The theory has been most often applied to crystals of aromatic hydrocarbons such as naphthalene (2), anthracene (3), and phenanthrene (4).

With the exception of the 2500 Å system of anthracene the Davydov splittings that have been measured are usually from 10 cm^{-1} to 500 cm^{-1}, the actual value depending on the oscillator strength of the transition involved. In the intense short wavelength system of anthracene the splitting is much greater than this (ca. 15,400 cm^{-1}) (5) although in this case detailed examination of the structure is difficult because of the awkward spectral location of the bands.

Perylene has an intense absorption in the visible region and it is the purpose of this paper to present measurements of the polarized absorption spectra of single crystals of perylene and to compare these with the above-mentioned theory.

THE CRYSTAL STRUCTURE OF PERYLENE

Perylene is monoclinic prismatic (6). There are 4 molecules per unit cell occupying the general positions in the space group $C_{2h}^5(P2_1/a)$. The unit cell dimensions are as follows: $a = 11.35$, $b = 10.87$, $c = 10.31$ Å, $\beta = 100.8°$.

The angles which the molecular axes L (long) and M (short) make with the crystal axes a and b are denoted by χ and ψ. The calculated values of these angles along with the oriented gas ratios for absorption intensity along the a and b crystallographic axes for light incident perpendicular to the ab (001) face of the crystal are given in Table I.

TABLE I

The orientation of the molecules in the crystal and the oriented gas ratios

Molecular axis	χ	ψ	Da/Db
L	83.3°	89.2°	73:1
M	55.4°	35.0°	1:2.08

[1]*Manuscript received November 14, 1960.*
Contribution from the Chemistry Department, University of British Columbia, Vancouver, B.C. Work supported by the National Research Council, Ottawa, Canada.

Can. J. Chem. Downloaded from www.nrcresearchpress.com by 210.87.254.6 on 09/05/12
For personal use only.

The Energy Levels of the Crystal

It is assumed that the allowed $^1(\pi\pi^*)$ electronic states of perylene are polarized in the molecular plane. In this event the lowest energy molecular singlet level will have the symmetry B_{2u} (short axis polarized) or B_{3u} (long axis polarized). The site symmetry in the crystal is lower than the D_{2h} symmetry of the molecule and each of the molecular levels will split into two allowed crystal states. The polarizations and relative energies of these states—the A_u and B_u representations in the space group C_{2h}^5—can be calculated if the oscillator strength of the molecular transition and the dipole interaction integral summations are known (5). Table II gives the intermolecular interaction integrals within the dipole–dipole approximation. Only the sums over non-translationally equivalent molecules are given; p runs over molecules related by the operation C_2^b (twofold screw along the b-axis) and q runs over molecules related by σ^{ac} (glide reflection in the ac-plane). The geometry factors used were calculated to convergence by Craig and Walmsley (7).

Figure 1 illustrates the type of splitting expected for B_{2u} and B_{3u} molecular levels. In the former case the splitting is 196 cm^{-1} $(Å)^{-2}$ with the B_u (a axis polarized) crystal state at lowest energy. For B_{3u} levels the lowest crystal state is also B_u and the splitting is 2592 cm^{-1} $(Å)^{-2}$. The shift of the crystal spectrum relative to that in solution was calculated from the data of Craig and Walmsley (7) and the results are included in Fig. 1. The B_{2u} and B_{3u} molecular levels are thus predicted to show widely different properties when these crystal interactions are taken into account.

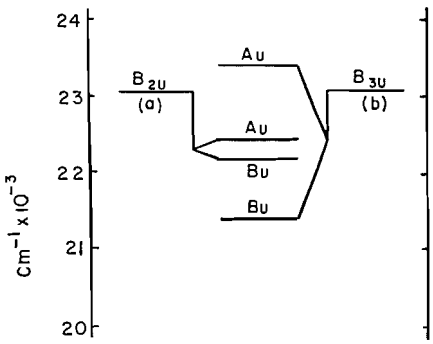


FIG. 1. The predicted arrangement of absorption bands of the perylene crystal for transitions to B_{2u} and B_{3u} molecular levels. Calculated for a dipole length of 1 Å.

EXPERIMENTAL

The perylene was purified further by recrystallization followed by sublimation *in vacuo*. Large rectangular plates were obtained when perylene was sublimed just below its melting point in an atmosphere of carbon dioxide. This was the only method whereby very thin crystals of this substance could be grown. Recrystallization from solution or the melt, sublimation *in vacuo*, and recrystallization between quartz disks all proved unsuccessful techniques in this case. The pure crystals were golden yellow. The thin crystals were pleochroic and exhibited symmetrical extinction under the polarizing microscope. A detailed examination of the isogyre patterns and the order of the interference colors indicated that the plates were basal sections with 001 as the most fully developed face. The b-axis was found to run parallel to the bisector of the slightly obtuse corner of the approximate rectangle. The optic plane of the crystal, containing the

Can. J. Chem. Downloaded from www.nrcresearchpress.com by 210.87.254.6 on 09/05/12
For personal use only.

a-axis, was normal to the exposed surface and bisected the acute-angled edge. Visual observations of the pleochroism indicated that the crystal absorbed most strongly when the electric vector of the light was made to vibrate parallel to the a-crystallographic axis.

The light source was a voltage-stabilized, air-cooled tungsten lamp. The spectrometer has been described previously. For the measurements at 77° K a metal cell was constructed with a copper holder in the nitrogen-free optical path. This cell has been described previously (8). The crystals were mounted over a pinhole by employing their own adhesive properties to metal or quartz. The analyzer was a Wollaston prism. In the low temperature experiments the polarized absorption spectra were obtained by spectrographic examination of each of the beams from the prism. For the experiments at room temperature the crystal was rotated relative to the prism and the optical system was not otherwise disturbed.

The f-number used in this work was determined by integration of the absorption spectrum of perylene in ethanol solution. A value of 5.4 ± 0.3 was obtained. The f-numbers of the vibronic components of the spectrum were obtained from the estimated areas of the individual vibronic bands of the spectrum in ethanol.

The Absorption Spectra

Figure 2 shows the absorption spectrum of a perylene crystal at room temperature. The relative intensities and exact spectral location of the bands were extremely sensitive to the crystal orientation. Figure 3 shows the spectrum of a thicker crystal at room temperature. The bands were much sharper at 77° K but even at this temperature (see Figs. 4 and 5) the details of the spectra were considerably altered by rotating the crystal through only fractions of a degree. This was understandable if the long axis of the molecule was active. This axis makes angles of 83.3° and 89.2° with the a- and b-crystallographic axes and very slight misorientations of the crystal would result in drastic changes of the expected oriented gas ratio of absorption intensities.

Table III shows the band positions measured in both crystal polarizations. The b-

TABLE II

Intermolecular interaction integrals (7)

	Integral sums [$cm^{-1}(Å)^{-2}$]	
Summations	$B_{3u} \leftarrow A_g$	$B_{2u} \leftarrow A_g$
$\sum_q I_{lq}/M^2$	−531	−774
$\sum_r I_{lr}/M^2$	−765	+876
Splitting	2592	204

polarized spectra were particularly difficult to interpret owing to the extreme weakness of some of the ill-resolved bands. The values which are quoted on Table III were seldom all observed with one crystal. It is for this reason that four representative spectra are shown.

Only a very broad, weak fluorescence emission was detected and the present experimental technique was not sensitive enough to enable a detailed study to be made. In this regard perylene resembles pyrene (9), a molecule that has also a similar crystal structure (6).

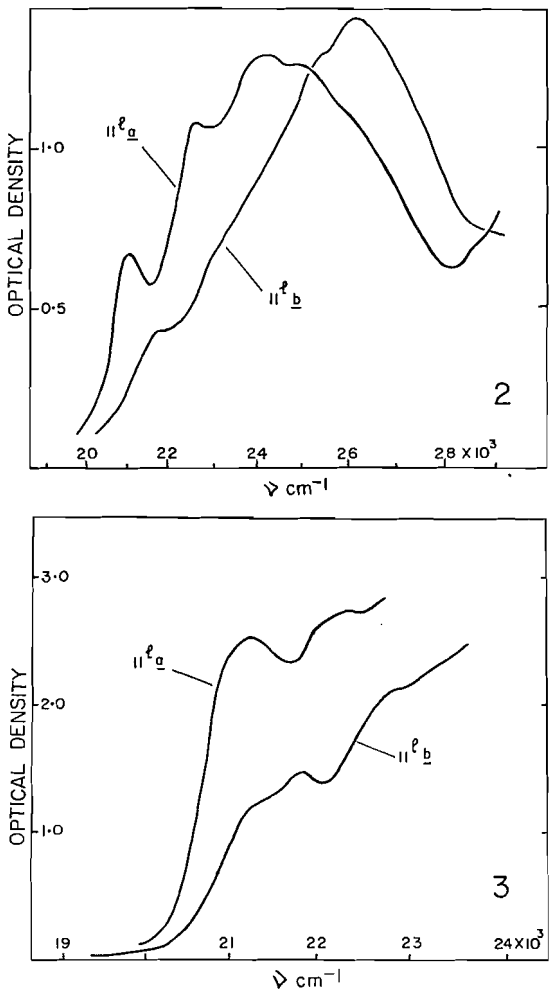
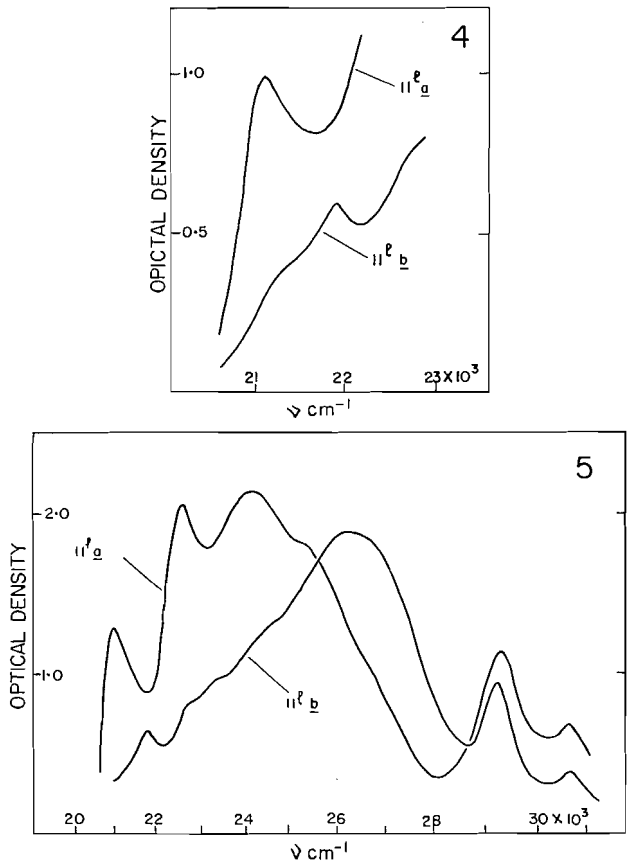


FIG. 2. Polarized absorption spectrum of perylene at room temperature.
FIG. 3. Polarized absorption spectrum of a thick perylene sublimation flake at room temperature.

DISCUSSION

The electronic levels of perylene have not yet received much theoretical attention. Platt (10) has predicted the polarizations of the transitions in this molecule using the simple free electron box model. The three lowest energy singlet states were calculated to have the same polarization properties; namely, they were all long axis polarized states thus belonging to the representation B_{2u} of the D_{2h} point group. A straightforward L.C.A.O.–A.S.M.O. calculation using Hückel orbitals yields the result that the lowest two excited molecular levels should have different symmetry. These two levels are predicted to lie at 19.8 kK (B_{2u}), and 28.4 kK (B_{3u}) respectively (1 kK ≡ 1000 cm^{-1}). A further intense level is expected at 42.4 kK with B_{3u} symmetry. These results are in fair agreement with the solution spectrum (11), which exhibits four separable absorptions in this spectral region. These were assigned on the basis of analogy, band structure, and intensity by Clar (11) as follows: 22.75 kK (p, B_{2u}); 29.60 kK (α, B_{3u}); 34.32 kK (β, B_{2u}); 39.86 (β, B_{3u}).

Can. J. Chem. Downloaded from www.nrcresearchpress.com by 210.87.254.6 on 09/05/12
For personal use only.



FIGS. 4 and 5. Polarized absorption spectrum of the perylene crystal at 77° K.

These predictions were substantiated by the results of Williams (11), who has shown that the lowest molecular level of perylene is polarized at right angles to the level at 39.86 kK.

In summary, it may be expected that absorption to the lowest excited singlet state of perylene will be intense and that the next lowest excited level will be active along the short molecular axis of the molecule (B_{3u}).

Figure 6 shows the observed energy scheme for the perylene crystal. A comparison with Fig. 1 clearly indicates that it is the B_{2u} molecular level from which the crystal spectrum is derived. The observed splittings are one order of magnitude too small to be accounted for by interactions between dipoles directed along the short molecular axes.

The over-all intensity of absorption in the *a*-polarized spectrum is greater than in the *b*-spectrum. This observation is in agreement with the predictions in Table I. The polarization ratios, however, were not expected to correlate with the oriented gas ratios in view of the large splitting. The poor agreement between theory and experiment in regard to polarization ratio is probably concerned with the near coincidence of the long molecular axis with the C′-crystallographic axis thus making it difficult to measure this quantity. In any case, the measured quantity in this work was the optical density ratio. This ratio may only be equal to the polarization ratio if the bands have similar shapes and have

Can. J. Chem. Downloaded from www.nrcresearchpress.com by 210.87.254.6 on 09/05/12
For personal use only.

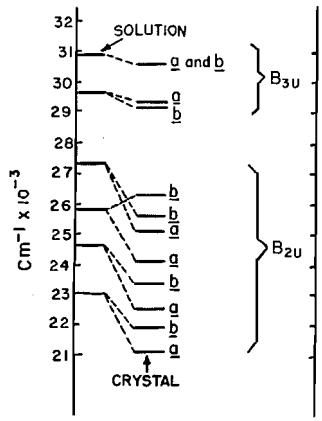


FIG. 6. Comparison of the observed data for perylene in solution and in the crystalline state.

nearly equal frequencies of maximum absorption. Clearly these conditions are not satisfied.

The absorption spectra show four bands in the region 20,000–28,000 cm^{-1}. The relationship between the *a*- and *b*-polarized spectra is apparent for the two lowest energy bands in each polarization (see Table III) but there may be some ambiguity regarding the

TABLE III

The band maxima in the absorption spectrum of the perylene crystal

Energy of band maximum ±40 cm^{-1}	Polarization	Assignment
21,160	*a*	B_u
21,930	*b*	A_u
22,510	*a*	$B_u \times a_g$
23,400	*b*	$A_u \times a_g$
24,110	*a*	$B_u \times (a_g)^2$
25,100	*a*	$B_u \times (a_g)^3$
25,575	*b*	$A_u \times (a_g)^2$
26,300	*b*	$A_u \times (a_g)^3$
29,130	*b*	Different crystal state; molecular $^1B_{3u}$ level?
29,300	*a*	
30,160	*a*	
30,160	*b*	

remaining bands. The frequency intervals other than that between the two lowest energy maxima do not correspond to a regularly spaced vibrational structure. Nor do the wave numbers between the centers of gravity of the pairs of A_u and B_u states follow any regular pattern. It is expected from the Davydov theory that in the crystal each molecular vibronic state will be split by an amount which depends on the strength of that separate oscillator. Accordingly Table IV gives the experimental *f*-numbers for the four principal vibronic levels of the perylene molecule. The *f*-numbers for the crystal vibronic levels could not be calculated as neither the crystal thickness nor the reflection corrections were known accurately.

Can. J. Chem. Downloaded from www.nrcresearchpress.com by 210.87.254.6 on 09/05/12
For personal use only.

TABLE IV

Comparison of crystal and solution data

Solution absorption maximum ν cm^{-1}	(ν_{cryst} + 1500 cm^{-1})* (cm^{-1})	f_{mol}	Splitting (cm^{-1})	
			Calc.	Expt.
23,050	23,050	1.4	1098	780
24,650	24,490	2.4	1764	820
25,850	26,340	1.2	844	1490
27,330	27,200	0.4	281	1200

*The values in this column refer to the centers of gravity of the pairs of *a*- and *b*-polarized bands which are shown in Fig. 6.

The Coupling Process

The coupling energy of the molecular vibronic forces in the perylene crystal by resonance force interaction is extremely large. The magnitude of the splitting is determined by the crystal geometry and the dipole strength of the crystal under study. It is therefore of interest to examine the applicability of the Davydov model, which was intended to treat only weakly coupled systems. Simpson and Peterson (13) have defined criteria in the form of inequalities which should distinguish one type of coupling from another. Clearly perylene falls into the class of strong to intermediate coupling as the band widths and interaction energies are of the same order of magnitude. The zeroth level splitting of 780 cm^{-1} was in fair agreement with the calculated value of 1098 cm^{-1}. This appears to imply that the Davydov theory is useful even in strongly coupled situations. On the other hand the higher vibronic levels, with the vibrational quantum number of the upper state greater than one, appear to split apart much more than is predicted by the Davydov theory. This suggests that it is the introduction of strong vibrational–electronic coupling which causes the deviations from the simple picture.

If the oscillator strength for a single vibronic transition is f_v then the total oscillator strength of the electronic transition is given by $\sum f_v$. The energy of interaction (splitting) between vibronic states with electronic symmetry B_{2u} is given by θm_v^2 where θ is the appropriate geometry factor and m_v is the dipole length corresponding to f_v. Thus the total interaction energy ΔE is

$$\Delta E = e^2\theta\sum m_v^2 = e^2\sum(\theta m_v^2).$$

The calculated value of ΔE, which is the sum of the splittings in the second last column of Table IV, was found to be 3987 cm^{-1}. Experimentally observed was a total interaction energy of 4290 cm^{-1}, which is in excellent agreement with that calculated within the dipole–dipole approximation.

Thus it is safe to conclude that the lack of agreement between theory and experiment for the individual vibronic transitions did not arise because of the use of a dipole–dipole approximation. Instead it appeared that a drastic redistribution of intensity compared to that in solution had occurred.

The Spectrum at Higher Energies

Above 28,000 cm^{-1} there appears to commence a new electronic transition. This transition is weaker than the first transition and virtually no splitting was observed. In solution there is a weak band at 29,600 cm^{-1}, which Clar assigned as the α'-band. The

Can. J. Chem. Downloaded from www.nrcresearchpress.com by 210.87.254.6 on 09/05/12
For personal use only.

absorption in this region is then expected to be due to the excitation of a state belonging to the $^1B_{3u}$ representation of the D_{2h} point group. This band appears to be much stronger in the crystal than in solution. Neither the small splitting nor the polarization ratio would fit with the assignment of the bands as absorption to a short axis polarized level. This region of the crystal spectrum was experimentally difficult to study and some reflection data is needed before the intensity may be measured more accurately.

A more complete account of the absorption spectrum of perylene sublimation flakes, including calculations of the band intensities and the emission spectrum at liquid helium temperature is in preparation.

REFERENCES

1. A. S. DAVYDOV. Zhur. Eksptl. i Teoret. Fiz. **18**, 210 (1948).
2. D. S. MCCLURE and O. SCHNEPP. J. Chem. Phys. **23**, 1575 (1955).
3. D. P. CRAIG and P. C. HOBBINS. J. Chem. Soc. 2309 (1955).
4. D. S. MCCLURE. J. Chem. Phys. **25**, 481 (1956).
5. D. P. CRAIG and P. C. HOBBINS. J. Chem. Soc. 539 (1955).
6. D. M. DONALDSON, J. M. ROBERTSON, and J. G. WHITE. Proc. Roy. Soc. (London), A, **220**, 311 (1952).
7. D. P. CRAIG and S. H. WALMSLEY. In course of publication; private communication.
8. R. M. HOCHSTRASSER. Spectrochim. Acta. In press.
9. J. FERGUSON. J. Chem. Phys. **28**, 765 (1958).
10. J. R. PLATT. J. Chem. Phys. **22**, 1448 (1954).
11. E. CLAR. Aromatische Kohlenwasserstoffe. Springer-Verlag, Berlin. 1952. p. 284.
12. R. WILLIAMS. J. Chem. Phys. **26**, 1186 (1956).
13. W. T. SIMPSON and D. L. PETERSON. J. Chem. Phys. **26**, 588 (1957).

Can. J. Chem. Downloaded from www.nrcresearchpress.com by 210.87.254.6 on 09/05/12
For personal use only.

Can. J. Chem. Downloaded from www.nrcresearchpress.com by 210.87.254.105 on 09/05/12
For personal use only.

THE EFFECT OF INTRAMOLECULAR TWISTING ON THE EMISSION SPECTRA OF HINDERED AROMATIC MOLECULES

PART I. 1,1′-BINAPHTHYL[1]

ROBIN M. HOCHSTRASSER

ABSTRACT

The fluorescence spectrum of 1,1′-binaphthyl has been examined in solution, in rigid glass, and in the crystal. It is found that in rigid media the spectral location of the emission is very sensitive to temperature. At 300° K the band is broad and structureless with a maximum at 26,700 cm^{-1} and a zero–zero band at about 30,200 cm^{-1} with very low intensity. The same is true at 273° K and 195° K. At temperatures below 157° K structure starts to appear until at 77° K the center of gravity of the emission is around 29,000 cm^{-1} and the 0–0 band at 31,270 cm^{-1} is quite clear and strong. Even at 77° K there is apparent a broad, but now weak band at 27,260 cm^{-1}. In the crystal the spectrum is broad and structureless at 300° K with a maximum emission intensity at 26,300 cm^{-1}. On lowering the temperature to about 142° K the intensity is built up on the high energy side of this band until eventually a new peak at 27,850 cm^{-1} becomes apparent at 77° K.

These results are interpreted on the basis of unsymmetrical potential energy variations with angle of twist which permit two origins for the fluorescence spectra of double molecules of this type.

INTRODUCTION

Aromatic molecules which consist of two identical planar aromatic systems joined through a single carbon–carbon bond may exhibit ultraviolet spectra which are either very different from or virtually identical with the known spectrum of one half of the molecule. If the rings are coplanar then resonance interaction is strong and the spectrum of the double molecule is vastly different from that of the isolated chromophores. If the molecular planes are perpendicular, the systems are essentially non-interacting, within a π-electron approximation, and the double-molecule spectrum does not appear different from that of one ring of the system. Perhaps the most extensively studied group of compounds in this regard are the biphenyls (1).

The binaphthyls were studied by Friedel and Orchin (2) and the ultraviolet spectra in solution at room temperature indicated that resonance interaction was at a minimum for 1,1′-binaphthyl whose spectrum was quite similar to that of naphthalene. 2,2′-Binaphthyl on the other hand exhibited a spectrum which extended much further to the red than did that of naphthalene, and in this case the steric inhibition of resonance was presumed to be at a minimum.

Unfortunately the spectra of these materials at room temperature are characteristically broad, and exact spectral comparisons are out of the question. The same is true of the luminescence spectra (phosphorescence and fluorescence) so that from such spectra little can be explained of the exact spectral shifts or of the true degree of interaction between the ring systems.

In this work a detailed study has been made of the low temperature absorption spectrum of 1,1′-binaphthyl and of the fluorescence and phosphorescence spectra of this compound at a variety of temperatures and in various rigid media.

[1]*Manuscript received November 14, 1960.*
Contribution from the Chemistry Department, University of British Columbia, Vancouver, B.C. Research supported by a grant from the National Research Council of Canada.

Can. J. Chem. Downloaded from www.nrcresearchpress.com by 210.87.254.105 on 09/05/12
For personal use only.

EXPERIMENTAL

The low temperature absorption spectra were taken on a Cary 14 recording spectrophotometer. The low temperature cell has been previously described (3). Extinction coefficients were calculated after corrections for contraction on cooling from 300° K to 77° K.

The fluorescence and phosphorescence spectra were excited by one of the mercury 3131 Å group of lines from a G.E. AH6 arc. A good monochromatic source was obtained by using a high aperture Bausch and Lomb grating monochromater with the entrance and exit slits at 1 mm in conjunction with the mercury arc. The parallel beam from the monochromater was directed onto the sample, which was contained in a quartz test tube, itself immersed in an unsilvered quartz Dewar flask. When the coolant was transparent to 3130 Å an immersed region of the solution was irradiated, otherwise the region just above the coolant surface was used.

The emission was focused on the slit of a medium Hilger quartz spectrograph. In order to obtain comparative fluorescence and phosphorescence curves the emission was recorded automatically. The travelling photomultiplier (R.C.A. 1P28) photocurrent was amplified by a Keithley (200B) vacuum tube micromicroammeter.

The solvents used were E.P.A. (ether, 5 parts; isopentane, 5 parts; ethyl alcohol, 2 parts); ethyl alcohol, which forms a slightly strained but nevertheless useful rigid glass at liquid nitrogen temperature; *n*-heptane, which when freshly distilled forms transparent crystals at 77° K; glycerol, which is virtually transparent to 3131-Å radiation (log I_0/I 0.12 in 1-cm path) and forms a rigid glass over the range 273° K–150° K. Dextrose and *n*-hexadecane were also used as solvents.

The following were employed as coolants: boiling nitrogen (77° K); *n*-pentane (142° K); diethyl ether (157° K); solid carbon dioxide (195° K); and melting ice (273° K).

RESULTS

Figure 1 shows the absorption spectrum of 1,1′-binaphthyl in ethyl alcohol at 300° K and in E.P.A. at 77° K. Only the long wavelength region is shown in the figure. Figure 2 shows the total emission spectra of naphthalene and 1-1′-binaphthyl in alcohol at 77° K. These spectra emphasize the similarity of vibrational structure in each tracing. The intensity scale in Fig. 2 was chosen such that the area under each of the fluorescence curves was comparable.

Figure 3 shows the fluorescence spectra of 1,1′-binaphthyl in glycerol at 273° K and 142° K; the fluorescence of 1,1′-binaphthyl in alcohol at 77° K is also shown in Fig. 3. Again, the curves were adjusted until they had similar areas on the drawn scale.

The 0–0 band of the lowest energy transition was measured at room temperature in ethyl alcohol and in the same solvent at 77° K. The crossing point of the broad high temperature absorption and emission curves was taken as the 0–0 band energy in this case. At low temperatures the mirror relationship between the long wavelength absorption and the fluorescence permitted accurate measurement of the 0–0 band energy. Table I

TABLE I

Substance	Temperature (°K)	Solvent	0–0 energy (cm^{-1})	Emission maximum (cm^{-1})
Naphthalene	77	Alcohol	31,730	30,000±100
1,1′-Binaphthyl	300	Glycerol	30,200±150	26,700±20
1,1′-Binaphthyl	77	Alcohol	31,270±20	29,100±100
1,1′-Binaphthyl	77	*n*-Heptane	31,230±20	29,000±100

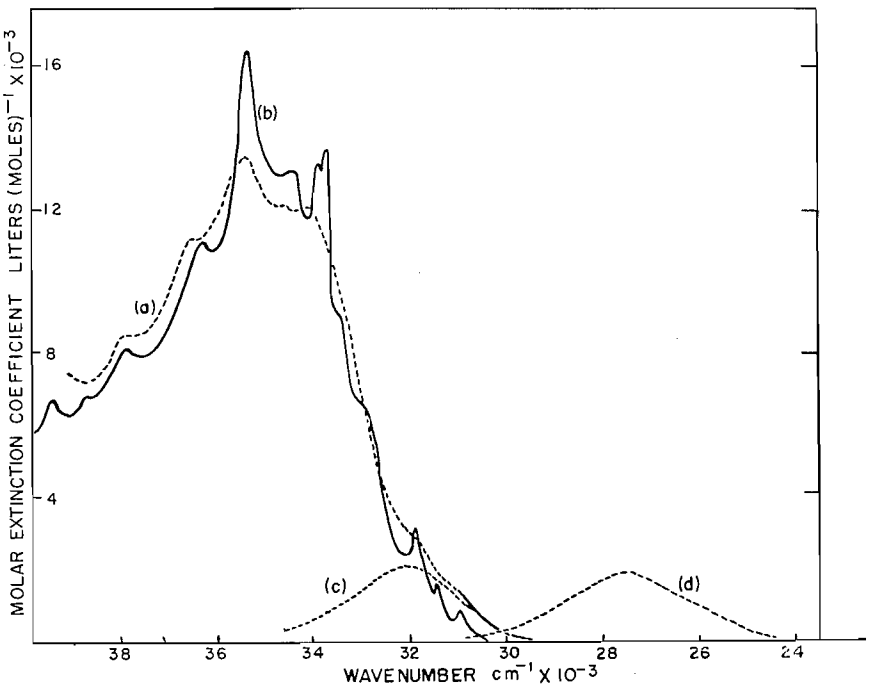


FIG. 1. The absorption spectra of 1,1′-binaphthyl. (*a*) In E.P.A. at 300° K. (*b*) In E.P.A. at 77° K. (*c*) The absorption to the lowest energy state after subtracting the long-wavelength tail of the first strong band. (*d*) The fluorescence spectrum at 300° K drawn in arbitrary units as the mirror image of curve (*c*).

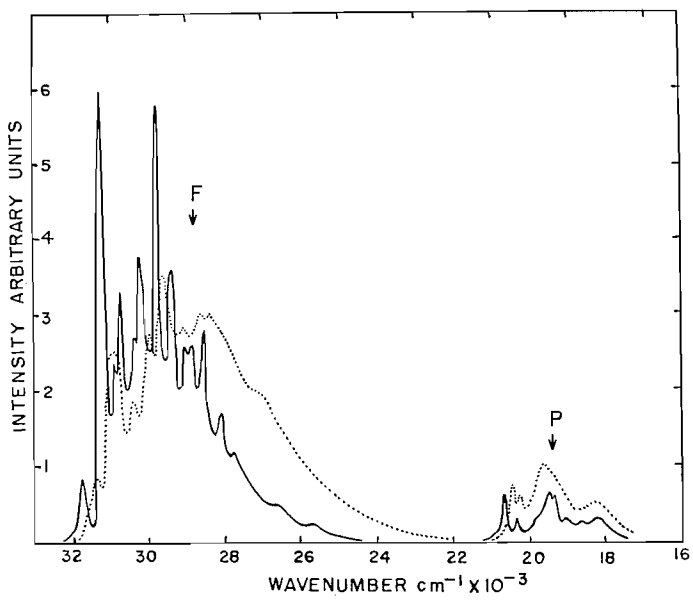


FIG. 2. The total emission spectra of naphthalene and 1,1′-binaphthyl in ethyl alcohol at 77° K. ..... 1,1′-Binaphthyl. ——— Naphthalene. F = Fluorescence region. P = Phosphorescence region.

Can. J. Chem. Downloaded from www.nrcresearchpress.com by 210.87.254.105 on 09/05/12
For personal use only.

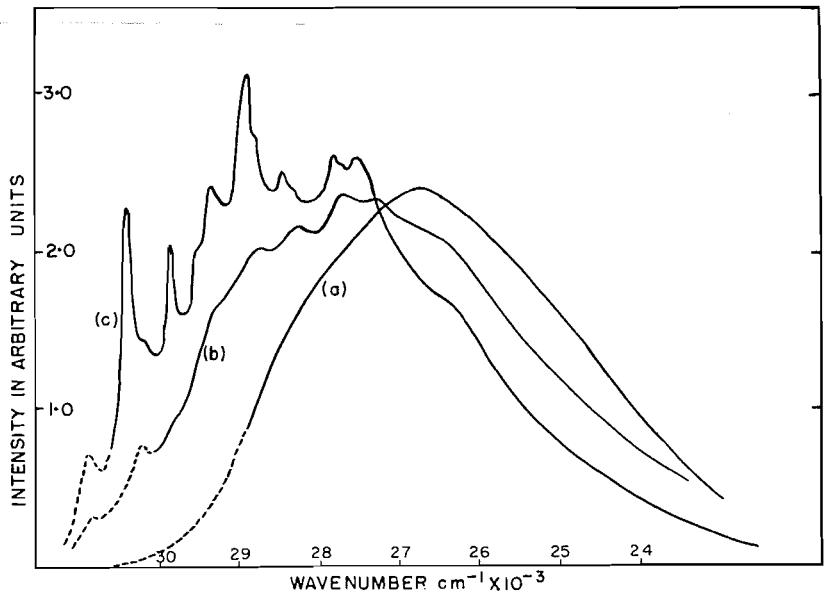


FIG. 3. The effect of temperature on the fluorescence spectrum of 1,1′-binaphthyl. (*a*) Glycerol, 273° K. (*b*) Glycerol, 142° K. (*c*) Ethyl alcohol, 77° K. The regions where very slight corrections for reabsorption of fluorescence may be necessary are covered by dashed curves.

summarizes these measurements. In all the experiments described so far the concentration of 1,1′-binaphthyl (10^{-4} *M*) and the optical arrangement, as far as possible, were uniformly maintained. When necessary, proper corrections were made for reabsorption of the fluorescence emission. The spectral response of the photomultiplier was not linear over the whole spectral range of phosphorescence plus fluorescence. However, the naphthalene spectra were so similar to those of the double molecule that accurate comparisons could be made without a complete spectral response curve. The phosphorescence emission spectra of naphthalene and 1,1′-binaphthyl were similarly located in the spectrum so that they also could be compared without a detailed knowledge of the spectral response curve.

The following is a summary of the experimental results including a few observations which may not be clear from the foregoing figures and description.

(1) The 0–0 band position was different at 300° K to that at 77° K. However, the error on the former measurement was large (see Table I).

(2) The center of gravity of the fluorescence band lay at $27{,}370 \pm 80$ cm^{-1} at 300° K, 273° K, or 194.7° K; the band was then broad and devoid of vibrational structure. At 77° K and 142° K vibrational structure was evident and the center of gravity of the spectrum was around 29,000 cm^{-1}.

(3) No radical changes were effected in the spectra at any temperature by altering the medium. This is clear from Table II. There were, however, marked changes in the phosphorescence – fluorescence yield ratios which will be discussed in a later paper.

(4) The 0–0 band of 1,1′-binaphthyl in alcohol was found to lie only 460 cm^{-1} to lower energies than that of the corresponding transition in naphthalene.

(5) Apart from the more subtle changes in the relative intensities of some vibrational bands in the low temperature fluorescence spectra, there was a shoulder at 27,260 cm^{-1}

Can. J. Chem. Downloaded from www.nrcresearchpress.com by 210.87.254.105 on 09/05/12
For personal use only.

TABLE II

The effect of solvent and temperature on the energy of maximum emission of 1,1′-binaphthyl

Solvent	Structure of the solvent	Temperature (°K)	Emission maximum (cm^{-1})
Crystal lattice		300	26,300±20
Dextrose	Rigid glass	300	27,000±150
Ethyl alcohol	Strained glass	77	27,260±100[a]
n-Heptane	Crystalline	77	27,260±100[a]
Hexadecane	Rigid	273	27,340±20
Glycerol	Rigid	273	27,340±20
Ethyl alcohol	Viscous	142	27,460±20
Ethyl alcohol	Liquid	300	27,380±20
Nujol	Very viscous	273	27,500±20
Crystal lattice		77	27,850±20
Glycerol	Strained glass	142	28,170±20[b]

[a]Shoulder.
[b]To be compared to the 28,540 cm^{-1} band at 77° K.

in all of the liquid nitrogen temperature spectra. There is no such shoulder in the naphthalene spectrum. The emission in this region was thus at about the same energy as the emission maximum of the higher temperature spectra.

(6) A similar set of phenomena have been observed for 1-phenylnaphthalene and to a lesser extent for biphenyl and 2,2′-binaphthyl. These results are being prepared for publication.

The Fluorescence Spectrum of the Crystal

The crystal emission was broad and structureless at 300° K with a peak at 26,300 cm^{-1}. At 77° K a little structure appeared at the high energy side of the band but the band maximum was shifted to 27,850 cm^{-1}. This blue shift amounted to 1550 cm^{-1} and was comparable to the shift of the center of gravity of the rigid glass fluorescence over the same temperature range. These spectra, which are shown in Fig. 4, were from randomly oriented crystals and they were not corrected for reabsorption of fluorescence. The spectra were taken under conditions which would minimize the reabsorption, i.e. front face illumination, and this correction probably becomes important at about 29,000 cm^{-1}. The third spectrum of Fig. 4 is of the crystal fluorescence at 194.7° K and the fourth was taken with the crystals at 157° K. From these spectra it was apparent that the 26,300 cm^{-1} band was not actually shifting to the blue with decreasing temperature but rather the intensity of the emission in this region was dropping as the intensity in the 27,850 cm^{-1} region was increasing.

The crystal spectra, solution spectra, and the fluorescence spectra in rigid glasses and their variations with temperature strongly indicate that emission is arising from two origins in the molecule of 1,1′-binaphthyl and that the *lower* energy level is favored at room temperature.

Vibrational Analysis of the Fluorescence in Alcohol

Table III compares the spectra of naphthalene and 1,1′-binaphthyl. It is quite clear from this analysis that the naphthalene state from which the emission occurs and the ground state at this same instant are not much affected by the presence of another α-naphthyl group. Thus at low temperatures the molecule behaves like two virtually non-interacting naphthalene molecules. Clearly there is no naphthalene analogue for the

Can. J. Chem. Downloaded from www.nrcresearchpress.com by 210.87.254.105 on 09/05/12
For personal use only.

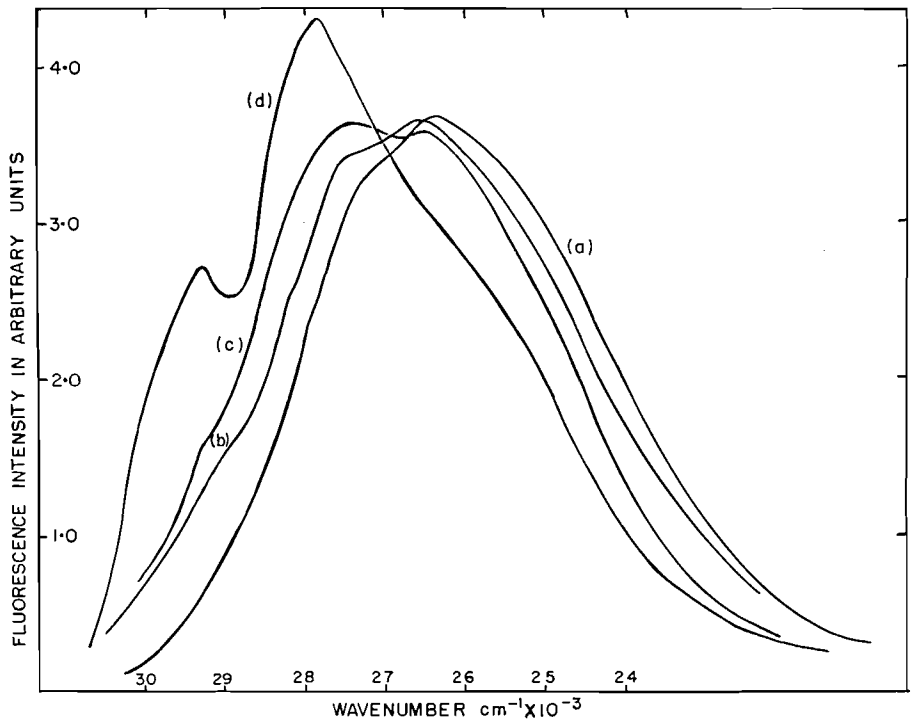


FIG. 4. The fluorescence of crystalline 1,1′-binaphthyl. (*a*) 300° K. (*b*) 195° K. (*c*) 157° K. (*d*) 77° K. No correction was applied to take into account the reabsorption of fluorescence.

TABLE III

Comparison of the vibrational structure of the fluorescence of naphthalene and 1,1′-binaphthyl

Naphthalene* (cm^{-1})	1,1′-Binaphthyl (cm^{-1})	$\Delta\nu$ (cm^{-1})	Analysis Naphthalene;* 1,1′-Binaphthyl
31,731 (w)	31,270 (w)	460	0–0
31,236 (vs)	30,910 (vs)	326	495 ; 360 b_{1g}
30,804 (s)	30,440 (s)	364	927 ; 830 b_{1g}
30,464 (s)	29,900 (s)	560	495+772 ; 360+(1010)
29,850 (s)	29,540 (vs)	310	495+1386 ; 360+1370
29,419 (s)	29,080 (s)	339	927+1386 ; 830+1360
28,824 (s)	28,540 (w)	284	Ill-resolved doublet
28,465 (s)	28,310 (w)	150	495+2×1386 ; 360+2×1300
	27,260 broad		
Only very weak bands			

*See reference 4; the emission spectrum of naphthalene in *n*-pentane at 77° K.

shoulder of medium intensity which appeared at 27,260 cm^{-1}. The analysis is based on the more complete findings of Bolotnikova (4), who studied naphthalene in pentane at 77° K.

Of the more subtle differences between the spectrum of 1,1′-binaphthyl and naphthalene is the large change in the frequency of the b_{1g} vibration (495 cm^{-1} in naphthalene ground state), which is lowered to 360±20 cm^{-1} in 1,1-binaphthyl. It has been suggested that this vibration is one of those responsible for the appearance of short axis polarized

Can. J. Chem. Downloaded from www.nrcresearchpress.com by 210.87.254.105 on 09/05/12
For personal use only.

absorption in the spectrum of the lowest energy $B_{2u} \leftarrow A_{1g}$ (long axis polarized) transition in naphthalene (4). If this in fact is the case, vibrations of this symmetry would be more modified in the double molecule than the totally symmetric ones because at interplanar angles around 90° the dipole–dipole interaction – vibronic coupling between the rings can only be significant for short axis polarized levels. In future experiments at higher resolution these discrepancies may be cleared up.

DISCUSSION

Firstly it is of interest to discuss the results in terms of known models. Jaffé and Orchin (5) have recently proposed a model to explain the wavelength shifts and intensity variations in hindered stilbenes. In this model the potential energy curves for the upper and lower states have double minima. These arise after the superimposition of a rotation barrier on the usual resonance potential versus angle of twist curve. The barrier is assumed small compared to the resonance stabilization at zero twist, and because the resonance interaction is not the same in both states it follows that the equilibrium angle of twist is not the same in the upper and lower states. The 1,1′ bond is most likely shorter in the upper state so the ground and excited state rotation barriers may not be identical.

If such a model is accepted for 1,1′-binaphthyl then the fluorescence spectrum would not be expected to alter markedly with temperature. Certainly the center of gravity of the emission would remain at the same energy at all temperatures in view of the Franck–Condon principle. Besides this, the experiments show that the spectral location of the bulk of the emission intensity red shifts as the temperature is raised, which would imply that the ground state potential curves were steeper than those of the upper state. This is contradictory to an increase of resonance interaction in the upper state. Even the postulate that emission may occur from highly excited twisting modes does not explain the observed phenomena on this model.

The Probable Configuration of 1,1′-Binaphthyl

In the trans planar configuration the 2–8′ and 8–2′ repulsions must be very great. In this configuration (see Fig. 5(*a*)) the molecule could be likened to 3,4-benzphenanthrene, which is known to be distorted from the planar configuration (6). In the cis planar configuration the interactions are akin to those in biphenyl (for the 2–2′ positions) and

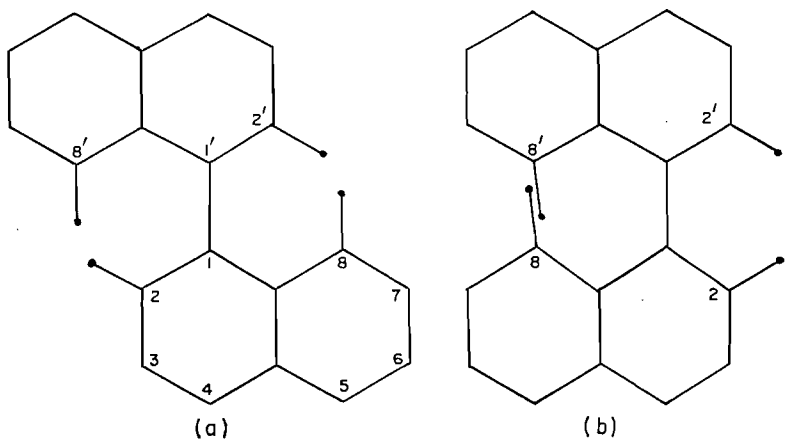


FIG. 5. 1,1′-Binaphthyl: (*a*) Trans-planar, (*b*) Cis-planar. C—H bands were drawn to terminate at the hydrogen nucleus in each case.

Can. J. Chem. Downloaded from www.nrcresearchpress.com by 210.87.254.105 on 09/05/12
For personal use only.

3,4-5,6-dibenzphenanthrene (for the 8–8′ positions). Certainly in the latter there is a large repulsion as dibenzphenanthrene is non-planar (7). The repulsions in 1,1′-binaphthyl will be smaller than those of the above analogies as the 1–1′ bond is presumably longer than for the condensed hydrocarbons.

Calculation has shown that when the H—H and C—C repulsions are minimized, i.e. the molecule is rotated about 1–1′ until each H—H and C—C distance is maximized and as near as possible equalized, then the most stable configuration on this basis is with the rings inclined to cis with an angle of 78° between the ring planes. Trotter (8) has recently determined the configuration from X-ray data at room temperature; the cis configuration was confirmed and the angle was 72°. The angle of twist was measured from 0° at the cis planar configuration.

It was also clear, both from the above discussion of the polynuclear hydrocarbon analogues and from geometrical calculations, that the energy required to reduce the angle by any given amount from 78° is much greater than the energy required to increase the angle by the same amount. This implies that the repulsion energy versus angle of twist curve will be *much steeper on the low angle (or cis) side of the equilibrium situation* than on the high angle (or trans) side.

The 1,1′-binaphthyl-5,5′-dicarboxylic acid has been resolved into optically active isomers at room temperature (9). This indicates that the rotation barrier is extremely large both at the trans and cis planar configurations.

The Resonance Energy of Interaction between Rings

There is some confusion regarding the resonance interaction between the two naphthalene units. On the one hand Magnus and Becker (10) have found an experimental resonance energy of 174.4 kcal for 1,1′-binaphthyl. From this they concluded that the molecule was planar. This result is at variance with conclusions from the optical activity of the 5,5′-dicarboxylic acid and the X-ray data, both of which indicate a severely twisted molecule. The ultraviolet absorption spectrum does not differ considerably from that of naphthalene, nor does the low temperature fluorescence spectrum; these results indicate that neither in the ground nor the excited state are the two rings strongly interacting. The broadness of the absorption spectrum in solution is most likely caused by librations about the equilibrium angle rather than by a permanent, strong, resonance force interaction.

The assumption will be held here that the resonance stabilization energy in the ground state is small in comparison to the van der Waals repulsive energy in either of the planar situations. In biphenyl the experimental resonance interaction energy is about 6 kcal/mole (2080 cm^{-1}) in the gas phase where the interplanar angle is probably near 45°. Thus the planar form should be stabilized by at least 12 kcal/mole.

After electronic excitation it is likely that the 1–1′ bond will be shortened because of the redistribution of charge at the 1 and 1′ carbon atoms. The resonance interactions in the excited state will therefore be greater than in the ground state.

The Potential Curves for the Ground and Excited States

Figure 6 shows the approximate variation of van der Waals repulsion energy with the interplanar angle. The curve is drawn steeper to the cis side in accordance with the above discussion. The dotted curve in Fig. 6 indicates the variation of the resonance interaction energy with interplanar angle and the extent of this variation is assumed to be larger in the excited state.

The van der Waals repulsive curves are drawn approximately in order that the ground

Can. J. Chem. Downloaded from www.nrcresearchpress.com by 210.87.254.105 on 09/05/12
For personal use only.

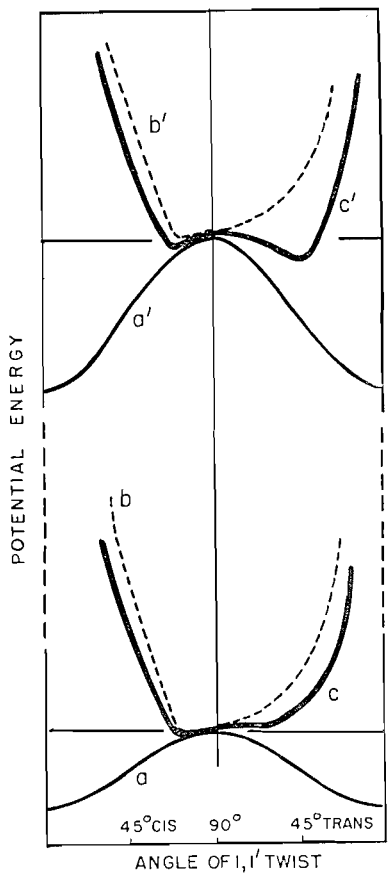


FIG. 6. The potential curves of the ground and excited states of a sterically hindered double molecule. Dashed curve: the non-uniform van der Waals repulsive energy. Thin line curve: resonance interaction. Thick line curve: resultant variation of potential with angle of twist.

NOTE: *The resonance interaction potential may not, in the general case, be symmetric about* $\theta = 90°$. *However, this is probably the case for molecules such as biphenyl, 1-phenylnaphthalene, and 2,2'-binaphthyl for which comparable experimental data has been collected. Therefore the particular case of 1,1'-binaphthyl, where the resonance interaction is greatest in the trans planar configuration and non-zero when the interplanar angle is 90° is avoided in this more general diagram. The curves on Fig. 7, on the other hand, refer specifically to 1,1'-binaphthyl. The resonance interaction energy discussed above is taken to be the potential energy of interaction of two dipoles (dipole-induced dipole) each of which is directed along the long axis and in the plane of one half of the molecule.*

state minimum occurs when there is about 72° between the ring planes. The same curves have been drawn in the upper state although in fact the repulsive forces in the upper state may be considerably altered. The equilibrium angle may also be different in the excited state but in the absence of detailed information on this point the minimum at 72° is drawn for both the ground and excited states. It is not thought that these assumptions will seriously affect the ensuing discussion.

In Fig. 6 the curve of the upper state has two potential minima while the ground state curve has only one. The trans-side minimum in the upper curve is probably lower than the cis-side minimum and it is certainly broader. This implies that molecules in this configuration are flapping with greater amplitude than molecules with the same thermal energy in the cis configuration.

Can. J. Chem. Downloaded from www.nrcresearchpress.com by 210.87.254.105 on 09/05/12
For personal use only.

It should be emphasized that potential energy curves of this type will arise even if the molecule under consideration does not have the trans and cis planar configurations. All that is required is that the equilibrium configuration is different from 90°. This condition may also be satisfied in phenylnaphthalene. For this molecule the 2 and 6 phenyl positions are subject to different repulsion energies at the planar position. Phenylnaphthalene would therefore be at least less planar than biphenyl on the basis of atom – atom repulsion energy.

The Fluorescence Spectra

It is proposed that there are two fluorescence origins in double molecules of this type. The origins arise because of the asymmetry of the potential energy in relation to angle of twist. Figure 7 shows one arrangement of ground and excited state potential curves

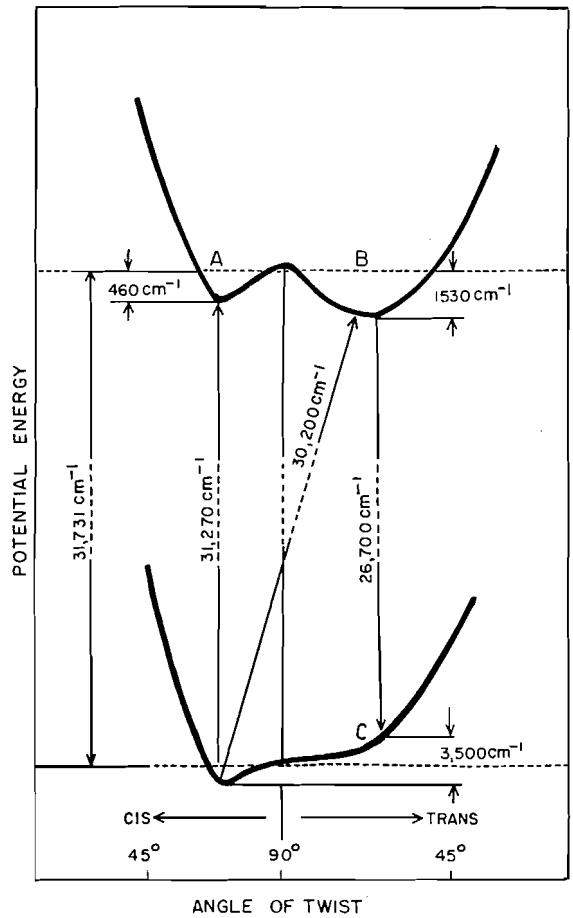


FIG. 7. The potential energy versus angle of twist relationships for 1,1′-binaphthyl: a model which accounts for the emission spectrum.

which may account for all the observed features of the fluorescence spectra of 1,1′-binaphthyl. It has been shown in the foregoing that curves of this type can arise from a combination of van der Waals and resonance forces which have slightly dissimilar angular variations in the ground and excited electronic states.

Can. J. Chem. Downloaded from www.nrcresearchpress.com by 210.87.254.105 on 09/05/12
For personal use only.

Can. J. Chem. Downloaded from www.nrcresearchpress.com by 210.87.254.105 on 09/05/12
For personal use only.

The difference in energy between the zero-point vibrational levels in the minima A and B is given by the difference in 0–0 band frequencies at 77° K and 300° K, that is 1050 cm^{-1}. This is necessarily approximate due to the uncertainty in the measurement at 300° K. The upper limit to the depth of minimum A is given to a first approximation by the difference in 0–0 band energies of naphthalene and 1,1′-binaphthyl at 77° K, that is 480 cm^{-1}. Thus the depth of the potential minimum B is approximately the sum of these two derived quantities (1050 + 480) cm^{-1} yielding 1530 cm^{-1}. The energy difference between the configuration represented by C in Fig. 7 and the zeroth vibrational level in the ground state is then 3500 cm^{-1} assuming vertical transitions (31,730–26,700–1,530 cm^{-1}).

At temperatures below room temperature virtually all molecules have a cis-inclined configuration and this configuration must be maintained immediately after light absorption in accordance with the Franck–Condon principle. Thus newly formed excited molecules have A-type configurations with an excess of vibrational energy. Within an extremely short time after this, the excited molecule will be vibrationally deactivated while retaining the cis configuration. This will arise because the twisting frequency should be small and hence the twisting time large (10^{-11}–10^{-12} seconds) in comparison to the time of vibrational deactivation (10^{-13} seconds). At a short time after light absorption the excited molecules will be in thermal equilibrium with the surrounding medium and the configuration A will be preferred. The potential barrier between A and B then determines the number of excited molecules which will remain in state A.

The height of this potential barrier is, however, not the only factor which will determine the relative yields of emission from state A and state B. It is unlikely that the rates of fluorescence emission will be the same in each of these states. Although the natural radiative lifetimes between the excited states and the ground state may be about equal in each configuration, any difference in the form of the potential minima, which describe the amplitude of any particular twisting mode, will alter the actual lifetimes of emission from these levels. Due to the different ring orientations in each minimum the internal conversion processes which bring about non-radiative transitions to the ground electronic state will not necessarily be identical for type A and B situations.

The following situations are envisaged after light absorption: (*a*) At 300° K—the thermal energy ($kT \doteqdot 200$ cm^{-1}) is comparable to the barrier height (<480 cm^{-1}) and the rate of emission from state A is considerably slower than from state B. Thus nearly all the radiatively lost energy originates from state B where the barrier height (1530 cm^{-1}) is large in comparison to kT. (*b*) At 77° K—the thermal energy ($kT \doteqdot 48$ cm^{-1}) is now small in comparison with the barrier height. Thus only about 5% of the emission will originate from state B (for a barrier of 480 cm^{-1}). (*c*) At intermediate temperatures both states will emit to some degree. The critical temperature appeared to be about 130° K ($2kT \doteqdot 140$ cm^{-1}), which may mean that the barrier height was overestimated by spectral measurements.

On the basis of the model presented here the experimental value of the zero–zero band energy at 300° K must lose significance. Instead the measured value is an upper limit of the actual value of the difference in energy between the zeroth level of the ground state and the zero-point vibrational level of the type B potential energy situation of Fig. 7. This stipulation is necessary because of the impossibility of knowing the exact form of the absorption to state B at the higher temperatures. The curve (*c*) in Fig. 1 is almost certainly composed of absorption to both A and B. In this event the zero (ground state) to zero (state B) energy can only be at lower energy than the measured value.

In conclusion, and in conjecture, it may be possible to say which of the potential curves has the greatest amplitude for the low frequency twist. The configuration which occupies the greatest volume (i.e. the trans) would probably exchange vibrational energy most rapidly with the surrounding medium. Thus the internal conversion from this to the ground level might be greater than for the cis configuration. This would imply that the curves A and B should be interchanged such that A is at lowest energy while B becomes shallow and flat-bottomed. The phosphorescence results do indicate that intersystem crossing is more favorable from the emitting level in 1,1′-binaphthyl than from the lowest singlet state of naphthalene (see Fig. 2). This problem will be treated more fully in Part II of this series.

CONCLUSIONS

Still many questions remain to be answered in regard to the effect of intramolecular twisting on the spectra of molecules of this type. Similar studies to the above on biphenyl, stilbene, 1-phenylnaphthalene, and 2,2′-binaphthyl and on the phosphorescence spectra of these materials are in preparation for publication. It is believed that much detailed information, some of this previously unforeseen, may be extracted from a study of the luminescence of such compounds.

It is not inconceivable that two emission origins A and B could arise for some other reason than has been presented here. The upper state of naphthalene would certainly be split into two double-molecule states of different polarization and radiative lifetime (11). It is also conceivable that one of these states is preferred over the other only at certain interplanar angles. Polarized fluorescence measurements will help to clear up these points. Preliminary calculations within a dipole–dipole approximation have, however, strengthened the present interpretation. The resonance interactions between the rings in the excited state at the cis, 90°, and trans configurations are in the respective ratios 0:1:5. These calculations indicate that the resonance interaction potential also varies in a non-uniform manner with angle of twist. The inclusion of this refinement in Fig. 7 would pull the minimum B down even further below A.

REFERENCES

1. STERIC EFFECTS IN CONJUGATED SYSTEMS. Chemical Society Symposium, Hull, 1958. *Edited by* G. W. GRAY. Butterworth Scientific Publications, London. 1958.
2. R. A. FRIEDEL, M. ORCHIN, and L. REGGEL. J. Am. Chem. Soc. **70**, 199 (1948).
3. R. M. HOCHSTRASSER. In press.
4. T. N. BOLOTNIKOVA. Optics and Spectroscopy, **7**, 24 (1959).
5. H. H. JAFFÉ and M. ORCHIN. J. Chem. Soc. 1078 (1960).
6. F. H. HERBSTEIN and G. M. J. SCHMIDT. J. Chem. Soc. 3302 (1954).
7. A. D. MCINTOSH, J. M. ROBERTSON, and V. VAND. J. Chem. Soc. 1661 (1954); Nature, **169**, 322 (1952).
8. J. TROTTER. Private communication.
9. F. BELL, W. H. D. MORGAN, and J. F. B. SMYTH. Chem. & Ind. (London), 634 (1951); F. BELL and W. H. D. MORGAN. J. Chem. Soc. 1716 (1954).
10. A. MAGNUS and F. BECKER. Erdöl u Kohle, 4, 115 (1951).
11. D. S. MCCLURE. Can. J. Chem. **36**, 59 (1958).

Can. J. Chem. Downloaded from www.nrcresearchpress.com by 210.87.254.105 on 09/05/12
For personal use only.

Can. J. Chem. Downloaded from www.nrcresearchpress.com by 210.87.254.5 on 09/05/12
For personal use only.

THE INFRARED FREQUENCIES AND INTENSITIES OF THE HYDROXYL BAND IN ORTHO-SUBSTITUTED PHENOLS[1]

K. U. INGOLD AND D. R. TAYLOR[2]

ABSTRACT

The infrared frequencies, intensities, and half-band widths of the fundamental stretching vibration of the hydroxyl group have been measured for a large number of ortho-alkyl phenols. It has been found that phenols containing a single ortho-alkyl substituent exist as cis and trans isomers in unequal amounts, the trans isomer being the more abundant. The difference in free energy between the two isomers in dilute solution in carbon tetrachloride at 24° C has been measured for ortho-cresol, 2,3-dimethyl phenol, and several ortho-*tert*-alkyl phenols.

INTRODUCTION

The fundamental frequencies of the hydroxyl group in *o*-alkyl-substituted phenols have been reported for a rather limited range of alkyl substituents by a number of workers (1, 2, 3, 4), but, with the exception of 2,6-di-*t*-butyl-4-substituted phenols (5), there has been no systematic study of the effect of these substituents on band intensities. The present work describes a comprehensive examination of both the frequencies and the intensities over a large range of *o*-alkyl substituents.

The O—H vibrational frequency, in carbon tetrachloride solution, of 2,6-di-*t*-butyl phenol is 36 cm^{-1} higher than phenol (5) and since the O—H band is coplanar with the ring in both cases (5) it should therefore be possible to observe two bands in the spectra of *o*-*t*-butyl phenol, and perhaps in other *o*-*t*-alkyl phenols as well. The two bands would correspond to geometrical isomers i.e. cis and trans structures in which the O—H group points towards the alkyl substituent and away from it, respectively. These two bands were, in fact, observed in all *o*-*t*-alkyl phenols, and while this work was being prepared for publication Goddu (6) reported finding two bands in *o*-*t*-butyl phenols and in 2-*t*-butyl-6-methyl phenols.

The possibility of detecting geometrical isomerism in non-tertiary-alkyl-*o*-substituted phenols was also examined.

EXPERIMENTAL

A Beckman I. R. 4 spectrophotometer with lithium fluoride optics was used to measure the O—H bands, the frequencies being calibrated by the standard absorption lines of water vapor. The effective slit width was about 4 cm^{-1}. Carbon tetrachloride was employed as the solvent and solution concentrations (C) were in the range 0.01 to 0.002 molar. Three cells of thickness (l), 1, 5, and 10 mm were used. Throughout this paper the term "intensity" (A) refers to the ratio, for the substituted phenol to phenol, of the apparent integrated absorption intensities, i.e. the band areas, and numerical values of A are given relative to the intensity of phenol. The band areas were obtained from the product of the half-band width ($\Delta\nu_{\frac{1}{2}}$) and the molecular extinction coefficient ($E_{max} = (1/Cl) \log_{10} (I_0/I)\nu_{max}$) (7).

Many of the phenols employed were commercial products which were purified by recrystallization or distillation before use. The purity of the liquid samples was checked

[1]*Manuscript received November 1, 1960.*
Contribution from the Division of Applied Chemistry, National Research Council, Ottawa, Canada. Issued as N.R.C. No. 6145.
[2]*National Research Council Summer Student, 1960. Present address: College of Science and Technology, Manchester, England.*

by gas chromatography and some of the phenols were purified on a preparatory column. The phenols 2-*t*-amyl-4-methyl; 2,6-di-*t*-amyl-4-methyl (8); 2-*t*-*t*-octyl-4-methyl (m.p. 50–51.2°) (9);* 2,6-di-*t*-*t*-octyl-4-methyl (m.p. 53.2–54.2°) (9); 2-triethylmethyl-4-methyl (m.p. 43–44°); and 2,6-di-triethylmethyl-4-methyl (m.p. 44°) were obtained by alkylation of *p*-cresol with the appropriate olefin by the method of Stillson, Sawyer, and Hunt (8). The hindered (2,6-substituted) and partially hindered (2-substituted) *p*-cresols were separated by adsorption chromatography on alumina. The yield of the last two hindered phenols was only 5 or 10%. 2-*t*-Butyl-5,6-dimethyl phenol (m.p. 52–53°) was obtained by alkylation of 2,3-dimethyl phenol with the theoretical amount of isobutylene. 2,6-Di-*t*-*t*-octyl-4-formyl phenol (white needles, m.p. 157–158°) was prepared in 25% yield from the 4-methyl derivative by oxidation with bromine (10). The main product of this reaction is a yellow crystalline material m.p. 124° C, the infrared spectrum of which suggests a para-quinolide structure (11). Since it appears to contain an equimolar quantity of HBr the analysis suggests it is 4-bromo-4-methyl-2,6-di-*t*-*t*-octyl-cyclohexadiene-2,5-one-1, hydrobromide. Analysis: Found C, 56.4; H, 8.15; Br, 32.6. Calculated for $C_{23}H_{40}OBr_2$: C, 56.1; H, 8.19; Br, 32.4.

2-*t*-*t*-Octyl-4-methyl-6-*t*-butyl phenol (m.p. 33–34°) was prepared by butylating 2-*t*-*t*-octyl-4-methyl phenol.

We are indebted to the Eastman Kodak Co. for gifts of the following phenols: 2,4,6-tri-*sec*-butyl; 2,4-di-*n*-amyl; 2,4,6-tri-*n*-amyl; 2-*n*-decyl-4-methyl; and 2-*sec*-dodecyl-4-methyl.

RESULTS

It has been shown previously (5) that the frequencies of the O—H band maxima (ν_m) for 4-substituted phenols and for 4-substituted-2,6-di-*t*-butyl phenols can be correlated by a Hammett $\rho\sigma$ relation. Two parallel straight lines were obtained whose slopes (ρ) were both -13.7 cm^{-1}. The intensities of the two groups of substituted phenols relative to phenol and to 2,6-di-*t*-butyl phenol respectively can be represented on a Hammett plot by a single straight line whose slope equals 0.37 (5). The measured values of ν_m and of the intensity relative to phenol (A) for the phenols studied here have therefore been compared with the values calculated from the Hammett equation to show up any departures from the predicted values. $\Delta\nu_m$ represents the difference between the measured and calculated values of ν_m and ΔA represents the difference between the measured and calculated values of A. It has been assumed in the calculations that the σ constant for an ortho substituent is the same as that for a para substituent (12). The σ values for the *t*-*t*-octyl and triethylmethyl groups have been assumed to be -0.19 and -0.18 respectively for structural reasons. All results are averages of at least two experiments.

The frequencies of single bands and of the main band in those phenols which show a double band are probably relatively correct to within 1 cm^{-1}.† Relative intensities should be correct to within about ± 0.05. The absolute intensity of phenol obtained by graphical integration over the absorption band using $\log_{10}(I_0/I)$ and applying Ramsey's correction for the wing absorption (7) has been redetermined to be 5.30 (1×10^4 mole^{-1} liter cm^{-2}). If the band is measured only to the flat wings of the curve (13) the intensity is 4.35 in the same units. These values are in good agreement with other recent estimates (13).

The results obtained with those phenols which were substituted with at least one *t*-alkyl group in an ortho position are given in Table I. The symmetrically substituted

*The *t*-*t*-octyl group is* $(CH_3)_3CCH_2(CH_3)_2C$—.

†*Frequencies given in reference 5 were low by 2 or 3 cm^{-1} owing to an error in the spectrometer calibration.*

Can. J. Chem. Downloaded from www.nrcresearchpress.com by 210.87.254.5 on 09/05/12
For personal use only.

phenols show only a single band but the asymmetrically substituted compounds show a complex band which consists of a main band at approximately the same frequency as phenol and a smaller, incompletely resolved band at a frequency approximately that of the 2,6-di-*t*-alkyl phenol. The value of ν_m for the side band is probably correct only to 2 or 3 cm^{-1}, owing to the difficulty of separating the contribution from the main band. Typical spectra are shown in Fig. 1. Table I also includes the ratio of the intensities of the two bands (denoted by $A(\text{trans})/A(\text{cis})$).

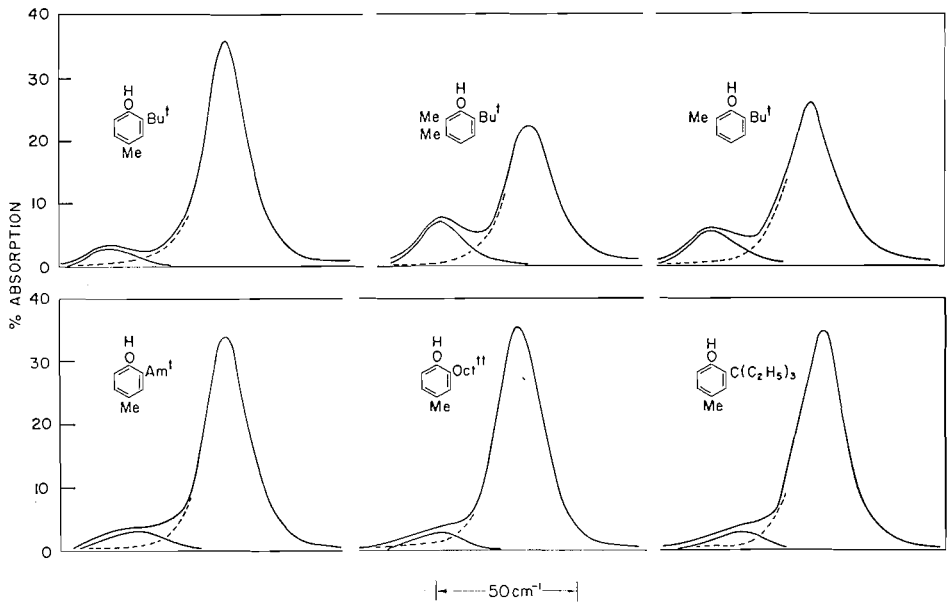


FIG. 1. The fundamental O—H vibration bands of ortho-*tert*-alkyl phenols.

The results obtained with phenols which do not contain an ortho-*t*-alkyl substituent are given in Table II.

DISCUSSION

The increases in frequency observed with 2,6-di-*t*-alkyl phenols compared with phenol are too large to be explained by the polar contributions of the *t*-alkyl groups. It has been shown previously (5) that the increase associated with 2,6-di-*t*-butyl phenols cannot be attributed to the twisting of the O—H bond out of the plane of the benzene ring. Similar evidence that the O—H bond is coplanar with the ring, or at least is nearly coplanar, has now been extended to 2,6-di-*t*-*t*-octyl phenols.

The fundamental stretching frequency of the C=O group in substituted benzaldehydes has been shown to follow a Hammett $\rho\sigma$ relation (14). If the O—H group is coplanar in 2,6-di-*t*-alkyl-4-formyl phenols the effective σ will be the sum of $\sigma_{para}(OH) = -0.36$ plus σ_{meta} for two *t*-alkyl groups $= 2\times -0.12$, i.e. -0.60. The shift in C=O frequency from benzaldehyde to *p*-hydroxybenzaldehyde and to 2,6-di-*t*-alkyl-4-formyl phenol should therefore be in the ratio 0.36:0.60, i.e., 3:5. If, however, the O—H bond is twisted away from the plane by the *t*-alkyl groups its effective σ will be increased i.e. become more

Can. J. Chem. Downloaded from www.nrcresearchpress.com by 210.87.254.5 on 09/05/12
For personal use only.

TABLE I

Frequencies and intensities of *t*-alkyl phenols

Substituents	$\Sigma\sigma$	ν_m cm^{-1}	$\Delta\nu_m$ cm^{-1}	A	ΔA	$\Delta\nu_{\frac{1}{2}}$ cm^{-1}	$\frac{A(\text{trans})}{A(\text{cis})}$
Phenol	0	3612.5	—	1.00	—	18.5	—
2-Bu^t	−0.20	3607.5	−8	0.92	0.07	18	11.0
		3647.5	32	0.08_4		18.5	
2-Bu^t-4-Me	−0.37	3610	−7.5	0.85	0.06	17.5	12.3
		3649.5	32	0.06_9		17.5	
2-Bu^t-4-MeO	−0.47	3614	−5	0.79	0.02	17	13.9
		3653	34	0.05_7		16.5	
2-Bu^t-5-Me	−0.27	3608	−8	0.86	0.04	17.5	9.5
		3648	32	0.09_0		18	
2,4-Bu$_2^t$	−0.39	3610	−8	0.86	0.09	18	11.5
		3648	30	0.07_5		19	
2-Bu^t-4-OH	−0.52 av.	3616.5	−3	1.62/2	0.06	19	26.8/2
		3651	31.5	0.06_0		19	=13.4
2,5-Bu$_2^t$-4-OH	−0.67	3614	−8	1.50/2	0.11	16.5	13.7
		3652	30	0.10_9/2		16	
2,6-Bu$_2^t$	−0.39	3648	30	1.02	0.17	17.5	
2,6-Bu$_2^t$-4-Me	−0.56	3650	29.5	0.95	0.16	19	
2,6-Bu$_2^t$-4-CHO	+0.73	3633	30.5	1.43	0.16	17.5	
4,4′-bis(2,6-Bu$_2^t$)	−0.30*	3645	28.5	2.40/2	0.31	17	
4,4′-CH$_2$bis(2,6-Bu$_2^t$)	−0.47*	3649	30	2.06/2	0.20	19	
2-Bu^t-6-Me	−0.37	3617	−1	0.67	−0.05	17.5	4.8_5
		3649.5	31.5	0.13_8		18	
2,4-Bu$_2^t$-6-Me	−0.56	3618	−2.5	0.63	−0.03	17.5	4.8_5
		3652.5	32	0.13		17.5	
4,4′-bis(2-Bu^t-6-Me)	−0.28*	3616	0	1.54/2	−0.04	18	5.0
		3650	33.5	0.31/2		17	
4,4′-CH$_2$bis(2-Bu^t-6-Me)	−0.45*	3618.5	0	1.38/2	0.01	20	5.1
		3653	34.5	0.27/2		19.5	
4,4′-Thio bis(2-Bu^t-6-Me)	−0.26*	3615	−1	1.62/2	0.1	19.5	4.5
		3648	32	0.36/2		19	
2-Bu^t-5,6-Me$_2$	−0.44	3621	2	0.56	−0.09	18.5	3.0
		3652	33	0.18_7		18	
2-Am^t	−0.19	3608	−7	0.92	0.06	20	12.4
		3643	28	0.07_4		21	
2,4-Am$_2^t$	−0.38	3609	−9	0.86	0.07	17	12.3
		3645	27	0.07_0		18.5	
2-Am^t-4-Me	−0.36	3609.5	−8	0.83	0.03	17	12.4_5
		3644.5	27	0.06_7		18	
2,6-Am$_2^t$-4-Me	−0.55	3642.5	22.5	1.15	0.35	19.5	
2,4,6-Am$_3^t$	−0.57	3642	21.5	1.13	0.34	20	
2-Oct^{tt}-4-Me	−0.36	3608.5	−9	0.86	0.06	18	13.0
		3639.5	22	0.06_6		19.5	
2,6-Oct$_2^{tt}$-4-Me	−0.55	3635.5	15.5	1.18	0.38	19	
2,6-Oct$_2^{tt}$-4-CHO	+0.75	3617	14.5	1.70	0.42	20.5	
2-(C$_2$H$_5$)$_3$C-4-Me	−0.35	3608	−9.5	0.86	0.06	17.5	13.2
		3638.5	21	0.06_5		18	
2,6-((C$_2$H$_5$)$_3$C)$_2$-4-Me	−0.52	3635	15	1.21	0.40	18	
2-Oct^{tt}-4-Me-6-Bu^t	−0.56	3647 (max)	27	1.22	0.43	25.5	See text
		3642 (center)	22				

*$\Sigma\sigma$ assigned on basis of ν_m and A.

positive (12, 15). The observed C=O frequencies were benzaldehyde 1710 cm^{-1}, *p*-hydroxybenzaldehyde 1701 cm^{-1}, 2,6-di-*t*-butyl-4-formyl phenol 1695 cm^{-1} (5), and 2,6-di-*t*-*t*-octyl-4-formyl phenol 1695 cm^{-1}; the frequency differences are in the ratio 9:15 in agreement with the ratio predicted for a coplanar hydroxyl group.

Can. J. Chem. Downloaded from www.nrcresearchpress.com by 210.87.254.5 on 09/05/12
For personal use only.

TABLE II

Frequencies and intensities of non-tertiary alkyl phenols

Substituents	$\Sigma\sigma$	ν_m cm^{-1}	$\Delta\nu_m$ cm^{-1}	A	ΔA	$\Delta\nu_{\frac{1}{2}}$ cm^{-1}
Phenol	0	3612.5		1.00		18.5
3-Me	−0.07	3613.5	0	0.99	0.02	18
4-Me	−0.17	3615	0	0.94	0	17
3,4,5-Me_3	−0.31	3617	0	0.90	0.01	17.5
2-Me	−0.17	3615	0	0.95	0.01	19.5
2,4-Me_2	−0.34	3617	0	0.92	0.05	19.5
2-Me-4-Cl	+0.06	3612	0	1.08	0.06	20.5
2,4,5-Me_3	−0.41	3618	0	0.89	0.04	19.5
2,6-Me_2	−0.34	3622.5	5.5	0.76	−0.11	18.5
2,6-Me_2-4-Cl	−0.11	3618	4	0.93	−0.03	21
2,4,6-Me_3	−0.51	3624.5	4.5	0.72	−0.09	18
2,3-Me_2	−0.24	3616	0	0.94	0.03	19
2,3,5-Me_3	−0.31	3617	0	0.90	0.02	19
2,3,6-Me_3	−0.41	3623	5	0.75	−0.10	18
2,3,4,6-Me_4	−0.58	3625.5	5	0.69	−0.10	18
2,3,5,6-Me_4	−0.48	3626	7	0.68	−0.14	18.5
2,3,4,5,6-Me_5	−0.65	3630	8.5	0.61	−0.15	20.5
2-Et	−0.15	3614.5	−0.5	0.97	0.03	19.5
2,6-Et_2	−0.30	3623	6	0.84	−0.05	18
2-Pr^n	−0.13	3614.5	0	0.99	0.04	19.5
2-Pr^n-4-Me	−0.30	3616.5	−0.5	0.90	0.01	19
2,6-Pr^n_2	−0.25	3621	5	0.82	−0.09	18.5
2-Pr^n-6-Me	−0.30	3623	6	0.78	−0.11	19
2-Pr^i	−0.15	3614.5	−0.5	0.91	−0.03	19.5
2-Pr^i-4-Me	−0.32	3616.5	−0.5	0.88	0	19
2,6-Pr^i_2	−0.30	3623	6	0.72	−0.17	19
2-Bu^s	−0.12	3614	0	0.89	−0.06	18.5
2,4-Bu^s_2	−0.25	3616	0	0.87	−0.04	18.5
2,4,6-Bu^s_3	−0.37	3622	5	0.71	−0.15	18
2,4-Am^n_2	−0.32	3616.5	−0.5	0.88	0	18
2,4,6-Am^n_3	−0.48	3622	3	0.67	−0.15	18
2-Am^i	−0.23	3615.5	−0.5	0.86	−0.06	18
2,4-Am^s_2	−0.25	3615.5	−0.5	0.89	−0.02	19.5
2-*n*-decyl-4-Me	−0.33	3616	−1	0.88	0	19
2-*sec*-dodecyl-4-Me	−0.29	3615.5	−1.5	0.79	−0.10	18

Although the OH group is coplanar in the presence of strong electron-attracting groups such as CHO this does not necessarily imply that it is also coplanar when the 4-substituent is electron releasing (e.g. CH_3). However, the differences in frequency between the hydroxyl groups of the 4-methyl and 4-formyl derivatives of phenol, 2,6-di-*t*-butyl phenol, and 2,6-di-*t*-*t*-octyl phenol are 16.5 (5), 17, and 18.5 cm^{-1} respectively compared with a calculated difference of 17.5 cm^{-1}.* That is, within the limits of experimental error the plots of ν_m against σ for these three classes of phenols are parallel (5) and therefore the OH group has the same orientation, independent of the 4-substituent, in all cases.

The intensities of the hindered phenols give further confirmation that they are true phenols and not "pseudo" phenols containing a non-planar hydroxyl group. The intensity of phenol is two or three times as great as the intensities of alcohols (13, 16), and, therefore, since the hindered phenols have even higher intensities than phenol, they must be true phenols. Moreover, the ratio of the intensities of the 4-formyl to 4-methyl derivatives of phenol; 2,6-di-*t*-butyl phenol; and 2,6-di-*t*-*t*-octyl phenol are 1.66 (5), 1.51, and 1.44

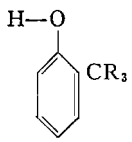
**An interesting difference between the OH bands of 2,6-di-t-butyl and 2,6-di-t-t-octyl phenols is that their half-band widths appear to change in opposite directions with a change in σ (Table I) (5).*

Can. J. Chem. Downloaded from www.nrcresearchpress.com by 210.87.254.5 on 09/05/12
For personal use only.

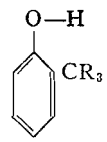
respectively, compared with a calculated ratio of 1.48, again suggesting that the structure of the phenols is independent of the 4-substituent.

Although the results quoted above strongly suggest that the OH group is coplanar with the ring, the accuracy of the experiments does not preclude the possibility that it is slightly twisted away from the plane. Both the resonance energy and the charge density at the carbon atom para to the resonance-inhibited group vary approximately as $\cos^2\theta$ (15, 17, 18) where θ is the angle of twist. That is, the resonance energy and charge density fall off rather slowly for small values of θ and therefore we could not detect small angles of twist in our experiments.

The conclusion that the OH group is in the plane, or at least close to it, makes the interpretation of the results obtained with single ortho-*t*-alkyl substituents comparatively straightforward. The results given in Table I and Fig. 1 clearly demonstrate the presence of two forms of *o*-*t*-alkyl phenols, as was predicted. Since the frequencies of the two bands are fairly close the one to the frequency of phenol, and the other to that of the corresponding 2,6-di-*t*-alkyl phenol, it is logical to suppose that the two forms represent geometrical isomers. The more intense band at the lower frequency will correspond to the trans isomer (T) and the less intense band at the higher frequency to the cis isomer (C).



(T)



(C)

Geometrical isomerism has been reported previously (19, 20) for *o*-substituted phenols in which the substituent can form an intramolecular hydrogen bond with the phenolic hydrogen (e.g. *o*-chlorophenol). This isomerism, which was deduced from infrared spectra, arises from the attraction of the phenolic hydrogen towards the *o*-substituent since the main band occurs at a much lower frequency than in phenol and the minor band occurs near the phenol frequency. In other words, the cis form is the most stable, whereas in *o*-*t*-alkyl phenols it is the trans form that is more stable. This suggests the presence of a steric repulsion between the phenolic hydrogen and the *t*-alkyl group, as might be expected.

Substitution of a methyl group in the 6-position increases the proportion of the isomer cis to the *t*-alkyl group. Substitution of a second methyl at the 5-position increases the proportion of the cis isomer even further, presumably because of its "buttressing" action on the methyl in the 6-position.

It should be pointed out that the occurrence of two bands does not necessarily imply that they correspond to geometrical isomers, since the low intensity band could conceivably be due to Fermi resonance (21) as has been postulated for hydroxy compounds containing the $—CH_2OH$ group (13). This possibility can, however, be discarded since the intensity of the subsidiary (cis) band decreases slightly as the two bands get closer together on going from *o*-*t*-butyl to *o*-*t*-amyl phenol, which is contrary to what would be expected from Fermi resonance. The results obtained with 2-*t*-butyl-6-methyl phenols and with 2-*t*-butyl-5,6-dimethyl phenol would also be difficult to explain on this basis. Furthermore, the spectra of structurally similar phenols e.g. *p*-*t*-butyl phenol, 2,6-diethyl phenol, 2,6-di-isopropyl phenol, etc. do not show any subsidiary bands.

The difference in free energy (ΔG) between the two isomers can be calculated from the

Can. J. Chem. Downloaded from www.nrcresearchpress.com by 210.87.254.5 on 09/05/12
For personal use only.

Can. J. Chem. Downloaded from www.nrcresearchpress.com by 210.87.254.5 on 09/05/12
For personal use only.

ratio of the intensities of the trans to cis bands in an *o*-*t*-alkyl phenol. This energy difference should be independent of the presence or absence of a 4-substituent, since any change in resonance energy produced by a 4-substituent will presumably alter the depths of the two coplanar potential minima by the same amount. However, the measured ratio of the intensities should be corrected for the fact that when the O—H group is cis to the *t*-alkyl group, as it must be in 2,6-di-*t*-alkyl phenols, the intensity is higher than phenol, whereas when it is trans to the substituent the intensity probably approximately follows the Hammett equation (5) and will be lower than phenol. For example, the average calculated cis intensity for 2-*t*-butyl phenol (1.09) is obtained from the intensities of 2,6-di-*t*-butyl phenol (1.02), and 2,6-di-*t*-butyl-4-methyl phenol (0.95) by applying corrections for the polar effects of an *o*-*t*-butyl group ($-(-0.20\times0.37)$) and for the effect of an *o*-*t*-butyl group and a *p*-methyl group ($-(-0.20-0.17)\times0.37$). The calculated trans intensity is based on phenol (1.00) less the effect of an *o*-*t*-butyl group i.e. 0.93. For 2-*t*-butyl-6-methyl phenol the calculated intensity cis to the *t*-butyl group is based on the calculated cis intensity of *o*-*t*-butyl phenol corrected for the polar effect of the 6-methyl group, and the calculated trans intensity is based in the same way on the measured intensities of 2,6-dimethyl and 2,4,6-trimethyl phenol. The measured trans to cis intensity ratio must be multiplied by the calculated cis to trans intensity ratio in order to obtain the true relative amounts of the two isomers. Table III gives the steps in the calculations

TABLE III

Cis – trans isomerism of *o*-alkyl phenols

o-Substituents	Av. calc. cis intensity	Av. calc. trans intensity	Calc. $\frac{A(\text{cis})}{A(\text{trans})}$	Measured $\frac{A(\text{trans})}{A(\text{cis})}$	$\frac{[\text{trans}]}{[\text{cis}]}$	ΔG kcal/ mole	% trans isomer	% cis isomer
2-Bu^t	1.09	0.93	1.17	12.3	14.39	1.5_7	93.5	6.5
2-Am^t	1.27_5	0.93	1.37	12.4_5	17.06	1.6_7	94.5	5.5
2-Oct^t	1.31	0.93	1.41	13.0	18.30	1.7_1	94.8	5.2
2-$(C_2H_5)_3C$	1.34	0.93	1.44	13.2	19.01	1.7_4	95.0	5.0
2-Bu^t-6-Me	1.03	0.83	1.24	4.8_5	6.01	1.0_6	85.7	14.3
2-Bu^t-5,6-Me_2	1.00	0.76_5	1.31	3.00	3.92	0.8_0	79.7	20.3
2-CH_3						0.5_1	70.5	29.5
2,3-$(CH_3)_2$						0.7_7	78.6	21.4

of the percentage of cis and trans isomers and the difference in free energy (ΔG) in kcal/mole between the two isomers in dilute solution in carbon tetrachloride at 24° C. ΔG is obtained in calories from the relation

$$\log_{10}\frac{[\text{trans}]}{[\text{cis}]} = \frac{\Delta G}{2.3RT}.$$

The measured trans/cis ratio for 2-*t*-butyl and 2-*t*-amyl have been taken from the values found for their 4-methyl derivatives; and for 2-*t*-butyl-6-methyl the ratio obtained with this phenol has been used. This was done since these compounds were known to be very pure and since the measurements were repeated at least six times, including once on a high-resolution Perkin–Elmer prism-grating spectrometer, model 112 G. Average values of the ratio for the other phenols of these types are in quite good agreement with the values chosen. The measured trans/cis ratio for 2-*t*-butyl and 2-*t*-butyl-6-methyl phenols are in good agreement with the values of Goddu (6), although our frequencies are from 3 to 8 cm^{-1} higher than the values he reported, the differences being most pronounced for 2,6-di-*t*-butyl phenols and for the cis isomers of various *o*-*t*-butyl phenols.

Can. J. Chem. Downloaded from www.nrcresearchpress.com by 210.87.254.5 on 09/05/12
For personal use only.

The percentages of the cis isomers given in Table III show, as would be expected, that the cis isomer decreases as the size of the *t*-alkyl substituent is increased, but is increased by substitution of a methyl at the 6-position or by two methyls at the 5- and 6-positions.

The values of ΔG obtained for 2-*t*-butyl-6-methyl phenol and for 2-*t*-butyl-5,6-dimethyl phenol can be combined with the value for 2-*t*-butyl phenol to give the differences in free energy between the cis and trans isomers of *o*-cresol and 2,3-dimethyl phenol. These values are also included in Table III. It was also possible to obtain a rough estimate of ΔG for the two forms of 2-*t*-*t*-octyl-4-methyl-6-*t*-butyl phenol. The OH band of this compound is asymmetric and from the degree of asymmetry observed on the prism-grating instrument ΔG was estimated to be 0.17 kcal/mole. The intensity of the band was also compared with the intensity of the combined band of mixtures of different proportions of 2,6-di-*t*-*t*-octyl-4-methyl phenol and 2,6-di-*t*-butyl-4-methyl phenol. A value of ΔG of 0.30 kcal/mole was obtained in this way. These values are in reasonably good agreement with the value of 0.14 kcal/mole obtained by difference from 2-*t*-*t*-octyl and 2-*t*-butyl phenol.

The ratio of the intensities of the cis to trans isomers of *o*-chlorophenol is about 50:1 in carbon tetrachloride at room temperature (22, 23), corresponding to $\Delta G \sim 2.3$ kcal/mole. We have found that for 2-chloro-6-methyl phenol this ratio increases to $\geqslant 100{:}1$ ($\Delta G \geqslant 2.7$ kcal/mole). The two values of ΔG can be combined to obtain ΔG for *o*-cresol $\geqslant 0.4$ kcal/mole, in reasonable agreement with the value given in Table III.

The results given in Table II show that a single non-tertiary alkyl group substituted in the ortho position gives a measured increase in frequency and decrease in intensity in good agreement with the values calculated from the Hammett equation (5). However, the results given in Table III show that these phenols must exist as cis–trans isomers in unequal amounts. The only direct evidence for this is that the half-band widths ($\Delta\nu_{\frac{1}{2}}$) are definitely greater for these *o*-alkyl phenols than for phenol or for the corresponding 2,6-dialkyl phenols. This suggests the presence of two unresolved bands, particularly since the half-band widths would be expected to decrease below the value for phenol with alkyl substitution (5) (see also results for 3-methyl, 4-methyl, and 3,4,5-trimethyl phenol in Table II). Failure to resolve these bands is not surprising since the band maxima would appear to be less than 10 cm^{-1} apart in general and even the prism-grating spectrometer would not resolve the two bands of 2-*t*-*t*-octyl-4-methyl-6-*t*-butyl phenol where a separation of about 15 cm^{-1} is expected.

The positive values of $\Delta\nu_m$ observed with the 2,6-dialkyl phenols in Table II (and which are also encountered with 2,6-di-*t*-alkyl phenols) suggest a steric interaction between these non-tertiary alkyl groups and the hydroxyl group. On the other hand, the values of ΔA are negative for these phenols, whereas positive values were obtained with the 2,6-di-*t*-alkyl phenols. This shows that the intensities cannot be simply related to the extent of steric interference by the alkyl groups. However, for the phenols listed in Table II the values of $\Delta\nu_m$ and ΔA both tend to increase with the expected increase in steric interaction (see 2,6-dimethyl; 2,3,6-trimethyl; 2,3,4,6-tetramethyl; 2,3,5,6-tetramethyl; and pentamethyl phenol). This result cannot be due to any saturation of the electronic effects produced by the increasing number of substituents (5) since this would cause both $\Delta\nu_m$ and ΔA to decrease. The magnitude of these differences may, however, have been reduced because of saturation effects; somewhat larger values would smooth out the curves in Fig. 2 (see below).

In Fig. 2 values of $\Delta\nu_m$ and ΔA for 2,6-dialkyl phenols have been plotted against the values of ΔG obtained from the *o*-alkyl phenols. There is no direct justification for this

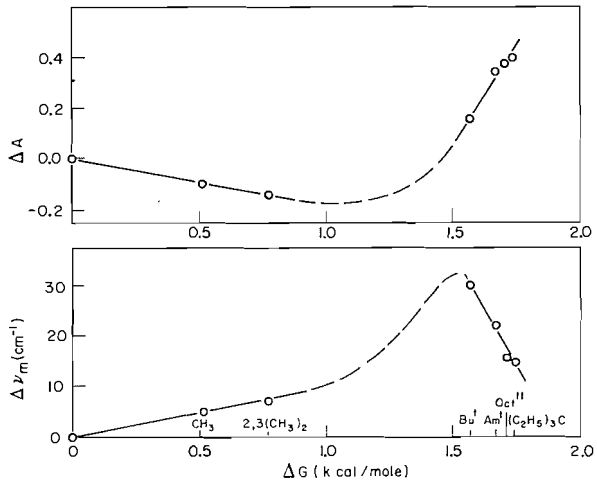


FIG. 2. Differences between measured and calculated frequencies, and intensities, of 2,6-dialkyl phenols plotted against ΔG.

procedure, but it is obvious that the values of ν_m and A for these phenols must be related in some way to the steric interaction of the alkyl groups with the hydroxyl group, and that this is measured approximately by ΔG. Both plots apparently show a discontinuity between the methyl phenols and the *t*-alkyl phenols, the curves going through a maximum or minimum. This shows that ortho-alkyl groups have two different effects on the hydroxyl, the magnitude of the two effects varying with the size of the alkyl groups.

A possible explanation of these results is that mild steric interaction between the alkyl and hydroxyl groups narrows the potential-energy well of the stretching mode of the O—H bond; this will increase the vibration frequency and decrease its amplitude and hence decrease the intensity. Stronger steric repulsions will begin to separate the proton from the electrons of the O—H bond since the repulsion is exerted primarily on the electrons of the phenolic hydrogen and only through them on the proton itself. This will tend to polarize the bond (i.e. $\overset{\delta-}{O}—\overset{\delta+}{H}$) and increase the intensity, and at the same time will weaken the internal force constant and so decrease the frequency. Incidentally the values of ΔG do not increase with the size of the *t*-alkyl substituent as rapidly as might be expected, which may be because the energy is minimized by an increase in the $C—\hat{O}—H$ angle. This forcing of the phenolic hydrogen away from its equilibrium position, as the substituents become larger than *t*-butyl, would also tend to decrease the O—H bond strength and hence ν_m.

The frequencies of the trans isomers of *o*-*t*-alkyl phenols, which are appreciably below their calculated values, are obviously much more readily influenced by the alkyl substituent than are the intensities (cf. small values of ΔA for these phenols in Table I); i.e. the intensities, but not the frequencies, follow the usual Hammett $\rho\sigma$ relations. The low frequencies observed must mean that an *o*-*t*-alkyl substituent has an effect on the hydroxyl group even when the latter is pointing away from it. This effect might be due to a more rigid geometry in the trans isomer compared to phenol (5). An alternative explanation that appears to be more consistent with the results is that *t*-alkyl groups exert van der Waals attraction on the lone pairs of electrons on the oxygen. This withdrawal of electrons from the oxygen would be transmitted to the O—H bond, the

Can. J. Chem. Downloaded from www.nrcresearchpress.com by 210.87.254.5 on 09/05/12
For personal use only.

frequency of which would be decreased. This suggestion helps to explain why $\Delta\nu_m$ is higher for the cis isomer of *o*-*t*-alkyl phenols than for the corresponding 2,6-di-*t*-alkyl phenol. In the cis isomer the only effect on the hydroxyl is one of steric repulsion, whereas in di-*t*-alkyl phenols there is also the attraction of the oxygen's electrons by the second *t*-alkyl group, which will decrease the frequency. The same effect may also be operating in ortho halophenols since the frequency, in carbon tetrachloride solution, of the trans isomer decreases by 5 cm^{-1} on increasing the size of the substituent from bromine to iodine, whereas the corresponding decrease for these two para-substituted phenols is only 1 cm^{-1} (22, 23).

An *o*-methyl or 2,3-dimethyl group has no effect, other than the calculated polar effect, on the frequency of the trans isomer (Table II). Therefore in 2-*t*-butyl-6-methyl and in 2-*t*-butyl-5,6-dimethyl phenol $\Delta\nu_m$ for the cis (to *t*-butyl) isomer has about the same value as for 2-*t*-butyl phenols (Table I). On the other hand, $\Delta\nu_m$ values for the trans (to *t*-butyl) isomers of these phenols are below $\Delta\nu_m$ values for 2,6-dimethyl and 2,3,5,6-tetramethyl phenol because of the influence of the *t*-butyl group. Non-tertiary alkyl groups in the ortho position apparently, therefore, only affect the hydroxyl group when it points towards them.

The barrier to rotation of the hydroxyl group in 2,4,6-tri-*t*-butyl phenol has been estimated from dielectric measurements to be 2.8 kcal/mole (24). The rotational barrier in this compound will be lower than in phenol owing to steric repulsion by the *t*-butyl groups ($\sim$1.6 kcal/mole) and also, perhaps, to a decrease in the resonance interaction between the hydroxyl and the ring because of the polar effects of the alkyl substituents. The barrier in phenol is, therefore, $\geqslant$4.4 kcal/mole.

ACKNOWLEDGMENTS

The authors are indebted to Dr. R. N. Jones for the spectra on the prism-grating spectrometer, and to Dr. D. Davidson and Dr. I. E. Puddington for several helpful discussions.

REFERENCES

1. P. J. Krueger and H. W. Thompson. Proc. Roy. Soc. (London), A, **250**, 22 (1959).
2. W. C. Sears and L. J. Kitchen. J. Am. Chem. Soc. **71**, 4110 (1949).
3. L. J. Bellamy and R. L. Williams. Proc. Roy. Soc. (London), A, **254**, 119 (1960).
4. N. A. Puttnam. J. Chem. Soc. 486 (1960).
5. K. U. Ingold. Can. J. Chem. **38**, 1092 (1960).
6. R. F. Goddu. J. Am. Chem. Soc. **82**, 4533 (1960).
7. D. A. Ramsay. J. Am. Chem. Soc. **74**, 72 (1952).
8. G. H. Stillson, D. W. Sawyer, and C. K. Hunt. J. Am. Chem. Soc. **67**, 303 (1945).
9. L. J. Kitchen. J. Am. Chem. Soc. **70**, 1290 (1948).
10. L. A. Cohen. J. Org. Chem. **22**, 1333 (1957).
11. E. Müller and K. Ley. Chem. Ber. **88**, 601 (1955).
12. R. W. Taft. Steric effects in organic chemistry. John Wiley & Sons, Inc., New York. 1956. Chap. 13.
13. T. D. Flynn, R. L. Werner, and B. M. Graham. Australian J. Chem. **12**, 575 (1959).
14. H. W. Thompson, R. W. Needham, and D. Jameson. Spectrochim. Acta, **9**, 208 (1957).
15. R. W. Taft and H. D. Evans. J. Chem. Phys. **27**, 1427 (1957).
16. R. Moccia and H. W. Thompson. Proc. Roy. Soc. (London), A, **243**, 154 (1957).
17. C. A. Coulson. Conference on quantum mechanical methods in valence theory. U.S. Govt. Printing Office. 1951. p. 47.
18. E. G. McRae and L. Goodman. J. Mol. Spectroscopy, **2**, 464 (1958).
19. O. R. Wulf, U. Liddel, and S. B. Hendricks. J. Am. Chem. Soc. **58**, 2287 (1936).
20. L. Pauling. J. Am. Chem. Soc. **58**, 94 (1936).
21. E. Fermi. Z. Physik, **71**, 250 (1931).
22. G. Rossmy, W. Lüttke, and R. Mecke. J. Chem. Phys. **21**, 1606 (1953).
23. A. W. Baker. J. Am. Chem. Soc. **80**, 3598 (1958).
24. M. Davies and R. J. Meakins. J. Chem. Phys. **26**, 1584 (1957).

Can. J. Chem. Downloaded from www.nrcresearchpress.com by 210.87.254.5 on 09/05/12
For personal use only.

Can. J. Chem. Downloaded from www.nrcresearchpress.com by 210.87.254.5 on 09/05/12
For personal use only.

THE EFFECT OF SOLVENT AND TEMPERATURE ON THE CIS–TRANS ISOMERISM OF ORTHO-*tert*-ALKYL PHENOLS[1]

K. U. INGOLD AND D. R. TAYLOR[2]

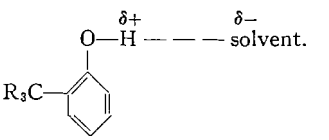
ABSTRACT

The effects of different solvents and of a change of temperature on the infrared band due to the fundamental hydroxyl stretching vibration in several 2,6-di-*t*-alkyl phenols and in the corresponding ortho-*t*-alkyl phenols have been examined. The conclusion that the two bands observed in ortho-*t*-alkyl phenols represent cis and trans isomers has been confirmed. The differences in enthalpy and entropy between the two isomers have been measured for six different phenols.

INTRODUCTION

The conclusions reached in the previous paper (1) as to the nature of the two hydroxyl stretching bands observed in *o-t*-alkyl phenols has been confirmed by an examination of the effects of different solvents and of changes in temperature on the ratios of the intensities of the two bands.

It was predicted, on the basis that the two bands represent cis and trans isomers, that an increase in the polarity or polarizability of the solvent would decrease the percentage of the cis isomer owing to the increased stability of structures of the type



It was also predicted that the trans/cis intensity ratio should decrease with increasing temperature. Both the predictions have been experimentally verified.

EXPERIMENTAL

The spectrometer and slit conditions have been described previously (1). The high-temperature cell consisted simply of a 5-mm cavity cell enclosed by an electrically heated glass tube, the ends of which were sealed by NaCl windows. Hexachloro-1,3-butadiene (HXB) was used as the solvent because of its high boiling point and because frequencies and intensities in this solvent are closely similar to their values in carbon tetrachloride. The concentration of the solute phenol was 0.005 *M*.

RESULTS

Bellamy and Williams (2) have shown that the effect of various solvents on the frequency of the O—H band (ν_m) of 2,6-di-*t*-butyl-4-methyl phenol is quite different from the solvent effect on phenol and on 2,6-dialkyl phenols in which the substituents are not tertiary alkyl groups. Their results have been confirmed with a limited number of solvents for phenol and 2,6-di-*t*-butyl-4-methyl phenol and the measurements have been extended to other 2,6-di-*t*-alkyl-4-methyl phenols. Pentamethyl phenol was also

[1]*Manuscript received November 1, 1960.*
Contribution from the Division of Applied Chemistry, National Research Council, Ottawa, Canada.
Issued as N.R.C. No. 6148.
[2]*National Research Council Summer Student, 1960. Present address: College of Science and Technology, Manchester, England.*

examined in order to discover whether this phenol behaved like the 2,6-di-tertiary or non-tertiary alkyl phenols. The frequencies (ν_m cm^{-1}) are given in Table I, which also includes intensities relative to phenol in carbon tetrachloride (A) and half-band widths ($\Delta\nu_{\frac{1}{2}}$ cm^{-1}). Intensities were obtained from the product of $\Delta\nu_{\frac{1}{2}}$ and the molecular extinction coefficient (1), they are probably not very accurate as they are based only on a single measurement in each case. Results are also included in Table I for the effect of solvent on the cis and trans bands of 2-*t*-butyl-4-methyl phenol.

TABLE I

Effect of solvent on O—H band of alkyl-substituted phenols

Substituent		Hexane	CCl_4	HXB	CS_2	1,2-Dichloro-ethane	Nitro-methane
None (phenol)	ν_m	3622.5	3612.5	3609	3593.5	3565	3511
	A	0.90	1.00	1.02	0.97	1.47	4.27
	$\Delta\nu_{\frac{1}{2}}$	15	18.5	23	29	58	133
$(Me)_5$	ν_m	3637.5	3630	—	3618.5	3596.5	3582
	A	0.55	0.61	—	0.60	0.73	~2.12
	$\Delta\nu_{\frac{1}{2}}$	16.5	20.5	—	26	42	54
2,6-Bu_2^t-4-Me	ν_m	3656	3650	3648.5	3645	3637.5	3629.5
	A	0.91	0.95	0.93	0.96	1.13	1.86
	$\Delta\nu_{\frac{1}{2}}$	16	19	22	19.5	28	42
2,6-Am_2^t-4-Me	ν_m	3647	3642.5	3643	3636	3631	3624.5
	A	0.93	1.15	1.05	1.00	1.04	1.50
	$\Delta\nu_{\frac{1}{2}}$	17	19.5	19.5	18.5	30	40
2,6-Oct_2^{tt}-4-Me	ν_m	3639	3635.5	3637.5	3633	3627	3622.5
	A	1.08	1.18	1.12	1.01	1.20	1.60
	$\Delta\nu_{\frac{1}{2}}$	18.5	19	21	19.5	31	39
2,6-$((C_2H_5)_3C)_2$-4-Me	ν_m	3638.5	3635	3636	3631.5	3625.5	3621
	A	1.18	1.21	1.14	0.96	1.35	1.76
	$\Delta\nu_{\frac{1}{2}}$	17.5	18	20.5	18.5	32.5	37
2-Bu^t-4-Me							
Trans	ν_m	3619.5	3610	3607.5	3591	3567	3506
	A	0.58	0.85	0.89	0.90	1.44	3.58
	$\Delta\nu_{\frac{1}{2}}$	16	17.5	19.5	27.5	50	118
Cis	ν_m	3658.5	3649.5	3649	3643.5	~3634	?
	A	0.06_0	0.06_9	0.07_2	0.06_2	0.05_9	<0.04
	$\Delta\nu_{\frac{1}{2}}$	17	17.5	20.5	20	~30	40*
$\frac{A(\text{trans})}{A(\text{cis})}$		9.6	12.3	12.3	14.5	25	>85
$\frac{[\text{trans}]}{[\text{cis}]}$		11.5	14.4	14.3	17	23	>45

*See text.

For the work at different temperatures it was necessary to examine not only the *o*-*t*-alkyl phenols, but also the corresponding dialkyl phenols and an unhindered phenol in order to find out whether the correction for the intrinsic differences in intensity between cis and trans isomers varied with temperature. 4-*t*-Butyl phenol was used in place of phenol because of its lower volatility—the presence of a para-substituent would not be expected to affect the results.

The intensities of symmetrically substituted phenols in HXB relative to phenol in HXB at room temperature (i.e. A_{HXB}) decrease linearly with increasing temperature within the accuracy of the measurements (Fig. 1). The points plotted in this figure have not been corrected for expansion of the solvent nor for changes in the path length. Over

Can. J. Chem. Downloaded from www.nrcresearchpress.com by 210.87.254.5 on 09/05/12
For personal use only.

Can. J. Chem. Downloaded from www.nrcresearchpress.com by 210.87.254.5 on 09/05/12
For personal use only.

the temperature range studied the former effect will cause values of A_{HXB} to decrease by about 10%. The percentage absorptions ($\log(I_0/I)_{max}$) of the bands decreased (3, 4) and their half-band widths increased as the temperature was raised. In contrast to a previous report (3) ν_m was found to increase regularly with temperature. The values of ν_m and $\Delta\nu_{\frac{1}{2}}$ at room temperature are given in Table I except for 4-*t*-butyl phenol ($\nu_m = 3610.5\ cm^{-1}$, $A = 0.94$, $\Delta\nu_{\frac{1}{2}} = 22.5\ cm^{-1}$) and 2,3,5,6-tetramethyl phenol ($\nu_m = 3626\ cm^{-1}$, $A = 0.64$, $\Delta\nu_{\frac{1}{2}} = 21.5\ cm^{-1}$). The increases in ν_m and $\Delta\nu_{\frac{1}{2}}$ in cm^{-1} on raising the temperature from 24° to 150° C are respectively: 4-*t*-butyl 7.5 and 3; 2,3,5,6-tetramethyl 4 and 2; 2,6-di-*t*-butyl-4-methyl 2.5 and 5.5; 2,6-di-*t*-amyl-4-methyl 2 and 4; 2,6-di-*t*-*t*-octyl-4-methyl 1.5 and 3; 2,6-di-triethylmethyl-4-methyl phenol 1.5 and 3.5.

Table II shows the effect of temperature on *o*-*t*-alkyl phenols. The temperatures are only approximately (±5° C) those at which the measurements were made, in order to simplify the Table. ν_m values for cis isomers are less accurate than for the trans isomers (1). The increases in ν_m and $\Delta\nu_{\frac{1}{2}}$ appear to follow the same relations as were observed with the symmetrically substituted phenols, i.e. ν_m and $\Delta\nu_{\frac{1}{2}}$ increase by about 6 cm^{-1} and 3 cm^{-1} respectively in the range 24° to 150° C for the trans band and by about 2.5 cm^{-1} and 3 cm^{-1} respectively for the cis band. However, the plots of A_{HXB} against temperature for trans isomers have much steeper slopes than are observed with the symmetrically substituted phenols, presumably because of the relative increase in the amount of cis isomers as the temperature rises. These plots appear, in general, to be slightly convex towards the temperature axis. As the temperature is raised it becomes increasingly difficult to separate the cis band since not only are both bands smeared out owing to the increase in $\Delta\nu_{\frac{1}{2}}$, but also the two band maxima move slightly closer together.

The parallel straight lines shown in Fig. 1 for symmetrically substituted phenols indicate that the correction factors for the intrinsic differences in intensity between cis and trans isomers are independent of temperature. The intensities of substituted phenols relative to phenol when plotted against Hammett σ constants are independent of solvent for a small range of solvent types (5). This means that ρ is independent of solvent and therefore the correction factors in HXB can be readily obtained (1). These factors are

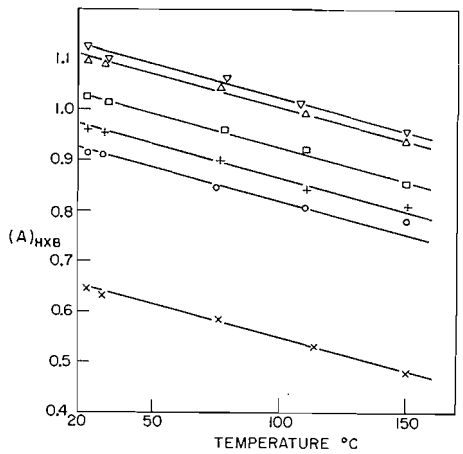


FIG. 1. Effect of temperature on the relative intensities of symmetrically substituted phenols. Key: 2,3,5,6-tetramethyl ×; 2,6-di-*t*-butyl-4-methyl ○; 4-*t*-butyl +; 2,6-di-*t*-amyl-4-methyl □; 2,6-di-*t*-*t*-octyl-4-methyl △; 2,6-di-triethylmethyl-4-methyl phenol ▽.

TABLE II

Effect of temperature on *o*-*t*-alkyl phenols in hexachlorobutadiene

Phenol		Approximate temperature (°C)							
		24°		75°		110°		150°	
		Trans	Cis	Trans	Cis	Trans	Cis	Trans	Cis
2-Bu^t-4-Me	ν_m	3607.$_5$	3649	3611	3649.$_5$	3612.$_5$	3651	3615	3652
	A	0.88	0.07$_2$	0.79	0.09$_0$	0.72	0.10$_2$	0.67	0.113
	$\Delta\nu_{\frac{1}{2}}$	19.$_5$	20.$_5$	20.$_5$	23	21.$_5$	24	23	24
2-Bu^t-6-Me	ν_m	3615.$_5$	3649	3618	3650	3619	3651	3620.$_5$	3652
	A	0.65	0.12$_8$	0.58	0.14$_9$	0.53	0.16$_1$	0.48	0.15$_9$
	$\Delta\nu_{\frac{1}{2}}$	22	21	23	22	24	23	25	24
2-Bu^t-5,6-Me$_2$	ν_m	3622	3652	3623.$_5$	3652	3625	3653	3626	3654
	A	0.54	0.17$_7$	0.48	0.19$_2$	0.42	0.18$_7$	0.37	0.18$_3$
	$\Delta\nu_{\frac{1}{2}}$	21.$_5$	21	22	22	22.$_5$	23	23	24
2-Am^t-4-Me	ν_m	3607	3645.$_5$	3609	3646	3611	3646.$_5$	3613	3647
	A	0.88	0.07$_0$	0.80	0.09$_4$	0.69	0.09$_9$	0.63	0.10$_5$
	$\Delta\nu_{\frac{1}{2}}$	19	18.$_5$	20.$_5$	22.$_5$	22	24.$_5$	23	25
2-Oct^{tt}-4-Me	ν_m	3607	3637	3609	3638	3610	3638	3612	3638
	A	0.92	0.06$_5$	0.82	0.09$_0$	0.77	0.10$_4$	0.70	0.11$_8$
	$\Delta\nu_{\frac{1}{2}}$	18.$_5$	20.$_5$	19.$_5$	22	21.$_5$	23	22.$_5$	25
2-(C_2H_5)$_3$C-4-Me	ν_m	3606	3637	3607.$_5$	3638	3609	3638.$_5$	3610.$_5$	3639
	A	0.89	0.06$_6$	0.78	0.09$_1$	0.71	0.10$_1$	0.64	0.10$_8$
	$\Delta\nu_{\frac{1}{2}}$	19.$_5$	20.$_5$	20.$_5$	22	21.$_5$	23	22.$_5$	24.$_5$

given in Table III; they are only slightly different from the values calculated in carbon tetrachloride (1). The measured ratios A(trans)/A(cis), which will, of course, be independent of solvent expansion etc., were multiplied by these factors to give the true concentration ratios of the two isomers at each temperature. The logarithms of the true concentration ratios have been plotted against $1/T$ (°K) in Fig. 2, since the relation

$$\log_{10}\frac{[\text{trans}]}{[\text{cis}]} = \frac{\Delta G}{2.3\,RT} = \frac{\Delta H}{2.3\,RT} - \frac{\Delta S}{2.3\,R}$$

should be obeyed. That is, the slopes of the lines in Fig. 2 give ΔH, the enthalpy difference between the cis and trans isomers, and the intercepts give ΔS, the entropy difference. These results, as well as values of ΔG obtained at room temperatures in carbon tetrachloride (1) are given in Table III.

TABLE III

Enthalpy difference between cis and trans isomers of *o*-*t*-alkyl phenols

Phenol	Correction factor in HXB	ΔS e.u. (HXB)	ΔH kcal/mole (HXB)	ΔG kcal/mole (CCl_4) (1)
2-Bu^t-4-Me	1.16	−0.2	1.5$_5$	1.5$_7$
2-Am^t-4-Me	1.24	−0.2	1.5$_5$	1.6$_7$
2-Oct^{tt}-4-Me	1.32	−0.2	1.6$_5$	1.7$_1$
2-(C_2H_5)$_3$C-4-Me	1.35	−0.2	1.6$_5$	1.7$_4$
2-Bu^t-6-Me	1.23	−0.1	1.0$_5$	1.0$_6$
2-Bu^t-5,6-Me	1.28	0	0.8$_0$	0.8$_0$

Owing to the increased difficulty of separating the two bands with increasing temperature the accuracy of the results was such that there is no real difference between the

Can. J. Chem. Downloaded from www.nrcresearchpress.com by 210.87.254.5 on 09/05/12
For personal use only.

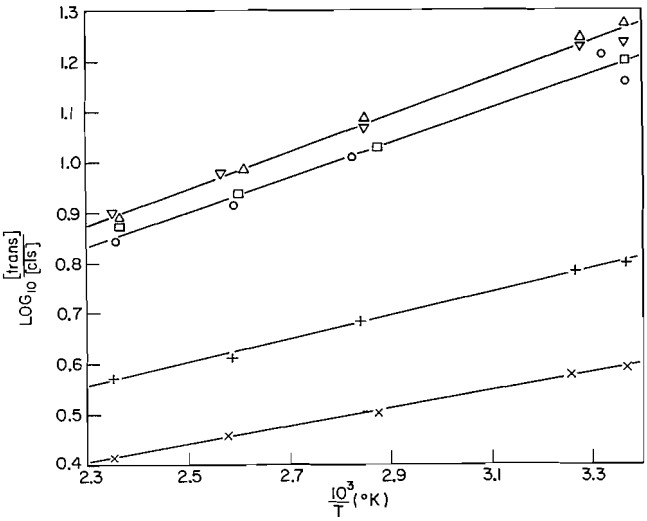


FIG. 2. Effect of temperature on $\log_{10}$[trans]/[cis] for ortho-alkyl phenols. Key: 2-*t*-butyl-5,6-dimethyl ×; 2-*t*-butyl-6-methyl +; 2-*t*-butyl-4-methyl ○; 2-*t*-amyl-4-methyl □; 2-*t*-*t*-octyl-4-methyl △; 2-triethyl-methyl-4-methyl phenol ▽.

plots of 2-*t*-butyl-4-methyl and 2-*t*-amyl-4-methyl phenol and between 2-*t*-*t*-octyl-4-methyl and 2-triethylmethyl-4-methyl phenol, a single line has therefore been drawn through each pair.

Although a small positive intercept is obtained in each case, it may well be due to an overestimation of the correction factors. Moreover, the intercepts are sufficiently small that the data for each phenol could be fitted almost equally well by straight lines passing through the origin. That is, ΔS is certainly small in each case and is very probably zero.

DISCUSSION

Bellamy and Williams (2) have shown that the changes in ν_m for phenol and 2,6-dialkyl phenols on passing from one solvent to another are due to local association effects, which occur even in non-polar solvents. By comparing ν_m for 2,6-dimethyl, -diethyl, and -diisopropyl phenol in different solvents with ν_m for phenol, these workers concluded that there is no significant steric hindrance to solvent effects in these phenols, the small effects observed being ascribed to the polar effects of the alkyl substituents. The results given in the previous paper (1) suggest that two *o*-methyl groups backed up by *m*-methyl groups may exert a greater effect on the hydroxyl group than is exerted by, for example, two *o*-isopropyl groups. For this reason it was considered of interest to study the effect of solvents on ν_m for pentamethyl phenol to see whether any steric hindrance to solvent effects could be observed. The results obtained (Table I) are not significantly different from the results reported for dialkyl phenols (2), the small differences that are observed are very likely due to the increased polar effect of five methyl substituents. Therefore, on the basis of Bellamy and Williams' work it could be concluded that steric hindrance to solvent effects does not occur in pentamethyl phenol. However, the changes in $\Delta\nu_{\frac{1}{2}}$ (which were not reported by Bellamy and Williams) of pentamethyl phenol compared to phenol do suggest some small steric effects are present, and therefore small effects may also have been operating in the dialkyl phenols they studied.

Can. J. Chem. Downloaded from www.nrcresearchpress.com by 210.87.254.5 on 09/05/12
For personal use only.

For 2,6-di-*t*-butyl-4-methyl phenol, however, Bellamy and Williams have shown that there is a very noticeable steric hindrance to the approach of solvent molecules. Our results confirm this, and also show that this hindrance increases with increasing size of the alkyl substituents, as would be expected. The comparatively small changes in A and $\Delta\nu_{\frac{1}{2}}$ for 2,6-di-*t*-alkyl phenols compared with phenol or pentamethyl phenol can also be ascribed to a steric hindrance of solvent effects.

The results obtained with 2-*t*-butyl-4-methyl phenol are in agreement with theory. That is, in terms of changes in ν_m, A, and $\Delta\nu_{\frac{1}{2}}$ the trans band behaves similarly to phenol and the cis band similarly to 2,6-di-*t*-butyl-4-methyl phenol, although the cis band does not appear to be quite as highly protected from solvent effects as is the band in the di-*t*-butyl phenol.

As the polarizability or polarity of the solvent increases the two band maxima move further apart, but the resolution of the two bands becomes more difficult owing to the increase in half-band widths. The values obtained for $A(\text{trans})/A(\text{cis})$ with 2-*t*-butyl-4-methyl phenol in the different solvents are given in Table I. In nitromethane no separate cis band was observed. A maximum value was estimated for this band from the value of $\Delta\nu_{\frac{1}{2}}$ for 2,6-di-*t*-butyl-4-methyl phenol and the maximum contribution to $\log(I_0/I)$ at the expected ν_m that could be due to the cis band. The trend in the ratio of $A(\text{trans})/A(\text{cis})$ overemphasizes the true increase in the percentage of the trans isomer since the solvent effect on this isomer will be greater than on the cis isomer, (cf. effect of solvent on A for phenol and 2,6-di-*t*-butyl-4-methyl phenol in Table I). However, even after this effect is approximately allowed for (i.e. [trans]/[cis] in Table I), the results still show the predicted increase in the concentration of the trans isomer with increasing solvent interaction. The results also show that even in carbon tetrachloride the percentage of trans isomer is greater than would be present in the vapor phase at the same temperature. A similar result has been observed with the isomers of *o*-halophenols by Rossmy, Lüttke, and Mecke (6). These workers, found, for example, that the trans isomer of *o*-iodophenol is stabilized by solvent interaction in carbon tetrachloride by about 1.4 kcal/mole with respect to the gaseous state. The values of ΔG and ΔH recorded in Table III must, therefore, be larger than they would be in the vapor state.

The increase in ν_m with temperature is probably related to the decreasing density of the solvent. That is, as the temperature is raised the solvent molecules are, on average, further removed from the solute molecules and therefore their influence will decrease and ν_m will increase. The smaller effect of temperature on ν_m for di-*t*-alkyl phenols compared with non-hindered phenols is to be expected since the effect of the solvent even at room temperature is greatly reduced by the shielding afforded to the OH group by the *t*-alkyl substituents.

As was mentioned above, ΔS values given in Table III are zero within the limits of experimental error, which suggests equal, a priori, probability for the two isomers and supports isomerization of the cis–trans type with the OH group coplanar in both isomers. If the O—H bond were twisted out of the plane in 2,6-di-*t*-alkyl phenols and also, therefore, in the cis isomer of *o*-*t*-alkyl phenols there would be two equivalent cis isomers and the a priori probability for this isomer would be twice that of the trans. Since ΔS is close to zero there is good agreement between ΔH and ΔG for the different phenols.

All the results obtained in this work support our original interpretation that the two infrared OH bands observed in *o*-*t*-alkyl phenols represent cis and trans isomers, the latter being thermodynamically more stable.

Can. J. Chem. Downloaded from www.nrcresearchpress.com by 210.87.254.5 on 09/05/12
For personal use only.

REFERENCES

1. K. U. INGOLD and D. R. TAYLOR. Can. J. Chem. This issue.
2. L. J. BELLAMY and R. L. WILLIAMS. Proc. Roy. Soc. (London), A, **254**, 119 (1960).
3. R. H. HUGHES, R. J. MARTIN, and N. D. COGGESHALL. J. Chem. Phys. **24**, 489 (1956).
4. T. L. BROWN. J. Chem. Phys. **24**, 1281 (1956).
5. K. U. INGOLD. Can. J. Chem. **38**, 1092 (1960).
6. G. ROSSMY, W. LÜTTKE, and R. MECKE. J. Chem. Phys. **21**, 1606 (1953).

Can. J. Chem. Downloaded from www.nrcresearchpress.com by 210.87.254.5 on 09/05/12
For personal use only.

Can. J. Chem. Downloaded from www.nrcresearchpress.com by 210.87.254.40 on 09/05/12
For personal use only.

PHOTOCHEMICAL SYNTHESES

I. THE REACTION OF ALDEHYDES AND KETONES WITH CYCLOALKENES[1]

P. DE MAYO,[2] J. B. STOTHERS,[2] AND W. TEMPLETON

ABSTRACT

The irradiation of dialkyl ketones in cyclohexene leads to the formation of cyclohexenyldialkylcarbinols. The use of aldehydes leads to the formation of the corresponding secondary alcohols, but the reaction is more complex because of concomitant Kharasch addition which can, however, be suppressed. The mechanism of the alcohol formation has been elucidated by the use of an optically active substrate, carvomenthene, and has been shown to involve the intermediacy of a cyclohexenyl radical. The structure and genesis of a biscarbinol by-product is discussed.

It was first observed by Bowen and Horton (1) that the irradiation of acetone in cyclohexane gave, in poor yield, an alcohol which was presumed to be cyclohexyldimethylcarbinol. More recent investigations (2) confirmed this, but the yield (12%) was not such as to render the reaction preparatively a very useful one.

It seemed probable that if the reaction proceeded by initial hydrogen atom abstraction by the photoactivated carbonyl compound, then any functional group designed to stabilize that radical should render the reaction more facile; and indeed there were indications in the literature (see, for instance, refs. 3, 4, 5) that in related transformations this was so.

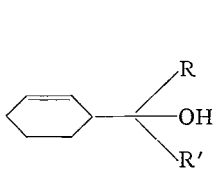
A simple function that would fulfill the requirements was the ethylenic linkage and to this end the symmetrical hydrocarbon cyclohexene was selected. Irradiation at room temperature of a solution of acetone in this hydrocarbon until no carbonyl band could be detected in the infrared gave, after removal of excess hydrocarbon and distillation from a polymeric residue, a colorless oil. This could be separated by gas–liquid chromatography into an alcohol, shown to be the desired carbinol, and 3,3′-bicyclohexenyl. The latter was characterized as the known two tetrabromides (6).

The alcohol showed bands in the infrared at 3322 (hydroxyl), 1378 and 1368 (geminal dimethyl), and 733 cm^{-1} (cis disubstituted ethylene) in accordance with structure (I, R = R′ = Me), and had the required analysis. It was characterized as the 3,5-dinitrobenzoate, and an authentic specimen of the alcohol was synthesized from cyclohexene-3-carboxylic acid by esterification (diazomethane) and Grignard reaction with methyl magnesium iodide. The alcohol so obtained and the derived 3,5-dinitrobenzoate were identical in every respect with the corresponding photoproducts.

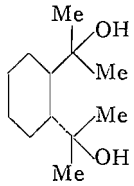
Under similar conditions the carbinols (I, R = R′ = Et) and (I, R = R′ = Pr) were obtained employing diethyl and dipropyl ketone respectively.

When the cyclohexene–acetone irradiation was performed at reflux temperature there was isolated in poor yield an additional substance, a saturated alcohol, which was readily characterized as a crystalline 3,5-dinitrobenzoate. The analysis indicated the condensation of two molecules of acetone with one of cyclohexene. The absence of unsaturation suggested structure (II) and comparison with an authentic specimen (see Experimental) confirmed this.

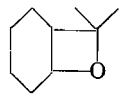
[1]*Manuscript received November 8, 1960.*
Contribution from the Departments of Chemistry, Imperial College, London, S.W.7, England, and the University of Western Ontario, London, Ontario. Part of the contents of this paper were contained in a preliminary communication (26).
[2]*Present address: Department of Chemistry, University of Western Ontario, London, Ontario.*



(I)



(II)



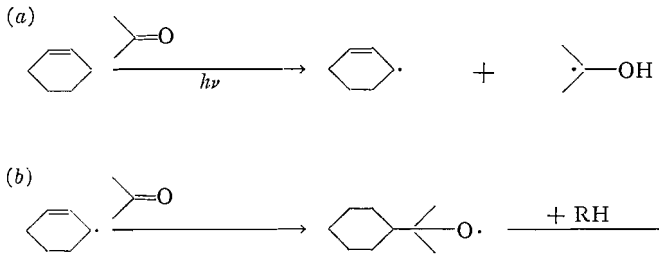
(III)

The formation of this interesting substance appears to be without photochemical parallel. Its genesis would not appear to involve, as expected, cyclohexenyl or, more probably, substituted cyclohexyl radicals, because when no attempt was made to exclude oxygen in the irradiation the formation of (I) was *totally suppressed*, all the cyclohexenyl radicals being trapped by the excess oxygen as cyclohexene hydroperoxide. The latter was characterized by conversion to cyclohexenone 2,4-dinitrophenylhydrazone. The yield of (II) remained, however, unaffected.

If such radicals are to be excluded a 'molecular' reaction must be presumed: one such reaction, known to occur with more-substituted ethylenes, is oxetane formation (7, 8). In the present case the oxide (III), not, however, isolated, would be the product. Bimolecular homolytic substitution at the cyclohexyl terminus of the oxide ring could then lead to (II). Radical displacements on carbon are rare, but are known to occur (cf. ref. 9). This possibility is being further investigated.

It has been the tacit assumption that the alcohols of type I were produced by the following steps:

Mechanism A

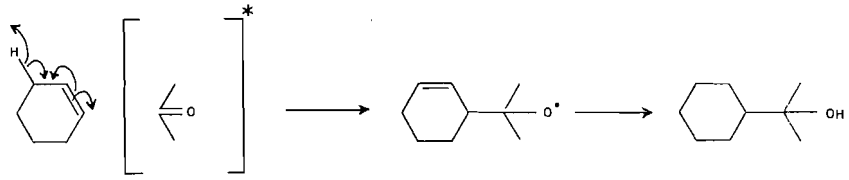


Evidence for step (*a*) lies in the formation of cyclohexene hydroperoxide in the presence of air, and in the formation of 3,3′-bicyclohexenyl as an important by-product. Although it is possible that in step (*b*) the cyclohexenyl radical may react with some other species than acetone in the ground state the assumption appears unnecessary since it is known (10) that chemically generated cyclohexyl radicals will add to carbonyl compounds in such a manner.

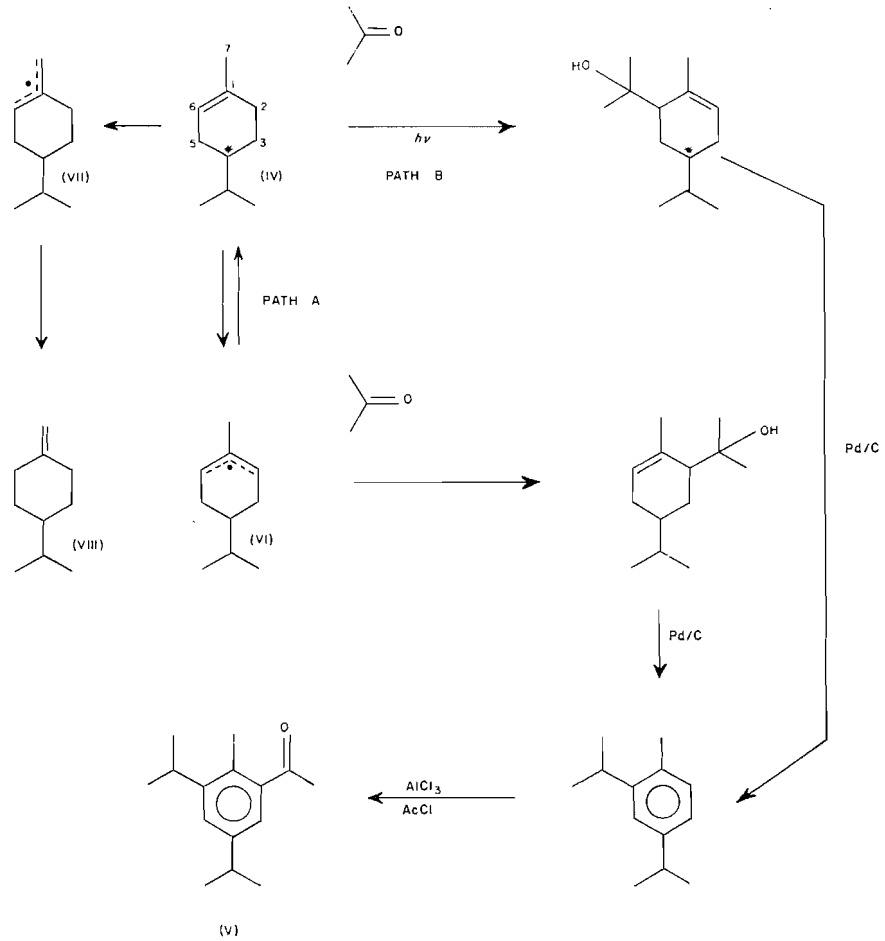
Nevertheless, although the evidence for step (*a*) is good it did not follow that the alcohol (I) was necessarily derived from a species produced in it. An alternative process, involving attack on the π-electrons of the cycloalkene appeared admissible, and such a mechanism has been proposed in radical substitutions in dienes and trienes (see, for instance, refs. 11, 12). This mechanism, in the present case, may be represented as follows:

Can. J. Chem. Downloaded from www.nrcresearchpress.com by 210.87.254.40 on 09/05/12
For personal use only.

Mechanism B



A distinction between these two mechanisms was arrived at in the following manner. (+)-Carvomenthene (IV), prepared by the hydrogenation of limonene, was irradiated in admixture with acetone. The alcoholic fraction, a mixture of stereoisomers, was completely racemized. The gross structure of the product was established by dehydrogenation and acylation to (V) characterized as the known 2,4-dinitrophenylhydrazone. The racemization of the active center during the photoreaction implies the intermediacy of the symmetrical allylic radical (VI), and supported mechanism A.



Can. J. Chem. Downloaded from www.nrcresearchpress.com by 210.87.254.40 on 09/05/12
For personal use only.

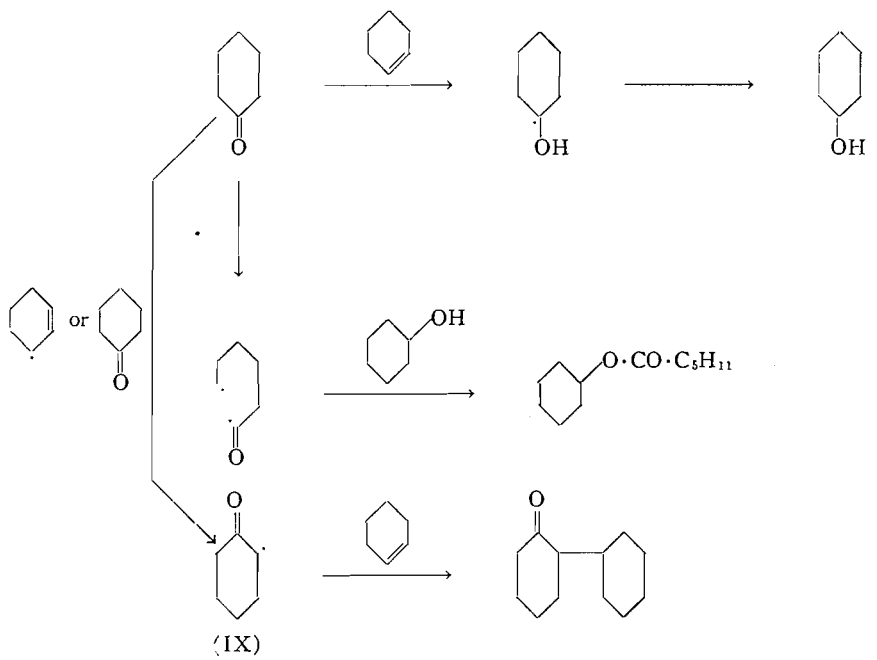
A possible criticism of the foregoing conclusions might rest on the fact that the zero rotation may have been a fortuitous combination of positive and negative rotations in stereoisomers. Since the separation of these isomers appeared difficult an alternative approach was sought.

It appeared possible that the radical (VI) might compete with the photoactivated ketone for allylic hydrogen abstraction in (IV), thus regenerating (inactive) carvomenthene on one hand and a new, equivalent, radical on the other. If this occurred, racemization could precede (apparent) reaction. In the event, interruption of the reaction before completion and recovery of carvomenthene by gas–liquid chromatography gave material which was approximately 30% racemized thus providing compelling evidence for the intermediacy of (VI). Carvomenthene, in the absence of acetone, was unaffected under the irradiation conditions.

By gas–liquid chromatography, also, a small amount of *p*-menth-1,7-ene (VIII) (13) was also isolated during the same experiment. This hydrocarbon is evidently formed by allylic hydrogen abstraction at the (alternative) primary (C_7) position, and provides further general support for the present thesis.

The irradiation of cyclohexanone in cyclohexene led to entirely different results. No alcohol of the required type was isolated, but instead, in addition to the 3,3′-bicyclohexenyl, two further liquid substances were obtained by chromatography of the total volatile product on alumina.

The first of these was readily identified as cyclohexyl *n*-caproate by hydrolysis to its components, each being characterized by a solid derivative. Evidently the cyclohexanol (or equivalent) derives from the hydrogen-abstraction step, but the cyclohexene is, however, apparently too bulky a molecule to allow of backside attack of the cyclohexenyl radical on the cyclohexanone carbonyl. Such reaction is presumably controlled by the 1,3-axial hydrogen interactions in the transition state. Under these circumstances, and



(IX)

Can. J. Chem. Downloaded from www.nrcresearchpress.com by 210.87.254.40 on 09/05/12
For personal use only.

in the presence of cyclohexanol, the slower solvolytic fission may then take place. Such fission in cyclic ketones is unexceptional (14).

The resistance of the cyclohexanone carbonyl to attack by the cyclohexenyl radical is also demonstrated by the nature of the second product. This substance showed a single carbonyl band in the infrared at 1715 cm^{-1}, whilst the empirical formula indicated it to be a 1:1 adduct of cyclohexanone and cyclohexene. The presumption that it was cyclohexyl cyclohexanone was justified by comparision of the ketone and its 2,4-dinitrophenylhydrazone with authentic specimens. The cyclohexenyl radical or, perhaps, activated ketone has, therefore, abstracted an α-hydrogen atom to give (IX), which has then added to a further molecule of cyclohexene. These observations parallel those of Kharasch, Kuderna, and Nudenberg, who noted the addition of cyclohexanone to oct-1-ene (15).

The irradiation of cyclohexene with aldehydes led to similar results. Propionaldehyde for instance gave (I, R = Et, R′ = H), characterized as the 3,5-dinitrobenzoate, and identified by comparison with an authentic specimen.[3] The latter was prepared by reaction of cyclohexene-3-carbonyl chloride with dimethyl cadmium followed by lithium aluminum hydride reduction. The expected product of Kharasch addition (16) was also obtained.

In the case of acetaldehyde it was found, because of the volatility of the substance, more convenient to work in a closed system. Here, again, the desired alcohol (I, R = Me, R′ = H) was obtained, together with the Kharasch addition product methylcyclohexyl ketone.

The 60 Mc N.M.R. spectra of the alcohol and its 3,5-dinitrobenzoate were obtained in CCl_4 solution (ca. 15%). The characteristic peaks observed (in p.p.m. from tetramethylsilane)[4] were as follows: alcohol: CH_3 group, 1.14 (doublet, J = 6 c.p.s.); OH, 2.9 (concentration-dependent); H on carbon bonded to oxygen, a multiplet centered at 3.6, and olefinic Hs, 5.7 (a multiplet); the 3,5-dinitrobenzoate: CH_3 group, 1.5 (doublet, J = 7 c.p.s.); H on carbon bonded to oxygen, 5.3 (center of multiplet); olefinic Hs, 5.8 (center of multiplet), and aromatic Hs, 9.1–9.4. The areas of the last three bands were in the ratio 1:2:3. These assignments are entirely compatible with the proposed structure. This is most clearly demonstrated in the paramagnetic shift of the methine hydrogen on carbon bonded to oxygen from 3.6 to 5.3 on esterification.

Since the Kharasch addition is a chain reaction (24) involving most probably the following steps:

(i) $R\cdot CHO \rightarrow \dot{R} + \dot{C}HO,$

(ii) $R\cdot + RCHO \rightarrow RH + R\dot{C}O,$

(iii) $R\dot{C}O + R_2C{=}CR_2 \rightarrow RCOR_2C{-}\dot{C}R_2,$

(iv) $RCOR_2C{-}\dot{C}R_2 + RCHO \rightarrow RCOR_2C{-}CHR_2 + R\dot{C}O$ etc.;

its perpetuation ((step ii)+(step iv)) should be favored by a high ratio of aldehyde to cyclohexene. On the other hand the process leading to the alcohol should require that the concentration of hydrocarbon be high so that hydrogen atom abstraction by the photoactivated aldehyde may compete with homolysis (step i). In the event, when the concentration (w/v) of acetaldehyde in cyclohexene was decreased from 20% to 2% the ratio of ketone to alcohol changed from about 1:1 to 1:9.

[3]*The alcohols from the aldehydes may possibly be mixtures of diastereoisomers. These did not resolve on the silicone column used. The synthetic specimens, also possibly diastereoisomers, were indistinguishable from these in chromatographic behavior as in other respects.*

[4]*For τ values (25) these figures should be subtracted from 10.*

Can. J. Chem. Downloaded from www.nrcresearchpress.com by 210.87.254.40 on 09/05/12
For personal use only.

Can. J. Chem. Downloaded from www.nrcresearchpress.com by 210.87.254.40 on 09/05/12
For personal use only.

EXPERIMENTAL

Materials were reagent grade and were dried over magnesium sulphate and distilled before use. Cyclohexene was purified by shaking with aqueous ferrous sulphate, dried, and distilled. Before use it was filtered through a short column of alumina. Gas–liquid chromatography was conducted on a silicone–celite column at 175°. Unless otherwise specified irradiations were carried out under dry oxygen-free nitrogen in a quartz immersion apparatus (8*b*), the light source being a 125-watt Compton mercury arc lamp or a Hanovia 85-watt AH-8, both of which had the outer envelope removed. The yields recorded are based on carbonyl compound employed (*not* that consumed) and are in no way optimum values. Light petroleum was b.p. 60–80°.

Irradiations

Acetone–Cyclohexene (i)

A solution of acetone (50 g) in cyclohexene (275 ml) was irradiated at approximately 20° for 100 hours. After evaporation of the solvents the residue was distilled *in vacuo* to give a colorless oil (70 g). Gas–liquid chromatography of a portion (0.65 g) gave two fractions. The first cyclohex-2-enyl dimethylcarbinol (0.34 g; 30%) had b.p. 82°/30° mm, n_D^{21} 1.4740. Calc. for $C_9H_{16}O$: C, 77.09; H, 11.50%. Found: C, 77.02; H, 11.82%. The 3,5-dinitrobenzoate crystallized from chloroform–methanol, and had m.p. 121–124°. Calc. for $C_{16}H_{18}O_6N_2$, 0.5 CH_3OH: C, 56.55; H, 5.75; N, 8.00. Found: C, 56.94; H, 5.38; N, 8.07%. The substance was identical in every respect with an authentic synthetic specimen (see below).

The second fraction 3,3′-bicyclohexenyl (0.28 g) had b.p. 167–170/130 mm, n_D^{24} 1.5050, λ_{max} 190 mμ (ϵ 14,300) expected for two cis disubstituted ethylenes,[5] ν_{max} 701 cm^{-1}. Bromination in carbon tetrachloride gave a crystalline mixture of bromides from which, by fractional crystallization from chloroform, the two tetrabromides of 3,3′-bicyclohexenyl, m.p. 158–160° and 191.5–192.5°, were obtained. These were identical in every respect with specimens of the same melting point prepared by the method of Farmer and Michael (6).

Acetone–Cyclohexene (ii)

Irradiation at reflux temperature, in a quartz vessel over a 500-watt Hanovia lamp, of a solution of acetone (25 g) in cyclohexene (225 ml) for 38 hours gave, after evaporation of the solvent and distillation, an oil (27 g). Gas–liquid chromatography revealed the presence of a further substance in addition to the 3,3′-bicyclohexenyl and the alcohol (I, R = R′ = Me). This component was obtained as a concentrate by fractional distillation (b.p. 133–138°/150 mm) and was converted into the 3,5-dinitrobenzoate, m.p. (from methanol) 112–115°. Calc. for $C_{26}H_{28}O_{12}N_4$: C, 53.06; H, 4.80; N, 9.52%. Found: C, 53.26; H, 4.45; N, 9.95%. It was identical in every respect with an authentic synthetic specimen of *trans*-1,2-di(2′-hydroxy-2′-propyl) cyclohexane prepared as described below. The corresponding alcohols had identical retention times on the silicone column.

Acetone–Cyclohexene (iii)

A solution of acetone (16 g) in cylohexene (200 ml) was irradiated at room temperature for 40 hours in the presence of excess oxygen. By fractional distillation an oil (2.5 g) b.p. 119–130°/140 mm was isolated. Gas–liquid chromatography showed the presence of two substances in approximately equal amounts. One was identified as *trans*-1,2-di(2′-hydroxy-2′-propyl) cyclohexane by retention time and conversion to the 3,5-dinitrobenzoate, m.p. and mixed m.p. 111–113°. The second substance cyclohex-2-ene

[5]*We are indebted to Dr. D. Turner (Imperial College) for the determination of this spectrum between 170 and 200 mμ.*

hydroperoxide was isolated by chromatography of the distillate (2 g) on silica gel (100 g). Elution with benzene–ether (1:1) gave a fraction (600 mg) which was optically transparent in the ultraviolet, gave a strong starch–iodide reaction, and had ν_{max} 3365 and 702 cm^{-1}. On treatment with 6 *N* sulphuric acid a maximum appeared in the ultraviolet at 228 mμ and rose to ϵ 8000. To convert the hydroperoxide into the α,β-unsaturated ketone 2,4-dinitrophenylhydrazone it was mixed with reagent hydrochloride at room temperature in dioxan–water and left to stand overnight; its melting point and mixed m.p. 163° were identical with those of an authentic specimen of cyclohexenone 2,4-dinitrophenylhydrazone.

Acetone – Diethyl Ketone

A solution of diethyl ketone (40.8 g) in cyclohexene (300 ml) was irradiated at room temperature for 138 hours. Fractional distillation of the product then gave a colorless oil (28 g). Chromatography of a portion (5 g) on alumina (Brockman Grade 3, 200 g) gave (eluted with light petroleum) 3,3′-bicyclohexenyl (3.5 g) identified by retention time and infrared spectrum. Elution with 4:1 benzene–ether then gave 3-cyclohex-2′-enylpentan-3-ol, b.p. 140°/50 mm, n_D^{23} 1.4823. Calc. for $C_{11}H_{20}O$: C, 78.51; H, 11.98%. Found: C, 78.25; H, 11.76%. The retention time and infrared spectrum were identical with those of an authentic specimen (see below).

Acetone - Dipropyl Ketone

A solution of di-*n*-propyl ketone (40 g) in cyclohexene (300 ml) was irradiated at room temperature for 72 hours. Fractional distillation yielded an oil (67 g) a sample of which (5 g) was chromatographed on alumina (Brockman Grade 3, 200 g). Elution with light petroleum gave 3,3′-bicyclohexenyl (4.0 g) identified as previously. Elution with ether – benzene (1:9) gave a mixture from which, by gas–liquid chromatography, the required alcohol could be isolated. It had n_D^{23} 1.4790. Calc. for $C_{13}H_{24}O$: C, 79.53; H, 12.32%. Found: C, 78.77; H, 12.27%. It was identical in infrared spectrum, retention time, and refractive index with a specimen prepared by an unambiguous route as described below.

Acetone – (+)-Carvomenthene (i)

A solution of acetone (80 g) in carvomenthene (270 g) ($[\alpha]_D$ +76°) (17) was irradiated at room temperature for 290 hours. Fractional distillation gave a crude product (41 g) which on gas–liquid chromatography gave an oil, $[\alpha]_D$ ±0°, ν_{max} 3434. Calc. for $C_{13}H_{24}O$: C, 79.53; H, 12.32%. Found: C, 79.43; H, 12.17%.

The crude alcohol (1.7 g) was refluxed with palladized charcoal (10%, 0.4 g) for 4 hours. The hydrocarbon (100 mg) was then acetylated in the manner described by Pines (23), and converted to the known 2,4-dinitrophenylhydrazone in the usual manner. The product, crystallized from chloroform–ethanol, had m.p. 161–165° undepressed on admixture with an authentic specimen of the same melting point (23).

Acetone – (+)-Carvomenthene (ii)

A solution of carvomenthene ($[\alpha]_D$+105°; 3.1 g) in acetone (60 ml) was irradiated at room temperature for 45 hours during which time the rotation of the solution fell from 102° to 43°. Distillation gave an oil b.p. 65–115°/14 mm. Gas–liquid chromatography then afforded carvomenthene ($[\alpha]_D$ +74° (*c*, 0.43)) identical in all respects except rotation with the starting material. A substance with lower retention time than carvomenthene was isolated and shown to be *p*-menth-1,7-ene. It had maxima in the infrared at 6.08 (s), 9.35, 9.62, 9.85, 10.07, 10.22, 11.07, and 11.26 (s) μ, and n_D^{25} 1.4578. The literature records (13) maxima in the infrared at 6.08 (s), 9.37, 9.62, 9.85, 10.07, 10.22, 11.07, 11.26 (s) μ and n_D^{25} 1.4575.

Carvomenthene was unaffected under the irradiation conditions in the absence of acetone.

Can. J. Chem. Downloaded from www.nrcresearchpress.com by 210.87.254.40 on 09/05/12
For personal use only.

Can. J. Chem. Downloaded from www.nrcresearchpress.com by 210.87.254.40 on 09/05/12
For personal use only.

Cyclohexanone–Cyclohexene

A solution of cyclohexanone (25 g) in cyclohexene (100 ml) was irradiated at reflux temperature over a 500-watt Hanovia lamp for 40 hours. Distillation then gave a colorless oil (15 g) b.p. 72–197°/25 mm. A portion (5 g) of the oil was chromatographed on alumina (Brockman Grade 5, 200 g). Three fractions were obtained. Fraction (i) (1 g) eluted with light petroleum had b.p. 108–109°/18 mm, n_D^{24} 1.5062, and was identical in every respect with 3,3′-bicyclohexenyl. Fraction (ii) (1.3 g) also eluted with light petroleum had b.p. 125°/7 mm, n_D^{24} 1.4513. Calc. for $C_{12}H_{22}O_2$: C, 72.68; H, 11.18%. Found: C, 72.68; H, 10.98%. The substance was identified as cyclohexyl *n*-caproate by hydrolysis, the caproic acid being characterized as the *p*-bromophenacyl ester (m.p. and mixed m.p. 70–71°) and the cyclohexanol as the 3,5-dinitrobenzoate (m.p. and mixed m.p. 109–111°). Fraction (iii) (1.5 g) eluted with benzene–light petroleum (1:4) had b.p. 145–146°/20 mm, n_D^{23} 1.4970, ν_{max} 1715 cm^{-1}. It gave an orange 2,4-dinitrophenylhydrazone, m.p. 172–5° from ethanol–chloroform. Calc. for $C_{18}H_{24}O_4N_4$: N, 15.55%. Found: N, 15.56%. It was undepressed in melting point on admixture with the 2,4-dinitrophenylhydrazone of cyclohexyl cyclohexanone prepared by the method of Hückel *et al.* (18), and the infrared spectra in chloroform solution were superposable.

The same substances were produced by irradiation at room temperature in similar yields.

Propionaldehyde–Cyclohexene

A solution of propionaldehyde (40 g) in cyclohexene (200 ml) was irradiated at reflux temperature over a 500-watt Hanovia lamp for 24 hours. Distillation gave a colorless oil (25 g). A portion of the oil (5 g) was chromatographed on alumina (Brockman Grade 5, 175 g) to give three fractions. Fraction (i) (650 mg), eluted with light petroleum, was identified, as previously, as 3,3′-bicyclohexenyl. Fraction (ii), also eluted with light petroleum, had b.p. 71–73°/15 mm, n_D^{25} 1.4547, ν_{max} 1709 cm^{-1}. It gave a 2,4-dinitrophenylhydrazone, m.p. 149–151° (from benzene). Calc. for $C_{15}H_{20}O_4N_4$: C, 56.24; H, 6.29; N, 17.49%. Found: C, 56.46; H, 6.40; N, 17.43%. This, and its derivative, were identical in every respect with a specimen of ethylcyclohexyl ketone and its 2,4-dinitrophenylhydrazone prepared by the method of Morris and Lusth (19). Fraction (iii) (1.05 g), eluted with benzene–ether (19:1) had b.p. 87–88°/11 mm, n_D^{25} 1.4772. It gave a 3,5-dinitrobenzoate, m.p. 74–8°. Calc. for $C_{16}H_{16}O_6N_2$: C, 57.48; H, 5.43; N, 8.38%. Found: C, 57.65; H, 5.50; N, 8.22%. It was identical with the derivative of 1-cyclohex-2′-enylpropan-1-ol from the alcohol prepared by an unambiguous route prepared as described below.

The same products, with a somewhat lower yield of ketone, were obtained by irradiation at room temperature.

Acetaldehyde–Cyclohexene

A solution of acetaldehyde (10.2 g) in cyclohexene (50 ml) in a sealed quartz tube was irradiated for 65 hours with an AH-8 lamp, the tube being cooled in a current of air. The crude oil, b.p. 60–120°/14 mm (4.9 g), on gas–liquid chromatography gave three main components. The last (retention time 110 minutes) was shown, as in previous cases, to be 3,3′-bicyclohexenyl. The first (retention time 32 minutes) had n_D^{25} 1.4498 and gave a semicarbazone m.p. 172.5–173.5° undepressed on admixture with the semicarbazone of methylcyclohexyl ketone of the same melting point. The infrared spectrum of the first component and that of a methylcyclohexyl ketone were superposable.

The second component (retention time 45 minutes) was most readily isolated in larger amounts by heating, under reflux, of the crude distillate (2.4 g) with Girards 'T' reagent

(3.3 g) in 95% ethanol (15 ml) containing acetic acid (0.5 ml) for 12 hours. Isolation of the non-ketonic material (1.6 g) followed by chromatography on alumina (Brockman Grade 1, 50 g) gave, on elution with benzene–ether (3:1) 1-cyclohex-2′-enylethan-1-ol, n_D^{21} 1.4798, b.p. 88–90°/13 mm. Calc. for $C_8H_{14}O$: C, 76.14; H, 11.18%. Found: C, 75.21; H, 11.59%. The substance was identical in infrared spectrum with that of the alcohol prepared by an unambiguous route described below. The substance gave a 3,5-dinitrobenzoate, m.p. 75.5–76.5° (from light petroleum). Calc. for $C_{15}H_{16}O_6N_2$: C, 56.25; H, 5.04; N, 8.75%. Found: C, 55.76; H, 5.07; N, 8.59%.

Under these conditions the yields of alcohol and ketone were approximately 6%. A similar irradiation employing a more dilute solution of acetaldehyde (1.2 g) in cyclohexene (55 ml) gave the same products, but whereas the yield of ketone was essentially unchanged, the yield of alcohol was now 38%.

2-Cyclohex-2′-enylpropan-2-ol, 3,5-Dinitrobenzoate

Cyclohexene-3-carboxylic acid (20) (2 g) was esterified with excess diazomethane. After evaporation of the excess diazomethane the ester in ether (50 ml) was added to a solution of methyl magnesium iodide (from methyl iodide (5 g) and magnesium (0.8 g)) and the mixture stirred for 1 hour. Isolation of the neutral material gave 2-cyclohex-2-enylpropan-2-ol (2 g) (identical in retention time with the photochemical product), which was converted directly into the 3,5-dinitrobenzoate. Crystallized from chloroform – light petroleum this had m.p. 122–125°.

trans-1,2-Di(2′-hydroxy-2′-propyl)cyclohexane, 3,5-Dinitrobenzoate

trans-Cyclohexan-1,2-dicarboxylic acid (21) (3 g) was esterified with excess diazomethane, the excess diazomethane reagent removed by evaporation, and the ester in ether (50 ml) added to methyl magnesium iodide prepared from methyl iodide (213 g) and magnesium (45 g) in ether (1l.) and the mixture refluxed for 150 hours. Isolation of the neutral material in the usual way gave an oil (2 g). A portion (1.5 g) of the oil was converted into the 3,5-dinitrobenzoate by the method of Brewster and Ciotti (22). Chromatography of the product on silica gel (100 g) gave on elution with benzene–ether (9:1) and crystallization from methanol and from ethyl acetate – light petroleum the bis 3,5-dinitrobenzoate, m.p. 110–112.5°, undepressed on admixture with the 3,5-dinitrobenzoate of the product obtained by irradiation.

4-Cyclohex-2′-enylheptan-4-ol and 3-Cyclohex-2′-enylpentan-3-ol

Methyl cyclohexene-3-carboxylate (2.15 g) was added to the Grignard reagent prepared from *n*-propyl iodide (18.5 g) and magnesium (2.4 g) in dry ether (100 ml). After 1-hour stirring the neutral material was isolated in the usual way, and purified by gas–liquid chromatography. Its retention time on the silicone column, its refractive index, and its infrared spectrum were identical with those of the photochemical product.

3-Cyclohex-2′-enylpentan-3-ol, n_D^{23} 1.4800, was prepared in a similar manner. It was identical in retention time and infrared spectrum with the photochemical product.

1-Cyclohex-2′-enylpropan-1-ol

A solution of cyclohexane-3-carboxylic acid (2 g) and oxalyl chloride (3 g) in dry benzene (15 ml) was allowed to stand at room temperature for 2 days after which solvent and excess oxalyl chloride were removed *in vacuo*. The acid chloride was added to cadmium diethyl (from anhydrous cadmium chloride (6.25 g), ethyl bromide (15 g), and magnesium (1.75 g)) at 10° and the mixture stirred for 2 hours and allowed to stand at room temperature for 16 hours. Decomposition of the complex with water, and isolation of the

Can. J. Chem. Downloaded from www.nrcresearchpress.com by 210.87.254.40 on 09/05/12
For personal use only.

neutral material gave an oil which was filtered through a column of silica gel in light petroleum – benzene (4:1) to remove alcoholic impurities. The crude unconjugated ($\epsilon_{230} < 600$) ketone (1.8 g) in ether (50 ml) was then added to a solution of lithium aluminum hydride in ether (100 ml) at 0°. After 1 hour the mixture was decomposed with ethyl acetate and the neutral material isolated in the usual way. The alcohol had the same retention time as the photochemical product on the silicone column, and gave a 3,5-dinitrobenzoate m.p. 65–78° undepressed on admixture with the derivative of the photochemical product and having identical infrared spectrum. However, although the column used in the gas–liquid chromatography showed a single peak it is probable in view of the diffuse melting point of the derivative that the product is a mixture of diastereoisomers.

1-Cyclohex-2-enylethan-1-ol was prepared in a precisely analogous fashion. The product had ν_{max} in the infrared at 3580, 3380, and 722 cm^{-1} and n_D^{25} 1.4806. It was identical in retention time with the photochemical product.

ACKNOWLEDGMENTS

The authors wish to thank the British Petroleum Company for support (for W. T.) and the Imperial Oil Ltd., of Canada for generous financial support. The authors are indebted to Professor D. H. R. Barton for his interest and for many discussions.

REFERENCES

1. E. J. Bowen and A. T. Horton. J. Chem. Soc. 1685 (1936).
2. N. C. Yang and D-D. H. Yang. J. Am. Chem. Soc. **80**, 2913 (1958).
3. E. Bergman and S. Fujise. Ann. **483**, 65 (1930).
4. E. Paterno and G. Chieffi. Gazz. chim. ital. **39**, 415 (1909).
5. A. Schönberg and A. Mustafa. J. Chem. Soc. 551 (1945).
6. E. H. Farmer and S. E. Michael. J. Chem. Soc. 513 (1942).
7. E. Paterno and G. Chieffi. Gazz. chim. ital. **39**, 341 (1909).
8. (*a*) G. Büchi, C. G. Inman, and E. S. Lipinsky. J. Am. Chem. Soc. **76**, 4327 (1954). (*b*) P. de Mayo. Ultraviolet photochemistry of simple unsaturated systems. *In* Advances in organic chemistry. Vol. II. Interscience Pub. 1960. p. 367.
9. H. G. Oswin, R. Rebbert, and E. W. R. Steacie. Can. J. Chem. **33**, 472 (1955); R. A. Herrmann and R. M. Noyes. J. Am. Chem. Soc. **78**, 5764 (1956).
10. G. Fuller and F. F. Rust. J. Am. Chem. Soc. **80**, 6148 (1958).
11. E. C. Coyner and G. A. Ropp. J. Am. Chem. Soc. **70**, 2283 (1948).
12. K. Weiss and M. Lalande. J. Am. Chem. Soc. **82**, 3117 (1960).
13. R. L. Webb and J. P. Bain. J. Am. Chem. Soc. **75**, 4279 (1953).
14. G. Ciamician and P. Silber. Ber. **46**, 3077 (1913); D. Arigoni, D. H. R. Barton, R. Bernasconi, C. Djerassi, J. S. Mills, and R. Wolf. Proc. Chem. Soc. 306 (1959).
15. M. S. Kharasch, J. Kuderna, and W. Nudenberg. J. Org. Chem. **18**, 1225 (1953).
16. M. S. Kharasch, W. H. Urry, and B. M. Kuderna. J. Org. Chem. **14**, 248 (1949).
17. H. A. Smith, J. F. Fuzek, and H. T. Meriwether. J. Am. Chem. Soc. **71**, 3765 (1949).
18. W. Hückel, O. Neunhoffer, A. Gercke, and E. Frank. Ann. **477**, 99 (1930).
19. H. H. Morris and M. L. Lusth. J. Am. Chem. Soc. **76**, 1237 (1954).
20. E. J. Boorman and R. P. Linstead. J. Chem. Soc. 258 (1935).
21. D. L. Huttord, D. S. Tarbell, and T. L. Koszalka. J. Am. Chem. Soc. 74, 3014 (1952).
22. J. H.Brewster and C. J. Ciotti. J. Am. Chem. Soc. **77**, 6214 (1955).
23. H. Pines, A. Weizmann, and V. N. Ipatieff. J. Am. Chem. Soc. **70**, 3859 (1948).
24. E. W. R. Steacie. Atomic and free radical reactions. Vol. I. Reinhold. 1954. pp. 284 *et seq.*; C. R. Masson, V. Boekelheide, and W. A. Noyes. *In* Technique of organic chemistry. *Edited by* A. Weissberger. Vol. II. 2nd. ed. Interscience Publishers, Inc., New York. 1956. p. 375.
25. G. V. D. Tiers. J. Phys. Chem. **62**, 1151 (1958).
26. P. de Mayo, J. B. Stothers, and W. Templeton. Proc. Chem. Soc. 72 (1960).

Can. J. Chem. Downloaded from www.nrcresearchpress.com by 210.87.254.40 on 09/05/12
For personal use only.

Can. J. Chem. Downloaded from www.nrcresearchpress.com by 210.87.254.42 on 09/05/12
For personal use only.

KINETICS AND THERMODYNAMICS OF THE CRYSTAL STRUCTURE TRANSFORMATION OF SPECTROSCOPICALLY PURE ANATASE TO RUTILE[1]

C. N. R. RAO[2]

ABSTRACT

The transformation of spectroscopically pure anatase to rutile was first investigated by Czanderna, Rao, and Honig. But it was not possible, then, to provide the mechanism on a molecular scale because of the lack of very accurate kinetic data. The kinetics and thermodynamics of the transformation have now been carefully investigated.

EXPERIMENTAL

The preparation of the spectroscopically pure anatase and the procedure adopted in the kinetic studies and in the X-ray analysis of the samples have been described earlier (1). The accuracy of the analytical method is found to be rather poor at anatase concentrations of less than 5% or greater than 95%. In order to obtain reliable kinetic data for fitting them into the order plots, the proportion of anatase was always seen to be within these limits. The temperature fluctuation in a run was within 5°. The purity of the sample is the most important requisite in this study since impurities are known to affect the transformation markedly (2, 3).

The differential thermal analysis of the anatase (preheated to 250° C) was carried out using a high sensitivity (0.25–0.5 cal) apparatus similar to that described by Pask and Warner (4). A sufficiently fast and constant heating rate of 12.5 deg min^{-1} was employed since the peaks corresponding to crystal structure transformations are usually small.

RESULTS AND DISCUSSION

The kinetic results at different temperatures are shown in Fig. 1(*a*). In Fig. 1(*b*), the data are plotted for the first-order equation. The data follow the first-order law fairly well. The first-order rate constants at different temperatures are summarized in Table I.

TABLE I

Temperature, °C	Rate constant, hr^{-1} $k\times10^2$
625	2.9_9
643	6.2_2
684	36.9_0
698	76.7_0

The reaction rate constants in Table I follow the Arrhenius equation closely (Fig. 2). The energy of activation is about 80±10 kcal per mole. The frequency factor is about 4×10^{14} sec^{-1}, which is surprisingly of the same order as expected for the first-order gas or solution reactions. The entropy of activation calculated from Eyring's theory is about 27 e.u. at 643° C.

The kinetic data of this investigation give a value of 610±10° C for the infinite-time

[1]*Manuscript received September 26, 1960.*
Contribution from the Department of Inorganic and Physical Chemistry, Indian Institute of Science, Bangalore-12, India, and Department of Chemistry, Purdue University, Lafayette, Indiana, U.S.A.
[2]*All the correspondence should be addressed to the Department of Inorganic and Physical Chemistry, Indian Institute of Science, Bangalore-12, India.*

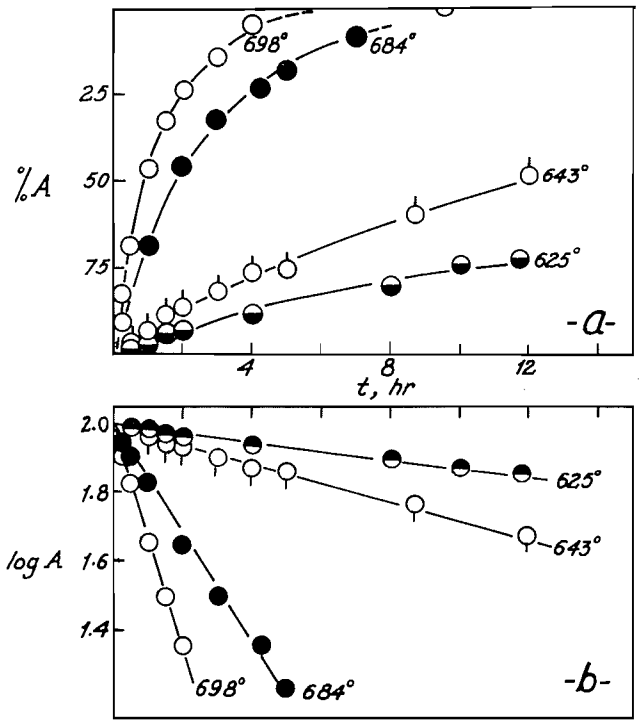


FIG. 1. (*a*) Plots of % anatase versus time at different temperatures. (*b*) First-order plots of the data in (*a*).

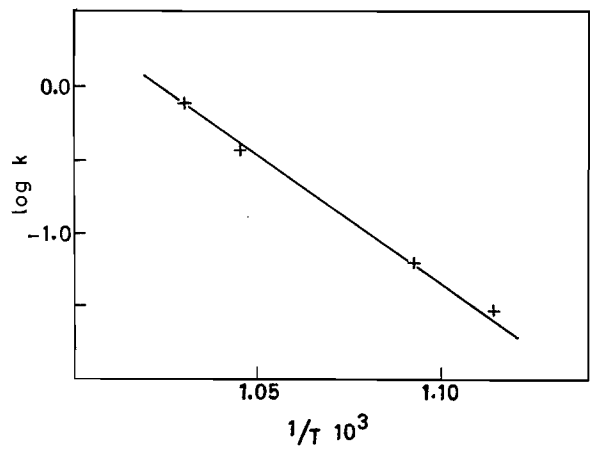


FIG. 2. Arrhenius plot.

temperature. That is, below 610° C, the transformation is immeasurably slow. This is in agreement with the value reported earlier (1).

The differential thermal analysis of the anatase showed a small exothermic peak starting around 630° C corresponding to the transformation to rutile. It was confirmed by X-ray analysis that the transformation was complete after the exothermic peak. This

Can. J. Chem. Downloaded from www.nrcresearchpress.com by 210.87.254.42 on 09/05/12
For personal use only.

temperature of 630° C corresponds excellently with the infinite-time temperature mentioned earlier.

The heat of the transformation, ΔH, was estimated by comparing the area of the exothermic peak with the α–β inversion peak of a known amount of quartz. The ΔH thus estimated was only -100 ± 50 cal per mole.

An interpretation of the data on the kinetics of this solid-state transformation may be obtained by drawing an analogy with the thermal decomposition of solids (1, 5). However, a more refined and satisfactory theoretical treatment has been possible, by the application of the order–disorder theory (6). The details of the theory will be discussed elsewhere (7). From the theory it can be shown that the ratio of the propagation rate constant to the nucleation rate constant is small. Also, the observed energy of activation seems to represent mainly the activation energy for the production of the nucleation sites.

ACKNOWLEDGMENT

The author's thanks are due to Prof. M. R. A. Rao for his keen interest.

REFERENCES

1. A. W. Czanderna, C. N. R. Rao, and J. M. Honig. Trans. Faraday Soc. **54**, 1069 (1958).
2. C. N. R. Rao, A. Turner, and J. M. Honig. J. Phys. Chem. Solids, **11**, 173 (1959).
3. C. N. R. Rao and M. P. Lewis. Current Sci. (India), **29**, 52 (1960).
4. J. A. Pask and M. F. Warner. Am. Ceram. Soc. Bull. **33**, 168 (1954).
5. P. W. M. Jacobs and F. C. Tompkins. *In* Chemistry of the solid state. *Edited by* W. E. Garner. Butterworth Scientific Publications, London. 1955. Chap. 7.
6. J. M. Honig. J. Chem. Phys. **28**, 723 (1958).
7. C. N. R. Rao and J. M. Honig. Symposium on rate processes. Indian Chemical Society, Bombay, January 1960. To be published in a special volume of J. Indian Chem. Soc.

Can. J. Chem. Downloaded from www.nrcresearchpress.com by 210.87.254.42 on 09/05/12
For personal use only.

Can. J. Chem. Downloaded from www.nrcresearchpress.com by 210.87.254.40 on 09/05/12
For personal use only.

NITRO- AND AMINO-IMIDAZOLESULPHONAMIDES[1]

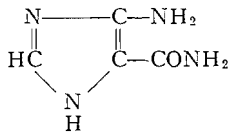
M. H. Fisher, W. H. Nicholson, and R. S. Stuart

ABSTRACT

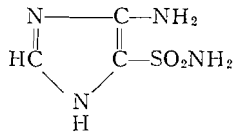
Several 4(5)-nitro- and 4(5)-amino-5(4)-sulphamylimidazoles have been synthesized as potential antagonists to 4(5)amino-5(4)-carbamylimidazole.

INTRODUCTION

There has recently been considerable interest in the role of 4(5)-amino-5(4)-carbamylimidazole (I) and related compounds in the biosynthesis of purines (1, 2, 3, 4). However, the preparation of imidazole analogues as potential antagonists has not been widely investigated (5). In this work compounds related to 4(5)-amino-5(4)-sulphamylimidazole (II) were synthesized for biological testing.[2]



(I)

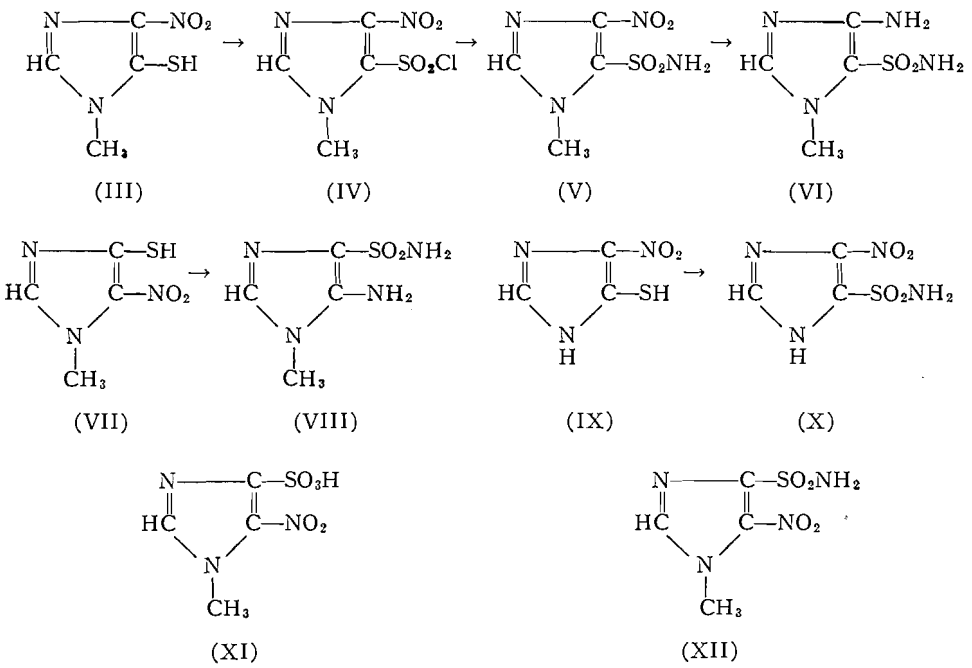


(II)

A number of unsuccessful attempts to prepare compounds of this type have been reported, e.g. chlorination of imidazole sulphonic acids, chlorosulphonation of nitro- or acylamino-imidazoles, amination of bromo-imidazoles, and conversion of imidazolethiols to sulphenamides followed by oxidation (5, 6, 7). 4(5)-Bromo-5(4)-sulphamylimidazole was prepared by chlorosulphonation of 4(5)-bromoimidazole (5), but it failed to react with ammonia.

The most attractive approach was the oxidative chlorination of the thiols, a general method described by Sprague and Johnson (8) and later used for the preparation of 2-sulphamylimidazoles (9, 10). 5-Mercapto-1-methyl-4-nitroimidazole (III) (5) was converted to the sulphonyl chloride (IV) by oxidative chlorination in dilute hydrochloric acid. The sulphonyl chloride with concentrated aqueous ammonia yielded 1-methyl-4-nitro-5-sulphamylimidazole (V). Catalytic reduction of this compound gave 4-amino-1-methyl-5-sulphamylimidazole (VI). In a similar manner 5-amino-1-methyl-4-sulphamylimidazole (VIII) was obtained from 1-methyl-4-mercapto-5-nitroimidazole (VII). 4(5)-Mercapto-5(4)-nitroimidazole (IX) (5) was converted to 4(5)-nitro-5(4)-sulphamylimidazole (X) but attempted catalytic reduction caused gross decomposition.

[1]*Manuscript received November 29, 1960.*
Contribution from the Research Department, Merck and Co. Ltd., Montreal, Que.
[2]*The compounds are being screened for anticancer activity at the Sloan-Kettering Institute for Cancer Research.*



(III) (IV) (V) (VI)

(VII) (VIII) (IX) (X)

(XI) (XII)

The oxidative chlorination of the 4-thiol (VII) yielded variable products. The desired sulphonyl chloride was obtained when the reaction temperature was maintained below 40° and the rate of addition of chlorine carefully controlled. Too rapid addition of chlorine at 20° or above resulted in the formation of 1-methyl-5-nitroimidazole-4-sulphonic acid (XI). Best results were obtained when the chlorine was added rapidly at 0° until the bright yellow starting material became white. The preparation was further complicated because the sulphonamide (XII) was isolated in two forms melting at 149° and 159°. Catalytic reduction of either form yielded the same amine. The oxidative chlorination of the other thiols (III) and (IX) gave good yields of the sulphonyl chlorides at 20°–30° and 0° respectively.

There was a pronounced difference in stability between the amines. 4(5)-Amino-5(4)-sulphamylimidazole was so unstable that it was neither isolated as the base nor a salt. 4-Amino-1-methyl-5-sulphamylimidazole (VI) was an unstable base and formed a moderately stable hydrochloride. 5-Amino-1-methyl-4-sulphamylimidazole (VIII) was stable either as the base or as the hydrochloride.

EXPERIMENTAL

1-Methyl-4-mercapto-5-nitroimidazole (VII)

4-Chloro-1-methyl-5-nitroimidazole (11) (10 g) was suspended in a warm solution of water (67 ml) and concentrated ammonia (33 ml). Hydrogen sulphide gas was passed into the stirred mixture until a clear, dark red solution was obtained (20 minutes). The ammonium salt of the product crystallized on standing (9 g), m.p. 139°–140°. Recrystallization by the addition of three volumes of isopropanol to a solution in a minimum volume of water yielded dark orange needles, m.p. 140°–141°. Found: C, 27.4; H, 4.5; N, 31.1; S, 18.3. Calc. for $C_4H_8N_4O_2S$: C, 27.3; H, 4.5; N, 31.8; S, 18.2%.

Can. J. Chem. Downloaded from www.nrcresearchpress.com by 210.87.254.40 on 09/05/12
For personal use only.

4(5)-Nitro-5(4)-sulphamylimidazole (X)

The ammonium salt of 4(5)-mercapto-5(4)-nitroimidazole (5) (1 g) was suspended in 1 *N* hydrochloric acid (10 ml) and cooled in an ice bath. Chlorine gas was passed into the stirred mixture until the suspended solids became buff colored (35 minutes). The sulphonyl chloride produced (m.p. 180°–183°) was collected, washed with a little ice water, and dissolved in concentrated ammonia (10 ml). After 15 minutes the excess of ammonia was evaporated *in vacuo* and the residual solution was acidified with hydrochloric acid. The sulphonamide, which precipitated, was collected and crystallized from water as jagged white needles (0.4 g), m.p. 261°–262°. Found: C, 18.8; H, 2.1; N, 29.3; S, 16.9. Calc. for $C_3H_4N_4O_4S$: C, 18.8; H, 2.1; N, 29.2; S, 16.7%.

1-Methyl-5-nitro-4-sulphamylimidazole (XII)

The ammonium salt of 4-mercapto-1-methyl-5-nitroimidazole (VII) (5.0 g) treated in a similar manner yielded the sulphonyl chloride (m.p. 104°), which was converted into the sulphonamide (3 g), m.p. 158°–159°. Found: C, 23.3; H, 2.9; N, 27.5; S, 15.7. Calc. for $C_4H_6N_4O_4S$: C, 23.3; H, 2.9; N, 27.2; S, 15.5%. The product was also isolated in another form, m.p. 149°–150°. Found: C, 23.4; H, 3.0; N, 26.6; S, 15.5%.

From a similar experiment in which the temperature was allowed to reach 50° there was isolated the ammonium salt of *1-methyl-5-nitroimidazole-4-sulphonic acid (XI)* m.p. 260°–265° (decomp.). Found: C, 21.4; H, 3.5; N, 25.0; S, 14.4. Calc. for $C_4H_8N_4O_5S$: C, 21.4; H, 3.6; N, 25.0; S, 14.3%. Acidification of a solution of the ammonium salt in water precipitated the acid m.p. 299°–300°. Found: C, 23.3; H, 2.4; N, 20.0; S, 15.5. Calc. for $C_4H_5N_3O_5S$: C, 23.2; H, 2.4; N, 20.3; S, 15.5%.

1-Methl-4-nitro-5-sulphamylimidazole (V)

The ammonium salt of 5-mercapto-1-methyl-4-nitroimidazole (5) (22 g) by similar oxidative chlorination at 20°–30° yielded the sulphonyl chloride (m.p. 106°–107°), which was converted into the sulphonamide (16.5 g), m.p. 176°–177°. Found: C, 23.4; H, 3.0; N, 27.0; S, 15.3. Calc. for $C_4H_6N_4O_4S$: C, 23.3; H, 2.9; N, 27.2; S, 15.5%. The acetyl derivative was prepared by refluxing the sulphonamide for 1 hour in an excess of acetic anhydride. Crystallization from water yielded white needles m.p. 219°–220° (decomp.). Found: C, 29.0; H, 3.3; N, 22.7. Calc. for $C_6H_8N_4O_5S$: C, 29.0; H, 3.2; N, 22.6%.

4-Amino-1-methyl-5-sulphamylimidazole (VI)

A suspension of 1-methyl-4-nitro-5-sulphamylimidazole (5 g) and Adams' platinum catalyst (0.1 g) in dry ethanol (250 ml) was hydrogenated at room temperature and atmospheric pressure. The theoretical volume of hydrogen was absorbed in 1 hour and a white solid was precipitated. The solid and the catalyst were collected, washed with ether, and suspended in ethanol (125 ml). Concentrated hydrochloric acid (5 ml) was added, the amine was dissolved, and the catalyst was filtered off immediately with the aid of filtercel. The hydrochloride salt of the product crystallized on standing as cream needles (1.9 g), m.p. 180° (decomp.), with sintering at 140°–150°. Found: C, 20.6; H, 4.0; Cl, 15.6; N, 23.9; S, 14.0. Calc. for $C_4H_8N_4O_2S,HCl,H_2O$: C, 20.8; H, 4.8; Cl, 15.4; N, 24.3; S, 13.9%. Attempts to obtain the base were unsuccessful and the hydrochloride salt itself darkened and finally decomposed on long standing.

5-Amino-1-methyl-4-sulphamylimidazole (VIII)

Catalytic reduction of 1-methyl-5-nitro-4-sulphamylimidazole (5 g) in a similar manner yielded the hydrochloride salt of the product as white needles (4.2 g), m.p. 185°–187°

Can. J. Chem. Downloaded from www.nrcresearchpress.com by 210.87.254.40 on 09/05/12
For personal use only.

(decomp.). Found: C, 22.6; H, 4.2; N, 26.3; S, 15.4. Calc. for $C_4H_8N_4O_2S$, HCl: C, 22.6; H, 4.2; N, 26.3; S, 15.0%.

An aqueous solution of the hydrochloride salt on addition of an excess of ammonia precipitated the base as white needles m.p. 208°–210° (decomp.).

Reduction of 4(5)-nitro-5(4)-sulphamylimidazole (X)

Catalytic reduction of 4(5)-nitro-5(4)-sulphamylimidazole with Adams' platinum catalyst was attempted in both dry ethanol and in a mixture of glacial acetic acid and acetic anhydride. In each case the solution became dark brown as hydrogen was absorbed. No crystalline products were isolated.

Infrared Spectra

The infrared spectrum of each of the compounds reported was examined. The nitroimidazole sulphonamides showed bands in the regions of 1540 and 1350 cm^{-1} characteristic of the nitro-group and bands in the regions of 1300 and 1175 cm^{-1} characteristic of the sulphonamide group. Reduction of the nitro-compounds caused a disappearance of the bands in the regions of 1540 and 1350 cm^{-1}. The spectra of the aminoimidazole sulphonamides showed two bands in the regions of 3385 and 3315 cm^{-1} characteristic of primary amine stretching absorptions and a band in the region of 1660 cm^{-1} characteristic of primary amine deformation vibrations. The bands in the regions of 1300 and 1175 cm^{-1} characteristic of sulphonamides were still evident.

The determination and interpretation of the infrared spectra was carried out by Professor A. Taurins, Department of Chemistry, McGill University.

REFERENCES

1. M. P. SCHULMAN and J. M. BUCHANAN. J. Biol. Chem. **196**, 513 (1952).
2. G. R. GREENBERG. Federation Proc. **13**, 745 (1954).
3. B. LEVENBERG and J. M. BUCHANAN. J. Am. Chem. Soc. **78**, 504 (1956).
4. H. FRIEDMAN and A. G. MOAT. Arch. Biochem. Biophys. **78**, 146 (1958).
5. L. L. BENNETT, JR. and H. T. BAKER. J. Am. Chem. Soc. **79**, 2188 (1957).
6. G. R. BARNES and F. L. PYMAN. J. Chem. Soc. 2711 (1927).
7. R. FORSYTH, J. A. MOORE, and F. L. PYMAN. J. Chem. Soc. **125**, 919 (1924).
8. T. B. JOHNSON and J. M. SPRAGUE. J. Am. Chem. Soc. **58**, 1348 (1936).
9. U. S. Patent No. 2,603,649 (1952).
10. R. O. ROBLIN, JR. and J. W. CLAPP. J. Am. Chem. Soc. **72**, 4890 (1950).
11. J. SARASIN and E. WEGMANN. Helv. Chim. Acta, **7**, 713 (1924).

Can. J. Chem. Downloaded from www.nrcresearchpress.com by 210.87.254.40 on 09/05/12
For personal use only.

Can. J. Chem. Downloaded from www.nrcresearchpress.com by 210.87.254.105 on 09/05/12
For personal use only.

N.M.R. SPECTRA OF SOME α–β UNSATURATED ESTERS[1]

ROBERT R. FRASER AND DONALD E. MCGREER

ABSTRACT

The results of analysis of methyl citraconate and mesaconate, methyl *cis*- and *trans*-crotonate, and methyl *cis*- and *trans*-2-pentenoate are reported. A previously reported analysis of the crotonates by first-order perturbation theory gave significantly different values for the 1,3 coupling constants. The discrepancy in results, which is due to the importance of second-order effects, emphasizes the need for caution in applying the first-order method. From values of 1,3 coupling constants reported here and elsewhere it is concluded that there is no simple relation between the magnitude of 1,3 coupling constants and geometrical configuration of the interacting nuclei.

Much attention has been devoted recently to the N.M.R. spectra of substituted propenes and butenes (1–7). Two aspects of the spectra have received special attention. The first is the magnitude of the 1,3 coupling constants.* Whipple *et al.* have reported 1,3 coupling to be consistently greater in the trans 2-substituted propenes ($J_{1,3\ cis}$) than in the cis isomers (2) ($J_{1,3\ trans}$). In tiglic and angelic acids and their methyl esters the opposite was found (1). Subsequently Jackman and Wiley (4) provided evidence which gave a different assignment to the protons of α-methacrolein from that of Whipple *et al.* and thus provided another case where $J_{1,3\ trans}$ was greater than $J_{1,3\ cis}$. The second aspect was the basis of Jackman's studies. He presented compelling evidence for the use of chemical shifts to assign configuration to α–β unsaturated esters. Among the compounds which he has studied were the methyl esters of mesaconic, citraconic, and *cis*- and *trans*-crotonic acids. We have examined these same four esters in addition to the methyl esters of *cis*- and *trans*-2-pentenoic acid. The more exact method of analysis employed in our case has provided some results of particular interest in this field.

Methyl Mesaconate and Methyl Citraconate

The olefinic and C-methyl protons in these esters comprise an AX_3 system. Analysis of such a system can be made by first-order perturbation theory. The complete results are listed in Table I. All coupling constants in this paper are reported with an estimated accuracy of ±0.05 cycle/sec as the standard deviation of each measurement was $\leqslant 0.05$ cycle/sec. The coupling constants in Table I are in agreement with those of Jackman and Wiley, who found values of 1.60±0.07 for each isomer. All chemical shift measurements are reported as τ values (8).

TABLE I

Compound	Coupling constants		Chemical shifts		
	$J_{1,3\ cis}$	$J_{1,3\ trans}$	β-H	β-CH_3	$COOCH_3$
Methyl mesaconate	—	1.56	3.32	7.75	6.22, 6.27
Methyl citraconate	1.64	—	4.23	7.97	6.28, 6.32

[1]*Manuscript received October 17, 1960.*
Joint contribution from the Departments of Chemistry of the University of Ottawa, Ottawa, Ontario, and the University of British Columbia, Vancouver, British Columbia.
**The term 1,3 coupling constant is used to denote the energy of interaction between protons separated by three carbon atoms.*

Methyl cis-Crotonate and Methyl trans-Crotonate

The results of analysis by first-order perturbation theory and also by the ABX_3 treatment of Waugh and Fessenden (9) are given in Table II. The relative signs of the coupling constants in these compounds could not be conclusively established from the observed spectra. It was therefore assumed that $J_{1,3}$ has the opposite sign to $J_{1,2}$ and $J_{2,3}$. Both experimental evidence (9, 10, 11, 17) and theoretical calculations (6) on relative signs in olefinic compounds justify this assumption.

The spectrum of the olefinic and β-methyl protons of cis methyl crotonate is shown in Fig. 1 and illustrates the nearly first-order appearance of this spectrum. The slight

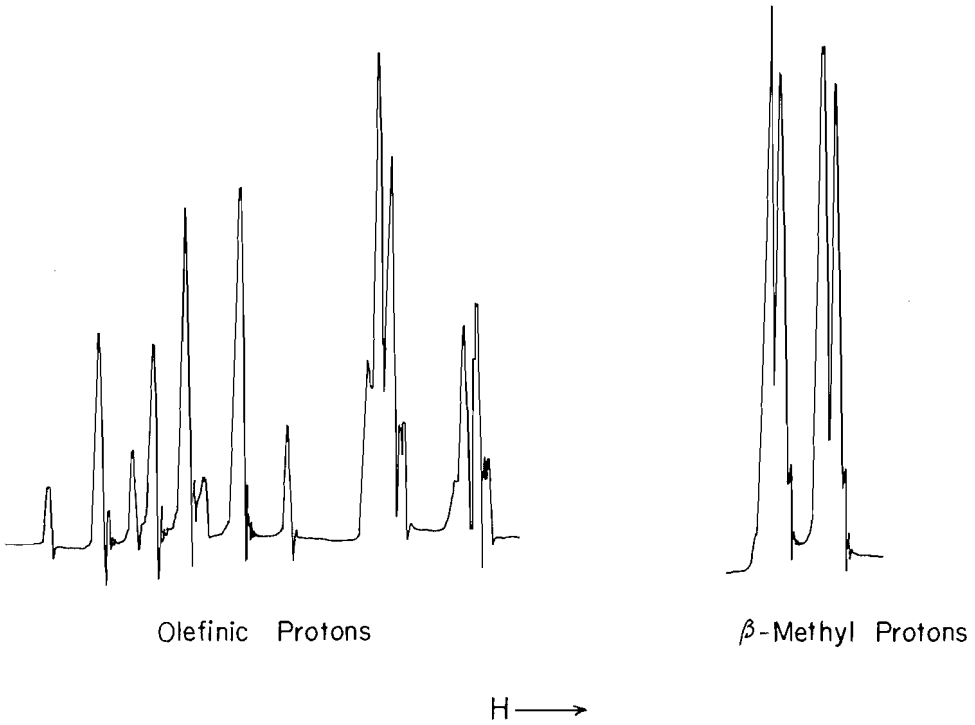


FIG. 1.

skewing of intensities is the only obvious indication of the mixing of proton spin states. Nevertheless, the observed splitting of the methyl group and the average of the three splittings in the weakly split quartets are 0.25 cycle/sec less than the actual interaction energy, $J_{1,3}$. While this error is usually, although not always, small in the determination of large coupling constants, it becomes important when dealing with the weaker long-range interactions. This effect, which was underestimated by one of us (R.R.F.) in the spectra of tiglic and angelic acids (1), emphasizes the need for caution in assuming first-order calculations to be applicable. Unfortunately exact analysis of the tiglic and angelic acids, which are A_3B_3X systems, is too tedious to warrant exact solution. Therefore the previously reported results for the coupling constants in tiglic and angelic acid and their esters must be considered as approximate. The results of first-order analysis of the crotonates agree with those of Jackman and Wiley. However, we found the values for the olefinic protons to be 0.15 p.p.m. to higher field.

Can. J. Chem. Downloaded from www.nrcresearchpress.com by 210.87.254.105 on 09/05/12
For personal use only.

Can. J. Chem. Downloaded from www.nrcresearchpress.com by 210.87.254.105 on 09/05/12
For personal use only.

TABLE II

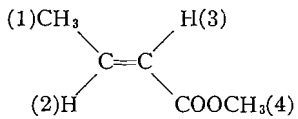
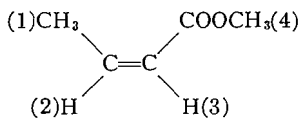
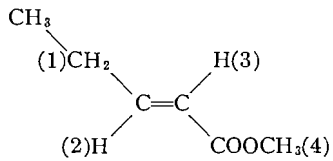
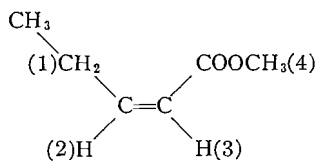
Compound	1st order			ABX$_3$			Chemical shifts			
	$J_{1,3}$	$J_{1,2}$	$J_{2,3}$	$J_{1,3}$	$J_{1,2}$	$J_{2,3}$	H_1	H_2	H_3	H_4
	−1.58	6.75	15.5	−1.67	6.85	15.5	8.12	3.10	4.24	6.33
	−1.57	7.03	11.4	−1.82	7.27	11.4	7.86	3.72	4.28	6.36

TABLE III

Compound	1st order			ABX$_2$			Chemical shifts				
	$J_{1,3}$	$J_{1,2}$	$J_{2,3}$	$J_{1,3}$	$J_{1,2}$	$J_{2,3}$	H_1	H_2	H_3	H_4	C—CH_3
	−1.60	6.26	15.6	−1.69	6.35	15.6	7.78	3.07	4.27	6.33	8.90
	−1.26	7.13	11.5	−1.56	7.43	11.5	7.35	3.83	4.35	6.36	8.95

Methyl cis-2-Pentenoate and Methyl trans-2-Pentenoate

The spectra of the pentenoates are further complicated by the presence of an extra methylene group. Analysis of the olefinic absorption was carried out by treating the olefinic and methylene protons as an ABX_2 system whose solution has been reported in detail by Mortimer (12). Again it was assumed that the sign of $J_{1,3}$ was opposite to that of the other coupling constants. By employing the ABX_2 method we have neglected two factors. First, the effect of the methyl group will be important if it is not sufficiently separated from the methylene protons. In the trans isomer, where this effect is greater, the J/δ ratio for the methyl–methylene interaction is <0.1 and therefore can be neglected. The possibility that the ABC_2 treatment should be employed was eliminated since the calculated second-order perturbation theory corrections (12), which were of the order of 0.02 cycle/sec, were negligible. The results are given in Table III.

DISCUSSION

It has been suggested that geometrical configuration might be the predominant factor in determining the relative magnitudes of $J_{1,3\ cis}$ and $J_{1,3\ trans}$ (1). It can be seen that in the three pairs of isomeric esters studied $J_{1,3\ trans}$ is equal to, greater than, and less than $J_{1,3\ cis}$. Furthermore Jackman and Wiley have found that in the 2-substituted propenes $J_{1,3\ cis} > J_{1,3\ trans}$ in all compounds except methacrolein whereas there was little or no difference in the magnitude of 1,3 couplings in five 1-substituted isobutenes (4). Since Whipple, Goldstein, and Mandell (2) had earlier made an assignment to the olefinic protons of methacrolein in opposition to Jackman and Wiley's rule we examined the effect of changing solvent on the spectrum of methacrolein* in order to confirm one assignment or the other. It was found that both olefinic protons were shifted by 0.88 p.p.m. to higher field in changing from cyclohexane to benzene, whereas the methyl shift was +0.56 p.p.m. Thus this method is not applicable to the assignment of proton structure in α-methacrolein and Jackman's assignment has been accepted.

From the work herein and that of Whipple *et al.* and Jackman and Wiley it is therefore clear that the geometrical configuration about the double bond will not determine the relative magnitude of 1,3 coupling constants. This does not mean that geometry is unimportant. Whipple, Goldstein, and McClure have shown that the coupling constants in 2,3-dihalopropenes vary with solvent composition (3) and have attributed this observation in a reasonable way to changes in geometry which result from a change in the population of conformations with change in solvent polarity.

EXPERIMENTAL

The spectra were obtained with a Varian V-4302 N.M.R. spectrometer at a frequency of 60 Mc/sec. Each measurement reported is the average of at least five determinations. Spectra for determination of coupling constants and chemical shifts were made on 40% (wt.:vol.) solutions in carbon tetrachloride. τ values were obtained from the spectra of 10% solutions in carbon tetrachloride containing 1% tetramethylsilane as internal reference. No difference in chemical shift at the two concentrations was observed.

The preparation of methyl *cis-* and *trans*-crotonate and methyl *cis-* and *trans*-2-pentenoate has been reported elsewhere (13, 14). Methyl citraconate and methyl mesaconate were prepared by conversion of itaconic acid to citraconic and mesaconic acids (15), followed by esterification to the known esters (16).

**Their assignment rested on the assumption that the preferential solvent shift of one olefinic proton and the methyl protons was approximately the same if the two were cis. This was applied to 2-chloropropene from which $J_{1,3\ cis}$ was found to be greater than $J_{1,3\ trans}$. From this observation assignments in other structures were made on the basis of the relative magnitudes of $J_{1,3\ cis}$ and $J_{1,3\ trans}$.*

Can. J. Chem. Downloaded from www.nrcresearchpress.com by 210.87.254.105 on 09/05/12
For personal use only.

ACKNOWLEDGMENTS

The authors wish to thank the National Research Council for their grants-in-aid of research. The technical assistance of Mrs. V. Nicolson is gratefully acknowledged.

REFERENCES

1. R. R. FRASER. Can. J. Chem. **38**, 549 (1960).
2. E. B. WHIPPLE, J. H. GOLDSTEIN, and L. MANDELL. J. Am. Chem. Soc. **82**, 3010 (1960).
3. E. B. WHIPPLE, J. H. GOLDSTEIN, and G. R. McCLURE. J. Am. Chem. Soc. **82**, 3812 (1960).
4. L. M. JACKMAN and R. H. WILEY. J. Chem. Soc. 2881 (1960).
5. L. M. JACKMAN and R. H. WILEY. J. Chem. Soc. 2886 (1960).
6. M. KARPLUS. J. Am. Chem. Soc. **82**, 4431 (1960).
7. R. A. HOFFMAN. Mol. Phys. **1**, 326 (1958).
8. G. V. D. TIERS. J. Phys. Chem. **62**, 1151 (1958).
9. R. W. FESSENDEN and J. S. WAUGH. J. Chem. Phys. **30**, 944 (1959).
10. S. ALEXANDER. J. Chem. Phys. **28**, 358 (1958).
11. J. A. ELVIDGE and L. M. JACKMAN. Proc. Chem. Soc. 89 (1959).
12. J. S. MORTIMER. J. Mol. Spectroscopy, **3**, 335 (1959).
13. D. E. McGREER. J. Org. Chem. **25**, 852 (1960).
14. D. E. McGREER, W. WAI, and G. CARMICHAEL. Can. J. Chem. **38**, 2410 (1960).
15. ORGANIC SYNTHESES. Coll. Vol. II. pp. 140, 382.
16. L. VAN DER STRAETE. Bull. classe sci., Acad. roy. Belg. **21**, 226 (1935).
17. A. D. COHEN and N. SHEPPARD. Proc. Roy. Soc. (London), A, **252**, 488 (1959).

Can. J. Chem. Downloaded from www.nrcresearchpress.com by 210.87.254.105 on 09/05/12
For personal use only.

Can. J. Chem. Downloaded from www.nrcresearchpress.com by 210.87.254.5 on 09/05/12
For personal use only.

SPECTROPHOTOMETRIC STUDY OF THE REACTION BETWEEN IRON (III) AND KOJIC ACID[1]

W. A. E. McBryde[2] and G. F. Atkinson[3]

ABSTRACT

A method introduced by Vareille enables calculation of formation constants of colored metallic complexes in solution by making appropriate deductions from the presence of isobestic points in the spectra of suitably chosen solutions. The rationale of this method is derived rigorously, and its application extended to include cases where three complexes are present together in certain regions of pH. These principles are applied to derive for the ferric kojates the following formation constants, at 25° C and ionic strength 0.5: $\log K_1 = 10.16$, $\log K_2 = 8.29$, $\log K_3 = 6.90$. The relationship between pH and pL for the experimental conditions is calculated, thereby enabling the estimation of the distribution of the metal among the several species in each solution and the absorption spectrum of each complex.

INTRODUCTION

Vareille (1) has derived and applied a method for obtaining formation constants of metallic complexes which consists in measuring the absorption spectra of solutions of fixed total concentration of metal, $[M]_T$, and ligand, $[L]_T$, and of various pH's; and then in locating, if they are present, isobestic points at which three or more of the spectral curves intersect at a single wavelength. This author interprets the presence of such isobestic points as evidence of the metal being distributed in solution between not more than two species in the ranges of pH in which the isobestic points are found. If the identity of these particular species can be established, it is possible, as Vareille has shown, to deduce the equilibrium constants governing their interconversion. In the first part of this communication we offer a generalized discussion of the principle of the method, showing in particular the conditions necessary or desirable for its application. From this discussion it will be seen that the systems of complexes to which the method may be applied are limited to those which possess a moderately large spread in magnitudes of the successive formation constants. The three systems examined by Vareille are ideal in this respect; but in this paper it is shown that the method may be extended to sets of complexes with less favorable spacing of formation constants.

PRINCIPLE OF THE METHOD

Many of the experimental methods for deriving the formation constants of the successive complexes formed by a metallic ion and a ligand molecule or ion depend on finding corresponding values of $\bar{n}$, the degree of complex formation, and [L], the molar concentration of free ligand. These are related to the formation constants of the several complexes by Bjerrum's formation function:

$$[1] \qquad \bar{n} = \frac{\sum_1^N n\beta_n[L]^n}{1+\sum_1^N \beta_n[L]^n}.$$

[1]*Manuscript received November 1, 1960.*
Contribution from the Department of Chemistry, University of Toronto, Toronto, Ont., and (in part) University of Waterloo, Waterloo, Ont.
[2]*Present address: Department of Chemistry, University of Waterloo, Waterloo, Ontario.*
[3]*Present address: Department of Chemistry, University of Western Ontario, London, Ontario.*

In this,

β_n is a cumulative formation constant $= K_1K_2 \ldots K_n$

$$= \prod_1^n K_n.$$

K_n is the equilibrium constant for the reaction

$$ML_{n-1} + L = ML_n.$$

Following common practice, charges on individual species are omitted. The so-called equilibrium constants discussed in this paper are, with the exception of hydrogen ion, based on concentrations of the reacting species; they are therefore "formal" or "conditional" constants, applying in theory only to the medium in which they have been determined.

A plot of $\bar{n}$ vs. pL ($= -\log [L]$) yields the formation curve for the system of complexes. From experimentally determined formation curves it is possible to extract the individual formation constants by various numerical methods. The shape of the formation curve depends on the relative magnitudes of the several K's. Two distinct possibilities occur, and these are illustrated in Fig. 1, showing formation curves calculated by means of equation 1 and the appropriate formation constants for (*a*) the ferric 5-sulphosalicylates (one of the systems examined by Vareille), and (*b*) the ferric 5-sulpho-oxinates. The wide spacing in the constants for case (*a*) results in regions of pL in which each complex, ML, ML_2, and ML_3, has exclusive existence; and these correspond to the plateaux in this formation curve. Where the constants are not so widely spaced, as with case (*b*), the formation curve contains no plateau, and often shows only one point of inflection. For case (*b*) one may calculate that the quantity

$$[2] \qquad \alpha_n = \frac{[ML_n]}{[M]_T} = \frac{\beta_n[L]^n}{1+\beta_n[L]^n}$$

falls considerably short of the value unity for $n = 1$ or 2, so that the metal can never exclusively be in the form of ML or ML_2. This difference is illustrated for the same two sets of complexes in Fig. 2. Examination of these plots shows that, in case (*a*) only, as pL changes one complex gives way to another in such a way that no more than two species at a time make up practically the entire total concentration of metal.

For any system of metallic complexes with $\bar{n}_{max} = 3$, such as the foregoing two examples, and such as commonly occurs with many of the bi- and ter-valent transition metals of co-ordination number 6 when coupled with bifunctional ligands to form chelate complexes, the solution may contain, in addition to free and protonated ligand, the following species containing metal: M, ML, ML_2, and ML_3. It might also contain protonated metallic species, e.g. MHL, or polynuclear species, e.g. M_2L_2; but these will be assumed absent for this description. By introducing the assumption that, at the wavelengths under consideration, the ligand or any protonated form of it absorbs no significant amount of radiation, we may write for the molar extinction coefficient of the solution, ϵ_M, calculated from the total concentration of metal,

$$[3] \qquad \epsilon_M = \epsilon_0\alpha_0 + \epsilon_1\alpha_1 + \epsilon_2\alpha_2 + \epsilon_3\alpha_3$$

$$[4] \qquad = \frac{\epsilon_0 + \epsilon_1\beta_1[L] + \epsilon_2\beta_2[L]^2 + \epsilon_3\beta_3[L]^3}{1+\beta_1[L]+\beta_2[L]^2+\beta_3[L]^3}$$

in which α is defined by equation 2.

Can. J. Chem. Downloaded from www.nrcresearchpress.com by 210.87.254.5 on 09/05/12
For personal use only.

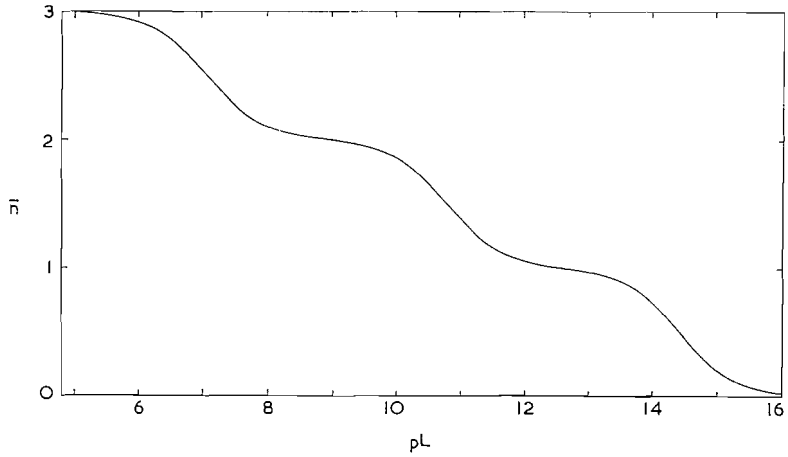


FIG. 1(*a*). Formation curve for the ferric sulphosalicylates.
$\log K_1 = 14.42$ $\log K_2 = 10.76$ $\log K_3 = 7.06$

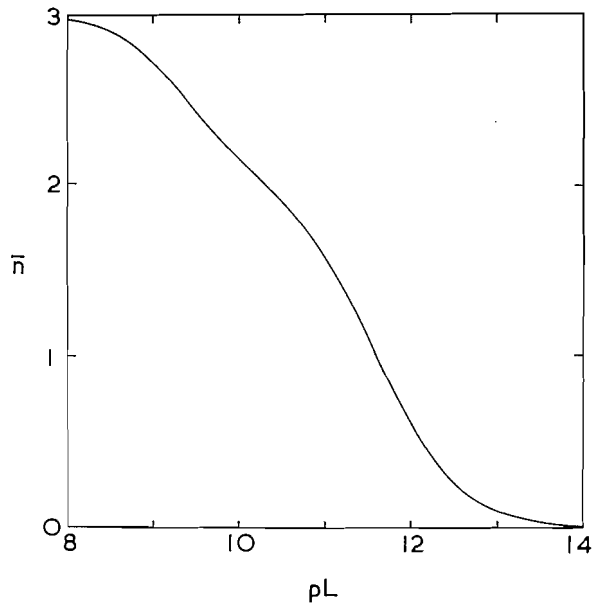


FIG. 1(*b*). Formation curve for the ferric sulpho-oxinates.
$\log K_1 = 12.0$ $\log K_2 = 11.2$ $\log K_3 = 9.4$

If the spectra of a series of solutions of these complexes differing only in pL reveal one or more isobestic points, then, at the wavelengths at which these points occur, plots of ϵ_M vs. pL will show horizontal regions which, in the discussion following, we may refer to as isobestic regions. We may derive an expression for the value of $d\epsilon_M/d\text{pL}$, and inquire into the conditions that will give this expression the value zero. Differentiating equation 4 with respect to [L], and simplifying, we get:

$$\frac{d\epsilon_M}{d[L]} = \{(\epsilon_1-\epsilon_0)\beta_1+2(\epsilon_2-\epsilon_0)\beta_2[L]+3(\epsilon_3-\epsilon_0)\beta_3[L]^2+(\epsilon_2-\epsilon_1)\beta_1\beta_2[L]^2 +2(\epsilon_3-\epsilon_1)\beta_1\beta_3[L]^3+(\epsilon_3-\epsilon_2)\beta_2\beta_3[L]^4\}(1+\beta_1[L]+\beta_2[L]^2+\beta_3[L]^3)^{-2}.$$

Can. J. Chem. Downloaded from www.nrcresearchpress.com by 210.87.254.5 on 09/05/12
For personal use only.

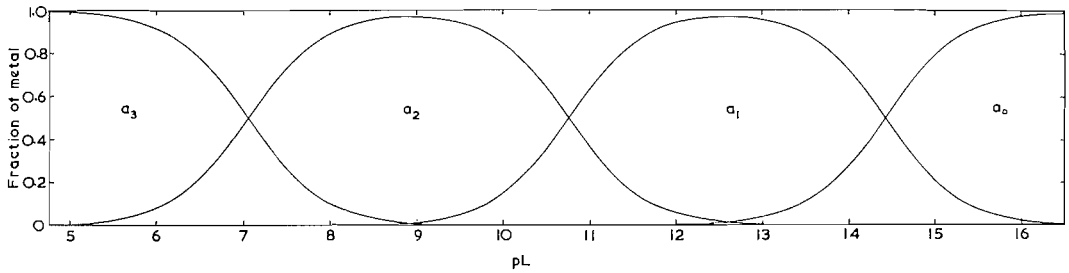


FIG. 2(*a*). Distribution of metal among simple and complex species: iron (III) + 5-sulphosalicylic acid.

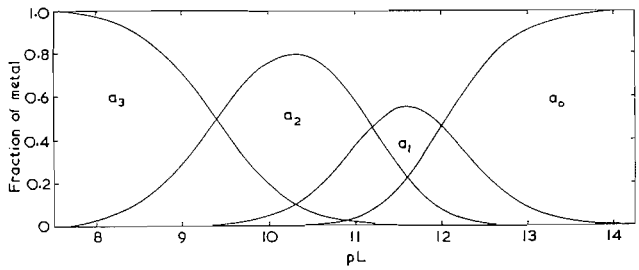


FIG. 2(*b*). Distribution of metal among simple and complex species: iron (III) + 8-hydroxyquinoline-5-sulphonic acid.

Multiplying both sides by [L], and applying equation 2, this becomes

$$[5] \qquad -0.4343\frac{d\epsilon_M}{d\mathrm{pL}} = (\epsilon_1-\epsilon_0)\alpha_0\alpha_1+2(\epsilon_2-\epsilon_0)\alpha_0\alpha_2+3(\epsilon_3-\epsilon_0)\alpha_0\alpha_3 + (\epsilon_2-\epsilon_1)\alpha_1\alpha_2+2(\epsilon_3-\epsilon_1)\alpha_1\alpha_3+(\epsilon_3-\epsilon_2)\alpha_2\alpha_3.$$

The expression on the right side of this equation will be zero if any one of the values of α becomes unity, since then the other three must be zero. This corresponds to the fact that ϵ_M will not change with pL as long as all the metal is present as a single constituent in solution. The same expression will be zero given the concurrence of any of the following pairs of relationships:

[6*a*]	$\epsilon_0 = \epsilon_1$	and	$\alpha_0+\alpha_1 \sim 1$
[6*b*]	$\epsilon_1 = \epsilon_2$	and	$\alpha_1+\alpha_2 \sim 1$
[6*c*]	$\epsilon_2 = \epsilon_3$	and	$\alpha_2+\alpha_3 \sim 1$
[7*a*]	$\epsilon_0 = \epsilon_1 = \epsilon_2$	and	$\alpha_0+\alpha_1+\alpha_2 \sim 1$
[7*b*]	$\epsilon_1 = \epsilon_2 = \epsilon_3$	and	$\alpha_1+\alpha_2+\alpha_3 \sim 1$

These are the conditions necessary for the generation of isobestic points in a series of absorption spectra of solutions differing only in pL.

The left-hand equations in 6 and 7 depend on wavelength only, and imply that each metallic species must obey Beer's law. The right-hand equations in each pair are independent of wavelength, but do depend on pL. From Fig. 2 it is seen that the relationships given by the right-hand members of the pairs of equations 6*a*, *b*, *c* are actually found for the ferric sulphosalicylates over practically the entire range of pL depicted. However, for the ferric sulpho-oxinates the same conditions are found only within comparatively narrow ranges of pL, especially that corresponding to equation 6*b*. Instead, for these complexes, the relationships of equations 7*a*, *b* are seen to obtain over most of the range of pL shown.

Can. J. Chem. Downloaded from www.nrcresearchpress.com by 210.87.254.5 on 09/05/12
For personal use only.

Can. J. Chem. Downloaded from www.nrcresearchpress.com by 210.87.254.5 on 09/05/12
For personal use only.

One may reasonably expect that any two adjacent members of a series of metallic complexes will have absorption spectra that intersect at some wavelength (see, for example, Fig. 6); that is, at some particular wavelength $\epsilon_n = \epsilon_{n+1}$. For as many such intersections as occur there will be corresponding isobestic points in a group of spectral curves for solutions differing only in pL, provided that the spacing of formation constants insures adherence to the relationships given by the right-hand members of equations 6*a*, *b*, *c* over moderate ranges of pL. For isobestic points to occur in a system of complexes having a distribution of species such as that shown in Fig. 2(*b*) is possible only within the narrow regions of pL in which equations 6*a*, *b*, *c* are valid. Where only equations 7*a*, *b* apply, the occurrence of isobestic points would require that three ionic species of differing complexity have the same molar extinction coefficient (not zero) at one wavelength; this possibility cannot be ruled out, but it seems to be exceedingly improbable.

In the systems of ferric complexes studied by Vareille, as well as in that considered in this paper, $\epsilon_0 \sim 0$ at the wavelengths under consideration, so that equation 6*a* does not apply and only two isobestic points are observed. All three sets of complexes in Vareille's work possess formation constants widely enough spaced so that the individual species are distributed as shown in Fig. 2(*a*). Thus as $\bar{n}$ increases the species ML essentially disappears from the solution before ML_3 forms in appreciable concentration. Also, the isobestic region for $\epsilon_1 = \epsilon_2$ ends at about the same pL (actually pH, but see below) as that for $\epsilon_2 = \epsilon_3$ begins; at this pL the metal is present almost exclusively as ML_2. At some wavelength (λ_{12}) $\epsilon_1 = \epsilon_2$; and a plot of ϵ_M vs. pL will show a horizontal region in which $\epsilon_M = \epsilon_1 = \epsilon_2$, and also, at lower pL, a horizontal region in which $\epsilon_M = \epsilon_3$. Between these horizontal regions there will be a skew-shaped curve in which $\epsilon_M = \epsilon_2\alpha_2 + \epsilon_3\alpha_3$. For the value of $\epsilon_M = \frac{1}{2}(\epsilon_2 + \epsilon_3)$ the corresponding value of pL = log K_3. Similarly at another wavelength (λ_{23}) $\epsilon_2 = \epsilon_3$; and when ϵ_M is plotted against pL two horizontal regions are noted, one in which $\epsilon_M = \epsilon_1$ and the other where $\epsilon_M = \epsilon_2 = \epsilon_3$. Between these horizontal regions $\epsilon_M = \epsilon_1\alpha_1 + \epsilon_2\alpha_2$, and the value of pL corresponding to $\epsilon_M = \frac{1}{2}(\epsilon_1 + \epsilon_2)$ is the value of log K_2. The identity between pL and log K in these two instances is based on the assumption that the logarithmic term in

$$\log K_n = \mathrm{pL} + \log \frac{[ML_n]}{[ML_{n-1}]}$$

is zero when $\epsilon_M = \frac{1}{2}(\epsilon_n + \epsilon_{n-1})$. However, this assumption is only valid if $\alpha_n + \alpha_{n-1} \sim 1$, that is, if the solution contains the metal in no more than two complex species in the region of pL in which ϵ_M is changing. It is evident, then, that Vareille's procedure for obtaining K_2 or K_3 cannot be applied without modification to sets of complexes in which the several species are distributed as portrayed in Fig. 2(*b*). Before introducing a proposal for dealing with such systems of complexes we must comment on the relationship between pL and pH in these solutions.

The majority of the ligands whose attachment to metallic ions is of interest are bases, i.e. proton acceptors, in aqueous solution. Accordingly there is frequently competition between metallic ions and protons for combination with a given ligand. We may derive a relationship between pL and pH in solutions of such complex species, provided we know the relevant equilibrium constants, by the following general equation:

$$[8] \qquad [L]_T = [L]\left(1 + \frac{[H]}{K_I} + \frac{[H]^2}{K_I K_{II}} \ldots .\right) + \bar{n}[M]_T.$$

(The acid dissociation constants, in order of increasing degree of protonation, are K_I, K_{II}, etc.) Corresponding values of pL and pH for a given $[M]_T$ and $[L]_T$ have been

calculated for solutions of the ferric kojates, and are shown graphically in Fig. 5. For purposes of the present discussion it is sufficient to remark that, for fixed total concentrations of metal and ligand, there must be curves similar in shape to those of Fig. 2 showing the relationship between pH and the fractions of metal in the various species. Experimentally pH is usually more readily measured than pL, and any observed shift of absorption spectra then considered as a function of pH. The occurrence of isobestic points among such spectra will result in horizontal regions in a plot of ϵ_M vs. pH. It is in this form that Vareille's data and ours are shown.

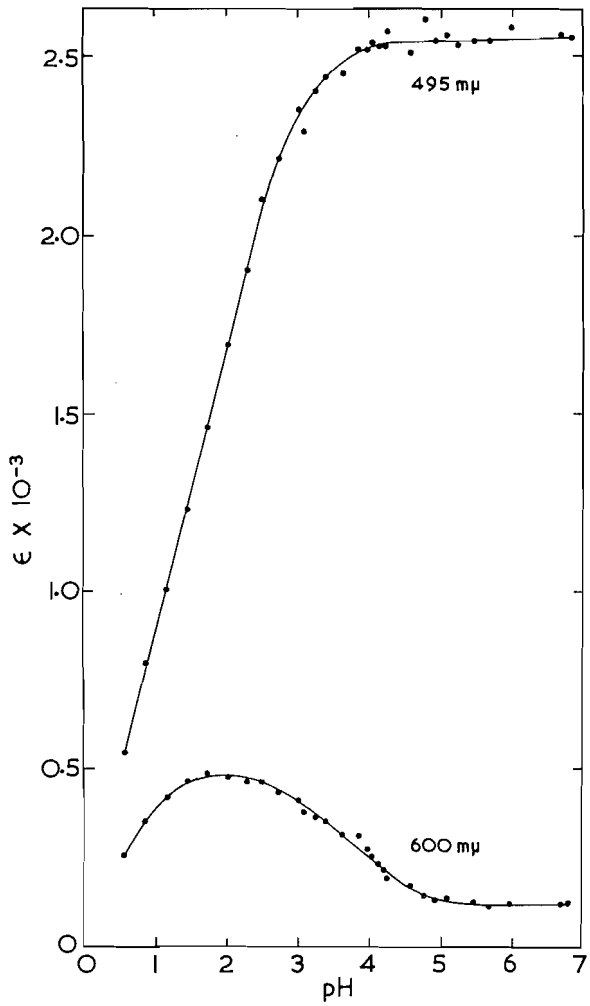


FIG. 3. Vareille curves, showing variation of molar extinction coefficient at isobestic wavelengths with pH.

Considering now the results of our experiments with the ferric kojates, we have confirmed the occurrence of isobestic points, first shown in the spectra published by Moss and Mellon (4), at 495 mμ and at 600 mμ. We have also confirmed, by the method of continuous variations, Moss and Mellon's finding that the complex formed at the highest pH is ML_3; we have assumed, by analogy with a great many other sets of ferric complexes, that with decreasing pH the species present are ML_2 and ML. We show in Fig. 3 our values of ϵ_M at the isobestic wavelengths plotted against pH. From the horizontal regions in these curves we may deduce as follows:

Can. J. Chem. Downloaded from www.nrcresearchpress.com by 210.87.254.5 on 09/05/12
For personal use only.

(i) above pH 5.2 only one species is present: $[M]_T = [ML_3]$; and at 600 mμ $\epsilon_3 = 120$ M^{-1} cm^{-1}.

(ii) between pH 4.0 and 5.2 $[M]_T = [ML_2]+[ML_3]$; and at 495 mμ $\epsilon_2 = \epsilon_3 = 2540$.

(iii) between pH 1.45 and 2.50 $[M]_T = [ML]+[ML_2]$; and at 600 mμ $\epsilon_1 = \epsilon_2 = 470$.

The absence of any isobestic region between pH 2.50 and 3.85 indicates that in this region $[M]_T = [ML]+[ML_2]+[ML_3]$. This is a difference from the cases investigated by Vareille, and presumably indicates a distribution of species similar to that shown in Fig. 2(*b*).

The consequence of the foregoing is that, for calculating equilibrium constants, we could not assume as Vareille had done that, at the mid-points of the curved portions of these plots, $[ML_3] = [ML_2]$ or $[ML_2] = [ML]$. Instead, we were obliged to estimate our formation constants by a series of successive approximations; the rapid convergence of the values for the constants with each cycle of approximations encouraged the belief that our extension of Vareille's procedure was valid.

The experimental data permitted calculation, not of the formation constants of the complexes, but of the equilibrium constants for the reaction

$$ML_{n-1}+HL = ML_n+H \qquad (n = 1, 2, 3)$$

and we designate these constants as $\mathscr{K}_n$. The method of evaluating these is now shown in detail.

Evaluation of $\mathscr{K}_3$

At pH 3.73 the value of ϵ_M at 600 mμ $= 295 = \frac{1}{2}(\epsilon_2+\epsilon_3)$. At this pH the solution may contain ML, ML_2, and ML_3, but since $\epsilon_1 = \epsilon_2$ we may put

[9] $$[ML_3] = [ML_2]+[ML] = [ML_2]\left(1+\frac{[H]}{\mathscr{K}_2[HL]}\right)$$

[10] $$[HL] = \frac{[HL]_T-\bar{n}[M]_T}{1+K_a/[H]} \sim [HL]_T-\bar{n}[M]_T$$

[11] $$\bar{n} = \frac{5+\dfrac{4[H]}{\mathscr{K}_2[HL]}}{2+\dfrac{2[H]}{\mathscr{K}_2[HL]}}$$

[12] $$\mathscr{K}_3 = \left(1+\frac{[H]}{\mathscr{K}_2[HL]}\right)\left(\frac{[H]}{[HL]_T-\bar{n}[M]_T}\right).$$

The value of $\mathscr{K}_3$ thus depends on the value of $\mathscr{K}_2$ obtained by the method described below. A cycle of approximations is introduced to find the best values of $\bar{n}$ and [HL]. This is begun by putting $\bar{n} = 2.5$ into equation 10, and the consequent value of [HL] into equation 11. When these values became constant, $\mathscr{K}_3$ was calculated by equation 12.

Evaluation of $\mathscr{K}_2$

For this purpose Vareille found the pH at which $\epsilon_M = \frac{1}{2}(\epsilon_1+\epsilon_2)$, and at which $[ML] = [ML_2]$. Our data give no direct indication of ϵ_1, so that we have had to estimate this quantity in order to calculate $\mathscr{K}_2$. Subsequently, with the aid of this value of $\mathscr{K}_2$, we were able to refine our estimate of ϵ_1. This cycle of approximations was repeated until constant values were obtained.

Can. J. Chem. Downloaded from www.nrcresearchpress.com by 210.87.254.5 on 09/05/12
For personal use only.

The lower limit of the isobestic region at 600 mμ, corresponding to $\epsilon_1 = \epsilon_2$ and $\alpha_1+\alpha_2=1$, occurs at pH 1.45. If, at this pH, α_1 became nearly unity we should have observed some horizontal region in the plot of ϵ_M vs. pH at 495 mμ; it was, in fact, from just such a horizontal that Vareille took his value of ϵ_1. We must assume for our solutions that, at and below pH 1.45, some ML_2 remains in solution. For all solutions below pH 2.5 we may write $\epsilon_M = \epsilon_1\alpha_1+\epsilon_2\alpha_2$, and for 495 mμ this becomes

$$\epsilon_1 = \frac{\epsilon_M - 2540\alpha_2}{\alpha_1}. \qquad [13]$$

The following data apply to the solutions of low pH.

pH	ϵ_M (600 mμ)	ϵ_M (495 mμ)	$\alpha_1+\alpha_2$
1.45	463	1230	1
0.57	254	545	0.548
0.86	350	794	0.758

Somewhat arbitrarily, in order to make an estimate of $\mathcal{K}_2$, we put ϵ_1 at 495 mμ = 1100 as a trial value.

Now, while at pH 1.45 $(\alpha_1+\alpha_2) = 1$, at any pH below this $(\alpha_1+\alpha_2) < 1$; and its value is given by the ratio of ϵ_M at this pH to ϵ_M at pH 1.45 measured at 600 mμ. In this way we get the values in the last column of the above table. But $\alpha_1+\alpha_2 = \alpha_1\{1+(\mathcal{K}_2[HL]/[H])\}$, and $[ML]+[ML_2] = (\alpha_1+\alpha_2)[M]_T = [ML]\{1+\mathcal{K}_2[HL]/[H]\}$. The conservation equation for L is

$$[HL]_T = [L] + [HL] + [ML] + 2[ML_2] + 3[ML_3] \qquad [14]$$

in which, for these solutions, the first and last terms on the right-hand side are relatively negligible. Hence we put

$$\begin{aligned}[HL] &= [HL]_T - [ML] - 2[ML_2] \\ &= [HL]_T - [ML] - 2([M]_T - [M] - [ML]) \\ &= [HL]_T + [ML] - 2[M]_T + 2[M].\end{aligned} \qquad [15]$$

The first estimate of [HL] was made by temporarily assuming $[ML_2] = 0$, and assigning [ML] the value calculated for $([ML]+[ML_2])$. Subsequent estimates were made using trial values of $\mathcal{K}_2$, since

$$[ML] = \frac{[ML]+[ML_2]}{1+\mathcal{K}_2([HL]/[H])}. \qquad [16]$$

The calculations quickly showed that the trial value of ϵ_1 had been too high, causing the first estimate of $\mathcal{K}_2$ to be too low.

The validity of this method of calculating $\mathcal{K}_2$ rests upon the inference from the isobestic region at 600 mμ that, at the pH at which $\epsilon_M = \frac{1}{2}(\epsilon_1+\epsilon_2)$, the metal in solution is present in only the two species, ML and ML_2.

Evaluation of $\mathcal{K}_1$

Once a steady value for [HL] in the solutions of pH 0.57 and 0.86 had been obtained from equations 15 and 16, and for [ML] from equation 16, the quantities in the expression for $\mathcal{K}_1$ could all be evaluated. In this way two estimates of this constant were obtained.

Can. J. Chem. Downloaded from www.nrcresearchpress.com by 210.87.254.5 on 09/05/12
For personal use only.

A third estimate, from the solution at pH 1.16, was not considered as reliable since, in this solution, the quantity [M] is obtained as a difference of two similar magnitudes.

The foregoing development of the principles underlying this method of obtaining formation constants of metal complexes does not support Vareille's claim that points of inflection on a plot of λ_{max} vs. pH will indicate values of pH at which two metallic species are present in equal concentrations.

We may summarize the conditions and assumptions required by this method:

(i) Each metallic complex must have distinctively different absorption spectra, and different also from the simple metallic ion. The spectral curves of each adjacent species must cross at some wavelength in order that an isobestic point may be generated.

(ii) The ligand and its protonated forms must show negligible absorption in the range of wavelengths considered.

(iii) Beer's law must be obeyed by all the metallic species.

(iv) Protonated or polynuclear species must not form to any appreciable extent.

(v) The formation constants sought must be widely enough separated that regions of pH (or pL) shall occur in which the metal is distributed between only two of the possible species at a time. In the method as originally described by Vareille it is a requirement that at some pH practically all of the metal should be present as a single one of the various possible species.

(vi) Since the mass law must be applied, at least in part, to concentrations, measurements should be made in solutions of constant and preferably moderately high ionic strength.

EXPERIMENTAL

Reagents

Kojic acid of purity suitable for this investigation was not found commercially. The available material, consisting of one lot purchased from Matheson, Coleman, and Bell, and a second generously contributed by Charles Pfizer and Co., was purified as follows. The crude acid was recrystallized once from a minimum of hot water. The resulting yellow, crystalline mass was then subjected to two, or in some cases three, extractions with warm ether in a modified Soxhlet apparatus. White needlelike crystals accumulated in the pot, and were from time to time removed by filtration, washed with ether, and air-dried. Product of acceptable purity was dead-white, with m.p. 152–3° C (uncorrected), and neutralization equivalent 142. Aqueous solutions of this material retained full potency in reaction with ferric salts for at least a week, and showed no darkening on standing. Off-white crystals obtained after one, or in some cases two, extractions gave drifting pH values when titrated in aqueous solutions with alkali (see below), and the aqueous solutions became yellow on standing.

The following solutions were prepared from analytical reagent grade chemicals (except for chloracetic acid), and standardized as noted:

Ferric nitrate, 2×10^{-3} $M+8\times10^{-3}$ M in HNO_3, standardized gravimetrically as Fe_2O_3,

Sodium hydroxide, 0.25 M, carbonate-free, standardized titrimetrically with potassium hydrogen phthalate,

Potassium nitrate, 1.25 M, by direct weighing,

Acetic acid, 0.25 M, standardized titrimetrically with 0.25 M alkali,

Chloracetic acid, 0.25 M, prepared from Eastman White Label reagent, passed through a $\frac{1}{2}\times24$ in. column of Dowex-50 in the hydrogen form, then standardized titrimetrically with 0.25 M alkali,

Can. J. Chem. Downloaded from www.nrcresearchpress.com by 210.87.254.5 on 09/05/12
For personal use only.

Hexamethylenetetramine, 0.25 *M*, by direct weighing,
Nitric acid, 0.50 *M*, standardized titrimetrically with 0.25 *M* alkali,
Potassium tetroxalate, 0.05 *M*, standard for pH 1.67 (25° C),
Potassium hydrogen phthalate, 0.05 *M*, standard for pH 4.00,
Sodium tetraborate decahydrate, 0.05 *M*, standard for pH 9.18,
Radiometer buffer, diluted 1 to 25 from concentrate, standard for pH 6.50.

Apparatus

Optical densities of solutions were measured with a Beckman Model DU spectrophotometer in matched Corex-glass cells of 1-cm path length. The cell compartment was enclosed by thermospacers through which water thermostatted at 25.0° C was circulated.

Measurements of pH were made with commercially available glass and calomel electrodes fitted to either a Beckman Model G or a Radiometer Model 22 meter. The meter assembly was standardized by the buffer solution of pH closest to the range being examined, and the response of the glass electrode was routinely checked by one or two other buffer solutions; this calibration was repeated hourly during periods while pH measurements were being made.

Ionization Constant of Kojic Acid

Aqueous solutions containing accurately weighed portions of purified acid dissolved in known amounts of freshly boiled and cooled doubly distilled water were titrated with standard alkali. The pH was observed throughout the titration, and from 10 points on the titration curve (between 15% and 85% neutralization) values of pK_a calculated by means of the Henderson equation. The end point in the titration was also determined, and a neutralization equivalent for the acid calculated. To examine the influence of ionic strength on the value of pK_a, weighed portions of potassium nitrate were introduced into most of the solutions prior to titration. The ionic strength obviously varies throughout the titration; the value recorded is based on the amount of salts present when the acid is half neutralized.

It was found that substantial drifting toward lower pH values occurred during titration of any sample of the kojic acid that was not pure white, and that in such titrations the solution became somewhat amber as the sample became alkaline. The cause of this observation is not known.

Spectral Curves

A considerable number of solutions were prepared containing fixed amounts of ferric nitrate and kojic acid, various amounts of acid, alkali, or buffers, as noted below, to give a distribution of pH values from 0.57 to 6.82, and a sufficient amount of potassium nitrate to give a final ionic strength of 0.5. These solutions were all made up to known volume and allowed to stand at room temperature (23 to 26° C) for 1 hour. The optical density of each was then measured at intervals of 10 mμ from 350 mμ to 700 mμ. Immediately after the spectrum of each solution was obtained, its pH was measured.

Regulation of pH in these solutions was secured by the addition of the following reagents:

pH 0.57 to 3.01: varying amounts of HNO_3,
2.03 to 3.40: 0.10 *M* $CH_2ClCOOH$ + varying amounts of NaOH,
3.20 to 5.73: 0.10 *M* CH_3COOH + varying amounts of NaOH,
3.09 to 3.62: varying small amounts of NaOH,
3.85 to 6.82: 0.10 *M* hexamine + varying amounts of HNO_3.

Can. J. Chem. Downloaded from www.nrcresearchpress.com by 210.87.254.5 on 09/05/12
For personal use only.

Continuous Variations

A series of 12 solutions was prepared from a (different) standard iron solution and a kojic acid solution in various proportions adjusted so that the total molarity of these remained constant. In our experiments $[M]_T+[HL]_T = 0.001$, and of this molarity the fraction of iron varied from 0.03 to 0.58. Each solution was buffered by the addition of a fixed amount of sodium acetate and varying amounts of nitric acid to a pH of 5.1 ± 0.2, and contained sufficient potassium nitrate to make the total ionic strength 0.5. The optical density of each solution was measured, and the values plotted against "mole fraction" of iron in the solution.

RESULTS AND DISCUSSION

Ionization Constant of Kojic Acid

Table I gives the values of pK_a found at the various ionic strengths investigated. Graphical extrapolation to zero ionic strength suggests a value of 7.88 for pK_a and this may provisionally be taken as the thermodynamic constant. The variation in pK_a with ionic strength may be largely accounted for by the variation in activity coefficient of the kojate ion, the magnitude of which, from the above measurements, appears to be comparable to those of other univalent ions. Okáč (5) has reported the value 7.75 for this constant.

As all solutions of the ferric kojates studied absorptiometrically were prepared to be of ionic strength 0.5, the value 7.73 was taken for pK_a when calculating their formation constants.

TABLE I

Ionization constant of kojic acid

Ionic strength	pK_a
0.03	7.83 ± 0.007
0.23	7.77 ± 0.005
0.53	7.73 ± 0.005
1.03	7.81 ± 0.007

Isobestic Points and Vareille Curves

Moss and Mellon (4) have given spectra for solutions containing fixed concentrations of iron (III) and kojic acid but differing in pH, and these show isobestic points at 495 mμ and 600 mμ. The spectra of our solutions that do not contain acetate or chloroacetate confirm theirs, including the same isobestic points. In Fig. 3 we show our values of ϵ_M at these two wavelengths for all these solutions. The interpretation of the various regions of these curves has been discussed previously.

Composition of Highest Complex

In the absence of acetate the spectra of the ferric kojate solutions was not altered by increasing the pH above 5. We assume that at and above this pH the maximum co-ordination of kojate ion has occurred. The experiment applying the method of continuous variations (6) showed maximum optical density when the "mole fraction" of iron in the prepared solutions was 0.25. This shows that the complex of maximum co-ordination is ML_3, as is the case with many other phenolic reagents capable of chelation to the metal. The same observation has been recorded by Moss and Mellon (4).

Can. J. Chem. Downloaded from www.nrcresearchpress.com by 210.87.254.5 on 09/05/12
For personal use only.

Formation Constants of Complexes

The method of deriving the equilibrium constants, $\mathscr{K}_n$, from the data of Fig. 3 has been described previously. For all these solutions $[M]_T = 2.05\times10^{-4}$ and $[L]_T = 15.00\times10^{-4}$ M. The first calculation was that of $\mathscr{K}_2$, based on the initial assumption that ϵ_1 (495 mμ) = 1100. The successive estimates were:

ϵ_1 (495 mμ)	Mid-point pH	$\mathscr{K}_2$
1100 (assumed)	2.18	5.53
964	2.10	6.65
946	2.09	6.82
946	2.09	6.82

The estimation of $\mathscr{K}_1$ and ϵ_1 was based on the following data:

Points	[H]	[ML] + [ML$_2$]	[M]	[HL]
1	2.70×10^{-1}	1.12×10^{-4}	0.93×10^{-4}	12.76×10^{-4} + [ML]
2	1.38×10^{-1}	1.55×10^{-4}	0.50×10^{-4}	11.90×10^{-4} + [ML]

Refinement in the value of ϵ_1 resulted from changes in the value of [ML], which in turn depended on the value assigned to $\mathscr{K}_2$. The successive values obtained in these calculations were:

Point 1				Point 2			
α_1	α_2	ϵ_1	$\mathscr{K}_1$	α_1	α_2	ϵ_1	$\mathscr{K}_1$
0.534	0.014	954	229	0.719	0.039	973	304
0.530	0.018	942	227	0.712	0.046	951	301
0.530	0.018	942	227	0.711	0.047	950	301

The average value of $\mathscr{K}_1$ was taken as 264.

The solution of equations 10 and 11, beginning with the trial value $\bar{n} = 2.5$, led to steady values at pH 3.73 of $[HL] = 9.90\times10^{-4}$ and $\bar{n} = 2.49$. Putting these values, and the final value of $\mathscr{K}_2 = 6.82$, into equation 12, gave $\mathscr{K}_1 = 0.191$.

To transform these equilibrium constants into formation constants, as more commonly are reported for metallic complexes we employ the relationship:

$$\log K_n = \log \mathscr{K}_n + pK_a.$$

From this the following values were obtained: $\log K_1 = 10.16$, $\log K_2 = 8.29$, and $\log K_3 = 6.90$. Previous values determined for these constants are assembled in Table II, with the present values for comparison.

TABLE II

Formation constants for ferric kojate complexes

	$\log K_1$	$\log K_2$	$\log K_3$	Ref.
Okáč, Sommer, Rády	3.13	3.99	4.00	(7)
Okáč, Kolařík	9.2	8.0	7.2	(5)
This work	10.16	8.29	6.90	—

Can. J. Chem. Downloaded from www.nrcresearchpress.com by 210.87.254.5 on 09/05/12
For personal use only.

The values of Okáč, Sommer, and Rády, which differ signally from the other two, were obtained by the method of continuous variations. Various authors, especially Woldbye (8), have criticized the application of this method to the measurement of formation constants whenever the possibility arises of one complex passing gradually into the next as the ligand concentration is gradually increased. From the formation curve of the ferric kojates, calculated from our constants with equation 1, shown as Fig. 4, it is apparent that such will be the case with these complexes.

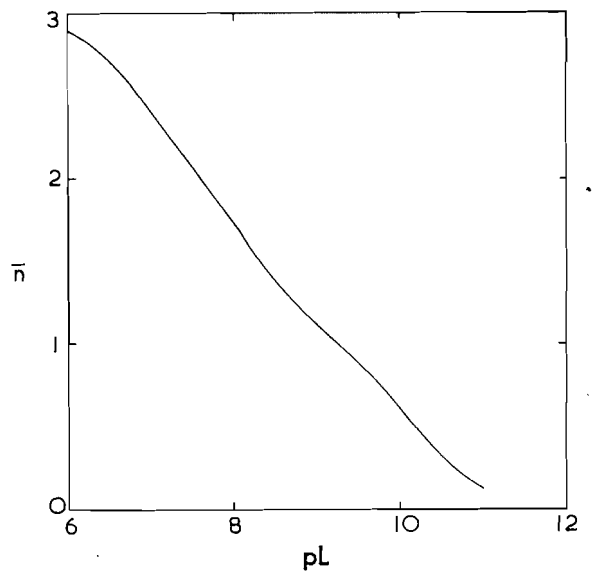


FIG. 4. Formation curve for the ferric kojates calculated from formation constants derived from this investigation.

In order to test the consistency between the conclusions drawn from Fig. 3 and the implications of the formation curve, we have calculated the relationship between pH and pL for our experimental solutions. For each value of pL at which a point on the formation curve was calculated, a value of pH was also obtained by means of equation 17

$$[17] \qquad 1 + \frac{[H]}{K_a} = \frac{[L]_T - \bar{n}[M]_T}{[L]}.$$

The results of these calculations are summarized in Table III, and shown graphically in Figs. 4 and 5.

Spectra of Single Complex Species

Since the spectra of a number of solutions of the ferric kojate complexes were available, and since the knowledge of the formation constants of these makes possible a calculation of their individual concentrations in the various solutions prepared, we undertook to extract from our data values of the molar extinction coefficients of the individual complexes. For these solutions, whose pH had been measured, a value of pL could be secured from Fig. 5, and with this, values of $\bar{n}$, α_0, α_1, etc. calculated. In the solution of highest pH, $\alpha_3 = 1$, and values of ϵ_3 were immediately available. In the solution of lowest pH the principal absorbing species was ML, but $\alpha_2 \sim 0.01$, so that a small contribution

Can. J. Chem. Downloaded from www.nrcresearchpress.com by 210.87.254.5 on 09/05/12
For personal use only.

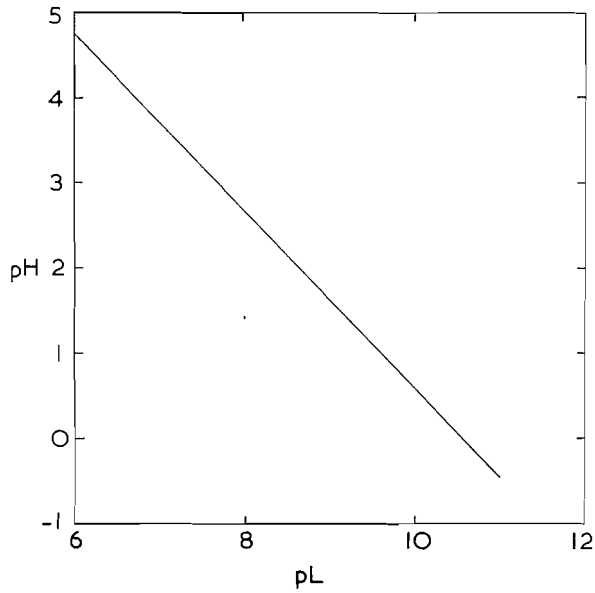


FIG. 5. Relationship between pL and pH for experimental conditions of this investigation
$[M]_T = 2.05 \times 10^{-4}$ molar.
$[L]_T = 15.00 \times 10^{-4}$ molar.

TABLE III
Formation curve for ferric kojates

pL	$\bar{n}$	α_0	α_1	α_2	α_3	pH
11.0	0.126	0.877	0.123	—	—	−0.44
10.7	0.224	0.776	0.224	—	—	−0.13
10.3	0.420	0.580	0.420	—	—	0.28
10.0	0.607	0.405	0.585	0.010	—	0.59
9.7	0.778	0.250	0.722	0.028	—	0.90
9.3	0.968	0.112	0.808	0.079	—	1.32
9.0	1.10	0.054	0.790	0.154	0.001	1.63
8.7	1.26	0.024	0.700	0.272	0.004	1.94
8.3	1.49	0.007	0.492	0.482	0.019	2.35
8.0	1.72_5	0.002	0.322	0.626	0.050	2.67
7.7	1.93	—	0.182	0.707	0.112	2.99
7.3	2.20	—	0.068	0.666	0.266	3.41
7.0	2.38	—	0.028	0.542	0.430	3.73
6.7	2.60	—	0.010	0.384	0.606	4.05
6.3	2.79_5	—	0.002	0.200	0.798	4.46
6.0	2.89	—	—	0.112	0.888	4.77

from ML_2 was included in the observed spectrum. A first estimate of ϵ_1 was made from the spectrum of this solution, neglecting the contribution of ϵ_2. Later, when a value of ϵ_2 had been extracted, a second, modified estimate of ϵ_1 was calculated with equation 3.

The estimate of ϵ_2 was, in this case, based on the spectrum of a solution of pH 2.52, for which we calculate $\alpha_0 = 0.004$, $\alpha_1 = 0.394$, $\alpha_2 = 0.569$, and $\alpha_3 = 0.033$. Values of ϵ_2 were calculated from the expression

$$\epsilon_2 = \frac{\epsilon_M - 0.394\epsilon_1 - 0.033\epsilon_3}{0.569}$$

using in turn the raw and improved estimates of ϵ_1 as described previously.

Can. J. Chem. Downloaded from www.nrcresearchpress.com by 210.87.254.5 on 09/05/12
For personal use only.

The results are shown plotted as Fig. 6. It is recognized that the values of ϵ obtained in this way are not very accurate, since their calculation involves taking differences of experimental numbers. The spectra show, with increase in ligand number of the complexes, a hypsochromic shift in λ_{max}, and a roughly proportionate increase in ϵ_{max}, typical of numerous other complexes formed by ferric iron with phenolic chelating agents.

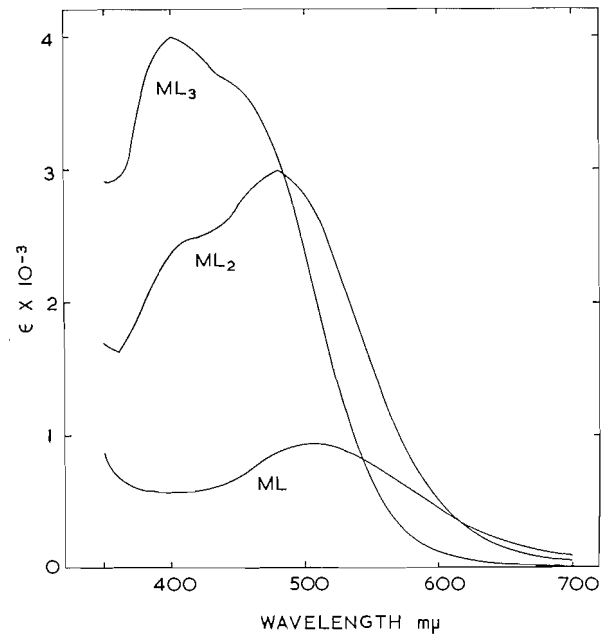


FIG. 6. Spectra of individual species for system iron (III) – kojic acid.

Effect of Acetate and Chloracetate

To prepare solutions of stabilized pH for spectral measurements it was planned to use buffering mixtures of acetic acid or chloracetic acid and sodium hydroxide. The use of acetate buffers is implied in the preparation of the solutions whose spectra had previously been examined by Moss and Mellon. The spectra of our solutions prepared with these buffering agents failed to give sharply defined isobestic points, and plots of ϵ_M vs. pH failed to give the expected horizontal regions. The effect observed is illustrated in Fig. 7, in which our experimental points at 495 mμ are shown together with the Vareille curve ultimately obtained for solutions not containing acetate or chloracetate (cf. Fig. 3). A similar drop in ϵ_M with increasing pH is observed with each set of solutions containing either acetate or chloracetate. This is attributed to a competition between acetate or chloracetate and the kojate ion for co-ordination to the metallic ion. As the concentration of the anion of either buffering acid increases with increase in pH, ferric acetate or chloracetate forms at the expense of the colored kojate. The fact that the experiments for continuous variations indicated a fairly robust 3:1 complex in the presence of a moderate concentration of acetate appears to rule out the likelihood of the formation of stable mixed acetate – kojate complexes.

Can. J. Chem. Downloaded from www.nrcresearchpress.com by 210.87.254.5 on 09/05/12
For personal use only.

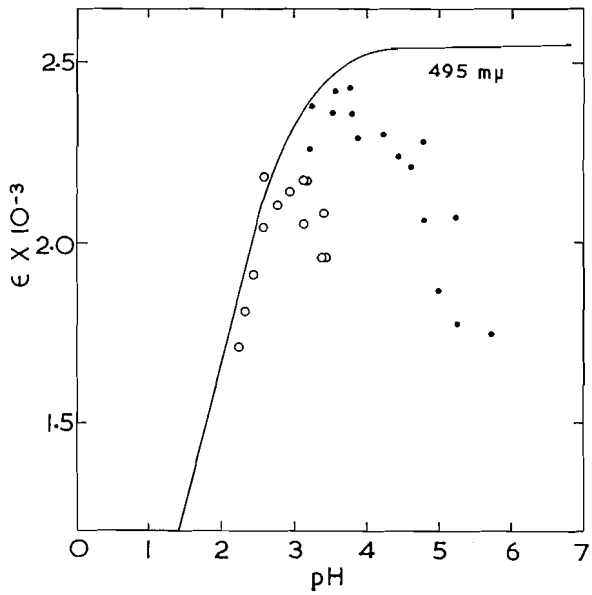


FIG. 7. Influence of acetate and chloracetate on formation of ferric kojates. The solid line shows the Vareille curve at 495 mμ taken from Fig. 3. Open circles show experimental observations for solutions buffered with chloracetic acid and alkali; solid circles refer to similar solutions buffered with acetic acid and alkali.

Implications of Results

Apart from any theoretical significance that may be attached to a knowledge of the formation constants and spectra of the three ferric kojate complexes, this study has certain practical consequences in analytical chemistry. Kojic acid has been proposed as a colorimetric reagent and as an indicator for complexometric titrations for iron (III). This work has revealed the superior stability of solutions of the highly purified reagent. It has demonstrated the significance of control of pH and of excess reagent necessary to insure that the solutions prepared for photometric measurement should have the same degree of complex formation. Finally, it has disclosed the deleterious effect of acetate in preventing complete formation of the colored complexes, and demonstrated that hexamine is a preferable buffering agent.

ACKNOWLEDGMENT

The authors gratefully acknowledge financial assistance from the National Research Council for this investigation. One author (G. F. A.) was holder of a Union Carbide Research Fellowship in 1958–59, for which thanks are hereby expressed.

REFERENCES

1. L. VAREILLE. Bull. Soc. Chim. France, 870, 872, 1493, 1496 (1955).
2. L. VAREILLE. Bull. Soc. Chim. France, 872 (1955).
3. A. ALBERT. Biochem. J. **54**, 646 (1953).
4. M. L. Moss and M. G. MELLON. Ind. Eng. Chem., Anal. Ed. **13**, 612 (1941).
5. A. OKÁČ and Z. KOLAŘÍK. Chem. listy, **51**, 2017 (1957); Collection Czech. Chem. Commun. **24**, 266 (1959).
6. P. JOB. Ann. Chim. **9** (10), 113 (1928).
7. A. OKÁČ, L. SOMMER, and G. RÁDY. Chem. listy, **48**, 828 (1954).
8. F. WOLDBYE. Acta Chem. Scand. **9**, 299 (1955).

Can. J. Chem. Downloaded from www.nrcresearchpress.com by 210.87.254.5 on 09/05/12
For personal use only.

Can. J. Chem. Downloaded from www.nrcresearchpress.com by 210.87.254.42 on 09/05/12
For personal use only.

THE COMPLEX DIELECTRIC CONSTANT OF SOLUTIONS OF TRIMETHYLPENTANE AND NITROBENZENE NEAR THE CONSOLUTE TEMPERATURE[1]

B. D. RIPLEY[2] AND R. MCINTOSH

ABSTRACT

The complex dielectric constants of three compositions of trimethylpentane and nitrobenzene have been measured as a function of temperature for a range near the consolute temperature. The frequency employed was 3300 Mc/sec. The experimental procedure involved the study of the standing wave established in a coaxial line. The chemical systems showed maxima in both the real and imaginary parts of the complex dielectric constant at temperatures above those at which phase separation occurs. The finding of Semenchenko and Azimov is thus confirmed. A discussion of the validity of applying thermodynamic formulae to dielectrics showing loss is given and some qualitative remarks are offered concerning the change of the systems as they are cooled. These remarks are based upon the effect of the applied field upon the entropy of the solutions.

INTRODUCTION

The properties of one-component systems at the critical temperature and of multicomponent systems at the consolute temperature are unusual, and have been frequently studied. Classical thermodynamics suffices to predict much of the behavior, such as the approach of c_p to an infinite value for a one-component system at the critical temperature (1). In the case of such systems the existence of turbidity, the occurrence of marked density gradients due to the extreme value of compressibility (2, 3), and the persistence of liquid-like properties above the temperature of the disappearance of the meniscus have been remarked frequently. Partially miscible liquid systems also show turbidity (4) and other interesting properties near the consolute temperature. Semenchenko and his associates have studied such properties as the viscosity (5), the specific heat (6), and the dielectric constant (7) for systems above the temperature at which phase separation occurs.

In all cases maxima of the physical properties were observed at a temperature between 0.5 and 1.5° C above that of the formation of layers. The magnitudes of the maxima were dependent upon composition and were greatest in each system for the composition corresponding to the consolute temperature. Semenchenko and Azimov (7) investigated the dielectric constant for low frequencies at which the liquids show no loss. Semenchenko (8, 9) has explained the occurrence of the maximum on the basis of the Gibbs' criteria for the existence of critical phases (10). Very briefly, the development follows the course outlined below.

The condition of a system of fixed mass, existing in one phase, is determined by the variables S, entropy, V, volume, and D, the dielectric displacement, which are taken as the independent variables. T, temperature, p, pressure, and E, electric field intensity are taken as dependent variables. The variations of these as a function of the independent variables may be written.

[1]*Manuscript received November 17, 1960.*
Contribution from the Chemistry Department, University of Toronto, based upon a thesis presented for the M.A. degree.
[2]*Graduate Student; present address: c/o International Nickel Co., Port Colborne, Ontario.*

$$dT = \left(\frac{\partial T}{\partial S}\right)_{m,V,D} dS + \left(\frac{\partial T}{\partial V}\right)_{m,S,D} dV + \left(\frac{\partial T}{\partial D}\right)_{m,S,V} dD,$$

$$dp = \left(\frac{\partial p}{\partial S}\right)_{m,V,D} dS + \left(\frac{\partial p}{\partial V}\right)_{m,S,D} dV + \left(\frac{\partial p}{\partial D}\right)_{m,S,V} dD,$$

$$dE = \left(\frac{\partial E}{\partial S}\right)_{m,V,D} dS + \left(\frac{\partial E}{\partial V}\right)_{m,S,D} dV + \left(\frac{\partial E}{\partial D}\right)_{m,S,V} dD.$$

The restriction of constant mass assures variations of the properties of the phase.

Keeping T and p constant also, the value of $(\partial E/\partial D)_{m,p,T}$ is determined and is given by

$$\begin{vmatrix} \left(\frac{\partial T}{\partial S}\right)_{m,V,D} & \left(\frac{\partial T}{\partial V}\right)_{m,S,D} & \left(\frac{\partial T}{\partial D}\right)_{m,V,S} \\ \left(\frac{\partial p}{\partial S}\right)_{m,V,D} & \left(\frac{\partial p}{\partial V}\right)_{m,S,D} & \left(\frac{\partial p}{\partial D}\right)_{m,V,S} \\ \left(\frac{\partial E}{\partial S}\right)_{m,V,D} & \left(\frac{\partial E}{\partial V}\right)_{m,S,D} & \left(\frac{\partial E}{\partial D}\right)_{m,V,S} \end{vmatrix}$$

divided by

$$\begin{vmatrix} \left(\frac{\partial T}{\partial S}\right)_{m,V,D} & \left(\frac{\partial T}{\partial V}\right)_{m,S,D} \\ \left(\frac{\partial p}{\partial S}\right)_{m,V,D} & \left(\frac{\partial p}{\partial V}\right)_{m,S,D} \end{vmatrix}.$$

The numerator can be shown by a general argument to become zero at the critical condition, since a system in that condition is at the limit of stability for continuous changes (10). Thus $(\partial E/\partial D)_{m,p,T} = 1/\epsilon = 0$ at the consolute temperature and composition. Since E is neither a maximum nor a minimum, it follows that $(\partial^2 E/\partial D^2)_{m,p,T} = 0$. Since the phase is stable, the necessary condition is that $(\partial E/\partial D)_{m,p,T} \geqslant 0$. Semenchenko (11) gives the conditions for what he calls false critical points as $(\partial E/\partial D)_{m,p,T} > 0$, $(\partial^2 E/\partial D^2)_{m,p,T} > 0$ and predicts finite values of the maximum.

For time-dependent electrical fields and dielectrics showing power absorption, careful consideration must be given to the validity of applying thermodynamic arguments. It would appear, however, on the basis of the discussion concerning entropy which is given later, that the prediction of a maximum of the real part of the complex dielectric constant can still be made.

The present work is therefore largely a repetition of Semenchenko's (7, 11), except that the imaginary part of the dielectric constant has also been measured and the second component is 2,2,4-trimethylpentane instead of octane. A discussion of the validity of thermodynamic treatments for lossy systems is offered, as well as a description of a convenient and precise system of measuring the parts of the complex dielectric constants of such liquid systems.

EXPERIMENTAL

The dielectric cell is shown in Fig. 1. The outer conductor was German silver tubing 13/128 in. thick; the inner conductor was the same metal 6/1000 in. thick down to the region marked E, which had a copper plug 3/8 in. in diameter and $3\frac{3}{16}$ in. in length

Can. J. Chem. Downloaded from www.nrcresearchpress.com by 210.87.254.42 on 09/05/12
For personal use only.

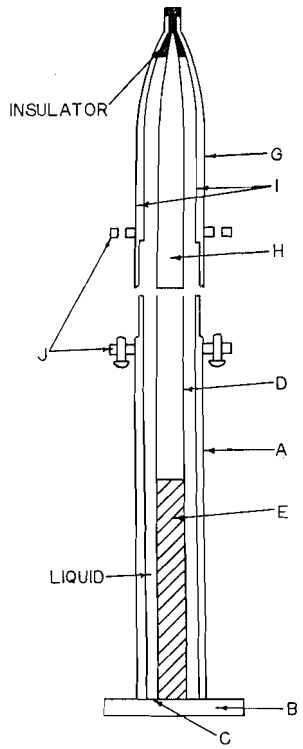


FIG. 1. Schematic representation of the experimental cell.

soldered inside the central conductor. The shorting plate was brass. The cell was designed in this way to provide good thermal conductivity to the fluid of the thermostat, but to reduce heat transfer to the air above the thermostat through the connector at the top of the cell. The cell was $6\frac{3}{16}$ in. long and 1 in. in diameter. A Caro UG-32U adaptor was used to make the connection between the cell and slotted line. The adaptor was designed so that no discontinuity occurred along either the inner or outer conductor surfaces. As indicated in the diagram, the adaptor was held to the cell by screws passing through plates, and these plates formed a tight fit to prevent evaporation of the liquids or absorption of water by them from the air. The oil thermostat was electrically heated and its temperature controlled by means of an adjustable mercury thermoregulator and a relay system. Temperatures were readily controlled to $\pm 0.01°$ C over a period of several hours, and because of the period of heating and cooling, the temperature of the liquid in the cell was more closely constant than this.

The coaxial line used was a Hewlett Packard model 805A, mounted vertically above the cell. In series with the line was a length of RG-21/U attenuating cable to reduce reflections to the generator. The generators were FXR L771B and S771B oscillators designed to work into a 50-ohm load. The generators were fitted with a series N, UG 107B/U tee adaptor providing connection from one side to the slotted line, and from the other, again through attenuating cable, to an FXR crystal mount. Connectors in both lines were series N, UG-18C/U plugs. Rectification of the r.-f. voltage was achieved by means of 1N21B crystals which were tested and found to provide square-law response in the range of voltages used.

The signal from the crystal of the slotted line was applied to one terminal of a Leeds

Can. J. Chem. Downloaded from www.nrcresearchpress.com by 210.87.254.42 on 09/05/12
For personal use only.

Can. J. Chem. Downloaded from www.nrcresearchpress.com by 210.87.254.42 on 09/05/12
For personal use only.

and Northrup mirror galvanometer of 0.05 μv/mm sensitivity mounted on a vibration-free table. The signal of the crystal in the FXR mount was sent to a voltage-dividing Muirhead resistance box of 10,000 ohms. The output of this box was sent through variable resistors, in series (which served as protective resistances for the galvanometer) to the other terminal of the galvanometer. Very careful shielding of all elements in the circuit was necessary, and an efficient ground connection had to be provided.

The purpose of comparing the rectified signal from the slotted line with a signal from a reference source fed by the same oscillator was to compensate for both long and short term fluctuations of the amplitude of the signal generator. The same technique was used by McCowan and McIntosh (12), but in the present instance no amplification was employed. As the signal is read as a fraction of the oscillator output at the time of measurement, and as both P_x and $P_{\min}$ are so recorded, (where P_x is the output at position x), the ratio between them is immediately given. Power is here considered to be measured because of the square-law response of the detector.

The data obtained were those necessary for the application of the equation given in Von Hippel (13, p. 68)

$$\frac{\tanh \gamma_2 d}{\gamma_2 d} = \frac{-j\lambda_1}{2\pi d} \frac{\frac{E_{\min}}{E_{\max}} - \frac{j \tan 2\pi X_0}{\lambda_1}}{1 - j\frac{E_{\min}}{E_{\max}} \frac{\tan 2\pi X_0}{\lambda_1}}$$

where λ_1 is the wavelength of the signal in the guide, d the depth of liquid in the cell, $E_{\min}$ and $E_{\max}$ the magnitudes of the standing wave at a node and at maximum amplitude, and X_0 the distance of the first minimum from the short. The position of the short as experienced by the electric wave had, of course, to be determined initially with no liquid in the cell. This was done relative to the scale readings of the line by determining the distance between successive minima and considering the electrical short position to be at the distance given by the smallest integral number of nodes required to approximate to the geometrical distance of the short from the scale. The average for three frequencies was 39.318 ± 0.004 whereas the corresponding geometrical distance was 33.9 cm. It should be noted also that attenuation along the line proved negligible as the amplitude of the minimum was constant along the line.

Although it would have been feasible to measure the ratio $P_{\min}/P_{\max}$ directly, this was not done because the crystal response departed somewhat from the square-law response near the maximum. The distance $\Delta X/2$ between the position of the minimum and the position for twice the amplitude of the minimum was measured and employed in the formula $E_{\min}/E_{\max} = \pi\Delta X/\lambda_1$ (13, p. 67). The small errors arising from this practice are discussed by Purcell (14) but could not influence the qualitative nature of the results given below. A matter giving rise to some error of unknown and variable extent was the use of the charts in Von Hippel (13, p. 88 *et seq.*) to evaluate $\tanh \gamma_2 d/\gamma_2 d$. This error arose in interpolating, but is again too small to affect the results seriously. Finally, to ensure good performance, the liquid level was changed to give the best depth of liquid for any particular frequency, that is $\lambda_1/4$, where λ_1 is the wavelength. Densities of the liquid compositions at the limits of the temperature range were measured, and the height of liquid at any intermediate temperature computed using the density obtained by linear interpolation between the extreme values.

The 2,2,4-trimethylpentane was British Drug Houses spectroscopic Grade, Laboratory Reagent. The nitrobenzene was B.D.H. Microanalytical Reagent, Organic Standard. Both

substances were stored over "Drierite" and transferred to the cell by the pressure of dry air.

RESULTS

Three experiments using nitrobenzene at 30.0° C were carried out using a variety of frequencies and the frequency of maximum loss established for pure nitrobenzene as 3300 Mc/sec. The average of the values is plotted in Fig. 2.

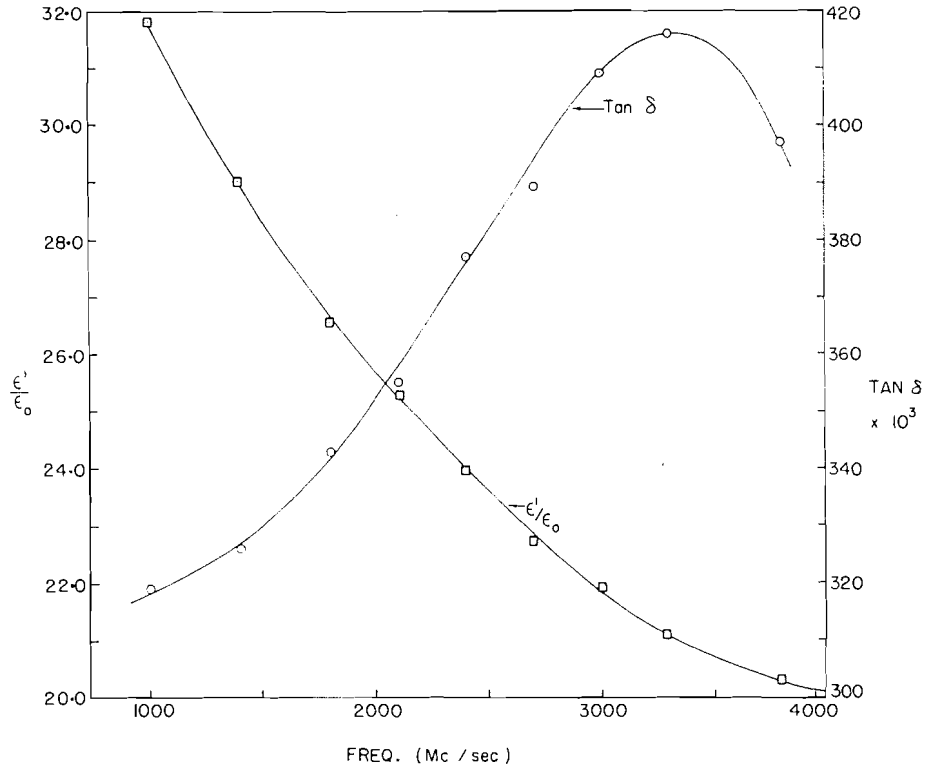


FIG. 2. The values of the real part of the dielectric constant and of tan δ of pure nitrobenzene as a function of frequency at 30.0° C.

Three two-component systems were also studied. These were nitrobenzene and trimethylpentane and the concentrations were 25.4%, 48.2%, and 77.1% nitrobenzene, respectively. The frequency used was 3300 Mc/sec. Table I shows the temperatures at

TABLE I

Temperatures of pronounced turbidity and of separation of phases

System	Temperature of turbidity, °C	Temperature of separation of phases, °C
I	22.6–22.7	21.0–21.1
II	29.6–29.7	27.6–27.7
III	23.1–23.2	21.4–21.5

which turbidity became marked and the temperatures at which phase separation occurred. For each of these three systems three series of determinations of complex dielectric constant versus temperature were carried out. The mean deviation never exceeded 0.3% and was usually 0.15% or less for the real part, with error up to 1% in tan δ. The averages of the real and imaginary parts of the complex dielectric constant are plotted as ϵ'/ϵ^0 (i.e. relative to vacuum) and as tan δ in Figs. 3, 4, and 5. It is clear from these plots that

Can. J. Chem. Downloaded from www.nrcresearchpress.com by 210.87.254.42 on 09/05/12
For personal use only.

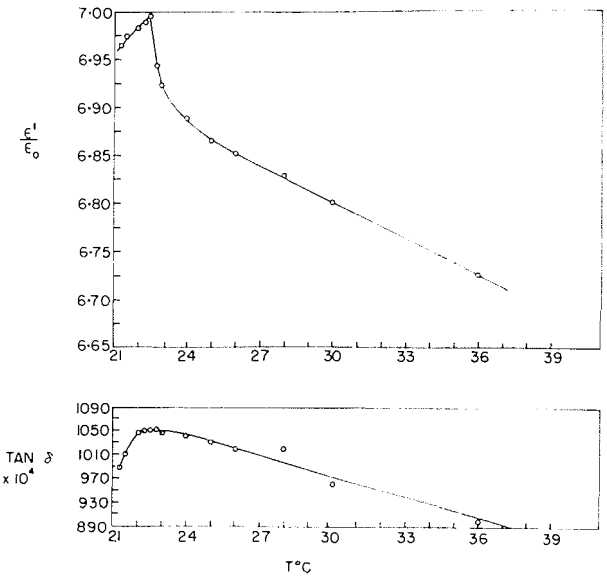


FIG. 3. The values of the real part of the dielectric constant and of tan δ of a solution of 25.4% nitrobenzene in trimethyl pentane. Frequency 3300 Mc/sec.

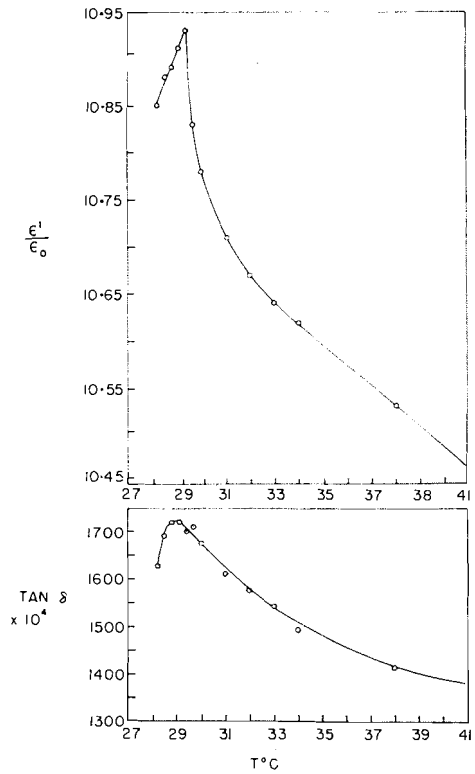


FIG. 4. The values of the real part of the dielectric constant and of tan δ of a solution of 48.2% nitrobenzene in trimethyl pentane. Frequency 3300 Mc/sec.

Can. J. Chem. Downloaded from www.nrcresearchpress.com by 210.87.254.42 on 09/05/12
For personal use only.

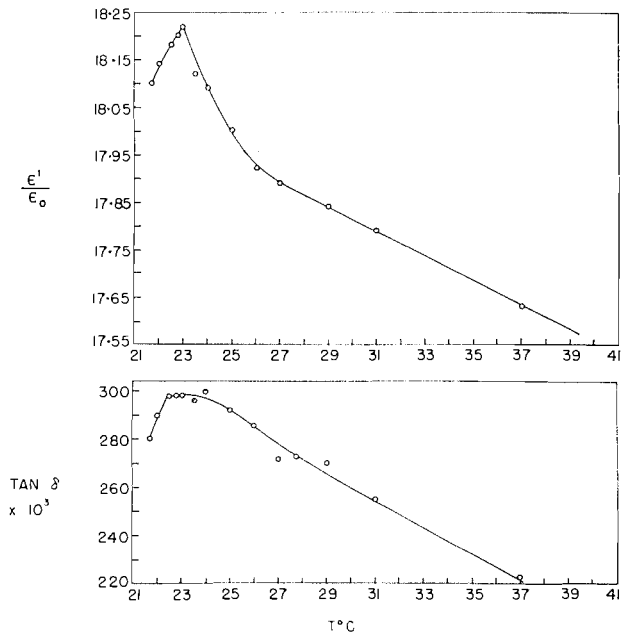


FIG. 5. The values of the real part of the dielectric constant and of tan δ of a solution of 77.1% nitrobenzene in trimethyl pentane. Frequency 3300 Mc/sec.

both ϵ' and ϵ'' show maxima at the temperatures where turbidity becomes apparent. The magnitude of the maximum is greatest for the system corresponding most closely to the composition of the system at the consolute condition. The consolute temperature for this system is 30.38° C (15) and the consolute composition was estimated by us as 56% nitrobenzene. The maxima of $\hat{\epsilon}$ confirm findings by Semenchenko and Azimov (7, 11).

DISCUSSION

Fröhlich (16) shows that the entropy per unit volume of a dielectric in a static field may be written

$$S = S_0 + \frac{1}{8\pi}\frac{\partial \epsilon}{\partial T}E^2,$$

where S_0 is the entropy of the dielectric at the particular temperature but with no field applied. If $\partial\epsilon/\partial T < 0$, the effect of the field is to reduce the entropy, and if $\partial\epsilon/\partial T > 0$, the effect of the field is to increase it. Fröhlich states that the treatment of the general case of time-dependent fields is complex and does not discuss it further. On the basis of the following considerations it appears that a very similar relation should be valid for time-dependent fields and dielectrics which absorb power.

In the case of lossy dielectrics an irreversible process is occurring due to the absorption of the power, namely the extraction of energy from the field at some temperature $T+\delta T$ and its elimination to the thermostat at T. The value of the energy absorbed per second is given by the imaginary part of $1/t\int_0^t \hat{E}\cdot d\hat{D}$. The real part of the expression represents energy stored by the dielectric and returned to the field twice during each cycle. In spite of the irreversible process and the generation of entropy, the condition of the

Can. J. Chem. Downloaded from www.nrcresearchpress.com by 210.87.254.42 on 09/05/12
For personal use only.

dielectric is specified by its temperature, assumed to be T, and by the time-average value of its polarization, which is a function of the value of the applied field at fixed frequency. We may thus consider the dielectric to exchange energy with its surroundings and to be maintained at constant volume, when, analogously with the equation given by Fröhlich (16), one may write $dU = TdS + (1/4\pi)$ r.p. $\overline{\hat{E} \cdot d\hat{D}}$, where S is a function of T and the real part of the applied field, and $\hat{D}$ is a function of temperature only at fixed frequency. The bar designates the time-average value and r.p. is the real part of the expression. Since $\hat{D} = \epsilon\hat{E}$ (magnitudes are employed since the vectors are parallel),

$$d\hat{D} = \epsilon d\hat{E} + \hat{E} d\hat{\epsilon}.$$

On substitution in the differential equation for energy, and using $\hat{E}^2$ as the variable

$$dU = \left(T\frac{\partial S}{\partial T} + \frac{1}{4\pi}\text{r.p.}\,\overline{\hat{E}^2\frac{\partial\hat{\epsilon}}{\partial T}}\right)dT + \left(T\frac{\partial S}{\partial \bar{\hat{E}}^2} + \frac{1}{8\pi}\text{r.p.}\,\hat{\epsilon}\right)\overline{d\hat{E}^2}.$$

Since,

$$\frac{\partial}{\partial \bar{\hat{E}}_2}\left(T\frac{\partial S}{\partial T} + \frac{1}{4\pi}\text{r.p.}\,\overline{\hat{E}^2\frac{\partial\hat{\epsilon}}{\partial T}}\right) = \frac{\partial}{\partial T}\left(T\frac{\partial S}{\partial \bar{\hat{E}}^2} + \frac{1}{8\pi}\text{r.p.}\,\hat{\epsilon}\right)$$

on integration, with $\hat{\epsilon}$ independent of $\hat{E}^2$, and on evaluation of the time average of the complex field, one obtains

$$S = S_0 + \frac{1}{16\pi}E_0^2\frac{\partial\epsilon'}{\partial T}$$

where E_0 is the maximum amplitude of the field. As in the static case, the system loses entropy or gains entropy in the presence of the field depending upon the sign of $\partial\epsilon'/\partial T$.

DISCUSSION OF EXPERIMENTAL RESULTS

Semenchenko (8, 9) has pointed out that the prediction of a maximum of the dielectric constant of one-phase systems at the condition of the limit of stability with respect to continuous changes is inherent in the general criteria established by Gibbs (10). He has obtained experimental confirmation of this prediction (7, 11). Using frequencies of measurement from 1000 to 3300 Mc/sec and the system nitrobenzene–trimethylpentane, we have confirmed Semenchenko's finding and have shown also that ϵ'' shows a maximum at the same temperature within the limits of experimental error. Analogous concepts to those of cybotactic groups (17) and regional orientation (18) which have been used to distinguish the liquid from the gaseous state of aggregation may also be employed to permit qualitative descriptions of the transition between single-phase and two-phase systems of several components. In the present instance, if the conclusion is correct that lossy dielectrics in alternating fields are amenable to discussion in terms of the usual thermodynamic treatment, then the maximum of the dielectric constant as a function of temperature permits the following qualitative description of the behavior of the system.

As the temperature is reduced towards the temperature of the maximum, association of the molecules into some type of structure is occurring. That this association is not complete is evident from the fact that the entropy of the system may be further reduced by the application of a field. At temperatures lower than that of the maximum, however, the reaction has occurred to a sufficient extent that application of a field will increase

Can. J. Chem. Downloaded from www.nrcresearchpress.com by 210.87.254.42 on 09/05/12
For personal use only.

the entropy, presumably by the destruction of structures which exist when no field permeates the sample. As the value of $\partial\epsilon'/\partial T$ remains constant or increases slightly with diminishing temperature, the application of a field remains effective in destroying order down to the temperature at which separation into phases occurs. As the existence of discrete phases suggests an increasing stability of ordered regions within the fluid as temperature is lowered, and as the effectiveness of the field persists, it is suggested that the amount of ordered matter increases with lowered temperature.

The range of frequency investigated was not sufficiently broad for us to learn much about the nature of the loss in the system. Pure nitrobenzene does not reveal a loss curve of the Debye type. The three solutions of nitrobenzene can only be discussed on the basis of their behavior as a function of temperature. The diminishing values of ϵ'' on both sides of the temperature of maximum ϵ' could be reconciled with the hypothesis of a smaller amount of ordered matter, but the likelihood of this being correct for lower temperatures is small in view of the remarks made earlier. Moreover, a wider distribution of relaxation times or the variation of loss with temperature even for a fixed amount of a single type of molecular aggregate could also explain the experimental facts. The last possibility follows from the knowledge that even for systems of a single relaxation time, the loss curve goes through a maximum for a given frequency as temperature is varied. It therefore seems clear that a much more thorough examination of these systems using a wide range of measuring frequencies would be required to increase the present understanding of their behavior.

ACKNOWLEDGMENTS

We are indebted to the Advisory Committee on Research, University of Toronto, and to the National Research Council, Ottawa, for financial support. It is a pleasure to thank Professors J. M. Anderson and R. H. McKay of the Physics Department, University of Toronto, and Dean A. R. Gordon of this Department for reading the discussion concerning the thermodynamics of lossy dielectrics.

REFERENCES

1. MOLECULAR THEORY OF GASES AND LIQUIDS. J. O. Hirschfelder, C. F. Curtiss, and R. B. Bird. John Wiley & Son, Inc., New York. 1954. p. 369.
2. R. MCINTOSH, J. R. DACEY, and O. MAASS. Can. J. Research, B, **17**, 241 (1939).
3. H. B. PALMER. Doctoral Dissertation, University of Wisconsin. 1952. As quoted in Molecular theory of gases. p. 373.
4. F. E. MURRAY and S. G. MASON. Can. J. Chem. **36**, 415 (1958).
5. V. K. SEMENCHENKO and E. L. ZORINA. Doklady Akad. Nauk. S.S.S.R. **80**, 903 (1951); National Research Council Technical Translation TT298.
6. V. K. SEMENCHENKO and V. P. SKRIPOV. Zhur. Fiz. Khim. **25**, 362 (1951); National Research Council Technical Translation TT243.
7. V. K. SEMENCHENKO and M. AZIMOV. Zhur. Fiz. Khim. **30**, 2228 (1956).
8. V. K. SEMENCHENKO. Zhur. Fiz. Khim. **25**, 121 (1951).
9. V. K. SEMENCHENKO. Doklady Akad. Nauk. S.S.S.R. **99**, 1045 (1954).
10. J. A. V. BUTLER. *In* Commentary of the scientific writings of J. Willard Gibbs. Vol. I. Yale University Press. 1936. p. 146 *et seq.*
11. V. K. SEMENCHENKO and M. AZIMOV. Zhur. Fiz. Khim. **30**, 1821 (1956).
12. J. D. MCCOWAN and R. MCINTOSH. Can. J. Chem. **39**, 425 (1961).
13. A. VON HIPPEL. Dielectric materials and applications. The Technology Press of M.I.T. and John Wiley & Sons. 1954.
14. E. M. PURCELL. Technique of microwave measurements. M.I.T. Radiation Laboratory Series. McGraw-Hill, 1947. Chap. 8.
15. H. M. WOODBURN, K. SMITH, and H. TETEWSKY. Ind. Eng. Chem. **36**, 588 (1944).
16. H. FRÖHLICH. Theory of dielectrics. Oxford, Clarendon Press. 1949. p. 9 *et seq.*
17. C. A. BENZ and G. W. STEWART. Phys. Rev. **46**, 703 (1934).
18. O. MAASS and L. A. GEDDES. Phil. Trans. Roy. Soc. London, Ser. A, **236**, 303 (1937).

Can. J. Chem. Downloaded from www.nrcresearchpress.com by 210.87.254.42 on 09/05/12
For personal use only.

Can. J. Chem. Downloaded from www.nrcresearchpress.com by 210.87.254.40 on 09/05/12
For personal use only.

INFRARED SPECTRA OF GASES CHEMISORBED ON ZINC OXIDE

I. CO AND CO_2[1]

J. H. TAYLOR[2] AND C. H. AMBERG

ABSTRACT

The infrared spectra of CO and CO_2 adsorbed on zinc oxide have been observed in the region 2–9 μ. The results show that CO does not exist as such on the surface at 155° C, but is immediately oxidized to CO_2. There is no evidence for carbonate formation in the adsorption of CO, the spectra corresponding to structures of the carboxylate type. A band is observed at 2174 cm^{-1} for CO at 25° C which may correspond to dipole interaction or to an oxidation step.

INTRODUCTION

Previous work (1–5) on the chemisorption of CO on surfaces of zinc oxide has shown that there are two distinct types: one, a weak reversible adsorption occurring at room temperature with a negligible activation energy, the other a stronger adsorption occurring at higher temperature with an activation energy of 5 to 16 kcal/mole (4), in which the CO can be removed only as CO_2. It was thought that the infrared method might give information on the nature of the adsorbed species.

EXPERIMENTAL

The zinc oxide was prepared by the precipitation of either the carbonate from nitrate solution, with subsequent decomposition at 350°, or the oxalate from acetate solution, the oxalate being decomposed by heating at 400° C in air. The oxide was pressed at 40 tons/sq. in. into plates containing about 100 mg/sq. cm, which had a B.E.T. nitrogen area of 25–30 sq. m/g and transmitted approximately 50% of the incident infrared radiation before outgassing. These plates were mounted in a cell similar to that described by Little, Klauser, and Amberg (6). This cell with a path length of 11.0 cm was fitted with a winding device which enabled the sample to be removed from the beam and the background spectrum to be run. A matched cell containing gas at a pressure equal to that in the sample cell was placed in the reference beam. In all experiments the pressure of CO and CO_2 was 20 mm Hg. The instrument was a Beckman IR-4 double beam spectrometer used with sodium chloride optics.

RESULTS

Figure 1 (*a*, *b*, *c*) shows a sequence of spectra taken as the sample was outgassed. It was found that the transmission slowly decreased until after pumping at 320° C for several hours, the sample became completely opaque. The transmission could be entirely restored, as shown in Fig. 1*d*, by heating for 5 minutes at 350° C under 1 cm oxygen, cooling to room temperature, and pumping to 10^{-5} mm Hg. All the spectra reported here were taken from samples pretreated in this manner.

Figure 2 shows the spectra of CO and CO_2 adsorbed on zinc oxide, with the zinc oxide spectrum subtracted.

The CO at 25° C shows a sharp band at 2174 cm^{-1} and a weaker one at 1333 cm^{-1}, which were formed immediately upon admission of the gas (Fig. 2*a*). On standing, the

[1]*Manuscript received September 26, 1960.*
Contribution from the Division of Applied Chemistry, National Research Council, Ottawa, Canada. Issued as N.R.C. No. 6163.
[2]*National Research Council Postdoctorate Fellow 1959–61.*

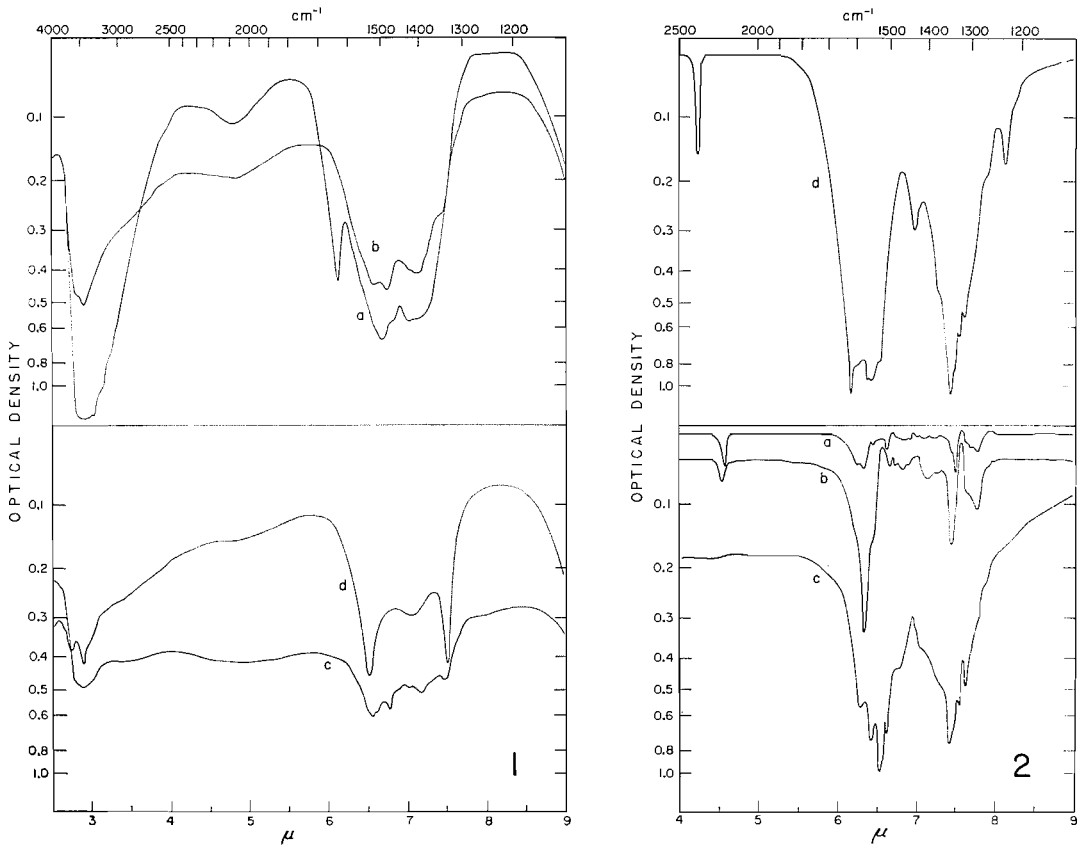


FIG. 1. Spectrum of zinc oxide on outgassing: (*a*) in air, (*b*) 3 hours at 150° C, (*c*) 18 hours at 150° C, (*d*) 18 hours at 320° C and treatment with 1 cm O_2 at 350° C. Spectra run at 25° C.

FIG. 2. Spectra of adsorbed gases with the zinc oxide spectrum subtracted: (*a*) CO at 25° C initially, (*b*) CO at 25° C after 24 hours, (*c*) CO at 155° C after 3 hours, (*d*) CO_2 at 25° C after 0.5 hour.

peak at 2174 cm^{-1} shifted slightly to a higher frequency, usually about 2198 cm^{-1}, and decreased in intensity. At the same time, three strong maxima appeared at 1575, 1342, and 1287 cm^{-1} and a slow increase in the background absorption was observed (Fig. 2*b*). The band at 2174 cm^{-1} disappeared as soon as evacuation was commenced, but those at 1575, 1342, and 1287 cm^{-1} were removed only by prolonged pumping at 320°.

Figure 2*c* is the spectrum obtained by admitting CO to zinc oxide at 155° C. In this case there was no peak at 2174 cm^{-1}, but the growth of the spectrum and increase in background absorption was much more rapid than in the cold. After some time at 155° C, a small peak at 2198 cm^{-1} was observed in some cases.

The adsorption of CO_2 at 25° was very rapid, and as can be seen from Fig. 2*d* the structure is somewhat complex. On opening of the system to the pumps the band at 2364 cm^{-1} was immediately removed, and that at 1618 cm^{-1} shifted to 1600 cm^{-1}. The bands at 1600, 1431, and 1230 cm^{-1} decreased quite rapidly in intensity and were almost entirely removed after 3 hours pumping at 25° C. The rest of the spectrum was removed only by several hours outgassing at 320° C.

Can. J. Chem. Downloaded from www.nrcresearchpress.com by 210.87.254.40 on 09/05/12
For personal use only.

Can. J. Chem. Downloaded from www.nrcresearchpress.com by 210.87.254.40 on 09/05/12
For personal use only.

DISCUSSION

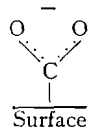
The spectrum shown in Fig. 1*a* corresponds to those we have obtained from mulls of basic zinc carbonate, and it is thought that in the presence of atmospheric water and CO_2, a surface carbonate was formed. This was decomposed on outgassing and simultaneously a steady decrease in the transmission of the sample occurred (Fig. 1, *b*, *c*). The latter phenomenon has been observed in previous work (7, 8, 9) and is generally ascribed to absorption by electrons in the conduction band. These may be produced by an increase in non-stoichiometry caused by loss of oxygen or the introduction of excess zinc. This readily explains why oxygen treatment restored the transmission since adsorbed oxygen atoms or molecules are known to act as electron traps. As the outgassing proceeded, three bands appeared at 1527, 1389, and 1333 cm^{-1}, those at 1527 and 1333 cm^{-1} in particular being apparently enhanced by the oxygen treatment (Fig. 1*d*). These peaks are unlikely to be due to nitrate impurity, as has been suggested by Matsushita and Nakata (7), as the same structure was obtained for samples prepared from the carbonate or the oxalate. The spectrum resembles that described by these authors, but a close correlation is not to be expected in view of the very different samples under investigation. The possibility that the two strong bands at 1527 and 1333 cm^{-1} arise from carboxylate residues can probably be discounted on the grounds that a sample outgassed at 570° C for 19 hours, and treated with oxygen as described above, still showed these two bands together with a third which appeared at 1350 cm^{-1}. In the unlikely event that CO_2^- surface impurities would remain stable under these conditions one would have to presume that the kinetic experiments which we are attempting to elucidate were similarly performed on samples containing the carboxylate group. We are at present unable to make definite assignments for the bands in question, but since they do not appear in the spectra of single crystals of zinc oxide, we believe that they may be associated with the defect structure of our material. During the adsorption of CO and CO_2 the two bands were apparently unchanged.

In the course of the outgassing treatment the physically adsorbed water was removed, but as can be seen from Fig. 1 a small concentration of hydroxyl groups remained. During the adsorption these bands were unperturbed and apparently took no part in the reaction.

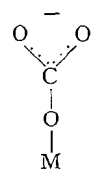
In the spectrum of CO at 25° (Fig. 2*a*) the peak at 2174 cm^{-1} appears similar to that observed at 2193 cm^{-1} (4.56 μ) by Eischens and Pliskin (10) in the oxidation of CO over NiO. They attributed this frequency to the asymmetric vibration of a structure of the type Ni—O⁻—C⁺≡O but failed to find any absorption in the 6- or 7-μ region corresponding to the symmetric vibration. In the present work, a band is observed at 1333 cm^{-1} (7.5 μ) which would be at the limit of their working range with Cabosil-supported samples and which may be considered a confirmation of their assignment. However, for symmetric and asymmetric vibrations to occur, the two bonds should be of similar order, which is not compatible with the observed fact that the peak at 2174 cm^{-1} is easily removed by pumping at room temperature. It would appear more likely that the interaction is of a weak dipolar nature, rather than a covalent one as suggested by Eischens. Since the small dipole in CO is $^-C{\equiv}O^+$, structures in which the oxygen is interacting with the negatively charged surface cannot be neglected. (For a discussion of oxygen chemisorption on zinc oxide surfaces and the resulting negatively charged surface species, see, for instance, Stone (11, 12) and Terenin and Solonitzin (8).) In a separate experiment, the gas desorbed after CO had been adsorbed on zinc

oxide for 10 minutes was examined mass spectrometrically. It was found to contain very little CO_2 (10^{-5} of the gas adsorbed), which favors the second interpretation.

The two principal regions of absorption at 1560 and 1330 cm^{-1} are close to the maxima shown by carboxylate ions such as formate and oxalate, and probably correspond to structures of the type:



The fact that a number of peaks is observed in each of these two regions may be because adsorption is occurring at different sites, giving species of essentially the same geometrical structure, but with a variety of surface-adsorbate bond strengths. Bicarbonates have been shown (13) to have a band between 1610 and 1630 cm^{-1} and another in the 1390–1410 cm^{-1} region. Eischens has observed bands at 1640 and 1390 cm^{-1} (6.1 and 7.2 μ) in the adsorption of CO_2 on NiO (10), which he attributes to structures of the type:



Although in our case CO_2 gave a band at 1618 cm^{-1} (6.18 μ) no absorption was found in the region 1430–1350 cm^{-1} (7.0–7.4 μ). However, it is difficult to assess how closely the spectra of structures of this type might be expected to resemble that of the bicarbonate ion and our failure to observe a band in the latter region does not necessarily rule out the existence of such structures. Apart from the bands at 2364, 1618, 1431, and 1230 cm^{-1}, all of which are strongly influenced by the removal of the ambient gas, the spectrum of CO_2 at 25° C corresponds very closely to that of CO at 155° C. This indicates that at 155°, CO does not exist on the surface, but is immediately oxidized to CO_2.

No absorption was observed in the region 1820–2080 cm^{-1}, which is normally associated with the C—O stretching mode in metallic carbonyls, nor was there any evidence for $\rangle C{=}O$ which might arise from bridged structures in which the carbon monoxide was adsorbed at dual sites. Carbonates normally give rise to strong absorption in the 7 μ region. Thus the band at 1431 cm^{-1} in the adsorbed CO_2 spectrum may be due to zinc carbonate, while the absence of bands in this region in either of the CO spectra would indicate that in these cases no carbonate was formed.

In order to assess the validity of a comparison between our results and those reported in the literature, the following facts should be taken into consideration: (*a*) The general qualitative aspects are the same in all cases, comprising fast room-temperature chemisorption which is reversible, and a slow chemisorption step above about 150°. (*b*) Kubokawa (5) has shown that oxygen pretreatment has no effect on either of the CO chemisorption steps, and he has concluded that CO chemisorption is independent of the

Can. J. Chem. Downloaded from www.nrcresearchpress.com by 210.87.254.40 on 09/05/12
For personal use only.

electronic state of the zinc oxide. However, it should be noted that his initial outgassing temperature (500°) was higher than ours, thus possibly giving rise to a higher Zn:O ratio in the bulk lattice. Also his outgassing temperature after exposure to oxygen (260°) would leave a smaller fraction of adsorbed oxygen on the surface. Our need for high surface areas coupled with infrared transparency has precluded duplication of this author's conditions. Although we do not at present believe the uncertainty arising out of this to be a serious one, it is hoped that work in progress may throw more light on this question.

REFERENCES

1. W. E. GARNER and J. MAGGS. Trans. Faraday Soc. **32**, 1744 (1936).
2. T. I. BARRY and F. A. BRIMELOW. United Kingdom Atomic Energy Authority Research Group. Atomic Energy Research Establ. 1/R 2745 (1958).
3. W. E. GARNER and F. J. VEAL. J. Chem. Soc. 1487 (1935).
4. Y. KUBOKAWA. Bull. Chem. Soc. Japan, **33**, 555 (1960).
5. Y. KUBOKAWA. Bull. Chem. Soc. Japan, **33**, 743 (1960).
6. L. H. LITTLE, H. E. KLAUSER, and C. H. AMBERG. Can. J. Chem. **39**, 42 (1961).
7. S. MATSUSHITA and T. NAKATA. J. Chem. Phys. **32**, 982 (1960).
8. A. TERENIN and YU. SOLONITZIN. Discussions Faraday Soc. **28**, 28 (1959).
9. A. REINHOLD. Naturwiss. **45**, 282 (1958).
10. R. P. EISCHENS and W. A. PLISKIN. Advances in Catalysis, **9**, 662 (1957).
11. F. S. STONE. Discussions Faraday Soc. **28**, 72 (1959).
12. T. I. BARRY and F. S. STONE. Proc. Roy. Soc. A, **255**, 124 (1960).
13. F. A. MILLER and C. H. WILKINS. Anal. Chem. **24**, 1253 (1952).

Can. J. Chem. Downloaded from www.nrcresearchpress.com by 210.87.254.40 on 09/05/12
For personal use only.

Can. J. Chem. Downloaded from www.nrcresearchpress.com by 210.87.254.40 on 09/05/12
For personal use only.

HIGH-TEMPERATURE STUDIES OF METALLURGICAL PROCESSES

PART I. THE THERMAL REDUCTION OF MAGNESIUM OXIDE WITH SILICON[1]

J. M. TOGURI[2] AND L. M. PIDGEON[3]

ABSTRACT

The rate of reaction (*a*) has been studied over the temperature range 1140–1460° C, by following the loss in weight of the reactants in high vacuum.

$$4MgO_{(s)} + Si_{(s)} = 2Mg_{(g)} + Mg_2SiO_{4(s)} \qquad (a)$$

The loss in weight of the reactants was found to be greater than that which can be accounted for by the above reaction. The excess weight loss was found to be due to a brownish, glassy deposit which appeared outside the reaction zone. This material was analyzed by X-ray diffraction and found to be an intimate mixture of Mg_2SiO_4 and Si. Experiments conducted showed that both of these materials are not appreciably volatile at 1350° C. This transfer of silicon and silicate is postulated to occur by the formation of gaseous SiO formed from the reaction mixture. Based on this assumption a possible mechanism for this reaction is postulated.

INTRODUCTION

The reduction of alkaline earth oxides by means of silicon proceeds theoretically according to the equation,

$$2MO_{(s)} + Si_{(s)} = SiO_{2\,(s)} + 2M_{(g)}. \qquad (I)$$

The reaction is reversible and generally proceeds from right to left at low temperatures with emission of heat and from left to right only at high temperatures with the absorption of heat. However, this simple equation is not followed and a secondary reaction always occurs in which the resulting silica combines with a certain amount of unreacted alkaline earth oxide, forming a silicate. Hence, when a theoretical reaction mixture is used according to reaction (I), only 1 mole of oxide is reduced from 2 moles of metal oxide and 1 mole of silicon and 1 mole of metal is formed, and $\frac{1}{2}$ mole silicon remains unused. In order to attain complete utilization of the reducing agent, it is necessary to have twice the amount of oxide as shown in equation (II).

$$4MO_{(s)} + Si_{(s)} = 2MO\cdot SiO_{2\,(s)} + 2M_{(g)}. \qquad (II)$$

In general, the reaction ceases when a dibasic silicate $2MO\cdot SiO_2$ has been formed. Jander (1) has shown that in a system of alkaline earth oxide – silica, the dibasic silicate is preferably formed.

Consequently, in the case of MgO, the reaction follows equation (II) where Mg replaces M.

This method of reduction of alkaline earth oxides by reducing agents producing a volatile metal and non-volatile oxide was known as early as 1878 (2). Schneider and Hesse (3) have studied this particular equilibrium, measuring the equilibrium pressure of magnesium using the transportation method with hydrogen as a carrier gas. From X-ray diffraction studies they identified the solid product as Mg_2SiO_4.

This reaction, however, has been found to be not as simple as is shown in equation (II). And, in order to have a better understanding of this reaction, it was investigated as a preliminary to the study of the calcined dolomite – silicon reaction.

[1]*Manuscript received October 21, 1960.*
Contribution from the Metallurgical Engineering Laboratory, based on a thesis submitted by J. M. Toguri in partial fulfillment of the requirements for the degree of Doctor of Philosophy to the School of Graduate Studies, of the University of Toronto, Toronto, Ontario.
[2]*Now at Norges Technishe Hogskole, Trondheim, Norway.*
[3]*Professor and Head of Department of Metallurgy, University of Toronto.*

Can. J. Chem. Downloaded from www.nrcresearchpress.com by 210.87.254.40 on 09/05/12
For personal use only.

EXPERIMENTAL PROCEDURES

The experimental method adopted for the determination of the reaction rate was to measure the weight loss of a briquetted mixture of reactants. By holding constant the particle size of the reactants and size and shape of the briquettes, the effect of rate-controlling factors could be determined.

The apparatus used in this investigation was described in detail in a previous paper (4). Briefly, it consists of a high-temperature vacuum furnace incorporating a thermobalance. The thermobalance was constructed from a helical wire spring such that continuous measurements of weight changes could be observed.

Finely powdered magnesium oxide of C.P. grade was used for all experiments. The silicon used was in the form of ferrosilicon, 200 mesh, the analysis of which was 96.7% Si. Briquettes of the reaction mixture were made in a 1-in. diameter mold at a pressure of 1500 p.s.i.

The reaction mixture contained 82% magnesium oxide and 18% ferrosilicon. This corresponds to a MgO:Si ratio of 3.33:1 or an excess of Si according to equation (II).

Three briquettes each weighing 10 g were placed in a graphite retort (Fig. 1) which was suspended in the furnace chamber from the helical wire spring. With this spring balance a weight change of 0.020 ± 0.005 g could be observed.

Blank runs using only MgO briquettes, prepared in the same manner as the reaction mixture, showed negligible weight losses due to reactions with the graphite retort over the temperature range 1100–1440° C. Thus, the weight loss of the briquetted reaction mixture was assumed to be due to the reaction between MgO and Si only. It is interesting

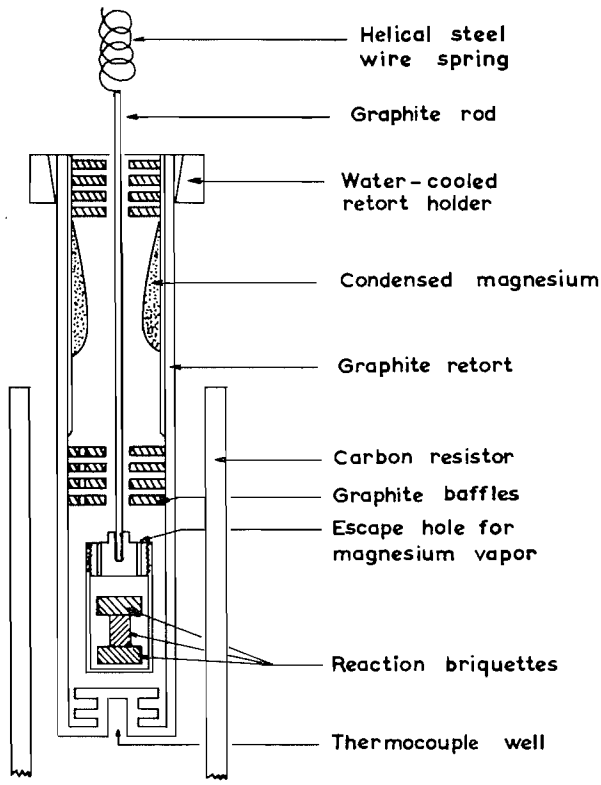


FIG. 1. Diagram of graphite retort.

to note that Kroll and Schlecten (5) found that, under high vacuum, carbon begins to react with MgO at a temperature of 1350° C. This value is lower by approximately 90° C than that determined above. This is to be expected, however, since Kroll and Schlecten used an intimate mixture of MgO and carbon, while in the present investigation a solid briquette of MgO was simply placed on the top of a surface of solid graphite.

The samples were in all cases heated to 750° C for 10 minutes, in order to effect degassing. After degassing, the length of the helical spring was measured by a cathetometer and the temperature of the furnace was increased to the required value. The time for reaching the operating temperature varied from 2 to 5 minutes. Loss in weight of the sample was then measured at constant intervals of time. During the experiments the vacuum of the system was maintained at a pressure of approximately one micron.

The bulk of the magnesium which evolved was successfully condensed as a dense deposit on the water-cooled walls of the condenser. There was no evidence of magnesium condensing on the graphite rod which supports the retort.

RESULTS AND DISCUSSION

The experimental results of this investigation are shown in Fig. 2 and Fig. 3. In Fig. 2

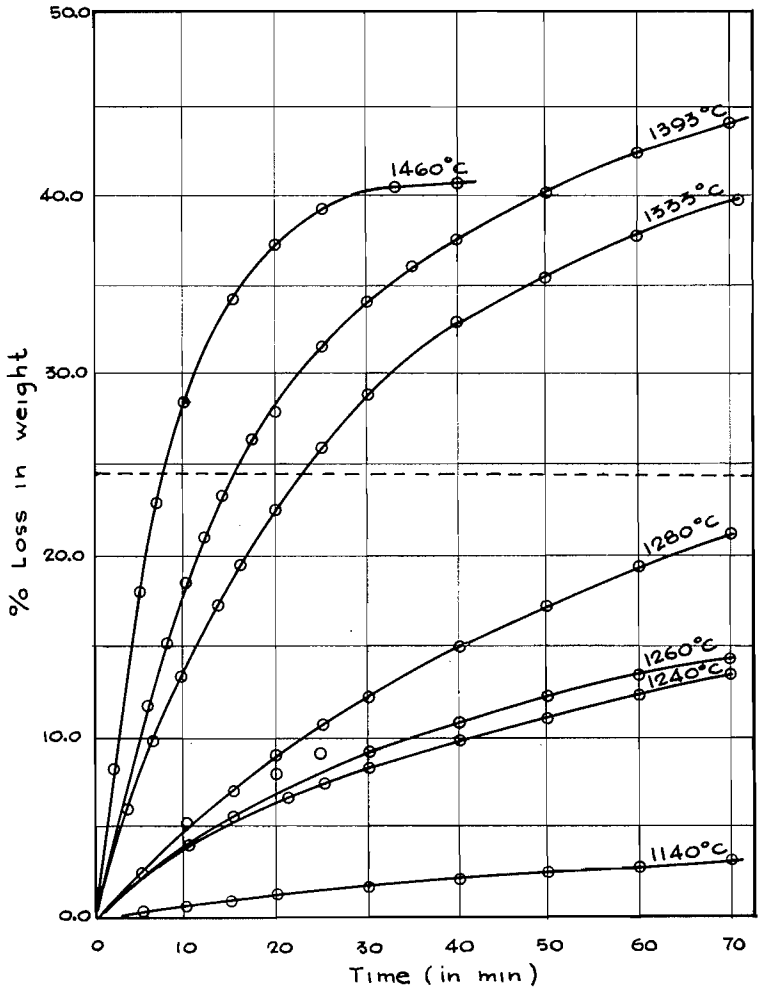


FIG. 2. Rate of reaction.

Can. J. Chem. Downloaded from www.nrcresearchpress.com by 210.87.254.40 on 09/05/12
For personal use only.

the percentage loss in weight of the reactant is plotted against time in minutes, while in Fig. 3 the percentage loss in weight of the reactant is plotted against temperature at

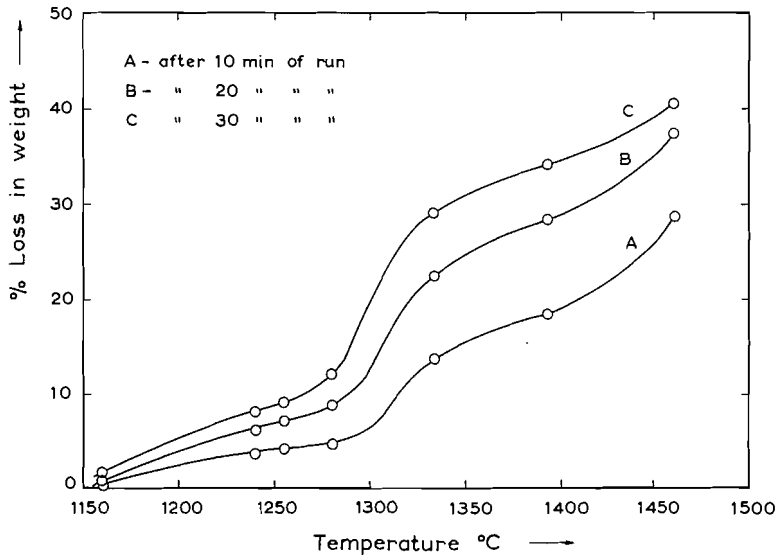


FIG. 3. Effect of temperature at constant time.

various constant times. A horizontal line is drawn through Fig. 2 to represent the maximum theoretical loss in weight, based on the magnesium evolution expected if MgO completely reacted according to equation (II).

The results at 1460° C show a tendency to level off after 25 minutes at temperature. This can be explained by the formation of liquid silicon at 1420° C which tends to agglomerate and thereby decrease the effective reaction surface.

Figure 3 shows a sharp change in the curve at about 1300° C. This suggests that another reaction involving a loss in weight becomes significant at this temperature.

After each experiment, the condenser containing the magnesium was weighed and it was found that the weight loss of the retort was always greater than the magnesium collected. Observation of the reaction retort after all experiments above 1280° C revealed a hard, glassy, brownish condensate on the baffles and condenser, the weight of which corresponded to the excess loss in weight.

On X-ray diffraction analysis, this material was found to be an intimate mixture of Mg_2SiO_4 and Si (compared with the A.S.T.M. Index), as shown in Fig. 4. The volatility of Mg_2SiO_4 and Si was independently investigated by heating each to a temperature of 1350° C. No measurable loss in weight could be observed after 1 hour of heating. The vapor pressure of silicon at 1350° C is approximately 10^{-3} mm of Hg (6). Thus, it was concluded that Mg_2SiO_4 and Si are not volatile at this temperature.

The presence of Mg_2SiO_4 and Si in the regions away from the reactor can be explained by the formation of gaseous silicon monoxide. It is known that when SiO_2 is heated with C, Si, and SiC or by the reduction of various silicates *in vacuo*, a brown distillate corresponding to the composition of SiO is produced. Zintl (7, 8) has suggested using solid SiO as a reducing agent for removing silica from siliceous compounds, or for reducing alkaline earth oxides according to the equation

$$3MO + SiO = M_2SiO_4 + M. \qquad (III)$$

Can. J. Chem. Downloaded from www.nrcresearchpress.com by 210.87.254.40 on 09/05/12
For personal use only.

Can. J. Chem. Downloaded from www.nrcresearchpress.com by 210.87.254.40 on 09/05/12
For personal use only.

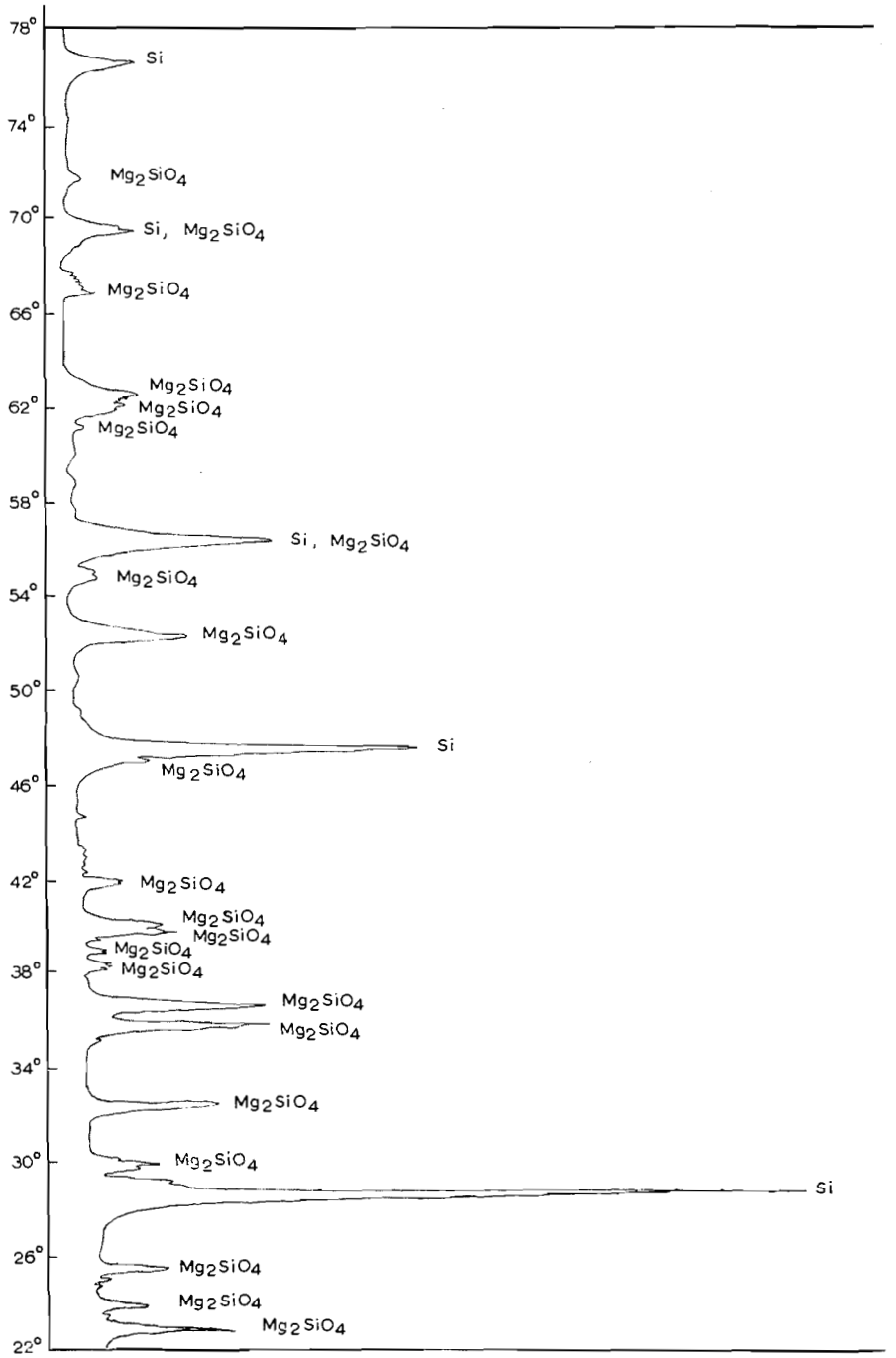


FIG. 4. X-Ray of brown condensate.

However, Brewer *et al.* (9, 10) reported in their extensive review of the literature on silicon monoxide that SiO solid appeared to be thermodynamically unstable at all temperatures, and that it disproportionated readily to Si and SiO_2. Spectrographic

TABLE I

The free-energy change for reactions under consideration

Eq. No.	Reaction	$\Delta G°$1550° K	Equilibrium pressure in mm Hg
IV	$MgO + Si = Mg + SiO$	47.8 kcal/mole Si	$P_{SiO} = 3.26\times10^{-1}$
V	$(4n+1)MgO+(1+n)Si = nMg_2SiO_4 + (1+2n)Mg + SiO$	44.9 kcal/mole Si	$P_{SiO} = 2.27\times10^{-1}$
VII	$2SiO + 2MgO = Mg_2SiO_4 + Si$	−27.0 kcal/mole MgO	$P_{SiO} = 1.18\times10^{-1}$

investigations have established unequivocally the existence of gaseous SiO. Kubaschewski and Evans (15) have recently summarized the thermodynamic data on gaseous SiO and their suggested value has been used in this discussion.

Of the number of reactions from which SiO can be formed, from a system containing MgO, Si, Mg_2SiO_4, and Mg gas, the most likely one according to thermodynamic calculations is

$$MgO + Si = Mg_{(g)} + SiO_{(g)}, \qquad (IV)$$

$$\Delta G°_{1550° K} = 47.8 \text{ kcal/mole Si.}$$

The over-all reaction can then be expressed by equation (V)

$$(4n + 1)MgO + (1 + n)Si = nMg_2SiO_4 + (1 + 2n)Mg_{(g)} + SiO_{(g)}, \qquad (V)$$

$$\Delta G°_{1550° K} = 44.9 \text{ kcal/mole Si when } n = 1.$$

The mole ratio of MgO:Si in equation (II) is 4:1, whereas in equation (V), assuming $n = 1$, the ratio is 2.5:1. The experimental ratio was 3.33:1. Therefore, according to equation (II) the reaction mixture should have an excess of silicon while according to equation (V) the reaction mixture should have an excess of magnesium oxide.

That the reaction between MgO and Si proceeds by equation (V) is substantiated by X-ray diffraction analysis of the residue. The diffraction patterns obtained in all experiments below 1280° C showed MgO, Mg_2SiO_4, and Si, while those above 1280° C showed only MgO and Mg_2SiO_4 even though excess Si was added to the reaction mixture according to equation (II). Since the residue shows in effect excess MgO, the formation of SiO cannot be due to the presence of excess silicon which might have continued its reducing action after most of the magnesium oxide had been removed from the system.

Reaction (V) would also explain the discrepancy in the weight loss of the reactants and the weight of the magnesium collected. The silicon monoxide gas that leaves the reaction zone disproportionates on reaching the cooler sections of the retort. The disproportionated product reacts with the magnesium gas coming from the reaction mixture as follows:

$$2SiO \rightarrow SiO_2 + Si,$$

$$2Mg + 2SiO_2 \rightarrow MgSiO_4 + Si,$$

the over-all reaction being represented by equation (VI).

$$4SiO + 2Mg = 3Si + Mg_2SiO_4. \qquad (VI)$$

The calculated equilibrium pressure of SiO above reaction (V) is 3.25×10^{-1} mm of Hg at 1300° C. The pressure of the system is of the order of 10^{-2} mm. Therefore one would expect the gaseous SiO to distill readily from the reactor. The discontinuity in the rate curve (Fig. 3) corresponds to the temperature at which the SiO distillation becomes significant.

Can. J. Chem. Downloaded from www.nrcresearchpress.com by 210.87.254.40 on 09/05/12
For personal use only.

Possible Reaction Mechanism

Although the present investigation does not permit a complete evaluation of the mechanism, a possible mechanism for the reaction between magnesium oxide and silicon, which accounts for the observed facts, may be expressed by the following equations. The initial reaction that occurs is that represented by equation (IV). The SiO that forms reacts with MgO according to

$$2SiO + 2MgO = Mg_2SiO_4 + Si, \qquad (VII)$$

$$\Delta G^\circ_{1550^\circ K} = -27.0 \text{ kcal/mole MgO.}$$

The calculated P_{SiO} over reactions (IV) and (VII) are 3.26×10^{-1} mm and 1.18×10^{-1} mm of Hg respectively at 1550° K. P_{SiO} must therefore be 1.18×10^{-1} mm of Hg before reaction (VII) will proceed. It is possible that the pressure of SiO is sufficient inside a reacting briquette for reaction (VII) to occur even though the residual pressure of the system is approximately 10^{-2} mm of Hg. At higher temperatures, however, SiO must be evolved faster by reaction (IV) than it can be removed by reaction (VII), thus resulting in distillation of SiO.

The reaction thus proceeds by a solid–solid and solid–gas mechanism. In both reactions (IV) and (VII), the silicons presumably occupy the magnesium sites in the oxide lattice, forming the orthosilicate. As this orthosilicate layer builds up around the silicon, diffusion of the oxygen anion outward to the silicon or diffusion of silicon to the magnesium oxide is necessary. Jander (1, 11) has indicated the rapidity at which alkaline earth oxides diffuse through the orthosilicate structure and this fact may also account for the diffusion process in the present reaction. According to equation (VII) any SiO molecules that react with MgO produce free silicon, which can act as a nucleus for further reaction. This phenomenon would decrease the diffusion path discussed above and may contribute in part to the explanation for the rapidity of this reaction.

The formation of Mg_2Si has been suggested as an intermediate in the reaction between magnesium oxide and silicon (12, 13). The phase diagram of the Mg–Si system shows only one-compound formation, Mg_2Si, with no solid solubility (14). In the present investigation Mg_2Si was heated to 1100° C in vacuum and complete dissociation according to equation (VIII) was observed on X-ray analysis.

$$Mg_2Si = 2Mg_{(g)} + Si. \qquad (VIII)$$

Furthermore when Si was replaced by Mg_2Si in the MgO–Si reaction, no difference in the rate was observed. X-Ray analysis of the residue from the MgO–Si reaction at various stages of the reaction showed no presence of magnesium silicides.

CONCLUSION

In the reaction between magnesium oxide and silicon, gaseous SiO is produced as well as magnesium. The reaction can be expressed by the equation

$$(4n + 1)MgO_{(s)} + (1 + n)Si_{(s)} = nMg_2SiO_{4\,(s)} + (1 + 2n)Mg_{(g)} + SiO_{(g)}.$$

The pressure of SiO appears to be appreciable above 1300° C.

A solid–solid, and solid–gas mechanism involving SiO is postulated for this reaction. An intermediate formation of Mg_2Si appears to be unlikely.

ACKNOWLEDGMENT

Support of this work through a fellowship (to J. M. T.) from the Steel Company of Canada is gratefully acknowledged.

Can. J. Chem. Downloaded from www.nrcresearchpress.com by 210.87.254.40 on 09/05/12
For personal use only.

REFERENCES

1. W. JANDER and E. HOFFMANN. Z. anorg. Chem. **218**, 211 (1934).
2. J. W. MALLET. Liebigs Ann. Chem. **190**, 62 (1878).
3. A. SCHNEIDER and E. HESSE. Z. Elektrochem. **46**, 279 (1940).
4. J. M. TOGURI and D. H. LAING. To be published.
5. W. J. KROLL and A. W. SCHLECTEN. J. Electrochem. Soc. **93**, 247 (1948).
6. J. L. MARGRAVE. Physico-chemical measurements at high temperature. *Edited by* Bockris, White, and Mackenzie. Butterworth Scientific Publications, London. 1959.
7. E. ZINTL. Z. anorg. Chem. **245**, 1 (1940).
8. E. ZINTL. U.S. Patent No. 2,286,663.
9. L. BREWER and R. K. EDWARDS. J. Phys. Chem. **58**, 35 (1954).
10. L. BREWER and F. T. GREENE. J. Phys. Chem. Solids, **2**, 286 (1957).
11. W. JANDER and E. WUHRER. Z. anorg. Chem. **226**, 225 (1936).
12. W. J. KROLL. U.S. Bureau of Mines I. C. 7327. 1945.
13. W. J. KROLL. Rev. mét. **48**, 929 (1951).
14. C. J. SMITHELLS. Metals reference book. Butterworth Scientific Publ., London. 1955.
15. O. KUBASCHEWSKI and E. L. L. EVANS. Metallurgical thermochemistry. Pergamon Press Ltd., London. 1958.

Can. J. Chem. Downloaded from www.nrcresearchpress.com by 210.87.254.40 on 09/05/12
For personal use only.

Can. J. Chem. Downloaded from www.nrcresearchpress.com by 210.87.254.6 on 09/05/12
For personal use only.

STEROIDS

I. 12β-METHYL-12a-HYDROXYPROGESTERONE[1]

GEORGE JUST AND R. NAGARAJAN

ABSTRACT

Lithium aluminum hydride reduction of 3α,12α-diacetoxypregnan-20-one (I*a*) gives as the major product pregnane-3α,12α,20β-triol (III), whereas the reduction of the corresponding dihydroxypregnanone I affords mainly the epimeric 3α,12α,20α-triol II. Triol III was transformed to 12β-methyl-12α-hydroxyprogesterone (VIII).

As part of a continuing study of the chemistry of steroids bearing functional groups in ring C, and of the interaction between substituents located at positions 12 and in the side-chain (1, 2), the preparation of 12-methyl-12-hydroxypregnane derivatives such as VI and VII was undertaken.

Engel and Huculak (3) have recently described the preparation of 3α,20β-dihydroxypregnan-12-one bis-methyl succinate (V*b*) through the sequence I*a* → III → III*b* → V*b*. This ketone V*b* appeared to us a useful intermediate for the introduction of a 12-methyl substituent.

Lithium aluminum hydride reduction of 3α,12α-diacetoxypregnan-20-one (I*a*) gave pregnane-3α,12α,20β-triol (III) and a small amount of material which Engel and Huculak (3) had tentatively formulated as pregnane-3α,12α,20α-triol (II). Chromic acid oxidation of this material to pregnane-3,12,20-trione (IV) confirmed this assignment of structure. In accordance to the findings of Sarett (4, see also refs. 3 and 5), the difference of increment of molecular rotation due to the acetylation of the 20β- and the 20α-hydroxy group was of the order of 200°.

Surprisingly, lithium aluminum hydride reduction of 3α,12α-dihydroxypregnan-20-one (I) gave as the major product pregnane-3α,12α,20α-triol (II). A more detailed study of the reduction revealed that the yield of the epimeric triols II and III depended on the solvent and on the nature of the functional group attached at position 12. The results are summarized in Table I.

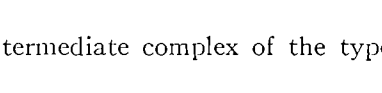
TABLE I

Starting material	Solvent	%II(20α-OH)	%III(20β-OH)
1. Diol I	Tetrahydrofuran	58.5	27.0
2. Diol I	Diethyl ether	65.8	10.2
3. Diacetate I*a*	Tetrahydrofuran	9.2	69.7*
4. Diacetate I*a*	Tetrahydrofuran	5.8	81 (3)
5. Diacetate I*a*	Diethyl ether	37	46.8

*No attempt was made in this case to obtain the maximum yield.

The reduction of the 20-keto diacetate I*a* to the 20β-triol III proceeds according to Cram's rule of steric control of asymmetric induction (6). The stereochemistry of the reduction of the 20-keto diol I to the 20α-triol II can be readily explained, if one assumes

[1]*Manuscript received November 7, 1960.*
Contribution from the Department of Chemistry, McGill University, Montreal, Que. This paper forms a part of the Ph.D. thesis of R. Nagarajan, to be presented to the Faculty of Graduate Studies, McGill University.

the formation of an intermediate complex of the type  . The carbonyl group is then reduced by another hydride molecule. Sicher *et al.* (7) have postulated a similar complex to explain why dehydrochloramphenicol and its *O*-acetate form threo- and erythro-chloramphenicol, respectively, upon Meerwein-Ponndorf reduction.

The co-ordination of the aluminum hydride alcoholate by the carbonyl group is competing with solvation by ether and tetrahydrofuran (8). As tetrahydrofuran is more basic than ether (9), one would expect less co-ordination of the 20-carbonyl oxygen in the lithium aluminum hydride reduction in tetrahydrofuran, and hence more 20β-alcohol III would be formed in that solvent. This hypothesis is confirmed by experimental evidence (Table I, columns 1 and 2).

An explanation of the solvent effect in the reduction of the diacetoxy ketone I*a* would follow similar lines. The only assumption which would have to be made is that the 20-keto group is reduced at a similar rate as the 12-acetate group. Reduction of keto diol I with a fivefold excess of sodium borohydride indicated the hindered nature of the 20-carbonyl group, since even after 20 hours it was not complete, as evident from infrared measurements. This experiment does lend some weight to the assumption made, without, however, proving it.

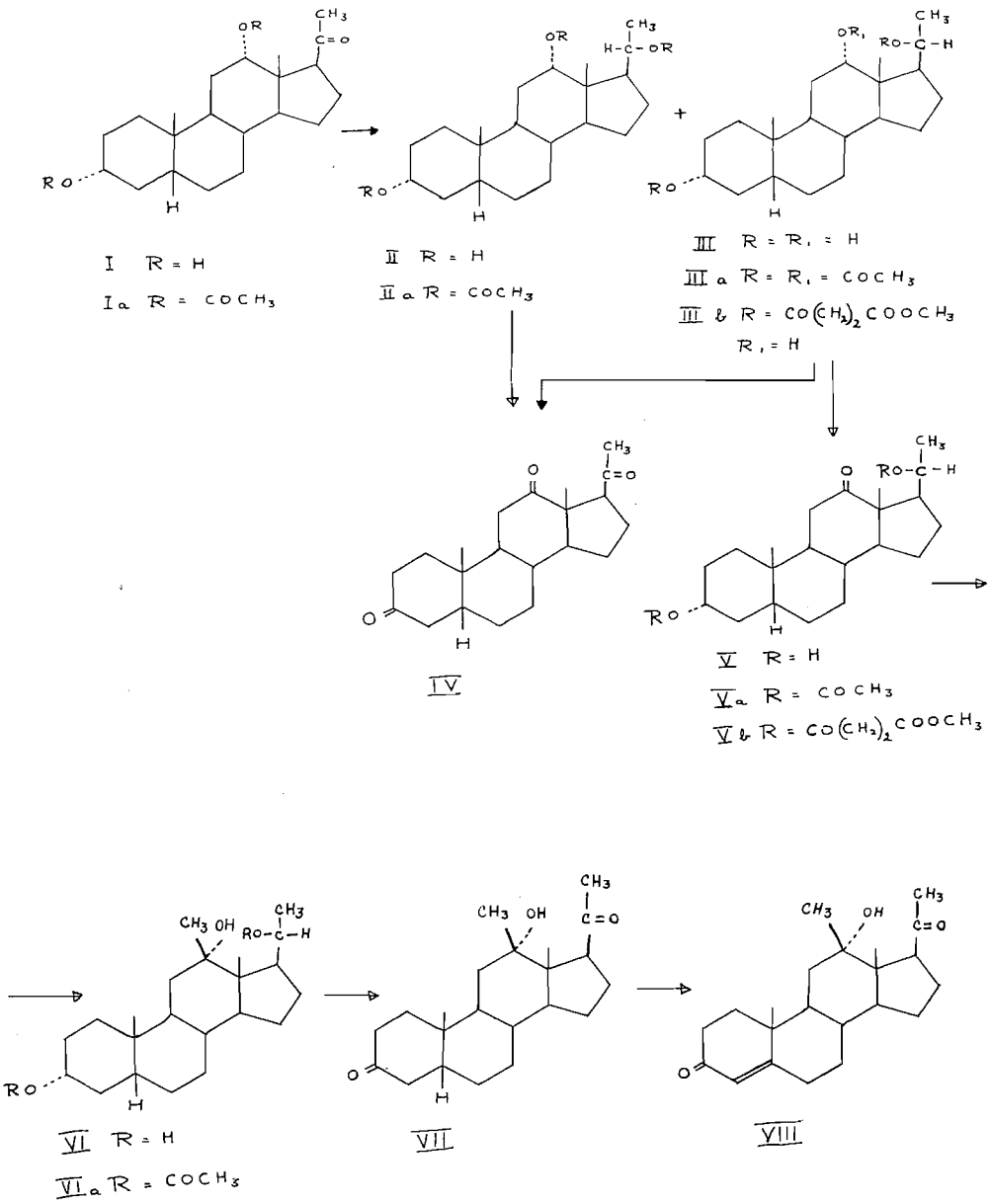
A co-ordination complex involving aluminum hydride would also account for the conversion of 17α-hydroxypregnan-20-ones by the action of lithium aluminum hydride to a mixture of 20β- and 20α-dihydroxypregnane derivatives, in which the latter predominated (5).

Succinylation of triol III to the succinate III*b* (3), followed by oxidation, afforded the 12-keto disuccinate V*b* (3). Prolonged treatment of the ketone V*b* with methyl magnesium iodide in diethyl ether led to a reaction mixture containing sizable amounts of starting material. The keto disuccinate V*b* was therefore hydrolyzed with methanolic potassium hydroxide to the dihydroxy ketone V, which was converted to the corresponding diacetate V*a*. Treatment of the 12-keto diacetate V*a* with excess ethereal methyl magnesium iodide for 20 hours gave a 73% yield of the desired 12β-methylpregnane-3α,12α,20β-triol VI. Triol VI formed a diacetate VI*a*, and was easily oxidized to 12β-methyl-12α-hydroxypregnane-3,20-dione (VII), thus establishing the tertiary nature of the 12-hydroxy group. The assignment of configuration of the 12-methyl group will be substantiated in a following paper. It is in disagreement with the assignment of configuration made by Levine and Wall (10) and Bladon and McMeekin (11), who transformed hecogenin to "12α-methyl-12β-hydroxy tigogenin".

Because of the considerable interest in steroid hormone analogues containing alkyl and other substituents in the steroid nucleus (see, e.g. 10, 11, 12), we decided to transform 12β-methyl-12α-hydroxypregnane-3,20-dione (VII) into the closely related 12β-methyl-12α-hydroxyprogesterone (VIII). This was readily achieved by bromination in position 4, followed by dehydrobromination (13). The progesterone analogue thus obtained did not exhibit any notable progestational, androgenic, diuretic, hypotensive, or anabolic properties.[2]

[2]*Biological tests were carried out by Dr. C. I. Chappel and Dr. Clara Revesz, Ayerst, McKenna and Harrison, Montreal.*

Can. J. Chem. Downloaded from www.nrcresearchpress.com by 210.87.254.6 on 09/05/12
For personal use only.



EXPERIMENTAL[3, 4, 5, 6]

Reduction of 3α,12α-Diacetoxypregnan-20-one (Ia) in Ether

A solution of the diacetate I*a* (14) (30.0 g, 0.0717 mole, m.p. 122–123°) in absolute ether (500 ml) was added with stirring to a solution of lithium aluminum hydride (33 g) in absolute ether (1500 ml). The reaction mixture was heated under reflux for 1 hour and

[3]*All the melting points were corrected.*
[4]*Only the best yields were reported.*
[5]*The commercially available aluminum oxide (Woelm) was used.*
[6]*The microanalyses were carried out by Dr. Alfred Bernhardt, Germany.*

Can. J. Chem. Downloaded from www.nrcresearchpress.com by 210.87.254.6 on 09/05/12
For personal use only.

left at room temperature overnight. The excess lithium aluminum hydride was destroyed by adding ethyl acetate (175 ml) and then 2 *N* sulphuric acid (450 ml). The solvents were removed by distillation and the reaction mixture extracted with chloroform. The chloroform layer was washed with 5% sodium bicarbonate solution, water, saturated sodium chloride solution, and dried over magnesium sulphate.

Repeated crystallizations from chloroform gave the 20α-alcohol II (8.902 g, 37.0%), m.p. 225–226°, $[\alpha]_D^{29}$ 46° (*c* 0.59 in $CHCl_3$). The substance was slightly hygroscopic. Crystallization from acetone did not change the melting point. Calcd. for $C_{21}H_{36}O_3$: C 74.98%, H 10.78%. Found: C 74.94%, H 10.66%.

Crystallization of the mother liquors from acetone gave the 20β-alcohol III (3) (11.260 g, 46.8%), m.p. 236–238°, $[\alpha]_D^{29}$ 34° (*c* 0.78 in $CHCl_3$).

Calcd. for $C_{21}H_{36}O_3$: C 74.98, H 10.78%. Found: C 74.84, H 10.61%.

Reduction of 3α,12α-Dihydroxypregnan-20-one (I) in Ether

A solution of the diol I (14) (1.414 g, 0.00423 mole, m.p. 168–172°; crude product obtained by alkaline hydrolysis of the diacetate I*a*) in absolute ether (200 ml) was added with stirring to a solution of lithium aluminum hydride (1.5 g) in absolute ether (100 ml). The reaction mixture was worked up as described above. The yields of 20α-alcohol II, m.p. 225–226°, and of 20β-alcohol III, m.p. 236–238°, were 65.5% and 10.5% respectively. The alcohols were identified by mixed melting point and comparison of I.R. spectra.

Reduction of 3α,12α-Dihydroxypregnan-20-one (I) in Tetrahydrofuran

A solution of the diol I (2.635 g, 0.00789 mole, m.p. 168–172°, crude product obtained by alkaline hydrolysis of the diacetate I*a*) in absolute tetrahydrofuran (200 ml) was added dropwise, with stirring, to a solution of lithium aluminum hydride (3.0 g) in absolute tetrahydrofuran (250 ml). The reaction mixture was worked up as described above. The yields of the 20α-alcohol II, m.p. 225–226°, and of 20β-alcohol III, m.p. 236–238°, were 58.5% and 27.2% respectively. The identity of the alcohols was confirmed by mixed melting point and superimposability of I.R. spectra.

Reduction of 3α,12α-Diacetoxypregnan-20-one (Ia) in Tetrahydrofuran (3)

A solution of the diacetate I*a* (30.9 g, 0.0739 mole, m.p. 122–123°) in absolute tetrahydrofuran (200 ml) was reduced with lithium aluminum hydride (36 g) in 1500 ml of absolute tetrahydrofuran (3). Chloroform extraction afforded 21.1 g (85% yield) of the crude product. Separation of the triols, as described above, afforded 2.40 g of the 20α-triol II (m.p. 221–224°, 9.5% yield), and 17.3 g of the 20β-triol III (m.p. 231–233°, 69.7% yield).

3α,12α,20α-Triacetoxypregnane (IIa)

Triol II (130 mg, m.p. 225–226°) was heated under reflux for 1 hour in pyridine (3 ml) and acetic anhydride (1 ml). The reaction mixture was worked up as usual and afforded, on crystallization from ether–hexane, the triacetate II*a*, m.p. 147–148°, $[\alpha]_D^{28}$ 95° (*c* 0.73 in $CHCl_3$).

Calcd. for $C_{27}H_{42}O_6$: C 70.09%, H 9.15%. Found: C 70.27%, H 9.20%.

3α,12α,20β-Triacetoxypregnane (IIIa)

Triol III (130 mg, m.p. 236–38°) was treated as described above. Crystallization of the crude product from ether–hexane yielded the triacetate III*a* (3), m.p. 201–202°, $[\alpha]_D^{28}$ 127° (*c* 0.81 in $CHCl_3$). The melting point was not depressed upon admixture with an authentic sample[7] and the I.R. spectra were identical.

[7]*Kindly supplied by Dr. C. R. Engel, Department of Chemistry, Laval University, Quebec.*

Can. J. Chem. Downloaded from www.nrcresearchpress.com by 210.87.254.6 on 09/05/12
For personal use only.

Pregnane-3,12,20-trione (IV)

In parallel runs, a solution of triol II and of triol III (300 mg) in acetic acid (15 ml) was treated with a solution of chromium trioxide (300 mg) in 3 ml of 90% acetic acid at room temperature for 20 hours. Extraction and crystallization gave in each case an 80–90% yield of IV (15), m.p. 203–205°. The identity of the samples in both cases was confirmed by mixed melting point and superimposability of I.R. spectra.

3α,12α,20β-Trihydroxypregnane 3α,20β-bis-Methyl Succinate (IIIb)

To a solution of the triol III (4.38 g) in pyridine (40 ml), succinic anhydride (10.2 g) was added. The reaction mixture was heated at 90° on a water bath for 4 hours, and left overnight at room temperature. It was diluted with ice-cold water (1500 ml) and left for 1 hour. The solution was extracted with ether, washed with 2 *N* sulphuric acid, and twice with water. The ethereal extract was dried over magnesium sulphate. Upon evaporation of the solvent to 250 ml, 4.054 g of the bis-hemisuccinate, m.p. 188–189°, crystallized.

Crystallization of mother liquors from acetone–hexane afforded 2.192 g, m.p. 188–189°.

Recrystallization for analysis raised the m.p. to 190–191° (m.p. 182–184° (3)).

Calcd. for $C_{29}H_{44}O_9$: C 64.91%, H 8.26%. Found: C 64.79%, H 8.35%.

A solution of the bis-hemisuccinate (6.152 g) in ether (1500 ml) was methylated with an excess of diazomethane in ether. One crystallization from ether–hexane afforded 5.855 g of III*b* (3), m.p. 96–97°, $[\alpha]_D^{29}$ 67° (*c* 0.97 in $CHCl_3$). Crystallization of the mother liquors gave 0.257 g of III*b*, m.p. 94–95° (yield 84%).

3α,20β-Dihydroxypregnan-12-one bis-Methyl Succinate (Vb)

Oxidation with chromium trioxide in acetic acid of the bis-methyl succinate III*b* (6.025 g) afforded 5.971 g of the keto bis-methyl succinate V*b* (3), m.p. 112–113°, $[\alpha]_D^{29}$ 110° (*c* 0.91 in $CHCl_3$).

3α,20β-Dihydroxypregnan-12-one (V)

To a solution of the keto bis-methyl succinate V*b* (10.0 g) in methanol (700 ml) and water (100 ml) was added potassium carbonate (12.5 g) and the mixture was refluxed for 17 hours. The major part of the methanol was distilled off *in vacuo*. The reaction mixture was worked up as usual and on crystallization from acetone–hexane, 2.868 g of the hydroxy ketone V, m.p. 221–222°, was obtained. The I.R. spectrum of the mother liquors showed that the hydrolysis was not complete. The mother liquors were further hydrolyzed with 5% methanolic potassium hydroxide for 8 hours at reflux temperature and worked up as usual. Crystallization from acetone–hexane afforded 3.044 g of the hydroxy ketone V, m.p. 220–222° (yield 96%).

A portion of the hydroxy ketone V was crystallized twice from acetone–hexane for analysis, m.p. 222–223°, $[\alpha]_D^{29}$ 131° (*c* 0.95 in $CHCl_3$).

Calcd. for $C_{21}H_{34}O_3$: C 75.41, H 10.24. Found: C 75.20, H 10.06.

3α,20β-Diacetoxypregnan-12-one (Va)

A solution of the hydroxy ketone V (400 mg) in pyridine (10 ml) and acetic anhydride (10 ml) was kept in a water bath at 90° overnight. Ether extraction gave 511 mg of crude product. One crystallization from ether–hexane yielded 416 mg of the ketone V*a*, m.p. 136–137°. Crystallization of mother liquors afforded 53 mg of V*a*, m.p. 135–136° (yield 93%).

Can. J. Chem. Downloaded from www.nrcresearchpress.com by 210.87.254.6 on 09/05/12
For personal use only.

A portion of ketone V*a* was crystallized twice from ether–hexane for analysis, m.p. 136–137°, $[\alpha]_D^{29}$ 179° (*c* 1.09 in $CHCl_3$).

Calcd. for $C_{35}H_{28}O_5$: C 71.73, H 9.15. Found: C 71.91, H 9.25.

12β-Methyl-3α,12α,20β-trihydroxypregnane (VI)

To 200 ml of an ethereal solution of methyl magnesium iodide (from 270 mg of magnesium and 0.7 ml of methyl iodide) was added with stirring 575 mg of the ketone V*a*, dissolved in 200 ml of absolute ether. The reaction mixture was refluxed for 20 hours. A solution of ammonium chloride (10 g) in water (200 ml) was added to the reaction mixture. It was then extracted with ether and the organic solution washed with water until neutral. The ethereal extract was dried over magnesium sulphate. On evaporating the major part of the ether, crystals of the triol VI (110 mg, m.p. 213–214°) were obtained. Crystallization of mother liquors afforded 98 mg of the triol VI, m.p. 210–213°.

Recrystallizations from aqueous methanol and methanol raised the m.p. to 213–215°, $[\alpha]_D^{29}$ 39° (*c* 0.88 in $CHCl_3$).

Calcd. for $C_{22}H_{38}O_3$: C, 75.37, H 10.92. Found: C 75.21, H 10.92.

The mother liquors were acetylated and the resulting oil (435 mg) chromatographed on alumina (4.5% water). The hexane–benzene (4:1) fractions consisted mainly of the unreacted ketone. Hexane–benzene (1:1) fractions were collected and on crystallization from hexane gave 73 mg of the diacetate VI*a*, m.p. 119–121°. The mother liquors on crystallization from hexane afforded 15 mg of the diacetate VI*a*, m.p. 119–121°.

A portion of the diacetate VI*a* was crystallized twice from hexane for analysis, m.p. 122–124°, $[\alpha]_D^{29}$ 78° (*c* 1.01 in $CHCl_3$).

Calcd. for $C_{26}H_{42}O_5$: C 71.86, H 9.74. Found: C 71.66, H 9.99.

The mother liquors of the hexane–benzene (1:1) fractions and the remainder of the fractions of the chromatogram afforded upon alkaline hydrolysis and crystallization from ether–hexane 71 mg of the triol VI, m.p. 208–210° (yield 73%).

12β-Methyl-12α-hydroxypregnane-3,20-dione (VII)

Chromium trioxide (490 mg) in 90% acetic acid (5 ml) was added with stirring to a solution of the triol VI (750 mg) in acetic acid (50 ml) and left at room temperature overnight. Ether extraction afforded 723 mg of the crude hydroxy ketone VII, m.p. 184–186°. One crystallization from acetone–hexane gave 663 mg of the hydroxy ketone VII, m.p. 187–188°. Crystallization of mother liquors afforded 15 mg of VII, m.p. 186–187° (yield 92%).

A portion of the hydroxy ketone VII was crystallized twice from acetone–hexane for analysis, m.p. 187–188°, $[\alpha]_D^{29}$ 102°, (*c* 1.05 in $CHCl_3$).

Calcd. for $C_{22}H_{34}O_3$: C 76.25, H 9.89. Found: C 76.10, H 9.87.

12β-Methyl-12α-hydroxyprogesterone (VIII)

A solution of bromine (141 mg) in acetic acid (9.4 ml) was added to a solution of the hydroxy ketone VII (300 mg) in acetic acid (10 ml) with stirring. After 5 minutes, the reaction mixture was poured into ice-water (500 ml), and extracted with ether. The organic layer was washed with water and dried. There was obtained 395 mg of an oil which resisted crystallization.

The crude bromo ketone was dehydrobrominated according to the method of McGuckin and Kendall (13). The crude product (240 mg of oil) on crystallization from ether–hexane afforded 125 mg of the progesterone derivative VIII, m.p. 140–150°. Repeated

Can. J. Chem. Downloaded from www.nrcresearchpress.com by 210.87.254.6 on 09/05/12
For personal use only.

crystallizations gave 97 mg of analytically pure VIII, m.p. 152–153°, $[\alpha]_D^{29}$ 182° (*c* 1.01 in $CHCl_3$), λ_{max}^{EtOH} 239 mμ, (ε 17500), $\nu_{max}^{CCl_4}$ 1710 cm^{-1} (20-ketone), 1680 cm^{-1}, 1620 cm^{-1} (Δ^4-3-ketone).

Calcd. for $C_{22}H_{32}O_3$: C 76.68, H 9.37. Found: C 76.40, H 9.40.

ACKNOWLEDGMENTS

We wish to thank the National Research Council, Messrs. Ayerst, McKenna and Harrison, and the Department of Chemistry, McGill University, for generous financial support.

REFERENCES

1. Ch. R. Engel, K. F. Jennings, and G. Just. J. Am. Chem. Soc. **78**, 6153 (1956).
2. G. Just and Ch. R. Engel. J. Org. Chem. **23**, 12 (1958).
3. Ch. R. Engel and W. Huculak. Can. J. Chem. **37**, 2031 (1959).
4. L. H. Sarett. J. Am. Chem. Soc. **71**, 1175 (1949).
5. D. K. Fukushima and E. D. Meyer. J. Org. Chem. **23**, 174 (1958), and references cited therein.
6. D. J. Cram and F. A. Abd Elhafez. J. Am. Chem. Soc. **74**, 5828 (1952).
7. J. Sicher, M. Svoboda, M. Hrdá, J. Rudinger, and F. Šorm. Collection Czechoslov. Chem. Commun. **4**, 487 (1953).
8. N. L. Paddock. Chem. & Ind. (London), 63 (1953).
9. H. C. Brown and R. M. Adams. J. Am. Chem. Soc. **64**, 2557 (1942).
10. S. G. Levine and M. E. Wall. J. Am. Chem. Soc. **82**, 3391 (1960).
11. P. Bladon and W. McMeekin. J. Chem. Soc. 2191 (1960).
12. B. G. Christensen, R. G. Strachan, N. R. Trenner, B. H. Arison, R. Hirschmann, and J M. Chemerda. J. Am. Chem. Soc. **82**, 3995 (1960).
13. W. F. McGuckin and E. C. Kendall. J. Am. Chem. Soc. **74**, 5811 (1952).
14. W. H. Hoehn and H. L. Mason. J. Am. Chem. Soc. **60**, 1493 (1938).
15. T. Reichstein and E. v. Arx. Helv. Chim. Acta, **23**, 747 (1940).

Can. J. Chem. Downloaded from www.nrcresearchpress.com by 210.87.254.6 on 09/05/12
For personal use only.

Can. J. Chem. Downloaded from www.nrcresearchpress.com by 210.87.254.105 on 09/05/12
For personal use only.

THE DEMETHYLATION OF SUGARS WITH HYDROGEN PEROXIDE[1]

B. FRASER-REID, J. K. N. JONES, AND M. B. PERRY

ABSTRACT

Demethylation of methylated sugars can be achieved using hydrogen peroxide and ferrous iron (Fenton's reagent). The reaction is not specific and further oxidation of the sugar also occurs. The preparation of 3,4-di-*O*-methyl-D-mannose from the corresponding mannitol derivative is described. Mono-*O*-methyl derivatives of D-mannose and of D-mannitol as well as D-mannose and D-mannitol were also produced. The course of the demethylation of 2,3,4,6-tetra-*O*-methyl methyl α-D-glucoside by Fenton's reagent has been examined.

Hydrolysis of methylated yeast mannan yields 3,4-di-*O*-methyl-D-mannose as a major component of the methylated sugars (1, 2). No simple method is available for the synthesis of this sugar but Aspinall and Zweifel (3) have shown how it may be obtained from D-mannose by a rather long and involved route.

As early as 1894, Fenton (4) showed that ferrous iron had a specific influence on the oxidation of hydroxyl-containing compounds by hydrogen peroxide and other oxidizing agents. He showed, for example, that it was possible to convert various polyhydric alcohols into the corresponding aldoses (5). This method suggested itself to us as convenient for the conversion of 3,4-di-*O*-methyl-D-mannitol to 3,4-di-*O*-methyl-D-mannose, the starting material being readily available from 1,2-5,6-di-*O*-isopropylidene-D-mannitol. An attraction of this scheme is the symmetry of the dimethyl mannitol, which ensures that only one aldohexose would be produced regardless of which end of the molecule was oxidized.

It was surprising, therefore, to find that, when 3,4-di-*O*-methyl-D-mannitol was oxidized by Fenton's reagent in ice-cold solution and the resulting solution analyzed chromatographically, sugars corresponding to mannitol, mannose, and their mono-*O*-methyl and di-*O*-methyl derivatives were detected, as well as methylated pentoses and uronic acids. Repetition of this experiment under a variety of conditions confirmed these observations.

Because of the strangeness of these findings we investigated the action of the reagent on a fully methylated sugar. It was observed that 2,3,4,6-tetra-*O*-methyl methyl α-D-glucoside was demethylated to yield among other products D-glucose and the possible mono-, di-, tri-, and tetra-*O*-methyl-D-glucoses. Our analyses of the mixture of monomethyl glucoses so obtained indicate that the methoxyl groups on carbons 2 and 4 are most strongly attacked, those on carbon 6 next strongly, and those on carbon 3 least strongly attacked.

Saunders (6) has shown that, under the catalytic influence of the enzyme ferriperoxidase, hydrogen peroxide will oxidize *p*-anisidine to 2-amino-5-*p*-anisidino benzoquinone di-*p*-methoxyphenylimine with elimination of one methoxyl group. But as far as we are aware the observations described above are the first in which the elimination of methoxyl groups by oxidation from sugar residues has been described.

It is well established that the ferrous–peroxide system produces hydroxyl radicals and the reaction sequence first formulated by the Haber–Weiss theory (7) was later confirmed and expanded by Evans (8). Waters *et al.* (9, 10) have shown that the kinetics of the system is consistent with the thesis that the oxidizing species is the free radical. Grinstead

[1]*Manuscript received November 23, 1960.*
Contribution from the Department of Chemistry, Queen's University, Kingston, Ontario.

(11, 12) has suggested how they may attack various substrates and Waters (9, 10) has postulated that the radical attacks primary hydroxyl groups as follows (scheme A).

$$RCH_2OH + OH\cdot \rightarrow R\dot{C}HOH + H_2O$$
$$R\dot{C}HOH + HO{-}{-}OH \rightarrow \cdot OH + RCH(OH)_2$$
$$R\dot{C}HOH + OH\cdot \rightarrow RCH(OH)_2$$
$$RCH(OH)_2 \rightarrow RCHO + H_2O$$

SCHEME A

This scheme explains the oxidation of hexitol to hexose. The latter may then be further oxidized to a hexonic acid, and if oxidized further a pentose may arise by oxidative decarboxylation, a well-known reaction in carbohydrate chemistry.

We suggest that the hydroxyl free radical is also the demethylating species and that the scheme operates as follows (scheme B).

1. $R\cdot OCH_3 + OH\cdot \rightarrow RC\cdot OH_2\cdot + H_2O$
2. $ROCH_2\cdot + HO{-}{-}OH \rightarrow ROCH_2OH + OH\cdot$
3. $ROCH_2\cdot + OH\cdot \rightarrow ROCH_2OH$
4. $ROCH_2OH \rightarrow ROH + HCHO$

SCHEME B

Cleavage of the $R{-}{-}OCH_3$ bond seems unlikely because (*a*) this would involve the more complex radical abstraction of $-{-}OCH_3$ and (*b*) some inversion of configuration at the reaction center might be expected, especially in view of the absence of steric hindrance in the zigzag form of the hexitol in solution. No products resulting from such an inversion have been detected. The electronegativity of the hydroxyl radical should render it capable of such hydrogen abstraction (cf. ref. 13). Quantitative experiments with 2,3,4,6-tetra-*O*-methyl methyl-α-D-glucoside indicated that the reducing power of the reaction mixture, after acidic hydrolysis, was increased only by 27% of the theoretical value. This indicated that the glucosidic methoxyl group was attacked to the extent of 73%. In neutral solution demethylation proceeds only to a limited extent.

If the hydroxyl radical is engaged in both oxidation and demethylation then some competition for the radical to be involved in either of the processes (schemes A and B) is to be expected. Tables I and II record the conditions and results of experiments. In these tables the relative order of intensity of sugars as detected chromatographically is given in the form 1 > 2 > 3, etc. The reaction was initially exothermic and was accompanied by a considerable evolution of carbon dioxide. The solution rapidly became acidic

TABLE I

Experiment	Dimethyl mannitol (g)	Ferrous sulphate (g)	15% H_2O_2 (ml)	Temp. (°C)
A	1.0	—	5	23–25
B	1.0	1.0	5	"
C	1.0	0.1	5	"
D	1.0	0.1	5	0–5
E	1.0	0.1	10	0–5
F	1.0	0.1	2.5	0–5

Can. J. Chem. Downloaded from www.nrcresearchpress.com by 210.87.254.105 on 09/05/12
For personal use only.

TABLE II

Experiment	Mannose	Monomethyl mannose	Dimethyl mannose	Pentose*	Unreacted dimethyl mannitol	Reducing group†
A	None	None	None	None	1	<1
B	1	2	3	Trace	4	40
C	3	3	3	2	1	20
D	4	3	2	Trace	1	36
E	2	Trace	None	1	None	13
F	2	2	2	Trace	1	54

*Free, mono-, and di-methyl.
†As percentage from available primary alcohol.

(pH 6 → pH 1) (cf. ref. 14). From the percentage of reducing groups produced it is clear that much of the hexitol is converted into reducing sugars and then further oxidized to aldonic acids. Osones were not detected, nor was formaldehyde. The latter was presumably further oxidized to carbon dioxide. After completion of the reaction, the solution in certain cases (see Experimental Section) was neutralized and deionized and the products separated chromatographically. It is clear that in the absence of ferrous sulphate no demethylation occurs and that a decrease in the concentration of ferrous sulphate or in the temperature of the reaction mixture results in less demethylation. High concentration of hydrogen peroxide and high temperatures favor the formation of pentoses and non-reducing acidic materials.

We have also investigated the fate of anisole when subjected to Fenton's reagent at 0–3° C. The reaction is only very slightly exothermic and an immediate dirty-green color is produced on the addition of peroxide. At least four phenolic products have been obtained, one being identified (by paper chromatography) as guaiacol. Infrared analyses indicate that very little of the methoxyl group is removed. Thus it appears that the aromatic nucleus is much more readily attacked than is the methoxyl group.

The removal of the methyl group from a methoxyl group by hydroxyl radicals is of biochemical interest because a similar mechanism may be operative in some organisms.

EXPERIMENTAL

The following solvent systems were used to separate sugars on paper chromatograms: (i) butan-1-ol, ethanol, water (3:1:1) and (ii) butan-1-ol, pyridine, water (10:3:3) (all vol/vol). Reducing sugars were detected with (*a*) the *p*-anisidine hydrochloride spray (15) and components with adjacent hydroxyls (reducing and non-reducing) were detected with (*b*) 0.1 *M* sodium periodate followed after about 5 minutes with the *p*-anisidine spray (cf. ref. 16).

Phenols were separated by reverse phase chromatography on paper (Whatman No. 1) previously impregnated with 10% tetrahydro naphthalene in methanol and allowed to dry in air. The irrigant was water:methanol (8:2) and the phenols on the air-dried chromatogram were sprayed with a solution of sulphanilic acid followed immediately after with 20% sodium bicarbonate solution (17).

Paper electrophoresis was performed on Whatman 3mm paper saturated with borate buffer pH 10 at ca. 1500 volts for 1–1½ hours (18, 19).

Deionizations were effected by passing the solution down columns of Amberlite IR120 (H^+ form) followed by passage through Duolite A4 (OH^- form). All solutions were concentrated under diminished pressure below 50° C.

Can. J. Chem. Downloaded from www.nrcresearchpress.com by 210.87.254.105 on 09/05/12
For personal use only.

Melting points and mixed melting points were determined simultaneously on a standard Fischer-Johns block and the values quoted are uncorrected. Optical rotations were determined in water ($C = 1$).

Chromatographic fractionations were effected by placing the syrup on a cellulose column in the usual manner (20). The columns were irrigated with butan-1-ol, light petroleum mixture (4:1) to remove tri-*O*- and higher methylated sugars; butan-1-ol – water mixture (95:5) was used to remove the lower methylated and free sugars. In every case the combined fractions were concentrated to a syrup which was purified by deionization and by refluxing their solutions in methanol with decolorizing charcoal.

PART I

Preparation of 3,4-Di-O-methyl-D-mannitol

3,4-Di-*O*-methyl-D-mannitol (m.p. 145–147° C) was prepared by methylation (Kuhn's method (21,22)) of 1,2–5,6-di-*O*-isopropylidene-D-mannitol, the latter being prepared from D-mannitol (23).

Oxidation of 3,4,Di-O-methyl-D-mannitol

To a solution of dimethyl mannitol (15 g) in water (100 ml) ferrous sulphate (45 g) was added with stirring. When solution was complete hydrogen peroxide (75 ml, 15%) was added gradually during 1½ hours and the temperature of the solution was maintained between 20–25° C by use of an ice-water bath. After the addition the reaction mixture was kept with stirring at room temperature for an additional 2 hours. The solution was neutralized and the precipitate was removed by filtration and the light-green-colored filtrate deionized. The solution was concentrated to give a syrup (9.5 g) which was fractionated on a cellulose column.

Fraction I gave a syrup which chromatographed as a single spot corresponding to authentic 3,4-di-*O*-methyl-D-mannose. This was crystallized from ethanol–ether. The crystals so deposited melted between 90–95° C and were possibly a mixture of the hydrated and anhydrous forms. The mixture was redissolved in dry acetone–ether and after about 6 weeks spherically shaped crystals had deposited, m.p. 77–79° C, mixed m.p. 78–81° C, $[\alpha]_D^{20} = 16.6°$ (initial) $\rightarrow 8°$ (after 24 hours, constant value) (cf. Aspinall and Zwiefel (3)).

Fraction II was identified as unchanged 3,4-di-*O*-methyl-D-mannitol.

Fraction III was identified chromatographically as a mixture of mono-*O*-methyl-D-mannoses. The purified syrup was dissolved in water (100 ml) (solution A) and the solution was used for further experiments.

Preparation and Analysis of Monomethyl Mannosides

The above solution (20 ml corresponding to 65 mg of syrup) was removed and evaporated to a syrup which was converted to the glycosides in the usual manner (see glycosidation of monomethyl glucoses below). The syrupy glycosides were purified by twice extracting them under reflux with ethanol, and once with water in the presence of decolorizing charcoal. The product was dried at 50° C (P_2O_5) to a constant weight (40.9 mg). This syrup was dissolved in water, diluted to 50 ml and periodate oxidation studies were conducted on 40 ml (≡ 32.7 mg) of the solution so prepared (31, 32). (See experimental on monomethyl glucose below.) After 35 hours the periodate uptake had a constant value of 0.41 mole, and the formic acid liberation was negligible (0.01 mole). These results indicate that approximately 40% of the monomethyl mannose is present as the 4-*O*-methyl isomer.

Can. J. Chem. Downloaded from www.nrcresearchpress.com by 210.87.254.105 on 09/05/12
For personal use only.

The oxidized solution was deionized and the deionized solution hydrolyzed with 2 *N* sulphuric acid. The hydrolyzate was neutralized with barium carbonate, filtered, deionized, and analyzed qualitatively by paper electrophoresis using authentic 3-*O*-methyl-D-mannose as standard. The presence of this isomer was clearly indicated.

Reduction of Monomethyl Mannose

Potassium borohydride (0.2 g) was added to solution A (30 ml) and the mixture was left at room temperature overnight, after which it gave a negative reaction to Fehling's solution. The solution was neutralized by adding Amberlite resin IR120 (H^+ form), filtered, and the filtrate was evaporated to dryness. The boric acid was removed by repeated codistillation with methanol. The resulting product was twice crystallized from ethanol, and then dried at 65° C to give white crystals; m.p. 133–134° C; $[\alpha]_D^{25} = +18°$, in good agreement with Hudson's constants for 3(4)-*O*-methyl-D-mannitol (24). Thus both sugars give one product upon reduction and this indicates conclusively that the two components are 3-*O*-, and 4-*O*-monomethyl-D-mannoses.

Fraction IV was monomethyl mannitol. The clear syrup was crystallized from ethanol. The dried crystals melted at 131–133° C and when mixed with the reduced monomethyl mannose above melted at 131–133° C. This fraction therefore contains only one component, which was identified as 3-*O*-monomethyl-D-mannitol (equivalent to the 4-*O*-methyl isomer).

Fraction V was identified as D-mannose. To the syrup obtained after purification 0.23 g phenylhydrazine reagent (6 ml) (1 g phenylhydrazine hydrochloride, 2.4 g sodium acetate, 0.6 ml acetic acid, and 25 ml water) was added. An almost immediate precipitate of D-mannose phenylhydrazone formed. The crystals were removed and recrystallized from ethanol. They had m.p. 190–191° C, mixed m.p. 191–192° C.

Fraction VI was identified as D-mannitol. The purified syrup was crystallized from methanol; m.p. 166–168° C, mixed m.p. 165–168° C.

PART II

Preparation of 2,3,4,6-Tetra-O-methyl Methyl-α-D-glucoside

Tetramethyl methyl glucoside was prepared by a Kuhn (21, 22) type methylation of reagent grade methyl-α-D-glucoside. The product had a refractive index of 1.4449 at 20° C [the accepted value is 1.4454 (25)].

Oxidation of 2,3,4,6-Tetra-O-methyl Methyl-α-D-glucoside

The glucoside (6 g) was dissolved in water (30 ml) and ferrous sulphate (36.6 g) was added with stirring. Hydrogen peroxide (50 ml, 15%) was added cautiously with stirring and the temperature was maintained between 20–25° C. After 18 hours at room temperature the mixture was neutralized with barium carbonate. The solution was filtered and the pale green filtrate was made 2 *N* with respect to sulphuric acid and the solution was boiled under reflux for 3½ hours. The cooled solution was neutralized (barium carbonate), filtered, and deionized and the solution evaporated to a syrup (0.992 g). A second oxidation was carried out using the same quantities of reagents but a smaller quantity of hydrogen peroxide.

The combined syrups (2.55 g) were fractionated on a cellulose column.

Fraction I was identified by paper chromatography as 2,3,4,6-tetra-*O*-methyl-D-glucose (260 mg). A partial crystallization occurred overnight. The crystals were removed and converted to the *N*-phenyl glucosylamine by the method of Wolfrom (26). The product had m.p. 133–135° C; mixed m.p. 132–135° C.

Can. J. Chem. Downloaded from www.nrcresearchpress.com by 210.87.254.105 on 09/05/12
For personal use only.

Fraction II (tri-*O*-methyl-D-glucoses) yielded a syrup (274 mg) which was a mixture. It was made up to a known volume (solution A) in water.

Detection of 2,3,4-Tri-O-methyl-D-glucose

A portion of solution A equivalent to ca. 20 mg of sugars was evaporated to a syrup which was then dissolved in phosphate buffer (10 ml, pH 7.4). The solution was then saturated with sodium periodate and left overnight at room temperature (solution B). To the oxidized solution (5 ml) excess inositol was added to destroy excess of periodate and acetyl acetone (3 ml) added. Within 1 minute a strong fluorescence developed indicative of the presence of formaldehyde (27). A blank of water treated similarly failed to show any fluorescence even when viewed under ultraviolet light.

Bell has shown (28) that 2,3,4-tri-*O*-methyl-D-glucose is attacked by periodate with non-quantitative liberation of formaldehyde. The presence of 2,3,4-tri-*O*-methyl-D-glucose is therefore established.

Detection of 3,4,6-Tri-O-methyl-D-glucose

The remainder of solution B (5 ml) was deionized and studied by paper chromatography in solvent systems (i) and (ii). A spot running evenly with 2,3,5-tri-*O*-methyl-D-arabinose indicated the presence of the latter in the periodate-oxidized material. This therefore confirms the presence of 3,4,6-tri-*O*-methyl-D-glucose as one of the components in the mixture.

The residue of tri-*O*-methyl-D-glucoses which had not been attacked by periodate was examined on the chromatogram and presumably contained the 2,3,6- and the 2,4,6-isomers since no color developed when the oxidized sample was treated with the triphenyl tetrazolium chloride spray (29, 30) (see Experimental Section on 3,4-di-*O*-methyl-D-glucose).

Fraction III contained di-*O*-methyl-D-glucoses.

Detection of 2,3- and 4,6-Di-O-methyl-D-glucoses

The syrup obtained (340 mg) was compared with authentic specimens of dimethyl glucose isomers by means of chromatograms run in solvent systems (i) and (ii) for 65 hours (*p*-anisidine spray). A major spot was revealed; but immediately ahead of it and immediately behind it, two distinct components were identifiable as 2,3- and 4,6-di-*O*-methyl-D-glucose respectively. The syrup (ca. 100 mg) was separated on paper in solvent system (i) and strips corresponding to the "major spot" removed and extracted with water, the extract now being evaporated to give a syrup (syrup B). Attempts to induce crystallization from ethanol, ethyl acetate, isopropyl acetate, and methanol were all unavailing.

Detection of 3,4- and 3,6-Di-O-methyl-D-glucoses

An electrophoretic analysis on a portion of syrup B against authentic samples of 3,4- and 4,6-di-*O*-methyl-D-glucoses revealed four components:

(i) a trace of a sugar which moved at the speed of the 4,6-isomer;

(ii) a large percentage of a sugar which corresponded with the 3,4-isomer;

(iii) a fast-moving constituent;

(iv) material which had remained on the base line.

A second electrophoretogram similarly prepared but developed with triphenyl tetrazolium chloride showed characteristic red coloration indicating free adjacent hydroxyls at carbons 1 and 2 (29, 30) and corresponding to (i), (ii), and (iii) above. Component (iii) was therefore probably the 3,6-di-*O*-methyl isomer.

Can. J. Chem. Downloaded from www.nrcresearchpress.com by 210.87.254.105 on 09/05/12
For personal use only.

Detection of 2,4-Di-O-methyl-D-glucose

A portion of syrup B was oxidized overnight at room temperature with sodium periodate solution. It was then deionized and the solution was chromatographed and showed residual sugar to be present. 2,4-Di-*O*-methyl-D-glucose is the only isomer in syrup B which is not oxidized by periodate and is therefore probably present in the mixture. The 2,6-di-*O*-methyl isomer was the only one not positively identified.

Fraction IV contained mono-*O*-methyl glucoses.

Preparation of Glucosides

A portion of the syrup obtained (250 mg) was converted to the glucosides by refluxing it with 5% methanolic hydrogen chloride for 18 hours. After neutralization with dry silver carbonate and removal of the precipitate by filtration, the methanolic solution was saturated with hydrogen sulphide, and the precipitated silver sulphide was filtered off through Celite. The filtrate, after decolorizing with charcoal, was evaporated to give a semicrystalline mass which was dried *in vacuo* over phosphorus pentoxide to a constant weight of 78 mg. It had a negative reaction to Fehling's solution.

The syrupy glucosides were made up to a volume of 25 ml with water. Of this, 10 ml (equivalent to 31.2 mg) was removed and 10 ml 0.1 *M* sodium periodate was added and the whole diluted to 100 ml. A blank of water was similarly prepared. Aliquots (5 ml) were removed at various time intervals and analyzed for periodate uptake by the method of Neumuller and Vasseur (31) and for formic acid liberation by that of Andrews *et al.* (32). The 3-*O*-methyl isomer is the only one which will survive attack (if all are pyranosides). (See Table III and Fig. 1.)

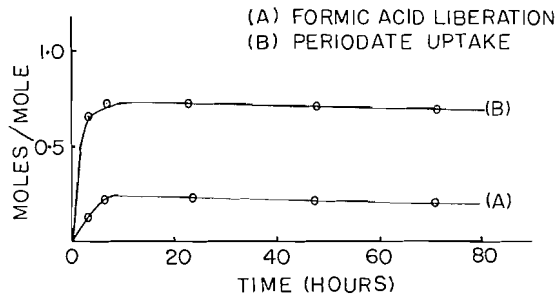


FIG. 1.

6-O-Monomethyl-D-glucose.—The molar production of formic acid is equivalent to the molar concentration of this isomer. This value is seen to be 0.23 mole, i.e. 23% of the mixture is present as 6-*O*-methyl-D-glucose.

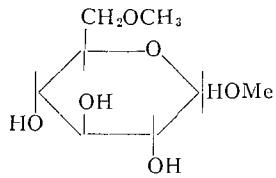
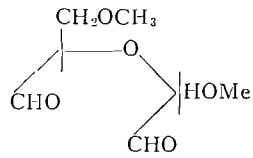
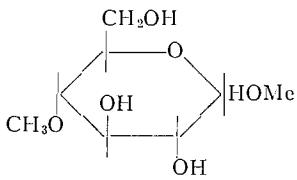
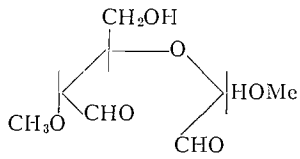
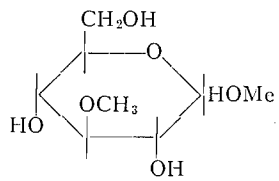
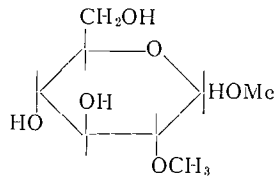
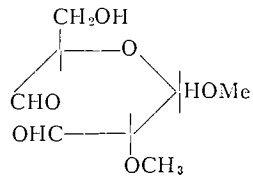
4- and 2-O-Methyl-D-glucose.—The total periodate consumption (0.68 mole) minus the molar concentration of the 6-*O*-methyl isomer (0.23 mole) gives the molar concentrations of both the 4- and 2-*O*-methyl isomers. Hence these two are present to the extent of 45% in the mixture.

3-Mono-O-methyl-D-mannose.—The remaining 32% of the mixture must be the 3-mono-*O*-methyl isomer.

Fraction V was identified as free glucose. The semicrystalline syrup (20 mg) obtained was dissolved in methanol (1 ml) and *p*-nitroaniline (20 mg) was added. The mixture was

Can. J. Chem. Downloaded from www.nrcresearchpress.com by 210.87.254.105 on 09/05/12
For personal use only.

TABLE III

Possible constituents	Oxidation products	IO_4' uptake (moles)	HCOOH liberation (moles)
		2	1
		1	0
	No reaction	0	0
		1	0

transferred to a bulb blown in glass tubing (3 mm in diameter), one drop of 13% methanolic hydrogen chloride was added, the tube was sealed and heated at 70° C for 20 minutes. After the mixture had been allowed to stand in the cold overnight, crystals of D-glucose-*N*-*p*-nitrophenylglucosylamine separated, m.p. 179–181° C, mixed m.p. 179–182° C.

Oxidation of Anisole.—Ferrous sulphate (2 g) was dissolved in water (15 ml) and reagent grade anisole (5 ml) added and the mixture was cooled to 0° C. Hydrogen peroxide (15 ml, 15%) was then added during 45 minutes and the whole was allowed to stand for 1½ hours (at 0° C), after which excess sodium arsenite was added to reduce excess peroxide. A copious green precipitate was removed by centrifugation during 1 hour at 0° C, and the green supernatant liquid was saturated with sodium chloride and repeatedly extracted with chloroform. The orange-colored chloroform phase was washed with (*a*) 5% sodium bicarbonate solution, then (*b*) with 5% sodium hydroxide solution, and finally evaporated to dryness, to give a residue (i) smelling strongly of anisole. Both the sodium bicarbonate and sodium hydroxide washings were then neutralized with dilute hydrochloric acid, and each extracted with chloroform, and the extracts were evaporated to dryness to give two residues (ii) and (iii) respectively. When chromatographed, (i)

Can. J. Chem. Downloaded from www.nrcresearchpress.com by 210.87.254.105 on 09/05/12
For personal use only.

and (ii) showed only traces of phenols which had escaped extraction, but at least four components were recognized in (iii), one being identifiable as guaiacol, and another as hydroquinone.

ACKNOWLEDGMENTS

The authors wish to thank Mr. C. R. Willis for undertaking the experimental work leading to the results shown in Tables I and II. One of us (B.F.-R.) is grateful to Queen's University for a Reuben Wells Leonard Foundation Fellowship and to the National Research Council for a grant, which made this work possible.

REFERENCES

1. W. N. HAWORTH, E. L. HIRST, and F. A. ISHERWOOD. J. Chem. Soc. 784 (1937).
2. W. N. HAWORTH, R. L. HEATH, and S. PEAT. J. Chem. Soc. 833 (1941).
3. G. O. ASPINALL and G. ZWIEFEL. J. Chem. Soc. 2271 (1957).
4. H. J. H. FENTON. J. Chem. Soc. **65**, 899 (1894).
5. H. J. H. FENTON and H. JACKSON. J. Chem. Soc. **75**, 1 (1899).
6. D. G. DANIELS and B. F. SAUNDERS. J. Chem. Soc. 2112 (1951).
7. F. HABER and J. WEISS. J. Proc. Roy. Soc. A, **147**, 332 (1934).
8. M. G. EVANS. J. Chem. Soc. 266 (1947).
9. J. H. MERZ and W. A. WATERS. J. Chem. Soc. 2427 (1949).
10. J. H. MERZ and W. A. WATERS. J. Chem. Soc. S15 (1949).
11. R. GRINSTEAD. J. Am. Chem. Soc. **82**, 3472 (1960).
12. R. GRINSTEAD. J. Am. Chem. Soc. **82**, 3464 (1960).
13. A. F. TROTMAN-DICKENSON. Free radicals. Methuen & Co. Ltd., London. 1959. p. 90.
14. N. URI. Chem. Revs. **50**, 375 (1952).
15. L. HOUGH, J. K. N. JONES, and W. H. WADMAN. J. Chem. Soc. 1702 (1950).
16. J. A. CIFONELLI and F. SMITH. Anal. Chem. **26**, 1132 (1954).
17. B. N. AMES and N. K. MITCHELL. J. Am. Chem. Soc. **74**, 252 (1952).
18. D. R. BRIGGS *et al.* Anal. Chem. **28**, 1333 (1956).
19. A. B. FOSTER. Chem. & Ind. (London), 1050 (1952).
20. J. K. N. JONES and H. SEPHTON. Can. J. Chem. **38**, 753 (1960).
21. R. KUHN. Angew. Chem. **67**, 32 (1955).
22. R. KUHN. Ber. **88**, 1540 (1955).
23. BIOCHEMICAL PREPARATIONS. Vol. 2. John Wiley & Sons, Inc., New York. 1952. p. 33.
24. C. HUDSON *et al.* J. Am. Chem. Soc. **65**, 70 (1943).
25. W. N. HAWORTH. J. Chem. Soc. **107**, 8 (1915).
26. M. L. WOLFROM. J. Am. Chem. Soc. **50**, 2822 (1928).
27. T. NASH. Biochem. J. **55**, 416 (1953).
28. D. J. BELL. J. Chem. Soc. 992 (1948).
29. K. WALLENFELS. Naturwiss. **37**, 491 (1950).
30. D. J. BELL and R. DEDONDER. J. Chem. Soc. 2866 (1954).
31. G. NEUMULLER and E. VASSEUR. Arkiv Kemi, **2**, 235 (1953).
32. P. ANDREWS, L. HOUGH, and J. K. N. JONES. J. Chem. Soc. 806 (1954).

Can. J. Chem. Downloaded from www.nrcresearchpress.com by 210.87.254.105 on 09/05/12
For personal use only.

Can. J. Chem. Downloaded from www.nrcresearchpress.com by 210.87.254.6 on 09/05/12
For personal use only.

CHEMISTRY OF THE TRIFLUOROMETHYL GROUP

PART III. PHENYLBISTRIFLUOROMETHYLPHOSPHINE AND RELATED COMPOUNDS[1]

M. A. A. Beg and H. C. Clark

ABSTRACT

The reaction of trifluoroiodomethane with tetraphenylcyclotetraphosphine leads to the formation of phenylbistrifluoromethylphosphine and phenyltrifluoromethyliodophosphine. The mechanism of the reaction is discussed and the physical and chemical properties of these compounds are reported. Bromine reacts with phenylbistrifluoromethylphosphine to form phenylbistrifluoromethyldibromophosphorane which is hydrolyzed to phenyltrifluoromethylphosphinic acid, $C_6H_5(CF_3)P(O)OH$.

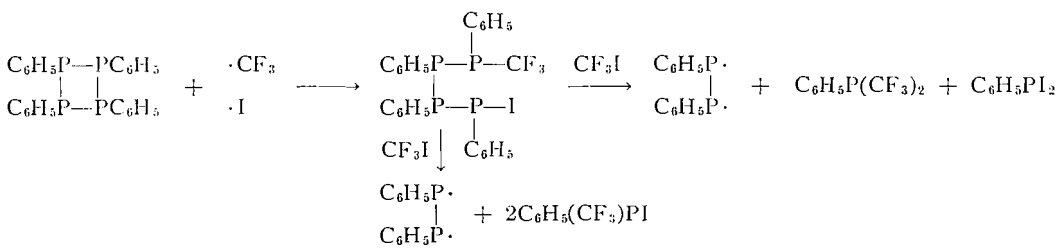
INTRODUCTION

In previous papers in this series, the donor properties of methyl-trifluoromethyl-phosphines were studied by the investigation of their ability to form complexes with boron trifluoride and platinum (II) chloride (1), and with a series of nickel (II) salts (2). Since much is known of the corresponding complexes of aryl phosphines, it seemed worthwhile to study the donor properties of aryl-trifluoromethyl-phosphines. Unlike the methyl-trifluoromethyl-phosphines which have been known for some time (3, 4, 5), the phenyl-trifluoromethyl-phosphines had not been previously reported, although their arsine analogues had been prepared (6). We now report the preparation of phenylbistrifluoromethylphosphine.

DISCUSSION AND RESULTS

Phenylbistrifluoromethylphosphine has been prepared by the reaction of trifluoroiodomethane with tetraphenylcyclotetraphosphine, the properties of which have been reported by other workers (7, 8, 9). The reaction was performed at 185°, above the melting point of the tetraphosphine, and the other reaction products, besides phenylbistrifluoromethylphosphine, are phenyltrifluoromethyliodophosphine, which is a very involatile reddish brown liquid, and small amounts of fluoroform and hexafluoroethane.

The mechanism of this reaction, involving the interaction of a perfluoroiodoalkane with a four-membered phosphorus ring is of some interest. A free-radical mechanism involving fission of phosphorus–phosphorus bonds by the attack of CF_3 radicals seems probable. This is supported by the fact that the reaction will occur thermally or on ultraviolet irradiation of the tetraphosphine with trifluoroiodomethane. Since the simultaneous breaking of four P—P bonds is unlikely, the following reaction scheme may be suggested.



$$2C_6H_5(CF_3)PI \rightleftharpoons C_6H_5P(CF_3)_2 + C_6H_5PI_2.$$

[1]*Manuscript received December 5, 1960.*
Contribution from the Department of Chemistry, University of British Columbia, Vancouver, B.C. From part of the thesis presented by M.A.A.B. in partial fulfillment of the requirements for the Ph.D. degree.

Can. J. Chem. Downloaded from www.nrcresearchpress.com by 210.87.254.6 on 09/05/12
For personal use only.

This scheme is supported by the observation that the reaction products contain phenylbistrifluoromethylphosphine and phenyltrifluoromethyliodophosphine in an approximately 2:1 ratio, and also by the results of a separate experiment which indicated extensive disproportionation of the iodophosphine at 200° as indicated above.

Phenylbistrifluoromethylphosphine is a colorless liquid boiling at 148–150°; it is stable at 200° and prolonged heating to 300° causes only partial decomposition. It is not hydrolyzed by acids, but reacts very slowly with water at 100° and much more rapidly with aqueous sodium hydroxide at 80°. The hydrolysis products are fluoroform and either phenylphosphonous acid $C_6H_5PO_2H_{27}$, or its sodium salt.

Phenylbistrifluoromethylphosphine does not react with iodine at room temperature, but at 185° the trifluoromethyl groups are cleaved as trifluoroiodomethane. There is no evidence of the formation of the diiodophosphorane, $C_6H_5(CF_3)_2PI_2$. However, the phosphine reacted vigorously with bromine at room temperature to form phenylbistrifluoromethyldibromophosphorane. This is in agreement with the usual decrease in stability for dichloro-, dibromo-, and diiodo-phosphoranes. Phenylbistrifluoromethyldibromophosphorane is readily hydrolyzed by water losing only one of the two trifluoromethyl groups per molecule as fluoroform and producing phenyltrifluoromethylphosphinic acid, $C_6H_5(CF_3)P(O)OH$.

Phenyltrifluoromethyliodophosphine is a reactive liquid which is readily hydrolyzed. Whereas alkaline hydrolysis produced fluoroform and the sodium phenylphosphonate, treatment with water gives phenyltrifluoromethylphosphine and phenyltrifluoromethylphosphinic acid, $C_6H_5(CF_3)P(O)OH$.

The production of phenyltrifluoromethylphosphinic acid from the aqueous hydrolysis of phenylbistrifluoromethyldibromophosphorane provides an interesting link between the trifluoromethyl- and aryl-phosphorus compounds. Whereas hydrolysis of triaryldichlorophosphoranes yields phosphine oxides (10), hydrolysis of tristrifluoromethyldichlorophosphorane (11) gives bistrifluoromethylphosphinic acid and one equivalent of fluoroform.

$$(CF_3)_3PCl_2 \xrightarrow{H_2O} [(CF_3)_3P(OH)_2] \rightarrow (CF_3)_2P(O)OH + CF_3H$$

The hydrolysis of phenylbistrifluoromethyldibromophosphorane shows that the intermediate compound $C_6H_5(CF_3)_2P(OH)_2$ is unstable.

$$C_6H_5(CF_3)_2PBr_2 \xrightarrow{H_2O} [C_6H_5(CF_3)_2P(OH)_2] \rightarrow C_6H_5(CF_3)P(O)OH + CF_3H$$

The trifluoromethyl groups behave in the same way as in the hydrolysis of tristrifluoromethyldichlorophosphorane and the phenyl group shows its customary resistance to hydrolytic attack.

The formation of phenyltrifluoromethylphosphinic acid from the hydrolysis of phenyltrifluoromethyliodophosphine is consistent with the general reactions of halophosphines (12). The spontaneous oxidation–reduction of the apparently unstable hydrolysis product leads to the production of phenyltrifluoromethylphosphine and phenyltrifluoromethylphosphinic acid.

$$2C_6H_5(CF_3)PI \xrightarrow{H_2O} [2C_6H_5(CF_3)POH] \rightarrow C_6H_5(CF_3)PH + C_6H_5(CF_3)P(O)OH$$

The infrared spectra of these phenyl-trifluoromethylphosphorus compounds show the expected features. Absorption associated with the strong carbon–fluorine stretching vibrations occurred in the 1100–1200 cm^{-1} region. However, it is of interest to notice

that the spectrum of silver phenyltrifluoromethylphosphinate, $C_6H_5(CF_3)P(O)OAg$, showed absorption at 1225 cm^{-1} corresponding to the P:O vibration. This absorption occurs in the same region for the aryl and alkyl phosphinic acids $R_2P(O)OH$, which are weak acids. For the strong acid, trifluoromethylphosphonic acid, this vibration is shifted to the higher frequency of 1300 cm^{-1} (13, 14). This might suggest that phenyltrifluoromethylphosphinic acid is a fairly weak acid.

EXPERIMENTAL

The preparations of the starting materials were carried out in a nitrogen atmosphere. Reactions with trifluoroiodomethane were carried out in sealed evacuated Pyrex tubes and the products and reactants were manipulated by standard vacuum techniques, out of contact with air and moisture.

Preparation of Tetraphenylcyclotetraphosphine

Phenyldichlorophosphine was obtained by the method of Buchner and Lockhart (15). The preparation of phenylphosphine by the Michaelis method (16, 17) is very cumbersome and gives a low yield. A much easier method (9, 18) is by reduction of phenyldichlorophosphine with lithium aluminum hydride. Phenyldichlorophosphine (18.8 g) dissolved in 100 ml diethyl ether was added cautiously to a well-stirred suspension of lithium aluminum hydride (3 g) in 100 ml ether. The reaction was vigorous and cooling was necessary. After the addition of phenyldichlorophosphine had been completed, the mixture was refluxed for 30 minutes and 5 ml of water were added dropwise. After being refluxed for an hour, the mixture was distilled and the resulting phenylphosphine, distilling at 160°, was dried over calcium chloride (yield 55%).

The preparation of tetraphenylcyclotetraphosphine by the Michaelis' method (19) is not convenient and the compound was prepared by adding phenylphosphine (11 g) in 50 ml ether to a well-stirred solution of phenyldichlorophosphine (18 g) in 50 ml ether. The solution gradually turned yellow but solid was not immediately deposited. After the addition was complete, the solution was refluxed for 3 hours during which time a white solid was deposited. The ether solution was decanted and the remaining solid was washed and dried. The yield of tetraphenylcyclotetraphosphine (m.p. 149–50°) was 90%.

Reaction of Tetraphenylcyclotetraphosphine with Trifluoroiodomethane

Tetraphenylcyclotetraphosphine (1.0 g) was sealed with trifluoroiodomethane (2.025 g) and left at room temperature for 24 hours. The solid phosphine was insoluble in trifluoroiodomethane. No reaction occurred at 70° C over 24 hours, nor at 150° C for 12 hours, but on heating at 185° C for 12 hours a dark-red involatile liquid was obtained and 0.558 g of unreacted trifluoroiodomethane was recovered. The dark-red liquid was shaken with mercury and the remaining liquid extracted with ether. After removal of the ether, a liquid (0.45 g) of low volatility was obtained and identified as phenylbistrifluoromethylphosphine (Found: C, 39.35%; H, 2.10%; F, 45.40%; P, 12.30%. Calculated for $C_8H_5F_6P$: C, 39.03%; H, 2.03%; F, 46.36%; P, 12.60%).

Phenylbistrifluoromethylphosphine is a colorless oily liquid whose odor is not as obnoxious as those of other phosphines. It boils at 148–150° and its vapor pressure is given by the equation $\log p_{mm} = 7.5606 - (1985/T)$, whence the latent heat of vaporization is 9054 cal $mole^{-1}$ and the Trouton's constant is 21.37. It is stable in air and does not react with water up to 100° C. It does not react with silver iodide, a solution of silver iodide in potassium iodide, or with carbon disulphide.

Can. J. Chem. Downloaded from www.nrcresearchpress.com by 210.87.254.6 on 09/05/12
For personal use only.

Can. J. Chem. Downloaded from www.nrcresearchpress.com by 210.87.254.6 on 09/05/12
For personal use only.

Two separate experiments were performed to investigate the mechanism of the above reaction and to characterize the other reaction products.

(1) Tetraphenylcyclotetraphosphine (2 g) was sealed with trifluoroiodomethane (5 g) in a Pyrex tube and was irradiated with ultraviolet radiation from a 200-watt U.V. lamp. The reaction was slow (possibly because of the heterogeneous phases), but after 15 days phenylbistrifluoromethylphosphine (0.899 g) and unreacted trifluoroiodomethane (2.192 g) were obtained. The rest of the product was a thick reddish syrup which showed strong absorption in the I.R. between 8–9 μ, characteristic of C—F stretching frequencies. This was not identified.

(2) Tetraphenylcyclotetraphosphine (7.5 g) was sealed with 18 g trifluoroiodomethane and heated at 185° C for 12 hours. A volatile mixture of hexafluoroethane and fluoroform (0.022 g), and 5.5 g of unreacted trifluoroiodomethane were recovered. The remaining liquid was subjected to fractional distillation under 20 mm pressure. Two fractions were obtained, one boiling at 62–65° (4.9 g) and the other boiling at 112–116° (3.8 g). A thick liquid which solidified on standing remained in the distillation flask. This showed strong absorption in the I.R., corresponding to the C—F stretching frequencies. Another experiment to identify this completely involatile liquid showed that it contained some iodides, including phosphorus triiodide. When treated with a large excess of trifluoroiodomethane and mercury, some pure phenylbistrifluoromethyl phosphine was obtained, but the main product was a very viscous pale-yellow liquid, presumably polymeric.

The liquid distilling at 62–65° was identified as phenylbistrifluoromethylphosphine and the fraction distilling at 112–114° was identified as phenyltrifluoromethyliodophosphine. (Found: I, 41.2%. Calculated for $C_7H_5F_3PI$: I, 41.78%.)

Reactions of Phenylbistrifluoromethylphosphine

(a) Hydrolysis

Phenylbistrifluoromethylphosphine (0.277 g) was sealed with water (1.28 g). There was no reaction at room temperature and the reactants formed two separate layers. After heating at 80° for 24 hours, only a trace of fluoroform was obtained, while after 36 hours at 110°, 0.038 g fluoroform was evolved. Traces of benzene were also identified spectroscopically. There remained a white crystalline solid which melted at 69° and was identified as phenylphosphonous acid.

Phenylbistrifluoromethylphosphine (0.273 g) was sealed with 5 ml of 20% aqueous sodium hydroxide solution. The reaction was slow at room temperature with the evolution of fluoroform. The tube was heated to 80° for 24 hours. The production of 0.149 g fluoroform (mol. wt. obtained 70.0, calculated 70.0) showed that the hydrolysis was 96.4% complete (CF_3 obtained as CF_3H: 54.8%; calculated for $C_6H_5P(CF_3)$: 56.1%). The solid obtained on evaporation of the solution was identified spectroscopically as the sodium salt of phenylphosphonous acid.

Phenylbistrifluoromethylphosphine (0.372 g) and 36 *N* hydrochloric acid (2 g) were sealed. There was no reaction at room temperature and the reactants formed separate layers. There was no reaction at 80° for 24 hours and at 110° for 48 hours. The tube was finally heated to 185° for 120 hours. At the end of this period the amount of fluoroform evolved was only 0.0022 g and the phosphine was recovered almost quantitatively.

(b) Reaction with Halogens

(1) Iodine.—Phenylbistrifluoromethylphosphine (0.389 g) and iodine (1.163 g) did not react at room temperature, nor after heating at 150° for 24 hours. The mixture was finally heated to 185° for 48 hours. The products obtained, were fluoroform (0.032 g),

trifluoroiodomethane (0.481 g), (mol. wt. 194, calculated 196), benzene (0.055 g), and traces of unreacted phosphine. The conversion into fluoroform and trifluoroiodomethane accounted for 91.5% of the trifluoromethyl group. The formation of fluoroform and benzene may be due to the presence of small traces of moisture on the iodine which is not removed even on extensive drying. The solid left in the tube, after pumping off the volatiles, contained phosphorus triiodide and no phenyltrifluoromethyliodophosphine.

(2) Bromine.—Phenylbistrifluoromethylphosphine (0.6965 g) and bromine (0.450 g) were combined. The ensuing vigorous reaction was controlled by performing the experiment in carbon tetrachloride solution and pumping off the volatiles after the reaction was complete. This was marked by the persistence of the bromine color. The reaction gave an orange-yellow solid which was very reactive towards moisture and was identified as phenylbistrifluoromethyldibromophosphorane (Found: Br, 38.93%. Calculated for $C_8H_5F_6PBr_2$: Br, 39.41%). On reacting the dibromophosphorane with water, one equivalent of CF_3 was lost and a white solid was left. The dibromophosphorane (0.324 g) was sealed with water (1.0 g) and left at room temperature overnight. Fluoroform (0.060 g) was evolved corresponding to a loss of one equivalent of CF_3 per mole (Found: CF_3, 18.4%. Calculated for $C_8H_5F_6PBr_2$:CF_3, 34.5%). A white solid was obtained by pumping off the liquids, recrystallizing the residue from water, and finally drying over phosphorus pentoxide. The solid was identified spectroscopically as phenyltrifluoromethylphosphinic acid, $C_6H_5(CF_3)P(O)OH$. The acid melted at 84–86°. The silver salt of the acid was obtained as needle-shaped crystals by treating the aqueous solution of the acid with silver oxide. The same salt could also be obtained from the reaction mixture of phenylbistrifluoromethyldibromophosphorane and water which had stood overnight and had lost one equivalent of CF_3. The silver salt $C_6H_5(CF_3)P(O)OAg$ (Found: Ag, 33.81%. Calculated for $C_7H_5F_3PO_2Ag$: Ag, 34.06%) melted at 294–96° and was very sensitive to light.

(c) Pyrolysis of the Phosphine

Phenylbistrifluoromethylphosphine (1.058 g) was heated to 210° for 48 hours; 1.004 g of the phosphine and traces of fluoroform and silicon tetrafluoride (identified spectroscopically) were obtained. Phosphine (0.639 g) was heated to 300° for 48 hours. The tube walls were etched but the phosphine was not all pyrolyzed: 0.48 g was recovered unchanged. The other volatile materials were fluoroform, silicon tetrafluoride, and some benzene trifluoride.

Reactions of Phenyltrifluoromethyliodophosphine

Phenyltrifluoromethyliodophosphine is a reddish-brown liquid which boils at 112–114° at 20 mm. It fumes in air and reacts slowly with water. The solution obtained by absorption of water is highly acidic. It disproportionates on heating.

(a) Hydrolysis

Phenyltrifluoromethyliodophosphine (0.334 g) was treated with 5 ml of 20% sodium hydroxide. There was immediate reaction at room temperature. The tube was heated to 100° for 15 hours. Fluoroform (0.0694 g) (mol. wt. found 69.8, calculated 70.0) was evolved (CF_3 found, 20.75%; calculated for $C_7H_5F_3PI$, 23.03%). The hydrolysis was only 90% complete. The residue contained a hygroscopic sodium salt whose I.R. spectrum corresponded with that of sodium phenylphosphonate.

Phenyltrifluoromethyliodophosphine (0.334 g) was treated with 0.125 g water and left in a sealed tube overnight. When water and other liquids were removed, a white solid was left. The melting point was 84–86° and in all respects the compound was similar to

Can. J. Chem. Downloaded from www.nrcresearchpress.com by 210.87.254.6 on 09/05/12
For personal use only.

Can. J. Chem. Downloaded from www.nrcresearchpress.com by 210.87.254.6 on 09/05/12
For personal use only.

that obtained from the hydrolysis of phenylbistrifluoromethyldibromophosphorane. The silver salt was also prepared by reacting more of the iodophosphine with water and precipitating the iodide as silver iodide. The solution was concentrated *in vacuo* and the solid dried over P_2O_5. The silver salt was identified analytically (Found: Ag, 33.80%. Calculated: Ag, 34.06%) by its melting point of 294–96°, and also spectroscopically.

The above treatment of the iodophosphine also gave a small amount of a liquid whose I.R. spectrum showed the presence of P—H, P—C_6H_5, and P—CF_3 bonds. The hydrolysis with water therefore appears to give some phenyltrifluoromethylphosphine.

(b) Reaction with Trifluoroiodomethane

The iodophosphine (2.347 g) was heated with trifluoroiodomethane (2.299 g) at 200° for 12 hours. Trifluoroiodomethane (2.210 g, 96.1%) was recovered and the main products of reaction, presumably from the disproportionation of the iodophosphine, were phenylbistrifluoromethylphosphine (0.617 g), phosphorus triiodide, and benzene. Some of the unreacted iodophosphine was also identified among the products.

(c) Reactions with Trifluoroiodomethane and Mercury

The iodophosphine (2.8 g) and trifluoroiodomethane (10 g), with 54 g mercury, were sealed in a tube and shaken for 24 hours. Trifluoroiodomethane (8.9 g) was recovered and phenylbistrifluoromethylphosphine (1.5 g) was obtained. The loss of 1.1 g of trifluoroiodomethane indicated that the reaction $C_6H_5PCF_3I + CF_3I \xrightarrow{Hg} C_6H_5(CF_3)_2P$ had occurred. Besides the phosphine, some polymers were also obtained as mentioned earlier.

Pyrolysis of phenyltrifluoromethylphosphine iodide: The iodophosphine (2.003 g) was heated in a sealed tube to 220° for 12 hours. Fluoroform (0.02 g) and trifluoroiodomethane (0.06 g) were obtained as the volatile products and there remained phenylbistrifluoromethylphosphine, benzene, phosphorus triiodide, and some unreacted phenyltrifluoromethyl iodophosphine.

The I.R. spectra were taken on a Perkin–Elmer model 21 double-beam instrument with rock salt optics. Liquid films were used for liquids and KBr pellets for solids. The following absorption bands were noted for the compounds mentioned.

Phenylbistrifluoromethylphosphine					
3080 (w)	2920 (w)	2320 (w)	1980 (w)		
1870 (w)	1835 (w)	1810 (w)	1770 (w)	1745 (w)	
1730 (w)	1670 (w)	1645 (w)	1590 (w)	1490 (w)	
1445 (m)	1330 (w)	1265 (w)	1190 (s)	1140 (s)	
1100 (s)	1070 (m)	1030 (w)	1000 (m)	875 (w)	
805 (w)	750 (m)	745 (m)	690 (m)		
Phenyltrifluoromethyliodophosphine					
3060 (w)	2900 (w)	2340 (w)	1880 (w)	1800 (w)	
1725 (w)	1710 (w)	1690 (w)	1675 (w)	1660 (w)	
1585 (w)	1490 (w)	1440 (m)	1385 (w)	1335 (w)	
1310 (w)	1270 (w)	1210 (m)	1150 (s)	1115 (s)	
1070 (m)	1025 (m)	1000 (m)	830 (w)	745 (s)	
715 (w)	690 (m)				
Silver phenyltrifluoromethyl phosphinate					
3080 (w)	2900 (w)	2300 (w)	1860 (w)		
1815 (w)	1725 (w)	1710 (w)	1690 (w)	1756 (w)	
1640 (w)	1630 (w)	1590 (w)	1555 (w)	1485 (w)	
1440 (m)	1335 (w)	1225 (s)	1200 (m)		
1140 (s)	1110 (s)	1045 (m)	1015 (m)	995 (m)	
970 (m)	870 (w)	760 (w)	740 (m)	715 (m)	695 (m)

ACKNOWLEDGMENTS

We gratefully acknowledge the support of the National Research Council, and one of us (M.A.A.B) expresses thanks for a scholarship received from C.S.I.R. (Pakistan) under the auspices of the Colombo Plan.

REFERENCES

1. M. A. A. Beg and H. C. Clark. Can. J. Chem. **38**, 119 (1960).
2. M. A. A. Beg and H. C. Clark. Can. J. Chem. This issue.
3. R. N. Haszeldine and B. O. West. J. Chem. Soc. 3631 (1956).
4. R. N. Haszeldine and B. O. West. J. Chem. Soc. 3880 (1957).
5. A. B. Burg and G. Brendel. J. Am. Chem. Soc. **80**, 3198 (1958).
6. W. R. Cullen. Can. J. Chem. **38**, 445 (1960).
7. J. W. B. Reesor and G. F. Wright. J. Org. Chem. **22**, 385 (1957).
8. W. Kuchen and H. Buchwald. Chem. Ber. **91**, 2296 (1958).
9. P. R. Bloomfield and K. Parvin. Chem. & Ind. 541 (1959).
10. G. M. Kosolapoff. Organophosphorus compounds. John Wiley & Sons, Inc., New York. 1950. p. 70.
11. H. J. Emeleus, R. N. Haszeldine, and R. C. Paul. J. Chem. Soc. 563 (1955).
12. G. M. Kosolapoff. Organophosphorus compounds. John Wiley & Sons, Inc., New York. 1950. p. 137.
13. L. W. Daasch and D. C. Smith. Anal. Chem. **23**, 853 (1957).
14. F. W. Bennett, H. J. Emeleus, and R. N. Haszeldine. J. Chem. Soc. 3598 (1954).
15. B. Buchner and L. B. Lockhart. J. Am. Chem. Soc. **73**, 755 (1951).
16. A. Michaelis. Chem. Ber. **7**, 6 (1874).
17. A. Michaelis. Ann. **265**, 181 (1876).
18. T. Weil, B. Prijs, and H. Erlenmeyer. Helv. Chim. Acta, **35**, 616 (1952).
19. A. Michaelis and H. Kohler. Chem. Ber. **10**, 807 (1877).

Can. J. Chem. Downloaded from www.nrcresearchpress.com by 210.87.254.6 on 09/05/12
For personal use only.

Can. J. Chem. Downloaded from www.nrcresearchpress.com by 210.87.254.6 on 09/05/12
For personal use only.

DIELECTRIC RELAXATION IN LIQUIDS

I. THE REPRESENTATION OF RELAXATION BEHAVIOR[1]

D. W. DAVIDSON

ABSTRACT

Methods are described for the determination from experimental data of the parameters used in the skewed-arc representation in the complex dielectric constant plane of dielectric relaxation in liquids. Graphs give the frequency dependence of the real and imaginary parts of the dielectric constant predicted by the skewed-arc equation. Evidence, which includes an analysis of published data and of some new data, is presented for the frequent occurrence of this type of relaxation behavior in liquids. The resolution of the effects of different relaxation processes is discussed.

The recent defect-diffusion model of Glarum is found to lead, under some conditions, to complex dielectric constant loci which are practically indistinguishable from skewed-arc loci over much of the frequency range of dispersion. It predicts departures from skewed-arc behavior at relatively high frequencies which are possibly related to experimentally observed departures.

It is concluded that skewed-arc characteristics arise from the presence of co-operative relaxation processes, possibly aided by the diffusion of disordered regions, in which the individual mechanisms of relaxation cannot be resolved by application of the superposition principle.

I. INTRODUCTION

The question of the accuracy with which empirical representations fit the experimental dielectric relaxation data is of considerable importance in the development of adequate models of liquid relaxation. In a recent publication of the National Bureau of Standards (1), Buckley and Maryott have collected dielectric dispersion and absorption data for some 193 compounds in the liquid state, as found in the literature to the end of 1956. The dielectric behavior of many of these compounds has been represented analytically, either in terms of the simple Debye equation involving only a single relaxation time and a semicircular locus in the complex dielectric constant plane, or in terms of the equation due to Cole and Cole which is an arc of a circle in the complex plane and involves a logarithmically symmetrical distribution of relaxation times about a most probable value. Among the liquids whose relaxation parameters are tabulated by Buckley and Maryott, two (glycerol and 1,2-propanediol) were described by a third representation, the skewed-arc locus proposed by Cole and Davidson which corresponds to an asymmetrical distribution of relaxation times.

More recently, however, comparatively accurate data for a considerable number of other liquids have been fitted to this third representation. These include most of the liquids originally cited by Cole and Cole (2) as evidence for their symmetrical circular arc description in the complex dielectric constant plane. Moreover, many other liquids have been characterized by Cole–Cole parameters (1) on the basis of rather inaccurate and incomplete relaxation data. This is particularly true for measurements in the experimentally difficult frequency range above 100 Mc/sec. In fact, unlike many solids, no liquid seems to have a principal dispersion region appreciably broader than that given by the Debye equation for which the adequacy of the Cole–Cole representation has been established.

It is the purpose of the present paper to consider the application of the Cole–Davidson equation in some detail. Methods of analyzing experimental results are discussed and

[1]*Manuscript received October 11, 1960.*
Contribution from the Division of Applied Chemistry, National Research Council, Ottawa, Canada.
Issued as N.R.C. No. 6128.

applied to data in the literature as well as to some new data. In subsequent papers the results of studies of other liquids will be presented.

II. THE DEBYE EQUATION

According to the classical Debye equation (3) the complex dielectric constant $\epsilon(i\omega) = \epsilon' - i\epsilon''$ is given by

$$\epsilon(i\omega) - \epsilon_1 = (\epsilon_0 - \epsilon_1)/(1 + i\omega\tau) \quad [1]$$

in which ϵ_0 and ϵ_1 are the values of the dielectric constant on the low- and high-frequency sides of the dispersion region, ω is the angular frequency, and τ the (single) relaxation time. This equation appears to be applicable (4) to the cases of relaxation of polar molecules in dilute solution in non-polar solvents, at least when the solute molecules are large in comparison with those of the solvent. Individual polar molecules are then in similar environments and a single relaxation time for rotation is adequate.

The Debye equation also describes the principal dielectric dispersion of water, at least to a high level of approximation (5), and of a large number of undiluted monohydroxy alcohols, within the accuracy of the measurements (6). In these liquids hydrogen bonding between molecules leads to a regularity of environment which may again account for the presence of only one relaxation time, although there is evidence (see VI(*b*) below) that here relaxation occurs by a co-operative process involving a large number of molecules.

Between these two extremes, a large number—probably the majority—of polar liquids show broader dielectric dispersion and absorption than can be attributed to a single relaxation time. There has been tendency to treat such departures from Debye behavior in terms of the symmetrical Cole–Cole locus (1), a procedure which has been reasonably successful in some cases. However, the data generally seem inadequate to show preference for this representation over other possible representations, in particular over that to be discussed in subsequent paragraphs.

III. THE SKEWED-ARC REPRESENTATION

The equation of the skewed-arc locus

$$\epsilon(i\omega) - \epsilon_1 = (\epsilon_0 - \epsilon_1)/(1 + i\omega\tau_0)^\beta \quad [2]$$

in which β is a positive parameter no greater than unity, was originally used (7) to represent, within the experimental accuracy, the relaxation behavior of glycerol and 1,2-propanediol and, subsequently, 1,3-propanediol (8). More recently, it has been successfully applied to accurate bridge data obtained for a variety of chemically dissimilar liquids (see IV below).

Methods of Applying the Equation to Extensive Data

The complex locus given by equation [2] is illustrated in Fig. 1. The imaginary part of the complex dielectric constant is plotted against the real part. It is an asymmetrical locus which resembles a semicircle on the low-frequency side and approaches asymptotically a line making an angle of $\beta\pi/2$ with the real axis on the high-frequency side. This behavior is apparent from an examination of the real and imaginary parts of equation [2]:

$$\frac{\epsilon' - \epsilon_1}{\epsilon_0 - \epsilon_1} = (\cos\phi)^\beta \cos\beta\phi \quad [3]$$

Can. J. Chem. Downloaded from www.nrcresearchpress.com by 210.87.254.6 on 09/05/12
For personal use only.

and

$$[4] \qquad \frac{\epsilon''}{\epsilon_0 - \epsilon_1} = (\cos \phi)^\beta \sin \beta\phi,$$

where ϕ is the principal value of $\tan^{-1} \omega\tau_0$. The ratio of these is

$$[5] \qquad \frac{\epsilon''}{\epsilon' - \epsilon_1} = \tan \beta\phi.$$

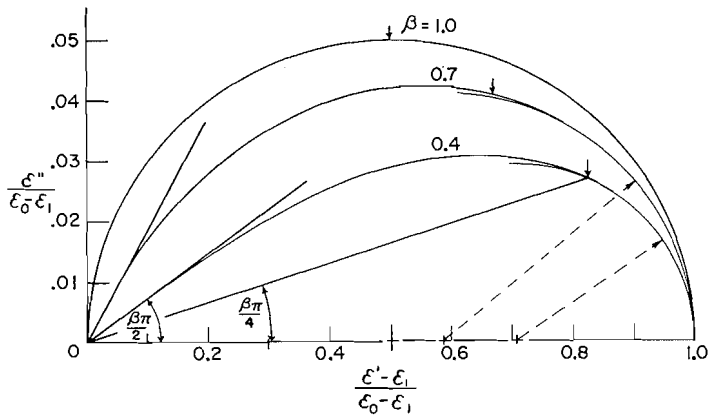


FIG. 1. Skewed-arc loci on the complex dielectric constant plane. Arrows indicate frequencies at which $\omega = 1/\tau_0$, broken lines the radii of circular arcs which coincide with the loci at low frequencies.

When an experimental locus has the characteristic shape of Fig. 1 the appropriate value of β may be obtained from the limiting slope at high frequencies. Since, for $\omega = 1/\tau_0$, $\epsilon''/(\epsilon' - \epsilon_1) = \tan \beta\pi/4$, τ_0 may be obtained as the reciprocal of the estimated radian frequency at which the bisector of the limiting angle cuts the locus. A more accurate method of evaluating the relaxation time τ_0, which is not dependent merely upon a few experimental points at values of ω in the vicinity of $1/\tau_0$, is to plot $\tan\{\tan^{-1}[\epsilon''/(\epsilon' - \epsilon_1)]/\beta\} = \omega\tau_0$ versus frequency, whence τ_0 may be evaluated from the frequency for which this function is unity. This also serves as a check of how well the data fit the predicted straight-line relationship. The plot is best made logarithmic in view of the large frequency range over which dispersion takes place. However, the validity of equation [5] is not a sufficient condition for the validity of equations [3] and [4]. Moreover, in many cases only one of ϵ' or ϵ'' (often only ϵ'') is accurately measured. Figures 2 and 3 show the individual variation of ϵ' and ϵ'' with frequency for a number of values of β and may be used to facilitate direct comparison with experiment.

Analysis of Less Extensive Data

The above methods for checking the agreement between experiment and the skewed-arc locus are applicable only when data are available for a considerable range of frequencies which includes the dispersion region. In cases where the data are less complete it is sometimes possible to use less straightforward methods. This may sometimes be done for data available at only a limited number of fixed frequencies provided that they are obtained over a considerable interval of temperature.

Can. J. Chem. Downloaded from www.nrcresearchpress.com by 210.87.254.6 on 09/05/12
For personal use only.

An aggregate complex locus may be drawn by plotting $\epsilon''/(\epsilon_0-\epsilon_1)$ versus $(\epsilon'-\epsilon_1)/(\epsilon_0-\epsilon_1)$ for data obtained at different temperatures. This method requires evaluation of ϵ_0 at the required temperatures by extrapolation of high temperature values and of ϵ_1 by extrapolation from low temperatures. Provided that β is not strongly temperature dependent (the evidence is that it increases slightly with increasing temperature), equation [2] requires that the points fall on a common skewed locus, from which β may

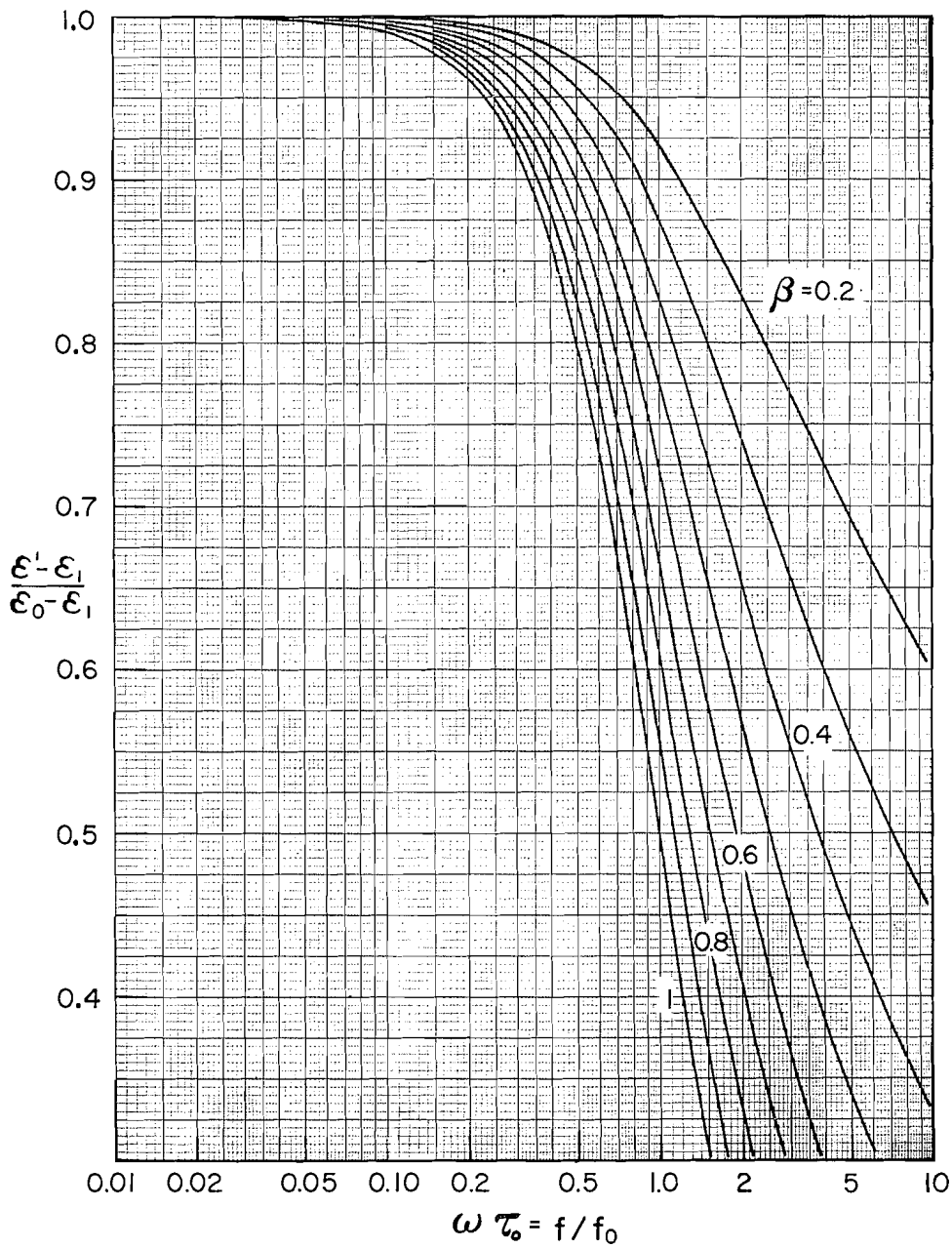


FIG. 2(*a*). Variation of ϵ' with frequency for skewed-arc behavior.

Can. J. Chem. Downloaded from www.nrcresearchpress.com by 210.87.254.6 on 09/05/12
For personal use only.

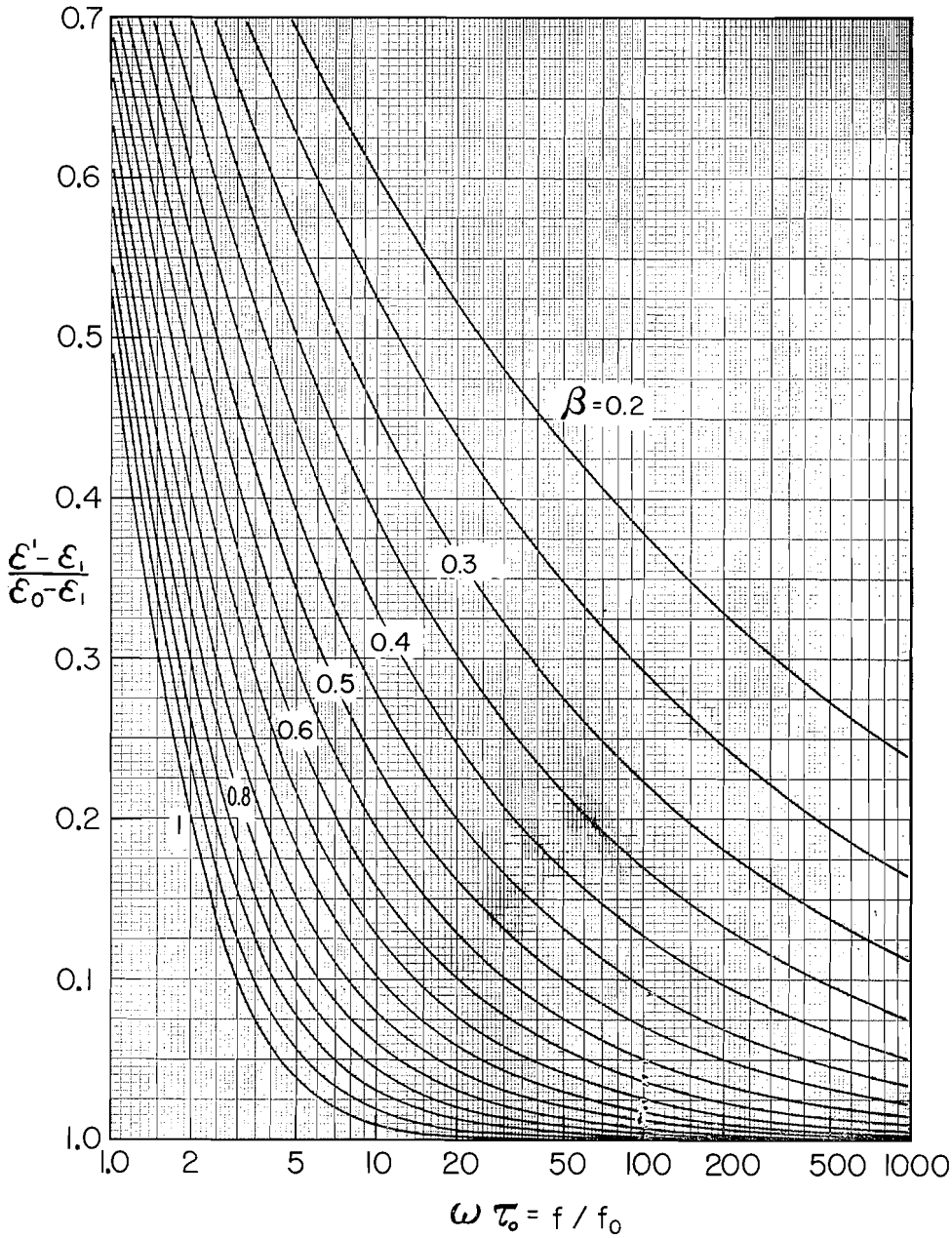


FIG. 2(*b*). Variation of ϵ' with frequency for skewed-arc behavior.

be determined. A value of τ_0 may then be obtained for each frequency of measurement at the estimated temperature at which the locus for that frequency is intercepted by the bisector of the limiting angle. A more complete analysis is possible if some reasonable assumption may be made about the variation of τ_0 with temperature. For example, τ_0 is sometimes proportional to the viscosity η, especially for viscous liquids (7, 9, 10), or, with more justification (11), to η/T.

Can. J. Chem. Downloaded from www.nrcresearchpress.com by 210.87.254.6 on 09/05/12
For personal use only.

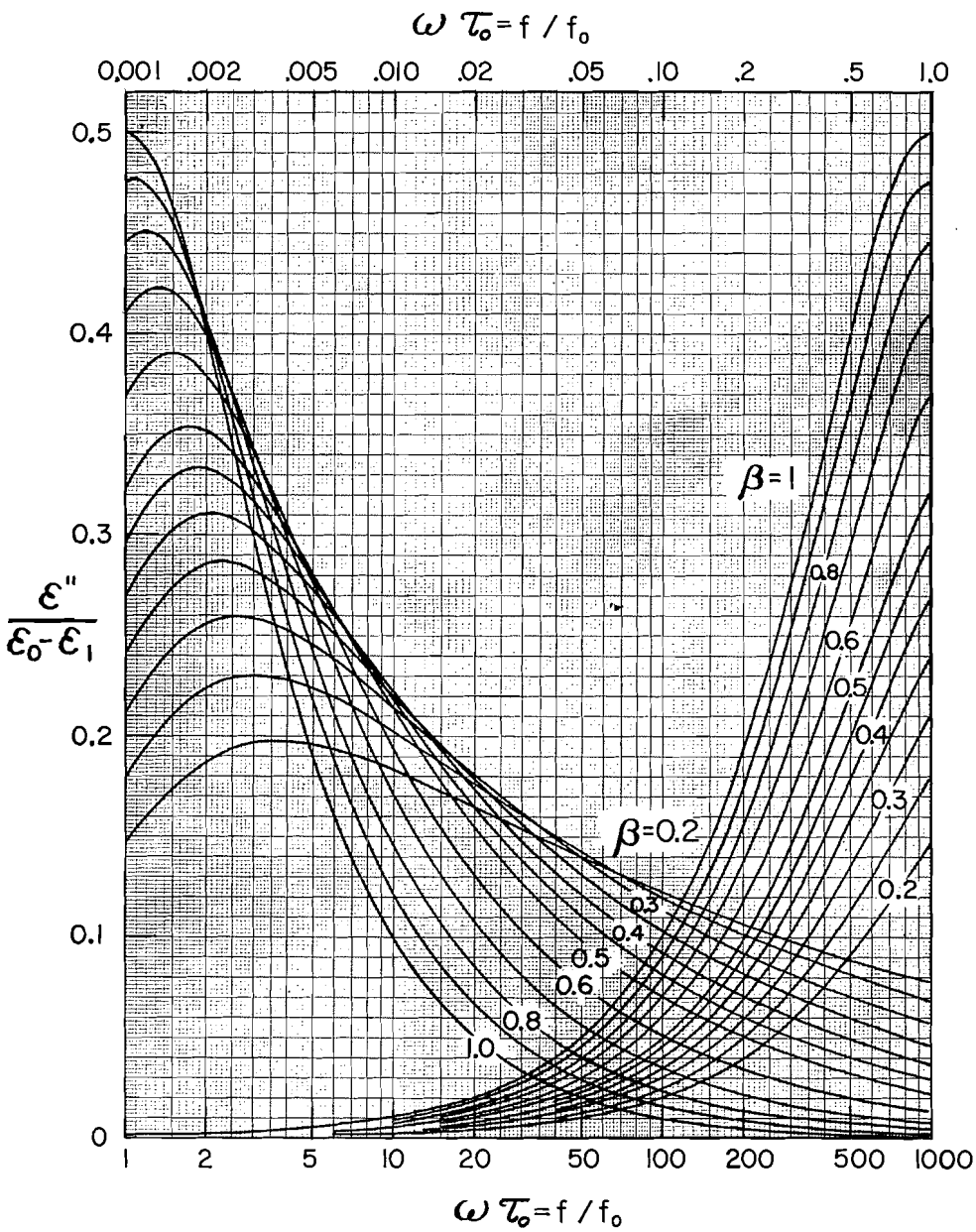


FIG. 3. Variation of ϵ'' with frequency for skewed-arc behavior.

An alternative method may be applied to data obtained at a fixed frequency over an adequate temperature range. The maximum in a plot of $\epsilon''/(\epsilon_0-\epsilon_1)$ versus temperature occurs at a temperature (T_0) such that the value of τ_0 is related to the fixed frequency of measurement $\omega_t/2\pi$ by

$$[6] \qquad \omega_t\tau_0 = \tan\frac{\pi}{2(1+\beta)} \qquad (\text{at } T_0).$$

Can. J. Chem. Downloaded from www.nrcresearchpress.com by 210.87.254.6 on 09/05/12
For personal use only.

At the same temperature (T_0) equations [3] and [4] become

$$[7] \qquad \frac{\epsilon' - \epsilon_1}{\epsilon_0 - \epsilon_1} = \left[\cos \frac{\pi}{2(1+\beta)}\right]^{1+\beta} \tan \frac{\pi}{2(1+\beta)} \qquad (\text{at } T_0),$$

and

$$[8] \qquad \frac{\epsilon''}{\epsilon_0 - \epsilon_1} = \left[\cos \frac{\pi}{2(1+\beta)}\right]^{1+\beta} \qquad (\text{at } T_0).$$

The variations of these functions with β are shown in Fig. 4. The simplest method of

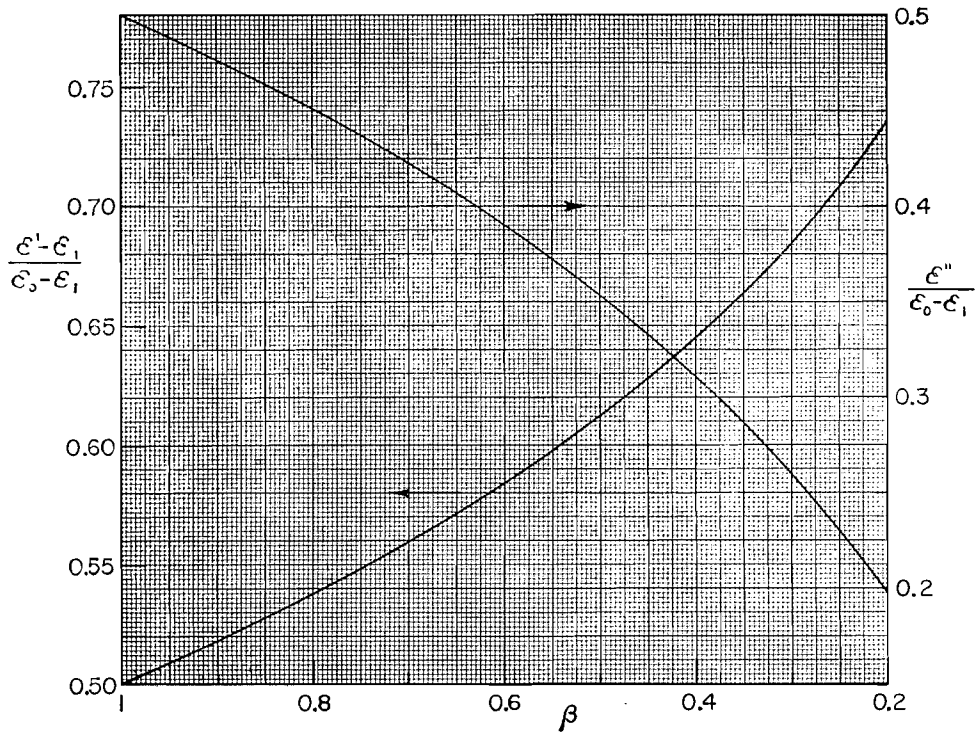


FIG. 4. Variation of reduced ϵ' and ϵ'' with β under conditions of maximum loss.

estimating β and τ_0 is from

$$[9] \qquad \frac{\epsilon' - \epsilon_1}{\epsilon''} = \omega_f \tau_0 = \tan \frac{\pi}{2(1+\beta)} \qquad (\text{at } T_0).$$

Determination of β and τ_0 from values of ϵ' and ϵ'' for a fixed frequency at the temperature of maximum loss, however, is meaningful only if there is some reason to believe that the behavior is of the skewed-arc type. This may be tested by considering the data at other temperatures. In one approach that has proved useful, the temperature dependence of the relaxation time τ_0 is assumed to be given by

$$[10] \qquad \tau_0 = Ae^{B/T}$$

over a narrow temperature range about T_0 and β is considered constant over this same temperature range. Suppose that two temperatures T_1 and T_2 are defined by $1/T_1$

Can. J. Chem. Downloaded from www.nrcresearchpress.com by 210.87.254.6 on 09/05/12
For personal use only.

$= 1/T_0 - \Delta$ and $1/T_2 = 1/T_0 + \Delta$. Δ may be chosen, for example, to make ϵ'' of the order of $\epsilon_{max}''/2$. The values of $\epsilon''/(\epsilon' - \epsilon_1)$ at T_1 and T_2, according to equation [5], are then

$$\tan \beta[\tan^{-1}(\omega_f \tau_0^0 e^{-B\Delta})] \quad \text{and} \quad \tan \beta[\tan^{-1}(\omega_f \tau_0^0 e^{B\Delta})],$$

respectively, in which τ_0^0 is the value of τ_0 at T_0. τ_0^0 and β are assumed to have been determined by the method of the previous paragraph. A necessary condition for the skewed-arc locus is that for some value of $B\Delta$ a pair of $\epsilon''/(\epsilon' - \epsilon_1)$ values can be computed which agree, within the experimental uncertainty, with the measured values at T_1 and T_2. Such pairs of values are given, for different values of β and $B\Delta$, in Fig. 5. If the data warrant it, the value of B so obtained may be used to calculate the dependence of ϵ' and ϵ'' on temperature, with the help of Figs. 2 and 3.

Under similar assumptions, the Cole–Cole symmetrical-arc locus gives rise to values of ϵ'' which are symmetrical in $1/T$ about the temperature of maximum loss and $\epsilon' - \epsilon_1$ at T_1 is equal to $\epsilon_0 - \epsilon'$ at T_2.

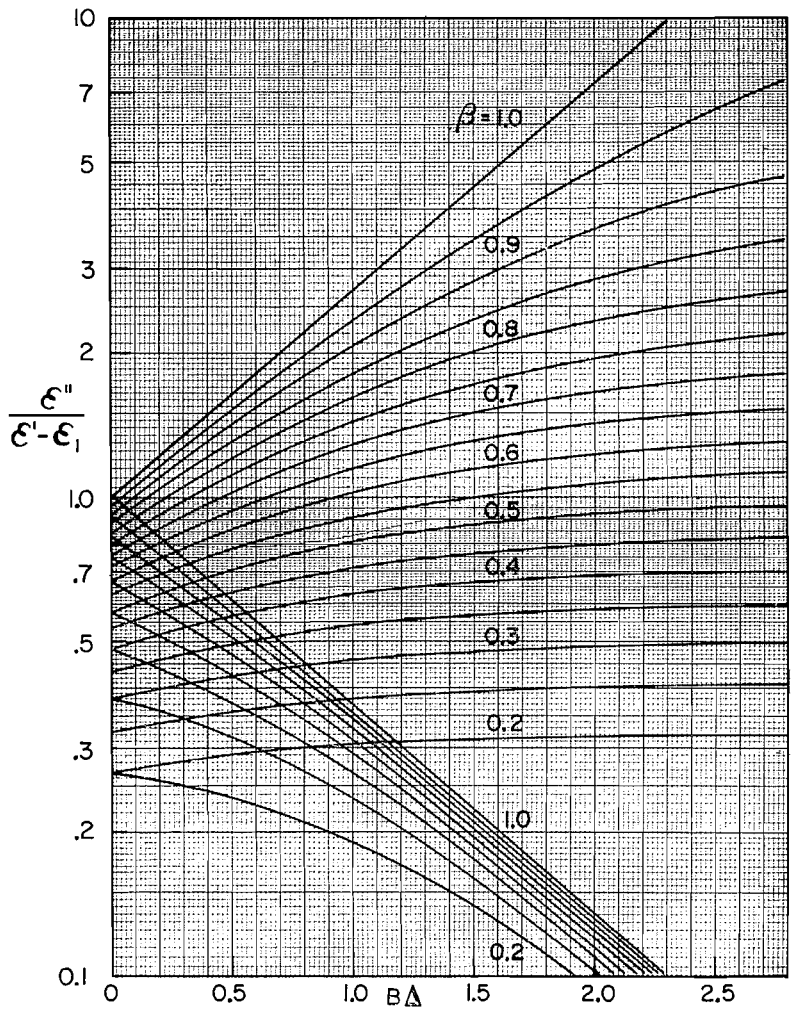


FIG. 5. Compatibility relationships for skewed-arc behavior at temperatures other than those of maximum loss.

Can. J. Chem. Downloaded from www.nrcresearchpress.com by 210.87.254.6 on 09/05/12
For personal use only.

Transient Measurements

At temperatures sufficiently low that polarization takes place too slowly to follow the changing phase of a low-frequency voltage, transient methods may be substituted for bridge methods. In these the charging or discharging current is measured as a function of time following application or removal of a suitable voltage.

TABLE I

Applied voltage	Transient current $I(t)$, $t \geqslant 0$, for: Debye locus	Skewed-arc locus
$V(t) = 0, \quad t < 0$ $= V_0, \quad t \geqslant 0$	(1) $V_0C_0\left[\epsilon_1\delta_0+\frac{\epsilon_0-\epsilon_1}{\tau}e^{-t/\tau}\right]$	(2) $V_0C_0\left[\epsilon_1\delta_0+\frac{\epsilon_0-\epsilon_1}{\tau_0\Gamma(\beta)}\left(\frac{t}{\tau_0}\right)^{\beta-1}e^{-t/\tau_0}\right]$
$V(t) = 0, \quad t < 0$ $= at, \quad t \geqslant 0$	(3) $aC_0\left[\epsilon_1+(\epsilon_0-\epsilon_1)(1-e^{-t/\tau})\right]$	(4) $aC_0\left[\epsilon_1+(\epsilon_0-\epsilon_1)\frac{\Gamma t/\tau_0(\beta)}{\Gamma(\beta)}\right]$

Table I summarizes the transient currents which follow the application of step and ramp voltage pulses to dielectrics having the Debye and skewed-arc characteristics. These equations result from application of the method of Fourier transforms (12, 13) to the equations for the frequency-dependent loci. The time variation of charge on the sample for a step voltage has the same form as the variation of current through the sample for a ramp voltage.

In Table I C_0 is the capacitance of the empty cell, δ_0 the delta function or unit impulse at $t = 0$, $\Gamma_{t/\tau_0}(\beta)$ and $\Gamma(\beta)$ the incomplete and complete gamma-function, respectively. The ratio of the two gamma-functions has been tabulated by Pearson (14), whose parameters are related to the present ones by $u = t/(\tau_0\sqrt{\beta})$ and $p = \beta-1$.

The ramp pulse is the more convenient since it does not give rise to the initial current surge which accompanies application of the step voltage and since it is somewhat simpler to evaluate the required parameters from the experimental transient behavior. However, it is easier to generate a constant voltage than a linearly rising one and the former may be used to advantage in the investigation of comparatively slow relaxation (as has been done, for example, with *n*-propanol at low temperatures (15)). An approximate method has been given by Hamon (16) for converting the results of time-dependent direct-current measurements to the equivalent frequency-dependent dielectric loss form.

In general transient methods do not seem capable of the same accuracy as bridge methods. They are, however, useful for extending the range of temperatures over which measurements of relaxation can be made by some 10 or 20°.

IV. EXPERIMENTAL EVIDENCE FOR THE SKEWED-ARC LOCUS

Hydroxyl Compounds

Practically all monohydroxyl alcohols that have been so far investigated are satisfactorily represented by the Debye semicircle in the complex plane (6), except for secondary dispersion regions (to be discussed below) at comparatively high frequencies which usually make a minor contribution to the value of the static dielectric constant. This semicircular behavior may be regarded as a limiting case of either the circular-arc locus of Cole and Cole (with $\alpha = 0$) or of the skewed-arc locus (with $\beta = 1$). At least one monohydroxyl alcohol, tetrahydrofurfuryl alcohol, exhibits an asymmetric dispersion locus of the skewed type. This is illustrated by Fig. 6 for which the data were obtained by L. Kuhi in this laboratory.

Can. J. Chem. Downloaded from www.nrcresearchpress.com by 210.87.254.6 on 09/05/12
For personal use only.

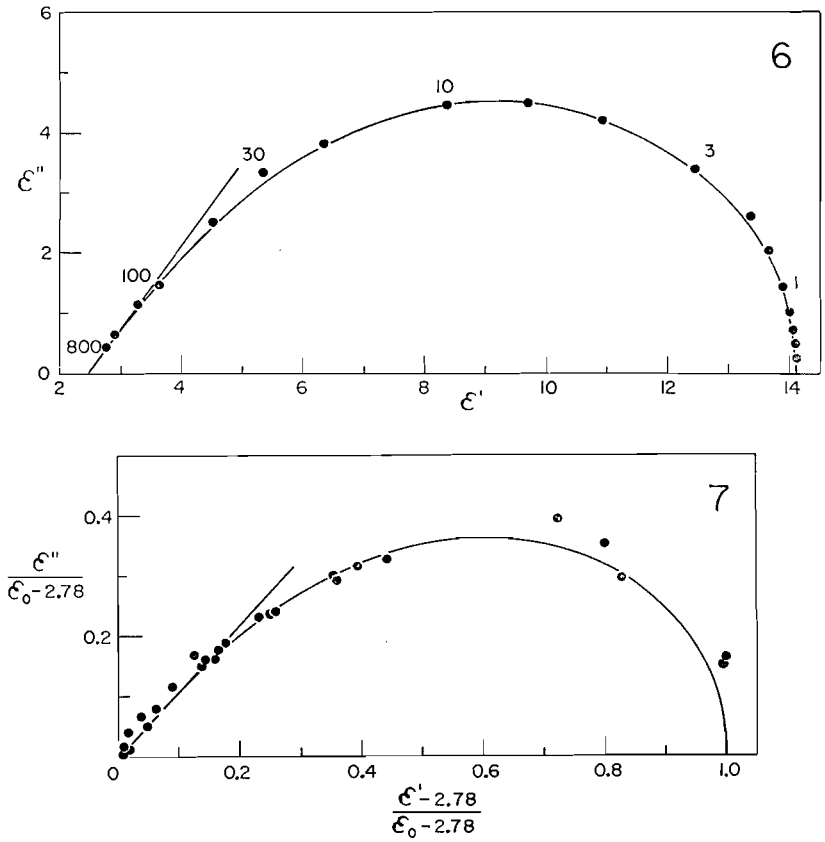


FIG. 6. Tetrahydrofurfuryl alcohol at −105.9° C. Skewed-arc locus is drawn for $\beta = 0.592$. Numbers beside points are frequencies in kc/sec.

FIG. 7. Aggregate plot for 2-methyl-2,4-pentanediol at temperatures between −45 and −79° C and frequencies of 1, 10, 30, and 100 kc/sec. Locus is drawn with $\beta = 0.525$.

The skewed-arc locus was originally used to describe the dispersion–absorption behavior of the polyhydroxyl liquids glycerol (7), 1,2-propanediol (7), and 1,3-propanediol (8). Data for the first two of these liquids are included in Fig. 11. The predicted form of transient current for systems giving skewed-arc loci (formula (4) of Table I) has been shown (12) to fit the transient behavior of glycerol at temperatures at which τ_0 is of the order of milliseconds. Koizumi and Hanai (17) expressed the results of a study of supercooled tetraethylene glycol by the skewed arc.

The dispersion of five isomeric pentanediols is accurately represented by equation [2] (18). 2-Methyl-2,4-pentanediol was examined by White and Morgan (19) whose data for four frequencies and a number of temperatures are shown in the aggregate plot of Fig. 7. The skewed-arc locus drawn represents the results in a satisfactory manner when it is considered that the variation of β with temperature is ignored. Data are not reported at sufficiently small temperature intervals to make analysis by the maximum loss method possible.

Halogen Compounds

Denney (20) has used the skewed-arc locus to describe the dielectric behavior of isobutyl bromide, isoamyl bromide, and isobutyl chloride at low temperatures. Winslow,

Can. J. Chem. Downloaded from www.nrcresearchpress.com by 210.87.254.6 on 09/05/12
For personal use only.

Good, and Berghausen (21) found it fitted the behavior of pentachlorobiphenyl (a mixture of isomers bearing the trade name Arochlor 1254) and hexachlorobiphenyl (Arochlor 1260), at temperatures below room temperature. Examination of the Massachusetts Institute of Technology data at 25° C (22), though reported only at frequencies which differ, for the most part, by a factor of 10, shows that in all probability the same behavior extends to higher temperatures. The M.I.T. tables indicate that the other polychlorodiphenyls probably exhibit skewed-arc-locus behavior. This is true also for Arochlor 4465 (a mixture of chlorinated bi- and ter-phenyls) and Arochlor 5460 (nonochloroterphenyls) for which β appears to be of the order of 0.2 and lower frequency measurements show the presence of d-c. conductance.

The skewed-arc behavior of 1,2-dibromopentane is illustrated in Fig. 8(*a*), which gives the results of bridge measurements at $-112°$ where τ_0 is of the order of a millisecond, and in Fig. 8(*b*), which presents transient results at $-127°$ where τ_0 is of the order of 10 seconds.

The method based on the temperature of maximum loss (see III) may be applied to the data of Turkevich and Smyth (23) for 2-methyl-1,2-dichloropropane, shown for low

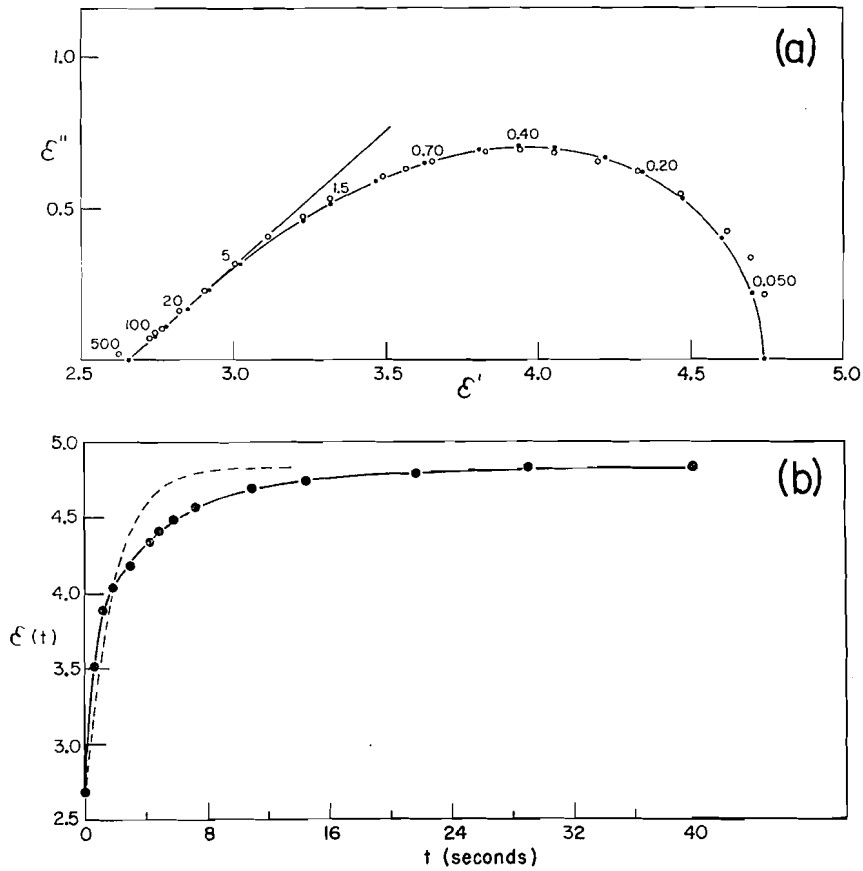


FIG. 8(*a*). ○ Data for 1,2-dibromopentane at $-112.0°$ C, ● calculated points for $\beta = 0.463$, $\tau_0 = 7.58 \times 10^{-4}$ sec.

FIG. 8(*b*). Transient data for 1,2-dibromopentane at $-127.2°$ C. Solid curve is the incomplete Γ-function with $\beta = 0.35$, $\tau_0 = 8.6$ sec, broken curve the exponential which rises to $(1-e^{-1})(\epsilon_0-\epsilon_1)$ in the same time.

Can. J. Chem. Downloaded from www.nrcresearchpress.com by 210.87.254.6 on 09/05/12
For personal use only.

temperatures in Fig. 9. The 50-kc points show a loss maximum of about 5.45 at −137.9° C. At this temperature and frequency $\epsilon' = 12.65$ and, taking $\epsilon_1 = 2.30$ (a reasonable value since ϵ' approaches 2.36 at −188° C), one finds $(\epsilon' - \epsilon_1)/\epsilon'' = 1.901$. The relaxation time τ_0 (at −137.9° C) is then $1.90/(2\pi \times 50{,}000)$ or 6.1×10^{-6} seconds and $\beta = 0.446$ (equation [9]). For $\Delta = 2 \times 10^{-4}$, T_1 is −141.5° C and T_2 is −134.1° C, which correspond to $\epsilon''/(\epsilon' - \epsilon_1)$ values of about 0.756 and 0.177, respectively. Inspection of Fig. 5, for $\beta = 0.45$ shows a value of $B\Delta$ at T_1 of about 1.37 and at T_2 of about 1.51. This is satisfactory agreement, which may be improved by allowing β to assume values slightly smaller than 0.45. B is then 7.2×10^3 and the "energy of activation" (BR) some 14 kcal/mole. Application of the same technique to the 5-kc points leads to a similar value of β. The loss maximum at 500 c, however, of the order of $(\epsilon_0 - \epsilon_1)/2$, is anomalously high. A similar anomaly for isobutyl chloride at the same frequency (23) is not confirmed by the results of Denney (20).

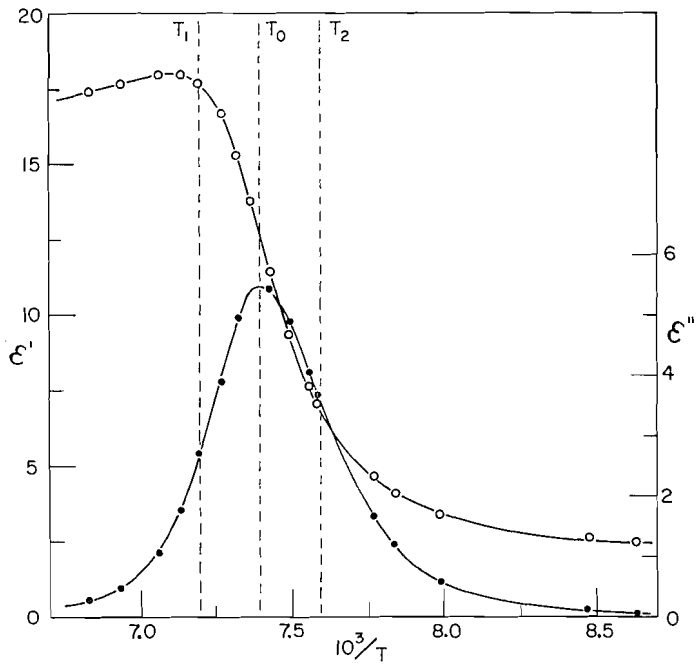


FIG. 9. Low-temperature dielectric behavior of 2-methyl-1,2-dichloropropane at 50 kc/sec.

Miscellaneous Compounds

Grant, Davidson, and Gray (24) found *n*-propyl nitrite at low temperatures to fit the skewed locus (see Fig. 11) as did Winslow, Good, and Berghausen (21) in the case of tolyl xylyl sulphone.

Schallamach's data at 9 Mc for the aldehyde citral (25), analyzed by the method of maximum loss, give results consistent with the skewed-arc locus, with β of the order of 0.75 and an activation energy of some 11 kcal/mole. The same author's results for the corresponding alcohol, geraniol, on the other hand, are adequately described by a single relaxation time ($\beta = 1$).

Polymers

Polar polymers in general exhibit very broad loss spectra (see, for example, the M.I.T.

Can. J. Chem. Downloaded from www.nrcresearchpress.com by 210.87.254.6 on 09/05/12
For personal use only.

tables (22)) which, although they may resemble the skewed-arc behavior in some respects, do not accurately conform to it. Dielectric relaxation in polymers proceeds by orientation of chain segments (26) and therefore differs from that in simple liquids.

The case of the poly(vinyl acetates) has been investigated by the author in some detail. Seven Gelvas (Shawinigan Chemicals Limited) ranging in Gelva number from 1.5 to 134 and in number-average molecular weight from 5,000 to ca. 200,000 were studied. The locus shown in Fig. 10, in which the ordinates are in arbitrary capacitance units, is

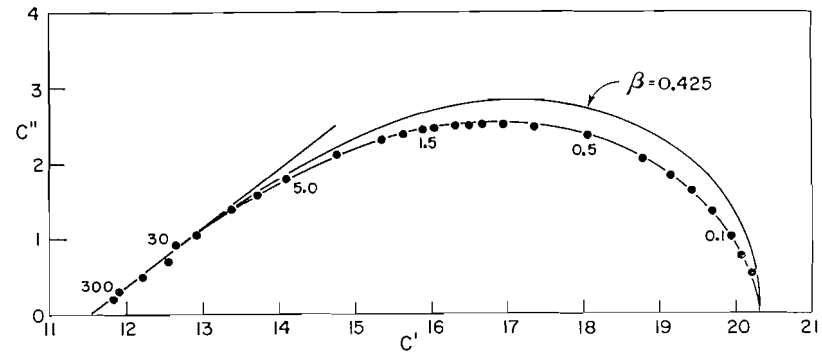


FIG. 10. Poly(vinyl acetate) (Gelva 134) at 68° C.

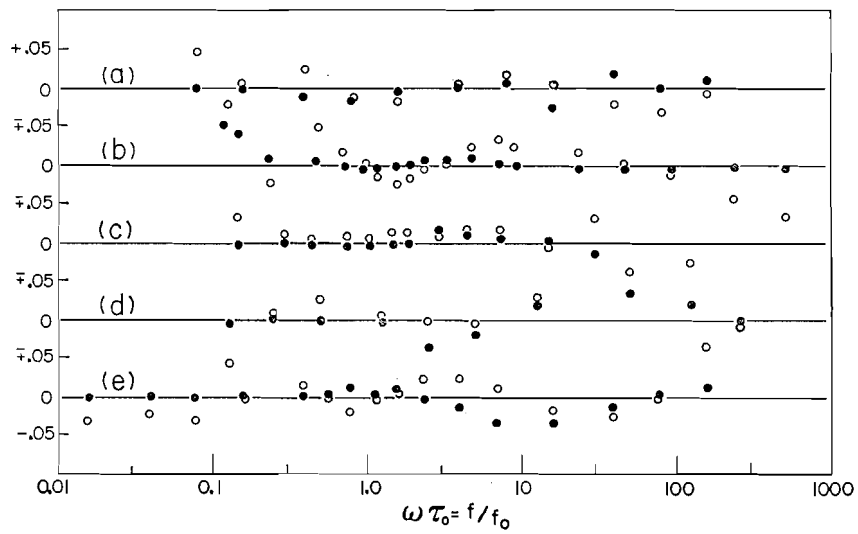


FIG. 11. $(\epsilon_{obs}' - \epsilon_{calc}')/\epsilon_{obs}'$ (●) and $(\epsilon_{obs}'' - \epsilon_{calc}'')/\epsilon_{obs}''$ (○) vs. frequency, for the liquids and parameters listed in Table II.

typical. The loss in the vicinity of the maximum and at lower frequencies is less than would be predicted by equation [2] for a β determined by the high frequency behavior, generally between 0.40 and 0.45. There appears to be no consistent dependence of this high frequency β on molecular weight. There is evidence that the presence of traces of benzene may broaden the loss spectrum.

Figure 11 illustrates the extent of the agreement for five liquids between the experimental values of ϵ' and ϵ'' and those computed from equation [2] with the parameters

Can. J. Chem. Downloaded from www.nrcresearchpress.com by 210.87.254.6 on 09/05/12
For personal use only.

shown in Table II. There appears to be no systematic disagreement. Periodic variations seem to be due to temperature fluctuations of the sample.

TABLE II

Parameters used to calculate $\epsilon(i\omega)$ in Fig. 11

	Liquid	T (° K)	ϵ_0	ϵ_1	β	τ_0 (sec)	Reference
(*a*)	Glycerol	223.2	64.1	4.10	0.603	1.26×10^{-4}	42
(*b*)	1,2-Dibromopentane	161.2	4.73_9	2.65_4	0.463	7.58×10^{-4}	This work
(*c*)	Isoamyl bromide	133.8	13.16	2.84	0.60	2.36×10^{-6}	20
(*d*)	*n*-Propyl nitrite	95.9	40.13	3.58	0.705	3.93×10^{-4}	This work
(*e*)	1,2-Propanediol	209.0	53.71	3.68	0.693	1.24×10^{-5}	8

V. THE EFFECT OF TEMPERATURE ON THE DISPERSION

There is therefore good experimental evidence for the rather general occurrence in liquids of a relaxation behavior that can be characterized by the skewed-arc locus. Most of this evidence has been obtained at low temperatures where the relaxation processes are sufficiently slow to be studied by accurate techniques. Whether these observations are valid only at low temperatures or may be extended to higher temperatures as well remains to be determined. Unfortunately many of the experimental results presented in the literature are not sufficiently complete to enable the shape of the dispersion–absorption locus to be adequately defined.

An interesting example of what might be a change in the shape of the dispersion locus with temperature is provided by the case of tetraethylene glycol. In the supercooled state, at temperatures between -44 and $-71°$ C, this glycol shows (17) a dielectric relaxation behavior very near that represented by the skewed arc with a β value of the order of 0.4. Koizumi (27) extended the measurements to higher temperatures and to microwave frequencies and found that the new results could be best represented by the symmetrical-arc locus. The parameter α of the Cole–Cole representation for tetraethylene glycol assumed values ranging from 0.23 at 5° C to 0.14 at 50° C (see Fig. 12(*a*)). An attempt is made to represent Koizumi's microwave data for tetraethylene glycol by the skewed locus in Fig. 12(*b*) by assuming values of β of about 0.60 at 5° and about 0.70 at 50°. It can be seen that this representation is not quite as successful as the circular-arc one, although there is not sufficient data near the top and on the low-frequency side of the locus to establish the preference of either representation with any certainty.

Glarum (28) has recently extended the low temperature measurements of Denney (20) on isoamyl bromide to the temperature range between $-75°$ and 25° and to microwave frequencies. He has concluded that for this liquid the skewed-arc representation probably remains valid at these higher temperatures.

VI. THE RESOLUTION OF RELAXATION PROCESSES

The separation of the effects of different relaxation processes is of obvious importance if the individual mechanisms of relaxation are to be studied. It is necessary to distinguish between (*a*) the case in which each relaxation process is independent of the others and the principle of superposition may be applied to the polarization or the complex dielectric constant and (*b*) the case in which two or more relaxation mechanisms occur either as successive stages or alternate routes in the relaxation process and superposition may not be used to separate the individual components of relaxation. Examples of case (*a*) include orientation of a polar group within the molecule by a different mechanism from

Can. J. Chem. Downloaded from www.nrcresearchpress.com by 210.87.254.6 on 09/05/12
For personal use only.

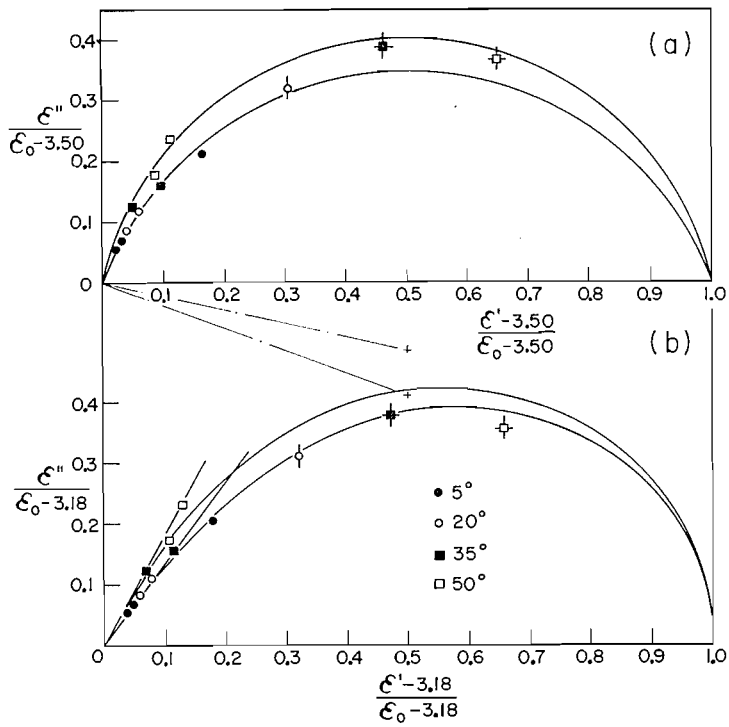


FIG. 12. Comparison of symmetric-arc (*a*) and skewed-arc (*b*) representations of microwave data for tetraethylene glycol.

orientation of the molecule as a whole, and orientation of different molecules in different *fixed* environments by different mechanisms. For each of these examples, assuming only two modes of relaxation, the total polarization decays as

$$P(t) = P_1 e^{-t/\tau_1} + (P_0 - P_1) e^{-t/\tau_2},$$

in which P_0 is the initial polarization, P_1 the polarization contributed by the first process, and τ_1 and τ_2 are the relaxation times of the two processes, each assumed to decay exponentially. An example of case (*b*) is provided by the orientation of molecules whose environments are subject to change during the period of relaxation and whose relaxation rates change with the environment. If there are only two types of environment, the simplest form of the polarization is

$$P(t) = P_0 e^{-t/\tau_1} e^{-t/\tau_2},$$

which is indistinguishable from a simple exponential decay function. Brot has proposed a model to account for the failure of superposition when the resolved dispersion regions apparently overlap (29).

(a) Independent Polarization Processes

Discontinuous Relaxation

Even in this case, the nature of relaxation spectra is such that resolution of different processes is difficult unless the corresponding relaxation times are widely different. This is illustrated in Fig. 13 for the most favorable case possible, that of two independent

Can. J. Chem. Downloaded from www.nrcresearchpress.com by 210.87.254.6 on 09/05/12
For personal use only.

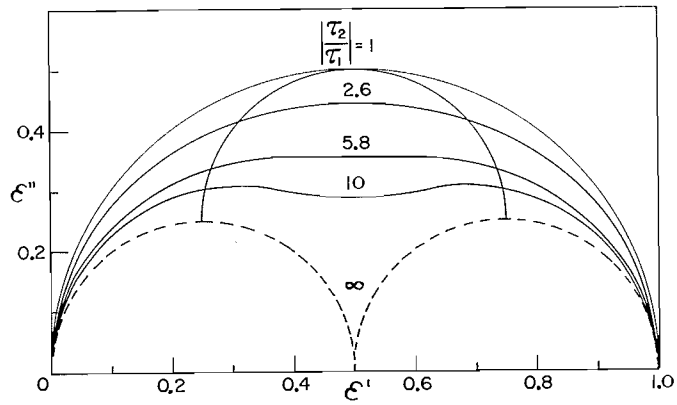


FIG. 13. Dependence of locus of $\epsilon'-i\epsilon'' = 0.5(1+i\omega\tau_1)^{-1}+0.5(1+i\omega\tau_2)^{-1}$ on τ_2/τ_1. Upper semicircle is locus of points at which $\omega = 1/\tau_1$ and $1/\tau_2$.

polarization processes each characterized by a single relaxation time and by the same amplitude of dispersion. Separate loss maxima occur only for relaxation times which differ by more than a factor of 5.8 (strictly, $3+2\sqrt{2}$). If the individual dispersion regions are considerably broader than this and are considerably different in amplitude, separate loss peaks may appear only when the appropriate relaxation times or critical frequencies differ by a factor of 100 or more. It is not surprising that the results may sometimes be analyzed in more than one way.

Examples of solutions for which the relaxation spectra are readily resolvable have been given (30, 31, 32), but most of the liquids that have been extensively studied exhibit broad dispersion–absorption behavior in which separate loss peaks do not occur.

The monohydroxyl alcohols, in addition to the principal (semicircular) dispersion region, show at considerably higher frequencies one or more additional dispersion regions of relatively small amplitude. Although in general not showing separate ϵ'' peaks, the high-frequency data for some alcohols have been reduced to a Cole–Cole arc by subtracting the contributions of the Debye relaxation region. A second dispersion region has been defined in this way for the alcohols from ethanol through the butanols (except for *t*-butanol) (33, 34, 35), for *n*-hexanol (36), cyclohexanol (37), *n*-heptanol (36), and four isomeric octanols (36, 38, 39, 40) and for *n*-propanol-*d* (15) and *n*-octanol-*d* (36). Most of these results also show signs of further dispersion at still higher frequencies which, by a further subtraction of the effects of the second dispersion, has been shown to be representable, within rather large experimental uncertainties, by an additional arc in the cases of *n*-propanol, *n*-propanol-*d*, and the octanols.

The question naturally arises as to whether behavior such as has been described by the asymmetric locus of equation [2] can be represented by the superposition of several discrete relaxation processes. Poley (41) first suggested that the main relaxation properties of glycerol could be attributed to the combined effects of a low-frequency semicircle and a high-frequency symmetric arc. Cole (42) has indicated that a detailed examination of the experimental data for glycerol does not support this suggestion. A number of glycols (1,2-ethanediol, 1,2-propanediol, 1,3-butanediol, and 1,5-pentanediol), which exhibit asymmetric loci have recently been analyzed (43, 44) in terms of one or more high-frequency arcs and a low-frequency semicircle or arc. The relaxation behavior of 1,2-propanediol, for example, over the range of frequencies between 0.1 and 25,000 Mc/sec,

Can. J. Chem. Downloaded from www.nrcresearchpress.com by 210.87.254.6 on 09/05/12
For personal use only.

has been expressed by the superposition of a symmetric arc and a semicircle. The reported (43) parameters at −40° C have been used to construct the locus shown in Fig. 14(*a*).

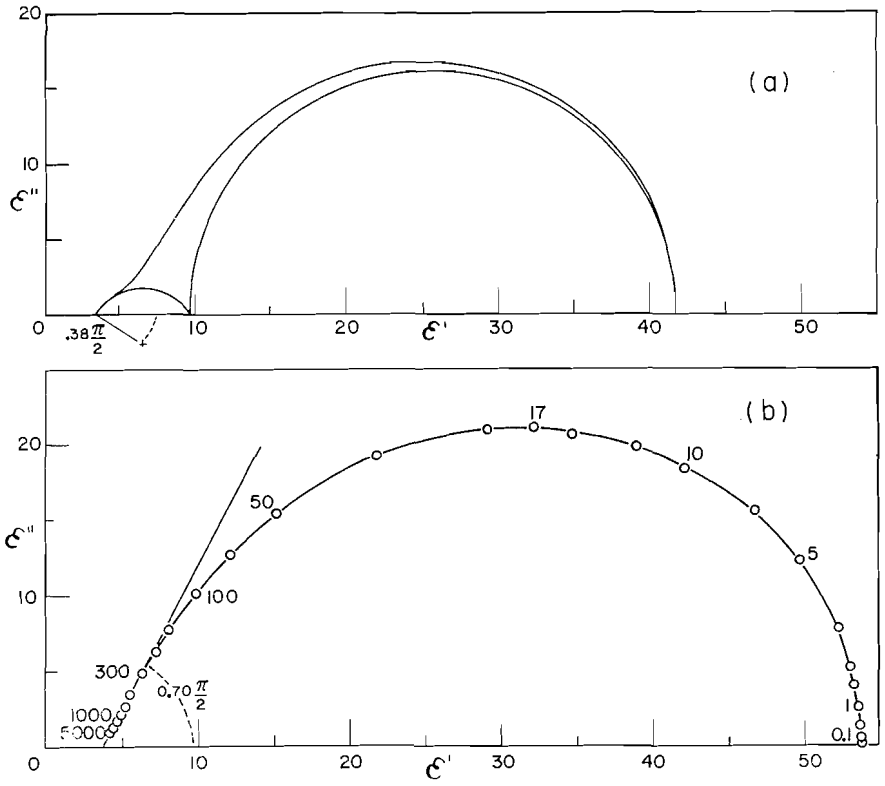


FIG. 14. Comparison for 1,2-propanediol of (*a*) the representation of the behavior at −40° suggested in reference 43 with (*b*) experimental data at −64.2° (●) and skewed-arc locus with $\beta = 0.70$.

From comparison with the locus shown in Fig. 14(*b*), from measurements at −64°C, it must be concluded that either the experimental behavior changes markedly with temperature or that the type of resolution proposed is not justified by the data for this liquid.

In some cases the proposed resolution has led to an overlapping of the resolved regions (29, 38, 44, 45). For example, the low-frequency limiting value of the dielectric constant for the second dispersion region may be appreciably greater than the limiting high-frequency value for the first (low-frequency) dispersion region. Brot (29, 38) has proposed on this basis that the superposition principle, in the form that assumes direct additivity of contributions to the complex dielectric constant from the individual relaxation processes, is violated. Although limitations of space have usually prevented publication of the full experimental data, it appears possible that in at least some cases the data may be adequately described by equation [2] or some other asymmetric representation. It is evident from inspection of Fig. 14(*a*) that a better approximation to the behavior of Fig. 14(*b*) may be realized by allowing the low-frequency side of the arc to overlap the high-frequency side of the semicircle, but it is doubtful whether this will lead to as good a fit of the data as equation [2].

Can. J. Chem. Downloaded from www.nrcresearchpress.com by 210.87.254.6 on 09/05/12
For personal use only.

In most liquids to which the skewed-arc behavior has been attributed there is a slight "tailing-off" of the high-frequency end of the experimental locus which is not described by equation [2] (Fig. 15). Although this behavior may correspond to a separate, very broad relaxation process, it is at least qualitatively predicted by the Glarum model to be considered below.

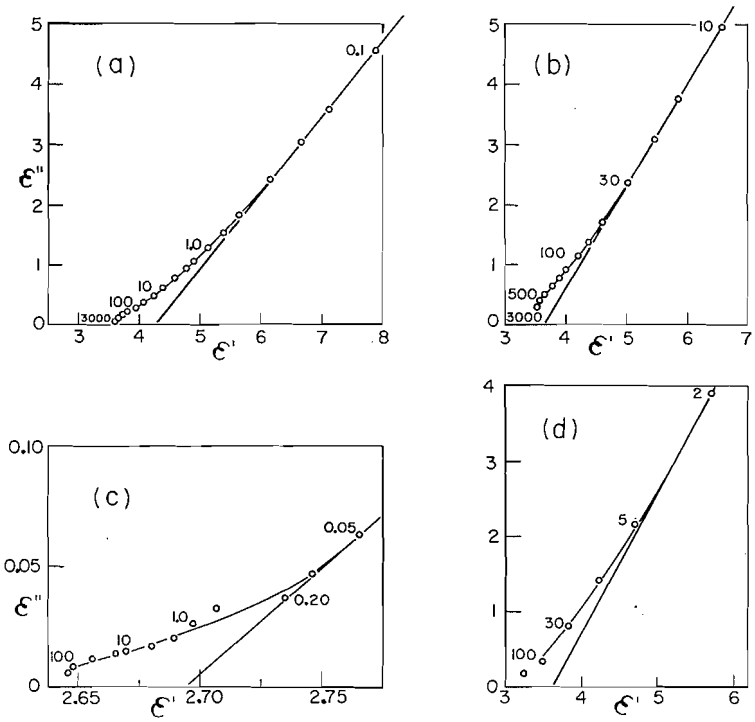


FIG. 15. Departures of dispersion behavior from skewed-arc type (straight lines) at relatively high frequencies for (*a*) glycerol at −70.0°, (*b*) 1,2-propanediol at −77.9°, (*c*) 1,2-dibromopentane at −127.1°, and (*d*) *n*-propyl nitrite at −179°.

Continuous Relaxation

The previous section has mentioned examples of the resolution of dispersion effects into different dispersion regions, some of which are much broader than predicted by the Debye equation. The principle of superposition may be applied to such a dispersion region, assumed to arise from a continuum of simple exponential decay functions, in the form

$$\epsilon(i\omega) = \epsilon_1 + (\epsilon_0 - \epsilon_1) \int_{-\infty}^{\infty} \frac{G(\tau) d \ln \tau}{1 + i\omega\tau}, \qquad [11]$$

which defines, along with $\int_{-\infty}^{\infty} G(\tau) d \ln \tau = 1$, a distribution function $G(\tau)$ such that $G(\tau)\, d \ln \tau$ represents the fractional contribution to $\epsilon_0 - \epsilon_1$ arising from that part of the relaxation process having relaxation times whose logarithms lie between $\ln \tau$ and $\ln \tau + d \ln \tau$.

For the $\epsilon(i\omega)$ of equation [2], $G(\tau)$ becomes (7)

$$G(\tau) = \frac{\sin \beta\pi}{\pi} \left(\frac{\tau}{\tau_0 - \tau} \right)^{\beta}, \qquad \tau \leqslant \tau_0 \qquad [12]$$

$$= 0, \tau > \tau_0,$$

Can. J. Chem. Downloaded from www.nrcresearchpress.com by 210.87.254.6 on 09/05/12
For personal use only.

a function with a singularity at $\tau = \tau_0$. This form of $G(\tau)$ has been criticized (41) as being physically unrealistic. Such a criticism may be applied with equal relevance to the classical Debye behavior, for which $G(\tau) = \delta[\ln(\tau/\tau_0)]$, the delta function. This is an improper function, with discontinuities on both sides of $\tau = \tau_0$. It is nevertheless of use in quantum mechanics where, as in the present case, it occurs as an integrand (46).

It may be argued that the presence of either a unique relaxation time or of a distribution of relaxation times which ends abruptly at its most probable value is inconsistent with the variations in molecular environment that occur in liquids. They do, however, lead formally to expressions for $\epsilon(i\omega)$ which are capable for many liquids of describing the experimental results within the accuracy of the measurements. It may be that additional accuracy will lead to modifications of these distribution functions. The results of Grant, Buchanan, and Cook (6) suggest that a finite distribution of relaxation times is present in water, although the departure from Debye dispersion is barely detectable. It would be possible to modify equation [12] by replacing the abrupt cutoff at $\tau = \tau_0$ by a rapid but monotonic decline to zero for $\tau > \tau_0$ without producing much change in the resulting form of $\epsilon(i\omega)$.

Figure 16 illustrates the integral distribution function

$$F(\tau) = \int_0^{\tau} G(\tau) d \ln \tau$$

for $G(\tau)$ defined by equation [12]. $F(\tau)$ is a special case of the incomplete β-function (7):

$$[13] \qquad F(\tau) = \frac{\sin \beta\pi}{\pi} \int_0^{\tau/\tau_0} (\tau/\tau_0)^{\beta-1}(1-\tau/\tau_0)^{-\beta} d(\tau/\tau_0), \qquad \tau \leqslant \tau_0,$$
$$= 1, \qquad \tau > \tau_0,$$

which may be evaluated by graphical integration. Pearson (47) has tabulated the incomplete β-function for parameters related to those of equation [13] by $p = \beta$, $q = 1-\beta$, and $x = \tau/\tau_0$, but the large intervals between successive entries make these tables of little use for the range of parameters of interest here.

In Fig. 17 the integrated distribution function for $\beta = 0.70$ is compared with the sum of the integrated functions for the Cole–Cole arc and Debye semicircle suggested (see above) for 1,2-propanediol.

The picture of relaxation which results from the assumption of the physical reality of the distribution function of equation [12] is one of molecular rotation which takes place at rates which differ widely and continuously with the molecular environment by mechanisms each of which makes an additive contribution to the dielectric constant and shows a simple exponential dependence on time. The maximum relaxation time in the distribution may then be the orientation time of molecules in surroundings of greatest order. It is not easy to reconcile this picture with the evidence that liquid relaxation is a co-operative process (see next paragraph) nor with the observation that relaxation in many different liquids may be represented by the same simple analytic expression.

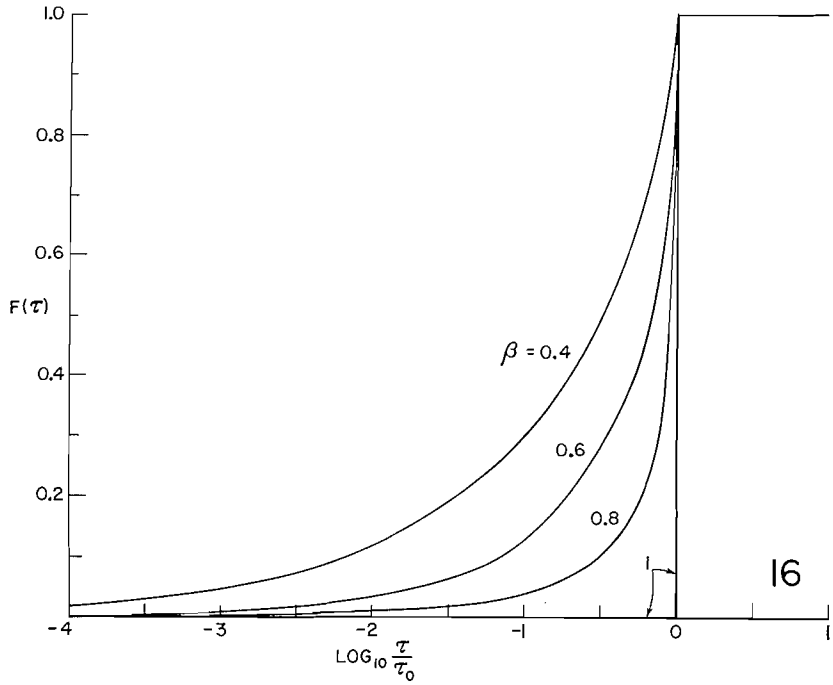
(b) Relaxation Processes not Resolvable by Superposition

It is likely that the behavior characterized by the skewed-arc locus arises from the presence of co-operative processes in which individual molecules in general do not rotate independently of one another.

The evidence for co-operative effects involving many molecules in the relaxation process may be summarized as follows:

Can. J. Chem. Downloaded from www.nrcresearchpress.com by 210.87.254.6 on 09/05/12
For personal use only.

Can. J. Chem. Downloaded from www.nrcresearchpress.com by 210.87.254.6 on 09/05/12
For personal use only.



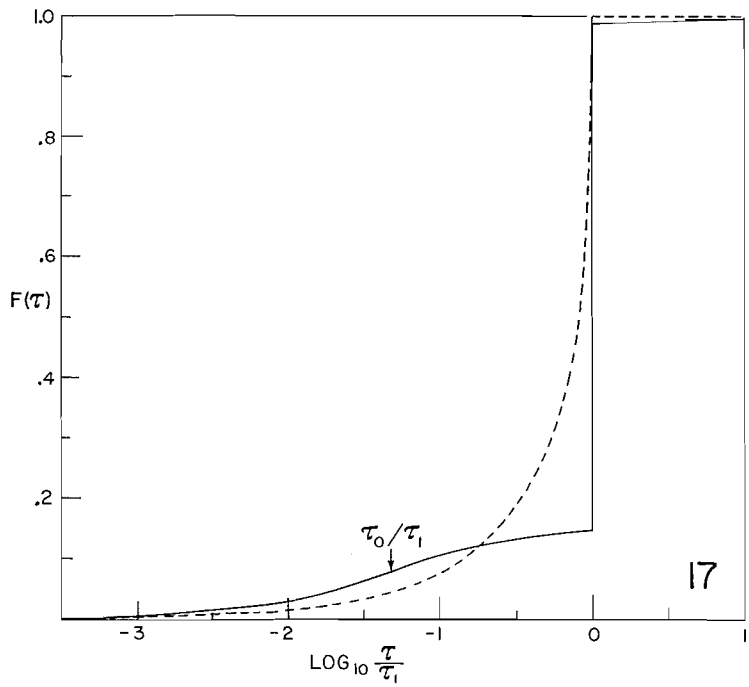


FIG. 16. The integral distribution function of relaxation times for various values of β.
FIG. 17. Comparison of integral distribution function arising from superposition of a semicircle (relaxation time τ_0) and a circular arc ($\alpha = 0.38$, $\tau_1 = 20.9\tau_0$) (solid curve) with that for a skewed arc ($\beta = 0.70$, broken curve).

(*a*) The temperature dependence of the relaxation times of many liquids leads to very large positive entropies of activation (48).

(*b*) Solutions of similar liquids in one another (e.g., alcohols (49) or halides (31)) lead to only one principal dispersion process, with little or no change in the shape of the dispersion. This suggests that the relaxing unit is large enough to contain the different molecules in the same proportion as in bulk solution.

(*c*) A similar inference may be drawn from the effect of electrolytes in changing the relaxation times of water and alcohols (50) without appreciably changing the width of the dispersion region.

(*d*) The similarity between the temperature dependence of such properties as dielectric relaxation time, macroscopic shear viscosity, and d-c. conductance in many liquids at low temperatures (see, for example, references 7 and 9) suggests that a common rate-determining process is involved. Such a process which involves only single molecules is difficult to envisage.

An interesting model which, under some conditions, leads approximately to a skewed-arc locus, has been recently proposed by Glarum (28). The polarization equation is

$$P(t) = P_0 e^{-t/\tau_0}[1-x(t)]$$

where τ_0 is the relaxation time of molecular orientation when there are no defects in the vicinity and $x(t)$ is the mole fraction of molecules which have relaxed completely as a result of the diffusion of defects. For the one-dimensional diffusion of randomly distributed defects in which only the defect initially nearest the molecule is permitted to reach it, the theory (28) leads to

$$\frac{\epsilon(i\omega)-\epsilon_1}{\epsilon_0-\epsilon_1} = \frac{1}{1+i\omega\tau_0} + \frac{i\omega\tau_0}{(1+i\omega\tau_0)[1+\sqrt{a_0(1+i\omega\tau_0)}]}$$

with $a_0 = l_0^2/D\tau_0$, where l_0 is the average distance over which the nearest defect must diffuse to reach the molecule when the diffusion coefficient is D. Since l_0^2/D represents an average diffusion time, a_0 may be considered to be the ratio of a relaxation time arising from the diffusion of defects to a relaxation time in the absence of defects. The locus changes gradually with increasing a_0 from a skewed-arc locus with $\beta = 0.5$ for $a_0 = 1$ to a simple Debye semicircle for $a_0 \gg 1$. The behavior at some intermediate values of a_0 is illustrated in Fig. 18. It is apparent that there is significant departure from a skewed arc only at high frequencies.

As plotted in Fig. 18 the Glarum locus approaches the origin at an angle of 45° with the real axis at high frequencies, a feature which gives the appearance of a small additional dispersion region for values of a_0 greater than unity. Since experimental results frequently show effects of roughly this type (compare Fig. 15), the value of ϵ_1 for "best fit" of the Glarum locus to experimental data is somewhat lower than that which is used for the skewed-arc representation (by an amount $\Delta\epsilon_1$). A more realistic comparison of the two representations than is shown in Fig. 18 is possible if the Glarum locus is expanded by a factor $1+\Delta\epsilon_1/(\epsilon_0-\epsilon_1)$ and the high-frequency intercept shifted a distance of $-\Delta\epsilon_1/(\epsilon_0-\epsilon_1)$ from the origin. The Glarum locus for $a_0 = 8$ has been modified in this way for $\Delta\epsilon_1 = 0.0175(\epsilon_0-\epsilon_1)$, and the results compared with the skewed-arc representation for $\beta = 0.756$ in Table III. For values of $\omega\tau_0$ up to about 30 the differences are well within the likely error of any comparable experimental data.

Can. J. Chem. Downloaded from www.nrcresearchpress.com by 210.87.254.6 on 09/05/12
For personal use only.

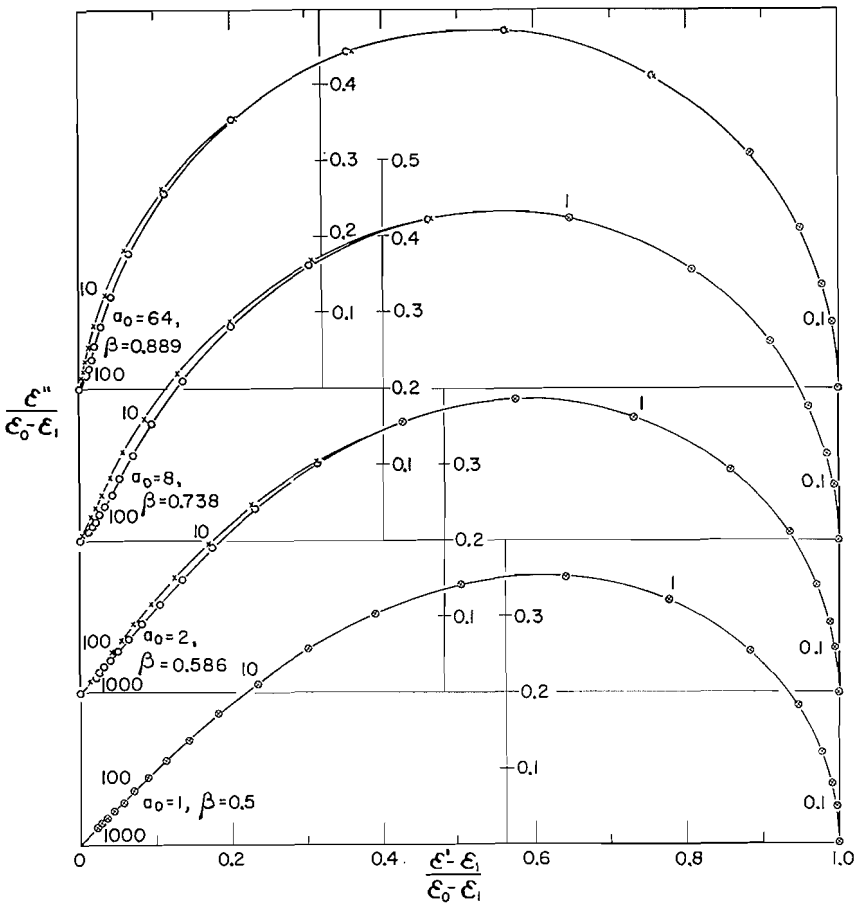


FIG. 18. Comparison of Glarum plots (O) for various values of a_0 with skewed-arc plots (×) for values of $\beta = \sqrt{a_0}/(1+\sqrt{a_0})$. Successive frequencies increase by a factor of 1.585.

As may be inferred from Fig. 18, $\Delta\epsilon_1$ becomes very small as a_0 either gets very large or approaches 1. The Glarum model therefore cannot account for the high-frequency dispersion effects appearing in the spectra of the alcohols (VI(a)) nor for some of the effects illustrated in Fig. 15. It is apparent, however, that a more critical experimental examination of the frequency range above $\omega\tau_0 = 100$ is required.

The Glarum theory shows, for the first time, that relaxation (which may be relatively slow) by an alternative mechanism to simple molecular orientation in a fixed environment may lead to a broadening of the Debye locus in the sense of increased dispersion and absorption on the high-frequency side, that is, in the sense required for skewed-arc behavior. The theory also predicts the Cole–Cole arc behavior in the case in which a_0 is very small (that is, relaxation proceeds by a defect diffusion mechanism only) and has possible application to relaxation in solids, for which symmetric-arc behavior is common.

It is formally possible for the Glarum model to take into account such co-operative effects as are mentioned above. Thus, τ_0 may be identified with the (macroscopic) relaxation time for co-operative molecular orientation in highly ordered regions of the liquid, a concept which requires further elaboration by a statistical approach.

Can. J. Chem. Downloaded from www.nrcresearchpress.com by 210.87.254.6 on 09/05/12
For personal use only.

TABLE III

Comparison of Glarum and skewed-arc representations

	Modified Glarum locus ($a_0 = 8$)		Skewed-arc locus ($\beta = 0.756$)	
$\omega\tau_0$	Reduced ϵ'	Reduced ϵ''	Reduced ϵ'	Reduced ϵ''
1.000×10^{-2}	0.9999	0.0075	0.9999	0.0076
1.000×10^{-1}	.9936	.0746	.9934	.0750
2.512	.9608	.1799	.9604	.1808
6.310	.8042	.3638	.8024	.3638
1.000×10^{0}	.6394	.4313	.6377	.4306
1.585	.4502	.4303	.4498	.4294
2.512	.2922	.3694	.2925	.3696
3.981	.1858	.2881	.1853	.2895
6.310	.1205	.2144	.1184	.2156
1.000×10	.0803	.1566	.0773	.1566
1.585	.0546	.1140	.0516	.1123
2.512	.0371	.0833	.0351	.0800
3.981	.0247	.0612	.0242	.0568
6.310	.0154	.0454	.0168	.0402
1.000×10^{2}	.0084	.0340	.0117	.0284
1.585	.0029	.0257	.0082	.0201
2.512	−0.0014	.0195	.0058	.0142
3.981	−0.0047	.0149	.0041	.0103
6.310	−0.0074	.0115	.0029	.0071
1.000×10^{3}	−0.0095	.0089	.0020	.0050
∞	−0.0175	0	0	0

VII. OTHER RELAXATION PHENOMENA

Distributions of relaxation times have long been used in the interpretation of relatively slow viscoelastic or mechanical relaxation processes. More recently (51, p. 454) the need for distributions of relaxation times has been demonstrated by the results of measurements of the dispersion of sound velocity and the absorption of ultrasonic energy in liquids. Although the measurements are not of sufficient accuracy to preclude other possible distributions, and the distribution function is not defined in quite the same way, it is interesting to find that the application of the distribution function of equation [12] to the complex compressional modulus leads to an adequate description of the main aspects of ultrasonic relaxation in a number of polyhydroxyl compounds (51, p. 479).

The classical theory of the nuclear magnetic resonance correlation time has been modified (52) to provide better agreement with experiment by the introduction of a distribution of correlation times. For two of the liquids showing the skewed-arc-locus type of dielectric behavior (glycerol (53) and isobutyl bromide (54)), the "most probable" correlation times are in surprisingly good agreement with dielectric relaxation times derived from the maxima of the dielectric loss curves. A rectangular distribution function is assumed for the correlation times although other distribution functions are equally possible.

It is likely that such a comparison of dielectric, ultrasonic, and n.m.r. relaxation behavior as has been initiated by Powles (53, 54), will facilitate attempts to devise an adequate mechanism of structural relaxation in liquids.

ACKNOWLEDGMENTS

The author is greatly indebted to Dr. S. D. Baxter for computations on which Figs. 1 to 5 and 18 are based and to Professor R. H. Cole for the opportunity to examine the manuscript of reference 28 in advance of publication.

Can. J. Chem. Downloaded from www.nrcresearchpress.com by 210.87.254.6 on 09/05/12
For personal use only.

Can. J. Chem. Downloaded from www.nrcresearchpress.com by 210.87.254.6 on 09/05/12
For personal use only.

REFERENCES

1. F. BUCKLEY and A. A. MARYOTT. Tables of dielectric dispersion data for pure liquids and dilute solutions. Natl. Bur. Standards Circular 589. 1958.
2. K. S. COLE and R. H. COLE. J. Chem. Phys. **9**, 341 (1941).
3. C. P. SMYTH. Dielectric behavior and structure. McGraw-Hill Book Co., Inc., New York. 1955. p. 56.
4. F. BUCKLEY and A. A. MARYOTT. Tables of dielectric dispersion data for pure liquids and dilute solutions. Natl. Bur. Standards Circular 589. 1958. Table 5.
5. E. H. GRANT, T. J. BUCHANAN, and H. F. COOK. J. Chem. Phys. **26**, 157 (1957).
6. F. BUCKLEY and A. A. MARYOTT. Tables of dielectric dispersion data for pure liquids and dilute solutions. Natl. Bur. Standards Circular 589. 1958. Table 2 (see entries to individual alcohols).
7. D. W. DAVIDSON and R. H. COLE. J. Chem. Phys. **19**, 1484 (1951).
8. D. W. DAVIDSON. Unpublished results. R. H. COLE. J. Chem. Phys. **23**, 493 (1955).
9. D. J. DENNEY. J. Chem. Phys. **30**, 159 (1959).
10. C. P. SMYTH. Dielectric behavior and structure. McGraw-Hill Book Co., Inc., New York. 1955. p. 103.
11. J. A. SAXTON. Proc. Roy. Soc. (London), A, **213**, 473 (1952).
12. D. W. DAVIDSON, R. P. AUTY, and R. H. COLE. Rev. Sci. Instr. **22**, 678 (1951).
13. G. A. CAMPBELL and R. M. FOSTER. Fourier integrals for practical application. Bell Telephone System Tech. Publs. Monograph B 584. 1931.
14. K. PEARSON. Tables of the incomplete gamma-function. H.M. Stationery Office, London. 1922.
15. D. W. DAVIDSON and J. WHEELER. J. Chem. Phys. **30**, 1357 (1959).
16. B. V. HAMON. Proc. Inst. Elec. Engrs. (London), Pt. IV, **99**, 1 (1952).
17. N. KOIZUMI and T. HANAI. J. Phys. Chem. **60**, 1496 (1956).
18. D. W. DAVIDSON. To be published.
19. A. H. WHITE and S. O. MORGAN. Physics, **2**, 313 (1932).
20. D. J. DENNEY. J. Chem. Phys. **27**, 259 (1957).
21. J. W. WINSLOW, JR., R. J. GOOD, and P. E. BERGHAUSEN. J. Chem. Phys. **27**, 309 (1957).
22. A. R. VON HIPPLE. Dielectric materials and applications. The Technology Press of M.I.T., and John Wiley & Sons, Inc., New York, 1954. pp. 363, 364, 315.
23. A. TURKEVICH and C. P. SMYTH. J. Am. Chem. Soc. **64**, 737 (1942).
24. R. F. GRANT, D. W. DAVIDSON, and P. GRAY. J. Chem. Phys. **33**, 1713 (1960).
25. A. SCHALLAMACH. Trans. Faraday Soc. A, **42**, 180 (1946).
26. J. G. KIRKWOOD and R. M. FUOSS. J. Chem. Phys. **9**, 329 (1941).
27. N. KOIZUMI. J. Chem. Phys. **27**, 625 (1957).
28. S. H. GLARUM. J. Chem. Phys. **33**, 639 (1960).
29. C. BROT. J. chim. phys. **55**, 451 (1956).
30. M. DAVIES and R. J. MEAKINS. J. Chem. Phys. **26**, 1584 (1957).
31. D. J. DENNEY. J. Chem. Phys. **30**, 1019 (1959).
32. C. P. SMYTH. Dielectric behavior and structure. McGraw-Hill Book Co., Inc., New York. 1955. p. 129.
33. F. X. HASSION and R. H. COLE. J. Chem. Phys. **23**, 1756 (1955).
34. R. H. COLE and D. W. DAVIDSON. J. Chem. Phys. **20**, 1389 (1952).
35. W. DANNHAUSER and R. H. COLE. J. Chem. Phys. **23**, 1762 (1955).
36. M. BRUMA. Thesis, Paris. 1952.
37. R. ARNOULT, A. LEBRUN, and C. BOULLET. Arch. sci. (Geneva), (spec. no.), **9**, 44 (1956).
38. C. BROT. Thesis, Paris. 1956.
39. R. ARNOULT, A. LEBRUN, C. MORIAMEZ, M. MORIAMEZ, and R. WEMELLE. Arch. sci. (Geneva), (spec. no.) **10**, 48 (1957).
40. R. WEMELLE. Compt. rend. **246**, 3232 (1958).
41. J. PH. POLEY. Physica, **19**, 301 (1953).
42. R. H. COLE. J. Chem. Phys. **23**, 493 (1955).
43. C. MORIAMEZ-BOULLET. Compt. rend. **246**, 2364 (1958).
44. C. MORIAMEZ. Arch. sci. (Geneva), (spec. no.) **11**, 77 (1958).
45. R. WEMELLE. Compt. rend. **244**, 775 (1957).
46. P. A. M. DIRAC. Quantum mechanics. 3rd ed. Clarendon Press, Oxford. 1947. p. 58.
47. K. PEARSON. Tables of the incomplete beta-function. University Press, Cambridge, 1934.
48. W. KAUZMANN. Revs. Modern Phys. **14**, 12 (1942).
49. D. J. DENNEY and R. H. COLE. J. Chem. Phys. **23**, 1767 (1955).
50. J. B. HASTED and G. W. RODERICK. J. Chem. Phys. **29**, 17 (1958).
51. K. F. HERZFELD and T. A. LITOVITZ. Absorption and dispersion of ultrasonic waves. Academic Press, New York. 1959.
52. H. S. GUTOWSKY, A. SAIKA, M. TAKEDA, and D. E. WOESSNER. J. Chem. Phys. **27**, 534 (1957).
53. K. LUSZCZYNSKI, J. A. E. KAIL, and J. G. POWLES. Proc. Phys. Soc. (London), **75**, 243 (1960).
54. K. LUSZCZYNSKI and J. G. POWLES. Proc. Phys. Soc. (London), **74**, 408 (1959).

Can. J. Chem. Downloaded from www.nrcresearchpress.com by 210.87.254.40 on 09/05/12
For personal use only.

NOTES

CHEMISTRY OF THE TRIFLUOROMETHYL GROUP
PART II. NICKEL (II) COMPLEXES OF TRIFLUOROMETHYL PHOSPHINES*

M. A. A. Beg and H. C. Clark

The ability of tri-alkyl and -aryl phosphines to form co-ordination compounds with transition metal salts is well established. However, this ability is considerably modified when the phosphine contains the highly electronegative trifluoromethyl group. This has been shown in the reactions of methyl-trifluoromethyl-phosphines with boron trifluoride and platinum (II) chloride (1), where the results have been interpreted in terms of the effect of the electron-withdrawing power of the trifluoromethyl group on the donor properties of the phosphines, and of the large steric requirements of the trifluoromethyl group.

These two factors of the perturbing power or ligand field strength of the phosphines, and their steric requirements are just those that have been considered important in producing tetrahedral nickel (II) complexes (2). The first example of an apparently tetrahedral complex was $(PEt_3)_2Ni(NO_3)_2$ (3), although the lack of a full structure determination left room for alternative configurations. For the triphenylphosphine complexes $(PPh_3)_2NiX_2$ where $X = NO_3^-$, Cl^-, Br^-, I^-, detailed studies (4) leave no doubt that they possess tetrahedral structures. Other examples of tetrahedral nickel (II) complexes are now known (5). It therefore seemed of interest to examine the nickel (II) complexes of $(CH_3)_3P$, $(CH_3)_2PCF_3$, $CH_3P(CF_3)_2$, and $P(CF_3)_3$ wherever stable compounds could be isolated. Only the first two of these phosphines gave stable complexes and there were no indications of reaction between nickel (II) salts and either methyl-bistrifluoromethylphosphine or tristrifluoromethylphosphine. The complexes of dimethyl-trifluoromethylphosphine were considerably less stable than those of trimethylphosphine. The properties of the newly prepared compounds are shown in the table.

Compound	Magnetic moment (B.M.)	Color	Absorption maxima
$(Me_3P)_2Ni(NO_3)_2$	3.17	Dark red	4850(m), 3950(s), 3325(s)
$(Me_3P)_2NiCl_2$	Diamagnetic	Crimson	5320(s), 3880(m), 3650(m), 2650(s)
$(Me_3P)_2NiBr_2$	"	Crimson	5400(m), 3800(m), 2700(s), 2425(w)
$(Me_3P)_2NiI_2$	"	Dark brown	5175(m), 3875(w), 2850(vs), 2600(s)
$(Me_3P)_2Ni(SCN)_2$	"	Orange-yellow	4600(sh), 3550(vs), 2975(s), 2600(s)
$(Me_2PCF_3)_2Ni(NO_3)_2$	2.93	Dark red	5550(w), 4850(s), 4150(s), 3270(s)
$(Me_2PCF_3)_2NiCl_2$	Diamagnetic	Pink	4800(w), 4050(m), 3450(s), 2550(s)
$(Me_2PCF_3)_2NiBr_2$	"	Black	4875(s), 3950(s), 2625(s), 2400(s)
$(Me_2PCF_3)_2NiI_2$	"	Dark brown	3750(m), 3550(m), 3140(m), 2280(s)
$(Me_2PCF_3)_2Ni(SCN)_2$	"	Yellow	4600(m), 3675(vs), 2550(s)

The trimethylphospine complexes have not been reported previously and it is not surprising that the nitrate is paramagnetic and like its triethylphosphine analogue may be considered to be tetrahedral. The halogen and thiocyanate complexes are diamagnetic in accordance with the greater ligand strengths of these anions. The complexes of dimethyltrifluoromethyl phosphine are very similar to the trimethylphosphine compounds, only the nitrate is paramagnetic and possibly tetrahedral.

**From part of a thesis submitted by M.A.A.B. in partial fulfillment of the requirements for the Ph.D. degree.*

The intensity of the colors of the solid compounds and of the observed absorption bands suggest that charge-transfer transitions are involved.

The fact that a nickel (II) complex of tristrifluoromethyl phosphine could not be obtained is consistent with its inability to give a platinum (II) compound (1). The smaller size of the nickel atom compared with platinum may explain why the latter but not the former can give a complex with methylbistrifluoromethyl phosphine.

EXPERIMENTAL

The methyl-trifluoromethyl-phosphines were prepared as described previously (1). All nickel salts were prepared in the anhydrous state, except the nitrate which was used as the hexahydrate. The trimethylphosphine complexes were prepared by direct reaction of the phosphines with the nickel salts in 2:1 ratio in sealed evacuated tubes, and were purified by refluxing with butanol for about 30 minutes when crystals of the complexes separated. In the case of nickel nitrate, the product could not be crystallized satisfactorily and solutions of the complex were used where necessary. For the dimethyltrifluoromethyl-phosphine complexes, crystallization was not possible owing to their instability. The preparations in these cases were therefore performed in the presence of excess phosphine which acted as a solvent and gave reasonably pure products. The analyses of the compounds are given in the table.

	% Ni		% X	
Compound	Found	Calc. for $NiX_2(PR_3)_2$	Found	Calc. for $NiX_2(PR_3)_2$
$(PMe_3)_2Ni(NO_3)_2$	17.33	17.37	—	—
$(PMe_3)_2NiCl_2$	20.05	20.56	25.14	25.27
$(PMe_3)_2NiBr_2$	16.01	15.68	42.70	43.24
$(PMe_3)_2NiI_2$	11.85	12.50	54.30	54.72
$(PMe_3)_2Ni(SCN)_2$	17.27	17.79	34.45	34.60
$(Me_2PCF_3)_2Ni(NO_3)_2$	13.22	13.12	—	—
$(Me_2PCF_3)_2NiCl_2$	14.72	14.91	18.15	18.25
$(Me_2PCF_3)_2NiBr_2$	11.84	12.14	34.10	33.47
$(Me_2PCF_3)_2NiI_2$	9.76	10.14	43.80	44.40
$(Me_2PCF_3)_2Ni(SCN)_2$	13.42	13.36	26.25	26.73

All the complexes except the iodides and thiocyanates decomposed in the presence of moisture. Although stable in dry solvents, wet polar solvents caused decomposition. Magnetic measurements were made on a Gouy magnetic balance, using powdered samples except for the nitrates for which solutions were used. Spectra were determined in carbon tetrachloride or methanol solutions using a Cary model 14 spectrophotometer.

ACKNOWLEDGMENTS

The financial support of the National Research Council is gratefully acknowledged as is the award of a Colombo Plan scholarship to M.A.A.B.

1. M. A. A. Beg and H. C. Clark. Can. J. Chem. **38**, 119 (1960).
2. L. M. Venanzi. J. Inorg. & Nuclear Chem. **8**, 137 (1958).
3. K. A. Jensen. Z. anorg. u. allgem. Chem. **229**, 225 (1936).
4. L. M. Venanzi and H. M. Powell. Proc. Chem. Soc. 6 (1956).
5. N. S. Gill and R. S. Nyholm. J. Chem. Soc. 3997 (1959).

Received December 5, 1960.
Chemistry Department,
University of British Columbia,
Vancouver, B.C.

Can. J. Chem. Downloaded from www.nrcresearchpress.com by 210.87.254.40 on 09/05/12
For personal use only.

Can. J. Chem. Downloaded from www.nrcresearchpress.com by 210.87.254.40 on 09/05/12
For personal use only.

PRESSURE EFFECT AND MECHANISM IN ACID CATALYSIS
VI. HYDROLYSIS OF α-D-GLUCOSE-1-PHOSPHATE[1]

A. R. OSBORN[2] AND E. WHALLEY

INTRODUCTION

α-D-Glucose-1-phosphate hydrolyzes by acid catalysis (1) with carbon–oxygen fission (2, 3). It is usually assumed that there is a pre-equilibrium proton transfer to the ester, and that the slow step is either a unimolecular decomposition of the protonated form or a bimolecular attack of water. The conclusion (3) on the basis of the Zucker-Hammett hypothesis that the slow step is unimolecular is invalid because the Zucker-Hammett hypothesis is invalid (4–6). We have measured the effect of pressure on the rate of hydrolysis in order to determine the mechanism. The effect of temperature was also measured.

EXPERIMENTAL METHODS AND RESULTS

Dipotassium α-D-glucopyranose-1-phosphate was obtained from General Biochemicals, Inc. It was about 96% pure according to both optical rotation (7) and hydrolyzable organic phosphate determined by Fiske's method (8). The hydrolyses were carried out at 25° C in at least 2-*M* perchloric acid to suppress the ionization of α-D-glucose-1-phosphate, which has a pK_a of 1.10 (9). The initial concentration of the ester was about 0.1 *M* and so potassium perchlorate was precipitated if the potassium salt was used. Potassium ions were therefore removed by passing a solution of the salt through an ion-exchange column of Dowex 50W-X-8 in the acid form.

The hydrolysis was followed by the change of optical rotation. The rate constants are accurate to about 5%. The high-pressure technique has been described elsewhere (10, 11).

The first-order rate constants are summarized in Table I. At normal pressure the

TABLE I

Acid-catalyzed hydrolysis of α-D-glucose-1-phosphate

p/bar	Temp.	$c°_{HClO_4}$/mole l.$^{-1}$*	$10^6\ k_1$/sec^{-1}
1	25.00°C	2.00	126
1	25.00°	3.00	328
1	30.00°	2.00	290
1	35.00°	2.00	580
500	25.00°	2.00	126
1000	25.00°	2.00	118
1500	25.00°	2.00	105

*$c°_{HClO_4}$ is the concentration of perchloric acid at room pressure and temperature.

ratio of the rates in 3-*M* and 2-*M* perchloric acid is much greater than 1.5, and is near the ratio of the acidity function h_0 of the two solutions, so confirming Barnard *et al.*'s observation (3) that the rate is approximately proportional to h_0. The second-order

[1]*Issued as N.R.C. No. 6164.*
[2]*National Research Council Postdoctorate Fellow 1958–60.*

constants in 2-*M* perchloric acid at normal pressure and 25, 30, and 35° C followed the Arrhenius law and yielded

$$E_A = 27.8 \text{ kcal mole}^{-1},$$

$$\log_{10} A/\text{sec}^{-1} = 16.5, \qquad \Delta S^{\ddagger} = 14.8 \text{ cal deg}^{-1} \text{ mole}^{-1}.$$

From the effect of pressure up to 1500 bar at 25.00° C we find graphically

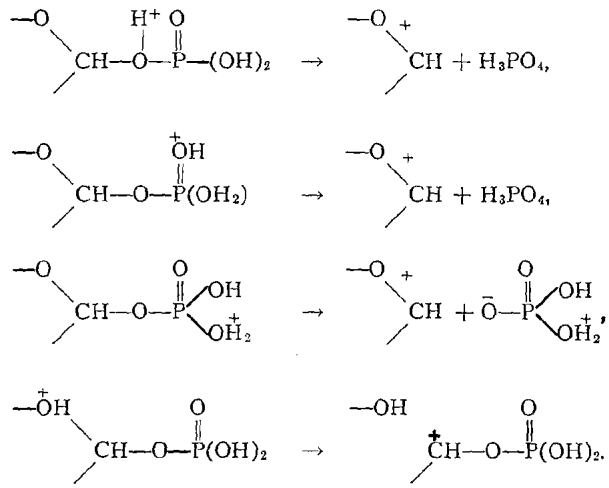
$$\partial \ln k_1/\partial p = 3.2 \pm \sim 1.2 \text{ cm}^3 \text{ mole}^{-1},$$

and assuming the compressibility χ of 2-*M* perchloric acid to be the same as that of water, remembering that $RT\,\partial \ln k_1/\partial p = -\Delta V^{\ddagger} + \chi RT$,

$$\Delta V^{\ddagger} = 4.3 \pm \sim 1.6 \text{ cm}^3 \text{ mole}^{-1}.$$

DISCUSSION

There are many protonated α-D-glucose-1-phosphates and it is not known which of them undergo hydrolysis. The following reactions and their bimolecular counterparts, in which a molecule of water attacks the carbon atom of the pyranose ring, seem to be the most likely. For clarity only the oxygen and one carbon atom of the pyranose ring are shown, and each reaction is presumed to be followed by the usual rapid steps.



The first and last of these were mentioned by Barnard *et al.* (3).

The first, second, and last mechanisms do not result in major changes of polarity and so the volumes of activation should depend mainly on the volume changes of the reactants. According to arguments and experiments in earlier papers in this series they should therefore have small positive volumes of activation if unimolecular, and negative volumes, about -10 cm^3 mole^{-1}, if bimolecular. The measured volume of activation of $4.3 \pm \sim 1.6$ cm^3 mole^{-1} eliminates the bimolecular reactions. In the third mechanism there is a great increase in polarity and so the volume of activation of either the unimolecular or the bimolecular mechanism would be negative because of electrostriction of solvent. Both these can therefore be eliminated. Thus the unimolecular first, second, or last mechanisms are consistent with the measured pressure effect.

The entropy of activation is 14.8 cal deg^{-1} mole^{-1}. Although all or nearly all entropies

Can. J. Chem. Downloaded from www.nrcresearchpress.com by 210.87.254.40 on 09/05/12
For personal use only.

of activation of unimolecular acid-catalyzed reactions are positive, it is not easy to understand why they should be (12), and so while the entropy is certainly consistent with the proposed mechanisms, it does not confirm them strongly.

REFERENCES

1. C. P. Cori, S. P. Colowick, and G. T. Cori. J. Biol. Chem. **121**, 465 (1937).
2. M. Cohn. J. Biol. Chem. **180**, 771 (1949).
3. P. W. C. Barnard, C. A. Bunton, D. R. Llewellyn, K. G. Oldham, L. B. Silver, and C. A. Vernon. Chem. & Ind. (London), 760 (1955).
4. J. Koskikallio and E. Whalley. Trans. Faraday Soc. **55**, 815 (1959).
5. J. Koskikallio and E. Whalley. Can. J. Chem. **37**, 788 (1959).
6. G. Archer and R. P. Bell. J. Chem. Soc. 3228 (1959).
7. M. L. Wolfram and D. E. Pletcher. J. Am. Chem. Soc. **63**, 1050 (1941).
8. C. H. Fiske. J. Biol. Chem. **46**, 285 (1921).
9. W. D. Kumler and J. J. Eiler. J. Am. Chem. Soc. **65**, 2355 (1943).
10. J. Koskikallio and E. Whalley. Trans. Faraday Soc. **55**, 809 (1955).
11. A. R. Osborn and E. Whalley. To be published.
12. E. Whalley. Trans. Faraday Soc. **55**, 798 (1959).

Received December 12, 1960.
Division of Applied Chemistry,
National Research Council,
Ottawa, Canada.

Can. J. Chem. Downloaded from www.nrcresearchpress.com by 210.87.254.40 on 09/05/12
For personal use only.

OXIDATION OF CHOLEST-4-EN-3-ONE WITH PERIODATE–PERMANGANATE

J. T. Edward, D. Holder, W. H. Lunn,[1] and I. Puskas[1]

For stereochemical studies (1) we required large quantities of the keto acid, 5-oxo-3,5-seco-A-norcholestan-3-oic acid, first prepared by Windaus (2) by oxidizing cholest-4-en-3-one with alkaline permanganate. Later workers (3, 4) had obtained better yields (60–85%) by oxidizing 2–3 g of the unsaturated ketone with ozone, but we found yields low and capricious when oxidation with this reagent was carried out on a larger scale. However, 50 g of the ketone could be oxidized to the acid in 79–81% yield with the permanganate–periodate reagent of Lemieux and von Rudloff (5, 6), while with 5 g of the ketone the yield rose to 88%.

EXPERIMENTAL

Potassium carbonate (28 g) in water (800 ml) was added with vigorous stirring to a solution of cholest-4-en-3-one (50 g) in *t*-butanol–water azeotrope (3 l.), followed by 500 ml of a solution prepared from sodium metaperiodate (200 g) and water (2.5 l.), and then 50 ml of 0.8% aqueous potassium permanganate. The remainder of the periodate was added at the rate of 110 ml/minute for 10 minutes, and then at 30 ml/minute for the next 30 minutes. Permanganate solution was added when necessary to maintain the permanganate color, 50 ml being usually required after the first 5 minutes and a further 75 ml at intervals over the next 30 minutes.

After 2 hours, the excess permanganate was destroyed with sodium bisulphite. The resultant iodine-colored solution was concentrated at reduced pressure to a volume of about 4 l., cooled to 4° C, acidified with ice-cold 50% sulphuric acid, and extracted with ether (2.5 l., 1.5 l., and 1.5 l.). The ethereal extract was washed with sodium bisulphite solution until free from iodine, with water until neutral, and dried (magnesium

[1]*Holder of National Research Council of Canada Studentships, 1958–60.*

of activation of unimolecular acid-catalyzed reactions are positive, it is not easy to understand why they should be (12), and so while the entropy is certainly consistent with the proposed mechanisms, it does not confirm them strongly.

REFERENCES

1. C. P. Cori, S. P. Colowick, and G. T. Cori. J. Biol. Chem. **121**, 465 (1937).
2. M. Cohn. J. Biol. Chem. **180**, 771 (1949).
3. P. W. C. Barnard, C. A. Bunton, D. R. Llewellyn, K. G. Oldham, L. B. Silver, and C. A. Vernon. Chem. & Ind. (London), 760 (1955).
4. J. Koskikallio and E. Whalley. Trans. Faraday Soc. **55**, 815 (1959).
5. J. Koskikallio and E. Whalley. Can. J. Chem. **37**, 788 (1959).
6. G. Archer and R. P. Bell. J. Chem. Soc. 3228 (1959).
7. M. L. Wolfram and D. E. Pletcher. J. Am. Chem. Soc. **63**, 1050 (1941).
8. C. H. Fiske. J. Biol. Chem. **46**, 285 (1921).
9. W. D. Kumler and J. J. Eiler. J. Am. Chem. Soc. **65**, 2355 (1943).
10. J. Koskikallio and E. Whalley. Trans. Faraday Soc. **55**, 809 (1955).
11. A. R. Osborn and E. Whalley. To be published.
12. E. Whalley. Trans. Faraday Soc. **55**, 798 (1959).

Received December 12, 1960.
Division of Applied Chemistry,
National Research Council,
Ottawa, Canada.

Can. J. Chem. Downloaded from www.nrcresearchpress.com by 210.87.254.105 on 09/05/12
For personal use only.

OXIDATION OF CHOLEST-4-EN-3-ONE WITH PERIODATE–PERMANGANATE

J. T. Edward, D. Holder, W. H. Lunn,[1] and I. Puskas[1]

For stereochemical studies (1) we required large quantities of the keto acid, 5-oxo-3,5-seco-A-norcholestan-3-oic acid, first prepared by Windaus (2) by oxidizing cholest-4-en-3-one with alkaline permanganate. Later workers (3, 4) had obtained better yields (60–85%) by oxidizing 2–3 g of the unsaturated ketone with ozone, but we found yields low and capricious when oxidation with this reagent was carried out on a larger scale. However, 50 g of the ketone could be oxidized to the acid in 79–81% yield with the permanganate–periodate reagent of Lemieux and von Rudloff (5, 6), while with 5 g of the ketone the yield rose to 88%.

EXPERIMENTAL

Potassium carbonate (28 g) in water (800 ml) was added with vigorous stirring to a solution of cholest-4-en-3-one (50 g) in *t*-butanol–water azeotrope (3 l.), followed by 500 ml of a solution prepared from sodium metaperiodate (200 g) and water (2.5 l.), and then 50 ml of 0.8% aqueous potassium permanganate. The remainder of the periodate was added at the rate of 110 ml/minute for 10 minutes, and then at 30 ml/minute for the next 30 minutes. Permanganate solution was added when necessary to maintain the permanganate color, 50 ml being usually required after the first 5 minutes and a further 75 ml at intervals over the next 30 minutes.

After 2 hours, the excess permanganate was destroyed with sodium bisulphite. The resultant iodine-colored solution was concentrated at reduced pressure to a volume of about 4 l., cooled to 4° C, acidified with ice-cold 50% sulphuric acid, and extracted with ether (2.5 l., 1.5 l., and 1.5 l.). The ethereal extract was washed with sodium bisulphite solution until free from iodine, with water until neutral, and dried (magnesium

[1]*Holder of National Research Council of Canada Studentships, 1958–60.*

sulphate). It was then concentrated to 700 ml, diluted with hexane, and further concentrated to 250 ml. After standing for 8 hours at room temperature and 8 hours at 4° C, the solution yielded white needles (36.6–38.3 g) of the keto acid, m.p. 153–154° C (lit. m.p. 154–155.5° C (4)). The mother liquors, on being concentrated to about 60 ml and chilled, gave after several days a second crop of impure acid, from which pure acid (4.2–4.9 g), m.p. 153–154° C, was obtained by recrystallization from ether–hexane.

1. J. T. EDWARD and P. F. MORAND. Can. J. Chem. **38**, 1316, 1325 (1960).
2. A. WINDAUS. Ber. **39**, 2008 (1906).
3. C. C. BOLT. Rec. trav. chim. **57**, 905 (1938).
4. R. B. TURNER. J. Am. Chem. Soc. **72**, 579 (1950).
5. R. U. LEMIEUX and E. VON RUDLOFF. Can. J. Chem. **33**, 1701, 1710 (1955).
6. E. VON RUDLOFF. Can. J. Chem. **33**, 1714 (1955); **34**, 1413 (1956).

RECEIVED NOVEMBER 23, 1960.
DEPARTMENT OF CHEMISTRY,
MCGILL UNIVERSITY,
MONTREAL 2, QUE.

Can. J. Chem. Downloaded from www.nrcresearchpress.com by 210.87.254.105 on 09/05/12
For personal use only.

Can. J. Chem. Downloaded from www.nrcresearchpress.com by 210.87.254.40 on 09/05/12
For personal use only.

Symposium on Nuclear Chemistry and Radiochemistry

The papers that follow were presented at a symposium held at Atomic Energy of Canada Limited, Chalk River, Ontario, on September 6, 7, and 8, 1960, under the joint auspices of the Inorganic Chemistry Subject Division of the Chemical Institute of Canada, and Atomic Energy of Canada Limited. The meeting was organized by Dr. R. H. Betts of A.E.C.L. Some of the papers presented are not published here because of prior commitments.

The symposium committee wishes to express its appreciation to the sponsoring organizations for their generous support and co-operation, and to the Editor-in-Chief and staff of the Canadian Journal of Chemistry for their valuable assistance.

THE RANGE OF Na^{24} IONS OF KILOELECTRON VOLT ENERGIES IN ALUMINUM[1]

J. A. Davies and G. A. Sims

ABSTRACT

Detailed studies are reported for the depth of penetration in aluminum of monoenergetic Na^{24} ions over the energy region 0.7–60 kev. Below 20 kev the median range (R_M) increases linearly with energy as predicted by the Bohr–Nielsen equation. As was observed in a previous study with Cs^{137} ions in aluminum, the experimental distribution curves are not Gaussian in shape, but consist of a markedly asymmetric peak followed by a pronounced exponential "tail". The results of a Monte Carlo calculation show that the observed distribution curves correspond quite closely to those predicted by an isotropic elastic-scattering model.

Above 20 kev, a slight deviation from the linear range–energy relationship is observed; also, the distribution curves become narrower and more symmetrical, suggesting that electronic interactions are starting to play a significant role in the stopping process. Some preliminary results for the range of accelerated ions of Rb^{86} and K^{42} in aluminum are also included for comparison. Median ranges for each of the alkali metal ions are compared with those predicted by the Bohr–Nielsen treatment.

INTRODUCTION

A program of research on the penetration depth and range straggling of heavy ions in solids at bombardment energies up to 100 kev has been under way in this laboratory for the past three years. Previous papers (1, 2) have described the development of a sufficiently sensitive technique for measuring the extremely small depths of penetration involved, and its application to the study of Cs^{137} ions in aluminum. The present paper extends these measurements in aluminum to other alkali metal ions, particularly Na^{24}, in an attempt to further our understanding of the mechanism of the elastic-scattering process and its dependence on the energy, mass, and atomic number of the bombarding ion. One important advantage of this technique is that it provides detailed information not only on the range but also on the extent of range straggling.

Until recently, there had been almost no reliable experimental results reported for heavy particles below 100 kev. The situation has now improved considerably, particularly as a result of papers being presented at this conference (see footnote 1). Powers (3) has used proton scattering to study accurately the range of several rare-gas ions in carbon, beryllium, boron, and aluminum targets; Schmitt and co-workers (4, 5), by a recoil-atom technique, have determined the average range of the radioactive atoms produced by (γ,n) processes in various solids. However, neither of these methods was sufficiently sensitive to give detailed information on the shape of the range–distribution curve.

[1]*Manuscript received November 3, 1960.*
Contribution from Research Chemistry Branch, Atomic Energy of Canada Limited, Chalk River, Ontario. Presented at the Third Symposium on Nuclear Chemistry and Radiochemistry held at Atomic Energy of Canada Limited, Chalk River, Ontario, September 6–8, 1960.
Issued as A.E.C.L. No. 1150.

Can. J. Chem. Downloaded from www.nrcresearchpress.com by 210.87.254.40 on 09/05/12
For personal use only.

EXPERIMENTAL PROCEDURE

Our experimental approach consists simply in bombarding an optically flat aluminum target with a monoenergetic beam of radioactive ions, and then measuring the depth of penetration of the incident beam by dissolving successive uniform layers of aluminum from the target surface and measuring the amount of radioactivity in each layer. The ion bombardments were carried out using an electrostatic accelerator specially designed for the purpose (2). The development of a sufficiently sensitive technique for dissolving extremely thin layers of known thickness from the surface of an aluminum foil has already been described in detail (1). The technique consists essentially of two steps: electrochemical oxidation at constant voltage in aqueous ammonium citrate, followed by chemical removal of the anodic oxide film in a phosphoric acid chromium trioxide solution. Due to the highly protective nature of the anodic oxide film, this process permits highly reproducible surface layers of metal as thin as 37 Å to be removed, the thickness of the layer increasing linearly with the anodic voltage. Furthermore, the process may be repeated as often as desired, so that it is possible to obtain the complete range–distribution curve from a single bombardment.

RESULTS

The results for a typical run, illustrating the determination of the Na^{24} distribution in a bombarded target, are shown in Table I. The thickness W per layer (column 3)

TABLE I

Distribution of 10-kev Na^{24} ions in an aluminum target

Layer No.	Anodic voltage	Amount of Al removed		Residual target activity (c.p.m.)	Na^{24} activity per layer (calculated from col. 5)	
		Per layer ($\mu g/cm^2$)	Total ($\mu g/cm^2$)		(c.p.m.)	(c.p.m./μg Al)
(1)	(2)	(3)	(4)	(5)	(6)	(7)
0				20,174		
1	4.2	1.8+0.5*	2.3	16,817	3,357	1,460
2	4.2	1.8	4.1	13,726	3,091	1,717
3	4.2	1.8	5.9	10,484	3,242	1,801
4	4.1	1.8	7.7	7,924	2,560	1,422
5	8.0	2.9	10.6	4,407	3,517	1,213
6	10.2	3.6	14.2	2,461	1,946	541
7	25.0	8.0	22.2	966	1,495	187
8	25.0	8.0	30.2	417	549	68.6
9	51.5	16.0	46.2	108	309	19.3
10	50.5	15.7	61.9	30	78	5.0

*An extra 0.5 $\mu g/cm^2$ is added to the first layer in each run to take account of the oxygen that was present during the bombardment as an oxide layer on the target surface.

was calculated from the anodic voltage V by using the previously established relationship (1) $W = 0.30\ (V+1.8)$.

As was observed in the earlier study with Cs^{137} (2), the distribution of Na^{24} ions in the target is markedly asymmetric. This may be seen more clearly in Fig. 1, in which the Na^{24} content in each layer is plotted against the total depth beneath the original surface. The distribution curves show a characteristic highly penetrating "tail"; as a result, the most probable range R_P is somewhat less than the median value R_M. It will

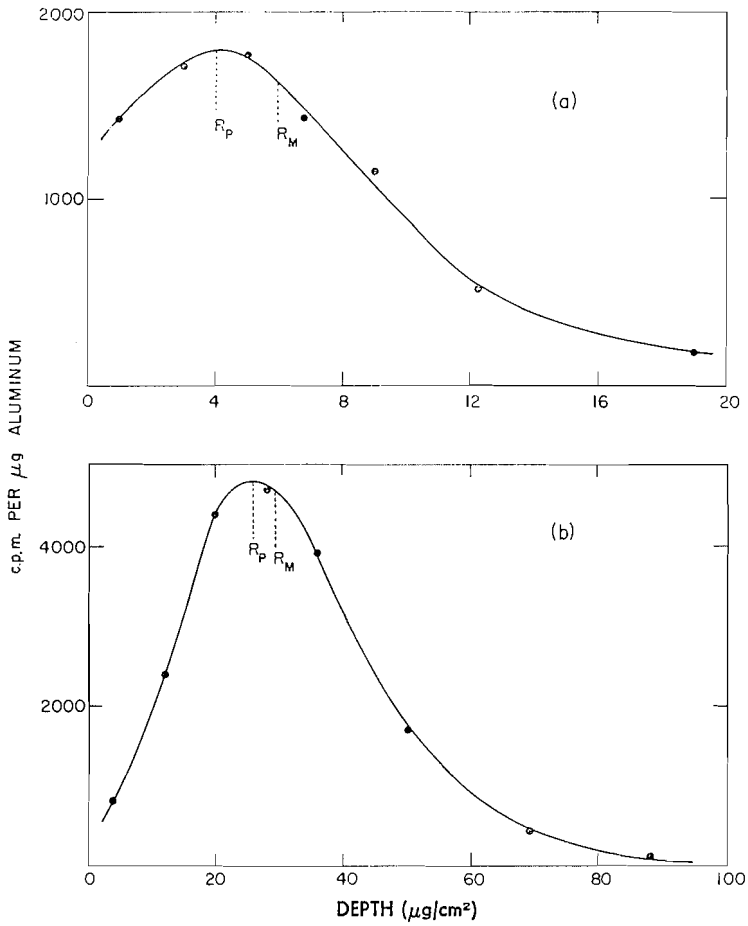


FIG. 1. Depth of penetration of Na^{24} ions in aluminum: (*a*) 10-kev Na^{24} ions, (*b*) 60-kev Na^{24} ions.

be noted, however, that with Na^{24} the asymmetry becomes less pronounced at high energy (Fig. 1*b*), and the peak becomes much sharper. The possible significance of this will be discussed in the next section; it suggests strongly that some process other than elastic scattering is starting to contribute to the rate of energy loss.

Typical distribution curves for the residual target activity (column 5, Table I) at various energies are shown in Fig. 2. In each case, the activity eventually falls off exponentially with depth.

Values of R_P, R_M, and the half-thickness ($X_{1/2}$) of the exponential region are shown as a function of energy in Table II, together with previous results for Cs^{137} (2). It will be noted that, over the energy region studied, the range increases approximately linearly with energy. However, a careful analysis of the data shows that at higher energies, a slight deviation from linearity occurs, and R_P and R_M gradually approach one another (see Table III). Some preliminary data for K^{42} and Rb^{86} have been included for comparison.

Can. J. Chem. Downloaded from www.nrcresearchpress.com by 210.87.254.40 on 09/05/12
For personal use only.

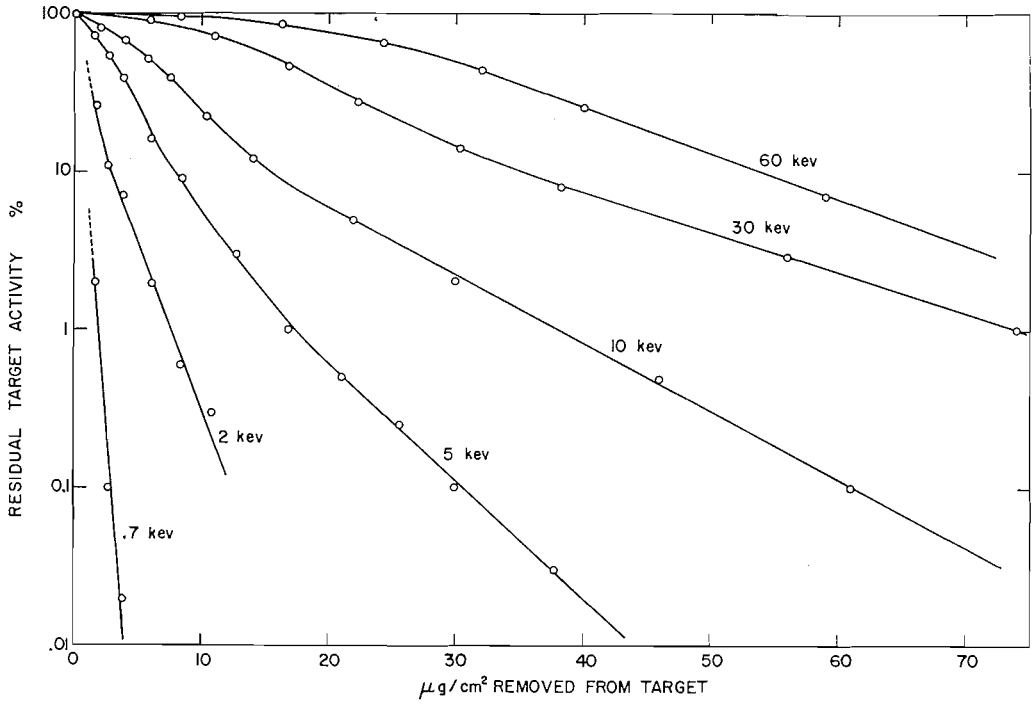


FIG. 2. Distribution curves of residual target activities for Na^{24} ions of various energies in aluminum.

TABLE II

Range of alkali metal ions in aluminum

Ion	Energy (kev)	R_P (μg/cm^2)	R_M (μg/cm^2)	$X_{1/2}$ (μg/cm^2)
Na^{24}	0.7	—	0.4±.2	0.4±.1
	1.0	—	0.5±.2	0.7±.1
	2.0	0.7±.3	1.1±.2	1.6
	5.0	1.6±.4	3.0	3.6
	10.5	3.9±.4	6.2	8.3
	15.0	—	7.8	9.0
	24	9.8	12.0	—
	30	13.1	15.0	15.5
	60	26	29.5	16
K^{42}	2	—	0.6_5±.2	0.6_7±.1
	30	6.8	9.0	9.2
Rb^{86}	30	6.6	8.1	5.4
Cs^{137}	2	—	0.6±.3	0.4±.1
	5	—	0.9±.3	0.6±.1
	20	4.0±.4	4.8	2.9
	30	5.7±.4	7.4	4.0
	50	9.5	11.3	6.5

NOTE: The estimated experimental error is ±6% except where otherwise noted.

DISCUSSION OF RESULTS

The most striking feature about these results—the marked asymmetry in the distribution curves—can be explained quite readily. Nielsen (6) has pointed out that scattering in a screened Coulomb field should be approximately isotropic in the center-of-mass

Can. J. Chem. Downloaded from www.nrcresearchpress.com by 210.87.254.40 on 09/05/12
For personal use only.

system. This means that, even with Cs^{137} in aluminum, the average energy loss per collision is almost 30%; hence, only the first few collisions contribute significantly to the total range.

Under such conditions, it has been shown (2), by a somewhat oversimplified mathematical approach, that the predicted distribution curve would in fact consist of an asymmetric peak, followed eventually by an exponential region of half-thickness identical with that for the first collision. The problem was treated analytically in a manner analogous to that used by Bateman (7) for resolving growth and decay curves of successive radioactive transformations, only with distance replacing time as the independent variable. This analytical treatment provides a qualitative explanation for the experimentally observed distribution curves, but is not suitable for quantitative comparison: it makes no allowance for variations in energy transfer from one collision to another (all collisions were assumed to transfer exactly the average energy), nor for the difference between the total path length and the depth of penetration. The latter difference may quite easily be taken into account by replacing the mean free path λ by its projection λ in the forward direction,

i.e.

$$\lambda_0 = \lambda_0,$$

$$\lambda_1 = \lambda_1 \cos \bar{\psi},$$

and

$$\lambda_n = \lambda_n \cos^n \bar{\psi},$$

where the subscript refers to the number of collisions which the incident ion has undergone and $\bar{\psi}$ is the scattering angle in laboratory co-ordinates for an "average collision". When this relationship is inserted into the Bateman equation (see appendix to reference 2), the following series of exponential terms is obtained:

$$\sum_{n=1}^{n=\infty} \frac{1}{a_n} \left\{ \exp -[(1-\bar{T}) \cos \bar{\psi}]^n \cdot \frac{r}{\lambda_0} \right\}.$$

This series is rapidly convergent and leads to the distribution curves shown as (*a*) in Fig. 3. It has been assumed that the mean free path λ decreases linearly with the ion energy, and that the average energy transfer per collision ($\bar{T}$) is equal to $0.5T_{max}$. The dotted line represents the distribution of incident particles which have not yet had a single collision.

A much more satisfactory method of calculating the shape of the distribution curve has recently been developed (8), viz. a Monte Carlo type of calculation, which permits both the angular scattering and the fractional energy transfer to be varied at random from one collision to another. The resulting distribution curves (*b*) are shown in Fig. 3. In order to test the validity of Nielsen's prediction (6), the scattering process was assumed to be isotropic in center-of-mass co-ordinates. The close agreement between curves (*a*) and (*b*), particularly at the higher mass ratio, suggests that one may use the much simpler "average collision" method to predict the approximate shape of range–distribution curves. Experimental results for two runs (10-kev Na^{24}, and 30-kev Cs^{137}) have been included for comparison; the abscissa scales were normalized by letting $\lambda_0 = 3.9$ $\mu g/cm^2$ and 5.7 $\mu g/cm^2$ for the Na^{24} and Cs^{137} runs, respectively. It will be noted that the isotropic scattering model predicts both the height and the shape of the experimental peaks extremely well, even in the extreme case of Na^{24} in aluminum, where the masses of the incident ion and the target atom are approximately equal. In such a case, T_{max} is

Can. J. Chem. Downloaded from www.nrcresearchpress.com by 210.87.254.40 on 09/05/12
For personal use only.

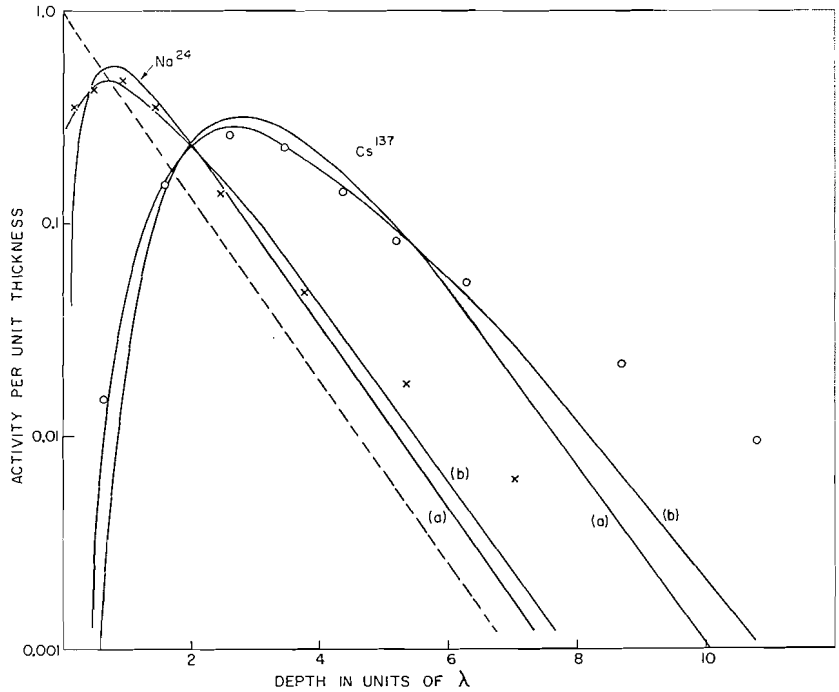


FIG. 3. Calculated distribution curves for Na^{24} and for Cs^{137} in aluminum using: (*a*) "average" collision method, (*b*) Monte Carlo method. Experimental results: ×, 10.5-kev Na^{24}; O, 30-kev Cs^{137}.

equal to 0.997, and hence the incident ion may lose almost all its energy in a single collision.

For both Na^{24} and Cs^{137} ions, a significant deviation between the predicted and observed distribution curves occurs at large depths of penetration. At about twice the median range, the experimental curve exhibits a point of inflection (see Fig. 2) which is not predicted by either the Monte Carlo or the "average collision" calculations. The half thickness ($X_{1/2}$) of the subsequent exponential "tail" is almost exactly a factor of two larger than the predicted value. A satisfactory explanation for this deviation has not yet been found. However, it involves less than 5% of the incident particles and hence should not appreciably affect the determination of R_P and R_M.

One very sensitive test of the agreement between the observed distribution and that predicted by the isotropic scattering model is to determine, for different mass ratios, how rapidly the curve falls off on either side of the maximum. The usual criterion for making such a comparison is the straggling parameter; however, with a markedly asymmetric peak, the normal definition of a straggling parameter has little theoretical significance.

Instead, let us consider the relative height (N/N_{max}) of the distribution curve at two selected abscissa values: at $x = \frac{1}{4}R_P$ and at $x = 2R_P$. In Fig. 4, the two solid lines represent the variation of N/N_{max} with the mass ratio, as determined by the Monte Carlo calculations. Typical experimental values for each of the alkali metal ions have been plotted, together with an estimate of the experimental error. With the exception of the higher-energy Na^{24} runs, the isotropic scattering model fits the observed straggling.

Furthermore, the discrepancy with Na^{24} at higher energies may quite reasonably be

Can. J. Chem. Downloaded from www.nrcresearchpress.com by 210.87.254.40 on 09/05/12
For personal use only.

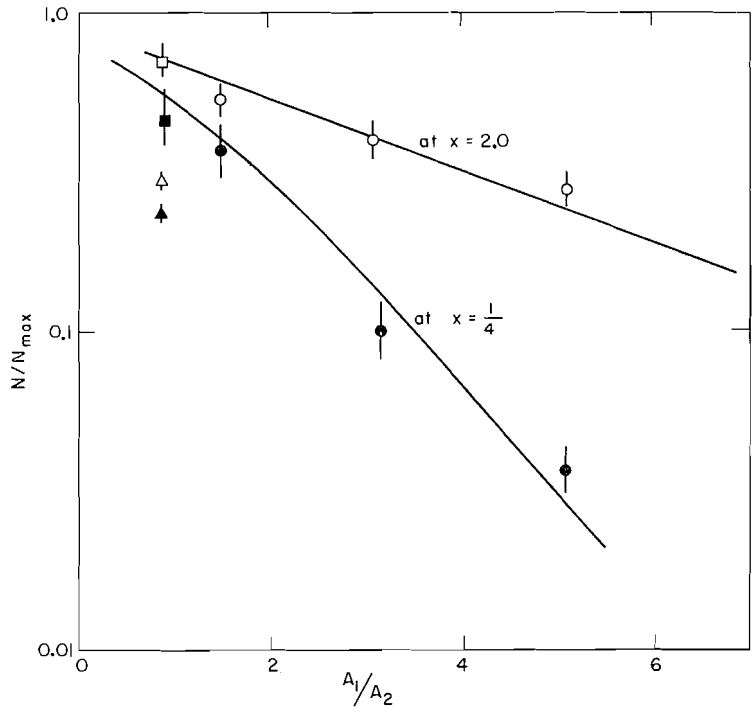


FIG. 4. Relative activity (N/N_{max}) vs. mass ratio. Solid lines are calculated from Monte Carlo distribution curves. Experimental points: ■□, 10.5 kev; ●○, 30 kev; ▲△, 60 kev; solid points at $x = \frac{1}{4}R_P$; open points at $x = 2R_P$.

attributed to a gradual increase in the significance of electronic interactions as a slowing-down process at higher velocities. It has been shown (9, 10) that heavy recoil atoms from α-decay undergo significant electronic interactions along their path, dissipating perhaps 20% of their energy in this manner. Yet these atoms have an initial velocity less than that of a 60-kev Na^{24} atom. Electronic stopping involves extremely small energy transfers per "collision", and so would tend to produce a narrower, more symmetrical peak. Such a trend was in fact observed (Fig. 1), and would account, at least qualitatively, for the low relative activity of 60-kev Na^{24} in Fig. 4.

Another convenient parameter for describing the degree of asymmetry is the ratio (R_P/R_M) of the most probable range to the median range (Table III). For electronic

TABLE III

Ratio (R_P/R_M) for alkali metal ions in aluminum

Energy (kev)	Na^{24}	K^{42}	Rb^{86}	Cs^{137}
2	.6			
5	.5			
10	.6$_3$			
20	.81			.83
30	.87	.75	.81	.77
60	.88			.85
Predicted value (isotropic scattering)	.57	.68	.79	.87

Can. J. Chem. Downloaded from www.nrcresearchpress.com by 210.87.254.40 on 09/05/12
For personal use only.

scattering (where the fractional energy transfer is extremely small), the ratio should be almost exactly unity, whereas for elastic scattering (where large fractional energy transfers occur), the ratio would be much less. Once again, with the exception of the higher-energy Na^{24} runs, the agreement with the isotropic scattering model is quite reasonable. In the case of Na^{24}, the measured ratio at 30 kev is approximately halfway between the theoretical values for elastic nuclear collision and for electronic interactions. It would seem therefore that at this energy the two processes are of roughly equal importance. Since velocity rather than energy is the significant criterion for determining the relative importance of the two processes, it is not surprising that no such discrepancy was observed in the earlier work with Cs^{137}.

So far, we have discussed only the shape of the range–distribution curve; the actual magnitude of the range is much more difficult to predict. The most commonly used theoretical approach is based on Bohr's (11) treatment of collisions in a screened Coulomb field, from which Nielsen (6) has derived the familiar range–energy relationship,

$$[1] \qquad \frac{R}{E} = 0.60\,\frac{A_1+A_2}{A_1}\cdot\frac{A_2}{Z_2}\cdot\frac{(Z_1^{2/3}+Z_2^{2/3})^{1/2}}{Z_1},$$

where R is the range in micrograms per square centimeter, E is the energy of the incident ion in kiloelectron volts, A_1, A_2 are the masses, and Z_1, Z_2 are the atomic numbers of the incident and target atoms respectively.

One necessary criterion for screened-field scattering is that the collision diameter, or minimum distance of approach in a head-on collision, must be somewhat larger than the screening parameter. Otherwise, unscreened or Rutherford-type scattering can occur. Using Bohr's value for the screening parameter, viz. $0.528\times10^{-8}/(Z_1^{2/3}+Z_2^{2/3})^{1/2}$, it can be shown that this criterion is fulfilled at the energies used in the present work, except for some of the Na^{24} runs where the critical energy is only 25 kev. For Cs^{137}, on the other hand, the critical energy is over 500 kev. Since, as noted above, the runs with Na^{24} at higher energies also involve a significant contribution from electronic stopping, their interpretation is obviously much more complicated and will not be discussed further at this time.

Unfortunately, in testing the validity of Bohr's screened-field model, it is not possible to use the above range–energy relationship for a direct comparison with our experimental data; this is because the equation may be applied only when $A_1 \gg A_2$. This restriction arises because equation [1] was obtained by integrating an expression for the stopping power ($\Delta E/\Delta R$). Such an integration assumes that the energy decrease per collision is small enough that the stepwise slowing-down process may be replaced by a smooth curve. Secondly, the expression predicts the total path length travelled rather than the actual depth of penetration. Neither of these assumptions holds true when using an aluminum target. Even with Cs^{137} ions, where $A_1 = 5.1A_2$, the energy transfer per collision can be as large as 55%; with Na^{24}, up to 99.7% of the energy may be lost in a single collision and the average angular deflection in laboratory co-ordinates is approximately 45°.

However, by a somewhat modified theoretical treatment combined with the results of the Monte Carlo calculations (Fig. 3), it is possible to develop a completely general expression for the depth of penetration, one which is applicable for any value of A_1/A_2. Nielsen's expression for the stopping power may be written as follows:

$$[2] \qquad -\frac{\Delta E}{\Delta R} = 1.68\,\frac{A_1}{(A_1+A_2)A_2}\cdot\frac{Z_1Z_2}{(Z_1^{2/3}+Z_2^{2/3})^{1/2}}$$

Can. J. Chem. Downloaded from www.nrcresearchpress.com by 210.87.254.40 on 09/05/12
For personal use only.

where $(\Delta E/\Delta R)$ is expressed in kev cm^2 μg^{-1}. Instead of integrating, we may write an alternative expression for the stopping power in terms of the average fractional energy transfer $\bar{T}$ per collision and the mean free path λ of the particle,

$$[3] \qquad -\frac{\Delta E}{\Delta R} = \frac{\bar{T}E}{\lambda}.$$

λ must be expressed in the same units as R, viz. micrograms per square centimeter. If the scattering process is approximately isotropic, then $\bar{T}$ may be expressed as $2A_1A_2/(A_1+A_2)^2$ and hence

$$[4] \qquad -\frac{\Delta E}{\Delta R} = \frac{2A_1A_2}{(A_1+A_2)^2}\cdot\frac{E}{\lambda}.$$

Combining equations [2] and [4], we obtain the following expression for the mean free path of the incident ion:

$$[5] \qquad \lambda = 1.19\frac{A_2^{\,2}}{A_1+A_2}\cdot\frac{(Z_1^{\,2/3}+Z_2^{\,2/3})^{1/2}}{Z_1Z_2}\cdot E.$$

It should be recognized that λ is only an "effective" mean free path: it applies to the approximately isotropic scattering process, but does not include the increased frequency of very small angular deflections which, according to Nielsen, have a negligible influence on the over-all rate of energy loss.

To calculate R_P, R_M, or the mean range $\bar{R}$ from equation [5], one simply multiplies λ by a numerical factor (k_P, k_M, or $\bar{k}$) for each mass ratio. These factors are computed from Monte Carlo distribution curves such as those in Fig. 3. Appropriate values for various mass ratios are given in Table IV.

In Table V, these factors are used to compare the predicted and experimental ranges

TABLE IV

k-Factors for various mass ratios

Mass ratio	Ion	k_P	k_M	$\bar{k}$
0.889	Na^{24} in Al^{27}	0.70	1.23	1.50
1.556	K^{42} in Al^{27}	1.00	1.49	1.79
3.185	Rb^{86} in Al^{27}	1.75	2.21	2.55
5.074	Cs^{137} in Al^{27}	2.70	3.10	3.46

TABLE V

Experimental and predicted values of R/E (μg cm^{-2} kev^{-1})

Ion	Energy region (kev)	R_P/E		R_M/E	
		Exptl.	Calc.	Exptl.	Calc.
Na^{24}	0.7–10	.36	.27	.59	.47
K^{42}	30	.23	.18	.30	.27
Rb^{86}	30	.22	$.11_5$	.27	$.14_5$
Cs^{137}	2.0–30	.19	.09	.25	.10

for each of the alkali metal ions. Clearly, although the theoretical values do have the correct order of magnitude, the observed variation from Na^{24} to Cs^{137} is much less than that predicted by the Bohr–Nielsen screened-field treatment. Holmes and Leibfried (12)

Can. J. Chem. Downloaded from www.nrcresearchpress.com by 210.87.254.40 on 09/05/12
For personal use only.

have recently criticized Nielsen's replacement of the Bohr screened-field potential by an $(1/r^2)$ potential. They also point out that the predicted range is extremely sensitive to the choice of screening parameter "a", since "a" occurs in the exponential term determining the interaction potential.

However, while it is interesting to speculate on possible causes for the discrepancy between experiment and theory, it is felt that further discussion should be postponed until more data become available.

ACKNOWLEDGMENTS

It is a pleasure to acknowledge our gratitude to Dr. R. H. Betts for his advice and encouragement throughout this work. We are also particularly indebted to Dr. J. M. Kennedy and B. Miles for suggesting and programing the Monte Carlo calculations used in interpreting the experimental results.

REFERENCES

1. J. A. DAVIES, J. FRIESEN, and J. D. MCINTYRE. Can. J. Chem. **38**, 1526 (1960).
2. J. A. DAVIES, J. D. MCINTYRE, R. L. CUSHING, and M. LOUNSBURY. Can. J. Chem. **38**, 1535 (1960).
3. D. POWERS. Unpublished. Paper presented at Third Symposium on Nuclear and Radiochemistry, held at A.E.C.L., Chalk River, Ontario, Sept. 6–8, 1960.
4. R. A. SCHMITT, V. A. J. VANLINT, and C. S. SUFFREDINI. Unpublished. Paper presented at Third Symposium on Nuclear and Radiochemistry, held at A.E.C.L., Chalk River, Ontario, Sept. 6–8, 1960.
5. R. A. SCHMITT and R. A. SHARP. Phys. Rev. Letters, **1**, 445, (1958).
6. K. O. NIELSEN. *In* Electromagnetically enriched isotopes and mass spectrometry. Academic Press, Inc., New York. 1956. pp. 68–81.
7. H. BATEMAN. Proc. Cambridge Phil. Soc. **15**, 423 (1910).
8. J. A. DAVIES, J. KENNEDY, and B. Miles. To be published.
9. W. G. STONE and L. W. COCHRAN. Phys. Rev. **107**, 702 (1957).
10. W. P. JESSE and J. SADAUSKIS. Phys. Rev. **102**, 389 (1956).
11. N. BOHR. Kgl. Danske Videnskab. Selskab, Mat-fys. Medd. **18** (8) (1948).
12. D. K. HOLMES and G. LEIBFRIED. J. Appl. Phys. **31**, 1046 (1960).

Can. J. Chem. Downloaded from www.nrcresearchpress.com by 210.87.254.40 on 09/05/12
For personal use only.

Can. J. Chem. Downloaded from www.nrcresearchpress.com by 210.87.254.40 on 09/05/12
For personal use only.

ISOTOPE EFFECT IN HEAVY ION RANGE STUDIES[1]

J. A. DAVIES, J. D. MCINTYRE,[2] AND G. A. SIMS

ABSTRACT

From measurements of the isotope ratio (Na^{22}/Na^{24}) at various depths of penetration, it has been possible to determine at 24 kev the small difference in the median ranges of the sodium isotopes. Na^{22} has the slightly larger median range, as is predicted by the Nielsen equation. Monte Carlo calculations show that an isotropic elastic-scattering model provides a reasonable explanation for the magnitude of the range difference and for the observed variation in the isotope ratio as a function of depth.

INTRODUCTION

The preceding paper on the range of alkali metal ions of kiloelectron volt energies in aluminum (1) showed that although the mean depth of penetration increases linearly with ion energy as predicted by Bohr (2), the variation with mass and atomic number of the incident ion was considerably smaller than would be expected on theoretical grounds.

In order to determine the relative contribution of each term to the observed depths of penetration, it was decided to investigate the possible existence and magnitude of an isotope effect, i.e. to study the effect of a variation in mass without varying the atomic number.

The sodium isotopes, Na^{22} and Na^{24}, were selected for this experiment for three reasons: (*a*) the fractional mass difference is large; (*b*) the mass ratio between the incident ion and the target atoms (Al^{27}) is close to unity, a situation where one might expect to observe the maximum effect; (*c*) both isotopes are radioactive and can be readily detected and measured.

According to the Nielsen equation (3), the ratio of the mean ranges for two isotopes of the same ion is given by

$$\frac{R_1}{R_2} = \frac{A_2}{A_1} \cdot \frac{A_1 + A_T}{A_2 + A_T}$$

where A_T is the mass of the target atoms. For the case of sodium ion in aluminum, R_{22}/R_{24} would be 1.048. However, the Nielsen equation is applicable only as a limiting case, i.e. when A_1 (and A_2) $\gg A_T$. If the more general treatment outlined in the preceding paper (1) is used, then the predicted ratio is even smaller.

Since the reproducibility between duplicate runs in our previous range studies was no better than $\pm 5\%$, it was obviously not feasible to study such a small isotope effect by measuring R_{22} and R_{24} independently in separate runs. However, by bombarding the target simultaneously with a mixture of Na^{22} and Na^{24} ions, and then measuring the Na^{22}/Na^{24} activity ratio at various depths beneath the surface, it is possible to obtain R_{22}/R_{24} directly from a single run. In this way, most of the sources of error are eliminated, except those involved in the actual counting process.

[1]*Manuscript received November 3, 1960.*
Contribution from the Research Chemistry Branch, Atomic Energy of Canada Limited, Chalk River, Ontario. Presented at the Third Symposium on Nuclear Chemistry and Radiochemistry held at Atomic Energy of Canada Limited, Chalk River, Ontario, September 6–8, 1960.
Issued as A.E.C.L. No. 1149.
[2]*Present address: Frick Chemical Laboratory, Princeton University, Princeton, N.J., U.S.A.*

Can. J. Chem. Downloaded from www.nrcresearchpress.com by 210.87.254.40 on 09/05/12
For personal use only.

EXPERIMENTAL PROCEDURE

The method used for bombarding aluminum targets with monoenergetic radioactive ions, and for subsequently removing thin, uniform layers of aluminum of accurately known thickness has been described in detail elsewhere (4, 5).

The ion source for each run was prepared by evaporating a small volume of aqueous Na_2SO_4 containing appropriate amounts of the radiochemical isotopes Na^{22} and Na^{24}. For maximum statistical accuracy during the subsequent counting operations, the initial relative activity was chosen to be approximately 20% Na^{22} and 80% Na^{24}. Immediately after the bombardment, a series of thin layers were removed successively from the target; the thickness of each layer was chosen so that approximately equal amounts of radioactivity were present in each one. The anodizing and film-stripping solutions from each layer were combined and γ-counted in a 5-ml volumetric flask using a 3×3 in. NaI well-type scintillation counter.

The total activity ($Na^{22}+Na^{24}$) in each flask was measured immediately after the bombardment. The samples were then set aside for 2 weeks to allow the Na^{24} to decay completely, and carefully recounted to obtain the Na^{22} activity. The original Na^{24} activity was determined by difference.

On each occasion the sample was counted at least three times, for a total period sufficient to reduce the standard deviation to less than 0.5%. The Na^{24} counts were corrected for decay to a standard time, using a value of 15.0 hours for the half-life. The maximum decay time involved in such corrections never exceeded 6 hours; furthermore, the samples were counted in random sequence in order to reduce the contribution from any subjective counting errors.

Sets of 5-ml counting flasks were carefully selected from a much larger number on the basis of uniformity of weight, bulb diameter, and position of graduation mark. To test their reproducibility, several flasks from each set were used to measure the isotopic composition of the Na_2SO_4 stock solution. The ratios of Na^{22}/Na^{24} activity obtained with different flasks from any one set agreed within the statistical counting error. A different set was used for each complete run.

RESULTS

Results for a typical run, illustrating the variation of isotope ratio with depth of penetration, are shown in Table I. The estimated standard deviation for the normalized isotope ratios is $\pm.005$. Three runs have been carried out, all using 24-kev sodium ions in aluminum. In each case, an abnormally high Na^{22} content was observed in the first

TABLE I

Distribution of 24-kev sodium ions in aluminum

Depth beneath surface ($\mu g/cm^2$)	c.p.m. per μg aluminum		Isotope ratio Na^{22}/Na^{24}	
	Na^{22}	Na^{24}	Observed	Normalized
0.6	371	1160	·320	1.12_0
2.9	348	1233	.282	0.98_6
6.4	586	2095	.279	0.97_5
9.9	664	2340	.284	0.99_3
13.4	520	1810	.287	1.00_3
18.1	312	1070	.292	1.02_1
36.0	$47._8$	164	.292	1.02_1
Total target	11,720	40,840	.286	1.000

layer; the subsequent variation with depth agrees at least qualitatively with the prediction that Na^{22} has a slightly longer mean range.

By plotting the distribution curves on an expanded scale and interpolating, it is possible to obtain the ratio of the median ranges quite accurately. The results of this interpolation are shown in Table II. The absolute value of each median range has a

TABLE II

Median range (R) of 24-kev sodium ions in aluminum

Run No.	R_{22}	R_{24}	R_{22}/R_{24}
1	13.6_8	13.4_4	1.018
2	13.0_2	12.7_3	1.023
3	13.0_6	12.8_8	1.014
			1.018±.004

probable error of at least ±5%, but, as noted above, most of this error cancels out in determining the isotope ratio R_{22}/R_{24}.

DISCUSSION OF RESULTS

In order to obtain a theoretical estimate for the magnitude of the isotope effect, let us apply the generalized treatment of the elastic-scattering process outlined in the preceding paper (1), viz.

$$R_M = k_M\lambda,$$

where λ is the mean free path of the incident ion and k_M, a numerical factor, is a function only of the mass ratio of the incident ion to the target atom. Appropriate values of k_M for each of the sodium isotopes in aluminum have been evaluated by using a Monte Carlo calculation based on an isotropic scattering model (details of this calculation will be described in a later paper). The resulting values are 1.204 for Na^{22} and 1.230 for Na^{24}.

Hence, the isotope effect may be expressed as

$$\frac{R_{22}}{R_{24}} = \frac{1.204\lambda_{22}}{1.230\lambda_{24}} = 0.979\left(\frac{\lambda_{22}}{\lambda_{24}}\right).$$

But, from equation 5 in the preceding paper

$$\lambda \propto \frac{A_T^2}{A_{ion}+A_T}.$$

Therefore,

$$\frac{\lambda_{22}}{\lambda_{24}} = \frac{24+27}{22+27} = 1.041$$

and

$$R_{22}/R_{24} = 0.979\times1.041 = 1.019.$$

It will be noted that this predicted ratio agrees with the measured values of 1.018, 1.023, and 1.014 within the estimated experimental error of ±0.5%.

Can. J. Chem. Downloaded from www.nrcresearchpress.com by 210.87.254.40 on 09/05/12
For personal use only.

Can. J. Chem. Downloaded from www.nrcresearchpress.com by 210.87.254.40 on 09/05/12
For personal use only.

In the preceding paper, the Na^{24} range studies indicated that, above 10 kev, elastic scattering is not the only significant process contributing to the slowing down of the incident ion, but that electronic interactions become increasingly important at higher energies. Unfortunately, the existence of significant electronic interactions at such low energies was not fully realized when these isotope effect measurements were undertaken; as a result, the energy selected for the present study is somewhat higher than would now seem desirable. However, it is probably safe to conclude that, even at 24 kev, elastic scattering is still the more significant mechanism.

A qualitative explanation for the observed variation in isotope ratio as a function of depth (Table I) can quite readily be found: Na^{22} has the larger velocity, and hence the longer mean free path; this produces a normalized Na^{22}/Na^{24} ratio slightly less than unity at depths less than the median range, and slightly greater than unity at depths greater than the median range. The only abnormal result is the very large Na^{22} content in the surface layer. This may be attributed to the fact that Na^{22}, being the lighter ion, suffers larger angular deflections per collision. It can be shown that, if the scattering process is approximately isotropic in center-of-mass co-ordinates, then in the laboratory co-ordinate system approximately 20% of the Na^{22} ions are deflected through 90° or more in a single collision, whereas the corresponding figure for Na^{24} is only 15%. This considerable difference in the frequency of large-angle deflections is sufficient to produce the enhanced Na^{22} content observed in the first layer. The sodium content in the first layer is caused almost entirely by those ions that undergo large angular deflections in their *first* collision, and that have this collision near the surface. In such a collision, more than 95% of the energy is lost, and hence these ions do not travel much further.

A modification of the Monte Carlo method for calculating the shape of distribution curves (1) may be used to put the above explanation on a more quantitative basis. The statistical accuracy obtainable in Monte Carlo calculations is determined by the number of individual particle tracks followed; and it would require a prohibitive amount of computer time to reduce the statistical error to $\pm 0.5\%$ for the Na^{22} and Na^{24} abundances in each of the seven layers in Table I. However, the random numbers used to characterize each collision in the calculation are not truly random in that they are generated by some arithmetical device: in other words, they are only "pseudo-random", and it is possible to regenerate exactly the same sequence if desired.

Therefore, in order to compute the isotope ratio theoretically, a reasonable number of particles ($\sim 10^4$) were followed through a random sequence of collisions (six collisions per particle) with the mass ratio set at 0.81, i.e. the Na^{22} ion case; then, with the mass ratio set at 0.89 (the Na^{24} case), the same number of particles were followed through exactly the same "random" sequence. Since we are interested only in the *ratio* of the Na^{22} activity to the Na^{24} activity at various depths, most of the statistical fluctuations cancel out.

These Monte Carlo calculations give the isotopic distribution (Na^{22}/Na^{24}) at various multiples of the mean free path (λ) of the incident ion. In order to compare the calculated and experimentally measured ratios at various depths, it is necessary to introduce the ratio of the mean free paths ($\lambda_{22}/\lambda_{24}$). The value of 1.041 obtained above in computing the ratio of median ranges was used for this purpose. The resulting values for the predicted variation of isotope ratio with depth are compared with experiment in Table III. Considering the errors involved both in the calculation and in the experimental measurement, the agreement between the observed and calculated ratios is quite satisfactory, and provides further support for the approximate validity of the isotropic

TABLE III

Variation in isotope ratio with depth of penetration

Depth ($\mu g/cm^2$)	Na^{22}/Na^{24} activity ratio	
	Observed	Calculated
0.6	1.120	1.080
2.9	0.986	0.972
6.4	0.975	0.960
9.9	0.993	0.964
13.4	1.003	0.998
18.1	1.021	1.009
36.0	1.021	1.048

scattering assumption. In particular, the theoretical treatment accounts for the anomalously high Na^{22} content in the surface layer.

ACKNOWLEDGMENTS

It is a pleasure to acknowledge the invaluable assistance of Dr. J. M. Kennedy and B. Miles in the development and programing of the special Monte Carlo calculations used in this work.

REFERENCES

1. J. A. DAVIES and G. A. SIMS. Can. J. Chem. **39**, 601 (1961).
2. N. BOHR. Kgl. Danske Videnskab. Selskab, Mat-fys. Medd. **18** (8) (1948).
3. K. O. NIELSEN. *In* Electromagnetically enriched isotopes and mass spectrometry. *Edited by* M. L. SMITH. Academic Press, New York. 1956. p. 73.
4. J. A. DAVIES, J. D. MCINTYRE, R. L. CUSHING, and M. LOUNSBURY. Can. J. Chem. **38**, 1535 (1960).
5. J. A. DAVIES, J. FRIESEN, and J. D. MCINTYRE. Can. J. Chem. **38**, 1526 (1960).

Can. J. Chem. Downloaded from www.nrcresearchpress.com by 210.87.254.40 on 09/05/12
For personal use only.

Can. J. Chem. Downloaded from www.nrcresearchpress.com by 210.87.254.6 on 09/05/12
For personal use only.

THE KINETIC ENERGY OF Cs^{136} PRIMARY FRAGMENTS FROM FISSION OF U^{235} [1]

F. Brown and B. H. Oliver

ABSTRACT

The ranges of Cs^{136}, Cs^{137}, and Ba^{140} fission fragments in aluminum have been measured using an anodizing technique to strip layers from the aluminum together with radiochemical methods to determine the fission products. The mean ranges are, in milligrams per square centimeter: Cs^{136}, 2.64; Cs^{137}, 2.91; and Ba^{140}, 2.82. The range distributions were of near-Gaussian form with the following percentage full widths at half height; Cs^{136}, 17.7; Cs^{137}, 17.0; and Ba^{140}, 17.5. The range–energy relationship of Bohr, R = const. $A^{1/2}E^{1/2}Z^{-2/3}$, was tested using the range data of Katcoff (7) and of Niday (2) together with the kinetic energy data of Milton and Fraser (15) and found to be accurate, within experimental error, over any limited range of fragment masses. Using this formula it then appears that the total kinetic energy in the fission mode leading to Cs^{136} is ~21 Mev less than normal.

INTRODUCTION

The general features of the distribution of nuclear charge in low-energy fission are well known. The situation is usually described in terms of the distribution in primary charge of fragments having a fixed mass. It is then found that the charge distribution is, at least approximately, independent of the particular mass chosen and can be represented by a Gaussian-like distribution around a most probable charge Z_p. The value of Z_p for any mass can be found using the empirical rule due to Glendenin (1) known as the "equal chain length hypothesis". An alternative, but equivalent, description is obtained by considering the distribution in mass of fragments having a fixed primary charge.

This latter distribution emphasizes the fact that the observed charge distribution can be modified by neutron emission from the fragments (a phenomenon which is well known in high-energy fission). The number of neutrons emitted in fission is not constant, and one can therefore ask whether those primary fragments found relatively close to stability (i.e. having less than the most probable mass for a fixed primary charge) have emitted more than the average number of neutrons. One associates a more than average neutron emission with fragments which possess more than average internal excitation and, if the total energy release for the formation of these fragments is normal, one then expects them to have less than normal kinetic energy.

Ideally one would like to have measurements of the total energy release, the kinetic energy, the γ-ray energy, and the neutron emission for fragments formed close to stability (and likewise for those formed exceptionally far from stability) but such fragments are rare and the present techniques for such measurements, by time of flight and so on, are not applicable. This suggests the use of radiochemical methods, which are highly specific. In particular it is possible, in principle, to measure the range of any fission fragment and given the range–energy relationship to obtain its kinetic energy. The paper presents the results of experiments to measure the kinetic energy of the fragment Cs^{136} which, being a shielded nuclide, is a primary fragment.

A collimated beam of fission fragments was directed into an aluminum catcher foil.

[1]*Manuscript received November 3, 1960.*
Contribution from the Research Chemistry Branch, Atomic Energy of Canada Limited, Chalk River, Ontario. Presented at the Third Symposium on Nuclear Chemistry and Radiochemistry held at Atomic Energy of Canada Limited, Chalk River, Ontario, September 6–8, 1960.
Issued as A.E.C.L. No. 1151.

Successive layers of the foil were dissolved by an anodizing technique and analyzed for Cs^{136}, Cs^{137}, and Ba^{140}. The relationship between range and energy was derived from theory and confirmed by the Cs^{137} and Ba^{140} data together with other data from the literature.

The results of these experiments show that, as anticipated, the range of Cs^{136} fragments is abnormally low. During the preparation of this work for publication a new set of range measurements, for U^{235} fragments in uranium, has become available (Niday (2)). These measurements also show that Cs^{136} and Rb^{86} (another shielded nuclide) have abnormally low ranges. The significance of these observations on shielded nuclides is discussed at the end of this paper.

EXPERIMENTAL

Apparatus

An electropolished aluminum plate approximately 1.5×4.0 cm was covered with a layer of U^{235} as oxide deposited using the lacquer technique and of thickness ~100 μg U^{235}/cm^2. This plate was covered with an aluminum collimating plate 3/16 in. thick drilled with 1/16 in. diameter holes. Against this was placed the catcher foil, a plate of electropolished, high-purity aluminum. The assembly was placed in an irradiation container, filled with hydrogen at atmospheric pressure, and hermetically sealed. The hydrogen was introduced to provide some cooling to the container walls. An irradiation of 1 week was made in a vacant fuel rod position of the NRX reactor at a neutron flux of $\sim 5 \times 10^{13}$ neutrons/cm^2 sec.

Sampling

After removal from the reactor and disassembly by remote handling the catcher foil was "stripped" using the anodizing technique developed by Davies (3). In this technique the specimen is anodized by applying a known voltage in a citrate buffer solution which causes an oxide layer to form whose thickness is proportional to the voltage and essentially independent of time after the first 5 minutes. The specimen is then removed, washed, and placed in a hot (95° C) stripping solution of chromic oxide and phosphoric acid which rapidly dissolves the oxide (2 minutes) but does not attack the metal. The process is then repeated as required. In the present case the anodizing voltage was 100 volts, which results in the stripping of ~25 μg/cm^2 of aluminum in each cycle. Since this is an unnecessarily small layer two oxide layers were dissolved in each sample of stripping solution so that each sample contained ~50 μg/cm^2 of the specimen. The actual amount stripped was determined by weighing the specimen after every seven samples and was found to be 54.3 μg/cm^2 per sample (in agreement with the data obtained by Davies). This figure could be in error by about 3% due to a possible error in measuring the area of the foil; the electropolishing process caused the edges of the foil to be somewhat rounded. This error would affect only the absolute values of the ranges measured.

The consistency in sampling was indicated by comparing the weights removed in each group of seven samples. The standard deviation from the mean was 1.4%. The weight loss for seven samples was ~5.0 mg, the error in the weighings ~0.05 mg, so that within the accuracy of measurement there were no significant variations between the groups of seven samples.

Purification

Each sample of stripping solution contained measured quantities of cesium and barium carriers. The barium was precipitated as carbonate, purified by the hydrochloric acid – ether method of Glendenin (4), collected on weighed filter papers, weighed as $BaCl_2 . 2H_2O$,

Can. J. Chem. Downloaded from www.nrcresearchpress.com by 210.87.254.6 on 09/05/12
For personal use only.

and finally mounted for γ-ray counting. The cesium was purified by the sodium tetraphenyl boron method of Handley and Burros (5). It was found necessary to apply this procedure twice in order to obtain sufficient radiochemical purity. Thus the precipitate of cesium tetraphenyl boron obtained from the first purification cycle was destroyed by fuming nitric acid and the whole cycle was repeated. The final precipitate was collected, weighed, and mounted for γ-ray counting as in the barium case.

Counting

The samples were counted by a 3×3 in. sodium iodide crystal mounted as recommended by Heath (6). For the cesium counting this was connected to a 100-channel kicksorter equipped with typewriter readout. The stability of both counting rate and energy scale was checked using Cs^{137} and Co^{60} standards and no corrections were found to be necessary. The spectra, corrected for background, showed the 661-kev peak from Cs^{137} and peaks from Cs^{136} at 822 kev, 1.04 Mev, and higher energies. The Cs^{136} counting rate was taken as the total rate in the 822-kev and 1.04-Mev peaks corrected for the high-energy tail from the 661-kev Cs^{137} peak. This correction was actually negligible except in the few samples which contained a very high Cs^{137}/Cs^{136} ratio when it amounted to $\sim$3%. The Cs^{137} counting rate was taken as the rate in the 661-kev peak corrected for the Compton contribution from the higher-energy Cs^{136} γ-rays. This contribution was estimated by comparing spectra of pure Cs^{137} with those from various Cs^{136}–Cs^{137} mixtures. The correction varied from $\sim$1% to $\sim$25% depending on the Cs^{136}/Cs^{137} ratio. In the samples of greatest interest it was $\sim$5%. These data were then corrected for the chemical yield and for decay of the Cs^{136} to obtain the results shown in Fig. 1.

For the Ba^{140} counting the crystal was connected to a discriminator and the total γ-ray count above 700 kev was recorded. All samples had been allowed to decay sufficiently before counting so that the La^{140} had reached secular equilibrium. The rates were corrected for background and chemical yield and are shown in Fig. 1. No corrections for decay were required since all the samples were counted within a short space of time and only relative rates were required.

RESULTS

The experimental data are shown in Fig. 1 where the activity for each nuclide, in arbitrary units, is plotted against the sample number. In each case the distribution shows the expected Gaussian-type distribution plus a tail of approximately constant level on the low-range side. This tail could arise from U^{235} lost from the source during irradiation and deposited on the surface of the catcher foil. The experiment was repeated with the uranium covered by $\sim$700 $\mu g/cm^2$ of aluminum in order to prevent transfer of uranium. The intensity of the tail was reduced to about one half. The remaining tail is presumably caused by scattering but it would seem desirable to perform experiments specifically designed to study this effect before attempting to draw any firm conclusions. Corrections for these tails were made by assuming they consisted of a square distribution smeared by a Gaussian of the same width as the main peak. The data so corrected are shown on Fig. 2. Typical errors are shown by the vertical bars. In the case of Ba^{140} and Cs^{137} they arise mainly from the chemical yield determinations, but in the Cs^{136} case the uncertainty in background correction is also involved and thus the errors are relatively larger for the low-activity points.

In order to test the shape of the distributions the data were integrated and plotted on probability paper; it was found that the mean range was, in all cases, slightly less

Can. J. Chem. Downloaded from www.nrcresearchpress.com by 210.87.254.6 on 09/05/12
For personal use only.

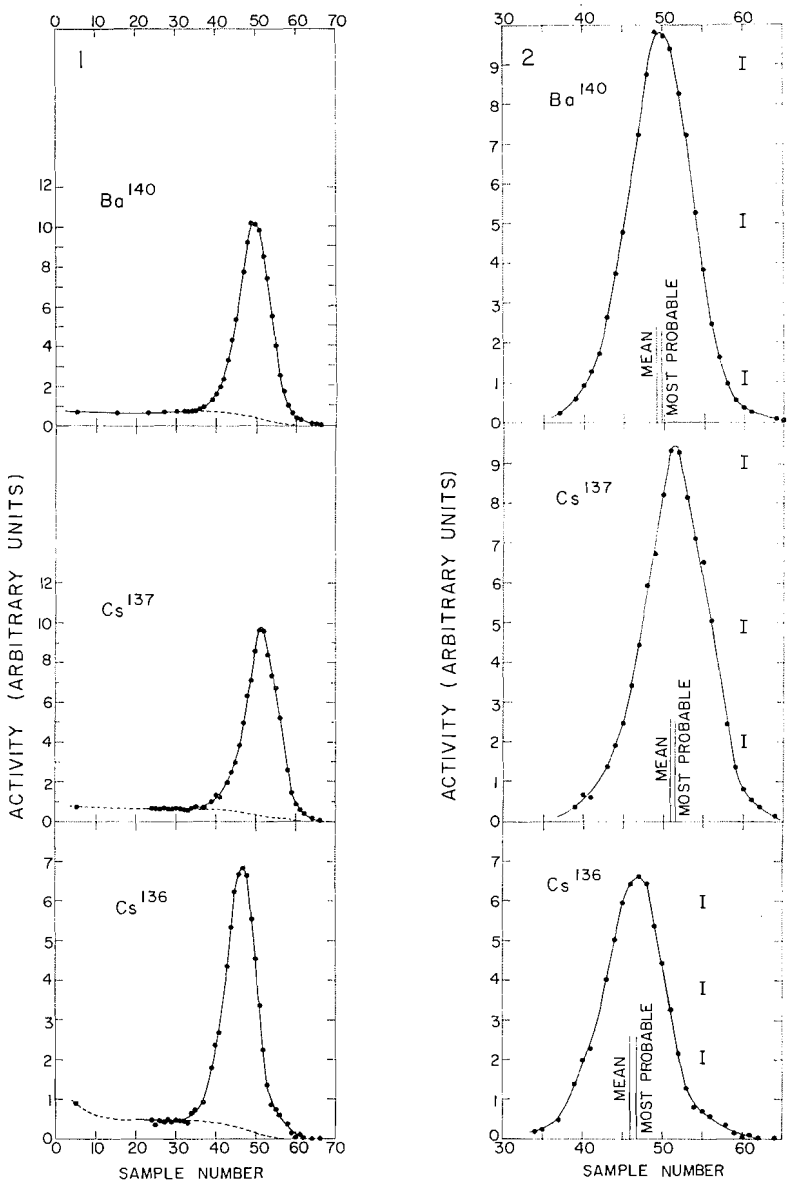


FIG. 1. Range distributions, uncorrected.
FIG. 2. Range distributions, corrected.

than the most probable, the difference being between 1 and 2%. This agrees qualitatively with the results of Katcoff *et al.* (7), who found, for Pu^{239} fission fragments in air, that the distributions were slightly steeper on the high-range side. As in the case of the Katcoff experiment it is not clear whether this small effect is fundamental or is caused by the experimental setup.

To convert sample number to range in aluminum it is necessary to multiply by 54.3 $\mu g/cm^2$ and to add a small correction for the weight of hydrogen in the collimator holes and for the source thickness. This correction amounts to the equivalent of ~2.3

Can. J. Chem. Downloaded from www.nrcresearchpress.com by 210.87.254.6 on 09/05/12
For personal use only.

samples and although it is not accurately established it has no significant effect on the final analysis. After making this correction one obtains the results shown in Table I for the mean ranges and full widths at half maximum of the distributions.

TABLE I

Ranges and range dispersions in aluminum

Nuclide	Range (mg/cm²)	Width (%)
Ba^{140}	2.82	17.5
Cs^{137}	2.91	17.0
Cs^{136}	2.64	17.7

The precision of the mean range values is ~0.4%; their absolute accuracy is about 4%. This is set by the error in correcting for source thickness and hydrogen absorption (~2%) and the error in the value for the weight removed per sample (~3%). The precision of the widths is ~3% and thus the variation in widths between the three nuclides is not significant.

The present experiments were designed primarily to detect differences in ranges rather than to set absolute values. The absolute range of the Ba^{140} fragments can be compared directly with the value obtained by Finkle *et al.* (8) for Ba^{140} from U^{235} stopping in aluminum, viz. 2.75 mg/cm². A recent measurement by Alexander and Gallagher (9) gives a value of 2.98 mg/cm².

The widths obtained by Good and Wollan (10) for I^{137} fragments from U^{235} stopping in various gases are: H_2, 4.3%; D_2, 8.0%; He, 6.3%; air, 15.7%; A, 18.2%. The width obtained by Katcoff *et al.* for the Ba^{140} fragments from Pu^{239} stopping in air was 12.6%. The widths obtained with the present technique appear therefore to be reasonable.

It should be noted that the range dispersion in all but the lightest stopping media is due almost entirely to straggling; the contributions from the variations in kinetic energy and nuclear charge are small in comparison. In the present experiment the contributions from source thickness (~1%) and finite collimator angle (~2.5%) are also very small.

DISCUSSION

The following discussion is presented in three parts: (*a*) range–energy relationships for fission fragments, (*b*) calculation of the kinetic energy released in forming Cs^{136}, and (*c*) the significance of the kinetic energy deficit which is found in the formation of Cs^{136}.

(a) Range–Energy Relationships for Fission Fragments

It is clear from the present experiment and from the results of Niday (2) that the Cs^{136} fragments have abnormally low ranges. Before discussing the significance of this fact it is necessary to know what this amounts to in terms of the kinetic energy of the fragment and it is in this question that the greatest difficulty arises. The only range data for particles of fission product masses and initial energies are those obtained on fission products themselves. Whilst, in principle, these range data can be combined with fragment energy data obtained by time-of-flight techniques in order to establish some relationship between fragment mass A, nuclear charge Z, and initial energy E, in practice it is difficult to draw any unambiguous conclusions. The difficulty is that, for normal fission fragments, A, Z, and E are correlated, viz. Z is approximately proportional

Can. J. Chem. Downloaded from www.nrcresearchpress.com by 210.87.254.6 on 09/05/12
For personal use only.

Can. J. Chem. Downloaded from www.nrcresearchpress.com by 210.87.254.6 on 09/05/12
For personal use only.

to A and E is very approximately inversely proportional to A. Another set of potentially useful data are those concerning the rate of energy loss dE/dx or rate of velocity loss dV/dx obtained by Lassen (11), Leachman and Schmitt (12), and Fulmer (13). Apart from the fact these studies involve only the "median light" and "median heavy" fragments there is also a fundamental difficulty in using them to establish a range–energy relationship, viz. the range–energy relationship changes as the fission fragments slow down. This is due to the change in effective charge as the fragment slows down, which means that the mechanism of energy loss changes from being predominantly ionization at high velocities to predominantly screened field scattering at low velocities. For the present purpose we are interested in the effect on the range when the initial energy is changed by only a rather small amount from the normal. We should also pay special attention to the effect of nuclear charge because the nuclear charge of a Cs^{136} fragment is abnormally high in relationship to its mass.

An approximate formula for the range, R, can be obtained from Bohr's theoretical discussions (14),

$$[1] \qquad R = k\frac{A^{1/2}E^{1/2}}{Z^{2/3}}$$

where k is a constant depending on the stopping material. This can be approximated to $R = E^{1/2}A^{-1/6}$ (see reference 7) by assuming Z proportional to A; however, for the present, it is preferable to retain the Z dependence. The validity of the expression can be checked to some extent by using the range data of Katcoff *et al.* (7) for fragments from Pu^{239} stopping in air and the range data of Niday (2) for U^{235} fission fragments stopping in uranium together with the fragment kinetic energy data obtained by time-of-flight techniques. We have used here the energy data obtained by Milton and Fraser (15), corrected for neutron emission as follows. Let E_p be the total prompt kinetic energy measured at prompt mass ratio A_H/A_L. The prompt kinetic energies of the separate fragments are given as usual by $E_p/(1+A_L/A_H)$ and $E_p/(1+A_H/A_L)$ but the kinetic energies of interest in range studies are those after neutron emission, which are given by

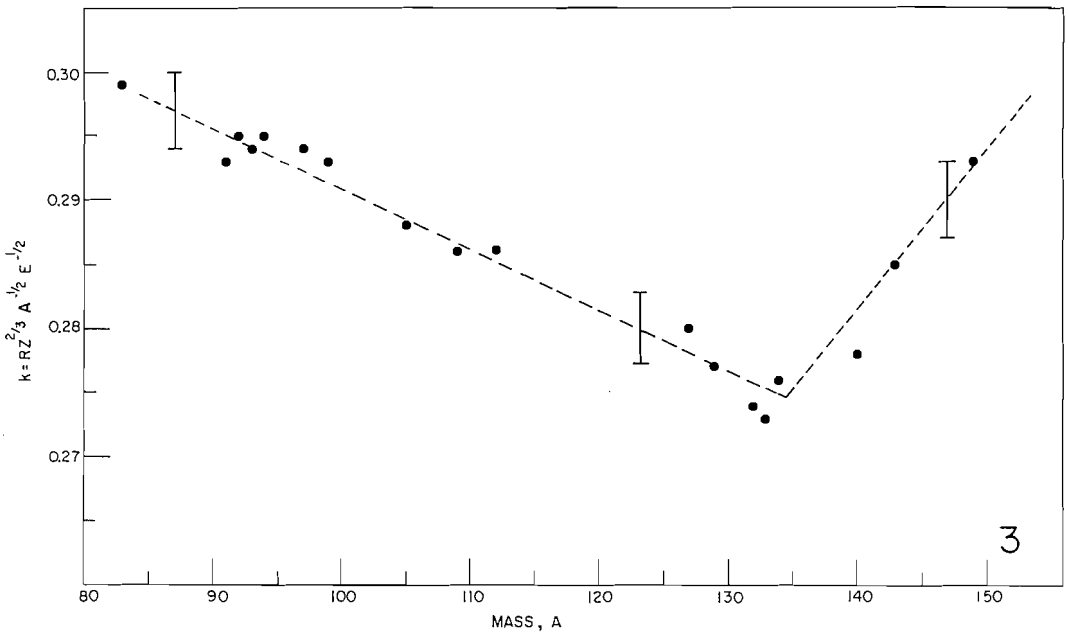
$$\left[\frac{E_p}{(1+A_L/A_H)}\right]\frac{A_L-\nu_L}{A_L} \quad \text{and} \quad \left[\frac{E_p}{(1+A_H/A_L)}\right]\frac{A_H-\nu_H}{A_H}$$

where ν_L and ν_H are the numbers of neutrons emitted by the light and heavy fragments respectively. The corresponding masses, as observed in range studies are of course $A_L-\nu_L$ and $A_H-\nu_L$. In the case of U^{235} the value of ν_L and ν_H was obtained from the data of Apalin *et al.* (16); in the Pu^{239} case the following relationships, due to Milton (17), were employed:

$$\nu_L = \frac{2.89}{2} + (A_L-100)\,0.045 \quad \text{and} \quad \nu_H = \frac{2.89}{2} + (A_H-140)\,0.067.$$

The appropriate values of Z are the most probable charges Z_p and were obtained from the empirical Z_p function of Wahl (18). We have then calculated the values of the constant k for each fragment measured and we have plotted the results in Fig. 3 (Katcoff's data (7) for fragments stopping in air) and Fig. 4 (Niday's data (2) for fragments stopping in uranium). Both figures show small but significant trends in the "constant" k, but for fragments whose masses differ by only a few units the formula is as good as the data used to check it. (The lines in Figs. 3 and 4, which have been drawn only for illustration,

Can. J. Chem. Downloaded from www.nrcresearchpress.com by 210.87.254.6 on 09/05/12
For personal use only.



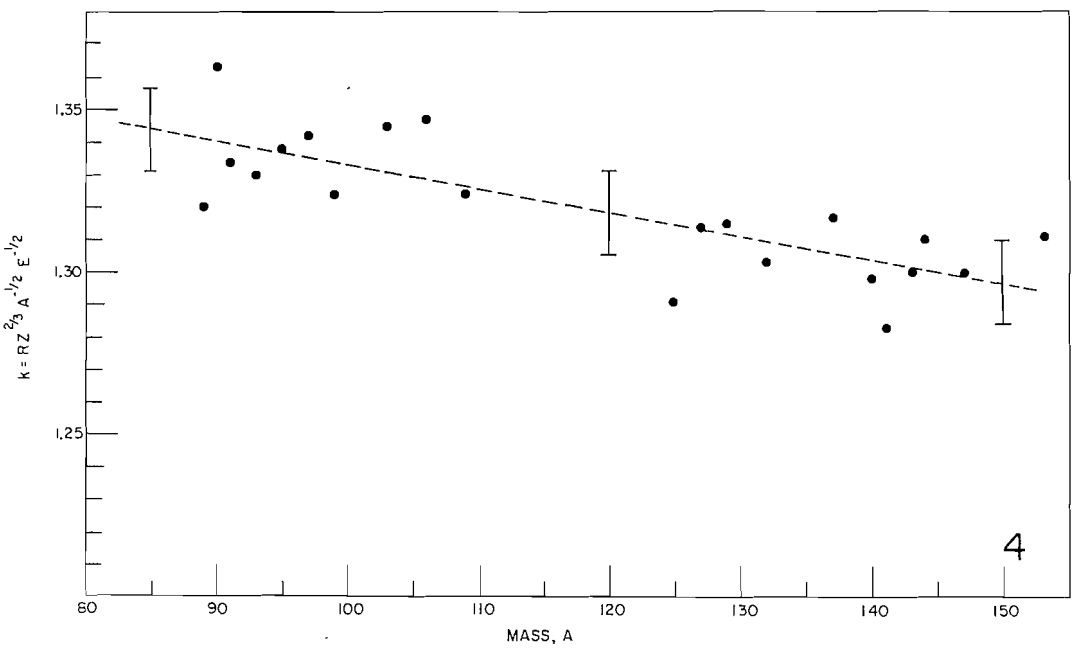


FIG. 3. Values of $k = RZ^{2/3}A^{-1/2}E^{-1/2}$; data of Katcoff *et al.* (7) for Pu^{239} fragments in air.
FIG. 4. Values of $k = RZ^{2/3}A^{-1/2}E^{-1/2}$; data of Niday (2) for U^{235} fragments in uranium.

have slopes of 0.12 and 0.06% per mass unit respectively. The vertical bars show deviations of $\pm 1.0\%$ in k.)

Niday (2) in the interpretation of his data for fission fragment ranges in uranium has

discussed Bohr's treatment of ranges and used the theoretical expressions as a basis for a semiempirical range formula as follows:

[2] $$R = \frac{A(V_1 - V_c)}{2.411(K + 4.762K^{5/3})}$$

where V_1 is the initial fragment velocity, V_c the velocity at which the collision diameter becomes greater than the screening parameter (see reference 2 for definition of these quantities), and $K = 1.077Z^{1/3}$. This formula was fitted to the range data and the velocity data of Stein (19). With the numerical constants given it applies to ranges in uranium. It may be noted that this expression, equation [2], approximates to the simpler expression, equation [1]. Thus V_c is small compared with V_1, the term K is small compared with the term $4.762K^{5/3}$, and since $V_1 = (2E/A)^{1/2}$ we then have

$$R = \text{const.} \frac{A^{1/2}E^{1/2}}{Z^{5/9}}.$$

Alexander and Gallagher (9) have considered the range–energy relationship for "median heavy" and "median light" fragments. Leachman and Schmitt's data (12) give the velocity (V) of these "average" fragments after passing through aluminum foils of known thickness, whilst Fulmer's data (13) give their energies (E), measured by a cesium iodide crystal, after passing through known thicknesses of various materials including aluminum. Alexander and Gallagher found that for these "average" fragments whose mass and charge, although not precisely defined, are constant, the range–energy data are fitted by either of two relationships,

[3] $$R = kV - \Delta$$

or

[4] $$R = KE^{2/3},$$

where k, K, and Δ are constants. Both these expressions fit the available data reasonably well over a rather *wide range* of energies. However, if we consider data for fragments slowed down only *slightly* we find that the range is more nearly proportional to $E^{1/2}$. This is of course implied by equation [3] since for fragments having their normal initial velocities or thereabouts the term Δ is small compared to kV; compare also equation [2]. This point is demonstrated by the data in Table III. To obtain this we have proceeded as follows. Let R_1 be the range of the unslowed fragment in aluminum and let E_1 be its initial energy. After passing through a given thickness of aluminum, t, its energy is E_2 (as given by Leachman and Schmitt (12) or by Fulmer (13)) and its range R_2 is just $R_1 - t$. We used our value for the Ba^{140} range as representative of the median heavy fragment to which Table III applies. The table lists (R_1/R_2), $(E_1/E_2)^{1/2}$, and $(E_1/E_2)^{2/3}$ and although the $E^{2/3}$ dependence gives the best over-all fit the $E^{1/2}$ dependence is better when E_2 is close to E_1. This test is of course of poor sensitivity when E_2 is close to E_1 and we present the table to illustrate the trend.

When equations [3] and [4] are applied to the ranges of fragments of different masses it is found that the "constants" Δ and K vary with mass. This is to be expected since the equations have no allowance for the effect of A and Z, but provided the variation is smooth and can be established, as was done by Alexander and Gallagher, it is possible to interpolate for K or Δ. It is interesting to note that equation [1] becomes equation [4] if we make the approximation that Z is proportional to A and A is inversely proportional to E.

Can. J. Chem. Downloaded from www.nrcresearchpress.com by 210.87.254.6 on 09/05/12
For personal use only.

TABLE III
Range-energy relationship for "median heavy" fragment

$(E_1/E_2)^{1/2}$	R_1/R_2	$(E_1/E_2)^{2/3}$
1.12	1.10	1.17*
1.22	1.22	1.30*
1.44	1.55	1.60*
1.50	1.60	1.67†
1.72	2.14	2.06*
1.96	2.82	2.46†

*Using reference 13 (Fulmer).
†Using reference 12 (Leachman and Schmitt).

(b) The Kinetic Energy Released in the Formation of Cs^{136}

We have used equation [1] to obtain the kinetic energy of the Cs^{136} fragments because (*a*) it contains terms for the Z and A dependence and (*b*) the constant of proportionality k is established by our own data on Cs^{137} and Ba^{140}. The Z dependence is important because the change from $Z = 52.6$ (Z_p for mass 136) to $Z = 55.0$ (Z for Cs^{136}) accounts for a change in range of some 2.8% (for a $1/Z^{2/3}$ dependence) out of an observed range anomaly of some 10%.

Z_p values were taken from Wahl (18). Kinetic energies were obtained from the data of Milton and Fraser (15) corrected for neutron emission as before. From the measured Cs^{137} and Ba^{140} ranges the constant k in equation [1] was obtained: the values were 0.418 and 0.419, respectively, in excellent agreement. The kinetic energy of the Cs^{136} fragment was then calculated using $k = 0.418$ and found to be 61.0 Mev. Assuming that two neutrons were emitted in the formation of this fragment, the kinetic energy of the prompt fragment (Cs^{138}) was 61.9 Mev and by conservation of momentum the total kinetic energy (for the two fragments) was 149.0 Mev. The total kinetic energy for a normal fission into prompt masses 138 and 98 is, according to Milton and Fraser, 169.8 Mev; by normal we mean having the normal charge distribution appropriate to the masses involved. The fission to produce Cs^{136}, whose Z is 55 compared with a Z_p of 52.6 for mass 136, has therefore about 21 Mev less kinetic energy than the normal fission to mass 136.

This conclusion relies on the range formula and although we have data (12, 13) to show that the energy dependence of the range is not likely to be in *serious* error we do not have any direct evidence for the relationship between range and charge or between range and mass. It is, however, encouraging to note that Niday (2), using his own range data and equation [2], calculated the kinetic energy of the Cs^{136} fragment to be 61.6 Mev, compared with our value of 61.0 Mev. It is also interesting to find that using energies from Milton and Fraser, range data from the present work and Alexander's range–energy relationship (equation [4], above) we find the kinetic energy of the Cs^{136} to be 60.5 Mev. If Niday's range data are used with this equation the result is again 60.5 Mev.

It is clear, therefore, that if we trust our present ideas on fission fragment ranges and energies we must conclude that the production of Cs^{136} involves some 21 Mev less total kinetic energy than is normal for this mass ratio. Niday's results show that the situation is similar in the production of Rb^{86}, another shielded nuclide; the deficit in total kinetic energy is again ~20 Mev. The following sections of this paper are an attempt to discuss the significance of these facts.

Can. J. Chem. Downloaded from www.nrcresearchpress.com by 210.87.254.6 on 09/05/12
For personal use only.

(c) The Kinetic Energy Deficit in the Formation of Cs^{136}

We expect the fissions which produce Cs^{136} as a primary fragment to produce less kinetic energy than normal for two reasons. (*a*) Because Cs^{136} is neutron deficient (for a fission fragment) it will be associated with events which involve greater than average neutron emission, which means greater than average internal excitation of the fragments and hence less kinetic energy for any given total energy release. (*b*) Because the charge division required to produce Cs^{136} is a long way from the most probable charge division there will be less total energy release.

We shall next attempt to make quantitative estimates of these two effects beginning with the question of neutron emission in the formation of Cs^{136}. Ideally we wish to know the distribution of neutron emission probabilities for heavy fragments in the mass range 136 to about 140. The distribution of neutron emission probabilities averaged over *all pairs* of fragments is known; Terrell (20) has shown that this distribution can be represented by a Gaussian with standard deviation $\sigma_{H+L} = 1.08$. We also know from the work of Apalin *et al.* (16) that the average numbers of neutrons from the heavy and light fragments are approximately the same at the mass ratio corresponding to Cs^{136}. To obtain the distribution for the heavy fragment alone we shall make two alternative assumptions. (*a*) Assume that the distributions for the light and heavy fragments are not correlated to each other. In this case the standard deviation for the heavy fragment is $\sigma_H = \sigma_{H+L}/\sqrt{2} = 1.08/\sqrt{2}$. (*b*) Assume that the distributions for heavy and light fragments are correlated in a positive sense, i.e. if the heavy fragment emits more than the average number of neutrons the light fragment also does; this implies that the two fragments share the available excitation energy in a constant proportion. In this case $\sigma_H = \sigma_{H+L}/2 = 1.08/2$. Using these distributions we can now calculate the probabilities, P_ν, that a fragment of mass 136 is formed from fragments of prompt mass 136, 137, 138, etc. by emission of 0, 1, 2, etc. neutrons.

In order to say how many of these mass 136 fragments so formed will actually be Cs^{136} we must know the probability P_{55} that each of the prompt mass precursors will have a nuclear charge 55. We thus need the charge distribution before neutron emission. The charge distribution after neutron emission is known; Nethaway and Wahl (21) have shown that it can be presented by a Gaussian with standard deviation σ_{obs} where $2\sigma_{obs}^2 = 1.0$. We can correct the charge distribution for neutron emission as follows. The fluctuations in the mass of the heavy fragment due to neutron emission have a standard deviation σ_H (defined above) and since for the heavy fragments $\Delta Z/\Delta A = 0.49$ this corresponds to a fluctuation in charge of $\sigma_Z = \sigma_H \times 0.49$. The corrected charge distribution will thus have a standard deviation σ_{cor} given by $\sigma_{cor}^2 = \sigma_{obs}^2 - \sigma_Z^2$ where $2\sigma_{obs}^2 = 1.0$, $\sigma_Z = \sigma_H \times 0.49$, and σ_H is either $1.08/\sqrt{2}$ or $1.08/2$ according to the alternative assumptions discussed above. It is interesting to see that the effect of neutron emission in broadening the observed charge distribution is not negligible.

From the corrected charge distribution we now obtain the probabilities P_{55} that each prompt mass, 136, 137, 138, etc., will have $Z = 55$. We have previously calculated the probabilities P_ν that each of these precursors will yield a fragment of mass 136 by emission of ν neutrons. The product $P_\nu P_{55}$ is the probability that Cs^{136} will be formed by emission of ν neutrons. The number of neutrons emitted in forming Cs^{136} is thus $\Sigma \nu P_\nu P_{55}$, the number of Cs^{136} fragments formed is $\Sigma P_\nu P_{55}$, and the average number of neutrons $\bar{\nu}_{Cs^{136}}$ emitted in forming Cs^{136} is given by

$$\bar{\nu}_{Cs^{136}} = \frac{\Sigma \nu P_\nu P_{55}}{\Sigma P_\nu P_{55}}.$$

Can. J. Chem. Downloaded from www.nrcresearchpress.com by 210.87.254.6 on 09/05/12
For personal use only.

These calculations show that for assumption (*a*) (uncorrelated neutron emissions from light and heavy fragments) $\bar{\nu}_{Cs^{136}}$ is 2.52. The normal neutron emission from the heavy fragment at this mass ratio is 1.21 neutrons (16) and thus the *extra* neutron emission in forming Cs^{136} is $\Delta\nu_{Cs^{136}} = 2.52-1.21 = 1.31$ neutrons. If we assume that the emission of each neutron involves the expenditure of 6.7 Mev (Terrell (22)) this requires an extra 8.8 Mev of excitation and leaves, correspondingly, 8.8 Mev less kinetic energy. For assumption (*b*) (correlated neutron emission from light and heavy fragments) the value of $\bar{\nu}_{Cs^{136}}$ is 2.01 and thus $\Delta\nu_{Cs^{136}}$ is $2.01-1.21 = 0.80$. Since we have assumed correlated neutron emissions the light fragment will also emit an equal number of extra neutrons so that the extra neutron emission involved is $2\times0.80 = 1.60$ neutrons. This involves 10.7 Mev extra excitation and thus 10.7 Mev less kinetic energy.

Having estimated the deficit in kinetic energy due to extra neutron emission we must add to it the deficit in total energy release caused by unfavorable charge division in order to obtain the total deficit in kinetic energy. The deficit in total energy release can be obtained using the mass tables of Cameron (23) provided we know the prompt masses involved. We have assumed $\bar{\nu}_{Cs^{136}} = 2.0$, i.e. a prompt mass ratio of 138:98. The most probable charge division for this mass ratio is almost exactly 53:39 and gives a total energy release of 183.9 Mev. The production of cesium by a charge division of 55:37 releases 176.2 Mev, i.e. 7.7 Mev less.

Thus our estimates for the deficit in kinetic energy involved in forming Cs^{136} are, for assumption (*a*), $8.8+7.7 = 16.5$ Mev and, for assumption (*b*), $10.7+7.7 = 18.4$ Mev. The measured deficit is 21 Mev.

Both estimates are low, but the agreement is reasonable considering the assumptions involved. We derived the number of neutrons emitted in forming Cs^{136} from the average distribution of neutron emission probabilities measured for all fissions. This could be a mistake, due, for example, to the existence of the 82-neutron shell in the precursor Cs^{137}. We have also assumed that the emission of each neutron requires an energy of 6.7 Mev; again this figure is an average for all fissions and could be quite inappropriate for the particular fragments we are discussing. Finally, in estimating the deficit in total energy release by means of Cameron's mass formula we have taken a unique prompt mass ratio, 138:98 and compared two unique charge divisions 53:39 and 55:37. We should have considered suitably weighted averages over several mass ratios and charge divisions but the uncertainty regarding neutron emissions makes it impossible to do this rigorously. We could also account for the difference between our estimates and measurement if we assumed that the internal excitation of the fragments is greater when the charge division is unfavorable.

In summary, considering the uncertainties in the estimates and the reliance we have placed on the range formula, we can say that the results of this experiment are in general agreement with expectations based on our present knowledge of the fission process.

ACKNOWLEDGMENTS

The authors wish to thank Dr. J. A. Davies of A.E.C.L., for advice concerning the anodizing technique and for helpful discussions on the ranges of heavy ions. They are also very grateful to Mr. G. C. Hanna, of A.E.C.L., who has contributed much to the interpretation and discussion of the experimental results.

REFERENCES

1. L. E. Glendenin. M.I.T. Tech. Rept. No. 35. 1949.
2. G. B. Niday. University of California Radiation Laboratory, UCRL-5816. 1960.
3. J. A. Davies. Can. J. Chem. **38**, 1526 (1960).

Can. J. Chem. Downloaded from www.nrcresearchpress.com by 210.87.254.6 on 09/05/12
For personal use only.

4. L. E. GLENDENIN. National Nuclear Energy Series. Vol. 9, Paper 288. McGraw-Hill. 1951.
5. T. H. HANDLEY and C. L. BURROS. Anal. Chem. **31**, 332 (1959).
6. R. L. HEATH. IDO-16408. 1957.
7. S. KATCOFF, J. A. MISKEL, and C. W. STANLEY. Phys. Rev. **74**, 631 (1948).
8. B. FINKLE, E. J. HOAGLAND, S. KATCOFF, and N. SUGARMAN. National Nuclear Energy Series. Vol. 9, Paper 46. McGraw-Hill. 1951.
9. J. M. ALEXANDER and M. F. GALLAGHER. University of California Radiation Laboratory, UCRL-8978. 1960.
10. W. M. GOOD and E. O. WOLLAN. Phys. Rev. **101**, 249 (1956).
11. N. O. LASSEN. Kgl. Danske Videnskab. Selskab, Mat-fys. Medd. **25**, No. 11 (1949).
12. R. B. LEACHMAN and H. W. SCHMITT. Phys. Rev. **96**, 1366 (1954).
13. C. B. FULMER. Phys. Rev. **108**, 1113 (1957).
14. N. BOHR. Phys. Rev. **59**, 270 (1941); Kgl. Danske Videnskab. Selskab, Mat-fys. Medd. **18**, No. 8 (1948).
15. J. C. D. MILTON and J. S. FRASER. Private communication.
16. V. F. APALIN, U. P. DOBRININ, V. P. ZAHAROVA, I. E. KUTIKOV, and L. A. MIKHAYLAN. Atomic Energy U.S.S.R. **8**, 15 (1960).
17. J. C. D. MILTON. Private communication.
18. A. C. WAHL. J. Inorg. & Nuclear Chem. **6**, 263 (1958).
19. W. E. STEIN. Phys. Rev. **108**, 94 (1957).
20. J. TERRELL. Phys. Rev. **108**, 783 (1957).
21. D. R. NETHAWAY and A. C. WAHL. *Quoted by* E. K. HYDE. University of California Radiation Laboratory, UCRL-9036. 1960.
22. J. TERRELL. Phys. Rev. **113**, 527 (1959).
23. A. G. W. CAMERON. Can. J. Phys. **35**, 1021 (1957).

Can. J. Chem. Downloaded from www.nrcresearchpress.com by 210.87.254.6 on 09/05/12
For personal use only.

Can. J. Chem. Downloaded from www.nrcresearchpress.com by 210.87.254.105 on 09/05/12
For personal use only.

THE THERMAL NEUTRON FISSION YIELDS OF U^{233} [1]

D. R. Bidinosti, D. E. Irish, and R. H. Tomlinson

ABSTRACT

Using the mass spectrometer and isotope dilution technique, 27 cumulative fission yields from the thermal neutron fission of U^{233} along with 13 other fission product chains relative to each other have been determined. After normalization of the latter, values are obtained for all but seven fission decay chains whose yields are in excess of 0.5%.

INTRODUCTION

Numerous studies have been made of the thermal neutron fission yields of U^{233}. Katcoff (1) has summarized the work preceding 1958, but since this time further mass spectrometric studies by Ivanov *et al.* (2) and radiochemical studies by Santry and Yaffe (3) and Bartholomew *et al.* (4) have been published.

In the present work, fission yields have been determined for isotopes of the elements rubidium, strontium, zirconium, molybdenum, ruthenium, cesium, cerium, neodymium, and samarium. These yields, together with the relative yields of the isotopes of krypton and xenon previously published from this laboratory (5), make the most complete study of the fission yields of U^{233} that have been made up to this time.

EXPERIMENTAL

Samples of U^{233} diluted with U^{238} were irradiated as U_3O_8 in quartz capsules along with cobalt flux monitors in the NRX Chalk River reactor. The U^{238} was added as a diluant to minimize flux depression in the samples. Since the U^{238} was a separated isotope obtained from the Oak Ridge National Laboratories, the U^{235} present in the samples was found to be less than 1% of the U^{233}.

The cobalt flux monitors, weighing approximately 1.14 mg, were made of 0.13 mm diameter cobalt wire which was sealed in aluminum tubing. After irradiation the activity of the cobalt monitors was measured with a well-type ionization chamber (Harwell type T.P.A. Mk II) relative to standards provided by R. C. Hawkins of Chalk River. The evaluation of the neutron flux by this method has been previously described (6). Sample 3 was not monitored in this manner, an approximate flux value being obtained from the extent of depletion of Cs^{135} which results from neutron absorption during the irradiation. Sample 4 was irradiated in a thermal column at a flux less than 10^{11} neutron/cm^2 sec. This sample was used to obtain the relative yield of the mass 135 and 137 chains, since at this flux Xe^{135} removal is small. The irradiation data for the various samples is shown in Table I.

The number of fissions (F) in samples 1 and 2 were computed from the relation

$$F = N^{233}\frac{\hat{\sigma}_f}{\hat{\sigma}_a}(1-e^{-\hat{\sigma}_a\phi t})$$

where N^{233} is the number of U^{233} atoms in each sample, $\hat{\sigma}_f$ and $\hat{\sigma}_a$ are the effective fission and absorption cross sections of uranium as defined by Westcott (7), and ϕt the integrated flux. The effective cross sections for samples 1 and 2 have been obtained from the tables of Westcoff (7) assuming the thermal neutron cross section values of $\sigma_f = 534$ barns and $\sigma_a = 589$ barns (8), and Westcott's r values of 0.026 and 0.018 which were appropriate to the irradiation positions in the reactor. Values of 6.91×10^{17} and 1.036×10^{17} have been estimated for the number of fissions in samples 1 and 2.

[1]*Manuscript received November 3, 1960.*
Contribution from the Chemistry Department, McMaster University, Hamilton, Ontario. Presented at the Third Symposium on Nuclear Chemistry and Radiochemistry held at Atomic Energy of Canada Limited, Chalk River, Ontario, September 6–8, 1960.

TABLE I
Irradiation data for U^{233} samples

Sample	U^{238}/U^{233}	Weight of U_3O_8 sample (grams)	Time in reactor (days)	ϕt, neutrons/cm^2 $\times 10^{-19}$
1	13.30±0.05	0.04085	55.9	2.16
2	18.54±0.10	0.03641	30.4	4.77
3	18.54±0.10	0.02938	30.4	2
4	13.30±0.05	0.07335	309	0.23

The analysis of the fission products in the samples were carried out by means of the mass spectrometer and isotope dilution techniques as has been previously described (9). Essentially complete recovery of the fission products was obtained by dissolution of the end of the quartz ampoule, which contained the sample, with hydrogen fluoride. After most of the contents had fallen from the ampoule, the remainder was obtained by rinsing the quartz until all radioactivity had been recovered.

Relative yields of masses 85 and 87 have been obtained from rubidium fission products; 88, 89, and 90 from strontium; 91, 92, 93, 94, 95, and 96 from zirconium; 95, 97, 98, and 100 from molybdenum; and 101, 102, 104, and 106 from ruthenium. The relative yields of the six zirconium isotopes were normalized to the four molybdenum isotopes by means of the common measurement at mass 95. Two samples of zirconium fission products were analyzed at less than the Zr^{95} half-life from the time of their formation. The yield of the mass 95 chain relative to other zirconium chains was therefore obtained after decay corrections were applied to the observed mass spectrometric ratios. The molybdenum 95 was observed from the samples after the Zr^{95} had decayed. The ruthenium yields have been normalized to the molybdenum and zirconium yields by the radiochemical normalization given by Katcoff (1). The rubidium yields were normalized to the previously published yields (5) of the krypton isotopes through the mass 85 fission chain, which is common to both elements. The absolute yields of these isotopes were obtained from the previously published (5) ratio of Kr^{86} to Cs^{133} = 0.567 and the absolute yield of Cs^{133} = 5.77%, which is obtained below. The absolute yields of the three strontium isotopes were obtained by isotope dilutions.

The present work together with the previously reported mass spectrometric work from this laboratory therefore gives absolute yields of mass chains 83–90 constituting 32.04% of the light mass fission products. Yields of chains below mass 83 have been obtained by extrapolation and when added to the measured yields give a total of 32.94% yield for fragments of mass 90 or less. The yields of masses 91–117 must therefore total 67.06%. The yields of the zirconium, molybdenum, and ruthenium isotopes which had been normalized to each other along with interpolated yields at 99, 103, 105 and extrapolated yields between 107 and 117 have been forced to total 67.06%. Although there are many assumed yields in this grouping their total is only 6.94% of which the assumed yield of 4.84% for mass 99 is the major contribution. The fission yields of the light mass fragments obtained in this manner together with some of the recent literature values are given in Table II. Graphical representation of the present data is given in Fig. 1.

For the heavy mass fragments yields the following procedures were followed. The relative yields of the cesium isotopes 133 and 137 to those of the xenon isotopes 131, 132, and 134 have been previously measured in this laboratory (5). The fission products used in this previous study were formed at high fluxes and the observed Cs^{135} was highly depleted and the observed Xe^{136} equally enhanced by Xe^{135} burning. It was therefore only possible in this work to obtain the sum of the 135 and 136 yields. From sample 4

Can. J. Chem. Downloaded from www.nrcresearchpress.com by 210.87.254.105 on 09/05/12
For personal use only.

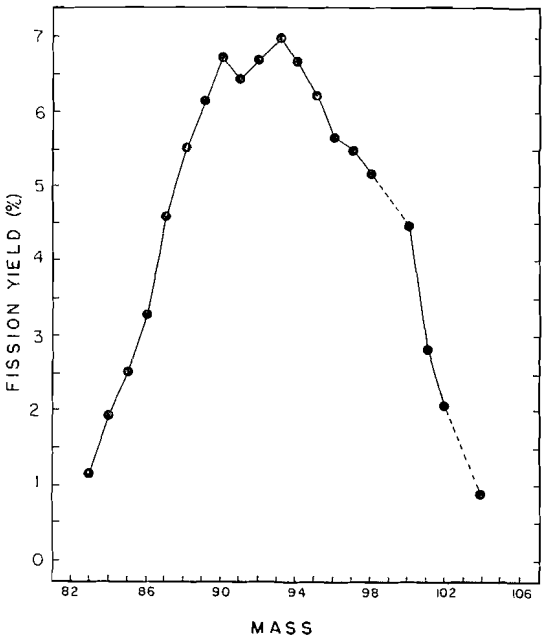


FIG. 1. Light mass yields in thermal neutron fission of U^{233}.

TABLE II

The cumulative yields of the light mass fragments formed in the thermal neutron fission of U^{233}

		Literature values		
Mass chain	Cumulative fission yield	Katcoff (1)	Yaffe (3)	Bartholomew *et al.* (4)
<80	0.15*			
81	0.25*			
82	0.50*			
83	1.18	1.14		
84	1.97	1.90		
85	2.54	2.45		
86	3.30	3.18		
87	4.61			
88	5.54			
89	6.15	6.5	5.56	5.87
90	6.75		6.19	
91	6.45†	6.53	{4.82 (Sr^{91}) {3.55 (Y^{91})	5.61
92	6.72†	6.70		
93	7.01†	7.10		
94	6.68†	6.82		
95	6.23†	6.10	{5.01 (Zr^{95}) {5.16 (Nb^{95})	
96	5.67†	5.60		
97	5.51†	5.35		
98	5.22†	5.18		
99	4.84*	4.8		
100	4.49†	4.40		
101	2.87†	3.00		
102	2.10†	2.37		
103	1.56*	1.6	2.02	
104	0.94†	0.96		
105	0.43*			
106	0.22†	0.28	0.264	
107–117	0.11*			

*Assumed yields; obtained by interpolation or extrapolation of observed data.
†Relative yield normalized to measured yield in such a manner that total of all yields is 100%.

Can. J. Chem. Downloaded from www.nrcresearchpress.com by 210.87.254.105 on 09/05/12
For personal use only.

it was possible to obtain the relative yields of the 133, 135, and 137 chains since the correction for Xe^{135} burning was only 1.4%. With the relative yield of the 135 chain it was possible to correct the previously published Xe^{136} yields. The relative yields of Cs^{133} and Cs^{137} found in the fission products of the present samples were essentially the same as those previously published.

Relative yields of the 140, 142, and 144 chains were obtained from cerium isotopes and these were normalized to the relative neodymium yields of isotopes 143, 144, 145, 146, 148, and 150 by means of the isobaric 144 nuclides. The values for the relative yields of the samarium isotopes 149, 151, 152, and 154 have been taken from previously published work from this laboratory (10) since the high neutron cross sections of Sm^{149} and Sm^{151} together with the large integrated fluxes severely altered the measured yields. The sum of Sm^{149} and Sm^{150} relative to the sum of Sm^{151} and Sm^{152} did correspond to the same ratio obtained in the earlier work.

Isotope dilution of the samarium made possible the determination of the number of atoms of Sm^{149} and Sm^{150}, which, together, are the cumulative number of atoms of the mass 149 fission chain. This made possible the normalization of the relative samarium yields to those of neodymium and cesium since both of the latter elements were also isotope diluted. The yields of isotopes of xenon, cesium, cerium, neodymium, and samarium were therefore all normalized to each other.

The atom yields of mass chains 138, 139, 141, 147, and 153 were obtained by interpolation and the yields between 117 and 131 as well as those above 154 were obtained by extrapolation. The atom yields obtained in this manner for the samples 1, 2, and 3 have normalized to total 100%. The average yields obtained from these three determinations are shown in Table III along with some of the recent literature values. The maximum difference between the three values obtained for any yield in the mass region 131–150 was less than 2.0% of the average value for that yield. The yields given in Table I are shown graphically in Fig. 2.

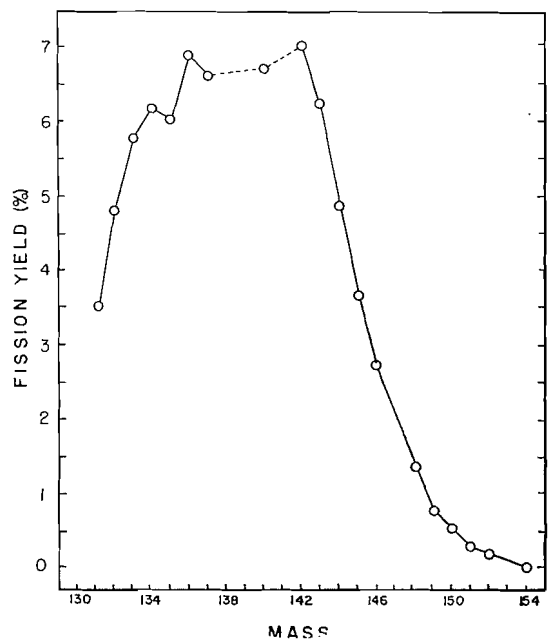


FIG. 2. Heavy mass yields in the thermal neutron fission of U^{233}.

Can. J. Chem. Downloaded from www.nrcresearchpress.com by 210.87.254.105 on 09/05/12
For personal use only.

TABLE III

The cumulative yields of the heavy mass fragments formed in the thermal neutron fission of U^{233}

Mass chain	Cumulative fission yield	Literature values			
		Katcoff (1)	Ivanov (2)	Yaffe (3)	Bartholomew *et al.* (4)
117–130	3.02*†				
131	3.52	3.74		2.84	
132	4.82	5.10		4.64	
133	5.77	6.18	5.5	3.40	
134	6.18	6.54			
135	6.02	>4.9			
136	6.89	<8.9			
137	6.58	7.16	6.16	5.39	
138	6.73†				
139	6.71†				5.59
140	6.72	5.6	6.16	5.48	5.60
141	6.92†			5.30	6.17
142	7.00	5.6	6.06		
143	6.22	5.2	5.19	6.99	
144	4.87	4.0	3.84	3.69	
145	3.66	3.0	2.88		
146	2.74	2.3	2.24		
147	2.08†	1.71			
148	1.40	1.15	1.07		
149	0.790	0.61	0.70		
150	0.567	0.48	0.49		
151	0.334	0.26	0.54		
152	0.222	0.17			
153	0.122†	0.095			
154	0.048	0.037			
155– –	0.033†				
	99.97%				

*Average of three independent determinations of which greatest difference in individual yields was about 2%.
†Assumed yields; obtained by interpolation or extrapolation of observed data.

DISCUSSION

It is difficult to assess the absolute accuracy of the yields of the light mass fragments shown in Table II. Only those values between masses 82 and 90 may be considered as absolute, the remainder being relative yields whose normalization has been chosen so that all yields total 100%. It is believed that the values should be within 4% error at each mass.

In general, the yields obtained in the present work are in very good agreement with those listed by Katcoff (1). With the exception of the ruthenium normalization, which involves about 8 fission yield per cent, the yields in this work are independently normalized from those given by Katcoff. The absolute zirconium, molybdenum, and ruthenium yields given by Katcoff are mass spectrometric relative yields by Steinberg *et al.* (11) normalized to the Steinberg radiochemical values for Sr^{89}, Zr^{95}, and Ru^{103}. With these yields and the relative krypton yields of Fleming *et al.* (5), Katcoff has drawn a smooth curve so that the total of the yields is 100%. It is to be noted that Katcoff's zirconium yields are in general higher than those reported in this work, whereas his molybdenum yields are slightly lower. The zirconium–molybdenum normalization given in the present work, through mass spectrometric relative yields determined for mass 95, should be more reliable. The absolute strontium yields, as determined by isotope dilution,

Can. J. Chem. Downloaded from www.nrcresearchpress.com by 210.87.254.105 on 09/05/12
For personal use only.

along with the relative rubidium yields, normalized to the krypton yields, give a more complete picture of the left side of the light mass curve than was given by Katcoff.

The data as plotted in Fig. 1 indicates fine structure in the mass 90 region. Since the break from a smooth curve occurs at the mass where the zirconium yields are normalized to the strontium yields, this fine structure may not be real. It is worth noting, however, that the yield of the complementary fragment (approximately mass 142) is also high. A similar fine structure at masses 90 and 144 are observed in U^{235} fission (12) which may lend some weight to the reality of that found in this work. Bartholomew *et al.* (4) have given the ratio of Sr^{89} to Zr^{91} as 1.05:1.00. This is considerably greater than the ratio of 0.95:1.00 found in this work. Had the Bartholomew value been used to normalize the strontium and zirconium yields, the yield of mass 90 would be 15% greater than that of mass 91 and the total of the fission yields would be only 94%.

The yields of the heavy mass fragments given in Table III are considered accurate to within 3%. There are various reasons for considering this to be the case. Firstly, there was excellent correspondence between the yields obtained from the three independent measurements, no yield being as much as 2.0% different from the mean. Secondly, the methods used to normalize the yields of the isotopes of the various elements to each other were direct. Isobaric yield determinations were used to normalize the isotopes of xenon to those of cesium as well as the cerium to the neodymium. Isotope dilution was used to normalize the cesium, neodymium, and samarium element yields. Thirdly, in the cases of samples 1 and 2, whose flux had been monitored, it was possible to estimate the number of fissions and compare these values to the total number of atoms found in all heavy mass fission chains. In samples 1 and 2 the number of fissions estimated were lower than the sum of the atoms found by 4% and 2% respectively. With the possible errors in monitoring the flux and the uncertainty of the fission cross section for the neutron spectra of the irradiation positions, these differences are considered slight. The importance of estimating the number of fissions from the flux and cross section is that this serves as a check against gross errors in normalizing by isotope dilution procedures. Had the differences been greater than were found, considerably less faith would have been given to the yields in Table III.

The yields of the heavy mass fragments found in this work are smaller for the 131–139 mass region and larger for the chains of mass greater than 140 than estimated by Katcoff (1). Since the Katcoff values are largely relative mass spectrometric yields from this laboratory that have been normalized by arbitrary means, there is no inconsistency with the present data. On the other hand the values reported more recently by Yaffe (3) are much lower at every mass with significant yield as are those of Bartholomew *et al.* (4) and Ivanov (2).

There are several criteria for concluding that the present values are approximately correct. Firstly the values measured, together with a relatively small percentage of interpolated values, total 100%. It is difficult to see how this condition can be met by any of the other recent measurements. A critical test of any fission yield curve is the estimation of the total number of neutrons liberated per fission. For U^{233} this may be obtained from the relation

$$\nu = 234 - \frac{\sum \text{mass} \times \text{yield}}{\text{yield}}$$

where ν is the average number of neutrons, including delayed neutrons, liberated per fission. This relation should be valid provided that insignificant amounts of light particles

Can. J. Chem. Downloaded from www.nrcresearchpress.com by 210.87.254.105 on 09/05/12
For personal use only.

and ternary fission products are formed. Since ν obtained from this relation is the difference between two comparable numbers it is very sensitive to small errors in the values of the yields used. With the yields given in Tables II and III a value of 2.32 is obtained which may be considered in fair agreement with the accepted value of 2.51 given by Hughes and Harvey (8).

Careful normalization of the xenon and cesium yields, and cesium ratios obtained from a thermal column irradiation, ensure the reality of the fine structure appearing at mass 134 (Fig. 2). Although it is much smaller in magnitude, it is similar to that found in the thermal neutron fission of U^{235} and other nuclides. The apparently high yield at mass 136 can in part be smoothed out by correction for delayed neutron emission.

Keepin *et al.* (13) attribute a 0.197% chain transfer to delayed neutron emission by I^{137}. Together with delayed neutron emission in the mass 138 and 139 chains (13) most of the mass 136 fine structure would be removed.

ACKNOWLEDGMENTS

We wish to thank the Atomic Energy of Canada Limited for the neutron irradiations and the National Research Council of Canada for financial assistance.

REFERENCES

1. S. KATCOFF. Nucleonics, **16**, 78 (1958).
2. R. N. IVANOV, V. K. GORSHKOV, M. P. ANIKINA, G. M. KUKAVADZE, and B. V. ERSHLER. J. Nuclear Energy, **9**, 46 (1959).
3. D. C. SANTRY and L. YAFFE. Can. J. Chem. **38**, 421 (1960).
4. R. M. BARTHOLOMEW, J. S. MARTIN, and A. P. BAERG. Can. J. Chem. **37**, 660 (1959).
5. W. FLEMING, R. H. TOMLINSON, and H. G. THODE. Can. J. Phys. **32**, 522 (1954).
6. H. R. FICKEL and R. H. TOMLINSON. Can. J. Phys. **37**, 926 (1959).
7. C. H. WESTCOTT. Atomic Energy of Canada Limited, CRRP-787. 1958.
8. D. J. HUGHES and J. A. HARVEY. Brookhaven National Laboratory, BNL-325. 1958.
9. J. A. PETRUSKA, E. A. MELAIKA, and R. H. TOMLINSON. Can. J. Phys. **33**, 640 (1955).
10. E. A. MELAIKA, M. J. PARKER, J. A. PETRUSKA, and R. H. TOMLINSON. Can. J. Chem. **33**, 830 (1955).
11. E. P. STEINBERG, L. E. GLENDENIN, M. G. INGHRAM, and R. J. HAYDEN. Phys. Rev. **95**, 867 (1954).
12. J. A. PETRUSKA, H. G. THODE, and R. H. TOMLINSON. Can. J. Phys. **33**, 693 (1955).
13. G. R. KEEPIN, T. F. WIMETT, and R. K. ZEIGLER. J. Nuclear Energy, **6**, 1 (1957).

Can. J. Chem. Downloaded from www.nrcresearchpress.com by 210.87.254.105 on 09/05/12
For personal use only.

Can. J. Chem. Downloaded from www.nrcresearchpress.com by 210.87.254.40 on 09/05/12
For personal use only.

DISTRIBUTION OF NUCLEAR CHARGE IN THE PROTON-INDUCED FISSION OF Th^{232}

PART II[1]

A. KJELBERG,[2] H. TANIGUCHI,[3] AND L. YAFFE

ABSTRACT

The fractional chain yields of Ga^{72}, Br^{82}, Ag^{112}, and La^{140}, formed in the proton-induced fission of Th^{232}, have been measured at proton energies ranging between 12.8 and 82.4 Mev. The yields are compared with data previously obtained by others from uranium and thorium fission, and with predictions made by Coryell.

During the course of this investigation, the half-life of Zn^{72} was checked and found to be 46.5 ± 0.1 hours, rather than 49 hours as previously reported.

INTRODUCTION

A great deal of data has been amassed dealing with the distribution of nuclear mass in fission. Nevertheless, studies in this aspect are still going on since many of the data published are in disagreement, especially those obtained by mass spectrometry as compared with those obtained radiochemically. While the above state of affairs is semisatisfactory, that of the charge distribution in fission is as yet highly unsatisfactory. A small amount of data has been accumulated for thermal fission and very much less for higher-energy fission.

One attempts to obtain a value for the most probable charge, Z_p, by reference to various postulates regarding the mechanism in which the fission act takes place. These postulates are summarized below:

(1) Unchanged Charge Distribution (UCD)

This suggests that, by analogy to the simplest form of the liquid drop model, the charge divides in the same manner as it was present in the fissioning nucleus, i.e. the neutron-to-proton ratio is the same in the fragments as in the parent nucleus.

(2) Minimum Potential Energy (MPE)

This proposes that the fission act is preceded by a nucleonic rearrangement such that the fission will take place in a manner to minimize the sum of the binding energies, the decay energies, and the electrostatic energy of mutual repulsion (calculated from two spheres in contact).

The thermal fission data collected did not support either hypothesis, although some evidence purported to show that the former held true for higher-energy fission.

(3) The Postulate of Equal Charge Distribution (ECD)

This suggestion was empirically derived by Glendenin, Coryell, and Edwards (1). In effect, mathematically, it tells us that

$$Z_{p_L} - Z_{A_L} = Z_{p_H} - Z_{A_H}$$

where L and H refer to the heavy and light fragments, Z_p again is the most probable charge, and Z_A is the non-integral value of the most stable charge for nuclides of mass A.

[1]*Manuscript received November 7, 1960.*
Contribution from the Radiochemistry Laboratory, Department of Chemistry, McGill University, Montreal, Que., with financial assistance from the National Research Council of Canada, Ottawa, Canada. Presented at the Third Symposium on Nuclear Chemistry and Radiochemistry held at Atomic Energy of Canada Limited, Chalk River, Ontario, September 6–8, 1960.
[2]*Present address: Nuclear Chemistry Division, Department of Chemistry, Oslo University, Blindern, Norway.*
[3]*Present address: Department of National Health and Welfare, Ottawa, Ontario.*

(4) The Postulate of Non-Uniform Charge Distribution (NUCD)

This theory, proposed originally by Present (2), proposes a division of charge calculated on the basis of two spherical nuclei in contact. The charge distribution in such a system is expected to be non-uniform radially due to the tendency of the charge to collect at the surface of a body and will result in the smaller fraction of an asymmetric division having a greater charge-to-mass ratio than the larger.

The latter two postulates give predictions which, at thermal energies, are reasonably concordant with the data. Inherent in the third postulate is the assumption that the same symmetrical charge distribution curve can be used to describe all fission-product chains. Indeed it has been used for all heavy fissioning nuclei.

A great deal of discussion has taken place regarding the proper value of Z_A to be used. Glendenin *et al.* (1) used a continuous Z_A function while Pappas (3) and others have suggested a Z_A function that was discontinuous at shell edges. This controversy is still raging.

Wahl (4) suggested the use of an empirical Z_p curve obtained directly from independent and cumulative yield values and the universal charge distribution curve. This showed a good degree of success for thermal fission as most data were found to lie on the empirical Z_p curve.

Unfortunately very little of the above-mentioned reasoning applies in the case of higher-energy fission. No satisfactory postulate for determining Z_p has as yet appeared. No universal charge distribution curve is known. Neutron emission soon begins to compete favorably with fission so that a variety of fissioning nuclei have to be taken into account.

The problem is made more difficult because of the paucity of high-energy independent yield data available. The paper by Pate, Foster, and Yaffe (5) summarizes those up to the beginning of 1958. Other papers of interest are those of Alexander and Coryell (6) and Stevenson *et al.* (7), which give some later references. It rapidly becomes apparent that one cannot use a single-charge distribution curve to fit all the data. Thus it is of some interest then to accumulate independent yield data to determine the best method of finding Z_p.

The paper by Pate, Foster, and Yaffe gave values for independent yields of isotopes of iodine and tellurium in the mass range 130 to 135. A study of this mass range permitted conclusions to be drawn regarding the variation with energy of the charge distribution, neglecting possible effects of mass number.

The previous work has been extended to give information about the range of mass numbers 72 to 140. Similar results at higher energies are now available for the proton-induced fission of uranium. These enable one to study the variation of charge distribution with atomic number of target and mass number of the products.

For the study of charge distribution the relatively few shielded nuclides are best suited. There are, however, also some semishielded nuclides, with a precursor of a long half-life compared with that of the daughter, and these can, under specific conditions, give valuable information. A study of the shielded nuclide Br^{82}, and the semishielded nuclides Ga^{72}, Ag^{112}, and La^{140}, in the energy interval of 15 to 85 Mev, is reported here.

EXPERIMENTAL TECHNIQUES

(a) Target and Irradiation

The target and irradiation details were essentially as reported by Pate *et al.* (5). Three thorium metal foils of about 200 mg/cm^2 superficial density were carefully aligned and

Can. J. Chem. Downloaded from www.nrcresearchpress.com by 210.87.254.40 on 09/05/12
For personal use only.

bombarded in the internal proton beam of the McGill 82-in. synchrocyclotron. The outer foils, serving as guard foils correcting for recoil losses, were discarded and the central foil was used for chemical processing. As the calculations of fractional yields were independent of absolute yield determinations, no monitoring of the proton beam was necessary.

The energy of the bombarding protons was obtained from a known radius–energy relation (8). Corrections for energy loss for the protons in the target itself were calculated using data from Aron *et al.* (9). Bombardments were of $\frac{1}{2}$- to 1-hour duration.

(b) Chemical Processing and Measurement

In the case of the semishielded isotopes, two separations of the nuclide in question were performed from the same master solution. The first sample contained the activity formed independently and that produced by decay during bombardment and in the short time interval before the separation from the precursor in the chain. The second sample contained activity formed by decay of the precursor only and gave information on the chain yield. Complete separation of the nuclide from its precursor and accurate timing of the separations were essential.

(i) Ga^{72}

This nuclide occurs in the following fission product chain:

$$Zn^{72} \xrightarrow[46.5\ \text{hours}]{\beta^-} Ga^{72} \xrightarrow[14.1\ \text{hours}]{\beta^-} Ge^{72}\ (\text{stable}).$$

The thorium target foil was dissolved in concentrated hydrochloric acid (with SiF_6^{--} catalyst present) shortly after bombardment. The separation occurred essentially as described by Siegel and Glendenin (10), except for the elimination of $Ga_4[Fe(CN)_6]_3$ precipitation, which had been found to be unsatisfactory (11). Briefly, gallium and zinc carriers were added and gallium was separated from zinc and most fission products by twice extracting with ethyl ether from 6 *N* hydrochloric acid. The time of the second ether extraction was used as the time of separation of Ga^{72} from Zn^{72}. Gallium was further purified by a number of scavenging precipitations and repeated extractions. Care was taken in all operations to avoid any loss of Zn^{72}. Gallium carrier was added to the master solution containing the zinc, and after about 1 day a second separation was performed using the same procedure. The two samples obtained, Ga-I and Ga-II, were made to equal volume in counting vials and the activity determined using a well-type gamma scintillation counter. Since all measurements were relative, absolute disintegration rates did not have to be determined.

By tracer experiments it was found that the loss of zinc by coextraction with gallium, and the retention of gallium with zinc, were 1% or less under the experimental conditions used. Chemical yields were determined by EDTA titrations (12).

(ii) Br^{82}

This nuclide (35.9 hours) is shielded. Br^{83}, which occurs in the chain,

$$Se^{83} \xrightarrow[\beta]{\substack{67\ \text{seconds} \\ 25\ \text{minutes}}} Br^{83} \xrightarrow[2.4\ \text{hours}]{\beta^-} Kr^{83m} \xrightarrow[1.9\ \text{hours}]{\gamma} Kr^{83}\ (\text{stable}),$$

was used as an internal monitor for Br^{82} (see section "Treatment of Data"). After dissolution of the target (ice-cooled), bromine was separated about 4 hours after bombardment. This allowed complete decay of Se^{83} to Br^{83}. The chemical method used was,

Can. J. Chem. Downloaded from www.nrcresearchpress.com by 210.87.254.40 on 09/05/12
For personal use only.

with minor modifications, that of Glendenin *et al.* (13), and is based on cyclic extractions of bromine into and out of carbon tetrachloride by successive oxidation and reduction steps.

Two points were specifically checked, namely possible loss of bromine during dissolution of the target, and completeness of exchange between carrier and active bromine. In one experiment, during dissolution, air was slowly bubbled through the ice-cooled solution and any bromine possibly escaping was trapped in sulphurous acid. No evidence of bromine activity was found in the trap, as determined by measurement of the activity of the chemically separated bromine. Also in one case the initial separation was carried out in duplicate using bromine and bromate carriers, respectively, to check the exchange. The bromate portion was reduced with hydrogen sulphide and the separation was continued in a manner identical with that used with the bromide carrier. No detectable difference attributable to the different carriers was found in the resultant samples. This is similar to results obtained for iodine when the irradiated material is a metallic matrix. Therefore the direct use of bromide carrier was chosen for subsequent separations.

The final solution was slightly acidic with the activity in the form of bromide. To prevent losses due to volatilization, the solution was neutralized with a measured amount of lithium hydroxide. The chemical yields were determined by titration according to Volhard's method.

The activity was measured with a 4π β-counter (14–18). To prevent loss of bromine during preparation of the samples (heating under an infrared lamp), about 100% excess silver nitrate was added. This is the same technique used by Pate *et al.* (5). It was found that the Kr^{83m} formed by decay of Br^{83} contributed significantly to the count rate of the sample through the conversion electrons from its 0.033-Mev gamma transition.

This krypton activity could not be removed by reheating the sample. Fresh samples therefore were periodically prepared to construct the decay curve of Br^{83}. This introduced a slight uncertainty in the time for the last separation from krypton, as the drying of the sample required about 30 minutes. It was later found that the addition of silver nitrate to the bromide solution was unnecessary, provided a slight excess of lithium hydroxide was present. The lithium bromide sources were much thinner and more uniform and permitted the krypton to diffuse out of the sample completely. No loss of bromine activity was detected using this technique. The thinner sources were also better suited for accurate self-absorption corrections. Incidentally, a similar technique was found to work well for iodine samples in so far as lithium iodide continually released xenon formed by decay of iodine activity, in contrast to what was found for silver iodide (5). No measurable loss of iodine activity was found.

(iii) Ag^{112}

This nuclide occurs in the following fission product chain:

$$Pd^{112} \xrightarrow[21 \text{ hours}]{\beta^-} Ag^{112} \xrightarrow[3.2 \text{ hours}]{\beta^-} Cd^{112} \text{ (stable).}$$

The target foil was dissolved in concentrated nitric acid containing silver carrier to prevent adsorption losses of active silver (19). The separation essentially followed the procedure of Glendenin (20) and was based on silver chloride precipitations alternated by scavenging precipitations. The time of separation of Ag^{112} from Pd^{112} was taken as the time of centrifugation of the silver chloride first precipitated, about 2 minutes after precipitation. This should therefore take care of exchange between silver chloride and active silver after precipitation.

Can. J. Chem. Downloaded from www.nrcresearchpress.com by 210.87.254.40 on 09/05/12
For personal use only.

The second sample was separated by adding silver carrier to the hot master solution. After 2 minutes of vigorous stirring, the silver chloride was centrifuged and further purified. The time for separation of Ag^{112} from Pd^{112} was again taken as the time at the start of centrifugation.

Tracer experiments showed that less than 2% of Pd^{112} was lost from the collected master solution by the silver chloride precipitations. Another point of concern was whether complete exchange was obtained between Ag^{112} and silver carrier added for the second silver sample, Ag-II. As this carrier was added to a solution containing some hydrochloric acid (less than 1 *N*), one inevitably had precipitation of silver chloride before complete mixing took place. Sunderman and Meinke (21) have found that the exchange between freshly precipitated inactive silver chloride and active silver tracer is very rapid at high temperatures. Their data indicate that, under the conditions used, well above 95% exchange was obtained. The reproducibility of the experiments was quite good, confirming a rapid exchange. The chemical yields were determined by titration according to Volhard's method. In a few ammoniacal samples, EDTA titrations (22) were used.

The two samples Ag-I and Ag-II were made up of equal volume and the activity determined by gamma-ray measurement. Ag^{112} and Ag^{113} have half-lives which are fairly close, 3.2 and 5.3 hours respectively. Since Ag^{113} was reputed to have no gamma ray with energy greater than 0.3 Mev, an attempt was made to measure only the high-energy gamma rays of Ag^{112}. It was soon found that a considerable portion of the Ag^{113} decay took place via high-energy gamma transitions (23). Subsequent measurements were performed using a 3 in.×3 in. NaI (Tl) crystal coupled to a 100-channel pulse-height analyzer. Gamma rays of 1.3 Mev and higher gave a pure 3.2-hour decay curve for Ag^{112}.

(iv) La^{140}

This nuclide occurs in the following fission product chain:

$$Xe^{140} \xrightarrow[16\text{ seconds}]{\beta^-} Cs^{140} \xrightarrow[66\text{ seconds}]{\beta^-} Ba^{140} \xrightarrow[12.8\text{ days}]{\beta^-} La^{140} \xrightarrow[40.2\text{ hours}]{\beta^-} Ce^{140}\text{ (stable).}$$

The target foil was dissolved in nitric acid in the presence of lanthanum and barium carriers. Barium chloride was then separated from the ice-cooled solution by addition of hydrochloric acid – ether mixture. Twice again barium carrier was added to complete the removal of Ba^{140}. The combined barium chloride precipitates were dissolved and a small precipitate formed by the addition of ammonia (caused by traces of thorium and lanthanum). This precipitate was further purified to remove barium and combined with the master solution for later separation of La-I. To the combined solutions containing barium was added lanthanum carrier, and this was stored for subsequent separation of La-II. According to Sunderman and Meinke (21) the above procedure should separate barium from lanthanum without loss.

The La-I was further purified by removal of thorium by precipitation as iodate. The solution was allowed to stand for 2 days so that short-lived activities could die away, cerium carrier was added, oxidized with bromate, and removed by precipitation as iodate. Ruthenium sulphide was next precipitated, and the final purification performed by passing a solution in 9 *N* hydrochloric acid through a Dowex-1 anion exchange column. The time of the first precipitation with ammonia in the barium solution was taken as the time of separation of La^{140} from Ba^{140} in La-I.

The samples were made to equal volume. It was found, despite the fact that no attempt had been made to effect a separation of lanthanum from the rest of the rare

Can. J. Chem. Downloaded from www.nrcresearchpress.com by 210.87.254.40 on 09/05/12
For personal use only.

earth elements, that a measurement of the 1.6-Mev gamma peak gave a decay curve with a 40.2-hour half-life (less than 1% long-lived contamination).

RESULTS AND DISCUSSION

(a) Decay Curves

The gallium samples Ga-I showed a very high proportion of the 4.87-hour Ga^{73}. When this was allowed to decay, the 14.1-hour Ga^{72} could be quite easily measured, although at the very lowest bombardment energies the activity of Ga^{72} was very low. A few samples showed long-lived contaminating activities, for which corrections were made. The Ga-II samples generally showed a pure 14.1-hour decay curve.

The half-life of Zn^{72} was checked and was found to be 46.5 ± 0.1 hours rather than 49.0 ± 1 hours as reported (24).

The bromine samples showed only the 35.9-hour Br^{82} and 2.4-hour Br^{83} activities, with 1.9-hour Kr^{83m} contributing in some samples, as discussed previously.

In the silver samples which were measured on the gamma spectrometer, only the 3.2-hour Ag^{112} was observed, with a trace of a long-lived tail in the Ag-I samples, presumably the 270-day Ag^{110m}.

The lanthanum samples showed a decay of 40.2 hours, the half-life of La^{140}, with the La-I samples containing less than 1% of longer-lived activities.

(b) Treatment of the Data

Using the same symbols as Pate *et al.* (5), the general case under consideration is

$$\begin{array}{l} \xrightarrow{\sigma_a} A \xrightarrow{\lambda_a} B \xrightarrow{\lambda_b} C, \\ \qquad\quad \xrightarrow{\sigma_b} B \xrightarrow{\lambda_b} C, \\ \qquad\qquad\quad \xrightarrow{\sigma_c} C. \end{array}$$

The fractional chain yield of B is then given by

$$[1] \qquad f = \frac{\sigma_b}{\sigma_a+\sigma_b+\sigma_c}$$

where it is assumed that σ_a represents the total yield of A formed independently and by decay of the short-lived precursors in the chain. These are assumed to have disintegration constants very much larger than A and will not be present at the time of chemical separation.

The rate of formation of any nuclide n is given by

$$[2] \qquad r_n = Nf\sigma_n$$

where N and f are the number of target nuclei and bombarding particle flux, respectively, and σ_n is the appropriate cross section.

The bombardment time is T, the time between the end of bombardment and the first separation of the nuclide B from its precursor A is t_1, the time between the first and second separation t_2. Generally, the disintegration rate $D_b(T,t_1)$ of B at time t_1 is

$$[3] \qquad D_b(T,t_1) = Nf\left[\sigma_a\left[\frac{\lambda_b}{\lambda_b-\lambda_a}(1-e^{-\lambda_a T})e^{-\lambda_a t_1} - \frac{\lambda_a}{\lambda_b-\lambda_a}(1-e^{-\lambda_b T})e^{-\lambda_b t_1}\right] + \sigma_b[(1-e^{-\lambda_b T})e^{-\lambda_b t_1}]\right].$$

Can. J. Chem. Downloaded from www.nrcresearchpress.com by 210.87.254.40 on 09/05/12
For personal use only.

For a shielded nuclide, where A is stable, this reduces to

$$[4] \qquad D_b(T,t_1) = Nf\sigma_b(1-e^{-\lambda_b T})e^{-\lambda_b t_1}.$$

If $\lambda_a > \lambda_b$, and $t_1 \gg \ln 2/\lambda_a$, equation [3] can be transformed into

$$[5] \qquad D_b(T,t_1) = Nf(\sigma_a+\sigma_b)(1-e^{-\lambda_b T})e^{-\lambda_b t_1}\times P$$

where

$$[6] \qquad P = \frac{\lambda_a}{\lambda_a-\lambda_b}\left(1-\frac{\lambda_b}{\lambda_a}\frac{\sigma_b}{\sigma_a+\sigma_a}\right).$$

The factor P is always larger than unity and less than $\lambda_a/(\lambda_a-\lambda_b)$.

If $\lambda_a < \lambda_b$ and $t_1 < (\ln 2/\lambda_a)$, equation [3] applies and gives the amount of B formed independently and by decay from A.

A second separation of B from A at the time t_2 after the first separation will give B formed by decay from A only and will be given by

$$[7] \qquad D_b(t_2) = Nf\sigma_a(1-e^{-\lambda_a T})e^{-\lambda_a t_1}\frac{\lambda_b}{\lambda_b-\lambda_a}(e^{-\lambda_a t_2}-e^{-\lambda_b t_2}).$$

In the experiments with Ga^{72}, Ag^{112}, and La^{140}, the appropriate equations are [3] and [7]. Here, N, f, σ_a, and σ_b are unknown, the rest are experimentally determinable terms. If therefore for these determinable terms one inserts 'constants' k_i as follows, equations [3] and [7] become

$$[8] \qquad k_1 = Nf(\sigma_a k_2+\sigma_b k_3),$$

$$[9] \qquad k_4 = Nf\sigma_a k_5.$$

If equation [8] is divided by equation [9] and terms are rearranged, then

$$[10] \qquad \frac{\sigma_b}{\sigma_a} = \frac{1}{k_3}\left(\frac{k_1 k_5}{k_4}-k_2\right) = k_6.$$

Substitution in equation [10] to solve for k_6 gives

$$[11] \qquad k_6 = \frac{1}{\lambda_b-\lambda_a}\left\{\lambda_b\frac{1-e^{-\lambda_a T}}{1-e^{-\lambda_b T}}e^{(\lambda_b-\lambda_a)t_1}\left[\frac{D_b(T,t_1)}{D_b(t_2)}(e^{-\lambda_a t_2}-e^{-\lambda_b t_2})-1\right]+\lambda_a\right\}.$$

The fractional chain yield as defined in equation [1] becomes

$$[12] \qquad f = \frac{\sigma_b}{\sigma_a+\sigma_b+\sigma_c} \simeq \frac{\sigma_b}{\sigma_a+\sigma_b} = \frac{k_6}{1+k_6}$$

provided $\sigma_c \ll \sigma_a+\sigma_b$, which generally is the case in these experiments. For the worst possible case, La^{140} at the highest energy, this would give a yield about 4% too high.

It is seen that only the ratio between the disintegration rates for two samples is required, thus facilitating the simple sample preparation and counting method used.

In the case of the shielded nuclide Br^{82}, the Br^{83} was used as an internal monitor for the beam. In equations [4] and [5] the factors N and f are the same for Br^{82} and Br^{83}, but the cross sections refer to different chains. Provided a relation between the yields for the chains 82 and 83 were known, such as

$$[13] \qquad (\sigma_a+\sigma_b)_{82} = R(E)(\sigma_a+\sigma_b)_{83}$$

where $R(E)$ is an energy-dependent function, equations [4] and [5] can be used directly.

Can. J. Chem. Downloaded from www.nrcresearchpress.com by 210.87.254.40 on 09/05/12
For personal use only.

With the previous notation, if $x = Br^{82}$, $y = Br^{83}$, and $z = Se^{83}$, then

$$[14] \qquad \frac{D_x(T, t_1)}{D_y(T,t^1)} = \frac{\sigma_x(1-e^{-\lambda_x T})e^{-\lambda_x t}}{P(\sigma_z+\sigma_y)(1-e^{-\lambda_y T})e^{-\lambda_y t^1}}$$

or

$$[15] \qquad f = \frac{\sigma_x}{R(E)(\sigma_z+\sigma_y)} = \frac{PD_x(T, t_1)(1-e^{-\lambda_y T})e^{-\lambda_y t^1}}{R(E)D_y(T, t^1)(1-e^{-\lambda_x T})e^{-\lambda_x t}}$$

where t and t^1 are times after bombardment when the activities of Br^{82} and Br^{83} were measured. According to equation [6], for this specific chain

$$[16] \qquad P = \frac{\lambda_{Se^{83}}}{\lambda_{Se^{83}}-\lambda_{Br^{83}}}\left[1-\frac{\lambda_{Br^{83}}\sigma_{Br^{83}}}{\lambda_{Se^{83}}(\sigma_{Se^{83}}+\sigma_{Br^{83}})}\right].$$

An estimate of the function $R(E)$ as defined in equation [13] can be made using the rather limited chain yield data available for thorium and uranium proton-induced fission at higher energies. For thorium, data are available only for the energy interval 8 to 21 Mev (25), except for one value at 450 Mev (26). Therefore data for uranium have been used to establish a trend, and a somewhat idealized curve for the function $R(E)$ for uranium has been established. The same curve shape has been assumed valid for thorium, with a shift in ordinate as shown in Fig. 1. The equation for $R(E)$ for

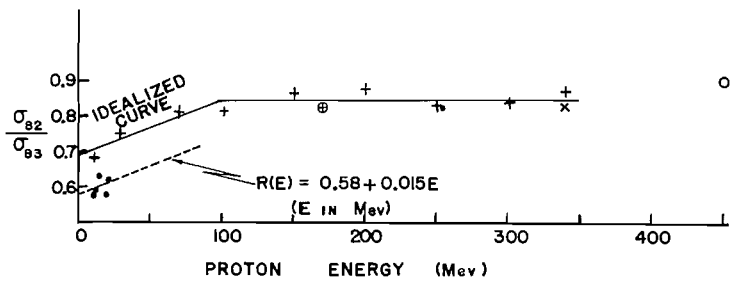


FIG. 1. Variation of the ratio of yields of Br^{82} to Br^{83} with proton-bombarding energy: ● Th fission (25), ○ Th fission (26), + U fission (7), × U fission (30), ⊕ U fission (27).

thorium deduced on this basis is

$$[15] \qquad R(E) = 0.58+0.015E$$

where E is in Mev. The energy interval of interest was 15 to 85 Mev, and here $R(E)$ varies between 0.60 and 0.71, and the absolute uncertainty in these values is probably not more than about 10%.

The factor P in equation [14] has also been estimated. Inserting values for the disintegration constants one gets

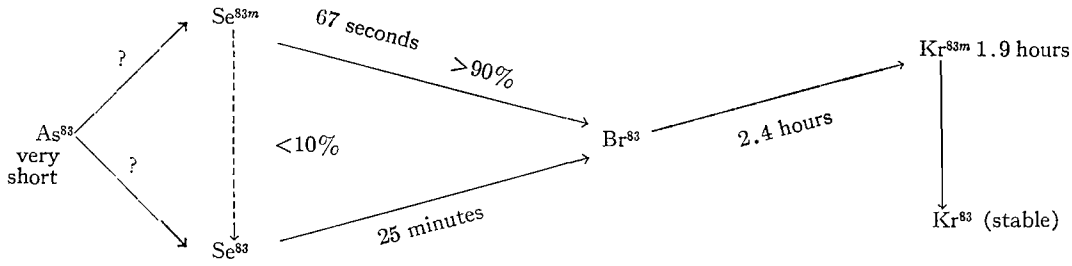
$$[16] \qquad P = 1.21\left(1-0.174\frac{\sigma_{Br^{83}}}{\sigma_{Se^{83}}+\sigma_{Br^{83}}}\right).$$

The ratio of the independent cross section of Br^{83} to that of the chain up to and including that nuclide can be estimated from Fig. 8 in reference 5 to be about 0 to 0.19 for the energy interval of concern. (Allowance has been made for the finding in the present

Can. J. Chem. Downloaded from www.nrcresearchpress.com by 210.87.254.40 on 09/05/12
For personal use only.

work that the abscissa scale should be shifted about 1.0 unit to the left for the mass number 83, i.e. to indicate a longer chain.) P therefore varies from 1.17 to 1.21 for the energy interval 15 to 85 Mev.

A more difficult factor to evaluate is the effect of the short-lived isomer Se^{83m}. The decay scheme for the 83-chain is



The factor P as already calculated is a maximum value, as it is assumed that all of Br^{83} is produced via Se^{83}. Any Se^{83m} in the chain produced by decay or by independent formation will make P approach 1.00.

No general conclusion as to the variation of the yields of isomers with energy can presently be drawn from the limited amount of experimental data available (26). In addition, the chain contribution from As^{83} is unknown. Therefore, a mean value for P of 1.10 for the whole energy interval was used, a factor which at most can have an error of 10%.

The fractional yields for Ga^{72}, Br^{82}, Ag^{112}, and La^{140} are given in Table I. Figure 2 gives these results together with similar data taken from reference 5. Also given are the values of $Z_A - Z$, the distance of the nuclide from the most stable charge for the mass number A (27, 28). For comparison, Fig. 3 gives similar data for uranium fission (7, 29).

TABLE I

Fractional chain yields, in per cent

Energy in Mev	12.8	17.2	18.6	25.8	36.1	39.5	40.7	55.5	82.4
Ga^{72}					2.1		3.3	6.8	13.2
Br^{82}	0.43		0.67			3.5		6.2	10.9
									12.5
Ag^{112}		1.8		3.5			5.8	7.7	15.4
								8.9	15.8
La^{140}				4.3				22	22

The errors associated with the fractional yield data are due mainly to (*a*) uncertainty in the exact proton energy at which the bombardments were made due to the radial distribution of the proton beam and (*b*) energy losses in the target itself as calculated (9). Nevertheless the beam energy was probably known to 2–5 Mev. The disintegration rates were measured relatively so that errors associated with these are small (~1%). The graphical decay curve analyses, associated extrapolation data and chemical analyses, present no difficulties and these errors are certainly less than 5%. It is believed that an uncertainty of ±10–15% on an over-all basis would cover the above and include systematic errors.

Can. J. Chem. Downloaded from www.nrcresearchpress.com by 210.87.254.40 on 09/05/12
For personal use only.

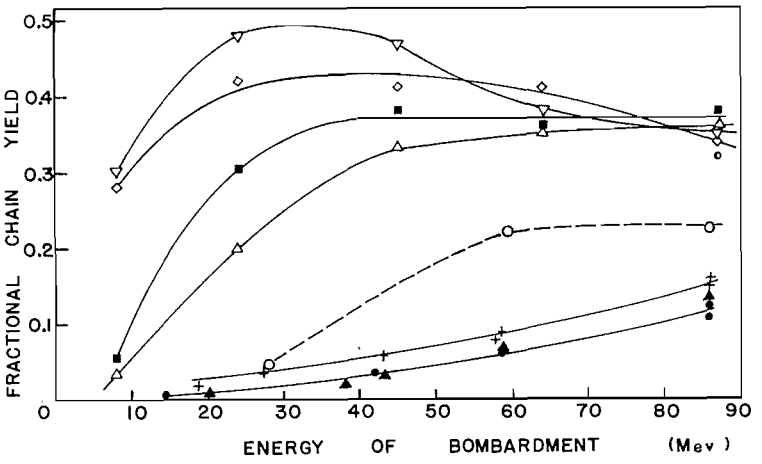


FIG. 2. Fractional chain yield in Th^{232} proton fission. (Values of $Z_A - Z$ in parentheses.)
This work: ▲ Ga^{72} (1.0), ● Br^{82} (0.8), + Ag^{112} (1.4), ○ La^{140} (1.0).
Pate *et al.* (5): ◐ I^{130} (0.8), △ I^{131} (1.1), ▽ Te^{131} (2.1), ■ I^{132} (1.5), ◇ I^{134} (2.2).

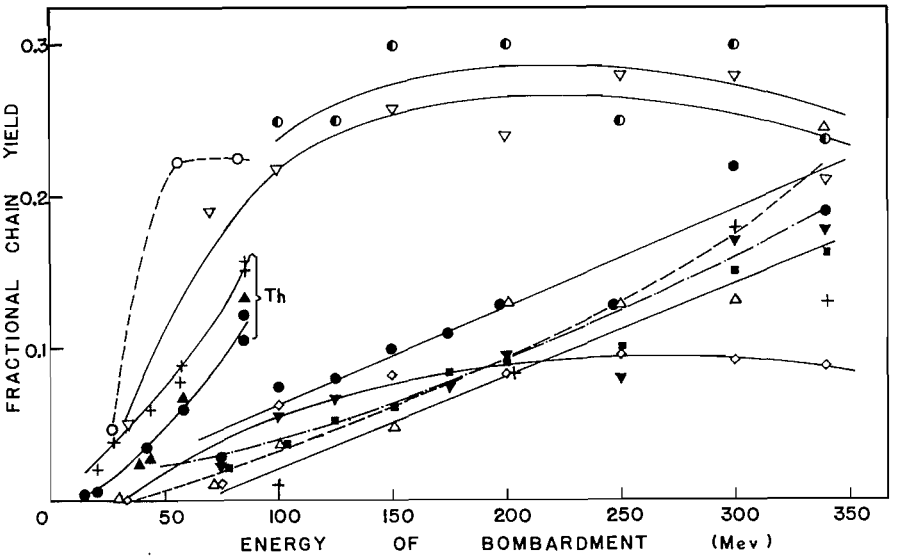


FIG. 3. Fractional chain yields in the proton-induced fission of thorium and uranium. (Values of $Z_A - Z$ in parentheses.)
This work: ▲ Ga^{72} (1.0), ● Br^{82} (0.8), + Ag^{112} (1.4), ○ La^{140} (1.0).
Hicks and Gilbert (29): U^{238} (p, f): ▼ Br^{80} (0.0), ● Br^{82} (0.8), ■ Nb^{96} (1.2), + Ag^{112} (1.4), ◐ Cs^{136} (0.9).
Stevenson *et al.* (7): U^{238} (p, f): △ Y^{90} (0.6), ▽ La^{140} (1.0), ◇ Pr^{143} (0.9).

It is very difficult at this point, with the scarcity of data available in this energy range, to discuss the results theoretically. One cannot draw reasonable charge distribution curves to obtain a Z_p value at each energy as Pate, Foster, and Yaffe (5) did since the range of $Z_A - Z$ values covered here is so small.

Coryell (31) has devised an elegant method for deriving Z_p values for any nuclide formed in fission at the energies with which we are concerned. Essentially he assumes that the excited nucleus, after bombardment, will de-excite by neutron emission and,

Can. J. Chem. Downloaded from www.nrcresearchpress.com by 210.87.254.40 on 09/05/12
For personal use only.

after neutron boil-off, fission then occurs. He then used the Z_p values obtained from U^{235} thermal fission and derives the appropriate Z_p value for another mode of fission by the following equation:

$$Z_{p_{corr}} = Z_p - \tfrac{1}{2}(Z_c - 92) + 0.21(A_c - 236) - 0.19 \times 0.12(E^* - 6.5)$$

where $Z_{p_{corr}}$ and Z_p are the most probable charges for that mass for the mode of fission being investigated and for U^{235} fission respectively.

Z_c and A_c are charge and mass of the compound nucleus, and E^* is the excitation energy calculated by means of an appropriate mass formula.

No complete application of this equation has been made to our data, but qualitatively the fit on this basis between the Pate, Foster, and Yaffe (5) data and those presented in this paper is good. Further data are now being accumulated to enable an appropriate check of this equation at these medium energies.

REFERENCES

1. L. E. GLENDENIN, C. D. CORYELL, and R. R. EDWARDS. Phys. Rev. **75**, 337 (1949).
2. R. D. PRESENT. Phys. Rev. **72**, 7 (1947).
3. A. C. PAPPAS. U.S. Atomic Energy Commission Report AECU-2806. 1953.
4. A. C. WAHL. J. Inorg. & Nuclear Chem. **6**, 263 (1958).
5. B. D. PATE, J. S. FOSTER, and L. YAFFE. Can. J. Chem. **36**, 1691 (1958).
6. J. M. ALEXANDER and C. D. CORYELL. Phys. Rev. **108**, 1274 (1957).
7. P. C. STEVENSON, H. G. HICKS, W. E. NERVIK, and D. R. NETHAWAY. Phys. Rev. **111**, 886 (1958).
8. R. E. BELL. Private communication.
9. W. A. ARON, B. G. HOFFMAN, and F. C. WILLIAMS. U.S. Atomic Energy Commission Report AECU-663. 1951.
10. J. M. SIEGEL and L. E. GLENDENIN. National Nuclear Energy Series. Div. IV, Vol. 9, Paper 227, Book 3. McGraw-Hill Book Co., Inc., New York. 1951.
11. W. W. MEINKE. U.S. Atomic Energy Commission Report AECD-2738. 1949.
12. H. FLASCHKA and H. ABDINE. Mikrochim. Acta, 657 (1954).
13. L. E. GLENDENIN, R. R. EDWARDS, and H. GEST. National Nuclear Energy Series, Div. IV, Vol. 9, Paper 232, Book 3. McGraw-Hill Book Co., Inc., New York. 1951.
14. B. D. PATE and L. YAFFE. Can. J. Chem. **33**, 15 (1955).
15. B. D. PATE and L. YAFFE. Can. J. Chem. **33**, 610 (1955).
16. B. D. PATE and L. YAFFE. Can. J. Chem. **33**, 929 (1955).
17. B. D. PATE and L. YAFFE. Can. J. Chem. **33**, 1656 (1955).
18. B. D. PATE and L. YAFFE. Can. J. Chem. **34**, 265 (1956).
19. R. L. FOLGER and H. G. HICKS. U.S. Atomic Energy Commission Report UCRL-432. 1949.
20. L. E. GLENDENIN. National Nuclear Energy Series. Div. IV, Vol. 9, Paper 267, Book 3. McGraw-Hill Book Co., Inc., New York. 1951.
21. D. N. SUNDERMAN and W. W. MEINKE. Anal. Chem. **29**, 1578 (1957).
22. H. FLASCHKA. Mickrochim. Acta, 38 (1952).
23. A. KJELBERG, H. TANIGUCHI, and L. YAFFE. Can. J. Phys. **38**, 866 (1960).
24. J. W. SIEGEL and L. E. GLENDENIN. National Nuclear Energy Series, Div. IV, Vol. 9, Paper 53, Book 2. McGraw-Hill Book Co., Inc., New York. 1951.
25. H. A. TEWES and R. A. JAMES. Phys. Rev. **88**, 860 (1952).
26. P. KRUGER and N. SUGARMAN. Phys. Rev. **99**, 1459 (1955).
27. A. KJELBERG and A. C. PAPPAS. Nuclear Phys. **1**, 322 (1956).
28. C. D. CORYELL. Ann. Rev. Nuclear Sci. **2**, 305 (1953).
29. H. G. HICKS and R. S. GILBERT. Phys. Rev. **100**, 1286 (1955).
30. R. L. FOLGER, P. C. STEVENSON, and G. T. SEABORG. Phys. Rev. **98**, 107 (1955).
31. C. D. CORYELL. Can. J. Chem. **39**, 000 (1961).

Can. J. Chem. Downloaded from www.nrcresearchpress.com by 210.87.254.40 on 09/05/12
For personal use only.

Can. J. Chem. Downloaded from www.nrcresearchpress.com by 210.87.254.105 on 09/05/12
For personal use only.

SEARCH FOR CORRELATIONS OF MOST PROBABLE NUCLEAR CHARGE Z_P OF PRIMARY FISSION FRAGMENTS WITH COMPOSITION AND EXCITATION ENERGY[1]

CHARLES D. CORYELL, MORTON KAPLAN,[2] AND RICHARD D. FINK[3]

ABSTRACT

The repartition of nuclear charge in fission has a narrower dispersion than almost any other property connected with the fission process. To a crude approximation, the distribution of nuclear charge between light and heavy partners L and H leads to the most probable charges $(Z_P)_L$ and $(Z_P)_H$ displaced from the respective charges Z_A of β-stability by the same amount for the two fragments (Glendenin rule of equal charge displacement ECD, 1946). The existence of shell offsets in the Z_A vs. A function for different neutron- and proton-shell regions must be considered. All available data for thermal fission $U^{235}(n_{th},F)$ are examined critically. The data show sudden offset-like drifts (fine structure) that may well be associated with shell properties of the products before the "neck" has dissolved. It is shown that these data eliminate naive equal charge displacement ECD, also an older competitive prescription of constant charge ratio CCR for the products, and an empirical Russian prescription (Apalin *et al.*, 1960). The data are also examined in the light of the postulate that fission gives minimum nuclear plus coulombic potential energy (Present 1947, Fong 1955, Swiatecki-Blann 1960), and it is shown that the present mass formulas give too much uncertainty three to four β-decays from stability to give a useful test, but that shell effects in masses must be retained. Data from charged-particle fission with energy deposit up to 40–50 Mev are in reasonable accord with the low-energy data on correcting for composition and neutron boil-off. It is concluded from experiment that Z_P is a single-valued function of A, known to about ± 0.15 unit for low-energy fission and ± 0.25 unit for medium-energy fission, and that the fine structure very probably present is an indication of intrinsic nuclear chemistry.

The early thinking on the wartime Manhattan Project about nuclear charge distribution in low-energy fission, before any yield data were available, was based on the concept (1, 2) of constant charge ratio CCR. Professor Wheeler had suggested (4) a search for positron emitters to see how wide the charge dispersion might be: the results of crude searches in the products of U^{235} (n_{th},F) were, of course, negative (5). Way and Wigner (7) postulated that the charge would distribute to give a minimum nuclear potential energy, and Present (8) postulated a minimum for the sum of nuclear potential energy plus coulombic energy (equal to final kinetic energy). Present took considerable pains to handle the coulombic term for polarizable spheres with non-uniform proton density.

The identification of shielded nuclides[4] 36-hour Br^{82}, 19-day Rb^{86}, and 13-day Cs^{136} among the fission products gave the first experimental leverage on charge distribution. The first detailed treatment of the problem (5) established the classical rule, or prescription (3, 6) of equal charge displacement ECD; namely that the nuclear charge distribution between light and heavy partners L and H leads to most probable charges Z_P displaced from stability Z_A by about the same amount for the two fragments,

$$[1] \qquad (Z_A - Z_P)_L = (Z_A - Z_P)_H.$$

[1]*Manuscript received November 3, 1960.*
Contribution of the Department of Chemistry and Laboratory for Nuclear Science of the Massachusetts Institute of Technology, Cambridge 39, Mass., with financial support from the U.S. Atomic Energy Commission. Presented at the Third Symposium on Nuclear Chemistry and Radiochemistry held at Atomic Energy of Canada Limited, Chalk River, Ontario, September 6–8, 1960.
[2]*Present address: Ernest Orlando Lawrence Radiation Laboratory, University of California, Berkeley 4, California.*
[3]*With partial support as National Science Foundation Summer Fellow, 1960, and Eastman Kodak Fellow 1960–61.*
[4]*A shielded nuclide is one unlikely to be formed by negatron decay since the isobar of $Z-1$ is stable, with little prospect of having a β-unstable isomer.*

There is often ambiguity about whether the prescription is meant for usage before or after prompt neutron emission. Equation [1] may be sharpened to give the most probable charge Z_P of a fission product of final mass number A_1 after the emission of ν_1 neutrons,

$$[2] \qquad Z_P(A_1) = Z_{(A_1+\nu_1)} - \tfrac{1}{2}[Z_{(A_1+\nu_1)} + Z_{(A_C-A_1-\nu_1)} - Z_C],$$

where Z_C and A_C denote the charge and mass of the compound nucleus formed by the target plus bombarding particle, and Z_A is the most stable charge associated with mass number A.

This first treatment was based on the fractional chain yields of the three species mentioned above and 9.2-hour Xe^{135}, a quasi-shielded nuclide[5] in U^{235} (n_{th},F), together with the roughly 10-fold higher fractional chain yield of Cs^{136} in Pu^{239}(n_{th},F). It was postulated that the charge dispersion curve, f_1 vs. $Z-Z_P{}^j$ would be an A-independent curve, symmetric about zero abscissa, if a reasonable j-th prescription $Z_P{}^j$ were found. The area under the curve must be unity. The very low yields found for Br^{82} and Rb^{86} showed that f_1 falls very rapidly with $|Z-Z_P|$ when this is more than 2.0. The analytical method usually employed was to invoke a rule for some $Z_P{}^j$, and test the experimental f_1 values against $Z-Z_P{}^j$ for coherence, continuity, and reasonable shape. The charge-dispersion curve for correlation of $\log f_1$ with $Z-Z_P$ seems to be approximately Gaussian when $\log f_1 > -2.0$, and linear when $\log f_1$ is < -2.0.

The CCR rule for products after the emission of ν_T total prompt neutrons (both fragments) is

$$[3] \qquad Z_P = \frac{Z_C A_1}{A_C - \nu_T}.$$

Low-energy fission data do not agree with this rule (5, 18, 19, 20), but evidence has been cited for high-energy data, beginning with the Goeckermann and Perlman study (9) of bismuth fission with 190-Mev deuterons, Bi^{209}(d_{190},F). A number of papers (10–16), mostly at Berkeley, examine this rule in the intermediate energy region (~50 Mev), and give it partial support. Pate (17) has, however, established a strong case against CCR and for ECD even up to very high-energy deposition before fission.

The postulate of minimal nuclear potential energy (7) seemed to have been eliminated by the first test (5), but question should be raised as to the validity of the mass equation[6] used in the calculations of Z_P. These were based on Bohr and Wheeler data (21). The related postulate of Present (8) was later tested by Glendenin (22); this was found to be in fair accord with the apparent empirical observation (5) of ECD except for very light or very heavy fragments, where data still are few.[7]

The ECD rule (eq. [1]) received substantial support in 1955 in two major reviews (19, 22). Pappas and Coryell (18) had raised the question of how discontinuities in Z_A

[5] *A quasi-shielded nuclide is one formed by the negatron decay of a moderately long-lived precursor of charge Z–1, whose half-life is long enough that daughter growth during irradiation and separation does not prevent estimation of the activity independently formed in fission. It may be shown that the ratio of the activity $A_2{}^d$ formed in decay to that $A_2{}^i$ formed independently is $\lambda_1 t/f_2$, where λ_1 is the disintegration constant of the precursor, t is the time to chemical separation after a very short burst of fission, and f_2 is the fractional chain yield of the quasi-shielded nuclide (Z,A).*

[6] *All available data indicate that nuclear potential energy is essentially parabolic with Z at constant A, with pairing terms p.t. for oddness or evenness of Z and N, namely,*

$$M(Z,A) = M(Z_A,A) + (B_A/2)(Z_A - Z)^2 + \text{p.t.}$$

Numerous evaluations of B_A and p.t. are available; see especially Coryell (23, 24), Fix (25), Green (26), Levy (27), and Cameron (28).

[7] *The senior author has weighted the ECD (equal charge displacement) postulate more heavily than that of minimum potential energy MPE, although both were given similar weight in an earlier review (22).*

Can. J. Chem. Downloaded from www.nrcresearchpress.com by 210.87.254.105 on 09/05/12
For personal use only.

caused by the crossing of neutron- and proton-shell edges[8] should effect Z_P. If ECD (eq. [1]) holds strictly, then Z_P is set solely by properties of the primary products. One would expect by eq. [1] frequent discontinuities in Z_P as A increases, whenever the composition of the fragment crosses a neutron- or proton-shell number, the discontinuities being half of those given in footnote 8. Correspondingly, discontinuities should occur when the complementary fragment crosses any shell number. Dispersion in neutron emission should change the discontinuities from breaks to sudden steep drifts in the Z_P vs. composition curve. Note, however, that the point in Z_P vs. composition diagrams where steep drifts occur for shell crossings in the complementary fragment are dependent on Z_C and A_C of the fissioning nucleus.

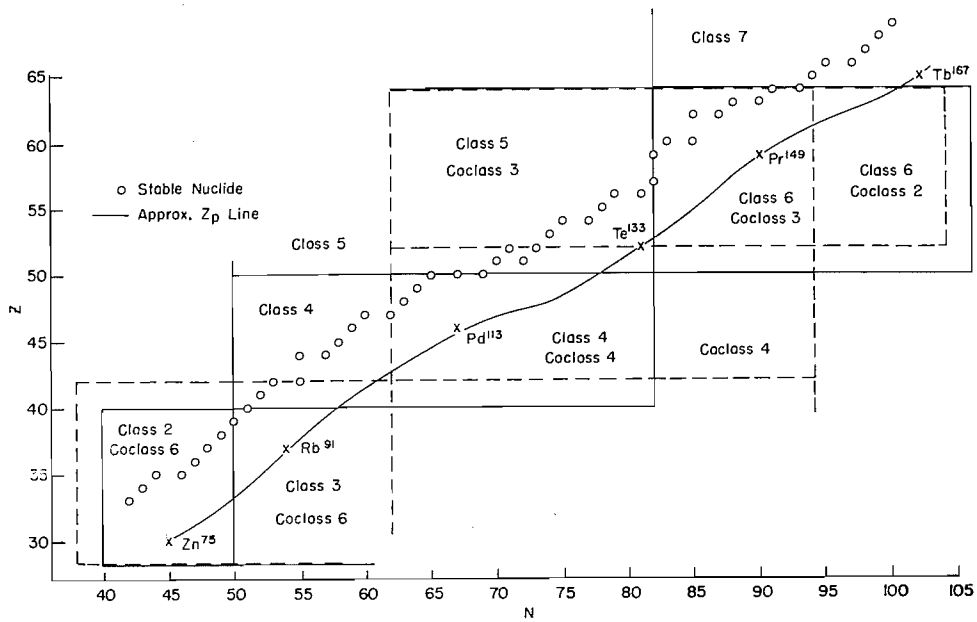


FIG. 1. Designation for $U^{235}(n,F)$ of shell classes for fragment and complement.

Figure 1 is a graphical breakdown of the shell classes of the pairs of fragments in the products of fission of U^{236} (as from thermal neutron fission of U^{235} at excitation energy $E^* = 6.5$ Mev) before neutron emission. The various rectangles designate classes: solid lines for the nucleus in question, broken lines for the complement (coclasses). The shell crossings designated are from the successive lines in Levy's master tables (27),[9] but the chart covers principally regions of interest in fission chemistry. Going to larger Z_C raises the ordinates of the Z-coclass lines; similarly going to larger $N_C = A_C - Z_C$ raises the abscissas of the N-coclass lines.

For reference, the stable odd-A nuclides ($Z_{stable} = Z_A \pm 0.5$) are shown, together with a rough idea of Z_P given as the sinuous curve. This Z_P line is taken from Glendenin (5) to avoid shell-edge prejudice.

[8]*It is well established (18, 23) that Z_A is essentially linear with A in a given nucleon-shell region, with slope ~0.4, but that Z_A undergoes upward discontinuity on crossing a neutron-shell edge, and downward discontinuity on crossing a proton-shell edge, the discontinuities ΔZ for $N = 50$, $N = 82$, and $Z = 50$ being (23) +0.9, +1.4, and −1.3 charge units, respectively.*

[9]*Levy's shell class distinctions (27) can be represented in the array: cl.1 ($N = 40$) cl.2 ($N = 50$) cl.3 ($Z = 40$) cl.4 ($Z = 50$) cl.5 ($N = 82$) cl.6 ($Z = 64$) cl.7 ($Z = 82$, $N = 126$) cl.8 ($N = 140$) cl 9. The numbers in parentheses are the shell crossings dividing the classes.*

Can. J. Chem. Downloaded from www.nrcresearchpress.com by 210.87.254.105 on 09/05/12
For personal use only.

Can. J. Chem. Downloaded from www.nrcresearchpress.com by 210.87.254.105 on 09/05/12
For personal use only.

Pappas (18) tried to determine how shell-crossings affect Z_P with few data to guide him (see Coryell (29) for criticism of paucity of data). He made the *ad hoc* decision, now not considered necessary, that the shell class and coclass that are to be used are those at the end of the decay chains. Steinberg and Glendenin (20) assumed that ECD was valid with a drift over three to four units of A in going from one shell-class set to the next.

It was established fairly well (18, 19, 20) that the data from thermal neutron fission of U^{235}, U^{233}, and Pu^{239} were compatible on a plot of $\log f_1$ vs. $Z-Z_P$ when Z_P is computed by eq. [1], assuming ECD. Similar analyses of the fission of U^{238} and Th^{232} with 14-Mev deuterons (30) and of U^{235} with 14-Mev deuterons and 24-Mev alpha particles (31) showed that fission with excitation energy near 20 Mev gave compatible results on the assumption of reasonable values for neutron emission ν_1.

In 1958 Wahl (32) made a very significant contribution. He used data for 28 fission products in the reaction U^{235} (n_{th},F) to show that one can reverse the conventional procedure of using consistency in the dispersion of f_1 with $Z-Z_P$ to check $Z_P{}^1$ values. He proposed using the Glendenin (5) charge-dispersion curve to obtain $Z-Z_P$ values from experimental f_1 values. This method established empirical Z_P values. He found a continuous but somewhat winding curve in a plot of Z_P vs. A and that the $(Z_P)_L$ values and the $(Z_P)_H$ values intercompare well using average neutron emission $\bar{\nu} = 2.5$. Until Wahl's paper, no firm values existed for cumulative fractional chain yields f_c for very early members of chains, obtained for example by gas sweeping of krypton and xenon (2), or by rapid quantitative precipitation of short-lived halogens, with yields determined by radiochemical assay of long-lived descendants. Yield values for such species, which will be called "swept-out" nuclides, would give the first measurements[10] on the left side of the curve for $\log f_1$ vs. $Z-Z_P$. Wahl (32) obtained results for krypton isotopes up to 3-second Kr^{92} and xenon isotopes up to 1-second Xe^{143} and ~1-second Xe^{141}. This study provided the first examples of even-Z species except for Xe^{135}, and the first even-Z – even-N species. It failed to show evidence for the odd–even sawtooth in observed fission yields that Herrington (33) predicted by simple evaporation theory from an assumed primordial yield-mass curve smooth in A. Further data have been obtained by Wahl and co-workers on other krypton and xenon isotopes (34), strontium, barium, and cerium isotopes (35, 36), and other species of odd Z, including (37) the three niobium isotopes[11] of mass number 96, 97, and 98.

This new body of data (32, 34–37) has led to a reanalysis of the charge dispersion curve (38). Figure 2 shows the Glendenin curve (5), labelled GCE, together with three Gaussian curves

$$y_1 = \frac{1}{\sqrt{\pi C}} e^{-(Z-Z_P)^2/C} \qquad [4]$$

with the parameter C for variance as 0.8, 1.0, and 1.43. It is seen that the Glendenin curve is very close to the Gaussian of $C = 1.43$ for $|Z-Z_P| < 1.8$. At high values of $|Z-Z_P|$ it is found that the curve is exponential,

$$\frac{d \log_{10} f_1}{d(Z-Z_P)} \cong \pm 3.2 \qquad \text{for } (|Z-Z_P| > 2.2), \qquad [5]$$

as far as experimental calibrations exist.[12] Wahl reports (38) that most data for chains

[10] *The change from observed f_c to computed f_i is obvious (32).*

[11] *Considerations of isomerism indicate that in niobium only the yields of high-spin isomers of even A are being measured.*

[12] *The curve is calibrated at present out to about $Z-Z_P = 3.2$, and extrapolations to ~4 are made.*

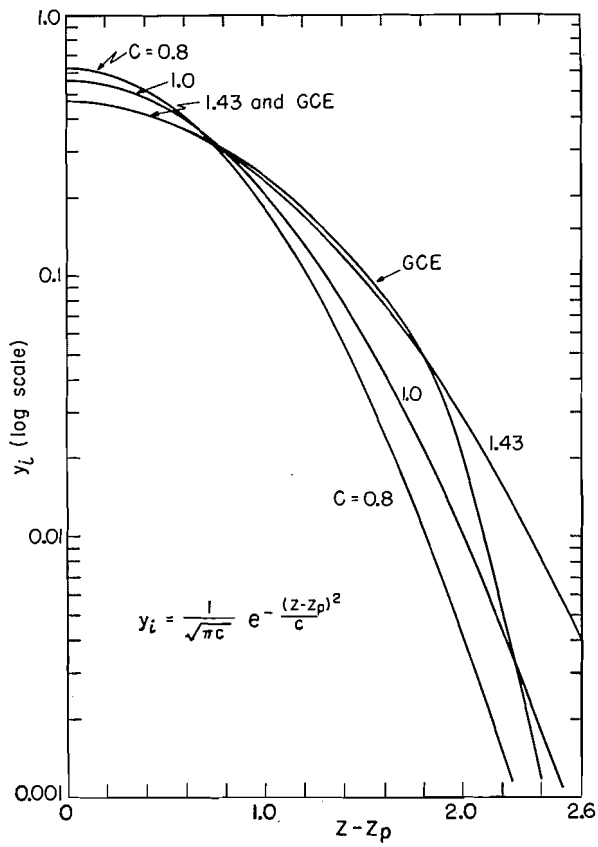


FIG. 2. Charge dispersion.

with several f_1 points at different Z values follow Gaussians with $0.8 < C < 1.0$. He now uses this type of curve (38) to measure Z_P by the 1958 method (32); the present paper is based on this method (32) but we still use the Glendenin curve (5, 32), one which gives a somewhat larger scatter in Z_P values.

It will be of interest to search for correlation of Z_P with Z_A, particularly with reference to fine structure (breaks or sudden drifts) in the former data, which are treated as a continuous curve in Z_P vs. A co-ordinates for a given type of fission. The type of fission chosen is $U^{235}(n_{th},F)$, the one best studied and most accessible. It may be noted that in the fission-product region, the average slope dZ_A/dA in a given shell region is 0.37_5 (23, 24, 25). It is clear that dZ_P/dA must be about the same. It is therefore useful to present all Z_A and Z_P data as $Z_A - 0.4A$ and $Z_P - 0.4A$ when plotting against A as abscissa as this function removes most of the drift present. This procedure will be used throughout this paper.

It is useful to check various prescriptions against the fairly comprehensive body of data for f_1 values for shielded, quasi-shielded, and swept-out nuclides formed in the reaction $U^{235}(n_{th},F)$. A summary of these data is presented in Table I; half-lives are from Katcoff (39) and most of the yield data are given in the Croall review (40), except that values obtained by difference (35, 36) are not included.

In Fig. 3 is a test by which eq. [3] for CCR fails for $U^{235}(n_{th},F)$. The ordinate is

Can. J. Chem. Downloaded from www.nrcresearchpress.com by 210.87.254.105 on 09/05/12
For personal use only.

TABLE I

Independent fractional chain yields, f_i, for the thermal neutron fission of U^{235}

Species	f_i	or	f_c	$Z-Z_P$	Z_P	$Z_P-0.4A$	References
$_{33}As^{78}$	$(8.5\pm2.5)10^{-3}$			2.12	30.88	−0.32	41*a*
$_{35}Br^{82}$	3×10^{-4}			2.64	32.3	−0.50	32
$_{37}Rb^{86}$	1.5×10^{-5}			3.08	33.92	−0.48	32
$_{36}Kr^{89}$			0.960±0.009	0.82	35.18	−0.42	32
$_{36}Kr^{90}$			0.86	0.35	35.65	−0.35	32
$_{36}Kr^{91}$			0.59±0.01	−0.32	36.32	−0.08	32
$_{38}Sr^{91}$	0.06±.04			1.70	36.30	−0.10	36
$_{36}Kr^{92}$			0.31	−0.90	36.90	0.10	32
$_{36}Kr^{93}$			0.075	−1.65	37.65	0.45	34
$_{36}Kr^{94}$			0.015	−2.02	38.02	0.42	34
$_{36}Kr^{95}$			1.12×10^{-3}	−2.40	38.40	0.40	34
$_{41}Nb^{96}$	$(1.0\pm0.2)\times10^{-4}$			2.80	38.20	−0.20	37
$_{41}Nb^{97}$	$(1.7\pm1.3)\times10^{-3}$			2.35	38.65	−0.15	37
$_{41}Nb^{98}$	0.011±0.004*			2.00	39.00	−0.20	37
$_{53}I^{128}$	$(9.8\pm1.0)\times10^{-5}$			2.78	50.22	−0.98	32
$_{53}I^{130}$	2.8×10^{-4}			2.62	50.38	−1.62	32
$_{52}Te^{131}$	0.11			1.4	50.6	−1.8	32
$_{52}Te^{132}$	0.36±0.017			0.0 to 1.2	50.9	−1.9	32
$_{53}I^{133}$	<0.05			>1.8	<51.2	<−2.0	32
$_{53}I^{134}$	0.12			1.44	51.56	−2.04	32
$_{54}Xe^{135}$	0.037			1.88	52.1	−1.9	32
$_{55}Cs^{136}$	9.5×10^{-4}			2.43	52.57	−1.83	32
$_{55}Cs^{138}$	0.045±0.005			1.84	53.16	−2.04	34
$_{54}Xe^{139}$			0.82	0.20	53.80	−1.80	32
$_{56}Ba^{139}$	0.011±0.005			2.08	53.92	−1.68	36
$_{54}Xe^{140}$			0.59	−0.32	54.32	−1.68	32
$_{57}La^{140}$	$(7.0\pm0.4)\times10^{-4}$			2.68	54.32	−1.68	35
$_{54}Xe^{141}$			0.205	−1.1	55.1	−1.3	34
$_{57}La^{141}$	$(4\pm2)\times10^{-3}$			2.23	54.77	−1.63	35
$_{56}Ba^{141}$	0.27±0.06			0.92	55.08	−1.32	35
$_{54}Xe^{142}$			0.059	−1.73	55.73	−1.07	34
$_{57}La^{142}$	0.018±0.006			2.00	55.00	−1.80	35
$_{54}Xe^{143}$			8.5×10^{-3}	−2.13	56.13	−1.07	32
$_{58}Ce^{143}$	0.010±0.004			2.10	55.90	−1.30	35
$_{54}Xe^{144}$			1.1×10^{-3}	−2.40	56.40	−1.20	32
$_{61}Pm^{150}$	0.0022			2.32	58.68	−1.32	41*b*

*Cumulative yield (37).

$Z-0.4A$, the upper set of tilted lines corresponding to different shell regions of Z_A, with N- and Z-shell numbers indicated. The lower line is the prediction of eq. [3], the crosses marking computed points for products after neutron emission.[13] The double circle at $Z_P = 46.0$, $A = 116.75$ represents the requirement in exactly symmetric fission that $Z_P = Z_C/2$.

We prefer to treat the experimental data in three categories:

(i) Early members of chains (here only krypton and xenon isotopes) where $Z-Z_P$ is negative: these come from fissions where the fragment of interest has had very low neutron boil-off.

(ii) Low-yield species ($f_i < 0.1$ or $Z-Z_P > 1.5$): these come from fissions of rather high neutron boil-off.

(iii) High-yield species ($f_i > 0.1$), where the Glendenin curve is less precise in setting $Z-Z_P$.

There is no evidence, however, in Fig. 3 that the data from any of these three classes diverge from the others.

[13]*The average value of 1.25 is taken for ν_1 throughout this paper for $U^{235}(n_{th},F)$, ignoring for the present the Whetstone–Vladimirskii effect (42, 43, 44), namely that ν_A is a double sawtooth function of A. Incorporation of this effect would make little difference.*

Can. J. Chem. Downloaded from www.nrcresearchpress.com by 210.87.254.105 on 09/05/12
For personal use only.

The remarkable part of Fig. 3 is that it reveals that the large body of data on $Z_P-0.4A$ from Table I represents a coherent body, in that checks agree well except at $A \cong 141$. There is a sharp drift up in Z_P (or $Z_P-0.4A$) between $A = 90$ and 93, and a sudden drop between Kr^{95} and Nb^{96}, Kr^{97}, and Nb^{97}, the latter two species not being affected by isomerism (see footnote 11). Another sharp fall is apparent between the Kennett and Thode data (45) for I^{128} and I^{130} (reflected also in $U^{233}(n_{th},F)$ and $Pu^{239}(n_{th},F)$). The blurred rise near $A = 141$ has been mentioned, and problems with $A = 141$ are discussed elsewhere (35).

The present authors consider that the data, as presented here, show that

(i) *Z_P is a single-valued function of A.*

(ii) *Z_P is known to about ± 0.15 unit.*[14]

(iii) *Z_P shows fine structure* (an indication of nuclear chemistry).

In Fig. 4 there is provided a test for a recent Russian prescription, given casually by Apalin *et al.* (44). This prescription is based on eq. [3] for CCR after neutron boil-off with a correction term vanishing for symmetric fission; it is

$$[6] \qquad (Z_P)_L = \frac{A_L}{A_H} Z_{P_H} + 5.90 - 0.05A_L.$$

This can be expressed in explicit form as

$$[7a] \qquad (Z_P)_L = 5.90 + 0.319A_L + 0.000214A_L^2,$$

$$[7b] \qquad (Z_P)_H = 0.419A_H - 0.000214A_H^2.$$

It is seen that the curve in the lower part of Fig. 4 for $Z_P-0.4A$ (Russian Z_P), based on crosses for computed points, fits the experimental data better than does CCR (Fig. 3). The prescription carries no provision for the fine structure which we admire. The average deviation would be lower if the coefficient of A_L in the last term of eq. [6] were taken near 0.033.

Figure 5 presents a test of an unpublished empirical (essentially graphical) prescription of Wahl (38). This prescription is based on a composite of data (32, 38, 40) for thermal neutron fission (U^{235}, U^{233}, Pu^{239}) and a few points (38) for spontaneous fission (Cm^{244}, Cf^{252}). The fit to the data is excellent; it is even better if the improved Wahl Z_P values (see footnote 14) are taken. It would seem, however, that the Wahl prescription is characteristic of the fission process, not of the composition of the products, as is indicated in Fig. 6, where there is given a schematic representation of the prescription as applied to $U^{235}(n_{th},F)$, $U^{235}(\alpha_{40},F)$, and Cf^{252}(spont. F), characterized by their compound nuclei and excitation energy E^*.

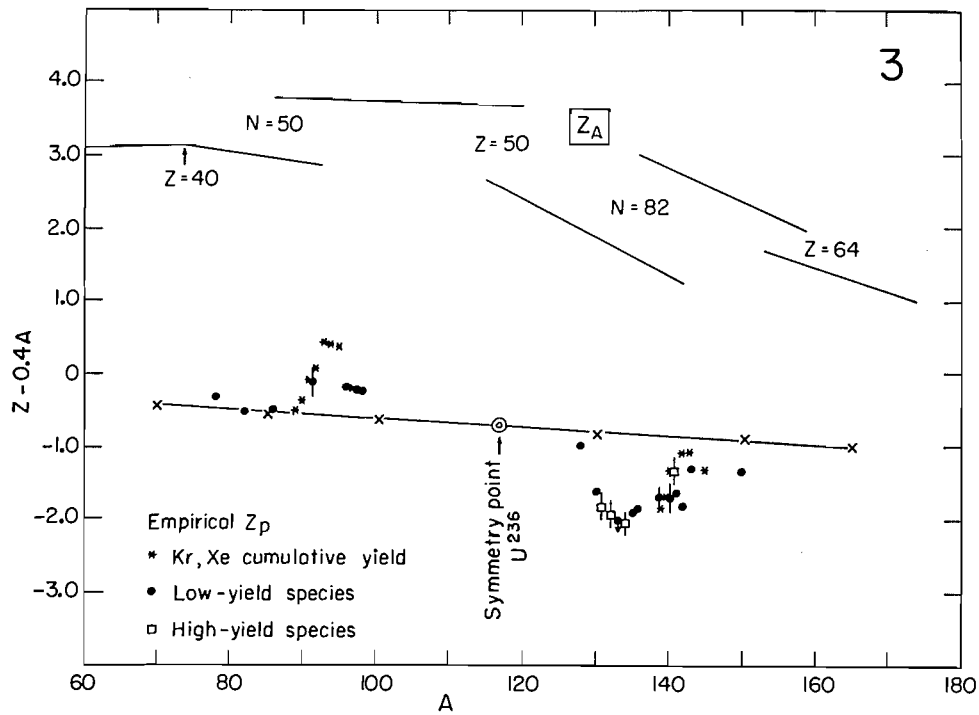
Figure 7 represents a treatment of the same data in the framework of the classical ECD approach of eqs. [1] and [2], with full recognition of shell effects (18, 19, 23, 24). Near-vertical broken lines represent the divisions between different shell regions for the Z and A values of the nucleus in question and its complement, denoted as "comp." The plot refers to $U^{235}(n_{th},F)$ with (see footnote 13) $\nu_T = 2.5$, so the sum of the charges is 92 and the sum of the A values is 233.5. Going to compound nuclides of higher Z_C or $N_C - \nu_T$ for the fission source leads to a rightward motion of the proton complementary lines or a rightward motion of the neutron complementary lines.

The Pappas prescription (18, 19) that the shell structure at the end of decay chain

[14]*Professor Wahl reports (38) that the new empirical Z_P curve is within 0.1 charge unit of the sums of the uncertainties (in the calculated Z_P values) due to experimental error and to the charge distribution curve ($C=0.8$ to 1.0) for greater than 80% of the points (Wahl 1960 method of determining Z_P).*

Can. J. Chem. Downloaded from www.nrcresearchpress.com by 210.87.254.105 on 09/05/12
For personal use only.

Can. J. Chem. Downloaded from www.nrcresearchpress.com by 210.87.254.105 on 09/05/12
For personal use only.



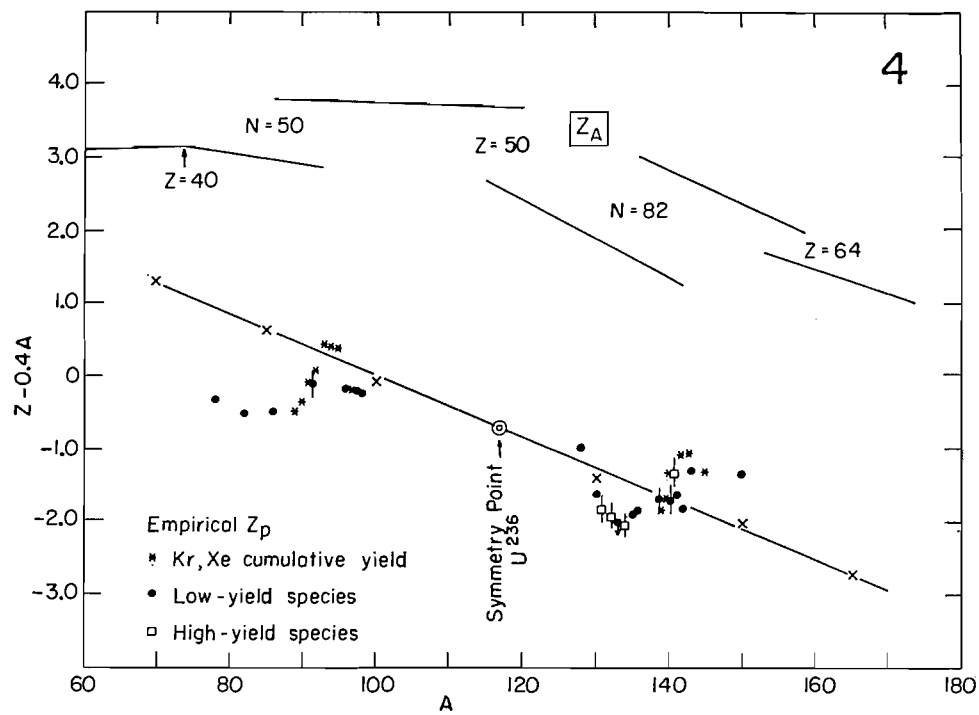
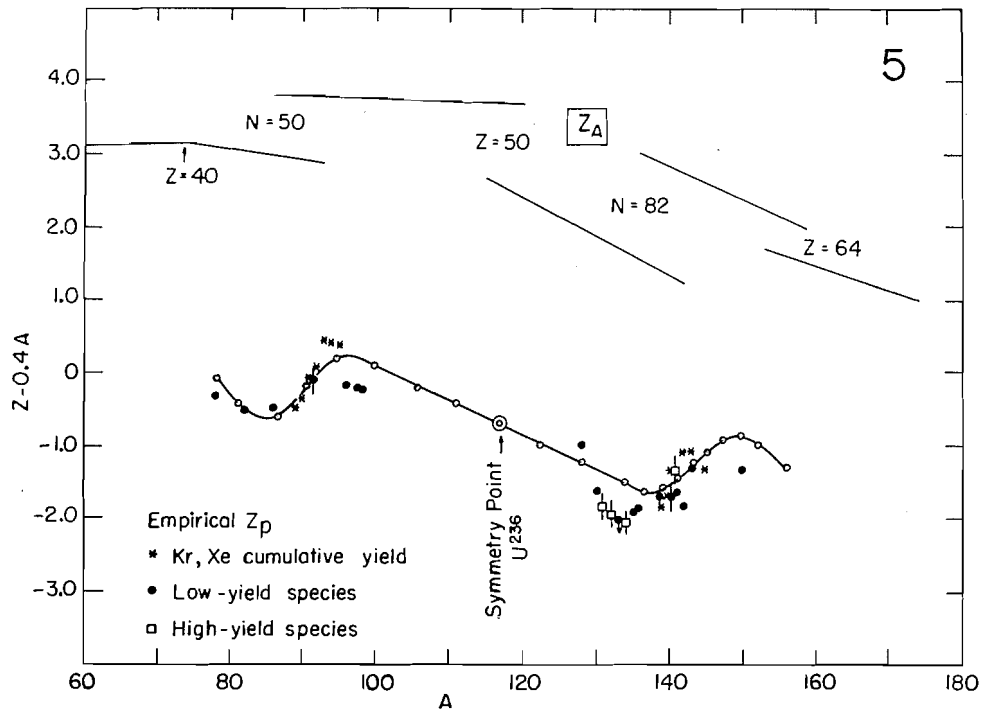


FIG. 3. Most probable charge Z_P in fission: constant charge ratio (CCR) for U^{235} (n,F).
FIG. 4. Most probable charge Z_P in fission: Russkaya formula (Apalin–Dobrynin–Zakharova–Kutikov–Mikaelyan (1960) for U^{235} (n,F)).



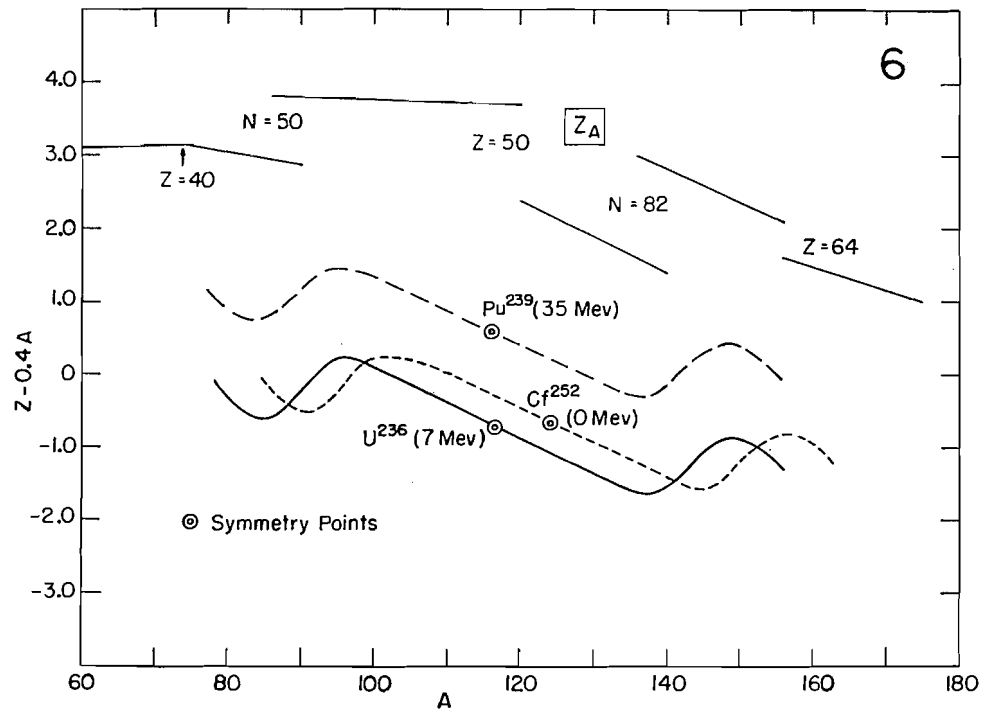


FIG. 5. Most probable charge Z_P in fission: Wahl prescription (1960) for $U^{235}(n,F)$.
FIG. 6. Wahl prescriptions for most probable charge Z_P in fission of various types: $U^{235}(n,F)$, $U^{235}(\alpha_{40},F)$, Cf^{252}(spont. F).

Can. J. Chem. Downloaded from www.nrcresearchpress.com by 210.87.254.105 on 09/05/12
For personal use only.

Can. J. Chem. Downloaded from www.nrcresearchpress.com by 210.87.254.105 on 09/05/12
For personal use only.

sets the Z_A from which Z_P is calculated by ECD from eq. [1] or [2] would require that neutron-shell breaks in the data occur to the right of the offsets shown in the Z_P lines, not inconsistent with the observations. It also requires neutron breaks for shell in the complement to occur to the left. Opposite effects are required for proton shell-breaks in species and complement. Difficulties are seen at $A = 96$, ~129, and 150. If on the other hand it be considered, as del Marmol and Coryell suggest (31), that occurrence of neutron or proton shells is "sensed" by the two nascent nuclei before contact is lost, underestimation of neutrons and protons should occur by the number of each coming from the neck. Thus breaks should be expected to occur to the right of the offsets shown in the Z_P lines for both neutron and proton shells and to the left for the complements. This new prescription is not inconsistent with the breaks at 91, 95, and 141, but has trouble with I^{128} and probably Pm^{150}. The identification of "breaks" is considered more important than the verification of eq. [1] or [2] (ECD) for predicting absolute values of Z_P.

Regarding the broken Z_P lines in the lower part of Fig. 7 (related to the breaks in the Z_A lines in the upper part), it should be noted that the breaks for the different shell crossings are comparable in magnitude to the sudden drifts in the experimental Z_P values shown as points. The approach of Fig. 7 differs greatly from that of Fig. 5, in that it presumes that all of the fine structure comes from composition of the fission products. Little change in the breaks would come from considering the effects of the sawtooth ν_1 function (see footnote 13, Whetstone–Vladimirskii effect (42, 43, 44)).

It should be pointed out also that the general closeness of the experimental Z_P points to the various segments of Z_P lines predicted by ECD, as shown in Fig. 7, is an empirical justification for the Glendenin ECD rule.[15] The rule is totally *ad hoc*, however, with no theoretical justification, as Halperin (6) also decides.

Until recently there has been no convenient and attractive way to intercompare $Z_P(A)$ among various types of fission differing in Z_C, A_C, and E^* or ν_T. The regularities in Z_A, and the approximate parallel relation between Z_P and Z_A (Fig. 7), show an easy way to handle changes in Z_C and A_C. Recalling (23, 24, 25) that

$$[8] \qquad \frac{dZ_A}{dA} = \frac{dZ_A}{d\nu} \cong 0.38$$

it can be shown that eq. [2] transforms to

$$[9] \qquad Z_P(A) = \tfrac{1}{2}[Z_A + 0.38\nu_1 - Z_{(A_C - A - \nu_T)} - 0.38\nu_2 + Z_C].$$

Using the approximation (see footnote 13)

$$[10] \qquad \nu_1 = \nu_T - \nu_2 \cong \nu_2$$

we find that

$$[11] \qquad Z_P(A) = \tfrac{1}{2}[Z_C + Z_A - Z_{(A_C - A - \nu_T)}].$$

Consider as a reference type of fission that of $U^{235}(n_{th},F)$, for which $A_C = 236$, $Z_C = 92$, and $\nu_T = 2.5$, for which eq. [11] is

$$[12] \qquad Z_P(A)^{ref} = \tfrac{1}{2}[92 + Z_A - Z_{(233.5-A)}].$$

By subtracting eq. [12] from eq. [11], it is seen that the difference $\Delta Z_P(A)$ is

$$[13a] \qquad \Delta Z_P(A) = Z_P(A) - Z_P(A)^{ref} = \tfrac{1}{2}(Z_C - 92) - \tfrac{1}{2}[Z_{(A_C - A - \nu_T)} - Z_{(233.5-A)}].$$

[15] *This means that the drifts are not very far from the breaks in predicted Z_P lines.*

The effect of increasing energy deposit on the type of fission is assumed to be only that of increasing the total neutron boil-off, in the amount

$$[14] \qquad \frac{d\nu_T}{dE} = 0.12\ \text{Mev}^{-1},$$

as shown by Leachman (46, 53) for spontaneous fission and for neutron-induced fission in the energy region 0 to 14 Mev. Thus the last term on the right of eq. [13] can be expressed as

$$[15] \qquad [Z_{(A_C-A-\nu_T)} - Z_{(233.5-A)}] = 0.38(A_C-236) - 0.38(\nu_T-2.5).$$

Thus eq. [13] for the shift $\Delta Z_P(A)$ for a given chain A by changing A_C, Z_C, and ν_T from that for the reference state of $U^{235}(n_{th},F)$ becomes[16]

$$[16] \qquad \Delta Z_P(A) = \tfrac{1}{2}(Z_C-92) - 0.19(A_C-236) + 0.19(\nu_T-2.5).$$

Equation [16] can be used to correct a $Z_P(A)$ value for a given type of fission (determined by the Wahl 1958 method (see footnote 14) (32)) to the reference state $U^{235}(n_{th},F)$:

$$[13b] \qquad Z_P{}^{corr} = Z_P(A) - \Delta Z_P(A).$$

The ΔZ_P values are independent of A and can be computed at once for a given Z_C, A_C, and E^* (or given target and projectile energy).

In Fig. 8 are shown $Z_P{}^{corr}$ values for various shielded and quasi-shielded nuclides from typical studies of medium-energy fission: del Marmol (31), $U^{235}(d_{14},F)$ and $U^{235}(\alpha_{25},F)$; Chu (14), $U^{235}(\alpha_{46},F)$; and Yellin (47), $U^{235}(d_{14},F)$ for 3.2-hour Ag^{112}. In our experience, most other recent data with energy deposit of 20 to 60 Mev fall in the same general region. These data are presented in a framework like that of Fig. 7, and the general course of the $U^{235}(n_{th},F)$ data are presented as a cross-hatched background.

It is concluded from Fig. 8 that $Z_P{}^{corr}$ values for medium-energy fission (with E^* up to about 50 Mev) show a somewhat greater scatter than for low-energy fission (E^* up to 7 Mev), but that they lie near the low-energy fission $Z_P{}^{corr}$ curve. It seems that there is a filling in of the Z_P hollow near $A = 135$. For further specific results on 13-day Cs^{136}, see Appendix I.

It has been proposed by Swiatecki (48, 49) that earlier theories of Way and Wigner (7), Present (8), and Fong (50) hold considerable promise, i.e., that the most probable division of charge in fission is that which leads to a minimum in the sum of nuclear potential energy and coulombic energy. This corresponds to maximizing the excitation energy and, in a rough way, the level density (50). The contribution of the coulombic term is less important than that of the nuclear potential energy.

Blann (49) has shown the comparison between Z_P data for $U^{235}(n_{th},F)$ and predictions of CCR by eq. [3], ECD by eq. [1], and the Swiatecki (48) prescription, a simplification of that of Present (8). The energy to be minimized for each mass split can be visualized roughly as the sum of the two steep concave-up energy parabolas (see footnote 6) for the light and heavy fragments, the first centered on $(Z_A)_L$, the second on $(Z_A)_H$, plus an inverted flat parabola for the coulombic term centered on $Z_C/2$. The net result, except for small pairing terms p.t. and shell offsets (23–29), is essentially a parabola, whose

[16] *Dr. J. P. Butler has pointed out that there is a fairly steady rise in ν_T for various fissioning species with A (46), so that the coefficient of the second term on the right should be raised to about 0.21 with ν_T as the nominal value of $0.12(E^*-6.5)$.*

Can. J. Chem. Downloaded from www.nrcresearchpress.com by 210.87.254.105 on 09/05/12
For personal use only.

Can. J. Chem. Downloaded from www.nrcresearchpress.com by 210.87.254.105 on 09/05/12
For personal use only.

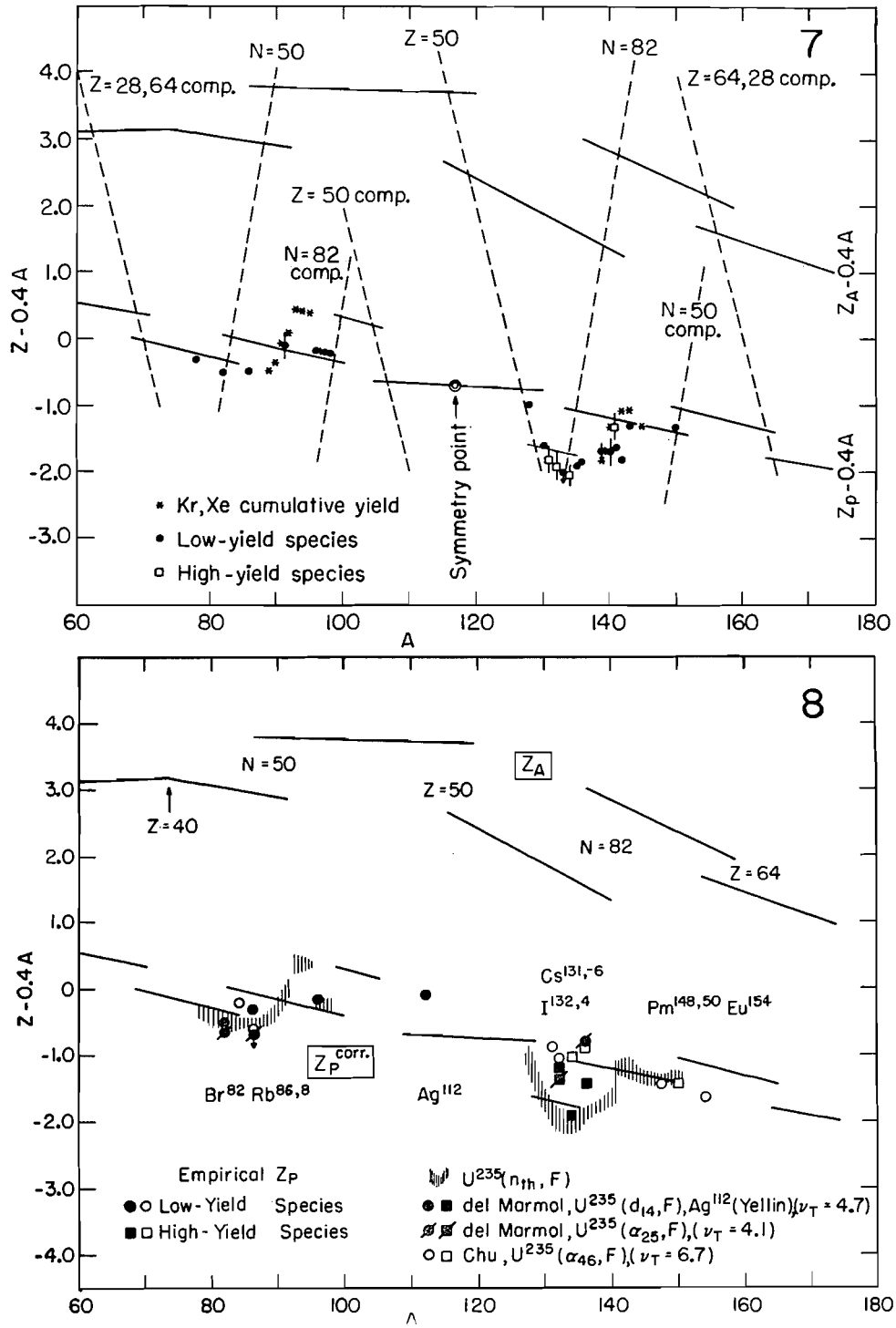
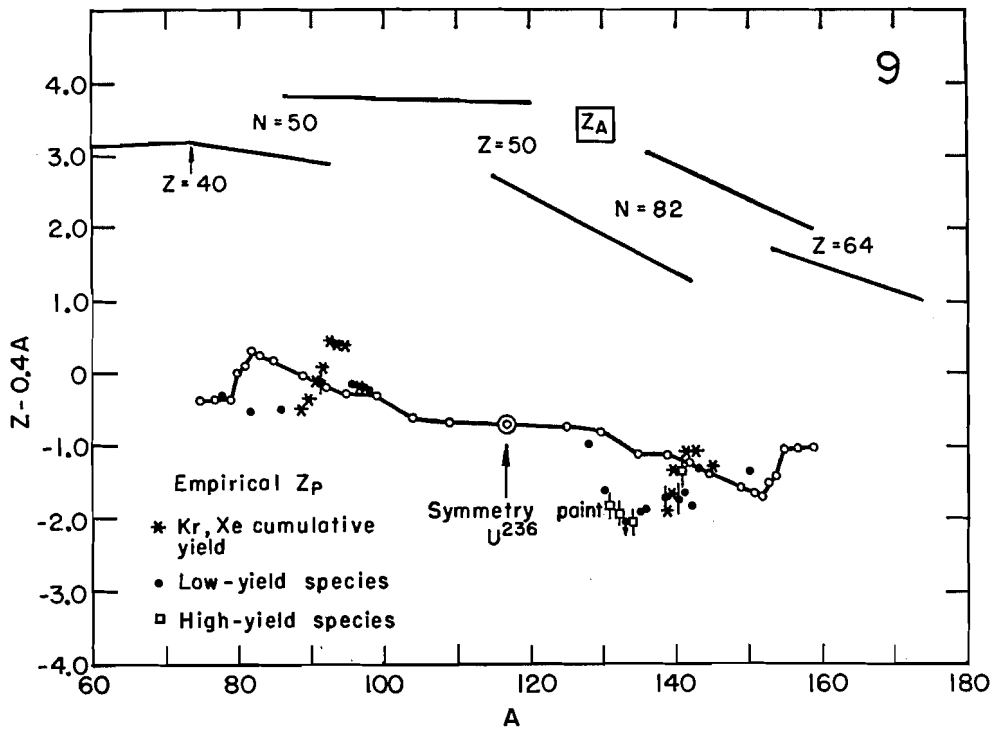


FIG. 7. The function $Z_A - 0.4A$ vs. A and its application to thermal neutron fission of U^{235}.
FIG. 8. Most probable charge Z_P in fission: change with fissile nuclide. Medium energy; $Z_P^{corr} = Z_P - 0.5(Z_C - 92) + 0.19(A_C - 236) - 0.19(\nu_T - 2.5)$.



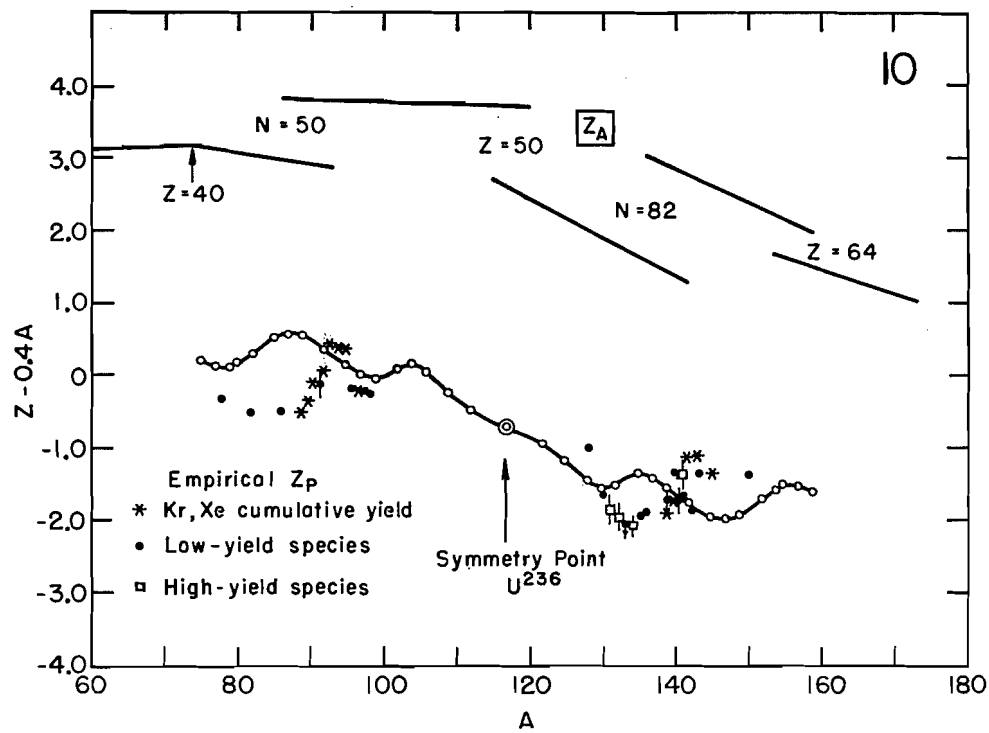


FIG. 9. Most probable charge Z_P in fission: minimum potential energy and Levy mass equation for $U^{235}(n,F)$.

FIG. 10. Most probable charge Z_P in fission: minimum potential energy and Cameron mass equation for $U^{235}(n,F)$.

Can. J. Chem. Downloaded from www.nrcresearchpress.com by 210.87.254.105 on 09/05/12
For personal use only.

Can. J. Chem. Downloaded from www.nrcresearchpress.com by 210.87.254.105 on 09/05/12
For personal use only.

minimum (called Z_0) is hopefully to be identified as Z_P. Swiatecki and Blann (49) computed Z_P by this prescription for maximum excitation energy. They selected the Grummitt and Milton (51) continuous Z_A values and basic B_A values of Green (26) before shell corrections were evaluated (a so-called liquid-drop formula). This odd prescription for Z_P (on graphical correlation with experiment) fits the low-energy data fairly well and agrees rather well with ECD. Part of its promise lies in the fact that it represents fairly well the Z_P function for the high-energy fission of gold with 112-Mev C^{12} ions, Au^{197} ($C_{112}{}^{12}$,F).

The dropping of shell terms from the mass equation (nuclear potential energy) removes all chance of representing fine structure in the Z_P vs. A correlation in low-energy fission. The apparent filling in Fig. 8 of the hollow at $A = 135$ with medium-energy fission (E^* of 20 to 40 Mev) may reflect the decrease in shell effects with increasing excitation, culminating in the Blann success (49) in the 110-Mev region.

The basic idea, however, of maximum excitation computed with shell terms included would seem to be an attractive one for further study. We have explored this in Fig. 9 using the tabulated Levy (27) mass data. Fine structure is present to some degree, principally in the region of highly asymmetric fission, in the opposite direction from the Present prediction (8). In Fig. 10 is given the same type of calculation using the tabulations of the Cameron mass equation (28). The fine structure is quite different. This shows that randomly chosen mass equations differ greatly in predictions of nuclear mass in regions about three to four β-decays from stability.

The parabolas in Fig. 11 emphasize differences between two popular, readily accessible

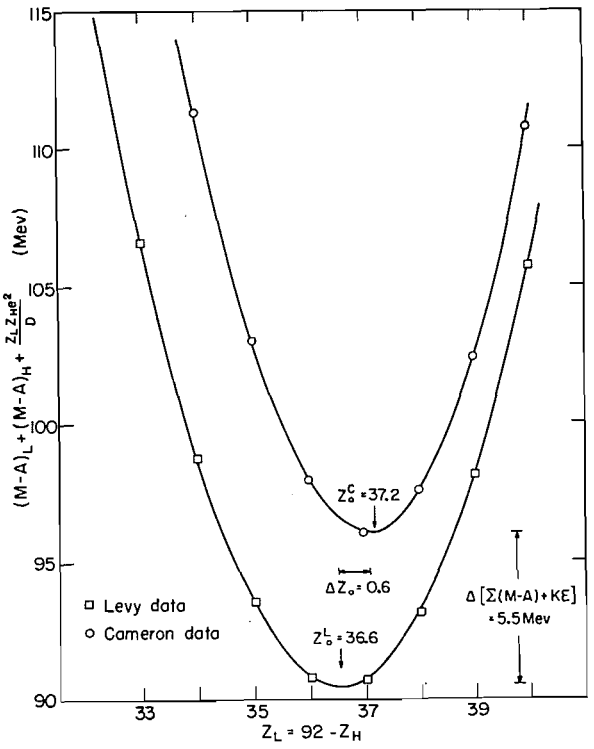


FIG. 11. Swiatecki prescription. Nuclear P.E.+(coulombic P.E. = K.E.) is at minimum for $Z = Z_P$, called Z_0. Prescription largely dependent on mass formula used. Total energy for split $A_L = 93$, $A_H = 143$ (no shell crossing).

mass tabulations for the mass split $A_L = 93$, $A_H = 143$, as from $U^{235}(n_{th},F)$ before prompt neutron emission. This split was chosen to avoid shell effects in the Z_L region near known Z_P. The energy function we wish to minimize is plotted in Fig. 11 against the charge Z_L of the light fragment,

$$[17] \qquad F(P.E.+K.E.) = (M-A)_L+(M-A)_H+\frac{Z_L(92-Z_L)e^2}{D}$$

where value of D is an internuclear distance (53) parameter, larger than $r_0(A_L^{1/3}+A_H^{1/3})$ by about 15% to account for the experimental kinetic energy of 167 Mev (46, 53).

The upper parabolic curve in Fig. 11 is the curve for the Cameron masses (28), with a minimum for eq. [17] at $Z_0 = 37.2$ at about 96 Mev. The lower parabola is that for the Levy masses (27), with a minimum at $Z_0 = 36.6$ at about 90.5 Mev. These two modern mass formulas give results for Z_0 (which we would like to call Z_P) differing by 0.6 charge unit, far beyond the uncertainty of the experimental data. The energy difference between the minima (5.5 Mev) is equally surprising.

It may not be too much to hope that the experimental course of Z_P as a function of A may be used to derive a more reliable mass formula. It will be interesting to see how firm the evidence is for fine structure, and how this relates to mass and nuclear shells, if the principle of maximum excitation (48) is established as a good approximation. These prospects make fission radiochemistry exciting.

ACKNOWLEDGMENTS

We are indeed grateful to Professor Arthur C. Wahl of the Washington University of St. Louis for providing us with the latest information from his group, for advance information on his correlation of Z_P, and for many fruitful discussions. The senior author wishes to express his gratification with the sessions on fission at the very constructive Chalk River Conference on Nuclear Chemistry and Radiochemistry. It was a great help that Atomic Energy of Canada, Ltd., furnished photo-offset preprints of the figures for this paper.

Many other people have given substantial help, especially Drs. John M. Alexander, Glen E. Gordon, Lawrence E. Glendenin, Ellis P. Steinberg, Leo Yaffe, and Nathan Sugarman. We also thank Mrs. Virginia Ekman, Grace Rowe, and Norma Osborne for indispensable aid.

APPENDIX I

Intercomparison of $Z_P(A)$ Values: Z_P^{corr} for 13-day Cs^{136}

Reference to Fig. 8 shows considerable drift in Z_P^{corr}, filling in the hollow around $A = 135$ on moving the type of fission into the medium-energy region. It is interesting to explore this effect, and it is useful to provide the reader with explicit examples of the method of calculating Z_P^{corr} from Z_P values derived either by Wahl's 1958 or 1960 formulas, (32) or (38).

We anticipate the improvement of eq. [16] by the suggestion (see footnote 16) of Butler, and offer the prescription

$$[18] \qquad Z_P^{corr} = Z_P-\tfrac{1}{2}(Z_C-92)+0.21(A_C-236)-0.19\times 0.12(E^*-6.5).$$

We choose $A = 136$, where coherence among the data is poor, but where numerous data on f_I for Cs^{136} are to be found. Typical values are given in Table II.

Can. J. Chem. Downloaded from www.nrcresearchpress.com by 210.87.254.105 on 09/05/12
For personal use only.

TABLE II

Data for fractional chain yield and Z_P for Cs^{136} in various fission types

Type	E^*(Mev)	Fractional chain yield	$Z-Z_P$	Z_P^{corr}	$Z_P^{corr}-0.4A$	Reference
$U^{235}(n_{th},F)$	6.5	$1.\times10^{-2}$	2.42	52.58	−1.82	32
$U^{233}(n_{th},F)$	6.76	0.0181	2.02	52.55	−1.85	39
Cm^{242}(sp.F)	0	0.123	1.50	52.80	−1.60	20
$Pu^{239}(n_{th},F)$	6.38	0.0166	2.03	52.81	−1.59	39
Cf^{252}(sp.F)	0	5.69×10^{-3}	2.18	52.92	−1.48	55
$U^{235}(n_{14},F)$	20.5	0.040	1.87	52.97	−1.43	54
$Th^{232}(d_{13.6},F)$	21.93	0.033	1.91	52.99	−1.41	30
$U^{238}(\alpha_{24},F)$	19.00	0.0292	1.93	53.03	−1.37	14
$U^{235}(\alpha_{24},F)$	18.76	0.2847	0.86	53.48	−0.98	14
$U^{235}(\alpha_{24},F)$	18.76	0.084	1.60	52.74	−1.66	31
$U^{238}(d_{14},F)$	22.10	0.037	1.88	53.09	−1.31	30
$U^{235}(\alpha_{45.7},F)$	40.50	0.4435	0.28	53.55	−0.85	14

The first column gives the type of fission; subscripts for the projectiles denote the projectile energy in million electron volts. The second column gives the excitation energy based on the nuclear masses of Everling *et al.* (52). The third column gives values of the fractional chain yield found by workers cited in the last column. The $Z-Z_P$ values of the fourth column were found by using the Glendenin curve given in Fig. 2, or taken from the literature (5, 19, 20, 32), reading the $Z-Z_P$ abscissa corresponding to the observed $\log f_1$ ordinate. (The Wahl 1960 method (38) should be better (see footnote 14).) The fifth column gives Z_P^{corr}, using the revised eq. [18], which differs but slightly from the eq. [16] used for Fig. 8. The sixth column is $Z_P^{corr}-0.4A$, column five diminished by 54.4, giving values like those plotted in Figs. 3–10.

The data in Table II have been presented in order of increasing Z_P or $Z_P-0.4A$. The low-energy fission data are in fair agreement, although the values seem to rise about 0.3 unit with A going up 16 units to Cf^{252} (spont. F). There is a discrepancy of factor 3.4 between f_1 data of Chu (14) and del Marmol (31) for Cs^{136} in $U^{235}(\alpha_{24},F)$ leading to a difference in Z_P of 0.7. It is hard to see a dependence of A in the medium-energy region, but there may be a dependence on E^*.

As is noted in Fig. 8, the Z_P^{corr} values for say Br^{82} scatter far less than the values around $A = 136$.

APPENDIX II

An Alternative E^* Treatment of ΔZ_P

An alternative to eq. [16] was outlined by Kaplan (56), using an empirical calibration for the effect of excitation energy E^* rather than using eq. [14] to estimate ν_T. He used the energy dependence of Z_P established by Pate, Foster, and Yaffe (57) based on f_1 values of tellurium and iodine isotopes for the reaction $Th^{232}(p,F)$. This gave a term $\delta_2 Z_P(E^*)$ to replace the ν_T term in eq. [16]. This new term is thought to be valid up to $E^* \sim 40$ Mev, since the charge dispersion seems to be independent of E^* for this energy region.

When all available data in the energy region $0 < E^* < 40$ are so treated, average deviations of Z_P^{corr} from a median curve are about ±0.2 charge unit, slightly larger than that from the treatment based on eq. [16] as given above.

Can. J. Chem. Downloaded from www.nrcresearchpress.com by 210.87.254.105 on 09/05/12
For personal use only.

Can. J. Chem. Downloaded from www.nrcresearchpress.com by 210.87.254.105 on 09/05/12
For personal use only.

REFERENCES

1. N. SUGARMAN and A. TURKEVICH. Private communication, 1944.
2. W. RUBINSON. Chicago Report CC-3146. September, 1945; National Nuclear Energy Series. Div. IV, Vol. 9, Paper 314. McGraw-Hill Book Co., New York. 1951.
3. C. D. CORYELL and N. SUGARMAN (*Editors*). Radiochemical studies: the fission products. National Nuclear Energy Series. Div. IV, Vol. 9. McGraw-Hill Book Co., New York. 1951.
4. J. A. WHEELER. Private communication, 1943.
5. L. E. GLENDENIN, R. R. EDWARDS, and C. D. CORYELL. Clinton Laboratory Report CL-LEG-1. July, 1946. L. E. GLENDENIN, C. D. CORYELL, and R. R. EDWARDS. National Nuclear Energy Series. Div. IV, Vol. 9, Paper 52. McGraw-Hill Book Co., New York. 1951.
6. I. HALPERIN. Ann. Rev. Nuclear Sci. **9**, 321 (1959).
7. K. WAY and E. P. WIGNER. Private communication, 1944; Chicago Report CC-3032. June, 1945; Phys. Rev. **73**, 1318 (1948); National Nuclear Energy Series. Div. IV, Vol. 9, Paper 43. McGraw-Hill Book Co., New York. 1951.
8. R. D. PRESENT. Private communication, 1946; Phys. Rev. **72**, 7 (1947).
9. R. H. GOECKERMANN and I. PERLMAN. Phys. Rev. **76**, 628 (1949).
10. W. M. GIBSON. University of California Radiation Laboratory, UCRL-3493. 1956.
11. B. M. FOREMAN. University of California Radiation Laboratory, UCRL-8223. 1958.
12. R. VANDENBOSCH. University of California Radiation Laboratory, UCRL-3858. 1957. R. VANDENBOSCH, T. D. THOMAS, S. E. VANDENBOSCH, R. A. GLASS, and G. T. SEABORG. University of California Radiation Laboratory, UCRL-8032. Revised 1958.
13. R. M. LESSLER. University of California Radiation Laboratory, UCRL-8439. 1958.
14. Y. Y. CHU. University of California Radiation Laboratory, UCRL-8926. 1958.
15. L. J. COLBY. Ph.D. Thesis in Chemistry, Purdue University, Lafayette, Ind. 1960.
16. H. M. BLANN. University of California Radiation Laboratory, UCRL-9190. 1960.
17. B. D. PATE. Can. J. Chem. **36**, 1707 (1958).
18. A. C. PAPPAS. Ph.D. Thesis in Chemistry, University of Oslo, Oslo, Norway. Given as Technical Report No. 63, Massachusetts Institute of Technology Laboratory for Nuclear Science. 1953; also United States Atomic Energy Commission, AECU-2806. 1953.
19. A. C. PAPPAS. Proceedings of the International Conference on the Peaceful Uses of Atomic Energy, 1955. Vol. 7. United Nations, New York. 1956. p. 19.
20. E. P. STEINBERG and L. E. GLENDENIN. Proceedings of the International Conference on the Peaceful Uses of Atomic Energy, 1955. Vol. 7. United Nations, New York. 1956. pp. 3–14, 31–35.
21. N. BOHR and J. A. WHEELER. Phys. Rev. **56**, 426 (1939).
22. L. E. GLENDENIN. Ph.D. Thesis in Chemistry, Massachusetts Institute of Technology, Cambridge, Mass. August, 1949.
23. C. D. CORYELL. Ann. Rev. Nuclear Sci. **2**, 305 (1953).
24. C. D. CORYELL. Lecture Notes for Massachusetts Institute of Technology Course 5.09. October, 1956.
25. R. C. FIX. Ph.D. Thesis in Chemistry, Massachusetts Institute of Technology, Cambridge, Mass. September, 1956.
26. A. E. S. GREEN and N. A. ENGLER. Phys. Rev. **91**, 40 (1953). A. E. S. GREEN and D. F. EDWARDS. Phys. Rev. **91**, 46 (1953). A. E. S. GREEN. Nuclear physics. McGraw-Hill Book Co., New York. 1955. pp. 244–270; Revs. Modern Phys. **30**, 569 (1958).
27. H. B. LEVY. University of California Radiation Laboratory, UCRL-4588 and UCRL-4713 Livermore Laboratory. 1955; Phys. Rev. **106**, 1265 (1957); J. RIDDELL. Numerical tables. Atomic Energy of Canada Ltd. Report AECL-339. 1956.
28. A. G. W. CAMERON. Can. J. Phys. **35**, 1021 (1957); Numerical tables. Atomic Energy of Canada Ltd. Report AECL-433. 1957.
29. C. D. CORYELL. Dedication U.S. Naval Radiological Defense Laboratory, San Francisco, Calif. August, 1957.
30. J. M. ALEXANDER and C. D. CORYELL. Phys. Rev. **108**, 1274 (1957).
31. P. DEL MARMOL. Ph.D. Thesis in Chemistry, Massachusetts Institute of Technology, Cambridge, Mass. January, 1959.
32. A. C. WAHL. J. Inorg. & Nuclear Chem. **6**, 263 (1958).
33. A. C. HERRINGTON. D.Sc. Thesis in Chemical Engineering, Massachusetts Institute of Technology, Cambridge, Mass. 1957.
34. K. WOLFSBERG. Ph.D. Thesis in Chemistry, Washington University, St. Louis, Mo. 1959.
35. D. R. NETHAWAY. Ph.D. Thesis in Chemistry, Washington University, St. Louis, Mo. 1959.
36. R. L. FERGUSON. Ph.D. Thesis in Chemistry, Washington University, St. Louis, Mo. 1959.
37. D. E. TROUTNER. Ph.D. Thesis in Chemistry, Washington University, St. Louis, Mo. 1959.
38. A. C. WAHL. Private communication.
39. S. KATCOFF. Brookhaven National Laboratory Report BNL-4977. 1960; Nucleonics, **16**, No. 4, 78 (1958).
40. I. F. CROALL. Harwell Report AERE-R3209. 1960.
41*a*. A. KJELBERG and A. C. PAPPAS. J. Inorg. & Nuclear Chem. **11**, 173 (1959).
41*b*. Y. Y. CHU. Private communication.
42. S. L. WHETSTONE. Phys. Rev. **114**, 581 (1959).
43. V. V. VLADIMIRSKII. J. Exptl. Theoret. Phys. (U.S.S.R.) **32**, 822 (1957); Soviet Phys. JETP, **5**, 673 (1957).
44. V. F. APALIN, U. P. DOBRYNIN, V. P. ZAKHAROVA, I. E. KUTIKOV, and L. A. MIKAELYAN. Atomnaya Energ. **8**, 15 (1960).

45. T. J. KENNETT and H. G. THODE. Phys. Rev. **103**, 323 (1956).
46. R. B. LEACHMAN. Proceedings of the International Conference on the Peaceful Uses of Atomic Energy, Geneva. Vol. 15. United Nations, Geneva, 1958. p. 229. (cf. Fig. 17); Phys. Rev. **101**, 1005 (1956).
47. E. YELLIN. Ph.D. Thesis in Chemistry, Massachusetts Institute of Technology, Cambridge, Mass. June, 1960.
48. W. SWIATECKI. Private communication.
49. H. M. BLANN. University of California Radiation Laboratory, UCRL-9190. 1960.
50. P. FONG. Phys. Rev. **102**, 434 (1956).
51. W. E. GRUMMITT and G. M. MILTON. J. Inorg. & Nuclear Chem. **5**, 93 (1957).
52. F. EVERLING, L. A. KÖNIG, J. H. E. MATTAUCH, and H. A. WAPSTRA. Nuclear Phys. **18**, 529 (1960).
53. E. K. HYDE. University of California Radiation Laboratory, UCRL-9036. 1960.
54. G. P. FORD. Report AECD-3597. 1952.
55. W. E. NERVIK and P. C. STEVENSON. *Quoted in* ref. 53, p. 169.
56. M. KAPLAN. Ph.D. Thesis in Chemistry, Massachusetts Institute of Technology, Cambridge, Mass. January, 1960.
57. B. D. PATE, J. S. FOSTER, and L. YAFFE. Can. J. Chem. **36**, 1691 (1958).
58. A. C. WAHL. Phys. Rev. **99**, 730 (1955).

Can. J. Chem. Downloaded from www.nrcresearchpress.com by 210.87.254.105 on 09/05/12
For personal use only.

Can. J. Chem. Downloaded from www.nrcresearchpress.com by 210.87.254.105 on 09/05/12
For personal use only.

THE ATTACHMENT OF INERT GASES TO POWDERS FOLLOWING (n,γ) EVENTS[1]

ROGER KELLY

ABSTRACT

It has been found that, when argon, krypton, and xenon are irradiated with neutrons in the presence of various powders, a portion of the inert-gas activity becomes "attached" to the powder. The attached activity was shown to be highly enriched, and to be distinguishable from adsorbed activity. Expressing the attachment in terms of the *attachment efficiency*, $A \equiv$ (inert-gas activity attached to target)/(total inert-gas activity), it was found that A was independent of irradiation time and neutron flux, and for fine powders was also independent of pressure between 0.7 and 700 mm. The use of a very coarse powder or no powder at all led to a decrease in A, on the basis of which it was estimated that the maximum distance from a surface that attached activity can originate is about 200 mean free paths. The following miscellaneous relations were observed to hold: (i) $A \ll 1$, (ii) $A_{Ar} > A_{Kr} > A_{Xe}$, (iii) $A_{oxide} > A_{metal}$ (approximate). The results were in general consistent with a mechanism of attachment based on electrical attraction: inert-gas atoms first acquire a high charge due to vacancy cascades initiated by the conversion of capture gamma rays; they then wander about, and, upon approaching a solid surface, are accelerated electrically into it.

In accordance with I.U.P.A.C. recommendations (1), the symbol "Ar" has been used for argon. In addition, left superscripts are used for mass numbers, thus leaving the right superscript position free for indicating ionic charge (cf. equations [4]).

The chemical effects of beta and gamma emission from radioactive atoms have been studied from several points of view. Most of the work has been done on the breaking of chemical bonds due either to the recoil of the emitting atom or to the state of charge acquired by the emitting atom (2). A limited amount of work on "release"[2] effects has also been described; for example, Yosim and Davies (4) have considered the release of ^{116}In and ^{198}Au from the surfaces of the metal lattices following (n,γ) events, while, in a related study, Baulch and Duncan (5) observed the release of ^{212}Bi from PbO and Pb_3O_4 following the beta decay of adsorbed ^{212}Pb. Complementary to the release work is that in which the "attachment"[2] of the products of beta or gamma emission to a target is studied. Species with which attachment studies have been made include: (i) metal atoms released from a metal film which is being irradiated with neutrons (4, 6), (ii) atomic bromine and iodine formed in neutron-irradiated ethyl bromide and iodide (7), and (iii) atomic tellurium formed in the decay of gaseous $^{127m}Te(C_2H_5)_2$ and $^{129m}Te(C_2H_5)_2$ (8).

The present work was concerned with attachment, in particular attachment following (n,γ) events in the inert gases. It was anticipated that the use of inert gases would yield information not obtainable with more reactive substances, such as were used in references 4, 6, 7, and 8. The reason is the difference in exchangeability. Material which becomes attached to a target in connection with (n,γ) events (e.g. ^{198}Au) will at first contain a smaller proportion of the parent isotopes (e.g. ^{197}Au) than does the unattached material; i.e. it will be *isotopically enriched* in the products of the (n,γ) event. With a reactive substance, the enrichment will tend to persist regardless of whether the attachment is

[1]*Manuscript received November 3, 1960.*
Contribution from the Development Chemistry Branch, Atomic Energy of Canada Limited, Chalk River, Ontario. Presented at the Third Symposium on Nuclear Chemistry and Radiochemistry, held at Atomic Energy of Canada Limited, Chalk River, Ontario, September 6–8, 1960.
Issued as A.E.C.L. No. 1165.

[2]*The terms "release" and "attachment" are used in preference to "emanation" and "penetration" since they are more general. For example, "emanation" is usually applied strictly to the release of inert gases (3).*

due to penetration into the lattice of the target or simply to surficial adsorption or reaction, for the chemical or physical differences between the attached and unattached material will inhibit exchange. In other words, the details of the attachment will be obscured. With substances which are simultaneously *unreactive*, *monatomic*, and *gaseous*, on the other hand, it is likely that enrichment will persist only under conditions of penetrative attachment. A distinction between penetrative and surficial attachment is then possible, and the mechanism of the attachment can be developed in detail.

The method used was quite simple. Inert gases were irradiated with neutrons in the presence of fine powders, and the distribution of inert-gas activity between the gas phase and the powder was then determined.

EXPERIMENTAL

For each experiment, a capsule was made from thin-walled quartz tubing having an I.D. of about 0.47 cm. The capsule was filled to a depth of between 2.5 and 3 cm with a given powder, drawn down close above the surface of the powder, and attached to a vacuum system with black wax. The inert gas (argon, krypton, or xenon) was now added, and the capsule was sealed off by applying a flame to the drawn portion.

After irradiation in a thermal neutron flux of between 2 and 27×10^{12} neutrons cm^{-2} sec^{-1} for a period of about 12 hours, the capsule was loaded into the "sample holder" as shown in Fig. 1A, and the sample holder was evacuated to about 40 mm. The capsule was cracked open by lifting a nail magnetically and dropping it, the residual air helping to prevent dispersal of the powder. The gases in the sample holder, including that portion of the inert-gas activity still remaining in the gas phase, were led to a trap containing activated charcoal and cooled with liquid nitrogen, henceforth called the "counting trap" (Fig. 1B). The unattached activity was now measured with a single-channel gamma counter. (The presence of activated charcoal was found to be essential for a quantitative collection of inert-gas activities. Thus, without charcoal, xenon activity was lost at the rate of 18% per hour when the counting trap was pumped upon, and the other activities were lost even more rapidly.)

After no further activity could be drawn from the sample holder, the counting trap was freed from activity. With argon and krypton this was accomplished simply by heating the trap with a carbonizing flame, though the charcoal generally had to be changed to eliminate the last traces of xenon activity. A furnace (F in Fig. 1A) was now drawn up over the bottom of the sample holder and the latter was heated, first to about 200° C to confirm that the powder was truly free of *unattached* activity, and then to about 1000° C to remove the *attached* activity. The adequacy of a temperature of 1000° C in removing attached activity was demonstrated by the fact that there was no appreciable release of activity when powder, previously heated to 700° C, was (i) heated to 1000° C (cf. Fig. 2) or (ii) dissolved in a suitable acid or flux.

Several points concerning the counting techniques require comment. With the irradiation and decay times used, the only readily countable isotopes were ^{41}Ar (1.83 hours), ^{85m}Kr (4.4 hours), and ^{125}Xe (18 hours), though ^{133}Xe (5.27 days) was easily distinguished after the shorter-lived ^{125}Xe had decayed for several days. While ^{135}Xe (9.2 hours) was presumably also present, the photopeak could not be resolved from the larger ^{125}Xe photopeak. Activities were expressed in terms of the integrated count, less background, in the region of the photopeak. It was not necessary to consider absolute counting rates, since ratios of activities were used. Resolving-time errors in high activities and background errors in low activities were minimized by the appropriate positioning of the

Can. J. Chem. Downloaded from www.nrcresearchpress.com by 210.87.254.105 on 09/05/12
For personal use only.

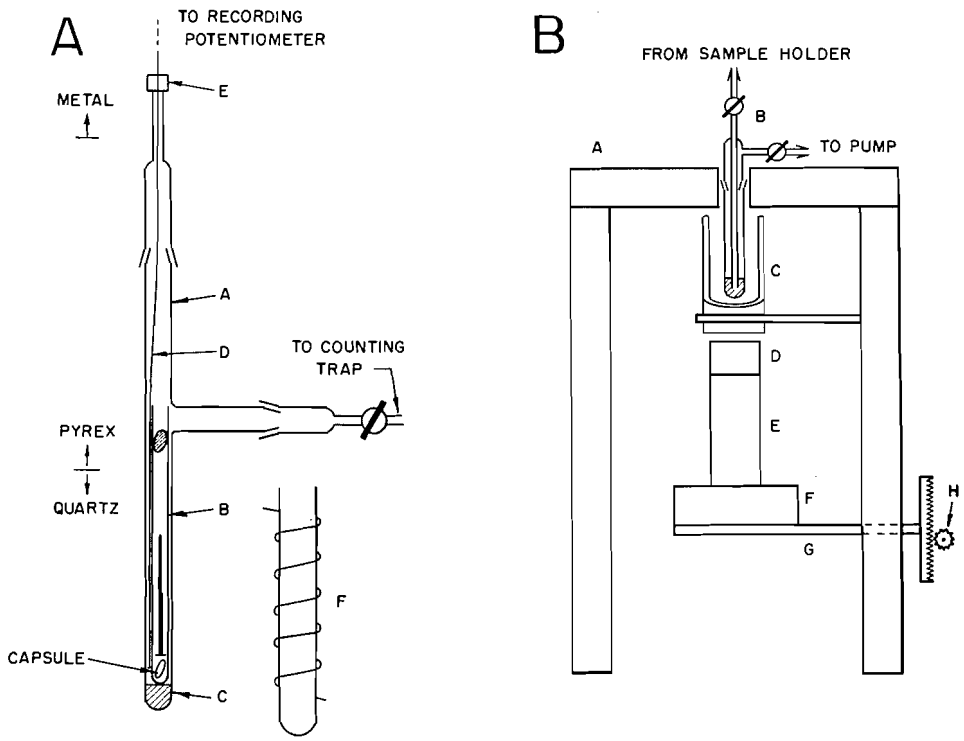


FIG. 1.
(A) The "sample holder". A = body of sample holder. B = disposable quartz tube. The tube is shown loaded with a capsule, a nail, and a wad of Pyrex wool. C = powdered SiO_2 to protect the bottom of A. D = thermocouple wires. E = assembly for admitting the thermocouple wires. The assembly consists of a perforated Teflon plug which can be shrunk around the wires by means of a suitably shaped brass fitting, the latter being soldered to the copper portion of a tubular "Housekeeper" seal. F = furnace. The temperature of the furnace was regulated by feeding the output of a thermocouple (*not* D) located outside A into a Minneapolis-Honeywell "Pulse Pyrovane" controller.

(B) System for trapping and counting (drawn to 2/3 the scale used in (A)). A = lead castle with lid split into two parts such that one part can be slid aside. The inside of the castle, including the lid, is lined with 0.15 cm of cadmium and 0.051 cm of copper. B = counting trap containing activated charcoal. C = Dewar for liquid nitrogen. D = 2-in. NaI(Tl) scintillation crystal. E = photomultiplier. F = preamplifier. G = supporting piece which extends through a vertical slit in the castle wall and bears a 14-cm rack at the end. H = pinion to move rack and thence scintillation crystal. The counting rate could be varied by a factor of 7.7 according to the position of the crystal.

scintillation crystal using the elevating mechanism shown in Fig. 1B (G and H). Errors due to the unreproducible dispersion of activity throughout the charcoal of the counting trap amounted to about $\pm 10\%$ for high crystal positions. Occasional experiments were ruined due to the attached activity being increased by krypton and xenon activities formed by the fission of uranium impurities. (The possible presence of fission activities was indicated whenever the integrated count *above* the photopeak was excessive.)

RESULTS

It soon became apparent in the course of the experiments that when the inert gases argon, krypton, and xenon were irradiated with neutrons in the presence of a powder, a portion of the inert-gas activity became attached to the powder.

Can. J. Chem. Downloaded from www.nrcresearchpress.com by 210.87.254.105 on 09/05/12
For personal use only.

Can. J. Chem. Downloaded from www.nrcresearchpress.com by 210.87.254.105 on 09/05/12
For personal use only.

Enrichment

The activities attached to the powders were shown to be highly enriched in the products of the (n,γ) reactions. A Xe–TiO_2 mixture was irradiated with neutrons, the xenon activity attached to the TiO_2 was released at 1000° C, and the ^{125}Xe was counted. The activity was then transferred to a quartz capsule containing a small amount of charcoal, allowed to decay for several weeks, and finally reirradiated under conditions similar to those of the original irradiation. It was found that the amount of gaseous activity with gamma energies in the region of the ^{125}Xe photopeak was now only 2 to 3% of the original attached activity. The experiment was done in duplicate.

Release of Attached Activity

Attached activity was shown to be released much less readily than adsorbed activity. Thus, activity which had become attached to a powder did not come off at a measurable rate until the powder was heated, a temperature of between 600 and 700° C being necessary to drive off 95% of the activity (Fig. 2). By contrast, activity which had been frozen down with liquid nitrogen to a glass or charcoal surface, i.e. to either an empty trap or a trap filled with activated charcoal, was 95% released within a few minutes after the coolant was removed (Fig. 3). Note how the rate of release was independent of whether or not the activity was enriched. The 8-minute induction period observed in the release of activity from charcoal presumably represents the time required for the charcoal to warm up.

The characteristic plateaus observed in the release of attached activity (Fig. 2) are evidently not an idiosyncrasy of the system Xe–TiO_2, for similar plateaus were observed in the release of argon from TiO_2 and xenon from silver.

Time and Flux Variation

Before considering further results, it is convenient to define the *attachment efficiency*,

$$[1] \qquad A \equiv \frac{(\text{inert-gas activity attached to target})}{(\text{total inert-gas activity})}.$$

The results given in Tables I and II show that A is independent of irradiation time

TABLE I

Effect on A of variation in irradiation time

System*	Time (hours)	A (equation [1])
Ar–Al	2	.019
Ar–Al	6	.014
Ar–Al	110	.021
Xe–Al	2	.010
Xe–Al	27	.0088
Xe–Al	110	.0095

*Inert gas at about 700 mm.

and neutron flux, at least for the times and fluxes used. In addition, A is unaffected by an increase in the proportion of fast neutrons (Table II, fifth line).

Variation in Pressure and Particle Size

The attachment efficiency, A, was found to be independent of pressure using a fine powder, but to vary in an inverse manner with pressure when a very coarse powder or no powder at all was used. Thus, referring to Table III, it is seen that the values of A

TABLE II

Effect on A of variation in neutron flux

System*	Position†	Approximate neutron flux (neutrons cm^{-2} $sec^{-1} \times 10^{-12}$)	A (equation [1])
Ar–TiO_2	S-15-1	2	.16, .16
Ar–TiO_2	S-15-3	6	.16
Ar–TiO_2	S-3-5	13	.10, .12, .12
Ar–TiO_2	NRU-J	27	.13
Xe–TiO_2	S-15-3+Cd	0.7	.020, .025
Xe–TiO_2	S-15-3	6	.016, .017
Xe–TiO_2	S-9-5	17	.016, .016, .017 .019, .025

*Inert gas at about 700 mm.
†Positions with designations such as "S-15-1" refer to the "self-serve" facility of the Chalk River NRX reactor. The position "NRU-J" refers to the "self-serve J-rod" of the Chalk River NRU reactor. The designation "+Cd" means that the sample was wrapped in 0.038 cm of cadmium to reduce the thermal neutron flux.

TABLE III

Effect on A of variation in pressure and particle size

Solid	Dimensions of solid (microns)	Pressure (mm)	A* (using Ar)	A (using Kr)	A* (using Xe)
TiO_2	<10	700	.14†	.026, .031 .036, .043	.019†
TiO_2	<10	70	.18, .18	.042	.014, .019, .025
TiO_2	<10	7	$.1_5$		
TiO_2	<10	0.7	$.1_3$		
Al	590–840 (i.e. 20–30 mesh)	700	.0035, .0037		
Al	590–840	70	.014, .021, $.02_5$		
Al	<10	700	.018†		
Empty quartz capsule	4700 (I.D.)	700	$.0002_9$, $.0005_3$		$.0001_3$, 0001_7 $.0003_1$
Empty quartz capsule	4700 (I.D.)	72			$.0006_1$, $.0008_8$
Empty quartz capsule	4700 (I.D.)	11			$.008_5$
Empty quartz capsule	4700 (I.D.)	7.6			$.01_1$
SiO_2 powder	<75	700	.055, .057		.014, .023, .026
Crushed quartz tubing	Indefinite	7			$.02_6$

*Whenever the attached activity was very low (<2000 counts min^{-1}), and the value of A therefore uncertain, the second figure of A is written as a subscript.
†Mean value based on data given in Tables I and II.

for systems involving $<10\ \mu$ TiO_2 were essentially the same whether the inert gas was at 700 or 70 mm (or even at a lower pressure in the case of the system Ar–TiO_2). On the other hand, with 590–840 μ aluminum, A increased by a factor of 5 when the pressure was lowered from 700 to 70 mm. The value of A observed at the lower pressure was evidently the limiting value, since it agrees with the value obtained with $<10\ \mu$ aluminum. To further demonstrate the effect of using a coarse powder, inert gases were irradiated in the usual quartz capsules *but without any powder present.* A was now exceedingly low at 700 mm, though it increased rapidly as pressure was decreased. The values of A obtained with powdered SiO_2 or crushed quartz tubing presumably represent the limits

Can. J. Chem. Downloaded from www.nrcresearchpress.com by 210.87.254.105 on 09/05/12
For personal use only.

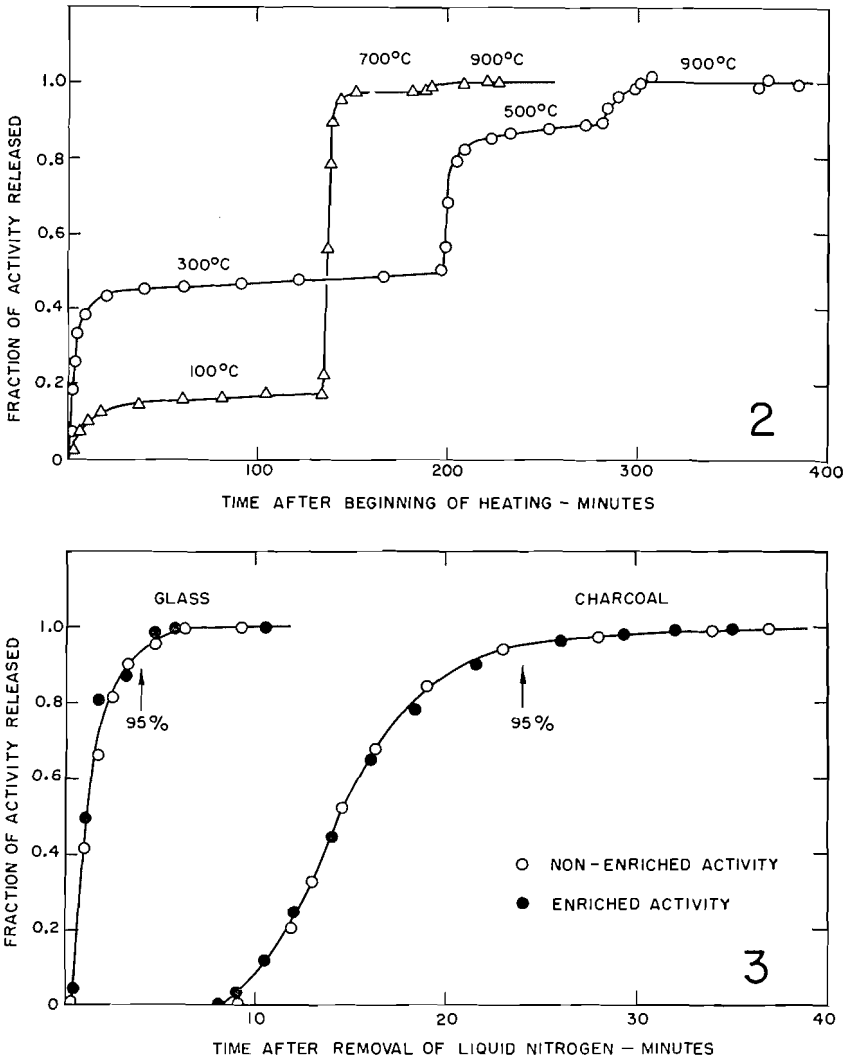


FIG. 2. Release of ^{125}Xe activity which has become attached to TiO_2. Two typical experiments out of a total of 11 are shown. In each experiment the temperature was raised rapidly (i.e. within 2 to 3 minutes) to a given value, was held constant until a well-defined plateau was reached, and was then raised to the next value indicated.

FIG. 3. Release of ^{125}Xe activity from glass and charcoal surfaces. The activity was frozen down to the surfaces at liquid-nitrogen temperature, and at zero time the liquid nitrogen was removed. The enriched activity was obtained by driving attached activity out of silicon.

of the increase. (The possibility that the small activities attached to the quartz capsules were due to ^{135}Xe formed by the fission of uranium impurities was tentatively eliminated in blank experiments, i.e. by irradiating evacuated quartz capsules.)

The "Collection Distance"

The results of the experiments on pressure and particle-size variation will be more suited for subsequent discussion if they are expressed in terms of the "collection distance", i.e. the apparent maximum distance from which attached activity can originate. Consider the empty-quartz-capsule experiments. The capsules were cylinders with an

Can. J. Chem. Downloaded from www.nrcresearchpress.com by 210.87.254.105 on 09/05/12
For personal use only.

I.D. ($2r$) of 0.47 cm and a length (l) of about 2.5 cm. Assuming that one half of the activity in a layer the thickness of the collection distance (d) will reach the capsule in an attachable state, then

$$[2] \qquad A_{\text{observed}} = \left(\frac{A_0}{2}\right)\left(\frac{2\pi rld + 2\pi r^2 d}{\pi r^2 l}\right),$$

where A_0 is the attachment efficiency under conditions when the limiting value is observed, i.e. using a fine powder. Interpreting the experimental data (Table III) in terms of equation [2], one obtains $d = 16\ \mu$ for argon at 700 mm and $d = 15\ \mu$ for xenon at 700 mm. (The figure for xenon represents the mean of all relevant experiments, with A corrected to 700 mm where necessary.) A collection distance is less readily derived from the powder experiments in Table III, since it is difficult to define the pore spacing in a loosely packed powder. However, assuming that the spacing is comparable to the grain size, it follows that $d > 10\ \mu$ (i.e. there was *no* pressure effect with $<10\ \mu$ TiO_2), $d < 590$–$840\ \mu$ (i.e. there *was* a pressure effect with 590–840 μ aluminum).

The mean free path at 700 mm is 0.11 μ in argon, 0.07 μ in xenon. The values obtained for the collection distance are therefore about 200 times larger than the mean free paths.

Trends among the Different Gases and Powders

The values of A for a number of different systems involving argon and xenon are given in Table IV; data for the system Kr–TiO_2 were included in Table III. In assessing these results, it should be noted that the experimental variables had values such that A will be largely unaffected (i) by differences in irradiation time, neutron flux, pressure, and particle size, or (ii) by activity attached to the quartz capsule or formed from uranium impurities in the quartz. Any trends among the different systems should therefore be real.

The most obvious trends are the following:

(i) $A \ll 1$. Thus for systems involving argon, A generally lies between 0.011 and 0.14; when xenon is used, the range is 0.0025 to 0.026.

(ii) $A_{\text{Ar}} > A_{\text{Xe}}$. Judging from the one system in which krypton was used, this relation can likely be extended to $A_{\text{Ar}} > A_{\text{Kr}} > A_{\text{Xe}}$.

(iii) $A_{\text{oxide}} > A_{\text{metal}}$. There is a fair number of exceptions to this trend.

(iv) Considering just the systems involving elemental solids, it appears that A does *not* vary systematically with the atomic weight of the solid.

DISCUSSION

It has been found that, when the inert gases argon, krypton, and xenon are irradiated with neutrons in the presence of various powders, a portion of the inert-gas activity becomes attached to the powder. A number of empirical characteristics of the attachment has already been considered, and it remains only to discuss certain general matters.

Mechanism of Attachment

It was pointed out in the introductory section that material which becomes attached to a target in connection with (n,γ) events will, at the moment of attachment, be isotopically enriched in the products of the (n,γ) event. However, if the attached material is an inert gas, the enrichment will persist only if the attachment is penetrative, as distinct from surficial. The high degree of enrichment observed in the present work therefore points to attachment which (i) is due to (n,γ) events, and (ii) is penetrative. Penetrative attachment is also suggested by the fact that the attached activity was released much less readily than adsorbed activity.

Can. J. Chem. Downloaded from www.nrcresearchpress.com by 210.87.254.105 on 09/05/12
For personal use only.

TABLE IV

Values of A for various systems involving argon and xenon*

Solid	Atomic weight of solid	A (using Ar)	A (using Xe)
B	11	$\{.002_3, .0024 = .002_9, .0045$	.0043, .0089
C (diamond)	12	.012	
C (graphite)	12	.054, .063	
Al	27	.018†	‖.0095†
Al_2O_3		.037, .041	‖.0033, .0039
Al_2O_3 (hydrated)		.032	
Si	28	.032, .033	.012, .018
SiO_2		.055, .057	.014, .023, .026
CaF_2		.052	
Ti	48	.022, .034	.0027, .0044
TiO_2		.14†	.019†
V_2O_5		.050, .069	
Fe	56	‖.045, .076	
Fe_2O_3		‖.036	
Co	59	.027	
Ni	59	.011, .012	
Ni_2O_3		.064	
Zn	65	.027	
Se	79	.0035, $.009_1$	
Nb	93	.014	.0080
Nb_2O_5		.14	.018
Rh	103	.019	
Ag	108	‖$.003_4$, .0053	‖.0025, .0033
Ag_2O		‖$.001_1$	‖.0004, .0007
Sn	119	.021	.0026
Ta	181	.029	
Pb	207	.018	‖.0028
PbO		.079	‖.0031
PbF_2		.014	

NOTE: Pairs of systems which are exceptions to the trends $A_{Ar} > A_{Xe}$ and $A_{oxide} > A_{metal}$ are indicated with double lines.

*The inert gas was always at about 700 mm. The powders generally had assorted grain sizes ranging up to about 75 μ, though in certain cases the grains were consistently smaller than 10 μ (C-graphite, Al, TiO_2, Co, Se, and Rh). In one case (Al_2O_3), the grains were consistently coarse. See also footnote * of Table III.

†Mean value based on data given in Tables I and II.

At least two mechanisms can be envisaged by which penetrative attachment could come about following (n,γ) events. According to what may be called the "recoil mechanism", the emission of the capture gamma rays might cause the capturing atoms to recoil directly into the target. Gamma-recoil energies are given by

$$[3] \qquad E_{recoil} = 536E_\gamma^2/M,$$

where E_{recoil} is in electron volts, E_γ in million electron volts, and M in atomic mass units. The recoil energies thus vary in the right direction to explain the trend $A_{Ar} > A_{Kr} > A_{Xe}$. Consider, however, the actual values of E_{recoil}. Assuming capture gamma energies of 4 Mev (there is nothing published on the capture spectra of the inert gases), E_{recoil} works out to about 210 ev for argon and 70 ev for xenon. Energies this low would probably

Can. J. Chem. Downloaded from www.nrcresearchpress.com by 210.87.254.105 on 09/05/12
For personal use only.

be degraded below the level at which penetration is possible within a few collisions.[3] Accordingly, it appears that a recoil mechanism would *by itself* be quite incompatible with the experiments on pressure and particle-size variation, for, as has been shown, these experiments require that attached activity be able to originate from a distance about 200 times larger than the mean free path.

An alternative mechanism of penetration is the "attraction mechanism", which is based on the electrical attraction between charged inert-gas atoms and solid surfaces. Atoms undergoing (n,γ) reactions not only gain recoil energy (equation [3]), but may also become highly charged. The charge is acquired due to the twofold effect of inner electrons being expelled by the conversion of capture gamma rays (7, 10), plus the vacancy-cascade process which occurs whenever there is an inner electron vacancy and in which still further electrons are expelled ("Auger electrons"). Thus, the conversion of a single inner electron has been observed to lead to mean charges of +4.3 for argon (11)[4] and +8 for krypton and xenon (12, 13). The steps leading to the build-up of charge are summarized in equations [4]:

$$[4] \qquad \begin{cases} n + {}^{124}\mathrm{Xe} \rightarrow {}^{125*}\mathrm{Xe} \rightarrow \begin{cases} {}^{125}\mathrm{Xe} + m\gamma \\ {}^{125}\mathrm{Xe}^{+} + (m-1)\gamma + \mathrm{e}^{-} \end{cases} \\ {}^{125}\mathrm{Xe}^{+} \rightarrow {}^{125}\mathrm{Xe}^{(p+1)+} + p\mathrm{e}^{-}, \end{cases}$$

where m is a number between 1 and 6 (14), and p is a number between 0 and about 20 (13). Suppose that the charged atoms escaped neutralization in the gas phase for a sufficient number of collisions that they finally found themselves in the vicinity of a solid surface. Then, *regardless of whether or not recoil energy was still present*, they would be accelerated electrically towards the surface. The acceleration might come about in several ways: (i) electric-image attraction, (ii) attraction between the charged atoms and their separated electrons (the latter would presumably accumulate on surfaces), or (iii) attraction between the charged atoms and electrons formed as a result of the passage of pile gamma rays through the sample. The acceleration would continue until, at a distance of a few angstroms from the surface, the atoms would probably lose their charge due to electron transitions (15). The neutral atoms would then coast the remaining distance to the surface, and, provided sufficient energy had been gained, might penetrate.

The main requirement of the attraction mechanism is seen to be that the charged atoms formed in the (n,γ) events must escape neutralization in the gas phase; in other words, the charge-exchange cross sections must be small. While the cross sections for charge exchange between ions and the corresponding neutral species have, unfortunately, not been studied beyond charges of +3 (16), there is reason to believe that they become exceedingly small with increasing charge.[5] The attraction mechanism is therefore more nearly compatible than the recoil mechanism with the large values observed for the collection distance.

On the other hand, the attraction mechanism has several weaknesses. The extent to which the capture gamma rays are converted may be very low in the nuclides with which the present work is concerned. Also, the trend $A_{\mathrm{Ar}} > A_{\mathrm{Kr}} > A_{\mathrm{Xe}}$ is the reverse to what might be expected: (i) the nuclear-level density increases with mass (17, p.

[3]*The minimum energy at which penetration can occur is perhaps to be identified with the displacement energy,* E_d. *The value of* E_d *is about 25 ev (9).*

[4]*It was shown in the work of reference 11 that the* ^{37}Cl *atoms formed by* electron capture *in* ^{37}Ar *have a mean charge of 3.3. Other things being equal,* conversion *in argon would accordingly lead to a mean charge of 4.3.*

[5]*This view was expressed by Dr. J. B. Hasted (University College, London, England) in a private communication. Further discussion of charge exchange will be postponed for a subsequent paper.*

Can. J. Chem. Downloaded from www.nrcresearchpress.com by 210.87.254.105 on 09/05/12
For personal use only.

406), so that heavy atoms should have a greater number of low-energy capture gamma rays than light atoms (conversion coefficients vary inversely with gamma energy (17, p. 222)); (ii) the conversion coefficients at a given gamma energy increase with atomic number (17, p. 223); (iii) the charge produced in vacancy cascades is greater for krypton and xenon than for argon (11, 12, 13). A more detailed discussion of the attraction mechanism will be possible when work currently underway at this laboratory on the capture spectra of the inert gases is completed.

The observation that A is independent of time and flux is compatible with either of the mechanisms that has been considered, for it implies simply that the rate of attachment is independent of time and directly dependent on flux. It is conceivable, however, that for very large values of (time)$\times$(flux) the rate of attachment, and thence A, will decrease to zero due to the surfaces of the powder becoming saturated.

Sample Heating

If a powder became heated to much over 200° C while under irradiation, the penetrated inert gas would be partially released (cf. Fig. 2). That sample heating is not ordinarily important is shown both by the fact that A is independent of neutron flux when TiO_2 is used, and the fact that the selenium and tin did not melt. On the other hand, sample heating might well account for the unusually low values of A in systems involving boron, silver, and Ag_2O. Boron will heat up owing to the prominent (n,α) reaction in ^{10}B, and silver and Ag_2O owing to the high cross sections with which the short-lived beta emitters ^{108}Ag and ^{110}Ag are formed. Similarly, the fact that three of the six exceptions to the trends $A_{Ar} > A_{Xe}$ and $A_{oxide} > A_{metal}$ are associated with boron, silver, and Ag_2O may be due to non-uniformity in the effects of sample heating among different systems. (Rhodium should also heat up, though the value of A for the system Ar–Rh appears to be normal.)

Enrichment and Storage of Activity

It is difficult to see how bond-breaking or release effects could be applied to enriching inert-gas activities. The present work indicates that *attachment*, on the other hand, is quite effective in bringing about enrichment with the inert gases. An attachment technique has the added advantage that the enriched activity is in a form convenient for handling or storing. (Compare the method of introducing ^{85}Kr into clathrate compounds (18).)

The possibility of using attachment for enriching activities with substances other than the inert gases was previously suggested by Magnusson (6), who succeeded in applying an attachment technique to gold.

ACKNOWLEDGMENTS

The writer wishes to acknowledge the contributions to the present work made by Drs. J. A. Davies and W. H. Stevens, who assisted in the interpretation of the results. The method of sealing thermocouple wires shown in Fig. 1A (E) was devised by Mr. V. T. Buckley, and the latter also helped design the castle and elevating mechanism.

REFERENCES

1. INTERNATIONAL UNION OF PURE AND APPLIED CHEMISTRY. Nomenclature of inorganic compounds. Butterworths Publications Ltd., London. 1959.
2. J. W. BARNES, W. H. BURGUS, and J. A. MISKEL. *In* Radioactivity applied to chemistry. *Edited by* A. C. WAHL and N. A. BONNER. John Wiley & Sons, Inc., New York. 1951.
3. A. C. WAHL. *In* Radioactivity applied to chemistry. *Edited by* A. C. WAHL and N. A. BONNER. John Wiley & Sons, Inc., New York. 1951.
4. S. YOSIM and T. H. DAVIES. J. Phys. Chem. **56**, 599 (1952).

Can. J. Chem. Downloaded from www.nrcresearchpress.com by 210.87.254.105 on 09/05/12
For personal use only.

5. D. L. BAULCH and J. F. DUNCAN. Proceedings of the Second United Nations International Conference on the Peaceful Uses of Atomic Energy. Vol. 29. United Nations, Geneva, 1958. p. 400.
6. L. B. MAGNUSSON. Phys. Rev. **81**, 285 (1951).
7. S. WEXLER and T. H. DAVIES. J. Chem. Phys. **20**, 1688 (1952).
8. G. T. SEABORG, G. FRIEDLAENDER, and J. W. KENNEDY. J. Am. Chem. Soc. **62**, 1309 (1940).
9. G. J. DIENES. Proceedings of the First United Nations International Conference on the Peaceful Uses of Atomic Energy. Vol. 7. United Nations, New York, 1956. p. 634.
10. C. T. HIBDON and C. O. MUEHLHAUSE. Phys. Rev. **88**, 943 (1952).
11. A. H. SNELL and F. PLEASONTON. Phys. Rev. **100**, 1396 (1955).
12. S. WEXLER. Phys. Rev. **93**, 182 (1954).
13. F. PLEASONTON and A. H. SNELL. Proc. Roy. Soc. (London), A, **241**, 141 (1957).
14. C. O. MUEHLHAUSE. Phys. Rev. **79**, 277 (1950).
15. L. J. VARNERIN. Phys. Rev. **91**, 859 (1953).
16. I. P. FLAKS and L. G. FILIPPENKO. Soviet Phys.—Tech. Phys. **4**, 1005 (1960).
17. R. D. EVANS. The atomic nucleus. McGraw-Hill Book Co., Inc., New York. 1955.
18. D. J. CHLECK and C. A. ZIEGLER. Intern. J. Appl. Radiation and Isotopes, **7**, 141 (1959).

Can. J. Chem. Downloaded from www.nrcresearchpress.com by 210.87.254.105 on 09/05/12
For personal use only.

Can. J. Chem. Downloaded from www.nrcresearchpress.com by 210.87.254.105 on 09/05/12
For personal use only.

HALF-LIVES OF Rb^{94}, Sr^{94}, Y^{94}, Rb^{95}, Sr^{95}, Y^{95} [1]

K. FRITZE, T. J. KENNETT, AND W. V. PRESTWICH[2]

ABSTRACT

The existence of a new rubidium isotope, Rb^{94}, has been established and its half-life measured. The half-life of this fission product was determined using the technique of timed precipitations. The value obtained for Rb^{94} was 2.9 ± 0.3 seconds. With this same technique only an upper limit of 2.5 seconds could be assigned to Rb^{95}. The half-lives of the strontium and yttrium daughters were also determined. The strontium isotopes were studied both by timed precipitations and direct measurements. The half-lives of Sr^{94} and Sr^{95} were found to be 1.36 ± 0.06 minutes and 0.8 ± 0.15 minute, respectively. Direct measurements lead to half-lives of 20.35 ± 0.20 minutes for Y^{94} and 10.9 ± 0.2 minutes for Y^{95}.

Experiments, carried out by Hahn and Strassmann (1, 2) and Dillard *et al.* (3, 4), showed the existence of krypton ancestors of Y^{94} and Zr^{95}. Since essentially all fission products decay by β-emission, these experiments also proved the existence of all the intermediate members of the two decay chains (Rb^{94}, Sr^{94} and Rb^{95}, Sr^{95}, Y^{95}, respectively). More direct measurements of some of these nuclides were done by Hahn and Strassmann (1, 2) and Knight *et al.* (5) for Sr^{94}, by Hoffman *et al.* (6) for Sr^{95}, and by Knight *et al.* for Y^{95} (7). This paper reports the first measurement of the Rb^{94} half-life as well as remeasurements of the half-lives of Sr^{94}, Sr^{95}, Y^{94}, and Y^{95}. In addition an estimate for the upper limit of the Rb^{95} half-life is given.

(A) Rubidium 94

The timed precipitation technique as described previously (8) was used to determine the half-life of Rb^{94}. Briefly, this method proceeds as follows: U^{235} is irradiated in a solution which is divided into two portions after the end of the irradiation and rubidium precipitated as perchlorate in both samples at two different times. The two precipitates are later (after almost complete decay of the 1.36-minute Sr^{94}) analyzed radiochemically for Y^{94}. From the amount of Y^{94} in each precipitate, the time interval between the two precipitations and the chemical yields, the half-life of Rb^{94} can be calculated. The experimental details as far as the chemistry is concerned were essentially the same as in the determination of the half-lives of Rb^{92} and Rb^{93} (8). However, the whole procedure had to be accelerated because of the relatively short 20-minute half-life of Y^{94}. Furthermore, the rubidium carrier was added to the uranium solution before the start of the irradiation in order to save time. Counting was usually started approximately 30 minutes after the end of the irradiation.

A gross β-decay curve of yttrium isolated from quickly precipitated rubidium perchlorate clearly shows the following components: 20.35-minute Y^{94}, 3.53-hour Y^{92}, 10.1-hour Y^{93}, and some long-lived Y^{91}. These decay curves, however, are not particularly suitable to determine the relative quantities of Y^{94} in two different samples since these amounts are rather small in comparison with the Y^{92} and Y^{93} present. This arises from the low independent yield and the short half-life of Rb^{94} compared with both the Rb^{92} and Rb^{93} half-lives. For this reason the Y^{94} was counted in a way which would discriminate against the other yttrium isotopes. In the first run this was done by com-

[1]*Manuscript received November 3, 1960.*
Contribution from McMaster University, Hamilton, Ontario. Presented in part at the Third Symposium on Nuclear Chemistry and Radiochemistry held at Atomic Energy of Canada Limited, Chalk River, Ontario, September 6–8, 1960.
[2]*Holder of an Ontario Research Foundation Scholarship 1960–61.*

paring the intensities of the 920-kev γ-ray associated with the decay of Y^{94} (5) in the two yttrium samples. A 3×3 in. NaI(Tl) crystal and a 256-channel analyzer was employed. The two samples were counted for a total time of 20 minutes. The samples were alternated in such a way as to cancel the half-life effects. The events of sample No. 1 were stored in the first 128 channels and those of sample No. 2 in channels 129–256. Each group of 128 channels covered the energy region from 0.2 to 1.5 Mev. In run No. 2 the counting was done similarly. However, the selected energy range was from 0.5 to 4.0 Mev and the samples were directly attached to the aluminum can of the NaI(Tl) crystal. Consequently a large number of high-energy β-rays were counted in addition to any γ-rays of this energy range. The decay of the yttrium samples was followed for several half-lives. The high-energy end of this type of spectrum contained only a 20-minute component. This was to be expected since Y^{94} emits β-rays of up to 5.0 Mev and γ-rays of up to 3.5 Mev (5) whereas the β- and γ-energies of the other three yttrium isotopes are considerably lower (5, 9). The counting rates of all channels which contained only events due to the decay of Y^{94} were added and used as a measure of the relative content of Y^{94} in the two rubidium perchlorate precipitates. This second method was also used for runs Nos. 3 and 4. The results of the four half-life measurements for Rb^{94} are given in Table I.

TABLE I

Summary of Rb^{94} half-life data

Run	U^{235} (μg)	Flux (neutrons cm^{-2} sec^{-1})	Duration of irradiation (seconds)	$RbClO_4$ precipitation times (seconds)		Rb^{94} half-life (seconds)
				1st ppt.	2nd ppt.	
1	200	3×10^{12}	10	9.0	11.7	2.8_1
2	400	3×10^{12}	10	7.6	11.1	2.6_5
3	400	3×10^{12}	10	8.9	12.9	3.1_5
4	300	3×10^{12}	10	6.1	9.1	2.8_5

The half-life values given in Table I are seen to have good internal consistency. The suggested value is 2.9 ± 0.3 seconds. The sources of error which may not effect this consistency have been discussed previously (8).

In order to check the reliability of the method, the yttrium samples can be analyzed for both Y^{93} and Y^{94} from which one can obtain the ratios of the Rb^{93} and Rb^{94} half-lives. This ratio is, of course, independent of the precipitation times provided that the half-lives and independent yields of the precursors are similar. This ratio $T_{1/2}(Rb^{94})/T_{1/2}(Rb^{93})$ was determined for runs No. 2, 3, and 4, and yielded a value of 0.48 ± 0.05. Using 5.6 seconds (8) for the half-life of Rb^{93} one obtains 2.7 ± 0.3 seconds for Rb^{94}. This value is expected to be somewhat low because of precursor effects.

(B) Strontium 94

Hahn and Strassmann (1) showed the existence of a decay period of approximately 2 minutes among the strontium isotopes produced in fission. They also were able to establish the genetic relationship to the 20-minute Y^{94} (1). Knight *et al.* (5) measured the half-life of Sr^{94} by milking yttrium from a purified fission product strontium sample and obtained 1.3 ± 0.2 minutes. Two methods were used in this work; the timed precipitation technique and direct counting. Strontium can be precipitated quickly and in sufficient purity as the nitrate. The coprecipitation of yttrium was found to be around 0.1%. The procedure employed is completely analogous to the one used for the half-life

Can. J. Chem. Downloaded from www.nrcresearchpress.com by 210.87.254.105 on 09/05/12
For personal use only.

determination of Rb^{94} with one exception; the strontium nitrate precipitate was separated from the supernatant solution of 80% nitric acid by means of glass filter crucibles having medium porosity and selected for fast filtration speed. A separation in approximately 15 seconds was achieved when a precipitating volume of 10 ml was used. The strontium nitrate was analyzed for its Y^{94} content starting approximately 8 minutes after the end of the irradiation. The amounts of Y^{94} were either obtained by unravelling gross β-decay curves using a least-squares method (runs No. 1 and No. 2) or by comparing the intensities of the 920-kev γ-ray (5) associated with the decay of Y^{94} (run No. 3). The results of these measurements are:

(1) 1.37 minutes,
(2) 1.31 minutes,
(3) 1.45 minutes,
average 1.38 ± 0.07 minutes.

This half-life, although short, makes feasible the observation of the γ-rays associated with the decay of Sr^{94}. To do this the following procedure was used. Immediately after the irradiation of U^{235}, strontium and barium were precipitated as nitrates. The barium was removed as the chromate and the filtrate was counted using a 3×3 in. NaI(Tl) crystal and a 256-channel pulse-height analyzer. The counting began about 1.7 minutes after the end of the irradiation. The spectrum, which was rather complex, extended to about 3.5 Mev. The two major periods associated with the spectrum were about 1 minute ($Sr^{94}+Sr^{95}$) and 7.5 minutes (Sr^{93}). A prominent γ-ray of 1.42 Mev was assigned to Sr^{94} on the basis of apparent half-life. Consequently this transition was used to determine the half-life of Sr^{94} by direct measurement. A series of measurements was carried out in which the spectra were recorded as a function of time, using the four 64-channel subgroups of the analyzer. Three such runs were done and the area of the 1.42-Mev photopeak was determined for each spectrum.

The half-lives determined from these runs are:

(1) 1.34 minutes,
(2) 1.33 minutes,
(3) 1.36 minutes,
average 1.34 ± 0.04 minutes.

The direct measurement agrees very well with the results of the timed precipitation experiment. The combined values give a half-life of 1.35 ± 0.05 minutes, which is entirely consistent with the results of Knight (5).

(C) Yttrium 94

Most authors agree that the half-life of this nuclide is 20 minutes (1, 5, 10) with the exception of Brown and Katcoff, who report 16.5 minutes (11). The decay of Y^{94} was measured by observing the rate of disappearance of the 920-kev line in the γ-spectrum of Y^{94} (5). The counting system for this purpose has been described previously (8). This method has the obvious advantage of discriminating strongly against other yttrium isotopes. The yttrium was isolated from fission product strontium which had been precipitated as a nitrate. Since the half-life of Sr^{95} is about half that of Sr^{94} one can by proper choice of the separation time discriminate against ingrowing Y^{95}. The radiostrontium was allowed to decay for a few minutes and then the yttrium was separated as the hydroxide. In this way the Y^{92} and Y^{93} content of the final sample was kept as

Can. J. Chem. Downloaded from www.nrcresearchpress.com by 210.87.254.105 on 09/05/12
For personal use only.

low as possible. The yttrium was then purified using standard procedures (12). A decay curve is shown in Fig. 1 and the results of two such measurements obtained from a least-squares analysis of the data were:

(1) 20.4 minutes,
(2) 20.3 minutes,
average 20.35±0.2 minutes.

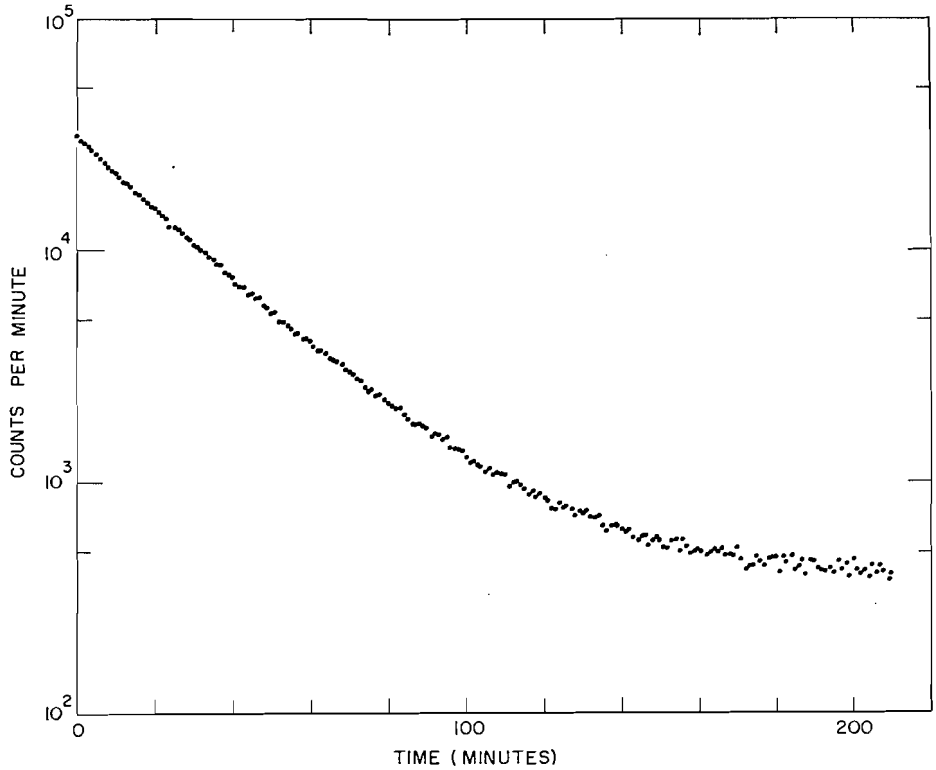


FIG. 1. A decay curve obtained for Y^{91}. The only events recorded were those whose pulse height fell within a 6% window centered about the 920-kev γ-ray line.

This value is in very good agreement with most of the previously reported measurements. An explanation for the lower value of 16.5 minutes is the undetected presence of 10.9-minute Y^{95}.

(D) Rubidium 95

An attempt was made to prove the existence of Rb^{95} directly. Rubidium perchlorate was precipitated 8 seconds after the end of a 10-second irradiation of 400 μg of U^{235} at a flux of 3×10^{12} neutrons/cm^2 sec. The rubidium isotopes and their respective strontium daughters were then allowed to decay for 10 minutes after which the sample was analyzed for radioyttrium. The sample was directly mounted on the face of a 3×3 in. NaI(Tl) crystal. A single-channel analyzer was set to accept γ-rays in the interval 2.0 to 3.7 Mev. The thin aluminum can of the crystal also permits β-counting. The decay of the combined radiations was followed for 220 minutes and the decay curve is shown in Fig. 2. It can be seen from Fig. 2 that there is no indication of a 10.9-minute Y^{95}

Can. J. Chem. Downloaded from www.nrcresearchpress.com by 210.87.254.105 on 09/05/12
For personal use only.

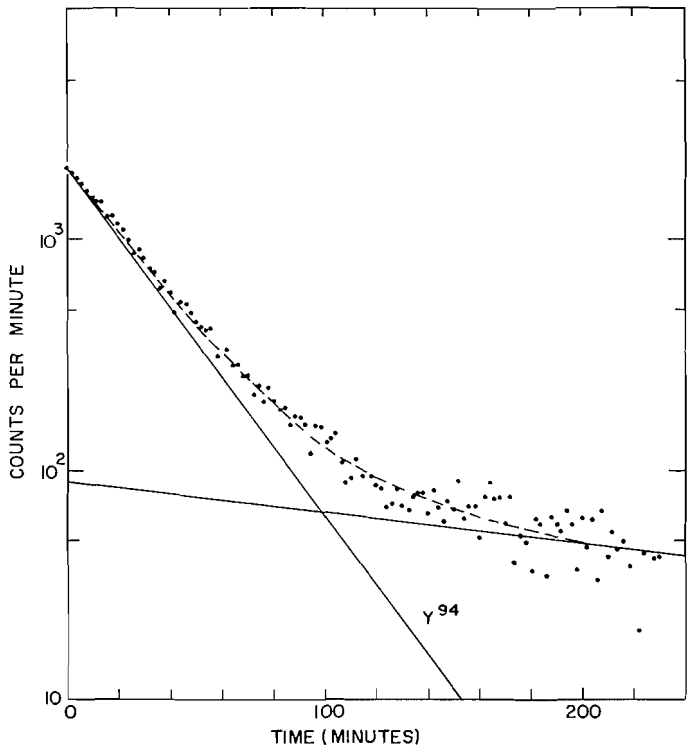


FIG. 2. This decay curve was used to infer that the half-life of Rb^{95} is less than 2.5 seconds. If Rb^{95} had a half-life greater than or equal to 2.5 seconds, the decay curve shown would have had a 10.9-minute Y^{95} component with an initial counting rate of 500 c.p.m. Since the curve is represented quite well by 20-minute Y^{94} and 3.5-hour Y^{92} components, the Y^{95} component must be small.

component, although its decay characteristics do satisfy the imposed counting conditions. From the time schedule of the whole experiment and the independent yields of Rb^{94} and Rb^{95} (13) an upper limit of 2.5 seconds for the Rb^{95} half-life can be estimated. This is based on the assumption that a 25% contribution of Y^{95} to the original counting rate would have been found.

(E) Strontium 95

So far the only half-life measurement of Sr^{95} was done by Hoffman *et al.* (6), who obtained approximately 0.7 minute. It can be assumed that their method was the same as the one used by Knight *et al.* (5) for Sr^{94}.

Two values for the half-life of Sr^{95} were obtained from the relative quantities of Y^{95} in the yttrium samples of runs No. 1 and No. 2 which are mentioned in Section (*B*). The values obtained were:

(1) 0.6_8 minute,
(2) 0.8_8 minute,
average 0.8 ± 0.15 minute.

An attempt was made to measure the half-life directly by observing the high-energy β-rays emitted from rapidly separated strontium. The results were consistent with the value quoted above. However, the technical difficulties encountered restricted the usefulness of the method.

Can. J. Chem. Downloaded from www.nrcresearchpress.com by 210.87.254.105 on 09/05/12
For personal use only.

(F) Yttrium 95

Only two values for the half-life of Y^{95} have been reported. Knight, Burgus, and Prestwood (7) quote 10.5 minutes in private communication and Knight *et al.* (5) mention a 9.5 minute Y^{95} activity as a low-intensity component in gross β-decay curves of fission product yttrium.

In order to remeasure the decay period of Y^{95} a sample was prepared in the following way. Immediately after the irradiation of U^{235} and the addition of strontium carrier, strontium nitrate was precipitated, centrifuged, and washed with 80% nitric acid. The strontium nitrate was dissolved in water, reprecipitated as the nitrate, and centrifuged. The supernate was directly used for a tributylphosphate extraction (12) of the yttrium which had grown in during the 3-minute interval between the two strontium nitrate precipitations. In this way the Y^{95} was enriched as much as chemically possible. The yttrium was further purified and finally β-counted as the oxalate long enough to allow a correction to be made for the small contribution due to the long-lived components. The data were then subjected to a least-squares analysis for two components. Half-lives of 10.9 ± 0.2 minutes and 20.4 ± 0.3 minutes were obtained for Y^{95} and Y^{94} respectively. The value of 20.4 ± 0.3 minutes agrees very well with the results given in Section (*C*) for Y^{94}.

ACKNOWLEDGMENTS

We wish to acknowledge the financial assistance given by the National Research Council and one of us (W.V.P.), that from the Ontario Research Foundation. We also appreciate the co-operation received from the McMaster University Reactor staff.

REFERENCES

1. O. Hahn and F. Strassmann. Naturwiss. **31**, 249 (1943).
2. O. Hahn and F. Strassmann. Z. Physik, **121**, 729 (1943).
3. C. R. Dillard, R. M. Adams, H. Finston, and A. Turkevich. National Nuclear Energy Series-PPR. Vol. 9. McGraw-Hill Book Co., Inc., New York. 1951. p. 616.
4. C. R. Dillard, R. M. Adams, H. Finston, and A. Turkevich. National Nuclear Energy Series-PPR. Vol. 9. McGraw-Hill Book Co., Inc., New York. 1951. p. 624.
5. J. D. Knight, D. C. Hoffman, B. J. Dropesky, and D. L. Frasco. J. Inorg. & Nuclear Chem. **10**, 193 (1959).
6. D. C. Hoffman, J. D. Knight, D. L. Frasco, and B. J. Dropesky. Unpublished data quoted in D. Strominger, J. M. Hollander, and G. T. Seaborg. Revs. Modern Phys. **30**, 866 (1958).
7. J. D. Knight, W. H. Burgus, and R. J. Prestwood. Private communication listed in National Nuclear Energy Series-PPR. Vol. 9. McGraw-Hill Book Co., Inc., New York. 1951. p. 2063.
8. K. Fritze and T. J. Kennett. Can. J. Phys. **38**, 1614 (1960).
9. W. A. Cassatt and W. V. Meinke. Phys. Rev. **99**, 760 (1955).
10. C. R. Dillard, R. M. Adams, H. Finston, and A. Turkevich. National Nuclear Energy Series-PPR. Vol. 9. McGraw-Hill Book Co., Inc., New York. 1951. p. 692.
11. L. J. Brown and S. Katcoff. J. Chem. Phys. **17**, 497 (1949).
12. C. H. Stanley. Atomic Energy Commission Report L.A.-1721. p. 104.
13. A. C. Wahl. J. Inorg. & Nuclear Chem. **6**, 263 (1958).

Can. J. Chem. Downloaded from www.nrcresearchpress.com by 210.87.254.105 on 09/05/12
For personal use only.

Can. J. Chem. Downloaded from www.nrcresearchpress.com by 210.87.254.42 on 09/05/12
For personal use only.

HALF-LIFE OF Cs^{137} [1]

H. FARRAR, A. K. DASGUPTA, AND R. H. TOMLINSON

ABSTRACT

The half-life of Cs^{137} was found to be 30.4 ± 0.4 years by determining the amount of Ba^{137} produced in various times from a known number of Cs^{137} atoms. The numbers of barium and cesium atoms were determined from isotope dilution data obtained with a mass spectrometer.

INTRODUCTION

In recent years there have been numerous measurements of the half-life of Cs^{137}. The original estimate by Glendenin and Metcalf (1) was 33 ± 3 years. Wiles and Thode (2) later published a value 33 ± 2 years which was obtained with a mass spectrometer by observing, over a period of years, the decrease in the relative amount of Cs^{137} with respect to Cs^{133} in fission product cesium.

Later experiments used the isotope dilution technique with a mass spectrometer to determine the number of Cs^{137} atoms in a given sample, and 4π absolute β-counting to determine the activity. In this way, values of 26.6 ± 0.4 years (3), 30.0 ± 0.4 years (4), $28.6 \pm {}^{2}_{1}$ years (5), and 32.6 ± 1.6 years (6) were obtained. Owing to the considerable disagreement in these values, a new method was desirable.

Rather than determine the rate of decay of Cs^{137} by counting the radiation released, the present work reports on the determination of the half-life by measuring the rate of formation of the daughter nuclide, Ba^{137}, from a known amount of Cs^{137}. Both measurements use isotope dilution technique with a mass spectrometer, and do not require any absolute counting procedures. It is also important that the present method is independent of the decay scheme and of radioactive contaminants.

EXPERIMENTAL

About 0.5 mg of fission product cesium was used for this experiment, amounting to about 20 mc of activity and generating about 1×10^{-8} grams of Ba^{137} per day.

Preliminary experiments with a 0.4-ml column of Dowex 50 cation exchange resin (100–200 mesh) in the acid form were made to determine conditions for the separation of barium from cesium. Using 0.5 mg of Cs^{133} with tracer Cs^{137}, and also the radioisotope Ba^{139}, it was found that when the column was eluted with 1 *M* HCl, virtually all the cesium was removed within the first 15 ml, the maximum coming off in the 9th ml, whereas the barium remained adsorbed until after the 90th ml. It was found that after the 22nd ml, an increase in concentration to 3 *M* HCl removed the barium tracer within a further 30 ml of eluate.

The fission product cesium was adsorbed on a new column and eluted as previously described. The eluate was set aside to allow the accumulation of Ba^{137}. While this was taking place, a weighed aliquot of isotope-enriched Ba^{134} solution was added. At the end of a measured period, the cesium plus the mixture of Ba^{137} and Ba^{134} were adsorbed on a new column. The cesium was eluted as before with 1 *M* HCl and was retained for a further period. The concentration of the elutriant was increased after the 22nd ml to 3 *M*, and the Ba^{137} plus the Ba^{134} were collected. Complete elution of the barium was

[1]*Manuscript received November 3, 1960.*
Contribution from Hamilton College, McMaster University, Hamilton, Ontario. Presented at the Third Symposium on Nuclear Chemistry and Radiochemistry held at Atomic Energy of Canada Limited, Chalk River, Ontario, September 6–8, 1960.

unnecessary since only the ratio of the Ba^{134} and Ba^{137} isotopes was needed to determine the number of Ba^{137} formed in the period. The barium solution was evaporated first in a pyrex beaker and then on a teflon sheet to one drop, which was placed on the filament of a 90° solid source mass spectrometer, for isotopic analysis.

RESULTS

Small amounts of natural barium were evident in the mass spectrograms. Since the isotopic content of natural barium is principally Ba^{138}, which is very different from the enriched Ba^{134} solution, a measurement of the ratio of Ba^{134} to Ba^{138} in any sample gives a precise knowledge of the amount of Ba^{137} contamination present. This correction varied almost linearly from 20% for the shortest period of growth to 0.8% for the longest.

Measurements of the amount of Ba^{137} formed in eight different periods have been made. The period in each case was the time between similar parts of consecutive cesium elutions. In case the rate of elution were to vary from one separation to the next, these parts were chosen when the 9th ml of eluate, which included most of the cesium, left the column.

Apart from the correction to the Ba^{137} for natural barium contamination, which already has been mentioned, the only correction made was that due to the loss and decay of Cs^{137} during the series of separations. To obtain this correction, the relative activity of the total sample was counted between each separation with a 4π ionization chamber.

The original number of Cs^{137} atoms, found by three independent isotope dilutions with natural cesium, had an average value of 7.592×10^{17} atoms. The maximum deviation from this was 0.4%. To prevent excessive increases of Cs^{133} in the sample, the first two isotope dilutions were performed with a small known fraction of the total. In the third case, the total sample was used.

The concentration of the barium isotopes in the Ba^{134} enriched isotope dilution solution was found by three independent isotope dilutions using natural barium. The average concentration was found to be 5.861×10^{14} atoms of Ba^{134} per gram of solution, the maximum deviation from this being 0.7%.

One cesium and one barium isotope dilution were performed without the use of the electron multiplier in the mass spectrometer. These results showed no difference from those obtained with the electron multiplier. Furthermore, a careful determination of the relative abundances of natural barium isotopes has been made both with and without the electron multiplier. Since both sets of results were identical and also in agreement with the values obtained by Nier (7), it can be concluded that no significant mass discrimination occurred at the electron multiplier.

The results of the data obtained for each separation are shown in Table I.

TABLE I

Accumulation of Ba^{137} for various periods

Period, days	Number of Ba^{137} formed
0.924	$0.459\pm0.008\times10^{14}$
2.975	$1.415\pm0.005\times10^{14}$
5.046	$2.338\pm0.014\times10^{14}$
6.074	$2.968\pm0.021\times10^{14}$
8.215	$3.948\pm0.043\times10^{14}$
10.085	$4.794\pm0.044\times10^{14}$
16.715	$7.91\pm0.10\times10^{14}$
48.960	$23.25\pm0.13\times10^{14}$

Can. J. Chem. Downloaded from www.nrcresearchpress.com by 210.87.254.42 on 09/05/12
For personal use only.

Column 2 gives the numbers of Ba^{137} formed from the initial amount of Cs^{137}, which are corrected to allow for loss and decay of the Cs^{137}. This correction accumulated to 5.00% for the final period. Of this, approximately 1% was due to decay and almost all the rest was lost in the separation between the fifth and sixth periods. A linear least-squares plot of the data in Table I is shown in Fig. 1. The slope for points obtained before

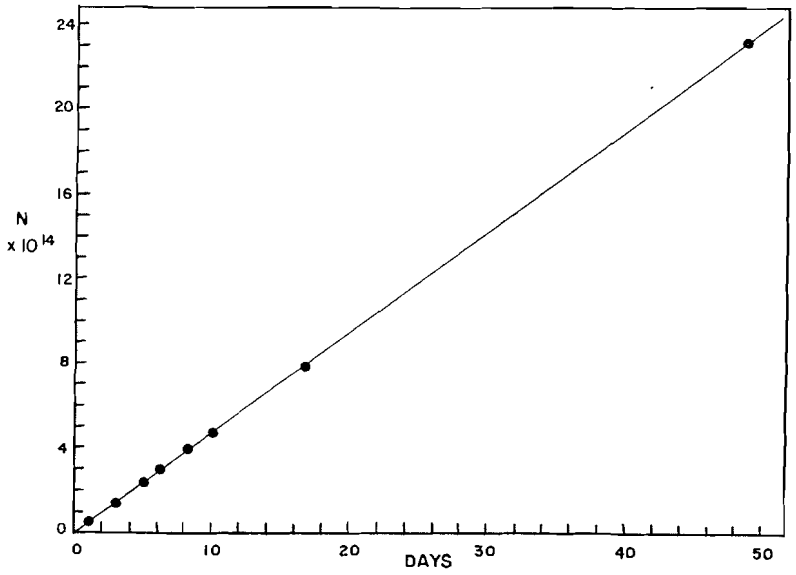


FIG. 1. Rate of growth of Ba^{137}.

the loss of cesium is the same as the slope for points obtained after, the appropriate corrections having been made. The slope thus obtained was found to be 4.746×10^{13} Ba^{137} per day. An error of $\pm 1.2\%$ has been arbitrarily assigned to this slope noting that six of the nine points, including (0,0), lie within these limits. The least-squares plot passes close to the origin, giving, at $t = 0$, 33 minutes of growth of Ba^{137}, which is small compared with the time intervals.

From these data, the half-life was calculated to be 30.4 ± 0.4 years. The error in the half-life has been estimated from the assigned errors in each of the measured quantities.

ACKNOWLEDGMENTS

This research was supported by the National Research Council of Canada. One of us (H. F.) is indebted to the Eldorado Mining and Refining Limited for the award of the Charles G. Williams Fellowship.

REFERENCES

1. L. E. GLENDENIN and R. P. METCALF. National Nuclear Energy Series. Vol. 9, Paper 152. McGraw-Hill Book Co., Inc., New York. 1951.
2. D. R. WILES, B. W. SMITH, R. HORSLEY, and H. G. THODE. Can. J. Phys. **31**, 419 (1953).
3. D. M. WILES and R. H. TOMLINSON. Phys. Rev. **99**, 188 (1955).
4. F. BROWN, G. R. HALL, and A. J. WALTER. J. Inorg. & Nuclear Chem. **1**, 241 (1955).
5. A. J. MOSES and H. D. COOK. United States Atomic Energy Commission, TID-7568. 1958.
6. L. E. GLENDENIN and E. P. STEINBERG. Private communication.
7. A. O. NIER. Phys. Rev. **54**, 275 (1938).

Can. J. Chem. Downloaded from www.nrcresearchpress.com by 210.87.254.42 on 09/05/12
For personal use only.

Can. J. Chem. Downloaded from www.nrcresearchpress.com by 210.87.254.40 on 09/05/12
For personal use only.

SEARCH FOR THE (n,t) REACTION AT 14 MEV IN SOME MEDIUM WEIGHT NUCLEI[1]

A. P. BAERG AND G. C. BOWES

ABSTRACT

The (n,t) reaction at 14.6 Mev has been observed to occur in S^{32} with a cross section of 4 ± 1 microbarns. Upper limits for the cross section of this reaction are also given for Ca^{40}, Cr^{50}, Fe^{54}, and Zn^{64} and the results are discussed qualitatively in the light of recently reported (10) (n,He^3) reactions.

INTRODUCTION

Among various types of nuclear reactions which are energetically possible with 14-Mev neutrons, the (n,t) reaction has been studied only in very light nuclei (1, 2, 3, 4). In accordance with the reciprocity theorem such reactions should be important in some cases since reactions of the type (t,n) are known to occur at 2.65 Mev in medium weight nuclei (5, 6).

Intuitively the emission of a complex loosely bound structure such as a triton seems much less probable than that of single-particle emission. In early work on (p,t) reactions, however, Cohen and Handley (7) already concluded that the inherent probability for triton emission, in the breakup of a compound nucleus at least, was little, if any, less than that for protons or neutrons. Reactions of the type (n,t) are in general characterized by large negative Q values and on the statistical theory the cross sections are expected to be generally very small. In lighter elements, however, a strong component of direct interaction is evident in Li^6 and Li^7 (1) as well as in Be^9 (3). More recent work by Cohen and others (8, 9) on the (p,t) reaction at 23 Mev shows strong evidence for a pickup mechanism for this reaction in heavier elements.

Recently Kumabe *et al.* (10) have reported the occurrence of (n,He^3) reactions at 14.8 Mev in Mn^{55}, Co^{59}, As^{75}, and Rh^{103}. The cross sections observed range in value from 1 to 6 millibarns and the authors have suggested several possible direct interaction mechanisms to account for the cross-section magnitudes.

In view of the accumulating evidence of significant contributions from direct interaction in 14-Mev neutron reactions, we have made a cursory search for the (n,t) reaction in medium weight elements. Several isotopes were selected for study by the activation method, from a consideration of reaction Q values and unambiguous identification of the product nucleus with the (n,t) reaction. This has restricted us to stable even–even target nuclei of low neutron number, to avoid interference from (n,p) or (n,d) reactions on other isotopes.

EXPERIMENTAL

The various targets were bombarded with neutrons of average energy 14.6 Mev (11) from the $T(d,n)He^4$ reaction using about 1 ma of 120-kev deuterons incident on a thick tritium-loaded titanium target.* Cross sections were measured by comparison of the positron activity induced in the sample with that induced in a fluorine "flux monitor"

[1]*Manuscript received November 3, 1960.*
Contribution from the Division of Applied Physics, National Research Council, Ottawa, Ontario. Presented at the Third Symposium on Nuclear Chemistry and Radiochemistry held at Atomic Energy of Canada Limited, Chalk River, Ontario, September 6–8, 1960.
Issued as N.R.C. No. 6140.
**A 150-kilovolt Texas Nuclear Corporation neutron generator was used.*

from the (*n*,2*n*) reaction on F^{19} giving 112-minute F^{18}. The cross section for the latter reaction was taken to be 53 millibarns (cf. 61 millibarns ref. 12), as measured in separate experiments relative to 556 millibarns for the (*n*,2*n*) reaction on Cu^{63} (13). The fluorine monitors were used in the form of sheets of "teflon", $(C_2F_4)_n$, placed on either side of the samples for the irradiation. During the irradiation the neutron flux was maintained constant within 5% as determined by continuous monitoring with a BF_3-filled ionization chamber and a $B^{10}F_3$ "long counter".

The positron activities were detected by scintillation counting of the annihilation radiation and identified by half-life measurements. Chemical separations were not made. The radiations from samples and fluorine monitors were measured under conditions identical, as nearly as possible, with respect to geometry and absorber material. (For the type of detector used see reference 14.) It is estimated that a maximum systematic error of 15% may be applicable to the relative activity measurements.

The samples were prepared from the elements or from suitable compounds such as hydrides, oxides, or organic salts which do not produce interfering activities. In several cases atmospheric nitrogen adsorbed in the sample produced interfering 10-minute N^{13} from the (*n*,2*n*) reaction on N^{14}. This was reduced to tolerable levels by evacuation of the samples and irradiation in an atmosphere of pure methane or helium.

RESULTS AND DISCUSSION

Among the five isotopes studied (S^{32}, Ca^{40}, Cr^{50}, Fe^{54}, and Zn^{64}) the (*n*,*t*) reaction was observed to occur only in S^{32}, producing the 2.5-minute P^{30} positron emitter with, however, a very small cross section. The gamma-ray spectrum of the irradiated sulphur is shown in Fig. 1 in which only the 0.511-Mev photopeak ascribed to P^{30} is present. In

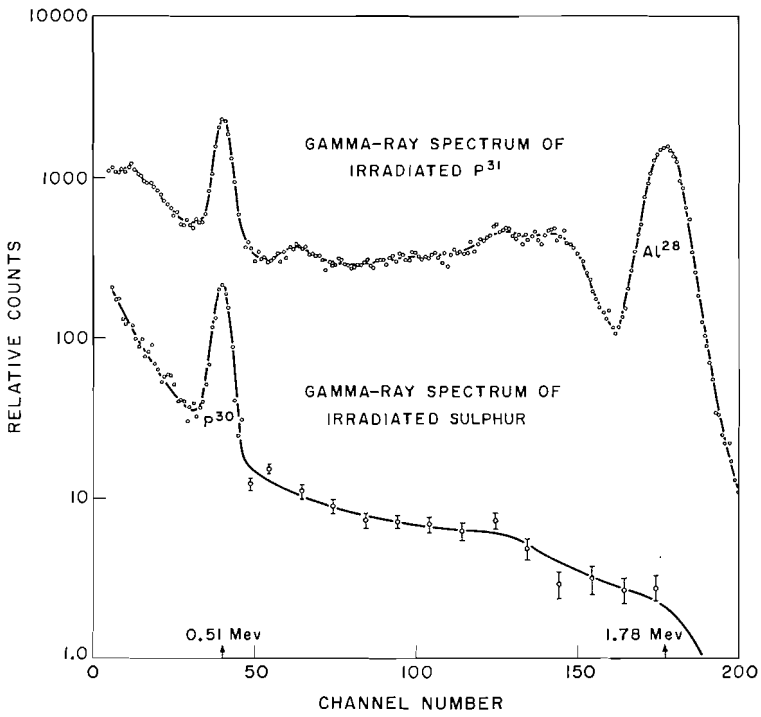


FIG. 1. Gamma-ray spectra of irradiated sulphur and phosphorus.

Can. J. Chem. Downloaded from www.nrcresearchpress.com by 210.87.254.40 on 09/05/12
For personal use only.

order to demonstrate that this activity did not arise from an $(n,2n)$ reaction on possible phosphorous impurity, the gamma-ray spectrum of irradiated P^{31} is given as well in this figure. This shows, in addition to the 0.511-Mev line, a strong peak at 1.78 Mev due to Al^{28} from the (n,α) reaction, which, however, is absent in the irradiated sulphur spectrum.

The decay of the 0.511-Mev photopeak showed a half-life of about 2.5 minutes with a smaller 10-minute component. This longer-lived component is ascribed to N^{13} resulting from an $(n,2n)$ reaction on a small amount of residual nitrogen in the samples. A typical decay curve is shown in Fig. 2.

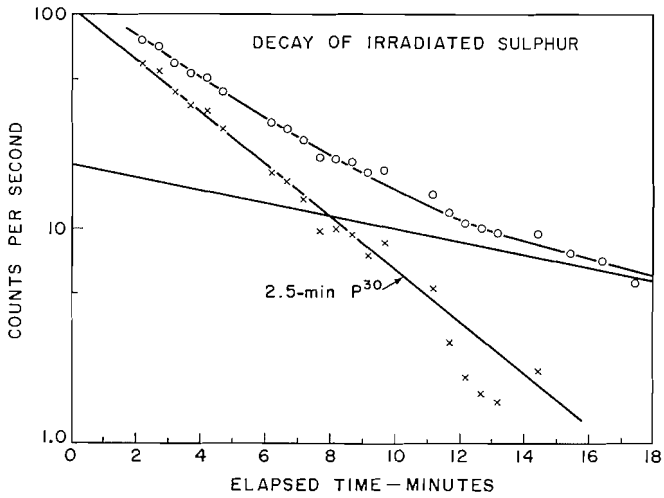


FIG. 2. Decay of 0.511-Mev photopeak in irradiated sulphur.

The experimental data and calculated cross sections for six irradiations of different samples are given in Table I. The cross sections are given relative to 53 millibarns for

TABLE I

Experimental results for (n,t) reaction on S^{32}

Sample	Duration of irradiation, minutes	P^{30} activity, c.p.m./g S^{32}	F^{18} activity, c.p.m./g F^{19}	Cross section, barns$\times 10^6$
Elemental sulphur	2.5	80.1	55.5×10^3	4.0
Elemental sulphur	2.5	73.4	54.3×10^3	3.7
Carbon disulphide	3.0	23.3	21.1×10^3	3.2
Carbon disulphide	3.0	60.1	37.8×10^3	4.6
Carbon disulphide	3.0	43.6	34.1×10^3	3.7
Carbon disulphide	2.5	56.0	35.5×10^3	4.3

the $(n,2n)$ reaction on F^{19}.

Activities resulting from the (n,t) reaction on the other nuclides studied were not definitely observed and upper limits only have been assigned for the cross sections. These assignments were made on the basis of a careful analysis of counting data and gamma spectra, taking into account isotopic abundances and positron branching ratios (15). The results for the various reactions sought are given in Table II together with the reaction

Can. J. Chem. Downloaded from www.nrcresearchpress.com by 210.87.254.40 on 09/05/12
For personal use only.

TABLE II

Cross sections for (n,t) reactions

Reaction	Q, Mev	$t_{\frac{1}{2}}$ of residual nucleus	$\sigma(n,t)$ observed, barns$\times 10^6$	Estimated theoretical $\sigma(n,t)$, barns$\times 10^6$
S^{32} (n,t) P^{30}	−12.56	2.5 minutes	4±1	5
Ca^{40} (n,t) K^{38}g.s.	−12.59	7.7 minutes	<20	0.002
Cr^{50} (n,t) V^{48}	−13.00	16.0 days	<200	0.06
Fe^{54} (n,t) Mn^{52}g.s.	−13.16	5.6 days	<75	0.001
Zn^{64} (n,t) Cu^{62}	−9.72	9.7 minutes	<100	2

Q values taken from the nuclear mass and binding energy tabulation given by Cameron (16). The sulphur experiments yield an average cross-section value of 4±1 microbarns with the error based on a standard deviation of 10% and a possible systematic error of 15% in the relative activity measurements.

The last column in Table II gives approximate theoretical cross sections calculated on the compound nucleus formalism (17, 18). Since there are rather large uncertainties (~200 kev) associated with the reaction Q values, approximate solutions only have been given but these are believed reliable to within a factor of 5. These calculated values are thus intended as a guide to the order of magnitude expected on the compound nucleus model. Since cross-section upper limits only were obtained experimentally for most of the reactions, the comparison with calculated values has some significance only in the case of S^{32} where the agreement is very satisfactory.

Perhaps a more instructive comparison is that with the (n,He^3) cross sections recently reported by Kumabe *et al.* (10) in Mn^{55}, Co^{59}, As^{75}, and Rh^{103}. The cross sections lie in the range 1 to 6 millibarns while the reaction Q values are comparable with those for the (n,t) reactions in the present study (e.g. for $Mn^{55}(n,He^3)V^{53}$, $Q = -12.65$ Mev). Thus the (n,He^3) cross sections given by Kumabe *et al.* are at least one or two orders of magnitude greater than the (n,t) cross sections for the nuclides studied here. This result seems surprising in view of the generally higher coulomb barriers for the nuclides studied by Kumabe *et al.* and the lower barrier penetrability to be expected for He^3 particles relative to that for tritons.

On the basis of evidence given by Wilkinson (19) for nucleon clustering in the nuclear surface, Kumabe *et al.* have suggested a direct interaction mechanism for the (n,He^3) reactions in which the incident neutron knocks out a preformed He^3 cluster. In this concept, the results on (n,t) reactions would imply a much lower probability for triton clusters relative to He^3 clusters.

As a further possibility these authors suggest a double-proton pickup mechanism. McManus (20) notes that the two protons would, in the usual case, be picked up from a given shell model state, i.e. from the last shell being filled. In deuteron pickup, however, i.e. in the (n,t) reaction, the neutron and proton picked up would normally occupy states of quite different energy in the target nucleus. On these grounds, since rather little energy is available for the reactions under consideration, the deuteron pickup might be expected to be a much less probable event. In this connection it is interesting to note that in N^{14}, with an odd proton and an odd neutron outside of the stable C^{12} core, a large (n,t) cross section is observed at 7 to 8.2 Mev (4). It is perhaps also noteworthy that the analogous (p,t) reactions are well-known while (p,He^3) reactions, involving deuteron pickup, appear generally to be inhibited (21).

Can. J. Chem. Downloaded from www.nrcresearchpress.com by 210.87.254.40 on 09/05/12
For personal use only.

In order to decide on the mechanism involved in the (n,He^3) reactions and to arrive at the explanation for the apparent difference with (n,t) reactions, further information such as angular and energy distributions of outgoing particles is obviously required. Unfortunately this is difficult to obtain with presently available neutron sources and measuring techniques.

ACKNOWLEDGMENTS

The authors wish to thank Dr. H. McManus and Dr. E. Vogt for valuable discussions in connection with this work.

REFERENCES

1. G. M. FRYE. Phys. Rev. **93**, 1086 (1954).
2. J. BENVENISTE, A. C. MITCHELL, C. D. SCHRADER, and J. H. ZENGER. U.S. Atomic Energy Commission Report UCRL-5596.
3. S. S. VASELEV, V. V. KOMAROV, and A. M. POPOVA. Soviet Phys. "Doklady", **3**, 354 (1958).
4. F. GABBARD, H. BICHSEL, and T. W. BONNER. Proceedings of the International Congress of Nuclear Physics, Paris. July, 1958. p. 406.
5. J. D. KNIGHT, T. B. NOVEY, C. V. CANNON, and A. TURKEVITCH. National Nuclear Energy Series. Div. IV, Vol. 9, Paper 326. McGraw-Hill Book Company, Inc., New York. 1951.
6. T. A. EASTWOOD. Atomic Energy of Canada Limited. Private communication.
7. B. L. COHEN and T. H. HANDLEY. Phys. Rev. **93**, 514 (1954).
8. B. L. COHEN and A. G. RUBIN. Phys. Rev. **114**, 1143 (1959).
9. J. B. BALL and C. D. GOODMAN. Phys. Rev. To be published.
10. I. KUMABE, A. D. POULARIKAS, I. L. PREISS, D. G. GARDNER, and R. W. FINK. Phys. Rev. **117**, 1568 (1960).
11. J. D. SEAGRAVE. Los Alamos Scientific Laboratory Report LAMS-2162.
12. E. B. PAUL and R. L. CLARK. Can. J. Phys. **31**, 267 (1953).
13. SHINJIRO YASUMI. J. Phys. Soc. Japan, **12**, 443 (1957).
14. R. L. HEATH. U.S. Atomic Energy Commission Report IDO-16408.
15. D. STROMBERGER, J. M. HOLLANDER, and G. T. SEABORG. Revs. Modern Phys. **30**, 585 (1958).
16. A. G. W. CAMERON. Atomic Energy of Canada Limited Report CRP-690.
17. L. M. BLATT and V. F. WEISSKOPF. Theoretical nuclear physics. John Wiley & Sons, New York. 1952.
18. A. M. LANE and R. G. THOMAS. Revs. Modern Phys. **30**, 257 (1958).
19. D. H. WILKINSON. Phil. Mag. 4, 215 (1959).
20. H. MCMANUS. Atomic Energy of Canada Limited. Private communication.
21. B. L. COHEN, A. G. RUBIN, and C. B. FULMER. Proceedings of the International Congress of Nuclear Physics, Paris. July, 1958. p. 392.

Can. J. Chem. Downloaded from www.nrcresearchpress.com by 210.87.254.40 on 09/05/12
For personal use only.

Th^{232} $(n,2n)$ Th^{231} CROSS SECTION FROM THRESHOLD TO 20.4 MEV[1]

J. P. BUTLER AND D. C. SANTRY

ABSTRACT

The excitation curve for the reaction Th^{232} $(n,2n)$ Th^{231} has been measured by the activation method from the threshold energy, 6.34 Mev, to 20.4 Mev, relative to the known cross section for the S^{32} (n,p) P^{32} reaction. Monoenergetic neutrons were obtained from the D (d,n) He^3 and T (d,n) He^4 reactions employing a Tandem Van de Graaff accelerator. From threshold to 9.0 Mev, the $(n,2n)$ cross section rises rapidly, reaching its maximum value of 1.88 ± 0.09 barns in the region of 9.5 to 11.0 Mev. Above 11.5 Mev the $(n,2n)$ cross section decreases due to competition of the $(n,3n)$ and $(n,2nf)$ reactions and at 20.4 Mev it has a value of $0.22_5\pm0.01_5$ barns.

INTRODUCTION

Although many measurements of fast neutron cross sections $(n,2n)$, (n,p), and (n,α) have been made with 14-Mev neutrons, relatively few data have been published over a range of neutron energies for which these reactions have appreciable cross sections. Due to the scarcity of data on neutron cross sections as a function of energy and the lack of agreement among existing results, a program has been initiated to measure fast neutron cross sections from threshold energies to about 21 Mev. These cross sections will be determined whenever possible with an accuracy of $\pm5\%$.

The recent development of the Tandem Van de Graaff accelerator now makes it possible to obtain measurements of fast neutron cross sections over a greater energy range. By accelerating deuterons to a precise energy, the reactions D (d,n) He^3 and T (d,n) He^4 can be used to produce monoenergetic neutrons at any energy from about 5 to 21 Mev.

Results have been published on the cross section for absorption reactions of fast neutrons with Th^{232}. The (n,γ) reaction has been measured up to 14 Mev (1) and the fission cross section has been measured by several investigators from threshold energies up to 11 Mev (1, 2) and at 14.5 Mev (1, 3). However, data on the significant $(n,2n)$ cross section are only available at a few energies (4, 5). The present investigation was undertaken to determine the cross section for the reaction Th^{232} $(n,2n)$ Th^{231} from threshold, 6.34 Mev, to 20.4 Mev. The reaction S^{32} (n,p) P^{32} was used to monitor the fast neutron flux. After the irradiation, thorium was purified radiochemically, and the Th^{231} as well as the P^{32} produced were determined by absolute beta counting. The $(n,2n)$ cross section at a particular neutron energy was then calculated from the Th^{231}- and P^{32}-activity measurements and the known cross section for the sulphur (n,p) reaction (6).

EXPERIMENTAL METHOD

A. Neutron Sources

Neutrons with energies from 6 to 11.6 Mev were obtained from the reaction D (d,n) He^3 employing the Chalk River Tandem Van de Graaff accelerator. A gas target cell similar to that described by Johnson and Banta (7) and illustrated in the lower part of Fig. 1 was used to contain the deuterium. The bombarding deuteron beam was magnetically analyzed, focused with a set of quadrupole magnets, and collimated by a 0.125-in. gold aperture. Deuterons scattered off the edge of the collimating aperture were

[1]*Manuscript received November 3, 1960.*
Contribution from the Research Chemistry Branch, Atomic Energy of Canada Limited, Chalk River, Ontario. Presented at the Third Symposium on Nuclear Chemistry and Radiochemistry held at Atomic Energy of Canada Limited, Chalk River, Ontario, September 6–8, 1960.
Issued as A.E.C.L. No. 1180.

Can. J. Chem. Downloaded from www.nrcresearchpress.com by 210.87.254.42 on 09/05/12
For personal use only.

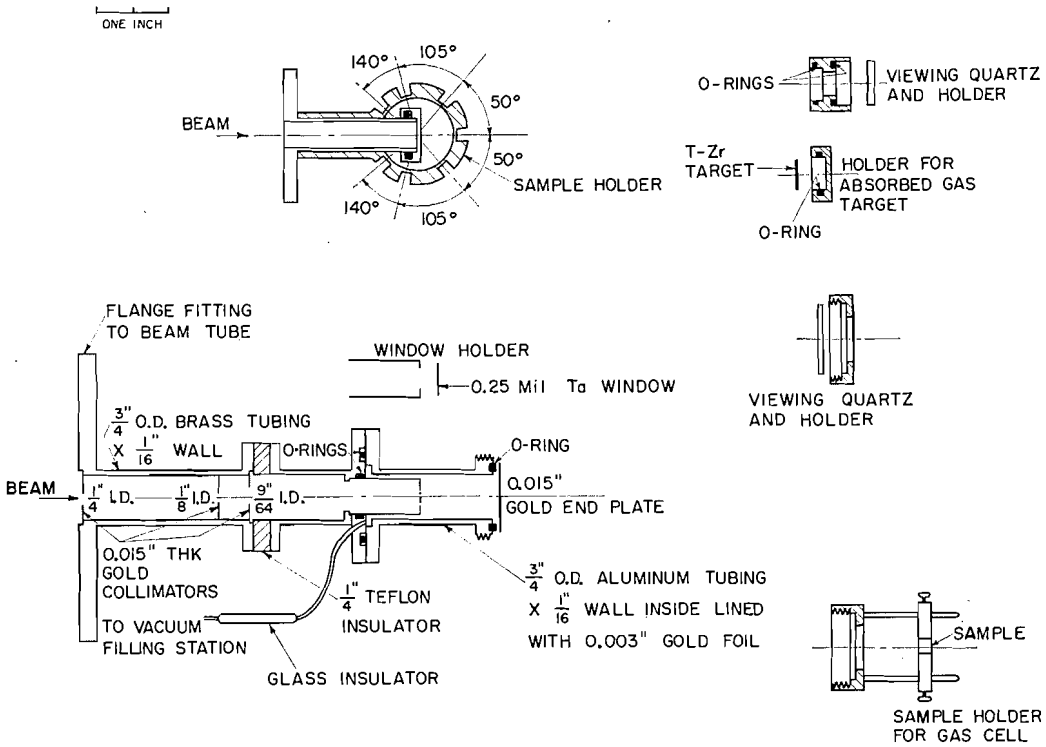


FIG. 1. Irradiation assemblies. The lower section of the diagram shows the deuterium gas target cell with the beam collimators and sample holder; the upper section shows the tritium–zirconium target and the arrangement of the samples.

prevented from entering the gas cell by a second gold aperture of slightly larger diameter, 0.140 in. The target cell was insulated from the beam tube by a 1/4 in. thick teflon ring. This enabled the cell to be used as a Faraday cup to measure the beam current during an irradiation. The cell consisted of three parts: a brass connecting section which is attached to the rest of the assembly with bolts passing through nylon insulating bushings, a brass window holder, and the outer aluminum chamber with a gold end plate. The deuteron beam enters the gas target cell through a 0.00025-in. tantalum foil which is cemented with Araldite to the brass window holder. Tantalum was found to be very suitable as a window material because of its high tensile strength. It has the added advantage that its high atomic number reduces the number of extraneous neutrons formed from (d,n) reactions. The window holder, which is held as a push fit, is aligned by a flange and makes a vacuum seal with the inner O-ring. The holder can readily be replaced if the tantalum foil ruptures. The gas chamber slips over the window holder and forms a vacuum seal with the outer O-ring. Deuterium gas enters the cell through a small hole between the O-rings and through the annular region between the chamber and the window holder. The gas target cell, which is 1.6 cm in diameter and 2.7 cm in length, was filled with deuterium to a pressure of 225 cm of Hg. The cell is made of aluminum to minimize neutron scatter and it was lined with 0.003-in. gold foil to prevent deuterons scattered in the entrance foil from striking the aluminum side walls and producing extraneous neutrons. The deuteron beam

Can. J. Chem. Downloaded from www.nrcresearchpress.com by 210.87.254.42 on 09/05/12
For personal use only.

was stopped in a 0.015-in. gold end plate which is held in position with the sample holder. For aligning and focusing the deuteron beam the gold end plate could be replaced by a piece of optical quartz.

Neutrons with energies from 12.5 to 20.4 Mev were produced by the T (d,n) He^4 reaction using a zirconium–tritium target with the Tandem accelerator providing a beam of 4.0-Mev deuterons. The target consisted of a 0.020 in. thick tungsten foil onto which was melted a thin layer of zirconium metal, 8 mg/cm². Tritium containing about 2% normal hydrogen was absorbed in the zirconium layer, the tritium content being about 1.2 cm³/cm² at N.T.P. or 3.1 curies/cm².* The deuteron energy loss in passing through the zirconium layer was about 600 kev and this was taken into account in determining the average deuteron energy. The irradiation assembly is illustrated in the upper part of Fig. 1. The neutron energy was varied by selecting the angular position of the sample relative to the deuteron beam. Data were obtained for the various energies in a single irradiation with the samples placed on a circular arc at a distance of 1.4 cm from the center of the Zr–T target. The samples were irradiated at angles of 50°, 105°, and 140° on both sides of the axis of the deuteron beam and at 0°. Any slight misalignment of the deuteron beam was corrected by averaging the activities produced in the samples at duplicate angles.

Neutrons of 14.5 Mev were also obtained from a 100-kev accelerator using the T (d,n) He^4 reaction. For these irradiations a Zr–T target as described above was used.

B. Irradiations

The Th^{232} was irradiated as metal disks of 3/16-in. diameter and 0.040-in. thickness. For irradiations employing the deuterium gas target, two thorium disks were stacked together in the sample holder at 0° to the deuteron beam and at a distance of 1.4 cm from the end of the gas target cell. To obtain the required neutron fluxes without excessive energy spread, the samples were only exposed at this position and a separate run was carried out for each neutron energy. At this position the half-angle subtended by the thorium disks from the average point of origin of the neutrons was about 6°. For irradiations using Zr–T targets the corresponding angle was about 9°. Irradiation times varied from 3 to 6 hours and the deuteron beam current from 0.4 to 1.0 μa.

In the irradiations performed with the 100-kev accelerator the thorium and sulphur samples were irradiated at 45° to the beam and at deuteron beam current of 10 to 30 μa.

The neutron beam was monitored with the reaction S^{32} (n,p) P^{32}. The sulphur monitors were prepared by compressing sulphur at 25 tons per square inch into pellets of the same dimensions as the thorium disks. In the irradiations the thorium samples were sandwiched between two sulphur monitors. The neutron beam was also monitored with a neutron long counter identical with that described by McTaggart (8). Besides obtaining a total neutron count for each irradiation, the output of the counter went to a counting rate meter which was connected to a chart recorder. This gave a continuous record of the neutron intensity throughout the irradiation. Normally, the neutron intensity was constant within 10%. Since the half-life of the product nuclide Th^{231} is longer than the irradiation times, it could be assumed that the neutron flux was constant during the irradiation. However, in several irradiations the neutron intensity varied more markedly and in these irradiations the chart record was divided into time increments and each

**The zirconium–tritium targets were obtained from the Radiochemical Centre, United Kingdom Atomic Energy Authority, Amersham, Bucks, England.*

Can. J. Chem. Downloaded from www.nrcresearchpress.com by 210.87.254.42 on 09/05/12
For personal use only.

portion was weighted by the neutron intensity and the exponential decay factor. The fraction of the radioactive nuclei which survived to the end of the irradiation calculated in this manner did not differ by more than 2% from that calculated assuming a constant neutron flux.

C. Radiochemical Analysis

After the irradiation, the thorium samples were dissolved and the thorium was radiochemically purified from fission products and the decay products of natural thorium by a modification of the procedure given by Prestwood (9). The method involved the precipitation of thorium as the iodate, oxalate, and the hydroxide as well as a mesityl oxide solvent extraction. The purified thorium was mounted as ThO_2 and beta counted in a methane flow beta proportional counter of about 2π geometry. The actual counting was done by an automatic sample changer coupled with automatic scaling, timing, and printout devices.

After the samples of thorium had decayed about a day there was considerable radioactivity due to the decay products of Th^{232}–Th^{228}. To correct for this activity, unirradiated thorium was separated from daughter activities and counted as a function of time to determine the growth in activity. The activity of Th^{231} in the irradiated samples was obtained by subtracting the activity due to the growth of the natural decay products of Th^{232}–Th^{228}. The Th^{231} decayed with an accepted value of 25.52 hours (10). The counter was calibrated for Th^{231}, by separating Th^{231} from a weighed amount of its parent U^{235} by means of an anion exchange resin (Dowex A1 100–200 mesh). The separation was performed with a known weight of natural thorium and the counter was calibrated for various weights of ThO_2.

The irradiated sulphur pellets were placed on counting trays and ignited. By measuring the activity ratio of unburnt to burnt sulphur pellets for pellets irradiated in a uniform neutron flux as a function of the pellet thickness, it was determined that $93.0\pm0.5\%$ of the P^{32} activity is left behind on the counting tray as essentially a weightless source. The efficiency of the counter for P^{32} was determined from aliquots of a solution of P^{32} standardized by 4π counting. The P^{32} samples were found to decay with the accepted half-life of 14.22 days (11).

RESULTS AND DISCUSSION

Values of the Th^{232} $(n,2n)$ Th^{231} cross sections were calculated from the observed activities of Th^{231} and P^{32} corrected to the end of the irradiation and the measured cross section for the reaction S^{32} (n,p) P^{32}, as reported by Allen *et al.* (6). Separate analyses were performed on the two thorium disks so that in each irradiation two measurements of the $(n,2n)$ cross section were obtained. Before the measured P^{32} activity could be used to calculate the neutron flux at the position of the thorium samples several corrections were necessary. These corrections took into account: (1) the difference in distance from the neutron source to the thorium and to the sulphur pellets, (2) neutron losses due to absorption and scattering in the pellets, (3) background neutrons which arise from neutrons generated in the beam plumbing, collimators, target window, and the gold end plate, (4) breakup neutrons produced by the reaction $D(d,np)D$, which has a threshold in the laboratory system of 4.45 Mev. The first two corrections were both calculated and measured experimentally by performing irradiations in which the thorium disks were replaced by sulphur pellets.

Can. J. Chem. Downloaded from www.nrcresearchpress.com by 210.87.254.42 on 09/05/12
For personal use only.

Typical corrections that were applied for the extraneous neutrons (corrections 3 and 4) in the neutron beam at various neutron energies are listed in Table I. The effect of

TABLE I

Typical corrections for extraneous neutrons

Deuteron energy (Mev)	Neutron energy (Mev)	% Various types of neutrons at 0° to deuteron beam			% Correction applied to P^{32} activity for	
		Monoenergetic $D(d,n)He^3$	Background	Breakup $D(d,np)D$	Background neutrons (obs.)	Breakup neutrons (calc.)
3.25	6.50	99.0	1.0	0	−0.5	0.0
5.30	8.50	95.4	2.6	2.0	−1.7	0.0
7.50	10.62	67.2	4.5	28.3	−4.0	−10.0

background neutrons was determined by performing irradiations with the gas cell evacuated. For T + D neutrons, zirconium targets without absorbed tritium were used. The percentage of breakup neutrons in the beam was calculated from the measurements of Cranberg *et al.* (12). From the table it is seen that their number increases rapidly as the deuteron energy is increased over the threshold for the reaction. The correction applied to the observed P^{32} activity due to the presence of breakup neutrons is listed in the last column of the table. It was calculated by graphical integration from the known spectrum of breakup neutrons (12) and the sulphur cross section. At the highest deuteron energy (8.55 Mev) this correction was 20%. It was not necessary to correct the observed Th^{231} activity for background and breakup neutrons since these neutrons have energies below the threshold for the $(n,2n)$ reaction.

For the angle irradiations, relative cross sections were obtained at various energies (12.5 to 20.4 Mev) by employing the differential cross section data of Bame and Perry (13) for the T (d,n) He^4 reaction to account for the variation in the neutron yield with angle. The values were normalized at a neutron energy of 14.45 Mev (sample at 105° to the deuteron beam) with the Th^{232} $(n,2n)$ cross section measured at this energy with sulphur monitors using the 100-kev accelerator.

The $(n,2n)$ cross section data are tabulated in Table II and displayed in Fig. 2. The cross sections are the average of at least two determinations. The errors quoted refer to the counting data, plus a 4% uncertainty in the absolute counting of Th^{231} and a 2% uncertainty in the counting of P^{32}. The errors do not include any error in the sulphur cross section. The sulphur (n,p) cross sections used in the calculations are also listed in the table and it is seen that the cross section is nearly constant in the energy range in which it was used.

For each irradiation an average neutron energy was calculated using the tables of Fowler and Brolley (14). The neutron energy is a direct function of the deuteron energy and the angle between the incident deuteron beam and the emitted neutron. To obtain the neutron energy, the following factors were considered: the deuteron energy loss in passing through the tantalum window or zirconium layer (15), the energy degradation in the deuterium gas, and the angular spread of the neutrons irradiating the thorium disks, as defined by the finite dimensions of both the disks and the deuteron beam. For each irradiation the effective neutron spectrum at the thorium disks was estimated. For irradiations employing the deuterium gas target, the spectrum was approximately

Can. J. Chem. Downloaded from www.nrcresearchpress.com by 210.87.254.42 on 09/05/12
For personal use only.

TABLE II

Summary of Th^{232} $(n,2n)$ Th^{231} cross section data

Neutron energy (Mev) average spread	Sulphur (n,p) cross section (barns)*	Th^{232} $(n,2n)$ cross section (barns)
$6.51^{+1.10}_{-0.14}$	0.338	0.015±0.007
$6.68^{+0.10}_{-0.13}$	0.336	0.036±0.003
$6.79^{+0.09}_{-0.13}$	0.336	0.094±0.008
$7.01^{+0.09}_{-0.13}$	0.338	0.271±0.013
$7.28^{+0.08}_{-0.12}$	0.340	0.603±0.028
$7.59^{+0.08}_{-0.12}$	0.342	0.976±0.045
$7.84^{+0.32}_{-0.32}$	0.344	1.20±0.07
$8.01^{+0.07}_{-0.11}$	0.346	1.39±0.07
$8.61^{+0.05}_{-0.11}$	0.350	1.61±0.07
$9.02^{+0.05}_{-0.11}$	0.353	1.75±0.08
$9.63^{+0.05}_{-0.11}$	0.357	1.94±0.09
$10.03^{+0.05}_{-0.11}$	0.359	1.83±0.08
$10.62^{+0.05}_{-0.11}$	0.356	1.91±0.09
$11.61^{+0.05}_{-0.11}$	0.345	1.72±0.08
12.53±0.26	—	1.51±0.08
14.45±0.20	0.229	1.23±0.06
18.52±0.5	—	0.459±0.027
20.40±0.20	—	0.225±0.015

*Allen *et al.* Phys. Rev. **107**, 1363 (1957).

trapezoidal with a greater number of lower-energy neutrons. An average energy was obtained by graphical analysis. The neutron energies given in Table II are average values and the spread quoted represents the standard deviation in the energy as seen by the thorium pellets.

In the graph of the data, Fig. 2, results from Los Alamos (4) at 7.5 and 8.5 Mev are also plotted. They appear to be consistent with the present measurements. However, the Russian value report by Zysin *et al.* (5) at 14.7 Mev lies outside the experimental errors quoted.

From the graph it is seen that the threshold for the reaction is 6.4±0.1 Mev in agreement with the value of 6.34±0.4 Mev (16) determined for the reaction Th^{232} (γ,n) Th^{231}. The decrease in cross section at about 12 Mev is attributed to competition with $(n,3n)$ and $(n,2nf)$ processes which have thresholds at 11.43 and 11.6 Mev respectively.

Can. J. Chem. Downloaded from www.nrcresearchpress.com by 210.87.254.42 on 09/05/12
For personal use only.

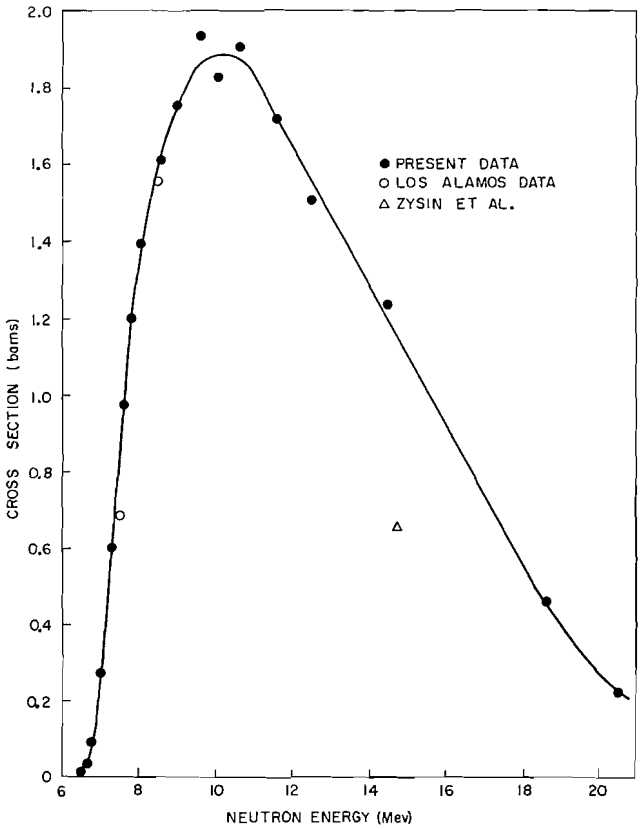


FIG. 2. $Th^{232}(n,2n)Th^{231}$ cross section versus neutron energy.

ACKNOWLEDGMENTS

We wish to express our appreciation to Mr. P. G. Ashbaugh and his staff for the operation of the Tandem Van de Graaff accelerator and to Drs. R. J. Clarke and W. G. Cross for the many helpful discussions and for the use of their 100-kev accelerator.

REFERENCES

1. D. J. HUGHES and R. B. SCHWARTZ. Neutron cross sections. 2nd ed. Brookhaven National Laboratory Report, BNL-325. 1958.
2. S. P. KALININ and V. M. PANKRATOV. Proceedings of the International Conference on the Peaceful Uses of Atomic Energy, Geneva. Vol. 16. 1958. p. 136.
3. A. A. BEREZIN, G. A. STOLIAROV, IU.V. NIKOL'SHII, and I. E. CHELNOKOV. J. Nuclear Energy, **11**, 175 (1960).
4. R. J. HOWERTON. Tabulated neutron cross sections. Part 1, Vol. III. University of California Radiation Laboratory, UCRL-5226. 1958.
5. IU.A. ZYSIN, A. A. KOVRIZHNYKH, A. A. LBOV, and L. I. SEL'CHENKOV. Atomnaya Energ. **8**, 360 (1960).
6. L. ALLEN, JR., W. A. BIGGERS, R. J. PRESTWOOD, and R. K. SMITH. Phys. Rev. **107**, 1363 (1957).
7. C. H. JOHNSON and H. E. BANTA. Rev. Sci. Instr. **27**, 132 (1956).
8. M. H. MCTAGGART. AWRE Report NR/A-1. 1959.
9. R. J. PRESTWOOD. Los Alamos Report LA-1721. 1958.
10. M. J. CABELL. Can. J. Phys. **36**, 989 (1958).
11. O. U. ANDERS and W. W. MEINKE. Nucleonics, **15** (12), 68 (1957).
12. L. CRANBERG, A. H. ARMSTRONG, and R. L. HENKEL. Phys. Rev. **104**, 1639 (1956); and private communications with Dr. L. Cranberg.

Can. J. Chem. Downloaded from www.nrcresearchpress.com by 210.87.254.42 on 09/05/12
For personal use only.

13. S. J. BAME, JR. and J. E. PERRY, JR. Phys. Rev. **107**, 1616 (1957).
14. J. L. FOWLER and J. E. BROLLEY, JR. Revs. Modern Phys. **28**, 103 (1956).
15. J. H. COON. *In* Fast neutron physics. Part I. *Edited by* J. B. MARION and J. L. FOWLER. Interscience Publishers Inc., New York. 1960. Chap. IV.D.
16. L. B. MAGNUSSON, J. R. HUIZENGA, P. R. FIELDS, M. H. STUDIER, and R. B. DUFFIELD. Phys. Rev. **84**, 166 (1951).

Can. J. Chem. Downloaded from www.nrcresearchpress.com by 210.87.254.42 on 09/05/12
For personal use only.

Can. J. Chem. Downloaded from www.nrcresearchpress.com by 210.87.254.105 on 09/05/12
For personal use only.

EVIDENCE FOR LOW-MOMENTUM-TRANSFER PROCESS IN K^{41} (α,n) $Sc^{44m,g}$ REACTIONS FROM RANGE MEASUREMENTS OF PRODUCTS[1]

TAKU MATSUO AND T. T. SUGIHARA

ABSTRACT

Average forward ranges have been measured for the product nuclides Sc^{43}, Sc^{44m}, and Sc^{44g} as produced in the reactions $K^{41}(\alpha,xn)$ with alpha particles in the energy region 23 to 39 Mev. These ranges, which are determined by a thick target – thick catcher technique, indicate that the (α,n)-produced isomers are formed in part by a low-momentum-transfer process above 30 Mev, its contribution being larger for the ground-state nuclide Sc^{44g}. From a thick target – thin catcher experiment at 40 Mev, it is found that the range distribution for Sc^{43} is that expected for a compound-nucleus reaction. Normalizing the Sc^{44m} and Sc^{44g} activity distributions to that of Sc^{43} for the catchers farthest from the target, we estimate the lower limits for the contribution of a direct-reaction low-momentum-transfer process to the formation of Sc^{44m} and Sc^{44g} at 40 Mev to be about 30% and 46% respectively.

A. INTRODUCTION

The ratio of formation cross sections of Sc^{44m} and Sc^{44g} (the "isomeric ratio") as produced in the reaction K^{41} (α,n) has previously been reported for the alpha energy region 6–30 Mev (1). These experiments have been extended to 40 Mev, and the excitation function for the reaction K^{41} $(\alpha,2n)$ Sc^{43} has also been measured (2). The results are summarized in Fig. 1.

The increase in the isomeric ratio from threshold to 26 Mev can be accounted for by a compound-nucleus mechanism, and the decrease in the region above 26 Mev was interpreted as resulting from the contribution of a non-compound-nucleus reaction (2). The latter reaction is expected to impart less linear momentum to the target nucleus than a compound-nucleus reaction. The linear momentum of the target nucleus is directly related to the recoil range of the product nucleus (3). Thus, a study of the recoil ranges of the Sc^{44} isomers should be useful in understanding the mechanisms by which these nuclides are produced. In this work, we report the average forward ranges in potassium chloride and aluminum of Sc^{43}, Sc^{44m}, and Sc^{44g} as produced by (α,xn) reactions on K^{41} in the alpha energy region 23–40 Mev.

In work by others, the recoil technique has recently been used by Winsberg and Alexander (3) in heavy-ion reactions, by Valyocsik (4) and by Harvey and co-workers (5) in deuteron and alpha reactions of heavy elements.

B. EXPERIMENTAL

Potassium chloride targets were prepared by evaporation on aluminum foil, and their thicknesses measured by weighing a target of known area. Fluctuations in thickness from point to point on the target were estimated to be less than 10%. Aluminum foils of high purity were used as recoil catchers. Stacks made up of target, catchers, and energy-degrading aluminum foils were bombarded in the deflected alpha beam of the 60-in. cyclotron at Brookhaven National Laboratory. The alpha-particle energy at each target foil was calculated from the range-energy curves of Aron (6). Schematic views of the

[1]*Manuscript received November 3, 1960.*
Contribution from Jeppson Laboratory of Chemistry, Clark University, Worcester, Massachusetts, with financial assistance from U.S. Atomic Energy Commission under contract AT(30-1)-1930. Presented at the Third Symposium on Nuclear Chemistry and Radiochemistry held at Atomic Energy of Canada Limited, Chalk River, Ontario, September 6–8, 1960.

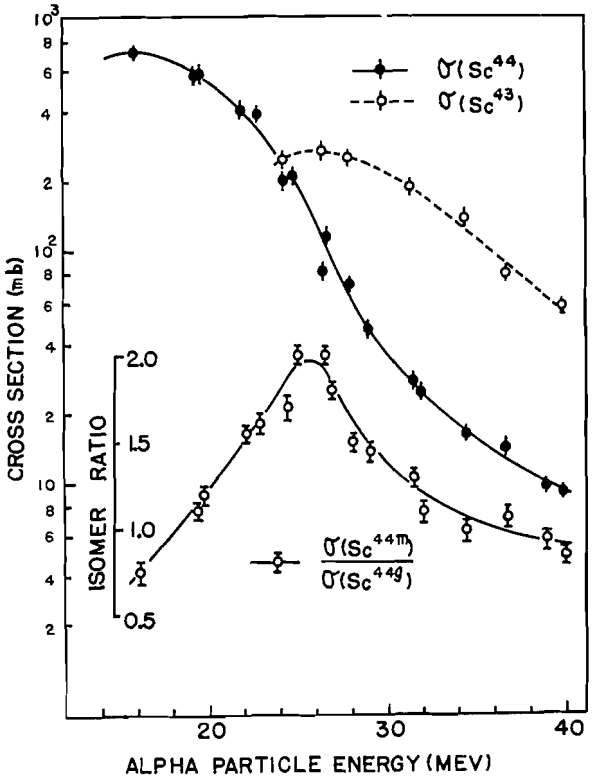


FIG. 1. Excitation functions for the $K^{41}(\alpha,n)$ (solid circles) and $K^{41}(\alpha,2n)$ (open circles) reactions. The (α,n) points include the contribution of both Sc^{44} isomers. The inset curve gives the isomeric ratio $\sigma(Sc^{44m})/\sigma(Sc^{44g})$.

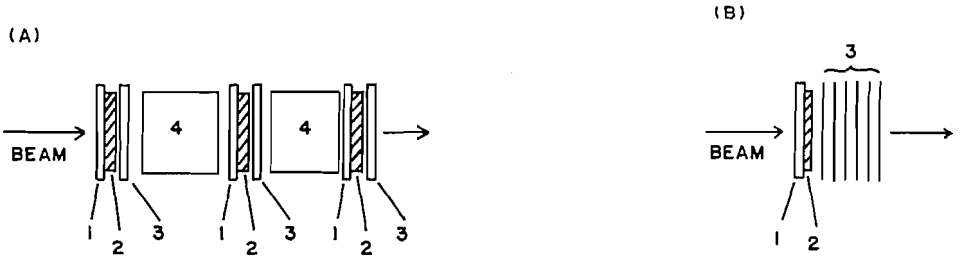


FIG. 2. Schematic diagram of target and catcher arrangement for (A) the thick – target thick catcher experiment and (B) the thick target – thin catcher experiment. 1 refers to an aluminum backing on which the KCl target 2 had been evaporated. The aluminum recoil catchers 3 are thick with respect to the range (A), or thin (B), where several such thin catchers are used. In (A) 4 refers to aluminum absorbers that were used to degrade the alpha-particle energy.

target and catcher arrangement are shown in Figs. 2*a* and 2*b*, and the details are discussed below.

After irradiation, target foils (on their aluminum backing) and catcher foils were separately dissolved in 8 *M* hydrochloric acid. Scandium carrier was added and extracted into tributyl phosphate, back extracted into 0.1 *M* hydrochloric acid, and precipitated as the hydroxide. The hydroxide was dissolved in minimum dilute hydrochloric acid.

Can. J. Chem. Downloaded from www.nrcresearchpress.com by 210.87.254.105 on 09/05/12
For personal use only.

Excess sodium carbonate was added, and lanthanum carbonate was precipitated. Scandium remains in solution as a carbonato complex. The supernate was acidified, and carbon dioxide was removed by boiling. Scandium hydroxide was precipitated again, dissolved in dilute hydrochloric acid, and finally precipitated as the salt of hypophosphorous acid (7).

Counting was done on a 3 in.×3 in. sodium iodide crystal, Sc^{43} being detected by its 0.38-Mev γ ray and Sc^{44g} by its 1.16-Mev γ ray. Since Sc^{44m} decays to Sc^{44g}, measurements of the 1.16-Mev γ ray as a function of time lead to a determination of both isomers. The γ-ray spectra of Sc^{43} and Sc^{44g} in equilibrium with Sc^{44m} are shown in Fig. 3. The Sc^{43} spectrum was obtained from a pure sample made by the reaction Ca^{40} (α,n) $Ti^{43} \xrightarrow{\beta^+} Sc^{43}$. From Fig. 3 it is clear that even when the Sc^{43} activity is 10 times that of Sc^{44g}, the 1.05-Mev γ ray of Sc^{43} does not appreciably contribute to the 1.16-Mev photopeak of Sc^{44g}.

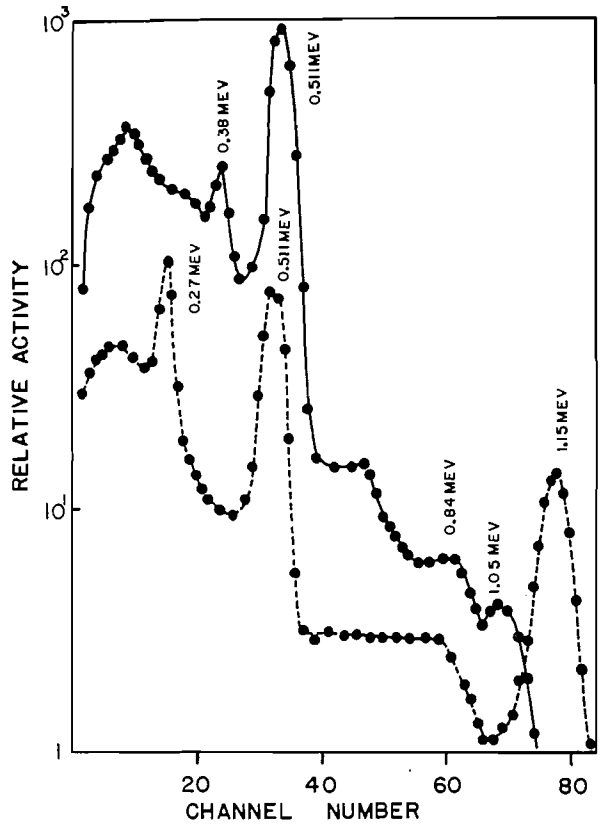


FIG. 3. Gamma-ray spectra of 4.0-hr Sc^{44g} in equilibrium with 2.4-day Sc^{44m} (dashed line) and of 3.9-hr Sc^{43} (solid line), as taken on a 3 in.×3 in. NaI crystal using a 100-channel analyzer. The Sc^{43} source was prepared by the reaction $Ca^{40}(\alpha,n)$ $Ti^{43} \xrightarrow{\beta^+} Sc^{43}$ and was free of Sc^{44}. Sc^{43} does not interfere with the determination of Sc^{44g} (and hence Sc^{44m}) at 1.15 Mev even if Sc^{43} has a 10-fold higher abundance. Sc^{43} was followed by its 0.38-Mev γ ray.

C. RESULTS

The average range (in the target material) of a nuclide can be measured in a thick target – thick catcher experiment such as that shown schematically in Fig. 2*a*. If the target

Can. J. Chem. Downloaded from www.nrcresearchpress.com by 210.87.254.105 on 09/05/12
For personal use only.

thickness is T and the fraction of the activity found in forward catcher is F, the average range R_0 is given (3) by

$$[1] \qquad R_0 = FT.$$

"Thick" in this context means considerably greater than R_0.

The results obtained for R_0 with a target thickness of 2.47 mg/cm² potassium chloride and an aluminum catcher of 7.3 mg/cm² are shown in Table I for alpha energies 23, 32, and 39 Mev. The estimated error in the determination of F is less than 5%; combined with possible fluctuations in the target thickness T, we estimate the over-all error in R_0 to be about 10%.

TABLE I

Thick-target ranges in KCl (μg/cm²)*

	E_α(Mev)		
Nuclide	23	32	39
Sc^{43}	380	423	575
Sc^{44m}	408	396	495
Sc^{44g}	413	361	430

*The errors are estimated to be about 10%.

The recoil behavior of the scandium nuclides was also studied in a thick target – thin catcher experiment at 40 Mev. A stack of foils similar to that shown schematically in Fig. 2*b* was irradiated. The target was 1.23 mg/cm² potassium chloride and each aluminum catcher 0.17 mg/cm².

The amount of the three nuclides found in each catcher, corrected for chemical yield, is shown in Table II and Fig. 4. The data in Table II and Fig. 4 are in arbitrary units,

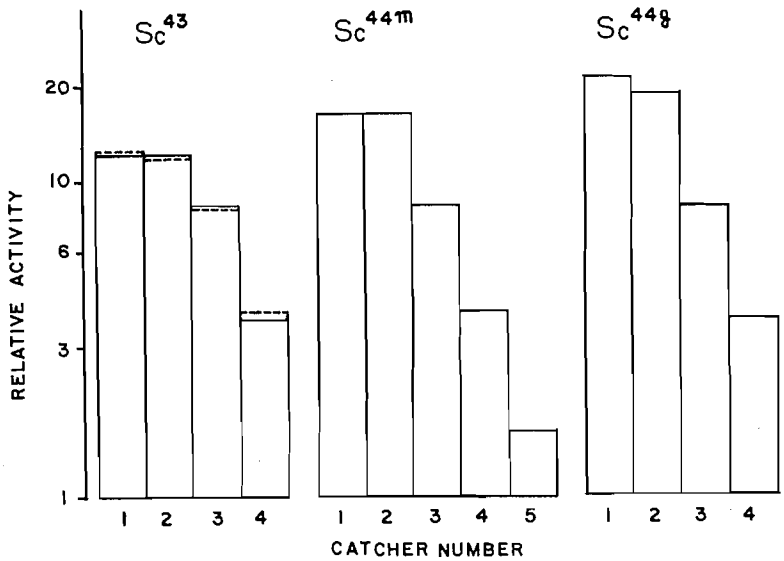


FIG. 4. The activity distribution of Sc^{43}, Sc^{44m}, and Sc^{44g} in thin forward catchers at 40 Mev. The dotted lines in the Sc^{43} distribution are the values expected from equation [7] for $n = 2.1$, $R_0 = 580$ μg/cm², and $\bar{\rho} = 0.45$.

Can. J. Chem. Downloaded from www.nrcresearchpress.com by 210.87.254.105 on 09/05/12
For personal use only.

TABLE II

Normalized differential distribution of products at E_α = 40 Mev*

	Catcher number (each 0.17 mg/cm² Al)				
Nuclide	1	2	3	4	5
Sc^{43}	12.2	12.1	8.30	3.62	—
Sc^{44m}	16.3	16.3	8.30	3.87	1.6
Sc^{44g}	21.0	18.6	8.30	3.60	—

*The errors are estimated to be about 5%.

normalized to give the same activity of all three nuclides in catcher number 3. The reason for this normalization procedure is discussed below.

D. DISCUSSION

The distribution in the forward range R of a product nucleus can be expressed (3) as

$$[2] \qquad P(R)dR = \frac{dR}{\sqrt{2\pi}\rho R_0} \exp\left[- \frac{(R - R_0)^2}{2\rho^2 R_0^2} \right]$$

where R_0 is the average range and ρ the straggling parameter. R_0 contains contributions from the momentum imparted by the incident particle, in this case an alpha particle, and from that resulting from emission of nucleons leading to the product nucleus. In reactions such as (α,n) or $(\alpha,2n)$ at relatively low energies, the latter contribution is small and is neglected here. The straggling parameter also consists of two terms (3), one characteristic of the stopping process and the other dependent on the angular distribution of the outgoing particles. The first term predominates over the latter (3).

The thick catcher experiment can give only R_0 as indicated in equation [1]. The data in Table I indicate that the ranges of Sc^{43}, Sc^{44m}, and Sc^{44g} differ from each other at energies above 30 Mev. It will be assumed that Sc^{43} is formed in a compound-nucleus reaction. Evidence to support this assumption is presented below. Lower R_0 values for Sc^{44m} and Sc^{44g} as compared to that for Sc^{43} indicate the contribution of a low-momentum-transfer or non-compound-nucleus reaction. This result is consistent with the interpretation for the decrease in isomeric ratio (2).

It has been shown (8) that R_0 is related to the kinetic energy E (in Mev) of a recoiling atom in a stopping material of atomic weight m and atomic number z in the following way:

$$[3] \qquad \frac{R_0}{E} = 0.600 \frac{m(m + M)}{M} \frac{(z^{2/3} + Z^{2/3})^{1/2}}{zZ} \text{ mg/cm}^2$$

where M and Z are the atomic weight and atomic number of the recoiling atom. R_0 values have been calculated from equation [3] for the compound nucleus formed by complete transfer of alpha-particle momentum to the K^{41} nucleus. These values as well as the observed Sc^{43} ranges are summarized in Table III. The ratio of the values calculated to those observed is about 2.5 and constant within experimental error at the three energies. Other workers (3, 4) have found also that observed ranges are substantially less than those

Can. J. Chem. Downloaded from www.nrcresearchpress.com by 210.87.254.105 on 09/05/12
For personal use only.

TABLE III
Comparison of calculated and observed ranges

	Ranges in KCl (mg/cm²)		
	E_α(Mev)		
	23	32	39
R_0 calculated for compound nucleus (eq. [3])	0.847	1.18	1.44
R_0 observed for Sc^{43}	0.380	0.423	0.575
Ratio calculated/observed	2.2	2.8	2.5

calculated by equation [3], particularly when the recoiling atom and stopping material are of nearly the same atomic weight and number, as is the case here. The constancy in the ratio implies that the range of Sc^{43} nuclei is increasing with energy in a manner consistent with equation [3]. Since the calculated R_0 assumes compound-nucleus formation, we consider the data of Table III to be evidence that Sc^{43} is formed chiefly by a compound-nucleus mechanism at all three energies. The fluctuations in the ratio are attributed primarily to variations in thickness of the target.

The differential-catcher method gives the straggling parameter ρ as well as R_0. If the recoiling atom traverses both target material and catcher, the probability that the atom will be found at some point x in the catcher is given by

$$[4] \qquad P(x)dx = \frac{dx}{\sqrt{2\pi}\bar{\rho}R_0}\int_0^T \exp\left[-\frac{(cx+t-R_0)^2}{2\bar{\rho}^2R_0^2}\right]dt$$

where x and t are the path lengths in catcher and target respectively as measured in the beam direction, $\bar{\rho}$ is the straggling parameter averaged over the target and catcher material, T is the target thickness, and c is a factor that converts range in catcher to that in the target material as follows:

$$[5] \qquad c = \frac{m_1(m_1+M)}{m_2(m_2+M)}\left(\frac{z_1^{2/3}+Z^{2/3}}{z_2^{2/3}+Z^{2/3}}\right)^{1/2}\frac{z_2}{z_1}.$$

The subscripts 1 and 2 refer to target and catcher respectively; the other symbols are as in equation [3].

The straggling parameter is given by (8)

$$[6] \qquad \rho = [2mM/3(m+M)^2]^{1/2}.$$

In our case both the target material and catcher material affect ρ; their relative importance depends on the ratio of t to x. However, since ρ_{KCl} and ρ_{Al} are 0.405 and 0.396 from equation [6], it is permissible to use an average value $\bar{\rho}$ without introducing appreciable error.

The integrand of equation [4] can be transformed into that of a normal distribution by making the substitution $u = (cx + t - R_0)/R_0$.

$$[7] \qquad P(x)dx = \frac{dx}{\sqrt{2\pi}\bar{\rho}}\int_{(cx-R_0)/R_0}^{[cx+R_0(n-1)]/R_0} \exp\left(-\frac{u^2}{2\bar{\rho}^2}\right)du$$

Can. J. Chem. Downloaded from www.nrcresearchpress.com by 210.87.254.105 on 09/05/12
For personal use only.

where $n = T/R_0$. The function $P(x)$ of equation [7] is shown in Fig. 5* for several values

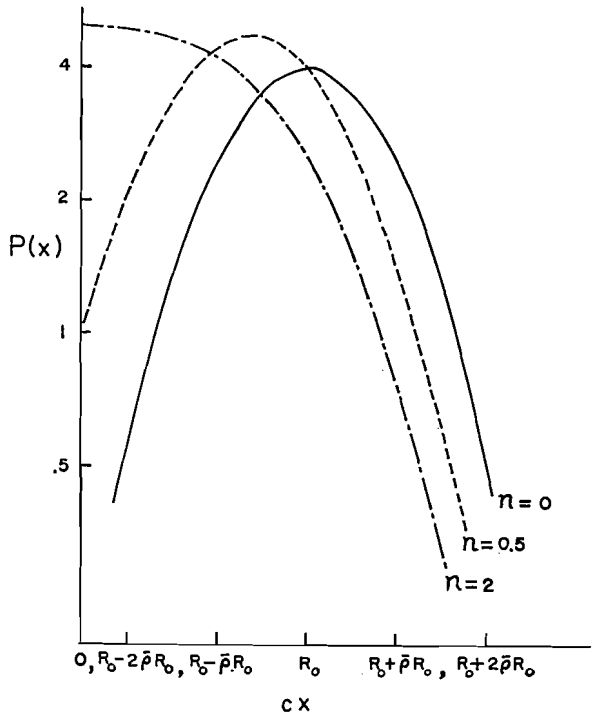


FIG. 5. The distribution function $P(x)$, equation [7], plotted as a function of cx. The various curves indicate the change in shape with reduced target thickness $n = T/R_0$. $\bar{\rho}$ has been taken to be 0.4.*

of n, indicating the shape of the distribution for various target thicknesses. For a given n value, if a nuclide is produced by several mechanisms of different momentum transfer and different R_0, a range distribution different in shape from those of Fig. 5 is expected.

When $n > 2$ and $\bar{\rho} \leqslant 0.45$,

$$[8] \qquad \frac{1}{\sqrt{2\pi}\bar{\rho}} \int_{(n-1)}^{\infty} \exp\left(-\frac{u^2}{2\bar{\rho}^2}\right) du \leqslant 0.013.$$

That is, the range distribution given by equation [7] is represented to a good approximation by

$$[9] \qquad P(x)dx = \frac{dx}{\sqrt{2\pi}\bar{\rho}} \int_{(cx-R_0)/R_0}^{\infty} \exp\left(-\frac{u^2}{2\bar{\rho}^2}\right) du.$$

The change in the upper limit of the integral does not appreciably affect the value of $P(x)$.

Thus it is apparent that probability paper should be used to determine $\bar{\rho}$ from the data of the thin-catcher experiment. The relative activity of a given nuclide found in catcher 1 (Table II) is plotted at $x_1 = 1/2$ thickness of catcher 1. That in catcher 2 is plotted at x_2 = thickness of catcher 1 + 1/2 thickness of catcher 2 and so on. The relative activity for $x = R_0/c$ is estimated by interpolation. The R_0 value is taken from the thick-catcher

*NOTE ADDED IN PROOF: The ordinate scale is in arbitrary units.

Can. J. Chem. Downloaded from www.nrcresearchpress.com by 210.87.254.105 on 09/05/12
For personal use only.

experiment (Table I). If this activity is taken to be 50%, then the range distribution is suitably normalized. This process was followed for each of the nuclides, and the resulting plot on probability paper is shown in Fig. 6. We see that $\bar{\rho} = 0.45 \pm 0.02$ is a reasonable value for all three nuclides, and in fair agreement with the calculated values of $\bar{\rho}$ from equation [6].

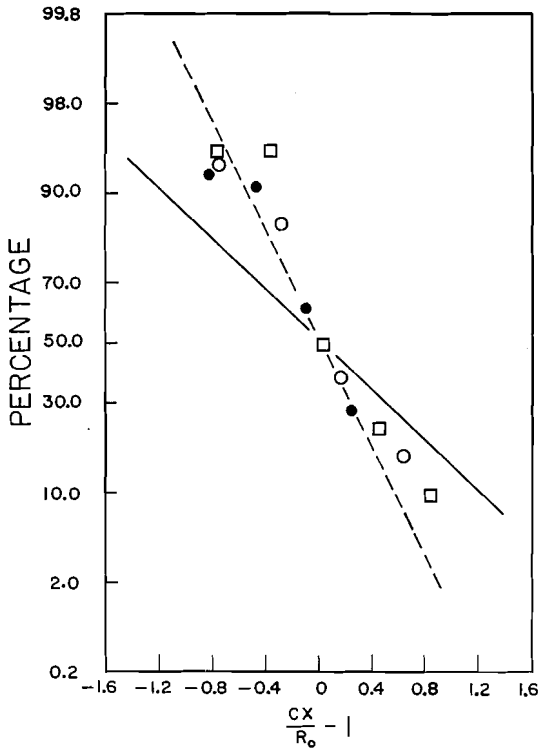


FIG. 6. Probability-paper plot of activity distribution in catchers as a function of $(cx/R_0) - 1$. The open circles refer to Sc^{44g}, the solid circles to Sc^{43}, and the squares to Sc^{44m}. The dashed line corresponds to $\bar{\rho} = 0.45$ and the solid line to $\bar{\rho} = 1.0$.

The activity distribution of Sc^{43} (Fig. 4) corresponds to that expected from equation [7] for $n = 2.1$. Other evidence (isomeric ratio and R_0 values) suggests that above 26 Mev a low-momentum-transfer process contributes to the formation of Sc^{44m} and Sc^{44g}. If we assume that at 40 Mev all of the Sc^{43} nuclei and some of the Sc^{44m} and Sc^{44g} nuclei are formed by a compound-nucleus mechanism, the observed range distributions should be the same for large values of x. Differences in range distribution should appear only for small values of x since a low-momentum-transfer contribution of smaller R_0 value is postulated. Thus the observed yields of the three nuclides in the various catcher foils have been normalized in Table II such that the distributions coincide for large values of x.

These data can now be used to estimate the amount of contribution of non-compound-nucleus reactions. The quantities used in this calculation are summarized in Table IV. The fraction found in the catcher, column (2), is obtained for each nuclide from measured R_0 values (Table I) and the target thickness T (1.23 mg/cm² KCl). Column (3) lists the sum of the activity found in the catchers, and column (4) is the calculated amount left in the target. In columns (3) through (8), the activity units are the normalized units of

Can. J. Chem. Downloaded from www.nrcresearchpress.com by 210.87.254.105 on 09/05/12
For personal use only.

Table II. Column (5) is simply the sum of (3) and (4), the total activity produced. In column (6) the activity in the catchers attributed to a direct reaction is calculated, assuming that this is obtained by subtracting the Sc^{43} activity in the catchers from that of Sc^{44m} and Sc^{44g}. The direct-reaction contributions to Sc^{44m} and Sc^{44g} are similarly calculated for the activity remaining in the target in column (7). Column (8), which is the sum of (6) and (7), represents the total contribution of direct reactions. The fractions of Sc^{44m} and Sc^{44g} activity that can be attributed to a direct reaction (column (8)/column (5)) are listed in column (9).

TABLE IV

Direct-reaction contribution to formation of Sc^{44m} and Sc^{44g} at 40 Mev

Nuclide	Fraction out*	Activity†						Fraction by direct reaction
		A	B	C	D	E	F	
Sc^{43}	0.467	37.8‡	43.2	81	—§	—§	—§	—§
Sc^{44m}	0.402	46.4	69.0	115	9	26	35	0.30
Sc^{44g}	0.350	53.1‡	98.6	152	15	55	70	0.46

NOTE: A = Activity in catchers. B = Activity in target. C = Total activity, target and catchers. D = Direct-reaction activity, catchers. E = Direct-reaction activity, target. F = Direct-reaction activity, total.

*Calculated from R_0 values of Table I at 39 Mev and T = 1.23 mg/cm² KCl.

†Normalized activity units used in Table II.

‡Assumed that 1.6 activity units of Sc^{43} and Sc^{44g} would have been found in catcher 5 (as in the case of Sc^{44m}) if detection sensitivity had been higher.

§Sc^{43} assumed to be formed only by compound-nucleus mechanism.

The calculated direct-reaction contributions, 30% for Sc^{44m} and 46% for Sc^{44g}, are only lower limits. It is conceivable that a direct reaction producing products of intermediate or long range could have contributed to the Sc^{44m} and Sc^{44g} activity found in catcher 3 and beyond. In this calculation, it has been assumed that all activity in these catchers could be attributed to a compound-nucleus reaction. If Sc^{43} is formed partially by a direct reaction at 40 Mev, the calculated direct-reaction contributions to Sc^{44m} and Sc^{44g} would also be low.

ACKNOWLEDGMENTS

We are greatly indebted to Dr. R. W. Dodson and Dr. G. Friedlander for their generous hospitality in making available to us many of the facilities of Brookhaven National Laboratory and to Dr. C. P. Baker and members of the cyclotron operating crew for their assistance in irradiations. We gratefully acknowledge some illuminating discussions with Dr. J. M. Alexander.

REFERENCES

1. T. MATSUO and T. T. SUGIHARA. Bull. Am. Phys. Soc. II, 4, 141 (1959).
2. T. MATSUO. Annual Progress Report, Clark University, Worcester, Mass. Contract AT(30-1)-1930. 1960.
3. L. WINSBERG and J. M. ALEXANDER. Lawrence Radiation Laboratory Reports UCRL-8618 (1959) and UCRL-8997 (1960).
4. E. W. VALYOCSIK. Lawrence Radiation Laboratory Report UCRL-8855. 1960.
5. B. G. HARVEY, W. H. WADE, and P. F. DONOVAN. Phys. Rev. **119**, 225 (1960).
6. W. A. ARON, B. G. HOFFMAN, and F. C. WILLIAMS. U.S. Atomic Energy Commission Report AECU-663. 1949.
7. D R. BOMBERGER. Anal. Chem. **30**, 1907 (1958).
8. J. LINDHARD and M. SCHARFF. Private communication quoted in R. B. LEACHMAN and H. ATTERLING. Arkiv Fysik, **13**, 101 (1959).

Can. J. Chem. Downloaded from www.nrcresearchpress.com by 210.87.254.105 on 09/05/12
For personal use only.

Can. J. Chem. Downloaded from www.nrcresearchpress.com by 210.87.254.42 on 09/05/12
For personal use only.

A GAS-CHROMATOGRAPHIC APPARATUS FOR THE STUDY OF THE HOT-ATOM CHEMISTRY OF ORGANIC HALIDES[1]

M. D. Silbert and R. H. Tomlinson

ABSTRACT

The construction of an easily assembled and inexpensive gas-chromatographic apparatus is described. This system has been designed to determine β-active materials. The operation of this instrument involves the use of a temperature program in order to resolve materials boiling over a wide range of temperature.

INTRODUCTION

Libby (1, 2) made the first attempts to isolate and identify the individual organic products from neutron-irradiated alkyl halides. From the reaction, $Br^{81}(n,\gamma)Br^{82}$, in *n*-propyl bromide he separated some eight active organic products using the technique of fractional distillation. Willard (3) using the same compound and separational method later increased the number of products to 11.

The technique of fractional distillation suffers from one great disadvantage. It cannot operate at the tracer level; carriers must be added for all components present. If carriers are not added the tracers will tend to contaminate each other or any carriers that are present.

Willard and Evans (4, 5) were the first to adapt gas-chromatographic methods to the study of hot-atom reactions of alkyl halides. From neutron-irradiated *n*-propyl bromide they obtained more than 20 active organic products without prior addition of macro amounts of inactive carrier. They had thus shown that gas chromatography was a method of analysis that was suitable not only for operation at the macro level, but also at a tracer level.

EXPERIMENTAL

In Fig. 1 is shown a schematic diagram of the gas-chromatographic apparatus constructed for determination of the β-active products from the hot-atom reactions of alkyl halides. The detection system employed was one designed for detection of active products; it is conceivable, however, that it could be substituted by or complemented with a conventional type of gas-chromatographic detection system for detection of inactive materials or added carriers.

The gas entered through a fine capillary (A) whose resistance to flow was greater than that of the column; thus it determined the flow rate of carrier through the entire system. With this device it was possible to program the column temperature with a minimum variation in flow rate.

The sample introduction system (D) shown in Fig. 2 had been designed to make use of the micropipettes commonly used in gas-chromatographic analysis. The pipette, filled by capillary action, was inserted through the rubber seal up to the stopcock. The stopcock was then opened and the pipette inserted until its tip plugged the hole in the silicone rubber disk. This blocked the normal carrier gas flow and thus forced the carrier gas to flow through the pipette, blowing the measured volume of liquid into the system. The pipette could then be withdrawn.

[1]*Manuscript received November 3, 1960.*
Contribution from the Department of Chemistry, Hamilton College, McMaster University, Hamilton, Ontario. This paper was presented at the Third Symposium on Nuclear Chemistry and Radiochemistry held at Atomic Energy of Canada Limited, Chalk River, Ontario, September 6–8, 1960.

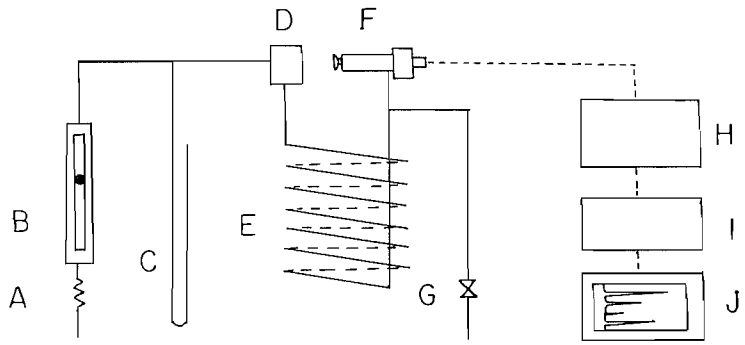


FIG. 1. Schematic diagram of gas-chromatographic apparatus.
A. Capillary flow restriction. B. Flowmeter. C. Mercury manometer. D. Sample introduction system. E. Column. F. Flow counter. G. Methane inlet. H. High-voltage supply and linear pulse amplifier. I. Rate meter. J. Recorder.
Solid lines indicate gas flow. Broken lines indicate electrical connections.

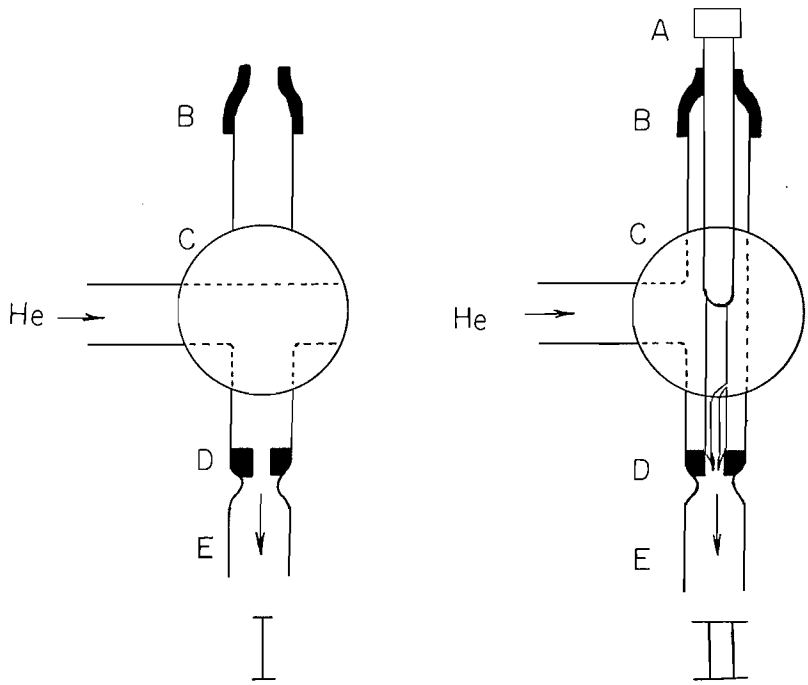


FIG. 2. Sample introduction system. I. Normal flow. II. Sample introduced.
A. Micropipette. B. Rubber seal. C. Large stopcock. D. Silicone rubber disk. E. Column.

A second sample-introduction system made use of a microsyringe and a puncture seal. The sample volume could be increased as a function of time thereby correcting for radioactive decay and normalizing all chromatograms to the same starting time after irradiation.

The column (E in Fig. 1) was heated by an air oven. This consisted of a metal can 30 cm high and 13 cm in diameter. It was wrapped with asbestos, nichrome wire, and aluminum foil. Temperature programing was achieved by increasing the voltage to the nichrome wire heater at preset time intervals.

Can. J. Chem. Downloaded from www.nrcresearchpress.com by 210.87.254.42 on 09/05/12
For personal use only.

The column was a helix of 6-mm O.D. pyrex tubing coiled to an outside diameter of 6.5 cm. Lengths of 2 and 4 meters were used. The packing was 30% by weight General Electric SF-96 (40) silicone oil coated on Johns–Manville Chromosorb P (30–60 mesh). This packing gave good resolution and short analysis times for alkyl halides. It also had the property of allowing the components to emerge in order of their boiling points, a help in identification.

The outlet of the column was connected to the flow counter (F in Fig. 1) which is shown in detail in Fig. 3. The connection was kept at 200° C in order to prevent condensa-

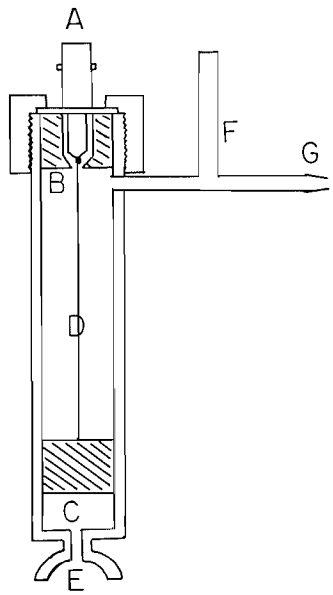


FIG. 3. Cross section of flow counter.
A. UG 931/U high-voltage connector. B. Teflon plug. C. Teflon plug grooved to permit flow of gas. D. 0.05-mm tungsten wire. E. Ball joint. F. Methane inlet. G. Connection to column, 7/25 standard taper joint.

tion of the high-boiling components. The carrier gas was mixed with methane (natural gas was also found suitable) before entering the active volume of the counter. The active components present in the carrier gas were then counted as part of the counting gas, inside the counter with a very high efficiency. This system was the most sensitive of all present day systems of monitoring gas streams. The relative sensitivity and resolution could be varied by adjusting the flow of the methane relative to the carrier gas as this determined the length of time the active fraction remains in the counter. A trap was connected to the exit of the counter using a spherical ground joint; this was necessary to dispose of the active waste.

The output of the flow counter was fed into a linear pulse amplifier and rate meter. The rate meter ran a standard 10-mv potentiometer recorder which plotted the radiochromatogram.

RESULTS

Figure 4 shows chromatograms of the products from the reaction Br^{79} (n,γ) Br^{80} in pure *n*-propyl bromide. Results are shown for irradiation at liquid air temperature

Can. J. Chem. Downloaded from www.nrcresearchpress.com by 210.87.254.42 on 09/05/12
For personal use only.

Can. J. Chem. Downloaded from www.nrcresearchpress.com by 210.87.254.42 on 09/05/12
For personal use only.

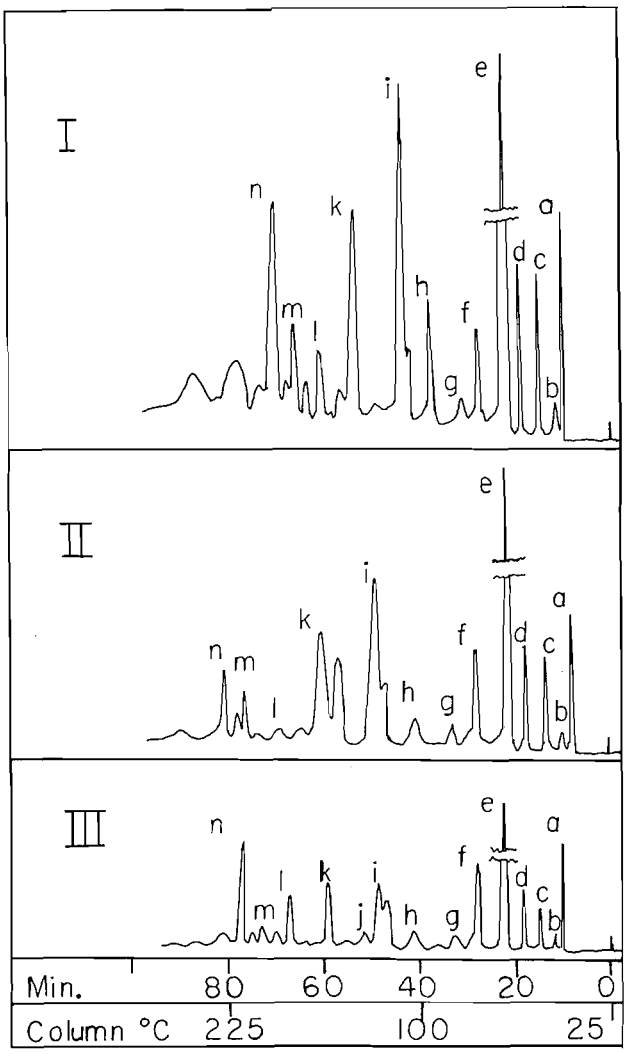


FIG. 4. Radiochromatograms of the products of the $Br^{79}(n,\gamma)Br^{80}$ reaction in *n*-propyl bromide. I, at liquid N_2 temperature (−196° C). II, at core temperature (30° C). III, elemental bromine scavenged (30° C).

IDENTIFICATION OF PRODUCTS:

(*a*)	Methyl bromide	(*h*)	1,2-Dibromoethane
(*b*)	Vinyl bromide	(*i*)	1,2-Dibromopropane
(*c*)	Ethyl bromide	(*j*)	Bromoform
(*d*)	*i*-Propyl bromide	(*k*)	1,3-Dibromopropane
(*e*)	*n*-Propyl bromide	(*l*)	1,1,2-Tribromoethane
(*f*)	Methylene bromide	(*m*)	Carbon tetrabromide
(*g*)	1,1-Dibromoethane	(*n*)	1,2,3-Tribromopropane

Vertical axis represents relative response of the recorder.

(−196° C) and at the reactor temperature (30° C). At the reactor temperature the effects of elemental bromine scavenger are also shown.

The samples sealed in quartz were irradiated in the Rabbit System of the McMaster Nuclear Reactor for 30 seconds at a flux of 5×10^{12} n/cm² sec. The background γ field, as determined by cobalt glass, was 10^5 r integrated over this 30-second irradiation period.

DISCUSSION

The detection system used in this apparatus was a gas-flow proportional counter designed to operate with a mixture of helium and methane. It was of similar design to the counter described by Wolfgang and Rowland (6) for studies of tritiated compounds.

The great advantage of this detection method was its great sensitivity. As the counting was done internally the counter was essentially 100% efficient for β radiation.

Both Willard (4, 5) and Herr (7) passed the carrier gas through external tubing close to scintillation crystals, thereby incurring loss due to both geometry and crystal efficiency. The literature also described several other systems which externally monitor the gas stream; these, however, lose sensitivity by geometrical losses. These included both Geiger–Müeller (7, 9) and scintillation (10) detection systems.

Harris (8) collected fractions in charcoal traps which were counted in a well-type crystal. Although this method is very sensitive it does not give continuous chromatograms and is not as convenient.

Ionization chambers have been described (11, 12) using continuous flow systems. The geometrical losses have thus been reduced but the sensitivity remains less than that of a proportional counting system.

The proportional counter suffers from the big disadvantage that it can not be used at elevated temperatures. In general, Geiger–Müeller and proportional counters do not perform satisfactorily above 75° C. Wolfgang and Rowland (6) have found, however, that their design performed satisfactorily up to 200° C, the only change having been a shortening in the length of the plateau. This result was confirmed with the flow counter used in this laboratory.

REFERENCES

1. L. W. Friedman and W. F. Libby. J. Chem. Phys. **17**, 647 (1949).
2. M. S. Fox and W. F. Libby. J. Chem. Phys. **20**, 487 (1952).
3. J. C. W. Chien and J. E. Willard. J Am. Chem. Soc. **79**, 4872 (1957).
4. J. B. Evans and J. E. Willard. J. Am. Chem. Soc. **78**, 2908 (1956).
5. J. B. Evans. Ph.D. Thesis, University of Wisconsin. 1957. University Microfilms, Ann Arbor, Mich.
6. R. Wolfgang and F. S. Rowland. Anal. Chem. **30**, 903 (1958).
7. W. Herr, F. Schmidt, and G. Stöcklin. Z. Anal. Chem. **170**, 301 (1959).
8. W. E. Harris. Paper presented at the Third Symposium on Nuclear and Radiochemistry, Chalk River, Ontario. Sept. 6–8, 1960. Can. J Chem. **39**, 121 (1961).
9. G. Blyholder. Anal. Chem. **32**, 572 (1960).
10. G. L. Grandy and R. C. Koch. Rev. Sci. Instr. **31**, 786 (1960).
11. L. H. Mason, H. J. Dulton, and L. R. Bair. J. Chromatog. **2**, 322 (1959).
12. Nuclear Chicago Corporation. Model DCF gas flow ion chambers.

Can. J. Chem. Downloaded from www.nrcresearchpress.com by 210.87.254.42 on 09/05/12
For personal use only.

Can. J. Chem. Downloaded from www.nrcresearchpress.com by 210.87.254.6 on 09/05/12
For personal use only.

SCINTILLATION COUNTING WITH ORGANIC PHOSPHORS[1]

B. LIONEL FUNT

ABSTRACT

Current techniques employed in scintillation detection of beta emitters are reviewed. Internal liquid scintillation counting, with a number of homogeneous mixed solvent systems, is described. Heterogeneous counting systems containing radioactive material in the dispersed phase include scintillating gels, thickened scintillators, and emulsions, and a number of methods embodying direct counting of active deposits on filter paper. Heterogeneous systems with the radioactive material in the continuous phase are described and include plastic capillary counters, plastic filaments, or organic crystals wetted with aqueous solutions.

INTRODUCTION

Internal sample scintillation counting provides inherent advantages of high sensitivity, energy discrimination, 4π geometry, and lower background for a given sample size.

Comparisons between different counting methods are often misleading, but it is nevertheless instructive to try to assess the potentialities and merits of different counting techniques.

Guinn (1), for example, compared Geiger and liquid scintillation counting of beta emitters. He drew the distinction between "absolute sensitivity" i.e. the minimum amount of an isotope detectable to a given standard deviation in a reasonable counting time, and "concentration sensitivity", which represents the minimum concentration detectable under the same conditions. Gas counting methods furnished superior or equal absolute sensitivities to those attainable with liquid scintillation counting. The merits of liquid scintillation counting were evident when the concentration sensitivities were compared. Here results that were superior by orders of magnitude to those attainable with gas counting methods were obtained for isotopes of low energy. The superiority of liquid scintillation counting in this comparison is primarily a reflection of the much larger quantity of isotope which can be introduced into the counting volumes with this method.

The technical problems encountered in the application of internal scintillation counting methods stem primarily from two sources: (1) sample insolubility and (2) quenching effects. The potentialities of the counting technique cannot, in general, be realized if the sample cannot be incorporated effectively into the counting volume. Since the choice of liquid scintillator solvent is limited to relatively non-polar compounds, the assay of many samples is hindered by the relative insolubility of the material in the scintillator solution. The use of mixed solvents may in many instances partially overcome these difficulties, but generally, this is at the expense of a decreased luminescent output with accompanying losses in counting efficiency (2, 3, 4, 5).

Even when the sample is directly soluble in the scintillator solution the quenching effects of various polar groups may result in a serious reduction in luminescent efficiency and of detection sensitivity (6). Furthermore, light absorption, particularly by colored compounds, will reduce the effectiveness of the counting methods (7).

Many of these difficulties have been overcome successfully by a variety of ingenious methods. Although an ideal counting technique cannot be said to exist, an intelligent

[1]*Manuscript received November 3, 1960.*
Contribution from the Chemistry Dept. University of Manitoba, Winnipeg, Manitoba. Paper presented at the Third Symposium on Nuclear Chemistry and Radiochemistry held at Atomic Energy of Canada Limited, Chalk River, Ontario, September 6–8, 1960.

choice of a counting method from those recently described can provide a simple, reproducible, and sensitive solution to most counting problems.

Homogeneous Liquid Scintillation Counting

This method provides the greatest inherent sensitivity and is most adaptable to samples of any size. Frequently the sample is directly soluble in the scintillator solution. For example, in our work on C-14-labelled polystyrene it was sufficient to dissolve the sample directly in the scintillator solution (8). For non-polar hydrocarbons surprisingly little quenching of the scintillations is found. Where quenching is suspected, compensating corrections may be applied. Frequently this is accomplished by the addition of an internal standard (9, 10) of known activity to the sample volume after the completion of the sample count. The counting efficiency of the sample plus standard is assumed to be equal to that for the standard alone.

Dilution of the sample solution with additional liquid scintillator will also serve to determine quenching effects and allow correction by extrapolation to zero concentration of quencher (10). Recently a novel suggestion for correction for quenching in H-3 counting has been made (11). A source of Co-60 on a platinum needle is inserted into the liquid scintillator where the 14-kev beta energy is detected. This procedure eliminated the contamination of the sample inherent in the use of an internal standard.

Where ultimate sensitivity is of the utmost importance, as in archaeological dating of natural radiocarbon, simplicity may be sacrificed to elaborate sample preparation. In such work the sample may be burned and the CO_2 synthesized to an aromatic hydrocarbon, or more simply to a soluble compound of moderate quenching action. The preparation of toluene (12), paraldehyde (13), methyl borate (14), and *p*-cymene (15) for such purposes has been reported.

In the more usual analysis, particularly of inorganic substances, such syntheses cannot be employed. There the expedient of using multicomponent homogeneous solvents is often practiced and solutions containing water–ethanol–toluene (16) or water–dioxane (2, 17, 18) have been described. The addition of naphthalene, as a secondary solvent, greatly reduces quenching effects in such systems (18, 19, 20). A composition employed frequently is that due to Kinard (21) which utilizes xylene–dioxane–ethanol and naphthalene. For inorganic salts, tributylphosphate can be employed in scintillator systems (22). Since this compound is a common extracting agent in various liquid–liquid extractions, its direct use appears to offer potentialities which do not appear to have been fully explored.

The use of the metal salts of 2-ethyl-hexanoic acid offers another method of incorporating many metallic substances into solution at concentrations ranging up to 10% of the metal by weight (23, 24). This procedure, although more elaborate than direct counting of aqueous solutions, will accommodate much greater amounts of the desired isotope, with a lower quenching effect. The weak natural activities of Sm-147, for example, have been studied by this method (25).

Several new solvents, including monoisopropylbiphenyl (26) and silicones (27) have recently been reported, and these deserve special consideration because of their lower quenching behavior and different solvent properties.

Heterogeneous Counting Systems

For routine counting of numerous samples some new methods offer an effective compromise between maximum sensitivity and minimum sample preparation. The use of heterogeneous counting systems circumvents the problems of quenching action and

Can. J. Chem. Downloaded from www.nrcresearchpress.com by 210.87.254.6 on 09/05/12
For personal use only.

Can. J. Chem. Downloaded from www.nrcresearchpress.com by 210.87.254.6 on 09/05/12
For personal use only.

sample insolubility but introduces new difficulties in the forms of light collection and self-absorption of energy.

Suspensions of solids in aluminum stearate gel scintillators were described by Funt and Hetherington (28) and their method can be applied to the assay of a wide variety of colorless salts or insoluble inorganic materials. The aluminum stearate gel scintillators were modified by White and Helf to suspensions in Thixcin (29), a castor oil derivative, and to liquid scintillators thickened with polymers, by Fleishman and Shadkidzhanyan (30). Another suspending agent, Cab-O-Sil, a finely divided form of silica was suggested by Ott *et al.* (31) and Gordon (32). In addition we have found that the original aluminum stearate gels can be replaced by aluminum-2-ethyl hexanoate which gels immediately without heating in the liquid scintillation medium (23). Alternatively the aluminum stearate suspensions may be gelled by the addition of phenols or cresols without the application of heat (23).

Scintillating emulsions have been described recently by Shapira and Perkins (33). As with suspensions in gels and thickened systems, the opacity of the scintillator does not greatly reduce the counting efficiency, and counting has been performed with 10% efficiency for H^3 and 52% for C^{14}.

We have considered the use of transparent emulsions in order to overcome the opalescence associated with the usual emulsion systems. Bowcott and Schulman (34) have described the preparation of such systems, and their possible application to scintillation detection is obvious.

Another interesting and effective method of scintillation counting in heterogeneous systems employs direct counting on filter paper. In many instances the active material is collected on filter paper or separated on a filter paper chromatogram. Roucayrol (35) reported that wetting the filter paper with a liquid scintillator solution rendered it transparent and made direct counting of the collected material possible. Funt and Hetherington (36) modified this technique by employing monoisopropylbiphenyl as the scintillator solvent thus reducing air quenching effects and overcoming variations in detection sensitivity due to solvent evaporation. Wang and Jones (37) found that the suspension of filter paper strips in counting vials containing liquid scintillator gave good counting efficiencies and reproducibilities and was eminently suitable for the counting of numerous samples in a commercial liquid scintillation spectrometer. The question of the best orientation of the strips was raised by Loftfield (38), who claimed differences in counting efficiency dependent upon orientation which are, however, disputed by other workers (39). Davidson (40) recently reported excellent results with this technique when circles of filter paper were arranged parallel to the phototube surface and this is very similar to the filter paper counting methods described above (36).

An alternative method of heterogeneous counting employs the organic phosphor in the dispersed phase with the active material in the continuous phase. Naphthalene and anthracene crystals were first suggested for the gaseous counting of tritium in 1950, (41, 42, 43) but an adaptation of these methods has only recently gained favor. Steinberg (44) described the use of packed broken filaments of plastic scintillator wetted with active material in aqueous solution. Powdered anthracene crystals were later reported for the same purpose (45). Best reproducibility is achieved when the counting vial is packed with the powdered phosphor and filled above the level of the phosphor with excess active solution.

A device for the counting of active aqueous solutions or gases in flow or static systems was described by Funt and Hetherington (46), who employed a spiral capillary of plastic

scintillator. The wall thickness and bore diameter were designed to provide maximum interaction with the betas and minimum self absorption in the aqueous medium. This device is now available commercially* and has found application in monitoring effluents from chromatographic columns. Its use in the detection of Ca^{45} (47) has recently been described.

Some particularly effective techniques limited to $C^{14}O_2$ counting employ liquid scintillator solutions containing long chain quaternary amines. Passmann, Radin, and Cooper introduced this technique (48) and valuable modifications have since appeared (49, 50, 51). Oppermann, Nystrom, Nelson, and Brown (52) and Radin and Fried (53) described the use of Primene 81-R (a mixture of tertiary alkyl primary C^{12}–C^{14} amines) obtained commercially from Rohm and Haas Co.

The reactions involved in the trapping of $C^{14}O_2$ in such systems are:

$$RNH_2 + C^{14}O_2 \rightarrow RNHC^{14}OOH$$

$$RNH_2 + RNHC^{14}OOH \rightarrow RNHC^{14}OOH_3NR.$$

The complexes formed are stable, particularly at low temperatures, and only moderate quenching action, which is attributed to the methanol employed as solvent, is observed.

Sheets of plastic scintillator have obvious applications for direct counting of beta emitters. Evaporation of an aqueous solution and the resultant deposition of radioactive material may be employed, or a flow system may be utilized (54). Special plastic well units for beta-ray spectroscopy have also been devised (55).

CONCLUSIONS

A comparison of the various counting systems is presented in Table I. It is evident that

TABLE I

Comparisons of counting systems

Method	Advantages	Disadvantages	Typical application	Sample size
Internal liquid scintillation counting	Highest ultimate sensitivity	Limited sample solubility; quenching	C^{14}, H^3 isotopes of low specific activity	Unlimited
Suspension of radioactive substance in gel or thickened liquid scintillator	Little sample preparation; no quenching	Reduced optical transmission	Inorganic salts and organic substances insoluble in aromatic solvents	Sample thickness limited by opacity; 1 g
Filter paper counting	Little sample preparation; no quenching	Self-absorption	Inorganic salts and organic substances insoluble in aromatic solvents	Milligram quantities
Anthracene or plastic scintillator filaments in aqueous medium	Direct analysis of aqueous sample	Self-absorption in aqueous phase. Low efficiency	Aqueous solutions of energetic beta emitters	Three milliliters of aqueous solution
Quaternary ammonium salts or amines in liquid scintillator	Direct absorption of $C^{14}O_2$	$C^{14}O_2$ only	Direct analysis of combustion products	Milligram quantities of $C^{14}O_2$
Plastic scintillator capillary	Continuous analysis of flow systems	Self-absorption in aqueous phase	Chromatographic effluents	<1 ml volume

**Nuclear Enterprises, Winnipeg, Manitoba.*

Can. J. Chem. Downloaded from www.nrcresearchpress.com by 210.87.254.6 on 09/05/12
For personal use only.

each of the counting methods has its particular merits and that the choice of the most suitable counting system must represent a delicate balance between maximum convenience and efficiency. Nevertheless it is obvious that the development of new alternative methods has hastened the adoption of scintillation detectors for many applications dependent upon the routine analysis of numerous samples. While the homogeneous liquid scintillator still represents the method of choice for extreme sensitivity, filter paper strips, or suspensions can be effectively employed in commercially available scintillation counters capable of automatically measuring many dozens of samples per day. For very small amounts of substance of high specific activity the heterogeneous detector systems also possess advantages in lower gamma backgrounds due to small scintillator size, and the elimination of quenching effects.

REFERENCES

1. V. P. GUINN. Liquid scintillation counting. C. G. Bell and F. N. Hayes (*Editors*). Pergamon Press, New York. 1958. p. 179.
2. E. C. FARMER and I. A. BERSTEIN. Science, **115**, 460 (1952).
3. B. N. AUDRIC and J. V. P. LONG. Research (London), **5**, 46 (1952).
4. J. C. ROUCAYROL and E. OBERHAUSEN. Naturwissenschaften, **42**, 411 (1955).
5. E. MATSUKAWA and E. EABORN. Research (London), Research Correspondence Suppl. **9**, 537 (1956).
6. F. N. HAYES, B. S. ROGERS, and P. C. SANDERS. Nucleonics, **13** (1), 46 (1955).
7. J. HERBERG. Anal. Chem. **32**, 42 (1960).
8. B. L. FUNT and W. M. PASIKA. Can. J. Chem. **38**, 1865 (1960).
9. F. N. HAYES, B. S. ROGERS, and W. H. LANGHAM. Nucleonics, **14** (3), 48 (1956).
10. J. D. DAVIDSON and P. FEIGELSON. Intern. J. Appl. Radiation and Isotopes, **2**, 1 (1957).
11. J. KAUFMAN, A. NIR, G. PARKS, and R. M. HOURS. Studies of low level liquid scintillation counting of tritium. University of New Mexico Conference on Organic Scintillation Detectors, Albuquerque, New Mexico. August, 1960.
12. R. W. PRINGLE, W. TURCHINETZ, and B. L. FUNT. Rev. Sci. Instr. **26**, 859 (1955).
13. C. LEGER and L. PICHAT. Compt. rend. **244**, 190 (1957).
14. R. W. PRINGLE, W. TURCHINETZ, B. L. FUNT, and S. DANYLUK. Science, **125**, 69 (1957).
15. F. N. HAYES, D. L. WILLIAMS, and B. ROGERS. Phys. Rev. **92**, 512 (1953).
16. G. T. OKITA, J. SPRATT, and G. V. LEROY. Nucleonics, **14** (3), 76 (1956).
17. F. N. HAYES and R. G. GOULD. Science, **117**, 480 (1953).
18. F. N. HAYES, W. J. EVERSOLE, W. H. LANGHAM, and T. T. TRUJILLO. J. Lab. Clin. Med. **47**, 819 (1956).
19. M. FURST, H. KALLMANN, and F. H. BROWN. Nucleonics, **13** (4), 58 (1955).
20. M. FURST and H. KALLMANN. Phys. Rev. **97**, 583 (1955).
21. F. E. KINARD. Rev. Sci. Instr. **28**, 293 (1957).
22. R. C. AXTMANN and L. CATHEY. Intern. J. Appl. Radiation and Isotopes, **4**, 26, 261 (1959).
23. B. L. FUNT and R. W. PRINGLE. Defence Research Board of Canada Report Contract P69-5-276. 1955.
24. A. R. RONZIO. Intern. J. Appl. Radiation and Isotopes, 4, 196 (1959).
25. G. B. BEARD and W. H. KELLY. Contract AF 49(638)-AD-158307 Michigan State University AFOSR-TN-58-497. June 18, 1958.
26. W. L. BUCK and R. K. SWANK. Rev. Sci. Instr. **29**, 252 (1958).
27. H. A. MIRANDA, JR. and H. SCHIMMEL. Rev. Sci. Instr. **30**, 1128 (1959).
28. B. L. FUNT and A. HETHERINGTON. Science, **125**, 986 (1957).
29. C. G. WHITE, S. HELF, and R. N. SHELLY. Anal. Chem. **32**, 238 (1960).
30. D. G. FLEISHMAN and L. G. SHADKIDZHANYAN. Atomnaya Energ. **6**, 669 (1959).
31. D. G. OTT, C. R. RICHMOND, T. T. TRUJILLO, and H. FOREMAN. Nucleonics, **17** (9), 106 (1959).
32. C. F. GORDON and A. L. WOLFE. Anal. Chem. **32**, 574 (1960).
33. J. SHAPIRA and W. H. PERKINS. Science, **131**, 414 (1960).
34. J. E. BOWCOTT and J. H. SCHULMAN. Z. Elektrochem. **59**, 283 (1955).
35. J. C. ROUCAYROL, E. OBERHAUSEN, and R. SCHULER. Radioisotopes in scientific research. Proceedings of the First UNESCO International Conference. Vol. 1. Pergamon, New York. 1958. p. 648.
36. B. L. FUNT and A. HETHERINGTON. Science, **131**, 1608 (1960).
37. C. H. WANG and D. E. JONES. Biochem. Biophys. Research Commun. **1**, 203 (1959).
38. R. B. LOFTFIELD. Atomlight, No. 13, 1, June (1960).
39. J. W. GEIGER and L. D. WRIGHT. Biochem. Biophys. Research Commun. **2**, 282 (1960).
40. J. D. DAVIDSON. Some recent developments in liquid scintillation counting of biochemical samples. University of New Mexico Conference on Organic Scintillation Detectors, Albuquerque, New Mexico. August 16–17, 1960.
41. R. F. TASCHEK and H. T. GITTINGS. Phys. Rev. **74**, 1553 (1948).
42. D. K. BUTT. Physica, **18**, 1142 (1952).
43. W. J. RAMLER and M. S. FREEDMAN. Rev. Sci. Instr. **21**, 784 (1950).

Can. J. Chem. Downloaded from www.nrcresearchpress.com by 210.87.254.6 on 09/05/12
For personal use only.

44. D. STEINBERG. Nature, **182**, 740 (1958).
45. D. STEINBERG. Nature, **183**, 1253 (1959).
46. B. L. FUNT and A. HETHERINGTON. Science, **129**, 1429 (1959).
47. E. D. PICKERING, H. L. REED, and R. L. MORRIS. Anal. Chem. **32**, 1214 (1960).
48. J. M. PASSMANN, N. S. RADIN, and J. A. D. COOPER. Anal. Chem. **28**, 484 (1956).
49. M. VAUGHAN, D. STEINBERG, and J. LOGAN. Science, **126**, 446 (1951).
50. D. STEINBERG, M. VAUGHAN, C. B. ANFINSEN, J. D. GORRY, and J. LOGAN. Liquid scintillation counting. C. G. Bell and F.N. Hayes (*Editors*). Pergamon Press, New York. 1958. pp. 230–236.
51. R. J. HERBERG. Anal. Chem. **32**, 42 (1960).
52. R. A. OPPERMANN, R. F. NYSTROM, W. O. NELSON, and R. E. BROWN. Intern. J. Appl. Radiation and Isotopes, **7**, 38 (1959).
53. N. S. RADIN and R. FRIED. Anal. Chem. **30**, 1926 (1958).
54. E. SCHRAM and R. LOMBAERT. Anal. Chim. Acta, **17**, 417 (1957).
55. D. G. GARDNER and W. W. MEINKE. Intern. J. Appl. Radiation and Isotopes, **3**, 232 (1958).

Can. J. Chem. Downloaded from www.nrcresearchpress.com by 210.87.254.6 on 09/05/12
For personal use only.

Can. J. Chem. Downloaded from www.nrcresearchpress.com by 210.87.254.40 on 09/05/12
For personal use only.

DETERMINATION OF THE DISINTEGRATION RATE OF NUCLIDES DECAYING BY ELECTRON CAPTURE[1]

J. R. S. DROUIN[2] AND L. YAFFE

ABSTRACT

In an attempt to determine disintegration rates of nuclides decaying by electron capture, various properties of a 2π proportional counter spectrometer were studied. These included gas multiplication, energy resolution, and energy linearity. The result of varying anode size, gas pressure, and nature of the gas was also investigated. An experimentally determined average path length for characteristic X-ray energies between 4 and 24 kev was found.

INTRODUCTION

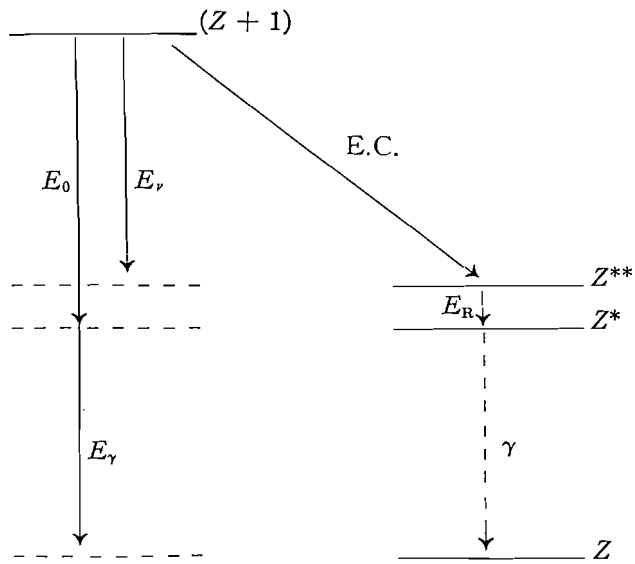
Charged-particle irradiations normally lead to the formation of a new nucleus where the proton-to-neutron ratio is greater than that required for stability. In turn, the proton in excess will decay by one or two different modes, namely positron emission and(or) capture of one of the orbital electrons.

The two transformations can be represented as a nuclear transition from a proton state to a neutron state with accompanying neutrino emission (ν) in the following schematic picture:

$$p \rightarrow n + \beta^+ + \nu,$$
$$p + e^-_{K,L,M\ldots} \rightarrow n + \nu.$$

The first transformation can be ascertained by measuring the radiation due to the annihilation of the positron or by measuring the positrons themselves.

The second transformation can be described by the following energy diagram wherein a parent nucleus with atomic number $(Z + 1)$ captures one of its own orbital electrons and emits a neutrino transforming itself to the nucleus with atomic number Z.



[1]*Manuscript received November 3, 1960.*
Contribution from the Radiochemistry Laboratory, Department of Chemistry, McGill University, Montreal, Que., with financial assistance from the National Research Council of Canada. Presented at the Third Symposium on Nuclear Chemistry and Radiochemistry held at Atomic Energy of Canada Limited, Chalk River, Ontario, September 6–8, 1960.

[2]*Holder of National Research Council Bursary 1956–57, and National Research Council Studentships 1957–58, 1958–59, and 1959–60.*

Subsequent de-excitation by γ-ray emission may occur with energy E_γ. Thus the total energy for the transition equals $E_0 + E_\gamma$, where E_γ may be zero. Further,

$$E_0 = E_\nu + E_R$$

where E_ν is the energy available for the neutrino and E_R is the energy of the radiation characteristic of an atomic shell rearrangement, i.e. a characteristic X-ray or Auger electron.

In a small fraction of the cases, a continuous spectrum of internal bremsstrahlung results from the sudden change of nuclear charge. In this case the energy is shared between the bremsstrahlung and the neutrino.

One can attempt to standardize electron-capture transitions in three ways. The first relies on the absolute measurement of the primary radiations due to the internal bremsstrahlung. The second and third methods are based on the absolute measurement of the secondary radiations due to characteristic Auger electrons or characteristic X-rays.

In 1955, Rasmussen (1) suggested an elegant method which involved direct coincidence counting of the internal bremsstrahlung and the shell rearrangement radiation. However, Hayward demonstrated in 1958 (2) that the method was not entirely reliable, especially for low-energy transitions and for high atomic number elements, where the apportioning of the radiations due to capture of K-electrons becomes very difficult. Also, interference by radioactive impurities, background, and gamma de-excitation radiation, and the low probability ($\sim 0.001\%$) (3) of internal bremsstrahlung do not militate in favor of such a method.

A more convenient way would be the absolute measurement of the Auger electrons or the characteristic X-rays. For low atomic number elements (< 30) the Auger electrons give a major contribution but their energies are very low (few kiloelectron volts). With normal source preparation methods, absolute measurement is rendered very difficult due to source absorption problems. The situation is much less difficult if one tries to measure the characteristic X-rays emerging after shell rearrangement. We have attempted to investigate the variables concerned with the operation of a 2π-proportional counter spectrometer. This would then enable the standardization of nuclides, decaying by electron capture, by measure of the characteristic X-rays.

EXPERIMENTAL TECHNIQUE AND RESULTS

The design of the counter is, with minor modifications, similar to that used by others, and is shown in Fig. 1. Curran, Angus, and Cockcroft in 1948 (4) and simultaneously Kirkwood, Pontecorvo, and Hanna (5) used gaseous sources with counters of this type and were the first to apply the spectrometric properties of such counters in the study of low energy β^-- and X-ray spectra. Our instrument is a windowless counter, of 2π-geometrical efficiency, which can be operated at elevated pressures. The experimental data reported here deal only with solid sources.

Various fundamental properties of proportional counters were investigated. These important criteria for performance were checked with a mixture of argon–methane (9:1) as counter gas, although some work was done with krypton–methane (9:1).

First of all the voltage plateaux were studied. Their respective shapes are critically dependent on the counter gas (pressure and nature), the anode to cathode ratio, and the electronic circuit. A block diagram of the electronic arrangement is shown in Fig. 2. It was found necessary to incorporate a White cathode follower (6) with the proper

Can. J. Chem. Downloaded from www.nrcresearchpress.com by 210.87.254.40 on 09/05/12
For personal use only.

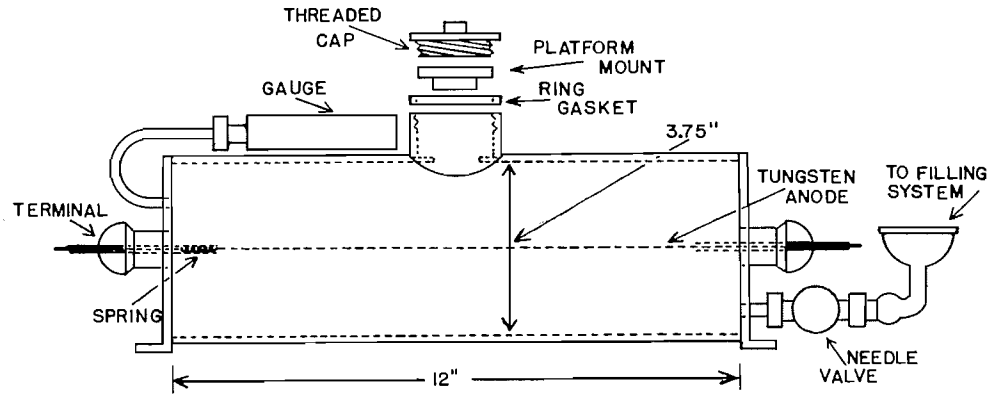


FIG. 1. 2π-Proportional counter.

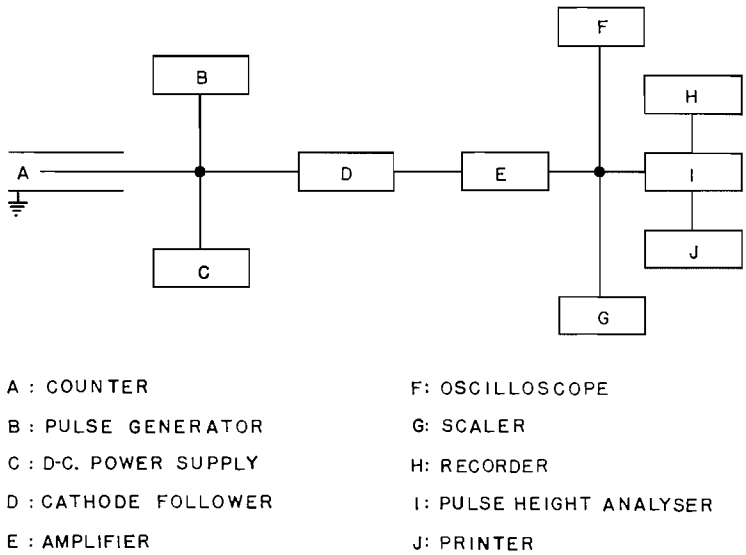


FIG. 2. Block arrangement of electronic equipment.

coupling constant for adequate performance. Figure 3 shows the plateau lengths obtained for different gas pressures and anode sizes. At a pressure of one atmosphere, for example, plateau lengths of about 600 volts with negligible slope were attainable when the anode diameters were 0.002 in., 0.003 in., 0.004 in., and 0.005 in. An anode diameter of 0.002 in. was used in the course of our work, unless otherwise mentioned.

Another intrinsic property of a proportional counter is the gas multiplication factor which is governed by the voltage across the chamber, the pressure and type of gas, and the anode-to-cathode ratio. In 1941, Rose and Korff (7) developed a theoretical treatment of this factor assuming an ionization cross section linear with electron energy up to 40 volts above the ionization threshold. They obtained experimental verification of the following equation, for amplification factors between 10^2 and 10^3 over a small voltage range ($\sim$ 150 volts).

Can. J. Chem. Downloaded from www.nrcresearchpress.com by 210.87.254.40 on 09/05/12
For personal use only.

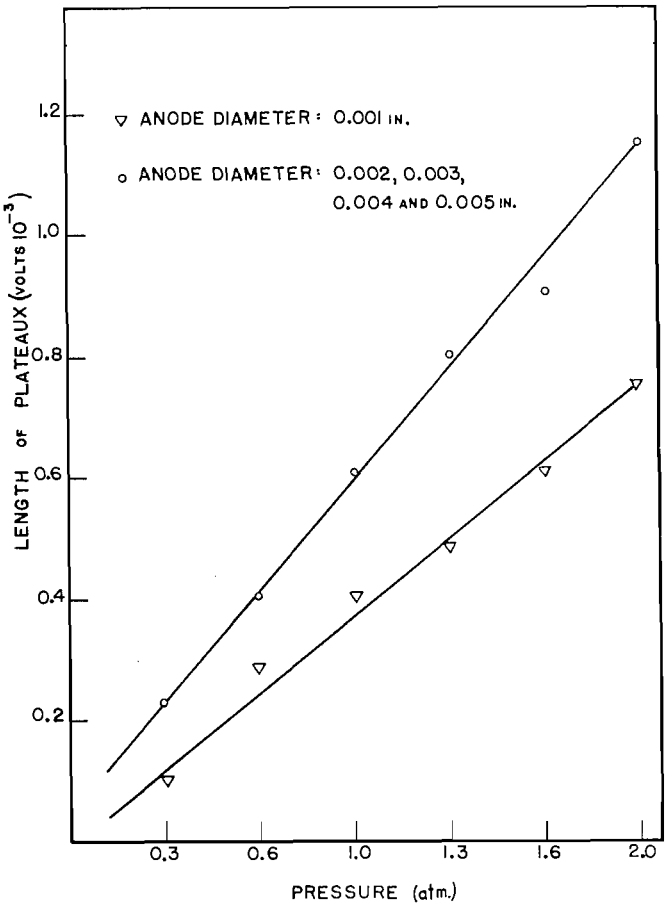


FIG. 3. Variation of length of voltage plateaux with counter gas pressure for various anode sizes.

$$A = \exp 2[a \,.\, N \,.\, c \,.\, r_1 V_0]^{\frac{1}{2}} \,.\, \left[\left(\frac{V_0}{V_p}\right)^{\frac{1}{2}} - 1\right]$$

where a = rate of increase of the ionization cross section with incident energy,
N = number of atoms or molecules inside the sensitive volume,

$$c = \frac{1}{\log_e \frac{r_2}{r_1}}$$

where r_2 is radius of the cathode and r_1 is radius of the anode,
V_0 = operating voltage, and
V_p = proportional threshold voltage.

For amplification factors greater than those used by Korff, it was found necessary to modify this equation by introducing another variable $f(0)$ into the exponential factor as follows:

$$A = \exp 2[a \,.\, N \,.\, c \,.\, r_1 \,.\, f(0) \,.\, V_0]^{\frac{1}{2}} \,.\, \left[\left(\frac{V_0}{V_p}\right)^{\frac{1}{2}} - 1\right]$$

Can. J. Chem. Downloaded from www.nrcresearchpress.com by 210.87.254.40 on 09/05/12
For personal use only.

Fig. 4 shows the variation of $f(0)$ when the anode size and gas pressure are varied over a wide range. From these data one can now calculate amplification factors between 10^3 and 10^6 for voltage ranges up to 1000 volts.

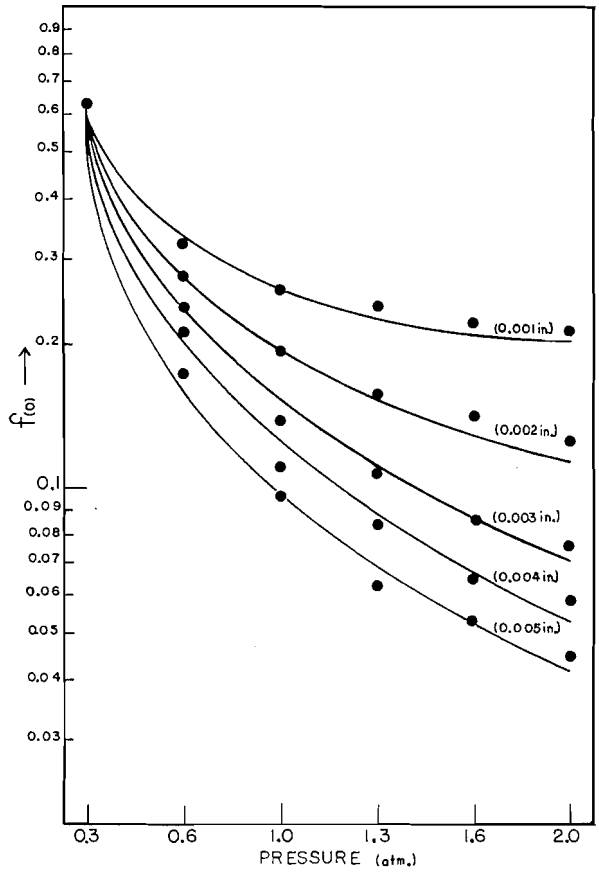


FIG. 4. Variation of $f(0)$ with pressure and anode size.

The energy linearity of the system was investigated for energy pulses between 3 and 24 kev as shown in Fig. 5. Only a very small departure from linearity at high energies was found.

Another important criterion for the operation of the device is the energy resolution. This was checked for anode wires of varying radii at different gas pressures. A standard source of Fe^{55} (5.9-kev X-rays) was used. The results in Fig. 6(*a*) show the variation of the energy resolution when five different anode sizes were employed.

If the anode size is kept constant and the pressure is varied, the mean free path of the electrons producing secondary ionizations will invariably be altered. According to calculations made by Korff (8), the mean free path should approximately be inversely proportional to the pressure. Then, as the pressure is decreased, statistical fluctuations in the pulse formations will increase. The energy resolution of the spectrometer was found to vary with pressure in the manner described in Fig. 6(*b*).

The pulse-size distribution from monoenergetic radiations in the energy range between 4 and 24 kev was analyzed. The size of every output pulse of a proportional counter,

Can. J. Chem. Downloaded from www.nrcresearchpress.com by 210.87.254.40 on 09/05/12
For personal use only.

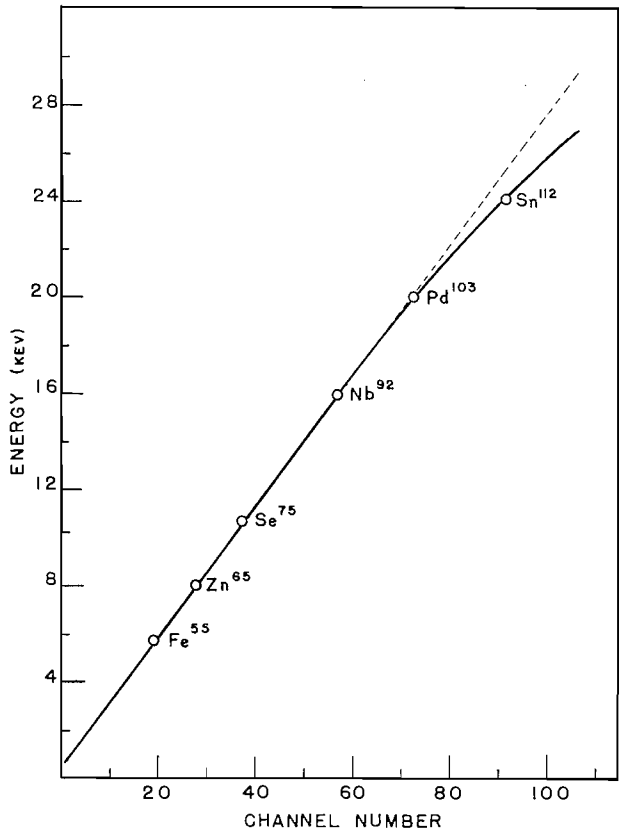


FIG. 5. Energy calibration of system.

arising from absorption of the full energy in the counter gas, is subject to statistical fluctuations. These fluctuations are mainly introduced by the statistics of the multiplication process in the counter.

A theoretical treatment by Frisch (9) and experimental results by Hanna *et al.* (10) have demonstrated that the relative variance (mean square relative standard deviation) of the output pulse size is practically independent of the multiplication factor. The pulse-size distributions produced by the radiations under investigation were studied. They could be fitted with Gaussian curves, at least in an interval of about ± 3 standard deviations.

The standard deviation (σ_P) can therefore be obtained by measuring the width (ΔE) of the peak at half maximum. This leads to $\Delta E = 2.36\ \sigma_P$, where $(\sigma_P/P)^2$ is the relative variance of the output pulse.

As may be seen from Fig. 7, (σ_P/P), the root mean square of the relative variance of the output pulse size, is plotted against the energy (E) of the radiations. The distribution was found to be slightly smaller than would be expected from a Poisson distribution.

The relationship derived from these experimental data can be described by

$$(\sigma_P/P) = 0.17\ E^{-\frac{1}{2}}.$$

Thus, resolving power $= 0.42\ E^{-\frac{1}{2}}$.

Now that the criteria for performance of the counter are ascertained, one needs to define the geometrical properties.

Can. J. Chem. Downloaded from www.nrcresearchpress.com by 210.87.254.40 on 09/05/12
For personal use only.

Can. J. Chem. Downloaded from www.nrcresearchpress.com by 210.87.254.40 on 09/05/12
For personal use only.

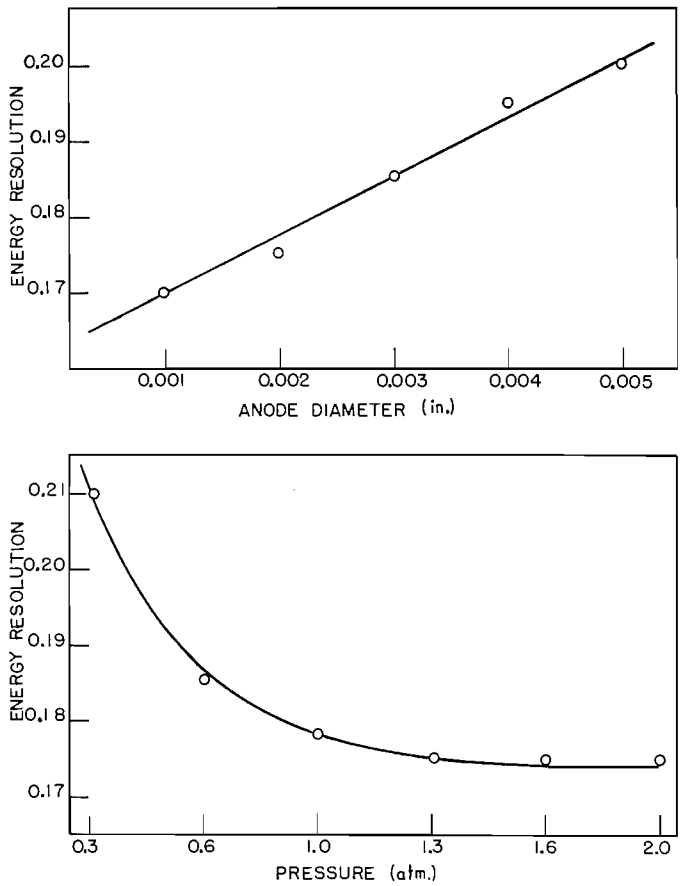


FIG. 6. (*a*) Variation of energy resolution with anode diameter (pressure = 1 atm). (*b*) Variation of energy resolution with pressure.

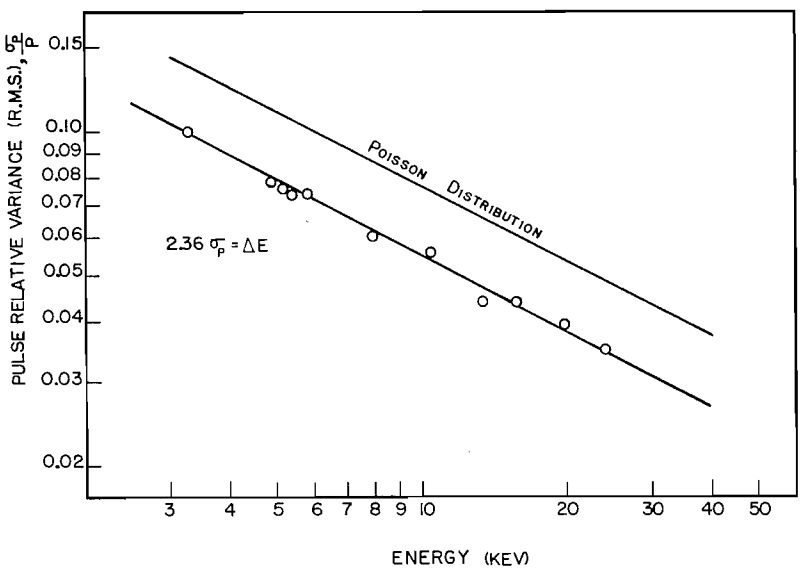


FIG. 7. Relation between the relative variance of the pulse and the X-ray energy.

The first factor is the geometrical efficiency. This was evaluated as 2π steradians when intercomparison was made with two other counters, (*a*) a high pressure proportional counter calibrated by Campion (11) and (*b*) a 4π β-counter calibrated by Pate and Yaffe (12). For this purpose, two different types of radiations were used, namely 5.9-kev X-rays from Fe^{55} and β^- particles emitted by H^3, Ni^{63}, and C^{14}. The values obtained are summarized in Table I.

TABLE I

Geometrical efficiency

Nuclides	This work (c.p.m.$\times 10^{-3}$)	High-pressure proportional counter (c.p.m.$\times 10^{-3}$)	4π β-counter (bottom half) (c.p.m.$\times 10^{-3}$)
Fe^{55}	34.00±0.05	34.07±0.07	—
H^3	41.2±0.2	—	41.5±0.2
Ni^{63}	47.3±0.2	—	47.5±0.2
C^{14}	46.2±0.2	—	46.7±0.2

A second correction which has to be introduced is that for the escape peak. For energies between 3 and 20 kev, Fig. 8 shows the ratio of the area under the escape peak to that of

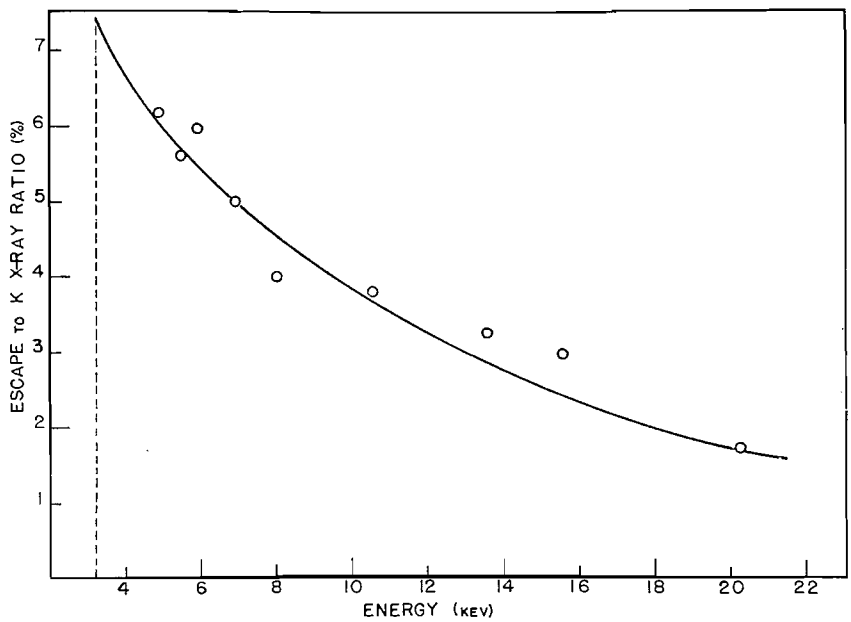


FIG. 8. Relation between the ratio of the escape peak to *K* X-ray and energy of the X-ray emitter.

the area under the *K* X-ray photopeak when the counter is operated at 1 atmosphere.

The third correction which has to be made resides in the absolute transmission of the X-rays through the finite sensitive volume of the counter. An average path length for these radiations in the counter was measured.

This was experimentally determined when four different radionuclides, namely Mn^{54} (5.4 kev), Fe^{55} (5.9 kev), Co^{57} (6.4 kev), and Zn^{65} (8.0 kev) were used. The pressure of the counter gas was increased up to a value where, if the relative count rates were plotted

Can. J. Chem. Downloaded from www.nrcresearchpress.com by 210.87.254.40 on 09/05/12
For personal use only.

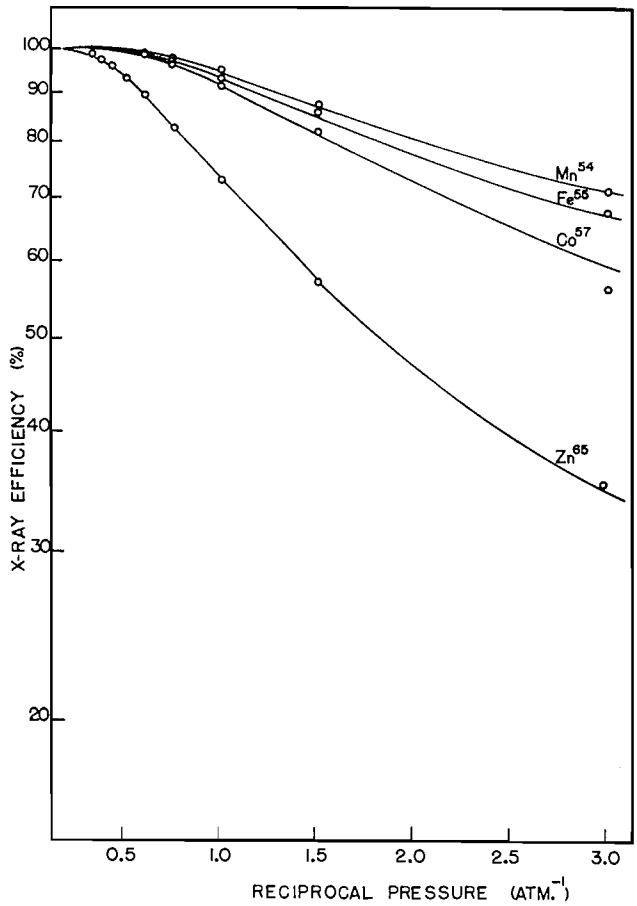


FIG. 9. Relation between X-ray counter efficiency and reciprocal pressure.

against the reciprocal pressures, as shown in Fig. 9, a plateau occurred. This was taken as total absorption in the counter. Such plots were originally investigated by Allen in 1957 (13). From these experimental data, an average path length can be derived from the equation for the absorption of photons passing through matter:

$$I = I_0 \exp -\mu t.$$

I and I_0 are the transmitted and incident radiation respectively, and t is the path length. The values for the linear absorption coefficient μ were obtained from Hagedoorn and Wapstra (14).

The results are summarized in Table II and give an average path length of 6.8 cm. Four of them were obtained from the plateau counting rates, while the other four were derived from integrating the counting rate beneath the K X-ray photopeaks.

With the above experimental path length, the efficiency of the 2π-proportional counter spectrometer was derived for K X-ray energies between 5 and 25 kev when the counter is operated at one atmosphere, argon–methane (9:1). Experimental relative efficiencies are shown in Fig. 10 when the pressure of the counter gas is varied. The contribution due to the escape peak has been included.

Can. J. Chem. Downloaded from www.nrcresearchpress.com by 210.87.254.40 on 09/05/12
For personal use only.

TABLE II

Average-path-length determination

Nuclides	t_p (cm)	t_s(cm)	$\bar{t}$ (cm)
Mn^{54}	6.18	6.05	
Fe^{55}	6.75	6.95	6.8
Co^{57}	7.35	7.10	
Zn^{65}	6.90	7.05	

NOTE: t_p = average path length based on calculations on the plateaux. t_s = average path length based on calculations on the spectra.

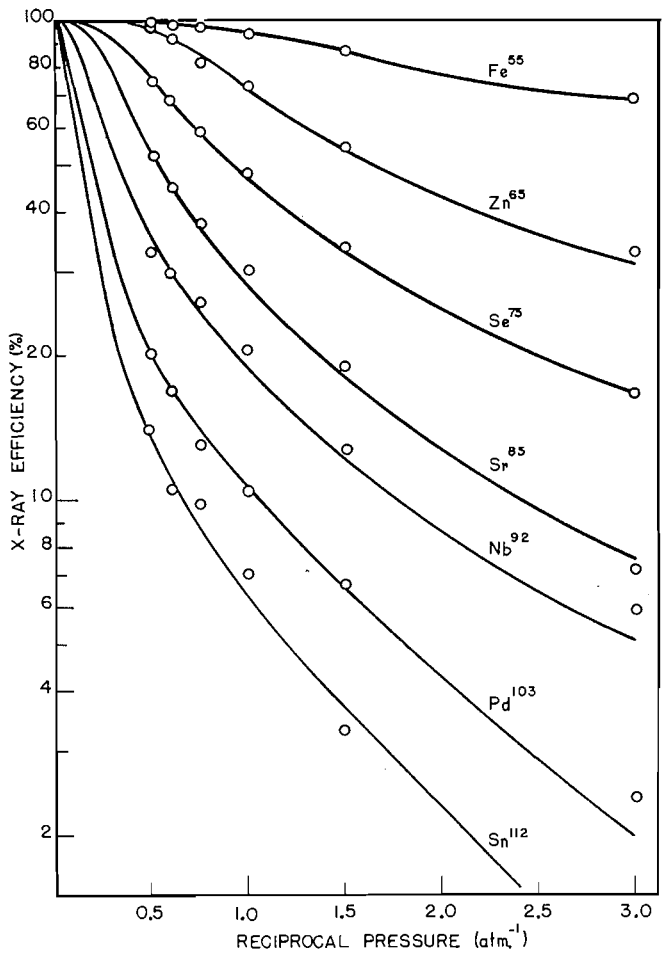


FIG. 10. Relation between X-ray counter efficiency and reciprocal pressure for argon–methane (9:1) (escape peak included).

For higher energy X-ray emitters, it is desirable to use a krypton–methane (9:1) mixture in order to take advantage of the enhanced absorption. These data are shown in Fig. 11 and again include the escape peak contribution.

Can. J. Chem. Downloaded from www.nrcresearchpress.com by 210.87.254.40 on 09/05/12
For personal use only.

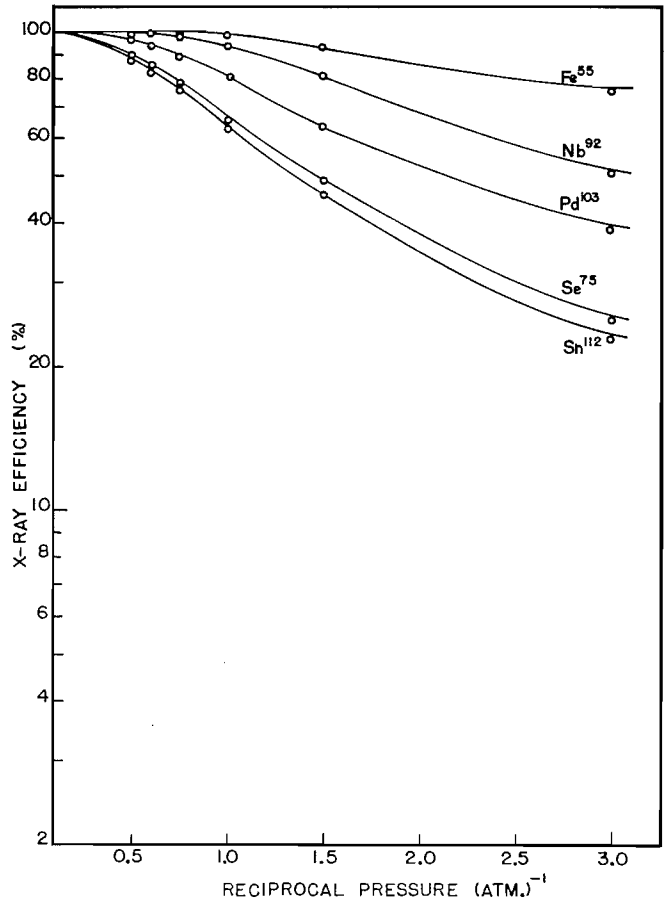


FIG. 11. Relation between X-ray counter efficiency and reciprocal pressure for krypton–methane (9:1) (escape peak included).

Figure 12 gives the ratio of the X-ray efficiencies for the two counter gases as a function of energy.

With a solid source, screened by sufficient aluminum to cut out the Auger electrons, a knowledge of the operational characteristics of the instrument and the evaluation of the correction factors necessary as described, one can now establish an equation for the disintegration rate N_0 of radionuclides decaying by electron capture when the counting rate R has been measured. The following equation applies:

$$R = N_0.G.f_a.f_t.f_{w_k}.f_r$$

where

G = defined source-to-counter geometrical efficiency (Table I).
f_a = factor correcting for total absorption inside the counter (Figs. 10 and 11).
f_t = factor for the transmission of K X-rays through the Auger electron absorber (11).
f_{wk} = factor due to the K-fluorescence yield (15).
f_r = factor due to L-capture events (16, 17).

Can. J. Chem. Downloaded from www.nrcresearchpress.com by 210.87.254.40 on 09/05/12
For personal use only.

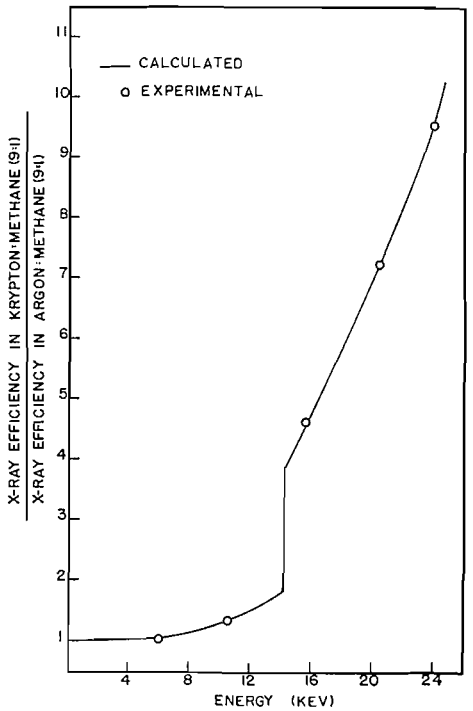


FIG. 12. Ratio between the X-ray efficiencies for the two counter gases at various energies.

REFERENCES

1. N. C. RASMUSSEN. Circular to National Research Council of U.S.A. Subcommittee on Beta and Gamma-Ray Measurement and Standards. April, 1955.
2. R. H. HAYWARD. Measurements and standards of radioactivity. Nuclear Science Series Report No. 24. National Academy of Sciences, National Research Council of U.S.A. Publication 573. 1958.
3. P. MORRISON and L. I. SCHIFF. Phys. Rev. **58**, 24 (1949).
4. S. C. CURRAN, J. ANGUS, and A. L. COCKCROFT. Nature, **162**, 302 (1948).
5. D. H. W. KIRKWOOD, B. PONTECORVO, and G. C. HANNA. Phys. Rev. **74**, 497 (1948).
6. E. L. C. WHITE. U.S. Patent No. 2,358,428 (September 19, 1944).
7. M. E. ROSE and S. A. KORFF. Phys. Rev. **59**, 850 (1941).
8. S. A. KORFF. Handbuch der Physik. Vol. XLV. 1958. p. 52.
9. O. R. FRISCH. Progr. in Nuclear Phys. **30**, 18 (1953); Statistics of multiplicative processes. Unpublished lectures. 1948.
10. G. C. HANNA, D. H. W. KIRKWOOD, and B. PONTECORVO. Phys. Rev. **75**, 985 (1949).
11. P. J. CAMPION and W. F. MERRITT. Atomic Energy of Canada Limited Report No. 532. 1957.
12. B. D. PATE and L. YAFFE. Can. J. Chem. **33**, 610 (1955).
13. R. A. ALLEN. Intern. J. Appl. Radiation and Isotopes, **1**, 289 (1957).
14. H. L. HAGEDOORN and A. H. WAPSTRA. Nuclear Phys. **15**, 146 (1960).
15. C. D. BROYLES, D. A. THOMAS, and S. K. HAYNES. Phys. Rev. **89**, 715 (1953).
16. H. BRYSK and M. E. ROSE. Revs. Modern Phys. **30**, 1169 (1958).
17. B. L. ROBINSON and R. W. FINK. Revs. Modern Phys. **32**, 117 (1960).

Can. J. Chem. Downloaded from www.nrcresearchpress.com by 210.87.254.40 on 09/05/12
For personal use only.

Can. J. Chem. Downloaded from www.nrcresearchpress.com by 210.87.254.105 on 09/05/12
For personal use only.

Canadian Journal of Chemistry

Issued by THE NATIONAL RESEARCH COUNCIL OF CANADA

VOLUME 39 APRIL 1961 NUMBER 4

THE STRUCTURE OF DI-*tert*-BUTYLNAPHTHALENESULPHONIC ACIDS[1]

MARCEL MENARD, LEONARD MITCHELL, JACQUELINE KOMLOSSY, AVERIL WRIGLEY, AND FRANCIS L. CHUBB

ABSTRACT

Commercial sodium di-*tert*-butylnaphthalenesulphonate has been resolved into its isomers, which were shown to be sodium 2,6- and 2,7-di-*tert*-butylnaphthalene-4-sulphonates.

Sodium di-*tert*-butylnaphthalenesulphonate is known as an effective central inhibitor of the cough reflex (1). Although some authors (1) refer to this antitussive drug as sodium 2,6-di-*tert*-butylnaphthalenesulphonate, its mode of preparation suggests that it is a mixture of at least two different isomers. It is prepared (2) by a Friedel–Crafts alkylation of naphthalene with 2 moles of *tert*-butyl chloride followed by sulphonation of the butylation product. Since several workers (3) have shown that *tert*-butylation of naphthalene gives a mixture containing about equal parts of 2,6- and 2,7-di-*tert*-butylnaphthalene, the commercial product can be inferred to consist of approximately equal quantities of the corresponding sulphonates. The purpose of this work was to isolate the isomers of sodium di-*tert*-butylnaphthalenesulphonate and to determine their structure.

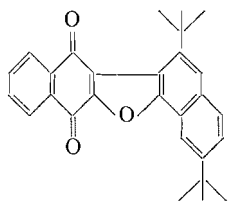
Reaction of commercial sodium di-*tert*-butylnaphthalenesulphonate with thionyl chloride according to a procedure recently developed by Bosshard *et al.* (4) gave a mixture from which two isomeric sulphonyl chlorides could be isolated by fractional crystallization: one melting at 167–169°, insoluble in cold ligroin; the second melting at 117–118°, moderately soluble in ligroin. Hydrolysis of these sulphonyl chlorides with sodium hydroxide regenerated the pure sulphonates. The sulphonate obtained from the higher-melting isomer was shown to be sodium 2,7-di-*tert*-butylnaphthalenesulphonate by conversion to 2,7-di-*tert*-butylnaphthalene (3) with 60% sulphuric acid. In the same way the sulphonate obtained from the lower-melting sulphonyl chloride was related to 2,6-di-*tert*-butylnaphthalene.

In order to determine the position of the sulphonic acid group of these compounds, sulphonation of 2,6- and 2,7-di-*tert*-butylnaphthalene under conditions which usually bring about α-sulphonation of naphthalene and naphthalene derivatives (5) was carried out. Reaction of these sulphonic acids with thionyl chloride gave the same sulphonyl chlorides as those isolated from the commercial product. On the other hand alkaline fusion of the sulphonates yielded naphthols which readily coupled with phenyldiazonium chloride to give orange-red azo dyes; these were easily reduced by stannous chloride to aminonaphthols, which in turn gave yellow quinones on oxidation. The quinone obtained from the 2,6-di-*tert*-butylnaphthol was found to be identical with the quinone obtained by Fieser and Price (6) from a chromic acid oxidation of 2,6-di-*tert*-butylnaphthalene.

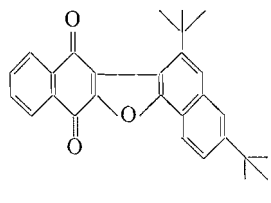
[1]*Manuscript received December 8, 1960.*
Contribution from the Research Laboratories, Frank W. Horner Limited, Montreal, Quebec.

This quinone was later shown by Crawford and Glesmann (3) to be 2,6-di-*tert*-butyl-1,4-naphthoquinone. Chromic acid oxidation of 2,7-di-*tert*-butylnaphthalene under similar conditions also gave a quinone, identical with that resulting from the coupling reaction of the 2,7-di-*tert*-butylnaphthol, reduction of the azo dye, and oxidation of the aminonaphthol. Furthermore, we found that the disubstitution product obtained by Buu-Hoi and Demerseman (7) from the alkylation of α-naphthol with *tert*-butyl bromide, which they suggest may be a 4,*x*-di-*tert*-butyl-1-naphthol, was identical with the naphthol obtained from the alkaline fusion of 2,6-di-*tert*-butylnaphthalenesulphonate. Thus the sulphonic acid group of the starting sulphonates can only be in the 1 or 4 positions.

Of the two possible α-positions, position 4 seemed more probable: sulphonation of 2,6- and 2,7-dimethylnaphthalene occurs preferentially in position 4 (8) and furthermore position 1 is subjected to the steric effect of the tertiary butyl group. Position 1 was finally eliminated by the fact that yellow di-*tert*-butyldinaphthofuranquinones, I and II, giving an intense blue color with sulphuric acid, could be isolated from the reaction of 2,6- and 2,7-di-*tert*-butylnaphthols with 2,3-dichloro-1,4-naphthoquinone. This cyclization reaction was shown by Buu-Hoi and Demerseman (7) to be characteristic of naphthols having an unsubstituted position adjacent to the OH group, which holds only if the hydroxyl group of the 2,6- and 2,7-di-*tert*-butylnaphthol occupies position 4. Consequently the sulphonic acid group in the starting sulphonates must occupy position 4.



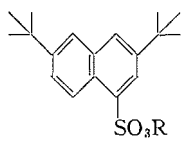
I



II

Reaction of 2,7-di-*tert*-butylnaphthalene-4-sulphonyl chloride with alcohols in pyridine solution afforded a series of esters which are reported in Table I. The methyl and ethyl ester of 2,6-di-*tert*-butylnaphthalene-4-sulphonic acid were prepared by reaction of the acid with diazomethane and diazoethane in ether solution.

TABLE I



R	M.p. (solvent)	Analysis			
		% C, calc.	% H, calc.	% C, found	% H, found
Ethyl	138–139° (EtOH)	68.93	8.10	69.32	8.20
n-Propyl	109–110° (EtOH)	69.57	8.35	69.57	8.36
n-Butyl	74–75° (EtOH)	70.17	8.57	70.54	8.49
n-Hexyl	77–78° (EtOH)	71.24	8.97	71.28	8.99
Cyclohexyl	124° (EtOH)	71.60	8.51	71.77	8.48
Phenyl	78–79° (EtOH)	72.69	7.12	72.86	7.12
Glycolyl	85–87° (CCl_4 – pet. ether)	65.90	7.74	66.93	8.31
Glyceryl	135–136° (CCl_4 – pet. ether)	63.93	7.67	64.47	7.72

Can. J. Chem. Downloaded from www.nrcresearchpress.com by 210.87.254.105 on 09/05/12
For personal use only.

Can. J. Chem. Downloaded from www.nrcresearchpress.com by 210.87.254.105 on 09/05/12
For personal use only.

EXPERIMENTAL

2,6- and 2,7-Di-tert-butylnaphthalene-4-sulphonyl Chloride

The commercial mixture of sodium di-*tert*-butylnaphthalenesulphonate (34.6 g, 0.1 mole), thionyl chloride (25 ml), and dimethylformamide (0.8 ml) were heated for 1 hour on the steam bath. The excess of thionyl chloride was evaporated under reduced pressure and the residue was triturated with 100 ml of cold water, filtered, and dried over sulphuric acid. The dried mixture of sulphonyl chlorides (36.2 g) was recrystallized in 100 ml of ligroin, with the aid of 3 g of decolorizing charcoal; there was so obtained 12.3 g (36%) of 2,7-di-*tert*-butylnaphthalene-4-sulphonyl chloride, m.p. 163–165°. The analytical sample, recrystallized from ligroin, had a melting point of 167–169°. Calc. for $C_{18}H_{23}O_2SCl$: C, 63.79; H, 6.84%. Found: C, 63.97; H, 7.01%.

Concentration of the mother liquors and repeated recrystallization of the residue from isopropanol gave 8.2 g (24.3%) of 2,6-di-*tert*-butylnaphthalene-4-sulphonyl chloride, m.p. 117–118°. Calc. for $C_{18}H_{23}O_2SCl$: C, 63.79; H, 6.84%. Found: C, 64.03; H, 6.97%.

Sodium 2,7-Di-tert-butylnaphthalene-4-sulphonate

To a boiling solution of 5 g of 2,7-di-*tert*-butylnaphthalene-4-sulphonyl chloride in 20 ml of ethanol there was slowly added a solution of 1.2 g of sodium hydroxide in 40 ml of water. The mixture was refluxed for 4 hours, the solvents removed, and the residue recrystallized from water to give 4.8 g (85%) of colorless waxy plates. Calc. for $C_{18}H_{23}O_3SNa.2H_2O$: C, 57.15; H, 7.20; S, 8.47%. Found: C, 57.44; H, 7.12; S, 7.49%.

Sodium 2,6-Di-tert-butylnaphthalene-4-sulphonate

Hydrolysis of 2,6-di-*tert*-butylnaphthalene-4-sulphonyl chloride with sodium hydroxide gave 90% of colorless needles from nitromethane, m.p. >360°. Calc. for $C_{18}H_{23}O_3SNa.2H_2O$: C, 57.15; H, 7.20; S, 8.47%. Found: C, 57.51; H, 7.09; S, 8.08%.

2,7-Di-tert-butylnaphthalene

A mixture of 8 g of sodium 2,7-di-*tert*-butylnaphthalene-4-sulphonate and 100 ml of a 60% solution of sulphuric acid was stirred and heated at 150–160° for 5 hours, cooled, poured into 1 liter of cold water, and extracted with ether. The ether extracts were washed with water, dried, and concentrated. After recrystallization from ethanol the residue yielded 2.8 g of colorless needles, m.p. 103–104°; these gave no depression of melting point when mixed with a sample prepared according to Price *et al.* (3).

2,6-Di-tert-butylnaphthalene

Hydrolysis of 5 g of sodium 2,6-di-*tert*-butylnaphthalene-4-sulphonate in 60% sulphuric acid gave 1.7 g of flat needles, m.p. 145–146°. Identity of this material with pure 2,6-di-*tert*-butylnaphthalene (3) was confirmed by a mixed melting point.

2,6-Di-tert-butylnaphthalene-4-sulphonic Acid

Chlorosulphonic acid (56 g, 0.48 mole) was slowly added, with stirring and cooling, to a solution of 116 g (0.48 mole) of pure 2,6-di-*tert*-butylnaphthalene in 240 ml of dichloroethane. The reaction mixture was allowed to stand for 2 hours at 0–5° and the solvent was removed at room temperature under reduced pressure. The residue, a heavy oil, started to crystallize upon the addition of 0.5 mole of water; recrystallization from dichloroethane gave 155 g (95%) of the hydrate of 2,6-di-*tert*-butylnaphthalene-4-sulphonic acid as colorless plates, m.p. 158°. Calc. for $C_{18}H_{24}O_3S.H_2O$: C, 63.87; H, 7.74%; M.W., 338.5. Found: C, 63.45; H, 7.76%; N.E., 339.3.

2,7-Di-tert-butylnaphthalene-4-sulphonic Acid

2,7-Di-*tert*-butylnaphthalene (3.3 g) dissolved in 7 ml of dichloroethane and treated, as described for the 2,6-isomer, with 1.8 g of chlorosulphonic acid gave 2.6 g (55%) of the hydrate of 2,7-di-*tert*-butylnaphthalene-4-sulphonic acid, m.p. 140–142° (chloroform – petroleum ether). Calc. for $C_{18}H_{24}O_3S.H_2O$: C, 63.87; H, 7.74%; M.W., 338.5. Found: C, 62.54; H, 7.82%; N.E., 339.4.

2,6-Di-tert-butylnaphthalene-4-sulphonyl Chloride

The anhydrous residue obtained from the reaction of 56 g of chlorosulphonic acid and 116 g of 2,6-di-*tert*-butylnaphthalene as described above was mixed, in a distillation apparatus, with 91 ml of thionyl chloride and 3 ml of dimethylformamide. The mixture was stirred and heated on the steam bath until it became homogeneous ($\frac{1}{2}$ hour). During that time most of the excess of thionyl chloride had distilled over; the remainder was removed under reduced pressure. The residue was triturated with cold water and extracted with ether. The combined ether extracts were dried and concentrated; the solid residue, recrystallized from alcohol, gave 133.5 g (86%) of colorless prisms, m.p. 117–118°. These gave no depression of melting point when mixed with a sample of the sulphonyl chloride obtained from the commercial mixture of sulphonates.

The amide was prepared by passing dry ammonia through a solution of the chloride in tetrahydrofuran, removing the solvent, triturating the residue with water, and recrystallizing the dried solid from ligroin: m.p. 160–161°. Calc. for $C_{18}H_{25}O_2NS$: C, 67.67; H, 7.89; N, 4.38%. Found: C, 67.70; H, 7.89; N, 4.37%.

2,7-Di-tert-butylnaphthalene-4-sulphonyl Chloride

The anhydrous 2,7-di-*tert*-butylnaphthalene-4-sulphonic acid, treated as described above with thionyl chloride and dimethylformamide, gave 90% of colorless prisms, m.p. 167–169°; this melting point was not depressed by mixing with the 2,7-di-*tert*-butylnaphthalene-4-sulphonylchloride obtained from the commercial mixture of sulphonates.

The amide was prepared as above, m.p. 165°. Calc. for $C_{18}H_{25}O_2NS$: C, 67.67; H, 7.89; N, 4.38%. Found: C, 67.17; H, 8.06; N, 4.59%.

2,7-Di-tert-butyl-4-naphthol

Potassium 2,7-di-*tert*-butylnaphthalene-4-sulphonate (30 g), 100 g of potassium hydroxide, and 30 ml of water were heated slowly in an iron crucible until the mixture melted and the potassium salt of the naphthol floated on the surface of the melt as a dark-brown oil. The mixture was cooled, dissolved in water, acidified with hydrochloric acid, and extracted three times with ether. The combined ether extracts were washed with water, dried, and concentrated. The residue, a heavy black oil, was distilled under reduced pressure and yielded 14.2 g of a yellow oil, b.p. 170–180°/4 mm. Crystallization of this oil in ligroin afforded 8 g (41%) of colorless needles, m.p. 125–126°. The analytical sample, recrystallized from ligroin, had a melting point of 127–128°. Calc. for $C_{18}H_{24}O$: C, 84.32; H, 9.44%. Found: C, 84.47; H, 9.43%.

2,6-Di-tert-butyl-4-naphthol

Alkaline fusion of potassium 2,6-di-*tert*-butylnaphthalene-4-sulphonate carried out as described above for the 2,7-isomer, gave 63% of a reddish oil, b.p. 190°/3 mm, which afforded 25% of colorless crystals, m.p. 142°. The identity of this compound with the one obtained by Buu-Hoi and Demerseman (7) from *tert*-butylation of α-naphthol was confirmed by a mixed melting point.

2,7-Di-tert-butyl-1-phenylazo-4-naphthol

Aniline (3.4 g), dissolved in 11 ml of concentrated hydrochloric acid and 11 ml of water,

Can. J. Chem. Downloaded from www.nrcresearchpress.com by 210.87.254.105 on 09/05/12
For personal use only.

Can. J. Chem. Downloaded from www.nrcresearchpress.com by 210.87.254.105 on 09/05/12
For personal use only.

was diazotized with a solution of 2.8 g of sodium nitrite in 14 ml of water. The resultant solution of phenyldiazonium chloride was added dropwise to a well-stirred mixture of 8 g of 2,7-di-*tert*-butyl-4-naphthol, 30 ml of 10% sodium hydroxide solution, and 20 ml of tetrahydrofuran cooled to 5°. The mixture was then stirred for 30 minutes at 5° and allowed to stand overnight. Most of the tetrahydrofuran was removed under reduced pressure and the water was decanted from the heavy dark oil, which was then boiled with 40 ml of glacial acetic acid and filtered hot. After cooling and filtering, the crude precipitate was recrystallized from 200 ml of acetic acid to yield 2.6 g (28%) of red crystals, m.p. 229–239°. Calc. for $C_{24}H_{28}ON_2$: C, 79.96; H, 7.83; N, 7.77%. Found: C, 79.91; H, 7.88%; N, 7.74%.

2,6-Di-tert-butyl-phenylazo-4-naphthol

The coupling reaction of 4 g of 2,6-di-*tert*-butyl-4-naphthol with phenyldiazonium chloride was carried out as described above for the 2,7-isomer. After removal of the tetrahydrofuran, a solid was obtained which was filtered and recrystallized from acetic acid to give 2.2 g of the orange-red azo compound, m.p. 204–206°. Calc. for $C_{24}H_{28}ON_2$: C, 79.96; H, 7.83; N, 7.77%. Found: C, 79.80%; H, 7.80%; N, 7.42%.

2,7-Di-tert-butyl-1,4-naphthoquinone

(a) From 2,7-Di-tert-butylnaphthalene

A solution of 2.6 g of chromium trioxide in 4.4 ml of acetic acid and 2.9 ml of water was added dropwise to a stirred slurry of 2.0 g of 2,7-di-*tert*-butylnaphthalene in 11 ml of acetic acid maintained at 60°. After the addition was complete, the mixture was stirred for ½ hour at 60°, poured into 150 ml of cold water and extracted with ether. The ether extracts were washed with water, dried, and concentrated; the residue crystallized from dilute alcohol and yielded 2.0 g (89%) of yellow needles, m.p. 72°. Calc. for $C_{18}H_{22}O_2$: C, 79.96; H, 8.20%. Found: C, 79.71%; H, 7.92%.

Reaction of the quinone with 2,4-dinitrophenylhydrazine gave a compound which crystallized from acetic acid as orange-red needles, m.p. 250–251°. Calc. for $C_{24}H_{26}O_6N_4$: C, 63.98; H, 5.82; N, 12.44%. Found: C, 63.79; H, 5.90; N, 12.41%.

(b) From 2,7-Di-tert-butyl-1-phenylazo-4-naphthol

A solution of 8 g of stannous chloride in 24 ml of concentrated hydrochloric acid was added to a boiling slurry of 1.9 g of 2,7-di-*tert*-butyl-1-phenylazo-4-naphthol in 80 ml of methanol; the azo compound slowly dissolved and after 1½ hours the solution was colorless. It was concentrated to a volume of approximately 30 ml and cooled. The crystalline 2,7-di-*tert*-butyl-1-amino-4-naphthol hydrochloride was filtered and slurried in a solution of 0.6 ml of sulphuric acid in 12 ml of water. A solution of 0.4 g of potassium dichromate in 6 ml of water was added to the resultant mixture and the whole was heated at steam-bath temperature for 5 minutes, cooled, diluted with water, and extracted with ether. The ether extracts were washed with water, dried, and concentrated. Upon reaction with 2,4-dinitrophenylhydrazine the liquid residue gave an orange-red compound, m.p. 250–251°, found by a mixed melting point determination to be identical with the addition compound obtained as under (*a*).

2,6-Di-tert-butyl-1,4-naphthoquinone

(a) From 2,6-Di-tert-butylnaphthalene

Oxidation of 13.8 g of 2,6-di-*tert*-butylnaphthalene with 18 g of chromium trioxide as described above for the 2,7-isomer yielded a solid compound after the reaction mixture was poured into water. Recrystallization of this solid from ethanol gave 7.4 g (48%) of yellow needles, m.p. 85–86° (lit. (6) m.p. 83.5–84.5°).

(b) From 2,6-Di-tert-butyl-1-phenylazo-4-naphthol

Reduction of this azo compound (0.23 g) with stannous chloride and oxidation of the aminonaphthol with potassium dichromate gave 0.1 g (60%) of yellow needles, m.p. 85–86°, not depressed when mixed with a sample prepared according to (*a*).

Esters of 2,7-Di-tert-butylnaphthalene-4-sulphonic Acid

A solution of 0.15 mole of the appropriate alcohol in 80 ml of anhydrous pyridine was cooled to −10°; 0.08 mole of powdered 2,7-di-*tert*-butylnaphthalene-4-sulphonyl chloride was added at such a rate that the temperature would not exceed −5°; the resultant mixture was stirred for 2 hours at 0–5° and poured into water (500 ml). In those cases where a solid ester was obtained it was separated by filtration and recrystallized from the appropriate solvent; when an oil was obtained, the ester was extracted with ether and isolated by the usual procedure. Physical data for the esters involved are included in Table I.

Esters of 2,6-Di-tert-butylnaphthalene-4-sulphonic Acid

A slight excess of an ethereal solution of the appropriate diazoalkane was added to a cooled solution of the monohydrate of 2,6-di-*tert*-butylnaphthalene-4-sulphonic acid in ether. After standing overnight the solvent was removed and the ester isolated. The methyl ester was obtained as a solid which crystallized from methanol as colorless prisms, m.p. 123–124°. Calc. for $C_{19}H_{26}O_3S$: C, 68.22; H, 7.84; S, 9.58%. Found: C, 68.58; H, 7.95; S, 9.94%.

The ethyl ester was obtained as a colorless oil, b.p. 180–185/1 mm. Calc. for $C_{20}H_{28}O_3S$: C, 68.93; H, 8.10%. Found: C, 68.92%; H, 8.26%.

3′,7′-Di-tert-butyldinaphtho(1′,2′-2,3)(2″,3″-4,5)furan-1″,4″-quinone

A solution of 2.6 g of 2,6-di-*tert*-butyl-4-naphthol and 2.3 g of 2,3-dichloro-1,4-naphthoquinone in 15 ml of anhydrous pyridine was stirred and refluxed for 18 hours. After cooling, the mixture was diluted with methanol and filtered. Recrystallization of the filter cake from toluene gave 0.52 g (13%) of yellow needles, m.p. 354–355°. Calc. for $C_{28}H_{26}O_3$: C, 81.92; H, 6.38%. Found: C, 81.78; H, 6.53%.

3′,6′-Di-tert-butyldinaphtho(1′,2′-2,3)(2″,3″-4,5)furan-1″,4″-quinone

A solution of 4.6 g of 2,3-dichloro-1,4-naphthoquinone and 5.2 g of 2,7-di-*tert*-butyl-4-naphthol in 30 ml of pyridine was stirred and refluxed for 18 hours. After cooling, the mixture was filtered and the filtrate concentrated to a volume of approximately 10 ml. The pyridine solution was then diluted with methanol and allowed to stand overnight. Filtration and recrystallization of the filter cake in toluene–methanol afforded 1.1 g (15%) of orange-yellow needles, m.p. 217–218.° Calc. for $C_{28}H_{26}O_3$: C, 81.92; H, 6.38%. Found: C, 82.21; H, 6.57%.

REFERENCES

1. G. R. DE VLEESCHLOUVER. Arch. intern. pharmacodynamie, **97**, 34 (1954); A. GRAVENITZ. Arch. exptl. Pathol. Pharmakol. **224**, 384 (1955); N. K. CHAKRAVARTY, A. MONTALLANA, R. JENSEN, and H. L. BORISON. J. Pharmacol. Exptl. Therap. **117**, 127 (1956).
2. SOCIÉTÉ BELGE DE L'AZOTE ET DES PRODUITS CHIMIQUES DU MARLY, BELG. 520,742 (1953).
3. W. GRUMP. J. Am. Chem. Soc. **53**, 380 (1931); C. C. PRICE, H. M. SHAFER, M. F. HUBERT, and C. BERNSTEIN. J. Org. Chem. **7**, 517 (1942); N. E. NURSTEN and A. T. PETERS. J. Chem. Soc. 729 (1950); H. M. CRAWFORD and M. C. GLESMANN. J. Am. Chem. Soc. **76**, 1108 (1954).
4. H. H. BOSSHARD, R. MORY, M. SCHMID, and HCH. ZOLLINGER. Helv. Chim. Acta, **42**, 1653 (1959).
5. C. M. SUTER and A. W. WESTON. Organic reactions. Vol. 3. John Wiley & Sons, New York. 1946. pp. 142–196.
6. L. F. FIESER and C. C. PRICE. J. Am. Chem. Soc. **58**, 1838 (1936).
7. NG PH. BUU-HOI and P. DEMERSEMAN. J. Chem. Soc. 4699 (1952).
8. R. WEISSGERBER and O. KURBER. Ber. **52**B, 346 (1919).

Can. J. Chem. Downloaded from www.nrcresearchpress.com by 210.87.254.105 on 09/05/12
For personal use only.

Can. J. Chem. Downloaded from www.nrcresearchpress.com by 210.87.254.40 on 09/05/12
For personal use only.

THE EQUILIBRIUM DIAGRAMS, HEATS OF MIXING, DIPOLE MOMENTS, DENSITIES, AND BOILING POINTS OF THE SYSTEM ACETONE–CHLOROFORM–BENZENE[1]

A. N. Campbell, E. M. Kartzmark, and H. Friesen

ABSTRACT

The equilibrium diagrams show that a compound, stable in the solid state, is formed in the system chloroform–acetone, but no compound is formed in the binary systems chloroform–benzene and acetone–benzene. The ternary equilibrium diagram, the heats of mixing, and the dipole moments, all show that this compound continues to exist in the presence of benzene, up to a high concentration of benzene. Since a series of ternary mixtures is shown to exist having zero heat of mixing, it was thought that this series of mixtures might behave in a pseudoideal manner, but the determinations of density (molar volume) and boiling point show that this is not so.

The existence of a compound, $CHCl_3$—$(CH_3)_2CO$, in mixtures of chloroform and acetone has been shown to be probable (1): the compound is an obvious example of hydrogen bonding. We thought it would be interesting to investigate the effect of adding the non-polar liquid benzene to the acetone–chloroform system. The systems benzene–chloroform, benzene–acetone, chloroform–acetone, and the ternary system benzene–chloroform–acetone, were investigated in regard to the following properties: freezing point diagrams, heats of mixing, dipole moments, densities, and boiling points.

EXPERIMENTAL

Freezing-Point Diagrams

The technique has often been described. It consisted essentially of a double-jacketed vessel containing a system of known composition. By controlling the degree of vacuum in the jacket, any desired rate of cooling could be obtained. The cooling agent was liquid nitrogen. Temperatures were measured by means of a copper–constantan thermocouple and a recording potentiometer.

Heats of Mixing

Heats of mixing were determined by having a weighed amount of one liquid in a magnetically stirred vacuum-walled calorimeter and the second liquid, also weighed, in a second such vessel. One set of junctions of a 20-junction copper–constantan thermopile was in the calorimeter and the other in the other vessel so that the thermopile measured the difference in temperature of the two vessels; allowance was made for slight original difference in temperature. The thermopile had a sensitivity of about 0.2° C, corresponding to the minimum reading of the recorder chart. A suitable quantity of the second liquid was forced through a course capillary into the calorimeter, the amount being determined by weighing at the end of the experiment.

The average rise in temperature was about 7°. The usual method of radiation correction was applied and the water equivalent of calorimeter and contents was determined electrically for each individual experiment. Current through the immersed platinum heating coil was determined from the voltage drop over a standard resistance. By this method temperatures are not measured as such; the electrical input is multiplied by the ratio of two vertical lines on the recorder graph.

[1]*Manuscript received December 1, 1960.*
Contribution from the Chemistry Department of the University of Manitoba, Winnipeg, Manitoba.

The ternary system was treated in the following way. Stock solutions were made up containing fixed mole fractions of benzene, e.g.

$$0.1\ N_{C_6H_6} \qquad 0.9\ N_{CHCl_3}$$

$$0.1\ N_{C_6H_6} \qquad 0.9\ N_{(CH_3)_2\cdot CO}.$$

These were mixed in varying proportions and the heat effect measured, corrections being applied for the heat exchange that had occurred in the original mixing of the quantities of stock solution used. This procedure was reported for each 1/10th mole fraction benzene; the results were plotted as in Fig. 5. The presence of benzene lowered the heat effect (evolution) with regard to acetone–chloroform because, on mixing benzene with acetone a small quantity of heat is absorbed, and in the case of benzene–chloroform, although heat is evolved, the quantity is small.

Dipole Moments

Dielectric constants of known mixtures of acetone, chloroform, and benzene were determined on a General Radio capacitance bridge, using an audio-frequency oscillator at 1000 cycles to energize the bridge and amplifying the signal to headphones. The arrangement worked well for low dielectric constants. Thus, it reproduced exactly the dielectric constants of pure benzene and pure chloroform but not the relatively high dielectric constant of acetone. Since, however, we were only interested in ternary solutions containing at least 90 mole% benzene, we experienced no trouble.

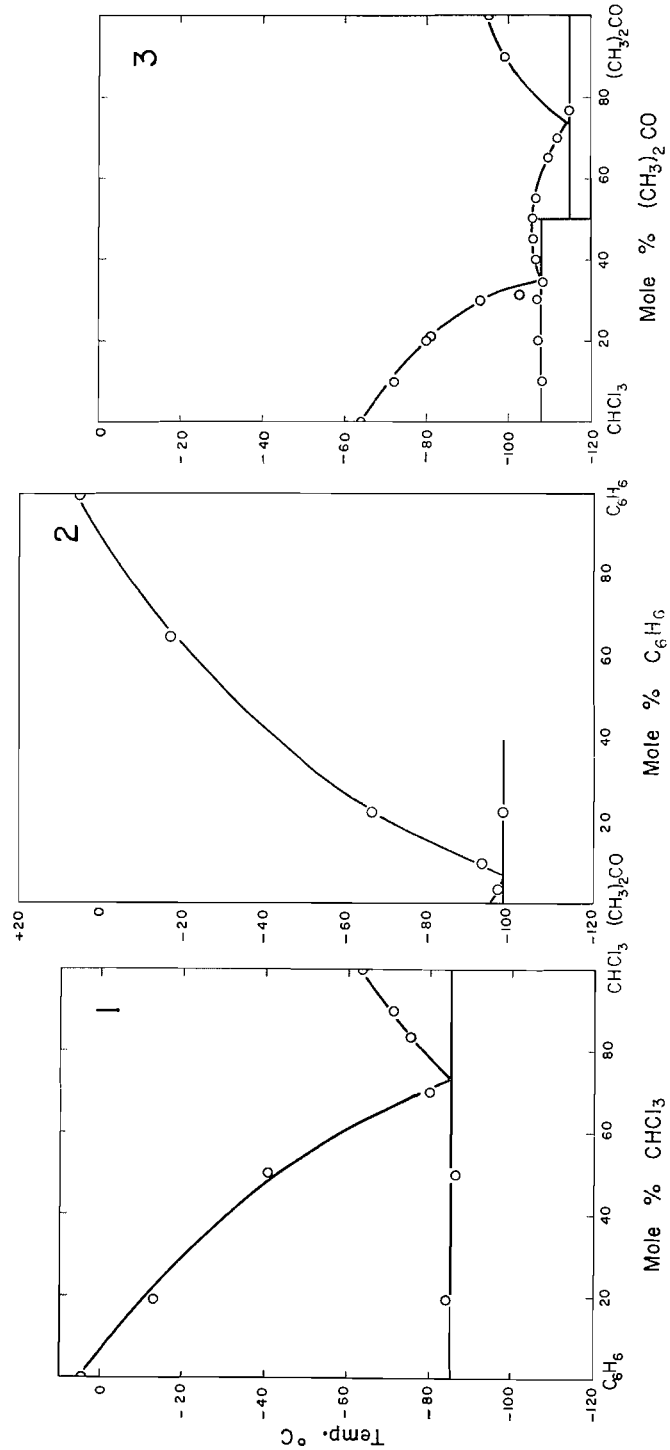
We argued in our paper on the energy of hydrogen bonding (2) that, however highly dissociated the compound of acetone and chloroform may be when the components are present in equimolecular proportion, the dissociation must be reduced to zero, when one or other component is present in infinite excess. A similar argument should apply to the dipole moment but here both components should be in the presence of an infinite excess of benzene, if the true molecular polarization is to be deduced. For this purpose we determined the dielectric constants over a range of chloroform–acetone ratios, in benzene as solvent. Two series of measurements were made: (1) in 90 mole% benzene; (2) in 95 mole% benzene. Measurements were not carried to greater dilution because the magnification of the experimental error rendered the final result of little value.

Boiling Points

A very complete investigation of the boiling points of the ternary system has been made by Reinders and de Minjer (3). The system is non-ideal, an azeotropic maximum occurring in the acetone–chloroform system. It seemed to us, however, from our measurements of heat of mixing that a curve of pseudoideal behavior might traverse the ternary diagram. At least, there certainly exists such a series of solutions which are formed with zero heat of mixing. If this series were really ideal, members of it would form from the components without volume change and the partial pressures would agree with Raoult's law. For this purpose, we re-established the apparatus previously used by Campbell and Dulmage (4), which comprises the Scatchard equilibrium still and a barostat made up from various suggestions. The apparatus works very well, since there is no detectable fluctuation in pressure and the boiling-point fluctuation is only $\pm 0.01°$ C (at most). Equilibrium liquid and vapor phases were analyzed by density and refractive index determinations using the graphs of Reinders and de Minjer.

Can. J. Chem. Downloaded from www.nrcresearchpress.com by 210.87.254.40 on 09/05/12
For personal use only.

Can. J. Chem. Downloaded from www.nrcresearchpress.com by 210.87.254.40 on 09/05/12
For personal use only.



FIGS. 1–3. Freezing-point diagrams. System benzene–chloroform (Fig. 1); acetone–benzene (Fig. 2); chloroform–acetone (Fig. 3).

EXPERIMENTAL RESULTS

Equilibrium Diagrams

The binary systems benzene–chloroform, benzene–acetone, and chloroform–acetone are represented in Figs. 1, 2, and 3 and the ternary system in Fig. 4.

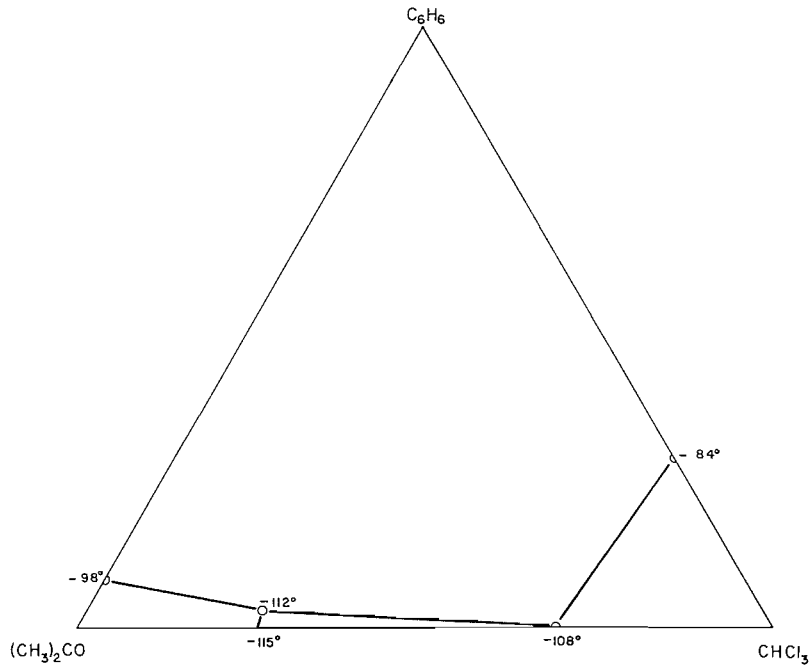


FIG. 4. Ternary freezing-point diagram of system benzene–acetone–chloroform.

Heats of Mixing

The heats of mixing of acetone–chloroform and of acetone – carbon tetrachloride have been published previously (2).

TABLE I

Heats of mixing

(*a*) Acetone–benzene			(*b*) Benzene–chloroform		
Mole fr. acetone	ΔH/mole mixture (cal)	ΔH/mole benzene (cal)	Mole fr. $CHCl_3$	ΔH/mole mixture (cal)	ΔH/mole benzene (cal)
0.230	28	41	0.218	−60	−77
0.374	40	65	0.358	−91	−140
0.492	46	91	0.455	−106	−190
0.548	46	102	0.528	−108	−230
0.618	41	107	0.598	−103	−260
0.708	30	104	0.691	−90	−290
0.829	18	108	0.817	−69	−380
			0.881	−59	−490
			0.917	−47	−570

Can. J. Chem. Downloaded from www.nrcresearchpress.com by 210.87.254.40 on 09/05/12
For personal use only.

TABLE I *(Concluded)*

(*c*) Acetone–chloroform–benzene

Mole fractions in mixtures		Mole fractions in absence of benzene		ΔH/mole mixture (cal)*
Acetone	Chloroform	Acetone	Chloroform	
	Series i. 0.1 mole fraction benzene present in all solutions			
0.799	0.101	0.887	0.113	−85
0.718	0.182	0.798	0.202	−170
0.627	0.273	0.697	0.303	−250
0.545	0.355	0.605	0.395	−330
0.450	0.450	0.501	0.499	−380
0.314	0.586	0.350	0.650	−410
0.190	0.710	0.211	0.789	−300
0.151	0.749	0.168	0.832	−290
0.106	0.794	0.118	0.882	−210
	Series ii. 0.20 mole fraction benzene present in all solutions			
0.681	0.119	0.851	0.149	−100
0.620	0.180	0.774	0.226	−170
0.506	0.294	0.632	0.368	−280
0.415	0.385	0.399	0.601	−350
0.302	0.498	0.377	0.623	−350
0.201	0.599	0.251	0.749	−320
0.095	0.705	0.119	0.881	−210
	Series iii. 0.30 mole fraction benzene present in all solutions			
0.595	0.105	0.850	0.150	−66
0.518	0.182	0.740	0.260	−160
0.441	0.259	0.630	0.370	−240
0.361	0.339	0.516	0.484	−270
0.200	0.500	0.286	0.714	−260
0.117	0.583	0.167	0.833	−220
	Series iv. 0.40 mole fraction benzene present in all solutions			
0.510	0.090	0.850	0.150	−45
0.408	0.192	0.680	0.320	−130
0.300	0.300	0.500	0.500	−190
0.208	0.392	0.347	0.653	−220
0.100	0.500	0.167	0.833	−180
	Series v. 0.50 mole fraction benzene present in all solutions			
0.384	0.116	0.768	0.232	−57
0.312	0.188	0.624	0.376	−130
0.218	0.282	0.436	0.564	−170
0.123	0.379	0.246	0.754	−180
	Series vi. 0.60 mole fraction benzene present in all solutions			
0.297	0.103	0.742	0.258	−54
0.236	0.164	0.590	0.410	−95
0.169	0.231	0.422	0.578	−120
0.107	0.293	0.267	0.733	−140
	Series vii. 0.70 mole fraction benzene present in all solutions			
0.211	0.089	0.703	0.297	−34
0.152	0.148	0.507	0.493	−68
0.091	0.209	0.303	0.697	−90
	Series viii. 0.80 mole fraction benzene present in all solutions			
0.101	0.099	0.505	0.495	−41

*These figures include the heats of mixing of the benzene with the acetone and with the chloroform.

Can. J. Chem. Downloaded from www.nrcresearchpress.com by 210.87.254.40 on 09/05/12
For personal use only.

TABLE II

Dielectric constants and apparent molar polarization of acetone–chloroform mixtures in large excess of benzene at 25° C

Composition		Density	Dielectric	Molar polarization of solutions and apparent molar polarization of acetone, chloroform, or compound			
Mole fr. acetone	Mole fr. chloroform	($d_4^{25°}$)	constant	Soln.	Acetone	Chloroform	Comp.
		Series i.	Mole fraction benzene = 0.90				
0.1000	0.0000	0.8662	3.329	38.40	144.1	—	—
0.0909	0.0000	0.8668	3.250	37.33	144.1	—	—
0.0900	0.0100	0.8734	3.247	37.62	—	—	210
0.0816	0.0000	0.8677	3.159	36.87	151.8	—	—
0.0800	0.0200	0.8794	3.159	37.23	—	—	206.5
0.0722	0.0000	0.8682	2.979	35.09	157.3	—	—
0.0700	0.0300	0.8867	3.087	36.07	—	—	194.7
0.0625	0.0000	0.8691	2.917	34.47	151.7	—	—
0.0600	0.0400	0.8906	2.982	35.09	—	—	201.8
0.0526	0.0000	0.8698	2.806	33.30	153.0	—	—
0.0500	0.0500	0.8977	2.907	34.28	—	—	205.8
0.0000	0.1000	0.9258	2.456	29.02	—	50.3	—
0.0000	0.0910	0.9219	2.438	28.77	—	49.9	—
0.0100	0.0900	0.9207	2.554	30.24	—	—	226
0.0000	0.0820	0.9168	2.423	28.01	—	50.5	—
0.0200	0.0800	0.9150	2.045	31.36	—	—	217
0.0000	0.0720	0.9120	2.400	28.29	—	49.31	—
0.0300	0.0700	0.9092	2.751	32.59	—	—	221.0
0.0000	0.0630	0.9074	2.386	28.12	—	49.84	—
0.0400	0.0600	0.9030	2.833	33.50	—	—	212.8
0.0000	0.0530	0.9012	2.370	27.93	—	53.77	—
0.0500	0.0500	0.8961	2.904	34.30	—	—	206.2
		Series ii.	Mole fraction benzene = 0.95				
0.0452	0.0000	0.8698	2.733	32.50	159.7	—	—
0.0450	0.0050	0.8728	2.717	32.28	—	—	208
0.0404	0.0000	0.8698	2.687	31.98	162.6	—	—
0.0400	0.0100	0.8751	2.693	32.04	—	—	200
0.0355	0.0000	0.8703	2.632	31.33	163.1	—	—
0.0350	0.0150	0.8763	2.653	31.64	—	—	214.7
0.0320	0.0000	0.8710	2.577	30.65	156.9	—	—
0.0300	0.0200	0.8813	2.609	31.02	—	—	214.5
0.0256	0.0000	0.8712	2.537	30.18	171.1	—	—
0.0250	0.0250	0.8850	2.555	30.34	—	—	207.2
0.0000	0.0452	0.8963	2.354	27.95	—	54.89	—
0.0050	0.0450	0.8968	2.407	27.36	—	—	210.0
0.0000	0.0404	0.8942	2.343	27.57	—	54.0	—
0.0100	0.0400	0.8938	2.452	29.03	—	—	225.0
0.0000	0.0355	0.8921	2.338	27.52	—	55.57	—
0.0150	0.0350	0.8912	2.489	29.47	—	—	212.7
0.0000	0.0306	0.8915	2.324	27.20	—	51.96	—
0.0200	0.0300	0.8876	2.542	30.19	—	—	225.5
0.0000	0.0256	0.8880	2.320	27.24	—	56.25	—
0.0250	0.0250	0.8859	2.558	30.34	—	—	207.2

When the molar polarizations of acetone in benzene, in the absence of chloroform, and of chloroform in benzene, in the absence of acetone, are extrapolated to zero concentration, in the usual way, and the dipole moments calculated, using the refractive indices to calculate the distortion polarization, the following values are obtained.

Acetone 2.79 (lit. 2.70 (5))

Chloroform 0.97 (lit. 1.10 (6))

The values for the molar polarization of the "compound", that is of an equimolecular

Can. J. Chem. Downloaded from www.nrcresearchpress.com by 210.87.254.40 on 09/05/12
For personal use only.

mixture of acetone and chloroform, are necessarily difference figures and are so scattered that no extrapolation was possible. The average value was used to calculate the dipole moment, which resulted as 2.9, as against 3.76 for the sum of the dipole moments of the constituents.

TABLE III

Densities and molar volumes

Comp. of liquid (mole fr.)		Density	Exptl.	Calc.	%
Acetone	Chloroform	(g/ml)	volume	volume	deviation
0.882	0.018	0.8080_9	75.7022	75.6822	+0.026
0.768	0.032	0.8284_3	77.2322	77.2406	−0.011
0.665	0.035	0.8400_6	78.8834	78.8763	+0.009
0.552	0.048	0.8577_8	80.4641	80.5084	−0.055
0.450	0.050	0.8677_9	82.0044	82.0553	−0.062
0.349	0.050	0.8753_6	83.5993	83.6111	−0.014
0.256	0.045	0.8795_0	85.0634	85.0908	−0.032
0.164	0.036	0.8816_2	86.5763	86.5917	−0.018
0.551	0.048	0.8583_9	80.4635	80.5193	−0.069
0.552	0.048	0.8581_3	80.4478	80.5062	−0.068
0.539	0.060	0.8665_9	80.5398	80.5889	−0.061

DISCUSSION

Figures 1 and 2 show that the binary systems benzene–chloroform and benzene–acetone are of the simple eutectic type. Figure 3 shows that acetone and chloroform form a compound, stable in the solid state, but, judging from the flatness of the maximum rather highly dissociated in the molten state. Figure 4 represents the ternary freezing point diagram; it shows that the ternary eutectics occur at very small percentages of benzene. The compound characteristic of the acetone–chloroform system continues to exist in the ternary system.

The heats of mixing of acetone–chloroform mixtures with fixed benzene content are plotted in Fig. 5. It is to be noted that the curves cross at the chloroform end, as they must necessarily do, since the heats of mixing of chloroform with benzene and of acetone with benzene themselves pass through a maximum with changing benzene concentration. The maximum in the heat of mixing curve of acetone–chloroform persists in the presence of benzene, at about the same concentration of chloroform, viz. about 60 mole%, but it becomes increasingly flattened with increasing benzene content, a necessary consequence of the decrease in the ternary heat of mixing.

It is readily possible by drawing horizontals across Fig. 5 to obtain the loci of solutions having identical heat of mixing, including zero heat of mixing. The loci thus obtained have been plotted in Fig. 6.*

The curve of zero heat of mixing was of particular interest to us, since it seemed to indicate a narrow region of pseudo-ideality, in a very non-ideal system. This curve runs from pure acetone to pure benzene, with a very small chloroform content. Accordingly, we performed some rather accurate density determinations on this series of mixtures to determine whether or not the change in volume on mixing was zero. Inspection of Table III shows that this is not so and that there is always a slight but definite contraction when the components are mixed. An inspection of Table IV, which gives the boiling points of mixtures under a fixed pressure of 705.6 mm and the partial pressures as derived from

**These curves of equal heat effect might perhaps be called "idemcals", a term derived from the Latin, since the Greek term "isotherm" has a different and well-known meaning.*

Can. J. Chem. Downloaded from www.nrcresearchpress.com by 210.87.254.40 on 09/05/12
For personal use only.

Can. J. Chem. Downloaded from www.nrcresearchpress.com by 210.87.254.40 on 09/05/12
For personal use only.

TABLE IV

Liquid–vapor equilibria, $P^{\circ} = 705.6$ mm

Liquid comp. mole fr.			Vapor comp. mole fr.			Partial pressure calc. by Raoult's law (P')			Exp. partial pressure (P'')			Ratio = P''/P'			Temp. (°C)
$(CH_3)_2CO$	$CHCl_3$	C_6H_6	$(CH_3)_2CO$	$CHCl_3$	C_6H_6	$(CH_3)_2CO$	$CHCl_3$	C_6H_6	$(CH_3)_2CO$	$CHCl_3$	C_6H_6	$(CH_3)_2CO$	$CHCl_3$	C_6H_6	
0.891	0.015	0.094	0.936	0.007	0.057	648.5	9.4	30.8	660.4	4.9	40.2	1.018	0.521	1.305	55.03
0.803	0.028	0.169	0.869	0.011	0.120	609.4	18.2	57.7	613.2	7.8	84.7	1.006	0.429	1.468	56.18
0.704	0.032	0.264	0.823	0.016	0.161	556.0	21.7	94.4	620.7	11.3	113.6	1.116	0.521	1.203	57.35
0.542	0.039	0.419	0.744	0.027	0.228	450.9	27.8	158.4	525.0	19.0	160.9	1.164	0.504	1.016	58.98
0.469	0.048	0.483	0.709	0.027	0.264	419.8	36.9	197.4	500.3	19.1	186.3	1.192	0.518	0.944	61.14
0.319	0.048	0.633	0.672	0.027	0.301	309.6	40.0	276.9	474.2	19.1	212.4	1.532	0.478	0.767	63.63
0.124	0.048	0.828	0.622	0.035	0.343	144.6	48.0	450.4	438.9	24.7	242.0	3.035	0.515	0.537	69.38
0.128	0.038	0.834	0.300	0.038	0.662	154.0	39.2	468.9	211.7	26.8	467.1	1.375	0.684	0.996	70.36

Can. J. Chem. Downloaded from www.nrcresearchpress.com by 210.87.254.40 on 09/05/12
For personal use only.

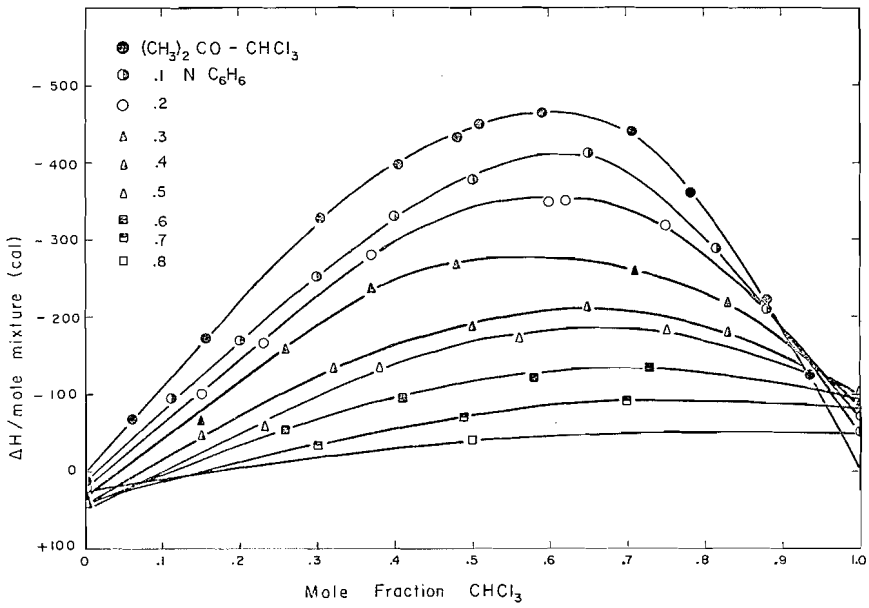


FIG. 5. Heat of mixing per mole of mixture vs. mole fraction of chloroform. Mole fraction calculated for the absence of benzene.

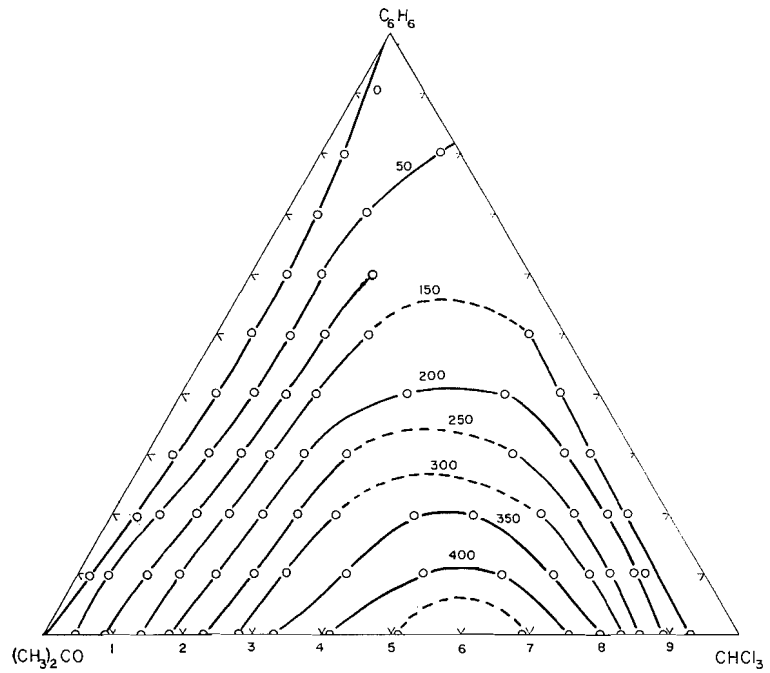


FIG. 6. Curves of equal heats of mixing. Figures on curves give the heat of mixing in negative calories.

Raoult's law and as calculated from the vapor composition, shows that these solutions are far from being ideal. It appears then that this series of solutions is not even pseudo-ideal and that the zero heat of mixing is merely a result of compensating factors.

The dielectric-constant measurements show that the dipole moment of the compound, or rather of a solution of equimolar proportions of acetone and chloroform in benzene, is greater than those of either acetone or chloroform, but considerably less than the sum of the two.

Since it was not possible to extrapolate our measurements to infinite excess of acetone or chloroform, our values must all refer to a compound which is highly dissociated. In view of the high dipole moment of the dissociated acetone, the figure given for the dipole moment of the compound is certainly too high and must be considered as purely qualitative evidence that the compound exists in benzene solution.

REFERENCES

1. F. DOLEZALEK. Z. Physik. Chem. **64**, 734 (1908); A. N. CAMPBELL and E. M. KARTZMARK. Can. J. Chem. **38**, 652 (1960).
2. A. N. CAMPBELL and E. M. KARTZMARK. Can. J. Chem. **38**, 652 (1960).
3. W. REINDERS and C. H. DE MINJER. Rec. trav. chim. **59**, 369 (1940).
4. A. N. CAMPBELL and W. J. DULMAGE. J. Am. Chem. Soc. **70**, 1723 (1948).
5. I. KUCHMA and J. W. WILLIAMS. J. Am. Chem. Soc. **49**, 2408 (1927); J. W. WILLIAMS. Physik. Z. **29**, 204 (1928).
6. J. W. WILLIAMS and I. KUCHMA. J. Am. Chem. Soc. **49**, 1676 (1927).

Can. J. Chem. Downloaded from www.nrcresearchpress.com by 210.87.254.40 on 09/05/12
For personal use only.

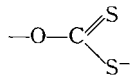
Can. J. Chem. Downloaded from www.nrcresearchpress.com by 210.87.254.42 on 09/05/12
For personal use only.

INFRARED SPECTRA OF XANTHATE COMPOUNDS

II. ASSIGNMENT OF VIBRATIONAL FREQUENCIES[1]

L. H. LITTLE,[2] G. W. POLING,[3] AND J. LEJA[3]

ABSTRACT

Discrepant interpretations regarding the frequency of the C=S stretching mode are reviewed and assignments of frequencies for the vibrational modes of the xanthate group,  , are presented.

A band at 1020–1070 cm^{-1} is assigned to the C=S stretching mode. Bands at 1200 cm^{-1} and 1110–1140 cm^{-1} are ascribed to the stretching vibrations of the C—O—C linkage.

The effects of the alkyl hydrocarbon chain length and of metal atoms (alkali metals, copper, and zinc) in displacing some of the frequencies are recorded.

In studying adsorption of xanthates on metals and their sulphide minerals by infrared spectroscopy, it became necessary to assign the spectral frequencies to the vibrational modes of the xanthate group. Previous studies of the spectra of xanthates (1, 2) and similar compounds (3, 4) were mainly exploratory in nature, due largely to the uncertain assignment of the C=S stretching mode for thiocarbonyl compounds (5, p. 293; 6; 7), in general.

Spectra of xanthates and similar compounds have been recorded and compared with recent studies of the thiocarbonyl stretching vibration (8, 9). Assignments of the xanthate vibrational frequencies have been made and conclusions reached with respect to the structures of dixanthogens, heavy metal xanthates, and alkali metal xanthates.

PROCEDURE

The spectra were recorded on Perkin–Elmer 21 and 221 double beam infrared spectrophotometers using sodium chloride prisms and on a Beckman IR4 infrared spectrophotometer using a cesium bromide prism. The solid samples were studied as mulls in nujol or in hexachlorobutadiene.

The intensities of the bands given in Table III, measured with the cesium bromide prism, are directly comparable with those of the bands shown in Figs. 1–4 for spectra measured with the sodium chloride prism.

The Raman spectrum of $(n\text{-}C_4H_9\text{—}S)_2C\text{=}O$ was recorded on a Cary Raman spectrophotometer. The other compounds are colored and, thus, are unsuitable for study by Raman spectroscopy.

*(1) Xanthates**

Potassium xanthate homologues, C_nH_{2n+1}—O—C(=S)—SK, listed in Table I, were prepared

[1]*Manuscript received November 17, 1960.*
Contribution from the Division of Applied Chemistry, National Research Council, Ottawa, Canada, and the Department of Mining and Metallurgy, University of Alberta, Edmonton, Alberta.
Issued as N.R.C. No. 6222.
[2]*Postdoctorate Research Fellow, National Research Council, Ottawa.*
[3]*Department of Mining and Metallurgy, University of Alberta, Edmonton, Alberta.*
**The dotted bands shown in Fig. 1 occur where bands due to the compounds being studied are masked by those of the nujol mulling agent.*

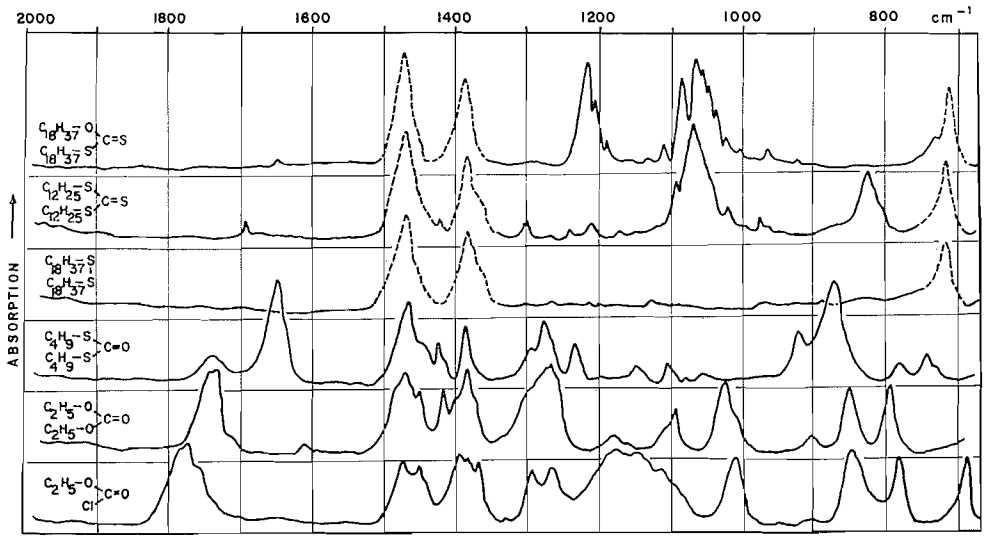


FIG. 1. Selected carbonyl and thiocarbonyl compounds.

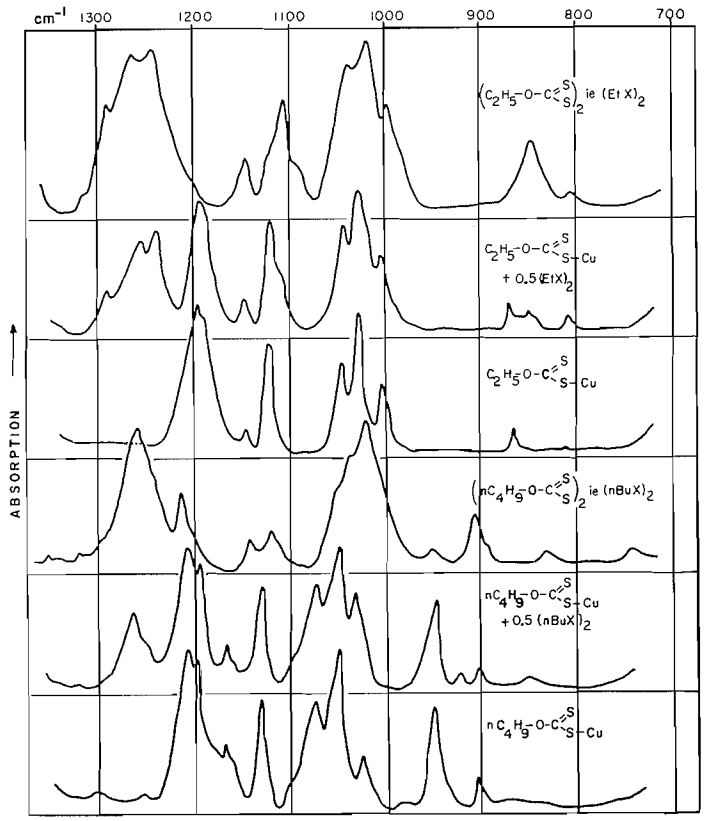


FIG. 2. Ethyl and butyl xanthates of copper and dixanthogens.

Can. J. Chem. Downloaded from www.nrcresearchpress.com by 210.87.254.42 on 09/05/12
For personal use only.

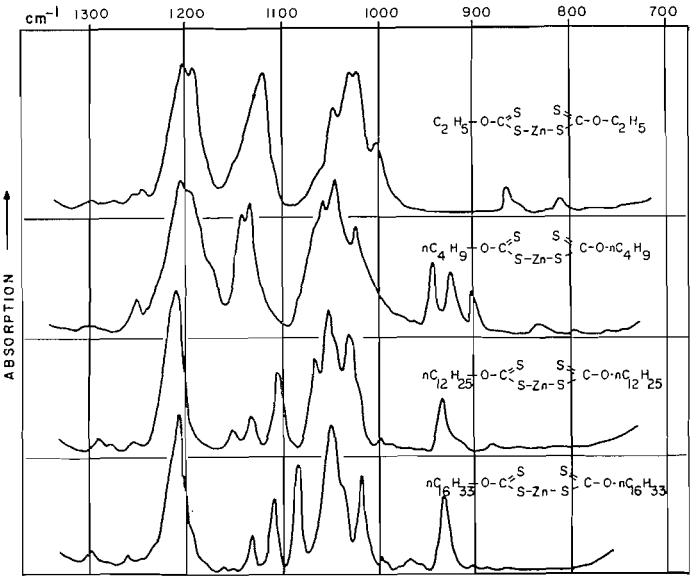


FIG. 3. Zinc alkyl xanthates.

TABLE I
Analysis of xanthates

Potassium salt of alkyl xanthate	% C		% H		% S	
	Calc.	Chem. anal.	Calc.	Chem. anal.	Calc.	Chem. anal.
K-methyl xanthate	16.45	16.38	2.07	2.10	43.84	43.59
K-ethyl xanthate	22.48	22.62	3.14	3.20	40.01	38.04
K-*n*-propyl xanthate	27.56	27.14	4.05	4.01	36.79	36.50
K-*n*-butyl xanthate	31.89	30.97	4.82	4.63	34.05	33.19
K-*n*-amyl xanthate	35.61	34.79	5.48	4.78	31.69	28.83
K-*n*-hexyl xanthate	38.85	38.78	6.05	6.04	29.73	29.40
K-*n*-nonyl xanthate	46.47	46.53	7.41	7.35	24.81	23.77
K-*n*-cetyl xanthate	57.25	55.63	9.32	9.15	17.98	17.86

as described previously (1).

AnalaR grade cupric sulphate and zinc sulphate were used to prepare heavy metal xanthates from solutions of alkali xanthates. It has been shown previously (1) by spectroscopic methods that dixanthogen is produced during the precipitation of copper xanthate from solutions of cupric salts, while no dixanthogen is produced during the precipitation of zinc xanthate. These findings are now confirmed by analytical results (see Table II).

(2) S,S-di-n-butyl Dithiocarbonate n-C_4H_9—S, C=O, n-C_4H_9—S

The dithiocarbonate was prepared by the method described by Bulmer and Mann (10). Phosgene was passed through a solution of sodium *n*-butyl mercaptide in ethanol

Can. J. Chem. Downloaded from www.nrcresearchpress.com by 210.87.254.42 on 09/05/12
For personal use only.

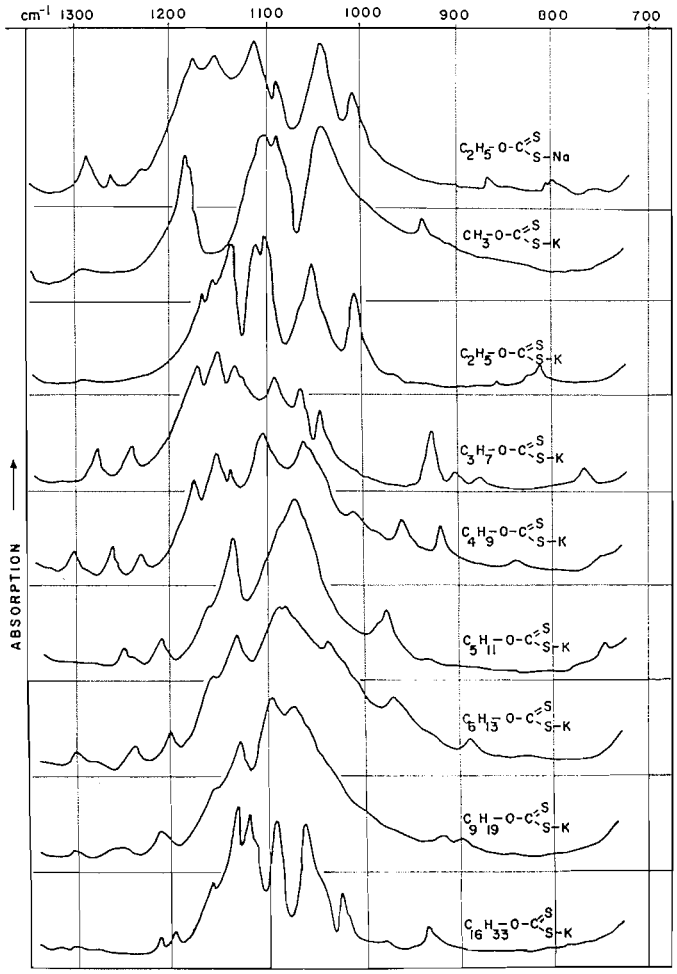


FIG. 4. Alkali metal xanthates.

and the resulting material was fractionally distilled (133° C at 20 mm Hg). Analysis: Calculated: 52.38% C; 8.79% H; 31.08% S. Found: 52.35% C; 8.75% H; 31.17% S.

*(3) S,S-didodecyl Trithiocarbonate** $n\text{-}C_{12}H_{25}\text{—}S$, $n\text{-}C_{12}H_{25}\text{—}S$, $C{=}S$

Analysis: Calculated: 67.20% C; 11.28% H; 21.53% S. Found: 67.93% C; 11.15% H; 19.40% S.

(4) O,S-dioctadecyl dithiocarbonate† $n\text{-}C_{18}H_{37}\text{—}O$, $n\text{-}C_{18}H_{37}\text{—}S$, $C{=}S$

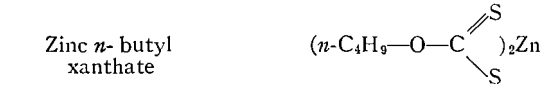
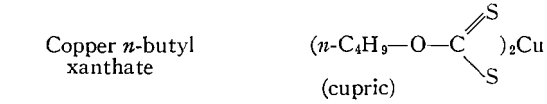
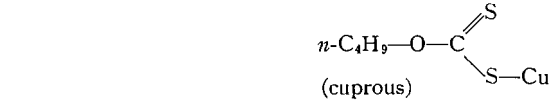
**Sample from B.D.H., Poole, England.*
†*Sample provided by D.S.I.R., Warren Spring Laboratory, Stevenage, Herts, England.*

Can. J. Chem. Downloaded from www.nrcresearchpress.com by 210.87.254.42 on 09/05/12
For personal use only.

Can. J. Chem. Downloaded from www.nrcresearchpress.com by 210.87.254.42 on 09/05/12
For personal use only.

TABLE II

Analysis of Zn and Cu xanthates

Material	Formula for calculations	% C		% H		% S		% metal	
		Calc.	Chem. anal.	Calc.	Chem. anal.	Calc.	Chem. anal.	Calc.	Chem. anal.
Zinc *n*- butyl xanthate		33.00	33.21	4.98	5.19	35.25	34.80	% Zn 17.97	% Zn 18.03
Copper *n*-butyl xanthate	 (cupric)	33.17		5.01		35.43		% Cu 17.55	% Cu
	 (cuprous)	28.22		4.26		30.14		29.86	
Ether-extracted copper xanthate precipitate			28.67		4.26		29.79		28.37
Non-extracted fresh precipitate			33.07		5.11		35.02		18.44
Mixture of 2:1 moles cuprous xanthate–dixanthogen (calculated)		33.17		5.01		35.43		17.55	

The original sample has been purified by Al_2O_3 column chromatography and gave the following analysis: Calculated: 74.18% C; 12.45% H; 10.70% S. Found: 73.80% C; 12.00% H; 10.97% S.

(5) Dialkyl Carbonates

Dialkyl carbonates (ethyl, *n*-butyl, and *n*-amyl) were commercial high-purity reagents.

(6) Alkyl Chloroformates

Alkyl chloroformates (ethyl and *n*-butyl) were commercial high-purity reagents.

INFRARED SPECTRA OF CARBONYL AND THIOCARBONYL COMPOUNDS

C=S Stretching Mode

Figure 1 shows the spectra of thiocarbonate compounds of the types R—O—C(=S)—S—R and $(RS)_2C{=}S$. It is seen that spectra of both types of compounds have strong bands at 1060–1070 cm^{-1}. Intense bands in this region are absent in molecules which do not contain the C=S group, although some weaker bands appear in this region for diethyl carbonate and ethyl chloroformate (Fig. 1).

The shape of the band at 1060 cm^{-1} is similar throughout the series of spectra of molecules containing the C=S group (Figs. 1, 2, and 3) and is composed of several peaks. This band has been assigned to the C=S stretching mode.

The C=S stretching mode has been assigned over a wide range of frequencies by different workers. Jones *et al.* (11) have discussed the variation of frequencies, depending on the environment of the C=S group, over the range 1000–1400 cm^{-1}. Hazeldine and Kidd (6) assigned to the C=S stretching vibration a band at 1050–1120 cm^{-1} in the spectra of the compounds $(RO)_2C{=}S$ and $(RS)_2C{=}S$, while Marvel *et al.* (7) assigned to this vibration a band at 1170–1195 cm^{-1}. Recently, Mecke *et al.* (8, 9) have investigated the spectra of a considerable number of molecules containing the C=S group and they ascribed its stretching frequency to the range 1053–1234 cm^{-1}; in the trithiocarbonate compounds the range was 1050–1060 cm^{-1}. An extremely intense absorption band between 1110 and 1145 cm^{-1} in the spectra of two mercaptopyridines has been assigned by Spinner (12) to the stretching vibration of conjugated C=S groups.

Felumb (3, 4) studied the spectra of many thiocarbonate molecules and assigned the C=S stretching mode to a band occurring at 1200–1250 cm^{-1}. The series of compounds studied by Felumb was, however, incomplete insofar as the compounds $(RS)_2C{=}S$ and $(RS)_2C{=}O$ were omitted. The former molecule, which contains the C=S group, has no strong absorption band in the region 1200–1250 cm^{-1} (Fig. 1). Moreover, all the molecules studied by Felumb contained the C—O—C linkage, which would be expected to show strong absorption bands at about 1200 cm^{-1} (5, p. 161). The molecule $(RS)_2C{=}O$, which has neither C—O—C nor C=S groups, has no strong bands between 1000 cm^{-1} and 1300 cm^{-1} (Fig. 1).

C—O—C Stretching Modes

Thompson and Torkington (13) have assigned two bands in the region of 1200 cm^{-1} to the stretching of the C—O bonds in esters. The assignment of absorption bands in the range 1000–1200 cm^{-1} in molecules containing the C—O—C group has been discussed

Can. J. Chem. Downloaded from www.nrcresearchpress.com by 210.87.254.42 on 09/05/12
For personal use only.

by Hales *et al.* (14). Their conclusion was that the two bands in this region may be associated with the stretching vibrations of the C—O—C group.

The spectra of copper and zinc xanthates, dixanthogens, and O,S-dioctadecyl xanthate (Figs. 1, 2, and 3) show two bands in the region 1100–1250 cm^{-1}: an intense band at 1200–1250 cm^{-1} and a weaker band at 1110–1140 cm^{-1}. The latter band is of variable intensity, being sensitive to the length of the hydrocarbon chain and the nature of the metal atoms incorporated in the compounds. It can be seen from the spectra of the zinc alkyl xanthates (Fig. 3) that the intensity of this band decreases as the chain length increases.

In the spectra of ethyl and *n*-butyl dixanthogens (Fig. 2), the frequency of the intense band is shifted to 1250 cm^{-1} (from 1200 cm^{-1} for copper and zinc xanthates) and the intensity of the band at lower frequency (1110 cm^{-1}) is greatly decreased for the dixanthogens. These bands appear at 1220 cm^{-1} and 1110 cm^{-1} for O,S-dioctadecyl xanthate (Fig. 1).

The spectra of compounds which do not contain the C—O—C linkage, i.e., $(RS)_2C{=}O$ and $(RS)_2C{=}S$ (Fig. 1) do not have strong bands between 1100 cm^{-1} and 1250 cm^{-1}.

The spectra of ethyl chloroformate and diethyl carbonate (Fig. 1) show the intense high-frequency bands at 1160 cm^{-1} and 1260 cm^{-1}, respectively, for these two compounds, and a considerably weaker band at a lower frequency, 1020 cm^{-1}. This band is weaker than the intense band ascribed to the C=S stretching mode of xanthates.

The bands at 1120 cm^{-1} and 1200 cm^{-1} appearing in the spectra of xanthates are here ascribed to the stretching vibrations of the C—O—C linkage.

C=O Stretching Mode

The intense band at 1650–1780 cm^{-1}, which occurs in the spectra of compounds containing the C=O group, viz. dialkyl carbonates, alkyl chloroformates, and $(n\text{-}C_4H_9S)_2C{=}O$, (Fig. 1), is absent from the spectra of trithiocarbonate and of all the xanthate compounds. This band has been ascribed to the C=O stretching mode of the carbonyl compounds.

In addition to the carbonyl absorption of $(n\text{-}C_4H_9S)_2C{=}O$, which occurs as a very intense band at 1650 cm^{-1} (Fig. 1), a weaker band is found at 1750 cm^{-1}. This is probably an overtone or combination band of the intense bands at 870 cm^{-1} and 920 cm^{-1}.

Structure of Xanthates

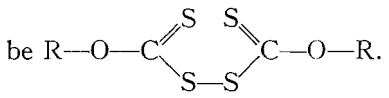
The spectra of copper and zinc xanthates (Figs. 2 and 3) show well-defined bands at 1200 cm^{-1} and 1120 cm^{-1}, which have been attributed to vibrations of the C—O—C linkage, while the intense band at 1060 cm^{-1} has been assigned to the C=S stretching mode.

The resonance hybrid $\left[R{-}O{-}C(=S){-}S \right]^-$ may be considered to represent the structure of the metal xanthates (2). However, the xanthate esters (Fig. 1), which do not exist as resonance hybrids, have the same C=S band at 1060 cm^{-1} as all the heavy metal xanthates. Consequently the structure of the heavy metal xanthates must be

$$R{-}O{-}C(=S){-}S^-\ .$$

Can. J. Chem. Downloaded from www.nrcresearchpress.com by 210.87.254.42 on 09/05/12
For personal use only.

For similar reasons the structure of the dixanthogens, retaining the C=S group, must

be  .

C—S and S—S Stretching Modes

Intense absorption bands occur at 830 cm^{-1} and 870 cm^{-1} in the spectra of $(n\text{-}C_{12}H_{25}S)_2C{=}S$ and $(n\text{-}C_4H_9S)_2C{=}O$ respectively (Fig. 1), while a band of medium intensity appears at 850 cm^{-1} in the spectrum of ethyl dixanthogen (Fig. 2). The intensities of the bands for $(n\text{-}C_4H_9S)_2C{=}O$ and ethyl dixanthogen are far greater than those of bands at lower frequencies (Table III). It is probable, therefore, that the bands at lower frequencies are associated with fundamental vibrations and not with overtones or combinations. An intense band also occurs at 870 cm^{-1} in the Raman spectrum of $(n\text{-}C_4H_9S)_2C{=}O$ (Table III).

The frequencies of these bands are considerably higher in value than those usually associated with the stretching of C—S or S—S bonds. Bellamy (5, p. 290) has discussed the assignments of C—S and S—S stretching modes to weak bands in the spectrum, occurring between 600–700 cm^{-1} and 400–500 cm^{-1}, respectively.

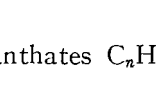
The intense bands (830 to 870 cm^{-1}) may be associated with an asymmetric C—S stretching mode of the C—S—C—S—C chain in the molecules $(n\text{-}C_{12}H_{25}S)_2C{=}S$ and $(n\text{-}C_4H_9S)_2C{=}O$ or the C—S—S—C chain in ethyl dixanthogen. It must be noted, however, that the disulphide $(n\text{-}C_{18}H_{37}S)_2$ (Fig. 1) does not have an intense absorption band in this region. Moreover, the metal xanthates, which have only one C—S bond also show bands in the region 800–950 cm^{-1} (Figs. 2 and 3), although these bands are generally weaker than those discussed above.

Jones *et al.* (11) have tentatively assigned bands occurring at 880–700 cm^{-1} in the spectra of "carbon sulphoxy chloride" and dimeric thiocarbonyl chloride to the stretching of the C—S bond. It is possible that, due to the environment of the C—S bond in the xanthate group, the frequency of the C—S stretching mode may be raised above the normal limits discussed by Bellamy.

An intense band appearing at 600 cm^{-1} in the Raman spectrum of $(n\text{-}C_4H_9S)_2C{=}O$ is probably due to a C—S stretching mode of this compound (5, p. 290).

Several bands appear between 300 and 550 cm^{-1} in the spectra of xanthates (Table III). Although the spectrum of ethyl dixanthogen has more bands in this region than those of the metal xanthates, no definite assignment can be given to the S—S stretching mode of dixanthogens.

Precipitation of Copper Xanthate

Pearson and Stasiak (2) have published spectra of potassium xanthates, heavy metal (Cu, Pb, Zn) xanthates, and potassium oxyxanthates C_nH_{2n+1}—O—  . In general, their spectra of corresponding xanthates are identical with those shown previously (1) and with those reported here. However, their spectrum of cupric xanthate corresponds to our spectrum of cuprous xanthate. The latter material was obtained after washing off the dixanthogen, which was coprecipitated with cuprous xanthate during the addition of cupric salts to solutions of alkali xanthates (1).

Can. J. Chem. Downloaded from www.nrcresearchpress.com by 210.87.254.42 on 09/05/12
For personal use only.

Can. J. Chem. Downloaded from www.nrcresearchpress.com by 210.87.254.42 on 09/05/12
For personal use only.

TABLE III

Cesium bromide infrared and Raman spectra of thiocarbonates

C_2H_5—O—C(=S)—S—Cu	$[C_2H_5$—O—C(=S)—S$]_2$Zn	$[C_2H_5$—O—C(=S)—S$]_2$	C_2H_5—O—C(=S)—SK	C_2H_5—O—C(=S)—SNa	$[n$-C_4H_9—O—C(=S)—S$]_2$Zn	n-C_4H_9—O—C(=S)—SK	$(n$-$C_4H_9S)_2C{=}O$

																			Infrared spectrum			Raman spectrum	
ν*	$\Delta\nu_{\frac{1}{2}}$†	% A‡	ν	$\Delta\nu_{\frac{1}{2}}$	% A	ν	$\Delta\nu_{\frac{1}{2}}$	% A	ν	$\Delta\nu_{\frac{1}{2}}$	% A	ν	$\Delta\nu_{\frac{1}{2}}$	% A	ν	$\Delta\nu_{\frac{1}{2}}$	% A	ν	$\Delta\nu_{\frac{1}{2}}$	% A	ν	$\Delta\nu_{\frac{1}{2}}$	% A	ν	% A
									290	~4	6													170	8
300	9	8				312	~25	7	308	9	15	308	~10	10	308	10	26	~295	~10	sh					
			345	~7	~20							327	2	10				~303	~5	15				220	11
350	9	8							350	~5	2							395	~10	3				440	8
			360	~15	~20	380	17	14							390	10	9				475	7	3		
453	9	10	452	10	18	425	13	11	447	8	29				405	11	18	435	9	20					
						470	15	3				470	~90	55	500	9	17	505	7	16	573	10	11	600	40
547	10	8				525	15	5	540	~15	2							~670	~10	~3				660	24
						565	10	2										750	10	~4					
667	~10	6	655	10	9	647	~25	6	655	~15	10	620	~60	30	665	10	10				747	~25	17	740	17
						673	~20	6										842	~10	~3					
						695	~15	8	672	~20	9				740	8	18				790	~20	11	800	12
815	~10	4	820	~10	7	815	17	15	820	~10	9	805	~15	6				925		13					
									840	~15	2	850	~10	2	840	~	2	962		11	870	~30	86	870	21
873	10	13	875	~15	11	850	22	41	875	~10	2	865	~10	3	904	10	12				920	~15	35	900	19
															927	7	13	1065		70					
															945	8	37				1050	20	7	1060	24
1015		43							1015		43							1107		78	1080	10	4		
															1026		38	1153		70	1105	10	11	1100	24
1040		80	1035		78	1020		~90				1040		74	1040		93				1147	15	11		
1053		37							1055		75										1235	15	17	1220	12
									1107		78										1280	15	24	1280	17
1127		66	1130		72	1110		67	1122		78	1115		74	1135		70				1300	~20	13	1310	25
						1153		31	1145		79	1153		70	1210		90				1345	~10	4		
1200		82	1213		80	1245		~90				1170		69							1387	10	15		
																					1420	10	18	1420	43
																					1470	~25	37	1460	64
																					1650	17	78	1650	44
																					1737	~40	20	1750	6

*Band frequency (cm^{-1}).

†Half-band width (cm^{-1}).

‡% absorption at band maximum.

Pearson and Stasiak do not state whether their copper xanthate precipitate was washed with solvents, yet in their spectrum no band appears at 1250 cm^{-1}, characteristic of dixanthogen in the precipitate. Nor do they state whether their elemental analysis was made before or after washing with solvents. Results of the analysis of the precipitate both before and after ether extraction are shown in Table II. In the absence of knowledge that the precipitate was a mixture of cuprous xanthate and dixanthogen, the results would indicate that it was cupric xanthate.

Infrared spectra (Fig. 2) and chemical analysis (Table II) suggest that the reaction between cupric ions and xanthate ions results in the coprecipitation of cuprous xanthate and dixanthogen in the molar ratio 2:1; $4\ RX^- + 2\ Cu^{++} \rightarrow 2\ RXCu + (RX)_2$ where X^- denotes the $-O-C(=S)-S^-$ group. With zinc ions a zinc dixanthate, but no dixanthogen, is formed.

Alkali Metal Xanthates

Spectra of some alkali metal xanthates are shown in Fig. 4. The absorption bands in the region 1000–1200 cm^{-1} are not well resolved but it is possible to distinguish three more or less distinct groups of bands, corresponding to the bands at 1200 cm^{-1}, 1130 cm^{-1}, and 1060 cm^{-1} for the heavy metal xanthates in Figs. 2 and 3.

If such a grouping of bands in the spectra of alkali metal xanthates is accepted, then the frequencies of the C—O—C linkage, discussed earlier, would appear to be displaced to lower values than those given for the C—O—C linkage in the heavy metal xanthates. The frequency of the band assigned to the C=S stretching mode varies from 1040 to 1080 cm^{-1} in the spectra of alkali metal xanthates. The presence of this band suggests that the C=S bond is preserved in the structure of the alkali metal xanthates.

ACKNOWLEDGMENTS

The authors gratefully acknowledge the assistance of Dr. K. Noack, Dr. E. C. Horswill, Mr. A. E. Castagne, and Mr. J. A. H. Desaulniers. G. W. Poling and J. Leja express their appreciation for the grants A699 and E140 received from the National Research Council of Canada.

REFERENCES

1. L. H. Little and J. Leja. Proceedings of the Second International Congress of Surface Activity. Vol. III. Butterworth Scientific Publications, London. 1957. p. 261.
2. F. G. Pearson and R. B. Stasiak. Appl. Spectroscopy, **12**, 116 (1957).
3. R. Felumb. Compt. rend. **244**, 2038 (1957).
4. R. Felumb. Bull. soc. chim. France, Ser. 5, **24**, 890 (1957).
5. L. J. Bellamy. The infrared spectra of complex molecules. 1st ed. Methuen & Co., Ltd., London. 1954.
6. R. N. Hazeldine and J. M. Kidd. J. Chem. Soc. 3871 (1955).
7. C. S. Marvel, P. DeRadzitzky, and J. J. Brader. J. Am. Chem. Soc. **77**, 5997 (1955).
8. R. Mecke, R. Mecke, and A. Lüttringhaus. Z. Naturforsch. Pt. *b*, **10b**, 367 (1955).
9. R. Mecke, R. Mecke, and A. Lüttringhaus. Chem. Ber. **90**, 975 (1957).
10. G. Bulmer and F. G. Mann. J. Chem. Soc. 666 (1945).
11. J. I. Jones, W. Kynaston, and J. L. Hales. J. Chem. Soc. 614 (1957).
12. E. Spinner. J. Org. Chem. **23**, 2037 (1958).
13. H. W. Thompson and J. Torkington. J. Chem. Soc. 640 (1945).
14. J. L. Hales, J. I. Jones, and W. Kynaston. J. Chem. Soc. 618 (1957).

Can. J. Chem. Downloaded from www.nrcresearchpress.com by 210.87.254.42 on 09/05/12
For personal use only.

Can. J. Chem. Downloaded from www.nrcresearchpress.com by 210.87.254.105 on 09/05/12
For personal use only.

STUDIES ON CHLOROBIUM CHLOROPHYLLS

II. THE RESOLUTION OF OXIDATION PRODUCTS OF CHLOROBIUM PHEOPHORBIDE (660) BY GAS-LIQUID PARTITION CHROMATOGRAPHY[1]

H. V. MORLEY[2] AND A. S. HOLT

ABSTRACT

Methylethylmaleimide, methyl-*n*-propyl maleimide, and dihydrohematinic acid imide are obtained from *Chlorobium* pheophorbide (660) on chromic acid oxidation. The separation and isolation of these products and of other imides and pyrroles by gas–liquid partition chromatography is described.

INTRODUCTION

It has been reported that *Chlorobium* chlorophyll (660) gives a negative Molisch phase test and fails to undergo methanolysis with ring opening (1). These observations and others to be published shortly indicate that this pigment differs from other known chlorophylls. An investigation involving degradation of the molecule to identifiable, substituted monocyclic compounds corresponding to the original pyrrole nuclei was therefore undertaken.

Each of the degradative methods described in the literature has disadvantages. Reduction by hydriodic acid (2) greatly complicates the analytical problem since each nucleus can yield up to four different pyrroles. Oxidation by chromic acid (3), while theoretically producing one imide per nucleus, causes loss of nuclei which possess unstable β-groups, e.g. vinyl, formyl, and hydroxyethyl groups (4). In this laboratory, oxidation by permanganate (5) gave yields of pyrroledicarboxylic acids which were too low to permit their isolation for elementary analysis.

Oxidation by chromic acid was chosen as the most suitable method of degrading *Chlorobium* pheophorbide (660). For the resolution of the resulting mixture of imides, gas–liquid partition chromatography (GLPC) required less starting material and proved to be faster and more convenient than previously described methods (3, 4, 6, 7, 8). A study of the separation of synthetic and analytical pyrroles by GLPC was initiated (Table I) but discontinued when imides were shown to be separable by the same technique (9).

TABLE I

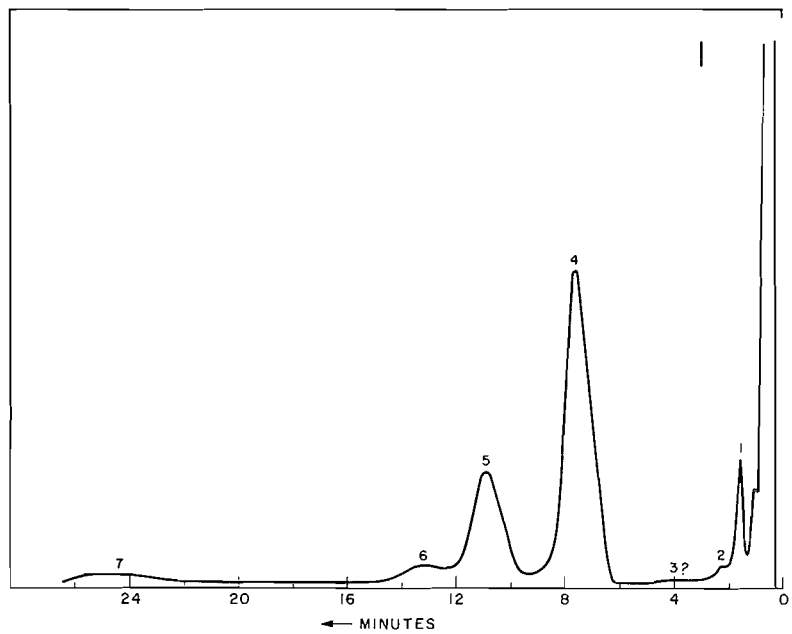
Retention volumes of pyrroles at 180°
relative to that of 2,4-dimethylpyrrole = 1

Pyrrole	0.50
2-Methylpyrrole	0.69
2,4-Dimethylpyrrole	1.00
3-Methyl-4-ethylpyrrole (opsopyrrole—fraction 1)	1.56
2,4-Dimethyl-3-ethylpyrrole (cryptopyrrole—fraction 2)	2.18
2,3-Dimethyl-4-ethylpyrrole (hemopyrrole—fraction 3)	2.48
2,4,5-Trimethyl-3-ethylpyrrole (phyllopyrrole—fraction 4)	3.38

Oxidation of *Chlorobium* pheophorbide (660) yielded "neutral" and "acid" fractions. The chromatogram of the "neutral" fraction (Fig. 1) shows two major peaks (4 and 5)

[1]*Manuscript received November 28, 1960.*
Contribution from the Division of Applied Biology, National Research Council, Ottawa, Canada.
Issued as N.R.C. No. 6185.
[2]*National Research Council Postdoctorate Research Fellow, 1957–59. Present address: Analytical Chemistry Research Service, Research Branch, Canada Agriculture, Ottawa.*

Can. J. Chem. Downloaded from www.nrcresearchpress.com by 210.87.254.105 on 09/05/12
For personal use only.



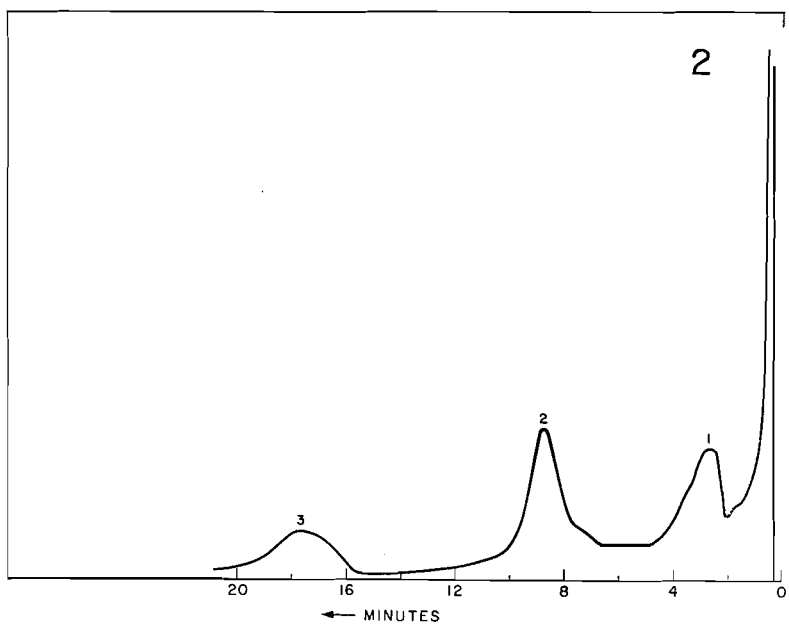


FIG. 1. Gas–liquid partition chromatogram of the "neutral" fraction from *Chlorobium* pheophorbide (660).

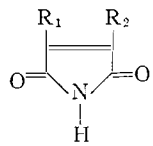
FIG. 2. Gas–liquid partition chromatogram of the "acid" fraction from *Chlorobium* pheophorbide (660).

and several minor ones. The compound responsible for peak 4 was readily shown, by GLPC, to be methylethylmaleimide by comparison with an authentic sample prepared from mesoporphyrin IX. From the retention volume (R_v, Table II), the compound

TABLE II

Retention volumes of maleimides at 200° relative to that of quinoline = 1

Maleimide	0.22	Methyl-*n*-propylmaleimide (III)	0.84
Citraconimide (I)	0.30	Bromocitraconimide	1.00
Succinimide	0.53	Hematinic acid imide methyl ester (IV)	2.90
Methylethylmaleimide (II)	0.59	Dihydrohematinic acid imide methyl ester	3.03



		R_1	R_2
I	Citraconimide	H	CH_3
II	Methylethylmaleimide	CH_3	C_2H_5
III	Methyl-*n*-propylmaleimide	CH_3	C_3H_7
IV	Hematinic acid imide	CH_3	$(CH_2)_2COOH$

responsible for peak 5 could be assumed to contain one more methylene group than methylethylmaleimide. This assumption was confirmed by elementary analysis. The melting point agreed with that of methyl-*n*-propylmaleimide (10); this structure was also deduced from the proton magnetic resonance spectrum. Subsequently, a synthetic sample of methyl-*n*-propylmaleimide (10) proved to be identical with the analytical sample. It is of interest to note that this is the first time a *n*-propyl side chain has been found in a natural tetrapyrrole.

The chromatogram of a small sample of the methylated "acid" fraction is given in Fig. 2. The products responsible for each of the three main peaks have infrared spectra not unlike those of methylethyl- and methyl-*n*-propylmaleimide. Because no reference specimen was available, dihydrohematinic acid imide was not identifiable among the products. It was thus necessary to isolate it from the remaining "acid" fraction by partition chromatography on silica gel. The eluent samples which were acidic and gave a positive imide test (11, 12) were combined and converted to the benzylamine salt. Analysis, melting point, and infrared spectrum confirmed that the product was the salt of *trans*-dihydrohematinic acid imide obtained previously by Linstead *et al.* (6). The above salt was converted to the free acid and esterified with only a slight excess of diazomethane. Such care was necessary in order to eliminate the possibility of methylating the imide nitrogen atom (13). The infrared spectrum of the colorless oil obtained after removing the solvent and excess diazomethane still showed the NH absorption band at 3390 cm^{-1} indicative of the intact imide nitrogen. A sample subjected to GLPC showed that dihydrohematinic acid imide methyl ester was responsible for peak 3 ($R_v = 3.03$) of Fig. 2. This result was to be expected since hematinic acid imide methyl ester has an R_v value of 2.90 (Table II). The substances responsible for peaks 1 and 2 were not recovered in sufficient quantity, after purification by GLPC, to permit their identification.

The above results identify at least three of the four pyrrole nuclei present in *Chlorobium* pheophorbide (660). Recent studies have shown that *Chlorobium* pheophorbide (650) possesses a hydroxyethyl group which is readily oxidized to an acetyl group, and that *Chlorobium* pheophorbide (660) possesses a similar group (14). Until these studies have been completed, the nature of the fourth nucleus in *Chlorobium* pheophorbide (660) remains in question.

Can. J. Chem. Downloaded from www.nrcresearchpress.com by 210.87.254.105 on 09/05/12
For personal use only.

Can. J. Chem. Downloaded from www.nrcresearchpress.com by 210.87.254.105 on 09/05/12
For personal use only.

EXPERIMENTAL

The preparation and purification of *Chlorobium* pheophorbide (660) from *Chlorobium* chlorophyll will be outlined in a forthcoming publication. Mesoporphyrin IX was obtained from hemin by a standard procedure (15, 16). Except where stated otherwise, infrared spectra were determined in chloroform on a Perkin–Elmer Model 21 double-beam instrument. Melting points were determined on the Koffler Hot Stage. The instrument used for GLPC was a modified Podbelniak "Chromacon" (Series 9475-3V) described previously (17). Pyrroles were separated on a column (8 ft long, 7-mm I.D.) packed with a mixture (1:4 w/w) of Apiezon M and alkali-washed Celite 545 (60–80 mesh). The operating temperature was 180° C; the carrier gas was helium with a flow rate of 75 ml/minute. The number of theoretical plates was 1300. Imides were separated as described earlier (9). The proton magnetic resonance spectrum of methyl-*n*-propylmaleimide was recorded at 60 Mc/s with a Varian V-4032 high-resolution spectrometer.

Oxidative Degradation of Chlorobium Pheophorbide (660)

The oxidation procedure and the separation of the imides into "neutral" and "acid" fractions followed closely the directions of Linstead *et al.* (6). *Chlorobium* pheophorbide (1.0 g) was dissolved in sulphuric acid (70 ml, 50% v/v); the solution was then diluted with ice (70 g) and cooled to −10° C. Chromic acid (3.3 g) in water (30 ml, 0° C) was added dropwise with stirring during 1 hour. The solution was maintained at −10° C for 2 hours with continued stirring. By this time carbon dioxide evolution had diminished. The mixture was allowed to warm slowly to room temperature with stirring until a total of 5 hours had elapsed since the first addition of chromic acid. The mixture was then extracted and fractionated (6). Later work showed that after a total period of $3\frac{1}{2}$ hours no further increases in the yields of the neutral imides were indicated by GLPC.

"Neutral" Fraction

Since fractions 1, 2, and 3 (Fig. 1) did not separate well they were not investigated intensively. ν_{max} of a crude sample of fraction 1: 3500 (m), 3375 (m), 1698 (s), 1600 (w), and 1565 (m) cm^{-1}. The R_V value (0.59) of fraction 4 agreed with that of methylethylmaleimide obtained from mesoporphyrin IX (see below). Initially 32 mg were obtained; further purification by GLPC yielded 16 mg as white blades, mixed m.p. 67–68°. The infrared spectrum was superposable upon that of an authentic sample. Found: C, 60.2; H, 6.39. $C_7H_9O_2N$ requires: C, 60.4; H, 6.52%.

Fraction 5 (ca. 13 mg) was further purified by GLPC (white needles, 6.7 mg); recrystallized (chloroform–ether), m.p. 52–54°. The yields from several oxidations were bulked. Found: C, 62.6; H, 7.38; N, 8.80. $C_8H_{11}O_2N$ requires: C, 62.7; H, 7.24; N, 9.14%. The proton magnetic resonance spectrum of a 10% (w/v) solution was consistent with the methyl-*n*-propylmaleimide structure. The following shifts, given as τ values (18) and compared to tetramethylsilane as an internal standard were observed: a broad band at 1.04 (=N*H*), a triplet at 7.57 (=C—CH_2CH$_2$—), a sharp singlet at 8.01 (=C—CH_3), six unresolved peaks at 8.47 (—CH$_2$—CH_2—CH$_3$), and at 9.02 a triplet (—CH$_2$—CH$_2$—CH_3). ν_{max} (CCl_4): 3430 (w), 1769 (w), and 1725 (s) cm^{-1}. On comparison with a synthetic specimen (10) this product was found to be identical with respect to mixed melting point, infrared spectrum, nuclear magnetic resonance spectrum, and X-ray powder diagram.

The small quantities of fractions 6 and 7 permitted only the examination of the infrared spectrum. ν_{max} of both were at: 3418 (w), 1768 (w), and 1720 (s) cm^{-1}.

Can. J. Chem. Downloaded from www.nrcresearchpress.com by 210.87.254.105 on 09/05/12
For personal use only.

"Acid" Fraction

A small sample (ca. 5 mg) of the acid fraction was esterified with distilled diazomethane. The R_v values of the three main products (Fig. 2) in this sample were 0.49, 1.49, and 3.03 respectively.

The remainder was partitioned on a wet silica gel column (55×2 cm) and eluted with ethyl acetate (6). Six-milliliter samples were collected (50 tubes). Paper chromatograms were developed in ethanol–NH_4OH–water (7:1:2) and sprayed with Universal indicator spray (British Drug Houses Ltd.) for acids or with an imide spray (11, 12). The results showed that tubes 4–8 contained traces of neutral imides and that tubes 8–16 contained the bulk of the acidic imides.

Tubes 8–16 were combined and evaporated to dryness. The residue was converted to the benzylamine salt(s) of the imide acid(s). Recrystallization from methanol – ethyl acetate yielded white needles. The infrared spectrum (nujol mull) had maxima at 1298 (m); 1265 (m); 1217 (m); 1190 (s); 1168 (w); 1160 (w); 888 (w); 872 (m); 823 (m); 795 (m); 772 (m); 755 (s); 741 (m); 719 (w); 696 (m); 686 (w) cm^{-1}, which agree well with data given by Linstead *et al.* (6) for the benzylamine salt of *trans*-dihydrohematinic acid imide, m.p. 158–161° (lit. 164–165° (6)). Found: C, 61.7; H, 6.97; N, 9.71. $C_{15}H_{20}O_4N_2$ requires: C, 61.6; H, 6.90; N, 9.58%. The benzylamine salt was dissolved in a little water and the free acid was extracted into ethyl acetate and ether after acidification. The extracts were combined, dried over sodium sulphate, and evaporated to dryness *in vacuo*. The free acid in the residue from the extract was carefully esterified with distilled diazomethane in ether, by dropwise addition until a faint yellow color persisted for 15 minutes. The R_v value of the resulting colorless oil was 3.03. ν_{max}: 3390 (w), 1775 (w), 1723 (s) cm^{-1}. Found: C, 54.3; H, 6.65. $C_9H_{13}O_4N$ requires: C, 54.3; H, 6.58%.

Oxidative Degradation of Mesoporphyrin IX

Mesoporphyrin IX (250 mg) was oxidized and separated into "neutral" and "acid" fractions essentially by the method of Muir and Neuberger (8). About 5 mg of the "neutral" fraction was analyzed by GLPC; the main fraction (R_v 0.59) was collected as crystals. Methylethylmaleimide was crystallized from an aqueous solution of the remainder of the "neutral" fraction (m.p. 67–68° (lit. 68° (8)). Yield, 45 mg. This sample proved to be identical (mixed melting point, R_v value, and infrared spectrum) with that obtained as crystals from the GLPC separation described above. ν_{max}: 3430 cm^{-1}, (w); 1768, (w); and 1718 (s) cm^{-1}.

Ten milligrams of the "acid" fraction was esterified with diazomethane. Three main fractions with the following R_v values were observed: (1) 0.387, (2) 1.49, and (3) 2.90 respectively. Fraction (3) was shown by comparison with an authentic sample (R_v value and infrared absorption spectrum) to be hematinic acid imide methyl ester. ν_{max}: 3430 (w), 1768 (w), and 1722 (s) cm^{-1}. Fractions (1) and (2) have not been identified. The spectra of each contained N—H bands but differed from those of other available imides in the double bond stretching region. ν_{max}: fraction (1), 1823 (w), 1758 (s), 1720 (s), 1673 (m), and 1600 (w) cm^{-1}; fraction (2), 1815 (w) (shoulder), 1762 (s), 1723 (s), and 1673 (m) cm^{-1}.

Reductive Degradation of Hemin

Hemin (250 mg, British Drug Houses Ltd.) was heated in glacial acetic acid (4.5 ml) containing hydriodic acid (5 g; s.g. 1.96) according to the method given by Willstätter and Stoll (19). Free iodine was reduced by hypophosphorous acid which was added

dropwise during ½ hour. The reaction mixture was adjusted to pH 11 (Na_2CO_3) and pyrroles were then extracted into ether. Strongly basic reduced pyrroles were removed from the ether by aqueous monosodium phosphate. The ether solution was dried (Na_2SO_4) and evaporated.

A sample of the residue from the ether solution was analyzed by GLPC and gave four main peaks, numbered 1 to 4 in the order of their emergence from the column. These products were collected as colorless oils, which darkened rapidly upon exposure to air.

Product 2 was shown to be cryptopyrrole by comparison of its R_v value (Table I) with that of an authentic sample. Product 1 was deduced to be opsopyrrole as follows: an ether solution of the reaction mixture was extracted with 12% (w/w) hydrochloric acid. This strength acid is known to remove crypto-, phyllo- and hemo-pyrrole and leave opsopyrrole in the ether phase (20). The material in the residue from the ether solution was analyzed by GLPC and gave peak 1, with only traces of the other three peaks. Product 4 was presumed to be phyllopyrrole because: (1) it gave a positive Ehrlich test only after heating (21) (products 1, 2, and 3 gave immediate positive tests at room temperature); and (2) it is reasonable to presume it would emerge last from the column since it possesses the highest molecular weight of the four pyrroles obtained from hemin. By elimination, product 3 was assumed to be hemopyrrole. It was later found that steam distillation of the pyrroles from the alkaline solution eliminated some impurities which otherwise appeared on the chromatogram.

ACKNOWLEDGMENTS

The authors are most grateful to the following members of the Division of Pure Chemistry, National Research Council, for gifts of samples: Drs. S. F. MacDonald and E. Bullock and Mr. Keith Chambers. Gas–liquid partition chromatographic separations were performed by Mr. F. Cooper; analyses were determined by Mr. A. Castagne; and infrared absorption spectra were measured by Mr. F. Rollin. For the measurement of the proton magnetic resonance spectrum of methyl-*n*-propylmaleimide the authors are indebted to Dr. R. R. Fraser, Department of Chemistry, University of Ottawa.

REFERENCES

1. A. S. Holt and H. V. Morley. J. Am. Chem. Soc. **82**, 500 (1960).
2. H. Fischer and H. Orth. Chemie des pyrroles. Vol. I. Leipzig. 1934. p. 48.
3. W. Kuster. Ber. **35**, 2498 (1902).
4. H. Fischer and H. Wenderoth. Ann. **537**, 170 (1939).
5. R. A. Nicolaus, L. Mangoni, and L. Caglioti. Ann. Chim. (Rome), **46**, 793 (1956).
6. G. E. Ficken, R. B. Johns, and R. P. Linstead. J. Chem. Soc. 2272 (1956).
7. H. Fischer and H. Wenderoth. Ann. **545**, 140 (1940).
8. H. M. Muir and A. Neuberger. Biochem. J. **45**, 163 (1949).
9. H. V. Morley, F. P. Cooper, and A. S. Holt. Chem. & Ind. (London), **32**, 1018 (1959).
10. H. Fischer, M. Goldschmidt, and W. Nüssler. Ann. **486**, 1 (1931).
11. H. N. Rydon and P. W. G. Smith. Nature, **169**, 922 (1952).
12. F. Reindel and W. Hopper. Ber. **87**, 1103 (1954).
13. F. Wrede and A. Rothaas. Z. physiol. Chem. **215**, 67 (1933).
14. A. S. Holt and D. W. Hughes. In preparation.
15. H. Fischer and H. Putzer. Z. physiol. Chem. **154**, 40 (1926).
16. S. Granick. J. Biol. Chem. **172**, 717 (1948).
17. A. G. McInnes, D. H. Ball, F. P. Cooper, and C. T. Bishop. J. Chromatog. **1**, 556 (1958).
18. G. V. D. Tiers. J. Phys. Chem. **62**, 1151 (1958).
19. R. Willstätter and A. Stoll. Untersuchungen über Chlorophyll. J. Springer, Berlin. 1913. Chap. 22.
20. H. Fischer and A. Treibs. Ann. **450**, 132 (1926).
21. A. Triebs and H. Derra-Scherer. Ann. **598**, 196 (1954).

Can. J. Chem. Downloaded from www.nrcresearchpress.com by 210.87.254.105 on 09/05/12
For personal use only.

Can. J. Chem. Downloaded from www.nrcresearchpress.com by 210.87.254.40 on 09/05/12
For personal use only.

FURTHER STUDIES ON THE REACTION BETWEEN HALOGEN-SUBSTITUTED NITRILES AND AMINES[1]

JOHN C. GRIVAS[2] AND ALFRED TAURINS

ABSTRACT

The scope of the reaction of halogen-substituted nitriles and amines was extended by including trifluoro- and dichloro-acetonitrile. Trifluoroacetonitrile reacts easily with primary and secondary aliphatic, primary aromatic, and heterocyclic amines to give the corresponding amidines. N-Mono- and N-di-substituted dichloroacetamidines were prepared from dichloroacetonitrile and amines. Trichloroacetonitrile also affords N-substituted amidines with heterocyclic amines.

INTRODUCTION

The reaction of trichloroacetonitrile with primary and secondary amines has been investigated and discussed (1). The present work deals with the extension of the reaction, using trifluoroacetonitrile and di- and mono-chloroacetonitrile, and a variety of amines. Trifluoroacetonitrile is expected to react even faster than trichloroacetonitrile owing to the stronger inductive effect ($-I_s$) of the trifluoromethyl group. Husted (2) synthesized a series of perfluoroalkylamidines by allowing the corresponding nitriles to react with liquid ammonia in sealed tubes for 2 weeks. Reilly and Brown (3) isolated some N-methyl-, and N,N-dimethyl-perfluoroalkylamidines by treating nitriles with methyl- and dimethyl-amine at $-60°$. They assumed that aniline, being a weak base, could not produce any amidines. There are no literature data concerning the addition of amines to the carbon–nitrogen triple bond of dichloroacetonitrile.

RESULTS AND DISCUSSION

The formation of amidines from nitriles and amines depends on both the basicity of the amine and the electron deficiency of the carbon atom of the nitrile group. The mechanism of this reaction (1) implies that the more mobile the electron pair of the amino nitrogen atom, the stronger will be the interaction between the two reactive centers and the faster the reaction will go. On the other hand, the greater the electron deficiency of the carbon atom, the faster the reaction will be. Acetonitrile does not react with amines because the mesomeric effect of the nitrile group is compensated by the ($+I_s$) inductive effect of the methyl group.

$$CH_3 \rightarrow - C \equiv \overset{\curvearrowright}{N}: \qquad CF_3 - \leftarrow C \equiv \overset{\curvearrowright}{N}:$$

Evidence for this was obtained by conducting a series of reactions involving primary and secondary amines and four α-halogen-substituted nitriles, of decreasing inductive ($-I_s$) effect as follows:

$$F_3C{-}CN > Cl_3C{-}CN > Cl_2HC{-}CN > ClCH_2{-}CN.$$

Trifluoroacetonitrile was found to react not only with primary and secondary aliphatic but also with primary aromatic and heterocyclic amines at room temperature providing excellent yields of products in each case. Trichloroacetonitrile also afforded mono-substituted amidines when treated with 2-amino-5-methylpyridine and 2-aminothiazole

[1]*Manuscript received November 10, 1960.*
Contribution from the Department of Chemistry, McGill University, Montreal, Quebec, with financial assistance from the National Research Council of Canada, Ottawa.
[2]*Holder of a National Research Council Studentship, 1957–58 and 1958–59.*

at room temperature. The monosubstituted amidines derived from both nitriles on the basis of infrared spectroscopic studies (4, 5) exist in the imino form (I):

$$\underset{\text{(I)}}{\underset{\displaystyle \underset{\displaystyle \underset{\displaystyle \

The present work has lead to the following conclusions:

(*a*) At least two strongly electronegative atoms are necessary to promote the non-catalyzed addition of amines to the nitrile group. It is of interest to note that ethyl cyanotartronate (V) adds amines in a manner identical with that of trichloro- and trifluoro-acetonitriles (7):

$$N\equiv C-\underset{\underset{OH}{|}}{C}(CO_2C_2H_6)_2.$$

(V)

(*b*) Methanol cannot be used as a solvent in the reaction of trichloroacetonitrile with secondary aliphatic amines, owing to the formation of methyl trichloroacetimidate. This would also occur with trifluoro- and dichloro-acetonitrile.

(*c*) Acetonitrile is an excellent solvent.

(*d*) The reaction between primary aromatic amines and the three nitriles used in these studies does not occur in non-polar solvents.

(*e*) Primary aliphatic amines react much faster than primary aromatic amines. Secondary aliphatic amines react more slowly than primary aliphatic amines, even though the former are the stronger bases. This discrepancy can be attributed to stereochemical factors.

(*f*) Secondary aliphatic amines containing alkyl groups with more than three carbon atoms react preferentially by substitution at the α-carbon atom of trichloroacetonitrile:

$$(n\text{-}C_5H_{11})_2NH + CCl_3—CN \rightarrow (n\text{-}C_5H_{11})_2NCCl_2CN + HCl.$$

EXPERIMENTAL

A. Preparation of Trifluoroacetamidines

1. N-Butyl-α,α,α-trifluoroacetamidine.—A slow stream of trifluoroacetonitrile was passed through pure *n*-butylamine (2.9 g) in a tube which was immersed in an ice-water bath. An exothermic reaction took place. The crude product was distilled in a nitrogen atmosphere to give a colorless liquid (5.5 g, 82% yield) boiling at 39–40°/2 mm. Analysis of this compound is recorded in Table I.

2. N-Benzyl-α,α,α-trifluoroacetamidine.—In a long glass tube was placed 1.9 g of trifluoroacetonitrile (0.02 mole). The tube was cooled in a dry ice – acetone mixture and was connected by a Tygon tubing to a 100-ml pear-shaped flask containing a solution of 2.15 g (0.02 mole) of benzylamine in 10 ml of benzene. The solution was stirred by a magnetic stirrer while a slight pressure of trifluoroacetonitrile was maintained in the closed system. This was achieved by keeping the surface of the liquid trifluoroacetonitrile slightly above the surface of the cooling mixture. After ½ hour the nitrile had been used up but the stirring was continued for an additional 30 minutes. The solvent was evaporated under reduced pressure and the remaining liquid fractioned to give 3.84 g (91%) of a colorless liquid boiling at 88–90°/3 mm. In a few hours, the liquid solidified to white transparent crystals which, after two sublimations at 2 mm pressure, gave pure N-benzyl-α,α,α-trifluoroacetamidine, m.p. 51°.

3. N-Phenyl-α,α,α-trifluoroacetamidine.—A solution of 5 g of aniline in 20 ml of methanol was added to a Pyrex glass tube (20×709 mm) which was cooled in a dry ice – acetone mixture. An equimolar amount of trifluoroacetonitrile was condensed in the tube, which was then sealed and left for 4 days at room temperature. The tube was cooled to condense any unreacted trifluoroacetonitrile and opened. The reaction product was precipitated by addition of distilled water, or by evaporation of methanol at reduced

Can. J. Chem. Downloaded from www.nrcresearchpress.com by 210.87.254.40 on 09/05/12
For personal use only.

pressure, washed twice with distilled water, and dried. After sublimation the amidine (9.2 g, 91% yield) melted at 81°.

4. N,N-Diethyl-α,α,α-trifluoroacetamidine.—Equimolar quantities of trifluoroacetonitrile and diethylamine were allowed to react in a sealed Pyrex tube at room temperature for 24 hours. The mixture was then fractionated to give a colorless amidine (90% yield) boiling at 119°.

5. N-(5-Methyl-2-pyridyl)-α,α,α-trifluoroacetamidine.—Equimolar quantities of trifluoroacetonitrile and 2-amino-5-methylpyridine in acetonitrile were kept in a sealed Pyrex tube at room temperature for 4 to 6 days. The addition of water caused the separation of a liquid layer which solidified in a few minutes. The crude yellowish product was dissolved in a small volume of acetonitrile and precipitated by addition of water (yield 71%). After sublimation the amidine melted at 102°.

B. Preparation of Dichloroacetamidines

1. N-Methyl-α,α-dichloroacetamidine.—Dichloroacetonitrile (6.87 g, 0.062 mole) was added to an aqueous 25% solution of methylamine containing an equivalent amount of the amine, and the mixture was shaken for a few minutes. The lower reddish-brown layer was separated and distilled in a nitrogen atmosphere to give an almost colorless liquid (4.8 g, 55% yield) boiling at 80–85°/6 mm. Some decomposition of the product occurred during distillation and the pure amidine which was isolated turned black in 2 days.

2. Piperidino-α,α-dichloroacetamidine.—Piperidine (3.15 g, 0.037 mole) was added to a benzene solution (15 ml) of dichloroacetonitrile (4.7 g, 0.037 mole) and left at room temperature for 3 days. The mixture was then fractionated under reduced pressure in a nitrogen atmosphere to give a colorless liquid (6.4 g, 88% yield) at 63–66°/1 mm. The pure amidine changed to a black tar in 3 weeks.

3. N-Phenyl-α,α-dichloroacetamidine.—A mixture of dichloroacetonitrile (0.025 mole), aniline (0.025 mole), and 16 ml of methanol was left in a stoppered flask at room temperature for 1 week. After the evaporation of the solvent under reduced pressure a dark-brown solid was obtained. The product was then sublimed. Unreacted aniline together with a portion of the amidine was collected first but continued sublimation gave colorless N-phenyl-α,α-dichloroacetamidine (3 g, 60% yield), m.p. 62°.

C. Preparation of Heterocyclic Trichloroacetamidines

1. N-(5-Methyl-2-pyridyl)-α,α,α-trichloroacetamidine.—Trichloroacetonitrile (2.88 g, 0.02 mole) was added to a solution of 2-amino-5-methylpyridine (2.16 g, 0.02 mole) in 6 ml of acetonitrile and the mixture was left at room temperature for 4 days. Then addition of 10 ml of water caused the separation of a yellowish liquid layer which solidified in a few minutes. The compound was filtered off, and dissolved in a small volume of methanol. Addition of water to the methanol solution resulted in the isolation of a colorless product (4.1 g, 81% yield) melting at 78–79°. Sublimation at 70°/2 mm raised the melting point to 83.5°.

2. N-(2-Thiazolyl)-α,α,α-trichloroacetamidine.—This compound was prepared by a method similar to that outlined above, m.p. 87°.

REFERENCES

1. J. C. GRIVAS and A. TAURINS. Can. J. Chem. **36**, 771 (1958).
2. D. HUSTED. U.S. Patent No. 2,676,985 (1954); Chem. Abstr. **49**, 5511 (1955).
3. W. L. REILLY and H. C. BROWN. J. Am. Chem. Soc. **78**, 6032 (1956).
4. J. C. GRIVAS and A. TAURINS. Can. J. Chem. **37**, 795 (1959).
5. J. C. GRIVAS and A. TAURINS. Can. J. Chem. **39**, 414 (1961).
6. L. HENRY and A. DEWAEL. Bull. acad. roy. méd. Belg. 904 (1904); Chem. Zentr. **8**, 1377 (1904).
7. R. CURTIS and L. NICKELL. J. Am. Chem. Soc. **35**, 887 (1913).

Can. J. Chem. Downloaded from www.nrcresearchpress.com by 210.87.254.40 on 09/05/12
For personal use only.

Can. J. Chem. Downloaded from www.nrcresearchpress.com by 210.87.254.42 on 09/05/12
For personal use only.

THE ABSORPTION SPECTRUM OF DIPHENYLENE IN THE NEAR-ULTRAVIOLET[1]

ROBIN M. HOCHSTRASSER

ABSTRACT

The absorption spectrum of diphenylene has been measured in the vapor at a variety of temperatures, in solution at room temperature, and in an EPA rigid glass at 90° K. From a consideration of the band structure and intensity distribution it was concluded that the weak absorption at 25,041 cm^{-1} (vapor; $f \approx 10^{-3}$) is due to a symmetry-forbidden electronic transition. The theoretical prediction that the excited level is of species B_{1g} was supported by the presence of a strong infrared band at 732 cm^{-1} corresponding to observed perturbing vibration of frequency 792 cm^{-1}. The solution spectrum was found to exhibit a vibrational structure typical of a g–g forbidden excitation.

The electronic levels of diphenylene are somewhat anomalous when compared to those of other alternant hydrocarbons such as the structurally similar naphthalene or phenanthrene and anthracene. The solution spectrum of diphenylene was studied by Carr, Pickett, and Voris (1) and the electronic transitions involved were subsequently classified by Clar (2, p. 279) on the basis of intensity and band position and by analogy with other alternant hydrocarbons. Recently, using the technique of mixed crystal spectroscopy the symmetry of the second molecular level, the absorption to which commences at 27,910 cm^{-1} in liquid solution, was determined (3). This level was found to belong to the $^1B_{3u}$ (long axis polarized) representation in the point group D_{2h}. Such an assignment is at variance with the systematic classification by Clar. The p-band, by analogy with other alternants, would involve excitation to a short axis polarized level. In view of this a closer study of the weak lower-energy band was prompted.

During the past few years the symmetry types of the molecular levels of most of the polyacenes have been determined experimentally. The theorists have correctly predicted both the symmetry and energy of these levels. However, this success is not yet known to extend to the pericondensed hydrocarbons such as pyrene and perylene or to hydrocarbons containing other than six-membered rings such as diphenylene.

There are certain features which become apparent during a qualitative examination of the absorption spectrum of diphenylene in liquid solution at room temperature. There are three obviously separated absorption regions which are taken to be due to absorption to three different electronic levels. The highest energy absorption commences at about 40,250 cm^{-1} with $\epsilon_{max} = 10^5$. This band has little structure and in both band position and intensity resembles the ^1B_b ($^1B_{2u}$) transitions of the polyacenes. The intermediate band occurs at 27,910 cm^{-1} with $\epsilon_{max} = 10^4 - 10^3$. This band resembles the $^1L_a(^1B_{3u})$ transitions of the polyacenes in these respects; however, the vibrational structure is neither regular nor similar to that observed in the ^1L_a bands of polyacenes. The lowest energy transition at 25,530 cm^{-1} with $\epsilon_{max} = 10^2$ has even lower intensity than the ^1L_b bands of benzene ($^1B_{2u}$; $\epsilon_{max} = 500$), naphthalene ($^1B_{2u}$; $\epsilon_{max} = 310$), and phenanthrene (B_1; $\epsilon_{max} = 800$).

Simple molecular orbital theory does predict that transitions to the lowest lying level of diphenylene will be forbidden by molecular symmetry. In this paper we have examined

[1]*Manuscript received November 14, 1960.*
Contribution from the Chemistry Department, the University of British Columbia, Vancouver, B.C. This research was supported by a grant from the National Research Council of Canada.

the lowest energy band of diphenylene in the vapor and in rigid glassy solution at liquid nitrogen temperature and have obtained results which are in accord with the predictions of simple theory.

EXPERIMENTAL

Vapor Spectra

Diphenylene is a reasonably volatile solid and appreciable concentrations of vapor were obtained in a 10-cm cell at around 100° C. A small heating compartment was made which fitted into the Cary spectrophotometer (Model 14). A small crystal of diphenylene was contained in an evacuated quartz cell which could be maintained at temperatures around 100° to within 0.5°. The cell windows were always at a slightly higher temperature than the body so that no crystals could interfere with the light beam. An identical quartz path was placed in the reference beam.

Spectra at Liquid Nitrogen Temperature

The solvent used was a mixture of ether (5 parts), isopentane (5 parts), and alcohol (1 part) to be referred to as EPA. This formed an optically clear glass at the temperature of boiling nitrogen.

The low-temperature cell was constructed to fit into the sample compartment of the Cary spectrophotometer. The Dewar system was made of metal to which was fitted a copper block. The liquid was contained in a cylindrical cell with copper walls and quartz windows which fitted tightly into the copper block of the Dewar. The windows were held in by means of steel springs and the vacuum seal was obtained by pressing the windows onto indium rings. In this way spectra could be run with a perfect optical path at any temperature between 25° C and −190° C. The window assembly used was a modification of that described by Willis (4). The cell thickness was 0.33 cm. In calculating extinction coefficients at liquid nitrogen temperature correction was made for the contraction of the solution on cooling from room temperature.

The wavelength scale of the Cary was calibrated absolutely to within 2 Å in the spectral region which was covered. Often the peaks were sharp enough such that wavelength differences could be measured to ±0.4 Å, which corresponds to ±2.5 cm^{-1} at 4000 Å and ±3.1 cm^{-1} at 3600 Å. The Cary was used with a maximum slit width of 0.015 mm.

RESULTS

Vapor Spectrum

The spectrum of diphenylene vapor at two temperatures is shown in Fig. 1. The main features are as follows:

(1) The weak band system is superimposed on the long wavelength tail of the 3600 Å transition.

(2) Although not well resolved by the instrument, the spectrum at 95° C appears as a typical electronic band system with some indication of red shading.

(3) At higher temperature the very weak member at 3880 Å has gained in relative intensity. Above 125° C all the diphenylene in the cell had vaporized and further temperature increases had little effect apart from broadening and an over-all intensification of the spectra due to an increase in the hot-band intensity from the higher energy transition.

(4) No accurate vapor pressure data were available for diphenylene so it was not possible to measure extinction coefficients or oscillator strengths.

Can. J. Chem. Downloaded from www.nrcresearchpress.com by 210.87.254.42 on 09/05/12
For personal use only.

Can. J. Chem. Downloaded from www.nrcresearchpress.com by 210.87.254.42 on 09/05/12
For personal use only.

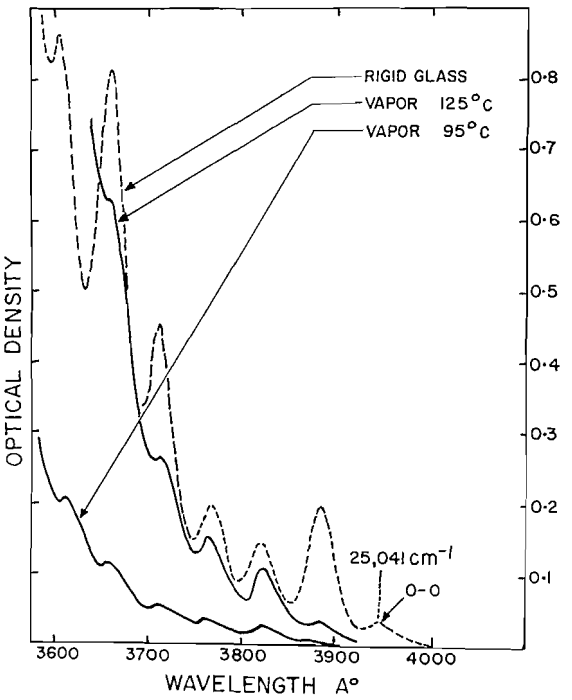


FIG. 1. The absorption spectra of diphenylene in vapor and rigid glass: the lowest energy transition.

Comparison of Vapor and Rigid Glass Spectra

The spectrum of diphenylene in EPA glass at −183° C is shown as a dotted curve on Fig. 1. The whole spectrum was shifted about 370 cm^{-1} to the blue in order to clarify the more important features. The essential dissimilarities between the vapor and rigid glass spectra were as follows:

(1) The 25,780 cm^{-1} lowest-energy vapor band now appears strongly at 3934.9 Å (25,414 cm^{-1}). The one–one correspondence between the bands in the vapor and rigid glass spectra is clearly shown in Table I.

TABLE I

Comparison of the vapor and rigid glass spectra of the weak system of diphenylene

ν_{max} (cm^{-1})		Relative intensity		
Vapor	Glass	Vapor	Glass	$\Delta\nu$ (cm^{-1})
25,407*	25,041	0	0.3	366 (calc.)
25,780	25,414	0.2	1.6	366
26,171	25,833	1.0	1.0	338
26,582	26,195	1.1	1.0	387
26,941	26,578	1.4	2.5	363
27,342	26,928	2.3	5.25	414
27,686	27,320	3.1	2.5	366

*See Table III.

(2) A new band is present at 25,041 cm^{-1} (3993.4 Å). This band is weak in the glass

but does not appear at all in the vapor spectra even at the highest temperatures studied (190° C).

(3) The intensity distribution throughout the band system is quite different to that in the vapor (see Table I). The relative intensities were measured after first subtracting out an estimated contribution from the tail of the higher energy transition.

(4) Each vibrational envelope is shifted to the red of the corresponding vapor band by 366 ± 24 cm^{-1}.

Higher Electronic Transitions

The vapor spectrum of diphenylene at 95° C down to 3000 Å is shown on Fig. 2.

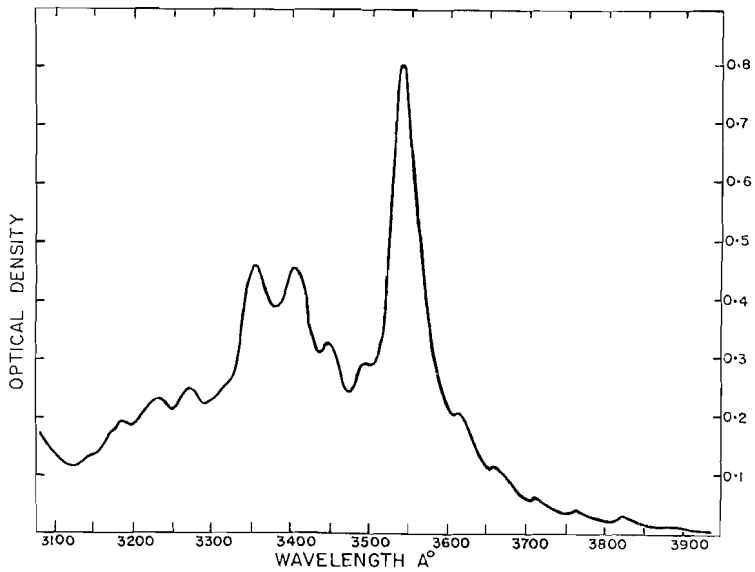


FIG. 2. Vapor spectrum of diphenylene.

Each band in this spectrum correlates with a band in the spectrum of diphenylene in liquid solution.

DISCUSSION

A proposed vibrational analysis of the absorption spectrum is given in Table II. The

TABLE II

Vibrational assignments in the weak system of diphenylene in a rigid EPA glass at 90° K

λ_{max} (Å)	ν_{max} (cm^{-1})	Assignment	$\nu_{obs} - \nu_{calc}$ (cm^{-1})
3993.4	25,041	0–0	0
3934.9	25,414	0+365	+8
3871.2	25,833	0+792	0
3817.6	26,195	*b*+365	+3
3762.6	26,578	*b*+2×365	−5
3713.6	26,928	*b*+3×365	+10
3660.4	27,320	*b*+4×365	−17

band origin was taken as 25,833 cm^{-1} in the glass and 26,171 cm^{-1} in the vapor. This band starts a long progression of what is almost certainly a symmetric vibration of

Can. J. Chem. Downloaded from www.nrcresearchpress.com by 210.87.254.42 on 09/05/12
For personal use only.

Can. J. Chem. Downloaded from www.nrcresearchpress.com by 210.87.254.42 on 09/05/12
For personal use only.

frequency 365 cm^{-1} in the upper state. The intensity distribution shows that the nuclear configurations are probably very different in the ground and excited states. The band due to the excitation of three quanta of 365 cm^{-1} is the most intense in the rigid glass. The vibrational interval was about 30 cm^{-1} greater in the spectrum of the vapor. The value of 365 cm^{-1} most probably corresponds to an a_g skeletal mode of diphenylene and may be compared with similar modes in naphthalene (485 cm^{-1} in $^1B_{2u}$) (5) and anthracene (399 cm^{-1} in $^1B_{2u}$) (6) and tetracene (309 cm^{-1} in $^1B_{2u}$) (7).

The 0–0 band of the electronic transition is taken to lie at 25,407 cm^{-1} in the vapor and 25,041 cm^{-1} in the rigid glass. The change in relative intensity of this band between the two media is taken as evidence of a symmetry-forbidden transition. Under these conditions the origin of the totally symmetric sequence was not the 0–0 band but instead was the band at 25,833 cm^{-1}, which is removed by 792 cm^{-1} from the 0–0 band. It is very likely that this interval represents one quantum of an antisymmetric vibration in the upper state. This vibration (represented as b in Table II) makes the electronic transition allowed and thus appears added to each of the other vibrational transitions. If the pure electronic part of the transition was symmetry-forbidden then of course the 0–0 band would not appear at all in the vapor at low pressure. However, in the rigid glass the environmental interactions will probably remove symmetry restrictions to some degree. The same could happen through intramolecular interactions in the vapor at higher pressures or through the excitation of low-lying ground state vibrations at the higher temperatures. The band at 25,414 cm^{-1} (rigid glass) was very weak in the vapor but much stronger in the rigid glass and in liquid solution at room temperature. This band was assigned to an excitation of one totally symmetric vibrational quantum in the upper state. Such a transition is symmetry-forbidden in vibronic symmetry and would either not appear or appear only weakly in the vapor. However, in asymmetric solvent fields a transition of this type might gain considerable intensity over that in the vapor. In other words the intensity of this band is derived from the relaxation of symmetry selection rules due to solvent-induced asymmetry. The lack of detail in the spectra does not permit other than a tentative acceptance of this explanation. The appearance of a vibronic level of this nature could evidence the fact that the molecule has changed its shape during excitation.

To summarize, there were five factors which, when considered together, provided an indication that this lowest electronic transition of diphenylene was forbidden by symmetry and made allowed by the simultaneous excitation of a vibration of the appropriate symmetry. These were as follows:

(1) The extremely low intensity of the electronic absorption. Because of the interference from the higher-energy band it was not possible to obtain an exact value for the f-number of the transition. However, this was estimated to be less than 10^{-3} at liquid nitrogen temperature. This factor alone, although at first sight convincing, was not sufficient evidence of a forbidden transition. The lowest-energy bands in naphthalene and phenanthrene have f-numbers of 2×10^{-3} and 3×10^{-3} (8) respectively and yet are apparently allowed by molecular symmetry. According to the Free Electron Perimeter model (9) these low intensities may be accounted for by the large change in orbital angular momentum associated with these transitions.

(2) The absence of the ascribed 0–0 transition in the vapor phase. Once again this is not a sufficient criterion for symmetry forbiddenness. The 0–0 band of naphthalene is extremely weak or absent in the vapor of naphthalene although it does appear in solution due to the asymmetry field of solvent molecules (2, p. 134). However, the non-appearance

of the 0–0 transition strongly suggests that the electronic transition being studied is forbidden by symmetry.

(3) The marked change in intensity distribution; in particular, the gain in intensity of the 0–0 band in the rigid glass compared to that in the vapor. The over-all intensity distribution and the changes which occur between vapor and rigid glass suggest that Franck–Condon limitations, imposed by a change of symmetry in the upper state, are in operation.

(4) The vibrational analysis, although severely limited by the resolution of the instrument, fully supports the interpretation of a symmetry-forbidden electronic transition. The observed frequencies fit well into the classical series for an electronic transition which is only given intensity by electronic–vibrational coupling in the upper state.

(5) One further piece of evidence which supports our interpretation can be gleaned from the absorption spectrum of diphenylene in solution at room temperature. Figure 3

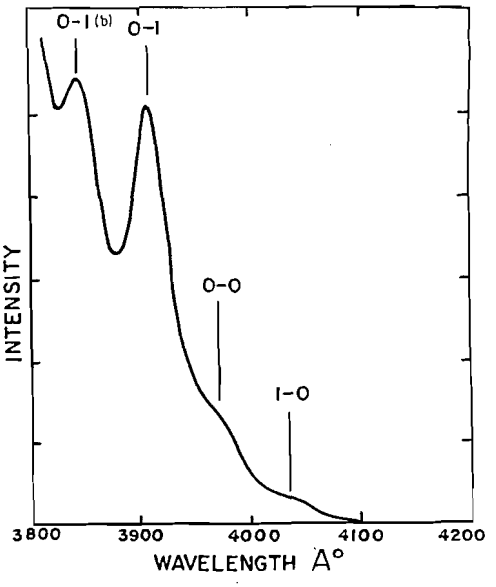


FIG. 3.

shows the absorption spectrum of the long wavelength tail of a highly purified sample of diphenylene in hexane. The two shoulders on the edge are characteristic of the spectra of molecules exhibiting forbidden transitions. In the usual case, when the absorption is to an allowed level, the 0–0 band is very strong. Thus the weak 1–0 band is seldom observed, even as a shoulder, as it is hidden by the strong 0–0 band. In the forbidden case the 0–0 band usually appears very weakly under solvent perturbations and the 1–0 band may then be observed as a shoulder or as a well-defined peak. Thus absorption to a forbidden level would give rise to a strong band (0–1) and then two shoulders corresponding to 0–0 and 1–0 transitions. This is shown quite clearly on Fig. 3. The 1–0 band was naturally not observed in the rigid glass at −183° C because of the Boltzmann factor in the ground state.

Comparison with Theory

The known data for diphenylene is summarized in Table III. The theoretical computations were made by Rowlands (10) using the ASMO–LCAO method. The symmetries were predicted from the table of orbital symmetries of Coulson and Daudel (11).

Can. J. Chem. Downloaded from www.nrcresearchpress.com by 210.87.254.42 on 09/05/12
For personal use only.

TABLE III

Comparison of theory and experiment for diphenylene

Theory (9)		Experiment	
0–0 energy (cm^{-1})	Symmetry	0–0 energy (cm^{-1})	Symmetry
17,660	$^1B_{1g}$(forbidden)	25,407*	Forbidden
25,760	$^1B_{3u}$(long axis)	28,200†	$^1B_{3u}$§
39,410	$^1B_{3u}$(long axis)	40,250‡	—

*In the vapor; calculated as 25,041 (glass) −366 cm^{-1}.
†Vapor ±25 cm^{-1}.
‡Solution at room temperature: see reference 1.
§See reference 3.

On the assumption that diphenylene is a planar molecule (see Fig. 4) belonging to

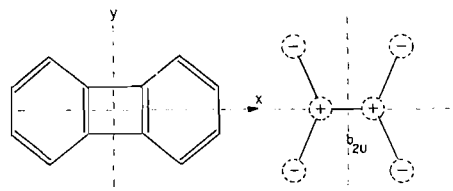


FIG. 4. Diphenylene, $C_{12}H_8$. The axes chosen are those of reference 11. The circles indicate the motion of the nuclei during the execution of a B_{2u} normal vibration within a D_{2h} nuclear framework. The b_{3u} normal vibrations involve asymmetric in-plane motions.

the point group D_{2h} then the lowest excited singlet molecular level is predicted to be $^1B_{1g}$. Transitions from the $^1A_{1g}$ ground state to this level are forbidden by symmetry. They may, however, be made allowed by vibrations of appropriate symmetry which in this case could be b_{2u} or b_{3u}. The symmetry of the resulting vibronic state will be either B_{3u} ($= b_{2u} \times B_{1g}$), which is long axis polarized or B_{2u} ($= b_{3u} \times B_{1g}$), which is short axis polarized. Fundamental vibrations belonging to the representations b_{2u} and b_{3u} should appear in the infrared spectrum of diphenylene.

Our analysis has assumed that the perturbing vibration has frequency 792 cm^{-1}. The infrared spectrum of diphenylene in carbon tetrachloride solution has only two very strong bands in this region. These infrared vibration frequencies are 963 cm^{-1} and 732 cm^{-1}.

The closeness of the 732 cm^{-1} infrared frequency to that of the observed perturbing vibration supports the contention that the electronic transition is of g–g character and made allowed by this b_u vibration. If this deduction is correct then the spectrum should exhibit *two* strong progressions; the first involving the excitation of 1, 2, 3, 4, etc. quanta of an a_g vibration in combination with one b_u quantum; the second involving the successive excitation of 1, 3, 5, etc. quanta of the symmetric b_u vibration. Unfortunately the energy of $0+3b_u$, which is 27,417 cm^{-1}, would place this band right under the strong 27,910 cm^{-1} origin of the next highest electronic state. Such a band could probably not be (and was not) observed in absorption.

The wide discrepancy between the observed and calculated energy of the weak 25,407 cm^{-1} band cannot be explained at the moment. The results of the present experiments do not completely exclude the possibility that this band corresponds to the calculated 25,760 cm^{-1}, $^1B_{3u}$ level.

A detailed examination of the infrared spectrum and of the crystal spectrum should make possible an unambiguous decision as to the nature of the perturbing vibration.

Can. J. Chem. Downloaded from www.nrcresearchpress.com by 210.87.254.42 on 09/05/12
For personal use only.

ACKNOWLEDGMENTS

The author would like to thank Dr. J. R. Rowlands both for the sample of diphenylene and some interesting discussions.

REFERENCES

1. E. P. CARR, L. W. PICKETT, and D. VORIS. J. Am. Chem. Soc. **63**, 3230 (1941).
2. E. CLAR. Aromatische Kohlenwasserstoffe. Springer-Verlag, Berlin. 1952.
3. R. M. HOCHSTRASSER. J. Chem. Phys. **33**, 950 (1960).
4. J. WILLIS. Rev. Sci. Instr. **29**, 1053 (1958).
5. H. SPONER and C. D. COOPER. J. Chem. Phys. **23**, 646 (1955).
6. J. W. SIDMAN. J. Chem. Phys. **25**, 115 (1956).
7. J. W. SIDMAN. J. Chem. Phys. **25**, 122 (1956).
8. D. P. CRAIG. Ann. Revs. Pure Appl. Chem. **3**, 207 (1953).
9. J. R. PLATT. J. Chem. Phys. **17**, 484 (1949).
10. J. R. ROWLANDS. Ph.D. Thesis, University of Bristol, Bristol, England. 1958.
11. C. A. COULSON and R. DAUDEL. Dictionary of values of molecular constants. Vol. II.

Can. J. Chem. Downloaded from www.nrcresearchpress.com by 210.87.254.42 on 09/05/12
For personal use only.

Can. J. Chem. Downloaded from www.nrcresearchpress.com by 210.87.254.6 on 09/05/12
For personal use only.

ELECTRODE POTENTIALS OF THE URANIUM CHLORIDES IN FUSED ALKALI CHLORIDE SOLUTIONS[1]

S. N. FLENGAS[2]

ABSTRACT

Using a silver – silver chloride reference electrode, the electrode potentials of the system U, UCl_3(KCl, NaCl) and the redox potentials of the system Pt, UCl_3, UCl_4(KCl, NaCl) were measured at various concentrations of the uranium chlorides and at temperatures between 650 and 850° C.

From the results, the electrode potential of the system U, UCl_4(KCl, NaCl) was calculated. In addition, the activity coefficients and partial molal properties of dilute solutions of UCl_3 and UCl_4 in the equimolar mixture of potassium and sodium chlorides were calculated.

INTRODUCTION

In previous publications (1–7) from the Mines Branch, measurements of the "apparent standard electrode potentials" of several metal – metal chloride systems in dilute solutions in fused alkali chlorides were reported. These measurements were made to provide fundamental information on the activities in fused alkali chloride solutions, to determine the equilibrium constants of chemical reactions in fused salts, and to provide some of the necessary data for studies of the electrolytic reduction of metals from alkali chloride melts.

In determining the electrode potentials, an equimolar mixture of potassium and sodium chlorides was used as the solvent for the metal chlorides, and a silver – silver chloride electrode developed earlier in this work (1) was used as a zero potential reference electrode.

In the experimental work reported here, the technique has been applied to the determination of the potentials of the uranium chlorides dissolved in an equimolar mixture of potassium and sodium chlorides. There are only two stable uranium chlorides at temperatures above 500° C, namely uranium trichloride and uranium tetrachloride. The electrode potentials of the two uranium ions and the redox potentials of the tri- and tetra-valent uranium ions were determined.

EXPERIMENTAL

The cells used for the measurement of the electrode potentials of uranium trichloride, and for the measurement of the redox potentials of the tri- and tetra-valent uranium chlorides, were similar in design to those described in the previous publications (6, 7).

The cell for measuring the electrode potential of uranium trichloride can be represented as follows:

$$\begin{array}{c|c|c|c|c} U_{(s)} & UCl_3\,(x_2) & \text{Asbestos fiber} & AgCl\,(x_1) & Ag_{(s)} \\ (-) & KCl + NaCl\,(1/1\text{ mole}) & \text{diaphragm} & KCl + NaCl\,(1/1\text{ mole}) & (+) \end{array}$$

The cell reaction is:

$$U_{(s)} + 3Ag^{+}_{(AgCl\text{ in }KCl + NaCl)} = U^{3+}_{(UCl_3\text{ in }KCl + NaCl)} + 3Ag_{(s)}$$

[1]*Manuscript received June 27, 1960.*
Contribution from the Extraction Metallurgy Division, Mines Branch, Department of Mines and Technical Surveys, Ottawa, Canada. Published with the permission of the Director, Mines Branch.
[2]*Present address: Department of Metallurgical Engineering, University of Toronto, Toronto, Ontario.*

The relationship between the electromotive force and the metal ion concentration in the cell is given by the Nernst equation in the form:

$$[1] \quad E_{cell} = (E^\circ_{UCl_3} - E^\circ_{AgCl}) - (2.303RT/3\mathcal{F}) \log(x_2/x_1^3) - (2.303RT/3\mathcal{F}) \log(\gamma_2/\gamma_1^3)$$

where $E^\circ_{UCl_3}$ and E°_{AgCl} are the formation potentials of uranium trichloride and silver chloride in their standard states. The standard state will be defined as the state of the pure metal chloride at the temperature of the experiments.

The γ and x terms are respectively the mean activity coefficients and the conventional mole fractions of the metal chlorides in the solutions in the two half-cells. The activity coefficient of silver chloride in these solutions was determined and found to be unity in a previous investigation (6), using a chlorine electrode.

Following the same method as used previously (6, 7), it is possible, from equation [1], to calculate the "apparent standard cell potential" of the system, by plotting the experimental potential E_{cell} against log (x_2/x_1^3) and extrapolating the linear relationship to zero log term. The "apparent standard cell potential" obtained in this way is a constant of the system investigated, and is related to the formation potentials of the metal chlorides and the activity coefficient of uranium trichloride by the equation:

$$[2] \quad E^\circ_{app} = (E^\circ_{UCl_3} - E^\circ_{AgCl}) - (2.303RT/3\mathcal{F}) \log \gamma_2.$$

Since the formation potentials of the metal chlorides in their pure state are listed in the literature (8), equation [2] can be used for the determination of the activity coefficient of UCl_3 in the chloride melt.

The cell for measuring the "redox potentials" of the tri- and tetra-valent uranium ions can be represented as follows:

$$\begin{array}{c|l||l||l|c} Pt_{(s)} & UCl_3\,(x_2) & \text{Asbestos fiber} & AgCl\,(x_1) & Ag_{(s)} \\ (-) & UCl_4\,(x_3) & \text{diaphragm} & KCl + NaCl\,(1/1\text{ mole}) & (+) \\ & KCl + NaCl\,(1/1\text{ mole}) & & & \end{array}$$

The cell reaction is:

$$U^{3+}_{(UCl_3 \text{ in } KCl + NaCl)} + Ag^{+}_{(AgCl \text{ in } KCl + NaCl)} = U^{4+}_{(UCl_4 \text{ in } KCl + NaCl)} + Ag_{(s)}.$$

The relationship between the cell potential and the metal ion concentration in the cell is given by the Nernst equation in the form:

$$[3] \quad E_{cell} = (E^\circ_{UCl_3/UCl_4} - E^\circ_{AgCl}) - (2.303RT/\mathcal{F}) \log (x_3/x_1 . x_2) - (2.303RT/\mathcal{F}) \log (\gamma_3/\gamma_1 . \gamma_2)$$

where the $E^\circ_{UCl_3/UCl_4}$ is the standard redox potential of the system UCl_3, UCl_4 in the standard state. The x and γ terms are, respectively, the mole fractions and the activity coefficients of the metal chlorides.

The "apparent standard redox" potential of the system is determined by plotting the experimental cell potentials against log $(x_3/x_1 . x_2)$ and then extrapolating the linear relationship to zero log term.

It should be noted that the above-mentioned cells were operated in an inert atmosphere of purified argon gas.

PREPARATION OF MATERIALS

The equimolar mixture of potassium and sodium chlorides was prepared from analytical grade reagents, and was dehydrated by heating under vacuum at 500° C for 12 hours.

Anhydrous uranium trichloride was prepared in a tubular furnace at 500° C, by the reaction between reactor grade uranium metal and oxygen-free anhydrous hydrogen

Can. J. Chem. Downloaded from www.nrcresearchpress.com by 210.87.254.6 on 09/05/12
For personal use only.

chloride (9). Very pure and dry gaseous hydrogen chloride was prepared in a suitable apparatus by the reaction between concentrated hydrochloric acid and concentrated sulphuric acid (10). The product of the reaction, between uranium metal and hydrogen chloride, was finely divided uranium trichloride which adhered to the surface of the metal. This finely powdered product, which was separated from the coarse unreacted uranium by sieving in a dry box, was of a purity of 98.5%.

Anhydrous uranium tetrachloride was prepared by the reaction between hydrated uranium trioxide ($UO_3.2H_2O$) and hexachloropropene (11). The product obtained from this reaction was purified by sublimation *in vacuo*, and was of a purity of 99.0%.

The uranium chlorides were pelletized in an argon-filled dry box and were transferred to the cell using the piston-type feeding apparatus described previously (7).

The uranium electrode for these experiments was a rod of reactor grade uranium which had been swaged down to $\frac{1}{2}$-in. diameter, and was about 3 in. long. It was connected to a platinum wire. Prior to its use, the electrode was polished to a silver-like finish in a dilute solution of nitric acid. The polished electrode was then washed with distilled water and dried with acetone.

The silver electrode was a rod of pure silver (99.9%) connected to a silver wire. The inert platinum electrode used for the redox potential measurements was a hollow platinum cylinder of $\frac{1}{2}$-in. diameter and 3-in. long. It was connected to a platinum wire.

The thermoelectric potentials due to the bimetallic systems of these electrodes were measured separately, and the appropriate corrections were applied to the measurements of the electrode potentials.

RESULTS

1. *Electrode Potentials of the U/U^{3+} System*

In the preliminary experiments, the stability of a system consisting of uranium metal immersed in a solution of uranium trichloride in molten potassium and sodium chlorides was investigated by following the change of the cell potential with time.

The solutions of uranium trichloride were prepared *in situ* during the run, by adding weighed pellets of the anhydrous salt to the melt in the indicator electrode compartment. After each addition, the equilibrium potential was attained in about 30 minutes. Potential readings were then taken at regular time intervals over a period of about 20 hours. It was found that the shift of potential was of the order of only 1 mv. Furthermore, after the end of the run there was no indication of a chemical attack on the uranium electrode.

It was concluded that uranium metal is insoluble in dilute solutions of uranium trichloride under the conditions of the experiment. However, it was observed that electrodes which accidentally had been placed in contact with the side walls of the silica tubing in the cell were heavily corroded. The potentials obtained under these conditions were erratic and non-reproducible. In all probability, the observed solubility of uranium metal in the melt was due to the formation of a soluble uranium oxide or oxychloride through the exchange reaction between uranium metal and silica. For this reason, during the experiments, the uranium electrode was suspended by the platinum wire in the center of the cell.

The electromotive force of the U/U^{3+} cell was measured first as a function of temperature, at various mole fractions of uranium trichloride.

The variation of the cell potential with temperature, at mole fractions varying between 10^{-4} and 10^{-2}, is shown in Fig. 1. The results in this graph represent three independent runs. It is apparent that the curves are linear over the temperature range between 650

Can. J. Chem. Downloaded from www.nrcresearchpress.com by 210.87.254.6 on 09/05/12
For personal use only.

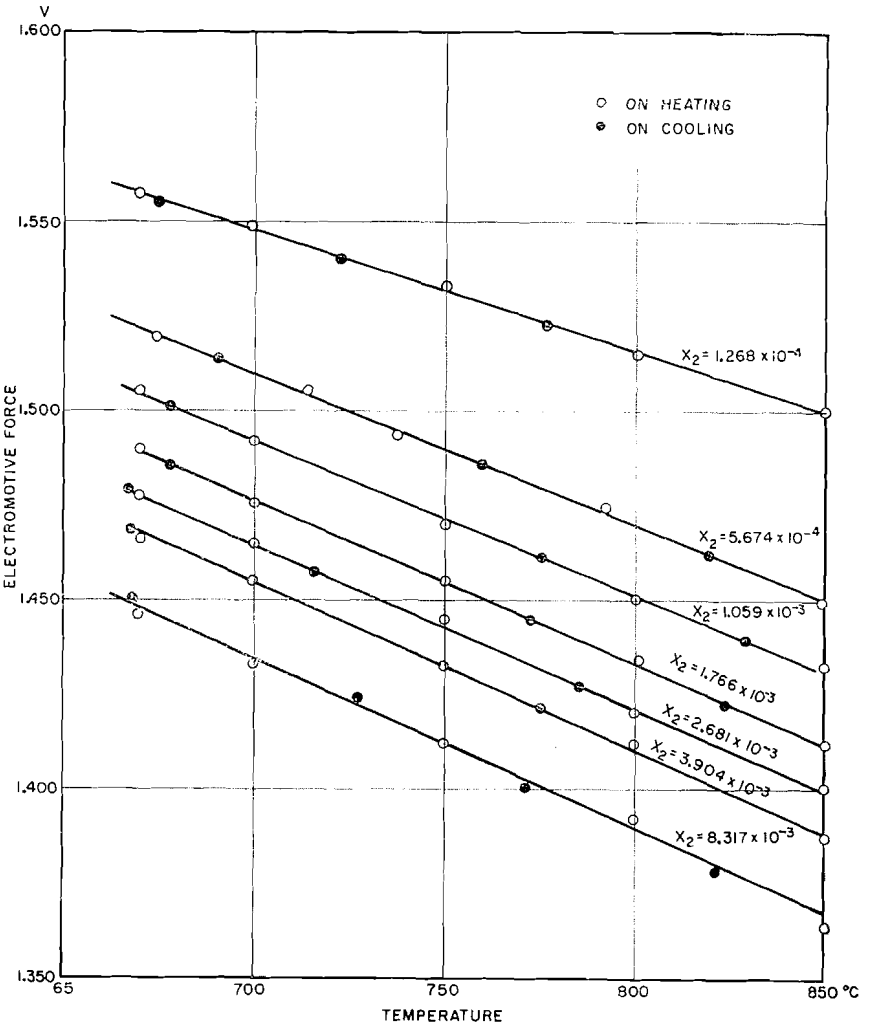


FIG. 1. Electromotive force of the cell:

$$\begin{matrix} \text{U} \\ (-) \end{matrix} \;\Big|\; \begin{matrix} UCl_3\ (x_2) \\ \text{KCl + NaCl (1/1 mole)} \end{matrix} \;\Big\|\; \begin{matrix} \text{AgCl}\ (x_1 = 5.0 \times 10^{-2}) \\ \text{KCl + NaCl (1/1 mole)} \end{matrix} \;\Big|\; \begin{matrix} \text{Ag} \\ (+) \end{matrix}$$

as a function of temperature.

and 850° C, and the cell potentials have a negative temperature coefficient. Potential readings made while temperature was being increased were in good agreement with those made while the temperature was decreasing.

The relationship between the cell potential and the logarithm of the mole fractions, at temperatures between 670 and 850° C, is shown in Fig. 2. In this graph the straight lines through the experimental points are the best straight lines that can be drawn with a slope equal to the slope of the Nernst equation for a three-electron electrode reaction at these temperatures. It is seen that the results are in agreement with the Nernst equation. The linearity of the curves indicates that the activity coefficient of uranium trichloride in these dilute solutions is independent of concentration. The "apparent standard cell potential" of uranium trichloride was obtained by extrapolation of the curves to zero log (x_2/x_1^3) term. These results are given in Table I.

Can. J. Chem. Downloaded from www.nrcresearchpress.com by 210.87.254.6 on 09/05/12
For personal use only.

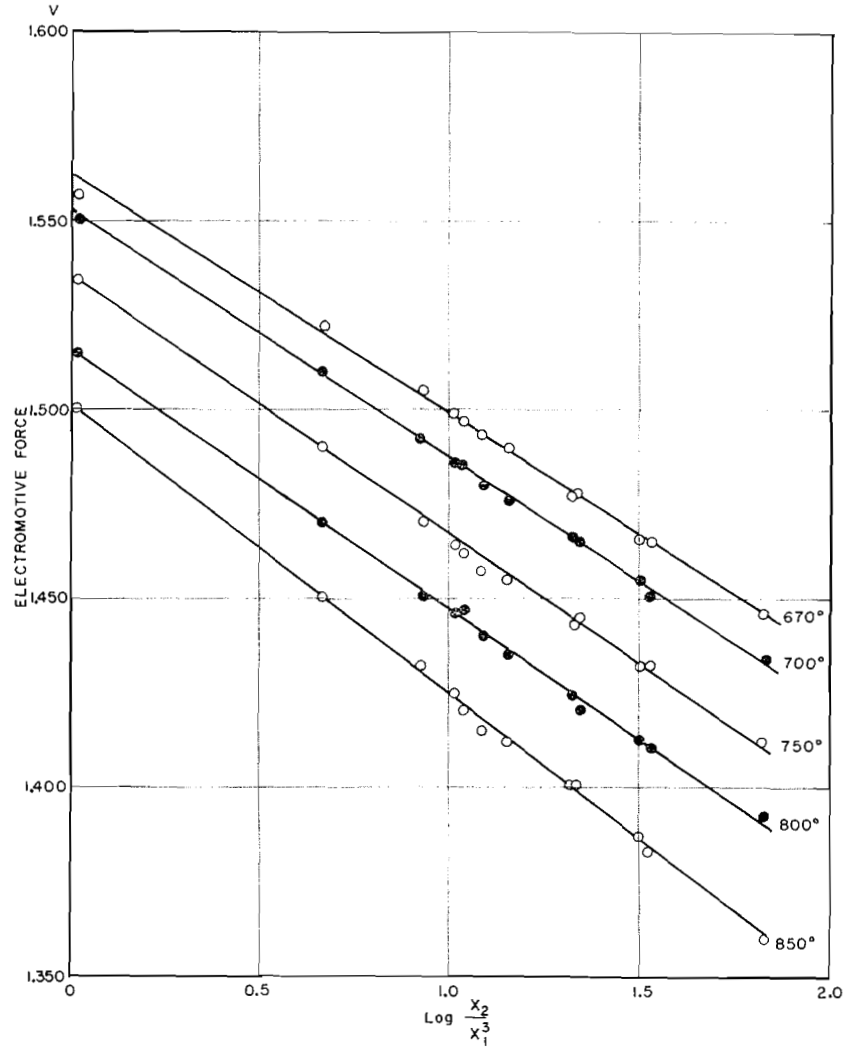


FIG. 2. Electromotive force of the cell:

$$\begin{array}{c|c|c|c|c} \text{U} & \text{UCl}_3\ (x_2) & & \text{AgCl}\ (x_1 = 5.0\times10^{-2}) & \text{Ag} \\ (-) & \text{KCl} + \text{NaCl}\ (1/1\ \text{mole}) & \| & \text{KCl} + \text{NaCl}\ (1/1\ \text{mole}) & (+) \end{array}$$

as a function of log (x_2/x_1^3), at various temperatures.

2. *"Redox" Potentials of the U^{3+}/U^{4+} System*

The electromotive force of the U^{3+}/U^{4+} redox cell was measured, as a function of temperature, at various mole fractions of uranium tri- and tetra-chlorides. The stability of the potential measurements over a period of time exceeding 12 hours indicated that solutions of uranium tri- and tetra-chlorides in the equimolar mixture of potassium and sodium chlorides are very stable.

The results of the redox potential measurements at temperatures between 650 and 850° C, for mole fractions of uranium tri- and tetra-chlorides varying between 10^{-3} and 10^{-2}, are shown in Fig. 3.

It is seen that the curves are linear over the temperature range investigated, and that the potentials of the redox cells have a negative temperature coefficient.

Can. J. Chem. Downloaded from www.nrcresearchpress.com by 210.87.254.6 on 09/05/12
For personal use only.

TABLE I

Apparent standard potentials in 1/1 mole KCl + NaCl

Indicator electrode	E_0' (volts)*				
	670° C	700° C	750° C	800° C	850° C
U, U^{3+}	−1.563	−1.554	−1.535	−1.519	−1.502
U, U^{4+}	−1.295	−1.285	−1.269	−1.252	−1.239
U^{3+}, U^{4+}	−0.494	−0.483	−0.473	−0.459	−0.450
Ag, Ag^+	0	0	0	0	0
Cl^-, Cl†	+0.852	+0.845	+0.832	+0.820	+0.807

*It will be noted that the sign of the experimentally obtained apparent standard potentials shown in this table has been altered to conform with the recommendations of the IUPAC Stockholm convention, as reported by Light and deBethune (12).

†The potential of the chlorine electrode against the silver – silver (6) chloride electrode was determined in a previous investigation, and the results are shown here for comparison.

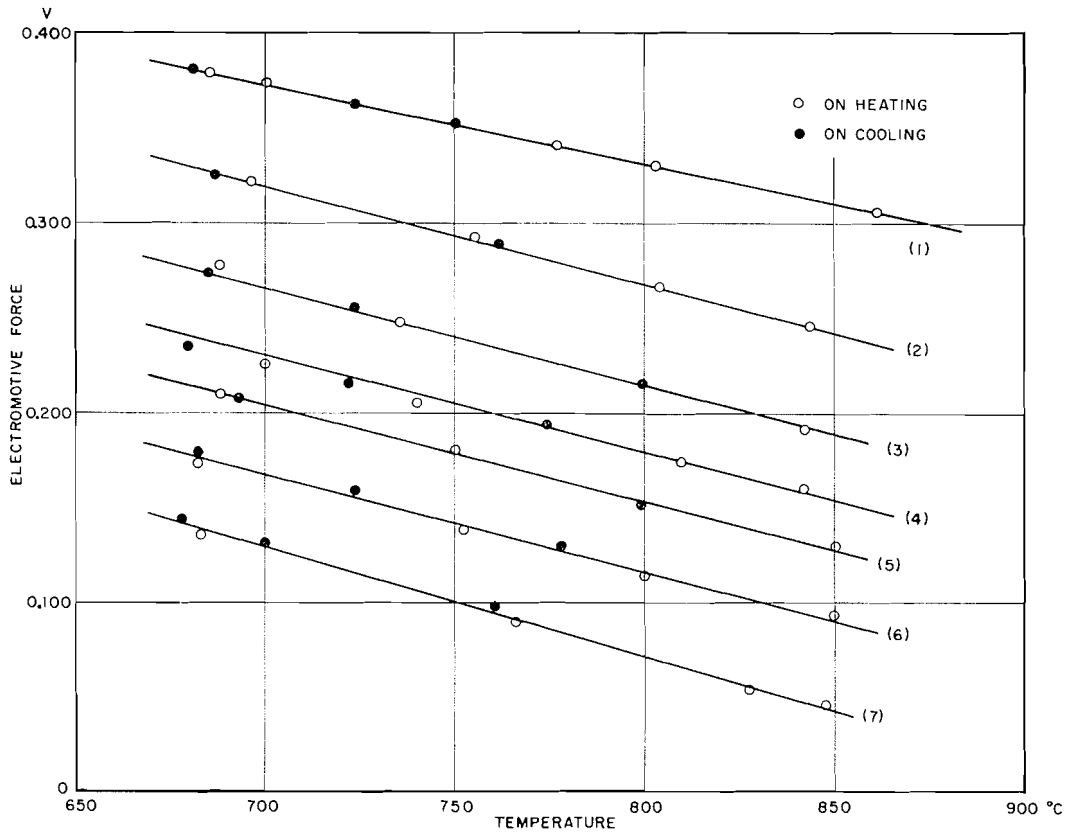


FIG. 3. Electromotive force of the cell:

Pt (−)	UCl_3 (x_2) UCl_4 (x_3) KCl + NaCl (1/1 mole)	‖	AgCl ($x_1 = 5.0\times10^{-2}$) KCl + NaCl (1/1 mole)	Ag (+)

as a function of temperature at mole fractions:

(1) $x_2 = 8.303\times10^{-3}$, $x_3 = 1.703\times10^{-3}$

(2) $x_2 = 8.287\times10^{-3}$, $x_3 = 3.527\times10^{-3}$

(3) $x_2 = 8.232\times10^{-3}$, $x_3 = 6.254\times10^{-3}$

(4) $x_2 = 2.445\times10^{-3}$, $x_3 = 2.671\times10^{-3}$

(5) $x_2 = 5.697\times10^{-3}$, $x_3 = 9.601\times10^{-3}$

(6) $x_2 = 2.447\times10^{-3}$, $x_3 = 5.723\times10^{-3}$

(7) $x_2 = 2.438\times10^{-3}$, $x_3 = 9.629\times10^{-3}$

Can. J. Chem. Downloaded from www.nrcresearchpress.com by 210.87.254.6 on 09/05/12
For personal use only.

The relationship between the cell potential and the logarithm of the mole fractions, at temperatures between 670 and 850° C, is shown in Fig. 4. In this graph the straight

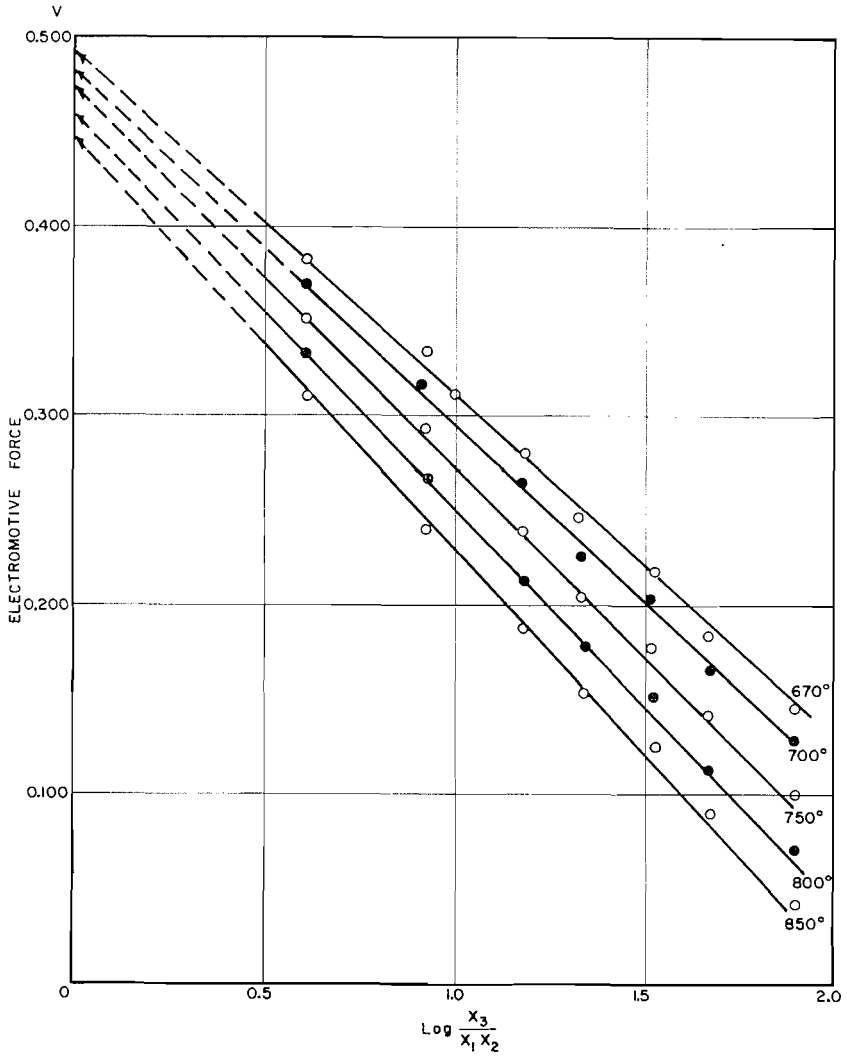


FIG. 4. Electromotive force of the cell:

Pt	UCl_3 (x_2)		$AgCl$ ($x_1 = 5.0\times10^{-2}$)	Ag
(−)	UCl_4 (x_3)	‖	KCl + NaCl (1/1 mole)	(+)
	KCl + NaCl (1/1 mole)			

as a function of $\log (x_3/x_1.x_2)$, at various temperatures.

lines through the experimental points are the best straight lines that can be drawn with a slope equal to the slope of the Nernst equation for a one-electron electrode reaction at these temperatures. It is seen that the results agree well with the Nernst equation. The linearity of these curves indicates that the activity coefficient of uranium tetrachloride in these dilute solutions is independent of concentration.

The "apparent standard redox potential" of the system was obtained by extrapolation of the curve to zero $\log (x_3/x_2.x_1)$. These results are given in Table I.

Can. J. Chem. Downloaded from www.nrcresearchpress.com by 210.87.254.6 on 09/05/12
For personal use only.

Can. J. Chem. Downloaded from www.nrcresearchpress.com by 210.87.254.6 on 09/05/12
For personal use only.

DISCUSSION

From the experimental values for the apparent standard potentials of the system $U/UCl_3(KCl + NaCl)$ and the apparent standard redox potential of the system $UCl_3/UCl_4(KCl + NaCl)$, the apparent standard potential of the system U/UCl_4 $(KCl + NaCl)$ was calculated by application of the equation:

$$[4] \qquad E^\circ_{UCl_4} = (3E^\circ_{UCl_3} + E^\circ_{UCl_3/UCl_4})/4.$$

The results of these calculations are shown in Table I.

The potentials of the chlorine electrode which were measured against the silver – silver chloride reference electrode in a previous investigation (6) are also included in this table. To refer the potentials of the uranium system to a chlorine reference electrode, it is only necessary to subtract the potential of the chlorine electrode, as given at the bottom of the table, from the corresponding uranium potential.

The graph of the "apparent standard potentials" of the uranium chlorides, as a function of temperature, is given in Fig. 5. In this graph, calculated standard potentials of the pure salts (8) are also included for comparison.

Apparent standard cell potentials of uranium tri- and tetra-chlorides, in a melt of potassium and lithium chlorides at 450° C, have been reported recently by Gruen and Osteryoung (13), and by Hill, Ferand, and Osteryoung (14). Inman, Hills, Young, and Bockris (15, 16) also investigated the potentials of uranium trichloride in the potassium chloride – lithium chloride eutectic.

When the results in Fig. 5 were extrapolated to 450° C, the "apparent standard cell potentials" of the uranium tri- and tetra-chlorides were found to be respectively 1.632 and 1.365 volts. These compare well with 1.611 volts for uranium trichloride, and 1.363 volts for uranium tetrachloride given by Gruen *et al.* (13), and Hill *et al.* (14). Also the "apparent standard cell potential" at 450° C, of uranium trichloride which can be calculated from the results of Inman *et al.* (15, 16), is of the same order of magnitude, i.e. about 1.66 volts.

For a variety of metal – metal chloride systems, the agreement between the apparent standard potential measured at 450° C in the eutectic of potassium and lithium chlorides (17), and those measured in the equimolar mixture of potassium and sodium chlorides, has been pointed out in a previous investigation (6). Furthermore, the same agreement was observed by Hill *et al.* (14) in their study of the uranium potentials in chloride melts containing comparatively light metal cations such as potassium, lithium, and magnesium. It appears that the partial molal free energy of mixing of the uranium chlorides is almost independent of the size of the cations present in the solvent, provided that these cations are much smaller than the uranium ions.

From the apparent standard potentials shown in Table I, it is possible to calculate the thermodynamic functions and the equilibrium constants of various reactions of metallurgical interest. The results of these calculations are given in Table II.

The magnitude of the equilibrium constant for reaction [4], shown in Table II, indicates that in the presence of uranium metal, uranium tetrachloride would be reduced quantitatively to the trichloride.

The equilibrium constants of reactions [1] to [3] indicate that uranium metal will displace silver ions from solution, and that at equilibrium, the predominant species will be uranium tetrachloride.

Using the results in Fig. 5, the partial molal properties and the activity coefficients

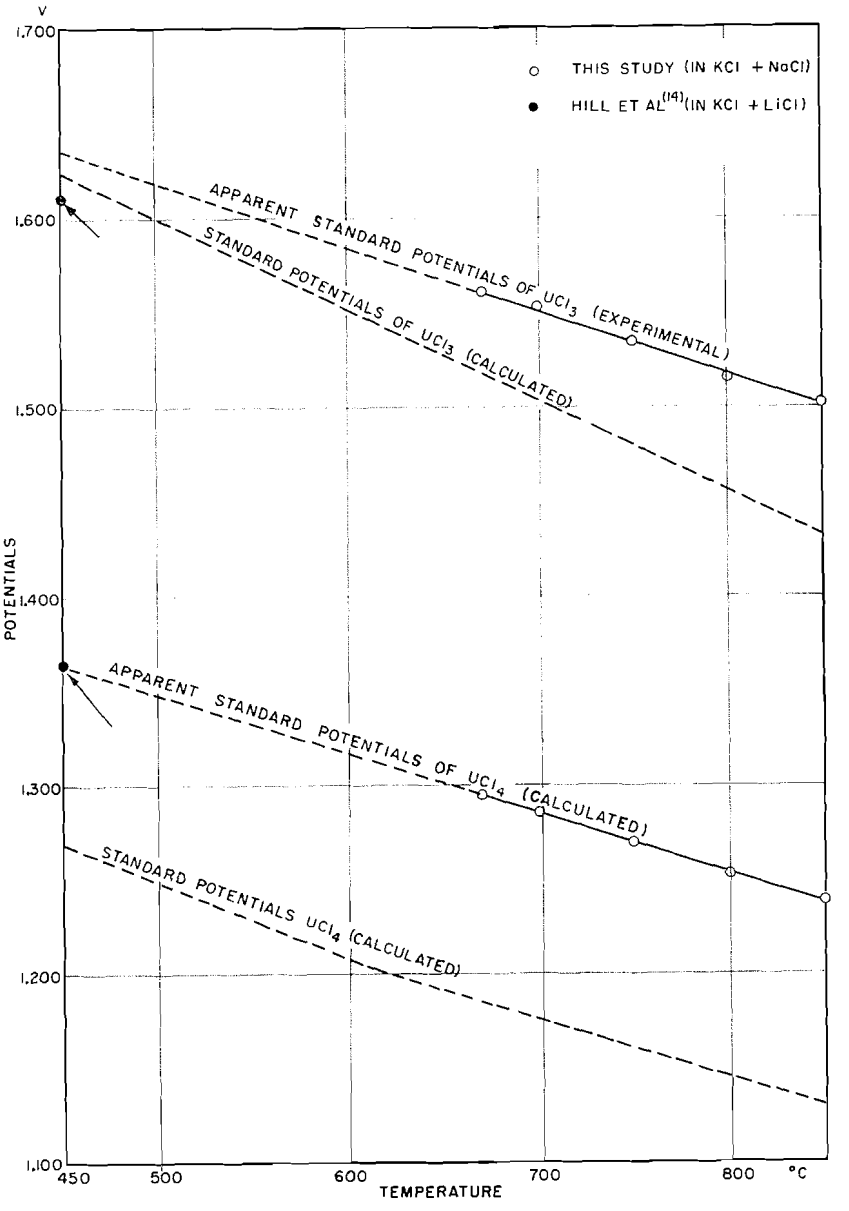


FIG. 5. Apparent standard potentials of UCl_3 and UCl_4 and the corresponding standard state potentials at various temperatures.

of the uranium chloride solutions were calculated from the differences between the "standard potentials" of the pure uranium tri- and tetra-chlorides and the "apparent standard potentials" in the fused salt solution. The results of these calculations are given in Table III.

The partial molal free energy of solution ($\Delta\bar{F}$), given in Table III, represents the difference between the free energy of the salt in its hypothetical standard state as a solute, i.e., "a solution containing a unit mole fraction of the salt but having in all other

Can. J. Chem. Downloaded from www.nrcresearchpress.com by 210.87.254.6 on 09/05/12
For personal use only.

Can. J. Chem. Downloaded from www.nrcresearchpress.com by 210.87.254.6 on 09/05/12
For personal use only.

TABLE II

Thermodynamic calculations for reactions involving the uranium ions

	Reaction in 1/1 mole KCl + NaCl		Temperature			
			670° C	750° C	800° C	850° C
(1)	$U_{(s)} + 3Ag^{+}_{(AgCl \text{ in } KCl + NaCl)} = U^{3+}_{(UCl_3 \text{ in } KCl + NaCl)} + 3Ag_{(s)}$	$\Delta\bar{H}$ (kcal/mole)	−130.2	−130.2	−130.2	−130.2
		$\Delta\bar{F}$ (kcal/mole)	−108.1	−106.2	−105.1	−103.9
		$\Delta\bar{S}$ (e.u.)	− 23.4	− 23.4	− 23.4	− 23.4
		K	1.1×10^{25}	4.8×10^{22}	2.5×10^{21}	1.6×10^{20}
(2)	$U_{(s)} + 4Ag^{+}_{(AgCl \text{ in } KCl + NaCl)} = U^{4+}_{(UCl_4 \text{ in } KCl + NaCl)} + 4Ag_{(s)}$	$\Delta\bar{H}$ (kcal/mole)	−136.0	−136.0	−136.0	−136.0
		$\Delta\bar{F}$ (kcal/mole)	−119.4	−117.0	−115.5	−114.3
		$\Delta\bar{S}$ (e.u.)	− 17.6	− 18.5	− 19.1	− 19.3
		K	4.7×10^{27}	1.0×10^{25}	3.3×10^{23}	1.7×10^{22}
(3)	$U^{3+}_{(UCl_3 \text{ in } KCl + NaCl)} + Ag^{+}_{(AgCl \text{ in } KCl + NaCl)} = U^{4+}_{(UCl_4 \text{ in } KCl + NaCl)} + Ag_{(s)}$	$\Delta\bar{H}$ (kcal/mole)	− 16.7	− 16.7	− 16.7	− 16.7
		$\Delta\bar{F}$ (kcal/mole)	− 11.4	− 10.9	− 10.9	− 10.4
		$\Delta\bar{S}$ (e.u.)	− 5.6	− 5.6	− 5.6	− 5.6
		K	4.3×10^{2}	3.3×10^{2}	1.4×10^{2}	1.0×10^{2}
(4)	$3U^{4+}_{(UCl_4 \text{ in } KCl + NaCl)} + U_{(s)} = 4U^{3+}_{(UCl_3 \text{ in } KCl + NaCl)}$	$\Delta\bar{H}$ (kcal/mole)	−112.8	−112.8	−112.8	−112.8
		$\Delta\bar{F}$ (kcal/mole)	− 74.2	− 73.8	− 73.9	− 72.7
		$\Delta\bar{S}$ (e.u.)	− 40.8	− 38.1	− 36.3	− 35.7
		K	1.5×10^{17}	5.4×10^{15}	1.1×10^{15}	1.4×10^{14}

TABLE III

Partial molal properties of dilute solutions of uranium chlorides in 1/1 mole KCl + NaCl

	UCl_3 in KCl + NaCl				UCl_4 in KCl + NaCl			
t (°C)	$\Delta\bar{F}$ (kcal/mole)	$\Delta\bar{H}$ (kcal/mole)	$\Delta\bar{S}$ (e.u.)	$\gamma\times10^4$	$\Delta\bar{F}$ (kcal/mole)	$\Delta\bar{H}$ (kcal/mole)	$\Delta\bar{S}$ (e.u.)	$\gamma\times10^3$
670	−2.97	+6.170	+9.7	2.05	−10.15	+10.60	+22.0	4.46
750	−3.80	+6.170	+9.7	1.54	−10.05	+10.60	+20.1	7.14
800	−4.50	+6.170	+9.7	1.21	−10.05	+10.60	+19.2	8.97
850	−4.70	+6.170	+9.7	1.22	−10.05	+10.60	+18.4	11.1

respects the thermodynamic properties of the state of infinite attenuation of the solute", as defined by Lewis and Randall (18), and the free energy of the salt in its actual standard state of the pure salt. It is of interest to note that the partial molar free energy of solution of uranium tetrachloride is much greater than that of uranium trichloride.

The activity coefficients and the partial molal entropies of mixing indicate that uranium trichloride and uranium tetrachloride form complexes in solution. A comparison of the activity coefficients indicates that the uranium tetrachloride complex is stronger than the uranium trichloride complex. The variation of the activity coefficients of uranium tetrachloride with temperature shows the expected behavior; i.e., they increase with temperature. On the contrary, the activity coefficients of uranium trichloride decrease with increasing temperature, which indicates that the complexity of uranium trichloride is greater at higher temperatures.

The presence of complexes of tetravalent uranium ions in chloride melts has also been observed by Gruen and McBeth from spectrophotometric studies (19).

The constancy of the activity coefficients over the mole fraction range 10^{-4} to 10^{-2} indicates that the solutions of uranium tri- and tetra-chlorides in fused salts obey Henry's law.

ACCURACY OF RESULTS

It is rather difficult to evaluate the absolute accuracy of the potentials shown in Table I. Individual potential measurements shown in Figs. 1 and 3 were stable and reproducible. The slight scattering of the experimental points, which can be seen in the figures, is probably due to other side effects which are always present in high-temperature systems. These effects are: concentration gradients due to thermal convection currents; difficulties in obtaining a completely oxygen-free uranium metal surface; and slight impurities in the electrolyte. However, judging from the results presented in Figs. 1 to 4, it is reasonable to assume that the potential values obtained in this investigation are accurate to within ±2 mv. This variation would also affect the calculation of the free energy listed in Tables II and III. It has been estimated that the variation of the free energy change should be about ±0.3 kcal/mole for the uranium trichloride system, and about ±0.4 kcal/mole for the uranium tetrachloride system.

ACKNOWLEDGMENTS

The author thanks Dr. T. R. Ingraham for his helpful advice and many useful discussions during the course of this work.

Can. J. Chem. Downloaded from www.nrcresearchpress.com by 210.87.254.6 on 09/05/12
For personal use only.

REFERENCES

1. S. N. FLENGAS and T. R. INGRAHAM. Can. J. Chem. **35**, 1139 (1957).
2. S. N. FLENGAS and T. R. INGRAHAM. Can. J. Chem. **35**, 1254 (1957).
3. S. N. FLENGAS and T. R. INGRAHAM. Can. J. Chem. **36**, 780 (1958).
4. S. N. FLENGAS and T. R. INGRAHAM. Can. J. Chem. **36**, 1103 (1958).
5. S. N. FLENGAS and T. R. INGRAHAM. Can. J. Chem. **36**, 1662 (1958).
6. S. N. FLENGAS and T. R. INGRAHAM. J. Electrochem. Soc. **106** (8), 714 (1959).
7. S. N. FLENGAS. Ann. N.Y. Acad. Sci. **79** (11), 853 (1959).
8. W. HAMER, M. MALMBERG, and B. RUBIN. J. Electrochem. Soc. **103**, 8 (1956).
9. J. J. KATZ and E. RABINOWICH. The chemistry of uranium, part 1. National Nuclear Energy Series, Div. VII, Vol. 5, Part 8. McGraw-Hill Book Co., Inc., New York. 1951. pp. 450–461.
10. INORGANIC SYNTHESES. Vol. 1. H. S. Booth. McGraw-Hill Book Co., Inc., New York. 1939. p. 147.
11. INORGANIC SYNTHESES. Vol. 5. T. Moeller. McGraw-Hill Book Co., Inc., New York. 1957. pp. 145–148.
12. T. S. LIGHT and A. J. DEBETHUNE. J. Chem. Educ. **34**, 443 (1957).
13. D. M. GRUEN and R. A. OSTERYOUNG. Ann. N.Y. Acad. Sci. **79** (11), 897 (1959).
14. D. L. HILL, J. FERAND, and R. OSTERYOUNG. An electrochemical study of uranium in fused chlorides. Rensselaer Polytechnic Institute, Troy, New York. Private communication.
15. D. INMAN, G. J. HILLS, L. YOUNG, and J. O'M. BOCKRIS. Trans. Faraday Soc. **55** (11), 1904 (1959).
16. D. INMAN, G. J. HILLS, L. YOUNG, and J. O'M. BOCKRIS. Ann. N.Y. Acad. Sci. **79** (11), 803 (1959).
17. H. A. LAITINEN and C. H. LIU. J. Am. Chem. Soc. **80**, 1015 (1958).
18. G. N. LEWIS and M. RANDALL. Thermodynamics. McGraw-Hill Book Co., New York. 1923. Chap. XXII.
19. D. M. GRUEN and R. L. MCBETH. Spectrophotometry applied to the analysis of fused salts. Paper presented at the 11th Ann. Summer Symposium, Div. Anal. Chem., Am. Chem. Soc. June 19, 1958.

Can. J. Chem. Downloaded from www.nrcresearchpress.com by 210.87.254.6 on 09/05/12
For personal use only.

Can. J. Chem. Downloaded from www.nrcresearchpress.com by 210.87.254.40 on 09/05/12
For personal use only.

CARBOXYMETHYLMERCAPTO AND CARBOXYMETHYLSULPHONYL DERIVATIVES OF NITROIMIDAZOLE[1]

M. H. Fisher, W. H. Nicholson, and R. S. Stuart

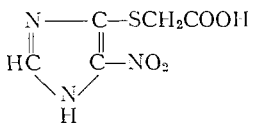
ABSTRACT

Several carboxymethylmercapto and carboxymethylsulphonyl derivatives of nitroimidazole were prepared for biological testing. Reduction or reductive cyclization of these compounds was unsuccessful.

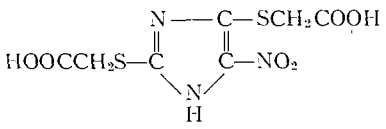
INTRODUCTION

In a previous communication (1) the syntheses of a number of nitro- and amino-imidazolesulphonamides as potential antimetabolites were described. This work has now been extended to the related carboxymethylmercapto compounds and oxidized derivatives. It was hoped that the nitro compounds could be reduced and cyclized but all attempts led to the formation of colored reaction mixtures from which no pure compounds could be isolated.

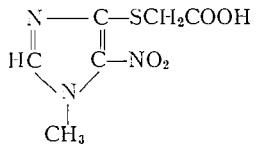
4(5)-Bromo-5(4)-nitroimidazole (2), 2,4(5)-dibromo-5(4)-nitroimidazole (2), 4-chloro-1-methyl-5-nitroimidazole (3), and 5-chloro-1-methyl-4-nitroimidazole (3) on treatment with thioglycolic acid in ammoniacal solution gave the carboxymethylmercapto compounds (I), (II), (III), and (IV).



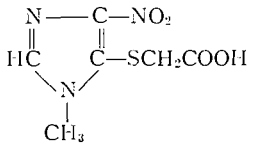
(I)



(II)

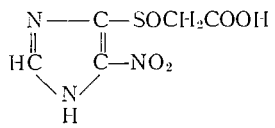


(III)

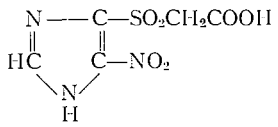


(IV)

Oxidation with hydrogen peroxide in glacial acetic acid yielded the sulphones (V), (VI), and (VII). The disulphide (II) gave an oil which could not be crystallized. The non-methylated compound (I) was somewhat more resistant to oxidation than the others. An intermediate sulphoxide (VIII) was isolated and further oxidized to the sulphone under more vigorous conditions.

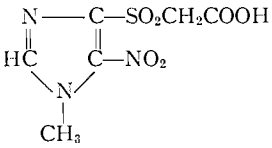


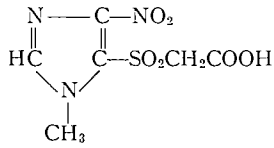
(VIII)



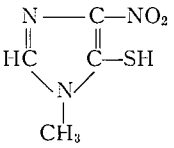
(V)

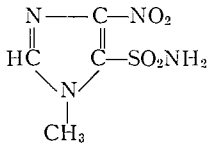
[1]*Manuscript received December 27, 1960.*
Contribution from the Research Department, Merck & Co. Ltd., Montreal, Que.


(VI)


(VII)

Treatment of the sulphide (IV) or the sulphone (VII) with bromine yielded mixtures containing some brominated material. Either mixture with hydrogen sulphide in ammoniacal solution gave 5-mercapto-1-methyl-4-nitroimidazole (IX) (4) as the major product.


(IX)


(X)

It was subsequently found that hydrogen sulphide readily displaced the carboxymethylmercapto, the carboxymethylsulphonyl, or the sulphonamide groups from compounds (IV), (VII), or (X). In each case the thiol (IX) was produced in good yield.

EXPERIMENTAL

Carboxymethylmercapto Compounds

2,4(5)-Bis-(carboxymethylmercapto)-5(4)-nitroimidazole (II)

Thioglycolic acid (11 ml) was added to a solution of 2,4(5)-dibromo-5(4)-nitroimidazole (20 g) in water (100 ml) and concentrated ammonia (50 ml). The mixture was allowed to stand at room temperature for 64 hours. Addition of isopropyl alcohol (300 ml) precipitated the yellow ammonium salt (12 g), m.p. 136°.

The ammonium salt was converted to the free acid with Amberlite resin IR-120(H^+). Crystallization from water gave yellow needles, m.p. 212–213°. Found: C, 28.5; H, 2.38; N, 14.1; S, 21.9. Calc. for $C_7H_7N_3O_6S_2$: C, 28.6; H, 2.39; N, 14.3; S, 21.8%.

4-Carboxymethylmercapto-1-methyl-5-nitroimidazole (III)

Thioglycolic acid (7.5 ml) was added dropwise with stirring to a suspension of 4-chloro-1-methyl-5-nitroimidazole (15 g) in water (100 ml) and concentrated ammonia (50 ml). After storage at 5° for 16 hours the ammonium salt was collected as yellow needles (18.5 g), m.p. 185°.

The ammonium salt was converted to the free acid by precipitation from water with hydrochloric acid. Crystallization from ethanol gave pale yellow needles, m.p. 163–164°. Found: C, 33.2; H, 3.26; N, 18.6; S, 14.7. Calc. for $C_6H_7N_3O_4S$: C, 33.2; H, 3.22; N, 19.3; S, 14.7%.

5-Carboxymethylmercapto-1-methyl-4-nitroimidazole (IV)

This compound was prepared from 5-chloro-1-methyl-4-nitroimidazole (15 g) in a similar manner. Addition of isopropanol (300 ml) and ether (150 ml) and storage for 18 hours at 5° precipitated the ammonium salt (16.5 g), m.p. 153–154°. The free acid crystallized from ethanol as jagged white lathes (8.5 g), m.p. 209–210°. Found: C, 33.5; H, 3.25; N, 19.3; S, 14.5. Calc. for $C_6H_7N_3O_4S$: C, 33.2; H, 3.22; N, 19.3; S, 14.7%.

Can. J. Chem. Downloaded from www.nrcresearchpress.com by 210.87.254.40 on 09/05/12
For personal use only.

4(5)-Carboxymethylmercapto-5(4)-nitroimidazole (I)

This compound was prepared from 4(5)-bromo-5(4)-nitroimidazole (9 g) in a similar manner. The ammonium salt (9.2 g) was collected after 1 hour. After crystallization from methanol it had a melting point of 193–194°. The free acid crystallized from water as yellow needles (6.7 g), m.p. 185–186°. Found: C, 29.6; H, 2.41; N, 20.4; S, 15.7. Calc. for $C_5H_5N_3O_4S$: C, 29.6; H, 2.48; N, 20.6; S, 15.8%.

Oxidations with Hydrogen Peroxide

4(5)-Carboxymethylsulphoxy-5(4)-nitroimidazole (VIII)

4(5)-Carboxymethylmercapto-5(4)-nitromidazole (2 g) in glacial acetic acid (10 ml) and 30% hydrogen peroxide (10 ml) was heated for 1 hour at 75°. The solution was cooled and the product crystallized as white needles (1.6 g), m.p. 219–220° (decomp.). Recrystallization from water raised the m.p. to 220–221° (decomp.). Found: C, 27.3; H, 2.26; N, 18.8; S, 14.8. Calc. for $C_5H_5N_3O_5S$: C, 27.4; H, 2.28; N, 19.2; S, 14.6%.

4(5)-Carboxymethylsulphonyl-5(4)-nitroimidazole (V)

The sulphoxide (VIII) (1 g) in glacial acetic acid (5 ml) and 30% hydrogen peroxide (5 ml) was heated for 4 hours at 90° until a clear solution was obtained. Evaporation to dryness yielded the product (0.8 g), m.p. 284–286°. Recrystallization from water gave white needles, m.p. 295–296°. Found: C, 25.0; H, 2.20; N, 18.0; S, 13.8. Calc. for $C_5H_5N_3O_6S$: C, 25.5; H, 2.12; N, 17.9; S, 13.6%.

4-Carboxymethylsulphonyl-1-methyl-5-nitroimidazole (VI)

Similar oxidation of 4-carboxymethylmercapto-1-methyl-5-nitroimidazole (5 g) for 1 hour at 85° yielded the product (4 g), m.p. 181–182° (decomp.) as white needles from water. Found: C, 28.9; H, 2.83; N,16.5; S, 13.0. Calc. for $C_6H_7N_3O_6S$: C, 28.9; H, 2.81; N, 16.8; S, 12.8%.

5-Carboxymethylsulphonyl-1-methyl-4-nitroimidazole (VII)

Similar oxidation of 5-carboxymethylmercapto-1-methyl-4-nitroimidazole (2 g) for 1 hour at 80° yielded the product (1.25 g), m.p. 170–171° (decomp.) as white needles from water. Found: C, 29.1; H, 2.81; N, 16.8; S, 13.0. Calc. for $C_6H_7N_3O_6S$: C, 28.9; H, 2.81; N, 16.8; S, 12.8%.

Brominations

5-Carboxymethylmercapto-1-methyl-4-nitroimidazole (0.01 mole) or 5-carboxymethylsulphonyl-1-methyl-4-nitroimidazole (0.01 mole) in 1 *N* sodium hydroxide (10 ml) was treated with bromine (0.012 mole). In both cases the precipitated product was a difficultly separable mixture of partially brominated materials.

Displacements with Hydrogen Sulphide

The partially brominated mixtures, 5-carboxymethylmercapto-1-methyl-4-nitroimidazole, 5-carboxymethylsulphonyl-1-methyl-4-nitroimidazole, or 1-methyl-4-nitro-5-sulphamylimidazole (1) were each dissolved in 5 *N* ammonia (1 g in 10 ml) and hydrogen sulphide passed through for 10 minutes. In each case the product was the ammonium salt of 5-mercapto-1-methyl-4-nitroimidazole.

Reductions

Each of the nitroimidazoles was reduced either with hydrogen and Adams platinum catalyst in ethanol or glacial acetic acid or with powdered zinc and glacial acetic acid. In all cases the solutions became highly colored and only dark brown tars could be isolated.

Can. J. Chem. Downloaded from www.nrcresearchpress.com by 210.87.254.40 on 09/05/12
For personal use only.

REFERENCES

1. M. H. FISHER, W. H. NICHOLSON, and R. S. STUART. Can. J. Chem. In press.
2. I. E. BALABAN and F. L. PYMAN. J. Chem. Soc. **121**, 947 (1922).
3. J. SARASIN and E. WEGMANN. Helv. Chim. Acta, **7**, 713 (1924).
4. L. L. BENNETT, JR. and H. T. BAKER. J. Am. Chem. Soc. **79**, 2188 (1957).

Can. J. Chem. Downloaded from www.nrcresearchpress.com by 210.87.254.40 on 09/05/12
For personal use only.

Can. J. Chem. Downloaded from www.nrcresearchpress.com by 84.22.46.98 on 09/08/12
For personal use only.

COUPLING CONSTANTS IN RIGID FIVE-MEMBERED RINGS

N.M.R. SPECTRA OF THE CAMPHANE-2,3-DIOLS[1]

F. A. L. ANET

ABSTRACT

The proton nuclear magnetic resonance (N.M.R.) spectra of the four diastereoisomers of camphane-2,3-diol are reported. The coupling constants between the 2-, 3-, and 4-protons agree with the values predicted by Karplus for ethane derivatives. In particular, the cis (0° dihedral angle) coupling constants (7.7 and 8.9 c.p.s.) are much larger than the trans (120° dihedral angle) coupling constants (2.2 and 2.3 c.p.s.). Unexpected 1,3-coupling between *exo*-hydrogen atoms occurs in some of the compounds studied.

INTRODUCTION

Indirect spin–spin coupling constants in substituted ethane derivatives have attracted attention because of the dependence of their values on the dihedral angle between the CH bonds involved (1–7). The dihedral angles are 60° and 180° in non-cyclic substituted ethanes, which, in general, exist in staggered rather than eclipsed forms. These are also the dihedral angles between vicinal CH bonds in six-membered rings existing in chair conformations. In each case the observed coupling constants may be weighted averages if more than one conformation exists to an appreciable extent.

Karplus (8) has used a semiempirical method to calculate the coupling constants with variation of the dihedral angle in the system CH–CH. The values for angles from 0° to 180° are plotted (cf. ref. 7) in Fig. 1. Most of the experimental evidence, as already mentioned, relates to the values of coupling constants for angles of 60° and 180°. Although

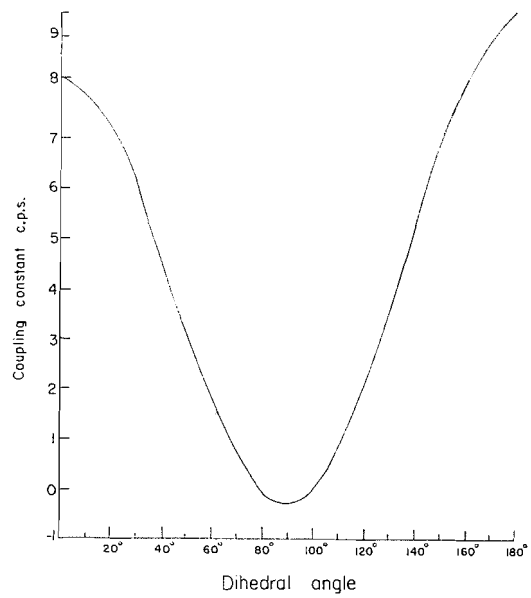


FIG. 1. Variation of coupling constants with dihedral angle in ethane derivatives, as calculated by Karplus (8).

[1]*Manuscript received November 29, 1960.*
Contribution from the Department of Chemistry, University of Ottawa, Ottawa, Canada.

the calculated values for these angles are in satisfactory agreement with the experimental values, it would be highly desirable to determine coupling constants for a whole series of angles from 0° to 180°. The results have a bearing not only in the N.M.R. field (9), but also in other problems, such as that of the origin of the energy barrier in ethane derivatives (10).

There are a few cases in the literature where zero coupling constants have been observed in the case of dihedral angles of about 90°, and these will be referred to at the end of this paper. No case seems to have been reported, however, for 0° or for very small angles. The spectra discussed in this paper provide data for determining coupling constants of the type required for angles of about 0°, 44°, 79°, and 120°.

Owing to the kindness of Dr. S. J. Angyal in providing samples, it has been possible to examine the N.M.R. spectra of the four diastereoisomers of camphane-2,3-diol (11, 12), which are ideal compounds for the present purpose because of the rigid structures of these molecules.

EXPERIMENTAL

The spectra were taken at a frequency of 60 Mc/sec on a Varian V-4302 high-resolution spectrometer. Solutions (10–15%) in pyridine containing a small amount of deuterium oxide and tetramethylsilane were used. Calibration of the spectra was carried out by the usual side-band method. Pyridine solutions were used because the trans isomers were only sparingly soluble in carbon tetrachloride or chloroform. The addition of a small amount of deuterium oxide had the effect of removing the coupling between the OH groups and the adjacent CH groups, thus simplifying the spectra. The OH peak, which had been broad before the addition of deuterium oxide, became quite sharp after the addition. As the OH groups should be strongly hydrogen-bonded with the nitrogen atoms of the pyridine molecules, their occurrence at lower field (ca. 4.6 τ) (5) than the other protons of the camphane diols is not surprising.

RESULTS AND DISCUSSION

The spectra (with the exception of the OH peaks) of the four diols (Fig. 2) are shown in Fig. 3. Slower sweeps of the bands of the 2- and 3-protons are shown in Fig. 4.

In each isomer there are appreciable chemical shifts between the three methyl groups

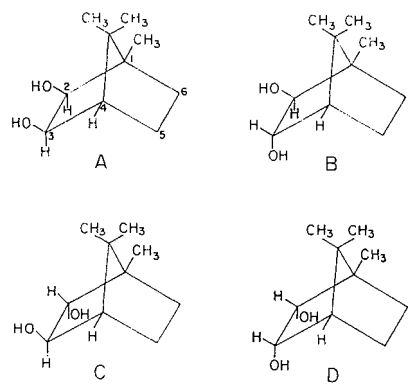


FIG. 2. Stereochemistry of the four camphane-2,3-diols. The diastereoisomers studied were optically active and of the same absolute configuration as (+) camphor (11). A, 2-*exo*,3-*exo*-isomer. B, 2-*exo*,3-*endo*-isomer. C, 2-*endo*,3-*exo*-isomer. D, 2-*endo*,3-*endo*-isomer.

Can. J. Chem. Downloaded from www.nrcresearchpress.com by 84.22.46.98 on 09/08/12
For personal use only.

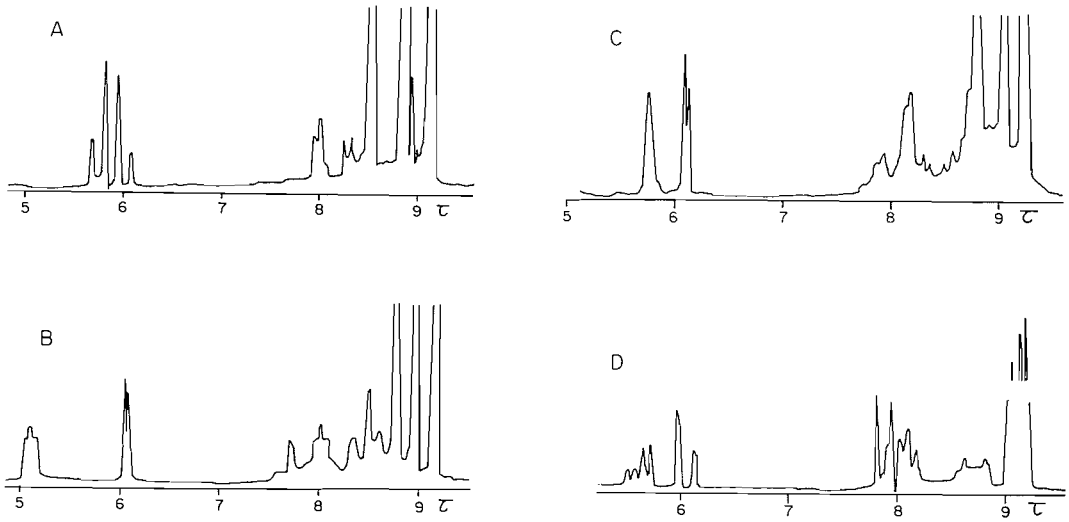


FIG. 3. N.M.R. spectra of the camphane-2,3-diols. A, 2-*exo*,3-*exo*-isomer. B, 2-*exo*,3-*endo*-isomer. C, 2-*endo*,3-*exo*-isomer. D, 2-*endo*,3-*endo*-isomer.

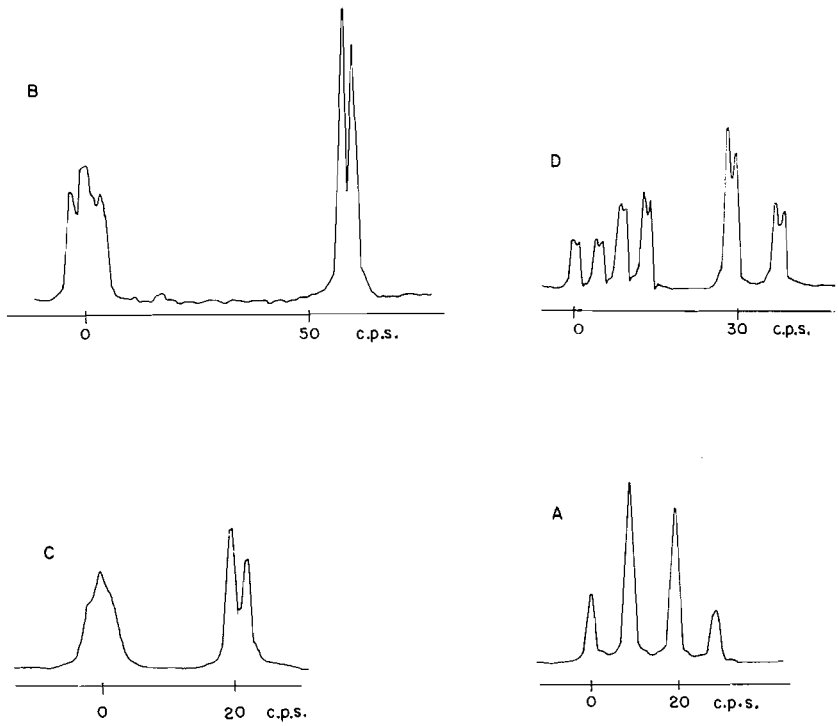


FIG. 4. Slow sweep of the 2- and 3-protons of the camphane-2,3-diols. A, 2-*exo*,3-*exo*-isomer. B, 2-*exo*,3-*endo*-isomer. C, 2-*endo*,3-*exo*-isomer. D, 2-*endo*,3-*endo*-isomer.

and these shifts are different for the various isomers. However, it is not easy to correlate the chemical shifts with structure. In the solutions used, it would be expected that the diamagnetic anisotropy of the pyridine molecules, especially those hydrogen-bonded to

Can. J. Chem. Downloaded from www.nrcresearchpress.com by 84.22.46.98 on 09/08/12
For personal use only.

the solute, would result in chemical shifts in the solute which would not occur in an isotropic solvent. Slomp and MacKellar (13) have in fact shown that pyridine can be a useful solvent in inducing chemical shifts between protons which otherwise have accidentally the same chemical shifts. Furthermore, the chemical shifts of the methyl groups differ appreciably when the solvent is wet pyridine instead of dry pyridine.

Protons on C4, C5, and C6 lie mostly to low field of the methyl groups. As these five protons are all different, but are not very chemically shifted from one another, an analysis would be extremely difficult and has not been attempted.

The greatest interest in the spectra lies in the bands (Fig. 4) given by the 2- and 3-protons. In the 2-*exo*,3-*exo*-diol,[2] the bands corresponding to these protons form a symmetrical quartet of the easily recognizable AB type (2, 5). The coupling constants obtained are $J_{23} = 7.7$ c.p.s. and $J_{24} = J_{34} = 0$.

In the other cis isomer, the 2-*endo*,3-*endo*-diol, the bands of the 2- and 3-protons have 12 lines. If one ignores for the moment the two smallest spacings, the pattern can be recognized as that of the AB part of an ABX system (2, 5). From this it is calculated that $J_{23} = 8.0$ c.p.s., $J_{34} = 4.4$ c.p.s., and $J_{24} = 0$. It is extremely unlikely that the alternative assignment of $J_{34} = 0$ and $J_{24} = 4.4$ c.p.s. is correct. The additional spacing present in the bands of the 2-proton might be explained as being due to J_{24}, but this cannot explain the fact that there is a similar spacing in the bands of the 3-proton. In that case there must be coupling of the 3-proton to one proton other than the 2- or 4-proton. None of the protons on the methyl groups can be implicated since the rapid internal rotation of the methyl groups (2) means that three protons would be the minimum number involved, and this could not give rise to the observed splitting. Furthermore, none of the methyl bands shows any sign of splitting.

The most reasonable explanation is that there is a small coupling between *exo*-protons on C2 and C6 and also on C3 and C5. The absence of coupling of the *endo*-protons on C2 and C3 in the 2-*exo*,3-*exo*-diol to either the *exo*- or the *endo*-protons on C6 and C5 (not necessarily respectively) makes it unlikely that in the present case the *exo*-protons on one side of the molecules are coupled with *endo*-protons on the other side. This leaves only the *exo*-protons for consideration. The molecular framework of the [1,2,2]-bicycloheptane system possesses symmetry, so that one would expect that if the 2-*exo*-proton is coupled to the 6-*exo*-proton then the 3-*exo*-proton should be coupled to the 5-*exo*-proton, even though the molecule as a whole has no symmetry. Similarly, if the 2-*exo*-proton is coupled to the 5-*exo*-proton, then the 3-*exo*-proton should be coupled to the 6-*exo*-proton. Of these two possibilities the first is preferable as it involves coupling through a lesser number of bonds.

Although 1,3-coupling does not seem to have been observed previously between protons in saturated systems (5), with the exception of three-membered rings, its presence in the [1,2,2]-bicycloheptane system may reflect the strain present and the closeness of the carbon atoms 2 and 6 and of 3 and 5. As in the case of 1,2-coupling, there is a strong angular dependence for only two *exo*-protons 1,3 to one another are coupled to an observable extent. The values of the coupling constants ($J_{24} = 0$, $J_{2\text{-}exo6\text{-}exo} = 1.4$, $J_{3\text{-}exo5\text{-}exo} = 1.0$, $J_{3\text{-}endo4} = 0$, $J_{3\text{-}exo4} = 4.4$ c.p.s.) found for the cis isomers should also hold approximately for the trans isomers. It will be assumed that this is so in the analysis of the remaining two spectra.

[2]*The terms exo and endo are used to indicate a substituent cis and trans respectively to the one carbon bridge of the bicycloheptane system. In the naming of the compounds the substituents are, of course, the hydroxyl groups. The terms exo and endo will also be used as required to denote the position of a proton. Thus in the present case the 2- and 3-protons are both endo.*

Can. J. Chem. Downloaded from www.nrcresearchpress.com by 84.22.46.98 on 09/08/12
For personal use only.

In the 2-*exo*,3-*endo*-diol the doublet at high field must be due to the 2-*endo*-proton and this gives J_{23} = 2.3 c.p.s. The 3-*exo*-proton at low field is coupled to the 4-proton, and presumably, also to the 5-*exo*-proton. The band obviously contains many unresolved lines, which are most probably due to the 4-proton (and also perhaps the 5-proton) being very little chemically shifted from protons on C5 and C6 to which it is coupled. Nevertheless, we may ascribe the large spacing (ca. 4 c.p.s.) to J_{34}; this will be at least a minimum value.

In the 2-*endo*,3-*exo*-diol the doublet at high field can be assigned to the 3-*endo*-proton. This gives J_{23} = 2.2 c.p.s. and J_{34} = 0. The 2-*exo*-proton gives a wide band, roughly a poorly resolved triplet of intensity 1:2:1, indicating that it is not only coupled to the 3-proton but also to another proton, presumably the 6-*exo*-proton. The poor aspect of the band can again be ascribed, as for the 3-*exo*-proton of the previous isomer, to insufficient chemical shift between the 6-*exo*-proton and other protons on C5 and C6.

The chemical shifts of the 2- and 3-protons of the camphane-2,3-diols are difficult to correlate with structure and this difficulty is at least partly due to the reasons previously mentioned in the case of the chemical shifts of the methyl groups. The τ values of the 2- and 3-protons (Fig. 3) are close to the value (6.15) for CH groups of secondary alcohols (5), but exact comparisons cannot be made because pyridine is used as the solvent in the present case.

The observed coupling constants and those calculated from the dihedral angles (Table I) and Karplus' data (8) are given in Table II. The dihedral angles in Table I were

TABLE I

Dihedral angles in the camphane system

CH bonds	Dihedral angle
2-*exo* and 3-*exo*	0°
2-*endo* and 3-*endo*	0°
2-*exo* and 3-*endo*	ca. 120°
2-*endo* and 3-*exo*	ca. 120°
3-*endo* and 4	ca. 79°
3-*exo* and 4	ca. 44°

TABLE II

Observed and calculated coupling constants (in c.p.s.) for the camphane-2,3-diols

	J_{23}		J_{34}		J_{26}	J_{35}
Diastereoisomer	Obs.	Calc.	Obs.	Calc.	Obs.	Obs.
2-*exo*,3-*exo*	7.7	8.2	0	0	0	0
2-*exo*,3-*endo*	2.3	2.1	ca. 4.0	4.1	?	0
2-*endo*,3-*exo*	2.2	2.1	0 (?)	0	0	?
2-*endo*,3-*endo*	8.9	8.2	4.4	4.1	1.4	1.0

obtained by measurements made on Barton molecular models. Some bending of the bonds is required to make the models and this results in a change of bond angles from the tetrahedral value. Some of the dihedral angles are uncertain because it is not known exactly how the distortion is spread through the molecule. In the model all bonds are slightly bent so that the strain is distributed more or less uniformly. The uncertainties in dihedral bond angles are most unlikely to affect the conclusions made in this paper.

Can. J. Chem. Downloaded from www.nrcresearchpress.com by 84.22.46.98 on 09/08/12
For personal use only.

The distortion of the molecule does not change the 0° dihedral angles, but does increase, for example, the dihedral angle which would have been 120° otherwise. Unfortunately, no very accurate structure determination seems to have been carried out in the [1,2,2]-bicycloheptane series. The structure of 3-cyanocamphor has been determined (14) but the positions of all the atoms are not accurately known. The [1,2,2]-bicycloheptane system can be considered as two fused five-membered rings. Each ring is approximately in the C_s (15) or envelope (16) conformation. The assumption of complete (or almost complete) eclipsing of carbons 2 and 3 is probably a good one in this case, as any staggering increases the considerable strain already present.

The results shown in Table II also agree with coupling constants found in α- and α'-chlorocamphor (17). In the α-isomer the 3-proton, which is *exo*, is coupled to the 4-proton by 5 c.p.s., whilst in the α'-isomer, where the 3-proton is *endo*, J_{34} is zero. Similarly, in 3,8-cyclocamphor (18) the coupling constant of the 3-*endo*-proton to the 4-proton is zero.

The very good agreement between calculated and observed coupling constants found in Table II is strong support for the validity of Karplus' calculations. It is to be noted that coupling constants in three-membered and four-membered rings (5, 19, 20) do not agree very well with those expected from Karplus' work, in contrast to the situation which exists in most five- and six-membered rings.

It is obvious from the results presented here that in non-rigid cyclopentane derivatives (15, 16) the coupling constants will depend very markedly on the conformation(s) which the molecules adopt. If the stereochemistry and coupling constants are known, it may become possible to deduce the conformation of such rings. In fact, attempts to do this have already been made by Jardetzky (9) in the case of the ribose nucleosides and nucleotides. The conclusions drawn in that paper derive support from the present work.

ACKNOWLEDGMENTS

I wish to thank Dr. S. J. Angyal of the University of New South Wales, Australia, for gifts of the camphane diols which made this work possible.

REFERENCES

1. R. U. Lemieux, R. K. Kullnig, H. G. Bernstein, and W. G. Schneider. J. Am. Chem. Soc. **80**, 6098 (1958).
2. J. A. Pople, W. G. Schneider, and H. J. Bernstein. High-resolution nuclear magnetic resonance. McGraw-Hill Book Co., New York. 1959.
3. A. D. Cohen, N. Sheppard, and J. J. Turner. Proc. Chem. Soc. 118 (1958).
4. C. N. Banwell, A. D. Cohen, N. Sheppard, and J. J. Turner. Proc. Chem. Soc. 266 (1959).
5. L. M. Jackman. Applications of nuclear magnetic resonance spectroscopy in organic chemistry. Pergamon Press, New York. 1959.
6. F. A. L. Anet. Proc. Chem. Soc. 327 (1959).
7. F. A. L. Anet. J. Am. Chem. Soc. **82**, 994 (1960).
8. M. Karplus. J. Chem. Phys. **30**, 11 (1959).
9. C. D. Jardetzky. J. Am. Chem. Soc. **82**, 229 (1960).
10. M. Karplus. J. Chem. Phys. **33**, 316 (1960).
11. S. J. Angyal and R. J. Young. J. Am. Chem. Soc. **81**, 5467 (1960).
12. T. Takeshita and M. Kitajima. Bull. Chem. Soc. Japan, **32**, 985 (1959).
13. G. Slomp and F. MacKellar. J. Am. Chem. Soc. **82**, 999 (1960).
14. E. H. Wiebenga and J. C. Krom. Rec. trav. chim. **65**, 663 (1946).
15. K. S. Pitzer and W. E. Donath. J. Am. Chem. Soc. **81**, 3213 (1959).
16. F. V. Brutcher, Jr., T. Roberts, S. J. Barr, and N. Pearson. J. Am. Chem. Soc. **81**, 4915 (1959).
17. W. D. Kumber, J. N. Shoolery, and F. V. Brutcher, Jr. J. Am. Chem. Soc. **80**, 2533 (1958).
18. E. J. Corey, M. Ohno, S. W. Chow, and R. A. Scherrer. J. Am. Chem. Soc. **81**, 6305 (1959).
19. F. S. Mortimer. J. Mol. Spectroscopy, **5**, 199 (1960).
20. C. A. Reilley and J. D. Swalen. J. Chem. Phys. **32**, 1378 (1960).

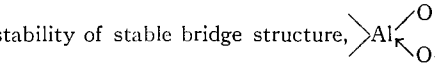
Can. J. Chem. Downloaded from www.nrcresearchpress.com by 84.22.46.98 on 09/08/12
For personal use only.

Can. J. Chem. Downloaded from www.nrcresearchpress.com by 210.87.254.5 on 09/05/12
For personal use only.

REACTIONS OF ALUMINUM ALKOXIDES WITH ACETYLACETONE, BENZOYLACETONE, AND ETHYL ACETOACETATE[1]

R. K. MEHROTRA AND R. C. MEHROTRA

ABSTRACT

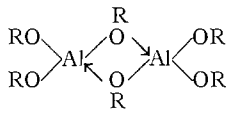
The observed stability of stable bridge structure,  , in aluminum alkoxides has been explained on the powerful tendency of aluminum to attain co-ordination number 4. This would predict the monomeric nature of the derivatives of the type, $(OR)_2Al(lig)$, where ligand (lig) is a diketone like acetylacetone (acac), benzoylacetone (bzac), or ketoester like ethyl acetoacetate (etac). This has been confirmed by actual synthesis of these compounds by reactions between aluminum alkoxides (ethoxide and isopropoxide) and acetylacetone, benzoylacetone, and ethyl acetoacetate in equimolecular ratios. These and also $(OR)Al(lig)_2$ as well as $Al(lig)_3$ have been shown to be monomeric in boiling benzene. The volatility of the derivatives was found in the order $[(OPr^i)_3Al]_2 > (OPr^i)_2Al(acac) > (OPr^i)Al(acac)_2$. This leads to the conclusion that chelation lowers the volatility and the direct relationship between volatility and molecular complexity, observed in the case of simple alkoxides, is not applicable in these derivatives. Further mixed derivatives of the type $Al(acac)(etac)_2$ and $Al(etac)(acac)_2$ have also been synthesized during the course of the above work.

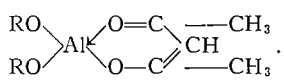
INTRODUCTION

Aluminum alkoxides are generally prepared by the reaction of corresponding alcohols with metallic aluminum with the help of catalysts (1). Mehrotra (2, 3) described the preparation of higher aluminum alkoxides by treating aluminum ethoxide and isopropoxide with the corresponding alcohol and removing the ethanol or isopropanol produced, azeotropically with benzene. The technique has now been extended to prepare acetylacetonate, benzoylacetonate, and ethyl acetoacetate derivatives of aluminum by the simple reactions of the type:

$$Al(OR)_3 + x\text{H lig} \rightarrow Al(OR)_{3-x}(lig)_x + x\text{ROH}$$

(where ligand is acetylacetone, benzoylacetone, or ethyl acetoacetate).

The main interest of the above study arose from earlier observations of one of us (2), that the bridge structure  is very stable in aluminum alkoxides and exists even in the vapor phase. On aging, alkoxides were shown to exhibit greater molecular complexity (2) and this phenomenon has been explained by Bradley (4) to be due to the tendency of 4-co-ordination aluminum to change to the 6-co-ordination. In view of the above, it was conjectured that a monosubstituted product like $Al(OR)_2(lig)$ should be monomeric as co-ordination number 4 would be easily satisfied in the structure:

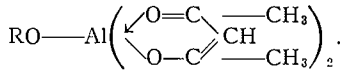


The above has been confirmed for the mono acetylacetone, benzoylacetone, and ethyl acetoacetate products with R as C_2H_5 (Et) or C_3H_7 (Pr^i). The derivatives further do not show any tendency of polymerization, even after aging for a few weeks. The di and tri derivatives have also shown to be monomeric in benzene. It is of particular interest

[1]*Manuscript received November 25, 1960.*
Contribution from the Chemical Laboratories, University of Gorakhpur, Gorakhpur, U.P., India.

Can. J. Chem. Vol. 39 (1961)

to note that the di derivatives would have a co-ordination number 5 as depicted by the following simple structure:



A point of further interest was the volatility of the above derivatives. This was of special interest as in a number of aluminum (2), titanium, zirconium (5), and other alkoxide derivatives, it has been shown that the decreasing volatility has, in general, a simple relationship with increasing molecular complexity or weights. The above derivatives could be distilled at higher temperatures compared to aluminum alkoxides, indicating that the chelation has the expected effect of lowering the volatility and overcomes the opposite effect of simpler molecular complexity.

EXPERIMENTAL

Materials

Aluminum ethoxide was prepared by the method of Chalmers (6). Aluminum isopropoxide was prepared as described by Young, Hartung, and Crossley (7). Both were purified by distillation under reduced pressure.

Acetylacetone and ethyl acetoacetate (E. Merck) were dried by refluxing with aluminum isopropoxide and fractionating. Benzoylacetone was synthesized (8) and purified by distillation.

Benzene (B.D.H.) was dried by distilling over metallic sodium and carefully fractionated before use.

All glass apparatus fitted with interchangeable joints was used throughout and special precautions were taken to exclude the moisture. Fractionations were carried out in a column packed with Raschig rings.

Analytical Methods

Aluminum was determined as oxinate gravimetrically except in benzoylacetonate derivatives in which cases ignition to oxide was employed.

The amount of alcohol in benzene–alcohol azeotrope was estimated by a back titration method of Bradley and Wardlaw (9).

Alkoxy group in the presence of acetylacetone, benzoylacetone, or ethyl acetoacetate was estimated by liberating the isopropanol or ethanol from the compound by boiling it in benzene with an excess of acetylacetone or ethyl acetoacetate and subsequently estimating the ethanol or isopropanol liberated in benzene alcohol azeotrope.

Molecular Weights

The molecular weights of compounds were determined ebullioscopically in boiling benzene by using a Gallenkamp ebulliometer with a sensitive transistor principle. The elevations (ΔT) were plotted against the weight of solute added and in all cases a straight line was obtained. The constant K for the solvent was determined with naphthalene. The results are recorded in Table I.

Synthetic Reactions

The general method of synthesis was the same in every case and so the details will be given only for acetylacetone compounds with aluminum isopropoxide and mixed acetylacetone – ethyl acetoacetate derivatives. In cases of all other derivatives described in Table II, the method was the same as with acetylacetone derivatives; the amount of alcohol collected in the azeotrope was, within experimental error, equal to the amount expected from the stoichiometry of the reaction. The yields of the pure distilled or crystallized derivatives are also included in Table II.

Can. J. Chem. Downloaded from www.nrcresearchpress.com by 210.87.254.5 on 09/05/12
For personal use only.

Can. J. Chem. Downloaded from www.nrcresearchpress.com by 210.87.254.5 on 09/05/12
For personal use only.

TABLE I

Results of molecular weight determination

No.	Formula of the compound	Concn. range (g), per 15 cc of benzene	Molecular weight	
			Found	Calcd.
1.	$Al(OEt)_2(acac)$	.102–.274	209	216
2.	$Al(OEt)_2(etac)$	.094–.431	261	246
3.	$Al(OEt)_2(bzac)$	.058–.227	262	278
4.	$Al(OEt)(acac)_2$	.124–.453	297	270
5.	$Al(OEt)(bzac)_2$	.052–.168	412	394
6.	$Al(OEt)(etac)_2$	.116–.292	344	330
7.	$Al(OPr^i)_2(acac)$	.062–.162	253	244
8.	$Al(OPr^i)_2(bzac)$	.041–.173	293	306
9.	$Al(OPr^i)_2(etac)$	.217–.471	283	274
10.	$Al(OPr^i)(acac)_2$	.046–.198	275	284
11.	$Al(OPr^i)(bzac)_2$	.058–.158	388	408
12.	$Al(OPr^i)(etac)_2$	.165–.564	360	344
13.	$Al(acac)_3$	.087–.336	316	324
14.	$Al(bzac)_3$	.080–.287	501	510
15.	$Al(etac)_3$	.102–.306	425	414

TABLE II

Properties of the compounds

No.	Formula	Appearance	% yield of distilled or purified compound	B.p.	Analyses			
					Al%		OR %	
					Found	Calcd.	Found	Calcd.
1.	$Al(OEt)_2(acac)$	Yellow liquid	96	188°/4 mm	12.52	12.49	41.2	41.6
2.	$Al(OPr^i)_2(acac)$	Yellow solid	81	160°/5 mm	11.18	11.06	47.6	48.3
3.	$Al(OEt)(acac)_2$	Yellow crystals	95	—	10.2	10.0	16.1	16.6
4.	$Al(OPr^i)(acac)_2$	Yellow crystals	96	—	9.38	9.5	19.6	20.7
5.	$Al(OEt)_2(bzac)$	Yellow crystals	95	—	9.9	9.7	31.6	32.3
6.	$Al(OPr^i)_2(bzac)$	Yellow crystals	97	—	8.9	8.8	39.1	38.5
7.	$Al(OEt)(bzac)_2$	Yellow crystals	97	—	6.9	6.8	11.0	11.4
8.	$Al(OPr^i)(bzac)_2$	Yellow crystals	97	—	6.53	6.61	13.7	14.4
9.	$Al(OEt)_2(etac)$	Yellow liquid	98	200°/5 mm	10.79	10.9	35.8	36.5
10.	$Al(OPr^i)_2(etac)$	Yellow liquid	94	205°/10 mm	9.83	9.80	44.6	43.06
11.	$Al(OEt)(etac)_2$	Yellow liquid	82	188°/3 mm	8.10	8.17	14.07	13.6
12.	$Al(OPr^i)(etac)_2$	Yellow liquid	67	225°/10 mm	7.7	7.8	17.3	17.1
13.	$Al(acac)_3$	Yellow crystals	91	—	8.5	8.32	—	—
14.	$Al(bzac)_3$	Yellow crystals	95	—	5.40	5.29	—	—
15.	$Al(etac)_3$	Yellow powder	93	—	6.80	6.51	—	—
16.	$Al(acac)(etac)_2$	Yellow semisolid	94	—	7.18	7.02	—	—
17.	$Al(etac)(acac)_2$	Yellow mass	94	—	7.7	7.6	—	—

I. Reaction of Aluminum Isopropoxide with Acetylacetone in Molar Ratio of 1:1

Acetylacetone (3.28 g) was added to a solution of aluminum isopropoxide (6.70 g) in dry benzene (60 g). Heat was evolved during mixing of reactants. The mixture was refluxed for 3 hours at bath temperature of 120–30°. Benzene–isopropanol azeotrope was distilled slowly between 72–80°, followed by benzene, leaving a yellow liquid in the reaction flask. No crystallization occurred even after standing overnight. The remaining benzene was distilled out under reduced pressure and the compound was distilled at 160°/5 mm to give a light yellowish mobile liquid (6.5 g) which solidified on being kept for 3–4 days. The total amount of isopropanol in the azeotrope was found to be 1.90 g against 1.97 g, calculated for 1 mole. (Found: Al, 11.18; OPr^i, 47.6. Calcd. for $Al(acac)(OPr^i)_2$: Al, 11.06; OPr^i, 48.3%.)

II. Reaction of Aluminum Isopropoxide with Acetylacetone in Molar Ratio of 1:2

Acetylacetone (5.89 g) was added to a solution of aluminum isopropoxide (6.01 g) in benzene (80 g). Heat was evolved. The mixture was refluxed for 4 hours and the benzene–isopropanol azeotrope was taken between 72–80°. Pure benzene was distilled out till a light yellowish residue was left. On cooling it gave crystals (8 g) which were dried under reduced pressure for 3 hours. The total amount of isopropanol found in the azeotrope was 3.35 g, against 3.46 g, calculated for 2 moles. (Found: Al, 9.38; OPr^i, 19.6. Calcd. for $Al(OPr^i)(acac)_2$: Al, 9.5; OPr^i, 20.7%.)

The above compound was sublimed at a bath temperature of 300°/5 mm to give a yellowish mass (Found: Al, 9.34%).

III. Reaction of Aluminum Isopropoxide with Acetylacetone in Molar Ratio of 1:>3

Acetylacetone (12.56 g) was added to a solution of aluminum isopropoxide (7.6 g) in benzene (80 g) and the mixture refluxed for 3 hours. Benzene–isopropanol azeotrope was taken out slowly. Afterwards, pure benzene was distilled out, till a light yellowish liquid remained in the reaction flask which on cooling gave crystals. Total amount of isopropanol was found to be 6.6 g, against 6.7 g, calculated for 3 moles, in the azeotrope. (Found: Al, 8.5. $Al(acac)_3$ requires Al, 8.33%.)

IV. Reaction of Aluminum Diisopropoxy Monoacetylacetonate with Ethyl Acetoacetate in Molar Ratio of 1:2

Ethyl acetoacetate (2.34 g) was added to a solution of aluminum diisopropoxy monoacetylacetonate (2.19 g) in benzene (50 g). The mixture was refluxed for 2 hours. Benzene–isopropanol azeotrope was collected slowly between 72–80°; followed by pure benzene leaving a yellow liquid in the reaction flask, which was dried under reduced pressure at 50° to give a yellow semisolid (3.2 g). The total amount of isopropanol in the azeotrope was found to be 1.1 g against 1.07 g calculated for 2 moles. (Found: Al, 7.18. Calcd. for $Al(etac)_2(acac)$, 7.02%.)

V. Reaction of Aluminum Diisopropoxy Monoethyl Acetoacetate with Acetylacetone in Molar Ratio of 1:2

Acetylacetone (3.26 g) was added to a solution of aluminum diisopropoxy monoethyl acetoacetate (4.45 g) in benzene (50 g). Heat was evolved as a result of reaction. The mixture was refluxed for 2 hours and the benzene–isopropanol azeotrope was taken between 72–80°. Pure benzene was distilled out till there was left a yellow liquid which was dried under reduced pressure for 4 hours to give a yellow mass (5.5 g). The total amount of isopropanol was found to be 1.9 g, against 1.94 g required for 2 moles. (Found: Al, 7.7. Calcd. for $Al(etac)(acac)_2$, 7.6%.)

ACKNOWLEDGMENT

The authors are grateful to the Council of Scientific and Industrial Research, India, for providing a research fellowship to one of them (R.K.M.). It is a pleasure to acknowledge the fruitful discussion by R.C.M. on the topic with Prof. D. C. Bradley, University of Western Ontario, London, Ontario.

REFERENCES

1. W. E. Tistschenko. J. Russ. Phys. Chem. Soc. **31**, 694, 784 (1899).
2. R. C. Mehrotra. J. Indian Chem. Soc. **30**, 585 (1953).
3. R. C. Mehrotra. J. Indian Chem. Soc. **31**, 85 (1954).
4. D. C. Bradley. Nature, **182**, 1211 (1958).
5. D. C. Bradley, R. C. Mehrotra, and W. Wardlaw. J. Chem. Soc. 2027, 4204, 5020 (1952).
6. W. Chalmers. Organic syntheses. Vol. 15. John Wiley & Sons, Inc., New York. 1935. p. 82.
7. W. G. Young, W. H. Hartung, and F. S. Crossley. J. Am. Chem. Soc. **58**, 100 (1936).
8. A. I. Vogel. A text book of practical organic chemistry. Longmans, Green & Co., London. 1956. p. 865.
9. D. C. Bradley and W. Wardlaw. J. Chem. Soc. 3450 (1950).

Can. J. Chem. Downloaded from www.nrcresearchpress.com by 210.87.254.5 on 09/05/12
For personal use only.

Can. J. Chem. Downloaded from www.nrcresearchpress.com by 210.87.254.42 on 09/05/12
For personal use only.

POTASSIUM DERIVATIVES OF FLUORENE AS INTERMEDIATES IN THE PREPARATION OF C_9-SUBSTITUTED FLUORENES

III. THE INFLUENCE OF SOLVENT AND METAL IN THE FORMATION OF C_9-SUBSTITUTED FLUORENES FROM 9-FLUORENYL METALS[1]

G. W. H. Scherf and R. K. Brown

ABSTRACT

Equimolar quantities of 9-fluorenyl-potassium, -sodium, or -lithium and alkyl or aralkyl halides at room temperature in ether solvents yielded a mixture of unchanged fluorene, C_9-monosubstituted fluorene, and C_9-disubstituted fluorene. The amount of disubstitution never exceeded that of unchanged fluorene, and was found to be maximum (~35%) for the potassium compound in 1,2-dimethoxyethane, somewhat less for the sodium analogue, and small (~5%) for the lithium compound. In hydrocarbon solvents such as hexane, 9-fluorenylpotassium gave only 7% of C_9-disubstituted fluorene. The lithium compound, upon reaction with methyl iodide or ethyl iodide gave, along with unreacted fluorene, only C_9-monosubstituted fluorene. But reaction of 9-fluorenyllithium with benzyl chloride in hexane gave a small quantity (~5%) of disubstituted fluorene as well as the monosubstituted product.

The results are explained in terms of (*a*) the solubilities of the organometallic compounds in ether and hydrocarbon solvents, (*b*) the polarity of the metal carbon bond, and (*c*) the acidity of the hydrogen on C_9 of fluorene.

INTRODUCTION

A recent publication described the infrared spectra of a number of C_9-mono- and -di-substituted fluorenes (1). For the infrared work the 9,9-disubstituted fluorenes were prepared by treating one mole of fluorene in dioxane with two gram equivalents of potassium metal. The metalated product was then brought into reaction with two moles of the appropriate halide. Contaminating monosubstituted and unsubstituted fluorene was then removed either by crystallization, or by chromatography.

Attempts to prepare C_9-monosubstituted fluorene from the reaction between equimolar proportions of fluorene and potassium in dioxane, followed by the addition of an equivalent amount of alkyl or aralkyl halide led to a mixture of C_9-monosubstituted, C_9-disubstituted, and unsubstituted fluorene whose separations were frequently somewhat tedious for routine synthesis. Accordingly, the C_9-monosubstituted compounds required for the absorption studies were prepared more conveniently by the procedure developed by Greenhow, White, and McNeil (2).

This paper describes the results of a study of mono- versus di-substitution at carbon 9 of fluorene when 9-fluorenyl-lithium, -sodium, or -potassium was allowed to react with an equimolar quantity of an alkyl or aralkyl halide in the solvents hexane (or heptane), dioxane, 1,2-dimethoxyethane (DME), 1,2-diethoxyethane (DEE), and tetrahydrofuran (THF).

RESULTS

The Reaction of 9-Fluorenylpotassium with Alkyl and Aralkyl Halides in Ether andHydrocarbon Solvents

The 9-fluorenylpotassium required for this work was prepared from equimolar amounts of potassium and fluorene (1). This could be readily isolated and transferred to the solvent chosen for study.

[1]*Manuscript received September 12, 1960.*
Contribution from the Department of Chemistry, University of Alberta, Edmonton, Alberta. Taken from the thesis of G. W. H. Scherf to be submitted to the Graduate School of the University of Alberta in partial fulfillment of the requirements for the degree of Doctor of Philosophy.

Can. J. Chem. Downloaded from www.nrcresearchpress.com by 210.87.254.42 on 09/05/12
For personal use only.

Two outstanding differences were observed between the reactions at room temperature of 9-fluorenylpotassium with organic halides in *ether* solvents and its reaction with these halides in hydrocarbon solvents. *Firstly*, when dioxane, diethyl ether, diisopropyl ether, or di-*n*-butyl ether was the solvent, reaction of the organometallic compound with the organic halide was relatively fast. Within 5 minutes nearly all of the solid suspension of 9-fluorenylpotassium had disappeared. On the other hand, when *n*-heptane was the suspending solvent, much of the 9-fluorenylpotassium was still unchanged after an interval of 30 minutes. The marked difference in the rate of reaction was no doubt due to the partial solution of the 9-fluorenylpotassium which occurred in the ethers but not in heptane. This was borne out by the observation that the depth of the reddish color of the ether solution could be correlated, if only roughly, with the rate of reaction when, for the experiments concerned, equivalent quantities of reagents were used. No color was observed in the solvent for the heptane suspension, hence, in this medium, the reaction with the halide is considered to occur heterogeneously on the surface of the suspended solid, resulting in a much slower reaction dependent in part upon diffusion rate and efficiency of stirring. *Secondly*, reaction of 9-fluorenylpotassium with an organic halide in molar ratio 1:1 in *ethers* gave considerable quantities of 9,9-disubstituted fluorene along with C_9-monosubstituted and also unchanged fluorene while the same reaction in *heptane* gave essentially monosubstitution with relatively little 9,9-disubstituted fluorene. The amount of disubstituted material obtained from the reaction in dioxane was about 25% of the fluorene originally used to form the potassium compound and fell somewhat short of equivalence to the amount of unchanged fluorene. This extra quantity of fluorene most likely was that which had originally failed to react with the metal. From an examination of the results of alkylation in dioxane solvent with methyl iodide, ethyl bromide, allyl bromide, and benzyl chloride, the ratio of disubstitution to monosubstitution appears to be independent of the size of the alkyl or aralkyl group (Table I).

TABLE I

Conversion of fluorene into the mono- and di-substituted derivatives by reaction of 9-fluorenylpotassium with various alkyl halides in dioxane solvent

Alkyl halide	% disubstitution	% monosubstitution	% fluorene
Methyl iodide	26	43	31
Ethyl bromide	27	43	30
Allyl bromide	27	40	33
Benzyl chloride	23	(*)	(*)

*Accurate amounts unknown since quantitative separation of the monobenzylfluorene from fluorene was not achieved either by crystallization or chromatography.

With heptane as solvent, only about 5% of the original fluorene was converted to 9,9-disubstituted fluorene while the quantity of C_9-monosubstituted product actually isolated was 75 to 85%. The remainder of the product was unchanged fluorene.

The characteristic absorption bands used to identify the presence of C_9-mono- and C_9-di-substitution (1) and to follow the extent of separation are given in Table II. The absorption spectra of 9-ethylfluorene and 9,9-diethylfluorene, previously unreported (1) are shown in Figs. 1 and 2. The small region from 1050 to 1110 cm^{-1} is quite helpful for the determination of mono- versus di-methylfluorene. The absorption is not intense but quite sharp and distinct. Dimethyl fluorene shows a band at 1078 cm^{-1} (with a smaller one at 1085 cm^{-1}). Monomethylfluorene shows no absorption at these positions

TABLE II

Characteristic absorption bands in the infrared for C_9-substituted fluorenes (cm^{-1})

Methyl		Ethyl†		Benzyl		Allyl	
mono-	di-	mono-	di-	mono-	di-	mono-	di-
		658 m	Nil				
						681 mw*	681 mw*
				700 s*	700 s*		
719 m	Nil	Nil	Nil				
				Nil	720 ms		
						727 ms	Nil
		735–40 (broad)	735–40 (narrow)				
				746–48	746–48		
				754 s	Nil	754 s	—
758 s*	758 s*						
				Nil	761–64 s	—	761–64 s
793 s	Nil	Nil	Nil				
Nil	Nil	820 w	Nil				
Nil	Nil	838 w	Nil				
		869 mw*	869 mw*				
				905–9 m*	905–9 w		
						913 s*	913 s*
			925 m*				
932 m	932 m						

m = medium; s = strong; w = weak

*The disubstituted compounds absorb approximately twice as much as do the monosubstituted fluorenes and have broader bands.

†In addition, the monoethyl compound shows two strong bands at 748 cm^{-1} and 760 cm^{-1}, the former more intense than the latter. The diethyl compound shows strong adsorption at 754 cm^{-1} and 760 cm^{-1} the latter stronger than the former.

but in turn exhibits sharp though weak absorption at 1098 cm^{-1}. Fluorene absorbs only at 1089 cm^{-1} in this region (Fig. 3).

Influence of Solvent and Metal in C_9-Mono- and -Di-substitution

Table III shows the results of the reaction of methyl iodide and 9-fluorenylpotassium

TABLE III

Products of the reaction of equimolar amounts of 9-fluorenylpotassium and methyl iodide in various solvents

Solvent	Time§ (hr)	Apparent extent of metalation	Dimethyl-fluorene, %	Mono-methyl-fluorene, %	Fluorene, %
DME	1	Complete	35	30	35
DEE	1–2	Complete	25	22	53
THF	4	Complete	20	20	60
Dioxane	4	Complete	25	40	35
Toluene–DME*	4	Complete	20	20	60
Toluene–DEE*	4	Complete	—	—	—
Toluene–THF*	4	Complete	10	25	65
Toluene–dioxane*	4	Incomplete	5	40	55
Heptane–DME*†	3	Complete	33	30	37
Hexane or heptane‡	4	—	7	40	53

*The ratio of ether to toluene was 1:4 by volume.

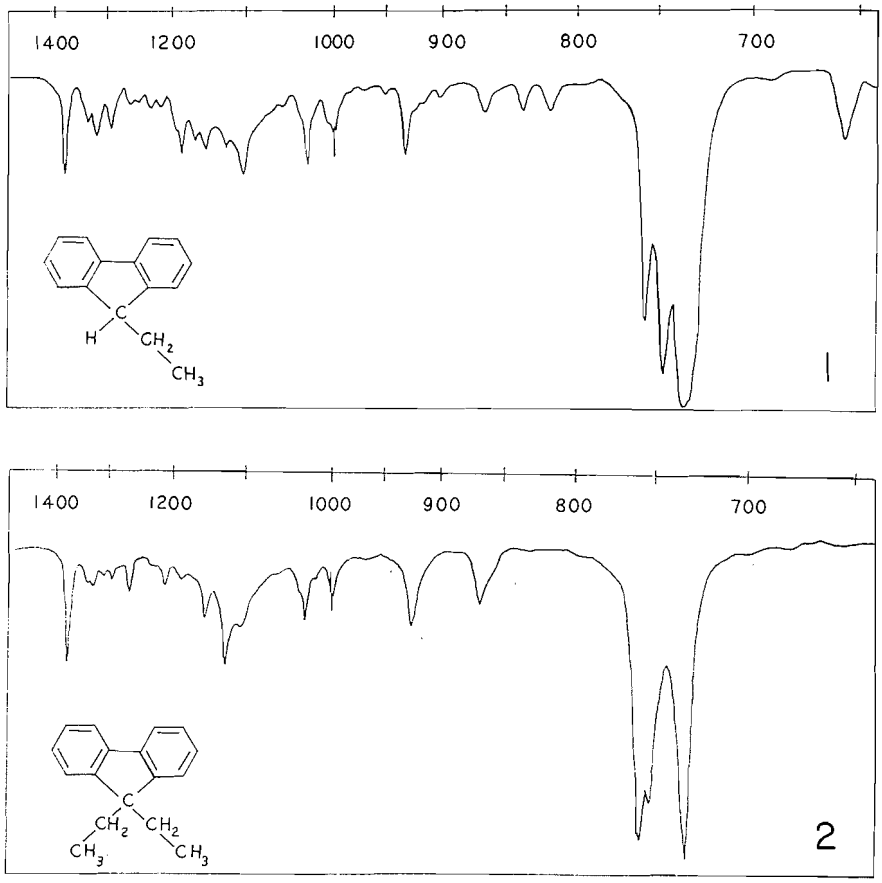
†Two layers were formed during the reaction, the lower one containing the ether and the metal organic compound (ref. 3).

‡The potassium fluorenyl was prepared in dioxane, isolated by filtration, and suspended in the hydrocarbon for the reaction with CH_3I.

§The time allowed for the formation of the organometallic compound at reflux temperature of the solution.

in cyclic- and poly-ethers, in hydrocarbons, and in mixtures of ethers and hydrocarbons. In Tables IV and V are listed the results of similar reactions of the sodium and lithium analogues with methyl iodide.

Can. J. Chem. Downloaded from www.nrcresearchpress.com by 210.87.254.42 on 09/05/12
For personal use only.



FIGS. 1 and 2.

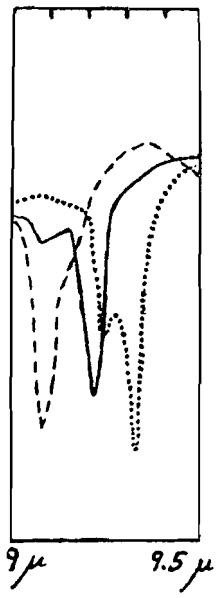


FIG. 3. The 9μ to 9.5μ region (1110 cm^{-1} to 1050 cm^{-1}) of the infrared spectrum of fluorene ——, 9-methylfluorene – – – –, and 9,9-dimethylfluorene . . . . . , taken in CS_2 solution.

Can. J. Chem. Downloaded from www.nrcresearchpress.com by 210.87.254.42 on 09/05/12
For personal use only.

TABLE IV

Products of the reaction of equimolar amounts of 9-fluorenylsodium and methyl iodide in various solvents

Reagent	Solvent	Time* (hr)	Apparent extent of metalation	Dimethyl-fluorene, %	Mono-methyl-fluorene, %	Fluorene, %
Na	DME	36	Complete	35	30	35
Na	DEE	40–50	Incomplete	20	40	40
Na	THF	48	†			
Na	Dioxane	36	‡			
$NaNH_2$	DME	3	Incomplete	15	40	45
$NaNH_2$	Dioxane	3	See experimental	10	35	55
	n-Heptane	§		None found	65	35

*Time allowed for the reaction between the metal or amide and fluorene in the refluxing solvents.
†The metalation with sodium metal was incomplete in all cases (ref. 3).
‡The extent of metalation was too small for separation of products.
§The sodamide was allowed to react with fluorene in refluxing dioxane for 3 hours. The precipitate was removed from the cooled solution, washed free of dioxane with hexane, and suspended in heptane.

TABLE V

Products from the reaction of equimolar amounts of 9-fluorenyllithium and methyl iodide in various solvents

Solvent	Time*	Apparent extent of metalation	Dimethyl-fluorene, %	Mono-methyl-fluorene, %	Fluorene, %
DME	4–5	Complete	5	80–85	15–10
DEE	5–6	Complete	5	60	35
THF	8	Complete	1–2	~85	14–13
Hexane†	—		0	80	20

*Time allotted for the formation of the organometallic compound in the refluxing solvent.
†9-Fluorenyllithium was prepared in DEE, then isolated, suspended in hexane, and treated with methyl iodide.

In general, it can be seen that in dimethoxyethane (DME), diethoxyethane (DEE), and tetrahydrofuran (THF), 9-fluorenylpotassium and 9-fluorenylsodium, treated with equimolar amounts of methyl iodide, gave from 20 to 35% disubstitution. In addition, at *least* the same amount of unreacted fluorene was formed along with 20 to 40% of monosubstitution. The efficiency of the solvent in promoting conversion to the dimethylated product is, in decreasing order, DME > DEE > THF. This is the same solvent order which was found previously in the study of the influence of solvent on the extent of reaction of potassium with fluorene (3). Hydrocarbon solvents, or ethers mixed with hydrocarbon solvents, generally gave less dimethylation but somewhat more monomethylation than was found when the pure ethers were used.

The exception was the reaction of 9-fluorenylpotassium with methyl iodide in a mixture of heptane and DME (Table III). However, that one obtained results similar to those found when pure DME was employed, can be explained. When the metal had reacted with the fluorene in this mixed solvent, two liquid layers appeared—the lower being essentially that due to the ether containing 9-fluorenylpotassium, while the upper was primarily heptane contaminated with some DME but containing no 9-fluorenylpotassium. Hence, the lower layer, where further reactions with methyl iodide occurred, approximated the conditions which held in the case where the solvent was DME only.

The 9-fluorenyllithium (prepared by precipitation from cold DEE (3)) treated with an equimolar amount of methyl iodide, gave little or no dimethylation in ether or hydrocarbon solvents. In all cases a high yield of monosubstituted fluorene was obtained.

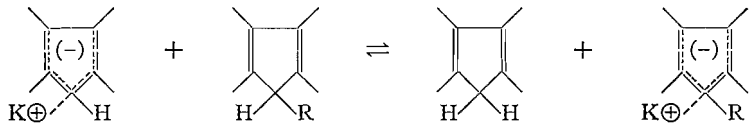
Can. J. Chem. Downloaded from www.nrcresearchpress.com by 210.87.254.42 on 09/05/12
For personal use only.

Can. J. Chem. Downloaded from www.nrcresearchpress.com by 210.87.254.42 on 09/05/12
For personal use only.

DISCUSSION

The results of the reaction of 9-fluorenyl-lithium, -sodium, or -potassium can be rationalized on the basis of (*a*) the insolubility of the organometallic compound in hydrocarbons such as hexane, but solubility, though limited in some cases, in ethers, (*b*) the relative electropositive nature of the three metals thus giving rise to both the ionic character and reactivity of the carbon–metal bond in fluorene in the order K—C > Na—C > Li—C, (*c*) the acidic properties of fluorene and C_9-monosubstituted fluorenes.

In non-polar and non-ionizing solvents such as hexane, all three alkali metal salts possess closely associated cations and anions having a considerable amount of covalent character in the metal–carbon bond. The degree of covalency is expected to be in the order Li > Na > K. The reaction of the organic halide (RX) in hexane occurs by attack at the surface of the insoluble and suspended solid. The more polar C—K bond should react with the organic halide more quickly than does the C—Li bond. The monosubstituted fluorene, as soon as it is formed, can escape from the surface of the solid into solution. However, if the newly formed 9-monosubstituted fluorene possesses an acidic hydrogen, there will occur on the surface of the solid a reaction such as shown in A



A

between this product and more of the salt, the extent of which depends upon the acidity of the monosubstituted fluorene. This would lead to disubstitution after further reaction with the alkyl halide. Since little or no disubstitution occurred in the reaction of 9-fluorenyl-lithium, and very little 9,9-disubstituted fluorene was formed when the potassium and sodium analogues reacted with alkyl or aralkyl halides in hexane or heptane, it is apparent that the polar halide was absorbed from the solution and reacted with the organometallic compound much more readily than did the 9-monoalkylated fluorene which escaped into solution before it reacted further. The small amount of disubstituted fluorene actually observed in the case of the potassium salt in hexane arose no doubt from a scheme such as that suggested in reaction A due to the greater ionic character of the K—C bond.

The electron-donor properties of ethers, however, causes some of the salt to be soluble in some cases (e.g. dioxane) while most or all of the alkali metal compound is dissolved in others (e.g. DME). In solution, because of this association of the ether and the organometallic compound (3), the ionic character of the metal–carbon bond is increased—more so for the more electropositive metals potassium and sodium than for the lithium. Reaction in solution between the salt and the organic halide therefore is expected to, and actually did, occur more rapidly. The newly formed 9-monosubstituted compound, which is also in solution, is thus able to set up an equilibrium similar to that shown in A but involving the solvated organometallic compound and that portion of the 9-fluorenyl metal as yet unreacted. The 9-alkyl-9-fluorenyl-potassium (-sodium or -lithium) can then react with a second molecule of the organic halide to give the disubstituted fluorene. Thus, there is produced one molecule of unchanged fluorene for every molecule of disubstituted fluorene. In all our experiments, there has been no case where more disubstituted than unsubstituted product has been produced, in agreement with the reaction

shown in A. The position of equilibrium will then depend upon the relative acidities of the fluorene and monosubstituted fluorene and upon the rapidity with which the organic halide reacts with the monometalated fluorene. The assumption that disubstitution is obtained via the above equilibrium occurring primarily *in solution* is supported by the greater extent of disubstitution actually found in solvents wherein almost all, if not all, the organometal was dissolved (Tables III and IV). Since the lithium derivative gave very little disubstitution in any solvent (Table V), even in those wherein it is quite soluble, it is obvious that the extent of ionic character of the carbon–metal bond is an important factor which establishes the degree to which such an equilibrium as portrayed by A can be established in competition with the direct reaction of the monometalated compound with the alkyl halide. Usually alkylation at a carbon atom reduces the acidity while arylation increases the acidity of the remaining hydrogen(s) at the same carbon atom. The greater acidity of 9-phenylfluorene over that of fluorene has been recorded (4, 5), but to our knowledge no report compares the acidity of 9-alkylated fluorenes with that of the parent substance. Since disubstitution was actually observed in this work, especially in the case of the more effective ethers, the acidity of 9-alkylfluorenes should be at least of the same order as, but is more likely greater than, that of the unsubstituted fluorene. The tendency of the C_9-substituent to become coplanar with the planar fluorene molecule would lend stability to the 9-substituted fluorenyl anion. A substituent on C_9 may prefer this coplanar arrangement due to steric factors and thus enhance the acidity of the C_9—H. Furthermore, the acidity of the 9-monoalkylated fluorene must be greater than that of fluorene to compete as successfully as it does with the polar bond in the organic halide for the organometallic compound. That the 9-monoalkylated compound should be more acidic than is fluorene due to steric considerations, is not clearly shown from the results of the reaction of 9-fluorenylpotassium with the halides, methyl iodide, ethyl bromide, allyl bromide, and benzyl chloride in dioxane (Table I) since approximately the same extent of disubstitution occurred in each regardless of the size of the group. This lack of differentiation might be due to the highly reactive and therefore less discriminating, K—C bond. But the results of reaction of the 9-fluorenyllithium and 9-fluorenylsodium with methyl iodide and benzyl chloride do support this point of view. Equimolar mixtures of 9-fluorenylsodium and benzyl chloride gave 16% of the 9,9-disubstituted fluorene while only 10% of the dimethylated fluorene was obtained when the halide was methyl iodide. In the case of 9-fluorenyllithium, although reaction with methyl iodide in hexane gave no detectable disubstituted fluorene, nearly 5% of dibenzylfluorene was obtained from the reaction of the lithium salt with benzyl chloride in hexane. The question of the relationship of the size of the C_9-substituent and the ratio of di- to mono-substituted product obviously requires further study.

There exists the possibility that some, if not all, of the disubstitution might be due to unreacted metal, occluded in the organometallic compound, which would react with the monosubstituted fluorene during the process of the addition of the alkyl halide. A report is to be found in the literature that describes such a highly dispersed state of potassium metal in a solvent so as to render it indiscernible to the eye when the solution is cooled (6). Our rate of stirring certainly would not lead to such an ultrafine state of division of the metal—hence any substantial quantity of it which remained unreacted should be readily seen. In order to determine if the presence of unreacted metal actually does play a part in producing disubstituted fluorene, an experiment was performed in which the reaction between equimolar quantities (0.05 mole) of fluorene and potassium in 50 ml of DME was allowed to proceed for just 15 minutes. To the mixture, containing

Can. J. Chem. Downloaded from www.nrcresearchpress.com by 210.87.254.42 on 09/05/12
For personal use only.

definitely some unreacted potassium, was added 0.05 mole of methyl iodide. By chromatography of the isolated solid on alumina using hexane as eluant, there was obtained 30% dimethylfluorene, 18% monomethylfluorene, and the remainder as unchanged fluorene. Since the experiments in which all the metal had apparently reacted to form 9-fluorenylpotassium gave 35% di- and 30% mono-methylfluorene, the conclusion must therefore be made that in those cases where unreacted metal does remain, the metal does cause dialkylation, somewhat more readily than in those reactions where only 9-fluorenylpotassium is present. This requires that the monomethylfluorene be more acidic than is fluorene. However, in those solutions where complete reaction of the metal with fluorene has occurred, dialkylation would proceed via an exchange such as shown in equation A.

In this connection, attempts to increase above 65% the yields of dialkylated fluorene, from the reaction with alkyl halides of the "9,9-fluorenyldipotassium" reported in the first of this series of articles (1), have met with consistent failure. Further experimentation has shown that the first atom of potassium reacted with fluorene to produce 9-fluorenylpotassium and an equivalent amount of hydrogen. However, treatment of the 9-fluorenylpotassium with a second equivalent of potassium in dioxane evolved *no hydrogen*. The metal, finely dispersed in the precipitated 9-fluorenylpotassium could not be readily perceived as unreacted metal. However, the reaction of two equivalents of potassium metal with one of fluorene in *DME* gave a clear solution of 9-fluorenylpotassium. Under these conditions the second equivalent of potassium remained unreacted and could be clearly seen suspended in the solvent if less vigorous stirring was employed. The existence of this second equivalent of potassium as unreacted metal, which would then react competitively with the alkyl halide and with the monoalkylated product, probably more rapidly with the former than with the latter, would thus account for the inability to produce more than 65% yield of 9,9-dialkylated fluorene (1). If this is so then at least some of the disubstituted fluorenes observed in the present work could arise from direct interaction of the monoalkylated fluorene and the residual metal in those cases of incomplete metalation.

EXPERIMENTAL

The various alkali metal salts of fluorene were prepared essentially according to published procedures (1, 3). For the present experiments a mixture of 0.05 mole of the metal, and 0.05 mole of fluorene in 50 ml of the appropriate refluxing solvent was used. The reaction times for preparation of the organometallic compound depended upon the particular experiment and are listed in the accompanying tables.

The alkyl halide (0.05 mole) was added to the cooled product (22°) slowly in order to avoid uncontrollable reaction. A 1-hour period of stirring at room temperature ensured complete reaction of the salt with the halide. The mixture was then poured into a separatory funnel containing water slightly acidified with dilute hydrochloric acid. The ether layer was separated and then dried over calcium chloride. After removal of the ether, a portion (1 g or less) of the product was passed through an 80 to 200 mesh alumina column, 60 cm × 1 cm, and eluted with pentane or hexane. Identification and estimation of the product in each small fraction (50 to 100 mg) was made by infrared spectroscopy using the absorption bands reported in Table II.

Crude benzylated fluorene was treated repeatedly with small portions of cold ethanol, thus effecting a separation of the soluble fluorene and monobenzylfluorene from the

Can. J. Chem. Downloaded from www.nrcresearchpress.com by 210.87.254.42 on 09/05/12
For personal use only.

sparingly soluble dibenzylated fluorene. Complete separation of fluorene from the monobenzylfluorene was not achieved.

Experiments using the metal amides instead of metals were carried out similarly using the same quantities of reagents.

Greenhow's method (2) for the preparation of 9-fluorenylsodium was not successful in our hands (1). Since the solid material was required in experiments, the reaction of sodium metal and fluorene in DME, DEE, and THF, although quite facile was of no assistance because the salt failed to precipitate. The reaction of equimolar quantities of fluorene and powdered sodamide in refluxing dioxane gave satisfactory results. From deuteration experiments (1) approximately two thirds of the fluorene had metalated when a mixture of 8.3 g of fluorene, 1.95 g of sodamide, and 25 ml of dioxane was refluxed for 4 hours. Longer reaction time increased the extent of metalation. The 9-fluorenylsodium was readily separated from dioxane, but unreacted sodamide was also retained as a contaminant which could not be removed. Hence, the results of all reactions with 9-fluorenylsodium prepared by this method must be considered with this in mind.

ACKNOWLEDGMENTS

The authors wish to thank the National Research Council of Canada for financial assistance throughout the course of this work. One of us (G. S.) thanks the Council for support during the summer months.

REFERENCES

1. G. W. H. SCHERF and R. K. BROWN. Can. J. Chem. **38**, 697 (1960).
2. E. J. GREENHOW, E. N. WHITE, and D. MCNEIL. J. Chem. Soc. 2848 (1951).
3. G. W. H. SCHERF and R. K. BROWN. Can. J. Chem. **38**, 2450 (1960).
4. W. K. MCEWEN. J. Am. Chem. Soc. **58**, 1124 (1936).
5. J. B. CONANT and J. W. WHELAND. J. Am. Chem. Soc. **54**, 1212 (1932).
6. A. A. MORTON. J. Org. Chem. **20**, 984 (1955).

Can. J. Chem. Downloaded from www.nrcresearchpress.com by 210.87.254.42 on 09/05/12
For personal use only.

Can. J. Chem. Downloaded from www.nrcresearchpress.com by 210.87.254.5 on 09/05/12
For personal use only.

THE INTERACTION OF DISILOXANE WITH BORON TRIFLUORIDE AND TRICHLORIDE[1]

M. ONYSZCHUK

ABSTRACT

Disiloxane does not form stable adducts with boron trifluoride and trichloride, but cleavage of an Si—O bond occurs with formation of the corresponding monohalogenosilane and siloxyboron dihalide. Although siloxyboron dichloride is stable at room temperature, siloxyboron difluoride disproportionates into silyl fluoride, boron trifluoride, and boron trioxide. A stepwise mechanism involving four-center cyclic transition states is postulated for the over-all reaction.

Disilthian does not react with boron trifluoride. This indicates that the sulphur atom in the Si—S—Si linkage system has little, if any, electron-donor activity. The absence of electron-donor activity for oxygen and sulphur in Si—O—Si and Si—S—Si linkages is discussed.

In a previous paper (1) it was reported that boron trifluoride and trichloride do not form stable addition compounds with 1,1′-dimethyl-, 1,1′,2,2′-tetramethyl-, or hexamethyl-disiloxane: instead cleavage of an Si—O bond occurs with formation of the methylhalogenosilane and the methylsiloxyboron dihalide:

$$(CH_3SiH_2)_2O + BF_3 = CH_3SiH_2OBF_2 + CH_3SiH_2F.$$

The methylsiloxyboron dihalides are unstable at room temperature, decomposing into the methylhalogenosilane, boron trihalide, and boron trioxide:

$$3CH_3SiH_2OBF_2 = 3CH_3SiH_2F + BF_3 + B_2O_3.$$

Similarly, the interaction of hexamethyldisiloxane with aluminum chloride or bromide produces trimethylsiloxyaluminum dihalides, but these are much more stable than the boron analogues (2). However, the siloxyaluminum dihalides, SiH_3OAlX_2, which result from the reaction of disiloxane with aluminum halides, are non-volatile, presumably polymeric solids, which appear to react with silyl halide forming silylene halide, SiH_2X_2, and silane, especially when a large proportion of aluminum halide is used initially (3).

The experiments described in this paper were made to examine the interaction of disiloxane and disilthian with boron trifluoride and trichloride.

RESULTS AND DISCUSSION

It was not possible to confirm the formation of a 1:1 adduct between disiloxane and boron trifluoride when they were combined at −78°, since Si—O bond cleavage at this temperature produced silyl fluoride and siloxyboron difluoride:

$$(SiH_3)_2O + BF_3 = SiH_3F + SiH_3OBF_2. \quad [1]$$

Siloxyboron difluoride, which was a white solid at −78°, decomposed gradually at higher temperatures into silyl fluoride, boron trifluoride, and boron trioxide, probably according to the equation:

$$3SiH_3OBF_2 = 3SiH_3F + BF_3 + B_2O_3. \quad [2]$$

An infrared spectrum of the decomposition mixture (Fig. 1, Table I), however, suggested

[1]*Manuscript received December 16, 1960.*
Contribution from the University Chemical Laboratory, Cambridge, England, and the Inorganic Chemistry Laboratory, McGill University, Montreal 2, Que.

TABLE I

Infrared absorption bands for silyl halides and siloxyboron dihalides

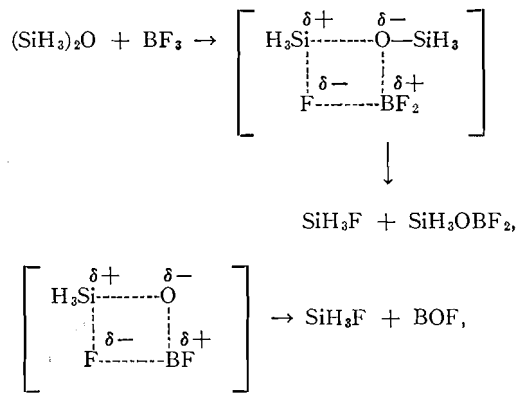
SiH_3F cm^{-1}	SiH_3OBF_2* cm^{-1}	SiH_3Cl cm^{-1}	SiH_3OBCl_2 cm^{-1}	Assignment
2225s 2210s	2200s	2215s 2195s	2210m	ν_{sym}(Si—H) and ν_{asym}(Si—H)
	1500m 1450vs			$\nu_{sym}(^{10}B—F)$ for BF_3 $\nu_{sym}(^{11}B—F)$ for BF_3
	1385m 1375m		1413m 1375s	ν(B—F) for —BF_2 and ν(B—O)
1100†vw	1105w	1100†vw	1100m	ν(Si—O)
1000vs	992s	952vs 940vs	996s 957vs	δ(Si—H)
			900m 885m	ν(B—Cl) for —BCl_2
874m 730m	875m 742m	675m	730w	ν(Si—F) for SiH_3F SiH_3 rock
	720m 692m			$\nu(^{11}B—F)$ for BF_3 $\nu(^{10}B—F)$ for BF_3

s = strong m = medium w = weak v = very

*Decomposition mixture.
†Due to disiloxane impurity.

the presence of siloxyboron difluoride in addition to silyl fluoride and boron trifluoride. Siloxyboron dichloride was much more stable than the difluoride, and a pure sample of the dichloride could be isolated so that its composition was confirmed by analysis.

These results show that cleavage of Si—O bonds in disiloxane by boron trihalides occurs in two stages, each of which probably involves a four-center cyclic transition state similar to those postulated for the interaction of boron trihalides with alkyl ethers (4), alkyldisiloxanes (5), and hexamethyldigermoxane (6). For example, the mechanism for the interaction of disiloxane with boron trifluoride can be represented as follows:



The initial step is thought to produce a 1:1 adduct which is stable only well below −78° and does not dissociate into the original reactants, but decomposes with cleavage of an Si—O bond presumably due to strong polar interactions in the four-center cyclic transition

Can. J. Chem. Downloaded from www.nrcresearchpress.com by 210.87.254.5 on 09/05/12
For personal use only.

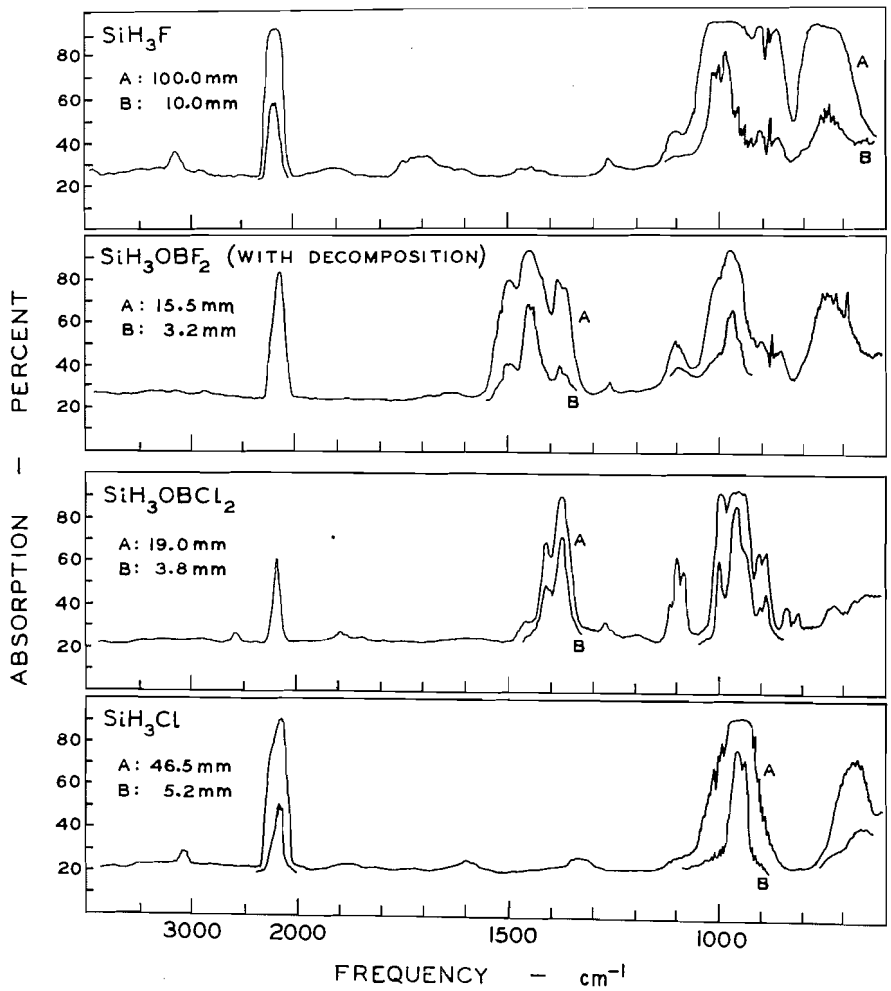


FIG. 1. A comparison of the infrared spectra of siloxyboron dihalides and silyl halides.

state. Probably the instability of siloxyboron difluoride also arises from intramolecular interaction between silicon and fluorine atoms, as indicated in the second step of the mechanism, although intermolecular disproportionation is equally probable. The higher thermal stability of siloxyboron dichloride compared with the difluoride might be attributed to weaker polar interaction between silicon and chlorine than that between silicon and fluorine, since chlorine is less electronegative than fluorine. The fact that boron oxyfluoride, resulting from the decomposition of siloxyboron difluoride, was not isolated is not surprising, because boron oxyfluoride exists as a cyclic trimer only below $-140°$ and disproportionates rapidly at higher temperatures into boron trifluoride and trioxide (7).

The over-all reaction of disiloxane with boron trifluoride at room temperature, which occurs almost quantitatively according to the following stoichiometric equation, provides a new convenient method for the preparation of silyl fluoride in high purity and yield:

$$3(SiH_3)_2O + 2BF_3 = 6SiH_3F + B_2O_3. \quad [3]$$

Can. J. Chem. Downloaded from www.nrcresearchpress.com by 210.87.254.5 on 09/05/12
For personal use only.

Can. J. Chem. Downloaded from www.nrcresearchpress.com by 210.87.254.5 on 09/05/12
For personal use only.

Silyl fluoride was first prepared by Emeléus and Maddock (8) in 79% yield and in only 98% purity from the reaction of silyl chloride with antimony trifluoride. Sujishi and Witz (9) obtained tensiometrically pure silyl fluoride in good yield from the reaction of trisilylamine with boron trifluoride.

The failure of disiloxane to form stable adducts with boron trifluoride and trichloride does not necessarily indicate a complete lack of electron-donor activity of the oxygen atom in disiloxane, since Si—O bond cleavage probably concealed the initial formation of a 1:1 adduct. The electron-donor power of disiloxane cannot be high because d_π–p_π back co-ordination between silicon and oxygen atoms might greatly decrease the availability of the electron pairs at the oxygen atom for donation. This partial double bonding effect is thought to be the reason for the Si—O—Si bond angle being approximately 150° (10, 11), much larger than the tetrahedral angle expected if only σ bonding occurs between silicon and oxygen atoms. Since the Si—O—Si bond angle is definitely not 180°, it seems reasonable to suppose that the lone electron pairs on oxygen are not entirely back-bonded to silicon and therefore should still be available for donation, at least to a detectable degree. Co-ordination probably occurs between disiloxane and boron trifluoride or trichloride, but it is difficult to detect due to simultaneous Si—O bond cleavage. Similarly, iodine does not appear to form an oxonium complex with disiloxane, and only Si—O bond splitting is observed (12). Although Kriner, MacDiarmid, and Evers (3) observed a solid adduct when they combined disiloxane with dimethylaluminum bromide at −50°, the adduct did not dissociate at higher temperatures but decomposed instead, with cleavage of the Si—O—Si linkage. In order to determine precisely the degree of electron-donor activity of disiloxane, it will be necessary to examine its behavior with less polarizable acceptor molecules, which are less likely to cause Si—O bond rupture.

Since disilthian did not undergo any recognizable interaction with boron trifluoride, the sulphur atom in disilthian has little, if any, electron-donor activity. This conclusion is in complete agreement with the previous observation that disilthian does not form co-ordination compounds with silyl iodide, methyl iodide, iodine, mercuric iodide, or mercuric chloride (12). It has been suggested that d_π–p_π bonding between silicon and elements of groups V, VI, and VII is greater the more electronegative the donor atom (13). Accordingly, there should be less d_π–p_π bonding in the Si—S bond than in the Si—O bond, since sulphur is less electronegative than oxygen. This, together with the fact that the sulphur atom is larger than the oxygen atom, suggests that in silyl derivatives the lone electron pairs on sulphur should be more available for donation than those on oxygen. It is surprising, therefore, that disilthian does not form an adduct with boron trifluoride, one of the most powerful electron-acceptor molecules.

The infrared spectrum of the siloxyboron difluoride decomposition mixture (Fig. 1, Table I) shows absorption bands at 1385 and 1105 cm^{-1} in addition to those characteristic of silyl fluoride and boron trifluoride. The band at 1385 cm^{-1} undoubtedly includes the B—O stretching vibration, which occurs in the range 1350–1310 cm^{-1} in a large number of borates, boronates, and boronites (14). The 1385 cm^{-1} band probably also contains the B—F stretching mode of the $—BF_2$ group in SiH_3OBF_2 since this vibration is found at 1363 cm^{-1} in methyldifluoroborane (15). The band at 1105 cm^{-1} in the SiH_3OBF_2 decomposition mixture must be the Si—O stretching frequency in SiH_3OBF_2, because the same vibration occurs at 1106 cm^{-1} in disiloxane (12). These assignments are confirmed by comparison with the spectrum of SiH_3OBCl_2, which shows B—O and Si—O stretching frequencies at 1375 and 1100 cm^{-1} respectively. By analogy with the spectra of alkylphenylchloroboronites in which the B—Cl stretching mode is found between 909 and

893 cm^{-1}, the band with peaks at 900 and 885 cm^{-1} in the spectrum of SiH_3OBCl_2 is attributed to B—Cl stretching vibration of the —BCl_2 group. The spectra of SiH_3F and SiH_3Cl shown in Fig. 1 are essentially the same as those previously reported (16, 17, 18, 19), and they are included here for comparison with the spectra of SiH_3OBCl_2 and the SiH_3OBF_2 decomposition mixture.

EXPERIMENTAL

Apparatus and Methods

A glass high-vacuum apparatus of the conventional type with stopcocks lubricated with Apiezon L grease was used for the transfer, separation, and characterization of volatile substances. Prolonged contact of volatile substances with stopcock grease was avoided by using all-glass reaction vessels (100 ml) fitted with break seals, which could be opened magnetically.

Hydrogen bonded to silicon was determined by measurement of the hydrogen liberated after rapid hydrolysis with potassium hydroxide (30%) of an accurately weighed sample of the unknown. Halide ion in the hydrolyzate was estimated gravimetrically. Boron trioxide was determined by titration, to the phenolphthalein end point, of its aqueous solution with standard alkali in the presence of mannitol.

The infrared spectra of the compounds were recorded in the range 4000–650 cm^{-1} on a Perkin–Elmer model 21 double-beam spectrophotometer equipped with a rock-salt prism. The substances were examined in the vapor phase at measured pressures in a cylindrical cell of 5-cm diameter and 10-cm length fitted with 5-mm-thick sodium chloride end plates.

Materials

Samples of disilthian and silyl iodide were kindly provided by Dr. Allan G. MacDiarmid. Disiloxane was prepared by hydrolysis of silyl iodide and disilthian (12). Commercial grade boron trifluoride and trichloride were purified by fractional distillation in the vacuum apparatus. The purity of each substance was checked immediately before use by measurement of its vapor pressure and molecular weight (M).

Reaction of Disiloxane with Boron Trifluoride

When boron trifluoride (0.0581 g, 0.85 mmole) and disiloxane (0.1010 g, 1.28 mmole) were condensed together and kept at −78° for 12 hours, a white solid and a volatile substance were obtained. The latter was removed by distillation at −78° and then it was redistilled at −132°. The component volatile at −132° was silyl fluoride (0.0378 g, 1.44 mmole. Found: M, 51.2. Calc. for SiH_3F: M, 50.1), and the fraction not volatile at −132° but volatile at −78° was unreacted disiloxane (0.0139 g, 0.18 mmole. Found: M, 78.4. Calc. for $(SiH_3)_2O$: M, 78.0). The yield of silyl fluoride was 12% in excess of that calculated for reaction [1], and this additional silyl fluoride probably resulted from decomposition of some siloxyboron difluoride according to reaction [2].

The white solid product, which remained after removal of volatile products by distillation at −78°, decomposed gradually without melting when warmed to 25°. It gave a white non-volatile residue of boric oxide (0.0166 g) and a volatile fraction. The latter decomposed partially, during the measurement of its molecular weight at 25°, into boric oxide and a volatile component (0.0504 g, found: M, 72.4), which was thought to contain mainly siloxyboron difluoride (calc. M, 95.7) and lesser amounts of silyl fluoride (calc. M, 50.1) and boron trifluoride (calc. M, 67.8). Unfortunately this mixture decomposed

Can. J. Chem. Downloaded from www.nrcresearchpress.com by 210.87.254.5 on 09/05/12
For personal use only.

Can. J. Chem. Downloaded from www.nrcresearchpress.com by 210.87.254.5 on 09/05/12
For personal use only.

further with each trap-to-trap transfer, leaving white deposits of boric oxide in each trap and therefore a pure sample of siloxyboron difluoride could not be isolated. An infrared spectrum of the decomposition mixture (Fig. 1, Table I) confirmed the presence of silyl fluoride and boron trifluoride, and showed Si—O and B—O stretching bands which were attributed to siloxyboron difluoride.

The over-all yield of pure silyl fluoride (0.110 g, 2.18 mmole. Found: M, 50.4; v.p. 121.0 mm at −112°, lit. (9) v.p. 120.0 mm at −112.3°) was 85%, calculated on the amount of boron trifluoride used in the over-all reaction [3].

Reaction of Disiloxane with Boron Trichloride

After 12 hours at −78°, disiloxane (0.1001 g, 1.28 mmole) and boron trichloride (0.1507 g, 1.28 mmole) gave a colorless, transparent solid and a volatile substance. The latter was distilled at −96° and was found to be silyl chloride (0.1142 g, 1.71 mmole. Found: M, 66.9. Calc. for SiH_3Cl: M, 66.6). Since the yield of silyl chloride was 25% in excess of that calculated for the reaction: $(SiH_3)_2O+BCl_3 \rightarrow SiH_3Cl+SiH_3OBCl_2$, it was thought that the additional silyl chloride had been formed by decomposition of some siloxyboron dichloride. The substance which remained after the distillation at −96°, on distillation at −64°, gave a fraction (0.1167 g, found: M, 119; v.p. 24.0 mm at −45.5° and 55.7 mm at −27.5°) which contained mainly siloxyboron dichloride (calc. M, 128.8) and a small amount of silyl chloride (calc. M, 66.6). The residue was non-volatile white flaky boron trioxide (0.0101 g). A pure sample of siloxyboron dichloride was obtained after several distillations at −112° of the fraction with a molecular weight of 119 (0.0505 g, found: M, 130.0; H, as Si–H, 2.31%; Cl, 61.3%. Calc. for SiH_3OBCl_2: M, 128.8; H, as Si—H, 2.35%; Cl, 61.4%).

Attempted Reaction of Disilthian with Boron Trifluoride

There was no reaction between disilthian (0.1281 g, 1.34 mmole) and boron trifluoride (0.0916 g, 1.35 mmole) at −132°, −78°, or 20°, and in each case unchanged reactants were recovered quantitatively by distillation of the mixture at −132°. Because of this negative result, it did not seem practical to investigate the behavior of disilthian with boron trichloride.

ACKNOWLEDGMENTS

I am grateful to Professor H. J. Emeléus for his advice and many helpful discussions while this work was done in his laboratory at Cambridge University. I am indebted to the Royal Commission for the Exhibition of 1851 for the award of an Overseas Scholarship.

REFERENCES

1. H. J. Emeléus and M. Onyszchuk. J. Chem. Soc. 604 (1958).
2. A. H. Cowley, F. Fairbrother, and N. Scott. J. Chem. Soc. 717 (1959).
3. W. A. Kriner, A. G. MacDiarmid, and E. C. Evers. J. Am. Chem. Soc. **80**, 1546 (1958).
4. W. Gerrard and M. F. Lappert. J. Chem. Soc. 2545 (1951).
5. C. Eaborn. Organosilicon compounds. Butterworth Scientific Publications, London. 1960. p. 265.
6. J. E. Griffiths and M. Onyszchuk. Can. J. Chem. **39**, 339 (1961).
7. H. D. Fisher and I. Shapiro. Abstracts of the 138th Meeting, Am. Chem. Soc., Div. Inorg. Chem. 1960. p. 39N.
8. H. J. Emeléus and A. G. Maddock. J. Chem. Soc. 293 (1944).
9. S. Sujishi and S. Witz. J. Am. Chem. Soc. **79**, 2447 (1957).
10. D. C. McKean. Spectrochim. Acta, **13**, 38 (1958).
11. R. F. Curl and K. S. Pitzer. J. Am. Chem. Soc. **80**, 2371 (1958).
12. H. J. Emeléus, A. G. MacDiarmid, and A. G. Maddock. J. Inorg. & Nuclear Chem. **1**, 194 (1955).

13. D. P. CRAIG, A. MACCOLL, R. S. NYHOLM, L. E. ORGEL, and L. E. SUTTON. J. Chem. Soc. 332 (1952).
14. L. J. BELLAMY, W. GERRARD, M. F. LAPPERT, and R. L. WILLIAMS. J. Chem. Soc. 2412 (1958).
15. H. J. BECHER. Z. anorg. Chem. **291**, 151 (1957).
16. F. A. ANDERSEN and B. BAK. Acta Chem. Scand. **8**, 738 (1954).
17. C. NEWMAN, J. K. O'LOANE, S. R. POLO, and M. K. WILSON. J. Chem. Phys. **25**, 855 (1956).
18. J. M. MEAL and M. K. WILSON. J. Chem. Phys. **24**, 385 (1956).
19. D. W. MAYO, H. E. OPITZ, and J. S. PEAKE. J. Chem. Phys. **23**, 1344 (1955).

Can. J. Chem. Downloaded from www.nrcresearchpress.com by 210.87.254.5 on 09/05/12
For personal use only.

Can. J. Chem. Downloaded from www.nrcresearchpress.com by 210.87.254.6 on 09/05/12
For personal use only.

ENZYMIC HYDROLYSIS OF A GLUCOMANNAN FROM JACK PINE (PINUS BANKSIANA LAMB.)[1]

O. PERILA[2] AND C. T. BISHOP

ABSTRACT

A crude glucomannan was isolated from jack pine holocellulose in 17% yield. Repeated delignification and copper complexing of this product provided a purified glucomannan (5% of the holocellulose) containing glucose, mannose, galactose, and xylose in a molar ratio of 10:25:1:1. This polysaccharide was hydrolyzed by a commercial hemicellulase preparation, the cleavage products being removed by continuous dialysis of the reaction mixture. The following oligosaccharides were isolated from the hydrolyzate and identified; yields are based on the glucomannan:

(*a*)	4-*O*-(β-D-mannopyranosyl)-D-mannopyranose	18.5%,
(*b*)	4-*O*-(β-D-glucopyranosyl)-D-mannopyranose	1.4%,
(*c*)	4-*O*-(β-D-mannopyranosyl)-D-glucopyranose	0.7%,
(*d*)	6-*O*-(α-D-xylopyranosyl)-D-glucopyranose	0.5%,
(*e*)	*O*-β-D-mannopyranosyl (1 → 4)-*O*-β-D-mannopyranosyl (1 → 4)-D-mannopyranose	6.5%,
(*f*)	*O*-β-D-mannopyranosyl (1 → 4)-*O*-β-D-glucopyranosyl (1 → 4)-D-glucopyranose	0.7%,
(*g*)	*O*-α-D-xylopyranosyl (1 → 6)-*O*-β-D-glucopyranosyl (1 → 4)-D-glucopyranose	0.1%,
(*h*)	*O*-β-D-mannopyranosyl (1 → 4)-*O*-β-D-mannopyranosyl (1 → 4)-D-glucopyranose	0.04%,
(*i*)	*O*-β-D-glucopyranosyl (1 → 4)-*O*-β-D-mannopyranosyl (1 → 4)-D-mannopyranose	0.03%,
(*j*)	a trisaccharide containing arabinose, glucose, and mannose	0.01%,
(*k*)	a trisaccharide containing two units of arabinose and one of galactose	0.01%.

The constitutions of glucomannans from a variety of softwoods have been studied extensively during the past 10 years and much of this work has been summarized in a review by Aspinall (1). References to later work may be found in some of the more recent papers (2–5). All of these studies have shown that the glucomannans consist basically of β-D-mannose and β-D-glucose residues joined together in a chain by 1 → 4 linkages. Differences between the glucomannans from different woods occur in the presence or absence of small amounts of D-galactose which, when it occurs, has been found as terminal, non-reducing units. There is also some uncertainty about the presence of a slight degree of branching in the main chain of these polysaccharides.

Until recently, every one of the fully defined oligosaccharides obtained by partial acid hydrolysis of glucomannans was found to contain 1 → 4 linkages exclusively (4–10). However, Meier (3) has now reported the isolation of 6-*O*-α-D-galactopyranosyl-D-mannopyranose and this was the first unequivocal evidence of a linkage other than 1 → 4 in a glucomannan. Relative rates of acid hydrolysis of methyl glycopyranosides differ considerably (11) and it may be assumed that various linkages in a polysaccharide are also hydrolyzed at different rates. Oligosaccharides obtained by partial acid hydrolysis of polysaccharides will therefore contain primarily the most stable linkages. Relative rates of hydrolysis of glycosidic linkages by enzymes can be quite different from the rates of hydrolysis by acids because the former are more specific catalysts. Oligosaccharides obtained by enzymic hydrolysis can therefore differ considerably from those obtained by acid hydrolysis of the same polysaccharide and an examination of such products can

[1]*Manuscript received December 28, 1960.*
Contribution from the Division of Applied Biology, National Research Council, Ottawa, Canada. Issued as N.R.C. No. 6205.
[2]*N.R.C. Postdoctorate Fellow 1960.*

yield new information about the linkages in the polymer. It is also possible to obtain higher yields of oligosaccharides through enzymic hydrolysis than acid hydrolysis by using dialysis for continuous removal of partly hydrolyzed fragments before they are degraded further (12).

A previous publication (2) described the gross structural features of a glucomannan from jack pine: this paper reports the isolation and identification of some of the oligosaccharides obtained by enzymic hydrolysis of that polysaccharide.

The crude polysaccharide was obtained in 17% yield from jack pine holocellulose prepared by the chlorine–monoethanolamine method (13). The crude product was purified by alternate delignification and precipitation as its copper complex, this cycle being repeated three times. The resulting polysaccharide (5% of the holocellulose) contained glucose, mannose, galactose, and xylose in a molar ratio of 10:25:1:1. Further precipitations as the copper complex gave products with a lower xylose content but recoveries fell off so sharply that it was difficult to decide whether this was removal of a xylan or simply fractionation of glucomannan molecules to which were attached small and varying amounts of galactose and xylose units. Croon, Lindberg, and Meier (14) have reported that a glucomannan from Scots pine could be freed from galactose- and xylose-containing impurities after further delignification. They believed that different polysaccharides were joined to the same lignin molecule thus preventing their separation prior to delignification. It is unlikely that this could explain the presence of galactose and xylose in the glucomannan used in the present study because the product was delignified three times after its isolation from the holocellulose. The glucomannan isolated from jack pine in the present work differed from that used in the previous study (2) in containing xylose; the molar ratios of the other three monosaccharides were in good agreement. This difference could conceivably be attributed to the two different methods of delignification. Acid chlorite (15) is known to degrade polysaccharides (16) and its use for delignification in the earlier work may have caused hydrolysis of the xylose units. The chlorine–monoethanolamine method (13) causes little degradation (16) and was used here specifically to preserve labile linkages which might then be detected in the products from enzymic hydrolysis.

The enzyme used was a commercially available hemicellulase which undoubtedly contained a variety of enzymes. However, it was lacking in cellulase activity and did not attack the cellophane tubing used for dialysis. Hydrolyses were carried out in dialysis tubing, a technique first developed by Painter (12). The apparatus used in the present work (Fig. 1) permitted stirring of the hydrolysis mixture and continuous removal of the dialyzable products. A purified cellulase (17) did not yield any dialyzable products from the glucomannan and a commercial pectinase yielded only monosaccharides.

Yields of products from hemicellulase hydrolysis of jack pine glucomannan are given in Table I. A mixture of higher oligosaccharides (8.2% of the glucomannan) was also recovered but was not examined further.

The following methods were used, where necessary, to establish identities of the oligosaccharides: total hydrolysis followed by paper chromatography revealed the component monosaccharides; reduction with potassium borohydride (18) followed by hydrolysis and paper chromatography showed which monosaccharide formed the reducing end groups; oxidation by lead tetraacetate and by periodate (19, 20), followed in some cases by reduction, hydrolysis, and paper chromatography (20–22), gave information about specific linkages; partial hydrolysis of trisaccharides yielded disaccharides which were identified by paper chromatography and provided further evidence for the location of linkages; anomeric configurations were based on specific rotations and, for some of the

Can. J. Chem. Downloaded from www.nrcresearchpress.com by 210.87.254.6 on 09/05/12
For personal use only.

TABLE 1

Products from enzymic hydrolysis of jack pine glucomannan

Monosaccharides (39.9%)	
D-Glucose	14.7%
D-Mannose	21.8%
D-Galactose	2.1%
D-Xylose	1.6%
Disaccharides (20.9%)	
(*a*) 4-*O*-(β-D-Mannopyranosyl)-D-mannopyranose	18.5%
(*b*) 4-*O*-(β-D-Glucopyranosyl)-D-mannopyranose	1.4%
(*c*) 4-*O*-(β-D-Mannopyranosyl)-D-glucopyranose	0.7%
(*d*) 6-*O*-(α-D-Xylopyranosyl)-D-glucopyranose	0.5%
Trisaccharides (7.6%)	
(*e*) *O*-β-D-Mannopyranosyl(1 → 4)-*O*-β-D-mannopyranosyl(1 → 4)-D-mannopyranose	6.5%
(*f*) *O*-β-D-Mannopyranosyl(1 → 4)-*O*-β-D-glucopyranosyl(1 → 4)-D-glucopyranose	0.7%
(*g*) *O*-α-D-Xylopyranosyl(1 → 6)-*O*-β-D-glucopyranosyl(1 → 4)-D-glucopyranose	0.1%
(*h*) *O*-β-D-Mannopyranosyl(1 → 4)-*O*-β-D-mannopyranosyl(1 → 4)-D-glucopyranose	0.04%
(*i*) *O*-β-D-Glucopyranosyl(1 → 4)-*O*-β-D-mannopyranosyl(1 → 4)-D-mannopyranose	0.03%
(*j*) A trisaccharide containing arabinose, glucose, and mannose	0.01%
(*k*) A trisaccharide containing two units of arabinose and one of galactose	0.01%

trisaccharides, were inferred from the identities of products of partial hydrolysis with disaccharides of known configuration; methylation and methanolysis yielded methyl-*O*-methyl glycosides which were identified and estimated by gas–liquid partition chromatography (23, 24) giving qualitative and quantitative data on the specific linkages. The latter method was used on a microscale (0.5–2.0 mg) after it was found that methylation by the Kuhn (25) procedure did not require protection of the reducing groups by prior glycosidation. Neither D-glucose or cellobiose, when methylated by this procedure, yielded any acidic products which would have resulted from oxidation of the reducing group by silver oxide. Furthermore, the fully methylated cellobiose yielded equimolar amounts of 2,3,4,6-tetra-*O*-methyl- and 2,3,6-tri-*O*-methyl-D-glucose on methanolysis proving that no oxidation of the reducing group had occurred.

Oligosaccharide (*a*) was isolated in crystalline form having the same physical constants as an authentic sample of 4-*O*-(β-D-mannopyranosyl)-D-mannopyranose. In addition to the crystalline anhydrous product a crystalline monohydrate (m.p. 122–124° C) was isolated which does not appear to have been reported previously.

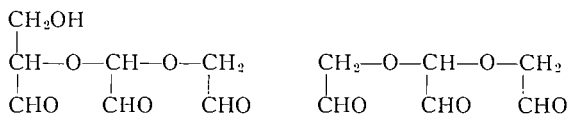
Oligosaccharide (*b*) was also obtained as crystals and had the same physical constants as an authentic sample of 4-*O*-(β-D-glucopyranosyl)-D-mannopyranose. Hydrolysis of the oligosaccharide yielded equal amounts of glucose and mannose while hydrolysis after reduction yielded glucose as the only reducing monosaccharide.

Oligosaccharide (*c*) was obtained as an amorphous product having a specific rotation within the range reported for 4-*O*-(β-D-mannopyranosyl)-D-glucopyranose. The compound was chromatographically pure in five different solvent systems and showed the same rates of movement as an authentic sample of this disaccharide. Hydrolysis yielded equimolar amounts of glucose and mannose; reduction and hydrolysis yielded mannose as the only monosaccharide. Oxidation with lead tetraacetate gave 1.3 moles of carbon dioxide per mole disaccharide with consumption of 3.7 moles of oxidant; calculated values are 1.0 and 4.0 moles/mole respectively. Reduction and hydrolysis of the oxidized product yielded erythritol and glycerol in approximately equal amounts. Methylation and methanolysis of the disaccharide yielded methyl glycosides of 2,3,4,6-tetra-*O*-methyl-D-mannose and 2,3,6-tri-*O*-methyl-D-glucose; the molar ratio of these *O*-methyl ethers was 1:1. Oligosaccharide (*c*) was therefore 4-*O*-(β-D-mannopyranosyl)-D-glucopyranose.

Can. J. Chem. Downloaded from www.nrcresearchpress.com by 210.87.254.6 on 09/05/12
For personal use only.

Can. J. Chem. Downloaded from www.nrcresearchpress.com by 210.87.254.6 on 09/05/12
For personal use only.

Oligosaccharide (*d*) was an amorphous product, chromatographically pure in three different solvent systems. Hydrolysis yielded equal amounts of xylose and glucose; hydrolysis of the reduced disaccharide yielded xylose as the only reducing sugar. Methylation and methanolysis of the disaccharide yielded glycosides of 2,3,4-tri-*O*-methyl-D-xylose and 2,3,4-tri-*O*-methyl-D-glucose, the two compounds being present in a molar ratio of 1:1. This evidence together with the high positive rotation ($[\alpha]_D+70°$) showed that oligosaccharide (*d*) was 6-*O*-(α-D-xylopyranosyl)-D-glucopyranose. Zemplen and Bognar (26) have reported the synthesis of this compound and obtained it in crystalline form, m.p. 200.5–201.5° C, $[\alpha]_D^{20}+150 \rightarrow 121°$ (16 hours in water). The assigned structure for oligosaccharide (*d*) is supported by the fact that when the compound was treated with lead tetraacetate in the presence of potassium acetate, 4.8 moles of oxidant were consumed per mole and 3.5 moles of carbon dioxide were evolved per mole, without the production of formaldehyde. These data eliminate any likelihood that the D-glucose reducing end unit was substituted at position 2, 3, or 4, and correspond to those expected for a $1 \rightarrow 6$ linked xylopyranosyl-glucose containing about 20% of non-oxidizable impurity.* The fact that the compound was extremely hygrosopic may account for the



I II

low oxidation, as well as rotational values.

Oligosaccharide (*e*) was obtained in two crystalline forms having melting points of 166–167° C and 214–216° C. Whistler and Smith (27) have reported the trihydrate of mannotriose as having a melting point of 137–137.5° C. Aspinall *et al.* (28) obtained the same melting point with rapid heating of the sample but noted that slow heating gave a melting point of 166.5–169.5° C and presumed that this was the anhydrous form of the trisaccharide. The lower melting form of oligosaccharide (*e*) did not depress the melting point of an authentic sample of *O*-β-D-mannopyranosyl $(1 \rightarrow 4)$-*O*-β-D-mannopyranosyl $(1 \rightarrow 4)$-D-mannopyranose having a melting point of 166–167° C. Elementary analysis showed that this compound was the monohydrate of the trisaccharide. Recrystallization of this product from hot, absolute ethanol yielded a crystalline compound with a melting point of 214–216° C. Analysis showed that this was the anhydrous form of mannotriose which does not appear to have been reported previously. It is apparent that the $1 \rightarrow 4$-β-linked mannotriose can be isolated as the trihydrate (m.p. 137–137.5° C), the monohydrate (m.p. 166–169° C), or the anhydrous sugar (m.p. 214–215° C). The specific rotation of oligosaccharide (*e*) was within the range of those reported for *O*-β-D-mannopyranosyl$(1 \rightarrow 4)$-*O*-β-D-mannopyranosyl$(1 \rightarrow 4)$-D-mannopyranose and methylation and methanolysis yielded glycosides of 2,3,4,6-tetra-*O*-methyl-D-mannose and 2,3,6-tri-*O*-methyl-D-mannose in a molar ratio of 1:2.

Oligosaccharide (*f*) was an amorphous product, chromatographically pure in five different solvent systems, and yielding on hydrolysis mannose and glucose in a molar

Other structures not inconsistent with these oxidation data are 6-O-(D-xylofuranosyl)-D-glucose and 5-O-(D-xylopyranosyl)-D-glucose. When oxidized by periodate such compounds should yield trialdehyde I (free aldehyde form) having $[\alpha]_D \pm 85°$ to 100° (the sign and value depending on the stereochemistry); however, 6-O-(D-xylopyranosyl)-D-glucose should yield optically inactive trialdehyde II (A. J. Charlson and A. S. Perlin, Can. J. Chem. **34, 1804 (1956)). When oligosaccharide (d) was oxidized with excess periodate the rotation dropped rapidly to a constant value of zero, evidence for formation of II (A. S. Perlin, Private communication).*

Can. J. Chem. Downloaded from www.nrcresearchpress.com by 210.87.254.6 on 09/05/12
For personal use only.

ratio of 1:2. The hydrolyzate of the reduced trisaccharide contained mannose and glucose in a molar ratio of 1:1 showing that the reducing end group in the trisaccharide was a glucose unit. Partial hydrolysis yielded glucose, mannose, and two disaccharides that were chromatographically identical with cellobiose and 4-*O*-(β-D-mannopyranosyl)-D-glucopyranose. Lead tetraacetate oxidation of the trisaccharide yielded 1.0 mole of formic acid and oxidant consumption was 3.7 moles. Assuming oxidation of a pyranosyl non-reducing end and a C_4-substituted reducing end the required values are 1.0 mole of formic acid and 4.0 moles of oxidant consumed. It has been shown that 2,3-trans glycols on the central residues of $1 \rightarrow 4$ linked trisaccharides are not oxidized by lead tetraacetate (29). Reduction and hydrolysis of the oxidation product from oligosaccharide (*f*) yielded glycerol, erythritol, and glucose which arose from the non-reducing unit, the C_4-substituted reducing group, and the central unit respectively of the trisaccharide. Methylation and methanolysis yielded glycosides of 2,3,4,6-tetra-*O*-methyl-D-mannose and 2,3,6-tri-*O*-methyl-D-glucose which were present in a ratio of 1:2. The foregoing results established that oligosaccharide (*f*) was *O*-β-D-mannopyranosyl$(1 \rightarrow 4)$-*O*-β-D-glucopyranosyl $(1 \rightarrow 4)$-D-glucopyranose.

Oligosaccharide (*g*) was isolated as an amorphous product, chromatographically pure in four different solvent systems. A sample crystallized after being kept for several weeks but was too small to permit recrystallization; melting point of the crude product was 147–150° C. Hydrolysis of oligosaccharide (*g*) yielded xylose and glucose in a molar ratio of 1:2 and hydrolysis of the reduced trisaccharide yielded xylose and glucose in a ratio of 1:1. Methylation and methanolysis yielded equimolar amounts of methyl glycosides of 2,3,4-tri-*O*-methyl-D-xylose; 2,3,4-tri-*O*-methyl-D-glucose; and 2,3,6-tri-*O*-methyl-D-glucose. The 2,3,6-tri-*O*-methyl-D-glucose was not present after methylation and methanolysis of the reduced trisaccharide. These results indicated that oligosaccharide (*g*) was *O*-α-D-xylopyranosyl$(1 \rightarrow 6)$-*O*-β-D-glucopyranosyl$(1 \rightarrow 4)$-D-glucopyranose. The anomeric configurations were assumed to be the same as in the other oligosaccharides where these linkages were found; i.e., the xylosyl–glucose $(1 \rightarrow 6)$ linkage was α in oligosaccharide (*d*) because of the high positive rotation and the glucosyl–glucose $(1 \rightarrow 4)$ linkage was β in oligosaccharide (*f*) because cellobiose was obtained on partial hydrolysis.

Oligosaccharide (*h*) was isolated in quantities too small for completely unequivocal identification. Hydrolysis yielded mannose and glucose with the former predominating. Hydrolysis after reduction yielded only mannose. Methylation and methanolysis gave methyl glycosides of 2,3,4,6-tetra-*O*-methyl-D-mannose; 2,3,6-tri-*O*-methyl-D-mannose; and 2,3,6-tri-*O*-methyl-D-glucose. Assuming the anomeric configurations and ring forms to be the same as found previously for these units it appeared that the oligosaccharide was *O*-β-D-mannopyranosyl $(1 \rightarrow 4)$-*O*-β-D-mannopyranosyl $(1 \rightarrow 4)$-D-glucopyranose.

Oligosaccharide (*i*) was also obtained in only small amounts. Hydrolysis yielded mannose and glucose with the former predominating. Methylation and methanolysis yielded glycosides of 2,3,4,6-tetra-*O*-methyl-D-glucose and 2,3,6-tri-*O*-methyl-D-mannose in a molar ratio of 1:2. Making the same assumptions as above this oligosaccharide was *O*-β-D-glucopyranosyl $(1 \rightarrow 4)$-*O*-β-D-mannopyranosyl $(1 \rightarrow 4)$-D-mannopyranose.

Oligosaccharide (*j*) yielded approximately equal amounts of arabinose, glucose, and mannose on hydrolysis and oligosaccharide (*k*) yielded galactose and arabinose in a ratio of 1:2. Both of these oligosaccharides were obtained in quantities too small for further investigation.

With a few notable exceptions the results of enzymic hydrolysis were similar to those

obtained by partial acid hydrolysis of glucomannans. The major products, mannobiose and mannotriose (oligosaccharides *a* and *e*) were obtained in a total yield of 25% from the glucomannan and showed the presence of extensive chains of $1 \rightarrow 4$ linked β-D-mannopyranose units. The significance of the relative amounts of oligosaccharides containing more than one monosaccharide is rather difficult to assess because the enzyme system used for hydrolysis contained enzymes of unknown specificities and reactivities. Oligosaccharides (*b*), (*c*), (*f*), (*h*), and (*i*) each contained β-D-glucose and β-D-mannose units joined by $1 \rightarrow 4$ linkages in various combinations. These results support the premise that the backbone of glucomannans is linear and confirm results found by partial acid hydrolysis (3–10); they also confirm the results of periodate oxidation of the glucomannan from jack pine which showed that there was no branching through C_2 or C_3 of any of the units (2). No cellobiose was found among the disaccharides but two trisaccharides (*f* and *g*) were obtained in which two glucose residues were joined together. The yield of trisaccharide (*f*) was of the same order as the other products of hydrolysis with exception of mannobiose and mannotriose, and indicated that some of the glucose residues in the polysaccharide were present in blocks of two or more units. The enzymic hydrolysis must have enriched these components because the enzyme used did not have any cellulase activity and a purified cellulase (17) of known specificity did not yield any dialyzable products from the polysaccharide.

The significance of oligosaccharides (*j*) and (*k*) is doubtful because the quantities were so small that polysaccharide impurities from the paper chromatograms (30) could contribute to the hydrolysis products.

To our knowledge oligosaccharides (*d*) and (*g*) represent the first evidence of a linkage between xylose and glucose units in wood polysaccharides. It was unlikely that these two oligosaccharides were products of enzymic synthesis or transfer reactions because the yields were as high or higher than other oligosaccharides which contained the $1 \rightarrow 4$ linkage. Also, no oligosaccharides were formed from monosaccharides that were incubated with the enzyme mixture under the same conditions used for the hydrolysis. The possibility seems remote that "transferases", if present, would transfer only xylose units and with glucose as the exclusive acceptor. It would therefore appear that oligosaccharides (*d*) and (*g*) were real hydrolysis products of a polysaccharide, either a xyloglucan or a xyloglucomannan, the presence of which has not been suspected before. A number of publications dealing with glucomannans have reported the presence of xylose in the polysaccharide, the amounts ranging from trace amounts to 3.0% (3, 4, 7–10, 14). This xylose has been ascribed to the presence of small amounts of acidic xylans which occur in those woods and which were not removed completely by the fractionation procedures used. The present work indicates that at least some of the xylose units in these preparations may have been attached to a glucose-containing polysaccharide and this could explain the failure to remove them completely by fractionation. Neither a pure mannan or a pure glucan (other than cellulose) has ever been isolated from wood; the evidence available at the present time indicates that glucomannans in the native state exist as linear molecules composed of glucose and mannose residues and containing small and varying amounts of xylose and galactose units as short side chains. This situation is remarkably similar to the xylans where small and varying amounts of 4-*O*-methyl-D-glucuronic acid and L-arabinose are attached to linear xylan molecules. The separation of "pure" polysaccharides from such mixtures, e.g. a glucomannan from a glucomannan containing 2–3% galactose or xylose, is extremely difficult by present methods.

Can. J. Chem. Downloaded from www.nrcresearchpress.com by 210.87.254.6 on 09/05/12
For personal use only.

Can. J. Chem. Downloaded from www.nrcresearchpress.com by 210.87.254.6 on 09/05/12
For personal use only.

EXPERIMENTAL

Paper chromatograms were run at room temperature (25°±2° C) by the descending method on Whatman No. 1 paper using the following solvent systems (v/v):

(A) butan-1-ol:pyridine:water—6:4:3; 2–3 days for di- and 4–6 days for tri-saccharides;

(B) butan-1-ol:pyridine:benzene:water—5:3:1:3; organic phase, 3–5 days for di- and 6–10 days for tri-saccharides;

(C) propan-1-ol:ethyl acetate:water—7:1:2; 3–5 days for di- and 6–10 days for tri-saccharides;

(D) ethyl acetate:pyridine:water—5:2:5; organic phase, 2–3 days for di- and 4–6 days for tri-saccharides;

(E) ethyl acetate:acetic acid:water—3:1:3; organic phase, 1–2 days for monosaccharides;

(F) ethyl acetate:pyridine:water—8:2:1; 1–2 days for monosaccharides;

(G) ethyl acetate:acetic acid:water—9:2:2; 5–10 days for di- and 10–20 days for tri-saccharides.

Sugars on the chromatograms were detected by aniline hydrogen phthalate (31) or *p*-anisidine hydrochloride (32) spray reagents or by successive dipping in methanolic silver nitrate, ethanolic sodium hydroxide, and aqueous sodium thiosulphate (33). The R_c values cited are migrations of sugars relative to that of cellobiose.

Evaporations were carried out under reduced pressure at 35° C, specific rotations are equilibrium values unless stated otherwise, and melting points are corrected.

Isolation of Glucomannan

Extractive-free jack pine wood was delignified by the chlorine–monoethanolamine procedure to yield holocellulose amounting to 63% of the extractive-free wood. The holocellulose (100 g) was extracted by stirring with 4% aqueous sodium hydroxide (1500 ml) in an atmosphere of nitrogen at 25° C for 24 hours. The residue was filtered and washed with 4% aqueous sodium hydroxide (1500 ml). The extract and washings were discarded. The residue was then extracted with alkaline borate solution (1500 ml) containing 17.5% sodium hydroxide and 4% boric acid (34) under the same conditions used before. The mixture was cooled in ice, filtered, and the residue was washed rapidly with cold, distilled water (1500 ml). Addition of freshly prepared Fehling's solution (250 ml) to the combined extract and washings caused precipitation of a polysaccharide copper complex (35). The precipitate was centrifuged and washed, twice with alkaline borate containing a small amount of Fehling's solution; twice with water containing a small amount of Fehling's solution; and finally twice with water. The copper complex was then dissolved in an ice-cold solution of *N* acetic acid and *N* hydrochloric acid (1:1). The clear solution was poured into an equal volume of ethanol and the precipitated polysaccharide was washed twice with ethanol and twice with water. Yield, determined on an aliquot of the aqueous suspension, was 17% of the holocellulose.

Purification of Glucomannan

Fresh chlorine water (10 g chlorine per liter) was added to the aqueous suspension of the crude glucomannan and the mixture was stirred thoroughly for 5 minutes. Hot 3% ethanolic monoethanolamine was added and the glucomannan was recovered by centrifugation. The precipitate was washed twice with the hot ethanolic monoethanolamine, twice with ethanol, twice with water and dissolved again in alkaline borate from which

it was precipitated as its copper complex by addition of Fehling's solution. The copper complex was washed and the glucomannan was recovered exactly as described above. The delignification and copper complexing were repeated two more times to yield a purified glucomannan, 5% of the holocellulose.

This polysaccharide had $[\alpha]_D^{26} = -25°$ (C, 1.2% in *N* sodium hydroxide) and upon hydrolysis by 30% formic acid in a sealed tube at 97° C for 15 hours yielded glucose, mannose, galactose, and xylose in a molar ratio of 10:25:1:1. The monosaccharides were separated chromatographically in solvent F and were estimated by the colorimetric procedure of Perila and Seppa (36).

Enzymic Hydrolysis of Glucomannan

The glucomannan was suspended in water at a concentration of 1–2% and dialyzed against distilled water through cellophane tubing for 24 hours. Hemicellulase (Nutritional Biochemicals Corporation) was added (10% of the dry weight of glucomannan) and the dialysis tube, closed at one end, was inserted into the large tube (A) of the dialysis apparatus (Fig. 1). The stirrer (B) was placed inside the dialysis tubing, the top of which was then fastened to the stirrer bearing (C), which was clamped in a fixed position. The

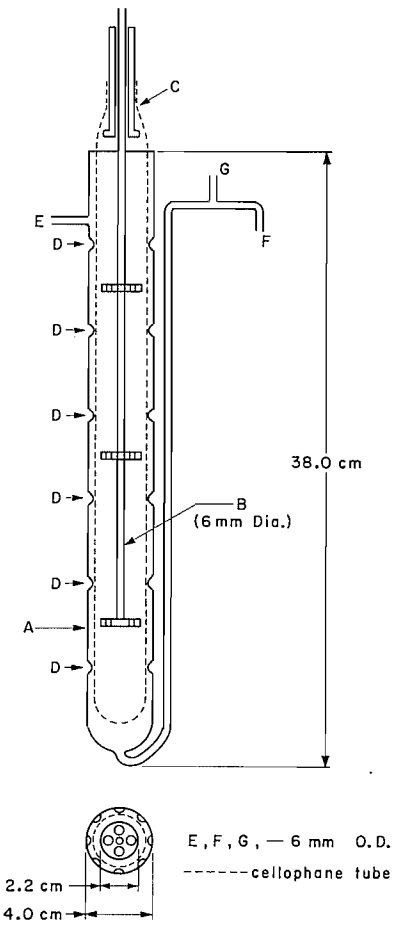


FIG. 1. Apparatus for continuous dialysis of enzymic hydrolyzates of polysaccharides.

Can. J. Chem. Downloaded from www.nrcresearchpress.com by 210.87.254.6 on 09/05/12
For personal use only.

stirrer was fastened to a concentric cam mounted on a stirring motor and of such size that the amplitude of the vertical movement of the stirrer was within the distance between the rings of indentations (D). The indentations served to hold the dialysis tubing away from the walls and permitted the passage of water around the entire surface. Water was introduced at E and collected at F at a rate of 1–2 ml per minute; the opening G prevented siphoning. Hydrolyses were carried out at 35° C, pH 6 without buffer, and were stopped when there was a drop in osmotic pressure within the dialysis tubing (100 hours). The dialyzate was evaporated and dried over anhydrous calcium chloride at 0.03 mm pressure. The yield of dialyzable products was 95±2% of the glucomannan.

Isolation of Oligosaccharides

The mixture of dialyzable products was chromatographed on a column of charcoal: Celite (37) using gradient elution (38) with water to 50% ethanol. The 500 fractions that were collected were examined by paper chromatography (solvent D) and similar fractions were combined to give 15 different fractions. Individual components were isolated from these fractions by chromatography on cellulose columns using butan-1-ol nearly saturated with water and by chromatography on large sheets of Whatman No. 3MM paper using solvents D and C. The isolated oligosaccharides were deionized by Amberlite IR-120 and IR-45, filtered through charcoal, and extracted with ether to remove any oils, fats, or waxes.

Hydrolysis of Oligosaccharides

Samples (ca. 0.5 mg) were heated in sealed tubes with 0.3 *N* hydrochloric acid at 97° C for 4 hours. Hydrolyzates were examined by paper chromatography using solvent E.

Reduction of Oligosaccharides

The oligosaccharide (1–2 mg) in water (0.5 ml) was added slowly to a solution of potassium borohydride (0.05 g) in water (1 ml) and the reaction was kept at room temperature for 18 hours. Amberlite IR-120 ion exchange resin was added until gas evolution ceased. The resin was filtered off, the filtrate was evaporated to dryness, and the residue was evaporated to dryness three times from methanol solution.

Methylation of Oligosaccharides

The oligosaccharide (0.5–2.0 mg) was shaken with methyl iodide (0.2 ml), dimethylformamide (0.2 ml), and silver oxide (0.2 g) at room temperature in the dark for 18 hours (25). The mixture was filtered and the residue was washed with chloroform. The combined filtrate and washings were dried (anhydrous calcium sulphate) and evaporated to dryness under 0.03 mm pressure at room temperature. The methylated oligosaccharides were refluxed in 2% methanolic hydrogen chloride for 20 hours and the resulting methyl glycosides were analyzed by gas–liquid partition chromatography (24). Separations were carried out using the following columns:

(*a*) 10% by weight of methylated hydroxyethylcellulose (39) on acid-washed Celite, 60–80 mesh, at 150° C and 180° C;

(*b*) 10% by weight of butanediol succinate polyester on Chromosorb W, 60–80 mesh, at 150° C;

(*c*) 10% by weight of Apiezon M on alkali-washed Celite, 60–80 mesh, at 150° C;

(*d*) 15% by weight of polyphenyl ether, *m*-bis(*m*-phenoxy-phenoxy)-benzene, on Celite, at 150° C.

The instrument used was a Pye Argon Chromatograph and gas flow rates were ca. 200 ml/min for columns (*a*), (*b*), and (*c*), ca. 100 ml/min for column (*d*). The methyl

Can. J. Chem. Downloaded from www.nrcresearchpress.com by 210.87.254.6 on 09/05/12
For personal use only.

O-methyl glycosides were identified by comparing their retention volumes with those of authentic samples run under the same conditions. The gas–liquid chromatographic behavior of most of the compounds found had been established previously by their isolation from the effluent gas stream (2, 23, 24, 40).

Oxidation of Oligosaccharides

Dr. A. S. Perlin kindly carried out the lead tetraacetate and periodate oxidations on 5–10 mg samples according to methods described previously by him and his colleagues (19, 20, 29).

Monosaccharides

Monosaccharides in the enzymic hydrolyzate were separated from the aqueous eluate of the charcoal column by paper chromatography in solvent E. Estimation (36) of the component sugars gave glucose, mannose, galactose, and xylose in a molar ratio of 10:15:1:1 respectively.

Oligosaccharides

M = mannopyranose; G = glucopyranose; X = xylopyranose.

Oligosaccharide (a) (M1 $\xrightarrow{\beta}$ 4M)

This component was eluted from the charcoal column by 0–5% ethanol. It was chromatographically identical with 4-*O*-(β-D-mannopyranosyl)-D-mannopyranose and had the following R_c values: solvent A, 1.0; B, 1.1; C, 1.2; D, 1.0; and G, 1.25. Crystallized from ethanol containing a little water the compound had a melting point of 122–124° C. Anal. Calc. for $C_{12}H_{22}O_{11}.H_2O$: C, 40.00%; H, 6.72%. Found: C, 40.32%; H, 6.82%. Crystallized from cold methanol the compound had a melting point of 190–191° C, undepressed by admixture with authentic mannobiose, $[\alpha]_D^{25} = -8.5°$ (*c*, 1.3% in water). Reported values are melting points within the range 193–210° C (4, 5, 8–10, 27, 28) and specific rotations from −5° to −9° (4, 5, 8–10, 28).

Oligosaccharide (b) (G1 $\xrightarrow{\beta}$ 4M)

This component was eluted from charcoal by 5–10% ethanol and was chromatographically identical with an authentic sample of 4-*O*-(β-D-glucopyranosyl)-D-mannopyranose. R_c values in different solvents were: A, 1.15; B, 1.25; C, 1.3; D, 1.2; and G, 1.6. Crystallized from methanol it had a melting point and mixed melting point of 133–135° C, $[\alpha]_D^{25} = +5.5°$ (*c*, 1.9% in water). Reported values (4, 5, 8–10) are for melting points within the range 133–139° C and specific rotations from +5° to +16°.

Oligosaccharide (c) (M1 $\xrightarrow{\beta}$ 4G)

This compound was eluted from charcoal by 0–5% ethanol and was chromatographically identical with an authentic sample of 4-*O*-(β-D-mannopyranosyl)-D-glucopyranose. R_c values in different solvents were: A, 0.8; B, 0.85; C, 0.75; D, 0.7; and G, 0.85. The product could not be crystallized and had $[\alpha]_D^{25} = +12°$ (*c*, 1.0% in water). Reported values range from +5° to +29° (4–10).

Oligosaccharide (d) (X1 $\xrightarrow{\alpha}$ 6G)

This compound was eluted from charcoal by 5–10% ethanol and had the following R_c values in different solvents: A, 1.1; B, 1.15; C, 1.25. The product was extremely hygroscopic but a specific rotation on the crude material showed $[\alpha]_D^{25} = +70°$ (*c*, 0.7% (?) in water; reported (26) for 6-*O*-(α-D-xylopyranosyl)-D-glucopyranose, $[\alpha]_D^{20} = +150° \rightarrow 121°$ (16 hours in water).

Can. J. Chem. Downloaded from www.nrcresearchpress.com by 210.87.254.6 on 09/05/12
For personal use only.

Oligosaccharide (e) (M1 $\xrightarrow{\beta}$ 4 M1 $\xrightarrow{\beta}$ 4M)

This compound was contained in the 5% ethanol eluate from the charcoal column and was chromatographically identical with an authentic sample of *O*-β-D-mannopyranosyl (1 → 4)-*O*-β-D-mannopyranosyl (1 → 4)-D-mannopyranose. R_c values in different solvents were: A, 0.5; B, 0.45; C, 0.5; D, 0.45; and G, 0.3. Crystallized from cold ethanol containing a small amount of water the product had m.p. 166–167° C undepressed by admixture with an authentic specimen. Reported melting points range between 155 and 169° C (4, 5, 8, 10, 28).

Anal. Calc. for $C_{18}H_{32}O_{16}.H_2O$: C, 41.39%; H, 6.58%. Found: C, 41.35%; H, 6.72%. Crystallized from hot ethanol the compound had a melting point of 214–216° C.

Anal. Calc. for $C_{18}H_{32}O_{16}$: C, 42.86%; H, 6.39%. Found: C, 42.71%; H, 6.38%. Specific rotation, calculated for the anhydrous compound, was the same for both forms: $[\alpha]_D^{25} = -23°$ (*c*, 2% in water); reported values range from −15° to −26° (4, 5, 8–10, 27, 28).

Oligosaccharide (f) (M1 $\xrightarrow{\beta}$ 4 G1 $\xrightarrow{\beta}$ 4G)

This component was eluted from the charcoal column by 15% ethanol and had the following R_c values in different solvents: A, 0.4; B, 0.35; C, 0.3; D, 0.25; and G, 0.25. Partial hydrolysis was done with 0.03 *N* oxalic acid for 10 hours at 97° C in a sealed tube. The amorphous compound had $[\alpha]_D^{28} = +9.5°$ (*c*, 1% in water).

Oligosaccharide (g) (X1 $\xrightarrow{\alpha}$ 6 G1 $\xrightarrow{\beta}$ 4G)

This compound was eluted from the charcoal column by 20% ethanol and had the following R_c values in different solvents: A, 0.8; B, 0.7; C, 0.75; and D, 0.5. A small sample crystallized after being kept for several weeks; melting point of the crude product was 147–150° C, $[\alpha]_D^{24} = +150°$ (*c*, 0.2% in water).

Oligosaccharide (h) (M1 $\xrightarrow{\beta}$ 4 M1 $\xrightarrow{\beta}$ 4G)

This compound was contained in the 10% ethanol eluate from the charcoal column and had R_c 0.8 in solvent C.

Oligosaccharide (i) (G1 $\xrightarrow{\beta}$ 4 M1 $\xrightarrow{\beta}$ 4M)

This compound was also in the 10% ethanol eluate and had R_c values in different solvents as follows: A, 0.6; B, 0.5; and C, 0.65.

Oligosaccharides (j) and (k)

These were eluted from charcoal by 5% ethanol and had the following R_c values: oligosaccharide (*j*), A, 0.45; B, 0.4; and C, 0.8; oligosaccharide (*k*), A, 0.40; B, 0.35; and C, 0.8.

Higher Oligosaccharides

Two further fractions were obtained from the charcoal column. One, eluted by 10–25% ethanol, contained mainly tetrasaccharides and amounted to 8.6% of the glucomannan. The other, eluted by 15–30% ethanol was 6% of the glucomannan and contained higher oligosaccharides (penta-, hexa-, hepta-). These two fractions were not examined further at this time.

ACKNOWLEDGMENTS

The authors are very grateful to Mr. F. P. Cooper for carrying out the gas–liquid partition chromatography and to Dr. A. S. Perlin, National Research Council, Prairie Regional Laboratories, Saskatoon, Sask., for performing and interpreting the lead tetraacetate and periodate oxidations. We wish to thank Dr. L. E. Wise, Institute of Paper

Can. J. Chem. Downloaded from www.nrcresearchpress.com by 210.87.254.6 on 09/05/12
For personal use only.

Chemistry, Appleton, Wisconsin; and Dr. T. E. Timell, Pulp and Paper Research Institute, Montreal, Que., for donations of the authentic samples of oligosaccharides. Microanalyses were carried out by Mr. A. E. Castagne.

REFERENCES

1. G. O. ASPINALL. Advances in Carbohydrate Chem. **14**, 429 (1959).
2. C. T. BISHOP and F. P. COOPER. Can. J. Chem. **38**, 793 (1960).
3. H. MEIER. Acta Chem. Scand. **14**, 749 (1960).
4. A. TYMINSKI and T. E. TIMELL. J. Am. Chem. Soc. **82**, 2823 (1960).
5. M. O. GYAW and T. E. TIMELL. Can. J. Chem. **38**, 1957 (1960).
6. A. ANTHIS. Tappi, **39**, 401 (1956).
7. G. O. ASPINALL, R. A. LAIDLAW, and R. B. RASHBROOK. J. Chem. Soc. 4444 (1957).
8. J. K. N. JONES and T. J. PAINTER. J. Chem. Soc. 669 (1957).
9. J. K. HAMILTON and H. W. KIRCHER. J. Am. Chem. Soc. **80**, 4703 (1958).
10. E. MERLER and L. E. WISE. Tappi, **41**, 80 (1958).
11. M. L. WOLFROM and A. THOMPSON. *In* The carbohydrates. *Edited by* W. PIGMAN. Academic Press Inc., New York. 1957. p. 208.
12. T. J. PAINTER. Can. J. Chem. **37**, 497 (1959).
13. P. BLOOM, E. C. JAHN, and L. E. WISE. Paper Trade J. **115**, TS107 (1942).
14. I. CROON, B. LINDBERG, and H. MEIER. Acta Chem. Scand. **13**, 1299 (1959).
15. L. E. WISE, M. MURPHY, and A. A. D'ADDIECO. Paper Trade J. **122**, 35 (1946).
16. T. E. TIMELL and E. C. JAHN. Svensk Papperstidn. **54**, 831 (1951).
17. D. R. WHITAKER. Arch. Biochem. Biophys. **43**, 253 (1953).
18. M. ABDEL-AKHER, J. K. HAMILTON, and F. SMITH. J. Am. Chem. Soc. **73**, 4691 (1951).
19. A. S. PERLIN. Anal. Chem. **27**, 396 (1955).
20. A. J. CHARLSON and A. S. PERLIN. Can. J. Chem. **34**, 1200 (1956).
21. G. JAYME, M. SÄTRE, and S. MARIS. Naturwissenschaften, **29**, 768 (1941).
22. M. ABDEL-AKHER, J. K. HAMILTON, R. MONTGOMERY, and F. SMITH. J. Am. Chem. Soc. **74**, 4970 (1952).
23. A. G. MCINNES, D. H. BALL, F. P. COOPER, and C. T. BISHOP. J. Chromatog. **1**, 556 (1958).
24. C. T. BISHOP and F. P. COOPER. Can. J. Chem. **38**, 388 (1960).
25. R. KUHN, H. TRISCHMANN, and I. LÖW. Angew. Chem. **67**, 32 (1955).
26. G. ZEMPLEN and R. BOGNAR. Ber. **72B**, 1160 (1939).
27. R. L. WHISTLER and C. SMITH. J. Am. Chem. Soc. **74**, 3795 (1952).
28. G. O. ASPINALL, R. B. RASHBROOK, and G. KESSLER. J. Chem. Soc. 215 (1958).
29. A. S. PERLIN and A. R. LANSDOWN. Can. J. Chem. **34**, 451 (1956).
30. G. W. HUFFMAN, P. A. REBERS, D. R. SPRIESTERSBACH, and F. SMITH. Nature, **175**, 990 (1955).
31. S. M. PARTRIDGE. Nature, **164**, 443 (1949).
32. L. HOUGH, J. K. N. JONES, and W. H. WADMAN. J. Chem. Soc. 1702 (1950).
33. W. E. TREVELYAN, D. P. PROCTER, and J. S. HARRISON. Nature, **166**, 444 (1950).
34. J. K. N. JONES, L. E. WISE, and J. P. JAPPE. Tappi, **39**, 139 (1956).
35. E. SALKOWSKI. Ber. **27**, 497 (1894).
36. O. PERILÄ and T. SEPPÄ. Suomen Kemistilehti, B**31**, 383 (1958).
37. R. L. WHISTLER and D. R. DURSO. J. Am. Chem. Soc. **72**, 677 (1950).
38. R. S. ALM, R. J. P. WILLIAMS, and A. TISELIUS. Acta Chem. Scand. **6**, 826 (1952).
39. H. W. KIRCHER. Anal. Chem. **32**, 1103 (1960).
40. C. T. BISHOP, F. BLANK, and P. E. GARDNER. Can. J. Chem. **38**, 869 (1960).

Can. J. Chem. Downloaded from www.nrcresearchpress.com by 210.87.254.6 on 09/05/12
For personal use only.

Can. J. Chem. Downloaded from www.nrcresearchpress.com by 210.87.254.6 on 09/05/12
For personal use only.

A COUNTER FOR MEASUREMENT OF TRITIUM EXCHANGE IN SOLIDS[1]

O. SEPALL,[2] A. R. G. LANG, AND S. G. MASON

ABSTRACT

An apparatus for measuring the exchange of tritium (H^3) between water vapor and solids such as cellulose has been developed which is simpler, less expensive, and more precise than an earlier model.

Both the exchange reaction and the determination of sample tritium activity are performed in a windowless, proportional counter. The background activity in sorbed water on counter surfaces is measured independently of sample activity. Satisfactory reduction of the effect of the electrostatic charge on the sample upon counting rate is achieved by the geometry of the counter.

INTRODUCTION

An exchange of hydrogen usually occurs between water and the hydroxyl groups of other substances, the extent of which can be determined by using tritiated water. The apparatus described in this paper is suitable for the measurement of exchange between water vapor and solid substances such as cellulose and is a much simpler version of a device previously described (1). The measurement consists of (1) exposing the sample to water vapor enriched with tritium, (2) removal of adsorbed water by evacuating, and (3) determination of tritium activity in the sample by a counting technique. The two main difficulties with the method are (1) the measurement of low-energy beta radioactivity from nonconductive solids and (2) elimination from the measurement, of significant background radioactivity from sorbed water on counter surfaces.

Low-energy beta radioactivity is preferably measured with a windowless counter so as to avoid attenuation of the radiation. In such a counter a nonconductive sample such as cellulose can accumulate electrostatic charge which may affect the measurement. The charge is produced by positive ions formed in the counting gas and tends to lower the counting rate by reducing the electric field intensity in the counter. An electrostatic charge was avoided in the earlier model by isolating the sample from the counting chamber by a thin conductive window (1). Bank *et al.* (2) have eliminated the charge by mixing the sample with graphite to render it conductive. The counter described here requires neither conductive window nor modification of the sample; reduction of the charge effect to an acceptable level is achieved by suitable dimensioning of the counter chamber. Windowless flow counters of special design for the detection of tritium in paper chromatograms have been described before (3, 4), but whether electrostatic charges affected counting performance could not be ascertained from the reported results.

The sorption of water on counter surfaces can result in a high contamination background activity which is included in the measurement of activity from the sample. The present counter permits the determination of the background for each measurement, and in this respect possesses a distinct advantage over the previous model (1).

DESCRIPTION

General Description of Apparatus

The apparatus shown schematically in Fig. 1 consists of the methane-filled counter and an arrangement for exposing the samples to tritiated water vapor. The counter is shown

[1]*Manuscript received November 29, 1960.*
Contribution from the Physical Chemistry Division, Pulp and Paper Research Institute of Canada and the Department of Chemistry, McGill University, Montreal, Quebec.
[2]*Holder of a C-I-L Fellowship 1960–61.*

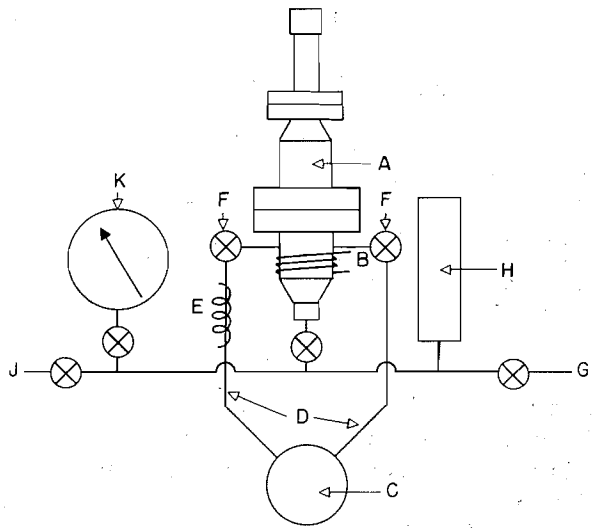


FIG. 1. Schematic drawing of apparatus.
A. Counter (methane-filled)
B. Electrical heater
C. Tritiated water reservoir
D. Copper tube
E. Electrical heater
F. High-vacuum bellows-type valve
G. Vacuum connection
H. Pirani gauge
J. Methane inlet
K. Pressure gauge (0 to 100 mm)

at A with an electrical heater on the lower section at B. The 100-ml Pyrex flask C contains 50 ml of tritiated water (1.5 μc/mg) which is stirred magnetically and is immersed in a water bath at constant temperature. Water vapor enriched with tritium is conducted over the sample through the copper tubes indicated at D. Circulation of vapor is assisted by the convection created by heating one of the tubes electrically at E. The vacuum valves F enable the counter to be isolated from the tritiated water reservoir. At G the apparatus is connected with a vacuum system consisting of a liquid-air trap, a single-stage oil diffusion pump, and a mechanical backing pump. The vacuum in the counter is measured during drying of the sample by the Pirani gauge H. The pressure of the methane gas, which is admitted through line J, is measured by gauge K.

Counter

A vertical section of the counter, which consists almost entirely of commercial fittings, is shown to scale in Fig. 2.

The body E of the counter is a copper bushing, soft soldered to the brass vacuum flanges G and C. Flange G provides access to the counter for inserting samples. Flange C supports the alloy glass insulator B, which carries the high voltage electrode with the 1-mil tungsten collector anode D. At A is shown the standard Amphenol connector for the associated preamplifier. The sample is mounted in holder F and is exposed to tritiated water vapor circulated through tubes H. The counter is evacuated through outlet J and methane counting gas is admitted through inlet K.

The sample holder is supported by two pins fitting into slots cut in the lower vacuum flange and can be rotated on the pins. Figure 3*a* shows the holder assembly in more detail. In the sectional view (A–A) the sample is shown at B, clamped in the steel ring F by the aluminum annulus C. A copper disk D is held centrally in the holder by another

Can. J. Chem. Downloaded from www.nrcresearchpress.com by 210.87.254.6 on 09/05/12
For personal use only.

Can. J. Chem. Downloaded from www.nrcresearchpress.com by 210.87.254.6 on 09/05/12
For personal use only.

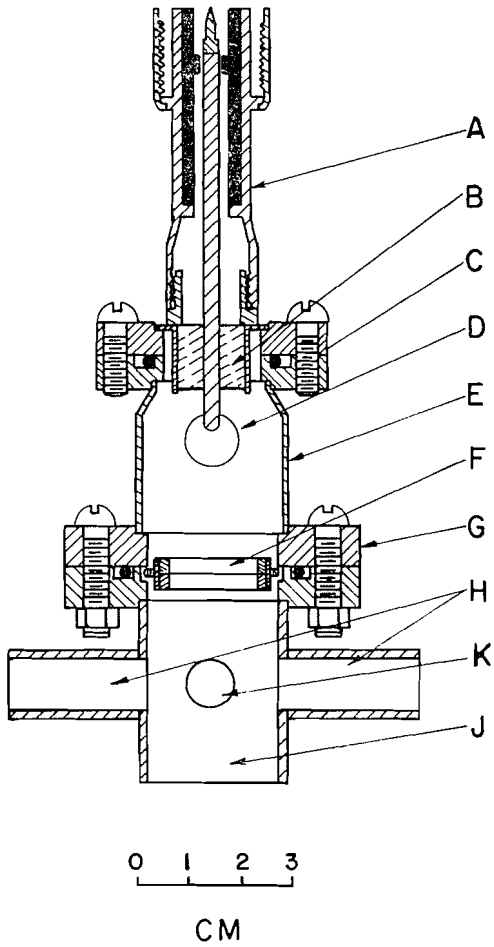


FIG. 2. Sectional view of counter.
A. Amphenol connector
B. Alloy-glass insulator (Stupakoff No. 95.0047)
C. Brass vacuum flange
D. Collector electrode
E. Copper bushing
F. Sample holder
G. Vacuum flange
H. Vapor circulation line
K. Methane inlet
J. Outlet to vacuum system

aluminum annulus G and serves to limit the electric field in the counter to the space above the sample holder.

The holder was positioned in the counter so that the closest distance from collector to copper disk was 20 mm or 74% of the diameter of the counter chamber, to satisfy a geometry requirement discussed later.

The sample is rotated and positioned from outside the counter by a magnetic field which interacts with the steel ring of the sample holder. To turn the sample over, a horseshoe magnet is directed along the axis of rotation of the holder and is rotated close to the counter through 180°. The holder is positioned by the arrangement shown in Fig. 3*b*. The vacuum flange which supports the holder is shown at L. Two iron pins K are soldered in holes drilled through the flange and extend to the inside surface. The pins are so positioned that the air gap between them and the steel ring of the sample holder

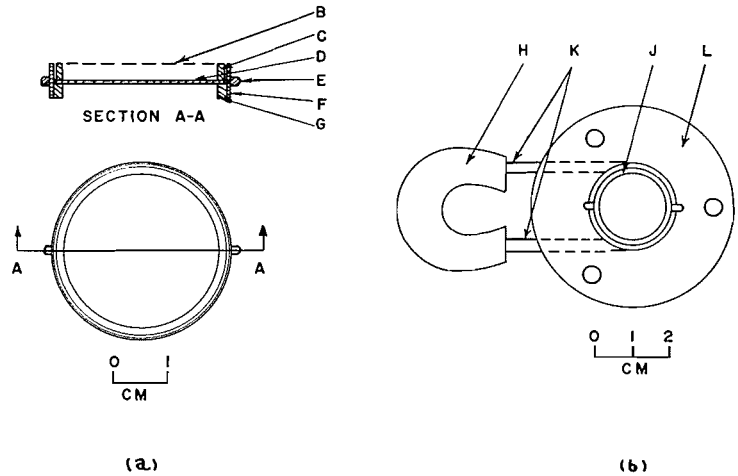


FIG. 3. (*a*) Sample holder.
B. Sample
C. Sample clamping ring
D. Copper disk
E. Supporting pin
F. Outside retaining ring
G. Clamping ring
(*b*) Sample positioning device.
H. Horseshoe magnet
K. Iron pins
J. Sample holder
L. Vacuum flange

is minimal when the holder is in the required position for counting. When the magnet H is placed on the ends of the iron pins, as shown in Fig. 3*b*, the magnetic field causes the sample holder to rotate to the counting position. There are thus two stable positions of the holder which differ by a rotation of 180° and permit the measurement of radioactivity from the sample and from the copper disk.

Experimental Procedure

The use of the apparatus is illustrated by considering the steps in a typical measurement. The sample (e.g. cellophane) was used in sheet form with a superficial density of 3 to 5 mg/cm^2, which corresponded to infinite thickness for beta particles from tritium.

The sample was mounted in the holder (Fig. 3*a*) and the counter assembled and evacuated. Tritiated water vapor was circulated over the sample and the relative humidity was kept constant at a desired value during the treatment. The relative humidity was determined by the sample temperature, which was kept constant by heating the counter, and by the vapor pressure in the vessel, which depended upon the temperature of the tritiated water reservoir. After the desired reaction time the counter was evacuated. It has been shown that the complete removal of water from cellulose requires heating the sample at 70° C at 1 μ Hg for many hours (5). It was possible to use these conditions for drying in the present counter, which could be heated to over 100° C, and thus to avoid the error in previous measurements from extraneous activity in sorbed water in the sample. Tritium activity was measured by counting in methane gas at 90 mm pressure. From the counting rates measured from the sample and from the copper disk, the counting rate for the sample only, was calculated by the following relationship:

$$S = M_s - (0.77 \times M_d)$$

where S is the counting rate for the sample, M_s is the counting rate measured from the sample, and M_d is the counting rate measured from the copper disk. The factor 0.77 was

Can. J. Chem. Downloaded from www.nrcresearchpress.com by 210.87.254.6 on 09/05/12
For personal use only.

determined from measurements of the background counting rate for the sample, which was found to be 77% of the counting rate measured from the copper disk and is discussed later.

GENERAL CONSIDERATIONS

Preliminary Remarks

The counter design was based on the results of preliminary studies of (1) the relationship between counter geometry and the effect of electrostatic charges on the sample upon counting rate, and of (2) the reduction of contamination background activity by the selection of a suitable counter material.

The following consideration of factors contributing to the formation of an electrostatic charge on the sample suggested its reduction by adopting a suitable geometry for the counter. The electrostatic charge is produced by positive gaseous ions which drift from the region of the collector electrode to negatively charged surfaces. Some ions strike the sample, which acquires a charge if it is nonconductive, the magnitude of the charge depending on the flux of ions impinging on the sample. To decrease this flux a greater fraction of ions must be constrained to drift to the metal wall of the counter by intensifying the electric field from collector to wall. The required modification of the electric field is achieved by decreasing the distance from collector to wall or by increasing the distance from collector to sample. The reduction of the flux of ions drifting to the sample is therefore related to a parameter $R = h/d$, where h is the least distance from collector to base at the sample position and d is the diameter of the counter. Larger values of R are associated with a more intense electric field between collector and wall. A brief study of the influence of R on the counting characteristics of a windowless counter with a cellophane source is outlined below.

Effect of Counter Geometry on Counting Performance

Four counters were constructed similar to the design described above and having values of R ranging from 0.16 to 4.6. For the two counters with lower values of R, d was 35 mm, while for the other two, d was 27 mm. The source was prepared by exposing cellophane to tritiated water vapor and drying. Counting rates were measured in methane at 90 mm pressure.

Counting rates measured in the region of the plateau with sources of equal activity are shown in Fig. 4*a* for counters with $R = 0.16$ and 0.37. The steeply rising portions

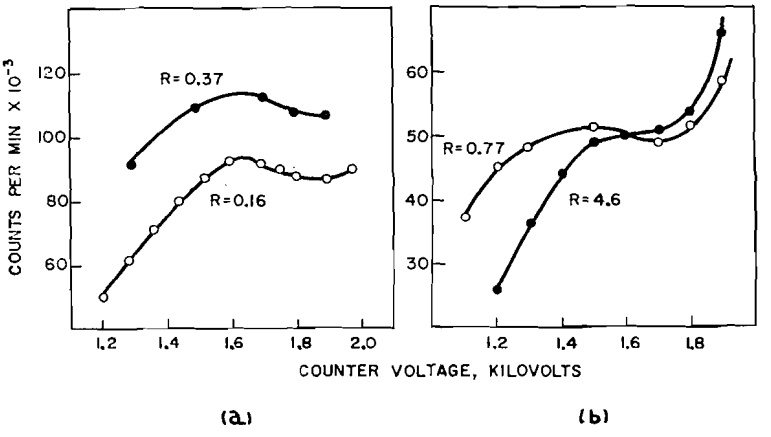


FIG. 4. Effect of R on plateau curves for cellophane sources. Source activities are different for (*a*) and (*b*).

Can. J. Chem. Downloaded from www.nrcresearchpress.com by 210.87.254.6 on 09/05/12
For personal use only.

of the curve at low and high voltages have been omitted in order to use an expanded scale for counting rates and to accentuate the differences from the usual plateau shape. A lower electrostatic charge is indicated on the sample in the counter with higher R by the higher counting rate found at all voltages. The negative slope along part of both curves suggests that a higher counter voltage results in a greater charge on the sample and the reduction of counting rate in the plateau region.

For larger values of R, the counting rates in the plateau region reach a limiting value as shown in Fig. 4*b* by the approximately equal rates measured near counter voltages of 1.55 kv for sources of equal activity and in counters with $R = 0.77$ and 4.6. For the counter with larger R, a negative slope is not found in the shortened plateau region. Although a counter with the larger R would be desirable because of the smaller effect of sample charge, the corresponding greater inside surface area results in increased background activity. The counter with $R = 0.77$ was therefore selected for use.

Counter Material

The influence of counter metal on the level of background activity was estimated by comparing background counting rates in a counter lined with a sheet of each metal. In each case the counter was exposed to tritiated water vapor and evacuated as for the measurement of tritium exchange. The measured counting rates are listed in Table I

TABLE I

Background activity from counter surfaces
$R = 0.37$

Counter material	Counts per minute
Aluminum	15,000
Nickel	57,000
Stainless steel 306	19,000
Copper	7,000

and show copper to be least contaminated of the materials tried, and for this reason was selected.

PERFORMANCE OF COUNTER

Counter Plateau

Plateau curves for the final counter with $R = 0.77$ are shown in Fig. 5 for a benzidine source with tritium incorporated by the method due to Wilzbach (6) and for a tritiated cellophane source prepared by exposing the cellophane to tritiated water and drying. The plateau for the benzidine source has a length of about 400 v and a slope of 4.4%/100 v. The plateau for cellophane appears distorted; it is displaced to higher voltage than the benzidine plateau and has a negative slope presumably because cellophane, unlike benzidine is nonconductive and acquires a residual electrostatic charge. A voltage of 1.5 kv, which corresponded to a counting rate least sensitive to changes in counter voltage, was chosen for measurement of tritium activities in cellophane.

Estimation of Background Activity

To determine the background activity from the counting rate measured from the copper disk, it was necessary to (1) estimate the counting rate resulting from the sample when the sample holder was inverted, and (2) to determine the activity on the copper disk.

Can. J. Chem. Downloaded from www.nrcresearchpress.com by 210.87.254.6 on 09/05/12
For personal use only.

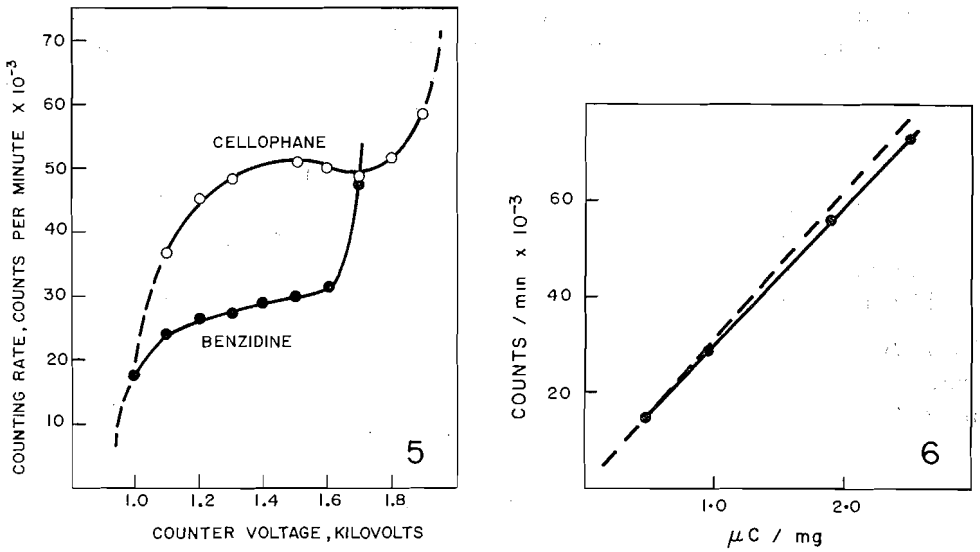


FIG. 5. Plateau curves for counter with $R = 0.77$.
FIG. 6. Sample counting rate vs. specific activity in water.

The transfer of radioactivity through the annular space between holder and counter was estimated by the following experiment. The counting rate from the copper disk was measured with and without a benzidine source of high activity (6×10^5 counts/minute) placed in the inverted sample position. The difference between the two measurements, which was ascribed to transfer of radioactivity to the counter, corresponded to less than 0.05% of source activity and could be neglected. The measured counting rates from sample and from copper disk therefore represented activities for (sample+background) and (copper disk+background), respectively.

To determine the background, a sample of zero activity was used. It was assumed that films of polyethylene, Teflon, and Saran would have no tritium activity after being exposed to tritiated water vapor and drying. Counting rates measured from the films are listed in Table II as percentage of the counting rate from the copper disk. Polyethylene

TABLE II

Ratio of background activity to activity measured with copper disk

Film used for measurement	Ratio %
Polyethylene	77
Teflon	78
Saran	80

was found to be the least contaminated and the value obtained in this case was taken to be the background. For the conditions described, the background count was 20 to 25% of the value for cellophane samples.

Calibration

Since there were indications that the counting rate measured from cellophane was affected by the residual electrostatic charge on the sample, it was desirable to determine

Can. J. Chem. Downloaded from www.nrcresearchpress.com by 210.87.254.6 on 09/05/12
For personal use only.

whether counting rate was proportional to sample activity. It was assumed that the activity of tritium in a cellophane sample, after the exchange reaction and drying, would be proportional to the isotopic concentration in the water vapor. Exchange measurements were conducted with samples of tritiated water ranging in activity from 0.5 to 2.5 μc/mg. The measured counting rates, which are plotted in Fig. 6, were found to vary linearly with specific activity in the water. An increase of specific activity by a factor 2.00 resulted in the increase of counting rate by the factor 1.96 and indicates a small deviation from proportionality between sample activity and counting rate. A correction can be readily applied to measured counting rates to eliminate the error. The dotted line in Fig. 6 shows the ideal relationship where exact proportionality exists between the two quantities.

Reproducibility

Measurements of tritium exchange were repeated with one sample of amylose film and with different samples of cellophane taken from a single sheet and are listed in Table III.

TABLE III

Reproducibility of exchange measurements on cellophane and amylose film

	Counts per minute	
Measurement	Cellophane*	Amylose†
1	43,400	55,650
2	42,100	55,710
3	43,300	55,700
4	43,500	55,400
Mean	43,100	55,620
Range	3.2%	0.54%

*Cellophane samples taken from one sheet.
†Same Amylose film used for each measurement.

The range of 0.54% in the results for amylose is indicative of good precision for the measurement. The greater range of 3.2% found in the measurements on cellophane was probably due to actual differences between samples.

REFERENCES

1. A. R. G. LANG and S. G. MASON. Intern. J. Applied Radiation and Isotopes, **7**, 251 (1960).
2. T. E. BANKS, J. C. CRAWHALL, and D. G. SMYTH. Biochem. J. **64**, 411 (1956).
3. J. M. LOWENSTEIN and P. P. COHEN. Nucleonics, **14**, 98 (1956).
4. A. HARRISON and F. P. W. WINTERINGHAM. Nucleonics, **13** (3), 64 (1955).
5. A. R. G. LANG and S. G. MASON. Can. J. Chem. **37**, 1829 (1959).
6. K. E. WILZBACH. J. Am. Chem. Soc. **79**, 1013 (1957).

Can. J. Chem. Downloaded from www.nrcresearchpress.com by 210.87.254.6 on 09/05/12
For personal use only.

Can. J. Chem. Downloaded from www.nrcresearchpress.com by 210.87.254.42 on 09/05/12
For personal use only.

DÉRIVÉS DU TRIMÉTHYL-1,8,8 BICYCLO[3.2.1]OCTANE

VI. SYNTHÈSE DU (+)-TRIMÉTHYL-5,8,8 BICYCLO[3.2.1]OCTÈNE-2[1]

J. M. BILLY,[2] H. FAVRE ET J. M. LALANCETTE[3]

RÉSUMÉ

Les (+)-triméthyl-5,8,8 amino-2α (et 2β) bicyclo[3.2.1]octanes, le (+)-triméthyl-5,8,8 bicyclo[3.2.1]octène-2 et le (+)-triméthyl-1,8,8 bicyclo[3.2.1]octane exempts d'isomères sont décrits.

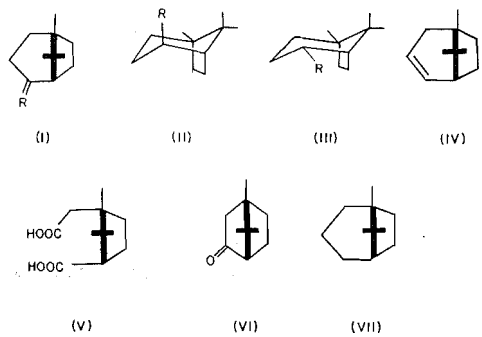
Au cours de l'étude de certaines réactions d'élimination à partir des alcools II et III (R = OH) nous avons eu besoin de triméthyl-5,8,8 bicyclo[3.2.1]octène-2 très pur et de configuration identique à celle du (+)-homoépicamphre I (R = O).[4] Pour obtenir cet hydrocarbure nous avons mis en œuvre la réaction de Tschugaeff et celle d'Hofmann.

L'un et l'autre des xanthogénates II et III (R = OCS_2CH_3), ayant un hydrogène cis par rapport à R en position 3, devaient conduire à l'hydrocarbure IV.[5, 6] Nous avons choisi de préparer et de pyrolyser le xanthogénate issu du triméthyl-5,8,8 bicyclo[3.2.1]-octanol-2α (III, R = OH), parce qu'étant équatorial l'alcool devait s'estérifier facilement. Le xanthogénate de méthyle en question se prépare aisément et sa pyrolyse conduit au (+)-triméthyl-5,8,8 bicyclo[3.2.1]octène-2 (IV) exempt d'isomères et d'une grande pureté stérique. La constitution et la pureté stérique de cet hydrocarbure furent établies par ozonolyse en acide β-homocamphorique (V) et cyclisation du sel de plomb de ce diacide en épicamphre VI, $[\alpha]_D = -57.4°$. Le pouvoir rotatoire de l'épicamphre VI, de configuration absolue identique à celle du (+)-homoépicamphre et du (+)-camphre (5, 6), est de −58°.

L'amine II (R = NH_2) nécessaire à la dégradation d'Hofmann a été préparée à partir de l'oxime de l'homoépicamphre (I, R = =N—OH). En manipulant de grandes quantités de cette oxime, nous avons pu en isoler deux variétés: p.f. 107.5–108.5°, $[\alpha]_D$ +168° et p.f. 104.5–105.5°, $[\alpha]_D = +107.8°$; il pourrait s'agir des isomères syn et anti, car les deux donnent de l'homoépicamphre par hydrolyse. Ainsi se trouve levée toute ambiguité au sujet de la différence entre les points de fusion et les pouvoirs rotatoires de l'oxime de l'homoépicamphre rapportés par Salmon-Legagneur (6) et par notre groupe; l'oxime que nous avons décrite (7) $[\alpha]_D = +125°$, est un mélange des deux isomères.

Dans un mémoire antérieur (1) notre groupe décrivait les alcools secondaires issus de la réduction du (+)-homoépicamphre I (R = O): l'alcool au platine et l'alcool au sodium reçurent respectivement les formules II (R = OH) et III (R = OH). En partant du fait—montré plusieurs fois (8, 9, 10)—que les réductions des cétones et des oximes suivent

[1]*Manuscrit reçu le 14 décembre 1960.*
Contribution du Département de Chimie de l'Université de Montréal, Montréal, Qué. Ce mémoire est tiré du rapport de maîtrise de J.M.L. et de la thèse de doctorat de J.M.B.
[2]*Boursier de l'Office de Recherches Scientifiques de la Province de Québec, 1959–1960. Adresse: Monsanto Canada Ltd., Montréal.*
[3]*Boursier du Conseil National de Recherches du Canada, 1957–1960. Adresse: Université de Sherbrooke, Sherbrooke, Qué.*
[4]*Pour la configuration absolue du (+)-homoépicamphre, voir référence 1.*
[5]*La formation de l'isomère à double liaison sur la tête de pont est interdite (règle de Bredt).*
[6]*Pour le mécanisme d'élimination cis, voir référence 2 et pour des pyrolyses de xanthogénates sans réarrangement de squelette, voir références 2, 3, 4.*



le même cours stérique, nous attribuons la formule II (R = NH_2, axial) à l'amine au platine et la formule III (R = NH_2, équatorial) à l'amine au sodium; fraîchement préparées, ces amines sont des solides; celle au platine est plus dextrogyre que celle au sodium, résultat en accord avec ce que nous avons observé chez les alcools II et III (R = OH) (1); elles sont exemptes d'isomères comme le montre la chromatographie sur papier; elles sont cependant très sensibles à l'air et à l'humidité, ce qui fait que nous n'avons pu obtenir des valeurs analytiques (carbone, hydrogène et azote) satisfaisantes. Les dérivés *p*-nitrobenzoylés sont toutefois stables et facilement cristallisables: ils confirment bien la structure des amines. L'amide issu de l'amine au platine (NH_2, axial) est plus dextrogyre que celui de l'amine au sodium (NH_2, équatorial) ($[\alpha]_D$ +86.4° et +35.1° respectivement), comme c'était le cas pour les *p*-nitrobenzoates issus des alcools correspondants—$[\alpha]_D$ +78.5° (axial) et +24.5° (équatorial) (1).

Haworth, McKenna et Powell (11), puis Gent et McKenna (10) ont montré que les hydroxydes de triméthylammonium quaternaires stéroïdaux (position 3, séries 5α et 5β; position 6, série 5α) ne donnent, par pyrolyse, des hydrocarbures non saturés que s'ils sont axiaux; lorsqu'ils sont équatoriaux les auteurs ont observé une élimination de méthanol avec régénération des diméthylamino-stéroïdes correspondants. McKenna et Slinger (12), dans leur étude de la décomposition des iodures et des hydroxydes de bornyl-, et de néobornyl-, triméthylammonium quaternaires, signalent que seule la pyrolyse des hydroxydes secs conduit au bornène-2 (réaction E_2, sans réarrangement); toute autre forme de traitement augmente la proportion de camphène, de tricyclène et d'amine tertiaire correspondante. À la lumière de ces résultats il était clair qu'il fallait pyrolyser l'hydroxyde d'ammonium quaternaire issu de l'amine axiale: seul le triméthyl-5,8,8 bicyclo[3.2.1]octène-2 était à prévoir.[5]

Nous avons donc préparé l'amine diméthylée II (R = $N(CH_3)_2$) par la méthode à la formaldéhyde/acide formique; il s'est formé au cours de cette opération 49% de cétones, caractérisées par spectroscopie infrarouge; cette formation de cétones est typique pour les amines empêchées (10). La quaternisation a été effectuée par l'iodure de méthyle, à la manière habituelle; l'iodure ainsi obtenu a été transformé en hydroxyde par l'oxyde d'argent; la pyrolyse de cet hydroxyde donne 83% de (+)-triméthyl-5,8,8 bicyclo-[3.2.1]octène-2 (IV) pur, identique à celui obtenu plus haut par la méthode de Tschugaeff.

L'hydrogénation catalytique de l'oléfine IV donne le (+)-triméthyl-1,8,8 bicyclo-[3.2.1]octane (VII), que l'on obtient également par hydrogénolyse du thioacétal I (R = —S—CH_2—CH_2—S—). L'hydrocarbure saturé VII montre de petites variations dans ses propriétés physiques suivant le mode de préparation.

Can. J. Chem. Downloaded from www.nrcresearchpress.com by 210.87.254.42 on 09/05/12
For personal use only.

Can. J. Chem. Downloaded from www.nrcresearchpress.com by 210.87.254.42 on 09/05/12
For personal use only.

PARTIE EXPÉRIMENTALE[7]

1. *Préparation des amines* II *et* III ($R=NH_2$)

1.1. *Oximes du (+)-homoépicamphre*

On chauffe à l'ébullition à reflux: 50 g d'homoépicamphre, 50 g de chlorhydrate d'hydroxylamine, 250 ml d'éthanol et 500 ml d'une solution aqueuse d'hydroxyde de sodium à 2%. Après 10 minutes de reflux, on abandonne à 5°. Les cristaux sont essorés, lavés à l'eau et dissous dans de l'éther. La solution éthérée est lavée avec Na_2CO_3 aqueux 2% et avec de l'eau, séchée sur sulfate de sodium anhydre et évaporée; on recueille 48.5 g d'oxime brute p.f. 103.5–104°, $[\alpha]_D = +137.8°$ ($c = 4.3$; benzène).

En cristallisant cette oxime dans le mélange éthanol–eau on obtient une oxime p.f. 107.5–108.5°, $[\alpha]_D = +168.0°$ ($c = 2.2$; benzène). Calculé pour $C_{11}H_{19}ON$: C, 72.88; H, 10.56; N, 7.73%. Trouvé: C, 72.69; H, 10.44; N, 7.78%. Dans les eaux-mères on recueille, après deux cristallisations dans le mélange éthanol–eau, l'oxime p.f. 104.5–105.5°, $[\alpha]_D = +107.8°$ ($c = 2.5$; benzène). Trouvé: C, 72.70; H, 10.51; N, 7.68%.

Chacune de ces oximes (500 mg), chauffée pendant 4 heures à reflux avec 20 ml d'une solution aqueuse d'acide oxalique à 20%, donne du (+)-homoépicamphre. Les spectres infrarouges des deux oximes sont identiques, quant aux nombres d'onde des bandes; on remarque toutefois de légères différences dans les intensités des bandes situées à 873, 1007 et 1320 cm^{-1}.

1.2. *Triméthyl-5,8,8 amino-2β bicyclo[3.2.1]octane* (II, $R=NH_2$)

Une solution de 40 g d'oxime d'homoépicamphre ($[\alpha]_D^{23} = +137.5°$) dans 250 ml d'acide acétique glacial fraîchement distillé est agitée en atmosphère d'hydrogène, à pression ordinaire, en présence de 900 mg d'oxyde de platine. Au bout de 18 heures, on filtre et neutralise le filtrat par NaOH aqueux 20%. On épuise par de l'éther, extrait la solution éthérée par HCl aqueux 5%; on neutralise la solution aqueuse et extrait par de l'éther; on lave la couche éthérée jusqu'à neutralité, évapore et recueille 33.3 g d'amine brute solide.

Picrate.—Les 33.3 g d'amine brute sont dissous dans 700 ml d'éthanol; à cette solution bouillante on ajoute une solution bouillante d'acide picrique (45.6 g dans 600 ml d'éthanol). Le picrate cristallise lentement: rendement 54.5 g (69%), p.f. 253–254°, $[\alpha]_D = +30.0°$ ($c = 3.54$; DMF). Un échantillon pour l'analyse présente les constantes suivantes, après cristallisation dans le mélange DMF–méthanol 1–30: p.f. 253–254°, $[\alpha]_D = +30.7°$ ($c = 3.6$; DMF). Calculé pour $C_{17}H_{24}O_7N_4$: C, 51.51; H, 6.10; N, 14.13%. Trouvé: C, 51.41; H, 6.31; N, 14.18%. On peut obtenir jusqu'à 90% de picrate $[\alpha]_D = +30.4°$. Le rendement stérique de la réduction est donc supérieur à 90%.

Amine libre.—On traite 11.0 g du picrate par NaOH aqueux 5% (excès 100%). On extrait par de l'éther, lave à l'eau, sèche et évapore l'éther. L'amine fond à 162°, $[\alpha]_D = +61.0°$ ($c = 1.0$; EtOH 95%). Chromatographie ascendante, papier Whatman No. 1, toluène – acide acétique – eau 50–3–47, développement à la ninhydrine: tache rouge, R_f 0.88.

p-Nitrobenzamide.—Préparé par l'action du chlorure de *p*-nitrobenzoyle sur l'amine libre dans du benzène. Fines aiguilles (MeOH–eau), p.f. 125°, $[\alpha]_D^{25} = +86.4°$ ($c = 1.0$;

[7]*Les points de fusion (p.f.) ont été déterminés dans des tubes capillaires, dans un bloc chauffé électriquement et en utilisant un thermomètre étalonné avec les standards du Bureau des Standards de Washington. Les spectres infrarouges ont été mesurés à l'aide d'un spectromètre "Perkin–Elmer", modèle 21, prisme* NaCl. *Les analyses sont de M. W. Manser, Herrliberg, Suisse. Les pouvoirs rotatoires* $[\alpha]_D$ *sont à* $\pm 2°$ *près, température 23–25°. DMF = diméthylformamide.*

$CHCl_3$). Calculé pour $C_{18}H_{24}N_2O_3$: C, 68.33; H, 7.65; N, 8.85%. Trouvé: C, 68.25; H, 7.69; N, 8.92%.

1.3. Triméthyl-5,8,8 amino-2α bicyclo[3.2.1]octane (III, R=NH_2)

À une solution de 24 g d'oxime d'homoépicamphre ($[\alpha]_D^{23}$ = +137.8°) dans 1500 ml d'éthanol anhydre on ajoute 92 g de sodium, en 15 minutes, par portions de 5 g. Après l'addition on chauffe à l'ébullition à reflux pendant 30 minutes. Le tout est refroidi à 25° et dilué par un égal volume d'eau. On épuise par de l'éther et isole, comme en *1.2*, 18 g d'amine brute.

Picrate (voir section 1.2).—Dix-huit grammes d'amine brute dans 50 ml d'éthanol et 25 g d'acide picrique dans 45 ml d'éthanol donnent 30 g de picrate. Après cinq cristallisations dans le mélange DMF–méthanol (1:30) le picrate fond à 263–265° (décomposition), $[\alpha]_D$ = +22.5° (*c* = 2.9; DMF). Calculé pour $C_{17}H_{24}O_7N_4$: C, 51.51; H, 6.10; N, 14.13%. Trouvé: C, 51.42; H, 6.17; N, 14.23%.

Amine libre (voir section 1.2).—Le picrate (13 g) est traité à la manière décrite en *1.2*; l'amine fond à 83–84°, $[\alpha]_D$ = +25.4° (*c* = 1.5; EtOH 95%). R_f 0.79, tache brune (conditions expérimentales, voir section *1.2*).

p-Nitrobenzamide (voir section 1.2).—Fines aiguilles (EtOH–eau), p.f. 188–190°, $[\alpha]_D^{23}$ = +35.1° (*c* = 3.0; $CHCl_3$). Calculé pour $C_{18}H_{24}N_2O_3$: C, 68.33; H, 7.65; N, 8.85%. Trouvé: C, 68.23; H, 7.64; N, 8.78%.

2. Réaction de Tschugaeff

2.1. Triméthyl-5,8,8 bicyclo[3.2.1]octyl-2α xanthogénate de méthyle

Méthode de Tschugaeff (13). Dix grammes de triméthyl-5,8,8 bicyclo[3.2.1]octanol-2 (III, R=OH) (59.4 mmoles) dans 25 g de toluène anhydre sont chauffés à reflux pendant 20 heures avec 1.5 g de sodium (65 mmoles). La solution de l'alcoolate est ensuite décantée dans 100 ml d'éther anhydre et traitée par 5.0 g de sulfure de carbone (66 mmoles). Le xanthogénate de sodium qui précipite immédiatement est essoré et lavé à l'éther; il est repris dans un mélange de 100 ml d'éther et de 20 ml de méthanol et chauffé à reflux pendant 5 heures en présence de 9.6 g d'iodure de méthyle (67.5 mmoles). On lave le mélange réactionnel à l'eau, on sèche la phase éthérée sur sulfate de sodium anhydre et distille l'éther: on recueille 14.8 g de résidu; huile légèrement jaune qui, à froid, abandonne de grosses aiguilles. Le xanthogénate a été recristallisé dans de l'éthanol aqueux jusqu'à indice de rotation constant: p.f. 48.5–49.5°, $[\alpha]_D^{23}$ = +82.2° (*c* = 1.33; benzène), rendement 11.0 g (72%). Calculé pour $C_{13}H_{22}OS_2$: C, 60.39; H, 8.58; S, 24.81%. Trouvé: C, 60.30; H, 8.52; S, 24.97%.

2.2. Pyrolyse du xanthogénate

Sept grammes de xanthogénate (décrit en section *2.1*) sont chauffés à pression ordinaire dans un appareil à sublimation jusqu'à 220° (température du bain d'huile). Le produit de cette pyrolyse est sublimé quatre fois, afin de compléter la décomposition du xanthogénate qui contamine l'hydrocarbure isolé. On retrouve ainsi 2.0 g (49%) d'un solide blanc, $[\alpha]_D$ = +6.9° (*c* = 2.7; chloroforme). Ce composé est repris dans 25 ml d'éther de pétrole, et fixé sur une colonne d'alumine de 60 g préparée dans le même solvant. Une première élution par 150 ml d'éther de pétrole donne 1.75 g de triméthyl-5,8,8 bicyclo-[3.2.1]octène-2 pur (43% de la théorie); il faut l'isoler par distillation lente du solvant sous une colonne de Widmer et évaporation finale sous vide à froid; $[\alpha]_D$ = +7.0° (*c* = 1.8; chloroforme), p.f. 143.5–145° (tube scellé). Spectre infrarouge (nujol): Bande forte à 3030 cm^{-1} (C=C—H); bande faible à 1647 cm^{-1} (double liaison C=C); bande très forte à 710 cm^{-1}; bande forte à 680 cm^{-1}. Calculé pour $C_{11}H_{18}$: C, 87.93; H, 12.08%. Trouvé: C, 87.87; H, 12.09%.

Can. J. Chem. Downloaded from www.nrcresearchpress.com by 210.87.254.42 on 09/05/12
For personal use only.

2.3. Ozonolyse du triméthyl-5,8,8 bicyclo[3.2.1]octène-2

(Adaptation des méthodes (14, 15, 16).) Une solution de 425 mg de l'alcène décrit en section *2.2*, dans 25 ml d'éther de pétrole, est refroidie dans un bain de CO_2 et d'acétone. Un courant d'oxygène de 300 ml par minute contenant 1.2% d'ozone est amené dans la solution; l'ozonide se dépose sous forme de solide blanc amorphe. Après 20 minutes, la couleur bleue qui apparaît indique la fin de la réaction. Le solvant est évaporé à froid par un jet d'air sec et l'ozonide (masse visqueuse) est agité pendant 18 heures en présence de 8 ml d'acide acétique glacial, 8 ml d'éther, 2 ml d'eau et 500 mg de zinc en poudre.

Après l'hydrolyse, le zinc en excès et l'acétate de zinc sont essorés et lavés à l'éther; les produits organiques dans le filtrat sont isolés par addition d'eau et décantation de la phase éthérée. Après séchage sur sulfate de sodium anhydre, l'éther est éliminé par distillation lente sous une colonne de Widmer.

Le résidu aldéhydique de cette évaporation, qui contient un peu d'acide acétique, est repris dans 25 ml d'acétone; 700 mg de permanganate de potassium pulvérisé sont ajoutés à la solution bien agitée, par petites portions, à température ambiante. Après 30 minutes d'agitation, l'excès d'oxydant est détruit par 5 ml d'acide chlorhydrique aqueux 5% et quelques cristaux de bisulfite de sodium. Le bioxyde de manganèse est essoré et lavé à l'éther; l'acide β-homocamphorique brut (454 mg) est isolé du filtrat par deux lavages à la soude caustique aqueuse 5%, acidification (HCl 10%) de cette solution alcaline et réextraction par de l'éther. Après cristallisation dans l'eau on retrouve 327 mg d'acide (54% de rendement qui fond à 244–245°, $[\alpha]_D = +21.5°$ ($c = 1.8$; éthanol 95%). Une seconde recristallisation dans 3 ml de nitrobenzène (rendement de 88%) donne un échantillon d'acide qui apparaît sous la forme de fines aiguilles. P.f. 246–246.5°, $[\alpha]_D = +22.0°$ ($c = 3.1$; éthanol 95%). Calculé pour $C_{11}H_{18}O_4$: C, 61.66; H, 8.47%. Trouvé: C, 61.64; H, 8.41%.

Cet acide ne donne pas de dépression de point de fusion en mélange avec l'acide β-homocamphorique, p.f. 245.5–246.5°, $[\alpha]_D = +22.5°$ ($c = 3.5$; éthanol 95%), obtenu dans ce laboratoire d'après le mode de synthèse de Salmon-Legagneur (6). Cet auteur indique dans son mémoire: $[\alpha]_D^{18} = +27.2°$ ($c = 2.2$; éthanol), p.f. 220–222°.

2.4. Calcination du β-homocamphorate de plomb

Par la méthode de Salmon-Legagneur (6), 514 mg d'acide β-homocamphorique obtenu par ozonolyse en section *2.3* donnent un mélange d'un liquide brun et d'un solide qui est soumis à un entraînement à la vapeur d'eau: 194 mg d'un solide blanc sont entraînés. Ce solide est repris dans 15 ml d'éther de pétrole, fixé sur une colonne d'alumine de 10 g; on élue par 200 ml du même solvant: cette première fraction contient 40 mg d'un solide blanc non étudié. Une seconde élution par 100 ml d'un mélange d'éther éthylique et d'éther de pétrole (1:3) fournit 120 mg d'épicamphre (34% de rendement). Après une sublimation à pression ordinaire à 100° on retrouve 83 mg (23.4%) d'épicamphre, $[\alpha]_D = -55.2°$ ($c = 0.8$; benzène), p.f. 181–183°. Une deuxième sublimation donne un échantillon d'épicamphre; $[\alpha]_D = -57.4°$ ($c = 0.6$; benzène). Le spectre infrarouge (en solution dans CCl_4) montre une bande carbonyle à 1750 cm^{-1}. Salmon-Legagneur (6) donne p.f. 182°, $[\alpha]_D^{23} = -57.5°$ ($c = 3.6$; benzène).

3. Réaction d'Hofmann

3.1. Chlorhydrate de triméthyl-5,8,8 diméthylamino-2β bicyclo[3.2.1]octane
(II, $R = N(CH_3)_2.HCl$)

On dissout 9.64 g (57.6 mmoles) de triméthyl-5,8,8 amino-2β bicyclo[3.2.1]octane (préparé selon section *1.2*) dans 44 ml d'acide formique 98%; on chauffe à reflux pendant 2.5 heures avec 47 ml d'une solution aqueuse de formaldéhyde à 37% et 96 ml d'eau.

Can. J. Chem. Downloaded from www.nrcresearchpress.com by 210.87.254.42 on 09/05/12
For personal use only.

Le mélange réactionnel est ensuite refroidi dans un bain de glace et neutralisé par de la soude caustique aqueuse 10% (400 ml). La solution légèrement alcaline est épuisée deux fois par de l'éther; ces phases éthérées sont réunies et lavées trois fois à l'eau, puis par deux portions de 100 ml d'HCl aqueux à 5%. On obtient ainsi une fraction A (HCl aqueux) et une fraction B (éther).

Étude de la fraction A.—Par évaporation sous vide on recueille 7.036 g de chlorhydrate de triméthyl-5,8,8 diméthylamino-2β bicyclo[3.2.1]octane (II, R=$N(CH_3)_2$.HCl). Après deux recristallisations, (MeOH–éther) on obtient 1.71 g de fines aiguilles blanches, p.f. 267° (décomp.), $[\alpha]_D = +39.2°$ ($c = 2.14$; éthanol 95%). Calculé pour $C_{13}H_{26}NCl$: C, 67.36; H, 11.31; N, 6.05%. Trouvé: C, 67.22; H, 11.22; N, 6.08%.

Étude de la fraction B.—L'éther est lavé avec du carbonate de sodium aqueux à 5%, puis deux fois à l'eau et enfin séché sur sulfate de sodium anhydre. On isole, par distillation de l'éther à travers une colonne de Widmer, 4.757 g d'un solide blanc. Cette fraction neutre, qui montre dans son spectre infrarouge des bandes à 1712 cm^{-1} et 1623 cm^{-1}, n'a pas été étudiée.

3.2. Picrate du triméthyl-5,8,8 diméthylamino-2β bicyclo[3.2.1]octane

La mise en contact d'un échantillon du chlorhydrate de l'amine tertiaire obtenu en section *3.1* avec NaOH aqueux 5% en excès a donné l'amine tertiaire libre (liquide à odeur d'amine). Le picrate de cette base préparé comme en section *1.2* et recristallisé dans un mélange de méthanol et de DMF fondait à 168–169°, $[\alpha]_D = +27.4°$ ($c = 1.81$; DMF). Calculé pour $C_{19}H_{28}O_7N_4$: C, 53.76; H, 6.65; N, 13.20%. Trouvé: C, 53.68; H, 6.58; N, 13.30%.

3.3. Iodure de (triméthyl-5,8,8 bicyclo[3.2.1]octyl-2β) triméthyl ammonium quaternaire

L'amine tertiaire (686 mg; 3.52 mmoles) (isolée du chlorhydrate comme en section *3.2*) est dissoute dans 15 ml d'acétone et abandonnée en présence de 10 ml d'iodure de méthyle à température ambiante pendant 15 heures. L'iodure se dépose à l'état pur en grosses paillettes blanches allongées, p.f. 232° (décomp.), $[\alpha]_D = -16.2°$ ($c = 2.66$; méthanol). Rendement: 861 mg soit 73% de la théorie.

3.4. Triméthyl-5,8,8 bicyclo[3.2.1]octène-2 (IV)

À une solution de 1.00 g (2.95 mmoles) de l'iodure (préparé en section *3.3* ci-dessus) dans 50 ml d'eau on ajoute 1.73 g d'oxyde d'argent fraîchement précipité. Après 24 heures d'agitation à la température de la pièce, le mélange est filtré sur de la terre de diatomées et le filtrat est évaporé sous 11 mm à 60° (température du bain). L'hydroxyde du triméthyl-5,8,8 bicyclo[3.2.1]octyl-2β triméthyl ammonium obtenu de cette évaporation est chauffé à 150° dans un ballon de 200 ml surmonté d'un réfrigérant pendant 30 minutes. L'alcène solide, qui s'est déposé au bas du réfrigérant est repris par de l'éther de pétrole. La phase organique est lavée avec HCl aqueux 2%, avec du carbonate de sodium aqueux à 2% et à l'eau, puis séchée sur sulfate de sodium. La distillation lente du solvant à travers une colonne de Widmer abandonne 367 mg de triméthyl-5,8,8 bicyclo[3.2.1]-octène-2 (83% de rendement).

Une sublimation à 100° à pression ordinaire donne 292 mg d'alcène pur, p.f. 144°, $[\alpha]_D = +7.04°$ ($c = 6.45$; chloroforme). Le spectre infrarouge de cet échantillon est identique à celui du même alcène obtenu en section *2.2*. Calculé pour $C_{11}H_{18}$: C, 87.93; H, 12.08%. Trouvé: C, 87.89; H, 12.14%.

4. (+)-Triméthyl-1,8,8 bicyclo[3.2.1]octane (VII)

4.1. Hydrogénation du triméthyl-5,8,8 bicyclo[3.2.1]octène-2

À 438 mg de triméthyl-5,8,8 bicyclo[3.2.1]octène-2 en solution dans 15 ml d'éthanol

Can. J. Chem. Downloaded from www.nrcresearchpress.com by 210.87.254.42 on 09/05/12
For personal use only.

95% on ajoute 500 mg de nickel de Raney. Après 2 heures d'hydrogénation à pression ordinaire, 77 ml d'hydrogène sont fixés (calculé 74.6 ml; 743 mm, 23°). Le catalyseur est essoré et le produit de réduction précipité du filtrat par addition d'eau. Le triméthyl-1,8,8 bicyclo[3.2.1]octane (VII) est repris par de l'éther de pétrole. L'évaporation du solvant sous une colonne de Widmer (rendement 286 mg) et une sublimation à pression ordinaire, à 100°, conduisent à l'hydrocarbure, p.f. 168.5–169.5° (tube scellé), $[\alpha]_D$ = +20.3° (c = 1.5; chloroforme). Calculé pour $C_{11}H_{20}$: C, 86.67; H, 13.32%. Trouvé: C, 86.65; H, 13.15%.

4.2. Triméthyl-5,8,8 éthylène-thio-acétal-2 bicyclo[3.2.1]octane
(I, R=—S—CH_2—CH_2—S—)

On refroidit à 0° un mélange de 6.5 g (42 mmoles) de (+)-homoépicamphre et de 4.4 g (47 mmoles) d'éthanedithiol dans un ballon de 50 ml. On y fait passer un courant de HCl sec pendant 2 heures. L'excès d'acide chlorhydrique est éliminé en plaçant le ballon dans un dessicateur contenant des pastilles d'hydroxyde de sodium, et dans lequel on maintient une pression de 11 mm. On agite ensuite le mélange avec une solution aqueuse de soude caustique à 2%, on sèche sur sulfate de sodium anhydre et distille. On recueille 8.39 g (rendement de 83%) de thio-acétal p. éb. 125° sous 0.7 mm, n_D = 1.5642. Calculé pour $C_{13}H_{22}S_2$: S, 26.05%. Trouvé: 26.21%.

4.3. Hydrogénolyse du thio-acétal

On chauffe à l'ébullition à reflux une solution de 0.543 g du thio-acétal décrit en section *4.2* dans 35 ml de dioxanne en présence de 15 g de nickel Raney saturé d'hydrogène. Ce catalyseur fut préparé selon les indications de Mozingo *et al.* (17). Temps de chauffage: 12 heures. La réduction terminée, on essore le catalyseur et précipite le triméthyl-1,8,8 bicyclo[3.2.1]octane (VII) du filtrat par addition d'eau. Après essorage et sublimation, cet hydrocarbure présente les constantes suivantes: p.f. 163–164°, $[\alpha]_D$ = +15.5° (c = 2.75; EtOH 95%). Calculé pour $C_{11}H_{20}$: C, 86.67; H, 13.32%. Trouvé: C, 86.76; H, 13.24%.

REMERCIEMENTS

Nous remercions le Conseil National de Recherches du Canada de son aide financière (subvention de recherche, H.F., et bourse d'étude, J.M.L.) et l'Office de Recherches Scientifiques de la Province de Québec d'une bourse d'études, J.M.B. Nous remercions aussi la Maison Ayerst, McKenna et Harrison, Produits Pharmaceutiques, Montréal, de son aide financière.

BIBLIOGRAPHIE

1. H. Favre, M. Lefebvre et J-C. Richer. Can. J. Chem. **37**, 403 (1959).
2. G. L. O'Connor et H. R. Nace. J. Am. Chem. Soc. **74**, 5454 (1952).
3. P. G. Stevens. J. Am. Chem. Soc. **54**, 3732 (1932).
4. W. Fomin et N. Sochanski. Ber. **46**, 244 (1913).
5. J. Bredt et W. H. Perkin, Jr. J. Chem. Soc. 2182 (1913).
6. F. Salmon-Legagneur. Bull. soc. chim. France, **51**, 807 (1932).
7. H. Favre, B. Marinier et J-C. Richer. Can. J. Chem. **34**, 1329 (1956).
8. C. W. Shoppee, D. E. Evans et G. H. R. Summers. J. Chem. Soc. 97 (1957).
9. C. W. Bird et R. C. Cookson. Chem. & Ind. (London), 1479 (1955).
10. B. B. Gent et J. McKenna. J. Chem. Soc. 137 (1959).
11. R. D. Haworth, J. McKenna et R. G. Powell. J. Chem. Soc. 1110 (1953).
12. J. McKenna et J. B. Slinger. J. Chem. Soc. 2759 (1958).
13. L. Tschugaeff. Ber. **32**, 3332 (1899).
14. D. G. M. Diaper. Can. J. Chem. **33**, 1720 (1955).
15. C. R. Noller et R. Adams. J. Am. Chem. Soc. **48**, 1074 (1926).
16. W. F. Symes et C. R. Dawson. J. Am. Chem. Soc. **75**, 4952 (1953).
17. R. Mozingo, D. E. Wolf, S. A. Harris et K. Folkers. J. Am. Chem. Soc. **65**, 1013 (1943).

Can. J. Chem. Downloaded from www.nrcresearchpress.com by 210.87.254.42 on 09/05/12
For personal use only.

Can. J. Chem. Downloaded from www.nrcresearchpress.com by 210.87.254.5 on 09/05/12
For personal use only.

SYNTHESIS OF SYMMETRICAL AND UNSYMMETRICAL DIALKYLPHOSPHINOUS CHLORIDES[1]

J. L. FERRON

ABSTRACT

A series of compounds with the generalized formula RR'PCl have been obtained by the metal (antimony or zinc) reduction of $[RR'PCl_2]^+[AlCl_4]^-$. The yields of symmetrical and unsymmetrical dialkylphosphinous chlorides obtained by this method are superior to those obtained in previous syntheses.

INTRODUCTION

The original synthesis of symmetrical dialkylphosphinous chlorides (R = C_2H_5, *i*-C_3H_7, *i*-C_4H_9) has been the pyrolysis of R_3PCl_2 (1),

$$R_3PCl_2 \xrightarrow{\text{heat}} R_2PCl + RCl.$$

The diethyl analogue has also been obtained in 38% yield by the action of lead tetraethyl upon ethylphosphonous dichloride (2),

$$C_2H_5PCl_2 + (C_2H_5)_4Pb \rightarrow (C_2H_5)_2PCl + (C_2H_5)_3PbCl.$$

The complex resulting from alkyl chlorides, phosphorus trichloride, and aluminum chloride was first prepared by Clay (3) and formulated as

$$RCl + PCl_3 + AlCl_3 \rightarrow [RPCl_3]^+ [AlCl_4]^-.$$

The above complexes have been used in these laboratories for the preparation of alkylphosphonous dichlorides (4). These dichlorides have been obtained in good yield when the aluminum chloride complex is dissolved in a high-boiling electron-donating solvent such as diethyl phthalate (DEP) and reduced with antimony powder. The diethyl phthalate apparently forms a more stable complex with the aluminum chloride and the liberated $RPCl_4$ is then reduced by the antimony powder as follows:

$$[RPCl_3]^+[AlCl_4]^- + DEP \rightarrow [DEP][AlCl_3] + RPCl_4$$

$$3RPCl_4 + 2Sb \rightarrow 3RPCl_2 + 2SbCl_3.$$

Since then Ivin and Karavanov (5) have shown that alkylphosphonous dichlorides react with aluminum chloride in an analogous fashion,

$$RPCl_2 + AlCl_3 + R'Cl \rightarrow [RR'PCl_2][AlCl_4],$$

and it occurred to us that the reduction of this complex might provide a simple and direct route to dialkylphosphinous chlorides. The reduction of a DEP solution of these aluminum chloride complexes by zinc dust at room temperature or by antimony powder at 75–80° C has provided dialkylphosphinous chlorides in yields of 60–73%.

EXPERIMENTAL

Apparatus

The apparatus used is shown in the figure and allows dialkylphosphinous chlorides to be prepared and distilled without coming in contact with air. The 10/30 Standard

[1]*Manuscript received December 19, 1960.*
Contribution from the Chemistry Section, Suffield Experimental Station, Ralston, Alberta. Work carried out under Defence Research Board Project No. D52-20-20-20. This paper constitutes Suffield Technical Paper No. 206.

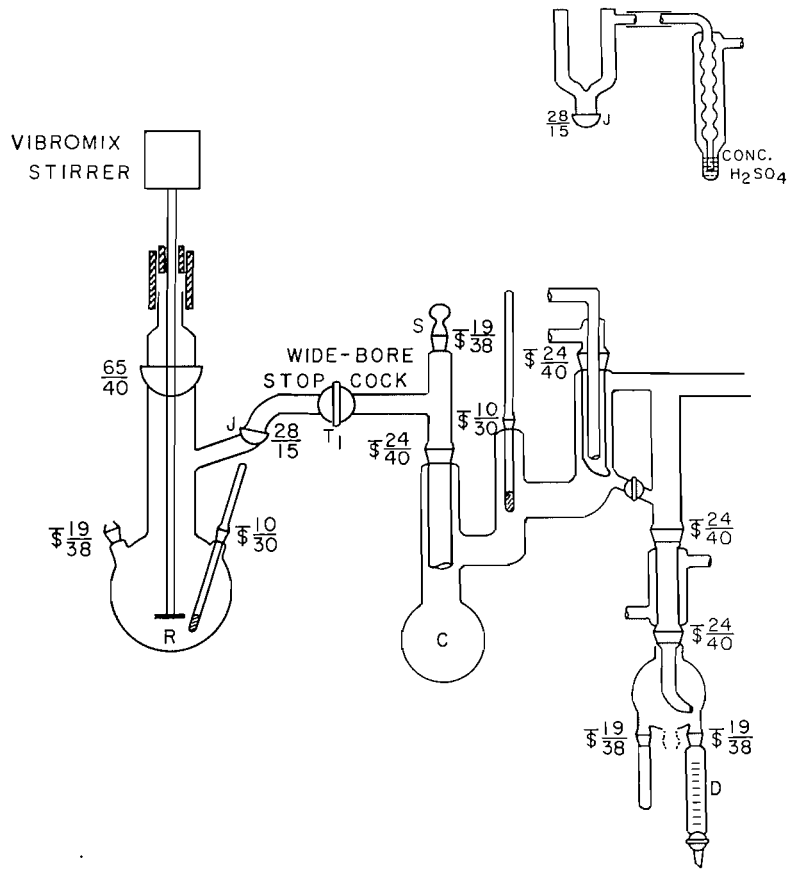


FIG. 1. Apparatus for the preparation of dialkylphosphinous chlorides.

Taper joint carries a thermometer and the 19/38 joint can be used for fitting an inlet tube, a dropping funnel, a bleed for distillations under reduced pressure, or for adding the powdered metal for the reduction. The 28/15 ball joint, J, accommodates the dry ice condenser (upper right of figure) during methyl chloride addition, or a water-cooled condenser during the addition of less volatile alkyl chlorides, as well as the distillation unit shown in the figure. Complexes described under (*a*) and (*b*) were formed in a pressure bottle and transferred into the flask R under a stream of dry N_2; those described under (*c*) and (*d*) were formed at atmospheric pressure directly in the reaction vessel R. All reactions were carried out under a dry N_2 atmosphere.

Reagents

All the reagents were of Reagent Grade and were used as supplied from the manufacturers without further purification. Antimony in lump form was ground in a mortar, pulverized in a ball mill, and sieved through a 250 mesh sieve immediately prior to use.

(*a*) *Preparation of Chloromethyl-methylphosphinous Chloride* $(ClCH_2)(CH_3)PCl$

Aluminum chloride (100 g, 0.75 mole) was weighed directly into a pressure bottle and cooled in a dry ice–acetone mixture. To the cold contents were then added chloromethylphosphonous dichloride (113.8 g, 0.75 mole) and liquid methyl chloride (40 ml,

Can. J. Chem. Downloaded from www.nrcresearchpress.com by 210.87.254.5 on 09/05/12
For personal use only.

Can. J. Chem. Downloaded from www.nrcresearchpress.com by 210.87.254.5 on 09/05/12
For personal use only.

0.80 mole). The bottle was stoppered and left standing at room temperature for 16 hours by which time the mixture had turned solid except for a small liquid layer in the bottom of the container. The contents were then heated at 100–102° C for a further 72 hours. After cooling in dry ice–acetone mixture the bottle was opened, the solid broken into pieces and transferred into the reaction flask R under a stream of dry N_2. Diethyl phthalate (DEP) (500 ml) was then added and violent stirring maintained until the solid had completely dissolved. The solution was then degassed under reduced pressure (water vacuum) while the temperature was gradually raised to 60° C. After the solution was cooled to room temperature, dry N_2 was admitted into the system, a dry ice–acetone cooling mixture placed under the receiver C, the wide-bore isolation stopcock closed, and the system evacuated to 0.1–0.5 mm. Finely powdered antimony (60.9 g, 0.5 mole) was added all at once through a Standard Taper joint, a bleed inserted, and the suspension vigorously stirred. The reaction flask R was rapidly evacuated by opening the wide-bore stopcock. The reduction of the complex by antimony was exothermic and the temperature rose slowly from 33° C to 49° C while the chloromethyl-methylphosphinous chloride distilled over into the distillation flask C. When the evolution of heat had stopped, the temperature of the solution was brought up to 80–85° C with the help of a heating mantle and maintained in that range for ½ hour. After all the dialkylphosphinous chloride had been collected, dry N_2 was admitted into the system, a bleed inserted in place of the stopper S, the isolation stopcock closed, and the product redistilled under reduced pressure, and the main fraction collected in one of the receivers. The yield of $(ClCH_2)(CH_3)PCl$ (b.p. 59° C/9 mm) was 72 g (73%). Most of the dialkylphosphinous chlorides are very reactive and cannot be handled readily in an open atmosphere. Analyses are thus cumbersome to perform and most of the compounds prepared have been identified by the formation of derivatives. $(ClCH_2)(CH_3)PCl$ was reacted with sulphur and the chloromethyl-methylthionophosphonic chloride analyzed. Calculated for $(ClCH_2)(CH_3)P(S)Cl$: C, 14.73%; H, 3.10%. Found: C, 14.84%; H, 3.20%.

(b) Preparation of Dimethylphosphinous Chloride $(CH_3)_2PCl$

This compound was prepared on a 0.75 mole scale by mixing in the cold methylphosphonous dichloride, aluminum chloride, and methyl chloride in a pressure bottle and shaking the mixture at room temperature. The complex formed readily and after transfer of the solid into the flask R and solution in DEP, the reduction by antimony (60.9 g, 0.50 mole) at 85–90° C gave 43.7 g (60%) of dimethylphosphinous chloride (b.p. 72–74° C/697 mm). The oxygen addition compound was analyzed for identification purposes. Calculated for $(CH_3)_2P(O)Cl$: C, 21.35%; H, 5.38%. Found: C, 21.33%; H, 5.33%.

(c) Preparation of Isopropyl-methylphosphinous Chloride $(i\text{-}C_3H_7)(CH_3)PCl$

For this preparation the reaction flask R was fitted with a dropping funnel in the 19/38 Standard Taper joint and the dry-ice condenser on the 28/15 ball joint J. Aluminum chloride (66.7 g, 0.5 mole) was placed in the reaction flask and isopropylphosphonous dichloride (73.0 g, 0.5 mole) was added dropwise while stirring violently. The addition was exothermic and the aluminum chloride dissolved completely. The solution was cooled to room temperature and the dropping funnel replaced by an inlet tube extending below the surface of the liquid. Slow addition of gaseous methyl chloride was started while the temperature of the reaction mixture was kept below 45° C by intermittent immersion of the flask in a cold-water bath. The addition of methyl chloride was stopped after the reaction was completed as evidenced by a fast reflux rate of methyl chloride on the dry ice condenser. The addition was complete in approximately 1½ hours. After

cooling to room temperature, the complex was dissolved in DEP (300 ml), degassed under reduced pressure, and the reduction carried out in the usual way using a theoretical amount of freshly powdered antimony (40.5 g, 0.33 mole). The yield of isopropylmethylphosphinous chloride (b.p. 82–85° C/208 mm) was 44.0 g (65.5%).

(d) Preparation of Diisopropylphosphinous Chloride (i-$C_3H_7)_2PCl$

Aluminum chloride (68.5 g, 0.51 mole) was placed in the flask R and isopropylphosphonous dichloride (74.8 g, 0.52 mole) added dropwise, the temperature being kept below 30° C by occasional immersion in a dry ice–acetone cooling bath. After the aluminum chloride had dissolved, isopropyl chloride (40.5 g, 0.51 mole) was added dropwise maintaining the temperature below 30° C. After about two-thirds of the isopropyl chloride had been added, the reaction mixture became very viscous and stirring became inefficient. The addition of isopropyl chloride was stopped, methylene chloride (50 ml) was added after which the addition of isopropyl chloride was resumed. This addition could be carried out rapidly as no appreciable heat was evolved. Once the addition was completed, the solution was heated to reflux for 1 hour, cooled to room temperature, DEP (300 ml) added with stirring, and the solution degassed in the usual way. After degassing, zinc dust (32 g, 0.51 mole) was added and the suspension heated to 45° C. An exothermic reaction set in, the heating source was removed and the reaction mixture reached a temperature of 78° C. The liquid collected in flask C was then redistilled, giving a yield of 51.2 g (67.2%) of product (b.p. 69° C/697 mm).

ACKNOWLEDGMENTS

The author is indebted to Mr. S. A. Gibbens for his technical assistance on the project, and to Mr. T. Stewart for the microanalytical work.

Thanks are due to the Chairman, Defence Research Board for kind permission to publish these results.

REFERENCES

1. G. M. Kosolapoff. Organophosphorus compounds. John Wiley & Sons, Inc., New York. 1950. pp. 42–51.
2. M. H. Beeby and F. G. Mann. J. Chem. Soc. **172**, 411 (1951).
3. J. P. Clay. J. Org. Chem. **17**, 892 (1952).
4. J. L. Ferron, B. J. Perry, and J. B. Reesor. Nature, **188**, 227 (1960).
5. S. Z. Ivin and K. V. Karavanov. J. Gen. Chem. U.S.S.R. **28**, 2988 (1958).

CORRECTIONS

Volume 39, 1961

Page 844. In line 22, "9 mm" should read "59 mm".
Line 35, which reports analytical data, should be deleted.

Page 845. In line 20, "697 mm" should read "35 mm".

Can. J. Chem. Downloaded from www.nrcresearchpress.com by 210.87.254.5 on 09/05/12
For personal use only.

Can. J. Chem. Downloaded from www.nrcresearchpress.com by 210.87.254.105 on 09/05/12
For personal use only.

HYDROXY FATTY ACID GLYCOSIDES OF SOPHOROSE FROM TORULOPSIS MAGNOLIAE[1]

P. A. J. GORIN, J. F. T. SPENCER, AND A. P. TULLOCH

ABSTRACT

The oil formed during fermentation by a strain of *Torulopsis magnoliae* consisted mainly of partly acetylated 2-*O*-β-D-glucopyranosyl-D-glucopyranose units attached β-glycosidically to 17-L-hydroxyoctadecanoic and 17-L-hydroxy-9-octadecenoic acids.

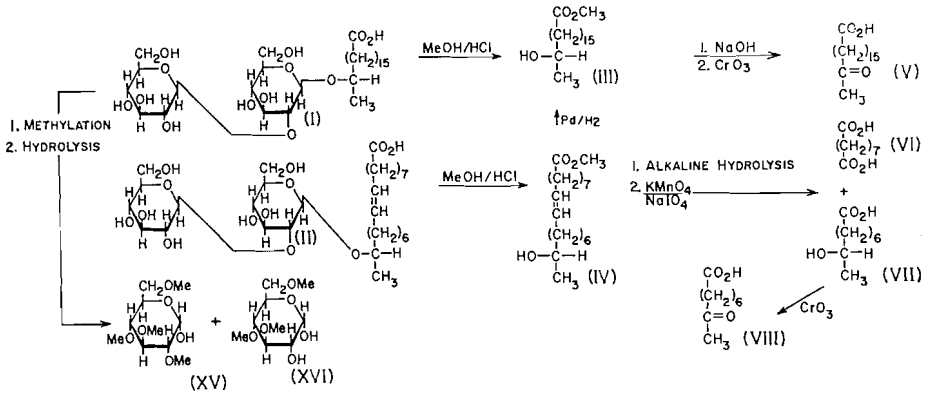
A strain of osmophilic yeast, *Torulopsis magnoliae*, isolated from sow thistle petals, was found to produce (1) an extracellular, heavier than water oil. The main components of the oil are now shown to be glycolipids (I and II) consisting of 2-*O*-β-D-glucopyranosyl-D-glucopyranose units linked β-glycosidically to 17-L-hydroxyoctadecanoic and 17-L-hydroxy-9-octadecenoic acids, the sugar moieties being partly acetylated.

The oil was labile both to acid and alkali. Hot methanolic sodium methoxide removed the acetyl groups, which constituted about 1.5 substituent groups per mole (the positions of these substituents were not determined). The deacetylated product, after fractionation, yielded a solid (I and II),which contained almost equal quantities of lactonic and acidic glycolipids, and it was on this mixture that the characterization studies of the sugar portion were carried out.

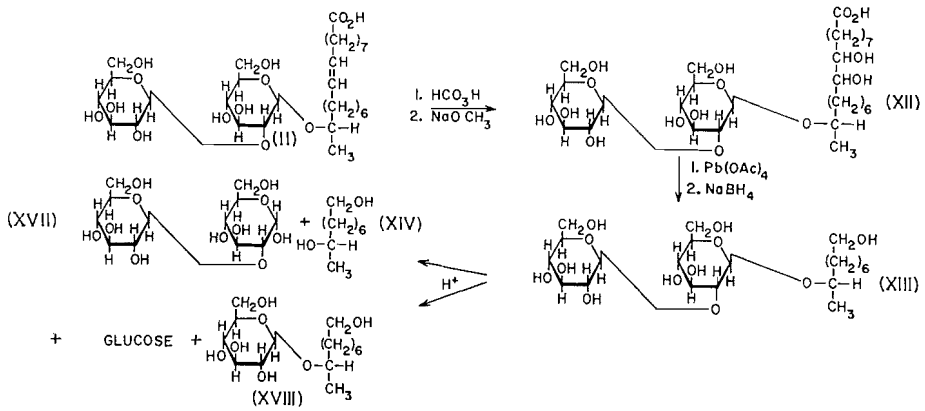
Acid methanolysis of the deacetylated oil yielded 2 moles of methyl-α-D-glucopyranoside and 1 mole of a mixture of fatty acid methyl esters. Gas – liquid phase chromatography of the esters on a silicone column showed one principal peak at the C_{20} saturated position with a shoulder suggesting partial resolution of saturated and unsaturated esters (2). However, on a butanediol succinate column (3) no peaks appeared after 2 hours (normal emergence time for a C_{20} ester was 30 minutes). The properties suggested that the major compounds present were C_{18} esters containing a polar substituent, such as a hydroxyl group (4) and the presence of the latter group was confirmed by infrared spectroscopy. From the quantity of permanganate–periodate reagent (5) consumed, the mixture was shown to contain 65% of monoolefinic ester. Fractional crystallization of the methyl esters also yielded 65% unsaturated and 35% saturated ester. However, later fermentations contained only about 10% of the saturated material. Catalytic hydrogenation showed that the unsaturated C_{18} ester (IV) contained one double bond and the product obtained was identical with the saturated C_{18} component (III). The position of the hydroxyl group in these compounds was shown to be at C_{17}, by the formation of 17-oxostearic acid (V) when the saturated acid was oxidized with chromium trioxide. An authentic specimen of V was synthesized by the method of Bergström *et al.* (6) from 15-bromopentadecanoic acid. The latter was prepared from 15-hydroxypentadecanoic acid which was in turn obtained from the 15,16-dihydroxypalmitic acid described by Lemieux (7).

The unsaturated component (IV) was shown to be 17-hydroxy-9-octadecenoic acid methyl ester since the acid on oxidation with permanganate–periodate (5) yielded azelaic

[1]*Manuscript received December 30, 1960.*
Contribution from the National Research Council of Canada, Prairie Regional Laboratory, Saskatoon, Saskatchewan. Presented at the 43rd Canadian Chemical Conference of The Chemical Institute of Canada, Ottawa, June 1960.
Issued as N.R.C. No. 6199.



1*a*



1*b*

FIGS. 1*a* and 1*b*. Degradation of sophorosides of 17-hydroxyoctadecanoic and 17-hydroxy-9-octadecenoic acids.

(VI) and 8-hydroxy-pelargonic acids (VII). These oxidation products could not be separated by crystallization and an attempt to separate the mixture of monomethyl azelate and hydroxy acid obtained by oxidation of the methyl ester in aqueous tertiary butanol (8) was also unsuccessful. Dimethyl azelate and methyl hydroxypelargonate were not well resolved by gas chromatography on a silicone column but conversion to the corresponding *n*-butyl esters gave a mixture which was easily separated preparatively. Oxidation of sirupy 8-hydroxypelargonic acid gave crystalline 8-oxopelargonic acid (VIII) with the same melting point as that reported by Barger *et al.* (9) for the synthetic acid. The double bond (IV) was considered to have the cis configuration as the infrared spectrum had no band in the 10.36 μ region (10).

The asymmetric center at carbon-17 has been provisionally assigned the L-configuration since the specific rotation of 17-hydroxyoctadecanoic acid was +4.4°. Assuming that the carboxyl group at the end of a long methylene chain has no more effect on the specific rotation than a methyl group the saturated C_{18} hydroxy acid can be regarded as a D-carbinol (IX) of which all known members of the type depicted are dextrorotatory (XI) (11). When the structure is written as (X) it has the L-configuration according to the usual rules of nomenclature (12). Further the acid might be expected to have the

Can. J. Chem. Downloaded from www.nrcresearchpress.com by 210.87.254.105 on 09/05/12
For personal use only.

same configuration as synthetic 12-L-hydroxyoctadecanoic acid ($[\alpha]_D$ +0.8°) (13) as the sign of rotation is the same.

15-D-16-Dihydroxy- and 2-D-15-D-16-trihydroxyhexadecanoic acids isolated from ustilagic acid also possess a hydroxyl group on the penultimate carbon atom and all

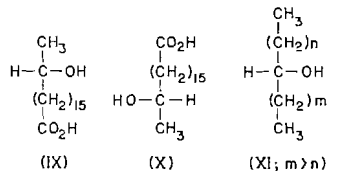


FIG. 2. Hydroxyl configuration in 17-L-hydroxydecanoic acid when regarded as an alcohol.

the optical centers were assigned the D-configuration (7), otherwise acids hydroxylated in this position do not seem to have been found in nature. For saturated acids the common positions for hydroxyl substitution are C_2, C_9, C_{10}, and the terminal carbon atom (14). Only two hydroxy monoenoic C_{18} acids have been reported, 12-hydroxy-9-octadecenoic acid, the major component of castor oil (14), and also occurring in ergot oil (15), which has been assigned the D-configuration (13), and 9-hydroxy-12-octadecenoic acid which is found in the seed fat of *Strophanthus* species (16).

To characterize the linkage types and configurations of the glycosidic linkages in the two disaccharide-C_{18} hydroxy acid glycolipids (I and II) it was necessary to separate them. Since fractionation was difficult the unsaturated portion was modified by oxidation. Treatment of the mixture with performic acid, followed by alkaline hydrolysis, gave *threo*-9,10-dihydroxy derivatives (XII) which were then oxidized by lead tetraacetate in acetic acid. The uptake of oxidant was almost immediate and indicated that 30% of the mixture was olefinic.* The resulting aldehydes were reduced with sodium borohydride, mainly to ω-hydroxypelargonic acid and a crystalline nonanediol sophoroside (XIII). These components were readily separable from the water-insoluble solid containing the 17-hydroxyoctadecanoic acid sophoroside (I). Complete acid hydrolysis of the nonanediol sophoroside yielded glucose and syrupy 1,8-nonanediol (XIV) from which a crystalline bis-*p*-nitrobenzoate was derived. The specific rotation of the diol was positive (+6.5°) indicating an L-hydroxy configuration (11) thus agreeing with the L-configuration already assigned to 17-hydroxy-9-octadecenoic acid. Complete methylation of the nonanediol sophoroside followed by acid hydrolysis gave equimolar amounts of 2,3,4,6-tetra-*O*-methyl-D-glucose (XV) and 3,4,6-tri-*O*-methyl-D-glucose (XVI), which would be expected from two glucose units linked 1,2-glycosidically. Partial acid hydrolysis of nonanediol sophoroside furnished a mixture, from which sophorose (XVII; 2-*O*-β-D-glucopyranosyl-D-glucose) and 1,8-L-nonanediol-β-D-glucopyranoside (XVIII) were isolated by cellulose chromatography (17). The negative rotation of the glycoside indicated a β-configuration for the glucose – fatty acid linkage, as well as that of the glucose-to-glucose linkage. This agrees with the observation that the nonanediol sophoroside was totally hydrolyzed by emulsin, a β-glucosidase.

The amorphous material containing mainly 17-hydroxyoctadecanoic acid sophoroside (I) was similarly methylated and hydrolyzed to yield equimolar amounts of 2,3,4,6-tetra-*O*-methyl-D-glucose (XV), 3,4,6-tri-*O*-methyl-D-glucose (XVI), and 17-L-hydroxyoctadecanoic acid. Although this evidence showed an analogous structure to the 17-L-hydroxy-9-octadecenoic acid sophoroside, the sodium salt was not hydrolyzed by emulsin.

**Since the proportion of unsaturated acid in the solid glycolipid is much less than in the parent oil (65%) it was evident that fractionation had taken place during isolation.*

Can. J. Chem. Downloaded from www.nrcresearchpress.com by 210.87.254.105 on 09/05/12
For personal use only.

However, Pigman and Richtmyer (18) note that the effect of emulsin on *n*-alkyl glucosides begins to decrease when the alcoholic aglycones have more than seven carbon atoms. The molecular rotations of the 17-hydroxyoctadecanoic acid (−14,200°, sodium salt) and 1,8-nonanediol sophorosides (−14,500°) agree closely and point to the likelihood that all the glucosidic linkages present are of the β-type.

The 2-*O*-β-D-glucopyranosyl-D-glucopyranose disaccharide unit is a unique structure in microbial metabolites. However, polysaccharides consisting of 1,2-β-D-glucopyranose units are known to be formed by various species of agrobacteria (19, 20, 21). The glycolipid molecule is similar in over-all structure to the ustilagic acids of Haskins (22) characterized by Lemieux *et al.* (7, and references cited therein) as partly acylated β-cellobiosides of 15-D-16-dihydroxyhexadecanoic and 2-D-15-D-16-trihydroxyhexadecanoic acids. Also similar is the acidic glycolipid formed by *Pseudomonas aeruginosa* which was isolated and identified by Jarvis and Johnson (23). This compound consists of a 3-*O*-L-rhamnopyranosyl-L-rhamnopyranose moiety attached glycosidically to a dimeric form of 3-D-hydroxydecanoic acid.

EXPERIMENTAL

Evaporations were carried out under reduced pressure using a bath temperature of 50° C. Optical rotations were measured at 26° C.

Method of Oil Production

The osmophilic yeast, obtained from the petal portion of a sow thistle, was shown to be a strain of *Torulopsis magnoliae* by carbon assimilation tests (1), and was designated strain N_1c.

The medium used consisted of glucose (20%), yeast extract (1.25%), and urea (0.2%) and was agitated at 385 r.p.m. for 8–10 days with an air flow rate of 500 ml/min, and incubated at 30° C in 5-l. New Brunswick fermentors (3-l. working volume). The maximum yield of the oil was about 5% of the volume of the medium and was recovered by allowing it to stand in a separatory funnel until it all settled out.

The aqueous portion of the solution was shown to contain D-mannitol, which is a common product of *Torulopsis magnoliae*, and this was obtained by crystallization of the evaporated residue from methanol. It had m.p. and mixed m.p. 166–167° C.

Deacetylation of the Oil

The oil (240 g), which contained a considerable proportion of water, was dissolved in 10 volumes of ethyl acetate. The solution was dried with $MgSO_4$, filtered, and evaporated to a yellow-brown viscous acidic syrup (148 g); C, 57.2%; H, 8.2%. It was shown to contain C—H, O—H, and carbonyl groups by infrared analysis. When saponified with alkali in aqueous ethanol it had a sap. equiv. of 226. The hydrolyzate was acidified and distilled to give acetic acid (10.2% of oil by weight).

The purified oil (115 g) was dissolved in refluxing methanol (2 l.) and sodium metal was added until the solution became alkaline. Refluxing was continued for 30 minutes, then the solution was evaporated to a syrup and the methanol distillate, which contained the methyl ester of the acetic acid, was collected in a dry-ice trap. Potassium hydroxide (1 g) dissolved in water (5 ml) was added to part of the methanol distillate and refluxed for 2 hours; after the methanol was taken off the residue was diluted with water and made just acid to phenol red by addition of hydrochloric acid. This solution was allowed to react with S-benzyl thiouronium chloride and gave S-benzyl thiouronium acetate, m.p. 131–134° C, which was not depressed by an authentic sample.

Can. J. Chem. Downloaded from www.nrcresearchpress.com by 210.87.254.105 on 09/05/12
For personal use only.

The deacetylated syrup was dissolved in water and acidified with formic acid. A gelatinous precipitate formed and after storage of the liquid at 3° C for a week it was filtered off, washed with cold water, and dried *in vacuo*. The light brown powder (44 g) had m.p. 137–139° C and analyzed as a hexose disaccharide attached glycosidically to a C_{18} hydroxy fatty acid. Roughly half of the material appeared to be in a lactonic form. Calculated for the saturated acid glycoside $C_{30}H_{56}O_{13}$: C, 57.6%; H, 9.0%; sap. equiv., 624. Found: C, 58.2%; H, 8.9%; sap. equiv., 652; neutral equiv., 1213.

Acid Hydrolysis of the Deacetylated Oil

The deacetylated syrup was refluxed with a large excess of 4% methanolic hydrogen chloride for 18 hours, then diluted with water and the fatty acid esters extracted with chloroform. The aqueous layer was neutralized (silver carbonate), filtered, and concentrated to a syrup which on crystallization from ethanol gave methyl-α-D-glucopyranoside, m.p. and mixed m.p. 166–167° C and $[\alpha]_D$ +160° (*c*, 1.0, H_2O).

Gas–liquid chromatography of the crude methyl ester on 1:6 silicone on Celite in a 6 ft×$\frac{1}{4}$ in. copper column at 235° C suggested the presence of 75% saturated and unsaturated hydroxy C_{18} esters. On oxidation with permanganate–periodate the crude acid, obtained by saponification, consumed 2.6 moles of oxidant corresponding to 65% of unsaturated esters.

17-Hydroxystearic Acid

A solution of the crude fatty acid methyl esters (15.62 g) in petroleum (b.p. 60–80° C) (225 ml) was stored at +2° C for 2 days and a crystalline product (3.97 g) was obtained. This solid was distilled, b.p./0.08 mm 180° C (bath), and repeatedly crystallized from petroleum (b.p. 60–80° C) but did not yield a completely pure ester. Saponification, isolation of the acid, and crystallization from acetone gave 17-hydroxystearic acid, m.p. 78–80° C. Calculated for $C_{18}H_{36}O_3$: C, 71.9%; H, 12.1%; neutral equiv., 300.5. Found: C, 71.8%; H, 11.95%; neutral equiv., 298; $[\alpha]_D$ +4.4° (*c*, 7.9, CH_3COOH). Methyl-17-hydroxystearate was prepared from the acid with diazomethane and crystallized from petroleum (b.p. 60–80° C) as platelets, m.p. 51–53° C. Calculated for $C_{19}H_{38}O_3$: C, 72.6%; H, 12.2%. Found: C, 72.2%; H, 12.1%; $[\alpha]_D$ +4.6° (*c*, 7.3, MeOH).

17-Hydroxy-cis-9-octadecenoic Acid

The solvent was removed from part of the mother liquors of the first crystallization of the crude saturated ester and the residue distilled, b.p./0.1 mm 150° C. After saponification a further small quantity of saturated acid was removed by crystallization from petroleum (b.p. 60–80° C) containing 8% acetone at 0° C and crystallization at −20° C gave almost pure unsaturated acid, m.p. 5° C. Distillation gave the pure acid as a colorless viscous oil, b.p./0.04 mm 160° C (bath). Calculated for $C_{18}H_{34}O_3$: C, 72.4%; H, 11.5%. Found: C, 72.35%; H, 11.3%; $[\alpha]_D$ +4.3° (*c*, 6.1, MeOH). There was no absorption band in the 10.36 μ region of the infrared spectrum. The methyl ester was prepared and had b.p./0.04 mm 145° C (bath). Calculated for $C_{19}H_{36}O_3$: C, 73.0%; H, 11.6%. Found: C, 72.8%; H, 11.5%; $[\alpha]_D$ +3.5° (*c*, 6.5, MeOH).

Hydrogenation of Methyl-17-hydroxy cis-9-Octadecenoate

The crude unsaturated ester (4.95 g) was recovered from the solvent remaining after crystallization of the saturated ester and was hydrogenated in ethanol (60 ml) in the presence of 5% palladium on charcoal (0.5 g). The volume of hydrogen absorbed at N.T.P. was 293 ml; calculated for the reduction of one double bond 353 ml. 17-Hydroxystearic acid was obtained on saponification and crystallized from acetone, m.p. 78.5–80.5° C,

Can. J. Chem. Downloaded from www.nrcresearchpress.com by 210.87.254.105 on 09/05/12
For personal use only.

mixed m.p. with natural saturated acid was 78–80° C. Calculated for $C_{18}H_{36}O_3$: C, 71.9%; H, 12.1%; neutral equiv., 300.5. Found: C, 71.8%; H, 11.95%; neutral equiv., 300; $[\alpha]_D$ +4.1° (*c*, 10.0, CH_3COOH). The derived methyl ester had a melting point of 50.5–51.5° C and the mixed melting point with natural saturated ester was 50.5–52.5° C. Calculated for $C_{19}H_{38}O_3$: C, 72.6%; H, 12.2%. Found: C, 72.4%; H, 12.0%; $[\alpha]_D$ +4.2° (*c*, 9.5, MeOH).

17-Oxostearic Acid

A solution of chromic oxide (2.4 g) in water (5 ml) was diluted with glacial acetic acid (25 ml) and added portionwise to a solution of 17-hydroxystearic acid (8.0 g), prepared by hydrogenation of the unsaturated ester, in acetic acid (80 ml) maintained at room temperature. After 30 minutes the mixture was poured into water (500 ml), the excess oxidant was reduced with sulphur dioxide and the product (6.8 g) was collected, washed, and dried. Crystallization from ethanol gave the pure acid, m.p. 86–87.5° C. Calculated for $C_{18}H_{34}O_3$: C, 72.4%; H, 11.5%. Found: C, 72.2%; H, 11.35%. The acid gave a positive iodoform test. A mixed melting point with 15-oxostearic acid (24) (m.p. 83° C) was depressed to 76–85° C. The melting point was not depressed by synthetic 17-oxostearic acid (m.p. 86.5–87.5° C) and the X-ray powder photographs were indistinguishable. The methyl ester was prepared and crystallized from petroleum as leaflets, m.p. 55–57.3° C, undepressed by admixture with the synthetic ester of m.p. 54.5–56.5° C. Calculated for $C_{19}H_{36}O_3$: C, 73.0%; H, 11.6%. Found: C, 72.9%; H, 11.5%. The infrared spectra and the X-ray powder photographs of the synthetic and natural esters were indistinguishable. 17-Oxostearic acid was similarly prepared from the naturally saturated acid and did not depress the melting point of the above oxo acid.

Oxidation of 17-Hydroxy-cis-9-octadecenoic Acid

The acid (1.73 g) was dissolved in 2% potassium carbonate solution (200 ml) and added all at once to the stock oxidant solution (400 ml, containing 20.86 g sodium metaperiodate and 0.4 g potassium permanganate per liter (5)) diluted with water (1400 ml) and shaken for 4 hours. The excess oxidant was destroyed with sodium metabisulphite, the mixture acidified with sulphuric acid, and the products extracted with ether and the ether removed without drying leaving the mixture of acids (1.88 g). The mixture was taken up in ethyl acetate (10 ml) when part of the azelaic acid (0.25 g) crystallized, recrystallization from the same solvent gave the pure dicarboxylic acid, m.p. 104–107° C undepressed when mixed with authentic azelaic acid. After removing the ethyl acetate the remaining acids were converted to the *n*-butyl esters by 4 hours' reflux with excess *n*-butanol containing 4% HCl. The butyl 8-hydroxypelargonate was separated from the dibutyl azelate by gas chromatography of 100-mg batches using 1:6 silicone on Celite (60–80 mesh) in a 6 ft×¼ in. copper column. The apparatus was operated at 200° C with injector at 225° C, and a flow rate of 75 ml of helium per minute. The *n*-butyl 8-hydroxypelargonate was distilled, b.p./0.05 mm 115° C (bath). Calculated for $C_{13}H_{26}O_3$: C, 67.8%; H, 11.4%. Found: C, 67.2%; H, 11.3%; $[\alpha]_D$ +4.8° (*c*, 6.8, MeOH). Alkaline hydrolysis of this ester yielded 8-hydroxypelargonic acid as a colorless syrup, b.p./0.04 mm 110° C (bath); $[\alpha]_D$ +6.7° (*c*, 10.1, MeOH). Calculated for $C_9H_{18}O_3$: C, 62.0%; H, 10.4%. Found: C, 62.1%; H, 10.3%. Oxidation of the acid with chromic oxide in the same way as for 17-hydroxystearic acid gave 8-oxopelargonic acid, m.p. 41–42° C (lit. (9) gives m.p. 40–41° C). Calculated for $C_9H_{16}O_3$: C, 62.8%; H, 9.4%. Found: C, 62.9%; H, 9.4%. The semicarbazone crystallized from aqueous methanol and had a melting point of 136.5–138.5° C (lit. (10) gives m.p. 136° C).

Can. J. Chem. Downloaded from www.nrcresearchpress.com by 210.87.254.105 on 09/05/12
For personal use only.

Can. J. Chem. Downloaded from www.nrcresearchpress.com by 210.87.254.105 on 09/05/12
For personal use only.

Hydroxylation of the Solid Glycolipid Mixture (I and II)

The mixed glycosides (44 g) were dissolved in formic acid (120 cc) and then 30% hydrogen peroxide (10 cc) added. After storage at 0° C for 18 hours the solution was evaporated to a dry crust which was then dissolved in refluxing methanol (1 l.). Sodium metal was added until the solution became alkaline and after 30 minutes the solvent was removed by evaporation. The solid was then dissolved in water and cations removed by shaking with Amberlite IR-120. Precipitation of glycosides on the resin took place, but redissolution was effected by adding an excess of methanol. Filtration and evaporation afforded a crusty light-yellow solid (39.5 g) containing unaffected glycoside and its *threo*-dihydroxy counterparts.

The amount of olefin in the original glycoside mixture was then estimated by lead tetraacetate oxidation of the hydroxylated product. The solid (100 mg) was dissolved in acetic acid (5 cc) and to this solution 1% lead tetraacetate (10 cc) was added. The uptake of oxidant after 3, 10, and 25 minutes corresponded to oxidation equivalents, based on 1 molar uptake of lead tetraacetate, of 2260, 2140, and 1940 respectively indicating 30% of olefinic glycoside.

Isolation of 17-Hydroxyoctadecanoic Acid β-Sophoroside, 1,8-Nonanediol β-Sophoroside, and ω-Hydroxypelargonic Acid

The mixed dihydroxy- and unhydroxylated 17-hydroxy-octadecanoic acid sophorosides (23 g) containing 30% of the former was dissolved in acetic acid (250 cc). Lead tetraacetate (13 mM.) in acetic acid (500 cc) was added and after 30 minutes oxalic acid dihydrate (13 mM.) in acetic acid (50 cc) was added and the precipitate filtered off. Evaporation to a residue and addition of water gave a solution from which 17-hydroxyoctadecanoic acid β-sophoroside precipitated. This material was isolated, dried, and boiled in ether to remove fatty acid fragments. It (11.1 g) had a melting point of 139–140° C and $[\alpha]_D$ −22° (*c*, 1.3, aqueous $NaHCO_3$). Calculated for $C_{30}H_{56}O_{13}$: C, 57.6%; H, 9.0%; sap. equiv., 624. Found: C, 57.7%; H, 9.0%; sap. equiv., 566; neutral equiv., 1050. The product was methanolyzed with 4% methanolic hydrogen chloride overnight under reflux. The methyl ester, obtained by neutralization (Ag_2CO_3), filtration, and evaporation, consisted mainly of the C_{18} ester with traces of other hydroxy methyl esters as shown by gas – liquid phase chromatography.

The mother liquor of the above glycoside precipitation was evaporated to a syrup and reduced with sodium borohydride (1.0 g) in water (100 cc). After 1 hour excess reductant was destroyed with acetic acid, cations removed with Amberlite IR-120, and the resulting filtrate evaporated to a crust. Boric acid was removed by repeated evaporation of the solid with methanol to give nonanediol β-sophoroside, which was recrystallized twice from ethanol to give material (3.2 g) with m.p. 188–190° C and $[\alpha]_D$ −30° (*c*, 1.0, H_2O). Calculated for $C_{21}H_{40}O_{12}$: C, 52.1%; H, 8.3%. Found: C, 51.9%; H, 8.3%.

In order to characterize the other fission fragment of the olefin 858 mg of the mixed hydroxylated glycosides was oxidized with lead tetraacetate in a similar manner to that described above, except that after filtration of the lead oxalate the filtrate was evaporated to a syrup to which sodium borohydride (250 mg) in water (25 cc) was added. After 1 hour the mixture was worked up and the product extracted with boiling ether to give a syrup (0.13 g) which crystallized. Two recrystallizations from ether afforded ω-hydroxypelargonic acid, m.p. and mixed m.p. 48–50° C. Calculated for $C_9H_{18}O_3$: C, 62.0%; H, 10.4%. Found: C, 62.1%; H, 10.1%. The material not extractable by ether was dissolved in methanol and precipitated by addition of excess water. Filtration

afforded a powder which gave on methanolysis (4% MeOH–HCl under reflux overnight) mainly two ether-soluble compounds corresponding to a C_{18} hydroxy methyl ester and an octadecanediol (by G.L.P.C.) thus indicating that reduction of a lactone had taken place.

Hydrolysis of 1,8-Nonanediol Sophoroside

The sophoroside (296 mg) was hydrolyzed by heating on a steam bath for 18 hours in *N* sulphuric acid (5 cc). The solution was neutralized ($BaCO_3$), filtered, and evaporated to a syrup which was extracted with boiling ether. Evaporation of the ether afforded the nonanediol (85 mg) with $[\alpha]_D$ +6.5° (*c*, 2.3, H_2O) and 40 mg of this was dissolved in pyridine (2 cc) containing *p*-nitrobenzoyl chloride (300 mg), and kept at 80° C for 30 minutes. To this an excess of aqueous sodium bicarbonate was added and after shaking for 2 hours the precipitate was collected, washed, and dried, and twice recrystallized from ethyl acetate – hexane. The 1,8-nonanediol bis-*p*-nitrobenzoate (93 mg) had a melting point of 94–96° C and $[\alpha]_D$ +21° (*c*, 2.1, $CHCl_3$). Calculated for $C_{23}H_{26}O_8N_2$: C, 60.3%; H, 5.7%; N, 6.1%. Found: C, 60.4%; H, 5.7%; N, 6.1%.

The residual glucose (233 mg) was crystallized from methanol to give crystals (168 mg) with m.p. and mixed m.p. 146–149° C.

Partial Hydrolysis of 1,8-Nonanediol Sophoroside

Nonanediol sophoroside (2.0 g) was partially hydrolyzed by keeping a solution in *N* sulphuric acid (10 cc) for 4 hours at 75° C. After neutralization ($BaCO_3$), filtration, and evaporation the residual syrup was chromatographed on a cellulose column using *n*-butanol one-half saturated with water as the mobile phase. The solvent eluted firstly 1,8-nonanediol β-D-glucopyranoside (396 mg), which was recrystallized twice from ethyl acetate to give material with m.p. 102–104° C and $[\alpha]_D$ −27° (*c*, 1.8, H_2O). Calculated for $C_{15}H_{30}O_7$: C, 55.9%; H, 9.4%. Found: C, 55.7%; H, 9.4%. This was followed by unhydrolyzed glycoside (670 mg) and glucose (396 mg), which were not positively identified. *n*-Butanol – ethanol – water (4:1:1 v/v) was then passed through the column to elute sophorose (163 mg), which after two crystallizations from methanol–ethanol, gave 80 mg of the α-anomer with m.p. 198–202° C (25) and $[\alpha]_D$ +27° → 19° (*c*, 0.9, H_2O; constant, 42 hours). Calculated for $C_{12}H_{22}O_{11}$: C, 42.1%; H, 6.5%. Found: C, 41.9%; H, 6.5%. Acetylation of the disaccharide gave the β-octaacetate with m.p. 192–195° C (25).

Methylation of 1,8-Nonanediol β-Sophoroside

Nonanediol sophoroside (647 mg) was methylated six times by the dimethyl sulphate – aqueous sodium hydroxide method (26). At the end of the methylation excess reagent was destroyed by heating the solution on a steam bath for 3 hours. It was then cooled and neutralized with aqueous sulphuric acid and then shaken three times with chloroform. The extract was dried ($MgSO_4$), filtered, and evaporated to a syrup (754 mg) which was methylated further with silver oxide – methyl iodide under reflux (27). The methylated product (623 mg) had —OCH_3: 39.1% (calculated for $C_{21}H_{32}O_4(OCH_3)_8$: OCH_3, 41.6%), n_D^{27} 1.4583 and $[\alpha]_D$ −4° (*c*, 2.6, hexane).

The fully methylated glycoside was refluxed overnight in 4% methanolic hydrogen chloride (20 cc) and then *N* hydrochloric acid (10 cc) was added and the methanolic component boiled off. After 20 hours heating on a steam bath the solution was shaken with hexane to remove 1-methoxy-8-nonanol (57 mg), which had n_D^{24} 1.4410 and $[\alpha]_D$ +8° (*c*, 1.9, hexane) after vacuum distillation. The aqueous portion was neutralized (Ag_2CO_3), filtered, and taken down to a syrup (443 mg) which was chromatographed

Can. J. Chem. Downloaded from www.nrcresearchpress.com by 210.87.254.105 on 09/05/12
For personal use only.

on cellulose using benzene–ethanol–water (500:50:1 v/v) as solvent. 2,3,4,6-Tetra-*O*-methyl-D-glucose (164 mg) was eluted and recrystallized twice from hexane to give crystals, m.p. and mixed m.p. 80–81° C. Calculated for $C_6H_8O_2(OCH_3)_4$: OCH_3, 51.6%. Found: OCH_3, 51.4%. 3,4,6-Tri-*O*-methyl-D-glucose (144 mg) (28) came off later and two recrystallizations from ether–hexane gave 37 mg of product with m.p. 77–79° C and $[\alpha]_D$ +107° (3 minutes) → 75° (*c*, 0.9, H_2O; 16 hours, constant value). Calculated for $C_6H_9O_3(OCH_3)_3$: OCH_3, 41.9%. Found: OCH_3, 41.4%. On treatment with 1% lead tetraacetate in acetic acid (0.9 molar equivalents) the sugar consumed 0.24, 0.47, and 0.68 molar equivalents of oxidant after 3, 10, and 25 minutes respectively, thus indicating that the 1 and 2 positions of the sugar are not substituted with methoxyl groups (29).

Methylation of 17-Hydroxyoctadecanoic Acid β-Sophoroside

The glycoside (2 g) was methylated with dimethyl sulphate – sodium hydroxide and Purdie's reagent as described for the nonanediol sophoroside. The fully methylated product (1.94 g) n_D^{25} 1.4620 had OCH_3, 32.9%. Calculated for $C_{30}H_{28}O_5(OCH_3)_8$: OCH_3, 33.7%. The fully methylated glycoside was also hydrolyzed under similar conditions and the insoluble residue which accumulated was washed with water and hydrolyzed for 2 hours in 50% aqueous ethanol (20 cc) containing sodium hydroxide (0.5 g). The solution was added to excess water which was acidified (dil. H_2SO_4) and extracted with ether which was dried ($MgSO_4$), filtered, and evaporated to a solid (767 mg). Two recrystallizations from acetone gave 310 mg of 17-hydroxyoctadecanoic acid with m.p. 77–79° C and $[\alpha]_D$ +4.3° (*c*, 10.4, acetic acid). Calculated for $C_{18}H_{36}O_3$: C, 71.9%; H, 12.1%. Found: C, 71.6%; H, 12.0%. Two further recrystallizations from acetone elevated the melting point to 80.5–82° C (constant m.p.).

The aqueous portion of the hydrolyzate was neutralized and chromatographed on a cellulose column as described for the previous methylation. The products consisted of 2,3,4,6-tetra-*O*-methyl-D-glucose (0.43 g), which was crystallized twice from hexane to give a product, m.p. and mixed m.p. 79–80° C, and 3,4,6-tri-*O*-methyl-D-glucose (0.30 g), m.p. and mixed m.p. 77–80° C (two recrystallizations from ether – *n*-hexane).

ACKNOWLEDGMENTS

The authors wish to thank Mr. N. R. Gardner, Mr. L. L. Hoffman, and Miss S. F. Lubin for technical assistance, Miss I. M. Gaffney for infrared measurements and X-ray diffraction diagrams, and Mr. M. Mazurek for microanalytical determinations.

REFERENCES

1. J. F. T. SPENCER. Unpublished results.
2. B. M. CRAIG and N. L. MURTY. Can. J. Chem. **36**, 1297 (1958).
3. B. M. CRAIG and N. L. MURTY. J. Am. Oil Chemists' Soc. **36**, 549 (1959).
4. A. P. TULLOCH, B. M. CRAIG, and G. A. LEDINGHAM. Can. J. Microbiol. **5**, 485 (1959).
5. R. U. LEMIEUX and E. VON RUDLOFF. Can. J. Chem. **33**, 1701 (1955).
6. S. BERGSTRÖM, G. AULIN-ERDTMAN, B. ROLANDER, E. STENHAGEN, and S. ÖSTLING. Acta Chem. Scand. **6**, 1157 (1952).
7. R. U. LEMIEUX. Can. J. Chem. **31**, 396 (1953).
8. E. VON RUDLOFF. Can. J. Chem. **34**, 1413 (1956).
9. G. BARGER, R. ROBINSON, and L. H. SMITH. J. Chem. Soc. 718 (1937).
10. O. D. SHREVE, M. R. HEETHER, H. B. KNIGHT, and D. SWERN. Anal. Chem. **22**, 1498 (1950).
11. J. A. MILLS and W. KLYNE. *In* Progress in stereochemistry. Vol. I. *Edited by* W. Klyne. Butterworth Ltd., London. 1954. p. 205.
12. E. J. CRANE. Chem. Eng. News, **26**, 1623 (1948).
13. K. SERCK-HANSSEN. Chem. & Ind. (London), 1554 (1958).
14. T. P. HILDITCH. The chemical constitution of natural fats. John Wiley & Sons, Inc., New York. 1956. pp. 517–520.

Can. J. Chem. Downloaded from www.nrcresearchpress.com by 210.87.254.105 on 09/05/12
For personal use only.

15. K. E. BHARUCHA and F. D. GUNSTONE. J. Chem. Soc. 610 (1957).
16. F. D. GUNSTONE. J. Chem. Soc. 1274 (1952).
17. L. HOUGH, J. K. N. JONES, and W. H. WADMAN. J. Chem. Soc. 2511 (1949).
18. W. W. PIGMAN and N. K. RICHTMYER. J. Am. Chem. Soc. **64**, 369 (1942).
19. E. W. PUTMAN, A. L. POTTER, R. HODGSON, and W. Z. HASSID. J. Am. Chem. Soc. **72**, 5024 (1950).
20. R. E. REEVES. J. Biol. Chem. **154**, 49 (1944).
21. P. A. J. GORIN and J. F. T. SPENCER. Unpublished results.
22. R. H. HASKINS and J. A. THORN. Can. J. Botany, **29**, 585 (1951).
23. F. G. JARVIS and M. J. JOHNSON. J. Am. Chem. Soc. **71**, 4124 (1949).
24. A. T. CROSSLEY and B. M. CRAIG. Can. J. Chem. **33**, 1426 (1955).
25. J. RABATÉ. Bull. soc. chim. France, **7**, 565 (1940).
26. W. N. HAWORTH. J. Chem. Soc. 8 (1915).
27. T. PURDIE and J. C. IRVINE. J. Chem. Soc. 1021 (1903).
28. R. L. SUNDBERG, C. M. MCCLOSKEY, D. E. REES, and G. H. COLEMAN. J. Am. Chem. Soc. **67**, 1080 (1945).
29. A. J. CHARLSON and A. S. PERLIN. Can. J. Chem. **34**, 1200 (1956).

Can. J. Chem. Downloaded from www.nrcresearchpress.com by 210.87.254.105 on 09/05/12
For personal use only.

Can. J. Chem. Downloaded from www.nrcresearchpress.com by 210.87.254.6 on 09/05/12
For personal use only.

DEUTERATION OF FLUORENE AT C_9 AND THE ASSIGNMENT OF CERTAIN BANDS IN THE INFRARED SPECTRUM TO THE $\rangle CDH$ AND $\rangle CD_2$ GROUPS[1]

G. W. H. Scherf and R. K. Brown

ABSTRACT

Equimolar amounts of 9-fluorenylpotassium and deuterium oxide, or potassium deuteroxide and fluorene, or potassium hydroxide, fluorene, and deuterium oxide gave a mixture of unchanged fluorene, 9-deuterofluorene, and 9,9-dideuterofluorene. In 1,2-dimethoxyethane (DME) deuteration occurs more readily and dideuteration is more extensive than in dioxane. Lithium deuteroxide and fluorene in DME show no exchange, but upon addition of deuterium oxide some monodeuteration occurs. 9-Fluorenyllithium and deuterium oxide in DME gives as much as 80% of 9-deuterofluorene accompanied by a small amount of dideuteration. Dideuteration is practically eliminated, and monodeuteration correspondingly increased when the same reaction is carried out in hexane.

The bands at 667 cm^{-1}, 827 cm^{-1}, and 974 cm^{-1} have been assigned definitely to the $\rangle CD_2$ group while those at 677 cm^{-1} and 832 cm^{-1} are due to the $\rangle CDH$ group in fluorene.

Recently six absorption bands in the infrared spectrum of fluorene have been assigned to the $\rangle CH_2$ group of that molecule (1). Evidence for such assignment was obtained from the study of the spectra of C_9-mono- and -di-alkylated as well as C_9-mono- and -di-deuterated fluorene. Mono- or di-deuteration at C_9 reduced or eliminated the absorption at the frequencies designated but in turn produced new bands at lower frequencies in the positions expected when a deuterium atom replaces an hydrogen atom attached to carbon (2). The new frequencies associated with the C_9—D bond were located at least tentatively, if not definitely, at 2150, 974, 939, 827, and 667 cm^{-1}, respectively. In addition, a band at 677 cm^{-1} was thought to be due to a vibration of the remaining C_9—H group in the monodeuterated molecule but shifted slightly from its normal frequency of

$$\begin{array}{c} | \\ \text{692 cm}^{-1} \text{ by the presence of the deuterium atom (i.e. DC—H). Also, the band at 939 cm}^{-1} \\ | \end{array}$$

was believed to contain a contribution due to the same structural feature.

For the work mentioned above, the 9-deuterofluorene was made by the reaction of excess deuterium oxide with 9-fluorenylpotassium in dioxane at room temperature. The 9,9-dideuterofluorene was prepared by similar addition of excess deuterium oxide to the substance formed when two equivalents of potassium metal reacted with one of fluorene in dioxane (1).

During a more detailed study of the preparation of 9-fluorenylpotassium in various solvents (3) the measurement of the extent of metalation by means of deuterating the organometallic compound (particularly with excess deuterium oxide) was shown to be questionable. It was observed that equimolar quantities of potassium deuteroxide and fluorene in dioxane, under anhydrous conditions, when kept at room temperature for 1 hour, gave 10 to 15% C_9-deuteration while equimolar amounts of potassium hydroxide,

[1]*Manuscript received September 16, 1960.*
Contribution from the Department of Chemistry, University of Alberta, Edmonton, Alberta. Taken from the thesis of G. W. H. Scherf to be submitted to the Graduate School of the University of Alberta in partial fulfillment of the requirements for the Degree of Doctor of Philosophy.

Can. J. Chem. Downloaded from www.nrcresearchpress.com by 210.87.254.6 on 09/05/12
For personal use only.

fluorene, and deuterium oxide in dioxane at room temperature for 3 hours produced 5 to 8% C_9-deuteration.

In addition the "9-deuterofluorene" previously prepared was shown to be contaminated with a trace of fluorene and a larger amount of 9,9-dideuterofluorene attributed to exchange due to the presence of potassium deuteroxide and excess deuterium oxide (1). From the tentative assignment of the 677 cm^{-1} and 667 cm^{-1} bands to the structural group DC—H and HC—D, respectively, both these bands should appear in the spectrum of 9-deuterofluorene. However, in the spectrum of 9,9-dideuterofluorene the 677 cm^{-1} band should be absent and the band at 667 cm^{-1} should double its intensity. As actually observed from the spectra of the mono- and di-deuterated fluorenes (Figs. 2 and 3, ref. 1) the 677 cm^{-1} band did nearly vanish while that at 667 cm^{-1} increased considerably, although not to twice its original magnitude. From this information, along with data from N.M.R. analyses of the "9-deuterofluorene", the purity of the monodeuterated compound had been estimated to be about 75%, the bulk of the remainder being the dideuterated material. This was in keeping with the greater area of the 667 cm^{-1} band. Although the N.M.R. spectrum could be interpreted as containing a somewhat greater proportion of the dideuterated fluorene than stated above, the broad but low signal was sufficient to agree fairly well with the above assignments in the infrared. An implicit assumption in this reasoning is that the 677 cm^{-1} and 667 cm^{-1} bands due respectively to the DC—H and HC—D are of about equal intensity for equal concentrations.

Support or modifications of the interpretations outlined above would be gained from the preparation and examination of authentic C_9-monodeuterated fluorene, uncontaminated as much as possible by fluorene and especially by 9,9-dideuterofluorene.

This paper presents results of the study of C_9-mono- and -di-deuteration of fluorene and gives the exact assignment of certain bands in the infrared associated with 9-mono- and 9,9-di-deuterofluorene.

RESULTS AND DISCUSSION

Since 9-fluorenyllithium, prepared by the reaction of fluorene with lithium (or lithium amide) preferably in ethers of ethylene glycol (4), produced essentially C_9-monosubstituted fluorene when treated with an equivalent amount of alkyl halide (5), the lithium salt was thought to be the most promising substance for the production of 9-deuterofluorene. The addition of deuterium oxide to an equimolar portion of 9-fluorenyllithium prepared in 1,2-dimethoxyethane (DME) (4) gave a product whose spectrum is shown in Fig. 1. It is clearly seen that a strong band appears at 677 cm^{-1} while the one at 667 cm^{-1} is quite small. The bands at 692 cm^{-1}, 952 cm^{-1}, and 1400 cm^{-1} show that there is some unchanged fluorene present, roughly to the extent of 12%. The N.M.R. analysis of this compound* shows a signal for the proton at C_9 (Fig. 2*a*) which is nearly half that found for the proton at C_9 of the parent fluorene (Fig. 2*b*). The broadening of the signal in Fig. 2*a* is probably due to spin coupling of the proton with the deuterium atom. Both the infrared and N.M.R. spectra are in agreement with the interpretation that the substance contains a high percentage of 9-deuterofluorene. The band at 677 cm^{-1} is thus due to the group $\rangle$CDH while that at 667 cm^{-1} arises from the structural feature $\rangle CD_2$. The

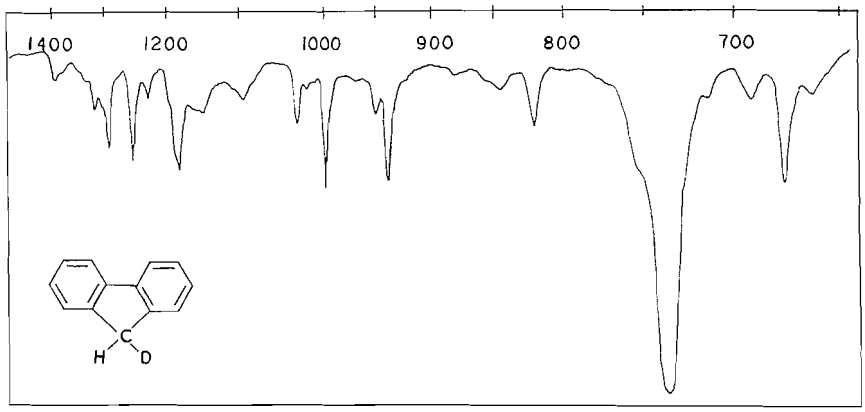


FIG. 1. I. R. spectrum in CS_2 of 9-deuterofluorene prepared from 9-fluorenyllithium and D_2O in 1,2-dimethoxyethane.

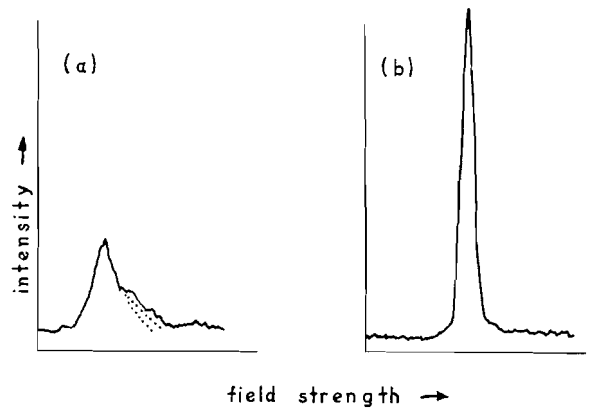


FIG. 2. Partial N.M.R. spectra showing only $\rangle$CHD and $\rangle CH_2$ bands of fluorene. (*a*) 9-Deuterofluorene. (*b*) Fluorene. The 9-deuterofluorene was prepared from 9-fluorenyllithium + D_2O in 1,2-dimethoxyethane.

product, described in the first paper of this series (1) and obtained from the reaction of 9-fluorenylpotassium with excess deuterium oxide in dioxane, therefore must have been composed of a mixture of C_9-mono- and -di-deuterated fluorene in the approximate ratio of 2 to 3. This mixture clearly contained a small amount of unchanged fluorene as a contaminant (Fig. 2, ref. 1).

Comparison of the spectrum of the 80% monodeuterated fluorene (Fig. 1, this paper) with that of the mixture of C_9-mono- and C_9-di-deuterated fluorene (Fig. 2, ref. 1) and 9,9-dideuterated fluorene (Fig. 3, ref. 1) shows that the band at 827 cm^{-1} is due to $\rangle CD_2$ while that at 823 cm^{-1} arises from the group $\rangle$CDH. The 974 cm^{-1} band, which appears much more clearly in the 9,9-dideuterofluorene and is nearly absent in the 80% 9-deuterofluorene, must then also be due to the structure $\rangle CD_2$ rather than to $\rangle$CDH. The band at 939 cm^{-1} appears in both C_9-mono- and C_9-di-deuterofluorene and is due to the carbon–deuterium bond in both $\rangle CD_2$ and $\rangle$CDH.

Can. J. Chem. Downloaded from www.nrcresearchpress.com by 210.87.254.6 on 09/05/12
For personal use only.

With the knowledge of the exact assignment of these bands due to $\rangle CD_2$, $\rangle CDH$, and $\rangle CH_2$ now available, some experiments on the deuteration of fluorene were carried out. The mixtures, conditions of reaction, and results are presented in Table I. The

TABLE I

Mono- and di-deuteration of fluorene

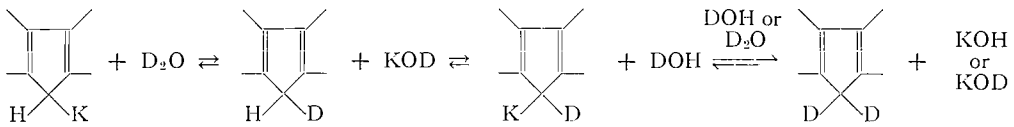
(Except where specified equivalent amounts of reagents were refluxed in 5 ml of solvent for 1 hour. DME = 1,2 dimethoxyethane)

Reagents	Solvent and conditions	% C_9H_2	% C_9DH	% C_9D_2
9-Fluorenylpotassium + D_2O (excess)*	Dioxane (room temperature, 1 hour)	2	38	60
9-Fluorenylpotassium + D_2O	Dioxane	35	50	15
9-Fluorenylpotassium + D_2O	DME	15	45	40
9-Fluorenylsodium + D_2O	DME	5	45	50
9-Fluorenyllithium + D_2O	Dioxane and trace DME	20	70	10
9-Fluorenyllithium + D_2O	DME	12	80	8
KOD + fluorene + D_2O	Dioxane (all KOD dissolved)	15	45	40
KOD + fluorene + D_2O†	DME (all KOD dissolved)	20	50	30
KOH + fluorene + D_2O	Dioxane (all KOH dissolved)	90	10	0
KOH + fluorene + D_2O	DME (all KOH dissolved)	45	50	5
KOD + fluorene	Dioxane (KOD not dissolved)	70	30	0
KOD + fluorene	DME (KOD not dissolved)	45	50	5
LiOD + fluorene‡	DME (LiOD not dissolved)	100	0	0
LiOD + fluorene + D_2O	DME (LiOD not dissolved)	90	10	0
LiOD + fluorene + D_2O (3-fold excess)	DME (LiOD not dissolved)	85	15	0
9-Fluorenyllithium§ and D_2O	Hexane	8	90	2

*From Fig. 2, ref. 1.
†The red color of 9-fluorenylpotassium became evident within the first 3 minutes.
‡Repeated twice with same results.
§Made in DEE (4), isolated, and transferred to hexane.

yields of mono- and di-deuterated fluorene, and unchanged fluorene were estimated from the magnitude of the bands at 677 cm^{-1}, 667 cm^{-1}, and 692 (or 952) cm^{-1}, 667 cm^{-1}, and 692 (or 952) cm^{-1}, respectively.

It is clearly seen that 9-fluorenylpotassium, when treated with an equimolar amount of deuterium oxide, produced less unchanged fluorene and more dideuteration in DME than in dioxane. Such deuteration no doubt occurred via the sequence shown below:



Unchanged fluorene might have come from (*a*) incomplete metalation, (*b*) a small amount of water in the deuterium oxide, (*c*) a combination of 9-fluorenylpotassium with the water or deuterium hydroxide produced in the first part of the reaction. The more extensive dideuteration which occurred in the solvent DME agrees with the greater effectiveness of DME as a solvent in the preparation and reactions of 9-fluorenylpotassium (4, 5) due to the more effective solvation of the ether with potassium deuteroxide, enhancing the latter's basicity.

9-Fluorenyllithium in DME, on the other hand, gave largely C_9-*mono*deuteration accompanied by only a small proportion of dideuterated and unchanged fluorene. But with the solvent hexane rather than DME, dideuteration was practically eliminated and the extent of monodeuteration increased correspondingly (Fig. 3).

Can. J. Chem. Downloaded from www.nrcresearchpress.com by 210.87.254.6 on 09/05/12
For personal use only.

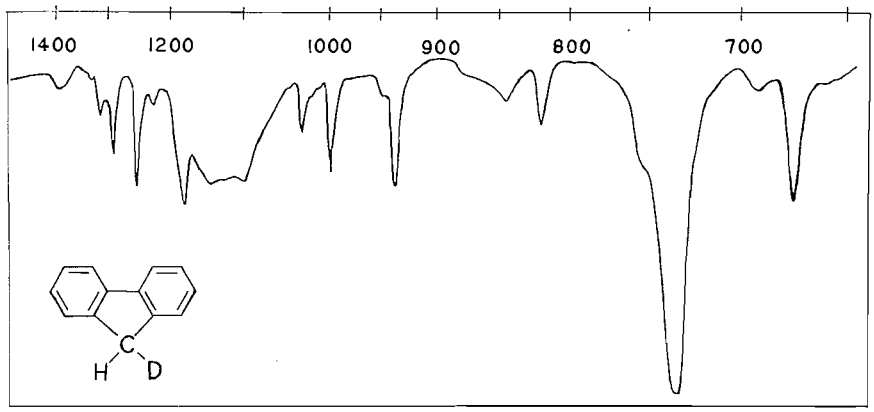
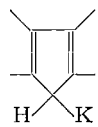


FIG. 3. I. R. spectrum in CS_2 of 9-deuterofluorene prepared from 9-fluorenyllithium and D_2O in hexane.

Potassium deuteroxide and fluorene in dioxane gave more extensive dideuteration than did a mixture of potassium hydroxide, fluorene, and deuterium oxide, in dioxane. This is probably due to the fact that in the reaction of potassium deuteroxide with fluorene, the products of the first step in the exchange,  + HOD, are in close proximity, thus facilitating the next step of exchange, whereas the product of the reaction of potassium hydroxide and fluorene requires time for collision with the solvated deuterium oxide. With DME as solvent, such differences appear to be minimized.

Lithium deuteroxide and fluorene failed to show any exchange, but when deuterium oxide was added, exchange did occur and increased in magnitude with the amount of deuterium oxide added. This agrees with the interpretation that lithium deuteroxide under anhydrous conditions is a much weaker base than is either potassium deuteroxide or sodium deuteroxide and hence will not initiate the first step of the reaction—that of transient formation of the 9-fluorenyllithium. The addition of deuterium oxide yields a solvent which promotes the ionization of lithium deuteroxide and enhances its basicity. Such a levelling effect of solvents has been observed before (6).

EXPERIMENTAL

The 9-fluorenyl-potassium, -sodium, and -lithium were made according to previous directions (1, 4).

Preparation of Potassium Deuteroxide and Lithium Deuteroxide

Into 100 ml of dry hexane was pipetted 1 ml of 98% D_2O. A piece of freshly cut potassium in excess of the amount required to react with all the D_2O was suspended on a length of wire and immersed in the hexane and cautiously allowed to touch the surface of the D_2O at the bottom of the flask and then was immediately withdrawn but not removed from the hexane. This "dipping" process was repeated until a coating of KOD was developed on the surface of the metal. The reaction was quite vigorous at first but soon moderated. The solid was allowed to remain overnight in the flask in contact with the

Can. J. Chem. Downloaded from www.nrcresearchpress.com by 210.87.254.6 on 09/05/12
For personal use only.

small amount of D_2O in the lower layer. The KOD was then removed from the metal and, following the elimination of hexane, was weighed for use.

LiOD was prepared by a similar manner but required somewhat longer contact with the traces of D_2O for complete reaction.

Deuteration Experiments

All reactions were carried out under the same conditions. A typical reaction is described.

Equimolar amounts of the reagents, KOD, fluorene, and D_2O (0.01 mole of each) were allowed to react for 1 hour in 5 ml of refluxing solvent. An atmosphere of pure, dry nitrogen was maintained throughout. The cooled solution was then treated with a mixture of ether and water. The ether extract, dried over calcium chloride, was freed from solvent and the solid crystallized from alcohol.

ACKNOWLEDGMENTS

The authors wish to thank the National Research Council of Canada for financial assistance which enabled this work to be carried out. Grateful acknowledgment is made to Dr. W. Schneider who kindly performed the N.M.R. analyses.

REFERENCES

1. G. W. H. SCHERF and R. K. BROWN. Can. J. Chem. **38**, 697 (1960).
2. A. WEISSBERGER. Chemical applications of spectroscopy. Vol. 9. Interscience Publishers, Inc., New York. 1956.
3. G. W. H. SCHERF and R. K. BROWN. Unpublished work.
4. G. W. H. SCHERF and R. K. BROWN. Can. J. Chem. **38**, 2450 (1960).
5. G. W. H. SCHERF and R. K. BROWN. Can. J. Chem. In press.
6. J. HINE. Physical organic chemistry. McGraw-Hill Book Co., Inc. 1956.

Can. J. Chem. Downloaded from www.nrcresearchpress.com by 210.87.254.6 on 09/05/12
For personal use only.

Can. J. Chem. Downloaded from www.nrcresearchpress.com by 210.87.254.105 on 09/05/12
For personal use only.

CONTRIBUTION À L'ÉTUDE DE LA RÉACTION DE VON RICHTER

IV. COMMENTAIRES CONCERNANT LA RÉACTION[1]

E. CULLEN[2] ET PH. L'ÉCUYER

RÉSUMÉ

Il existe une relation entre l'anhydride carbonique et les composés azoxyques formés au cours de la réaction. Ces composés azoxyques, dans la série du benzène, ne donnent pas les acides benzoïques attendus, lorsqu'ils sont soumis aux conditions de la réaction. Par contre, dans la série du naphtalène, les composés qui ont été isolés et dont la formule empirique correspond aux composés azoxyques attendus se transforment en acides naphtoïques. Enfin, le 2-nitro-5-chlorobenzonitrile ne produit pas de composé azoxyque, ni d'acide *m*-chlorobenzoïque.

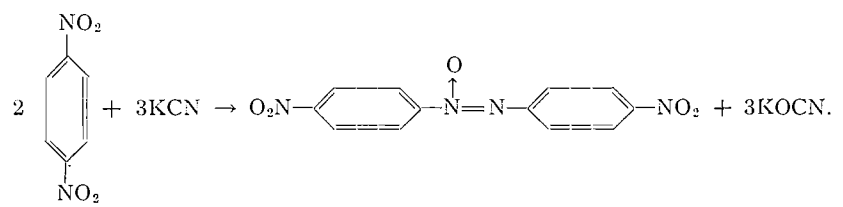
Durant la réaction de von Richter,[3] il se forme de l'ammoniac. Celui-ci peut provenir de l'hydrolyse de la fonction nitrile qui se fixe à l'anneau benzénique et d'une certaine quantité de cyanure ou de cyanate de potassium. L'hydrolyse du cyanure de potassium (*a*) est, toutefois, extrêmement lente à la température d'ébullition. Nous avons constaté que seulement 7% du cyanure s'hydrolyse en acide formique et en ammoniac, lorsqu'on fait bouillir à reflux pendant 48 heures une solution de cyanure de potassium dans l'éthanol à 50%.

$$KCN + 2H_2O \rightarrow HCO_2K + NH_3 \qquad (a)$$

En milieu aqueux, le cyanure de potassium s'oxyde en cyanate aux dépens d'un groupe nitré (1) et le cyanate s'hydrolyse ensuite en ammoniac et bicarbonate de potassium (*b*). Ainsi, dans la réduction du *p*-dinitrobenzène en 4,4′-dinitroazoxybenzène, le rendement du composé azoxyque est proportionnel à la quantité de cyanate qui se forme durant la réaction. Cependant en solution alcoolique, le rendement du composé azoxyque est beaucoup plus faible, le groupe nitré étant en majeure partie substitué par la fonction oxalcoyle. Durant la réaction de von Richter dans l'éthanol à 50%, il se forme aussi de l'anhydride carbonique. Nous l'avons dosé pour nous rendre compte de la proportion de la substance nitrée de départ qui est réduite de cette façon.

$$KCN \xrightarrow{[O]} KOCN \xrightarrow{2H_2O} NH_3 + KHCO_3 \qquad (b)$$

Après 4 heures d'ébullition à reflux dans le 2-éthoxyéthanol à 50%, il s'est formé pour 1 mole de *p*-chloronitrobenzène, 0.148 mole de gaz carbonique et 0.031 mole de 3,8-dichloro-6-iminoquinazolo[1,2,2′,3′]indazol (III) (2). D'après la quantité d'anhydride carbonique dégagé, il aurait dû théoriquement s'être formé 0.049 mole du composé azoxyque II, si on se réfère à (*c*):



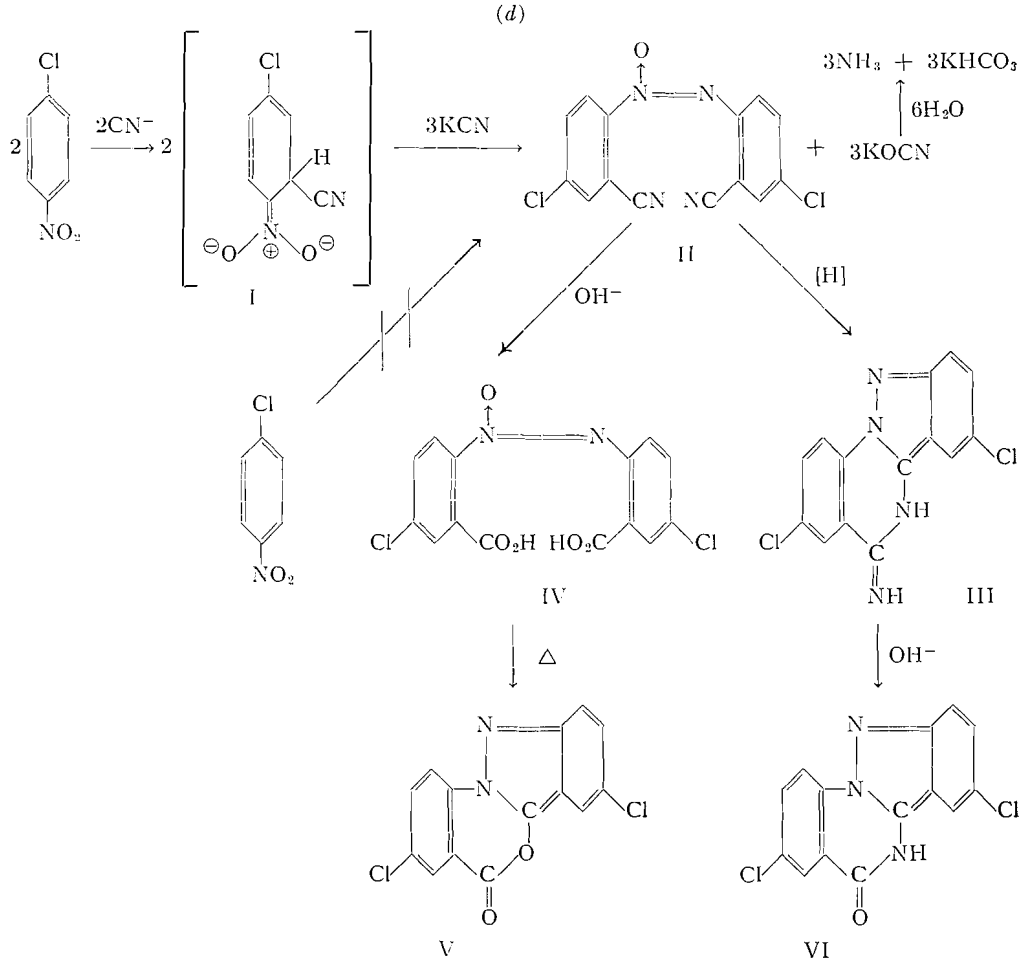
(*c*)

[1]*Manuscrit reçu le 11 octobre 1960.*
Contribution du Département de Chimie, Faculté des Sciences, Université Laval, Québec, Qué.
[2]*Bénéficiaire de bourses d'études accordées par le Conseil national de Recherches du Canada, les firmes C.I.L. et Shell Oil et l'Office de Recherches scientifiques de la Province de Québec.*
[3]*Consulter la référence 8 pour la bibliographie des mémoires antérieurs concernant cette réaction.*

La différence de 0.018 mole peut provenir d'une part, de l'hydrolyse d'une certaine quantité du composé azoxyque II en l'acide correspondant IV, qui par sublimation se transforme en la lactone de l'acide 5-chloro-2-[5-chloro-3-oxy-indazyl-(2)]-benzoïque (V), et d'autre part, de l'hydrolyse partielle du produit neutre III en 3,8-dichloro-6-cétoquinazolo[1,2,2′,3′]indazol (VI) (3).

La formation de la substance neutre III qui dépend de celle du 4,4′-dichloro-2,2′-dicyanoazoxybenzène (II) (ou du dicarbamyle correspondant), est ainsi, d'après les résultats précédents, indirectement reliée à celle du cyanate et partant de l'anhydride carbonique (*d*).

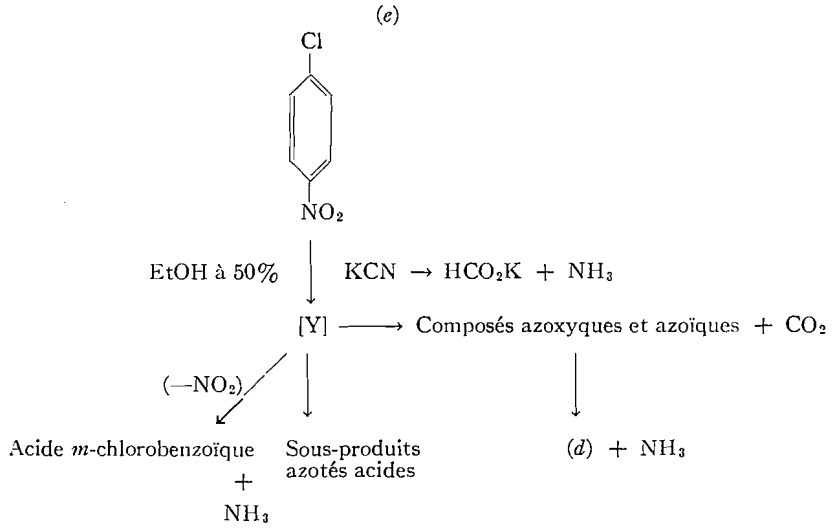
Nous avons aussi dosé l'ammoniac qui se dégage au cours de la réaction du *p*-chloronitrobenzène avec le cyanure de potassium dans l'éthanol à 50% ou le 2-éthoxyéthanol à 50%. Dans l'un ou l'autre solvant, la quantité d'ammoniac dégagé correspond à environ 75% de la substance nitrée de départ, les corrections étant faites pour l'apport de l'ammoniac attribuable aux réactions secondaires (*a*) et (*b*).



Ces réactions secondaires enlèvent à la réaction de von Richter toute valeur synthétique, parce qu'une réaction d'oxydo–réduction entre le groupe nitré et le cyanure de potassium

Can. J. Chem. Downloaded from www.nrcresearchpress.com by 210.87.254.105 on 09/05/12
For personal use only.

accompagne la fixation du groupement nitrile au noyau aromatique. En nous basant sur les observations précédentes et d'autres faites jusqu'ici concernant cette réaction, nous pouvons déduire que celle-ci, en plus de donner naissance à un acide dans lequel le groupe nitré est éliminé, engendre divers composés azotés plus ou moins réduits selon les transformations indiquées en (*e*), Y représentant un intermédiaire.



Excepté l'acide 4,4′-dichloroazoxybenzène-2,2′-dicarboxylique qui se transforme en la lactone de l'acide 5-chloro-2-[5-chloro-3-oxy-indazyl-(2)]-benzoïque, les sous-produits acides (80% du total) ne se subliment pas. Ceci porte à croire que la majeure partie des substances à caractère acide qui accompagnent l'acide *m*-chlorobenzoïque dans le produit de la réaction ne sont pas des dérivés réduits azoïques, azoxyques, hydrazoïques, indazylbenzoïques ou anthraniliques; car ceux-ci sont tous sublimables.

Dans le but d'observer si un intermédiaire s'accumule durant la réaction, nous avons déterminé la quantité des principales substances qui se trouvent dans le produit de la réaction après une ébullition plus ou moins prolongée des réactifs. Nous présentons au Tableau I les résultats de cette série d'expériences.

Après 2 heures d'ébullition à reflux d'une solution de 0.01 mole de *p*-chloronitrobenzène et de 0.1 mole de cyanure de potassium dans le tétrahydrofurfurol à 50%, tout le *p*-chloronitrobenzène est disparu et le poids des acides bruts ne varie plus, quel que soit le temps de chauffage. Cependant, l'acide *m*-chlorobenzoïque continue de se former lentement pendant encore plusieurs heures au détriment, semble-t-il, des autres produits acides, car le poids de ces derniers diminue proportionnellement à celui de l'acide *m*-chlorobenzoïque qui se forme. De 2 heures à 48 heures, le rendement de l'acide *m*-chlorobenzoïque augmente de 6% alors que celui du résidu acide diminue de 5%. Pendant le même temps, le pourcentage du produit neutre, le 3,8-dichloro-6-iminoquinazolo[1,2,2′,3′]indazol (V), décroît aussi après avoir atteint un maximum. C'est qu'il s'hydrolyse très lentement dans le milieu réactionnel en 3,8-dichloro-6-cétoquinazolo[1,2,2′,3′]indazol (VI) (2).

Rauhut et Bunnett ont observé qu'une solution alcoolique diluée de *m*-nitroanisole et de cyanure de sodium donne du 4,4′-diméthoxy-2,2′-dicarbamylazoxybenzène sans acide *m*-anisique, lorsqu'elle est bouillie à reflux (4), mais qu'elle produit 3% d'acide anisique en plus d'un composé neutre non-identifié, lorsqu'elle est chauffée en tube scellé,

Can. J. Chem. Downloaded from www.nrcresearchpress.com by 210.87.254.105 on 09/05/12
For personal use only.

TABLEAU I

Pourcentage des produits formés par la réaction du *p*-chloronitrobenzène et du cyanure de potassium dans le tétrahydrofurfurol à 50% en fonction du temps d'ébullition

Temps d'ébullition, heures	*p*-Chloro-nitrobenzène récupéré, %	Produits neutres		Produits acides		
		Bruts %	*k** %	Bruts %	Acide *m*-chloro-benzoïque	Résidu %
¼	45.5	2.0	—	20.2	3.0	17.2
½	29.1	12.0	1.6	38.0	8.0	30.0
¾	14.8	15.8	3.5	52.0	14.6	37.4
1	4.5	17.8	5.2	58.0	18.0	40.0
1½	3.5	14.2	4.5	58.0	20.0	38.0
2	0.0	15.0	4.5	70.0	22.0	48.0
4	0.0	13.0	—	70.0	24.0	46.0
8	0.0	11.5	3.6	70.8	25.0	45.0
24	0.0	—	—	—	29.0	—
48	0.0	9.0	2.6	71.0	28.0	43.0

*6-Iminoquinazolo[1,2,2′,3′]indazol.

à 180° (5). Ceci laisse supposer que le 4,4′-diméthoxy-2,2′-dicarbamylazoxybenzène peut se transformer en acide *m*-anisique en présence de cyanure de sodium; mais, nous avons vérifié que cela ne se produit dans l'éthanol aqueux, ni à l'ébullition dans le glycol à 50%, ni en tube scellé à 180°. Lorsqu'il est bouilli à reflux dans le méthanol avec de l'hydroxyde de potassium, le 4,4′-diméthoxy-2,2′-dicarbamylazoxybenzène se transforme en acide 4,4′-diméthoxybenzène-2,2′-dicarboxylique et non en acide *m*-anisique (4).

Soumis aux conditions de la réaction de von Richter, l'acide 4,4′-dichloroazoxybenzène-2,2′-dicarboxylique ne subit aucune transformation (5); le 2,2′-dicyanoazoxybenzène donne du 6-iminoquinazolo[1,2,2′,3′]indazol, mais non de l'acide benzoïque (2); le 2-nitro-4-chlorobenzonitrile ne fournit pas d'acide *p*-chlorobenzoïque (6) et nous avons constaté que l'acide 2-nitro-5-chlorobenzoïque, le 2-nitro-5-chlorobenzonitrile et la 2-nitro-5-chlorobenzamide n'engendrent ni l'acide *m*-chlorobenzoïque, ni aucun des produits azoxyques que fournit normalement la réaction. Ceux-ci sont donc formés au cours de la réaction par la réduction de l'intermédiaire dihydroaromatique I et non des substances aromatiques correspondantes (*d*).

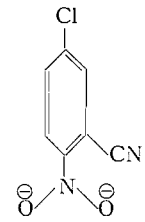
Von Richter a proposé un mécanisme de la réaction (7), qui a été temporairement accepté par Bunnett et quelques collaborateurs (8). Ce mécanisme supposait qu'un intermédiaire dihydroaromatique (I) se transforme en nitrile par l'addition et l'élimination successive d'un proton, puis qu'il se produit le départ nucléofuge de l'ion nitrite.

Bunnett et Rauhut (6) ont ensuite suggéré que l'élimination du groupement nitré sous forme de l'ion nitrite passe par l'intermédiaire d'un "imino-anhydride" (imino-isoxazoline) et d'un anhydride mixte de l'acide nitreux et de l'acide carboxylique. Dernièrement, Samuel (9) a observé que, lorsque la réaction est exécutée dans un solvant dont l'eau a été enrichie en isotope ^{18}O, l'acide carboxylique obtenu ne contient que la moitié de l'oxygène ^{18}O qu'il devrait posséder si les deux atomes d'oxygène du groupe carboxylique provenaient de l'eau. Il en conclut que l'un des atomes d'oxygène doit provenir du groupement nitré et que cela confirme le mécanisme proposé par Bunnett et Rauhut.

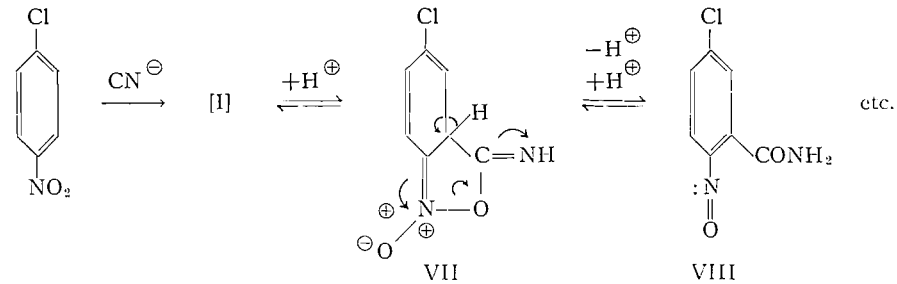
Tout récemment, après avoir constaté qu'il se trouve dans le produit de la réaction du *p*-chloronitrobenzène 50% d'azote et pas plus de 3% de l'ion nitrite qui devrait se former selon le mécanisme précédent, Rosenblum (10) a proposé une ingénieuse modification pour expliquer l'élimination de l'azote qui accompagnerait la formation de l'acide

Can. J. Chem. Downloaded from www.nrcresearchpress.com by 210.87.254.105 on 09/05/12
For personal use only.

m-chlorobenzoïque; mais néanmoins, il y a lieu de douter de l'existence de l'anion aromatique bivalent

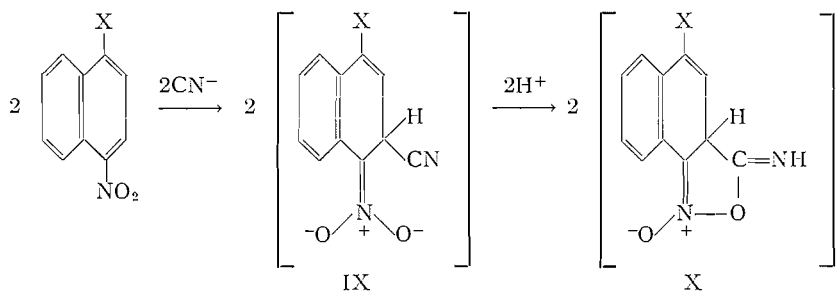


que cet auteur considère comme un intermédiaire de la réaction et qui n'est d'ailleurs pas nécessaire pour interpréter la formation du 4-nitroso-3-carbamylchlorobenzène (VIII), clef de ce nouveau mécanisme. En effet, nous sommes d'avis que la formation de l'intermédiaire VIII peut s'expliquer normalement par l'intermédiaire dihydroaromatique I des mécanismes précédents (6, 8, 9), de la façon suivante:



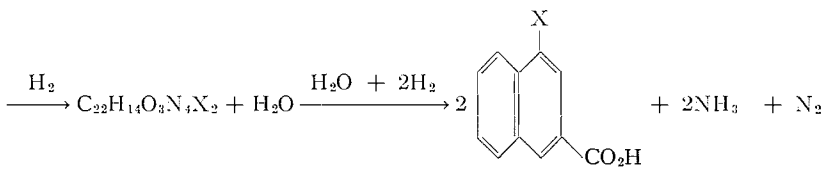
Quoi qu'il en soit, il est certain que dans la série du benzène, lorsque la substance nitrée est réduite en composés azoxyques ou azoïques, ces derniers ne peuvent pas se transformer en acides benzoïques dans les conditions de la réaction et ils sont isolés tels quels ou sous la forme de dérivés de l'indazol (2, 3). Par contre, dans la série du naphtalène, les substances, $C_{22}H_{14}O_3N_4Cl_2$ et $C_{22}H_{16}O_3N_2$, que nous avons respectivement isolées à la suite de réactions de von Richter avec le 4-chloro-1-nitronaphtalène et le nitronaphtalène suivant des conditions quelque peu modifiées, donnent naissance aux acides 4-chloro-2-naphtoïque et 2-naphtoïque (11), lorsqu'elles sont soumises aux conditions normales de la réaction.

À un atome d'oxygène près, la formule brute $C_{22}H_{14}O_3N_4X_2$ (X = H ou Cl) est le double de l'intermédiaire X, analogue à l'intermédiaire imino-anhydride proposé par Bunnett pour la réaction dans la série du benzène. Elle suppose l'union de deux molécules du dérivé nitré du naphtalène par réduction (*f*).



(*f*)

Can. J. Chem. Downloaded from www.nrcresearchpress.com by 210.87.254.105 on 09/05/12
For personal use only.



X = Cl ou H

Si ces composés sont vraiment des intermédiaires de la réaction, il faudrait convenir que le mécanisme (du moins dans la série du naphtalène) fait intervenir un composé de réduction qui réunit deux molécules du produit de départ. Nous tentons présentement de trancher cette question.

PARTIE EXPÉRIMENTALE[1]

La réaction de von Richter a été exécutée en faisant bouillir à reflux une solution de *p*-nitrochlorobenzène et de cyanure de potassium.

Rendement en fonction du temps

On fait bouillir à reflux une solution comprenant une partie de *p*-nitrochlorobenzène et quatre parties de cyanure de potassium dans 10 parties de tétrahydrofurfurol à 50% (en volume). Au moment désiré, la réaction est interrompue. Les produits sont isolés et purifiés selon le mode opératoire déjà décrit (3). Les résultats sont présentés au Tableau I.

Dosage de l'anhydride carbonique

Du *p*-chloronitrobenzène (2.0 g), du cyanure de potassium (6.0 g) et du 2-éthoxyéthanol à 50% (30 ml) sont introduits dans un ballon de 100 ml à trois cols dont l'un est pourvu d'un réfrigérant, un autre d'un entonnoir à décantation et le troisième d'un tube de verre qui plonge dans le mélange réactionnel et peut être fermé à l'aide d'un robinet. Le mélange est bouilli à reflux pendant 4 heures, les robinets de l'entonnoir et du tube de verre étant fermés. Une fois la réaction terminée, après quelques minutes de repos à la température ambiante, on relie le réfrigérant à un flacon contenant 225 ml d'eau de baryte par un tube de verre qui plonge dans la solution de baryte. Tout en faisant barbotter un courant d'azote dans le mélange réactionnel, on y introduit, à l'aide de l'entonnoir, un excès d'acide chlorhydrique concentré suffisant pour rendre acide le produit de la réaction et on chauffe pour en chasser tout l'anhydride carbonique.

Le précipité de carbonate de baryum est filtré, lavé à l'eau, suspendu dans 50 ml d'eau, puis transformé en sulfate. Le précipité de sulfate de baryum est essoré, lavé par l'eau, séché et calciné. On obtient 0.4415 g de sulfate de baryum correspondant à 0.00189 mole (0.083 g) d'anhydride carbonique ou à 0.148 mole pour une mole de *p*-chloronitrobenzène. Dans une expérience témoin, sans *p*-chloronitrobenzène, il ne se forme pas d'anhydride carbonique.

Dosage de l'ammoniac

On introduit dans un ballon de 100 ml à deux tubulures, 2.0 g de *p*-chloronitrobenzène, 6.0 g de cyanure de potassium et 20 ml d'éthanol à 50%. L'un des cols du ballon est muni d'un tube de verre qui s'arrête au-dessus de la surface des réactifs et l'autre, d'un réfrigérant dont l'extrémité est reliée à un flacon laveur renversé et de là à une fiole conique par un tube qui plonge dans 100 ml d'acide chlorhydrique 0.5 *N*. On chauffe à

[1]*Les points de fusion ont été déterminés en tubes capillaires et ne sont pas corrigés.*

Can. J. Chem. Downloaded from www.nrcresearchpress.com by 210.87.254.105 on 09/05/12
For personal use only.

reflux pendant 47 heures et laisse ensuite reposer pendant quelques minutes à la température ambiante, tout en faisant circuler un courant d'azote dans l'appareil pour éviter les retours. On ajoute ensuite au mélange réactionnel, 10 ml d'une solution d'hydroxyde de potassium à 50% et fait bouillir de nouveau à reflux pendant une heure.

Pour neutraliser l'excès d'acide chlorhydrique 0.5 *N*, il faut 64.3 ml de soude 0.5 *N*. La différence, 35.7 ml (100−64.3), équivaut à 0.0179 mole (0.304 g) d'ammoniac ou 1.41 mole pour 1 mole de *p*-chloronitrobenzène. Une expérience témoin, en l'absence de *p*-chloronitrobenzène, a fourni 0.10845 g d'ammoniac. Ceci indique que 0.4301 g ou 7.18% du cyanure de potassium est hydrolysé durant la réaction.

Traitement de diverses substances dans les conditions de la réaction de von Richter

(a) 2,2′-Dicyanoazoxybenzène

À une solution de 9.0 g de 2-nitrobenzonitrile dans 75 ml d'acide acétique et 10 ml d'anhydride acétique on ajoute petit à petit (environ $1\frac{1}{4}$ heures) 12.0 g de zinc en poudre, sous agitation mécanique et en maintenant la température du mélange entre 30 et 35°. La pâte est ensuite versée dans 1 litre d'eau glacée et essorée. Le précipité est traité par 300 ml d'une solution de carbonate à 10% pendant 15 minutes à 40°, filtré et lavé à l'eau. Le solide est dissous dans de l'éthanol et la solution traitée au noir animal et filtrée. Le 2,2′-dicyanoazoxybenzène (3.9 g; 53% de la théorie) cristallise en fines aiguilles fondant à 192–193° (p.f. lit. 194° (12)).

Une solution de 1.0 g de 2,2′-dicyanoazoxybenzène et de 30 g de cyanure de potassium dans 200 ml de glycol d'éthylène aqueux (90%) est bouillie à reflux pendant 3 heures. Le produit de la réaction traité de la façon habituelle (2) a fourni 0.08 g de 6-iminoquinazolo-[1,2,2′,3′]indazol, mais pas d'acide benzoïque.

(b) 4,4′-Diméthoxy-2,2′-dicarbamylazoxybenzène

Le *p*-nitrophénol est méthylé, avec un rendement de 70% de la théorie, par le sulfate de méthyle, suivant les données d'Ullman (13) pour la méthylation de l'*o*-nitrophénol, et transformé en 4,4′-diméthoxy-2,2′-dicarbamylazoxybenzène (4). Ce dernier composé (1.0 g) se décompose, lorsqu'il est traité par la potasse (0.05 g) dans le glycol (10 ml) et ne réagit pas, en tube scellé à 150°, avec du cyanure de potassium (3.0 g) dans l'éthanol à 50% (10 ml).

(c) 2-Nitro-5-chlorobenzamide

De la 2-nitro-5-chlorobenzamide (3.5 g), obtenue à partir de l'acide 2-nitro-5-chlorobenzoïque préparé selon Bunnett (4), est bouillie à reflux pendant 24 heures avec 10.0 g de cyanure de potassium en solution dans 35 ml d'éthanol à 50%. Le produit de la réaction traité de la façon habituelle (2) ne fournit que des traces d'un produit acide qui n'est pas de l'acide *m*-chlorobenzoïque et un sublimé différent de la lactone de l'acide 5-chloro-2-[5-chloro-3-oxy-indazyl(2)]-benzoïque.

(d) 2-Nitro-5-chlorobenzonitrile

Du pentoxyde de phosphore (8.0 g) est intimement mélangé à de la 2-nitro-5-chlorobenzamide (4.0 g) et chauffé sous pression réduite. Le 2-nitro-5-chlorobenzonitrile distille à 120°/20 mm Hg. Il cristallise dans l'éthanol en aiguilles jaune pâle et on en recueille 1.53 g (40% de la théorie) fondant à 94°. Calculé pour $C_7H_3O_2N_2Cl$: C, 46.30%; H, 1.82%; N, 15.50%. Trouvé: C, 46.20%; H, 1.65%; N, 15.40%. Lorsque 0.70 g de 2-nitro-5-chlorobenzonitrile est bouilli à reflux pendant 24 heures avec 3.0 g de cyanure de potassium dans 20 ml d'éthanol à 50%, il se dégage de l'ammoniac, mais il ne se forme pas d'acide *m*-chlorobenzoïque. Des produits acides (0.346 g) seule une petite quantité (0.086 g)

Can. J. Chem. Downloaded from www.nrcresearchpress.com by 210.87.254.105 on 09/05/12
For personal use only.

d'une substance de p.f. 320° est obtenue par sublimation. Celle-ci n'est pas la lactone de l'acide 5-chloro-2-[5-chloro-3-oxy-indazyl-(2)]-benzoïque.

Après avoir bouilli à reflux pendant 24 heures 5.0 g d'acide 5-chloroanthranilique (5) avec 15.0 g de cyanure de potassium dans 50 ml d'éthanol à 50%, 3.0 g (60%) d'acide 5-chloroanthranilique peuvent être récupérés, mais il ne se trouve pas d'acide *m*-chlorobenzoïque.

REMERCIEMENTS

Nous remercions le Conseil national de Recherches du Canada, les firmes C.I.L. et Shell Oil, ainsi que l'Office de Recherches scientifiques de la Province de Québec, pour des bourses d'études accordées à l'un de nous (E.C.).

BIBLIOGRAPHIE

1. C. A. De Bruyn et J. W. van Guens. Rec. trav. chim. **23**, 29 (1904).
2. E. Cullen et Ph. L'Écuyer. Can. J. Chem. **39**, 155 (1961).
3. E. Cullen et Ph. L'Écuyer. Can. J. Chem. **39**, 144 (1961).
4. M. M. Rauhut et J. F. Bunnett. J. Org. Chem. **21**, 939 (1956).
5. J. F. Bunnett, J. F. Cormack et F. C. McKay. J. Org. Chem. **15**, 481 (1950).
6. J. F. Bunnett et M. M. Rauhut. J. Org. Chem. **21**, 944 (1956).
7. V. von Richter. Ber. **8**, 1418 (1875).
8. J. F. Bunnett, M. M. Rauhut, D. Kutson et G. E. Bussell. J. Am. Chem. Soc. **76**, 5755 (1954).
9. D. Samuel. J. Chem. Soc. 1318 (1960).
10. M. Rosenblum. J. Am. Chem. Soc. **82**, 3796 (1960).
11. E. Cullen et Ph. L'Écuyer. Can. J. Chem. **39**, 382 (1961).
12. J. Pinnow et E. Müller. Ber. **28**, 149 (1895).
13. F. Ullmann. Ann. **327**, 114 (1903).

Can. J. Chem. Downloaded from www.nrcresearchpress.com by 210.87.254.105 on 09/05/12
For personal use only.

Can. J. Chem. Downloaded from www.nrcresearchpress.com by 210.87.254.6 on 09/05/12
For personal use only.

FRIEDEL–CRAFTS REARRANGEMENTS IN BRANCHED CONDENSED RING SYSTEMS

I. OCTAMETHYLOCTAHYDROANTHRACENE[1]

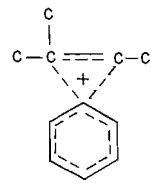
L. R. C. Barclay, A. H. Gray, and C. E. Milligan

ABSTRACT

Treatment of 1,1,4,4,5,5,8,8-octamethyl-1,2,3,4,5,6,7,8-octahydroanthracene ($C_{22}H_{34}$, I) with aluminum chloride produced a new hydrocarbon ($C_{22}H_{32}$, II) containing a conjugated olefinic double bond. Hydrocarbon II was proved to be 1,1,5,5,8,8-hexamethyl-3-isopropyl-5,6,7,8-tetrahydrobenzindene by spectral data, by oxidative studies, and by a synthesis of its reduction product, 1,1,5,5,8,8-hexamethyl-3-isopropyl-5,6,7,8-tetrahydrobenzindane (III). A benzenonium ion mechanism is postulated to explain the 1,2-phenyl shift accompanied by dehydrogenation in the formation of II from I. The detection of hydrogen in the off gas of the rearrangement supports this mechanism. A similar benzenonium ion mechanism can be applied to elucidate the mechanism of isomerization of tertiary to secondary alkylbenzenes reported in the literature.

INTRODUCTION

The branched condensed hydrocarbon octamethyloctahydroanthracene (I) provides an interesting system for conducting isomerizations under Friedel–Crafts conditions. Since in I the tertiary alkyl groups are part of a ring system, the nature of the products of rearrangement is expected to provide information on the mechanism of isomerization of tertiary to secondary alkylbenzenes. Such isomerizations were observed by Schmerling and West (1), who made the general observation that the formation of a tertiary alkylbenzene in the presence of catalysts such as aluminum chloride was really the exception rather than the general rule even when the alkyl halide used was tertiary. In the case of alkylation of benzene with *t*-pentyl chloride, they proposed that the tertiary alkylate is formed first and this is subsequently isomerized to the secondary alkylate by migration of a methyl or of a phenyl group. Schmerling and co-workers (2) later suggested that the rearrangement could take place through the cyclic bridged benzenonium ion—*



Roberts and Han (3) proposed the same mechanism to explain the conversion of *t*-pentylbenzene into 2-methyl-3-phenylbutane. Essentially this mechanism requires that the phenyl group is the migrating species in this arrangement rather than methyl migration. In a recent communication, however, Slaugh and Raley (4) made the general statement that Lewis acids produce no 1,2-phenyl migrations but rather lead to methyl migration processes.

In a system such as octamethyloctahydroanthracene (I) where the tertiary alkyl groups are in a ring system, a rearrangement where the phenyl group migrates through a benzenonium ion mechanism would lead to ring contraction. On the other hand if methyl groups migrate there would be no change in ring size. For this reason I was

[1]*Manuscript received December 1, 1960.*
Contribution from the Department of Chemistry, Mount Allison University, Sackville, New Brunswick. Reported in part at the 43rd Annual Conference of the Chemical Institute of Canada, Ottawa, Ontario, June 14, 1960.

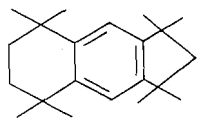
The term "benzenonium ion" introduced by W. von E. Doering. Tetrahedron, **4, 178 (1958) is used on the recommendation of the referee.*

selected for some initial experiments on isomerization of tertiary alkylbenzenes under Friedel–Crafts conditions.

DISCUSSION OF RESULTS

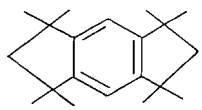
Treatment of octamethyloctahydroanthracene ($C_{22}H_{34}$, I) with aluminum chloride in tetrachloroethane or carbon disulphide converted it into a new crystalline compound, $C_{22}H_{32}$, II. The ultraviolet spectrum of II indicated the presence of a substituted conjugated olefinic double bond. There was a broad band at 260 mμ, ϵ = 11,220 and weaker bands at 288 mμ, ϵ = 2884 and 299 mμ, ϵ = 3162. The infrared spectrum of II showed a strong band at 11.3 microns attributed to 1,2,4,5-tetrasubstitution since this band was also observed for I. High-temperature mass spectral analysis of II established the parent mass to be 296, compared to 298 for I. There was also a strong peak in the mass spectrum of II at mass 253 corresponding to the loss of a C_3H_7 fragment. On catalytic reduction, II was converted into a compound III, $C_{22}H_{34}$, isomeric with I. This reduction product also lost a propyl fragment on high-temperature mass spectral analysis.

An important lead to the structure of III was provided by its ultraviolet spectrum. This spectrum was very similar to that of 1,1,3,3,5,5,8,8-octamethyl-5,6,7,8-tetrahydrobenzindane (IV) prepared by alkylating 1,1,3,3-tetramethylindane with 2,5-dichloro-2,5-dimethylhexane.



(IV)

Hydrocarbon IV showed bands at 279 mμ, ϵ = 2408; 273.5 mμ (side band), ϵ = 1815; 270 mμ, ϵ = 2007; and a shoulder at 265.5 mμ. Hydrocarbon III showed bands at 280.5 mμ, ϵ = 2371; 275 mμ (side band), ϵ = 1908; 271.5 mμ, ϵ = 2067; and a shoulder at 267 mμ. The curves for III and IV had the same shape, the only significant difference was a shift in the spectrum of III of 1.5 mμ to longer wavelengths. On the other hand the spectrum of III showed distinct differences from that of octamethyloctahydroanthracene (I). The latter showed only two bands, at 278 mμ, ϵ = 1096, and 270 mμ, ϵ = 955. Furthermore the ultraviolet spectrum of I was practically identical with that of some other methylated octahydroanthracenes which we have synthesized such as the hexamethyl- and heptamethyl-octahydroanthracenes. The spectra of I and IV are both somewhat different from the spectrum of 1,1,3,3,5,5,7,7-octamethylhydrindacene (V) (5) —

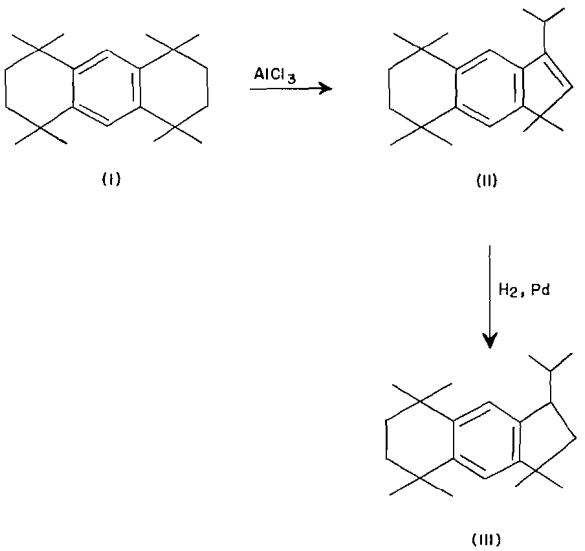


(V)

The latter had bands at 281 mμ, ϵ = 4725; 276 mμ, ϵ = 4243; 271.5 mμ, ϵ = 3760; and 267 mμ, ϵ = 2700. This shows that the degree of substitution around the non-aromatic rings has little effect on the character of ultraviolet absorption of the condensed ring systems. On the other hand the size of the non-aromatic rings has a more pronounced effect on the intensity and shape of the curves. Thus ultraviolet analysis provides a convenient means of deciding whether these ring systems are 6,6,6-, 6,6,5-, or 5,6,5-tricyclic systems.

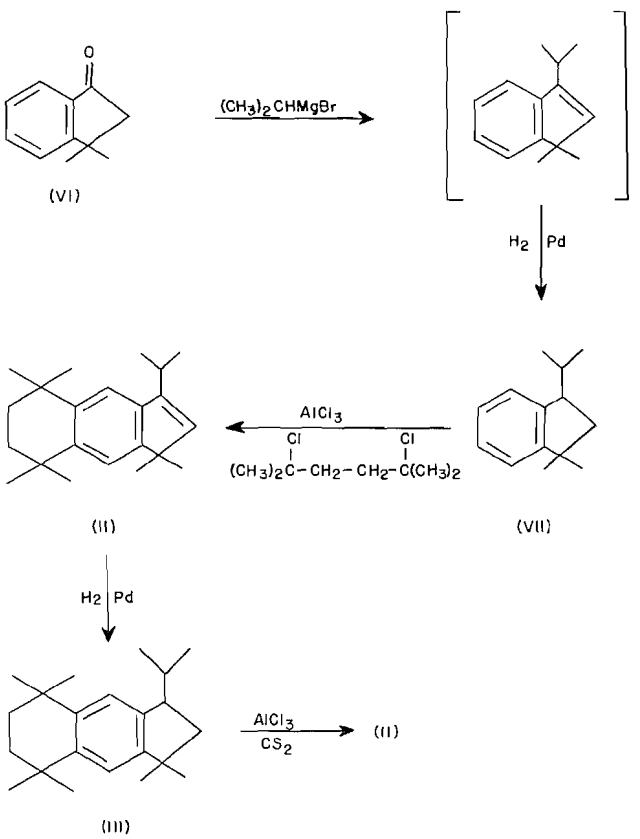
Can. J. Chem. Downloaded from www.nrcresearchpress.com by 210.87.254.6 on 09/05/12
For personal use only.

The structures shown below for II and III seemed reasonable from the spectral evidence.



(I) (II) (III)

Compound II was tentatively assigned the endocyclic formulation since the exocyclic form would not be expected to lose a C_3H_7 fragment on mass spectral analysis. The structure suggested for III was confirmed by a classical synthesis which is outlined below—



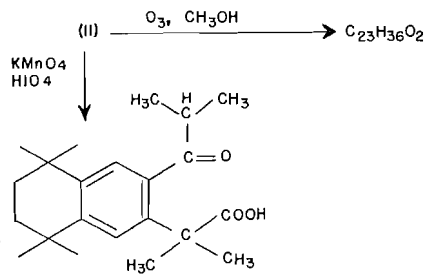
(VI) (II) (VII) (III) (II)

Can. J. Chem. Downloaded from www.nrcresearchpress.com by 210.87.254.6 on 09/05/12
For personal use only.

Can. J. Chem. Downloaded from www.nrcresearchpress.com by 210.87.254.6 on 09/05/12
For personal use only.

Friedel–Crafts alkylation of 3,3-dimethyl-1-isopropylindane (VII) with 2,5-dimethyl-2,5-dichlorohexane actually yielded the conjugated olefin II instead of the expected reduction product (III). This synthetic product was reduced for further identification and the reduction product proved to be identical with III.

The above synthesis confirmed the structure suggested for III but the position of the olefinic double bond in II remained to be established. The endocyclic formulation is in agreement with the work of Myhre (6), who produced a compound identical with our II by treatment of I with aluminum chloride. Although Myhre did not arrive at the structure of II, he hydroxylated it with permanganate followed by lead tetraacetate cleavage to produce a single product whose infrared spectrum indicated two carbonyl groups, an unconjugated aldehyde and a conjugated ketone. Our attempts to convert II into this dicarbonyl compound by ozonolysis in methanol yielded instead a mixture. By chromatography and recrystallization there was isolated from this mixture a compound of melting point 114–115° which had an ultraviolet spectrum practically identical with that of I. The infrared spectrum of this compound showed no carbonyl absorption but rather had two strong bands in the region of ether absorption at 8.85 and 9.45 microns. The compound analyzed for a methoxyl group and the ultimate analysis corresponded to $C_{23}H_{36}O_2$. The structure of this ozonolysis product was not definitely established. The spectral and ultimate analyses indicate a six-membered cyclic ether containing in addition a methoxyl group. Such a compound could only have formed from an endocyclic olefin, II.



The endocyclic formulation for II was confirmed in a more regular manner by permanganate–periodate oxidation. This oxidation yielded an aldehydic compound and an acidic compound both of which showed two strong carbonyl bands in the infrared at 5.90 and 5.75 microns. The acid had a strong band in the ultraviolet at 253 mμ attributed to the conjugated ketone. Its neutralization equivalent corresponded to the theoretical value for $C_{21}H_{31}OCOOH$. The conclusion arrived at by these degradative studies was later confirmed by the nuclear magnetic resonance spectrum* of II. This spectrum had a peak at −348 c.p.s. removed from tetramethylsilane, the internal standard. This peak was attributed to an olefinic proton which confirms the endocyclic formula II since the alternative exocyclic olefin could not have a hydrogen on the olefinic double bond.

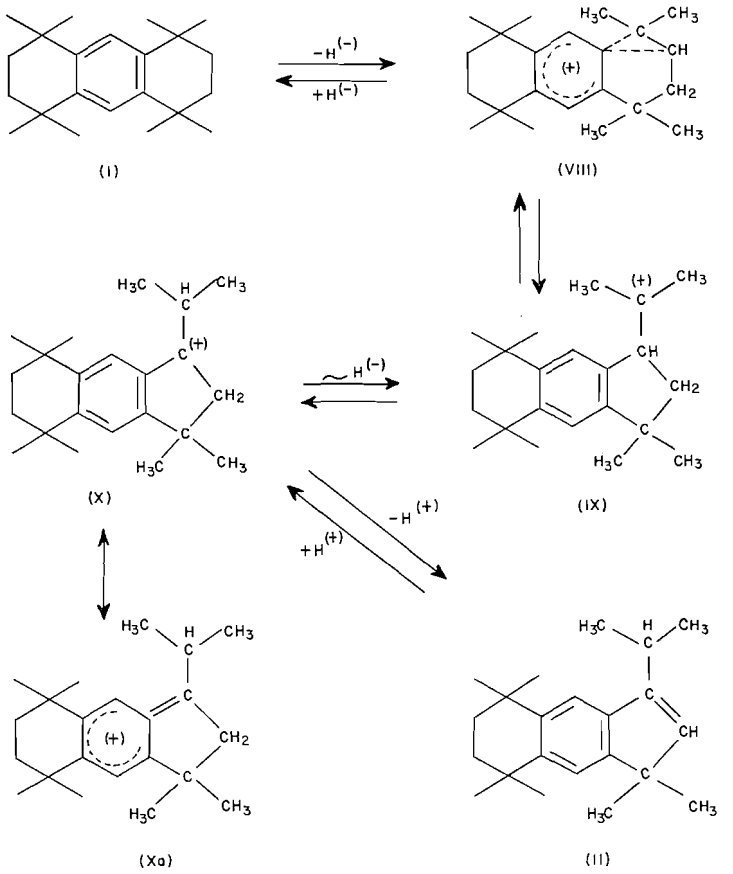
It is apparent that the more substituted exocyclic olefin is not favored in this reaction. A molecular model of the exocyclic olefin was made using Stuart and Briegleb models. In this model the methyl groups on the olefinic double bond are coplanar with the benzene ring resulting in a very strong steric interaction between one methyl and an ortho hydrogen. There is, of course, no such unfavorable interaction in the endocyclic compound II, which is therefore the principal product.

*We are indebted to Dr. Robert R. Fraser of the Chemistry Department, University of Ottawa, who measured and interpreted this spectrum.

Treatment of I with aluminum chloride in benzene did not yield the rearrangement compound (II). In this case the main product was 1,1,4,4-tetramethyltetralin. Thus, in benzene solution, the main reaction is disproportionation of I instead of rearrangement.

THE MECHANISM OF THE REARRANGEMENT

In a preliminary communication (7) it was suggested that the rearrangement of I to II proceeded via a hydrogen-bridged π-complex involving opening of a ring by displacement of a side chain with a proton. A more attractive mechanism for this 1,2-phenyl migration is a benzenonium ion mechanism. In this mechanism it is proposed that the catalyst extracts a hydride ion from a —CH_2— group of a side chain to initiate the reaction. The benzene ring could participate in the displacement of the hydride ion by anchimeric assistance through a cyclic bridged benzenonium ion (VIII). The mechanism is outlined below:



The carbonium ion X would be more stable than IX because the former is stabilized by resonance interaction with the directly attached benzene ring (X*a*). Loss of a proton from X produces the product isolated (II). It is not necessary for the reduction product III to be an intermediate in this reaction. We were unable to detect any of III by chromatographic fractionation of the reaction product. Of course this does not rule out the possibility of III being an intermediate especially since we found that aluminum chloride

Can. J. Chem. Downloaded from www.nrcresearchpress.com by 210.87.254.6 on 09/05/12
For personal use only.

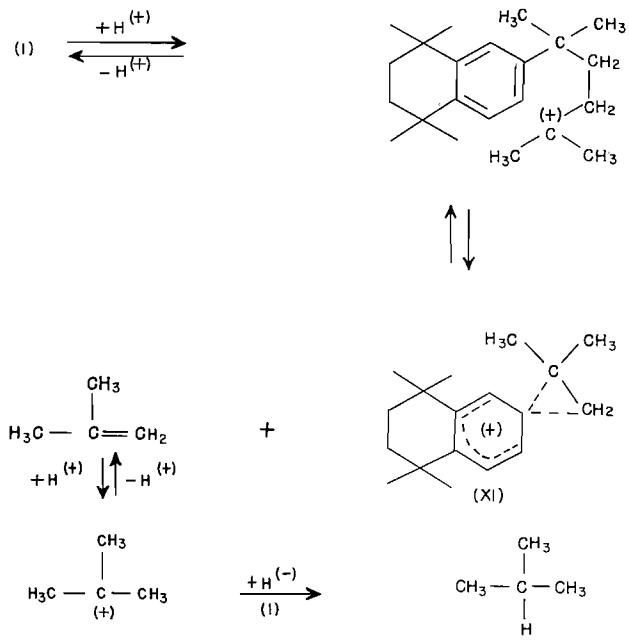
Can. J. Chem. Downloaded from www.nrcresearchpress.com by 210.87.254.6 on 09/05/12
For personal use only.

treatment of III in carbon disulphide produced II. Treatment of III with aluminum chloride in tetrachloroethane alone did not yield sufficient II for characterization. The product in this case was a complex mixture containing some unchanged III, some non-crystalline products with strong absorption in the 260 mμ region, and a new crystalline compound with a strong band at 241 mμ and bands at 291 and 302 mμ. Such a spectrum is typical of extended conjugation. This material was not available in sufficient amount for a characterization but this spectrum indicates that it may have been formed by a rearrangement–dehydrogenation of both of the non-aromatic rings. Treatment of III with aluminum chloride and *t*-butyl chloride as a promoter in tetrachloroethane yielded II accompanied by the evolution of isobutane.

Nenitzescu (8) proposed that aluminum chloride exerts its strong catalytic action by formation of a strong acid $H^+AlCl_3\bar{O}H$ with traces of water. This strong acid initiates rearrangements by extraction of a hydride ion as follows:

$$R{-}H + H^+AlCl_3\bar{O}H \rightarrow R^+AlCl_3\bar{O}H + H_2.$$

The reaction can then be propagated as a chain reaction through carbonium ions which act as hydride ion acceptors. To support this concept they found traces of molecular hydrogen in the off gases from isomerizations. In this case the hydrogen was detected by combustion to water. Despite this discovery, Deno and co-workers (9) made the general observation that the hydride ion transfer reaction has the characteristic of *not* reacting with labile protons of the medium to form molecular hydrogen. It therefore was desirable to attempt to confirm the findings of Nenitzescu and co-workers by analyzing the off gases from our reaction directly for hydrogen. Vapor phase chromatographic and mass spectral analyses definitely showed the presence of hydrogen in the off gases. The major fraction of the off gases consisted of the hydrocarbons, isobutane and isopentane. Isobutane could have originated from I by side reactions as outlined below:



Elimination of isobutylene takes place by displacement of a side chain by the catalyst followed by fragmentation to yield isobutylene and the intermediate XI. The isobutylene could then be protonated by the catalyst to form a *t*-butyl cation which also would act as a hydride ion acceptor in promoting rearrangement of I. The production of isobutane thus takes place by a process which is just the reverse of the reaction proposed recently (5) to explain the cyclialkylation of 1,3,5-tri-*t*-butylbenzene through a benzenonium ion intermediate analogous to XI yielding I. When a trace of D_2O was added to the reaction during rearrangement of I, the infrared spectrum of the evolved isobutane showed a band in the C—D region at 4.6 microns. Deuterated isobutane would be expected to form if the isobutane originated as postulated. The isopentane could have originated by a process similar to that suggested for isobutane except that rearrangement must have taken place in a displaced side chain before the C_5 fragment was split off. No products were isolated from the rearrangement corresponding to the aromatic fragment XI. This intermediate probably undergoes polymerization to account for the resinous by-product formed in the reaction.

In order to substantiate the proposed mechanism for the conversion of I to II, attempts are being made to isolate the benzenonium ion intermediate as a stable salt.

EXPERIMENTAL

Apparatus and Procedures

The melting points are uncorrected. Ultraviolet spectra were recorded on a Beckman DK-2 ratio recording spectrophotometer using spectro-grade cyclohexane as solvent. Infrared spectra were recorded on a Perkin–Elmer Model 136 Infracord. Mass spectroscopic analyses were determined in an independent laboratory. A high-temperature inlet mass spectrometer was used for solids. The aluminum chloride was Fisher Certified Reagent, anhydrous sublimed, used as received. The rearrangement reactions were carried out at room temperature in an atmosphere of pure nitrogen. The apparatus was attached to a Perkin–Elmer Model 154-D vapor fractometer for direct analysis of the off gases. The product from the aluminum chloride – solvent mixture was worked up in the usual way and then in each case subjected to chromatography from petroleum ether on Fisher chromatographic alumina. The progress of the fractionation was followed by periodic analysis of the eluate from the column on the recording ultraviolet spectrophotometer. In this way the various possible components of the hydrocarbon mixture such as compounds I, II, and III could quite easily be detected and separated.

The Action of Aluminum Chloride on Octamethyloctahydroanthracene (I)

(A) In Tetrachloroethane

Octamethyloctahydroanthracene (10) (m.p. 220°) (5.00 g, 0.017 mole) was dissolved in 100 ml of purified tetrachloroethane and aluminum chloride (7.50 g, 0.056 mole) was added. The reaction was continued with stirring for 24 hours. Gas chromatographic analysis of the off gases showed that isobutane was slowly evolved throughout the course of the reaction. When a trace of water was added to the reaction, hydrogen gas was also detected on the vapor fractometer. Mass spectroscopic analysis of a sample of the off gases gave the following results:

nitrogen + air	98.5%,	*n*-pentane	0.1,
isobutane	0.7,	C_5 olefinic	0.1,
isopentane	0.5,	hydrogen	0.1.

Can. J. Chem. Downloaded from www.nrcresearchpress.com by 210.87.254.6 on 09/05/12
For personal use only.

Can. J. Chem. Downloaded from www.nrcresearchpress.com by 210.87.254.6 on 09/05/12
For personal use only.

Chromatograph fractionation of the crystalline residue (4.80 g) recovered from the reaction yielded 3.0 g, 60% of compound II from fractions 1 to 3. Fractions 4–8 (0.75 g) apparently consisted of a mixture of compounds. Recrystallization of fraction 4 (0.56 g) from ethanol followed by sublimation yielded colorless crystals, m.p. 96–97°.

Anal. Calcd. for $C_{22}H_{32}$: C, 89.12; H, 10.88. Found:* C, 89.07, 89.29; H, 10.99, 11.00.

The ultraviolet spectrum of this compound shows a broad band at 261 mμ, ϵ = 21,727 and a broad band at 298 mμ, ϵ = 6215. The infrared spectrum of this compound was clearly distinguishable from that of II. They both had a strong band at 11.3 microns attributed to 1,2,4,5-tetrasubstitution but there were differences in the 8–10 micron region and a strong band in II at 12.1 microns was absent in the lower melting compound. This band is most likely due to an out-of-plane =C—H deformation of the olefinic proton in II and its absence in the compound of melting point 96–97° indicates that the latter is the exocyclic isomer of II since this isomer would have no olefinic proton. A sample of this compound was dissolved in methanol and reduced with hydrogen at 4 atm over a palladium – calcium carbonate catalyst. This reduction product proved identical with III (below) by mixed melting point and ultraviolet spectrum. The remainder of the original reaction product was strongly adsorbed on the alumina column. It was removed by elution with acetone to yield 1.0 g of resinous material.

The crystalline material from chromatograph fractions 1 to 3 was recrystallized from ethanol to yield colorless plates, m.p. 133–134°.

Anal. Calcd. for $C_{22}H_{32}$: C, 89.12; H, 10.88. Found: C, 89.15; H, 10.51.

A 0.21-g sample of pure II was dissolved in methanol and reduced with hydrogen at 4 atm over 0.10 g of palladium – calcium carbonate catalyst to give a quantitative yield of product, m.p. 98–99°.

Anal. Calcd. for $C_{22}H_{34}$: C, 88.51; H, 11.49. Found: C, 88.35, 88.85; H, 11.37, 11.26.

This reduction product (III) showed a parent mass of 298 in the mass spectrum. There was also a strong peak at mass 255 corresponding to the loss of a C_3H_7 fragment. The infrared spectrum of III in carbon disulphide lacked the 12.1 micron band which was attributed to the olefinic proton in the infrared spectrum of II.

Another aluminum chloride reaction was carried out on I in tetrachloroethane as described above. In this case, 5 ml of water was added slowly to the reaction mixture and a deep blue-green solution resulted. This solution had an absorption band in the visible at 640 mμ. On standing, a solid separated from the tetrachloroethane solution. This solid was removed by centrifugation and washed twice with tetrachloroethane and three times with carbon tetrachloride. The solvents were removed by centrifugation to leave a blue crystalline powder. This material could be stored for several hours in a vacuum desiccator but it decomposed to a brown amorphous material on exposure to air. The infrared spectrum on a Nujol mull of this material showed strong hydroxyl absorption in the region of 3 microns. There was also a strong band in the unsaturation region at 6.1 microns and a band at 8.3 microns.

(B) In Carbon Disulphide

A rearrangement of I (5.0 g) was carried out in carbon disulphide under essentially the same conditions as described in section (*A*). Isobutane and hydrogen were detected in the off gases. On working up as in section (*A*), there was obtained 30% of the rearrangement product II, 60% of unreacted I and the remainder was resinous material. When the carbon disulphide solution was refluxed, the yield of II was at least 50%.

**Analyses by Geller Laboratories, Bardonia, New York.*

(C) In Benzene

Aluminum chloride (1.0 g) was added to a solution of I (2.0 g) in 50 ml of benzene and the mixture was stirred overnight. On working up the benzene layer, there was obtained 1.4 g of a clear oil. This oil was proved to be tetramethyltetralin by comparison of its ultraviolet spectrum and gas chromatographic analysis with synthetic tetramethyltetralin.

Synthesis of 1,1,5,5,8,8-Hexamethyl-3-isopropyl-5,6,7,8-tetrahydrobenzindane (III)

(A) 3,3-Dimethyl-1-isopropylindane (VII)

To the Grignard reagent, prepared from 6.76 g of isopropyl bromide (0.055 mole) and 1.36 g of magnesium (0.056 mole) in 25 ml of anhydrous ether, was added over 1 hour at 5° a solution of 8.5 g of 3,3-dimethyl-1-indanone (11) in 25 ml of dry benzene. The reaction mixture was refluxed for 2 hours with continuous stirring and worked up in the usual manner to yield 6.7 g (68.5%) of 3,3-dimethyl-1-isopropylindene, b.p. 80–84°/1.5 mm, $N_D^{28} = 1.5295$. This oil was reduced in methanol over a palladium catalyst with hydrogen at 2 atm yielding 6.5 g (98%) of 3,3-dimethyl-1-isopropylindane (VII). Distillation of this product yielded a colorless oil, b.p. 78–80°/2.5 mm. The ultraviolet spectrum of VII showed bands at 272 mμ, $\epsilon = 1175$ and at 265 mμ, $\epsilon = 933$ and was typical of similar indanes.

(B) Alkylation of VII with 2,5-Dimethyl-2,5-dichlorohexane. Characterization of III

To a solution of 1 g of VII (0.0053 mole) and 0.98 g of the dichloride (0.0054 mole) in 25 ml of carbon disulphide, was added 0.70 g of aluminum chloride (0.0053 mole) over a period of ½ hour with stirring which was continued for 3 hours. The product was worked up and chromatographed on alumina from petroleum ether to yield 1.3 g (80%) of white plates of melting point 125°. The ultraviolet and infrared spectra of this compound were identical with those of the rearrangement product II of octamethyloctahydroanthracene.

The alkylation product was reduced (in methanol solution) with hydrogen over palladium catalyst yielding 1.2 g (94%) of colorless needles. Purification was carried out by recrystallization from ethanol followed by sublimation yielding colorless needles, m.p. 100–101°. This compound was proved to be identical with the reduction product of II by mixed melting point and ultraviolet and infrared spectra.

Synthesis of 1,1,3,3,5,5,8,8-Octamethyl-5,6,7,8-tetrahydrobenzindane (IV)

Tetramethylindane (12) (5.00 g, 0.028 mole) and 2,5-dichloro-2,5-dimethylhexane (5.70 g, 0.031 mole) were dissolved in 10 ml of carbon disulphide and the mixture was cooled in an ice–salt bath. Anhydrous aluminum chloride (0.25 g, 0.002 mole) was added with stirring and the mixture allowed to warm to room temperature (2½ hours). The product was worked up and purified by recrystallization from ethanol to yield colorless needles (5.9 g, 74%) m.p. 195–198°; λ_{max} 279, $\epsilon = 2408$; 274.5 (side band), $\epsilon = 1815$; 270, $\epsilon = 2007$; and a shoulder at 265.5 mμ.

The Action of Aluminum Chloride on III

(A) In Carbon Disulphide

A 0.60-g sample of III was dissolved in 100 ml of carbon disulphide and reacted with 1.0 g of aluminum chloride under similar conditions as described for the reaction of aluminum chloride on I. Chromatographic fractionation of the reaction product yielded 45% of II.

Can. J. Chem. Downloaded from www.nrcresearchpress.com by 210.87.254.6 on 09/05/12
For personal use only.

(B) In Tetrachloroethane. The Effect of t-Butyl Chloride

A 1.0-g sample of III was dissolved in 100 ml of tetrachloroethane and treated with aluminum chloride as before. Chromatography of the product yielded 20% of III in the first fractions and a new compound (0.17 g, m.p. 177°) in later fractions. This compound had an intense band in the ultraviolet at 241.5 mμ and bands at 291 and 302 mμ. None of the hydrocarbon II was detected in the product.

Another aluminum chloride treatment of III was carried out under similar conditions except that, in this case, an equimolar amount of *t*-butyl chloride was added with the hydrocarbon. The reaction was allowed to continue for 8 hours during which time isobutane gas was detected in the off gases. Chromatographic fractionation of the reaction mixture from this run yielded 61% of the hydrocarbon II. None of the starting hydrocarbon (III) could be detected in the reaction mixture.

Oxidative Studies on II

(A) Ozonolysis

A 0.55-g sample of II was dissolved in 100 ml of absolute methanol. This solution was cooled to −25° and ozone (3%) was passed in slowly until a slight excess of ozone was detected. The ozonide was decomposed by shaking with hydrogen over a palladium – calcium carbonate catalyst. Distillation of the solvent left a non-crystalline residue. This was dissolved in petroleum ether and chromatographed on alumina. Elution with petroleum ether containing methanol removed a crystalline compound (0.1 g) m.p. 114–115°; λ_{max} 278, ϵ = 1222; 270 mμ, ϵ = 1056. The infrared spectrum of this compound in carbon tetrachloride showed no carbonyl absorption but had strong bands at 8.85 and 9.45 microns in the region of ether absorption.

Anal. Calcd. for $C_{23}H_{36}O_2$: C, 80.18; H, 10.05; O, 9.77; OCH_3, 9.01. Found: C, 80.15, 80.04; H, 10.40, 10.22; O, 9.72, 9.50; OCH_3, 11.60, 11.89.

(B) Permanganate–Periodate Oxidation

The hydrocarbon (1.40 g, 0.0047 mole) was dissolved in 200 ml of pyridine and oxidized with permanganate–periodate according to the method of Lemieux (13). The reaction mixture was worked up to yield 0.70 g (45%) of viscous neutral material and 0.50 g (31%) of crystalline acid. Recrystallization of the latter from petroleum ether yielded colorless crystals, m.p. 210°; λ_{max} 253 mμ, ϵ = 10,434. The infrared spectrum showed two strong bands in the carbonyl region, at 5.90 and 5.75 microns.

Anal. Calcd. for $C_{22}H_{32}O_3$: Neut. equiv. 344. Found: Neut. equiv. 344.

N.M.R. Spectrum of II

The N.M.R. spectrum was run on an 11% solution of II dissolved in carbon tetrachloride containing 1% of tetramethylsilane as internal standard. A peak appeared at −348 c.p.s. removed from tetramethylsilane and this peak was assigned to an olefinic proton.

ACKNOWLEDGMENTS

Acknowledgment is made to the donors of The Petroleum Research Fund, administered by the American Chemical Society, for support of this research.

REFERENCES

1. L. SCHMERLING and J. P. WEST. J. Am. Chem. Soc. **76**, 1917 (1954).
2. L. SCHMERLING, R. W. WELCH, and J. P. LUVISI. J. Am. Chem. Soc. **79**, 2636 (1957).
3. R. M. ROBERTS and Y. W. HAN. Tetrahedron Letters, No. 6, 5 (1959).

Can. J. Chem. Downloaded from www.nrcresearchpress.com by 210.87.254.6 on 09/05/12
For personal use only.

4. L. H. SLAUGH and J. H. RALEY. J. Am. Chem. Soc. **82**, 1259 (1960).
5. L. R. C. BARCLAY, J. W. HILCHIE, A. H. GRAY, and N. D. HALL. Can. J. Chem. **38**, 94 (1960).
6. P. C. MYHRE. Private communication. Dept. of Chem., Univ. of Washington, Seattle.
7. L. R. C. BARCLAY and A. H. GRAY. Chem. & Ind. (London), 1350 (1959).
8. C. D. NENITZESCU, M. AVRAM, and E. SLIAM. Bull. soc. chim. France, 1266 (1955).
9. N. C. DENO, H. J. PETERSON, and G. S. SAINES. Chem. Revs. **7**, 60 (1960).
10. H. A. BRUSON and J. W. KROEGER. J. Am. Chem. Soc. **62**, 41 (1940).
11. C. F. KOELSCH and C. LECLAIRE. J. Org. Chem. **6**, 526 (1941).
12. M. T. BOGERT and D. DAVIDSON. J. Am. Chem. Soc. **63**, 2033 (1934).
13. R. U. LEMIEUX and E. RUDLOFF. Can. J. Chem. **33**, 1701 (1955).

Can. J. Chem. Downloaded from www.nrcresearchpress.com by 210.87.254.6 on 09/05/12
For personal use only.

Can. J. Chem. Downloaded from www.nrcresearchpress.com by 210.87.254.40 on 09/05/12
For personal use only.

THE HYDROLYSIS OF A SERIES OF STRAIGHT-CHAIN ALKYL METHANESULPHONIC ESTERS IN WATER[1]

P. W. C. BARNARD[2] AND R. E. ROBERTSON

ABSTRACT

Rate data for the hydrolysis of methyl, ethyl, *n*-propyl, *n*-butyl methanesulphonate have been determined over sufficient range of temperature to permit an evaluation of the corresponding enthalpy, entropy, and heat capacity terms for the activation process. Changes in these derived parameters are related to characteristic differences in solvation and mechanism as a consequence of changes in the structure of the hydrolyzing ester.

Our knowledge concerning the details of hydrolysis of simple alkyl esters of strong acids in water have been extended recently by a study of isotope effects arising from changing the medium from H_2O to D_2O (1, 2, 3) and from various secondary deuterium isotope effects (4, 5, 6). In principle, further information should be made available from a consideration of the changes in the derived parameters, $\Delta H^{\ddagger}$, $\Delta S^{\ddagger}$, $\Delta C_p^{\ddagger}$ but the theoretical basis for the interpretation of changes in these parameters suffers from such uncertainty that to an important degree, relating changes in these parameters with changes in structure amounts to no more than confirming changes anticipated from other evidence of mechanism. The greatest uncertainty would appear to lie in $\Delta H^{\ddagger}$ and $\Delta C_p^{\ddagger}$, differences in $\Delta S^{\ddagger}$ being somewhat easier to interpret. Our purpose in this paper, therefore, was to determine the rate data for hydrolysis of a series of alkyl methanesulphonates over sufficient range of temperature that reliable values of the enthalpy, entropy, and heat capacity of activation could be determined, and to show how changes in these parameters are consistent with the solvation of sulphonates and with changes to be expected in mechanism from lengthening the carbon chain.

EXPERIMENTAL METHODS AND MATERIALS

The methanesulphonic esters used in this study were synthesized by conventional methods (7, 8). The physical constants are given in Table I. The method used in determining rates of hydrolysis, in temperature measurement and control were identical in all respects with those used in determining kinetic data for the benzenesulphonates (9)

TABLE I

Physical properties of the methanesulphonic esters

Alkyl group	n_D^{25}	% purity*	d_4^{24}
Methyl†	1.4138	99.8	1.30056
Ethyl	1.4151	100.3	1.20492
n-Propyl	1.4210	99.1	1.11483
n-Butyl	1.4255	99.6	1.10853
n-Amyl	1.4298	101.6	1.08242
n-Octyl	1.4378	97.1	1.01521

*Based on the neutral equivalent % purity

$$= \text{neutral equivalent} \left[\frac{\text{calculated}}{\text{observed}}\right] \times 100.$$

†B.p. 2mm, 55–55.5° C.

[1]*Manuscript received December 16, 1960.*
Contribution from the Division of Pure Chemistry, National Research Council, Ottawa, Canada. Issued as N.R.C. No. 6212.
[2]*Present address: Chelsea College of Science and Technology. (National Research Council Postdoctorate Fellow 1956–57.)*

with the obvious change that sodium methanesulphonate (0.003 M) was used as the backing electrolyte. The conductance cells were the ones used in our study of the benzenesulphonates and initially good agreement between parallel runs in different cells or successive runs in the same cells was not possible. These discrepancies disappeared, however, following repeated washings with the backing electrolyte, interspersed with several hours "aging" at 100° C in the presence of a reaction solution. Similar treatment was found to be necessary for "new" cells, but here the aging process required fewer "dummy" runs to satisfy what was assumed to be the absorptive capacity of the walls. When such equilibrium was established, reproducibility of the rate appears to be independent of the cell within the stated limits shown in the tables.

The temperature was controlled to ±0.01° C or better and was determined with a platinum thermometer and a Mueller bridge (L. and N. 8069).

First-order rates were calculated by the Guggenheim method as described in our earlier paper (9).

RESULTS AND DISCUSSION

The rate data for a series of temperatures together with the average deviation of n repetitive runs at the same temperature are given for the methyl, ethyl, n-propyl, and n-butyl esters in Table II. It was found that the temperature dependence of the rates

TABLE II

Kinetic data for the hydrolysis of a series of methanesulphonic esters

Temp., °C	$k_1\times10^5$, sec^{-1}	n
(*a*) Methyl methanesulphonate		
0.00_0	$0.159_6\pm0.0009$	3
5.00_0	$0.333_1\pm0.0022$	4
9.95_0	$0.691_3\pm0.0034$	4
14.99_8	1.38_2 ±0.001	3
19.99_4	2.69_5 ±0.002	3
24.90_8	5.00_4 ±0.015	4
29.99_5	9.33_0 ±0.031	3
34.99_9	16.7_0 ±0.05	4
39.85_2	28.7_9 ±0.14	4
44.78_6	49.2_4 ±0.28	4
49.93_1	84.0_2 ±0.12	2
49.92_3	83.9_5 ±0.06	2
59.70_4	$217._5$ ±0.2	3
$\log_{10} k = 7125.354/T - 17.9380 \log T + 62.9900$		
(*b*) Ethyl methanesulphonate		
9.81_7	$0.497_8\pm0.0008$	3
19.85_2	2.01_1 ±0.006	4
29.41_0	6.80_8 ±0.006	3
39.83_9	23.6_5 ±0.29	3
50.04_9	71.6_3 ±0.08	3
60.03_4	$197._4$ ±0.11	4
70.00_3	$501._2$ ±0.5	7
79.76_9	116_9 ±3.0	3
$\log_{10} k = 7204.552/T - 17.4479 \log T + 61.9329$		
(*c*) n-Propyl methanesulphonate		
89.98_9	182.8 ±0.6	4
89.97_8	182.6	1
84.97_5	123.2 ±0.1	2
79.99_6	82.2_8 ±0.05	2
79.98_7	82.1_7 ±0.18	4
74.13_4	49.9_1 ±0.2	4
70.00_0	34.6_8 ±0.02	4
64.99_5	22.0_3 ±0.01	4
60.00_0	13.8_3 ±0.05	4
54.99_8	8.51_4 ±0.01	4
49.99_8	5.16_4 ±0.03	3
44.96_4	3.05_4 ±0.016	4
40.30_9	1.83_8 ±0.001	3
29.98_4	$0.560_3\pm0.003$	3
20.16_2	$0.164_7\pm0.0004$	4
$\log_{10} k = -6498.02712/T - 13.1105373 \log T + 48.719322_5$		
(*d*) n-Butyl methanesulphonate		
89.91_7	186.3 ±0.5	3
84.99_0	127.6 ±0.2	3
79.97_8	85.38 ±0.08	4
74.98_4	56.32 ±0.05	3
69.94_1	36.38 ±0.04	3
65.05_8	23.55 ±0.0	2
59.98_4	14.80 ±0.03	3
49.89_5	5.54_8 ±0.009	4
44.75_3	3.25_2 ±0.003	4
40.00_0	1.96_4 ±0.001	4
$\log_{10} k = -6163.0693/T - 11.319_4 \log T + 43.2238$		
(*e*) n-Amyl methanesulphonate		
84.973	124.1 ±0.2	2
84.967	124.0 ±0.1	2
74.97_1	54.26 ±0.1	3
64.95_1	22.6_0 ±0.05	3
(*f*) n-Octyl methanesulphonate		
65.00_2	23.68 ±0.1	2
74.95_4	58.1_7 ±0.1	2
85.06_2	131.7 ±0.5	2

Can. J. Chem. Downloaded from www.nrcresearchpress.com by 210.87.254.40 on 09/05/12
For personal use only.

in every case could be expressed within the accuracy of reproducibility of the rate determination by an empirical equation of the form

$$[1] \qquad \log k = A/T + B \log T + C$$

and the equations immediately under each section, Table II, give the corresponding constants for each ester as determined by the method of least squares. If we accept the usual transition-state hypothesis for the case where $d\Delta H^{\ddagger}/dT$ is non-zero, but $d\Delta C_p^{\ddagger}/dT$ is invariant with temperature, then the constant of equation [1] may be interpreted as follows: $A = -(\Delta H_0^{\ddagger}/2.303\ R)$; $B = (\Delta C_p^{\ddagger}/R - 1)$; $C = \{(\Delta S_0^{\ddagger} - \Delta C_p^{\ddagger})/2.303\ R + \log_{10} k/h\}$. Thermodynamic parameters characterizing the hydrolysis of the four esters, calculated according to the above assumptions are given in Table III. No claim is made here that

TABLE III

Thermodynamic parameters for the hydrolysis of a series of methanesulphonates for 50.0° C

Ester	$H^{\ddagger}$, cal/mole	$S^{\ddagger}$, cal/mole deg	$C_p^{\ddagger}$, cal/mole deg
Methyl	20,441	−14.08	37.6
Ethyl	21,120	−12.31	36.7
n-Propyl	20,672	−16.43	28.0
n-Butyl	20,289	−15.37	24.5
n-Amyl	20,440	−15.1	—
n-Octyl	20,100	−15.9	—

the assumption that $d\Delta C_p/dT = 0$ is not in some measure arbitrary; and it may well be that when data over a wider range and with greater precision are available, $\Delta C_p^{\ddagger}$ will be found to vary with temperature. The present data do not suggest, however, that $d\Delta C_p/dT > 0.1$ cal/deg mole. Estimated values of $\Delta H^{\ddagger}$ and $\Delta S^{\ddagger}$ values for *n*-amyl and *n*-octyl methanesulphonate from limited rate data (Table II) are included in Table III but these terms have much larger probable errors than those determined for the preceding compounds.

In the hydrolysis of the alkyl methanesulphonates there seems no basis to doubt that bond fission occurs at the C—O bond just as in the hydrolysis of the alkyl benzenesulphonates (10, 11). This conclusion is supported by product analysis and neutral equivalent determinations which also indicate that the reaction goes to virtual completion under the experimental conditions. The possibility that elimination would become a competing reaction path in this series of straight-chain alkyl methanesulphonates is discounted by the small proportion of olefine found (Table IV) and it is by no means

TABLE IV

Olefine production in the hydrolysis of a series of methanesulphonic esters in water

Ester	Temp., °C	% olefine*
Ethyl	60	0.52±0.05†
n-Propyl	100	1.26±0.03
n-Butyl	60	1.60±0.16

*As determined by the method of Byrne and Johnstone (13).
†Reproducibility from parallel determinations.

certain that the olefine so formed represents a competing path and is not formed subsequently to the transition state.

Can. J. Chem. Downloaded from www.nrcresearchpress.com by 210.87.254.40 on 09/05/12
For personal use only.

In current terminology, the hydrolysis of the methyl methanesulphonate in water occurs by an "intermediate" mechanism, i.e., an S_N2 mechanism in which the solvent provides the nucleophile and in which solvation of the forming anion is assumed to be a significant driving force. Evidence from relative rates of hydrolysis with and without the presence of OH^- (k_{OH^-}/k_{H_2O}) (12) and the relative deuterium isotope effect derived by replacing the methyl hydrogens by deuterium (k_H/k_D) (4, 5) support the contention that in hydrolysis, nucleophilic interaction between oxygen of one particular water molecule and the methyl carbon is less in hydrolysis for the methyl methanesulphonate than for the methyl halides in the transition state, but is not absent. Both methyl halides and sulphonates show an inverse α-deuterium isotope effect on hydrolysis which can be rationalized in terms of interference with the C—H out-of-plane bending frequency by the partially bonded water molecule on the side opposite to the leaving group (Table V).

TABLE V

Deuterium isotope effects for the hydrolysis of the methanesulphonates

Ester	αd_2	βd_2	γd_3	Ref.
Methyl*	0.95	—	—	4
Ethyl	1.037	1.027	—	6
n-Propyl	1.036	1.074	0.94	6

*αd_3

Deuterium substitution of ethyl and *n*-propyl esters in the β-position leads to k_H/k_D values greater than unity. The effect is small and it would be difficult, on the basis of these isotope effects alone, to distinguish between the possibility that the observed effect arises from some weak interaction between the β-H and the partially empty *p*-orbital developing at the rear of α-C or is the consequence of a reduction in non-bonded interactions or arises from other causes. The empirical observation that deuterium substitution on the γ-carbon gives an inverse isotope effect ($k_H/k_D > 1$) analogous to the effect of α-substitution is an indication that the activation process requires a configuration which reduces the freedom of γ-C—H vibration. In a recent paper Leffek, Llewellyn, and Robertson discuss these problems in greater detail (6). Here we shall examine the very much larger indications of mechanistic changes with chain lengthening apparent in the derived parameters, $\Delta H^{\ddagger}$, $\Delta C_p^{\ddagger}$, and $\Delta S^{\ddagger}$, particularly the latter.

Entropy of Activation

The relation of structure to the derived values of $\Delta S^{\ddagger}$ for hydrolysis will be considered in this section with reference to two specific examples (1) a comparison of $\Delta S^{\ddagger}$ values for the hydrolysis of MeBr and MeMes and (2) the changes in $\Delta S^{\ddagger}$ with chain lengthening within the methanesulphonate series.

Example I

The difference in the rate of hydrolysis of methyl bromide and methanesulphonate ($k_{MeBr}/k_{MeMes}=7.6$) is much less than would be expected from differences in $\Delta H^{\ddagger}$ or $\Delta S^{\ddagger}$ alone (Table VI), a circumstance frequently observed (14, 15, 16, 17, 18) and usually associated with solvation differences either in the initial or transition states or both. It is known, of course, from differences in k_{OH^-}/k_{H_2O} ratios (12) that the hydrolysis of methyl bromide requires a greater degree of nucleophilic interaction than methyl methanesulphonate but this could hardly contribute as much as 1–2 e.u. to $\delta_{RX}\Delta S^{\ddagger}$. Hence some 5–6 e.u. must be associated with $\delta_{RX}\Delta S^{\ddagger}$ solvent.

Can. J. Chem. Downloaded from www.nrcresearchpress.com by 210.87.254.40 on 09/05/12
For personal use only.

TABLE VI

A comparison of kinetic parameters for the hydrolysis of MeBr and MeMes

	$k_1 \times 10^{-5}$, sec^{-1}	$\Delta H^{\ddagger}$, cal/mole	$\Delta C_p^{\ddagger}$, cal/mole deg	$\Delta S^{\ddagger}$, cal/mole deg	Ref.
MeBr	1.11	24,142	46.5	−2.91	14
MeMes	8.44	20,441	37.6	−10.83	This work

Following the argument of Robertson, Heppolette, and Scott (17) the charge development on Br^- at the transition state will be about 0.8 e. Hence applying Laidler's hypothesis (19) that $\Delta S_0^0 \alpha z^2$, the entropy change to be associated with the quasi-ionic Br^- will be about $(0.8)^2 \times 12 = -8$ e.u. where the entropy of solvation for Br^- ion is −12 e.u. for a standard state of 1 mole/l. in both phases (20). The corresponding parameter for the methanesulphonate ion is not known but may be estimated from Altschuler's empirical equation (21) for oxy anions. Assuming the same charge development for the methanesulphonate as for the bromide the corresponding entropy change will be −14.3 e.u.

If the above assumptions are correct, there is here a difference of about 6 e.u. in the solvation of the quasi-ionic anions in the transition state and this will account for the major observed differences in $\Delta S^{\ddagger}$. To infer that the initial states are comparably solvated, however, would be incorrect.

In aqueous solutions it is now accepted that a non-electrolyte may be described as being surrounded by a solvation shell in which water–water interaction is greater than the interaction in bulk water or of water–solute interaction in solution (22, 23, 24). The formation of this initial-state solvation shell is characterized by a negative component in the entropy which appears to bear some inverse relationship to the polarity of the solute. Thus the entropy of solution for the gas solution equilibrium for MeBr and methane are both about −18 e.u. (17), indicating that in substituting —Br for —H in methane, the increased size of the substituent, which would imply a more negative shift in entropy of solvation, is cancelled by the increased polarity of the substituent.

Obviously the fraction of this value which must be associated with increased water–water interaction about the Br atom is difficult to judge, but it would seem that a value of 5–6 e.u. implied by the difference

$\Delta S^{\ddagger}_{\text{solvent}}$ (transition state for Br^-)	−8 e.u.
$\Delta S^{\ddagger}$	−2.91
	−5.09

would not be unreasonable. Evidence both from the solvent isotope effect (3) and particularly from the temperature dependence of the solvent isotope effect (25) suggests that the water molecules adjacent to the sulphonic group are already interacting with the sulphonic oxygens in the initial state with a corresponding loss in rotational entropy. The same inference may be drawn from the enhanced solubility in water which the sulphonic groups introduce into organic molecules. Taking the calculated entropy loss associated with the quasi-ionic sulphonic transition state (−14.3 e.u.) and subtracting the observed value of $\Delta S^{\ddagger}$, we may estimate that this initial-state loss corresponds to about 3–4 e.u. Hence, summing up, the entropy difference observed in the hydrolysis of the two esters probably arises largely in the transition state. The differences in the initial state are smaller but the physical characteristics of the initial-state solvation are quite different.

Can. J. Chem. Downloaded from www.nrcresearchpress.com by 210.87.254.40 on 09/05/12
For personal use only.

We have noted above that $(S^0_{solv})^{gas}_{soln}$ for MeBr and methane are both about -18 e.u. but so far have neglected to consider the contribution to $\Delta S^{\ddagger}$ from reorganization about the Me group. The initial-state solvation shell has a large negative component due to increased water–water interaction. Granted that the entropy assignments to the anionic moiety are correct, any change in entropy about the methyl group will have to come out of the respective residuals (-5.09 and -3, or -4). For simplicity we have assumed such differences to be small for the methyl esters.

Example II

In hydrolysis, the structural change Me $\rightarrow$ Et may be assumed to lead to a more ionic transition state and an increase in steric hindrance to nucleophilic interaction. This conclusion based largely on relative rates in solvolysis and the effect of added bases on such rates (12) has gained further support from the results for secondary deuterium isotope effects (6). In the present series the difference in rates of hydrolysis between the methyl and ethyl esters ($k_{Et}/k_{Me} = 0.85$) is much smaller than normal for S_N2 displacements and tends to belie larger changes in the detailed mechanism suggested by differences in $\Delta H^{\ddagger}$ and $\Delta S^{\ddagger}$ (Table III).

A more ionic transition state for the ethyl ester would seem to require a more negative $\Delta S^{\ddagger}$ and this is probably true for that component of $\delta_R \Delta S^{\ddagger}$ associated with the quasi-anion even though the net $\delta_R \Delta S^{\ddagger}$ for the structural change Me $\rightarrow$ Et is 1.7 e.u. positive. Of the sources of positive entropy which could contribute to the positive residual in $\delta_R \Delta S^{\ddagger}$ that due to the diminished nucleophilic interaction is probably small. A more likely source is associated with the breakdown of a larger initial-state solvation shell but it is not clear how to estimate this contribution.

The introduction of a γ-methyl group to Et— (to give *n*-propyl) need not produce added steric hindrance to nucleophilic interaction (26) and would not be expected to have a large direct electronic effect on the seat of reaction; nor would the change in reactivity ($k_{n\text{-Pro}}/k_{Et} = 0.72$) lead us to anticipate the observed shift in $\Delta S^{\ddagger}(\delta_R \Delta S^{\ddagger} = -4.12$ e.u.). Such a change in entropy appearing suddenly in a straight-chain series is not unusual and has been attributed to loss of rotational freedom in the transition state (6, 27) due to either increased crowding or to solvent exclusion. The latter is the hypothesis adopted by Evans and Hamann (28) and by Everett, Landsman, and Pinsent (29) to account for the gradual negative shift in entropy with chain lengthening in the ionization of a series of straight-chain acids and amines. While "solvent exclusion" may be a factor here, the contrast between the gradual shift in entropy for ionization of the amines and acids and the abrupt shift at *n*-propyl and also the results of secondary deuterium isotope studies are evidence of some other larger contributing factor. Leffek, Llewellyn, and Robertson (6) showed that whereas the β-H deuterium isotope effect is greater than unity, the γ-substitution led to a value of $k_H/k_D < 0.95$ for four different displaced groups —a result consistent with increased crowding in the transition state. It is suggested that this alteration in spacial relationships is the direct consequence of rehybridization of α-C in the activation process. The normal secondary deuterium isotope effect for β-H is small and may either arise from the same cause or be taken as possible evidence of some degree of weak interaction between the β-H and the partially empty *p*-orbital but is of the wrong sign were solvent exclusion the source of loss of rotational freedom.

The constancy of $\Delta S^{\ddagger}$ for the hydrolysis of the longer straight-chain alkyl mesalates suggests that the above discussion for *n*-propyl may be applied to the higher members of the series and further that solvation changes are not influenced by chain length beyond the second or third member of the series.

Can. J. Chem. Downloaded from www.nrcresearchpress.com by 210.87.254.40 on 09/05/12
For personal use only.

Heat Capacity of Activation

The temperature dependence of $\Delta H^{\ddagger}$ is assumed to be linear in T. Although in some measure arbitrary the range of temperature covered by the investigation and the accuracy of the rate determinations would not justify a more-refined treatment.

The actual values of the temperature coefficients of $\Delta H^{\ddagger}$ for the hydrolysis of the methanesulphonic esters are of the same magnitude and sign as for the benzenesulphonates and less negative than for the halides (17). The major factor determining the latter difference would appear to be the same: the temperature dependence for the "stability" of the initial-state solvation shell or that part thereof which must be broken down in the activation process. The change in $\Delta C_p^{\ddagger}$ with the change Me $\rightarrow$ Et is negligible, but there is a significant reduction in the negative value of $\Delta C_p^{\ddagger}$ for the structural change Et $\rightarrow$ *n*-Pro.

Such a change is in qualitative agreement with the shift to be expected where there is a decrease in rotational freedom for a simple model of a harmonic oscillator (31), the entropy becoming more negative and the $\Delta C_p^{\ddagger}$ more positive. The stiffening here, however, arises from a different cause than that suggested by Kirkwood and adopted by Evans and Hamann (26) and by Everett, Landsman, and Pinsent (27) since in the work described by the latter authors chain stiffening was assumed to arise as a consequence of the exclusion of the low polar hydrocarbon from the charge center by the solvent. Here the loss of rotational freedom appears to arise at least in part as an incidental to the decrease in $\Delta H^{\ddagger}$ as a consequence of the β-hydrogen interaction with the forming empty p-orbital coupled with a possible change in the non-bonded interaction between the terminal methyl and the leaving group.

The Enthalpy of Activation

The $\Delta H^{\ddagger}$ values reported in Table III are similar to the corresponding values for the benzenesulphonates and some 4–5 kcal lower than for the halides. The latter difference may be attributed to solvation differences in the initial state, in particular, to the evidence of strong solute–water interaction in the initial state for the sulphonates compared to the enhanced water–water interaction about the halide. Granted this explanation for the difference, we are left with the uncomfortable question of why the residuals are so similar.

The change in $\Delta H^{\ddagger}$ with increasing length of the alkyl group, while small, follows the same pattern as for the benzenesulphonates, with an increase from Me $\rightarrow$ Et where the α-methyl increased the steric hindrance to nucleophilic interaction without supplying through electron release or hydrogen interaction a driving force sufficient to compensate for this loss. The further lengthening of the chain (Et $\rightarrow$ *n*-Pro) leads to increased β-hydrogen interaction, loosening of the β-C—H bond, and a lowering of $\Delta H^{\ddagger}$ which partially compensates the negative shift in $\Delta S^{\ddagger}$ attributed to loss of rotational freedom. The influence of the specific nature of the leaving group is apparent here; $\delta_R \Delta H^{\ddagger}$ having values (17) (in kcal) for I^- of 0.1, Br^- −0.98, methanesulphonate −0.4, and benzenesulphonate −0.56.

ACKNOWLEDGMENTS

The authors wish to acknowledge the assistance of Mr. R. Maillet for the olefine determinations, and of Mr. S. Sugamori for least-square determinations, and other technical assistance.

REFERENCES

1. P. M. LAUGHTON and R. E. ROBERTSON. Can. J. Chem. **34**, 1714 (1956).
2. R. E. ROBERTSON and P. M. LAUGHTON. Can. J. Chem. **35**, 1319 (1957).

Can. J. Chem. Downloaded from www.nrcresearchpress.com by 210.87.254.40 on 09/05/12
For personal use only.

3. P. M. LAUGHTON and R. E. ROBERTSON. Can. J. Chem. **37**, 1491 (1959).
4. J. A. LLEWELLYN, R. E. ROBERTSON, and J. M. W. SCOTT. Chem. & Ind. (London), 723 (1959).
5. J. A. LLEWELLYN, R. E. ROBERTSON, and J. M. W. SCOTT. Can. J. Chem. **38**, 222 (1960).
6. K. LEFFEK, J. A. LLEWELLYN, and R. E. ROBERTSON. Am. Chem. Soc. Meeting, Cleveland, April 12, 1960.
7. M. S. MORGAN and L. H. CRETCHER. J. Am. Chem. Soc. **70**, 375 (1948).
8. R. S. TIPSON. J. Org. Chem. **9**, 235 (1949).
9. R. E. ROBERTSON. Can. J. Chem. **33**, 1536 (1955).
10. G. ADER. Ph.D. Thesis. London. 1949.
11. C. A. BUNTON and Y. F. FREI. J. Chem. Soc. 1872 (1951).
12. S. HARTMAN and R. E. ROBERTSON. Can. J. Chem. **38**, 2033 (1960).
13. R. E. BYRNE and J. B. JOHNSTONE. Anal. Chem. **28**, 126 (1956).
14. E. TOMMILA, M. TILLIKAINEN, and A. VOILIO. Ann. Acad. Sci. Fennicae Ser. A. II. **65**, 125 (1955).
15. S. WINSTEIN and A. H. FAINBERG. J. Am. Chem. Soc. **79**, 5937 (1957).
16. K. J. LAIDLER. Soumen Kemistilehti, **33**, 44 (1960).
17. R. E. ROBERTSON, R. L. HEPPOLETTE, and J. M. W. SCOTT. Can. J. Chem. **37**, 803 (1959).
18. J. B. HYNE. J. Am. Chem. Soc. **82**, 5129 (1960).
19. K. J. LAIDLER. Can. J. Chem. **34**, 1107 (1956).
20. R. A. ROBINSON and R. H. STOKES. Electrolyte solutions. Butterworth Scientific Press, London. 1955. p. 69.
21. A. P. ALTSHULLER. J. Chem. Phys. **24**, 642 (1956).
22. D. D. ELEY. Trans. Faraday Soc. **40**, 184 (1944).
23. H. S. FRANK and M. G. EVANS. J. Chem. Phys. **13**, 507 (1945).
24. D. N. GLEW and E. A. MOELWYN-HUGHES. Discussions Faraday Soc. **15**, 150 (1953).
25. R. L. HEPPOLETTE and R. E. ROBERTSON. In press.
26. A. G. EVANS and S. D. HAMANN. Trans. Faraday Soc. **41**, 25 (1951).
27. D. H. EVERETT, D. A. LANDSMAN, and B. R. W. PINSENT. Proc. Roy. Soc. London, A, **215**, 403 (1952).
28. C. K. INGOLD. Structure and mechanism in organic chemistry. Cornell University Press, Ithaca, N.Y. 1953. Chap. VII.
29. N. IVANOFF and M. MAGAT. J. chim. phys. **47**, 914 (1950).
30. E. S. LEWIS, J. L. KINSEY, and R. R. JOHNSON. J. Am. Chem. Soc. **78**, 4294 (1956).
31. D. H. EVERETT. Ind. chim. belge, **16**, 647 (1951).
32. F. P. PRICE and L. P. HAMMETT. J. Am. Chem. Soc. **62**, 2387 (1941).

Can. J. Chem. Downloaded from www.nrcresearchpress.com by 210.87.254.40 on 09/05/12
For personal use only.

Can. J. Chem. Downloaded from www.nrcresearchpress.com by 210.87.254.5 on 09/05/12
For personal use only.

CONSTITUTION OF A GLUCOMANNAN FROM TAMARACK (LARIX LARICINA)[1]

P. KOOIMAN[2] AND G. A. ADAMS

ABSTRACT

A hemicellulose fraction containing D-mannose, D-glucose, and D-galactose in a ratio of 70:25:3 has been isolated from tamarack wood. The product was homogeneous under conditions of free boundary electrophoresis and of sedimentation in the ultracentrifuge. Hydrolysis of the fully methylated hemicellulose yielded 2,3,4,6-tetra-*O*-methyl-D-glucose (1.2%); 2,3,4,6-tetra-*O*-methyl-D-galactose (2.2%); 2,3,6-tri-*O*-methyl-D-glucose (24.0%); 2,3,6-tri-*O*-methyl-D-mannose (68.8%); 2,3-di-*O*-methyl-D-mannose (1.6%); and 2,3-di-*O*-methyl-D-glucose (1.7%). This data and that from periodate oxidation indicated that the glucomannan had a linear backbone of approximately 35 ($1 \rightarrow 4$) linked β-D-glucopyranose and β-D-mannopyranose units; approximately two thirds of the chains were terminated at the non-reducing ends by D-galactose and the remainder by D-glucose. Branching, if present, must occur through C_6 of the hexoses in the main chain.

Investigations of glucomannans from various gymnosperms have shown a similar basic structure (1–5). They consist of D-glucose and D-mannose units (ratio 1:3–4) joined by β-1,4-glucosidic bonds into linear chains. Two additional structural features about which there are divided opinions concern the presence of branching in the molecule, and the presence and structural attachment of D-galactose units associated with glucomannans. Much of the evidence for branching has been based on the presence of the dimethyl sugars found during methylation studies. It is well known that such evidence may be of questionable significance and the general consensus of opinion at the present time is that most glucomannans are unbranched (2, 6, 7, 8). Galactose units, when present, occur predominantly as non-reducing end groups (2, 7, 8, 9).

The present investigation of the glucomannan of tamarack was undertaken as part of a systematic study of the polysaccharides of this species. It was desirable also to compare the composition and structure of the glucomannan from tamarack with those from other coniferous species.

Extraction of tamarack holocellulose with 17.5% sodium hydroxide yielded a crude hemicellulose fraction which on acid hydrolysis gave D-mannose, D-glucose, D-galactose, D-xylose, L-arabinose, and a uronic acid component. The acidic xylan was precipitated as its "Cetavlon" (cetyl trimethyl ammonium hydroxide) complex. From the soluble residue, the glucomannan was recovered by gradient addition of ethanol. The yield of glucomannan was approximately 20% of the crude hemicellulose, a relatively large proportion having coprecipitated with the xylan–"Cetavlon" complex. Acid hydrolysis of the glucomannan and chromatographic examination of the sugars showed galactose, glucose, and mannose with only traces of xylose and arabinose. Quantitative estimations showed that galactose, glucose, and mannose occurred in the hemicellulose in a ratio of 3:25:70. The hemicellulose behaved as a single compound on examination in the ultracentrifuge and in moving boundary electrophoresis.

The methyl ethers obtained from methanolysis of the fully methylated glucomannan were analyzed by gas–liquid partition chromatography (10, 16). This method provided not only a means of identification of the methylated sugar glycosides but also yielded

[1]*Manuscript received December 29, 1960.*
Contribution from the Division of Applied Biology, National Research Council, Ottawa 2, Canada. Issued as N.R.C. No. 6202.
[2]*National Research Council of Canada Postdoctorate Fellow 1960.*

quantitative data as to the relative amounts of methylated sugars. The free methylated sugars were separated by paper chromatography using the appropriate solvents and the results are shown in Table I. The main methylated sugars were found to be 2,3,6-tri-*O*-methyl-D-mannose and 2,3,6-tri-*O*-methyl-D-glucose which showed that the glucose and mannose residues were joined by 1,4 glycosidic bonds in the original hemicellulose. The linkage was presumably of the β type because of the negative specific rotations both of the original and the methylated hemicellulose; these values were increased on hydrolysis. The 2,3,4,6-tetra-*O*-methyl-D-galactose was the only methylated galactose found and therefore the galactose units must have occurred exclusively as non-reducing end groups. Although less than the required amount of galactose was recovered as 2,3,4,6-tetra-*O*-methyl-D-galactose, no evidence for any other methylated galactose was found. A small amount of glucose occurred as non-reducing end groups as shown by the presence of 2,3,4,6-tetra-*O*-methyl-D-glucose. Apparently mannose did not constitute any end groups as no tetramethyl mannose was detected. Approximately two thirds of the glucomannan chains were terminated by D-galactose and the remainder by D-glucose. One tetramethyl sugar residue was present for every 32 hexose residues. This value is of the same general order as the 34 hexose residues per reducing end group as found by hypoiodite oxidation and the value of 40 as determined by gas–liquid chromatography of the methylated sugars.

Periodate oxidation of the hemicellulose showed that 1.10 moles of periodate per mole of anhydrohexose sugar was consumed. Formic acid production was 0.11 mole per anhydro sugar unit and indicated a chain length of 33 hexose units. The absence of any glucose or mannose in the hydrolyzate of the product obtained by borohydride reduction of the periodate-oxidized hemicellulose showed that all monosaccharide units had been oxidized and there was no branching through C_2 or C_3 of these units. If any branching occurred it would have to be through C_6. The erythritol and glycerol produced in the degradation reactions must have come from $1 \rightarrow 4$ linked sugar units and non-reducing terminal residues respectively.

At variance with the prediction of a straight-chain structure is the finding of dimethyl sugars which may be interpreted as indicating branch points in the molecule. If the amounts of dimethyl sugars found on hydrolysis had their origin from branch points in the hemicellulose, then the amount of recovered tetramethyl sugars which represents terminal groups becomes insufficient. Even allowing for less than a quantitative yield of tetramethyl galactose, there would still be a shortage of end groups. The conclusion that the amount of end groups found is substantially correct is supported by the fact that estimation of the degree of polymerization using these values is in good agreement with that found by periodate oxidation, by gas–liquid chromatography, and also by reducing end group estimation. It seems likely then that the dimethyl sugars do not represent branch points in the molecule but are products of demethylation or incomplete methylation.

It is apparent that D-galactose is an integral part of the glucomannan molecule. If it were to occur as a separate entity, then methylated galactoses other than tetra-*O*-methyl-D-galactose should be found on hydrolysis. So far, these have not been found even by the sensitive gas–liquid chromatographic method. Terminal galactose units could originate from an admixture of galactoglucan or (and) galactomannan with the present polysaccharide. While the presence of such polysaccharides is not excluded no positive evidence for them has been found.

It is apparent that the tamarack glucomannan is similar to most glucomannans of coniferous origin. The glucose-to-mannose ratio, specific rotation, and general structural features correspond clearly to those of other glucomannans (2, 4, 11, 12). While species

Can. J. Chem. Downloaded from www.nrcresearchpress.com by 210.87.254.5 on 09/05/12
For personal use only.

Can. J. Chem. Downloaded from www.nrcresearchpress.com by 210.87.254.5 on 09/05/12
For personal use only.

differences may well account for variations in composition and structure of the glucomannans, the methods of preparation may also contribute to the differences. For example, a glucomannan prepared from Sitka spruce by Dutton and Hunt (7) had a glucose-to-mannose ratio of 1:9; using another method of preparation Aspinall *et al.* (6) obtained a glucomannan from the same species having a glucose-to-mannose ratio of 1:2.5.

Evidence for branching through C_2 and C_3 in the glucomannans of western hemlock (13), Norwegian spruce (14), and Scots pine (12) have been provided through examination by the Smith degradation procedure (15). Examination of the glucomannan of jack pine (2) yielded neither D-glucose nor D-mannose after periodate oxidation, a result which is in agreement with that reported above for tamarack.

Further differences between the glucomannan of tamarack and those of some other species are the sugars constituting the non-reducing terminal group. Western hemlock (13) and Scots pine (12) have non-reducing terminal units of both D-glucose and D-mannose while Norwegian spruce (14), Sitka spruce (6), and loblolly pine (9) have non-reducing terminal units of D-mannose but none of D-glucose. Some of these differences may have been caused by the difficulty in separating the 2,3,4,6-tetra-*O*-methyl ethers of D-glucose and D-mannose (6) a difficulty which is obviated by the use of gas–liquid partition chromatography (16).

The occurrence of D-galactose in glucomannans has been noted by several investigators and it has not always been found to be a part of the glucomannan molecule. A polysaccharide from loblolly pine (17) having a composition similar to that of tamarack was considered to be a mixture of galactomannan and glucomannan. Further investigation (9) of the same polysaccharide showed that the chains of 27–33 sugar units were terminated by non-reducing units of D-galactose and D-mannose. The methyl ethers of D-galactose obtained from the hydrolysis of methylated glucomannan from western red cedar were considered to have originated from a contaminating galactoglucomannan (8). D-Galactose was found in glucomannans isolated from Sitka spruce (7) and Scots pine (12) but in each instance further purification removed it. Glucomannans prepared from western hemlock (13), Norwegian spruce (14), Sitka spruce (6), and white spruce (4) were devoid of D-galactose.

Fragmentation analyses of the tamarack glucomannan are being undertaken in this laboratory to determine the structural relationships of the D-galactose units and the sequence of the hexose residues in the molecule.

EXPERIMENTAL

All specific rotations are equilibrium values unless otherwise stated, melting points are corrected, and all evaporations were done at 35° C or less.

Paper Chromatography

Chromatographic separations were carried out on filter paper using the following solvent systems (v/v):

(A) pyridine:ethyl acetate:water (2:1:2),
(B) methyl ethyl ketone:water:ammonia (100:50:3),
(C) ethanol:benzene:water:ammonia (47:200:14:1),
(D) *n*-butanol:ethanol:water (40:11:19),
(E) *n*-butanol:pyridine:water (5:4:5).

Separations were made by the descending method on either Whatman No. 1 or No. 3MM filter paper. Sugars were located on the paper by the *p*-anisidine spray reagent (18);

non-reducing sugar derivatives were detected by silver nitrate and sodium hydroxide sprays (19).

Preparation of the Hemicellulose

Starting material for the preparation was a crude hemicellulose obtained from tamarack (*Larix laricina* (Du Roi) Koch) chlorite holocellulose by extraction with sodium hydroxide solution (17.5%). Chromatographic examination of an acid hydrolyzate showed galactose, glucose, mannose, arabinose, xylose, and a uronic acid were present.

Crude hemicellulose (50 g) was added gradually to water (2.5 liters) and stirring was continued at 0° C for 3 days. Undissolved material (4.6 g) was removed by centrifuging and the supernatant was diluted to 4.5 l. with water. An aqueous solution of 2% "Cetavlon" (cetyl trimethyl ammonium hydroxide) (1 liter), hydroxide form was prepared from the bromide form by stirring with silver oxide (13 g) for 1/2 hour and then removing the silver salts by filtration. Addition of "Cetavlon" to the solution of the hemicellulose with stirring gave a sticky precipitate which settled out on standing overnight. The supernatant was removed by decantation and its pH adjusted to 5.0 by acetic acid. The first hemicellulose fraction (I) was precipitated by adding ethanol to a concentration of 24%, after its removal a second fraction (II) was precipitated by adding ethanol to 50% concentration. The precipitates were recovered by centrifuging, washed successively with 50% ethanol (3 times), 100% ethanol (3 times), and ethyl ether (3 times). Ether was removed on the steam bath and the hemicellulose was dried *in vacuo* at room temperature. The yields were: fraction I, 2.14 g, fraction II, 10.0 g. Chromatographic examination of hydrolyzates showed that fraction II contained galactose, glucose, and mannose, fraction I contained xylose in addition to galactose, glucose, and mannose. On the basis of these results, fraction II, which appeared to be a galactoglucomannan, was selected for subsequent investigations.

The polysaccharide was dissolved in dilute alkali to give a clear solution $[\alpha]_D^{25}$ $-30°$ (*c*, 1% in 0.5 *N* sodium hydroxide). Hydrolysis of a sample (12 mg) in a sealed tube with *N* sulphuric acid for 12 hours and examination of the sugars by paper chromatography (solvents A and E) showed the presence of mannose, glucose, a small amount of galactose, and a trace of xylose. No uronic acids could be detected.

The ratio of the sugars in the hydrolyzate was determined using the method of Dubois *et al.* (20) and was found to be mannose:glucose:galactose, 70:25:4. A more accurate measurement of the amount of galactose present was provided by using gas–liquid chromatographic determination of the fully methylated sugars as described by Adams and Bishop (21). This latter method gave the previous ratio of mannose and glucose but the galactose content was 2.7%. Xylose was present in only trace amounts.

Examination of the hemicellulose in a 0.05 *M* borate buffer by moving boundary electrophoresis carried out in a Spinco model H Tiselius-type apparatus showed only a single sharp peak. Mobility measurements gave the value, $\mu = 6.71 \times 10^{-5}$ cm^2 volts^{-1} sec^{-1}. The same solution was centrifuged in a Spinco model E ultracentrifuge at 59,000 r.p.m. and showed only one symmetrical peak which is indicative of a single compound.

End Group Determination by Hypoiodite

A slightly modified Willstätter–Schudel method (22) was used for reducing end group determination of the hemicellulose. Samples in triplicate (50 mg each) were dissolved in 5 ml of *N* sodium hydroxide and then 2.5 ml of 0.02 *N* iodine was added. The solutions along with suitable controls were kept in stoppered flasks in the dark for 3 hours. After acidification with 10 ml of *N* sulphuric acid, the iodine was titrated with 0.01 *N* sodium thiosulphate. One reducing group was found to occur per 34 anhydrohexose units.

Can. J. Chem. Downloaded from www.nrcresearchpress.com by 210.87.254.5 on 09/05/12
For personal use only.

Periodate Oxidation

Duplicate samples of the hemicellulose (100 mg) were dissolved in water (50 ml) and oxidized by 0.1 *M* sodium metaperiodate (50 ml) in the dark at room temperature. Suitable reagent blanks were prepared under the same conditions. At the intervals shown in the table below, analyses were made for periodate consumption and formic acid production (23). The results given in moles per mole anhydrohexose unit were as follows.

Time, hours	26	77	130	179	221	300
Periodate consumption	0.84	0.98	1.07	1.10	1.15	1.18
Formic acid production	0.027	0.067	0.078	0.094	0.103	0.130

In a separate experiment, the hemicellulose was degraded according to Smith's procedure (15) as follows: hemicellulose (200 mg) was dissolved in water (100 ml) and oxidized with 0.1 *M* sodium metaperiodate (100 mg) for 240 hours at room temperature. Excess periodate was destroyed by the addition of ethylene glycol and the solution was dialyzed for 24 hours. The non-dialyzable material was concentrated to 25 ml and potassium borohydride (250 mg) was added. After 72 hours, the solution was neutralized with acetic acid and deionized by Amberlite IR-120 and IR-45. The resulting solution was evaporated *in vacuo* to dryness and the boric acid removed by repeated evaporation with methanol. The dried residue (65 mg) was dissolved in water (10 ml) and an aliquot (1 ml) was hydrolyzed with *N* hydrochloric acid for 6 hours at 100° C. Paper chromatography of the hydrolyzate in solvent D showed erythritol as the main component with glycerol present in small amounts. No monosaccharides were detected in the hydrolyzate.

Methylation of the Hemicellulose

Hemicellulose (5.0 g) was dissolved in 20% sodium hydroxide (50 ml) and methylated by the dropwise addition of dimethyl sulphate (50 ml) and 45% sodium hydroxide (100 ml). The methylation procedure was repeated four more times and the partially methylated product recovered by dialysis. Repetition of the methylation gave a product which was extracted by chloroform. Fractionation from chloroform solution by the addition of light petroleum (b.p. 30–60°) gave a methylated fraction (5.1 g) having a methoxyl content of 40.6%. Four further methylations were carried out using Purdie's reagents (methyl iodide (75 ml) and silver oxide (10 g)). The methylated hemicellulose (4.3 g) $[\alpha]_D^{25}$ −25.2° (*c*, 1% in chloroform) had a methoxyl content of 43.5% (theoretical for fully methylated hexosan 45.6%) and showed no hydroxyl absorption in the infrared.

Methanolysis and Hydrolysis of the Methylated Hemicellulose

A solution of the methylated hemicellulose (4.0 g) in 8% methanolic hydrogen chloride (60 ml) was refluxed on a boiling-water bath for 15 hours. A sample of the mixture of the methyl glycosides (5 mg) was removed for examination by gas–liquid partition chromatography (16).

The presence of the methyl glycosides of the following methyl sugars was indicated:

2,3,4,6-tetra-*O*-methyl-D-glucose,
2,3,4,6-tetra-*O*-methyl-D-galactose,
2,3,6-tri-*O*-methyl-D-glucose,
2,3,6-tri-*O*-methyl-D-mannose.

Smaller peaks which were not resolved were glycosides of dimethyl sugars.

The methanolysis mixture was freed of methanol and then hydrolyzed by heating it

Can. J. Chem. Downloaded from www.nrcresearchpress.com by 210.87.254.5 on 09/05/12
For personal use only.

with 0.5 *N* hydrochloric acid (25 ml) at 100° C for 22 hours. The acid was neutralized with silver carbonate and the methylated sugars were recovered as a clear syrup (4.1 g), $[\alpha]_D^{25}$ +11.3° (*c*, 1% in water). Chromatographic examination on filter paper (solvent B) indicated the same methyl sugars as found by gas–liquid chromatography, but in addition the dimethyl portion had been resolved into two components.

Separation of Methylated Sugars

The mixture of methylated sugars was separated on sheets of Whatman No. 3MM filter paper using solvent B. The sugars were eluted with water and the solutions were taken to dryness. The residues were extracted with methanol, clarified with charcoal, and the syrups were recovered and dried. Yields of methylated sugars along with their R_g values are given in Table I.

TABLE I

Methylated sugars from hydrolysis of methylated hemicellulose

Methylated sugars	R_g solvent B	Yield (mg)	%
2,3,4,6-Tetra-*O*-methyl-D-glucose	0.98	27	1.2
2,3,4,6-Tetra-*O*-methyl-D-galactose	0.81	50	2.2
2,3,6-Tri-*O*-methyl-D-glucose	0.66	557	24.1
2,3,6-Tri-*O*-methyl-D-mannose	0.55	1587	68.8
Dimethyl sugar 1	0.30	38	1.6
Dimethyl sugar 2	0.23	40	1.7

Identification of Methylated Sugars

*2,3,4,6-Tetra-O-methyl-*D*-galactose*

The syrup had the same R_g value (0.81) in solvent B as an authentic sample of 2,3,4,6-tetra-*O*-methyl-D-galactose. The sugar (24 mg) was dissolved in ethanol (1 ml), freshly distilled aniline (20 mg) was added, and the mixture was refluxed for 3 hours. Removal of the solvent in a desiccator yielded white needles which were recrystallized from ethanol to yield 2,3,4,6-tetra-*O*-methyl-*N*-phenyl-D-galactosylamine (17 mg), m.p. and mixed m.p. 196–197° C, $[\alpha]_D^{25}$ −138° (*c*, 0.9% in pyridine).

*2,3,4,6-Tetra-O-methyl-*D*-glucose*

This sugar had the same mobility on a paper chromatogram in solvent B and on paper electrophoresis in borate buffer as authentic 2,3,4,6-tetra-*O*-methyl-D-glucose.

The sugar (9 mg) was dissolved in ethanol, aniline (6 mg) was added, and the mixture was refluxed for 2 hours. The fine needles which formed on removal of the solvent had a melting point of 128–130° C. Two recrystallizations from ethyl ether – light petroleum yielded 2,3,4,6-tetra-*O*-methyl-*N*-phenyl-D-glucosylamine, m.p. 136–137°; reported value 137–138° (24).

*2,3,6-Tri-O-methyl-*D*-glucose*

The sugar separated on paper chromatograms was decolorized with charcoal. The solution was concentrated to a syrup, ethanol was added, and on slow evaporation a portion of the sugar crystallized. Recrystallization several times from ethanol – ethyl ether – light petroleum yielded 2,3,6-tri-*O*-methyl-D-glucose, m.p. 121° C, $[\alpha]_D^{24}$ +70.0° (*c*, 0.5% in water); reported values m.p. 121–123° C, $[\alpha]_D$ +70° (25).

Preparation of the 1,4-di-*p*-nitrobenzoate according to Rebers and Smith (32) yielded the crystalline derivative, m.p. 189–190° after recrystallization from methanol. Reported value m.p. 189–190° (26).

Can. J. Chem. Downloaded from www.nrcresearchpress.com by 210.87.254.5 on 09/05/12
For personal use only.

2,3,6-Tri-O-methyl-D-mannose

This sugar had the same mobility on a paper chromatogram (Solvent B) as an authentic sample of 2,3,6-tri-*O*-methyl-D-mannose. The aniline derivative was prepared as described above and yielded the crystalline 2,3,6-tri-*O*-methyl-*N*-phenyl-mannosylamine, which on repeated recrystallization from ethyl acetate – petroleum ether, had a melting point of 131–133° C (reported value 133° (28)). The 1,4-di-*p*-nitrobenzoate derivative was prepared as described above and after one recrystallization from methanol had a melting point of 187–188°; reported value 187–188° (26).

2,3-Di-O-methyl-D-mannose

Demethylation of a small amount of the syrup (5 mg) with boron trichloride (17) showed that mannose was the main product with minor amounts of glucose also present. On paper electrophoresis in borate buffer the main di-*O*-methyl mannose had an M_g value of 0.11. It was separated from other minor components on paper chromatograms using solvent C. The sugar (32 mg) was converted into the 1,4,6-tri-*p*-nitrobenzoate derivative using the same procedure described above. After several recrystallizations from methanol the melting point was 192°, reported value 194° (29).

2,3-Di-O-methyl-D-glucose

Glucose was the main product found on demethylation along with a minor amount of mannose. Paper chromatography (solvent C) separated the main component which on paper electrophoresis in borate had an M_g value of 0.12. The sugar which appeared to be 2,3-di-*O*-methyl-D-glucose could not be obtained in crystalline form. On refluxing it in ethanol solution with aniline, crystalline 2,3-di-*O*-methyl-*N*-phenyl-D-glucosylamine was obtained. Recrystallization from ethyl acetate gave a product having m.p. 132°; reported value 134° (30).

Other Dimethyl Sugars

Along with the two di-*O*-methyl sugars described above, two others, a di-*O*-methyl mannose (M_g 0.07) (solvent C) and a di-*O*-methyl glucose were recovered in trace amounts. They were tentatively identified as 2,4-di-*O*-methyl-D-mannose and 2,4-di-*O*-methyl-D-glucose on the basis of demethylation and paper electrophoretic and chromatographic evidence.

ACKNOWLEDGMENTS

The authors wish to thank Professor J. K. N. Jones, Queen's University, Kingston, who generously provided a sample of 2,3-di-*O*-methyl-D-glucose. Thanks are also due to Mr. F. P. Cooper for assistance with the gas–liquid chromatography, to Mr. A. E. Castagne for analyses, and to Mr. R. W. Rowsome for electrophoresis measurements.

REFERENCES

1. G. O. Aspinall. Advances in Carbohydrate Chem. **14**, 429 (1959).
2. C. T. Bishop and F. P. Cooper. Can. J. Chem. **38**, 793 (1960).
3. H. Meier. Acta Chem. Scand. **14**, 749 (1960).
4. A Tyminski and T. E. Timell. J. Am. Chem. Soc. **82**, 2823 (1960).
5. M. O. Gyaw and T. E. Timell. Can. J. Chem. **38**, 1957 (1960).
6. G. O. Aspinall, R. A. Laidlaw, and R. B. Lashbrook. J. Chem. Soc. 4444 (1957).
7. G. G. S. Dutton and K. Hunt. J. Am. Chem. Soc. **80**, 5697 (1958).
8. J. K. Hamilton and E. V. Partlow. J. Am. Chem. Soc. **80**, 4880 (1958).
9. J. K. N. Jones and T. J. Painter. J. Chem. Soc. 573 (1959).
10. A. G. McInnes, D. H. Ball, F. P. Cooper, and C. T. Bishop. J. Chromatog. **1**, 556 (1958).
11. J. K. Hamilton, H. W. Kircher, and N. S. Thompson. J. Am. Chem. Soc. **78**, 2508 (1956).
12. I. Croon, B. Lindberg, and H. Meier. Acta Chem. Scand. **13**, 1299 (1959).
13. J. K. Hamilton and H. W. Kircher. J. Am. Chem. Soc. **80**, 4703 (1958).
14. I. Croon and B. Lindberg. Acta Chem. Scand. **12**, 453 (1958).

Can. J. Chem. Downloaded from www.nrcresearchpress.com by 210.87.254.5 on 09/05/12
For personal use only.

15. M. ABDEL-AKHER, J. K. HAMILTON, R. MONTGOMERY, and F. SMITH. J. Am. Chem. Soc. **74**, 4970 (1952).
16. C. T. BISHOP and F. P. COOPER. Can. J. Chem. **38**, 388 (1960).
17. D. H. BALL, J. K. N. JONES, W. H. NICHOLSON, and T. J. PAINTER. Tappi, **39**, 438 (1956).
18. L. HOUGH, J. K. N. JONES, and W. H. WADMAN. J. Chem. Soc. 1702 (1950).
19. W. E. TREVELYAN, D. P. PROCTER, and J. S. HARRISON. Nature, **166**, 444 (1950).
20. M. DUBOIS, K. A. GILLIES, J. K. HAMILTON, P. A. REBERS, and F. SMITH. Anal. Chem. **28**, 350 (1956).
21. G. A. ADAMS and C. T. BISHOP. Can. J. Chem. **38**, 2380 (1960).
22. R. WILLSTÄTTER and G. SCHUDEL. Ber. **51**, 780 (1918).
23. S. K. CHANDA, J. K. N. JONES, and E. G. V. PERCIVAL. J. Chem. Soc. 1289 (1950).
24. J. C. IRVINE and A. M. MOODIE. J. Chem. Soc. **93**, 95 (1908).
25. J. C. IRVINE and J. W. H. OLDHAM. J. Chem. Soc. **119**, 1744 (1921).
26. P. A. REBERS and F. SMITH. J. Am. Chem. Soc. **76**, 6097 (1954).
27. S. ALLEN, T. G. BONNER, E. J BOURNE, and N. M. SAVILLE. Chem. & Ind. (London), 630 (1958).
28. E. L. HIRST and J. K. N. JONES. J. Chem. Soc. 1278 (1948).
29. F. SMITH and R. MONTGOMERY. Chemistry of plant gums and mucilages. Am. Chem. Soc. Monograph No. 141. New York. 1959. p. 539.
30. E. SCHUCHTERER and M. STACEY. J. Chem. Soc. 776 (1945).

Can. J. Chem. Downloaded from www.nrcresearchpress.com by 210.87.254.5 on 09/05/12
For personal use only.

Can. J. Chem. Downloaded from www.nrcresearchpress.com by 210.87.254.105 on 09/05/12
For personal use only.

CHALKOGENIDES OF THE TRANSITION ELEMENTS

III. MOLYBDENUM DITELLURIDE[1,2]

OSVALD KNOP AND RODERICK D. MACDONALD[3]

ABSTRACT

$MoTe_2$ prepared by dry synthesis from the elements at 460° C and annealed at 600° C has a layer structure of the *C7* type with $a_0 = 3.5182 \pm 14$ Å and $c_0 = 13.9736 \pm 40$ Å. The parameter of the tellurium atom has been determined from closely reproducible X-ray diffractometer powder intensities as 0.621 ± 1. The nearest-neighbor co-ordination polyhedron of the molybdenum atom is a trigonal prism with a Mo—Te distance of 2.716 ± 12 Å. The distance of nearest approach of the tellurium atoms between layers is 3.945 ± 25 Å and thus greater than the similar distance between chains in metallic tellurium. It is shown that the observed intensities are not compatible with a stacking sequence of the *C27* type, which differs from the *C7* arrangement in the geometry of the co-ordination polyhedra of the metal atoms.

INTRODUCTION

It has been recently reported that molybdenum disulphide does not always have a crystal structure of the *C7* type, whose prototype it is, but that it can exist as at least two, and possibly three, polymorphs (1, 2, 3, 4). The two structures of the sulphide which are known in detail, i.e., the hexagonal *C7* structure and the rhombohedral form first described by Bell and Herfert (3) and later structurally reinterpreted by Jellinek *et al.* (4), are both layer structures consisting of planar sheets of superposable hexagonal networks of molybdenum and sulphur atoms stacked parallel to the basal plane. They differ in the sequence and period of displacement of the molybdenum and sulphur networks with respect to each other. The sequence is . . .AMABNBAMABNBAMA . . . for the *C7* form and . . . APACMCBNBAPACMCBNBAPA . . . for the rhombohedral form (A, B, C refer to sulphur layers, M, N, P, to molybdenum layers), but in both cases the stacking sequences result in trigonal-prismatic nearest-neighbor co-ordination of the molybdenum atom. Other sequences are theoretically possible, in some of which the environment of the metal atom is trigonal antiprismatic (distorted octahedral). A structure of this type would be, for example, the *C27*-type structure known from β-CdI_2, which Hägg and Schönberg (1) proposed as a possible MoS_2 structure to account for the observed X-ray intensities of some of their MoS_2 samples showing reportedly large disagreement between I_o and $I_c(C7)$.*

Although the crystal structure of the corresponding telluride, $MoTe_2$, has not been determined before, it was usually assumed that it belonged to the *C7* group; in reference 5, for instance, this follows by implication. When evidence for the polymorphism of MoS_2 appeared, it became clear that the telluride need not necessarily have the stacking arrangement of a *C7* compound and even if it does, the structure may be of lower symmetry, as has been found to be probably the case with the corresponding wolfram compound (6).

[1]*Manuscript received January 9, 1961.*
Contribution from the Department of Chemical Engineering, Nova Scotia Technical College, Halifax, N.S., with financial assistance from the National Research Council of Canada.
[2]*Part II of this series appeared in Can. J. Chem.* **39**, *297 (1961).*
[3]*Present address: Fuels Development Branch, Atomic Energy of Canada, Ltd., Chalk River, Ontario.*
**The relationship between the C7 and the rhombohedral form of* MoS_2 *is the same as that between the C27 and the C19* ($CdCl_2$) *structure, except that the metal co-ordination is trigonal prismatic in the first pair and distorted octahedral in the second.*

Can. J. Chem. Downloaded from www.nrcresearchpress.com by 210.87.254.105 on 09/05/12
For personal use only.

As far as we know, the occurrence of the *C7* type of structure is restricted to chalkogenides of niobium (4), molybdenum, tantalum (7), wolfram, rhenium (8), and possibly hafnium.* These compounds and the rhombohedral polymorphs of the disulphides of molybdenum, niobium, and tantalum are, moreover, almost the only known instances of structures in which the metal atom has trigonal-prismatic nearest-neighbor co-ordination,† which would seem to indicate a strong preference for this rather than for octahedral co-ordination. The observed bulk diamagnetism of MoS_2 (11) (and also of WTe_2 (13)) is in agreement with the assumption that the trigonal-prismatic co-ordination is the result of d^4sp bonding. Further support of this contention comes from the appreciable diamagnetic anisotropy of single crystals of molybdenite, the negative susceptibility parallel to the hexagonal axis being almost twice as large as that in the direction normal to the axis (12). Such magnetic behavior with its strong temperature dependence and the appreciable electrical conductivity of molybdenite along the basal plane both point to the presence of a system of largely delocalized mobile π electrons within the MoS_2 layers; the existence of such a system can again be explained from the d^4sp orbital configuration on the molybdenum atom, or more particularly from its $\pi(p^2d)$ system of trigonal symmetry. The telluride, which, too, has been shown to be diamagnetic (13), can accordingly be expected to have a *C7* structure or its rhombohedral modification. Furthermore, unless Hägg and Schönberg's MoS_2 preparations were paramagnetic, an explanation of the observed discrepancies in the diffraction intensities of these samples cannot be advanced on the basis of a *C27*-type structure with its sp^3d^2 (or d^2sp^3) bonding and its associated magnetic moment.

On the other hand, ReS_2 (14) and WS_2 (15) have been reported to be paramagnetic. The effective magnetic moment of ReS_2 is small and independent of temperature, but natural WS_2, tungstenite, has been stated to be strongly paramagnetic with a curious temperature dependence and a pronounced anisotropy. The effective moment of tungstenite at room temperature was found higher than would correspond to the "spin-only" value for two unpaired 5*d*-electrons. The *ad hoc* explanation for the paramagnetism of tungstenite profered by Dutta and Chowdhury (15) and based on the assumption of a *C7* structure, fails to establish why molybdenite, for which the same qualitative arguments apply, is diamagnetic. If the reported magnetic behavior of tungstenite is genuine and not caused by ferromagnetic or strongly paramagnetic impurities in the natural material‡ the orbital configuration on the tungsten atom cannot be d^4sp. The paramagnetism could be due to d^3p^3 or d^3sp^2 bonding, but then the stereochemistry of the WS_6 group would not be consistent with the $\bar{6}$ symmetry of the regular trigonal prism. The difference in co-ordination could be brought to light by crystal-structure analysis, but a sufficiently accurate detailed study of WS_2 has not yet been made. If orbital configurations of geometries different from that of d^4sp are, however, admitted to explain the paramagnetism of WS_2, one should bear in mind that this last configuration is not the only one to account for the observed diamagnetism of $MoTe_2$, but that this telluride might conceivably exist with a d^4p^2 configuration on the molybdenum atom. Since neither the magnetic properties of WS_2 nor its crystal structure has been established beyond doubt

*This case is now under investigation in this laboratory.

†In the *B8* (nickel arsenide) structure the atoms with trigonal-prismatic co-ordination are the non-metal atoms. A similar situation obtains, for instance, in Re_3B, Ru_7B_3, and other borides (9), and also in some carbides and phosphides. In the borides $RhB_{\sim 1.1}$ and PtB, however, which have been reported to have anti-NiAs structures, the nearest-neighbor co-ordination of the metal atoms is trigonal prismatic (10).

‡The tungstenite used by Dutta and Chowdhury was, to the authors' own admission, impure, but chemical analyses of the mineral are not shown. The impurity content varied with the source of the material; the spread of the experimental densities of the individual crystals (method not stated) was very appreciable, 7.00–8.2.

to either eliminate or include the possibility of co-ordination other than trigonal prismatic in the above group of dichalkogenides, prediction of the crystal structure of $MoTe_2$ is not entirely straightforward.

As for the differences caused by the stacking sequences of MX_2 layers of a particular type, either trigonal-prismatic or octahedral, polymorphs of this kind would not be expected to have widely dissimilar lattice energies. This is borne out by the relative readiness with which mixed sequences are formed in, for instance, cadmium or nickel bromides, although the ratio of the atomic radii does to some extent determine the stacking arrangement (cf. α-CdI_2 and $CdCl_2$).

In view of the contradicting statements in the literature concerning the molybdenum etc. dichalkogenides and since the tellurides of the above elements have so far received only scanty attention, we thought it of interest to investigate whether the trigonal-prismatic co-ordination of molybdenum, which is apparently characteristic for the typical molybdenum disulphide and diselenide, is preserved in the ditelluride; and if this is the case, whether the structure corresponds to the *C7* type, with or without distortion, or to another stacking arrangement.

EXPERIMENTAL

The ditelluride was prepared by dry synthesis from the elements *in vacuo* in much the same way as previously WTe_2 (6). Fansteel molybdenum powder type 352 of average particle size of 4–5 microns and of specified minimum purity of 99.9% and specified minimum impurity content of 0.015% C, 0.125% O, and 0.02% Ni, was reduced before use with purified hydrogen at 690–700° C. The tellurium metal was kindly donated by Canadian Copper Refiners, Ltd., and contained, according to the supplied analysis (in p.p.m.), 0.4 Cu, 3.0 Al, and 0.5 Mg. Hg (detection limit 2 p.p.m.), Pb (0.5), Fe (1), As (10), Sb (0.5), Sn (0.5), Bi (0.5), Ni (1), Cr (0.5), Zn (10), Ag (0.1), Na (4), and Si (1) were not detected.

A stoichiometric mixture of molybdenum and tellurium powders totalling 15 g was sealed in a degassed, evacuated tube of clear quartz and kept at 460° C for 16 hours. On removal from the furnace the tube was opened and the reacted mixture crushed lightly to pass a 125-mesh screen. The thoroughly mixed powder was then resealed and annealed at 600° C for 48 hours. The product was a loose dark-gray powder of uniform appearance consisting of very fine needles and platelets. The crystals were too small and often intimately intergrown to be suitable for a single-crystal study. No foreign particles were detected under magnifications up to 30 diameters.

Specimens for X-ray powder diffraction were prepared by mounting $MoTe_2$ powder that had been crushed to pass completely a 325-mesh screen, on very thin pyrex fibers coated thinly and uniformly with vacuum grease. Powder photographs were taken in 114.6-mm Straumanis-type cameras with filtered Cu K, Fe K, and Cr K radiations. Powder specimens for the Norelco diffractometer were prepared by sifting the annealed powder through a 325-mesh screen on a cylindrical aluminum specimen mount coated evenly with a thin, flat layer of stiff silicon grease. The diffractometer patterns were obtained with rotating specimens using 1/2, 1, and 4° slits and a pulse-height analyzer. They were used for the integrated intensities only. The same wavelengths were used as are quoted in the second paper of this series.

RESULTS

The films were of surprisingly good quality, considering the frequently poor definition of the diffraction lines obtained with tellurides of the transition elements. As could be

Can. J. Chem. Downloaded from www.nrcresearchpress.com by 210.87.254.105 on 09/05/12
For personal use only.

expected, the photographs taken with filtered Cu K radiation had the best appearance and were used in the final determination of lattice parameters. All lines could be indexed on a hexagonal unit cell (Table I). After six cycles of refining a and c by least squares

TABLE I

Observed and calculated $\sin^2\theta$ values and X-ray powder intensities for $MoTe_2$ (Cu $K\alpha$ radiation)

	$10^4 \cdot \sin^2\theta$					$10^4 \cdot \sin^2\theta$			
*hkl**	calcd.	obs.	I_c†‡§	I_o‡§	*hkl**	calcd.	obs.	I_c†‡§	I_o‡§
002	0122	0124	22.0	21.0	218	6429	6427	5.0	5.1
004	0487	0493	12.7	13.0	10.14	6605	6611	0.7	1.0
100	0640	0641	37.0	40.4	306	6858	6852	1.5	2.3
101	0670	0673	9.0	10.9	20.12	6944	—	0.4	—
102	0762	0764	3.7	3.3	219	6947		0.2	
103	0914	0918	100	100	10.15	7488	7494	1.3	2.1
006	1096	1109	3.4	3.8	21.10(*1*)	7512		0.0	
104	1127	1141	6.2	6.3	21.10(*2*)	7550	7533		
105	1401	1403	36.8	36.9	220	7682	7679	5.6	
106	1736	1753	2.4	2.8	20.13(*1*)	7690	7706	3.1	
110	1921	1922	27.3	41.8	308(*1*)	7696		11.1	
008	1948	1967	8.6		20.13(*2*)	7730	7739		
112	2043	2048	3.0	3.4	308(*2*)	7736			31.2‖
107	2132	2147	3.2	3.8	00.16(*1*)	7777	—	1.7	
114	2408	2414	7.6	7.7	222(*1*)	7791	7796	0.7	
200	2561	2568	4.3	5.1	222(*2*)	7829	7835		
108	2588	2608	7.6	8.8	11.14(*1*)	7871	7887	3.3	
201	2591		1.1		11.14(*2*)	7913	7928		
202	2683	—	0.3	0.4	21.11(*1*)	8159	8159	15.6	
203	2835	2843	14.4	15.2	224(*1*)	8155		2.4	19.3
116	3017	3030	3.8	5.9	21.11(*2*)	8191	8202		
00.10	3044		0.0		224(*2*)	8196			
204	3048		1.3		310(*1*)	8303	8307		
109	3106	—	0.2	—	310(*2*)	8350	8348	3.2	3.8
205	3322	3336	8.2	8.8	311(*1*)	8338		0.9	
206	3657	3676	0.7	0.8	10.16(*1*)	8416	8430	2.9	
10.10	3684		0.0		312(*1*)	8430		0.4	4.1
118	3869	3887	16.2	18.4	10.16(*2*)	8469	8480		
207	4053	4063	1.2	1.2	312(*2*)	8472			
10.11	4323	4351	8.9	11.5	20.14(*1*)	8510	8525	1.0	14.9
00.12	4383	—	0.4		313(*1*)	8581	8581	14.6	
210	4481	4505	3.4	7.8	313(*2*)	8625	8625		
208	4509		3.3		226(*1*)	8763	8766	2.3	
211	4511		1.0		30.10(*1*)	8790	8802	0.1	
212	4603	—	0.4	0.4	314(*1*)	8794		1.6	3.5¶
213	4755	4768	13.0	13.3	30.10(*2*)	8835	8856		
11.10	4965	4974	0.1	2.0	314(*2*)	8839			
214	4968		1.2		21.12(*1*)	8849		1.3	
10.12	5023	5042	0.5		315(*1*)	9068	9065	13.1	12.6
209	5027		0.1		315(*2*)	9114	9109		
215(*1*)	5234	5249	8.8	8.7	20.15(*1*)	9392	9404	2.5	
215(*2*)	5260	5267			316(*1*)	9402		1.6	
216	5577	5592	0.8	1.0	10.17(*1*)	9420		0.0	4.0¶
20.10	5605		0.0		20.15(*2*)	9441	9451		
300	5762	5760	5.3	8.8	316(*2*)	9449			
10.13(*1*)	5773	5789	2.9		10.17(*2*)	9468			
10.13(*2*)	5803	5815			21.13(*1*)	9608	9613	15.0	
302	5884	—	0.6	0.7	228(*1*)	9613		27.3	37.0
00.14	5966	5971	0.5	2.6	21.13(*2*)	9657	9659		
217	5973		1.5		228(*2*)	9662			
20.11(*1*)	6232	6247	6.4		11.16(*1*)	9694	9706	28.7	29.8**
304(*1*)	6238		2.1		11.16(*2*)	9745	9754		
20.11(*2*)	6264	6281		11.3	317(*1*)	9797	9797	6.1	
304(*2*)	6270				317(*2*)	9846	9844	0.0	
11.12	6304		1.7		00.18(*1*)	9843			

*Resolved α-doublets are indicated by (*1*) and (*2*). †For $z = 0.621$; temperature factor not included. ‡Normalized to $I(103)$. §Intensities of the α_1 and α_2 components are taken together. ‖Overlap. ¶Extent of maxima uncertain. **Diffractometer cutoff.

Can. J. Chem. Downloaded from www.nrcresearchpress.com by 210.87.254.105 on 09/05/12
For personal use only.

using Nelson–Riley extrapolation for reflections with $\theta > 30°$ the final values of the lattice parameters were $a_0 = 3.5182 \pm 14$ Å, $c_0 = 13.9736 \pm 40$ Å, and $c_0/a_0 = 3.972$. The volume of the unit cell is 149.79 ± 17 Å^3.

The density of $MoTe_2$ (125−) was determined in the same way as described in Part II of this series. Average of three determinations gave $d_4^{25} = 7.681 \pm 18$ g/cm^3, which corresponds to 1.974 $MoTe_2$ per unit cell. This density compares rather more favorably with the density calculated from the lattice parameters, 7.784 ± 9 g/cm^3, than the value quoted by Morette (13), $d_4^{15} = 7.60 \pm 1$ g/cm^3, and is only −1.28% lower than the X-ray density. It is difficult to say whether the discrepancy has a real significance as regards the existence of molybdenum and tellurium vacancies in the structure.* Unreacted molybdenum and tellurium in amounts lower than the minimum amounts capable of producing observable diffraction lines cannot be detected in a stoichiometric $MoTe_2$ sample by density measurement because of the almost identical densities of $MoTe_2$ and a 1:2 mixture of molybdenum and tellurium.

Reflections of the (hkl) type with $h-k = 3n$, $l = 2n+1$ were absent. This condition is satisfied in eight space groups, viz., D_{6h}^4—$P\,6_3/mmc$, D_{3h}^4—$P\,\bar{6}2c$, C_{6v}^4—$P\,6_3mc$, D_6^6—$P\,6_322$, C_{6h}^2—$P\,6_3/m$, C_6^6—$P\,6_3$, D_{3d}^2—$P\,\bar{3}1c$, and C_{3v}^4—$P\,3/c$, but the symmetries and equipoints of these space groups are compatible not only with the *C7*, but also with, for instance, the *C27* structure, which has been claimed as possible for some MoS_2 samples (cf. Introduction).

The first model tried was a *C7* structure (space group D_{6h}^4—$P\,6_3/mmc$) with 2 Mo in $2(c)$: $\pm(1/3, 2/3, 1/4)$ and 4 Te in $4(f)$: $\pm(1/3, 2/3, z)$; $\pm(1/3, 2/3, 1/2-z)$, $z_{Te} = 0.625$ $(= 5/8)$. A set of intensities was calculated for Cu $K\alpha$ radiation using Thomas–Fermi atomic scattering factors tabulated in reference 18. The agreement between I_o and I_c was good, but it was felt that the integrated powder intensities, which had been obtained by careful planimetering of several diffractometer charts, would justify further refinement. Six other values of z varying from 0.618 to 0.628 were then tried. Since out of the 70 observable reflections with $I_c \geqslant 0.5$ (normalized to $I_o(103)$) only 26 were fully resolved, the extent of agreement could not be assessed from the reliability index, $R = \sum ||F_o| - |F_c|| / \sum |F_o|$, customary in structure analysis from single-crystal data. However, the sum $\sum |I_o - I_c|$, though not an unambiguous measure of the progress of refinement, was found to be quite sensitive to variations in z. The agreement of I_o and I_c for $z = 0.621 \pm 1$, which was the value corresponding to the minimum of the difference sum located analytically for a parabolic least-squares fit, was indeed remarkably good (Table I). The *C7* structure adopted in the first trial can thus be considered correct, the existence of homometric structures compatible with the observed dimensions and symmetry of the unit cell being not very probable.

The close agreement of the intensities also demonstrates that the diffractometer specimens were free from orientation effects which are frequently present in specimens of compounds with fully developed layer structures. Stacking disorder in our $MoTe_2$ preparation must have been negligible for the same reason. The increase of $|I_c - I_o|$ with θ for individual reflections was so small that it did not justify inclusion of an isotropic temperature factor. In particular, there was no systematic weakening of I_o for reflections with $h-k \neq 3n$ with increasing l, nor was there selective line-broadening affecting particular orders.

As for the possibility that $MoTe_2$ has a *C27*-type structure (space group $C_{6v}^4 - P\,6_3mc$),

*Similar, and even greater, differences between pycnometric and X-ray densities have been reported for wolfram disulphide (16, 17).

Can. J. Chem. Downloaded from www.nrcresearchpress.com by 210.87.254.105 on 09/05/12
For personal use only.

it is readily seen that a model structure with 2 Mo in 2(*b*): ±(1/3, 2/3, 1/4), 2 Te in 2(*b*): (1/3, 2/3, *z*), (2/3, 1/3, 1/2+*z*), 2 Te in 2(*a*): (0, 0, −*z*), (0, 0, 1/2−*z*), and z_{Te} = 5/8* is not isovectorial with *C7* and cannot account satisfactorily for the observed intensities. In particular, the calculated intensities of the reflections {100} and {200}, whose geometrical structure factors do not contain *z*, differ very considerably from the corresponding I_o values, the ratios $F_{100}(C27)/F_{100}(C7)$ and $F_{200}(C27)/F_{200}(C7)$ being −0.072 and −0.081, respectively, and thus far from unity. A similar situation is obtained with another conceivable model structure, viz. that based on the structure of the recently described hexagonal NbS_2 (4), even though the nearest-neighbor co-ordination of the metal atom is trigonal prismatic.

The interatomic distances and bond angles in the $MoTe_2$ structure are as follows (Fig. 1):

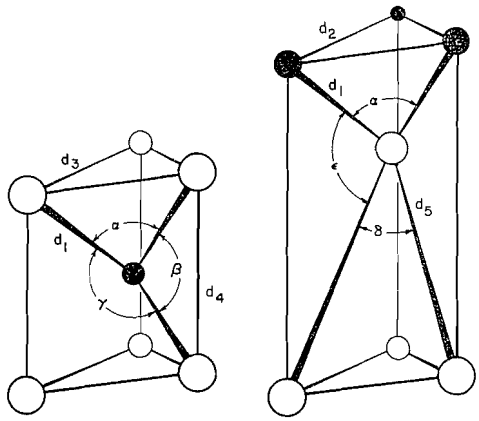


FIG. 1. Nearest-neighbor co-ordination of the molybdenum and tellurium atoms in molybdenum ditelluride. Full circles, molybdenum; open circles, tellurium.

d_1(Mo—Te) = 2.716±12 Å
d_2(Mo—Mo) = d_3(Te—Te) = a_0 = 3.5182±14 Å
d_4(Te—Te) = 3.603±25 Å
d_5(Te—Te) = 3.945±25 Å
d_6(Mo—Mo, between layers) = 7.276±5 Å

α(Te—Mo—Te) = α(Mo—Te—Mo) = 80.74±0.50°
β(Te—Mo—Te) = 83.10±0.60°
γ(Te—Mo—Te) = 135.95±0.60°
δ(Te—Te—Te) = 52.96±0.40°
ϵ(Mo—Te—Te) = 100.59±0.60°.

The Te—Te distance d_5 is about 14% longer than the distance of nearest approach between chains in metallic tellurium, 3.468 Å (19), and the similar Te—Te distance, 3.46±8 Å, in $NiTe_2$(*C6*) (20), but it is fairly close to the Te—Te distance between layers in γ(V, Te)(*C6*), 3.82–3.85 Å (21). The asymmetric Te_I—Te_{II}—Te_I angle between neighboring chains I and II in tellurium which subtends the shortest Te—Te distance in a chain, 2.864 Å, is only 35.4° and thus appreciably smaller than the corresponding angle δ in $MoTe_2$. A symmetric Te_I—Te_{II}—Te_I angle in tellurium is equal to 80.0°, but it subtends not the shortest Te—Te distance but the distance between next-nearest neighbors in the tellurium helix, 4.864 Å. The bond angle δ in $MoTe_2$ is thus almost the arithmetic average of these two bond angles. The Te—Mo—Te angles are very nearly the same as the corresponding S—Mo—S angles in MoS_2(*C7*).

**Origin shifted by (0, 0, 1/4) with respect to the original description of the C27 type as represented by β-CdI_2.*

Can. J. Chem. Downloaded from www.nrcresearchpress.com by 210.87.254.105 on 09/05/12
For personal use only.

Since the distances d_3 and d_4 are not equal, the axial ratio of the trigonal prism is not exactly unity, as claimed by Pauling (22, p.175) for molybdenite, but slightly different, $d_4/d_3 = 1.024$.

The shortest Mo—Te distance, d_1, agrees quite well with the sum of the appropriate atomic radii, which is between 2.64 and 2.74 Å, depending on whether the value for Te is taken as the "single-bond" or the "double-bond" radius (22).

Allowing for the fact that WTe_2 is orthorhombic with $b \sim a\sqrt{3}$ (6) and taking the unit-cell dimensions for MoS_2 and WS_2 from (23) and (24), respectively, the square roots of the ratio of the basal areas and the cube roots of the unit-cell volumes are nearly the same for corresponding pairs:

	(basal area)$^{1/2}$	(volume)$^{1/3}$
$(WS_2)/(MoS_2)$	0.998	1.008
$(1/2\ WTe_2)/(MoTe_2)$	1.014	1.009
$(MoTe_2)/(MoS_2)$	1.113	1.121
$(1/2\ WTe_2)/(WS_2)$	1.131	1.122.

Since the estimated radius of Mo in molybdenite is 1.37 Å and that of W in tungstenite is 1.44 Å (22), the difference amounting to about 5%, it is clear that the dimensions of the unit cells of these compounds are determined essentially by the chalkogen atoms.

The stability of $MoTe_2$ on heating under orthobaric conditions is greater than that of WTe_2. There is no isothermal transition between room temperature and 1200° C (cf. (6)). The failure to observe melting in this temperature range is in full agreement with the result of Morette (13), who heated a sample of $MoTe_2$ with excess tellurium *in vacuo* up to 1130° without fusion.

The trigonal-prismatic co-ordination of the molybdenum atom in $MoTe_2$ established in this investigation and the observed diamagnetism of $MoTe_2$ and WTe_2 (13) as well as of MoS_2 throw some doubt on the strong paramagnetism of WS_2 reported for natural material in reference 15. Work is in progress in this laboratory to determine whether MoS_2 and WS_2 form mixed phases; and if so, how the magnetic properties of such phases depend on their composition. It is also intended to re-examine the crystal structure of WS_2 in the light of the conceivable structural ambiguities discussed in the introduction and to obtain a more accurate value for the sulphur parameter than the approximate value of 5/8 first proposed by van Arkel in 1926 (25) and quoted ever since.

ACKNOWLEDGMENTS

One of the authors (R. D. M.) wishes to express his gratitude to the Eldorado Mining and Refining Limited for the award of the Charles G. Williams Fellowship, and to Atomic Energy of Canada, Ltd., for leave of absence. The assistance of Dr. R. H. Tuxworth of Atomic Energy of Canada, Ltd., Chalk River, Ontario, who provided the preliminary diffraction charts, and of Mr. Muntaz Ali, who carried out some of the calculations and determined the density of molybdenum ditelluride, is hereby gratefully acknowledged.

REFERENCES

1. G. HÄGG and N. SCHÖNBERG. Arkiv Kemi, **7**, 376 (1955).
2. J. R. STUBBLES. PhD. Thesis. Imperial College, London, England. 1957; J. R. STUBBLES and F. D. RICHARDSON. Trans. Faraday Soc. **56**, 1460 (1960).
3. R. E. BELL and R. E. HERFERT. J. Am. Chem. Soc. **79**, 3351 (1957).
4. F. JELLINEK, G. BRAUER, and H. MÜLLER. Nature, **185**, 376 (1960).
5. R. C. EVANS. An introduction to crystal chemistry. Cambridge University Press, London. 1946. p. 137.

Can. J. Chem. Downloaded from www.nrcresearchpress.com by 210.87.254.105 on 09/05/12
For personal use only.

6. O. KNOP and H. HARALDSEN. Can. J. Chem. **34**, 1142 (1956).
7. F. JELLINEK. Private communication.
8. J. LAGRENAUDIE. J. phys. radium, **15**, 299 (1954).
9. B. ARONSSON, M. BÄCKMAN, and S. RUNDQVIST. Acta Chem. Scand. **14**, 1001 (1960); B. ARONSSON. Acta Chem. Scand. **13**, 109 (1959); R. KIESSLING. Acta Chem. Scand. **4**, 209 (1950).
10. B. ARONSSON, E. STENBERG, and J. ÅSELIUS. Acta Chem. Scand. **14**, 733 (1960).
11. B. T. TJABBES. Proc. Acad. Sci. Amsterdam, **35**, 693 (1932).
12. A. K. DUTTA. Indian J. Phys. **18**, 249 (1944); **19**, 225 (1945).
13. A. MORETTE. Ann. chim. **19** (11), 130 (1944); Compt. rend. **215**, 86 (1942).
14. W. SCHÜTH and W. KLEMM. Z. anorg. u. allgem. Chem. **220**, 193 (1934).
15. A. K. DUTTA and B. C. R. CHOWDHURY. Indian J. Phys. **23**, 131 (1949).
16. O. GLEMSER, H. SAUER, and P. KÖNIG. Z. anorg. u. allgem. Chem. **257**, 241 (1948).
17. P. EHRLICH. Z. anorg. u. allgem. Chem. **257**, 247 (1948).
18. INTERNATIONALE TABELLEN ZUR BESTIMMUNG VON KRISTALLSTRUKTUREN. Bd. 2. Gebr. Borntraeger, Berlin. 1935.
19. M. STRAUMANIS. Z. Krist. **102**, 432 (1940).
20. S. TENGNÉR. Z. anorg. u. allgem. Chem. **239**, 126 (1938).
21. F. GRØNVOLD, O. HAGBERG, and H. HARALDSEN. Acta Chem. Scand. **12**, 971 (1958).
22. L. PAULING. The nature of the chemical bond. 3rd ed. Cornell Univ. Press, Ithaca, N.Y. 1960.
23. H. SWANSON, N. T. GILFRICH, and G. UGRINIC. Natl. Bur. Standards Circ. 539, Vol. 5. Washington, D.C. 1955. p. 47.
24. H. SWANSON, N. T. GILFRICH, and M. I. COOK. Natl. Bur. Standards Circ. 539, Vol. 8. Washington, D.C. 1958. p. 65.
25. A. E. VAN ARKEL. Rec. trav. chim. **45**, 442 (1926).

Can. J. Chem. Downloaded from www.nrcresearchpress.com by 210.87.254.105 on 09/05/12
For personal use only.

Can. J. Chem. Downloaded from www.nrcresearchpress.com by 210.87.254.6 on 09/05/12
For personal use only.

THE PROTON RESONANCE SPECTRA OF SOME SUBSTITUTED FURANS AND PYRROLES[1]

R. J. ABRAHAM[2] AND H. J. BERNSTEIN[3]

ABSTRACT

The proton magnetic resonance spectra of some substituted furans and pyrroles have been analyzed for spin coupling constants and chemical shifts.

The relative insensitivity of the spin coupling constants to the nature of the substituent makes it possible to estimate their values in the parent molecules furan and pyrrole. The magnitude of the spin coupling constants is correlated with the angles made by the CH bonds with the CC bonds of the ring.

The chemical shifts are interpreted in terms of an effect due to the electronegativity of the substituent together with the effect due to conjugation with the ring.

The proton resonance spectra of the heterocyclic compounds furan, pyrrole, and thiophene and of their derivatives have been the subject of a number of investigations (1, 2, 3, 4). The present work is an attempt to determine more systematically the effects of substitution on the chemical shifts and spin coupling constants of the ring protons in substituted furans and pyrroles.

These compounds are well suited to a proton magnetic resonance investigation since their spectra are usually capable of a unique interpretation and assignment. The simplest spectra are those of the substituted furans. Here, due to the large difference in the chemical shifts of the α and β protons of the ring, any monosubstituted furan can be classed as an ABX-type spectrum for which a complete analysis is readily achieved. In some cases, where fewer lines are observed than theoretically expected, the spectrum obtained does not give explicit values of any of the coupling constants. This type of spectrum, which is obtained not only for some monosubstituted furans but also for the parent compounds furan and pyrrole, has been the subject of a previous publication (5). The spectra of the substituted pyrroles are complicated by the additional interaction of the N—H proton with the other ring protons. However, a possible interpretation of the spectra of some monosubstituted pyrroles is presented.

EXPERIMENTAL

The compounds used were the commercial samples except for the following. 2-Nitro furan was prepared by nitrating furan with fuming nitric acid and acetic anhydride following the procedure of Marquis (6). 5-Chlormethyl furfural was prepared from sugar and concentrated HCl following the procedure of Aso (7). 3-Furoic acid and its derivatives were kindly supplied by Prof. H. Gilman. The specimen of 2-cyano pyrrole was kindly supplied by Prof. H. J. Anderson.

The spectra of the compounds demonstrated their purity. Only in one case, 2-furoyl-trifluoromethyl ketone, was there any sign of any impurity.

The spectrometer and the techniques for measuring the spectra have been described fully in a previous paper (1). The spectra are shown for 40 Mc/s operation except where stated otherwise, and the convention adopted is that high applied field is positive.

[1]*Manuscript received December 12, 1960.*
Contribution from the National Physical Laboratory, Teddington, Middlesex, England and the Division of Pure Chemistry, National Research Council, Ottawa, Canada.
Issued as N.R.C. No. 6230.
[2]*Present address: National Physical Laboratory, Teddington, Middlesex, England.*
[3]*Present address: Division of Pure Chemistry, National Research Council, Ottawa, Canada.*

The Analysis of Spectra

The spectra of the monosubstituted furans studied fall into three distinct classes.

The spectrum of 2-furanmethanethiol (Fig. 1) is given as an example of the type of

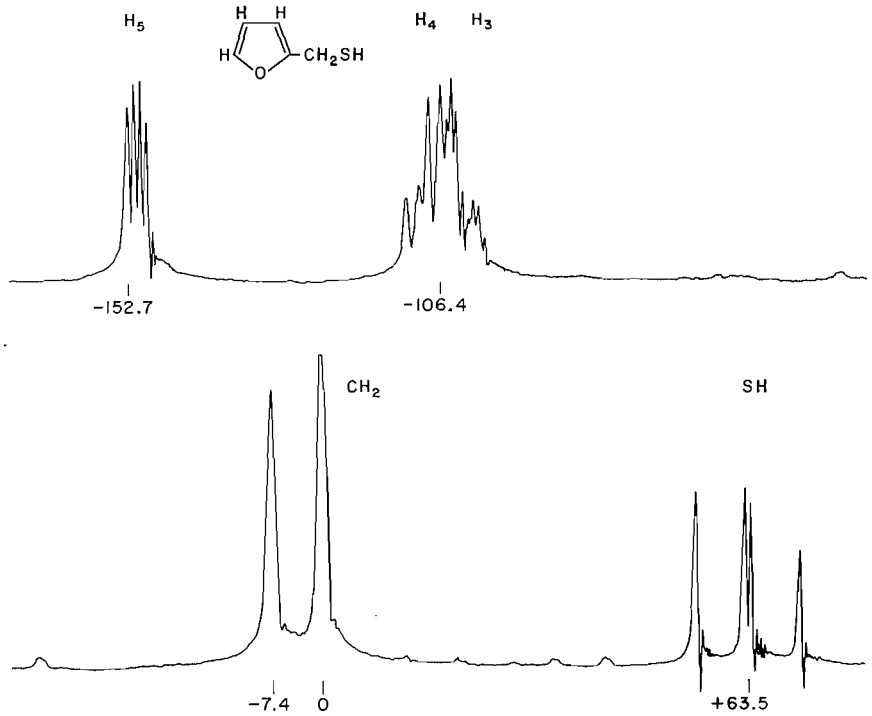


FIG. 1. The proton resonance spectrum of 2-furanmethanethiol (liquid) at 40 Mc/s. (The chemical shifts are in c.p.s. from a dioxane internal reference.)

spectrum obtained from a 2-furfuryl derivative. This is an ABX pattern with one of the normal quartets split into 12 unresolved lines by coupling with the CH_2 group. This interaction would be expected to take place between the methylene group and proton 3 of the ring, identifying the H_3 signals. This assignment is confirmed by the chemical shift data, as the methyl mercapto group is electron donating with respect to the furan ring and thus proton 3 would be expected to be more shielded than proton 4.

The spectrum of 2-nitro furan (Fig. 2) demonstrates the influence of a powerful electron-attracting group in position 2 of the ring. The electron shielding of proton 3 is decreased considerably. Thus the signal due to this proton moves to low field to such an extent that the spectrum is a simple first-order one, with the coupling constants given directly by the separations of the lines in each group. Any strongly electronegative group in position 2, e.g., the carbonyl group, gives the same type of spectrum.

The spectrum of 2-furanacrolein (Fig. 3) is an example of the third class of spectrum. Here the ring proton spectrum is very similar to that of 2-nitro furan, but is partially obscured by the side chain spectrum. The assignment shown in Fig. 3 was confirmed by the spectrum of 2-furanacrylic acid, which is identical with the one shown except that in this case the aldehyde splitting of one of the side chain protons is removed leaving a simple quartet.

The remaining spectra are straightforward examples of one of these classes or are

Can. J. Chem. Downloaded from www.nrcresearchpress.com by 210.87.254.6 on 09/05/12
For personal use only.

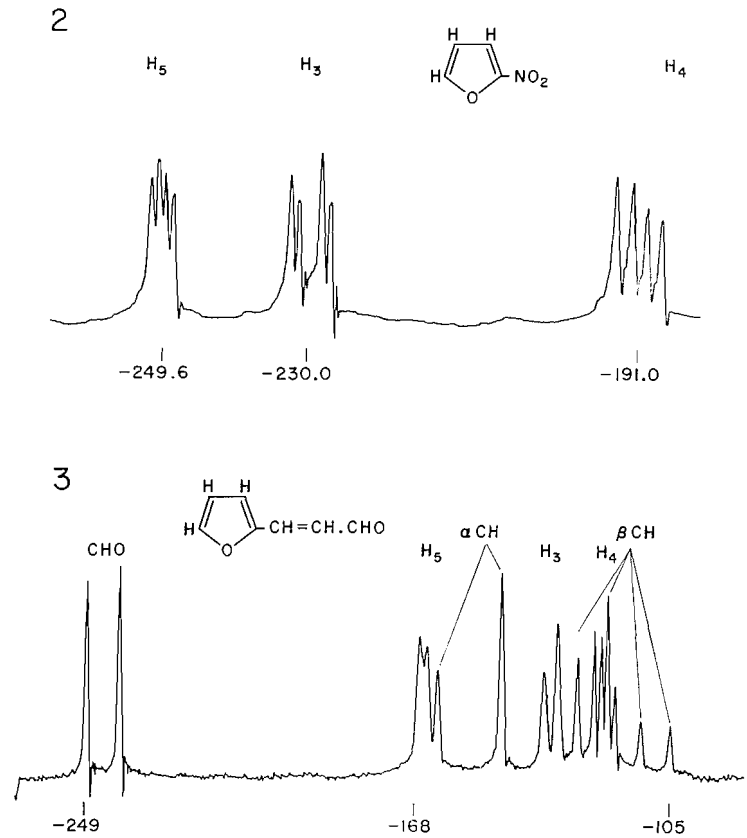


FIG. 2. The proton resonance spectrum of 2-nitro furan (liquid) at 60 Mc/s. The chemical shifts are in c.p.s. from a dioxane internal reference.

FIG. 3. The proton resonance spectrum of 2-furanacrolein in acetone solution at 40 Mc/s. α and β refer to the carbon atoms of the substituent. The chemical shifts are in c.p.s. from a dioxane internal reference.

even more simple spectra, as in the case of the disubstituted furans, and are not reproduced.

The spectra of the 2-substituted pyrroles can be analyzed and assigned in the same general manner as in the furan derivatives; however, there are two additional factors involved. There is the spin coupling of the N—H proton with each of the ring protons which doubles the number of peaks in each spectrum. Also, the chemical shift separation between the α and β protons in the pyrroles is not significantly larger than the change in the chemical shifts due to the substituent group. Thus the assignment of the groups in these spectra is not as certain as the assignments in the furan spectra.

The spectrum of 2-pyrrole aldehyde is shown in Fig. 4. The groups in the spectrum are labelled from left to right, A, B, and X. The problem of the analysis of this spectrum consists in picking out from the observed signals those due to the couplings of the ring protons to the N—H proton and a further coupling of one proton to the aldehyde proton (known to be 1.1 c.p.s. from the doublet separation of the aldehyde proton peak). This process is shown in Table I. The result of this is to leave the three quartets characteristic of an ABX spectrum. The numbering of the lines in these quartets (given in Table I) is unusual due to the fact that J_{AB} is less than J_{AX} or J_{BX}. Apart from this, it is a straightforward ABX analysis (8).

Can. J. Chem. Downloaded from www.nrcresearchpress.com by 210.87.254.6 on 09/05/12
For personal use only.

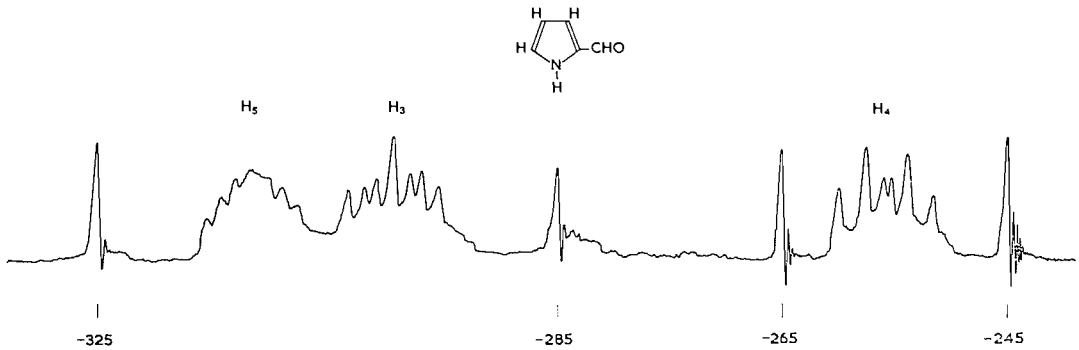


FIG. 4. The proton resonance spectrum of 2-aldehydo pyrrole in acetone solution at 60 Mc/s. The marker side bands are in c.p.s. from the acetone signal.

TABLE I

The analysis of the proton resonance spectrum of 2-pyrrole aldehyde

			A Obs. energy		*B* Obs. energy 12.30+			*X* Obs. energy 55.45+			
			0	1.26		0			0		
			0.63					12. 1.18		2.35	
			1.26		4. 1.21	1.40	2.42		2.35		
8. 1.87	2.48		1.88	1.23							
			2.49		2. 2.65	2.42	2.50	11. 3.49	3.92	2.28	
6. 3.12	2.47		3.11	1.24							
			3.73			3.90		10. 4.99	4.63	2.14	
			4.35								
			Unresolved		3. 5.13	5.37	2.47		6.06		
7. 4.74	(2.45)		4.78					9. 7.19		2.26	
			5.40	1.12	1. 6.61	6.37	2.48		8.32		
5. 5.98	2.41		5.96								
			6.52			7.85					
			7.19	1.34							
			7.86								

$J_{A-NH} = 2.45\ (\pm 0.02)$ $J_{A-CHO} = 1.24\ (\pm 0.05)$ $J_{B-NH} = 2.47\ (\pm 0.02)$ $J_{X-NH} = 2.26\ (\pm 0.06)$

The remaining problem is the assignment of the groups in the spectrum. The *X* peak is readily assigned to proton 4 of the ring, from chemical shift and coupling constant data (1). This leaves two possible assignments for the remaining groups. Here the *A* group is assigned to proton 5. This is supported by (*a*) the values of the coupling constants obtained from this assignment agree with the previous values of the coupling constants in the pyrrole ring (1) and with the values of the analogous coupling constants in the furan and thiophene rings (Table IV), and (*b*) the J_{A-CHO} coupling is analogous to the J_{5-CHO} coupling in 2-furfural (1). The effect of the alternative assignment would be to interchange the subscripts 3 and 5 in the δ and J values given for this spectrum.

The analysis of the spectrum of 2-cyano pyrrole (Fig. 5) is very similar to the analysis of Table I, but simpler due to the fact that the J_{5-CHO} coupling is not present. The assignment of the groups in this spectrum also follows the above assignment. In the spectrum of the pure liquid (not shown) the chemical shift difference between protons 3 and 5 is so small that the groups of peaks overlap. This is analogous to the small chemical shift difference in liquid pyrrole and the shift of the α-proton signal to low field with respect to the β-proton signal on dilution in acetone (9). This is further support for the assignment of the low field signal to proton 5.

Can. J. Chem. Downloaded from www.nrcresearchpress.com by 210.87.254.6 on 09/05/12
For personal use only.

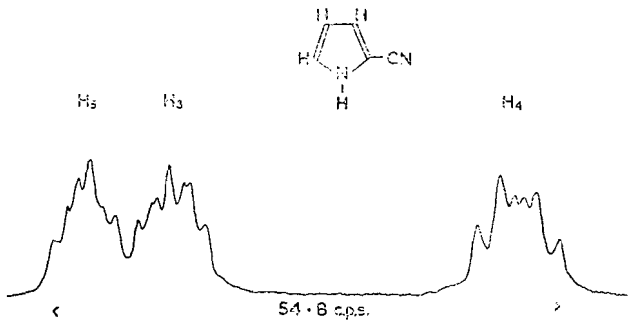


FIG. 5. The proton resonance spectrum of 2-cyano pyrrole in acetone solution at 60 Mc/s.

RESULTS AND DISCUSSION

(a) The Proton–Proton Coupling Constants

The values of the coupling constants which have been derived from the above analyses are shown in Tables II and III, together with the estimated mean deviations. The mean

TABLE II

Proton–proton coupling constants in substituted furans (c.p.s.)

Substance	J_{24}	J_{25}	J_{34}	J_{35}	J_{45}	
2-Methyl furan			3.12(.10)	1.03(.07)	1.90(.08)	$J_{CH_3-3} = 0.91$
2-Furanmethanethiol			3.25	0.73	1.91	$J_{CH_2-3} = 0.79$
2-Furfurylamine			3.18(0.10)	0.76(.10)	1.94(0.10)	$J_{CH_2-3} = 0.84$
2-Furfurol			3.17(.05)	0.84(.07)	1.90(.05)	
2-Furanacrylic acid			3.44(.07)		1.84(.08)	
2-Furanacrolein			3.46(.08)		1.83(.04)	
2-Furamide			3.57(.07)	0.72(.07)	1.76(.04)	
Ethyl 2-furoate			3.47(.09)	0.91(.06)	1.76(.05)	
2-Furoic acid			3.51(.07)	0.86(.09)	1.73(.08)	
Ethyl 2-furoylacetate			3.60(.09)	0.82(.10)	1.72(.05)	
2-Furfural			3.62(.05)	0.82(.06)	1.65(.08)	$J_{CH-5} = 0.81$
2-Nitro furan			3.66(.10)	0.98(.07)	1.92(.07)	
2-Furoyl trifluoromethyl ketone			3.70(.06)	0.76(.06)	1.70(.04)	
2-Furoyl chloride			3.79(.07)	0.79(.07)	1.70(.05)	
5-Chlormethyl furfural			3.67(.07)			
3-Furoic acid	0.8(.1)	1.5(.1)			1.8 (.1)	
2-Methyl-3-furoic acid					1.94(.1)	
4-Methyl-3-furoic acid		1.6(.1)				$J_{CH_3-5} = 1.4$
2,3-Difuroic acid					1.83(.1)	

TABLE III

Proton–proton coupling constants in substituted pyrroles

Substance	J_{13}	J_{14}	J_{15}	J_{34}	J_{35}	J_{45}	
2-Cyano pyrrole	2.25(0.2)	2.42(.2)	2.70(.2)	3.74(.2)	1.45(.2)	2.62(.2)	
2-Aldehydo pyrrole	2.47(.1)	2.26(.1)	2.45(.1)	3.73(.1)	1.36(.1)	2.68(.1)	$J_{CHO-5} = 1.17$
3,4-Dimethyl pyrrole			2.3 (.1)				
2,3,5-Trimethyl pyrrole		2.1 (.1)					

deviations measure the extent to which the line separations, and thus coupling constants, are reproducible in different parts of the spectrum. The mean deviations given in Table II for the substituted furans are solely due to experimental difficulties. The larger values given in Table III are due to an additional error caused by the overlapping of many lines

Can. J. Chem. Downloaded from www.nrcresearchpress.com by 210.87.254.6 on 09/05/12
For personal use only.

in each part of the spectrum (e.g. see Figs. 4 and 5), so that the actual positions of the individual lines may not be at the center of the component line.

The average values of the coupling constants in the five-membered ring systems of furan, pyrrole, and thiophene are shown in Table IV. The furan coupling constants are

TABLE IV

Spin coupling constants in five-membered hetercyclic aromatics

Ring system	J_{12} (=J_{15})	J_{13} (=J_{14})	J_{23} (=J_{45})	J_{24} (=J_{35})	J_{34}	J_{25}
Furan			1.80 (.09)	0.80 (.10)	3.53 (.13)	1.55 (.1)
Pyrrole	2.43 (.16)	2.43 (.24)	2.63 (.03)	1.44 (.05)	3.42 (.42)	
Thiophene			5.2 (.3)	1.3 (.3)	3.6 (.3)	2.7 (.3)

the mean of the results of Table II, the pyrrole coupling constants the mean of the results of Table III and reference 1, and the thiophene coupling constants the mean of the values obtained from the analysis of the thiophene spectrum (10) and those obtained from substituted thiophenes (4).

Considering first the results given in Tables II and IV for the substituted furans. The spin coupling constants are in agreement with the less accurate results of reference 1 and also with the less extensive measurements of Leane and Richards (3). The average values of the coupling constants in the furan ring are also fully consistent with the observed furan spectrum and the 2-furfural 40 Mc/s spectrum (5). The results for the 2-substituted furans of Table II, however, do show one striking feature. Although the variations in the magnitudes of the coupling constants J_{35} and J_{45} are not significantly greater than the experimental error, the magnitude of the coupling constant J_{34} changes markedly over a range of substituent groups. The 2-substituted furans in Table II are listed in the order of increasing "electronegativity" of the substituent group (as determined by the ring proton chemical shifts (see Table V)). It can be seen that, although the total

TABLE V

Coupling constants (c.p.s.) and angles (degrees) in unsaturated cyclic compounds

	θ_2	θ_3	$\theta_2+\theta_3$	J_{23}	ref. for θ_1, θ_2	θ_1	$2\theta_1$	J_{34}
Furan	126	134	260	1.8	*a*	128	256	3.5
Pyrrole	126	$131\frac{1}{2}$	$257\frac{1}{2}$	2.6	*b*	$126\frac{1}{2}$	253	3.4
Thiophene	$124\frac{3}{4}$	$127\frac{1}{2}$	$252\frac{1}{4}$	5.2	*c*	$123\frac{1}{2}$	247	3.6
Ethylene	120	120	240	11	*d*			
		Hydrocarbons	2θ	J				
5 members			252	3	*e*			
6 members			240	7	*e*			
7 members			231.4	11	*e*			

a. B. Bak, L. Hansen, and J. Rastrup-Hansen. Discussions Faraday Soc. **19**, 30 (1955).
b. B. Bak *et al.* J. Chem. Phys. **24**, 720 (1956).
c. B. Bak *et al.* J. Chem. Phys. **25**, 892 (1956).
d. θ taken as 120°. Coupling constant from ref. 8 p. 242.
e. Coupling constant from ref. 8 p. 193.

variation of J_{24} is only of the order of 0.5 c.p.s., there is a close correlation between the magnitude of J_{34} and the "electronegativity" of the substituent group. The measurements on substituted pyrroles (Table III and ref. 1) support this correlation, but since the experimental error is much larger in this case and only a few compounds have been measured, this effect is not seen so clearly.

Can. J. Chem. Downloaded from www.nrcresearchpress.com by 210.87.254.6 on 09/05/12
For personal use only.

One more point that might be enlarged upon is the magnitude of the coupling constants J_{23} and J_{34} in the various heterocyclic rings. The angular dependence of the gem coupling constants (11) suggests that there may be a correlation between the sum of the angles $\theta_1+\theta_2$ and the H—H coupling constant J_{34}, and $\theta_2+\theta_3$ with J_{23} (see Fig. 6). Further, this

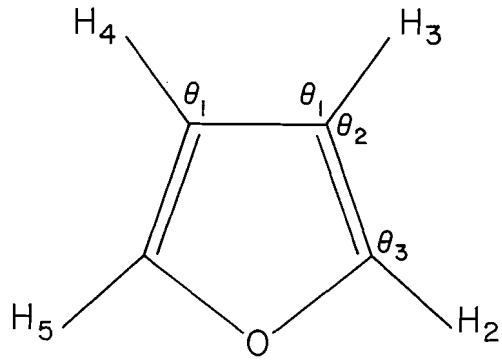


FIG. 6.

correlation might be expected to be different for the two types of coupling constants since J_{23} operates through essentially a double bond (of length 1.35 Å) whereas J_{34} operates over a 'single' bond (of length ~1.44 Å).

In Table V the values of the coupling constants are shown along with the angle sums for coupling constants acting through double bonds, 'single' bonds, and aromatic bonds. The angle θ for the hydrocarbons was calculated on the assumption that the 5-, 6-, and 7-membered rings are regular polygons. These data are plotted in Fig. 7 showing the rather good correlation with the angle sum.

A further point of interest is the interaction between the side-chain protons and the ring protons. It can be seen from Tables II and III that in all cases except 2-furfural and 2-aldehydo pyrrole the side chain protons couple with the neighboring ring proton.

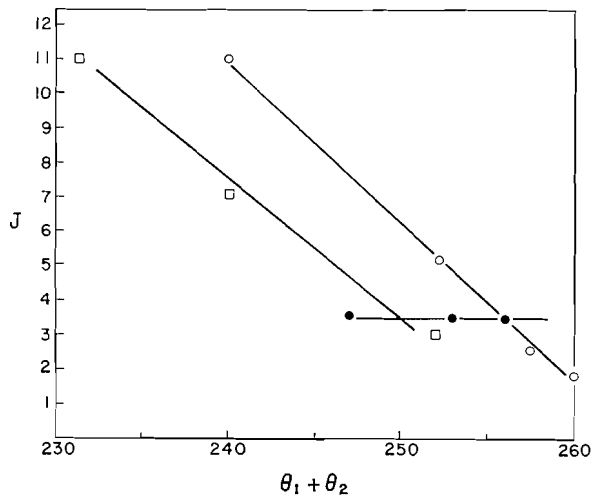


FIG. 7. The relation between spin coupling constant and angle sum. ○ CC length 1.35 Å (double bond). ● CC length ~1.43 Å ('single' bond). □ CC length ~1.40 (aromatic CC bonds).

Can. J. Chem. Downloaded from www.nrcresearchpress.com by 210.87.254.6 on 09/05/12
For personal use only.

Thus the apparent coupling of the aldehyde proton to proton 5 of the ring is rather remarkable. There are, however, further experimental facts in this case, in particular there is a change in the fine structure of the signal due to proton 5 of the ring on going from 30 Mc/s (3) to 40 Mc/s (1). Thus this effect may not be a straightforward long-range coupling interaction of the same type as that observed in substituted thiophenes (12). However, more data is necessary before this question can be answered.

(b) The Ring-Proton Chemical Shifts

The results of the chemical shift measurements are shown in Tables VI and VII. The

TABLE VI

Substituent effects in the ring-proton chemical shifts of furans
(Results are given in parts per 10^7)

Compound	(a) Pure liquids			(b) In 10% acetone solution				(c) 10% CH_2Cl_2 solution		
	δ_3	δ_4	δ_5	δ_2	δ_3	δ_4	δ_5	δ_3	δ_4	δ_5
2-Methyl furan	+3.8	+0.8	+1.0	—	+4.35	+1.53	+2.05	+4.3	+1.5	+2.3
2-Furanmethanethiol	+1.5	+0.3	+0.3	—						
2-Furfurylamine	+1.3	−0.5	−0.8	—	+2.42	+1.00	+1.37			
2-Furfurol	−0.4	−0.1	−0.5	—	+1.51	+0.76	+0.89	+1.5	+1.5	+0.5
Furan	0.0	0.0	0.0	0.0	0.00	0.00	0.00	0.0	0.0	0.0
2-Furanacrylic acid				—	−4.08	−1.44	−1.36			
2-Furanacrolein				—	−5.51	−2.09	−2.26			
Ethyl furoate	−8.5	−1.8	−3.3	—	−7.74	−1.83	−2.26			
2-Furoic acid				—	−7.95	−1.81	−2.20	−8.8	−1.0	−0.8
Ethyl 2-furoylacetate	−11.3	−3.5	−3.3	—	−9.59	−2.55	−2.98			
Furfural	−11.0	−3.5	−4.8	—	−9.87	−2.94	−3.66	−8.3	−1.5	−2.3
2-Nitro furan	−10.8	−4.3	−3.3	—	−10.65	−4.02	−3.18			
2-Furoyl trifluoromethyl ketone				—	−11.98	−3.73	−4.54			
2-Furoyl chloride	−12.0	−3.8	−4.8	—	—	—	—			
5-Chloromethyl furfural	−11.0	−4.5	—	—	—	—	—			
2,5-Dimethyl furan	+5.0	+5.0	—	—			—			
3-Furoic acid*				−7.0	—	−3.9	−1.7			
2-Methyl-3-furoic acid*				—	—	−2.9	+0.8			
4-Methyl-3-furoic acid*				−5.2	—	—	+2.0			
2,3-Difuroic acid*				—	—	−6.4	−4.2			

(*a*) Actual furan value −38.3 (α protons); −27.5 (β protons).
(*b*) Actual furan value −54.82 (α protons); −43.58 (β protons).
*Unknown concentration, very dilute; experimental error ±0.3.

TABLE VII

Ring-proton chemical shifts of substituted pyrroles

Compound	δ_3	δ_4	δ_5
2-Methyl pyrrole	+3.58	+1.75	+2.06
Pyrrole	0.00	0.00	0.00
2-Cyano pyrrole	−7.47	−1.42	−3.31
2-Aldehydo pyrrole	−8.87	−1.95	−4.56

NOTE: All compounds measured in 10% solutions in acetone, with the solvent peak as reference. Results are in parts per 10^7. Actual pyrrole values are −47.08 (α protons), −40.43 (β protons).

chemical shifts are given in parts per 10^7 from the chemical shift of the corresponding proton in the parent compound furan and pyrrole. These chemical shift differences will be designated by δ values in the following discussion.

Can. J. Chem. Downloaded from www.nrcresearchpress.com by 210.87.254.6 on 09/05/12
For personal use only.

Can. J. Chem. Downloaded from www.nrcresearchpress.com by 210.87.254.6 on 09/05/12
For personal use only.

Table VI gives the results for the substituted furans. Three series of measurements are given. The first set of results (Table VI*a*) was determined by measurements at 40 Mc/s on the pure liquid samples using an internal dioxane reference. They are accurate to ± 1 c.p.s. i.e. to ± 0.3 parts per 10^7. In the second set (Table VI*b*) the compounds were remeasured (at 60 Mc/s) in 10% solutions in acetone, using the acetone signal as reference. From three independent spectra for each solution, the reproducibility of the latter results was ± 0.2 c.p.s. i.e. ± 0.03 parts per 10^7. Also in Table VI*c* are given some measurements of Corey *et al.* (2) using CH_2Cl_2 as solvent.

The three sets of results in Table VI provide a means of estimating the effect of dilution (in acetone) on the δ values and also how the δ values change in different solvents. A comparison of the δ values of the compounds in acetone (VI*b*) and the pure liquids (VI*a*) shows that there is a constant shift to high field in the former case, of 0.9 ± 0.5 parts per 10^7 and this shift is the same for protons 3, 4, and 5 of the ring and is nearly independent of the substituent group. This shows that dilution in acetone does not give rise to a significant change in the internal δ values for these compounds. This is probably due to the fact that the environment of a substituted furan molecule in the pure liquid state is very similar to the environment of the same molecule in acetone. However, when the δ values in the two very different solvents acetone and dichloromethane are compared (Tables VI*b* and VI*c*), a different result is obtained. Here the differences in the δ values depend markedly on the substituent group. For 2-methyl furan and 2-furfurol there is reasonably good agreement but there are larger differences of about 1.5 parts in 10^7 for 2-furfural and 2 furoic acid. This is to be expected since the COOH and CHO groups give rise to much larger δ values than the CH_3 or CH_2OH groups and thus changes due to different solvents would give larger absolute changes in the δ values. It is evident then that the effect of the substituent group on the ring-proton chemical shifts is to some extent a function of the solvent used (13). Further, the chemical shift of proton 3 could be influenced by different neighboring anisotropic effects due to the different substituents. A discussion of the relative chemical shifts of H_3, H_4, and H_5 with substitution can therefore at best be roughly qualitative.

From the data for the 2-substituted furans in acetone (Table VI*b*) the chemical shifts are found to be linearly related. That is

$$\delta_3 = 3.08\delta_4 - 0.42 \text{ with a mean deviation of } \pm 0.8 \times 10^7,$$

$$\delta_5 = 1.23\delta_4 + 0.10 \text{ with a mean deviation of } \pm 0.1 \times 10^7.$$

This implies that the effect of substitution is different from that in a benzene ring where the *m* signals are chiefly due to inductive effects and the *o*, *p* to resonance effects. This difference could arise because in the parent molecule furan, the resonance effect influences *both* the α and β positions (14). The effect of substitution in 5-membered rings is twofold. Firstly, the substituent (due to the electronegativity difference between it and H) tends to shift all signals to low field if more electronegative than H, the closest proton being shifted most and the effect being attenuated as the distance from the substituent increases. Secondly, because of its power to donate or withdraw electrons from "aromatic" rings the substituent can cause the signals to move to high field or low field respectively. Again, the largest effect is felt by the proton closest to the substituent. This mesomeric effect probably behaves in a fashion analogous to that in the parent compound affecting all positions in the same qualitative way (that is, all increase in π-electron density or all decrease). This is consistent with the linear dependences of δ_3, δ_4, and δ_5. Semi-

quantitatively, we may distinguish between the effect of electron-donating and -withdrawing substituents. In the case of the former, the electronegativity of the substituent shifts the signals to low field but the mesomeric effect increases the π-electron density causing greater shielding, which causes the signals to appear at higher field. In the case of electron-withdrawing substituents, however, both the electronegativity and mesomeric effects operate to shift the signals to low field. We expect therefore for 2-methyl furan, where the electronegativity effect is small, that the donor property of the methyl group will cause high field shifts relative to furan. Since all of the substituents used here are more electronegative than CH_3, we expect for the donors (e.g. NH_2, OH) that the shifts will be at lower field than in 2-me-furan, and, as one progresses to electron-withdrawing substituents, that the proton signals appear at increasingly low fields. This is indeed the order of the chemical shifts data given in Table VI*b*. Also as anticipated, the largest changes are exhibited by δ_3. The less complete results for the 2-substituted pyrroles seem to show a similar behavior of the effect of substitution on chemical shift.

It is of interest also to note that the effect of multiple substitution is very nearly additive. For example, if the chemical shifts relative to furan for a $2-x$-substituted furan are δ_{3x}, δ_{4x}, δ_{5x} and for $3-y$, are δ_{4y}, δ_{5y} then for the $2-x$, $3-y$-disubstituted furan the shifts are $\delta_{4x}+\delta_{4y}$ for H_4 and $\delta_{5x}+\delta_{5y}$ for H_5. For example, the calculated shifts for 2,3-difuroic acid are $\delta_3=\delta_5=-5.7$ and $\delta_2=\delta_4=-3.9$, and the observed shifts are -6.4 and -4.2 respectively. Similarly the calculated shifts for 2-methyl-3-furoic acid are $\delta_3=\delta_5=-2.4$ and $\delta_4=\delta_5=+0.4$, which may be compared with the observed shifts of -2.9 and 0.8 respectively.

REFERENCES

1. R. J. ABRAHAM and H. J. BERNSTEIN. Can. J. Chem. **37**, 1056 (1959).
2. E. J. COREY, G. SLOMP, S. DEV, S. TOBINAGA, and E. R. GLAZIER. J. Am. Chem. Soc. **80**, 1204 (1958).
3. J. B. LEANE and R. E. RICHARDS. Trans. Faraday Soc. **55**, 518 (1959).
4. S. GRONOWITZ and R. A. HOFFMAN. Arkiv Kemi, **13**, 279 (1958).
5. R. J. ABRAHAM and H. J. BERNSTEIN. Can. J. Chem. **39**, 216 (1961).
6. R. MARQUIS. Ann. Chim. et Phys. [8], **4**, 216 (1905).
7. K. ASO. J. Agr. Chem. Soc. Japan, **16**(3), 249.
8. J. A. POPLE, W. G. SCHNEIDER, and H. J. BERNSTEIN. High resolution nuclear magnetic resonance. McGraw-Hill Book Co., New York. 1959.
9. M. FREYMANN and R. FREYMANN. Compt. rend. **248**, 677 (1959).
10. R. J. ABRAHAM and H. J. BERNSTEIN. Can. J. Chem. **37**, 2095 (1959).
11. M. KARPLUS. J. Chem. Phys. **30**, 11 (1959).
12. P. L. CORIO and I. WEINBERG. J. Chem. Phys. **31**, 569 (1959).
13. A. D. BUCKINGHAM, T. SCHAEFFER, and W. G. SCHNEIDER. J. Chem. Phys. **32**, 1227 (1960).
14. S. NAGAKURA and T. HOSAYA. Bull Chem. Soc. Japan, **25**, 179 (1952).

Can. J. Chem. Downloaded from www.nrcresearchpress.com by 210.87.254.6 on 09/05/12
For personal use only.

Can. J. Chem. Downloaded from www.nrcresearchpress.com by 210.87.254.105 on 09/05/12
For personal use only.

THE ELECTRICAL CONDUCTIVITY OF LIQUID TIN (II) SULPHIDE[1]

DENIS BOUTIN AND MARCEL BOURGON

ABSTRACT

The electrical conductivity "σ" of tin (II) sulphide in the liquid state has been measured using a capillary type cell. Both a-c. and d-c. methods were used. The conductivity of SnS increases regularly with temperature, from approximately 24 $ohm^{-1}\,cm^{-1}$ at 895° C to 31.2 $ohm^{-1}\,cm^{-1}$ at 930° C. The similarity of results obtained with both a-c. and d-c. methods, the positive temperature coefficient of conductivity, the high value of the conductivity and the absence of electrolysis effects when passing heavy currents in the melt lead to the conclusion that SnS remains a semiconductor in the liquid state. The value of the energy gap has been calculated to be 1.9 ev for the liquid as compared to the value 1.2 ev for the solid. Conductivity measurements have been limited to the temperature of approximately 935° C because of the decomposition of SnS at higher temperatures.

INTRODUCTION

Study of the electrical properties of liquid inorganic salts and oxides has shown that these chemical compounds are often ionic in the liquid state as evidenced by the high value of the conductivities, the positive temperature coefficients of conductivity, and the high current efficiencies (1, 2, 3). The electrical conductivity of a few metallic sulphides in the liquid state has been investigated: NiS (9), Bi_2S_3 (9), and FeS (4, 5, 7) have been reported to behave as typical metallic conductors while Cu_2S (4, 5, 6) and Tl_2S (10) have been shown to be semiconductors. Liquid antimony (III) sulphide Sb_2S_3 has a mixed conductivity, ionic and electronic (8).

Tin (II) sulphide SnS is known to be a semiconductor in the solid state (11) and has been reported to possess mixed conductivity in the liquid state (9). In order to determine whether this compound retains its semiconductivity in the liquid state it was planned to study its electrical conductivity more thoroughly than was done by previous workers.

EXPERIMENTAL

Preparation of SnS

The tin (II) sulphide used in this study was prepared by direct synthesis from the elements: "Reagent" grade tin and recrystallized sulphur were used. The tin sulphide so obtained contains free sulphur and some SnS_2. Consequently, the crude sulphide was heated under vacuum at 450° C to eliminate the free sulphur and melted under a nitrogen atmosphere at 1000° C, this temperature being maintained between 1 and 2 hours in order to decompose the tin (IV) sulphide to tin (II) sulphide and sulphur. The furnace temperature was then brought down to 890° C and a partial vacuum was maintained over the melt to eliminate the last traces of sulphur. The tin (II) sulphide was then distilled at the same temperature under high vacuum using a graphite condenser. The tin (II) sulphide thus prepared has a metallic appearance and is completely soluble in concentrated HCl. Two batches of sulphide were prepared and showed identical X-ray powder patterns (114.8-mm camera, Cu radiation, Ni filter): these patterns were strictly identical with the known X-ray powder pattern of SnS (12). The characteristic X-ray

[1]*Manuscript received December 12, 1960.*
Contribution from the Department of Chemistry, University of Montreal, Montreal, Que. This paper was taken from the thesis of D. Boutin, presented in partial fulfillment of the requirements for the degree of M.Sc., May 1960. Presented at the 43rd Annual Conference, Chemical Institute of Canada, Ottawa, Ontario, June 1960.

lines of SnS_2 and SnO_2 were absent from the X-ray diagrams. The first batch was nevertheless rejected because chemical analysis showed it to contain graphite particles. The second batch was analyzed for tin using the potassium iodate method: found $78.58 \pm 0.05\%$, theoretical 78.73%. According to the analysis figure the tin sulphide used in this study, although very near the stoichiometric composition, is slightly enriched in sulphur.

The Conductivity Cell

The cell used for measuring the electrical conductivity was of the capillary type and is shown in Fig. 1. It is made entirely of "Vitreosil" tubing and has four electrodes made

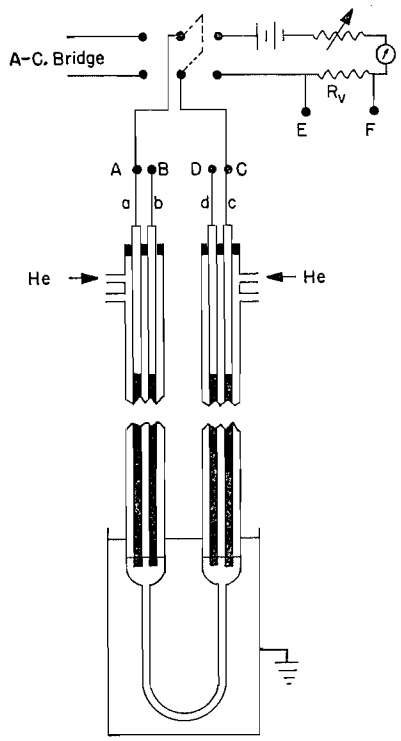


FIG. 1. Cell for measuring the electrical conductivity.

of spectrographic graphite rods: two of these electrodes carry current into the melt and the two others serve as potential probes, this system having the advantage of eliminating lead resistances. The cell is approximately 50 cm long and the over-all length of the capillary tube is approximately 10 cm. In order to obtain good temperature control and to eliminate stray currents in the melt the cell was placed in a liquid tin bath which was connected to ground. The cell and the liquid tin bath were contained in a "Mullite" tube which, in turn, was placed in a furnace heated by means of silicon carbide rods and controlled by a Weston Celectray Controller. Temperature measurements were made by means of calibrated Pt, 10% Rh–Pt thermocouples. The measuring thermocouple was contained in a sheath made of pure recrystallized alumina and placed between the two tubes of the cell so that the junction was in the middle of the capillary portion of the cell. Provisions were made to introduce purified helium gas into the cell. Because

Can. J. Chem. Downloaded from www.nrcresearchpress.com by 210.87.254.105 on 09/05/12
For personal use only.

of the rather high vapor pressure of tin (II) sulphide the helium gas was not circulated in the cell but a slightly positive static atmosphere was maintained over the melt.

The measuring cells were calibrated at room temperature using 0.1 *N* KCl. The cell constants were determined using an a-c. bridge operated at 1000 cycles/sec (13). With cells having a 10-cm-long capillary (I.D. 1 mm or lower) cell constants as high as 1200–1500 were obtained.

Resistance Measurements

Two methods were used to measure the resistance of the melt: a direct-current method and an alternating-current method. With the d-c. method the potential drops were measured across the potential probes of the cell and across a calibrated resistance in series with the latter using a potentiometer. By this method the lead resistances are eliminated.

The a-c. measurements were made using the same bridge as was used for calibrating the cells. This bridge measures the resistance of the melt and the resistance value thus found includes the resistance of the leads. A correction was made for the lead resistances at the different temperatures by using the following procedure.

Referring to Fig. 1, the d-c. potential drops across AC, BD, and EF are respectively:

$$E_{AC} = (R_x + r_a + r_c)i, \quad [1]$$

$$E_{BD} = R_x i, \quad [2]$$

$$E_{EF} = R_v i \quad [3]$$

where R_x, r_a, and r_c are the resistances of the melt and the electrodes respectively and R_v is the standard resistance in series with the cell. The d-c. resistance between points A and C is thus:

$$R_{AC} = R_x + r_a + r_c = R_v \cdot E_{AC}/E_{EF}. \quad [4]$$

The d-c. resistance of the melt is given by:

$$R_x = R_v \cdot E_{BD}/E_{EF}. \quad [5]$$

The difference between [4] and [5] gives the resistance of the electrodes:

$$r_a + r_c = R_v(E_{AC} - E_{BD})/E_{EF}. \quad [6]$$

The a-c. resistance across points A and C as measured by the bridge is:

$$R'_{AC} = R_x + r_a + r_c + r \quad [7]$$

where r is the residual resistance of the bridge and was found to be 0.4 ohm. The a-c. resistance of the melt R″ is thus given by [7]−[6].

RESULTS

Typical curves obtained by measuring the conductivity of liquid tin (II) sulphide as a function of temperature are shown in Fig. 2. Curve A shows the results obtained while increasing the temperature; curve B gives the conductivity values of the same sample obtained while decreasing the temperature from a maximum of approximately 1050° C. Curve C was obtained using a different sample and a different cell while decreasing the temperature: all these results were obtained by means of d-c. measurements. It is noticeable that the results obtained while decreasing the temperature are always

Can. J. Chem. Downloaded from www.nrcresearchpress.com by 210.87.254.105 on 09/05/12
For personal use only.

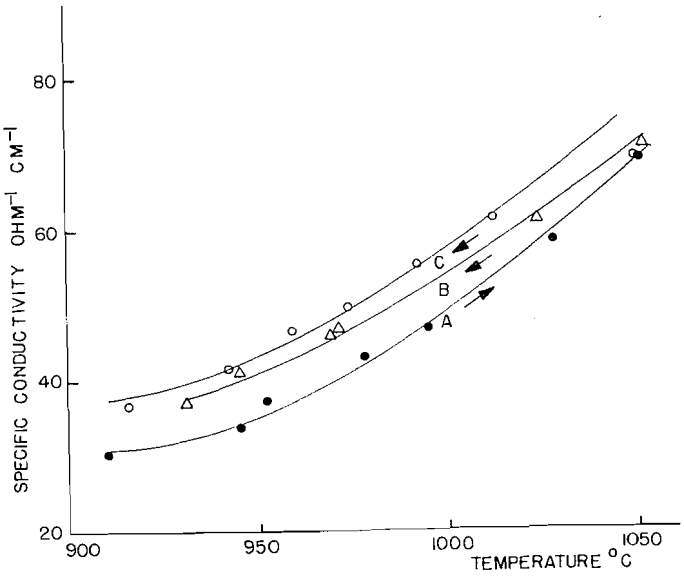


FIG. 2. Specific conductivity of liquid SnS as a function of temperature.

higher than those obtained while increasing the temperature. It is to be noticed also that curves B and C do not coincide and this could be due to the non-reproducibility of the different cells. This latter point was checked by mounting two cells with identical samples in the furnace so that both of them would follow the same thermal program. Conductivity measurements were made while increasing and decreasing the temperature and although the conductivity values obtained during the cooling cycle were, as in earlier experiments, higher than those obtained during the heating cycle the conductivity values obtained while decreasing the temperature were identical in both cells.

The different values of the conductivity obtained when heating or cooling the sample could be due to an increase in the tin content of the melt during the heating cycle. This increase in the tin content could be due to a reduction of the SnS by the graphite electrodes, to a partial electrolysis of the melt caused by the direct current or to the decomposition of the SnS. The first of these hypotheses was verified by heating SnS samples in closed quartz tubes for a few hours at approximately 1050° C; one of the tubes contained in addition a piece of the graphite used for electrodes. After the experiment sulphur deposits could be seen in the upper parts of both tubes showing that SnS does decompose independently of the presence of carbon.

To determine the decomposition temperature it was planned to do conductivity measurements as a function of time. To determine also whether there was partial electrolysis of the melt when using direct current the circuit permitting simultaneous a-c. and d-c. measurements and described in the experimental section was set up.

The results of these experiments are shown in Table I and Fig. 3 where the specific conductivity of the melt is shown as a function of time at several temperatures. Many such time–conductivity curves were determined on different samples in different cells: in the preliminary runs the heating time was extended for at least 30 hours at each temperature. The curves shown in Fig. 3 are those obtained under the best experimental conditions. The same cell was used throughout but because of the volatilization of the

Can. J. Chem. Downloaded from www.nrcresearchpress.com by 210.87.254.105 on 09/05/12
For personal use only.

Can. J. Chem. Downloaded from www.nrcresearchpress.com by 210.87.254.105 on 09/05/12
For personal use only.

TABLE I

Conductivity of tin (II) sulphide

Time, hours	T, °C	R'_{AC}, ohms	R_{AC}, ohms	R_X, ohms	$R_{AC}-R_X$, ohms	R'', ohms	σ, $ohm^{-1}\,cm^{-1}$
0	894	41.1	40.63	40.12	0.51	40.2	23.90
4.0	896	41.0	40.50	39.98	0.52	40.1	23.99
14.0	895	41.1	40.54	40.03	0.51	40.2	23.96
18.0	895	41.1	40.52	40.00	0.52	40.2	23.98
0	908	37.1	36.59	36.08	0.51	36.2	26.58
5.5	907	37.0	36.52	36.01	0.51	36.1	26.64
8.8	908	37.1	36.61	36.07	0.54	36.2	26.59
18.0	907	37.0	36.50	36.00	0.50	36.1	26.64
21.0	907	37.0	36.56	36.04	0.52	36.1	26.61
0	915	35.0	34.48	33.96	0.52	34.1	28.24
1.0	916	34.8	34.31	33.82	0.49	33.9	28.36
1.8	915	35.0	34.38	33.87	0.51	34.1	28.31
4.5	915	35.0	34.48	33.99	0.49	34.1	28.21
8.5	916	34.9	34.30	33.81	0.49	34.0	28.36
0	930	31.6	31.16	30.70	0.46	30.7	31.24
12.3	929	31.7	31.35	30.85	0.50	30.8	31.08
13.5	930	31.5	31.13	30.65	0.48	30.6	31.29
14.5	930	31.5	31.08	30.61	0.47	30.6	31.33
0	937	29.7	29.22	28.76	0.46	28.8	33.36
4.3	939	29.3	28.73	28.29	0.44	28.5	33.90
23.8	938	29.1	28.52	28.07	0.45	28.2	34.16
24.5	939	28.9	28.45	27.98	0.47	28.0	34.27
48.5	944	19.8	x	x	x	x	x

Sulphur deposited at top of the cell.

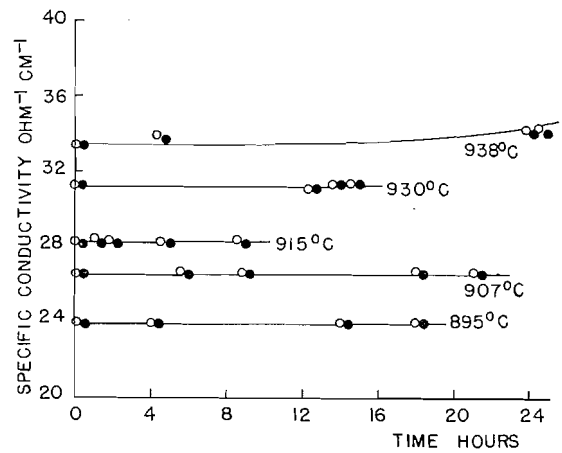


FIG. 3. Specific conductivity of liquid SnS as a function of time at constant temperature. ● a-c. data. ○ d-c. data.

sample additional SnS was added periodically. It was found necessary to bubble helium through the melt before each measurement in order to obtain reproducible results.

As can be seen from the curves an increase in the conductivity of the melt as a function of time occurs at a temperature of approximately 938° C. This is attributed to an increase in the tin content due to the decomposition of the tin sulphide. After completing the measurements the cell was maintained at a few degrees above the decomposition temperature for many hours at the end of which period the conductivity had increased to the point where it was difficult to measure: determination of the tin content of the melt

at the completion of the experiment showed that the latter had increased from 78.58 to 79.80%. The decomposition temperature was reproducible from sample to sample within 3 or 4 degrees. Resistance measurements made at temperatures higher than the decomposition temperature, using uncalibrated cells, showed that the decomposition rate increased as the temperature increased. In all cases sulphur deposition could be observed in the cooler parts of the cell.

The curves plotted in Fig. 3 show the results obtained with both alternating and direct currents. The conductivity values given in Table I are those calculated from the d-c. measurements, which are thought to be more precise. There is a small difference between the resistance values obtained with alternating current as compared with those obtained with direct current: this is probably due in part to a certain uncertainty in the residual resistance of the a-c. bridge and we do not believe it to be significant.

Electrolysis experiments were made on liquid SnS using a graphite crucible which served as the cathode and a graphite rod enclosed in a quartz tube which served as the anode. These experiments were made at 910° C using heavier currents (approximately 2 amperes) than were employed during the conductivity measurements. Preliminary experiments showed that it was difficult to distinguish the tin, which could be produced by electrolysis, from the tin sulphide. The anode compartment was instead observed for signs of sulphur evolution: there was no sulphur deposit in the cool part of the quartz tube even after the current had been passed for 2 hours.

DISCUSSION

Delimarskii and Velikanoff (9) have reported values for the conductivity of liquid SnS; their values range from 69 $ohm^{-1}cm^{-1}$ at 900° C to 103 $ohm^{-1}cm^{-1}$ at 1000° C with a temperature coefficient of 3.8×10^{-3}. They conclude from these results that liquid SnS has a mixed conductivity, ionic and electronic. The high results obtained by these workers are most probably due to the contamination of the melt by metallic tin: they prefused their sulphide at a probably too high temperature as evidenced by the stated analytical figures: they report an initial tin content of 79.7%, which increased to 80.6% at the end of the measurements.

Our results show that the conductivity of liquid tin (II) sulphide increases from approximately 24 $ohm^{-1}cm^{-1}$ at 895° C to 31.2 $ohm^{-1}cm^{-1}$ at 930° C with a temperature coefficient of 6.5×10^{-3}. The conductivity of SnS is somewhat high to be due to the migration of ions under the influence of an electric field. The absence of a considerable amount of ions is indicated by the fact that the d-c. and a-c. values of the conductivity are identical within experimental errors. The absence of sulphur evolution during the electrolysis experiments corroborates these conclusions.

Anderson and Morton (11) have shown SnS to be a semiconductor in the solid state. The conductivity follows the law:

$$\sigma = A_1 \exp(-E_1/kT) + A_2 \exp(-E_2/kT)$$

where the first term is preponderant at low temperatures and is attributable to an excess of non-metal in the lattice (*p*-type semiconduction) while the second term takes importance at high temperatures and is attributed to the intrinsic conduction of the lattice. From the high-temperature term, Anderson and Morton have calculated the width of the forbidden energy gap for intrinsic conduction to be 1.2 ev. These workers also showed that solid SnS can act as a *n*-type semiconductor when treated by hydrogen at high temperature, this operation having the effect of increasing the tin content.

Can. J. Chem. Downloaded from www.nrcresearchpress.com by 210.87.254.105 on 09/05/12
For personal use only.

The conductivity values of liquid tin sulphide plotted in Fig. 3 have been replotted in Fig. 4 as a function of the inverse of the absolute temperature to give a straight line.

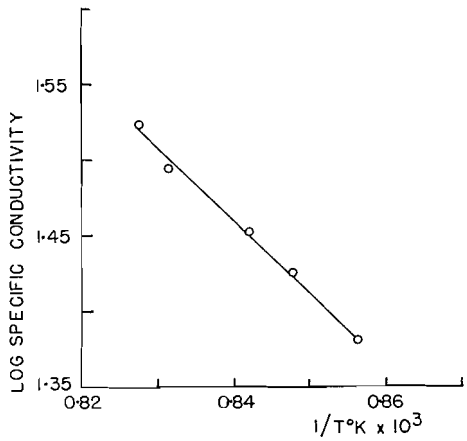


FIG. 4. Log specific conductivity as a function of the inverse of the absolute temperature for liquid SnS.

This line follows the law:

$$\sigma = A \exp(-E/kT).$$

All the facts stated above lead to the conclusion that tin (II) sulphide remains a semiconductor in the liquid state. The width of the forbidden energy gap as calculated from the slope of the line in Fig. 4 is 1.9 ev.

Attempts were made to determine the change in conductivity of SnS as it passes from the liquid state to the solid state. Although the cell design did not permit quantitative estimation of the conductivity, it was observed, in many cases, that the resistance of SnS increases sharply at the freezing point. Comparison of our results for the liquid state with the high-temperature results obtained by Anderson and Morton (11) for the solid state also indicates a sharp decrease of the conductivity at the freezing point.

It should be mentioned that the tin (II) sulphide used in this study is slightly richer in sulphur then the stoichiometric compound. One way of determining the influence of this excess sulphur on the conductivity would be to measure the conductivity of SnS as a function of sulphur pressure using hydrogen – hydrogen sulphide atmospheres: this is somewhat difficult because of the volatility of the tin sulphide.

Besides the liquid semiconductors mentioned in this paper other occurrences of semiconductivity in liquids have been reported. By measuring the electrical conductivity and the thermoelectric power of liquid selenium Henkels and Maczuk (14, 15) have shown this elementary substance to be a semiconductor in the liquid state with a forbidden energy gap of 2.31 ev as compared to 1.8 ev for the solid. Epstein, Fritzsche, and Lark-Horovitz (16, 17, 18) have measured the electrical conductivity, the thermoelectric power and the Hall coefficient of pure tellurium at the melting point and in the liquid state: they find a sharp decrease in conductivity on passing from the liquid to the solid state. Their experimental results indicate that the semiconducting properties persist in the liquid state and that a graded transition to metallic properties takes place at higher temperatures. Inouye, Tomlinson, and Chipman (19) conclude, from conductivity measurements, that FeO remains a semiconductor in the liquid state. Liquid HgSe (20)

Can. J. Chem. Downloaded from www.nrcresearchpress.com by 210.87.254.105 on 09/05/12
For personal use only.

has been reported to be a semiconductor with an energy gap of 2.3 ev. Ioffe (10) has reported the compounds Sb_2O_3, Bi_2O_3, Na_2Te_3, Na_2Te_6 to be semiconductors in the liquid state.

ACKNOWLEDGMENTS

The financial assistance of the National Research Council of Canada is gratefully acknowledged. One of us (D. B.) wishes to thank the "Office de Recherches scientifiques de la Province de Québec" for assistance in the form of a bursary. Thanks are due also to Dr. Guy Perreault of the École Polytechnique for determining the X-ray diagrams.

REFERENCES

1. J. O'M. Bockris and H. Bloom. Modern aspects of electrochemistry. Vol. 2. Butterworth Scientific Publications, London. 1959. p. 160.
2. G. J. Janz, C. Solomons, and H. J. Gardner. Chem. Revs. **58** (3), 461 (1958).
3. G. Watelle-Marion. J. chim. phys. **56**, 302 (1959).
4. G. M. Pound, G. Derge, and G. Osuch. AIME Trans. **203**, 481 (1955).
5. Ling Yang, G. M. Pound, and G. Derge. AIME Trans. **206**, 783 (1956).
6. M. Bourgon, G. M. Pound, and G. Derge. AIME Trans. **209**, 454 (1957).
7. D. Argyriades, G. Derge, and G. M. Pound. AIME Trans. **215**, 909 (1959).
8. T. Yanagase and G. J. Derge. Electrochem. Soc. **103**, 303 (1956).
9. J. K. Delimarskii and A. A. Velikanoff. Zhur. Neorg. Khim. **3**, 1075 (1958).
10. A. F. Ioffe. Izvest. Akad. Nauk S.S.S.R. Ser. Fiz. **15**, 477 (1951); Chem. Abstr. **46**, 3820 (1952).
11. J. S. Anderson and M. C. Morton. Proc. Roy. Soc. (London), A, **184**, 83 (1945).
12. J. D. Hanawalt. Ind. Eng. Chem. Anal. **10**, 457 (1938).
13. J. Archambault. Thèse de Maîtrise, Université de Montréal. 1952.
14. H. W. Henkels. J. Appl. Phys. **21**, 725 (1950).
15. H. W. Henkels and J. Maczuk. J. Appl. Phys. **24**, 1056 (1953).
16. A. S. Epstein, H. Fritzsche, and K. Lark-Horovitz. Phys. Rev. **107**, 412 (1957).
17. A. Epstein and H. Fritzsche. Phys. Rev. **93**, 922 (1954).
18. A. Epstein and H. Fritzsche. Phys. Rev. **94**, 1426 (1954).
19. H. Inouye, J. W. Tomlinson, and J. Chipman. Trans. Faraday Soc. **49**, 796 (1953).
20. A. I. Blum, N. P. Mokrovskii, and A. R. Regel. Izvest. Akad. Nauk S.S.S.R. Ser. Fiz. **16**, 139 (1952); Chem. Abstr. **46**, 10753 (1952).

Can. J. Chem. Downloaded from www.nrcresearchpress.com by 210.87.254.105 on 09/05/12
For personal use only.

Can. J. Chem. Downloaded from www.nrcresearchpress.com by 210.87.254.6 on 09/05/12
For personal use only.

TETRAHYDROFURANS

I. 2,2-DIMETHYL-4-SUBSTITUTED-4-HYDROXYMETHYLTETRAHYDROFURANS AND RELATED COMPOUNDS[1]

B. K. Wasson, C. H. Gleason, I. Levi, J. M. Parker, L. M. Thompson, and C. H. Yates

ABSTRACT

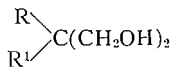
Substituted methallylmalonic esters (I) were reduced with lithium aluminum hydride to the corresponding 2-methallyl-1,3-propanediols (II). These diols II underwent cyclization on treatment with a mineral acid to the isomeric 2,2-dimethyl-4-substituted-4-hydroxymethyltetrahydrofurans (IV). II and IV were converted to the respective carbamates III and V, which exhibited pharmacological activity. The assigned structures of the cyclic compounds IV were proved by infrared analyses and the following transformations. Ring scission of 2,2-dimethyl-4-allyl-4-hydroxymethyltetrahydrofuran (IV*e*) with acetic anhydride – pyridine hydrochloride yielded 2-allyl-2-methallyl-1,3-propanediol diacetate (X*e*). Catalytic reduction of IV*e* gave 2,2-dimethyl-4-*n*-propyl-4-hydroxymethyltetrahydrofuran (IV*d*). Reductive cleavage of the tosylate VIII*b* of 2,2,4-trimethyl-4-hydroxymethyltetrahydrofuran (IV*b*) with lithium aluminum hydride yielded the known 2,2,4,4-tetramethyltetrahydrofuran (IX*b*).

While preparing 2,2-disubstituted-1,3-propanediol dicarbamates, it was noted that an intermediate, 2-allyl-2-methallyl-1,3-propanediol (II*e*), was labile to hydrochloric acid affording a compound assumed to be 2,2-dimethyl-4-allyl-4-hydroxymethyltetrahydrofuran (IV*e*). This assignment, made by analogy with a known method of preparing tetrahydrofurans (1–3), was subsequently verified. Since IV*e* possessed interesting pharmacological activity it was decided to prepare additional 2,2-dimethyl-4-substituted-4-hydroxymethyltetrahydrofurans (IV). Thus substituted methallylmalonic esters (I) were reduced to the corresponding 2-substituted-2-methallyl-1,3-propanediols (II) and subsequently cyclized by means of mineral acid. Both II and IV were converted to the corresponding carbamates III and V (Fig. 1).

Substituted methallylmalonic esters (I) were reduced by lithium aluminum hydride (4) to 2-substituted-2-methallyl-1,3-propanediols (II) (Table I). The use of sodium and

TABLE I

Substituted-1,3-propanediols



No.	R	R^1	% Yield	B.p. °C	B.p. mm
XI	H	$CH_2CH{=}CH_2$	73.5	110–112°	5
II*a*	H	$CH_2C(CH_3){=}CH_2$	74.4	75–83°	0.2–0.3
II*b*	CH_3	$CH_2C(CH_3){=}CH_2$	92.3	137–143°	27–30
II*c*	CH_2CH_3	$CH_2C(CH_3){=}CH_2$	75.0	140–147°	15–20
II*d*	$CH_2CH_2CH_3$	$CH_2C(CH_3){=}CH_2$	87.8	121–154°	15–16
II*e*	$CH_2CH{=}CH_2$	$CH_2C(CH_3){=}CH_2$	81.8	151–156°	14–15
II*f*	$CH_2C{\equiv}CH$	$CH_2C(CH_3){=}CH_2$	95.6	84–104°	0.05–0.10
II*g*	C_6H_5	$CH_2C(CH_3){=}CH_2$	61.6	128–141°	0.27–0.50

[1]*Manuscript received May 4, 1960.*
Contribution from the Research Laboratories, Charles E. Frosst & Co., Montreal, Quebec.

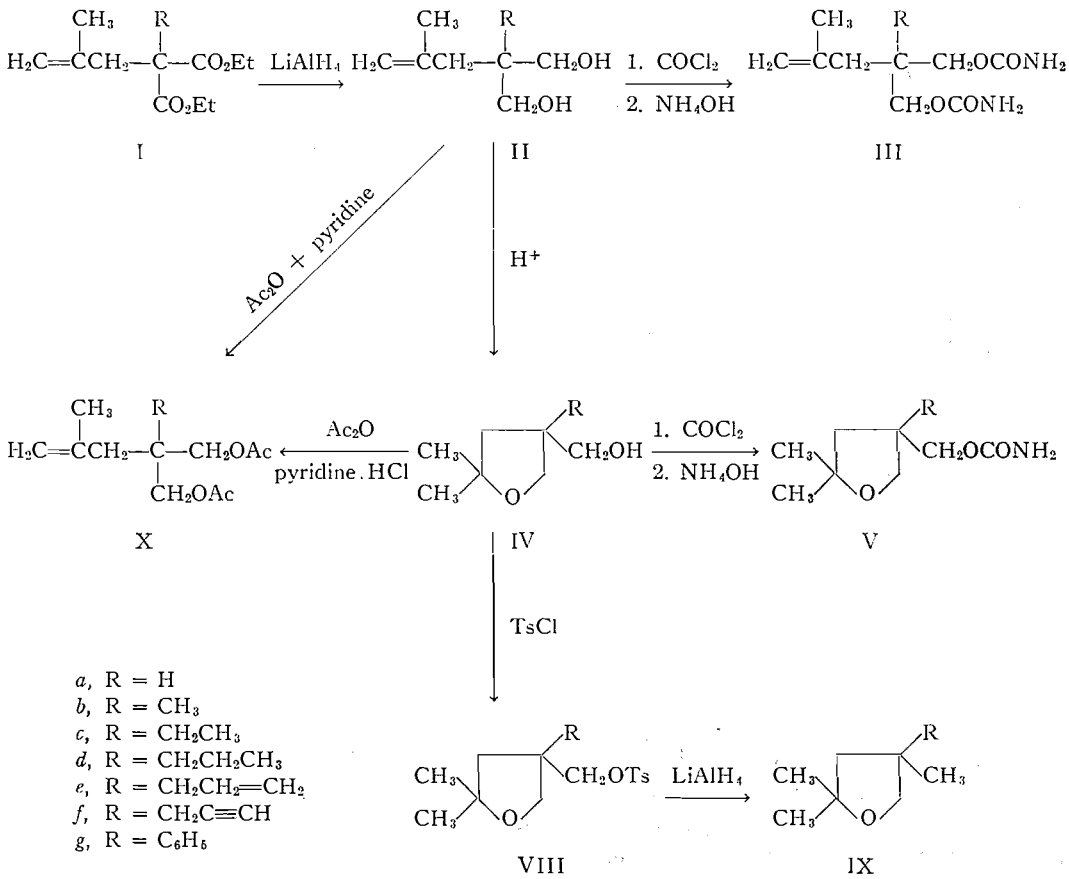


FIG. 1.

an alcohol (ethanol, 1-propanol, 1-butanol) (5) was unsatisfactory. Decomposition of the excess hydride was effected in two stages by the successive addition of methanol and water. Mineral acid was omitted in order to preclude possible ring closure between a hydroxyl and the methallyl group. The diols II were converted to the crystalline dicarbamates III (Table II).

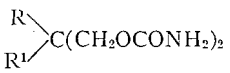
Tetrahydrofurans have been prepared by the acid-catalyzed ring closure of γ-unsaturated monoalcohols (1–3). When 2-substituted-2-methallyl-1,3-propanediols (II) were contacted with concentrated hydrochloric or sulphuric acid, the hitherto unreported cyclic 2,2-dimethyl-4-substituted-4-hydroxymethyltetrahydrofurans (IV) were obtained. This conversion occurred most satisfactorily when the diols II were treated with 1–3 volume per cent of concentrated hydrochloric acid in the presence of a solvent. Tetrahydrofuran was particularly suitable since the cyclization was readily controlled and the reaction mixture could be used directly in the preparation of carbamates. When methanol was used as a diluent, there was no indication that it supplanted or competed with the primary alcoholic function of II because IV was the sole product. This is an interesting finding in view of the mechanism of cyclization proposed below. The use of a larger amount of acid led to a decrease in the yield of IV. For example, with 2-allyl-2-

Can. J. Chem. Downloaded from www.nrcresearchpress.com by 210.87.254.6 on 09/05/12
For personal use only.

Can. J. Chem. Downloaded from www.nrcresearchpress.com by 210.87.254.6 on 09/05/12
For personal use only.

TABLE II

Substituted 1,3-propanediol dicarbamates

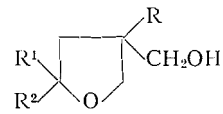


No.	R	R¹	% Yield	M.p., °C	Formula	Carbon %		Hydrogen %		Nitrogen %	
						Calcd.	Found	Calcd.	Found	Calcd.	Found
—	H	$CH_2CH{=}CH_2$	62.8	112.5–114°	$C_8H_{14}N_2O_4$	47.52	47.39	6.98	6.71	13.86	13.80
III*a*	H	$CH_2C(CH_3){=}CH_2$	54.5	161–163°	$C_9H_{16}N_2O_4$	50.00	50.59	7.46	7.54	12.96	13.11
III*b*	CH_3	$CH_2C(CH_3){=}CH_2$	67.0	155–156°	$C_{10}H_{18}N_2O_4$	52.15	51.80	7.88	7.48	12.17	12.25
III*c*	CH_2CH_3	$CH_2C(CH_3){=}CH_2$	65.9	161–163°	$C_{11}H_{20}N_2O_4$	54.07	53.74	8.25	8.18	11.47	11.59
III*d*	$CH_2CH_2CH_3$	$CH_2C(CH_3){=}CH_2$	44.5	147–148°	$C_{12}H_{22}N_2O_4$	55.79	55.80	8.59	8.54	10.85	11.07
III*e*	$CH_2CH{=}CH_2$	$CH_2C(CH_3){=}CH_2$	43.8	130–131.5°	$C_{12}H_{20}N_2O_4$	56.22	56.29	7.87	7.80	10.93	11.00
III*f*	$CH_2C{\equiv}CH$	$CH_2C(CH_3){=}CH_2$	37.4	178–181°	$C_{12}H_{18}N_2O_4$	56.66	56.53	7.13	6.98	11.02	11.34
III*g*	C_6H_5	$CH_2C(CH_3){=}CH_2$	9.5	101.5–103°	$C_{15}H_{20}N_2O_4$	61.63	61.47	6.90	6.89	9.59	9.46

methallyl-1,3-propanediol (II*e*), not only did the expected cyclization occur, but also the allyl group and the remaining hydroxyl group tended to interact. Whereas methallyl-substituted diols underwent facile isomerization, 2-allyl-1,3-propanediol (XI) required prolonged treatment with a larger amount of acid. The cyclized products IV (Table III) were converted to the crystalline carbamates V (Table IV).

TABLE III

Substituted 4-hydroxymethyltetrahydrofurans



No.	R	R¹	R²	% Yield	B.p. °C	B.p. mm
XII	H	CH_3	H	66.3	75–78°	5
IV*a*	H	CH_3	CH_3	65.0	—	—
IV*b*	CH_3	CH_3	CH_3	72.0	92–105°	15
IV*c*	CH_2CH_3	CH_3	CH_3	96.4	118–124°	15–20
IV*d*	$CH_2CH_2CH_3$	CH_3	CH_3	94.2	120–127°	15
IV*e*	$CH_2CH{=}CH_2$	CH_3	CH_3	91.9	122–126°	15
IV*f*	$CH_2C{\equiv}CH$	CH_3	CH_3	76.5	110–125°	8
IV*g*	C_6H_5	CH_3	CH_3	47.2	95–140°	0.1–0.2

The cyclization of 2-substituted-2-methallyl-1,3-propanediols (II) may be shown as occurring via an ionic mechanism (Fig. 2). Thus a proton adds to the olefin II to give a

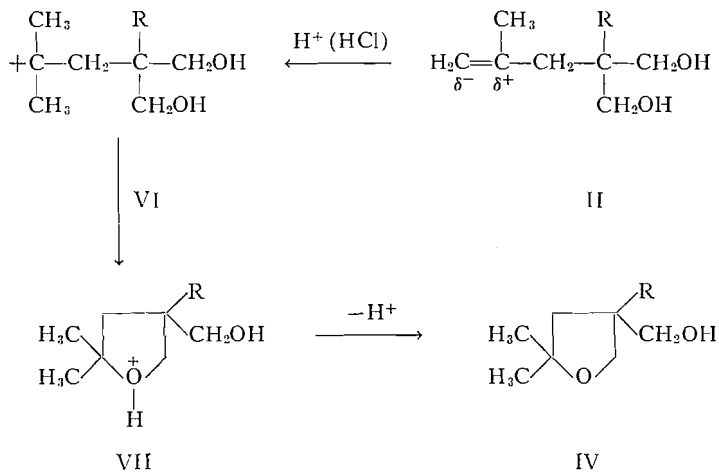


FIG. 2.

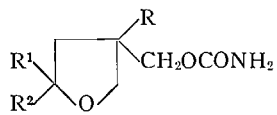
tertiary carbonium ion VI. Intramolecular reaction between the charged carbon atom of VI and one of the primary hydroxyl groups affords an oxonium ion VII from which a proton is expelled giving IV. Such a mechanism allows for the formation, via a Markownikoff addition, of a tetrahydrofuran rather than a tetrahydropyran ring and also depicts the catalytic role of hydrogen ion in promoting such a reaction.

Can. J. Chem. Downloaded from www.nrcresearchpress.com by 210.87.254.6 on 09/05/12
For personal use only.

Can. J. Chem. Downloaded from www.nrcresearchpress.com by 210.87.254.6 on 09/05/12
For personal use only.

TABLE IV

Substituted 4-carbamyloxymethyltetrahydrofurans



No.	R	R¹	R²	% Yield	M.p., °C	Formula	Carbon %		Hydrogen %		Nitrogen %	
							Calcd.	Found	Calcd.	Found	Calcd.	Found
—	H	CH_3	H	63.6	75–76.5°	$C_7H_{13}NO_3$	52.81	52.99	8.23	8.12	8.80	8.88
V*a*	H	CH_3	CH_3	41.5	99–101°	$C_8H_{15}NO_3$	55.47	55.51	8.73	8.56	8.09	8.19
V*b*	CH_3	CH_3	CH_3	83.1	46.5–47.5°	$C_9H_{17}NO_3$	57.75	57.79	9.16	9.08	7.48	7.36
V*c*	CH_2CH_3	CH_3	CH_3	74.5	53.5–54.0°	$C_{10}H_{19}NO_3$	59.66	59.63	9.51	9.50	6.96	7.17
V*d*	$CH_2CH_2CH_3$	CH_3	CH_3	57.7	59.0–59.5°	$C_{11}H_{21}NO_3$	61.36	61.28	9.83	9.44	6.51	6.56
V*e*	$CH_2CH{=}CH_2$	CH_3	CH_3	89.1	55–57°	$C_{11}H_{19}NO_3$	61.93	62.01	8.98	8.85	6.57	6.70
V*f*	$CH_2C{\equiv}CH$	CH_3	CH_3	66.2	88–92°	$C_{11}H_{17}NO_3$	62.54	62.48	8.11	7.89	6.63	7.06
V*g*	C_6H_5	CH_3	CH_3	34.9	85–86°	$C_{14}H_{19}NO_3$	67.43	67.52	7.68	7.24	5.62	5.53

Assignment of structure IV to the products of cyclization was supported by infrared absorption data. The isomerization of 2-substituted-2-methallyl-1,3-propanediols (II) to IV required an increase in the number of methyl groups from one to two, the appearance of a cyclic ether group, and the loss of the methallyl and a hydroxyl group. An inspection of the infrared spectra of II and IV showed that these changes did occur. They were exhibited by the appearance in the 7.25–7.35 μ region of a doublet (*gem*-dimethyl) in place of a single band (methyl), the loss of the 11.2 μ band (methallyl), the narrowing and shifting of the hydroxyl band from 3.0 to 2.95 μ, and finally the shifting of the 9.6–9.8 μ band (hydroxyl) to 9.5–9.6 μ (hydroxyl, cyclic ether) (6). In addition IV possessed a strong unassigned band at 12.95 μ.

Supporting evidence for the formulation of the cyclic compounds IV was obtained by cleaving the ring of IV*e*, a typical member of the group. Surprisingly, in this instance, the use of methods that have been described for the cleavage of tetrahydrofurans (7–11) led to intractable mixtures. However, the conversion was effected by applying a method used successfully in the field of sapogenin chemistry (12–14). Thus acetic anhydride – pyridine hydrochloride (12) readily converted IV*e* in excellent yield to 2-allyl-2-methallyl-1,3-propanediol diacetate (X), identical with a sample prepared by the acetylation of II*e* (Fig. 1). Hence, the methallyl and hydroxyl groups that had disappeared during the cyclization of the diol II to the isomeric IV, have reappeared upon ring opening.

Additional chemical evidence for the structures of 2,2-dimethyl-4-substituted-4-hydroxymethyltetrahydrofurans (IV) was obtained by the elimination of the hydroxyl group. Thus IV*b* was tosylated and the ester VIII*b* reduced with lithium aluminum hydride (15) to 2,2,4,4-tetramethyltetrahydrofuran (IX*b*) (Fig. 1). The infrared absorption curve and boiling point of IX*b* were the same as those previously reported (16). The 4-allyl analogue IV*e* was similarly converted to the expected 2,2,4-trimethyl-4-allyltetrahydrofuran (IX*e*) as judged by infrared analysis, where bands typical of the tosyl group appeared in the spectrum of VIII*e*, and disappeared in that of IX*e*. IV*e*, VIII*e*, and IX*e* exhibited bands denoting the presence of the allylic double bond, methyl groups, and the cyclic ether linkage.

2,2-Dimethyl-4-allyl-4-hydroxymethyltetrahydrofuran (IV*e*) was hydrogenated over platinum giving 2,2-dimethyl-4-*n*-propyl-4-hydroxymethyltetrahydrofuran (IV*d*). IV*d* was also obtained when diethyl *n*-propylmethallylmalonate (I*d*) was reduced with lithium aluminum hydride to 2-*n*-propyl-2-methallyl-1,3-propanediol (II*d*) and subsequently ring-closed with mineral acid.

The monocarbamates V were more active than the dicarbamates III upon the central nervous system of animals. The allyl derivative V*e* was particularly effective as an anticonvulsant (17). More comprehensive results of the pharmacological evaluation will be reported elsewhere.

EXPERIMENTAL

Boiling points and melting points (Fisher–Johns apparatus) are uncorrected. Infrared absorption spectra were obtained with a Beckman IR-5 spectrophotometer equipped with a sodium chloride prism. Solids were examined in potassium bromide pellets and liquids either as thin films or as solutions in carbon disulphide.

Preparation of Mono- and Di-substituted Malonates

Diethyl sodiomalonate and diethyl sodio-alkyl- (and -alkenyl-) malonates were treated

Can. J. Chem. Downloaded from www.nrcresearchpress.com by 210.87.254.6 on 09/05/12
For personal use only.

with the appropriate alkyl halide (bromide or chloride) in the customary manner giving the corresponding mono- and di-substituted malonates. These were purified by distillation *in vacuo*. The preparation of some of these malonates has been described (18). Diethyl methylmalonate (Sapon), diethyl ethylmalonate (Distillation Products Industries), diethyl *n*-propylmalonate (Sapon), and diethyl phenylmalonate (Benzol Products) were used without further purification.

Preparation of Substituted 1,3-Propanediols

The following procedure illustrates the general method used for preparing the 1,3-propanediols listed in Table I. A solution of 100 g of diethyl allylmethallylmalonate (I*e*) in 246 ml of anhydrous ethyl ether was added dropwise over a 3-hour period to a well-dispersed and vigorously stirred mixture of 22.5 g of lithium aluminum hydride in 554 ml of anhydrous ethyl ether maintained below 25° C in an atmosphere of nitrogen. The reaction mixture was stored overnight at room temperature. Excess hydride was discharged by the addition of 27.2 ml of methanol in 66 ml of ethyl ether; the resulting complexes were decomposed by the successive addition of 15.6 ml of 50% methanol and 31.2 ml of water while maintaining the temperature of the mixture below 25° C. The ethereal phase was separated and the residual solids were washed four times with ethyl ether. The combined ethereal extracts were washed with water twice, filtered, and evaporated, leaving 65.2 g (97.5%) of crude 2-allyl-2-methallyl-1,3-propanediol (II*e*). Infrared: λ_{max} 3.0 (hydroxyl), 3.25, 6.1 (unsaturation), 7.25 (methyl), 9.6–9.8 (hydroxyl), 10.9 (allyl), 11.25 (methallyl) μ. This product was distilled *in vacuo* and used directly for the preparation of either 2,2-dimethyl-4-allyl-4-hydroxymethyltetrahydrofuran (IV*e*) or 2-allyl-2-methallyl-1,3-propanediol dicarbamate (III*e*).

Cyclization of 2-Methallyl-1,3-propanediols (II)

The general procedure used for the cyclization of 2-methallyl-1,3-propanediol and 2-substituted-2-methallyl-1,3-propanediols to give the 2,2-dimethyl- and 2,2-dimethyl-4-substituted-4-hydroxymethyltetrahydrofurans, listed in Table III, is illustrated by the following example.

A solution of 65.2 g of 2-allyl-2-methallyl-1,3-propanediol (II*e*) in 40.5 ml of dry tetrahydrofuran was treated at room temperature with 1 ml of concentrated hydrochloric acid. The solution was warmed gently until, at approximately 50° C, an exothermic reaction occurred. External heating was discontinued while the temperature of the reaction mixture rose spontaneously to 94° C. The solution was then refluxed for 2 hours. The solvent was removed under reduced pressure and the residue distilled giving 59.9 g of 2,2-dimethyl-4-allyl-4-hydroxymethyltetrahydrofuran (IV*e*), b.p. 122–126° C/5 mm. The cyclization of II*e* was also effected with 0.5–1.0 volume per cent of hydrochloric acid in the absence of solvent. However, the reaction was extremely vigorous and difficult to control by external cooling. The yield of IV*e* was substantially decreased.

Cyclization of 2-Allyl-1,3-propanediol (XI)

2-Allyl-1,3-propanediol (XI) was cyclized by more drastic conditions than those described above. Thus a mixture of 11 g of XI and 1 ml of concentrated hydrochloric acid was refluxed for 17 hours. Following removal of the hydrochloric acid, distillation of the product (10.9 g) yielded 7.3 g (66.3%) of 2-methyl-4-hydroxymethyltetrahydrofuran (XII), b.p. 75–78° C/5 mm. The infrared spectrum possessed a strong band at 7.25 μ (C—CH_3) but no band indicative of a double bond.

Can. J. Chem. Downloaded from www.nrcresearchpress.com by 210.87.254.6 on 09/05/12
For personal use only.

Preparation of 2,2-Disubstituted 1,3-Propanediol Dicarbamates (III)

The procedure using tetrahydrofuran as solvent (19) was found to be superior to that wherein chloroform–toluene served as solvent and antipyrine was included as a hydrogen chloride acceptor (20). The products III (Table II) were recovered from the reaction mixtures by chilling the aqueous solutions after evaporating the organic solvent, and were recrystallized from aqueous alcohol. (Infrared: λ_{max} 2.95, 5.85, 6.2 μ (primary amide).)

Preparation of 2,2-Dimethyl-4-substituted-4-carbamyloxytetrahydrofurans (V)

The method used for preparing V (Table IV) was a modification of that applied above. The following example was typical of the procedure. A solution of 57.3 g of IV*e* in 77.6 ml of tetrahydrofuran was added dropwise during 1 hour to 55.2 g of phosgene dissolved in 63.1 ml of cold tetrahydrofuran (−8 to 4° C). The mixture was stirred for 30 minutes at this temperature and then stored overnight at room temperature. The solution was added over a 1-hour period to a stirred mixture of 276 ml of concentrated ammonium hydroxide and 3.4 g of sodium bisulphite maintained at 10–27° C (subsequent study showed that bisulphite could be omitted). After stirring for ½ hour, sufficient water was added to dissolve the solids. Distillation afforded a residue that was extracted four times with ether. The combined ethereal extracts were washed twice with 25-ml portions of water and the ether removed. The residue (72.6 g) was distilled giving 67.7 g of V*e*, b.p. 111–119° C/0.02–0.04 mm, solidifying at room temperature. The material was crystallized from ether – petroleum ether giving 64 g (89.1%) of V*e*, m.p. 55–57° C. When the distillation of crude material was omitted, V*e* was obtained in lower yield. The substance could also be crystallized from acetone – petroleum ether, aqueous methanol, or methanol – petroleum ether. Molecular weight (Rast): calc. 213; found 211, 216. Infrared: λ_{max} 3.0, 5.8, 6.2 (primary amide), 3.25, 6.1 (unsaturation), 10.95 (allyl), 7.25, 7.35 (*gem*-dimethyl), 12.95 μ.

Preparation of 2,2-Dimethyl-4-allyl-4-hydroxymethyltetrahydrofuran (IVe) from the Carbamate Ve

A mixture of 16 g of 2,2-dimethyl-4-allyl-4-carbamyloxymethyltetrahydrofuran (V*e*) (m.p. 54.0–55.5° C), 12 g of sodium hydroxide, and 250 ml of ethanol was refluxed for 8 hours. After dilution with water, the ethanol was removed by distilling *in vacuo*. The aqueous residue was cooled, saturated with sodium chloride, and extracted five times with ethyl ether. The ethereal extracts were washed with water and reduced to dryness. The resulting oily product was vacuum-distilled, yielding 8.2 g (64%) of IV*e*, b.p. 116–117° C/10–15 mm. Analysis: Calc. for $C_{10}H_{18}O_2$: C, 70.56; H, 10.66. Found: C, 70.17; H, 10.45. Main infrared absorption bands: λ_{max} 2.95, 3.25, 3.40, 3.50, 6.10, 6.90, 7.08, 7.23, 7.78, 8.24, 8.40, 8.56, 8.90, 9.4–9.75, 10.05, 10.95, 11.42, 11.60, 12.94 μ.

Preparation of 2-Allyl-2-methallyl-1,3-propanediol Diacetate (Xe)

(a) From 2-Allyl-2-methallyl-1,3-propanediol (IIe) by Acetylation

A solution of 20 g of 2-allyl-2-methallyl-1,3-propanediol (II*e*) in 110 ml of acetic anhydride and 22 ml of anhydrous pyridine was heated for 1 hour on a steam bath and then allowed to stand for 18 hours at room temperature. The solution was poured into 400 ml of cold water and the mixture stirred for 1 hour at room temperature. The mixture was extracted five times with ethyl ether and the combined ethereal extracts washed successively with water, 5% hydrochloric acid, saturated saline solution, 5% sodium bicarbonate, and finally with water. After drying over sodium sulphate, the solvent was

Can. J. Chem. Downloaded from www.nrcresearchpress.com by 210.87.254.6 on 09/05/12
For personal use only.

removed leaving 28.42 g (95%) of the crude acetate. Distillation of this product afforded 2-allyl-2-methallyl-1,3-propanediol diacetate (X*e*), b.p. 153–157° C/16 mm, λ_{max} 5.78, 8.0–8.2, 9.6–9.7 (ester), 3.25, 6.1, 10.9–11.2 (unsaturation) μ.

(b) From 2,2-Dimethyl-4-allyl-4-hydroxymethyltetrahydrofuran (IVe) by Treatment with Acetic Anhydride – Pyridine Hydrochloride

A stream of hydrogen chloride was passed into a mixture of 150 ml of acetic anhydride and 12 ml of pyridine until 5.2 g had been absorbed. After adding 22.86 g of 2,2-dimethyl-4-allyl-4-hydroxymethyltetrahydrofuran (IV*e*) the solution was refluxed for 5 hours and then stored overnight at 5° C. Excess anhydride was decomposed by adding 2000 ml of water and stirring the mixture for 1 hour. The mixture was worked up as described in procedure (*a*) to give 33.8 g (98.9%) of crude product. Several distillations of this material gave X*e*, b.p. 155–160° C/17 mm. The infrared spectrum was identical with that of the product from procedure (*a*).

Catalytic Reduction of 2,2-Dimethyl-4-allyl-4-hydroxymethyltetrahydrofuran (IVe)

A solution of 23.53 g of 2,2-dimethyl-4-allyl-4-hydroxymethyltetrahydrofuran (IV*e*) in 300 ml of ethanol was shaken with hydrogen and 0.5 g of platinum oxide under slightly positive pressure. Approximately 1 mole of hydrogen was absorbed within 30 minutes. Following removal of the catalyst, the solvent was evaporated giving 23.6 g of a yellow oil. Distillation *in vacuo* afforded 20.6 g (87.4%) of 2,2-dimethyl-4-*n*-propyl-4-hydroxymethyltetrahydrofuran (IV*d*) as a colorless oil, b.p. 50–65° C/0.06–0.07 mm. The infrared spectrum of IV*d* indicated the absence of unsaturation and was indistinguishable from that of a sample prepared from diethyl *n*-propylmethallylmalonate (I*d*) by reduction and subsequent ring closure.

Conversion of 2,2,4-Trimethyl-4-hydroxymethyltetrahydrofuran (IVb) to 2,2,4,4-Tetramethyltetrahydrofuran (IXb)

(a) 2,2,4-Trimethyl-4-tosyloxymethyltetrahydrofuran (VIIIb)

p-Toluenesulphonyl chloride (79 g) dissolved in 140 ml of redistilled pyridine was added during 1 hour to a vigorously stirred solution of 39.3 g of 2,2,4-trimethyl-4-hydroxymethyltetrahydrofuran (IV*b*) in 140 ml of redistilled pyridine, maintained at 5° C. The mixture was stirred with cooling for an additional 3 hours and left overnight at room temperature. It was poured onto crushed ice and acidified with concentrated hydrochloric acid. The mixture was extracted six times with ethyl ether, and the combined ethereal extracts washed to neutrality with water and evaporated, affording 79.5 g (97.7%) of crude tosylate VIII*b*. The substance was not purified but used directly for the following reduction. Infrared: λ_{max} 6.25, 7.3–7.4, 8.4–8.5, 10.3–10.5, 10.95, 11.3, 12.7, 14.2, 15.0 μ (aromatic, tosyl).

(b) Lithium Aluminum Hydride Reduction of 2,2,4-Trimethyl-4-tosyloxymethyltetrahydrofuran (VIIIb)

A solution of 79.5 g of tosylate VIII*b* in 400 ml of anhydrous ethyl ether was added dropwise during 1 hour at 25–30° C to 16.2 g of lithium aluminum hydride dissolved in 800 ml of anhydrous ethyl ether. The mixture was refluxed for 8 hours with vigorous stirring, cooled, and decomposed with ice and water. The solids were repeatedly extracted with ethyl ether, and the combined ethereal extracts washed with water and concentrated, yielding 27.8 g of yellow oil. Two distillations of this oil gave 12.9 g of 2,2,4,4-tetramethyltetrahydrofuran (IX*b*) boiling at 116–118° C, n_D^{20} 1.422; reported (16) boiling

Can. J. Chem. Downloaded from www.nrcresearchpress.com by 210.87.254.6 on 09/05/12
For personal use only.

point 120° C and n_D^{20} 1.4061. The infrared spectrum of IX*b* was identical with that reported (16).

ACKNOWLEDGMENTS

The authors are indebted to Dr. G. W. Holden and E. B. Dechene for their many valuable discussions, to Dr. A. Taurins of McGill University for preliminary infrared spectra, and to H. Williams for invaluable suggestions concerning the possible role of acid in promoting cyclization. We also wish to acknowledge the capable assistance of A. Franck, O. Kristiansen, the late U. Liepins, J. Pollard, and P. Thibodeau, and S. Watanabe for elemental analyses and infrared spectra.

REFERENCES

1. J. COLONGE and A. LAZIER. Bull. soc. chim. France, 17 (1949).
2. R. PAUL and M. NORMANT. Compt. rend. **216**, 689 (1943).
3. O. WALLACH. Ann. **275**, 169 (1893).
4. R. F. NYSTROM and W. G. BROWN. J. Am. Chem. Soc. **69**, 1197 (1947).
5. L. BOUVEAULT and G. BLANC. Bull. soc. chim. France, **31** (3), 1206 (1904).
6. L. J. BELLAMY. Infra-red spectra of complex molecules. 2nd ed. Methuen & Co. Ltd., London. 1958.
7. O. MOLDENHAUER, G. TRAUTMANN, W. IRION, R. PFLUGER, H. DOSER, D. MASTAGLIO, H. MARWITZ, and R. SCHULTE. Ann. **580**, 169 (1953).
8. H. SCHMID, A. MASCHKA, and H. FRAUENSCHILL. Monatsh. **80**, 670 (1949).
9. K. ALEXANDER and H. V. TOWLES. Org. Syntheses, **30**, 27 (1950).
10. H. STONE and H. SHECHTER. J. Org. Chem. **15**, 491 (1950).
11. M. E. SYNERHOLM. J. Am. Chem. Soc. **69**, 2581 (1947).
12. W. G. DAUBEN and G. J. FONKEN. J. Am. Chem. Soc. **76**, 4618 (1954).
13. D. H. GOULD, H. STAEUDLE, and E. B. HERSHBERG. J. Am. Chem. Soc. **74**, 3685 (1952).
14. M. E. WALL, S. SEROTA, and C. R. EDDY. J. Am. Chem. Soc. **77**, 1230 (1955).
15. R. T. BLICKENSTAFF and F. C. CHANG. J. Am. Chem. Soc. **80**, 2726 (1958).
16. F. F. RUST and D. O. COLLAMER. J. Am. Chem. Soc. **76**, 1055 (1954).
17. J. M. PARKER, B. K. WASSON, and R. H. HALL. Federation Proc. **18**, 431 (1959).
18. W. J. DORAN and H. A. SHONLE. J. Am. Chem. Soc. **59**, 1625 (1937).
19. A. O. GEISZLER and M. A. SPIELMAN. U.S. Patent No. 2,806,053 (September 10, 1957).
20. R. E. OESPER, W. BROKER, and W. A. COOK. J. Am. Chem. Soc. **47**, 2609 (1925).

Can. J. Chem. Downloaded from www.nrcresearchpress.com by 210.87.254.6 on 09/05/12
For personal use only.

Can. J. Chem. Downloaded from www.nrcresearchpress.com by 210.87.254.6 on 09/05/12
For personal use only.

RADIATION-INDUCED EXCHANGE REACTIONS IN SOLUTIONS OF HYDROGEN IN WATER[1]

P. J. Dyne, J. W. Fletcher, W. M. Jenkinson, and L. P. Roy[2]

ABSTRACT

The exchange of H, D, and T atoms between water and dissolved hydrogen has been studied in both heavy and light water solutions. Values of the "exchange yield", G_{tracer}, for the isotopic hydrogen atoms have been deduced and are identified with the yield of D atoms from HDO in H_2O, H atoms from HDO in D_2O, T atoms from HTO in H_2O and from DTO in D_2O. These values are correlated by assuming that the medium, H_2O or D_2O, affects the total probability of dissociation of the tracer molecule (HDO, HTO, DTO) and that in HDO H atoms are more readily dissociated than D atoms.

INTRODUCTION

The radiation-induced exchange of hydrogen atoms (H, D, or T) between water and dissolved hydrogen is a direct observation of the presence and reaction of these atoms and provides a further method of studying the difference in radiolytic yields between heavy and light water.

This exchange was first studied by Gordon and Hart (1), who irradiated a solution of D_2 in H_2O with Co^{60} γ rays and found that HD and H_2 appeared in the dissolved gas. The initial yield of HD in neutral solution was found to be about 2.7 molecules/100 ev, equal to the yield of hydrogen atoms in pure water. They advanced the mechanism:

$$H_2O \sim\sim\sim\rightarrow H + OH \quad [1]$$

$$H_2O \sim\sim\sim\rightarrow \tfrac{1}{2}H_2 + \tfrac{1}{2}H_2O_2 \quad [2]$$

$$H + D_2 \rightarrow HD + D \quad [3]$$

$$OH + D_2 \rightarrow HOD + D \quad [4]$$

$$D + D \rightarrow D_2 \quad [5]$$

In this scheme every hydrogen atom produced in reaction [1] is detected by exchange in reaction [3]. Hydrogen is produced with the "molecular" yield, $G \simeq 0.4$ by reaction [2], but the total amount of dissolved hydrogen ($H_2 + HD + D_2$) remains constant.

If the dissolved hydrogen is a mixture of isotopic species, H_2 and D_2 say, then reaction [3] may be followed by

$$D + H_2 \rightarrow HD + H \quad [6]$$

and this H atom may react again by reaction [3]. A chain reaction is now observable in which the yield of HD is about 60, much greater than the initial yield of H atoms. Chain reactions in this system have been studied in detail by Friedman and Zeltman (2) whose results were in agreement with Gordon and Hart where comparison was possible.

Bardwell and Dyne (3) followed the initial exchange reaction (3) by a tracer technique. Hydrogen gas was dissolved in H_2O containing about 1% HDO. The only exchanges observed are those in which an HDO molecule is dissociated and gives a D atom; on a statistical basis these amount to $\sim$1/200 of the total number of initial exchanges (reactions [1] and [3] in the above scheme). The results were calculated on the assumption

[1]*Manuscript received December 8, 1960.*
Contribution from Research Chemistry Branch, Atomic Energy of Canada Limited, Chalk River, Ontario.
Issued as A.E.C.L. No. 1200.
[2]*Present address: Laval Industrial Association, 10510 Notre Dame Street East, Montreal, Que.*

that there was no isotopic discrimination in the production or reaction of the tracer D atoms; the initial "total exchange" yield was found to be much less than the primary yield of H atoms in H_2O.

In a subsequent paper (5) it was suggested that an excited HDO molecule dissociated less frequently to give D atoms than H atoms. The "total exchange" yield calculated from data obtained with D atoms as tracers would therefore be less than the hydrogen atom yield in pure water. This paper describes further tracer experiments using H and T atoms in which the interest centers on the differing availability of H, D, and T atoms from the mixed molecules, HTO, HDO, and DTO.

EXPERIMENTAL

The technique used for isolating gases dissolved in water was that described by Bardwell and Dyne (3). In this method one sample of water is used for several determinations. A check on the consistency of these experiments is obtained when different samples of water, with different concentrations of tracer atoms, give compatible results, when plotted as in Figs. 1 and 2. Reproducible results, comparable with those obtained in other laboratories, were obtained when the following method was used: water was purified by distillation, followed by distillation from alkaline permanganate followed by distillation in a stream of oxygen, the mixture of steam and oxygen being passed through a quartz tube heated to 700° C. In a private communication E. J. Hart tells us that small amounts of peroxide may be formed above 700° C. The water was degassed by freezing with solid CO_2, pumping, and thawing several times using a vacuum system

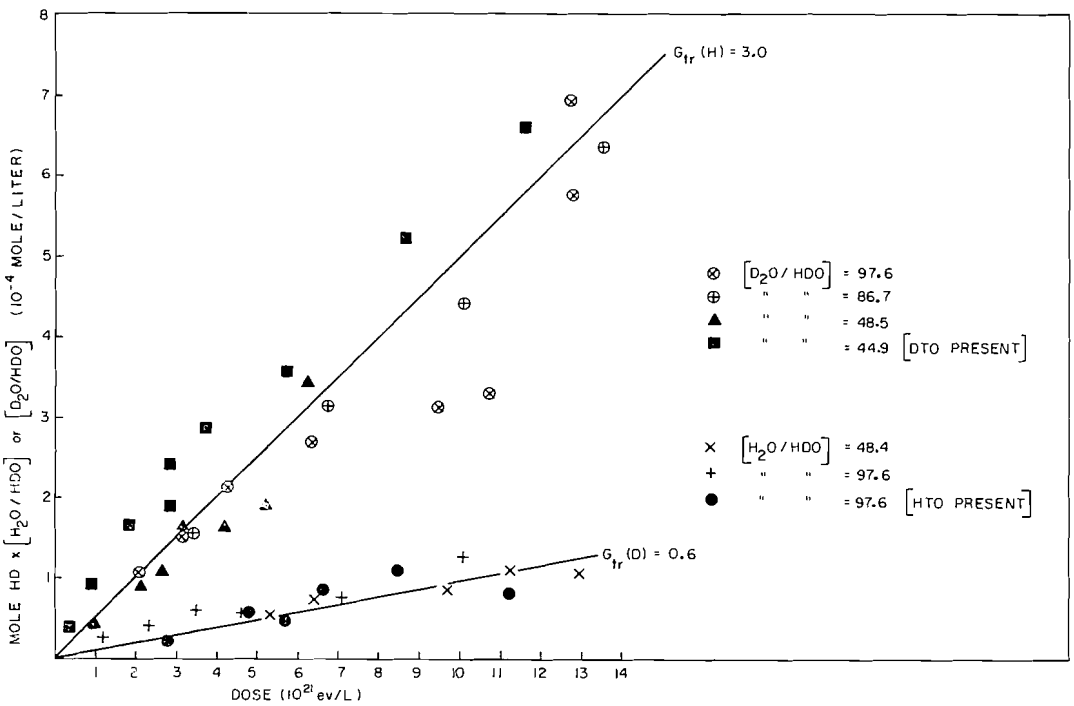


FIG. 1. Formation of HD in tracer experiments on the radiolysis of solutions of H_2 in H_2O and D_2 in D_2O. The upper line is for experiments using H atoms as a tracer in D_2O, the lower line is for D atoms as a tracer in H_2O.

Can. J. Chem. Downloaded from www.nrcresearchpress.com by 210.87.254.6 on 09/05/12
For personal use only.

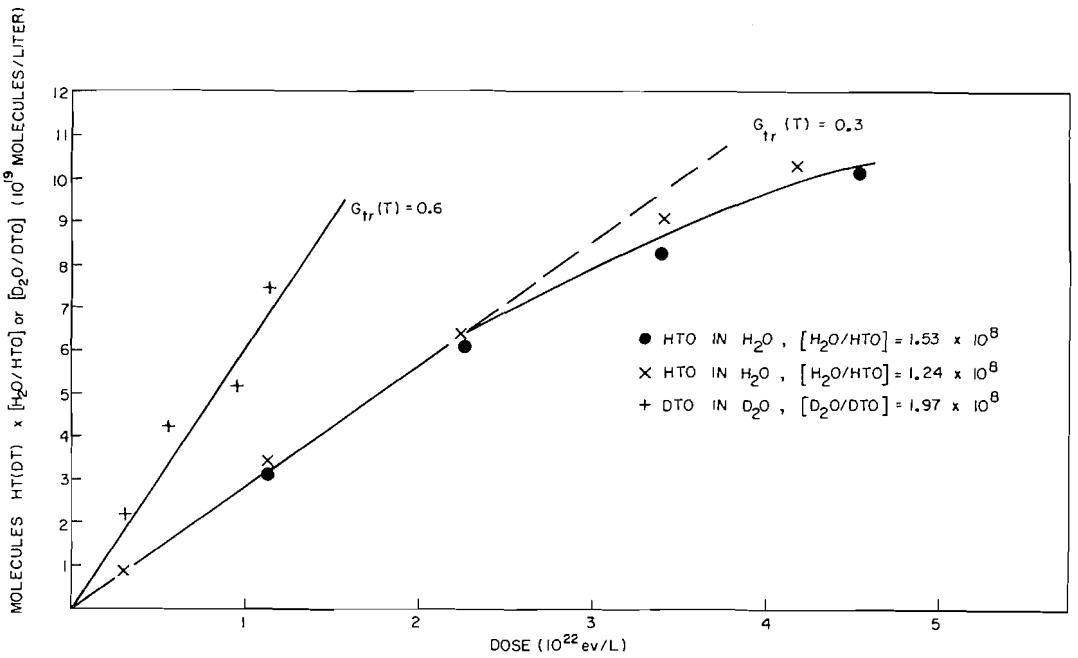


FIG. 2. Exchange of tritium atoms between water, H_2O or D_2O, containing tritium with dissolved hydrogen or deuterium.

with stopcock joints lubricated by Kel-F grease. The sample of water was saturated with H_2 or D_2 which had been passed into the system through a charcoal trap cooled with liquid air, and the saturated solution irradiated overnight. The dissolved hydrogen was pumped away and the cell was then filled with H_2 or D_2 for the first run. Without this preirradiation, low yields were invariably obtained.

Tritiated water with a specific activity of 4.5 mc/g was diluted to give solutions containing in the order of $\sim$10 μcuries T/ml and was purified by distillation as described above. The absolute tritium content was determined by gas-counting a sample of electrolyzed water (10). In the exchange experiments the whole sample of dissolved gas was pumped into the counter. Total counting rates were in the range 100–1000 c.p.m. in a system which detected $\frac{1}{3}$ of the total disintegrations. Corrections were made for the tritium content of the D_2 and D_2O used.

Mass spectrometric analysis for HD, H_2, and D_2 was carried out on a Consolidated 21-610 instrument. The analytical precision at a concentration of 0.5% HD in D_2 is about 10% and improves as the concentration increases.

Irradiations were carried out in the Co^{60} source described previously (3). The dose rate, $\sim 1 \times 10^{22}$ ev/l./hr, was determined by the Fricke dosimeter taking $G(Fe^{3+}) = 15.5$ ions/100 ev.

EXPERIMENTAL RESULTS

Results of tracer experiments are expressed as "total exchanges": the number of exchanges observed (number of atoms T appearing in dissolved gas per liter of solution or the number of HD molecules formed per liter of solution) multiplied by the ratio of unlabelled molecules to labelled molecules e.g. H_2O/HDO, D_2O/HDO, H_2O/HTO,

Can. J. Chem. Downloaded from www.nrcresearchpress.com by 210.87.254.6 on 09/05/12
For personal use only.

D_2O/DTO as the case may be. For experiments with H or D as a tracer this ratio is between 40 to 100, for experiments with tritium it is of the order of 1.5×10^8. We call the G values obtained in this way G(tracer) or G_{tr}. G_{tr}(D) from HDO may be thought of as the yield of D atoms from HDO per 100 ev absorbed in the HDO molecule. In terms of the "reactivity" of H or D atoms, values of G_{tr} must be compared with $\frac{1}{2}G$(H) in H_2O or $\frac{1}{2}G$(D) in D_2O since these molecules contain two labile atoms/molecule.

As will be seen in the discussion, G_{tr} is a quantity determined both by the tracer atom, H, D, or T, and by the solvent. For rigorous definition we refer to G_{tr}(H, D_2O) or G_{tr}(T, H_2O) giving both the tracer atom and the solvent in which the exchange is observed.

In the discussion we estimate values of G_{tr}(H, H_2O) and G_{tr}(D, D_2O), the "total exchange" yields of H atoms from HDO in H_2O, and of D atoms from HDO in D_2O; these quantities are, of course, unobservable but have considerable theoretical significance.

Values of G(tr) determined from the slopes of lines in Figs. 1 and 2 are given in Table I.

TABLE I

Values of G(tracer)

Tracer molecule	Solvent	Solute	G(tr)
HDO	D_2O	D_2	$G_{tr}(H,D_2O) = 3.0\pm0.5$
HDO	H_2O	H_2	$G_{tr}(D,H_2O) = 0.6\pm0.1$
HTO	H_2O	H_2	$G_{tr}(T,H_2O) = 0.3\pm0.05$
DTO	D_2O	D_2	$G_{tr}(T,D_2O) = 0.6\pm0.1$

The limits of error are arbitrarily determined from the scatter of the points and the slopes of the most extreme lines that could reasonably be drawn through them. The experimental points for G_{tr}(H, D_2O) show the largest scatter and it is also noteworthy that some of the initial points lie on a line of significantly greater slope. (G(tr) = 5.0 or more.) In series of results in which this was observed, such as those with (D_2O/HDO) = 44.9, the points for greater doses lay on a line parallel to that drawn in the figure. We have no explanation of this but conclude that G_{tr}(H, D_2O) = 3.0 can be taken as a minimum value.

The value of G_{tr}(D, H_2O) agrees well with that obtained by Bardwell and Dyne (3). It should be noted that their "exchange yield" is twice G(tr) as defined here; consequently their exchange yield of 1.0 is equivalent to G_{tr}(D, H_2O) = 0.5.

Experiments in which D_2 was dissolved in pure H_2O and H_2 dissolved in pure D_2O were also carried out. These experiments are of course not "tracer" experiments, since every exchange is observed. The results are given in Table II. The first series of experiments is simply a repetition of Gordon and Hart's original experiment, and the results are in good agreement with their results. The value of G(HD) from D_2O is the first determination of this quantity in neutral solution.

TABLE II

Values of G(HD) in H_2O and D_2O

Solvent	Solute	G(HD)	$\frac{1}{2}G$ ($\equiv G_{tr}$)
H_2O	D_2	2.9 ± 0.1	1.45
D_2O	H_2	3.7 ± 0.1	1.85

Can. J. Chem. Downloaded from www.nrcresearchpress.com by 210.87.254.6 on 09/05/12
For personal use only.

A small pressure dependence was observed in these experiments. Yields measured at small doses (1×10^{21} ev/l.) are shown in Fig. 3. This is negligible in the range of dissolved

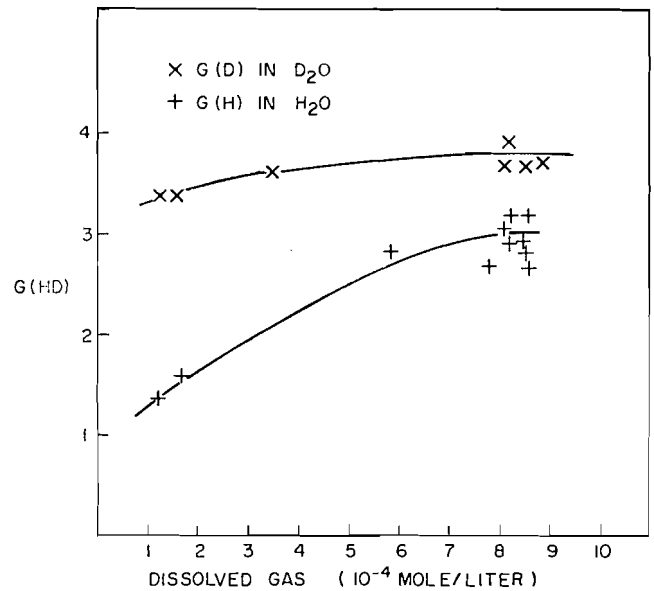


FIG. 3. Variation of G(HD) with partial pressure of dissolved D_2 in H_2O or dissolved H_2 in D_2O. Doses of $\sim1\times10^{21}$ ev/l. were given for all the data presented.

gas concentrations of $5–10\times10^{-4}$ mole/liter but is appreciable at lower concentrations. In this matter our data are not in serious disagreement with other workers who were working in the higher-pressure ranges.

In agreement with Gordon and Hart, yields of H_2 in H_2O solutions and D_2 in D_2O solutions were also observed which are identified with the molecular process, reaction [2]. Values of $G(H_2)$ lay in the range 0.4–0.5, and values of $G(D_2)$ in the range 0.3–0.35. $G(H_2)$ increased as the pressure of dissolved deuterium decreased.

DISCUSSION

In comparing values of G_{tr}, G(H), and G(D) two effects must be distinguished: there are effects of the medium (H_2O or D_2O) on the effective probability of dissociation of the tracer molecule, and effects due to the differing detachment probabilities of, for instance, H and D atoms from an excited HDO molecule.

The first effect, the influence of the properties of the medium on the initial radiolytic steps, is possibly the origin of the isotope effects in the primary yields in heavy and light water. These isotope effects have been discussed by many workers (4, 5, 7, and 8): the current conclusions are firstly that differences in the rate constants and diffusion constants between H and D atoms and between OH and OD radicals will not affect the product yields. Secondly, Armstrong, Collinson, and Dainton (4) suggest that a more extended initial distribution of D atoms in spurs in D_2O, relative to the initial distribution of H atoms in H_2O, would give the observed isotope effect, viz. $G(D_2) < G(H_2)$ and $G(D) > G(H)$; in the more extended, dilute distribution the probability of atom recombination to give molecular products is smaller and the probability of escape and reaction with the solute is greater. These workers suggested that the distribution of H or D atoms

Can. J. Chem. Downloaded from www.nrcresearchpress.com by 210.87.254.6 on 09/05/12
For personal use only.

was, at least in part, determined by rate of thermalization of the ~100-ev electrons formed in the initial ionization and by the time required for capture by the solvent molecules to form H_2O^- ions (which subsequently dissociate to give H and OH^-). The rates of these processes are intimately connected with the dielectric properties of H_2O and D_2O and may differ appreciably in the two media.

It follows from this suggestion that hydrogen atoms produced from the dissociation of HDO in a D_2O medium will be formed in a distribution characteristic of D_2O. They will have a greater probability of escape from the spur and of reacting with a solute than D atoms produced from the same molecule in a H_2O medium. Calculations have shown that there are no isotopic separations resulting from the reactions of H and D atoms in the same spur (5).

The magnitude of this effect of the medium can be estimated from the values of G(D) and G(H) (given in Table II). In neutral solution the present measurements give $G(D)/G(H) = 1.27$. In acid solution lower values, 1.11 (8) and 1.08 (9) are reported. We conclude that, in the absence of any isotopic discrimination in the detachment of H and D atoms from an HDO molecule, $G_{tr}(H, D_2O)$ would be 10–30% greater than $G_{tr}(D, H_2O)$.

The differing detachment probabilities of H and D atoms from an excited molecule can only be discussed qualitatively and by inference from mass-spectral studies on partially deuterated hydrocarbons. Isotope effects in mass spectra are fully summarized by Field and Franklin (6); the general conclusions are that in a partially deuterated hydrocarbon, detachment of H atoms is more probable than the detachment of D atoms, that detachment of an H atom in a partially deuterated molecule is more probable than the detachment of an H atom in the fully protonated molecule and, lastly, that there are no large changes in the total yields of molecular ions and fragments on isotopic substitution. We postulate that these conclusions are applicable to HDO.

To correlate our experimental results with these ideas, we have to eliminate the effect of the medium, i.e. $G_{tr}(D, H_2O)$ is to be compared with the "unobservable" quantity $G_{tr}(H, H_2O)$. Using our experimental ratio of $G(D)/G(H) = 1.27$ we put $G_{tr}(H, H_2O) = 1/1.27\, G_{tr}(H, D_2O)$. Similarly we correlate results in heavy water by comparing $G_{tr}(H, D_2O)$ with $G_{tr}(D, D_2O) = 1.27\, G_{tr}(D, H_2O)$.

With these corrections the ratio $G_{tr}(D)/G_{tr}(H)$ should be the same in H_2O and D_2O since it expresses a molecular property of HDO and not a property of the medium. The data should also be consistent with our expectation that there are no large isotope effects in the *total* probability of dissociation to give, for instance H and D atoms from HDO or to give two H atoms from H_2O. The approximate equalities $G_{tr}(H, H_2O)+G_{tr}(D, H_2O) \simeq G(H)$, and $G_{tr}(H, D_2O)+G_{tr}(D, D_2O) \simeq G(D)$ should be observed.

Values of $G_{tr}(H, H_2O)$ and $G_{tr}(D, D_2O)$ calculated using our ratio of $G(H)/G(D) = 1.27$ are given in brackets in Table III together with values of the sums and ratios referred to above.

The values of the sums agree well with the values of G(H) and G(D).

While the value of the ratio $G_{tr}(D)/G_{tr}(H)$ is, indeed, independent of the solvent this agreement is probably fortuitous. The limits of error on the ratio are large if upper and lower limiting values of G_{tr} are combined in this ratio; in D_2O for instance the values are 0.25 (+0.12, −0.07). It can only be claimed that the data are consistent with the postulate that the discrimination is analogous to "mass-spectral" isotope effects. The ratio $G_{tr}(D)/G_{tr}(H)$ is, in our interpretation, equivalent to the π factor (probability of dissociation of a D atom from HDO/probability of dissociation of an

Can. J. Chem. Downloaded from www.nrcresearchpress.com by 210.87.254.6 on 09/05/12
For personal use only.

TABLE III
Correlations of G(tracer)

	Medium	
	H_2O	D_2O
$G_{tr}(H)$	$(2.3_6 \pm 0.5)$	3.0 ± 0.5
$G_{tr}(D)$	0.6 ± 0.1	$(0.7_6 \pm 0.1)$
$G_{tr}(H) + G_{tr}(D)$	$2.9_6 \pm 0.6$	$3.7_6 \pm 0.6$
$G(H)$ or $G(D)$	2.9 ± 0.1	3.7 ± 0.1
$G_{tr}(D)/G_{tr}(H)$	0.25	0.25

H atom from HDO) for the mass spectrum of HDO. The mass spectrum of HDO is unknown but values of the π factor of 0.3–0.5 are observed in light hydrocarbons (6).

The experimental values of $G_{tr}(T)$ are also, in a more limited sense, consistent with the same postulate. No detailed comparison is possible without values of $G(T)$ in pure T_2O. In H_2O solutions one would expect T atoms to be less labile than D atoms in HDO and so $G_{tr}(T) < G_{tr}(D)$, as observed; in D_2O solutions again H from HDO would be much more labile than T in DTO and $G_{tr}(H) > G_{tr}(T)$ as observed.

ACKNOWLEDGMENTS

It is a pleasure to acknowledge the many helpful discussions we had with Dr. R. H. Betts on this problem.

REFERENCES

1. S. GORDON and E. J. HART. J. Am. Chem. Soc. **77**, 3981 (1955).
2. H. L. FRIEDMAN and A. H. ZELTMANN. J. Chem. Phys. **28**, 878 (1958).
3. J. BARDWELL and P. J. DYNE. Can. J. Chem. **35**, 82 (1957).
4. D. A. ARMSTRONG, E. COLLINSON, and F. S. DAINTON. Trans. Faraday Soc. **55**, 1375 (1959).
5. P. J. DYNE and J. M. KENNEDY. Can. J. Chem. **36**, 1518 (1958).
6. F. H. FIELD and J. L. FRANKLIN. Electron impact phenomena. Academic Press Inc., New York. 1957.
7. P. J. DYNE and J. M. KENNEDY. Can. J. Chem. **38**, 61 (1960).
8. K. COATSWORTH, E. COLLINSON, and F. S. DAINTON. Trans. Faraday Soc. **56**, 1008 (1960).
9. H. A. MAHLMAN and J. W. BOYLE. J. Am. Chem. Soc. **80**, 773 (1958).
10. L. P. ROY. Can. J. Chem. In press.

Can. J. Chem. Downloaded from www.nrcresearchpress.com by 210.87.254.6 on 09/05/12
For personal use only.

Can. J. Chem. Downloaded from www.nrcresearchpress.com by 210.87.254.105 on 09/05/12
For personal use only.

THE MECHANISM OF THE ALCOHOLYSIS OF ALIPHATIC NITRITES

I. ALCOHOLYSIS OF 1-METHYLHEPTYL NITRITE IN ALKALINE AND NEUTRAL SOLUTION[1]

A. D. ALLEN[2] AND G. R. SCHONBAUM[3]

ABSTRACT

A polarimetric study of the kinetics of the alcoholysis of 1-methylheptyl nitrite in alkaline solution has shown that the reaction rate is proportional to both the nitrite and alkoxide ion concentration. The asymmetric carbon center is not involved in the reaction. In strictly neutral solution no reaction occurs; the commonly observed "neutral" reaction is attributed to traces of acid formed in the decomposition of the nitrite ester. The mechanism of the reactions is discussed.

In a previous paper (1) the mechanism of the acid- and base-catalyzed hydrolysis of some organic nitrite esters was discussed, and some preliminary work on alcoholysis reported. With perchloric acid as the catalyst the rapid reaction was first order with respect to both the nitrite and acid concentrations, but with hydrochloric acid or added halide salts an additional catalysis, proportional to the halide ion concentration, was observed. In alkaline solution the much slower reaction was approximately first order with respect to both the nitrite and hydroxide ion concentration, but the second-order rate coefficient decreased slightly with increasing hydroxide concentration. Since this decrease was not a simple salt effect it indicated the possibility of a solvolytic reaction between the nitrite and water. It had been reported earlier that nitrite esters react readily with methanol, in the absence of added catalysts, evolving gaseous methyl nitrite (2). These observations prompted the present investigation into the uncatalyzed alcoholysis reaction. The indications, from our work using aqueous media, were that the solvolytic reaction would be too slow to account for the apparently rapid reaction with methanol.

The reversible reaction between an aliphatic nitrite and an alcohol may be written:

$$RONO + R'OH \rightleftarrows R'ONO + ROH \qquad R,\ R' = \text{alkyl.}$$

Some physical method must be used to follow the course of such a reaction, and the polarimetric method was chosen as the most suitable one. From our previous work (1) it was known that the specific rotation of (+)- or (−)-1-methylheptyl nitrite is just over half that of its hydrolysis product (+)- or (−)-octan-2-ol, and it seemed likely that, under the conditions to be used, complete retention of configuration would be observed. Preliminary experiments confirmed the following relationships, which had to be known precisely before any rate measurements could be made: (*a*) the optical rotations of solutions of the alcohol and nitrite are proportional to their concentrations, (*b*) the total rotation of mixtures of the two optically active compounds in solution is given by the sum of their individual rotations, and (*c*) the asymmetric center is not involved in the reactions to be studied, so that the optical configurations are preserved. During repeated esterification, hydrolysis, and alcoholysis in a wide variety of acidic and basic solutions, the optical purity of the alcohol recovered was always unchanged, confirming exclusive fission of the nitrosyl-oxygen bond. The rotations of these compounds in various solvents are given in Table I.

[1]*Manuscript received November 18, 1960.*
Contribution from the Department of Chemistry, University College, London, England.
[2]*Present address: Department of Chemistry, University of Toronto, Toronto 5, Ontario, Canada.*
[3]*Present address: Johnson Foundation, University of Pennsylvania, Philadelphia, Pa., U.S.A.*

TABLE I

Optical rotations of 10% (by weight) solutions at 25°

Solvent	(+)-Octan-2-ol α_D^{25} (l = 2)	(+)-1-Methylheptyl nitrite α_D^{25} (l = 2)
1-Propanol	1.58	0.59
1-Pentanol	1.65	0.60
2-Propanol	1.46	—
2-Methyl-2-butanol	1.45	0.56
Dioxane	2.27	—
Nitromethane	—	0.11

It is of interest to note that, whereas the rotation of 1-methylheptyl nitrite in alcoholic solution is relatively insensitive to the alcohol used, it is smaller by a factor of about five in nitromethane solution; also the rotation of octan-2-ol in dioxane is significantly higher than in alcoholic solution.

Equilibrium Measurements

The position of equilibrium for the over-all reaction

$$R^*ONO + R'OH \overset{H^+}{\rightleftharpoons} R^*OH + R'ONO$$

where R* = (+)- or (−)-1-methylheptyl, R′ = alkyl, was determined. The measurements were carried out in acid solution to reduce the time needed to reach equilibrium, and it was shown that the concentration and the nature of the acid present had no effect on the final result. Values obtained for the concentration equilibrium constant $K_c = [R^*OH][R'ONO]/[R^*ONO][R'OH]$ at 25° were as follows.

R′OH	K_c
2-Methyl-2-butanol	0.28
2-Propanol	0.51
1-Propanol	1.6 (In dioxane)

With the tertiary and secondary alcohols the equilibrium position could be determined from simple mixtures of the alcohols and nitrite, but with the primary alcohol the reaction was displaced too far to the right for accurate measurement. Dioxane was used as a solvent to reduce the concentration of the alcohol. These results show that the equilibrium is shifted towards the products as the reagent is changed from tertiary, through secondary, to primary alcohol. Two mutually supporting effects would account for this trend, (*a*) the reactivity of nitrites in acid solution decreases in the order tertiary > secondary > primary, and (*b*) the nucleophilic strength of the alcohols decreases in the order primary > secondary > tertiary (11).

Kinetics and Mechanism of Alcoholysis in Alkaline Solution

The alcoholysis of 1-methylheptyl nitrite in alkaline solution was studied using 1-propanol as the solvent, in the presence of small concentrations of sodium propoxide. It was found that secondary and tertiary alcohols and alkoxides could not be used as reagents, for the following reason. The reversible reaction in alkaline solutions

$$R^*ONO + R'O^- \overset{\text{slow}}{\rightleftharpoons} R^*O^- + R'ONO \qquad (a)$$

is complicated by the further equilibrium

$$R^*O^- + R'OH \overset{\text{fast}}{\rightleftharpoons} R^*OH + R'O^-. \qquad (b)$$

Can. J. Chem. Downloaded from www.nrcresearchpress.com by 210.87.254.105 on 09/05/12
For personal use only.

Can. J. Chem. Downloaded from www.nrcresearchpress.com by 210.87.254.105 on 09/05/12
For personal use only.

If reaction (*b*) is displaced strongly towards the right the reagent alkoxide will be quantitatively regenerated and its concentration will remain constant throughout the reaction. Thus, if the reaction rate is given by $v = k_2$ [R*ONO][R'O$^-$], (as in alkaline hydrolysis) the kinetics observed would be pseudo first order, the rate coefficient being proportional to the (constant) concentration of alkoxide. Alternatively, if reaction (*b*) is displaced strongly towards the left, the reagent alkoxide would be consumed and second-order kinetics could, in principle, be observed. However, since in our experiments the nitrite is in very large excess over the alkoxide, the reaction would cease after a small fraction of the ester had reacted. Finally, if reaction (*b*) has an intermediate equilibrium position it will be difficult to determine with sufficient accuracy the concentrations of the two alkoxides at any point in the reaction and the kinetic order will be obscured. Displacement of equilibrium (*b*) to the left or right will depend on the relative basicities of the two alkoxides. The following order of decreasing basicity has been given (3): tertiary > secondary > primary alkoxide > hydroxide. The position of hydroxide at the lower end of this sequence presents a further problem, since, if there is any water present in the reaction mixture some hydroxide ion will be formed, which will give rise to the irreversible hydrolysis reaction

$$R^*ONO + HO^- \rightarrow R^*OH + NO_2^-.$$

Conversion of alkoxide to hydroxide, followed by production of nitrite ion, would again lead to early termination of the reaction. Extreme precautions were therefore necessary to ensure that all the solutions used were perfectly dry.

The alkoxide of octan-2-ol formed in the reaction is secondary, and it follows from the above that clear kinetic results could only be expected if the reagent were a much more weakly basic primary alkoxide. We should then expect to observe pseudo first-order kinetics. The results obtained are shown in Table II. Good first-order kinetics were

TABLE II

Reaction of 1-methylheptyl nitrite with sodium propoxide in 1-propanol at 25° C

$[R^*ONO]_0$ (M)	$[PrO^-]_0$ (10^2 M)	10^4 k_1 (sec^{-1})	$k_2 = \frac{k_1}{[PrO^-]}$
0.826	1.07	0.091	8.5
0.744	2.14	0.221	10.3
0.772	2.60	0.253	9.7
0.596	4.34	0.432	9.9
0.827	5.24	0.509	9.7

observed, the first-order rate coefficient (k_1) being satisfactorily proportional to the concentration of alkoxide. Several conclusions may be drawn from these results: (*a*) propoxide must be much less basic than octan-2-oxide, (*b*) the solutions were satisfactorily dry, (*c*) any contribution to the total reaction rate by reaction of the nitrite with the solvent alcohol is negligible, since otherwise the second-order rate coefficients would decrease with increasing alkoxide concentration. From this it follows that the alcoholysis reaction in neutral solution should be immeasurably slow, unless some other mechanism is possible which is inhibited by alkali.

Since the alkaline reaction proceeds without disturbing the asymmetric center, we envisage a bimolecular nucleophilic attack by alkoxide on the nitrogen atom of the ester molecule:

$$R'O^- + R^*ONO \underset{\text{fast}}{\overset{\text{slow}}{\rightleftharpoons}} \left[R^*O \cdots \overset{O}{\overset{\|}{N}} \cdots OR' \right]^- \underset{\text{slow}}{\overset{\text{fast}}{\rightleftharpoons}} R'ONO + R^*O^-,$$

followed by

$$R^*O^- + R'OH \xrightarrow{\text{fast}} R^*OH + R'O^-.$$

Alcoholysis Reactions in Neutral Solution

At the beginning of this investigation many kinetic runs were attempted using (+)- or (−)-1-methylheptyl nitrite prepared and purified in the usual way, with various alcohols and solvents similarly purified and dried. Reaction always occurred as soon as the reagents were mixed, but the rates of these reactions were quite random and could not be reproduced. Improvements in experimental technique, e.g. complete exclusion of oxygen, moisture, light, and nitrite decomposition products, gradually reduced the speed of the spontaneous reactions until, under optimum conditions, no reaction occurred on mixing the reagents. Generally a variable induction period of up to 48 hours was observed: reaction then started and in some cases it was possible to follow it kinetically. The results are given in Table III. The initial rates of these spontaneous reactions did not

TABLE III

Solvolysis of 1-methylheptyl nitrite at 25° C

$[R^*ONO]_0$ (M)	Solvent	Induction period (hr)	Approx. initial rate $10^4\ k_1$ (sec^{-1})
0.635	1-Propanol	—	0.35
0.564	"	48	0.35
0.503	"	—	0.55
0.360	2-Methyl-2-butanol	3	0.12
0.421	"	15	0.15
0.856	"	3	0.12
0.590	"	—	0.14
0.530	"	24 days	—*
0.447	85 Dioxane:7 propanol	18	—
0.488	70 Dioxane:15 nitromethane:7 propanol	3	—
0.466	35 Dioxane:50 nitromethane:7 propanol	2	1.2
0.461	25 Dioxane:60 nitromethane:7 propanol	—	4.0
0.455	5 Dioxane:80 nitromethane:7 propanol	—	Very fast

*In presence of 10^{-4} M sodium alkoxide.

depend on the length of the induction period, but were generally faster in 1-propanol than in 2-methyl-2-butanol. Induction periods were more usually observed in the tertiary than in the primary alcohol. Addition of traces (10^{-4} M) of alkali prolonged the induction period greatly. The use of mixed solvents containing varying proportions of dioxane and nitromethane showed that the trend is towards shorter induction periods and faster rates as the nitromethane content of the mixture is increased. It is thought that this trend is connected with the decreasing basicity of the medium rather than the increase in its dielectric constant.

It seemed most likely that the reaction was being initiated by the spontaneous production of an acid in the reaction mixture. The following tests were made which confirmed this belief. To a solution of 1-methylhepytl nitrite in 2-methyl-2-butanol was added just enough lacmoid indicator to give a recognizable color. This solution was divided

Can. J. Chem. Downloaded from www.nrcresearchpress.com by 210.87.254.105 on 09/05/12
For personal use only.

into two. One half was placed in the polarimeter and the rotation observed. After an induction period of about 5 hours reaction started and it was observed that the indicator had changed color. To the other half was added sodium 2-methyl-2-butoxide to give a concentration of about 10^{-4} M. This alkaline solution was further divided into two. After 24 hours both alkaline solutions were unchanged. One of these was then irradiated with a mercury lamp until the color changed; reaction began at once. Addition of just enough alkali to restore the indicator color immediately stopped the reaction.

From our other work (4) it is estimated that a concentration of approximately 10^{-6} M of a strong acid is all that is needed to account for the observed reaction rates. A weak acid, such as nitrous acid, would have to be present in very much higher concentrations, as was shown by the investigation of formic acid as a catalyst (4). A concentration of approximately 0.1 M of this acid, which is comparable in strength to nitrous acid, is needed to produce the observed rate. The most likely catalyst is nitric acid, which could be formed in sufficient quantity if traces of oxygen remained in the solutions or apparatus. The following is a possible reaction sequence;

$$\mathrm{RONO} \rightleftarrows \mathrm{RO}\cdot + \mathrm{NO} \quad \text{(thermal or photochemical decomposition (5))}$$

$$\mathrm{NO} + \mathrm{O} \rightarrow \mathrm{NO_2}$$

$$2\mathrm{NO_2} \rightleftarrows \mathrm{N_2O_4}$$

$$\mathrm{R'OH} + \mathrm{N_2O_4} \rightarrow \mathrm{R'ONO} + \mathrm{HNO_3}. \qquad (6)$$

It is also possible that a much more complex decomposition of the nitrite could produce nitric acid in the absence of oxygen (7). Under normal atmospheric conditions it is obvious that the above reactions could occur readily. The presence of nitric acid in samples of 1-methylheptyl nitrite that had been exposed to the atmosphere was demonstrated by the addition of a small amount of pyridine, which gave a fine white precipitate, m.p. 118°, which gave a positive test for nitrate ion and which did not depress the melting point of synthetic pyridinium nitrate. Samples of the nitrite prepared and preserved as described in the experimental section gave no precipitate with pyridine.

CONCLUSIONS

Our results show that the commonly observed 'uncatalyzed' reaction of an alkyl nitrite with alcohols is caused by traces of nitric acid arising from the thermal or photochemical decomposition of the nitrite in the presence of atmospheric oxygen. In acid-free solutions no reaction occurs. The results in alkaline solution show that the unprotonated ester molecule can only be attacked by strong nucleophilic reagents such as alkoxide, since no solvolytic component of the reaction rate could be detected. The mechanism of the reaction with alkoxide in alcoholic solution appears to be the same as that with hydroxide in aqueous solution, and involves a nucleophilic attack by alkoxide ion on the nitrogen atom of the nitrite molecule.

EXPERIMENTAL

Resolution of Octan-2-ol

Octan-2-ol was resolved into its (+) and (−) optical isomers by Kenyon's phthalic anhydride – brucine method (8). From several such resolutions the following average values were obtained: b.p. 86°/20 mm, $n_D^{25°}$ 1.4244, $[\alpha]_D^{25°}$ +9.53, −9.33°.

Preparation of (+)- and (−)-1-Methylheptyl Nitrite

These were prepared from the (+)- or (−)-octan-2-ol by esterification with nitrous

Can. J. Chem. Downloaded from www.nrcresearchpress.com by 210.87.254.105 on 09/05/12
For personal use only.

acid in weakly acid solution. The procedure of Chretien and Longi (9), using aluminum sulphate as the source of acid, was found to be greatly superior to the more commonly used methods. Yields were generally better than 90% if the temperature was kept below 5° throughout the preparation. The crude product was dried and fractionally distilled at reduced pressure in a nitrogen atmosphere, giving b.p. 61–62°/15 mm, 34°/2.5 mm, $n_D^{25°}$ 1.4067, $d_4^{25°}$ 0.8602, $[\alpha]_D^{25°} \pm 5.00°$ (mean value, no solvent). The pure product was stored over potassium carbonate in a dark flask at 0° to minimize decomposition.

Purification of Solvents

The solvents used were purified and thoroughly dried by standard procedures, and fractionally distilled at high reflux ratio using a 48-in. helix packed column. Purity and dryness were checked by constancy of the boiling point on changing to total reflux. The absence of water in the dried solvents was confirmed by Karl Fischer titration (10). All solvents were collected and stored in an atmosphere of dry nitrogen, and samples for use were taken by siphon, using dry nitrogen pressure.

Equilibrium Measurements

1-Methylheptyl nitrite was mixed with the appropriate alcohol. Acid was added and the change in rotation followed until a constant value was obtained. The rotation for 100% reaction was calculated and hence the position of equilibrium was found. The results are shown in Table IV.

TABLE IV

1-Methylheptyl nitrite:alcohol equilibria at 25°

$[R^*ONO]_0$ (M)	$[R'OH]_0$ (M)	α_D^{25} at t_∞ (observed)	α_D^{25} 100% (calculated)	% reaction	K_e
(*a*) R'OH = 2-methyl-2-butanol					
0.512	8.30	1.080	1.18	83.5	0.28
0.421	8.47	0.90	0.975	85.0	0.25
0.638	8.08	1.34	1.47	83.0	0.34
0.451	8.41	0.97	1.05	85.0	0.28
0.251	8.74	0.555	0.585	90.0	0.24
(*b*) R'OH = 2-propanol					
0.528	11.7	1.225	1.280	92.0	0.49
0.745	11.2	1.70	1.80	89.5	0.53
(*c*) R'OH = 1-propanol (in dioxane solution)					
0.522	1.3	1.21	1.50	78.5	1.6

NOTE: [Acid] = 10^{-3}–10^{-4} M.

Alkaline Alcoholysis

Stock solutions of sodium propoxide in 1-propanol were prepared by dissolving clean sodium in the dry alcohol, in an atmosphere of dry nitrogen. The solution was standardized against standard hydrochloric acid. The reagents for each kinetic run were separately brought to 25°, mixed at zero time, and transferred to the polarimeter tube under dry nitrogen. Details of a typical run were as follows:

$[R^*ONO]_0 = 0.596$ M $[\text{Propoxide}]_0 = 4.34 \times 10^{-2}$ M $\alpha_D^{25}(t = \infty, \text{calc.})$ 1.510

Time (min)	6	13	22	42	53	65	120	210	20 hours
α_D^{25} (obs.)	.74	.76	.78	.82	.83	.85	.94	1.06	1.465

$k_1 = 0.43 \times 10^{-4}$ sec^{-1} $k_2 = k_1/[RO^-]_0 = 9.9 \times 10^{-4}$ sec^{-1} $M.^{-1}$ l.

Can. J. Chem. Downloaded from www.nrcresearchpress.com by 210.87.254.105 on 09/05/12
For personal use only.

Alcoholysis in Neutral Solution

To obtain solutions free from acid and oxygen for this part of the work the following precautions were found to be necessary: (*a*) Small samples of 1-methylheptyl nitrite from stock preparations were freshly distilled from potassium carbonate in the dark at low pressures immediately before each kinetic run. Static distillation into a liquid-air trap at about 10^{-4} mm pressure was used, the distillate being collected in a calibrated tube and used immediately. (*b*) All operations were carried out in an atmosphere of dry nitrogen. (*c*) All solvents were thoroughly degassed and stored in an atmosphere of dry nitrogen. (*d*) The reaction mixture was shielded from light, except for occasional exposure to the sodium lamp during measurement of the rotation. In the following example an induction period of about 3 hours was observed. The first-order rate coefficient for the initial part of the reaction which followed was approximately 0.12×10^{-4} sec^{-1}.

$[R^*ONO]_0 = 0.856\ M$ Solvent: 2-methyl-2-butanol, 25°

Time (hr)	0	1	2	3	$4\frac{1}{2}$	5	$6\frac{3}{4}$	$7\frac{3}{4}$	∞ (calc.)
α_D^{25} (obs.)	0.95	.95	.945	.955	.985	1.005	1.07	1.125	1.96

REFERENCES

1. A. D. ALLEN. J. Chem. Soc. 1968 (1954).
2. W. M. FISCHER. Z. physik. Chem. **65**, 61 (1908).
3. J. HINE and M. HINE. J. Am. Chem. Soc. **74**, 5266 (1952).
4. A. D. ALLEN and G. R. SCHONBAUM. Can. J. Chem. In press.
5. F. O. RICE and G. L. RODOWSKAS. J. Am. Chem. Soc. **57**, 350 (1935).
6. A. M. FAIRLIE, J. J. CARBERRY, and J. C. TREACY. J. Am. Chem. Soc. **75**, 3786 (1953).
7. N. KORNBLUM and E. P. OLIVETO. J. Am. Chem. Soc. **71**, 226 (1949).
8. J. KENYON. Organic syntheses. Coll. Vol. I. 1941. p. 418.
9. A. CHRETIEN and Y. LONGI. Compt. rend. **220**, 746 (1948).
10. R. H. PRINCE. Analyst, **78**, 607 (1953).
11. A. STREITWEISER. Chem. Revs. **56**, 581 (1956); A. D. ALLEN *et al.* J. Chem. Soc. 3668 (1957).

Can. J. Chem. Downloaded from www.nrcresearchpress.com by 210.87.254.105 on 09/05/12
For personal use only.

Can. J. Chem. Downloaded from www.nrcresearchpress.com by 210.87.254.5 on 09/05/12
For personal use only.

THE MECHANISM OF THE ALCOHOLYSIS OF ALIPHATIC NITRITES

II. ACID-CATALYZED ALCOHOLYSIS OF 1-METHYLHEPTYL NITRITE[1]

A. D. ALLEN[2] AND G. R. SCHONBAUM[3]

ABSTRACT

The acid-catalyzed alcoholysis of 1-methylheptyl nitrite has been studied kinetically. The reaction rate is first order with respect to both the nitrite and the hydrogen ion concentration, and the reaction does not involve the asymmetric carbon center. Addition of lithium salts (chloride and perchlorate) indicates catalysis by chloride ion. Addition of water in low concentrations inhibits the reaction strongly. These results and the mechanism of the reactions are discussed in terms of the properties of the alcohols and the dissociation of the acid catalysts in the alcohols used.

In a previous paper (1) it was reported that the alcoholysis of 1-methylheptyl nitrite in "neutral" solution was, in fact, catalyzed by traces of a strong acid, probably nitric acid, formed in the decomposition of the nitrite ester. The sensitivity of this reaction to very small concentrations of acid led to a study of the mechanism of the acid-catalyzed reaction.

The polarimetric method was again used, and the alcoholysis of (+)- or (−)-1-methylheptyl nitrite in 1-propanol, 1-pentanol, and 2-methyl-2-butanol was studied, using various acids as catalysts.

Catalysis by Strong Acids

In very dilute solutions of perchloric, hydrochloric, or methanesulphonic acid the reaction rate was found to be first order with respect to both the acid and ester concentration, giving the rate expression $v = k_2[H^+][R^*ONO]$ (R*— = (+)- or (−)-1-methylheptyl-). Since the hydrogen ion concentration was constant during each kinetic run, first-order kinetics were observed, the first-order rate coefficient being proportional to the acid concentration. The reagent alcohol was in large excess over the other reagents and does not, therefore, appear in the rate equation. A comparison of the results obtained in 1-propanol with the three strong acids used is shown in Table I.

TABLE I

Catalysis by strong acids in 1-propanol at 25°

(*a*) Hydrochloric acid							
[HCl] 10^5 *M*	3.60	5.26	6.30	8.30	10.70	12.20	13.0
$10^4 k_1$ sec^{-1}	3.6	5.5	7.1	8.9	12.8	14.6	15.5
k_2 sec^{-1} M.$^{-1}$ l.	10.0	10.4	11.3	10.7	12.0	12.0	11.9
(*b*) Perchloric acid							
[$HClO_4$] 10^5 *M*	1.70	5.35	8.10	8.85	11.4	12.5	
$10^4 k_1$ sec^{-1}	1.82	5.55	8.7	9.45	14.1	14.2	
k_2 sec^{-1} M.$^{-1}$ l.	10.7	10.4	10.7	10.7	12.4	11.4	
(*c*) Methanesulphonic acid							
[Acid] 10^5 *M*	3.05	4.50	6.05	8.40	9.35		
$10^4 k_1$ sec^{-1}	3.12	4.55	7.30	8.95	10.95		
k_2 sec^{-1} M.$^{-1}$ l.	10.2	10.1	12.0	10.6	11.4		

NOTE: $[R^*ONO]_0 \simeq 0.5$ *M*.

[1]*Manuscript received November 18, 1960.*
Contribution from the Department of Chemistry, University College, London, England.
[2]*Present address: Department of Chemistry, University of Toronto, Toronto 5, Ontario, Canada.*
[3]*Present address: Johnson Foundation, University of Pennsylvania, Philadelphia, Pa., U.S.A.*

Can. J. Chem. Downloaded from www.nrcresearchpress.com by 210.87.254.5 on 09/05/12
For personal use only.

It is evident that perchloric, hydrochloric, and methanesulphonic acids are equally efficient as catalysts for the reaction. This indicates that, in 1-propanol at these very low (10^{-4}–10^{-5} M) concentrations, all three acids are virtually completely dissociated. It also follows that the hydrogen ion is the only significant catalyst, since changes in the nature of the anion do not affect the rate. Previously (2) we observed catalysis of the hydrolysis reaction by halide ion in aqueous dioxane, resulting in faster rates in hydrochloric acid than in perchloric acid solutions of the same concentration. In the present case, however, the acid concentrations are very much smaller and it is probable that any catalysis by chloride ion would be too small to be detected. The effect of added chloride ion will be discussed later.

In 1-pentanol and the tertiary alcohol 2-methyl-2-butanol a similar dependence of rate on acid concentration was observed. The results obtained are given in Table II.

TABLE II

Catalysis by perchloric acid in 1-pentanol and 2-methyl-2-butanol at 25°

1-Pentanol			2-Methyl-2-butanol		
[Acid] 10^5 M	$10^4 k_1$ sec^{-1}	k_2 sec^{-1} $M.^{-1}$ l.	[Acid] 10^5 M	$10^4 k_1$ sec^{-1}	k_2 sec^{-1} $M.^{-1}$ l.
5.91	6.30	10.6	1.80	4.00	22.2
7.06	8.01	11.2	3.90	8.65	22.2
10.6	13.2	12.4	5.0	10.95	21.9
15.1	17.8	11.8	8.1	17.1	20.9
			12.8	26.8	21.0

NOTE: $[R^*ONO]_0 \simeq 0.5$ M.

The rate of the reaction with the tertiary alcohol is about twice as fast as that with the two primary alcohols. The mechanism appears to be the same in each case, and is also the same as that observed in aqueous dioxane (2). The rate-determining step is preceded by a proton transfer equilibrium:

$$R^*ONO + SH^+ \overset{\text{fast}}{\rightleftharpoons} (R^*ONOH)^+ + S, \qquad (S = \text{solvent})$$

which is established rapidly and is maintained throughout the reaction. This is followed by the rate-determining step:

$$(R^*ONOH)^+ + R'OH \overset{\text{slow}}{\rightleftharpoons} (R'ONOH)^+ + R^*OH.$$

For this we envisage a bimolecular nucleophilic attack by the alcohol on the nitrogen atom of the protonated ester, preserving the configuration of the asymmetric carbon center:

$$R'OH + (R^*ONOH)^+ \underset{\text{fast}}{\overset{\text{slow}}{\rightleftharpoons}} \left[R'O\overset{H}{\ldots}\overset{O}{\overset{\|}{N}}\ldots\overset{H}{OR^*} \right]^+ \underset{\text{slow}}{\overset{\text{fast}}{\rightleftharpoons}} (R'ONOH)^+ + R^*OH.$$

Two important factors will influence the rate of this reaction, (*a*) the nucleophilic power of the reagent alcohol, and (*b*) the concentration of the protonated ester. The nucleophilic power of the alcohols used decreases in the order 1-propanol $\sim$ 1-pentanol $>$ 2-methyl-2-butanol, steric factors being the main reason for the relatively weak nucleophilic power of the tertiary alcohols. If this were the only factor it would result in a

much slower rate in the tertiary alcohol, contrary to our observations. To explain the observed faster rate we propose that, at equivalent acid concentrations, the concentration of the protonated ester is much greater in 2-methyl-2-butanol than in the primary alcohols. This means that the equilibrium:

$$R^*ONO + R'OH_2^+ \rightleftarrows R^*ONOH^+ + R'OH$$

is displaced to the right when R′ changes from primary to tertiary. Thus the tertiary alcohol is apparently much more weakly basic than the primary alcohol, despite the obvious inductive effects of the tertiary amyl group. There is much evidence to support this view. Absence of significant hydrogen bonding in liquid 2-methyl-2-butanol has been shown by infrared and dipole moment studies (3, 4). The relation between hydrogen bonding and basicity has been studied by Gordy and Stanford (5, 6), who found that the shift to lower frequencies of an infrared band of CH_3OD, due to deuterium bonding, is proportional to the basicity of the solvent used. The available data (7, 8) indicate that the basicity of hydroxy compounds decreases in the order: water $\gg$ primary $>$ secondary $>$ tertiary alcohols. It should be noted that this sequence is quite different from the order of relative basicities of the corresponding alkoxides, illustrating the importance of steric strain in the protonated molecule, ROH_2^+ (8, 9).

Catalysis by Organic Acids

As part of the investigation into the cause of the so-called "neutral" reaction, a study was made of the catalytic effect of trichloroacetic and formic acids. Reaction rates in 1-propanol and 2-methyl-2-butanol, in the presence of trichloroacetic acid, are shown in Table III.

TABLE III

Catalysis by trichloroacetic acid at 25°

1-Propanol			2-Methyl-2-butanol		
[Acid] $10^3\ M$	$10^4\ k_1$ sec^{-1}	$10^2\ k_2$ $sec^{-1}\ M.^{-1}\ l.$	[Acid] $10^3\ M$	$10^4\ k_1$ sec^{-1}	$10^2\ k_2$ $sec^{-1}\ M.^{-1}\ l.$
1.31	1.11	8.5	2.90	0.94	3.2
2.84	2.27	8.0	5.40	1.75	3.2
3.75	3.02	8.1	8.40	2.82	3.4
5.41	4.54	8.4			

NOTE: $[R^*ONO]_0 \simeq 0.5\ M$.

In both alcohols the rates are again first order with respect to both the ester and acid concentrations. For a given acid concentration, however, the rate is some 100 times slower than that found when the catalyst is a strong acid. This shows that trichloroacetic acid is only weakly ionized in these solvents, as would be expected. The faster rate in 1-propanol than in 2-methyl-2-butanol (in contrast to the previous results with strong acids) is readily explained on the basis of greater acid ionization in the medium of higher dielectric constant. The linearity of the dependence of rate on acid concentration is, however, surprising. From mass law considerations, we would expect a deviation from linearity due to a decrease in the degree of dissociation of the weak acid with increasing concentration. This will only be found, however, if the acid dissociation constant is independent of concentration. In solvents of moderately low dielectric constant, such as these alcohols, an increase in acid concentration has a marked effect on the activity

Can. J. Chem. Downloaded from www.nrcresearchpress.com by 210.87.254.5 on 09/05/12
For personal use only.

coefficient of the ionic species, resulting in an increase in the classical dissociation constant of the acid. For example, the dissociation constant for iodic acid (which is similar to that of trichloroacetic acid) in methanol increases from 2.4 to 14×10^{-8} when the acid concentration is raised from 9 to 64×10^{-4} M (10). It appears that a similar increase occurs with trichloroacetic acid in the alcohols used in our experiments, and that the linearity between rate and acid concentration is fortuitous. Assuming that hydrogen ion is the only catalyst, we can calculate the following dissociation constants (K_c) for trichloroacetic acid in these solvents at 25°.

[Acid] 10^3 M	1-Propanol 10^8 K_c	2-Methyl-2-butanol 10^8 K_c
1	8.1	—
3	19	0.83
5	31	—
6	—	1.5
9	—	2.2

A value of $K_c=34\times10^{-8}$ has been given (11) for this acid in 1-butanol at 25°, which is in good agreement with our results.

Formic Acid Catalysis

In 2-methyl-2-butanol the addition of formic acid in concentrations up to 0.01 M gave no measurable initial reaction. At 0.1 M acid concentration reaction occurred with a first-order rate coefficient of 0.29×10^{-4} sec^{-1}. Thus formic acid is about 100 times less effective as a catalyst than trichloroacetic acid. This is approximately the figure that would be expected if hydrogen ion were the only catalyst, bearing in mind the increase in the dissociation constant of formic acid at the very much higher concentrations used. The results with trichloroacetic and formic acids indicate that catalysis by the undissociated acid is negligible, even, in the case of formic acid, at concentrations of some 10^5 times greater than that of the hydrogen ion concentration. It also follows that, since formic acid is comparable in strength to nitrous acid, the spontaneous "neutral" reaction is not caused by traces of nitrous acid in the reaction mixture.

Salt Effects: (1) Strong Acids

The effect of added salts (lithium perchlorate and lithium chloride) on the reactions catalyzed by hydrochloric and perchloric acids in 1-propanol are given in Table IV.

TABLE IV

Salt effects on catalysis by strong acids at 25°
$[R^*ONO]_0 \simeq 0.6$ M; $[HClO_4] = 6.5\times10^{-5}$ M; solvent: 1-propanol

Lithium chloride		Lithium perchlorate	
[Salt] 10^3 M	10^4 k_1 sec^{-1}	[Salt] 10^3 M	10^4 k_1 sec^{-1}
0	7.0	0	7.0
.99	10.2	3.11	9.9
1.44	11.6	4.69	11.0
2.52	13.1	6.70	11.2
4.10	14.4		
4.72	14.6		
9.02	14.5		

Can. J. Chem. Downloaded from www.nrcresearchpress.com by 210.87.254.5 on 09/05/12
For personal use only.

Lithium chloride has a much greater effect on the rate than lithium perchlorate, but the increase in rate is not linear with respect to concentration. The rate reaches a maximum value at about 4×10^{-3} *M* chloride ion, i.e. at about 60 times the concentration of acid used. It is not possible, on the basis of these few results, to attempt a full analysis of these salt effects, but the results are at least consistent with (*a*) significant catalysis by chloride ion, as observed in hydrolysis, and (*b*) depression of the hydrogen ion concentration by its association with chloride ion to form hydrogen chloride. The results obtained are consistent with a dissociation constant of between $3–4\times10^{-3}$ for hydrogen chloride in this medium. Owen and Waters (12) give a value of 2×10^{-4} for this acid in 82% dioxane–water, which has a lower dielectric constant than 1-propanol.

Salt Effects: (2) Trichloroacetic Acid

Addition of lithium chloride and lithium perchlorate to reactions catalyzed by trichloroacetic acid in 1-propanol and 2-methyl-2-butanol gave the following results (Table V).

TABLE V

Salt effects on catalysis by trichloroacetic acid at 25°

1-Propanol				2-Methyl-2-butanol			
[Acid] = 2.5×10^{-3} *M*				[Acid] = 2.8×10^{-3} *M*			
[LiCl] 10^3 *M*	$10^4 k_1$ sec^{-1}	[$LiClO_4$] 10^3 *M*	$10^4 k_1$ sec^{-1}	[LiCl] 10^3 *M*	$10^4 k_1$ sec^{-1}	[$LiClO_4$] 10^3 *M*	$10^4 k_1$ sec^{-1}
0	2.10	0	2.10	0	0.95	0	0.95
0.98	3.60	1.68	3.75	0.50	4.67	0.79	1.85
1.70	4.95	3.03	4.90	1.01	7.45	1.61	2.15
2.42	6.25	4.16	6.15	1.26	10.55	2.32	3.20
				1.62	12.5	2.95	3.75

NOTE: $[R^*ONO]_0 \simeq 0.5$ *M*.

Addition of lithium perchlorate produces an increase in rate in both alcohols, the relative increase being greater in the tertiary alcohol. These increases are presumably due to an increase in the dissociation of the weak acid with increasing ionic strength of the medium, and would be expected to be greater in the medium of lower dielectric constant.

Addition of lithium chloride produces a greater effect in both solvents, but the effect is particularly marked in the tertiary alcohol. This is consistent with catalysis by chloride ion, which would be greater in the system involving the combination of a greater concentration of the protonated ester and a weaker nucleophilic reagent. It was argued earlier that the reaction in the tertiary alcohol fulfills both these requirements in comparison with the reaction in the primary alcohol.

Effect of Added Water on the Acid-Catalyzed Reaction

The difference in the rates of the acid-catalyzed reactions in the primary and tertiary alcohols was attributed to a marked difference in the basicity of the reagents. If this is so, then the addition of a small amount of a very much more basic substance to the reaction mixture should decrease the rate strongly, and should have the most marked effect on the system involving the weakest base. Since water is very much more basic

Can. J. Chem. Downloaded from www.nrcresearchpress.com by 210.87.254.5 on 09/05/12
For personal use only.

than these alcohols, addition of small amounts of water to the reaction mixture will set up the following equilibria, which will be displaced strongly towards the right:

$$R'OH_2^+ + H_2O \rightleftarrows R'OH + H_3O^+,$$
$$R^*ONOH^+ + H_2O \rightleftarrows R^*ONO + H_3O^+.$$

Thus addition of water should result in a decrease in the concentration of the protonated nitrite, which will retard the reaction rate strongly, provided that the concentration of water is sufficiently low to prevent its being able to act significantly as a nucleophilic reagent. In this connection it has been shown (10) that addition of water to dilute alcoholic solutions of strong acids decreases the conductivity, the decrease being linear with water concentration up to about 1% water, above which concentration the conductivity begins to increase.

The effect of addition of small amounts of water on the reaction in 1-propanol, 1-pentanol, and 2-methyl-2-butanol, catalyzed by perchloric acid, is shown in Fig. 1.

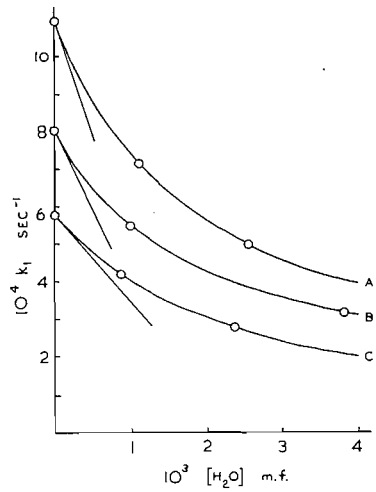


FIG. 1. Effect of added water on acid catalysis. First-order rate constants at 25° in A = 2-methyl-2-butanol, B = 1-propanol, and C = 1-pentanol, at constant (5.66×10^{-6}) acid mole fraction.

Significant decreases in rate were observed even at very low (10^{-3} *M*) concentrations of water. From the smooth curves obtained it is possible to estimate the slope at zero water concentration. The steepest slope occurs with the least basic alcohol, 2-methyl-2-butanol, and it appears that 1-pentanol is more basic than 1-propanol. These results, together with the effects of added salts, provide strong support for the argument that the basicity of the reagents is one of the important factors in these reactions. They also emphasize the importance of carrying out any alcoholysis reaction rate studies in perfectly dry solvents, since random traces of water would completely invalidate any results obtained.

EXPERIMENTAL

(1) Materials

Octan-2-ol was resolved into its (+) and (−) optical isomers, (+)- and (−)-1-methylheptyl nitrite was prepared and purified, and all solvents and reagents were purified and dried as described previously (1).

Can. J. Chem. Downloaded from www.nrcresearchpress.com by 210.87.254.5 on 09/05/12
For personal use only.

(2) Optical Rotations of Reaction Mixtures

The results previously reported (1) were used to determine the progress of the various reactions from changes in optical rotation and in the calculation of rate constants.

(3) Kinetic Measurements

All operations were carried out in an atmosphere of dry nitrogen. The (+)- or (−)-1-methylheptyl nitrite and the reagent alcohol were separately brought to thermostat temperature (25°) and then mixed. After allowing 1–2 minutes to regain thermostat temperature the appropriate acid solution was added at zero time. The mixture was then transferred rapidly to the polarimeter tube, using a self-sealing rubber diaphragm cap. Changes in optical rotation (sodium D line) with time were observed, the following being typical examples:

Example 1

$[R^*ONO]_0 = 0.560\ M$ $[HCl] = 5.26\times10^{-5}\ M$ 25° Solvent = 1-propanol

Time (min)	2	4	6	8	10	15	20	25	30	40	∞
α_D	.700	.755	.800	.840	.895	.960	1.035	1.085	1.135	1.24	1.42

$k_1 = 5.48\times10^{-4}\ sec^{-1}$

Example 2

$[R^*ONO]_0 = 0.574\ M$ $[HClO_4] = 6.60\times10^{-5}\ M$ 25° Solvent: 2-methyl-2-butanol

Time (min)	2½	4	6	8	10	12	17	21	50	∞
α_D	.805	.865	.940	.995	1.045	1.075	1.145	1.170	1.220	1.220

$k_1 = 15.5\times10^{-4}\ sec^{-1}$

Example 3

$[R^*ONO]_0 = 0.611\ M$ $[HClO_4] = 6.20\times10^{-5}\ M$ $[H_2O] = 0.047\ M$ 25° Solvent: 1-propanol

Time (min)	2¼	4	9	15½	22	30	45	60	73	∞
α_D	0.735	.78	.85	.925	.995	1.075	1.185	1.280	1.335	1.545

$k_1 = 3.07\times10^{-4}\ sec^{-1}$

REFERENCES

1. A. D. ALLEN and G. R. SCHONBAUM. Can. J. Chem. In press.
2. A. D. ALLEN. J. Chem. Soc. 1968 (1954).
3. R. M. BADGER and S. H. BAUER. J. Chem. Phys. **5**, 839 (1937).
4. S. R. PHADKE, N. L. PHALNIKAR, and B. V. BHIDE. J. Indian Chem. Soc. **22**, 239 (1945).
5. W. GORDY and S. C. STANFORD. J. Chem. Phys. **8**, 170 (1940); **9**, 204 (1941).
6. W. GORDY. J. Chem. Phys. **7**, 93 (1939); **9**, 215 (1941).
7. B. O. HESTON and N. F. HALL. J. Am. Chem. Soc. **56**, 1463 (1934).
8. P. D. BARTLETT and J. D. MCCOLLUM. J. Am. Chem. Soc. **78**, 1441 (1956).
9. H. C. BROWN, H. BARTHOLOMAY, and M. D. TAYLOR. J. Am. Chem. Soc. **66**, 435 (1944).
10. D. M. MURRAY-RUST and H. HARTLEY. Proc. Roy. Soc. A, **126**, 84 (1929).
11. R. B. MASON and M. KILPATRICK. J. Am. Chem. Soc. **59**, 572 (1937).
12. B. B. OWEN and G. W. WATERS. J. Am. Chem. Soc. **60**, 2371 (1938).

Can. J. Chem. Downloaded from www.nrcresearchpress.com by 210.87.254.5 on 09/05/12
For personal use only.

Can. J. Chem. Downloaded from www.nrcresearchpress.com by 210.87.254.40 on 09/05/12
For personal use only.

ISOTOPE EFFECTS IN CARBONIUM ION REACTIONS
V. SOLVOLYSIS OF METHYL AND ETHYL *p*-BROMOBENZENESULPHONATES

EDWARD S. LEWIS, JUDITH C. BROWN, AND WILLIAM C. HERNDON

It has been suggested that various secondary hydrogen isotope effects in solvolytic reactions are related to changes in hyperconjugation (1), to alterations in vibrational frequencies on change of hybridization (2), and to changes in extent of non-bonded interactions (3) on activation. Among the data leading to these conclusions were those showing solvent dependence of the effect of β-hydrogens on solvolysis rates (4). The reverse hydrogen isotope effects (5) in the reactions of methyl esters were attributed to increases in bending force constants resulting from steric interactions of the methyl hydrogens with the attacking and leaving groups, and this suggestion was supported by more extensive studies on the reactions of methyl halides in water (6).

Table I shows some rates and isotope effects for the solvolysis of methyl and ethyl

TABLE I

Isotope effects in solvolysis of methyl and ethyl *p*-bromobenzenesulphonates

Alkyl group*	Solvent	Temp., °C	$k_H \times 10^5$ sec^{-1}	k_H/k_D
CD_3CH_2†	CH_3CO_2H	116.8	10.56	1.01
CH_3CD_2‡	CH_3CO_2H	100	2.72	1.09±.03
CH_3CD_2‡	CH_3OH	56.2	3.25	1.04±.01
CD_3	CH_3CO_2H	100	2.66	0.92±.03
CD_3§	CH_3OH	70.25	25.13‖	0.940‖

*Alkyl groups are shown with deuterium. Reference compounds for which k_H is reported are normal methyl or ethyl *p*-bromobenzenesulphonates. †Deuterium analysis not precise, at least 75% deuterated. ‡Deuterium analysis not precise, almost no CH_2 n.m.r. spectrum visible. §2.88 D per molecule by mass spectra. ‖R. R. Johnson. Ph.D. Thesis, William M. Rice University, Houston, Texas. 1958, and ref. 5.

p-bromobenzenesulphonates in two solvents of widely differing nucleophilic character. These results can be shown to be consistent with explanations in terms of either electronic or essentially steric factors. We need only assume that there is virtually no carbonium ion character in any methyl ester solvolytic transition state, but that the transition state for the ethyl compound has a little carbonium ion character in acetic acid but less in the more nucleophilic methanol. This assumption then leads to the prediction that the isotope effect with methyl *p*-bromobenzenesulphonate will be insensitive to solvent, whereas in the ethyl case the value of k_H/k_D should increase as the nucleophilic character of the solvent decreases. The values in the table, although not highly precise, support this idea. The very small effect on β-substitution also is consistent with only minor carbonium ion character, even in acetic acid. This result is the same as that reported recently for water solutions (7).

EXPERIMENTAL

Materials

Ethyl *p*-bromobenzenesulphonate was prepared from the alcohol by conventional procedures (8). Ethanol-2-d_3 was prepared by the lithium aluminum hydride reduction of sodium acetate-d_3 (Isotopes Specialties Corp.). A rather crude deuterium analysis by

combustion indicated 75% D in the β-position, but the n.m.r. spectrum indicated a much larger extent of deuteration.

Ethanol-1-d_2 was prepared by the reduction of cyclohexyl acetate with sodium and acetic acid-*d* in dibutyl ether (9). Infrared and n.m.r. showed nearly complete deuteration, but the exact extent is not established.

Methyl-d_3 *p*-bromobenzenesulphonate was prepared by R. R. Johnson, by the sequence

$$\text{methyl bromide-}d_3\ (10) \xrightarrow[\text{acetone}]{\text{NaI}} \text{methyl iodide-}d_3 \rightarrow \text{methyl-}d_3\ p\text{-bromobenzenesulphonate,}$$

using silver *p*-bromobenzenesulphonate. It was the same material reported in ref. 5.

Rate Measurements

All rates were measured by titration of the acid produced using an electrometric end point by familiar methods. Solvents were Reagent Grade materials and the hydrogen and deuterium compounds were run concurrently to avoid errors attributable to variations in water content of the solvents, thermostat temperatures, and the clock. The rates in Table I are therefore not known absolutely as well as are the isotope effects. All entries are the averages of at least two runs, agreeing in isotope effect within the estimated precision.

1. E. S. Lewis. Tetrahedron, **5**, 143 (1959); V. J. Shiner, Jr. Tetrahedron, **5**, 243 (1959).
2. A. Streitwieser, Jr., R. H. Jagow, R. C. Fahey, and S. Suzuki. J. Am. Chem. Soc. **80**, 2326 (1958).
3. L. S. Bartell. Tetrahedron Letters, **6**, 13 (1960).
4. E. S. Lewis and C. E. Boozer. J. Am. Chem. Soc. **76**, 791 (1954).
5. R. R. Johnson and E. S. Lewis. Proc. Chem. Soc. 52 (1958).
6. J. A. Llewellyn, R. E. Robertson, and J. M. W. Scott. Can. J. Chem. **38**, 222 (1960).
7. K. T. Leffek, J. A. Llewellyn, and R. E. Robertson. Can. J. Chem. **38**, 2171 (1960).
8. W. F. Edgell and L. Parts. J. Am. Chem. Soc. **77**, 4899 (1955).
9. D. G. Hill, W. A. Judge, P. S. Skell, S. W. Kantor, and C. R. Hauser. J. Am. Chem. Soc. **74**, 5599 (1952); A. Streitwieser, Jr. and W. D. Schaeffer. J. Am. Chem. Soc. **78**, 5597 (1956).
10. R. Renaud and L. C. Leitch. Can. J. Chem. **34**, 179 (1956).

Received January 10, 1961.
The Department of Chemistry,
William M. Rice University,
Houston, Texas.

ARSENIDES OF THE TRANSITION METALS
IV. A NOTE ON THE PLATINUM METAL ARSENIDES*

R. D. Heyding and L. D. Calvert

In the current literature increasing attention is given to the binary compounds formed by the VA elements (pnigogens†) and the platinum metals. Rundqvist has undertaken a systematic study of the phosphides (1), and Zhuravlev and Zhdanov the antimonides and bismuthides (e.g., 2, 3, 4). To our knowledge there are no reports on the formation and structure of platinum metal arsenides, with the exception of Thomassen's early study of palladium and platinum arsenides (5), Schubert's recent note on the compound Pd_3As

Issued as N.R.C. No. 6197.

†*The terms pnigogen and pnictide have been suggested by Prof. A. E. van Arkel for the elements and compounds of the nitrogen family, N, P, As, Sb, and Bi. The root is the Greek word to choke, and the allusion to the Germanic name for nitrogen, Stickstoff, or choking gas.*

Can. J. Chem. Downloaded from www.nrcresearchpress.com by 210.87.254.40 on 09/05/12
For personal use only.

combustion indicated 75% D in the β-position, but the n.m.r. spectrum indicated a much larger extent of deuteration.

Ethanol-1-d_2 was prepared by the reduction of cyclohexyl acetate with sodium and acetic acid-d in dibutyl ether (9). Infrared and n.m.r. showed nearly complete deuteration, but the exact extent is not established.

Methyl-d_3 p-bromobenzenesulphonate was prepared by R. R. Johnson, by the sequence

$$\text{methyl bromide-}d_3\ (10) \xrightarrow[\text{acetone}]{\text{NaI}} \text{methyl iodide-}d_3 \rightarrow \text{methyl-}d_3\ p\text{-bromobenzenesulphonate,}$$

using silver p-bromobenzenesulphonate. It was the same material reported in ref. 5.

Rate Measurements

All rates were measured by titration of the acid produced using an electrometric end point by familiar methods. Solvents were Reagent Grade materials and the hydrogen and deuterium compounds were run concurrently to avoid errors attributable to variations in water content of the solvents, thermostat temperatures, and the clock. The rates in Table I are therefore not known absolutely as well as are the isotope effects. All entries are the averages of at least two runs, agreeing in isotope effect within the estimated precision.

1. E. S. Lewis. Tetrahedron, **5**, 143 (1959); V. J. Shiner, Jr. Tetrahedron, **5**, 243 (1959).
2. A. Streitwieser, Jr., R. H. Jagow, R. C. Fahey, and S. Suzuki. J. Am. Chem. Soc. **80**, 2326 (1958).
3. L. S. Bartell. Tetrahedron Letters, **6**, 13 (1960).
4. E. S. Lewis and C. E. Boozer. J. Am. Chem. Soc. **76**, 791 (1954).
5. R. R. Johnson and E. S. Lewis. Proc. Chem. Soc. 52 (1958).
6. J. A. Llewellyn, R. E. Robertson, and J. M. W. Scott. Can. J. Chem. **38**, 222 (1960).
7. K. T. Leffek, J. A. Llewellyn, and R. E. Robertson. Can. J. Chem. **38**, 2171 (1960).
8. W. F. Edgell and L. Parts. J. Am. Chem. Soc. **77**, 4899 (1955).
9. D. G. Hill, W. A. Judge, P. S. Skell, S. W. Kantor, and C. R. Hauser. J. Am. Chem. Soc. **74**, 5599 (1952); A. Streitwieser, Jr. and W. D. Schaeffer. J. Am. Chem. Soc. **78**, 5597 (1956).
10. R. Renaud and L. C. Leitch. Can. J. Chem. **34**, 179 (1956).

Received January 10, 1961.
The Department of Chemistry,
William M. Rice University,
Houston, Texas.

ARSENIDES OF THE TRANSITION METALS
IV. A NOTE ON THE PLATINUM METAL ARSENIDES*

R. D. Heyding and L. D. Calvert

In the current literature increasing attention is given to the binary compounds formed by the VA elements (pnigogens†) and the platinum metals. Rundqvist has undertaken a systematic study of the phosphides (1), and Zhuravlev and Zhdanov the antimonides and bismuthides (e.g., 2, 3, 4). To our knowledge there are no reports on the formation and structure of platinum metal arsenides, with the exception of Thomassen's early study of palladium and platinum arsenides (5), Schubert's recent note on the compound Pd_3As

Issued as N.R.C. No. 6197.

†*The terms pnigogen and pnictide have been suggested by Prof. A. E. van Arkel for the elements and compounds of the nitrogen family, N, P, As, Sb, and Bi. The root is the Greek word to choke, and the allusion to the Germanic name for nitrogen, Stickstoff, or choking gas.*

Can. J. Chem. Downloaded from www.nrcresearchpress.com by 210.87.254.42 on 09/05/12
For personal use only.

(6), and Kjekshus' redetermination of the unit cell dimensions of $PtAs_2$ (7). We have prepared binary alloys corresponding to M_3As, M_2As, MAs, MAs_2, and MAs_3 with all of the platinum metals, and have examined their structures by X-ray powder diffraction techniques. The results of this preliminary survey are reported here.

All alloys were formed by reaction of the elements in sealed vycor tubes at 700° C in the usual manner. High-purity metal sponge was obtained from Baker Platinum, and semiconductor grade arsenic from ASARCO and COMINCO. The products were ground and annealed for a minimum of 2 days at 700° C and cooled slowly to room temperature. Debye–Scherrer patterns were obtained in 11-cm Norelco cameras using copper K_α radiation.

Two compounds are formed in the ruthenium/arsenic system: RuAs, with the orthorhombic B31 (MnP) structure, and $RuAs_2$, with the orthorhombic C18 (marcasite) structure. With the single annealing scheme followed no other compounds could be detected.

$OsAs_2$, also with the marcasite structure, was the only compound observed in the osmium/arsenic system.

At least four compounds are formed in the rhodium/arsenic system: The compound Rh_2As has the f.c.c. C1 (antifluorite) structure; RhAs, the orthorhombic B31 structure; and $RhAs_3$ the cubic DO_2 (skutterudite) structure. The structure of the fourth compound, $RhAs_2$, is complicated and as yet unknown.

Iridium and arsenic form $IrAs_3$ with the cubic DO_2 structure. In this system there are two other phases, the diarsenide $IrAs_2$ whose structure has not been determined, and apparently one other compound in the composition region between $IrAs_2$ and $IrAs_3$.

There are at least two compounds in the palladium/arsenic system. Pd_3As has the b.c. tetragonal Fe_3P structure, which confirms Schubert's description, and $PdAs_2$ has the cubic C2 (pyrite) lattice, in agreement with Thomassen's data. A complicated series of phases has been observed in the region between Pd_3As and Pd_2As.

Only one compound has been obtained in the platinum/arsenic system, $PtAs_2$ with the C2 structure, again in agreement with Thomassen's data.

Unit cell dimensions for the compounds whose structures have been identified are given in Table I.

TABLE I

Structures and unit cell dimensions of platinum metal arsenides

Structure type	Compound	a (Å)	b (Å)	c (Å)	Ref.
Tetragonal DO_e (Fe_3P) S_4^2, $I\bar{4}$	Pd_3As	$9.95_1\pm0.01$ (9.98_6)		$4.81_7\pm0.01$ (4.83_6)	(6)
Cubic C1 (antifluorite) O_h^5, $Fm3m$	Rh_2As	5.674 ± 0.001			
Rhombic B31 (MnP) V_h^{16}, $Pnma$	RuAs	5.70 ± 0.01	3.25 ± 0.01	6.27 ± 0.01	
	RhAs	5.62 ± 0.01	3.58 ± 0.01	6.00 ± 0.01	
Rhombic C18 (marcasite) V_h^{12}, $Pnnm$	$RuAs_2$	5.41 ± 0.01	6.17 ± 0.01	2.96 ± 0.01	
	$OsAs_2$	5.40 ± 0.01	6.16 ± 0.01	3.00 ± 0.01	
Cubic C2 (pyrite) T_h^6, $Pa3$	$PdAs_2$	5.983 ± 0.001 (5.970)*			(5)
	$PtAs_2$	5.966 ± 0.001 (5.957)*			(5)
		(5.9665)			(7)
Cubic DO_2 (skutterudite) T_h^5, $Im3$	$RhAs_3$	8.453 ± 0.001			
	$IrAs_3$	8.467 ± 0.001			

*Thomassen's values are probably in kX units.

Can. J. Chem. Downloaded from www.nrcresearchpress.com by 210.87.254.42 on 09/05/12
For personal use only.

It is remarkable that all of the 1:1 compounds crystallize in the distorted NiAs (MnP) structure rather than the NiAs structure itself. In the palladium and platinum systems where one might anticipate the NiAs structure no 1:1 compounds were obtained.

The diphosphides, diarsenides, and diantimonides of ruthenium and osmium have the marcasite structure, while the corresponding compounds of palladium and platinum have the pyrite structure. The rather complicated diffraction patterns of $RhAs_2$ and $IrAs_2$ are most certainly related, and bear a distinct similarity to the pattern of $CoAs_2$ (8). A strong low-order reflection in the $CoAs_2$ pattern is split in the $RhAs_2$ and $IrAs_2$ patterns; this leads us to doubt the orthorhombic cell we proposed earlier for $CoAs_2$. These diarsenides may prove to be isostructural with the rhodium and iridium diphosphides mentioned by Rundqvist.

Since the triphosphides and triantimonides of cobalt, rhodium, and iridium are known to have the cubic $CoAs_3$ structure, it is not surprising that $RhAs_3$ and $IrAs_3$ have the same structure. The list of compounds crystallizing in the skutterudite system now stands at 11, and insofar as binary pnictides are concerned, can be considered to be complete. With the exception of NiP_3 and PdP_3 they are formed only by the cobalt family of transition metals. Bismuthides with this structure have not been observed.

These systems are now being studied in some detail.

We are indebted to Miss M. McClellan and Mr. G. J. G. Despault for their assistance in preparing alloys and obtaining diffraction patterns.

1. S. Rundqvist. Nature, **185**, 31 (1960).
2. N. N. Zhuravlev and G. S. Zhdanov. Zhur. Eksptl. i Teoret. Fiz. **25**, 485 (1953).
3. N. N. Zhuravlev and L. Kertes. Zhur. Eksptl. i Teoret. Fiz. **32**, 1313 (1957).
4. R. N. Kuz'min, N. N. Zhuravlev, and S. A. Losievskaya. Soviet Physics Crystallography, **5**, 202 (1960).
5. L. Thomassen. Z. physik. Chem. B, **4**, 279 (1929).
6. K. Schubert, S. Bahn, W. Burkhardt, R. Gohle, H. G. Meissner, M. Pötzschke, and E. Stolz. Naturwiss. **13**, 303 (1960).
7. A. Kjekshus. Acta Chem. Scand. **14**, 1450 (1960).
8. R. D. Heyding and L. D. Calvert. Can. J. Chem. **38**, 313 (1960).

Received December 29, 1960.
Division of Applied Chemistry,
National Research Council,
Ottawa, Canada.

SOLVATION EFFECTS AND RELATIVE RATES
III. SALT EFFECTS IN THE SOLVOLYSIS OF exo-NORBORNYL BROMIDE*

Kirk D. McMichael and Robert A. Clement

As part of our study of solvation effects in organic reactions (1, 2), it seemed desirable to examine the nature of the kinetic salt effect for a simple organic reaction in a typical organic solvent. The system we chose for study was exo-norbornyl bromide in 85% (w/w) aqueous dioxane at 25.06°, and our approach was that used in an earlier paper (1) in which analysis of kinetic and thermodynamic data is in terms of the Bronsted rate law (3).

**This paper is abstracted from a portion of the Ph.D. dissertation of Kirk D. McMichael, University of Chicago, 1960, and was presented before the Organic Division, American Chemical Society, at the 138th National Meeting, New York, September 11–16, 1960.*

Can. J. Chem. Downloaded from www.nrcresearchpress.com by 210.87.254.42 on 09/05/12
For personal use only.

It is remarkable that all of the 1:1 compounds crystallize in the distorted NiAs (MnP) structure rather than the NiAs structure itself. In the palladium and platinum systems where one might anticipate the NiAs structure no 1:1 compounds were obtained.

The diphosphides, diarsenides, and diantimonides of ruthenium and osmium have the marcasite structure, while the corresponding compounds of palladium and platinum have the pyrite structure. The rather complicated diffraction patterns of $RhAs_2$ and $IrAs_2$ are most certainly related, and bear a distinct similarity to the pattern of $CoAs_2$ (8). A strong low-order reflection in the $CoAs_2$ pattern is split in the $RhAs_2$ and $IrAs_2$ patterns; this leads us to doubt the orthorhombic cell we proposed earlier for $CoAs_2$. These diarsenides may prove to be isostructural with the rhodium and iridium diphosphides mentioned by Rundqvist.

Since the triphosphides and triantimonides of cobalt, rhodium, and iridium are known to have the cubic $CoAs_3$ structure, it is not surprising that $RhAs_3$ and $IrAs_3$ have the same structure. The list of compounds crystallizing in the skutterudite system now stands at 11, and insofar as binary pnictides are concerned, can be considered to be complete. With the exception of NiP_3 and PdP_3 they are formed only by the cobalt family of transition metals. Bismuthides with this structure have not been observed.

These systems are now being studied in some detail.

We are indebted to Miss M. McClellan and Mr. G. J. G. Despault for their assistance in preparing alloys and obtaining diffraction patterns.

1. S. Rundqvist. Nature, **185**, 31 (1960).
2. N. N. Zhuravlev and G. S. Zhdanov. Zhur. Eksptl. i Teoret. Fiz. **25**, 485 (1953).
3. N. N. Zhuravlev and L. Kertes. Zhur. Eksptl. i Teoret. Fiz. **32**, 1313 (1957).
4. R. N. Kuz'min, N. N. Zhuravlev, and S. A. Losievskaya. Soviet Physics Crystallography, **5**, 202 (1960).
5. L. Thomassen. Z. physik. Chem. B, **4**, 279 (1929).
6. K. Schubert, S. Bahn, W. Burkhardt, R. Gohle, H. G. Meissner, M. Pötzschke, and E. Stolz. Naturwiss. **13**, 303 (1960).
7. A. Kjekshus. Acta Chem. Scand. **14**, 1450 (1960).
8. R. D. Heyding and L. D. Calvert. Can. J. Chem. **38**, 313 (1960).

Received December 29, 1960.
Division of Applied Chemistry,
National Research Council,
Ottawa, Canada.

SOLVATION EFFECTS AND RELATIVE RATES
III. SALT EFFECTS IN THE SOLVOLYSIS OF exo-NORBORNYL BROMIDE*

Kirk D. McMichael and Robert A. Clement

As part of our study of solvation effects in organic reactions (1, 2), it seemed desirable to examine the nature of the kinetic salt effect for a simple organic reaction in a typical organic solvent. The system we chose for study was exo-norbornyl bromide in 85% (w/w) aqueous dioxane at 25.06°, and our approach was that used in an earlier paper (1) in which analysis of kinetic and thermodynamic data is in terms of the Bronsted rate law (3).

**This paper is abstracted from a portion of the Ph.D. dissertation of Kirk D. McMichael, University of Chicago, 1960, and was presented before the Organic Division, American Chemical Society, at the 138th National Meeting, New York, September 11–16, 1960.*

Can. J. Chem. Downloaded from www.nrcresearchpress.com by 210.87.254.40 on 09/05/12
For personal use only.

Can. J. Chem. Downloaded from www.nrcresearchpress.com by 210.87.254.40 on 09/05/12
For personal use only.

Existing information (4, 5) on the solvolyses of exo-norbornyl derivatives indicates the operation of unimolecular reactions possibly complicated, however, by internal return from a reactive ion-pair intermediate. Hence, the appropriate form of the Bronsted rate law for the system under study is equation [1] (1, 6)

$$k'/k = (H'/H)F$$

where k is the observed first-order specific rate constant for the production of acid, H is the Henry's law constant for distribution of exo-norbornyl bromide between the solution and the gas phase, F is a factor of constitution dependent upon the precise course of reaction (1), the primed symbols refer to a salt solution, and the unprimed symbols to the reference solution, the pure solvent. The ratio k'/k is the total kinetic salt effect and the ratio H'/H is that portion of the kinetic salt effect due to the influence of salt on the activity coefficient of the substrate. It is the factor F, alone, which yields information on the effect of salt upon the stability(ies) of the critical complex(es); in general, it will be greater than unity if salt stabilizes the critical complex(es) and less than unity if salt destabilizes the critical complex(es).

In the present study, initial first-order specific rate constants, k, for the production of strong acid were obtained for solutions of exo-norbornyl bromide in 85% (w/w) aqueous dioxane in the absence of salt and in the presence of lithium chloride, bromide, and perchlorate and sodium perchlorate at concentrations of 0.100 M and of magnesium perchlorate at a concentration of 0.0333 M. The results are recorded in Table I. From

TABLE I

First-order specific rate constants for the development of acid, Henry's law constants for exo-norbornyl bromide, and related data for exo-norbornyl bromide in 85% (w/w) aqueous dioxane at 25.06° in the presence of various salts at ionic strengths of 0.100 molar

Salt	$10^5 k$, sec^{-1}	H, $mm(mole/l.)^{-1}$	p_{H_2O}, mm	$p_{dioxane}$, mm	k'/k	H'/H	F
None	3.57	0.72	18.5	29.1	(1.000)	(1.000)	(1.000)
LiCl	5.0	0.68	17.7	29.4	1.40	0.94	1.49
LiBr	5.2	0.69	17.9	29.4	1.46	0.96	1.52
$LiClO_4$	7.4	0.72	18.1	29.2	2.07	1.00	2.07
$NaClO_4$	7.0	0.71	18.1	29.0	1.96	0.99	1.98
$Mg(ClO_4)_2$	6.2	0.70	18.1	29.0	1.74	0.97	1.80

the ratios k'/k it is apparent that the solvolysis of exo-norbornyl bromide in this solvent is subject to very large kinetic salt effects.

Henry's law constants, H, for the distribution of exo-norbornyl bromide between the vapor phase and the same solutions utilized for the kinetic experiments were obtained by the dynamic vapor pressure technique essentially as described earlier (2), and are also recorded in Table I. The Henry's law constant for exo-norbornyl bromide in this solvent is *essentially insensitive to the presence of salts.*

Although irrelevant to the use of equation [1], the vapor pressures of water (p_{H_2O}) and of dioxane ($p_{dioxane}$) above the various solutions were obtained, necessarily, during the measurements of the Henry's law constants and are recorded in Table I. They are also insensitive to the presence of salts.

Consideration of the entries in Table I in terms of equation [1] shows clearly that for the solvolysis of exo-norbornyl bromide in 85% (w/w) aqueous dioxane the kinetic salt effect is due, almost exclusively, to the factor F. In this system, then, it is proper to

regard the kinetic salt effect as a reflection of the nature of the critical complex(es), and the usual qualitative deduction that a positive kinetic salt effect identifies a critical complex that is more ionic than the reactant is completely justified.

It should be noted that the result of this study stands in marked contrast to the results of previous studies (1, 6, 7, 8, 9, 10, 11) where, in every case, the ratio H'/H was found to make a significant contribution to the over-all kinetic medium effect, k'/k. Further investigation is necessary to ascertain whether this result is general for reactions in mixed aqueous–organic media or is due to a peculiarity of the present system.

EXPERIMENTAL

Kinetic and thermodynamic measurements were made at a temperature of 25.06+0.02° as established by an N.B.S.-calibrated thermometer.

Materials

Anhydrous salts were prepared from commercial reagent-grade materials which were dried to constant weight in an oven at the appropriate temperatures and were stored in a desiccator over anhydrous magnesium perchlorate.

Dioxane was purified by the method of Fieser (12) and was stored frozen, in the dark and under nitrogen, in glass-stoppered bottles which were sealed with paraffin.

exo-Norbornyl bromide (exo-2-bromobicyclo[2.2.1]heptane) was prepared by the method of Roberts (13) from purified norbornene, m.p. 43–44°, sealed cap. (lit. (14) m.p. 44–46°). In order to remove reactive impurities, the exo-norbornyl bromide (b.p. 81.0–81.8° (30 mm)) obtained initially was mixed with ethylene glycol and heated on the steam bath for 20 minutes, at the end of which ca. 25% (by acidimetry) of the bromide had been destroyed. The mixture was then poured into water, the organic layer was isolated, washed twice with water, and dried over magnesium sulphate. Distillation afforded pure exo-norbornyl bromide, b.p. 78.7–79.5° (29 mm), n_D^{25} 1.5124 (lit. (13) b.p. 82° (29 mm), n_D^{25} 1.5126). The kinetic homogeneity of the material was demonstrated by solvolysis of a sample in 80% (v/v) aqueous ethanol at the boiling point of acetone. Precise conformation to first-order kinetics was observed with a specific rate constant of 5.3×10^{-5} sec^{-1} (lit. (15) $k = 5.6\times10^{-5}$ sec^{-1} at 55°) and an experimental infinity titer (10 half lives) 98% of the calculated value.

Kinetic and Vapor Pressure Measurements

Kinetic and vapor pressure measurements were made in tandem on portions of the same solution which was prepared by diluting to volume with freshly prepared solvent (85 parts of dioxane and 25 parts of water, by wt.) weighed amounts of exo-norbornyl bromide and anhydrous salt. The final solutions were all 0.100±0.001 M in exo-norbornyl bromide and the salt solutions possessed molar ionic strengths of 0.100±0.001. Solvent was prepared as required for each run, and as a check on the reproducibility of its composition, the kinetic behavior of exo-norbornyl bromide was determined in each preparation; the average deviation of the first-order specific rate constants obtained from 12 such determinations was less than 2%.

The rate of development of strong acid was followed titrimetrically as before (2), the reactions being followed to 1.5–5% completion. First-order specific rate constants were determined by the increment method (1), plotted vs. % reaction and extrapolated back to 0% to yield the initial first-order specific rate constants, k, reported in Table I. Each k in Table I is the average of at least two runs involving different batches of solution and possesses an average deviation of 2–4%. The slopes of the plots of the first-order

Can. J. Chem. Downloaded from www.nrcresearchpress.com by 210.87.254.40 on 09/05/12
For personal use only.

specific rate constants vs. % reaction were all close to zero, and in most cases the average rate constant was within the limits defined by the average deviation of the extrapolated value.

Vapor pressure measurements were made by the dynamic method essentially as described before (2) except that nitrogen was the entraining gas and that mass flow was induced by a hydrostatic head of mercury which could not exceed 1 mm. The contents of the distillate trap was analyzed for exo-norbornyl bromide by precipitation of silver bromide with acidic aqueous ethanolic silver nitrate and for water by the Karl Fischer technique; dioxane was determined by difference. The values of the Henry's law constant, H, for exo-norbornyl bromide, and of the partial pressures of water, p_{H_2O}, and of dioxane, p_{dioxane}, obtained for each solution are recorded in Table I as the averages of at least two separate determinations which involved different flow rates (6.5–9.5 l./hr) of the entraining gas and different batches of solution. The average deviations noted were 1–2%.

ACKNOWLEDGMENTS

It is a pleasure to acknowledge the support of this work by the National Science Foundation under grants no. G-5116 and G-12305.

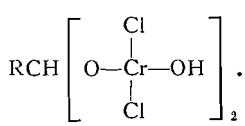
1. R. A. CLEMENT and M. R. RICE. J. Am. Chem. Soc. **81**, 326 (1959).
2. R. A. CLEMENT, J. N. NAGHIZADEH, and M. R. RICE. J. Am. Chem. Soc. **82**, 2449 (1960).
3. J. N. BRONSTED. Z. physik. Chem. **102**, 169 (1922).
4. S. WINSTEIN and D. TRIFAN. J. Am. Chem. Soc. **74**, 1154 (1952).
5. J. D. ROBERTS, C. C. LEE, and W. H. SAUNDERS, JR. J. Am. Chem. Soc. **76**, 4501 (1954).
6. E. GRUNWALD and S. WINSTEIN. J. Am. Chem. Soc. **70**, 846 (1948)
7. A. R. OLSON and R. S. HALFORD. J. Am. Chem. Soc. **59**, 2644 (1937).
8. M. L. BIRD, E. D. HUGHES, and C. K. INGOLD. J. Chem. Soc. 255 (1943).
9. A. R. OLSON and L. K. J. TONG. J. Am. Chem. Soc. **66**, 1555 (1944).
10. F. A. LONG, F. B. DUNKLE, and W. F. MCDEVIT. J. Phys. Chem. **55**, 829 (1951).
11. E. F. J. DYNSTEE, E. GRUNWALD, and M. L. KAPLAN. J. Am. Chem. Soc. **82**, 5654 (1960).
12. L. F. FIESER. Experiments in organic chemistry. 3rd ed. D. C. Heath & Co., Boston. 1955. p. 284.
13. J. D. ROBERTS, E. R. TRUMBULL, JR., W. BENNETT, and R. ARMSTRONG. J. Am. Chem. Soc. **72**, 3116 (1950).
14. L. M. JOSHEL and L. W. BUTZ. J. Am. Chem. Soc. **63**, 3350 (1941).
15. J. D. ROBERTS, W. BENNETT, and R. ARMSTRONG. J. Am. Chem. Soc. **72**, 3329 (1950).

RECEIVED OCTOBER 26, 1960.
GEORGE HERBERT JONES LABORATORY,
DEPARTMENT OF CHEMISTRY,
UNIVERSITY OF CHICAGO,
CHICAGO 37, ILLINOIS.

KINETICS OF ETARD'S REACTION

R. A. STAIRS AND J. W. BURNS*

The oxidation of toluene and similar compounds to aldehydes by chromyl chloride has been known (1) since Etard's work (1877–1893, see reference 2) but has never been thoroughly understood. It is characterized by the formation of a brown, insoluble substance, readily hydrolyzed to the aldehyde (and inorganic substances). Etard formulated the precipitate:



Note that the oxidation state of chromium is IV (see ref. 7). This structure has been much criticized, but never discredited.

**Department of Chemistry, University of Western Ontario, London, Ont.*

Can. J. Chem. Downloaded from www.nrcresearchpress.com by 210.87.254.40 on 09/05/12
For personal use only.

specific rate constants vs. % reaction were all close to zero, and in most cases the average rate constant was within the limits defined by the average deviation of the extrapolated value.

Vapor pressure measurements were made by the dynamic method essentially as described before (2) except that nitrogen was the entraining gas and that mass flow was induced by a hydrostatic head of mercury which could not exceed 1 mm. The contents of the distillate trap was analyzed for exo-norbornyl bromide by precipitation of silver bromide with acidic aqueous ethanolic silver nitrate and for water by the Karl Fischer technique; dioxane was determined by difference. The values of the Henry's law constant, H, for exo-norbornyl bromide, and of the partial pressures of water, p_{H_2O}, and of dioxane, $p_{dioxane}$, obtained for each solution are recorded in Table I as the averages of at least two separate determinations which involved different flow rates (6.5–9.5 l./hr) of the entraining gas and different batches of solution. The average deviations noted were 1–2%.

ACKNOWLEDGMENTS

It is a pleasure to acknowledge the support of this work by the National Science Foundation under grants no. G-5116 and G-12305.

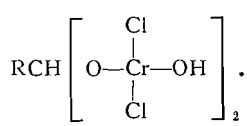
1. R. A. CLEMENT and M. R. RICE. J. Am. Chem. Soc. **81**, 326 (1959).
2. R. A. CLEMENT, J. N. NAGHIZADEH, and M. R. RICE. J. Am. Chem. Soc. **82**, 2449 (1960).
3. J. N. BRONSTED. Z. physik. Chem. **102**, 169 (1922).
4. S. WINSTEIN and D. TRIFAN. J. Am. Chem. Soc. **74**, 1154 (1952).
5. J. D. ROBERTS, C. C. LEE, and W. H. SAUNDERS, JR. J. Am. Chem. Soc. **76**, 4501 (1954).
6. E. GRUNWALD and S. WINSTEIN. J. Am. Chem. Soc. **70**, 846 (1948)
7. A. R. OLSON and R. S. HALFORD. J. Am. Chem. Soc. **59**, 2644 (1937).
8. M. L. BIRD, E. D. HUGHES, and C. K. INGOLD. J. Chem. Soc. 255 (1943).
9. A. R. OLSON and L. K. J. TONG. J. Am. Chem. Soc. **66**, 1555 (1944).
10. F. A. LONG, F. B. DUNKLE, and W. F. MCDEVIT. J. Phys. Chem. **55**, 829 (1951).
11. E. F. J. DYNSTEE, E. GRUNWALD, and M. L. KAPLAN. J. Am. Chem. Soc. **82**, 5654 (1960).
12. L. F. FIESER. Experiments in organic chemistry. 3rd ed. D. C. Heath & Co., Boston. 1955. p. 284.
13. J. D. ROBERTS, E. R. TRUMBULL, JR., W. BENNETT, and R. ARMSTRONG. J. Am. Chem. Soc. **72**, 3116 (1950).
14. L. M. JOSHEL and L. W. BUTZ. J. Am. Chem. Soc. **63**, 3350 (1941).
15. J. D. ROBERTS, W. BENNETT, and R. ARMSTRONG. J. Am. Chem. Soc. **72**, 3329 (1950).

RECEIVED OCTOBER 26, 1960.
GEORGE HERBERT JONES LABORATORY,
DEPARTMENT OF CHEMISTRY,
UNIVERSITY OF CHICAGO,
CHICAGO 37, ILLINOIS.

KINETICS OF ETARD'S REACTION

R. A. STAIRS AND J. W. BURNS*

The oxidation of toluene and similar compounds to aldehydes by chromyl chloride has been known (1) since Etard's work (1877–1893, see reference 2) but has never been thoroughly understood. It is characterized by the formation of a brown, insoluble substance, readily hydrolyzed to the aldehyde (and inorganic substances). Etard formulated the precipitate:



Note that the oxidation state of chromium is IV (see ref. 7). This structure has been much criticized, but never discredited.

**Department of Chemistry, University of Western Ontario, London, Ont.*

Can. J. Chem. Downloaded from www.nrcresearchpress.com by 210.87.254.6 on 09/05/12
For personal use only.

Some mechanisms have been proposed (3, 4) for other reactions of chromyl chloride, but no work has been done on the kinetics or the mechanism of the Etard reaction proper. The present note records an attempt to fill this gap.

EXPERIMENTAL

Three compounds were chosen that were expected to show significant differences in rate. They were toluene, diphenylmethane (which yields benzophenone), and triphenylmethane (which yields triphenylcarbinol). In addition one run was done with benzyl chloride. Carbon tetrachloride was the solvent.

The reactions were carried out in 10 or 12 Hinton flasks. The flasks were supported on a simple stand in a thermostat. Aliquot portions of chromyl chloride solution were pipetted into one compartment of each flask, the other reactant into the other, and the flasks stoppered. When the stand was shaken, the contents of all the flasks were simultaneously mixed. The reaction was then stopped in each flask in turn by the addition of 50 ml of a 1% aqueous sodium hydroxide solution. The color of chromyl chloride was rapidly discharged.

The contents of the flasks were then analyzed for residual Cr (VI) by iodometric titration. Assuming that the precipitate contains Cr (IV), which would give, on hydrolysis, 2/3 Cr (III) + 1/3 Cr (VI), one can calculate the concentration of CrO_2Cl remaining. It was shown that this method leads correctly to $[CrO_2Cl_2]_\infty = 0$ when the hydrocarbon is in excess.

Chromyl chloride was prepared by Sisler's method (5), and probably contained some sulphate (1). Reagent grade toluene, diphenylmethane, triphenylmethane, and benzyl chloride (Eastman) were used without further purification. Reagent grade carbon tetrachloride was dried over calcium sulphate and once distilled.

The reaction curves found with toluene were not of any simple form. For example, the curve reproduced in Fig. 1, is concave downwards in the early portion. Diphenylmethane yielded apparently normal, second-order curves (Fig. 2). Triphenylmethane

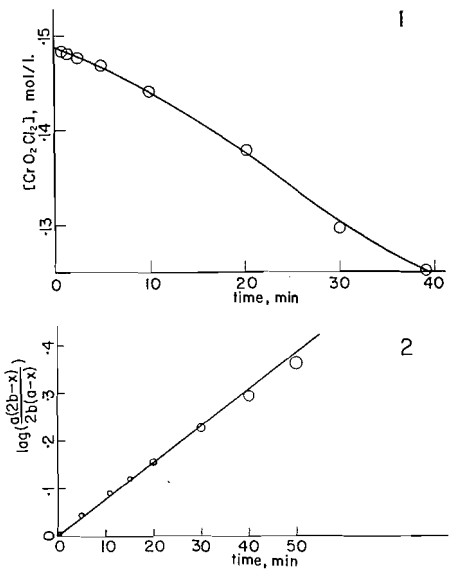


FIG. 1. Typical reaction curve with toluene (run I-A).
FIG. 2. Second-order plot for run II-D, diphenylmethane. ($\text{Log}_{10}\,[a(2b-x)]/[2b(a-x)]$ vs. time, where a and b are the initial concentrations of chromyl chloride and diphenylmethane, respectively, and x is the concentration of chromyl chloride consumed at time t.)

Can. J. Chem. Downloaded from www.nrcresearchpress.com by 210.87.254.6 on 09/05/12
For personal use only.

yielded curves that appeared normal at first but levelled out before reaching zero concentration (Fig. 3). A separate experiment showed that this was due to an oxidizing

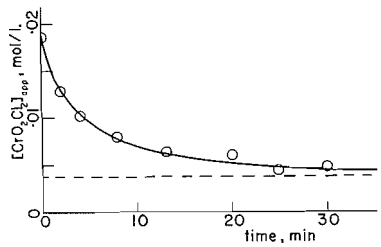


FIG. 3. Typical reaction curve with triphenylmethane (run III-B).

agent formed during the reaction, which was not extracted from the CCl_4 solution by aqueous NaOH, but which reacted slowly with aqueous KI. Such an agent could be a peroxide, resulting from air oxidation.

In view of these two complications, it was decided to base most of the conclusions on the initial rates. The partial order with respect to each reactant was determined for the three reactions by varying the initial concentrations one at a time, and noting the effect on the initial rates. The orders found are shown in Table I. They were considered close enough to unity, and the totals to two, to justify calculation of second-order rate constants. Some typical values of the rate constants are also shown in Table I, the

TABLE I

Hydrocarbon	T, °C	Order			k, l. mole^{-1} sec^{-1}	ΔH^*, kcal	p
		CrO_2Cl_2	HC	Total			
$PhCH_3$	22.1	0.94	0.98	1.92	1.28×10^{4}	14.9	10^{-4}
Ph_2CH_2	21.8	1.04	0.83	1.87	1.67×10^{-2}	12.5	10^{-2}
Ph_3CH	13.7	1.14	0.82	1.96	0.11	~3	—
$PhCH_2Cl$	30.0	—	—	(2)	1.02×10^{-4}	—	—

best known for each reaction, irrespective of temperature. For comparison, the value of k for Ph_3CH at 22° C is 0.16. That for $PhCH_2Cl$ is presumably somewhat less than 1×10^{-4}. All data are summarized in Table II.

DISCUSSION

It is clear from the reaction curves that the attack mechanism for triphenylmethane is different from that for toluene and diphenylmethane and probably involves a free radical, possibly thus:

$$(a) \quad CrO_2Cl_2 + Ph_3CH \rightarrow Ph_3C + HOCrOCl_2,$$

$$(b) \quad Ph_3C + HOCrCl_2 \rightarrow Ph_3C.O.CrCl_2OH \text{ etc.}$$

This suggestion would account for the observed oxygen absorption and would be in agreement with the known stability of the Ph_3C radical.

Ionic attack by the reagent has been postulated already by Cristol and Eilar (4) in the olefin reaction. Involvement of Cl^+ in this case is unlikely as ring attack is not observed, although it does take place in polar solvents (Carstanjen, see Hartford and

Can. J. Chem. Downloaded from www.nrcresearchpress.com by 210.87.254.6 on 09/05/12
For personal use only.

TABLE II
Summary of data

	Run	$(CrO_2Cl_2)_0$	$(HC)_0$, moles/l.	T, °C	k, l./mole-sec
Toluene	I-A	.149	.150	11.6	5.25×10^{-5}
	I-B	.149	.150	22.1	1.39×10^{-4}
	I-D	.147	.152	30.0	2.37×10^{-4}
	I-C	.148	.150	39.9	5.62×10^{-4}
	I-E	.154	.152	29.9	2.26×10^{-4}
	I-F	.309	.335	22.1	1.15×10^{-4}
	I-G	.307	.152	22.1	1.63×10^{-4}
	I-H	.311	.624	22.1	1.20×10^{-4}
	I-J	.308	1.002	22.1	1.14×10^{-4}
Diphenylmethane					
	II-B	.0495	.050	0.2	0.32×10^{-2}
	II-C	.0486	.050	21.8	1.71×10^{-2}
	II-D	.0477	.050	15.7	1.10×10^{-2}
	II-E	.0928	.115	21.8	1.55×10^{-2}
	II-F	.0928	.0573	21.8	1.74×10^{-2}
Triphenylmethane					
	III-A	.0195	.020	0.4	0.107
	III-B	.0188	.020	22.0	0.16
	III-C	.0191	.020	13.7	0.117
	III-D	.00908	.020	13.7	0.101
	III-E	.00908	.010	13.7	0.115
Benzyl chloride					
	IV-A	.1450	.159	30.0	1.02×10^{-4}

Darrin (1)). If $(CrO_2Cl)^+$ is the attacking species and if it is formed from chromyl chloride so rapidly that this ionic dissociation is not rate-determining, the kinetic data would be consistent with the following two-step process:

$$(CrO_2Cl)^+ + \text{hydrocarbon} \rightarrow \text{complex I} \qquad (k_1),$$

$$\text{complex I} + CrO_2Cl_2 \rightarrow \text{complex II} \qquad (k_2).$$

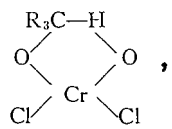
Complex I contains one chromyl chloride residue for each hydrocarbon molecule; complex II contains two for one. Such a kinetic system (6) of two consecutive, second-order steps, gives rate curves of forms dependent on the relative magnitudes of k_1 and k_2. When $k_2 \gg k_1$, the over-all reaction should approach first order with respect to chromyl chloride. This is the form of the diphenylmethane result (Fig. 2). The reaction of chromyl chloride with toluene (Fig. 1), of variable apparent order would be accommodated by having k_1 and k_2 the same order of magnitude.

The single experiment with benzyl chloride indicates a rate constant comparable with that found for toluene whereas the ionic mechanism above might be expected to predict a faster reaction. A free radical mechanism, such as that postulated for triphenylmethane, would also be expected to be faster.

Attack by the neutral chromyl chloride molecule could also fit these kinetic data. Such an attack may result in proton expulsion thus:

$$CrO_2Cl_2 + R_3CH \rightarrow (R_3C.O.CrOCl_2)^+ + H^+$$

or it may make a "four-center" activated complex of the form



Can. J. Chem. Downloaded from www.nrcresearchpress.com by 210.87.254.6 on 09/05/12
For personal use only.

which in turn could rearrange to $R_3C.O.CrCl_2OH$, or, if R_3C is a stable radical, decompose by a homolytic route. Wheeler (7) favors a π complex in solution, changing to a precipitate with two moles of chromyl chloride for each mole of hydrocarbon and with the chromium tetravalent. Both hypotheses of neutral chromyl chloride attack, as well as the $(CrO_2Cl)^+$ postulate, are in agreement with the two-step kinetic scheme advanced above.

1. W. H. HARTFORD and M. DARRIN. Chem. Revs. **58**, 1 (1958).
2. A. ETARD. Compt. rend. **116**, 434 (1893).
3. J. SWORD. Chem. News, **133**, 1 (1926).
4. S. J. CRISTOL and K. R. EILAR. J. Am. Chem. Soc. **72**, 4353 (1950).
5. H. H. SISLER. Inorganic syntheses. Vol. II. *Edited by* W. C. Fernelius. McGraw-Hill Book Co., Inc., New York. 1946. p. 205.
6. A. A. FROST and R. G. PEARSON. Kinetics and mechanism. John Wiley & Sons, Inc., New York. 1953. pp. 165–171.
7. O. H. WHEELER. Can. J. Chem. **38**, 2137 (1960).

RECEIVED JUNE 17, 1960.
DEPARTMENT OF CHEMISTRY,
QUEEN'S UNIVERSITY,
KINGSTON, ONTARIO.

Can. J. Chem. Downloaded from www.nrcresearchpress.com by 210.87.254.6 on 09/05/12
For personal use only.

Can. J. Chem. Downloaded from www.nrcresearchpress.com by 210.87.254.105 on 09/05/12
For personal use only.

Canadian Journal of Chemistry

Issued by THE NATIONAL RESEARCH COUNCIL OF CANADA

VOLUME 39 MAY 1961 NUMBER 5

THE SYNTHESIS OF ACETAMIDO-DEOXY KETOSES BY ACETOBACTER SUBOXYDANS

PART I[1]

J. K. N. JONES, M. B. PERRY, AND J. C. TURNER

ABSTRACT

The microbiological oxidation of 2-acetamido-2-deoxy-D-glucitol by *Acetobacter suboxydans* yielded a crystalline ketose which is shown to be 5-acetamido-5-deoxy-L-xylohexulose.

INTRODUCTION

The oxidation of unsubstituted polyhydric alcohols by proliferating cells of *Acetobacter suboxydans* has been studied intensively (1, 2, 3, 4, 5, 6), and has given rise to the Bertrand–Hudson rule for oxidations occurring in the pH range 5 to 6.5 (7, 8). Thus, a polyhydric alcohol possessing the D-erythro configuration (I) is oxidized mainly at the secondary alcohol group adjacent to the terminal primary alcohol to give a ketose (II). Bollenback and Underkofler (9), Richtmyer, Stewart, and Hudson (10), Hough, Jones, and Mitchell (11), and Jones and Mitchell (12) investigated the microbiological oxidation of terminal-substituted polyhydric alcohols. The latter authors reported the oxidation of several alcohols, giving chromatographic evidence for the presence of oxidation products, and characterizing completely the ketoses produced from 1-deoxy-1-*S*-ethyl-D-glucitol (11) and 1-deoxy-1-*S*-ethyl-D-arabitol (12).

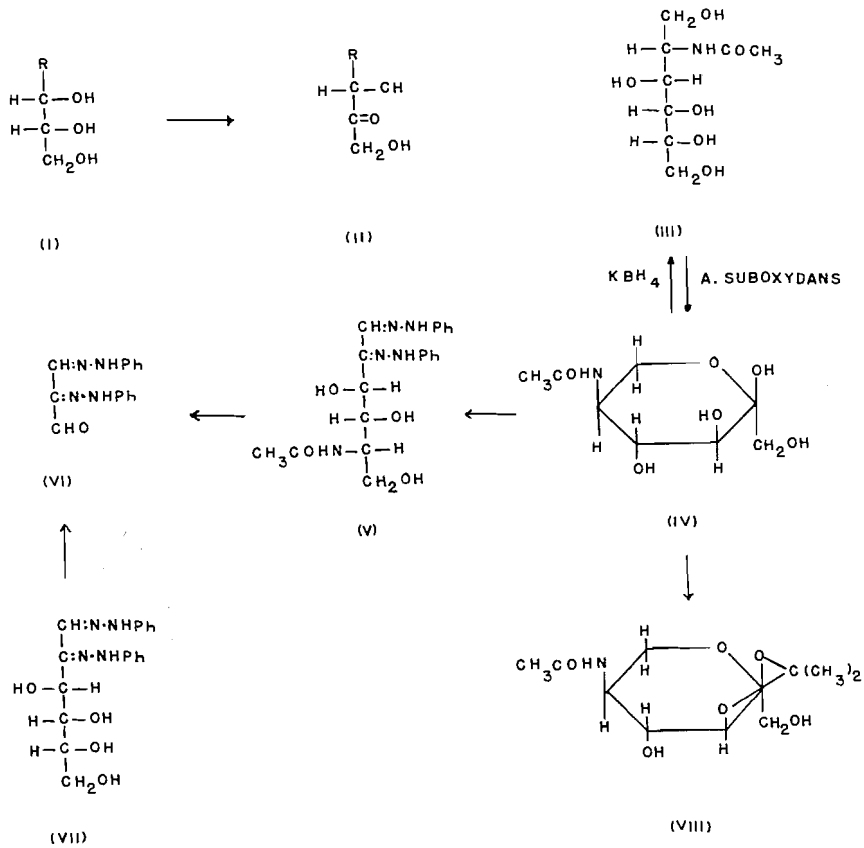
We now wish to report the isolation and proof of structure of the ketose 5-acetamido-5-deoxy-L-xylohexulose (IV), produced by microbiological oxidation at pH 5 to 6.5 of 2-acetamido-2-deoxy-D-glucitol (III). Oxidation was slow when the culture medium contained only 2-acetamido-2-deoxy-D-glucitol, and was more rapid when glycerol (0.3%) was included. However, oxidation was not complete after 21 days.

The product (IV) was obtained as a white crystalline solid. Analysis indicated an acetamido-deoxy hexulose and the compound gave absorptions in the infrared corresponding to OH, NH, and the amide linkage. On periodate oxidation of (IV) in unbuffered solution it was found to consume 2.85 moles of periodate with the liberation of 0.85 mole formic acid and 0.8 mole formaldehyde per mole of sugar, which indicated that the ketose (IV) possessed a pyranose ring form. The ketose (IV) gave a crystalline phenylosazone (5-acetamido-5-deoxy-L-xylohexose phenylosazone) (V, acyclic form) which possessed an acetamido-deoxy group and gave absorptions in the infrared corresponding to OH, NH, the aromatic ring, and the amide linkage. The phenylosazone (V), when oxidized with periodate by the method of Hough, Powell, and Woods (13), consumed 1 mole of periodate immediately and released no formic acid or formaldehyde. Periodate oxidation gave an immediate precipitate of the 1,2-bisphenylhydrazone of mesoxalaldehyde (VI) (14),

[1]*Manuscript received January 12, 1961.*
Contribution from the Department of Chemistry, Queen's University, Kingston, Ontario.

which was identified by mixed melting point and comparison of its infrared spectrum with that of an authentic sample obtained from the periodate oxidation of D-glucose phenylosazone (VII, acyclic form). These results indicated that the osazone (V) possessed hydroxyl groups at carbons 3 and 4 and that the acetamido-deoxy group was located at carbon 5. Considered with the preceding evidence, these results indicate that the site of biological oxidation in 2-acetamido-2-deoxy-D-glucitol (III) was at carbon 5, in accordance with the well-known enzyme specificity for oxidations at pH 5 to 6.5.

The ketose (IV) was shown to be a derivative of L-sorbose by its reduction with sodium borohydride to 2-acetamido-2-deoxy-D-glucitol, which had melting point, optical rotation, and infrared spectrum identical with those of an authentic specimen. The ketose (IV) gave, with acidified acetone, a non-reducing *O*-isopropylidene derivative (VIII) which was not attacked by periodate under unbuffered conditions, indicating that the mono-*O*-isopropylidene group spanned carbons 2 and 3 as in the case of 2,3-mono-*O*-isopropylidene-L-sorbose.



The microbiological oxidations of 1-acetamido-1-deoxy-*N*-methyl-D-glucamine and 1,2-dideoxy-2-acetamide-D-glucitol have been carried out and structural studies are in progress on the ketoses isolated.

EXPERIMENTAL

Solutions were concentrated under reduced pressure (ca. 15 mm) below 40° C. Melting points are uncorrected and optical rotations were determined in water at 23±3° C unless

400106

Can. J. Chem. Downloaded from www.nrcresearchpress.com by 210.87.254.105 on 09/05/12
For personal use only.

otherwise stated. Paper chromatography was carried out on Whatman No. 1 paper using the descending method (15). The following solvent systems were used (v/v):

(*a*) ethyl acetate – acetic acid – formic acid – water (18:3:1:4);
(*b*) butan-1-ol – pyridine – water (5:3:2);
(*c*) butan-1-ol – ethanol – water (9:3:3).

Reducing compounds were detected with the *p*-anisidine hydrochloride spray reagent (16) and ketoses with the orcinol/trichloroacetic acid spray reagent (17). Non-reducing compounds were detected with the alkaline silver nitrate spray reagent (18). Rates of movement of the sugars on paper chromatograms are given relative to that of rhamnose (R_{rh}). Infrared spectra were measured as a 6% solution in chloroform or as a 0.8% dispersion in a potassium bromide disk, using a Perkin–Elmer Model 21 spectrophotometer.

Acetobacter suboxydans (A.T.C.C. No. 621) was obtained from the American type culture collection and maintained at 5° C on slopes of agar (3% w:v) containing sorbitol (5% w:v), yeast extract powder (0.5% w:v), potassium dihydrogen phosphate (0.05% w:v), and D-glucose (0.05% w:v). At approximately 2-month intervals a broth containing sorbitol (7% w:v), yeast extract powder (0.5% w:v), and potassium dihydrogen phosphate (0.05% w:v) in tap water was inoculated from the slopes. After 72 hours, when growth of the organism was apparent, fresh slopes were inoculated from the broth and left 2–3 days at room temperature when cream-colored colonies became visible. The slopes were then stored at 5° C.

*5-Acetamido-5-deoxy-*L*-xylohexulose*

A broth consisting of 2-acetamido-2-deoxy-D-glucitol (8.5 g), prepared by sodium borohydride reduction of 2-acetamido-2-deoxy-D-glucose, glycerol (0.5 g), yeast extract powder (0.8 g), and potassium dihydrogen phosphate (0.16 g) in tap water (160 ml) was distributed among eight 250-ml conical flasks giving a surface:volume ratio of ca. 2.5:1. The broths were then autoclaved at 15 p.s.i. for 30 minutes, allowed to cool, and each inoculated with one drop of a 48-hour culture of *Acetobacter suboxydans* grown in glycerol (6%). The broths were stored at room temperature in the dark, without agitation, for 21 days. At intervals small samples (2 ml) were withdrawn using sterile pipettes and the broth examined on paper chromatograms. The gradual disappearance of glycerol and the appearance of dihydroxyacetone (1,3-dihydroxypropanone) and a spot which had R_{rh} 0.59 (solvent (*c*)), 0.73 (solvent (*a*)), 0.65 (solvent (*b*)), and gave a yellow color with orcinol/trichloroacetic acid spray were noted. A quantitative measure of the rate of oxidation was obtained by estimation of the copper-reducing power of the broth using the Somogyi method (19). The results are recorded in Table I. After 21 days the broths

TABLE I

Time (days)	% yield of ketose (corrected for the presence of dihydroxyacetone)
3	4.5
11	11.25
17	14.55

were combined and poured into 2 volumes of ethanol. The cell debris was removed by filtration and the filtrate was evaporated to about 20 ml and then deionized by

Can. J. Chem. Downloaded from www.nrcresearchpress.com by 210.87.254.105 on 09/05/12
For personal use only.

passage through columns of Amberlite IR 120 (H) and Duolite A4 (OH) resins. The eluate was concentrated to a syrup which crystallized. The crystalline material was washed with ethanol and dried, m.p. 154–155° C, mixed m.p. with 2-acetamido-2-deoxy-D-glucitol, 154–155° C. The mother liquors from the crystallization were concentrated to a syrup (2.4 g) which was deposited on cellulose powder and packed as a level band on top of a cellulose column (54 cm × 4.5 cm). The column was irrigated with butan-1-ol half saturated with water, and 5-ml fractions of the eluate were collected using an automatic fraction collector (20). The fractions were examined on paper chromatograms run in solvent (*c*) and sprayed with alkaline silver nitrate spray reagent. A good separation of the sugars was obtained and the appropriate fractions were evaporated to dryness yielding crystalline 5-acetamido-5-deoxy-L-xylohexulose. One recrystallization from ethanol/ether gave crystals m.p. 174–176° C, $[\alpha]_D$ −62. Anal. Calc. for $C_8H_{15}O_6N$: C, 43.4; H, 6.8; N, 6.3. Found: C, 43.3; H, 6.9; N, 6.35. Absorptions in the infrared due to OH and NH (broad fused peak at 3300 cm^{-1}) and the amide linkage (1625 cm^{-1} and 1570 cm^{-1}) were observed. For infrared spectrum see Appendix (A).

Periodate Oxidation of 5-Acetamido-5-deoxy-L-xylohexulose

The ketose (50.62 mg) was dissolved in about 40 ml of water, 0.3 *M* sodium metaperiodate (5.0 ml) was added, and the volume was made up to 50 ml with water. A blank was prepared with 0.3 *M* sodium metaperiodate (5.0 ml), which was made up to 50 ml with water. The solutions were stored in the dark at room temperature and 5-ml aliquots were removed at intervals from each of the two solutions for the determination of periodate uptake (21) and formic acid production (22). Formaldehyde production was measured by the chromotropic acid method (23). The results are recorded in Tables II and III.

TABLE II

Oxidation of 5-acetamido-5-deoxy-L-xylohexulose

Time (hr)	Periodate uptake (moles/mole)	Formic acid production (moles/mole)
0.12	1.15	0.31
1.83	1.79	0.59
8.5	2.68	0.82
24	2.85	0.85

TABLE III

Time (hr)	Formaldehyde production (moles/mole)
0.2	0.36
1	0.53
25	0.62
45	0.80

5-Acetamido-5-deoxy-L-xylohexose Phenylosazone

5-Acetamido-5-deoxy-L-xylohexulose (45 mg) was dissolved in water (2.4 ml), and acetic acid (0.24 ml) and freshly distilled phenylhydrazine (0.24 ml) were added. The mixture was heated in a boiling-water bath for 15 minutes, after which time the phenylosazone had crystallized. The solution was cooled and the phenylosazone was collected by filtration, washed with ice-cold dilute acetic acid, ice water, and cold (−60° C)

Can. J. Chem. Downloaded from www.nrcresearchpress.com by 210.87.254.105 on 09/05/12
For personal use only.

methanol, and then dried. One recrystallization from ethanol gave a yellow powder (small needles) m.p. 202–203° C (decomposes). (An optical rotation could not be measured due to the intense color of the osazone.) Anal. Calc. for $C_{20}H_{25}O_4N_5$: C, 60.15; H, 6.3; N, 17.5. Found: C, 59.7; H, 6.35; N, 17.3.

Absorptions in the infrared due to OH and NH (broad fused peak at 3300 cm^{-1}), the aromatic ring (3030 cm^{-1}, 1605 cm^{-1}, 1500 cm^{-1}, 745 cm^{-1}, 690 cm^{-1}), and the amide linkage (1647 cm^{-1}, 1583 cm^{-1}) were observed. The infrared spectrum is given in the Appendix (B).

*Periodate Oxidation of 5-Acetamido-5-deoxy-*L*-xylohexose Phenylosazone*

The method of Hough, Powell, and Woods (13) was used. The results are shown in Table IV. (Formaldehyde was estimated by the chromotropic acid method (23).)

TABLE IV

Time (hr)	Periodate uptake (moles/mole)	Formic acid (moles/mole)	Formaldehyde (moles/mole)
0.25	1.1	0.00	0.00
3.15	1.14	0.00	0.00
18.65	1.22	0.00	0.00
40.65	1.18	0.00	

On oxidation a bright yellow precipitate of the 1,2-bisphenylhydrazone of mesoxalaldehyde was obtained. The material was collected by filtration, washed with water, recrystallized from aqueous ethanol, and obtained as orange needles, m.p. 188–189.5° C.

1,2-Bisphenylhydrazone of Mesoxalaldehyde (14)

D-Glucose phenylosazone was prepared (300 mg) and dissolved in 50% aqueous ethanol (500 ml). Sodium metaperiodate (20 ml; 0.3 *M*) was added with vigorous stirring and after about 15 seconds a curdy mass of fine orange-yellow needles was precipitated. The mixture was allowed to stand for 15 minutes, then the crystals were collected by filtration, and washed with cold 50% aqueous ethanol and dried. One recrystallization from aqueous ethanol gave orange needles, m.p. 188.5–190.5° C.

The two specimens of the 1,2-bisphenylhydrazone of mesoxalaldehyde had mixed m.p. 188–189.5° C and had identical R_{rh} values on paper chromatograms run in solvents (*a*), (*b*), and (*c*) (R_{rh} 2.03, 1.58, and 2.9 respectively). The infrared spectra were identical and showed absorptions due to NH (3310 cm^{-1}), the aromatic ring (3050 cm^{-1}, 1605 cm^{-1}, 1500 cm^{-1}, 745 cm^{-1}, 687 cm^{-1}), and the unsaturated aldehyde group (1675 cm^{-1}). Further details of the infrared spectrum are given in the Appendix (C).

*Potassium Borohydride Reduction of 5-Acetamido-5-deoxy-*L*-xylohexulose to 2-Acetamido-2-deoxy-*D*-glucitol*

5-Acetamido-5-deoxy-L-xylohexulose (100 mg) was dissolved in water (10 ml) and the solution was cooled in ice. A solution of potassium borohydride (100 mg) in water (10 ml) was added dropwise, with stirring, over a period of 30 minutes and the solution was then stirred at 0° C for 3 hours, after which time it was non-reducing towards Fehling's solution. Amberlite IR-120 (H) resin was added to decompose excess potassium borohydride and the solution was then passed through a column of Amberlite IR-120 (H). The eluate and washings from the column were concentrated to a white amorphous residue which was repeatedly evaporated to dryness with methanol to remove boric acid as

Can. J. Chem. Downloaded from www.nrcresearchpress.com by 210.87.254.105 on 09/05/12
For personal use only.

methyl borate. The residue was dissolved in hot methanol and ether added to incipient turbidity. On cooling, white needles (57 mg) of 2-acetamido-2-deoxy-D-glucitol were deposited. A further crop of crystals (30 mg) was obtained on concentration of the mother liquors. The material had m.p. 154–156° C, mixed m.p. with an authentic specimen of 2-acetamido-2-deoxy-D-glucitol, 153–156° C, and $[\alpha]_D$ −10.8°. The crystalline material gave one spot when run on paper chromatograms in solvents (*a*), (*b*), and (*c*), detected with the alkaline silver nitrate reagent. The spot had R_{rh} values identical with those of the authentic specimen (solvent (*a*) 0.79; solvent (*b*) 0.62; solvent (*c*) 0.50). The infrared spectra of the derived and authentic specimens were identical and showed absorptions due to OH and NH (very broad peak at 3300 cm^{-1}) and the amide linkage (1645 cm^{-1}, 1587 cm^{-1}). Further details are given in the Appendix (D).

2,3-Mono-O-isopropylidene-5-acetamido-5-deoxy-L-xylohexulose

5-Acetamido-5-deoxy-L-xylohexulose (100 mg) was shaken with dry acetone (50 ml) containing concentrated sulphuric acid (2 drops) for 24 hours. At the end of this time the clear solution was neutralized with barium carbonate, filtered, and the filtrate was concentrated to a clear colorless syrup (120 mg) which was examined on paper chromatograms run in solvents (*a*), (*b*), and (*c*). The *p*-anisidine hydrochloride spray reagent showed only a very faint spot due to 5-acetamido-5-deoxy-L-xylohexulose. However, the orcinol/trichloroacetic acid spray reagent revealed also a strong spot due to the *O*-isopropylidene compound with the following R_{rh} values (Table V). An ethanol solution of

TABLE V

Solvent	R_{rh} (f = faint, s = strong)	
	p-Anisidine hydrochloride	Orcinol/trichloroacetic acid
(*a*)	0.73 (f)	0.73 (f)+1.86 (s)
(*b*)	0.65 (f)	0.65 (f)+1.73 (s)
(*c*)	0.59 (f)	0.59 (f)+1.95 (s)

the syrup was applied to Whatmann 3 mm paper and developed in solvent (*a*) overnight. The section containing the *O*-isopropylidene ketose was cut out and eluted with 50% aqueous ethanol. The eluate was passed through Amberlite IR-120 (H) and Duolite A-4 (OH) resins and then concentrated to a clear colorless syrup (108 mg) which was chromatographically pure. The syrup had $[\alpha]_D$ −51° (*c*, 2.16 in ethanol), and was non-reducing towards Fehling's solution. The infrared spectrum showed absorptions due to OH and NH (broad peak at 3360 cm^{-1}), the amide linkage (1665 cm^{-1}, 1560 cm^{-1}), and the C-methyl group (1460 cm^{-1}, 1380 cm^{-1}). A considerable reduction of the OH peak as compared to that of 5-acetamido-5-deoxy-L-xylohexulose was observed. Further details are given in the Appendix (E).

Periodate Oxidation of 2,3-Mono-O-isopropylidene-5-acetamido-5-deoxy-L-xylohexulose

The *O*-isopropylidene ketose (75 mg) was dissolved in 50% aqueous ethanol (ca. 40 ml). A 0.3 *M* quantity of sodium metaperiodate (2 ml) was added and the volume made up to 50 ml with 50% aqueous ethanol. A blank solution was prepared containing 0.3 *M* sodium metaperiodate (2 ml), which was made up to 50 ml with 50% aqueous ethanol. The solutions were stored in the dark at room temperature and 5-ml aliquots removed at intervals for estimation of periodate uptake (22). No periodate was taken up by the *O*-isopropylidene ketose.

Can. J. Chem. Downloaded from www.nrcresearchpress.com by 210.87.254.105 on 09/05/12
For personal use only.

ACKNOWLEDGMENTS

We wish to thank the National Research Council for financial assistance (NRC T-39), and Queen's University for the award of a scholarship to one of us (J.C.T.).

REFERENCES

1. R. L. WHISTLER and L. A. UNDERKOFLER. J. Am. Chem. Soc. **60**, 2507 (1938)
2. W. BOSSHARD and T. REICHSTEIN. Helv. Chim. Acta, **18**, 959 (1935).
3. L. C. STEWART, N. K. RICHTMYER, and C. S. HUDSON. J. Am. Chem. Soc. **71**, 3532 (1949).
4. J. W. PRATT, N. K. RICHTMYER, and C. S. HUDSON. J. Am. Chem. Soc. **74**, 2210 (1952).
5. L. C. STEWART, N. K. RICHTMYER, and C. S. HUDSON. J. Am. Chem. Soc. **74**, 2206 (1952).
6. J. W. PRATT and N. K. RICHTMYER. J. Am. Chem. Soc. **77**, 6326 (1955).
7. R. M. HANN, E. B. TILDEN, and C. S. HUDSON. J. Am. Chem. Soc. **60**, 1201 (1938).
8. G. BERTRAND. Ann. chim. **3**(8), 209, 287 (1904).
9. G. N. BOLLENBACH and L. A. UNDERKOFLER. J. Am. Chem. Soc. **72**, 741 (1950).
10. N. K. RICHTMYER, L. C. STEWART, and C. S. HUDSON. J. Am. Chem. Soc. **72**, 4934 (1950).
11. L. HOUGH, J. K. N. JONES, and D. L. MITCHELL. Can. J. Chem. **37**, 725 (1959).
12. J. K. N. JONES and D. L. MITCHELL. Can. J. Chem. **37**, 1561 (1959).
13. L. HOUGH, D. B. POWELL, and B. M. WOODS. J. Chem. Soc. 4799 (1956).
14. E. CHARGAFF and B. MAGASANIK. J. Am. Chem. Soc. **69**, 1459 (1947).
15. S. M. PARTRIDGE. Biochem. J. **42**, 238 (1948).
16. L. HOUGH, J. K. N. JONES, and W. H. WADMAN. J. Chem. Soc. 1702 (1950).
17. R. KLEVSTRAND and A. NORDAL. Acta Chem. Scand. **4**, 1320 (1950).
18. W. E. TREVELYAN, D. P. PROCTOR, and J. S. HARRISON. Nature, **166**, 444 (1950).
19. M. SOMOGYI. J. Biol. Chem. **160**, 61, 69 (1945).
20. L. HOUGH, J. K. N. JONES, and W. H. WADMAN. J. Chem. Soc. 2511 (1949).
21. G. NEÜMULLER and E. VASSEUR. Arkiv Kemi, **5**, 235 (1953).
22. D. M. W. ANDERSON, C. T. GREENWOOD, and E. L. HIRST. J. Chem. Soc. 225 (1955).
23. J. F. O'DEA and R. A. GIBBONS. Biochem. J. **55**, 580 (1953).

APPENDIX

Infrared Spectra

The following abbreviations are used: s = strong, m = medium, w = weak; wave numbers expressed in cm^{-1}.

*(A) 5-Acetamido-5-deoxy-*L*-xylohexulose (0.8% in KBr)*

3300 (s), 2950 (m), 2880 (m), 1625 (s), 1570 (s), 1510 (m), 1475 (m), 1440 (s), 1400 (m), 1380 (m), 1360 (m), 1330 (s), 1310 (m), 1280 (m), 1255 (m), 1225 (w), 1185 (m), 1160 (s), 1120 (s), 1100 (s), 1065 (s), 1030 (s), 955 (m), 905 (m), 825 (s), 785 (m), 685 (m), 670 (m).

*(B) 5-Acetamido-5-deoxy-*L*-xylohexose Phenylosazone (0.8% in KBr)*

3300 (s), 3030 (m), 2960 (m), 2910 (m), 1647 (s), 1605 (s), 1583 (s), 1540 (s), 1500 (s), 1450 (m), 1420 (m), 1385 (m), 1305 (m), 1257 (s), 1170 (m), 1150 (m), 1105 (m), 1055 (m), 1010 (s), 960 (w), 890 (w), 880 (w), 785 (w), 745 (m), 690 (m).

(C) 1,2-bis Phenylhydrazone of Mesoxalaldehyde (Authentic and Derived Specimens) (0.8% in KBr)

3310 (s), 3050 (w), 2840 (w), 1675 (s), 1605 (s), 1550 (s), 1535 (s), 1500 (s), 1355 (m), 1280 (s), 1245 (s), 1200 (m), 1170 (m), 1165 (m), 1155 (m), 745 (s), 705 (m), 687 (m).

*(D) 2-Acetamido-2-deoxy-*D*-glucitol (Authentic and Derived Specimens) (0.8% in KBr)*

3300 (s), 2940 (s), 1645 (s), 1587 (s), 1447 (s), 1385 (s), 1315 (s), 1277 (s), 1255 (m), 1215 (w), 1145 (w), 1130 (w), 1090 (s), 1065 (s), 1010 (s), 970 (m), 940 (w), 895 (w), 880 (m), 765 (m), 690 (s).

Can. J. Chem. Downloaded from www.nrcresearchpress.com by 210.87.254.105 on 09/05/12
For personal use only.

*(E) 2,3-Mono-O-isopropylidene-5-acetamido-5-deoxy-*L*-xylohexulose (6% in Chloroform)*
3360 (s), 3100 (w), 3030 (m), 2970 (w), 2910 (w), 1725 (w), 1665 (s), 1560 (s), 1460 (m), 1435 (m), 1390 (s), 1380 (s), 1315 (m), 1240 (s), 1190 (s), 1115 (s), 1095 (s), 1075 (s), 1035 (m), 975 (m), 950 (w), 900 (s), 885 (s), 835 (w), 815 (w), 685 (w), 657 (w).

Can. J. Chem. Downloaded from www.nrcresearchpress.com by 210.87.254.105 on 09/05/12
For personal use only.

Can. J. Chem. Downloaded from www.nrcresearchpress.com by 210.87.254.40 on 09/05/12
For personal use only.

THE PREPARATION OF SOME THIOSEMICARBAZONES AND THEIR COPPER COMPLEXES

PART II[1]

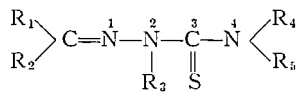
B. A. GINGRAS, R. L. SOMORJAI,[2] AND C. H. BAYLEY

ABSTRACT

Reactions of N- and S-substituted thiosemicarbazones with Cu(I) have been examined. No complexes are formed when the S atom is substituted and(or) when the N^2 hydrogen atom is replaced by Me. 4,4-Dimethyl derivatives not only give the usual 1:1 complexes, but also 2:1 complexes (2 thiosemicarbazones to 1 copper) in which copper has been oxidized to Cu(II). Reactions of thiosemicarbazones with Cu(II) give 1:1, 2:1, and probably a mixture which corresponds to 2:3 complexes. A discussion on the possible structures for the 1:1 complexes is given and they are best represented as polymers, the metal being bonded to the sulphur and to a nitrogen atom of the thiosemicarbazide portion of the molecule. Infrared spectra of these compounds have been examined, particularly in the 1100 cm^{-1} region where a strong to medium band disappears in going from thiosemicarbazones to copper complexes. It is suggested that this band is due to the C=S vibration.

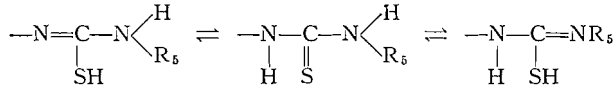
Various metallic complexes of organic sulphur compounds are described in the literature (1–10). Many of these were prepared for physiological studies and their structures are not discussed fully (7, 10). In earlier publications we have reported the preparation of Cu(I) complexes of thiosemicarbazones* (1 tsc:1 Cu) (11) and their fungicidal action (12). This paper presents a discussion of the possible structures for these complexes based mainly on the reactions of several *N*-methyl thiosemicarbazones with copper ions in ammoniacal and neutral media.

Thiosemicarbazones have the structure (I) (R = alkyl, aryl, or H).

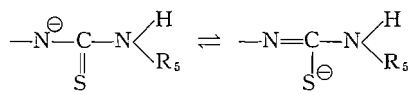


(I)

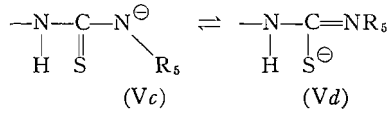
When R_3 and R_4 and(or) R_5 are hydrogen atoms, tautomeric thiols (II) and (IV) and thione (III) forms are possible, these being interconvertible through their common anions (V) and cations (VI). The dipolar structures (III*a*) and (III*b*) may contribute to (III).



(II) (III) (IV)

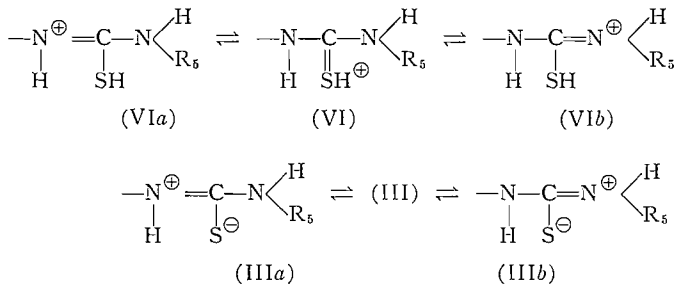


(V*a*) (V*b*)



(V*c*) (V*d*)

[1]*Manuscript received November 28, 1960.*
Contribution from the Division of Applied Chemistry, National Research Council, Ottawa, Canada. Issued as N.R.C. No. 6244.
[2]*Present address: Chemistry Department, Princeton University, Princeton, New Jersey, U.S.A.*
* *tscs.*



(VI*a*) (VI) (VI*b*)

(III*a*) (III*b*)

Infrared absorption spectra of tscs in the solid state indicate the absence of tautomerism, the thione form (III) being the exclusive structure (13). On the other hand most tscs dissolve in alkali (13, 14) and form metallic complexes in alkaline solution (5, 8, 11) thus suggesting the important role of one of the anions (V) in solution. The observation that N^2-methyl tscs (I, R_3 = Me) do not dissolve in alkali (13) and that hydrazides of type (R—CO—NH—NRR) do not form copper complexes if the H atom is replaced by Me (15), suggest that the N^2 hydrogen atom is essential for the complex formation in these compounds. Apparently the resonance structure (III*a*) and consequently anion (V*b*) are the main contributing forms in alkaline solutions. This is plausible because of the greater stability conferred on anion (V*b*) through the formation of a conjugated unit, C=N—N=C, where the delocalization of the π electrons lowers the free energy of the system. Anion (V*a*) is probably less important as a contributing form partly because of the lack of the above-stated conjugation and partly because the sulphur atom has more available orbitals to accommodate extra electrons than the nitrogen atom (16). These observations agree with a number of published data. Wilson and Burns (14) found that the sodium salt of acetone tsc had retained the terminal NH_2 group. Jensen *et al.* prepared several substituted thiosemicarbazides (4, 5, 6) and found that neither in alkaline nor in acidic media did S-substituted thiosemicarbazides form complexes (6), indicating the necessity of a metal–sulphur bonding. Jensen also concluded that co-ordination in M(II)-thiosemicarbazide and M(II)-semicarbazide complexes is through the N^1 atom (4, 5, 6, 17). He arrived at this conclusion from the observation that 1-aryl thiosemicarbazide, ($ArN^1H—N^2H—C^3S—N^4H_2$), did not form Ni(II) complexes, and 1-acyl ($RCON^1H—N^2H—C^3S—N^4H_2$), 1,1-disubstituted thiosemicarbazides ($R_1R_2N^1—N^2H—C^3S—N^4H_2$) as well as tscs (I) gave no Cu(II) complexes in acidic media (6).

The fact that thiobenzhydrazide (Ph—CS—$NHNH_2$) forms a Ni(II) complex similar to the corresponding thiosemicarbazide complex, supports the theory of co-ordination through the N^1 atom (1).

In Part I (11) it has been found that Cu(I) ions in ammoniacal solution formed 1:1 complexes with tscs, one hydrogen atom being presumably replaced by Cu. We have now prepared a series of *N*-methyl and S-substituted tscs (Table I) and examined their reaction with Cu(I) ions in ammoniacal solution (Table II) and with Cu(II) ions in alcoholic solution (Table III).

With Cu(I) ions, complexes were formed in all instances, except with the N^2-methyl (I, R_3 = Me) and *S*-methyl tscs. These various reactions are summarized in Table II. These observations support the conclusions concerning the importance of anion (V*b*) (N^2-hydrogen being replaced) and the S–metal linkage.

Can. J. Chem. Downloaded from www.nrcresearchpress.com by 210.87.254.40 on 09/05/12
For personal use only.

Can. J. Chem. Downloaded from www.nrcresearchpress.com by 210.87.254.40 on 09/05/12
For personal use only.

TABLE I

Substituted thiosemicarbazones

No.	Name	m.p., °C	Yield, %	Solvent used in recryst.	Formula	Found, %	Calc., %	I.R. bands in cm^{-1}*			Reference for preparation of substituted thiosemicarbazides
								3500–3000	1630–1515	1130–1010	
1	Benzaldehyde 2-methyl tsc	175	78	EtOH	$C_9H_{11}N_3S$	C, 56.19 H, 5.78 N, 21.50 S, 16.35	C, 56.00 H, 5.70 N, 21.72 S, 16.58	3460 m 3280 m 3130 w	1582 s	1083 m 1050 w 1010 s	28
2	Benzaldehyde 4-methyl tsc	163	93	EtOH–C_6H_{14}	$C_9H_{11}N_3S$	C, 55.57 H, 6.30 N, 21.90 S, 16.40	C, 56.00 H, 5.70 N, 21.72 S, 16.58	3325 m 3150 m	1550 b	1090 m 1070 m 1035 s	29
3	Benzaldehyde 2,4-dimethyl tsc	117.5	100	EtOH–C_6H_{14}	$C_{10}H_{13}N_3S$	C, 58.19 H, 6.21 N, 20.40 S, 15.30	C, 57.97 H, 6.28 N, 20.29 S, 15.46	3370 m	1605 w 1580 w 1530 s	1060 s 1050 w	30
4	Benzaldehyde *S*,4-dimethyl tsc	66	55	C_6H_{14}	$C_{10}H_{14}N_3S$	C, 58.10 H, 6.19 N, 20.20 S, 15.30	C, 57.80 H, 6.73 N, 20.20 S, 15.40	3290 m	1615 s 1583 s	1085 m 1055 w 1035 m	
5	Benzaldehyde 4,4-dimethyl tsc	148 s	77	MeOH	$C_{10}H_{13}N_3S$	C, 57.98 H, 6.45 N, 20.20 S, 15.08	C, 57.97 H, 6.28 N, 20.29 S, 15.46	3260 w 3180 m	1610 m 1565 s	1080 m 1065 m 1030 m	31
6	*p*-Chlorobenzaldehyde-2,4-dimethyl tsc	146 s	100	MeOH–acetone	$C_{10}H_{12}ClN_3S$	C, 49.64 H, 5.08 Cl, 14.95 N, 17.35 S, 13.34	C, 49.68 H, 4.97 Cl, 14.72 N, 17.39 S, 13.24	3340 m	1605 m 1595 m	1093 v 1060 s 1040 w 1015 w	30
7	*p*-Chlorobenzaldehyde-4,4-dimethyl tsc	132	96	*n*-Hexane	$C_{10}H_{12}ClN_3S$	C, 50.56 H, 4.51 Cl, 14.46 N, 17.18 S, 13.00	C, 49.68 H, 4.97 Cl, 14.72 N, 17.39 S, 13.24	3120 m	1595 m 1515 m	1090 m 1060 m 1015 m	31
8	Heptanal-2-methyl tsc	52	40	*n*-Hexane	$C_9H_{19}N_3S$	C, 53.45 H, 9.13 N, 21.35 S, 16.44	C, 53.7 H, 9.45 N, 20.85 S, 15.9	3420 m 3260 m 3120 m	1585 m	1085 vw 1040 w	28

Can. J. Chem. Downloaded from www.nrcresearchpress.com by 210.87.254.40 on 09/05/12
For personal use only.

TABLE I

Substituted thiosemicarbazones (*concluded*)

No.	Name	m.p., °C	Yield, %	Solvent used in recryst.	Formula	Found, %	Calc., %	I.R. bands in cm^{-1}*			Reference for preparation of substituted thiosemicarbazides
								3500–3000	1630–1515	1130–1010	
9	Octanal-2-methyl tsc	45	35	*n*-Hexane†	$C_{10}H_{21}N_3S$	C, 56.57 H, 8.82 N, 19.61 S, 14.85	C, 55.9 H, 9.76 N, 19.54 S, 14.92	3190 vw 3120 w	1592 s 1505 s	1040 m 1030 m 1007 w	28
10	Octanal-4-methyl tsc	51	47	*n*-Hexane	$C_{10}H_{21}N_3S$	C, 55.85 H, 10.32 N, 19.55 S, 14.60	C, 55.9 H, 9.76 N, 19.54 S, 14.92	3280 m 3180 m	1560 b 1535 w	1080 m 1045 m 1025 w	29
11	Nonanal-2-methyl tsc	62.5	73	*n*-Hexane	$C_{11}H_{23}N_3S$	C, 57.59 H, 9.86 N, 18.41 S, 14.02	C, 57.61 H, 10.12 N, 18.32 S, 13.95	3400 m 3200 m 3100 m	1585 s	1055 sh 1035 w	28
12	Decanal-2-methyl tsc	45	64	*n*-Hexane	$C_{12}H_{25}N_3S$	C, 59.60 H, 10.30 N, 16.95 S, 13.31	C, 59.25 H, 10.37 N, 17.28 S, 13.16	3420 m 3250 m 3120 w	1585 m	1050 m	28
13	Undecanal-2-methyl tsc	73.5	75	EtOH	$C_{13}H_{27}N_3S$	C, 60.53 H, 10.43 N, 16.25 S, 12.86	C, 60.7 H, 10.5 N, 16.3 S, 12.45	3420 m 3250 m 3120 m	1588 s (Nujol)	1090 w 1068 w 1050 w 1025 vw	28
14	9-Undecenal-2-methyl tsc	33	20	*n*-Hexane	$C_{13}H_{25}N_3S$	C, 61.57 H, 9.64 N, 16.65 S, 12.60	C, 61.25 H, 9.8 N, 16.45 S, 12.50	3460 m 3300 m 3140 m	1580 b	1075 w	28
15	Acetone-*S*-benzyl tsc	50	50	*n*-Hexane	$C_{11}H_{15}N_3S$	C, 59.70 H, 6.90 N, 18.95 S, 14.30	C, 59.68 H, 6.84 N, 19.00 S, 14.47	3500 m 3300 m 3130 m	1545 m 1505 m	1075 m 1035 m	14

*From KBr pellets.
†After purification by chromatography.

Can. J. Chem. Downloaded from www.nrcresearchpress.com by 210.87.254.40 on 09/05/12
For personal use only.

TABLE II

Reactions between methyl derivatives of tscs and Cu(I) in ammoniacal solution

tsc No. from Table I	Type of complex formed	m.p., °C decomp.	Yield, %	Formula	Found, %	Calc., %	I.R. bands in cm^{-1}*		
							3500–3000	1630–1515	1130–1010
1	None								
2	1:1	207–208.5	85	$C_9H_{10}N_3SCu$	C, 42.23 H, 4.00 N, 16.20 S, 11.99 Cu, 25.2	C, 42.30 H, 3.91 N, 16.42 S, 12.6 Cu, 24.85	3380 s 3060 vw 3030 vw	1580 m 1550 b	1065 s 1013 m
3	None								
4	None								
5	(*a*) 1:1	225	25	$C_{10}H_{12}N_3SCu$	C, 43.73 H, 3.69 N, 14.81 S, 11.38 Cu, 23.4	C, 44.57 H, 4.49 N, 15.58 S, 11.87 Cu, 23.55	3060 vw	1600 m 1575 m	1080 w 1035 m
	(*b*) 2:1	185–187	40	$C_{20}H_{24}N_6S_2Cu$	C, 50.50 H, 5.80 N, 17.59 S, 13.18 Cu, 13.33	C, 50.42 H, 5.08 N, 17.64 S, 13.44 Cu, 13.33	3070 vw	1590 w 1570 m 1510 s	1065 m 1040 m
6	None								
7	2:1	232	60	$C_{20}H_{22}Cl_2N_6S_2Cu$	C, 43.66 H, 3.88 Cl, 13.15 N, 15.18 S, 11.69 Cu, 12.26	C, 44.00 H, 4.25 Cl, 13.02 N, 15.40 S, 11.68 Cu, 11.65	3120 vw	1595 m 1560 w 1515 s	1085 m 1060 w 1025 m
8	None								
9	None								
10	Not attempted								
11	None								
12	None								
13	None								
14	Not attempted								
15	Unidentified compound								

*From KBr pellets.

Can. J. Chem. Downloaded from www.nrcresearchpress.com by 210.87.254.40 on 09/05/12
For personal use only.

TABLE III

Reaction of tscs with Cu(II) in alcoholic solution

tscs	Type of complex	m.p., °C decomp.	Yield, %	Formula	Found, %	Calc., %	Remarks
Benzaldehyde tsc	1:1	184–185	49	$C_8H_8N_3SCu$			Identical with the one described in Part I (11)
Benzaldehyde-4,4-dimethyl tsc	1:1	225	40	$C_{10}H_{12}N_3SCu$			Identical with the one described in Table II
	2:1	185	40	$C_{20}H_{24}N_6S_2Cu$			Identical with the one described in Table II
o-Chlorobenzaldehyde tsc	1:1	198	52	$C_8H_7ClN_3SCu$			Identical with the one described in Part I (11)
m-Fluorobenzaldehyde tsc	1:1	162	58	$C_8H_7FN_3SCu$			Identical with the one described in Part I (11)
n-Octanal tsc	2:1	122	Trace	$C_{18}H_{37}N_6S_2Cu$	Cu, 15.4	Cu, 13.75	Not enough material for further purification and complete analysis
n-Nonanal tsc	2:3	135–138	42	$C_{20}H_{40}N_6S_2Cu_3$	C, 37.27 H, 5.73 N, 13.35 S, 10.45 Cu, 31.0	C, 38.85 H, 6.48 N, 13.58 S, 10.34 Cu, 30.8	
Undecanal tsc	1:1						Identical with the one described in Part I (11)
9-Undecenal tsc	2:3	134–137	58		Cu, 30.7	Cu, 28.9	
Laurylaldehyde tsc	2:1	125	18	$C_{26}H_{52}N_6S_2Cu$	C, 55.17 H, 9.33 N, 14.71 S, 10.75 Cu, 11.66	C, 54.23 H, 9.12 N, 14.60 S, 11.11 Cu, 11.03	
	2:3	137–140	52.5	$C_{26}H_{52}N_6S_2Cu_3$	N, 12.25 S, 9.60 Cu, 27.8	N, 11.95 S, 9.12 Cu, 27.1	

Magnetic moment measurements on two typical complexes indicated zero magnetic moment, and thus the presence of monovalent copper.

Crystal field theory shows that d^{10} ions may co-ordinate octahedrally (sp^3d^2), tetrahedrally (sp^3), or linearly (sp), depending on the nature of the surrounding field (18). Although linear co-ordination occurs in cuprite (19), cuprous chromite (20), and cuprous ferrite (21), only one example of this type of co-ordination with an organic ligand is well-known (e.g. diazoaminobenzene-Cu(I) (22).

Since most Cu(I) ions co-ordinate tetrahedrally (23) and in many cases, the resulting complexes were found to be polymers (24), it is possible that in the case of tsc copper complexes, the metal is bonded to a sulphur and an N^1 atom and co-ordinated further tetrahedrally to a sulphur and N atom of another molecule in a polymeric chain.

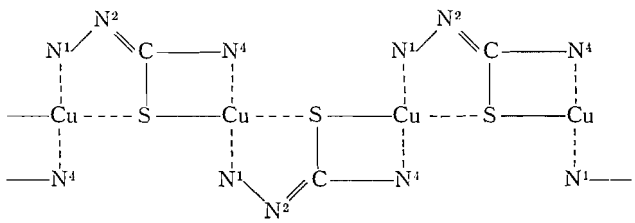
Experimental results obtained with 4,4-dimethyl derivatives of tscs indicate that N^4 nitrogen is probably involved in this co-ordination.

It was found that 4,4-dimethyl tscs form mostly 2:1 complexes when they react in the usual manner with Cu(I). Magnetic moment measurements on (benzaldehyde-4,4-dimethyl tsc)$_2$-copper showed one unpaired electron indicating oxidation of the Cu(I) ion to the Cu(II) state. This change was brought about by an extra Me group on the N^4 atom, since 4-methyl tscs behave normally giving 1:1 complexes only. These observations are difficult to explain unless the Cu ion is actually co-ordinated to the N^4 atom. Oxidation of the metal could have happened by disproportionation (25) as follows:

$$2\text{Cu(I)} \rightarrow \text{Cu(II)} + \text{Cu(0)}.$$

Material balance of starting materials and products in the case of benzaldehyde-4,4-dimethyl tsc supports this view.

Molecular models of various polymeric structures were examined and a few were discarded because of steric factors and(or) too much strain particularly in small rings. Two possible structures are (VII) and (VIII) below.



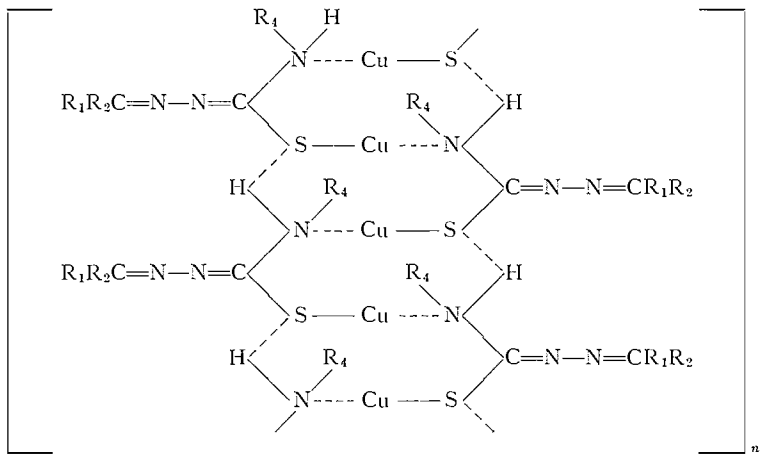
(VII)

Structure (VII) comprises a series of 5- and 4-membered rings in which Cu(I) is co-ordinated tetrahedrally to a sulphur and N^1 atoms of a tsc and a sulphur and N^4 atoms of another molecule. Molecular model of this structure shows a certain amount of strain in the 4-membered ring. Although such a structure accounts for many of the experimental facts, it does not explain easily the anomalous behavior of 4,4-dimethyl tscs.

Structure (VIII) in which copper is linearly co-ordinated to N^4 and sulphur atoms is even more likely and is completely strainless. Molecular models show that the copper atoms lie in a straight line very close to each other suggesting that there may be bonds between them. This would contribute to the insolubility of the complexes as pointed

Can. J. Chem. Downloaded from www.nrcresearchpress.com by 210.87.254.40 on 09/05/12
For personal use only.

out by Frasson *et al.** Structure (VIII) accounts for all the facts including the reaction of 4,4-dimethyl tscs and is to be favored.



(R_4 = H or Me)

(VIII)

Several attempts to determine the molecular weight of these complexes failed, but a polymeric structure would conveniently explain their stability and their high insolubility.

Table I lists the various derivatives of tscs prepared and examined in the present work. They were made by the usual method (11) using an aldehyde and the appropriate substituted thiosemicarbazide. The reactions proceeded as expected in all cases except with 2-methyl-*S*-methyl thiosemicarbazide which did not give the corresponding 2,*S*-dimethyl tscs. Instead, benzaldehyde and *p*-chlorobenzaldehyde when treated with that reagent gave the corresponding 2-methyl semicarbazones, the S—Me group being obviously replaced by an oxygen atom. The reaction proceeded normally, however, in the case of *S*-methyl-4-methyl thiosemicarbazide.

Table II is a summary of the reactions of these substituted tscs with Cu(I) ions in alkaline solution, and the products obtained. In all cases where the N^2-hydrogen atom has been replaced by Me, there were no complexes formed. Only about 50% of the original tsc could be recovered as there was some decomposition. Likewise, when the sulphur atom was substituted with a methyl or benzyl group, there were no complexes formed. The fact that, with all other derivatives complexes of some kind were obtained, emphasizes the importance of the N^2-hydrogen atom, and the S—Cu bond and thus the significance of anion (V*b*).

We have also examined the reaction of various tscs with Cu(II) acetate in alcoholic solution (see Table III). The results were quite surprising since, instead of obtaining the expected 2:1 complexes, aromatic tscs gave 1:1 complexes identical with those obtained using Cu(I) in ammoniacal solution. Benzaldehyde 4,4-dimethyl tsc gave a mixture of 2:1 and 1:1 complexes identical with those obtained using Cu(I) as the reagent. Aliphatic tscs gave an insoluble compound which analyzed fairly close to a 2 tsc

**Reference added in proof: E. Frasson, R. Zannetti, R. Bardi, S. Bezzi, and G. Giacometti. The chemistry of the co-ordinate compounds, a symposium. Edited by H. Taube and A. G. Maddock. Pergamon Press. 1958. p. 452.*

Can. J. Chem. Downloaded from www.nrcresearchpress.com by 210.87.254.40 on 09/05/12
For personal use only.

to 3 Cu, and in some cases, in addition, the usual 1:1 complexes. The yields were, in every case, much lower than with Cu(I). Kuhn and Zilliken (8) had also found that aromatic tscs gave the same complexes both with Cu(I) and Cu(II), the yield being lower with the latter. It is likely that tscs reduce part of the Cu(II) to Cu(I) which then reacts with the unoxidized tscs. This type of reduction is quite common with organic sulphur compounds containing an oxidizable sulphur (2, 6, 8, 26, 27).

$$2R—S^- + 2Cu^{++} \rightarrow R—S—S—R + 2Cu^+$$

In some cases the disulphides and their copper complexes were obtained (2, 26). We did not isolate the disulphide–Cu complexes but we have identified from the soluble part of the reaction mixture some 2:1 complexes.

Infrared spectra of all these compounds have been taken in Nujol (Part I) and(or) KBr (Tables I, II, and IV). Table IV lists the typical bands in three regions, obtained from KBr disks, of a few tscs and their corresponding Cu(I) complexes. Contrary to the results reported in Part I from infrared spectra taken in Nujol mulls, it can be seen that both classes of compounds show three bands in the N—H stretching region. It appears that the very strong absorption of Nujol overlaps with the band at around 3100 cm^{-1} in certain cases. The two bands at about 3400 and 3200 cm^{-1} are shifted to higher frequencies by about 70 cm^{-1} in the complexes and the third band at 3150 cm^{-1} remains constant or is shifted down by 50 to 70 cm^{-1}. It is known that if a metal co-ordinate bond is formed with a nitrogen atom already bonded to H atoms, a shift of the N—H stretching bands to lower frequencies occurs, probably due to the increase in the polarity of the N—H bond (32). Although the shift to higher frequencies is difficult to explain, there is no doubt that the electronic environment of the NH_2 group has changed.

By examination of the spectra of various methyl-substituted tscs (Table I), it can be seen that differentiation between those three bands is difficult. The N^2-methyl compounds, although they have one less N—H group than free tscs, show the same number of bands in this region. The 2,4-dimethyl derivatives show only one band at around 3370–3340 cm^{-1} while the 4,4-dimethyl derivative of benzaldehyde tsc, with only one N—H group in the molecule shows two bands at 3260 and 3180 cm^{-1}. 4-Methyl compounds have two bands in this region.

The complexes in general show one additional band in the 1600 cm^{-1} region which can be attributed to an extra —C=N— as would be expected from any of the structures discussed above.

Tables I, II, and IV, also contain the region 1130–1010 cm^{-1} where a tentative assignment for the C=S vibration can be made. This vibration has been studied widely with many types of thio compounds and its assignment varies from about 1500 to 800 cm^{-1}. Davies and Jones (33), from a study of thioformamide, point out the difficulty of assigning a characteristic frequency for the C=S. The range 1400–1300 cm^{-1} has been suggested (34), and in thioacetamide the C=S was assigned at 1302 cm^{-1} (35). Lieber *et al.* (36) suggest the region 1395–1346 cm^{-1} in 4-substituted thiosemicarbazides. The band at 1100 cm^{-1} was assigned to C=S in thiopeptides (37), while the region 1200–1000 cm^{-1} was suggested for this vibration in thiocarbonyl compounds (38), and the region 1000 cm^{-1} in secondary thioamides (39). More recently, Bellamy (40) suggested the band at 1080 cm^{-1} in cyclic trithiocarbonates, 1200 cm^{-1} in dithioesters, and near 1000 cm^{-1} in some thioamides.

By comparing the spectra of tscs and their copper complexes (Tables I, II, and IV), it can be seen that a band disappears in the 1130–1080 cm^{-1} region. It is reasonable to

Can. J. Chem. Downloaded from www.nrcresearchpress.com by 210.87.254.40 on 09/05/12
For personal use only.

Can. J. Chem. Downloaded from www.nrcresearchpress.com by 210.87.254.40 on 09/05/12
For personal use only.

TABLE IV

Infrared absorptions in three regions of some typical tscs and their 1:1 copper complexes*

Compounds	tscs			1:1 copper complexes		
	3500–3000 cm^{-1}	1630–1515 cm^{-1}	1130–1010 cm^{-1}	3500–3000 cm^{-1}	1630–1515 cm^{-1}	1130–1010 cm^{-1}
Acetone	3400 m 3220 m 3150 m	1600 s	1115 m 1085 w 1035 m	3470 m 3300 m 3160 m	1625 m 1600 m	1080 w 1015 m
o-Fluorobenzaldehyde	3440 m 3250 m 3140 m	1600 s	1090 m 1070 m 1040 m	3460 m 3340 m 3140 vw	1620 m 1580 b	1040 w 1025 m
m-Fluorobenzaldehyde	3390 m 3230 m 3140 m	1600 s 1580 w	1100 m 1070 m	3460 m 3360 m 3070 w	1610 m 1575 b	1025 m
o-Chlorobenzaldehyde	3420 m 3250 m 3150 m	1600 m	1080 m 1055 m 1040 m	3490 m 3360 m 3150 vw	1600–1550 b	1060 m 1035 m
2,4-Dichlorobenzaldehyde	3480 m 3280 m 3160 m	1600 s	1120 m 1105 m 1060 m	3460 m 3380 m 3160 m	1600–1550 b	1110 m 1060 m
Nonanal	3400 m 3200–3100 b	1600 s	1110 s 1050 m	3450 m 3270 m 3100 m	1635 s 1610 m	1030 m
Octanal	3400 m 3250 m 3150 m	1600 s	1110 s 1050 m	3450 m 3280 m 3100 m	1610 w 1580 m	1030 m
Undecanal	3440 m 3300 m 3180 m	1610 s	1130 s 1050 m 1015 m	3450 m 3280 m 3100 m	1630 w 1610 m	1030 m

*From KBr pellets.

assume that this band is due to the C=S of the free tsc. Yamaguchi *et al.* (9) found that a strong band at 1083 cm^{-1} in thiourea is extremely weakened or disappears upon complex formation with a metal and they attributed this band to C=S.

In the region where the "thioureide" band has been assigned by Randall (41) between 1613 and 1471 cm^{-1}, Ettlinger (42) at 1508 cm^{-1} and at 1495 cm^{-1} (43), there are no noticeable differences between spectra of tscs and their copper complexes.

EXPERIMENTAL

Thiosemicarbazones were generally prepared by the method of Sah and Daniels (44). Preparations of the various substituted thiosemicarbazides were carried out according to the procedures referred to in Table I, except for *S*-methyl-4-methyl thiosemicarbazide, which is described below. Reactions of substituted tscs with Cu(I) (Table II) were carried out as described in Part I (11). Melting points (corrected), yields, solvents used in purification, bands in three regions of the infrared spectrum, and analyses are shown in the tables.

Preparation of S-Methyl-4-methyl Thiosemicarbazide.HI

A mixture of 4-methyl thiosemicarbazide (32) (14.3 g, 0.1 mole) and methyl iodide (20.5 g, 0.15 mole) dissolved in isopropyl alcohol (115 ml) and acetone (200 ml) was refluxed for 1.5 hours. The solution became yellow and after cooling, the white solid that precipitated out was collected by filtration and recrystallized from absolute alcohol. It had m.p. 164° C; yield: 15 g, 59%. The compound is sensitive to moisture and was kept in dry alcohol and recovered only before use in the next step.

Preparation of Benzaldehyde-S,4-dimethyl tsc (No. 4, Table I)

S,4-Dimethyl thiosemicarbazide.HI (4.94 g, 0.02 mole, corresponding to 2.38 g, 0.02 mole free base) was dissolved in water (60 ml) and neutralized with NaOH *N*/1 (20 ml). The solution turned dark yellow probably due to some liberated iodine. Two drops of acetic acid were added followed by 50 ml of an alcoholic solution of benzaldehyde (2.12 g, 0.02 mole). The clear solution obtained was heated for 15 minutes on the steam bath and cooled. The dark red oil that separated was taken up in ether and dried over drierite. After evaporation of the solvent, the residue was dissolved in *n*-hexane and after cooling, benzaldehyde-*S*,4-dimethyl tsc crystallized out.

Reaction between Benzaldehyde-4,4-dimethyl tsc and CuCl

To a boiling solution of benzaldehyde-4,4-dimethyl tsc (2.4 g, 0.11 mole) in MeOH (50 ml) was added, dropwise, a solution of CuCl (1.16 g, 0.11 mole) in ammonia (25 ml, sp. gr. 0.9). A brown precipitate was formed and heating and stirring were continued for 15 minutes after the addition had been completed. The mixture was allowed to cool and the precipitate was collected by filtration and washed with HCl 3% and water. Part of this solid was soluble in acetone from which it was recrystallized; this was the 2:1 complex (No. 5*b*, Table II). The insoluble fraction was washed successively with ammonia, water, HCl 3%, water, acetone, ether, and alcohol, after which it gave fairly good analysis for the 1:1 complex (No. 5*a*, Table II).

Reaction between p-Chlorobenzaldehyde-4,4-dimethyl tsc and CuCl

This was carried out as above except that the precipitate obtained was not too soluble in acetone. It was dissolved in toluene from which it was recovered by evaporation. This corresponds to the 2:1 complex (No. 7, Table II). No 1:1 complex was isolated in this case from the insoluble residue.

Can. J. Chem. Downloaded from www.nrcresearchpress.com by 210.87.254.40 on 09/05/12
For personal use only.

Attempt to React Benzaldehyde-2-methyl tsc with CuCl

The following is typical of attempts made to react 2-methyl-substituted tscs with CuCl.

To a refluxing solution of benzaldehyde-2-methyl tsc (5.8 g, 0.03 mole) in MeOH (200 ml) was added, dropwise, a solution of CuCl (4 g, 0.04 mole) in ammonia (50 ml). A small amount of a precipitate was observed and this when collected was found to be inorganic and had a high copper content (50%). The remaining solution was neutralized with HCl, diluted with water, and cooled. The starting material (3 g) crystallized out; m.p. and mixed m.p. 175° C.

Reaction between p-Chlorobenzaldehyde tsc and Copper Acetate

To a boiling solution of *p*-chlorobenzaldehyde tsc (5.3 g, 0.025 mole) in ethanol (200 ml) was added slowly a solution of cupric acetate (5 g, 0.025 mole) in the same solvent (150 ml). A light yellow compound precipitated out and, after cooling, was collected by filtration and washed on the filter with hot acetone. This precipitate was found to be the 1:1 complex, identical with the one described in Part I; m.p., mixed m.p., and infrared spectra. No other products were isolated from the mother liquor.

Other reactions with cupric acetate were carried out in a similar manner and the various products obtained are described in Table III.

ACKNOWLEDGMENTS

We are indebted to Mr. E. C. Goodhue of the Analytical Section for the copper analyses and infrared spectra, and also to Dr. M. L. Hair of the Chemical Engineering Section for the magnetic moment measurements.

REFERENCES

1. K. A. JENSEN and J. F. MIGUEL. Acta Chem. Scand. **6**, 189 (1952).
2. R. WEISS and H. VENNER. Z. physiol. Chem. **317**, 82 (1959).
3. S. ÅKERSTRÖM. Arkiv Kemi, **14**, 387 (1959).
4. K. A. JENSEN. Z. anorg. u. allgem. Chem. **221**, 6 (1934).
5. K. A. JENSEN. Z. anorg. u. allgem. Chem. **221**, 11 (1934).
6. K. A. JENSEN and E. RANCKE-MADSEN. Z. anorg. u. allgem. Chem. **219**, 243 (1934).
7. G. N. MAHAPATRA. J. Proc. Inst. Chemists (India), **31**, 113 (1959).
8. R. KUHN and F. ZILLIKEN. U.S. Patent No. 2,695,911 (November, 1954).
9. A. YAMAGUCHI, R. B. PENLAND, S. MIZUSHIMA, T. J. LANE, C. CURRAN, and J. V. QUAGLIANO. J. Am. Chem. Soc. **80**, 527 (1958).
10. F. T. COUNTER, JR., R. N. DUVALL, W. O. FOYE, and R. W. VANDERWYK. J. Am. Pharm. Assoc. Sci. Ed. **49**, 140 (1960).
11. B. A. GINGRAS, R. W. HORNAL, and C. H. BAYLEY. Can. J. Chem. **38**, 712 (1960).
12. B. G. BENNS, B. A. GINGRAS, and C. H. BAYLEY. Appl. Microbiol. **8**, 353 (1960).
13. S. G. BOGOMOLOV, E. A. POSTOVSKI, and U. H. SCHEINKER. Doklady Akad. Nauk S.S.S.R. **91**, 1111 (1953).
14. F. J. WILSON and R. BURNS. J. Chem. Soc. 870 (1922).
15. J. CYMERMAN-CRAIG, D. WILLIS, S. D. RUBBO, and J. EDGAR. Nature, **176**, 34 (1955).
16. H. G. MAUTNER and W. D. KUMLER. J. Am. Chem. Soc. **78**, 97 (1956).
17. K. A. JENSEN and E. RANCKE-MADSEN. Z. anorg. u. allgem. Chem. **227**, 25 (1936).
18. H. J. EMELÉUS and A. G. SHARPE. Advances in inorganic chemistry and radiochemistry. Vol. II. Academic Press Inc., New York. 1960. p. 38.
19. P. NIGGLI. Z. Krist. **57**, 253 (1922).
20. W. DANNHAUSER and P. A. VAUGHAN. J. Am. Chem. Soc. **77**, 896 (1955).
21. W. SOLLER and A. J. THOMPSON. Phys. Rev. **47**, 644 (1935).
22. I. D. BROWN and J. D. DUNITZ. Abstr. Papers Intern. Conf. on Co-ordination Chem. London. 1959.
23. J. C. BAILAR, JR. The chemistry of the coordination compounds. Reinhold Publishing Corp., New York. 1956. p. 167.
24. H. J. EMELÉUS and J. S. ANDERSON. Modern aspects of inorganic chemistry. 2nd ed. Routledge and Kegan Paul Ltd., London. 1952. p. 140.
25. G. BODLÄNDER and O. STARBECK. Z. anorg. Chem. **31**, 1 (1902).
26. E. CATTELAIN. Bull. soc. chim. 49 (1945).

Can. J. Chem. Downloaded from www.nrcresearchpress.com by 210.87.254.40 on 09/05/12
For personal use only.

27. V. N. POCHAĬNOVA, E. I. KRYLOV, and D. I. RYABCHIKOV. Zhur. Neorg. Khim. **1**, 406 (1956).
28. A. H. GREER and G. B. L. SMITH. J. Am. Chem. Soc. **72**, 874 (1950).
29. J. BERNSTEIN, W. A. LOTT, and F. Y. WISELOGLE. U.S. Patent No. 2,635,115 (April, 1953).
30. G. TRAVERSO. Gazz. chim. ital. **83**, 1027 (1953).
31. K. A. JENSEN. J. prakt. Chem. **159**, 189 (1941).
32. G. F. SVATOS, C. CURRAN, and J. V. QUAGLIANO. J. Am. Chem. Soc. **77**, 6159 (1955).
33. M. DAVIES and W. J. JONES. J. Chem. Soc. 955 (1958).
34. N. B. COLTHUP. J. Opt. Soc. Am. **40**, 397 (1950).
35. R. MECKE and H. SPIESECKE. Chem. Ber. **89**, 1110 (1956).
36. E. LIEBER, C. N. R. RAO, C. N. PILLAI, J. RAMACHANDRAN, and R. D. HITES. Can. J. Chem. **36**, 801 (1958).
37. R. MECKE, JR. and R. MECKE. Chem. Ber. **89**, 343 (1956).
38. R. MECKE, JR., R. MECKE, and A. LUTTRINGHAUS. Chem. Ber. **90**, 975 (1957).
39. D. HADŽI. J. Chem. Soc. 847 (1957).
40. L. J. BELLAMY and P. E. ROGASH. J. Chem. Soc. 2218 (1960).
41. H. M. RANDALL, R. G. FOWLER, N. FUSON, and J. R. DANGL. Infrared determination of organic structures. D. Van Nostrand Co., Inc., New York. 1949.
42. M. G. ETTLINGER. J. Am. Chem. Soc. **72**, 4699 (1950).
43. J. MANN. Trans. Inst. Rubber Ind. **27**, 232 (1951).
44. P. T. SAH and T. C. DANIELS. Rec. trav. chim. **69**, 1545 (1950).

Can. J. Chem. Downloaded from www.nrcresearchpress.com by 210.87.254.40 on 09/05/12
For personal use only.

Can. J. Chem. Downloaded from www.nrcresearchpress.com by 210.87.254.42 on 09/05/12
For personal use only.

THE INTERACTION OF BORON TRIFLUORIDE WITH HYDRAZINE[1]

W. G. PATERSON[2] AND M. ONYSZCHUK

ABSTRACT

Boron trifluoride and anhydrous hydrazine react rapidly at 25° *in vacuo* yielding a 1:1 complex compound, $BF_3 \cdot N_2H_4$ (m.p. 87°), while at higher temperatures, or with diethyl ether as solvent, they form complex mixtures containing 52.2 to 63.5 mole percent BF_3; but in tetrahydrofuran solution the 2:1 adduct, $2BF_3 \cdot N_2H_4$ (m.p. 260°) is formed. The X-ray powder diffraction pattern of $BF_3 \cdot N_2H_4$ consists of 28 lines from which a unit cell with triclinic symmetry was calculated. The thermal decomposition of $BF_3 \cdot N_2H_4$ is complex, yielding in part N_2, NH_3, NH_4BF_4, and BN. Hydrolysis of $BF_3 \cdot N_2H_4$ yields a mixture of hydroxyfluoroborate ions. At −80°, $BF_3 \cdot N_2H_4$ absorbs NH_3 to form a diammoniate which liberates NH_3 slowly at higher temperatures. Partial displacement of BF_3 from $BF_3 \cdot N_2H_4$ by HCl and partial absorption of HCl by $BF_3 \cdot N_2H_4$ occur simultaneously at 110°.

Infrared spectra of $BF_3 \cdot N_2H_4$ and $2BF_3 \cdot N_2H_4$ have been measured in the range of 4000 to 650 cm^{-1} and frequency assignments have been made.

Boron trifluoride forms co-ordination complexes with a variety of nitrogen compounds such as ammonia, amines, imines, amides, nitriles, and nitrogen-containing heterocyclics (1, 2, 3). The lone electron pair on the nitrogen atom in these compounds readily forms a co-ordinate bond with the electron-deficient boron trifluoride molecule. Since hydrazine has two available electron pairs, one on each nitrogen atom, it is interesting to determine whether this molecule will co-ordinate with one or two molecules of boron trifluoride. In two independent studies (4, 5) it was found that diborane reacted with hydrazine to form the addition compound $H_3B \cdot NH_2NH_2 \cdot BH_3$, indicating that both nitrogen atoms in hydrazine are capable of co-ordinating with borane groups. This paper is the first of a series dealing with the reactions of electron-deficient molecules with hydrazine. Since boron trifluoride is one of the most active electron acceptors, its reaction with hydrazine was investigated first.

RESULTS AND DISCUSSION

It was found that the reaction of boron trifluoride with anhydrous hydrazine at −80°, in the absence of a solvent, was extremely slow. At room temperature, however, a solid white 1:1 complex compound, boron trifluoride-hydrazine, $BF_3 \cdot N_2H_4$ (m.p. 87°), was formed within a few minutes. With reaction times of 2 and 3 hours, complexes having ratios of boron trifluoride to hydrazine of 1.09 and 1.16, respectively, were obtained. The latter complex, when treated with additional boron trifluoride in diethyl ether as solvent for 11 hours, gave a substance with an empirical composition of $(BF_3)_{1.72}N_2H_4$. The reaction of boron trifluoride with hydrazine in diethyl ether produced complexes of different stoichiometry. Depending upon such experimental conditions as efficiency of mixing, reaction time, and temperature, substances were obtained with boron trifluoride to hydrazine ratios in the range 1.42 to 1.88, but the ratio was never 2.* Similar results were obtained for the reaction of boron trifluoride with hydrazine at 140 and 200°. With tetrahydrofuran as solvent, however, the product was 2-boron trifluoride-hydrazine, $2BF_3 \cdot N_2H_4$ (m.p. 260°). It is noteworthy that tetrahydrofuran also promoted the for-

[1]*Manuscript received November 18, 1960.*

Contribution from the Inorganic Chemistry Laboratory, McGill University, Montreal, Quebec, with financial assistance from the Defence Research Board of Canada, under Grant Number 9530-20, Project D46-95-30-20.

[2]*Holder of National Research Council Studentships, 1957–59. Present address: Physical Chemistry Laboratory, Oxford, England.*

*One of the referees has suggested that the non-stoichiometric mixtures were possibly solid solutions.

Can. J. Chem. Downloaded from www.nrcresearchpress.com by 210.87.254.42 on 09/05/12
For personal use only.

mation of 2-boron trifluoride-ethylenediammine (6), whereas the 1:1 adduct resulted in diethyl ether solution.

The formation of 1:1 and 2:1 addition compounds between boron trifluoride and hydrazine indicates that both nitrogen atoms in hydrazine are strong electron-pair donors. This is expected on the basis of the configuration of the hydrazine molecule (7), which shows that the electron pairs on each of the two nitrogen atoms are probably located in tetrahedral (sp^3) hybrid orbitals and are readily accessible for the formation of one or two co-ordinate bonds with suitable acceptor molecules. While the 1:1 adduct formed easily by direct interaction of boron trifluoride with hydrazine, the 2:1 adduct could not be obtained in the same way. Apparently the formation of one co-ordinate link reduces the availability of the lone electron pair on the other nitrogen atom for bonding with a second boron trifluoride molecule. The decreased reactivity of the second electron pair in hydrazine seems to be a general rule (8). In tetrahydrofuran solution both electron pairs appear to be readily available so that the 2:1 complex was the only product.

The hydrazine – boron trifluoride phase diagram in the range 46.5 to 66.7 mole% boron trifluoride (Fig. 1) clearly shows a maximum at 50 mole% boron trifluoride corresponding

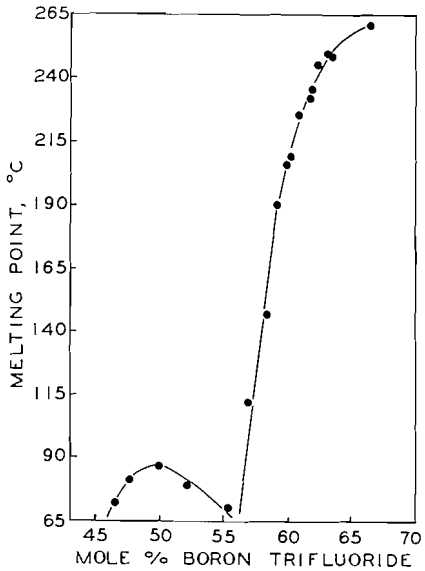


FIG. 1. A portion of the phase diagram of the system hydrazine – boron trifluoride.

to the 1:1 adduct. A second maximum at 66.7 mole% boron trifluoride, corresponding to the 2:1 adduct, is inferred since at the extreme right of the complete phase diagram, i.e. at 100 mole% boron trifluoride, the curve must drop to −127°, the melting point of pure boron trifluoride. The absence of a peritectic point in the region investigated rules out the possibility of incongruently melting compounds of intermediate stoichiometry, such as, $3BF_3 \cdot 2N_2H_4$. The phase diagram was investigated only in the range 46.5 to 66.7 mole% boron trifluoride because it was not possible to obtain, by direct interaction or by reaction in a solvent, solid complex compounds with boron trifluoride contents outside this range.

The compound boron trifluoride-hydrazine was insoluble in diethyl ether and slightly

soluble in acetone. The compound 2-boron trifluoride-hydrazine was soluble in tetrahydrofuran. Both new compounds were hygroscopic and dissolved readily in water yielding acidic solutions, which retained the reducing properties of hydrazine in that these aqueous solutions decolorized instantly an aqueous solution of potassium permanganate.

Infrared spectra of the 1:1 and 2:1 complex compounds (Fig. 2), obtained by the

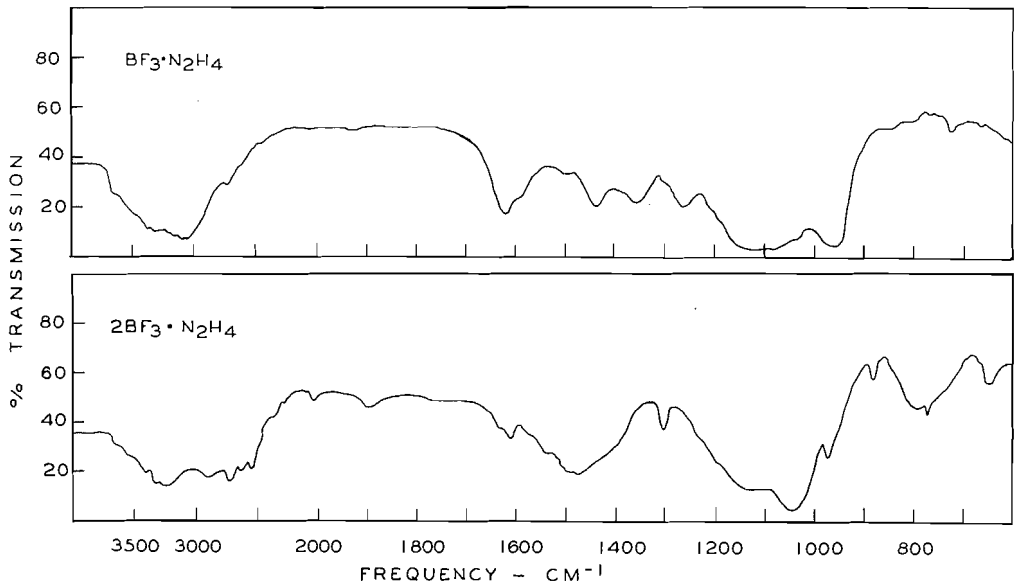


FIG. 2. Infrared spectra of $BF_3 \cdot N_2H_4$ and $2BF_3 \cdot N_2H_4$ in KBr disks.

potassium bromide pellet technique, consist of broad and unresolved bands which nevertheless indicate vibration frequencies (Table I) characteristic of the constituent BF_3 and N_2H_4 molecules together with a B—N stretching frequency in the vicinity of 1035 cm^{-1}. The assignments in Table I have been made by analogy with the infrared spectra

TABLE I

Infrared absorption bands of $BF_3 \cdot N_2H_4$ and $2BF_3 \cdot N_2H_4$

$BF_3 \cdot N_2H_4$ (cm^{-1})	$2BF_3 \cdot N_2H_4$ (cm^{-1})	Assignment
3650 to 3050, s, b	3650 to 2550, s, b	N—H stretching
1620 s	1610 m	NH_2 deformation (asym.)
1440 s	1475 s, b	NH_2 deformation (sym.)
1355 m	1300 m	NH_2 rocking
1260 m		Unidentified
1100 vs, vb; 1035 s, sh, u	1200 to 1040, s, u	B—F asym. stretching and B—N stretching (BF_4^-?)
965 s	970 s	N—N stretching
	883 w	Unidentified
725 w	775 m	NH_2 wagging and BF_3 bending

s = strong, m = medium, w = weak, b = broad, u = unresolved

Can. J. Chem. Downloaded from www.nrcresearchpress.com by 210.87.254.42 on 09/05/12
For personal use only.

of N_2H_4 (7), $BF_3 \cdot NH_3$ (9), $C_5H_5N \cdot BF_3$ (10), $N_2H_4 \cdot HCl$ (11), and $N_2H_4 \cdot 2HCl$ (12). It is not possible to confirm or deny the presence of BF_4^- since its characteristic band at 1020–1100 cm^{-1} (13) might be superimposed on the B—F and B—N stretching frequencies which also occur in this region.

The Debye–Scherrer X-ray powder diffraction pattern of $BF_3 \cdot N_2H_4$ consists of 28 lines, the intensities and interplanar spacings of which are given in Table II. From these

TABLE II

X-ray powder diffraction data for $BF_3 \cdot N_2H_4$*

Line	Intensity	d_{obs} (Å)	d_{calc} (Å)	*hkl*
1	vvw	5.50	5.52	100
2	vvw	4.87	4.87	010
3	vs	4.27	4.23	001
4	vs	3.47	3.47	$\bar{1}01$
5	vw	3.25	3.25	101
6	vw	3.11	3.10	$2\bar{1}0$
7	vvw	2.96	2.99	110
8	s	2.78	2.76	200
9	s	2.43	2.43	011, 020
10	m	2.31	2.31	$3\bar{2}1$
11	vw	2.22	2.24	$1\bar{2}\bar{2}$
12	w	2.11	2.11	002
13	w	2.03	2.03	210, 111
14	w	1.93	1.93	$10\bar{2}$
15	vvw	1.80	1.80	$1\bar{3}0$
16	vvw	1.76	1.76	$\bar{1}21$
17	vvw	1.65	1.65	021
18	w	1.57	1.56	$01\bar{2}$
19	vvw	1.48	1.49	$04\bar{1}$
20	vvw	1.44	1.44	$\bar{3}02$
21	vvw	1.39	1.39	130
22	vvw	1.34	1.34	103, 302
23	vvw	1.26	1.26	$21\bar{2}$
24	vvw	1.23	1.24	$01\bar{4}$
25	vvw	1.19	1.19	$\bar{4}10$
26	vvw	1.16	1.16	$\bar{3}03$
27	vvw	1.13	1.13	$\bar{2}13$
28	vvw	1.11	1.10	500

s = strong, m = medium, w = weak, v = very

*A 57.30-mm camera was used.

measurements the following dimensions of a crystallographic unit cell with triclinic symmetry were calculated by applying Ito's reciprocal lattice method (14): $a = 6.93$ Å, $b = 5.50$ Å, $c = 6.78$ Å; $\alpha = 111.5°$, $\beta = 64.0°$, $\gamma = 88.3°$. While these dimensions represent a solution of the observed X-ray powder pattern, they must be confirmed by X-ray pattern measurements on a single crystal of $BF_3 \cdot N_2H_4$ before they can be accepted as the dimensions of the true unit cell. Other boron trifluoride adducts such as $BF_3 \cdot NH_3$, $BF_3 \cdot CH_3NH_2$, and $BF_3 \cdot (CH_3)_3N$ have orthorhombic, monoclinic, and hexagonal symmetry respectively (15).

Boron trifluoride-hydrazine was stable indefinitely *in vacuo* at room temperature. Decomposition occurred slowly at 190° and was almost complete at about 300° after 5 hours, yielding mainly nitrogen, ammonia, ammonium fluoroborate, and boron nitride. Since the boron–nitrogen bond is probably the weakest one in the addition compound, it seems reasonable to assume that the first step in the pyrolysis was the dissociation reaction,

$$N_2H_4 \cdot BF_3 \rightarrow BF_3 + N_2H_4.$$

Can. J. Chem. Downloaded from www.nrcresearchpress.com by 210.87.254.42 on 09/05/12
For personal use only.

Boron trifluoride is stable at 300° (1) while hydrazine decomposes slowly at this temperature into ammonia and nitrogen (16, 17)

$$3N_2H_4 \rightarrow 4NH_3 + N_2.$$

Subsequent interaction of ammonia with boron trifluoride to give a 1:1 adduct,

$$NH_3 + BF_3 \rightarrow NH_3 \cdot BF_3$$

could be followed by its thermal decomposition into ammonium fluoroborate and boron nitride (18),

$$4(NH_3 \cdot BF_3) \rightarrow 3NH_4BF_4 + BN.$$

The over-all reaction, taken as the sum of the above reactions,

$$12(BF_3 \cdot N_2H_4) \rightarrow 4N_2 + 4NH_3 + 9NH_4BF_4 + 3BN$$

accounted quantitatively for the nitrogen production (the ratio of $BF_3 \cdot N_2H_4$ used to N_2 produced was 2.98), but only qualitatively for the other observed products.

The apparent molecular weight of $BF_3 \cdot N_2H_4$ in aqueous solution (49.5 and 54.5 in separate experiments) was approximately one half of the calculated formula weight (99.9), suggesting that the initial action of water gave two ions per formula weight, probably by the following reaction:

$$BF_3 \cdot N_2H_4 + H_2O \rightleftarrows N_2H_5^+ + BF_3OH^-.$$

Since positive tests for fluoroborate ion, BF_4^-, were obtained, it appeared that the hydroxyfluoroborate ion might have been involved in a disproportionation reaction:

$$2BF_3OH^- \rightleftarrows BF_4^- + BF_2(OH)_2^-.$$

Disproportionation of $BF_2(OH)_2^-$, as represented by (19):

$$2BF_2(OH)_2^- \rightleftarrows BF_4^- + B(OH)_4^- \quad \Updownarrow \quad B(OH)_3 + OH^-$$

was presumed to occur in view of the fact that the basicity of the aqueous solution increased slightly on standing. Although the various ionic species (except BF_4^-) were not identified, the results were consistent with the observation that the hydrolysis of boron trifluoride itself yields a mixture of hydroxyfluoroboric acids (1).

No significant reaction occurred between anhydrous hydrogen chloride and boron trifluoride-hydrazine either at −96° or at 25°, but at 110°, the results shown in Table III were obtained. Three points seem noteworthy: (i) evidently HCl displaced BF_3

TABLE III

Results for the interaction of HCl with $BF_3 \cdot N_2H_4$

Experiment number	1	2
Initial HCl, mmole	8.05	2.73
Initial $BF_3 \cdot N_2H_4$, mmole	3.73	2.71
Reaction time, hr	15	15
Recovered HCl, mmole	4.36	0.60
Consumed HCl, mmole	3.69	2.13
Liberated BF_3, mmole	0.61	0.23
% BF_3 displaced	16.4	8.6

from $BF_3 \cdot N_2H_4$, (ii) the amount of HCl absorbed by the complex was much greater than the amount of BF_3 liberated, suggesting that 1:1:1 complex $BF_3 \cdot N_2H_4 \cdot HCl$ was

Can. J. Chem. Downloaded from www.nrcresearchpress.com by 210.87.254.42 on 09/05/12
For personal use only.

formed in substantial quantities, and (iii) the extent of displacement of BF_3 decreased when the initial amount of HCl was lower.

At −80°, $BF_3 \cdot N_2H_4$ readily absorbed ammonia, forming a diammoniate, $BF_3 \cdot N_2H_4 \cdot 2NH_3$. On warming to room temperature ammonia was evolved in two stages, but it was not possible to isolate complexes of definite stoichiometry such as $BF_3 \cdot N_2H_4 \cdot NH_3$. Ammonia was thought to be bound to $BF_3 \cdot N_2H_4$ by weak dipole–dipole forces.

EXPERIMENTAL

Since most of the materials used in this work are gaseous and react rapidly with atmospheric moisture, it was necessary to manipulate them in a standard vacuum system (20) equipped with stopcocks and ground-glass joints lubricated with Kel-F grease. Prolonged contact of vapors with this grease was avoided by using all-glass reaction vessels and storage bulbs fitted with capillary break-seals instead of stopcocks. The purity of a volatile compound was checked by determination of its vapor pressure and molecular weight (M). Molecular weights were determined by the vapor density method with an accuracy usually better than 1%. Debye–Scherrer X-ray powder diffraction patterns were obtained from samples sealed in glass tubes of 0.01-mm wall thickness. The pictures were taken on a Seifert apparatus using the Cu $K\alpha$ radiation filtered by nickel. Infrared spectra were measured with a Perkin–Elmer Model 21 double-beam spectrophotometer fitted with sodium chloride optics.

Anhydrous hydrazine was prepared by refluxing the 95+% material (Eastman Kodak) for 3 hours over potassium hydroxide pellets in an atmosphere of dry nitrogen. The fraction boiling in the range 111–113° was found to be 100% pure by the iodate method (8). Commercial boron trifluoride, hydrogen chloride, and ammonia were purified by low-temperature fractionation.

Interaction of Boron Trifluoride with Hydrazine

In a typical experiment boron trifluoride (11.63 mmoles) and anhydrous hydrazine (5.89 mmoles) were brought together *in vacuo* and kept at room temperature for 30 minutes before the mixture was frozen with liquid air. A vigorous exothermic reaction yielded a white solid which was involatile at room temperature and contained boron trifluoride and hydrazine in a 1:1 ratio, corresponding to the compound $BF_3 \cdot N_2H_4$ (found: N_2H_4, 33.3%. $BF_3 \cdot N_2H_4$ requires: N_2H_4, 32.1%). The amount of unchanged boron trifluoride (5.81 mmoles. Found: M, 67.8. Calc. for BF_3: M, 67.8) recovered by distillation at −80°, also indicated that boron trifluoride (5.82 mmoles) had reacted with hydrazine (5.89 mmoles) in a 1:1 ratio. The melting point of the adduct was 87°. Using identical procedures and longer reaction times, complex mixtures with BF_3/N_2H_4 ratios of 1.09 and 1.16 were obtained (Table IV). The latter product (0.237 g) was treated with additional

TABLE IV

Boron trifluoride-hydrazine complex mixtures

Composition ratio BF_3/N_2H_4	Reaction conditions	Analysis % N_2H_4
1.09	2 hr *in vacuo* at 25°	30.4
1.16	3 hr *in vacuo* at 25°	28.3
1.40	Diethyl ether solution	25.2
1.70	Diethyl ether solution	21.8
1.84	Diethyl ether solution	20.4
1.88	Diethyl ether solution	20.1

Can. J. Chem. Downloaded from www.nrcresearchpress.com by 210.87.254.42 on 09/05/12
For personal use only.

boron trifluoride (15.3 mmoles) in diethyl ether (15 ml) for 11 hours. A substance of empirical composition $(BF_3)_{1.72}\cdot N_2H_4$ (found: N_2H_4, 21.6%) was recovered after distillation of the solvent and excess boron trifluoride at room temperature.

Additional complexes with different compositions, were obtained by the interaction of boron trifluoride and hydrazine in diethyl ether as solvent (Table IV). Similar results were obtained for the reaction *in vacuo* of boron trifluoride with hydrazine above room temperature. In a typical experiment, boron trifluoride (11.7 mmoles) and hydrazine (3.87 mmoles) were sealed in an all-glass reaction vessel and kept for 4 hours at 140°. The amount of boron trifluoride recovered (4.67 mmoles; found: M, 67.5; calc. for BF_3: M, 67.8) by distillation at room temperature showed that the white solid reaction product contained BF_3 and N_2H_4 in a ratio of 1.84:1 (found: N_2H_4, 20.9%; calc. for $(BF_3)_{1.84}\cdot N_2H_4$: N_2H_4, 19.8%).

In another experiment boron trifluoride (34.5 mmoles), hydrazine (10.1 mmoles), and anhydrous tetrahydrofuran (25 g) were condensed together in an all-glass reaction vessel which was then sealed off *in vacuo*. The reactants were stirred (magnetically) overnight at room temperature; a clear solution resulted. The solvent and the excess of boron trifluoride were removed by distillation under low pressure at room temperature; this left a white crystalline deposit of a new compound, 2-boron trifluoride-hydrazine, $2BF_3\cdot N_2H_4$ (found: N_2H_4, 19.25%; calc. for $2BF_3\cdot N_2H_4$: N_2H_4, 19.12%). Its melting point was 260°.

Pyrolysis of $N_2H_4\cdot BF_3$

Vapor pressure measurements in the range 140 to 220° showed that the compound decomposed irreversibly, with nitrogen and ammonia as the only volatile products. Pyrolysis of the adduct (5.65 mmoles) at 275–300° for 4.5 hours in an all-glass vessel gave nitrogen (1.72 mmoles; M: found, 27.8; calc., 28.0) together with a white solid residue which contained some unchanged 1:1 compound (0.52 mmole). An X-ray powder diffraction pattern showed that ammonium fluoroborate and boron nitride were the major components, with the former present in much larger amount. The presence of at least one unidentified solid compound in the residue was suggested by the X-ray data. Although reproducible analytical results were obtained for fluoroborate ion, these were considered unreliable in view of the fact that the hydrolysis of unchanged 1:1 compound yields an uncertain amount of fluoroborate ion.

Hydrolysis of $BF_3\cdot N_2H_4$

Two aqueous freezing point depression measurements indicated apparent molecular weights in solution of 49.5 and 54.5, or approximately one half the formula weight of $BF_3\cdot N_2H_4$, which is 99.9. Potassium chloride (1), cesium sulphate (1), and nitron acetate (21) solutions all gave precipitates when added to an aqueous solution of $BF_3\cdot N_2H_4$, thus confirming the presence of fluoroborate ion, BF_4^-. It was also noted that the initial acidity (pH = 4.35) of a dilute aqueous solution of $BF_3\cdot N_2H_4$ decreased slightly (pH = 4.65) on standing for 35 minutes.

Interaction of $BF_3\cdot N_2H_4$ with Hydrogen Chloride

Anhydrous hydrogen chloride (8.05 mmoles) and boron trifluoride-hydrazine (3.73 mmoles) were sealed in an all-glass vessel and left overnight at 110°. The products of the reaction were a non-volatile solid and a gas which was recovered by distillation at −80° (4.97 mmoles; found: M, 40.3; calc. for HCl: M, 36.5; calc. for BF_3: M, 67.8). The infrared spectrum of the gas showed clearly that it was a mixture of HCl (22) and BF_3 (23).

Can. J. Chem. Downloaded from www.nrcresearchpress.com by 210.87.254.42 on 09/05/12
For personal use only.

From the molecular weight value of 40.3, it was calculated, assuming ideal gaseous behavior, that this volatile fraction consisted of 4.36 mmoles HCl and 0.61 mmole BF_3. Thus 3.69 mmoles of HCl reacted with 3.73 mmoles of $BF_3 \cdot N_2H_4$ yielding a solid residue and 0.61 mmoles BF_3. The solid residue was probably a complex mixture of $BF_3 \cdot N_2H_4 \cdot HCl$, $N_2H_4 \cdot HCl$, and $N_2H_4 \cdot 2HCl$, which could not be separated by fractional sublimation.

In an attempt to prepare pure $BF_3 \cdot N_2H_4 \cdot HCl$, $BF_3 \cdot N_2H_4$ (2.71 mmoles) and HCl (2.73 mmoles) were condensed together and kept overnight at 110° in an all-glass reaction vessel. Again the products were a non-volatile solid and a gas (0.835 mmole; found: M, 45.2), which was shown by its infrared spectrum to be a mixture of BF_3 and HCl. The composition of this volatile mixture was estimated to be 0.60 mmole of HCl and 0.23 mmole of BF_3. Thus, as before, it appeared that both displacement of BF_3 from $BF_3 \cdot N_2H_4$ by HCl and absorption of HCl by $BF_3 \cdot N_2H_4$ occurred simultaneously.

Interaction of $BF_3 \cdot N_2H_4$ with Ammonia

When anhydrous ammonia (10.38 mmoles) and $BF_3 \cdot N_2H_4$ (1.86 mmoles) were left in contact for 1 hour at −80°, the amount of ammonia (6.66 mmoles; found: M, 17.0; calc. for NH_3: M, 17.03) recovered by distillation at −80° indicated that the diammoniate, $BF_3 \cdot N_2H_4 \cdot 2NH_3$, had been formed at −80°. Above −80°, this crystalline compound dissociated irreversibly, evolving ammonia in what appeared to be two distinct stages as evident from the results summarized in Table V, but it was not possible to confirm the

TABLE V

Dissociation of the diammoniate of $BF_3 \cdot N_2H_4$

Distillation temperature, °C	Ammonia recovered, mmole	Molecular weight of recovered ammonia (calc. M, 17.03)
−64	0.64	17.1
−46	0.81	17.9
−26	None	—
0	1.50	17.4
+28	0.75	17.2

presence of the monoammoniate. Measurements of the dissociation pressure were not reproducible and the conventional plot of log $p_{(mm)}$ against $1/T$ was always concave to the reference axes.

ACKNOWLEDGMENTS

We are grateful to the Defence Research Board for financial assistance and to the National Research Council for the award of two Studentships to one of us (W.G.P.). We are indebted to Dr. R. St. J. Manley of the Pulp and Paper Research Institute of Canada for X-ray diffraction measurements and for assistance in their interpretation.

REFERENCES

1. H. S. Booth and D. R. Martin. Boron trifluoride and its derivatives. John Wiley & Sons, Inc., New York. 1949. p. 43.
2. N. N. Greenwood and R. L. Martin. Quart. Revs. (London), **8**, 1 (1954).
3. F. G. A. Stone. Chem. Revs. **58**, 101 (1958).
4. M. J. Steindler and H. I. Schlesinger. J. Am. Chem. Soc. **75**, 756 (1953).
5. H. J. Emeléus and F. G. A. Stone. J. Chem. Soc. 840 (1951).
6. C. A. Brown, E. L. Muetterties, and E. G. Rochow. J. Am. Chem. Soc. **76**, 2537 (1954).
7. P. A. Giguère and I. D. Liu. J. Chem. Phys. **20**, 136 (1952).

Can. J. Chem. Downloaded from www.nrcresearchpress.com by 210.87.254.42 on 09/05/12
For personal use only.

8. L. F. AUDRIETH and B. A. OGG. The chemistry of hydrazine. John Wiley & Sons, Inc., New York. 1951.
9. J. GOUBEAU and H. MITSCHELEN. Z. physik Chem. (Frankfurt), **14**, 61 (1958).
10. H. LUTHER, D. MOOTZ, and F. RADWITZ. J. prakt. Chem. **5**, 242 (1958).
11. J. C. DECIUS and D. P. PEARSON. J. Am. Chem. Soc. **75**, 2436 (1953).
12. R. G. SNYDER and J. C. DECIUS. Spectrochim. Acta, **13**, 280 (1959).
13. G. L. COTE and H. W. THOMPSON. Proc. Roy. Soc. (London), A, **210**, 217 (1951).
14. L. V. AZAROFF and M. J. BUERGER. The powder method in X-ray crystallography. McGraw-Hill Book Co., New York. 1958. p. 106.
15. J. L. HOARD, S. GELLER, and T. B. OWEN. Acta Cryst. **4**, 405 (1951).
16. J. C. ELGIN and H. S. TAYLOR. J. Am. Chem. Soc. **51**, 2059 (1929).
17. P. J. ASKEY. J. Am. Chem. Soc. **52**, 970 (1930).
18. A. W. LAUBENGAYER and G. F. CONDIKE. J. Am. Chem. Soc. **70**, 2274 (1948).
19. I. G. RYSS and L. P. BOGDANOVA. Zhur. Neorg. Khim. **1**, 2264 (1956).
20. R. I. SANDERSON. Vacuum manipulation of volatile compounds. John Wiley & Sons, Inc., New York. 1948.
21. W. LANGE. Ber. **59**, 2107, 2432 (1926).
22. R. H. PIERSON, A. N. FLETCHER, and E. ST. C. GANTZ. Anal. Chem. **28**, 1218 (1956).
23. C. R. BAILEY, J. B. HALE, and J. W. THOMPSON. Proc. Roy. Soc. (London), A, **161**, 107 (1937).

Can. J. Chem. Downloaded from www.nrcresearchpress.com by 210.87.254.42 on 09/05/12
For personal use only.

Can. J. Chem. Downloaded from www.nrcresearchpress.com by 210.87.254.5 on 09/05/12
For personal use only.

ORTHO-SUBSTITUTED CHLOROBENZENES RELATED TO METAMECONINE[1]

J. A. McRae,[2] Marjorie Allen,[3] and R. Y. Moir[4]

ABSTRACT

Chlorinated derivatives of metameconine were formed for the first time. Partial demethylation of the derivatives with sulphuric acid occurred in highly selective fashion at the methoxyl ortho to the halogen, without regard to the relative position of the carbonyl group which is known to be highly directive for demethylations in the absence of halogen. The phenolic products of the demethylations are needed for the synthesis of sterically hindered diphenyl ethers. They showed a type of intermolecular hydrogen bonding in the crystal which was markedly subject to steric interference by the halogen atoms.

Our work with the chlorinated derivatives of metameconine (X) was first undertaken many years ago as a check upon the results we had obtained in the corresponding bromine series (1, 2, 3); these results had differed sharply from those reported by others (4). The need for a check was emphasized when our more recent work (5) led to somewhat surprising conclusions as to the direction of bromination, nitration, and selective demethylation in the metameconines. This paper reports the independent characterization of the chlorine series of compounds, shows that the chlorine series is an almost exact parallel to the bromine series, and therefore thoroughly verifies our previous results.

Two more reasons for proceeding with the chlorine series appeared later in our work. (*a*) A subject of continuing interest to us is the study of steric hindrance in diphenyl ethers (3, 6); obviously the ortho-chloro- and ortho-bromo-phenols obtained in this work will allow the preparation of corresponding diphenyl ethers with blocking groups of different sizes. (*b*) We hope to study the effect of crowding upon the quadrupole resonance frequency of the halogens; measurement of these frequencies is, of course, easier for chlorine compounds than for bromine or iodine compounds.

The main novelty of the present work lies in the description of an interesting steric hindrance of hydrogen bonding in the solid phase.

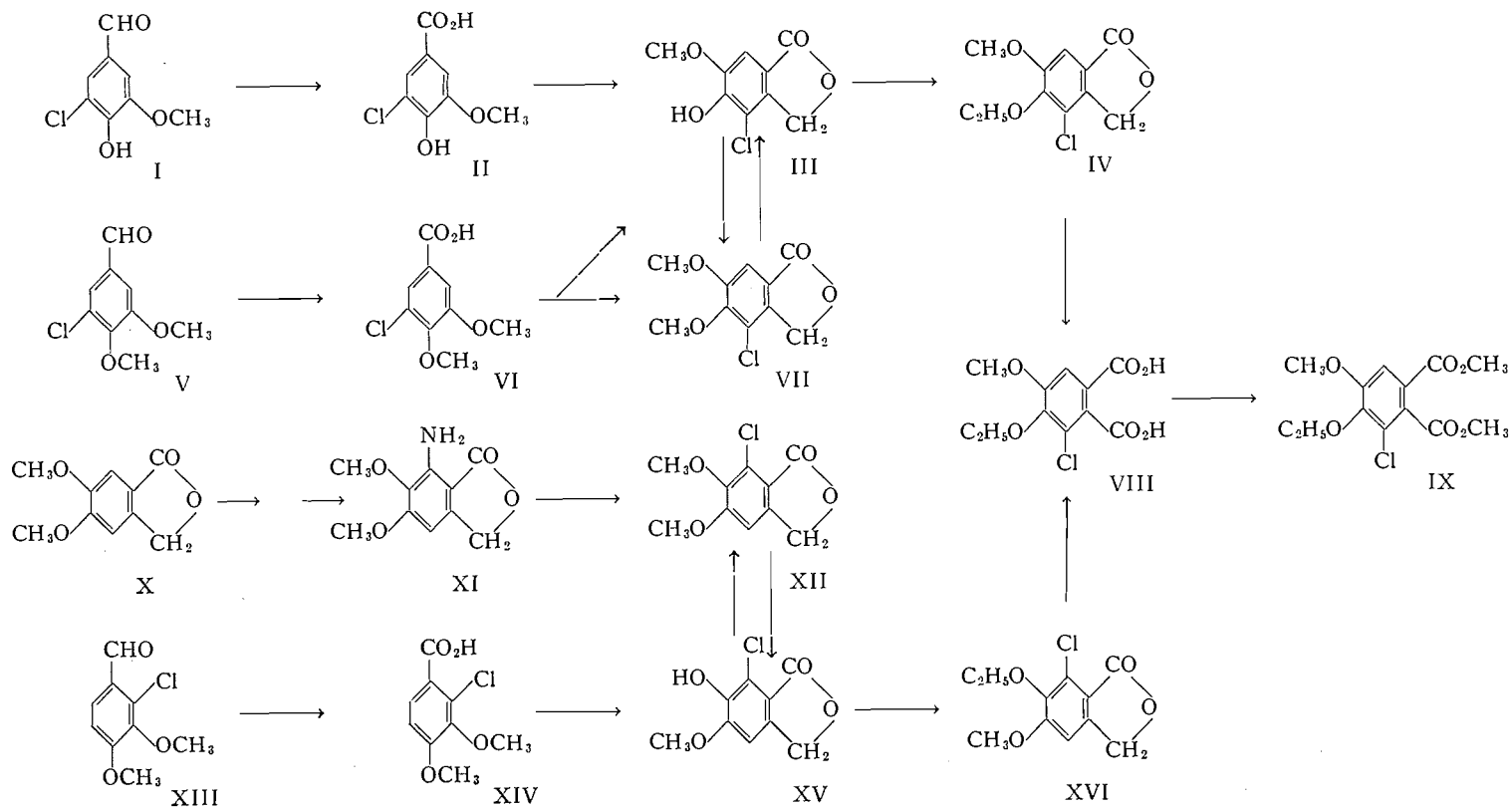
Synthesis and Structure

The most easily available of the chlorine derivatives was 7-chlorometameconine[5] (XII), made from metameconine (X) by nitration, reduction to the amine (XI) (1, 2, 4), diazotization of the amine, and the Sandmeyer reaction. No doubt the structure was obvious, since 7-bromometameconine (1, 2, 4) and 7-iodometameconine (1, 3), formed in corresponding ways, have had their structures thoroughly verified. Nevertheless the present work offered a quite independent proof that the new substance was indeed 7-chlorometameconine, its indirect formation from 2-chloroveratric acid (XIV), as shown in the chart, leaving no room for doubt as to its structure.

The isomeric 4-chlorometameconine (VII) was formed by the action of formaldehyde upon 5-chloroveratric acid (VI) in acid solution. The structure of the resulting phthalide

[1]*Manuscript received January 12, 1961.*
Contribution from the Department of Chemistry, Queen's University, Kingston, Ontario, Canada. The material in this paper is taken from the Report of the C.I.L. Fellow, Part I (R.Y.M., Queen's University, May, 1944) and from a forthcoming thesis for the degree of Doctor of Philosophy at Queen's University, by Mrs. Marjorie Allen.
[2]*Died April 8, 1960.*
[3]*Holder of Canadian Industries Limited Fellowship 1958–60.*
[4]*Holder of Canadian Industries Limited Fellowship 1942–43.*
[5]*A different numbering scheme was used in some earlier papers.*

Can. J. Chem. Downloaded from www.nrcresearchpress.com by 210.87.254.5 on 09/05/12
For personal use only.



Can. J. Chem. Downloaded from www.nrcresearchpress.com by 210.87.254.5 on 09/05/12
For personal use only.

was not immediately obvious, since the phthalide ring might have closed on either of the positions ortho to the carbonyl group in VI. That it did actually close as shown in structure VII followed from the fact that the phthalide could be converted to the phthalic ester IX which (as shown on the chart) could also be formed from metameconine (X) or from 2-chloroveratric acid (XIV).

Interesting phenolic compounds were obtained by selective demethylation of the chlorinated metameconines with sulphuric acid. Preparative yields were obtained of the easily purified products, much desired for future synthetic work. From 4-chlorometameconine (VII) there was obtained 4-chloro-5-hydroxy-6-methoxyphthalide (III), and from 7-chlorometameconine (XII) the isomeric 7-chloro-6-hydroxy-5-methoxyphthalide (XV). Just as in the bromine series, demethylation of both VII and XII occurred overwhelmingly at the methoxyl group ortho to the halogen, and without regard to the position of the carbonyl group, even though with veratraldehyde (7), veratric acid (7), and metameconine (5), highly selective demethylation occurred at the methoxyl meta to the carbonyl.

The methods used to show the structures of the phenolic compounds will be obvious from the transformations shown on the chart, the properties given in the experimental part, and the description of the corresponding bromine compounds (5).

Formaldehyde and 2-chloroveratric acid in acid solution gave none of the expected 7-chlorometameconine (XII); instead, very small amounts of 7-chloro-6-hydroxy-5-methoxyphthalide (XV) were obtained, along with large amounts of tars; the product was exceedingly difficult to purify. This miserable reaction was of central importance in our investigation, since it formed an exact parallel with the corresponding reaction of formaldehyde and 2-bromoveratric acid (1, 6), one of the main points in which our previous work disagreed with that of Rây and Robinson (4). Formaldehyde and 5-chloroveratric acid gave a mixture of the expected 4-chlorometameconine (VII) and the partially demethylated product, 4-chloro-5-hydroxy-6-methoxyphthalide (III). This too was an exact parallel with our experience with the corresponding 5-bromoveratric acid (2, 5). Even the infrared spectra of corresponding bromine and chlorine compounds are very similar throughout the two series, a further confirmation of the work in both. In fact the parallelism of the series broke down in only one respect: reductive dehalogenation, easy and convenient in the bromine series (5), in our hands failed completely in the chlorine series.

The correct orientation of the compounds of the metameconine series (1, 2, 3, 5, 6) has rested upon the correct orientation of the derivatives of vanillin used as reference compounds. It seems proper to point out how heavily we have relied upon the careful work of Dr. Raiford[6] and his students; of some 25 derivatives of vanillin needed in our structure proofs, only two (noted in the experimental part) have differed significantly from the descriptions given by these workers. One of the necessary intermediates, 5-chlorovanillic acid (II), has been made for the first time by Pearl's method (10), as shown in the experimental part.

Physical Properties

Jones, Angell, Ito, and Smith (12) reported that unsaturated lactones in solution sometimes show double peaks in the region of the carbonyl stretching frequency, though the two phthalides they investigated both showed single peaks. When their paper appeared

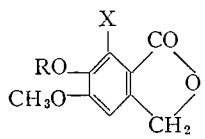
[6]*We especially wish to acknowledge the kindness of Professor Raiford in sending us an authentic sample of 2-chloroveratric acid nearly a year before its description was published (8), at a time when our work was delayed by the erroneous description of the acid then available (9), and not long before Professor Raiford's death (11).*

we had already observed, among the spectra of about 20 *solid* phthalides, a number of double peaks as well as some exceptionally large displacements of the carbonyl stretching frequency. A suggestion by Dr. R. N. Jones then enabled us to gain some understanding of the phenomena we had observed. Repetition of the spectra of the phthalides, but using solutions in tetrahydrofuran rather than solid samples in potassium bromide, immediately eliminated both the doubling of the peaks and the large displacements. Both factors were therefore due to intermolecular effects in the crystals; they were not due to impurities, incorrectly determined structures, or to unusual situations within the molecules.

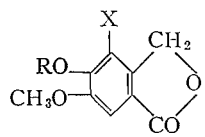
If one is interested in infrared spectra only for the determination of molecular structures, then the spectra of the crystals might simply be dismissed as inferior to the spectra of solutions. But the crystal effects are interesting in themselves, and had a special urgency for us, since quadrupole resonances *must* be observed in the solid state. We were able to make some progress in understanding the crystal effects because of the very large number of closely related phthalides at our disposal.

Spectra of Phthalides in Tetrahydrofuran

No double peaks were observed in the carbonyl stretching region, even in the acetylated derivatives (XVII A*d*, XVII C*d*, and XVIII C*d*) which have two different carbonyl groups. The peaks were all at positions normal for phthalides (13). In view of the results



XVII



XVIII

Substituent code

A: X = H	*a*: R = H
B: X = Cl	*b*: R = Me
C: X = Br	*c*: R = Et
D: X = I	*d*: R = Ac

Examples: XVII A*b* is structure X; XVII B*c* is XVI.

with the solid phthalides reported below, it was especially noteworthy that the phthalides bearing free phenolic groups had their peaks in the normal position, in agreement with previous work on related compounds (13, 14). Twelve halogenated phthalides (XVII and XVIII, with all possible combinations of B, C, *a*, *b*, and *c*) had their maxima in the region 1769–1773 cm^{-1}. Three unhalogenated phthalides (XVII A*a*, XVII A*b*, and XVIII A*a*) absorbed in the region 1766–1769 cm^{-1}. The available acetylated phthalides (XVII A*d*, XVII C*d*, and XVIII C*d*) showed absorption at the noticeably higher values of 1775–1777 cm^{-1}.

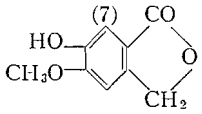
Spectra of Solid Phthalides in Potassium Bromide

We discuss only effects which are both large and reproducible, since the peaks were, of course, broader and had less sharply defined maxima than those obtained with solutions, and because of the well-known smaller spectral variations possible with this technique. Two remarkable phenomena were noticed.

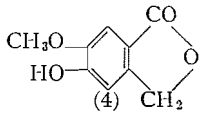
(*a*) *Steric interference with intermolecular hydrogen bonding.*—The reality of this effect was evident because the effect was reproducible, extremely large, and beautifully correlated with structure. Two phthalides (XVII A*a* and XVIII A*a*) (5) both showed absorption at the abnormally low frequency of 1715 cm^{-1}. The displacement of the band was

Can. J. Chem. Downloaded from www.nrcresearchpress.com by 210.87.254.5 on 09/05/12
For personal use only.

due to an intermolecular effect, since it vanished in solution; even phthalides having hydroxyl ortho to the carbonyl show but little intramolecular association (13, 14). Clearly too the displacement involved the hydroxylic hydrogen since methylation of the free hydroxylic group returned the maximum absorption (of solid XVII A*b*) to 1755 cm^{-1};



XVII A*a*



XVIII A*a*

acetylation of the free phenolic group brought the peak (in solid XVII A*d*) to 1753 cm^{-1}. Both values represent complete elimination of the effect. Direct hydrogen bonding from the phenolic group to the carbonyl group of another molecule would in any case be suspected from the great effect on the carbonyl stretching frequency, and confirmation of this was afforded by a most interesting steric effect. Substitution of either chlorine or bromine at position 7 in XVII A*a* also abolished the displacement effect, even though the hydroxyl group was still present, since solid XVII B*a* absorbed at 1760 cm^{-1}, and solid XVII C*a* at 1768 cm^{-1}. In view of our other results, by far the main effect of halogen at position 7 must have been due to steric blocking of the carbonyl group. Halogen at position 4 was very much less effective in interfering with the hydrogen bonding, solid XVIII B*a* absorbing at 1726 cm^{-1}, and solid XVIII C*a* at 1730 cm^{-1}, and this comparatively small increase from the values for unsubstituted XVIII A*a* may have been due to a combination of effects: a partial steric interference with the phenolic group, a general increase in lattice dimensions, and a small direct effect of halogen on the carbonyl group (see solution values, and reference 13). We have not yet been able to form phthalides having halogen ortho to carbonyl and meta to hydroxyl, so that these three effects cannot yet be separated from each other. Nevertheless, the displacement of the carbonyl peak in the solid phenolic compounds is so clear cut that it might have been used in the structure proofs to fix the relative positions of halogen and carbonyl. Eight solid phthalides in which intermolecular hydrogen bonding was absent showed a single peak in the carbonyl stretching region in the range 1753–1768 cm^{-1}. The rather wide range may be correlated with the lattice effects discussed in the next section.

(*b*) *Double carbonyl peaks with solid phthalides.*—Seven solid phthalides showed very distinct double carbonyl peaks; of the seven all were halogenated, none was phenolic, and none was acetylated. The lower peaks were all in the region 1748–1755 cm^{-1}, but the upper peaks were more variable in position. Four phthalides halogenated at position 4 (XVIII B*b*, B*c*, C*b*, and C*c*) had the upper peak at 1776–1782 cm^{-1}, and three phthalides halogenated at position 7 (XVII B*b*, C*b*, and D*b*) had the upper peak in the noticeably lower range of 1764–1767 cm^{-1}. The peaks varied considerably in relative amplitudes, without any obvious correlation with structure.

The double peaks were certainly due to effects of crystal structure, since only a single peak appeared in the spectra of solutions. For at least one phthalide, the double peak was associated with dimorphism. Fresh preparations of XVIII C*c* (5) consisted of feathery needles and showed peaks at 1753 and 1781 cm^{-1}. Older preparations consisted of heavy prisms and showed only a single peak at 1758 cm^{-1}. We have been unable to obtain a single peak in the spectrum of the less stable form. On the other hand the phthalide XVIII C*d* (5) showed only a single peak at room temperature, though it showed dimorphism at higher temperatures, the long needles melting at 140°, then resolidifying to

Can. J. Chem. Downloaded from www.nrcresearchpress.com by 210.87.254.5 on 09/05/12
For personal use only.

small prisms which melted again at 165°. Although these have been our only direct observations of dimorphism, the phenomenon cannot be ruled out as the explanation of all the double peaks observed with our phthalides.

Double Carbonyl Peaks in the Phthalic Esters

The dimethyl ester of 3-chloro-4-ethoxy-5-methoxyphthalic acid showed double peaks both in solution (at 1730 and 1744 cm^{-1}) and in the solid state (at 1720 and 1735 cm^{-1}); the corresponding bromine compound (5) was very similar in its spectra. The corresponding phthalic acids showed double peaks in the solid state, and single, very wide peaks in solution.

EXPERIMENTAL

All identities claimed in this paper were checked by comparison of the infrared spectra. The spectra were obtained using potassium bromide disks containing 0.8% by weight of sample, and tetrahydrofuran solutions containing up to 6% depending on the solubility of the sample. The spectrometer (a Perkin–Elmer Model 21, using a sodium chloride prism) was repeatedly calibrated by the use of the polystyrene bands at 1802 cm^{-1} and 1603 cm^{-1}. Most melting points were determined in an instrument of high precision (15) and the rest were performed on a Koffler Micro Hot Stage and lowered 3–5° to agree with precision capillary melting points within less than 1° up to 250°.

5-Chlorovanillic Acid (II)

The oxidation of 5-chlorovanillin (I) (m.p. 162.6–163.2°) (16) was accomplished following the method described by Pearl (10) for the preparation of vanillic acid. The product melted at 252–254°. The recorded (17) melting point is 244–245°. Found: C, 47.58; H, 3.39; Cl, 17.25%. Calc. for $C_8H_7ClO_4$: C, 47.42; H, 3.48; Cl, 17.52%.

5-Chloroveratraldehyde (V)

The method described for veratraldehyde (18) was adapted to the methylation of 5-chlorovanillin. The product melted at 55–55.6°; the recorded (11) melting point is 48–49°. Found: Cl, 18.2%. Calc. for $C_9H_9ClO_3$: Cl, 17.69%.

5-Chloroveratric Acid (VI)

5-Chloroveratraldehyde (17.0 g) and sodium bicarbonate (3.0 g) in water (100 ml) were heated to 60°. With vigorous stirring a solution, also heated to 60°, of potassium permanganate (20.2 g) in water (200 ml) was slowly added over 30 minutes whilst the temperature was maintained at 60–80°. The reaction was allowed to proceed for another 30 minutes, and then the reaction mixture was cooled, saturated with sulphur dioxide, and strongly acidified with hydrochloric acid (20 ml, conc.). The white precipitate was recovered by filtration, washed with a small volume of cold water and crystallized from ethyl alcohol to yield the product (15.6 g) with a melting point of 189.0–189.6°. Two more crystallizations from ethyl alcohol raised the melting point to 189.8–190.4°. The recorded (11) melting point is 188–189°. Found: C, 50.14; H, 4.00; Cl, 16.38%. Calc. for $C_9H_9ClO_4$: C, 49.88; H, 4.19; Cl, 16.38%.

2-Chloroveratric Acid (XIV)

This acid was obtained from 2-chlorovanillin by methylation according to the procedure recorded for veratraldehyde (18) followed by oxidation by the method described above for the isomeric 5-chloroveratric acid. The product purified by crystallization from aqueous ethyl alcohol had a melting point of 202°–203°. A mixed melting point determination with an authentic sample supplied by Professor Raiford gave a melting point of 202.5–204.5°.

Can. J. Chem. Downloaded from www.nrcresearchpress.com by 210.87.254.5 on 09/05/12
For personal use only.

4-Chloro-5-hydroxy-6-methoxyphthalide (III)

(*a*) 5-Chlorovanillic acid (II) (2.0 g, m.p. 247–249°), glacial acetic acid (80 ml), hydrochloric acid (40 ml, conc.), and formaldehyde (20 ml, 36–38%) were mixed and heated at 80–85° for 2 days. The cooled reaction mixture was poured onto ice (200 g) and after 2 hours the resulting precipitate was recovered by filtration, washed with a little cold water, and dried. The product (1.18 g) had a melting point of 204–206° which was raised to 236.4–237.2° by three crystallizations from ethyl alcohol. Found: C, 50.55, 50.78; H, 3.55, 3.46; Cl, 16.21, 16.55; —OCH_3, 15.45, 15.37 and on the same sample by a different analyst 13.64%. Calc. for $C_9H_7ClO_4$: C, 50.37; H, 3.29; Cl, 16.54; —OCH_3, 14.46%.

(*b*) 5-Chloroveratric acid (VI) (10 g, m.p. 186–187°), glacial acetic acid (400 ml), hydrochloric acid (200 ml, conc.), and formaldehyde solution (100 ml, 36–38%) were combined and heated at 95–100° for 2 days. The white precipitate obtained after pouring the reaction mixture onto ice was extracted with sodium bicarbonate solution. The insoluble fraction yielded after one crystallization from ethyl alcohol 4-chlorometameconine (VII) (1.66 g) with a melting point of 168–171°. (For further details see below.) The sodium bicarbonate extract was acidified and the resulting precipitate recovered and crystallized from ethyl alcohol. The product (2.77 g) had a poor melting point of 168–220°, but a second crystallization raised the melting point to 234–235°. A mixed melting point with the product from method (*a*) showed no depression.

(*c*) 4-Chlorometameconine (VII) (0.13 g, m.p. 171.2–171.8°) was heated in sulphuric acid (1 ml, conc.) at 60° for 2 days. The solution was poured onto ice and the precipitate recovered by filtration and washed with water. The product after two crystallizations from ethyl alcohol melted at 234–235° and gave no depression in melting point when mixed with the product from method (*a*).

The infrared spectra of the three samples of 4-chloro-5-hydroxy-6-methoxyphthalide produced by these methods, are identical throughout the range 4000–600 cm^{-1}.

4-Chlorometameconine (VII)

(*a*) This method of preparation is the same as method (*b*) described for 4-chloro-5-hydroxy-6-methoxyphthalide. The product (1.66 g) was crystallized twice from ethyl alcohol to give the analytical sample with a melting point of 171.2–171.8°. Found: C, 52.77, 52.71; H, 4.11, 4.25; Cl, 15.62, 15.65%. Calc. for $C_{10}H_9ClO_4$: C, 52.50; H, 3.97; Cl, 15.52%.

(*b*) 4-Chloro-5-hydroxy-6-methoxyphthalide (III) (0.2 g, m.p. 234–235°) from method (*a*) above was added to an ether solution of diazomethane (20 ml, 2%) and the mixture was left to stand overnight. The solution was evaporated and the easily solidified residue crystallized from ethyl alcohol to give fluffy needles (0.13 g) which melted at 171.2–171.8°. A mixed melting point with the product from (*a*) gave no depression, and the infrared spectra of the two products were identical.

4-Chloro-5-ethoxy-6-methoxyphthalide (IV)

4-Chloro-5-hydroxy-6-methoxyphthalide (III) (1.63 g, m.p. 234–235°), from method (*a*) above, ethyl iodide (30 ml), and dry acetone (75 ml) were refluxed and stirred in dry apparatus protected from moisture by drying tubes. Drierite (1.0 g) was added and the mixture stirred for 30 minutes. Freshly prepared silver oxide (5.0 g) was added in portions (1.0 g) at intervals over 7 hours, the reaction was allowed to proceed for a further 2 hours, and then the reaction mixture was cooled and filtered to remove the silver compounds. The filtrate was evaporated to dryness and the solid residue crystallized from ethyl alcohol to give white crystals (1.48 g) which melted at 138–139°. Three more

Can. J. Chem. Downloaded from www.nrcresearchpress.com by 210.87.254.5 on 09/05/12
For personal use only.

crystallizations raised the melting point to 141.4–141.8°. Found: C, 54.72, 54.67; H, 4.70, 4.45; Cl, 14.30%. Calc. for $C_{11}H_{11}ClO_4$: C, 54.44; H, 4.57; Cl, 14.63%.

7-Chlorometameconine (XII)

(*a*) 7-Aminometameconine (XI) (2) (15 g crude) was dissolved in hydrochloric acid (45 ml, conc.) and water (300 ml). The solution was mechanically stirred and cooled in an ice and salt bath to −5°. Sodium nitrite (7.5 g) in water (60 ml) was added from a dropping funnel over 20 minutes, and then the mixture was stirred and cooled for 3.5 hours longer. The excess nitrous acid was destroyed with urea and the reaction mixture was slowly poured, with stirring, into a well-cooled solution of cuprous chloride (from 19 g $CuSO_4.5H_2O$) in hydrochloric acid (21 ml, conc.) and water (8 ml). When the frothing had subsided, the reaction mixture was gently heated on a boiling-water bath. The precipitate which settled out of the cooled solution, was recovered by filtration, washed with water, and crystallized once from dilute acetic acid (3:2) and three times from *n*-butanol to yield white needles (5.0 g) with a melting point of 193–193.5°. Two more crystallizations of corresponding material from another preparation gave the analytical sample with a melting point of 195.8–196.6°. Found: C, 52.48, 52.32; H, 3.97, 3.96; Cl, 15.22, 15.37%. Calc. for $C_{10}H_9ClO_4$: C, 52.50; H, 3.97; Cl, 15.52%.

(*b*) 5-Methoxy-6-hydroxy-7-chlorophthalide (XV) (0.5 g, m.p. 234–235°) from method (*a*) below, when methylated with diazomethane yielded white needles (0.42 g), with a melting point of 194.2–195.2° after one crystallization from ethyl alcohol. The infrared spectra of these two samples of 7-bromometameconine are identical, and a mixed melting showed no depression. The material made by method (*b*) below was methylated with methyl sulphate and gave 7-chlorometameconine proved by mixed melting point determination and infrared spectra.

5-Methoxy-6-hydroxy-7-chlorophthalide (XV)

(*a*) 7-Chlorometameconine (XII) (2.0 g, m.p. 193–194°) was heated with sulphuric acid (10 ml, conc.) for 3.5 days at 60°. The cooled viscous solution was poured onto ice and the resulting precipitate recovered by filtration, washed with water, and dried. The solid (1.87 g) was extracted with sodium bicarbonate solution and the soluble fraction recovered by acidifying the extracts. This procedure yielded a solid (1.47 g) with a melting point of 230–231°, which was raised to 235–235.8° by three crystallizations from ethyl alcohol. Found: C, 50.66, 50.48; H, 3.42, 3.28; Cl, 16.23, 16.53; —OCH_3, 14.44%. Calc. for $C_9H_7ClO_4$: C, 50.37; H, 3.29; Cl, 16.54; —OCH_3, 14.46%. A mixed melting point with the isomer 4-chloro-5-hydroxy-6-methoxyphthalide (III) showed a large depression.

(*b*) 2-Chloroveratric acid (XIV) (5.0 g), formaldehyde solution (9.0 ml, 36–38%), hydrochloric acid (31 ml, conc.), and glacial acetic acid (45 ml) were heated at 80–90° for 76 hours and at 100° for 7 hours longer. The combined solutions from three similar experiments were cooled and decanted from a small amount of tar, diluted with water (85 ml), and filtered to remove more tar. A second dilution with water (50 ml) precipitated unchanged 2-chloroveratric acid which after successive crystallizations from ethyl alcohol, aqueous ethyl alcohol, *n*-butyl alcohol, and aqueous acetic acid melted at 200–201.5°. The filtrate was again diluted with water (500 ml) and the solution evaporated to less than 150 ml under a slight vacuum, neutralized with sodium bicarbonate, made very slightly acid with hydrochloric acid, and the resulting precipitate collected after 24 hours. The precipitate (1.95 g) was washed with hot and cold water, and crystallized three times from *n*-butanol to give a product with a melting point of 231–232.5°. Found: C, 51.98; H, 3.84; Cl, 16.85, 16.50%. Calc. for $C_9H_7ClO_4$: C, 50.37; H, 3.29; Cl, 16.54%.

Can. J. Chem. Downloaded from www.nrcresearchpress.com by 210.87.254.5 on 09/05/12
For personal use only.

Better material, m.p. 234.2–234.8°, was obtained by a further recrystallization from ethyl alcohol. The infrared spectra given by these two products from methods (*a*) and (*b*) were identical.

5-Methoxy-6-ethoxy-7-chlorophthalide (XVI)

5-Methoxy-6-hydroxy-7-chlorophthalide (XV) (2.0 g, m.p. 234–235°) was ethylated by the method described above for 4-chloro-5-hydroxy-6-methoxyphthalide. The product (1.59 g) after one crystallization from ethyl alcohol melted at 174–175°. Three more crystallizations raised the melting point to 177.2–177.6°. Found: C, 54.43, 54.52; H, 4.70, 4.56; Cl, 14.63%. Calc. for $C_{11}H_{11}ClO_4$: C, 54.44; H, 4.57; Cl, 14.63%.

3-Chloro-4-ethoxy-5-methoxyphthalic Acid (VIII)

(*a*) Potassium permanganate (2.5 g) was added over a period of 15 minutes to a well-stirred solution of 4-chloro-5-ethoxy-6-methoxyphthalide (IV) (1.0 g, m.p. 140.6–141.2°) in potassium hydroxide solution (110 ml, 5%) heated on a steam bath. The reaction was allowed to proceed another 45 minutes, and then cooled. Sulphur dioxide was passed until a clear solution was obtained. The solution was evaporated to half volume and after standing at room temperature, crystals with a poor melting point settled out of the solution. The product crystallized from water containing a few drops of hydrochloric acid in two modifications which were separated by hand: (A) long needles (0.2 g) with a melting point of 200–201° and a second melting point due to the anhydride of 133.5–134°; (B) small prisms (0.02 g) with a melting point of 203–207° and a second melting point of 133.5–134°. The infrared spectra in potassium bromide disks of these two modifications showed slight differences in the intensity of the peaks in the region 1500–1450 cm^{-1}, and differences in the positions of the peaks in the region 1000–850 cm^{-1}, which are probably due to variations in the crystalline structure. The two forms were methylated separately (see below) to give identical products as determined by infrared spectra and mixed melting points.

(*b*) 5-Methoxy-6-ethoxy-7-chlorophthalide (XVI) (1.0 g, m.p. 174–175°) was oxidized as above, and the product after one crystallization from water melted at 192–194° and the second melting point was 133.5–134°. This product appeared to be homogeneous, and the infrared spectrum was identical with that given by the modification B above.

Dimethyl 3-Chloro-4-ethoxy-5-methoxyphthalate (IX)

(*a*) 3-Chloro-4-ethoxy-5-methoxyphthalic acid (0.2 g, crystals A) were added to diazomethane solution (20 ml, 2% in ether) and left to stand overnight. The colorless solution was evaporated to dryness and the easily solidified residue was crystallized from petroleum ether (b.p. 30–60°) to give heavy needles which melted at 68.8–70.4°.

The product from crystals B melted at 70.4–70.6°, and a mixed melting point was 68.8–70.4°.

(*b*) 3-Chloro-4-ethoxy-5-methoxyphthalic acid (0.44 g from (*b*) above) yielded white needles (0.38 g) with a melting point of 70.4–71.4°, which did not depress the melting point of the above products. Found: C, 51.70, 51.66; H, 5.12, 4.86; Cl, 12.29, 12.42%. Calc. for $C_{13}H_{15}ClO_6$: C, 51.56; H, 4.99; Cl, 11.72%.

The infrared spectra given by the three samples of dimethyl 3-chloro-4-ethoxy-5-methoxyphthalate were identical.

Attempted Dechlorinations

5-Chlorovanillic acid (II) was used as a model compound in experiments designed to find the conditions for removal of the chlorine atom. The methods tried were: (*a*) sodium

Can. J. Chem. Downloaded from www.nrcresearchpress.com by 210.87.254.5 on 09/05/12
For personal use only.

amalgam in aqueous medium, (*b*) zinc dust and potassium hydroxide, (*c*) preformed chromous chloride, (*d*) chromous chloride prepared *in situ*. All experiments failed, the only compound isolated being unchanged 5-chlorovanillic acid. The last two series of experiments were repeated with 4-chloro-5-hydroxy-6-methoxyphthalide (III) and once again there was no evidence that chlorine had been successfully removed.

ACKNOWLEDGMENTS

We wish to thank Dr. A. L. Promislow for the preparation of some intermediates used in this work, Miss Shelagh Courtenay for the determination of the infrared spectra, and Dr. C. A. Sankey for a generous gift of vanillin, the ultimate source of all the new compounds produced in our work. The work was made possible by the financial support of the National Research Council of Canada, and by the grants of Fellowships to two of us by Canadian Industries Limited.

REFERENCES

1. J. A. McRae, R. B. VanOrder, F. H. Griffiths, and T. E. Habgood. Can. J. Chem. **29**, 482 (1951).
2. R. H. Manske, J. A. McRae, and R. Y. Moir. Can. J. Chem. **29**, 526 (1951).
3. J. A. McRae, R. Y. Moir, J. J. Ursprung, and H. H. Gibbs. J. Org. Chem. **19**, 1500 (1954).
4. J. N. Rây and R. Robinson. J. Chem. Soc. **127**, 1618 (1925).
5. M. Allen, A. L. Promislow, and R. Y. Moir. J. Org. Chem. In press.
6. M. Allen and R. Y. Moir. Can. J. Chem. **37**, 1799 (1959).
7. A. Lovecy, R. Robinson, and S. Sugasawa. J. Chem. Soc. 817 (1930).
8. L. C. Raiford and D. E. Floyd. J. Org. Chem. **8**, 358 (1943).
9. K. Feist, W. Awe, and W. Völksen. Ber. **69**, B, 2743 (1936).
10. I. A. Pearl. J. Am. Chem. Soc. **68**, 429 (1946).
11. L. C. Raiford and F. B. Wittmer. J. Org. Chem. **10**, 527 (1945).
12. R. N. Jones, C. L. Angell, T. Ito, and R. J. D. Smith. Can. J. Chem. **37**, 2007 (1959).
13. W. R. Allison and G. T. Newbold. J. Chem. Soc. 3335 (1959).
14. L. A. Duncanson, J. F. Grove, and J. Zealley. J. Chem. Soc. 1331 (1953).
15. F. C. Merriam. Anal. Chem. **20**, 1246 (1948).
16. L. C. Raiford and J. G. Lichty. J. Am. Chem. Soc. **52**, 4579 (1930).
17. L. C. Raiford and D. J. Potter. J. Am. Chem. Soc. **55**, 1682 (1933).
18. G. Barger and R. Silberschmidt. J. Chem. Soc. **133**, 2924 (1928).

Can. J. Chem. Downloaded from www.nrcresearchpress.com by 210.87.254.5 on 09/05/12
For personal use only.

Can. J. Chem. Downloaded from www.nrcresearchpress.com by 210.87.254.6 on 09/05/12
For personal use only.

THE CARBOHYDRATE–PROTEIN LINKAGE IN GLYCOPROTEINS

PART I. THE SYNTHESES OF SOME MODEL SUBSTITUTED AMIDES AND AN L-SERYL-D-GLUCOSAMINIDE[1]

J. K. N. JONES, M. B. PERRY, B. SHELTON, AND D. J. WALTON[2]

ABSTRACT

The syntheses of *N*-L-seryl-D-glucosamine, *N*-glycyl-D-glucosamine, *N*-L-glutamyl-D-glucosamine, and 1-*O*-β-L-seryl-*N*-acetyl-D-glucosaminide are described. These D-glucosamine derivatives may result from the fragmentation of some glycoproteins. The chemical properties of these compounds indicate that *N*-peptides are relatively stable in acid solution but unstable in neutral and alkaline solution. The seryl glucosaminide is relatively stable in alkaline solution but is hydrolyzed by acid.

INTRODUCTION

The mode of the linkage of sugars to amino acids in glycoproteins and mucoproteins which contain small amounts of carbohydrate, is obscure. Examples of this group are collagen and reticulin. Reticulin (1) is found in fairly large amounts in some internal organs (e.g. kidney and lung), and contains 3–4% of neutral sugars and 0.2% of hexosamine. Collagen (2) contains 0.3–0.7% of glucose and galactose. Several collagens which have been investigated (3) have been shown to contain D-glucosamine. Histochemical work has demonstrated that in some diseases, such as rheumatoid arthritis, there appear to be increases in the carbohydrate content of the glycoprotein of the subcutaneous tissue, which is rich in collagen. It was therefore of interest to investigate the mode of linkage of carbohydrate to amino acid in glycoproteins and mucoproteins. Bovine subcutaneous tissue, which is rich in collagen and elastic fibers, when degraded by proteolytic enzymes yielded a complex mixture of peptides to which were attached sugar residues. It was clear that this subcutaneous tissue did not contain any appreciable quantities of high molecular weight polysaccharides (4). This suggested that carbohydrate residues of low molecular weight were covalently linked to the amino acid residues of the proteins. It was therefore decided to attempt the syntheses of carbohydrate–amino acid derivatives which might result from the degradation of glycoproteins. A survey of the literature indicates that little was known about the type of linkage in such a derivative, but that linkages through glycine, aspartic acid, serine, threonine, and amides have been implicated (5, 6, 7). Many glycoproteins contain D-glucosamine and the possible biological role of *N*-peptides of this amino sugar have been investigated. The syntheses of *N*-glycyl-D-glucosamine (8) and of *N*-L-alanyl-D-glucosamine (9) have been reported in which they were isolated either as the hydrochloride or as some alternative derivative, with the amino group protected. *N*-(L-Alanyl-L-alanyl)-D-glucosamine has been found to be stable (10), as have several other similar dipeptides, the syntheses of which have been reported. A peptide composed of D-glucosamine and L-glutamic acid has been synthesized (11) but this was reported to be unstable even when the amino group was protected. It was of particular interest to examine these *N*-peptides, rather than their more stable substituted derivatives to determine whether they might be expected to survive during the hydrolysis

[1]*Manuscript received October 26, 1960.*
Contribution from the Department of Organic Chemistry, Queen's University, Kingston, Ontario. Abstracted in part from the thesis submitted by D. J. Walton in partial fulfillment of the requirements for the Ph.D. degree, Queen's University, 1959.
[2]*Present address: 18, Maiden Castle Road, Dorchester, Dorset, England.*

of glycoproteins. Accordingly, we have attempted the syntheses of several amino acids amide linked to D-glucosamine, in order to examine their properties. The *N*-peptide of L-serine was chosen as it had been reported by Masamune (12) to be present in gastric mucin together with glucosamine. Glycine has been reported by Gross (13) to constitute about 30–35% of all collagens investigated, and may therefore be linked to sugar residues. The *N*-peptide of L-glutamic acid was prepared in order to investigate whether the presence of a free carboxylic acid end group might confer stability to the derivative. L-Serine contains a primary hydroxyl group, and is therefore capable of being united glycosidically with a sugar residue: an L-seryl-*N*-acetyl-D-glucosaminide has been synthesized and its properties examined.

N-L-*Seryl*-D-*glucosamine*

N-(*N*-Carbobenzoxy-L-alanyl)-1,3,4,6-tetra-*O*-acetyl-β-D-glucosamine hydrochloride and the corresponding *N*-glycyl compound were synthesized by Bergmann and Zervas (8) by treating 1,3,4,6-tetra-*O*-acetyl-β-D-glucosamine with *N*-carbobenzoxy-L-alanyl chloride or with *N*-carbobenzoxyglycyl chloride. L-Serine, however, contains a primary hydroxyl group which must be protected before a reaction of this type can be used. Accordingly we turned our attention to the possibility of condensing a suitably substituted D-glucosamine derivative with *N*-carbobenzoxy-L-serine by the carbodiimide method (14). Unfortunately the L-serine derivative was not soluble in methylene chloride which is the solvent usually employed in this type of reaction. To overcome this difficulty the primary hydroxyl group of the L-serine derivative was protected by a tetrahydropyranyl group which led to the formation of two separable optical isomers which were soluble in methylene chloride. Racemization does not occur in the formation of the tetrahydropyranyl derivatives (15). Each isomer was then condensed with the suitably substituted 1-*O*-α-acetyl- and 1-*O*-β-acetyl-D-glucosamine derivatives, resulting in the formation of four isomers. The yields were poor when dicyclohexyl carbodiimide was used because of the difficulty in separating dicyclohexyl urea from the products. When diisopropyl carbodiimide was used as a condensation agent, better yields were obtained since the product was more readily separable from the diisopropyl urea by-product. When these isomers were warmed in dilute acetic acid solution, dihydropyran was eliminated and *N*-(*N*-carbobenzoxy-L-seryl)-1,3,4,6-tetra-*O*-acetyl-α- (and β-) D-glucosamine were produced, respectively. When the carbobenzoxy grouping was removed by reduction the resulting *N*-L-seryl-1,3,4,6-tetra-*O*-acetyl-α- (and β-) D-glucosamine decomposed to a brown tar within a few minutes. Presumably this was due to the basic character of the amino group of the amino acid moiety. Despite this instability it was possible to prepare the fully acetylated derivative. However, it was found that in the presence of hydrochloric acid the deacetylated product yielded a stable hydrochloride on removal of the carbobenzoxy grouping by hydrogenolysis.

N-Glycyl-D-*glucosamine*

Bergmann (8) synthesized the hydrochloride of this material but the parent compound has not been reported. *N*-(*N*-Carbobenzoxyglycyl)-D-glucosamine was obtained by the deacetylation of *N*-(*N*-carbobenzoxyglycyl)-1,3,4,6-tetra-*O*-acetyl-β-D-glucosamine. This compound was prepared by Bodanszky and Du Vigneaud's method (16) for condensing amino groups and carboxylic acid groups to form peptide linkages. The condensation is effected between the hydrogen halide of an amine and the *p*-nitrophenyl ester of a carboxylic acid. In this case the amine salt used was 1,3,4,6-tetra-*O*-acetyl-β-D-glucosamine hydrobromide, and the ester was glycyl *p*-nitrophenyl ester. The fully

Can. J. Chem. Downloaded from www.nrcresearchpress.com by 210.87.254.6 on 09/05/12
For personal use only.

substituted product was then deacetylated and reduced in the presence of hydrochloric acid to give *N*-(glycyl hydrochloride)-D-glucosamine. Hydrogenolysis in neutral solution caused both the acetylated and the deacetylated derivative to decompose rapidly.

N-L-Glutamyl-D-glucosamine

In the synthesis of this compound the method of Bodanszky and Du Vigneaud (16) was again used in an analogous manner to that used in the preparation of the *N*-glycyl-D-glucosamine. The amino acid was converted into *N*-carbobenzoxy-α-*p*-nitrophenyl ester-γ-L-glutamine by condensation of *N*-carbobenzoxy-L-glutamic acid with *p*-nitrophenol, using diisopropyl carbodiimide as a dehydrating agent, to form the diester. The diester was then treated with the calculated amount of methanolic ammonia solution to form the monoester–monoamide. It is reasoned from steric considerations that the replacement is effected in the less hindered γ-position. When the derivative had been formed and the terminal amide group removed, attempts to synthesize the free amine by hydrogenolysis of the carbobenzoxy group yielded very unstable products which could not be isolated. This was also true of the *N*-peptide after deacetylation. The hydrogen reduction was also carried out in the presence of hydrochloric acid, and in this case the stable *N*-peptide hydrochloride was formed.

1-O-β-L-Seryl-N-acetyl-D-glucosaminide

The glucosaminide was formed using a modified Koenigs–Knorr (17) type synthesis. 1-Chloro-1-deoxy-*N*-acetyl-3,4,6-tri-*O*-acetyl-D-glucosamine was prepared by the action of titanium tetrachloride on fully acetylated D-glucosamine in the manner described by Inouye and his co-workers (18). The acetohalogen sugar was allowed to react with *N*-carbobenzoxy-L-seryl methyl ester, using anhydrous alcohol-free chloroform as a solvent, and employing the Koenigs–Knorr conditions.

The initial yields of the product were low owing to steric hindrance, but when the reaction was allowed to proceed for 6 days with vigorous shaking, better yields were obtained. The product was not purified at this stage, but was de-*O*-acetylated with barium methylate. The deacetylated material was purified by chromatography, and was then subjected to hydrogenolysis, under neutral conditions, to remove the carbobenzoxy group. The over-all yield was small and the product at this stage, 1-*O*-β-(L-seryl methyl ester)-*N*-acetyl-D-glucosaminide, was stable and the corresponding hydrochloride was synthesized. The substituted D-glucosaminide was then saponified using sodium hydroxide solution to give the free acid, 1-*O*-β-L-seryl-*N*-acetyl-D-glucosaminide, which was found to be stable.

EXPERIMENTAL

All melting points reported are uncorrected. Solutions were concentrated by rotary evaporation under reduced pressure below 40°, unless otherwise stated.

Paper chromatography was performed by the descending method on Whatman No. 1 paper, using 1-butanol/ethanol/water (3:1:1 v/v) as the mobile phase. The following sprays were used to detect the compounds on the paper chromatograms: (A) 2% solution of *p*-anisidine hydrochloride in 1-butanol, (B) 1% solution of silver nitrate in acetone, followed by 2% ethanolic sodium hydroxide, and (C) 2% ninhydrin in 1-butanol. The rate of movement of the compounds on the chromatograms is given relative to that of D-glucosamine hydrochloride ($R_{GN.HCl}$), *N*-acetyl-D-glucosamine (R_{GNAc}), or pentaacetyl-D-glucosamine (R_{GNpAc}).

The infrared spectra of crystalline compounds were measured as 0.8% dispersions

Can. J. Chem. Downloaded from www.nrcresearchpress.com by 210.87.254.6 on 09/05/12
For personal use only.

in potassium bromide disks, and non-crystalline materials were examined as 6% solutions in chloroform, using a Perkin–Elmer Model 21 spectrophotometer.

Elemental analyses were carried out by the Schwarzkopf Microanalytical Laboratory, Woodside, New York.

*1. N-*L*-Seryl-*D*-glucosamine*

(a) Carbobenzoxychloride

The reagent was prepared by the method of Carter *et al.* (19). Benzyl alcohol (65 ml) was added to a solution of phosgene (69 g) in toluene (200 ml) at 0°. After 3 hours the excess benzyl alcohol and the toluene were removed by distillation under reduced pressure. The remaining solution (104 g) contained 76 g of carbobenzoxychloride.

*(b) N-Carbobenzoxy-*L*-serine*

The method of Moore *et al.* (14) was used in a slightly modified form. Between the additions of the reactants the alkaline solution was transferred to a tap funnel and vigorously shaken, then returned to the reaction vessel. The product (98% yield) had m.p. 116°.

*(c) N-Carbobenzoxy-*L*-seryl Methyl Ester*

N-Carbobenzoxy-L-serine (20 g) was dissolved in 2.5 *N* methanolic hydrogen chloride solution (200 ml). The solution was allowed to stand overnight and it was then deacidified with Duolite A4(OH^-) exchange resin. The solution was concentrated to a syrup (20 g; 94% yield) which was kept in a desiccator.

*(d) N-Carbobenzoxy-O-tetrahydropyranyl-*L*-seryl Methyl Ester*

The procedure of Iselin and Schwyzer (15) was followed. *N*-Carbobenzoxy-L-seryl methyl ester (12.6 g) was dissolved in purified 2,3-dihydro-4-pyran (6 g) and a solution of 2.2 *N* hydrogen chloride in dry ethyl acetate (0.7 ml) was added. The reaction mixture was allowed to stand for 3 hours at room temperature after which it was diluted with ether and then washed with dilute sodium bicarbonate solution followed by water. The solution was dried (anhyd. sodium sulphate), filtered, and then concentrated to a yellow oil (15 g; 88% yield).

*(e) N-Carbobenzoxy-O-tetrahydropyranyl-*L*-serine*

The methyl ester (*d*) was dissolved in methanol (50 ml) and saponified by the method of Iselin and Schwyzer (15). Addition of ether to the final product in ethyl acetate resulted in the separation of one isomer in a crystalline form (I_{e1}), in 14% yield, which had m.p. 129°.

The second isomer (I_{e2}) was obtained from the concentrated mother liquor which gave crystals after 2 days (30% yield) which had m.p. 150°.

The infrared spectra of the products showed absorption bands at 987 cm^{-1} and 1130 cm^{-1} (in chloroform solution). These bands are due to the tetrahydropyranyl group, and are not present in the spectrum of *N*-carbobenzoxy-L-serine. The phenyl band at 695 cm^{-1} was also present.

*(f) 1,3,4,6-Tetra-O-acetyl-N-acetyl-β-*D*-glucosamine*

D-Glucosamine hydrochloride (30 g) was dissolved in a solution of zinc chloride (36 g) in acetic anhydride (250 ml). The solution was kept at 70–80° for 10 minutes and was then poured into ice water (400 ml). Sodium bicarbonate was slowly added to neutralize the excess acid and on allowing the reaction mixture to stand overnight in a refrigerator, a white precipitate of the pentaacetate separated. The material was collected, washed with water, dried, and recrystallized from ethanol solution to give the product (30.8 g;

Can. J. Chem. Downloaded from www.nrcresearchpress.com by 210.87.254.6 on 09/05/12
For personal use only.

52% yield) which had m.p. 187° which rose to m.p. 190–192° after recrystallization. $[\alpha]_D^{25}$ +3° (*c*, 4.0 chloroform).

The infrared spectrum of the product showed the following absorption bands: carbonyl of *O*-acetyl (1740 cm^{-1}); amide I (1682 cm^{-1}); and amide II (1512 cm^{-1}). Important bands referred to later occurred at 1238, 1078, 1042, and 900 cm^{-1}.

The corresponding α-anomer was prepared in a similar manner, but the reaction was carried out at room temperature. Yield 56%, m.p. 139°, $[\alpha]_D^{22}$ +91° (*c*, 4.0 chloroform).

(g) 1,3,4,6-Tetra-O-acetyl-α- (and β-) D-*glucosamine Hydrobromide*

The technique of Inouye *et al.* (18) was used. 1,3,4,6-Tetra-*O*-acetyl-*N*-acetyl-α-D-glucosamine (10 g) was added to a stirred ice-cold solution of dry hydrogen bromide in acetic acid (30 ml) to give the product (4.5 g; 45% yield), which had $[\alpha]_D^{22}$ +129° (*c*, 4.0 water), chars at 205–220°.

The β-anomer was prepared in a similar manner from 1,3,4,6-tetra-*O*-acetyl-*N*-acetyl-β-D-glucosamine and the product (4.5 g; 45% yield) had $[\alpha]_D^{21}$ +12.1° (*c*, 4.0 water), chars above 200°.

(h) 1,3,4,6-Tetra-O-acetyl-α- (and β-) D-*glucosamine*

The hydrobromides (1 g) were respectively dissolved in a slurry of Amberlite IR45 ($CO_3^=$) exchange resin (4 g hydrobromide to 50 ml resin). The mixture was stirred at 5° for 1 hour and then filtered. The filtrates were extracted with chloroform (4×80 ml) and the combined extracts were dried (anhyd. sodium sulphate) and then concentrated to a small volume. On the addition of ether to the concentrates, the products separated as needle-like crystals, which were collected and recrystallized from ethanol. The α-anomer (65% yield) had m.p. 118° and $[\alpha]_D^{23}$ +145.5° (*c*, 4.0 chloroform). The β-anomer (65% yield) had m.p. 143° and $[\alpha]_D^{22}$ +27° (*c*, 3.6 chloroform).

*(i) N-(N-Carbobenzoxy-O-tetrahydropyranyl-*L-*seryl)-1,3,4,6-tetra-O-acetyl-α- (and β-)* D-*glucosamine*

N-Carbobenzoxy-*O*-tetrahydropyranyl-L-serine (isomer I_{c1}) (2.0 g; 6.2 mmoles), 1,3,4,6-tetra-*O*-acetyl-β-D-glucosamine (2.3 g; 6.2 mmoles), and diisopropyl carbodiimide (0.8 g; 6.2 mmoles) were dissolved in methylene chloride (25 ml) and the solution was shaken mechanically for 20 hours at room temperature. One drop of dilute acetic acid was added, and the shaking was continued for a further 1 hour. The diisopropyl urea by-product was filtered off, and the filtrate was stored at −10° for 24 hours. The solution was refiltered, and the filtrate then washed with dilute hydrochloric acid, followed by 2 *N* sodium carbonate solution and finally with water. The solution was dried (anhyd. sodium sulphate) and the methylene chloride removed by distillation to leave a syrup. The syrup was taken up in the minimum amount of hot ethanol from which the α-anomer was obtained as crystals (40% yield) which had m.p. 201° and $[\alpha]_D^{23}$ +10° (*c*, 4.0 chloroform). Anal. Found: C, 55.8; H, 6.16; N, 4.3%. $C_{30}H_{40}O_{14}N_2$ requires: C, 55.2; H, 6.18; N, 4.3%.

The above synthesis was repeated using 1,3,4,6-tetra-*O*-acetyl-α-D-glucosamine to give the α-anomer as a syrup (35% yield) which could not be crystallized and which had $[\alpha]_D^{23}$ +91° (*c*, 4.0 chloroform).

The second isomer (I_{c2}) of *N*-carbobenzoxy-*O*-tetrahydropyranyl-L-serine was treated in the same way as described above with 1,3,4,6-tetra-*O*-acetyl-β-D-glucosamine to yield a crystalline product (29% yield) which had m.p. 160° and $[\alpha]_D^{23}$ +2° (*c*, 5.0 chloroform). Anal. Found: C, 55.5; H, 6.18; N, 4.6%.

The infrared absorption spectra of the products showed absorption band at the following wave numbers: carbonyl of *O*-acetyl (1745 cm^{-1}), amide I (1682 cm^{-1}), and amide II

Can. J. Chem. Downloaded from www.nrcresearchpress.com by 210.87.254.6 on 09/05/12
For personal use only.

(1495 cm^{-1}). The spectra showed the following absorption bands in common with 1,3,4,6-tetra-*O*-acetyl-β-D-glucosamine: 1235 (s), 1078 (s), 1041 (s), and 900 cm^{-1} (s). Bands characteristic of *N*-carbobenzoxy-*O*-tetrahydropyranyl-L-serine were detected at 1130, 987, and 695 cm^{-1}. The spectra of the isomers were almost identical.

*(j) N-(N-Carbobenzoxy-*L*-seryl)-1,3,4,6-tetra-O-acetyl-α- (and β-)* D*-glucosamine*

The *O*-tetrahydropyranyl group was removed from the products (*i*) by the following method. *N*-(*N*-Carbobenzoxy-*O*-tetrahydropyranyl-L-seryl)-1,3,4,6-tetra-*O*-acetyl-β-D-glucosamine (600 mg) was boiled for 10 minutes in 50% aqueous acetic acid (10 ml) and the cooled solution was then diluted with water (50 ml). The solution was extracted with chloroform (4×20 ml), the combined extracts were washed with water, dried (anhyd. sodium sulphate), and concentrated to a small volume. The residue was dissolved in the minimum quantity of hot ethanol from which the product crystallized slowly in the form of long colorless needles (75% yield) which had m.p. 168° and $[\alpha]_D^{23}$ +25° (*c*, 4.0 chloroform). Anal. Found: C, 53.3; H, 5.73; N, 5.0%. $C_{25}H_{32}O_{13}N_2$ requires: C, 52.8; H, 5.67; N, 4.93%.

The α-anomer was similarly prepared from *N*-(*N*-carbobenzoxy-*O*-tetrahydropyranyl-L-seryl)-1,3,4,6-tetra-*O*-acetyl-α-D-glucosamine as a crystalline product (65% yield) which had m.p. 145° and $[\alpha]_D^{23}$ +102° (*c*, 3.7 chloroform).

The infrared absorption spectra of these products were the same as those of the precursors except that the bands at 1130 cm^{-1} and 987 cm^{-1} due to the tetrahydropyranyl group were absent. The isomerism due to the forms (I_{e1}) and (I_{e2}) disappeared, as the same product was obtained from both isomers.

*(k) N-(N-Carbobenzoxy-*L*-seryl)-α- (and β-)* D*-glucosamine*

N-(*N*-Carbobenzoxy-L-seryl)-1,3,4,6-tetra-*O*-acetyl-α-D-glucosamine (0.4 g) dissolved in anhydrous methanol (8 ml) was treated with 0.4 *N* barium methoxide in methanol (2 ml) at 5° for 20 hours. After testing for the presence of excess barium, a little water was added and the remaining alkali was precipitated by carbonation of the solution. The barium carbonate was removed by centrifugation, and the clear supernatant was concentrated to a small volume. The residue gave a crystalline product (24% yield) from ethanol solution which had m.p. 195° and $[\alpha]_D^{20}$ +75° (*c*, 4.0 chloroform).

The β-anomer was similarly prepared from *N*-(*N*-carbobenzoxy-L-seryl)-1,3,4,6-tetra-*O*-acetyl-β-D-glucosamine as a crystalline product (30% yield) which had m.p. 198° and $[\alpha]_D^{21}$ +8° (*c*, 4.0 chloroform).

The products had R_{GNAc} 2.10 on paper chromatograms and was free from D-glucosamine and L-serine.

The infrared spectra of the two products were very similar, and differed from the spectra of the precursors in that the carbonyl of *O*-acetyl at 1750 cm^{-1} had disappeared, and the hydroxyl band at 3460 cm^{-1} appeared very strongly. The amide linkage bands at 1682 cm^{-1} and 1495 cm^{-1} were still present, though the latter was slightly displaced.

*(l) N-(*L*-Seryl hydrochloride)-*D*-glucosamine*

The carbobenzoxy group was removed from (1*k*) by hydrogenolysis using palladized charcoal as a catalyst. The catalyst was prepared by adding palladous chloride (0.1 g) in a little water to animal charcoal (2 g) and the mixture was then heated to 130° to remove water. Hydrazine sulphate was added, followed by a little *N* sodium hydroxide and the mixture was then stored for 24 hours at −5°. The charcoal was then collected by filtration and dried.

Can. J. Chem. Downloaded from www.nrcresearchpress.com by 210.87.254.6 on 09/05/12
For personal use only.

N-(*N*-Carbobenzoxy-L-seryl)-D-glucosamine (26 mg) was dissolved in a mixture of methanol and chloroform (5 ml) and the solution was added to water (5 ml) containing *N* hydrochloric acid (0.07 ml). Palladized charcoal was added and the mixture was shaken mechanically for 20 hours at room temperature under a slight pressure of hydrogen (2 lb above atmospheric pressure). The charcoal was removed from the product by filtration and the filtrate was concentrated to a syrup which was insoluble in chloroform and alcohol, but soluble in water.

The product was obtained from methanol/ether mixture as fine colorless crystals (19 mg; 86% yield) which decomposed over the temperature range 200–250°. On paper chromatograms developed in the 1-butanol/ethanol/water system the compound was revealed by the ninhydrin spray reagent as an orange spot which reddened on standing, and had $R_{GN\cdot HCl}$ 0.55. Anal. Found: N, 8.9; Cl, 11.7%. $C_9H_{19}O_7N_2Cl$ requires: N, 9.2; Cl, 11.7%.

The infrared spectrum showed a strong hydroxyl band at 3460 cm^{-1} which was very wide due to the amino group absorption. Amide I absorption was present at 1682 cm^{-1}, but was absent at 1495 cm^{-1}. Evidence for the ionic nitrogen was found at 1495 cm^{-1}.

The product prepared from the α-anomer failed to crystallize, and the yield of crude material was very poor.

(m) N-L-Seryl-D-glucosamine

Attempts to synthesize the free amine from *N*-(*N*-carbobenzoxy-L-seryl)-β-D-glucosamine by direct hydrogenolysis in aqueous solution failed, owing to the rapid decomposition of the product in the atmosphere. An indirect method was investigated. A little of the hydrochloride (*l*) (15 mg) was dissolved in an aqueous slurry of Amberlite IR 45 ($CO_3^=$) exchange resin (5 ml) and after removal of the resin the water was removed by distillation under reduced pressure at 30°, methanol being added to speed the evaporation of the water. The product which was a solid, blackened before it could be isolated.

(n) N-(N-Acetyl-O-acetyl-L-seryl)-1,3,4,6-tetra-O-acetyl-β-D-glucosamine

N-(L-Seryl hydrochloride)-β-D-glucosamine (10 mg) was acetylated with pyridine/acetic anhydride mixture (5 ml) at 0° for 2 days. The product was obtained as a syrup (10 mg) which had R_{GNpAc} 1.08 on paper chromatograms developed in the neutral solvent system. The infrared absorption spectrum of the product showed strong carbonyl of *O*-acetyl absorption at 1750 cm^{-1} but no band due to hydroxyl at 3460 cm^{-1}.

2. N-Glycyl-D-glucosamine

(a) N-Carbobenzoxyglycine

Glycine (25 g) was treated with carbobenzoxy chloride in toluene (60 g) using the method of Moore *et al.*, to give *N*-carbobenzoxyglycine (70 g).

(b) N-Carbobenzoxyglycyl p-Nitrophenyl Ester

N-Carbobenzoxyglycine (10 g) was dissolved in ethyl acetate (100 ml) containing *p*-nitrophenol (6.4 g) and dicyclohexycarbodiimide (9.2 g), and the mixture was kept at 0° for 1 hour and was then allowed to rise to room temperature. The precipitated dicyclohexyl urea by-product was removed by filtration and was washed free from the mother liquor with ethyl acetate. The combined filtrate and washings were concentrated and the ethanol solution of the residue gave the crystalline product (15 g; 95% yield) which had m.p. 127°. The infrared spectrum of the product showed the characteristic sharp absorption peaks due to the *p*-nitrophenyl group at 1775, 1635. 1600, 1540, 1500, 1355, and 695 cm^{-1}.

Can. J. Chem. Downloaded from www.nrcresearchpress.com by 210.87.254.6 on 09/05/12
For personal use only.

(c) N-(N-Carbobenzoxyglycyl)-1,3,4,6-tetra-O-acetyl-β-D-glucosamine

N-Carbobenzoxyglycyl *p*-nitrophenyl ester (1 g) was condensed with 1,3,4,6-tetra-*O*-acetyl-β-D-glucosamine hydrobromide (1.25 g) in the presence of dimethylformamide containing triethylamine (0.3 g) by Bodanszky and Du Vigneaud's (16) procedure to give the product, obtained as crystals (0.9 g) from methanol solution, which had m.p. 168°, and $[\alpha]_D^{22}$ +49° (*c*, 4.0 methanol).

The infrared spectrum of the product resembled that of the corresponding L-serine derivative (1*j*) showing absorption bands due to amide at 1675 cm^{-1} and carbonyl of *O*-acetyl at 1750 cm^{-1}. The "fingerprint" regions of the spectra were also similar, with peaks at 1375, 1250, 1058, and 695 cm^{-1}.

(d) N-(N-Carbobenzoxyglycyl)-D-glucosamine

N-(*N*-Carbobenzoxyglycyl)-1,3,4,6-tetra-*O*-acetyl-β-D-glucosamine (0.5 g) in dry methanol (10 ml) was treated with 0.4 *N* barium methylate (1 ml) at −5° for 20 hours and the deacetylated product was isolated as described for (1*k*), as crystals (0.2 g) which had m.p. 188° and $[\alpha]_D^{24}$ +39.5° (*c*, 4.0 methanol).

(e) N-(Glycyl hydrochloride)-D-glucosamine

N-(*N*-Carbobenzoxyglycyl)-D-glucosamine (0.15 g), dissolved in dioxan/water mixture (1:1 v/v) containing palladized charcoal (0.1 g), was placed under a slight pressure of hydrogen (2 lb above atmospheric pressure) and shaken for 24 hours. Hydrochloric acid (1 ml, 10%) was added to the mixture, the charcoal removed by filtration, and the filtrate was concentrated *in vacuo* to a syrup. The syrup was dissolved in hot ethanol from which the product was obtained as crystals (70 mg) which had m.p. 172° and $[\alpha]_D^{23}$ +31.5° (*c*, 1.0 water). Reported constants (8) for the product obtained by a different route are: m.p. 170° and $[\alpha]_D^{18}$ +29.7° (water).

The product was detected on paper chromatograms, developed in the neutral solvent system, by the ninhydrin and silver nitrate spray reagents as a single spot which had $R_{GN.HCl}$ 0.53.

(f) N-Glycyl-D-glucosamine

Attempts to remove the carbobenzoxy group from *N*-(*N*-carbobenzoxyglycyl)-1,3,4,6-tetra-*O*-acetyl-β-D-glucosamine and *N*-(*N*-carbobenzoxyglycyl)-D-glucosamine by hydrogenolysis in neutral solution, to form the free base, failed owing to the rapid decomposition of the product when it was exposed to the atmosphere. Attempts were made to deionize the salt (2*e*) with Amberlite IR 45($CO_3^=$) exchange resin but the product decomposed immediately on isolation.

3. N-L-Glutamyl-D-glucosamine

(a) N-Carbobenzoxy-L-glutamic Acid

L-Glutamic acid (25 g) was treated with 75% carbobenzoxychloride in toluene (44 ml) according to the procedure of Moore *et al.* (14), to give the crystalline product (51 g; 95% yield), which had m.p. 124°.

(b) N-Carbobenzoxy-L-glutamic Acid Di-p-nitrophenyl Ester

The ester was prepared by treating *N*-carbobenzoxy-L-glutamic acid (21 g) dissolved in ethyl acetate (200 ml) with *p*-nitrophenol (26 g) and dicyclohexylcarbodiimide (32 g) for 30 minutes at 0°. The reaction mixture was then kept at room temperature for 1 hour, the precipitated dicyclohexyl urea by-product was filtered off, and the filtrate was concentrated to a syrup which was dissolved in hot ethanol. On cooling, the crystalline product was obtained (21 g), which had m.p. 210° and $[\alpha]_D^{23}$ +17.1° (*c*, 4.0 benzene).

Can. J. Chem. Downloaded from www.nrcresearchpress.com by 210.87.254.6 on 09/05/12
For personal use only.

Can. J. Chem. Downloaded from www.nrcresearchpress.com by 210.87.254.6 on 09/05/12
For personal use only.

The infrared spectrum of the product showed no absorption due to hydroxy group, but showed bands due to the *p*-nitrophenyl group at 1775, 1540, 1500, 1355, and 1135 cm^{-1}.

(c) N-Carbobenzoxy-γ-L-glutamide α-p-Nitrophenyl Ester

The diester (3*b*) (10 g) dissolved in benzene/methanol mixture (100 ml; 1:1 v/v) was treated with the calculated amount of *N* methanolic ammonia, sufficient to react with one ester group, and the solution was allowed to stand overnight at room temperature. A small amount of precipitated material, identified as the diamide derivative, was removed and on the addition of benzene the crystalline monoamide was obtained (4.6 g; 60% yield) which after recrystallization from methanol had m.p. 158° and $[\alpha]_D^{21}$ −25.1° (*c*, 4.0 DMF). Anal. Found: N, 10.6%. $C_{19}H_{19}O_7N_3$ requires: N, 10.5%.

(d) 1-(1′,3′,4′,6′-Tetra-O-acetyl-β-D-glucosaminyl)-2-N-carbobenzoxy-L-glutamine

1,3,4,6-Tetra-*O*-acetyl-β-D-glucosamine hydrobromide (0.4 g) and the monoamide ester (3*c*) (0.4 g) dissolved in dimethylformamide (2 ml) were treated with excess triethylamine (0.2 g) at 95° for 20 minutes and the reaction mixture was then cooled to room temperature. Ether (4 ml) was added to precipitate the triethylamine hydrobromide which was removed by filtration, and the filtrate was then washed with *N* hydrochloric acid (3×20 ml) followed by water until the yellow color due to *p*-nitrophenol was removed. An ethanol solution of the product, diluted with chloroform, was dried (anhyd. sodium sulphate) and concentrated to a syrup which was dissolved in ethyl acetate and ether was added. The product was obtained as crystals (0.23 g) from the cooled solution which had, after recrystallization from ethanol, m.p. 178° and $[\alpha]_D^{20}$ −6.0° (*c*, 4.0 pyridine). The infrared spectrum of the product showed absorption bands in common with the D-glucosamine reactant at 1750, 1480, 1250, and 1050 cm^{-1}, and in common with the substituted amino acid at 3360, 1650, 1530, 1460, 1090, 1050, 900, and 695 cm^{-1}. The characteristic *p*-nitrophenyl bands were absent.

(e) 1-(1′,3′,4′,6′-Tetra-O-acetyl-β-D-glucosaminyl)-2-N-carbobenzoxy-L-glutamic Acid

The condensation product (3*d*) (50 mg) was treated with an excess of nitrous acid and when the reaction had subsided the solution was diluted with water and extracted with chloroform (3×10 ml). The dried (anhyd. sodium sulphate) chloroform extract was concentrated to a syrup (41 mg) which was purified by cellulose column partition chromatography using 1-butanol half saturated with water as the mobile phase. The final product (30 mg), obtained crystalline from ethanol solution, had m.p. 218° (decomp.) and $[\alpha]_D^{18}$ −7.4° (*c*, 2.0 pyridine).

(f) 1-(N-D-Glucosaminyl)-2-N-carbobenzoxy-L-glutamic Acid

The compound (3*e*) (30 mg) was treated with barium methoxide in the usual way to yield the deacetylated product (9 mg), which had m.p. 184°, and $[\alpha]_D^{18}$ +70° (*c*, 1.0 pyridine).

(g) 1-(N-D-Glucosaminyl)-L-glutamic Acid Hydrochloride

The deacetylated product (3*f*) (63 mg) dissolved in aqueous methanol (4 ml) containing 2 *N* hydrochloric acid (2 ml) was reduced with hydrogen in the presence of palladized charcoal as described for (1*l*). The product, crystallized from ethanol – light petroleum (b.p. 60–80°) mixture (30 mg), had $[\alpha]_D^{24}$ +14.1° (*c*, 1.5 water) and decomposed above 200°. Anal. Found: C, 37.9; H, 6.2; N, 8.0; Cl, 10.0%. $C_{11}H_{21}N_2O_8Cl$ requires: C, 38.3; H, 6.1; N, 8.1; Cl, 10.3%.

*4. 1-O-β-*L*-Seryl-N-acetyl-*D*-glucosaminide*

*(a) 1-Chloro-1-deoxy-N-acetyl-3,4,6-tri-O-acetyl-α-*D*-glucosamine*

The compound was prepared in 25% yield by the method of Inouye (18) and his co-workers. It had m.p. 124° and $[\alpha]_D^{25}$ +116° (*c*, 4.0 chloroform).

*(b) N-Carbobenzoxy-*L*-seryl Methyl Ester*

The methyl ester was synthesized by the action of diazomethane on the carboxylic acid (20). *N*-Carbobenzoxy-L-serine (8 g) dissolved in an alcohol/ether mixture (50 ml; 1:1 v/v) was treated with a solution of diazomethane (3 g) in ether (100 ml) and after the esterification was completed, the excess diazomethane was removed with hydrogen chloride gas. The solution was deacidified with Duolite A4(OH^-) exchange resin and then concentrated under reduced pressure to give the product as a pale yellow syrup (7 g).

*(c) 1-O-β-(N-Carbobenzoxy-*L*-seryl methyl ester)-N-acetyl-*D*-glucosaminide*

The substituted *O*-glucosaminide was synthesized by the Koenigs and Knorr (17) procedure, followed by deacetylation and hydrogenolysis of the product. Dried samples of 1-chloro-1-deoxy-*N*-acetyl-3,4,6-tri-*O*-acetyl-α-D-glucosamine (3.23 g) and *N*-carbobenzoxy-L-seryl methyl ester (2.5 g) were dissolved in anhydrous alcohol-free chloroform (50 ml) containing Drierite (10 g). Silver oxide (3 g) and iodine (5 mg catalyst) were added and the reaction mixture was shaken in the dark at room temperature for 140 hours. The insoluble material was removed by filtration through a Celite pad, the residue washed with chloroform, and the combined filtrate and washings were concentrated to a syrup. Paper chromatographic examination of the syrup in the neutral solvent system revealed the product as the major component having R_{GNAc} 3.2. The syrup was fractionated by cellulose column partition chromatography using 1-butanol half saturated with water as the mobile phase to give the chromatographically pure product (1.78 g) as a syrup which could not be crystallized. The product was deacetylated in absolute methanol (30 ml) containing 0.4 *N* barium methylate (2 ml) for 22 hours at −5°. The syrupy product (0.94 g) was found by paper chromatography to contain the required compound, which had R_{GNAc} 1.88, and *N*-acetylglucosamine. The faster-moving component was isolated by cellulose column partition chromatography using 1-butanol half saturated with water as the mobile phase. The product was crystallized from ethanol/light petroleum (b.p. 60–80°) mixture (219 mg). It had R_{GNAc} 1.89 and R_{GNDAc} 0.50, m.p. 133° and $[\alpha]_D^{23}$ +6.4° (*c*, 10 ethanol).

*(d) 1-O-β-(*L*-Seryl methyl ester)-N-acetyl-*D*-glucosaminide*

1-*O*-β-(*N*-Carbobenzoxy-L-seryl methyl ester)-*N*-acetyl-D-glucosaminide (140 mg) dissolved in aqueous ethanol (4 ml) containing palladized charcoal (200 mg), was placed under a slight pressure of hydrogen and shaken for 24 hours. The charcoal was removed by filtration and the filtrate was concentrated to a syrup (100 mg) which was shown by paper chromatography to contain the product contaminated with *N*-acetylglucosamine. The syrup was fractionated by chromatography on large sheets of Whatman 3MM paper in the neutral solvent system to give the pure derivative (60 mg) which had $R_{GN.HCl}$ 0.28, m.p. 230° (decomp.) and $[\alpha]_D^{24}$ +1.7° (*c*, 1.0 methanol).

The substituted D-glucosaminide was much more stable in air than the corresponding *N*-peptide.

*(e) 1-O-β-(*L*-Seryl methyl ester hydrochloride)-N-acetyl-*D*-glucosaminide*

1-*O*-β-(*N*-Carbobenzoxy-L-seryl methyl ester)-*N*-acetyl-D-glucosaminide (25 mg) was treated in the cold with 0.1 *N* hydrochloric acid (5 ml) for 6 hours, the excess acid was removed on Duolite A4(OH^-) exchange resin and the solution concentrated to dryness.

Can. J. Chem. Downloaded from www.nrcresearchpress.com by 210.87.254.6 on 09/05/12
For personal use only.

The product was twice recrystallized from ethanol/light petroleum (b.p. 60–80°) mixture. Anal. Found: C, 40.5; H, 6.7; N, 8.1; Cl, 9.8%. $C_{12}H_{23}N_2O_8Cl$ requires: C, 40.2; H, 6.4; N, 7.8; Cl, 9.90%.

The infrared spectrum of the product supported the assigned structure and showed absorption peaks at 1750 cm^{-1} due to ester carbonyl, 1610 cm^{-1} due to *N*-acetyl, and an ether-type absorption peak at 1100 cm^{-1}.

*(f) 1-O-β-*L*-Seryl-N-acetyl-*D*-glucosaminide*

The glucosaminide methyl ester (4*d*) (48 mg) dissolved in methanol (0.5 ml) was diluted with water (2 ml) and 0.5 *N* sodium hydroxide solution (3 ml) was slowly added and the saponification was allowed to proceed for 3 hours at room temperature. The solution was made slightly acidic by the addition of 0.1 *N* sulphuric acid (0.24 ml) and the solution was concentrated under reduced pressure. The residue was extracted with methanol from ionic material and the concentrated extract was dissolved in ethanol/light petroleum (b.p. 60–80°) mixture which on cooling gave the crystalline product (27 mg) which had m.p. 236°, and $[\alpha]_D^{24}$ −31.0° (*c*, 1.0 water). Anal. Found: C, 42.85; H, 6.4; N, 9.0%. $C_{11}H_{20}N_2O_8$ requires: C, 42.9; H, 6.5; N, 9.1%.

The infrared absorption spectrum of the product showed no absorption peak due to ester group at 1750 cm^{-1} but the strong absorption band at 1610 cm^{-1} due to *N*-acetyl was present.

DISCUSSION

The object of this investigation was to determine the properties of D-glucosamine derivatives of some amino acids, particularly their stability in solution.

The prepared derivatives were dissolved in acidic media in order to investigate their behavior under conditions of acid hydrolysis. The *N*-peptide hydrochlorides were found to be unaffected by *N* hydrochloric acid at 60° for 24 hours, but the 1-*O*-β-L-seryl-D-glucosaminide gave L-serine, *N*-acetyl-D-glucosamine, and D-glucosamine after 1 hour under the same conditions.

The *N*-peptides were stable in neutral or basic media but degraded rapidly in the presence of air, and immediately upon isolation. It is apparent that the *N*-peptides may only be obtained as their salts, from acid media, whereas the D-glucosaminides examined are relatively unstable in acid solution and should be separated only from neutral or basic media.

ACKNOWLEDGMENTS

We wish to thank the Ontario Department of Health, the Canadian Arthritis and Rheumatism Society, the National Research Council, The National Institutes of Health, Bethesda, Md., U.S.A. (Grant No. A4127), and Queen's University for financial assistance.

REFERENCES

1. G. M. Windrum, P. W. Kent, and J. E. Eastoe. Brit. J. Exptl. Pathol. **36**, 49 (1955).
2. Z. Dische and E. Borenfreud. Am. J. Ophthalmol. **38**, 165 (1954).
3. K. A. Piez and J. Gross. Biochim. et Biophys. Acta, **34**, 24 (1960).
4. D. J. Walton. Ph.D. Thesis, Queen's University, Kingston, Ontario. August 1960.
5. J. Mandelstam and H. G. Rogers. Nature, **181**, 956 (1958).
6. R. Hancock and J. T. Park. Nature, **181**, 1050 (1958).
7. J. M. Ghuysen and M. R. J. Salton. Biochim. et Biophys. Acta, **40**, 462 (1960).
8. M. Bergmann and L. Zervas. Ber. **65**, 1201 (1932).
9. A. Bertho, F. Holden, W. Weiser, and F. Huther. Liebigs. Ann. Chem. **485**, 127 (1931).
10. A. Bertho and J. Maier. Liebigs. Ann. Chem. **495**, 113 (1932).

Can. J. Chem. Downloaded from www.nrcresearchpress.com by 210.87.254.6 on 09/05/12
For personal use only.

11. D. G. DOHERTY, E. A. POPENOE, and K. P. LINK. J. Am. Chem. Soc. **75**, 3466 (1953).
12. H. MASAMUNE, S. HAKOMORI, and O. MASAMUNE. Tohoku. J. Exptl. Med. **65**, 63 (1956).
13. J. GROSS. Personal communication. February 1960.
14. J. A. MOORE, J. R. DICE, E. D. NICOLAIDES, R. D. WESTLAND, and E. L. WHITTLE. J. Am. Chem. Soc. **76**, 2884 (1954).
15. B. ISELIN and R. SCHWYZER. Helv. Chim. Acta, **39**, 57 (1956).
16. M. BODANSZKY and V. DU VIGNEAUD. J. Am. Chem. Soc. **81**, 5688 (1959).
17. W. KOENIGS and E. KNORR. Ber. **34**, 957 (1901).
18. Y. INOUYE, K. ONODERA, S. KITAOKA, and H. OCHIAI. J. Am. Chem. Soc. **79**, 4218 (1957).
19. H. E. CARTER, R. L. FRANK, and H. W. JOHNSTON. Organic syntheses. Collected Vol. III. John Wiley & Sons, Inc., New York. 1955. p. 167.
20. TH. J. DEBOER. Ph.D. Thesis. Groningen. 1953.

Can. J. Chem. Downloaded from www.nrcresearchpress.com by 210.87.254.6 on 09/05/12
For personal use only.

Can. J. Chem. Downloaded from www.nrcresearchpress.com by 210.87.254.42 on 09/05/12
For personal use only.

GUANIDINE COMPOUNDS

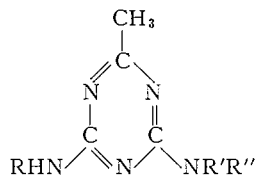
IV. ACETYLATION OF SOME ALKYL-SUBSTITUTED GUANIDINES WITH ACETIC ANHYDRIDE AND ETHYL ACETATE[1,2]

R. GREENHALGH AND R. A. B. BANNARD

ABSTRACT

The acetylation of some mono-, N,N-, and N,N′-dialkylguanidines was studied using ethyl acetate and acetic anhydride. Except for the N,N-dialkylguanidines, the action of ethyl acetate on the free bases gave monoacetyl derivatives. Acetic anhydride with the acetate salts gave diacetyl derivatives with monoalkylguanidines, acetamido-1,3,5-triazines with N,N-dialkylguanidines, and unstable di- and tri-acetyl derivatives with N,N′-dialkylguanidines. The assignment of symmetrical structures to the mono- and tri-acetyl derivatives and an asymmetrical structure to the diacetyl derivatives was supported by nuclear magnetic resonance spectra. The ultraviolet spectra of the monoacetyl derivatives exhibited one peak in the region 230–235 mμ whilst the diacetyl derivatives showed two peaks in the regions 220–230 mμ and 253–263 mμ. Some comments are made on the infrared spectra of these compounds.

In an earlier paper in this series Cockburn and Bannard (1) reported the formation of amino- (I) and acetamido-*s*-triazines (II) on acetylation of alkylguanidine salts under vigorous conditions.



I. R = H; R′, R″ = H or alkyl
II. R = CH_3CO; R′, R″ = H or alkyl
III. R = CH_3CO; R′, R″ = CH_3

Ryabinin (2) had previously shown that the products obtained on acetylation of guanidine acetate were dependent on the conditions used. Under mild conditions, an acetylated guanidine derivative was obtained rather than an *s*-triazine derivative. The present study, in which the acetylation of several mono-, N,N-, and N,N′-dialkylguanidines with ethyl acetate and acetic anhydride was examined, revealed that the type of alkyl substitution also influenced the product obtained. The opportunity was taken to examine the infrared and ultraviolet spectra of the acetylated guanidines isolated.

Various conditions for the acetylation of *trans*-2-guanidocyclohexanol with acetic anhydride were examined to determine which gave the highest yield of acetylated products. The addition of sodium acetate did not influence the yields and was therefore omitted, since it merely complicated isolation of the products. It was found that a shorter time of heating at 100° than that previously employed for the acetylation of guanidine (3) was beneficial, since even the relatively stable diacetyl derivatives were degraded or cyclized on prolonged heating with acetic anhydride at this temperature.

[1]*Manuscript received January 3, 1961.*
Contribution from Defence Research Chemical Laboratories, Ottawa, Canada. Presented at the 43rd Annual Conference of the Chemical Institute of Canada, Ottawa, Ontario, June 13–15, 1960.
Issued as D.R.C.L. Report No. 339.
[2]*Part III, Can. J. Chem.* **37**, *1810 (1959).*

The use of the readily soluble acetate salts rather than the more insoluble hydrochlorides, nitrates, or sulphates enabled a reaction period of 30 minutes to be used.

Acetylation of the monoalkylguanidines under these conditions gave the diacetyl derivatives in yields exceeding 79%, together with small amounts of the corresponding acetylated amino compounds. The latter products were shown to result from degradation of the diacetyl derivatives by acetic anhydride, since on warming of diacetyl cyclohexylguanidine for 1 hour at 100° with acetic anhydride, acetyl cyclohexylamine was isolated in 50% yield.

The N,N-dialkylguanidines gave, in general, acetamido-*s*-triazines, although in the case of N,N-dimethylguanidine a diacetyl derivative was also isolated. The results given in Table I show that the amount of diacetyl derivative (IV) decreases as the amount of acetamido-*s*-triazine (III) increases when the heating period is prolonged. It thus appears that diacetyl derivatives are intermediates in the formation of triazines from N,N-dialkylguanidines. This behavior contrasts with that of the diacetyl derivatives of the monoalkylguanidines, which, on being heated with acetic anhydride, are degraded rather than cyclized. The formation of triazines from monoalkylguanidine acetates or monoacetyl derivatives has been reported (4) but more drastic conditions were involved (0.5 hour at 200°).

TABLE I

Variation of product composition on heating N,N-dimethylguanidine with acetic anhydride at 100° for various periods of time

Heating period (min)	Percentage yield of products	
	III	IV
15	24	46
30	32	31
60	49	23

NOTE: III = 2-dimethylamino-4-acetamido-6-methyl-1,3,5-triazine. IV = diacetyl N,N-dimethylguanidine.

With N,N′-dialkylguanidines, the products obtained were very dependent on the individual structure of the guanidine. Both six-membered ring compounds gave unstable diacetyl derivatives which could only be isolated by vacuum distillation. Attempts to purify them by chromatography on alumina, or recrystallization from alcohol gave the more stable monoacetyl derivatives. N,N′-Dimethylguanidine together with 2-iminoimidazolidine gave compounds whose analysis indicated a triacetyl derivative. Because of the peculiar spectral and chemical properties of triacetyl 2-iminoimidazolidine it is discussed more fully later in the paper.

Acetylation of alkylguanidines with ethyl acetate was studied with the object of preparing monoacetyl derivatives. Ostrogovich (5) reported the acetylation of aminotriazines by boiling them with ethyl acetate or acetic acid. The reaction most likely occurs by nucleophilic attack of the π electrons of the guanidine on the ester, similar to the mode of action formulated by Gordon *et al.* (6) for the ammonolysis of esters. Simons and Weaver (4) showed that ethyl acetate reacts with monoalkylguanidine free bases in the cold to give the monoacetyl derivatives. We modified their procedure by using Amberlite IRA-400 (OH) resin prepared in absolute alcohol to generate the free base. This procedure had the advantage over the usual one in which the hydrochloride

Can. J. Chem. Downloaded from www.nrcresearchpress.com by 210.87.254.42 on 09/05/12
For personal use only.

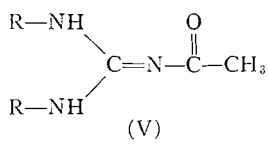
is treated with sodium ethoxide in that it gave quantitative conversion to the pure free base, uncontaminated with inorganic material. The type of alkyl substituents again affected the type of product obtained. With the exception of the N,N-dialkylguanidines all the alkylguanidines gave monoacetyl derivatives by this method. Since Angyal and Warburton (7) and Neivelt *et al.* (8) have shown that methyl guanidines, regardless of the type and degree of alkyl substitution have a pK_a greater than 13.4, basicity is obviously not the reason for lack of reactivity. It is interesting to note that 2-imino-5-hydroxyhexahydropyrimidine gave only a mono-N-acetyl derivative, indicating that the method could be used to selectively monoacetylate a guanidine moiety in a molecule also possessing a hydroxyl function. Acetylation of guanidine itself gave a monoacetyl derivative which is still basic (pK_a 8.2) but would not form a diacetyl derivative on further treatment with ethyl acetate.

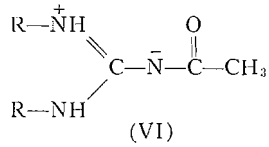
TABLE II

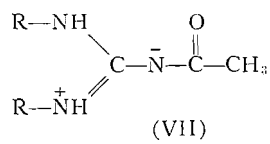
Ultraviolet absorption of monoacetyl guanidines in absolute alcohol

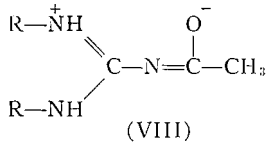
Compound	λ_{max} (mμ)	log ϵ_{max}
Acetyl guanidine	230	4.24
Acetyl methylguanidine	234	4.31
Acetyl cyclohexylguanidine	232	4.30
N-Acetyl guanidocyclohexanol	234	4.26
Acetyl N,N′-dimethylguanidine	234	4.23
Acetyl 2-iminoimidazolidine	230	4.24
Acetyl 2-iminohexahydropyrimidine	234	4.23
Acetyl 2-imino-5-hydroxyhexahydropyrimidine	235	4.31
Acetyl guanidine acetate	230	3.92

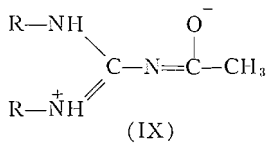
The ultraviolet spectra of the monoacetyl guanidines, when measured in ethanol, all exhibit one peak in the range 230–235 mμ as shown in Table II. This absorption is independent of the type of alkyl substitution possessed by the guanidine moiety. A similar observation was reported by McKay *et al.* (9) for alkyl nitroguanidines.


(V)


(VI)


(VII)


(VIII)


(IX)

Since neither guanidine nor primary or secondary amides absorb strongly above 210 mμ, the absorption indicates conjugation of the acetyl carbonyl group with the guanidine moiety. It was therefore concluded that monoacetyl guanidines exist in the acetylimino form (V, R = alkyl or H) and this was confirmed in the case of acetyl 2-iminoimidazolidine by measurement of its nuclear magnetic resonance spectrum.

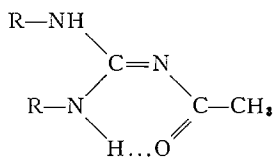
Some contribution to the structure from the other canonical forms of the guanidine moiety (VI) and (VII), together with a small contribution from forms (VIII) and (IX)

Can. J. Chem. Downloaded from www.nrcresearchpress.com by 210.87.254.42 on 09/05/12
For personal use only.

would also be expected. Bryden *et al.* (10), from crystallographic studies, showed this to be the case for nitroguanidine, which is best formulated as a resonance hybrid which combines both the forms postulated by McKay *et al.* (9) and by Kirkwood and Wright (11).

The infrared spectra of monoacetyl guanidines would be expected to show two bands in the region 1700–1500 cm^{-1} corresponding to the stretching vibrations of the C=N and the C=O of the acetyl group (amide I (12)). Table III shows the results obtained.

The spectra mainly show one very strong broad band at 1620–1580 cm^{-1} with shoulders on the high and low frequency sides. This strong band is presumably due to the unresolved vibrations of the C=N and C=O groups. Two bands are observed only in the cases of the monoacetyl derivatives of 2-iminoimidazolidine and 2-imino-5-acetoxyhexahydropyrimidine. The stronger band, at 1580 cm^{-1} and 1595 cm^{-1} respectively, was assigned to amide I vibrations, since it is doubtful whether the intensity of the C=N vibration, even though it is known to increase on conjugation (13), would approach that of an amide I. Also, the amide I is known to be more susceptible to displacement than the C=N vibration. The large shift found for the amide I band can be attributed partly to intramolecular hydrogen bonding as shown in X and partly to conjugation. Examination of the spectrum of triacetyl 2-iminoimidazolidine, a compound which contains no NH bond shows a normal amide I vibration with no absorption around 1600 cm^{-1}.



(X)

The second band found in the spectra of both monoacetyl 2-iminoimidazolidine and monoacetyl 2-imino-5-acetoxyhexahydropyrimidine occurs at 1620 cm^{-1} and is assigned to the C=N stretching vibration, the shift to lower frequency resulting from conjugation with the acetyl group. In the literature, the C=N vibration for substituted nitroguanidines is variously assigned, Leiber *et al.* (14) give 1680–1661 cm^{-1}, Randall *et al.* (15) 1695–1639 cm^{-1}, and Kumler (16) 1689–1618 cm^{-1}. Kumler's assignment for the C=N vibration in 2-nitriminoimidazolidine at 1618 cm^{-1} agrees closely with that of the acetyl analogue, but his assignment of a band at 1664 cm^{-1} in nitroguanidine itself seemed high. Monoacetyl guanidine also shows a band at 1660 cm^{-1} which we thought was most likely due to the NH_2 deformation vibrations as suggested by Jones (17) for guanidine. Attempts to deuterate acetyl guanidine resulted in hydrolysis, but deuteration of nitroguanidine caused the band at 1664 cm^{-1} to disappear whilst another band appeared at 1290 cm^{-1}. Hence Kumler's assignment of the 1664 cm^{-1} band in nitroguanidine to the C=N appears to be in error and it must appear at lower frequencies together with the vibration for the nitro group.

The diacetyl guanidines possess characteristic ultraviolet spectra by means of which they can be readily distinguished from mono- or tri-acetyl guanidines. All the diacetyl guanidines show two peaks in the regions 212–225 $m\mu$ and 243–263 $m\mu$ as shown in Table V.

In all cases examined the extinction coefficient of the low wavelength peak was just

Can. J. Chem. Downloaded from www.nrcresearchpress.com by 210.87.254.42 on 09/05/12
For personal use only.

Can. J. Chem. Downloaded from www.nrcresearchpress.com by 210.87.254.42 on 09/05/12
For personal use only.

TABLE III

Infrared absorption of some monoacetyl guanidines in the region 1700–1550 cm^{-1}

Compound	Absorption (cm^{-1})				Type of spectrum
Acetyl guanidine	1660 (m)	1605 (sh)	1600 (vs)	—	KBr pellet
Acetyl cyclohexylguanidine	—	1615 (sh)	1590 (vs)	1565 (sh)	KBr pellet
	—	1640 (sh)	1595 (vs)	1575 (sh)	Chloroform solution
Acetyl *trans*-2-guanidocyclohexanol	—	1640 (sh)	1600 (vs)	1580 (sh)	KBr pellet
Acetyl 2-iminohexahydropyrimidine	—	1620 (sh)	1595 (vs)	1560 (sh)	KBr pellet
	—	1620 (sh)	1595 (vs)	1570 (sh)	Chloroform solution
Acetyl 2-iminoimidazolidine	1660 (w)	1620 (sh)	1595 (vs)	1565 (sh)	KBr pellet
	—	1620 (s)	1580 (vs)	—	Chloroform solution
Acetyl 2-imino-5-acetoxyhexahydropyrimidine	—	1620 (s)	1595 (vs)	1575 (sh)	KBr pellet

TABLE IV

Infrared absorption of some diacetyl guanidines in the region 1750–1550 cm^{-1}

Compound	Absorption frequencies (cm^{-1})					Type of spectrum
Diacetyl guanidine	—	1700 (s)	1625 (s)	1585 (vs)	1550 (m)	KBr pellet
Triacetyl *trans*-2-guanidinocyclohexanol	1740 (s)	1705 (s)	1620 (sh)	1595 (vs)	1570 (m)	KBr pellet
Diacetyl cyclohexylguanidine	—	1700 (s)	1615 (sh)	1600 (vs)	1565 (m)	KBr pellet
Diacetyl N,N-dimethylguanidine	—	1705 (m)	1620 (sh)	1595 (vs)	1550 (m)	KBr pellet
Diacetyl 2-iminohexahydropyrimidine	—	1670 (m)	—	1595 (s)	—	KBr pellet
	—	1680 (m)	—	1605 (s)	—	Chloroform solution
Diacetyl 2-imino-5-acetoxyhexahydropyrimidine	1725 (s)	1680 (m)	1620 (m)	1595 (vs)	—	KBr pellet

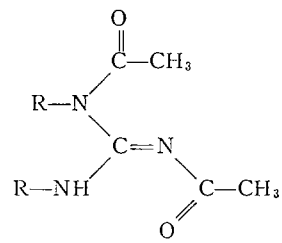
TABLE V

Ultraviolet absorption of diacetyl guanidines

Compound	λ_{max} (mμ)	log ϵ_{max}	λ_{max} (mμ)	log ϵ_{max}	Solvent
Diacetyl guanidine	212	3.95	243	4.25	Abs. ethanol
Diacetyl guanidocyclohexanol	222	3.99	255	4.23	Abs. ethanol
Diacetyl cyclohexylguanidine	221	4.03	254	4.25	Abs. ethanol
Diacetyl methylguanidine	218	4.01	254	4.24	Cyclohexane
Diacetyl N,N'-dimethylguanidine	225	3.87	263	4.29	Abs. ethanol
Octa-acetyl streptidine	220	4.27 (3.99)*	254	4.55 (4.25)*	Abs. ethanol
Diacetyl 2-iminohexahydropyrimidine	223	3.95	256	4.24	Cyclohexane
Diacetyl 2-imino-5-acetoxyhexahydropyrimidine	225	3.97	254	4.17	Cyclohexane

*Log ϵ_{max}/guanidine moiety.

about half that for the peak at higher wavelength. Unlike monoacetyl guanidines, alkyl substitution does affect the chromophore for the diacetyl guanidines, resulting in a variation of 13 mμ for the first peak and 20 mμ for the second. The bathochromic shift observed in the ultraviolet spectra in going from mono- to di-acetyl derivatives is compatible with a further lengthening of the π electron path. An asymmetrical structure XI was assigned to the diacetyl derivatives based on nuclear magnetic resonance studies with the diacetyl derivative of 2-iminohexahydropyrimidine.



(XI)

Korndorfer (18) postulated the existence of both symmetrically and asymmetrically substituted diacetyl guanidines. Later Ryabinin (2) established that only one isomer exists, but did not specify which one. The infrared spectra of the diacetyl guanidines also give ample evidence for the asymmetric structure, the results being given in Table IV.

The spectra exhibit a very strong broad band in the region 1620–1585 cm^{-1} together with a strong band in the region 1705–1670 cm^{-1}. The first band is similar to that exhibited by the monoacetyl guanidines and, as in that case, is ascribed to the unresolved stretching frequencies of the C=N and the C=O of the acetylimino group. The second band is assigned to the amide I vibration of the second acetyl group by analogy with the absorption observed for the acetamido group in 6-methyl-2-cyclohexylamino-4-acetamido-1,3,5-triazine at 1680 cm^{-1}, 6-methyl-2-dimethylamino-4-acetamido-1,3,5-triazine at 1685 cm^{-1}, and 6-methyl-2-piperidino-4-acetamido-1,3,5-triazine at 1690 cm^{-1}. The shift to higher frequencies of the amide I band of the second acetyl group is expected, since Richards and Thompson (19) showed that substitution of an amide nitrogen with an electrophilic group produces this effect. We found the amide I band above 1700 cm^{-1}

Can. J. Chem. Downloaded from www.nrcresearchpress.com by 210.87.254.42 on 09/05/12
For personal use only.

Can. J. Chem. Downloaded from www.nrcresearchpress.com by 210.87.254.42 on 09/05/12
For personal use only.

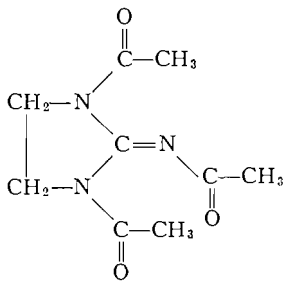
if the second acetyl group is present as a secondary amide and below if present as a tertiary amide, e.g. diacetyl N,N-dimethylguanidine absorbs at 1705 cm^{-1} (KBr) and diacetyl hexahydropyrimidine at 1670 cm^{-1} (KBr). Since the main difference between the amides is in the nature of the third group attached to the amide nitrogen, i.e. either a hydrogen or an alkyl group, the spectral data can be explained in terms of the electron-donating power of the third group. The alkyl group is able to contribute a greater share of its electrons to the amide nitrogen than the hydrogen, thus reducing the demand placed on the nitrogen by the acetyl and acetylimino groups. Hence the increase in frequency is not as great for the tertiary amide. In diacetyl guanidines possessing a secondary amide group, a third band in the range 1575–1560 cm^{-1} is found, due to the amide II vibration.

The ultraviolet spectra of the triacetyl derivatives obtained from N,N′-dimethylguanidine and 2-iminoimidazolidine were similar, showing only one peak at 232 $m\mu$ and 234 $m\mu$ respectively. This absorption is similar to that obtained with the monoacetyl derivatives, although it seems unlikely that the same chromophore is involved. The infrared spectra showed no absorption above 3000 cm^{-1} or near 1600 cm^{-1} in either case, and this was interpreted as evidence for intramolecular hydrogen bonding between the N—H and acetylimino groups in mono- and di-acetyl guanidines. The spectra differed in that triacetyl N,N′-dimethylguanidine shows two strong bands at 1690 and 1620 cm^{-1} (film), whereas triacetyl 2-iminoimidazolidine shows three in chloroform solution at 1745, 1690, and 1645 cm^{-1} and four for a KBr pellet at 1725, 1690, 1680, and 1620 cm^{-1}. The band at lowest frequency is thought to be due to the amide I of the non-hydrogen-bonded acetylimino group, whilst bands at 1690 cm^{-1} are due to the amide I of the tertiary amides. The band found at 1745 cm^{-1} (chloroform) and 1725 cm^{-1} (KBr) in triacetyl 2-iminoimidazolidine appears to be associated with the C=N, since it is missing from the methanol adduct of triacetyl 2-iminoimidazolidine where addition has taken place across the C=N bond. Since it is also missing from triacetyl N,N′-dimethylguanidine, it appears to be associated with the cyclic structure. The shift in the amide I frequently observed for the lactam group in ethylene urea from 1652 cm^{-1} to 1752 cm^{-1} (KBr) in the diacetyl ethylene urea lends credence to this idea.

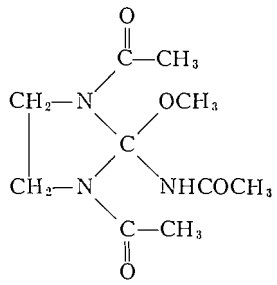
The proof that triacetyl 2-iminoimidazolidine has a symmetrical structure (XII) was obtained from its nuclear magnetic resonance spectrum, which showed three peaks at 3.41, 4.96, and 5.12 p.p.m. upfield from chloroform with relative intensities 4:6:3. The first peak was assigned to the methylene hydrogens and as no splitting was apparent, it was taken as evidence that they were equivalent. The two remaining peaks were assigned to the methyl hydrogens of the acetyl groups, the intensities indicating that two of the three methyl groups were similar. Formation of an addition product on warming of triacetyl 2-iminoimidazolidine with alcohol is of interest in view of the fact that dinitro-2-iminoimidazolidine also exhibits such a property with alcohols and amines (20). The cyclic structure (XIII) was assigned to it on the basis of its analysis and infrared spectrum. The presence of bands at 3142(m), 1650(s), and 1525(m) cm^{-1} (KBr pellet) was taken as indicative of the formation of a secondary amide. The absence of the C=N group was indicated by the stability of the addition product to boiling water, since under these conditions triacetyl 2-iminoimidazolidine readily yields diacetyl ethylene urea.

To summarize, this work has shown that the products obtained on acetylation of alkylguanidines depend on the degree and position of alkyl substitution, as well as the

conditions used. Analogies have been shown to exist between the chemistry of the nitro and acetyl derivatives of alkylguanidines. This is to be expected, since a similarity does exist between the inductive and mesomeric effects of the two groups, although it is of a qualitative nature. However, the extent to which a guanidine moiety is nitrated or acetylated is not necessarily the same, e.g. 2-iminoimidazolidine forms a dinitro (20) but a triacetyl derivative.



(XII)



(XIII)

The difference in reactivity of the five- and six-membered cyclic N,N′-dialkylguanidines on acetylation must be attributed to the effect of the geometry of the ring on the guanidine moiety, since no difference exists in the basicity of these guanidines.

EXPERIMENTAL

All melting points are uncorrected unless otherwise stated. Microanalyses are by Micro-Tech Laboratories, Skokie, Ill., and J. Helie of these laboratories. Ultraviolet spectra were measured on a Cary Model 14 P.M. recording spectrophotometer, while the infrared spectra were measured on a Baird double beam recording spectrophotometer.

Starting Materials

Methylguanidine was purchased from Mann Research Laboratories. Cyclohexylguanidine, 2-guanidocyclohexanol, N,N-dimethylguanidine, guanylpyrrolidine, and guanylpiperidine were prepared from the corresponding amines by the action of 1-guanyl-3,5-dimethylpyrazole nitrate as described by Bannard *et al.* (21). The method of Mold *et al.* (22), employing cyanogen bromide and methylamine, was used to prepare N,N′-dimethylguanidine. Synthesis of 2-iminoimidazolidine, 2-iminohexahydropyrimidine, and 2-imino-5-hydroxyhexahydropyrimidine involved first preparation of the corresponding cyclic nitrimines as described by McKay and Wright (23), followed by treatment of the nitrimines with liquid ammonia as reported by Stefanye and Howard (24). We isolated these compounds as the acetate salts, which are described in Table VI.

All the other alkylguanidines were converted into the acetate salts by ion exchange and dried prior to acetylation with acetic anhydride.

Acetylation of Guanidine Free Bases with Ethyl Acetate

An Amberlite IRA-400 (OH^-) resin column (15 ml) was prepared in the usual manner, then washed for 24 hours with absolute ethanol excluding carbon dioxide. Guanidine hydrochloride (500 mg, 5.2 millimoles) was dissolved in absolute ethanol (15 ml) and the solution passed through the column, after which the column was washed with absolute ethanol, a total of 100 ml eluate being collected. Evaporation of the latter to dryness

Can. J. Chem. Downloaded from www.nrcresearchpress.com by 210.87.254.42 on 09/05/12
For personal use only.

Can. J. Chem. Downloaded from www.nrcresearchpress.com by 210.87.254.42 on 09/05/12
For personal use only.

TABLE VI

Cyclic guanidine acetates

Compound	Formula	m.p.	C		H		N	
			Calc.	Found	Calc.	Found	Calc.	Found
2-Iminoimidazolidine acetate	$C_5H_{11}O_2N_3$	186–188°	41.37	41.51	7.64	7.81	28.95	28.66
2-Iminohexahydropyrimidine acetate	$C_6H_{13}O_2N_3$	141–143°	45.27	45.32	8.37	8.30	26.30	26.17
2-Imino-5-hydroxyhexahydropyrimidine acetate	$C_6H_{13}O_3N_3$	134–135°	41.13	40.90	7.48	7.65	23.99	23.91

TABLE VII

Monoacetyl guanidines

Compound	Formula	m.p.	C		H		N		Yield (%)
			Calc.	Found	Calc.	Found	Calc.	Found	
Acetyl guanidine	$C_3H_7ON_3$	188–190°	35.63	35.62	6.95	7.07	41.56	41.56	89
Acetyl methylguanidine	$C_4H_9ON_3$	158–160°	41.72	41.45	7.88	7.62	36.50	36.63	73
Acetyl 2-iminoimidazolidine	$C_5H_9ON_3$	227–229°	47.23	47.05	7.13	7.11	33.05	32.93	84
Acetyl cyclohexylguanidine	$C_9H_{17}ON_3$	163–165°	59.98	59.96	9.35	9.28	22.93	23.10	92
Acetyl 2-guanidinocyclohexanol	$C_9H_{17}O_2N_3$	183–185°	54.25	54.34	8.60	8.57	21.09	21.26	80
Acetyl 2-imino-5-hydroxyhexahydropyrimidine	$C_6H_{11}O_2N_3$	213–215°	45.85	45.84	7.05	7.25	26.74	26.82	87
Acetyl 2-iminohexahydropyrimidine	$C_6H_{11}ON_3$	189–191°	51.04	51.07	7.85	8.00	29.77	29.55	71

in vacuo gave a colorless oil which was dissolved in absolute alcohol (0.5 ml), to which solution freshly distilled ethyl acetate (0.5 ml, 5.2 millimoles) was slowly added. Although colorless crystals formed instantly, the solution was allowed to stand overnight at room temperature before they were filtered off, washed with ethyl acetate/ethanol and finally recrystallized from ethanol/acetone to give 475 mg (89%) of monoacetyl guanidine as colorless prisms, m.p. 188–190°. The compound was characterized by its acetate, m.p. 178–180°, lit. 180° (3), picrate m.p. 237–239°, lit. 238° (2).

All the other monoacetyl derivatives shown in Table VII were prepared in a similar manner.

Acetylation of Guanidine Acetate Salts with Acetic Anhydride

Cyclohexylguanidine

Cyclohexylguanidine hydrochloride (500 mg) was converted to the acetate salt by ion exchange using Amberlite IRA-400 (OAc) resin. The acetate salt was thoroughly dried *in vacuo* (0.05 mm) at room temperature before addition of acetic anhydride (5 ml). The mixture was heated at 100° for 1/2 hour, after which the acetic anhydride was removed *in vacuo* leaving 493 mg of brown oil. The oil was chromatographed on Woelm IV neutral alumina and gave two fractions. Elution with 2:1 hexane/benzene yielded a crystalline material, which, after recrystallization from pentane, gave colorless prisms, m.p. 71–72°, and analyzed for diacetyl cyclohexylguanidine. Calc. for $C_{11}H_{19}O_2N_3$: C, 58.64; H, 8.50; N, 18.65. Found: C, 58.87; H, 8.64; N, 18.36%. Yield: 445 mg (86%). Further elution with ether gave more crystalline material which was recrystallized from ether/pentane yielding fine white needles, m.p. 106–107°, lit. 107° (25), yield 37 mg (10%). Analysis and melting point indicated it to be N-acetyl cyclohexylamine, and this was confirmed by preparation of an authentic sample and comparison of the infrared spectra.

2-Guanidocyclohexanol

2-Guanidocyclohexanol sulphate (500 mg) was acetylated as described above yielding 530 mg of light brown oil which gave two products on chromatography. The first was obtained by elution with 2:1 hexane/benzene, and after recrystallization from pentane yielded colorless crystals, m.p. 69–70°, which analyzed for a triacetyl derivative, the infrared spectrum indicating O,N,N′ substitution. Calc. for $C_{13}H_{21}O_4N_3$: C, 55.11; H, 7.47; N, 14.83. Found: C, 55.04; H, 7.53; N, 14.53%. Yield: 498 mg (79%). The second product which was eluted with 1:1 ether/chloroform, appeared from analysis, infrared spectrum, and m.p. 117–118°, lit. 117° (26), to be O,N-diacetyl *trans*-2-aminocyclohexanol. Yield: 26 mg (5%). Verification was obtained by synthesis of the compound and comparison of the infrared spectra.

N,N-Dimethylguanidine

N,N-Dimethylguanidine sulphate (475 mg) was acetylated as above and the crude material chromatographed on neutral alumina yielding two products. The first product was obtained by elution with 1:1 pentane/benzene and after recrystallization from benzene/ether gave colorless prisms, m.p. 115–117°, which analyzed for 4-acetamido-2-dimethylamino-6-methyl-1,3,5-triazine. Calc. for $C_8H_{13}ON_5$: C, 49.22; H, 6.77; N, 35.88. Found: C, 49.44; H, 6.83; N, 35.83%. Yield: 77 mg (32%). The infrared spectrum was in agreement with this assignment. A second substance was obtained by elution with 2:1 chloroform/ether which gave colorless prisms after recrystallization from methanol/ether, m.p. 176–178°, and analyzed for diacetyl N,N-dimethylguanidine. Calc. for

Can. J. Chem. Downloaded from www.nrcresearchpress.com by 210.87.254.42 on 09/05/12
For personal use only.

$C_8H_{13}O_2N_5$: C, 49.11; H, 7.65; N, 24.55. Found: C, 49.24; H, 7.74; N, 24.90%. Yield: 92 mg (31%).

2-Iminoimidazolidine

2-Iminoimidazolidine hydrochloride (500 mg) was acetylated as above and the oily product remaining after removal of the acetic anhydride slowly crystallized. Further recrystallization from acetone gave long white needles, m.p. 141–142°, which, from its analysis, appeared to be triacetyl 2-iminoimidazolidine. Calc. for $C_9H_{13}O_3N_3$: C, 51.17; H, 6.20; N, 19.9; CH_3CO, 61.13. Found: C, 51.25; H, 6.33; N, 19.85; CH_3CO, 60.82%. Yield: 441 mg (51%).

Warming the triacetyl derivative with methanol for 20 minutes at 50° gave a quantitative yield of the methanol adduct, which was recrystallized from the same solvent, giving white rhombohedral crystals, m.p. 165–167°. Calc. for $C_{10}H_{17}O_4N_3$: C, 49.39; H, 7.04; N, 17.28; CH_3CO, 53.60; CH_3O, 12.77. Found: C, 49.56; H, 7.00; N, 17.06; CH_3CO, 53.63; CH_3O, 12.43%.

2-Iminohexahydropyrimidine

2-Iminohexahydropyrimidine acetate (500 mg) on acetylation under the usual conditions gave an oily product which distilled at 105–110° at 0.01 mm, giving a clear oil which slowly crystallized. Recrystallization from pentane/ether gave colorless thick prisms, m.p. 61–63°, which after drying *in vacuo* analyzed for diacetyl 2-iminohexahydropyrimidine. Calc. for $C_8H_{13}O_2N_3$: C, 52.44; H, 7.15; N, 22.94. Found: C, 52.70; H, 6.91; N, 22.61%. Yield: 371 mg (65%).

Attempts to chromatograph the crude product on neutral alumina or to recrystallize the diacetyl derivative from solvents containing alcohol led to the isolation of monoacetyl 2-iminohexahydropyrimidine, m.p. 187–189°, identified by its infrared spectrum.

2-Imino-5-hydroxyhexahydropyrimidine

The acetate salt (500 mg) was acetylated in the usual manner giving an oily product which distilled at 115–125° at 0.01 mm. The oil crystallized from pentane/ether giving fine white needles, m.p. 117–119°, which analyzed for a triacetyl derivative, with the infrared spectrum indicating O,N,N′ substitution. Calc. for $C_{10}H_{15}O_4N_3$: C, 49.78; H, 6.27; N, 17.42. Found: C, 49.49; H, 6.92; N, 17.62%. Yield: 325 mg (57%).

Recrystallization of the triacetyl derivative from solvents containing alcohol, or chromatography on alumina, caused decomposition. The resulting product could be purified either by sublimation *in vacuo* at 140–150° at 0.01 mm or by recrystallization from methanol/ether, which gave white microprisms, m.p. 230–232°, analyzing for a diacetyl derivative. The infrared spectrum indicated the compound to be the O,N-diacetyl derivative. Calc. for $C_8H_{13}O_3N_3$: C, 48.23; H, 6.58; N, 21.18. Found: C, 48.28; H, 6.53; N, 21.40%.

Methylguanidine

Methylguanidine acetate (500 mg) was acetylated at 100° for only 15 minutes, and the oily product was chromatographed on neutral alumina. Elution with benzene, followed by recrystallization from ether/pentane furnished colorless thick needles, m.p. 80–82°, analysis of which indicated diacetyl methylguanidine. Calc. for $C_6H_{11}O_2N_3$: C, 45.85; H, 7.05; N, 26.74. Found: C, 46.15; H, 6.91; N, 26.99%. Yield: 289 mg (49%). Further elution with 1:1 chloroform/benzene gave a solid, which, after recrystallization from methanol/ether, had m.p. 158–160° and was identified as monoacetyl methylguanidine by comparison of infrared spectra. Yield: 53 mg (12%).

Can. J. Chem. Downloaded from www.nrcresearchpress.com by 210.87.254.42 on 09/05/12
For personal use only.

Guanylpiperidine

Guanylpiperidine hydrochloride (500 mg) was converted to the acetate salt by ion exchange, after which it was acetylated with excess acetic anhydride for 30 minutes at 100°. The resulting yellowish oil was chromatographed on Woelm IV neutral alumina yielding only one product which was eluted with 1:1 pentane/ether and gave colorless crystals, m.p. 147–148°, from acetone/hexane. Comparison of its infrared spectrum with that of an authentic sample (1) together with its analysis proved it to be 4-acetamido-6-methyl-2-piperidino-1,3,5-triazine. Yield: 202 mg (56%).

Guanylpyrrolidine

Guanylpyrrolidine acetate (500 mg) was acetylated as described above producing a dark red oil together with some crystals. Treatment with cold acetone removed the oil leaving yellow needle-like crystals, which after recrystallization from methanol/ether had m.p. 173–175° and analyzed for 4-acetamido-6-methyl-2-pyrrolidino-1,3,5-triazine. Calc. for $C_{10}H_{15}ON_5$: C, 54.28; H, 6.83; N, 31.66. Found: C, 54.40; H, 6.25; N, 31.38%. Yield: 203 mg (67%).

N,N'-Dimethylguanidine

Dimethylguanidine acetate (500 mg) was acetylated in the usual manner, giving a clear oily product. Chromatography on neutral alumina caused decomposition so the product was purified by distillation at 100–110° at 0.05 mm, giving a colorless oil which analyzed for the triacetyl derivative. Calc. for $C_9H_{15}O_3N_3$: C, 50.69; H, 7.09; N, 19.71. Found: C, 50.39; H, 7.32; N, 19.92%. (λ_{max} 234 mμ, log ϵ 4.2.) Yield: 444 mg (61%).

ACKNOWLEDGMENTS

We are indebted to Miss S. Head and Mr. R. Gravelle for the ultraviolet and infrared spectra and to Miss M. Green for assistance with the experimental work. Finally we also express our gratitude to Dr. M. A. Weinberger for the nuclear magnetic resonance spectra and their interpretation.

REFERENCES

1. W. F. Cockburn and R. A. B. Bannard. Can. J. Chem. **35**, 1285 (1957).
2. A. A. Ryabinin. J. Gen. Chem. U.S.S.R. **22**, 541 (1952).
3. R. Greenhalgh and R. A. B. Bannard. Can. J. Chem. **37**, 1810 (1959).
4. J. K. Simons and W. I. Weaver. U.S. Patent No. 2,408,694; Chem. Abstr. **41**, 1239i (1947).
5. A. Ostrogovich. Chem. Zentr. II, 1358 (1905).
6. M. Gordon, J. G. Miller, and A. R. Day. J. Am. Chem. Soc. **70**, 1946 (1948).
7. S. J. Angyal and W. K. Warburton. J. Chem. Soc. 2492 (1951).
8. B. Neivelt, E. C. Mayo, J. M. Tiers, D. M. Smith, and G. W. Wheland. J. Am. Chem. Soc. **73**, 3475 (1951).
9. A. F. McKay, J. P. Picard, and P. E. Brunet. Can. J. Chem. **29**, 746 (1951).
10. J. H. Bryden, L. A. Burkardt, E. W. Hughes, and J. Donohue. Acta Cryst. **9**, 573 (1956).
11. M. W. Kirkwood and G. F Wright. J. Org. Chem. **18**, 629 (1953).
12. L. J. Bellamy. The infrared spectra of complex molecules. Methuen, London. 1958. Chap. 12.
13. P. L. Pickard and G. W. Polly. J. Am. Chem. Soc. **76**, 5169 (1954).
14. E. Lieber, D. R. Levering, and L. J. Patterson. Anal. Chem. **23**, 1594 (1951).
15. M. M. Randall, R. G. Fowler, N. Fuson, and J. R. Dangl. Infrared determination of organic structures. D. Van Nostrand Co., New York. 1949.
16. W. D. Kumler. J. Am. Chem. Soc. **76**, 814 (1954).
17. W. J. Jones. Trans. Faraday Soc. **55**, 524 (1959).
18. G. Korndorfer. Arch. Pharm. **241**, 449 (1903).
19. R. E. Richards and H. W. Thompson. J. Chem. Soc. 1248 (1947).
20. A. F. McKay and G. F Wright. J. Am. Chem. Soc. **70**, 3990 (1948).
21. R. A. B. Bannard, A. A. Casselman, W. F. Cockburn, and G. M. Brown. Can. J. Chem. **36**, 1541 (1958).

Can. J. Chem. Downloaded from www.nrcresearchpress.com by 210.87.254.42 on 09/05/12
For personal use only.

22. J. D. MOLD, J. M. LADINO, and E. J. SCHANTZ. J. Am. Chem. Soc. **75**, 6321 (1953).
23. A. F. MCKAY and G. F WRIGHT. J. Am. Chem. Soc. **70**, 430 (1948).
24. D. STEFANYE and W. L. HOWARD. J. Am. Chem. Soc. **77**, 761 (1955).
25. A. SKITA and H. ROLFES. Ber. **53**, B, 1242 (1920).
26. L. C. RAIFORD and F. C. MORTENSEN. J. Am. Chem. Soc. **50**, 1201 (1928).

Can. J. Chem. Downloaded from www.nrcresearchpress.com by 210.87.254.42 on 09/05/12
For personal use only.

Can. J. Chem. Downloaded from www.nrcresearchpress.com by 210.87.254.42 on 09/05/12
For personal use only.

CO-ORDINATION COMPOUNDS OF NICKEL (II)

PART II. NEW SPECIES OF NICKEL (II) – SALICYLALDIMINE COMPLEXES[1]

H. C. Clark and R. J. O'Brien

ABSTRACT

The preparation of two solid paramagnetic forms, one light green and the other buff-colored, of bis-N-methyl-5-chloro-salicylaldimine nickel (II) is reported. Their magnetic and spectral properties are correlated with those of solutions of the originally diamagnetic complex, and it is concluded that in both of these species and also in some of the solutions association of the complex occurs. On this basis a general explanation of the properties of bis-N-alkyl-salicylaldimine nickel (II) complexes is given.

INTRODUCTION

The ability of certain nickel (II) – salicylaldimine complexes, which are diamagnetic as solids, to become paramagnetic when dissolved in organic solvents has been examined by many workers (1–4). As indicated in the first paper of this series (5), several different explanations have been proposed. The earliest suggestion (1) was that in non-co-ordinating solvents such as chloroform, a temperature-dependent, partial conversion from a square planar to a tetrahedral configuration occurred. Later views required either the formation of distorted octahedral species as a result of solvent interaction, or a sufficient modification of the crystal field to give essentially a paramagnetic square planar form.

Recent work has ruled out any possibility that the complexes assume tetrahedral configurations. Dielectric polarization measurements (6) give values of the dipole moments which are too low for tetrahedral forms, and also the spectra of the salicylaldimine complexes (1–5, 7) show no similarities to those of known tetrahedral nickel (II) complexes (8, 9). That paramagnetism may arise from solvent interaction with the square planar complexes to give a distorted octahedral configuration has been concluded by Maki (10) on the basis of detailed quantum mechanical calculations. With a suitable choice of parameters, this approach appears to explain satisfactorily the spectra both of the solid complexes and of their solutions. However, Maki's interpretation of the solution paramagnetism is really based on calculations of the distribution of the planar molecules between singlet and triplet states, between which a small, temperature-dependent energy separation is produced by an axial perturbation of the molecule. Such a situation may result from any suitable axial perturbation, of which solvent interaction is just one possibility. Moreover, if solvent interaction occurred in all solvents, one might expect there to be some correlation between the base strength of the solvent and the degree of occupation of the triplet state. Magnetic measurements of a series of bis-N-alkyl-salicyl-aldimine nickel (II) complexes in various solvents (4) show no relation between base strength of the solvent and the degree of paramagnetism. Also, bis-N-methyl-salicyl-aldimine nickel (II) can be converted to a buff-colored, paramagnetic form on heating to 180° (11, 12) in the complete absence of solvent. Although the very low solubility of this form, as well as its color, suggest that it is not the species responsible for solution paramagnetism, it is clear that solvent interaction is not necessary to produce paramagnetism. The low solubility has been taken (12) as an indication that this species is an associated form of the planar complex, association possibly occurring through Ni—O intermolecular links.

Ballhausen and Liehr (13) have also examined the problem theoretically and have concluded that paramagnetism may result from a decrease in the effective crystalline field seen by the complexes on melting, or on dissolution in "non-complexing" solvents.

[1]*Manuscript received December 12, 1960.*
Contribution from the Chemistry Department, University of British Columbia, Vancouver 8, B.C.

Can. J. Chem. Downloaded from www.nrcresearchpress.com by 210.87.254.42 on 09/05/12
For personal use only.

Such a decrease may well lower the splitting between the low-lying singlet and triplet states so that $h\nu$ is comparable with thermal energies. In this event the complex will show paramagnetism, and these authors presented an equation which would describe such a system. This is a general equation of state describing the thermal distribution of electrons between two energy levels. Although the application of this equation to the results of some magnetic measurements (14) leads to reasonable values of the energy separation between the two levels, this does not "prove" the equation nor is it possible to draw any conclusions from these measurements as to the true state of co-ordination of the nickel atoms in this situation.

There is general agreement, then, that the partial paramagnetism of the nickel (II) – salicylaldimine complexes arises from a distribution between singlet and triplet states, but there is still no agreement as to the geometry of the paramagnetic species. The occurrence of paramagnetism in the absence of a solvent is attributed to association giving an octahedral configuration about the Ni (II) atoms. Ferguson (15) has very recently found that spectroscopic and molecular weight studies of benzene and chloroform solutions of bis-N-methyl-salicylaldimine nickel (II) show that associated forms are present at the concentrations at which partial paramagnetism is observed. Hence the axial perturbation of the planar complex, causing a thermal distribution between singlet and triplet states, may be due to association of the molecules in "non-complexing" solvents, rather than to direct solvent interaction. With this in mind, it seemed worth while to attempt to isolate paramagnetic species from solutions of these complexes, and also to investigate the formation of paramagnetic species by heating of the solid complexes.

EXPERIMENTAL

Of 14 complexes prepared and studied, only three showed interesting features. They were bis-N-methyl-salicylaldimine nickel (II) and its 5-chloro and 5-bromo analogues; their preparation has been described previously (5).

The species of bis-N-methyl-5-chloro-salicylaldimine nickel (II) obtained were as follows.

(i) On heating the dark green diamagnetic complex (A) at 165° for 30 minutes, conversion to a light green form (B) occurred. This was very soluble in organic solvents, and paramagnetic. Values of the molar susceptibility at temperatures in the range 80° to 298° K are listed in Table I, and the resultant plot of $1/\chi_M$ versus T_1 gives a value of

TABLE I
Corrected molar susceptibilities $\times 10^6$ c.g.s. units

Temperature (°K)		110	177	231	298
Species (B)		19080	8950	5965	4606
Temperature (°K)	80	118	157	221	298
Species (C)	20370	12910	9489	6606	4909
Temperature (°K)	81	104	151	208	298
Species (G)	18650	13550	8905	6389	4494

NOTE: Species (G) = buff-colored form of bis-N-methyl-salicylaldimine nickel (II).

+72° for the molecular field constant, whence the effective magnetic moment at 25° is 2.90 Bohr magnetons. That this product has the same composition as the original compound was shown by analysis. (Found: Ni, 14.46; N, 6.89; C, 48.51; H, 3.41. Calc. for $NiC_{16}H_{14}O_2N_2Cl_2$: Ni, 14.83; N, 7.07; C, 48.51; H, 3.56%.)

(ii) Exposure to temperatures of 200–205° for 4 hours, or considerably longer periods at 170°, converted bis-N-methyl-5-chloro-salicylaldimine nickel (II) into a buff-colored

solid (C) almost insoluble in all common organic solvents. The values of molar magnetic susceptibilities over a temperature range are also shown in Table I, from which the molecular field constant is found to be $+10°$ and $\mu_{(eff)}$ (25°) = 3.38 Bohr magnetons.

Analysis showed it to have the same empirical formula as both the original compound (A) and the light green form (B). (Found: Ni, 14.22; N, 7.17. Calc. for Ni $C_{16}H_{14}O_2N_2Cl_2$: Ni, 14.83; N, 7.07%.)

(iii) Since earlier magnetic measurements (2, 3) have shown that the paramagnetism of this type of complex in chloroform solution approaches the normal value for two unpaired electrons as the temperature is lowered towards −78°, such solutions provide an alternative means of isolating paramagnetic species. Repeated partial freezing of chloroform solutions of bis-N-methyl-5-chloro-salicylaldimine nickel (II) in solid CO_2–ethanol mixtures, followed by decantation of the concentrated solution from the solid chloroform, eventually caused precipitation of a light green species (D), quite different in properties from the original form (A). The same product was obtained by the removal of the solvent under vacuum from a cooled (−46° to −64°) chloroform solution, or by precipitation from a cooled chloroform solution by the addition of ligroin. Each of these procedures gave only small amounts of species (D) which in all instances contained a small amount of the original diamagnetic complex (A). It was therefore not possible to make accurate magnetic measurements, although a measurement at 25° gave a gram susceptibility of 8.3×10^{-6} c.g.s. and therefore an approximate effective magnetic moment of 2.8 Bohr magnetons. Species (D) was not a solvate since there was a negligible weight loss on heating at 100° and conversion to the diamagnetic form (A) occurred.

The positions of the absorption bands in the diffuse reflectance spectra of these various species are listed in Table II together with the bands observed for solutions of bis-N-methyl-salicylaldimine nickel (II) in chloroform and pyridine (10). The diffuse reflectance spectra were kindly determined by Dr. M. C. R. Symons by a procedure previously described (16).

TABLE II

Species	Observed maxima(mμ)			
A	440	620	—	—
B	480 (sh)	630	820 (sh)	ca. 1000
C	420 (sh)	560	780 (sh)	900
D	430 (sh)	610	780 (sh)	ca. 930
A* in $CHCl_3$	490 (sh)	610	(800 (sh)?)	1150
A* in C_5H_5N		570	785 (sh)	960

NOTE: A* = bis-N-methyl-salicylaldimine nickel (II); sh = shoulder.

The X-ray diffraction powder photographs of the various solid species were obtained with a G. E. model XRP-SF11 X-ray diffraction unit. The photographs of species (B) and (D) were very similar in line spacings and relative intensities, although not completely identical. Both were quite different from that of either species (A) or (C). Some slight differences might be expected in the crystal packings of (B) and (D) in view of the very different conditions under which they were obtained.

Previous reports (11, 12) of the effect of heat on bis-N-methyl-salicylaldimine nickel (II) are in disagreement. Harris, Lenzer, and Martin (12) obtained a buff-colored compound, while Sacconi *et al.* (11) reported the isolation of a light green product. An examination of the magnetic measurements of Sacconi's product shows that their original sample was slightly paramagnetic, presumably due to traces of bis-salicylaldehyde nickel (II), which would certainly give the final product a green color. We have found that on

Can. J. Chem. Downloaded from www.nrcresearchpress.com by 210.87.254.42 on 09/05/12
For personal use only.

heating a sample of the diamagnetic complex ($\chi_g = -0.307\times10^{-6}$ c.g.s.) to 200° for 2 hours conversion to a paramagnetic, buff-colored product occurred. There was no sign of the formation of any green paramagnetic product in the temperature range 150–210° and our results entirely confirm those of Harris *et al.* Measurements of the magnetic susceptibility are indicated in Table I, and these give a value of 10° for the molecular field constant and hence μ_{eff} (25°) is 3.23 Bohr magnetons in good agreement with the results of Harris *et al.*

Bis-N-methyl-5-bromo-salicylaldimine nickel (II) was converted to a light green form (at 175°) and then to a buff-colored form (at 220°). For both this complex and bis-N-methyl-salicylaldimine nickel (II), light green products were obtained from their chloroform solutions at low temperatures but no detailed studies of these were made. The heating of 14 other nickel (II) – salicylaldimine complexes to 350° for several hours did not cause conversion to other forms, although in certain cases decomposition occurred.

Analyses of nickel were made gravimetrically by precipitation with dimethylglyoxime. Nitrogen was determined by the standard semimicro Kjeldahl method.

Magnetic susceptibilities were measured with a Gouy magnetic balance fitted with a cryostat similar to that described by Figgis and Nyholm (17). The magnetic balance consisted of a Varian 4-in. electromagnet, model V4084, with 2-in. tapered pole caps, in conjunction with a Spoerhaese Model 10 M microbalance with a sensitivity of ±0.01 mg. Current regulation was provided by a Varian Model U 2300 A power supply and Model 2301 A current regulator. The cryostat used for temperature control of the sample is shown in Fig. 1. The general principles of design and the associated electrical circuits

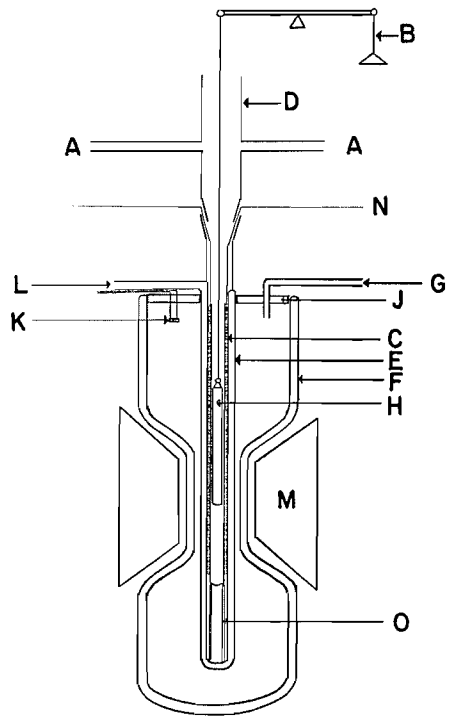


FIG. 1. Cryostat for the magnetic balance. A, nitrogen gas inlet and outlet; B, balance; C, heater and platinum resistance thermometer wound on brass former; D, draught shield; E, inner Dewar; F, outer Dewar; G, liquid nitrogen inlet; H, sample tube; J, icing shield; K, thermistor; L, to the pump for evacuation of the inner Dewar; M, magnet pole caps; N, connection to the heater and resistance thermometer; O, support for heater former.

Can. J. Chem. Downloaded from www.nrcresearchpress.com by 210.87.254.42 on 09/05/12
For personal use only.

of the cryostat are the same as described by Figgis and Nyholm. With this apparatus, temperatures can be maintained constant at any point in the range 78°–300° K by suitable control of the current passing through the electrical heating coil and of the pressure within the inner Dewar. A device is provided for maintaining constant the level of liquid nitrogen in the outer Dewar. The main modification of Figgis and Nyholm's design is in the shape of the outer Dewar. In our apparatus, the outside diameter of the outer Dewar is only 2.6 cm between the pole caps, compared with 7 cm. This makes it much simpler to obtain a reasonably large homogeneous region of the field and still use tapered pole caps and a shorter sample. Moreover the temperature control is perhaps improved by having a reservoir of refrigerant both above and below the constriction. The sample tube and apparatus were calibrated using mercury (II) cobaltitetrathiocyanate (18) as standard. Magnetic moments were calculated using the formula $\mu = 2.839 \sqrt{\{\chi_M \times (T+\theta)\}}$ Bohr magnetons.

DISCUSSION

The above results indicate the ability of bis-N-methyl-5-chloro-salicylaldimine nickel (II), and its 5-bromo analogue, to become paramagnetic under four sets of conditions, namely (i) heating to 165° to give the light green species (B), (ii) heating to 200–205° to form the buff-colored product (C), (iii) dissolution of the diamagnetic complex in organic solvents, and (iv) separation as a light green species (D) from such solutions in organic solvents. The experimental results show that there is considerable similarity between species (B) and (D). Their absorption spectra are very similar, both in the positions of the bands and in their relative intensities. Their X-ray diffraction powder photographs are also very similar although not quite identical. It is then reasonable to conclude that forms (B) and (D) are identical and also that they are probably identical with the paramagnetic species present in the chloroform solution from which form (D) was obtained. Species (C), the buff-colored product, is quite different from the other forms, as shown by its color, its very low solubility in organic solvents, and its very different diffraction pattern. For bis-N-methyl-salicylaldimine nickel (II), only the buff-colored form was obtained on heating the solid diamagnetic complex, and it seems that quite minor differences in the properties of the complexes determine whether conversion to this buff form will take place directly or through the light green form. In general, it seems a reasonable conclusion that these complexes are capable of existing as diamagnetic species, as green, paramagnetic soluble forms, or as buff-colored paramagnetic insoluble forms. Since both paramagnetic species exist in the absence of solvent, they presumably have distorted octahedral configurations about the nickel atoms as a result of association of the complex molecules. This has already been suggested for the buff form of bis-N-methyl-salicylaldimine nickel (II) (12) and the results of Ferguson, indicating association of the complex in chloroform solution, make it probable also for the green paramagnetic species.

Satisfactory explanations can now be made for all observations of these anomalous complexes. Clearly the paramagnetism of their solutions in strongly co-ordinating solvents such as pyridine results from the formation of octahedral, presumably monomeric species, some of which have been isolated (3, 19). In solvents which are normally considered non-co-ordinating (e.g. chloroform, cyclohexane, carbon tetrachloride), the removal of the crystalline forces which have restrained the molecule in its diamagnetic form, allows association of the complex and a decrease of the energy separation between

Can. J. Chem. Downloaded from www.nrcresearchpress.com by 210.87.254.42 on 09/05/12
For personal use only.

Can. J. Chem. Downloaded from www.nrcresearchpress.com by 210.87.254.42 on 09/05/12
For personal use only.

singlet and triplet states. Thus, an axial perturbation does occur, not through solvent interaction but rather by association. The same effect occurs on heating the solid when some breakdown of the crystal structure leads to the formation of the same associated green product. These conclusions are consistent with the dielectric polarization measurements (6), with the spectra of the complexes and their solutions (1, 15, 20), and with the magnetic measurements (3, 6).

Sacconi *et al.* (14), from magnetic and viscosity measurements, conclude that there is no evidence for the association of the nickel (II) – N-alkyl-salicylaldimine complexes. They report a practically linear relationship, for bis-N-octyl- and bis-N-nonyl-salicylaldimine nickel (II) in the molten state, between ln η and $1/T$ over a wide temperature range. However, examination of their results shows that while there is certainly linearity for temperatures above about 120° C, below this temperature there are small but definite departures from linearity. Moreover, magnetic measurements of the N-octyl complex in dibutyl phthalate solution (14) show, in a plot of μ versus T, a minimum in μ which is shifted towards higher temperatures and approaches 120° at higher concentration. Both this concentration effect and the non-linearity of viscosity can be explained in terms of association of the complex. It is interesting to note that magnetic measurements (21) of the melts of many of these N-alkyl-salicylaldimine complexes give a minimum value of the magnetic moment at approximately 120° in the plots of μ versus T.

Different effects therefore seem to be occurring below and above 120°. At temperatures below and up to approximately 120°, we conclude that there is a distribution between singlet and triplet states, the small energy separation between these two states being a consequence of association. The degree of association will be concentration dependent and also temperature dependent, so that as the temperature increases towards 120°, the population of the triplet state will decrease. Above approximately 120°, it is possible that the energy separation between the two energy levels may remain practically constant, as suggested by Sacconi *et al.* (14) so that an increase in thermal energy may increase the population of the lowest triplet state. Alternatively the observed increase in magnetic moments (14) for temperatures higher than 120° may be due to conversion to the insoluble buff-colored species. However, this conversion has only been observed for the N-methyl compounds and not for the higher members of the alkyl series.

The question of the manner of association of the complexes cannot be settled unambiguously without complete structure determinations of both the buff-colored and light green paramagnetic species of bis-N-methyl-5-chloro-salicylaldimine nickel (II). The magnetic moments unfortunately do not allow a distinction to be made between tetrahedral and octahedral configurations since although tetrahedral nickel complexes containing four identical ligands have moments of 3.5 Bohr magnetons or higher (9), tetrahedral complexes with several different ligands about the nickel atom are known to have moments of about 3.0 Bohr magnetons (22). However, the large values of the molecular field constant, at least in one case, can be explained as due to distortion from a regular octahedral arrangement and also by the fact that the splitting between the lower triplet and next singlet state is not large. It has already been suggested (12) that the buff-colored species of bis-N-methyl-salicylaldimine nickel (II) is polymeric with a six-covalent arrangement about each nickel atom due to interaction of each such atom with oxygen atoms of the molecules above and below it. If this be accepted, then the associated light green paramagnetic forms may involve interaction between the nitrogen atoms of one molecule with the nickel atoms of other molecules to give an octahedral arrangement. It is also interesting to notice that Ferguson (15) has recently prepare and orthogonal

form of bis-N-methyl-salicylaldimine nickel (II) in which the Ni—Ni distance is 3.30 Å, compared with 5.32 Å in the monoclinic form, emphasizing the possibility of quite close packing of the molecules in associated forms.

ACKNOWLEDGMENTS

A grant from Research Corporation for the purchase of the magnetic balance, and the financial support of the National Research Council is gratefully acknowledged.

REFERENCES

1. J. B. Willis and D. P. Mellor. J. Am. Chem. Soc. **69**, 1237 (1947).
2. S. Fujii and M. Sumitani. Sci. Repts. Tôhoku Univ. First. Ser. **37**, 49 (1953).
3. H. C. Clark and A. L. Odell. J. Chem. Soc. 3431 (1955).
4. L. Sacconi, P. Paoletti, and G. Del Re. J. Am. Chem. Soc. **79**, 4062 (1957).
5. H. C. Clark and R. J. O'Brien. Can. J. Chem. **37**, 436 (1959).
6. L. Sacconi, M. Ciampolini, F. Maggio, and G. Del Re. J. Am. Chem. Soc. **82**, 815 (1960).
7. H. C. Clark and A. L. Odell. J. Chem. Soc. 520 (1956).
8. D. M. Gruen and R. L. McBeth. J. Phys. Chem. **63**, 393 (1959).
9. N. S. Gill and R. S. Nyholm. J. Chem. Soc. 3997 (1959).
10. G. Maki. J. Chem. Phys. **29**, 1129 (1958).
11. L. Sacconi, P. Paoletti, and R. Cini. J. Am. Chem. Soc. **80**, 3683 (1958).
12. C. H. Harris, S. H. Lenzer, and R. L. Martin. Australian J. Chem. **11**, 331 (1958).
13. C. J. Ballhausen and A. D. Liehr. J. Am. Chem. Soc. **81**, 538 (1959).
14. L. Sacconi, R. Cini, M. Ciampolini, and F. Maggio. J. Am. Chem. Soc. **82**, 3487 (1960).
15. J. Ferguson. Private communication.
16. T. R. Griffiths, K. A. K. Lott, and M. C. R. Symons. Anal. Chem. **31**, 1338 (1959).
17. B. N. Figgis and R. S. Nyholm. J. Chem. Soc. 331 (1959).
18. B. N. Figgis and R. S. Nyholm. J. Chem. Soc. 4190 (1958).
19. F. Basolo and W. Matoush. J. Am. Chem. Soc. **75**, 5663 (1952).
20. H. C. Clark and A. L. Odell. J. Chem. Soc. 3435 (1955).
21. L. Sacconi, R. Cini, and F. Maggio. J. Am. Chem. Soc. **79**, 3933 (1957).
22. L. M. Venanzi. J. Chem. Soc. 719 (1958).

Can. J. Chem. Downloaded from www.nrcresearchpress.com by 210.87.254.42 on 09/05/12
For personal use only.

Can. J. Chem. Downloaded from www.nrcresearchpress.com by 210.87.254.40 on 09/05/12
For personal use only.

ARYLATION OF QUINONES BY DIAZONIUM SALTS

VII. SYNTHESIS AND STRUCTURE OF SOME ARYL-CHLORO-*p*-BENZOQUINONES[1]

JEHANBUX F. BAGLI[2] AND PH. L'ÉCUYER

ABSTRACT

A careful re-examination of the arylation (P. Brassard and P. L'Écuyer. Can. J. Chem. **36**, 814 (1958)) reaction with chlorobenzoquinone[3] has revealed in its products the presence of all the three possible disubstituted isomeric quinones. Arylation using diazotized *p*-nitroaniline has resulted in the isolation of the three new isomeric quinones, whose structures are assigned, based on chemical and spectral evidences. Mechanistic implications in the arylation and halogenation of benzoquinones are discussed.

The Meerwein reaction (2) provides a general method of arylation of activated double bonds, using aryl diazonium salts, in the presence of copper salts as catalysts. Arylation of benzoquinone by diazotized aniline using typical Meerwein conditions (80% acetone–water solvent system, cupric chloride catalyst, and acetate buffer) is found to give crude phenylbenzoquinone in poor yield (<10% of crude product). Modified Meerwein conditions[4] (variation of the solvent system or the type of buffer) have been used for the arylation of benzoquinones. It has been recently (3) demonstrated that excellent yields of monoaryl benzoquinones are obtained by conducting the reaction in a completely aqueous medium, in the presence of an acetate buffer, and without the copper catalyst. An application of the procedure to the arylation of the monosubstituted benzoquinones has also been described (1, 4). However, the latter reactions are complicated by the fact that theoretically three isomers can be formed. The substituent present in the starting quinone and the stability of the diazonium salt are the major factors responsible for influencing the yields of these isomers. The arylation of toluquinone and phenylbenzoquinone with $ArN_2^+Cl^-$ (Ar = *p*-chlorophenyl) yields a single isolable disubstituted benzoquinone in reasonable yield (86% and 43% respectively) as against that of chlorobenzoquinone (1) which gives two isomeric chloro-*p*-chlorophenylbenzoquinones (III*a* and III*c*). The last mentioned result strongly suggests the possibility of the formation of all three isomers in the course of this reaction.

The investigation of the arylation of chlorobenzoquinone was therefore resumed with a view to the preparation of these isomers using benzene, *p*-chlorobenzene, and *p*-nitrobenzene diazonium chlorides as the arylating agents.

In the previous studies (1, 4) and in synthetic studies with benzoquinones in general little or no attempt has been made to use chromatography as a means of separation of the products. The use of ordinary alumina is impeded by the ease with which a molecule of benzoquinone can accept two electrons from a nucleophile to go over to the dianion of the corresponding hydroquinone. We found that such a conversion on acid alumina is slow but nevertheless unavoidable. Silica gel has proved to be a satisfactory adsorbent for the separation of substituted benzoquinones with complete inhibition of reduction on the column. It is of interest to note that the order of elution of the chloro-aryl-

[1]*Manuscript received August 22, 1960.*
Contribution from the Department of Chemistry, Laval University, Quebec, Que.
[2]*National Research Council postdoctoral fellow 1959–60.*
[3]*The term "benzoquinone" throughout this publication refers to p-benzoquinone.*
[4]*For earlier references see reference 3.*

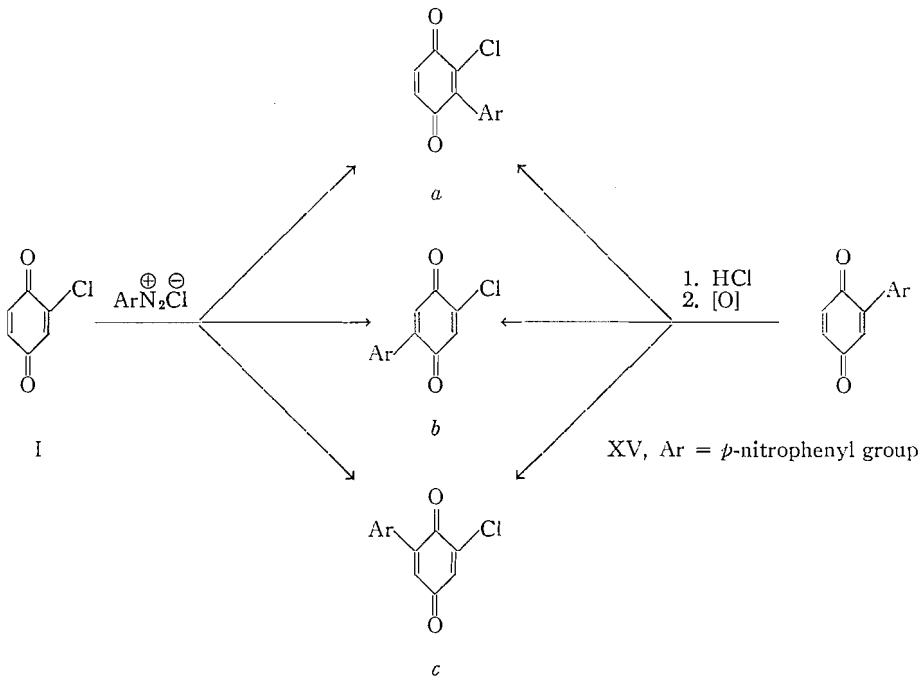
benzoquinones from a column bears a definite relationship to their structure. In all the cases studied, the degree of adsorbability of the disubstituted isomers follows the order: 2,3 > 2,6 > 2,5.

RESULTS AND DISCUSSION

Arylation of chlorobenzoquinone (I) (Chart I) with diazotized aniline gives the three isomers: 2-chloro-3-phenylbenzoquinone (II*a*), 2-chloro-5-phenylbenzoquinone (II*b*), and 2-chloro-6-phenylbenzoquinone (II*c*), in contrast to one isomer (II*b*) reported before (1).

CHART I

Arylation of chloroquinone and chlorination–oxidation of quinone XV



I

XV, Ar = *p*-nitrophenyl group

II, III, or IV

II, Ar = phenyl group

III, Ar = *p*-chlorophenyl group

IV, Ar = *p*-nitrophenyl group

Their structures are proven by their unequivocal synthesis (5). From the reaction of *p*-chlorobenzene diazonium chloride with I, besides 2-chloro-3-*p*-chlorophenylbenzoquinone (III*a*) and 2-chloro-6-*p*-chlorophenylbenzoquinone (III*c*) already described (1), the third isomer, 2-chloro-5-*p*-chlorophenylbenzoquinone (III*b*) is also isolated. The structures of all the three isomers of this series are confirmed by their infrared spectra (6).

Can. J. Chem. Downloaded from www.nrcresearchpress.com by 210.87.254.40 on 09/05/12
For personal use only.

Can. J. Chem. Downloaded from www.nrcresearchpress.com by 210.87.254.40 on 09/05/12
For personal use only.

The arylation of I with diazotized *p*-nitroaniline yields three disubstituted benzoquinones: 2-chloro-3-*p*-nitrophenylbenzoquinone (IV*a*), 2-chloro-5-*p*-nitrophenylbenzoquinone (IV*b*), and 2-chloro-6-*p*-nitrophenylbenzoquinone (IV*c*). The same three compounds are also obtained from the chlorination of *p*-nitrophenylbenzoquinone (XV) with concentrated hydrochloric acid, followed by oxidation with ferric chloride. The ratio of the isomers IV*a*, IV*b*, IV*c* obtained from the arylation of chloroquinone is 2:1:1; whereas that of the isomers secured from the chlorination–oxidation of *p*-nitrophenylquinone is about 0.1:2:1. Variation of the conditions for chlorination, e.g. passing dry HCl gas in a benzene or chloroform solution of the quinone XV, gave essentially the same results. The structures of these three isomers are assigned on the basis of their infrared (6) and nuclear magnetic resonance spectra. The N.M.R. spectrum of the compound IV*a* showed a nine-cycle spin coupling between the two adjacent quinoid hydrogen atoms whereas that of compound IV*c* showed a relatively weaker coupling of 2.5 cycles. Benzoquinone IV*b*, on the other hand, does not exhibit spin coupling between the two adjacent quinoid hydrogen atoms.

The above structural assignments are further substantiated by chemical evidence, obtained from the results of chlorination–oxidation experiments with each of these isomers (Chart II). Compound IV*c* on treatment with HCl followed by oxidation yields 2,3-dichloro-6-*p*-nitrophenylbenzoquinone (X) and 2,5-dichloro-3-*p*-nitrophenylbenzoquinone (VIII) in the ratio 1:5. Isomers IV*a* and IV*b* under identical treatment give respectively as a predominant product quinones VIII and X, together with traces of 2,6-dichloro-3-*p*-nitrophenylbenzoquinone (IX) as evidenced by infrared spectra (*vide*: Experimental). Trichloro-5-*p*-nitrophenylbenzoquinone is also isolated in small amounts (10–20%) from the chlorination–oxidation experiments with IV*a*, IV*b*, and IV*c*. Authentic samples of VIII, IX, and X are prepared by coupling diazotized *p*-nitroaniline with the corresponding 2,5-dichlorobenzoquinone (V), 2,6-dichlorobenzoquinone (VI), and 2,3-dichlorobenzoquinone (VII).

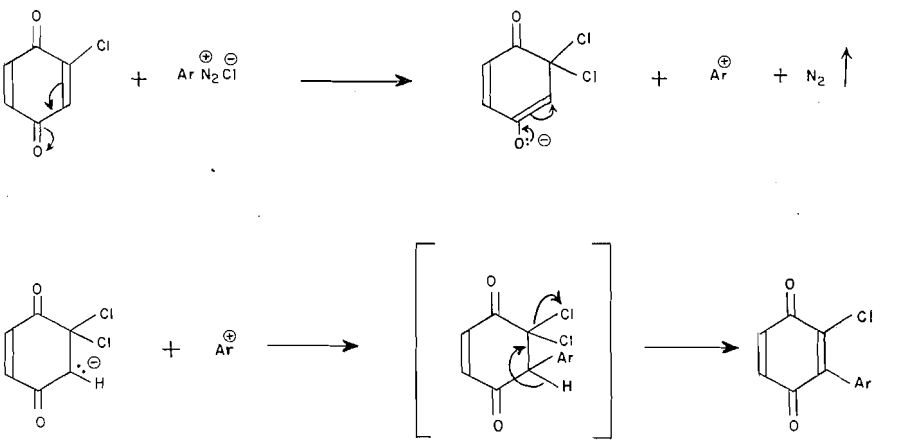
Treatment of hydroquinone with bromine as described (18), followed by oxidation with ferric chloride, results in the formation of 2,5-dibromobenzoquinone (XII), 2,3-dibromobenzoquinone (XIII), and tribromobenzoquinone (XIV), which are separated chromatographically.

The free radical nature of the Meerwein reaction is conclusively established by the recent work of Kochi (7). The oxidation–reduction capacity of the copper catalyst in presence of acetone is a unique feature of this mechanism. Absence of both the acetone and the copper catalyst makes such a mechanism highly improbable for the arylation under consideration. However, the problem of whether the arylation in the aqueous acidic medium proceeds via a free radical or an ionic pathway is still unresolved.

It is observed (from infrared spectra) that the decomposition of the diazonium salts into phenols and azo compounds according to their stability and the conversion of the quinones into quinhydrones (8) according to their redox potential compete with the main reaction.

It has been demonstrated by DeTar *et al.* (9) that the course of SN_1-type decomposition of the diazonium salts is largely governed by the pH of the mixture. The reaction follows a free radical pathway (10) under basic conditions, in contrast to an ionic pathway in an aqueous acidic medium. In view of these facts, a possible ionic mechanism for

the arylation may be formulated as follows:



Ar = aryl group

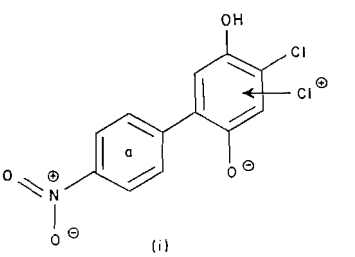
The experimental results from the chlorination–oxidation treatment of arylated chloroquinones IV*a*, IV*b*, and IV*c* are noteworthy.

In the predominant product X obtained from 2-chloro-5-*p*-nitrophenylbenzoquinone (IV*b*), the second chlorine atom enters ortho to the first one. On the other hand, in the formation of compound VIII from 2-chloro-6-*p*-nitrophenylbenzoquinone (IV*c*), the second chlorine atom enters ortho to the phenyl group. The substitution therefore seems to be independent of the bulk of the groups present. The generally accepted concept of 1,4 addition (11, 12) of HX (X = Cl or CN) to benzoquinone, by itself fails to explain the variation in the proportions of the isomers obtained from quinones XV, IV*a*, and IV*b*. This concept, however, assumes the prior chlorination of the quinone nucleus followed by aromatization to yield the chlorohydroquinones.

If one assumes that the aromatization of the quinone nucleus by an anion precedes the substitution as suggested by Clark (13) and more recently by Dewar (14), the subsequent substitution will then be governed by the principles of electrophilic aromatic substitution. The formation of compounds VIII and X as a major product from quinones IV*a* and IV*b*, now becomes readily explicable.[5]

The results of chlorination–oxidation of the quinone XV are, however, not explained by this latter view. Thus it seems reasonable that the addition of HX (X = Cl or CN) type reagents to benzoquinones does not involve either one or the other mechanism

[5]*The prior aromatization can generate a transition complex of the type (i) from IV*b*, in which the nitro group can exert its electronic influence through the phenyl ring (a).*

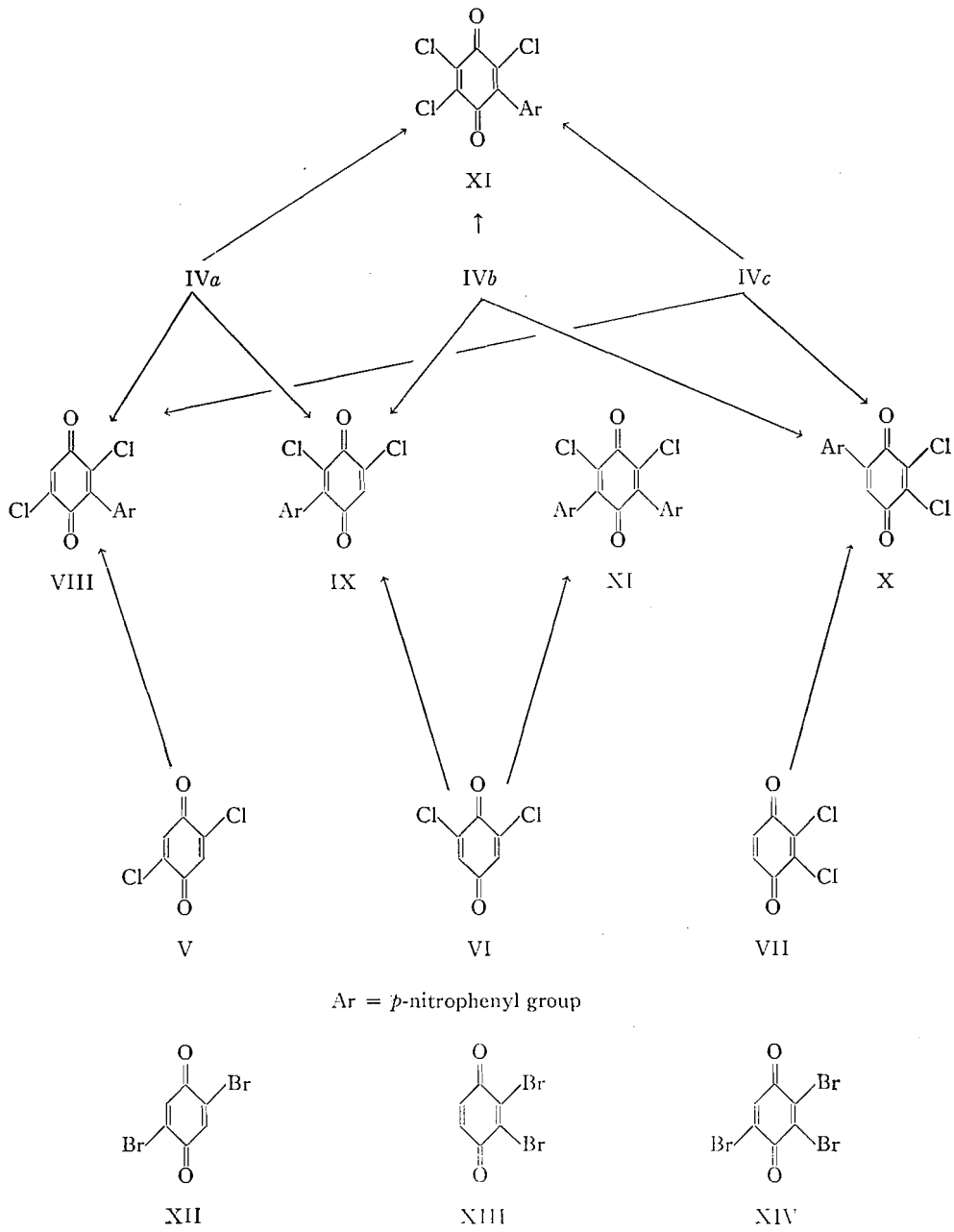


(i)

Can. J. Chem. Downloaded from www.nrcresearchpress.com by 210.87.254.40 on 09/05/12
For personal use only.

CHART II

Chlorination–oxidation of quinones IV*a*, IV*b*, and IV*c* and arylation of dichloroquinones V, VI, and VII



exclusively. It is suggested that both pathways may be operative, depending upon the substituents present on the quinone nucleus and therefore upon the oxidation–reduction potential of the benzoquinone involved.

Can. J. Chem. Downloaded from www.nrcresearchpress.com by 210.87.254.40 on 09/05/12
For personal use only.

Can. J. Chem. Downloaded from www.nrcresearchpress.com by 210.87.254.40 on 09/05/12
For personal use only.

EXPERIMENTAL

General

All the melting points are uncorrected. Davison grade-923 silica gel (100–200 mesh) and Woelm grade-I acid alumina were used for chromatography. Unless otherwise mentioned, the term pet. ether refers to that fraction of petroleum ether with b.p. 30–60°. Ether extracts were all dried over sodium sulphate and ether always removed under vacuum. All infrared (IR) spectra were recorded with a Beckman IR-4 spectrophotometer using a NaCl prism; and reported spectra were all calibrated by the use of a polystyrene film. Chloroform and carbon disulphide used for IR spectra were ANALAR grade (B. D. H.) and reagent grade (Merck) respectively. Ultraviolet spectra were all recorded with a Beckman DU spectrophotometer using hexane (B. D. H., spectroscopic grade) as a solvent. Unless otherwise stated, diazotization of amines was conducted using amine (1 mole), in approximately 8% hydrochloric acid (3 moles) and adding, to the precooled (0–5°) solution, a concentrated solution of sodium nitrite (1 mole), maintaining the temperature between 0–5°.

Oxidation with ferric chloride was conducted as follows: to a solution of hydroquinone in acetic acid, was added a solution (60%, w/v in water) of ferric chloride. The reaction mixture was heated for about 10 minutes on a steam bath, cooled, and diluted with water. The quinone thus precipitated was collected, washed with water, dried, and recrystallized.

Preparation of Isomeric Chloro-phenylbenzoquinones

A solution of benzene diazonium chloride (from aniline, 4.7 g) was added to a stirred suspension of chlorobenzoquinone (I) (7.15 g) in a solution of sodium acetate (15.3 g) in water (650 ml). The reaction mixture was stirred overnight at room temperature. The oil thus separated was extracted with ether, the ether extract was washed and dried, and the ether was removed. The residue (13 g) was dissolved in pet. ether – benzene (1:1) and chromatographed on acid alumina (390 g). Elution with the same solvent gave first 2-chloro-5-phenylbenzoquinone (II*b*) (1.3 g), which crystallized from ethanol in platelets, m.p. 129–130° (reported m.p. 130–131.5° (15)). Its identity was confirmed by a mixed melting point and IR spectra. Further elution with benzene and a mixture of benzene–ether of gradually increasing polarity up to 50% ether gave an oily eluate (5.4 g). This oil was mixed with the residue from the mother liquor obtained from the first crystallization of II*b* above. The mixture (5.7 g) was dissolved in benzene – pet. ether (33:67) and rechromatographed on acid alumina (174 g). Initial fractions gave more of II*b* (0.61 g). Further elution with the same solvent followed by pure benzene gave unidentified oils (1.73 g). Elution with benzene–ether (98:2) gave an oil (0.82 g) which was rechromatographed on silica gel (65 g). Elution with benzene – pet. ether (1:1) gave a solid (0.42 g) which, after two crystallizations from ethanol, yielded 0.3 g of 2-chloro-6-phenylbenzoquinone (II*c*), m.p. 106–110°. Further purification from the same solvent provided an analytical sample, m.p. 112–113°, ν^{CHCl_3}: 919, 1659, and 1688 cm^{-1}; ν^{CS_2}: 916 (=C—H deformation, on the quinone nucleus), 1656, and 1684 cm^{-1} (=C=O stretching). λ_{max}: 230 mμ (4.37), 300 mμ (3.87), 378 mμ (3.56). Calc. for $C_{12}H_7O_2Cl$ (218.63): C, 65.92; H, 3.21. Found: C, 66.10; H, 3.31. The proof of structure was provided by its unequivocal synthesis (5).

Further elution with the same solvent pair gave an eluate (0.29 g) which crystallized, when triturated with ether at dry-ice temperature. The solid (0.24 g) was dissolved in

benzene – pet. ether (1:3) and passed through silica gel (15 g). The eluate (0.2 g), crystallized from pet. ether (b.p. 65–110°), gave 2-chloro-3-phenylbenzoquinone (II*a*) (0.15 g), m.p. 115–116°. Two more crystallizations provided an analytical sample, m.p. 117–118°, ν^{CHCl_3}: 849, 1683 cm^{-1}; ν^{CS_2}: 844 (=C—H deformation, on quinone nucleus), 1681, 1669 cm^{-1} shoulder (=C=O stretching). λ_{max}: 250 mμ (4.19), 376 mμ (3.32). Calc. for $C_{12}H_7O_2Cl$ (218.63): C, 65.92; H, 3.21. Found: C, 65.95; H, 3.22. The structure of this compound was proved by mixed m.p. and infrared spectra of a sample synthesized by an unequivocal route (5).

Preparation of the Isomeric Chloro-p-chlorophenylbenzoquinones

A solution of *p*-chlorobenzene diazonium chloride (from *p*-chloroaniline, 6.4 g) was poured into a suspension of chlorobenzoquinone (I) (7.15 g) in a solution of sodium acetate (15.3 g) in water (675 ml). The reaction mixture was stirred overnight at room temperature. The oily solid which had then separated, was extracted with ether, the ether extract was washed and dried, and the ether was removed. The residue (13 g) was taken in benzene – pet. ether (1:3) and chromatographed on silica gel (420 g). The chromatogram was developed[6] over a period of 8 hours and eluted with the same solvent. Earlier fractions yielded an unidentified oil (0.43 g). Further elution gave 2-chloro-5-*p*-chlorophenylbenzoquinone (III*b*) as a crystalline solid (2.43 g), m.p. 135–140°. Crystallizations from acetone–ethanol afforded an analytical sample, m.p. 147–148°, ν^{CHCl_3}: 914, 1674 cm^{-1}; ν^{CS_2}: 910 (=C—H deformation, on quinone nucleus), 1674 cm^{-1} (=C=O stretching). λ_{max}: 239 mμ (4.34), 303 mμ (3.85), 380 mμ (3.51). Calc. for $C_{12}H_6O_2Cl_2$ (253.06): C, 56.96; H, 2.39; Cl, 28.02. Found: C, 56.98; H, 2.39; Cl, 27.98.

Further elution with solvents of increasing polarity up to benzene – pet. ether (2:3), yielded a crystalline solid (2.63 g). One crystallization from ethanol gave bright red needles of 2-chloro-6-*p*-chlorophenylbenzoquinone (III*c*) (1.73 g), m.p. 150–151°. A mixed melting point with an authentic sample (1) was undepressed and the I.R. spectra were superimposable. Elution with benzene – pet. ether (1:1) yielded an oily solid (4.0 g). Trituration of this solid with ether at dry-ice temperature followed by one crystallization from acetone – pet. ether provided golden yellow plates of 2-chloro-3-*p*-chlorophenylbenzoquinone (III*a*) (2.1 g), m.p. 104–105° (reported m.p. 103–104° (1)).

Preparation of the Isomeric Chloro-p-nitrophenylbenzoquinones

(a) By Arylation of Chlorobenzoquinone

p-Nitroaniline (3.45 g) was diazotized as described (16). The solution of *p*-nitrobenzene diazonium chloride was added to a stirred suspension of chlorobenzoquinone (I) (3.55 g) in a solution of sodium acetate (7.65 g) in water (325 ml) and the reaction mixture stirred overnight. The brown amorphous powder thus obtained was collected, washed thoroughly with water, and dried. This solid (5.3 g) was dissolved in benzene and chromatographed on silica gel (260 g). Eluates obtained were combined into three fractions based on I.R. analysis: I (1.14 g), II (1.70 g), and III (1.20 g).

Fraction II was dissolved in benzene and rechromatographed on silica gel (93 g). Initial eluates gave 2-chloro-6-*p*-nitrophenylbenzoquinone (IV*c*) (0.77 g) which crystallized in reddish-brown needles (0.31 g) from chloroform, m.p. 205–211°. An analytical sample recrystallized from acetone – pet. ether had m.p. 212–213°. ν^{CHCl_3}: (saturated

[6]*Preliminary development was found to be essential. Changing the solvent to the next higher polarity (benzene – pet. ether, 3:7) resulted in poorer separation.*

Can. J. Chem. Downloaded from www.nrcresearchpress.com by 210.87.254.40 on 09/05/12
For personal use only.

solution) 919 (=C—H deformation, on quinone nucleus), 1353, 1531 (N—O stretching), 1657, 1682 cm^{-1} (=C=O stretching). Calc. for $C_{12}H_6O_4NCl$ (263.63): C, 54.67; H, 2.24. Found: C, 54.63; H, 2.14.

The residue from the mother liquor of the chloroform crystallization above was pooled with fraction I. A first crystallization of their mixture from chloroform yielded 0.2 g more of IV*c*. The filtrate was evaporated to dryness and the residue, when crystallized from ethanol, yielded 2-chloro-5-*p*-nitrophenylbenzoquinone (0.47 g) (IV*b*), m.p. 129–132°. An analytical sample had m.p. 134–135°. ν^{CHCl_3}: 913 (=C—H deformation, on quinone nucleus), 1353, 1533 (N—O stretching), 1679 cm^{-1} (=C=O stretching). λ_{max}: 260 mμ (4.26), 360 mμ (3.26). Calc. for $C_{12}H_6O_4NCl$ (263.63): C, 54.67; H, 2.24; N, 5.31. Found: C, 54.99; H, 2.22; N, 5.53.

Further elution of fraction II with benzene gave a solid (0.72 g) which crystallized from acetone – pet. ether (b.p. 90–120°) in yellow rhombs (0.58 g), m.p. 147–155°. This was combined with 0.78 g of crystals, m.p. 146–157°, obtained from crystallization of fraction III, from the same solvent pair. The mixture was crystallized twice to yield 2-chloro-3-*p*-nitrophenylbenzoquinone (IV*a*) (1.0 g), m.p. 157–158°. An analytical sample melted at 160–161°. ν^{CHCl_3}: 845, 853 (=C—H deformation), 1354, 1533 (N—O stretching), 1686, inflection at 1671 cm^{-1} (=C=O stretching). λ_{max}: 256 mμ (4.33), 350 mμ (3.41). Calc. for $C_{12}H_6O_4NCl$ (263.63): C, 54.67; H, 2.24; N, 5.31. Found: C, 54.61; H, 2.34; N, 5.47.

(b) By Chlorination of p-Nitrophenylbenzoquinone (XV)

p-Nitrophenylbenzoquinone, m.p. 135–136°, (5 g) was refluxed with concentrated hydrochloric acid (500 ml) for 2 hours, cooled to room temperature, and the reaction product filtered. The precipitate was washed free of acid with water, dried, dissolved in acetic acid (78 ml), and oxidized with ferric chloride solution (50 ml), to give a mixture of quinones (5.3 g). The quinones were dissolved in benzene and chromatographed on silica gel (300 g). Initial fractions yielded a semisolid (0.43 g). This solid was crystallized three times from acetone–ethanol to give pale yellow crystals (0.18 g), m.p. 196.5–198° which proved to be identical with 2,5-dichloro-*p*-nitrophenylbenzoquinone (VIII) by a mixed melting point with an authentic sample and I.R. spectra. Further elution gave 2-chloro-5-*p*-nitrophenylbenzoquinone (IV*b*) which, after being purified through silica gel and crystallized from acetone–ethanol, gave crystals (1.0 g), m.p. 134–135°. Continued elution yielded a solid (0.74 g), m.p. 200–207°. Crystallization from acetone – pet. ether gave 2-chloro-6-*p*-nitrophenylbenzoquinone (IV*c*) (0.5 g), m.p. 208–211°. The residue (0.14 g) from the mother liquor of this crystallization was crystallized from acetone – pet. ether (b.p. 90–120°) and 2-chloro-3-*p*-nitrophenylbenzoquinone (IV*a*) (0.055 g), m.p. 153–156°, was isolated. The I.R. spectrum of this sample was essentially superimposable with that of the analytical sample of IV*a* obtained by method (*a*) above.

Preparation of 2,5-Dichloro-p-nitrophenylbenzoquinone (VIII)

To a stirred solution of 2,5-dichlorobenzoquinone, m.p. 160–161°, (1.77 g) in a mixture of acetic acid (130 ml), water (12 ml), and sodium acetate (3.06 g), was added a solution of diazotized (16) *p*-nitroaniline (1.38 g). The reaction mixture was stirred overnight and the temperature was then raised to 45° for 2.5 hours. The reaction mixture was cooled and filtered. The precipitate was thoroughly washed with water, dried, and

Can. J. Chem. Downloaded from www.nrcresearchpress.com by 210.87.254.40 on 09/05/12
For personal use only.

crystallized from acetone–ethanol. Pale yellow crystals (0.66 g), m.p. 196–198°, were isolated. The filtrate was then poured on ice while a solid (1.14 g) separated. This solid was crystallized from ethanol, dissolved in benzene, and passed through silica gel (25 g). The eluate was evaporated to dryness and the residue (0.28 g), m.p. 194–198°, was added to the first crop of 0.66 g of yellow crystals, m.p. 196–198°, and recrystallized from acetone–ethanol. Pure 2,5-dichloro-*p*-nitrophenylbenzoquinone melts at 197–198°.

ν^{CHCl_3}: 889 (=C—H deformation, on quinone nucleus), 1354, 1533 (N—O stretching), 1686 cm^{-1} (=C=O stretching). Calc. for $C_{12}H_5O_4NCl_2$ (298.08): C, 48.33; H, 1.69; N, 4.68. Found: C, 48.51; H, 1.87; N, 4.77.

Preparation of 2,6-Dichloro-p-nitrophenylbenzoquinone (IX)

To a stirred solution of sodium acetate (3.06 g) in acetic acid (80 ml) and water (100 ml) 2,6-dichlorobenzoquinone, m.p. 120–121° (1.77 g) and finally a solution of diazonium salt (16) obtained from *p*-nitroaniline (1.38 g) were added. The reaction mixture was stirred overnight and then the temperature raised to 50° for 45 minutes. After cooling, the precipitate was collected, washed with water, dried (1.63 g), dissolved in benzene, and chromatographed on silica gel (102 g). Initial fractions gave a solid (0.85 g), which was further purified by passing through silica gel. 2,6-Dichloro-*p*-nitrophenylbenzoquinone (0.65 g), m.p. 138–139°, thus obtained, crystallizes from acetone – pet. ether in pale yellow prisms, m.p. 140–141°. ν^{CHCl_3}: 890 (=C—H deformation, on quinone nucleus), 1353, 1533 (N—O stretching), 1663, 1698 cm^{-1} (=C=O stretching). Calc. for $C_{12}H_5O_4NCl_2$ (298.08): C, 48.33; H, 1.69; N, 4.68. Found: C, 48.19; H, 1.75; N, 4.66.

Further elution yielded a solid (0.44 g), which was crystallized twice from acetone – pet. ether to provide yellow crystals (0.22 g) of 2,6-dichloro-3,5-di-*p*-nitrophenylbenzoquinone (XI), m.p. 222–224°. An analytical sample had m.p. 229–230°. ν^{CHCl_3}: 1350, 1534 (N—O stretching), 1663, 1692 cm^{-1} (=C=O stretching). Calc. for $C_{18}H_8O_6N_2Cl_2$ (419.17): N, 6.68. Found: N, 6.67.

Preparation of 2,3-Dichloro-p-nitrophenylbenzoquinone (X)

2,3-Dichlorohydroquinone (16 g), prepared as described by Conant and Fieser (17), was dissolved in acetic acid (133 ml) and oxidized with ferric chloride solution (130 ml) into dichlorobenzoquinone (VII) (13.04 g), m.p. 100–101° (reported m.p. 100–101° (18)).

ν^{CHCl_3}: 840 (=C—H deformation), 1692 cm^{-1} (=C=O stretching).

To a stirred solution of 2,3-dichlorobenzoquinone (1.77 g) and sodium acetate (3.06 g) in acetic acid (100 ml) and water (63 ml) was added a solution of the diazonium salt (16) prepared from *p*-nitroaniline (1.38 g). The reaction mixture was stirred overnight and the temperature then raised to 50° for 45 minutes. After cooling, the mixture was filtered and the residue washed and dried. The solid (1.3 g) thus collected, was dissolved in pet. ether – benzene (3:7) and chromatographed on silica gel (104 g). Initial fractions yielded 2,3-dichloro-*p*-nitrophenylbenzoquinone (0.59 g), m.p. 162–164°, which after two crystallizations from acetone–ethanol melted at 164–165°. ν^{CHCl_3}: 906 (=C—H deformation, on quinone nucleus), 1353, 1533 (N—O stretching), 1688 cm^{-1} (=C=O stretching). Calc. for $C_{12}H_5O_4NCl_2$ (298.08): C, 48.33; H, 1.69; N, 4.68. Found: C, 48.20; H, 1.70; N, 4.67.

Can. J. Chem. Downloaded from www.nrcresearchpress.com by 210.87.254.40 on 09/05/12
For personal use only.

Chlorination of Isomeric Chloro-p-nitrophenylbenzoquinones

Chloro-*p*-nitrophenylbenzoquinones (IV*a*), m.p. 159–160°; (IV*b*), m.p. 134–135°; (IV*c*), m.p. 210–211°, were refluxed with concentrated hydrochloric acid (0.29 mole per mole of quinone) for 1.5 hours, cooled, diluted with water, and the reaction product extracted with ether. The ether extract was dried and the ether removed. The residue thus obtained was oxidized with ferric chloride solution into a mixture of quinones.

(*a*) 2-Chloro-3-*p*-nitrophenylbenzoquinone (IV*a*) (0.211 g) gave a crude mixture of quinones (0.17 g). This was dissolved in benzene – pet. ether (2:3) and chromatographed on silica gel (10 g). Eluate in the first three fractions gave a material (0.02 g) the I.R. spectrum of which showed no characteristic bands due to $=\overset{|}{C}—H$ out-of-plane deformation on the quinone nucleus. This observation, coupled with the fact that this material was present in small amount in the crude mixtures obtained from chlorination of all the three isomers, suggested it to be trichloro-*p*-nitrophenylbenzoquinone. This was further confirmed by chlorination of 2,5-dichloro-*p*-nitrophenylbenzoquinone (VIII) under the above conditions. The I.R. spectrum of the addition product was superimposable with that of the material obtained from the chromatogram. Further elution gave a quinone (0.11 g) which crystallized from acetone–ethanol, yielding crystals (0.08 g), m.p. 197–198°. A mixed melting point and I.R. spectra proved this to be 2,5-dichloro-*p*-nitrophenylbenzoquinone (VIII). The residue (0.02 g) from the mother liquor showed in its I.R. spectrum a band at 1056 cm^{-1} and a pronounced hump at 1664 and 1699 cm^{-1} on the carbonyl maxima at 1686 cm^{-1}. These are characteristic absorptions of 2,6-dichloro-*p*-nitrophenylbenzoquinone (IX). Further processing of this residue by one crystallization from acetone–ethanol gave another 0.012 g of 2,5-dichloro-*p*-nitrophenylbenzoquinone. The I.R. spectrum of the residue from the mother liquor of this last crystallization showed a marked increase in the intensity of the bands at 1056, 1664, and 1699 cm^{-1}, indicating strongly the presence of 2,6-dichloro-*p*-nitrophenylbenzoquinone (IX) in the crude product. Further elution gave 0.031 g of an oil which the I.R. spectrum (3560 cm^{-1}, O—H stretching) indicated it to be unchanged hydroquinone.

(*b*) 2-Chloro-6-*p*-nitrophenylbenzoquinone (IV*c*) (0.203 g), when treated with hydrochloric acid and oxidized as described previously, gave 0.205 g of a crude product. This was dissolved in benzene – pet. ether (1:1) and chromatographed carefully on silica gel (20 g). Fractions eluted were combined based on their I.R. spectra.

Fractions 1 to 17 (0.027 g) consisted exclusively of 2,5,6-trichloro-*p*-nitrophenylbenzoquinone. Fractions 18 to 23 (0.007 g) were found to be a mixture of this quinone and 2,3-dichloro-*p*-nitrophenylbenzoquinone (X) from the I.R. spectra of the intermediate fractions. From fractions 24 to 32 a solid was obtained which crystallized from acetone–ethanol to yield reddish brown needles of X (0.011 g), m.p. 160–163°, identified by a mixed melting point and the I.R. spectra. Fractions 33 to 45 (0.056 g) yielded in one crystallization a solid (m.p. 150–170°) suggested by its I.R. spectrum to be a mixture of X and 2,5-dichloro-*p*-nitrophenylbenzoquinone (VIII). Fractions 46 to 71 (0.076 g) were crystallized from acetone–ethanol to yield pale yellow needles (0.06 g) of a quinone, m.p. 192–194°, found to be VIII by mixed melting point and their I.R. spectra.

(*c*) 2-Chloro-5-*p*-nitrophenylbenzoquinone (IV*b*) (0.204 g), when treated with hydrochloric acid and ferric chloride as described above, yielded 0.206 g of crude quinones. This was dissolved in benzene – pet. ether (1:1) and carefully chromatographed on silica gel (20 g). Fractions eluted were pooled based on I.R. spectra.

Can. J. Chem. Downloaded from www.nrcresearchpress.com by 210.87.254.40 on 09/05/12
For personal use only.

Fractions 2 to 25 (0.049 g) consisted mainly of trichloro-*p*-nitrophenylbenzoquinone as identified by their I.R. spectra. Combination 26 to 65 (0.076 g) from the spectra of the intermediate fractions was found to contain 2,3-dichloro-*p*-nitrophenylbenzoquinone (X). It crystallized from acetone–ethanol in clusters of reddish-brown needles (0.07 g), m.p. 160–162°. A mixed melting point with an authentic sample and comparison of their I.R. spectra, confirmed its identity. An I.R. analysis of fractions 66 to 84 (0.048 g), eluted with pet. ether – benzene (3:7) showed the carbonyl band at 1688 cm^{-1} flanked by shoulders of varying intensities (increasing from 66 to 84) at 1663 and 1699 cm^{-1} and appearance of a band of increasing intensity in the same order at 890 cm^{-1}. These were strongly suggestive of the presence of 2,6-dichloro-*p*-nitrophenylbenzoquinone (IX) but crystallization of combination 66 to 84 from acetone–ethanol gave 0.02 g of 2,3-dichloro-*p*-nitrophenylbenzoquinone (X). An I.R. spectrum of the residue from the mother liquor showed marked increase in the intensity of the bands at 1663, 1699, and 890 cm^{-1}. However, an attempt to isolate IX either by chromatography or by crystallization proved fruitless.

Preparation of 2,5- and 2,3-Dibromobenzoquinones (XII and XIII)

Treatment of hydroquinone (11 g) with 2 moles of bromine as described (18), gave a mixture of dibromohydroquinones. This was oxidized with a ferric chloride solution (100 ml) to yield a mixture of quinones (26 g). A 5.1-g portion of this was crystallized from benzene – pet. ether to give 2,5-dibromobenzoquinone (XII) (2.7 g) which, after one crystallization from acetone–ethanol, melted at 189–190° (m.p. 191° (19)). The residue (2.13 g) from the mother liquor of the first crystallization was dissolved in benzene – pet. ether (1:1) and chromatographed on silica gel (126 g). Elution gave in the first two fractions a solid (0.27 g). After three crystallizations of this solid from acetone – pet. ether tribromobenzoquinone (XIV) (0.15 g) was obtained as pale yellow platelets, m.p. 152–153°, (m.p. 155° (19), 150° (20)). λ_{max}: 295 mμ (4.01), 375 mμ (2.75); reported (20) λ_{max}: 296 mμ (4.03), 375 mμ (2.76). ν^{CHCl_3}: 886 (=C–H deformation), 1674, 1696 cm^{-1} (=C=O stretching).

By further elutions more 2,5-dibromobenzoquinone (0.42 g) crystallized from acetone – pet. ether and finally 2,3-dibromobenzoquinone (XIII) was obtained. This quinone crystallized from pet. ether (b.p. 65–110°) in prismatic needles (0.5 g), m.p. 124–125°. ν^{CHCl_3}: 836 (=C–H deformation), 1681 cm^{-1} (=C=O stretching). λ_{max}: 256 mμ (4.28), 362 mμ (3.45). Calc. for $C_6H_2O_2Br_2$ (265.91): C, 27.10; H, 0.76; Br: 60.13. Found: C, 27.29; H, 0.77; Br, 60.54.

ACKNOWLEDGMENTS

We are grateful to Dr. Le Roy F. Johnson of the Varian Associates for taking nuclear magnetic resonance spectra. One of us (J.F.B.) is greatly indebted to the National Research Council of Canada for a postdoctorate fellowship.

REFERENCES

1. P. Brassard and P. L'Écuyer. Can. J. Chem. **36**, 814 (1958).
2. H. Meerwein, E. Buchner, and K. van Emster. J. prakt. Chem. **152**, 237 (1939).
3. P. Brassard and P. L'Écuyer. Can. J. Chem. **36**, 700 (1958).
4. P. Brassard and P. L'Écuyer. Can. J. Chem. **36**, 709 (1958); **36**, 1346 (1958); **37**, 1505 (1959).
5. P. Brassard and P. L'Écuyer. Unpublished results.

Can. J. Chem. Downloaded from www.nrcresearchpress.com by 210.87.254.40 on 09/05/12
For personal use only.

6. J. F. BAGLI. Unpublished results.
7. J. K. KOCHI. J. Am. Chem. Soc. **79**, 2942 (1957).
8. L. MICHAELIS and S. GRANICK. J. Am. Chem. Soc. **66**, 1023 (1944).
9. D. F. DETAR and S. V. SAGMANLI. J. Am. Chem. Soc. **72**, 965 (1950); D. F. DETAR and D. J. RELYEA. J. Am. Chem. Soc. **76**, 1680, 1686 (1954); **78**, 4302 (1956).
10. D. H. HEY and W. WATERS. Chem Revs. **21**, 169 (1937).
11. J. CASON, R. E. HARMAN, S. GOODWIN, and C. F. ALLEN. J. Org. Chem. **16**, 860 (1950).
12. C. F. ALLEN and C. V. WILSON. J. Am. Chem. Soc. **63**, 1756 (1939).
13. T. H. CLARK. Am. J. Chem. **14**, 571 (1892).
14. M. J. S. DEWAR. Electronic theory of organic chemistry. Oxford University Press, London, 1949. p. 195.
15. K. HOEGERLE and P. L'ÉCUYER. Can. J. Chem. **37**, 2068 (1959).
16. E. E. FIERZ-DAVID and L. BLANGEY. Farbenchemie. 6th ed. Springer-Verlag, Berlin. 1946. p. 235.
17. J. B. CONANT and L. F. FIESER. J. Am. Chem. Soc. **45**, 2194 (1923).
18. E. VON SARAUW. Ann. **209**, 93 (1881).
19. E. A. BRAUDE. J. Chem. Soc. 490 (1945).
20 M. KOHN and J. PFEIFER. Monatsh. **48**, 211 (1927).

Can. J. Chem. Downloaded from www.nrcresearchpress.com by 210.87.254.40 on 09/05/12
For personal use only.

Can. J. Chem. Downloaded from www.nrcresearchpress.com by 210.87.254.5 on 09/05/12
For personal use only.

THE EFFECT OF BETA-DECAY ON THE EXCHANGE PROPERTIES OF THE RARE EARTH–EDTA COMPLEX IONS[1]

P. GLENTWORTH[2] AND R. H. BETTS

ABSTRACT

It is shown that the rare earth ion Yb^{3+} is very resistant towards ordinary thermal exchange when it is complexed with the chelating agent EDTA in aqueous solution. However, when the complexed rare earth atom, as the 1.8-h Yb-177, emits a beta-particle, the daughter atom Lu-177 escapes readily from the chelate structure. Nuclear recoil arising from the beta-particle emission is shown not to be the cause of the escape of the daughter atom. It is suggested that the observed lability of the daughter atom is a result of a high degree of chemical reactivity of the chelate ion arising from the sudden change in atomic number of the central metal ion of the chelate structure.

INTRODUCTION

The emission of nuclear radiation from an atom is always accompanied by a corresponding recoil of the residual atom. Enhanced chemical reactivity of the daughter atom, as a result of the nuclear event, is also frequently observed. This paper reports the results of a preliminary study of these so-called "hot-atom" effects for the lanthanide isotope Lu-177, in a particular chemical environment, when it is formed as a result of β^- decay of its 1.8-h Yb-177 parent. The decay sequence may be written as:

$$^{177}\text{Yb} \xrightarrow[T_{1/2} = 1.8\ \text{h}]{\beta^- = 1.3\ \text{Mev}} {}^{177}\text{Lu} \xrightarrow[T_{1/2} = 6.8\ \text{d}]{\beta^-} {}^{177}\text{Hf}_{\text{stable}}.$$

As is shown above, the daughter Lu-177 is also radioactive, a fact which greatly facilitates observations of its chemical behavior.

The particular system examined was the exchange reaction in aqueous solution between hydrated Yb^{3+} cations and $^{177}LuX^-$, where X stands for the tetrabasic chelating agent ethylenediaminetetraacetic acid (EDTA). The entity $^{177}LuX^-$ was formed in solution as a result of the β^- decay of $^{177}YbX^-$. This system was chosen because previous work from this laboratory had shown that these complex ions are remarkably stable, and in particular the thermal exchange reaction between the chelated lanthanide ion and the simple ion is very slow (1, 2). Any enhancement of reactivity of the chelate ion, as a result of β^- decay of its central lanthanide atom, was therefore expected to be readily observable.

The parent nuclide, Yb-177, was made by neutron irradiation of samples of pure ytterbium which were highly enriched in the isotope of mass 176. The use of this enriched material, rather than natural ytterbium (for which Yb-177 is not the predominant radionuclide (3)) permitted some simplification in the experimental methods and also aided in the interpretation of the results.

EXPERIMENTAL METHODS AND RESULTS

Radioactive ytterbium was produced by neutron irradiation of a known quantity of ytterbium (as an aqueous solution of the nitrate salt) for 1 hour in an empty fuel rod

[1]*Manuscript received December 1, 1960.*
Contribution from the Research Chemistry Branch, Atomic Energy of Canada Limited, Chalk River, Ontario. Issued as A.E.C.L. No. 1213.
[2]*N.R.C. Fellow 1959–60. Present address: The Department of Chemistry, The University, Leeds 2, England.*

position of the NRX reactor. The nitrate solution was prepared from ytterbium oxide which had been mass-separated at Oak Ridge National Laboratories, and contained 97.5% Yb-176, and 1.81% Yb-174. It was initially free of lutetium. The principal activity formed was 1.8-h Yb-177, by neutron capture in the 97.5% abundant Yb-176. A minor activity, 4.2-d Yb-175, was also produced by neutron capture in Yb-174. It will be shown below that the presence of this Yb-175 activity permitted the correction for thermal exchange to be determined directly.

After the irradiation, sufficient Na_4EDTA solution was added to the irradiated solution to complex approximately two-thirds of the Yb^{3+} ions present. The remaining uncomplexed Yb^{3+} ions were quantitatively removed by absorption on a Dowex-50 cation resin column. This procedure ensured that all the radioactive atoms were initially complexed with EDTA and that no excess of EDTA was present. Non-radioactive Yb^{3+} ions were then added to the test solution, together with 0.01 *M* ammonium acetate, pH = 6.5. (The time at which these additions were made was recorded as "zero time".) The concentration of both ionic species YbX^- and Yb^{3+} was 2.5×10^{-4} *M*. The pH of 6.5 was chosen to minimize the normal thermal exchange between these two species, previous studies (1) having shown that the rate of the thermal exchange between M^{3+} and MX^- ions varies directly with the acidity of the solution.

The decay of the 1.8-h Yb-177, and the concurrent "hot-atom" or thermal exchange reactions in solution, were allowed to proceed for 4.6 hours. During this time, 81.2% of the Yb-177 atoms present had decayed to Lu-177. The free Yb^{3+} ions (and any $^{177}Lu^{3+}$ ions which had found their way into this so called free-ion fraction as a result of recoil or thermal exchange processes) were then quantitatively removed from the test solution by absorption onto a Dowex-50 resin column. The absorbed species were then eluted off the column with 0.4 *M* α-hydroxyisobutyric acid solution of pH 6.5. Sufficient time, approximately 24 hours, was then allowed for the residual Yb-177 to decay completely to Lu-177, and then the latter nuclide in the free-ion fraction was separated from 4.2-d Yb-175 by chromatographic elution from a Dowex-50 resin column; this method has been described by Choppin and Silva (4). The separated Yb-175 and Lu-177 were set aside for further measurements outlined below.

1. The Number of Yb-177 Atoms in the Test Solution at Zero Time

This quantity was determined by absolute 4π-β^- counting of an aliquot of the test solution, the radioactive decay of the Yb-177 being followed for 10 half-lives. A total of 11.37×10^{10} atoms of Yb-177 was present in solution as $^{177}YbX^-$ at zero time. Of this number, 81.2% or 9.23×10^{10} atoms had decayed to Lu-177 in the 4.6-hour period allowed.

2. Measurement of the Number of Lu-177 Atoms in the Free-ion Fraction

Lu-177 atoms in the free-ion fraction could have found their way there by one or more of the following routes:

(i) "Hot-atom" effects associated with the β^- decay of $^{177}YbX^-$.

(ii) Thermal exchange of Yb^{177}: $^{177}YbX^- + Yb^{3+} \rightarrow YbX^- + {}^{177}Yb^{3+}$, followed by β^- decay of the Yb-177 atoms so released.

(iii) Thermal exchange involving the reaction: $^{177}LuX^- + Yb^{3+} \rightarrow YbX^- + {}^{177}Lu^{3+}$.

(Lu-177 atoms in the form $^{177}LuX^-$ are present in significant and calculable amount at zero time as a result of β^- decay of Yb-177 during the irradiation in NRX, and also in the time between the end of the irradiation and the time at which the EDTA chelate was formed.) The sum of these three contributions was determined in the following

Can. J. Chem. Downloaded from www.nrcresearchpress.com by 210.87.254.5 on 09/05/12
For personal use only.

way. The Lu-177 activity isolated from the free-ion fraction was measured on a 100-channel γ-ray spectrometer which had been previously calibrated with an independently standardized Lu-177 source. A total of 5.85×10^{10} atoms of Lu-177 was found in the free-ion fraction. It is now necessary to distinguish between the "hot atom" and thermal exchange contribution to this quantity.

3. Extent of Thermal Exchange

Earlier studies (1) suggested that thermal exchange would not be a significant effect for the conditions used in the present work, and this was confirmed by measurements of the extent of transfer of Yb-175 from the chelate ion to the free-ion fraction. These measurements were made by comparing the areas under the photopeak characteristic of Yb-175 in the γ-ray spectra of an aliquot taken from the test solution and an aliquot of the Yb-175 part of the free-ion fraction referred to earlier. A value of 2.8% was obtained for the extent of thermal exchange, a result somewhat higher than would have been predicted from earlier studies (1) but not grossly inconsistent with these earlier results. This result can be used to estimate the contribution of process (ii) above (thermal transfer of Yb-177), to the appearance of Lu-177 in the free-ion fraction. Thus, the *average* number of Yb-177 atoms available for thermal exchange during the 4-hour period may be taken to a good approximation as one-half the original number present, i.e., $0.5\times11.37\times10^{10} = 5.68\times10^{10}$ atoms. Transfer of 2.8% of these represents 0.16×10^{10} atoms of Lu-177 contributed to the free-ion fraction.

A similar assessment can be made of the extent of thermal transfer of Lu-177 from the form $^{177}LuX^-$ to $^{177}Lu^{3+}$. Earlier studies (1, 2) showed that the rate of thermal exchange of the lanthanide elements in the form MX^- decreases slowly with increasing atomic number. The 2.8% transfer of Yb-175 therefore represents also an *upper* limit of the percentage of lutetium atoms present as $^{177}LuX^-$, which underwent normal thermal exchange during the experiment. The number of Lu-177 atoms present in this form at zero time was 7.44×10^{10} atoms. This number was readily calculated from the number of Yb-177 atoms present at zero time, together with the time of irradiation, and the time between the end of the irradiation and the formation of the EDTA chelate. The number of $^{177}LuX^-$ present at the end of the run was 10.8×10^{10}. An average value of 9.1×10^{10} may be used for estimating the extent of thermal transfer. A maximum of 2.8% of these 9.1×10^{10} atoms would be transferred to the free-ion fraction in 4.6 hours, i.e., 0.25×10^{10} atoms.

The pertinent numerical results obtained above are summarized in Table I. Comparison of items B and C in Table I shows clearly that the number of Lu-177 atoms found in

TABLE I

Source and distribution of Lu-177 atoms

	No. of atoms $\times10^{-10}$
A. Formed in solution from decay of $^{177}YbX^-$ in 4.6 hours	9.23
B. Found in free-ion fraction	5.85
C. No. expected in free-ion fraction from thermal exchanges:	
(i) $^{177}YbX^- + Yb^{3+} \rightarrow YbX^- + {}^{177}Yb^{3+}$, $^{177}Yb^{3+} \rightarrow Lu^{3+} + \beta^-$	0.16
(ii) $^{177}LuX^- + Yb^{3+} \rightarrow YbX^- + {}^{177}Lu^{3+}$	0.25
Total contribution to B from thermal exchange processes	0.41
D. No. transferred by "hot-atom" processes = (B–C)	5.44
Net fraction of A transferred by "hot-atom" processes = D/A =	0.590

Can. J. Chem. Downloaded from www.nrcresearchpress.com by 210.87.254.5 on 09/05/12
For personal use only.

the free-ion fraction was very much greater than can be accounted for by thermal exchange processes. The presence of these extra Lu-177 atoms in the free-ion fraction is ascribed to "hot-atom" processes associated with the β^- emission from Yb-177, when this nuclide is present in the chemical form $^{177}YbX^-$. A comparison of items D and A, shown in the last entry of Table I, shows that 59% of the Lu-177 atoms formed by β^- decay of $^{177}YbX^-$ escape from the chelate and turn up in solution in the cationic form $^{177}Lu^{3+}$.

The results described above appear to be quantitatively reproducible; a second essentially identical experiment gave a value of 56% for the percentage of the Lu-177 atoms escaping from the chelate ion as a result of β^- decay of $^{177}YbX^-$. This is in good agreement with the value of 59% listed in Table I.

DISCUSSION

The maximum energy of the β^- particle emitted by Yb-177 is 1.3 Mev. A free, isolated Lu-177 daughter atom then receives, as a result of nuclear recoil, a *maximum* of 9 ev of kinetic energy. This value is given by the expression

$$E_R = \frac{541\,E_\beta}{M} + \frac{536\,E_\beta^2}{M}.$$

E_R is the recoil energy in electron volts, E_β is the maximum energy of the beta particle in Mev, M is the mass of the recoiling atom.

However, it is well known that the average β^- energy is approximately 0.4 E_β, so that an isolated Lu-177 atom will receive on the average only 3.5 to 4.0 ev of recoil. (The relation between the average recoil energy given to an isolated atom and the maximum β^- energy of the disintegration has been discussed by several authors, e.g. Libby (5).) Moreover, in the present study, the daughter atom is in fact not a free, isolated atom, but is linked by at least four strong co-ordinate bonds to the chelating agent EDTA (2, 6). The recoil energy is therefore shared by a more massive configuration, with the result that the average kinetic energy of translation of the recoiling Lu-177 will be significantly less than 3–4 ev. On the other hand, 2–3 ev would be a reasonable estimate of the binding energy associated with each of the four co-ordinate bonds in the chelate. It appears highly unlikely therefore that nuclear recoil, as such, contributes appreciably to the observed escape of Lu-177 from the chelate environment.

A more likely cause for the observed escape is the abrupt change in atomic number of the central atom of the chelate. The loss of a negative charge from the nucleus produces a rearrangement of the electronic energy levels of the daughter atom, and thereby introduces a high degree of electronic excitation (see, for example, a recent review by Baulch and Duncan (7)). One may suppose therefore either that this excitation leads directly to dissociation, or alternatively that an excited species is formed. A necessary corollary of the latter alternative is that the excited species, during its lifetime, is very much more labile with respect to exchange than an ordinary lanthanide–EDTA chelate. Further speculations would appear unwarranted at present, in view of the limited amount of experimental evidence yet available. In this connection, a useful line for future investigation would be to discover whether or not changes in the chemical environment (pH, temperature, concentration of free lanthanide ions) have any effect on this "hot-atom" system.

Can. J. Chem. Downloaded from www.nrcresearchpress.com by 210.87.254.5 on 09/05/12
For personal use only.

ACKNOWLEDGMENTS

One of the authors, P. Glentworth, is indebted to the National Research Council of Canada for a Fellowship 1959–60, and to Atomic Energy of Canada Limited, in whose laboratories this work was carried out. Thanks are also due to Mrs. J. Merritt for providing the standard Lu-177 sources used in this work.

REFERENCES

1. R. H. BETTS, O. F. DAHLINGER, and D. M. MUNRO. Radioisotopes in scientific research. Proceedings of the First UNESCO International Conference, Paris, 1957. Vol. II. Pergamon Press, New York. 1958. p. 326.
2. R. H. BETTS and O. F. DAHLINGER. Can. J. Chem. **37**, 91 (1959).
3. R. H. BETTS, O. F. DAHLINGER, and D. M. MUNRO. Can. J. Phys. **36**, 73 (1958).
4. G. R. CHOPPIN and R. J. SILVA. J. Inorg. & Nuclear Chem. **3**, 153 (1956).
5. W. F. LIBBY. J. Am. Chem. Soc. **69**, 2523 (1947).
6. T. MOELLER, F. A. J. MOSS, and R. H. MARSHALL. J. Am. Chem. Soc. **77**, 3182 (1955).
7. D. L. BAULCH and J. F. DUNCAN. Quart. Revs. (London), **12**, 133 (1958).

Can. J. Chem. Downloaded from www.nrcresearchpress.com by 210.87.254.5 on 09/05/12
For personal use only.

Can. J. Chem. Downloaded from www.nrcresearchpress.com by 210.87.254.40 on 09/05/12
For personal use only.

SOME STABLE DIMERS OF SUBSTITUTED BENZYLCYANAMIDES[1]

D. L. Garmaise and A. Uchiyama

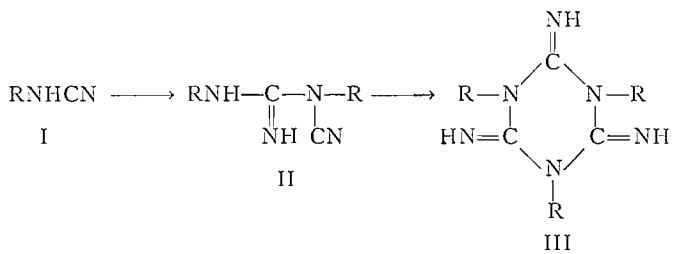
ABSTRACT

2,4- and 3,4-Dichlorobenzylcyanamides dimerize on standing to 1-cyano-1,3-di-(2,4-dichlorobenzyl)-guanidine and 1-cyano-1,3-di-(3,4-dichlorobenzyl)-guanidine respectively. Apart from dicyandiamide itself, no other cyanamide dimers appear to have been described. The dimers on heating are converted into the corresponding trisubstituted isomelamines. 1-Cyano-1,3-di-(3,4-dichlorobenzyl)-guanidine condenses with 4-nitrobenzylcyanamide to form 1,3-di-(3,4-dichlorobenzyl)-5-(4-nitrobenzyl)-isomelamine. No dimers were obtained from the 4-chloro-, 4-bromo-, 4-nitro-, or 4-methyl-benzylcyanamides.

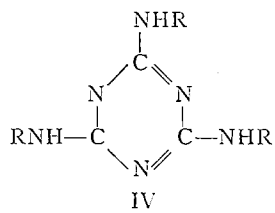
Monosubstituted cyanamides trimerize slowly on standing, more rapidly when heated, and, in some cases, when subject to the action of strong alkali (1).

Alkylcyanamides (2, 3) and aralkylcyanamides (4) give trisubstituted isomelamines, while arylcyanamides may also yield the corresponding melamines (5).

No stable intermediate would be expected in the formation of melamines (IV), but the formation of isomelamines (III) should involve as intermediates, 1,3-disubstituted dicyandiamides (II).



a: R = 3,4-$Cl_2C_6H_3CH_2$—
b: R = 2,4-$Cl_2C_6H_3CH_2$—
c: R = 4-$ClC_6H_4CH_2$—
d: R = 4-$BrC_6H_4CH_2$—
e: R = 4-$O_2NC_6H_4CH_2$—
f: R = 4-$H_3CC_6H_4CH_2$—



Derivatives of this type have not been previously reported.

It is now shown that when R = 3,4-dichlorobenzyl (*a*) or 2,4-dichlorobenzyl (*b*), the second step is sufficiently slow to permit the isolation and characterization of the dicyandiamides II*a* and II*b*.

Six substituted benzylcyanamides (Table I) were prepared by treating benzylamines with cyanogen bromide in ether (6). The products were readily isolated, generally in good yield, by operating at room temperature. The infrared spectra of the cyanamides showed the C≡N band at 2220–2240 cm^{-1} with no absorption in the C=N region except in the case of 3,4-dichlorobenzylcyanamide (I*a*). Even freshly prepared samples of I*a* showed a weak band at 1675 cm^{-1} in addition to the C≡N band.

[1]*Manuscript received January 31, 1961.*
Contribution No. 31 from the L. G. Ryan Research Laboratories of Monsanto Canada Limited, LaSalle, Quebec.

TABLE I
Benzylcyanamides RNHCN

R	Yield, %	M.p., °C	Formula	C Calc.	C Found	H Calc.	H Found	Hal. Calc.	Hal. Found	N Calc.	N Found
4-Chlorobenzyl	76	91–92	$C_8H_7ClN_2$	57.68	57.51	4.23	4.36	21.28	21.64	16.81	16.37
4-Bromobenzyl	70	99–101	$C_8H_7BrN_2$	45.52	46.39	3.34	3.36	37.86	38.39	13.27	13.70
4-Nitrobenzyl	37	120–121	$C_8H_7N_3O_2$	54.24	54.41	3.98	4.16			27.32	23.62
4-Methylbenzyl	95	79–80	$C_9H_{10}N_2$	73.94	74.16	6.89	7.23			19.17	18.97
2,4-Dichlorobenzyl	94	60–61	$C_8H_6Cl_2N_2$	47.80	47.78	3.01	3.16	35.27	35.64	13.93	13.72
3,4-Dichlorobenzyl	93	48–50*									

*Not isolated free of the dimer.

Birkofer (4) reported that in attempting to purify benzylcyanamide by extraction with 30% sodium hydroxide solution in accordance with an earlier procedure (7), he observed an immediate precipitation of tribenzylisomelamine. We have found that 4-methylbenzylcyanamide (I*f*) is slowly converted to the isomelamine in 30% sodium hydroxide solution, but that benzylcyanamides with electron-withdrawing substituents (I*a*, I*b*, I*c*, I*d*) hydrolyze in this medium to the corresponding ureas instead of trimerizing. The 4-nitro analogue (I*e*) did not yield an identifiable derivative.

All of the cyanamides are converted to the isomelamines (III) when heated at 100°. The infrared spectra of the isomelamines show characteristically strong C=N bands at 1610–1620 cm^{-1}, with no adsorption in the C≡N region. I*c*, I*d*, and I*f* also formed the corresponding isomelamines on standing at room temperature for periods of 10–30 days, while the nitro analogue (I*e*) was unchanged in 30 days. The 2,4-dichloro analogue (I*b*), m.p. 60–61°, on being allowed to stand in an open vessel for 3 days, gave a 95% yield of a substance melting at 142–143°. This product (II*b*) showed strong bands at both 2245 cm^{-1} and 1690 cm^{-1}, indicating the presence of both C≡N and C=N bands. II*b*, on being melted and then heated at 100° for 4 hours was converted to the isomelamine III*b*, m.p. 220–222° in 75% yield.

Similarly, the 3,4-dichloro analogue (I*a*) (m.p. 48–50°), on standing in an open dish for 24 hours, gave a 63% yield of II*a*, m.p. 138–139°. II*a* also showed strong bands at 2240 cm^{-1} and 1674 cm^{-1}, and was converted in refluxing methanol to the isomelamine III*a*, m.p. 170–171° (8) in 70% yield. Paper chromatography in butanol:acetic acid:water, with development by bromcresol green gave R_f values of 0.73, 0.86, and 0.93 for I*a*, II*a*, and III*a* respectively.

Although reliable molecular weight determinations could not be made, the dimeric nature of II*a* was established by benzoylation to a monobenzoyl derivative, m.p. 200–201°. The benzoyl derivative analyzed for the formula $C_{23}H_{16}Cl_4N_4O$, which could be derived only from a dimer of the formula $C_{16}H_{12}Cl_4N_4$. The structure of the benzoyl derivative was not established.

The dicyandiamide (II*a*) and 4-nitrobenzylcyanamide (I*e*) were allowed to stand in alcohol solution for 6 days, giving 1,3-di-(3,4-dichlorobenzyl)-5-(4-nitrobenzyl)-isomelamine in 20% yield. This result supports the assumption that 1,3-disubstituted dicyandiamides of the structure II are true intermediates in the trimerization of cyanamides to

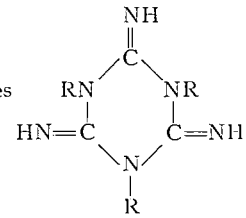
Can. J. Chem. Downloaded from www.nrcresearchpress.com by 210.87.254.40 on 09/05/12
For personal use only.

isomelamines. 4-Nitrobenzylcyanamide was chosen for this reaction because of its relative stability at room temperature.

For purpose of comparison, a number of N^2,N^4,N^6-tribenzylmelamines (IV*b*, IV*c*, and IV*f*) were prepared by the reaction between cyanuric chloride and benzylamines. N^2,N^4,N^6-Tri-(3,4-dichlorobenzyl)-melamine has been previously described (8). The infrared spectra of the melamines showed C=N absorption at 1613–1624 cm^{-1}.

TABLE II

Isomelamines



R	Yield, %	M.p., °C	Formula	C Calc.	C Found	H Calc.	H Found	Hal. Calc.	Hal. Found	N Calc.	N Found
4-Chlorobenzyl	80	165–167	$C_{24}H_{21}Cl_3N_6$	57.68	58.01	4.23	4.42	21.28	21.31	16.81	16.53
4-Bromobenzyl	90	207–208	$C_{24}H_{21}Br_3N_6$	45.52	45.90	3.34	3.63	37.86	38.39	13.27	13.71
4-Nitrobenzyl	19	228–229	$C_{24}H_{21}N_9O_6$	54.24	54.34	3.98	3.94			23.72	23.62
4-Methylbenzyl	90	203–204	$C_{27}H_{30}N_6$	73.94	73.43	6.89	7.04			19.17	18.63
2,4-Dichlorobenzyl	65	220–222	$C_{24}H_{18}Cl_6N_6$	47.80	47.42	3.01	3.16	35.27	35.40	13.93	13.88
3,4-Dichlorobenzyl	70	171–172*									

*Literature reported m.p. 171–172° (8).

EXPERIMENTAL[2]

Preparation of Benzylcyanamides

Example.—Cyanogen bromide (7.55 g, 0.075 mole) in ether (100 ml) was added to a stirred solution of 4-chlorobenzylamine (21.4 g, 0.15 mole) in ether (100 ml) at 5° during 15 minutes. The suspension was stirred for 1 hour, and the precipitated 4-chlorobenzylamine hydrochloride was filtered. The ether solution was washed with 1 *N* hydrochloric acid (2×200 ml) and with water, and was then dried and evaporated. The crystalline residue of 4-chlorobenzylcyanamide (12.3 g), m.p. 67–70°, was recrystallized from ether to a constant melting point of 91–92°, yield 9.5 g (76% of theory).

Preparation of Isomelamines

4-Chlorobenzylcyanamide (0.50 g) was heated at 100° for 4 hours. Trituration with methanol gave 1,3,5-tri-(4-chlorobenzyl)-isomelamine, m.p. 162–165°, yield 0.40 g (80% of theory). Recrystallization from methanol raised the melting point to 165–166°.

In the case of the 4-nitro analogue (III*e*), the product had to be separated from relatively large amounts of colored by-products. The 4-chloro, 4-bromo, and 4-methyl analogues (III*c*, *d*, and *f*) could also be obtained by allowing the cyanamides to stand at room temperature for periods of 10–30 days.

[2]*All melting points are uncorrected. Analyses were performed by Micro-Tech Laboratories, Skokie, Ill., and Dr. Claude Daessle, Montreal, Quebec.*

Can. J. Chem. Downloaded from www.nrcresearchpress.com by 210.87.254.40 on 09/05/12
For personal use only.

Behavior of Benzylcyanamides in Aqueous Alkali

4-Methylbenzylcyanamide.—A solution of 4-methylbenzylcyanamide (1.5 g) in 30% sodium hydroxide (35 ml) was allowed to stand for 3 days. 1,3,5-Tri-(4-methylbenzyl)-isomelamine, m.p. 203–204°, slowly precipitated, yield 1.0 g (67%). There was no depression on admixture with a sample prepared as described above.

4-Chlorobenzylcyanamide.—4-Chlorobenzylcyanamide (0.50 g, 0.003 mole) was allowed to stand in 30% sodium hydroxide solution (20 ml) overnight. The precipitated 4-chlorobenzylurea, m.p. 185–186°, was filtered, yield 0.30 g (48%). Recrystallization from methanol raised the melting point to 189–190°. Acidification of the alkaline filtrate gave 0.11 g of unchanged 4-chlorobenzylcyanamide. Anal. Calc. for $C_8H_9ClN_2O$: C, 52.05; H, 4.91; Cl, 19.20; N, 15.18. Found: C, 51.96; H, 4.99; Cl, 19.08; N, 14.92.

3,4-Dichlorobenzylcyanamide.—Under the same conditions as described above, 3,4-dichlorobenzylcyanamide gave 3,4-dichlorobenzylurea, m.p. 163.5–164.5° (from methanol) in 77% yield. Anal. Calc. for $C_8H_8Cl_2N_2O$: C, 43.81; H, 3.68; N, 12.78. Found: C, 43.67; H, 3.58; N, 13.01.

4-Bromobenzylcyanamide.—Similarly, 4-bromobenzylcyanamide gave 4-bromobenzylurea, m.p. 201–203° (from ethanol), in 52% yield. Anal. Calc. for $C_8H_9BrN_2O$: Br, 34.89; N, 12.23. Found: Br, 34.75; N, 12.64.

Preparation of Melamines

Example.—Cyanuric chloride (3.7 g, 0.020 mole) was added to 4-methylbenzylamine (20.0 g, 0.165 mole) in *o*-xylene (100 ml) during 15 minutes, and the mixture was refluxed for 4 hours. The precipitated 4-methylbenzylamine hydrochloride was filtered, and the filtrate was evaporated to dryness. Crystallization of the residue from ethanol gave N^2,N^4,N^6-tri-(4-methylbenzyl)-melamine, m.p. 123–127°, yield 8.8 g (quantitative). The analytical sample melted at 129–130° after recrystallization from ethanol and from acetone. Anal. Calc. for $C_{27}H_{30}N_6$: C, 73.90; H, 6.91; N, 19.18. Found: C, 73.92; H, 7.05; N, 19.38.

N^2,N^4,N^6-Tri-(4-chlorobenzyl)-melamine.—N^2,N^4,N^6-Tri-(4-chlorobenzyl)-melamine, m.p. 158–159° (from ethanol) was obtained in 69% yield. Anal. Calc. for $C_{24}H_{21}Cl_3N_6$: C, 57.67; H, 4.24; Cl, 21.28; N, 16.81. Found: C, 57.65; H, 4.17; Cl, 21.27; N, 16.79.

N^2,N^4,N^6-Tri-(2,4-dichlorobenzyl)-melamine.—N^2,N^4,N^6-Tri-(2,4-dichlorobenzyl)-melamine, m.p. 155–157°, was isolated in 88% yield. Anal. Calc. for $C_{24}H_{18}Cl_6N_6$: C, 47.81; H, 3.01; Cl, 35.26; N, 13.95. Found: C, 47.64; H, 3.08; Cl, 35.26; N, 13.95.

1-Cyano-1,3-di-(2,4-dichlorobenzyl)-guanidine

2,4-Dichlorobenzylcyanamide (1.0 g, m.p. 60–61°) was allowed to stand in an open crystallizing dish for 2 days. Trituration with ether yielded the product melting at 140–143°. The ethereal mother liquors on standing for 24 hours deposited an additional quantity of the same substance, m.p. 140–142°. Total yield 0.95 g (95%). Recrystallization from methanol (30 ml/g) raised the melting point to 142–143°. Anal. Calc. for $C_{16}H_{12}Cl_4N_4$: C, 47.80; H, 3.01; Cl, 35.27; N, 13.93. Found: C, 47.35; H, 3.04; Cl, 35.37; N, 13.70.

The product (0.20 g) was heated above its melting point (150–160°) for 10 minutes and then heated at 100° for 4 hours. Trituration with methanol yielded crude 1,3,5-tri-(2,4-dichlorobenzyl)-isomelamine, m.p. 210–217°, yield 0.15 g (75%). Recrystallization from dimethylformamide–methanol–water raised the melting point to 220–222°. There was no depression on admixture with an authentic sample prepared by direct trimerization of 2,4-dichlorobenzylcyanamide.

Can. J. Chem. Downloaded from www.nrcresearchpress.com by 210.87.254.40 on 09/05/12
For personal use only.

1-Cyano-1,3-di-(3,4-dichlorobenzyl)-guanidine

3,4-Dichlorobenzylcyanamide (13.0 g, m.p. 48–50°) was allowed to stand in an open crystallizing dish for 24 hours. During this period the starting material melted and later partially resolidified. Trituration with ether yielded the product, m.p. 128–134°, yield 8.2 g (63%). The product was recrystallized to a constant melting point of 138–139° by dissolving in preheated methanol (30 ml/g) and cooling rapidly. Anal. Calc. for $C_{16}H_{12}Cl_4N_4$: C, 47.80; H, 3.01; Cl, 35.27; N, 13.93. Found: C, 47.57; H, 3.24; Cl, 35.58; N, 13.93.

A solution of 1-cyano-1,3-di-(3,4-dichlorobenzyl)-guanidine (0.50 g) in methanol (50 ml) was refluxed for 3 hours. The solution was evaporated and the residue was crystallized from ether, giving 1,3,5-tri-(3,4-dichlorobenzyl)-isomelamine, m.p. 167–169°, yield 0.35 g (70%). There was no depression on admixture with a sample, m.p. 171–172°, prepared by direct trimerization of 3,4-dichlorobenzylcyanamide.

Benzoylation of 1-Cyano-1,3-di-(3,4-dichlorobenzyl)-guanidine

Benzoyl chloride (1.01 g, 0.00712 mole) was added to 1-cyano-1,3-di-(3,4-dichlorobenzyl)-guanidine (2.86 g, 0.00712 mole) in pyridine (25 ml) at 5° and the solution was allowed to stand overnight. The solution was diluted with ether (200 ml), washed with 1 *N* hydrochloric acid (3×200 ml) and with water (2×100 ml). The crude product, m.p. 173–180°, separated at the interface, yield 1.0 g (28%). Repeated recrystallization from methanol raised the melting point of the monobenzoylated derivative to 200–201°, yield 0.50 g (14%). Anal. Calc. for $C_{23}H_{16}Cl_4N_4O$: C, 54.56; H, 3.19; Cl, 28.02; N, 11.07. Found: C, 54.53; H, 3.26; Cl, 28.09; N, 11.18.

1,3-Di-(3,4-dichlorobenzyl)-5-(4-nitrobenzyl)-isomelamine

A solution of 1-cyano-1,3-di-(3,4-dichlorobenzyl)-guanidine (0.75 g, 0.00187 mole) and 4-nitrobenzylcyanamide (0.33 g, 0.00187 mole) in methanol (150 ml) was allowed to stand at 25° for 6 days. The solution was evaporated, and the residue was crystallized from ether (25 ml) to give 0.50 g of a gummy solid. Suspension of the crude product in ether (50 ml) at 5° for 1 week gave the product melting at 170–172°, yield 0.22 g (20%). Recrystallization from methanol raised the melting point to 177–179°. Anal. Calc. for $C_{24}H_{19}Cl_4N_7O_2$: C, 49.76; H, 3.30; Cl, 24.49; N, 16.93. Found: C, 49.90; H, 3.38; Cl, 24.07; N, 16.67.

ACKNOWLEDGMENT

The authors are grateful to Miss V. Falta for skilful technical assistance.

REFERENCES

1. E. M. SMOLIN and L. RAPOPORT. s-Triazines and derivatives. Interscience Publishers, Inc., New York. 1959. p. 379.
2. A. W. HOFMANN. Ber. **18**, 2781 (1885).
3. W. TRAUBE, F. KEGEL, and H. E. P. SCHULZ. Z. angew. Chem. **39**, 1465 (1926).
4. L. BIRKOFER. Ber. **75**, B, 429 (1942).
5. F. KURZER. J. Chem. Soc. 3033 (1949).
6. J. STRAKOSCH. Ber. **5**, 692 (1872).
7. R. H. MCKEE. Am. Chem. J. **36**, 208 (1906).
8. A. F. MCKAY, D. L. GARMAISE, G. Y. PARIS, and S. GELBLUM. Can. J. Chem. **38**, 343 (1960).

Can. J. Chem. Downloaded from www.nrcresearchpress.com by 210.87.254.40 on 09/05/12
For personal use only.

Can. J. Chem. Downloaded from www.nrcresearchpress.com by 210.87.254.40 on 09/05/12
For personal use only.

CONSTITUTION OF A 4-*O*-METHYLGLUCURONOXYLAN FROM THE WOOD OF TREMBLING ASPEN (POPULUS TREMULOIDES MICHX.)[1]

J. K. N. Jones, C. B. Purves, and T. E. Timell

ABSTRACT

A 4-*O*-methylglucuronoxylan has been isolated in almost quantitative yield from the wood of trembling aspen (*Populus tremuloides* Michx.). The hemicellulose was electrophoretically homogeneous and had a number-average degree of polymerization of 212. Partial hydrolysis gave D-xylose, galacturonic acid, 4-*O*-methylglucuronic acid, and 2-*O*-(4-*O*-methyl-α-D-glucopyranosyluronic acid)-D-xylopyranose. Methanolysis and hydrolysis of the fully methylated polysaccharide, which contained 108 xylose residues per average molecule, gave 2-*O*-methylxylose, 2,3-di-*O*-methyl-D-xylose, 2,3,4-tri-*O*-methyl-D-xylose, and methyl 2-*O*-(2,3,4-tri-*O*-methyl-α-D-glucopyranosyluronic acid)-3-*O*-methyl-D-xylopyranoside in a mole ratio of 0.2:95:1:11. It is concluded that the hemicellulose contained a linear framework of approximately 200 (1 → 4)-linked β-D-xylopyranose residues and that, on the average, every ninth xylose unit carried a (1 → 2)-linked 4-*O*-methyl-α-D-glucuronic acid residue directly attached to the xylan backbone. The polysaccharide is evidently similar to the 4-*O*-methylglucuronoxylans occurring in the wood of all arborescent angiosperms so far investigated.

The xylan present in trembling aspen was the first wood hemicellulose to be subjected to detailed structural investigations. Jones and Wise (1) on hydrolysis of aspen wood obtained several monosaccharides, xylobiose, xylotriose, D-galacturonic acid, 4-*O*-methyl-D-glucuronic acid, and 2-*O*-(4-*O*-methyl-α-D-glucopyranosyluronic acid)-D-xylopyranose, all of which were unequivocally identified. Milks and Purves (2) isolated from the same wood four fractions containing various amounts of hexuronic, 4-*O*-methylglucuronic and (1 → 4)-linked xylose residues. Partial hydrolysis yielded a crystalline aldotriuronic acid containing one 4-*O*-methylglucuronic acid and two xylose residues. The polysaccharide appeared to be extensively branched and was considered to possess non-reducing end groups of hexuronic acid rather than xylopyranose residues.

Jones, Merler, and Wise (3), on direct extraction of aspen wood with alkali, obtained a hemicellulose fraction in a yield of 19%. This material had a specific rotation of −75° and contained 1.7% methoxyl and 9.2% uronic anhydride groups. Hydrolysis yielded mostly xylose in addition to minor amounts of hexoses, arabinose, and rhamnose. On electrophoresis, the material was resolvable into two components, while on enzymic hydrolysis, 20% was enzyme-resistant. On the basis of results obtained by the methylation technique, the authors concluded that the xylose-containing hemicelluloses consisted of (1 → 4)-linked xylose residues to which were attached, through positions 2 and 3, end groups of L-arabinofuranose and side chains terminated by uronic acid residues. It was pointed out that the acid side chains might contain both glucose and xylose residues, since 2,3,6-tri-*O*-methyl-D-glucose and 3,4-di-*O*-methyl-D-xylose were obtained on hydrolysis of the methylated polysaccharide.

All other xylans so far isolated from the wood of arborescent angiosperms have been found to consist of a linear framework of (1 → 4)-linked β-D-xylose residues, approximately every tenth of which, on the average, carried a (1 → 2)-linked single, terminal side chain of a 4-*O*-methyl-α-D-glucuronic acid residue (4–6). While L-arabinofuranose residues are evidently integral parts of most softwood xylans (7, 8), no such residues have been detected in any hardwood xylan with the exception of that isolated from aspen wood.

[1]*Manuscript received December 5, 1960.*
Contribution from the Department of Chemistry, Queen's University, Kingston, Ontario, the Pulp and Paper Research Institute of Canada, and the Department of Chemistry, McGill University, Montreal, Quebec.

The rather exceptional characteristics of the aspen xylan prompted the present re-investigation of this hemicellulose. Another aim was to establish the degree of branching and the average length of the xylan backbone, properties which had not been dealt with in the earlier studies.

RESULTS

Aspen wood meal was delignified by alternate treatments with gaseous chlorine and alcoholic monoethanolamine (9), a procedure which, when applied to hardwoods, appears to cause no degradation of the polysaccharides (10). The resulting holocellulose was extracted with aqueous potassium hydroxide (11) to give a product in a yield of 21.4% of the wood. Besides xylose and uronic acids, this material also contained glucose, mannose, and arabinose residues. Complexing with copper lowered the yield to 15.0%, eliminating all hexose- and arabinose-containing polysaccharides. When the wood was directly extracted with aqueous potassium hydroxide, a product was obtained in a yield of 18.1% which gave only xylose and uronic acids on hydrolysis.

The yields and properties of the three products isolated are summarized in Table I.

TABLE I

Yields and characteristics of aspen hemicelluloses

Source	Yield, %*	$[\alpha]_D$†	Xylose per uronic acid calc. from:		
			Methoxyl	Uronic anh.	Equiv. wt.
Wood (A)	18.1	−81°	8.7	9.3	8.6
Holocellulose (B)	21.4	−75°	9.5	7.5	7.5
Copper complex (C)	15.0	−78°	9.5	8.2	7.1

*Based on extractive-free wood.
†In 10% aqueous sodium hydroxide.

It is evident that they differed little in specific rotation or chemical composition and that they contained on the average nine xylose units per *O*-methylglucuronic acid residue. The yields obtained are comparable to the *O*-methylglucuronoxylan content, 19%, calculated from the amount of xylose residues in the wood. The hexose and arabinose residues in the material obtained from the holocellulose were probably not integral parts of the glucuronoxylan since they could be eliminated by complexing with copper and did not appear when the wood was extracted without prior delignification.

The hemicellulose, on boundary electrophoresis, gave only one mobile peak which was very distinct, thus indicating the homogeneity of the material. On oxidation with periodate, the expected 9 moles of oxidant were consumed per repeating unit of the polysaccharide. Attempts to determine the weight-average molecular weight of the polymer by light scattering measurements (12) failed, the value obtained, 200,000, probably being a result of molecular association (13). Osmotic pressure measurements with the acetate derivative (14) gave a number-average degree of polymerization of 212.

A portion of the hemicellulose was partially hydrolyzed and the hydrolyzate was resolved on a column of anion exchange resin into a neutral and an acidic portion. The former crystallized and was identified as D-xylose. The sugar acids were separated on a charcoal–Celite column (15) by gradient elution. Two of the acids obtained were probably galacturonic acid, presumably derived from contaminating pectic material, and 4-*O*-methylglucuronic acid. A third acid had a methoxyl content and an equivalent weight

Can. J. Chem. Downloaded from www.nrcresearchpress.com by 210.87.254.40 on 09/05/12
For personal use only.

corresponding to that of an *O*-methylhexuronosyl pentose. This compound was identified through the crystalline tetraacetate of its methyl ester methyl glycoside (16) as 2-*O*-(4-*O*-methyl-α-D-glucopyranosyluronic acid)-D-xylopyranose, the same aldobiouronic acid as that first characterized by Jones and Wise (1).

Another portion of the hemicellulose was methylated to completion, first according to Haworth and subsequently by the procedure of Kuhn and co-workers (17). The fully methylated polysaccharide, $[\alpha]_D$ −67°, contained 108 xylose residues as estimated by osmotic pressure measurements, indicating that degradation had occurred during the methylation. The methylated hemicellulose was subjected to methanolysis under conditions known to effect no cleavage of aldobiouronic acids. The resulting mixture of glycosides was resolved into an acidic and a neutral portion on an anion exchange resin. The acid fraction, which contained only one component, was esterified and reduced with lithium aluminum hydride to yield a crystalline, partly methylated glycoside which was identified as methyl 2-*O*-(2,3,4-tri-*O*-methyl-α-D-glucopyranosyl)-3-*O*-methyl-α,β-D-xylopyranoside (18, 19).

The neutral portion was hydrolyzed to a mixture of reducing sugars which was resolved by gradient elution on a charcoal–Celite column. The three fractions obtained were 2-*O*-methyl-D-xylose, 2,3-di-*O*-methyl-D-xylose, and 2,3,4-tri-*O*-methyl-D-xylose. Paper electrophoresis of the di-*O*-methyl fraction indicated the absence of any 3,4-di-*O*-methyl-D-xylose. A minor portion of the mixture was resolved by paper chromatography and subjected to quantitative analysis (20), giving a molar ratio of 0.2:95:1 for the mono-, di-, and tri-*O*-methylxyloses.

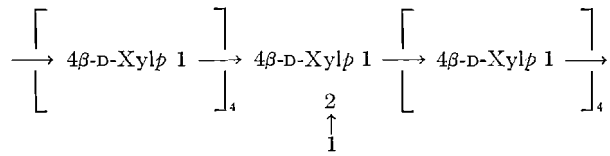
DISCUSSION

The large quantity of 2,3-di-*O*-methyl-D-xylose obtained, in conjunction with the high negative rotation of the original and the methylated hemicelluloses, showed that the xylose residues in the backbone of the macromolecule were linked together by β-(1 → 4)-glycosidic bonds. Methanolysis of the methylated xylan produced no monouronic acids and the partly methylated aldobiouronic acid was unsubstituted at C_4 in the xylose moiety. These facts, together with the absence of any 3,4-di-*O*-methylxylose in the neutral portion, showed that the xylose residues were attached *directly* to the (1 → 4)-linked xylan framework. The constitution of the aldobiouronic acid showed that the side chains were composed of (1 → 2)-linked 4-*O*-methyl-α-D-glucuronic acid residues.

The non-reducing end groups of the polysaccharide undoubtedly gave rise to the 2,3,4-tri-*O*-methyl-D-xylose. The results indicated that 107 xylose residues were present per non-reducing end group while the average macromolecule contained 108 such residues. Only one non-reducing end group was therefore present per average molecule and the xylan framework was accordingly linear. The very small quantity of mono-*O*-methylxylose isolated had probably been formed by demethylation during degradation of the methylated hemicellulose.

From the evidence adduced it is now possible to suggest a tentative structure for the 4-*O*-methylglucuronoxylan present in the wood of trembling aspen. This hemicellulose contains slightly more than 200 β-D-xylopyranose residues linked together by (1 → 4)-glycosidic bonds to a linear framework. Every ninth xylose residue, on the average, carries a single, terminal side chain of a 4-*O*-methyl-α-D-glucuronic acid residue attached to C_2. The acid groups are probably distributed at random along the macromolecules (14). In analogy with similar hemicelluloses present in two species of birch (21, 22), the aspen xylan probably contains *O*-acetyl groups in its native state.

Can. J. Chem. Downloaded from www.nrcresearchpress.com by 210.87.254.40 on 09/05/12
For personal use only.



4-*O*-Me-α-D-G*p*A

The xylan present in aspen wood is evidently very similar to the 4-*O*-methylglucuronoxylans previously isolated from the wood of various species of arborescent angiosperms, including American beech (*Fagus grandifolia*) (23), European beech (*F. sylvatica*) (24), Finnish birch (*Betula verrucosa*) (21, 25), white birch (*B. papyrifera*) (26), yellow birch (*B. lutea*) (27), white elm (*Ulmus americana*) (28), and sugar maple (*Acer saccharum*) (29, 30). It is also similar to the 4-*O*-methylglucuronoxylan occurring in the inner bark of white birch (31). The presence of fewer acid side chains and the absence of terminal L-arabinofuranose residues are the main characteristics in which these polysaccharides differ from the xylans present in the wood of most gymnosperms.

EXPERIMENTAL

All specific rotation are equilibrium values and were determined at 20° C. Melting points are corrected. Evaporations were carried out *in vacuo* at 40–50° C.

Paper Chromatography

Solvents (v/v) used for separating the sugars were (A) ethyl acetate – pyridine – water (8:2:1), (B) ethyl acetate – acetic acid – water (9:2:2), and (C) butanone–water (90:10). Separations were carried out on Whatman No. 1 filter paper. Paper electrophoresis was carried out on Whatman No. 3 MM filter paper in a 0.05 *M* borate buffer at 700 v for 4 hours. The spray reagent was *o*-aminodiphenyl. The same reagent was used for quantitative sugar analyses (32).

Composition of the Wood

Aspen wood (33), 40–60 mesh, was exhaustively extracted with ethanol–benzene (1:2). Analyses according to standard methods gave the following analytical data: cellulose (53.3%), pentosan (18.9%), lignin (16.3%), acetyl (3.4%), ash (0.2%), uronic anhydride (3.3%), residues of galactose (0.8%), glucose (57.3%), mannose (2.3%), arabinose (0.4%), and xylose (16.0%).

Isolation of Hemicelluloses

A. From wood.—Extractive-free wood meal (361 g) was treated with 24% (w/w) aqueous potassium hydroxide (2 liters) in an atmosphere of nitrogen at room temperature for 7 hours. The filtrate and washings were poured into four times their volume of ethanol containing an excess of acetic acid, cooled to 0° C. The precipitate formed was recovered by filtration and washed in succession with 70% ethanol, ethanol, and petroleum ether (b.p. 30–60° C). Drying *in vacuo* at room temperature gave a white powder (65.2 g, 18.1% of the wood), $[\alpha]_D$ −81° (*c*, 1.0 in aqueous 10% sodium hydroxide). Anal: OCH_3, 2.33%; uronic anhydride, 12.4%; equiv. wt., 1330. All analyses were carried out with the free acid form of the hemicellulose.

B. From chlorine holocellulose.—Wood meal (765 g) was subjected to three treatments with gaseous chlorine in ice water, followed by extraction with alcoholic monoethanolamine according to the procedure of Timell and Jahn (9). Yield: 692 g, 90.5% of the wood.

Can. J. Chem. Downloaded from www.nrcresearchpress.com by 210.87.254.40 on 09/05/12
For personal use only.

The holocellulose (688 g) was exhaustively extracted with 24% aqueous potassium hydroxide as described above to yield a white powder (163 g, 21.4% of the wood), $[\alpha]_D$ −75°. Anal: K salt: Potassium as potassium sulphate, 6.30%, corresponding to 8.7 xylose residues per acid group. Free acid: OCH_3, 2.10%; uronic anhydride, 15.0%; equiv. wt., 1170. Residues of glucose, 1.3%; mannose, 1.7%; arabinose, 1.2%; xylose, 82.4%; 4-*O*-methylglucuronic acid, 13.4%. Extraction of the solid residue with 17.5% aqueous sodium hydroxide to which 4% of boric acid had been added gave a crude glucomannan (20.6 g, 2.7% of the wood) containing 15% of *O*-methylglucuronoxylan, corresponding to 0.4% of the wood.

C. By copper complexing of xylan B.—A portion of xylan B (50 g) was dissolved in 5% aqueous sodium hydroxide (2 liters) and Fehling's solution (1300 ml) was added. The blue precipitate was washed with water until it started to swell, when it was decomposed with ice-cold 0.1 *N* hydrochloric acid in a Waring blendor. The aqueous mixture was poured into 15 liters of ethanol and the precipitate was washed five times on the centrifuge with 80% aqueous ethanol. The material, which was still green, was treated with aqueous ethylenediaminetetraacetic acid for removal of the last traces of copper salts. After neutralization with sodium bicarbonate, the solution (2 liters) was poured into ethanol (10 liters) to give a granular precipitate and a blue solution. The solids were recovered in the usual way and dried to give a white powder (35 g, 15.0% of the wood), $[\alpha]_D$ −78°. Anal: OCH_3, 2.10%; uronic anhydride, 13.9%; equiv. wt., 1130. Hydrolysis and subsequent examination by paper chromatography indicated the presence of uronic acid and xylose only.

Electrophoresis of the Hemicellulose

Free-boundary electrophoresis was carried out with a 2% solution of xylan A in an aqueous solution containing 7.5 g of boric acid and 4.0 g of sodium hydroxide per liter. The apparatus was a Spinco Model H instrument and photographs were taken at three stages of migration. Only one mobile peak was observed.

Determination of the Molecular Weight of the Hemicellulose

Attempts to determine the weight-average molecular weight of the polysaccharide by light scattering measurements with 0.2–1.0% solutions in dimethyl sulphoxide (12) failed. The value obtained, 200,000, was deemed to be the result of fortuitous molecular association.

A portion of the hemicellulose was converted to the fully substituted acetate derivative as described elsewhere (14) to give a product (4.0 g) containing 37.1% acetyl (34). Osmotic pressure measurements were carried out with a 9:1 mixture of chloroform and ethanol (v/v) at 30° C and with Stabin–Immergut (35) osmometers provided with gel cellophane membranes. The results obtained (Table II) gave a number-average molecular weight of 51,400, corresponding to 212 xylose residues in the xylan framework of the average molecule.

Periodate Oxidation of the Hemicellulose

Samples of hemicellulose (A, acid form, 150 mg) were shaken in the dark at 30° C for various lengths of time with 50 ml of 0.05 *M* sodium metaperiodate. The consumption of oxidant was determined by the excess arsenite method. The following moles of periodate were consumed per repeating unit (1378) of the polysaccharide during the first eight days: 1 (9.1), 3 (9.3), 4 (10.2), 6 (10.9), and 8 (11.3). Extrapolation to zero concentration gave a consumption of 9.0±0.1 moles of oxidant per repeating unit.

Can. J. Chem. Downloaded from www.nrcresearchpress.com by 210.87.254.40 on 09/05/12
For personal use only.

TABLE II
Osmometry data

Acetylated hemicellulose		Methylated hemicellulose	
w*	h/w†	w	h/w
2.435	0.502	2.575	1.390
2.029	0.513	2.063	1.364
1.644	0.527	1.675	1.301
1.401	0.518	1.386	1.324
1.125	0.470	1.170	1.329
0.853	0.527	0.759	1.300
0	0.50	0	1.27

*Concentration in g/kg solution.
†Osmotic height in cm solution.

Hydrolysis of the Hemicellulose

The hemicellulose (B, 80 g) was partially hydrolyzed as described earlier (16). After treatment with Amberlite IR-120 exchange resin (acid form), the solution (200 ml) was resolved into a neutral and an acid portion on a column with Dowex 1-X4 exchange resin (acetate form) (16). The neutral sugar fraction contained only D-xylose, m.p. and mixed m.p. 147.5–149° C, $[\alpha]_D$ +20.6° (c, 5.0 in water). The dibenzylidene dimethyl acetal derivative (36) had m.p. and mixed m.p. 211–212° C.

The acid fraction contained three sugar acids as indicated by paper chromatography (solvent B). A portion of the mixture (5 g) was added to the top of a Darco G-60 charcoal–Celite (15) column (1:1, 5.5×70 cm). Gradient elution was carried out with aqueous ethanol (37, 38) to give three fractions, corresponding in rate of movement on the paper chromatogram to galacturonic acid (900 mg), 4-*O*-methylglucuronic acid (500 mg), and an aldobiouronic acid (2.3 g). Anal. Calc. for $C_{12}H_{20}O_{11}$:OCH_3, 9.1%; equiv. wt., 340. Found: OCH_3, 9.5%; equiv. wt., 380; $[\alpha]_D$ +100° (c, 1.1 in water). The white solid had an infrared diagram identical with that of an authentic specimen of 2-*O*-(4-*O*-methyl-α-D-glucopyranosyluronic acid)-D-xylopyranose (7).

A portion of the aldobiouronic acid was converted to the methyl ester methyl glycoside of the tetraacetate derivative (16), as described earlier (27). Recrystallization from ethanol gave crystals, m.p. and mixed m.p. 199–200° C, $[\alpha]_D$ +100° (c, 1.3 in chloroform). Anal. Calc. for $C_{22}H_{32}O_{15}$: C, 49.2%; H, 6.02%; OCH_3, 17.3%. Found: C, 49.6%; H, 5.85%; OCH_3, 17.0%. The infrared spectrum of the compound was indistinguishable from that of an authentic sample of methyl 2-*O*-[methyl(2,3-di-*O*-acetyl-4-*O*-methyl-α-D-glucopyranosyl)uronate]-3,4-di-*O*-acetyl-D-xylopyranoside (16).

Methylation of the Hemicellulose

Hemicellulose (A, 24.0 g) was subjected to three methylations with dimethyl sulphate and sodium hydroxide as described earlier (27) to give a white powder (24.7 g). This product was further methylated according to Kuhn and co-workers (17) with methyl iodide, silver oxide, and dimethyl formamide in the presence of Drierite. The product was recovered in the usual way (17) to yield a white, fluffy material (21.5 g), $[\alpha]_D$ −67° (c, 2.0 in chloroform). Anal. Calc. for a product containing nine xylose and one 4-*O*-methylglucuronic acid residue: OCH_3, 39.2%. Found: OCH_3, 38.7%.

Methanolysis of the Methylated Hemicellulose and Identification of the Acidic Component

The methylated polysaccharide (15.0 g) was boiled under reflux with 0.8 N methanolic hydrogen chloride (650 ml) in the presence of some Drierite for 8 hours. The solution was

Can. J. Chem. Downloaded from www.nrcresearchpress.com by 210.87.254.40 on 09/05/12
For personal use only.

Can. J. Chem. Downloaded from www.nrcresearchpress.com by 210.87.254.40 on 09/05/12
For personal use only.

neutralized with silver carbonate, filtered through Celite, and evaporated to dryness to give a sirup (15.2 g) which was kept in aqueous barium hydroxide at 60° C for 2 hours. Barium hydroxide was removed by treatment with solid carbon dioxide followed by filtration through Celite. The aqueous solution was treated with Amberlite IR-120 exchange resin (acid form), filtered, and evaporated to a sirup (13.0 g). An aqueous solution of the latter was added to the top of a column with Dowex 1-X4 exchange resin (acid form) (8×20 cm). A mixture of neutral glycosides (10.1 g) was eluted with water (6 liters) after which an acid fraction (2.5 g) was recovered by elution with 30% aqueous acetic acid (4 liters).

The acid glycoside (2.5 g) was re-esterified by boiling with methanolic hydrogen chloride, dissolved in dry tetrahydrofuran (100 ml), and reduced with lithium aluminum hydride (3.0 g) (39). The product was recovered in the usual way to give a sirup (2.0 g) which crystallized spontaneously on evaporation from ethyl acetate. Two recrystallizations from ethyl acetate yielded pure crystals, m.p. and mixed m.p. 165–166° C, $[\alpha]_D$ +91° (*c*, 1.5 in water). Anal. Calc. for $C_{16}H_{30}O_{10}$: C, 50.3%; H, 7.92%; OCH_3, 40.6%. Found: C, 49.7%; H, 8.60%; OCH_3, 40.6%. The infrared spectrum of the compound was identical with that of an authentic specimen of methyl 2-*O*-(2,3,4-tri-*O*-methyl-α-D-glucopyranosyl)3-*O*-methyl-α,β-D-xylopyranoside (27).

Separation and Identification of the Neutral Sugars

The mixture of neutral glycosides eluted from the exchange resin was hydrolyzed with *N* sulphuric acid to give a pale yellow sirup (9 g). A portion of the mixture of reducing sugars (700 mg) was added to the top of a column (3.5×60 cm) containing a 1:1 mixture of Darco G-60 charcoal and Celite. The sugars were separated by gradient elution with 4 liters each of 5% aqueous ethanol → 20% ethanol and 20% ethanol → 40% ethanol. Three fractions were obtained in duplicate experiments in the order given below.

2-O-Methylxylose.—This fraction (2 mg) on electrophoresis had a rate of movement identical with that of 2-*O*-methylxylose.

*2,3-Di-O-methyl-*D*-xylose.*—The main fraction (500 mg) crystallized spontaneously. Two recrystallizations from ethyl acetate – petroleum ether gave crystals with m.p. 94–95° C (40), $[\alpha]_D$ −20° (2 minutes) → +22° (equilibrium, *c*, 2.0 in water). Anal. Calc. for $C_7H_{14}O_5$: OCH_3, 34.8%. Found: OCH_3,3 4.8%. The 2,3-di-*O*-methyl-*N*-phenyl-D-xylopyranosylamine had m.p. and mixed m.p. 124–125° C (41).

*2,3,4-Tri-O-methyl-*D*-xylose.*—This fraction (7 mg), $[\alpha]_D$ +20° C (*c*, 0.5 in water), could not be induced to crystallize. Its rate of movement on the paper chromatogram (solvent C) and its infrared spectrum were identical with those of an authentic sample of 2,3,4-tri-*O*-methyl-D-xylose.

Quantitative Analysis of the O-Methylxyloses

The mixture of neutral *O*-methylxyloses was resolved on filter papers with solvent C. The appropriate strips were excised and eluted with water. The concentration of the sugar solutions were determined by a recent modification of the phenol – sulphuric acid procedure of Smith and his co-workers (20, 42). The reagents used were 3% phenol in water (1 ml), concentrated sulphuric acid (5 ml), and sugar solution (1 ml). The following concentrations in mg/ml corresponded to one absorbance unit (10% transmittance): 2-*O*-methylxylose (118), 3-*O*-methylxylose (63), 2,3-di-*O*-methylxylose (139), and 2,3,4-tri-*O*-methylxylose (87). Paper blanks were analyzed for each compound and the absorbance obtained was deducted from that of the sugar. The average ratio between mono-, di-, and tri-*O*-methylxyloses from several analyses was 0.5:95:1.

ACKNOWLEDGMENTS

The authors wish to express their gratitude to Mr. E. Bleichert, who carried out a part of the experimental work. Financial assistance from the National Research Council of Canada is gratefully acknowledged.

REFERENCES

1. J. K. N. JONES and L. E. WISE. J. Chem. Soc. 2750, 3389 (1952).
2. J. E. MILKS and C. B. PURVES. J. Am. Chem. Soc. **78**, 3738 (1955).
3. J. K. N. JONES, E. MERLER, and L. E. WISE. Can. J. Chem. **35**, 634 (1957).
4. J. K. HAMILTON and N. S. THOMPSON. Pulp Paper Mag. Can. **59** (10), 233 (1958); Tappi, **42**, 752 (1959).
5. T. E. TIMELL, C. P. J. GLAUDEMANS, and A. L. CURRIE. Pulp Paper Mag. Can. **59** (10), 242 (1958); Tappi, **42**, 623 (1959).
6. G. O. ASPINALL. Advances in Carbohydrate Chem. **14**, 429 (1959).
7. A. JABBAR MIAN and T. E. TIMELL. Svensk Papperstidn. **63**, 884 (1960).
8. P. J. GAREGG and B. LINDBERG. Acta Chem. Scand. **14**, 871 (1960).
9. T. E. TIMELL and E. C. JAHN. Svensk Papperstidn. **54**, 831 (1951).
10. C. P. J. GLAUDEMANS and T. E. TIMELL. Svensk Papperstidn. **60**, 869 (1957).
11. J. K. HAMILTON and G. R. QUIMBY. Tappi, **40**, 781 (1957).
12. D. A. I. GORING and T. E. TIMELL. J. Phys. Chem. In press (1960).
13. H. SWENSON. Paper presented at the 3rd Cellulose Conference, Cellulose Research Institute, State University College of Forestry, Syracuse, N.Y., October, 1960.
14. C. P. J. GLAUDEMANS and T. E. TIMELL. Svensk Papperstidn. **61**, 1 (1958).
15. R. L. WHISTLER and D. F. DURSO. J. Am. Chem. Soc. **72**, 677 (1950).
16. T. E. TIMELL. Can. J. Chem. **37**, 827 (1959).
17. R. KUHN, H. TRISCHMANN, and I. LÖW. Angew. Chem. **67**, 32 (1955).
18. G. G. S. DUTTON and F. SMITH. J. Am. Chem. Soc. **78**, 2505, 3744 (1956).
19. R. MONTGOMERY and F. SMITH. J. Am. Chem. Soc. **79**, 695 (1957).
20. M. DUBOIS, K. GILLES, J. K. HAMILTON, P. A. REBERS, and F. SMITH. Nature, **168**, 167 (1951); Anal. Chem. **28**, 350 (1956).
21. H. O. BOUVENG, P. J. GAREGG, and B. LINDBERG. Acta Chem. Scand. **14**, 742 (1960).
22. T. E. TIMELL. J. Am. Chem. Soc. **82**, 5211 (1960).
23. G. A. ADAMS. Can. J. Chem. **35**, 556 (1957).
24. G. O. ASPINALL, E. L. HIRST, and R. S. MAHOMED. J. Chem. Soc. 1734 (1954).
25. J. SAARNIO, K. WATHEN, and CH. GUSTAFSSON. Acta Chem. Scand. **8**, 825 (1954).
26. C. P. J. GLAUDEMANS and T. E. TIMELL. J. Am. Chem. Soc. **80**, 941, 1209 (1958).
27. T. E. TIMELL. J. Am. Chem. Soc. **81**, 4989 (1959).
28. J. K. GILLHAM and T. E. TIMELL. Can. J. Chem. **36**, 410, 1467 (1958).
29. L. G. NEUBAUER and C. P. PURVES. Can. J. Chem. **35**, 388 (1957).
30. T. E. TIMELL. Can. J. Chem. **37**, 893 (1959).
31. A. JABBAR MIAN and T. E. TIMELL. Tappi, **43**, 775 (1960).
32. T. E. TIMELL, C. P. J. GLAUDEMANS, and A. L. CURRIE. Anal. Chem. **28**, 1916 (1956).
33. T. E. TIMELL. Tappi, **40**, 568 (1957).
34. L. B. GENUNG and R. C. MALLAT. Ind. Eng. Chem. Anal. Ed. **13**, 369 (1941).
35. J. V. STABIN and E. IMMERGUT. J. Polymer Sci. **14**, 209 (1954).
36. L. J. BREDDY and J. K. N. JONES. J. Chem. Soc. 581 (1939).
37. R. S. ALM. Acta Chem. Scand. **6**, 1186 (1952).
38. B. LINDBERG and B. WICKBERG. Acta Chem. Scand. **8**, 569 (1954)
39. F. SMITH. J. Chem. Soc. 2646 (1951).
40. J. K. HAMILTON, E. V. PARTLOW, and N. S. THOMPSON. Tappi, **41**, 811 (1958).
41. I. EHRENTHAL, M. C. RAFIQUE, and F. SMITH. J. Am. Chem. Soc. **74**, 1341 (1952).
42. T. E. TIMELL. Svensk Papperstidn. **63**, 668 (1960).

Can. J. Chem. Downloaded from www.nrcresearchpress.com by 210.87.254.40 on 09/05/12
For personal use only.

Can. J. Chem. Downloaded from www.nrcresearchpress.com by 210.87.254.40 on 09/05/12
For personal use only.

THE STRUCTURE AND RESISTANCE TO METHYLATION OF 1,2-β-GLUCANS FROM SPECIES OF AGROBACTERIA[1]

P. A. J. Gorin, J. F. T. Spencer, and D. W. S. Westlake

ABSTRACT

The structures of extracellular polysaccharides produced by the plant pathogens *Agrobacterium tumefaciens* (2 strains), *A. rhizogenes*, *A. radiobacter*, *A. rubi*, *A. gypsophilae*, and *A. pseudotsugae* were investigated. Polymeric material was formed in good yield from all organisms except *A. gypsophilae*. Periodate oxidations of the polysaccharides and their sodium borohydride reduction products indicated linear 1,2-glucopyranose structures for *A. tumefaciens* (2 strains), *A. rhizogenes*, *A. radiobacter*, and *A. rubi* polymers. Optical rotational considerations led to the assignment of β-configurations. The linear structure for the *A. radiobacter* polysaccharide was confirmed by the isolation, after partial acid hydrolysis, of five 1,2-linked oligosaccharides with chain lengths of two to six. Periodate and chromatographic data indicated that the polysaccharide from *A. pseudotsugae* contained glucose and galactose and 1,6- as well as 1,2-glycopyranose links. It is noteworthy that the polysaccharides from the genus *Agrobacterium* are shown to be mainly 1,2-β-glucans, a structure not yet found in other genera.

Treatment of linear 1,2-β-glucans from *A. tumefaciens*, *A. radiobacter*, and *A. rhizogenes* with sodium hydroxide – dimethyl sulphate, followed by silver oxide in methyl iodide – dimethyl formamide, did not cause full methylation. Some of the 3-hydroxyl groups were not substituted and possible reasons for this unreactivity are discussed.

Hassid and co-workers (1) have shown that *Agrobacterium tumefaciens* (*Phytomonas tumefaciens*) produces in artificial media a polysaccharide consisting mainly of 1,2-D-glucopyranose units joined with the β-configuration (2). It has now been found that several other species of phytopathogenic Agrobacteria form polysaccharides of a similar type. The organisms examined were strains of *Agrobacterium tumefaciens* (virulent and non-virulent), *A. rhizogenes*, *A. radiobacter*, *A. rubi*, *A. pseudotsugae*, and *A. gypsophilae*. The latter organism did not form appreciable amounts of polysaccharide. The yields of 2-linked glycans varied from 2 to 4 g per liter of crude material, depending on the run and the species of organism used.

A striking property of the glucan from *A. tumefaciens* was its resistance to complete methylation (1). Attempts in this laboratory to fully methylate the glucans from *A. tumefaciens* (virulent strain), *A. rhizogenes*, and *A. radiobacter* also did not succeed using, as the final step, the Kuhn procedure (3). In each case, after acid hydrolysis of the methylated product, no 2,3,4,6-tetra-*O*-methyl-D-glucose was isolated, the main product being 3,4,6-tri-*O*-methyl-D-glucose. The undermethylated component was 4,6-di-*O*-methyl-D-glucose, indicating, in the light of periodate data described later, unreactivity of the C_3 hydroxyl group. In the methylation of cellulose, starch, and xylan, the 3-hydroxyl groups are substituted less readily than the other positions, and Croon (4) has suggested that this lower activity is due to hydrogen bonding with the ring oxygen of the adjacent pyranose unit (attached by its reducing end). A molecular model (Courtauld) of 2-*O*-β-D-glucopyranosyl-D-glucopyranose, each unit having the C-1 conformation, shows that this type of bonding can take place in a 1,2-β-glucan. The infrared spectrum of the partly methylated 1,2-β-glucan from *A. radiobacter* contained a strongly hydrogen-bonded hydroxyl band with $\Delta\nu_s$ 195 cm^{-1}.* Since the magnitude of $\Delta\nu_s$ varies with the strength of the hydrogen

[1]*Manuscript received January 23, 1961.*
Contribution from the National Research Council of Canada, Prairie Regional Laboratory, Saskatoon, Saskatchewan.
Issued as N.R.C. No. 6261.
**Difference of frequency between hydrogen-bonded and non-bonded hydroxyl absorption bands.*

bond (5) it is noteworthy that methyl α,β-2,4,6-tri-*O*-methyl-D-glucopyranoside had $\Delta\nu_s$ 75 cm^{-1}, showing that the two possible hydrogen bonds between the C_3 hydroxyl group and the C_2 or C_4 methoxyl groups are weaker. However, this evidence does not rule out interaction between the C_3 hydroxyl in the polymer and the glycosidic oxygen at C_2, but a molecular model suggested that this oxygen atom cannot approach the hydroxyl group as closely as the ring oxygen when the pyranose ring is in the C-1 conformation.

The lower reactivity of the C_3 hydroxyl in a 2-linked glucose dimer can be found in work by Rabaté, who methylated kaempferol sophoroside (6) in a conventional way. Acid hydrolysis of the methyl ether yielded as an unidentified product crystals with m.p. 169° C and $[\alpha]_D$ +113° → 62°, constants corresponding to those of 4,6-di-*O*-methyl-D-glucose. However, when 17-L-hydroxyoctadecanoic acid- and 1,8-nonanediol-sophorosides were methylated under vigorous conditions, no undermethylation was noted (7). It is therefore apparent that the low reactivity of the C_3 hydroxyl in these disaccharide derivatives is merely one of degree. Although strongly hydrogen-bonded hydroxyl groups react more slowly than those less bonded, this property alone does not explain the total unreactivity to methylation of some of the C_3 hydroxyl groups in 1,2-β-glucans. Since there is no reason to believe that the strength of the hydrogen bonds should increase during the course of the methylation to a point of total unreactivity of the group, it is now suggested that the C_3 hydroxyl is increasingly hindered sterically by the rest of the molecule as the methylation proceeds until the group is blocked by the increased bulk of the surrounding methoxyl groups.

Sodium periodate oxidation of the 1,2-β-glucans and derivatives from *A. tumefaciens* (virulent and non-virulent), *A. rhizogenes*, *A. radiobacter*, *A. rubi*, and *A. pseudotsugae* provided more complete structural information than the methylation technique. Excepting the product from *A. pseudotsugae*, the polysaccharides each consumed approximately 1.0 molar equivalents of oxidant, and a little formic acid was produced. As would be expected, overoxidation took place over the observed time of 1–8 days excluding any accurate deductions. *A. pseudotsugae* polysaccharide, which contained galactose as well as glucose, consumed oxidant more gradually up to 0.99 mole after 6 days and gave a high initial production of 0.21 mole of formic acid. After oxidation the dialdehyde units in each of the products were reduced with sodium borohydride and the materials obtained were hydrolyzed with acid. Glycerol was the only detectable hydrolysis product, confirming the linear poly-1,2-D-glucopyranose structure for the polysaccharides from the two strains of *A. tumefaciens*, *A. rhizogenes*, *A. radiobacter*, and *A. rubi*. Since *A. pseudotsugae* polysaccharide gave formic acid on periodate oxidation, it must contain some 1,6-linkages also. The low consumption of oxidant compared with formic acid production therefore shows that the polysaccharide must be impure. All of the above-mentioned polysaccharides except the one from *A. pseudotsugae* have specific rotations near −10°, strongly suggesting β-linkages are present. The polysaccharides from *A. tumefaciens* (two strains), *A. rhizogenes*, *A. radiobacter*, and *A. rubi* were first reduced with sodium borohydride to the derived alcohols, which obviated overoxidation of the reduced end-units (8, 9). The observed consumption of periodate was then 1.0 mole per anhydroglucose unit and small yields of formic acid were produced. However, since no tetramethyl glucose was isolated from methylated polymers on hydrolysis the acid formed may not give a true indication of chain length and may only provide evidence to show that there are differences between the polysaccharides from different species.

The polysaccharide from *A. radiobacter* was examined further and evidence was found to show that the glucan contains at least five consecutive linear 1,2-links. Graded acid

Can. J. Chem. Downloaded from www.nrcresearchpress.com by 210.87.254.40 on 09/05/12
For personal use only.

hydrolysis of the polymer yielded a homologous series of oligosaccharides detected on paper chromatograms. Cellulose chromatography of the mixture gave six apparently pure components varying from glucose and sophorose (2-*O*-β-D-glucopyranosyl-D-glucose) to a hexasaccharide. Attempts to crystallize these components, their derived alcohols, or their acetates did not succeed except for sophorose and the trisaccharide identified as *O*-β-D-glucopyranosyl(1 → 2)-*O*-β-D-glucopyranosyl(1 → 2)-D-glucose. Periodate oxidation data on the amorphous alcohols obtained by sodium borohydride reduction of the tri-, tetra-, penta-, and hexa-saccharides, was consistent with linear 1,2-glucopyranosyl linkages only being present (Table I). Also, the oxidation products were reduced with sodium

TABLE I

Specific and molecular rotations and sodium periodate oxidation data of oligosaccharides from *A. radiobacter*

	Dimer	Trimer	Tetramer	Pentamer	Hexamer
Reducing oligosaccharides					
Specific rotations (*c*, 1.0, H_2O)	+15°	+11°	+10°	+7.5°	+5°
Molecular rotations	+5100°	+5500°	+6700°	+6300°	+5000°
Oligosaccharide alcohols					
Specific rotations (*c*, 1.0, H_2O)	−17.5°	−15°	−7.5°	+7.5°	+17.5°
Molecular rotations	−6000°	−5150°	−5000°	+6200°	+17,300°
Periodate consumed (moles/mole)	—	6.18 (6)*	7.01 (7)	8.12 (8)	9.25 (9)
Formic acid formed (moles/mole)	—	2.91 (3)*	3.08 (3)	3.00 (3)	3.21 (3)

*Figures in parentheses are the calculated values.

borohydride and hydrolyzed to yield glycerol only, thus confirming this observation. Although there is no evidence that there are α-linkages in the polysaccharide, the molecular rotations of the oligosaccharides (and derived alcohols) are not, as governed by the Freudenberg and Kuhn equation (10), proportional to their chain lengths (Table I), a situation which applies in other homologous series of oligosaccharides. Possibly this unusual behavior is related to the arrangement, which was such as to contribute to the over-all optical rotation of the molecule, of the sugar units in the chain.

Since *Agrobacterium* species are the only organisms that have yet been shown to produce 1,2-β-glucopyranose polysaccharides or to contain this linkage to some degree, this property provides further justification for placing these organisms in a particular genus. Other work, now at an early stage, on the polysaccharides produced by phytopathogenic organisms of the genera *Corynebacterium* and *Xanthomonas* indicates that in the main there are definite regularities in polysaccharide structure within the genera.

EXPERIMENTAL

Solutions were evaporated under reduced pressure using a bath temperature of 50° C and specific rotations were measured at 26° C. *A. tumefaciens*, strains IIBV7 and IIBNV6, were supplied by the Rockefeller Institute; *A. radiobacter*, strain 1000 by Dr. A. W. Hofer; *A. rhizogenes*, strain TR102, and *A. pseudotsugae*, strain TG102, by Dr. M. Starr; and *A. gypsophilae*, strain 13329, and *A. rubi*, strain 13335, by the American Type Culture Collection.

Isolation of Extracellular Polysaccharides of Agrobacteria

Stock cultures were maintained at 25° C on slants containing 1.5% glucose, 1% yeast extract, 0.2% calcium carbonate, and 1.3% agar. Shake cultures were grown in 500-ml

Can. J. Chem. Downloaded from www.nrcresearchpress.com by 210.87.254.40 on 09/05/12
For personal use only.

Erlenmeyer flasks containing 100 ml of the above medium, but without the agar (yeast extract was dialyzed to remove high molecular weight material). Flasks were incubated at 25° C on a rotary shaker having an eccentricity of 1/2 in., operated at 240 r.p.m. Larger volumes of culture were produced in stirred fermentors having volumes of 3 liters or 20 liters using the same medium and growing conditions as for the flask cultures. Cells were removed, after 5 days, by centrifugation in the Sharples supercentrifuge. In a 20-liter fermentation the solution was evaporated to 1 liter and ultracentrifuged to remove small amounts of gelatinous material. The supernatant liquid was added to 4 volumes of ethanol to precipitate the polysaccharide, which was then filtered off and washed with ethanol. The yields of crude polysaccharide varied from 2 to 4 g per liter of medium from *Agrobacterium tumefaciens* (virulent and non-virulent strains), *A. radiobacter*, *A. rhizogenes*, *A. rubi*, and *A. pseudotsugae*, which all proved to contain the 1,2-β-glucan structure. The yield from *A. gypsophilae* was less than 1 g per liter and gave galactose, glucose, and an aldobiuronic acid on acid hydrolysis.

The 1,2-β-glucan-containing polysaccharides were further purified for specific rotation and periodate oxidation measurements. Polysaccharides were dissolved in water, the solutions deionized with Amberlite IR-120 and Dowex-1 and then filtered and evaporated to a small volume. The polysaccharides were isolated by ethanol precipitation and in each case dissolved readily in water to yield non-viscous solutions. The only exception was the polysaccharide from *A. pseudotsugae*, which dissolved only with difficulty to form a somewhat viscous solution. This material was also different in having a higher specific rotation than the other polysaccharides (Table II). When polysaccharides from

TABLE II

Component sugars and specific rotations of Agrobacteria polysaccharides and periodate oxidation of the derived reduced polysaccharides

Source of polysaccharide	Component sugars	$[\alpha]_D$ in water	Time in hours: 18	42	66
			Periodate oxidation of reduced polysaccharide		
A. tumefaciens (virulent)	Glucose	−12° (*c*, 0.1)	1.01* (0.08)	1.01 —	— —
A. tumefaciens (non-virulent)	Glucose	−12° (*c*, 0.1)	0.98 (0.04)	0.98 —	— —
A. radiobacter	Glucose	−13° (*c*, 0.1)	0.99 (0.02)	0.99 —	— —
A. rhizogenes	Glucose	−19° (*c*, 0.1)	0.98 (0.08)	0.98 —	— —
A. rubi	Glucose	−8° (*c*, 0.1)	0.97 (0.12)	1.05 (0.13)	1.06 (0.14)
A. pseudotsugae	Glucose and galactose	+48° (*c*, 1.0)	— —	— —	— —

*These figures are molar periodate uptakes and those in parentheses the formic acid produced.

the other organisms were hydrolyzed with *N* sulphuric acid at 100° C overnight only glucose was detected on paper chromatograms and refluxing with 5% methanolic hydrogen chloride overnight yielded methyl α-D-glucopyranoside. The polysaccharide from *A. pseudotsugae* gave galactose as well as glucose on paper chromatograms after hydrolysis in *N* sulphuric acid at 100° C (spray: *p*-anisidine hydrochloride (11); solvent: ethyl acetate:pyridine:water, 10:4:3 v/v).

Can. J. Chem. Downloaded from www.nrcresearchpress.com by 210.87.254.40 on 09/05/12
For personal use only.

Can. J. Chem. Downloaded from www.nrcresearchpress.com by 210.87.254.40 on 09/05/12
For personal use only.

Sodium Periodate Oxidations of Polysaccharides

Twenty-five cubic centimeters of water containing 25 mg of polysaccharides was treated with 10 cc 0.1 *M* sodium periodate at 26° C. Uptake of oxidant was measured by addition to aliquots of buffered sodium arsenite containing potassium iodide followed by back-titration with iodine. Acid production was estimated by direct titration against sodium hydroxide. With each polysaccharide except that of *A. pseudotsugae* approximately 1.0 mole of periodate per mole of anhydroglucose unit was consumed within 21 hours reaction time; during the next 120 hours a further uptake of 0.1 mole was observed. Formic acid production increased from 0.10 mole/mole to 0.18 mole/mole when measured simultaneously. The *A. pseudotsugae* polysaccharide consumed 0.78 mole/mole of periodate releasing 0.21 mole/mole of formic acid after 21 hours, these values increasing gradually to 0.99 mole/mole and 0.36 mole/mole, respectively after a further 120 hours. After the oxidations were complete the solutions were deionized with Amberlite IR-120 and Dowex-1. The periodate-oxidized polysaccharides (10 mg) were reduced in the aqueous filtrate (20 cc) with sodium borohydride (10 mg) over a period of 3 hours. Excess reductant was destroyed with acetic acid, Amberlite IR-120 was added and, after shaking, the resin was filtered off and the filtrates evaporated to crusts. Boric acid was removed as trimethyl borate by repeated evaporations with methanol. The residues were hydrolyzed by heating in *N* sulphuric acid (5 cc) at 100° C for 3 hours. The acid was then neutralized with barium carbonate, the solutions filtered, and the filtrates evaporated. Paper chromatographic examination (solvent: butanol:ethanol:water, 40:11:19 v/v) of each hydrolyzate using the ammoniacal silver nitrate spray (12) showed that glycerol only was present. For the polysaccharides from *A. tumefaciens* (two strains), *A. rhizogenes*, *A. rubi*, and *A. radiobacter* 1,2-glucopyranose structures were indicated. However, the *A. pseudotsugae* polysaccharide gave a higher proportion of formic acid on periodate oxidation than the other polysaccharide, thus showing that some 1,6-linked glycopyranose units were present also.

Sodium Periodate Oxidations of Borohydride-Reduced Polysaccharides

Since the above described polysaccharides were overoxidized on treatment with aqueous sodium periodate, the reducing ends were modified with sodium borohydride in order to avoid the possibility of overoxidation starting from this site. Samples (1.00 g) of each polysaccharide were reduced with sodium borohydride (100 mg) in water (100 cc). After 6 hours the reaction mixture was worked up (in a similar manner to that described above for the reduction of the periodate-oxidized polysaccharides) to yield solids which were then oxidized with periodate. The same proportions of oxidant was used for the reduced polysaccharides, as in the oxidation of the unmodified polysaccharides. The results of this oxidation are recorded in Table II.

Methylation of Polysaccharides from A. tumefaciens (virulent), A. rhizogenes, and A. radiobacter

A portion of each polysaccharide (5.0 g) was dissolved in water (20 cc), dimethyl sulphate (3.3 cc) was added and the mixture was stirred vigorously. Sodium hydroxide (3.0 g) in water (10 cc) was introduced dropwise at such a rate as to keep the solution slightly alkaline over a period of 30 minutes. Then sodium hydroxide (30 g) in water (60 cc) was poured into the reaction mixture and methylation was effected using dimethyl sulphate which was added, in 11 separate aliquots of 3 cc each, once every 30 minutes. This process was repeated five times on successive days and then the solution was heated at 100° C for 3 hours. After it was cooled, the methylation mixture was neutralized with

Can. J. Chem. Downloaded from www.nrcresearchpress.com by 210.87.254.40 on 09/05/12
For personal use only.

dilute sulphuric acid, and then extracted by shaking four times with chloroform. The extract was dried ($MgSO_4$), filtered, and evaporated to a crust (—OCH_3, 35.8% for the *A. radiobacter* polysaccharide derivative).

The partially methylated polysaccharides (yields 3.9 g to 4.2 g) were dissolved in a dimethyl formamide (30 cc) – methyl iodide (30 cc) mixture and shaken vigorously with portions of silver oxide (100 g total), fresh additions of oxide being made when the suspension had become yellow-brown. After 5 days the solutions were filtered and evaporated to brittle crusts (—OCH_3 contents for *A. tumefaciens*, *A. rhizogenes*, and *A. radiobacter* derivatives, 38.7%, 39.8%, and 39.5% respectively). Remethylation of the partially methylated *A. radiobacter* polysaccharide over a further 9 days under identical conditions did not increase the methoxyl content appreciably. The yields of methylated polysaccharides at the end of the Kuhn procedure appeared to be quantitative.

Samples (2.5 g) of the three partially methylated polysaccharides were refluxed in 10% methanolic hydrogen chloride (25 cc) for 16 hours. The acid was neutralized with silver carbonate and the solutions filtered and evaporated. The sirupy products were hydrolyzed on a steam bath in *N* sulphuric acid (10 cc) for 16 hours and after cooling the solutions were neutralized with barium carbonate, filtered, and evaporated. Paper chromatographic examination with the *p*-anisidine hydrochloride spray showed that, with each hydrolyzate, the main product was trimethyl glucose with a relatively smaller quantity of dimethyl glucose. No tetramethyl glucose was detected. Portions of the hydrolyzates (250 mg) were fractionated on cellulose columns using benzene:ethanol:water (500:50:1 v/v) as the mobile phase, which gave a complete separation. The proportion of each sugar was estimated gravimetrically and the percentages present of the dimethyl hexoses (on a molar basis) in the mixtures from *A. tumefaciens*, *A. rhizogenes*, and *A. radiobacter* were 27%, 20%, and 21% respectively. The trimethyl glucoses were converted to 3,4,6-tri-*O*-methyl-D-gluconic acid phenylhydrazide by the method of Haworth and co-workers (13). This derivative from the polysaccharides of *A. tumefaciens* (virulent), *A. rhizogenes*, and *A. radiobacter* melted at 130–131° C, 130° C, and 129–130° C respectively, and the melting points were not depressed on mixing with an authentic specimen. Also, the X-ray diffraction patterns of these phenylhydrazides and known material were identical. The dimethyl components of the mixtures crystallized readily and were recrystallized from ethyl acetate. The constants obtained on the crystals were consistent with 4,6-di-*O*-methyl-D-glucose (14). Examination of the mother liquors showed that no other dimethyl glucose components were present. The product from *A. tumefaciens* (virulent) polysaccharide had m.p. 160–164° C and $[\alpha]_D$ +110° → +64° (*c*, 1.1, H_2O; 18 hours, constant value). Calculated for $C_6H_{10}O_4(OCH_3)_2$: —OCH_3, 29.8%. Found: —OCH_3, 29.3%. The 4,6-di-*O*-methyl-D-glucoses from *A. radiobacter* and *A. rhizogenes* polysaccharides melted at 161–164° C and 161–162° C respectively. The dimethyl glucoses from the three different sources did not have their melting points depressed on intermixture.

Infrared Spectrum of the Partially Methylated A. radiobacter Polysaccharide

The partially methylated polysaccharide was dissolved in dry chloroform as 0.04 *M* and 0.2 *M* solutions. At 27° C both of these solutions showed strong absorption at 3465 cm^{-1} and a weak band at 3660 cm^{-1}, thus giving a $\Delta\nu_s$ of 195 cm^{-1} between hydrogen-bonded and undissociated hydroxyl groups.

A sample of methyl α,β-2,4,6-tri-*O*-methyl-D-glucopyranoside had its infrared spectrum measured under similar conditions. In this case there was a strong band at 3605 cm^{-1} and a very weak one at 3680 cm^{-1} indicating a $\Delta\nu_s$ of 75 cm^{-1}.

Partial Hydrolysis of A. radiobacter Polysaccharide

The polysaccharide (8.75 g) was dissolved in *N* sulphuric acid (200 cc) and the hydrolysis mixture was kept at 70° C for 18 hours. The acid was neutralized ($BaCO_3$), the solution was filtered and evaporated to a syrup which was fractionated on a cellulose column. *n*-Butanol saturated with water eluted glucose (1.62 g); butanol:ethanol:water (4:1:1 v/v) gave a disaccharide (0.79 g) and a trisaccharide (0.37 g); butanol:ethanol:water (8:3:3 v/v) gave a tetrasaccharide (0.49 g); and butanol:ethanol:water (2:1:1 v/v) a pentasaccharide (0.27 g) and a hexasaccharide (0.13 g).

The disaccharide crystallized from methanol–ethanol to yield sophorose with m.p. and mixed m.p. 198–200° C and $[\alpha]_D$ +28° → +16° (*c*, 1.0, H_2O; 18 hours, constant value). The trisaccharide was twice crystallized from aqueous methanol to give *O*-β-D-glucopyranosyl-(1 → 2)-*O*-β-D-glucopyranosyl-(1 → 2)-D-glucose with m.p. 218–223° C and $[\alpha]_D$ +16° → +11° (*c*, 1.0, H_2O; 18 hours, constant value). Calculated for $C_{18}H_{32}O_{16}$: C, 42.9%; H, 6.4%. Found: C, 42.55%; H, 6.7%.

The tetra-, penta-, and hexa-saccharides and their acetates were amorphous as were the derived polyols (by sodium borohydride reduction) and their acetates. The specific and molecular rotations of the five reducing oligosaccharides and their derived alcohols are recorded in Table I. The polyols were oxidized in aqueous sodium periodate and the uptake of oxidant and formic acid production measured after 18 hours (Table I) using the proportions in the oxidation of the reducing polysaccharide described earlier in the paper. The values obtained correspond to the presence of 1,2-linked hexapyranose units only.

ACKNOWLEDGMENTS

The authors wish to thank Dr. M. Starr for cultures of *A. rhizogenes* and *A. pseudotsugae*. The technical assistance of Mr. N. R. Gardner and Mrs. S. F. Hector is appreciated, as were the services of Miss I. M. Gaffney and Mr. M. Mazurek, who determined infrared spectra and carbon, hydrogen, and methoxyl analyses respectively.

REFERENCES

1. E. W. PUTMAN, A. L. POTTER, R. HODGSON, and W. Z. HASSID. J. Am. Chem. Soc. **72**, 5024 (1950).
2. R. E. REEVES. J. Biol. Chem. **154**, 49 (1944).
3. R. KUHN, H. TRISCHMANN, and I. LOW. Angew. Chem. **67**, 32 (1955).
4. I. CROON. Svensk Papperstidn. **63**, 247 (1960).
5. R. F. BADGER. J. Chem. Phys. **8**, 288 (1940).
6. J. RABATÉ. Bull. soc. chim. France, **71** (5), 565 (1940).
7. P. A. J. GORIN, J. F. T. SPENCER, and A. P. TULLOCH. Can. J. Chem. In press.
8. A. N. O'NEILL. J. Am. Chem. Soc. **76**, 5074 (1954).
9. D. H. BALL and G. A. ADAMS. Can. J. Chem. **37**, 1012 (1959).
10. K. FREUDENBERG, W. KUHN, W. DURR, F. BOLZ, and G. STEINBRUNN. Ber. **63**, 1510 (1930).
11. L. HOUGH, J. K. N. JONES, and W. H. WADMAN. J. Chem. Soc. 1702 (1950).
12. S. M. PARTRIDGE. Nature, **158**, 270 (1946).
13. W. N. HAWORTH, E. L. HIRST, and L. PANIZZON. J. Chem. Soc. 154 (1934).
14. D. J. BELL and R. L. M. SYNGE. J. Chem. Soc. 1711 (1937).

Can. J. Chem. Downloaded from www.nrcresearchpress.com by 210.87.254.40 on 09/05/12
For personal use only.

Can. J. Chem. Downloaded from www.nrcresearchpress.com by 210.87.254.40 on 09/05/12
For personal use only.

A STUDY OF THE CN EMISSION FROM ACTIVE NITROGEN FLAMES[1]

KYLE D. BAYES[2]

ABSTRACT

When organic compounds are added to active nitrogen, the red and violet bands of the CN radical are emitted. The relative intensities of these red bands have been measured for a variety of added compounds, temperatures, and pressures. It is shown that there are at least three processes producing electronically excited CN radicals, two yielding CN($A^2\Pi$) and one yielding CN($B^2\Sigma$). The behavior of the flames indicates that a chain mechanism is involved. Adding ammonia, which does not react with nitrogen atoms, quenches the CN emission and inhibits the consumption of nitrogen atoms. It is concluded that a second reactive species in active nitrogen, possibly metastable $N_2(A^3\Sigma)$ molecules, initiates the reactions which result in light emission.

INTRODUCTION

When organic compounds are added to active nitrogen, a red or lilac flame appears which consists mostly of bands of the red ($A^2\Pi \rightarrow X^2\Sigma$) and violet ($B^2\Sigma \rightarrow X^2\Sigma$) systems of the CN radical (see Fig. 1). Winkler and co-workers have studied the products of the

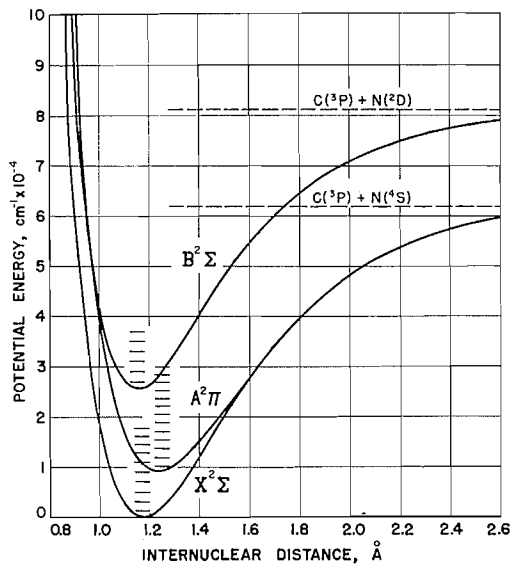


FIG. 1. The Morse potential energy curves for CN. The value 7.53 ev has been used for the dissociation energy of CN, the other constants are from G. Herzberg. Molecular spectra and molecular structure, I. Spectra of diatomic molecules. Van Nostrand, New York. 1950. The low-lying vibrational levels are indicated by the short horizontal lines within each curve.

reactions of active nitrogen with various compounds (1). They have proposed reaction mechanisms which could account for the observed products: however, they only speculate on the nature of the CN emission. Recently Kiess and Broida (2) have systematically studied the spectra of active nitrogen flames using various organic compounds. They concluded that there are at least two different reactions which produce electronically excited CN radicals. The present work was undertaken to learn more of these reactions which are responsible for the CN emission. In order to simplify the investigation as much as possible, only simple compounds have been used.

[1]*Manuscript received November 23, 1960.*
Contribution from Institut für physikalische Chemie der Universität Bonn, Bonn/Rh., Germany.
[2]*Present address: Department of Chemistry, University of California, Los Angeles 24, California, U.S.A.*

Can. J. Chem. Downloaded from www.nrcresearchpress.com by 210.87.254.40 on 09/05/12
For personal use only.

EXPERIMENTAL

The active nitrogen was formed in an electrodeless discharge (Deutsche Elektronik, 2500 Mc, 1000 w) operated at 0.6 to 30 mm Hg nitrogen pressure. A minimum of 0.5 second was required for the gas to flow from the discharge through 110 cm of Pyrex tubing (7-mm i.d.) to the reaction zone. The observation cell was a Pyrex tube of 30-mm inner diameter, 40 cm long, with a flat Pyrex window at the end where the active nitrogen stream entered. The organic compounds flowed through a capillary tube into the active nitrogen stream 3 cm before it entered the observation cell. A second capillary 40 cm upstream from the observation cell was used for adding ammonia and hydrogen in the quenching experiments. The pressure was measured by a small McLeod gauge at the exit of the observation cell. A cold trap prevented the products of the reaction from entering the rotary oil pump. All of the glass surfaces between the discharge and the cold trap were treated with a dilute solution of hydrofluoric acid in order to minimize atom recombination on the walls.

The observation cell and the entrance tubing were wrapped with Nichrome wire and asbestos so that spectra at elevated temperatures could be taken. A glass thermometer inside the cell measured the gas temperature. It was also possible to surround the cell with dry ice for low-temperature studies.

Commercially purified nitrogen (Nachgereinigter Stickstoff, Linde's Eismaschinen) was used without further purification. The CCl_4, $HCCl_3$, $HCBr_3$, and BrCN were chemically pure commercial products and were used without further purification. The HCN was produced by dropping concentrated sulphuric acid on NaCN and collecting the evolved gas in a dry-ice trap. The ClCN and $(CN)_2$ were prepared by standard procedures (3). The ClCN was redistilled twice, and only the most volatile half was retained, in order to separate it from the CCl_4 which was used in the preparation. Pressure drops across the flow capillaries were measured with mercury manometers. Gas flows were calculated using the Bernoulli equation for a compressible fluid. Standard viscosities were used when available (4). The viscosities of ClCN, BrCN, and HCN were assumed, for simplicity, to be equal to the viscosity of $(CN)_2$. The smaller capillaries were calibrated empirically by measuring the rate of pressure change in a known volume.

A small condensing lens focused the light from the observation cell onto the entrance slit of a Steinheil Universal Spectrograph which was equipped with $f/5$ glass optics and a plane grating (600 lines/mm). The reciprocal dispersion at the exit slit was 60 Å/mm. The spectrum was scanned by slowly turning the grating. Both entrance and exit slits were 0.5 mm wide, giving a resolution of about 30 Å. The use of glass optics should have resulted in some defocusing of the image as the grating was rotated; however, the effect was small and did not appreciably effect the resolution.

An infrared-sensitive photomultiplier tube (RCA 7102) was placed 4 cm behind the exit slit. A chopper between the cell and the condensing lens modulated the light at about 180 c.p.s. An ordinary 6-v bicycle generator was mounted on the same axis as the chopper to provide a reference signal of the same frequency and with a fixed phase difference compared to the light signal. The signal from the phototube and the reference signal were amplified and compared by a lock-in amplifier, the output going to a 5 mv Siemens strip chart recorder. The phototube was used at dry-ice temperature, and the other usual precautions were taken to minimize the noise level. A Jena OG 5"A" filter, which transmitted only wavelengths longer than 5300 Å, was used at the condensing lens to prevent the second-order blue spectrum from overlapping the red bands. For the very strong flames it was necessary to use neutral filters (Mikro-Siebblech) of 10

Can. J. Chem. Downloaded from www.nrcresearchpress.com by 210.87.254.40 on 09/05/12
For personal use only.

and 1.5% transmission in order to prevent overloading the amplifier. A pip marker was used to correlate the rotation of the grating with the strip chart record.

The spectral sensitivity of the system was measured by taking the spectrum of a calibrated Osram tungsten filament bulb, said to have a black-body temperature of 2300° K. A calcium sulphate reflector was used just before the observation cell window to simulate the intensity and position of the flames. Since the present study was more interested in changes in the relative intensities of the bands, the small corrections for the emissivity of tungsten or the reflectivity of calcium sulphate were not made. The system had a maximum sensitivity per quantum at about 7000 Å, which decayed to about 20% of maximum at 10,000 Å and 5% at 11,000 Å. Toward the end of this study the photocathode sensitivity beyond 10,000 Å decayed considerably, making the intensity of the $A(0)$–$X(0)$ band* much less certain.

The areas of the peaks on the strip chart were measured with a compensating planimeter. These areas were divided by the relative sensitivity determined in the calibration in order to obtain the relative band intensities. Since the sensitivity of the photomultiplier did not extend far enough into the infrared to measure all of the CN bands, and since for some of the conditions used in this study the overlapping nitrogen afterglow spectrum was of comparable intensity with the CN bands, only one band was used as a measure of the total emission from a given vibrational level of $A^2\Pi$. The bands used ($A(0)$–$X(0)$, $A(1)$–$X(0)$, $A(2)$–$X(1)$, $A(3)$–$X(1)$, $A(4)$–$X(2)$, $A(5)$–$X(1)$, $A(6)$–$X(2)$, $A(7)$–$X(3)$, $A(8)$–$X(3)$, $A(9)$–$X(3)$, $A(10)$–$X(4)$) were chosen to have a minimum of overlap by other bands. When necessary, corrections were made for overlapping by weak nitrogen afterglow bands. These corrections never amounted to more than 30% of the CN intensity, and were usually much less. Minor corrections were usually made on the spectra to account for slight changes in intensity or in the base line during a run. The emission curves were reproducible to within several per cent of the total emission.

The intensity of a measured band, $A(v')$–$X(v'')$, was converted to the total emission from the level $A(v')$ by using the previously measured intensities of the CN red system (5). The total emissions from the various levels $A^2\Pi(v')$ were then plotted against the vibrational quantum number v' to give an "emission" curve as is shown in Fig. 2. Such

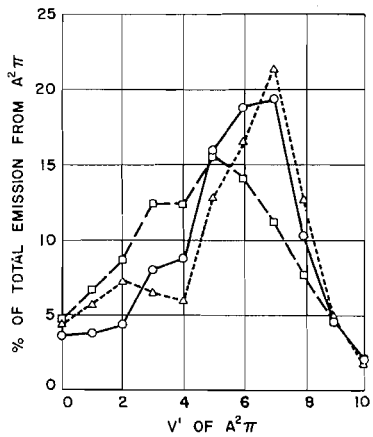


FIG. 2. Emission curves for the CCl_4 – active nitrogen flames. The percentage of the total emission from $A^2\Pi$ which originates in the level $A^2\Pi(v')$ is plotted against v'. Total pressure 3.0 mm Hg, CCl_4 flow 6×10^{-8} mole/sec. Temperature: □ 450° K; ○ 300° K; △ 200° K.

*This abbreviated notation will be used for the transition $A^2\Pi(v'=0) \rightarrow X^2\Sigma(v'=0)$.

a curve represents the relative number of quanta that are emitted from each vibrational level of $A^2\Pi$. If it can be assumed that the electronically excited molecules undergo no deactivating collisions, and that there is a steady-state concentration of excited CN molecules, then the emission curve would also represent the relative number of molecules which are being formed in the various vibrational levels of the $A^2\Pi$ state.

RESULTS

The spectrum of the CCl_4 – active nitrogen reaction was studied for a variety of conditions. For total pressures lower than about 5 mm Hg and CCl_4 flow rates lower than 10^{-7} mole/sec the spectral distribution of the CN red system did not change within the experimental error for changes in pressure (0.6 to 5 mm Hg) or CCl_4 flow.* There did appear to be a slight shift to higher vibrational levels with decreasing temperature as is shown in Fig. 2. At pressures greater than 5 mm and for higher flow rates of CCl_4 the distribution shown in Fig. 2 for 300° K (solid line) began to shift to lower vibrational quantum numbers in a manner which suggested that vibrational relaxation within the $A^2\Pi$ state was becoming important. Thus at 9.3 mm pressure (N_2 flow 2.6×10^{-5} mole/sec) and a CCl_4 flow of 2.4×10^{-8} mole/sec it was possible to obtain an emission distribution similar to that reported by Dixon and Nicholls (5) for similar conditions. Since vibrational relaxation masked the original distribution, further runs were limited to the lower pressures and flow rates.

The $HCCl_3$ flame at room temperature had an emission curve similar in shape to that of the CCl_4 flame, but with a less pronounced peak at $v' = 5$, 6, and 7. The emission curve for a $HCBr_3$ flame also had a peak centered on $v' = 6$ and 7, but it was significantly broader than the peak observed for the CCl_4 flame, especially toward higher vibrational levels. The stronger emission from the 10th vibrational level of $A^2\Pi$ for organic bromide flames has been noted previously (2).

In order to determine the effect of the reaction products on the spectral distribution of the CN emission, a study of the compounds XCN (X = H, Cl, Br, CN) was made. HCN is the main nitrogen-containing compound which is formed in active nitrogen–hydrocarbon reactions (1). The only detectable products of the CCl_4 flame were found to be ClCN and Cl_2 (6), so that it is expected that BrCN would be formed when organic bromides are used. Cyanogen is usually formed in small amounts in most of these reactions.

When HCN was added to active nitrogen, the CN emission was rather weak but the spectrum was very interesting and, therefore, was extensively studied. The distribution of the CN red emission for a HCN – active nitrogen mixture is shown in Fig. 3. A distribution almost identical with that shown in Fig. 3 was observed when ethylene at a flow rate of 1.9×10^{-8} mole/sec was added to active nitrogen at a pressure of 2.3 mm. In contrast to the CCl_4 flame, the relative intensities within the CN red system depended on both the flow rate of HCN and on the total pressure.

The curve of Fig. 3 can be divided up into two peaks. P_1 is arbitrarily defined as the emission from $A^2\Pi(v' = 0, 1, 2)$ and half of the emission from $v' = 3$, and P_2 is the remaining emission from $v' = 3$ and from the higher vibrational levels. It is believed that P_1 is not the result of vibrational relaxation of CN molecules originally formed in $A^2\Pi(5, 6, \text{and } 7)$. The pressure and flow of fuel are below the values mentioned above, at which vibrational relaxation is first apparent in the CCl_4 flame. Also the

**The spectra of reference 2 show a slight shift to lower v' in going from 1 mm to 4 mm Hg pressure. No reason for this disagreement is apparent.*

Can. J. Chem. Downloaded from www.nrcresearchpress.com by 210.87.254.40 on 09/05/12
For personal use only.

distribution in Fig. 3 is not what is theoretically expected for such a partially relaxed system (7).

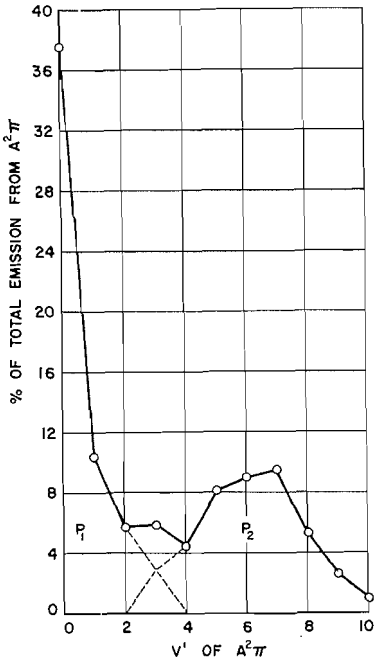


FIG. 3. Emission curve for a HCN – active nitrogen mixture. Pressure 3.3 mm Hg, temperature 300° K, HCN flow 8×10^{-8} mole/sec.

While holding the active nitrogen flow constant (total pressure 3 mm) and increasing the HCN flow, the ratio P_1/P_2 varied as is shown in Fig. 4. Adding HCN did not decrease the intensity of the nitrogen afterglow initially: however, there were gradual changes in intensity whenever hydrogen-containing compounds were added, probably because of changes in wall conditions. Therefore, it is necessary to compare the ratio of intensities within a given spectrum. The change of the inverse ratio, P_2/P_1, with nitrogen flow is shown in Fig. 5. It appears that in the limit of small HCN flow the ratio P_1/P_2 approaches

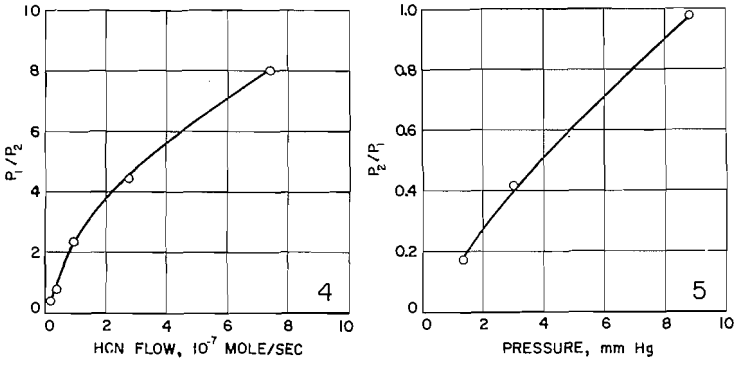


FIG. 4. The ratio P_1/P_2 for constant total pressure (3.0 mm Hg), constant temperature (300° K), and varying HCN flow.

FIG. 5. The ratio P_2/P_1 for constant HCN flow (9×10^{-8} mole/sec), constant temperature (300° K), and varying total pressure.

Can. J. Chem. Downloaded from www.nrcresearchpress.com by 210.87.254.40 on 09/05/12
For personal use only.

zero, while in the limit of low active nitrogen flow (or low pressure) the ratio P_2/P_1 approaches zero.

When cyanogen was added to active nitrogen the emission from the lowest vibrational levels of $A^2\Pi$ was comparable, both in intensity and spectral distribution to that observed with HCN. But the emission from the 5th, 6th, and 7th vibrational levels (P_2) was approximately 10 times weaker. In spite of this, the ratio of intensities $A(1)$–$X(0)/A(8)$–$X(3)$ showed the same shape curve as was found for P_1/P_2 with HCN (Fig. 4). Although small additions of cyanogen (10^{-8} mole/sec) did not reduce the normal afterglow intensity, larger flow rates quenched it almost completely, in agreement with previous work (8).

In contrast to the weak CN emission associated with HCN and $(CN)_2$, both ClCN and BrCN gave very bright flames, much brighter even than the CCl_4 flames. At 3 mm nitrogen pressure the reaction was so rapid that the flame was confined to the 7-mm tubing between the capillary and the observation cell. For this confined flame no afterglow could be observed downstream, and a brown deposit rapidly built up on the glass walls in contact with the flame. Thus it was necessary when studying these compounds to introduce the fuel capillary directly into the cell volume. When this was done, a roughly spherical flame formed, from 1 to 3 cm in diameter depending on the flow conditions. The distributions of CN emission from such ClCN and BrCN flames are shown in Fig. 6. Changing the ClCN or BrCN flow only changed the size of the flame, without

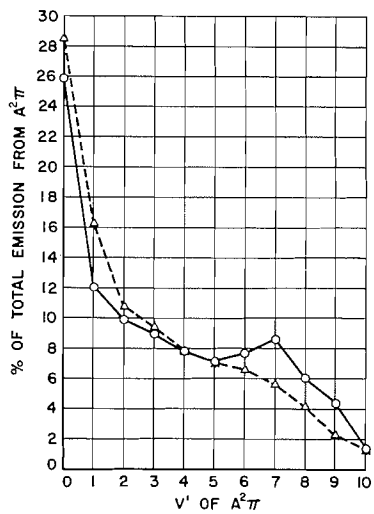


FIG. 6. Emission curves at 3.0 mm Hg pressure and 300° K, for ○ ClCN and △ BrCN flames.

changing the relative intensities of the emission. Runs at 1.3 mm nitrogen pressure, for which there was no bright flame but a diffuse emission throughout the cell volume, gave emission curves equal, within experimental error, to those shown in Fig. 6.

Since it is known that ammonia quenches certain of the first positive bands in the nitrogen afterglow faster than others (9), it was decided to test its quenching effect on the CN emission. With the nitrogen flow rate 1.4×10^{-5} mole/sec, the pressure in the cell was 3.0 mm and the Lewis–Rayleigh afterglow filled the entire system. Addition of 0.2% BrCN gave a bright flame and no afterglow could be observed downstream. Then 0.7% ammonia was added to the active nitrogen stream 40 cm (0.1 second) before it entered the observation cell. This weakened the CN emission by a factor of 62 and

Can. J. Chem. Downloaded from www.nrcresearchpress.com by 210.87.254.40 on 09/05/12
For personal use only.

the nitrogen afterglow could once again be observed downstream, although it was not quite as intense as for the pure nitrogen. Increasing the BrCN flow sevenfold increased the total CN emission by less than 10% although it did shift the distribution somewhat to low vibrational levels. Essentially complete quenching of the CN emission occurred for larger ammonia flows. When 0.2% BrCN was added to active nitrogen containing 2% ammonia, there was no change in the relative intensities of the nitrogen first positive bands (i.e., no overlapping CN emission) but the total intensity of the afterglow was reduced by about 20%. Similar quenching by ammonia was observed for the HCN and CCl_4 reactions.

When the filter was not used before the entrance slit, the CN blue system in the second order was superimposed on the red system. For the conditions of this study the emission from the lowest vibrational level of the $B^2\Sigma$ state was much stronger than the emission from higher vibrational levels. The photomultiplier tube was not calibrated in the blue region of the spectrum, but the intensity of the $B^2\Sigma(v' = 0) \rightarrow X^2\Sigma(v'' = 0)$ band, in arbitrary units, divided by the total emission in the red system is plotted in Fig. 7 against the total pressure for a constant flow of CCl_4.

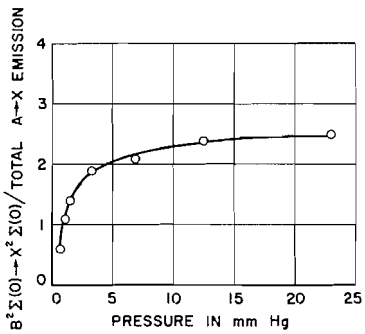


FIG. 7. The intensity of the $B^2\Sigma(0)$–$X^2\Sigma(0)$ band, in arbitrary units, divided by the total emission in the $A^2\Pi$–$X^2\Sigma$ system, plotted against the total pressure.

DISCUSSION

The variation of intensity of the $CN(B^2\Sigma(0) \rightarrow X^2\Sigma(0))$ band with total pressure (Fig. 7) was expected on the basis of the spectra previously reported by Kiess and Broida (2). They resolved the rotational structure of this band in a CH_2Cl_2 – active nitrogen flame, and showed that at low pressure (0.15 mm Hg) the blue emission originates almost entirely in those rotational levels of $B^2\Sigma(0)$ which are perturbed by rotational levels of $A^2\Pi(10)$. As the pressure was increased, the emission from the other, non-perturbed rotational levels of $B^2\Sigma(0)$ increased, until approximate rotational equilibrium was attained at 11 mm pressure. This behavior could be interpreted in the following way. The CN molecules are originally formed in the $A^2\Pi$ electronic state, some with 10 quanta of vibration. Because of the mixing of eigenfunctions (10) of the perturbed rotational levels of $A^2\Pi(10)$ and $B^2\Sigma(0)$, transitions between these two states can take place easily for certain J's. If the pressure is high enough, collisions can redistribute the $B^2\Sigma$ molecules among the other nonperturbed rotational levels before the allowed emission of radiation occurs. If one assumes a rapid equilibrium of molecules between the perturbed rotational levels of $A^2\Pi(10)$ and $B^2\Sigma(0)$, then the total emission from $B^2\Sigma(0)$ will depend on the rate of approach to equilibrium between the perturbed and unperturbed rotational levels of $B^2\Sigma(0)$, and thus on the total pressure. This mechanism

Can. J. Chem. Downloaded from www.nrcresearchpress.com by 210.87.254.40 on 09/05/12
For personal use only.

cannot explain the "tail bands" of CN, originating from high vibrational levels of $B^2\Sigma$, which sometimes appear in active nitrogen flames (11).

It is now generally accepted that active nitrogen contains nitrogen atoms in their ground state (12, 13). However, there is strong evidence that at least one other reactive species is present. Kaufman and Kelso (14) reported a temperature increase when N_2O, which is known not to react with nitrogen atoms (15), is introduced into active nitrogen. Freeman and Winkler (16) found that ammonia was decomposed by active nitrogen, and their experiments indicated that atomic nitrogen was not responsible. Kistiakowsky and Volpi (17) showed that the atomic nitrogen concentration was not reduced by additions of up to 7% ammonia. Since it was observed in this study that the intense CN emission could be completely quenched by the addition of 2% ammonia, it seems apparent that the second reactive species is important in at least initiating the reaction which leads to the CN emission.

Any of the electronic states of molecular nitrogen which participate in the afterglow mechanism might be the second reactive species. These include the proposed $^5\Sigma$, the $B^3\Pi$, and the $Y^3\Sigma$, which are the upper states of the afterglow emission, and the $A^3\Sigma$, which is the lower electronic state of the emitting molecules (9). Vibrationally excited ground state molecules should also be present since they will be formed by direct recombination of nitrogen atoms and by deactivation of $A^3\Sigma$ molecules. However, the observation that ammonia quenches the CN emission eliminates the possibility that the $^5\Sigma$, $B^3\Pi$, and $Y^3\Sigma$ states are the initiators of the CN emission. The small concentration of ammonia which was used quenches the nitrogen afterglow only slightly. This requires that the concentration of all the electronic states of nitrogen which precede the afterglow emission remain approximately constant. Since the CN emission is reduced drastically by the addition of ammonia, the concentration of the reactive species initiating the CN emission must also be changed significantly.

It has been suggested that ground state nitrogen molecules in high vibrational levels are responsible for the decomposition of ammonia by active nitrogen (18). If this is so, the ammonia molecules must absorb a large amount of the excess vibrational energy (since the ammonia is decomposed) and in this way prevent the reactions which result in the CN emission. To test this possibility, methane was substituted for ammonia in the quenching experiment previously described. Methane was chosen because it does not react significantly with active nitrogen at room temperature (19), and because its efficiency of transferring vibrational energy from N_2O is comparable to that of ammonia (20). The CN emission was reduced by a factor of two when 0.7% methane was added to a BrCN – active nitrogen flame, as compared with a factor of 62 for 0.7% ammonia. If vibrationally excited ground state nitrogen molecules are the second reactive species in active nitrogen, it is difficult to understand this large difference in the quenching effect of ammonia and methane. But because of the complexity of such an energy transfer, this experiment cannot be considered conclusive evidence against the vibrationally excited ground state hypothesis.

Nitrogen molecules in the lowest triplet state, the metastable $A^3\Sigma$, could also be the second reactive species in active nitrogen. Such molecules are certainly being formed in active nitrogen since this is the lower electronic state of the afterglow emission. Also it has been estimated that only 1 out of 20 recombining pairs of nitrogen atoms emits a quantum in the afterglow (21), the other pairs must recombine directly into the $X^1\Sigma$ and $A^3\Sigma$ states. On a statistical basis it is expected that three fourths of these recombining pairs will form $A^3\Sigma$ molecules. Thus approximately 16 molecules are formed in the $A^3\Sigma$ state for every quantum emitted in the Lewis–Rayleigh afterglow.

Can. J. Chem. Downloaded from www.nrcresearchpress.com by 210.87.254.40 on 09/05/12
For personal use only.

Can. J. Chem. Downloaded from www.nrcresearchpress.com by 210.87.254.40 on 09/05/12
For personal use only.

Several unsuccessful attempts have been made to observe $A^3\Sigma$ state molecules in active nitrogen. Exposures of 60 hours (22) failed to detect emission of the Vegard–Kaplan bands, $A^3\Sigma \rightarrow X^1\Sigma$, or the Lyman–Birge–Hopfield bands, $a^1\Pi \rightarrow X^1\Sigma$, from active nitrogen. But the latter have since been observed with much shorter exposures (13). Worley could find no absorption from the $A^3\Sigma$ state using a 13-m path length in active nitrogen (23), from which he concluded that the concentration of $A^3\Sigma$ was smaller than 10^{10} molecules/cm^3. However, mercury vapor was present in his experiments which might have reduced the concentration of triplet molecules by collisional deactivation.

It can be argued that if $A^3\Sigma$ molecules are the second reactive species, then Freeman and Winkler's estimate (16) that the second species is about one-sixth as abundant as nitrogen atoms is incompatible with the failures to observe the $A^3\Sigma$ state in emission or absorption. However, for the apparatus used in reference 16 the elapsed time between the discharge and the reaction cell was comparable with the radiative lifetime of the $A^3\Sigma$ state (0.026 second or longer (24)), so that metastable molecules formed in the discharge might be responsible for the high concentration of the second reactive species. This interpretation is consistent with their observation that increasing the voltage on the discharge increased the relative amount of the second reactive species (18).

The $N_2(A^3\Sigma)$ molecule could transfer its electronic energy to XCN, exciting it to a repulsive triplet state (I) which would then dissociate to CN and X radicals (II).

$$N_2(A^3\Sigma) + XCN \rightarrow N_2(X^1\Sigma) + XCN^* \quad (I)$$

$$XCN^* \rightarrow X + CN \quad (II)$$

It is known that such transfers in which the total spin is conserved can occur readily (25). The energy available from the triplet state of nitrogen, assuming a transition from $A^3\Sigma(0)$ to $X^1\Sigma(0)$, is 142 kcal/mole. The bond energy of X—CN has been calculated using the recently favored value for D(CN—CN) of 146 kcal (26) and accepted thermodynamic data (27, 28), and is presented in the second column of Table I. The energy necessary to break the X—CN bond and excite the CN radical to the $A^2\Pi(0)$ level (an additional 26 kcal) is shown in the last column in Table I. It is seen that the 142 kcal provided

TABLE I

The bond energies of X—CN (second column); the energies necessary to break the X—CN bond and excite the CN radical to the $A^2\Pi(v' = 0)$ level (third column)

Compound	Bond energy D in kcal	D + 26 kcal
$(CN)_2$	146	172
HCN	130	156
ClCN	107	133
BrCN	94	120

by the transition $A^3\Sigma(0)$–$X^1\Sigma(0)$ is sufficient to break the X—CN bonds, with the possible exception of $(CN)_2$. However, to break the X—CN bond and excite the CN radical to the $A^2\Pi$ state requires more than 142 kcal for HCN and $(CN)_2$. This might explain the weak CN emission associated with these compounds as compared to the more weakly bonded halogen cyanides. If the $A^3\Sigma$ molecules are vibrationally excited when they react, there would be correspondingly more energy available to excite the CN radical.

The decomposition of more complex molecules (at least those whose flames are quenched by ammonia) might occur by a similar mechanism. A transfer of electronic energy from

$N_2(A^3\Sigma)$ to the complex molecule, similar to step (I), could cause an initial bond rupture. Any polyatomic radicals formed should react rapidly with atomic nitrogen, yielding CN compounds or the CN radical directly.

The behavior of the flames observed in this work seemed to indicate that a chain reaction is involved. Sometimes, when adding very small amounts of fuel to the active nitrogen stream, an oscillating flame front would form. This was especially noticeable for the CCl_4 reaction at 80° C. This flame front, which gave the usual bright CN emission, would sometimes pulsate at about 5 c.p.s. with an amplitude of 1 cm. But it could be made to slowly sweep the entire length of the observation cell in an upstream direction once every several seconds, the flame completely disappearing at the window end of the cell before reforming again downstream. In between the passage of the flame the normal afterglow filled the tube, but the passing of the flame weakened it considerably. The effect was very sensitive to changes in fuel flow and total pressure, and was not entirely reproducible from day to day, possibly because of wall conditions. Such a lower concentration limit to a fast reaction is typical of a chain mechanism (29).

The complete consumption of nitrogen atoms in the BrCN and ClCN flames also suggests a chain mechanism. The second reactive species is, at most, one-sixth the concentration of nitrogen atoms (16), and is probably much less in these experiments because of the long flow time between the discharge and the reaction cell. But the removal of the second reactive species by ammonia prevents, essentially completely, the consumption of nitrogen atoms. Such behavior could be explained if the second reactive species initiates a chain reaction which consumes nitrogen atoms.

It was suspected, from the behavior of the CN emission in the HCN – active nitrogen mixtures, that the P_2 peak in Fig. 3 was associated with a reaction of free CN radicals. This possibility was tested by further experiments. It is known that CN radicals will react with molecular hydrogen (30). Therefore, the addition of hydrogen to a HCN – active nitrogen mixture should reduce the CN concentration, and thus the height of the P_2 peak, if the above suspicion is correct. With a total pressure of 3.0 mm and a flow rate of HCN of 2.5×10^{-8} mole/sec, the ratio P_2/P_1 was 1.1. Addition of 1.2×10^{-5} mole/sec of hydrogen between the discharge and the cell increased the total pressure to 3.3 mm and decreased the ratio P_2/P_1 to 0.2, as predicted above. The results of a similar experiment using ClCN instead of HCN are shown in Fig. 8. The response of the photomultiplier at 11,000 Å had decayed considerably by the time this experiment was done, so the intensity of the $A^2\Pi(0)$–$X^2\Sigma(0)$ band was rather uncertain. The two

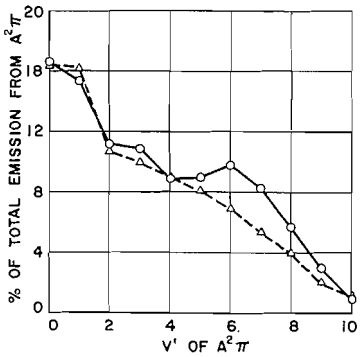


FIG. 8. Emission curves at 300° K. ○ Pressure 3.1 mm Hg, flow ClCN 7×10^{-8} mole/sec. △ Pressure 3.7 mm Hg, flow ClCN 7×10^{-8} mole/sec, flow hydrogen 2.4×10^{-5} mole/sec.

Can. J. Chem. Downloaded from www.nrcresearchpress.com by 210.87.254.40 on 09/05/12
For personal use only.

emission curves have been normalized so that the total emission from the lowest three vibrational levels of $A^2\Pi$ is equal. It is seen that the emission from the 5th through 8th vibrational levels is reduced by the addition of hydrogen, and the difference between the two curves has the same shape, within experimental error, as the P_2 peak for the HCN spectrum. It thus appears that the population curve for the ClCN flame shown in Fig. 6 could also be interpreted as consisting of a P_1 and a P_2 peak. But the P_1 peak for ClCN extends to higher vibrational levels than the P_1 peak for HCN.

One possible behavior of the free CN radical would be to catalyze the recombination of nitrogen atoms, as is shown in steps (III) and (IV).

$$N + CN \rightarrow CN_2 \qquad \text{(III)}$$

$$CN_2 + N \rightarrow CN + N_2 \qquad \text{(IV)}$$

The CN_2 radical should be stabilized by several resonance structures. If at least some of the nitrogen molecules formed in step (IV) were in the $A^3\Sigma$ state, this catalytic recombination could explain the chain characteristics of these flames since the $N_2(A^3\Sigma)$ molecule could initiate further reactions (step (I)). Two nitrogen atoms recombining into the lowest vibrational level of the $A^3\Sigma$ state provide 83 kcal, which could be used to excite the CN radical. Since the CN_2 radical would probably have a significant binding energy, and since it is possible to form $N_2(A^3\Sigma)$ molecules in vibrational levels other than the lowest, it is expected that any $CN(A^2\Pi)$ formed during such a cycle would have less than the full 83 kcal. The average amount of excitation energy of the CN molecules which are responsible for the P_2 emission peak is 56 kcal.

Since the emission curve for the CCl_4 flame (Fig. 2, solid line) is very similar to the P_2 peak in the HCN reaction (Fig. 3), it was thought that the same mechanism was responsible for both emissions. However, the addition of 1.2×10^{-5} mole/sec of hydrogen to a CCl_4 flame (CCl_4 flow 1.0×10^{-8}) did not strongly quench the CN emission. The emission from the 6th, 7th, and 8th vibrational levels of $A^2\Pi$ appeared to be reduced slightly, compared to the rest of the spectrum, but the effect was comparable with the experimental error. Thus it appears that the CN emission in the CCl_4 flame and the P_2 emission in the HCN reaction occur by different mechanisms, in spite of the similar spectral distributions.

The conclusions of this study can be summarized. (1) The second reactive species in active nitrogen, which is responsible for decomposing ammonia, initiates the reactions which cause the CN emission. (2) Chain reactions are involved in the CN emission. (3) There are at least three reactions producing electronically excited CN radicals, one yielding $B^2\Sigma$ state molecules and two yielding $A^2\Pi$ state molecules. (4) The CN emission from CCl_4, $HCCl_3$, and $HCBr_3$ flames cannot be accounted for by a reaction between active nitrogen and the products of the primary reactions.

The helpful discussions and criticism of Professor E. F. Greene and Professor W. Groth are gratefully acknowledged. Thanks are expressed to Dr. H. P. Broida and Dr. H. T. Knight for permission to see their data before publication. I wish to thank the National Science Foundation for the postdoctoral fellowship which made this work possible, and the personnel of the Institute für physikalische Chemie der Universität Bonn for their hospitality.

REFERENCES

1. H. G. V. Evans, G. R. Freeman, and C. A. Winkler. Can. J. Chem. **34**, 1271 (1956).
2. N. H. Kiess and H. P. Broida. Seventh symposium on combustion. Butterworth Publications, London. 1959. p. 207.

Can. J. Chem. Downloaded from www.nrcresearchpress.com by 210.87.254.40 on 09/05/12
For personal use only.

3. G. H. COLEMAN, R. W. LEEPER, and C. G. SCHULZE. Inorganic syntheses. Vol. II. McGraw-Hill, New York. 1946. p. 90. G. J. JANZ. Inorganic syntheses. Vol. V. McGraw-Hill, New York. 1957. p. 43.
4. HANDBOOK OF CHEMISTRY AND PHYSICS. Vol. 39. Chemical Rubber, Cleveland. 1957. p. 2043.
5. R. N. DIXON and R. W. NICHOLLS. Can. J. Phys. **36**, 127 (1958).
6. S. E. SOBERING and C. A. WINKLER. Can. J. Chem. **36**, 1223 (1958).
7. R. J. RUBIN and K. E. SHULER. J. Chem. Phys. **25**, 59 (1956).
8. C. HAGGART and C. A. WINKLER. Can. J. Chem. **38**, 329 (1960).
9. K. D. BAYES and G. B. KISTIAKOWSKY. J. Chem. Phys. **32**, 992 (1960).
10. A. T. WAGER. Phys. Rev. **64**, 18 (1943).
11. F. A. JENKINS. Phys. Rev. **31**, 539 (1928).
12. D. S. JACKSON and H. I. SCHIFF. J. Chem. Phys. **23**, 2333 (1955); J. BERKOWITZ, W. A. CHUPKA, and G. B. KISTIAKOWSKY. J. Chem. Phys. **25**, 457 (1956).
13. Y. TANAKA, A. JURSA, and F. LEBLANC. *In* M. Zelikoff. Threshold of space. Pergamon Press, New York. 1957. p. 89.
14. F. KAUFMAN and J. R. KELSO. J. Chem. Phys. **28**, 510 (1958).
15. G. B. KISTIAKOWSKY and G. G. VOLPI. J. Chem. Phys. **27**, 1141 (1957).
16. G. R. FREEMAN and C. A. WINKLER. J. Phys. Chem. **59**, 371 (1955).
17. G. B. KISTIAKOWSKY and G. G. VOLPI. J. Chem. Phys. **28**, 665 (1958).
18. H. G. V. EVANS and C. A. WINKLER. Can. J. Chem. **34**, 1217 (1956).
19. P. A. GARTAGANIS and C. A. WINKLER. Can. J. Chem. **34**, 1457 (1956).
20. A. EUCKEN and H. JAACKS. Z. physik. Chem. B, **30**, 85 (1935).
21. T. WENTINK, J. O. SULLIVAN, and K. L. WRAY. J. Chem. Phys. **29**, 231 (1958).
22. H. P. KNAUSS. Phys. Rev. **32**, 417 (1928).
23. R. E. WORLEY. Phys. Rev. **73**, 531 (1948).
24. P. G. WILKINSON and R. S. MULLIKEN. J. Chem. Phys. **31**, 674 (1959); N. P. CARLETON and O. OLDENBERG. Report to geophysics research directorate, Air Force Cambridge Research Center, Contract 19(604)-4984.
25. A. TERENIN and V. ERMOLAEV. Trans. Faraday Soc. **52**, 1042 (1956).
26. H. T. KNIGHT. To be published.
27. NATL. BUR. STANDARDS. Circ. No. 500. 1952. Selected values of chemical thermodynamic properties; L. BREWER and A. W. SEARCY. Ann. Rev. Phys. Chem. **7**, 259 (1956).
28. G. LORD and A. A. WOOLF. J. Chem. Soc. 2546 (1954).
29. B. LEWIS and G. VON ELBE. Combustion, flames and explosions of gases. Academic Press, New York. 1951. p. 27.
30. C. HAGGART and C. A. WINKLER. Can. J. Chem. **37**, 1791 (1959).

Can. J. Chem. Downloaded from www.nrcresearchpress.com by 210.87.254.40 on 09/05/12
For personal use only.

Can. J. Chem. Downloaded from www.nrcresearchpress.com by 210.87.254.6 on 09/05/12
For personal use only.

SOME NEW COMPONENTS OF ROYAL JELLY[1]

WILLIAM H. BROWN,[2] ETHEL E. FELAUER, AND ROBERT J. FREURE[3]

ABSTRACT

Two additional acids, 10-hydroxydecanoic and *p*-hydroxybenzoic, have been isolated from the ether-soluble fraction of royal jelly. A sterol, 24-methylenecholesterol, has been found in the ether-insoluble, methanol-soluble fraction of royal jelly.

Until recently, the only acid known to be present in royal jelly was 10-hydroxy-2-decenoic acid (I) isolated by Townsend and Lucas (1), and characterized by Butenandt and Rembold (2). In 1959 Brown and Freure (3) reported the isolation and identification of two additional acids, sebacic (II) and 2-decendioic (III).

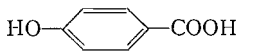
By further investigation of the ether-soluble fraction of royal jelly we have isolated and identified two more acids, 10-hydroxydecanoic (IV) and *p*-hydroxybenzoic (V).

$HOCH_2-(CH_2)_6-CH=CH-COOH$ I

$HOOC-(CH_2)_6-CH_2-CH_2-COOH$ II

$HOOC-(CH_2)_6-CH=CH-COOH$ III

$HOCH_2-(CH_2)_6-CH_2-CH_2-COOH$ IV

 V

When the mixture of ether-soluble acids from royal jelly, after removal of the neutral compounds and phenols as previously described (3), is allowed to stand at room temperature for a week a layer of water forms in the bottom of the container and the oil gives a positive ester test. From the oil a neutral compound (probably a mixture of lactones) can be separated which on saponification gives 10-hydroxydecanoic acid (IV). Lactone formation is undoubtedly due to the catalytic effect of residual sulphuric acid which is present in the mixture of acids, A (3). Lactones of IV have been prepared and described by Stoll and Rouvé (4). Authentic 10-hydroxydecanoic acid was prepared from castor oil by a modification of a patented procedure (5). No previous report of the finding of IV as a naturally occurring acid could be found although higher hydroxy acids such as 14-hydroxypalmitic acid are present as esters in common beeswax (6). Subsequent to the submission of this communication Weaver and Law (7) reported the presence of IV in royal jelly.

Following chromatographic methods as previously described (3) we have also isolated *p*-hydroxybenzoic acid (V) from royal jelly. This acid is widely distributed in nature. Borner (8) isolated V by chromatographic means from the aqueous extracts of straw from grains such as rye, wheat, and barley. Jarczynski, Kiermerier, and Gossel (9) have shown that V is a natural ripening agent of cheese. Also, Davis (10) in studies using *E. coli* and *A. aerogenes* associated with their enzyme systems has demonstrated vitamin activity with V. The concentration of V in royal jelly is very small (30 p.p.m.).

Table I gives the concentrations and R_f values of the acids which have been isolated from royal jelly to date.

[1]*Manuscript received August 17, 1960.*
Contribution from the Department of Chemistry, Ontario Agricultural College, Guelph, Ontario.
[2]*Associate Professor of Chemistry, Ontario Agricultural College, Guelph, Ontario.*
[3]*Graduate student, Department of Chemistry, Ontario Agricultural College, Guelph, Ontario. Present address: Naugatuck Chemicals, Elmira, Ontario.*

TABLE I

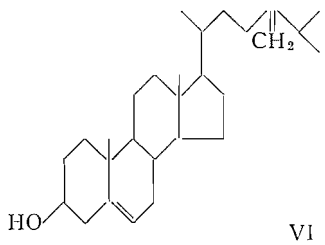
Concentrations and R_f values of acids present in royal jelly

Acid	Concn. in p.p.m. (basis lyophilized royal jelly)	R_f value*
I	70,000	0.79
II	200	0.44
III	300	0.39
IV	5,000	0.83
V	30	0.27

*Determined at 25° using a 7:3 ratio by volume of propanol and 28% aqueous ammonia solution as the developing solvent on Whatman No. 1 chromatography paper.

Methanol extraction of lyophilized royal jelly, previously extracted with ether, led to the isolation of a sterol, m.p. 139–141°, concentration 500 p.p.m.

The infrared absorption spectra of both the free sterol as well as its O-acetyl derivative are identical with those of authentic 24-methylenecholesterol (VI) and O-acetyl-24-methylenecholesterol, published by Barbier and Schindler (11). A mixture melting point between the O-acetyl derivatives was not depressed.



VI

Various melting points have been given for VI, depending upon the source from which it has been isolated. The reported melting points of the free sterol and the acetate derivative are listed in Table II.

TABLE II

Comparison of melting points of 24-methylenecholesterol (VI)

Source	Free sterol	Acetate derivative
From oysters (12)	142°	136°
From queen bees (13)	138–145°	131–136°
From worker bees (13)	138–140°	130–134°
Synthetic compound (14)	143°	135°
From royal jelly	139–141°	129–133°

The occurrence of VI in biological material has been reported twice. Barbier *et al.* (13) demonstrated the presence of VI in the neutral fraction of whole-bodied queen and worker bee extracts. Idler *et al.* (12) reported the isolation of VI from acetone extracts of the oyster (*Ostrea gigins*) and the clam (*Saxidomas giganteus*). Idler *et al.* (14) synthesized VI from 24-ketocholesterol and showed its identity with the natural product.

Can. J. Chem. Downloaded from www.nrcresearchpress.com by 210.87.254.6 on 09/05/12
For personal use only.

Can. J. Chem. Downloaded from www.nrcresearchpress.com by 210.87.254.6 on 09/05/12
For personal use only.

EXPERIMENTAL

All melting points reported by us have been corrected against reliable standards. Infrared data were determined by us on a Beckman IR5 instrument.

Isolation and Identification of 10-Hydroxydecanoic Acid (IV)

When 44 g of the mixture of ether-soluble acids, A (see Brown and Freure (3)), obtained from 390 g of lyophilized royal jelly, was allowed to stand at 25° for 1 week the oil did not crystallize but a second liquid phase appeared in the bottom of the flask. This liquid, 1.5 g, was removed and identified as water. The non-aqueous phase, which gave a positive test for sulphate ion, was processed again for the removal of neutral compounds as previously described (3). It yielded 1.85 g of a neutral colorless liquid, b.p. 270°; d_4^{20} 0.946; η_D^{20} 1.4472. The liquid gives a positive ester test.

Saponification of 1.5 g of the neutral liquid with 5% aqueous sodium hydroxide solution yielded 1.5 g of crude acid, m.p. 56–64°. One crystallization from water and two crystallizations from hexane (250 ml/g) gave 0.5 g of white needles melting at 71.5–72.5° both by itself and in admixture with authentic 10-hydroxydecanoic acid (IV).

Isolation and Identification of p-Hydroxybenzoic Acid (V)

The initial separation of V from the mixture of acids present in A (ether-soluble carboxylic acids. See Brown and Freure (3).) was carried out by chromatographing 0.30 g of A on 9×22.5 in. sheets of Whatman seed test paper as previously described (3). The area of paper, R_f 0.22–0.30, was cut out and extracted with propanol in a Soxhlet apparatus for 15 hours. The propanol extracts were combined, concentrated to a volume of 2 ml, and fractionated on four, 9×22.5 in. sheets of 3MM chromatography paper in order to remove residual amounts of the acids II and III. The area of paper, R_f 0.22–0.28, was cut out and extracted with propanol. The propanol extract was evaporated to dryness and the residue processed as described for the isolation of acids II and III (3). From 15 g of A, 0.014 g of crude V, m.p. 205–214°, was obtained. The crude V was washed with four 2-ml portions of cold chloroform (5°) to remove a sticky brown residue extracted from the chromatography paper. The resulting white residue, 0.011 g, had m.p. 211–215°. Crystallization from chloroform (55 ml/g) gave 0.0035 g of acid, m.p. 214–215°. Inspection of the infrared spectrum (KBr disk) of the sample suggested that it is *p*-hydroxybenzoic acid, a supposition which was confirmed by mixture melting point.

Blank determinations showed that V came from A and not from the possible breakdown of small amounts of lignin in the chromatography paper.

Isolation and Identification of 24-Methylenecholesterol (VI)

Ether-extracted, lyophilized royal jelly, 647 g, was placed in a Corning 3885 Soxhlet apparatus in 2-in. layers alternating with Pyrex glass fibers and extracted with absolute methanol for 2.5 hours. The dark orange extract was concentrated by distillation to 500 ml and cooled to 5°. White, plate-like crystals, which formed, were removed by filtration, weighed 0.278 g and had m.p. 122–135°. By concentrating the mother liquor and cooling, another 0.037 g of crystals, m.p. 125–137° was obtained. The crude product, 0.315 g, (500 p.p.m.) was crystallized twice from acetone (100 ml/g) including treatment with decolorizing charcoal. By this process there was obtained 0.029 g of white plates, m.p. 139–141°.

The compound gives a positive Liebermann–Burchard test and ferric chloride – sulphuric acid reaction (15) thus indicating that it is a sterol. The acetate, prepared according to the procedure of Barbier and Schindler (11), has m.p. 129–133°. A mixture melting point with authentic O-acetyl-24-methylenecholesterol was not depressed. Finally, the infrared spectra of the free sterol and the acetate are identical with those of authentic 24-methylenecholesterol and its acetate.

ACKNOWLEDGMENTS

Financial support for one of us (E.E.F.) was through a Public Health Research Grant. W. C. Hardesty Co. of Canada, Ltd. supplied generous amounts of 10-hydroxydecanoic acid. Professor G. F. Townsend, Department of Apiculture, O.A.C., Guelph, Ont., made available to us the lyophilized royal jelly used in the project. Dr. E. Reiner, Fisheries Research Board of Canada, Vancouver, B.C., kindly provided us with an authentic sample of 24-methylenecholesterol.

REFERENCES

1. G. F. Townsend and C. C. Lucas. Biochem. J. **34**, 1155 (1940).
2. A. Butenandt and H. Rembold. Z. physiol. Chem. Hoppe-Seyler's, **308**, 284 (1957).
3. W. H. Brown and R. J. Freure. Can. J. Chem. **37**, 2042 (1959).
4. M. Stoll and A. Rouvé. Helv. Chim. Acta, **18**, 1087 (1935).
5. U. K. Patent No. 675,434.
6. Y. Toyama and H. Hirai. Fette u. Seifen, **53**, 556 (1951).
7. N. Weaver and J. H. Law. Nature, **188**, 938 (1960).
8. H. Borner. Naturwissenschaften, **42**, 583 (1955).
9. F. Jarczynski, F. Kiermeirer, and I. Gossel. Z. Lebensm. Untersuch. u. Forsch. **100**, 195 (1955).
10. B. D. Davis. Harvey Lectures, **50**, 230 (1954–55).
11. M. Barbier and O. Schindler. Helv. Chim. Acta, **42**, No. 219, 1998 (1959).
12. D. R. Idler and U. H. M. Fagerlund. J. Am. Chem. Soc. **77**, 4142 (1955).
13. M. Barbier, T. Reichstein, and O. Schindler. Nature, **184**, 732 (1959).
14. D. R. Idler and U. H. M. Fagerlund. J. Am. Chem. Soc. **79**, 1988 (1957).
15. A. Zlatkis, B. Zak, and A. J. Boyle. J. Lab. Clin. Med. **41**, 486 (1953).

Can. J. Chem. Downloaded from www.nrcresearchpress.com by 210.87.254.6 on 09/05/12
For personal use only.

Can. J. Chem. Downloaded from www.nrcresearchpress.com by 210.87.254.5 on 09/05/12
For personal use only.

LYCOPODIUM ALKALOIDS

PART IV. ALKALOIDS OF JAMAICAN LYCOPODIUM CLAVATUM LINN.[1,2]

R. H. Burnell and B. S. Mootoo

ABSTRACT

Seven alkaloids have been isolated from *L. clavatum* Linn. collected in Jamaica, clavolonine $C_{16}H_{25}NO_2$, fawcettiine $C_{18}H_{29}NO_3$, base A (now named fawcettimine), lycopodine, dihydrolycopodine, and L.2 (acetyldihydrolycopodine). Fawcettimine is a secondary amine now shown to be $C_{16}H_{25}NO_2$. The isolation of deacetylfawcettiine $C_{16}H_{27}NO_2$ in quantity from a later extraction indicated that there was a seasonal variation in the alkaloid content of the plant. These bases differ from those obtained from *L. clavatum* of Canadian or European origin.

Lycopodium clavatum Linn. occurs in many areas of the world and at least two previous extractions are reported of the plant collected in Poland (1) and Canada (2). Since different bases were obtained from these previous extractions it seemed worth while to investigate material from a tropical source such as Jamaica. Club mosses do not grow in abundance in the tropics except at relatively high altitudes so the plant used for this work was collected in the Blue Mountains of Jamaica (ca. 5500 ft).

The extraction procedures follow closely the method used by us to extract *L. fawcettii* (3) and the yield of crude base amounted to 0.2% of the weight of dried plant when collected in April. Upon subjecting the crude alkaloid to a diagonal distribution between chloroform and buffer, three distinct fractions were obtained: (i) weak bases, (ii) a base of intermediate basicity, and (iii) strong bases. The latter afforded a crystalline base $C_{16}H_{25}NO_2$, m.p. 238°, which showed both hydroxyl and carbonyl absorption in the infrared and so was named clavolonine. The structure of the latter became apparent during work on fawcettiine (4).

The clavolonine mother liquors were acidified with perchloric acid and gave, in high yield, a perchlorate $C_{18}H_{29}NO_3.HClO_4$, m.p. 272–275°, which has been shown by the usual methods to be fawcettiine perchlorate, previously isolated from *L. fawcettii* (3, 5). Chromatography of the base regenerated from the mother liquors yielded more fawcettiine and clavolonine and another base, m.p. 168°, which proved to be dihydrolycopodine, $C_{16}H_{27}NO$.

The compound of intermediate basicity could not be crystallized but gave a methiodide, m.p. 240–242°, and a perchlorate, m.p. 225–226°, neither of which depressed the melting point of the corresponding derivative of base A, also obtained previously from *L. fawcettii*. Analyses of the free base, its hydrochloride, and perchlorate have prompted us to correct the molecular formula of base A to $C_{16}H_{25}NO_2$. We have named this compound fawcettimine since analysis of the methiodide, $C_{18}H_{30}NO_2I$ and the conversion of the base to an N-nitroso derivative (6) show it to be a secondary amine. Acetylation affords neutral N-acetylfawcettimine but this derivative has never been obtained crystalline. An infrared spectrum of the compound in carbon tetrachloride solution shows one carbonyl band at 1730 cm^{-1} whereas the methiodide shows two peaks at 1692 and 1730 cm^{-1}. The salts (perchlorate and hydrochloride) show only the 1690 cm^{-1} band in the carbonyl region.

[1]*Manuscript received November 7, 1960.*
Contribution from the Chemistry Department, University College of the West Indies, Jamaica.
[2]*Part III. Burnell and Taylor, Chem. & Ind. (London), 1239 (1960).*

Can. J. Chem. Downloaded from www.nrcresearchpress.com by 210.87.254.5 on 09/05/12
For personal use only.

The weak bases consisted of lycopodine, acetyldihydrolycopodine (Marion's L.2 (7, 8), and an extremely labile, feebly basic substance which has, as yet defied all attempts at characterization.

In a later extraction using plant material collected in the same locality, but in July (of the same year) the yield of crude base amounted to only a little over 0.1%. Clavolonine, fawcettiine, and lycopodine were obtained but fawcettimine, easily recognized by the green coloration it gives with the platinic chloride – potassium iodide spray used for chromatograms, was absent. The work-up of the strong bases from this extraction differed from that of the earlier work due to the presence of deacetylfawcettiine $C_{16}H_{27}NO_2$ in abundance. The latter was obtained in trace amounts from *L. fawcettii* (5) but it was felt at the time that the conditions used for the extraction could have hydrolyzed some of the fawcettiine present. Using a milder extraction such as employed in this case excludes this possibility.

EXPERIMENTAL

All infrared figures are for nujol mulls unless otherwise stated.

Crude Base (April)

Through the dried, ground plant (42 kg) was percolated 2% aqueous tartaric acid, which was then concentrated to about one-tenth of its volume and continuously extracted with chloroform. After basification with ammonia, the crude alkaloid (73.6 g) was obtained by further chloroform extraction. The crude base was distributed between chloroform and phosphate buffer, pH 6.98 in large separatory funnels in a diagonal manner to give 10 fractions. The buffer layers contained the strong bases (27 g) and the first two chloroform fractions the weak bases (25 g). The intermediate funnels contained only one base in abundance (14 g).

Clavolonine

The strong base (27 g) was dissolved in acetone and allowed to cool and the crystalline material filtered off (9.67 g). After recrystallization from acetone, the clavolonine was sublimed for analysis, m.p. 238°. Found: C, 72.9; H, 9.7; N, 5.1; O, 12.0; C—CH_3, 5.8. $C_{16}H_{25}NO_2$ requires: C, 73.0; H, 9.6; N, 5.3; O, 12.1; C—CH_3, 5.7.

Infrared peaks at 1693 cm^{-1} (C:O) and 3180 cm^{-1} (OH). A well-defined peak at 1412 cm^{-1} is indicative of the grouping —CH_2—CO—.

The methiodide was recrystallized from ethanol/acetone, m.p. 325–328° (decomp.). Found: C, 50.5; H, 6.6; N, 3.4; O, 8.2; I, 31.8; N—Me, 3.9. $C_{16}H_{25}NO_2.CH_3I$ requires: C, 50.4; H, 7.0; N, 3.4; O, 79; I, 31.3; N—Me, 3.7.

Fawcettiine Perchlorate

The clavolonine mother liquors were made acidic with an acetone solution of perchloric acid and a little ether added. The perchlorate was filtered and washed with acetone/ether and dried (11.3 g). The salt, recrystallized from acetone melted at 272–275° and showed no depression on admixture with fawcettiine perchlorate obtained from *L. fawcettii* (3). The infrared traces were superimposable.

Dihydrolycopodine

The base regenerated from the fawcettiine perchlorate mother liquors (8.0 g) was chromatographed over alumina in benzene. The first benzene eluate containing base afforded a pale yellow oil (1.28 g) which was taken up in ethyl acetate and cooled. The

lustrous prisms which separated (440 mg) were recrystallized from acetone, m.p. 168°. A second crop (170 mg) was obtained on further standing. Found: C, 77.4; H, 11.2; N, 5.4. $C_{16}H_{27}NO$ requires: C, 77.1; H, 10.9; N, 5.6.

The infrared showed hydroxyl absorption at 3150 cm^{-1}, showed no bands in the carbonyl region, and was identical with that of a sample of dihydrolycopodine prepared from lycopodine (9). Mixed melting points of the bases or the methiodides prepared from them (m.p. 283–287°) showed no depression. The methiodide was recrystallized from ethanol/acetone. Found: C, 52.3; H, 7.8; N, 3.7; I, 32.0. $C_{16}H_{27}NO.CH_3I$ requires: C, 52.2; H, 7.7; N, 3.6; I, 32.4.

Base A (Fawcettimine)

The intermediate funnels from the distribution yielded 14 g of crude base which was partitioned again between chloroform and phosphate buffer, pH 6.69, in a multiple extractor. The strong and weak bases were combined with the respective fractions from the first distribution and the intermediate base (4.48 g) run over alumina in benzene. The base obtained (4.07 g) was shown to be homogeneous by paper chromatography and sublimed as a glass (130° at 2 mm). Found: C, 72.7; H, 9.3; N, 5.6; O, 12.7; C—Me, 4.7. $C_{16}H_{25}NO_2$ requires: C, 73.0; H, 9.6; N, 5.3; O, 12.2; C—Me, 5.7.

The infrared spectrum of the base in carbon tetrachloride showed a carbonyl peak at 1730 cm^{-1} but in nujol mulls of the salts of fawcettimine the carbonyl peak was at 1690 cm^{-1}.

The methiodide was prepared in acetone and recrystallized from ethanol/acetone, m.p. 240–242°. Found: C, 51.5; H, 7.2; N, 3.1; I, 29.6. $C_{18}H_{30}NO_2I$ requires: C, 51.6; H, 7.2; N, 3.3; I, 30.3.

The hydrochloride was recrystallized from ethanol/acetone, m.p. 235° (decomp.). Found: C, 63.8; H, 8.7; N, 4.7; O, 10.8; Cl, 11.6. $C_{16}H_{25}NO_2.HCl$ requires: C, 64.1; H, 8.7; N, 4.7; O, 10.7; Cl, 11.8.

The perchlorate was recrystallized from isopropanol/acetone, m.p. 225–226°. Found: C, 52.4; H, 7.0; O, 26.7; Cl, 9.9. $C_{16}H_{25}NO_2.HClO_4$ requires: C, 52.8; H, 7.2; O, 26.4; Cl, 9.7.

N-Nitroso-fawcettimine

Fawcettimine (170 mg) was dissolved in glacial acetic acid (1 ml) and water (3 ml) and cooled in ice. A cold solution of sodium nitrite (170 mg) in water (2 ml) was added dropwise with stirring. Crystals appeared on standing in the cold (106 mg), m.p. 137–138°. The derivative was recrystallized from ethanol/water and showed a peak in the ultraviolet at 235 mμ (ϵ: 7000) (6). Found: C, 65.1; H, 8.8; N, 9.4; O, 16.4. $C_{16}H_{24}N_2O_3$ requires: C, 65.7; H, 8.3; N, 9.6; O, 16.4.

Active hydrogen determinations in anisole and pyridine gave 0%.

Lycopodine

The weak base (25 g) was distributed diagonally between chloroform and acetate buffer, pH 5.59, to remove traces of stronger bases and neutral materials. A portion of this purer base (4.15 g) was run over alumina in benzene and the first benzene eluate (2.97 g) dissolved in 2 *N* acetic acid and saturated potassium nitrate solution added. The turbid solution deposited crystals of lycopodine nitrate (1.2 g) on cooling (10). The base regenerated from the nitrate melted over the range 116–118° and showed a carbonyl peak in the infrared at 1710 cm^{-1}.

The methiodide was recrystallized from ethanol/acetone, m.p. 322–323° (inserted at

Can. J. Chem. Downloaded from www.nrcresearchpress.com by 210.87.254.5 on 09/05/12
For personal use only.

280°). Found: C, 52.5; H, 7.5; N, 3.8; O, 4.1. $C_{16}H_{25}NO.CH_3I$ requires: C, 52.4; H, 7.3; N, 3.6; O, 4.1.

Obtaining the lycopodine via the nitrate does not afford an effective separation since more of the base remains in solution than crystallizes out, so the weak base (8.5 g) regenerated from the nitrate solution and remaining on the column was shaken between chloroform and acetate buffer, pH 4.27, for 20 transfers. The lycopodine (plus one other base) was mostly in tubes 6–14 (3.09 g) and was obtained by conversion to the perchlorate (2.11 g). Tubes 17–19 contained a small amount of clavolonine (120 mg).

Acetyldihydrolycopodine (L.2)

Solution infrared spectra of the fractions from the weak base distribution showed that tubes 6–14 contained, in addition to lycopodine, another base containing an O-acetyl grouping and no hydroxyl. Fraction 8 (0.58 g) was hydrolyzed in methanolic sodium hydroxide and the product chromatographed over alumina. Lycopodine (0.29 g) was obtained and the only other base was dihydrolycopodine, m.p. 168° (105 mg). Since the latter is far too strong a base to be present as such the acetylated base in the plant must be L.2 (acetyldihydrolycopodine).

The first tubes of the distribution contained an extremely labile base which has, as yet, resisted all attempts at purification or characterization.

Crude Base (July)

The dried, ground plant (22 kg) was extracted as described above affording the crude base (25.0 g), which was diagonally distributed in funnels as described above. Funnels 1 and 2 (weak base: 9.9 g) contained lycopodine and funnels 3–8 (7.9 g) afforded clavolonine (2.22 g) and fawcettiine perchlorate (2.45 g). No fawcettimine was found.

Deacetylfawcettiine

Funnel 10 from the distribution (2.44 g) solidified on evaporation of the solvent and afforded a crystalline base (1.18 g) m.p. 205–208° from acetone. A second crop (300 mg) of the same base was obtained on further concentration. A comparison of the infrared spectrum of this base with that of deacetylfawcettiine and a mixed melting point determination showed that the two bases were identical.

ACKNOWLEDGMENTS

The authors would like to thank Mr. C. G. Chin for technical assistance.

REFERENCES

1. C. ACHMATOWICZ and W. UZIEBLO. Roczniki Chem. **18**, 88 (1938).
2. L. MARION and R. H. F. MANSKE. Can. J. Research, B, **22**, 137 (1944).
3. R. H. BURNELL, B. S. MOOTOO, and D. R. TAYLOR. Can. J. Chem. **38**, 1927 (1960).
4. R. H. BURNELL and D. R. TAYLOR. Chem. & Ind. (London), 1239 (1960).
5. R. H. BURNELL. J. Chem. Soc. 3091 (1959).
6. R. N. HAZELDINE and J. JANDER. J. Chem. Soc. 691 (1954).
7. R. H. F. MANSKE and L. MARION. Can. J. Research, B, **20**, 87 (1942).
8. B. DOUGLAS, D. G. LEWIS, and L. MARION. Can. J. Chem. **31**, 272 (1953).
9. D. B. MACLEAN, R. H. F. MANSKE, and L. MARION. Can. J. Research, B, **28**, 460 (1950).
10. A. BERTHO and A. STOLL. Ber. **85**, 663 (1952).

Can. J. Chem. Downloaded from www.nrcresearchpress.com by 210.87.254.5 on 09/05/12
For personal use only.

Can. J. Chem. Downloaded from www.nrcresearchpress.com by 210.87.254.105 on 09/05/12
For personal use only.

PRESSURE EFFECT AND MECHANISM IN ACID CATALYSIS

VII. HYDROLYSIS OF METHYL, ETHYL, AND *t*-BUTYL ACETATES[1]

A. R. OSBORN[2] AND E. WHALLEY

ABSTRACT

The effect of pressures up to 3 kbar on the rate of the acid-catalyzed hydrolysis of methyl, ethyl, and *t*-butyl acetates in dilute aqueous acid and of ethyl acetate in concentrated hydrochloric acid has been measured. The volume of activation for *t*-butyl acetate is zero within experimental error, showing that the mechanism is unimolecular. Those for methyl and ethyl acetates are near -9 cm^3 mole^{-1} in both dilute and concentrated acid. We deduce from this that the mechanism is the same in 9.2-*M* hydrochloric acid as in dilute acid, that the transition state is not highly polar, and that if the proton in the reactive protonated ester is on the carbonyl oxygen then the attacking water molecule adds, and if the proton is on the ether oxygen then the attacking water molecule substitutes.

1. INTRODUCTION

In spite of a large amount of experimental work, the hydrogen-ion-catalyzed hydrolysis of simple aliphatic esters is not well understood. There is little doubt, because, for example, of the relative rates in water and heavy water (1–3), that a pre-equilibrium proton transfer occurs, but the location of the proton in the reactive conjugate acid is not known. There is little doubt, mainly because of substituent effects (4, p. 770), that hydrolysis occurs by an attack of a water molecule on the conjugate acid, but it is not known whether the attack is an addition to a water molecule to form a stable intermediate or whether it is a simple substitution. It is, however, known that when ethyl benzoate is hydrolyzed by acid catalysis, the carbonyl oxygen of the unhydrolyzed ester exchanges with the oxygen of the solvent water (5, 6), but it is not known whether the hydrolysis and exchange follow similar or unrelated mechanisms. There are differing opinions (e.g. refs. 7–11) about whether the transition states that determine the rates have high dipole moments or not.

The effect of pressure on the rates of acid-catalyzed hydrolyses can provide useful information about the mechanisms (11–16), and a preliminary discussion of the hydrolysis of methyl acetate based on a few results reported by Bogojawlensky and Tammann (17) has already been given (11). In this paper we report measurements of the effect of pressures up to 3 kbar on the rates of hydrolysis of methyl and ethyl acetates in dilute hydrochloric acid.

Tal'vik and Pal'm (18) have argued that in concentrated acids ethyl acetate becomes essentially completely protonated, and that if allowance is made for the protonation, then the rate becomes nearly proportional to Hammett's acidity function h_0 rather than to the concentration of hydrogen ion. By using the Zucker–Hammett hypothesis (19, 20) they deduced that the slow step is

$$CH_3{-}C(=O)(H)({}^{+}OC_2H_5) \rightarrow CH_3CO^{+} + C_2H_5OH. \qquad [1]$$

An attempt to verify this mechanism in concentrated acids has been made by measuring the volume of activation in concentrated hydrochloric acid.

[1]*Manuscript received January 19, 1961.*
Contribution from the Division of Applied Chemistry, National Research Council, Ottawa, Canada. Issued as N.R.C. No. 6270.
[2]*N.R.C. Postdoctorate Fellow 1958–60.*

t-Butyl acetate hydrolyzes by acid catalysis (21–26) with alkyl–oxygen fission (26) and with an Arrhenius energy of 27.6 kcal $mole^{-1}$ and an entropy of activation of 14.2 cal deg^{-1} $mole^{-1}$ (22, 25) and it seems likely that the mechanism is unimolecular. The effect of pressure on the rate of hydrolysis in water has been measured to test this mechanism.

2. EXPERIMENTAL METHODS

The methyl and ethyl acetates used were of analytical grade and were not further purified. The *t*-butyl acetate was a commercial sample and it was distilled, the fraction b.p. 94–96.5° C being retained.

The high-pressure technique was similar to that used previously (12), except for the following modifications. In the original apparatus oil was pumped by hand into the pressure vessel to prevent loss of pressure when a sample was taken. We have added an air-driven oil pump to the apparatus, which automatically maintains the pressure constant when a sample is taken. The pump was modified from one made by the Sprague Engineering Co. by fitting it with a high-pressure end capable of generating a pressure of 4 kbar when 100 p.s.i.g. of compressed air is supplied to the low-pressure end.

In the original apparatus the reacting solution was in contact with an austenitic-stainless-steel capillary tube, which corrodes in strong acid. The sampling system was modified so that the solution is in contact with only glass, tantalum, Hastelloy B (Haynes Stellite Co.), and neoprene, all of which are unaffected for practical purposes by concentrated perchloric and hydrochloric acids up to at least 8 *M* near room temperature and will withstand more dilute acids up to at least 100° C. The new sampling system is shown in Fig. 1. The hypodermic syringe which is used as the reaction vessel is attached to the tantalum capillary sampling tube by means of the stainless-steel union and the small neoprene seal which isolates the reaction solution from the hydraulic oil. A small nut and lock nut at the upper end of the union allows the force on the neoprene seal to be adjusted. The union is held in place on the syringe by means of an o-ring which fits into a groove in the neck of the syringe. The two parts of the union are held together by means of a bayonet-and-socket device similar to that used on some lamp bulbs. The sampling valve is made of Hastelloy B, and the connection between the valve and the tantalum tube is shown in the upper part of Fig. 1. A metal–metal seal isolates the hydraulic oil from the atmosphere, and an o-ring seal isolates the oil from the sample. This connection can be easily dismantled when necessary. The stem of the valve is also made of Hastelloy B. The outlet of the valve is connected to a water-jacketed tantalum capillary tube.

The hydrolyses were followed by titration with standard alkali of the acid produced during the hydrolysis, using phenolphthalein as indicator.

3. RESULTS

The reactions follow first-order kinetics and the first-order constants were obtained graphically in the usual way. The accuracy was about 2%. For reactions in dilute aqueous acids, the second-order constants k_a were obtained by dividing the first-order constants by the concentration of acid at the temperature and pressure of the experiment, assuming that the compression and thermal expansion of the solution are the same as that of pure water (27). For reactions in concentrated acids the first-order constants k_1 are reported because the compressibility of concentrated hydrochloric acid has not been measured. The rate constants are given in Tables I and II and are shown graphically in Fig. 2.

Can. J. Chem. Downloaded from www.nrcresearchpress.com by 210.87.254.105 on 09/05/12
For personal use only.

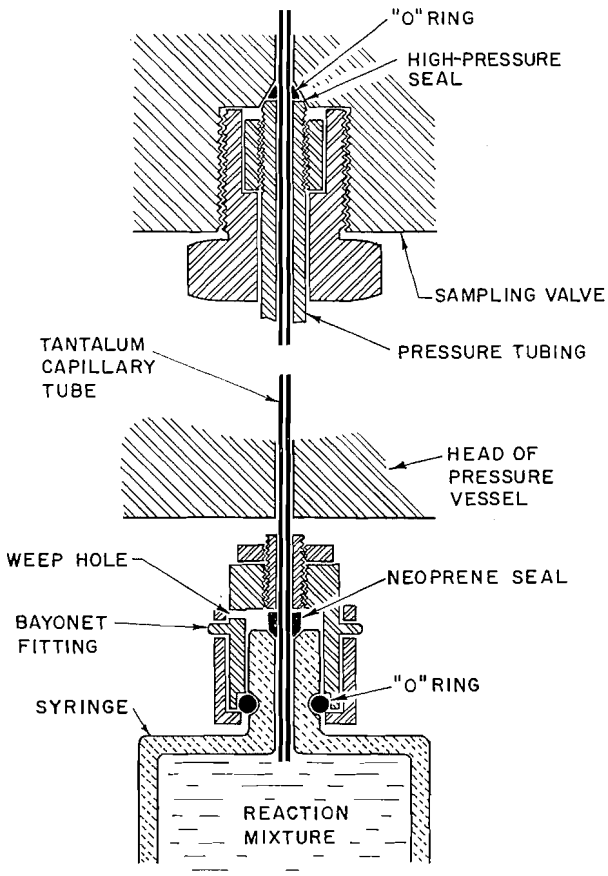


FIG. 1. Sampling system for high-pressure apparatus.

TABLE I

Acid-catalyzed hydrolysis of methyl acetate in aqueous solution at 35.00° C with 0.1-*M* HCl

p/bar	$10^6\ k_a$/l. mole^{-1} sec^{-1} in water
1	2.82
250	3.09
507	3.27
507	3.29
1000	3.98
1500	4.64
2000	5.24
2500	6.06
3000	6.90

For comparison, the second-order rate constant for the hydrolysis of methyl acetate at 35.00° C, is reported to be 277×10^{-6} l. mole^{-1} sec^{-1} in 0.1-*M* hydrochloric acid (28). For ethyl acetate interpolation of Tommila and Hella's (29) results gives 269×10^{-6} l. mole^{-1}

Can. J. Chem. Downloaded from www.nrcresearchpress.com by 210.87.254.105 on 09/05/12
For personal use only.

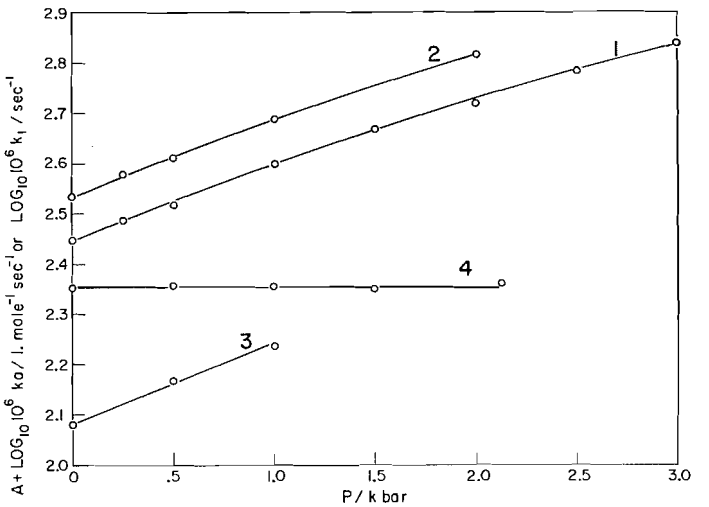


FIG. 2. Hydrolysis of acetates catalyzed by hydrochloric acid. Curve 1, k_a for methyl acetate in 0.1-M aq. HCl at 35.00° C, $A = 0$; curve 2, k_a for ethyl acetate in 0.1-M aq. HCl at 35.00° C, $A = 0.1$; curve 3, k_1 for ethyl acetate in 9.21-M aq. HCl at 0.00° C, $A = 0$; curve 4, k_a for t-butyl acetate in 0.01-M aq. HCl at 60.00° C, $A = -1.9$.

TABLE II

Acid-catalyzed hydrolysis of ethyl acetate in aqueous solution

p/bar	$10^6\ k_a$/l. mole^{-1} sec^{-1}	p/bar	$c°_{HCl}/M$	$10^6\ k_1$/sec^{-1}
1	273	1	2.35	21.7
250	301	1	4.63	51.5
500	325	1	7.18	98.3
1000	387	1	9.21	120
2000	520	1	9.21	120
		500	9.21	147
		1000	9.21	172
35.00° C, 0.1-M HCl		0.00° C, $c°_{HCl}$ = concn. of HCl at room temperature and pressure		

TABLE III

Acid-catalyzed hydrolysis of t-butyl acetate in water at 60.00° C with 0.01-M HCl

p/bar	$10^3\ k_a$/l. mole^{-1} sec^{-1}
1	17.9
500	18.0
1000	18.0
1500	17.8
2000	18.2

sec^{-1} for k_a at 35.00° C in water. For t-butyl acetate interpolation of Palomaa *et al.*'s results (22) gives 17.6×10^{-3} l. mole^{-1} sec^{-1}. The agreement is satisfactory.

The volumes of activation $\Delta V^{\ddagger}$ were obtained graphically (Fig. 2) using the usual relations

$$\partial \ln k_a/\partial p = -\Delta V^{\ddagger}/RT \text{ or } \partial \ln k_1/\partial p = -\Delta V^{\ddagger}/RT + \kappa,$$

Can. J. Chem. Downloaded from www.nrcresearchpress.com by 210.87.254.105 on 09/05/12
For personal use only.

where κ is the compressibility of the solution. For methyl acetate,

$$\Delta V^{\ddagger} = -9.1 \pm \sim 0.7 \text{ cm}^3 \text{ mole}^{-1} \text{ at } 35^\circ \text{ C in water.}$$

For ethyl acetate

$$\Delta V^{\ddagger} = -9.3 \pm \sim 0.7 \text{ cm}^3 \text{ mole}^{-1} \text{ at } 35^\circ \text{ C in water.}$$

These compare with -8.3 cm^3 mole^{-1} for methyl acetate in water at 30.5° C calculated (11) from Bogojawlensky and Tammann's (17) rate constants at 1 and 500 atm. Rothmund's (30) measurements, which were the second published on the effect of pressure on reaction rates in solution, yield -10.1 cm^3 mole^{-1} for methyl acetate and -8.4 cm^3 mole^{-1} for ethyl acetate at 14° C. The rates in 9.21-M hydrochloric acid yield graphically

$$RT\partial \ln k_1/\partial p = 9.1 \pm \sim 1.0 \text{ cm}^3 \text{ mole}^{-1}.$$

If the compressibility of 9.21-M hydrochloric acid is taken to be the same as that of pure water then

$$\Delta V^{\ddagger} = -7.9 \pm \sim 1.3 \text{ cm}^3 \text{ mole}^{-1},$$

where the error has been increased to allow for the uncertainty of the compressibility of the acid solution.

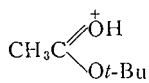
For t-butyl acetate

$$\Delta V^{\ddagger} = 0.0 \pm \sim 1.0 \text{ cm}^3 \text{ mole}^{-1} \text{ at } 60^\circ \text{ C.}$$

4. DISCUSSION

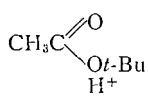
1. *t-Butyl Acetate*

The hydrolysis of t-butyl acetate is the simplest, and it is discussed first. The volume of activation of $0.0 \pm \sim 1.0$ cm^3 mole^{-1} is clearly consistent with either of the likely (see Section 1) unimolecular slow steps



$$\rightarrow CH_3CO_2H + t\text{-}Bu^+,$$

or

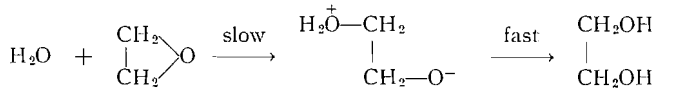


$$\rightarrow CH_3CO_2H + t\text{-}Bu^+.$$

2. *Polarity of the Transition States for Methyl and Ethyl Acetates*

The volumes of activation for the acid-catalyzed hydrolysis of methyl and ethyl acetates in dilute aqueous acid at 35° C are about -9.1 and -9.3 cm^3 mole^{-1}. As was pointed out earlier (11) these are approximately the values expected for a bimolecular reaction of a water molecule with a positively charged substrate if no major change in electrostriction due to changes in electrostatic moments occurs. In confirmation of this they are within about 1.5 cm^3 mole^{-1} of the volumes of activation for the acid-catalyzed hydrolysis of several aliphatic epoxides (13) and diethyl ether (14), for which the transition states are unlikely to have high dipole moments. They are much higher than the volume of activation for the spontaneous hydrolysis of ethylene oxide, which is -15.9 to -19.9 cm^3 mole^{-1} at 25 to 70° C (31), whose mechanism is

Can. J. Chem. Downloaded from www.nrcresearchpress.com by 210.87.254.105 on 09/05/12
For personal use only.



where the transition state is almost certainly very polar. In addition, all the volumes of activation so far measured of the reactions of small negative ions such as hydroxide and ethoxide with small neutral molecules lie in the range -5 to -10 cm^3 mole^{-1} (31). We conclude therefore that the transition state of the acid-catalyzed hydrolysis of simple esters is not highly polar and in particular that the carbonyl group is not appreciably ionized in the transition state.

Tal'vik and Pal'm's (18) mechanism, equation [1], should give a positive or zero volume of activation like *t*-butyl acetate, sucrose (11), formals and acetals (12), and α-D-glucose-1-phosphate (16), and it can be eliminated by these results, at least in dilute acid. The volume of activation of ethyl acetate appears to be little different in 9.21-*M* hydrochloric acid, in which the acidity function $-H_0$ is about 3.5, from that in dilute acid. In sulphuric acid the rate is reported (18) to be independent of acid concentration for $-H_0 > 2$ and it was deduced that the ester is essentially completely protonated. It is likely from the small change in the volume of activation that no change of mechanism has occurred in concentrated acid.

It has been argued (8–10) that the effect of solvent (7, 10, 29, 32, 33, 34) on the rates of these hydrolyses shows the transition states to be very highly polar, having dipole moments of 26.1 D. It has also been argued (e.g. 7, 34) that the same results show the transition state to be not highly polar. The solvent effects are small, the second-order rate constants typically decreasing by a few tens per cent in the range zero to 50% v/v acetone in water, and by similar amounts in other aqueous solvents. These are very much smaller effects than occur in reactions between two neutral molecules in which a highly polar transition state is formed, for which there is a large decrease in the rate constant as the dielectric constant of the solvent decreases (4, p. 345 *et seq.*). They are similar to, and in fact less than, the solvent effects for the acid-catalyzed hydrolysis of ethylene oxide in methanol–water mixtures (35) and in ethanol–water mixtures (36) for which the transition states are thought not to be highly polar. The solvent effects therefore confirm that the transition states for the acid-catalyzed hydrolysis of simple esters and of ethylene oxide have similar polarity.

Theories (8) that invoke highly polar transition states for the hydrolysis of esters suffer also from the following defects.

(i) They predict a large variation in entropy and enthalpy of activation with varying solvent, whereas the entropy of activation for the acid-catalyzed hydrolysis of methyl acetate differs by less than 10% between solvent water and solvent 50% v/v acetone–water (29).

(ii) They require radii of the transition states that seem too large. Thus, for the hydrolysis of ethyl acetate in dioxane–water mixtures the radius of the transition state is given (8) as 4.6 Å, which corresponds to a volume, calculated as $(4/3)\pi Na^3$ where a is the radius and adding one-third for the unoccupied volume, of 328 cm^3 mole^{-1}, and in methanol–water mixtures a radius of 5.7 Å is required (10), which corresponds to 620 cm^3 mole^{-1}.

Two other objections to the details of Laidler and Landskroener's mechanism are as follows. The hydrolyses are a good deal faster in heavy water than in ordinary water,

Can. J. Chem. Downloaded from www.nrcresearchpress.com by 210.87.254.105 on 09/05/12
For personal use only.

which is difficult to explain on the basis of the assumed transition states because they require two O—H bonds to be broken. However, a slight alteration of two O—H distances in their transition states would meet this objection. Also, the assumed transition state incorporates H_3O^+, H_2O, and ester and so the reaction should be third-order. The third-order rate constants *increase* with increasing concentration of organic solvent (7, 34).

We conclude therefore that the transition state for the hydrolysis of simple aliphatic esters is not very polar.

3. Location of the Proton

The conclusions that we can draw about the location of the proton in the reactive conjugate acid of the ester are intimately connected with the problem of whether the attack by water is a substitution or an addition. The exchange of ^{18}O between hydrolyzing ethyl benzoate and the solvent (5, 6) show that water can add reversibly to the ester, and though it is not unlikely that the adduct is an intermediate in the hydrolysis, this has not yet been conclusively demonstrated. It has been shown (11) that if the transition state is not very polar, then either the proton is on the carbonyl oxygen and the water molecule adds or the proton is on the ether oxygen and the water molecule substitutes. The demonstration given above that the transition state is not very polar confirms this conclusion.

ACKNOWLEDGMENTS

We are greatly indebted to Mr. A. Lavergne for help with the high-pressure apparatus.

REFERENCES

1. W. E. Nelson and J. A. V. Butler. J. Chem. Soc. 957 (1938).
2. J. C. Hornel and J. A. V. Butler. J. Chem. Soc. 1361 (1936).
3. K. Schwartz. Z. Elektrochem. **40**, 474 (1936).
4. C. K. Ingold. Structure and mechanism in organic chemistry. Cornell University Press, Ithaca. 1953.
5. M. L. Bender. J. Am. Chem. Soc. **73**, 1626 (1951).
6. M. L. Bender, R. D. Ginger, and J. P. Unik. J. Am. Chem. Soc. **80**, 1044 (1958).
7. J. L. Hockersmith and E. S. Amis. Anal. Chim. Acta, **9**, 101 (1953).
8. K. J. Laidler and P. A. Landskroener. Trans. Faraday Soc. **52**, 200 (1956).
9. K. J. Laidler. Suomen Kemistilehti, **33**, A, 44 (1960).
10. M. Sadek and M. I. A. Latif. Z. physik. Chem. (Frankfurt), **17**, 21 (1959).
11. E. Whalley. Trans. Faraday Soc. **55**, 798 (1959).
12. J. Koskikallio and E. Whalley. Trans. Faraday Soc. **55**, 809 (1959).
13. J. Koskikallio and E. Whalley. Trans. Faraday Soc. **55**, 815 (1959).
14. J. Koskikallio and E. Whalley. Can. J. Chem. **37**, 788 (1959).
15. J. Koskikallio, D. Pouli, and E. Whalley. Can. J. Chem. **37**, 1360 (1959).
16. A. R. Osborn and E. Whalley. Can. J. Chem. **39**, 597 (1961).
17. A. Bogojawlensky and G. Tammann. Z. physik. Chem. **23**, 13 (1897).
18. A. I. Tal'vik and V. A. Pal'm. Zhur. Fiz. Khim. **33**, 1214 (1959).
19. L. Zucker and L. P. Hammett. J. Am. Chem. Soc. **61**, 2791 (1939).
20. F. A. Long and M. A. Paul. Chem. Revs. **57**, 935 (1957).
21. A. Skrabal and A. M. Hugetz. Monatsh. **47**, 17 (1926).
22. M. H. Palomaa, E. J. Salmi, J. I. Jausson, and T. Salo. Ber. **68**, 303 (1935).
23. V. R. Stimson. J. Chem. Soc. 4020 (1955).
24. P. Salomaa. Acta Chem. Scand. **14**, 577 (1960).
25. P. Salomaa. Suomen Kemistilehti, B, **32**, 145 (1959).
26. C. A. Bunton, A. E. Comyns, and J. L. Wood. Research (London), 4, 383 (1951).
27. P. W. Bridgman. Proc. Am. Acad. Arts Sci. **48**, 309 (1912).
28. A. Lamble and W. C. MacLewis. J. Chem. Soc. **105**, 2330 (1914).
29. E. Tommila and A. Heller. Ann. Acad. Sci. Fennicae, A, II, **53** (1954).
30. V. Rothmund. Z. phys. Chem. **20**, 168 (1896).
31. J. Koskikallio and E. Whalley. Can. J. Chem. **37**, 783 (1959).
32. S. V. Anantakrishnan and S. Krishnamurti. Proc. Indian Acad. Sci. A, **14**, 270 (1941).
33. P. M. Nair and S. V. Anantakrishnan. Proc. Indian Acad. Sci. A, **32**, 85, 330 (1952).
34. P. M. Nair and E. S. Amis. Anal. Chim. Acta, **9**, 111 (1953).
35. A. M. Eastham and C. Newall. Unpublished results.
36. R. K. Brown and A. M. Eastham. Can. J. Chem. **38**, 2039 (1960).

Can. J. Chem. Downloaded from www.nrcresearchpress.com by 210.87.254.105 on 09/05/12
For personal use only.

Can. J. Chem. Downloaded from www.nrcresearchpress.com by 210.87.254.42 on 09/05/12
For personal use only.

PRESSURE EFFECT AND MECHANISM IN ACID CATALYSIS

VIII. HYDROLYSIS OF ACETAMIDE AND BENZAMIDE[1]

A. R. OSBORN,[2] T. C-W. MAK, AND E. WHALLEY

ABSTRACT

The effect of pressures up to 3 kbar on the rate of the acid-catalyzed hydrolysis of acetamide and benzamide in both dilute and concentrated perchloric acid has been measured. The volumes of activation in dilute acid are consistent with a transition state that is not highly polar. It follows from this that if the attacking water molecule adds to the amidium ion then the reactive amidium ion is the O-protonated form, and if the attacking water molecule substitutes then the reactive amidium ion is the N-protonated form.

The volume of activation for acetamide in concentrated acid provides no additional information about the mechanism. That for benzamide in concentrated acid is tentatively interpreted as favoring the O-protonated benzamidium ion as the reactive ion.

1. INTRODUCTION

The acid-catalyzed hydrolysis of amides is in many ways similar to the acid-catalyzed hydrolysis of carboxylic esters, and many of the questions that require solution are similar to those for esters (1). It seems certain that the mechanism is

$$RCONH_2 + H_3O^+ \rightleftharpoons RCONH_2.H^+ + H_2O, \quad \text{equilibrium} \quad [1]$$

$$RCONH_2.H^+ + H_2O \rightarrow \text{products}. \quad \text{slow} \quad [2]$$

The relative rates of hydrolysis of acetamide in dilute acid in water and heavy water (2) show that a pre-equilibrium proton transfer occurs, and mechanisms that omit this (3, 4, 5) are almost certainly wrong. The location of the proton is unknown. Substituent effects (6, 7) indicate that a bimolecular attack of water probably occurs, but it is not known whether the attack is by substitution or by addition. Hydrolyzing benzamide does not exchange its oxygen with the solvent (8, 9) but this does not, of course, prove that an intermediate molecule is not formed, but only that if one is formed then it decomposes to products much faster than it reverts to reactants. Useful information about the mechanism of hydrolysis of simple esters has been obtained by measuring the effect of pressure on the rate (1), and so the effect of pressure on the rate of hydrolysis of acetamide and benzamide has been measured.

It is well known that the rates of hydrolysis go through a maximum as the concentration of acid is increased, and there is no doubt that the amide becomes appreciably protonated in concentrated acids. So that something could be learned about the volume change of the proton-transfer reaction [1] and the volume of activation of the slow step [2], the effect of pressure on the rates in concentrated acid has also been measured.

2. EXPERIMENTAL METHODS

Reagent-grade acetamide was recrystallized from approximately 1:10 ether–ethanol (10). Eastman-Kodak benzamide was recrystallized from water to constant melting point.

The high-pressure technique was as described in previous papers (1). About five samples were taken for analysis during a run. The reaction mixtures were made from perchloric acid and amide solutions of known concentrations.

[1]*Manuscript received January 19, 1961.*
Contribution from the Division of Applied Chemistry, National Research Council of Canada, Ottawa, Canada. Issued as N.R.C. No. 6271.
[2]*N.R.C. Postdoctorate Fellow 1958–60.*

Can. J. Chem. Downloaded from www.nrcresearchpress.com by 210.87.254.42 on 09/05/12
For personal use only.

The hydrolysis of acetamide was followed by analyzing for the acetic acid produced. About 5 ml of reaction solution (initially either 0.2992 *M* in perchloric acid and 0.1980 *M* in acetamide or 3.99 *M* in perchloric acid and 0.0990 *M* in acetamide) were withdrawn and 3.00 ml pipetted into a 30-ml weighing bottle. One drop of thymol blue indicator was added and the solution was titrated with 2-*N* sodium hydroxide solution until the color of the indicator just changed from red to yellow (pH approximately 2.8–3.0). Six milliliters of methanol was added and the solution titrated potentiometrically with 0.1-*N* barium hydroxide solution, using a Beckman Model-G pH meter with a Beckman No. 40463 sleeve-type calomel electrode as reference. The first inflection, at about pH 4, corresponded to neutralization of the perchloric acid, and the second, at about pH 7.3, to neutralization of the acetic acid. The methanol was added to sharpen the first inflection. Both inflections were easily located to ±0.01 or 0.02 ml. A typical titration required 2 ml, so the error is about 1 to 2%.

The same method could not be used for benzamide because if its concentration was much greater than about 0.02 *M* benzoic acid precipitated and it may clog the high-pressure apparatus, and 0.02 *M* is too low a concentration for this method. The ammonia produced was therefore determined by the formol titration method (11, 12). About 5 ml of reaction mixture (initially about either 1 *M* or 4.08 *M* in perchloric acid and 0.02 *M* in benzamide) was withdrawn, weighed accurately, and neutralized approximately with 1-*N* sodium hydroxide solution. It was adjusted to pH 6.6 with 0.1-*N* barium hydroxide solution, using the pH meter described above. A 5-ml blank solution, identical with the above solution except that it contained no benzamide, was treated similarly. Five milliliters of formalin solution (50 ml of Merck formaldehyde (37.0–37.3%) plus 0.5 ml of phenolphthalein indicator (0.5% in 50% ethanol) neutralized to faint pink color with *N* sodium hydroxide) were added to each of the two solutions. The pH of the blank was determined, the sample titrated to the same pH with 0.1-*N* barium hydroxide, and the pH of the blank measured again. If the pH of the blank had changed, alkali was added to either sample or blank and the appropriate allowance made. The alkali was run in from a precision-bore capillary tube with a meter stick attached, so that the amount added was measured to ±0.005 ml. The titer gave the equivalent amount of acid liberated by the reaction of ammonia and formaldehyde to form hexamethylenetetramine. To obtain reproducible results the electrode was flushed frequently with saturated potassium chloride solution.

3. RESULTS

1. Acetamide

For the hydrolysis in dilute acid the second-order rate law is appropriate. The integrated form

$$k_a t = \frac{1}{a-b} \ln \frac{b(a-x)}{a(b-x)},$$

where a and b are the initial concentrations of perchloric acid and acetamide, x is the amount of each reacted per unit volume at time t, and k_a is the second-order rate constant, can be rewritten

$$\log_{10} \frac{a-x}{b-x} = \frac{a-b}{2.303} k_a(t-t_0) - \log_{10} \frac{a-x_0}{b-x_0},$$

where x_0 is the amount reacted per unit volume at any arbitrary starting time t_0. A plot of $\log_{10}[(a-x)/(b-x)]$ against t gives therefore a straight line of slope $k_a(a-b)/2.303$. The appropriate corrections for compression (13) and thermal expansion of the solution were made. The second-order rate constants are given in Table I.

TABLE I

Acid-catalyzed hydrolysis of acetamide at 55.00° C

p/bar	$10^6 k_a$/l. mole^{-1} sec^{-1} (initially 0.2992-M $HClO_4$ 0.1980-M acetamide)	$10^6 k_1$/sec^{-1} (3.99-M $HClO_4$ 0.0990-M acetamide)
1	195	109
500	228	130
1000	268	164
1500	332	205
1500	333	
2000	387	248

The volume of activation of the reaction

$$RCONH_2.H^+ + H_2O \rightarrow \text{products}$$

can, at least in principle, be obtained from rates in concentrated acid because in these solutions the amide becomes largely protonated. There is, however, a difficulty, that the rate does not become of zero order in acid, but the first-order (in amide) rate constant passes through a maximum at concentrations of acid that are dependent upon the acid and amide, but are often around 2 to 4 M. What allowance to make in the rate constant for the effect of pressure on the concentration is not entirely clear, and we have preferred to reduce the effect of this uncertainty by using acid concentrations not far above those corresponding to the maximum rate. This gain in using a low concentration of acid is partly offset by the lower degree of protonation of the amide, and the concentration chosen, which was 4 M, was a compromise.

For the hydrolysis in a solution initially 3.99 M in perchloric acid the first-order rate law is appropriate, and the first-order constants were obtained graphically in the usual manner; they are given in Table I. They were not converted to second-order constants because, as mentioned above, the reactions are not second-order in concentrated acid.

By interpolating Rabinovitch and Winkler's (14) results at atmospheric pressure we find that $10^6 k_a$/liter mole^{-1} sec^{-1} in 1-M hydrochloric acid is 186 compared with our 195 in 0.3-M perchloric acid, and that $10^6 k_1$/sec^{-1} in 4-M hydrochloric acid is 133 compared with our 109 in 4-M perchloric acid. The agreement is satisfactory considering that in concentrated acids exact agreement is not expected.

2. Benzamide

The concentration of benzamide was always low enough that the first-order law was followed. The rate constants are accurate to about 5%. The rate constants in 1-M perchloric acid were converted to second-order constants k_a in the usual way and they are given in Table II.

A few kinetic runs were made to determine approximately the acid concentration that gives the maximum rate of hydrolysis. The first-order constants are given in Table III. The high-pressure rate constants were determined in 4.08-M perchloric acid solution. Because the rate is not first order in acid in concentrated acid the first-order constants are listed in Table II.

Can. J. Chem. Downloaded from www.nrcresearchpress.com by 210.87.254.42 on 09/05/12
For personal use only.

TABLE II

Acid-catalyzed hydrolysis of benzamide at 80.00° C

p/bar	$10^6\ k_a$/l. mole^{-1} sec^{-1} (initially M $HClO_4$ 0.02-M amide)	$10^6\ k_1$/sec^{-1} (4-M $HClO_4$ 0.02-M amide)
1	60.4	99.4
500	73.3	129.2
	71.7	
1000	87.6	171
	87.6	
1500	107.7	228
	98.9	
2000	112.4	339
	109.9	
	114.6	

TABLE III

Hydrolysis of benzamide in different concentrations of acid at 80.00° C and atmospheric pressure (Initial concentration of benzamide was 0.02-M)

c_{HClO_4}/M	$10^6\ k_1$/sec^{-1}
1.02	60
2.04	104
2.86	114
4.08	99
4.08	99*

*Reaction carried out in pressure vessel.

For comparison, we find by interpolating Rabinovitch and Winkler's (14) results that in M hydrochloric acid $10^6\ k_1$/sec^{-1} is 59 compared with our 60.4 in M perchloric acid, and in 4-M hydrochloric acid $10^6\ k_1$/sec^{-1} is 219 compared with our 99 sec^{-1} in 4.08-M perchloric acid. The cause of the difference in concentrated acid is not immediately obvious.

3. Volumes of Activation

The rate constants as a function of pressure are shown in Fig. 1. The volumes of activation were obtained graphically from the slope of the graph of log k vs. p at zero pressure from the appropriate formula

$$\frac{\partial \ln k_a}{\partial p} = -\frac{\Delta V^{\ddagger}}{RT}, \quad \text{or} \quad \frac{\partial \ln k_1}{\partial p} = -\frac{\Delta V^{\ddagger}}{RT}.$$

The volumes of activation are given in Table IV.

TABLE IV

Volumes of activation for the acid-catalyzed hydrolysis of acetamide and benzamide

Amide	Concn. of $HClO_4/M$	Temp./ °C	$\Delta V^{\ddagger}$ / cm^3 mole^{-1}
Acetamide	0.299	55	$-9.4\pm\sim0.5$
Acetamide	3.99	55	$-11.3\pm\sim0.8$
Benzamide	1.00	80	$-12.1\pm\sim1.0$
Benzamide	4.08	80	$-16.0\pm\sim0.7$

Can. J. Chem. Downloaded from www.nrcresearchpress.com by 210.87.254.42 on 09/05/12
For personal use only.

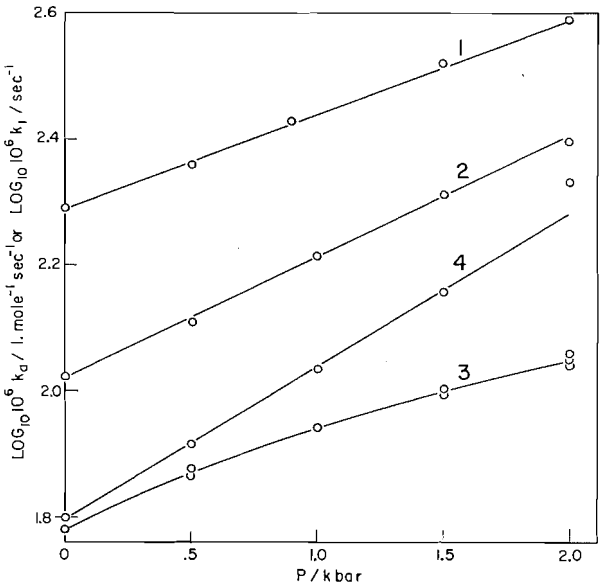


FIG. 1. Acid-catalyzed hydrolysis of acetamide and benzamide. Curve 1, k_a for acetamide at 35.00° C in 0.3-M $HClO_4$ and 0.2-M acetamide. Curve 2, k_1 for acetamide at 35.00° C in 4-M $HClO_4$ and 0.1-M acetamide. Curve 3, k_a for benzamide at 80.00° C in M $HClO_4$ and 0.02-M benzamide. Curve 4, k_1 for benzamide at 80.00° C in 4-M $HClO_4$ and 0.02-M benzamide, displaced downwards one unit for clarity.

4. Volume Changes of the Proton-Transfer Reactions

We assume for want of anything better that the volume change of reaction [1] and the volume of activation of reaction [2] are the same in dilute and in 4-M perchloric acid and that the pK_a's are independent of temperature (see, for example, ref. 7). There is some disagreement about the value of pK_a for the acetamidium ion (15, 16, 17, 18). The smallest pK_a, −1.40 (18), indicates that about two thirds of the amide is protonated in 4-M perchloric acid and the others indicate that more than this is protonated. It follows therefore that the volume change of the proton-transfer reaction (1) is $3.8 \pm \sim 2.5$ cm^3 mole^{-1} for acetamide.

The value of pK_a for the benzamidium ion has recently been revised from −1.85 (18) to −2.16 (19) and so it seems that benzamide is only about one-quarter protonated in 4-M perchloric acid, instead of about one-third as it seemed when this work was done. The volume change for the proton-transfer reaction [1] for benzamide appears to be therefore about $16 \pm \sim 8$ cm^3 mole^{-1}. These values are unfortunately rather rough, but they do seem to be significant.

4. DISCUSSION

1. Polarity of the Transition State

If the dipole moment of the transition state is much bigger than that of the amide, then there will be an increase in the electrostriction of the solvent when the transition state is formed (see, for example, preceding paper). The object of this section is to determine whether this occurs. Only the reaction

$$H_3O^+ + RCONH_2 \rightarrow \text{transition state}$$

need be considered for the present because in dilute acid, where the amide is only slightly protonated, the volume of activation is the difference between the partial volume of the

Can. J. Chem. Downloaded from www.nrcresearchpress.com by 210.87.254.42 on 09/05/12
For personal use only.

transition state and the sum of the partial volumes of the amide and the hydronium ion, and is independent of the partial volume of the protonated amide. This is important because the partial volume of the transition state can be discussed without reference to the partial volume of the protonated amide. This last shall be discussed in the next section.

The volume of activation for the hydrolysis of acetamide in dilute acids is $-9.4\pm\sim 0.5$ cm^3 mole^{-1}, which is almost identical with the volumes of activation for the hydrolysis of ethylene oxide (20), propylene oxide (20), isobutylene oxide (20), diethyl ether (21), methyl acetate (1), and ethyl acetate (1). The same arguments as those used in discussing the hydrolysis of esters (1) show that very little of the volume of activation can be accounted to increased electrostriction. It follows then that the dipole moment of the transition state is probably little different from that of the amide. The volume of activation for the hydrolysis of benzamide in dilute acid is somewhat lower, $-12.1\pm\sim 1.0$ cm^3 mole^{-1}, and it is possible that about 2 to 4 cm^3 mole^{-1} of this may be due to slightly increased electrostriction. It may also be due to the phenyl group's having a greater steric hindrance to the approach of a water molecule than the methyl group. We conclude therefore that no large separation of charges occurs in the transition states.

This conclusion is confirmed by the effect of solvent on the rate of the acid-catalyzed hydrolysis of acetamide in ethanol–water mixtures (4). This is very similar to that of the acid-catalyzed hydrolysis of ethylene oxide in the same solvent (22), confirming the conclusions drawn from the close similarity of the volumes of activation. Laidler and Landskroener (4) and Laidler (5) have argued that this solvent effect implies that the transition state for the hydrolysis of acetamide has a dipole moment of 18.4 D, but this is probably wrong. In addition, the detailed mechanism proposed by Laidler and Landskroener (4) requires two OH bonds to be broken in the transition state, and it is difficult to see how this can be reconciled with the observed faster rate in dilute acid in heavy water than in ordinary water. It seems certain that this demands a pre-equilibrium proton transfer to the amide. However, this can be accommodated in Laidler and Landskroener's transition states by altering two O—H distances.

2. Location of the Proton in the Reactive Amidium Ion

There has been much controversy about whether the extra proton in amidium ions is on the oxygen or the nitrogen atom. Proton resonance spectra (23, 24) appear to show conclusively that acetamide, N-methylacetamide, and N,N-dimethylacetamide are mainly O-protonated. There is no certain information about benzamide. The O-protonated form need not, of course, be the more reactive form.

The conclusions that we can draw about the location of the proton in the reactive form are intimately connected with the question whether the attack of water on the amidium ion is by addition to form a molecule followed by rapid elimination of NH_3 (or NH_2^-) or by direct substitution with simultaneous elimination of NH_3 (or NH_2^-), about which there is no direct evidence. Approximate representations of the transition states for the various mechanisms are given in Fig. 2. The only ones in which a great separation of charges has not occurred, and which therefore are consistent with the evidence discussed in the preceding section are substitution of the N-protonated form or addition to the O-protonated form.

3. Volume Change of the Proton-Transfer Reaction [1]

The evidence that will be discussed in this section is a good deal more uncertain than that discussed in preceding sections.

Can. J. Chem. Downloaded from www.nrcresearchpress.com by 210.87.254.42 on 09/05/12
For personal use only.

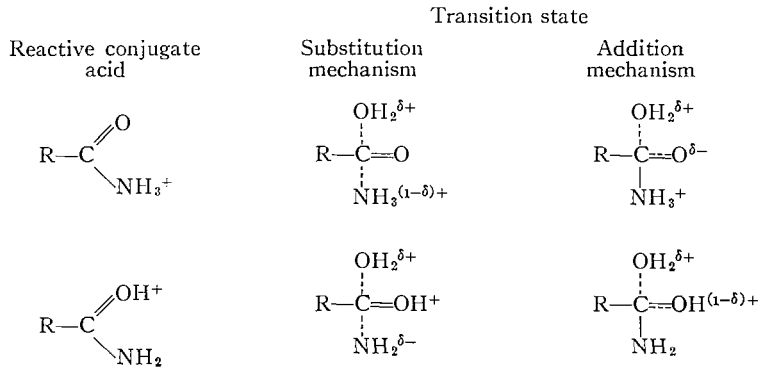
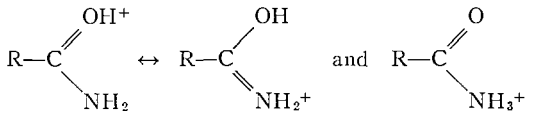


FIG. 2. Transition states for the acid-catalyzed hydrolysis of amides.

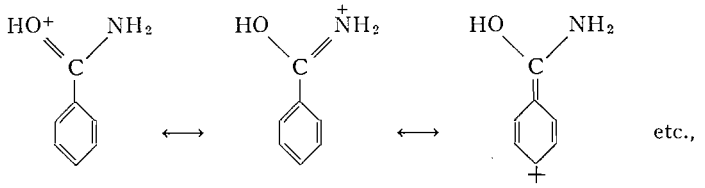
The two most likely amidium ions are



(the double-headed arrow indicates resonating forms). There will probably be an increase in volume when the O-protonated amidium ion is formed from amide and hydronium ion, because the positive charge becomes spread between the oxygen and the nitrogen atoms and this dispersion will decrease the electrostriction of the solvent. A similar, probably more complete, sharing of charge occurs when a proton is transferred from a carboxylic acid to a hydroxyl ion. The volume changes for this reaction for various acids, calculated from the data in the references quoted and the volume of ionization of water of -23.4 cm^3 $mole^{-1}$ (25) are as follows: formic, 15.4 (26); acetic, 10.9 (26); propionic, 9.7 (26); *n*-butyric, 9.7 (26); fumaric, 11.0 (27); benzoic, 12.8 (28); *o*-hydroxybenzoic, 16.2 (28) cm^3 $mole^{-1}$. The increase of volume for the O-protonation of acetamide may not be so great as these because the sharing of the charge between the oxygen and the nitrogen atoms may not be equal. When the N-protonated amidium ion is formed, little dispersion of charge will occur, and so little change of volume is expected (29).

The volume of protonation of acetamide, $3.8 \pm \sim 2.5$ cm^3 $mole^{-1}$, appears to be consistent with either of these protonations, and it does not allow us to choose between them.

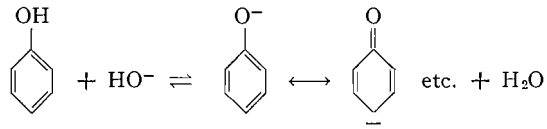
The volume change for the protonation of benzamide, $16 \pm \sim 8$ cm^3 $mole^{-1}$, appears to be too big for N-protonation. It is, however, quite consistent with O-protonation because in the O-protonated ion, which has the following main resonating forms



the charge is probably shared not only by the oxygen and the nitrogen atoms, but also

Can. J. Chem. Downloaded from www.nrcresearchpress.com by 210.87.254.42 on 09/05/12
For personal use only.

by the benzene ring. An example of the effect of dispersal of a charge into a benzene ring on the electrostriction of the solvent is the reaction



for which the volume change is 6.6 cm^3 $mole^{-1}$ (26).

This conclusion is certainly rather tentative at present. However, it does agree with Leisten's (7, 30) observation that while the rate of hydrolysis of substituted benzamides in dilute acid (31, 3) is practically uninfluenced by polar substituents, in concentrated acid, where the rate measured is largely the rate of reaction of the amidium ion with water, there are quite strong polar effects, electron-releasing substituents decreasing the rate and electron-withdrawing substituents increasing the rate. These are the effects that are expected if the attack of water results in the withdrawal of positive charge from the benzene ring.

ACKNOWLEDGMENTS

We are greatly indebted to Mr. A. Lavergne for help with the high-pressure apparatus.

REFERENCES

1. A. R. Osborn and E. Whalley. Can. J. Chem. **39**, 1094 (1961).
2. O. Reitz. Z. physik. Chem. A, **183**, 371 (1939).
3. I. Meloche and K. J. Laidler. J. Am. Chem. Soc. **73**, 1712 (1951).
4. K. J. Laidler and P. A. Landskroener. Trans. Faraday Soc. **52**, 200 (1956).
5. K. J. Laidler. Suomen Kemistilehti, **33**, A, 44 (1960).
6. C. K. Ingold. Structure and mechanism in organic chemistry. Cornell University Press, Ithaca. 1953. p. 784ff.
7. J. A. Leisten. J. Chem. Soc. 765 (1959).
8. M. L. Bender, R. D. Ginger, and K. C. Kemp. J. Am. Chem. Soc. **76**, 3350 (1954).
9. M. L. Bender and R. D. Ginger. J. Am. Chem. Soc. **77**, 348 (1955).
10. G. H. Coleman and A. N. Alvarado. Organic syntheses. Collective Vol. I. 2nd ed. John Wiley & Sons, Inc., New York. p. 3.
11. S. P. L. Sorensen. Biochem. Z. **1**, 45 (1907).
12. P. B. Hawk. Practical physiological chemistry. 13th ed. Blakiston, Philadelphia. p. 897.
13. P. W. Bridgman. Proc. Am. Acad. Arts Sci. **48**, 309 (1912).
14. B. S. Rabinovitch and C. A. Winkler. Can. J. Research, B, **20**, 73 (1942).
15. N. F. Hall. J. Am. Chem. Soc. **52**, 5115 (1930).
16. H. Lemaire and H. J. Lucas. J. Am. Chem. Soc. **73**, 5198 (1951).
17. A. R. Goldfarb, A. Mele, and N. Gutstein. J. Am. Chem. Soc. **77**, 6194 (1955).
18. J. T. Edward and S. C. R. Meacock. J. Chem. Soc. 2000 (1957).
19. J. T. Edward, H. S. Chang, K. Yates, and R. Stewart. Can. J. Chem. **38**, 2271 (1960).
20. J. Koskikallio and E. Whalley. Trans. Faraday Soc. **55**, 815 (1959).
21. J. Koskikallio and E. Whalley. Can. J. Chem. **37**, 788 (1959).
22. R. K. Brown and A. M. Eastham. Can. J. Chem. **38**, 2039 (1960).
23. G. Fraenkel and C. Niemann. Proc. Natl. Acad. Sci. U.S. **44**, 688 (1958).
24. G. Fraenkel and C. Franconi. J. Am. Chem. Soc. **82**, 4478 (1960).
25. B. B. Owen and S. R. Brinkley. Chem. Revs. **29**, 461 (1941).
26. S. D. Hamann and S. C. Lim. Australian J. Chem. **7**, 329 (1954).
27. E. Brander. Soc. Sci. Fennica. Commentationes Phys. Math. **6**(8), 1 (1932).
28. R. J. H. Clark and A. J. Ellis. J. Chem. Soc. 247 (1960).
29. E. Whalley. Trans. Faraday Soc. **55**, 798 (1959).
30. J. T. Edward, H. S. Chang, K. Yates, and R. Stewart. Can. J. Chem. **38**, 2271 (1960).
31. E. Reid. Am. Chem. J. **21**, 284 (1899); **24**, 397 (1902).

Can. J. Chem. Downloaded from www.nrcresearchpress.com by 210.87.254.42 on 09/05/12
For personal use only.

Can. J. Chem. Downloaded from www.nrcresearchpress.com by 210.87.254.5 on 09/05/12
For personal use only.

SPECTROPHOTOMETRIC DETERMINATION OF ALUMINUM IN URANIUM METAL AND ITS COMPOUNDS[1]

ALLAN W. ASHBROOK AND G. M. RITCEY

ABSTRACT

A rapid spectrophotometric method for the determination of small amounts of aluminum in uranium metal and uranium compounds is described. The method makes use of the yellow-colored complex formed between aluminum and 8-hydroxyquinoline (oxine) at pH 9.5–10; the complex is extracted with carbon tetrachloride. Elements which interfere are extracted with 8-hydroxyquinaldine. The method is suitable for the determination of up to 0.1% aluminum.

INTRODUCTION

Aluminum is found in trace amounts in uranium metal and its compounds. Specifications limit its amount to 30 p.p.m. in uranium metal; consequently a sensitive and accurate method was required to determine this amount.

Aluminum has been determined by Horton and Thompson (1) after separation of most of the interfering elements by ion-exchange. Aurine tricarboxylic acid (Aluminon) was used as the chromophoric reagent. This procedure gave erratic results in this laboratory, and also suffered from non-uniformity of the reagent. Of four samples of Aluminon used, each gave a different calibration curve for aluminum.

Methods employing mercury cathode electrolysis for the removal of interfering elements are time consuming. Of other reagents available, oxine showed the best sensitivity (2). The use of this reagent has produced a simple and sensitive method for the determination of aluminum in uranium metal and its compounds. With slight modifications, it has also been used for the determination of small amounts of aluminum in uranium-containing steels.

EXPERIMENTAL

Apparatus and Solutions

The spectrophotometer used in these experiments was a Beckman Model B, with matched 5-cm glass cells.

A standard aluminum solution was prepared by dissolving 0.1759 g of aluminum potassium sulphate ($AlK(SO_4)_2.12H_2O$) in water, and diluting to 1 liter. This solution contained 10 μg of aluminum per milliliter.

The buffer solution was a saturated solution of ammonium carbonate, adjusted to pH 9.5–10 with ammonium hydroxide.

The reagent was a 1% w/v solution of oxine in carbon tetrachloride. Other reagents included a 1% w/v solution of 8-hydroxyquinaldine in chloroform, a 10% w/v aqueous solution of potassium cyanide, and diethylammonium diethyldithiocarbamate.

All other chemicals used were of analytical reagent grade.

Development of the Method

Preliminary Studies

Oxine forms extractable complexes with over 40 elements. Of the trace elements usually to be found in uranium metal and its compounds, almost all will form extractable

[1]*Manuscript received January 30, 1961.*
Contribution from the Research and Development Division, Eldorado Mining and Refining Limited, Ottawa, Ontario.

Can. J. Chem. Vol. 39 (1961)

oxinates. It was therefore essential to remove or complex all elements whose oxinates are extracted at the pH at which the aluminum is extracted. Of the reagents studied for either extraction or complexing of these elements, 8-hydroxyquinaldine appeared to be the most suitable. Merritt and Walker (3) have found that 8-hydroxyquinaldine does not complex aluminum, due to steric hindrance, but otherwise behaves almost like oxine in its reactions. Hynek and Wrangell (4) used this reagent for the extraction of interfering elements from a solution buffered at pH 9.2. It was found in this laboratory that this pH was not critical. The removal of interfering elements with this reagent, at a pH of 9.5–10, was studied.

Aluminum Calibration

For extraction purposes, oxine is generally used in chloroform solution. In the presence of uranium a carbon tetrachloride solution was found to give lower blank values, and this solvent was used throughout these experiments.

A calibration curve was determined by adding known amounts of aluminum to an ammonium chloride – ammonia buffer solution, and extracting with 20 ml of the oxine solution. Absorbance measurements of the extracts were determined at 430 mμ, using 5-cm cells. A straight-line calibration curve was given.

Complexing of Uranium

Since uranium precipitates in an ammonia – ammonium chloride solution, various reagents were tried in order to keep the uranium in solution at pH 9–10. Ammonium tartrate and citrate, while keeping the uranium in solution, inhibited extraction of aluminum. Uranium is soluble in ammonium carbonate solutions at this pH, and this solution was found to have no effect on the extraction of aluminum. A saturated solution of ammonium carbonate, adjusted to pH 9.5–10 with ammonium hydroxide, was used, both to keep the uranium in solution and as a buffer solution.

Interfering Elements

Elements found in uranium metal and its compounds which are likely to interfere in the determination are cobalt, manganese, nickel, zinc, copper, and iron. A study of the removal of these elements by extraction with a 1% solution of 8-hydroxyquinaldine in chloroform was carried out.

Known amounts of these elements were added to ammonium carbonate – ammonia buffer solutions, containing uranium and 25 μg of aluminum. Extraction with 8-hydroxyquinaldine showed that up to 100 μg of cobalt, nickel, zinc, copper, lead, and iron could be extracted without effect on the aluminum recovery (Table I). Manganese, however, was

TABLE I

Extraction of elements with 8-hydroxyquinaldine

Element added	Amount added, μg	Aluminum* recovered, μg
Cobalt	100	24
Nickel	100	25
Zinc	100	25
Copper	100	25
Iron	100	25
Lead	100	26
Manganese	10	27
"	20	30
"	100	63

*Twenty-five micrograms of aluminum added in each case.

Can. J. Chem. Downloaded from www.nrcresearchpress.com by 210.87.254.5 on 09/05/12
For personal use only.

not extracted by the 8-hydroxyquinaldine, but was extracted by the oxine, giving large positive errors in the aluminum determination. The valency state of the manganese had no effect on its extraction. Small amounts of manganese (5 μg) had little or no effect on the aluminum determination. Larger amounts had to be removed.

Removal of Manganese

There appeared to be no reagent available which would complex manganese under the conditions of the experiments. A study of reagents suitable for its extraction prior to the determination of aluminum showed diethylammonium diethyldithiocarbamate to be the most suitable. This reagent had no effect on the recovery of aluminum. Sample solutions containing more than 5 μg of manganese were extracted with chloroform after the addition of solid diethylammonium diethyldithiocarbamate. Extraction of other interfering elements was completed by extraction with 8-hydroxyquinaldine.

In order to ensure the complete removal of deleterious effects of interfering elements which may not have been completely removed by the extraction with 8-hydroxyquinaldine, potassium cyanide solution was added before addition of the oxine solution. Potassium cyanide did not affect the extraction of aluminum.

Preparation of Samples

Samples of uranium metal and uranium compounds were dissolved in a 3:1 mixture of hydrochloric and nitric acids. The solutions were then boiled to remove oxides of nitrogen, and diluted to a suitable volume.

Recommended Procedure

Dissolve and dilute the sample as described under Preparation of Samples. Transfer by pipette an aliquot containing 5–50 μg of aluminum into a 125-ml, separatory funnel. Add 30 ml of the buffer solution and mix. If the aliquot contains more than 5 μg of manganese, add 1 g of diethylammonium diethyldithiocarbamate, mix thoroughly, and extract with 10-ml portions of chloroform until the extracts are colorless. Add 5 ml of the 8-hydroxyquinaldine solution and shake for 2 minutes. Allow the phases to separate and discard the organic phase. Repeat this extraction until little or no color is given in the organic phase. Extract the aqueous phase with 3×10-ml portions of chloroform. Discard the extracts. Add 5 ml of potassium cyanide solution and mix. By pipette, add 20 ml of the oxine solution into the funnel and shake the mixture for 2 minutes. Allow the phases to separate and filter the organic phase through a coarse, dry filter paper. Measure the absorbance of the extract at a wavelength of 430 mμ, using 5-cm cells, with the spectrophotometer set to zero on a blank.

Calibration Procedure

Measure from a burette 0-, 1-, 2-, 3-, 4-, and 5-ml volumes of the standard aluminum solution into 125-ml separatory funnels, and carry them through the procedure. Plot absorbance readings against micrograms of aluminum. Beer's law is obeyed.

Results and Precision

Table II presents some typical results obtained on uranium metal samples, together with results obtained on a New Brunswick Laboratories Analysed Sample (No. 16) of uranium metal. Also shown is the precision obtained on samples of uranium metal containing low and high quantities of aluminum.

The method gave a standard deviation of 0.8 p.p.m. aluminum at the 13 p.p.m. level, and the 95% confidence limits on a single determination of ±1.7 p.p.m. At the 600 p.p.m. level these were 7.5 and ±16 p.p.m. respectively.

Can. J. Chem. Downloaded from www.nrcresearchpress.com by 210.87.254.5 on 09/05/12
For personal use only.

TABLE II

Results obtained on samples of uranium metal and uranium dioxide

Sample		Aluminum, p.p.m.
NBL No. 16*		12, 12, 14, 13, 14, 13
UO_2	A	4, 4
	B	3, 3
	C	60, 61
	D	52, 54
Uranium	A	573, 570, 568, 572, 575
Metal	B	935, 945
	C	14, 14, 13

*NBL certificate, 10 p.p.m. (spectrographic analysis).

REFERENCES

1. A. D. HORTON and P. F. THOMPSON. Anal. Chem. **28**, 1326 (1956).
2. E. B. SANDELL. Colorimetric determination of traces of metals. 3rd ed. Interscience Publishers, New York. 1959. p. 227.
3. L. L. MERRITT and J. K. WALKER. Ind. Eng. Chem. Anal. Ed., **16**, 387 (1944).
4. R. J. HYNEK and L. J. WRANGELL. Anal. Chem. **28**, 1520 (1956).

Can. J. Chem. Downloaded from www.nrcresearchpress.com by 210.87.254.5 on 09/05/12
For personal use only.

Can. J. Chem. Downloaded from www.nrcresearchpress.com by 210.87.254.105 on 09/05/12
For personal use only.

A STUDY OF THE EMISSION INTENSITIES OF Cr LINES FROM SHOCKED GASES CONTAINING $Cr(CO)_6$[1]

S. H. Bauer, John H. Kiefer, and Brian E. Loader

ABSTRACT

Argon–nitrogen mixtures (9/1) were inoculated with traces of $Cr(CO)_6$ (0.026%) and shocked to temperatures in the range 3500° K to 5700° K. The intensities of a violet line ($^7P_2 \rightarrow {}^7S_3$) and a triplet of green lines ($^5P_{3,2,1} \rightarrow {}^5S_2$) were measured concurrently, with a dual-channel spectrograph. Exclusive of runs for which $T > 5000°$ K, the variation of intensity with temperature was brought to agreement with theoretical predictions under the assumption that the N_2 vibrations, the dissociation of $Cr(CO)_6$, and the ionization of Cr attained their equilibrium states, but allowance had to be made for self-absorption. The dependence of the rise times on temperature suggest that the excitation and ionization of Cr is predominantly due to collisions with electrons. The over-all shapes of the recorded light pulses were qualitatively accounted for. It is suggested that extraneous background radiation contributed to the measured intensities for samples shocked to temperatures above 5000° K.

INTRODUCTION

Studies of the excitation of atomic energy states by collisions with heavy particles in the thermal energy range have been limited experimentally by the difficulty of preparing sufficiently intense beams of incident atoms or molecules and theoretically by the inherent complexity of the potential energy hypersurfaces which must be considered in the treatment. Efficiencies for energy transfer in de-excitation processes have been measured for a number of target atoms from the quenching of radiation due to the introduction of a variety of incident molecules. The cross sections (Q) for the forward and reverse processes are, of course, related. For particles which have a high relative kinetic energy (primed),

$$Cr' + Ar' \leftrightarrows Cr^* + Ar,$$

let the p' be the momentum of relative motion prior to excitation and p of the excited pair. Then (1, p. 417),

$$[1] \qquad g_{Cr'}g_{Ar'}p'^2Q' = g_{Cr^*}g_{Ar}p^2Q,$$

where the g's designate the statistical weights, as indicated. Since $p'^2 > p^2$, the cross section for the superelastic process is generally greater than for the excitation process. However, the cross sections for collision-induced electronic transitions are very small unless the change of internal energy is very small. Per impact, the transition probability is low if

$$[2] \qquad a|\Delta E|/hv \gg 1,$$

where a is the range of interaction between the atoms, and v is their relative velocity, since such an event takes place at near-adiabatic conditions. Massey and Burhop (1, p. 515) suggest that the cross section for excitation should then vary as $\exp(-Ca|\Delta E|/v)$ and consequently would increase exponentially with temperature, for a thermalized system.

Investigations of the luminous front in shocked gases provide data on excitation processes in thermalized systems where the average relative kinetic energies of the participating particles are less than one volt. A theory for the excitation of atoms by

[1]*Manuscript received October 24, 1960.*
Contribution from the Department of Chemistry, Cornell University, Ithaca, New York. Presented at the Symposium on Fundamental Aspects of Atomic Reactions, McGill University, Montreal, Que., September 7, 1960.

collisions at elevated temperatures has been outlined by Nikitin (2). In this paper, we describe preliminary work on the excitation of resonance lines in chromium, introduced in trace amounts as $Cr(CO)_6$ in argon–nitrogen mixtures and shocked to temperatures from 3000–5500° K. The possible utility of chromium emission intensity ratios for the estimation of shock temperatures has been analyzed previously (3). Wilkerson (4) obtained time-resolved Cr(I) and Cr(II) emission spectra from incident and reflected shocks in Ne which had been inoculated with 0.3% of chromium carbonyl. Recent studies (5) of the delayed luminosity in highly purified xenon as induced by a shock have proved both interesting and puzzling, since the current predictions suggest that the potential curves for two xenon atoms do not cross over the energy range of collisions which are prevalent in shocked gases at 6000° K. It now appears that the diameter of the shock tube, the composition of the tube walls, and the purity of the driver gas play important roles in determining both the electrical and optical structure of the shock front.

The sensitivity to slight impurities, which appears in accentuated form when one measures the electrical conductivity of shocked gases, is due to free electrons, the concentration of which is probably determined by the lowest ionization potential of any impurity present in the gaseous sample and by the nature of the shock-tube walls. It also seems likely that these electrons play a dominant role in collision-induced electronic excitations. For the excitation of electronic states, the collision cross section becomes appreciable only when the *speed* of the incident particle approaches that of the atomic electron involved in the transition (1, p. 515). Hence, at the temperatures developed in the shocked gases, the average energy per pair is too low to provide an appreciable transition probability for excitation by atom–atom collisions. However, in that energy range, the efficiency of excitation by collision with electrons is much greater, perhaps by a factor of 10^3.

Insofar as there is *structure* to the shock front, no single measure of temperature can be specified. The very difficult problem of determining the velocity distribution of the electrons in this region has yet to be solved. One may argue, however, that beyond a distance of the order of 10 mean free paths following the steep pressure gradient in the shock front the electrons will have attained translation equilibrium and would then possess the same translational temperature as the massive particles present.

SPECTROSCOPIC MEASUREMENT OF SHOCK TEMPERATURES

The gas temperature behind a shock wave may be computed from the measured shock speed, the composition of the gas being subjected to the shock, and its initial temperature and pressure, provided one assumes that thermodynamic equilibrium is attained in the system for specified end products. One must postulate not only definite chemical species but also their allowed states of excitation, so that the thermodynamic state of the shocked gas is determined by a temperature, a density, and a set of mole fractions. When the chemical kinetics of a system are being studied in a shock tube, such detailed information and its dependence on distance behind the shock front are not available. However, it is meaningful to consider the translational temperature of the gas and to inquire whether the temperatures which may be associated with rotations, vibrations, and electronic states are in equilibrium with translation.

Various techniques have been developed for directly estimating temperatures in very hot gases. Stark shifts (6) and the broadening of spectral lines (7) have been used for very strong shocks and gases heated by electrical discharges. Gaydon and co-workers

Can. J. Chem. Downloaded from www.nrcresearchpress.com by 210.87.254.105 on 09/05/12
For personal use only.

Can. J. Chem. Downloaded from www.nrcresearchpress.com by 210.87.254.105 on 09/05/12
For personal use only.

(8) described a modified form of the sodium-line-reversal technique to deduce temperatures with an estimated accuracy of ±20° C. Although this method is capable of higher precision when long measuring times are available as in steady-state conditions for flames (9), it is accompanied by considerable difficulties when the data must be recorded with microsecond resolution. To produce a sufficiently dense suspension of sodium chloride particles in the gas to be shocked, they found it necessary to pass the sample through a hot tube (~800° C) over the molten salt. Very few gases of chemical interest may be treated in this manner. It is interesting to note that electronic temperatures deduced for flames by the reversal technique utilizing various spectral lines from iron, lead, etc. (10), were found to be higher than the maximum theoretical temperature for the specified composition. The origin of these excessive temperatures is not known, but it is surmised that they arise partly from chemical excitations.

The relative emission intensities of two atomic lines characteristic of a trace impurity are a measure of temperature, provided one may assume that the electronic states of the emitter have attained equilibrium with translation or vibration. Then, the intensities can be readily converted to a temperature from the known location of the corresponding upper states and the absolute f numbers or by a calibration procedure. If the concentration of emitter is sufficiently low so that self-absorption may be ignored, the results are independent of emitter density (3). Sobolev *et al.* (11), tested this procedure with lithium chloride and sodium chloride as trace emitters but obtained badly scattered results due to self-absorption, inhomogeneous gas distribution, etc.

To avoid the difficulty of working with crystallites of a nonvolatile material, we measured the emission intensities of the resonance lines of chromium at λ4290 and λ5206, derived from known concentrations of traces of chromium carbonyl in Ar–N_2 mixtures. Manganese, iron, tungsten, and nickel carbonyls can be similarly used as sources of metal atoms. Flame spectra (2200–3200° K) indicate that the spectral sensitivities of these chromium lines are of the order of 10^{-2} of that of NaD. We thus have controlled concentrations, with pressures which may be as high as 0.3 mm Hg of emitter gas.

THEORY

A rough numerical estimate shows that in the shock front the change of intensity with time is indeed a measure of the rates of excitation of the chromium atoms, that is, of the process:

$$Cr_{(g)}[a,\ ^7S] + X_{(g)} \xrightarrow[k_x]{} Cr_{(g)}^*[z,\ ^7P \text{ or } z,\ ^5P] + X$$

and not that due to the rate of dissociation of the carbonyl. The enthalpy change at 0° K for the reaction

$$Cr(CO)_{6(g)} = Cr_{(g)} + 6CO_{(g)}, \qquad \Delta H^\circ_0 = 173.23 \text{ kcal/mole} \qquad (12a).*$$

It follows that the average ⟨Cr—CO⟩ bond dissociation energy is 28.9 kcal. An order of magnitude for the unimolecular rate constant for the dissociation

$$Cr(CO)_n^* \xrightarrow[k_{uni}^{(n)}]{} Cr(CO)_{n-1} + CO$$

is:

$$[3] \qquad k_{uni}^{(n)} \approx 10^{18} e^{-29,000/RT}, \text{ sec}^{-1}.$$

**The authors reported that the standard heat of formation at 298.2° K of $Cr(CO)_{6(g)}$ is −257.57±0.51 kcal/mole. Correction for the heat of sublimation of $Cr(CO)_6$ (ΔH°_{sub} $Cr(CO)_6$ = 17.18 kcal, as reported in reference 12b), the heat of sublimation of $Cr_{(g)}$ (ΔH°_{sub} $Cr_{(s)}$ = 95 kcal/mole, as reported in reference 12c), and the heat of formation of 6CO molecules leads to ΔH°_{298} = 176.90 kcal for the indicated dissociation reaction.*

If one postulates that on the average this value is typical of each of the six steps, the time required for $(Cr)/(Cr)_{final}$ to reach 0.9 at 1000° K is $t_{0.9} \simeq 10/k_{uni}^{(n)} \simeq 10^{-10.7}$ sec. This is much less than the response times of currently available recording apparatus. For all practical purposes, the metal carbonyl is completely dissociated in the forward portion of relatively weak shocks.

The spectral radiancy from a distributed emitter in thermal equilibrium, of optical depth X ($= pL$, atm cm) and spectral absorption coefficient $P_\omega(\text{atm}^{-1}\,\text{cm}^{-1})$, is (13)

$$[4] \qquad R_\omega = R^\circ_\omega[1-\exp(-P_\omega X)].$$

The black-body radiancy at the specified temperature is given by

$$[5] \qquad R^\circ_\omega = 2\pi hc^2\omega^3[\exp(hc\omega/kT)-1]^{-1}.$$

Since the spectrometer–phototube–oscilloscope system integrates radiation over a selected line, with central position at ω_1, one should use the integral of the spectral absorption coefficient. For a Gaussian shape,

$$[6] \qquad P_\omega X = \alpha \exp\left[-\left(\frac{\omega-\omega_1}{\beta}\right)^2\right]; \qquad \int_{\text{line}} P_\omega d\omega = \frac{\sqrt{\pi}\alpha\beta}{X}.$$

However,

$$[7] \qquad \int_{\text{line}} P_\omega d\omega = \frac{\pi e^2}{mc^2}\frac{N_l}{p} f_{l\to u}\,(1-e^{-hc\omega_1/kT}),\ \text{cm}^{-2}\,\text{atm}^{-1}$$

where

$f_{l\to u}$ = oscillator strength for the transition from the lower (l) state to the upper (u) state (for Cr, refer to the report by Hill and King (14)),

$$\omega_1 = \frac{E_u - E_l}{hc},$$

N_l = number of molecules of emitting species per cubic centimeter, in the lower state,

p = pressure (atm) of emitting species.

Whence,

$$[8] \qquad \alpha = \frac{L}{\sqrt{\pi}\beta}\frac{\pi e^2}{mc^2} N_l f_{l\to u}\,(1-e^{-hc\omega_1/kT}).$$

If $P_\omega X$ is sufficiently small, the exponential in [4] may be expanded and the terms integrated (for the Gaussian shape), provided one assumes that $R^\circ_{\omega_1}$ is constant over the narrow band of wave lengths which is transmitted by the exit slit.

$$[9] \qquad V_{\omega_1} = K_{\omega_1} R^\circ_{\omega_1}\sqrt{\pi}\alpha\beta[1-\alpha/2\sqrt{2}+\ldots]$$

$$= K_{\omega_1}\frac{2\pi^2 he^2\omega_1^3}{m} N_l L f_{l\to u} e^{-hc\omega_1/kT}[1-\alpha/2\sqrt{2}+\ldots]$$

K_{ω_1} is a transmission-amplification constant which relates the oscilloscope-voltage output to the intensity of ω_1 picked up by the spectrometer. The term in α in the bracket is a measure of self-absorption; it is density and temperature dependent.

Can. J. Chem. Downloaded from www.nrcresearchpress.com by 210.87.254.105 on 09/05/12
For personal use only.

Can. J. Chem. Downloaded from www.nrcresearchpress.com by 210.87.254.105 on 09/05/12
For personal use only.

[10] $$N_i = \rho \frac{g_i}{Q} e^{-E_i/kT}$$

where Q is the total partition function, with the ground state taken as the zero; ρ is the total emitter density, in molecules per cubic centimeter.

[11] $$V_{\omega_1} \propto \frac{\rho g_i}{Q} f_{i\to u} \exp\left(-\frac{hc\omega_1 + E_i}{kT}\right)$$

For a given spectrometer setting, a plot of $\ln [V_{\omega_1} Q/\rho]$ vs. $1/T$ should be a line with slope $-(hc\omega_1 + E_i)/kT$. If appreciable ionization takes place, the concentration of atoms in state l will be depleted by an amount which depends sensitively on the temperature, as given by the Saha equation.

Provided self-absorption is in fact negligible, the 'two-color temperature' (15) is given by the ratio

[12] $$\frac{V_{\omega_1}}{V_{\omega_2}} = \frac{K_{\omega_1}}{K_{\omega_2}} \frac{g_{l_1} f_1}{g_{l_2} f_2} \exp\left[-\frac{E_{u_1} - E_{u_2}}{kT}\right]$$

since $E_{l_1} + \omega_1 = E_{u_1}$, etc. The unknown ratios may be lumped into a single constant which may be determined by calibration with shocks of measured speed under idealized conditions.

The observed rise time for each line depends on many factors. In addition to the response time of the recording electronics and particle passage time past the cone of observation, the rate of approach to the 'equilibrium' emission intensity may be limited by the vibrational and dissociation relaxation of nitrogen, if present, and by the finite rates for excitation and ionization of the chromium atoms. Since $dV(t)/dt \propto |f_{u\to l}| dN_u/dt$ and $V_e \propto g_l f_{l\to u} (N_u)_e / g_u$,

[13] $$\left[\frac{1}{V_e}\frac{dV(t)}{dt}\right]_{corr} \propto \frac{1}{(N_u)_e}\frac{dN_u}{dt}$$

is an experimental 'rise time' characteristic of the atomic state and of the excitation processes. There are at least three distinct processes which populate the specified upper state:

(a) excitation from a lower state by collision with a heavy particle:

$$Cr(i) + Ar' \xrightarrow[k_i]{} Cr(u) + Ar$$

(b) excitation by collision with an electron:

$$Cr(j) + e^- \xrightarrow[k_j]{} Cr(u) + e^-$$

(c) radiative recombination with an electron:

$$Cr^+ + e^- \xrightarrow[k_c]{} Cr(u) + h\nu.$$

The total rate is the sum over all states i and j.

The mechanism for ionization in shock fronts has been discussed by a number of authors (16, 17). Electron–atom processes have the largest cross sections. This is also the case for excitation reactions (b) (1, p. 515; 18). Some electrons are initially present in the unshocked gas; some of these may have been generated photoelectrically by

Can. J. Chem. Downloaded from www.nrcresearchpress.com by 210.87.254.105 on 09/05/12
For personal use only.

photons downstream from the shock front, others by residual radioactivity. Their concentration is rapidly increased when the gas is compressed by the shock. Because of their low mass, these electrons diffuse ahead of the shock front and establish a double layer across which there exists a considerable potential drop. In the co-ordinates of the moving shock, rapidly moving atoms enter from the upstream side and collide with relatively energetic electrons to produce excited atoms and more electrons.

The depopulation of the upper state can occur via:

(a') the reverse of (a):

$$\mathrm{Ar} + \mathrm{Cr(u)} \xrightarrow[k_i']{} \mathrm{Cr}(i) + \mathrm{Ar}'$$

(b') the reverse of (b):

$$\mathrm{e^-} + \mathrm{Cr(u)} \xrightarrow[k_j']{} \mathrm{Cr}(j) + \mathrm{e^-}$$

(d) radiation:

$$\mathrm{Cr(u)} \xrightarrow[f_{\mathrm{u}\to i}]{} \mathrm{Cr}(i) + hc\omega_i$$

(e) ionization from the excited state:

$$\mathrm{Cr(u)} + \mathrm{e^-} \xrightarrow[k_x]{} \mathrm{Cr^+} + 2\mathrm{e^-}.$$

Electrons are also produced via:

(f) ionization from all other states:

$$\mathrm{Cr}(j) + \mathrm{e^-} \xrightarrow[k_+]{} \mathrm{Cr^+} + 2\mathrm{e^-}.$$

Let n be the concentration of electrons in the shocked gas at $t = 0(+)$ and $c(t)$ the additional electrons generated via (e) and (f). For the early stages ($t < t_{\frac{1}{2}}$), one may write

$$\frac{d(n+c)}{dt} \approx [k_x(\mathrm{Cr_u}) + k_+(\mathrm{Cr}_j) - k_c(\mathrm{Cr^+})](n+c).$$

Then, since $(\mathrm{Cr^+}) \ll (\mathrm{Cr})$, an average value of the ionization rate constant may be used,

$$(n+c) \approx n \exp\,[\langle k\rangle \rho_{\mathrm{Cr}} t]; \qquad [14]$$

i.e., the electron concentration initially rises exponentially.

It is very likely that under shock conditions (b') and (e) are more effective in depleting the upper state than are (a') and (d). We estimated that in the experiments described below the mean time between collisions (kinetic-theory cross sections) is between 1×10^{-9} sec to 4×10^{-10} sec, whereas the radiative lifetimes of the ^7P and ^5P states of chromium are of the order of 10^{-8} sec. For the net rate of population of the upper state, assuming that atom–electron processes dominate,

$$\frac{d(\mathrm{Cr_u})}{dt} \approx (n+c)[k_j(\mathrm{Cr}_j) + k_c(\mathrm{Cr^+}) - (k_x + k_j')(\mathrm{Cr_u})]. \qquad [15]$$

Since, at $t = 0(+)$, $k_j(\mathrm{Cr}_j)^\circ \gg (k_x + k_j')\ (\mathrm{Cr_u})^\circ$, the population of the excited state may 'overshoot' its equilibrium value and thus produce a maximum in the emitted

intensity vs. time curve. For comparable rate constants, say $(k_r+k_j') = k_j(1+\alpha)$ with α small, $t_m = 1/k_j$. Whether the maximum is experimentally observable will depend on the temporal behavior of $(n+c)$. If the latter reaches its equilibrium value rapidly, the maximum will be recorded and will become more pronounced in amplitude as $(k_r+k_j')/k_j$ decreases.

There are insufficient data at present to permit a complete kinetic analysis of the above complex mechanism. However, as a preliminary approach, assume that the net rate of excitation to the upper level at the shock front may be expressed in terms of a single rate constant. Let

$$\left(\frac{dN_u}{dt}\right)_{net} = \rho_{Cr}{}^n A \exp(-E_u^*/kT). \quad [16]$$

Hence,

$$\frac{1}{\tau_0} \equiv \frac{1}{V_e}\left(\frac{dV}{dt}\right)_{initial} = \frac{AQ}{g_u} e^{-(E_u^*-E_{(\cdot)})/kT} \rho_{Cr}{}^{n-1}. \quad [17]$$

E_u^* has the significance of an activation energy* and corresponds to the energy at the crossover point of the unperturbed potential function curves for Cr-incident particle and $Cr_{(u)}$-incident particle. A plot of $\ln [1/QV_e\rho^{n-1}(dV/dt)_i]$ vs. $1/T$ should give a line with a slope $-(E_u^*-E_u)/k$. If process (a) dominates, the slope should be steep, whereas under conditions where (b) and (c) control the rate, $E_u^* \approx E_u$.

In the above formulation, it has been assumed that the temperature of the shocked gas was unambiguously defined and independent of time. This is the case for samples which consist solely of argon with traces of chromium carbonyl, since the depletion of energy by the dissociation of $Cr(CO)_6$ and ionization of Cr results in a temperature drop of no more than 10° K at the highest temperatures studied. However, when the ambient gas contains an appreciable amount of N_2 (circa 10%), the shock front consists of several relaxation zones, which are superposed, due to vibrational excitation and dissociation of the nitrogen, as well as the excitation and ionization of the chromium. In the samples shocked to temperatures above 4700° K, an appreciable fraction of the nitrogen is dissociated at equilibrium. Preliminary measurements by Byron (private communication) gave for the dissociation rate constant at 7000° K

$$N_2 + Ar \underset{k^d}{\overset{k^a}{\rightleftharpoons}} 2N + Ar$$

$$(dN/dt)_{initial} = k^d(N_2)(Ar); \quad \begin{aligned} k_{Ar}{}^d &= 2.8\times10^8, \text{ (mole/cc)}^{-1}\,\text{sec}^{-1} \\ k_{Ar}{}^a &= 1.7\times10^{14}, \text{ (mole/cc)}^{-2}\,\text{sec}^{-1} \end{aligned}$$

(As a third body, N_2 appears to be about 2.5 times as effective as Ar. In our system, however, the Ar rate dominates.) We estimated that at 5000° K, in a 10% N_2 – 90% Ar mixture, the half time for the attainment of dissociation equilibrium is 80 milliseconds.

*The product of the time elapsed between ionization onset and the attainment of its maximum value and the initial pressure of the shocked gas ($\tau_i p_1$) was found to decrease approximately linearly with increasing Mach number, for air (Y. Manheimer-Timnat and W. Low. J. Fluid Mech. **6**, 449 (1959); B. Niblett and V. H. Blackman. J. Fluid Mech. **4**, 191 (1958)). Generally, the Mach numbers correlate with the initial pressures. It is suggested, therefore, that these ionization–relaxation times might be more uniquely interpreted in terms of eq. [17].*

Can. J. Chem. Downloaded from www.nrcresearchpress.com by 210.87.254.105 on 09/05/12
For personal use only.

EXPERIMENTAL

The following experiments were performed in a stainless-steel tube, 6-in. I.D., Fig. 1.

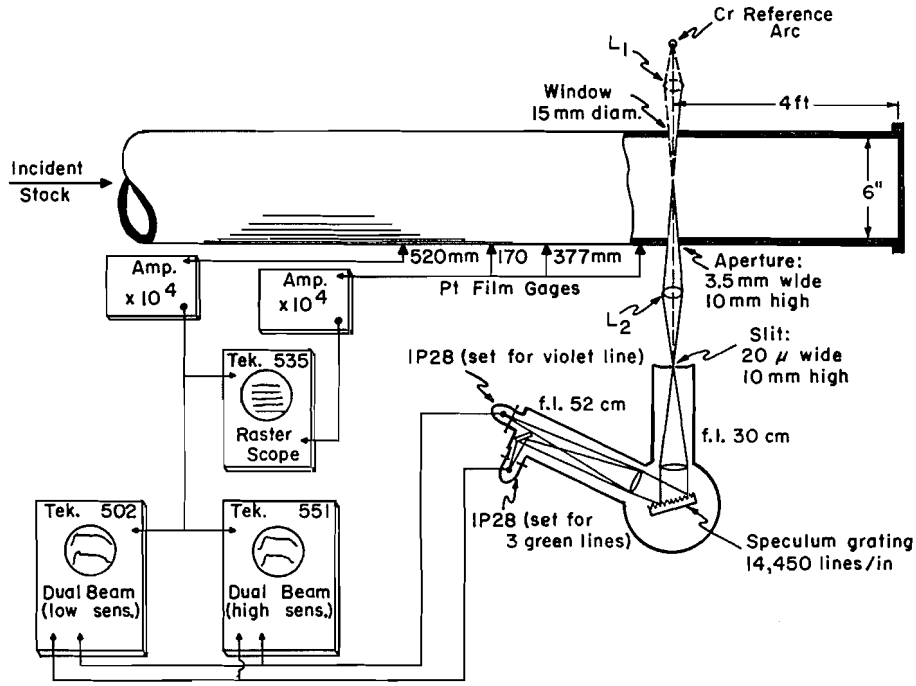


FIG. 1. Schematic arrangement of the optics and a block diagram of the electronic components. The spectrograph had an entrance slit 20 μ wide and 10 mm high. The dispersion at a camera focal length of 52 cm was 30 Å/mm. The exit slit for the violet line was set at 70 μ and for the green lines at 170 μ.

The driver section was 8 ft long. The windows through which the luminosity was observed were located 18 ft downstream from the diaphragm. Beyond the windows, the tube extended 4 ft, so that ample time was provided to avoid confusion with the reflected shock. The diaphragms were of half-hard brass, 0.032 in. thick, precision scribed through half their thickness. In all of the experiments described, the diaphragms were broken by exceeding the predetermined breaking pressure. Depending on the batch of sheet stock used, this was reproducible to within 5 lb. The windows were of quartz, and the aperture for observing the emitted light was limited to a section 3.5 mm wide and 10 mm high. Gauges for detecting shock arrival times were thin platinum films supported on Pyrex, placed at the indicated locations. Hydrogen was used as the driver gas at pressures of 200 to 230 p.s.i. The temperature of the shock was controlled by the pressure of the driven gas, which consisted of argon plus chromium carbonyl or a mixture of argon and nitrogen (9/1) plus the chromium carbonyl. The shock tube was evacuated with a 4-in. diffusion pump to 10^{-5} mm Hg; the leak rate was about one-half micron per minute.

We found it essential to premix the chromium carbonyl with the argon or argon–nitrogen mixture to insure uniformity of the sample. The mixtures consisted of chromium carbonyl vapor as derived from the solid maintained at room temperature and expanded into a 50-gal glass-lined tank to a pressure of 70 μ. To this, 27 cm of the carrier gas

Can. J. Chem. Downloaded from www.nrcresearchpress.com by 210.87.254.105 on 09/05/12
For personal use only.

Can. J. Chem. Downloaded from www.nrcresearchpress.com by 210.87.254.105 on 09/05/12
For personal use only.

was added and the mixture allowed to stand for several days prior to use. The concentration of chromium carbonyl in the test samples was 0.026%. Total pressures of the driven gas ranged from 0.65 cm to 3.15 cm to cover the full range of shock temperatures. Shock speeds were measured from a raster display. The optical arrangement is also diagramed in Fig. 1. The two channels of the grating spectrograph (dispersion, 30 Å/mm) were aligned with a chromium arc so set on the opposite side of the tube as to focus to a virtual source in the center of the tube. The violet line at λ4289.7 ($a\ ^7S_3 \leftarrow z\ ^7P_2^0$) was sent along the central axis of the receiver section and the receiving slit set to admit a region in wave length roughly twice the width of the line. The small side mirror was then positioned so that the green triplet [λ5208.4, 5206.0, 5204.5 ($a\ ^5S_2 \leftarrow z\ ^5P^0_{3,2,1}$)] passed through the side receiver; this slit also was set to collect a little more than the triplet (19).*

The two photomultipliers were powered by a single well-regulated voltage supply, and the output of these tubes was split and sent to two dual-beam oscilloscopes, so that the intensity of the two lines could be recorded simultaneously at two sensitivity levels. This was necessary because the level of emission intensity was not always predictable. The time constant for the phototubes, amplifiers, and recording oscilloscopes was of the order of 4 μseconds. In some of the experiments to be described below, another set of phototubes was used. These were constructed with cathode followers which gave an electronic time constant of 0.8 μsecond but were of limited utility since they were easily saturated. The experimental 'rise time' was not limited by the 2- to 3-μsecond passage time of the gas past the cone of observation as viewed by the spectroscope. Typical shock parameters are summarized in Table I for a high-temperature shock and for one

TABLE I

Shock parameters for typical experiments

(Driver: H_2, 200–220 p.s.i., gauge. Mixture: Ar (90%), N_2 (10%), $Cr(CO)_6$ (0.026%))

	Run No. 51		Run No. 50	
Initial sample pressure (total), cm at $T_1 = 300.5°$ K	3.15		0.65	
Initial density (total), in mole cc^{-1}	1.68×10^{-6}		3.38×10^{-7}	
Incident shock speed, in mm/μsec	1.974		2.556	
Incident shock T_2 (no N_2 vib. or dissoc.)	3560° K		5789° K	
p_2, cm	139		48.3	
ρ_2 (total), mole cc^{-1}	6.74×10^{-6}		1.35×10^{-6}	
Density of Cr atoms $(\rho_2)_{Cr}$, mole cc^{-1}	1.68×10^{-9}		3.48×10^{-10}	
Particle speed, in mm/μsec	1.21		1.79	
Particle passage time past cone of observation, in μsec	2.89		1.95	
Theoretical interval between shock front and contact interface, in μsec	920		700	
Light intensity at t_m (1000 v on dynodes, voltage output across 10K load resistor)	Green 0.888	Violet 1.475	Green 3.99	Violet 7.54
$[(1/V_m)(dV/dt)_i]^{-1}$ as measured, in μsec	34.5	30	13.0	13.9
Approx. width of light pulse (lab time), in μsec	480		360	

near the lower end of the temperature range studied. Figure 2 shows traces of typical oscillograms.

**The author gives energy levels and frequencies for chromium. Note that the $a\ ^5S_2$ state is 7593 cm^{-1} above the ground $a\ ^7S_3$ state.*

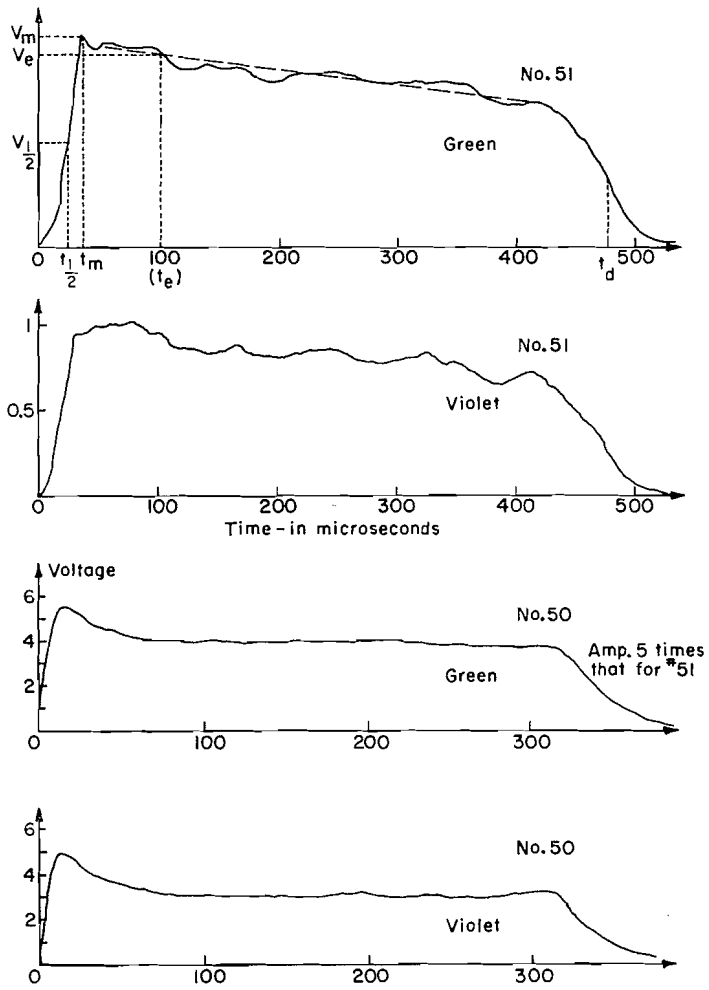


FIG. 2. Tracings of the oscilloscope records of the violet and green line photomultiplier outputs for two runs. Refer to Table I for a summary of the experimental conditions. The characteristic features of these voltage variations are designated in the top curve.

SUMMARY OF OBSERVATIONS

One of the first experiments performed was a spectroscopic examination of the total light emitted. The double-channel photomultiplier unit was replaced by a camera. In order to enhance the intensity of the emitted light, a fairly high concentration of chromium carbonyl was introduced and the spectrum taken in the reflected shock region. The plate showed a very large number of lines. On careful examination, all of the lines were identified and proved to be due to Cr(I). No other lines nor background intensities were observed under these conditions. On these plates, the lines of interest appeared reversed, which suggested that the amount of carbonyl should be reduced from the initial 300 μ to roughly 3 μ.

In another crucial experiment, the initiation of light emission was checked against the arrival time of the shock at the window. For this measurement, the phototube circuitry had a rise time of 0.8 μsecond. To within 1 microsecond, the incidence of light

Can. J. Chem. Downloaded from www.nrcresearchpress.com by 210.87.254.105 on 09/05/12
For personal use only.

emission coincided with the arrival time of the shock front at the central line of the viewing port; further inspection of the traces suggested that the luminosity started perhaps half to 1 microsecond earlier.

The oscillogram records show a number of features for analysis. Specifically, the following will be considered:

(*a*) for each line, the variation of intensity with shock temperature and density,
(*b*) the rise time of light emission at the shock front and its dependence on temperature, on the composition of the ambient gas (presence of 10% N_2 diluent), and on the specific levels involved, and
(*c*) the general shape of the emission output as a function of time; in particular, the presence of an initial maximum and the duration of the pulse.

ANALYSIS OF THE DATA

Since most of the shocks were run with the 9/1 Ar/N_2 mixture, the question arose as to whether the effective temperature in the shock front should be computed with the vibrational contribution of the nitrogen included or deleted. From Blackman's data (20), we estimated that the vibrational relaxation time for run No. 50 was 7 μseconds, and for No. 51 it was 10 μseconds (assuming no difference in efficiency between Ar–N_2 and N_2–N_2 collisions), with intermediate periods for the other runs. These times are more than twice that required for the particles to pass the cone of observation but about half of the observed rise time (lab. co-ordinates) for emission. Were the populations of the $^7P_2{}^0$ and $^5P^0{}_{3,2,1}$ states to rapidly attain equilibrium with the vibrational temperature (cf. Clouston and Gaydon (8)), the rise time for emission would be considerably shorter than that observed. The lag in the excitation of vibrations should at most affect the *initial* slope of the emission-time curve but should have no influence on the slope at the half-height position ($V_{\frac{1}{2}}$ at $t_{\frac{1}{2}}$, Fig. 2). In view of our estimate of the half time for the attainment of dissociation equilibrium, the temperatures used in Figs. 3–5 were computed on the assumption of partial equilibrium; i.e., we included the excitation of vibrations in N_2 (these reduced the translational temperatures by 60–180° K, over the range 3500–5800° K), the complete dissociation of the chromium carbonyl ($\sim$ 8° K), and the ionization of chromium atoms (0–7° K). The ionization of argon is negligible even at the highest temperatures.

An analysis of a number of runs is presented to illustrate features *a*, *b*, and *c*. In Figs. 3 and 4, eq. [11] was applied to the recorded intensities of the violet and green lines at t_m and t_e, respectively. The ordinates were computed on the assumption that the population of the upper states was proportional to the total chromium concentration. Within the scatter of the data, the slopes of the two sets of curves are independent of the time, for $t > t_m$, and for the lower third of the range in $1/T$ the observed slopes check the theoretical values. At the upper temperatures, the recorded intensities fall below the theoretical curves by a factor which increases with the temperature. This departure is considerably greater for the green line than for the violet lines and is more evident at t_e than at t_m. The same data were replotted on the assumption that the populations of the upper states were proportional to the concentration of chromium atoms which remain unionized; i.e., the abscissa was $\log [V_m Q/7\rho_{Cr}(1-x)]$, where x is the percentage ionized at the equilibrium shock temperature and density, as computed by means of the Saha equation; considerable ionization is present at equilibrium for $1/T \leqslant 2.1\times10^{-4}$. The points were found to lie on the theoretical slopes over the lower two thirds of the

Can. J. Chem. Downloaded from www.nrcresearchpress.com by 210.87.254.105 on 09/05/12
For personal use only.

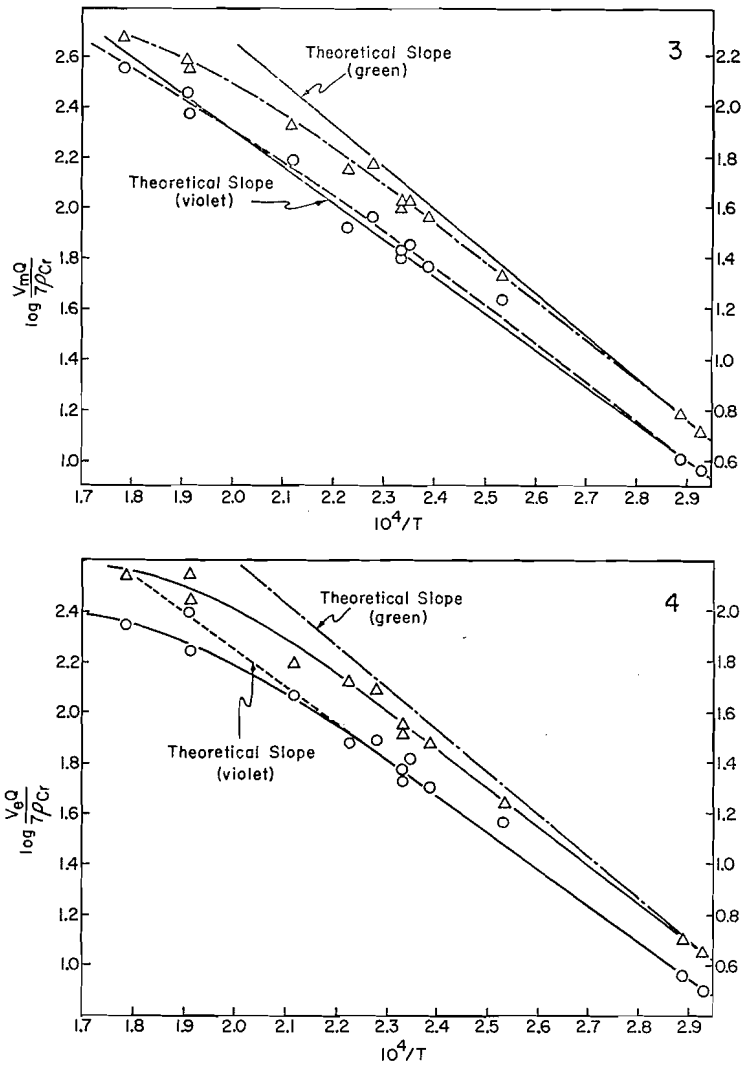


FIG. 3. Plots of $\log[(V_mQ)/(7\rho_{Cr})]$ vs. $10^4/T$ for the violet and green lines. The temperature and density were computed neglecting ionization of the chromium and dissociation of the nitrogen.
FIG. 4. Plots of V_e (at $t = 100$ μsec), similar to Fig. 3.

range in $1/T$. For the upper temperature range, it appears that the correction for ionization has 'overcompensated' the intensity function (Fig. 5 for V_m; a similar curve was obtained for V_e). Note also that the points for the violet line depart more from the theoretical slope than do those for the green lines.

Kinetic data presented below suggest that electron–atom processes control the rate of populating the upper levels and the production of ions. We then tested the possibility that the relaxation time for nitrogen dissociation was appreciably shortened by the presence of Cr^+. These ions, the few negative ions produced by attachment of the electrons, and even the chromium atoms should be highly efficient third bodies for the dissociation reaction. In Fig. 6, the intensities recorded at t_e have been plotted, per eq. [11], against the reciprocal temperatures computed on the assumption of complete

Can. J. Chem. Downloaded from www.nrcresearchpress.com by 210.87.254.105 on 09/05/12
For personal use only.

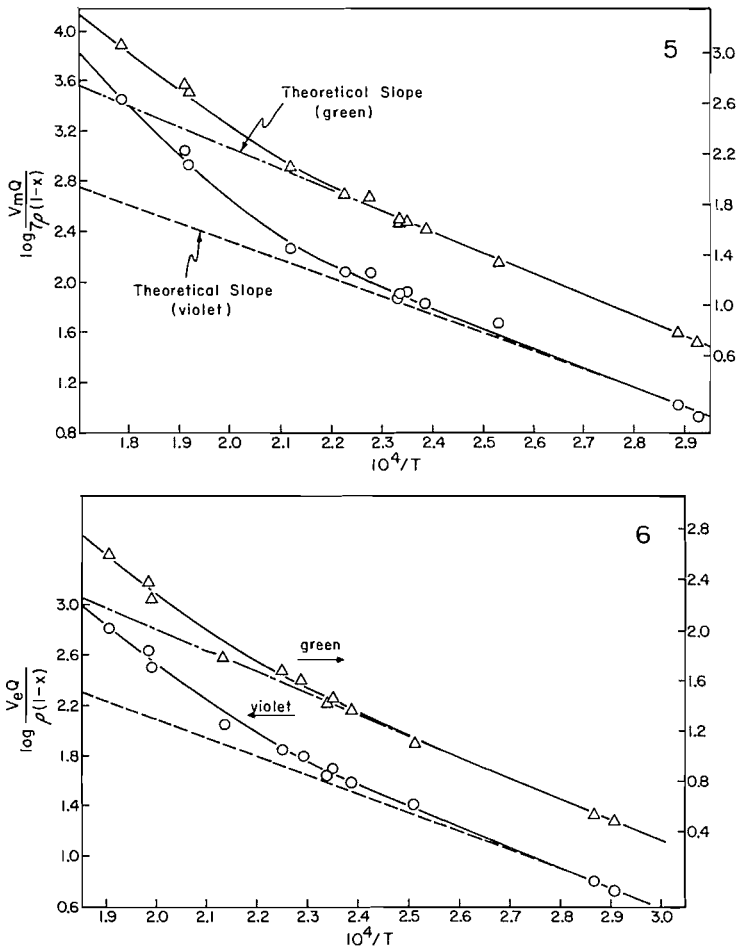


FIG. 5. Plots of $\log [(V_m Q)/7\rho(1-x)]$ vs. $10^4/T$ for the violet and green lines. The temperature and density were computed neglecting the dissociation of nitrogen but allowing for the depletion of chromium by ionization. The fraction ionized is denoted by x.

FIG. 6. Plots of $\log [(V_e Q)/\rho(1-x)]$ vs. $10^4/T$ for the violet and green lines. The temperature and density were computed allowing for the dissociation of N_2 and the ionization of Cr.

equilibrium. Dissociation of the nitrogen, at the highest shock speeds, reduced the computed temperature by $\sim 350°$ K and thereby the magnitude of x. However, the deviations from the theoretical slope were not eliminated due to the concurrent shift of the high-temperature points along the $1/T$ axis with an increase in $(1-x)$.

Except for the points obtained at the highest temperature, the departures from the theoretical slopes may be eliminated by introducing a correction for self-absorption (the term in α, eq. [9]). Since this correction is directly dependent on the population of the lower state, its magnitude for the violet line is proportional to $7\rho_{Cr}(1-x)\,(1-e^{-23,400hc/kT})/Q$ and for the green lines to $5\rho_{Cr}(1-x)e^{-7,593hc/kT}(1-e^{-26,800hc/kT})/Q$. Both functions depend linearly on the density. This is noticeable for the run at $10^4/T = 2.135$ (Fig. 6), which was at a higher density than the adjacent points. In general, the shock densities were lower for the higher-temperature runs. Due to the exp $(-7593hc/kT)$ factor, the green lines should self-absorb approximately 1/33 as much as the violet line, and the

Can. J. Chem. Downloaded from www.nrcresearchpress.com by 210.87.254.105 on 09/05/12
For personal use only.

over-all variation of the former for the different runs should be less than for the latter. In Fig. 7, V_e data have been replotted after they were corrected for self-absorption, of

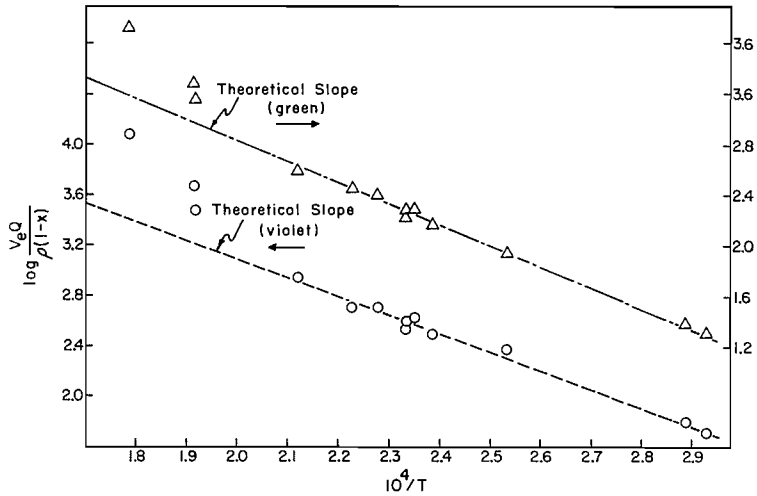


FIG. 7. Plots of $\log [(V_e Q)/\rho(1-x)]$ vs. $10^4/T$ corrected for self-absorption; N_2 dissociation was not included.

such magnitude as to optimize the agreement with the theoretical slope. It is evident that except for the three high-temperature points the experimental slopes coincide with the theoretical values. If these deviations are due to some rate process, a relatively long time constant is involved, since the points for V_m and V_e fall on similar curves; that it is not simply a relaxation in the effective temperature is demonstrated by Fig. 6. Qualitative estimates indicate that these deviations are not due to boundary-layer effects; these would be quite small and of a sign opposite to that observed.* An *ad hoc* explanation is to assume that for $T > 5000°$ K extraneous background radiation contributes appreciably to the recorded intensity due to the relatively broad band passed by the exit slits of the spectrometer.

RISE TIME OF EMISSION

In eq. [16], it is plausible to assume that $(dN_u/dt)_{net} = \rho(1-x)\rho x A \exp(-E_u^*/kT)$ with $(N_u)_e = \rho(1-x) \exp(-E_u/kT)/Q$. This implies that the net rate is proportional to the product of the equilibrium concentration of unionized chromium atoms by the concentration of chromium ions (equal to electrons). A plot of $\log [1/\rho x Q V_m (dV/dt)_{\frac{1}{2}}]$ vs. $1/T$ gave a curve with a suggestion of a minimum in the high-temperature region and a large positive slope as $1/T$ increased. Since no reasonable mechanism can be associated with such a temperature dependence, this assumption must be discarded.

A direct second-order dependence of $(dN_u/dt)_{net}$ on the total density leads to a plot of $\log [1/\rho Q V_m (dV/dt)_{\frac{1}{2}}]$ vs. $1/T$; Fig. 8 is such a graph for the violet line. The change in slope at $10^4/T = 2.3$ implies that two mechanisms are operative, with $(E_u^* - E_u) =$ 18 kcal mole^{-1} and 54 kcal mole^{-1} for the low- and high-temperature ranges, respectively. (A similar set of values was obtained for the green lines.) For these, we find no acceptable explanation. If the dominant processes for the attainment of the steady-state emission

*Roth and Hartunian (21) analyzed boundary-layer temperatures and densities.

Can. J. Chem. Downloaded from www.nrcresearchpress.com by 210.87.254.105 on 09/05/12
For personal use only.

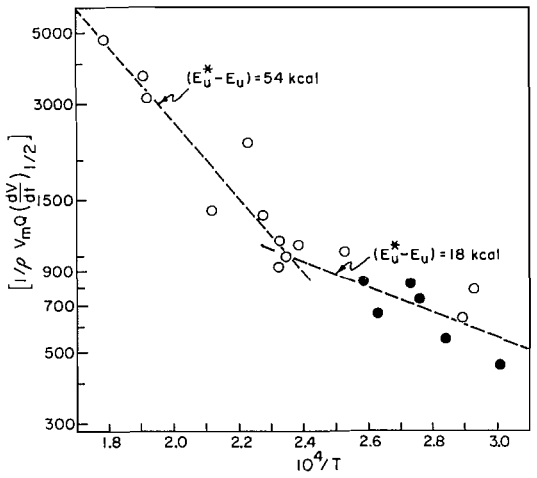


FIG. 8. A plot of $[1/(\rho V_m Q)][(dV/dt)_{\frac{1}{2}}]$, log scale, vs. $10^4/T$ for the *violet* line. The six solid points were taken during the early runs where there was insufficient mixing of $Cr(CO)_6$ and Ar.

involved atom–atom collisions, they would be much slower (18), and the activation energies for excitation, process (*a*), are expected to be much larger.

The simplest assumption is that the rate of excitation, $(dN_u/dt)_{net}$, is dominated by a single process which depends linearly on the density in the same manner as does $(N_u)_e$. This similarity of dependence on density is also imposed on the ionization factor. Graphs of log $[1/V_m Q(dV/dt)_{\frac{1}{2}}]$ vs. $1/T$ for the violet and green lines are shown in Fig. 9; six

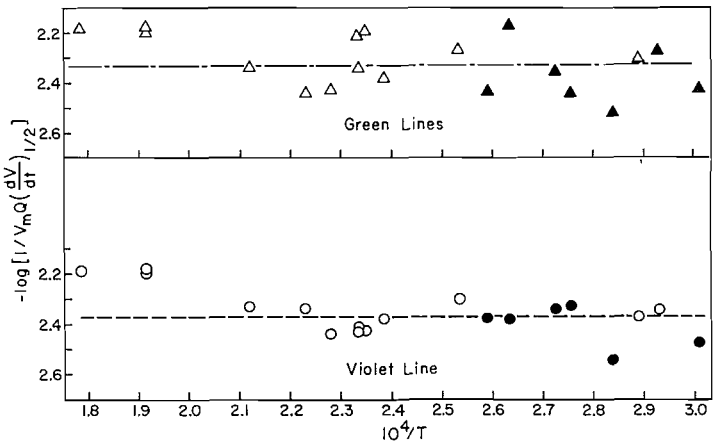


FIG. 9. Plots of $-\log[1/(V_m Q)][(dV/dt)_{\frac{1}{2}}]$ vs. $10^4/T$ for the violet and green lines. The six solid points were taken during the early runs where there was insufficient mixing of the $Cr(CO)_6$ and Ar. The dashed lines have zero slope.

additional points from early runs have been included (full circles and hexagons). Exclusive of the three points for which $1/T < 2\times10^{-4}$, the slopes are nearly zero within the scatter of the data. This is consistent with the postulate that the excitation and ionization of chromium atoms are due mostly to collisions with electrons, for which $E_u^* \approx E_u$ is expected. The initial rise should be exponential in character, as per eq. [14]. Suppose

Can. J. Chem. Downloaded from www.nrcresearchpress.com by 210.87.254.105 on 09/05/12
For personal use only.

extraneous background radiation did contribute appreciably to the recorded intensities for runs with $T > 5000°$ K; it may well have done so with a short relaxation time, so that the τ_0's for the three high-temperature points were somewhat shorter than for the others, as observed. Finally, in agreement with the above analysis, the τ_0's for the violet and green lines are equal to within the scatter of the data.

Rather crude measurements obtained with the short response-time circuitry indicate that the rise times for emission were somewhat longer when pure Ar was the ambient medium, compared with the N_2–Ar mixture. This is consistent with the observations of Clouston and Gaydon (8).

SHAPE OF THE LIGHT PULSE

The characteristic shapes of the recorded phototube outputs (Fig. 2) may be accounted for on a qualitative basis. Following the rapid rise, the intensity briefly passes through a slight maximum and levels off to a constant value for the high temperature runs but to a slowly declining magnitude at low temperatures. Finally, it falls rapidly at a time (t_d) which is roughly half the interval from shock front to contact surface, as estimated from ideal shock-tube theory (Table I). It has been established both experimentally (22) and theoretically (23)* that at low initial pressures the flow duration is considerably less than the time computed for ideal shock-tube operation due to effects of the laminar boundary layer behind the shock; low speed gas in the boundary layer near the wall leaks past the contact surface. Quantitative estimates show that this effect is very small for our experiments, even for the lowest initial pressures of 6.3 mm Hg, because of the large diameter of the shock tube. The major source of the short duration flow is the nonideal rupture of the diaphragms, which were comparatively massive (0.032-in. half-hard brass sheets, scored to a depth of 0.016 in., 6 in. in diameter). Under these circumstances, it probably takes more than 10 tube diameters to form the shock, resulting in an effective tube length considerably shorter than the geometrical 18 ft.

Inspection of all the oscilloscope traces showed that the initial maximum was more prominent for the green lines than for the violet line and that it increased in magnitude with rising shock temperature. Reference to Fig. 2 shows that in run No. 51 it is essentially absent for the violet line and of the same order of magnitude as the fluctuation for the green line. From the curves in Fig. 7, we have estimated that for the green line $(V_m - V_e)$ corresponds to 40–100° K for the upper temperature runs. The maximum in emission is accounted for by eq. [15]. In view of our conclusion that $E_u^* \approx E_u$, reasonable estimates of the rate constants are

	$^7P_2 \leftarrow {}^7S_3$	$^5P_2 \leftarrow {}^5S_2$
	(violet)	(green)
k_j	$A_j^v \exp(-23{,}305\ hc/kT)$	$A_j^g \exp(-26{,}796\ hc/kT)$
k_x	$A_x^v \exp(-31{,}236\ hc/kT)$	$A_x^g \exp(-27{,}745\ hc/kT)$
k_+	ground state: $A_+ \exp(-54{,}541\ hc/kT)$	

Since all the pre-exponential factors should be of comparable magnitude for these similar processes, k_j^v at low temperatures may be large enough to place t_m^v within the rising portion of $(n+c)$. As the temperature is raised, $(n+c)$ rises more rapidly to its final value than do other excitation processes (k_+ has the largest activation energy), and the maxima in intensity become more prominent.

We acknowledge with thanks permission to refer to the author's paper "On flow duration in low pressure shock tubes" prior to publication.

Can. J. Chem. Downloaded from www.nrcresearchpress.com by 210.87.254.105 on 09/05/12
For personal use only.

Can. J. Chem. Downloaded from www.nrcresearchpress.com by 210.87.254.105 on 09/05/12
For personal use only.

CONCLUSIONS

The use of dual-channel data to deduce two-color temperatures to the desired precision still awaits the development of techniques for the measurement of intensities with a reproducibility and precision to the order of 2% and with a time resolution of less than a microsecond. For the range 3000–5000° K, if a known trace concentration of $Cr(CO)_6$ is premixed with the test gas, measurement of the intensity of a single Cr emission line does permit the estimation of temperatures to roughly ±50° K, provided care is taken to calibrate the optical–electronic system. Above 5000° K, it appears that extraneous background radiation leads to too high a value, when the intensity is recorded with a spectroscope of modest resolution. Except at the lowest temperatures, the measured intensities had to be corrected for self-absorption.

The rate of excitation of chromium emission is independent of the carbonyl dissociation rate. Our data suggest that the excitation is due primarily to collision of chromium atoms with electrons. The over-all time dependence of the intensity can thus be accounted for in a qualitative manner.

ACKNOWLEDGMENTS

This work was supported by the Air Force (ARDC) under contract AF33(616)-6694. B. E. L. acknowledges with thanks a NATO Research Studentship Grant for the past year. We also thank Mr. Emmett Sutton and Miss Ann Walbran for the use of their program for the computation of equilibrium shock parameters for a dissociating gas and the Ethyl Corporation for the samples of chromium carbonyl used in these experiments. Finally, we gratefully acknowledge the kindness of Dr. R. E. Duff, who computed the thermodynamic functions of $Cr(CO)_6$ (cf. Appendix) and obtained the least-squares fit of coefficients for the free energy expansion via his IBM 704 program.

APPENDIX

Thermodynamic and Partition Functions

A. The thermodynamic functions of chromium carbonyl were recomputed for the ideal gas at one atmosphere, under the simple harmonic-oscillator, rigid-rotor approximation, over the temperature range 300–6000° K (cf. N. J. Hawkins *et al.* J. Chem. Phys. **23**, 2422 (1955)). The values for the free energy function were least-squares fitted to a polynomial in the temperature:

$$\frac{F^\circ_T - H^\circ_0}{RT} = a(1-\ln T) - bT - \frac{c}{2}T^2 - \frac{d}{3}T^3 - \frac{e}{4}T^4 - k.$$

Values for the coefficients were obtained over two ranges.

	Best fit over 300–2000° K	Best fit over 1500–6000° K
k	-3.8958892	$-5.7940996\times10^{+1}$
a	7.5396309	$2.0163532\times10^{+1}$
b	4.2072684×10^{-2}	9.0970966×10^{-3}
c	-3.6287469×10^{-5}	-2.5055972×10^{-6}
d	1.6024045×10^{-8}	3.3908588×10^{-10}
e	-2.7501040×10^{-12}	-1.7854329×10^{-13}

B. The ratio of the partition functions for chromium in the singly ionized and neutral states were computed, to facilitate estimation of the degree of ionization of the metal vapor, via the Saha equation.

T	$10^4/T$	Q_{Cr^I}	$Q_{Cr^{II}}$	$(Q_{Cr^{II}}Q_e)/(Q_{Cr^I})$
3448	2.900	8.07	6.20	1.5366
3704	2.700	8.37	6.29	1.5030
4000	2.500	8.75	6.42	1.4674
4348	2.300	9.25	6.62	1.4313
4762	2.100	9.92	6.93	1.3972
5263	1.900	10.89	7.39	1.3572
5882	1.700	12.38	8.13	1.3134

REFERENCES

1. H. S. W. Massey and E. H. S. Burhop. Electronic and ionic impact phenomena. Clarendon Press, Oxford. 1952.
2. E. E. Nikitin. Optics and Spectroscopy U.S.S.R. **8**, 82 (1960).
3. S. H. Bauer, N. C. Rol, and J. H. Kiefer. AFOSR-GE Conference on Physical Chemistry in Aerodynamics and Space Flight, Philadelphia. September, 1959. *Edited by* A. L. Myerson. Pergamon Press, London.
4. T. D. Wilkerson. Bull. Am. Phys. Soc. **5**, 131, 362 (1960).
5. W. Roth and P. Gloersen. J. Chem. Phys. **29**, 820 (1958); W. Roth. J. Chem. Phys. **31**, 844 (1959); P. Gloersen, T. I. S. Report R60SD364. M. S. V. D., General Electric Co., Philadelphia, April 26, 1960; J. N. Bradley and W. Roth. J. Chem. Phys. **32**, 1875, 1876 (1960).
6. H. E. Petschek *et al.* J. Appl. Phys. **26**, 83 (1955).
7. J. G. Clouston and A. G. Gaydon. Nature (London), **180**, 1342 (1957).
8. J. G. Clouston, A. G. Gaydon, and I. I. Glass. Proc. Roy. Soc. A, **248**, 429 (1958); J. G. Clouston, A. G. Gaydon, and I. R. Hurle. Proc. Roy. Soc. A, **252**, 143 (1959); A. G. Gaydon, G. N. Spokes, and J. L. Van Suchtelen. Proc. Roy. Soc. A, **256**, 323 (1960).
9. H. M. Strong and F. P. Bundy. J. Appl. Phys. **25**, 1521, 1527 (1954).
10. A. G. Gaydon. The spectroscopy of flames. J. Wiley & Sons, New York. 1957. pp. 138ff., 201.
11. N. N. Sobolev *et al.* Optics and Spectroscopy U.S.S.R. **6**, 185 (1959); W. H. Parkinson and R. W. Nicholls. Can. J. Phys. **38**, 715 (1960).
12*a*. F. A. Cotton, A. K. Fischer, and G. Wilkinson. J. Am. Chem. Soc. **78**, 5168 (1956).
12*b*. W. Hibber and E. Romberg. Z. anorg. u. allgem. Chem. **221**, 332 (1935).
12*c*. R. F. Porter. Private communication.
13. S. S. Penner. Quantitative molecular spectroscopy and gas emissivities. Addison-Wesley Publishing Co., Inc., Reading, Mass. 1959.
14. A. J. Hill and R. B. King. J. Opt. Soc. Am. **41**, 315 (1951).
15. S. S. Penner. J. Opt. Soc. Am. **41**, 457 (1951).
16. H. E. Petschek and S. Byron. Ann. Phys. **1**, 270 (1957).
17. J. Bond. Phys. Rev. **105**, 1683 (1957).
18. W. L. Fite. Proceedings of the Fourth International Conference on Ionization Phenomena in Gases. *Edited by* N. R. Nilsson. North-Holland Pub. Co., Amsterdam. 1960.
19. C. C. Kiess. J. Research Natl. Bur. Standards, **51**, 247 (1953).
20. V. H. Blackman. J. Fluid Mech. **1**, 61 (1956).
21. N. Rott and R. Hartunian. Report to AFOSR under Contract AF33(038)-2146, November, 1955. Grad. School Aero. Eng., Cornell University, Ithaca, N.Y.
22. R. E. Duff. Phys. Fluids, **2**, 207 (1959).
23. A. Roshko. Private communication.

Can. J. Chem. Downloaded from www.nrcresearchpress.com by 210.87.254.105 on 09/05/12
For personal use only.

Can. J. Chem. Downloaded from www.nrcresearchpress.com by 210.87.254.105 on 09/05/12
For personal use only.

LIGHT ABSORPTION STUDIES

PART XVIII. THE ULTRAVIOLET ABSORPTION SPECTRA OF BROMOBENZENES[1]

W. F. Forbes

ABSTRACT

The ultraviolet absorption spectra of bromobenzene in various solvents, and the spectra of a series of substituted bromobenzenes in cyclohexane solution, are reported. The *B*-band spectral data confirm the hypotheses postulated for the *B*-band spectra of chlorobenzenes in the previous part of this series of papers. That is, the bromine atom usually gives rise to greater steric effects than the chlorine atom and the apparent mesomeric interaction as judged from these spectra increases with the size of the halogen substituent.

Both bromobenzene and chlorobenzene *C*-band intensities are unusually small, and this is assumed to account for the frequent *C*-band similarity between the spectrum of a mono-substituted benzene derivative PhX, where X = OH, OCH_3, NH_2, and the spectrum of the corresponding chloro- or bromo-substituted PhX derivative.

INTRODUCTION

Following a study of the ultraviolet absorption spectra of chlorobenzenes (1) and of fluorobenzenes (2), it is intended to extend the discussion of the properties of halogen-substituted benzenes by the study of the spectra of bromobenzenes. It follows from this that the band nomenclature and other terms used in the present paper are identical with the terms as defined or used in the previous papers (1, 2).

THE SPECTRUM OF BROMOBENZENE

The absorption characteristics of bromobenzene in different solvents are listed in Table I.

Table I shows that the location of the *B*-band of bromobenzene is similar for cyclohexane, ether, ethanol, and aqueous solutions. Three points may be noted on comparing the *B*-band of bromobenzene and chlorobenzene. First, a slight wavelength displacement is observed between the *B*-band of bromobenzene in the vapor phase and in cyclohexane solution, whereas no such wavelength displacement was observed for chlorobenzene (1). Since the dipole moment data (3, and references cited therein), infrared data (4), and other data (which are determined by the ground state alone) are similar for chlorobenzene and bromobenzene, it is possible that the electronic excited state of chlorobenzene (which determines predominantly the observed absorption band) is practically independent of the C—Cl dipole but that the C—Br dipole makes some contribution to the relevant electronic excited state of bromobenzene.

Next, the bromobenzene *B*-band usually exists as a maximum accompanied by subsidiary inflections at longer wavelength, and these latter submerged maxima do not facilitate precise comparisons with the locations of absorption bands of other compounds, and in particular with that of chlorobenzene. However, using the absorption band occurring at the longest wavelength, namely the inflection occurring at ca. 222 mμ, or using the "center of gravity" of the bands, the data suggest that the *B*-band of bromobenzene occurs at slightly longer wavelength than the *B*-band of chlorobenzene (cf. ref. 1 and see Fig. 1).

Thirdly, the intensity of the *B*-band of bromobenzene in most solvents is also slightly greater than for the corresponding chlorobenzenes (see, for example, Fig. 1 and cf. also

[1]*Manuscript received November 28, 1960.*
Contribution from the Division of Protein Chemistry, C.S.I.R.O., Parkville N.2 (Melbourne), Victoria, Australia.

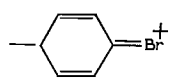
TABLE I

Main ultraviolet absorption maxima of bromobenzene in various solvents*

Solvent	*B*-band		*C*-band	
	λ_{max} (mμ)	ϵ_{max}	λ_{max} (mμ)	ϵ_{max}
Vapor phase	209 213 *218*	†	251 254 257 260 *263* 264 266	†
Cyclohexane	*211* 213 *215* ca. *222*	*8500* 9000 *8500* *6000*	245 252 *257* 259 262 265 272	130 140 *160* 180 180 200 130
Ether	212 *215* ca. *222*	8800 *8200* *5700*	244 *249* 251 *255* 258 261 264 *267* 272	130 *120* 135 *155* 160 175 180 *130* 115
Ethanol	212 ca. *215* ca. *222*	8100 *7500* *5000*	ca. *245* 251 ca. *255* 258 261 264 ca. *267* 271	*130* 135 *155* 160 175 180 *130* 110
Water	211 ca. *215* ca. *222*	4000 *4000* *2500*	ca. *244* 251 255 261 264	*100* 100 120 140 130

*Values in italics represent inflections in this and the subsequent table.
†Intensities not determined.

Table I and ref. 1). A simple explanation of these three effects (i.e., the increased solvent–solute interaction, the slight shift to longer wavelength, and the intensification of the *B*-band in bromobenzene compared with these effects in chlorobenzene) is to relate these *B*-band changes to mesomeric interaction as illustrated by resonance structures of type I and to assume that the apparent mesomeric effect is in the order I > Br > Cl



(I)

> F. Since this order of mesomeric interaction is different from that suggested by other data (except for some isolated infrared data (5, 6) which indicate an order of mesomeric interaction parallel to the order as suggested by the ultraviolet data), we refer to it as the *apparent* mesomeric effect of the halogen atoms. Further evidence of the order

Can. J. Chem. Downloaded from www.nrcresearchpress.com by 210.87.254.105 on 09/05/12
For personal use only.

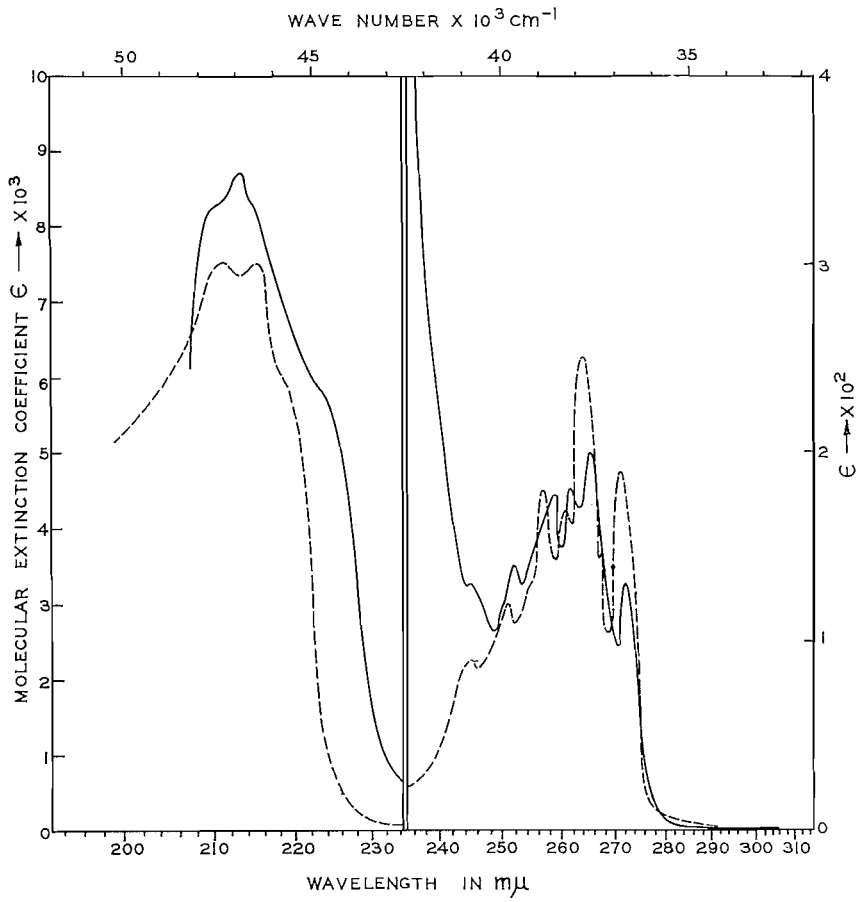


FIG. 1. The ultraviolet absorption spectra in cyclohexane solution of bromobenzene (full line) and chlorobenzene (dotted line).

Br > Cl for the apparent mesomeric effect of the halogen atoms will be presented in the next section.

On the other hand, it should be noted that the majority of ground state data indicate a reverse order of mesomeric interaction, namely F > Cl > Br > I. Moreover, even if the order of mesomeric interaction is as indicated by the present data in the electronically excited state of the observed spectra, it should be pointed out that the order of mesomeric interaction would still be different in these excited levels from the order prevailing in the activated complexes involved in chemical reactions.*

The *C*-bands of bromobenzene and chlorobenzene are similar (see, for example, Fig. 1 and cf. also Table I and ref. 1). Both *C*-bands are unusually weak and this may account for the frequent "overshadowing" of these *C*-bands when another substituent is present, as for example in the spectra of *p*- and *m*-bromofluorobenzenes, which show *C*-bands of comparable intensity to that of fluorobenzene (see Fig. 2).

**A referee has pointed out that ground state calculations have shown that the resonance integrals which measure the π-orbital overlap of two bonded atoms decrease in the order* F > Cl > Br > I *for* =C—X *systems. In support, however, of the arguments presented in this paper, the referee suggests that the excited states for the heavier halogens are more energetically stable and this might tend to reverse the series "in the excited state".*

Can. J. Chem. Downloaded from www.nrcresearchpress.com by 210.87.254.105 on 09/05/12
For personal use only.

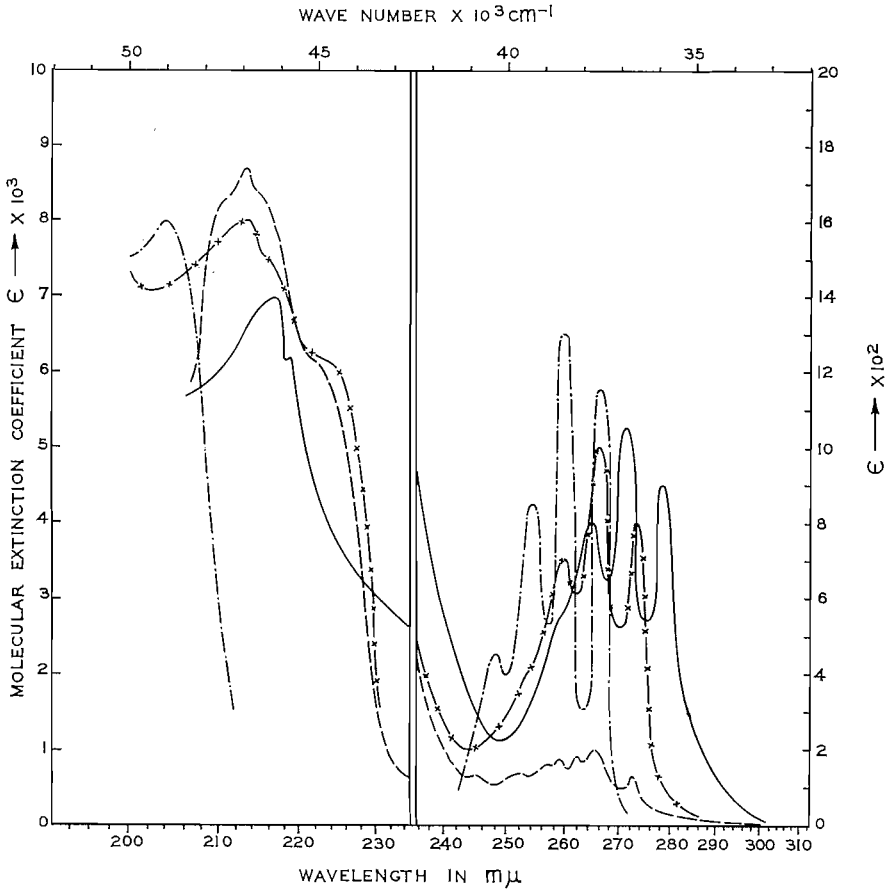
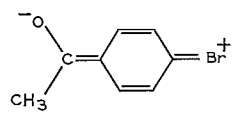


FIG. 2. The ultraviolet absorption spectra in cyclohexane solution of *p*-bromofluorobenzene (——) *m*-bromofluorobenzene (— ×), fluorobenzene (— ·), and bromobenzene (— —).

THE SPECTRA OF PARA-SUBSTITUTED BROMOBENZENES

Using the simplified resonance concept illustrated by structures of type I, electron-withdrawing substituents in the *p*-position of bromobenzene, which permit the extension of the conjugated system as illustrated by resonance structures of type II, would be



(II)

expected to lead to *B*-band absorption at longer wavelength and with increased absorption intensity. In fact, the *B*-band data for *p*-substituted bromobenzenes, where the *p*-substituent is —CHO, —$COCH_3$, or —NO_2, show that the *B*-band now occurs at longer wavelength and with increased absorption intensity (see Table II). Moreover, comparison with the *B*-band data of the related *p*-substituted chlorobenzenes, given in reference 1, shows that the *B*-bands of these *p*-substituted bromobenzenes absorb at slightly longer wavelength and with greater absorption intensity than the corresponding *p*-substituted

Can. J. Chem. Downloaded from www.nrcresearchpress.com by 210.87.254.105 on 09/05/12
For personal use only.

Can. J. Chem. Downloaded from www.nrcresearchpress.com by 210.87.254.105 on 09/05/12
For personal use only.

TABLE II

Main ultraviolet absorption maxima of substituted bromobenzenes in cyclohexane solution

	Para isomer				Meta isomer						Ortho isomer					
	B-band		*C*-band		Bromobenzene *B*-band		2nd *B*-band		*C*-band		Bromobenzene *B*-band		2nd *B*-band		*C*-band	
Substituent	λ_{max} (mμ)	ϵ_{max}	λ_{max} (mμ)	ϵ_{max}	λ_{max} (mμ)	ϵ_{max}	λ_{max} (mμ)	ϵ_{max}	λ_{max} (mμ)	ϵ_{max}	λ_{max} (mμ)	ϵ_{max}	λ_{max} (mμ)	ϵ_{max}	λ_{max} (mμ)	ϵ_{max}
—F	217	7,000	ca. *259*	*550*	213	8,000*			ca. *253*	*400*	211	9,000*			ca. *255*	*450*
			265	800	ca. *216*	*7,500*			260	700	ca. *215*	*8,500*			260	800
			271	1,050	ca. *225*	*6,000*			266	1,000	ca. *221.5*	*6,000*			266	1,200
			278	900					273	800					272.5	1,200
—Cl	224	13,500	ca. *260*	*250*	ca. *212*	*12,000**			251	120	ca. *212.5*	*13,000**			ca. *250*	*185*
	ca. *230*	*10,000*	267	340	ca. *218*	*10,500**			257	165	ca. *217*	*12,000*			257	170
			274	415	ca. *224*	*7,000*			264	300	ca. *220*	*9,500*			ca. *261*	*175*
			282	335	ca. *228*	*5,500*			271	400	ca. *227*	*6,000*			264	235
									278	325					ca. *268*	*210*
															271	315
															279	275
—Br	*225*	*14,000*	258	310							ca. *214.5*	*12,500**	—	—	ca. *257.5*	*280*
	229	15,000	260	315							219.5	12,500			264.5	260
	ca. *235*	*12,000*	267	365							ca. *223.5*	*11,000*			272	295
			273	*345*											279.5	230
			275	390												
			283	260												
—I	238	17,500	ca. *260*	*1,350*							210	25,000*	230	9,000	253	650
	243	18,000	ca. *265*	*1,150*							ca. *215*	*20,500*	235	10,000	263	600
			ca. *275*	*800*									ca. *238*	*9,500*	269	570
			ca. *285*	*400*											ca. *282*	*350*
—CH_3	218	10,400	257	225	ca. *214*	*10,000**			*248*	*130*	ca. *213*	*10,000**			ca. *253*	*195*
	221	10,500	264	315	ca. *225*	*5,500*			*255*	*165*	ca. *224*	*5,500*			ca. *260*	*315*
	227	*7,800*	271	425					262	235					267	460
			278	375					269	320					273.5	440
									275	275					ca. *277.5*	*280*
—OH	224	10,000	ca. *275*	*1,250*	210	7,500*			269	1,450	212.5	8,700*			ca. *268*	*1,750*
			281.5	1,750	ca. *216*	*6,500*			275	2,300					274	2,700
			289	1,500					282	2,250					281	2,650
—OCH_3	227	12,500	ca. *277*	*1,300*			ca. *218*	*8,500**	ca. *270*	*1,450*	ca. *218*	*8,300**			ca. *271*	*1,800*
			282	1,750					275.5	2,350	ca. *223*	*7,500*			276.5	2,750
			290	1,550					282.5	2,300					283.5	2,800
—NH_2	241	14,000	297	1,750	207	20,000*	237–238	7,800	290	2,400			235	8,500	289	3,000
			ca. *306*	*1,150*					*294*	*1,900*						
—$COCH_3$	253	19,500	*286*	*600*			240	10,000	ca. *282*	*900*			235	4,900	282	700
							ca. *245–246*	*8,000*	287	1,100						
									296	950						
—CHO	258.5	22,000	ca. *277*	*2,350*	212.5	20,000*	243.5	7,000	292	825	210	27,000*	246	12,500	ca. *287*	*1,500*
	264	19,000	290	1,250	218	18,000			302	700			ca. *252*	*10,000*	295	2,100
															304	1,750
—NO_2	270	13,000	ca. *285*	*9,000*	210	18,000*	254	7,500	293	1,300	211	15,000*	ca. *246*	*3,700*	293	1,300
			ca. *295*	*4,500*	214.5	18,500			301	1,300	ca. *218*	*13,500*				
					ca. *223*	*16,500*			ca. *313*	*750*						

*B-band assignment doubtful.

chlorobenzenes (cf. also refs. 7, 8 for the *B*-bands of the *p*-chloro and *p*-bromo derivatives of nitrobenzenes and acetanilides). This indicates that the bromine atom has a greater ability to release electrons in the electronic excited state than the chlorine atom and again confirms the order of apparent mesomeric interaction Br > Cl for the halogen atoms as suggested in the previous section. It is also worth noting that the reported dipole moment of compounds like *p*-bromonitrobenzene is slightly greater than that of *p*-chloronitrobenzene (3) although dipole moment data are determined only by the ground state.

A plot of the wavelength displacements (in cm^{-1} units) for four *p*-substituted bromobenzenes, where the *p*-substituent was —H, —CHO, —$COCH_3$, or —NO_2, against various functions such as σ^*, $(\sigma_p - \sigma')$ values for the above substituents did not give rise to a straight line. Nor was a straight line obtained when the wavelength displacements in cm^{-1} units for *p*-substituted acetophenones, when the *p*-substituent was H, F, Cl, Br, or I, were plotted against the σ^* or $(\sigma_p - \sigma')$ values of these substituents. However, as noted by Schubert and co-workers (9), a graph relating ν_{max} values of the *B*-band in the gas phase against molar refraction values does afford an approximately linear relationship for the *p*-halonitrobenzenes, *p*-haloacetophenones, and *p*-haloanisoles, in this way confirming the relationship between molecular polarizability (as measured by molar refraction values) and certain absorption spectra.

Table II not only includes the *p*-substituted bromobenzenes discussed in the previous paragraph, but also includes *p*-substituted bromobenzenes where the *p*-substituent does not extend the conjugation in the most probable resonance form. These spectra, as expected from simple resonance theory, involve so-called locally excited states; that is, these spectral data (which are listed at the beginning of Table II) indicate that the *B*-bands of these compounds usually resemble the *B*-band of one of the monosubstituted parent compounds. Of the two substituents, normally the substituent with the greater electron-donating power will predominantly determine the wavelength and intensity of the monosubstituted benzene *B*-band, while the other substituent will exert only a "secondary" effect on the *B*-band. For example, the *B*-band of *p*-bromoiodobenzene in cyclohexane solution shows the characteristic *B*-band doublet near 240 mμ fairly close to the *B*-band absorption doublet of iodobenzene, near 230 mμ, and the spectrum of *p*-bromoaniline resembles that of aniline. In both these examples the corresponding *C*-bands resemble the *C*-bands of iodobenzene and aniline respectively. This is further illustrated by Fig. 3, which shows the similarity of the spectra of *p*-bromoaniline and aniline and the dissimilarity from the absorption spectrum of bromobenzene.

For other compounds the assignments are more doubtful. For example, the *B*-band of *p*-bromofluorobenzene in cyclohexane solution resembles the band of bromobenzene more than the *B*-band of fluorobenzene (see Fig. 2) since the latter band occurs below 205 mμ (2); however, the *C*-band of *p*-bromofluorobenzene resembles the *C*-band of fluorobenzene more than the *C*-band of bromobenzene. Next, the *B*-bands of *p*-bromophenol, *p*-bromoanisole, and *p*-chlorobromobenzene are tentatively ascribed to phenol, anisole, and bromobenzene absorption respectively with the *p*-bromo or *p*-chloro substituents facilitating the transition by means of a secondary interaction (cf. also ref. 1). Partial support for these assignments is provided by the lack of fine structure in the *B*-bands of *p*-bromophenol and *p*-bromoanisole, and by the relevant *C*-bands (see Table II), which may readily be identified as phenol or anisole *C*-bands (see also Fig. 4, a fact that illustrates the similarity of the spectra of *p*-bromoanisole and anisole and the dissimilarity from the absorption spectrum of bromobenzene). On the other hand, *C*-band

Can. J. Chem. Downloaded from www.nrcresearchpress.com by 210.87.254.105 on 09/05/12
For personal use only.

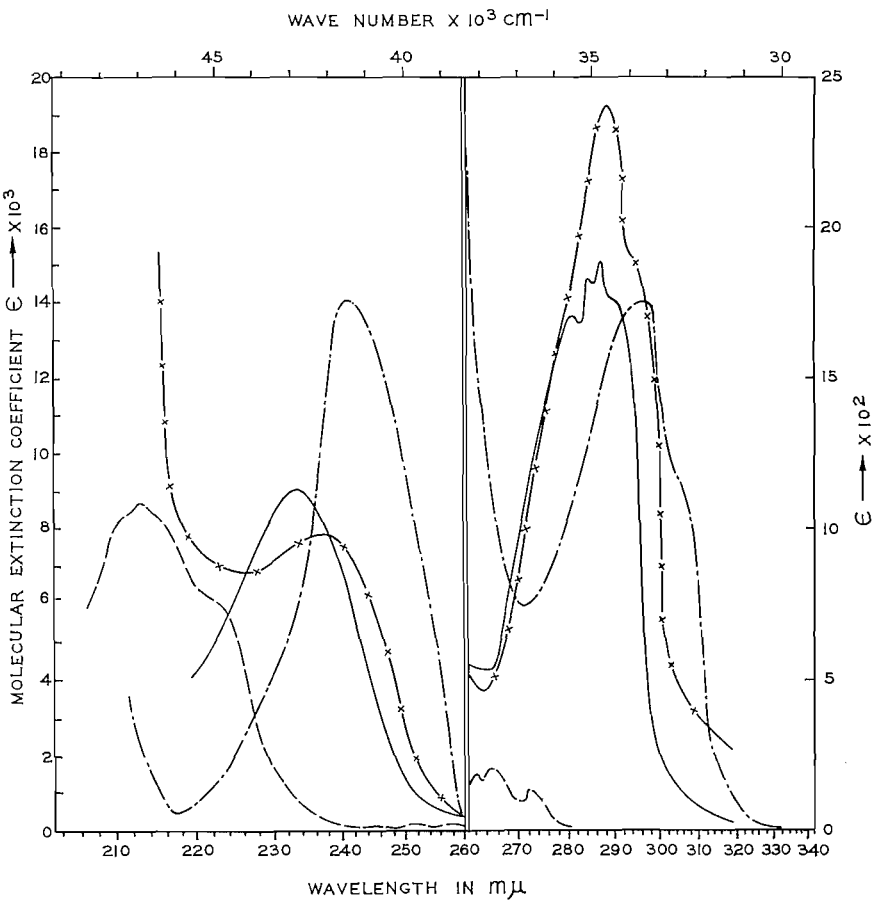


FIG. 3. The ultraviolet absorption spectra in cyclohexane solution of aniline (——), *p*-bromoaniline (—·), *m*-bromoaniline (—×), and bromobenzene (— —).

similarities can be misleading (see the preceding discussion of the spectra of *p*-bromofluorobenzene) and also some of the solvent changes suggest a different assignment. For example, the wavelength displacement observed on determining the *B*-band of *p*-bromoanisole in the vapor phase and in an inert solvent medium (2.8 mμ (9); 550 cm^{-1}) is closer to the wavelength displacements observed under similar conditions for bromobenzene (ca. 2 mμ (see Table I); 440 cm^{-1}) than to that observed for anisole (4.6 mμ (9); 980 cm^{-1}).

A *p*-bromo substituent generally appears to cause the *B*-band absorption to occur at longer wavelength even if both substituents are electron-donating as in *p*-dibromobenzene; the wavelength displacement relative to the non-bromo-substituted reference compound is usually not less than ca. 10 mμ and the absorption intensity is appreciably enhanced (see Table II and previous parts of this series of papers). This displacement may be visualized as the bromine atom donating electrons in the electronic excited state and this effect of the *p*-bromo substituent is again slightly larger than the previously noted similar effect of a *p*-chloro substituent (1).

Concerning *C*-band absorption it may be noted that a *p*-bromo substituent generally (except in examples where resonance structures of type II may be assumed to be involved)

Can. J. Chem. Downloaded from www.nrcresearchpress.com by 210.87.254.105 on 09/05/12
For personal use only.

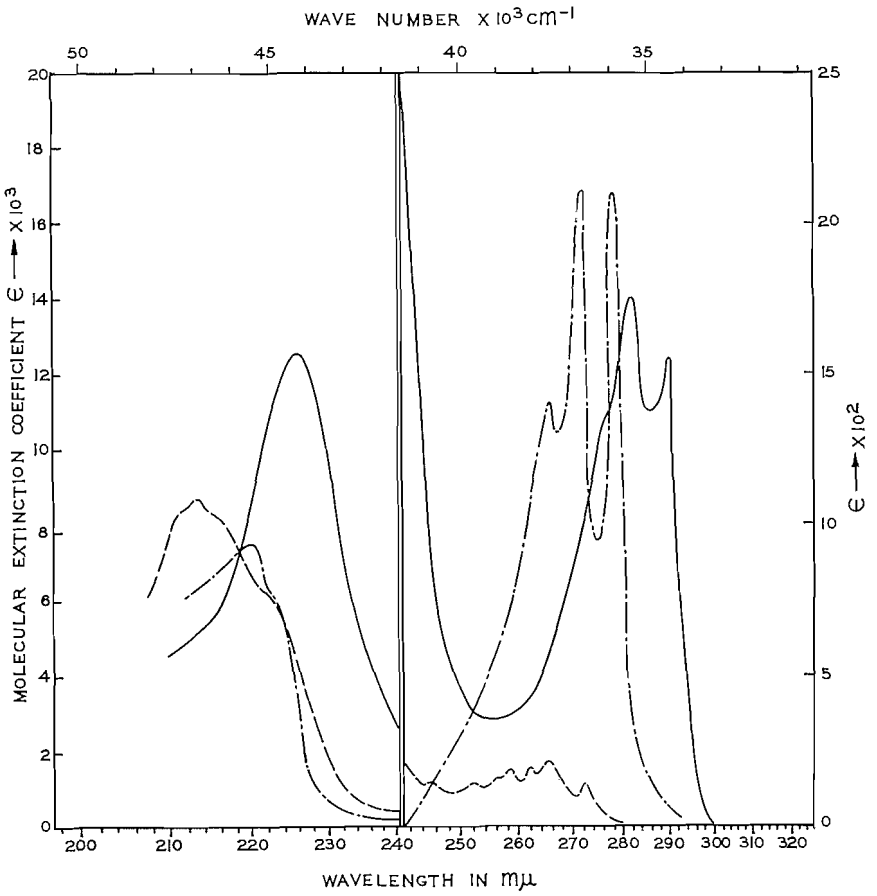


FIG. 4. The ultraviolet absorption spectra in cyclohexane solution of *p*-bromoanisole (——), anisole (—·), and bromobenzene (— —).

does not appear to affect the *C*-band structure of a number of *p*-substituted bromobenzenes; that is, the *C*-bands of these *p*-substituted bromobenzenes may occur at slightly longer wavelength and with slightly decreased absorption intensity but are otherwise similar to the *C*-bands of the corresponding non-bromo-substituted parent compounds (see, for example, Figs. 2, 3, and 4 and cf. ref. 10). The absence of any marked evidence of bromobenzene *C*-band absorption on the structure of the *C*-band may again be related to the low-intensity *C*-band absorption in bromobenzene. That is, the bromobenzene *C*-band absorption is normally hidden by other more intense *C*-band absorption except in compounds like *p*-bromochlorobenzene where both constituent *C*-bands, namely the *C*-bands of chlorobenzene and bromobenzene, are weak.

THE SPECTRA OF META-SUBSTITUTED BROMOBENZENES

For *m*-substituted bromobenzenes, a *B*-band associated with the bromobenzene *B*-band can usually be ascertained; the *C*-band only rarely corresponds to bromobenzene *C*-band absorption (cf. last paragraph of previous section). For example, for *m*-bromofluorobenzene the *B*-band absorption at 213 mμ is associated, at least partly, with bromobenzene *B*-band absorption (see Tables I and II), whereas the *C*-band absorption of

Can. J. Chem. Downloaded from www.nrcresearchpress.com by 210.87.254.105 on 09/05/12
For personal use only.

Can. J. Chem. Downloaded from www.nrcresearchpress.com by 210.87.254.105 on 09/05/12
For personal use only.

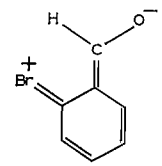
m-bromofluorobenzene is similar to that of fluorobenzene (see Fig. 2). Frequently the *C*-band similarity for *m*-substituted bromobenzenes and the corresponding non-bromo-substituted parent compounds is more pronounced than the previously referred to *C*-band similarity for *p*-substituted bromobenzenes and the corresponding non-bromo-substituted benzene derivatives (see Table II and the relevant reference compounds described in previous papers of this series). This may be interpreted in terms of resonance theory since electronic perturbations, such as may be associated with resonance interactions in the *p*-isomer, would be of less importance in a *m*-disubstituted benzene derivative.

For a number of *m*-substituted bromobenzenes, instead of the bromobenzene *B*-band, a "second" *B*-band—for example, the *B*-band of *m*-bromoaniline associated with the aniline *B*-band—is readily identified (see Fig. 3; reasons why *m*-disubstituted benzene derivatives sometimes show two *B*-bands have been discussed in previous papers of this series (e.g. refs. 1, 2)). The *m*-bromo substituent generally causes this *B*-band absorption to occur at slightly longer wavelength. This displacement is less pronounced than for a *p*-bromo substituent and about equally effective for *m*-chloro and *m*-bromo substituents. It may be noted that both *m*-chloro and *m*-bromo substituents have the effect of enhancing the integrated intensities of the O—H infrared absorption band in phenol (integrated absorption intensities are well known to relate to mesomeric interactions) to a similar extent (11).

The effect of the non-bromo substituent on the *location* of the maximal wavelength of the bromobenzene *B*-band absorption in *m*-substituted bromobenzenes appears to be small but the intensity of the bromobenzene *B*-band is sometimes enhanced (see Tables I and II for the relatively more intense "bromobenzene *B*-bands"). However, since the bromobenzene *B*-band occurs at shorter wavelength, it seems likely that *A*-band transitions contribute to the observed band (see Table II).

THE SPECTRA OF ORTHO-SUBSTITUTED BROMOBENZENES

The ultraviolet spectra of *o*-substituted bromobenzenes would be expected to show the effects of appreciable steric interactions. In fact, the second *B*-band (that is, the *B*-band *not* associated with bromobenzene absorption) of an *o*-bromo-substituted compound frequently occurs with decreased absorption intensity compared with the second *B*-band of the corresponding *o*-chloro-substituted compound.* (See Table II and ref. 1;



(III)

cf. also the data reported for nitrobenzenes (7), acetanilides (8), N,N-dimethylanilines (12), and 5-phenyltetrazoles (13), which show that the maximal extinction coefficient

**An example of an exception is the B-band of o-bromobenzaldehyde (see Table II) which is more intense than the corresponding B-band of o-chlorobenzaldehyde (1; cf. also the ε values reported (19) for o-chloro- and o-bromophenyl-2,5-diphenyloxazoles). This may be because in o-bromobenzaldehyde and related compounds the effect of mesomeric interactions, as illustrated by resonance forms of type III, is still appreciable and hence the greater apparent mesomeric effect of the bromo substituent leads to increased absorption intensity. For most other o-substituted bromobenzenes resonance structures of type III may be of little importance because the non-planarity of the molecule inhibits the necessary conjugation.*

of the *B*-band of the *o*-bromo derivative is less than the corresponding maximal extinction coefficient of the *o*-chloro derivative.) Moreover, in examples like *o*-bromoacetophenone, where the non-bromo substituent is large, the absorption intensity is also smaller than the intensity of the corresponding *m*-isomer (see Table II). This decreased extinction coefficient, relative to the *m*-isomer, is also accompanied by a hypsochromic wavelength displacement, which in this type of compound is assumed to be associated with steric interactions. Since non-planarity in *o*-bromo-substituted benzene derivatives is also suggested from other data (see, for example, refs. 3, 14, 15, 16, 17, 18), the above spectral data are assumed to indicate that the bromine atom, because of its larger size relative to the chlorine atom (cf. ref. 14), more effectively dislodges the non-bromo substituent from the plane of the benzene ring and in this way gives rise to the observed spectral changes.

However, the ultraviolet data do not consistently indicate that the bromo substituent exerts a greater steric effect than the chloro substituent (see footnote of previous paragraph). A similar lack of consistency is found when comparing the ϵ values of *o*-bromo-substituted benzene derivatives with the ϵ values of *o*-methyl-substituted benzene derivatives. For example, for acetanilides (8) the *o*-bromo derivative shows more intense *B*-band absorption than the *o*-methyl derivative (see also reference 20 for the spectra of the corresponding benzoic acids). However, more frequently, for example, for anilines (21), or benzaldehydes (22), the *o*-methyl derivative shows more intense *B*-band absorption than the *o*-bromo derivative (see also refs. 19, 23). The data thus indicate that the effective interference radius of the bromine atom is greater than that of the methyl group (or than that of the chlorine atom; cf. refs. 14, 15), but it remains to provide an explanation for the minority of anomalous data. This can be done by considering dipole moments. That is, a methyl substituent, which has a dipole moment in the opposite direction to that of the halogen atoms, may cause a considerably different over-all dipole moment and in this way compounds like *o*-toluic and *o*-bromobenzoic acids, for example, may possess appreciably different dipole moments. Moreover, steric interactions (which are assumed to be present) may increase the over-all dipole moment of one molecule while decreasing the dipole of another, similar molecule (cf. ref. 3, where it was pointed out for nitrobenzenes that an *o*-methyl substituent increases the dipole moment by increasing the angle between the C—N and C—Me bonds, whereas an *o*-bromo or *o*-chloro substituent may decrease the over-all dipole moment). Since absorption intensities are determined by transition probabilities which, in turn among other things, are governed by transition moments—which are related to the change in dipole moment on passing from the ground state to the excited state—it is evident that the absorption intensities of the above *o*-disubstituted benzene derivatives are not determined merely by steric interactions.

Although intramolecular hydrogen bonds have been postulated in *o*-substituted bromobenzenes because of evidence from other physical data (24, 25, 26), as for the previously discussed spectra of *o*-substituted chlorobenzenes or fluorobenzenes (1, 2), there is little evidence *from the above ultraviolet spectra* for such a hydrogen bond. That is, no unusual wavelength displacement or unusual change in ϵ_{max} values, such as may be ascribed to the presence of an intramolecular hydrogen bond, is observed in the spectrum of *o*-bromophenol compared with the spectrum of *m*-bromophenol or *o*-bromoanisole (see Table II); only for *o*-bromoaniline small intensity increases are observed in the ϵ_{max} values compared with the ϵ_{max} values of the *m*-isomer, but it is not certain that these intensity increases are caused by an intramolecular hydrogen bond.

Can. J. Chem. Downloaded from www.nrcresearchpress.com by 210.87.254.105 on 09/05/12
For personal use only.

The *C*-bands in *o*-substituted bromobenzenes usually occur with increased absorption intensity compared with the *C*-bands of the corresponding *m*-isomers, except in compounds, such as *o*-bromoacetophenone, which are believed to be appreciably non-planar because of steric interactions. For a number of *o*-chloro- and *o*-bromo-substituted compounds the *C*-bands are remarkably similar; for example, *o*-chloroaniline, λ_{max} 291 mμ, ϵ = 2900 and *o*-bromoaniline, λ_{max} 289 mμ, ϵ = 3000 (see ref. 1 and Table II). This *C*-band similarity has previously been discussed (see Introduction).

EXPERIMENTAL

The ultraviolet absorption spectra were determined by standard methods in 1-cm cells using either a Beckman DU or DK 2 spectrophotometer or Unicam SP 500 spectrophotometers calibrated against a didymium filter. Wavelength readings obtained on the Unicam and Beckman instruments were found to be within 1 mμ of each other. The accuracy of λ_{max} values is estimated to be $\pm$1 mμ, and the precision of ϵ_{max} values $\pm$5%, or better. Values of ϵ_{max} were reproducible in most cases to $\pm$2%. For each compound at least two independent sets of observations were made. The ultraviolet maxima are listed in Tables I and II. Some of the spectra have previously been described in this series and elsewhere. Whenever possible, the bromobenzene spectra were determined under conditions identical with those under which previous spectra in this series had been determined. Frequently, but not always, the data were in good agreement with recent values reported by other workers.

The bromobenzenes were mostly commercial materials, purified by distillation or recrystallization until their boiling points and refractive indices or melting points showed them to be sufficiently pure. The solvents used were spectroanalyzed cyclohexane (Fisher) and other commercially available spectroanalyzed solvents.

ACKNOWLEDGMENTS

The author is indebted to Miss V. R. Jellett and Mr. A. A. Sioumis for the careful determination of the spectral data. Some of the spectra have been determined by Mr. J. C. Dearden, assisted by Miss Florence Jackman, in preparation for his Ph.D. thesis at the Memorial University of Newfoundland and the author is indebted to Mr. Dearden for making these data available.

Grateful acknowledgment for financial assistance in support of that part of these studies which was carried out in Canada is made to the National Research Council.

REFERENCES

1. W. F. Forbes. Can. J. Chem. **38**, 1104 (1960).
2. W. F. Forbes. Can. J. Chem. **37**, 1977 (1959).
3. A. C. Littlejohn and J. W. Smith. J. Chem. Soc. 2476 (1957).
4. A. R. Katritzky and J. M. Lagowski. J. Chem. Soc. 4155 (1958).
5. F. Meda. Spectrochim. Acta, **13**, 75 (1958).
6. W. F. Forbes and W. A. Mueller. Can. J. Chem. **35**, 488 (1957).
7. H. E. Ungnade. J. Am. Chem. Soc. **76**, 1601 (1954).
8. H. E. Ungnade. J. Am. Chem. Soc. **76**, 5133 (1954).
9. W. M. Schubert, J. M. Craven, and H. Steadly. J. Am. Chem. Soc. **81**, 2695 (1959).
10. J. C. Dearden and W. F. Forbes. Can. J. Chem. **37**, 1294 (1959).
11. T. L. Brown. J. Phys. Chem. **61**, 820 (1957).
12. W. R. Remington. J. Am. Chem. Soc. **67**, 1838 (1945).
13. R. M. Herbst and K. R. Wilson. J. Org. Chem. **22**, 1142 (1957).
14. R. J. Francel. J. Am. Chem. Soc. **74**, 1265 (1952).
15. J. W. Smith. J. Chem. Soc. 4050 (1957).
16. G. H. Beaven and D. M. Hall. J. Chem. Soc. 4637 (1956).

Can. J. Chem. Downloaded from www.nrcresearchpress.com by 210.87.254.105 on 09/05/12
For personal use only.

17. S. BROWNSTEIN. J. Am. Chem. Soc. **80**, 2300 (1958).
18. R. D. KROSS, V. A. FASSEL, and M. MARGOSHES. J. Am. Chem. Soc. **78**, 1332 (1956).
19. D. G. OTT, F. N. HAYES, E. HANSBURY, and V. N. KERR. J. Am. Chem. Soc. **79**, 5448 (1957).
20. W. F. FORBES, W. A. MUELLER, A. S. RALPH, and J. F. TEMPLETON. Can. J. Chem. **35**, 1049 (1957).
21. W. F. FORBES and I. R. LECKIE. Can. J. Chem. **36**, 1371 (1958).
22. J. C. DEARDEN and W. F. FORBES. Can. J. Chem. **36**, 1362 (1959).
23. K. NAIKI. Bull. Chem. Soc. Japan, **32**, 1327 (1959).
24. W. F. ANZILOTTI and B. C. CURRAN. J. Am. Chem. Soc. **65**, 607 (1943).
25. A. W. BAKER and W. W. KAEDING. J. Am. Chem. Soc. **81**, 5904 (1959).
26. A. W. BAKER. J. Am. Chem. Soc. **80**, 3598 (1958).

Can. J. Chem. Downloaded from www.nrcresearchpress.com by 210.87.254.105 on 09/05/12
For personal use only.

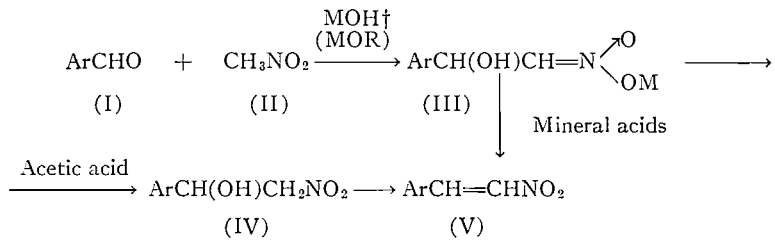
Can. J. Chem. Downloaded from www.nrcresearchpress.com by 210.87.254.40 on 09/05/12
For personal use only.

NOTES

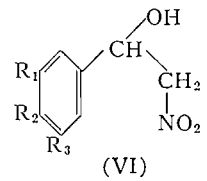
A NOTE ON THE PREPARATION OF SOME 1-PHENYL-2-NITROETHANOL DERIVATIVES

R. A. Heacock, O. Hutzinger, and C. Nerenberg*

It has been known for many years that aromatic aldehydes (I) and nitromethane (II) will undergo a condensation reaction, under alkaline conditions, to yield the alkali metal derivatives of the *aci*-form of the monohydric nitroalcohols (III). The free nitroalcohols (IV) can be liberated on acidification of the alkali metal derivative with acetic acid; however, the products will often dehydrate with extreme ease to form the corresponding ω-nitrostyrenes (V), unless certain precautions are taken (cf. ref. 1).



In this laboratory, we have been primarily interested in obtaining certain alkyl, acyl, and aroyl derivatives of 1-(3,4-dihydroxyphenyl)-2-nitroethanol and 1-(3,4,5-trihydroxyphenyl)-2-nitroethanol. A few of these nitroalcohols had previously been described in the literature namely: 3,4-methylenedioxy-α-nitromethylbenzyl alcohol (VI: R_1+R_2 = OCH_2O; R_3 = H) (2, 3, 4, 5); 3,4-diacetoxy-α-nitromethylbenzyl alcohol (VI: R_1 = R_2 =



(VI)

$OCOCH_3$; R_3 = H) (6); and 4-benzyloxy-3-methoxy-α-nitromethylbenzyl alcohol (VI: R_1 = OCH_3; R_2 = $OCH_2C_6H_5$; R_3 = H) (7). The 3,4-diacetoxy derivative was obtained using aqueous sodium bicarbonate as the condensing agent (6); however, the other nitroalcohols were prepared either using sodium methoxide under anhydrous conditions or aqueous alcoholic potassium hydroxide to effect the condensation (1, 2, 3, 4, 5, 7).

Some of the aforementioned procedures are rather tedious to carry out and this note reports a rapid and simple method for preparing nitroalcohols of this general type in good yield. The procedure involves the condensation of a suitable aldehyde with excess nitromethane at about 5° in the presence of sodium hydroxide in aqueous alcoholic solution. The optimum reaction time, which was of very short duration (⩾ 3 minutes), varied from case to case and was determined empirically.

As well as the nitroalcohols mentioned above, the following new 1-phenyl-2-nitroethanol

**Present address: Research Division, Columbus Psychiatric Institute and Hospital, Ohio State University Health Center, Columbus 10, Ohio, U.S.A.*

†M = Na *or* K.

TAB

Preparation of nitroalcohols

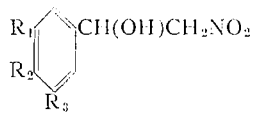
Nitroalcohol prepared				Reagents used and reaction conditions						
Name	R_1	R_2	R_3	Aldehyde*		(g)	CH_3NO_2 (ml)	95% C_2H_5OH (ml)	10% NaOH aq. (ml)	2% AcOH (ml)
3,4-Methylenedioxy-α-nitromethylbenzyl alcohol	OCH_2O		H	Piperonaldehyde	*a*	10	11	135	20	160
4-Acetoxy-3-methoxy-α-nitromethylbenzyl alcohol	CH_3O	CH_3COO	H	4-Acetoxy-3-methoxybenzaldehyde	*b*	5	3.5	35	10	80
3-Acetoxy-4-methoxy-α-nitromethylbenzyl alcohol	CH_3COO	CH_3O	H	3-Acetoxy-4-methoxybenzaldehyde	*b*	5	3.5	50	10	80
3,4-Diacetoxy-α-nitromethylbenzyl alcohol	CH_3COO	CH_3COO	H	3,4-Diacetoxybenzaldehyde	*c*	5	3	25	10	90
4-Benzyloxy-3-methoxy-α-nitromethylbenzyl alcohol	CH_3O	$C_6H_5CH_2O$	H	4-Benzyloxy-3-methoxybenzaldehyde	*d*	1	0.7	7	1.55	13
3,4,5-Trimethoxy-α-nitromethylbenzyl alcohol	CH_3O	CH_3O	CH_3O	3,4,5-Trimethoxybenzaldehyde	*e*	3	2.1	21	5.55	48
4-Acetoxy-3,5-dimethoxy-α-nitromethylbenzyl alcohol	CH_3O	CH_3COO	CH_3O	4-Acetoxy-3,5-dimethoxybenzaldehyde	*f*	1	0.7	18	1.65	13.5

*Sources of aldehydes: *a* = Eastman Kodak. *b* = Prepared by the acetylation of vanillin and isovanillin respectively by an adaptation of the method described by Kanao for the preparation of 3,4-diacetoxybenzaldehyde (6). *c* = Prepared by the method of Kanao (6). *d* = 4-Benzyloxy-3-methoxybenzaldehyde (m.p. 64°) was prepared from vanillin by benzylation with benzyl chloride in the presence of aqueous potassium hydroxide. This substance has previously been prepared by alternative routes and the melting point is quoted as 63–64° (9). *e* = Aldrich Chemical Company. *f* = Prepared by the acetylation of Syringaldehyde

derivatives have been prepared: 4-acetoxy-3-methoxy-α-nitromethylbenzyl alcohol (VI: $R_1 = OCH_3$; $R_2 = OCOCH_3$; $R_3 = H$); 3-acetoxy-4-methoxy-α-nitromethylbenzyl alcohol (VI: $R_1 = OCOCH_3$; $R_2 = OCH_3$; $R_3 = H$); 3,4,5-trimethoxy-α-nitromethylbenzyl alcohol ($R_1 = R_2 = R_3 = OCH_3$) and 4-acetoxy-3,5-dimethoxy-α-nitromethylbenzyl alcohol ($R_1 = R_3 = OCH_3$; $R_2 = OCOCH_3$). Attempts to prepare a number of related nitroalcohols by this method were not successful: (i) veratraldehyde gave mainly 3,4-dimethoxy-ω-nitrostyrene, even after cooling the reaction mixture below 0°; (ii) protocatechualdehyde, syringaldehyde, vanillin, and isovanillin did not react with nitromethane under the above conditions. This is not altogether surprising in view of the fact that three of these aldehydes have a para hydroxyl group, which has been reported by several workers to hinder this type of condensation (1, 8); (iii) 3,4-dibenzoyloxybenzaldehyde, 3-benzyloxy-4-methoxybenzaldehyde, 3,4-diethoxycarbonyloxybenzaldehyde, and 3-ethoxycarbonyloxy-4-methoxybenzaldehyde gave oily products, for which satisfactory analyses could not be obtained (for the nitroalcohol) even after distillation in high vacuum. It would appear in these cases that condensation had occurred, but partial decomposition of the products took place in the isolation or distillation stages. The infrared spectra of thin films of these oils showed strong absorption in the 2.79 to 2.81 μ region, probably due to the stretching vibrations of the benzyl alcohol hydroxyl group. (The authenticated nitroalcohols all exhibited marked absorption in this region (2.75 to 2.88 μ).) Recently Axelrod, Senoh, and Witkop have reported the OH stretching fre-

Can. J. Chem. Downloaded from www.nrcresearchpress.com by 210.87.254.40 on 09/05/12
For personal use only.

LE I



Reaction time (sec)	Yield of purified product (g)	Crystalline form	m.p. (°C)	Literature m.p. (°C) (if known)	Analysis: Found C	Found H	Found N	Calculated C	Calculated H	Calculated N
60	9.3	Fine colorless needles from benzene	95	91(5),‡ 95–96(4), 91(3), 94(2)	51.34	4.41	6.61	51.19	4.30	6.63
45	5.5	Fine colorless needles from benzene	90.5		51.90	5.12	5.59	51.77	5.14	5.49
30	4	Fine colorless needles from benzene	103–104		51.87	5.21	5.43	51.77	5.14	5.49
30	4.9	Colorless plates from ethanol	153–155	155(6)	50.99	4.59	5.02	50.88	4.63	4.95
45	0.65†	Colorless small prisms from benzene	107–108.5	107–109(7)	63.44	5.71	4.13	63.36	5.65	4.62
45	2.4	Colorless fine needles from benzene	109		51.60	5.84	5.33	51.36	5.88	5.45
20	1	Fine colorless needles from ethanol	200		50.74	5.39	5.07	50.52	5.30	4.91

(Aldrich Chemical Company) by an adaptation of the method described by Kanao for the preparation of 3,4-diacetoxybenzaldehyde (6), m.p. 115°. Freudenberg and Hübner prepared this compound by a different route and quote m.p. 114° (10).

†The crude product, a yellow oil, was stirred with concentrated sodium bisulphite solution for 20 minutes before recrystallization from benzene.

‡The melting point has been incorrectly reported as 98–99° in Chem. Abstr. **48**, 13,653 (1954).

quency of 4-benzyloxy-3-methoxy-α-nitromethylbenzyl alcohol as 2.81 μ in chloroform solution (7).

In a few cases, the corresponding ω-nitrostyrenes had not been previously described in the literature and these derivatives were prepared in good yield, from the nitroalcohol in question, by an adaptation of the method described by Kanao for the preparation of 3,4-diacetoxy-ω-nitrostyrene from 3,4-diacetoxy-α-nitromethylbenzyl alcohol (6).

EXPERIMENTAL

*General Procedures**

(*i*) *Nitroalcohols.*—Aqueous sodium hydroxide (10%; 1.05 mole) was added with vigorous stirring to a mixture of the aldehyde (1.0 mole) and nitromethane (2–3 mole) dissolved in 95% ethanol at ca. 5°; the reaction mixture was vigorously stirred for a short time (⩾3 minutes), accurately timed on a stop watch. Aqueous acetic acid (2%) was added to arrest the reaction and decompose the sodium derivative of the nitroalcohol; the crude product precipitated out as a yellow or colorless solid or oil. After being allowed to stand at 4° for 4–5 hours, the crude product was filtered and purified by repeated recrystallization from a suitable solvent.

(*ii*) *ω-Nitrostyrenes.*—A suspension of the nitroalcohol and the same weight of fused

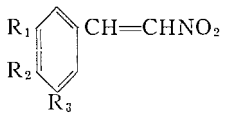
**The specific quantities of reagents used and reaction times employed are given in Tables I and II.*

Can. J. Chem. Downloaded from www.nrcresearchpress.com by 210.87.254.40 on 09/05/12
For personal use only.

Can. J. Chem. Downloaded from www.nrcresearchpress.com by 210.87.254.40 on 09/05/12
For personal use only.

TABLE II

Preparation of ω-nitrostyrenes



ω-Nitrostyrene prepared				Amount of nitro-alcohol used in g	Properties of product			Analysis					
					Yield of purified product (g)	Crystalline form (from 95% ethanol)	m.p. (°C)	Found			Calculated		
Name	R_1	R_2	R_3					C	H	N	C	H	N
4-Acetoxy-3-methoxy-ω-nitrostyrene*	CH_3O	CH_3COO	H	2	1.5	Fine yellow needles	166–167	55.62	4.62	5.90	55.69	4.68	5.91
3-Acetoxy-4-methoxy-ω-nitrostyrene	CH_3COO	CH_3O	H	0.85	0.7	Yellow needles	142	55.51	4.61	5.75	55.69	4.68	5.91
4-Acetoxy-3,5-dimethoxy-ω-nitrostyrene	CH_3O	CH_3COO	CH_3O	0.3	0.25	Pale yellow plates	177	54.01	4.87	5.21	53.93	4.90	5.24
3-Ethoxycarbonyloxy-4-methoxy-ω-nitrostyrene	C_2H_5OCOO	CH_3O	H	†	—	Fine yellow needles	116	54.13	4.98	5.22	53.93	4.90	5.24

*The preparation of this substance has been reported previously by Kobayashi; however, the original Japanese paper is not available to the authors and no preparative details or melting points are given in Chemical Abstracts, but according to Beilstein, the substance was obtained by acetylation of 4-hydroxy-3-methoxy-ω-nitrostyrene and had m.p. 161–162° (11).
†A small quantity of the crude reaction mixture from the attempted preparation of 3-ethoxycarbonyloxy-4-methoxy-α-nitromethylbenzyl alcohol was used.

sodium acetate in acetic anhydride (five times the weight of one of the other reagents) was boiled under reflux for 10 minutes. After cooling, the reaction mixture was poured into water; a yellow solid separated out, which was filtered off, washed with water, and recrystallized from 95% ethanol.

This investigation was supported by grants from the Department of National Health and Welfare (Ottawa), the Saskatchewan Department of Public Health, and the Rockefeller Foundation.

1. K. W. Rosenmund. Ber. **46**, 1034 (1913).
2. P. W. Neber, A. Burgard, and W. Thier. Ann. **526**, 277 (1936).
3. L. Canonica and C. Cardani. Gazz. chim. ital. **79**, 262 (1949).
4. T. A. Jacob, G. B. Bachman, and H. B. Hass. J. Org. Chem. **16**, 1572 (1951).
5. J. Boileau. Bull. soc. chim. France, 1007 (1953).
6. S. Kanao. J. Pharm. Soc. Japan, **49**, 239 (1929); Chem. Abstr. **23**, 5162 (1929).
7. J. Axelrod, S. Senoh, and B. Witkop. J. Biol. Chem. **233**, 697 (1958).
8. G. Hahn and K. Stiehl. Ber. **71**, 2154 (1938).
9. C. H. Boehringer and Sons. D.R.P. 65937 (1892).
10. K. Freudenberg and H. H. Hübner. Ber. **85**, 1181 (1952).
11. S. Kobayashi. Sci. Papers Inst. Phys. Chem. Research (Tokyo), **6**, 149 (1927); Chem. Abstr. **22**, 1345 (1928); Beilstein's Handbuch der Organischen Chemie. Vol. VI. 4th ed. 2nd suppl. *Edited by* F. Richter. Springer-Verlag, Berlin. 1944. p. 915.

Received December 9, 1960.
Psychiatric Research Unit,
University Hospital,
Saskatoon, Saskatchewan.

PREPARATION AND DEHYDRATION OF DI-(1-HYDROXYCYCLOALKYL)-ALKANES[1]

A. S. Bailey,[2] D. G. M. Diaper, and M. V. H. Schwemin

1-Alkylcycloalkanols have been employed (1, 2) as intermediates in the extension of monofunctional aliphatic chains. An obvious extension of this synthetic method would be the use of di-(1-hydroxycycloalkyl) compounds in chain extension of α,ω-dicarboxylic acids of the aliphatic series. Although there is no record (3) of the use of such intermediates for this purpose, diols of the requisite structural type have been made in isolated previous investigations. We have now prepared diols having five-, six-, seven-, and eight-membered rings and with 2 to 10 methylene groups connecting them, using procedures already described. The results are summarized in Table I.

Method A, reaction of a diester with two moles of a Grignard reagent from a dihalide, has been studied previously only in the synthesis of 1,1′-ethylenedicyclopentanol and 1,1′-ethylenedicyclohexanol from ethyl succinate and respectively tetramethylene dibromide and pentamethylene dibromide (4). We attempted to use hexamethylene dibromide and 1,3-dibromo-2,2-dimethylpropane in similar syntheses but in each case obtained no crystalline product but the major outcome was evidently a polymer. Diethyl 2,2-dimethylglutarate was successfully condensed with 2 moles of the derived Grignard reagent from pentamethylene dibromide although one might have expected the gem dimethyl group to hinder or deactivate one of the ester groups sterically.

[1]*Financial support for this work was supplied by Defence Research Board under Grant No. 9530-17.*
[2]*Defence Research Board Fellow 1958–59. Present address: The Dyson Perrins Laboratory, Oxford University, England.*

Can. J. Chem. Downloaded from www.nrcresearchpress.com by 210.87.254.40 on 09/05/12
For personal use only.

sodium acetate in acetic anhydride (five times the weight of one of the other reagents) was boiled under reflux for 10 minutes. After cooling, the reaction mixture was poured into water; a yellow solid separated out, which was filtered off, washed with water, and recrystallized from 95% ethanol.

This investigation was supported by grants from the Department of National Health and Welfare (Ottawa), the Saskatchewan Department of Public Health, and the Rockefeller Foundation.

1. K. W. Rosenmund. Ber. **46**, 1034 (1913).
2. P. W. Neber, A. Burgard, and W. Thier. Ann. **526**, 277 (1936).
3. L. Canonica and C. Cardani. Gazz. chim. ital. **79**, 262 (1949).
4. T. A. Jacob, G. B. Bachman, and H. B. Hass. J. Org. Chem. **16**, 1572 (1951).
5. J. Boileau. Bull. soc. chim. France, 1007 (1953).
6. S. Kanao. J. Pharm. Soc. Japan, **49**, 239 (1929); Chem. Abstr. **23**, 5162 (1929).
7. J. Axelrod, S. Senoh, and B. Witkop. J. Biol. Chem. **233**, 697 (1958).
8. G. Hahn and K. Stiehl. Ber. **71**, 2154 (1938).
9. C. H. Boehringer and Sons. D.R.P. 65937 (1892).
10. K. Freudenberg and H. H. Hübner. Ber. **85**, 1181 (1952).
11. S. Kobayashi. Sci. Papers Inst. Phys. Chem. Research (Tokyo), **6**, 149 (1927); Chem. Abstr. **22**, 1345 (1928); Beilstein's Handbuch der Organischen Chemie. Vol. VI. 4th ed. 2nd suppl. *Edited by* F. Richter. Springer-Verlag, Berlin. 1944. p. 915.

Received December 9, 1960.
Psychiatric Research Unit,
University Hospital,
Saskatoon, Saskatchewan.

PREPARATION AND DEHYDRATION OF DI-(1-HYDROXYCYCLOALKYL)-ALKANES[1]

A. S. Bailey,[2] D. G. M. Diaper, and M. V. H. Schwemin

1-Alkylcycloalkanols have been employed (1, 2) as intermediates in the extension of monofunctional aliphatic chains. An obvious extension of this synthetic method would be the use of di-(1-hydroxycycloalkyl) compounds in chain extension of α,ω-dicarboxylic acids of the aliphatic series. Although there is no record (3) of the use of such intermediates for this purpose, diols of the requisite structural type have been made in isolated previous investigations. We have now prepared diols having five-, six-, seven-, and eight-membered rings and with 2 to 10 methylene groups connecting them, using procedures already described. The results are summarized in Table I.

Method A, reaction of a diester with two moles of a Grignard reagent from a dihalide, has been studied previously only in the synthesis of 1,1′-ethylenedicyclopentanol and 1,1′-ethylenedicyclohexanol from ethyl succinate and respectively tetramethylene dibromide and pentamethylene dibromide (4). We attempted to use hexamethylene dibromide and 1,3-dibromo-2,2-dimethylpropane in similar syntheses but in each case obtained no crystalline product but the major outcome was evidently a polymer. Diethyl 2,2-dimethylglutarate was successfully condensed with 2 moles of the derived Grignard reagent from pentamethylene dibromide although one might have expected the gem dimethyl group to hinder or deactivate one of the ester groups sterically.

[1]*Financial support for this work was supplied by Defence Research Board under Grant No. 9530-17.*
[2]*Defence Research Board Fellow 1958–59. Present address: The Dyson Perrins Laboratory, Oxford University, England.*

Can. J. Chem. Downloaded from www.nrcresearchpress.com by 210.87.254.6 on 09/05/12
For personal use only.

Can. J. Chem. Downloaded from www.nrcresearchpress.com by 210.87.254.6 on 09/05/12
For personal use only.

TABLE I

Compound	M.p., °C	Method of prep.	Yield,* %	Lit. m.p.	Ref.	Analysis C Found	Analysis C Calc.	Analysis H Found	Analysis H Calc.	Dehydration product B.p.	Dehydration product n	Dehydration product H. equiv.¶
1,1′-Ethylenedicyclopentanol	134	A	65	131.2–1.4	12					85–9°/ 0.5 mm	1.4810 (21°)	27, 21%
		C	48	135	4							
1,1′-Ethylenedicyclohexanol	130–1	A	46	128–9	9					90–7°/ 0.5 mm	1.4821 (20°)	28, 33%
		C	42									
1,1′-Ethylenedicycloheptanol	123–4	C	16	Oil	10†	75.6	75.6	11.7	11.8			
1,1′-Ethylenedicyclooctanol	123–4	C	18			76.4	76.6	12.0	12.0			
1,1′-Trimethylenedicyclopentanol	119–21	A	58			73.4	73.6	11.4	11.3			
1,1′-Trimethylenedicyclohexanol	122–3	A	69	120	25					111–5°/ 14 mm	1.4916 (25°)	97%
1,1′-Tetramethylenedicyclopentanol	98–9	B	49	91.8–2.5	14‡							
		D	68									
1,1′-Tetramethylenedicyclohexanol	113.5–5	B	53	103	26					157–9°/ 15 mm	1.5104 (25°)	101%
		D	71									
1,1′-Tetramethylenedicycloheptanol	85–6	D	65			76.3	76.6	12.1	12.0			
1,1′-Pentamethylenedicyclopentanol	63.5–4	B	83			75.1	75.0	11.7	11.7	101–4°/ 0.5 mm	1.5103 (25°)	94%
1,1′-Pentamethylenedicyclohexanol	72–3	B	76			76.4	76.2	11.8	11.9			
1,1′-Hexamethylenedicyclopentanol	87–9	B	86			75.8	75.6	11.9	11.8	109–14°/ 0.5 mm	1.5092 (25°)	96%
1,1′-Hexamethylenedicyclohexanol	83–4	B	71			76.3	76.6	12.1	12.0			
1,1′-Octamethylenedicyclopentanol	83–4	A	52			76.4	76.6	11.8	12.0	141–5°/ 0.8 mm	1.4811 (25°)§	94%
1,1′-Octamethylenedicyclohexanol	87.5–8	A	31			77.4	77.5	12.2	12.3	157–61°/ 0.4 mm	1.4911 (25°)‖	96%
1,1′-Decamethylenedicyclohexanol	56–7	B	38			77.9	78.1	12.2	12.4			
$HO.C_6H_{10}.CH_2.CMe_2.CH_2.C_6H_{10}.OH$	146–7	B	18			76.1	76.2	11.9	11.9			
$HO.C_6H_{10}.CMe_2.CH_2.CH_2.C_6H_{10}.OH$	Liq.	A	47							165–9°/ 0.3 mm	1.4903 (25°)	96%

*The yield of the coupling reaction is given in methods A, B, and C. The hydrogenation steps of methods C and D and the oxidation step in method D were almost quantitative. The yield recorded for method D is for the ethynylation step.
†1,1′-Ethynylenedicycloheptanol (1,4-dihydroxy-1,1,4,4-bishexamethylene-2-butyne) had m.p. 81–2° (literature, 10, 78–80°).
‡1,1′-Diacetylenedicyclopentanol (1,6-dihydroxy-1,1,6,6-bistetramethylene-2,4-hexadiyne) had m.p. 136–7° (literature, 14, 133.2–134.2°).
§M.p. (thermometer immersed) 8°.
‖M.p. (thermometer immersed) 5°.
¶Hydrogenation equivalent, expressed as a percentage of the theoretical uptake for the diolefin.

Method B (18) was the conversion of a cyclic ketone to the symmetrical diol by reaction with the double Grignard reagent derived from an α,ω-dihalide having from 4 to 10 carbon atoms in the chain. In agreement with Lukes and Blaha (5), good results were obtained in this range, but it is generally recognized that aliphatic dihalides having three carbon atoms or fewer between the halogen atoms are useless in Grignard syntheses (6). We have, however, converted 1,3-dibromo-2,2-dimethylpropane (7) to a Grignard reagent and obtained a condensation product from it with cyclohexanone. The success of this reaction is the more remarkable in the light of the reaction of the dihalide with zinc (8) which gives dimethylcyclopropane in 96% yield. Whatever the reasons for the general failure of trimethylene halides in Grignard reactions, cyclopropane ring closure is evidently not one of them. In this instance it is suggested that the 2,2-dimethyl group functions either to limit polymeric coupling of the dihalide by steric hindrance or to preclude olefin formation as there are no hydrogen atoms α to the halogen.

Method C was the interaction of ethynylenemagnesium bromide (BrMgC≡CMgBr) with 2 moles of the appropriate cyclic ketone. Using cyclopentanone, cyclohexanone, and cycloheptanone, this reaction has been investigated previously (9, 10, 11, 12); we have used cyclooctanone also. The 1,1′-ethynylenedicycloalkanol thus obtained is hydrogenated in good yield to give the 1,1′-ethylenedicycloalkanol. It is possible to arrest the hydrogenation of the acetylenic diol in each case to give the olefinic derivative, but complete hydrogenation may be ensured by using either platinum or palladium catalysts in preference to nickel or by performing the hydrogenation over nickel at high pressures. The use of high temperatures in the hydrogenation must be avoided because the tertiary diols are susceptible to dehydration.

Method D, which also involved acetylenic intermediates, was confined to those diols having four methylene groups between the rings. By oxidation of 1-ethynylcycloalkanols, coupling of two molecules to give a diacetylene derivative results (13, 14, 15). This may be hydrogenated to a 1,1′-tetramethylenecycloalkanol. Both steps are practically quantitative.

All of the polymethylene diols were obtained as crystalline solids. One of the diols with a branched connecting chain, the symmetrical one, was also solid, but its unsymmetrical isomer was liquid. Many tenaciously retained sticky impurities, which were best removed by chromatography, and from the nature of the preparative methods adopted, one may infer that these impurities were polymeric. Attempts to prepare crystalline derivatives were unsuccessful, for the customary reagents for alcohol characterization are acidic and need heating. Under such conditions, dehydration of the diol results.

A detailed study of dehydration of ethylene and trimethylene diols of this series is still in progress. Members with four or more carbon atoms between the rings were found to give the expected olefinic dehydration products, and it may be assumed that they are of the alkylcycloalkene type rather than the less stable alkylidenecycloalkane type. It has been reported (4) that the product of dehydration of 1,1′-ethylenedicyclopentanol is also of this nature, although in this compound the presence of an α,δ-diol system might be expected to give a product with a butadienoid system, namely dicyclopentylidene-ethane. Previous studies also indicate that the dehydration of such an α,δ-diol might give a cyclic ether rather than a diolefin; for example, Henry (16) obtained 2,2,5,5-tetramethyltetrahydrofuran from 2,5-dimethylhexane-2,5-diol and Reppe (17) reported the conversion of 1,1′-ethylenedicyclohexanol to 7-oxaspiro-(5,1,5,2)-pentadecane. The quantitative microhydrogenation data on our dehydration products from both 1,1′-

Can. J. Chem. Downloaded from www.nrcresearchpress.com by 210.87.254.6 on 09/05/12
For personal use only.

ethylenedicyclohexanol and 1,1′-ethylenedicyclopentanol indicate that a mixture of diolefin and epoxide was obtained.

EXPERIMENTAL

All melting points, except where otherwise noted, were determined by the capillary-tube method on a thermometer calibrated against an Anschütz set with a National Bureau of Standards certificate. Melting points and other temperatures are recorded as degrees centigrade.

1,1′-Octamethylenedicyclohexanol (Method A, cf. ref. 4) and its Dehydration

Pentamethylenedimagnesium bromide and dimethyl sebacate were condensed by the known procedure (4) but benzene was added to the reaction mixture and it was worked up with ammonium chloride to minimize dehydration loss. The crude product was sticky and melted between 60 and 80°. It was adsorbed from benzene on alumina and eluted successively with benzene and diethyl ether. Crystals were deposited by evaporation of each eluate and these were united and crystallized once from heptane, m.p. 87.5–88°. Further elution of the column with ethyl acetate gave a viscous oil which was not further investigated.

The crystalline diol (7.0 g, 0.025 mole) was heated to 150° for 4 hours in the presence of iodine (10 mg). A further portion of iodine (5 mg) was then added and heating continued for 1 hour at 170°. The product, an oil, was taken up in ether and shaken with sodium thiosulphate solution. After drying, the solvent was removed and the residual oil distilled, yield 4.1 g, 67%, b.p. 157–161°/0.4 mm, n_D^{25}, 1.4911, m.p. (thermometer immersed) 5°. Other diols listed in Table I were dehydrated similarly.

1,1′-Ethylenedicyclooctanol (Method C)

Interaction of cyclooctanone and ethynylenemagnesium bromide (the Iotsitch reagent) (19) was achieved essentially by the method described by Pinkney and Marvel (11) for other ketones. Using ammonium chloride as described above for decomposition of the magnesium complex, 1,1′-ethynylenedicyclooctanol (1,4-dihydroxy-1,1,4,4-bisheptamethylene-2-butyne) was isolated in ether and finally obtained as a solid, m.p. 115°. Found: C, 77.8; H, 10.8, hydrogenation equivalent 132. Calc. for $C_{18}H_{30}O_2$: C, 77.8; H, 10.8%, hydrogenation equivalent 139.

By hydrogenation of the acetylenic diol in ethyl acetate as previously described, 1,1′-ethylenedicyclooctanol was obtained in nearly quantitative yield, m.p. 123–124°.

1,1′-Tetramethylenedicycloheptanol (Method D)

Ethynylation of cycloheptanone was performed in a manner analogous to the recorded ethynylation of cyclohexanone (20, 21). Oxidative coupling of this alcohol to yield the diacetylene derivative was accomplished by copper-catalyzed autoxidation in an experiment similar to that performed by Zal'kind and Aizikovich (13) on its lower homologue. 1-Ethynylcycloheptanol (70 g, 0.5 mole) in ethanol (75 ml) was added during 2 hours to a vigorously stirred solution of ammonium chloride (36 g), cuprous chloride (11.5 g), and hydrochloric acid (10 *N*, 2.5 ml) in water (100 ml) at 50° while a slow stream of oxygen bubbled through. The solution was stirred with oxygen passed in for 4 hours more, and then 250 ml of a saturated aqueous solution of ammonium chloride was added. Next day the solid product was collected by filtration and washed with ammonium chloride solution. It was then washed with hydrochloric acid (2 *N*) until the washings

Can. J. Chem. Downloaded from www.nrcresearchpress.com by 210.87.254.6 on 09/05/12
For personal use only.

were no longer colored. The crude product (70 g, an almost quantitative yield) melted at 164–166°. This was raised to 165–166° by one crystallization from ethanol.

This diacetylenic diol (2.5 g, 0.01 mole) was hydrogenated in ethyl acetate suspension (50 ml) over palladized calcium carbonate at ambient temperature and 32.5 p.s.i. Uptake was complete in 3 hours and the filtered solution deposited crystals of 1,1′-tetramethylenedicycloheptanol (2.5 g, quantitative yield, m.p. 80–84°). This product was stable to aqueous potassium permanganate and was purified by one crystallization from a mixture of petroleum ether and benzene, in which it is very soluble (m.p. 85–86°).

Diethyl 2,2-Dimethylglutarate

In our hands, the previously published procedures (e.g. ref. 22) for conversion of 2,2-dimethyl-4-cyanobutyraldehyde to 2,2-dimethylglutaric acid gave 55 to 60% yields of a sticky product melting at 55–60°. Such procedures employ nitric acid alone or mixed with concentrated sulphuric acid as the reagent for simultaneous hydrolysis and oxidation of the starting material and it is possible that side reactions of polymerization or further oxidation can take place. Much loss of material occurred during purification.

The method adopted resembled that employed by Bruson and Riener (23) for conversion of 2,2-diethyl-4-cyanobutyraldehyde to 2,2-diethylglutaric acid. 2,2-Dimethyl-4-cyanobutyraldehyde (24) was used as soon as possible after it was prepared, because it is unexpectedly susceptible to autoxidation and on one occasion an explosion occurred when a sample that had been kept for some months without precautions against peroxide formation was distilled. The cyanoaldehyde (60 g, 0.5 mole) was boiled with sodium hydroxide (25 g, 0.63 mole) in water (250 ml) until a homogeneous solution was obtained ($\frac{1}{2}$ hour). After cooling, a further 25-g portion of sodium hydroxide and a further 250 ml of water were added. Potassium permanganate (114 g, 0.7 mole) was ground to a slurry with water (1 liter) and added to the cooled, stirred solution at such a rate that the temperature was 35–40°. Following a further $\frac{1}{2}$ hour of stirring, sulphur dioxide was passed until all the manganese dioxide was reduced. The 2,2-dimethylglutaric acid was isolated by ether extraction of the solution (66 g, 86%, m.p. 74–76°). By recrystallizing from a mixture of benzene and petroleum ether the melting point was raised to 83–84°, but the bulk of the product was esterified without purification, yielding diethyl 2,2-dimethylglutarate, b.p. 147/46 mm, $n_D^{22.5}$, 1.4262. (Found: saponification equivalent, 107. Calc. for $C_{11}H_{20}O_4$: 108).

1. L. F. Fieser and J. Smuszkowicz. J. Am. Chem. Soc. **70**, 3352 (1948).
2. D. G. M. Diaper. Can. J. Chem. **33**, 1720 (1955).
3. D. G. M. Diaper and A. Kuksis. Chem. Revs. **59**, 90 (1959).
4. C. D. Nenitzescu and I. Necsoiu. J. Am. Chem. Soc. **72**, 3483 (1950).
5. R. Lukes and K. Blaha. Chem. listy, **46**, 683 (1952).
6. I. T. Millar and H. Heaney. Quart. Revs. (London), **11**, 109 (1957).
7. F. C. Whitmore. J. Am. Chem. Soc. **63**, 124 (1941).
8. R. W. Shortridge. J. Am. Chem. Soc. **70**, 946 (1948).
9. P. S. Pinkney, G. A. Nesty, D. E. Pearson, and C. S. Marvel. J. Am. Chem. Soc. **59**, 2666 (1937).
10. I. M. Gverdtsiteli, Sh. G. Mikadze, and T. D. Tsiklauri. Sbornik Statei Obshchei Khim. **2**, 956 (1953); Chem. Abstr. **49**, 6828h (1955).
11. P. S. Pinkney and C. S. Marvel. J. Am. Chem. Soc. **59**, 2669 (1937).
12. Yu. S. Zal'kind and I. M. Gverdtsiteli. J. Gen. Chem. U.S.S.R. **9**, 855 (1939); Chem. Abstr. **34**, 3876 (1940).
13. Yu. S. Zal'kind and M. A. Aizikovich. J. Gen. Chem. U.S.S.R. **7**, 227 (1937); Chem. Abstr. **31**, 42837 (1937).
14. Yu. S. Zal'kind and I. M. Gverdtsiteli. J. Gen. Chem. U.S.S.R. **9**, 971 (1939); Chem. Abstr. **33**, 85698 (1939).
15. A. S. Hay. J. Org. Chem. **25**, 1275 (1960).

Can. J. Chem. Downloaded from www.nrcresearchpress.com by 210.87.254.6 on 09/05/12
For personal use only.

16. L. HENRY. Compt. rend. **143**, 496 (1906).
17. W. REPPE. Ann. **596**, 25 (1955).
18. G. CHAVANNE and P. BECKER. Bull. soc. chim. Belg. **36**, 591 (1927).
19. R. LESPIEAU. Bull. soc. chim. **39**, [4], 991 (1926).
20. J. H. SAUNDERS. Org. Syntheses, Coll. Vol. III. 416 (1955).
21. I. HEILBRON, E. R. H. JONES, J. B. TOOGOOD, and B. C. L. WEEDON. J. Chem. Soc. 1827 (1949).
22. W. FRANKE and J. BUEREN. Z. Naturforsch. Pt. *b*, **5**, 122 (1950).
23. H. A. BRUSON and T. W. RIENER. J. Am. Chem. Soc. **66**, 56 (1944).
24. D. HOCH and P. KARRER. Helv. Chim. Acta, **37**, 397 (1954).
25. K. ZEILE and H. MEYER. Ber. **75**, B, 356 (1942).
26. J. COLONGE and G. POILANE. Compt. rend. **238**, 117 (1954); Bull. soc. chim. 499 (1955).

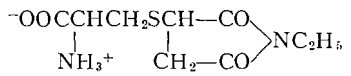
RECEIVED OCTOBER 27, 1960.
DEPARTMENT OF CHEMISTRY,
ROYAL MILITARY COLLEGE,
KINGSTON, ONT.

Can. J. Chem. Downloaded from www.nrcresearchpress.com by 210.87.254.6 on 09/05/12
For personal use only.

ADDUCTS FROM THE REACTION OF N-ETHYLMALEIMIDE WITH L-CYSTEINE AND WITH GLUTATHIONE

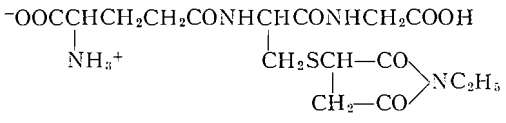
C. C. LEE AND E. R. SAMUELS

Since the first report of a quantitative reaction between thiols and N-ethylmaleimide (NEM) (1), a number of workers have described the use of NEM as a reagent for the assay of the sulphydryl group (2–6). However, it was only recently that the product from the reaction of L-cysteine and NEM was isolated and characterized as S-(N-ethylsuccinimido)-L-cysteine (I) (7). This note reports an independent isolation of I as well



(I)

as the preparation of S-(N-ethylsuccinimido)-glutathione (II), the adduct from the reaction of NEM with glutathione. Adduct II has not been recorded in any earlier publication.



(II)

The present work was undertaken as part of a project involving the determination of relative amounts of sulphhydryl and disulphide groups in certain proteins in which S^{35} has been incorporated. A suitable carrier for the reaction product between NEM and thiols was sought so that isotope dilution studies may be carried out. With this aim in mind, the behaviors of I and II on acid hydrolysis were studied. Somewhat surprisingly, it was found that after treatment for 18 hours in refluxing 6 *N* hydrochloric acid, I was recovered without change. The products from the hydrolysis of II were identified by paper chromatography as glycine, glutamic acid, and adduct I, exactly as expected for hydrolysis of the peptide bonds with I remaining unaffected. It was also noted that paper chromatographic separation of I from II, cysteine, and cystine can be easily accomplished. These observations indicate that it is likely feasible to use I as a

16. L. HENRY. Compt. rend. **143**, 496 (1906).
17. W. REPPE. Ann. **596**, 25 (1955).
18. G. CHAVANNE and P. BECKER. Bull. soc. chim. Belg. **36**, 591 (1927).
19. R. LESPIEAU. Bull. soc. chim. **39**, [4], 991 (1926).
20. J. H. SAUNDERS. Org. Syntheses, Coll. Vol. III. 416 (1955).
21. I. HEILBRON, E. R. H. JONES, J. B. TOOGOOD, and B. C. L. WEEDON. J. Chem. Soc. 1827 (1949).
22. W. FRANKE and J. BUEREN. Z. Naturforsch. Pt. *b*, **5**, 122 (1950).
23. H. A. BRUSON and T. W. RIENER. J. Am. Chem. Soc. **66**, 56 (1944).
24. D. HOCH and P. KARRER. Helv. Chim. Acta, **37**, 397 (1954).
25. K. ZEILE and H. MEYER. Ber. **75**, B, 356 (1942).
26. J. COLONGE and G. POILANE. Compt. rend. **238**, 117 (1954); Bull. soc. chim. 499 (1955).

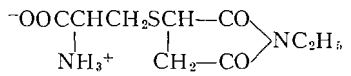
RECEIVED OCTOBER 27, 1960.
DEPARTMENT OF CHEMISTRY,
ROYAL MILITARY COLLEGE,
KINGSTON, ONT.

Can. J. Chem. Downloaded from www.nrcresearchpress.com by 210.87.254.5 on 09/05/12
For personal use only.

ADDUCTS FROM THE REACTION OF N-ETHYLMALEIMIDE WITH L-CYSTEINE AND WITH GLUTATHIONE

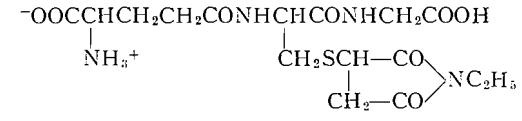
C. C. LEE AND E. R. SAMUELS

Since the first report of a quantitative reaction between thiols and N-ethylmaleimide (NEM) (1), a number of workers have described the use of NEM as a reagent for the assay of the sulphydryl group (2–6). However, it was only recently that the product from the reaction of L-cysteine and NEM was isolated and characterized as S-(N-ethylsuccinimido)-L-cysteine (I) (7). This note reports an independent isolation of I as well



(I)

as the preparation of S-(N-ethylsuccinimido)-glutathione (II), the adduct from the reaction of NEM with glutathione. Adduct II has not been recorded in any earlier publication.



(II)

The present work was undertaken as part of a project involving the determination of relative amounts of sulphhydryl and disulphide groups in certain proteins in which S^{35} has been incorporated. A suitable carrier for the reaction product between NEM and thiols was sought so that isotope dilution studies may be carried out. With this aim in mind, the behaviors of I and II on acid hydrolysis were studied. Somewhat surprisingly, it was found that after treatment for 18 hours in refluxing 6 *N* hydrochloric acid, I was recovered without change. The products from the hydrolysis of II were identified by paper chromatography as glycine, glutamic acid, and adduct I, exactly as expected for hydrolysis of the peptide bonds with I remaining unaffected. It was also noted that paper chromatographic separation of I from II, cysteine, and cystine can be easily accomplished. These observations indicate that it is likely feasible to use I as a

carrier in isotope dilution studies. If a protein containing S^{35} were allowed to react with NEM and then hydrolyzed in 6 *N* hydrochloric acid, any sulphydryl groups originally present in cysteine residues should give rise to S^{35}-labeled adduct I, which may be isolated with the aid of ordinary I as carrier.

EXPERIMENTAL

S-(N-Ethylsuccinimido)-L-cysteine (I)

Equal volumes of 0.1 *M* solutions of NEM and L-cysteine hydrochloride were mixed and allowed to stand at room temperature overnight. The resulting solution was concentrated under reduced pressure at 50–60° C. Ethanol was then added to precipitate the product. The latter was dissolved in distilled water, passed through a column packed with the anion exchanger, Dowex 1-x8, eluted with 0.5 *N* acetic acid, concentrated again under reduced pressure, and then crystallized with the addition of ethanol. The yield of purified S-(N-ethylsuccinimido)-L-cysteine, m.p. 194–195° C, decomp., was 85%. It gave a positive ninhydrin reaction and a negative nitroprusside test, which indicated the absence of the sulphydryl group.

Anal. Calc. for $C_9H_{14}O_4N_2S$: C, 43.89; H, 5.73; N, 11.38; S, 13.02. Found: C, 43.89; H, 5.78; N, 11.05; S, 12.90. This procedure for the preparation of I was essentially similar to that reported by Smyth and co-workers (7). However, it was noted that although, when the reactants were mixed, the pH was 1.8, it was not necessary to add sodium hydroxide to the reaction mixture as was done by Smyth *et al.* (7). It was found that inclusion of sodium hydroxide in the reaction mixture often gave a product containing detectable amounts of ash. The elimination of the base and final purification through the Dowex 1-x8 column proved to be quite satisfactory.

S-(N-Ethylsuccinimido)-glutathione (II)

Equal volumes of 0.1 *M* solutions of NEM and glutathione (reduced) were mixed and allowed to stand overnight. The resulting solution was worked up in the same way as in the isolation and purification of I. The product, S-(N-ethylsuccinimido)-glutathione, m.p. 204–206° C, decomp., was obtained in 90% yield. It also gave a positive reaction with ninhydrin and a negative test with nitroprusside.

Anal. Calc. for $C_{16}H_{24}O_8N_4S$: C, 44.44; H, 5.59; N, 12.96; S, 7.42. Found: C, 44.14; H, 5.59; N, 12.88; S, 7.13.

Acid Hydrolysis

One gram of I or II in 20 ml 6 *N* hydrochloric acid was refluxed for 18 hours. The resulting solution was concentrated to a small volume under reduced pressure, passed through a Dowex 1-x8 column, eluted with 0.5 *N* acetic acid, concentrated again and the product crystallized with the addition of acetone. After this treatment, unchanged I was almost quantitatively recovered. That I was the same before and after hydrolysis was established by mixed melting point; unchanged analyses for C, H, N, S; identical infrared absorption spectrum; and behavior in paper chromatography. Ascending paper chromatography on Whatman No. 1 paper with *t*-butanol – water – formic acid (69.5:29.5:1) as solvent was run for 16 hours and developed with 0.1% ninhydrin in acetone. The same spot was obtained for I before and after hydrolysis. On the other hand, paper chromatographic analysis of the hydrolyzate of II gave three spots. By comparison with behaviors of known compounds, these spots were identified as glycine, glutamic acid, and adduct I.

Can. J. Chem. Downloaded from www.nrcresearchpress.com by 210.87.254.5 on 09/05/12
For personal use only.

ACKNOWLEDGMENT

The financial aid given by the National Research Council of Canada is gratefully acknowledged.

1. E. FRIEDMANN, D. H. MARRIAN, and I. SIMON-REUSS. Brit. J. Pharmacol. **4**, 105 (1949).
2. J. D. GREGORY. J. Am. Chem. Soc. **77**, 2922 (1955).
3. R. BENESCH, R. E. BENESCH, M. GUTCHO, and L. LAUFER. Science, **123**, 981 (1956).
4. C. A. PRICE and C. W. CAMPBELL. Biochem. J. **65**, 512 (1957).
5. E. ROBERTS and G. ROUSER. Anal. Chem. **30**, 1291 (1958).
6. N. M. ALEXANDER. Anal. Chem. **30**, 1292 (1958).
7. D. G. SMYTH, A. NAGAMATSU, and J. S. FRUTON. J. Am. Chem. Soc. **82**, 4600 (1960).

RECEIVED DECEMBER 27, 1960.
DEPARTMENT OF CHEMISTRY,
UNIVERSITY OF SASKATCHEWAN,
SASKATOON, SASKATCHEWAN.

Can. J. Chem. Downloaded from www.nrcresearchpress.com by 210.87.254.5 on 09/05/12
For personal use only.

FINE STRUCTURE IN THE PROTON MAGNETIC RESONANCE SPECTRUM OF 6–6 NYLON

D. J. SHAW[1] AND B. A. DUNELL

Correlation of the nuclear magnetic resonance (n.m.r.) spectra of polymers with their physical properties and mechanical behavior has received considerable attention recently and has been reviewed by Slichter (1, 2) and by Sauer and Woodward (3). The existence of a narrow component of the n.m.r. spectrum superimposed on the broad line above certain temperatures has been associated with extensive molecular motion in the amorphous phase of such polymers as branched and straight-chain polyethylene (4–6) and isotactic polypropylene (7, 8). One might anticipate that a narrow component would also be observed in the n.m.r. spectrum of nylon in the vicinity of room temperature, corresponding to the onset in the amorphous part of the nylon of molecular motion which gives rise to energy dissipation and dispersion of elastic modulus in mechanical experiments (3, 9, 10). Although Slichter (11) had already reported the variation with temperature of line width and second moment of nylon 6–6 and given no indication of the existence of fine structure in the spectrum at any temperature, it was decided to reinvestigate this substance. Woodward, Glick, Gupta, and Sauer (12) have published detailed results of the change with temperature of the n.m.r. line width and second moment of a number of polyamides, both thoroughly dried and containing various H_2O and D_2O contents. They do not, however, mention the existence of any fine structure in the spectra. Illers and Kosfeld (13) have recently obtained evidence of a narrow component in the n.m.r. spectrum of a completely dry sample of nylon 6–12.

EXPERIMENTS AND RESULTS

The nylon used in this work was a multifilament commercial yarn containing no delustrant. It was extracted with boiling ether for 8 hours and dried in a vacuum desiccator over phosphorus pentoxide for 24 hours before any experiments were done on it. Initially, this nylon was sealed, without further treatment, into a sample tube under dry nitrogen and its n.m.r. spectrum taken with a broad-line spectrometer of the marginal oscillator type (14), operating at 28 Mc/sec, and a 6-in. Varian electromagnet.

[1]*Present address: Research Department, Unilever Ltd., Port Sunlight, Cheshire, England.*

ACKNOWLEDGMENT

The financial aid given by the National Research Council of Canada is gratefully acknowledged.

1. E. FRIEDMANN, D. H. MARRIAN, and I. SIMON-REUSS. Brit. J. Pharmacol. **4**, 105 (1949).
2. J. D. GREGORY. J. Am. Chem. Soc. **77**, 2922 (1955).
3. R. BENESCH, R. E. BENESCH, M. GUTCHO, and L. LAUFER. Science, **123**, 981 (1956).
4. C. A. PRICE and C. W. CAMPBELL. Biochem. J. **65**, 512 (1957).
5. E. ROBERTS and G. ROUSER. Anal. Chem. **30**, 1291 (1958).
6. N. M. ALEXANDER. Anal. Chem. **30**, 1292 (1958).
7. D. G. SMYTH, A. NAGAMATSU, and J. S. FRUTON. J. Am. Chem. Soc. **82**, 4600 (1960).

RECEIVED DECEMBER 27, 1960.
DEPARTMENT OF CHEMISTRY,
UNIVERSITY OF SASKATCHEWAN,
SASKATOON, SASKATCHEWAN.

Can. J. Chem. Downloaded from www.nrcresearchpress.com by 210.87.254.40 on 09/05/12
For personal use only.

FINE STRUCTURE IN THE PROTON MAGNETIC RESONANCE SPECTRUM OF 6–6 NYLON

D. J. SHAW[1] AND B. A. DUNELL

Correlation of the nuclear magnetic resonance (n.m.r.) spectra of polymers with their physical properties and mechanical behavior has received considerable attention recently and has been reviewed by Slichter (1, 2) and by Sauer and Woodward (3). The existence of a narrow component of the n.m.r. spectrum superimposed on the broad line above certain temperatures has been associated with extensive molecular motion in the amorphous phase of such polymers as branched and straight-chain polyethylene (4–6) and isotactic polypropylene (7, 8). One might anticipate that a narrow component would also be observed in the n.m.r. spectrum of nylon in the vicinity of room temperature, corresponding to the onset in the amorphous part of the nylon of molecular motion which gives rise to energy dissipation and dispersion of elastic modulus in mechanical experiments (3, 9, 10). Although Slichter (11) had already reported the variation with temperature of line width and second moment of nylon 6–6 and given no indication of the existence of fine structure in the spectrum at any temperature, it was decided to reinvestigate this substance. Woodward, Glick, Gupta, and Sauer (12) have published detailed results of the change with temperature of the n.m.r. line width and second moment of a number of polyamides, both thoroughly dried and containing various H_2O and D_2O contents. They do not, however, mention the existence of any fine structure in the spectra. Illers and Kosfeld (13) have recently obtained evidence of a narrow component in the n.m.r. spectrum of a completely dry sample of nylon 6–12.

EXPERIMENTS AND RESULTS

The nylon used in this work was a multifilament commercial yarn containing no delustrant. It was extracted with boiling ether for 8 hours and dried in a vacuum desiccator over phosphorus pentoxide for 24 hours before any experiments were done on it. Initially, this nylon was sealed, without further treatment, into a sample tube under dry nitrogen and its n.m.r. spectrum taken with a broad-line spectrometer of the marginal oscillator type (14), operating at 28 Mc/sec, and a 6-in. Varian electromagnet.

[1]*Present address: Research Department, Unilever Ltd., Port Sunlight, Cheshire, England.*

With this spectrometer the line widths obtained in the range from liquid nitrogen temperature to 400° K were substantially the same as those reported by Slichter (11), and no evidence of fine structure was obtained. The comparison of line widths is shown in Fig. 1. The widths that we obtained at the three highest temperatures are too great because of instrumental difficulties.

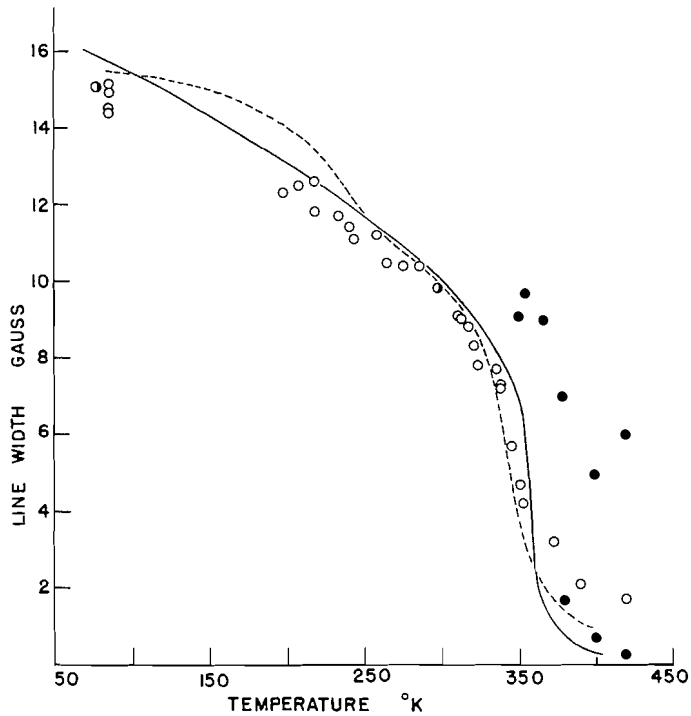


FIG. 1. Nuclear magnetic resonance line width of nylon 6–6 as a function of temperature. ○ This work, using sample dried at room temperature. ● This work, using exhaustively dried sample. ◑ Coincidence of open and filled points. ——— Results of Slichter (11). – – – Results of Glick *et al.* (12).

Since the α' dispersion region (found near 350° K for dry nylon 6–6) moves to lower temperature as nylon sorbs water, and is centered near room temperature when the relative humidity approaches 100% (10); evidence of fine structure in the n.m.r. spectrum of nylon was sought at room temperature using a sample that was in equilibrium with a number of different partial pressures of water vapor. An intense narrow component was obtained under these conditions, but it disappeared when the nylon was soaked in 99% D_2O for several hours, dried in a vacuum system, and exposed to D_2O vapor in the sealed sample tube. The marginal oscillator spectrometer gave the line width of the deuterated and dried nylon sample as 10.2 gauss and of the deuterated sample exposed to saturated D_2O vapor as 9.7 gauss, both at 295° K. The corresponding second moments were 16.3 and 14.4 gauss^2.

A second group of experiments was done using a Varian V-4250 combination high-resolution and broad-line spectrometer operating at 40 Mc/sec. When we used this apparatus we found that samples which were dried under vacuum at room temperature showed a narrow component which may be attributed to residual sorbed moisture in the sample. Illers has found that complete drying of the nylon can be achieved only by

Can. J. Chem. Downloaded from www.nrcresearchpress.com by 210.87.254.40 on 09/05/12
For personal use only.

heating at 100° C or more under vacuum (15). When we heated under these conditions for 6 hours, this narrow component observed at room temperature on the Varian spectrometer disappeared. The exhaustively dried sample was then run in the Varian spectrometer at temperatures up to 420° K. The sample was heated in a small Dewar vessel which fitted inside the spectrometer insert-tube by a stream of heated air, and the temperature measured by a thermocouple (16). The rather small sample and large insert-tube together with high sample temperature give rather poor signal to noise ratio. Nevertheless the appearance and growth in intensity with increasing temperature of a narrow component in the n.m.r. spectrum of exhaustively dried nylon can be distinguished in the traces reproduced in Fig. 2. Because the resolving of each spectrum

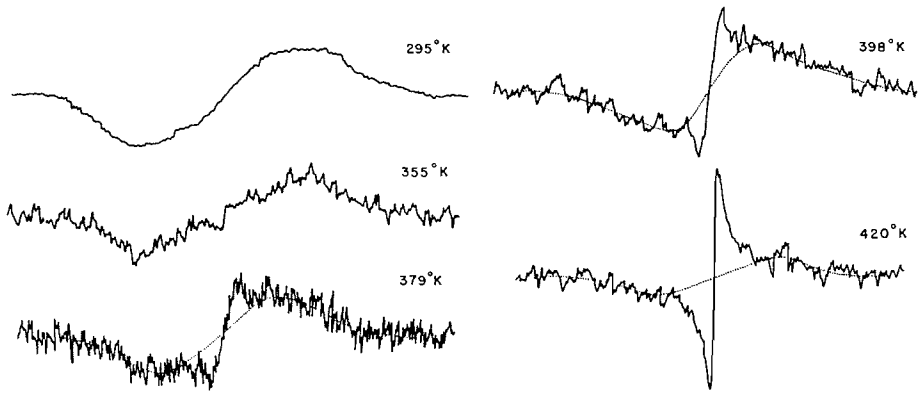


FIG. 2. Nuclear magnetic resonance spectra of exhaustively dried nylon 6–6 at various temperatures. The dotted lines show the assumed resolution into broad and narrow components.

into a broad and narrow component has been done arbitrarily, the width of the resolved broad line is, as Illers (13) points out in his corresponding case, subject to large error. It is estimated that the error may be as great as 40%. Line widths of the broad and narrow components are plotted in Fig. 1.

The deuterated sample was also re-examined on the Varian machine at room temperature. Dry, it gave a line width of 9.8 gauss and a second moment of 14.2 gauss^2; exposed to saturated vapor of D_2O, it gave 9.5 gauss and 13.0 gauss^2. These values are in satisfactory agreement with those obtained from the other spectrometer. A narrow component of very small intensity was observed with the deuterated system after the sample had been exposed to D_2O vapor for several days. This is attributed to traces of proton exchanging with sorbed heavy water.

The density of the nylon was measured in a density gradient tube (17) and used to obtain the percentage crystallinity from the correlation of Starkweather and Moynihan (18). The sample was found to be 35% crystalline.

DISCUSSION

In the exhaustively dried nylon the appearance of a narrow component near 380° K is attributed to the onset of very extensive molecular motion in part of the amorphous region of the substance. Such motion is considered to be the cause of the α' energy loss and dispersion mechanism (9, 10) which occurs at about 350° K at sonic frequencies in dry samples. Exhaustive drying would be expected to raise the temperature of the maximum in mechanical loss by several degrees (19), bringing it closer to 380° K. (An activation energy of 70 kcal/mole for the α' mechanism would correspond to a 20°

Can. J. Chem. Downloaded from www.nrcresearchpress.com by 210.87.254.40 on 09/05/12
For personal use only.

temperature difference between a correlation frequency of 10^5 for the n.m.r. experiment and a frequency of 650 c.p.s. (10) for the mechanical experiment.) As the temperature rises from 380° to 420° K the intensity of the narrow component increases, and its width decreases from 1.7 gauss (with modulation amplitude 1 gauss) at 379° K to approximately 0.3 gauss (modulation 0.12 gauss) at 420° K. The narrow-component line width indicated that although motion of the molecular chain segments becomes very extensive it is not liquid-like at least by 420° K. Further, it does not appear that even at this temperature the whole of the amorphous region is in the vigorous motion that produces the narrow line. Thus, although the percentage of amorphous component was found to be some 65%, the area under the narrow peak is only 20% of the area under both peaks at 420° K.

The width of the broad component at 420° K is somewhat less than half of the width at liquid nitrogen temperature, and the second moment of 6 gauss^2 is one quarter of the value at 77° K. Slichter (11) has calculated that if the chain segments in crystalline nylon 6–6 all rotate freely, the second moment should be 8.5 gauss^2. Thus both line-width and second-moment reduction are consistent with an interpretation that the part of the nylon which is not in extensive motion at 420° K is involved in motion which, on the average, is slightly more extensive than rotation of chain segments about their long axes.

When there is present even the very small amount of water remaining in a nylon sample dried at room temperature, the temperature at which very extensive motion begins must be reduced considerably and the amount of amorphous phase involved in the motion must be increased to such an extent that the broad component is masked by the now much more intense narrow component and no fine structure is distinguishable in the spectrum. The width of the line is that corresponding to the narrow component.

Our observation that exposure of a deuterated nylon sample to saturated D_2O vapor did not significantly reduce the line width at room temperature is entirely at variance with the results reported by Woodward and his co-workers (12), who found it decreased to about 1 gauss under approximately these conditions (i.e., 7.8 wt.% D_2O sorption at 295° K). We observed the same line width, 9.5 ± 0.1 gauss, 1, 14, 15, and 28 days after exposure to D_2O vapor, using the Varian spectrometer; and, as mentioned earlier, this width agreed with that obtained from the other spectrometer using a different sample. The discrepancy would not seem, therefore, to be of diffusional, equilibrium, or instrumental origin. One must conclude that the difference of results arises from the fact that we have used a drawn-filament sample rather than "bulk polymer". In the drawn filament it is possible that the chain segments in the amorphous regions are restricted in mobility to such an extent, because of great crystallite to crystallite distance in the direction of stretching, that only the first traces of water can be effective in increasing molecular motion at given temperature.

ACKNOWLEDGMENTS

We wish to thank the Defence Research Board for the financial assistance under Grant 7570-07 which made this work possible. Correspondence and discussion with Dr. K. H. Illers, Technische Hochschule, Aachen, was most helpful. We are indebted to Dr. R. D. Bennett of the du Pont Company of Canada (1956) Ltd. for supplying the nylon samples.

1. W. P. SLICHTER. Makromol. Chem. **34** (Sonderband 1), 67 (1959).
2. W. P. SLICHTER. Fortschr. der Hochpolymeren Forschung, **1**, 35 (1958).
3. J. A. SAUER and A. E. WOODWARD. Revs. Modern Phys. **32**, 88 (1960).

Can. J. Chem. Downloaded from www.nrcresearchpress.com by 210.87.254.40 on 09/05/12
For personal use only.

4. N. FUSCHILLO and J. A. SAUER. J. Appl. Phys. **28**, 1073 (1957).
5. R. C. REMPEL, H. E. WEAVER, R. H. SANDS, and R. L. MILLER. J. Appl. Phys. **28**, 1082 (1957).
6. D. W. MCCALL and W. P. SLICHTER. J. Polymer Sci. **26**, 171 (1957).
7. W. P. SLICHTER and E. R. MANDELL. J. Appl. Phys. **29**, 1438 (1958).
8. J. A. SAUER, R. A. WALL, N. FUSCHILLO, and A. E. WOODWARD. J. Appl. Phys. **29**, 1385 (1958).
9. K. SCHMIEDER and K. WOLF. Kolloid-Z. **134**, 149 (1953).
10. A. E. WOODWARD, J. A. SAUER, C. W. DEELEY, and D. E. KLINE. J. Colloid Sci. **12**, 363 (1957).
11. W. P. SLICHTER. J. Appl. Phys. **26**, 1099 (1955).
12. R. E. GLICK, R. P. GUPTA, J. A. SAUER, and A. E. WOODWARD. J. Polymer Sci. **42**, 271 (1960); **45** 367 (1960).
13. K. H. ILLERS and R. KOSFELD. Makromol. Chem. **42**, 44 (1960).
14. H. S. GUTOWSKY, L. H. MEYER, and R. E. MCCLURE. Rev. Sci. Instr. **24**, 644 (1953).
15. K. H. ILLERS. Private communication.
16. H. J. BERNSTEIN, W. G. SCHNEIDER, and J. A. POPLE. Proc. Roy. Soc. A, **236**, 515 (1956).
17. R. F. BOYER, R. S. SPENCER, and R. M. WILEY. J. Polymer Sci. **1**, 249 (1946).
18. H. W. STARKWEATHER, JR. and R. E. MOYNIHAN. J. Polymer Sci. **22**, 363 (1956).
19. K. H. ILLERS. Makromol. Chem. **38**, 168 (1960).

RECEIVED DECEMBER 12, 1960.
CHEMISTRY DEPARTMENT,
UNIVERSITY OF BRITISH COLUMBIA,
VANCOUVER 8, B.C.

Can. J. Chem. Downloaded from www.nrcresearchpress.com by 210.87.254.40 on 09/05/12
For personal use only.

THE PROTON MAGNETIC RESONANCE SPECTRUM AND THE CHARGE DISTRIBUTION OF THE PYRIDINIUM ION*

I. C. SMITH† AND W. G. SCHNEIDER

The protonation of pyridine by trifluoracetic acid has been examined by proton resonance techniques. In the presence of excess acid it has been found possible to observe the proton spectrum characteristic of the pyridinium ion. Figure 1 shows the spectrum of pyridine (in a 5 mole% cyclohexane solution) as well as those of trifluoracetic acid solutions containing 20, 10, and 5 mole% of pyridine respectively. A small amount ($\sim$ 3 mole%) of CH_2Cl_2 was added to each solution to serve as an internal reference signal. Modulation side bands of the reference at 140 and 240 cycles/sec are indicated on the individual traces. The assignment of the proton signals is based on the previously reported analysis of the pyridine spectrum (1). Figure 2 shows a more extended spectrum of the 5 mole% pyridine solution in trifluoracetic acid taken under conditions of lower resolution. It shows, in addition to the signal of the carboxyl group of the trifluoracetic acid and that of the α, β, and γ protons, a triplet signal characteristic of a proton bonded to a nitrogen atom. This confirms the presence of the pyridinium ion. The triplet splitting arises from spin coupling with the N^{14} nucleus having spin $S = 1$. The spin-coupling constant has the value 70 cycles/sec.

The position of the N—H proton signal, to the low-field side of the acid carboxyl group, is unusual for protons bonded to nitrogen. In neutral molecules this ordinarily appears at a much higher field. It is evident from Fig. 1 that there is also a low-field displacement, though smaller, for the signals of the protons of the pyridine ring when the ion is formed. Table I shows the actual chemical shifts (relative to CH_2Cl_2 internal reference) for the individual protons in pyridine and in the pyridinium ion. These shifts are necessarily approximate since an exact analysis of the pyridinium ion spectrum, which has broadened

**Issued as N.R.C. No. 6265.*
†*Research Student, Summer, 1960; University of Manitoba, Winnipeg, Manitoba.*

4. N. FUSCHILLO and J. A. SAUER. J. Appl. Phys. **28**, 1073 (1957).
5. R. C. REMPEL, H. E. WEAVER, R. H. SANDS, and R. L. MILLER. J. Appl. Phys. **28**, 1082 (1957).
6. D. W. MCCALL and W. P. SLICHTER. J. Polymer Sci. **26**, 171 (1957).
7. W. P. SLICHTER and E. R. MANDELL. J. Appl. Phys. **29**, 1438 (1958).
8. J. A. SAUER, R. A. WALL, N. FUSCHILLO, and A. E. WOODWARD. J. Appl. Phys. **29**, 1385 (1958).
9. K. SCHMIEDER and K. WOLF. Kolloid-Z. **134**, 149 (1953).
10. A. E. WOODWARD, J. A. SAUER, C. W. DEELEY, and D. E. KLINE. J. Colloid Sci. **12**, 363 (1957).
11. W. P. SLICHTER. J. Appl. Phys. **26**, 1099 (1955).
12. R. E. GLICK, R. P. GUPTA, J. A. SAUER, and A. E. WOODWARD. J. Polymer Sci. **42**, 271 (1960); **45** 367 (1960).
13. K. H. ILLERS and R. KOSFELD. Makromol. Chem. **42**, 44 (1960).
14. H. S. GUTOWSKY, L. H. MEYER, and R. E. MCCLURE. Rev. Sci. Instr. **24**, 644 (1953).
15. K. H. ILLERS. Private communication.
16. H. J. BERNSTEIN, W. G. SCHNEIDER, and J. A. POPLE. Proc. Roy. Soc. A, **236**, 515 (1956).
17. R. F. BOYER, R. S. SPENCER, and R. M. WILEY. J. Polymer Sci. **1**, 249 (1946).
18. H. W. STARKWEATHER, JR. and R. E. MOYNIHAN. J. Polymer Sci. **22**, 363 (1956).
19. K. H. ILLERS. Makromol. Chem. **38**, 168 (1960).

RECEIVED DECEMBER 12, 1960.
CHEMISTRY DEPARTMENT,
UNIVERSITY OF BRITISH COLUMBIA,
VANCOUVER 8, B.C.

Can. J. Chem. Downloaded from www.nrcresearchpress.com by 210.87.254.5 on 09/05/12
For personal use only.

THE PROTON MAGNETIC RESONANCE SPECTRUM AND THE CHARGE DISTRIBUTION OF THE PYRIDINIUM ION*

I. C. SMITH† AND W. G. SCHNEIDER

The protonation of pyridine by trifluoracetic acid has been examined by proton resonance techniques. In the presence of excess acid it has been found possible to observe the proton spectrum characteristic of the pyridinium ion. Figure 1 shows the spectrum of pyridine (in a 5 mole% cyclohexane solution) as well as those of trifluoracetic acid solutions containing 20, 10, and 5 mole% of pyridine respectively. A small amount ($\sim$ 3 mole%) of CH_2Cl_2 was added to each solution to serve as an internal reference signal. Modulation side bands of the reference at 140 and 240 cycles/sec are indicated on the individual traces. The assignment of the proton signals is based on the previously reported analysis of the pyridine spectrum (1). Figure 2 shows a more extended spectrum of the 5 mole% pyridine solution in trifluoracetic acid taken under conditions of lower resolution. It shows, in addition to the signal of the carboxyl group of the trifluoracetic acid and that of the α, β, and γ protons, a triplet signal characteristic of a proton bonded to a nitrogen atom. This confirms the presence of the pyridinium ion. The triplet splitting arises from spin coupling with the N^{14} nucleus having spin $S = 1$. The spin-coupling constant has the value 70 cycles/sec.

The position of the N—H proton signal, to the low-field side of the acid carboxyl group, is unusual for protons bonded to nitrogen. In neutral molecules this ordinarily appears at a much higher field. It is evident from Fig. 1 that there is also a low-field displacement, though smaller, for the signals of the protons of the pyridine ring when the ion is formed. Table I shows the actual chemical shifts (relative to CH_2Cl_2 internal reference) for the individual protons in pyridine and in the pyridinium ion. These shifts are necessarily approximate since an exact analysis of the pyridinium ion spectrum, which has broadened

*Issued as N.R.C. No. 6265.
†*Research Student, Summer, 1960; University of Manitoba, Winnipeg, Manitoba.*

Can. J. Chem. Downloaded from www.nrcresearchpress.com by 210.87.254.5 on 09/05/12
For personal use only.

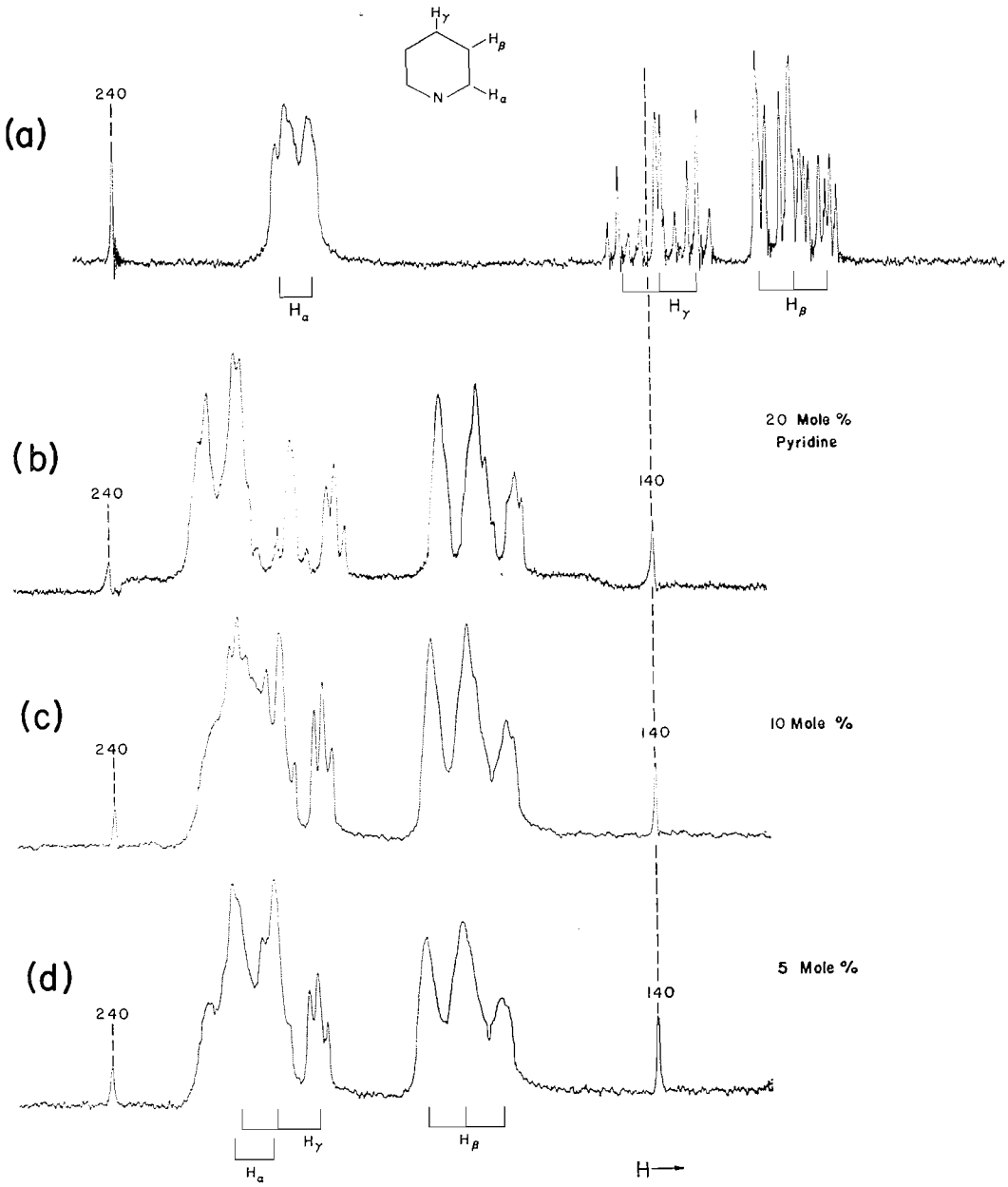


FIG. 1.

lines, is not possible. As shown by the differences listed in the last column, the largest low-field displacement occurs for the γ-proton, that for the β-protons is almost as large, while the corresponding displacement for α-protons is much smaller. These low-field displacements may be attributed to the decrease in electron charge density at the individual carbon nuclei as a result of adding the positively charged proton at the nitrogen atom. Assuming a simple proportionality between the proton resonance displacement

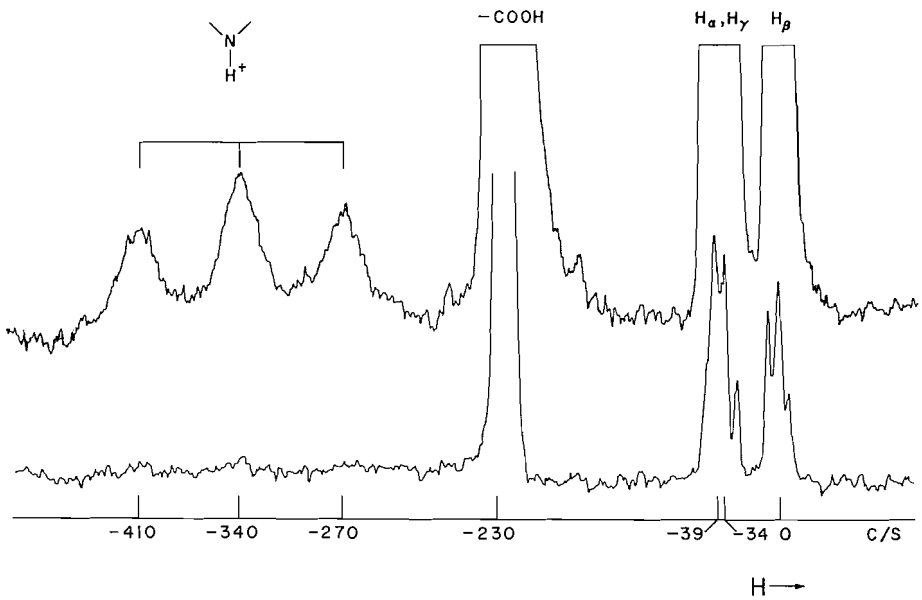


FIG. 2.

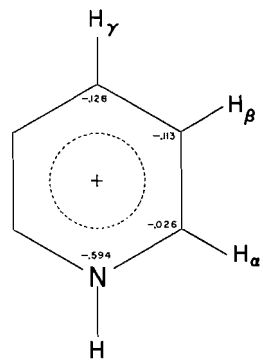
TABLE I

Proton chemical shifts of pyridine and pyridinium ion
(in cycles/sec at 60 Mc/sec relative to internal CH_2Cl_2)

	Pyridine*	Pyridinium† ion	Difference
H_α	−200	−215	−15
H_β	−112	−176	−64
H_γ	−137	−210	−73
N—H		−516	(−336)

*Measured in 5 mole% solution in cyclohexane.
†Measured in 5 mole% concentration in CF_3COOH.

and the electron charge deficiency on the carbon and nitrogen atom to which the proton is bonded* leads to a rough partitioning of the charge density in the pyridinium ion as follows.



**A simple proportionality of this type is supported by a recent study of* C^{13} *and* H^1 *resonances in aromatic systems. (H. Spiesecke and W. G. Schneider. To be published.)*

Can. J. Chem. Downloaded from www.nrcresearchpress.com by 210.87.254.5 on 09/05/12
For personal use only.

The local charges shown (in units of the electronic charge) are not the absolute charge densities, but represent the amount, $\Delta\rho$, by which the local charge density of pyridine is altered when the pyridinium ion is formed. In this process one unit positive charge is added to the pyridine nucleus resulting in a decrease in the local charge density, i.e. $\Delta\rho$ is negative. Employing the simple relation, $\Delta\delta = k\Delta\rho$, where $\Delta\delta$ is the observed change in the proton shift (in p.p.m.), the constant k was found to have the value 9.5 p.p.m. per electron. For the present purpose the low-field displacement of the N—H signal, resulting from the charge deficiency at the N atom, was taken to be 336 cycles/sec. This is the difference in chemical shift between the N—H group protons in the pyridinium ion and in pyrrole. The N—H shift in the latter is −96 cycles/sec relative to CH_2Cl_2 which, if pyrrole were an aromatic system, must be corrected for the "ring current effect" (2). This correction is approximately −84 cycles/sec, giving a total shift of −180 cycles/sec. On combining this with the N—H shift in the pyridinium ion, −516 cycles/sec, results in a net low-field displacement of 336 cycles/sec. The results, which are necessarily approximate, show that roughly 60% of the unit charge deficiency in the pyridinium ion is located at the N atom, the remainder being distributed on the carbon atoms in the ring as indicated.

Finally the relative line width of the resonance spectra under the experimental conditions employed are of some interest. In the spectrum of pyridine itself (Fig. 1(*a*)) the signals of the α-protons are significantly broader than those of β and γ protons. This broadening can be attributed to a shorter T_1 relaxation time of the α-protons caused by nuclear quadrupole relaxation effects of the N^{14} nucleus. Such effects are frequently encountered in nitrogen-containing compounds when a proton is directly bonded to the N atom, whereas in this instance the relaxation is evidently transmitted to protons two bonds removed. In the presence of trifluoracetic acid (Fig. 1(*b*), (*c*), and (*d*)), the α-proton signals remain broad, and in addition the β- and γ-protons are broadened. This additional broadening is no doubt due to proton exchange between the acid and the pyridine nitrogen atom. The fact that the triplet structure of the N—H proton is observable in the 5 mole% solution indicates that under these conditions the exchange rate must be considerably less than 400 times per second. With lower acid concentrations the proton exchange rate is much greater than this and the triplet N—H resonance cannot be observed.

1. W. G. Schneider, H. J. Bernstein, and J. A. Pople. Can. J. Chem. **35**, 1487 (1957).
2. J. A. Pople. J. Chem. Phys. **24**, 1111 (1956).

Received January 17, 1961.
Division of Pure Chemistry,
National Research Council,
Ottawa, Canada.

THE REVERSIBLE ELECTRODE POTENTIAL OF THE SYSTEM U/UCl_3 IN MOLTEN CHLORIDE SOLVENTS

D. Inman* and J. O'M. Bockris

This electrode potential has been measured with respect to various silver – silver chloride reference electrodes by Gruen and Osteryoung (1), Hill, Osteryoung, and Perano (2), Flengas (3), and Inman, Hills, Young, and Bockris (4). The results, expressed as $E^\circ_{UCl_3} - E^\circ_{AgCl}$, along with the theoretical values calculated from the data given by

*Present address: Chemistry Department, University of Reading, Reading, England.

Can. J. Chem. Downloaded from www.nrcresearchpress.com by 210.87.254.5 on 09/05/12
For personal use only.

The local charges shown (in units of the electronic charge) are not the absolute charge densities, but represent the amount, $\Delta\rho$, by which the local charge density of pyridine is altered when the pyridinium ion is formed. In this process one unit positive charge is added to the pyridine nucleus resulting in a decrease in the local charge density, i.e. $\Delta\rho$ is negative. Employing the simple relation, $\Delta\delta = k\Delta\rho$, where $\Delta\delta$ is the observed change in the proton shift (in p.p.m.), the constant k was found to have the value 9.5 p.p.m. per electron. For the present purpose the low-field displacement of the N—H signal, resulting from the charge deficiency at the N atom, was taken to be 336 cycles/sec. This is the difference in chemical shift between the N—H group protons in the pyridinium ion and in pyrrole. The N—H shift in the latter is −96 cycles/sec relative to CH_2Cl_2 which, if pyrrole were an aromatic system, must be corrected for the "ring current effect" (2). This correction is approximately −84 cycles/sec, giving a total shift of −180 cycles/sec. On combining this with the N—H shift in the pyridinium ion, −516 cycles/sec, results in a net low-field displacement of 336 cycles/sec. The results, which are necessarily approximate, show that roughly 60% of the unit charge deficiency in the pyridinium ion is located at the N atom, the remainder being distributed on the carbon atoms in the ring as indicated.

Finally the relative line width of the resonance spectra under the experimental conditions employed are of some interest. In the spectrum of pyridine itself (Fig. 1(*a*)) the signals of the α-protons are significantly broader than those of β and γ protons. This broadening can be attributed to a shorter T_1 relaxation time of the α-protons caused by nuclear quadrupole relaxation effects of the N^{14} nucleus. Such effects are frequently encountered in nitrogen-containing compounds when a proton is directly bonded to the N atom, whereas in this instance the relaxation is evidently transmitted to protons two bonds removed. In the presence of trifluoracetic acid (Fig. 1(*b*), (*c*), and (*d*)), the α-proton signals remain broad, and in addition the β- and γ-protons are broadened. This additional broadening is no doubt due to proton exchange between the acid and the pyridine nitrogen atom. The fact that the triplet structure of the N—H proton is observable in the 5 mole% solution indicates that under these conditions the exchange rate must be considerably less than 400 times per second. With lower acid concentrations the proton exchange rate is much greater than this and the triplet N—H resonance cannot be observed.

1. W. G. Schneider, H. J. Bernstein, and J. A. Pople. Can. J. Chem. **35**, 1487 (1957).
2. J. A. Pople. J. Chem. Phys. **24**, 1111 (1956).

Received January 17, 1961.
Division of Pure Chemistry,
National Research Council,
Ottawa, Canada.

THE REVERSIBLE ELECTRODE POTENTIAL OF THE SYSTEM U/UCl_3 IN MOLTEN CHLORIDE SOLVENTS

D. Inman* and J. O'M. Bockris

This electrode potential has been measured with respect to various silver – silver chloride reference electrodes by Gruen and Osteryoung (1), Hill, Osteryoung, and Perano (2), Flengas (3), and Inman, Hills, Young, and Bockris (4). The results, expressed as $E^\circ_{UCl_3} - E^\circ_{AgCl}$, along with the theoretical values calculated from the data given by

*Present address: Chemistry Department, University of Reading, Reading, England.

Can. J. Chem. Downloaded from www.nrcresearchpress.com by 210.87.254.5 on 09/05/12
For personal use only.

Hamer *et al.* (5), for the pure compounds, are shown in Fig. 1. These results are somewhat discrepant. Recently the present authors have repeated their previous measurements with an improved technique in an attempt to clarify the position.

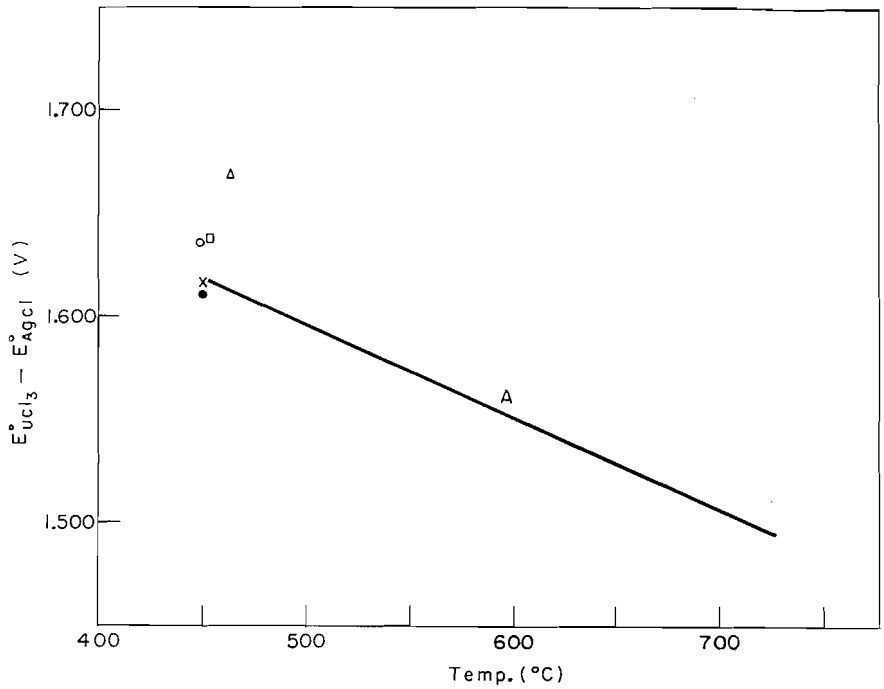


FIG. 1. $E^\circ_{(UCl_3)} - E^\circ_{(AgCl)}$ vs. temperature. (A) Electromotive force data of Hamer *et al.* (5). Experimental $E^\circ_{(UCl_3)} - E^\circ_{(AgCl)}$ values: △ Inman, Hills, Young, and Bockris (4). ● Hill, Perano, and Osteryoung (2). × Gruen and Osteryoung (1). ○ Flengas (3). □ Present work.

The experiments were performed at 453° C in a helium atmosphere. The LiCl–KCl eutectic solvent was purified by a modification (6) of the method described previously (4). The reference electrode was the same as that used before (7). The various concentrations of UCl_3 in LiCl–KCl were prepared by anodic dissolution of U wires into several similar glass diaphragm compartments to that used for the reference electrode. Both these compartments and the reference electrode compartment were immersed in a bath of purified LiCl–KCl eutectic.

The concentrations of UCl_3 in the separate compartments were determined by the dichromate method (8). A standard sample containing 1.025 mg of U was determined as 0.998 mg by this analytical method. The anodic dissolution process was ~100% efficient on the basis of $n = 3$, i.e., when 7.42 mg of uranium were expected in the compartment after the anodic dissolution, 7.60 mg were found.

The electromotive force results are shown in Table I.

A line of theoretical slope for $n = 3$ through these points gives $E^\circ_{(UCl_3)} - E^\circ_{(AgCl)} = 1.638$ v. This value is also shown in Fig. 1. (The previous value (4) at 463° C was 1.668 v.) The corresponding f_{UCl_3} values (standard state pure UCl_3 at the same temperature) are 3.8×10^{-1} and 0.8×10^{-1} respectively.

Can. J. Chem. Downloaded from www.nrcresearchpress.com by 210.87.254.5 on 09/05/12
For personal use only.

TABLE I

Electromotive force of the cell U^{-}/UCl_3, LiCl–KCl ¦ AgCl, LiCl–KCl/Ag^{+} at 453° C

e.m.f. (v)	N_{UCl_3}	$\text{Log}_{10}N_{UCl_3} - 3\ \log_{10}N_{AgCl}$	N_{AgCl}
1.472	$1.113.10^{-3}$	3.462	$7.27.10^{-3}$
1.450	$2.880.10^{-3}$	3.875	
1.431	$4.894.10^{-3}$	4.106	
1.416	$1.048.10^{-2}$	4.436	

The present result is seen to be in good agreement with the value obtained by Flengas (3) by extrapolation of his results obtained at a higher temperature. On the basis of the ionic sizes of Pb^{2+} and U^{3+} (9) the implied degree of complexing seems reasonable (10). The results of Gruen and Osteryoung (1) and Hill *et al.* (2), indicate positive deviations from ideality on the basis of the data of Hamer *et al.* (5).

ACKNOWLEDGMENTS

Thanks are due to the United States Atomic Energy Commission for support of this work under Contract No. AT(30-1)-1769.

1. D. M. Gruen and R. A. Osteryoung. Ann. N.Y. Acad. Sci. **79**, 897 (1960).
2. D. L. Hill, J. Perano, and R. A. Osteryoung. J. Electrochem. Soc. **107**, 698 (1960).
3. S. N. Flengas. Can. J. Chem. To be published.
4. D. Inman, G. J. Hills, L. Young, and J. O'M. Bockris. Trans. Faraday Soc. **55**, 1904 (1959); Ann. N.Y. Acad. Sci. **79**, 803 (1960).
5. W. J. Hamer, M. S. Malmberg, and B. Rubin. J. Electrochem. Soc. **103**, 8 (1956).
6. W. Inman and J. O'M. Bockris. To be published.
7. J. O'M. Bockris, G. J. Hills, D. Inman, and L. Young. J. Sci. Instr. **33**, 438 (1956).
8. I. M. Kolthoff and D. B. Sandell. Textbook of quantitative inorganic analysis. Macmillan. 1950.
9. Handbook of Chemistry and Physics. Chemical Rubber Publishing Co., Cleveland. 1958–59.
10. L. Yang and R. G. Hudson. Trans. Met. Soc. Am. Inst. Mining Engrs. **215**, 589 (1959).

Received January 13, 1961.
John Harrison Laboratory of Chemistry,
University of Pennsylvania,
Philadelphia 4, Pa.

Can. J. Chem. Downloaded from www.nrcresearchpress.com by 210.87.254.5 on 09/05/12
For personal use only.

Can. J. Chem. Downloaded from www.nrcresearchpress.com by 210.87.254.42 on 09/05/12
For personal use only.

Canadian Journal of Chemistry

Issued by THE NATIONAL RESEARCH COUNCIL OF CANADA

VOLUME 39 JUNE 1961 NUMBER 6

OLIGOSACCHARIDES FROM THE SAP OF SUGAR MAPLE (ACER SACCHARUM MARSH)[1]

S. HAQ[2] AND G. A. ADAMS

ABSTRACT

From the sap of the sugar maple (*Acer saccharum* Marsh) two trisaccharides have been isolated by column and paper chromatography. One was identified as *O*-β-D-fructofuranosyl-(2 → 6)α-D-glucopyranosyl(1 → 2)β-D-fructofuranoside (6^G-fructosylsucrose), the other was tentatively established as either 6^F-fructosylsucrose or 1^F-fructosylsucrose. These trisaccharides are not related in either composition or structure to the polysaccharides present in the sap and wood.

Maple sap is known to contain mainly sucrose, the percentage of which varies from season to season and from tree to tree. It was shown by Bois and Nadeau (1) that maple sap contains two enzymes, namely, "sucrogen-amylase" and "cellobiogen-amylase" which transform starch into sucrose and cellobiose respectively. The claim of these workers was later refuted by Meeuse (2), who found that maple sap contains an enzyme which produces maltose from starch and not sucrose and cellobiose. Porter *et al.* (3) have demonstrated the presence of five oligosaccharides in addition to sucrose in maple sap. The sugars found on complete hydrolysis were glucose, fructose, and galactose, and the presence of raffinose and a glucosylsucrose was also indicated. Smith and Zavarin (4) have investigated the mono- and oligo-saccharides of the heartwood, sapwood, and bark of nine conifers and reported the presence of several monosaccharides, raffinose, stachyose, and two unidentified oligosaccharides. In the foregoing investigations, identification of the sugars was based on chromatographic evidence and no information on the structure of the oligosaccharides was provided. The only proven structure for an oligosaccharide containing D-glucose and D-fructose from wood is that of 1^F-fructosylsucrose isolated from aspen wood by Pridham (5). In the course of an investigation in this laboratory on the polysaccharides of maple sap (6), it was observed on paper chromatograms that there were some oligosaccharides in the sap which had R_f values lower than that of sucrose. It was thought worth while to investigate the structure of these oligosaccharides to shed some light on their relationship to the polysaccharides of the sap and wood. The present paper describes the isolation of two trisaccharides and characterization of the major one.

The sap was collected from a commercial stand of sugar maples in the first week of April 1960. Collection of the sap early in the season and fresh from the tree precluded significant bacterial contamination (7). The sap was immediately concentrated at low

[1]*Manuscript received February 3, 1961.*
Contribution from the Division of Applied Biology, National Research Council, Ottawa 2, Canada. Issued as N.R.C. No. 6268.
[2]*National Research Council of Canada Postdoctorate Fellow, 1959–1961.*

temperature to a small volume and the inorganic material, and some sucrose, were removed by precipitation with ethanol. After removal of most of the sucrose by crystallization, the remaining syrup was fractionated on a charcoal–celite column. The individual sugars were eluted by stepwise increase in the concentration of ethanol (8). This procedure proved more advantageous than the gradient elution technique (9) because of the large amount of sucrose present in the syrup. It was found that 5% ethanol eluted sucrose completely from the column leaving the trisaccharides. Seven and one-half per cent ethanol was needed to elute one trisaccharide (component I, minor) and 10% and 20% ethanol were required for another trisaccharide (component II, major). The major trisaccharide proved to be neokestose, a name suggested by Gross, Blanchard, and Bell (10) for *O*-β-D-fructofuranosyl(2 → 6)α-D-glucopyranosyl(1 → 2)β-D-fructofuranoside which they isolated from sucrose solution which had been acted upon by yeast invertase. This trisaccharide has also been isolated from banana (11) as well as from sucrose solution acted upon by fructose-transferring enzymes of higher plants (*Beta vulgaris*) (12).

The proof of the structure of component II was based on the following evidence. The purity of the trisaccharide was established by paper chromatography and by paper electrophoresis. It had $[\alpha]_D$ +15° on the basis of dry syrup. It gave a positive Raybin (13) test with diazouracil, which is a test, essentially, though not exclusively, for derivatives of sucrose in which the fructose unit is unsubstituted (14). On the basis of its reaction with silver nitrate and orcinol – orthophosphoric acid spray reagents the trisaccharide was non-reducing and contained a ketose sugar. Complete hydrolysis with dilute acid gave D-fructose and D-glucose in the ratio of 2:1. On partial hydrolysis with dilute acetic acid it gave glucose, fructose, sucrose, and a reducing disaccharide, the latter moving on a paper chromatogram between sucrose and the original trisaccharide. This disaccharide is probably β-6-*O*-D-fructosyl-D-glucose (15, 16, 17), which would be produced if the glycosidic bond between glucose and fructose of the sucrose moiety in the trisaccharide were broken. On complete methylation the trisaccharide gave an undeca-*O*-methyl derivative. A portion of the methylated trisaccharide after methanolysis and examination by gas–liquid chromatography (18, 19) revealed the presence of tetra-*O*-methyl fructose (2 moles) and tri-*O*-methyl glucose (1 mole). Hydrolysis with dilute acid and separation of the methylated sugars by paper chromatography afforded 2 moles of tetra-*O*-methyl fructose and 1 mole of tri-*O*-methyl glucose. The tetra-*O*-methyl fructose and tri-*O*-methyl glucose were identified as 1,3,4,6-tetra-*O*-methyl-D-fructose and 2,3,4-tri-*O*-methyl-D-glucose by isolation of crystalline derivatives. The β-fructosylfuranoside linkages were established by the hydrolytic action of invertase (β-fructofuranosidase). The identity of the trisaccharide was established, therefore, as *O*-β-D-fructofuranosyl (2 → 6)α-D-glucopyranosyl(1 → 2)β-D-fructofuranoside (6^G-β-fructosylsucrose).

Component I (minor) was found to be a non-reducing trisaccharide composed of 2 moles of fructose and 1 mole of glucose. On partial hydrolysis it gave glucose, fructose, and sucrose. On methylation and hydrolysis the trisaccharide gave tetra-*O*-methyl glucose, tetra-*O*-methyl fructose, and a tri-*O*-methyl sugar on the basis of gas–liquid chromatographic evidence. The tri-*O*-methyl sugar, on the basis of its reaction on paper with orcinol – orthophosphoric acid spray reagent, was considered to be a tri-*O*-methyl fructose. Therefore, it seems likely that component I is a trisaccharide composed of sucrose and fructose in which the fructose unit is attached to the fructose moiety of the sucrose in the trisaccharide. The point of attachment could not be ascertained because of the lack of sufficient material but it is supposed that this trisaccharide is either 6^F-fructosylsucrose (20) or 1^F-fructosylsucrose (5, 21, 22, 23).

Can. J. Chem. Downloaded from www.nrcresearchpress.com by 210.87.254.42 on 09/05/12
For personal use only.

Can. J. Chem. Downloaded from www.nrcresearchpress.com by 210.87.254.42 on 09/05/12
For personal use only.

The possibility of component I being raffinose could easily be eliminated because of the absence of galactose in the hydrolyzate of the trisaccharide. The elution of component I before component II from the charcoal column suggested that component I was a kestose type sugar. This behavior has been previously observed by Gross, Blanchard, and Bell (10).

The present investigation has established the presence of 6^G-β-fructosylsucrose, which had not been reported previously as a constituent of maple sap. This trisaccharide may be one of the unidentified oligosaccharides containing glucose and fructose which were isolated from maple sap by Porter *et al.* (3). Raffinose has been reported as a constituent of the sapwood and inner bark of conifers (4), the xylem of aspen tissue (5), and possibly maple sap (3) but was not found in the present study. However, 1^F-β-fructosylsucrose, which has been identified as a component of aspen tissue (5), may be a component of maple sap, as indicated in the present study.

In general, the fructosylsucrose derivatives occur in plant storage tissues which have a high content of sucrose. Both 6^G-fructosylsucrose and 1^F-fructosylsucrose have been isolated from onion, leek, Italian rye grass, and oat grass (24). Since maple sap is a reservoir high in sucrose it is not unexpected that it should contain the same trisaccharide.

The oligosaccharides found in the maple sap undoubtedly have been formed from sucrose by transferase reactions. They bear no resemblance in either composition or structure to the polysaccharides found in the sap (6) and wood of the sugar maple (25, 26). These latter polysaccharides must have their origin from precursors unrelated to the sap oligosaccharides.

EXPERIMENTAL

The organic phase of the following solvent systems (v/v) was used for chromatography: A, ethyl acetate – pyridine – water (2.5:1:2.5); B, butan-1-ol – acetic acid – water (4:1:5); C, ethyl methyl ketone – water (2:1, water containing 2% ammonia).

Paper chromatography was done on Whatman No. 1 and No. 3 MM paper for qualitative and quantitative separations respectively. An ethanolic solution of *p*-anisidine hydrochloride (3%) (27) was used to detect reducing sugars; orcinol – orthophosphoric acid (28) was used for ketoses. All evaporations were done under reduced pressure at 34° C. Specific rotations were measured in water at 25° C unless otherwise stated.

Separation of the Sugars of Maple Sap

About 18 liters of maple sap, freshly collected in the first week of April 1960 from a commercial stand of sugar maples (*Acer saccharum* Marsh), was evaporated to a small volume (1 l.) and centrifuged to remove the suspended impurities. The clear supernatant liquid was poured into ethanol (4 l.) with constant stirring. The precipitate, which consisted mainly of inorganic matter, polysaccharides, and some sucrose, was removed by filtration. The filtrate on evaporation gave a syrup which was dissolved in 70% methanol (500 ml); on cooling of the solution most of the sucrose crystallized. The mother liquor on evaporation gave a thick syrup.

The syrup (13 g) was fractionated on a charcoal–celite (1:1) column (30 cm × 6.5 cm). Sucrose and monosaccharides (glucose and fructose) were eluted with 5% ethanol. Fractions (60 ml/hr each) were collected and from time to time were chromatographically examined to ensure that no trisaccharides were being eluted. When 8400 ml had been eluted all the sucrose had come off and the eluate up to 9900 ml contained no sugar. Then the column was washed successively with 7½% ethanol (3 l.) (fraction A), 10%

ethanol (2 l.) (fraction B), and 20% ethanol (2 l.) (fraction C). Evaporation of these eluates yielded the following products.

Fraction A. A syrup (47.5 mg) which contained traces of sucrose and a trisaccharide (component I) having $R_{sucrose}$ 0.65 in solvent A.

Fraction B. A syrup (106.0 mg) which consisted of component I and another trisaccharide (component II) R_{suc} 0.73 in solvent A.

Fraction C. A syrup (346.2 mg) which contained mainly component II and traces of very slow moving sugars which were not examined.

An additional quantity of syrup (12 g) was fractionated as above to obtain more sugars. The fractions from the two lots were further purified by paper chromatography in solvent A and chromatographically pure sugars, component I (53.5 mg) and component II (430 mg), were obtained.

Component II (Major)

The syrup ($[\alpha]_D$ +15° (*c*, 2.8)) could not be crystallized. About 50 mg of the syrup was hydrolyzed with 0.2 *N* H_2SO_4 for 4 hours, the products were separated on paper in solvent A, and the individual sugars were determined according to Nelson (29). The ratio of D-fructose to D-glucose was found to be 2:1.

Another portion of the sugar (3 mg) was hydrolyzed with 15% acetic acid (0.5 ml) for 10 minutes, 20 minutes, 30 minutes, and 40 minutes, and the hydrolyzates were examined by paper chromatogram in solvent B. The hydrolyzate for 10 minutes gave a spot of reducing disaccharide having R_{suc} 0.82 while the original trisaccharide had R_{suc} 0.64 in the same solvent. The other hydrolyzates did not show this disaccharide spot.

A solution of the trisaccharide (1%) was incubated with invertase (β-fructofuranosidase) for 3 hours at 35° C. Examination of the hydrolyzate by paper chromatography in solvent A showed complete conversion of the trisaccharide to glucose and fructose.

Methylation of Component II

The syrup (305.6 mg) was dissolved in water (3 ml) and 30% sodium hydroxide solution (2 ml) was added. The solution was stirred at room temperature and dimethyl sulphate (1 ml) was added dropwise. Following this procedure sodium hydroxide solution (8×2 ml) and dimethyl sulphate (8×1 ml) were added during 24 hours. Then the solution was heated at 60° for 1 hour to destroy any unreacted methyl sulphate. The partially methylated sugar was recovered by extraction with chloroform for 4 days. After removing the chloroform the partially methylated sugar was methylated three times with Purdie's reagent, whereby an undeca-*O*-methyl trisaccharide (252 mg) was obtained (Anal. OMe 49.33%; $C_{29}H_{54}O_{16}$ requires OMe 51.8%).

A portion of the methylated sugar (2 mg) was refluxed with 0.5% methanolic HCl (1 ml) for 30 minutes and the sample was examined by gas–liquid chromatography (15, 16). It showed peaks of a tetra-*O*-methyl sugar (α and β anomer) and of a tri-*O*-methyl sugar (α and β). The tetra-*O*-methyl sugar peaks corresponded to that of tetra-*O*-methyl fructose and the peaks of tri-*O*-methyl sugar corresponded to that of the tri-*O*-methyl glucose. The ratio of the areas of the peaks of tetra-*O*-methyl to that of tri-*O*-methyl sugar was approximately 2:1.

Another portion of the methylated trisaccharide (2 mg) was hydrolyzed with 0.04 *N* H_2SO_4 on a water bath for 1 hour. The hydrolyzate was examined by paper chromatography in solvent C and showed two spots having R_g 1.02 and R_g 0.71 respectively.

Can. J. Chem. Downloaded from www.nrcresearchpress.com by 210.87.254.42 on 09/05/12
For personal use only.

The main bulk of the methylated sugar was hydrolyzed as above giving a syrup (210 mg) which was separated on paper in solvent C. Two fractions were obtained, i, tetra-*O*-methyl fructose (115 mg) and ii, tri-*O*-methyl glucose (60.6 mg).

Identification of the Methylated Sugars

*(1) 1,3,4,6-Tetra-O-methyl-*D*-fructose*

The tetra-*O*-methyl fructose was identified as its tetra-*O*-methyl fructofuranamide derivative according to Avery, Haworth, and Hirst (30). The sugar (115 mg) was oxidized with concentrated nitric acid (1.2 ml, sp. gr. 1.42) at 70° for 1 hour and then the temperature of the bath was raised slowly to 93° and the oxidation continued for another $\frac{1}{2}$ hour. Nitric acid was removed by repeated distillation with water. The product was esterified by refluxing for 10 hours with methanol containing 3% HCl. After neutralization with Ag_2CO_3 and removal of the methanol the product was methylated with Purdie's reagent for 5 hours. The syrup obtained was fractionally distilled.

Fraction	i	0–90°	at .01 mm	34.5 mg
	ii	90–105°	"	43.2 mg
	iii	105–160°	"	6.8 mg

All the fractions were separately dissolved in methanolic ammonia (10 ml) and kept in the cold for 4 days. After removal of the methanol, fractions i and ii gave crystalline residues which after recrystallization from ethyl acetate had the same melting point 99–100° C (reported melting point of tetramethyl fructofuranamide is 99–100° C (30) and 100–101° (22)).

*(2) 2,3,4-Tri-O-methyl-*D*-glucose*

The sugar (60.6 mg) was heated with freshly distilled aniline (35 mg) in ethanol (5 ml) for 3 hours. Ethanol was removed by distillation and the residual syrup was extracted with hot ether. The extract was evaporated to a syrup which crystallized on seeding with 2,3,4-tri-*O*-methyl-*N*-phenyl-D-glucosylamine. After three crystallizations from ether it had m.p. 145–146°, undepressed on admixture with an authentic specimen of 2,3,4-tri-*O*-methyl-*N*-phenyl-glucosylamine (31).

Component I (Minor)

The syrup had $[\alpha]_D$ +22°, $R_{sucrose}$ 0.65 in solvent A. On complete hydrolysis it gave 2 moles of fructose and 1 mole of glucose. On partial hydrolysis with dilute acetic acid (15%) it gave glucose, fructose, sucrose; no other sugar could be detected.

The syrup (45 mg) was methylated as above with dimethyl sulphate (4 ml) and 30% sodium hydroxide solution (8 ml), followed by two methylations with Purdie's reagent. The methylated trisaccharide (36.4 mg) had MeO 49.03%; $C_{29}H_{54}O_{16}$ requires OMe 51.8%.

A portion of the methylated trisaccharide (3 mg) was heated with 0.5% methanolic HCl as above and examined by gas–liquid chromatography. It showed peaks corresponding to the methyl glycosides of 2,3,4,6-tetra-*O*-methyl-D-glucose, 1,3,4,6-tetra-*O*-methyl-D-fructose, and a tri-*O*-methyl sugar.

Another portion of the methylated trisaccharide (2 mg) was hydrolyzed by heating on a boiling-water bath for 1 hour with .04 *N* H_2SO_4 and examined by paper chromatography in solvent C. Two papers were irrigated, one was sprayed with *p*-anisidine hydrochloride and the other with orcinol – orthophosphoric acid spray reagent. The

Can. J. Chem. Downloaded from www.nrcresearchpress.com by 210.87.254.42 on 09/05/12
For personal use only.

tri-*O*-methyl sugar had R_g 0.86 in solvent C and gave an immediate reaction with orcinol spray reagent, which indicated that the sugar was a tri-*O*-methyl derivative of D-fructose. The quantity of methylated sugar was insufficient to permit further characterization.

ACKNOWLEDGMENTS

Thanks are due to Mr. A. Castagne for microchemical analysis and to Mr. F. P. Cooper for assistance in gas–liquid chromatography.

REFERENCES

1. E. Bois and A. Nadeau. Can. J. Research, B, **16**, 114 (1938).
2. D. Meeuse. Acta. Botan. Neerl. **1**, 216 (1952).
3. W. L. Porter, N. Hoban, and C. O. Willits. Food Research, **19**, 597 (1954).
4. L. V. Smith and E. Zavarin. Tappi, **43**(3), 218 (1960).
5. J. B. Pridham. Biochem. J. **76**, 13 (1960).
6. G. A. Adams and C. T. Bishop. Can. J. Chem. **38**, 2380 (1960).
7. G. A. Adams, C. T. Bishop, and I. J. McDonald. Can. J. Biochem. and Physiol. **37**, 507 (1959).
8. R. L. Whistler and D. F. Durso. J. Am. Chem. Soc. **72**, 677 (1950).
9. R. S. Alm, R. J. P. Williams, and A. Tiselius. Acta Chem. Scand. **6**, 826 (1952).
10. D. Gross, P. H. Blanchard, and D. J. Bell. J. Chem. Soc. 1727 (1954).
11. R. W. Henderson, R. K. Morton, and W. A. Rawlinson. Biochem. J. **72**, 340 (1959).
12. P. J. Allen and J. S. D. Bacon. Biochem. J. **63**, 200 (1956).
13. H. W. Raybin. J. Am. Chem. Soc. **55**, 2602 (1933); **59**, 1402 (1937).
14. I. Levi and C. B. Purves. Advances in Carbohydrate Chem. **4**, 35 (1949).
15. W. J. Whelan and D. M. Jones. Biochem. J. **54**, 34 (1953).
16. L. M. White and G. E. Secor. Arch. Biochem. Biophys. **36**, 490 (1952).
17. J. S. D. Bacon and J. Edelman. Arch. Biochem. **28**, 467 (1951).
18. A. G. McInnes, D. H. Ball, F. P. Cooper, and C. T. Bishop. J. Chromatog. **1**, 556 (1958).
19. C. T. Bishop and F. P. Cooper. Can. J. Chem. **38**, 388 (1960).
20. N. Albon, D. J. Bell, P. H. Blanchard, D. Gross, and T. J. Rundall. J. Chem. Soc. 24 (1953).
21. J. S. D. Bacon and D. J. Bell. J. Chem. Soc. 2528 (1953).
22. S. A. Barker, E. J. Bourne, and T. R. Carrington. J. Chem. Soc. 2125 (1954).
23. J. H. Pazur. J. Biol. Chem. **199**, 217 (1952).
24. J. S. D. Bacon. Biochem. J. **73**, 507 (1959).
25. L. G. Neubauer and C. B. Purves. Can. J. Chem. **35**, 388 (1957).
26. T. E. Timell. Can. J. Chem. **37**, 893 (1959).
27. L. Hough, J. K. N. Jones, and W. H. Wadman. J. Chem. Soc. 1702 (1950).
28. J. L. Bryson and T. J. Mitchell. Nature, **167**, 864 (1951).
29. N. Nelson. J. Biol. Chem. **153**, 375 (1944).
30. J. Avery, W. N. Haworth, and E. L. Hirst. J. Chem. Soc. 2308 (1927).
31. S. Peat, Elsa Schlüchterer, and M. Stacey. J. Chem. Soc. 581 (1939).

Can. J. Chem. Downloaded from www.nrcresearchpress.com by 210.87.254.42 on 09/05/12
For personal use only.

Can. J. Chem. Downloaded from www.nrcresearchpress.com by 210.87.254.6 on 09/05/12
For personal use only.

REDUCTIVE CLEAVAGE OF NITROGEN–NITROGEN BONDS WITH RANEY NICKEL AND HYDRAZINE[1]

F. P. Robinson and R. K. Brown

ABSTRACT

Raney nickel and hydrazine readily cleave the nitrogen–nitrogen bond of a number of N,N′-diacylated hydrazines to produce the corresponding amides in good yield.

INTRODUCTION

During the course of investigations under way in this laboratory it became necessary to prepare several mono- and di-acylated phenylhydrazines in which the specific position of the acyl group(s) on the nitrogen atom(s) was known with certainty. A promising method for this structural determination was thought to be a mild reductive cleavage of the nitrogen–nitrogen bond which would leave the amide linkage undisturbed. Reductive cleavage of the nitrogen–nitrogen bond in carboxylic acid hydrazides and in 1,2-diacylated hydrazines has been accomplished by refluxing these compounds in ethanol in the presence of a large excess of Raney nickel (1, 2). In a study of the scope of this reaction (3) Hinman found that several previously reported resistant compounds could be cleaved by extending the reaction time from the usual 3 hours to one of 15–20 hours. However, by either of these methods yields were generally only fair, ranging from 5 to 60%. In addition, several compounds, notably 1,2-diacetyl-1,2-dimethylphenylhydrazine and phthalhydrazide failed to reduce even after prolonged reaction.

Recent work on the facile reduction of nitro compounds to amines by hydrazine in the presence of Raney nickel (4, 5, 6) shows that the reduction proceeds, at least in part, by way of the bimolecular reduction intermediates, azoxybenzene and hydrazobenzene. Continued reduction readily converted these in turn to the corresponding amine. It was therefore thought that the combination of Raney nickel and hydrazine would reductively cleave nitrogen–nitrogen bonds much more readily than would Raney nickel alone. A series of experiments showed that this was indeed the case.

RESULTS AND DISCUSSION

When hydrazine hydrate was added dropwise over a period of 1 hour to refluxing methanol containing equal weights of acylated phenylhydrazine and Raney nickel, a smooth reaction occurred giving good yields of the expected products. Results of some typical reductions are shown in the accompanying table. The amides which formed were quite unaffected by the reducing medium hence it was possible to deduce the position of the acyl group(s) in mono- or di-acylated phenylhydrazines. By this means it was easily shown that the diacetylation of 2,6-dimethylphenylhydrazine with acetic anhydride did in fact form N,N′-diacetyl-2,6-dimethylphenylhydrazine rather than the unsymmetrically acylated isomer. The symmetrically acylated product had been expected in view of the N,N′-diacetylphenylhydrazine obtained by Michaelis and Schmidt from a similar acetylation of phenylhydrazine (7).

An interesting point is that the quality of the Raney nickel apparently is unimportant

[1]*Manuscript received February 21, 1961.*
Contribution from the Department of Chemistry, University of Alberta, Edmonton, Alberta. Taken from the thesis of F. P. Robinson to be submitted to the Graduate School of the University of Alberta as part of the requirements for the degree of Doctor of Philosophy.

Compound reduced	Reference to preparation	Product	Reference to preparation of product	% yield of product
N,N′-Diacetyl-2,6-dimethylphenylhydrazine	See exptl. section	N-Acetyl-2,6-dimethylaniline plus acetamide	*a*	68 45
Maleic acid phenylhydrazide	9	Maleamic acid anilide	10, 11	81
N,N′-Diacetylphenylhydrazine	7	Acetanilide plus acetamide	*b*	73 51
Maleic hydrazide	*c*	Maleamide	*d*	66 (*e*)
Phthalhydrazide	*f*	*g*		—

a. I. Heibron and H. M. Bunbury. Dictionary of organic compounds. Eyre & Spottiswoode Ltd., London. 1953.
b. L. F. Fieser. Experiments in organic chemistry. D.C. Heath & Co., Boston. 1957. p. 151.
c. H. Feuer, E. White, and J. Wyman. J. Am. Chem. Soc. **80**, 3790 (1958).
d. I. J. Rinkes. Rec. trav. chim. **46**, 272 (1927); Chem. Abstr. **21**, 2875 (1927).
e. Maleic acid hydrazide was also reduced according to Hinman's method (3) and yielded 36% of maleamide.
f. H. Drew and H. Hatt. J. Chem. Soc. 16 (1937).
g. Only starting material (~70%) could be isolated from the reaction mixture.

since freshly prepared W-2 Raney nickel (8) gave no better results than those obtained with Raney nickel which had been prepared previously (8) and kept for a period of 6 months under methanol in a refrigerator before use in this reaction. This aged Raney nickel had lost its pyrophoric activity completely.

The synthetic value of this reductive cleavage is shown in the simple *two-step* preparation of maleamic acid anilide (example 2 in the table) by reductive cleavage of maleic acid phenylhydrazide, the product of the reaction of phenylhydrazine and maleic anhydride (9). Maleamic acid anilide has been made previously by reaction of aniline with maleimide (10), the latter compound being formed in reasonable yield by a *five-step* synthesis devised by Berson *et al.* (11).

EXPERIMENTAL

N,N′-Diacetyl-2,6-dimethylphenylhydrazine

An aqueous solution of 8.6 g (0.05 mole) of 2,6-dimethylphenylhydrazine hydrochloride (12) was basified with dilute sodium hydroxide and extracted with 4×50 ml of benzene. To the combined benzene extracts, dried over anhydrous magnesium sulphate, was added 10.2 g (0.10 mole) of acetic anhydride and the resulting mixture refluxed for 30 minutes. When half the solvent had been removed, the solution deposited 8.1 g of crude product melting at 70–72°. Recrystallization from 95% ethanol yielded 7.2 g (65%) of product, m.p. 71–72°. Calculated for $C_{12}H_{16}N_2O_2$: C, 65.43; H, 7.32; N, 12.72%. Found: C, 65.33; H, 7.49; N, 12.77%.

Reduction Procedure

The following general procedure was used for all reductions. A solution of 50 ml of methanol, containing 1 g of the acylated phenylhydrazine and 1 g of W-2 Raney nickel (8) was stirred vigorously and gently refluxed for a period of 1 hour during which time an excess of hydrazine hydrate was added dropwise. At the end of the reaction time the catalyst was separated by filtration, and the solvent removed under reduced pressure. The product, crystallized from a suitable solvent, was identified by its melting point and mixed melting point with an authentic sample. With those compounds which yielded acetamide as one product, the residue obtained after removal of solvent was treated with 20 ml of cold water to dissolve and thus remove the acetamide. Subsequent treatment followed the usual procedure.

Can. J. Chem. Downloaded from www.nrcresearchpress.com by 210.87.254.6 on 09/05/12
For personal use only.

ACKNOWLEDGMENTS

The authors wish to thank the National Research Council of Canada for generous financial assistance throughout the course of this work.

REFERENCES

1. C. AINSWORTH. J. Am. Chem. Soc. **76**, 5774 (1954).
2. C. AINSWORTH. J. Am. Chem. Soc. **78**, 1636 (1956).
3. R. L. HINMAN. J. Org. Chem. **22**, 148 (1957).
4. B. E. LEGGETTER and R. K. BROWN. Can. J. Chem. **38**, 2363 (1960).
5. A. FURST and R. E. MOORE. J. Am. Chem. Soc. **79**, 5492 (1957).
6. P. M. G. BAVIN. Can. J. Chem. **36**, 238 (1958).
7. A. MICHAELIS and F. SCHMIDT. Ann. **250**, 300 (1889).
8. R. MOZINGO. Org. Syntheses, Coll. Vol. III, 181 (1955).
9. J. DRUEY, A. HÜNI, KD. MEIER, B. H. RINGIER, and A. STAEHELIN. Helv. Chim. Acta, **37**, 510 (1954).
10. R. ANSCHÜTZ. Ann. **259**, 138 (1890).
11. J. A. BERSON and R. SWIDLER. J. Am. Chem. Soc. **76**, 2835 (1954).
12. R. B. CARLIN and D. P. CARLSON. J. Am. Chem. Soc. **81**, 4673 (1959).

Can. J. Chem. Downloaded from www.nrcresearchpress.com by 210.87.254.6 on 09/05/12
For personal use only.

Can. J. Chem. Downloaded from www.nrcresearchpress.com by 210.87.254.5 on 09/05/12
For personal use only.

STUDIES ON THE PERVANADIUM COMPLEX[1]

G. A. DEAN[2]

ABSTRACT

The 'pervanadium complex' is investigated in a general manner. The kinetics of its thermal decomposition in acid solution are shown to be first order with respect to pervanadium, the apparent activation energy is 26.5±1.0 kcal/mole, and possible mechanisms are suggested. The effect of various acids upon the nature of the decomposition products is determined: almost quantitative yields of vanadium (V) or vanadium (IV) are obtained in very dilute or concentrated acid, respectively. Spectrophotometric studies indicate that in acid solution two separate complexes exist: a red (1:1) cationic complex and a yellow (1:2) anionic complex. The stoichiometry of the equilibrium between the two complexes in solutions of sulphuric acid is investigated by a method of 'discrete variations'. The equilibrium could be described by

$$\text{red} + H_2O_2 \overset{K_{r/y}}{\rightleftharpoons} \text{yellow} + 3/2H_2SO_4$$

where $K_{r/y} = 2.2 \pm 0.2$ at 22° C. The anion is shown to play an important part in determining the nature of the pervanadium complex.

INTRODUCTION

The formation and subsequent bleaching of a red-brown coloration when an excess of hydrogen peroxide is slowly added to an acid solution of vanadium (V) has been known for over a century. The original explanation of the reaction as a simple peroxidation of vanadate

$$HVO_3 + H_2O_2 \rightarrow HVO_4 + H_2O$$

was refuted by Meyer and Pawletta (1), who showed that both the original and peroxidized vanadium existed as cations. According to them, the reaction that occurs in solutions containing sulphuric acid is

$$(VO)_2(SO_4)_3 + 2H_2O_2 \rightarrow [V(O_2)]_2(SO_4)_3 + 2H_2O$$

and the following equilibrium exists on adding an excess of hydrogen peroxide:

$$\underset{\text{red-brown}}{[V(O_2)]_2(SO_4)_3} + 6H_2O \overset{H_2O_2}{\underset{H_2SO_4}{\rightleftharpoons}} \underset{\text{yellow}}{2V(O_2)(OH)_3} + 3H_2SO_4.$$

Although the last equation is often used in text books to explain the bleaching by an excess of peroxide it is difficult to see how it can be justified since peroxide does not occur on either side. In addition, the species (VO^{3+}) used by Meyer and Pawletta to represent vanadium (V) in acid solution does not agree with that currently accepted (VO_2^+) (see ref. 2).

The complex is unstable and decomposes readily on heating to give a mixture of vanadium (V) and vanadium (IV); the composition of the solution has a large influence upon the relative proportions of the latter but has hitherto received but brief mention in the literature (3, 4).

Wright and Mellon (5) performed the first spectrophotometric study of the complex and showed that an absorption maximum occurred in the region 450–460 mμ. Suitable conditions for its analytical use were determined empirically and although a decrease in the absorption maximum was confirmed to be due to an excess of peroxide no attempt

[1]*Manuscript received December 1, 1960.*
Contribution from the Department of Chemistry, Dalhousie University, Halifax, Nova Scotia.
[2]*National Research Council of Canada Postdoctorate Fellow, 1959–61.*

was made to determine quantitative relationships. A later study by Telep and Boltz (6) revealed a second (and larger) absorption maximum at 290 mμ, and this also was decreased by an excess of peroxide, but again no attempt was made to investigate further.

This paper investigates in a general manner various aspects of the complex which have long seemed to demand attention, particularly with regard to its decomposition and formulation.

EXPERIMENTAL

For the kinetic studies, reactions were followed colorimetrically with a Fisher electrophotometer fitted with cell-heating and -stirring devices. Spectrophotometric measurements were made with a Beckman DU spectrophotometer fitted with a photomultiplier attachment.

Vanadium (V) was determined by adding sulphuric and orthophosphoric acids to concentrations of about 1 *N* and 0.5 *M*, respectively, and then titrating with ferrous sulphate solution standardized against recrystallized potassium dichromate. An amperometric ('dead-stop') end point was used in conjunction with a synchronous magnetic stirrer and a Leeds and Northrup mirror-galvanometer type 2285*f* (maximum sensitivity: 0.03 μa for full scale deflection) allowing a very high sensitivity to be obtained. In all determinations comparative titrations were made using an untreated aliquot of stock solution as a reference. Hydrogen peroxide was determined by amperometric titration with permanganate previously standardized against ferrous sulphate.

Stock solutions of vanadium (V) (free from vanadium (IV)) were prepared by dissolving Fisher $NaVO_3$ ('purified') in water redistilled from dilute alkaline permanganate in an all-Pyrex-glass still fitted with splash guards. Solutions of hydrogen peroxide were prepared by dilution of Mallinckrodt reagent-grade 100-volume hydrogen peroxide (stabilized). All other reagents were of reagent-grade quality.

To avoid any reduction of vanadium (V) by traces of grease, organic matter, etc., all glassware was cleaned (where necessary) before use with permanganic – sulphuric acid cleaning mixture; it was then rinsed with dilute acidified hydrogen peroxide to remove any traces of manganese dioxide, rinsed thoroughly with distilled water, and finally steamed for 1 minute with steam evolved from boiling dilute alkaline permanganate.

RESULTS AND DISCUSSION

Thermal Decomposition of Pervanadium

The reactions which occur on heating an acid solution of pervanadium containing an excess of hydrogen peroxide are as follows: initially, the excess peroxide is decomposed catalytically by the vanadium, any decomposed pervanadium being regenerated by the excess peroxide, and the red color remaining unchanged; finally, when the excess peroxide has disappeared, the pervanadium complex itself undergoes decomposition and the red color fades rapidly. The last stage may be followed conveniently and, despite the oxygen evolved during the reaction, fairly accurately by determining colorimetrically the variation of [pervanadium] with time.

The results of experiments at different temperatures and acidities are plotted in Fig. 1. In all cases a linear relationship between log [pervanadium] and time was obtained, indicating that the decomposition is first order with respect to pervanadium and that

$$d[\text{pervanadium}]/dt = -k\,[\text{pervanadium}].$$

Expressing concentrations in mole/liter, k had the value 0.0100 ± 0.0005 sec^{-1} in 2 *N*

Can. J. Chem. Downloaded from www.nrcresearchpress.com by 210.87.254.5 on 09/05/12
For personal use only.

sulphuric acid at 90° C; it was not significantly altered by changing the concentration of sulphuric acid from 2 N to 0.2 N (Fig. 1, plots 1 and 2) or by adding iron (III) to a concentration of 10^{-4} M (plot 2).

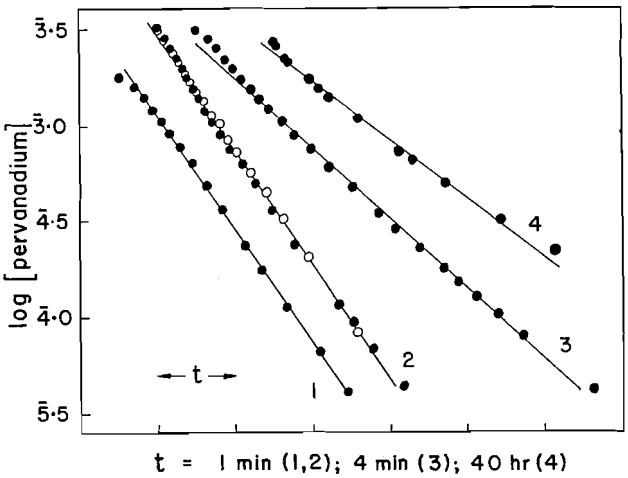


FIG. 1. Thermal decomposition of pervanadium.

	$[H_2SO_4]$, N	Temperature, °C
1.	0.2	90
2.	2	90
	(open circles: also 10^{-4} M to Fe (III))	
3.	2	70
4.	2	22

The products of the decomposition are vanadium (V) and vanadium (IV), the proportion of vanadium (V) being dependent upon the acid and its concentration; values for seven different acids are presented in Fig. 2. It is evident that the anion plays an important part in determining the behavior of the complex.

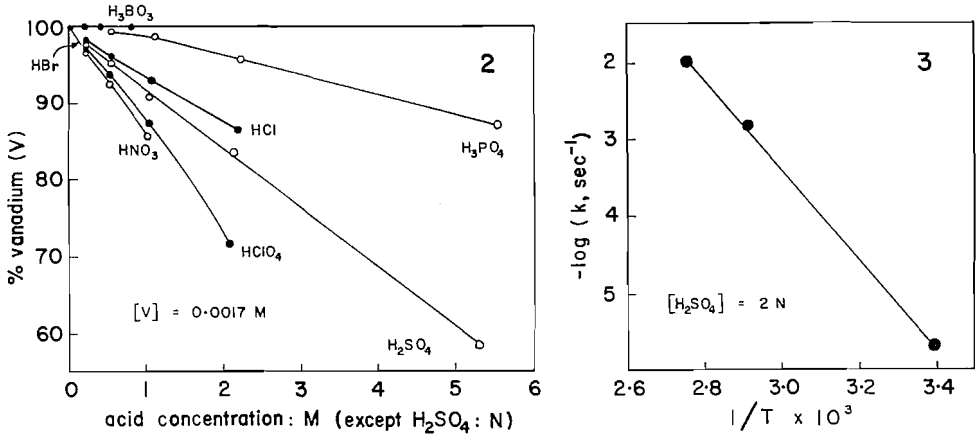


FIG. 2. Effect of various acids on the products from the decomposition of pervanadium in boiling solution.
FIG. 3. Plot of log k against $1/T$ for the thermal decomposition of pervanadium.

The logarithms of the various slopes depicted in Fig. 1 are plotted in Fig. 3 against the reciprocal of the absolute temperature. From the slope of this line the activation energy was calculated to be 26.5±1.0 kcal/mole.

Can. J. Chem. Downloaded from www.nrcresearchpress.com by 210.87.254.5 on 09/05/12
For personal use only.

The decomposition can be represented in two ways (in the subsequent account pervanadium is represented by perV$^+$): either as an initial dissociation

$$\text{perV}^+ \rightleftharpoons VO_2^+ + H_2O_2, \quad [1]$$

followed by subsequent reaction

$$2VO_2^+ + H_2O_2 + 2H^+ \rightarrow 2VO^{++} + 2H_2O + O_2, \quad [2]$$

$$2VO^{++} + H_2O_2 \rightarrow 2VO_2^+ + 2H^+, \quad [3]$$

or as a direct decomposition

$$\text{perV}^+ \rightarrow VO_2^+, \quad [4]$$

$$\text{perV}^+ + H^+ \rightarrow VO^{++}. \quad [5]$$

In each case an increase of $[H^+]$ is seen to favor the formation of vanadium (IV) in agreement with the results of Fig. 2.

Unfortunately there appears to be no way of distinguishing directly between these two schemes and it is necessary to consider indirect evidence as follows.

Considering the first scheme, the rate-determining step *in dilute acid* can be one of two consistent with the first-order dependence upon the pervanadium concentration:

(*a*) Dissociation of the pervanadium complex is rapid, when (see later)

$$[\text{perV}^+] \propto [VO_2^+]\,[H_2O_2],$$

suggesting that the kinetics of the rate-determining step (*in dilute acid*) are dependent upon $[VO_2^+][H_2O_2]$, which, in turn, suggests that the rate-determining step is reaction [2], and that, effectively,

$$d[VO_2^+]/dt = -k_1\,[VO_2^+][H_2O_2].$$

Unfortunately the kinetics of this reaction cannot be determined directly. In dilute acid pervanadium is formed at once, and in concentrated acid reduction is rapid (e.g., complete reduction occupies a few seconds in concentrated sulphuric acid at $-5°$ C) with but momentary formation of pervanadium. The kinetics of reaction [3] can be determined directly and were found to be as follows. For a constant $[H_2SO_4]$, the initial rate was proportional to $[VO^{++}]^2$ and to $[H_2O_2]$, giving

$$d[VO^{++}]/dt = -k_2\,[VO^{++}]^2[H_2O_2].$$

With concentrations expressed in mole/liter, and time in seconds, k_2 had the value 1.3×10^2 in 2 *N* sulphuric acid at 21° C. A few experiments were made to determine the effect of $[H_2SO_4]$, and the rate was found to be proportional to $[H_2SO_4]^{-x}$, where $x \sim 0.7$ for $[H_2SO_4] = 0.01-2$ *N*.

The final ratio of vanadium (IV) to vanadium (V) is remarkably constant despite large variations in initial vanadium concentration and temperature (Table I). No evidence

TABLE I

% Vanadium (V) produced by the decomposition of pervanadium

Conditions	[vanadium], $M\times10^4$		
	760	15.3	0.31
0.55 *M* H_3PO_4, boiling	99.42 99.45	99.02 98.98	99.08 99.08
0.53 *N* H_2SO_4, boiling	94.57 94.82	94.95 95.19	96.24 97.65
0.53 *N* H_2SO_4, 65° C		95.28	
0.53 *N* H_2SO_4, 22° C		94.58	

Can. J. Chem. Downloaded from www.nrcresearchpress.com by 210.87.254.5 on 09/05/12
For personal use only.

for the direct oxidation in dilute acid of vanadium (IV) by pervanadium was found and it seems reasonable to assume that the ratio of vanadium (IV) to vanadium (V) remains sensibly constant throughout the reaction. It follows from this that $(d[VO^{++}]/dt)/(d[VO_2^+]/dt)$ should also be constant, and hence

$$\frac{k_1[VO^{++}]^2[H_2O_2]}{k_2[VO_2^+][H_2O_2]} = \frac{k_1[VO^{++}]^2}{k_2[VO_2^+]}$$

should be constant, which is impossible. Hence mechanism (*a*) is unlikely.

(*b*) Dissociation of the pervanadium complex is slow and is rate-determining. Attempts to determine the rate of dissociation directly were inconclusive: permanganate solution added to a 0.01 *N* solution of vanadium (V) in *N* sulphuric acid containing an excess of hydrogen peroxide reacted rapidly with the excess, and then only slowly (over ~10 seconds at room temperature) with the 'combined' peroxide (a similar result was observed with the pertitanium complex); the slowness might be due either to slow dissociation or to the small equilibrium concentration of peroxide ($\sim 10^{-6}$ *M*, see later). However, the complexity of the over-all reaction produced by competing reactions [2] and [3] seems unlikely to result in a constant ratio of vanadium (IV) to vanadium (V) over large changes of both concentration *and* temperature, and on these grounds mechanism (*b*) is unlikely.

On the other hand, it is far easier to reconcile the experimental observations with a scheme involving a direct decomposition such as [4] and [5], and in the absence of direct evidence to the contrary is to be preferred. However, the complete explanation of the decomposition is likely to be far more complicated than the simple pictures presented here, and no further attempts to investigate the reaction were made.

Decomposition of Pervanadium at Extreme Concentrations of Acid

At very low acidities almost quantitative recovery of the vanadium as vanadium (V) is obtained (Table II).

TABLE II

Vanadium (V) produced by the decomposition of pervanadium in boiling dilute acid solution

0.050 *M* H_3BO_3	100.00 100.03
0.0112 *M* H_3PO_4	99.88 99.90
0.0099 *M* HBr	99.81 99.79
0.0105 *N* H_2SO_4	99.76 99.78
0.0110 *M* HCl	99.67 99.74
0.0101 *M* HNO_3	99.62 99.58
0.0103 *M* $HClO_4$	99.59 99.58

NOTE: [vanadium] = 0.00153 *M*; the acid concentrations have been corrected for the amount consumed by $NaVO_3 + 2H^+ \rightarrow VO_2^+ + Na^+ + H_2O$.

At very high acidities almost quantitative recovery of the vanadium as vanadium (IV) is obtained (Table III) although in this instance phosphoric acid, and not sulphuric

Can. J. Chem. Downloaded from www.nrcresearchpress.com by 210.87.254.5 on 09/05/12
For personal use only.

TABLE III

% vanadium (IV) produced by the decomposition of pervanadium in concentrated acid solution

Acid	Experiment A		Experiment B	
H_2SO_4	96.7	96.5	99.33	99.42
H_3PO_4	99.96	100.00	100.00	99.92
$H_2SO_4 + H_3PO_4$	29	35	14	19

NOTE: Ten milliliters of 0.01 *M* aqueous $NaVO_3$ and 4 ml of concentrated acid were evaporated right down; a few drops of 100-volume hydrogen peroxide were added to the cold solution with stirring, and the process repeated. The solution was then warmed to destroy any traces of peroxide. For experiment B the periods of heating were prolonged.

acid, as a simple extrapolation of the data of Fig. 2 might suggest, gives the higher yield. The reduction in sulphuric acid has long been proposed as a basis for the determination of vanadium by titration with permanganate but experiments using the specified procedure (4) always resulted in incomplete reduction with results similar to those of Table III.

The results of Tables II and III, and of Fig. 2, emphasize the importance of the anion in determining the behavior of the complex.

Nature of the 'Pervanadium Complex'

The absorption spectra of vanadium (V) in solutions of sulphuric acid containing various amounts of hydrogen peroxide were found to exhibit an isobestic point at about 402 mμ (Fig. 4) suggesting at once the formation of a second complex in the presence of

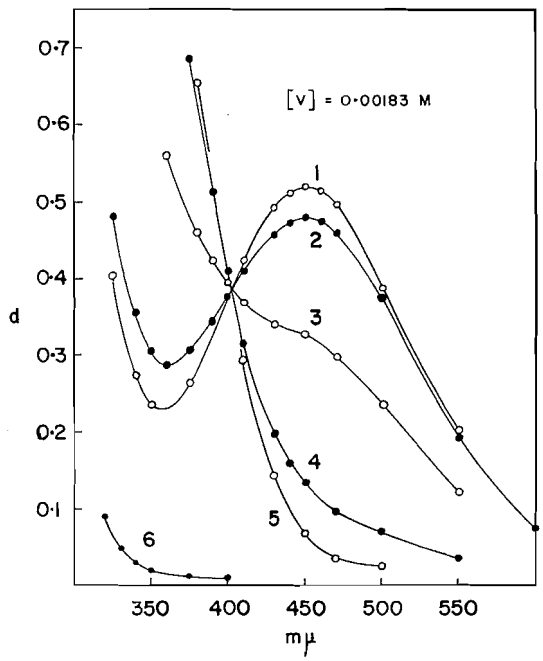


FIG. 4. Absorption spectra of pervanadium complexes.

	$[H_2O_2]$, *M*	$[H_2SO_4]$, *N*	
1.	0.005	2.0	
2.	0.02	0.5	
3.	0.005	0.05	
4.	0.02	0.05	
5.	0.12	0.05	
6.	0.25	0.8	(V absent)

Can. J. Chem. Downloaded from www.nrcresearchpress.com by 210.87.254.5 on 09/05/12
For personal use only.

an excess of peroxide. In the subsequent account the initial complex is called the 'red' complex and the second the 'yellow' complex.

Nature of the Red Pervanadium Complex

Shaeppi and Treadwell (7) have investigated the complex colorimetrically (using a mercury lamp with blue filters) by the method of continuous variations. In 7 *M* sulphuric acid the ratio of $V:H_2O_2$ in the complex was shown to be accurately 1:1 and

$$K = \frac{[\text{pervanadium}]}{[VO_2^+][H_2O_2]} = 8.2\times10^4\ M^{-1}.$$

No estimate of the experimental error was made and none of the experimental details or data necessary for its evaluation were given. From their results, however, it is estimated that the possible error in their value of *K* is likely to be about $\pm(5\text{–}10)\%$.

The acid concentration used by them was rather high, and the complex was studied by the same method, but for *N* acid, with the results shown in Table IV. These experiments confirmed the 1:1 nature of the complex; despite the large difference in acid

TABLE IV

Dissociation constant of the red pervanadium complex by the method of continuous variations

Acid	Position of d_{max}, mμ	d_{max}	d_{max}, extrapolated	$K\times10^{-4}$, M^{-1}
H_2SO_4	454	0.502	0.566	3.5±0.2
$HClO_4$	460	0.501	0.566	3.4±0.2

NOTE: Total concentration $[V+H_2O_2] = 0.00398\ M$; acid concentration = 1.0 *N*; temperature = 22° C. All values of *d* are corrected for blank and for the absorbance of the small amount of uncomplexed vanadium (V). Length of optical path = 1.000 cm.

concentration the results are reasonably in agreement with those of Shaeppi and Treadwell, indicating that H^+ does not enter the reaction to a significant extent. The latter may consequently be written in a simplified manner as

$$VO_2^+ + H_2O_2 \rightleftharpoons VO(O_2)^+ + H_2O$$

where (O_2) denotes a peroxy group. The shift in the position of maximum absorbance with a change of anion confirms the participation of the latter in determining the behavior of the complex. It was found that, under suitable conditions, the red complex was strongly absorbed by a cation-exchange resin and hence, in accordance with previous observations (1, 7) and the preceding equation, exists as a cation.

It is interesting to note that from 9 *M* hydrochloric acid rendered 0.1 *M* with respect to hydrogen peroxide the complex is about 50% extracted by an equal volume of methyl-*i*-butyl ketone, and 80–85% extracted by an equal volume of tri-*n*-butyl phosphate, and that in contrast with its bright red-brown color in the aqueous phase the complex is bright green in the organic phase (9). No extraction occurs from solutions in sulphuric acid (9, 10). No attempt is made to explain these observations.

Latimer (8) represents the formation of the red complex by

$$V(OH)_4^+ + H_2O_2 \rightarrow VO_4^- + 2H_2O + 2H^+, \quad \Delta F^0 = -29.8\ \text{kcal.}$$

The above value of ΔF^0 leads to the value

$$\frac{[VO_4^{4-}][H_2O]^2[H^+]^2}{[V(OH)_4^+][H_2O_2]} \sim 10^{22}\ M^3,$$

Can. J. Chem. Downloaded from www.nrcresearchpress.com by 210.87.254.5 on 09/05/12
For personal use only.

and on putting $[H^+] = 1$, and $[H_2O] = 56$, we get

$$\frac{[VO_4^{--}]}{[V(OH)_4^+][H_2O_2]} \sim 0.3\times10^{19}\ M^{-1}.$$

Even allowing for the use of concentrations in place of activities there is a very large discrepancy between the above value and the observed value.

Nature of the Yellow Pervanadium Complex

Meyer and Pawletta (1) observed that a clear yellow solution was obtained by adding hydrogen peroxide to an aqueous solution of V_2O_5 and that this color was the same as that produced in the presence of sulphuric acid by a large excess of hydrogen peroxide. By rather inaccurate distribution experiments they established that in the clear yellow solution at least one molecule of hydrogen peroxide was bound to each atom of vanadium (V); conductivity measurements indicated that an analogy with H_3PO_4 existed and accordingly it was postulated that the clear yellow solution contains $H_3[V(O_2)O_3]$, an orthoperoxy vanadic acid. These conclusions are not supported by the present work.

It is known that in solutions less than reasonably acid widespread changes occur in the nature of the species of vanadium (V) present (2). For this reason experiments were always conducted in strongly acid solutions and any deviation towards less acid conditions and the formation of complex species was carefully avoided.

The yellow complex cannot be investigated by the method of continuous variations, nor by any of the usual methods, owing to inevitable interference from the red complex at some stage. Fortunately, at the wavelength of maximum absorption for the red complex the absorption of the yellow complex is small, and it was found possible to study the stoichiometry of the equilibrium between red and yellow forms by a method of 'discrete variations'.

Assuming that the reaction in the presence of sulphuric acid can be represented by

[6] $$a\ (\text{red}) + b\ (H_2O_2) \rightleftharpoons c\ (\text{yellow}) + d\ (H_2SO_4),$$

then

[7] $$K_{r/y} = \frac{[\text{yellow}]^c[H_2SO_4]^d}{[\text{red}]^a[H_2O_2]^b}.$$

The red complex is known to obey Beer's law (5, 6); assuming that the yellow complex behaves similarly, that there is no interaction between the complexes in an optical sense, and that no additional complexes are formed, then the optical densities of the red and yellow forms, d_r and d_y, respectively, will be related to the observed optical density at 454 mμ, d_{obs}, by

[8] $$d_{obs} = d_r + d_y.$$

Provided, as in these experiments, that the concentration of hydrogen peroxide is sufficiently high to prevent significant dissociation of the red complex, then

[9] $$d_y = (1 - d_r/D_r) \times D_y,$$

where D_r and D_y represent the optical densities when the vanadium is present entirely in the red and yellow forms, respectively, and

[10] $$[\text{yellow}]/[\text{red}] = (D_r - d_r)/d_r.$$

Values of d_r may be calculated from equations [8] and [9] by successive approximation: d_{obs} is inserted for d_r in [9] and the value of d_y thereby obtained is used to calculate a

Can. J. Chem. Downloaded from www.nrcresearchpress.com by 210.87.254.5 on 09/05/12
For personal use only.

new value for d_r from [8]. This is then reinserted in [9], and the process repeated, until the value of d_r becomes sensibly constant. This was usually realized after one procedure. D_r may be determined or calculated as previously; D_y may be estimated fairly accurately by extrapolation of d_{obs} for large relative concentrations of hydrogen peroxide.

From equations [7] and [10] it follows that, with $[H_2SO_4]$ = constant,

$$(D_r-d_r)^c/(d_r)^a = K' \times [H_2O_2]^b.$$

Observed values of $(D_r-d_r)/d_r$ are plotted against $[H_2O_2]$ in Fig. 5. D_r and D_y were

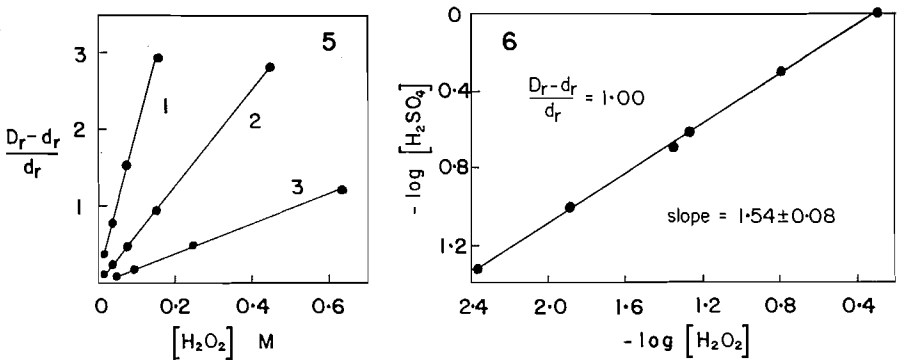


FIG. 5. Variation of $(D_r-d_r)/d_r$ with $[H_2O_2]$. $[H_2SO_4]$, N, = 0.245 (1); 0.502 (2); 1.010 (3). [V] = 0.00199 M.
FIG. 6. Variation of log $[H_2SO_4]$ with log $[H_2O_2]$.

assumed to be constant over the range of acid concentration involved; the concentration of hydrogen peroxide was corrected for the amount consumed by the formation of the red (1:1) and yellow (assumed to be 1:2) complexes; the concentrations of sulphuric acid were sufficiently high to swamp any variations produced by the reaction. The linear relationships obtained indicate that K' is a constant for any one value of $[H_2SO_4]$, and that

$$a = b = c,$$

thereby confirming that in the yellow complex $V:H_2O_2::1:2$.

The influence of sulphuric acid may be evaluated by putting [yellow]/[red] = constant, and by rearranging [7], when

$$\log [H_2O_2] = d/b \log [H_2SO_4] - 1/b \log K_{r/y}.$$

Observed values are plotted in Fig. 6. A linear relationship is again obtained, whence

$$d/b = 1.54 \pm 0.08.$$

No distinction can be made as to whether this result implies the existence of a real dependence on $[H_2SO_4]$ to this power or whether it merely reflects a relationship fortuitously produced by the participation of the anion.

Rearranging in terms of b, and putting $b = 1$, equation [6] may now be written

$$\text{red} + H_2O_2 \rightleftharpoons \text{yellow} + 3/2H_2SO_4;$$

with concentrations expressed as molar, except $[H_2SO_4]$, as normal,

$$K_{r/y} = \frac{[\text{yellow}][H_2SO_4]^{3/2}}{[\text{red}][H_2O_2]} = 2.2 \pm 0.2 \qquad \text{at } 22^\circ \text{ C.}$$

Can. J. Chem. Downloaded from www.nrcresearchpress.com by 210.87.254.5 on 09/05/12
For personal use only.

In contrast with the behavior of the red complex, the yellow complex was not absorbed by a cation-exchange resin, but was absorbed by an anion-exchange resin, and hence exists as an anion; this difference in behavior has been used as the basis for a separation of vanadium from chromium by ion exchange (9).

From the values of K (Table IV) and $K_{r/y}$, and putting $[VO_2^+]/[\text{red}] = [\text{yellow}]/[\text{red}] = n$, it can be shown that

$$n \sim 0.008/[H_2SO_4]^{3/4}.$$

The value of $(1-2n)$ represents the maximum possible amount of vanadium which can exist in the red form under these conditions and is about 0.991 for $[H_2SO_4] = 2\ N$. While this value is in no way directly related to the possible error involved in the colorimetric determination of vanadium with hydrogen peroxide by a *standardized* procedure it does emphasize the empirical basis upon which the method rests.

ACKNOWLEDGMENTS

Grateful acknowledgment is made to Dr. K. E. Hayes for helpful advice concerning kinetic problems, to Dr. D. E. Ryan for helpful discussion, and to the National Research Council for financial support.

REFERENCES

1. J. MEYER and A. PAWLETTA. Z. physik. Chem. **125**, 49 (1927).
2. F. J. C. ROSOTTI and H. ROSOTTI. Acta Chem. Scand. **10**, 957 (1956).
3. V. AUGER. Compt. rend. **172**, 1355 (1921).
4. J. R. CAIN and J. C. HOSTETTER. J. Am. Chem. Soc. **34**, 274 (1912).
5. E. R. WRIGHT and M. G. MELLON. Ind. Eng. Chem. Anal. Ed. **9**, 375 (1937).
6. G. TELEP and D. F. BOLTZ. Anal. Chem. **23**, 901 (1957).
7. Y. SHAEPPI and W. D. TREADWELL. Helv. Chim. Acta, **31**, 577 (1948).
8. W. M. LATIMER. The oxidation states of the elements and their potentials in aqueous solutions. 2nd ed. Prentice-Hall, Inc., New York. 1952.
9. G. A. DEAN. Ph.D. Thesis, University of London, London, England. 1959.
10. J. J. LINGANE and L. MEITES. J. Am. Chem. Soc. **68**, 2443 (1946).

Can. J. Chem. Downloaded from www.nrcresearchpress.com by 210.87.254.5 on 09/05/12
For personal use only.

Can. J. Chem. Downloaded from www.nrcresearchpress.com by 210.87.254.40 on 09/05/12
For personal use only.

INFRARED SPECTRA OF 2,6-DIMETHYL-4-PYRONE COMPLEXES[1]

DENYS COOK

ABSTRACT

The infrared spectra of 2,6-dimethyl-4-pyrone in solution, and in complexes with $HgCl_2$, $ZnCl_2$, BF_3, $SbCl_5$, and HBr have been recorded. A band at 1639 cm^{-1} in the free pyrone moves to progressively lower frequencies in the complexes as the Lewis acid strength increases, identifying this band as the carbonyl stretching frequency and the donor site as the carbonyl group. A higher-frequency band, at 1678 cm^{-1} in the free pyrone, moves to lower frequency on complex formation, but to a much smaller extent, and is to be identified with a stretching mode of the ring. The site of protonation in 2,6-dimethyl-4-pyrone salts has been unequivocally shown to be the carbonyl oxygen atom.

INTRODUCTION

The 4-pyrones form an interesting group of compounds whose basic constitution is still somewhat in doubt. An investigation of the structure of 2,6-dimethyl-4-pyrone by X-ray diffraction (1) could not be resolved, though a similar study on the sulphur analogue, 2,6-dimethyl-4-thiopyrone (2) revealed adjacent ring carbon–carbon bond lengths of 1.34_2 Å and 1.42_1 Å. The first value is close to the ethylene value (3), while the second is a little smaller than the value of a single bond between two coplanar, trigonally hybridized, carbon atoms (4). Conjugation, therefore, extends from the 2 to the 6 carbon atom. The degree to which the ring oxygen participates in conjugation, if any, is doubtful. The lengths of the C—O bonds, 1.37_8 and 1.36_7 Å are slightly larger than those of the C—O group in α-resorcinol, 1.34_9 Å (5), where the OH group is not coplanar with the ring and therefore the degree of conjugation, again, if any, is questionable.

Published data on the vibrational spectra of 4-pyrones and complexes is meager. An early work by Ross on the infrared spectrum suffers from experimental limitations (6), while Wolkenstein and Syrkin's Raman study unfortunately gave no polarization data (7). Tarbell and Hoffman (8) gave data on some pyrones and thiapyrones. Glusker and Thompson (9) investigated the spectra of 2,6-dimethyl-4-pyrone in solution in CCl_4 and CS_2 saturated with iodine and found some interesting shifts in certain bands. Some pyrones and some pyronium salts were studied by Tsubomura (10). The most complete data on 1,4-pyrone was the thesis of W. D. Phillips (11) from which some material was published by Lord and Phillips (12).

In a recent paper, Bellamy and Rogasch showed that the 4-pyridones exhibit a reversal of the C=C and C=O vibrational frequencies, the latter being of lower frequency, at ~1580 cm^{-1} (13). It was also suggested that 4-pyrones show the same effect. Solvent effects on the polar carbonyl group of the 4-pyridones were used to prove this point. In the present work we have used the extent to which the carbonyl frequency shifts when the pyrone is complexed with different Lewis acids as an indication of the site and extent of complex formation.

RESULTS AND DISCUSSION

Table I shows the main bands in the various spectra. The band marked $\nu_{C=C}$ decreases from 1678 to 1645 cm^{-1} over the complexes shown, a change of 33 cm^{-1}. The band marked

[1]*Manuscript received February 2, 1961.*
Contribution No. 40 from the Exploratory Research Laboratory, Dow Chemical of Canada, Limited, Sarnia, Ont.

TABLE I

Some bands in the infrared spectra of 2,6-dimethyl-4-pyrone

	In solution in:					In complexes with:				
	CCl_4	$CHCl_3$	Nujol	CCl_4+I_2	C_2H_5OH	$HgCl_2$	$ZnCl_2$	BF_3	$SbCl_5$	HBr
			1680					1662	1660	
$\nu_{C=C}$	1678	1677	1670	1668	1670	1664	1660	1652	1653	1645
						1659				
								1562	1560	
$\nu_{C=O}$	1639	1630	1612	1600	1597	1571	1530	1518	1496	1488
			1600							
	1394	1400	1396			1412	1420			
			1372			1368				
		1340	1342				1340	1350	1340	1337
			1200							
δ_{C-H}	1158	1163	1161			1168	1172	1181		1179
δ_{C-H}	1035	1040	1040			1039	1035	1056	1035	
			958			950				
γ_{C-H}	932	940	928							920
		905	900			907	910		911	900
γ_{C-H}	868	872				870	888		871	
							848			851

$\nu_{C=O}$ decreases from 1639 to 1488 cm^{-1}, a change of 151 cm^{-1}. This band is assigned to the carbonyl vibration from the following arguments.

It is widely accepted that when donor–acceptor complexes are formed between carbonyl compounds and Lewis acids, a lowering of bond order, force constant, and stretching frequency occur in the carbonyl group. Susz recently summarized the frequency changes occurring upon complex formation for many adducts of BF_3, $AlBr_3$, $TiCl_4$, etc. with ketones (14). The concomitant increase in the carbonyl bond distance has been observed in one case, the coumarin:$HgCl_2$ (and $HgBr_2$) complex (15), where it is about 0.1 Å. For a given Lewis acid the largest change in carbonyl frequency upon complex formation occurs for the compound with the most polarizable carbonyl bond. In this category are aromatic ketones and $\alpha\beta$-unsaturated ketones. It is likely that $\alpha\beta$-, $\alpha'\beta'$-unsaturated ketones (to which group 2,6-dimethyl-4-pyrone formally belongs) will have an even more polarizable carbonyl group, and will give larger shifts on complex formation. The 2,6-dimethyl-4-pyrone:BF_3 complex shows a shift of 121 cm^{-1} which is somewhat larger than that of the benzophenone:BF_3 complex, namely 112 cm^{-1}.

A similar lowering in frequency of a band at 1635 cm^{-1} has been described in some iodine complexes of 2,6-dimethyl-4-pyrone (9). A new band appeared at ~1584 cm^{-1}. The band in the free pyrone at 1674 cm^{-1} was located at 1658 cm^{-1} in the complex. The molecular arrangement in the 2,6-dimethyl-4-pyrone:iodine complex is probably similar to that in the acetone:bromine complex recently described (16). The iodine:pyrone complexes have been prepared here, using very dilute solutions* of 2,6-dimethyl-4-pyrone in CCl_4 and CS_2, and an iodine concentration equimolar with the pyrone concentration.

A difference spectrum (where the pyrone solution is placed in the reference beam, and the same solution, but with iodine, is placed in the sample beam) showed "negative bands" paired with normal bands of approximately the same intensity, thus identifying the perturbed band with the band in the free pyrone.

It is thus felt that considerable confidence can be placed in the frequencies assigned to the carbonyl bands in the complexes and in the free pyrone.

**A misprint must have occurred in this paper, since the pyrone is certainly not soluble to the extent of 15% in CCl_4; 0.15% by weight would be more reasonable.*

Can. J. Chem. Downloaded from www.nrcresearchpress.com by 210.87.254.40 on 09/05/12
For personal use only.

The higher-frequency band at 1678 cm^{-1} in the free pyrone, lowering progressively in the complexes to 1645 cm^{-1} must, therefore, be associated with a carbon–carbon stretching vibration or a nuclear vibration of the ring as a whole. Such a vibration might be similar to the one at 1585 cm^{-1} in benzene (ν_8 using the notation of Wilson (17) and Langseth and Lord (18)).

The lowering of $\nu_{C=C}$ as the Lewis acid in the complex gets stronger might at first sight be ascribed to a real alteration in the force constant and bond order of the C=C bond, as these quantities in the C=O bond alter in different complexes. This idea must be rejected, however, since in the Lewis acid complexes of similar molecules, such as pyridine 1-oxide and 4-pyridone, although the ring modes are different from the parent compound, there is hardly any variation in the ring frequencies as the Lewis acid varies. Because complex formation involves the oxygen atom $\nu_{C=O}$ and ν_{N-O} will vary in different complexes. Table II shows $\nu_{C=C}$ and $\nu_{C=O}$ (or ν_{N-O}) for these compounds (all in chloroform solution). The two bands for the pyrone are much closer together than the other two, and $\nu_{C=C}$ is at a much higher frequency. It is therefore thought that there is a mechanical interaction responsible for splitting two very similar frequencies.

TABLE II

Comparison of $\nu_{C=C}$ with $\nu_{C=O}(\nu_{N-O})$ ($CHCl_3$ solution)

Compound	$\nu_{C=C}$	$\nu_{C=O}(\nu_{N-O})$	Δ
2,6-Dimethyl-4-pyrone	1677	1630	47
N-Methyl-4-pyridone*	1646	1581	65
4-Pyridone	1636	1515	121
Pyridine-1-oxide	1612	1250	362

*Reference 11.

No frequency lower than ~1645 cm^{-1} has been observed for the $\nu_{C=C}$ vibration in any complex. For the strongest Lewis acid, $SbCl_5$, the lowered $\nu_{C=O}$ is at 1493 cm^{-1}, sufficiently removed from $\nu_{C=C}$ to preclude any interaction. It is very probable, therefore, that the unperturbed value of $\nu_{C=C}$ is at approximately 1645 cm^{-1}. In the free pyrone in solution in CCl_4, the separation of $\nu_{C=C}$ and $\nu_{C=O}$ is 39 cm^{-1}. This is similar in magnitude to that in some symmetrical acid anhydrides, where the unperturbed frequencies are identical due to symmetry. The unperturbed values of $\nu_{C=C}$ and $\nu_{C=O}$ are, therefore, probably close to 1645 cm^{-1}. These values seem very reasonable ones for the vibrations involved. The $\nu_{C=O}$ value is close to that in the following similar molecules: tropone, 1642 cm^{-1}; quinone, 1662 cm^{-1}. For the $\nu_{C=C}$ vibration, its precise identity prohibits critical comparison, but either a pure carbon–carbon double bond stretching mode, or a mode similar to the ν_8 in benzene would be at about the right frequency. Olefinic aldehydes and ketones have an absorption due to the C=C stretching vibration around 1624 cm^{-1} (19). The ν_{8a} band in benzene is at 1596; in pyridine at 1580 (20); in the pyridinium ion at 1639 (21); in *m*-xylene at 1618 cm^{-1} (22).

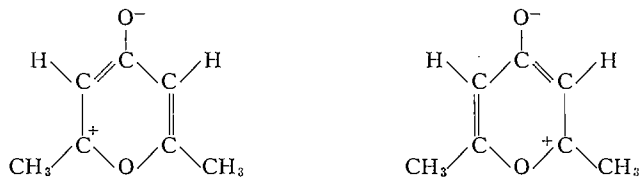
The existence of the interaction between $\nu_{C=C}$ and $\nu_{C=O}$ also does not help to identify $\nu_{C=C}$. Such interaction usually occurs between vibrations of the same species. Since $\nu_{C=O}$ must be of A_1 species, $\nu_{C=C}$ must be the same. However, both the ring mode (cf., ν_8 in benzene) and a symmetrical C=C stretch would also belong to an A_1 species (see Table II for selection rules), so that a decision between the two cannot be made.

Possibly the distinction between these two modes has been a little unduly stressed.

Can. J. Chem. Downloaded from www.nrcresearchpress.com by 210.87.254.40 on 09/05/12
For personal use only.

Examination of the normal co-ordinate displacements (23) of the ν_{8a} vibration in deuterobenzene (C_6H_5D has C_{2v} symmetry, as has 2,6-dimethyl-4-pyrone) shows this to be almost exclusively associated with stretching the bonds parallel to the C_{2v} axis. Little clarification of the vibrational assignments would arise from attempting to label it a pure double bond stretching vibration and it is probably best considered as a ring mode.

Usually when such interaction is present there will be alterations in intensity in one of the perturbed bands. In the present case, one would expect $\nu_{C=C}$ to borrow intensity from $\nu_{C=O}$ and as $\nu_{C=O}$ was lowered by complex formation a decrease in intensity might be expected. This is by no means the case as in most spectra both bands are of approximately the same intensity (in chloroform solution $\nu_{C=C}$ is a good deal stronger than $\nu_{C=O}$). What complicates the situation, unfortunately, is the difficulty of comparing solid-state intensities with solution ones. Additionally, as these two main bands are superimposed on other minor bands (the 2,6-dimethyl-4-pyrone molecule has 45 fundamentals), the question of intensity variations is not straightforward. The fact that in the BF_3 and $SbCl_5$ complexes (where presumably there is no interaction) $\nu_{C=C}$ is as intense as $\nu_{C=O}$, suggests that, in resonance language, an important contribution to the real nature of the pyrones must come from structures similar to the following.



A conclusion similar to this has also been drawn from proton-exchange experiments in 4-pyrone (11, 12).

Considering next the salts of 2,6-dimethyl-4-pyrone with mineral acids, it follows that the only site of protonation must be the carbonyl group. This is proved by the lowering of $\nu_{C=O}$ by some 151 cm^{-1} in the HBr salt indicative of a strong interaction at the carbonyl group. Protonation at the ether oxygen, as was earlier suggested (24), would have little or no effect on the carbonyl group vibration.

The strong broad band in the spectrum of 2,6-dimethyl-4-pyrone hydrobromide at 2380 cm^{-1}, shifting to 1860 cm^{-1} in the deuterobromide is identified as a hydrogen stretching motion of the protonated carbonyl group. It is not uncommon for carbonyl oxygen atoms to be sufficiently basic to accommodate a proton. Tropone (25), tropolone (26), N-methyl urea (27), urea (28), and acetamide (29) can all form ionized solids with certain mineral acids and the X-ray diffraction investigations have shown protonation to take place at the carbonyl oxygen atom. Furthermore, many dialkylamides show evidence of protonation at the same site (30). It is significant that those carbonyl compounds capable of forming solid salts with mineral acids are those with low carbonyl stretching frequencies (31).

In such a complicated molecule having 17 atoms, and, therefore, 45 fundamentals, it would be difficult to make a complete assignment, especially when the symmetry is C_{2v}, thus permitting all vibrations to occur in both infrared and Raman spectra with the exception of the A_2 species in the infrared. Table III lists the symmetry properties,

Can. J. Chem. Downloaded from www.nrcresearchpress.com by 210.87.254.40 on 09/05/12
For personal use only.

TABLE III
Selection rules for 2,6-dimethyl-4-pyrone

Class	Symmetry elements			Activity		Vibrations		
	$C_2(z)$	$\sigma_v(xz)$	$\sigma_v(yz)$	R	IR	C and O	H	Total
A_1	*s*	*s*	*s*	*p*	*a*	8	8	16
A_2	*s*	*as*	*as*	*dp*	*ia*	2	4	6
B_1	*as*	*s*	*as*	*dp*	*a*	7	8	15
B_2	*as*	*as*	*s*	*dp*	*a*	4	4	8

activity, and selection rules. It is possible though to make an approximate description of some bands as Table I shows.

EXPERIMENTAL

The spectra were recorded on a Perkin–Elmer Model 221 prism-grating double-beam spectrometer using sodium chloride optics. Frequencies are believed accurate to ± 2 cm^{-1}.

The complexes were prepared by mixing solutions of the two components, if liquid or solid, or, if the Lewis acid was a gas, by passing it through a solution of the pyrone.

2,6-Dimethyl-4-pyrone:SbCl$_5$.—2,6-Dimethyl-4-pyrone:$SbCl_5$ was prepared according to Meerwein (32).

2,5-Dimethyl-4-pyrone:HBr.—HBr passed into CCl_4 solution of the pyrone gave a white precipitate which was recrystallized from a methanol–acetone mixture. Melting point 185° decomp. % HBr, 39.1; theory, 39.4%.

2,6-Dimethyl-4-pyrone:BF$_3$.—BF_3 passed into a CCl_4 solution of the pyrone gave two phases from which a white solid was precipitated with ether. Melting point 135–137°.

2,6-Dimethyl-4-pyrone:ZnCl$_2$.—An acetone solution of the pyrone was mixed with a methanol–acetone solution of $ZnCl_2$, then poured into ether to give the solid complex. It was recrystallized from a methanol–acetone mixture.

2,6-Dimethyl-4-pyrone:HgCl$_2$.—Concentrated warm solutions of each component were mixed and on cooling gave a white solid. It was recrystallized from a methanol–acetone mixture.

ACKNOWLEDGMENTS

The assistance of Miss C. D. Anderson in preparing some of the compounds and taking their spectra is gratefully acknowledged.

REFERENCES

1. H. G. NORMENT. Ph.D. Thesis, University of Maryland, College Park, Maryland. 1956.
2. J. TOUSSAINT. Bull. soc. chim. Belges, **65**, 213 (1956).
3. L. S. BARTELL and R. A. BONHAM. J. Chem. Phys. **31**, 400 (1959).
4. D. COOK. J. Chem. Phys. **28**, 1001 (1958).
5. G. E. BACON and N. A. CURRY. Proc. Roy. Soc. A, **235**, 552 (1956).
6. A. ROSS. Proc. Roy. Soc. A, **113**, 208 (1926).
7. M. W. WOLKENSTEIN and J. K. SYRKIN. Acta Physicochim. U.R.S.S. **10**, 677 (1939).
8. D. S. TARBELL AND P. HOFFMAN. J. Am. Chem. Soc. **76**, 2451 (1954).
9. D. L. GLUSKER and H. W. THOMPSON. J. Chem. Soc. 471 (1955).
10. H. TSUBOMURA. J. Chem. Phys. **28**, 355 (1958).
11. W. D. PHILLIPS. Ph.D. Thesis, Massachusetts Institute of Technology, Cambridge, Massachusetts. 1951.
12. R. C. LORD and W. D. PHILLIPS. J. Am. Chem. Soc. **74**, 2429 (1952).
13. L. J. BELLAMY and P. E. ROGASCH. Spectrochim. Acta, **16**, 30 (1960).
14. B. P. SUSZ. Compt. rend. **248**, 2569 (1959).

Can. J. Chem. Downloaded from www.nrcresearchpress.com by 210.87.254.40 on 09/05/12
For personal use only.

15. J. T. STRUCKOV, A. I. KITAIGORODSKI, and T. L. CHOZIANOVA. Doklady Akad. Nauk U.S.S.R. **93**, 675 (1953).
16. O. HASSEL and K. O. STRØMME. Acta Chem. Scand. **13**, 275 (1959).
17. E. B. WILSON, JR. Phys. Rev. **45**, 706 (1934).
18. A. LANGSETH and R. C. LORD. Kgl. Danske Videnskab. Selskab, Mat. fys. Medd. **16**, 6 (1938).
19. R. MECKE and K. NOACK. Spectrochim. Acta, **12**, 391 (1958).
20. J. K. WILMSHURST and H. J. BERNSTEIN. Can. J. Chem. **35**, 1183 (1957).
21. D. COOK. Seventh Ottawa Symposium on Applied Spectroscopy. October 4, 1960.
22. D. COOK. Unpublished results.
23. C. R. BAILEY, R. R. GORDON, J. B. HALE, N. HERZFELD, C. K. INGOLD, and H. G. POOLE. J. Chem. Soc. 299 (1946).
24. J. N. COLLIE and T. TICKLE. J. Chem. Soc. **75**, 710 (1899).
25. H. W. DAUBEN, JR. and H. R. RINGOLD. J. Am. Chem. Soc. **73**, 876 (1951).
26. Y. SASADA and I. NITTA. Bull. Chem. Soc. Japan, **30**, 62 (1957).
27. J. H. BRYDEN. Acta Cryst. **10**, 714 (1957).
28. R. V. G. SUNDERA-RAO, J. W. TURLEY, and R. PEPINSKY. Acta Cryst. **10**, 435 (1957).
29. W. TAKEI. Ph.D. Thesis, California Institute of Technology, Pasadena, California. 1957.
30. D. COOK. Unpublished results.
31. D. COOK. J. Am. Chem. Soc. **80**, 49 (1958).
32. H. H. MEERWEIN. J. prakt. Chem. **134**, 51 (1932).

Can. J. Chem. Downloaded from www.nrcresearchpress.com by 210.87.254.40 on 09/05/12
For personal use only.

Can. J. Chem. Downloaded from www.nrcresearchpress.com by 210.87.254.40 on 09/05/12
For personal use only.

GAS–LIQUID CHROMATOGRAPHY OF TERPENES

PART III. THE USE OF OLEIC ACID ESTERS AS LIQUID PHASES[1]

E. VON RUDLOFF

ABSTRACT

The separation of several cyclic terpene hydrocarbons and some oxygenated derivatives was studied on a variety of triglyceride and dioleate ester columns. Use of rapeseed oil, partially hydrogenated rapeseed oil, olive oil, triolein, tristearin, methyl oleate, and potassium oleate as liquid phases led to the conclusion that the presence of an esterified mono-unsaturated long-chain acid is a desirable constituent of the liquid phase. Dioleate esters of 1,3-propanediol, 1,4-butanediol, 1,6-hexanediol, diethylene glycol, and polyethylene glycol showed useful differences in the degree of separation of both terpene hydrocarbons and oxygenated derivatives. Ether linkages, as in the di- and poly-ethylene glycol ester, also were associated with favorable separations. When the liquid phase contained free hydroxyl groups, the degree of separation of hydrocarbons and ketones was in general less favorable. The spacing of the ester groups was found to have some effect on retention data. The separation of such critical pairs of isomers as tricyclene and α-pinene, α-fenchene and camphene, and also geometrical isomers of oxygenated derivatives is facilitated by use of several of these liquid phases.

During an examination of the essential oil of the leaves of Eastern white cedar (*Thuja occidentalis* L.) by means of gas–liquid chromatography (GLC) (1), the peak corresponding in retention time to camphene was isolated and its infrared spectrum was found to correspond to that of synthetic camphene. Yet the sample failed to crystallize on seeding. Further examination on the rapeseed oil column (2) indicated a second component, presumably α-fenchene (3), to be present (partially resolved peak). There was no indication of this impurity on either the 6-ft adipate polyester (APEG) column or polyphenyl ether columns (2, 4). Other such unresolved or partially resolved pairs of isomeric terpenes are frequently encountered, e.g. tricyclene and α-pinene (3), terpinolene and $\Delta^{2,4(8)}$-*p*-menthadiene (2), or the many geometrical and positional isomers of oxygenated terpenes. Thus, for either qualitative or quantitative analyses by GLC of mixtures of terpenes and especially essential oils, improved separations over those previously obtained seem imperative. Slight improvements were obtained with the apparatus used in this study by some modification of the injector (see experimental part) and by using less than 5 μl amounts, but this did not lead to the desired results. Bernhard (5) has pointed out that the most useful experimental parameter is the choice of stationary liquid phase, and has investigated a large variety of compounds for use in the separation of lemon oil constituents. This aspect was further investigated in this study.

The use of polyesters as liquid phases in GLC separation has been studied fairly extensively (3–10) and the results obtained with adipate polyesters (4, 5) were a considerable improvement over older results. However, columns with these liquid phases failed to separate several of such critical pairs of isomers. In the previous paper of this series (2), it was shown that vegetable oils, such as rapeseed and olive oil, were very suitable for the separation of monocyclic terpene hydrocarbons and it was suggested that triolein may be useful as a liquid phase. This has now been found to be so, and it could also be shown that these triglyceride columns give useful retention data for oxygenated monocyclic terpenes.

[1]*Manuscript received January 30, 1961.*
Contribution from the National Research Council of Canada, Prairie Regional Laboratory, Saskatoon, Saskatchewan.
Issued as N.R.C. No. 6276.

During investigations on GLC separations of methyl esters of fatty acids in this laboratory, Craig (11) has observed that the spacing of the ester group along a polyester chain can have significant effects on the degree of separation. Thus, it is conceivable that the close proximity of three ester groups in the triglycerides is not necessarily the most favorable arrangement for the separation of terpenoid compounds. Therefore, a number of dioleate esters were prepared in which the ester groups were spaced progressively further from one another, viz. esters of 1,3-propanediol, 1,4-butanediol, 1,6-hexanediol, diethylene glycol, and polyethylene glycol. Oleate esters were chosen because the data obtained with the triglycerides suggested that oleic acid was the most desirable acidic component in these polyesters. In addition, the polyester of azelaic acid with diethylene glycol was tested to obtain further data on the spacing of the ester groups.

EXPERIMENTAL

Apparatus

A Beckman GC-2 chromatograph equipped with a thermal conductivity cell was modified by placing the injector as close as possible to the head of the column. The temperature of the injector was kept 20–25° C higher than that of the column and the detector cell. All experiments were carried out with an inlet pressure of 55 p.s.i. (3.74 atm) and the column outlet at atmospheric pressure (0.93 ± 0.02 atm). The flow rates were measured with a moving soap bubble at room temperature. The chart speed of the 1-mv recorder was 10 in. per hour, and samples were injected with a hypodermic syringe.

Preparation of Columns

All liquid phases were applied to the solid support Chromosorb W (Johns-Manville) in the ratio of 6 to 1 by weight. The liquid phase (2.0 g) was dissolved in chloroform (45 ml) and to the solution was added, with stirring, the solid support (12.0 g). The resulting thick slurry was stirred for 5–10 minutes, transferred to a shallow tray and stirred intermittently until the slurry became a dry powder. The material was then dried *in vacuo* at 50–60° C for 1 hour and packed with constant tapping into 6 ft by $\frac{1}{4}$ in. O.D. copper columns. The weights of liquid phase and solid support for each column are shown in Table I. All columns were used for a number of runs before critical measurements were taken.

Synthesis of Oleic Acid Esters

The technique described by Youngs *et al.* (12, 13) was followed throughout. In a typical example oleic acid (6.2 g, 22 mmoles, commercial 95%) was dissolved in dry petrol (b.p. 60–70° C) (65 ml) and to this was added phosphorus pentachloride (5.0 g, 24 mmoles). The mixture was heated under reflux with exclusion of moisture for 1 hour, then cooled and quickly washed twice with ice water (13). After the petrol solution was dried over anhydrous sodium sulphate, the solvent was evaporated. To the residual oleyl chloride was added 1,3-propanediol (0.76 g, 10 mmoles) and the mixture was heated on a rotary evaporator at 50–60° C for 6 hours, the initial vacuum being gradually increased to 10 mm Hg to remove the hydrochloric acid liberated. Any attempts to remove unreacted oleic acid by washing a solution of the crude reaction product with aqueous alkali resulted in very stable emulsions. Therefore, the residual reaction product was chromatographed on a 3×50 cm column of silicic acid, the ester being eluted with 100-ml aliquots of petrol:chloroform (1:1 v/v). The first three fractions had an infrared spectrum expected for the diester but acidic impurities could be detected, especially in

Can. J. Chem. Downloaded from www.nrcresearchpress.com by 210.87.254.40 on 09/05/12
For personal use only.

Can. J. Chem. Downloaded from www.nrcresearchpress.com by 210.87.254.40 on 09/05/12
For personal use only.

TABLE I

Physical constants of the 6 ft×¼ in. columns

Liquid phase	Abbrevn.	Weight with solid support (g)	80° C			110° C			Retention time of air peak	
			Flow rate*	*t* limonene†		Flow rate*	*t* camphor†			
				(*a*)	(*b*)		(*a*)	(*b*)	80° C	110° C
Rapeseed oil	—	10.0	113	31.1	32.3	94	37.2	39.0	0.4	0.4
Olive oil	—	9.5	103	29.3	30.5	85	32.8	35.0	0.4	0.4
Triolein	—	10.3	125	28.3	29.5	109	29.4	31.2	0.3	0.3
Hydrogenated rapeseed oil I	HRO I	11.1	110	33.1	34.5	100	40.3	42.9	0.4	0.5
Hydrogenated rapeseed oil II	HRO II	10.5	110	35.4	37.5	100	42.3	45.8	0.3	0.3
Tristearin	—	10.1	120	36.0	39.1	95	28.9	32.5	0.3	0.3
Methyl oleate	—	10.5	94	71.5	75.0	—	—	—	0.5	—
Potassium oleate	—	10.9	78	9.9	10.9	—	—	—	0.3	—
1,3-Propanediol dioleate	PDDO	10.0	81	64.1	66.5	66	51.9	56.6	0.4	0.4
1,4-Butanediol dioleate	BDDO	10.5	127	32.9	33.9	113	32.1	35.0	0.3	0.3
1,6-Hexanediol dioleate	HDDO	10.4	86	51.8	53.3	75	45.0	47.5	0.3	0.3
Diethylene glycol dioleate	DEGDO	10.8	88	23.5	24.5	80	27.5	28.8	0.4	0.4
Polyethylene glycol dioleate	PEGDO	10.6	113	25.3	26.3	100	35.1	37.0	0.3	0.4
Polyethylene glycol monooleate	PEGMO	11.0	100	32.4	34.1	85	39.0	41.5	0.4	0.4
Polyoxyethylene sorbitan trioleate	Tween 85	10.2	120	17.4	19.0	100	21.8	24.5	0.2	0.3
Polyethylene glycol polyadipate	APEG	12.5	100	10.2	11.3	95	30.7	32.5	0.3	0.3
Diethylene glycol polyazelate	AzDEG	11.6	103	12.0	13.0	104	24.3	24.0	0.2	0.3
Polyethylene glycol	PEG 1540	11.2	89	13.6	14.6	67	30.8	32.7	0.4	0.4
m-bis(*m*-Phenoxyphenoxy)-benzene	PPE	11.5	150	17.9	19.2	150	28.3	30.5	0.2	0.2

*In ml helium per minute.
†Retention time: (*a*) measured to peak base; (*b*) measured to peak maximum.

the third fraction. The material was combined by dissolving in chloroform (10 ml), solid anhydrous potassium carbonate (1.0 g) was added, and the mixture was stirred for 10–15 minutes. It was then rechromatographed on silicic acid to give the crude diester (3.6 g, 60% of theory). The infrared spectrum of the eluted material showed no longer the presence of free acid, but elementary analysis gave low values for the percentage carbon (up to 0.8%). On distilling the crude diester *in vacuo* (b.p. 195° C at 0.2 mm, air bath) the colorless diester was obtained practically pure. Found: C, 76.90%; H, 11.98%; neutral equivalent, 3; saponification equivalent, 297. Calculated for $C_{39}H_{76}O_4$: C, 76.91%; H, 12.58%; saponification equivalent, 304.50.

Where the yield of the diester was poor, a substantial amount of the corresponding monoester was recovered from the silicic acid column by eluting first any unreacted oleic acid with chloroform and then eluting further with chloroform – 2-butanone (1:1 v/v). The crude esters were all light to medium yellow in color and were obtained colorless only after distillation. Polyethylene glycol mono- and di-oleate failed to distill at a pressure of 0.1 mm Hg, and any residual oleic acid which may have been present after chromatography was converted to methyl oleate by treatment with an ethereal solution of diazomethane.

Materials

Triolein, tristearin, and the partially hydrogenated rapeseed oils were kindly donated by Dr. C. G. Youngs. Two different samples of partially hydrogenated rapeseed oil were used: I (HRO I), having a content of 14% saturated fatty acids, and II (HRO II) with 50% saturated acids. The adipate polyester of polyethylene glycol (APEG) and azelate polyester of diethylene glycol (AzDEG) were a gift kindly made by Dr. B. M. Craig (6). The polyphenyl ether [*m*-bis(*m*-phenoxyphenoxy)-benzene], "Tween 85" (polyoxyethylene sorbitan trioleate), and polyethylene glycol (Carbowax 1540) were commercial products.

The terpenes used in this study were either commercial samples or those previously prepared (2). The mixture of *trans*- and *cis*-dihydro-α-terpineol was prepared by hydrogenating α-terpineol with platinum oxide as catalyst (14). In addition a commercial sample of the essential oil of cedar leaf (*Thuja occidentalis* L.) was used.

PRESENTATION OF DATA

In 1958, Ambrose *et al.* (15) and Johnson and Stross (16) put forward proposals for a unified way of presenting GLC data. It was pointed out that reproduction of the actual recorder chart gave the least amount of information in a maximum amount of space. Tables of relative retention times with respect to a standard, or standards, were to be preferred, but far more useful presentation would result from calculation of retention volumes (corrected or uncorrected) and(or) partition coefficients. However, all such calculated data are obtained from the basic equation $V_R = F_c t'$ (15) where V_R is the retention volume, F_c the flow rate of carrier gas at column temperature, and t' the time of emergence of the peak maximum. Now it was shown (4, 17, 18, 19) that the position of the peak maximum of a given compound varies considerably with the size of the injected sample (over the practical range of about 0.1 to 50 μl used with the type of apparatus employed in this study). Also, the retention time may be longer if the compound is preceded by a much larger quantity of another compound (20). Thus, unless all measurements are carried out with identical sample sizes, considerable errors will

Can. J. Chem. Downloaded from www.nrcresearchpress.com by 210.87.254.40 on 09/05/12
For personal use only.

result in all of the calculated data. The use of equal sample sizes is not only time consuming but is a practical impossibility in essential oils and many mixtures of synthetic terpenes. Thus, for practical purposes at least, comparison of the actual recorder tracing (chromatogram) will remain the most reliable means of comparing column efficiencies. Next best, possibly, is the tabulation of relative retention times (with respect to a standard compound) *as measured from the point of injection to the initial emergence* of the peaks under consideration (2). The latter procedure is also subject to small errors when peaks are not completely separated. Further objections may be raised since the initial emergence is dependent upon detector sensitivity and thus small fluctuations in the base line may obscure detection of the initial emergence of a peak to some extent. These difficulties can be overcome, in part at least, by drawing the tangent to the peak and using the intercept at the base line as reference point. However, this is also subject to small variations with different sample sizes and the initial emergence point is to be preferred. Therefore, the data obtained in the present study was tabulated as relative retention times with respect to a standard and as measured to the initial emergence of each peak.

Retention times, or relative retention times, give no information on the peak width. Thus, whilst the relative retention times of two compounds may be the same on different columns, the actual separation achieved will only become apparent on comparing the recorder charts. Also, in separations involving essential oils different types of organic compounds are involved and the relative peak width of, for example, the hydrocarbons may be different from those of the ketones, alcohols, etc. Separation factors or functions have been put forward (21, 22, 23) to overcome this difficulty, and Jones and Kieselbach (24) have proposed the use of the ratio of retention time to peak width (relative peak sharpness) as a measure of the efficiency of a column. The latter quantity appears to offer advantages since it is a direct measure and not a theoretical concept relating to an idealized mode of operation. However, if the retention time is measured at the peak maximum, the error discussed above will once again make comparison between peaks of different sample sizes unreliable. Also, peak width varies with sample size and a smaller value for the relative peak sharpness will be obtained with larger sample size. These same observations apply to the use of retention indices as developed by Kováts (25). Thus, the visual examination of the charts still remains the most reliable means of determining column efficiency when peaks of varying sample size are involved. However, some measure of the degree of separation can be obtained by comparing the retention time of the point of initial emergence of a peak with that of the peak maximum. This is shown in Table I for all the columns studied for limonene (at 80° C) and for camphor (at 110° C). Flow rates, retention times of air, and the total weight of the liquid phase and solid support are also listed to allow other calculations, if desired.

RESULTS AND DISCUSSION

The relative retention times of monoterpene hydrocarbons, 1,8-cineole and *p*-cymene with respect to limonene as obtained on the rapeseed oil, tristearin, methyl oleate, and potassium oleate columns are compared in Table II with those obtained on a polyethylene glycol (PEG 1540) column. Only insignificant differences in the relative retention times were obtained with the rapeseed oil, olive oil, trioleate, and methyl oleate columns and only the data for the former are shown. Visual comparison showed a slightly better degree of separation for the triolein column, whilst that obtained with olive oil was

Can. J. Chem. Downloaded from www.nrcresearchpress.com by 210.87.254.40 on 09/05/12
For personal use only.

TABLE II

Relative retention times (limonene = 1.00) of cyclic terpene hydrocarbons on 6 ft × ¼ in. triglyceride columns at 80° C

l limonene† (minutes)	31.1	33.1	35.4	36.0	9.9	13.6
Liquid phase	Rapeseed oil	HRO I*	HRO II*	Tristearin	Potassium oleate	PEG* 1540
1. Tricyclene	0.35	0.39	0.39	0.37	0.40	0.32
2. α-Pinene	0.39	0.425	0.43	0.41	0.44	0.325
3. Unknown‡	0.44	0.47	0.50	0.48	0.505	0.44
4. Camphene	0.465	0.49				
5. β-Pinene	0.56	0.59	0.62	0.61	0.625	0.56
6. Unknown§	0.63	0.65	0.64			0.59
7. α-Phellandrene	0.80	0.82	0.80	0.80	0.78	0.775
8. α-Terpinene	0.87	0.89	0.89	0.87	0.81	0.88
9. Limonene	1.00	1.00	1.00	1.00	1.00	1.00
10. γ-Terpinene	1.30	1.28	1.29	1.27	1.22	1.30
11. Terpinolene	1.56	1.45	1.56	1.51	1.49	1.65
12. $\Delta^{2,4(8)}$-*p*-Menthadiene	1.64	1.50				
13. 1,8-Cineole	0.94	0.94	0.92	1.00	1.00	1.125
14. *p*-Cymene	1.06	1.08	1.07	1.01	1.01	1.50
15. Fenchone	1.82	1.52	—	—	—	3.40

*Abbreviations as used in Table I.
†Retention time of limonene as measured from injection to initial emergence of peak.
‡From cedar leaf oil, possibly α-fenchene.
§From cedar leaf oil, possibly myrcene.

slightly worse than that for rapeseed oil. Methyl oleate did not only give very high retention times (see Table I), but was found to bleed at higher temperatures. With the more saturated triglycerides a decrease in efficiency was noted with increasing concentrations of saturated esters. Quite different results were obtained with potassium oleate; the retention times were very low and the resolution was rather poor. Since more unsaturated vegetable oils, such as linseed and sunflower oils, gave also poorer results than rapeseed oil (2), there is little doubt that esterified oleic acid is the most desirable component in this type of liquid phase.

Pure oleate esters will not oxidize as rapidly as when they are contaminated with more unsaturated esters. However, this advantage of synthetic triolein over the vegetable oils may be offset by the difficulties encountered in preparing pure triolein. Deterioration of the vegetable oil columns was conveniently detected by a decrease in the separation between 1,8-cineole and limonene; a 6-month-old rapeseed oil column gave even slightly longer retention times for the oxide. No noticeable differences in the separation of isomeric hydrocarbons were detected, unless the deterioration was severe. This behavior of the oleate columns may be due to slow oxidation of the liquid phase resulting in a gradual increase in polarity and thus approaching the polyether or polyester type of separation. The results obtained with rapeseed oil, triolein, and partially hydrogenated rapeseed oil I (14% saturated fatty acids) show that the purity of the triglycerides with respect to saturation is not critical up to a content of about 10% of saturated acids. Also, small variations in the chain length of the unsaturated moiety (as found in rapeseed oil) do not appear to have a marked effect on the degree of separation of terpene hydrocarbons.

Table III shows the relative retention times of the same terpenes obtained with synthetic dioleates, polyethylene glycol monooleate, "Tween 85", azelate polyester (AzDEG), and adipate polyester (APEG) as liquid phase. 1,3-Propanediol dioleate gave

Can. J. Chem. Downloaded from www.nrcresearchpress.com by 210.87.254.40 on 09/05/12
For personal use only.

TABLE III

Relative retention times (limonene = 1.00) of cyclic terpene hydrocarbons at 80° C on 6 ft × $\frac{1}{4}$ in. dioleate columns

t limonene† (minutes)	32.9	51.8	23.5	25.3	32.4	17.4	10.2	12.0
Liquid phase	BDDO*	HDDO*	DEGDO*	PEGDO*	PEGMO*	Tween 85*	APEG polyester*	AzDEG polyester*
1. Tricyclene	0.36	0.37	0.36	0.345	0.35	0.345	0.31	0.30
2. α-Pinene	0.41	0.41	0.40	0.375	0.39	0.37	0.33	
3. Unknown‡	0.46	0.46	0.45	0.45	0.455	0.46	0.46	0.41
4. Camphene	0.48	0.48	0.47	0.47	0.47	0.47	0.47	0.49
5. β-Pinene	0.62	0.61	0.59	0.59	0.59	0.58	0.58	0.56
6. Unknown§	0.68	0.69	0.65	0.65	0.60		0.60	0.625
7. α-Phellandrene	0.82	0.84	0.80	0.79	0.81	0.83	0.80	0.79
8. α-Terpinene	0.88	0.90	0.86	0.855	0.88	0.86	0.83	0.87
9. Limonene	1.00	1.00	1.00	1.00	1.00	1.00	1.00	1.00
10. γ-Terpinene	1.27	1.29	1.25	1.28	1.28	1.28	1.33	1.33
11. Terpinolene	1.54	1.55	1.51	1.59	1.60	1.59	1.60	1.65
12. $\Delta^{2,4(8)}$-*p*-Menthadiene	1.62	1.61	1.58	1.63		1.64	1.63	1.71
13. 1,8-Cineole	1.05	0.98	0.95	1.14	0.99	1.02	1.06	1.21
14. *p*-Cymene	1.12	1.13	1.08	1.25	1.22	1.25	1.54	1.48
15. Fenchone	2.01	1.82	1.83	2.37	2.11	2.10	3.50	3.20

*Abbreviations as used in Table I.
†Initial emergence of peak.
‡From cedar leaf oil, possibly α-fenchene.
§From cedar leaf oil, possibly myrcene.

similar results to those obtained with the unsaturated triglycerides and the relative retention times are therefore not shown. All dioleates gave favorable separation, especially so for the critical pairs of peaks 5 and 6 and peaks 11 and 12. The separation in the α-terpinene to γ-terpinene range were especially good on the di- and poly-ethylene glycol dioleate columns. Noteworthy is also the finding that on most of these columns fenchone was eluted relatively later than on the triglyceride columns. The retention times of 1,8-cineole with respect to limonene varied considerably and no correlation between the degree of separation and the spacing of the two ester groups could be detected. Also, the much shorter retention times obtained on the 1,4-butanediol dioleate (BDDO) column (in part due to the higher flow rate in this column) as compared with those on the propanediol or hexanediol dioleate columns did not result in a markedly different degree of separation, except that 1,8-cineole was eluted later with limonene. The presence of free hydroxyl groups (polyethylene glycol monooleate, polyethylene glycol, and "Tween 85") results in a loss of over-all efficiency. This can also be seen from the data obtained earlier with a polyphenyl ether column (2). Together with the difference in separation obtained on the polyester (APEG and AzDEG), polyphenyl ether (PPE), and polyethylene (PEG 1540) columns these results lead to the conclusion that for the separation of isomeric terpene hydrocarbons, mono-unsaturated hydrocarbon chains and ester groups are favorable, but free hydroxyl groups not. The ether linkage of the polyethers is, in general, favorable, too, and results in a longer retention of 1,8-cineole and *p*-cymene.

For the study of the composition of essential oils, columns which are equally efficient for the separation of oxygenated compounds, including isomeric pairs, are required. The separation of the isomeric menthols on either polyethylene glycol (26) or silicone oil (27) has been reported, and Ofner *et al.* (28) have separated the cis–trans isomers of

Can. J. Chem. Downloaded from www.nrcresearchpress.com by 210.87.254.40 on 09/05/12
For personal use only.

Can. J. Chem. Downloaded from www.nrcresearchpress.com by 210.87.254.40 on 09/05/12
For personal use only.

aliphatic sesquiterpenoid alcohols on Apiezon. Also, the retention time of the fastest-moving monoterpenoid ketone (usually fenchone) should be such as to allow complete separation of the monoterpene fraction. For this reason the relative retention time of fenchone at 80° C on some of the columns investigated has been included in Tables II and III. The relative retention times with respect to camphor of a number of closely related ketones and alcohols and bornyl acetate as obtained with the above columns at 110° C are shown in Table IV. Though only a relatively small number of oxygenated monoterpenes were studied, the retention data obtained allow conclusions to be drawn as to which column or columns may be suitable for a specific separation. Since the differences obtained with the various triglycerides followed the same pattern as described above, only the results obtained with rapeseed oil and tristearin as liquid phase are shown as typical examples. It is noteworthy that the drop in efficiency in going from the unsaturated to the fully saturated triglyceride was not as marked as in the case of isomeric terpene hydrocarbons. However, this may no longer be true if unsaturated ketones or alcohols are involved. The triglyceride columns tend to separate approximately according to boiling point, showing that these columns are intermediate in polarity as compared with saturated hydrocarbon or silicone and the polyester type of columns.

Very marked differences in relative retention times were obtained on the various dioleate columns. On 1,3-propanedioleate (PDDO) the most remarkable difference is that *trans*-dihydro-α-terpineol and borneol as well as the cis isomer of the former and isoborneol were not separated from one another, whilst on the other oleate columns the cis isomer and borneol would fall together. The relative retention times on the 1,4-butanediol dioleate (BDDO) column were similar to those obtained with rapeseed oil, except that bornyl acetate was eluted more rapidly. This was also so on the polyethylene glycol dioleate (PEGDO) column, only here the separation between *cis*-dihydro-α-terpineol and borneol was superior. The hexanediol dioleate (HDDO) column eluted bornyl acetate more slowly. The most noticeable differences were obtained with diethylene glycol dioleate (DEGDO). Not only are the retention times lower than on the other oleate columns, but the relative retention times of the ketones are noticeably higher. The degree of separation on the polyethylene glycol monooleate column was of the same order as that obtained with tristearin, except that bornyl acetate was eluted ahead of α-terpineol.

Comparison of the retention data obtained on the triglyceride and oleate ester columns with those found on the polyester and polyether columns shows some useful differences. The former columns all gave better resolution of the hydrocarbons. This, however, appears to be at the expense of longer retention times. Regarding the polyester of azelaic acid (AzDEG), also studied in this series (see Tables III and IV), a slight but definite improvement in the separation of hydrocarbons with respect to the adipate polyester polyethylene glycol column was obtained. Since the retention time of limonene was less than half that of most of the oleate ester columns, this liquid phase offers advantages in routine analyses. The separation of oxygenated terpenes on this column was of the same order as that obtained on the adipate polyester column. Previously it was found (2) that succinate polyester was less efficient as liquid phase than adipate polyester as far as separation of terpenes is concerned. Thus, there appears to be a definite advantage in having the ester groups spaced more than four carbon atoms apart. This relationship will, of course, not hold for all types of compounds to be separated, but it confirms the observation made by Craig (11) that the distance of polar groups along the chain of the polymer may have a significant influence on the degree of separation.

Can. J. Chem. Downloaded from www.nrcresearchpress.com by 210.87.254.40 on 09/05/12
For personal use only.

TABLE IV

Relative retention times (camphor = 1.00) of oxygenated terpenes at 110° C

t camphor† (minutes)	39.0	30.4	30.8	28.3	30.7	24.3	51.9	32.1	45.0	27.5	35.1
Liquid phase	Rapeseed oil	Tristearin	PEG* 1540	PPE*	APEG*	AzDEG*	PDDO*	BDDO*	HDDO*	DEGDO*	PEGDO*
1. 1,8-Cineole	0.38	0.425	0.27	0.27	0.23	0.23	0.48	0.37	0.395	0.28	0.27
2. Limonene	0.43		0.215	0.23	0.19	0.19		0.39		0.32	0.305
3. Fenchone	0.62	0.61	0.56	0.57	0.52	0.555	0.66	0.62	0.64	0.76	0.59
4. α-Thujone	0.735	0.75	0.655	0.66	0.615	0.655	0.74	0.72	0.76	0.74	0.71
5. Isothujone	0.84	0.83	0.74	0.73	0.74	0.73	0.84	0.82	0.86	0.86	0.78
6. Menthone	1.02	0.84	0.74	0.90	0.75	0.78	1.05	1.02	1.06	0.99	0.96
7. Isomenthone	1.17	0.98	0.88	1.06	0.94	0.95	1.20	1.17	1.14	1.10	1.07
8. Camphor	1.00	1.00	1.00	1.00	1.00	1.00	1.00	1.00	1.00	1.00	1.00
9. *trans*-Dihydro-α-terpineol	1.25	1.40	1.22	0.78	1.09	1.275	1.38	1.33	1.29	0.985	1.20
10. *cis*-Dihydro-α-terpineol	1.40	1.53	1.43	0.90	1.30	1.46	1.51	1.51	1.40	1.13	1.51
11. Borneol	1.41	1.45	2.02	0.93	1.90	1.69	1.34	1.51	1.39	1.13	1.69
12. Isoborneol	1.60	1.63	2.48	1.05	2.24	2.08	1.52	1.71	1.53	1.28	1.93
13. α-Terpineol	1.88	2.04	2.43	1.31	2.45	2.41	2.02	2.13	1.90	1.52	2.17
14. Bornyl acetate	1.89	2.09	1.33	1.56	1.33	1.33	2.21	1.92	2.10	1.53	1.71

*Abbreviations as used in Table I.
†Initial emergence of peak.

The application of the liquid phases found to be most useful in the study of the components of the essential oil of cedar leaves is described in the following communication.

ACKNOWLEDGMENTS

The many helpful discussions with Drs. B. M. Craig and C. G. Youngs and the gifts of chemicals are gratefully acknowledged. Thanks are also due to Mr. M. Granat for technical assistance, to Miss I. M. Gaffney for recording the infrared spectra, and to Mr. M. Mazurek for the microanalyses.

REFERENCES

1. E. VON RUDLOFF. Can. J. Chem. In press.
2. E. VON RUDLOFF. Can. J. Chem. **39**, 1 (1961).
3. W. J. ZUBYK and A. Z. CONNER. Anal. Chem. **32**, 912 (1960).
4. E. VON RUDLOFF. Can. J. Chem. **38**, 631 (1960).
5. R. A. BERNHARD. Food Research, **25**, 531 (1960).
6. B. M. CRAIG and N. L. MURTY. Can. J. Chem. **36**, 1297 (1958).
7. C. H. ORR and J. E. CALLEN. J. Am. Chem. Soc. **80**, 249 (1958).
8. L. D. QUIN and M. E. HOBBS. Anal. Chem. **30**, 1400 (1958).
9. S. R. LIPSKY and R. A. LANDOWNE. Biochim. et Biophys. Acta, **27**, 666 (1958).
10. E. C. HORNING, E. A. MOSCATELLI, and C. C. SWEELEY. Chem. & Ind. (London), 751 (1959).
11. B. M. CRAIG. Unpublished information.
12. C. G. YOUNGS, A. EPP, B. M. CRAIG, and H. R. SALLANS. J. Am. Oil Chemists' Soc. **34**, 107 (1957).
13. C. G. YOUNGS. J. Am. Oil Chemists' Soc. **35**, 416 (1958).
14. R. H. EASTMAN and R. A. QUINN. J. Am. Chem. Soc. **82**, 4249 (1960).
15. D. AMBROSE, A. I. M. KEULEMANS, and J. H. PURNELL. Anal. Chem. **30**, 1582 (1958).
16. H. W. JOHNSON and F. H. STROSS. Anal. Chem. **30**, 1586 (1958).
17. P. E. PORTER, C. H. DEAL, and F. H. STROSS. J. Am. Chem. Soc. **78**, 2999 (1956).
18. R. M. BETHEA and M. SMUTZ. Anal. Chem. **31**, 1211 (1959).
19. E. M. BENS and W. R. MCBRIDE. Anal. Chem. **31**, 1379 (1959).
20. G. RAUPP. Z. anal. Chem. **164**, 135 (1958).
21. E. GLUECKAUF. Trans. Faraday Soc. **51**, 34 (1955).
22. J. H. PURNELL. J. Chem. Soc. 1268 (1960).
23. J. C. GIDDINGS. Anal. Chem. **32**, 1707 (1960).
24. W. L. JONES and R. KIESELBACH. Anal. Chem. **30**, 1590 (1958).
25. E. KOVÁTS. Helv. Chim. Acta, **41**, 1915 (1958).
26. H. J. PETROWITZ, F. NERDEL, and G. OHLOFF. J. Chromatog. **3**, 351 (1960).
27. W. TAGAKI and T. MITSUI. Bull. Agr. Chem. Soc. Japan, **24**, 217 (1960).
28. A. OFNER, W. KIMEL, A. HOLMGREN, and F. FORRESTER. Helv. Chim. Acta, **42**, 2577 (1959).

Can. J. Chem. Downloaded from www.nrcresearchpress.com by 210.87.254.40 on 09/05/12
For personal use only.

Can. J. Chem. Downloaded from www.nrcresearchpress.com by 210.87.254.6 on 09/05/12
For personal use only.

GAS–LIQUID CHROMATOGRAPHY OF TERPENES

PART IV. THE ANALYSIS OF THE VOLATILE OIL OF THE LEAVES OF EASTERN WHITE CEDAR[1]

E. VON RUDLOFF

ABSTRACT

The complete analysis of the neutral volatile oil of the leaves of Eastern white cedar (*Thuja occidentalis* L.) by means of gas–liquid chromatography was attempted. The mixture of terpenes was resolved into 28 monoterpenoid components and the major ones were isolated in 5- to 20-mg amounts. Comparison of infrared spectra and retention times with those of authentic specimens led to the positive identification of *d*-α-pinene, camphene, sabinene, *d*-limonene, *p*-cymene, γ-terpinene, *l*-fenchone, *l*-α-thujone, *d*-isothujone, camphor, and bornyl acetate. α-Thujene, β-pinene, myrcene, 1,8-cineole, terpinolene, and terpinen-4-ol were tentatively identified. The percentage composition of a commercial sample of the oil and of one obtained from a tree grown in Saskatoon was determined. The latter oil contained 7.0 to 7.5% of sesquiterpenoid components, which were resolved into four peaks on polyester columns at 180° C.

INTRODUCTION

In the analysis of essential oils difficulties are encountered which are due to the presence not only of a fairly large number of components (up to 40) with a relatively wide boiling point range (about 150° to 250° C), but also of position and geometric isomers and of compounds which isomerize, autoxidize, polymerize, or dehydrate quite readily. Thus, it is not surprising that the analysis of such oils by gas–liquid chromatography (GLC) has not advanced as rapidly as, for example, that of fatty acid or hydrocarbon mixtures. The direct analysis of a number of essential oils has been attempted (1–8) and several of the difficulties encountered have been discussed (1–13). To overcome such difficulties, various prefractionation techniques have been applied. Naves *et al.* (5, 12) have combined fractional distillation, GLC, and infrared spectroscopy, and the problems relating to commercial practices have been eminently discussed (13, 14). Fractional distillation was also used by Cvrkal and Janák (15). Liberti and Cartoni (16), as well as Stahl and Trennheuser (11), combined GLC with silicic acid column or "thin-layer" chromatography. Removal of specific components by use of molecular sieves was described by Brenner *et al.* (17), whereas removal by chemical means (1, 18, 19) has been criticized (8). Most of these techniques require larger amounts of material than GLC and the danger of decomposition or rearrangement of one or more components is increased.

With the finding by the author of several liquid phases which give improved separations of both terpene hydrocarbons and some of their oxygenated derivatives (20), it was hoped that the direct and complete analysis of essential oils by GLC may become feasible. Identification of individual components could then be carried out conveniently by comparison of retention data and infrared spectra of the constituents of an oil with those of authentic specimens. The volatile oil of cedar leaves (*Thuja occidentalis* L.) was chosen as a test mixture because this oil is readily available commercially, its chemical composition is well known (21–24), and this conifer species was available locally for the preparation of small quantities of the fresh oil. Also, its composition appeared to be sufficiently complex to tax the present technique. Since free acids can cause ester interchange in polyester columns (25), only the neutral steam-volatile oil was investigated.

[1]*Manuscript received January 30, 1961.*
Contribution from the National Research Council of Canada, Prairie Regional Laboratory, Saskatoon, Saskatchewan.
Issued as N.R.C. No. 6277.

Wallach (21) identified the major constituents of cedar leaf oil as *d*-α-thujone and *l*-fenchone and also isolated *d*-α-pinene and *l*-borneol (free and as the acetate). Recently, Shaw (23, 24) has carried out a more complete analysis by fractional distillation and identified, in addition to the above compounds, *l*-α-thujene, *l*-camphene, *d*-sabinene, myrcene, limonene, *d*-isothujone, *l*-camphor, and *d*-terpinen-4-ol. Camphor was also found by Wallach, but he considered this to be an artifact (21, 22). Shaw also obtained a small amount of sesquiterpenoid material (24), but he was not able to resolve the mixture into pure compounds.

EXPERIMENTAL

A modified Beckman GC-2 chromatograph with a thermal conductivity cell as detector was used and the experimental techniques employed have been described in the preceding paper (20). The various 6 ft by $\frac{1}{4}$ in. O.D. columns employed, with the liquid phase and solid support (Chromosorb W) in the ratio of 1 to 6, have also been described. In preparative work a 3 ft by $\frac{1}{4}$ in. column with polyphenyl ether (*m*-bis(*m*-phenoxyphenoxy)-benzene) in the ratio of 1 to 4 was used either alone or placed ahead of the 6-ft analytical columns. Two samples of *Thuja* leaf oil were obtained, one was from a commercial source (Fritzsche Brothers, Inc.) and the other was prepared by steam distillation of the leaves and terminal branches (217 g) of a locally grown Eastern white cedar tree; yield (1.9 g) 0.88% based on the fresh weight of the leaves. The two oils had n_D^{23} 1.4562, 1.4630 and $[\alpha]_D^{23}$ −13.0°, −7.9° respectively. The reference compounds were either of commercial origin or prepared by conventional methods and, where necessary, these were purified in 0.02- to 0.1-g amounts by preparative GLC. The sample of thujone was a mixture of α-thujone and isothujone and was used as such.

In the preparative experiments the runs were carried out "blind", i.e. with the detector current off (26), and the desired fractions were isolated by timing as determined in trial runs, using the same sample size. Collection of these fractions was carried out with the Beckman fraction collector (No. 92730), the traps being cooled with a dry ice–ethanol mixture. The infrared spectra of pure fractions were obtained with a Perkin–Elmer Model 21 spectrophotometer, using both the film technique and dilute solutions in chloroform.

In the analytical GLC experiments, 3–5 μl aliquots of the leaf oil were injected. The percentage composition was then calculated by means of the area under the peaks. Before and after each run, standard samples were run to determine the retention times of reference compounds. The retention times obtained on a 6-ft rapeseed oil column at 110° C and a flow rate of 93 ml helium per minute are shown in Table I. For complete, or nearly complete, resolution of the terpene hydrocarbons 12-ft rapeseed oil, polyethylene glycol dioleate (PEGDO), and azelate polyester (AzDEG) columns were used. High-boiling components (sesquiterpenes) were detected on the adipate (APEG) polyester column at 180° C and azelate (AzDEG) polyester column at 160 to 180° C.

RESULTS AND DISCUSSIONS

Aliquots of the commercial cedar leaf oil were analyzed at 80° C and 110° C on all of the columns described in the previous paper (20). The best over-all resolution was obtained with the rapeseed oil column at 110° C (Fig. 1); 25 peaks were recorded. All of the chromatograms were compared visually and it was concluded that useful differences in the separation of these peaks were obtained with the polyethylene or diethylene glycol dioleate (PEGDO, DEGDO), hexanediol dioleate (HDDO), polyethylene glycol (PEG

Can. J. Chem. Downloaded from www.nrcresearchpress.com by 210.87.254.6 on 09/05/12
For personal use only.

TABLE 1

Composition of the volatile oil of the leaves of Eastern white cedar

Components		Calculated composition (%)		Composition reported by A. C. Shaw (24)	Retention time* (minutes)
Peak No.	Compound	Commercial oil	Saskatoon oil		
1	Unknown	0.1– 0.2	—	—	4.0
2	Unknown	0.1– 0.2	Trace	—	5.4
3	α-Thujene†	0.2– 0.3	0.2– 0.4	0.8	6.0
4	*d*-α-Pinene	1.2– 1.5	1.0– 1.3	2.6	6.5
5	α-Fenchene†	0.7– 0.8	0.7– 0.8	—	7.5
6	Camphene	1.1– 1.3	0.9– 1.1	2.0	7.8
7	*d*-Sabinene	1.7– 1.9	3.3– 3.5	3.5	9.0
8	β-Pinene†	0.5– 0.6	1.2– 1.5		9.5
9	Myrcene†	0.4– 0.6	0.2– 0.3	0.9 (1.3)	10.4
10	1,8-Cineole†	0.2– 0.4	0.1– 0.2	—	12.4
11	*d*-Limonene	0.8– 1.0	0.8– 1.2	3.6	14.0
12	*p*-Cymene	1.2– 1.6	0.4– 0.5	—	15.2
13	γ-Terpinene	0.2– 0.4	0.2– 0.4	—	16.7
14	Terpinolene†	0.1– 0.2	Trace	—	19.5
15	*l*-Fenchone	13.5–14.5	10.6–11.5	7.8	22.5
16	*d*-α-Thujone	59.0–61.5	53.0–55.0	47.5	26.5
17	Isothujone	9.0–10.0	8.8– 9.5	9.2	31
18	Unknown	0.3– 0.5	0.4– 0.5	—	33
19	*l*-Camphor	1.9– 2.3	2.8– 3.5	2.5	37.4
20	Unknown	0.3– 0.4	0.2– 0.3	—	40.5
21	Unknown	0.1	—	—	44
22	Terpinen-4-ol†	0.9– 1.5	0.9– 1.4	2.7	47.5
23	Unknown	0.2– 0.3	—	—	51.5
24	Bornyl acetate	2.0– 2.5	0.5– 0.9	5.9	55.5
25	Unknown	0.2– 0.4	—	—	60
26–28	Unknown	0.2– 0.3	0.5– 0.7	6.8	—
29–32	Sesquiterpenoid	0.8– 1.2	7.0– 7.3		—

*On a 6-ft rapeseed oil column at 110° C and a flow rate of 93 ml helium per minute.
†Tentatively identified.

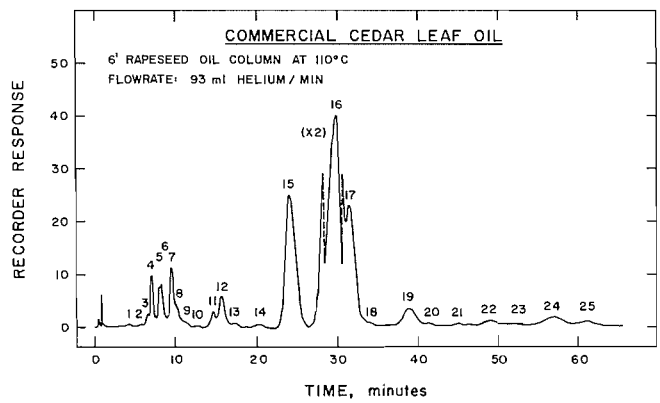


FIG. 1. Chromatogram of a commercial Eastern white cedar leaf oil on a 6-ft rapeseed oil column at 110° C.

1540), and diethylene glycol azelate polyester (AzDEG) columns, and these were used for the more detailed qualitative and quantitative analyses.

Whereas the oxygenated components (peaks 15 to 25 in Fig. 1) were separated readily on the 6-ft columns (at 110° C), the hydrocarbons (peaks 1 to 14) presented difficulties, a finding which is also apparent from the data of Zubyk and Conner (10). The resolution of components 3 and 4, 5 and 6, and 7, 8, and 9 was better at 80–90° C, but even then

Can. J. Chem. Downloaded from www.nrcresearchpress.com by 210.87.254.6 on 09/05/12
For personal use only.

tentative identification by comparison of retention times was difficult; e.g. whereas the retention time of component 4 corresponded to that of α-pinene on all columns, that of component 3 was the same as that of either tricyclene or α-thujene. The incomplete resolution of components 5 and 6 or 7 and 8 made the identification and isolation of these compounds also difficult. For this reason, the oils were also analyzed on 12-ft rapeseed oil, polyethylene glycol dioleate, and azelate polyester columns (at 100 to 110° C). Although this procedure resolved the monoterpene components satisfactorily (see Fig. 2) it was rather time consuming, since the higher-boiling compounds

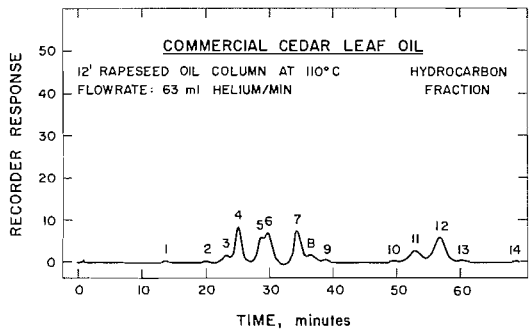


FIG. 2. Chromatogram of the monoterpene hydrocarbon fraction of the cedar leaf oil on a 12-ft rapeseed oil column at 110° C.

had to be eluted (or back-purged) before the next analysis could be carried out. Prefractionation into the monoterpenoid hydrocarbons (peaks 1 to 14), oxygenated monoterpenes (peaks 15 to 25), and higher-boiling components (if present) was thus desirable. This was carried out by preparative GLC on a 0.3- to 0.5-g scale (see below). To determine whether higher-boiling components were present, aliquots of the oils were analyzed on the polyester (APEG and AzDEG) columns at 180° C. The commercial oil showed only three trace components in the geraniol range and two minor components in the sesquiterpene alcohol range (26), but the oil from the local tree contained seven detectable compounds in this region, three of which were present in significant amounts.

Prefractionation was carried out on a 3-ft-long column at 110° C with polyphenyl ether and solid support in the ratio of 1 to 4. Individual peaks were not separated and skewing was very marked when 300- to 500-μl aliquots were used. However, components 1 to 13 or 14, 15 to 18 or 19, and 19 or 20 to 25 were obtained as distinct groups. The higher-boiling components were not recovered at this temperature. Experiments at 150 to 180° C allowed the recovery of the sesquiterpenoid compounds but several of the more labile monoterpenes decomposed to a considerable extent. When azelate or adipate polyester columns were used, decomposition was detected already at 130° C. Also, with all polyester columns trans esterification of the alcohols in the oil may take place (25). Therefore, prefractionation of 0.3- to 0.5-g aliquots was carried out with a polyphenyl ether column at 110° C. The fractions thus obtained were then separated into individual components on suitable analytical columns, when 5- to 20-mg amounts of components 3, 4, 5 and 6, 7, 8, 9, 11, 12, 15, 16, 17, 19, 22, and 24 were isolated. The amounts isolated allowed the determination of the infrared spectra and in some instances the sign of optical rotation. Comparison of the infrared spectra and retention times with those of authentic specimens led to the identification of components 4 (*d*-α-pinene), 6 (camphene),

Can. J. Chem. Downloaded from www.nrcresearchpress.com by 210.87.254.6 on 09/05/12
For personal use only.

Can. J. Chem. Downloaded from www.nrcresearchpress.com by 210.87.254.6 on 09/05/12
For personal use only.

7 (sabinene), 11 (*d*-limonene), 12 (*p*-cymene), 13 (γ-terpinene), 15 (*l*-fenchone), 16 (*l*-α-thujone), 17 (*d*-isothujone), 19 (camphor), and 24 (bornyl acetate). The separation of components 5 and 6 was incomplete and camphene failed to crystallize on seeding with the synthetic compound. The infrared spectrum of the mixture corresponded in all respects to that of camphene. Since component 5 is present in almost equal amount (see Fig. 2), it follows that its infrared spectrum must be very similar to that of camphene. This, together with the retention data, suggests that component 5 is α-fenchene. Components 3, 8, 9, 10, 14, and 22 were not obtained sufficiently pure to allow a positive identification, but the data agreed with those for α-thujene, β-pinene, myrcene, 1,8-cineole, terpinolene, and terpinen-4-ol respectively. The remaining components (peaks 1, 2, 18, 20, 21, 23, 25, 26 to 28, and the sesquiterpenes) could not be identified, mainly because suitable reference compounds were lacking.

The material having higher retention times than component 25 deserves some comment. Using the adipate polyester (APEG) column at 180° C and a flow rate of 60 ml helium per minute five minor components beyond peak 25 were recorded when 3 μl of the commercial oil was injected. The first three (peaks 26 to 28) amounted to less than 0.3% and had retention times (RT) of 6.2, 7.7, and 10.3 minutes respectively, which are in the geraniol range (RT 7.2 minutes). The other two peaks (RT 22.8 and 27.3 minutes) amounted to 0.4 to 0.6% each and were in the eudesmol range (RT 24.8 and 30.0 minutes). The fresh oil from the local tree showed not only a higher content of these higher-boiling components (7.5 to 8.0%), but had in addition two further components (RT 14.8 and 18.8 minutes). The amounts recorded for these seven components in order of their retention times were about 0.3, 0.1, 0.3, 1.1, 0.4, 1.7, and 4.0% respectively. The separation of these compounds on other columns which could be operated at 160 to 180° C was not as good (see also (26)). Sesquiterpene hydrocarbons, if present, would fall into the monoterpene alcohol range.

In the quantitative determinations, the main question was whether the detector response was the same for all compounds encountered. Zubyk and Conner (10) reported that when a thermal conductivity cell is used with helium as the carrier gas, the area under the peak is approximately proportional to the amount of the compound represented by that peak. Messner *et al.* (27) and Jamieson (28) have shown that the response varies with the molecular weight and branching of the molecule and proposed the use of correction factors to increase the accuracy of the calculated data. The determination of the amount of a compound present in a mixture by the various methods commonly employed (e.g. triangulation) may be subject to some errors in itself (29). For these reasons a mixture of representative terpenes was made up and the percentage composition was determined on all columns used by means of the triangulation method. The values obtained for the hydrocarbons were somewhat high and those for the less volatile oxygenated compounds correspondingly low. A source of this error was the amount of tailing, which was negligibly small for early peaks but increased for later peaks. When the area due to tailing was included in the calculations, the results (Table II) were within the limits of the error of this method, which is about 3 to 8% for the size of peak obtained (29). However, the values obtained for the hydrocarbons still tend to be high and those for the oxygenated compounds low. The use of correction factors would become very cumbersome since these would differ from column to column as well as for different types of compounds. Therefore, the quantitative composition of the essential oils under investigation was determined by calculation of the area under each peak (triangulation method) and including the amount due to tailing where this became

TABLE II

Composition of the synthetic mixture of terpenes as determined on a number of GLC columns

Compound	Weight (%)	% determined on different columns (at 110° C)				
		Rapeseed	PEG 1540*	AzDEG†	DEGDO‡	HDDO§
α-Pinene	6.7	7.2	7.4	6.85	7.2	7.5
β-Pinene	5.95	6.5	6.4	6.25	6.4	6.5
Limonene	9.1	10.35	10.1	10.5	11.0‖	10.5‖
1,8-Cineole	5.2	5.5	5.45	5.55	5.0‖	5.0‖
Fenchone	25.2	24.4	24.9	25.3	24.8	25.1
Thujone	28.5	15.2	15.6	15.3	15.8	15.6
Isothujone		11.9	12.0	11.2	11.4	11.4
Camphor	8.45	8.5	8.3	8.5	8.3	8.3
Bornyl acetate	10.8	10.4	9.85	10.5	9.8	10.1

*Polyethylene glycol (Carbowax 1540).
†Azelate polyester of diethylene glycol.
‡Diethylene glycol dioleate.
§1,6-Hexanediol dioleate.
‖Incomplete separation (approximate values only).

measurable. In Table I the range of the percentages calculated from the data obtained with five columns is shown for both the commercial and the local oils. Allowance was made for the presence of the sesquiterpenes when these were not eluted. This table also shows the composition of a cedar leaf oil analyzed by Shaw (24) by means of fractional distillation.

Comparison of the present data with that reported by Shaw shows that the analysis by GLC leads to more complete data and distinctly better separation of individual components. Since the difference in composition of the commercial oil and that isolated from a locally grown tree was only small, the smaller number of compounds identified by Shaw cannot be due to the source of material only. GLC analysis of the commercial oil at 180° C showed only five minor peaks after component 25 and amounting to about 1%. Thus, it is reasonable to assume that the analysis by GLC covers practically all of the volatile material. If one adds to this the very small amounts required (less than 5 ml in the present study), then the advantage over preceding techniques is considerable. However, the difficulties encountered in identifying 5- to 10-mg amounts of terpenes are a disadvantage, since at no time may agreement of retention times with known compounds be taken as a positive identification. Once the chemical composition of a particular oil has been established, the analysis of a similar oil is rapid and very convenient since only milligram amounts of the oil to be compared are required. In the present study, less than 50 mg of the oil from the locally grown tree was used. This fact should facilitate greatly studies of botanical variations, etc. and the method may become very useful in questions relating to plant physiology, morphology, and taxonomy.

Two observations which may affect the analysis by GLC must be pointed out. On some columns (e.g. with hexanediol dioleate as liquid phase) the retardation of components 17 to 25 due to the large amount of α-thujone (peak 16) in the oil was found to be outside of the error of measuring retention times. Raupp (30) reports similar findings due to preceding peaks. When the charts obtained with, for example, the 6-ft rapeseed oil column at 80° C and the 12-ft rapeseed oil column at 110° C were compared, the increase in separation obtained on the longer column was not very marked. However, the peak height resulting from the same amount of material was larger at the

Can. J. Chem. Downloaded from www.nrcresearchpress.com by 210.87.254.6 on 09/05/12
For personal use only.

higher temperature and thus the definition of the trace components was superior. Also, at the higher temperature somewhat larger samples could be used before a loss in the degree of separation became noticeable, making detection of trace components easier.

CONCLUSIONS

Using several columns with liquid phases having different separation properties, the volatile oil of cedar leaves was resolved into 30 to 32 components. Although comparison of retention data (obtained on columns having different polarities) facilitates the identification of individual components, such identifications should not be accepted without correlation with at least one other reliable technique. Isolation of individual components in more than milligram amounts is as yet difficult, unless the separation factor is relatively large. Prefractionation can overcome this difficulty only in part. Such small amounts of terpenes seldom allow chemical identification, and physical methods have to be relied upon. Positive identification may fail when two components are so closely related that differences in physical properties are too small to be detected.

The quantitative determination of individual components presents less difficulty, and the GLC technique becomes especially attractive when an oil of the same species is to be compared qualitatively and quantitatively with one from a different source.

ACKNOWLEDGMENTS

The author wishes to thank Mr. M. Granat for technical assistance and Miss I. M. Gaffney for recording the infrared spectra.

REFERENCES

1. E. BAYER, G. KUPFER, and K. H. REUTHER. Z. anal. Chem. **164**, 1 (1958).
2. M. L. DOMANGE and S. LONGUEVALL. Compt. rend. **247**, 209 (1958).
3. R. A. BERNHARD. Food Research, **23**, 213 (1958).
4. R. A. BERNHARD. J. Chromatog. **3**, 471 (1960).
5. Y. R. NAVES. Compt. rend. **246**, 1734 (1958).
6. Y. R. NAVES and A. ODERMATT. Compt. rend. **247**, 300, 687 (1958).
7. E. BAYER. Angew. Chem. **71**, 299 (1959).
8. W. MEYER ZU RECKENDORF. Z. anal. Chem. **175**, 350 (1960).
9. V. LUKEŠ, R. KOMERS, and V. HEROUT. J. Chromatog. **3**, 303 (1960).
10. W. J. ZUBYK and A. Z. CONNER. Anal. Chem. **32**, 912 (1960).
11. E. STAHL and L. TRENNHEUSER. Arch. Pharm. **293**, 826 (1960).
12. Y. R. NAVES, P. OCHSNER, and P. TULLEN. Helv. Chim. Acta, **43**, 1616, 1619 (1960).
13. Y. R. NAVES. Perfumery Essent. Oil Record, **49**, 290 (1958).
14. O. LAMPARSKY. Riechstoffe u. Aromen, No. 7/8, 1 (1959).
15. H. CVRKAL and J. JANÁK. Collection Czechoslov. Chem. Commun. **24**, 1967 (1959).
16. A. LIBERTI and G. P. CARTONI. *In* Gas chromatography. *Edited by* D. H. Desty. Butterworth Scientific Publications, London. 1958. p. 321.
17. N. BRENNER, E. CIEPLINSKI, L. S. ETTRE, and V. J. COATES. J. Chromatog. **3**, 230, 235 (1960).
18. R. BASSETTE and C. H. WHITNAH. Anal. Chem. **32**, 1098 (1960).
19. P. A. STADLER. Helv. Chim. Acta, **43**, 1601 (1960).
20. E. VON RUDLOFF. Can. J. Chem. In press.
21. O. WALLACH. Ann. **272**, 99 (1893); **275**, 182 (1893); **279**, 384 (1894).
22. E. GUENTHER. The essential oils. Vol. VI. D. Van Nostrand Co., Inc., New York. 1952. p. 328.
23. A. C. SHAW. Pulp Paper Mag. Can. **53** (4), 119 (1952).
24. A. C. SHAW. Can. J. Chem. **31**, 277 (1953).
25. R. G. ACKMAN, M. A. BANNERMAN, and F. A. VANDENHEUVEL. Anal. Chem. **32**, 1209 (1960).
26. E. VON RUDLOFF. Can. J. Chem. **38**, 631 (1960).
27. A. E. MESSNER, D. M. ROSIE, and P. A. ARGABRIGHT. Anal. Chem. **31**, 230 (1959).
28. G. R. JAMIESON. J. Chromatog. **3**, 464 (1960); **4**, 420 (1960).
29. J. JANÁK. J. Chromatog. **3**, 308 (1960).
30. G. RAUPP. Z. anal. Chem. **164**, 135 (1958).

Can. J. Chem. Downloaded from www.nrcresearchpress.com by 210.87.254.6 on 09/05/12
For personal use only.

Can. J. Chem. Downloaded from www.nrcresearchpress.com by 210.87.254.40 on 09/05/12
For personal use only.

SULPHONIUM SALT SOLVOLYSIS

PART I. EFFECT OF CONCENTRATION, ANION TYPE, AND SOLVENT VARIATION ON RATE OF REACTION[1]

J. B. HYNE

ABSTRACT

Previous work on the mechanism of sulphonium salt solvolysis is reviewed briefly. Rate data, determined by two independent methods, is presented for the solvolysis of dimethyl-*t*-butyl sulphonium iodide, bromide, and chloride in water and various ethanol–water mixtures. Rate dependence on the anion character and concentration of salt is shown to develop as the dielectric constant of the medium is lowered. The results are interpreted in terms of the increasing importance of an ion-pair mechanism as the composition of the medium is changed. The interpretation is substantiated by independent evidence for ion-pair formation.

INTRODUCTION

The solvolysis of sulphonium salts (R_3S^+, X^-) with the displacement of an electrically neutral thioether molecule (R_2S) represents a type of reaction where the formal charge of the initial state undergoes delocalization in the formation of the transition state. Such a delocalization phenomenon will be operative in solvolytic mechanisms of both the S_N1 and S_N2 type although to a different degree in each case.

S_N1 type:

$$R_3C{-}\overset{+}{S}R_2 \longrightarrow \left[R_3C^{d+}\cdots\cdots SR_2^{d+} \right] \longrightarrow \underset{\text{Solvolysis}}{\swarrow} R_3C^+ \underset{\text{Elimination}}{\searrow} + R_2S,$$

S_N2 type:

$$B^- + R_3C{-}\overset{+}{S}R_2 \longrightarrow \underset{\text{Transition state}}{\left[B^{d-}\longrightarrow R_3C^{d+}\cdots\cdots SR_2^{d+} \right]} \longrightarrow B{-}CR_3 + R_2S.$$

The effect of lowering the dielectric constant of the solvolytic medium on such a mechanism has been shown by various workers (1, 2, 3) to be an increase in the rate of solvolysis. This is as would be predicted on the basis of increased stability of the charge-dispersed transition state over the formally charged initial state as the dielectric constant is lowered. The behavior is the converse of that normally observed in the more fully studied solvolysis of alkyl halides and benzenesulphonates where charge is created on passing from the initial dipolar to the ion-like transition state.

One of the most thoroughly studied cases of sulphonium salt solvolysis has been that of dimethyl-*t*-butyl sulphonium chloride. In this particular system it is now generally accepted that the mode of solvolysis in media of high dielectric constant (e.g. water) is the S_N1 type mechanism (3, 4, 5, 6). Such a mechanism is reasonable in the case of the dimethyl-*t*-butyl sulphonium ion in water in view of the high solvating power of water and the stability of the intermediate *t*-butyl carbonium ion. It has also been shown (6) that the sulphur isotope effect in this solvolysis is considerable, an observation in keeping with the large distortion of the C—S bond in the S_N1 transition state. In cases such as tribenzyl (7) and trimethyl (7, 8) sulphonium halides, however, the stability of the

[1]*Manuscript received January 13, 1961.*
Contribution from the Department of Chemistry, University of Alberta in Calgary, Calgary, Alberta. Work done partly at Yale University.

incipient carbonium ion is reduced to the point where it is questionable whether an S_N1 mechanism could be operative even in high dielectric media such as pure water. This is especially true in the trimethyl sulphonium salt. Recent work on the ethanolysis of trimethyl sulphonium salts (8) has shown that the anion is intimately involved in the rate-determining step and that the S_N1 type mechanism is extremely improbable as might be expected from a combination of the instability of the methyl carbonium ion and the low dielectric constant of the ethanolic medium.

Although the solvolysis of dimethyl-*t*-butyl sulphonium halides in water proceeds by a predominantly S_N1 mechanism the question immediately arises as to whether this mode of reaction persists as the dielectric constant of the medium is lowered and the stability of the carbonium ion decreases. Swain and Kaiser (7) have suggested several other possible mechanisms including the participation of ion-pairs in the rate-determining step at lower dielectric constant. In order to check the possibility of such ion pairing these authors carried out conductimetric measurements on sulphonium salts in 90% acetone–water solution ($D = 25$) and concluded that the agreement between the measured equivalent conductances and those calculated by the Onsager equation for strong electrolytes was sufficiently close to preclude the presence of a significant degree of ion pairing. Jacobson and Hyne (9) have repeated the conductance study for trimethyl sulphonium iodide in various ethanol–water mixtures using the modified Fuoss method of analysis (10) to determine the degree of ion pairing involved. These latter workers found that, below a dielectric constant of 30, ion pairing in such a system *was* sufficiently significant to be observable as a kinetic effect if the ion pairs participated in a rate-determining step. The purpose of the work reported in this paper and subsequent papers of the series was to investigate the possibility of other mechanisms of solvolysis replacing the S_N1 type as the predominant mode of reaction as the dielectric constant of the solvolytic medium is reduced.

CONDUCTIMETRIC KINETIC MEASUREMENTS

Since the solvolysis of dimethyl-*t*-butyl sulphonium halides involves the replacement of the bulky sulphonium ion by a proton, the rate of reaction can be followed conductimetrically under pseudo first-order conditions with the solvent present in great excess.

$$X^- + (CH_3)_2S^+{-}C(CH_3)_3 + ROH \rightarrow \underset{\text{or olefine}}{(CH_3)_2S} + (CH_3)_3COR + HX \qquad (R = H, \text{ or alkyl})$$

Conductance measurements were made in the usual manner using a precision a-c. conductance bridge (11) and the data analyzed to obtain rate constants by the method of Guggenheim (12). Rate constants were reproducible to better than ±0.5%. Table I

TABLE I

Rates of solvolysis of 0.001 *M* dimethyl-*t*-butyl sulphonium salts in various ethanol–water mixtures at 78.4° C (conductimetric method)

Mole fraction ethanol	$k \times 10^4$, sec^{-1}		
	I^-	Br^-	Cl^-
0.000	3.55	3.52	3.54
0.125			4.02
0.236	4.52		
0.415			5.35
0.552	5.81	5.77	5.76
0.730	6.85		6.15
0.855	7.73	6.68	6.08

Can. J. Chem. Downloaded from www.nrcresearchpress.com by 210.87.254.40 on 09/05/12
For personal use only.

contains rate constants measured at several mole fractions of ethanol in water at 78.4° C for dimethyl-*t*-butyl sulphonium iodide, bromide, and chloride. These data are plotted in Fig. 1(*a*). As the dielectric constant of the solvolytic medium decreases, however,

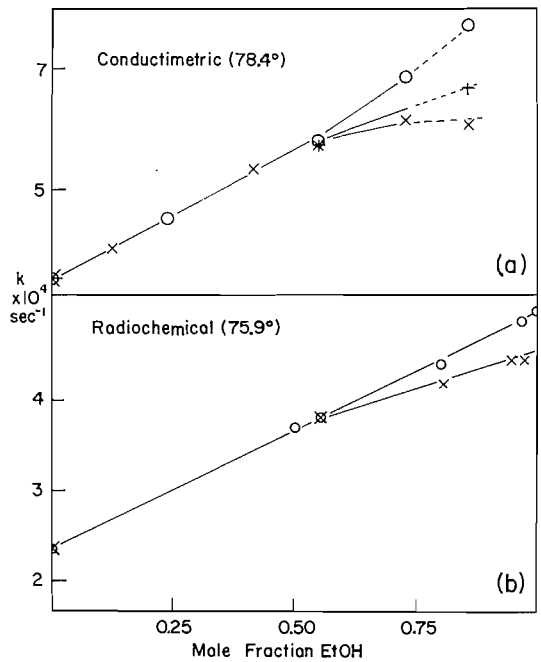


FIG. 1. Rate of solvolysis of 0.001 *M* dimethyl-*t*-butyl sulphonium salts in ethanol–water mixtures; O iodide, + bromide, × chloride.

the hydrohalic acid no longer behaves as a strong electrolyte. This condition is necessary for the valid application of the Guggenheim type of analysis since this method depends upon the assumption that the conductance is a linear function of the concentration. Furthermore at high ethanol compositions the conductance was found to *decrease* as the reaction proceeded, this being shown to be due to the reaction of HX with the alcohol. It is therefore clear that beyond a mole fraction of 0.75 ethanol the conductimetric method is not dependable. Such a back reaction of HX with the alcohol will also introduce errors in rate determinations involving titration of the hydrohalic acid released in the reaction. From Fig. 1(*a*), however, it is clear that it is particularly in this high ethanol composition region that the role of the anion becomes apparent in the rate-determining process.

RADIOCHEMICAL KINETIC MEASUREMENTS

In order to investigate the kinetic behavior of the various dimethyl-*t*-butyl sulphonium salts in the highly ethanolic range of solvent composition the continuous-flow-counting radiochemical technique of Hyne and Wolfgang was applied (13). This method has the advantage of the precision characteristics of the conductimetric technique, but does not suffer from breakdown in low dielectric media. The method depends essentially upon a continuous sampling of C^{14}-labelled dimethyl sulphide as it is produced and swept from the reaction mixture by a stream of inert gas. Labelled materials were prepared as described previously (13). Due to the fact that this method involves an open

Can. J. Chem. Downloaded from www.nrcresearchpress.com by 210.87.254.40 on 09/05/12
For personal use only.

reaction system it was not possible to work at 78.4° C as in the conductimetric case due to the proximity of the boiling point of ethanol. It is not necessary, however, to compare (at the same temperature) rate values determined conductimetrically with those determined radiochemically but rather to observe the effect of solvent change on the rates of solvolysis of different salts. Consequently the whole range of solvent compositions was scanned again at a lower temperature using the radiochemical method. In this work, only the chloride and the iodide salts were used. The rates so measured are shown in Table II and plotted in Fig. 1(*b*). It should be noted that the radiochemical

TABLE II

Rates of solvolysis of 0.001 *M* dimethyl-*t*-butyl sulphonium salts in various ethanol–water mixtures at 75.9° C (radiochemical method)

Mole fraction ethanol	$k \times 10^4$, sec^{-1}	
	I^-	Cl^-
0.000	2.52	2.53
0.501	3.70	
0.555	3.81	3.82
0.800	4.40	4.20
0.944		4.48
0.970	4.88	4.47
1.000	4.99	

method measures the rate of solvolysis of only the C^{14}-labelled salt.* Consequently if an isotope effect is present the radiochemical and conductimetric methods should not give precisely the same rate even under identical conditions. As was shown previously (13) there is no detectable isotope effect in the hydrolysis (pure water medium) as might be expected due to the fact that at best the effect would be secondary. This does not ensure, however, that the isotope effect might not become important if the mechanism were to change. As stated above, however, the phenomenon under study is the influence of the solvent medium on the rate of reaction, and provided that the labelled salt is used throughout the range of solvents investigated the kinetic data will be internally consistent.

DISCUSSION OF RESULTS

Effect of Anion Type

It is clear from the plots in Fig. 1 that within the solvent range 0.0 to 0.6 mole fraction ethanol any specific effect due to the anion type in the sulphonium salt is not of sufficient magnitude to be detected kinetically. At mole fractions of ethanol greater than 0.6, however, the differences in rates of solvolysis of the various salts become increasingly significant both in conductimetric and radiochemical methods of measurement. It should be noted that it was at approximately the same mole fraction of ethanol that ion pairing was found to become significant (i.e. $>2\%$) in the conductance measurements of Jacobson and Hyne (9).

Effect of Concentration of Salt

In Table III the rates of solvolysis of dimethyl-*t*-butyl sulphonium chloride in water

*This point was brought to the notice of the author by Dr. J. A. Llewellyn after the publication of reference 13.

Can. J. Chem. Downloaded from www.nrcresearchpress.com by 210.87.254.40 on 09/05/12
For personal use only.

TABLE III

Effect of concentration on rates of solvolysis of dimethyl-*t*-butyl sulphonium chloride in various media

		$k \times 10^4$, sec^{-1}		
t, °C	Concn. salt, *M*	H_2O	0.55 mole fraction EtOH	Reference
78.4	0.05	3.52	7.11	1, 2*
78.4	0.001	3.53	5.75	This work
50.4	0.05	0.064	0.131	1, 2*
50.4	0.006–0.013	0.065	0.115	3
50.4	0.001	0.063	0.105	This work†

*These rates interpolated from data at other temperatures.
†Additional rate measurement for comparison purposes.

and 0.55 mole fraction ethanol as reported by various workers are shown. The point of major interest in this data is the effect of change of initial concentration of the salt on the observed rate. At both 78.4° and 50.5° variation in concentration of salt has no measurable effect on the rate of solvolysis in water. In 0.55 mole fraction ethanol, however, the observed rates are significantly different at the three concentrations of the sulphonium chloride used and are higher for higher salt concentrations.

Interpretation of Observed Effects

All the evidence presented in this paper suggests the increasing participation of ion pairing in the rate-determining process as the dielectric constant of the solvolytic medium is reduced. The facts may be summarized as follows.

(*a*) The rate of solvolysis shows an increasing dependence upon the nature of the anion as the solvent dielectric is reduced.

(*b*) The value of the dielectric constant at which the rate begins to show a detectable dependence on the nature of the anion is approximately equal to that at which the degree of ion pairing in sulphonium salts has been shown to become significant.

(*c*) For a given anion the rate of solvolysis shows a dependence on the total initial concentration of salt in low-dielectric media but not in high-dielectric media.

These observations can be explained by the following mechanism.

$$\begin{array}{ccc} R_3S^+ + X^- & \overset{K_A}{\rightleftharpoons} & R_3S^+X^- \\ \downarrow k_+ & & \downarrow k_{ip} \end{array}$$

The sulphonium salt can solvolyze either from an initial free ion state (k_+) or from an initial ion pair state (k_{ip}). When the solvolysis proceeds predominantly from the ion the rate should be virtually independent of the nature of X^- since this species is not involved in the rate-determining transition state. This is as observed in water where K_A (ion association constant) has been shown to be very small (9). As the dielectric constant of the medium is reduced, however, K_A increases and the concentration of ion pairs becomes a significant fraction of the total. An increasing proportion of the reaction can therefore proceed via the ion-pair pathway. The conductance studies of ion pairing of trimethyl sulphonium iodide in ethanol–water mixtures (9) shows less

Can. J. Chem. Downloaded from www.nrcresearchpress.com by 210.87.254.40 on 09/05/12
For personal use only.

than 2% ion pairs in 10^{-3} M salt below mole fraction 0.55 ethanol, but this figure increases rapidly beyond 0.55 mole fraction ethanol to a value in excess of 10% at 0.95 mole fraction ethanol. It is in such solutions containing greater than 0.55 mole fraction ethanol that rate dependence on anion character is observed.

Although at 10^{-3} M and 0.55 mole fraction ethanol the degree of ion pairing is not sufficient to be kinetically measurable by varying the character of the anion (Fig. 1) higher total concentrations of a given anion will force the equilibrium to the right and the degree of ion pairing will be higher at higher salt concentrations. A greater proportion of the solvolysis will therefore proceed through the ion-pair mechanism. The data of Table III not only substantiate this reasoning by virtue of the variation of rate with concentration but show that the rate of solvolysis from the ion pair must be greater than that from the ion ($k_{ip} > k_+$) since the over-all rate increases with increasing concentration of ion pairs in the system. This relative order of rates is in keeping with the fact that the difference in charge character between the ion pair and the charge-dispersed transition state is less than that between the free ion and the charge-dispersed transition state. Consequently attainment of the transition state from the ion pair will be energetically favored and hence the rate by that path will be greater.

It is seen from Fig. 1 that at a given concentration, temperature, and solvent composition the order of rates of solvolysis, when differences are detectable, is $I^- > Br^- > Cl^-$. This phenomenon could be due to one or both of the following factors. If the order of magnitude of the association constants was $K_A(I^-) > K_A(Br^-) > K_A(Cl^-)$ then under a fixed set of conditions the proportion of the solvolysis proceeding through the ion-pair intermediate would be greatest in the case of the iodide and least in the chloride salt. Since $k_{ip} > k_+$ the observed order of rates would be as found. Assuming the relationship between association constant (K_A) and center-to-center distance (a) in the ion pair (14, 15), $\ln K_A = e^2/aDkT + \text{const.}$, K_A should decrease as the center-to-center distance increases. Presumably as the ionic radius of the anion increases the center-to-center distance in the pair with a fixed cation should also increase. Consequently K_A should *decrease* as the anion is changed from Cl^- through Br^- to I^-. Such an argument would suggest rejection of the explanation of the observed order of rates based on variation of K_A with anion type. However, very few tests have been made of the validity of the relationship where the anion has been varied through a series such as the halides. On the other hand, experimental determination of the degree of association of lithium halides in acetic acid (16) has revealed an order of K_A's LiI > LiBr > LiCl. Similarly the order of association constants for the reaction $Pb^{++} + X^- \rightleftharpoons PbX^+$ in water has been shown to be $I^- > Br^- > Cl^-$ (17). The second possible explanation lies in variation of k_{ip} with the nature of the anion in the ion pair. It would be very surprising if k_{ip} did not vary in such a manner but it is again difficult to predict the direction of the variation without a detailed knowledge of the mechanism of solvolysis of the ion pair. It is noteworthy, however, that the order of rates is that of the order of nucleophilicity of the anions, suggesting a nucleophilic role for these species in the solvolytic mechanism.

CONCLUSIONS

The role of a rate-determining step involving participation of the anion in the solvolysis of dimethyl-*t*-butyl sulphonium salts has been shown to become significant as the dielectric constant of the medium is reduced. Experimental evidence points to the participation being of the ion-pair type but a more thorough analysis of the details of the ion-pair mechanism is required.

Can. J. Chem. Downloaded from www.nrcresearchpress.com by 210.87.254.40 on 09/05/12
For personal use only.

ACKNOWLEDGMENTS

The technical assistance of Mr. David E. Pleasure in part of this work and financial support from Research Corporation is gratefully acknowledged.

REFERENCES

1. K. A. Cooper, E. D. Hughes, C. K. Ingold, and B. J. MacNulty. J. Chem. Soc. 2038 (1948).
2. K. A. Cooper, M. L. Dhar, E. D. Hughes, C. K. Ingold, B. J. MacNulty, and L. I. Woolf. J. Chem. Soc. 2843 (1948).
3. C. G. Swain, L. E. Kaiser, and T. E. C. Knee. J. Am. Chem. Soc. **80**, 4092 (1958).
4. E. D. Hughes and C. K. Ingold. J. Chem. Soc. 1571 (1933).
5. E. D. Hughes, C. K. Ingold, G. A. Maw, and B. J. MacNulty. J. Chem. Soc. 2049 (1948).
6. W. H. Saunders, Jr. and S. Asperger. J. Am. Chem. Soc. **79**, 1612 (1957).
7. C. G. Swain and L. E. Kaiser. J. Am. Chem. Soc. **80**, 4089 (1958).
8. E. D. Hughes, C. K. Ingold, and Y. Pocker. Chem. & Ind. (London), 1282 (1959).
9. A. L. Jacobson and J. B. Hyne. J. Am. Chem. Soc. **82**, 2418 (1960).
10. R. M. Fuoss. J. Am. Chem. Soc. **81**, 2659 (1959).
11. R. E. Robertson. Can. J. Chem. **33**, 1536 (1955).
12. E. A. Guggenheim. Phil. Mag. **2**, 538 (1926).
13. J. B. Hyne and R. Wolfgang. J. Phys. Chem. **64**, 699 (1960).
14. J. D. Denison and J. B. Ramsey. J. Am. Chem. Soc. **77**, 2615 (1955).
15. R. M. Fuoss. J. Am. Chem. Soc. **80**, 5059 (1958).
16. J. Kenttamma. Suomen Kemistilehti, B, **32**, 9 (1959).
17. A. I. Biggs, M. H. Panckhurst, and H. N. Parton. Trans. Faraday Soc. **51**, 802, 806 (1955).

Can. J. Chem. Downloaded from www.nrcresearchpress.com by 210.87.254.40 on 09/05/12
For personal use only.

Can. J. Chem. Downloaded from www.nrcresearchpress.com by 210.87.254.105 on 09/05/12
For personal use only.

AN INFRARED STUDY OF TRIMETHYLAMINE OXIDE, ITS HYDRATE, AND ITS HYDROCHLORIDE[1]

PAUL A. GIGUÈRE AND DAVID CHIN

ABSTRACT

The infrared spectra of trimethylamine oxide, its hydrate, and its hydrochloride in the solid state were measured over the range 300 to 3500 cm^{-1} to ascertain the nature of the bonds in these compounds. From the observed stretching frequencies, 937 cm^{-1} for N—O and 945 cm^{-1} for C—N, the corresponding bond lengths are calculated to be 1.44 and 1.50 Å in agreement with X-ray and electron diffraction data. Both these frequencies remain unchanged in the hydrate and the hydrochloride as could be expected for molecular compounds. However, in the hydrochloride most of the evidence points to an ionic constitution. In both the hydrate and the hydrochloride the hydrogen bonds are particularly strong presumably because of the formal charges.

INTRODUCTION

Trimethylamine oxide $(CH_3)_3NO$ offers the classical example of the so-called "co-ordinate link," an essentially covalent bond between two atoms with opposite formal charges. It was first pointed out by Pauling (1) that the distance between the atoms thus bonded, viz. N^+ and O^-, should not be affected appreciably by the electrical charges. Due to absence of other complicating factors, such as resonance among different valence bond structures, trimethylamine oxide is a suitable molecule to test this hypothesis. A first determination by electron diffraction (2) gave a N—O bond length of 1.36 Å, exactly the sum of the then accepted values (1) for the single-bond covalent radii of the N and O atoms. However, this result now appears inconclusive because, (*a*) the radial distribution method cannot resolve the very close C—N and N—O peaks and, (*b*) in the various models used for the visual comparison method, the N—O bond length was varied only between 1.30 and 1.40 Å since there is no obvious reason why this bond should be much longer than the sum of the covalent radii. In the meantime the latter parameters were found to require a sizable upward revision—to 0.74 Å for both atoms (3). This prompted a reinvestigation of the electron diffraction pattern of trimethylamine oxide (4). Preliminary results (5) indicated a longer N—O bond (1.44 Å) than the original one, and a C—N bond length (1.49 Å) just a little over the sum of the (revised) covalent radii. These two values have been confirmed by a recent X-ray study of the crystalline hydrochloride (6), which gives 1.424 Å for the N—O bond and 1.50 Å for the average of the C—N bond lengths.

The first spectroscopic investigations of trimethylamine oxide were done in Raman effect. Edsall (7) studied the hydrochloride in aqueous hydrochloric acid solution; from the marked resemblance with the spectrum of tertiary-butyl alcohol he concluded to the existence of a trimethylhydroxyl ammonium ion $[(CH_3)_3NOH]^+$. Later Goubeau and Fromme (8) measured the spectra of the oxide dissolved in methanol (Table I). Also by comparison with the spectra of tertiary-butyl alcohol they assigned the band at 947 cm^{-1} to the N—O stretching frequency and estimated the corresponding force constant to lie between 4 and 5×10^5 dynes cm^{-1}. An exploratory infrared study of the crystalline solid carried out in this laboratory (9) revealed some 10 bands between 700 and 3000 cm^{-1}; there also, a band at 943 cm^{-1}, one of the strongest, was assigned to

[1]*Manuscript received January 23, 1961.*
Contribution from the Department of Chemistry, Laval University, Quebec, Que.

TABLE I
Raman spectra of trimethylamine oxide and its hydrochloride

$(CH_3)_3NO$ (8)		$(CH_3)_3NO.HCl$ (7)	
Frequencies (in cm^{-1})	Relative intensities	Frequencies (in cm^{-1})	Relative intensities
244	0		
304	1/2	382	3
413	1		
439	1		
494	1	500	2
705	1		
759	5	754	7
947	4	947	7
984	0		
1029	0		
1135	1	1132	2
1281	1	1263	2
		1412	2
1453	3	1449	7
1593	0		
		1658	1 (water)
		2104	1
		2186	1
		2426	0
		2597	2
		2674	1/2
		2811	3
		2886	3
2960	3	2974	10
3031	4	3043	10

the N—O bond. While this work was in progress we came across two other communications on the same subject (10, 11) both relating in fact to the hydrate, as we shall see below.

EXPERIMENTAL

The sample of trimethylamine oxide was prepared by oxidation of a 25% aqueous solution of trimethylamine with 5% hydrogen peroxide (12). Repeated crystallizations in methanol gave needle crystals of the dihydrate, from which the anhydrous oxide was obtained by gentle heating under reduced pressure (13). The powder, resublimed twice, was placed in an evacuable absorption cell fitted with rock salt windows. By means of an electric heating tape a thin film of the solid was deposited on the windows. After recording of the spectra, air was admitted in the absorption cell, whereupon the film became hydrated fairly quickly. However, if the film was too thick, complete hydration was very slow. Upon hydration the white, powdery film became transparent. For comparison the spectra of dihydrate crystals were also obtained by the KBr pellet technique.

The same method was used for the hydrochloride, prepared by addition of hydrochloric acid to an aqueous solution of trimethylamine oxide. The crystals, purified by recrystallization, melted at 217–218° C with some decomposition. Two spectrometers were used: a Perkin–Elmer, Model 112, with NaCl and CsBr optics, and a Beckman, Model IR-4. Numerous attempts to secure the spectrum of the amine oxide in the vapor state were unsuccessful. A short (10 cm) glass absorption cell and a long-path (1 m) metal cell were tried in succession. Because of the low volatility of the oxide the sample had to be heated to about 180° C to produce measurable absorption. However, at that temperature the vapor decomposed rapidly and reacted with the salt windows.

Can. J. Chem. Downloaded from www.nrcresearchpress.com by 210.87.254.105 on 09/05/12
For personal use only.

DISCUSSION

In interpreting the spectra of trimethylamine oxide (Fig. 1) it is convenient to consider

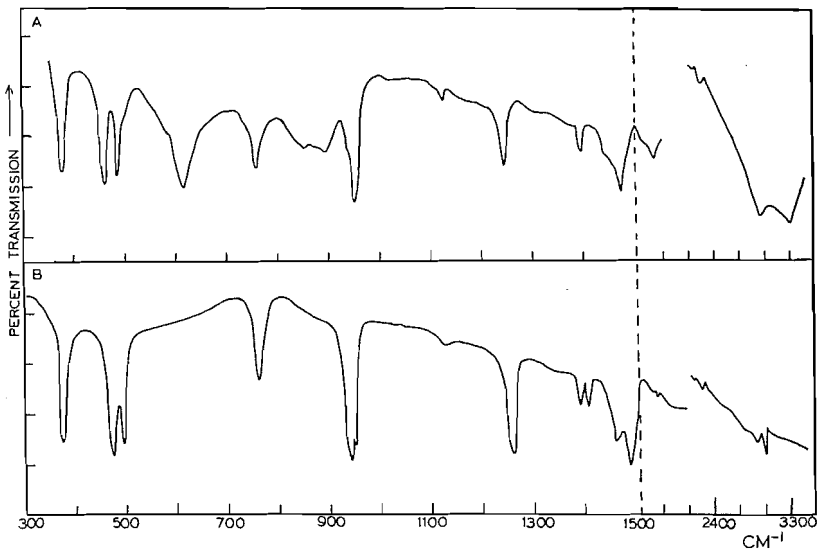


FIG. 1. Infrared spectra of the hydrated (A) and anhydrous (B) trimethylamine oxide.

the CH_3 groups as single atoms R of mass 15. The resulting XY_3Z type of molecule is of C_{3v} symmetry, with six fundamental frequencies all active in infrared and Raman. For further simplification frequencies above 1200 cm^{-1} (Table II) may be ignored here as they arise either from combination tones or from vibrations in the CH_3 groups. The latter are already well known from analysis of the spectra of trimethylamine (14, 15) and similar molecules. Assignment of the various fundamentals of the R_3NO molecule is best made by correlation with those of the isoelectronic tetramethyl ammonium ion R_4N^+ (15). As shown in Table III the two symmetrical vibrations ν_1 and ν_2 of that ion have practically the same frequencies in the oxide, ν_2 and ν_6. On the other hand the two triply degenerate vibrations ν_3 and ν_4 of RN_4^+ are split in the oxide molecule into one non-degenerate and one doubly degenerate vibration: viz. ν_3 at 955 cm^{-1} splits into a doublet at 937 cm^{-1} and 945 cm^{-1}, and ν_4 at 455 cm^{-1}, into a pair at 490 and 472 cm^{-1}.

Present assignment of the infrared frequency at 937 cm^{-1} (missing from the spectra of trimethylamine) to the N—O stretching mode follows that of the strong Raman shift at 947 cm^{-1} (8). Apparently it was not feasible in the latter spectra to separate the two very close stretching frequencies ν_1 and ν_4. Even in this work the doublet could be clearly resolved only in fairly thick samples and with the maximum resolving power available. Gallais and his co-workers (10) have reported a strong band at 1060 cm^{-1} which they assigned to ν_4. No significant absorption could be detected at that frequency in repeated recordings of our spectra of both the oxide and the hydrate (Table II); none was found either in an independent investigation of the latter compound (11). Since no experimental details were given by the French authors on preparation and purity of their samples it is not possible to account for that result. At any rate it is quite certain from the near identity of their reported spectra for trimethylamine oxide and its hydrate

Can. J. Chem. Downloaded from www.nrcresearchpress.com by 210.87.254.105 on 09/05/12
For personal use only.

Can. J. Chem. Downloaded from www.nrcresearchpress.com by 210.87.254.105 on 09/05/12
For personal use only.

TABLE II

Infrared spectra of trimethylamine oxide, its hydrate, and its hydrochloride

$(CH_3)_3NO$	$(CH_3)_3NO.2H_2O$		$(CH_3)_3NO.HCl$
This work	This work	Gallais (10)	This work
378 vs	381 vs		
472 vs	475 vs		
490 vs	490 vs		
	620 vs		620 w
757 s	757 s	756 vw	758 vs
765 sh	767 sh	773 vw	
		795 vw	
	852 m		
	893 m		
937 vs	937 s		939 s
945 s	950 vs	950 s	950 vs
		1020 s	
		1060 w	
1135 w	1125 m	1120 m	1122 m
		1170 w	
1256 vs	1244 s	1244 s	1255 s
		1265 w	
		1320 vw	
		1342 w	
1390 m	1395 m		1395 m
1405 m			
	1440 sh		1432 w
1458 s	1456 vw	1466 s	1453 vw
1488 s	1475 s		1468 m
			1530vs
	1620 w		
1668 w	1662 sh		
	1690 s		
1868 w	1868 w		
2175 w	2192 w		
2285 w	2275 w		
			2460 sh
			2615 vs
			2670 vs
			2790 s
2940 m	2975 m		2930 m
3012			3030 w
	3180 w		
	3330 s		
	4100 w		

TABLE III

Fundamental frequencies of the R_4N^+ ion and the R_3NO molecule

$(CH_3)_4N^+$				$(CH_3)_3NO$			
ν_1	(a_1)	752 cm^{-1}	→	ν_2	(a_1)	757 cm^{-1}	∥ sym. C—N stretch. non-deg.
ν_2	(e)	372 cm^{-1}	→	ν_6	(e)	378 cm^{-1}	⊥ asym. $\widehat{CNC}$ bend. doubly deg.
ν_3	(f_2)	955 cm^{-1}	→	ν_1	(a_1)	937 cm^{-1}	∥ sym. N—O stretch. non-deg.
			↘	ν_4	(e)	945 cm^{-1}	⊥ asym. C—N stretch. doubly deg.
ν_4	(f_2)	455 cm^{-1}	→	ν_3	(a_1)	490 cm^{-1}	∥ sym. $\widehat{ONC}$ bend. non-deg.
			↘	ν_5	(e)	472 cm^{-1}	⊥ asym. $\widehat{OCN}$ bend. doubly deg.

that they were actually working with the same compound, namely the latter, in both cases. Indeed, the partial pressure of water vapor over the hydrate is less than 2.5 mm Hg at room temperature (16) so that unless special precautions are taken, as described above, atmospheric humidity almost always will be sufficient to hydrate completely the very hygroscopic amine oxide.

An attempt was made to calculate from the above frequencies the two bond force constants f_{N-O} and f_{C-N}. Equations of a valence force systems for a tetrahedral XY_3Z molecule (17) were used assuming force constants for bending modes to be one-tenth of those for stretching modes. Unique values could not be obtained, but only the following estimates.

	f ($\times 10^{-5}$ dyne cm^{-1})	r (Å)
N—O	3.8 to 4.8	1.44±0.03
C—N	3.1 to 3.4	1.51±0.01

The bond lengths are from application of Badger's rule. These values agree exactly with the results of the more recent electron diffraction (5) and X-ray diffraction measurements (6). From comparison with other molecules such as NH_2OH, HNO_2, etc. (5) it is obvious that the N—O "co-ordinate link" in trimethylamine oxide has roughly the same length as a "normal" N—O single bond as predicted by Pauling. The relationship suggested by Schomaker and Stevenson (18) also yields a N—O bond length (1.435 Å) very close to the present result; for the C—N bond, however, it gives a slightly shorter distance (1.465 Å) than the experimental value, although the difference is still within the limits of uncertainty of the latter. On the contrary Pauling had predicted for that bond an appreciable shortening (about 0.03 or 0.04 Å) from the normal single-bond length.

The spectrum of the hydrate, or more correctly the dihydrate, is shown in Fig. 1A and the principal frequencies are listed in Table II. Essentially identical spectra were obtained with the two kinds of samples used, viz. thin hydrated films and KBr pellets. Since, in addition, they agreed closely with the results of an independent investigation over the NaCl range (11) there is little doubt about the identity of the compound studied. As may be gathered by comparison, the spectrum of the dihydrate bears strong resemblance to that of the anhydrous oxide; particularly the N—O stretching band which retains the same frequency, 937 cm^{-1}. (The reversed intensity ratio with the C—N band at 950 cm^{-1} may be due to hydrogen bonding.) From this it is safe to infer the molecular nature of the dihydrate crystal. Indeed, the trimethylhydroxide ammonium ion $[(CH_3)_3NOH]^+$ suggested before (7, 10) would normally have a somewhat different N—O stretching frequency from the above. Furthermore, one would expect for that ion an OH bending frequency and a low-lying OH wagging frequency not found in our spectra. The O—H stretching mode cannot, obviously, yield any conclusive evidence, being indistinguishable from that in H_2O. Lüttke found a slightly lower value (3236 cm^{-1}) than that reported here, but the nearness of the C—H stretching frequencies makes these figures rather uncertain.

On the other hand all the new features in the spectra of the dihydrate may be accounted for satisfactorily in terms of vibrations of the H_2O molecules. Besides a strong O—H band at 3 μ, of which there is no trace in the anhydrous oxide, the broad, rather weak band centering around 1690 cm^{-1} must belong to ν_2, the bending mode. This frequency

Can. J. Chem. Downloaded from www.nrcresearchpress.com by 210.87.254.105 on 09/05/12
For personal use only.

is appreciably higher than in pure water, 1650 cm^{-1} (19), which may be due to loss of symmetry of that mode because of unequal hydrogen bonds. In all probability one of the H atoms of each water molecule is hydrogen bonded to the O atom of trimethylamine oxide; now it is conceivable that the negative formal charge on the latter atom enhances its attraction for the proton, hence a strengthening of hydrogen bonds. The same explanation holds for the three separate broad bands at 893, 852, and 620 cm^{-1} attributable to the three libration modes of H_2O molecules. In pure water these appear to merge into a single broad band with center at about 710 cm^{-1} in the liquid and at 800–850 cm^{-1} in ice (19). Formation of especially strong hydrogen bonds between the two kinds of molecules may be linked with the great stability of the dihydrate as mentioned above. Finally, it is worth recalling here that the low electrical conductivity of aqueous solutions of trimethylamine oxide has long ago been interpreted as proof of non-ionization of the dihydrate (20).

On the contrary, the infrared spectrum of the hydrochloride (Fig. 2) shows some

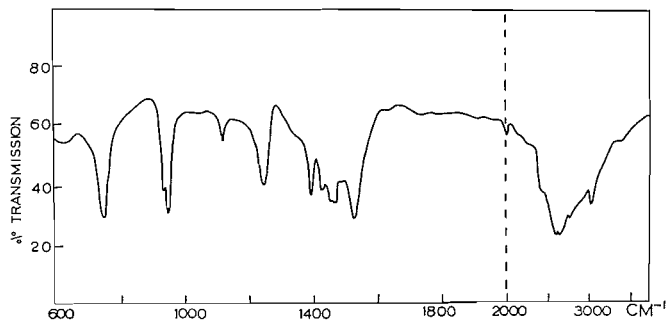


FIG. 2. Infrared spectrum of trimethylamine oxide hydrochloride, $(CH_3)_3NO.HCl$.

significant differences from those of the oxide and the dihydrate. True, the C—N and N—O stretching frequencies are unchanged (939 and 950 cm^{-1}) contrary to expectation for an ionic compound. (In hydroxylamine (21), for instance, the N—O frequency at 926 cm^{-1} is shifted to 1000 cm^{-1} in the hydrochloride.) However, the appearance of new, strong bands, notably at 1530 cm^{-1} and around 2600 cm^{-1}, is certainly due to OH vibrations of the $[(CH_3)_3NOH]^+$ species. Very strong hydrogen bonds between that ion and the chloride anion must be responsible for the rather high OH bending frequency and, correspondingly, for the low OH stretching frequency. Rérat (6) has deduced an ionic structure for the hydrochloride on the basis of his X-ray data, particularly (*a*) the measured O—Cl distance (2.94 Å), which is definitely shorter than the sum of the van der Waals radii (3.2 Å), and (*b*) the near tetrahedral (110.4°) NOCl angle. Yet it should be pointed out that these features are equally compatible with a molecular structure since (*a*) there is no reason a priori why the over-all distance in O—H . . . Cl should be any different from that in O . . . H—Cl and (*b*) hydrogen bonds have a tendency to become oriented along the direction of lone-pair orbitals (22). Thus sp^3 hybridization of the oxygen orbitals could account as well for the observed NOCl angle.

ACKNOWLEDGMENTS

The authors are grateful to the National Research Council for generous financial support of this project in the form of instrument grants and bursaries to one of them (D. C.).

Can. J. Chem. Downloaded from www.nrcresearchpress.com by 210.87.254.105 on 09/05/12
For personal use only.

RÉSUMÉ

On a étudié les spectres infrarouges de la triméthylaminoxyde, de son hydrate et son chlorhydrate afin de déterminer la nature de ces composés. La fréquence des vibrations N—O (937 cm^{-1}) et C—N (945 cm^{-1}) permet d'évaluer la longueur de ces liaisons à 1.44 Å et 1.50 Å respectivement en bon accord avec les résultats d'études récentes par diffraction des rayons X et des électrons. Le spectre du dihydrate indique qu'il s'agit d'un composé moléculaire, tandis que le chlorhydrate est très probablement ionique. Dans ces deux composés les charges nominales conduisent à des liaisons hydrogène particulièrement fortes.

REFERENCES

1. L. PAULING. Nature of the chemical bond. Cornell University Press, Ithaca, N.Y. 1939.
2. M. W. LISTER and L. E. SUTTON. Trans. Faraday Soc. A, **35**, 495 (1939).
3. P. A. GIGUÈRE and V. SCHOMAKER. J. Am. Chem. Soc. **75**, 2025 (1943).
4. R. E. RUNDLE. Unpublished results.
5. L. E. SUTTON (*Editor*). Tables of interatomic constants. Special publication No. 11, The Chemical Society, London. 1958.
6. C. RÉRAT. Acta Cryst. **13**, 63 (1960).
7. J. T. EDSALL. J. Chem. Phys. **5**, 225 (1937).
8. J. GOUBEAU and I. FROMME. Z. anorg. Chem. **258**, 18 (1949).
9. K. B. HARVEY. Ph.D. Thesis, Laval University. 1956.
10. R. MATHIS-NOËL, R. WOLF, and F. GALLAIS. Compt. rend. **242**, 1873 (1956).
11. W. LÜTTKE. Private communication.
12. W. R. DUNSTAN and E. GOULDING. J. Chem. Soc. **75**, 1004 (1899).
13. W. A. NOYES and J. H. HIBBEN. J. Am. Chem. Soc. **45**, 358 (1923).
14. R. ANANTHAKRISHNAN. Proc. Indian Acad. Sci. A, **4**, 204 (1936).
15. H. SIEBERT. Z. anorg. Chem. **273**, 161 (1953).
16. T. D. STEWART and S. MAESER. J. Am. Chem. Soc. **46**, 2585 (1924).
17. J. WAGNER. Z. physik. Chem. B, **40**, 36 (1938).
18. V. SCHOMAKER and D. P. STEVENSON. J. Am. Chem. Soc. **63**, 37 (1941).
19. P. A. GIGUÈRE and K. B. HARVEY. Can. J. Chem. **34**, 798 (1956).
20. W. A. NOYES. J. Am. Chem. Soc. **47**, 3025 (1925).
21. P. A. GIGUÈRE and I. D. LIU. Can. J. Chem. **30**, 948 (1952).
22. W. G. SCHNEIDER. J. Chem. Phys. **23**, 26 (1955).

Can. J. Chem. Downloaded from www.nrcresearchpress.com by 210.87.254.105 on 09/05/12
For personal use only.

Can. J. Chem. Downloaded from www.nrcresearchpress.com by 210.87.254.6 on 09/05/12
For personal use only.

THE KINETICS OF THE REACTION OF SILICA WITH GROUP I HYDROXIDES[1]

J. G. Hooley

ABSTRACT

A method is presented for preparing a reproducible silica glass or quartz surface that does not craze during rate of solution measurements in solutions of the five group I hydroxides. For silica glass, initial rates are a maximum at 8 *M* for at least NaOH and KOH and are an inverse function of ion size for the five cations and tetramethyl ammonium ion. A proposed mechanism of water addition followed by reaction with hydroxyl ion is used to explain the maximum rate and the effect of solution products and the substitution of methanol for water as a solvent. For quartz an explanation is offered for the lower rate and for the absence of a maximum rate below 27 *M* NaOH. A common temperature coefficient of 20 kcal mole^{-1} is reported for all reactions in water. The crazing of finely ground or polished silica glass surfaces is related to the presence of surface cracks and their enlargement by possible conversion of some silica to quartz in NaOH solution.

INTRODUCTION

The reactivity of commercial silicate glasses with a variety of aqueous solutions has been extensively studied (1) usually with the object of predicting the behavior of the glass under practical conditions. The reaction of colloidal silica with aqueous NaOH has also received considerable attention (2, 3). The behavior, however, of massive silica glass with alkali solutions has not been studied beyond measuring the rate in a few isolated cases. The object of the present work was therefore to investigate the rate of attack of one of the simplest glasses—fused silica—by alkali solution and thereby to elucidate the mechanism of the reaction. All the group I hydroxides were used as well as tetramethyl ammonium hydroxide and some runs were made with methanol as a cosolvent and others with quartz instead of silica glass.

MATERIALS

1. Silica and Quartz

All the vitreous silica samples were of Vycor 7900, a Corning Glass Works product which is about 97% SiO_2, 3% B_2O_3, 0.3% Al_2O_3, and <0.02% Na_2O. Samples 4×4 cm were cut from 6 mm thick panels and ground against a rotating iron disk using a water suspension of aluminum oxide grit. The edges and corners were rounded and they and all the flat surfaces were ground until perfectly uniform to the eye before etching with HF as described under Methods.

For crystalline silica, eight samples from 1.0 to 1.5 cm on an edge were cut from colorless crystals of natural quartz, ground as described above, and then polished with rouge in water on a rotating felt pad.

2. Basic Solutions

The hydroxides of Li, Na, and K were of the best commercial grade. Exposure to air was minimized to reduce CO_2 absorption and fresh solutions were used in all runs.

The RbOH was made from a mixture of nitrate and chloride of very high purity from atomic weight work. It was converted to the sulphate and then to the hydroxide with $Ba(OH)_2.8H_2O$. The filtered solution was evaporated to 100 ml in a large silver tube in

[1]*Manuscript received February 13, 1961.*
Contribution from the Department of Chemistry, University of B.C., Vancouver, B.C., with financial assistance from President N. A. M. MacKenzie's Research Fund.

a CO_2-free atmosphere. All runs were made with this solution, lower concentrations being obtained by dilution. The normality was determined for each run by titrating a pipetted sample.

The CsOH was prepared and used in a similar manner, the starting material being very pure $CsCl_2I$.

Tetramethyl ammonium hydroxide was prepared from the bromide with a suspension of freshly prepared silver oxide. The AgBr was filtered off and the clear solution was diluted to 1.40 *M*.

METHODS

The following experimental details were first studied in NaOH solution to arrive at a procedure that would give the initial rate of attack of a reproducible surface.

1. Surface Treatment

(a) Vitreous Silica

The surface of Vycor 7900 whether polished with rouge or ground only with fine grit crazed in 2 *N* NaOH at 80° C. Pure fused silica (Vitreosil) behaved similarly. That is, the surface became increasingly covered with visible cracks about 1 mm long and a fraction of a millimeter deep. The surface remained smooth to the touch, however, until the cracks began to shed small chips of glass anywhere from a few hours to a few days after the action began. Weight losses per unit area varied widely even when based on surfaces that had not lost any chips and it is perhaps for this reason that so little work has been done on the reactivity of silica glass with alkali solutions.

If a finely ground or polished surface was treated with a 50 volume% solution of concentrated H_2SO_4 and 60% HF for 15 minutes before immersion in alkali there was no sign of crazing until several days had elapsed in 2 *N* NaOH at 80° C. A surface freshly formed by breaking behaved in the same fashion as did the acid-etched sample. In all the above cases, crazing occurred sooner if the NaOH solution was contained in a tube of Pyrex than if it was in one of iron or silver. If crazing is initiated in the invisible cracks in the surface of ground or polished glass its elimination by etching is explained because this process removes the scratched surface and exposes a virgin one that indeed resembles a freshly formed surface. Whatever the cause of crazing it can be eliminated for the 15-hour runs employed in this work by etching the finely ground surface with HF. Prepolishing is unnecessary because the subsequent etching produces a translucent surface that resembles the nonpolished one and that exhibits the same weight loss in alkali solution.

(b) Quartz

A surface ground with fine grit also crazed in alkali but it was not possible even to try to prevent this by acid etching because the HF also caused crazing. It was found that unlike the surface of silica glass, however, a surface polished with wet rouge on felt showed crazing only after 200 hours in 2 *N* NaOH at 80° C. Polished quartz was therefore used in 72-hour runs and all samples were reground and polished before each run. The regrinding was necessary to remove the irregular surface pattern produced by NaOH solution. These patterns were observed to repeat themselves in subsequent runs.

Finally, for both silica glass and quartz the sample was suspended by a loop of silver wire near the center of a silver tube 5 cm in diameter and 30 cm long. The tube contained 300 ml of solution (less for some of the Rb and CsOH runs) and was immersed in a

Can. J. Chem. Downloaded from www.nrcresearchpress.com by 210.87.254.6 on 09/05/12
For personal use only.

constant temperature bath held to ±0.1° C. A fitted, water-cooled condenser prevented loss of solvent. In handling the samples great care was taken to prevent any scratching against glass or metal. The samples of quartz were warmed and cooled slowly in the reacting solutions to prevent cracking.

2. Stirring

Any effect of stirring on the rate of attack of Vycor by 1 *M* or 16 *M* NaOH at 80° C was found to be less than the experimental error of 3%. In one series of experiments the solution above the suspended sample was stirred at a speed that raised the level at the periphery of the tube about 7 cm. In another series the sample was a sealed Vycor tube 1 cm in diameter and 12 cm long which was rotated in the solution at a similar speed.

3. Time of Reaction

The effect of time and therefore of the dissolved silica on the rate of solution of Vycor in NaOH solution at 80° C was studied by using the same solution for a series of 8-hour runs. Between these runs measured weights of silica were allowed to dissolve from a weighed Vycor sample left in the solution. The concentration of NaOH in the reaction tube was kept constant by washing the samples with water as they were removed from the solution and then adjusting the volume to its original value by evaporating off the excess water introduced in this way. All samples were etched before each run to prevent crazing. In Fig. 1 the average rate for each 8-hour run is plotted against the total weight

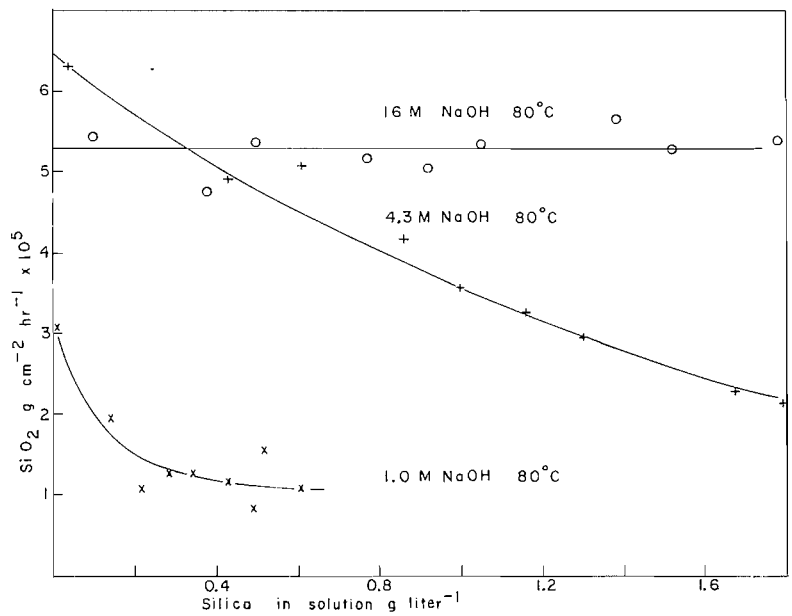


FIG. 1. Rate of solution of Vycor 7900 at 80° C vs. total silica in solution.

of silica that had accumulated in the solution. The reaction products are seen to have an inhibitory effect in 1 *M* NaOH, less in 4 *M*, and none in 16 *M*. Because initial rates are sought in this work the reaction times were later chosen so that the error introduced by dissolved silica would be less than 3%.

Can. J. Chem. Downloaded from www.nrcresearchpress.com by 210.87.254.6 on 09/05/12
For personal use only.

Can. J. Chem. Downloaded from www.nrcresearchpress.com by 210.87.254.6 on 09/05/12
For personal use only.

RESULTS

1. *Vitreous Silica*

(a) Reproducibility

In one duplicate series of eight concentrations from 0.1 to 10 *M* NaOH at 80° C for 15 hours the weight losses per sq. cm of the Vycor samples showed a root mean square deviation of 3% from the averages. In other duplicate runs the precision was at least that value as long as no crazing had occurred. Area differences between samples were never found to affect reproducibility.

(b) Vycor 7900 Compared with Vitreosil

Clear Vitreosil from the Thermal Syndicate Co. in England is made by fusing quartz and is therefore more pure than Vycor. Four samples of each in 2 *M* NaOH at 80° C showed the same rate of attack within experimental error. Hence for these conditions, at least, the 3% B_2O_3 in Vycor has no measureable effect on the rate.

(c) Concentration of Group I Hydroxide

The initial rate at 80° C is plotted against molarity in Fig. 2. For NaOH and KOH

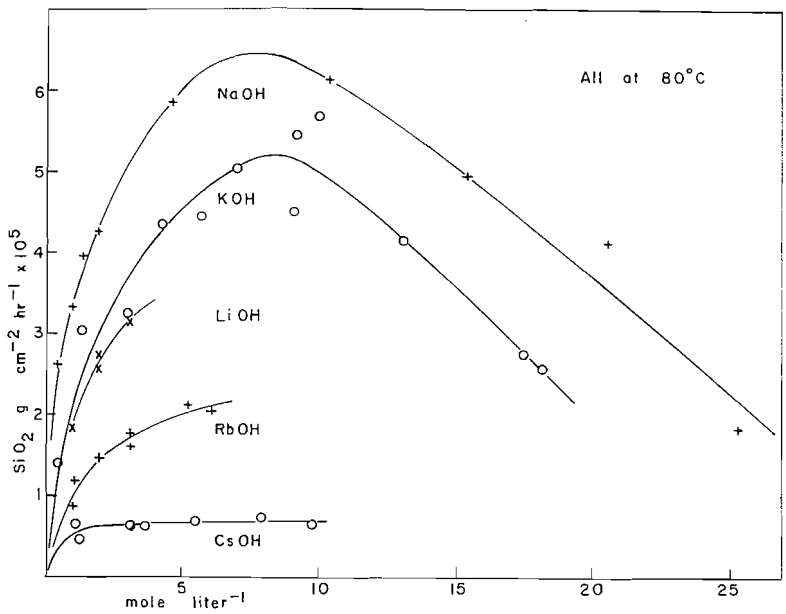


FIG. 2. Rate of solution of Vycor 7900 at 80° C vs. concentration for various alkali hydroxides.

there is a maximum rate at about 8 *M*. For the other three, data at high concentrations are not available because of a solubility limitation for LiOH and lack of material for Rb and CsOH. However, a maximum rate at 8 *M* would not be inconsistent with the data.

One run was made with the eutectic of 2.6% LiOH, 23.6% NaOH, and 73.8% KOH, which, because of impurities (probably water and carbonates), melted at 135° C instead of 70 to 80° C. Its molarity, assuming additive densities, was 41. In a 5-hour run at 146° C the rate was 91×10^{-5} g cm^{-2} hr^{-1}. If the temperature coefficient found in the next section is used to calculate the rate at 80° C, a value of 1×10^{-5} is obtained.

In 1.40 *M* tetramethyl ammonium hydroxide at 91.5° C, duplicate samples each lost 5.8×10^{-5} g cm^{-2} hr^{-1}, which is about the same as in 1.4 *M* KOH.

(d) Temperature Coefficient

The effect of temperature on the rate with NaOH is shown in Fig. 3. The Arrhenius

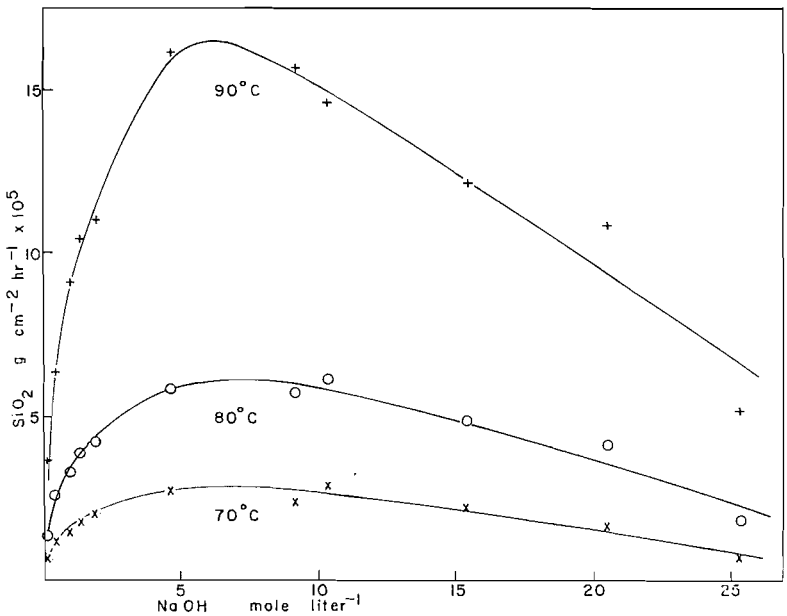


FIG. 3. Rate of solution of Vycor 7900 vs. NaOH concentration for three temperatures.

plots made from these curves at 2, 8, and 20 *M* are linear and give activation energies of 22 kcal at each concentration. For the reactions with KOH (2, 9, 18 *M*), RbOH (1, 3 *M*), and CsOH (1, 3 *M*) at 70°, 80°, and 90° C the Arrhenius plots show the same linearity as for NaOH and give activation energies of 20, 18, and 22 kcal $mole^{-1}$ respectively. The variation in calculated energy is not regarded as significant and an average value of 20 ± 2 kcal $mole^{-1}$ for all four hydroxides at all concentrations is suggested.

(e) Solvent

To study the effect of the concentrations of water and of NaOH separately, a mixed solvent of alcohol and water was used. In one series, the molar concentration of NaOH was held constant at 6.0 *M* and the concentration of water was varied by substituting methanol. The rate at 63.4° C is plotted in Fig. 4 against water concentration and is seen to increase smoothly from zero for pure methanol to the value for pure water. A similar curve was obtained for ethanol although the water concentration could not be taken below 750 g $liter^{-1}$ at 78° C because of solubility limitations.

In a second series, the water concentration was held constant at 800 g $liter^{-1}$ and the NaOH was varied, methanol being the third component. The rate at 63.4° C is plotted in Fig. 5 against NaOH concentration and is seen to go through a maximum at 8 *M*.

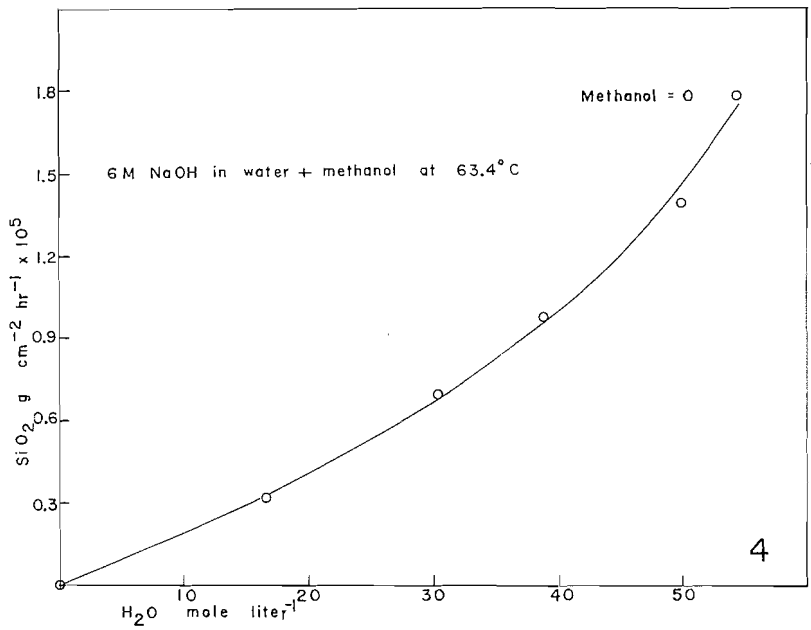
2. Quartz

(a) Concentration

The rates at 91.5° C plotted in Fig. 6 against concentration are each the average for four different quartz cubes, the standard deviation being equal to the length of the vertical line drawn through the point. The same four cubes were used for each of the

Can. J. Chem. Downloaded from www.nrcresearchpress.com by 210.87.254.6 on 09/05/12
For personal use only.

Can. J. Chem. Downloaded from www.nrcresearchpress.com by 210.87.254.6 on 09/05/12
For personal use only.



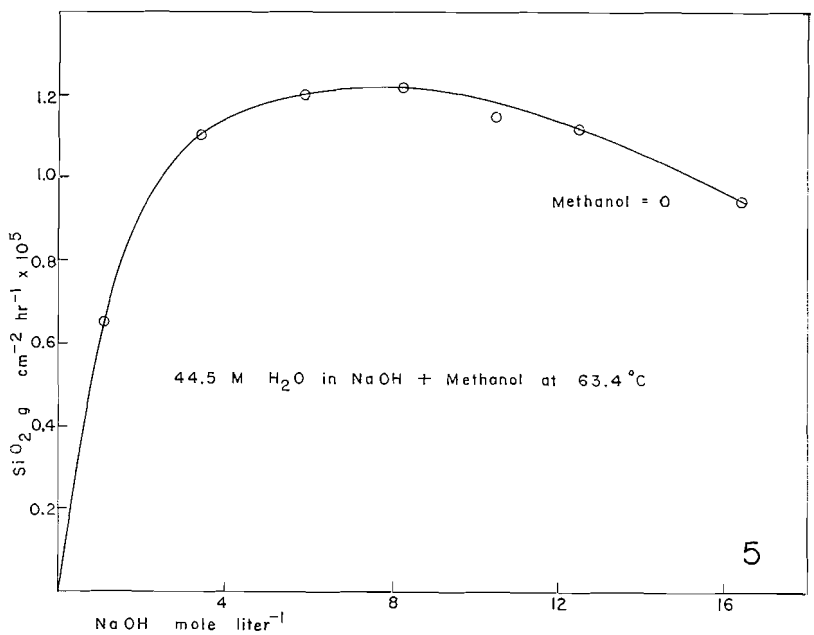


FIG. 4. Rate of solution of Vycor 7900 vs. water concentration for 6 *M* NaOH in water + methanol.
FIG. 5. Rate of solution of Vycor vs. NaOH concentration for 44.5 *M* H_2O in methanol.

three lowest concentrations and the other four for the remaining concentrations. The precision is less than for fused silica because of the much lower rate of reaction. There is, however, no evidence for a maximum rate below 27 *M*.

(b) Temperature

The rates for duplicate runs at two concentrations and three temperatures are listed

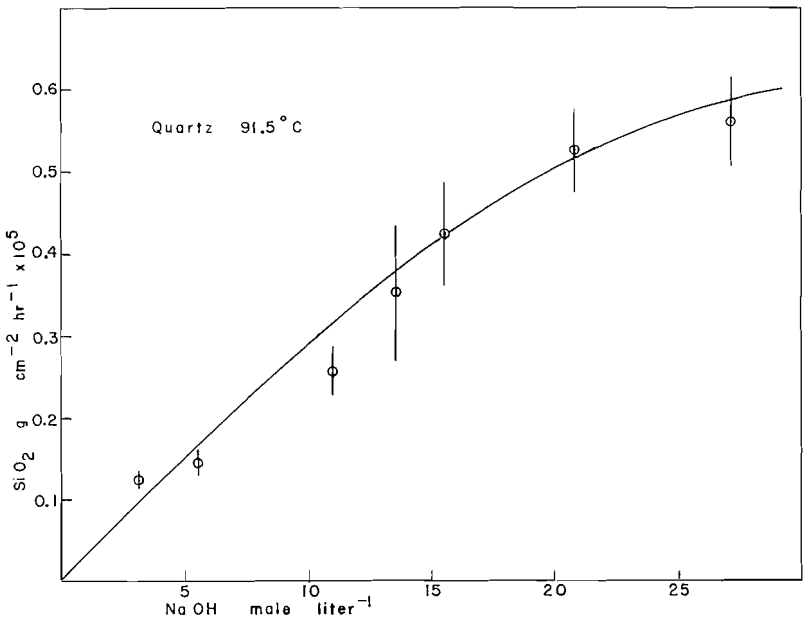


FIG. 6. Rate of solution of quartz vs. NaOH concentration.

in Table I along with the activation energies from an Arrhenius plot. Because of the low

TABLE I

Rate in mg cm^{-2} $hr^{-1} \times 10^5$ for quartz in aqueous NaOH

Sample	1	2	3	4
Concn., *M*	2.73	2.73	10.3	10.3
70.4° C	0.20	0.28	0.53	0.63
79.6° C	0.56	0.65	0.91	0.97
89.2° C	1.18	1.33	2.23	2.94
E, kcal $mole^{-1}$	25	22	19	18

rates, the data is only of sufficient accuracy to say that the activation energy is 21 ± 4 kcal $mole^{-1}$.

(c) Solvent

There was no measurable weight loss after 140 hours in 1.4 *M* NaOH in ethanol at 78° C.

DISCUSSION

Any reaction mechanism with silica glass must explain the following.

1. A maximum in the plot of rate against concentration.
2. The variation of rate with cation.
3. The inhibitory effect of dissolved silica at low NaOH concentrations but not at high ones.
4. The small or zero variation in temperature coefficient with concentration.
5. The experiments with NaOH in methanol–water mixtures.

Also of interest in the case of quartz are its low reactivity and the absence of a maximum rate below 27 *M* NaOH.

For both silica glass and quartz two consecutive reactions are proposed. First an

Can. J. Chem. Downloaded from www.nrcresearchpress.com by 210.87.254.6 on 09/05/12
For personal use only.

adsorption of water followed by reaction with hydroxyl ion to produce soluble products. The two can be represented in several simplified ways, one of which is:

$$SiO_2(s) + 2H_2O(l) \rightarrow SiO_2.2H_2O(s), \quad [1]$$

$$SiO_2.2H_2O(s) + 2OH^- \rightarrow [Si(OH)_6]^{-2} \text{ in solution.} \quad [2]$$

In more detail, the surface of the silica being exposed for reaction consists largely of oxygen ions because the small, more highly charged silicon ions are well shielded by the highly polarizable oxygen ions. This concept of the surface of an ionic crystal has been discussed by Weyl (4) and has been recently reviewed by Benson and co-workers (5). It is realized that the silica structure has considerable covalent character and that the actual charges on the "ions" are less than +4 and −2. The important point is that the silicon atom or ion is sufficiently buried below the surface so that hydroxyl ion alone will not react with it. This is supported by the zero rate in methanolic NaOH in which only OH^-, Na^+, and solvent are present. Now the addition of water causes reaction [1] to occur. This equation represents water adsorption on the silica surface by hydrogen bonding to the oxygen "ions" of that surface. This transfer of negative charge toward the water molecules decreases the screening so that the silicon "ions" can now combine with any hydroxyl ions present to form a soluble co-ordination complex. The formula suggested in equation [2] is only for illustrative purposes. If water and no hydroxyl ion is present as in NaCl solution the theory correctly predicts no attack. It also predicts for aqueous solutions of alkali hydroxides the observed maximum rate. Thus at low molarity and therefore high water concentration reaction [2] will be the rate-determining step and so the rate will increase with molarity as observed. However, at high molarity and therefore low water concentration reaction [1] becomes the rate step and hence the rate decreases as molarity increases as observed. A maximum rate at some intermediate concentration is the result. The rate should go to zero for the nonaqueous eutectic mixture of three hydroxides. That it did not quite do this is believed to be caused by a small amount of water in the system.

The theory predicts, of course, a maximum rate not only for silica glass but also for quartz which was not observed below 27 *M*. However, the rate did go to zero for methanolic NaOH in which there is hydroxyl ion but no water. It is therefore believed that for aqueous solutions a maximum rate would be reached above 27 *M*. That it is at a higher concentration than in the case of silica glass means that for quartz, reaction [2] has been slowed more than [1] and therefore remains the rate step to higher molarities. This is reasonable because the surfaces of the two forms of silica are predominately oxygen "ions" and so should react about equally with water as in reaction [1]. Reaction [2], however, involves the penetration of the surface and reaction with silicon ions. These ions have a higher potential energy in the glass and therefore react more rapidly than when in the crystalline quartz.

The variation of rate with cation size is difficult to explain. It may simply be that the larger the cation, the greater the interference with the above reactions by adsorption and the lower the rate as was observed. The apparent discrepancy with LiOH disappears when account is taken of its low dissociation—about 50% in 3 *M* solution (6, 7). Even tetramethyl ammonium ion fits in if the effective area is taken as that of the base of the tetrahedron.

The effect of dissolved silica on the rate is correctly predicted. Thus the inhibitory effect should be greatest at low molarity where [2] is the rate step and should disappear for concentrated solutions where [1] is the rate step.

The temperature coefficient would be expected to depend on whether reaction [1] or

Can. J. Chem. Downloaded from www.nrcresearchpress.com by 210.87.254.6 on 09/05/12
For personal use only.

[2] is the rate step and on whether silica glass or quartz is involved. The data, however, were not sufficiently precise to detect differences caused by these factors. Some recent work on finely divided silica (3) reports an activation energy of 18 kcal mole^{-1} for the solution of this material in dilute alkali and 17.8 for solution in water. The agreement of these with the 20 ± 2 for this work is rather good. The comparison, however, should be confined to reaction [2] for complete solution because reaction [1] is only a surface reaction and not a solution process.

In discussing the results with methanol as a solvent it is important to have an estimate of the concentration of hydroxyl ion in a solution of NaOH in pure methanol. Conductivity and transference-number data are available for a dilute solution of KOH in methanol plus 0–100 mole% water at 25° C (8, 9). In this range of solvents the conductivity increases from 90 to 260 ohm^{-1} cm^2 and the transference number of hydroxyl ion changes from 0.5 to 0.7. Hence for a given molarity of KOH the hydroxyl ion is conducting about 25% as much in pure methanol as in pure water. Thus in Fig. 4 the 6 *M* NaOH solution in pure methanol should contain of the order of 1 *M* hydroxyl ion. Because there is no water, however, theory predicts the observed zero rate of reaction. When water is added, the rate increases with water concentration because reaction [1] is the rate step. At a sufficiently high water concentration one would expect reaction [2] to become the rate step and, because the concentration of NaOH is constant, the rate to become constant. However, the dissociation of NaOH is increasing with water concentration so that the rate continues to increase in this region as well. For the other experiment in Fig. 5 at constant 44 *M* water concentration, theory predicts the initial zero rate at zero hydroxyl ion concentration and the subsequent increase. However, the rate should become constant as reaction [1] becomes the rate step. Instead, it goes through a maximum which may be explained by the removal of available water from the system to hydrate the increasing concentration of sodium ions.

Finally, the phenomenon of crazing should be discussed. This occurs on a silica glass surface, whether finely ground or polished, but not when etched with HF or when freshly formed as in breaking. Because the first two surfaces are known to contain invisible cracks and the latter two none, it is believed that crazing starts at or in such cracks. Their enlargement to visible dimensions must now be explained. A simple solution process would do this but if that is the mechanism, then one would also expect crazing in surfaces of Pyrex or soft glasses in general. But these surfaces never craze in alkali even though they are known to contain invisible cracks. Another mechanism that would enlarge cracks is the conversion of the glass to the crystalline form. The resultant volume decrease would explain the enlargement to visible dimensions and the eventual chipping out of a piece of glass from the crack. Such conversion has never been reported in solution for Pyrex or soft glass but is known to take place readily for silica glass at 400° C and 340 atm in solutions of sodium silicate (10) or NaOH (11). It is suggested that even at 80° C this conversion to α quartz occurs to some extent. The fact that crazing is more rapid when sodium silicate is present in the NaOH solution supports this theory. We are now left with the case of quartz for which a finely ground surface crazes in alkali and in HF solution and for which a polished surface does not craze in alkali until after at least 200 hours at 80° C. No theory for this is offered.

CONCLUSION

The rate of reaction of silica glass or quartz with solutions of group I hydroxides is chemically controlled by one or the other of two consecutive reactions depending on the

Can. J. Chem. Downloaded from www.nrcresearchpress.com by 210.87.254.6 on 09/05/12
For personal use only.

molarity of the base. In being chemically rather than diffusion controlled, it resembles the reaction with hydrofluoric acid (12). A theory is offered to explain the crazing of silica glass but not of quartz.

ACKNOWLEDGMENTS

To the following research students for their ideas and measurements: Miss A. Day and Miss R. Irish, and Messrs. J. R. G. Bryce, J. R. Colclough, D. W. Kay, and J. W. Wainwright. Also to Professor R. M. Barrer and the staff of Imperial College, London, for their hospitality during my study leave there when this was written.

REFERENCES

1. G. W. MOREY. The properties of glass. Reinhold, N.Y. 1954. Chap. IV.
2. R. K. ILER. The colloid chemistry of silica and silicates. Cornell Press, N.Y. 1955. Chap. 1.
3. T. L. O'CONNOR and S. A. GREENBERG. J. Phys. Chem. **62**, 1195 (1958).
4. W. A. WEYL. A new approach to surface chemistry and heterogeneous catalysis. Mineral Industries Experiment Station, State College, Penna. Bull. No. 57 (1951).
5. G. C. BENSON, H. P. SCHREIBER, and D. PATTERSON. Can. J. Phys. **34**, 265 (1956).
6. R. A. ROBINSON and R. H. STOKES. Electrolyte solutions. Butterworth, London. 1959. p. 491.
7. H. SPIRO. Trans. Faraday Soc. **55**, 1746 (1959).
8. T. ERDEY-GRUZ, E. KUGLER, and A. REICH. Acta Chim. Acad. Sci. Hung. **13**, 429 (1958).
9. T. ERDEY-GRUZ and L. MAJTHENYI. Acta Chim. Acad. Sci. Hung. **16**, 417 (1958).
10. N. WOOSTER and W. WOOSTER. Nature, **157**, 297 (1946).
11. J. F. CORWIN, A. H. HERZOG, G. E. OWEN, R. G. YALMAN, and A. C. SWINNERTON. J. Am. Chem. Soc. **75**, 3933 (1953).
12. W. G. PALMER. J. Chem. Soc. 1656 (1930).

Can. J. Chem. Downloaded from www.nrcresearchpress.com by 210.87.254.6 on 09/05/12
For personal use only.

Can. J. Chem. Downloaded from www.nrcresearchpress.com by 210.87.254.105 on 09/05/12
For personal use only.

PRIMARY METHOXY RADICAL FORMATION IN THE REACTION OF METHANOL VAPOR WITH Hg 6($^3P_1$) ATOMS[1]

ARTHUR R. KNIGHT AND HARRY E. GUNNING

ABSTRACT

A study has been made of the decomposition of methanol vapor by Hg 6($^3P_1$) atoms, under static conditions, at 25° C. A system constructed entirely of quartz was employed to eliminate the dark reaction between methanol vapor and pyrex glass to form trimethyl borate. Emphasis in this investigation was placed on the determination of the nature of the primary processes operative, and to this end, the reaction was studied in some detail in the presence of nitric oxide.

For pure methanol, the major primary products were found to be hydrogen and ethylene glycol. The primary quantum yield for hydrogen was 0.46. Minor products of primary origin were formaldehyde (0.01), ethane (0.005), and dimethyl ether (0.006), with the numbers in parentheses showing the primary quantum yields.

In the presence of nitric oxide, the major products became methyl nitrite, nitrous oxide, and water. The quantum yield of methyl nitrite rose steadily with increasing NO concentrations. For a 1:1 CH_3OH:NO mixture, the primary quantum yield for methyl nitrite was found to be 0.56. The behavior of the reaction in the presence of NO establishes fairly unequivocally that the major primary process involves O—H bond scission to form methoxy radicals and H atoms. These primary radicals then form hydroxymethyl radicals by abstraction reactions with the substrate. The ethylene glycol product arises by recombination of the secondary hydroxymethyl radicals. These conclusions were further substantiated by mass spectrometric analysis of the products of the decomposition of CD_3OH. It was shown that CD_2OD is a significant product of the reaction.

INTRODUCTION

The reaction of methanol vapor with Hg 6($^3P_1$) atoms has been studied previously (1, 2), and in detail by Phibbs and Darwent (3) from 25–500°. From the fact that H_2 ($\Phi = 0.43$) and $HOCH_2CH_2OH$ were the major products at 25°, they concluded (3) quite reasonably that the major primary process was:

$$CH_3OH + Hg\ 6(^3P_1) \rightarrow CH_2OH + H + Hg\ 6(^1S_0). \quad [1]$$

The observed products could also be explained by the two-step sequence:

$$CH_3OH + Hg\ 6(^3P_1) \rightarrow CH_3O + H + Hg\ 6(^1S_0) \quad [2]$$

$$CH_3O + CH_3OH \rightarrow CH_3OH + CH_2OH. \quad [3]$$

For both [1] and [2] the H atoms formed are assumed to attack the methyl group of the substrate:

$$H + CH_3OH \rightarrow H_2 + CH_2OH. \quad [4]$$

Phibbs and Darwent rejected [2] as an important primary process since they found that CH_3OD substrate produced little HD. However, the results of a number of more recent studies have indicated that the methanol reaction should be re-examined. Thus Takezaki and Takeuchi (4) showed that methanol is readily decomposed by CH_3O radicals from the pyrolysis of dimethyl peroxide. From detailed studies on the photolyses of CH_3COOCH_3 and CH_3COOCD_3, Wijnen (5) has concluded that CH_3O radicals are very efficient in abstraction reactions. For reaction [3] specifically, Gray and Williams (6) estimate an exothermicity of 7–8 kcal/mole.

[1]*Manuscript received January 20, 1961.*
Contribution from the Department of Chemistry, University of Alberta, Edmonton, Alberta.

In the photolysis of methanol vapor below 2000 Å, Porter and Noyes (7) found evidence that O—H bond scission is an important primary process. Their ethylene glycol product was attributed to combination of CH_2OH radicals from [3]. In this laboratory interest arose in the reaction of methanol with Hg $6(^3P_1)$ atoms, from an investigation of the decomposition of water vapor by ^{202}Hg $6(^3P_1)$ atoms, photoexcited in natural mercury vapor. Here Pertel and Gunning (8) found that the HgO product of the reaction was enriched in ^{202}Hg, indicating the formation of an Hg—O bond in the primary quenching reaction. Since the oxygen atom was a quenching site in the HOH reaction, it appeared likely that a similar process would be operative in the CH_3OH reaction.

In the present study, emphasis has been placed on the nature and relative importance of the primary reactions. In order to distinguish between reactions [1] and [2], it was decided to use nitric oxide as scavenger. It was presumed the CH_3O radicals would react readily with NO to form methyl nitrite, thereby suppressing reaction [3]. Since the alkyl nitrites are relatively stable compounds, the technique could be of general value in alkoxy radical reactions.

While the results of the present study were being prepared for publication, a paper appeared by Pottie, Harrison, and Lossing (9), wherein important data were reported on the reaction of Hg $6(^3P_1)$ atoms with methanol vapor, at a substrate partial pressure of 5 μ in helium carrier at 55°. The primary fragments from the reaction were identified by mass spectrometry via their combination products with CD_3 radicals from the *in situ* decomposition of $Hg(CD_3)_2$. With CD_3OH as substrate, CD_3OCD_3 was found to be the major combination product. It was estimated that CD_2OH could not account for more than 3% of the primary decomposition. Since CH_3, CH_4, C_2H_6, and CH_3OCH_3 were found as products from the reaction with CH_3OH alone, together with an amount of water roughly equivalent to the CH_3 yield, it was concluded that in addition to [2], a second primary process,

$$CH_3OH + Hg\ 6(^3P_1) \rightarrow CH_3 + OH + Hg\ 6(^1S_0), \qquad [5]$$

was occurring to an extent of ca. 18%. The results of Pottie *et al.* (9) will be compared with those of the present study later in this paper.

EXPERIMENTAL

Exploratory runs were first made in a conventional high-vacuum system of pyrex glass, using cylindrical quartz reaction cells. The reaction was studied under static conditions at 25°. Analyses were made by gas–liquid partition chromatography (G.L.P.C.) and mass spectrometry. Product yields were found to vary erratically under apparently constant experimental conditions. Mass spectrometry revealed the presence of trimethyl borate in the methanol, although this product was not detectable by G.L.P.C. It was confirmed, in agreement with Porter (10), that the trimethyl borate was formed by the reaction of methanol vapor with the pyrex glass of the storage bulb. At a gas pressure of 100 mm 9.7 mole% of this product was found after 24 hours of storage.

All results reported here were obtained from a system constructed entirely of quartz. A Hanovia, model 87A45, resonance tube was positioned 5 cm from the cylindrical quartz cell, which was 5 cm in length and of the same diameter. A Vycor 7910 filter was placed between lamp and cell to remove the 1849 Å line. The absorbed light intensity, with propane as actinometer (11), was found to be 1.92×10^{-6} einstein/min.

Can. J. Chem. Downloaded from www.nrcresearchpress.com by 210.87.254.105 on 09/05/12
For personal use only.

Methanol (Mallinckrodt, reagent grade) was purified by trap-to-trap distillation and stored in a quartz bulb. Neither G.L.P.C. analysis nor mass spectrometry revealed any impurities, including water. The nitric oxide (Matheson) was purified by repeated circulation over KOH, and stored over mercury in a bulb. Methyl nitrite was prepared after Gray and Style (12) and similarly stored.

G.L.P.C. analyses for hydrogen were performed on silica gel columns with N_2 carrier; for the condensable products, the column packings were "Ucon" on Celite and Apiezon "L" on firebrick, with H_2 carrier. Identification of products was made by retention times on two columns, and confirmed by mass spectrometry. The heavy product of the reaction with pure substrate was confirmed (3) to be ethylene glycol by comparing the infrared spectrum of its chloroform solution with that of an authentic sample. The spectra were essentially identical.

RESULTS

In the first series of runs, a substrate pressure of 50 mm and an exposure duration (t) of 105 minutes were used. The products were hydrogen, ethylene glycol, carbon monoxide, methane, ethane, dimethyl ether, formaldehyde, methyl formate, water, and a trace of ethanol. The mean quantum yield (Φ) for hydrogen was 0.24.

In the presence of NO, the only significant products were methyl nitrite, water, nitrous oxide, and formaldehyde. In Fig. 1, $\Phi(H_2)$, Φ(MeONO), and Φ(HOH) are shown

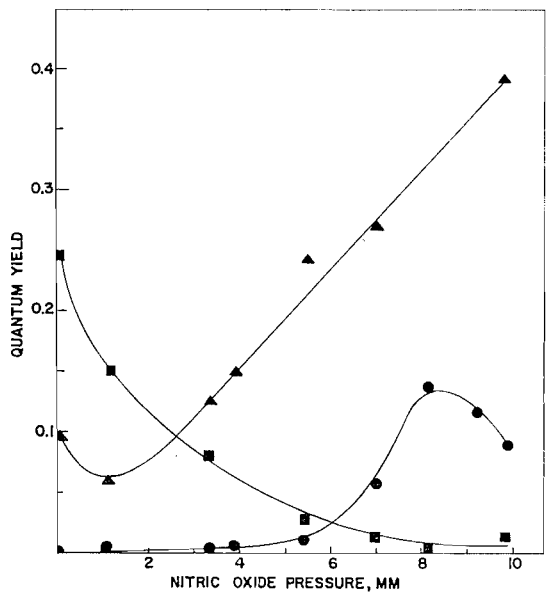


FIG. 1. Mean quantum yields for methyl nitrite ●, hydrogen ■, and water ▲ as a function of nitric oxide pressure, for a methanol pressure of 50 mm and an exposure time of 105 minutes.

as a function of P(NO) for P(MeOH) = 50 mm and t = 105 minutes. With increasing NO pressure, $\Phi(H_2)$ is seen to fall off rapidly, while Φ(HOH) rises linearly. Φ(MeONO) achieves a maximum value of 0.15 at P(NO) = 8 mm. By dissolving the cell deposit

Can. J. Chem. Downloaded from www.nrcresearchpress.com by 210.87.254.105 on 09/05/12
For personal use only.

in $CHCl_3$, and measuring the integrated absorbed intensity for the OH band in the infrared, it was shown that the ethylene glycol yield decreased with increasing P(NO). The minor products, formaldehyde and methyl formate, are shown in Fig. 2. It is

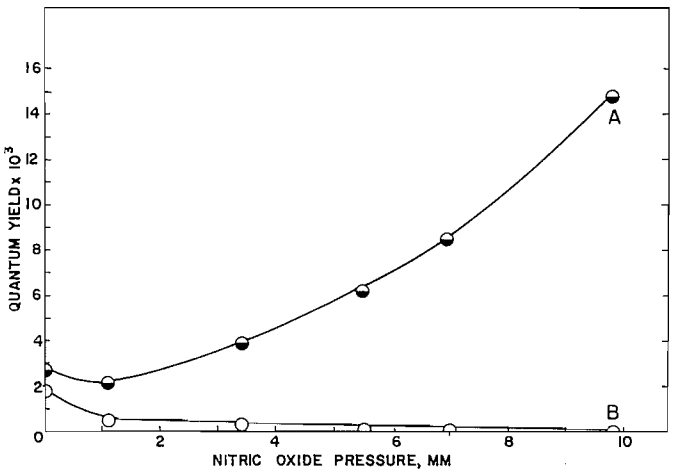


FIG. 2. Mean quantum yield of formaldehyde, curve A, and methyl formate, curve B, as a function of the nitric oxide pressure for a methanol pressure of 50 mm, and an exposure time of 105 minutes.

apparent with increasing P(NO) that Φ(HCHO) rises rapidly, while Φ(HCOOMe) becomes negligible.

To assess the importance of secondary reactions, the effect of exposure duration on the inhibited reaction was studied. For this series P(MeOH) = 50 mm and P(NO) = 5.5 mm. The exposure time was varied from 2 to 105 minutes. The results for Φ(MeONO) and $\Phi(H_2)$ are shown in Fig. 3, and Φ(HCHO) in Fig. 4. The rapid secondary decomposition of methyl nitrite is apparent, with a concomitant rise in Φ(HCHO). From Fig. 4, it can be further seen that formaldehyde is not a primary product of the inhibited reaction. The micromoles of water formed were found to be a linear function of t. At $t = 0$, Φ^0(MeONO) = 0.15 and $\Phi^0(H_2) = 0.012$. The rise in $\Phi(H_2)$ with increasing t was shown to be associated with a depletion of NO in the reaction zone. Thus two runs were made at the same substrate pressure, with P(NO) = 7.0 mm. $\Phi(H_2)$ was found to have values of 0.013 and 0.014 for t-values of 13 and 105 minutes, respectively.

The possibility of dark reaction between NO and substrate was checked by a duplicate run with P(MeOH) = 50 mm and P(NO) = 5.5 mm. The mixture was carried through all stages of the procedure except irradiation. In a second experiment, 2 mm of methyl nitrite—equivalent to the maximum amount formed in any of the exposures—was admixed with 50 mm N_2, and irradiated for 105 minutes. No products were detected in any of the above runs.

The effect of adding large quantities of NO is shown in Fig. 5. For these runs P(MeOH) = 50 mm and $t = 5.0$ minutes. For the equimolar MeOH:NO mixture, Φ(MeONO) = 0.56. The results are, of course, corrected in all cases for competitive quenching by NO.

The results of a series of runs on the uninhibited reaction at P(MeOH) = 50.0 mm

Can. J. Chem. Downloaded from www.nrcresearchpress.com by 210.87.254.105 on 09/05/12
For personal use only.

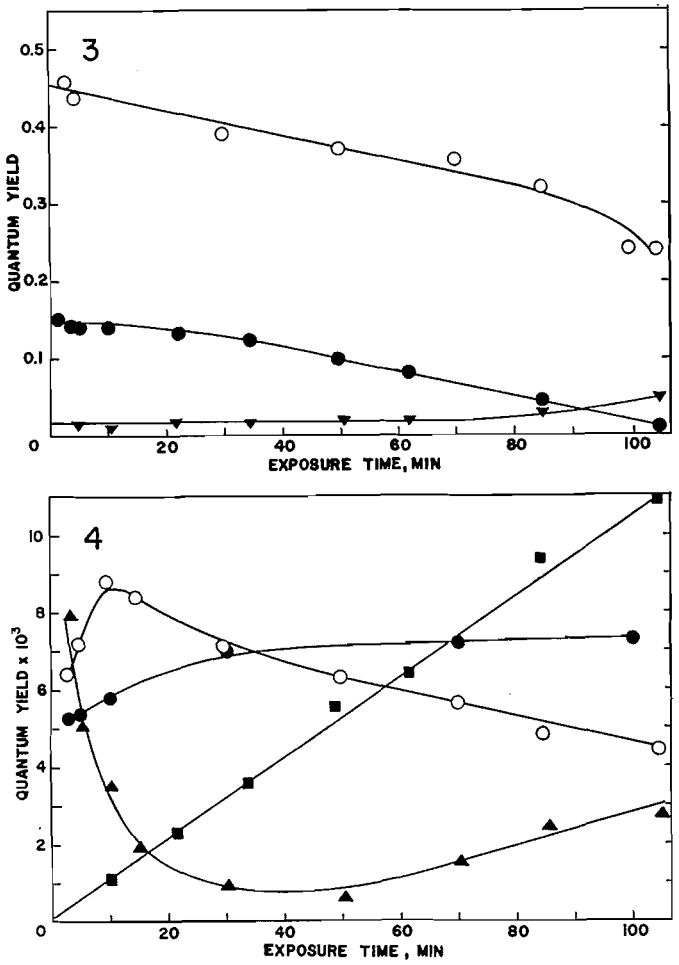


FIG. 3. Mean quantum yield of methyl nitrite ● and hydrogen ▼ as a function of exposure time for a mixture of 50 mm of methanol and 5.5 mm of nitric oxide. Mean quantum yield of hydrogen ○ as a function of exposure time for pure methanol at a pressure of 50 mm.

FIG. 4. Mean quantum yield of formaldehyde ■ as a function of exposure time for a mixture of 50 mm of methanol and 5.5 mm of nitric oxide. Mean quantum yield of formaldehyde ▲, ethane ●, and dimethyl ether ○ as a function of exposure time for pure methanol at a pressure of 50 mm.

are shown in Figs. 3 and 4. From Fig. 3, it is seen that $\Phi^0(H_2) = 0.46$. In Fig. 4, the trends in Φ for the minor products are shown. We obtain $\Phi^0(HCHO) = 0.01$; $\Phi^0(C_2H_6) = 0.005$, and $\Phi^0(CH_3OCH_3) = 0.006$. For water, $\Phi(HOH) = 0.095$ at $t = 105$ minutes. The values decreased rapidly to 0.035 at $t = 25$ minutes. Water is apparently not a primary product of the reaction. Similarly Φ(HCOOMe) fell from 0.0013 at $t = 105$ minutes to 0.0003 at $t = 25$ minutes. Again this product is not of primary origin.

Finally one qualitative run was done with CD_3OH (Merck, 99%). Mass spectrometric analysis of the residual substrate after 105 minutes of exposure showed the presence of appreciable amounts of CD_3OD.

Can. J. Chem. Downloaded from www.nrcresearchpress.com by 210.87.254.105 on 09/05/12
For personal use only.

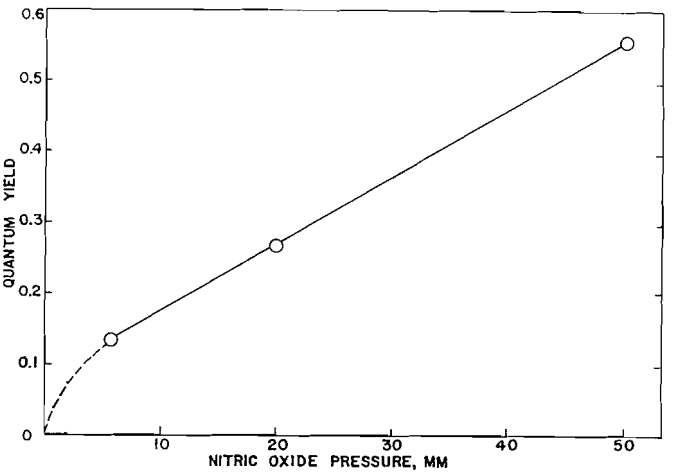


FIG. 5. Mean quantum yield of methyl nitrite, as a function of nitric oxide pressure for a methanol pressure of 50 mm, and an exposure time of 5.0 minutes.

DISCUSSION

The appearance of methyl nitrite as the major reaction product in the NO-inhibited reaction is strong evidence for the formation of CH_3O radicals in the primary reaction via step [2]. The presence of CD_3OD among the products of the CD_3OH run would suggest that both [2] and [3] are occurring. Our findings are therefore in qualitative agreement with the mass spectrometric results of Pottie, Harrison, and Lossing (9). While no evidence could be found for primary CH_2OH formation (3) via [1], the reaction could be occurring to a minor extent.

From the Φ^0's for C_2H_6 and CH_3OCH_3, we estimate that $\Phi^0(CH_3)$ would have a maximum value of ca. 0.02, while $\Phi(H)$ will be at least 0.46, the value for $\Phi^0(H_2)$. Furthermore it is likely that $\Phi^0(H)$ is actually near unity, since H atoms can be consumed by combination with themselves and with the CH_3O and CH_2OH radicals present in the reaction zone, without concomitant H_2 formation. Thus we conclude that reaction [5] cannot be more than five per cent of the primary reaction, and that it is more likely to be roughly two per cent of it. These conclusions would support the suggestion made by Pottie *et al.* (9) that CH_3 formation arises from atomic cracking:

$$CH_3O + H \rightarrow CH_3OH^* \rightarrow CH_3 + OH. \qquad [6]$$

Certainly [6] would be much more probable at the very low pressures (ca. 5 μ) used by Pottie *et al.* (9) than under the conditions of this study.

In the presence of nitric oxide, the significant products are methyl nitrite, nitrous oxide, water, and formaldehyde. With [2] as the primary process, the following secondary reactions are postulated to explain our findings.

$$CH_3O + NO \rightarrow CH_3ONO \qquad [7]$$

$$H + NO \rightarrow HNO \qquad [8]$$

$$CH_3O + HNO \rightarrow CH_3OH + NO \qquad [9]$$

$$HNO + HNO \rightarrow N_2O + H_2O \qquad [10]$$

$$CH_3O + CH_3ONO \rightarrow CH_3OH + CH_2O + NO \qquad [11]$$

Reactions [8] and [10] have been used by a number of investigators (12, 13, 14) to

Can. J. Chem. Downloaded from www.nrcresearchpress.com by 210.87.254.105 on 09/05/12
For personal use only.

Can. J. Chem. Downloaded from www.nrcresearchpress.com by 210.87.254.105 on 09/05/12
For personal use only.

explain the appearance of N_2O and H_2O in systems containing H atoms and NO. The analogous reaction to [9], for ethoxy radicals has been postulated by Levy (13) for the thermal decomposition of ethyl nitrite. The reaction should be highly exothermic. Reaction [11] forms a step in the Steacie–Sklar (13) mechanism for the decomposition of the alkyl nitrites. From Figs. 3 and 4, it is apparent that CH_3ONO is being consumed with increasing exposure, and that HCHO is being formed. Reaction [11] would explain this behavior. The fact that the quantum yield of CH_3ONO is only 0.56 with an equimolar mixture of CH_3OH and NO, whereas one would expect a value near unity, would point up the importance of [9] and to a much lesser extent [11]. It should be emphasized here that in mercury photosensitization the reaction zone is confined to a small volume near the incident window, owing to the high absorption coefficient of mercury for its own resonance radiation. Radical concentrations will therefore be high in this zone, and secondary reaction will be very difficult to eliminate. Finally, in the inhibited reaction, it will be noted from Fig. 3 that $\Phi^0(H_2)$ retains a small but finite value of ca. 0.01. Since this value is not appreciably reduced by increasing $P(NO)$, it is likely that hydrogen is forming by a step postulated by Levy (13):

$$NOH + NOH \rightarrow 2NO + H_2. \qquad [12]$$

For pure substrate, at a partial pressure of 5 μ, in 8 mm He carrier, Pottie, Harrison, and Lossing (9) at 55° find HCHO to be an important product whereas at 50 mm pressure, we find this product to be of minor significance with $\Phi^0(HCHO) = 0.01$ (cf. Fig. 4). This is what would be expected if HCHO is formed by the disproportionation of CH_3O radicals:

$$CH_3O + CH_3O \rightarrow CH_2O + CH_3OH. \qquad [13]$$

At high substrate pressures the CH_3O radicals would disappear largely by [3]. Hence it appears unlikely that CH_2OH radicals are involved in HCHO formation. With increasing duration of exposure, it is apparent from Figs. 3 and 4 that extensive secondary decomposition is occurring in the methanol reaction. It would seem unprofitable to discuss these reactions in detail here.

Since the bulk of the reaction in mercury photosensitization is confined to a zone near the incident window, as pointed out above, special techniques must be employed to study the rates of the primary reactions, without complication by secondary processes. In this laboratory chopped-beam techniques are being investigated to this end. During the dark period, products and radicals can diffuse away from the reaction zone, thereby decreasing the extent of secondary reaction. By such studies it is hoped to obtain information on the primary efficiency of the methanol reaction, and on other mercury-photosensitized reactions involving primary bond scission.

CONCLUSIONS

As a principal result of this investigation, it has been shown that the CH_2OH radicals responsible for ethylene glycol formation in the reaction of methanol with Hg $6(^3P_1)$ atoms arise by a secondary reaction of primary CH_3O radicals with the substrate. In this respect our findings are in agreement with the mass spectrometric results obtained by Pottie *et al.* (9). Our study also suggests that nitric oxide should be of value in trapping alkoxy radicals through the formation of the nitrite.

Similar studies on ethanol and isopropanol are in progress in this laboratory and will be published shortly.

ACKNOWLEDGMENTS

The authors would like to express their deep appreciation to Dr. W. F. Allen of this laboratory for valuable assistance and many helpful discussions, and to Mr. A. G. Sherwood for supplying the nitric oxide used in this investigation.

Our program was supported in part by the National Research Council under Block Term Grant No. BT-74. This assistance is most gratefully acknowledged.

REFERENCES

1. D. BERTHELOT and H. GAUDECHON. Compt. rend. **151**, 478 (1920).
2. R. BATES and H. S. TAYLOR. J. Am. Chem. Soc. **49**, 2436 (1927).
3. M. K. PHIBBS and B. DE B. DARWENT. J. Chem. Phys. **18**, 495 (1950).
4. Y. TAKEZAKI and C. TAKEUCHI. J. Chem. Phys. **22**, 1527 (1954).
5. M. H. J. WIJNEN. J. Chem. Phys. **27**, 710 (1957); **28**, 271 (1958).
6. P. GRAY and A. WILLIAMS. Chem. Revs. **59**, 240 (1959).
7. R. P. PORTER and W. A. NOYES, JR. J. Am. Chem. Soc. **81**, 2307 (1959).
8. R. PERTEL and H. E. GUNNING. Can. J. Chem. **37**, 35 (1959).
9. R. F. POTTIE, A. G. HARRISON, and F. P. LOSSING. Can. J. Chem. **39**, 102 (1961).
10. R. P. PORTER. J. Phys. Chem. **61**, 1260 (1957).
11. S. BYWATER and E. W. R. STEACIE. J. Chem. Phys. **19**, 319 (1951).
12. J. A. GRAY and D. W. G. STYLE. Trans. Faraday Soc. **48**, 1137 (1952).
13. J. B. LEVY. J. Am. Chem. Soc. **78**, 1780 (1956).
14. A. SEREWICZ and W. ALBERT NOYES, JR. J. Phys. Chem. **63**, 843 (1959).

Can. J. Chem. Downloaded from www.nrcresearchpress.com by 210.87.254.105 on 09/05/12
For personal use only.

Can. J. Chem. Downloaded from www.nrcresearchpress.com by 210.87.254.40 on 09/05/12
For personal use only.

RECOMBINATION OF ATOMS AT THE SURFACE OF THERMOCOUPLE PROBES[1]

KIN TSU AND M. BOUDART

ABSTRACT

When atoms produced by a discharge at one end of a closed cylindrical tube diffuse down the tube, their rate of recombination on the walls of the tube can be determined by measuring the temperature of a probe traveling along the axis of the tube. However, the catalytic activity of the probe may, under specified conditions, appear to be the same whatever the catalytic activity of the probe material. This effect is offered as a possible explanation of the findings of Wood and Wise, who recently reported essentially the same recombination probability for hydrogen atoms on 12 different metals.

INTRODUCTION

The rate of recombination of atoms on solid surfaces is a problem of considerable theoretical and practical interest. Recently, Wood and Wise (1), investigating the catalytic effect of various surfaces, have reported almost identical rates of recombination of hydrogen atoms on 12 different metals.*

This result is a very novel and interesting one. If confirmed by further work, it will require an explanation. While such an explanation may perhaps be found ultimately in the mechanism of recombination, it seems worth while to explore the possibility that this lack of catalytic specificity could actually be a result of the experimental technique used in the determination of rates of recombination.

It is shown below how this can happen. To this end, the method of Wood and Wise is reanalyzed first, for the sake of clarity, in an approximate way, then in more detailed fashion. The new solution presented is of general interest and its consequences are of special importance in investigations of recombination of atomic species.

DISK-SHAPED CATALYTIC PROBES: ONE-DIMENSIONAL APPROXIMATION

Consider a cylindrical reactor of radius R_0. It is closed at one end, filled with hydrogen at low pressure, and surrounded at the other end by a coil through which is sent a high-frequency a-c. current, so that an electrodeless discharge in the tube generates hydrogen atoms. These diffuse down the tube (dimensionless co-ordinate x equal to length divided by tube radius R_0). The walls of the tube are sufficiently inactive for recombination. Then there is no appreciable radial gradient in the concentration C of hydrogen atoms in the tube. Yet there is an axial gradient because atoms recombine on the walls of the tube. Transport of atoms is purely diffusive, if Stefan flow can be neglected, as is legitimate in suitable experimental situations where the concentration of atoms is not too high. The diffusivity of the atoms is D, and the probability of the first-order recombination on the walls is 2γ. The reason for the factor two is explained elsewhere (2).

Then, the equation of the problem is:

$$D\frac{d^2C}{dx^2} = R_0 v \gamma C$$

[1]*Manuscript received January 23, 1961.*
Contribution from the American Cyanamid Co., Stamford, Connecticut, and the Department of Chemical Engineering, Princeton, New Jersey. This paper was presented at the Symposium on Atomic Reactions, Montreal, Que., September 1960. This work was supported in part by the Office of Scientific Research, United States Air Force, under contract number AF-49-638-32. Reproduction, translation, publication, use, and disposal in whole or in part by or for the United States government is permitted.

**Aluminum was an exception. However, Dr. Wise kindly informs us that further work in his laboratory has not confirmed this anomalous behavior and that aluminum behaves very much like the other 12 metals tested.*

where v is the mean molecular speed of hydrogen atoms as given by gas-kinetic theory.

The first boundary condition, on the side of the discharge will be assumed to be, as usual:

$$C = C_0 \qquad \text{at} \qquad x = 0.$$

The second boundary condition is provided by a disk-shaped catalytic probe, filling the cross section of the tube, at a distance $x = L$ from the discharge. If the rate of recombination on the surface of the probe is first-order and characterized by a probability γ', the second boundary condition is:

$$-D\frac{dC}{dx} = R_0\frac{v}{4}\gamma' C \qquad \text{at} \qquad x = L.$$

With these boundary conditions, the equation of the problem admits the solution:

$$\frac{C}{C_0} = \frac{F e^{m(L-x)} - e^{-m(L-x)}}{F e^{mL} - e^{-mL}}$$

with the following values for F and m:

$$m = \left(\frac{R_0 v \gamma}{D}\right)^{1/2}; \qquad F = \frac{h+m}{h-m}; \qquad h = R_0\frac{v\gamma'}{4D}.$$

This solution gives immediately the concentration C_L of atoms at the surface of the probe, i.e. at $x = L$:

$$\frac{C_0}{C_L} = \frac{1}{2m}[(h+m)e^{mL} - (h-m)e^{-mL}].$$

Now, because of the heat of recombination, the temperature of the probe will be higher than the ambient temperature by the amount ΔT, which must be proportional to the rate of heat release at the probe, i.e. to the concentration of atoms at the probe surface and to the probability of recombination at the probe. Thus:

$$\Delta T = \gamma' K C$$

where K is a proportionality constant.

If the probe is at the origin, $C = C_0$ and $\Delta T_0 = K C_0 \gamma'$, while at a distance L from the origin $C = C_L$ and $\Delta T_L = K C_L \gamma'$. Therefore from measurements of ΔT_0 and ΔT_L at various distances L,

$$\frac{\Delta T_0}{\Delta T_L} = \frac{C_0}{C_L} = \frac{1}{2m}[(h+m)e^{mL} - (h-m)e^{-mL}],$$

it appears possible to determine both h and m and thus also both γ and γ', the probabilities of recombination on the walls of the tube and on the surface of the probe. This is how Wood and Wise (1) have determined the activity of different metal probes. In fact, they have made use of a three-dimensional solution, with probe geometry identical with that used here. If the activity of the wall is small, the difference between the solution shown here and the complete solution (1) is negligible.

The validity of this solution will now be questioned. Is it correct to assume that the concentration of atoms C in the discharge at the origin remains a constant C_0 irrespective of the position of the probe? Is it not expected that an active probe in the vicinity of the origin, that is near the discharge, will deplete the atomic concentration in the discharge? In other words, is the first boundary condition, $C = C_0$ at $x = 0$, a valid one?

Can. J. Chem. Downloaded from www.nrcresearchpress.com by 210.87.254.40 on 09/05/12
For personal use only.

In order to examine this question, a more refined analysis of the situation near the origin is necessary. Two distinct regions are now considered: the discharge zone for $x < 0$ and the measurement zone for $x > 0$. In the discharge, the number of atoms generated uniformly per unit volume per unit time will be represented by Q'. With $Q = R_0^2 Q'/D$, the equations of the problem become:

$$\frac{d^2C_1}{dx^2} + Q - m^2 C_1 = 0, \qquad -\infty < x < 0$$

$$\frac{d^2C_2}{dx^2} - m^2 C_2 = 0, \qquad 0 < x < L$$

$$\frac{dC_1}{dx} + h\,C_1 = 0 \qquad \text{at} \qquad x = L$$

$$C_1 = C_2 \qquad \text{and} \qquad \frac{dC_1}{dx} = \frac{dC_2}{dx} \qquad \text{at} \qquad x = 0.$$

The solution of these equations is:

$$C_L = \frac{Q}{m(m+h)}\, e^{-mL}.$$

Also:

$$C_0 = \frac{Q}{m(m+h)}.$$

Thus:

$$\frac{C_0}{C_L} = \frac{\Delta T_0}{\Delta T_L} = e^{mL}.$$

Consequently, it is seen that an experimental curve of $\Delta T_0/\Delta T_L$ versus distance L depends only on m, i.e., on the rate of recombination at the wall. But it will not depend on h, i.e., on the catalytic activity of the probe. Such profiles of temperature versus distance are therefore unsuitable for measurements of the activity of the probe. An analysis of the data, based on the previous boundary condition $C = C_0$ at $x = 0$, ignoring the effect of the probe on the concentration of atoms at the origin, would reveal an apparently identical catalytic activity of all probe materials.

SPHERICAL CATALYTIC PROBES: THREE-DIMENSIONAL SOLUTION

The analysis of the problem with a disk-shaped probe is only an approximation because, in practice, the catalytic probe is positioned along the axis of the tube and occupies only a small fraction of the cross-sectional area of the tube.

A more realistic analysis will now be attempted in order to corroborate the conclusion just arrived at on the basis of an approximate analysis.

The three-dimensional solution is obtained by first considering the following problem. Atoms are continuously liberated from a point source of unit strength located on the central axis of an infinite cylinder. An atomic sink of variable strength β is also placed on the central axis but at a variable distance from the source. Atoms may recombine on the cylinder walls in the usual manner. The radial co-ordinate r is dimensionless, equal to radial length divided by R_0.

Can. J. Chem. Downloaded from www.nrcresearchpress.com by 210.87.254.40 on 09/05/12
For personal use only.

The concentration of atoms in the cylinder is described by the differential balance:

$$\frac{\partial^2 C}{\partial r^2}+\frac{1}{r}\frac{\partial C}{\partial r}+\frac{\partial^2 C}{\partial x^2}=0, \qquad -\infty < x < \infty$$

with the boundary condition

$$\frac{\partial C}{\partial r}+BC=0 \qquad \text{at} \qquad r=1$$

where $B=\gamma v R_0/2D$. Further conditions are: a source of unit strength at $r=0$, $x=0$ and a sink of strength $-\beta$ at $r=0$, $x=L$. Thus β is expressed in number of atoms per unit time.

The solution is readily obtained from the principles discussed in reference 3.

[1] $$C=\frac{1}{2\pi DR_0}\sum_{i=1}^{\infty}\left[e^{-\alpha_i|z|}-\beta\, e^{-\alpha_i|z-L|}\right]\frac{\alpha_i J_0(\alpha_i r)}{(\alpha_i^2+B^2)J_0^2(\alpha_i)}$$

where α_i are the roots of

$$\alpha_i J_1(\alpha_i)-B J_0(\alpha_i)=0$$

and J_0, J_1 are Bessel functions in the usual nomenclature.

Now imagine a sphere of dimensionless radius r' surrounding the sink. This will represent the catalytic thermocouple probe whose surface is covered by a metal under study.

The net flux of atoms into the sink can be represented by the total rate of reaction of atoms on the probe surface.

$$J=-\oint\frac{v}{4}\gamma' C\, dS$$

The integral is taken over the surface of the sphere of radius r'. But the flux must be equal to the strength of the sink $-\beta$.

$$J=-\beta.$$

Therefore

[2] $$\beta=\oint\frac{v}{4}\gamma' C\, dS.$$

The concentration C under the integral in this last equation is evaluated from equation [1] using the relationship

[3] $$r^2+(x-L)^2=(r')^2$$

for all points on the surface of the sphere.

Thus (given the known physical constants: D, R_0, r', v) β can be evaluated in terms of γ, γ', and L by the use of equations [1], [2], and [3]. β is the sink strength and corresponds directly to the temperature measured by the thermocouple probe at any position L.

Fig. 1 shows some calculated results obtained from the present three-dimensional solution. The corresponding three-dimensional solution published by Wise *et al.* (1) is shown by the dashed curves. Our results are plotted as $1/\beta-1$ vs. L and are extrapolated to read zero for $L=0$ (curves 1 and 2). The results of Wise *et al.* are plotted as $n_0/n-1$ vs. L (curves 3 and 4). Following these authors, n stands for atomic concentration. The values of the parameters used in calculating the curves are listed in Table I.

Can. J. Chem. Downloaded from www.nrcresearchpress.com by 210.87.254.40 on 09/05/12
For personal use only.

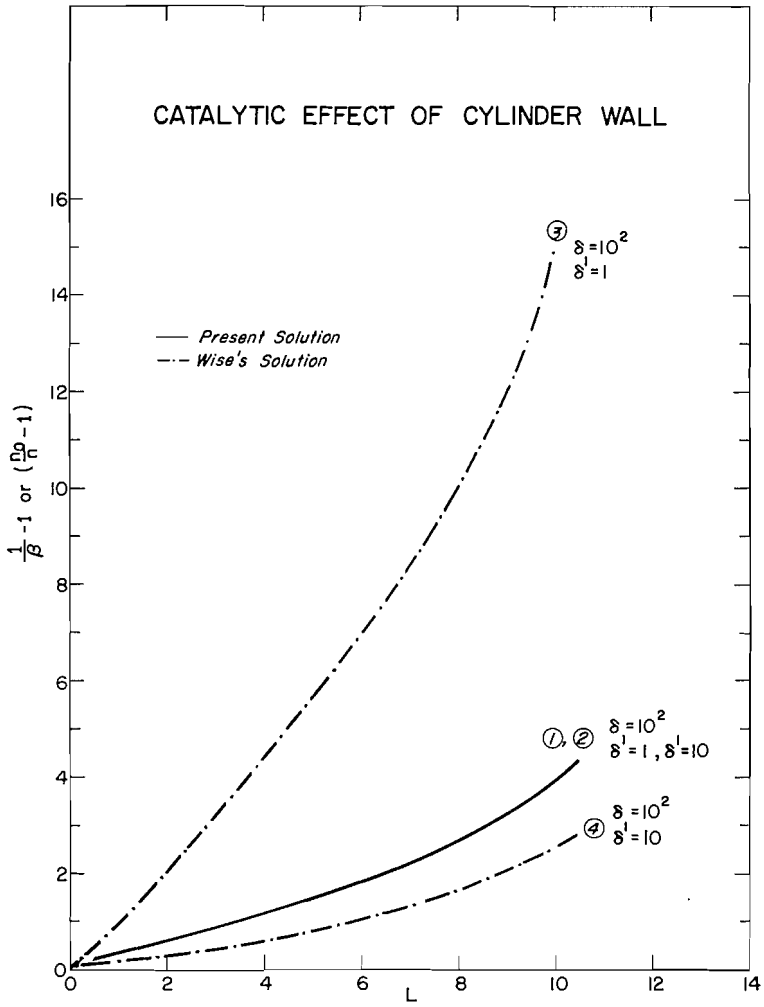


FIG. 1. Depletion of atoms, as expressed by $(n_0/n-1)$ or $1/\beta-1$, as a function of axial distance. Abscissae: L co-ordinate. Ordinates: broken curves, calculated following Wise *et al.*: $n_0/n-1$ vs. L with $\delta = 1/B = 10^2$; upper curve: $\delta' = 1/h = 1$; lower curve: $\delta' = 1/h = 10$; full curve, calculated from equations [1], [2], and [3]: superposed curves (1) and (2) $1/\beta-1$ vs. L for $\delta = 10^2$, $\delta' = 1$, *or* $\delta' = 10$.

TABLE I

Parametric values used in calculating curves in Figs. 1 and 2

Diffusivity, D_{H-H_2}, cm²/sec	2.3×10^4
Tube radius, R_0, cm	1.9
Velocity of H atoms, v, cm/sec	2.6×10^5
Probe radius, r', dimensionless	0.2
Recombination probability on tube walls, γ, dimensionless	9.3×10^{-4}

It is immediately seen that according to the present analysis, curves 1 and 2 are superposed to give a single curve for values of the catalytic activity of the probe differing by a factor of 10, namely $\gamma' = 0.186$ (curve 1) and $\gamma' = 0.0186$ (curve 2). The analysis of

Can. J. Chem. Downloaded from www.nrcresearchpress.com by 210.87.254.40 on 09/05/12
For personal use only.

Wise *et al.* based upon the doubtful boundary condition at the origin shows two separate curves for two different probe catalysts. This result had, of course, been anticipated by the one-dimensional solution. Thus the experiments carried out and analyzed by Wise *et al.* should indicate and do indicate that all metals possess the same catalytic activity for atom recombination, if probes of the same size r' are used in all cases.

It must be noted that minor differences in the catalytic activity of various probes may be explained, in the light of the present analysis, by differences in the size of the probes. Indeed, the size of the probe, in the more realistic model presented here, enters into the problem as one of the parameters of the system. This, of course, is not apparent in previous treatments using a hypothetical disk-shaped probe.

DISCUSSION

The present analysis of the technique of thermocouple probes does not purport to show that the technique does not provide a good way to measure catalytic recombination of atomic species.

First of all, for the measurement of the catalytic activity of the walls of the tube, when this activity is not too high, the method is indeed an excellent one as established in a definitive fashion by the work of Linnett *et al.* (4), who showed that identical results were obtained whether the atomic concentration in the tube was measured by a thermocouple catalytic probe or by a Wrede-Harteck gauge. The validity of the method will again be demonstrated below.

The possibility of measuring also the relative catalytic activity of probe materials by means of thermocouple probes is first suggested by the one-dimensional treatment. It was shown that

$$\Delta T = \gamma' K C_L$$

with

$$C_L = \frac{Q}{m(m+h)} e^{-mL}.$$

Therefore, if two different probes with efficiencies γ_1' and γ_2' are positioned in the tube at a distance L from a constant source Q, the value say of γ_2', if γ_1' is known, can be obtained from the temperature rise of the two probes ΔT_1 and ΔT_2:

$$\frac{\Delta T_1}{\Delta T_2} = \frac{\gamma_1'}{\gamma_2'} \frac{(m+h_2)}{(m+h_1)}.$$

The proper way to use the technique of the thermocouple probe in order to determine the catalytic activity of the probe is illustrated in Fig. 2 based on the three-dimensional treatment. Plots of β versus L are shown and the numbering of curves corresponds to that used in Fig. 1. It is noted that curves 1 and 2 of Fig. 2 have exactly the same shape; this is the reason why they become superimposed into one curve in Fig. 1. Results following Wise *et al.* are plotted as $\Delta T/\Delta T_0$ for comparison (curves 3 and 4). Curve 4 has been normalized to read 0.1 at $L = 0$ since the probe catalyst is 10 times less active than for curve 3.

The displacement between curves 1 and 2 (present solution) is the result of the different catalytic activity of the two probes. Thus, as already apparent from the one-dimensional solution, the ratio of the temperature rises measured by two different probes under the same experimental conditions is related to the relative catalytic activities of the two

Can. J. Chem. Downloaded from www.nrcresearchpress.com by 210.87.254.40 on 09/05/12
For personal use only.

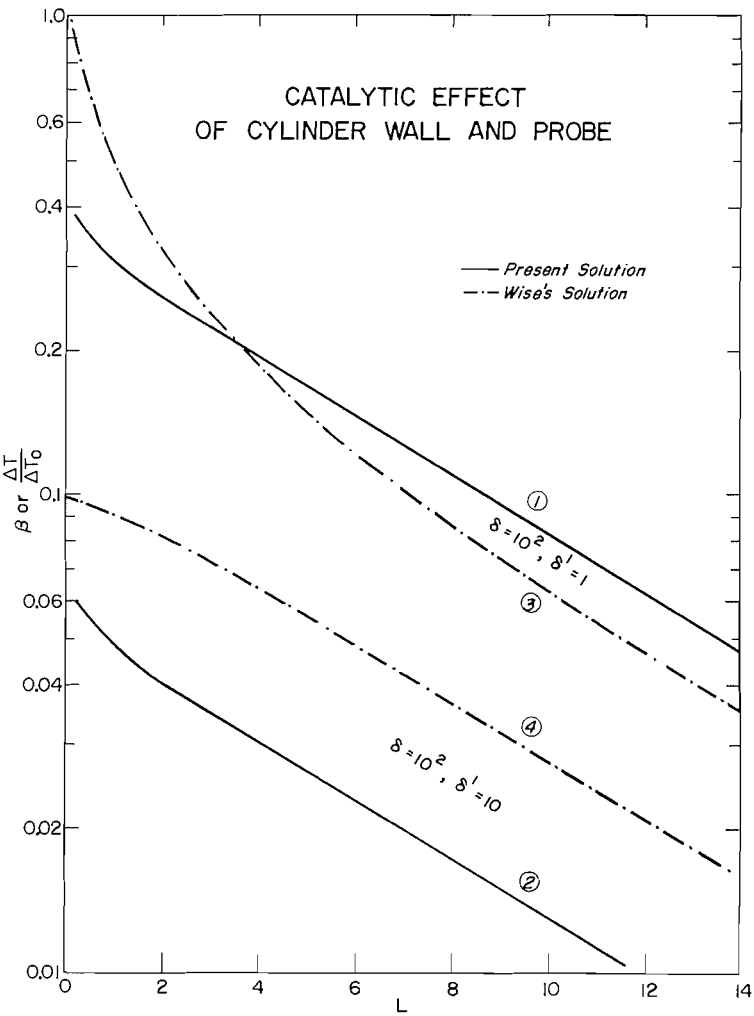


FIG. 2. Semilogarithmic plot showing depletion of atoms as a function of axial distance. Abscissae: L co-ordinate. Ordinates: full curves 1 (upper) and 2 (lower) calculated from equations [1], [2], and [3]: β vs. L for $\delta = 10^2$, $\delta' = 1$ (upper), and $\delta' = 10$ (lower); broken curves 3 (upper) and 4 (lower) calculated following Wise *et al.*: $\Delta T/\Delta T_0$ vs. L for $\delta = 10^2$, $\delta' = 1$ (upper), and $\delta' = 10$ (lower).

probes. It must be noted that this method of obtaining the relative catalytic activities of various surfaces is only an elaboration of the simpler technique used by Katz, Kistiakowsky, and Steiner (5). It is noted that the displacement between curves 3 and 4 (Wise's solution) is not the same as between curves 1 and 2. This is a reflection upon the fact that Wise *et al.* did not take into account the actual size and shape of the thermocouple probe. Since the displacement is also a function of probe radius, a convenient experimental verification of equations [1], [2], and [3] could be carried out by using different sized probes but the same metal catalyst.

In regard to Fig. 2, it is seen that the logarithmic slope at large L becomes identical for all curves.

This common slope is determined only by γ, the probability of recombination on the

Can. J. Chem. Downloaded from www.nrcresearchpress.com by 210.87.254.40 on 09/05/12
For personal use only.

tube walls. It is independent of probe activity or radius. Thus the more complete treatment presented here substantiates, as expected, the results of Linnett and Marsden (4): the experimental results of these and other authors (2) who have used a simplified analysis to calculate the small catalytic activity of tube walls remain perfectly valid.

CONCLUSION

When the perturbing effect of a catalytic probe on the concentration of atoms in a discharge is taken into account, thermocouple probes may indicate similar or even identical apparent catalytic activities of metals covering the probes under investigation.

A solution of the problem is presented which, for the first time, assumes a probe of realistic shape and size and not the hypothetical flat disk used in previous treatments. The conditions for the correct application of the probe method then become clearly delineated.

REFERENCES

1. J. B. Wood and H. Wise. J. Chem. Phys. **29**, 1417 (1958); H. Wise and C. M. Ablow. J. Chem. Phys. **29**, 634 (1958).
2. K. Tsu and M. Boudart. In press.
3. H. S. Carslaw and J. C. Jaeger. Conduction of heat in solids. Oxford University Press. 1959.
4. J. W. Linnett and D. G. H. Marsden. Proc. Roy. Soc. A, **234**, 489 (1956).
5. S. Katz, G. B. Kistiakowsky, and R. F. Steiner. J. Am. Chem. Soc. **71**, 2258 (1949).

Can. J. Chem. Downloaded from www.nrcresearchpress.com by 210.87.254.40 on 09/05/12
For personal use only.

Can. J. Chem. Downloaded from www.nrcresearchpress.com by 210.87.254.6 on 09/05/12
For personal use only.

DIPOLE MOMENTS AND STRUCTURE OF MOLECULAR COMPOUNDS

PART I. ALIPHATIC AND AROMATIC AMINE PICRATES[1]

R. RAMAN AND SUNDARESA SOUNDARARAJAN

ABSTRACT

Dipole moment measurements have been made for some aliphatic and aromatic amine picrates in dioxane solution. The fractional ionic character of these complexes in the ground state has been calculated from μ_N, the observed value of dipole moment; μ_0, the vector sum of the moments of the components of the complex; μ_1, the moment resulting from complete one-electron transfer; and known values of S, using the charge-transfer theory of Mulliken. For these complexes of the $n+h\sigma_d$ type, the charge-transfer process lies in the direction of the symmetry axis N^+O^-, the picture corresponding to an energy of interaction U, versus charge-transfer co-ordinate (C) curve with a shallow minimum showing an inner complex corresponding to ($C = 1$), $b \simeq a^2$ or $b^2 > a^2$, and an activated complex (roughly between $C = 0.3$ to 0.5) corresponding to an intermediate.

INTRODUCTION

Molecular compounds have long been known, and theoretical considerations like the formation to a considerable extent of covalent bonds between the two components (2, 19), saturation of residual valencies (23), electrostatic induction (4), and polarization mechanism similar to an oxidation–reduction reaction (11, 13) have been put forth to describe the forces which bind the components of such compounds. Recently Weiss (28) suggested that an extension of the last idea in terms of an electron transfer from the donor to the acceptor can explain their formation and structure in detail. Brackman (3) then put forth the concept of complex resonance, by which the donor can share an electron pair with the acceptor by a process comparable to Lewis acid interaction and suggested that the color of the complex is not determined by either component but is a characteristic feature of the complex itself. This idea is shared by Mulliken (20, 21), who has recently integrated the various views to provide a theory of complex bonding which seems compatible with the known chemical and physical properties of molecular compounds.

Picric acid forms two types of picrates, (*a*) with strong organic bases, compounds having some of the properties of substituted ammonium salts, (*b*) with very weak bases, molecular complexes, which show pronounced color deepening with none of the properties commonly associated with salts. The colored compounds of the picric acid have been the subject of many investigations (5, 9, 12, 24). However, the nature of the binding forces in the complexes are best deduced by a study of the dipole moments of these compounds, since the interaction products are frequently more polar than the constituents. Examples of such systems involving the donor–acceptor type of non-saltlike complexes are given in a review by Andrews (1). Dipole moments of many of the saltlike molecular compounds have also been investigated (10, 14, 17, 18, 27). In this paper dipole moments of some aliphatic and aromatic amine picrates have been reported and interpreted in terms of Mulliken's theory.

EXPERIMENTAL

Materials and Their Purification

Dioxane

This solvent, used in this investigation, was purified by Eigenberger's method (25).

[1]*Manuscript received December 19, 1960.*
Contribution from the Department of Inorganic and Physical Chemistry, Indian Institute of Science, Bangalore 12, India.

Aromatic Amine Picrates

Aniline and dimethylaniline picrates were obtained by mixing the base solutions in benzene with hot saturated solutions of picric acid in benzene, both being recrystallized from absolute alcohol. The naphthylamines were treated in alcoholic solutions and the products recrystallized twice from ethyl alcohol:

aniline picrate:	yellowish needles, decomposes on heating;
dimethylaniline picrate:	greenish-yellow glistening crystals, melting point 163° C;
α-naphthylamine picrate:	greenish-yellow prismatic crystals, melting point 181° C (decomposes);
β-naphthylamine picrate:	yellow needles, decomposes into components on heating.

Ethylamine Picrate

Anhydrous ethylamine was dissolved in ice-cold water and was gradually neutralized by adding solid picric acid with stirring. The mixture was kept overnight and the solid cake obtained was washed with alcohol and twice recrystallized from alcohol, melting point 167° C.

Apparatus and Methods of Measurement

Measurements of dielectric constant were made using an a-c. mains operated heterodyne beat apparatus, details of which are given in an earlier paper (25). Densities of the solutions were determined using an Ostwald–Sprengel pycnometer with closed, ground-in caps at both ends. The electron polarization was calculated by the additivity of the bond refractions of Denbigh (7). Atomic polarization was neglected and the polarization of the solute at infinite dilution was obtained using the mean values of the Hedestrand constants α and β (25). In the case of aromatic amine picrates in dioxane solution the variation of dielectric constant with mole fraction of the solute was found to be linear only at dilute concentrations. For very dilute solutions non-linearity was observed below the mole fraction range of 0.0009 for aniline picrate, 0.00055 for dimethylaniline picrate, 0.00088 for α-naphthylamine picrate, and 0.00016 for β-naphthylamine picrate, the trend of the curve being similar in all these cases. Consequently the polarization at infinite dilution in these cases has been calculated using values from the linear portion. The data are given in Tables I and II.

TABLE I

(Temperature 35°±0.01° C; solvent: dioxane)

Mole fraction	Dielectric constant	Density	Mole fraction	Dielectric constant	Density
Aniline picrate			α-Naphthylamine picrate		
0.000143	2.21338	1.01764	0.000314	2.21294	1.01690
0.000528	2.22243	1.01818	0.000884	2.22777	1.01765
0.000901	2.23450	1.01852	0.001639	2.25561	1.01870
0.001409	2.26164	1.01917	0.001740	2.25743	1.01881
0.002924	2.35211	1.02105	β-Naphthylamine picrate		
0.004414	2.45365	1.02295	0.000162	2.20727	1.01700
Dimethylaniline picrate			0.000574	2.21814	1.01751
0.000149	2.22042	1.01768	0.001752	2.29061	1.01906
0.000676	2.23952	1.01824	0.001293	2.25981	1.01854
0.000552	2.23248	1.01811	Ethylamine picrate		
0.000672	2.23851	1.01824	0.000274	2.25535	1.01868
0.001316	2.27068	1.01893	0.000428	2.28025	1.01884
			0.000525	2.29757	1.01898
			0.002536	2.59431	1.02116

Can. J. Chem. Downloaded from www.nrcresearchpress.com by 210.87.254.6 on 09/05/12
For personal use only.

TABLE II

Picrate	Mol. wt.	Hedestrand α	Hedestrand β	Total polarization (cm^3)	Molar refraction (cm^3)*	Orientation polarization (cm^3)	Dipole moment (Debye)
1. Aniline	322.23	28.31	1.218	977.09	78.09	899.00	6.74
2. Dimethylaniline	350.29	22.90	1.042	814.73	87.73	727.00	6.06
3. α-Naphthylamine	372.29	16.42	1.333	603.88	93.63	510.25	5.08
4. β-Naphthylamine	372.29	30.25	1.296	1052.63	93.63	959.00	6.96
5. Ethylamine	274.13	66.03	1.041	2188.02	63.05	2124.97	10.37

*Calculated from bond refractions of Denbigh (7).

THEORETICAL CALCULATIONS

Calculation of the Ionic Character Using Mulliken's Theory

The theory of Mulliken can be applied to a wide variety of donor D and acceptor A entities. In the present context, the donors are the neutral (n) onium bases (the aromatic and aliphatic amines), while the acceptor is the picric acid, which forms fairly stable compounds, viz. the amine picrates. For the donor–acceptor resonance complex, the wave function of the ground state N is

$$\psi_N = a\psi_0 + b\psi_1. \quad [1]$$

Here ψ_0 is the no-bond wave function of AD in the equilibrium separation r_{AD} without the consideration of exchange forces, i.e. the quantum mechanical first-order value. The wave function ψ_1 is the dative-bond wave function of the polar state D^+A^- corresponding to transfer of an electron from D to A and contains exchange forces; ψ_N is approximated by the sum of the two terms alone and, from the normalization condition $\int \psi_N^2 dv = 1$, the coefficients a and b in equation [1] are related by

$$a^2 + 2abS + b^2 = 1 \quad [2]$$

where S is evaluated from the Slater overlap integral S_{AD} (22) by means of the relationship

$$S \simeq 2^{\frac{1}{2}}[(1+S_{AD}^2)]^{-\frac{1}{2}} S_{AD}.$$

The dipole moment of the charge-transfer process lies in the direction of the symmetry axis N^+O^-. On account of the insignificant overlapping of ψ_A and ψ_D due to large distance (3.22 Å), S is very small. The moment μ_N (the experimentally determined value) is given by

$$\mu_N = \int \psi_N M \psi_N dv = a^2\mu_0 + b^2\mu_1 + 2ab\mu_{01} \quad [3]$$

where μ_0 is the vector sum of the component moments of A and D, $\mu_1 = er_{AD}$ (e, the electronic charge, and r_{AD}, the equilibrium distance between N^+ and O^- atoms, i.e. 3.22 Å taken from the X-ray data for hydroxylamine hydrochloride (16)) and

$$\mu_{01} = \tfrac{1}{2}(\mu_1 - \mu_0)S + S\mu_0 \quad [4]$$

so that

$$\mu_N = a^2\mu_0 + b^2\mu_1 + abS(\mu_1 - \mu_0) + 2abS\mu_0.$$

From known values of S, μ_1, μ_0, and μ_N, the coefficients a and b and the values of $b^2/(a^2+b^2)$ taken as corresponding to the ionic character of the compound have been calculated.

Can. J. Chem. Downloaded from www.nrcresearchpress.com by 210.87.254.6 on 09/05/12
For personal use only.

The values are given in Table III. (R_{ab} = 3.22 Å taken from N—O distance in hydroxylamine hydrochloride (16); $\mu_1 = 4.803 \times 3.22$ Å = 15.46 D; S = 0.0177, calculated from

TABLE III*

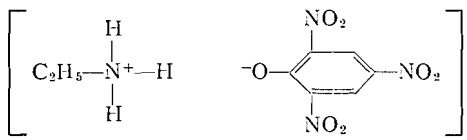
Picrate	Moment of the base	Covalent moment, μ_0	Moment of the complex	a	b	$b^2/(a^2 + b^2)$
Aniline	1.54	2.533	6.742	0.8114	0.5707	0.3310
Dimethylaniline	1.58	2.565	6.063	0.8448	0.5210	0.2751
α-Naphthylamine	1.49	2.492	5.079	0.8861	0.4469	0.2029
β-Naphthylamine	1.77	2.722	6.960	0.8067	0.5772	0.3386
Ethylamine	1.37	1.714	10.365	0.5954	0.7932	0.6396

*μ resultant of picric acid (1.57 D) (18) was taken as acting at an angle of 71° to the C—O bond. This angle was derived from the bond moment values of 0.8 D for the C—O link and 1.51 D for the H—O link, from which a resultant moment of 1.57 D and an angle of 101° was obtained for the COH angle. In all the aromatic amines the hydrogen or the methyl groups of the amino group were assumed to be in plane with the aromatic rings (consistent with the theoretical treatment of aniline by Coulson (6)) and the resultant moments were assumed to act from N → C (8). For ethylamine the resultant moment was assumed to act from the nitrogen atom in the direction of the lone pair orbital (N → :).

S_{ab}, Slater overlap integral using Slater μ values for N^+ and O^- ions (22); mainly because of its strong dependence on the uncertain quantity S, the value of b can only be relative.)

DISCUSSION

Though the stable compounds of the amine picrate type can be discussed in terms of the same general theoretical framework of Mulliken, there are some important differences. It is convenient to visualize that picric acid be placed near the amine with hydrogen directly between the nitrogen of the amine and the oxygen of picric acid at a distance approximately equal to that in the ionic but undissociated complex, i.e.



Mulliken has outlined the various possible modes of interaction of donor–acceptor pair by plotting the energy of interaction U against a co-ordinate C (called the charge-transfer co-ordinate) which increases continuously with the charge transfer, subject to the added specification that the nuclear skeleton be so adjusted for each value of C as to make U as small as possible. For the above situation C could still be only a little larger than zero. If C is allowed to increase, the hydrogen atom comes towards the nitrogen atom, the tendency being to set up tetrahedral angles around nitrogen (sp^3 hybridization). The N—O distance adjusted according to the above definition very nearly remains constant. According to Mulliken an increase in C corresponds to a likely increase in U because, (i) the non-bonded repulsions with ψ_0 increase, (ii) the amount b^2/a^2 of the higher-energy wave function ψ_1 increases. However, other factors that diminish U as C increases are (i) electrostatic polarization within ψ_0, (ii) decrease in the energy of ψ_1 due to increasing attractions and decreasing repulsions as the H moves towards the nitrogen atom, (iii) decrease in the energy of ψ_1 because of "dative polarization", and (iv) resonance between ψ_1 and ψ_0. In the present case the amine is the lone pair or onium donor (n) and the picric acid an even-bonding electron hydrogen acid ($h\sigma$) acceptor. The ultimate picture of these factors for complexes of the $n+h\sigma_d$ type should probably be a $U(C)$ curve with a shallow minimum showing an inner complex corresponding to (C = 1), $b^2 \approx a^2$ or $b^2 > a^2$, and an

Can. J. Chem. Downloaded from www.nrcresearchpress.com by 210.87.254.6 on 09/05/12
For personal use only.

activated complex (roughly between $C = 0.3$ to 0.5). The variation of ionic character values (b^2/a^2+b^2) from 0.640 for ethylamine picrate to 0.203 for α-naphthylamine picrate in dioxane solution shows that the structure of the picrates varies in between the inner complex with maximum transfer and the activated complex. According to Mulliken for such $n+h\sigma$ pairs the charge-transfer forces may be too weak to give rise to an outer complex.

If the inner complex becomes energetically the stable form, complete dissociation into solvated ions may result if the assisting agent is an ionizing solvent. This electrolytic dissociation occurs at a constant value of 1 for C, the inner complex corresponding to maximum charge transfer and 100% ionic character. In the present case of amine picrates where a σ bond is broken, even assuming that two ions are formed, they still cohere because of the presence of the non-ionizing solvent, dioxane.

Previously Kraus *et al.* (10) and Maryott (18) have determined independently the dipole moments of picrates of alkylamines in benzene and dioxane solutions, the observed moments lying between 12 and 18 D. They explained that these large dipole moments are due to the presence in solution of an ion pair A^-HD^+. Very recently Tsubomura (26) has measured the moments of a series of organic salts (viz. anilinium and pyridinium picrates, trimethylamine–phenol complexes, and trimethylamine–haloacetic acid complexes etc.) with a view to studying the proton transfer in these compounds. Tsubomura concluded that the picrates as well as the amine – haloacetic acid complexes are ion pairs on the basis of the differences in the moment $\Delta\mu$ between the observed moments and the structure moments, which are the vector sum of the component moments. The trimethylamine – acetic acid complex was characterized as having an incomplete proton transfer, whereas the other complexes studied (e.g. hexamethylene tetramine complexes) were characterized as belonging to that of the hydrogen-bonded type. However, his expectation of the possibility of determining whether an acid–base pair is an ion pair or a hydrogen-bonded complex is based on erroneous grounds because a molecular compound cannot be rigidly classified as belonging to one or other of the two types on the basis of the observed moments of the complex as has been pointed out by Sutton *et al.* (15).

ACKNOWLEDGMENTS

The authors wish to record their deep sense of gratitude to Professor K. R. Krishnaswami for his keen interest and guidance during the progress of this work, and to Professor M. R. Aswathanarayana Rao for his invaluable suggestions. One of the authors (R. Raman) is thankful to the Government of India for awarding him a senior research scholarship during the course of this study.

REFERENCES

1. L. J. ANDREWS. Chem. Revs. **54**, 713 (1954).
2. G. M. BENNETT and G. H. WILLIS. J. Chem. Soc. 256 (1929).
3. W. BRACKMAN. Rec. trav. chim. **68**, 147 (1949).
4. G. BRIEGLEB. Zwischen-molekulare Kräfte und Molekül-Struktur. G. Braun, Karlsruhe, Germany. 1949.
5. W. R. BURTON and R. E. RICHARDS. J. Chem. Soc. 1316 (1950).
6. C. A. COULSON. Valence. Oxford University Press, Amen House, London. 1952. pp. 244, 256.
7. K. G. DENBIGH. Trans. Faraday Soc. **36**, 936 (1940).
8. K. B. EVERARD and L. E. SUTTON. J. Chem. Soc. 2818 (1951).
9. R. FOSTER, D. LL. HAMMICK, and A. A. WARDLEY. J. Chem. Soc. 3817 (1953).
10. J. A. GEDDES and C. A. KRAUS. Trans. Faraday Soc. **32**, 585 (1936).
11. R. E. GIBSON and O. H. LOEFFLER. J. Am. Chem. Soc. **62**, 1324 (1940).
12. H. V. HALBAN and B. SZIGETI. Helv. Chim. Acta, **20**, 746 (1937).
13. D. LL. HAMMICK and R. B. M. YULE. J. Chem. Soc. 1539 (1940).

Can. J. Chem. Downloaded from www.nrcresearchpress.com by 210.87.254.6 on 09/05/12
For personal use only.

14. G. S. HOOPER and C. A. KRAUS. J. Am. Chem. Soc. **56**, 2265 (1934).
15. J. R. HULETT, J. A. PEGG, and L. E. SUTTON. J. Chem. Soc. 3901 (1955).
16. B. JERSLEV. Acta Cryst. **1**, 21 (1948).
17. G. KORTÜM and H. WALZ. Z. Elektrochem. **57**, 73 (1953).
18. A. A. MARYOTT. J. Research Natl. Bur. Standards (U.S.), **41**, 1, 7 (1948).
19. T. S. MOORE, F. SHEPHERD, and E. GOODALL. J. Chem. Soc. 1447 (1931).
20. R. S. MULLIKEN. J. Am. Chem. Soc. **74**, 811 (1952).
21. R. S. MULLIKEN. J. Phys. Chem. **56**, 801 (1952).
22. R. S. MULLIKEN, C. A. RIEKE, D. ORLOFF, and H. ORLOFF. J. Chem. Phys. **17**, 1248 (1949).
23. P. PFEIFFER. Organische Molekül verbindungen. 2nd ed. Ferdinand Enke, Stuttgart, Germany. 1927.
24. C. SHINOMIYA. Bull. Chem. Soc. Japan, **15**, 259, 309 (1940).
25. S. SOUNDARARAJAN. Trans. Faraday Soc. **53**, 159 (1957).
26. H. TSUBOMURA. Bull. Chem. Soc. Japan, **31**, 435 (1958).
27. H. TSUBOMURA and S. NAGAKURA. J. Chem. Phys. **27**, 819 (1957).
28. J. WEISS. J. Chem. Soc. 245 (1942); 462 (1943).

Can. J. Chem. Downloaded from www.nrcresearchpress.com by 210.87.254.6 on 09/05/12
For personal use only.

Can. J. Chem. Downloaded from www.nrcresearchpress.com by 210.87.254.105 on 09/05/12
For personal use only.

THE HELLMANN–FEYNMAN THEOREM AND CHEMICAL BINDING[1]

RICHARD F. W. BADER AND GLENYS A. JONES[2]

ABSTRACT

The advantages of the electrostatic interpretation of chemical binding are illustrated. It is shown that the forces exerted by the electrons in a molecular orbital may be determined by general expressions. These are functions of only one parameter, the value of which is easily specified for a particular case. From the general expressions it is possible to obtain quantitative measures of the bonding or antibonding power of a molecular orbital. It is shown that the usual interpretations of bonding and antibonding properties in molecular orbital theory are misleading and that few orbitals are, in actual fact, antibonding. If molecular orbitals are classified as *net bonding* or *net antibonding*, terms which are precisely defined and have a definite physical significance, a much closer correlation with previous concepts of bonding is obtained. The effects of mutual orthogonalization within a set of orbitals are studied. It is found that this procedure decreases the bonding ability of bonding orbitals, but increases that of antibonding orbitals. The dangers of disregarding such orthogonalization in a conventional calculation are clearly illustrated.

I. INTRODUCTION

The Hellmann–Feynman theorem permits one to relate the forces acting on a nucleus in a molecule to the classical electrostatic forces exerted on the nucleus by the other nuclei and by the particular distribution of electrons found in the molecule. This relationship may be expressed as

$$F_{\alpha x} = \frac{\partial}{\partial x_\alpha}\left(\sum_{\beta(\neq\alpha)} \frac{Z_\alpha Z_\beta e^2}{r_{\alpha\beta}}\right) - e\int \rho \mathscr{E}_{\alpha x} dr \qquad [1]$$

where $\rho(x, y, z,)$ is the electron density, $\mathscr{E}_{\alpha x}$ the electric field produced by the αth nucleus in the x direction at the position of the ith electron, and Z_α is the nuclear charge of atom α. In a previous paper (1) we have shown that equation [1] is capable of providing reasonable results for the binding energies of simple molecules. At that time it was stated that the Hellmann–Feynman theorem provides a qualitative interpretation of chemical binding that is perhaps more readily understandable than is the usual discussion which is couched in terms of energies. The reason for this is that the electron density present in a molecule is a real three-dimensional quantity. In employing the Hellmann–Feynman theorem one reduces a problem in molecular structure to a problem in classical electrostatics, a problem of the interaction of a system of nuclei and some continuous charge distribution. In this paper we wish to illustrate the advantages of this approach. Rather than press the Hellmann–Feynman theorem by attempting to calculate molecular energies through the use of approximately determined electron densities, we wish instead to demonstrate the ability of the theorem to provide us with useful semiquantitative results regarding the bonding character of various electron distributions.

II. THE HELLMANN–FEYNMAN THEOREM AND THE MOLECULAR ORBITAL APPROACH

When the molecular orbitals used in the description of the electronic structure of a molecule are all orthonormal, the electron density may be expressed as

$$\rho = \sum_i n_i \psi_i^* \psi_i$$

where the summation is over all of the occupied molecular orbitals and n_i (= 1 or 2) is

[1]*Manuscript received February 22, 1961.*
Contribution from the Department of Chemistry, University of Ottawa, Ottawa 2, Canada.
[2]*Recipient of a Commonwealth Scholarship.*

the occupation number. (In the general discussion which follows we shall confine ourselves to the case of a homonuclear diatomic molecule simply to avoid cumbersome notations. The extension to more complex molecules is straightforward.) Any of the products $\psi_i^*\psi_i$ may be expressed in terms of the atomic orbitals which are used to approximate the molecular orbital and, for a homonuclear diatomic molecule, this is

$$\psi_i^*\psi_i = N_i^2 (\phi_\alpha^2+\phi_\beta^2\pm 2\phi_\alpha\phi_\beta)$$

where the plus signs represent a bonding and the minus signs an antibonding combination, and N_i is the normalizing factor. The force F_i acting on nucleus α due to a pair of electrons in the ith molecular orbital is

$$F_i = 2e\int \mathscr{E}_{\alpha z}\psi_i^*\psi_i\, d\tau. \qquad [2]$$

The analytical expression for $\mathscr{E}_{\alpha z}$ is $Z_\alpha e \cos\theta_\alpha/r^2_{\alpha j}$. Therefore, the force exerted on nucleus α by a pair of electrons in the ith molecular orbital may be interpreted in terms of the interaction of an ideal dipole centered on nucleus α with the various atomic and overlap charge distributions,

$$F_i = \frac{Z_\alpha}{1\pm S}\left[\int \mathscr{D}_{\alpha z}\,\phi_\alpha^2 d\tau+\int \mathscr{D}_{\alpha z}\,\phi_\beta^2 d\tau\pm 2\int \mathscr{D}_{\alpha z}\,\phi_\alpha\phi_\beta d\tau\right] \qquad [3]$$

where $\mathscr{D}_{\alpha z} = \cos\theta_\alpha/r_{\alpha j}$, and F_i is expressed in atomic units. The total force in atomic units exerted on nucleus α is simply the sum of all the individual F_i's together with the repulsions due to the other nuclei present in the molecule,

$$F_{\alpha z} = \sum_\beta{}' \frac{Z_\alpha Z_\beta}{R^2} - \sum_i (n_i/2)F_i. \qquad [4]$$

By choosing suitable expressions for the molecular orbitals we may calculate the forces exerted on a nucleus. The bonding and antibonding characters of different electron distributions may be compared and semiquantitative predictions made with much greater ease than is possible with the usual discussion in terms of energies. We shall illustrate this with a discussion of the molecular orbitals which are responsible for the bonding found in the homonuclear diatomic molecules composed of the atoms in the first row of the periodic table.

We have chosen to employ Slater's expressions with variable screening constants for the atomic orbitals in a L.C.A.O. approximation to the molecular orbitals. Such expressions give results for the electron densities that are sufficiently accurate to allow meaningful comparisons to be made between the forces resulting from different molecular orbitals. We have previously demonstrated that such expressions give good estimates of bonding energies for simple molecules (1). To this approximation it is possible to write a completely general expression for the forces exerted on a nucleus due to the occupation of any particular type of molecular orbital.

Reference to equation [3] shows that F_i for a homonuclear diatomic molecule is composed of three terms. If the atomic orbital ϕ_α is centrosymmetric, the first integral $\int \phi_\alpha\phi_\alpha\mathscr{D}_{\alpha z}d\tau$ is zero since no force will be exerted on a nucleus by a symmetrically placed charge distribution. The second integral $\int \phi_\beta\phi_\beta\mathscr{D}_{\alpha z}d\tau$ is the force due to the penetration of nucleus α into the charge distribution about the second nucleus.[3] This penetration effect results in an imperfect screening of the second nucleus and, if no other effects

[3]*For example, integration of* $\int \phi_\beta\phi_\beta\mathscr{D}_{\alpha z}d\tau$ *from* R *to* ∞ *for* ϕ_β = *1s a.o. results in the so-called J integral which occurs in the regular molecular orbital calculation of the energies of* H_2^+ *and* H_2.

Can. J. Chem. Downloaded from www.nrcresearchpress.com by 210.87.254.105 on 09/05/12
For personal use only.

Can. J. Chem. Downloaded from www.nrcresearchpress.com by 210.87.254.105 on 09/05/12
For personal use only.

were operative, it would give rise to a resultant repulsive force between the two nuclei. The third contribution to F_i, $2\int \phi_\alpha\phi_\beta \mathscr{D}_{\alpha x}d\tau$ gives the magnitude of the force on nucleus α due to the charge which is built up between the two nuclei in a bonding orbital. It is well known that $2\phi_\alpha\phi_\beta/(1+S)$ (where S is the overlap integral) is a measure of the amount of charge transferred from regions where ϕ_α^2 and ϕ_β^2 are large to the region where $\phi_\alpha\phi_\beta$ is large. The total amount of charge transferred in the formation of the molecular orbital is simply $2S/(1+S)$. Thus $\int \phi_\alpha\phi_\beta \mathscr{D}_{\alpha x}d\tau$ gives a quantitative measure of the forces arising from the charge which is transferred due to the overlap of the atomic orbitals. (In an antibonding orbital an amount of charge $2S/(1-S)$ is, of course, removed from the overlap region and placed in regions where ϕ_α^2 and ϕ_β^2 are large.) It is this build-up of charge in a bonding orbital which counteracts the repulsive force mentioned above to give a resultant binding force.[4]

All of the integrals encountered in equation [3] may be expressed as a product of $(1/R^2)$ with a dimensionless expression which is a function only of Q where $Q = \beta R$, R being the internuclear separation and β a screening constant. Because of this property, general expressions may be derived from any type of molecular orbital as functions of Q alone, from which the forces are obtained simply by dividing by R^2. Before presenting these general expressions for the forces, it will be instructive to consider the dimensionless functions for the $\int \phi_\beta^2 \mathscr{D}_{\alpha x}d\tau$ and $\int \phi_\alpha\phi_\beta \mathscr{D}_{\alpha x}d\tau$ integrals separately. These we have plotted in Fig. 1 for the molecular orbital composed of $2s$ atomic orbitals. We can, for the sake of

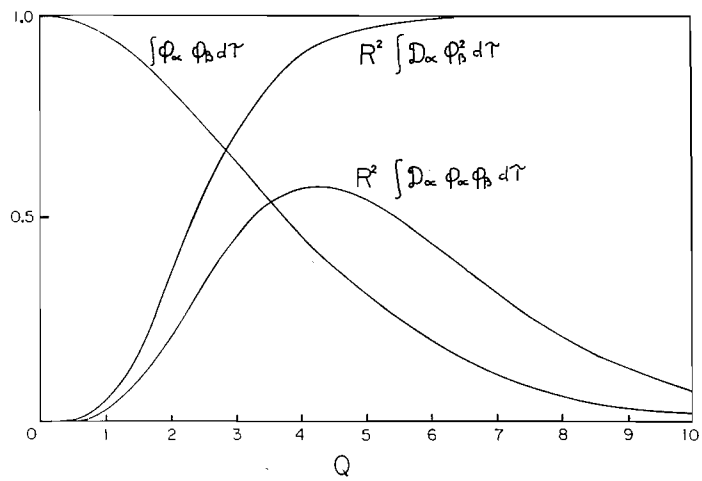


FIG. 1. The overlap integral and the dimensionless expressions for the components of the force due to the $\sigma_g 2s$ molecular orbital.

discussion, consider Q as equal to R, that is, give an arbitrary value of unity to the screening constant. Notice that as R is decreased the value of $\int \phi_\beta^2 \mathscr{D}_{\alpha x}d\tau$ falls steadily from unity to zero. In these same dimensionless units (i.e., multiplication by R^2) the nuclear repulsion is simply -1 for a pair of electrons. Thus for large values of R, the screening is complete and the forces are zero. However, as R is decreased and the penetration of the charge cloud on the second center begins, the net result of the nuclear repulsion and the penetration effect alone is a net repulsive force.

[4]*Hurley (2) has previously discussed the electrostatic interpretation of chemical binding as given in this paragraph.*

The form of $\int \phi_\alpha \phi_\beta \mathscr{D}_{\alpha x} d\tau$ as compared to that of simply S (which is also given in Fig. 1) is of great interest. It reaches a maximum and then returns to zero. That is, initially the charge which is transferred is placed in the binding region and the net attractive force is increased. However, as the overlap continues to increase, much of the charge is now placed in regions which are principally antibinding regions and the net attractive force begins to decrease. How this effect arises can be seen most simply and elegantly by a consideration of some views put forward by Berlin (3). Consider an element of charge which is placed at any point within the two full curves in the field of two nuclei of equal nuclear charge as indicated in Fig. 2. It is evident that the net force

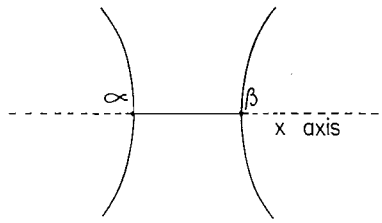


FIG. 2. A Berlin diagram showing the binding and antibinding regions in a diatomic molecule.

in the x direction which this element of charge exerts on the nuclei is one which draws them together. A similar element of charge placed at a point outside of the two curves (at either end of the molecule) produces an unbalanced resultant force in the x direction, one that tends to increase the distance between the two nuclei. It is also clear that there will be positions from which the forces acting on the nuclei will be equal with no net force tending to increase the nuclear separation. These positions in effect lie upon the two boundary curves which divide the "binding" region from the "antibinding" regions. Thus while the amount of charge transferred in the formation of a molecular orbital is proportional to the overlap integral, the position at which this charge is placed is of great importance. The great advantage of the present approach is that a quantitative estimate of the relative bonding or antibonding abilities of molecular orbitals may be made without the necessity of couching the discussion in terms of overlap integrals or other qualitative concepts.

All of the F_i's for the various types of molecular orbitals may be expressed in the form

$$F_i = (Z_\alpha/R^2) f_i(Q) \qquad [5]$$

where f_i is a dimensionless function of $Q(= \beta R)$. Specifically,

$$f_i/R^2 = \frac{1}{1 \pm S}\left[\int \phi_\beta^2 \mathscr{D}_{\alpha x} d\tau \pm 2 \int \phi_\alpha \phi_\beta \mathscr{D}_{\alpha x} d\tau\right] \qquad [6]$$

where again the plus and minus signs refer to the bonding and antibonding combinations respectively. We have derived analytical expressions for the f_i's due to the g and the u combinations of the $\sigma 1s$, $\sigma 2s$, $\sigma 2p$, $\pi 2p$, and sp hybrid molecular orbitals. Coulson (4) has previously given the expressions for the $\sigma 1s$ and $\sigma 2s$ molecular orbitals. All of the expressions are listed in the appendix for the sake of completeness. In Figs. 3 and 4 we have plotted the functions f_i for the various bonding and antibonding combinations. The actual force, expressed in atomic units, exerted on nucleus α by the electrons in the ith orbital in some particular molecule is obtained simply by multiplying the value of f_i as determined by the value of Q, by Z_α/R^2. The curves as shown when divided by R^2

Can. J. Chem. Downloaded from www.nrcresearchpress.com by 210.87.254.105 on 09/05/12
For personal use only.

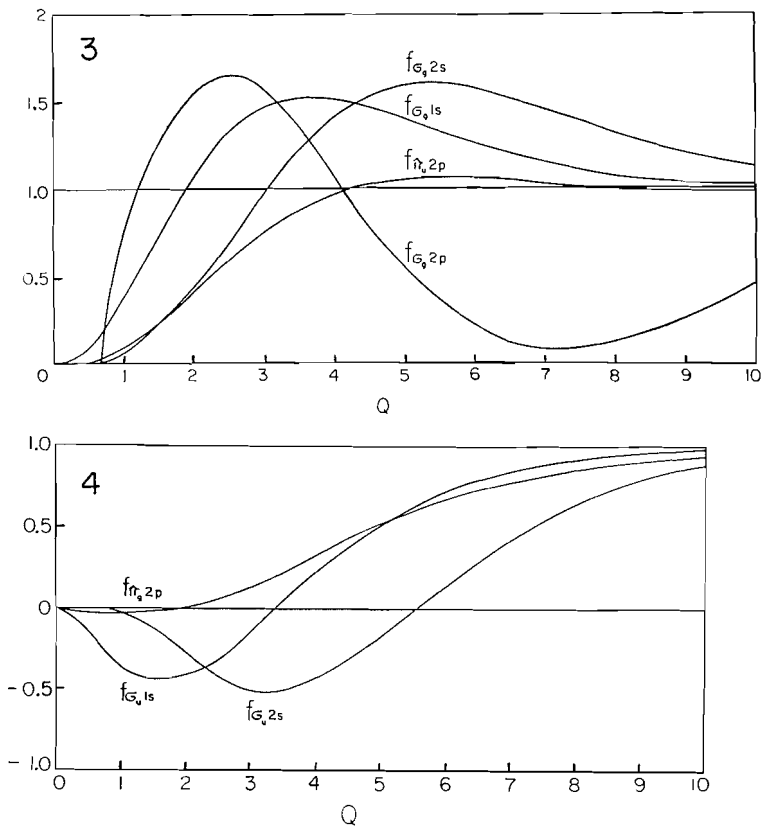


FIG. 3. The dimensionless expressions for the forces due to the bonding combinations $\sigma_g 1s$, $\sigma_g 2s$, $\sigma_g 2p$, and $\pi_u 2p$ ($\sigma_g 2p$ is orthogonal to $\sigma_g 2s$).

FIG. 4. The dimensionless expressions for the forces due to the antibonding combinations, $\sigma_u 1s$, $\sigma_u 2s$, and $\pi_g 2p$.

represent the forces exerted on a nucleus of unit charge by electrons distributed in molecular orbitals with a screening constant equal to unity for all values of R.

III. A DISCUSSION OF THE FORMS OF THE f_i CURVES

Many attempts have been previously made to relate the strengths of various bonds to the magnitude of the overlap between the atomic orbitals comprising the bond. Examples are Pauling's criterion of maximum overlap, the use of the overlap integral by Mulliken (5) and Maccoll (6), and discussions due to Mulliken (7) of atomic and overlap populations. All these discussions are qualitative in nature. By focusing our attention on the forces involved we may make the discussions more quantitative, and less speculative. A number of interesting points emerge from a consideration of Figs. 3 and 4. For instance, while the $\pi_u 2p$ molecular orbital possesses an overlap integral which, for any value of Q, is only slightly less than that for a $\sigma_g 2s$ molecular orbital, the π_u is much less bonding than is the σ_g orbital. A consideration of the forces involved illustrates why this should be expected. First, a comparison of the integrals $\int \mathscr{D}_{\alpha z} 2p\pi_\beta^2 d\tau$ and $\int \mathscr{D}_{\alpha z} 2s_\beta^2 d\tau$ shows that the π_u orbital is much less effective at screening the nucleus than is the σ_g orbital. Second, the π_u orbital, while possessing an appreciable overlap and transferring

Can. J. Chem. Downloaded from www.nrcresearchpress.com by 210.87.254.105 on 09/05/12
For personal use only.

Can. J. Chem. Downloaded from www.nrcresearchpress.com by 210.87.254.105 on 09/05/12
For personal use only.

a considerable amount of charge to the binding region, places most of the charge above and below the internuclear axis. It is evident from the form of the integral $\int \pi_\alpha \pi_\beta^* \mathscr{D}_{\alpha z} d\tau$ that the maximum force will be obtained when the charge is placed along the internuclear axis as it is in this position that the interaction with the nuclear dipole will be a maximum. While the total amount of charge transferred by the σ_g orbital is very nearly the same as for the π_u, the force exerted on the nucleus by this distribution of electrons is much greater since the maximum pile-up of charge is on the internuclear axis. This example illustrates why a mere comparison of the overlap integrals is insufficient to determine the relative bonding properties; one needs to know, rather, the amount of charge transferred and the point to which it is transferred, two facts which the f_t values take into account fully.

The force exerted by the electrons in a $\sigma_g 1s$ orbital reaches a maximum value for smaller values of Q than does that for the molecular orbitals composed of $2s$ and $2p$ atomic orbitals. This result is to be expected as maximum force should reflect the maximum in the radial density function.

The force curves illustrate in a very lucid manner the effect of mutual orthogonalization on the bonding properties of molecular orbitals. The $f_{\sigma_g 2p}$ curve is that for a $\sigma_g 2p$ molecular orbital which is orthogonal to the $\sigma_g 2s$ molecular orbital. Neither the $\sigma_g 2s$ nor the $\sigma_g 2p$ molecular orbitals have been made orthogonal to the $\sigma_g 1s$ orbital. The reasons for this procedure are as follows. When all 10 of the molecular orbitals are made mutually orthogonal the resulting picture is too complicated to be useful in making general observations. Thus one must decide between taking the $\sigma_g 2s$ and the $\sigma_g 2p$ orthogonal to each other and neglecting the non-orthogonality with respect to the $\sigma_g 1s$, or else make both the $\sigma_g 2s$ and $\sigma_g 2p$ orthogonal to the $\sigma_g 1s$ but then not to each other. Coulson and Lester (8) have pointed out the necessity of including the $1s$–$2s$ and $1s$–$2p$ orthogonalities in the calculation of molecular energies. It has been pointed out by them that when a $\sigma_g 2p$ molecular orbital is constructed so as to be non-orthogonal to the $\sigma_g 1s$ function the $2p$ function will contain a significant amount of $\sigma_g 1s$ character. Thus the energy obtained for this non-orthogonal $2p$ molecular orbital will be too large as it contains a contribution due to the $1s$ molecular orbital. This is a very serious discrepancy as the term value for the $1s$ molecular orbital lies about 10 ev below that for the $\sigma_g 2p$ molecular orbital even in H_2^+ and thus a small amount of $1s$ contribution to the $2p$ molecular orbital causes considerable error. Coulson and Lester (8) do not discuss the discrepancies which arise from the lack of orthogonality between the $2s$ and $2p$ molecular orbitals. In the calculation of the forces it is much more important to take into account this latter orthogonality than the former. The *forces* due to the $\sigma_g 1s$ orbital are actually slightly less than those due to the $\sigma_g 2s$ and $\sigma_g 2p$ molecular orbitals at the equilibrium internuclear distances and as can be seen from the graphs, all the curves approach unity for large values of Q. Thus a small amount of $1s$ character in the molecular orbitals constructed from the $2s$ and $2p$ orbitals will be much less serious than in the calculations of energies.[5] However, it is very important in these calculations to ensure orthogonality between the $2s$ and $2p$ functions. In Fig. 5 we show a plot of $f'_{\sigma_g 2p}$ which is the result obtained when the $\sigma_g 2p$ molecular orbital is not orthogonal to the $\sigma_g 2s$. The result is meaningless. The forces predicted by this curve are of such a magnitude as to actually make every other force operative in the molecule insignificant. When the condition of orthogonality is introduced, however, the result for $f_{\sigma_g 2p}$ is very reasonable, as illustrated in Fig. 3. Mulliken (9) has

[5]*It should be pointed out that when one employs the electrostatic method for the calculation of bond energies a mutually orthogonal set of molecular orbitals (including the 1s contribution) must be used.*

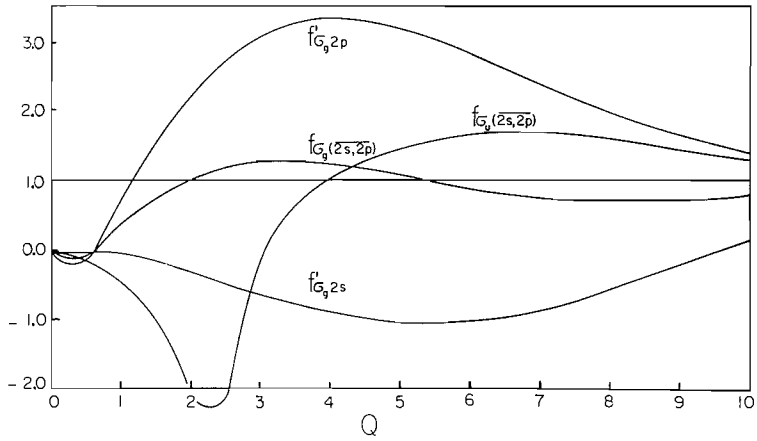


FIG. 5. The dimensionless expressions for the forces due to the $\sigma_g 2p$ and orthogonal $\sigma_g 2s$ molecular orbitals; also shown are the corresponding expressions due to the average electron densities of the mutually orthogonal pairs $\sigma_g 2s$, $\sigma_g 2p$ and $\sigma_u 2s$, $\sigma_u 2p$.

noted that when this "forced" hybridization (i.e., that due to the consequences of orthogonality) is taken into account the $\sigma_g 2p$ and $\sigma_g 2s$ orbitals become less bonding. Notice that the same trend is illustrated in the force curve for $\sigma_g 2p$. If the $\sigma_g 2p$ molecular orbital is made orthogonal to the $\sigma_g 2s$, the force exerted by the $\sigma_g 2p$ molecular orbital decreases to almost zero in the region of $Q = 7$. All this leads to an even more important observation. Included in Fig. 5 is the force curve for a $\sigma_g' 2s$ orbital which is now orthogonal to the $\sigma_g' 2p$ molecular orbital. That is, their roles have been reversed in the orthogonalization procedure. Now it is apparent that the $\sigma_g 2p$ molecular orbital is much more strongly binding than is the $\sigma_g 2s$ molecular orbital, which in fact becomes *antibinding*. Thus it is rather arbitrary to speak of the relative bonding properties of the $\sigma_g 2s$ and the $\sigma_g 2p$ molecular orbitals. When both of these orbitals are occupied there will be a resulting total force. This total force will have some meaning as it is the only contribution from the $n = 2$ orbitals with σ_g symmetry. This total force is, of course, the same as that obtained from the previous pair of orthogonal $\sigma_g 2s$ and $\sigma_g 2p$ orbitals, since an orthogonal transformation leaves the wave function and the total electron density unchanged. We have plotted, in Fig. 5, $f_{\sigma_g(\overline{2s},\overline{2p})}$, which is the average of the $f_{\sigma_g 2s}$ and the orthogonal $f_{\sigma_g 2p}$ curves (or equally well, the average of $f'_{\sigma_g 2s}$ and $f'_{\sigma_g 2p}$ curves), and $f_{\sigma_u(\overline{2s},\overline{2p})}$, which is the average of the values obtained from the orthogonal $\sigma_u 2s$ and $\sigma_u 2p$ molecular orbitals. By this consideration of the forces, we bring into sharp focus the fact that the concept of a molecular electronic configuration in terms of molecular orbitals does have definite limitations. The order of the orbital energies is at the complete mercy of the orthogonalization procedure and has no real significance. All that does possess significance is the total energy (or force) for the electronic state of the molecule, not how this energy is divided into contributions for the different orbitals.

IV. THE BONDING AND ANTIBONDING CHARACTER OF MOLECULAR ORBITALS

Much of what has been written about the bonding character of orbitals is based on spectroscopic observations, e.g., the ionization of an electron from the π_g orbital of the oxygen molecule results in the bond length of the O_2^+ ion being less than that for the neutral molecule. As Coulson (10) points out, this observation serves as the definition

Can. J. Chem. Downloaded from www.nrcresearchpress.com by 210.87.254.105 on 09/05/12
For personal use only.

Can. J. Chem. Downloaded from www.nrcresearchpress.com by 210.87.254.105 on 09/05/12
For personal use only.

of an antibonding electron. Nonetheless much more is inferred from the results of such observations, i.e., that the electron when present in the molecule actually did exert an antibinding force. This is rarely the case as we shall demonstrate.

The electrostatic calculations allow for an unusually clear and simple definition of an antibinding and binding molecular orbital.[6] The force curves f_i give immediately the net force due to any particular density distribution. The simplest definition of a binding or a bonding orbital is one for which f_i is positive at the particular value of Q which is of interest, and of an antibinding or an antibonding orbital one for which the pertinent value of f_i is negative. A negative value of f_i implies that the electrons are distributed in such a fashion as to exert a force on the nuclei which tends to draw them apart, and surely this is the simplest interpretation of an antibinding or antibonding electron. Reference to Fig. 4 illustrates that the so-called "antibonding orbitals" possess negative f_i values only for very small values of Q, corresponding to very close approach of the atoms (for values of R usually less than R_e). Charge of total amount $2S/(1-S)$ is transferred in the formation of these orbitals, but it is transferred primarily to binding regions. Figure 4 shows that it is only when a relatively large amount of charge has been transferred that the amount placed in antibinding regions exerts an effect which outweighs that due to the binding regions. Reference to equation [6] shows that the analytical requirement for antibonding is for $2\int \phi_\alpha\phi_\beta \mathscr{D}_{ax}d\tau > \int \phi_\beta{}^2\mathscr{D}_{ax}d\tau$.

An important orbital, which is classed as antibonding, is the π_g orbital of the homonuclear diatomic, and symmetrical linear triatomic molecules. These molecular orbitals are of the form $N(\pi_\alpha-\pi_\beta)$. There are no other orbitals of the same symmetry to be considered in these molecules which allows us to refer specifically to the bonding properties of this particular orbital.

(i) Carbon Dioxide

The ionization of a π_g electron from carbon dioxide results in an increase in the equilibrium bond length from 1.163 Å to 1.177 Å. Mulliken (11) assumed this to imply that the π_g orbital was in reality a bonding orbital. He, however, states that it is impossible for the orbital as ordinarily written ($\pi_g = N(\pi_\alpha-\pi_\beta)$) to be bonding and that if it is bonding it must be due to a participation of a $3d$ atomic orbital of carbon in the molecular orbital. Moffitt (12) excludes this possibility as he maintains that the mixing in of a $3d$ orbital would be energetically very unfavorable. Instead Moffitt (12) tendered the explanation that after the removal of a π_g electron the residual π electron distribution rearranges in such a way that the π-bond order decreases. We can obtain a good estimate of the bonding character of this orbital by the electrostatic method simply by assigning a reasonable value to the screening constant β.[7] Using the expression for β in the footnote we obtain a value of 2.28 for the screening constant, and thus a value of 10 for Q, as the equilibrium bond distance for the O—O separation in CO_2 is 4.396 a.u. Clearly the π_g orbital is well within the region where the electron density is principally in the binding region. The value of f_{π_g} at $Q = 10$ is $+0.94$ and, therefore, the force acting on the nuclei tends to draw them closer together. The orbital is thus binding and has no antibinding properties whatsoever in this range of values for Q. The removal of one electron will leave only three electrons

[6]*Following the suggestion of Berlin we use the terms binding and antibinding when referring to forces and bonding and antibonding when referring to energies.*

[7]*The screening constant β is given by*

$$\beta = Z_s - \Delta Z e^{-R}$$

where $\Delta Z = Z_s - Z_u$, Z_s is the value of the screening constant for the separated atoms ($R = \infty$) and Z_u is the screening constant for the united atom ($R = 0$). R is expressed in atomic units. Both Z_s and Z_u include the factor $1/n^*$ in the Slater recipe (1).

Can. J. Chem. Downloaded from www.nrcresearchpress.com by 210.87.254.105 on 09/05/12
For personal use only.

in the π_g orbital. To a first approximation this will decrease the amount of binding contributed by this orbital by 1/4. The C—O distance should therefore increase as is observed. The decrease in binding will not be as great as might at first be expected, for the removal of the electron has increased the value of the screening constant for the remaining electrons. Thus the value of Q increases *for the same value of* R, and the remaining electrons will exert a greater positive force per electron in the ion than in the neutral molecule. This is part of the effect which Moffitt has termed a rearrangement of the remaining π electrons. However, at $Q = 10$, f_{π_g} has already practically reached its maximum value of 1.00 and hence an increase in Q can result in only a small change in the force exerted per electron. Thus it is not necessary to invoke any special carbon participation to explain why the π_g orbital in carbon dioxide is bonding. The answer lies simply in the fact that at this value of the internuclear distance the atomic orbitals have not overlapped sufficiently to remove a significant amount of charge from the binding region, with the result that the force exerted on the nuclei is positive.

(ii) Oxygen

The ionization of a π_g electron from the oxygen molecule results in the formation of an O_2^+ ion which has a considerably shorter bond length and a higher energy of dissociation than the neutral molecule. This has always been interpreted as implying that the π_g orbital is in this case very strongly antibinding. The present interpretation does not bear this out. The screening constant for the π_g orbital in the oxygen molecule will be approximately 2.12, which places the π_g orbital in the region of Q equal to 4.82, i.e., in the region where the orbital is still definitely binding. Furthermore, it is in a region of the force curve where f_{π_g} is increasing rapidly with increasing Q. In the vertical ionization the screening constant and hence Q for the remaining π_g electron will be greater than the corresponding O_2 values for the same value of R. The force exerted on the nuclei per electron is thus considerably greater in the ion than in the neutral molecule for the same value of R. The end result of the removal of a π_g electron is the formation of an unbalanced force which draws the two nuclei together. This results even though the original molecular orbital itself was not antibinding. The molecule may now collapse and of course all of the deeper-lying orbitals will fall into regions of greater binding until the force due to the nuclear repulsion again matches that due to the electron density. (A glance at the force curves for the 1*s* and 2*s* orbitals will illustrate how these forces may well become appreciable as the value of R and thus Q is decreased.) The net result is an increase in force integrated over a significant distance, or a greater total bonding energy for the O_2^+ ion.

This discussion of the π_g orbital clearly shows the danger of attempting to extract detailed information regarding the binding character of an orbital solely from its spectroscopic behavior.

There is another manner in which the total force may be broken down into individual contributions, in such a way as to be useful in the interpretation of the trend in bond strengths. The values of the f_i's all tend to unity as Q increases. This occurs because the overlap between the atomic orbitals decreases to zero and the nuclei are simply screened by the electrons present in each atomic orbital. The total force thus approaches zero, for at large distances the screening will be complete. The interesting point is the behavior of the f_i values as Q (i.e., R) is decreased. A strongly "bonding" orbital will show an increase above unity in its f_i while an "antibonding" orbital will possess a f_i whose value drops below unity, eventually to a negative value for small values of Q. Thus

certain orbitals not only provide the shielding amount of force (equal to unity) but exceed this due to the favorable transfer of charge into the binding region. Because of this it is of interest to express the total force as

$$[7] \qquad F_{ax} = \frac{Z}{R^2} \sum_{i}^{n} (f_i - 1) \qquad \text{where } n = Z.$$

When written in this form we can see immediately which molecular orbitals provide electron densities which do more than simply screen their share of the nuclear charge.[8]

In fact the term $(f_i - 1)$ can be used as a new definition of bonding and antibonding. When the sign of $(f_i - 1)$ is negative it implies that the two electrons in the ith molecular orbital are distributed in such a way that the resulting density distribution is not sufficient to screen their share of the nuclear charge, and thus their presence contributes a resultant repulsive force to the molecular system. We term this a *net antibonding orbital.* When the sign of $(f_i - 1)$ is positive it implies that the pair of electrons in the ith molecular orbital exert a resultant binding force and hence such a molecular orbital is termed a *net bonding orbital.* According to these definitions, a doubly occupied orbital is bonding when its f_i value exceeds its share of the nuclear repulsive force. An orbital may thus be net antibonding even though its f_i value is positive. Reference to Figs. 3 and 4 illustrates that the definition of net antibonding coincides much more closely with the usual assignment of bonding and antibonding properties of the molecular orbitals. For example, the π_g molecular orbital is net antibonding for the value of Q found in the oxygen molecule. Thus a molecule which is forced to employ the π_g orbital must distribute these electrons in such a fashion that although the electron density in the binding region is still sufficient to result in a force which draws the nuclei together, is insufficient to overcome that portion of the nuclear repulsive force associated with their presence.

The statement is often made that there is no stable helium molecule because the $\sigma_u 1s$ orbital is more antibonding than the $\sigma_g 1s$ orbital is bonding. In fact, it is generally stated that for any molecular orbital, the antibonding combination is more antibonding than is the bonding combination bonding. This is in fact not true. The $\sigma_u 1s$ orbital is binding, that is, draws the nuclei together except for values of Q less than 3.4 (which would correspond to R values of less than 2.0 a.u. in He_2). It is less binding than the $\sigma_g 1s$ orbital but still binding, for values of $R > 2.0$ a.u. What causes the helium molecule to be unstable is that the $\sigma_u 1s$ orbital is *net antibonding.* On proceeding from the hydrogen molecule to the helium molecule we increase the nuclear repulsive force and add a pair of electrons to an orbital which while binding, is not sufficiently binding to meet the increased nuclear repulsion. This is not equivalent to the usual interpretation.

The $\sigma_g 1s$ and $\sigma_u 1s$ molecular orbitals for the homonuclear diatomic molecules, from Li_2 across, all possess a value of $Q > 10$ at R_e. In this region of Q, the quantity $(f_i - 1) = 0$ and this implies that the electrons in these molecular orbitals are doing nothing more than shielding the nuclei of each atom. They are not contributing to either the net bonding or net antibonding, but rather may be classed as *net nonbonding* as $(f_i - 1) = 0$ implies. The $\sigma_g 1s$ and $\sigma_u 1s$ orbitals are truly localized. The force curves illustrate that we are justified in labelling them simply as KK in the molecular orbital description of a molecule.

[8]*Equation [7] as written applies to a neutral molecule with all the molecular orbitals doubly occupied. For a molecule with two singly occupied molecular orbitals the pertinent measure would then be $(f_i/2 - 1/2)$ for each. Fully occupied π orbitals are counted twice.*

Can. J. Chem. Downloaded from www.nrcresearchpress.com by 210.87.254.105 on 09/05/12
For personal use only.

Reference to Fig. 5 shows that the result of making $\sigma_g 2p$ orthogonal to $\sigma_g 2s$ is to make the average contribution from these two orbitals net antibinding for large values of Q. However, making $\sigma_u 2s$ orthogonal to $\sigma_u 2p$ results in a net binding force from these orbitals for large values of Q. That is, when orthogonalization is taken into account, the "bonding" orbitals become net antibonding and the "antibonding" orbitals become net bonding above some value of Q.

In general, the f_i curves illustrate that *for any value of* Q, the process of orthogonalization reduces both the bonding properties of "bonding" orbitals and the antibonding properties of "antibonding" orbitals. Mulliken (9), from qualitative considerations of overlap integrals, has stated that the effect of forced hybridization "is to weaken very considerably the bonding power of bonding molecular orbitals but to strengthen markedly the antibonding power of antibonding molecular orbitals". We therefore disagree with Mulliken's predictions regarding the effects of forced hybridization on the antibonding orbitals.

The effect of orthogonalization on the forces and the f_i curves is again easier to see than is the effect it has on the energies. If the molecular orbital σ_2 is to be made orthogonal to another molecular orbital σ_1 of the same symmetry, the resulting electron density is

$$\rho = [\sigma_2^2 + S_{12}^2\sigma_1^2 - 2S_{12}\sigma_1\sigma_2]/(1 - S_{12}^2)$$

where $S_{12} = \int \sigma_2\sigma_1 d\tau$. The amount of density subtracted, $2S_{12}\sigma_1\sigma_2$, from the original density σ_2^2 is greater than the amount added, $S_{12}^2\sigma_1^2$, since S_{12} is less than unity. The orthogonalization diminishes the electron density and hence reduces the force. If σ_1 and σ_2 are of u symmetry, i.e., antibonding combinations, the correction $S_{12}\sigma_1\sigma_2$ is itself negative in sign and both corrections to σ_2 are positive. Thus the effect of "forced hybridization" on an antibonding orbital is to increase the electron density and hence the value of the force. Furthermore, an estimate of the exact extent of the effect of forced hybridization can readily be made by the use of f_i curves.[9]

The N_2 molecule possesses the strongest bond of all the homonuclear diatomic molecules formed from the elements of the first row of the periodic table. The dissociation energy of the O_2 molecule is 5.080 ev, as compared to 9.756 ev for N_2. It is a simple matter to account for this decrease in bond strength. The extra pair of electrons that is possessed by the O_2 molecule is placed in the π_g orbital. This orbital is net antibinding for all values of Q. The added pair of electrons on passing from nitrogen to oxygen does not yield a force large enough to overcome the added nuclear repulsion. The term $(f_{\pi_g} - 1)$ thus detracts from the total force F_{ax} at any value of Q, and will cause F_{ax} to equal zero at a value of Q larger than that found for N_2, corresponding to a weaker and a longer bond. As the fluorine molecule has four π_g electrons, the net antibinding contribution to F_{ax} is still greater for all values of Q, and thus one would predict an even larger value for R_e and a still smaller value for the dissociation energy in this case.

Proceeding in the other direction from N_2, the C_2 molecule should have a smaller dissociation energy than N_2 simply because it has one electron less in the π_u and $\sigma_g 2p$ orbitals, both of which are net bonding when integrated over a large enough range of Q. Thus carbon, in effect, obtains only 3/4 and 1/2 respectively of the net binding forces as does N_2 from these two orbitals, making F_{ax} for C_2 less than that for N_2 at any value of Q.

[9]*The effects of general (as opposed to forced) hybridization on bond strengths as determined by an analysis of the associated force curves will form the subject of a forthcoming publication.*

Can. J. Chem. Downloaded from www.nrcresearchpress.com by 210.87.254.105 on 09/05/12
For personal use only.

This explanation of the variation in the bond strengths of the diatomic molecules in terms of the forces involved is essentially the same as that obtained from the usual interpretations if one replaces the terms "bonding" and "antibonding" with the terms net bonding and net antibonding. The present discussion is necessarily less speculative than former ones because of the analytical definitions which may be obtained from the f_i curves for the terms net bonding and net antibonding. This is preferable to qualitative discussions based entirely on bonding abilities which were inferred from the forms of the molecular orbitals.

In addition to this we summarize the other advantages of the present approach: the simple electrostatic interpretation of the chemical bond, in terms of two easily understandable force integrals, one giving the effect of the nuclear penetration into the neighboring atomic charge cloud, and the other relating the magnitude of the forces to the extent of overlap, or to the amount of charge which is transferred in the formation of a molecule. An analytical definition of binding and antibinding, and the ease with which any molecular orbital may be so classified by the assignment of a single parameter. The clarification of the terms bonding and antibonding, together with the definition of net antibonding and net bonding. That the previous concept of bonding and antibonding actually fit in more closely with these later definitions, and that in most instances, the electrons are not distributed in such a way as to give an antibinding force, nor do they exert an antibonding effect on the energy of a molecule when they are placed in an orbital which by symmetry is usually classed as antibonding. The possibility of expressing the resultant forces in terms of the individual f_i functions, which may be plotted as a function of Q only, allows one to see clearly for the first time the total effect of orthogonalization or forced hybridization within a set of orbitals, and what effect this has on their bonding abilities.

Can. J. Chem. Downloaded from www.nrcresearchpress.com by 210.87.254.105 on 09/05/12
For personal use only.

REFERENCES

1. R. F. W. Bader. Can. J. Chem. **38**, 2117 (1960).
2. A. C. Hurley. Proc. Roy. Soc. (London), A, **235**, 228 (1956).
3. T. Berlin. J. Chem. Phys. **19**, 214 (1951).
4. C. A. Coulson. Proc. Cambridge Phil. Soc. **38**, 210 (1942).
5. R. S. Mulliken. J. Chem. Soc. **72**, 4502 (1950).
6. A. Maccoll. Trans. Faraday Soc. **46**, 369 (1950).
7. R. S. Mulliken. J. Chem. Phys. **23**, 1833, 1841 (1955).
8. C. A. Coulson and G. R. Lester. Trans. Faraday Soc. **51**, 1605 (1955).
9. R. S. Mulliken. J. Chem. Phys. **19**, 912 (1951).
10. C. A. Coulson. Valence. Oxford University Press, London. 1952. p. 143.
11. R. S. Mulliken. Revs. Modern Phys. **14**, 204 (1942).
12. W. Moffitt. Proc. Roy. Soc. (London), A, **196**, 524 (1949).

APPENDIX

$$1s_a = (\beta^3/\pi)^{1/2} \exp(-\beta r_a); \quad 2s_a = (\beta^5/3\pi)^{1/2} r_a \exp(-\beta r_a)$$

$$2p\sigma_a = (\beta^5/\pi)^{1/2} r_a \cos\theta_a \exp(-\beta r_a); \quad 2p\pi_a = (\beta^5/2\pi)^{1/2} r_a \sin\theta_a \exp(-\beta r_a) \exp i\phi$$

$$\int \mathscr{D}_{ax}\, 1s_b \cdot 1s_b d\tau = \frac{1}{R^2}\left[1-(1+2Q+2Q^2)\, e^{-2Q}\right]$$

$$\int \mathscr{D}_{ax}\, 2s_b \cdot 2s_b d\tau = \frac{1}{R^2}\left[1-\left(1+2Q+2Q^2+\frac{4}{3}Q^3+\frac{2}{3}Q^4\right) e^{-2Q}\right]$$

$$\int \mathscr{D}_{ax}\, 2p\sigma_b \cdot 2p\sigma_b d\tau = \frac{1}{R^2}\left[1+\frac{1}{Q^2}\{9-(9+18Q+19Q^2+14Q^3+8Q^4+4Q^5+2Q^6)\, e^{-2Q}\}\right]$$

$$\int \mathscr{D}_{ax}\, 2p\pi_b \cdot 2p\pi_b^* d\tau = \frac{1}{R^2}\left[1-\frac{1}{2Q^2}\{9-(9+18Q+16Q^2+8Q^3+2Q^4)\, e^{-2Q}\}\right]$$

$$\int \mathscr{D}_{ax}\, 2s_b \cdot 2p\sigma_b d\tau = \frac{1}{R^2}\cdot\frac{1}{\sqrt{3}Q}\,[5-(5+10Q+10Q^2+7Q^3+4Q^4+2Q^5)\,e^{-2Q}]$$

$$\int \mathscr{D}_{ax}\, 2s_a \cdot 2p\sigma_a d\tau = \frac{1}{R^2}\cdot\frac{Q^2}{3\sqrt{3}}$$

$$\int \mathscr{D}_{ax}\, 1s_a \cdot 1s_b d\tau = \frac{1}{R^2}\cdot 2\,\{e^{Q}\cdot E_i^*(2Q)(Q^2-3Q+3)+e^{-Q}(C+\ln 2Q)(Q^2+3Q+3)$$
$$-e^{-Q}(3Q^2+6Q)\}$$

$$\int \mathscr{D}_{ax}\, 2s_a \cdot 2s_b d\tau = \frac{1}{R^2}\cdot\frac{2}{3}\Big\{e^{Q}\cdot E_i^*(2Q)(Q^3-5Q^2+12Q-12)$$
$$-e^{-Q}(C+\ln 2Q)(Q^3+5Q^2+12Q+12)$$
$$+e^{-Q}\left(\frac{1}{3}Q^4+\frac{10}{3}Q^3+12Q^2+24Q\right)\Big\}$$

$$\int \mathscr{D}_{ax}\, 2p\sigma_a \cdot 2p\sigma_b d\tau = \frac{1}{R^2}\cdot 2\,\Big\{e^{Q}\cdot E_i^*(2Q)2\left(Q^3-9Q^2+45Q-150+\frac{315}{Q}-\frac{315}{Q^2}\right)$$
$$-e^{-Q}(C+\ln 2Q)\cdot 2\left(Q^3+9Q^2+45Q+150+\frac{315}{Q}+\frac{315}{Q^2}\right)$$
$$+e^{-Q}\left(\frac{1}{3}Q^4+8Q^3+55Q^2+250Q+630+\frac{1260}{Q}\right)\Big\}$$

$$\int \mathscr{D}_{ax}\, 2p\pi_a \cdot 2p\pi_b^* d\tau = \frac{1}{R^2}\cdot 2\Big\{e^{Q}\cdot E_i^*(2Q)\cdot 3\left(-Q^2+10Q-45+\frac{105}{Q}-\frac{105}{Q^2}\right)$$
$$-e^{-Q}(C+\ln 2Q)\cdot 3\left(Q^2+10Q+45+\frac{105}{Q}+\frac{105}{Q^2}\right)$$
$$+e^{-Q}\left(\frac{1}{3}Q^3+\frac{25}{2}Q^2+95Q+315+\frac{630}{Q}\right)\Big\}$$

$$\int \mathscr{D}_{ax}\, 2s_a \cdot 2p\sigma_b d\tau = \frac{1}{R^2}\cdot\frac{2}{\sqrt{3}}\Big\{e^{Q}\cdot E_i^*(2Q)\left(-Q^3+5Q^2-15Q+30-\frac{30}{Q}\right)$$
$$-e^{-Q}(C+\ln 2Q)\left(Q^3+5Q^2+15Q+30+\frac{30}{Q}\right)$$
$$+e^{-Q}\left(\frac{1}{3}Q^4+\frac{19}{6}Q^3+\frac{79}{6}Q^2+30Q+60\right)\Big\}$$

$$\int \mathscr{D}_{ax}\, 2p\sigma_a \cdot 2s_b d\tau = \frac{1}{R^2}\cdot\sqrt{3}\,\Big\{e^{Q}\cdot E_i^*(2Q)\cdot 4\left(-\frac{1}{3}Q^3+3Q^2-13Q+30-\frac{30}{Q}\right)$$
$$-e^{-Q}(C+\ln 2Q)\cdot 4\left(\frac{1}{3}Q^3+3Q^2+13Q+30+\frac{30}{Q}\right)$$
$$+e^{-Q}\left(\frac{2}{9}Q^4+\frac{49}{9}Q^3+\frac{337}{9}Q^2+120Q+240\right)\Big\}$$

C is Euler's constant and $E_i^*(x)$ is the exponential integral, defined by

$$E_i^*(x) = -E_i(-x) = \int_x^{\infty}(e^{-t}/t)dt.$$

$\mathscr{D}_{ax}$, the electric field due to a unit change on nucleus a, is $(\cos\theta_a)/r_a^2$ in atomic units.

Can. J. Chem. Downloaded from www.nrcresearchpress.com by 210.87.254.105 on 09/05/12
For personal use only.

Can. J. Chem. Downloaded from www.nrcresearchpress.com by 210.87.254.5 on 09/05/12
For personal use only.

THE SULPHURIC ACID SOLVENT SYSTEM

PART II. CONDUCTIVITY MEASUREMENTS ON SOLUTIONS OF SOME ACIDS[1]

J. Barr, R. J. Gillespie, and E. A. Robinson

ABSTRACT

Conductivity measurements have been made on solutions of the following substances in sulphuric acid: $HClO_4$, HSO_3F, HSO_3Cl, HPO_2F_2, $HAs(HSO_4)_4$, CH_3SO_3H, and CF_3CO_2H. Of these substances HSO_3F, HSO_3Cl, $HAs(HSO_4)_4$, and probably $HClO_4$, behave as acids, CF_3CO_2H is a non-electrolyte, and HPO_2F_2, and probably CH_3SO_3H, are bases of the sulphuric acid system. Acid dissociation constants for HSO_3F, HSO_3Cl, and $HAs(HSO_4)_4$ have been determined by comparing the conductivities of their solutions with those of $H_2S_2O_7$, whose dissociation constant is known from other measurements, and also by conductimetric titration with a strong base, e.g. $KHSO_4$. These acids of the sulphuric acid system decrease in strength in the order $HSO_3F > HAs(HSO_4)_4 > HSO_3Cl > HClO_4$.

INTRODUCTION

Very few substances are known that have a sufficiently great proton-donating ability to protonate sulphuric acid i.e., to ionize according to the equation

$$HA + H_2SO_4 = H_3SO_4^+ + A^- \qquad [1]$$

thereby behaving as acids of the sulphuric acid solvent system. It has been shown by cryoscopic measurements (1, 2) that disulphuric acid is partially ionized according to the equation

$$H_2S_2O_7 + H_2SO_4 = H_3SO_4^+ + HS_2O_7^- \qquad [2]$$

with a dissociation constant $K_a = [H_3SO_4^+]\,[HS_2O_7^-]/[H_2S_2O_7] = 0.014$ mole kg^{-1} over the range 10–25° C (2, 3). It was deduced from cryoscopic measurements (4) that tetra-(hydrogen sulphato)boric acid, $HB(HSO_4)_4$, is a rather strong acid ionizing according to the equation

$$HB(HSO_4)_4 + H_2SO_4 = H_3SO_4^+ + B(HSO_4)_4^-. \qquad [3]$$

By conductimetric titration with strong bases a value of $K_a = 0.3$ mole kg^{-1} was deduced (5). From the results of conductimetric and cryoscopic measurements on solutions of lead tetraacetate in sulphuric acid (6), it has been concluded that the $Pb(HSO_4)_6^{2-}$ ion is formed and that it undergoes considerable solvolysis, indicating that the corresponding acid, $H_2Pb(HSO_4)_6$, is rather weak, but solutions of the acid itself have not been investigated. Cryoscopic measurements on solutions of ammonium and nitronium perchlorates showed that they undergo essentially complete solvolysis and it was therefore concluded that perchloric acid is an exceedingly weak acid of the sulphuric acid system (7).

The present measurements were undertaken to extend our knowledge of acids of the sulphuric acid system by finding additional examples of acid behavior and by obtaining quantitative data on acid dissociation constants. The relative strengths of these extremely strong proton donors are of some theoretical interest; no information can be obtained from measurements on aqueous solutions since some of these acids are hydrolyzed by water and all of them would be so extensively ionized that it would not be possible to differentiate among their strengths.

[1]*Manuscript received February 14, 1961.*
Contribution from the Department of Chemistry, McMaster University, Hamilton, Ontario.

Can. J. Chem. Downloaded from www.nrcresearchpress.com by 210.87.254.5 on 09/05/12
For personal use only.

EXPERIMENTAL

The apparatus and general procedure for making the electrical conductivity measurements has been described elsewhere (8). The conductimetric titrations were carried out as previously described (5). The composition of the sulphuric acid solvent was adjusted until it had the conductivity corresponding to the composition 100% H_2SO_4 (κ = 0.010439 $ohm^{-1}\ cm^{-1}$) (8). Fluorosulphuric acid was redistilled twice in a closed system from which all moisture was rigorously excluded and had b.p. 161°. Chlorosulphuric and trifluoroacetic acids were purified by distillation and had boiling points 152° and 72° respectively. Perchloric acid was distilled under reduced pressure from a mixture of one part of 70% aqueous perchloric acid and four parts of 20% oleum and condensed in a trap at liquid-air temperature (9). Difluorophosphoric acid was a sample kindly provided by Dr. W. E. White of the Ozark Mahoning Company, Tulsa, Oklahoma. It was twice redistilled and had b.p. 44–46° at approximately 15 mm. The fluorine n.m.r. spectrum showed that there was no appreciable concentration of any other fluorine-containing compound (10). Solutions of tetra(hydrogen sulphato)arsenious acid $HAs(HSO_4)_4$ were prepared by dissolving arsenious oxide in an oleum (11), whose composition was known from its conductivity (12), in accordance with the equation:

$$As_2O_3 + 3H_2S_2O_7 + 2H_2SO_4 = 2HAs(HSO_4)_4. \quad [4]$$

RESULTS

The results of the conductivity measurements, which were made at 25°, are given in Table I and Fig. 1. Interpolated values from a previous publication (12) are included

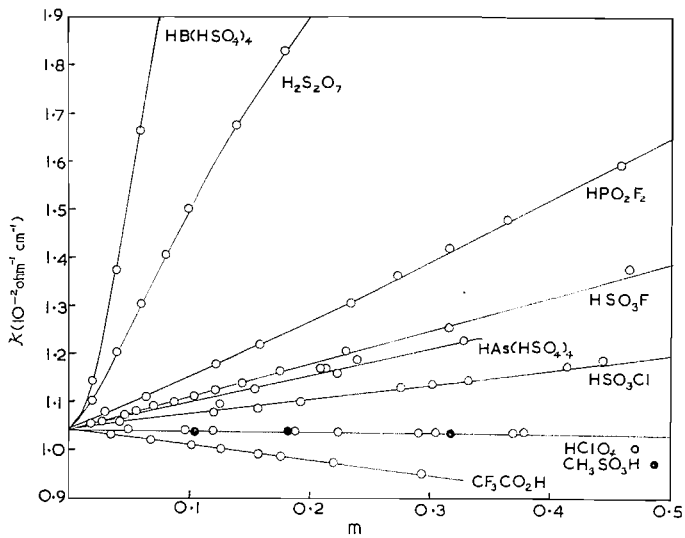


FIG. 1. Conductivities of solutions of acids.

for $HB(HSO_4)_4$ and a new value for its dissociation constant is calculated from these results. In the conductimetric titrations, solutions of the acids HSO_3F, HSO_3Cl, and $HAs(HSO_4)_4$ were titrated with the strong bases $KHSO_4$ or $NaHSO_4$, and disulphuric acid was titrated with the base HPO_2F_2, and in each case the composition of the solution

Can. J. Chem. Downloaded from www.nrcresearchpress.com by 210.87.254.5 on 09/05/12
For personal use only.

TABLE I

Conductivities of solutions in sulphuric acid

Molality (mole kg^{-1})	κ (10^{-2} ohm^{-1} cm^{-1})	Molality (mole kg^{-1})	κ (10^{-2} ohm^{-1} cm^{-1})	Molality (mole kg^{-1})	κ (10^{-2} ohm^{-1} cm^{-1})
HSO_3Cl		$HClO_4$		0.1755	0.986
0.1573	1.087	0.0172	1.0438	0.2194	0.973
0.3025	1.137	0.0966	1.0416	0.0353	1.034
0.4148	1.175	0.1878	1.0393	0.1025	1.012
0.6108	1.208	0.2902	1.0371	0.1574	0.994
0.7984	1.237	0.3704	1.0359	0.2761	0.977
0.8956	1.257	0.5034	1.0345	0.2934	0.950
0.0424	1.058	0.0070	1.0435		
0.1213	1.080	0.0489	1.0423	CH_3SO_3H	
0.1917	1.101	0.1209	1.0403	0.0507	1.041
0.2765	1.132	0.2237	1.0378	0.1047	1.040
0.3325	1.144	0.3049	1.0362	0.1819	1.038
0.4440	1.184	0.3771	1.0351	0.3173	1.037
HSO_3F		HPO_2F_2		$HAs(HSO_4)_4$	
0.0019	1.045	0.0042	1.111	0.0256	1.050
0.0055	1.047	0.1215	1.181	0.1257	1.095
0.0119	1.051	0.2344	1.318	0.1543	1.123
0.0175	1.055	0.3169	1.418	0.2101	1.169
0.0268	1.061	0.4585	1.592	0.2138	1.169
0.0471	1.074	0.6539	1.818	0.2228	1.161
0.0565	1.080	0.0305	1.080	0.2397	1.188
0.0700	1.090	0.1587	1.221	0.3288	1.230
0.0878	1.102	0.2741	1.365	0.3292	1.223
0.1036	1.113	0.3653	1.480		
0.1218	1.126	0.0703	1.831	$HB(HSO_4)_4$	
0.1434	1.141	0.8062	1.974	0.020	1.145
0.1750	1.163	1.028	2.216	0.040	1.375
0.0680	1.081	1.028*	2.423	0.060	1.665
0.1170	1.113			0.080	1.970
0.2301	1.205	CF_3CO_2H		0.100	2.29
0.3158	1.255	0.0165	1.035	0.140	2.81
0.4665	1.377	0.0692	1.021	0.180	3.19
0.6001	1.449	0.1264	1.002	0.240	4.01

*1.028 molal HPO_2F_2 + 0.0451 molal $KHSO_4$.

having a minimum conductivity was determined (5). This composition is conveniently expressed in terms of the ratio, $r_{min} = n_B/n_{HA}$, of the moles of base n_B that have to be added to n_{HA} moles of the acid to obtain the conductivity minimum. The results of the conductimetric titrations are given in Table II and Fig. 2.

TABLE II

Conductimetric titrations

Acid	Base	a	r_{min}	K_a
HSO_3Cl	$NaHSO_4$	0.44	0.065	9×10^{-4}
HSO_3F	$NaHSO_4$	0.60	0.14	2.2×10^{-3}
$HAs(HSO_4)_4$	$KHSO_4$	0.15	0.085	1.1×10^{-3}
$HAs(HSO_4)_4$	$KHSO_4$	0.17	0.085	1.1×10^{-3}
				K_b
$H_2S_2O_7$	HPO_2F_2	0.090	1.40	1.1×10^{-2}
$H_2S_2O_7$	HPO_2F_2	0.136	1.50	1.0×10^{-2}

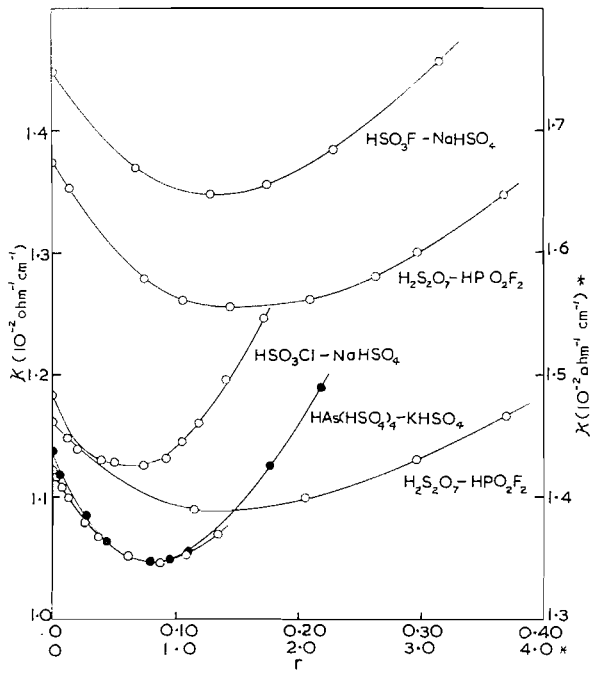


FIG. 2. Conductimetric titrations.

*$H_2S_2O_7 - HPO_2F_2$ only.

DISCUSSION

The $H_3SO_4^+$ and HSO_4^- ions conduct almost exclusively by a proton-transfer mechanism and they have much larger mobilities than all other ions which conduct by the ordinary diffusion process (13). Thus the conductivities of solutions of acids and bases in sulphuric acid can to a reasonable approximation be assumed to be due only to $H_3SO_4^+$ in solutions of acids and only to HSO_4^- in solutions of bases. The conductivity of a solution of an acid is therefore determined almost entirely by the concentration of $H_3SO_4^+$ and is a measure of its extent of ionization according to equation [1]. Thus it is immediately apparent from the conductivities of the acids shown in Fig. 1 that they decrease in strength in the order $HB(HSO_4)_4 > H_2S_2O_7 > HSO_3F > HAs(HSO_4)_4 > HSO_3Cl > HClO_4$.

The Acids HSO_3F, HSO_3Cl, $HAs(HSO_4)_4$, and $HB(HSO_4)_4$

That the electrolytes HSO_3F, HSO_3Cl, and $HAs(HSO_4)_4$ are acids of the sulphuric acid system is shown by the fact that the conductivities of their solutions are decreased by the addition of a base such as $NaHSO_4$ (Fig. 2) because of the neutralization reaction

$$H_3SO_4^+ + HSO_4^- = 2H_2SO_4 \qquad [5]$$

and the consequent diminution in the concentration of the highly conducting $H_3SO_4^+$ ion. Addition of sufficient base causes the conductivity to pass through a minimum and then increase and the value of r_{min} is related to the dissociation constants of the acid and the base, K_a and K_b respectively, by the expression

$$[6] \qquad r_{min} = (1+0.018/K_b).(1+0.013/K_a)^{-1}+0.0007/a$$

where a is the initial stoichiometric concentration of the acid (5). For a strong base such

Can. J. Chem. Downloaded from www.nrcresearchpress.com by 210.87.254.5 on 09/05/12
For personal use only.

as $NaHSO_4$ this simplifies to

[7] $$r_{min} = (1+0.013/K_a)^{-1}+0.0007/a.$$

Values of the dissociation constants of HSO_3F, HSO_3Cl, and $HAs(HSO_4)_4$ calculated from this expression are given in Table II.

Since the dissociation constant of disulphuric acid is known from cryoscopic measurements, values for the dissociation constants of acids can also be obtained by comparing the conductivities of their solutions with those of $H_2S_2O_7$ solutions. The method is similar to that used previously to determine the strengths of weak bases by comparison of the conductivities of their solutions with those of the strong base $KHSO_4$ (14). Assuming that the conductivity of a solution of any acid HA is determined only by the concentration of $H_3SO_4^+$ the concentration of this ion must be the same in solutions of any acids having the same conductivity. The concentration of $H_3SO_4^+$ in any solution of $H_2S_2O_7$ can be calculated from its known dissociation constant and the equilibrium constants for the self-dissociation reactions of the solvent. Concentrations of $H_3SO_4^+$ at round values of the stoichiometric concentration of $H_2S_2O_7$ taken from a previous publication (12) are given in column 3 of Table III. The stoichiometric concentrations $[HA]^s$ of

TABLE III

Dissociation constants from conductivities

$[H_2S_2O_7]$	$[HA]^s$	$[H_3SO_4^+]$	$[A^-]$	[HA]	K_a	
HSO_3Cl						
0.020	0.208	0.0189	0.0116	0.196	1.1×10^{-3}	
0.030	0.350	0.0213	0.0159	0.334	1.0	9×10^{-4}
0.040	0.550	0.0236	0.0195	0.530	0.9	
0.050	0.900	0.0256	0.0229	0.877	0.9	
HSO_3F						
0.020	0.102	0.0189	0.0116	0.090	2.5×10^{-3}	
0.030	0.167	0.0213	0.0159	0.151	2.3	
0.040	0.232	0.0236	0.0195	0.212	2.3	2.3×10^{-3}
0.050	0.306	0.0256	0.0229	0.283	2.2	
0.060	0.375	0.0277	0.0288	0.346	2.3	
$HAs(HSO_4)_4$						
0.020	0.113	0.0189	0.0116	0.1014	2.2×10^{-3}	
0.030	0.195	0.0213	0.0159	0.1791	1.9	1.9×10^{-3}
0.040	0.280	0.0236	0.0195	0.2005	1.8	
0.050	0.356	0.0256	0.0229	0.3331	1.8	
$HB(HSO_4)_4$						
0.050	0.028	0.0256	0.0229	0.0051	0.12	
0.100	0.047	0.0346	0.0360	0.0110	0.11	
0.150	0.063	0.0422	0.0459	0.0179	0.11	
0.200	0.076	0.0488	0.0541	0.0219	0.12	0.14
0.250	0.086	0.0547	0.0615	0.0245	0.14	
0.300	0.095	0.0601	0.0679	0.0271	0.15	
0.350	0.104	0.0651	0.0737	0.0303	0.16	
0.400	0.111	0.0698	0.0792	0.0318	0.17	
$[HPO_2F_2]^s$	$[KHSO_4]$	$[HSO_4^-]$	$[H_2PO_2F_2^+]$	$[HPO_2F_2]$	K_b	
HPO_2F_2						
0.100	0.023	0.035	0.023	0.077	0.9×10^{-3}	
0.200	0.036	0.044	0.036	0.164	0.9	
0.300	0.046	0.053	0.046	0.254	0.9	
0.400	0.057	0.062	0.057	0.343	0.9	1.0×10^{-3}
0.500	0.067	0.072	0.067	0.433	1.0	
0.600	0.077	0.082	0.077	0.623	1.1	
0.700	0.087	0.092	0.087	0.713	1.2	
0.800	0.097	0.102	0.097	0.803	1.2	

Can. J. Chem. Downloaded from www.nrcresearchpress.com by 210.87.254.5 on 09/05/12
For personal use only.

the acids HSO_3F, HSO_3Cl, $HAs(HSO_4)_4$, and $HB(HSO_4)_4$, having the same conductivities as solutions of these concentrations of $H_2S_2O_7$, were obtained from the plots shown in Fig. 1 and are given in column 2 of Table III. The concentrations of $H_3SO_4^+$ in solutions of these acids are then as given in column 3. The concentrations of A^- are not exactly equal to the concentrations of $H_3SO_4^+$ because of the self-dissociation equilibria of the solvent but the concentrations of A^- corresponding to given concentrations of $H_3SO_4^+$ have been previously calculated (Table 2 of ref. 13). By interpolating from these values the concentrations of A^- given in column 4 of Table III were obtained. From the relationship

$$[8] \qquad [HA]^s = [HA] + [A^-]$$

the corresponding concentrations of unionized acid [HA] were obtained (column 5) and finally the acid dissociation constants given in the last column were calculated from the expression

$$[9] \qquad K_a = [H_3SO_4^+]\,[A^-]/[HA].$$

In general the values of the dissociation constants determined by the two methods are in reasonable agreement considering the approximations involved in both methods. Table IV lists all the known acids of the sulphuric acid system and gives mean values for their dissociation constants.

TABLE IV

Dissociation constants of acids at 25° C

	K_a	Ref.
$HB(HSO_4)_4$	2×10^{-1}	*, 5
$H_2S_3O_{10}$ etc.	Moderately strong	
$H_2S_2O_7$	1.4×10^{-2}	1, 2
$H_2Pb(HSO_4)_6$	1.1×10^{-2}	6
HSO_3F	2.3×10^{-3}	*
$HPb(HSO_4)_6^-$	1.8×10^{-3}	6
$HAs(HSO_4)_4$	1.5×10^{-3}	*
HSO_3Cl	9×10^{-4}	*
$HClO_4$	Very weak	*, 7
H_2SO_4	2.4×10^{-5}	†

*This paper.
†$K_a(H_2SO_4) = K_{ap}/10.2$.

Trifluoroacetic Acid

This substance causes a slight decrease in the conductivity of sulphuric acid. A similar behavior has been observed previously for trichloroacetic acid and sulphuryl chloride (15) and for a number of polynitroaromatic compounds (14). It was concluded that these substances are non-electrolytes. The decrease in conductivity was attributed to a decrease in the concentration of the conducting ions $H_3SO_4^+$ and HSO_4^-, resulting partly from dilution by the solute and partly from a decrease in the extent of autoprotolysis and to a decrease in the mobilities of these ions resulting from interference with the proton-transfer mechanism of conduction by the non-electrolyte (14, 15). We conclude that trifluoroacetic acid is a non-electrolyte like trichloroacetic acid and sulphuryl chloride.

Perchloric Acid and Methanesulphonic Acid

These substances cause an almost negligible change in the conductivity of sulphuric

Can. J. Chem. Downloaded from www.nrcresearchpress.com by 210.87.254.5 on 09/05/12
For personal use only.

acid. This could be due either to their being non-electrolytes which, in contrast to other non-electrolytes, do not affect the conductivity of the solvent, or, more probably, to their being just sufficiently ionized to compensate for a decrease in conductivity caused by their non-ionized portions.

Since perchloric acid is more extensively ionized than sulphuric acid in solution in acetic acid (16) it seems reasonable to suppose that it behaves as an acid in solution in sulphuric acid, although it is evidently very weak. It is obviously not possible to calculate a dissociation constant for perchloric acid from the present results.

In contrast to perchloric acid, however, we suppose that the very slight ionization of methanesulphonic acid is as a base rather than as an acid. Benzenesulphonic acid and *p*-toluenesulphonic acid have been found to be weak bases (K_b = 0.011 and 0.026 respectively) (17) and, just as nitromethane (K_b = 0.002) is a somewhat weaker base than nitrobenzene (K_b = 0.01) (14, 18), so methanesulphonic acid might be expected to be a weaker base than benzenesulphonic acid but it is not possible, from the present results, to obtain a value for its dissociation constant.

Difluorophosphoric Acid

The conductivities of difluorophosphoric acid are greater than those of fluorosulphuric acid but in contrast to most of the other electrolytes discussed above it behaves as a base rather than as an acid, i.e. it is partially ionized according to the equation

$$HPO_2F_2 + H_2SO_4 = H_2PO_2F_2^+ + HSO_4^-. \quad [10]$$

Addition of $KHSO_4$ to a solution of HPO_2F_2 increases rather than decreases the conductivity (Table I) and addition of HPO_2F_2 to a solution of $H_2S_2O_7$ causes a decrease in the conductivity. In fact, disulphuric acid can be titrated conductimetrically with the base HPO_2F_2 (Fig. 2) and a value for the basic dissociation constant can be calculated from the value of r_{min} by means of equation [6] (Table II).

Another value for the basic dissociation constant of HPO_2F_2 can be obtained by comparing the conductivities of its solutions with those of the strong base $KHSO_4$ (12, 14). The concentrations of $KHSO_4$ solutions having the same conductivities as those of solutions of round concentrations of HPO_2F_2 were obtained from plots of the conductivities of the two substances and are given in Table III. The concentrations of HSO_4^- in these solutions of $KHSO_4$, which are not equal to the stoichiometric concentration of $KHSO_4$ because of the HSO_4^- ions resulting from the self-ionization of the solvent, were obtained from a previous paper (Table 3 of ref. 13). The corresponding concentrations of $H_2PO_2F_2^+$ were also obtained from this table. Then from the relation

$$[HPO_2F_2]^s = [H_2PO_2F_2^+] + [HPO_2F_2]$$

the concentration of unionized HPO_2F_2 was obtained and finally a value for the basic dissociation constant $K_b = [H_2PO_2F_2^+]\,[HSO_4^-]/[HPO_2F_2]$ was calculated (Table III). The basic strength of difluorophosphoric acid in sulphuric acid ($K_b = 1.0\times10^{-2}$) is the same as that of nitrobenzene. Phosphoric acid is a strong base in sulphuric acid (11); the substitution of two OH groups by more electronegative fluorine atoms has the expected effect of decreasing the base strength.

As difluorophosphoric acid is a base of the sulphuric acid system it is reasonable to conclude that its proton-donating power is less than that of either of the isoelectronic molecules HSO_3F and $HClO_4$. Thus the intrinsic strengths or proton-donating abilities of these acids are in the order $HSO_3F > HClO_4 > HPO_2F_2$. It has been suggested (19, 7)

Can. J. Chem. Downloaded from www.nrcresearchpress.com by 210.87.254.5 on 09/05/12
For personal use only.

that the strengths of inorganic oxyacids are determined largely by the number of equivalent oxygen atoms in the anion over which the negative charge may be spread, the strength increasing with the number of equivalent oxygen atoms. According to this viewpoint fluorosulphuric, chlorosulphuric, and sulphuric acids are all of the same general type, their anions, FSO_3^-, $ClSO_3^-$, and $HOSO_3^-$, each having three equivalent oxygen atoms. All three acids should be weaker than perchloric acid whose anion ClO_4^- has four equivalent oxygen atoms. On the other hand phosphoric acid and difluorophosphoric acid, whose anions, $(HO)_2PO_2^-$ and $F_2PO_2^-$, have only two equivalent oxygen atoms, should both be weaker than sulphuric acid. The observed strength of HPO_2F_2 is consistent with the above ideas but the strengths of HSO_3F and HSO_3Cl are not. It seems reasonable to suppose that some of the charge of the anion is also accommodated on the halogen atom; if the sharing of the charge between the oxygen atoms and the halogen were equal this would put HSO_3F and HSO_3Cl in the same class as perchloric acid, and their strengths would not then be anomalous. A similar sharing of charge would be expected in the anion of difluorophosphoric acid which would also put this acid in the same class as perchloric acid and it would then be expected to be stronger, rather than weaker, than sulphuric acid. It should be noted, though, that we have been comparing the acid strength of dilute solutions of various acids with that of sulphuric acid in bulk. The acid strength of sulphuric acid in bulk may, because of co-operative hydrogen-bonding effects, be considerably greater than that of sulphuric acid in dilute solution. Thus the observed strength of difluorophosphoric acid may not, after all, be anomalous. It would be interesting to compare the extents of dissociation of sulphuric acid and difluorophosphoric acid in dilute solution in some more basic solvent such as acetic acid.

ACKNOWLEDGMENTS

Financial assistance from the National Research Council is gratefully acknowledged. We thank Mr. R. Childs, who carried out the conductivity measurements on methanesulphonic acid.

REFERENCES

1. R. J. Gillespie. J. Chem. Soc. 2493 (1950).
2. S. J. Bass, R. J. Gillespie, and E. A. Robinson. J. Chem. Soc. 821 (1960).
3. R. J. Gillespie, E. A. Robinson, and C. Solomons. J. Chem. Soc. 4320 (1960).
4. R. H. Flowers, R. J. Gillespie, and J. V. Oubridge. J. Chem. Soc. 1925 (1956).
5. R. H. Flowers, R. J. Gillespie, and E. A. Robinson. Can. J. Chem. **38**, 1363 (1960).
6. R. J. Gillespie and E. A. Robinson. Proc. Chem. Soc. 145 (1957).
7. R. J. Gillespie. J. Chem. Soc. 2537 (1950).
8. R. J. Gillespie, J. V. Oubridge, and C. Solomons. J. Chem. Soc. 1804 (1957).
9. G. F. Smith. J. Am. Chem. Soc. **75**, 184 (1953).
10. D. P. Ames, S. Ohashi, C. F. Callis, and J. R. Van Wazer. J. Am. Chem. Soc. **81**, 6350 (1959).
11. R. J. Gillespie and E. A. Robinson. Unpublished work. See R. J. Gillespie and E. A. Robinson. Advances in inorganic chemistry and radiochemistry. Vol. 1. Academic Press, New York. 1959. p. 385.
12. S. J. Bass, R. H. Flowers, R. J. Gillespie, E. A. Robinson, and C. Solomons. J. Chem. Soc. 4315 (1960).
13. R. H. Flowers, R. J. Gillespie, E. A. Robinson, and C. Solomons. J. Chem. Soc. 4327 (1960).
14. R. J. Gillespie and C. Solomons. J. Chem. Soc. 1796 (1957).
15. R. J. Gillespie and S. Wasif. J. Chem. Soc. 231 (1953).
16. R. P. Bell. The proton in chemistry. Cornell University Press, Ithaca, New York. 1959. Chap. 4.
17. R. J. Gillespie. J. Chem. Soc. 2542 (1950).
18. R. J. Gillespie and E. A. Robinson. J. Chem. Soc. 4233 (1957).
19. L. Pauling. General chemistry. Freeman, San Francisco. 1947. p. 394.

Can. J. Chem. Downloaded from www.nrcresearchpress.com by 210.87.254.5 on 09/05/12
For personal use only.

Can. J. Chem. Downloaded from www.nrcresearchpress.com by 210.87.254.5 on 09/05/12
For personal use only.

STEROIDS

II. THE STEREOCHEMISTRY OF THE ADDITION OF GRIGNARD REAGENTS TO 12-KETOSTEROIDS[1]

R. NAGARAJAN AND GEORGE JUST

ABSTRACT

The action of methyl magnesium iodide on 3α,20α-diacetoxypregnan-12-one (II*a*) led to the formation of the epimeric 12-methyl-12-hydroxypregnanes III and V, in which the 12α-hydroxy-12β-methyl isomer III predominated.

Infrared measurements on the corresponding 12-hydroxy-12-methylpregnane-3,20-diones VI and IV permitted unambiguous assignment of configuration at C_{12}.

The pregnanedione IV was transformed to 12β-hydroxy-12α-methylprogesterone.

In the first paper of this series (1) we described the conversion of pregnane-3α,12α,20β-triol to 12α-hydroxy-12β-methylprogesterone. We should now like to report on the conversion of pregnane-3α,12α,20α-triol (I) to the epimeric 12-hydroxy-12-methyl-3,20-pregnanediones IV and VI and on the conversion of the former to 12β-hydroxy-12α-methylprogesterone (VII).

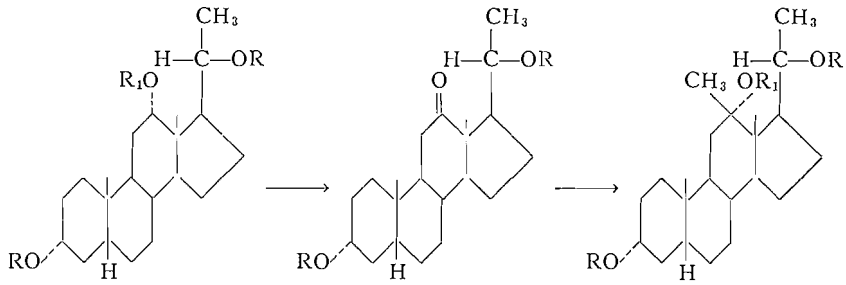
Partial succinylation (1) of pregnane-3α,12α,20α-triol (I) with succinic anhydride in pyridine, followed by methylation of the hemisuccinate with ethereal diazomethane, afforded a 91% yield of pregnane-3α,12α,20α-triol 3,20-bis-methyl succinate (I*a*). Oxidation of I*a* with chromium trioxide in acetic acid gave the corresponding 12-ketone II*b*. Our experience in the 20β-hydroxy series (1) indicated that the reaction of methyl magnesium iodide on pregnan-12-ones proceeded in better yield in the presence of a 20-acetate group rather than a 20-succinate function. Hence, the disuccinoxy ketone II*b* was hydrolyzed with methanolic potassium hydroxide to 3α,20α-dihydroxypregnan-12-one (II) and the latter acetylated with acetic anhydride in pyridine. The resulting diacetoxy ketone II*a* was treated with an excess of ethereal methyl magnesium iodide for 20 hours. Acetylation, chromatography, alkaline hydrolysis, and repeated crystallizations gave the epimeric 12-methylpregnane-3α,12,20α-triols III and V. The mono-, di-, and triacetates III*a–c* and V*a* were prepared and interrelated (see Experimental). Since the separation of the epimeric triols III and V by crystallization was tedious and incomplete, the mother liquors of the crystallization of the Grignard product containing the epimeric triols III and V were oxidized with chromic oxide in acetic acid. Chromatography on alumina of the oxidation product afforded 12β-methyl-12α-hydroxypregnane-3,20-dione (VI) and its 12α-methyl isomer IV. The total yield of the Grignard adducts III (VI) and V (IV) was 60.5% and 25.0% respectively. The hydroxy ketone VI was identical with the 12β-methyl-12α-hydroxypregnane-3,20-dione, isolated previously in the 20β-series (1) in 73% yield as the only product of the corresponding Grignard reaction. The infrared spectrum of this hydroxy diketone showed bands at 3680 cm^{-1} (free OH) and 1713 cm^{-1} (3,20-dione).[2]

[1]*Manuscript received January 6, 1961.*

Contribution from the Department of Chemistry, McGill University, Montreal, Que. Some of the results described in this paper were presented at the October 1960 meeting of ACFAS in Quebec. This paper forms a part of the Ph.D. thesis of R. Nagarajan, to be presented to the Faculty of Graduate Studies, McGill University.

[2]*The infrared spectra were taken in carbon tetrachloride solutions.*

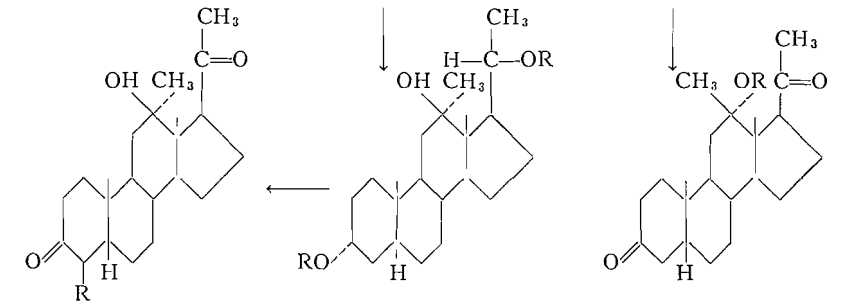
FLOWSHEET I



I R = R_1 = H
Ia R = $CO(CH_2)_2COOCH_3$, R_1 = H

II R = H
IIa R = $COCH_3$
IIb R = $CO(CH_2)_2COOCH_3$

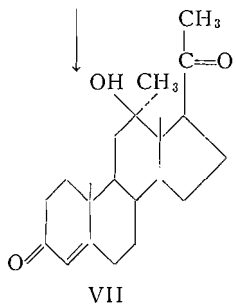
III R = R_1 = H
IIIa R = R_1 = $COCH_3$
IIIb R = $COCH_3$, R_1 = H
IIIc R = H, R_1 = $COCH_3$



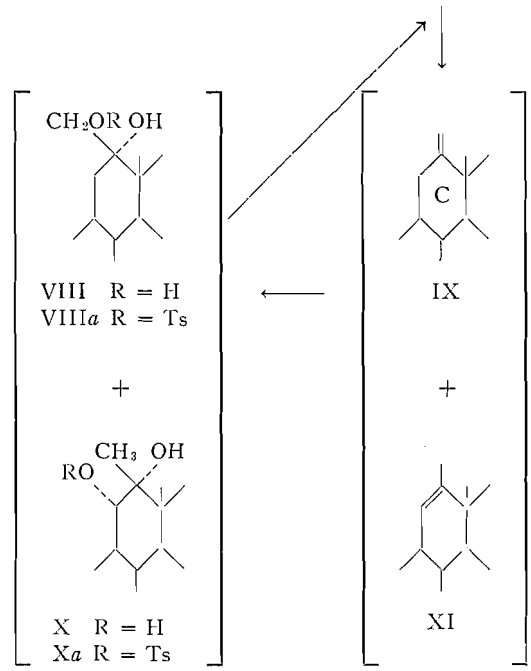
IV R = H
IVa R = Br

V R = H
Va R = $COCH_3$

VI R = H
VIa R = $COCH_3$



VII



VIII R = H
VIIIa R = Ts

IX

X R = H
Xa R = Ts

XI

Can. J. Chem. Downloaded from www.nrcresearchpress.com by 210.87.254.5 on 09/05/12
For personal use only.

The epimeric 12α-methyl-12β-hydroxypregnane-3,20-dione (IV), obtained as a minor product, absorbed in the infrared at 3450 cm^{-1} (LiF prism; change in concentration did not shift the frequency of absorption; intramolecularly bonded OH); 1716 cm^{-1} (3-ketone), and 1695 cm^{-1} ($\diagdown$C$_{20}$=O $\cdots$ H—O—C$_{12}$—).[2] Inspection of models indicated that only a 12β-hydroxy function would form an internal hydrogen bond to the 20-carbonyl group (minimal distance: 2 Å).[3]

These data made possible an unambiguous assignment of configuration for the epimeric tertiary alcohols IV and VI and proved that the attack of methyl magnesium iodide on pregnan-12-ones proceeded mainly from the β-side of the steroid molecule, contrary, in this case, to the well-known "rule of rear-attack" in steroids (3, 4). The validity of the assignment of configuration at the 12-position was confirmed as follows: The tertiary alcohol VI on treatment with acetic acid, acetic anhydride, and *p*-toluenesulphonic acid (5) gave the acetate VI*a*, m.p. 175–176° (also obtained by partial hydrolysis of the triacetate III*a* to the monoacetate III*c* followed by oxidation) and a product, m.p. 72–73°. Further crystallizations gave a compound, m.p. 100–101°, which was assigned the 12-methylene structure IX, since it showed characteristic bands at 3080 cm^{-1}, 1645 cm^{-1}, and 885 cm^{-1}. The infrared spectrum of the product, m.p. 72–73°, was virtually identical with that of the compound melting at 100°, so that it must have consisted mainly of olefin IX, probably contaminated with olefin XI (compare 8). Treatment of the olefinic product m.p. 72–73° with osmium tetroxide gave predominantly the diol VIII containing probably traces of the diol X, which on tosylation gave the tosylate VIII*a* with probably a minor amount of the tosylate X*a*. Lithium aluminum hydride reduction of the tosylates, followed by chromium trioxide oxidation, gave the hydroxy ketone VI, identified by melting point, mixed melting point, and superimposability of the infrared spectra. Since nucleophilic attack by a Grignard reagent on a 12-ketone, and electrophilic addition of OsO_4 on a 12-methylene pregnane gave rise to products of identical configuration at C$_{12}$, it must be concluded that the nucleophilic and electrophilic reagents add from opposite sides of the steroid molecule. It is suggested that this conclusion, at least as far as it concerns nucleophiles of the Grignard type, applies to all steroidal 12-ketones (A) and 17*a*-ketones (E) where the steric environments are very similar.

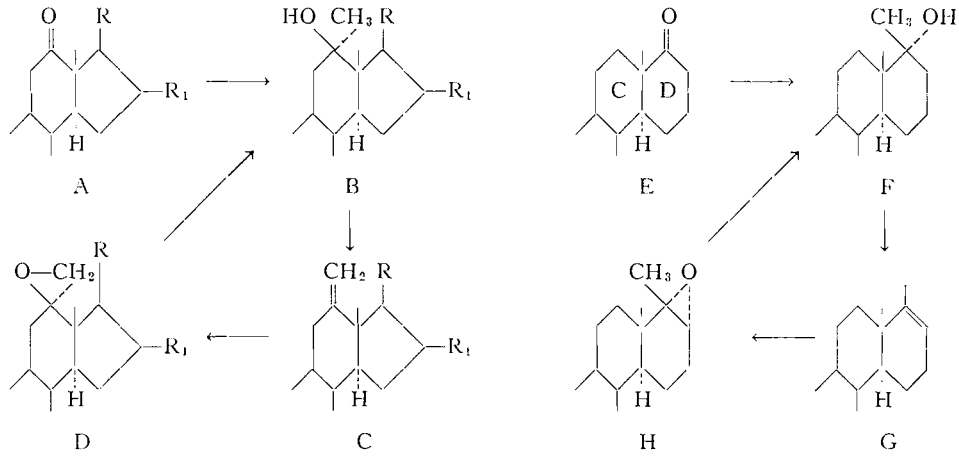
Indeed, Ruzicka *et al.* (6) described some time ago the conversion of Δ^5-3β-acetoxy-17*a*-D-homoandrosterone (E) to Δ^5-17*a*β-methyl-3β-17*a*α-D-homoandrostenediol (F) by the action of methyl magnesium bromide. In order to prove the stereochemistry of the Grignard adduct F, it was dehydrated to the olefin G, which was treated with perbenzoic acid. The epoxide H was then reduced with lithium aluminum hydride and gave the original Grignard product F. This meant that attack by the Grignard reagent and the peracid must have proceeded from opposite sides of the steroid molecule. Since the Grignard adduct (F) was biologically inactive, and since its 17*a*-epimer was expected to show androgenic activity, Ruzicka and co-workers assumed that methyl magnesium bromide attacked the carbonyl function from the β-side, and that perbenzoic acid attacked the double bond from the α-side.

Recently, Bladon and McMeekin (7) submitted the tetrahydropyranylether of hecogenin

[3]*Wall and Serota (2) have recently reported two instances of an intramolecular hydrogen bond between a 12β-hydroxy group and a 20-carbonyl function in 3β-acetoxy-12β-hydroxy-12α-methoxy, 5α,16-pregnen-20-one, and 3β-acetoxy-12β-hydroxy-12α-methoxy-5,16-pregnandiene-20-one.*

Can. J. Chem. Downloaded from www.nrcresearchpress.com by 210.87.254.5 on 09/05/12
For personal use only.

FLOWSHEET II



(A) to the action of methyl lithium. They assigned a 12α-methyl-12β-hydroxy configuration (B) to the tertiary alcohol obtained in the reaction. Dehydration (C), epoxidation (D), and reduction with lithium aluminum hydride led to the original tertiary alcohol B. Since it is extremely unlikely that both the nucleophilic and electrophilic additions on hecogenin derivatives should proceed differently from the corresponding addition reactions in the pregnane series, and since Bladon and McMeekin's assignment were arbitrary, we suggest that they be reversed.

Levine and Wall (8) have also recently reported the reaction of hecogenin acetate (A) with methyl magnesium bromide, which led to "12β-hydroxy-12α-methyltigogenin" (B). Their proof of configuration rested on a reaction sequence identical with that outlined on Flowsheet I (VI $\rightarrow$ IX $\rightarrow$ VIII, VIII*a* $\rightarrow$ VI). In contrast to the results obtained by Bladon and McMeekin (7), Ruzicka *et al.* (6), and ourselves, the two products obtained by Grignard reaction and osmium tetroxide addition were not identical, but epimeric.[4]

The experiments described lead to the conclusion that in most cases different factors govern the stereochemistry of additions of reagents which form complexes, such as Grignard reagents, and of electrophiles. This statement is corroborated by experiments involving reduction of steroidal 12-ketones with lithium aluminum hydride in which a 50% yield of 12α-hydroxy compound is obtained (β-attack, 9).

Bromination at the 4-position of 12α-methyl-12β-hydroxy-3,20-pregnandione IV afforded the bromoketone IV*a*, which was transformed to 12α-methyl-12β-hydroxyprogesterone VII by the method of McGuckin and Kendall (10). This progesterone analogue did not exhibit any notable progestational, androgenic, diuretic, hypotensive, or anabolic properties.[5]

[4]*Melting point, mixed melting point, and optical rotation of the two "epimers" of Levine and Wall (8) seem to indicate that their products are not epimeric. However, unpublished N.M.R. data (private communication by Dr. S. Levine) show that the two compounds are distinctly different. A clarification of the conflicting results of Levine and Wall (8) and Bladon and McMeekin (7) will probably only be achieved by further experimental work.*

[5]*Biological tests were carried out by Dr. C. I. Chappel and Dr. Clara Revesz, Ayerst, McKenna and Harrison, Montreal.*

Can. J. Chem. Downloaded from www.nrcresearchpress.com by 210.87.254.5 on 09/05/12
For personal use only.

Can. J. Chem. Downloaded from www.nrcresearchpress.com by 210.87.254.5 on 09/05/12
For personal use only.

EXPERIMENTAL[6, 7, 8, 9, 10]

3α,12α,20α-Pregnanetriol 3,20-bis-Methyl Succinate (Ia)

A solution of the triol I (7.0 g) and succinic anhydride (12.0 g) in absolute pyridine (40 ml) was heated on a water bath at 90° for 4 hours, and left overnight at room temperature. To the reaction mixture was added 1 liter of ice water and it was extracted with ether after 1 hour. The ethereal layer was washed with water, cold 2 *N* hydrochloric acid, and water. The organic solution was dried over magnesium sulphate, filtered, and treated with excess ethereal diazomethane solution. Crystallization from acetone–hexane afforded 10.10 g of the bis-methyl succinate I*a*, m.p. 109–110°. Repeated crystallizations of the mother liquors from acetone–hexane gave 0.571 g of I*a*, m.p. 109–110° (yield 90.8%). Recrystallization did not raise the melting point, $[\alpha]_D^{29}$ 43° (*c* 1.02 in $CHCl_3$).

Calc. for $C_{31}H_{48}O_9$: C 65.92, H 8.57. Found: C 66.09, H 8.41.

3α,20α-Dihydroxypregnan-12-one bis-Methyl Succinate (IIb)

A solution of chromium trioxide (1.19 g) in 90% acetic acid (12 ml) was added to a solution of the bis-methyl succinate I*a* (6.088 g) in glacial acetic acid (210 ml) and left overnight at room temperature. Methanol (5 ml) was added to the reaction mixture, which was then poured into 2 liters of water and extracted with ether. The ethereal layer was washed with 5% sodium bicarbonate solution and water until the washings were neutral. Evaporation of the solvent afforded 6.071 g of the crude keto bis-methyl succinate II*b*, m.p. 65–66°.

Two crystallizations from ether–hexane raised the melting point of the keto bis-methyl succinate II*b* to 65.5–66.5°, $[\alpha]_D^{29}$ 87° (*c* 0.84 in $CHCl_3$).

Calc. for $C_{31}H_{46}O_9$: C 66.16, H 8.24. Found: C 65.94, H 8.04.

3α,20α-Dihydroxypregnan-12-one (II)

A solution of the keto bis-methyl succinate II*b* (6.004 g, crude product obtained from the above reaction) in 5% methanolic potassium hydroxide (500 ml) was heated under reflux for 4 hours. The methanol was removed by distillation until the volume of the reaction mixture was about 150 ml. After cooling, it was poured into 1 liter of water with stirring. The hydroxy ketone II, which separated out, was filtered, washed with water, and dried (3.49 g, m.p. 260–261°). The filtrate was extracted with ether and the ethereal solution was washed with saturated sodium chloride solution. Evaporation of the solvent afforded 0.077 g of II, m.p. 250–260°.

The hydroxy ketone was recrystallized twice from methanol for analysis, m.p. 260–261°, $[\alpha]_D^{29}$ 120° (*c* 0.56 in $CHCl_3$). (A few drops of C_2H_5OH was added to bring the hydroxy ketone II into solution.)

Calc. for $C_{21}H_{34}O_3$: C 75.41, H 10.24. Found: C 75.70, H 10.14.

3α,20α-Diacetoxypregnan-12-one (IIa)

Absolute pyridine (30 ml) and acetic anhydride (25 ml) were added to 3.40 g of the hydroxy ketone II and the mixture heated under reflux for 10 minutes until the crystals dissolved. The reaction mixture was left overnight in a water bath at 90°. Ether extraction gave 4.243 g of the crude ketone II*a*, m.p. 210–212°. Crystallization from acetone–hexane

[6] *All the melting points were corrected.*
[7] *Only the best yields were reported.*
[8] *Unless otherwise stated, the infrared spectra were taken in carbon tetrachloride solution using a 1-mm sodium chloride cell.*
[9] *The commercially available aluminum oxide (Woelm) was used for chromatography.*
[10] *The microanalyses were carried out by Dr. Alfred Bernhardt, Mülheim, Germany and Dr. C. Daesslé, 5757 Decelles St., Montreal.*

afforded 4.082 g of crystals, m.p. 211–212°. Crystallization of mother liquors gave 0.127 g, m.p. 211–212°. The over-all yield for the reaction sequence I*a* → II*b* → II → II*a* was 99%.

Two recrystallizations of the ketone II*a* from acetone–hexane raised the melting point to 212–212.5°, $[\alpha]_D^{29}$ 103° (*c* 1.25 in $CHCl_3$).

Calc. for $C_{25}H_{38}O_5$: C 71.73, H 9.15. Found: C 71.54, H 8.97.

Reaction of Methyl Magnesium Iodide with 3α,20α-Diacetoxypregnan-12-one (II a)

To 300 ml of an ethereal solution of methyl magnesium iodide (from 4.984 g of magnesium and 13.0 ml of methyl iodide) was added with stirring 10.68 g of the ketone II*a*, dissolved in 2 liters of absolute ether. The reaction mixture was heated under reflux for 16 hours and cooled, and a solution of ammonium chloride (50 g) in water (1 liter) was added. Ether extraction afforded 10.28 g of a product, m.p. 194–202°, which was acetylated with 65 ml of pyridine and 55 ml of acetic anhydride at 90° for 14 hours. The usual extraction procedure afforded 12.25 g of foam, which was chromatographed on alumina (4.5% water). The hexane–benzene (3:1) eluates were crystallized from ether–hexane and there was obtained 520 mg of the triacetate III*a*, m.p. 171–172°. Recrystallization from ether–hexane raised the melting point to 172–173°, $[\alpha]_D^{28}$ 90° (*c* 1.11 in $CHCl_3$).

Calc. for $C_{28}H_{44}O_6$: C 70.57, H 9.32. Found: C 70.57, H 9.21.

The hexane–benzene (1:1) and benzene eluates (4.485 g) on hydrolysis with 5% methanolic potassium hydroxide gave 3.587 g of crystals, m.p. 208–216°. Repeated crystallization from methanol afforded 3.216 g of triol III, m.p. 240–241°, $[\alpha]_D^{28}$ 70° (*c* 0.97 in $CHCl_3$).

Calc. for $C_{22}H_{38}O_3$: C 75.37, H 10.92. Found: C 75.33, H 10.83.

The benzene–ether and ether–methanol eluates (4.273 g) were hydrolyzed with 5% methanolic potassium hydroxide and there was obtained 3.604 g of a mixture of epimeric triols III and V, m.p. 204–216°. Fractional crystallization from methanol afforded 1.22 g of the triol III, m.p. 240–241°, and 1.376 g of the triol V, m.p. 201–203°. Recrystallization from acetone did not raise the melting point of the triol V, $[\alpha]_D^{22}$ 38° (*c* 1.07 in $CHCl_3$).

Calc. for $C_{22}H_{38}O_3$: C 75.37, H 10.92. Found: C 75.50, H 10.96.

An ether solution of the mother liquors of the hexane–benzene (3:1) fractions and the hexane–benzene (9:1 and 4:1) eluates were deacetylated with lithium aluminum hydride, and the triol mixture thus obtained was combined with the mother liquors of crystallization of triols III and V. To a solution of the combined triol mixture (3.181 g) in 150 ml of glacial acetic acid was added a solution of 2.13 g of chromium trioxide in 25 ml of 90% acetic acid and the mixture left for 16 hours at room temperature. Ether extraction gave 2.85 g of a pale-brown semicrystalline product, which was chromatographed on 80 g of alumina (4.5% water).

The hexane–benzene (4:1) eluates (170 mg), on crystallization from acetone–hexane, gave 80 mg of pregnane-3,12,20-trione, m.p. 198–200° (1, 11), identified by mixed melting point and comparison of I.R. spectra with an authentic sample.

Hexane–benzene (3:1, 2:1, 1:1) and benzene eluates (950 mg) were crystallized from ether–hexane and there was obtained 741 mg of the hydroxy ketone IV, m.p. 125–126°. The mother liquors were combined with the benzene–ether (95:5) fractions and crystallization from ether–hexane gave 113 mg of IV, m.p. 122–123°.

A portion of the hydroxy ketone IV was crystallized from ether–hexane for analysis, m.p. 125–126°, $[\alpha]_D^{28}$ 30° (*c* 0.90 in $CHCl_3$), $\nu_{max}^{CCl_4}$ 1716 cm^{-1} (3-ketone), 1695 cm^{-1}, and 3480 cm^{-1} ($>C_{20}=O \cdots H-O-C_{12}-$).

Can. J. Chem. Downloaded from www.nrcresearchpress.com by 210.87.254.5 on 09/05/12
For personal use only.

Calc. for $C_{22}H_{34}O_3$: C 76.25, H 9.89. Found: C 76.16, H 9.90.

The rest of the benzene–ether and ether–methanol eluates on crystallization from acetone–hexane afforded 465 mg of the hydroxy ketone VI, m.p. 187–188°, $\nu_{max}^{CCl_4}$ 1713 cm^{-1} (3,20-dione), 3680 cm^{-1} (C_{12}-hydroxyl), found identical with 12β-methyl-12α-hydroxypregnane-3,20-dione (1) by mixed melting point and superimposability of I.R. spectra, thus confirming our assignment of configuration of the 12-hydroxy-12-methyl compound in our previous publication (1). Recrystallization of mother liquors gave 121 mg of VI, m.p. 184–186°.

Taking into consideration the isolation at different stages in the above experiment of the triacetate III*a* by chromatography, the triols III and V by crystallizations, and the hydroxy ketones VI and IV by chromatography, the over-all yields of 12β-methylpregnane-3α,12α,20α-triol and 12α-methylpregnane-3α,12β,20α-triol were 60.5% and 25.0% respectively.

*12β-Methylpregnane-3α,12α,20α-triol 12-Acetate (III*c*)*

A solution of 200 mg of the triacetate III*a* in 25 ml of 5% methanolic potassium hydroxide was heated at reflux temperature for 10 hours. Ether extraction gave 194 mg of oil. Fractional crystallization from ether–hexane afforded 56 mg of III*c*, m.p. 183–184° (yield 34%), and 10 mg of the triol III, m.p. 240–241°. The latter was identified by comparison of I.R. spectra and mixed m.p. with an authentic sample of triol III.

Recrystallization of III*c* with ether–hexane raised the m.p. to 184–185°, $[\alpha]_D^{28}$ 90° (*c* 1.07 in $CHCl_3$).

Calc. for $C_{24}H_{40}O_4$: C 73.40, H 10.27. Found: C 73.23, H 10.20.

*12β-Methyl-12α-acetoxypregnane-3,20-dione (VI*a*)*

To a solution of the monoacetate III*c* (165 mg, crude product obtained by alkaline hydrolysis of 170 mg of the triacetate III*a*) in 5 ml of acetic acid was added with stirring a solution of 112 mg of chromium trioxide in 2.5 ml of 90% acetic acid, and the reaction mixture left overnight at room temperature. Ether extraction gave 140 mg of oil, which was chromatographed on alumina (4.5% water). The hexane–benzene (1:1) and benzene eluates on crystallization from ether–hexane afforded 52 mg of the ketone VI*a*, m.p. 175–176°. Crystallization of mother liquors gave 16 mg, m.p. 174–175° (yield 49.1%). Two crystallizations of the ketone VI*a* from ether–hexane raised the m.p. to 175.5–176°, $[\alpha]_D^{22}$ 102° (*c* 1.04 in $CHCl_3$).

Calc. for $C_{24}H_{36}O_4$: C 74.18, H 9.34. Found: C 74.31, H 9.37.

The ether–methanol (9:1) fractions on crystallization from acetone–hexane gave 15 mg of the hydroxy ketone VI, m.p. 187–188°, identified by comparison of I.R. spectra and mixed melting point with an authentic sample of VI.

*12β-Methylpregnane-3α,12α,20α-triol 3,20-Diacetate (III*b*)*

A solution of 150 mg of the triol III in 5 ml of pyridine and 5 ml of acetic anhydride was left at room temperature for 16 hours. Ether extraction and crystallization from ether–hexane afforded 175 mg of the diacetate III*b*, m.p. 188–189°. Recrystallization of mother liquors gave 7 mg, m.p. 186–188° (yield 98%).

Recrystallization for analysis did not raise the melting point, $[\alpha]_D^{28}$ 80° (*c* 0.98 in $CHCl_3$).

Calc. for $C_{26}H_{42}O_5$: C 71.86, H 9.74. Found: C 71.69, H 9.67.

*12α-Methylpregnane-3α,12β,20α-triol 3,20-Diacetate (V*a*)*

Acetylation of 100 mg of the triol V at room temperature as described above gave upon crystallization from ether–hexane 117 mg of the diacetate V*a*, m.p. 189–190° (yield

Can. J. Chem. Downloaded from www.nrcresearchpress.com by 210.87.254.5 on 09/05/12
For personal use only.

94.4%). (Mixed melting point of the diacetate V*a* with the diacetate III*b* showed a depression in melting point.) Recrystallization for analysis did not raise the melting point, $[\alpha]_D^{28}$ 56° (*c* 0.99 in $CHCl_3$).

Calc. for $C_{26}H_{42}O_5$: C 71.86, H 9.74. Found: C 71.91, H 9.67.

Chromium Trioxide Oxidation of Triols III and V

To a solution of 200 mg of the triol III in 5 ml of glacial acetic acid was added with stirring 130 mg of chromium trioxide dissolved in 2.5 ml of 90% acetic acid and the mixture was left at room temperature for 18 hours. Ether extraction and crystallization from acetone–hexane gave 156 mg of the hydroxy ketone VI, m.p. 188–189°. Recrystallization of mother liquors afforded 5 mg, m.p. 187–188° (yield 86.5%). The identity of the above product was confirmed by the superimposability of I.R. spectra and mixed melting point with an authentic sample of VI.

Chromium trioxide oxidation of 200 mg of the triol V as described above gave 199 mg of an oil, which on chromatography on alumina and crystallization from ether–hexane afforded 83 mg of needles, m.p. 124–125°. Recrystallization of mother liquors gave 51 mg, m.p. 123–124° (yield 68%). The identity of this compound with the hydroxy ketone IV was proved by a comparison of I.R. spectra and mixed melting point.

12α-Methyl-12β-hydroxyprogesterone (VII)

A solution of bromine (306 mg) in acetic acid (15.2 ml) was added with stirring to a solution of the hydroxy ketone IV (600 mg) in acetic acid (5 ml) containing a drop of 50% (w/v) solution of hydrobromic acid. The reaction mixture was stirred for 5 minutes and poured in 250 ml of ice water. The solid which separated out was filtered, dried, and on crystallization from ether–hexane afforded 332 mg of the bromoketone IV*a*, melting point 172–173° (decomp.), λ_{max}^{EtOH} 285 mμ (ε 60), $\nu_{max}^{CCl_4}$ 1695 cm^{-1}, 3480 cm^{-1} ($>C_{20}{=}O \cdots H{-}O{-}C_{12}{-}$), 1735 cm^{-1} (4β-bromo-3-ketone).

The filtrate was extracted with ether and combined with the mother liquors of the crystallization of the bromoketone IV*a*. Since recrystallization was tedious and afforded only 114 mg of the bromoketone IV*a*, m.p. 168–169° (decomp.), the second crop and the mother liquors (533 mg of oil) were reduced by heating with 550 mg of zinc dust, 5.5 ml of acetic acid, and 0.5 ml of water at 90° for 1 hour. Ether extraction, chromatographic purification, and crystallization from ether–hexane gave 276 mg of the hydroxy ketone IV, m.p. 124–125°. Taking into consideration the recovery of the hydroxy ketone IV, the yield of pure bromoketone IV*a* was 83.2%.

The bromoketone IV*a* (330 mg, m.p. 172–173° decomp.) was dehydrobrominated according to the method of McGuckin and Kendall (10). The resulting oil was chromatographed on alumina (4.5% water). The benzene, benzene–ether, and ether eluates on crystallization from ether–hexane afforded 120 mg of the progesterone derivative VII, m.p. 142–143°. The mother liquors on crystallization afforded 19 mg of VII, melting point 139–142° (yield 48.4%). The second crop was recrystallized and added to the first batch. Recrystallization gave 126 mg of analytically pure VII, melting point 142–143°, $[\alpha]_D^{22}$ 113° (*c* 1.07 in $CHCl_3$), λ_{max}^{EtOH} 238 mμ (ε 18,600), $\nu_{max}^{CCl_4}$ 1695 cm^{-1} and 3480 cm^{-1} ($>C_{20}{=}O \cdots H{-}O{-}C_{12}{-}$), 1680 cm^{-1} and 1622 cm^{-1} (Δ^4-3-ketone).

Calc. for $C_{22}H_{32}O_3$: C 76.68, H 9.37. Found: C 76.68, H 9.41.

Can. J. Chem. Downloaded from www.nrcresearchpress.com by 210.87.254.5 on 09/05/12
For personal use only.

Reaction of 12β-Methyl-12α-hydroxypregnane-3,20-dione (VI) with Acetic Acid, Acetic Anhydride, and p-Toluenesulphonic Acid

To a solution of 500 mg of the hydroxy ketone VI in 25 ml of glacial acetic acid was added 5 ml of acetic anhydride and 500 mg of *p*-toluenesulphonic acid (5) and the suspension was stirred until the solid dissolved. The reaction mixture was left at room temperature for 4.5 hours, then poured into 250 ml of ice water and extracted with ether. The ethereal solution was washed with 5% sodium carbonate solution and water until the washings were neutral, and dried over magnesium sulphate. Evaporation to dryness afforded 565 mg of oil, showing bands in the infrared at 3070 cm^{-1}, 1645 cm^{-1}, 890 cm^{-1} ($\diagdown$C=CH_2) (12); 1750 cm^{-1}, 1215 cm^{-1} ($\Delta^{17(20)}$-enol acetate) (13); 1713 cm^{-1} (3-ketone). Under the above reaction conditions the $\Delta^{17(20)}$-enol acetate is known to be formed (14 and 15). The enol acetate was converted to the C_{20}-ketone by heating a solution of the crude reaction product in 25 ml of methanol with 750 mg of potassium carbonate in 10 ml of water under reflux for 2 hours. Ether extraction gave 555 mg of product showing no bands at 1750 cm^{-1} and 1215 cm^{-1} characteristic of enol acetates. It was chromatographed on alumina (4.5% water) and the hexane and hexane–benzene eluates on crystallization from hexane afforded 145 mg of needles, m.p. 72–73°. A portion of it was recrystallized from hexane for analysis, m.p. 73–74°, $[\alpha]_D^{22}$ 139° (*c* 1.03 in $CHCl_3$), $\nu_{max}^{CS_2}$ 3080 cm^{-1}, 1645 cm^{-1}, 885 cm^{-1} ($\diagdown$C=CH_2); 1713 cm^{-1} (3,20-dione).

Calc. for $C_{22}H_{32}O_2$: C 80.41, H 9.82. Found: C 80.02, H 9.66.

Recrystallization of mother liquors gave 45 mg of needles, m.p. 71–73° (yield 40.1%).

The mother liquors were dissolved in 5 ml of hexane and left in an ice box. After 1 week, 80 mg of crystalline compound was obtained. Repeated crystallization gave 63 mg of needles, m.p 100–101° (yield 13.3%). Recrystallization from hexane for analysis raised the melting point to 101–102°, $[\alpha]_D^{22}$ 130° (*c* 0.95 in $CHCl_3$), $\nu_{max}^{CS_2}$ 3080 cm^{-1}, 1645 cm^{-1}, 885 cm^{-1} ($\diagdown$C=CH_2); 1713 cm^{-1} (3,20-dione).

Calc. for $C_{22}H_{32}O_2$: C 80.41, H 9.82. Found: C 80.19, H 9.86.

In view of the close similarity of the infrared spectra of the compounds melting at 73–74° and 101–102° and the presence only of characteristic bands due to a vinylidene group, it was presumed that the compound melting at 73–74° contained, if any, only traces of the olefin XI, the major proportion being olefin IX.

The benzene eluates of the chromatogram on crystallization from acetone–hexane afforded 76 mg of VI*a*, m.p. 175–176° (yield 12.1%). (Also obtained by partial hydrolysis of the triacetate III*a* to the monoacetate III*c*, and subsequent oxidation.)

The later fractions consisted mainly of the starting material VI, as identified by infrared spectra. No attempt was made to recover it.

Conversion of the Olefin IX to 12β-Methyl-12α-hydroxypregnane-3,20-dione (VI)

To a solution of 175 mg of the crude olefin IX (m.p. 71–73°) in 20 ml of absolute ether containing 0.2 ml of pyridine was added 150 mg of osmium tetroxide (1.1 mole equivalent) and the reaction mixture was left at room temperature for 2 days (8). It was then heated under reflux for 30 minutes with 100 ml of an 80% ethanolic solution of sodium sulphite. After cooling, filtering through celite, and ether extraction, 208 mg of an oil was obtained.

Its infrared spectrum showed no characteristic bands due to a vinylidene group. Crystallization from acetone–hexane afforded 36 mg of the crude hydroxylation product

Can. J. Chem. Downloaded from www.nrcresearchpress.com by 210.87.254.5 on 09/05/12
For personal use only.

VIII (possibly containing traces of X). Two recrystallizations from acetone gave 13 mg of fine needles, m.p. 196–199°, $[\alpha]_D^{22}$ 22° (*c* 0.88 in $CHCl_3$).

Calc. for $C_{22}H_{34}O_4$: C 72.88, H 9.45. Found: C 72.81, H 9.42.

The mother liquors (170 mg of oil) were tosylated with 170 mg of *p*-toluenesulphonyl chloride and 5 ml of pyridine at room temperature for 18 hours. Ether extraction afforded 195 mg of oil, which showed absorption bands at 1375 cm^{-1}, 1193 cm^{-1}, and 1190 cm^{-1} in the infrared region, characteristic of tosyl groups (12*a*).

A solution of the oil in 20 ml of absolute tetrahydrofuran was heated under reflux for 16 hours with 200 mg of lithium aluminum hydride. The reduction product was worked up in the usual fashion, and there was obtained 155 mg of semicrystalline compound. Its infrared spectrum indicated the absence of tosyl groups.

To a solution of the above product (155 mg) in 5 ml of acetic acid was added with stirring a solution of 105 mg of chromium trioxide in 2 ml of 90% acetic acid and the mixture was left for 16 hours at room temperature. The reaction mixture was worked up in the usual manner, and when the ethereal extract was evaporated to about 5 ml, there was obtained 58 mg of plates, m.p. 188–189°. Admixture with an authentic sample of 12β-methyl-12α-hydroxypregnane-3,20-dione (VI) did not depress the melting point and the I.R. spectra were also identical. Chromatographic purification and crystallization from acetone–hexane of the mother liquors afforded an additional 27 mg of VI, m.p. 181–186° (yield 56.8%).

ACKNOWLEDGMENTS

We wish to thank the National Research Council, Ayerst, McKenna and Harrison Ltd., and the Department of Chemistry, McGill University, for generous financial support.

We should also like to thank Dr. C. Sandorfy, Department of Chemistry, Université de Montréal, for having taken and interpreted the infrared spectra with a lithium fluoride prism.

REFERENCES

1. G. Just and R. Nagarajan. Can. J. Chem. **39**, 548 (1961).
2. M. E. Wall and S. Serota. Tetrahedron, **10**, 238 (1960).
3. L. F. Fieser. Experientia, **6**, 312 (1950).
4. T. E. Gallagher and T. H. Kritchevsky. J. Am. Chem. Soc. **72**, 882 (1950).
5. R. B. Turner. J. Am. Chem. Soc. **75**, 3489 (1953).
6. L. Ruzicka, N. Wahba, P. Th. Herzig, and H. Heusser. Ber. **85**, 491 (1952).
7. P. Bladon and W. McMeekin. J. Chem. Soc. 2191 (1960).
8. S. G. Levine and M. E. Wall. J. Am. Chem. Soc. **82**, 3391 (1960).
9. R. Hirschmann, C. S. Snoddy, Jr., C. F. Hiskey, and N. L. Wendler. J. Am. Chem. Soc. **76**, 4013 (1954).
10. W. F. McGuckin and E. C. Kendall. J. Am. Chem. Soc. **74**, 5811 (1952).
11. T. Reichstein and E. v. Arx. Helv. Chim. Acta, **23**, 747 (1940).
12. L. J. Bellamy. The infrared spectra of complex molecules. John Wiley & Sons, Inc., New York. 1958. pp. 34, 364.
13. H. Vanderhaeghe, E. R. Katzenellenbogen, K. Dobriner, and T. F. Gallagher. J. Am. Chem. Soc. **74**, 2810 (1952).
14. C. W. Marshall, T. H. Kritchevsky, S. Lieberman, and T. F. Gallagher. J. Am. Chem. Soc. **70**, 1837 (1948).
15. P. Z. Bedoukian. J. Am. Chem. Soc. **67**, 1430 (1945).

Can. J. Chem. Downloaded from www.nrcresearchpress.com by 210.87.254.5 on 09/05/12
For personal use only.

Can. J. Chem. Downloaded from www.nrcresearchpress.com by 210.87.254.40 on 09/05/12
For personal use only.

π-BONDING IN INORGANIC COMPOUNDS

III. A MAGNETOCHEMICAL STUDY OF HEXAHALOOSMATES AND HEXACHLORORHENATE[1,2]

A. D. WESTLAND AND N. C. BHIWANDKER

ABSTRACT

The anomalously small magnetic moments of osmium(IV) and rhenium(IV) in their hexahalo complexes are investigated by measurement of the magnetic susceptibilities of the mixed crystal systems, K_2OsCl_6/K_2PtCl_6, K_2OsBr_6/K_2PtBr_6, and K_2ReCl_6/K_2PtCl_6. It is shown that only at high dilution is the magnetic behavior of the systems that which is expected from theory; therefore, extensive superexchange through the overlap of *d*-orbitals on the central atom and orbitals on the ligands takes place in the pure substances and in the concentrated systems. Determination of the spin–orbit coupling constant for $OsCl_6^{2-}$ provides a value in agreement with estimates based on spectra.

INTRODUCTION

In Parts I and II of this series, thermochemical aspects and mesomeric effects of d_π–d_π bonding were discussed. The present paper is concerned with π-bonding as manifested in the magnetic superexchange effect. Admittedly, it has been postulated that in this phenomenon the principal overlap is of d_π–p_π type (1) and if this is so, the bond is essentially different from that considered previously. It seems to the present authors, however, that in the compounds being considered in this paper, a contribution to the superexchange effect may be a secondary result of d_π–d_π bonding. Apparently, the superexchange is possible when the ligands possess orbitals of the appropriate symmetry (e.g., t_{2g} for octahedral co-ordination and e_g for tetrahedral co-ordination) and the central ion possesses *d*-electrons in an insufficient number to fill the d_ϵ, or respectively, the d_γ subshell. It is here suggested that unpaired electrons will be subject to "superexchange", i.e. quantum mechanical exchange between neighboring co-ordination groups, providing these groups are in sufficient proximity and are suitably oriented. These conditions are met by alkali hexahalo salts of rhenium (IV) and iridium (IV), for example.

Superexchange has been detected in K_2IrCl_6 and $(NH_4)_2IrCl_6$ by means of paramagnetic resonance spectra (2, 3). We shall proceed to show that superexchange and hence π-bonding does indeed occur in K_2OsCl_6, K_2OsBr_6, and K_2ReCl_6 as well.

A. Potassium Hexachloroosmate and Hexabromoosmate

Osmium(IV) compounds are of "low-spin" type in which there are four electrons in the t_{2g} orbital. Consequently, a moment corresponding to two unpaired electrons is expected, viz. 2.83 Bohr magnetons (B.M.). The observed effective moments are very much less than this, e.g. 1.44 B.M. for K_2OsCl_6. This is generally regarded as a result of the strong coupling between angular and spin moments which is observed in the spectra of the heavy elements. Kotani has predicted that when the coupling constant, *A*, is large with respect to *kT* in the d^4 configuration the magnetic susceptibility will be independent of temperature (4). Syrkin and Belova observed that the susceptibility of K_2OsCl_6 is, in fact, constant from 77° to 292° K (5). Similar results were obtained by Johansen and Lindberg for $(NH_4)_2OsBr_6$ (6).

Figgis and co-workers (7) have collected data for various Os (IV) compounds, part of which are reproduced in Table I. The values of the coupling constant were derived by

[1]*Manuscript received January 30, 1961.*
Contribution from the Department of Chemistry, University of Ottawa, Ottawa, Canada.
[2]*Part II. Can. J. Chem.* **39**, *324 (1961).*

TABLE I

Compound	μ_{eff}, B.M. at 300° K	Spin–orbit coupling constant, A, cm^{-1}
K_2OsF_6	1.30	8,800
K_2OsCl_6	1.50	6,700
K_2OsBr_6	1.20	10,300
K_2OsI_6	1.38	7,200
Cs_2OsCl_6	1.66	5,200

extrapolating the susceptibilities to zero temperature and applying Kotani's formula

$$\chi_M = \frac{24\,N\beta^2}{A} \qquad [1]$$

in which N is Avogadro's number and the other symbols have their usual significance. The values of A so obtained are rather greater than the value 3600 cm^{-1} obtained from the spectrum of $OsCl_6^{2-}$ (8). Griffith estimated a value of 4500 cm^{-1} for the free ion (9). The nephelauxetic effect of the ligands is expected to produce a 10 to 30% reduction in the latter value (10).

In order to account for their high values for A, Figgis and co-workers considered one of Kotani's assumptions invalid, namely, that the spin–orbit interaction is much smaller than the interelectronic repulsion and consequently adopted the view that an equivalent of j–j coupling holds within the d_ϵ subshell. On this assumption the susceptibility at zero temperature is given by

$$\chi_M = \frac{16}{3}\frac{N\beta^2}{A}. \qquad [2]$$

Accordingly, the values of A thus derived are smaller than those given in Table I by a factor of 9/2. The modified values are therefore somewhat low. Figgis and co-workers further remark that there should be a variation in the observed susceptibilities of the different haloosmates consistent with the differing degrees of delocalization of the electrons on the central atom and a consequent trend in the values of the coupling constant. However, it may be seen from the table that the distribution of the measured values of the susceptibility is random. We shall return to this point later.

The moments of the osmium in the cesium salts are invariably higher than those in the corresponding potassium salts. This led us to believe that there is a superexchange coupling between neighboring osmium atoms through the intervening chlorine atoms and that this coupling becomes weaker as the osmium atoms are forced apart by the introduction of the larger alkali ion. Further, if the theoretical treatment (11) of the exchange coupling in K_2IrCl_6 is to be accepted there is reason to expect that all analogous paramagnetic salts of the third transition series elements should be similar in this respect. It is evident that infinite isomorphous dilution in K_2PtCl_6 should provide magnetically isolated $OsCl_6^{2-}$ groups and only in such a state can their magnetic behavior be expected to conform to Kotani's expression.

Results for K_2OsCl_6 and K_2OsBr_6

The effective moment of the osmium atom in solid solutions of K_2OsCl_6 and K_2PtCl_6 is plotted against composition in Fig. 1. The marked rise in the moment at low concentrations of osmium indicates that the $OsCl_6^{2-}$ groups must be essentially isolated from

Can. J. Chem. Downloaded from www.nrcresearchpress.com by 210.87.254.40 on 09/05/12
For personal use only.

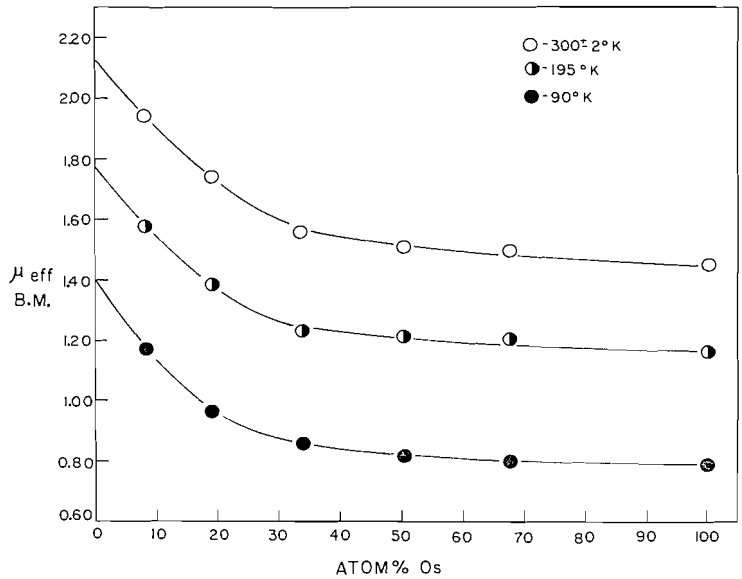


FIG. 1. Plot of the effective moments of osmium at various temperatures against composition of the system K_2OsCl_6/K_2PtCl_6.

other paramagnetic centers before they can exhibit their full paramagnetism. We take this as an indication of superexchange coupling in the concentrated systems. Table II

TABLE II

Temp., °K	Pure K_2OsCl_6		K_2OsCl_6 at infinite dilution	
	$\chi_M \times 10^3$	μ_{eff}, B.M.	$\chi_M \times 10^3$	μ_{eff}, B.M.
298	0.858	1.44	—	—
301	—	—	1.90	2.13
195	0.860	1.16	1.94	1.76
90	0.860	0.79	1.92	1.38

presents our results for pure K_2OsCl_6 and the results of extrapolation to infinite dilution. The results for pure K_2OsCl_6 agree with those of Mellor (12) although they differ slightly from those given in reference 7.

Upon substituting the values of the susceptibility at infinite dilution in equation [1] the value 3240 cm^{-1} is obtained for A. This is in good agreement with the values obtained from spectra which were mentioned earlier.

The uncertainty of extrapolation and the correction for diamagnetism are possible sources of error. The diamagnetism amounted to approximately 60% of the total susceptibility for the most dilute preparation. The value for K_2PtCl_6 was obtained from material prepared from the same stock and in the same manner as was used in the preparation of the solid solutions. The diamagnetism of K_2OsCl_6 was estimated from the value for K_2PtCl_6 by appropriate correction for the change in the central atom using Klemm's values (13). The possible error in the extrapolated values due to the large diamagnetic corrections is $\leqslant 4\%$. It should be emphasized that the measured values of

Can. J. Chem. Downloaded from www.nrcresearchpress.com by 210.87.254.40 on 09/05/12
For personal use only.

susceptibility may be in error due to possible inhomogeneity of the samples. This could only lead to negative errors, however, so the true values of the susceptibilities may be slightly higher. It is to be expected that error from this source is negligible at extreme dilution.

In order to see if bromine can transmit superexchange coupling to any appreciable extent, we have measured the change in atomic susceptibility of the osmium atom in the $OsBr_6^{2-}$ ion in K_2OsBr_6 and in a 10.4 mole% solution of K_2OsBr_6 in K_2PtBr_6. The results are shown in Table III. It is apparent that $OsBr_6^{2-}$ is subject to superexchange

TABLE III

Substance	Temp., °K	$\chi_M \times 10^3$	μ_{eff}, B.M.
K_2OsBr_6	300	0.99_1	1.55
	195	0.98_1	1.24
	90	0.98_2	0.84
K_2OsBr_6/K_2PtBr_6	302	1.59	1.96
	195	1.49	1.52
	90	1.32	0.97

to approximately the same extent as is $OsCl_6^{2-}$ for the increase in the room temperature value of μ_{eff} upon dilution to 10 atom% is about 0.4 B.M. in each case.

Our value of χ_M for K_2OsBr_6 is $9.86 \pm .05 \times 10^{-3}$ over the temperature range 90° to 300° K. This is much higher than the value 6.09×10^{-3} given in reference 7. However, it is very close to Johansen and Lindberg's value for $(NH_4)_2OsBr_6$, viz. 9.80×10^{-3} (6). Since the space requirements of the ammonium and potassium ions are very similar, one must expect the susceptibilities of the two salts to differ but little. We conclude therefore that the value of μ_{eff} for K_2OsBr_6 in Table I is incorrect. If our value of 1.55 B.M. is inserted in Table I it is seen that the magnetic moment increases with increasing atomic number of the halogen except in the case of the iodo compound. This is in good agreement with what was observed by Figgis and co-workers for the series of cesium salts. In order to rationalize this trend in magnetic moments it would be necessary to compare values for magnetically dilute systems. However, we may make a prediction about the direction of the trend for the isolated ions on the basis of the following considerations.

It may be doubted whether there can be superexchange in hexafluoro salts since the *p*-orbitals of the ligands on neighboring groups would overlap little, if at all, and moreover, fluorine cannot engage in d_π–d_π bonding. In fact, most salts containing discrete hexafluoro anions, e.g. RuF_6^{2-}, MnF_6^{2-}, FeF_6^{3-}, appear to be free from superexchange effects (14, 15, 16)* but the quinquevalent d_ϵ^3 fluorides, $MRuF_6$ and $MOsF_6$, give some indication of partial quenching of the magnetic moment (14). Thus it may well be that among the various hexahalo compounds superexchange is least pronounced in the case of fluorides. Moreover, the value of the Weiss constant, Δ, increases as does the change in moment upon dissolving in water, with change of halogen in going from K_2ReF_6 to K_2ReI_6 (7). According to the theory of Kotani, d_ϵ^3 compounds should exhibit a spin-only moment regardless of the value of the coupling constant and the temperature providing that they are free from superexchange. Consequently, if Kotani's theory is valid the trends in question must be due to an increasing degree of superexchange in going from the fluoro to the iodo compound. If these considerations are correct, it must be assumed

**It is suggested that in certain exceptions to this, namely K_3CoF_6 and K_3NiF_6, there may be a mixture of different spin states (17). This postulate is well justified by ligand field theory.*

Can. J. Chem. Downloaded from www.nrcresearchpress.com by 210.87.254.40 on 09/05/12
For personal use only.

that the reason for the effective moment of K_2OsI_6 being lower than that of K_2OsBr_6 is that at this point the superexchange supersedes the relatively small increase in the nephelauxetic effect. The increase in superexchange from chloro to iodo compounds is reasonable in view of the increase in spatial extension of *d*-orbitals with increasing atomic number. This matter is receiving further study.

B. Potassium Hexachlororhenate

As indicated above, Kotani's theory predicts a value of 3.87 B.M. for the moment of the d_ϵ^3 configuration at all temperatures. However, experimental values of the moment in rhenium compounds are appreciably lower. Penney and Schlapp have provided an alternative theory (18):

$$[3] \qquad \mu_{obs} = 3.87\left(1-\frac{4A}{30Dq}\right)$$

in which Dq is the ligand field splitting parameter. The measurements made by Figgis and co-workers (7), when applied to this expression, yield a value of 1800 cm^{-1} for A which is of the correct order of magnitude for ions of the third transition series.

Again we questioned the use of moments obtained from magnetically concentrated substances.

Results for K_2ReCl_6

The results of measurements on pure and dilute potassium chlororhenate appear in Table IV. The limits shown provide an estimate of the error to which the method of

TABLE IV

Substance	Temp., °K	$\chi_M \times 10^3$	μ_{eff}, B.M.	μ from Curie–Weiss law, B.M.	Δ
K_2ReCl_6	298	4.45	3.26	3.72	90
	195	6.05	3.07		
	90	9.54	2.62		
K_2ReCl_6/K_2PtCl_6	298	5.48±0.15	3.62	3.76	26
	195	7.9 ±0.2	3.52		
	90	15.3 ±0.4	3.34		

rhenium analysis is subject.

It is clear that in the case of K_2ReCl_6 also there is significant superexchange. The effective moments at infinite dilution would be higher still, but because of the inaccuracy of the method of analysis, it was deemed unprofitable to expend more effort on the system in an attempt to determine the limiting value.

EXPERIMENTAL

The Gouy method was used for the magnetic measurements. The balance was calibrated with purified Mohr's salt as a standard. The maximum field strength was 5320 gauss. The samples were contained in evacuated pyrex tubes.

Preparations

The samples were prepared from metal sponge supplied by Johnson, Matthey, and Mallory, Ltd. Solutions of the quadrivalent halo complexes in the appropriate halogen acid (19, 20) were mixed in various proportions and a solution of potassium chloride

Can. J. Chem. Downloaded from www.nrcresearchpress.com by 210.87.254.40 on 09/05/12
For personal use only.

added rapidly with stirring. The precipitate was removed immediately by filtration through a porous crucible. The products were washed with water and air-dried at 120° C. X-Ray diffraction photographs were unable to detect any inhomogeneity, had it occurred, because of the near identity of the lattice constant of each of the paramagnetic complexes and that of the corresponding platinum compound. The amount of ferromagnetic impurity in the preparations was so small as to be negligible.

Analyses

Duplicate determinations of the concentration of the paramagnetic ion were carried out in each case.

Osmium was separated from platinum by distillation from perchloric acid medium (21) and determined gravimetrically as described in a previous publication (22). Rhenium was separated by heating strongly in a slow stream of air in a quartz combustion tube fitted directly to a receiver which was cooled in liquid oxygen and followed by a bubbler containing 1% hydrogen peroxide. The heating was continued for 30 minutes after the potassium chloride remaining in the sample boat had entirely volatilized. The content of the first receiver was allowed to warm up and was dissolved in 1% hydrogen peroxide. The solutions so obtained were acidified and the rhenium precipitated and weighed as the nitrogen complex. As indicated earlier, the method is not considered highly accurate as the average error of the control analyses was −1.4% on amounts of rhenium between 11 and 23 mg.

ACKNOWLEDGMENTS

The authors greatly appreciate the financial support of the National Research Council of Canada.

REFERENCES

1. K. W. H. Stevens. Proc. Roy. Soc. (London), A, **219**, 542 (1953).
2. J. Owen and K. W. H. Stevens. Nature, **171**, 836 (1953).
3. J. H. E. Griffiths, J. Owen, J. G. Park, and M. F. Partridge. Proc. Roy. Soc. (London), A, **250**, 84 (1959).
4. M. Kotani. J. Phys. Soc. Japan, **4**, 293 (1949).
5. Ya. K. Syrkin and V. I. Belova. Doklady Akad. Nauk S.S.S.R. **105**, 517 (1955).
6. R. B. Johansen and A. R. Lindberg. J. Am. Chem. Soc. **76**, 5349 (1954).
7. B. N. Figgis, J. Lewis, R. S. Nyholm, and R. D. Peacock. Discussions Faraday Soc. **26**, 103 (1958).
8. C. K. Jorgensen. Discussions Faraday Soc. **26**, 176 (1958).
9. J. S. Griffith. Discussions Faraday Soc. **26**, 174 (1958).
10. J. Owen. Proc. Roy. Soc. (London), A, **227**, 183 (1955).
11. B. R. Judd. Proc. Roy. Soc. (London), A, **250**, 110 (1959).
12. D. P. Mellor. Proc. Roy. Soc. N. S. Wales, **77**, 145 (1944).
13. W. Klemm. Z. anorg. u. allgem. Chem. **244**, 377 (1940); **246**, 347 (1941).
14. R. D. Peacock. Rec. trav. chim. **75**, 576 (1956).
15. R. Hoppe and K. Blinne. Z. anorg. u. allgem. Chem. **291**, 269 (1957).
16. E. Cotton-Feytis. Ann. chim. (Paris), **4**, 9 (1925).
17. R. Hoppe. Rec. trav. chim. **75**, 569 (1956).
18. W. G. Penney and R. Schlapp. Phys. Rev. 666 (1932).
19. R. Gilchrist. J. Research Natl. Bur. Standards, **6**, 421 (1931).
20. G. Brauer. Handbuch der präparativen anorganischen Chemie. Ferdinand Enke Verlag, Stuttgart. 1953. p. 1104.
21. A. D. Westland and F. E. Beamish. Anal. Chem. **26**, 739 (1954).
22. A. D. Westland and F. E. Beamish. Mikrochim. Acta, 625 (1957).

Can. J. Chem. Downloaded from www.nrcresearchpress.com by 210.87.254.40 on 09/05/12
For personal use only.

Can. J. Chem. Downloaded from www.nrcresearchpress.com by 210.87.254.40 on 09/05/12
For personal use only.

PHYTIC ACID: AN ANALYTICAL INVESTIGATION[1]

E. C. Brown, M. L. Heit, and D. E. Ryan

ABSTRACT

Acid–base titrations in aqueous and non-aqueous solutions, titrations with metal ions, and analyses of various metal phytates support beyond question the 18-acid structure of phytic acid. Six of the hydrogens are too weakly acidic to be ordinarily titratable in water; in aqueous solution, two distinct breaks occur in the titration curve corresponding to the titration of 8 and 12 protons of phytic acid.

INTRODUCTION

The structure of phytic acid, a naturally occurring plant acid, has not been clearly demonstrated. Neuberg (1) has proposed a structure, $C_6H_{24}O_{27}P_6$, with 18 acid hydrogens about an inositol phosphate nucleus. Anderson (2) proposed a structure containing 12 acid hydrogens, $C_6H_{18}O_{24}P_6$. The two structures are shown in Fig. 1.

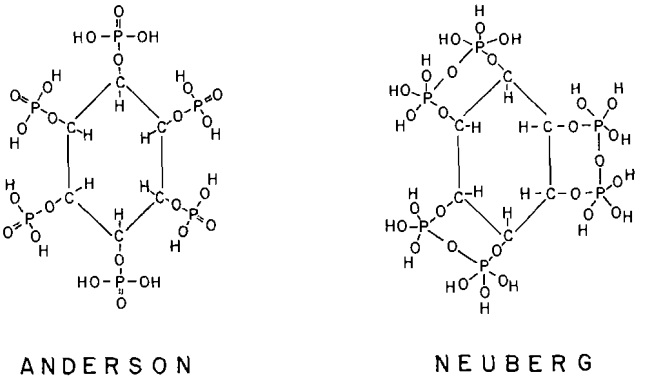


FIG. 1. Proposed structures of phytic acid.

Various studies of the chemistry of phytic acid have produced supporting arguments for both structures. A number of phytic acid salts have been prepared which, on the basis of analysis, have been used to support either the Neuberg (3, 4, 5, 6, 7) or the Anderson (2, 8, 9, 10, 11) structure. Courtois and Mason (12), on comparing acid and phytate hydrolysis curves, favored the Neuberg formula. Desjobert and Fleurent (13) concluded, from a study of chemical hydrolysis, that phytic acid behaved like the Anderson model but they noted certain anomalies. Barre, Courtois, and Wormser (14) produced titration and conductivity curves which they evaluated as indicative of the Anderson formula.

This wealth of conflicting results suggests that an undefined factor may be operative. Analytical difficulties may account for discrepancies in some of the salt analyses but certainly not all of them; nor will they explain the anomalous conclusions from hydrolysis and conductivity investigations. The possible diversity of starting materials used could be an important factor; the source of phytate has been neglected in many papers and purification procedures do not always account for possible contaminants (e.g. orthophosphate).

[1]*Manuscript received February 7, 1961.*
Contribution from the Chemistry Department, Dalhousie University, with financial assistance from the National Research Council.

From the analytical standpoint, phytic acid is of interest because it complexes or chelates metal ions and, by virtue of its many reaction sites, is extremely effective in precipitating or sequestering them. It has been applied to the determination of scandium (15), titanium (3), zirconium (3), and thorium (16); for the removal of copper (17) and iron (18, 19, 20); for corrosion prevention (21); and for stabilizing metal oxides in cooling waters (22).

It was thought, in view of the above considerations, that a further study of phytic acid would be worth while.

EXPERIMENTAL

Equipment and Materials

Measurements of pH were made using either a Beckman Zeromatic or Radiometer 4 pH meter with a glass-saturated calomel electrode pair. Titrations were performed in a pyrex vessel equipped with a water jacket and the temperature of the titration solution maintained at $25 \pm 0.1°$ C, by circulating water from a constant temperature bath through the jacket; a Wilkens–Anderson "Lo-Temp Bath" was used to control bath temperature. The titration vessel was covered with a plastic lid in which holes were drilled to accommodate a 10-ml microburette, two nitrogen inlet tubes, the electrodes, a thermometer, and a glass rod suitable for removing drops from the burette tip. A carbon-dioxide-free atmosphere was maintained by bubbling nitrogen both through the solution and above it.

The starting material was a commercial aqueous phytic acid solution (70%) obtained from the Staley Manufacturing Company, Decatur, Illinois. It is a by-product of the corn liquor industry and contains water-soluble contaminants identified by the company as "nitrogenous organic materials" and a stabilizer for these materials; it is to be expected that orthophosphate is also present.

Analysis of Materials

To study phytic acid it was essential to prepare pure materials and to characterize them by analysis. Phytic acid, sodium phytate, ammonium phytate, and various metal phytates were prepared but a number of difficulties were encountered in analyzing them. Since there are 6 phosphorus atoms in the phytic acid molecule, a method for the determination of total phosphorus was essential. A number of standard methods for the determination of phosphorus, dependent on hydrolysis of phytate and precipitation of orthophosphate, proved unsatisfactory. It was concluded that these procedures were impaired by attendant difficulties with hydrolysis of phytate and that, because of the stability of the phytate nucleus, ordinary methods of phosphorus analysis could not be used.

The phosphorus content of phytates was determined successfully by use of a method reported recently in the literature (23). The method, applicable to solid compounds, involved burning a weighed sample in oxygen and collecting the residue in nitric acid. The orthophosphate resulting from the combustion was then determined by magnesium ammonium phosphate precipitation; the precipitate was either ignited to the pyrophosphate or redissolved and the magnesium determined by an EDTA titration.

Sodium Phytate

Preparation and Analysis

In the preparation of sodium phytate, orthophosphate was first removed from the commercial phytic acid by ether extraction. Three portions of ether were used, each portion being at least equal in volume to the commercial product being treated. The

Can. J. Chem. Downloaded from www.nrcresearchpress.com by 210.87.254.40 on 09/05/12
For personal use only.

resulting aqueous solution was diluted with an equal volume of water and neutralized by small additions of concentrated sodium hydroxide solution. The reaction vessel was immersed in an ice bath and the reacting mixture stirred continuously to discourage hydrolysis to orthophosphate. The sodium phytate, after the addition of a large excess of sodium hydroxide, was precipitated by filtering the reaction mixture and allowing it to fall dropwise into a beaker of stirred methyl or ethyl alcohol. The white flocculent precipitate was filtered, washed with alcohol, and redissolved in dilute sodium hydroxide; the sodium phytate was reprecipitated, ground in a mortar under alcohol, and finally oven-dried at 80° C.

This product, analyzed by the combustion method for phosphorus (23), contained 16.5% P. The filtrates from these determinations were analyzed for sodium by uranyl salt precipitation (24) and gave 36.5±1% Na. The compound Na_{18} phytate contains 16.7% phosphorus and 37.3% sodium. The mole ratio of sodium to phosphorus as calculated from analyzed values was 3.0. These results show the prepared sodium phytate to be $Na_{18}Phy$.*

Potentiometric Titration of Sodium Phytate

Samples of sodium phytate were dissolved in water and titrated with hydrochloric acid; on completion of reaction, the reverse titration, of the phytic acid formed, was carried out with potassium hydroxide. Typical curves are shown in Fig. 2. In aqueous solution there were two end points; the first of these occurred at a mole ratio of 8 to 1 and the other was well defined at 12 moles of acid or base per mole of phytate or phytic acid.

In other titrations sodium phytate was dissolved in glacial acetic acid to which acetic anhydride, sufficient to react with contaminating water, was added. The sodium phytate was now titrated using a perchloric acid solution in acetic acid that had been standardized against potassium acid phthalate. Sodium phytate was not readily soluble in acetic acid but 0.1 g was dissolved in 80 ml of the acid when warmed and stirred for 5 hours; hydrolysis of the sodium phytate in this solution was considered possible but tests, both for orthophosphate and phytate, showed that little or no hydrolysis had occurred. A typical titration curve is shown in Fig. 2; only one end point is evident corresponding to 18 moles of hydrogen ion per mole of sodium phytate.

It follows from these titrations of sodium phytate in aqueous and non-aqueous media that there are 18 acid hydrogens in a molecule of the acid but only 12 of these are strong enough to be titratable in aqueous solution.

Phytic Acid

The previous titrations were carried out with samples of the sodium salt but comparable results were obtained when the free acid was titrated. Phytic acid is obtainable only in aqueous solution and different procedures have been used for producing the acid from one of the phytate salts (12, 13, 14). In the present work good results were obtained by passing a solution of sodium phytate through a column of strong cation exchange resin (Amberlite IR-120) in the acid form until the solution was strongly acid and the sodium content was insignificant; the amount of sodium in this acid solution, detected by flame photometry, was only slightly more than that found for a sample of deionized and distilled water. Titrations of phytic acid, however, were generally carried out on solutions of the sodium salt to which sufficient perchloric acid was added to ensure complete

*Phy *will be used to denote the phytate anion,* $C_6H_6O_{27}P_6^{-18}$, *throughout this paper.*

Can. J. Chem. Downloaded from www.nrcresearchpress.com by 210.87.254.40 on 09/05/12
For personal use only.

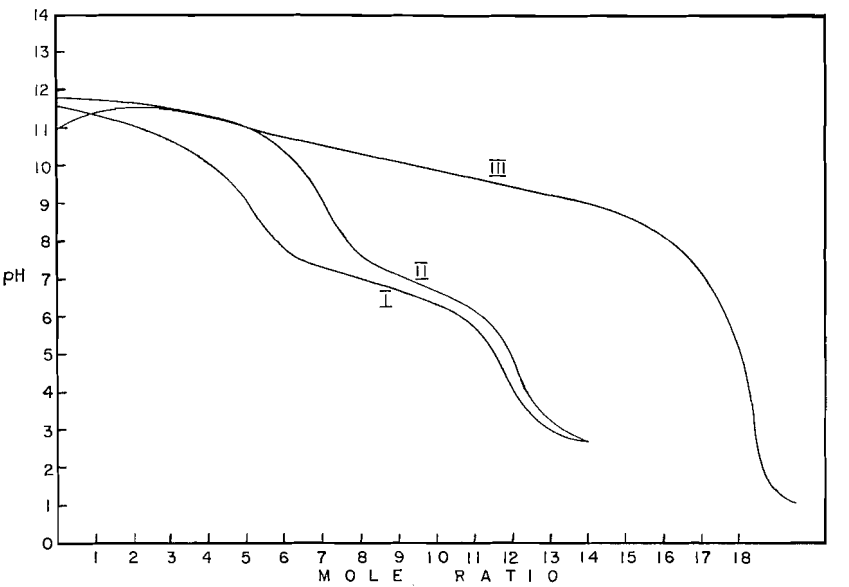


FIG. 2. Titration of sodium phytate. I, 0.4163 g sodium phytate in 50 ml water titrated with 0.1065 *N* HCl; II, resultant solution from titration I back-titrated with 0.0940 *N* KOH; III, 0.0780 g sodium phytate in 80 ml of glacial acetic acid titrated with 0.1040 *N* $HClO_4$ in glacial acetic acid.

conversion to the acid. The titration curve, shown in Fig. 3, was smooth with two inflection points corresponding to the liberation of 8 and 12 moles of hydrogen ion. In the presence of excess metal ion with strong complexing ability, a further 6 moles of hydrogen ion were liberated from a mole of phytic acid; with lead, for example, the inflection at 8 moles of hydrogen ion liberated disappeared completely and well-defined inflections occurred at 16 and 18 moles of hydrogen ion liberated. Results obtained in the titration of phytic acid in the presence of excess magnesium and when the mole ratio of lead to phytic acid was 9 to 1 are shown in Fig. 3; a white precipitate formed immediately upon addition of lead to the phytic acid solution but precipitation did not begin with magnesium until pH 7.5.

These titrations show that phytic acid has 18 acid hydrogens; of these acid hydrogens, 6 are not ordinarily titratable in water, being too weakly acidic to give a break in the titration curve. The first break in the titration curve, which corresponds to the consumption of 8 moles of base per mole of acid, shows that eight protons are more easily removed than the others; removal of a further four protons is also represented by only one break and their acid strengths cannot be very different.

Titration of Phytate with Metal Ions

Solutions of sodium phytate have a high pH due to hydrolysis of the phytate anion; since phytate is itself a base, the reaction of metal ions to form complexes or insoluble substances with it should be accompanied by a change in pH. The sudden decrease in the concentration of phytate ions at an end point, resulting from the addition of metal ion to a solution of the reagent, is accompanied by a sharp decrease in pH.

Since the constant for the reaction

$$Phy^{-x} + yH_2O \rightleftarrows H_yPhy^{-(x-y)} + yOH^-$$

Can. J. Chem. Downloaded from www.nrcresearchpress.com by 210.87.254.40 on 09/05/12
For personal use only.

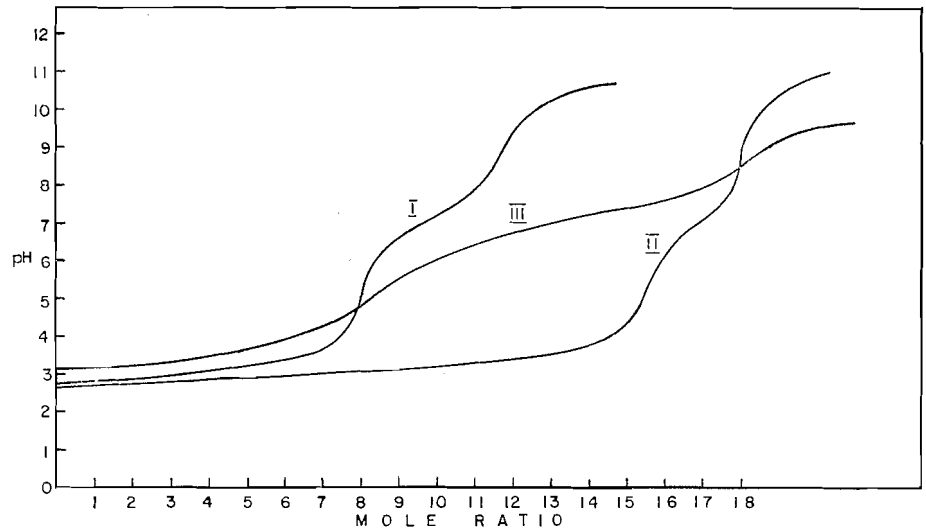


FIG. 3. Titration of phytic acid. I, 2.673×10^{-5} mole phytic acid titrated with 0.09968 *N* NaOH; II, 2.527×10^{-5} mole phytic acid + 2.284×10^{-4} mole Pb^{++} titrated with 0.1018 *N* NaOH; III, 8.48×10^{-6} mole phytic acid + 81.5×10^{-6} mole Mg^{++} titrated with 0.0094 *N* KOH.

is high, it is necessary for the solubility product constant of the metal phytate precipitated to be very small so that the change in the concentration of phytate ion (and thus pH change) at the equivalence point be large. A high stability of metal phytate will mean a sharp pH drop to a low value; if the complex stability is low the pH drop throughout the titration will be slight, the end point poorly defined, and resulting pH value will be high.

In these titrations, then, standard solutions of various metal ions were added dropwise, with stirring, to solutions containing a known quantity of sodium phytate. The change in pH as the metal phytate precipitated was noted and a graphical plot made of this pH change against mole ratio of metal ion added per mole of sodium phytate. Figure 4 shows titration curves obtained from examples of metal ions from each of four valence states—Ag^{+}, Pb^{+2}, Fe^{+3}, Zr^{+4}. Distinct breaks in the titration curves were obtained for 9 moles of lead, 6 moles of iron, and $4\frac{1}{2}$ moles of zirconium per mole of sodium phytate; the break in the silver titration curve was not so well defined but was indicative of 18 moles of silver reacting. The titrations all support the 18-acid form for phytic acid; the equivalence point pH's show an increasing stability order of Ag^{+}, Pb^{+2}, Fe^{+3}, Zr^{+4}.

A few constant pH titrations were carried out in which a solution of sodium phytate was adjusted to a desired pH and a solution of metal ion added to it; reaction of the metal ion with the acid formed caused a pH drop which could be readjusted with a base (potassium hydroxide was used). The point at which addition of metal ion did not lower the pH appreciably and at which addition of base greatly increased the pH was taken as an end point. The pH's chosen for these titrations corresponded generally to the two least-buffered regions of the acid–base titration curve for phytic acid when the dominant phytate species would be $H_{10}Phy^{-8}$ (pH$\sim$5) and H_6Phy^{-12} (pH$\sim$8.5). The method is limited because free acid must be absent in the original metal solution but acceptable end points were found for silver, magnesium, and lead ions.

Can. J. Chem. Downloaded from www.nrcresearchpress.com by 210.87.254.40 on 09/05/12
For personal use only.

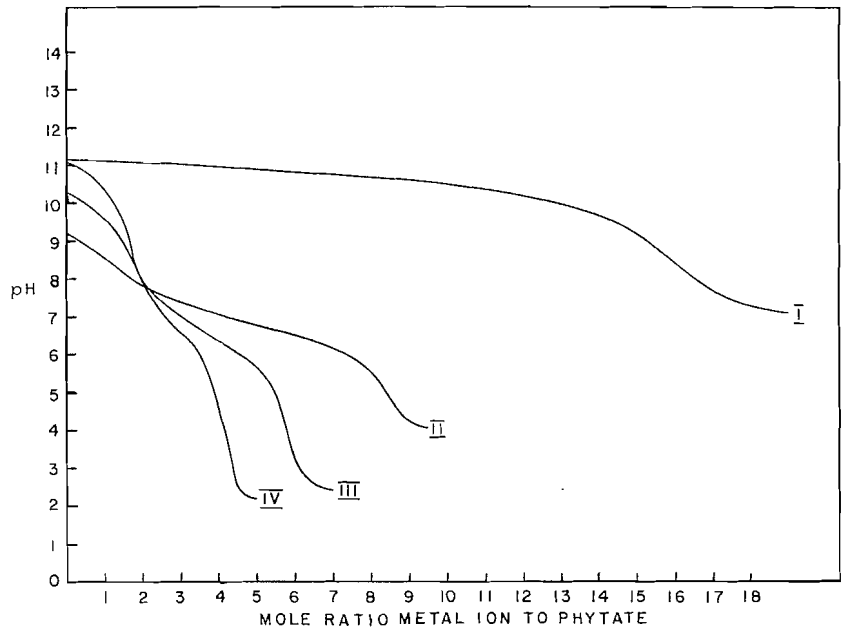


FIG. 4. Titration of sodium phytate with metal ions (solution volumes 100 ml). I, 1.41×10^{-4} mole sodium phytate with 0.201 *M* Ag^{+}; II, 0.728×10^{-4} mole sodium phytate with 0.0152 *M* Pb^{+2}; III, 1.61×10^{-4} mole sodium phytate with 0.0215 *M* Fe^{+3}; IV, 1.75×10^{-4} mole sodium phytate with 0.0440 *M* Zr^{+4}.

Description and Analyses of Some Metal Phytates

The composition of metal phytate precipitating from solution is, of course, dependent upon acidity. Normal salts, except for the most basic ions, would be uncommon; the acid strength of phytic acid suggests that salts containing $H_{10}Phy^{-8}$ and H_6Phy^{-12} should be an ordinary occurrence. A description of various phytates prepared, in the course of this work, follows.

Ammonium Phytate

Ammonium phytate was prepared from commercial phytic acid after extracting the commercial product with ether to remove orthophosphate. The aqueous residue was neutralized to pH 6 with 1:1 ammonia and the phytate precipitated with silver nitrate; no yellow orthophosphate was noted. The silver phytate, after washing with water, was ground in a mortar under a deficiency of 1:1 hydrochloric acid to remove silver as silver chloride and liberate the phytic acid. An equal quantity of methanol was added to the resulting solution and ammonia bubbled through the mixture. The white precipitate was filtered, washed with methanol, and dried in a desiccator under slight negative pressure. Analysis of the ammonium phytate for ammonium ion (by Kjeldahl) and for phosphorus (by combustion method) gave $16.5\pm0.5\%$ NH_4^+ and $20.9\pm0.5\%$ P; these figures give a mole ratio of ammonium ion to phytate of 8 to 1 and suggest the incompletely neutralized product $(NH_4)_8H_{10}Phy$.

Silver Phytate

Silver phytate formed as a white precipitate when silver nitrate was added to phytic acid (pH 2); addition of ammonia gave more precipitate up to pH 4 but dissolved when more ammonia was added to pH 8. The silver phytate was light sensitive, the color

Can. J. Chem. Downloaded from www.nrcresearchpress.com by 210.87.254.40 on 09/05/12
For personal use only.

changing from white through pink and brown to black. The precipitate resulting from the sodium phytate – silver nitrate titration was analyzed for silver by dissolving in nitric acid and precipitating the silver as silver chloride; the silver content of the dried precipitate was 70±1%, corresponding to a mole ratio of silver to phytate of approximately 16 to 1; this result was not unexpected in view of the titration curve obtained (Fig. 4).

Magnesium Phytate

Magnesium ion did not react with phytic acid below pH 3. Above this pH reaction was slight until about pH 7 where constant pH titrations indicated about 4 moles of magnesium ion reacting; however, the titration of phytic acid in the presence of excess magnesium ion showed the eventual reaction of 9 moles (Fig. 3). Precipitation did not begin until the pH was 7.5; the white precipitate was not easily separated from solution.

Lead Phytate

The lead phytate resulting from titration of sodium phytate with lead nitrate was filtered, washed with water, dried at 100° C, and weighed; the agreement between actual and theoretical weights, calculated as Pb_9Phy, was excellent (within 0.05%). The stability of lead phytate in mineral acids made direct determination of lead difficult but successful analyses were obtained after dissolving the lead phytate in aqua regia, destruction of organic matter by addition of sulphuric acid, and three evaporations to incipient dryness, and weighing as lead sulphate; a mole ratio of lead to phytate of 9 to 1 was found. The 9 to 1 phytate forms above pH 5.6 but in more acid solutions lower lead phytates are formed. Analysis of compounds precipitated at both pH 3 and pH 2 showed 4 moles of lead per mole of phytate.

Iron Phytate

Although ferrous phytate was not easily precipitated, ferric phytate separated immediately as a white precipitate on addition of ferric ion to a solution of phytic acid. The precipitate from the titration of sodium phytate with ferric chloride was analyzed for iron, after dissolution in hydrochloric acid, by adding excess potassium iodide and titrating the liberated iodine with thiosulphate (25). Analysis supported the composition shown by the titration curve (Fig. 4) giving an iron to phytate ratio of 6 to 1; the precipitate contained water that could not be removed completely without decomposition, and analysis calculations were based on iron content to phytate used in the titration. At pH 11 a soluble, wine-orange ferric phytate was formed.

Zirconium Phytate

The titration curve of sodium phytate with zirconium ion indicated formation of insoluble compounds containing 2 and 4.5 moles of zirconium per mole of phytate. The final precipitate was coagulated with ethanol, filtered, washed with ether, and dried at 80° C; the weight was 117% that expected for $Zr_{4.5}Phy$. Drying at higher temperatures decreased the weight, apparently by loss of water, but resulted in eventual decomposition of the compound. This phytate was only slightly soluble in concentrated hydrochloric, nitric, and sulphuric acids. Alimarin and Kozel (26) have used phytic acid to precipitate zirconium quantitatively in 0.5 *N* nitric and 6 *N* hydrochloric acid; the precipitate was ignited and weighed as $Zr_2P_6O_{19}$.

CONCLUSIONS

Phytic acid, prepared from the Staley Manufacturing Company product, has 18 acid hydrogens. Of these acid hydrogens, 6 are not titratable in water but are titratable in a more basic solvent. Analysis, titrations of sodium phytate with metal ions, and titration

Can. J. Chem. Downloaded from www.nrcresearchpress.com by 210.87.254.40 on 09/05/12
For personal use only.

of phytic acid solutions containing an excess of metal ions support the 18-acid structure and indicate that phytic acid has a structure corresponding to the Neuberg configuration.

It is necessary, in view of these results, to consider possible reasons for disagreement with workers who favor the Anderson model. Titrations in aqueous solution would, of course, support a 12-acid structure since six protons are not titratable in water. Under ordinary conditions normal salts are not readily formed and erroneous conclusions could readily be drawn on the basis of moles of metal ion contained per mole of phytate; the acid strength of phytic acid suggests that salts corresponding to $(M^{II})_4H_{10}Phy$, $(M^{II})_6H_6Phy$, or $(M^{III})_4H_6Phy$, in addition to the more difficultly formed $(M^{II})_9Phy$ or $(M^{III})_6Phy$, should be common. Such considerations would explain Otolski's iron phytates (5) which were analyzed to be A—Fe_4* but which reacted with 6 moles of monovalent amine. Wrenshall and Dyer's iron salt (7), which gave an intermediate analysis between A—Fe_4 and N—Fe_6, could easily be the result of an incompletely neutralized phytate. Bourdillon prepared a mixed calcium and sodium salt, A—$Ca_2Na_8.3H_3O$ (8); this could be written as $Ca_2Na_8H_6Phy$. The possible existence of two phytic acids should not be overlooked; an interesting thought, since they differ only by three water molecules, is that the Anderson phytate is simply the degradation product of Neuberg phytate.

ACKNOWLEDGMENTS

One of us (E.C.B.) gratefully acknowledges the assistance of the Defence Research Board of Canada in arranging special leave credits and in making laboratory space available for some of this work.

REFERENCES

1. C. NEUBERG. Biochem. Z. **9**, 557 (1908).
2. R. J. ANDERSON. J. Biol. Chem. **17**, 141 (1914).
3. G. BECK. Mikrochemie ver. Mikrochim. Acta, **34**, 62 (1948).
4. F. FISCHLER and F. KURTEN. Biochem. Z. **254**, 138 (1932).
5. S. OTOLSKI. J. pharm. chim. **21**, 170 (1935).
6. S. POSTERNAK. Helv. Chim. Acta, **12**, 1165 (1929).
7. C. WRENSHALL and W. DYER. Soil Sci. **51**, 235 (1941).
8. J. BOURDILLON. N.Y. State Dept. Health, Ann. Rept. Div. Labs. and Research, 23 (1953).
9. E. B. EARLEY. Ind. Eng. Chem. Anal. Ed. **16**, 389 (1944).
10. S. OTOLSKI. Arch. Chem. Farm. **3**, 231 (1937).
11. N. SELIGSON. Arch. Pharm. **268**, 104 (1930).
12. J. COURTOIS and M. MASSON. Bull. soc. chim. biol. **32**, 314 (1950).
13. A. DESJOBERT and P. FLEURENT. Bull. soc. chim. biol. **36**, 475 (1954).
14. R. BARRE, J. E. COURTOIS, and G. WORMSER. Bull. soc. chim. biol. **36**, 455 (1954).
15. G. BECK. Anal. Chim. Acta, **4**, 21 (1950).
16. D. J. RYABCHIKOV, O. K. BELYAEVA, and A. N. ERMAKOV. Zhur. Anal. Khim. **11**, 658 (1956).
17. E. NEGRE and B. CORDONNIER. Compt. rend. acad. agr. France, **39**, 776 (1953).
18. R. CORDONNIER. Ann. fals. et fraudes, **45**, 415 (1952).
19. F. PRILLINGER. Mitt. (Klosterneuberg), Ser. A, **4**, 30 (1954).
20. O. T. ROTINI. Accad. ital. vite e vino, Siena, Atti, **5**, 138 (1953).
21. N. E. ARTZ. U.S. Patent No. 2,626,238. (January 20, 1953); Chem. Abstr. **47**, 11620[a] (1953).
22. C. WOHLBERG. U.S. Pat. Appl. 17,122. Offic. Gaz. **646**, 1378 (1951); Chem. Abstr. **46**, 6778[d] (1952).
23. K. D. FLEISCHER, B. C. SOUTHWORTH, J. H. HODECKER, and M. M. TUCKERMAN. Anal. Chem. **30**, 152 (1958).
24. W. F. HILLEBRAND, G. E. F. LUNDELL, J. I. HOFFMAN, and H. A. BRIGHT. Applied inorganic analysis. John Wiley & Sons Inc., New York. 1953.
25. J. R. FOY and J. B. THOMPSON. Ind. Eng. Chem. Anal. Ed. **15**, 747 (1943).
26. I. P. ALIMARIN and L. Z. KOZEL. Inst. Obshchei i Neorg. Khim. **3**, 114 (1957).

*A— *denotes Anderson nucleus,* $C_6H_6O_{24}P_6$, *and* N— *the Neuberg nucleus,* $C_6H_6O_{27}P_6$.

Can. J. Chem. Downloaded from www.nrcresearchpress.com by 210.87.254.40 on 09/05/12
For personal use only.

Can. J. Chem. Downloaded from www.nrcresearchpress.com by 210.87.254.40 on 09/05/12
For personal use only.

PHOSPHATASE ALCALINE INTESTINALE: CINÉTIQUE DE L'HYDROLYSE DU PHOSPHATE DE *p*-NITROPHÉNYLE*

MICHEL LAZDUNSKI ET LUDOVIC OUELLET

ABSTRACT

The Michaelis constants and the rates at high substrate concentration for the system *p*-nitrophenyl phosphate – intestinal alkaline phosphatase have been measured at 15.3° C and 24.4° C from pH 7.5 to pH 10.4.

The experimental data can be interpreted as indicating the presence of three acid groups in the active center of the enzyme. The observed pK of ionization of these groups are 9.02, 8.39, and 7.65 at 15.3° C, and 9.75, 8.42, and 7.62 at 24.4° C.

These data stress the importance of electrostatic interactions between the groups in the active center and the rest of the enzyme molecule. A heat of ionization of 6 to 7 kcal/mole is attributed to each of these groups. At least one active group of the enzyme would be a thiol function and the other ones imidazole or thiol.

Quelques auteurs seulement ont cherché à identifier les composants du centre actif de la phosphatase alcaline. Les résultats les plus importants ont été obtenus par Morton (1) et Zittle et Bingham (2) dont les études cinétiques suggèrent la présence d'un hydroxyle phénolique essentiel ayant un pK de 9.2 à 38° C. En 1952, Koshland (3) a proposé un mécanisme d'action de la phosphatase alcaline, et en 1958, Engström (4) a réussi à isoler une P^{32} phosphorylsérine venant d'une préparation de phosphatase alcaline incubée avec du phosphate inorganique radioactif.

La présente publication traite, à deux températures, de l'influence du pH sur l'hydrolyse du phosphate de *p*-nitrophényle catalysée par la phosphatase alcaline. Les données permettront de déterminer: (*a*) le nombre de groupes actifs ionisables de l'enzyme; (*b*) les constantes et chaleurs d'ionisation de ces groupes.

PRÉAMBULE

Les hypothèses et définitions usuellement utilisées en cinétique enzymatique sont rapportées dans l'ouvrage de Laidler (5). Le schéma réactionnel fondamental est présenté dans la figure 1.

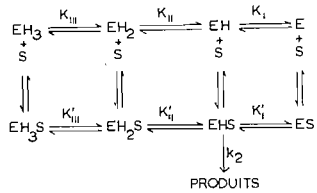


FIG. 1. Schéma représentant les états d'ionisation d'une enzyme E et du complexe enzyme–substrat lorsque le centre actif inclut trois groupes acides.

L'enzyme apparaît sous quatre formes ionisées: EH_3, EH_2, EH, E. Nous supposons que seul, parmi les différents complexes enzyme–substrat, EHS se décompose pour donner les produits. K_I', K_{II}', K_{III}', K_I, K_{II}, K_{III} sont des constantes apparentes d'ionisation.

*Manuscrit reçu le 1 mars 1961.
Contribution du Département de Chimie, Faculté des Sciences, Université Laval, Québec, Qué.

La vitesse de l'hydrolyse est donnée par l'équation de Michaelis–Menten:

$$[1] \qquad v = \bar{V}_m[S]/(\bar{K}_m+[S]).$$

Si le système est à l'état d'équilibre ou de quasi-équilibre (5), $\bar{V}_m$ représente la vitesse à concentration de substrat infinie, $\bar{K}_m$ est la constante de Michaelis. Ces deux grandeurs ont pour valeur:

$$[2] \qquad \bar{V}_m = V_m \Big/ \left(1+\frac{[H^+]}{K_{II}'}+\frac{K_I'}{[H^+]}+\frac{[H^+]^2}{K_{II}'K_{III}'}\right)$$

$$[3] \qquad \bar{K}_m = K_m\left(1+\frac{K_I}{[H^+]}+\frac{[H^+]}{K_{II}}+\frac{[H^+]^2}{K_{II}K_{III}}\right) \Big/ \left(1+\frac{K_I'}{[H^+]}+\frac{[H^+]}{K_{II}'}+\frac{[H^+]^2}{K_{II}'K_{III}'}\right).$$

Les techniques utilisées pour l'estimation des constantes d'ionisation ont été décrites par Dixon (6), Massey et Alberty (7) et Laidler (5). L'évaluation de $\bar{V}_m/\bar{K}_m$ en fonction du pH permet de déterminer les constantes relatives à l'enzyme (équation [4]).

$$[4] \qquad \bar{V}_m/\bar{K}_m = (V_m/K_m)\left(1/1+\frac{K_I}{[H^+]}+\frac{[H^+]}{K_{II}}+\frac{[H^+]^2}{K_{II}K_{III}}\right)$$

Si l'enzyme n'existe que sous trois formes ionisées EH_2, EH, E, les termes K_{III} et K_{III}' deviennent infinis et les équations [2] et [3] se simplifient:

$$[5] \qquad \bar{K}_m = K_m\left(1+\frac{K_I}{[H^+]}+\frac{[H^+]}{K_{II}}\right) \Big/ \left(1+\frac{K_I'}{[H^+]}+\frac{[H^+]}{K_{II}'}\right)$$

$$[6] \qquad \bar{V}_m = V_m\left(1/1+\frac{K_I'}{[H^+]}+\frac{[H^+]}{K_{II}'}\right).$$

PARTIE EXPÉRIMENTALE

Réactifs

Phosphate de paranitrophényle

Le sel disodique utilisé comme substrat provient de "Mann Research Laboratories Inc.". Sa richesse en phosphate de paranitrophényle est de 99.7%; il a été utilisé sans purification ultérieure. Les solutions à différentes concentrations de substrat ont été obtenues par dilution du sel dans l'eau distillée.

Enzyme

L'enzyme utilisée est une phosphatase alcaline intestinale purifiée, vendue par "Mann Research Laboratories". Les solutions à différentes concentrations d'enzyme ont été obtenues par dilution dans l'eau distillée.

Solutions tampons

Les tampons trishydroxyméthyle-amino-méthane (0.01 *M*) – HCl ont été utilisés au-dessous de pH 9 et éthanolamine (0.01 *M*) – HCl pour les valeurs de pH supérieures à 9.

L'éthanolamine provient de Eastman Organic Chemicals et le trishydroxyméthyle-amino-méthane de Fisher Scientific Co.

Les pH ont été mesurés avec un pHmètre Radiometer TTT1b utilisant une électrode de verre Radiometer type B.

Can. J. Chem. Downloaded from www.nrcresearchpress.com by 210.87.254.40 on 09/05/12
For personal use only.

Can. J. Chem. Downloaded from www.nrcresearchpress.com by 210.87.254.40 on 09/05/12
For personal use only.

Procédé

Détermination de la vitesse initiale d'hydrolyse v

L'hydrolyse du phosphate de *p*-nitrophényle est suivie par mesure colorimétrique du *p*-nitrophénol libéré lors de la réaction:

$$NO_2C_6H_4OPO_3^{=} + OH^- \rightarrow NO_2C_6H_4O^- + PO_4H^{=}.$$

Des essais préliminaires ont montré que la réaction d'hydrolyse s'arrêtait par passage en milieu très alcalin.

Le déroulement des opérations est le suivant: 14 ml d'une solution de phosphate de *p*-nitrophényle de concentration adéquate sont ajoutés à 15 ml de solution tampon. Ce mélange est porté dans un bain à thermostat (à 15.3° C ou 24.4° C ±0.1° C) et y est laissé pendant 30 minutes. Ce laps de temps écoulé, la réaction est démarrée par injection de 1 ml d'une solution de l'enzyme également à température voulue. La réaction est suivie pendant 5 à 10 minutes suivant les cas. Des prélèvements de 5 ml sont faits chaque minute et versés dans 0.3 ml d'une solution de soude 4 *N*. La réaction s'arrête. Le para-nitrophénol est, dans ces conditions de basicité, sous forme ionisée et les lectures sont faites au spectrophotomètre Beckman DU à la longueur d'onde de 407 mμ correspondant au maximum de densité optique.

RÉSULTATS

Les constantes de Michaelis expérimentales ont été déterminées à deux températures: de pH 7.46 à pH 10.43 à 15.3° C, et de pH 7.5 à pH 10.3 à 24.4° C.

La figure 2 représente trois courbes de Lineweaver–Burk (8) où l'inverse de la vitesse

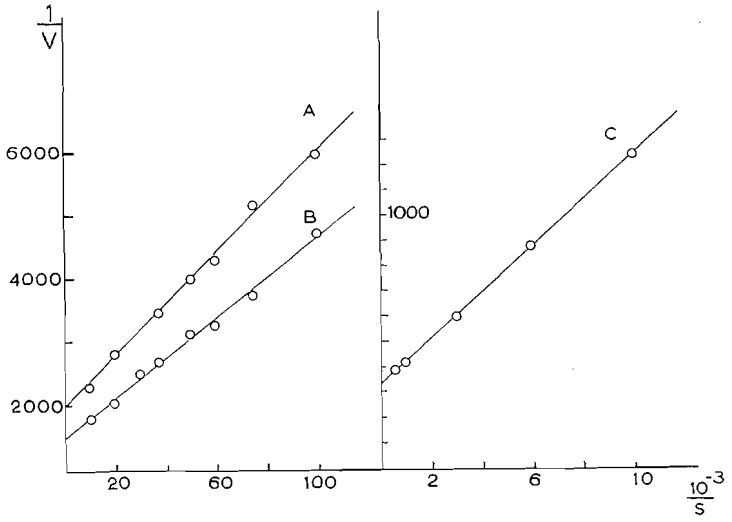


FIG. 2. Courbes de Lineweaver–Burk: (A) pH 8.15, température 24.4° C; (B) pH 8.0, température 24.4° C; (C) pH 9.87, température 15.3° C.

est porté en fonction de l'inverse de la concentration de substrat. Des rapports de 20 entre les valeurs les plus faibles et les plus élevées de 1/[S] ont été couramment atteints. Les valeurs de $\bar{K}_m$ obtenues sont reproductibles à mieux de 10%.

Les résultats expérimentaux confirment la validité de la loi de Michaelis–Menten aux températures et pH étudiés et quelles que soient les concentrations d'enzyme utilisées.

Influence du pH sur $\bar{K}_m$

Les représentations de Dixon traduisent, dans les figures 3 et 4, les variations de

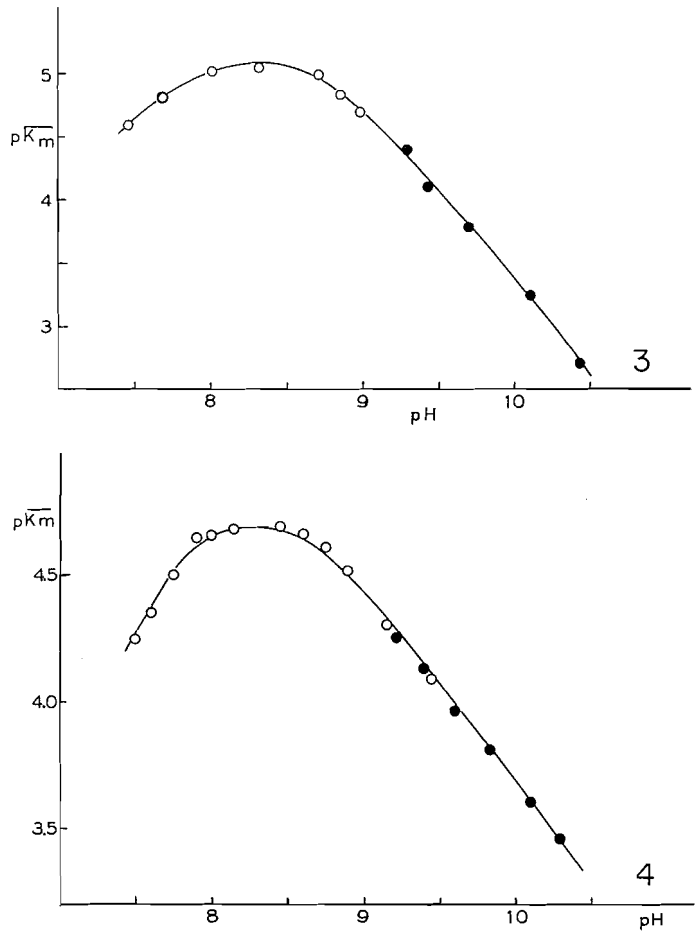


FIG. 3. Courbe de $p\bar{K}_m$ en fonction du pH à 15.3° C.
FIG. 4. Courbe de $p\bar{K}_m$ en fonction du pH à 24.4° C.

$p\bar{K}_m(-\log \bar{K}_m)$ en fonction du pH aux deux températures étudiées. Les courbes obtenues à 15.3° C et 24.4° C ont une allure semblable, seule peut être notée une différence de pente du côté alcalin du maximum.

Les points blancs ont été obtenus en utilisant un tampon trishydroxyméthyle-aminométhane–HCl; les points noirs, en utilisant un tampon éthanolamine–HCl. Le recouvrement des deux parties de la courbe représentée dans la figure 3, indique que, s'il y a effet spécifique du tampon, il est le même dans les deux cas.

Les constantes d'ionisation observées ne peuvent être attribuées au substrat dont le plus haut pK, 5.38, est très au-dessous du domaine de pH étudié (9).

La vitesse maximum est sensible aux variations de concentration de l'enzyme dues, soit à une qualité non-homogène, soit à un vieillissement de la phosphatase utilisée. La détermination de $\bar{V}_m$ a fait l'objet d'une série spéciale d'expériences, effectuée aussi rapidement que possible. A chaque pH étudié, la réaction a été faite à concentration

Can. J. Chem. Downloaded from www.nrcresearchpress.com by 210.87.254.40 on 09/05/12
For personal use only.

de substrat élevée. La valeur de $\bar{V}_m$ est calculée en multipliant la vitesse initiale ainsi obtenue par le terme correctif $(1+\bar{K}_m/[S])$.

Les figures 5 et 6 présentent les données expérimentales sous forme logarithmique

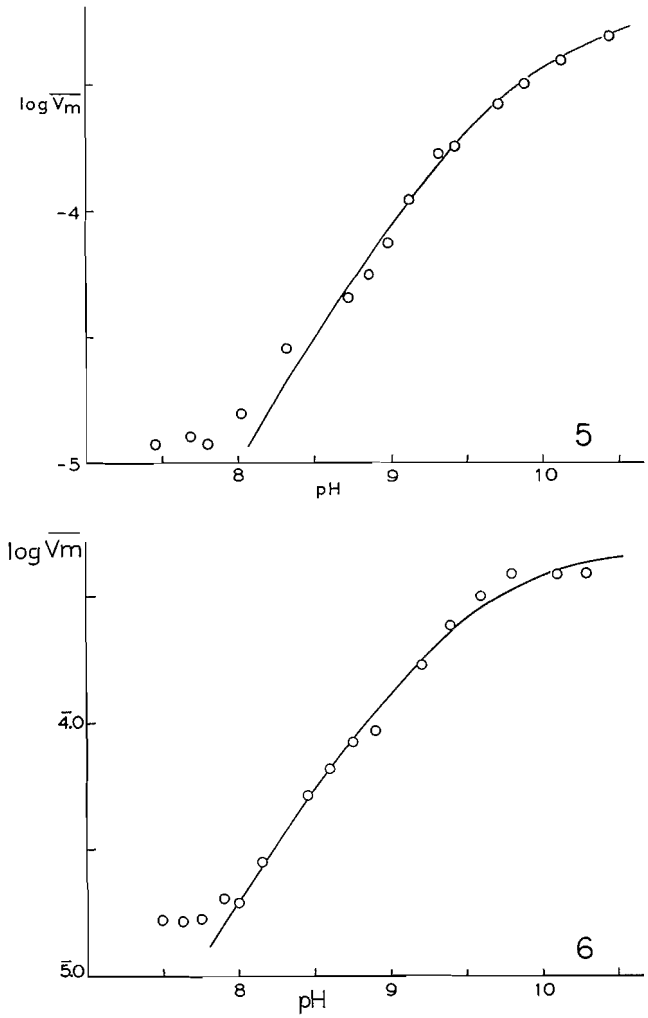


FIG. 5. Courbe de log $\bar{V}_m$ en fonction du pH à 15.3° C. Les vitesses sont en unités arbitraires.
FIG. 6. Courbe de log $\bar{V}_m$ en fonction du pH à 24.4° C. Les vitesses sont en unités arbitraires.

(log $\bar{V}_m$ en fonction du pH). Les points sont expérimentaux, les tracés sont théoriques et ont pour équations:

[7] à 15.3° C: $\log \bar{V}_m = \log [V_m/(1+[H^+]/10^{-9.7})]$

[8] à 24.4° C: $\log \bar{V}_m = \log [V_m/(1+[H^+]/10^{-9.37})]$.

Ces équations sont celles qui décrivent le mieux les données expérimentales.

La valeur de $pK_{II}' = 9.37$, déterminée à 24.4° C, est sujette à caution. Il semble qu'il se produise à cette température, au-delà de pH 9.8, un début de désactivation, peut-être réversible, de l'enzyme. Si, dans la figure 6, les vitesses à pH 10.1 et 10.3 n'ont pas la valeur qui leur est accordée, pK_{II}' pourrait augmenter sensiblement et se rapprocher ainsi de la valeur 9.7 obtenue à 15.3° C.

Can. J. Chem. Downloaded from www.nrcresearchpress.com by 210.87.254.40 on 09/05/12
For personal use only.

Deux possibilités se présentent pour K_I': (1) $K_I' = 0$; le complexe ES n'existe pas. Il y a compétition sur l'enzyme entre les ions hydroxyle et le substrat. (2) $K_I' \ll K_{II}'$: la pente des courbes de Dixon à haut pH (figs. 3 et 4) et l'allure des courbes de log $\bar{V}_m$ en fonction du pH (figs. 5 et 6) indiquent que la constante K_I', si elle existe, est certainement inférieure à 10^{-11}. Aux pH correspondant à pK_I' éventuel, l'enzyme se désactive et en rend la détermination impossible.

De la même manière K_{III}' peut être soit très supérieure aux plus grandes concentrations d'ions hydrogène étudiées, soit infinie, ce qui indiquerait une compétition entre les ions hydrogène et le substrat sur EH_3. Le complexe EH_3S ne pourrait alors exister.

DISCUSSION

Les figures 3 et 4 s'interprètent au moyen des règles établies par Dixon (6). Les changements de pente observés correspondent à l'ionisation de deux groupes essentiels du centre actif de l'enzyme. Leurs pK sont voisins des valeurs 7.8 et 8.6.

Pour la même phosphatase alcaline intestinale, Morton (1) et Zittle (2) obtenaient un changement de pente à pH 9.2 à 38° C et concluaient à la présence d'un hydroxyle phénolique au centre actif. Les courbes de Dixon obtenues par Zittle et Bingham avec la phosphatase du lait et par Motzok (10) avec la phosphatase du plasma ne présentent pas de changement de pente. Dans les trois cas, le domaine de pH étudié est trop étroit pour qu'on puisse prétendre déterminer les pK d'ionisation de tous les groupes ionisables du centre actif. Une étude semblable a permis à Lora-Tamayo et ses collaborateurs (11) de mettre en évidence trois groupes ionisables au centre actif de la phosphatase acide de la pomme de terre. Néanmoins, l'interprétation des courbes de Dixon présente deux inconvénients: (*a*) l'expression de K_m en fonction du pH (équation [3]) fait intervenir les constantes d'ionisation des complexes enzyme–substrat. Aussi bien, l'interprétation des figures 3 et 4 ne peut-elle conduire qu'à des valeurs approchées des constantes d'ionisation de l'enzyme. (*b*) Lorsque la présence de substrat sur l'enzyme a pour effet d'élever les pK des groupes du centre actif, il peut se produire un masquage de constante (figure 7). Seule l'étude de l'influence du pH sur la quantité $\bar{V}_m/\bar{K}_m$ donne le

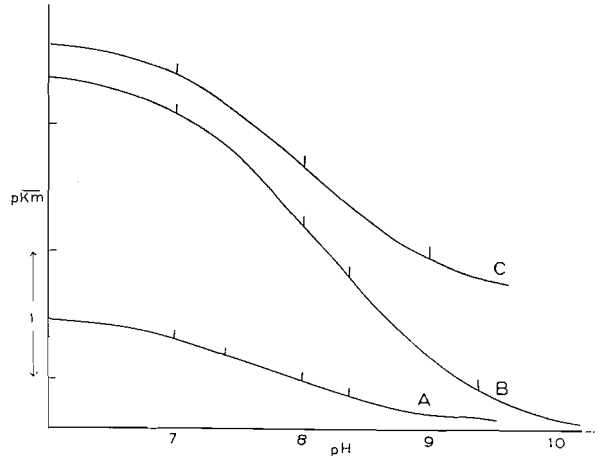


FIG. 7. Influence du pH sur $p\bar{K}_m$ pour un enzyme fictif possédant au centre actif deux groupes ionisables ayant pour pK: $pK_I = 8$ et $pK_{II} = 7$.

Les constantes d'ionisation des complexes enzyme–substrat sont: courbe A $pK_{II} = 7.4$, $pK_I' = 8.4$; courbe B $pK_{II}' = 8.4$, $pK_I' = 9.4$; courbe C $pK_{II}' = 8$, $pK_I' = 9$.

Les valeurs de $p\bar{K}_m$ sont portées en unités arbitraires.

Can. J. Chem. Downloaded from www.nrcresearchpress.com by 210.87.254.40 on 09/05/12
For personal use only.

nombre et les constantes d'ionisation exactes des groupes ionisables du centre actif. Tout pK qui apparaît dans les courbes de Dixon doit se retrouver dans les courbes de log $\bar{V}_m/\bar{K}_m$ en fonction du pH avec sa valeur exacte. Le nombre de groupes actifs ainsi déterminé doit être supérieur ou au moins égal à celui déterminé à partir des courbes de Dixon.

Les figures 8 et 9 traduisent l'influence du pH sur log $\bar{V}_m/\bar{K}_m$ à 15.3° C et 24.4° C. Les

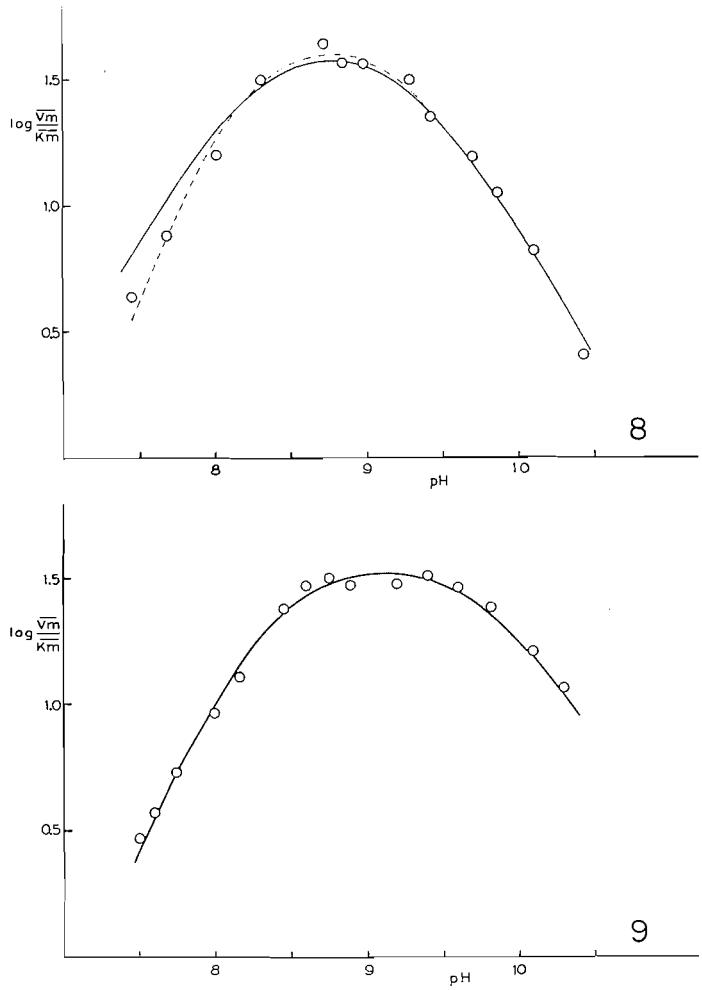


FIG. 8. Influence du pH sur la quantité log $\bar{V}_m/\bar{K}_m$ à 15.3° C. Les points représentent les données expérimentales, le tracé est théorique.

FIG. 9. Influence du pH sur la quantité log $\bar{V}_m/\bar{K}_m$ à 24.4° C. Les points représentent les données expérimentales, le tracé est théorique.

tracés sont théoriques et les points ont été obtenus en additionnant les valeurs expérimentales de log $\bar{V}_m$ et de p$\bar{K}_m$ en fonction du pH. Le tracé (A) de la figure 7 suppose deux groupes ionisables par centre actif et a pour équation:

$$[9] \qquad \log \bar{V}_m/\bar{K}_m = \log \left[(V_m/K_m) \Big/ \left(1+\frac{K_I}{[H^+]}+\frac{[H^+]}{K_{II}}\right)\right].$$

Can. J. Chem. Downloaded from www.nrcresearchpress.com by 210.87.254.40 on 09/05/12
For personal use only.

Les constantes K_I et K_{II} ont été déterminées par la méthode d'Alberty (12): $pK_I = 9.02$, $pK_{II} = 8.39$. Cette courbe (A) s'éloigne sensiblement des points pratiques du côté acide du maximum. Par contre, le tracé (B) qui suppose trois groupes ionisables par centre actif, et a pour équation l'expression logarithmique de l'équation [3], fournit une coincidence satisfaisante. Les valeurs K_I et K_{II} sont celles indiquées ci-dessus. La constante K_{III} est celle qui apparaît dans la courbe de Dixon (fig. 3) dans la région de 7.8. Nous lui avons assigné la valeur de $pK_{III} = 7.65$ pour obtenir un bon accord entre les données théoriques et expérimentales. Le tracé théorique de la figure 8 a été également calculé à partir de l'équation [3]. Les constantes K_I, K_{II} et K_{III} ont été déterminées comme pour le tracé (B) de la figure 7. Le tableau I récapitule les valeurs des constantes obtenues

TABLEAU I

Constantes d'ionisation des groupes actifs ionisables de la phosphatase alcaline intestinale et du complexe enzyme–substrat qu'elle forme avec le phosphate de *p*-nitrophényle

	24.4° C	15.3° C
pK_I	9.75	9.03
pK_{II}	8.42	8.39
pK_{III}	7.62	7.65
pK_{II}'	9.37	9.7

à 24.4° C et 15.3° C. Les valeurs de pK sont valables avec une erreur absolue de ± 0.05 unité de pK. Les trois groupes ionisables identifiés font partie du centre actif de l'enzyme et participent à la formation des complexes enzyme–substrat. Ils peuvent être tous différents, tous identiques ou l'un différent des autres.

Si les groupes sont identiques et s'il n'y a aucune influence électrostatique, les pK apparents pK_I, pK_{II}, pK_{III} doivent être séparés par 0.48 unité de pK (13). Si, les mêmes hypothèses étant posées, les groupes sont différents, leurs pK apparents doivent être séparés par plus de 0.48 unité de pK.

L'influence de la charge électrique sur le processus d'ionisation est en général beaucoup trop importante pour qu'elle puisse être négligée. Les groupes actifs peuvent d'une part s'influencer mutuellement, d'autre part être affectés par l'ionisation des groupes voisins qui ne participent pas directement à la formation du complexe enzyme–substrat. Cet effet électrostatique a pour résultat d'augmenter les différences entre les pK apparents de fonctions identiques. Les données de Britton (14) montrent l'amplitude du phénomène dans les molécules beaucoup plus simples que celles des protéines. Pour l'acide succinique $pK_a = 5.60$, $pK_b = 4.20$, ce qui donne un ΔpK, dû aux effets électrostatiques, de 0.8; pour l'acide glutarique le ΔpK électrostatique est égal à 0.47. L'équation [10] rend compte de l'influence de la charge électrostatique Z sur la constante d'ionisation d'un groupe acide de la protéine.

[10] $$pK = pK_0 - 2wZ/2.3$$

où w est donné par:

[11] $$w = \frac{e^2}{2DkT}\left(\frac{1}{b} - \frac{\kappa}{1+\kappa a}\right)$$

où e est la charge de l'électron, D la constante diélectrique du milieu, k la constante de Boltzman, T la température absolue, b le rayon de la molécule de protéine considérée comme sphérique, $\kappa/(1+\kappa a)$ est la fonction de Debye–Hückel.

Can. J. Chem. Downloaded from www.nrcresearchpress.com by 210.87.254.40 on 09/05/12
For personal use only.

Can. J. Chem. Downloaded from www.nrcresearchpress.com by 210.87.254.40 on 09/05/12
For personal use only.

Chaleurs d'ionisation

Les ionisations relatives à K_{II} et K_{III} sont pratiquement athermiques et pourraient —si ce n'était des valeurs de pK—être attribuées à la fonction carboxylique ou à un groupe phosphate. L'ionisation relative à K_I, exothermique par 32 kcal/mole, est d'interprétation beaucoup plus difficile. Les groupes ionisables des molécules de protéines ont des ionisations soit athermiques, soit endothermiques, mais jamais exothermiques.

L'interprétation des phénomènes électrostatiques permet d'expliquer ces valeurs anormales des chaleurs d'ionisation. La molécule de phosphatase alcaline est riche en lysine (15), le pK des groupes ϵ amino est environ 10 à 15.3° C et leur chaleur d'ionisation est environ 12 kcal/mole. À pH 8.39 (pK_{II} à 15.3° C), ces groupes contribuent à la charge de l'enzyme. Lorsque la température passe de 15.3° C à 24.4° C, le pK des groupes ϵ amino diminue d'environ 0.3 unités de pK. Si le groupe actif de pK 8.39 a une chaleur d'ionisation de 7 kcal/mole son pK diminue de 0.16 unité pK pour la même élévation de température. Au pH égal au nouveau pK du groupe actif, la protéine est plus négative qu'elle ne l'était à pH 8.39. Cette augmentation de la charge négative a pour effet d'élever le pK d'ionisation (équation [10]).

Les deux effets—abaissement du pK d'ionisation du groupe actif dû à l'élévation de température de 15.3° C à 24.4° C et l'augmentation de ce pK dû à l'accroissement de la charge négative—se compensent en milieu faiblement alcalin. C'est là l'explication des chaleurs d'ionisation nulles obtenues pour pK_{II} et pK_{III}.

À pH élevé, l'élévation de la température produit une telle augmentation de la charge négative de l'enzyme qu'il y a "surcompensation". La chaleur d'ionisation apparente sera négative. C'est certainement là l'explication de l'exothermicité considérable de l'ionisation relative à pK_I. Les influences du pH et de la température sur la charge de la phosphatase alcaline sont très mal connues. L'enzyme n'a pas été titrée et ceci élimine toute possibilité d'un traitement quantitatif des effets électrostatiques. Le point isoélectrique (16) de la phosphatase alcaline est environ 5.6; l'enzyme est riche en groupes carboxyliques, en résidus ϵ amino et possède de l'histidine en quantité appréciable (15). Nous admettrons, en première approximation, que sa courbe de titrage a la même allure que celle de la myosine qui possède des propriétés semblables. Les courbes de titrage obtenues par Mihalyi (17) montrent que l'influence de la température sur la charge négative de l'enzyme, bien qu'appréciable entre pH 7 et 9, est surtout sensible au-delà de pH 9. Ceci justifie l'interprétation donnée précédemment, qui veut que les groupes ionisables du centre actif de l'enzyme aient des chaleurs d'ionisation inférieures à celles des groupes ϵ amino. Des chaleurs d'ionisation de 6 à 7 kcal/mole semblent raisonnables.

Influence du pH sur la vitesse maximum

Aux deux températures et pour les valeurs de pH inférieures à 8, les points expérimentaux sont sensiblement au-dessus des courbes théoriques. Les paliers obtenus peuvent être dus à la décomposition des deux complexes EHS et EH_2S. La vitesse de réaction devient:

$$v = k_1[EH_2S] + k_2[EHS].$$

La participation d'un deuxième complexe à la formation des produits n'affecte que la valeur de $\bar{V}_m$ et n'influe pas sur $\bar{K}_m$.

Si l'enzyme fournit un mécanisme à la réaction, on imagine mal qu'il soit multiple ou comporte divers stades intermédiaires en parallèle. Il semble plus raisonnable d'admettre, ici encore, la participation des effets électrostatiques. La fixation du substrat, avec

ses deux charges négatives élève le pK de l'enzyme de 8.39 à 9.7 à 15.3° C. Il est possible qu'aux pH inférieurs à 8, la charge négative du complexe enzyme–substrat diminue suffisamment vite pour conserver au rapport $[H^+]/K_{II}'$ une valeur constante. Ceci a pour effet de maintenir constante l'expression de la vitesse maximum en fonction du pH:

$$\bar{V}_m = V_m\left(1/1+\frac{[H^+]}{K_{II}'}\right).$$

CONCLUSION

Identification des groupes ionisables du centre actif

Dans les molécules de protéines, les seuls groupes qui aient des chaleurs d'ionisation faibles sont: le groupe hydroxyle phénolique (6 kcal/mole), le groupe imidazole de l'histidine (18) (6.9 à 7.5 kcal/mole), le groupe sulfhydryle de la cystéine (19) ($\sim$7 kcal/mole).

Les pK_I, pK_{II}, pK_{III} apparents sont trop élevés pour pouvoir appartenir au groupe imidazole (pK 5.6 à 7.0) et trop faibles pour pouvoir appartenir au groupe hydroxyle phénolique (pK 9.6 à 10.9). Par contre, ils appartiennent tous au domaine d'ionisation des —SH (pK 7.5 à 10). Les données expérimentales conduisent donc à une seule conclusion: présence au centre actif de trois groupes ionisables qui sont tous des groupes thiols.

La charge négative de la protéine est probablement considérable dans le domaine de pH étudié. Toutes les expériences ont été faites en l'absence de quantités appréciables de cations. Les valeurs de pK obtenues sont des valeurs maximum; les pK_0 correspondants (équation [10]) sont sans doute sensiblement plus faibles. Une étude des courbes de titrage est en cours qui devrait permettre un traitement semi-quantitatif des effets électrostatiques. Il se pourrait qu'alors le ou les deux groupes actifs ayant les pK les plus bas soient attribués à l'imidazole de l'histidine et non plus au groupe thiol de la cystéine.

RÉSUMÉ

Les constantes de Michaelis et les vitesses maxima ont été évaluées à 15.3° C et 24.4° C, de pH 7.5 à pH 10.4.

Les données expérimentales permettent d'identifier trois groupes ionisables au centre actif de l'enzyme. Les pK apparents d'ionisation de ces groupes sont à 15.3° C: pK_I = 9.02; pK_{II} = 8.39; pK_{III} = 7.65; à 24.4° C: pK_I = 9.75; pK_{II} = 8.42; et pK_{III} = 7.62.

Ces résultats mettent en relief le rôle important des phénomènes électrostatiques. Les chaleurs d'ionisation attribuées aux trois groupes actifs sont de 6 à 7 kcal/mole.

L'un des groupes actifs au moins est une fonction thiol. Les deux autres peuvent être des thiols ou des imidazoles.

REMERCIEMENTS

Les auteurs désirent remercier le Conseil national des Recherches du Canada pour l'aide financière qui leur a permis d'exécuter ce travail. L'un de nous (M. L.) était bénéficiaire d'une bourse de la firme C. I. L.

BIBLIOGRAPHIE

1. R. K. Morton. Biochem. J. **65**, 674 (1957).
2. C. A. Zittle et E. W. Bingham. Arch. Biochem. Biophys. **86**, 25 (1960).
3. D. E. Koshland. Arch. Biochem. Biophys. **39**, 229 (1952).
4. L. Engström. Acta Soc. Med. Upsaliensis, **64**, 214 (1959).

Can. J. Chem. Downloaded from www.nrcresearchpress.com by 210.87.254.40 on 09/05/12
For personal use only.

5. K. J. LAIDLER. The chemical kinetics of enzyme action. Oxford University Press. 1958. p. 117.
6. M. DIXON. Biochem. J. **55**, 161 (1953).
7. R. A. ALBERTY et V. MASSEY. Biochim. et Biophys. Acta, **12**, 347 (1954).
8. H. LINEWEAVER et D. BURK. J. Am. Chem. Soc. **56**, 658 (1934).
9. J. M. STURTEVANT. J. Am. Chem. Soc. **77**, 255 (1955).
10. I. MOTZOK. Biochem. J. **72**, 169 (1959).
11. M. ANDREU, E. FERNANDEZ ALVAREZ et M. LORA-TAMAYO. Anales real soc. españ. fís y quím. (Madrid), B, **56**, 67 (1960).
12. R. A. ALBERTY. J. Cellular Comp. Physiol. **47**, 245 (1956).
13. I. M. KLOTZ. The proteins. Vol. 1-B. *Edité par* H. Neurath et K. Bailey. Academic Press Inc., New York. 1953. p. 753.
14. H. T. S. BRITTON. Hydrogen ions. 3rd ed. Van Nostrand & Co., New York. 1943. p. 248.
15. P. PORTMAN, R. ROSSIER et H. CHARDONNENS. Helv. Physiol. et Pharmacol. Acta, **18**, 414 (1960).
16. G. SCHRAMM et O. ARMBUSTER. Z. Naturforsch. b, **9**, 114 (1954).
17. E. MIHALYI. Enzymologia, **14**, 224 (1950).
18. E. J. COHN et J. T. EDSALL. Proteins, amino acids and peptides. Reinhold Publishing Corp., New York. 1943. p. 445.
19. R. E. BENESCH et R. BENESCH. J. Am. Chem. Soc. **77**, 5877 (1955).

Can. J. Chem. Downloaded from www.nrcresearchpress.com by 210.87.254.40 on 09/05/12
For personal use only.

Can. J. Chem. Downloaded from www.nrcresearchpress.com by 210.87.254.40 on 09/05/12
For personal use only.

SYNTHÈSES DE COURTS PEPTIDES RENFERMANT DES ACIDES AMINO-1 CYCLOALKYL CARBOXYLIQUES[1]

PATRICE TAILLEUR ET LOUIS BERLINGUET

ABSTRACT

Using classical methods of synthesis nine small peptides containing amino-1 cycloalkyl carboxylic acids have been synthesized. The cyclic acids have been placed either at the N-terminal or at the C-terminal positions or in between two natural amino acids, glycine and DL-phenylalanine.

The cyclization of two dipeptides into a substituted diketopiperazine, and the subsequent hydrolysis of this compound have been studied.

INTRODUCTION

L'acide amino-1 cyclopentane carboxylique présente un intérêt particulier puisqu'on a démontré qu'il pouvait inhiber la croissance de certains types de tumeurs (1, 2). Plusieurs dérivés ainsi que des homologues supérieurs et inférieurs de cet acide amino-1 cyclopentane carboxylique ont été récemment synthétisés (3, 4, 5). Mais il semble que de tous ces dérivés, seul l'acide amino-1 cyclopentane carboxylique ait un effet antitumoral appréciable.

Par ailleurs, l'acide aminé possède une toxicité assez marquée; nous avons alors pensé qu'en l'incorporant dans un court peptide, on pourrait à la fois diminuer sa toxicité et conserver son activité biologique. Connors et Ross (5) ont déjà synthétisé trois dipeptides dans lesquels l'acide amino-1 cyclopentane carboxylique est combiné soit à la glycine, soit à la DL-phénylalanine.

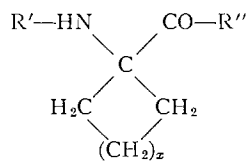
Nous avons voulu obtenir d'autres dipeptides, et surtout placer l'acide aminé cyclique entre des acides aminés naturels. Les peptides non-naturels ainsi obtenus devraient avoir des propriétés biologiques intéressantes, lesquelles seront rapportées ailleurs. Pour ce faire, nous avons surtout utilisé les méthodes classiques de synthèse des peptides, en passant par les dérivés carbobenzoxy et les esters benzyliques, qui ont été condensés par le N,N′-dicyclohexylcarbodiimide, suivant la méthode de Sheehan et Hess (6). Nous avons ainsi obtenu neuf peptides dont trois ont déjà été obtenus par Connors et Ross, mais par une méthode différente des nôtres. Ces neuf peptides contiennent soit l'acide amino-1 cyclopentane carboxylique, soit l'acide amino-1 cyclohexane carboxylique, lesquels sont placés soit à l'extrémité N-terminale de la chaîne, soit à l'extrémité C-terminale, soit entre deux acides aminés naturels. Les acides aminés naturels utilisés ont été la glycine et la DL-phénylalanine.

Les dérivés carbobenzoxy des deux acides aminés cycliques ont été préparés avec des rendements élevés, soit 75%. Mais lorsque nous avons voulu préparer les chlorures d'acides de ces dérivés, nous avons observé une cyclisation spontanée en anhydride correspondant. D'ailleurs MacDonald (7) avait aussi observé la formation spontanée du 3-oxa-1-azaspiro[4.4]nonanedione-2,4 correspondant à l'acide amino-1 cyclopentane carboxylique et du 3-oxa-1-azaspiro[4.5]décanedione-2,4 correspondant à l'acide amino-1

[1]*Manuscrit reçu le 25 janvier 1961.*
Contribution du Département de Biochimie, Faculté de Médecine, Université Laval, Québec, Qué. Présenté en partie aux congrès de l'ACFAS, Montréal et Québec, novembre 1959 et 1960.

cyclohexane carboxylique. Nous avons donc pensé à utiliser la méthode de Sheehan et Hess où l'on condense un dérivé carbobenzoxy avec un ester benzylique. Les esters benzyliques des deux acides aminés cycliques ont été synthétisés en modifiant quelque peu la méthode de Miller et Waelsch (8). Ces esters ont été isolés sous formes de *p*-toluènesulfonates et de chlorhydrates avec d'excellents rendements. La condensation avec le N,N′-dicyclohexylcarbodiimide nous a donné des peptides protégés qui ont ensuite été hydrogénés en peptides libres dont la liste apparaît dans le tableau I.

TABLEAU I



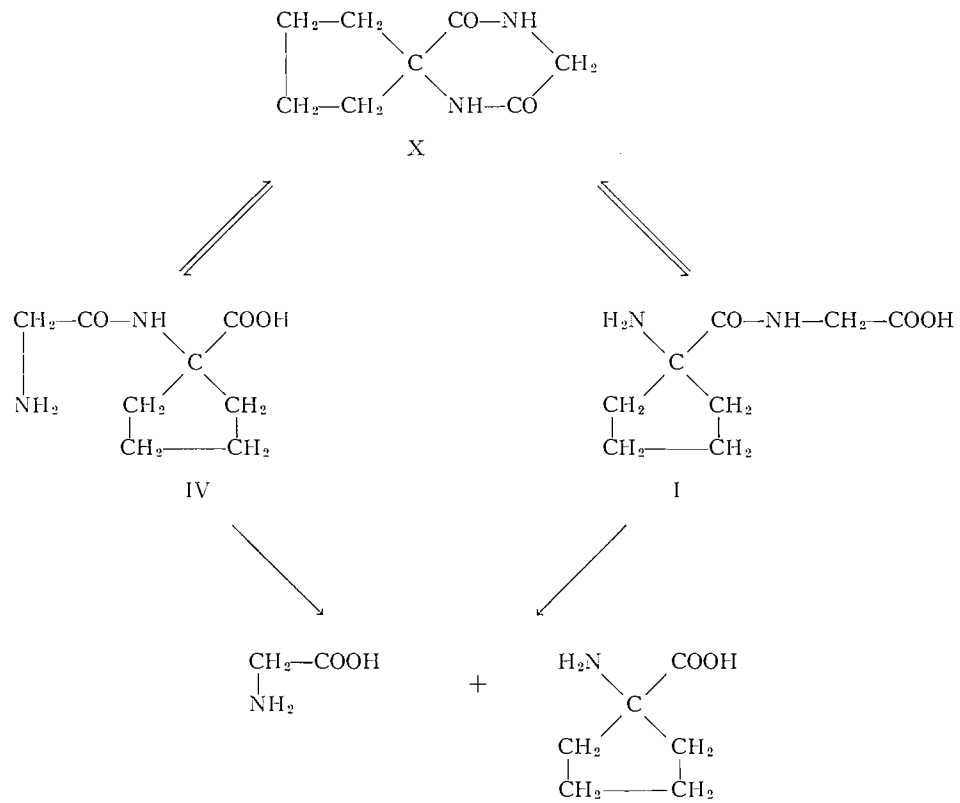
R′	R″	*x*	Nom	
H	Glycine	2	Amino-1 cyclopentane carboxyl-glycine	(I)
H	DL-Phénylalanine	2	Amino-1 cyclopentane carboxyl-DL-phénylalanine	(II)
H	DL-Phénylalanine	3	Amino-1 cyclohexane carboxyl-DL-phénylalanine	(III)
Glycyl	OH	2	Glycyl-acide amino-1 cyclopentane carboxylique	(IV)
Glycyl	OH	3	Glycyl-acide amino-1 cyclohexane carboxylique	(V)
DL-Phénylalanyl	OH	2	DL-Phénylalanyl-acide amino-1 cyclopentane carboxylique	(VI)
DL-Phénylalanyl	OH	3	DL-Phénylalanyl-acide amino-1 cyclohexane carboxylique	(VII)
Glycyl	DL-Phénylalanine	2	Glycyl-amino-1 cyclopentane carboxyl-DL-phénylalanine	(VIII)
Glycyl	DL-Phénylalanine	3	Glycyl-amino-1 cyclohexane carboxyl-DL-phénylalanine	(IX)

Pour obtenir des peptides renfermant une molécule de glycine placée à l'extrémité N-terminale, nous avons préparé les dérivés chloroacétylés des acides aminés cycliques. Ceux-ci, après amination, ont donné avec d'excellents rendements, les deux dipeptides suivants: le glycyl-acide amino-1 cyclopentane carboxylique et le glycyl-acide amino-1 cyclohexane carboxylique. Cette même méthode nous a permis d'obtenir deux tripeptides à partir de l'amino-1 cyclopentane carboxyl-DL-phénylalanine et de l'amino-1 cyclohexane carboxyl-DL-phénylalanine.

La très grande facilité de cyclisation des dérivés N-carbobenzoxy des deux acides aminés cycliques nous a amenés à étudier la formation d'une dicétopipérazine substituée à partir des deux dipeptides renfermant l'acide amino-1 cyclopentane carboxylique et la glycine. Connors et Ross (5) en chauffant à 180°, dans le vide, l'amino-1 cyclopentane carboxyl-glycine (I), ont obtenu la dicétopipérazine (X), sans mentionner le rendement. Théoriquement il était intéressant de comparer la facilité de cyclisation en dicétopipérazine des deux peptides, glycyl-acide amino-1 cyclopentane carboxylique (IV) et amino-1 cyclopentane carboxyl-glycine (I). Nous avons constaté que le glycyl-acide amino-1 cyclopentane carboxylique après un chauffage à 180° pendant 6 heures dans le vide se cyclisait facilement avec un rendement de 80% en dicétopipérazine. Dans des conditions expérimentales identiques, l'amino-1 cyclopentane carboxyl-glycine donne la même dicétopipérazine mais avec un rendement très faible de 10 à 15%.* Vu la différence marquée dans le comportement des deux peptides lors de la cyclisation, il nous a semblé possible que par hydrolyse acide, un des liens peptidiques soit plus facilement coupé que l'autre.

**Les cristaux obtenus lors de ces deux cyclisations ont des spectres aux rayons-X identiques, tel que déterminé par Madame Przybylska du Conseil National de Recherches à Ottawa.*

Can. J. Chem. Downloaded from www.nrcresearchpress.com by 210.87.254.40 on 09/05/12
For personal use only.



Connors et Ross ont observé que l'hydrolyse acide de la dicétopipérazine (X) conduit au peptide amino-1 cyclopentane carboxyl-glycine (I). Nous avons voulu étudier plus en détail cette hydrolyse dans de l'acide chlorhydrique 1 *N*, en identifiant, par chromatographie, les produits formés. Les deux dipeptides et les deux acides aminés qui les composent se séparent bien par chromatographie, mais leur détermination quantitative présente des difficultés. L'acide amino-1 cyclopentane carboxylique ne possède pas d'hydrogène en position α, et de ce fait, se comporte de façon anormale lors de la titration de Sörensen avec le formol (9), et ne réagit pas quantitativement avec la ninhydrine (10). Lorsque cet acide aminé cyclique est placé à l'extrémité N-terminale d'une chaîne peptidique, la fonction aminée semble être encore moins réactive. C'est ainsi que le dipeptide amino-1 cyclopentane carboxyl-glycine réagit très peu avec la ninhydrine et avec le fluoro-1, dinitro-2,4 benzène. Dans ces conditions, il devenait très difficile d'estimer avec précision la proportion relative des deux dipeptides provenant de l'hydrolyse de la dicétopipérazine. La dicétopipérazine ne donnant pas de coloration avec la ninhydrine nous avons alors utilisé la méthode au chlore de Rydon et Smith (11), puis étudié la marche de cette hydrolyse par chromatographie (voir la figure 1). Nous avons pu constater qu'après 10 minutes il ne restait que des traces de dicétopipérazine, et que déjà les deux dipeptides (I et IV) commençaient à s'hydrolyser en acides aminés. La dicétopipérazine était complètement ouverte après 20 minutes. Ludtke (12) et Levene (13) ont démontré déjà que l'hydrolyse d'une dicétopipérazine se faisait en deux étapes: l'une rapide, donnant un ou des dipeptides, et l'autre lente, libérant les acides aminés. Si les deux

Can. J. Chem. Downloaded from www.nrcresearchpress.com by 210.87.254.40 on 09/05/12
For personal use only.

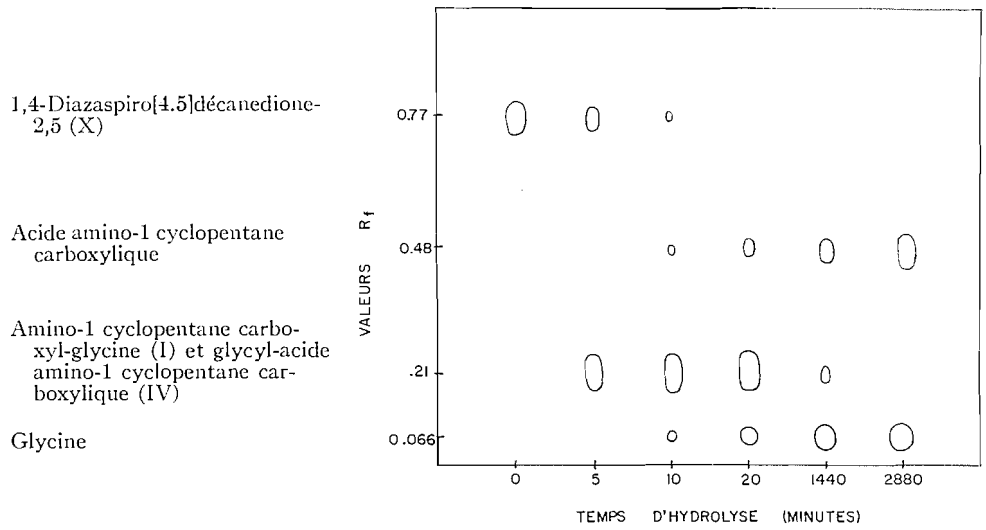


FIG. 1. Représentation du chromatogramme des produits d'hydrolyse de la dicétopipérazine (X). Le solvant est le suivant: *n*-butanol (225), acide acétique (75) et eau (25).

dipeptides se cyclisent en une même dicétopipérazine substituée avec des rendements bien différents, par contre, l'ouverture de cette dicétopipérazine donne naissance de façon indifférente aux deux peptides attendus, contrairement à ce qui a été rapporté (5).

PARTIE EXPÉRIMENTALE

Acide amino-1 cyclopentane carboxylique

On dissout 46.26 g (0.3 mole) de 1,3-diazaspiro[4.4]nonanedione-2,4 et 110.05 g (0.35 mole) d'hydroxyde de barium octahydraté dans 500 ml d'eau chaude. On porte ensuite à l'autoclave pendant une heure à 165°. Après refroidissement à 60°, on ajoute 35.5 g (0.37 mole) de carbonate d'ammonium pour précipiter l'excès de barium. Après filtration, on concentre la solution, et l'acide aminé cristallise par refroidissement. Rendement: 27.8 g (71.8%). Anal. Calc. pour $C_6H_{11}O_2N$: N, 10.84%. Trouvé: N, 10.70%.

Acide amino-1 cyclohexane carboxylique

On hydrolyse de façon analogue à la précédente, 50.46 g (0.3 mole) de 1,3-diazaspiro-[4.5]décanedione-2,4. L'acide amino-1 cyclohexane carboxylique obtenu est recristallisé avec de l'eau et de l'acétone. Rendement: 34.4 g (80%). Anal. Calc. pour $C_7H_{13}O_2N$: N, 9.77%. Trouvé: N, 9.80%.

Acide N-carbobenzoxy amino-1 cyclopentane carboxylique

On dissout 12.92 g (0.1 mole) de l'acide amino-1 cyclopentane carboxylique dans 25 ml (0.1 mole) d'hydroxyde de sodium 4 *N*. En agitant vigoureusement, dans un bain d'eau à 20°, on additionne simultanément, goutte-à-goutte, pendant 30 minutes, 27.5 ml (0.11 mole) d'hydroxyde de sodium 4 *N* et 22.8 ml (0.11 mole) d'une solution de chloroformate de benzyle dans le toluène et dont la concentration est de 8.3 g/10 ml. L'addition des réactifs étant terminée, on continue l'agitation pendant 30 minutes. On extrait avec 50 ml d'éther et on acidifie la fraction aqueuse refroidie avec 15 ml d'acide chlorhydrique concentré. On extrait ensuite le produit avec deux portions de 50 ml d'acétate d'éthyle qu'on sèche finalement sur du sulfate de magnésium anhydre. Après concentration de

Can. J. Chem. Downloaded from www.nrcresearchpress.com by 210.87.254.40 on 09/05/12
For personal use only.

Can. J. Chem. Downloaded from www.nrcresearchpress.com by 210.87.254.40 on 09/05/12
For personal use only.

la solution, le produit cristallise au froid par addition d'un excès d'éther de pétrole. Rendement: 19.5 g (74.3%). Le produit recristallisé fond à 92–93°.* Anal. Calc. pour $C_{14}H_{17}O_4N$: N, 5.33%. Trouvé: N, 5.43%.

Acide N-carbobenzoxy amino-1 cyclohexane carboxylique

On traite 14.32 g (0.1 mole) d'acide amino-1 cyclohexane carboxylique par le chloroformate de benzyle tel que décrit précédemment. On obtient ainsi 20 g (72.2%) du dérivé N-carbobenzoxy de l'acide amino-1 cyclohexane carboxylique. P.f. 154–156°. Anal. Calc. pour $C_{15}H_{19}O_4N$: N, 5.06%. Trouvé: N, 5.07%.

N-Carbobenzoxy glycine

On condense 7.5 g (0.1 mole) de glycine avec le chloroformate de benzyle tel que décrit plus haut, mais dans un bain d'eau à 0°. Le dérivé N-carbobenzoxy de la glycine est précipité par l'acide chlorhydrique puis filtré et recristallisé avec du chloroforme. Rendement: 17 g (81.3%). P.f. 119–120° (litt. p.f. 120°) (14). Anal. Calc. pour $C_{10}H_{11}O_4N$: N, 6.70%. Trouvé: 6.80%.

N-Carbobenzoxy DL-*phénylalanine*

On traite comme précédemment 16.5 g (0.1 mole) de DL-phénylalanine. La réaction se fait dans un bain d'eau à 0°. Le dérivé N-carbobenzoxy de la DL-phénylalanine obtenu pèse 23 g (76.8%). P.f. 98°. Après recristallisation avec de l'éther et de l'éther de pétrole, le produit fond à 103° (litt. p.f. 103°) (14). Anal. Calc. pour $C_{17}H_{17}O_4N$: N, 4.68%. Trouvé: 4.60%.

3-Oxa-1-azaspiro[4.4]nonanedione-2,4

A 2.63 g (0.1 mole) de l'acide N-carbobenzoxy amino-1 cyclopentane carboxylique, on additionne 5 ml d'anhydride acétique et 1 ml de chlorure de thionyle. On maintient à l'ébullition pendant une minute. On évapore à sec sous vide, et on cristallise l'anhydride formé en dissolvant le résidu dans un peu d'acétate d'éthyle chaud, et en ajoutant un excès d'éther de pétrole. Rendement: 1.1 g (73.3%). Le produit recristallisé fond à 128–129° (p.f. litt. 128°) (7). Anal. Calc. pour $C_7H_9O_3N$: N, 9.00%. Trouvé: N, 9.01%.

3-Oxa-1-azaspiro[4.5]décanedione-2,4

On traite 2.77 g (0.1 mole) de l'acide N-carbobenzoxy amino-1 cyclohexane carboxylique par le chlorure de thionyle tel que décrit plus haut. On obtient ainsi 1.3 g (76.8%) de l'anhydride. P.f. 112° (litt. p.f. 114.8–115.2°) (7). Anal. Calc. pour $C_8H_{11}O_3N$: N, 8.26%. Trouvé: N, 8.32%.

Acide N-chloroacétyl-amino-1 cyclopentane carboxylique

On dissout 5.46 g (0.05 mole) d'acide amino-1 cyclopentane carboxylique dans 12.5 ml (0.05 mole) d'hydroxyde de sodium 4 *N*. On ajoute à froid, en agitant violemment, simultanément et par portions, pendant 20 minutes, 13.75 ml (0.055 mole) d'hydroxyde de sodium 4 *N* et 6.21 g de chlorure de chloroacétyle. L'addition des réactifs terminée, on continue l'agitation pendant 15 minutes, et on ajoute à froid 10 ml d'acide chlorhydrique concentré. Après 3 heures au froid, on filtre le dérivé chloroacétylé et on le recristallise avec de l'acétate d'éthyle et de l'éther de pétrole. Rendement: 6 g (73%). P.f. 160°. Anal. Calc. pour $C_8H_{12}O_3NCl$: N, 6.80%, Cl, 17.25%. Trouvé: N, 6.89%, Cl, 17.54%.

Les autres dérivés chloroacétylés sont préparés de façon analogue.

**Les points de fusion ne sont pas corrigés.*

Acide N-chloroacétyl-amino-1 cyclohexane carboxylique

On traite comme ci-haut 6.45 g (0.05 mole) d'acide amino-1 cyclohexane carboxylique par le chlorure de chloroacétyle. Le dérivé chloroacétylé obtenu pèse 8 g (72.8%). P.f. 206°. Anal. Calc. pour $C_9H_{14}O_3NCl$: N, 6.37%; Cl, 16.18%. Trouvé: N, 6.48%; Cl, 16.23%.

Glycyl-acide amino-1 cyclopentane carboxylique (IV)

A 100 ml d'ammoniaque concentrée, on ajoute 3 g (0.015 mole) d'acide N-chloroacétyl-amino-1 cyclopentane carboxylique. Après 3 jours à la température de la chambre tout est dissous, et on laisse continuer la réaction une journée de plus. On évapore ensuite à sec sous vide sur un bain-marie. Le résidu est dissous dans un minimum d'eau bouillante et on additionne un excès de méthanol. Le glycyl-acide amino-1 cyclopentane carboxylique cristallise à froid. Rendement: 2 g (71.7%). P.f. 271–275°. On recristallise avec de l'eau et du méthanol. P.f. 276–278°. Anal. Calc. pour $C_8H_{14}O_3N_2$: N, 15.05%. Trouvé: 15.10%.

Tous les autres dérivés chloroacétylés sont traités de façon analogue par l'ammoniaque.

Chlorhydrate du glycyl-acide amino-1 cyclopentane carboxylique

On dissout 3.72 g (0.02 mole) du glycyl-acide amino-1 cyclopentane carboxylique dans 25 ml d'eau. Après refroidissement dans la glace on additionne 22 ml (0.022 mole) d'acide chlorhydrique 1 *N*. Après quelques minutes, on évapore à sec sous vide et on recristallise deux fois le chlorhydrate avec de l'eau et de l'acétone. Rendement: 3.5 g (78.7%). P.f. 214–215° (litt. p.f. 216°) (5). Anal. Calc. pour $C_8H_{14}O_3N_2.HCl$: N, 12.52%. Trouvé: N, 12.65%.

Glycyl-acide amino-1 cyclohexane carboxylique (V)

On traite comme ci-haut, 2.2 g (0.01 mole) d'acide N-chloroacétyl-amino-1 cyclohexane carboxylique par 100 ml d'ammoniaque concentrée. On obtient ainsi 1.5 g (75%) de glycyl-acide amino-1 cyclohexane carboxylique. Après une recristallisation avec de l'eau et de l'éthanol, le produit se décompose à une température supérieure à 300°. Anal. Calc. pour $C_9H_{16}O_3N_2$: N, 14.01%. Trouvé: N, 14.00%.

N-Carbobenzoxy glycyl-acide amino-1 cyclopentane carboxylique

On traite 18.6 g (0.1 mole) du glycyl-acide amino-1 cyclopentane carboxylique par le chloroformate de benzyle tel que décrit plus haut. Le dérivé N-carbobenzoxy du glycyl-acide amino-1 cyclopentane carboxylique, précipité par l'addition d'acide chlorhydrique concentré, est filtré et recristallisé avec de l'eau contenant 25% d'éthanol. Rendement: 26 g (81.2%). P.f. 176°. Anal. Calc. pour $C_{16}H_{20}O_5N_2$: N, 8.74%. Trouvé: N, 8.60%.

N-Carbobenzoxy glycyl-acide amino-1 cyclohexane carboxylique

On condense 20 g (0.1 mole) du glycyl-acide amino-1 cyclohexane carboxylique avec le chloroformate de benzyle tel que décrit plus haut. Le dérivé N-carbobenzoxy du glycyl-acide amino-1 cyclohexane carboxylique est précipité à un pH de 5–6 par addition d'acide chlorhydrique dilué. Le produit est filtré et recristallisé avec un minimum d'eau contenant 25% d'éthanol. Rendement: 31 g (92.5%). P.f. 263°. Anal. Calc. pour $C_{17}H_{22}O_5N_2$: N, 8.37%. Trouvé: N, 8.30%.

p-Toluènesulfonate de l'ester benzylique de l'acide amino-1 cyclopentane carboxylique

On suspend 6.46 g (0.05 mole) d'acide amino-1 cyclopentane carboxylique et 10.46 g (0.055 mole) d'acide *p*-toluènesulfonique monohydraté dans 100 ml d'alcool benzylique et 150 ml de toluène. On laisse bouillir le mélange pendant une nuit, en recueillant l'eau formée au moyen d'un tube de Dean et Stark. Après refroidissement, on filtre une partie

Can. J. Chem. Downloaded from www.nrcresearchpress.com by 210.87.254.40 on 09/05/12
For personal use only.

de l'ester qui pèse 10 g, et on évapore le filtrat à sec sous vide et à une température ne dépassant pas 130°. On reprend le résidu à chaud avec un minimum de chloroforme et on cristallise à froid en présence d'un excès d'éther. On obtient ainsi le reste de l'ester qui pèse 9 g. Rendement: 19 g (92.7%). P.f. 180–186° C. Après trois recristallisations, on obtient le *p*-toluènesulfonate de l'ester benzylique de l'acide amino-1 cyclopentane carboxylique pur qui fond à 193–195°. Anal. Calc. pour $C_{13}H_{17}O_2N.p\text{-}CH_3C_6H_4SO_3H$: N, 3.58%. Trouvé: N, 3.58%.

Chlorhydrate de l'ester benzylique de l'acide amino-1-cyclopentane carboxylique

On suspend 16.38 g (0.04 mole) de *p*-toluènesulfonate de l'ester benzylique de l'acide amino-1 cyclopentane carboxylique dans 100 ml d'eau glacée et 50 ml de chloroforme. On agite fortement pendant 10 minutes en neutralisant avec un léger excès d'une solution 1 *M* de bicarbonate de sodium. On décante le chloroforme et on extrait de nouveau avec 50 ml de chloroforme. Après avoir séché les deux fractions de chloroforme réunies sur du sulfate de magnésium anhydre, on sature la solution d'acide chlorhydrique gazeux, on évapore à environ 50 ml, et le produit cristallise au froid par addition d'une excès d'éther. Rendement: 9.7 g (95%). P.f. 162°. On recristallise avec du dioxane et de l'éther. P.f. 163°. Anal. Calc. pour $C_{13}H_{17}O_2N.HCl$: N, 5.48%; Cl, 13.88%. Trouvé: N, 5.53%; Cl, 14.00%.

p-Toluènesulfonate de l'ester benzylique de l'acide amino-1 cyclohexane carboxylique

On traite comme précédemment 7.2 g (0.05 mole) d'acide amino-1 cyclohexane carboxylique. Après refroidissement du mélange, rien ne cristallise. Après évaporation à sec et cristallisation du résidu avec du chloroforme et de l'éther, on obtient 19 g (85%) de *p*-toluènesulfonate de l'ester benzylique de l'acide amino-1 cyclohexane carboxylique qui fond à 160–163°. Après deux recristallisations avec du chloroforme et de l'éther, le produit fond à 167–169°. Anal. Calc. pour $C_{14}H_{19}O_2N.p\text{-}CH_3C_6H_4SO_3H$: N, 3.46%. Trouvé: N, 3.33%.

Chlorhydrate de l'ester benzylique de l'acide amino-1 cyclohexane carboxylique

On traite comme précédemment 16.94 g (0.04 mole) de *p*-toluènesulfonate de l'ester benzylique de l'acide amino-1 cyclohexane carboxylique. Le chlorhydrate de l'ester benzylique de l'acide amino-1 cyclohexane carboxylique ainsi obtenu pèse 9.6 g (90%) et est recristallisé avec du dioxane et de l'éther. P.f. 211°. Anal. Calc. pour $C_{14}H_{19}O_2N.HCl$: N, 5.21%; Cl, 13.18%. Trouvé: N, 5.40%; Cl, 13.60%.

p-Toluènesulfonate de l'ester benzylique de la glycine

On estérifie de façon analogue aux expériences précédentes, 30 g (0.4 mole) de glycine en présence de 83.6 g (0.44 mole) d'acide *p*-toluènesulfonique monohydraté dans 200 ml d'alcool benzylique et 200 ml de benzène. L'estérification terminée, on ajoute 200 ml d'éther de pétrole et le *p*-toluènesulfonate de l'ester benzylique de la glycine cristallise à froid. Rendement: 140 g (98.5%). P.f. 128–130°. On recristallise le produit avec du chloroforme et de l'éther de pétrole. P.f. 134–135°. Anal. Calc. pour $C_9H_{11}O_2N.p\text{-}CH_3C_6H_4SO_3H$: N, 4.15%. Trouvé: 4.20%.

Chlorhydrate de l'ester benzylique de la glycine

Comme précédemment, on suspend 6.7 g (0.02 mole) de *p*-toluènesulfonate de l'ester benzylique de la glycine dans 75 ml de chloroforme en présence de 50 ml d'eau glacée. Le chlorhydrate de l'ester benzylique de la glycine ainsi obtenu pèse 4 g (99%) et est recristallisé avec du chloroforme contenant 25% d'éthanol. P.f. 139–140° (litt. p.f. 139–140°) (15). Anal. Calc. pour $C_9H_{11}O_2N.HCl$: N, 6.95%. Trouvé: N, 7.00%.

Can. J. Chem. Downloaded from www.nrcresearchpress.com by 210.87.254.40 on 09/05/12
For personal use only.

p-Toluènesulfonate de l'ester benzylique de la DL-*phénylalanine*

On estérifie comme ci-haut 33 g (0.2 mole) de DL-phénylalanine en présence de 41.8 g (0.22 mole) d'acide *p*-toluènesulfonique monohydraté, de 200 ml d'alcool benzylique et de 100 ml de benzène. L'estérification terminée, on refroidit et on ajoute 200 ml d'éther de pétrole. Le *p*-toluènesulfonate de l'ester benzylique de la DL-phénylalanine cristallise au froid. Rendement: 84.5 g (95%). P.f. 142–146°. Après une recristallisation avec du chloroforme et de l'éther de pétrole le produit fond à 145–146°. Anal. Calc. pour $C_{16}H_{17}O_2N.p\text{-}CH_3C_6H_4SO_3H$: N, 3.14%. Trouvé: N, 3.09%.

Chlorhydrate de l'ester benzylique de la DL-*phénylalanine*

On neutralise comme précédemment 8.9 g (0.02 mole) de *p*-toluènesulfonate de l'ester benzylique de la DL-phénylalanine suspendus dans 75 ml de chloroforme et 50 ml d'eau glacée. On obtient finalement 5.5 g (94%) de chlorhydrate de l'ester benzylique de la DL-phénylalanine. P.f. 203–204°. On recristallise le produit deux fois avec de l'eau. P.f. 205–206° (litt. p.f. 196°) (8). Anal. Calc. pour $C_{16}H_{17}O_2N.HCl$: N, 4.80%. Trouvé: N, 4.88%.

Esters benzyliques libres des acides aminés

Pour effectuer les condensations par le N,N′-dicyclohexylcarbodiimide, les esters benzyliques qui sont synthétisés sous forme de chlorhydrates ou de *p*-toluènesulfonates doivent être obtenus à l'état libre. Le chlorhydrate ou le *p*-toluènesulfonate de l'ester benzylique est suspendu dans du chloroforme en présence de 25% en volume d'eau glacée. On additionne un excès d'une solution de bicarbonate de sodium 1 *M*. On agite fortement pendant 10 à 15 minutes et le chloroforme est décanté. On extrait de nouveau la solution aqueuse avec un peu de chloroforme qu'on décante ensuite. Après avoir séché les deux fractions de chloroforme réunies, sur du sulfate de magnésium anhydre, on évapore à sec sous vide. Les rendements moyens en esters libres sont de 90 à 99%.

N-Carbobenzoxy amino-1 cyclopentane carboxyl-glycinate de benzyle

On dissout dans 100 ml de chlorure de méthylène, 13.2 g (0.05 mole) de dérivé N-carbobenzoxy de l'acide amino-1 cyclopentane carboxylique et 9.08 g (0.055 mole) d'ester benzylique de la glycine. On additionne ensuite 11.4 g (0.055 mole) de N,N′-dicyclohexylcarbodiimide. Après 4 heures à la température de la chambre, on ajoute 5 ml d'acide acétique pour détruire l'excès de carbodiimide. Après 10 minutes, on filtre la N,N′-dicyclohexylurée formée qui pèse 12 g. On évapore le filtrat à sec sous vide et on reprend le résidu par un minimum d'acétate d'éthyle chaud. Le N-carbobenzoxy-amino-1-cyclopentane carboxyl-glycinate de benzyle cristallise à froid par addition d'un excès d'éther de pétrole. Rendement: 15 g (73.2%). P.f. 122–123°. Ce produit peut être hydrogéné directement sans être recristallisé. Après trois recristallisations avec de l'alcool et de l'éther de pétrole, le produit fond à 130–131°. Anal. Calc. pour $C_{23}H_{26}O_5N_2$: N, 6.83%. Trouvé: N, 6.83%. Les quatres condensations suivantes sont effectuées de façon analogue.

N-Carbobenzoxy DL-*phénylalanyl-amino-1 cyclopentane carboxylate de benzyle*

On dissout dans 50 ml de chlorure de méthylène, de façon analogue à la précédente, 8.98 g (0.03 mole) de dérivé N-carbobenzoxy de la DL-phénylalanine et 7.24 g (0.033 mole) d'ester benzylique de l'acide amino-1 cyclopentane carboxylique. On additionne ensuite 6.82 g (0.033 mole) de N,N′-dicyclohexylcarbodiimide. On obtient ainsi 12 g (80%) de N-carbobenzoxy DL-phénylalanyl-amino-1 cyclopentane carboxylate de benzyle. P.f. 107–110°. Ce produit peut être utilisé tel quel pour l'hydrogénation. Après deux recristallisations avec de l'alcool et de l'éther de pétrole, le produit fond à 123–124°. Anal. Calc. pour $C_{30}H_{32}O_5N_2$: N, 5.59%. Trouvé: 5.79%.

Can. J. Chem. Downloaded from www.nrcresearchpress.com by 210.87.254.40 on 09/05/12
For personal use only.

N-Carbobenzoxy DL-*phénylalanyl-amino-1 cyclohexane carboxylate de benzyle*

On dissout dans 40 ml de chlorure de méthylène, comme précédemment, 9.0 g (0.03 mole) de dérivé N-carbobenzoxy de la DL-phénylalanine et 7.7 g (0.033 mole) d'ester benzylique de l'acide amino-1 cyclohexane carboxylique. On additionne ensuite 6.82 g (0.033 mole) de N,N′-dicyclohexylcarbodiimide. On obtient ainsi 13 g (84.4%) de N-carbobenzoxy DL-phénylalanyl-amino-1 cyclohexane carboxylate de benzyle. P.f. 115–117°. On recristallise avec de l'alcool et de l'éther de pétrole. P.f. 117–118°. On peut hydrogéner subséquemment sans recristalliser. Anal. Calc. pour $C_{31}H_{34}O_5N_2$: N, 5.44%. Trouvé: N, 5.43%.

*Ester benzylique du N-carbobenzoxy amino-1 cyclohexane carboxyl-*DL-*phénylalanine*

On dissout comme ci-haut, dans 60 ml de chlorure de méthylène, 13.86 g (0.05 mole) de dérivé N-carbobenzoxy de l'acide amino-1 cyclohexane carboxylique et 14.05 g (0.055 mole) d'ester benzylique de la DL-phénylalanine. On additionne ensuite 16.85 g (0.056 mole) de N,N′-dicyclohexylcarbodiimide. On obtient ainsi 19.5 g (75.5%) d'ester benzylique du N-carbobenzoxy amino-1 cyclohexane carboxyl-DL-phénylalanine. P.f. 105–106°. Ce produit peut être hydrogéné tel quel. Après deux recristallisations avec de l'alcool et de l'éther de pétrole, le produit fond à 102–103°. Anal. Calc. pour $C_{31}H_{34}O_5N_2$: N, 5.44%. Trouvé: N, 5.44%.

*Ester benzylique du N-carbobenzoxy amino-1 cyclopentane carboxyl-*DL-*phénylalanine*

On dissout comme ci-haut, dans 200 ml de chlorure de méthylène, 13.2 g (0.05 mole) de dérivé N-carbobenzoxy de l'acide amino-1 cyclopentane carboxylique et 14.05 g (0.055 mole) d'ester benzylique de la DL-phénylalanine. On additionne ensuite 11.4 g (0.055 mole) de N,N′-dicyclohexylcarbodiimide. Après 4 heures à la température de la chambre, on filtre une partie de l'urée formée qui pèse 5 g. On additionne au filtrat 5 ml d'acide acétique et on évapore à sec sous vide. On reprend le résidu par 300 ml de dioxane à 50°. On filtre la solution. Il reste un résidu insoluble de 7 g constitué en grande partie du reste de l'urée. On évapore le filtrat jusqu'à un volume de 100 ml et le produit cristallise au froid par addition d'un excès d'éther de pétrole. Le rendement brût de l'ester benzylique du N-carbobenzoxy amino-1 cyclopentane carboxyl-DL-phénylalanine est de 21 g (84%). Ce produit fond à 154–157° et peut être utilisé tel quel pour l'hydrogénation. Après deux recristallisations avec de l'alcool additionné de 50% d'acide acétique, il fond à 165–166°. Anal. Calc. pour $C_{30}H_{32}O_5N_2$: N, 5.59%. Trouvé: 5.52%.

Amino-1 cyclopentane carboxyl-glycine (I)

On dissout 8.21 g (0.02 mole) de N-carbobenzoxy amino-1 cyclopentane-carboxyl-glycinate de benzyle dans 200 ml d'un mélange égal d'alcool et d'acide acétique bouillant. On refroidit à la température de la chambre et on additionne environ 0.1 g de palladium à 10% sur du carbone. On effectue ensuite l'hydrogénation pendant 6 heures sous une pression de départ de 30 livres. Après avoir filtré le catalyseur on évapore à sec sous vide. On reprend le résidu avec 20 ml d'acétate d'éthyle chaud. On laisse refroidir 15 minutes et on filtre le dipeptide insoluble. L'amino-1 cyclopentane carboxyl-glycine est recristallisé avec de l'eau et de l'acétone. P.f. 277°. Rendement: 3.5 g (94.5%). Anal. Calc. pour $C_8H_{14}O_3N_2$: N, 15.05%. Trouvé: 15.00%.

Pour les autres hydrogénations, on procède de façon analogue.

Chlorhydrate de l'amino-1 cyclopentane carboxyl-glycine

On dissout 2 g (0.017 mole) d'amino-1 cyclopentane carboxyl-glycine dans 20 ml d'eau bouillante. On refroidit dans la glace avant d'ajouter 17.4 ml (0.017 mole) d'acide chlorhydrique 1 *N*. On évapore à sec sous vide et après trois recristallisations avec de l'alcool

Can. J. Chem. Downloaded from www.nrcresearchpress.com by 210.87.254.40 on 09/05/12
For personal use only.

et de l'acétone on obtient un produit qui fond à 214–215° (p.f. litt. 200°) (5). Anal. Calc. pour $C_8H_{14}O_3N_2$.HCl: N, 12.52%; Cl, 15.75%. Trouvé: N, 12.38%; Cl, 15.70%.

DL-*Phénylalanyl-acide amino-1 cyclopentane carboxylique (VI)*

On dissout 10.01 g (0.02 mole) de N-carbobenzoxy DL-phénylalanyl-amino-1 cyclopentane carboxylate de benzyle dans 250 ml d'une solution chaude d'acide acétique à 25% dans l'éthanol. On refroidit à la température de la chambre et on fait l'hydrogénation comme précédemment. Le DL-phénylalanyl-acide amino-1 cyclopentane carboxylique est recristallisé avec de l'éthanol aqueux à 50%. Rendement: 5.0 g (90.4%). P.f. 270–272° (p.f. litt. 268–270°) (5). Anal. Calc. pour $C_{15}H_{20}O_3N_2$: N, 10.12%. Trouvé: 10.08%.

Amino-1 cyclohexane carboxyl-DL-*phénylalanine (III)*

On fait une hydrogénation comme ci-haut sur une solution contenant 10.29 g (0.02 mole) d'ester benzylique de N-carbobenzoxy amino-1 cyclohexane carboxyl-DL-phénylalanine. L'amino-1 cyclohexane carboxyl-DL-phénylalanine obtenu est recristallisé en le suspendant dans un peu d'eau chaude et en ajoutant à chaud de l'éthanol jusqu'à dissolution complète puis en portant au froid. Rendement: 5 g (86.2%). P.f. 286°. Après une recristallisation le produit fond à 292°. Anal. Calc. pour $C_{16}H_{22}O_3N_2$: N, 9.63%. Trouvé: 9.61%.

Amino-1 cyclopentane carboxyl-DL-*phénylalanine (II)*

On dissout 5 g (0.01 mole) de N-carbobenzoxy de l'ester benzylique de l'amino-1 cyclopentane carboxyl-DL-phénylalanine dans 200 ml d'un mélange égal d'éthanol et d'acide acétique bouillant. Avant que la solution ne refroidisse et que le produit de départ ne cristallise, on procède immédiatement à l'hydrogénation comme précédemment. L'amino-1 cyclopentane carboxyl-DL-phénylalanine ainsi obtenu est recristallisé en le suspendant dans 20 ml d'alcool bouillant et en additionnant de l'eau jusqu'à dissolution complète et en portant au froid. P.f. 272–273°. Rendement: 2 g (72.1%). Après recristallisation le peptide fond à 273°. Anal. Calc. pour $C_{15}H_{20}O_3N_2$: N, 10.13%. Trouvé: N, 10.14%.

Le produit est très insoluble dans l'eau et dans l'alcool, mais il se dissout dans un mélange des deux à chaud.

Chlorhydrate du DL-*phénylalanyl-acide amino-1 cyclohexane carboxylique (VII)*

Cette hydrogénation est analogue aux précédentes. On dissout 10.3 g (0.02 mole) de N-carbobenzoxy DL-phénylalanyl-amino-1 cyclohexane carboxylate de benzyle dans 100 ml d'alcool additionné de 25 ml d'acide acétique et de 10 ml d'acide chlorhydrique 3 *N*. L'hydrogénation terminée, on évapore le solvant à sec sous vide, après avoir filtré le catalyseur. Le résidu est traité par 20 ml d'acétone. Après 10 minutes on filtre le chlorhydrate du DL-phénylalanyl-acide amino-1 cyclohexane carboxylique insoluble qui pèse 5.0 g (77%). Le produit est recristallisé deux fois avec du méthanol et de l'éther. P.f. 281–282°. Anal. Calc. pour $C_{16}H_{22}O_3N_2$.HCl: N, 8.57%; Cl, 10.85%. Trouvé: N, 8.45%; Cl, 10.50%.

N-Chloroacétyl-amino-1 cyclopentane carboxyl-DL-*phénylalanine*

On dissout 2.76 g (0.01 mole) d'amino-1 cyclopentane carboxyl-DL-phénylalanine dans 50 ml d'éthanol aqueux (20%) bouillant. On refroidit vitement, et avant que le peptide ne cristallise on additionne 2.5 ml (0.01 mole) d'hydroxyde de sodium 4 *N*. On évapore à sec sous vide à une température ne dépassant pas 30° et on dissout le résidu dans un peu d'eau. On fait ensuite le Schotten-Baumann avec 2.75 ml (0.011 mole) d'hydroxyde

Can. J. Chem. Downloaded from www.nrcresearchpress.com by 210.87.254.40 on 09/05/12
For personal use only.

de sodium 4 *N* et 1.24 g (0.011 mole) de chlorure de chloroacétyle. Rendement: 2.5 g (71%). Le produit est recristallisé avec de l'alcool et de l'éther de pétrole. P.f. 189–191°. Anal. Calc. pour $C_{17}H_{21}O_4N_2Cl$: N, 7.94%; Cl, 10.05%. Trouvé: N, 7.85%; Cl, 10.21%.

*N-Chloroacétyl-amino-1 cyclohexane carboxyl-*DL*-phénylalanine*

On dissout 2.90 g (0.01 mole) d'amino-1 cyclohexane carboxyl-DL-phénylalanine dans 2.5 ml (0.01 mole) d'hydroxyde de sodium 4 *N*. Les réactifs additionnés sont les suivants: 2.75 ml (0.011 mole) d'hydroxyde de sodium 4 *N* et 1.24 g (0.011 mole) de chlorure de chloroacétyle. Rendement: 3 g (81.8%). Le dérivé chloroacétylé est recristallisé avec de l'alcool et de l'éther de pétrole. P.f. 172°. Anal. Calc. pour $C_{18}H_{23}O_4N_2Cl$: N, 7.64%; Cl, 9.72%. Trouvé: N, 7.75%; Cl, 10.00%.

*Glycyl-amino-1 cyclopentane carboxyl-*DL*-phénylalanine (VIII)*

On traite comme précédemment, 2.0 g (0.057 mole) de N-chloroacétyl-amino-1 cyclopentane carboxyl-DL-phénylalanine par 200 ml d'ammoniaque concentrée. On obtient alors 1.2 g (63.1%) de glycyl-amino-1 cyclopentane carboxyl-DL-phénylalanine qui fond à 243–244°. Anal. Calc. pour $C_{17}H_{23}O_4N_3$: N, 12.60%. Trouvé: 12.55%.

*Glycyl-amino-1 cyclohexane carboxyl-*DL*-phénylalanine (IX)*

On ajoute 2.5 g (0.0068 mole) de N-chloroacétyl-amino-1 cyclohexane carboxyl-DL-phénylalanine à 200 ml d'ammoniaque concentrée, comme précédemment. On obtient 2.0 g (84%) de glycyl-amino-1 cyclohexane carboxyl-DL-phénylalanine. On recristallise le tripeptide avec de l'eau et de l'éthanol. Le produit prend un aspect vitreux à environ 155°, commence à se décomposer à 200° et fond à 202–204°. Anal. Calc. pour $C_{18}H_{25}O_4N_3$: N, 12.10%. Trouvé: 11.92%.

1,4-Diazaspiro [4.5]décanedione-2,5 (X)

On traite 8.0 g (0.043 mole) de glycyl-acide amino-1 cyclopentane carboxylique à 180° et sous un vide de 0.03–0.04 mm pendant 6 heures, dans une fiole conique à succion de 1000 ml. On dissout le produit dans 100 ml d'eau bouillante et on traite par environ 0.5 g de noir animal. La solution purifiée est ensuite évaporée à environ 60 ml. La dicétopipérazine cristallise au froid. Rendement: 6.0 g (81%). P.f. 275–277° (p.f. litt. 275–280°) (5). Anal. Calc. pour $C_8H_{12}O_2N_2$: C, 57.12%; H, 7.20%; N, 16.67%. Trouvé: C, 57.39%; H, 7.23%; N, 16.65%.

1,4-Diazaspiro[4.5]décanedione-2,5 (X)

On traite 8.0 g (0.043 mole) d'amino-1 cyclopentane carboxyl-glycine à 180° et sous un vide de 0.03–0.04 mm pendant 6 heures, dans une fiole conique à succion de 1000 ml. On décante le produit non sublimé, constitué du peptide non cyclisé, et on dissout le produit sublimé sur les parois dans 25 ml d'eau bouillante. On traite par un peu de noir animal et on évapore la solution purifiée à environ 10 ml. La dicétopipérazine cristallise à froid. Rendement: 1 g (13.5%). P.f. 276–277° (p.f. litt. 275–280°) (5). Anal. Calc. pour $C_8H_{12}O_2N_2$: C, 57.12%; H, 7.20%; N, 16.67%. Trouvé: C, 57.33%; H, 7.29%; N, 16.58%.

Hydrolyse du 1,4-diazaspiro[4.5]décanedione-2,5

On laisse bouillir à reflux pendant 48 heures 0.3 g (0.0018 mole) de 1,4-diazaspiro[4.5]-décanedione-2,5 en présence de 30 ml d'acide chlorhydrique 1 *N*. On prélève un aliquot de 1 ml à différents intervalles de temps, et on identifie par chromatographie les produits d'hydrolyse de ces différents échantillons. Les acides aminés et les peptides soumis à la chromatographie l'ont toujours été sous forme de chlorhydrates.

Can. J. Chem. Downloaded from www.nrcresearchpress.com by 210.87.254.40 on 09/05/12
For personal use only.

Le chromatogramme illustré par la figure 1 montre que la dicétopipérazine s'hydrolyse rapidement et qu'après 20 minutes, un lien peptidique est ouvert complètement. Mais après 10 minutes les deux peptides (I) et (IV) formés commencent à s'hydrolyser très lentement et ce n'est qu'après 48 heures qu'ils disparaissent complètement. Le système de solvants utilisé est le suivant: *n*-butanol (225), acide acétique (75) et eau (25). Les deux peptides ayant des R_f à peu près identiques dans ce système de solvants, on doit, pour les séparer convenablement, utiliser d'autres solvants. Dans un mélange de *s*-collidine (1 partie), de lutidine-2,4 (85%) (1 partie) et d'eau (2 parties), le glycyl-acide amino-1 cyclopentane carboxylique (IV) a un R_f de 0.22 et l'amino-1 cyclopentane carboxyl-glycine a un R_f de 0.35.

Cette dernière chromatographie n'est utilisée que pour l'aliquot de 5 minutes, identifiant ainsi les deux peptides et prouvant que l'hydrolyse coupe de façon non spécifique une des deux liaisons de la dicétopipérazine. Il ne semble pas que la formation d'un peptide soit favorisée plus que l'autre.

REMERCIEMENTS

Les auteurs sont très reconnaissants envers le Conseil National de Recherches pour une bourse accordée à l'un d'eux (P.T.), et envers l'Institut National du Cancer pour aide financière. Ils remercient de plus le Dr Léo Marion, directeur de la division de chimie du Conseil National de Recherches à Ottawa, pour l'analyse aux rayons-X de deux échantillons.

BIBLIOGRAPHIE

1. F. MARTEL et L. BERLINGUET. Can. J. Biochem. and Physiol. **37**, 433 (1959).
2. T. A. CONNORS, L. A. ELSON et W. C. J. ROSS. Biochem. Pharmacol. **1**, 239 (1958).
3. L. NICOLE et L. BERLINGUET. Résultats non publiés.
4. C. J. NOLL et C. N. HABECKER. M.Sc. Thesis. The Pennsylvania State University. August, 1958.
5. T. A. CONNORS et W. C. J. ROSS. J. Chem. Soc. 2124 (1960).
6. J. C. SHEEHAN et G. P. HESS. J. Am. Chem. Soc. **77**, 1067 (1955).
7. R. N. MACDONALD. U.S. Patent No. 2,560,584 (July, 1951).
8. H. K. MILLER et H. WAELSCH. J. Am. Chem. Soc. **74**, 1092 (1952).
9. C. J. NOLL et H. C. TILLSON. M.Sc. Thesis. The Pennsylvania State University. June, 1948.
10. A. GAGNON et L. BERLINGUET. Résultats non publiés.
11. H. N. RYDON et P. W. G. SMITH. Nature, **169**, 922 (1952).
12. M. LUDTKE. Z. physiol. Chem. Hoppe-Seyler's, **141**, 100 (1924).
13. P. A. LEVENE, R. E. STEIGER et L. W. BAS. J. Biol. Chem. **81**, 697 (1929); P. A. LEVENE, R. E. STEIGER, A. ROTHEN et M. OSAKI. J. Biol. Chem. **86**, 723 (1930).
14. M. BERGMANN et L. ZERVAS. Ber. **65**, 1192 (1932).
15. C. R. HARINGTON et R. H. MEAD. Biochem. J. **30**, 1598 (1936).

Can. J. Chem. Downloaded from www.nrcresearchpress.com by 210.87.254.40 on 09/05/12
For personal use only.

Can. J. Chem. Downloaded from www.nrcresearchpress.com by 210.87.254.5 on 09/05/12
For personal use only.

THE RADIO-FREQUENCY DIELECTRIC DISPERSION IN SOLID ETHYL STEARATE[1]

D. W. DAVIDSON

ABSTRACT

The dielectric properties of solid ethyl stearate were studied between −100° and the melting point at frequencies between 100 cycles/sec and 80 Mc/sec. The circular-arc locus lying within this frequency range in the β (tilted) form consists of a time-dependent and a time-independent part. It is more likely to arise from rotational disorder of tilted molecules than from regions of vertically stacked molecules. The width of the relaxation-time distribution function appears to decrease somewhat more rapidly with increasing temperature than would be expected for a temperature-independent distribution of heights of rotational-energy barriers.

In spite of the common occurrence of dielectric-relaxation effects in the solid forms of polar derivatives of long-chained aliphatic compounds (1) there remains considerable doubt about their origin. One such compound is ethyl stearate, for which a number of experimental studies (2–4) have been published. In the most recent report (4), the radio-frequency dispersion in the β form of ethyl stearate has been attributed to the presence of metastable regions of vertically stacked molecules.

The present report gives some recent results which bear on this question.

EXPERIMENTAL METHODS

Two samples of ethyl stearate were used: one (EK) was the Eastman Kodak White Label product, the other (PRL) a purified product provided by Dr. Burton M. Craig of the Prairie Regional Laboratory. Melting points determined by the capillary-tube method were 31.9 and 30.0° for the β and α forms of the EK sample and 33.1 and 30.7° for the corresponding forms of the PRL sample. The latter are in close agreement with the values of Smith (33.3 and 30.9°, respectively) (5).

Measurements were made at frequencies between 0.1 and 800 kc/sec with a capacitance bridge, and at frequencies between 80 and 80,000 kc/sec by the voltage-resonance method of Hartshorn and Ward (6). Measurements were made to below −100° with the bridge and to −35° with the Hartshorn–Ward apparatus. In the latter the micrometer head containing the sample was enclosed in a Lucite box through which cold air was circulated.

All solid samples were prepared by cooling the melts in the dielectric cells. For examination at low temperatures the samples were rapidly cooled so as to "freeze-in" a sufficient number of defects to ensure sufficient dispersion for accurate measurement.

RESULTS

In Fig. 1 the dielectric constant of the EK sample is plotted vs. temperature for two separate cycles, starting from the liquid, at cooling and heating rates of ca. 3° per hour. In the first cycle freezing into the α phase ($\epsilon = \sim 2.95$) was followed by conversion into the β phase, which was complete at 20°. The shape of the curve in the $\alpha \rightarrow \beta$ transformation region depends on the rate of cooling and on the purity of the sample, the transformation being more rapid for the PRL than for the EK sample. In the second

[1]*Manuscript received February 16, 1961.*
Contribution from the Division of Applied Chemistry, National Research Council, Ottawa, Canada.
Issued as N.R.C. No. 6289.

Can. J. Chem. Downloaded from www.nrcresearchpress.com by 210.87.254.5 on 09/05/12
For personal use only.

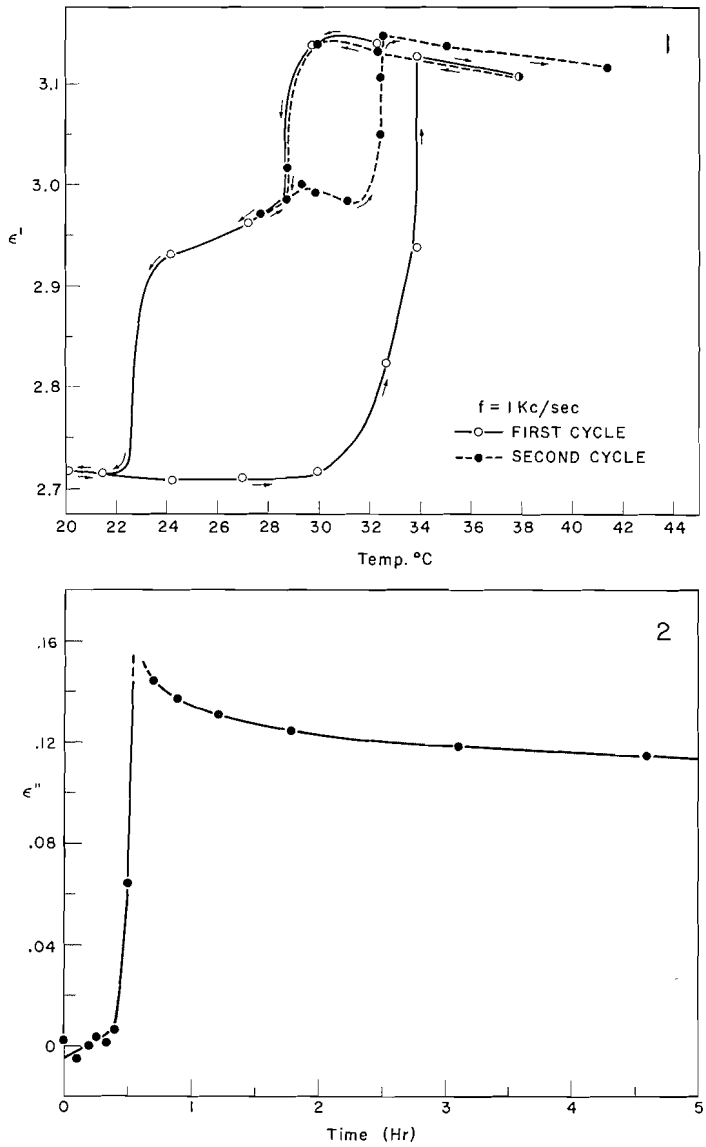


FIG. 1. Phase changes in ethyl stearate.
FIG. 2. Time dependence of ϵ'' at 15 Mc/sec and 24°, following freezing.

cycle the α form was melted before an appreciable amount of the β form had been formed. It is apparent that the melting point of the α form is lower by about 2° than that of the β form.

Figure 2 shows the dependence on time of the dielectric loss of the PRL sample at 24°, measured at a frequency near that of the loss maximum of the β form. The zero of time was taken at the first appearance of solid (α form) in the melt. At 24°, conversion to the β form starts within 30 minutes of freezing and is thereafter rapidly completed.

Typical complex plane loci for the PRL sample are illustrated in Fig. 3. Except for an upward turn at low frequencies (particularly marked for these rapidly cooled samples),

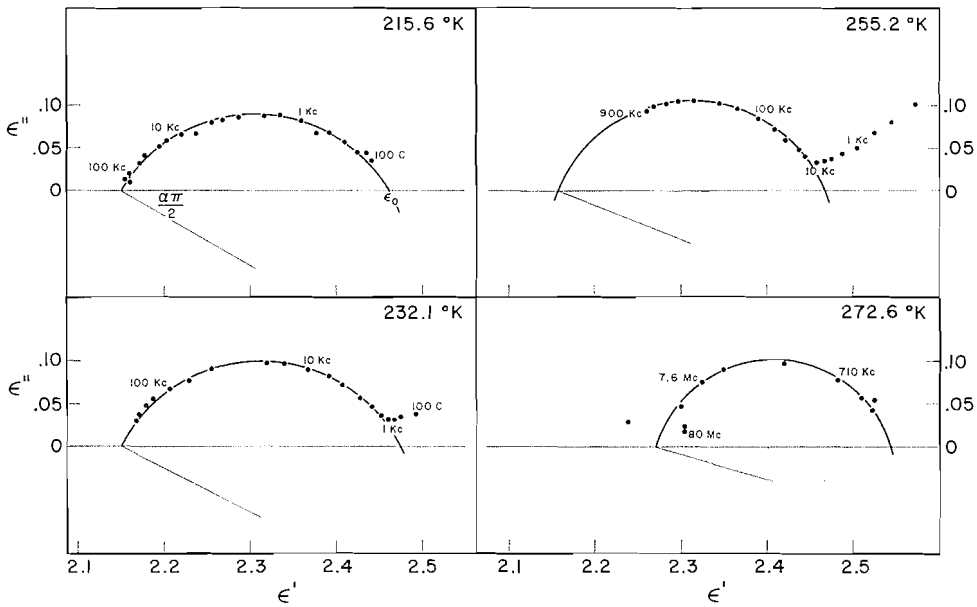


FIG. 3. Cole–Cole plots for β-phase ethyl stearate.

these loci are circular arcs, with centers below the real axis. Data obtained with the resonance device (like those shown at 272.6° K) give more uncertain arcs than bridge data. This arises primarily from the inaccuracy of the ϵ' values, as may be seen from the results shown in Fig. 4. Analysis of the resonance results was based on ϵ'' values alone.

Typical dielectric parameters are listed in Table I. For the bridge measurements,

TABLE I

Dielectric parameters of ethyl stearate (PRL sample)

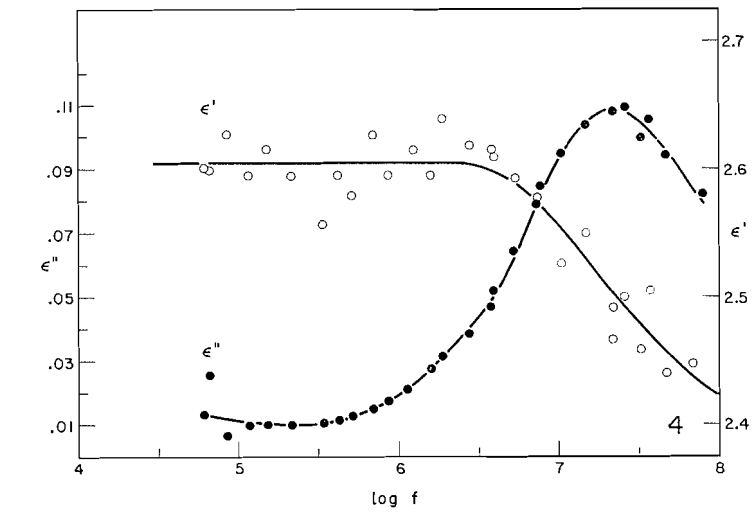
Phase	T (°K)	τ_0 (sec)	ϵ_0	$\Delta\epsilon$	α	ϵ''_{max}	Method
β	204.7	3.29×10^{-4}	2.517	.326	.37	.084	Bridge
	215.6	7.04×10^{-5}	2.461	.312	.34	.088	
	226.9	1.47×10^{-5}	2.469	.326	.31$_5$	.095	
	244.6	1.85×10^{-5}	2.486	.330	.29	.102	
	255.2	5.04×10^{-7}	2.467	.311	.25	.104	
	272.6	7.58×10^{-8}	~2.50	.27	~.21	.097	Resonance
	297.2	7.40×10^{-9}	~2.50*	.27*	~.12	.109*	
α			~2.95				
Liquid	301.4 (supercooled)		3.106				
	312.0		3.031				

*Sixteen hours after freezing.

ϵ_0 and ϵ_1 were the low- and high-frequency intercepts of the circular arcs with $\epsilon'' = 0$, and $\Delta\epsilon = \epsilon_0 - \epsilon_1$. The most probable relaxation time τ_0 and the distribution parameter α were determined from plots of $\log v/u$ vs. $\log f$, where $v^2 = (\epsilon_0-\epsilon')^2+(\epsilon'')^2$ and $u^2 = (\epsilon'-\epsilon_1)^2+(\epsilon'')^2$. For Cole–Cole arcs (7), $\log v/u = (1-\alpha)(\log f+\log 2\pi\tau_0)$. Figure 5 shows such a plot of the data at 215.6° K.

For the resonance data, $\Delta\epsilon$ was determined from the area of the ϵ'' vs. $\log f$ plot (8) and α from $\tan(1-\alpha)\pi/4 = 2\epsilon''_{max}/\Delta\epsilon$ (7).

Can. J. Chem. Downloaded from www.nrcresearchpress.com by 210.87.254.5 on 09/05/12
For personal use only.



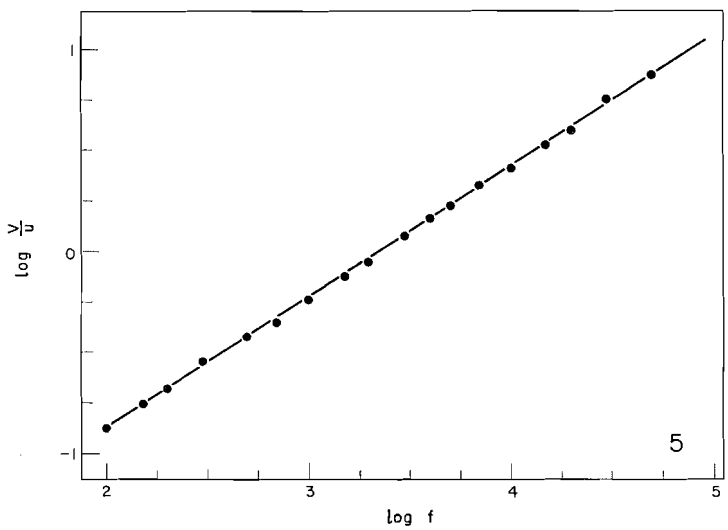


FIG. 4. β-Phase ethyl stearate at 24°.
FIG. 5. Method of determining τ_0 and α from bridge data.

The results given for bridge measurements in Table I refer to the same solid sample; no dependence on time was observed at these temperatures. The amplitude, but not the frequency characteristics, of the dispersion–absorption region varied considerably with the thermal history of the sample. At room temperature the magnitude of the dispersion decreased slowly with time, as is shown by the decay of the loss in Fig. 6. The decay was approximately exponential, with a time constant of some 24 hours. After several days the loss had fallen to about one half of its initial value and no further reduction was apparent.

The linear dependence of log τ_0 on $1/T$ (Fig. 7) formally gives an activation energy of 13.7 kcal/mole, in agreement with the value 13 kcal/mole reported by Dryden and Dasgupta (3) from measurements in the vicinity of room temperature and with the 12.7 kcal/mole value obtained by Broadhurst and Fitzgerald (4) for temperatures between ca. −80 and −30°.

Can. J. Chem. Downloaded from www.nrcresearchpress.com by 210.87.254.5 on 09/05/12
For personal use only.

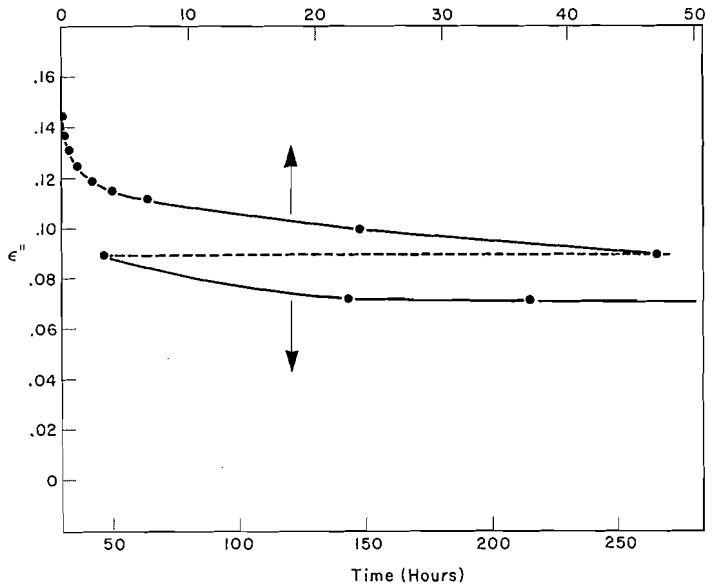


FIG. 6. Time dependence of ϵ'' of β-phase ethyl stearate at 24° and 15 Mc/sec.

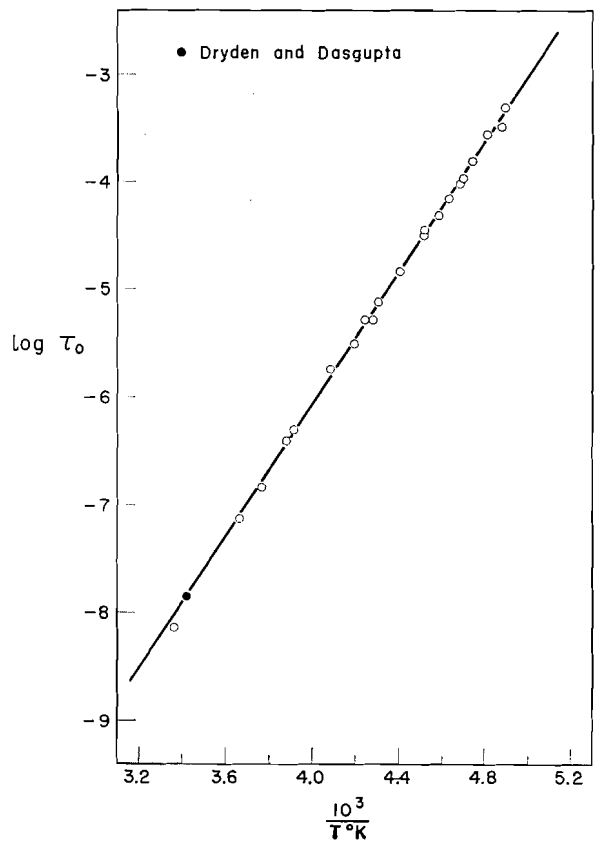


FIG. 7. Dependence of relaxation time on temperature.

Can. J. Chem. Downloaded from www.nrcresearchpress.com by 210.87.254.5 on 09/05/12
For personal use only.

Can. J. Chem. Downloaded from www.nrcresearchpress.com by 210.87.254.5 on 09/05/12
For personal use only.

DISCUSSION

Variation of Width of the Distribution Function of Relaxation Times with Temperature

Broadhurst and Fitzgerald reported (4) a value of 0.39 for the distribution parameter α, a value obtained from measurements at $-65°$ (private communication from Professor Fitzgerald). As is evident from Fig. 8, our results indicate that α decreases rapidly with

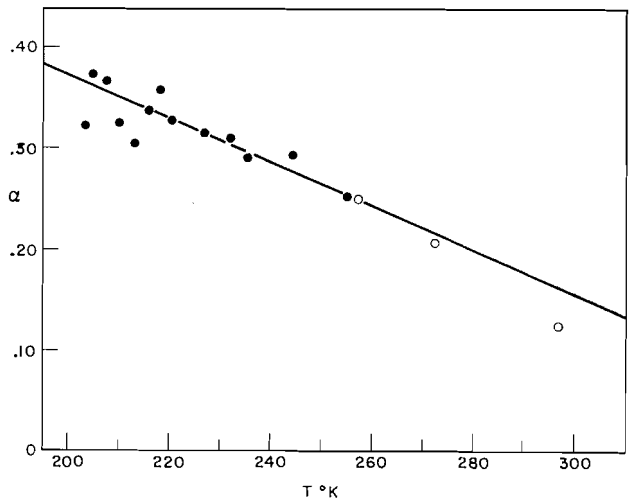


FIG. 8. Variation of α with temperature: ● bridge, ○ resonance measurements.

increasing temperature. Such a trend is to be expected from the presence of a finite distribution in heights of the energy barriers to orientation of dipoles. It is of interest to attempt to estimate quantitatively the temperature-dependence of α in such a case.

The distribution function (7) for relaxation times $G(s)ds$, where $s = \ln_e(\tau/\tau_0)$, may be replaced by a distribution in barrier heights B, where B is related to the relaxation time by $\tau/\tau_0 = \exp(B/T)$:

$$H(B)dB = \frac{\sin \alpha\pi}{2\pi T[\cosh (1-\alpha)B/T - \cos \alpha\pi]}\, dB.$$

If the distribution of barrier heights does not depend on temperature, the integral

$$\int_{-\infty}^{B} H(B)dB = 0.5 + \frac{1}{(1-\alpha)\pi} \tan^{-1}\left[\tanh \frac{(1-\alpha)B}{2T} \tan \frac{(1-\alpha)\pi}{2}\right]$$

is independent of temperature. If α is known at some temperature, α may then be computed for some other temperature for various assumed values of B. The value so obtained is found to be somewhat dependent on B, which implies that the assumption of a temperature-independent distribution of barrier heights is not strictly compatible with maintenance of the circular-arc locus as the temperature is changed. However, the variation of α with B is small for B's which contribute appreciably to the relaxation behavior.

It is evident from Table II that over-all values of α of 0.31 at 250° and 0.265 at 300° K lead to approximately the same integral distribution in B as that given by the experimental value of α (0.38) at 200° K. The experimental values of α (Fig. 8) decrease somewhat more rapidly than these "predicted" values. This suggests that the breadth of the barrier distribution function decreases as the temperature is raised.

TABLE II

Integrated distribution function $I(B) = \int_{-\infty}^{B} H(B)dB$

B	$\alpha = 0.38$, $T = 200°$	$\alpha = 0.31$, $T = 250°$	$\alpha = 0.265$, $T = 300°$
−2000	0.001	0.001	0.002
−1000	.022	.025	.029
− 600	.078	.081	.086
− 346	.179	.178	.182
− 200	.286	.283	.285
− 100	.386	.383	.384
0	.500	.500	.500

For positive values of B, $I(B) = 1 - I(-B)$.

It is worth noting that the range of barrier heights corresponding to the distribution of relaxation times is small in comparison with the actual magnitude of the barriers. Thus at 200° K half the relaxation occurs across barrier heights which lie within $BR = \pm 0.5$ kcal/mole of the 14 kcal/mole value of the most probable barrier height given by the energy of activation.

The variations with temperature of bridge values of $\Delta\epsilon$ and ϵ''_{max} for the same rapidly cooled sample are shown in Fig. 9. The fall in ϵ''_{max} with decreasing temperature, observed

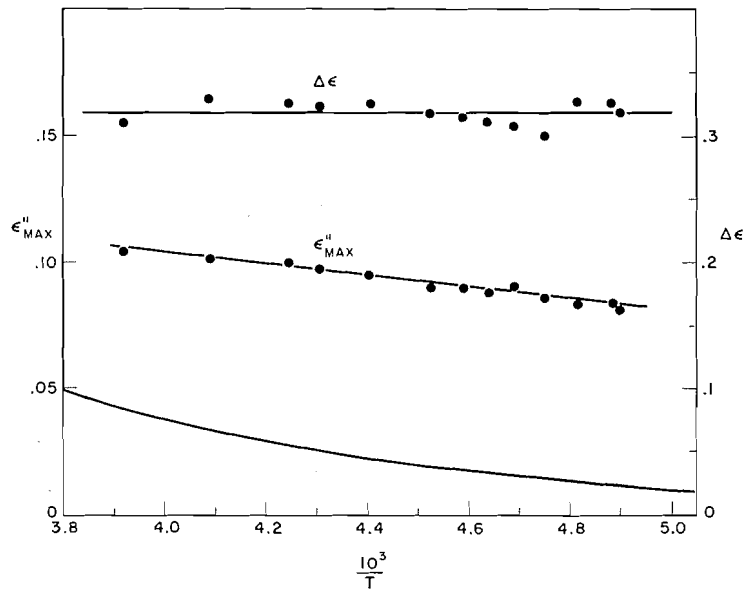


FIG. 9. Variations of ϵ''_{max} and $\Delta\epsilon$ with temperature.

also by Broadhurst and Fitzgerald, reflects the increase in α, since $\Delta\epsilon$ is approximately constant.

Origin of the Dispersion

There can be little doubt that the dispersion and absorption effects observed at radio frequencies are related to defects in the crystal structure. The amplitude of these effects, but neither the most probable relaxation time nor the width of the distribution of relaxation times, depends appreciably on the thermal history of the sample. Measurements in the vicinity of room temperature indicate that the amplitude of absorption ultimately

Can. J. Chem. Downloaded from www.nrcresearchpress.com by 210.87.254.5 on 09/05/12
For personal use only.

reaches a steady value, rather than falling to zero. This suggests that in general the absorption is the sum of two terms, one arising from the presence of defects intrinsic in the sample at the temperature of measurement, and the second from the presence of defects in excess of the "equilibrium" number by an amount which depends on the thermal history. At low temperatures the rate of disappearance of excess defects is so slow that they are effectively "frozen-in". The loss observed is then considerably higher than that corresponding to the "equilibrium" number of defects. In Fig. 9 the lowest curve is an extrapolation from higher temperatures of the equation for the equilibrium value of ϵ''_{max} reported by Dryden and Dasgupta (3). For a sample maintained several days at room temperature, however, our ϵ''_{max} agreed with the equilibrium value given by their equation (0.08) (but not with the value shown in their Fig. 1).

It is apparent that the dispersion cannot arise from the presence of regions of vertically stacked molecules of the type originally produced on freezing of the sample, since the latter phase shows no dispersion in this frequency range. The possibility has been considered (4) that a second vertical form may be responsible for the dispersion. This suggestion is not supported by a number of factors:

(1) The X-ray photographs of freshly frozen samples show (9) a single long spacing which is quite rapidly replaced completely by a second, somewhat shorter, long spacing. The size of the contribution of the dispersion to the static dielectric constant (0.2 to 0.4 or more at room temperature) is an appreciable fraction of the contribution of the rotating dipoles in the liquid state (0.8 to 0.9, extrapolated to room temperature). This seems to indicate that an appreciable fraction (of the order of one third) of the molecules in the β phase at room temperature are capable of contributing to the polarization, despite the X-ray evidence for the absence of a vertical form. This does not necessarily imply that, according to the model of vertical packing, about one third of the molecules need exhibit vertical packing, since one defect might affect the ability of several molecules to orient. However, the case in which the effective defect population is least, that of single, or small groups of, defect molecules, is precisely the case which is least attractive thermodynamically for defects which consist of molecules whose long axes are considerably inclined to the long axes of neighboring molecules.

(2) It appears unlikely that parts of the sample can remain indefinitely frozen into a vertical structure, when a good part of the dispersion disappears at a finite rate.

(3) Broadhurst and Fitzgerald (4) found that the dispersion shown by the solidified form of a 10% solution of ethyl stearate in heneicosane was similar to that shown by pure ester, except for the magnitude of the dispersion, which was only about 10% as great. These workers have inferred, since heneicosane exists only in vertical modifications, that ethyl stearate in the solid solution occurs in a vertical form. However, the effect of the ester on the crystal form of the hydrocarbon is not known. Moreover, one should have expected the dispersion, per ethyl stearate molecule, to be much greater in the solution (where all the molecules are vertically packed) than in the pure ester (where groups of vertically packed molecules constitute defects in a tilted form).

Perhaps the most satisfactory model is one which takes the defects to consist of molecules whose carbon chains lie in planes which make appreciable angles with the planes of neighboring molecules, that is, which have been considerably rotated about their long axes from their most stable positions. Positions of relative stability would occur at angles of rotation determined by the crystalline field but separated from coplanarity with neighboring molecules by a high rotational barrier. Dryden and Meakins (1) suggest that positions of relative stability exist for angles of rotation of about 90°.

Can. J. Chem. Downloaded from www.nrcresearchpress.com by 210.87.254.5 on 09/05/12
For personal use only.

Considerable uncertainty about the nature of the dispersion process remains. A vertical-type defect is not definitely excluded. It is possible that a detailed X-ray or wide-band nuclear magnetic resonance study would prove useful.

Interfacial polarization in the microcrystalline solid is probably responsible for the low-frequency effects (see Fig. 3), which seem to depend even more on rate of cooling than does the radio-frequency dispersion.

ACKNOWLEDGMENTS

The author is indebted to Dr. Burton M. Craig of the Prairie Regional Laboratory, Saskatoon, for a sample of ethyl stearate and to Professor E. R. Fitzgerald for helpful correspondence.

REFERENCES

1. J. S. DRYDEN and R. J. MEAKINS. Revs. Pure and Appl. Chem. (Australia), **7**, 15 (1957).
2. W. O. BAKER and C. P. SMYTH. J. Am. Chem. Soc. **60**, 1229 (1938).
3. J. S. DRYDEN and S. DASGUPTA. Trans. Faraday Soc. **51**, 1661 (1955).
4. M. G. BROADHURST and E. R. FITZGERALD. J. Chem. Phys. **33**, 210 (1960). M. G. BROADHURST. J. Chem. Phys. **33**, 221 (1960).
5. J. C. SMITH. J. Chem. Soc. 802 (1931).
6. L. HARTSHORN and W. H. WARD. J. Inst. Elec. Engrs. **79**, 597 (1936).
7. K. S. COLE and R. H. COLE. J. Chem. Phys. **9**, 341 (1941).
8. C. J. F. BÖTTCHER. Theory of electric polarisation. Elsevier Publishing Co., New York. 1952. p. 367.
9. T. MALKIN. J. Chem. Soc. 2796 (1931).

Can. J. Chem. Downloaded from www.nrcresearchpress.com by 210.87.254.5 on 09/05/12
For personal use only.

Can. J. Chem. Downloaded from www.nrcresearchpress.com by 210.87.254.6 on 09/05/12
For personal use only.

A NEW QUATERNARY APORPHINE FROM FAGARA TINGUASSOIBA HOEHNE[1]

N. V. RIGGS,[2] L. ANTONACCIO,[3] AND LÉO MARION

ABSTRACT

An alkaloid isolated as picrate from *Fagara tinguassoiba* gives rise on methylation to a derivative of glaucine. It has been shown to be the 6-hydroxy-2,3,5-trimethoxy-N,N-dimethylaporphinium ion.

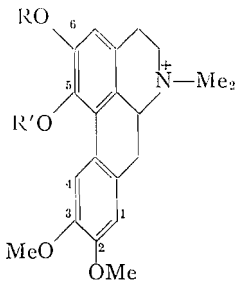
An extract of the bark of the Brazilian plant, *Fagara tinguassoiba* Hoehne, has yielded an alkaloid which has been isolated as a picrate. We have been able to investigate the structure of this alkaloid and are now reporting our results.

Passage of a solution of the crude picrate through a strong base ion-exchange resin gave a water-soluble base, $C_{21}H_{27}O_5N$, converted by hydriodic or hydrochloric acid into the corresponding halide, $C_{21}H_{26}O_4NX$, containing three methoxyl groups. The ultraviolet absorption spectra of the base and chloride in the absence of added alkali were nearly identical and resembled closely that of glaucine. The presence in the chloride of the fourth oxygen atom as a phenolic hydroxyl group was suggested by the large displacement to longer wavelength in its spectrum on addition of alkali; in agreement, a monoacetate was formed on gentle acetylation. The alkaloid was apparently a phenolic quaternary aporphine, probably oxygenated in positions 2, 3, 5, and 6, since oxygenation in positions 3, 4, 5, and 6 leads to light absorption of much lower intensity in the vicinity of 300 mμ than that observed in the present case (1, 2).

N-Methylisocorydine, a quaternary representative of the latter oxygenation class, has been isolated from *Fagara coca* (3), and from Australian *Zanthoxylum* species (4, 5), but its picrate has a much higher melting point, and its chloride a much greater optical rotation than the melting point and rotation of the corresponding derivatives of the *F. tinguassoiba* alkaloid. Confirmation of the suggested oxygenation pattern in the present case was obtained by O-methylation of the iodide to give a product which by m.p., mixed m.p., infrared spectra, and X-ray powder diagrams proved identical with N-methylglaucinium (I*a*) iodide. Two-stage Hofmann degradation of the O-methylated chloride gave 3,4,6,7-tetramethoxy-1-vinylphenanthrene (II*a*) (but see Experimental section).

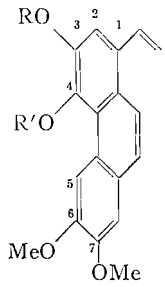
The phenolic hydroxyl group of the parent substance was not in position 5, since the product of O-ethylation of the phenolic quaternary iodide differed from O-ethyl-N-methylglaucentrinium (I*b*) iodide (6). A generous sample of the latter was kindly provided by Dr. R. H. F. Manske, but unfortunately the so-far unknown vinyl derivative II*b* of the two-stage Hofmann degradation polymerized during evaporation of its ethereal solution so that it could not be compared with the ethoxytrimethoxyvinylphenanthrene

[1]*Manuscript received March 15, 1961.*
Contribution from the Division of Pure Chemistry, National Research Council, Ottawa, Canada.
Issued as N.R.C. No. 6299.
[2]*National Research Council of Canada Postdoctorate Fellow. Present address: Department of Organic Chemistry, University of New England, Armidale, N.S.W., Australia.*
[3]*Instituto Nacional de tecnologia, Rio de Janeiro, Brazil.*



I

Ia: R = R′ = Me
Ib: R = Me, R′ = Et
Ic: R = H, R′ = Me
Id: R = Ac, R′ = Me
Ie: R = Et, R′ = Me



II

IIa: R = R′ = Me
IIb: R = Me, R′ = Et
IIc: R = Et, R′ = Me

obtained from our alkaloid.[4] This last degradation product from our alkaloid was, however, different from the known 6-ethoxy-3,4,7-trimethoxy- and 7-ethoxy-3,4,6-trimethoxy-1-vinylphenanthrene (7). It was oxidized to an acid which must be 3-ethoxy-4,6,7-trimethoxyphenanthrene carboxylic acid. Elimination of trimethylamine in the second stage of the Hofmann degradation incidentally showed the presence of an N,N-dimethyl group in the parent alkaloid; it is difficult to understand why exhaustive Herzig–Meyer analysis of the phenolic quaternary chloride gave a value close to that for only one N-methyl group, whereas a value close to the theoretical for two N-methyl groups was obtained with N-methylisocorydinium chloride (3).

The quaternary alkaloid isolated as picrate from *F. tinguassoiba* is therefore the 6-hydroxy-2,3,5-trimethoxy-N,N-dimethylaporphinium (Ic) ion.

EXPERIMENTAL

All melting points were taken on a hot-stage under a microscope. The ultraviolet absorption spectra were determined in 95% ethanol on a Carey Model 11 recording spectrophotometer. Infrared absorption spectra were measured on a Perkin–Elmer double-beam Model 21 spectrophotometer equipped with sodium chloride optics, and in Nujol mulls. Except as otherwise noted, samples for analysis were dried in a vacuum at 100° for up to 20 hours.

Isolation of the Alkaloid

The ground bark of *F. tinguassoiba* Hoehne (2K) was extracted with ethanol, the extract evaporated to a small bulk, acidified to Congo red with hydrochloric acid, and washed with ether. The residual viscous solution left after extraction with ether was diluted with water, alkalized with sodium hydroxide, and extracted with chloroform. The aqueous alkaline solution was acidified with hydrochloric acid and treated with mercuric chloride. The precipitated complex was filtered, and the regenerated base isolated as the crystalline picrate, wt. 55.3 g. The picrate was recrystallized from a large volume of ethanol from which it separated as yellow needles, m.p. 118–124°, which

[4]*Some polymerization of the vinylphenanthrene from authentic glaucine methiodide also occurred, but none was observed when Hofmann degradation of the O-alkylated chlorides was carried through to the vinylphenanthrenes without purification of the intermediates; some occurred, however, when purified O-ethylated iodide was degraded. It is possible that polymerization, perhaps initiated by traces of peroxide in the ether used for extraction, is inhibited by phenolic material that escapes alkylation and is extracted in trace amounts from the alkaline solutions.*

Can. J. Chem. Downloaded from www.nrcresearchpress.com by 210.87.254.6 on 09/05/12
For personal use only.

browned and became sticky on being dried at 100°. For analysis the picrate was dried at 56° at 0.5 mm for 20 hours. Found: C, 55.51; H, 5.39; N, 8.92. Calc. for $C_{21}H_{26}O_4N.C_6H_2O_7N_3.C_2H_5OH$: C, 55.25; H, 5.46; N, 8.89%. This product or the original picrate formed prisms from aqueous acetone, m.p. 146–151°. Found (after drying at 80° at 0.5 mm for 20 hours): C, 55.29; H, 5.06; N, 9.30. Calc. for $C_{21}H_{26}O_4N.C_6H_2O_7N_3$: C, 55.47; H, 4.83; N, 9.59%. N-Methylisocorydinium picrate has m.p. 202–204° (3).

6-Hydroxy-2,3,5-trimethoxy-N,N-dimethylaporphinium (Ic) Hydroxide

A solution of the picrate (2 g) in a mixture of acetone (80 ml) and methanol (20 ml) was passed down a column of Amberlite IRA 400 (OH) (16 g), the deep red band formed extending nearly to the bottom of the column. The darkening eluate was rapidly evaporated to dryness at 60° under reduced pressure. The crystalline residue was readily soluble in water, methanol, or ethanol. Addition of several volumes of acetone to the ethanolic solution caused separation of long needles which were promptly filtered, washed with acetone, and dried overnight in a vacuum desiccator over potassium hydroxide pellets and concentrated sulphuric acid. The dried product melted at ca. 120° (decomp.). Found: C, 67.03; H, 7.53; N, 3.62. Calc. for $C_{21}H_{27}O_5N$: C, 67.54; H, 7.23; N, 3.75%. Ultraviolet spectrum: λ_{max} 228 mμ, log ε 4.57; λ_{max} 270 mμ (sh), log ε 4.00; λ_{max} 281 mμ, log ε 4.10; λ_{max} 307 mμ, log ε 4.18; λ_{max} 321 mμ (sh), log ε 4.04. The base darkened on being kept, and discolored rapidly in ethanol solution. If the eluate from the column, or a suspension of the product in acetone were kept for several hours, the mixture became dark brown, presumably owing to condensation of the acetone in the presence of the strong quaternary base, and little or no crystalline product could be obtained. The sparing solubility of the picrate in any other of the common volatile solvents required the use of acetone containing some water or methanol on the ion-exchange column. (No exchange occurred with acetone alone as solvent.) Satisfactory results were obtained as described in the following sections.

6-Hydroxy-2,3,5-trimethoxy-N,N-dimethylaporphinium (Ic) Iodide

The eluate from the column was run directly into a slight excess of hydriodic acid diluted with methanol. The brownish eluate was evaporated to a gum which crystallized on treatment with warm methanol and ether. Recrystallization from acetone–methanol–ether gave buff-colored leaves, m.p. 226–229° (decomp.). Found: C, 52.04; H, 5.54; I, 26.40; OCH_3, 18.61. Calc. for $C_{21}H_{26}O_4NI$: C, 52.17; H, 5.42; I, 26.25; $3OCH_3$, 19.26%.

6-Hydroxy-2,3,5-trimethoxy-N,N-dimethylaporphinium (Ic) Chloride

The eluate from the column was run directly into a slight excess of hydrochloric acid. The eluate remained practically colorless for several hours. Evaporation to dryness as above and recrystallization of the residue from methanol–acetone gave the chloride as long colorless needles, m.p. 215–219° (decomp.), $[\alpha]_D^{25}$ +30.2° (*c*, 2.16 in water). Found: C, 63.73; H, 6.95; OCH_3, 23.59; (N).CH_3, 3.57. Calc. for $C_{21}H_{26}O_4NCl$: C, 64.35; H, 6.69; $3OCH_3$, 23.74; 1(N).CH_3, 3.83%. Ultraviolet absorption (in neutral 95% ethanol): λ_{max} 228 mμ, log ε 4.60; λ_{max} 271 mμ (sh), log ε 4.02; λ_{max} 281 mμ, log ε 4.12; λ_{max} 307 mμ, log ε 4.21; λ_{max} 321 mμ (sh), log ε 4.06. (In 0.3 *N* sodium hydroxide in 95% ethanol): very strong below 230 mμ, λ_{max} 250 mμ (sh), log ε 4.40; λ_{max} 265–270 mμ (sh), log ε 4.29; λ_{max} 347 mμ, log ε 4.19.

N-Methylisocorydinium chloride has m.p. 217–218° (decomp.) on slow heating, and $[\alpha]_D^{30}$ +169° (*c*, 0.22 in water) (3).

Can. J. Chem. Downloaded from www.nrcresearchpress.com by 210.87.254.6 on 09/05/12
For personal use only.

6-Acetoxy-2,3,5-trimethoxy-N,N-dimethylaporphinium (Id) Chloride

A sample (128 mg) of the above product was warmed with acetic anhydride (2 ml) and pyridine (0.25 ml) for 1 hour. Evaporation to dryness on the steam bath under reduced pressure, and recrystallization of the residue from methanol–acetone–ether gave small prisms, m.p. 234–238°. Found: C, 63.47; H, 6.39. Calc. for $C_{23}H_{28}O_5NCl$: C, 63.66; H, 6.54%.

2,3,5,6-Tetramethoxy-N,N-dimethylaporphinium (Ia) Iodide

A solution of the iodide of I*c* in ice-cold methanol was treated with an excess of ethereal diazomethane for 24 hours, gas evolution ceasing after 6 hours. More ethereal diazomethane was added and after 24 hours the yellow mixture was evaporated under reduced pressure to a brown gum. Treatment with methanol and ether gave a heavy brown oil, and nearly colorless needles appeared in the supernatant liquor. Recrystallization from methanol–ether gave needles softening in the range 200–210° then melting sharply at 216–217° to a dark brown liquid. Glaucine methiodide (prepared from an authentic sample of glaucine provided by Dr. R. H. F. Manske) and a mixture of the two specimens behaved identically on the hot-stage. Debye–Scherer diagrams of the two were identical and the infrared absorption spectra in Nujol mulls of glaucine methiodide and the product were superimposable.

3,4,6,7-Tetramethoxy-1-vinylphenanthrene (IIa)

A solution of the chloride of I*c* (1.00 g) in ice-cold methanol (20 ml) was treated with an excess of ethereal diazomethane (from 3.0 g N-nitrosomethylurea). After 18 hours the reaction mixture was evaporated to a syrup which was dissolved in methanol (10 ml) and heated on the steam bath with 10% aqueous sodium hydroxide (10 ml) for 1 hour in an open flask. The cooled aqueous residue was extracted with ether, heated again for 1 hour, and after being cooled extracted once more with ether. The combined ether extract on evaporation yielded a resinous methine base (380 mg) which was converted to the methiodide and treated as above with aqueous methanolic sodium hydroxide. The product (234 mg) formed plates, m.p. 141–143°, from methanol. Found: C, 73.94; H, 5.98. Calc. for $C_{20}H_{20}O_4$: C, 73.98; H, 6.22%. It was apparently identical (mixed m.p. and infrared spectrum) with a sample of 3,4,6,7-tetramethoxy-1-vinylphenanthrene (II*a*) obtained by similar two-stage Hofmann degradation of N-methylglaucinium iodide, but the Debye–Scherer diagrams of the two were not identical. The latter result may arise from a difference in crystal form, but repeated attempts to purify the reference sample by chromatography and recrystallization have given material contaminated by a persistent flocculent impurity, possibly polymerized compound. The product from the new alkaloid was oxidized by potassium permanganate in acetone solution to a carboxylic acid, m.p. 207–215°, after crystallization from aqueous methanol, and m.p. 220–223°, after recrystallization from benzene–hexane.

Barger and Silberschmidt (8) report for 3,4,6,7-tetramethoxy-1-vinylphenanthrene, m.p. 142°, and for the corresponding 1-carboxylic acid recrystallized from aqueous acetone or benzene–ligroin, m.p. 215°. The small quantity of our product did not crystallize well from aqueous acetone.

6-Ethoxy-2,3,5-trimethoxy-N,N-dimethylaporphinium (Ie) Iodide

A solution of the iodide of I*c* (1.00 g) in ice-cold ethanol (50 ml) was treated with an excess of ethereal diazoethane (from 1.5 g N-nitrosoethylurea) for 24 hours. The same quantity of ethereal diazoethane was then added and after 24 hours the mixture was

Can. J. Chem. Downloaded from www.nrcresearchpress.com by 210.87.254.6 on 09/05/12
For personal use only.

evaporated to dryness under reduced pressure. Twice crystallized from methanol–ether the residue formed colorless silky needles, m.p. 216–220° (decomp.), readily soluble in chloroform. Found: C, 54.10; H, 6.04; I, 24.71; OR (calc. as OCH_3), 23.94. Calc. for $C_{23}H_{30}O_4NI$: C, 54.04; H, 5.91; I, 24.81; 4×OR (calc. as OCH_3), 24.27%.

The product was different from O-ethyl-N-methylglaucentrinium (I*b*) iodide. Part of a sample of the latter provided by Dr. R. H. F. Manske was twice recrystallized from methanol–ether, and formed prisms, m.p. 205–207°, and was sparingly soluble in chloroform. It was also obtained in needles having a Debye–Scherer diagram identical with that of the prisms, and different from that of the above product.

3-Ethoxy-4,6,7-trimethoxy-1-vinylphenanthrene (IIc)

The iodide of I*e* was degraded with aqueous methanolic sodium hydroxide in two stages as in the preparation of 3,4,6,7-tetramethoxy-1-vinylphenanthrene (II*a*) to give some amorphous material, sparingly soluble in ether, together with a product extracted by ether and forming plates, m.p. 106–108°, from methanol. Similar degradation of the syrupy product of ethylation with ethereal diazomethane of the chloride of I*c* gave little amorphous material. The main product was extracted by ether. The extract was washed thoroughly with aqueous sodium hydroxide, dried, and chromatographed on basic alumina. The eluate yielded leaves, m.p. 106–108°, undepressed in admixture with the above vinyl derivative obtained from the iodide. Found: C, 73.92; H, 6.36; OR (calc. as OCH_3), 36.32. Calc. for $C_{21}H_{22}O_4$: C, 74.53; H, 6.56; 4×OR (calc. as OCH_3), 36.68%.

6-Ethoxy-3,4,7-trimethoxy-1-vinylphenanthrene has m.p. 141°, and 7-ethoxy-3,4,6-trimethoxy-1-vinylphenanthrene has m.p. 142°; these melting points are depressed on admixture of the compounds with one another or with 3,4,6,7-tetramethoxy-1-vinylphenanthrene, m.p. 142° (7).

The vapors of the second stage of the degradation were collected in methanolic picric acid. Evaporation of the solution to dryness and crystallization of the residue from ethyl acetate – ether gave yellow needles, m.p. 214–216°. (The recorded melting point for trimethylamine picrate is 216°.)

Similar degradation of O-ethyl-N-methylglaucentrinium (I*b*) iodide gave a product which at first crystallized on evaporation of its ethereal solution. Addition of a later extract and evaporation left an amorphous product which failed to crystallize from methanol and reduced potassium permanganate very slowly in acetone solution; a crystalline acidic product was not obtained from the oxidation mixture.

3-Ethoxy-4,6,7-trimethoxyphenanthrene-1-carboxylic Acid

The vinylphenanthrene (II*c*) (210 mg) in pure acetone (20 ml) at room temperature was oxidized with a saturated solution of potassium permanganate in pure acetone, added in portions (1 ml) until the color persisted for 30 minutes. The acidic product was obtained by addition of water and sulphur dioxide, evaporation of the acetone, and extraction into ether. The extract was washed with aqueous sodium hydrogen carbonate, dried, and chromatographed on silica. The eluate on evaporation left a residue which crystallized from a large volume of aqueous acetone as fawn needles, m.p. 196–198°. Found: C, 67.47; H, 5.49; OR (calc. as OCH_3), 34.75. Calc. for $C_{20}H_{20}O_6$: C, 67.40; H, 5.66; 4×OR (calc. as OCH_3), 34.82%. Prismatic needles of the same melting point, but retaining tenaciously a trace of orange coloring matter, were obtained from more concentrated solutions in aqueous acetone, and gels formed when solutions in hot benzene were cooled, with or without addition of hexane.

Can. J. Chem. Downloaded from www.nrcresearchpress.com by 210.87.254.6 on 09/05/12
For personal use only.

7-Ethoxy-3,4,6-trimethoxyphenanthrene-1-carboxylic acid has m.p. 213° (unsharp) when crystallized from acetone (7), or m.p. 222–223° when crystallized from benzene (9).

ACKNOWLEDGMENTS

We wish to thank Dr. R. H. F. Manske, Dominion Rubber Company, Guelph, Ontario, for providing generous samples of O-ethyl-N-methylglaucentrinium iodide and glaucine for comparison or degradation to reference compounds. Our indebtedness is also acknowledged to Dr. M. Przybylska for preparing the Debye–Scherer diagrams, to Mr. R. Lauzon for the infrared spectra, and Mr. M. Lesage for the ultraviolet spectra.

REFERENCES

1. L. KITASATO. Acta Phytochim. (Japan), **3**, 175 (1927).
2. A. GIRARDET. J. Chem. Soc. 2630 (1931).
3. J. COMIN and V. DEULOFEU. J. Org. Chem. **19**, 1774 (1954).
4. J. R. CANNON, G. K. HUGHES, E. RITCHIE, and W. C. TAYLOR. Australian J. Chem. **6**, 86 (1953).
5. R. G. COOKE and H. F. HAYNES. Australian J. Chem. **7**, 99 (1954).
6. R. H. F. MANSKE, E. H. CHARLESWORTH, and W. R. ASHFORD. J. Am. Chem. Soc. **73**, 3751 (1951).
7. G. BARGER, J. EISENBRAND, and L. EISENBRAND. Ber. **66**, 450 (1933).
8. G. BARGER and R. SILBERSCHMIDT. J. Chem. Soc. 2919 (1928).
9. E. SPÄTH and K. THARRER. Ber. **66**, 583 (1933).

Can. J. Chem. Downloaded from www.nrcresearchpress.com by 210.87.254.6 on 09/05/12
For personal use only.

Can. J. Chem. Downloaded from www.nrcresearchpress.com by 210.87.254.42 on 09/05/12
For personal use only.

IMIDAZOLE SULPHONAMIDES AND RELATED COMPOUNDS[1]

M. H. Fisher, W. H. Nicholson, and R. S. Stuart

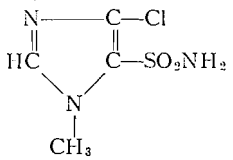
ABSTRACT

The preparations of a number of imidazole sulphonamides and related compounds are described.

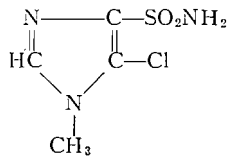
INTRODUCTION

The interest in heterocyclic sulphonamides as diuretic agents (1) prompted us to prepare a number of imidazole sulphonamides and related compounds for investigation. The syntheses of those compounds which have not been previously reported are described in this communication.

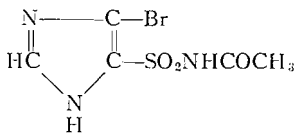
4-Chloro-1-methylimidazole (2) and 5-chloro-1-methylimidazole (3) were chlorosulphonated with chlorosulphonic acid and the sulphonyl chlorides were converted into the sulphonamides (I) and (II) with concentrated ammonia. 4(5)-Bromo-5(4)-sulphamylimidazole (4) was converted into the acetylsulphonamide (III) with acetic anhydride, in the usual way.



(I)



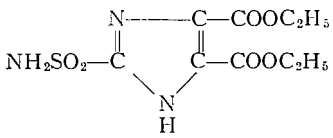
(II)



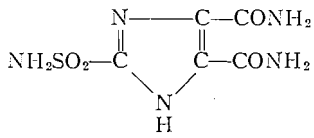
(III)

The halo compounds could not be converted into amines by treatment with alcoholic ammonia at an elevated temperature in a sealed tube. Bennett and Baker (4) showed similar inertness of the bromine atom in 4(5)-bromo-5(4)-sulphamylimidazole.

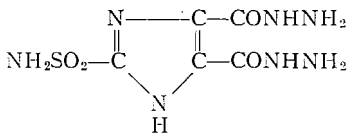
4,5-Bis(ethoxycarbonyl)-2-mercaptoimidazole (5) was converted into the sulphonyl chloride by oxidative chlorination in dilute hydrochloric acid. A brief treatment with concentrated ammonia gave the sulphonamide (IV). This ester on standing in concentrated ammonia or hydrazine for several hours was converted into the diamide (V) and the dihydrazide (VI).



(IV)



(V)



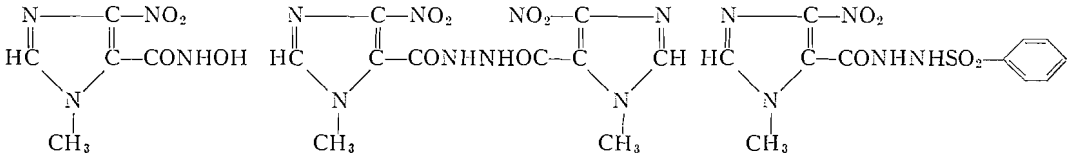
(VI)

Attempted conversion of the diamide into a xanthine with alkaline hypobromite (6) was unsuccessful. The dihydrazide with dilute hydrochloric acid gave a substance of undetermined structure rather than the expected dihydroxypyridazine (7).

The acid chloride of 5-carboxy-1-methyl-4-nitroimidazole (8) with hydroxylamine gave the expected hydroxamic acid (VII). However, with hydrazine under a variety of

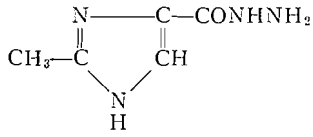
[1]*Manuscript received February 10, 1961.*
Contribution from the Research Department, Merck Sharp & Dohme of Canada Limited, Montreal, Que.

conditions only the 1,2-disubstituted hydrazine (VIII) could be isolated. Reaction with benzenesulphonylhydrazine gave the normal benzenesulphonylhydrazide (IX).



(VII) (VIII) (IX)

4(5)-Ethoxycarbonyl-2-methylimidazole (9) refluxed with hydrazine in methanol gave the hydrazide (X).



(X)

EXPERIMENTAL

4-Chloro-1-methyl-5-sulphamylimidazole (I)

4-Chloro-1-methylimidazole (8 g) dissolved in chlorosulphonic acid (48 ml) was refluxed for 2 hours. The solution was cooled and poured on to ice. The sulphonyl chloride was collected, washed with a little water, and dissolved in concentrated ammonia. After 15 minutes the excess of ammonia was evaporated and the solution was acidified with hydrochloric acid. The product was collected and crystallized from water as white needles (2.1 g), m.p. 164–165°. Found: C, 24.5; H, 3.22; N, 21.4; S, 16.4. Calc. for $C_4H_6ClN_3O_2S$: C, 24.6; H, 3.07; N, 21.5; S, 16.4%.

5-Chloro-1-methyl-4-sulphamylimidazole (II)

This compound was prepared from 5-chloro-1-methylimidazole (12 g) in a similar manner. Recrystallization from water gave white needles (5.4 g), m.p. 188–189°. Found: C, 24.9; H, 3.24; N, 21.3; Calc. for $C_4H_6ClN_3O_2S$: C, 24.6; H, 3.07; N, 21.5%.

4(5)-Acetylsulphamyl-5(4)-bromoimidazole (III)

4(5)-Bromo-5(4)-sulphamylimidazole (5 g) and acetic anhydride (50 ml) were refluxed for 1 hour and then cooled. The solid which crystallized was collected and recrystallized from water as white needles (2.4 g) m.p. 247–248°. Found: C, 22.3; H, 2.3; N, 15.4; S, 11.9. Calc. for $C_5H_6BrN_3O_3S$: C, 22.4; H, 2.2; N, 15.7; S, 12.0%.

4,5-Bis(ethoxycarbonyl)-2-sulphamylimidazole (IV)

4,5-Bis(ethoxycarbonyl)-2-mercaptoimidazole (1 g) was suspended in 2 *N* hydrochloric acid (10 ml) and cooled in an ice bath. Chlorine gas was passed gently through the solution for 25 minutes. The sulphonyl chloride was collected, washed with a little water, and dissolved in concentrated ammonia (10 ml). After 10 minutes the excess of ammonia was evaporated and the solution was acidified with hydrochloric acid. The product was collected and crystallized from water as white needles (0.65 g), m.p. 235–236°. Found: C, 37.4; H, 4.47; N, 14.4; S, 11.1. Calc. for $C_9H_{13}N_3O_6S$: C, 37.1; H, 4.96; N, 14.4; S, 11.0%.

4,5-Dicarbamyl-2-sulphamylimidazole (V)

4,5-Bis(ethoxycarbonyl)-2-sulphamylimidazole (0.4 g) was dissolved in concentrated ammonia (10 ml) and allowed to stand at room temperature for 3 days. The excess of

Can. J. Chem. Downloaded from www.nrcresearchpress.com by 210.87.254.42 on 09/05/12
For personal use only.

ammonia was evaporated and the solution was acidified with hydrochloric acid. The product was collected and crystallized from a large volume (100 ml) of water as white needles (0.2 g), m.p. >300°. Found: C, 25.5; H, 3.05; N, 29.6; S, 13.9. Calc. for $C_5H_7N_5O_4S$: C, 25.8; H, 3.01; N, 30.1; S, 13.8%.

4,5-Bis(hydrazinocarbonyl)-2-sulphamylimidazole (VI)

4,5-Bis(ethoxycarbonyl)-2-sulphamylimidazole (2.5 g) was dissolved in 30% hydrazine (50 ml) and allowed to stand at room temperature for 1 day. The solution was evaporated almost to dryness then diluted with water and acidified with glacial acetic acid. The product was collected and crystallized from water as small white needles (1.5 g), m.p. >300°. Found: C, 23.0; H, 3.45; N, 37.5; S, 12.3. Calc. for $C_5H_9N_7O_4S$: C, 22.8; H, 3.42; N, 37.2; S, 12.2%.

1-Methyl-4-nitroimidazole-5-hydroxamic acid (VII)

The acid chloride of 5-carboxy-1-methyl-4-nitroimidazole (11 g) dissolved in chloroform (25 ml) was added dropwise with stirring at 0–5° to a solution of hydroxylamine hydrochloride (5 g) and sodium hydroxide (9 g) in water (50 ml). The dark red solution was acidified at 0° with hydrochloric acid. The product which precipitated was collected and crystallized from "cellosolve" as white needles (3.5 g), m.p. 200° (sintered), 308° (decomp.). Found: C, 32.5; H, 3.31; N, 30.6; Calc. for $C_5H_6N_4O_4$: C, 32.3; H, 3.23; N, 30.2%.

1,2-Bis(1-methyl-4-nitro-5-imidazolylcarbonyl)-hydrazine (VIII)

The acid chloride of 5-carboxy-1-methyl-4-nitroimidazole (18 g) dissolved in chloroform (180 ml) was added dropwise, with stirring and cooling, to a solution of 95% hydrazine (7 ml) in chloroform (180 ml). After 30 minutes the orange product was collected, dissolved in water, and acidified with hydrochloric acid yielding white needles (10 g), m.p. 308°. Found: C, 36.1; H, 3.46; N, 33.6; Calc. for $C_{10}H_{10}N_8O_6$: C, 35.6; H, 2.96; N, 33.2%.

1-Methyl-4-nitro-5-phenylsulphonylhydrazinocarbonylimidazole (IX)

The acid chloride of 5-carboxy-1-methyl-4-nitroimidazole (11.1 g) dissolved in benzene (30 ml) was added dropwise, with stirring, to phenylsulphonylhydrazine (10 g) in pyridine (25 ml). After 10 minutes the solution was poured into an excess of ice-cold dilute hydrochloric acid to precipitate the product (10.5 g). Recrystallization from "cellosolve" gave small white needles, m.p. 248° (decomp.). Found: C, 40.7; H, 3.45; N, 21.4. Calc. for $C_{11}H_{11}N_5O_6S$: C, 40.6; H, 3.38; N, 21.5%.

4(5)-Hydrazinocarbonyl-2-methylimidazole (X)

4(5)-Ethoxycarbonyl-2-methylimidazole (0.7 g) was dissolved in a mixture of 85% hydrazine hydrate (5 ml) and methanol (5 ml) and refluxed for 1 hour. The solution was evaporated to dryness and the residue crystallized from methanol to give white needles (0.4 g), m.p. 210°. Found: C, 43.5; H, 5.70; N, 39.9. Calc. for $C_5H_8N_4O$: C, 42.9; H, 5.71; N, 40.0%.

The Reaction of 4,5-Dicarbamyl-2-sulphamylimidazole with Alkaline Hypobromite

4(5)-Dicarbamyl-2-sulphamylimidazole (1.17 g) was dissolved in a solution of bromine (1.6 g) and 10% sodium hydroxide (28 ml) at 0°. After 1 hour at 0° the solution was acidified with glacial acetic acid and the precipitate was collected. After several crystallizations from water the product was obtained as pale buff needles (0.15 g), m.p. >300°. Found: C, 20.6; H, 2.58; N, 24.8; S, 11.3; residue, 14.23%.

Can. J. Chem. Downloaded from www.nrcresearchpress.com by 210.87.254.42 on 09/05/12
For personal use only.

The Reaction of 4,5-Bis(hydrazinocarbonyl)-2-sulphamylimidazole with Hydrochloric Acid

4,5-Bis(hydrazinocarbonyl)-2-sulphamylimidazole (1.5 g) dissolved in 2 *N* hydrochloric acid (15 ml) was heated for 6 hours on a steam bath. The solid (0.7 g) which precipitated during the reaction was collected and purified by dissolution in dilute sodium hydroxide and precipitation with hydrochloric acid, as white needles, m.p. >300°. Found: C, 30.8; H, 2.55; N, 31.1; S, 5.29%.

REFERENCES

1. R. O. ROBLIN, JR. and J. W. CLAPP. J. Am. Chem. Soc. **72**, 4890 (1950). J. R. VAUGHAN, JR., J. A. EICHLER, and G. W. ANDERSON. J. Org. Chem. **21**, 700 (1956). R. V. FORD, C. L. SPURR, and J. H. MOYER. Circulation, **16**, 394 (1957).
2. J. SARASIN. Helv. Chim. Acta, **6**, 370 (1923).
3. F. F. BLICKE and H. C. GODT, JR. J. Am. Chem. Soc. **76**, 3653 (1954).
4. L. L. BENNETT, JR. and H. T. BAKER. J. Am. Chem. Soc. **79**, 2188 (1957).
5. R. G. JONES. J. Am. Chem. Soc. **74**, 1085 (1952).
6. R. A. BAXTER and F. S. SPRING. J. Chem. Soc. 232 (1945).
7. R. G. JONES. J. Am. Chem. Soc. **78**, 159 (1956).
8. F. G. MANN and J. W. GEOFFREY PORTER. J. Chem. Soc. 751 (1945).
9. R. G. FARGHAR and F. L. PYMAN. J. Chem. Soc. **115**, 1015 (1919).

Can. J. Chem. Downloaded from www.nrcresearchpress.com by 210.87.254.42 on 09/05/12
For personal use only.

Can. J. Chem. Downloaded from www.nrcresearchpress.com by 210.87.254.105 on 09/05/12
For personal use only.

THE CONVERSION OF α-KETO ACIDS AND OF α-KETO ACID OXIMES TO NITRILES IN AQUEOUS SOLUTION[1]

A. Ahmad and Ian D. Spenser

ABSTRACT

The conversion of α-oximino acids (anti HO— —COOH) to nitriles in aqueous solution is shown to be a general reaction. α-Keto acids are converted to nitriles in excellent yield in aqueous solution in the presence of hydroxylamine. Oxidation of α-oximino acids yields hydroxamic acids.

Recently we reported the facile conversion of indolyl-3-pyruvic acid oxime to indolyl-3-acetonitrile in aqueous solution at moderate temperature, and put forward the hypothesis that this reaction forms the missing link in the biosynthesis of this nitrile (1).

We have now extended our study to other α-keto acid oximes, all of which gave the lower nitrile and carbon dioxide on warming in dilute aqueous and also in dilute hydrochloric acid solution. A summary of the results obtained with 10 representative α-keto acid oximes is presented in Table I. In each case 25 mg acid was suspended in 10 ml water and refluxed 25 minutes under nitrogen. The system was protected from atmospheric carbon dioxide and the CO_2 generated in the reaction was collected quantitatively as $BaCO_3$. At the same time nitrile was isolated and identified by its infrared absorption. A similar series of experiments with 0.1 *M* HCl as the solvent gave substantially identical results. The rate of the reaction is lowered with rise in pH (1) and markedly affected by temperature. Thus α-oximinopropionic acid was stable at pH 4 below 45°, whereas at 55° it gave CO_2 corresponding to 79% decarboxylation in 6 hours.

The conversion $R—C(=NOH)COOH \rightarrow RCN+CO_2+H_2O$ thus constitutes a general reaction of α-keto acid oximes, and a general route to nitriles.

The general nature of the reaction in aqueous solution is further indicated by widely scattered observations of different authors. These are summarized in Table II. The general instability of α-oximino acids in aqueous solution at room temperature was also observed in the course of conductivity measurements (2).

In dilute mineral acid solution a similar conversion takes place, whose generality was recorded, without experimental evidence, by Waters (3, 4), who refers to a paper by Bouveault and Locquin (5). Table II presents a summary of reported instances of this reaction. It has also been found that under normal conditions of oxime formation indolyl-3-glyoxylic acid did not yield the corresponding oxime but 3-cyanoindole (6, 7), and that 2,6-dimethoxyphenylthiopyruvic acid gave a mixture of oximino acid and nitrile (8).

α-Oximino acids are stable in alkaline solution (3, 4); they may be obtained in good yields by alkaline hydrolysis of α-oximino esters (e.g. 9, 10) or amides (11).

No systematic experimental study of the reaction of α-oximino acids in aqueous solution has been reported, nor has it been used for the synthesis of nitriles.

Under anhydrous conditions this route of synthesis has been applied to prepare ring-substituted phenylacetonitriles from the corresponding phenylpyruvic acid oximes, either by pyrolysis (12) or in the manner of the Beckmann rearrangement, in acetic anhydride solution (13). The limitation to arylacetonitriles is surprising, since there is

[1]*Manuscript received February 21, 1961.*
Contribution from the Department of Chemistry, McMaster University, Hamilton, Ontario.

TABLE I

Yield of $BaCO_3$ on refluxing 25 mg α-oximino acid in 10 ml H_2O for 25 minutes

	α-Oximino acid	M.p. (decomp.)	$BaCO_3$ (mg)	% decarboxylation	Nitrile isolated and (or) identified by I.R. (ν(—C≡N) cm^{-1})
(1)	CH_3—C(=N—OH)—COOH	175–176°	45	94	CH_3—CN (2254 cm^{-1})
(2)	CH_3—CH_2—C(=N—OH)—COOH	154–155°	37	88	CH_3—CH_2—CN (2249 cm^{-1})
(3)	$(CH_3)_2$CH—C(=N—OH)—COOH	150°	33	87	$(CH_3)_2$=CH—CN (2251 cm^{-1})
(4)	HOOC—CH_2—C(=N—OH)—COOH	126–127°	43	128	HOOC—CH_2—CN isolated (2271 cm^{-1})
(5)	HOOC—CH_2—CH_2—C(=N—OH)—COOH	151–152°	28	91	HOOC—CH_2—CH_2—COOH isolated
(6)	C_6H_5—C(=N—OH)—COOH	144–145°	25	83	C_6H_5—CN isolated (2230 cm^{-1})
(7)	C_6H_5—C(=N—OH)—COOH	130–131°	10	33	C_6H_5—CN (2230 cm^{-1})
(8)	C_6H_5—CH_2—C(=N—OH)—COOH	166–167°	21	76	C_6H_5—CH_2—CN (2254 cm^{-1})
(9)	CH_3O—C_6H_4—CH_2—C(=N—OH)—COOH	158–159°	22	93	CH_3O—C_6H_4—CH_2—CN (2252 cm^{-1})
(10)	indole-CH_2—C(=N—OH)—COOH	157°	21	93	indole-CH_2—CN isolated (2250 cm^{-1})

overwhelming evidence in the early literature that both reaction conditions are of general applicability (14): Table II lists the α-keto acid oximes which have been shown to yield the lower nitrile on warming with acetic anhydride. Yet only one nitrile other than an arylacetonitrile appears to have been prepared in this manner (8). Evidence regarding the generality of the pyrolytic decomposition is similarly dispersed throughout the literature: Most α-oximino acids described are reported to decompose at their melting point with evolution of gas, which was recognized as CO_2 in some instances while in others the second product of pyrolysis was identified as the nitrile (Table II).

It would appear that the pyrolytic decomposition and the decomposition under Beckmann conditions, as well as the decomposition in aqueous solution, are general reactions.

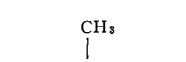
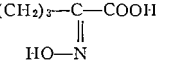
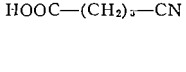
A further general property of α-oximino acids may be gleaned from the literature: A number of them have been reported to decompose to nitrile and CO_2 in aqueous solution

Can. J. Chem. Downloaded from www.nrcresearchpress.com by 210.87.254.105 on 09/05/12
For personal use only.

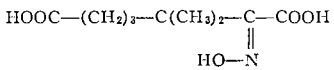
Can. J. Chem. Downloaded from www.nrcresearchpress.com by 210.87.254.105 on 09/05/12
For personal use only.

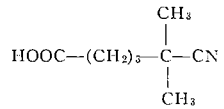
TABLE II

α-Oximino acids reported to decompose to nitrile and CO_2

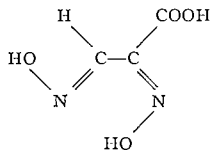
α-Oximino acid	In aqueous solution			In dilute hydrochloric acid solution			α-Oximino acids (other than aryl-pyruvic acid oximes) reported to yield nitrile on treatment with acetic anhydride		α-Oximino acids (other than aryl-pyruvic acid oximes) reported to yield nitrile on heating to their melting points	
	Temp.	Product	Ref.	Temp.	Product	Ref.	Product	Ref.	Product	Ref.
	100°	Stable	35						HCN	35
	120°	HCN	35							
	Room temp.	HCN	36							
	40°	$HCN + CO_2$	70							
	40°	$HOOC-CH_2-CN$	30	Room temp.	$HOOC-CH_2-CN$	30			$HOOC-CH_2-CN$	30
	100°	Stable	30		Stable	30			$HOOC-CH_2-CN$	30
	130°	$HOOC-CH_2-CN$	30							
	100°	$HOOC-CH_2-CH_2-CONH_2$	37				$HOOC-CH_2-CH_2-CONH_2$	37	$HOOC-CH_2-CH_2-CONH_2$	72
	100°	$HOOC-CH_2-CH_2-CN$	71							
			73							73
	Above 70°	$HOOC-(CH_2)_3-CN$	48				$HOOC-(CH_2)_3-CN$	48	$HOOC-(CH_2)_3-CN$	48
	100°		49					49		49
	Above 70°	$HOOC-(CH_2)_4-CN$	48				$HOOC-(CH_2)_4-CN$	48	$HOOC-(CH_2)_4-CN$	48

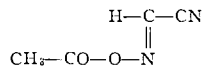
Can. J. Chem. Downloaded from www.nrcresearchpress.com by 210.87.254.105 on 09/05/12
For personal use only.



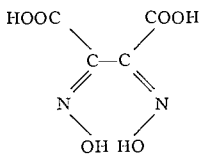


74

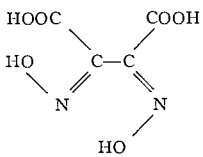


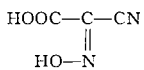


33

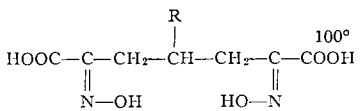


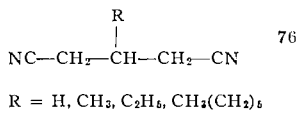
NC—CN 31





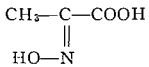
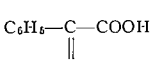
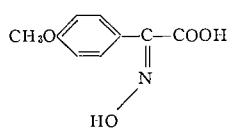
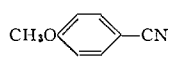
75





76

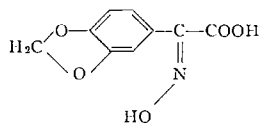
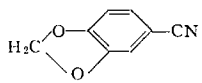
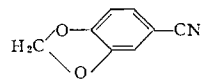
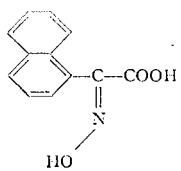
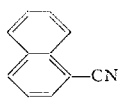
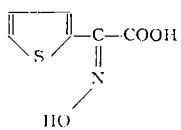
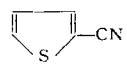
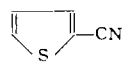
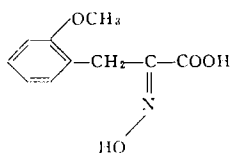
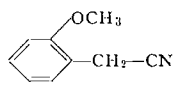
R = H, CH_3, C_2H_5, $CH_3(CH_2)_5$

	100°	Stable	15				CH_3—CN	15	Nitrile	54
	80°	Decomposes	77							
	100°	Stable	15	100°	C_6H_5—CN	15	C_6H_5—CN	15		
		C_6H_5—CN	This paper							
						78				

Can. J. Chem. Downloaded from www.nrcresearchpress.com by 210.87.254.105 on 09/05/12
For personal use only.

TABLE II (*Concluded*)

α-Oximino acids reported to decompose to nitrile and CO_2

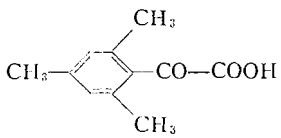
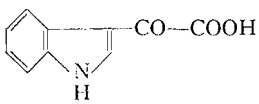
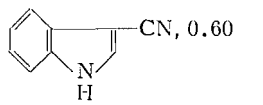
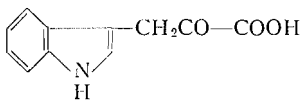
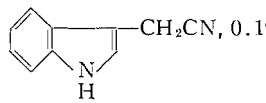
	In aqueous solution			In dilute hydrochloric acid solution			α-Oximino acids (other than aryl-pyruvic acid oximes) reported to yield nitrile on treatment with acetic anhydride		α-Oximino acids (other than aryl-pyruvic acid oximes) reported to yield nitrile on heating to their melting points	
α-Oximino acid	Temp.	Product	Ref.	Temp.	Product	Ref.	Product	Ref.	Product	Ref.
	100°		78					78		
			79							
	100°	Stable	15	100°		15		15		
			80							

more readily in the presence of hydroxylamine hydrochloride (15). This led us to investigate whether nitrile could be prepared by direct treatment of α-keto acid with hydroxylamine, without isolation of the intermediate oximino acid, according to the reaction

$$R{-}\underset{\underset{O}{\|}}{C}{-}COOH + NH_2OH \rightarrow R{-}\underset{\underset{HO{-}N}{\|}}{C}{-}COOH \xrightarrow{H^+} R{-}CN + CO_2 + H_2O.$$

Each of eight α-keto acids was refluxed under nitrogen with one equivalent hydroxylamine hydrochloride in aqueous solution, and in every case an almost quantitative yield of the corresponding nitrile was obtained. The results are summarized in Table III.

TABLE III

α-Keto acid Formula	Wt. (g)	NH_2OH—HCl (g)	H_2O (ml)	Nitriles (g)	Reaction (%)
CH_3CO—COOH	4.40 (0.05)*	3.50	10	CH_3CN, 2.00	98
CH_3CH_2CO—COOH	2.04 (0.02)	1.40	10	CH_3CH_2CN, 0.60	55
HOOC—CH_2CO—COOH	2.16 (0.016)	1.15	10	CH_3CN, 0.22 (33%) and CN—CH_2COOH, 0.82 (59%)	92
HOOC—$(CH_2)_2CO$—COOH	1.46 (0.01)	0.70	10	$(CH_2$—$COOH)_2$, 1.10	93
C_6H_5CO—COOH	1.23 (0.008)	0.57	5	C_6H_5CN, 0.84	99
$C_6H_5CH_2CO$—COOH	1.64 (0.01)	0.70	10	$C_6H_5CH_2CN$, 1.05	90
	1.92 (0.01)	0.70	10	No reaction	
	1.89 (0.01)	0.70	30		42
	0.40 (0.002)	0.14	30		62

*Values in parentheses are in moles.

α-Keto acids alone did not decarboxylate when refluxed in aqueous or 0.1 *M* HCl solution. The only acid amongst those tested which did not undergo conversion to nitrile under these conditions was 2,4,6-trimethylphenylglyoxylic acid. Di-ortho-substituted phenyl ketones do not form carbonyl derivatives under normal reaction conditions (16) and this failure serves as further indication for the required intermediary formation of oxime in the conversion to nitrile. Oxalacetic acid gave a mixture of cyanoacetic acid and, by further decarboxylation of the latter, acetonitrile. α-Ketoglutaric acid gave a quantitative yield of succinic acid, presumably by hydrolysis of the primary product, β-cyanopropionic acid.

Can. J. Chem. Downloaded from www.nrcresearchpress.com by 210.87.254.105 on 09/05/12
For personal use only.

Can. J. Chem. Downloaded from www.nrcresearchpress.com by 210.87.254.105 on 09/05/12
For personal use only.

The facile conversion to nitriles of α-keto acid oximes explains the finding (4) that standard methods for the hydrolysis of oximes fail in the case of α-oximino acids. α-Keto acid esters have been regenerated from their oximes by treatment with 85% formic acid and lead chamber crystals (5, 17), and α-keto acids from α-oximino acids by hydrolysis with concentrated HCl in the presence of formaldehyde (14, but cf. 18), but hydrolysis by dilute acid does not yield α-keto acid and hydroxylamine (4).

In view of this failure it is somewhat surprising that a method for the detection and estimation of oxime nitrogen, based on preliminary hydrolysis to hydroxylamine, has been repeatedly thought applicable to α-oximino acids (19, 20, 21). The procedure (19) and its modifications consists of the supposed acid hydrolysis of α-oximino acids to hydroxylamine, and detection of the latter (22) by oxidation to nitrite and treatment with sulphanilic acid and α-naphthylamine (Gries' reagent) to form an azo dye which may be estimated colorimetrically. In spite of the finding that very poor recoveries were obtained with α-oximino acids (21, 23) this procedure has been used in attempts to establish the occurrence of such compounds in living tissues. Evidence so obtained would appear to be questionable.

In another method of estimation of α-oximino acids (24), which gave almost quantitative results, acid hydrolysis was omitted. Instead the keto acid oxime was oxidized in alkaline solution with iodine, yielding nitrite ion, which was estimated as before. The tacit assumption was made that alkaline hydrolysis precedes oxidation in this case. In fact the reaction takes an entirely different course:

When α-oximino acids (R—C(=NOH)—COOH) were treated with hydrogen peroxide at pH 6 oxidative decarboxylation took place and the corresponding hydroxamic acids (R—CO—NHOH) were shown to be present in the reaction mixture. They were identified by paper chromatography (cf. 25, 26). The following α-keto acid oximes gave hydroxamates in this way: pyruvic, α-ketobutyric, oxalacetic, α-ketoglutaric, phenylglyoxylic (syn and anti), phenylpyruvic, *p*-methoxyphenylpyruvic, and 3-indolylpyruvic acid oximes. The pH of the reaction mixture was critical: below pH 4.0 and above pH 6.5, hydroxamic acids could not be detected; even under optimal conditions (pH 6.2) attempts to isolate the products have so far been successful in one case only (phenylacethydroxamic acid from phenylpyruvic acid oxime) in very poor yield.

This failure may be due either to the further oxidation of hydroxamic acid to nitrite ion (26, 27), or to a Lossen rearrangement of the hydroxamic acids to yield isocyanate which decomposes further (28).

Oxidation of α-oximino acids with iodine does not stop at the hydroxamic acid stage. The —NHOH moiety of hydroxamic acids is quantitatively converted to nitrite under these conditions (26, 27).

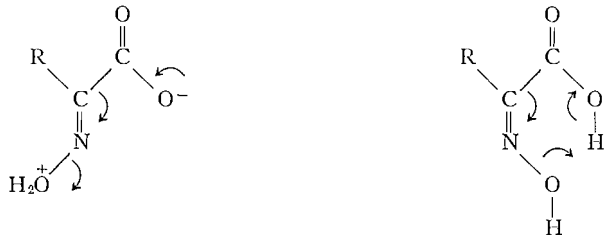
The steps in the estimation of α-oximino acids by means of iodine oxidation are thus as follows:

$$\mathrm{R{-}\underset{\underset{\mathrm{HO{-}N}}{\|}}{C}{-}COOH} \xrightarrow[-CO_2]{[O]} \mathrm{R{-}\underset{\underset{\mathrm{HO{-}N}}{\|}}{C}{-}OH} \rightleftharpoons \mathrm{R{-}CO{-}NHOH} \xrightarrow{[O]} NO_2^-.$$

The mechanism of the oxidative decarboxylation of α-oximino acids to hydroxamic acids, analogous to that proposed for the oxidative decarboxylation of α-amino acids (29), will be discussed in a separate communication.

Two types of mechanism for the conversion of α-oximino acids to nitriles may be considered, and have been discussed in connection with the failure of indolyl-3-glyoxylic

acid to yield oxime (7). The first, a concerted trans elimination, requires an anti (HO— —COOH) stereochemistry; the second, a concerted cyclic elimination, demands the syn (HO— —COOH) configuration of the α-oximino acids.



Initial decarboxylation to yield aldoxime, or initial hydrolysis to yield α-keto acid as intermediates in the reaction, may be excluded, since both aldoximes and α-keto acids are stable under conditions when the corresponding α-oximino acids yield nitrile.

Few pairs of geometrical isomers of α-oximino acids are well authenticated: Hantzsch and his collaborators isolated and studied the isomers of phenylglyoxylic acid oxime (15), of oxalacetic acid oxime (30), of dioximinosuccinic acid (31, 32), and of dioximinopropionic acid (33, 34). Isomers have also been reported, mostly on the basis of melting point differences, of oximinoacetic acid (35, 36), α-oximinoglutaric acid (37, 38), $NH{=}C(NH_2){-}C(=NOH)COOH$ (39), furan-2-pyruvic acid oxime (40), *p*-methoxyphenylpyruvic acid oxime (41, 42), and phenylpyruvic acid oxime (e.g., 14, 42).

We have prepared the two isomers of phenylglyoxylic acid oxime (15) and of oxalacetic acid oxime (30). One of the latter, however, was exceedingly unstable so that a pure sample could not be obtained. We failed to isolate more than one isomer of α-ketoglutaric acid oxime (38), of phenyl- (14, 42), and of *p*-methoxyphenylpyruvic acid oxime[2] (41, 42).

The only experimental attempt to assign configurations to the stereoisomers of α-oximino acids was that of Hantzsch and his collaborators (15, 30, 31, 33, cf. 43). By analogy with their work on benzaldoximes, they made their configurational assignment of the isomers of phenylglyoxylic acid oxime on the basis of the behavior of the O-acetyl derivatives on hydrolysis (44): The oxime (α-oxime) whose acetate on treatment with carbonate at 0° reverted to the oxime was assigned the anti (HO— —COOH) configuration, whereas the oxime (β-oxime), whose acetate under similar conditions gave nitrile, was assigned the syn (HO— —COOH) configuration. Since these assignments were based on the assumption of a cis elimination of the elements of acetic acid, an assumption which was proved erroneous by later experimental work (45), it is necessary to revise Hantzsch's assignments of the stereochemistry of phenylglyoxylic acid oximes (Table IV).

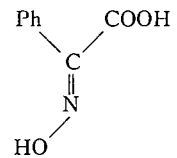
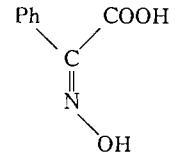
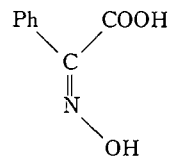
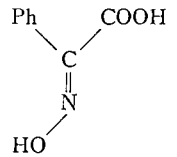
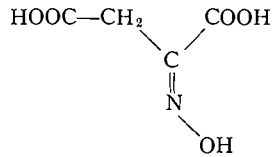
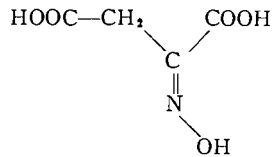
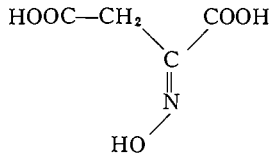
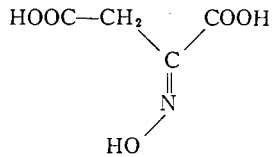
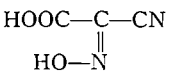
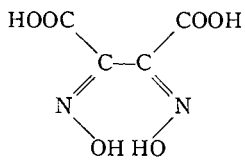
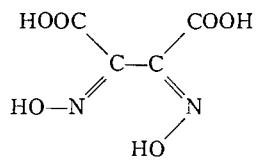
The decomposition of α-oximino acids in acetic anhydride is a special case of the "second-order" Beckmann rearrangement of α-oximinocarbonyl compounds (46), i.e.,

[2]*Dr. R. A. McIvor informs us that further work on his compounds (42) indicates that the phenylpyruvic acid oxime, decomp. 206°, was a molecular complex of the acid and its sodium salt, from which phenylpyruvic acid oxime, decomp. 166–167°, was obtained by high-vacuum sublimation; and that the isomer, decomp. 155°, had reducing properties and probably contained the hydroxylammonium salt of phenylpyruvic acid oxime. This also gave phenylpyruvic acid oxime, decomp. 166–167°, on sublimation at 10^{-3} mm. The isomer of p-methoxyphenylpyruvic acid oxime, decomp. 199°, gave p-methoxyphenylpyruvic acid oxime, decomp. 159°, on recrystallization from water and was a molecular complex of p-methoxyphenylpyruvic acid and its sodium salt. The "unknown compound", melting at 147.5–148° (decomp.), which had reducing properties, was shown to be the hydroxylammonium salt of p-methoxyphenylpyruvic acid oxime.*

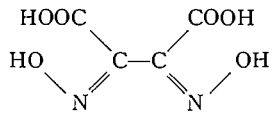
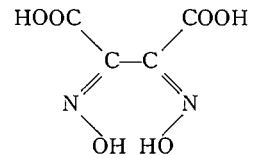
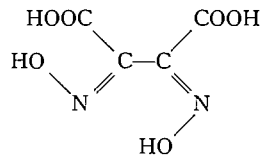
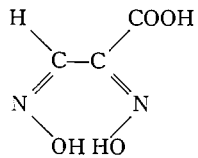
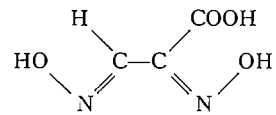
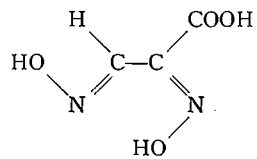
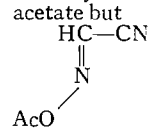
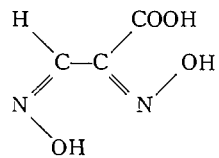
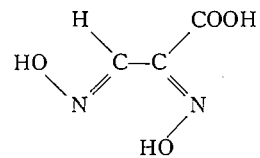
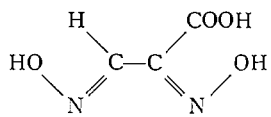
Can. J. Chem. Downloaded from www.nrcresearchpress.com by 210.87.254.105 on 09/05/12
For personal use only.

Can. J. Chem. Downloaded from www.nrcresearchpress.com by 210.87.254.105 on 09/05/12
For personal use only.

TABLE IV
Reported stereoisomers of α-oximino acids

Oxime of	Hantzsch's description	M.p. (decomp.)	Product obtained on treatment of: O-Acetyl deriv. with Na_2CO_3 at 0°	Product obtained on treatment of: Acid with dilute HCl	Hantzsch's assignment	Ref.	Revised assignment	Ref.
C_6H_5—CO—COOH	α	127°	Phenylglyoxylic acid oxime decomp. 127°	—	anti (HO— —COOH) 	15		43, 55
	β	145°	C_6H_5—CN	C_6H_5—CN	syn (HO— —COOH) 	15		43, 55
HOOC—CH_2—CO—COOH	α	125°		Stable at room temp.		30		
	β	88° Blue color with Fe^{+++}		NC—CH_2—COOH At room temp.		30		
HOOC—CO—CO—COOH	1ry, ββ	145–150° (hydrate m.p. 70°)			 "syn"	31, 75		

Can. J. Chem. Downloaded from www.nrcresearchpress.com by 210.87.254.105 on 09/05/12
For personal use only.

	2nd, αα	145–150°	Does not yield acetate but NC—CN	 "anti"	31	
		168–170°		 "amphi"	32	
CHO—CO—COOH	1ry, α	141–143°	Dioximino acid m.p. 172° (decomp.)	 "syn"	33	
				 "amphi"	53	
	2nd, β	172°, 185°	Does not yield acetate but 	 "amphi"	33	
				 "anti" but cf. ref. 34	53	

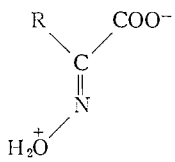
a trans fragmentation reaction requiring the anti (HO— —COOH) configuration (47), and stereochemical assignments must be made accordingly (Table IV).

Hantzsch (15) was able to convert phenylglyoxylic acid oxime, decomp. 127°, (α), into the β-isomer, decomp. 145°, at room temperature in aqueous solution. We observed a similar isomerization, accompanied by some decomposition to benzonitrile, when the low-melting oxime was distilled at 10^{-3} mm, just below its melting point. An attempt to prepare a pure specimen of the low-melting isomer of oxalacetic acid oxime (30) failed, since the crude product which gave a strong blue color with $FeCl_3$ (30), obtained by hydrolysis of diethyl oxalacetate oxime, was unstable at room temperature.

The isomer, decomp. 127°, of phenylglyoxylic acid oxime, decomposed much less readily to benzonitrile, on refluxing in aqueous solution, than the isomer, decomp. 145° (Table I). Since the former isomerizes slowly to the latter at room temperature in aqueous solution (15), it is probable that such a transformation preceded the decarboxylation of the isomer, decomp. 127°. Similarly, the isomer, decomp. 125°, of oxalacetic acid oxime yields cyanoacetic acid less readily in aqueous solution than the isomer, decomp. 88°. In both cases the isomer to which an anti (HO— —COOH) configuration is now assigned on the basis of the reactivity of the O-acetyl derivatives, undergoes elimination of CO_2 and water more readily than the corresponding syn isomer.

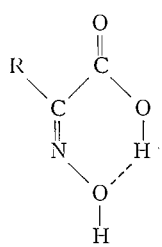
This leads us to favor a mechanism involving concerted trans elimination for the reaction in aqueous solution in the two cases where both syn and anti isomers are known, and prompts us to assign an anti (HO— —COOH) configuration to those α-oximino acids of which only one isomer has been described, which readily undergoes conversion to nitrile in aqueous solution (Table I).

The zwitterion form



would be most favorable for concerted trans elimination. The observations that α-oximino acids may be recovered unchanged from concentrated sulphuric (15, 30, 48, 49) and hydrochloric acid (50), that they are stable in alkaline solution (4), and that in one instance (1) the reaction in aqueous solution has been shown to have a pH optimum at pH 2, tend to support the zwitterion form as the reacting species in a concerted trans elimination.

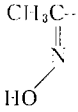
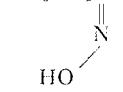
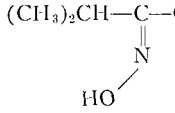
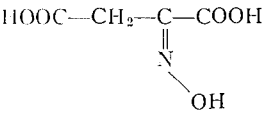
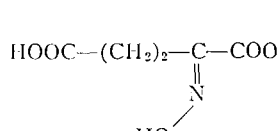
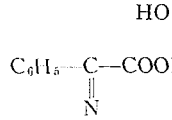
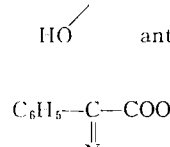
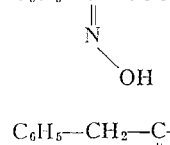
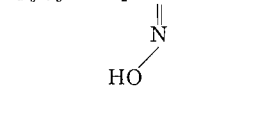
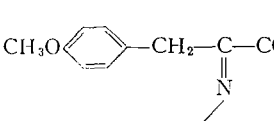
The pyrolytic decomposition is more likely to take place by a concerted cyclic mechanism (cf. 51) demanding the syn form of the α-oximino acid. Such a course of reaction would be favored by intramolecular hydrogen bonding, e.g.,



Can. J. Chem. Downloaded from www.nrcresearchpress.com by 210.87.254.105 on 09/05/12
For personal use only.

Can. J. Chem. Downloaded from www.nrcresearchpress.com by 210.87.254.105 on 09/05/12
For personal use only.

TABLE V

α-Oximino acid	M.p. (decomp.)	Infrared absorption bands (cm^{-1}) (Nujol)				
1. 	175–176°	700 (s) 755 (w) 810 (m) 900 (m) 985 (w)	1040 (s) 1180 (s) 1300 (m) 1370 (s) 1415 (m)	1465 (s) 1650 (m) 1690 (s)	2450 2570 (sh) 2700	3210 (broad)
2. 	154–155°	685 (s) 760 (s) 785 (s) 890 (s) 955 (w)	1000 (s) 1040 (s) 1065 (s) 1165 (s) 1250 (s)	1300 (m) 1370 (s) 1420 (s) 1450 (s) 1650 (s) 1690 (s)	2350 2500 (sh)	3210 (broad)
3. 	150°	695 (w) 760 (s) 793 (w) 900 (m) 1000 (s)	1030 (s) 1085 (w) 1110 (w) 1155 (w) 1210 (m)	1297 (m) 1360 (m) 1380 (s) 1450 (s) 1650 (m) 1690 (s)	2550 2650 (sh)	3210 (broad)
4. 	126–127°	680 (m) 700 (s) 730 (m) 750 (w) 820 (m) 865 (m) 930 (s)	1030 (s) 1120 (s) 1200 (s) 1275 (s) 1325 (w) 1360 (m) 1390 (s)	1410 (s) 1440 (s) 1670 (s) 1720 (s)	1800 2520 (sh) 2620	3280 (broad)
5. 	151–152°	830 (s) 995 (w) 1025 (s) 1115 (s) 1190 (s) 1210 (m)	1255 (s) 1375 (s) 1440 (s) 1660 (s) 1720 (s)	1850 (w & broad)	2350 2550 (sh)	3210 (broad)
6.  anti-	144–145°	680 (s) 707 (s) 760 (m) 790 (w) 850 (m) 940 (w)	1015 (s) 1030 (s) 1045 (s) 1210 (s) 1245 (w) 1300 (w)	1375 (s) 1410 (s) 1440 (s) 1460 (s) 1500 (w) 1630 (w) 1690 (s)	2487 2550 (sh) 2670	3210 (broad)
7.  syn-	130–131°	680 (s) 700 (s) 730 (m) 820 (m) 940 (s) 1025 (m)	1040 (m) 1210 (m) 1240 (s) 1300 (m) 1375 (s) 1415 (s)	1455 (s) 1500 (w) 1625 (s) 1660 (s) 1712 (s)	2510 2585 (sh) 2700	3250 (broad)
8. 	166–167°	690 (s) 740 (s) 755 (m) 785 (m) 825 (w) 835 (w) 885 (s)	920 (m) 1015 (s) 1070 (s) 1115 (m) 1130 (m) 1200 (s) 1215 (s)	1282 (s) 1375 (s) 1430 (s) 1460–70 (s) 1493 (s) 1600 (m) 1640 (m) 1693 (s)	2500 2565 (sh) 2670	3210 (broad)
9. 	156–157°	695 (m) 710 (m) 730 (w) 752 (s) 780 (m) 815 (s) 830 (s)	950 (m) 1030 (s) 1105 (m) 1140 (m) 1175 (s) 1225 (s) 1250 (s)	1280 (s) 1375 (s) 1405 (m) 1470 (s) 1510 (s) 1610 (s) 1650 (s) 1690 (s) 1880 (w & broad)	2465 2525 (sh) 2650	3210 (broad)
10. 	157°	715 (w) 750 (s) 840 (m) 1020 (s) 1100 (w)	1130 (m) 1220 (m) 1305 (m) 1375 (s) 1455 (s)	1620 (w) 1690 (s)	3360 (NH) (broad)	

Infrared data (Table V) show up similarities between anti (HO— —COOH) phenylglyoxylic acid oxime and those oximes of which only one isomer is known. The syn (HO— —COOH) isomers of phenylglyoxylic acid oxime and of oxalacetic acid oxime showed similarities in absorption, and their infrared curves differed in certain respects from those of all other α-oximino acids examined.

The —OH stretching frequency, found at 3210 cm^{-1} in all anti oximes, was displaced in the two syn isomers (3250, 3280 cm^{-1} respectively for phenylglyoxylic and oxalacetic acid oxime). This is in accord with the assignment of Palm and Werbin (52). The band near 1300 cm^{-1}, assigned to —OH deformation, was present in all compounds between 1280 and 1300 cm^{-1}, except in the two dicarboxylic acids, where it was displaced to higher wave numbers (1325 and 1375 cm^{-1} respectively). The N—OH stretching vibration of oximes is associated with bands near 920 cm^{-1} (52). The two syn (HO— —COOH) compounds showed strong absorption in this region (940 and 930 cm^{-1} for phenylglyoxylic and oxalacetic acid oxime, respectively), whereas the anti (HO— —COOH) isomers showed bands of weaker intensity. All the compounds examined showed one or more strong bands between 1000 and 1085 cm^{-1}. In general all oximino acids show the band due to C=N vibration at 1620–1650 cm^{-1}. This band was masked by broad carbonyl absorption in the dicarboxylic acids. All monocarboxylic anti oximino acids showed carbonyl absorption at 1690 cm^{-1}. In syn-phenylglyoxylic acid oxime this band was split, appearing at 1660 cm^{-1} and 1712 cm^{-1}. The dicarboxylic acids absorbed at 1670 and 1720 cm^{-1}.

Hantzsch (53) attempted to confirm his configurational assignment on the basis of conductivity measurements. The significance of these results has, however, been called into question (2, 54). Table VI summarizes the pK_a values of the α-oximino acids we have determined, together with those recalculated from reports in the early literature. Configurational assignments have also been made, using as a criterion differences in the readiness of the isomers of α-oximino acids to complex with metal ions (55). It is reported that complexing takes place through the oxime-N and not through the oxime-O, and that anti (HO— —COOH) oximino acids react readily with Cu^{++} and Ca^{++}, whereas the syn (HO— —COOH) isomers do so slowly, presumably only after isomerization.

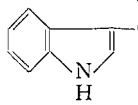
The general methods of synthesis of α-oximino acids have been listed (56). The compounds have been prepared from α-keto acids (e.g. 57) or α-thioketo acids (e.g. 14, 41, 42) by treatment with hydroxylamine, or from α-oximino esters by alkaline hydrolysis (e.g. 9, 10, 58). A more versatile method of preparation is by nitrosation, under a variety of conditions, of β-keto esters (9, 10, 48, 49, 58, 59, 60) or lactones (61), substituted malonic esters (62, 56), tetronic acids (63), phenylacetonitriles (64), or phenylacetic acid esters (65), followed by acid or alkaline hydrolysis of the resulting α-nitroso derivatives, with deacylation or decarboxylation respectively in the first two cases, and rearrangement to the α-oximino acid. Nitrosation of substituted malonic acids has also been used (66, 56). α-Oximino esters are obtained by treatment of α-halo esters (67) or α-nitro esters (68) with sodium nitrite. The mechanism of these two reactions has been elucidated (68).

Two other methods of preparation, whose route is puzzling, have been used: Treatment of α-halo acids with hydroxylamine (69) gave α-oximino acids, as did hydrolysis of α-hydroxylaminonitriles (11), i.e., of the addition products of aldoximes and HCN. The chemistry of these two reactions has now been clarified and will be discussed in a separate communication.

Can. J. Chem. Downloaded from www.nrcresearchpress.com by 210.87.254.105 on 09/05/12
For personal use only.

TABLE VI

pK_a values of α-oximino acids

α-Oximino acid	pK_a (pH at half equivalence in 0.03 *M* solution)	Reported value (converted to pK_a)
H—C(NOH)COOH	—	3.00 (53); 3.02 (54)
CH_3—C(NOH)COOH	3.38	3.29 (53); 3.33 (54) 3.30 (81)
CH_3—CH_2—C(NOH)COOH	3.20	3.08 (53); 3.16 (54)
CH_3—$(CH_2)_2$—C(NOH)COOH	—	3.16 (53); 3.22 (54)
$(CH_3)_2$=CH—C(NOH)COOH	3.05	2.94 (2)
CH_3—$(CH_2)_3$—C(NOH)COOH	—	3.19 (2)
$(CH_3)_2$=CH—CH_2—C(NOH)COOH	—	3.25 (2)
C_6H_5—C(NOH)COOH		
M.p. 144–145° (decomp.)	2.82	2.75 (53)
M.p. 130–131° (decomp.)	2.27	2.82 (2); 1.81 (?) (53)
	—	2.30 (53)
C_6H_5—CH_2—C(NOH)COOH	3.90	3.24 (2)
CH_3O	3.85*	—
	3.40*	—
NC—C(NOH)COOH	—	1.86 (53)
HOOC—CH_2—C(NOH)COOH		
M.p. 126–127° (decomp.)	2.90, 4.55	2.96 (53)
M.p. 88° (decomp.)	Cannot be measured. pK_a 2.43 is that of NC—CH_2—COOH (53, misquoted by 38).	
HOOC—$(CH_2)_2$—C(NOH)COOH	3.25, 4.95	—
H—C(NOH)—C(NOH)COOH		
M.p. 141–143° (decomp.)	—	2.38 (53)
M.p. 172° (decomp.)	—	2.55 (53)
CH_3—C(NOH)—C(NOH)COOH	—	1.86 (53)
HOOC—C(NOH)—C(NOH)COOH		
"Primary"	—	1.21 (53)
"Secondary"	—	1.98 (53)

*In 0.01 *M* solution.

EXPERIMENTAL

α-Oximino Acids

α-Oximino acids were prepared by well-established methods, either from suitably substituted β-keto or malonic esters or malonic acids, by nitrosation with freshly prepared butyl nitrite (82), or from the α-keto acid and hydroxylamine. Details are given only when modifications of reported methods were used.

Can. J. Chem. Downloaded from www.nrcresearchpress.com by 210.87.254.105 on 09/05/12
For personal use only.

α-Oximinopropionic Acid (Pyruvic Acid Oxime) (cf. 57)

A solution of hydroxylamine hydrochloride (3.50 g, 0.05 mole) in 15 ml water containing 4.20 g (0.05 mole) $NaHCO_3$ was cooled to 5° and poured, with cooling and stirring, into a cooled solution of pyruvic acid (4.40 g, 0.05 mole) in 30 ml water containing 4.20 g (0.05 mole) $NaHCO_3$. After standing 24 hours at room temperature the mixture was extracted with ether, cooled to 5°, carefully acidified with 3 *M* HCl, and repeatedly extracted with ether. The dried (Na_2SO_4) ether extract was evaporated at room temperature, yielding α-oximinopropionic acid, melting at 175–176° (decomp.); neutralization equivalent: found, 103; calculated, 103; pK_a, 3.38. Reported melting point 177° (decomp.) (9), 180–181° (decomp.) (54).

α-Oximinobutyric Acid (α-Ketobutyric Acid Oxime)

α-Oximinobutyric acid (α-ketobutyric acid oxime) was prepared by nitrosation of diethyl ethyl malonate with butyl nitrite under alkaline conditions (56) in 60% yield. After sublimation at 140° and 1.10^{-3} mm the product melted at 154–155° (decomp.); neutralization equivalent: found, 116; calculated, 117; pK_a, 3.20. Reported melting point 154° (decomp.) (69), 169–170° (decomp.) (59).

α-Oximino-β-methylbutyric Acid (α-Ketoisovaleric Acid Oxime)

α-Oximino-β-methylbutyric acid (α-ketoisovaleric acid oxime) was prepared from ethyl α-isopropylacetoacetate (83) by alkaline nitrosation. The ester (3.44 g, 0.02 mole) was dissolved in dry ethanol (15 ml) containing sodium metal (0.46 g, 0.02 mole). The solution was cooled to 5°, butyl nitrite (3.10 g, 0.03 mole) was added dropwise with stirring over 10 minutes, stirring was continued 20 minutes at 5° and then 30 minutes at room temperature. Ethanol was distilled off at room temperature, the residue mixed with crushed ice, acidified with 3 *M* H_2SO_4, and extracted with ether. The ether layer was extracted with 10% NaOH solution, the alkaline solution heated 15 minutes on the steam bath, cooled to 0°, acidified with dilute H_2SO_4, and repeatedly extracted with ether. The ether extract was dried (Na_2SO_4) and concentrated, yielding α-oximino-β-methylbutyric acid (1.78 g, 68%) as a white crystalline solid, melting point 150° (decomp.), after sublimation at 135° and 1.10^{-3} mm; neutralization equivalent: found, 130; calculated, 131; pK_a, 3.05. Reported melting point 163–165° (decomp.) (84), 171–172° (decomp.) (59), 151.5° (decomp.) (2).

α-Oximinosuccinic Acid (Oxalacetic Acid Oxime)

(*a*) syn (HO— α-COOH). This isomer was prepared by nitrosation of ethane-1,1,2-tricarboxylic acid (85). Butyl nitrite (1.03 g, 0.01 mole) was added to a solution of the tricarboxylic acid (1.62 g, 0.01 mole) in ether (30 ml) at 0°. A stream of dry HCl gas was passed through the solution for 10 minutes and the reaction mixture then evaporated. The residual oil was crystallized from chloroform – ethyl acetate, yielding 0.44 g (30%) syn (HO— α-COOH)-oximinosuccinic acid, melting at 126–127° (decomp.). Neutralization equivalent: found, 70; calculated, 73.5; pK_a, 2.90, 4.55. Reported melting point 125° (decomp.) (30), 126° (decomp.) (60). After 12 months at 5° a solid sample of this isomer had partially decomposed to cyanoacetic acid. Alkaline nitrosation of the triethyl ester failed to give the desired product. Treatment of oxalacetic acid with methanolic hydroxylamine at 0° yielded a product contaminated with hydroxylammonium salt.

(*b*) anti (HO— α-COOH) (cf. 30, 38). Sodium diethyl oxalacetate (10.5 g, 0.05 mole) in 50 ml methanol was treated with 3.5 g hydroxylamine hydrochloride (0.05 mole) in 30 ml methanol. The mixture was stirred at 40° for 1 hour, then rapidly cooled to 0° and

Can. J. Chem. Downloaded from www.nrcresearchpress.com by 210.87.254.105 on 09/05/12
For personal use only.

precipitated sodium chloride filtered off. The filtrate was evaporated at room temperature when an oily colorless liquid was obtained which was extracted into ether and dried (Na_2SO_4). The oily liquid, obtained by evaporation of the ethereal solution, which gave a sharp infrared peak at 1630 cm^{-1} (C=N), was dissolved in 15 ml methanol and treated with 10% NaOH to adjust the pH to 10.5. The solution was warmed for 30 minutes on the steam bath with occasional shaking, cooled to 0°, and acidified (pH 2) with 4 *M* HCl. The white solid which separated on acidification was rapidly filtered with cooling, washed with a little cold water, and dried *in vacuo* over caustic soda. After 24 hours the product was washed with dry ether to remove any unreacted oxalacetic acid, as well as any cyanoacetic acid, yielding impure anti (HO— α-COOH) α-oximinosuccinic acid, melting with violent decomposition at 71° (yield 4.59 g, 61.2%). Attempts to purify this isomer at room temperature led to extensive decomposition. Reported melting point 88° (30).

α-Oximinoglutaric Acid (α-Ketoglutaric Acid Oxime)

α-Oximinoglutaric acid (α-ketoglutaric acid oxime) was obtained from triethyl propane-1,1,3-tricarboxylate (86) by alkaline nitrosation. The triethyl ester (6.50 g, 0.025 mole) was dissolved in sodium ethoxide solution (0.575 g sodium metal (0.025 mole) in 40 ml dry ethanol); the solution was cooled to 10° and a solution of *n*-butyl nitrite (2.86 g, 0.0275 mole) in 15 ml dry ethanol was added dropwise with stirring over 15 minutes. The reaction mixture was stirred for another 30 minutes and concentrated at room temperature. Crushed ice was added to the brown viscous residue and the mixture acidified with 3 *M* H_2SO_4. The solution was extracted with ether, the ether layer washed with a little water, extracted with 15 ml 10% NaOH, and the alkaline extract warmed on the steam bath for 15 minutes. On completion of the saponification the solution was cooled to 0°, acidified with 3 *M* H_2SO_4, and the product extracted into ether. The ether extract was washed with water, dried (Na_2SO_4), and concentrated, yielding a brown residue which was taken up in dry ether. On addition of petroleum ether (30–40°) α-oximinoglutaric acid (1.21 g, 30%), melting at 151–152° (decomp.), crystallized. Neutralization equivalent: found, 81; calculated, 80.5; pK_a, 3.25, 4.95. Reported melting point 152° (decomp.) (72, 37), 156° (decomp.) (38), 140° (decomp.) (71, 38).

This oximino acid was also obtained in 13% yield from propane-1,3,3-tricarboxylic acid (87) by acid nitrosation. Treatment of α-ketoglutaric acid with methanolic hydroxylamine (cf. 38) gave the oximino acid contaminated with hydroxylammonium salt, accounting for the low melting point (140°) of the product.

α-Oximinophenylacetic Acid (Phenylglyoxylic Acid Oxime)

(*a*) syn (HO— —COOH) (cf. 15). Cooled solutions of phenylglyoxylic acid (1.50 g, 0.01 mole) in 30 ml water containing 0.84 g $NaHCO_3$ (0.01 mole) and of hydroxylamine hydrochloride (0.70 g, 0.01 mole) in 10 ml water containing 0.84 g $NaHCO_3$ (0.01 mole) were mixed at 5° and shaken 24 hours at room temperature. The mixture was extracted with ether, cooled, and acidified with dilute H_2SO_4, and the product extracted into ether. The dried (Na_2SO_4) ether extract was concentrated at room temperature and the solid residue washed with dry benzene to remove unreacted phenylglyoxylic acid. The product (1.353 g, 82%) melted at 130–131° (decomp.); neutralization equivalent: found, 161; calculated, 165; pK_a, 2.27. Reported melting point 127° (decomp.) (15).

(*b*) anti (HO— —COOH) (cf. 15). The syn isomer, decomp. 130–131° (0.15 g), was dissolved in 5 ml water and the solution allowed to stand 24 hours at room temperature and then at 5°, when the anti isomer crystallized (0.043 g, 26%). It melted at 144–145° with decomposition; neutralization equivalent: found, 160; calculated, 165; pK_a, 2.82.

Can. J. Chem. Downloaded from www.nrcresearchpress.com by 210.87.254.105 on 09/05/12
For personal use only.

Sublimation of the syn isomer at 120° and 2.10^{-3} mm gave the anti isomer in 90% yield, together with a small amount of benzonitrile. Reported melting point 145° (decomp.) (15).

α-Oximino-β-phenylpropionic Acid (Phenylpyruvic Acid Oxime)

α-Oximino-β-phenylpropionic acid (phenylpyruvic acid oxime) was obtained by nitrosation, under acidic conditions, of benzylmalonic acid (56) in 85% yield. Recrystallization from hot water was unsatisfactory due to decomposition to phenylacetonitrile. Sublimation at 145° and 10^{-3} mm gave the product, melting at 166–167° (decomp.), neutralization equivalent: found, 175; calculated, 179; pK_a, 3.90. Reported melting point: 159–160° (decomp.) (88), 167° (decomp.) (63).

α-Oximino-β-(p-methoxyphenyl)-propionic Acid (p-Methoxyphenylpyruvic Acid Oxime)

α-Oximino-β-(*p*-methoxyphenyl)-propionic acid (*p*-methoxyphenylpyruvic acid oxime), decomp. 156–157°, neutralization equivalent: found, 209; calculated, 209; pK_a, 3.85; was supplied by Dr. R. A. McIvor,[3] who prepared it from his sample, melting at 199° (42), by recrystallization from water. Reported melting point 159° (decomp.) (41).

α-Oximino-β-(3-indolyl)-propionic Acid (Indolyl-3-pyruvic Acid Oxime)

α-Oximino-β-(3-indolyl)-propionic acid (indolyl-3-pyruvic acid oxime), melting at 157° (decomp.), neutralization equivalent: found, 218; calculated, 218; pK_a, 3.40; was obtained from indolyl-3-pyruvic acid (7) and also by alkaline nitrosation of ethyl α-acetyl-β-(3-indolyl)-propionate (89). Reported melting point 155° (decomp.) (89), 158° (decomp.) (7).

Conversion of α-Oximino Acids to Nitriles

The α-oximino acid (25 mg) was suspended in 10 ml water in a 25-ml two-necked flask, supplied with condenser and gas inlet. Nitrogen was passed first through a $Ba(OH)_2$ trap and then through the reaction mixture; CO_2 was collected in a trap containing saturated $Ba(OH)_2$ solution and the reaction train was linked to a further baryta trap. All experiments were carried out at reflux temperature over 25 minutes. Barium carbonate was collected, washed with water, and methanol, and dried to constant weight. The reaction mixture was worked up for nitrile either by ether extraction or, in the case of non-volatile nitriles, by evaporation. Nitriles were purified by distillation and identified by comparison of their infrared absorption curves with those of authentic specimens. Results are summarized in Table I. In several cases the experiments were repeated with larger quantities to make isolation of nitrile possible.

Oxidation of α-Oximino Acids to Hydroxamic Acids

The α-oximino acid (1 mg) was dissolved in phthalate buffer (pH 6.2) (1 ml). One drop of 15% H_2O_2 was added and the solution kept at 90° for 20–30 minutes, when solvent had almost completely evaporated. The residue was cooled and dissolved in methanol (1 ml), and a sample of this solution was chromatographed (Whatman No. 1, butanol – acetic acid – water, 4:1:5 (25)). After development, the chromatogram was sprayed with 5% $FeCl_3$ in methanol, followed by 2% aqueous HCl. Hydroxamic acids appeared as wine-red spots.

α-Keto Acids

Pyruvic, α-ketobutyric, oxalacetic, and α-ketoglutaric acid were commercial samples. Phenylglyoxylic acid (90), indolyl-3-glyoxylic acid (7), phenylpyruvic acid (91), and

[3]*See footnote 2.*

Can. J. Chem. Downloaded from www.nrcresearchpress.com by 210.87.254.105 on 09/05/12
For personal use only.

indolyl-3-pyruvic acid (92) were prepared by established methods. Mesitylglyoxylic acid was prepared by oxidation of 2,4,6-trimethylacetophenone with alkaline potassium permanganate (93), interrupting the oxidation at the keto-acid stage. The solution was then acidified with 1.5 *M* H_2SO_4 and the product extracted into ether. Drying and evaporation yielded mesitylglyoxylic acid (48% yield), melting point 116–117°. Reported melting point 115–116.5° (94).

Conversion of α-Keto Acids to Nitriles

Equivalent amounts of α-keto acid and hydroxylamine hydrochloride in aqueous solution were refluxed for 1–1.5 hours. When CO_2 evolution was complete, the nitriles were isolated as before, either by ether extraction or by evaporation of the reaction mixture. Results are summarized in Table III.

Nitriles

Authentic specimens of nitriles were either redistilled commercial specimens (acetonitrile, propionitrile, isobutyronitrile, cyanoacetic acid, benzonitrile, and phenylacetonitrile) or were prepared by established methods (*p*-methoxyphenylacetonitrile (95), indolyl-3-cyanide (7), indolyl-3-acetonitrile (1)).

ACKNOWLEDGMENTS

We are indebted to Dr. R. A. McIvor, Defence Research Board, Ottawa, for samples of phenyl- and *p*-methoxyphenylpyruvic acid oxime, and for permission to quote his unpublished results.

Financial assistance by the National Research Council of Canada and by the Ontario Research Foundation is gratefully acknowledged. One of us (A. A.) wishes to thank the Colombo Plan authorities for financial support and the Pakistan Council of Scientific and Industrial Research for the award of a scholarship.

REFERENCES

1. A. Ahmad and I. D. Spenser. Can. J. Chem. **38**, 1625 (1960).
2. C. S. Hicks. J. Chem. Soc. **113**, 554 (1918).
3. K. L. Waters. Chem. Revs. **41**, 585 (1947).
4. K. L. Waters and W. H. Hartung. J. Org. Chem. **12**, 469 (1947).
5. L. Bouveault and R. Locquin. Bull. soc. chim. France, [3], **31**, 1142 (1904).
6. R. Majima, T. Shigematsu, and T. Rokkaku. Ber. **57**, 1453 (1924).
7. K. N. F. Shaw, A. McMillan, A. G. Gudmundson, and M. D. Armstrong. J. Org. Chem. **23**, 1171 (1958).
8. F. E. King and M. F. Grundon. J. Chem. Soc. 3547 (1950).
9. V. Meyer and J. Züblin. Ber. **11**, 692 (1878).
10. J. Schmidt and H. Dieterle. Ann. **377**, 30 (1910).
11. W. v. Miller and J. Plöchl. Ber. **26**, 1545 (1893).
12. H. Avenarius and R. Pschorr. Ber. **62**, 321 (1929). P. Pfeiffer, K. Quehl, and F. Tappermann. Ber. **63**, 1301 (1930).
13. G. A. Edwards. J. Chem. Soc. 740 (1926). H. E. Carter. Org. Reactions, **3**, 198 (1946).
14. Ch. Gränacher. Helv. Chim. Acta, **5**, 610 (1922).
15. A. Hantzsch. Ber. **24**, 36 (1891).
16. A. R. Gray and R. C. Fuson. J. Am. Chem. Soc. **56**, 739 (1934). R. G. Kadesch. J. Am. Chem. Soc. **66**, 1207 (1944).
17. L. Bouveault and R. Locquin. Compt. rend. **135**, 179 (1902). H. K. Sen. Biochem. Z. **143**, 195 (1923).
18. N. Hall, J. E. Hynes, and A. Lapworth. J. Chem. Soc. **107**, 132 (1915).
19. G. Endres. Ann. **518**, 109 (1935). G. Endres and L. Kaufmann. Ann. **530**, 184 (1937); Ann. **535**, 1 (1938).
20. A. I. Virtanen and T. Laine. Biochem. J. **33**, 412 (1939).
21. K. Yamafuji and T. Akita. Enzymologia, **15**, 313 (1952).
22. J. Blom. Ber. **59**, 121 (1926); Biochem. Z. **194**, 385 (1928).
23. R. Novak and P. W. Wilson. J. Bacteriol. **55**, 517 (1948).

Can. J. Chem. Downloaded from www.nrcresearchpress.com by 210.87.254.105 on 09/05/12
For personal use only.

24. K. YAMAFUJI and F. YOSHIHARA. Enzymologia, **16**, 161 (1953).
25. A. R. THOMPSON. Australian J. Sci. Research, Ser. B, **4**, 180 (1951).
26. F. BERGMANN and R. SEGAL. Biochem. J. **62**, 542 (1956).
27. S. SEIFTER, P. M. GALLOP, S. MICHAELS, and E. MEILMAN. J. Biol. Chem. **235**, 2613 (1960).
28. H. L. YALE. Chem. Revs. **33**, 209 (1943).
29. I. D. SPENSER, J. C. CRAWHALL, and D. G. SMYTH. Chem. & Ind. 796 (1956).
30. C. CRAMER. Ber. **24**, 1198 (1891).
31. H. G. SÖDERBAUM. Ber. **24**, 1215 (1891).
32. A. WAHL. Compt. rend. **144**, 922 (1907); Bull. soc. chim. France, [4], **3**, 31 (1908).
33. H. G. SÖDERBAUM. Ber. **25**, 904 (1892).
34. G. PONZIO and I. DE PAOLINI. Gazz. chim. ital. **56**, 247 (1926).
35. C. CRAMER. Ber. **25**, 713 (1892).
36. F. C. PALAZZO. Gazz. chim. ital. **43**, 51 (1913). F. C. PALAZZO and V. EGIDI. Gazz. chim. ital. **43**, 57 (1913).
37. L. WOLFF. Ann. **260**, 79 (1890).
38. J. G. WOOD, M. R. HONE, M. E. MATTNER, and C. P. SYMONS. Australian J. Sci. Research, Ser. B, **1**, 38 (1948).
39. C. ULPIANI. Gazz. chim. ital. **46**, 1 (1916).
40. J. PLUCKER and E. D. AMSTUTZ. J. Am. Chem. Soc. **62**, 1512 (1940).
41. CH. GRÄNACHER, M. GERÖ, A. OFNER, A. KLOPFENSTEIN, and E. SCHLATTER. Helv. Chim. Acta, **6**, 458 (1923).
42. R. GAUDRY and R. A. MCIVOR. Can. J. Chem. **29**, 427 (1951).
43. J. MEISENHEIMER and W. THEILACKER. *In* Stereochemie. Vol. 3. *Edited by* K. Freudenberg. F. Deuticke, Leipzig and Vienna. 1932. p. 1040.
44. A. HANTZSCH. Ber. **24**, 13, 31, 1192 (1891).
45. J. MEISENHEIMER and W. THEILACKER. *In* Stereochemie. Vol. 3. *Edited by* K. Freudenberg. F. Deuticke, Leipzig and Vienna. 1932. p. 974.
46. A. H. BLATT and R. P. BARNES. J. Am. Chem. Soc. **56**, 1148 (1934). A. F. FERRIS. J. Org. Chem. **25**, 12 (1960). A. F. FERRIS, G. S. JOHNSON, and F. E. GOULD. J. Org. Chem. **25**, 1813 (1960).
47. C. A. GROB. Bull. soc. chim. France, 1360 (1960).
48. W. DIECKMANN. Ber. **33**, 579 (1900).
49. W. DIECKMANN and A. GROENEVELD. Ber. **33**, 959 (1900).
50. W. STEINKOPF. Ann. **434**, 21 (1923).
51. C. H. DEPUY and R. W. KING. Chem. Revs. **60**, 431 (1960).
52. A. PALM and H. WERBIN. Can. J. Chem. **31**, 1004 (1953).
53. A. HANTZSCH and A. MIOLATI. Z. physik. Chem. **10**, 1 (1892).
54. J. K. H. INGLIS and L. E. KNIGHT. J. Chem. Soc. **93**, 1595 (1908).
55. W. HIEBER and F. LEUTERT. Ber. **62**, 1839 (1929).
56. R. H. BARRY and W. H. HARTUNG. J. Org. Chem. **12**, 460 (1947).
57. V. MEYER and A. JANNY. Ber. **15**, 1525 (1882).
58. J. SCHMIDT and K. TH. WIDMANN. Ber. **42**, 1886 (1909).
59. L. BOUVEAULT and R. LOCQUIN. Bull. soc. chim. France, [3], **31**, 1049, 1055, 1061 (1904). R. LOCQUIN. Bull. soc. chim. France, [3], **31**, 1068 (1904).
60. H. EBERT. Ann. **229**, 45 (1885).
61. V. V. FEOFILAKTOV and A. S. ONISHCHENKO. J. Gen. Chem. (U.S.S.R.), **9**, 304 (1939). H. MCILWAIN and G. M. RICHARDSON. Biochem. J. **33**, 44 (1939).
62. H. BERGREEN. Ber. **20**, 531 (1887).
63. L. WOLFF. Ann. **399**, 309 (1913).
64. A. MEYER. Ber. **21**, 1306 (1888).
65. W. WISLICENUS and R. GRÜTZNER. Ber. **42**, 1930 (1909).
66. A. S. ONISHCHENKO. J. Gen. Chem. (U.S.S.R.), **11**, 197 (1941).
67. G. LEPERCQ. Bull. soc. chim. France, [3], **9**, 630 (1893); [3], **11**, 295, 297, 883, 886 (1894). K. E. HAMLIN and W. H. HARTUNG. J. Biol. Chem. **145**, 349 (1942).
68. N. KORNBLUM and J. H. EICHER. J. Am. Chem. Soc. **78**, 1494 (1956). N. KORNBLUM, R. K. BLACKWOOD, and D. D. MOOBERRY. J. Am. Chem. Soc. **78**, 1501 (1956). N. KORNBLUM, R. K. BLACKWOOD, and J. W. POWERS. J. Am. Chem. Soc. **79**, 2507 (1957).
69. A. HANTZSCH and W. WILD. Ann. **289**, 285 (1896).
70. A. BAEYER. Ann. **131**, 291 (1864). M. CONRAD, C. A. BISCHOFF, and M. GUTHZEIT. Ann. **209**, 211 (1881).
71. E. E. BLAISE and H. GAULT. Bull. soc. chim. France, [4], **9**, 451 (1911).
72. R. SERDA and J. WIEDEMANN. Ber. **23**, 3284 (1890).
73. E. E. BLAISE and H. GAULT. Bull. soc. chim. France, [4], **9**, 458 (1911).
74. P. J. TARBOURIECH. Compt. rend. **156**, 75 (1913).
75. H. G. SÖDERBAUM. Ber. **24**, 1988 (1891).
76. E. E. BLAISE and H. GAULT. Bull. soc. chim. France, [4], **1**, 75 (1907).
77. C. GASTALDI. Gazz. chim. ital. **53**, 635 (1923).
78. F. GARELLI. Gazz. chim. ital. **21**, 173 (1891).
79. L. ROUSSET. Bull. soc. chim. France, [3], **17**, 302 (1897). *Quoted from* Beilstein, **10**, 745.
80. T. R. SESHADRI and S. VARADARAJAN. Proc. Indian Acad. Sci. A, **37**, 514 (1953).
81. P. WALDEN. Z. physik. Chem. **10**, 638 (1892).
82. W. A. NOYES. Org. Syntheses, **2**, 108 (1943).

Can. J. Chem. Downloaded from www.nrcresearchpress.com by 210.87.254.105 on 09/05/12
For personal use only.

83. E. FRANKLAND and B. F. DUPPA. Ann. **145**, 78 (1868).
84. L. BOUVEAULT and A. WAHL. Bull. soc. chim. France [3], **25**, 1031 (1901).
85. C. A. BISCHOFF. Ann. **214**, 38 (1882).
86. L. RUZICKA, A. BORGES DE ALMEIDA, and A. BRACK. Helv. Chim. Acta, **17**, 183 (1934).
87. F. DICKENS, G. A. R. KON, and J. F. THORPE. J. Chem. Soc. **121**, 1496 (1922).
88. E. ERLENMEYER. Ann. **271**, 137 (1892).
89. D. O. HOLLAND and J. H. C. NAYLER. J. Chem. Soc. 280 (1953).
90. T. S. OAKWOOD and C. A. WEISGERBER. Org. Syntheses, **3**, 114 (1955).
91. R. M. HERBST and D. SHEMIN. Org. Syntheses, **2**, 519 (1943).
92. J. A. BENTLEY, K. R. FARRAR, S. HOUSLEY, G. F. SMITH, and W. C. TAYLOR. Biochem. J. **64**, 44 (1956).
93. R. W. HUFFERD and W. A. NOYES. J. Am. Chem. Soc. **43**, 925 (1921).
94. A. R. GRAY and R. C. FUSON. J. Am. Chem. Soc. **56**, 1367 (1934).
95. J. B. NIEDERL and A. ZIERING. J. Am. Chem. Soc. **64**, 885 (1942).

Can. J. Chem. Downloaded from www.nrcresearchpress.com by 210.87.254.105 on 09/05/12
For personal use only.

Can. J. Chem. Downloaded from www.nrcresearchpress.com by 210.87.254.105 on 09/05/12
For personal use only.

ADSORPTION OF BENZENE AND ETHANOL UP TO HIGH RELATIVE PRESSURES ON FINELY DIVIDED SODIUM CHLORIDE

PART I. PARTICLE SIZE EFFECTS AND THE ADSORPTION OF BENZENE
PART II. THE LOWERING OF SURFACE FREE ENERGY BY ETHANOL[1]

R. R. WEILER,[2] J. BEECKMANS,[3] AND R. MCINTOSH

ABSTRACT

Adsorption of benzene has been studied using four samples of fine sodium chloride. The range of relative pressures employed extended to 0.99. The data were employed to show that a correction to the relative pressure should be applied because of the curvature of the surface. The correction was made in the form of a reduction of the apparent relative pressure by application of the Kelvin equation, since the relative pressure over a convex surface would be less than over a plane surface. The adsorption data at high relative pressures for several samples of salt could then be represented by a common curve. It was further concluded that the thick-layer theory of adsorption due to Frenkel, Halsey, and Hill was applicable to adsorption on salt. Adsorption data for ethanol were then obtained and the reduction of surface free energy of the salt by the saturated vapor was evaluated. This figure was then combined with van Zeggeren's and Benson's value of the solid–liquid interfacial free energy for salt and ethanol to provide a provisional value of the surface free energy of sodium chloride of 227 ergs cm^{-2}.

INTRODUCTION

Theoretical estimates of the total surface energy of ionic crystals at the absolute zero of temperature have been made many times, and the values are quite sensitive to the assumed model and to the interaction terms employed (1, 2, 3). The values may even change importantly with the values of the van der Waal's coefficients which are chosen (4). At $T = 0$, $E_s = \sigma_{so}$, where σ_{so} is the surface free energy of the solid. E_s at all temperatures closely approximates the value of the total surface enthalpy H_s, which can be measured by the method of Lipsett, Johnson, and Maass (5). Experimental values of H_s have been much greater than the computed values of E_s, and other procedures to measure either E_s or σ_{so} have been sought. One such possible procedure involves the determination of the enhanced solubility of small particles and the use of the Kelvin equation for an assumed spherical interface between particles and the solution saturated with respect to the particles. This measurement leads to a value of σ_{sl}. The additional relation

$$\sigma_{sv}^* - \sigma_{sl} = \sigma_{lv} \cos \phi$$

is available, and with many systems the wetting angle is small so that $\cos \phi \simeq 1.0$. σ_{sv}^* is the free energy of the solid-saturated vapor interface. Although the value of this quantity cannot be determined, the lowering of surface free energy from that of the clean solid surface may be determined from the Gibbs relation

$$\sigma_{so} - \sigma_{sv}^* = RT \int_0^{p^\circ} \Gamma \, d \ln p \qquad [1]$$

where Γ is the surface excess of adsorbed vapor in moles cm^{-2} and p° is the saturated vapor pressure. Thus a value of σ_{so} may be obtained. To summarize the state of knowledge of the total surface energy of sodium chloride one may note that the value of $E_s = \sigma_{so}$ (at $T = 0$) from the work of Benson, Schreiber, and Patterson (2), which takes into account surface distortion in conjunction with Shuttleworth's result in which

[1]*Manuscript received February 13, 1961.*
Contribution from the Department of Chemistry, University of Toronto, Toronto, Ontario.
[2]*Graduate Student. Present address: Institute of Oceanography, Dalhousie University, Halifax, Nova Scotia.*
[3]*Graduate Student. Present address: Ontario Research Foundation, Toronto, Ontario.*

Can. J. Chem. Downloaded from www.nrcresearchpress.com by 210.87.254.105 on 09/05/12
For personal use only.

dipole–dipole and dipole–quadrupole interactions were considered, leads to 113 ergs cm^{-2}. A more recent treatment by Benson, Balk, and White leads to the value 124 ergs cm^{-2} for the {100} face (3). Van Zeggeren and Benson's (6) quantum mechanical calculation leads to 187 ergs cm^{-2}. Experimental values of H_s for room temperature have been 386 ergs cm^{-2} by Lipsett, Johnson, and Maass (5), 395 ergs cm^{-2} by Boyd and Harkins (7), and 366 ergs cm^{-2} by Hutchison and Manchester (8). Benson and Benson (9) found a value of 305 ergs cm^{-2}, and with purer salt, Benson, Schreiber, and van Zeggeren (10) obtained a value of 276 ergs cm^{-2}. The surface specific heat C_{p_s} is not sufficient to account for the difference in values of 276 ergs cm^{-2} and 124 ergs cm^{-2}, which are the best experimental and theoretical values available.

Van Zeggeren and Benson (11) investigated the enhanced solubility of fine sodium chloride in ethanol and obtained 171 ergs cm^{-2} for σ_{s1}, which was considered to approximate σ_{so}. Since σ_{so} at room temperature must be less than E_s at $T = 0$, this result is inconsistent with the theoretical value of 124 ergs cm^{-2} but it is consistent with the experimental value of $E_s = 276$ ergs cm^{-2}. However, it is advantageous to obtain σ_{so} rather than σ_{s1}, and to this end an attempt has been made to evaluate $\sigma_{so} - \sigma_{sv^*}$. The attempt is described in Part II of this paper. As experimental observations cannot be made for relative pressures of 1.0, it is important to know something of the shape of the adsorption isotherm at relative pressures as close to 1.0 as feasible. Since sintering in the presence of water vapor is known to occur (12), and since Benson obtained some evidence of the sintering of salt in the presence of large pressures of ethanol (13), it was decided to study the adsorption of benzene at these high relative pressures. The study using benzene supports the contention of theory due to Frenkel (14), Halsey (15), and Hill (16) that adsorption approaches infinity as p/p° approaches 1.0 according to the expression $-a/\Gamma^3 = \ln (p/p^\circ)$, so that $-a/\Gamma^3$ is zero at $p/p^\circ = 1.0$. The study also reveals that the larger the specific surface of the powder sample, the less is the adsorption (in relative terms) at high relative pressures. The importance of the curvature of the surface of the particles has been recognized and discussed by Hill (17). Although discrepant results between two sets of samples remain to be clarified, the correction for surface curvature can apparently be made by application of the Kelvin equation and the assumption of spherical particles for which the surface free energy is taken to be that of bulk liquid. The details of this study are described in Part I.

PART I. PARTICLE SIZE EFFECTS AND THE ADSORPTION OF BENZENE

Experimental

The apparatus for measuring adsorption is shown schematically in Fig. 1. One part consisted of a McBain-type balance. The extension of the quartz spiral was observed by its movement relative to a pointer on a long quartz rod attached to the same support. Thus temperature effects and settling of the column were eliminated from the observations. Changes of weight of about 1 μg could be detected when extension of the spiral was small, and 6 μg was the limit of detection at large extension because the pointers moved out of the focal plane of the lens system. The weight of adsorbent varied between 0.05 and 0.13 g.

The temperature of the column was maintained at $92 \pm 1^\circ$ C by a control unit described by Benedict (18). The chamber holding the quartz bucket and sample was kept at a temperature of approximately 35° C with a variation of $\pm 0.1^\circ$ C as measured in the surrounding air bath.

The adsorbates benzene and ethanol were obtained purified and dried from the

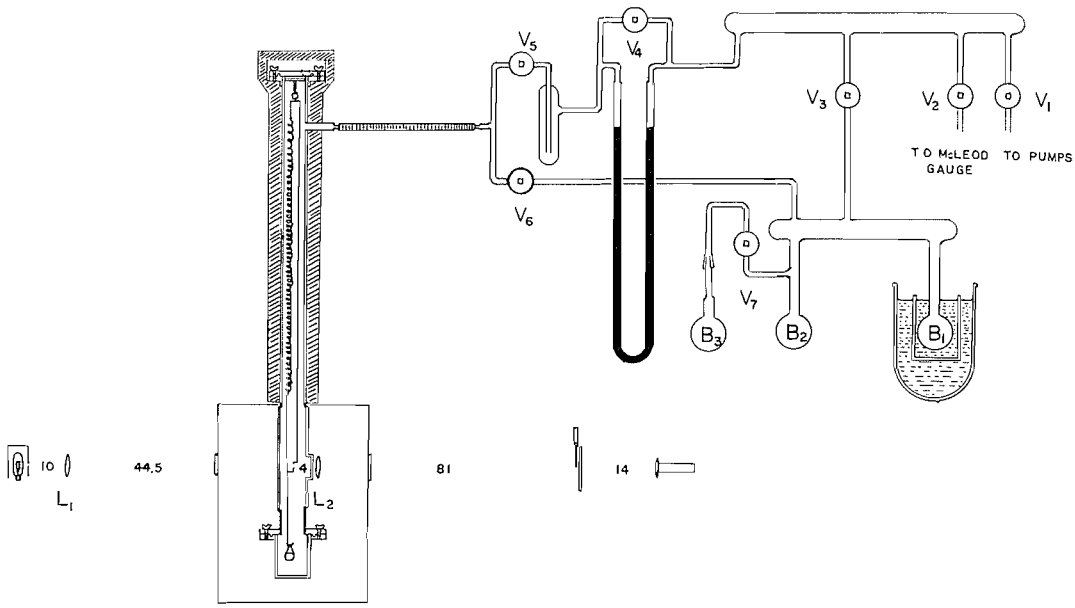


FIG. 1. Schematic representation of adsorption apparatus.

Organic Chemistry Section. After storage over Drierite they were distilled into the adsorption assembly under vacuum, and were repeatedly frozen and melted under vacuum to eliminate permanent gases. The desired adsorbate pressures were generated by fixing the temperature of the surrounding thermostat at the appropriate values. Temperature variations did not exceed $\pm 0.05°$ C. All glass tubing and Hoke 413 metal valves connecting the vapor reservoirs with the adsorption assembly were kept above 35° C to prevent condensation. The vapor pressures of the adsorbates were computed from the equations

$$\log_{10} p_{\text{mm}} = -\frac{1882.0}{244.0+t}+9.0963 \qquad \text{for } t < 4.5° \text{ C}$$

$$\log_{10} p_{\text{mm}} = -\frac{1206.35}{220.237+t} \qquad \text{for } t > 5.5° \text{ C}$$

for benzene (19) and from

$$\log_{10} p_{\text{mm}} = -\frac{2310.43}{273.2+t}+9.5171$$

based upon data in the *Handbook of Physics and Chemistry* (20) for ethanol.

Corrections for buoyancy, etc. in the extension of the spiral system were made by observing the extension without adsorbent in the sample bucket.

The salt samples were prepared in the apparatus described by Moffat and McIntosh (12) which had been modified so that the carrier stream was recycled nitrogen. One sample was obtained from Dr. J. A. Morrison and was an aliquot of the sample B studied by Morrison and Patterson (21). Analyses for nitrate were performed for all samples (22) and the percentage P of surface molecules that are sodium nitrate may be estimated from the approximate relation $P = 1200\,X/A$ where X is the weight% of sodium nitrate and A is the area (23). Obviously, this equation cannot apply to sample 45 and the detection of lines due to sodium nitrate in similar samples by X-ray examination certainly suggests that the impurities are not completely in the surface layers (12). The

Can. J. Chem. Downloaded from www.nrcresearchpress.com by 210.87.254.105 on 09/05/12
For personal use only.

surface area of the samples was usually obtained by the adsorption of carbon dioxide, and in the case of the sample received from Dr. Morrison, an area measured by nitrogen adsorption was available. The areas obtained using the different adsorbates differ and lead to a variety of estimates of particle size of which the effects are discussed later. In an adsorption experiment using benzene or ethanol the time to equilibrium was about 45 minutes. Both adsorption and desorption points were obtained and no hysteresis in the isotherms was discovered. The salt samples were not heated during the pumping for fear of sintering, so that evacuation was carried out in the main at about 30° C.

Results

Experiments using four samples will be discussed. These samples were labelled No. 7, No. 25, No. 45, and NRC. Relevant data concerning them are given in Table I. Areas

TABLE I

Sample No.	% nitrate	Area by benzene, $m^2 g^{-1}$	Area by N_2, $m^2 g^{-1}$	Area by CO_2, $m^2 g^{-1}$
7	0.5	8.97	39.9	30.0
25	0.5	4.90	21.8	21.6
45	5.0	14.9	66.5	70.0
NRC	0.05–0.10	11.7	52.0	—

determined using benzene were, of course, available for all the samples and were calculated using the familiar B.E.T. multilayer theory (24) and an area for the benzene molecule of 35.0 Å^2 (25). Nitrogen areas were obtained from the ratio of the nitrogen area to the benzene area for sample NRC. Areas using carbon dioxide were employed by us merely to select the samples, although it is interesting to note a reasonable measure of agreement between these values and the values computed for nitrogen. For the purposes to be discussed below, none of these values of area satisfactorily accounted for the effect of particle size. The nature of the problem and the attempts made to resolve it will now be outlined.

If various samples of an adsorbent differ only in specific surface area, and if the surface of each sample may be considered as planar, the adsorption isotherms should be identical except for a proportionality factor. This factor might be estimated by means of a reliable theory of adsorption, or determined empirically without reference to any adsorption theory. When such attempts to correlate the adsorptive properties of one sample with another have been attempted in this laboratory, it has been found that a proportionality factor would usually suffice to superimpose one curve upon another in the region of low relative pressures, but not in the high. Moreover, those samples with the large specific surfaces always showed less adsorption at high relative pressures when the scale factor obtained from the low relative pressure region was employed. This phenomenon was attributed to a particle-size effect, which for the higher relative pressure range, may be thought of as producing an enhanced vapor pressure over the curved surface of the liquidlike adsorbed layers. Hill has discussed the effect of curvature on the adsorption of thick layers (17). In dealing with the same problem we have found the use of the Kelvin equation satisfactory provided that a reasonable assessment of area and hence particle size can be achieved.

In the case of the adsorption of benzene, a mean particle size was calculated on the basis of the area determined by the use of the B.E.T. equation and the assumption that the particles were spherical. The value of the mean radius was then employed with the

Can. J. Chem. Downloaded from www.nrcresearchpress.com by 210.87.254.105 on 09/05/12
For personal use only.

Kelvin equation $RT \ln p/p^\circ = 2\sigma\bar{V}/r$, taking the value of the surface free energy of the curved interface to be 27.0 dynes cm^{-1} at 35.0° C. This provided a value of the pressure p over the curved surface which is greater than the value p° over a plane surface of the liquid adsorbate. On this basis the equilibrium pressure is a lower relative pressure, by the ratio p°/p, than the experimenter would expect to obtain if the particles were considered to have planar surfaces. A proportionality factor was also calculated on the basis of adsorption in the low relative pressure range. The proportionality factors for the four samples, in conjunction with the corrections to the relative pressures (which become important in the higher relative pressure range) should suffice to yield a common adsorption curve for the four samples. A comparison is given in Fig. 2. Clearly, samples 7 and 25 may be paired, and also samples 45 and NRC. Agreement is satisfactory in

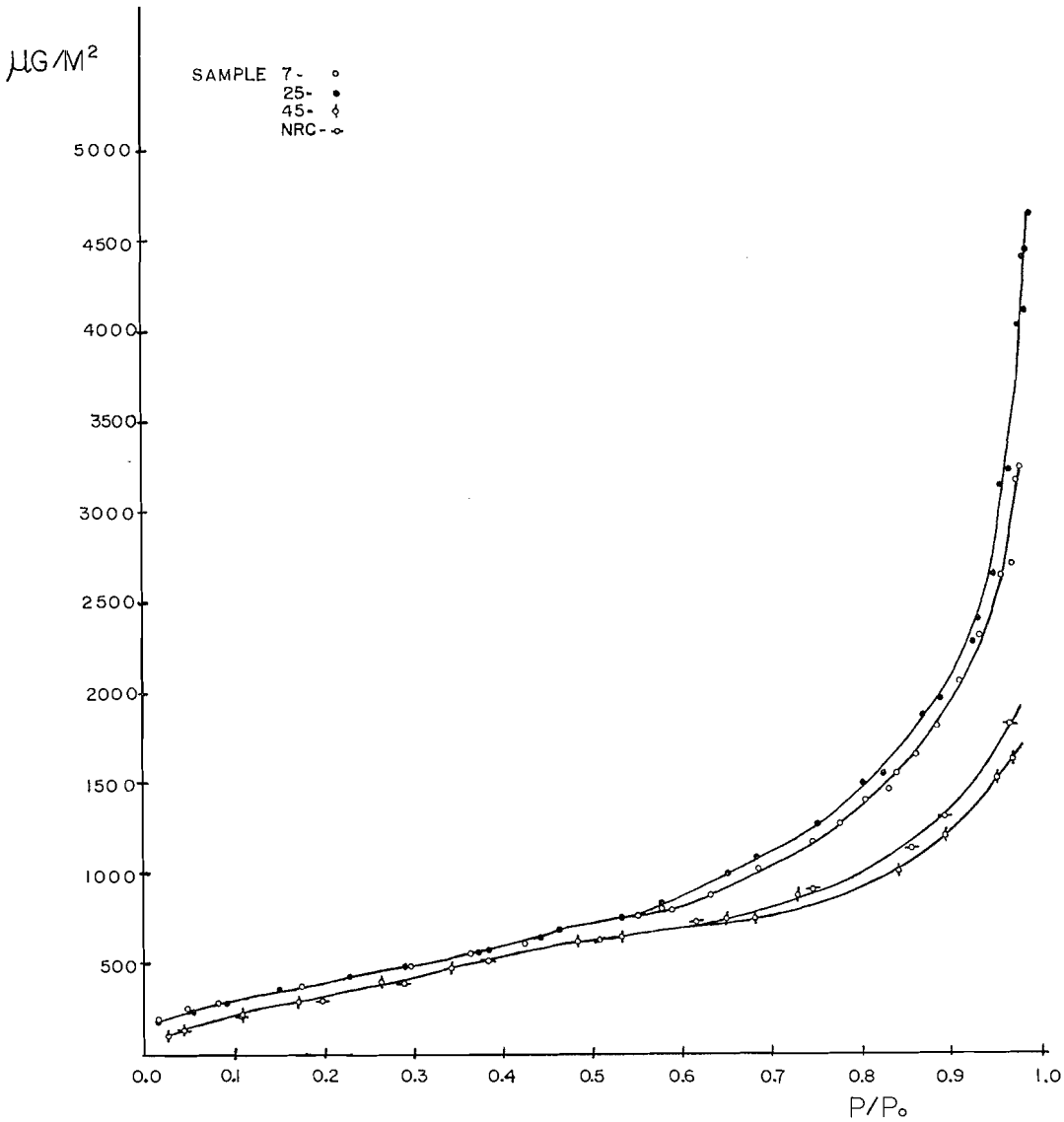


FIG. 2. Adsorption isotherms for benzene at 35° C represented after application of a scale factor and correction of p/p° based upon the area to benzene.

Can. J. Chem. Downloaded from www.nrcresearchpress.com by 210.87.254.105 on 09/05/12
For personal use only.

Can. J. Chem. Downloaded from www.nrcresearchpress.com by 210.87.254.105 on 09/05/12
For personal use only.

the low-adsorption range, which shows that the appropriate proportionality factor has been achieved for each pair of samples, although it has not been for all four samples. Leaving aside for the moment the fact that all four samples have not been made to show a common adsorption curve even in this range, it is also clear that success has not been achieved in the high-pressure range for either pair of samples.

The areas by nitrogen were next employed to obtain the mean particle radius, and as before, the value of the saturation pressure for particles of such curvature predicted by the use of the Kelvin equation. When this was done samples 7 and 25 showed a common adsorption curve and similar results were found for samples 45 and NRC. In spite of this partial success in correlating adsorption data for the samples, it was considered that the correction factor applied on the basis of nitrogen areas was somewhat too great, for the reason outlined below. Since the thick-layer theory of adsorption due to Frenkel (14), Halsey (15), and Hill (16), should be applicable in this range, a plot of $1/\Gamma^3$ vs. $\ln p/p^\circ$ should yield a straight line, and should pass through zero (Γ infinite) for a corrected relative pressure of 1.0. For samples 7 and 25, for which the data were more extensive, intercepts were found at a value of 0.966 when relative pressures corrected for the particle-size effect were employed. The saturation pressures estimated for particles of the size indicated by the nitrogen areas were 1.057 and 1.031 times that for a plane surface in the case of samples 7 and 25, respectively. It was therefore found that the predicted saturation pressures should have been 1.057×0.966 and 1.031×0.966, that is 1.022 and 0.996 times the usual saturation pressure for these two samples. The latter figure is well within experimental error of 1.0. Thus it was shown that the experimental equilibrium pressures over sample 7 were, on a relative pressure scale, 1/1.022 times those thought to have been generated. Using relative pressures corrected in this manner and a proportionality factor of 1.83, the data for samples 7 and 25 could be represented by a common curve, as shown in Fig. 3 and Table II. Although the data

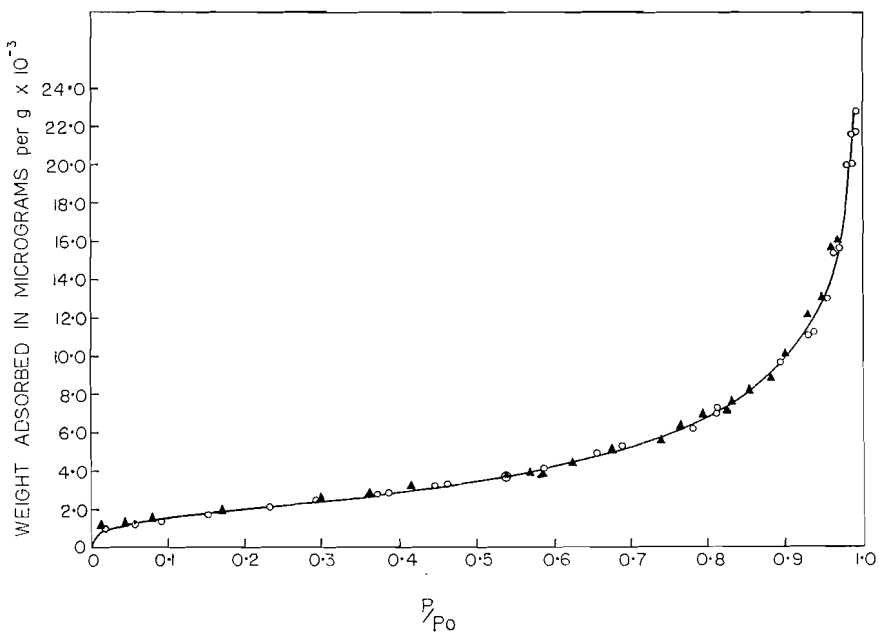


FIG. 3. Representation of the isotherms for samples 7 and 25 using a scale factor and a corrected value of p/p°.

TABLE II

Adsorption data for samples 25 and 7 at 35° C

Sample 25 (No corrections; T = 35.9° C)		Sample 7 (Relative pressure corrected by 1/1.022; T = 35.1°; col. 1, weight adsorbed g^{-1} is divided by 1.83; col. 2, weight adsorbed g^{-1} is increased by 3.0×10^3 μg)		
Weight, μg per g$\times10^{-3}$	Relative pressure	Weight, μg per g$\times10^{-3}$	Weight, μg per g$\times10^{-3}$	Relative pressure
0.83	0.018	0.95	4.75	0.017
1.11	0.055	1.20	5.21	0.047
1.34	0.091	1.40	5.56	0.080
1.72	0.150	1.83	6.35	0.171
2.09*	0.229	2.35	7.30	0.293
2.41	0.290	2.68	7.91	0.358
2.74	0.372	3.03	8.54	0.414
2.79*	0.384	3.72	9.82	0.538
3.16	0.442	3.92	10.2	0.570
3.37*	0.461	3.89*	10.1	0.586
3.67	0.537	4.31	10.9	0.624
4.08*	0.580	5.03	12.2	0.677
4.90	0.654	5.78*	13.6	0.738
5.32*	0.686	6.24	14.4	0.766
6.15	0.754	6.88*	15.6	0.795
7.31*	0.808	7.10	16.0	0.823
6.91	0.810	7.60	16.9	0.830
7.56	0.830	8.10*	17.8	0.853
9.14	0.876	8.90	19.3	0.878
9.62	0.893	10.1*	21.5	0.898
10.0	0.902	12.2	25.3	0.929
11.2	0.931	13.0*	26.8	0.948
11.8	0.938	15.6	31.5	0.962
13.0	0.954	15.9	32.1	0.967
15.4*	0.962			
15.8	0.969			
19.8	0.983			
21.6*	0.987			
20.1	0.988			
21.8	0.992			
22.8	0.994			

*Designates desorption.

were much less extensive for samples 45 and NRC, the correction factors were established as $1/1.05_6$ and $1/1.03_5$, respectively, for these two samples. The adsorption data for them are depicted in Fig. 4 and given in Table III. It is to be noted that in estimating these correction factors no account was taken of the thickness of the adsorbed layer, because that thickness was only a few per cent of the particle radius.

Several matters remain to be discussed. The two pairs of salt samples cannot be made to yield a common adsorption curve by means of a proportionality factor along with corrections to the relative pressure. However, as is illustrated in Fig. 5, samples 7 and 45 may be made to correspond from a relative pressure (corrected) of about 0.37 to the highest relative pressures, by addition of 3.0×10^3 μg per g to the data for sample 7 (see Table II). This means that adsorption data of all four samples may be made to fit a single curve above a relative pressure of 0.37. Chemical composition, as measured by nitrate content, does not appear to be the cause of the difference between pairs of samples. Similarly, surface area does not permit a grouping into pairs. From the experimental standpoint, the benzene, employed to generate the equilibrium pressures, was changed between the accumulation of the two sets of data. There is no independent reason, however, to believe that this is the cause. Possibly the structure of the particles

Can. J. Chem. Downloaded from www.nrcresearchpress.com by 210.87.254.105 on 09/05/12
For personal use only.

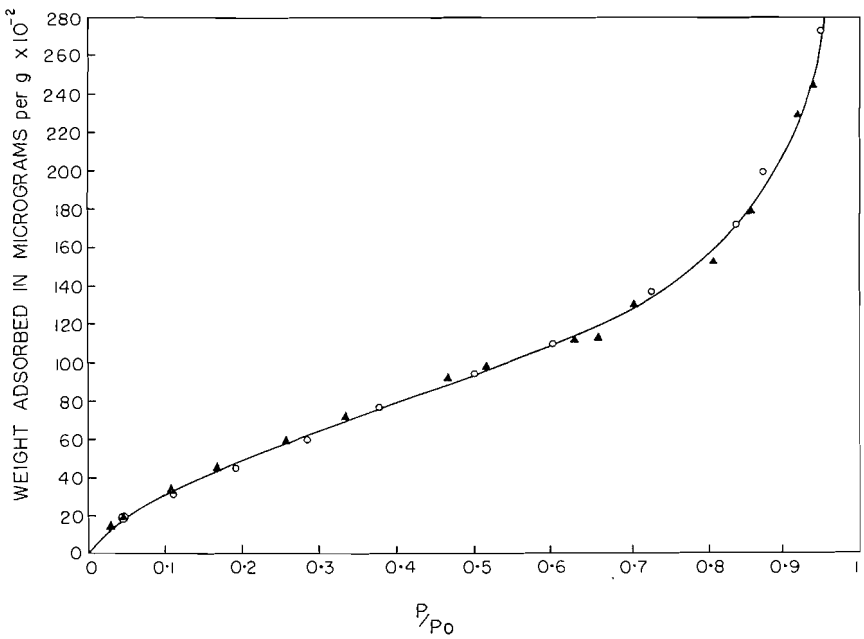


FIG. 4. Representation of the isotherms for samples 45 and NRC using a scale factor and a corrected value of $p/p°$.

TABLE III
Adsorption data for samples 45 and NRC at 35.2° C

Sample 45 (Relative pressure corrected by 1/1.056)		Sample NRC (Relative pressure corrected by 1/1.035)	
Weight, μg per g$\times 10^{-3}$	Relative pressure	Weight$\times$1.28, μg per g$\times 10^{-3}$	Relative pressure
1.43	0.025	1.87	0.041
1.89	0.042	3.10	0.108
3.30	0.106	4.39	0.194
4.43	0.165	5.89	0.285
5.90	0.255	7.64	0.376
7.04	0.331	9.36	0.500
9.21	0.465	11.0	0.602
9.71*	0.514	13.7	0.732
11.2	0.629	17.2	0.839
11.3	0.658	19.8*	0.877
13.2*	0.704	27.4	0.947
15.3	0.812		
18.0	0.862		
23.0	0.918		
24.5	0.938		

*Designates desorption.

in samples of widely differing areas is involved. Agreement in the high-pressure range could still be expected because the influence of the surface is small, apart from the effect of curvature.

Secondly, it should be noted that a value of particle size is employed which is not based upon the area obtained using nitrogen. Presumably this arises because there is a distribution of particle sizes and a variation of the curvature effect with particle size. The intercept method, based upon the thick-layer theory, provides a weighted average particle size dependent upon the Kelvin effect.

Can. J. Chem. Downloaded from www.nrcresearchpress.com by 210.87.254.105 on 09/05/12
For personal use only.

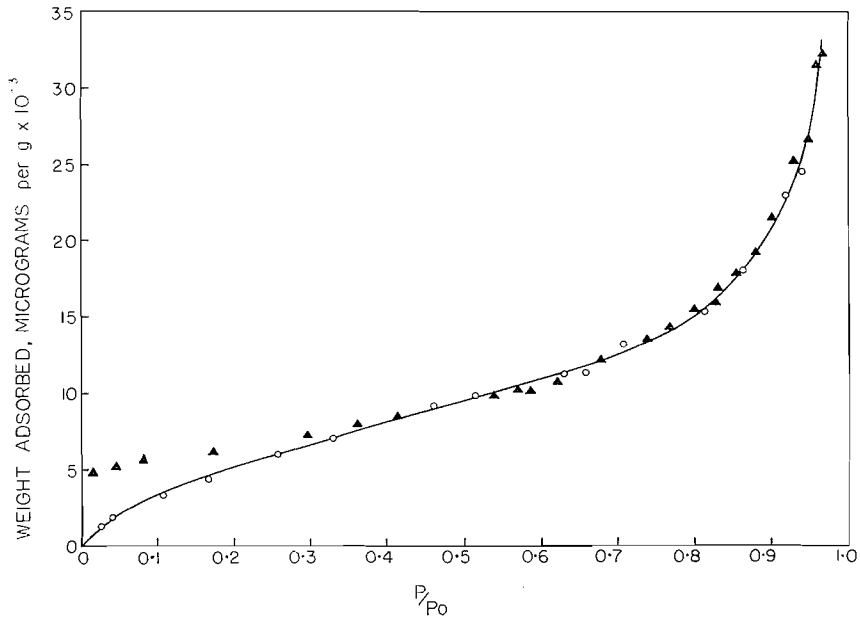


FIG. 5. Representation of the isotherms for samples 7 and 45 using an additive correction to amount adsorbed and a corrected value of p/p°.

Thirdly, there are undoubtedly other mechanisms which might be suggested to explain why the relative adsorption at high pressures is smaller for samples of relatively larger areas as these are normally determined by appeal to adsorption data up to relative pressures of about 0.4. The suggestion made here has the merit of simplicity, and is based upon the well-known phenomenon of enhanced vapor pressure of small droplets. It is important to observe that the adsorptions at high pressures are made to correspond well with one another by applying this idea. Further data are required to confirm its utility, but the initial results show promise.

Finally, on the basis of such data, it seems justified to employ the thick-layer adsorption theory for adsorption at high relative pressures. This conclusion is of importance in connection with the adsorption data for ethanol from which the lowering of surface free energy is calculated in Part II.

PART II. THE LOWERING OF SURFACE FREE ENERGY BY ADSORPTION OF ETHANOL

Four samples of sodium chloride were used in studying the adsorption of ethanol, and quite good agreement among the values of lowering of surface free energy was found. This agreement was somewhat fortuitous, however, since differences in the value of surface free energy lowering appeared over the three sections into which the data were subdivided. These sections were the low, the intermediate, and the high relative pressures, respectively. In our opinion the most reliable value was obtained with the sample designated NRC. There are two reasons for this view.

The first three samples were studied using an adsorption assembly which had less adequate temperature control along the column and within the chamber containing the sample. Moreover, the sample chamber was attached to the column by means of a greased taper joint, which might have caused some contamination of the surface. The assembly used to study sample NRC (and for the benzene adsorptions reported in

Can. J. Chem. Downloaded from www.nrcresearchpress.com by 210.87.254.105 on 09/05/12
For personal use only.

Part I), was free from any greased joints, as metal chambers or plates and indium gaskets were employed for those parts of the assembly which were removable.

To evaluate the Gibbs integral for the first region involving relative pressures less than 0.2, the equation

$$[2] \qquad \sigma_{so}-\sigma_{sv} = -\frac{RT}{(A+B)A_0}\ln\frac{B(p^\circ-p)}{Ap+Bp^\circ}$$

was employed.

This equation results from expressing the quantity adsorbed by the B.E.T. equation, and substituting the appropriate expression into equation [1]. The B.E.T. equation expressed the adsorption data admirably from 0.02 to 0.20 relative pressure. In equation [2] A is $(C-1)/(\Gamma_m C)$ and B is $1/(\Gamma_m C)$, where Γ_m is the number of moles required to complete a monolayer on 1 gram of adsorbent. A_0 is the area of the sample in square centimeters per gram. To check this procedure the Gibbs integral was also expressed as

$$\sigma_{so}-\sigma_{sv} = \frac{RT}{A_0}\int_0^{\Gamma} d\Gamma + \frac{RT}{A_0}\int_0^{p/\Gamma} \Gamma d \ln p/\Gamma,$$

and a plot of Γ versus $\ln p/\Gamma$ was integrated graphically from the extrapolated value of p/Γ at $\Gamma = 0$, up to the value at the relative pressure of about 0.2. The agreement between the two methods was, in the case of two separate experiments, 17.5 and 17.3 ergs cm^{-2}, and 20.5 and 18.7 ergs cm^{-2}, respectively.

Evaluation of the integral for the second section of data was performed graphically. The range of relative pressure over which graphical integration was performed was from about 0.2 to 0.97. In this range the contribution to the lowering of surface free energy fell between 13.8 and 15.6 ergs cm^{-2} for all runs, and as the limits of integration varied slightly for each run, the agreement was considered satisfactory.

Because of the conclusions derived from the study of the high relative pressure end of the benzene isotherms, the evaluation of the integral for the ethanol data from 0.97 to 1.0 of the relative pressure range was performed analytically. It should be noted that the value of the surface free energy lowering does not depend upon whether or not the Kelvin correction has been applied, but the upper limit of relative pressure at which Γ approaches infinity will exceed the experimental value of 1.0, and this fact should be considered if the limit of relative pressure is involved in the analytical form by which the evaluation is made.

Insufficient data at the very high experimental relative pressures above 0.97, introduced some uncertainty in the evaluation of the lowering of the surface free energy. With the data available three procedures were possible. These were: (1) To utilize the data obtained for relative pressures above 0.80 in the form of a Hill plot (i.e. $1/\Gamma^3$ vs. $\ln p/p^\circ$) and ignore the two values at the highest pressures (which might be considered incorrect, since they suggest that $\Gamma \rightarrow \infty$ at the experimental relative pressure 1.0) and thus obtain the slope a from the lower relative pressure data. This resulted in a value of $-\Delta\sigma$ from 0.97 relative pressure to Γ infinite of 2.1 ergs cm^{-2}. (2) To utilize the data for the four highest relative pressure points to obtain the slope a of the Hill plot. This yielded 0.35 ergs cm^{-2}. (3) To use the knowledge of the area determined with nitrogen to predict the required relative pressure to make Γ infinite, and employ this along with all data for relative pressures above 0.80 to obtain the slope a. This gives a value 1.2 ergs cm^{-2}.

If one separates the data obtained into two groups, namely those data found in the first adsorption run, and those found in subsequent adsorption runs after what appeared to be sintering of the salt by the ethanol, the total lowering of surface free energy would

Can. J. Chem. Downloaded from www.nrcresearchpress.com by 210.87.254.105 on 09/05/12
For personal use only.

be 31.6 to 33.3 ergs cm^{-2} for the first adsorption before sintering occurred, or 35.6 to 37.3 for subsequent adsorptions. Taking the mean of these results, the lowering of surface free energy is 34.5 ± 2.9 ergs cm^{-2}. In the estimate of this value, in addition to the uncertainties arising from the procedures outlined above, there is the conversion of values to unit surface on the basis of an area to nitrogen reported as 52 $m^2 g^{-1}$. The area as measured by ethanol before sintering was 16.5 $m^2 g^{-1}$ on the basis of 20.7 $Å^2$ for the area of the ethanol molecule. The conversion factor of 0.317 was retained in dealing with the sintered sample, of ethanol area 11.2 $m^2 g^{-1}$. Van Zeggeren's and Benson's value of σ_{s1} was obtained at 25° C, while the value of 34.5 ± 2.9 ergs cm^{-2} was obtained at 35.3° C. However, these may be combined to give an approximate value of σ_{so} on assuming $\cos \phi = 1.0$; thus $\sigma_{so} \simeq 21.5 + 171 + 34.5 = 227$ ergs cm^{-2}. This value is consistent with the value 276 ergs cm^{-2} for the total surface enthalpy, and leads to a value of about 0.16 ergs cm^{-2} deg^{-1} for $\partial\sigma_{so}/\partial T$. Similar experiments to determine σ_{s1} and $\sigma_{so} - \sigma_{sv^*}$ for solvents other than ethanol are required to establish that the value derived for σ_{so} is independent of the solvent employed. For the moment the provisional value of 227 ergs cm^{-2} is suggested.

TABLE IV

Ethanol adsorption

(Weight of sample, 0.0847 g; sample designation NRC; temp., 35.3° C)

$p/p°$, uncorrected	Weight adsorbed, μg	$p/p°$, uncorrected	Weight adsorbed, μg
First adsorption		Second adsorption	
0.020	325	0.428	455
0.050	446	0.538	471
0.093	509	0.760	519
0.150	557	0.805	535
0.231	553	0.883	578
0.366	592	0.948	645
0.497	608	0.979	797
0.640	617	0.983	834
0.797	639		
0.860	695	Third adsorption	
0.921	713	0.018	215
0.969	865	0.042	314
0.986	1178	0.091	373
		0.181	415
First desorption		0.335	458
0.046	307	0.511	488
0.076	333	0.673	519
0.127	360	0.751	539
0.408	462	0.795	552
0.624	499	0.860	565
0.908	624	0.874	583
0.937	708	0.962	717
		0.995	3435
		0.996	3591

ACKNOWLEDGMENTS

We are pleased to acknowledge the financial support of this work by the Advisory Committee on Research, University of Toronto, and the National Research Council.

REFERENCES

1. R. SHUTTLEWORTH. Proc. Phys. Soc. A, **62**, 167 (1949).
2. G. C. BENSON, H. P. SCHREIBER, and D. PATTERSON. Can. J. Phys. **34**, 265 (1956).
3. G. C. BENSON, D. BALK, and P. WHITE. J. Chem. Phys. **31**, 109 (1959).
4. G. C. BENSON and R. MCINTOSH. Can. J. Chem. **33**, 1677 (1955).
5. S. G. LIPSETT, F. M. G. JOHNSON, and O. MAASS. J. Am. Chem. Soc. **49**, 1940 (1927).

Can. J. Chem. Downloaded from www.nrcresearchpress.com by 210.87.254.105 on 09/05/12
For personal use only.

6. F. VAN ZEGGEREN and G. C. BENSON. Can. J. Phys. **34**, 985 (1956).
7. G. E. BOYD and W. D. HARKINS. J. Am. Chem. Soc. **64**, 1190 (1942).
8. E. HUTCHINSON and K. E. MANCHESTER. Rev. Sci. Instr. **26**, 364 (1955).
9. G. C. BENSON and G. W. BENSON. Can. J. Chem. **33**, 232 (1955).
10. G. C. BENSON, H. P. SCHREIBER, and F. VAN ZEGGEREN. Can. J. Chem. **34**, 1553 (1956).
11. F. VAN ZEGGEREN and G. C. BENSON. Can. J. Chem. **35**, 1150 (1957).
12. J. B. MOFFAT and R. MCINTOSH. Can. J. Chem. **35**, 1511 (1957).
13. G. C. BENSON. Private communication.
14. J. FRENKEL. Kinetic theory of liquids. Oxford University Press, Oxford. 1946.
15. G. HALSEY. J. Chem. Phys. **16**, 931 (1948).
16. T. L. HILL. *In* Advances in catalysis. Vol. IV. Academic Press, Inc., New York. 1952.
17. T. L. HILL. J. Phys. & Colloid Chem. **54**, 1186 (1950).
18. M. BENEDICT. Rev. Sci. Instr. **8**, 252 (1937).
19. T. E. JORDAN. The vapour pressure of organic compounds. Interscience Publishers, New York. 1954.
20. HANDBOOK OF CHEMISTRY AND PHYSICS. 40th ed. Chemical Rubber Publishing Co. 1958–59.
21. J. A. MORRISON and D. PATTERSON. Trans. Faraday Soc. **52**, 764 (1956).
22. F. FEIGL. Qualitative analysis by spot tests. Nordemann Publishing Co., New York. 1939.
23. F. VAN ZEGGEREN, H. P. SCHRIEBER, and G. C. BENSON. Can. J. Chem. **34**, 1501 (1956).
24. S. BRUNAUER, P. H. EMMETT, and E. TELLER. J. Am. Chem. Soc. **60**, 309 (1938).
25. C. KEMBAL and E. K. RIDEAL. Proc. Roy. Soc. A, **187**, 53 (1946).

Can. J. Chem. Downloaded from www.nrcresearchpress.com by 210.87.254.105 on 09/05/12
For personal use only.

Can. J. Chem. Downloaded from www.nrcresearchpress.com by 210.87.254.40 on 09/05/12
For personal use only.

CATALYTIC ACTIVATION OF MOLECULAR HYDROGEN BY RUTHENIUM (III) CHLORIDE COMPLEXES[1]

J. F. HARROD,[2] STEFANIA CICCONE, AND J. HALPERN

ABSTRACT

Ruthenium(III) chloride, in aqueous HCl solution, was found to activate H_2 homogeneously and to catalyze the reduction by H_2 of Ru(IV) and Fe(III). The kinetics of these reactions were examined and, in each case, the rate law was found to be $-d[H_2]/dt = k_1[H_2][Ru^{III}]$ where $k_1 = 4.0\times10^{14}\exp[-23{,}800/RT]\ M^{-1}\ sec^{-1}$. The mechanisms of these reactions are discussed and compared to those of other homogeneously catalyzed reactions of hydrogen. A special feature of the present system is the resistance of the catalytic species itself (i.e. Ru^{III}) to reduction by H_2.

INTRODUCTION

Among the metal ions and complexes which have previously been reported to activate molecular hydrogen homogeneously in solution are the chloride complexes of two group VIII metals, Pd^{II} and Rh^{III} (1, 2, 3). In extending these studies we have now found that the chloride complexes of another member of this group, Ru^{III}, exhibits similar catalytic activity. Thus Ru^{III}, in aqueous HCl solution, catalyzes, under relatively mild conditions, the homogeneous reduction by hydrogen of Ru^{IV} and of Fe^{III}. The present paper describes a kinetic study of these reactions.

EXPERIMENTAL

In most of the experiments, the source of ruthenium was Johnson, Matthey $(NH_4)_2RuCl_6$ (99.7%). Essentially similar results, however, were obtained using Johnson, Matthey specpure $(NH_4)_2RuCl_5.H_2O$ or $RuCl_3.3H_2O$ as starting materials. When dissolved in concentrated HCl all of these gave solutions having essentially the same spectra and exhibiting similar reactivity toward H_2. The spectrum in each case corresponded with that reported by Wehner and Hindman (4) for Ru^{IV}. The presence of all the ruthenium in these solutions as Ru^{IV} was further confirmed (*a*) by titration with Sn^{II} and (*b*) by measuring the volume of H_2 taken up by the solution. The latter corresponded to one atom of hydrogen for each atom of ruthenium and the spectrum of the resulting reduced solution agreed with that reported by Jörgensen (5) for Ru^{III}. The concentrations of Ru^{IV} determined by these various methods were in excellent accord with each other and (to within 5%) with the total ruthenium concentration estimated by spectrophotometric determination of perruthenate, following distillation as RuO_4 using bismuthate as oxidant (6).

Solutions of Ru^{III}, used to study the catalyzed reduction of Fe^{III}, were prepared by reducing solutions of Ru^{IV} with H_2.

Kinetic measurements were made by following the uptake of hydrogen using the apparatus and procedure described earlier (7, 1).

RESULTS AND DISCUSSION

Solutions of Ru^{IV} were found to absorb H_2 in an autocatalytic manner as shown in Fig. 1. The stoichiometry of the total H_2 uptake (Table I) corresponds to complete

[1]*Manuscript received February 10, 1961.*
Contribution from the Department of Chemistry, University of British Columbia, Vancouver, B.C.
[2]*Present address: Research Laboratory, General Electric Company, Schenectady, N. Y.*

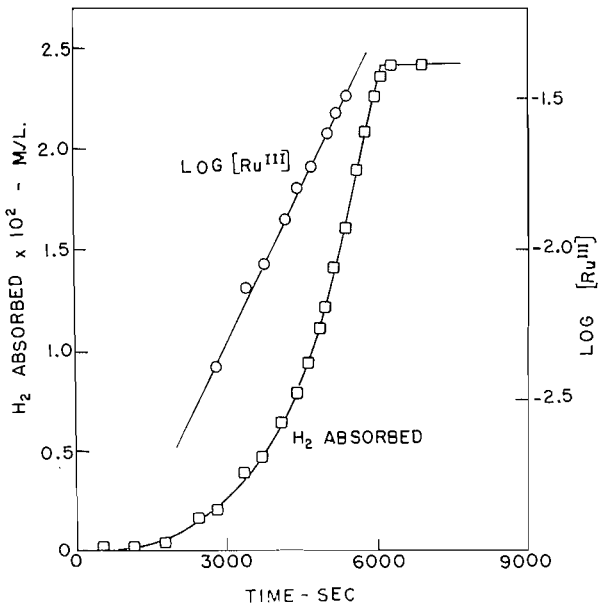


FIG. 1. Autocatalytic reduction of Ru^{IV} by H_2 at 80° C, 450 mm H_2, 3 M HCl.

TABLE I

Autocatalytic reduction of Ru^{IV}

(3 M HCl; 3.6×10^{-4} M H_2; 80° C)

Initial $[Ru^{IV}]$ (moles/l.)	Total H_2 uptake (moles/l.)	k_1 (l. $mole^{-1}$ sec^{-1})
0.037	0.019	1.07
0.048	0.024	1.08
0.055	0.030	0.91

reduction of Ru^{IV} to Ru^{III},

$$2Ru^{IV} + H_2 \rightarrow 2Ru^{III} + 2H^+ \qquad [1]$$

as do the spectra of the final solutions.

The autocatalytic behavior may be explained in terms of catalysis of the reaction by Ru^{III}, and fitted by a rate law of the form,

$$-d[H_2]/dt = \tfrac{1}{2}d[Ru^{III}]/dt = k_1[H_2][Ru^{III}]. \qquad [2]$$

With $[H_2]$ constant during the course of each experiment, this yields on integration,

$$\log [Ru^{III}] = \log [Ru^{III}]_{initial} + 2k_1[H_2]t/2.303. \qquad [3]$$

In accord with this, plots of log $[Ru^{III}]$ vs. time, such as that depicted in Fig. 1, were found to be linear over the major portion of each experiment and to yield consistent values of k_1 (Table I). About 3% of the Ru, initially present as Ru^{III}, sufficed to account for the initial rates observed in these experiments. Ru^{IV} itself appeared to be unreactive toward H_2 under these conditions. Thus the addition of a small amount of $Cr_2O_7^=$, which oxidizes the Ru^{III} initially present, inhibited completely the uptake of H_2. Conversely the initial rate of uptake of H_2 could be increased (and the total amount of H_2 taken up

Can. J. Chem. Downloaded from www.nrcresearchpress.com by 210.87.254.40 on 09/05/12
For personal use only.

correspondingly decreased) by prior reduction of a portion of the Ru^{IV} to Ru^{III} by Sn^{II}. These effects were completely reversible and the rate of uptake of H_2 under given conditions was found, in accord with equation [3], to depend only on the concentration of Ru^{III} and not on the method of attainment of the latter.

Although responsible for the activation of H_2 in this system, Ru^{III} itself showed little tendency to undergo reduction (i.e. to Ru^{II} or metallic Ru). Thus the uptake of hydrogen in the experiments described ceased abruptly when all the Ru^{IV} had been reduced to Ru^{III}. However, like Rh^{III} and Pd^{II}, which also activate hydrogen under these conditions, Ru^{III} proved to be an effective catalyst for the homogeneous reduction of Fe^{III}. (The latter, unlike $Cr_2O_7^=$, is not a sufficiently strong oxidant to oxidize Ru^{III} to Ru^{IV}.) Thus the reaction,

$$2Fe^{III} + H_2 \rightarrow 2Fe^{II} + 2H^+ \qquad [4]$$

proceeded readily in the presence of Ru^{III}. Since both $[H_2]$ and $[Ru^{III}]$ remained constant during the reaction, the uptake of H_2, while still conforming to equation [3], followed a pseudo zero-order rate law. Typical zero-order plots for such experiments are shown in Fig. 2. Values of k_1, computed from the slopes of these plots using equation [3] are listed

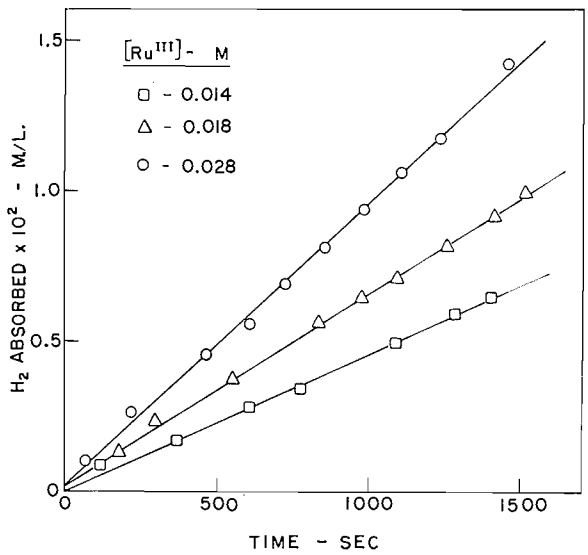


FIG. 2. Ru^{III}-catalyzed reduction of Fe^{III} by H_2 at 80° C, 450 mm H_2, 3 M HCl.

in Table II and are seen to be substantially independent of $[Ru^{III}]$, $[H_2]$, and $[Fe^{III}]$. At 80° C, in 3 M HCl these values range from 0.90 to 1.10 M^{-1} sec^{-1} and are thus in excellent agreement with the values of k_1 determined from the autocatalytic reduction of Ru^{IV} (Table I). There thus seems little doubt that the two reactions proceed by a common mechanism, the rate-determining step of which is a bimolecular reaction between H_2 and Ru^{III}. Since the kinetics of the Ru^{III}-catalyzed reduction of Fe^{III} are simpler than those of the autocatalytic reduction of Ru^{IV} and since both yield essentially the same information, most of the measurements were made on the former reaction.

Kinetic measurements over the temperature range 65° to 85° C yielded the values of k_1 listed in Table II. These gave a good Arrhenius plot fitted by the equation

$$k_1 = 4.0\times10^{14} \exp[-23{,}800/RT]\ M^{-1}\ \text{sec}^{-1}. \qquad [5]$$

Can. J. Chem. Downloaded from www.nrcresearchpress.com by 210.87.254.40 on 09/05/12
For personal use only.

TABLE II

Ru^{III}-catalyzed reduction of Fe^{III}

Temp. (°C)	$[Ru^{III}]$ (moles/l.)	$[FeCl_3]$ (moles/l.)	H_2 (mm)	$[H_2]\times10^4$ (moles/l.)*	Medium	Rate$\times10^6$ (mole l^{-1} sec^{-1})	k_1 (l. $mole^{-1}$ sec^{-1})
80.7	0.0145	0.074	450	3.60	3 *M* HCl	0.475	0.91
80.6	0.014	0.19	"	"	"	0.46	0.91
80.6	0.018	0.17	"	"	"	0.64	0.99
80.7	0.025	0.125	"	"	"	0.79	0.90
80.6	0.028	0.125	"	"	"	0.94	0.93
80.0	0.029	0.125	"	"	"	1.13	1.05
80.0	0.029	0.125	342	2.74	"	0.87	1.09
80.0	0.029	0.125	245	1.96	"	0.60	1.06
80.0	0.029	0.125	156	1.25	"	0.382	1.05
85.3	0.018	"	380	3.00	"	0.89	1.65
80.2	0.018	"	450	3.60	"	0.625	0.96
75.0	0.018	"	500	3.84	"	0.414	0.60
70.4	0.018	"	550	4.24	"	0.262	0.34
64.9	0.018	"	580	4.50	"	0.179	0.22
80.0	0.029	"	450	3.60	6 *M* HCl	1.14	1.11
"	0.019	"	"	"	4 *M* HCl	0.70	1.02
"	0.015	"	"	"	3 *M* HCl	0.56	1.09
"	0.0097	"	"	"	2 *M* HCl	0.19	0.54
"	0.0073	"	"	"	1.5 *M* HCl	0.088	0.33
"	0.053	"	"	"	3 *M* HCl	2.09	1.10
"	"	"	"	"	1.5 *M* HCl; 1.5 *M* LiCl	1.01	0.53
"	"	"	"	"	0.75 *M* HCl; 2.25 *M* LiCl	0.70	0.36

*Based on solubility of H_2 in 3 *M* HCl estimated as described earlier (1).

The corresponding values of $\Delta H^{\ddagger}$ and $\Delta S^{\ddagger}$, 23.1 kcal/mole and +6 e.u., respectively, are remarkably close to those (24.5 kcal/mole and +9 e.u.) found earlier (2) for the kinetically similar reduction of Fe^{III} by H_2, catalyzed by Rh^{III}.

Little change in k_1 was noted when the HCl concentration was varied between 3 *M* and 6 *M* (Table II). Available data (8) on the formation constants of Ru^{III}-chloride complexes suggest that, at least at room temperature, $RuCl_4^-$, $RuCl_5^{2-}$, and $RuCl_6^{3-}$ are all present in appreciable concentrations in this region and that there is a significant displacement of the complexing equilibrium toward $RuCl_6^{3-}$ as the HCl concentration is increased from 3 *M* to 6 *M*. The constancy of the rate thus implies either similar reactivities for the various complexes or, alternatively, a displacement of the complexing equilibrium at the higher temperature (80° C) of the reaction so that formation of $RuCl_6^{3-}$ is substantially complete at 3 *M* HCl. The former alternative is considered the more likely one.

Below 3 *M* HCl, k_1 exhibited a marked inverse dependence on the HCl concentration, which was only partially offset by addition of LiCl to maintain a constant ionic strength and total Cl^- concentration. A possible explanation of these effects is in terms of hydrolytic equilibria of the type

$$Ru(OH)Cl_{n-1}^{3-n} + H^+ + Cl^- \rightleftharpoons RuCl_n^{3-n} + H_2O, \qquad [6]$$

where the hydrolyzed species has the lower reactivity.

A common feature of the mechanisms of many of the homogeneously catalyzed hydrogenation reactions thus far examined (3) appears to be a rate-determining heterolytic splitting of H_2 by the catalytic species with the formation of a metal-hydride complex which reduces the substrate in a subsequent (generally fast) step. It seems highly likely

Can. J. Chem. Downloaded from www.nrcresearchpress.com by 210.87.254.40 on 09/05/12
For personal use only.

that the mechanism of activation of H_2 by Ru^{III} also is of this type and that the over-all reaction scheme in the system under consideration is as follows:

$$Ru^{III} + H_2 \underset{k_{-1}}{\overset{k_1}{\rightleftharpoons}} Ru^{III}.H^- + H^+ \quad [7]$$

$$Ru^{III}.H^- + 2Ru^{IV} \xrightarrow{k_2} 3Ru^{III} + H^+ \quad [8]$$

$$Ru^{III}.H^- + 2Fe^{III} \xrightarrow{k_3} Ru^{III} + 2Fe^{II} + H^+ \quad [9]$$

$$Ru^{III}.H^- + Ru^{III} \xrightarrow{k_4} 2Ru^{II} + H^+ \quad [10]$$

All the observations relating to these reactions are explained by this scheme, provided that,

$$k_2, k_3 > k_{-1} > k_1, k_4.$$

Thus step [7] is irreversible in the presence of Ru^{IV} or Fe^{III}, which react rapidly with $Ru^{III}.H^-$. However in the absence of such substrates most of the H_2 which reacts with Ru^{III} is regenerated since step [10] is too slow to compete effectively with reversal of step [7]. This situation is analogous in many respects to that already encountered in the Cu^I-catalyzed reduction of Cu^{II} (7).

ACKNOWLEDGMENTS

Grateful acknowledgment is made to the National Research Council of Canada and to the donors of the Petroleum Research Fund, administered by the American Chemical Society, for support of this research.

REFERENCES

1. J. HALPERN, J. F. HARROD, and P. E. POTTER. Can. J. Chem. **37**, 1446 (1959).
2. J. F. HARROD and J. HALPERN. Can. J. Chem. **37**, 1833 (1959).
3. J. HALPERN. J. Phys. Chem. **63**, 398 (1959); Advances in catalysis, **XI**, 301 (1959).
4. P. WEHNER and J. C. HINDMAN. J. Phys. Chem. **56**, 10 (1952).
5. C. K. JÖRGENSEN. Acta. Chem. Scand. **10**, 518 (1956).
6. R. P. LARSEN and L. E. ROSS. Anal. Chem. **31**, 176 (1959).
7. A. J. CHALK and J. HALPERN. J. Am. Chem. Soc. **81**, 5846, 5854 (1959).
8. D. A. FINE. Ph.D. Dissertation, University of California, Berkeley, California. 1960.

Can. J. Chem. Downloaded from www.nrcresearchpress.com by 210.87.254.40 on 09/05/12
For personal use only.

Can. J. Chem. Downloaded from www.nrcresearchpress.com by 210.87.254.105 on 09/05/12
For personal use only.

KINETICS OF THE OXIDATION OF HYDRAZOBENZENE BY IODINE AND TRIIODIDE[1]

J. W. MAY[2] AND J. HALPERN

ABSTRACT

The oxidation of hydrazobenzene (AH_2) to azobenzene by iodine in aqueous ethanol solution was found to be very rapid and in order to render the kinetics measurable it proved necessary to reduce the concentration of free iodine by complexing with iodide. This revealed a parallel oxidation path, much slower than for iodine, involving the triiodide ion. The overall rate law thus is: $-d[AH_2]/dt = k_1[AH_2][I_2]+k_2[AH_2][I_3^-]$ where the rate constants, in 60 volume% ethanol, are given by, $k_1 = 4.2\times10^{11}\exp[-10{,}000/RT]\ M^{-1}\,\text{sec}^{-1}$ and $k_2 = 2.5\times10^{11}\exp[-16{,}400/RT]\ M^{-1}\,\text{sec}^{-1}$. These and other features of the kinetics, including the inverse dependence of the rate constants on the ethanol concentration and the absence of effects due to added quinone and various metal ions, are interpreted in terms of a simple bimolecular mechanism for each path. Some measurements of the thermodynamics of triiodide formation in aqueous ethanol also are reported.

INTRODUCTION

This paper describes a kinetic study of the oxidation of hydrazobenzene (AH_2) to azobenzene (A), in aqueous ethanol solution, by iodine and triiodide. The oxidation by iodine,

[1] $$C_6H_5NHNHC_6H_5 + I_2 \rightarrow C_6H_5N{=}NC_6H_5 + 2HI,$$

was found to be rapid and, in order to render the kinetics measurable, it proved necessary to reduce the concentration of free iodine to a very low level by complexing with iodide. This revealed a parallel oxidation path, involving the triiodide ion, I_3^-, the kinetics of which also were examined. Some measurements of the thermodynamics of the triiodide equilibrium, required for the interpretation of the kinetic results, also are reported.

EXPERIMENTAL

Materials

AR grade KI and Eastman Kodak hydrazobenzene were recrystallized from aqueous ethanol, in the latter case until white crystals (m.p. 127° C) were obtained. Formic and acetic acids (C.P.) were redistilled. Iodine and other chemicals were of reagent grade. Water and ethanol used as solvents were redistilled, the former from alkaline permanganate.

Determination of the Triiodide Formation Constant

Although the triiodide equilibrium,

[2] $$I_2 + I^- \rightleftharpoons I_3^-,$$

has been examined in aqueous solution (1, 2) no data were available for aqueous ethanol and the equilibrium constants, K ($= [I_3^-]/[I_2][I^-]$), required for interpretation of the kinetic results were therefore determined experimentally. A spectrophotometric procedure, similar to that of earlier workers (1, 2) was used. This involved, essentially, determination of the equilibrium I_3^- concentration in a solution of KI and I_2, by measuring the absorption in the 3500–3600 Å region where I_3^- absorbs strongly ($\epsilon_{max} \sim 2.7\times10^4$) and I_2 and I^-, negligibly. From the initially known KI concentration, the

[1]*Manuscript received February 10, 1961.*
Contribution from the Department of Chemistry, University of British Columbia, Vancouver, B.C., with financial assistance from the National Research Council of Canada.
[2]*Present address: Inorganic Chemistry Laboratory, Oxford, England.*

equilibrium I^- concentration (generally in the range $0.5\text{–}20\times10^{-4}$ M) could be computed, while the equilibrium I_2 concentration (generally $0.5\text{–}2.5\times10^{-5}$ M) was determined (after the measurement of the I_3^- concentration) from the *increase* in I_3^-, on addition of an excess ($\sim$0.1 M) of KI sufficient to displace equilibrium [2] far to the right and convert essentially all the free I_2 to I_3^-. The I_3^- absorption spectrum exhibited a slight dependence on the solvent composition and was determined for each of the solvent mixtures used. A Beckman DU spectrophotometer with a thermostated cell compartment was used for the spectrophotometric measurements. The normal precautions (e.g. deaeration of solvents, use of stoppered spectrophotometer cells to which solutions were transferred with a hypodermic syringe after flushing with N_2) were taken in preparing the solutions and in making the spectrophotometric measurements, to minimize air oxidation of iodide. The effectiveness of the resulting procedure was confirmed by running a parallel blank (with a solution containing KI only) for each experiment and determining the amount of iodine formed by air oxidation. The latter was always small and the correction to K from this source generally amounted to less than 3%. In some experiments, notably at the higher temperatures, a small decrease in the total iodine concentration (due presumably to reduction by the solvent or buffer) during the period required for thermal equilibration of the solution and for the spectrophotometric measurement was noted and, where necessary, corrected for; this correction also was small, in every case less than 3%.

Kinetic Measurements

To minimize zero-time errors the reaction was started by adding 10 ml of a standard hydrazobenzene solution to 90 ml of a solution containing all the other reagents (KI, I_2, and buffer) after both solutions had already reached the reaction temperature. The reaction vessel, a darkened stoppered flask, was immersed in a water bath, thermostated to $\pm0.03°$ C. Aliquots of the reacting solution were withdrawn periodically and after the reaction was quenched by addition of an excess of thiosulphate (to reduce the unreacted iodine) the concentration of azobenzene produced was determined spectrophotometrically by measuring the absorption at 4300 Å where interference from other species was negligible. The spectrum of azobenzene exhibited an appreciable solvent dependence and was determined for each of the solvent mixtures used.

The choice of a mixed solvent, aqueous ethanol, was dictated by the requirement for simultaneous solubility of hydrazobenzene, azobenzene, KI, and buffer (0.26 M HOAc – 0.047 M KOAc, unless otherwise stated). The latter served to buffer the solution against the HI produced in the reaction and thus prevent the acid-catalyzed benzidine rearrangement of hydrazobenzene. A few unbuffered experiments were made, however, to check the reaction stoichiometry. In these it was found (by potentiometric titration with NaOH) that, in accord with equation [1] and with the corresponding equation for the oxidation of hydrazobenzene by I_3^-,

$$[3] \qquad AH_2 + I_3^- \rightarrow A + 2HI + I^-,$$

two equivalents of acid were produced for each molecule of azobenzene. Further support for the proposed stoichiometry and for absence of side reactions was provided by the excellent agreement always observed (in experiments in which the initial iodine concentration exceeded that of hydrazobenzene) between the initial hydrazobenzene and final azobenzene concentrations.

The spectrum of the azobenzene product corresponded to that of the trans isomer.

Can. J. Chem. Downloaded from www.nrcresearchpress.com by 210.87.254.105 on 09/05/12
For personal use only.

Can. J. Chem. Downloaded from www.nrcresearchpress.com by 210.87.254.105 on 09/05/12
For personal use only.

RESULTS

Thermodynamics of I_3^- Formation

Values of the I_3^- formation constant, K, determined over a range of temperatures and solvent compositions, are listed in Table I. From the temperature dependence of K

TABLE I

Equilibrium constants for I_3^- formation

Temp. (°C)	Volume% ethanol	Buffer concn.* (M)	$K\times10^{-4}$ (M^{-1})
16.8	0	0.31	0.082
14.9	0	"	0.086†
14.9	50	"	2.05
15.0	55	"	2.33
14.9	60	"	2.57
14.9	65	"	3.13
14.9	75	"	4.28
11.9	60	0.15	3.51 (2.88)‡
12.4	"	"	3.48 (2.86)‡
14.9	"	"	3.13§
17.9	"	"	2.71 (2.22)‡
22.8	"	"	2.02 (1.66)‡
27.4	"	"	1.58 (1.30)‡
32.3	"	"	1.19 (0.98)‡

*Buffer composition: [HOAc]:[KOAc] = 5.7:1.

†Computed from the measured value at 16.8° C using $\Delta H^0 = -4.8$ kcal/mole (1).

‡The values in parentheses are adjusted to the normal buffer concentration of 0.31 M.

§Obtained by interpolation from the data at the other temperatures.

in 60 volume% ethanol, the values of ΔH^0 and ΔS^0 for the formation of triiodide (reaction [2]) were found to be -9.5 kcal/mole and -13 e.u., respectively; the corresponding values in water are -4.8 kcal/mole and -3 e.u. (1).

The marked dependence of K on the ethanol content of the solvent (corresponding to a 50-fold increase in going from pure water to 75 volume% ethanol) is in the direction expected from a consideration of the polarities of the two solvents. Water, being the more polar solvent, undoubtedly solvates and stabilizes I^- (relative to the larger I_3^- ion) to a greater degree than ethanol and thus favors dissociation of I_3^-, relative to ethanol. The more negative ΔH^0 and ΔS^0 values for I_3^- formation in the mixed solvent, relative to pure water, also find explanation in these terms.

In the series of experiments made to determine the temperature dependence of K, the buffer concentration was reduced to half its normal value (0.15 instead of 0.31 M) in an attempt to eliminate a possible cause of the instability (referred to earlier) which the iodine solutions sometimes exhibited on prolonged standing at the higher temperatures. Where they overlap, the measurements at the two different buffer concentrations reveal a slight inverse dependence of K on the buffer concentration. Thus at 14.9° C and 60 volume% ethanol, the values of K for buffer concentrations of 0.15 and 0.31 M (i.e. 3.13×10^4 and 2.57×10^4 M^{-1}, respectively) differ by a factor of 0.82. This factor was assumed to be temperature independent and was applied to the data at other temperatures to obtain values of K (given in parentheses in Table I) for 0.31 M buffer, which were used in the kinetic calculations. The correction factor is small enough that the introduction of an appreciable error from this source is unlikely.

Kinetics

The over-all rate law for the oxidation of hydrazobenzene was found to be,

$$[4] \qquad -d[AH_2]/dt = k_1[AH_2][I_2]+k_2[AH_2][I_3^-]$$

$$[5] \qquad = (k_1/K[I^-]+k_2)[AH_2][I_3^-].$$

Under the conditions pertaining in all the experiments the triiodide equilibrium [2] was displaced far to the right, hence $[I_3^-] \sim [I_2]_T$, where $[I_2]_T$ $(= [I_2]+[I_3^-])$ is the total (i.e. stoichiometric) iodine concentration. Equation [5] thus reduces to a pseudo second-order rate law,

$$[6] \qquad -d[AH_2]/dt = k_{exp}[AH_2][I_2]_T$$

where,

$$[7] \qquad k_{exp} = k_1/K[I^-]+k_2.$$

On integration, this gives,

$$[8] \qquad \log ([I_2]_T/[AH_2]) = \log ([I_2]_T/[AH_2])_{initial}+([I_2]_T-[AH_2])_{initial}k_{exp}\,t/2.303.$$

In accord with equation [8] each experiment yielded a good plot (generally extending over at least 90% of the reaction) of log $([I_2]_T/[AH_2])$ vs. time (Fig. 1) from the slope of which k_{exp} was determined. Values of k_1 and k_2 were determined from the slopes and intercepts of linear plots (Figs. 2 and 3) of k_{exp} vs. $[I^-]^{-1}$ according to equation [7] using the values of K in Table I. The latter are uncorrected for ionic strength effects due to the varying KI concentration and the values of k_1 are thus subject to some systematic influence from this source whose magnitude is difficult to assess.

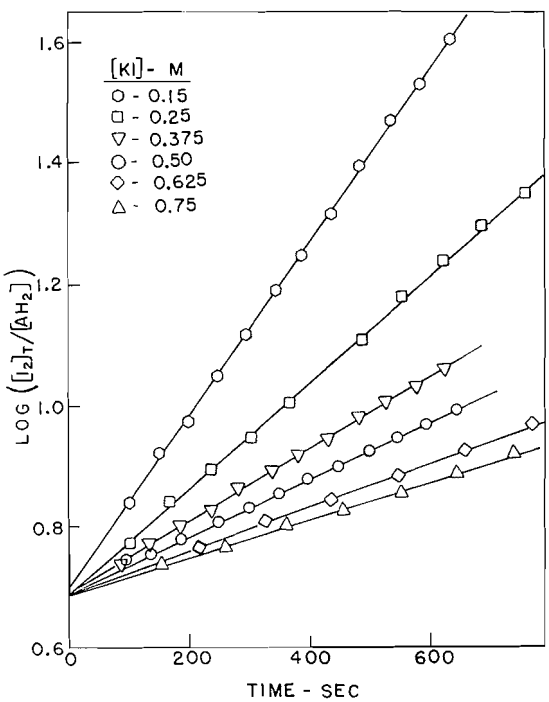


FIG. 1. Typical second-order rate plots. (15° C; 75 vol.% ethanol; 0.31 M buffer. Initial reactant concentrations: 1.20×10^{-3} M AH_2; 5.46×10^{-3} M total I_2.)

Can. J. Chem. Downloaded from www.nrcresearchpress.com by 210.87.254.105 on 09/05/12
For personal use only.

Can. J. Chem. Downloaded from www.nrcresearchpress.com by 210.87.254.105 on 09/05/12
For personal use only.

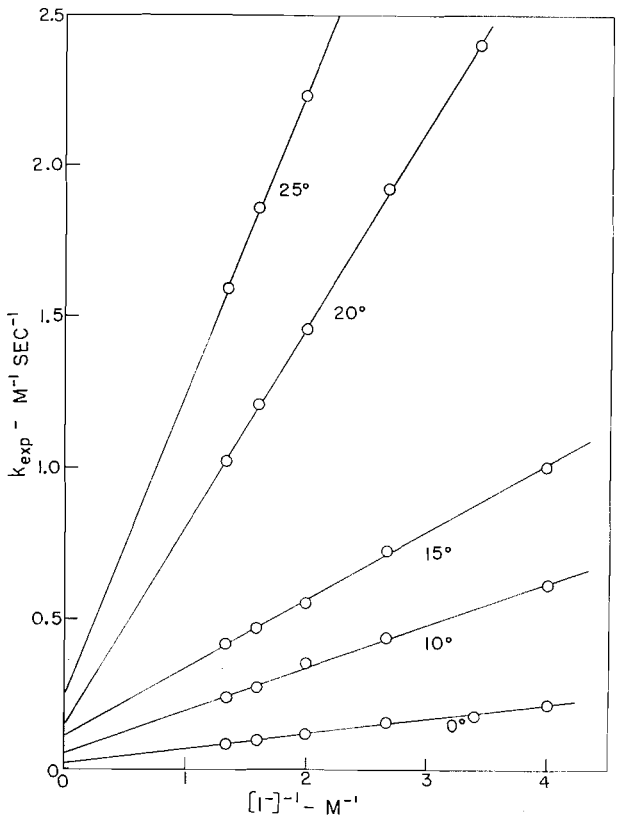


FIG. 2. Plots of k_{exp} vs. $[I^-]^{-1}$ according to equation [7]. Effect of temperature. (60 vol.% ethanol; 0.31 *M* buffer.)

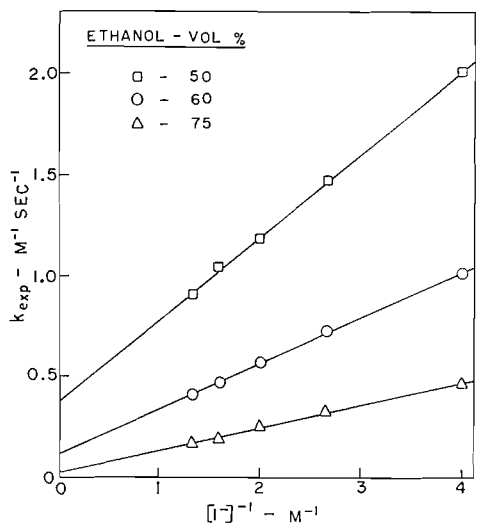


FIG. 3. Plots of k_{exp} vs. $[I^-]^{-1}$. Effect of solvent. (15° C; 0.31 *M* buffer.)

Values of k_{exp} listed in Table II are seen to be independent of the initial AH_2 concentration. Independence of the initial iodine concentration was observed only when the latter exceeded 3.0×10^{-3} *M*. At lower concentrations an apparent inverse dependence of k_{exp} on $[I_2]_T$ was noted which is believed to reflect the increasing *relative* importance of air oxidation of hydrazobenzene under these conditions. In view of this all the pertinent kinetic measurements were made with $[I_2]_T > 5\times10^{-3}$ *M*, i.e. in the region of constant k_{exp}.

TABLE II

Effects of initial reactant concentrations, buffer, and other solutes
([I⁻] = 0.25 *M*; Temp. = 15° C; 60 volume% ethanol)

Initial reactant concn. (*M*)				
$[AH_2]\times10^3$	$[I_2]_T\times10^3$	Buffer (*M*)	Other ($\times10^4$ *M*)	k_{exp} (M^{-1} sec^{-1})
0.66	5.46	0.26 HOAc–0.047 KOAc	—	0.92
0.91	"	"	—	1.00
1.20	"	"	—	0.98
1.52	"	"	—	1.00
1.82	"	"	—	1.12
2.66	"	"	—	0.99
3.03	"	"	—	1.03
1.20	0.33	"	—	1.79
"	0.98	"	—	1.32
"	3.00	"	—	1.11
"	4.10	"	—	0.98
"	4.46	"	—	1.02
"	6.20	"	—	1.00
"	7.05	"	—	1.00
1.80	5.65	"	1 Quinone	0.99
1.80	5.65	"	2 "	1.04
1.80	8.47	"	1 $Co(ClO_4)_2$	0.91
1.80	8.47	"	5 "	0.90
1.20	5.32	"	1 $FeSO_4$	0.82
1.20	5.32	"	1 $UO_2(OAc)_2$	0.98
1.20	5.32	"	1 $Cr(ClO_4)_3$	1.00
1.20	5.32	"	1 $Hg(OAc)_2$	0.98
1.20	6.35	0.13 HOAc–0.023 KOAc	—	0.66
1.20	6.20	0.26 " –0.047 "	—	1.00
1.20	6.35	0.39 " –0.070 "	—	1.13
1.20	4.48	0.088 HCOOH–0.162 NaOOCH	—	0.62
"	"	0.100 " –0.150 "	—	0.76
"	"	0.125 " –0.125 "	—	0.65
"	"	0.150 " –0.100 "	—	0.66
"	"	0.175 " –0.075 "	—	0.64
"	"	0.200 " –0.050 "	—	0.68

At least over a limited pH range, in weakly acid solution, the rate of reaction appeared to be pH independent. Thus no variation in k_{exp} was noted in a series of experiments with formic acid – formate buffer ratios ranging from 1:1.85 to 4:1 (corresponding to a pH variation of 4.02 to 3.15, in aqueous solution).* With increasing pH, however, marked acceleration of the reaction was noted indicating the emergence of an additional, base-catalyzed path, in neutral and basic solution. This region was not investigated.

With acetic acid – acetate buffers of constant ratio, some dependence of the rate on the total buffer concentration was noted (Table II), presumably due to an ionic strength effect.

**Formate buffers were used in place of acetate buffers in these experiments in order to achieve as large a variation of* pH *as possible, without approaching the* pH *range where base catalysis might begin to play some part.*

Can. J. Chem. Downloaded from www.nrcresearchpress.com by 210.87.254.105 on 09/05/12
For personal use only.

Values of k_1 and k_2 in 60 volume% ethanol for various temperatures ranging from 0° to 25° C are listed in Table III and yield the Arrhenius expressions,

[9] $$k_1 = 4.2\times10^{11} \exp[-10{,}000/RT]\ M^{-1}\ \text{sec}^{-1},$$

[10] $$k_2 = 2.5\times10^{11} \exp[-16{,}400/RT]\ M^{-1}\ \text{sec}^{-1}.$$

Both frequency factors are in the normal range for simple bimolecular reactions.

TABLE III

Temperature dependence of the rate constants
(60 volume % ethanol; 0.31 *M* 5.7:1 HOAc–KOAc buffer)

Temp. (°C)	k_1/K (sec^{-1})	$k_1\times10^{-3}$ ($M^{-1}\ \text{sec}^{-1}$)	k_2 ($M^{-1}\ \text{sec}^{-1}$)
0.0	0.049	3.2	0.020
10.0	0.141	5.0	0.050
15.0	0.220	5.7	0.12
20.0	0.655	12.8	0.14
25.0	1.00	14.6	0.25

Measurements in different solvent mixtures ranging from 45 to 85 volume% ethanol reveal a marked inverse dependence of k_{exp} on the ethanol content (Fig. 3, Table IV).

TABLE IV

Solvent effects
(15.0° C; 0.31 *M* 5.7:1 HOAc–KOAc buffer)

Volume % ethanol	k_{exp} (0.25 *M* KI) ($M^{-1}\ \text{sec}^{-1}$)	$k_1\times10^{-3}$ ($M^{-1}\ \text{sec}^{-1}$)	k_2 ($M^{-1}\ \text{sec}^{-1}$)
45	3.40		
50	2.02	8.4	0.38
55	1.36		
60	0.984	5.7	0.12
65	0.775		
70	0.610		
75	0.472	4.8	0.021
80	0.342		
85	0.248		

While k_1 and k_2 both contribute to this trend the solvent effect is much greater for the latter. Thus, on going from 75 to 50 volume% ethanol, k_1 increases by a factor of 1.75 and k_2 by a factor of 18.1.

Addition of 10^{-4} *M* benzoquinone and comparable concentrations of salts of a number of metal ions including Co^{2+}, Fe^{2+}, UO_2^{2+}, Cr^{3+}, and Hg^{2+}, were without marked effect on the rate (Table II). The largest effect, exhibited by $FeSO_4$, was a reduction of 18% in the rate.

DISCUSSION

Although hydrazobenzene is known to be oxidized readily by many oxidants only in a few other cases, notably for $S_2O_8^=$ (3) and O_2 (4), have the reaction kinetics been examined. In connection with each of these reactions, including the present ones, there arises the question of whether oxidation of hydrazobenzene occurs by a "molecular" (i.e. one-step) mechanism or by a multi-step mechanism involving the α,β-diphenylhydrazyl radical (AH) as an intermediate. A mechanism of the latter type, involving

Can. J. Chem. Downloaded from www.nrcresearchpress.com by 210.87.254.105 on 09/05/12
For personal use only.

a chain reaction propagated by the AH and SO_4^- radicals, has been demonstrated by Whalley, Evans, and Winkler (3) for the oxidation of hydrazobenzene by persulphate,

[11a] $$AH_2 + S_2O_8^= \rightarrow AH + HSO_4^- + SO_4^-,$$

[11b] $$AH_2 + SO_4^- \rightarrow AH + HSO_4^-,$$

[11c] $$AH + S_2O_8^= \rightarrow A + HSO_4^- + SO_4^-,$$

[11d] $$2AH \rightarrow A + AH_2.$$

For the oxidation by O_2, on the other hand,

[12] $$AH_2 + O_2 \rightarrow A + H_2O_2,$$

at least under certain conditions, a one-step mechanism has been suggested (4).

For the oxidation of hydrazobenzene by I_2 (and similarly by I_3^-), both a simple one-step mechanism (equation [1]) as well as a chain mechanism analogous to that for persulphate, i.e.

[13a] $$AH_2 + I_2 \rightarrow AH + HI + I,$$

[13b] $$AH_2 + I \rightarrow AH + HI,$$

[13c] $$AH + I_2 \rightarrow A + HI + I,$$

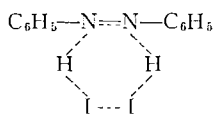
[13d] $$2AH \rightarrow A + AH_2,$$

appeared at the outset to be reasonable possibilities. The evidence accumulated in the present study, among which the following in particular may be cited, is considered to favor strongly the former alternative:

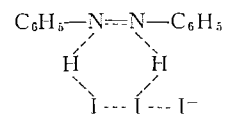
1. The second-order kinetics and normal frequency factors for both the AH_2–I_2 and AH_2–I_3^- reactions are most readily reconciled with a simple bimolecular rate-determining step in each case. A chain mechanism such as that considered above would be expected to exhibit marked departures from second-order kinetics such as are observed for the AH_2–$S_2O_8^=$ reaction (3).

2. The absence of significant effects due to addition of quinone and of various oxidizing and reducing metal ions which commonly catalyze or inhibit chain reactions (5). Failure to observe any such effects in the present case makes it very unlikely that a chain mechanism is involved.

The very low activation energy, notably for the I_2 reaction, is most readily reconciled with a "cyclic" activated complex, such as (I), which is stabilized both by incipient formation of the relatively strong H—I bonds and by a substantial portion of the resonance energy of the incipient azobenzene molecule.



(I)



(II)

An alternative mechanism, namely hydride transfer from AH_2 to I_2, leading to the formation, initially, of I^-, HI, and AH^+ (i.e. the conjugate acid of azobenzene) is considered less likely in view of the absence of evidence (e.g. a low frequency factor) for a highly polar transition state which would be expected for such a mechanism. Both mechanisms are consistent with the formation of *trans*-azobenzene, the more stable isomer, as the initial product.

Can. J. Chem. Downloaded from www.nrcresearchpress.com by 210.87.254.105 on 09/05/12
For personal use only.

An analogous path (II) may be envisaged for the I_3^- reaction. The lower reactivity of I_3^-, relative to I_2, is reflected largely in the activation energy difference (16.4 vs. 10.0 kcal/mole) between the two reactions. The additional activation energy of 6.4 kcal/mole represents a substantial portion of, though not quite all, the energy of 9.5 kcal/mole required to remove the extra I^- ion completely (i.e. to dissociate I_3^- into I_2 and I^-); this suggests that the extra I^- ion is nearly dissociated in the activated complex. Also in accord with this interpretation is the much greater accelerating effect of water on k_2 than on k_1, which may be explained in terms of an additional contribution to stabilization of the activated complex by solvation of the incipient I^- ion.

ACKNOWLEDGMENTS

The helpful advice of Dr. G. B. Porter is gratefully acknowledged.

REFERENCES

1. G. DANIELE. Gazz. chim. ital. **90**, 1068 (1960).
2. A. D. AWTREY and R. E. CONNICK. J. Am. Chem. Soc. **73**, 1842 (1951).
3. B. J. P. WHALLEY, H. G. V. EVANS, and C. A. WINKLER. Can. J. Chem. **34**, 1154 (1956).
4. W. J. ZUBYK. Ph.D. Dissertation, University of Delaware. 1957.
5. J. HALPERN and J. G. SMITH. Can. J. Chem. **34**, 1419 (1956).

Can. J. Chem. Downloaded from www.nrcresearchpress.com by 210.87.254.105 on 09/05/12
For personal use only.

Can. J. Chem. Downloaded from www.nrcresearchpress.com by 210.87.254.6 on 09/05/12
For personal use only.

THE PREPARATION OF ALKOXIDES AND TRIETHYLSILANOLATES OF Ti, Zr, V, Nb, Ta, AND Sn FROM THE DIALKYLAMIDES

I. M. THOMAS*

The chemical properties of the dialkylamides of titanium, zirconium, vanadium, niobium, tantalum, and tin have recently been studied in this laboratory (1), and it has been found that they are very reactive to reagents containing replaceable hydrogen atoms. Besides being extremely sensitive to moisture, they react smoothly and completely with alcohols and triethylsilanol at room temperature in benzene to give the corresponding alkoxides and triethylsilanolates with the liberation of the dialkylamine:

$$M(NR_2)_x + xR^1OH \rightarrow M(OR^1)_x + xR_2NH,$$
$$M(NR_2)_x + xEt_3SiOH \rightarrow M(OSiEt_3)_x + xR_2NH.$$

This method has been used by Gilman *et al.* (2) to prepare uranium^{IV} tetraalkoxides from tetrakis-diethylamido-uranium^{IV}.

Previous methods of preparation of transition metal alkoxides have utilized the metal chloride as starting material, and subsequent side reactions have reduced the yields in many cases. No niobium penta-*t*-alkoxides (3) or vanadium^{IV} tetraalkoxides have been reported.

The preparation of trialkylsilanolates from trialkylsilanols is also hindered by the ease with which the trialkylsilanols condense to a disiloxane and water under the influence of acidic or 'Lewis acidic' reagents (4), with subsequent hydrolysis of the product.

The absence of side reactions in this method enables near quantitative yields to be obtained in all cases, and it is particularly suitable for the preparation of all alkoxides of vanadium^{IV} and tin, and the tertiary alkoxides of zirconium and niobium.

It should be noted that niobium^{IV} tetra-dialkylamides on reaction with alcohols and triethylsilanol give pentavalent derivatives. Repeated attempts to prepare tetraalkoxides were unsuccessful, and it is evident that reduction of the alcohol by Nb^{IV} readily takes place even at 0° with subsequent formation of a pentavalent product. However, the comparative stability of vanadium in the tetravalent state enabled substantially pure tetra derivatives to be prepared from vanadium^{IV} tetra-dialkylamides.

EXPERIMENTAL

Special precautions, e.g. carefully dried all-glass apparatus, were adapted to avoid hydrolysis, and all experiments were conducted under an atmosphere of dry, oxygen-free nitrogen.

Analysis

Metals, except vanadium, were determined gravimetrically as the ignited oxides (4), and silicon as silica (4). An oxidation method (5) was used for the determination of ethoxy and isopropoxy groups, and basic nitrogen was estimated in a modified Kjeldahl apparatus (1). Estimation of vanadium and valency determination were carried out using a Jones reductor and ceric sulphate solution (6).

The alcohols and benzene were dried azeotropically prior to use.

*Present address: Stauffer Chemical Company, Anderson Chemical Division, Weston, Michigan, U.S.A.

Can. J. Chem. Downloaded from www.nrcresearchpress.com by 210.87.254.6 on 09/05/12
For personal use only.

The preparations of dialkylamido compounds of titanium, zirconium, and tantalum have been described (1, 7). Those of vanadium and niobium will be reported in another communication. Tetrakis-diethylamido-tin was prepared as described below.

Preparation of Tetrakis-diethylamido-tin

Stannic chloride (19.0 g) in benzene (50 ml) was added, over 20 minutes, to a stirred solution of lithium diethylamide in ether (300 ml of 1.18 *N* solution). The mixture was refluxed for 3 hours after the addition and then stirred overnight at room temperature. Evaporation of the solvent under reduced pressure, and distillation of the residue under high vacuum gave tetrakis-diethylamido-tin (8.90 g: 30% yield) as a pale yellow liquid, b.p. 90°/0.1 mm. Found: Sn, 29.1%; N, 13.4%; Cl, zero. Calc. for $Sn(NEt_2)_4$: Sn, 29.1%; N, 13.8%.

Since the technique used in the alcoholysis and silanolysis reactions was essentially the same in each experiment, the details are given for the preparation of zirconium tetra-*t*-butoxide and the other results summarized in Tables I and II.

TABLE I

Preparation of alkoxides

	Dialkylamide		Product			Found (%)		Calc. (%)	
Alkoxide	Type	Wt. (g)	Wt. (g)	% yield	B.p./mm	M	OR	M	OR
$Ti(OBu^n)_4$	$Ti(NPr^n_2)_4$	5.30	3.85	95	140°/0.1	13.9	—	14.1	—
$V(OBu^t)_4$	$V(NMe_2)_4$	3.10	4.07	87	55°/0.05	15.0*	—	14.8	—
$V(OPr^i)_4$	$V(NMe_2)_4$	6.65	8.10	98	55°/0.1§	17.9†	82.6	17.7	82.3
$Nb(OBu^t)_5$	$Nb(NEt_2)_4$	1.98	1.76	74	90°/0.1‡	20.4	—	20.3	—
$Nb(OPr^i)_5$	$Nb(NEt_2)_4$	5.44	3.90	72	80°/0.1‡	24.0	76.6	24.0	76.0
$Ta(OBu^n)_5$	$Ta(NPr^n_2)_3NPr^n$	6.44	6.15	98	210°/0.05	33.0	—	33.1	—
$Ta(OEt)_5$	$Ta(NPr^n_2)_3NPr^n$	4.75	3.16	92	145°/0.05	44.2	54.6	44.6	55.4
$Sn(OPr^i)_4$	$Sn(NEt_2)_4$	7.00	4.60	75	120°/0.05	33.3	66.6	33.4	66.6

*Valency 4.10, royal blue liquid.
†Valency 4.08, dark green solid.
‡Sublimation temperature.
§M.p. 40°.
NOTE: All products were analyzed for basic nitrogen content and this was found to be zero in every case. All products, except those of vanadium, were colorless solids or liquids.

TABLE II

Preparation of triethylsilanolates

	Dialkylamide		Product			Found (%)		Calc. (%)	
Triethyl-silanolate	Type	Wt. (g)	Wt. (g)	% yield	B.p./mm	M	Si	M	Si
$Ti(OSiEt_3)_4$	$Ti(NEt_2)_4$	4.95	7.60	90	150°/0.1*	8.41	19.5	8.36	19.6
$Zr(OSiEt_3)_4$	$Zr(NEt_2)_4$	4.07	6.17	93	150°/0.1	14.9	18.1	14.8	18.2
$V(OSiEt_3)_4$	$V(NEt_2)_4$	3.54	5.53	92	150°/0.1	9.10†	19.2	8.84	19.5
$Nb(OSiEt_3)_5$	$Nb(NPr^n_2)_4$	3.78	5.79	100	—‡	12.5	18.6	12.4	18.7
$Ta(OSiEt_3)_5$	$Ta(NEt_2)_3NEt$	4.93	8.67	95	210°/0.1§	21.7	16.9	21.6	16.8

*M.p. 110°.
†Valency 4.15, blue-green liquid.
‡This product decomposes on sublimation at 210°/0.1 mm.
§Sublimation temperature.
NOTE: All products, except those of vanadium, were colorless liquids or solids. All products were analyzed for basic nitrogen content, which was found to be zero in every case.

Preparation of Zirconium Tetra-t-butoxide

t-Butanol (12 ml: ca. 100% excess) was added dropwise to tetrakis-diethylamido-zirconium (5.63 g) in benzene (30 ml). An exothermic reaction took place and the solution

was left at room temperature for 20 minutes after the addition. Evaporation of the solvent under reduced pressure and distillation of the residue under high vacuum gave zirconium tetra-*t*-butoxide (5.00 g: 88% yield) as a colorless liquid, b.p. 60°/0.1 mm. Found: Zr, 23.7%; N, zero. Calc. for $Zr(OBu^t)_4$: Zr, 23.8%.

ACKNOWLEDGMENTS

The author is indebted to Professor D. C. Bradley for valuable discussion and to the National Research Council for financial assistance.

1. D. C. Bradley and I. M. Thomas. J. Chem. Soc. 3857 (1960).
2. R. G. Jones, G. Karmas, G. A. Martin, and H. Gilman. J. Am. Chem. Soc. **78**, 4285 (1956).
3. D. C. Bradley, B. N. Chakravarti, and W. Wardlaw. J. Chem. Soc. 4439 (1956).
4. D. C. Bradley and I. M. Thomas. J. Chem. Soc. 3404 (1959).
5. D. C. Bradley, F. M. Halim, and W. Wardlaw. J. Chem. Soc. 3450 (1950).
6. D. C. Bradley, R. K. Multani, and W. Wardlaw. J. Chem. Soc. 4647 (1958).
7. D. C. Bradley and I. M. Thomas. Proc. Chem. Soc. 225 (1959).

Received February 17, 1961.
The Chemistry Department,
The University of Western Ontario,
London, Ontario.

THE ACIDITY OF 9-MONOALKYL- (OR ARYL-) FLUORENES

G. W. H. Scherf and R. K. Brown

In a previous publication (1) it was shown that the reaction between equivalent amounts of alkyl halide and 9-fluorenyl-potassium (or -sodium) in ether solvents gave not only the expected 9-monoalkyl fluorene but as much as 35% yield of 9,9-dialkylfluorene. This latter product was considered to occur as result of cross metalation between unreacted 9-fluorenyl-potassium (or -sodium) and the 9-alkylfluorene initially produced. For the 9-alkylfluorene to compete with the alkyl halide for the remaining 9-fluorenyl-potassium as successfully as it apparently did, the postulation was made that the C_9-monoalkylated fluorene was at least as acidic as, and probably more acidic than, the parent unsubstituted fluorene. It is known that 9-phenylfluorene is more acidic than is fluorene (2, 3), but that an *alkyl* substituent at C_9 of fluorene should also lead to enhanced acidity of the remaining hydrogen at carbon 9 is unexpected. The explanation given (1) was that of a tendency of the C_9 substituent to become coplanar with the planar fluorene moiety, hence assisting the tendency to rehybridization of carbon 9 from sp^3 to sp^2, in agreement with the known capability of fluorene for carbanion formation (4). Such coplanarity is quite possible if the carbon atom attached to C_9 of fluorene is methyl or methylene.

Some evidence has now been obtained that certain 9-alkylfluorenes do in fact possess somewhat greater acidity than that of the parent fluorene. Several reports concerning nuclear magnetic resonance studies show that the chemical shift observed for the proton signal is related to the electronic environment and hence the acidity of the proton (5, 6). Accordingly an examination was made of the N.M.R. spectra of fluorene, 9-benzylfluorene, 9-methylfluorene, and 9-phenylfluorene in chloroform solution. The position of the C_9 proton signal, referred to the proton signal of the solvent, is shown for each of these compounds.

Can. J. Chem. Downloaded from www.nrcresearchpress.com by 210.87.254.6 on 09/05/12
For personal use only.

was left at room temperature for 20 minutes after the addition. Evaporation of the solvent under reduced pressure and distillation of the residue under high vacuum gave zirconium tetra-*t*-butoxide (5.00 g: 88% yield) as a colorless liquid, b.p. 60°/0.1 mm. Found: Zr, 23.7%; N, zero. Calc. for $Zr(OBu^t)_4$: Zr, 23.8%.

ACKNOWLEDGMENTS

The author is indebted to Professor D. C. Bradley for valuable discussion and to the National Research Council for financial assistance.

1. D. C. Bradley and I. M. Thomas. J. Chem. Soc. 3857 (1960).
2. R. G. Jones, G. Karmas, G. A. Martin, and H. Gilman. J. Am. Chem. Soc. **78**, 4285 (1956).
3. D. C. Bradley, B. N. Chakravarti, and W. Wardlaw. J. Chem. Soc. 4439 (1956).
4. D. C. Bradley and I. M. Thomas. J. Chem. Soc. 3404 (1959).
5. D. C. Bradley, F. M. Halim, and W. Wardlaw. J. Chem. Soc. 3450 (1950).
6. D. C. Bradley, R. K. Multani, and W. Wardlaw. J. Chem. Soc. 4647 (1958).
7. D. C. Bradley and I. M. Thomas. Proc. Chem. Soc. 225 (1959).

Received February 17, 1961.
The Chemistry Department,
The University of Western Ontario,
London, Ontario.

THE ACIDITY OF 9-MONOALKYL- (OR ARYL-) FLUORENES

G. W. H. Scherf and R. K. Brown

In a previous publication (1) it was shown that the reaction between equivalent amounts of alkyl halide and 9-fluorenyl-potassium (or -sodium) in ether solvents gave not only the expected 9-monoalkyl fluorene but as much as 35% yield of 9,9-dialkylfluorene. This latter product was considered to occur as result of cross metalation between unreacted 9-fluorenyl-potassium (or -sodium) and the 9-alkylfluorene initially produced. For the 9-alkylfluorene to compete with the alkyl halide for the remaining 9-fluorenyl-potassium as successfully as it apparently did, the postulation was made that the C_9-monoalkylated fluorene was at least as acidic as, and probably more acidic than, the parent unsubstituted fluorene. It is known that 9-phenylfluorene is more acidic than is fluorene (2, 3), but that an *alkyl* substituent at C_9 of fluorene should also lead to enhanced acidity of the remaining hydrogen at carbon 9 is unexpected. The explanation given (1) was that of a tendency of the C_9 substituent to become coplanar with the planar fluorene moiety, hence assisting the tendency to rehybridization of carbon 9 from sp^3 to sp^2, in agreement with the known capability of fluorene for carbanion formation (4). Such coplanarity is quite possible if the carbon atom attached to C_9 of fluorene is methyl or methylene.

Some evidence has now been obtained that certain 9-alkylfluorenes do in fact possess somewhat greater acidity than that of the parent fluorene. Several reports concerning nuclear magnetic resonance studies show that the chemical shift observed for the proton signal is related to the electronic environment and hence the acidity of the proton (5, 6). Accordingly an examination was made of the N.M.R. spectra of fluorene, 9-benzylfluorene, 9-methylfluorene, and 9-phenylfluorene in chloroform solution. The position of the C_9 proton signal, referred to the proton signal of the solvent, is shown for each of these compounds.

Can. J. Chem. Downloaded from www.nrcresearchpress.com by 210.87.254.42 on 09/05/12
For personal use only.

Compound	Signal relative to solvent, c.p.s.	Shift relative to fluorene, c.p.s.
Fluorene	+193	0
9-Phenylfluorene	+130	−63
9-Methylfluorene	+181	−12
9-Benzylfluorene	+181	−12

The large shift of 63 c.p.s. found for the proton signal in 9-phenylfluorene relative to that of fluorene is clearly an indication of the marked acidity actually found for 9-phenylfluorene (2, 3). Both 9-methylfluorene and 9-benzylfluorene show a shift of only 12 c.p.s. relative to fluorene *but in the same direction* as that found for 9-phenylfluorene. This supports the view that the proton on carbon 9 of these monoalkylated fluorenes is also more acidic than the proton in unsubstituted fluorene.

ACKNOWLEDGMENTS

The authors wish to thank Dr. W. Schneider of the National Research Council, Ottawa, for the N.M.R. analyses.

1. G. W. H. Scherf and R. K. Brown. Can. J. Chem. **39**, 799 (1961).
2. J. B. Conant and G. W. Wheland. J. Am. Chem. Soc. **54**, 1212 (1932).
3. W. K. McEwen. J. Am. Chem. Soc. **58**, 1124 (1936).
4. G. Rieveschl and F. E. Ray. Chem. Revs. **23**, 287 (1938).
5. L. H. Meyer, A. Saika, and H. S. Gutowsky. J. Am. Chem. Soc. **75**, 4567 (1953).
6. P. L. Corio and B. P. Dailey. J. Am. Chem. Soc. **78**, 3043 (1956).

Received February 20, 1961.
Department of Chemistry,
University of Alberta,
Edmonton, Alberta.

NUCLEAR MAGNETIC RESONANCE SPECTRA OF A VINYL PHOSPHATE AND THIONOPHOSPHATE ISOMERS (PHOSDRIN AND 'thionoPHOSDRIN')*

J. B. Stothers and E. Y. Spencer

Some substituted vinyl phosphates, because of their high biological activity, have been the subject of a number of recent investigations (1, 2, 3, 4). One systemic insecticide of this type, methyl 3-(O,O-dimethylphosphoryloxy)but-2-enoate, (Phosdrin), exists in two geometric isomeric forms, I*a* and I*b*, one of which has a much higher anticholinesterase activity. An assignment of the configuration about the double bond has been made previously on rather weak arguments based on relative water solubility, chromatographic behavior, and selective toxicity (1). By analogy, a similar assignment had been tentatively suggested for the thiono derivatives, II*a* and II*b*, since their properties were somewhat similar to those of the Phosdrins. The thiono derivatives were prepared as part of a continuing investigation on the biological activity of phosphate esters, and their preparation is described herein. The results of the toxicity studies will be reported elsewhere.

**Contribution No. 192.*

Can. J. Chem. Downloaded from www.nrcresearchpress.com by 210.87.254.42 on 09/05/12
For personal use only.

Compound	Signal relative to solvent, c.p.s.	Shift relative to fluorene, c.p.s.
Fluorene	+193	0
9-Phenylfluorene	+130	−63
9-Methylfluorene	+181	−12
9-Benzylfluorene	+181	−12

The large shift of 63 c.p.s. found for the proton signal in 9-phenylfluorene relative to that of fluorene is clearly an indication of the marked acidity actually found for 9-phenylfluorene (2, 3). Both 9-methylfluorene and 9-benzylfluorene show a shift of only 12 c.p.s. relative to fluorene *but in the same direction* as that found for 9-phenylfluorene. This supports the view that the proton on carbon 9 of these monoalkylated fluorenes is also more acidic than the proton in unsubstituted fluorene.

ACKNOWLEDGMENTS

The authors wish to thank Dr. W. Schneider of the National Research Council, Ottawa, for the N.M.R. analyses.

1. G. W. H. Scherf and R. K. Brown. Can. J. Chem. **39**, 799 (1961).
2. J. B. Conant and G. W. Wheland. J. Am. Chem. Soc. **54**, 1212 (1932).
3. W. K. McEwen. J. Am. Chem. Soc. **58**, 1124 (1936).
4. G. Rieveschl and F. E. Ray. Chem. Revs. **23**, 287 (1938).
5. L. H. Meyer, A. Saika, and H. S. Gutowsky. J. Am. Chem. Soc. **75**, 4567 (1953).
6. P. L. Corio and B. P. Dailey. J. Am. Chem. Soc. **78**, 3043 (1956).

Received February 20, 1961.
Department of Chemistry,
University of Alberta,
Edmonton, Alberta.

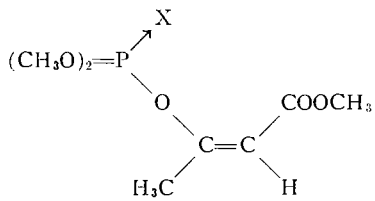
NUCLEAR MAGNETIC RESONANCE SPECTRA OF A VINYL PHOSPHATE AND THIONOPHOSPHATE ISOMERS (PHOSDRIN AND 'thionoPHOSDRIN')*

J. B. Stothers and E. Y. Spencer

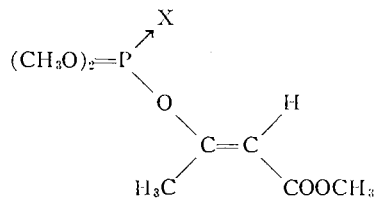
Some substituted vinyl phosphates, because of their high biological activity, have been the subject of a number of recent investigations (1, 2, 3, 4). One systemic insecticide of this type, methyl 3-(O,O-dimethylphosphoryloxy)but-2-enoate, (Phosdrin), exists in two geometric isomeric forms, I*a* and I*b*, one of which has a much higher anticholinesterase activity. An assignment of the configuration about the double bond has been made previously on rather weak arguments based on relative water solubility, chromatographic behavior, and selective toxicity (1). By analogy, a similar assignment had been tentatively suggested for the thiono derivatives, II*a* and II*b*, since their properties were somewhat similar to those of the Phosdrins. The thiono derivatives were prepared as part of a continuing investigation on the biological activity of phosphate esters, and their preparation is described herein. The results of the toxicity studies will be reported elsewhere.

**Contribution No. 192.*

Can. J. Chem. Downloaded from www.nrcresearchpress.com by 210.87.254.40 on 09/05/12
For personal use only.



Ia X = O
IIa X = S



Ib X = O
IIb X = S

Two methods utilized for the synthesis of Phosdrin yield different ratios of cis and trans isomers (1). One involving the reaction of trimethyl phosphite with methyl α-chloroacetoacetate (5) favors the "cis" isomer slightly while substituting benzyl α-chloroacetoacetate yields only the "cis" form (2). On the other hand, reaction of dimethyl phosphorochloridate with the sodium salt of methyl acetoacetate favors the "trans" isomer (1). It is of interest that in the synthesis of the thiono derivatives of Phosdrin, the latter method gave only the "trans" product from which the "cis" form was obtained by ultraviolet irradiation. Due to low solubilities, the Craig countercurrent extraction, employed in Phosdrin isomer separation (2), was replaced by selective elution from acid-washed activated alumina.

The earlier study had assigned the cis configuration, I*a*, to the more active isomer. (It should be noted that this assignment refers to the relative configuration of the carbomethoxyl and phosphoryloxy groupings.) Recently, Jackman (6) has shown that, in a number of β-methyl-α,β-unsaturated esters, an assignment of configuration can be made on the basis of a comparison of the N.M.R. spectra of cis and trans isomers. Therefore, the high-resolution proton magnetic resonance spectra of these four compounds have been determined in order to confirm or deny the original assignment.

Each compound was examined in dilute solution in carbon tetrachloride and the assignment of peaks from the observed chemical shifts was straightforward. The olefinic proton appeared at lowest field and the allylic methyl protons at highest field in each case. The methoxyl protons gave rise to three peaks, since the methoxyl groups on phosphorus are chemically shifted from the carbomethoxy group and are split into a doublet by spin–spin interaction with phosphorus. The distinction between the three peaks followed readily since the coupling constants, J_{H-P}, for both $CH_3OP \rightarrow O$ and $CH_3OP \rightarrow S$ are well known (7). The observed chemical shifts and J_{H-P} coupling constants are listed in Table I. It should be noted that the naming of these compounds arises from the previous assignment (1).

TABLE I

Proton chemical shifts and coupling constants (J_{H-P})

Compound	ν (cycles/sec)*				J (cycles/sec)
	Olefinic H	CH_3OP	CH_3OOC	CH_3	CH_3—OP→X
"cis" Phosdrin	347	232	222	145	10.4
"trans" Phosdrin	318	233	220	129	11.2
"cis" 'thionoPhosdrin'	341	233	222	142	14.6
"trans" 'thionoPhosdrin'	322	229	220	126	14.6

*Measured at 60 Mc/sec, expressed in cycles/sec from the single peak of tetramethylsilane.

Can. J. Chem. Downloaded from www.nrcresearchpress.com by 210.87.254.40 on 09/05/12
For personal use only.

From these results, it can be seen that the allylic methyl group appears at lower field in the previously assigned "cis" forms. Since it is reasonable to assume that the phosphoryl group will exert a similar effect on this methyl group in both the cis and trans structures, the difference in chemical shift must arise from the orientation of the carbomethoxyl grouping. Jackman and Wiley (6) have clearly demonstrated that in similar systems the allylic methyl group is found at lower field in that isomer having the carbomethoxyl group and the β-methyl group in a cis relation than in the corresponding trans isomer. Therefore, the N.M.R. spectra of these four compounds show the original assignment to be incorrect. The more active isomer, the so-called "cis" Phosdrin must be that form in which the *allylic methyl and carbomethoxyl* groupings are in a cis relation.

There is one further point of interest in this study. It was expected that each of the multiplets observed in these spectra could be analyzed by first-order treatment, since the relative chemical shift between interacting protons is large compared to the coupling constants. In each case, however, the observed pattern was more complex than the simple doublet and quartet pattern expected for the allylic methyl and olefinic protons, respectively. Only one of these compounds, trans thionoPhosdrin, II*a*, is a solid and so amenable to rigorous purification. Its spectrum exhibited a well-resolved quartet for the allylic methyl group. This appears to be clear evidence for H^1—P^{31} spin–spin interaction through *four* bonds. From this pattern, however, it is not possible to assign a coupling constant unequivocally to each of the two observed interactions. The P^{31} spectra of this and related compounds will undoubtedly allow the assignment of J's and work is being directed to this end.

EXPERIMENTAL

N.M.R. Spectra

All spectra were obtained using dilute solutions (10–12% w/v) in carbon tetrachloride containing ca. 0.5% tetramethylsilane (TMS) as an internal reference. A Varian Associates V-4302 spectrometer operating at 60 Mc/sec was employed and the usual audio side-band technique was used to measure the relative chemical shifts from the TMS peak. The audio oscillator was calibrated with an H-P 522B frequency counter. The chemical shift data are reported in cycles per second from TMS and are judged to be accurate to within ± 1 cycles/sec.

"cis" and "trans" Phosdrin

These compounds were prepared as previously described (2).

"cis" and "trans" 'thionoPhosdrin'

The reaction product of 2.3 g of sodium and 11.6 g of methyl acetoacetate was heated in refluxing benzene with 16.0 g of dimethyl phosphorothionochloridate for 24 hours. Subsequent removal of the precipitate, evaporation of the solvent, and final vacuum distillation yielded a crude fraction boiling between 92° and 112° C at 0.6 mm. Crystals later formed and were filtered off and recrystallized to yield 5.1 g (21%), m.p. 49–50° C. Allowing for recovery of unreacted starting materials, the yield of purified product was 30%. The absence of the P → O linkage was indicated by the lack of a band between 1275 and 1300 cm^{-1} in the infrared spectrum, while absorption at 913 cm^{-1}, and none at 897 cm^{-1}, indicated the presence of only the "trans" isomer. Bromide–bromate titration confirmed the theoretical thiono sulphur content and a satisfactory analysis was obtained.

Twenty-nine hours of ultraviolet irradiation of 'thionoPhosdrin' in carbon tetrachloride by a Hanovia lamp was required to give maximum isomerization as indicated

Can. J. Chem. Downloaded from www.nrcresearchpress.com by 210.87.254.40 on 09/05/12
For personal use only.

by the increase in absorption at 897 cm^{-1} and decrease at 913 cm^{-1}. Quantitative separation of the isomers was accomplished by absorption on Merck acid-washed activated alumina, triturated with 2% water, from hexane. This was followed by elution of the 'cis' isomer with carbon tetrachloride and then the 'trans' isomer by chloroform to yield 54% 'cis' isomer and 37% 'trans'. No absorption at 1285 cm^{-1} after ultraviolet irradiation indicated no P → S to P → O shift.

ACKNOWLEDGMENTS

Financial support provided by the National Research Council of Canada is gratefully acknowledged. Thanks are due Mrs. Ann Holmes for technical assistance, Mr. R. W. White for infrared spectra, and Mrs. Dorle Bongart for microanalyses.

1. J. E. Casida. Science, **122**, 597 (1955).
2. E. Y. Spencer, A. R. Todd, and R. F. Webb. J. Chem. Soc. 2968 (1958).
3. J. E. Casida, P. E. Gatterman, L. W. Getzin, Jr., and R. K. Chapman. J. Agr. Food Chem. **4**, 236 (1956).
4. E. Y. Spencer and J. R. Robinson. J. Agr. Food Chem. **8**, 293 (1960).
5. A. R. Stiles. U.S. Patent No. 2,685,552 (August, 1954).
6. L. M. Jackman and R. H. Wiley. J. Chem. Soc. 2881, 2886 (1960).
7. H. Finegold. Ann. N. Y. Acad. Sci. **70**, 875 (1958).

Received February 8, 1961.
Department of Chemistry,
University of Western Ontario and
Pesticide Research Institute,
Department of Agriculture,
London, Ontario.

Can. J. Chem. Downloaded from www.nrcresearchpress.com by 210.87.254.40 on 09/05/12
For personal use only.

THE HEAT OF FORMATION OF THE FORMYL RADICAL

T. W. Shannon and A. G. Harrison

As discussed by Cottrell (1) the bond dissociation energy D(CHO—H) in formaldehyde and consequently the heat of formation of the formyl radical appear to be in some doubt. From investigations of the photolysis of formaldehyde Gorin (2) and Klein and Schoen (3) have suggested D(CHO—H) = 77 kcal/mole, leading to ΔH_f(CHO) = −2.8 kcal/mole. From a study of the photolysis of a number of aldehydes, as summarized by Calvert (4), a value D(CHO—H) = 91 kcal/mole (ΔH_f(CHO) = 11.2 kcal/mole) has been obtained.

Both the direct and indirect mass spectrometric methods have been applied by Reed and co-workers to the formyl radical. Reed and Brand (5) have reported the ionization potential of the formyl radical to be 9.83 to 10.03 v. This ionization potential, when combined with the appearance potential of CHO^+ from formaldehyde, 13.10 v (6), gives D(CHO—H) = 70.8 to 75.4 kcal/mole, corresponding to ΔH_f(CHO) = −4.4 to −9.0 kcal/mole.

In the indirect method Reed (6) has measured the appearance potential of CH_3^+ from acetaldehyde. On the assumption that the process occurring is $CH_3CHO + e \rightarrow CH_3^+ + CHO + 2e$ the reported appearance potential, 13.12±0.06 v, may be combined with $\Delta H_f(CH_3^+)$ = 262 kcal/mole (7) and $\Delta H_f(CH_3CHO)$ = −39.8 kcal/mole (8) to give ΔH_f(CHO) = −0.8 kcal/mole. As discussed below we have not been able to confirm in this work the reported appearance potential of CH_3^+ from acetaldehyde.

by the increase in absorption at 897 cm^{-1} and decrease at 913 cm^{-1}. Quantitative separation of the isomers was accomplished by absorption on Merck acid-washed activated alumina, triturated with 2% water, from hexane. This was followed by elution of the 'cis' isomer with carbon tetrachloride and then the 'trans' isomer by chloroform to yield 54% 'cis' isomer and 37% 'trans'. No absorption at 1285 cm^{-1} after ultraviolet irradiation indicated no P → S to P → O shift.

ACKNOWLEDGMENTS

Financial support provided by the National Research Council of Canada is gratefully acknowledged. Thanks are due Mrs. Ann Holmes for technical assistance, Mr. R. W. White for infrared spectra, and Mrs. Dorle Bongart for microanalyses.

1. J. E. Casida. Science, **122**, 597 (1955).
2. E. Y. Spencer, A. R. Todd, and R. F. Webb. J. Chem. Soc. 2968 (1958).
3. J. E. Casida, P. E. Gatterman, L. W. Getzin, Jr., and R. K. Chapman. J. Agr. Food Chem. **4**, 236 (1956).
4. E. Y. Spencer and J. R. Robinson. J. Agr. Food Chem. **8**, 293 (1960).
5. A. R. Stiles. U.S. Patent No. 2,685,552 (August, 1954).
6. L. M. Jackman and R. H. Wiley. J. Chem. Soc. 2881, 2886 (1960).
7. H. Finegold. Ann. N. Y. Acad. Sci. **70**, 875 (1958).

Received February 8, 1961.
Department of Chemistry,
University of Western Ontario and
Pesticide Research Institute,
Department of Agriculture,
London, Ontario.

THE HEAT OF FORMATION OF THE FORMYL RADICAL

T. W. Shannon and A. G. Harrison

As discussed by Cottrell (1) the bond dissociation energy D(CHO—H) in formaldehyde and consequently the heat of formation of the formyl radical appear to be in some doubt. From investigations of the photolysis of formaldehyde Gorin (2) and Klein and Schoen (3) have suggested D(CHO—H) = 77 kcal/mole, leading to ΔH_f(CHO) = −2.8 kcal/mole. From a study of the photolysis of a number of aldehydes, as summarized by Calvert (4), a value D(CHO—H) = 91 kcal/mole (ΔH_f(CHO) = 11.2 kcal/mole) has been obtained.

Both the direct and indirect mass spectrometric methods have been applied by Reed and co-workers to the formyl radical. Reed and Brand (5) have reported the ionization potential of the formyl radical to be 9.83 to 10.03 v. This ionization potential, when combined with the appearance potential of CHO^+ from formaldehyde, 13.10 v (6), gives D(CHO—H) = 70.8 to 75.4 kcal/mole, corresponding to ΔH_f(CHO) = −4.4 to −9.0 kcal/mole.

In the indirect method Reed (6) has measured the appearance potential of CH_3^+ from acetaldehyde. On the assumption that the process occurring is $CH_3CHO + e \rightarrow CH_3^+ + CHO + 2e$ the reported appearance potential, 13.12±0.06 v, may be combined with $\Delta H_f(CH_3^+)$ = 262 kcal/mole (7) and $\Delta H_f(CH_3CHO)$ = −39.8 kcal/mole (8) to give ΔH_f(CHO) = −0.8 kcal/mole. As discussed below we have not been able to confirm in this work the reported appearance potential of CH_3^+ from acetaldehyde.

Can. J. Chem. Downloaded from www.nrcresearchpress.com by 210.87.254.5 on 09/05/12
For personal use only.

The present work reports the measurement of appearance potentials of ions of known heat of formation from a number of aldehydes in an attempt to obtain further information by the indirect mass spectrometric method for the heat of formation of the formyl radical. The results are given in Table I. Column six of Table I records values for

TABLE I

Energetics of the process RCHO + e → R^+ + CHO + 2e

R	$A_p(R^+)$, ev: This work	$A_p(R^+)$, ev: Lit.	$\Delta H_f(R^+)$, kcal/mole	ΔH_f(RCHO), kcal/mole	ΔH_f(CHO) + E, kcal/mole
CH_3	14.51±0.1	13.12±0.06[a]	262[c]	−39.8[f]	See text
i-Pr	10.62±0.1		190[c]	−55.2[g]	−0.2±2.3
n-Pr	10.65±0.1		190[c]	−53.9[g]	1.7±2.3
C_6H_5	13.37±0.1	13.51±0.12[b]	301[c]	−11.2[h]	−2.3±2.3
CCl_3	11.58±0.1		216[d]	−44[i]	6.9±2.3
C_2H_3	13.72±0.1	13.69±0.1[b]	283[e]	−20[h]	13.2±2.3

[a]Reference 6.
[b]R. I. Reed and M. B. Thornley. Trans. Faraday Soc. **54**, 949 (1958).
[c]Reference 7. The ion from *n*-PrCHO was assumed to have the isopropyl structure.
[d]J. B. Farmer, I. H. S. Henderson, F. P. Lossing, and D. G. H. Marsden. J. Chem. Phys. **24**, 348 (1956).
[e]A. G. Harrison and F. P. Lossing. J. Am. Chem. Soc. **82**, 519 (1960).
[f]Reference 8.
[g]Estimated by group orbital method (J. L. Franklin. Ind. Eng. Chem. **41**, 339 (1949)). Roberts and Skinner (footnote *h*) report an estimated value ΔH_f(*n*-PrCHO) = −52.5 kcal/mole.
[h]J. S. Roberts and H. A. Skinner. Trans. Faraday Soc. **45**, 339 (1949).
[i]H. O. Pritchard and H. A. Skinner. J. Chem. Soc. 1928 (1950).

ΔH_f(CHO) + E calculated from the relation

$$A_p(R^+) \text{ from RCHO} = \Delta H_f(R^+) + \Delta H_f(\text{CHO}) - \Delta H_f(\text{RCHO}) + E$$

by substituting the known values for $\Delta H_f(R^+)$ and ΔH_f(RCHO), where E is any excess energy which may be associated with either the charged or uncharged fragment. The above relation assumes that the lowest energy process occurring is

$$\text{RCHO} + e \rightarrow R^+ + \text{CHO} + 2e.$$

The appearance potential of CH_3^+ from acetaldehyde obtained in this work is over 1 v higher than that reported by Reed and discussed above. The measured appearance potential, 14.51±0.1 v, is only slightly greater than that calculated for the process

$$CH_3CHO + e \rightarrow CH_3^+ + CO + H + 2e \qquad A_p = 14.3 \text{ v}.$$

No evidence was obtained for formation of methyl ions in any significant amounts below this appearance potential. Until further independent evidence is obtained, the appearance potential of CH_3^+ from acetaldehyde cannot be considered as providing convincing evidence concerning the heat of formation of the formyl radical.

The appearance potentials of the $C_3H_7^+$ ion from *n*-butyraldehyde and isobutyraldehyde, as well as the appearance potential of the $C_6H_5^+$ ion from benzaldehyde, lead to mutually consistent values for ΔH_f(CHO) + E. If one assumes that in these cases no excess energy is involved these results lead to ΔH_f(CHO) = −0.3±3 kcal/mole, in essential agreement with the low value obtained from chemical kinetics. If excess energy is involved then the true heat of formation will be even lower; in any case the results are not consistent with the high value, ΔH_f(CHO) = 11.2 kcal/mole, derived from chemical kinetics.

Can. J. Chem. Downloaded from www.nrcresearchpress.com by 210.87.254.5 on 09/05/12
For personal use only.

On the basis of $\Delta H_f(CHO) = -0.3$ kcal/mole the appearance potentials of CCl_3^+ from chloral and $C_2H_3^+$ from acrolein appear to involve excess energy in both cases. It should be noted that the result reported for acrolein is the only one which provides support for the high value for the heat of formation of the formyl radical. If one assumes this value then one must conclude that the appearance potentials measured for the $C_3H_7^+$ ions and the $C_6H_5^+$ ion are too low by approximately 0.5 v. Such a possibility appears highly unlikely; rather the results are more consistent with excess energy being associated with the formation of the CCl_3^+ and $C_2H_3^+$ ions.

In conclusion, the results reported in Table I provide support for the low value for the heat of formation of the formyl radical as derived from chemical kinetics. The results further suggest that excess energy is involved in the formation of the CCl_3^+ and $C_2H_3^+$ ions from the corresponding aldehydes.

EXPERIMENTAL

The appearance potentials were measured using an Associated Electrical Industries MS-2 mass spectrometer. The electron-accelerating voltage could be read to ± 0.02 volts with a precision voltmeter and was varied in 0.2-v steps while determining the ionization-efficiency curves. The voltage scale was calibrated by admitting either krypton or xenon with the sample. The appearance potentials were evaluated by extrapolating the voltage-difference curves to zero ion current. The limits of error given in column two of Table I represent the average deviations of three or more determinations.

Note added in proof: J. R. Majer, C. R. Patrick, and J. C. Robb (Trans. Faraday Soc. **57**, 14, 1961) have recently reported the appearance potential of CH_3^+ from CH_3CHO to be 14.55 v, in excellent agreement with the value obtained in this work.

The financial support of the National Research Council of Canada is gratefully acknowledged.

1. T. L. COTTRELL. The strengths of chemical bonds. 2nd ed. Butterworth Scientific Publications, London. 1958.
2. E. GORIN. J. Chem. Phys. **7**, 256 (1939).
3. R. KLEIN and R. J. SCHOEN. J. Chem. Phys. **24**, 1094 (1956).
4. J. G. CALVERT. J. Phys. Chem. **61**, 1206 (1957).
5. R. I. REED and J. C. D. BRAND. Trans. Faraday Soc. **54**, 478 (1958).
6. R. I. REED. Trans. Faraday Soc. **52**, 1195 (1956).
7. F. H. FIELD and J. L. FRANKLIN. Electron impact phenomena and the properties of gaseous ions. Academic Press Inc., New York. 1957.
8. F. D. ROSSINI *et al.* Selected values of physical and thermodynamic properties of hydrocarbons and related compounds. Carnegie Press, Pittsburgh. 1953.

RECEIVED FEBRUARY 27, 1961.
DEPARTMENT OF CHEMISTRY,
UNIVERSITY OF TORONTO,
TORONTO, ONTARIO.

THE REACTION OF 2,2-DIPHENYL-1-PICRYLHYDRAZYL WITH 9,10-DIHYDROANTHRACENE AND 1,4-DIHYDRONAPHTHALENE

J. S. HOGG, D. H. LOHMANN, AND K. E. RUSSELL

The use of 2,2-diphenyl-1-picrylhydrazyl (DPPH) as a hydrogen acceptor in free radical reactions in solution has been the subject of a number of recent investigations.

Can. J. Chem. Downloaded from www.nrcresearchpress.com by 210.87.254.5 on 09/05/12
For personal use only.

On the basis of $\Delta H_f(CHO) = -0.3$ kcal/mole the appearance potentials of CCl_3^+ from chloral and $C_2H_3^+$ from acrolein appear to involve excess energy in both cases. It should be noted that the result reported for acrolein is the only one which provides support for the high value for the heat of formation of the formyl radical. If one assumes this value then one must conclude that the appearance potentials measured for the $C_3H_7^+$ ions and the $C_6H_5^+$ ion are too low by approximately 0.5 v. Such a possibility appears highly unlikely; rather the results are more consistent with excess energy being associated with the formation of the CCl_3^+ and $C_2H_3^+$ ions.

In conclusion, the results reported in Table I provide support for the low value for the heat of formation of the formyl radical as derived from chemical kinetics. The results further suggest that excess energy is involved in the formation of the CCl_3^+ and $C_2H_3^+$ ions from the corresponding aldehydes.

EXPERIMENTAL

The appearance potentials were measured using an Associated Electrical Industries MS-2 mass spectrometer. The electron-accelerating voltage could be read to ± 0.02 volts with a precision voltmeter and was varied in 0.2-v steps while determining the ionization-efficiency curves. The voltage scale was calibrated by admitting either krypton or xenon with the sample. The appearance potentials were evaluated by extrapolating the voltage-difference curves to zero ion current. The limits of error given in column two of Table I represent the average deviations of three or more determinations.

Note added in proof: J. R. Majer, C. R. Patrick, and J. C. Robb (Trans. Faraday Soc. **57**, 14, 1961) have recently reported the appearance potential of CH_3^+ from CH_3CHO to be 14.55 v, in excellent agreement with the value obtained in this work.

The financial support of the National Research Council of Canada is gratefully acknowledged.

1. T. L. COTTRELL. The strengths of chemical bonds. 2nd ed. Butterworth Scientific Publications, London. 1958.
2. E. GORIN. J. Chem. Phys. **7**, 256 (1939).
3. R. KLEIN and R. J. SCHOEN. J. Chem. Phys. **24**, 1094 (1956).
4. J. G. CALVERT. J. Phys. Chem. **61**, 1206 (1957).
5. R. I. REED and J. C. D. BRAND. Trans. Faraday Soc. **54**, 478 (1958).
6. R. I. REED. Trans. Faraday Soc. **52**, 1195 (1956).
7. F. H. FIELD and J. L. FRANKLIN. Electron impact phenomena and the properties of gaseous ions. Academic Press Inc., New York. 1957.
8. F. D. ROSSINI *et al.* Selected values of physical and thermodynamic properties of hydrocarbons and related compounds. Carnegie Press, Pittsburgh. 1953.

RECEIVED FEBRUARY 27, 1961.
DEPARTMENT OF CHEMISTRY,
UNIVERSITY OF TORONTO,
TORONTO, ONTARIO.

THE REACTION OF 2,2-DIPHENYL-1-PICRYLHYDRAZYL WITH 9,10-DIHYDROANTHRACENE AND 1,4-DIHYDRONAPHTHALENE

J. S. HOGG, D. H. LOHMANN, AND K. E. RUSSELL

The use of 2,2-diphenyl-1-picrylhydrazyl (DPPH) as a hydrogen acceptor in free radical reactions in solution has been the subject of a number of recent investigations.

Can. J. Chem. Downloaded from www.nrcresearchpress.com by 210.87.254.40 on 09/05/12
For personal use only.

As a result, information is now available concerning the rates of hydrogen abstraction by this polar radical from mercaptans (1, 2, 3), hydroaromatic compounds (4), amines (5, 6, 7), and phenols (7, 8). It has been confirmed in all these reactions that the major product is 2,2-diphenyl-1-picrylhydrazine, but only in the case of the hydroaromatic compounds has it been possible to isolate good yields of the dehydrogenation products (4). The kinetic results for hydroaromatic compounds do not, however, fit into the general pattern in that rates of reaction dependent upon the square of the DPPH concentration have been reported (4) in addition to activation energies as high as 33 kcal/mole. This note records the results of a new investigation of the kinetics of reaction of DPPH with 9,10-dihydroanthracene and 1,4-dihydronaphthalene.

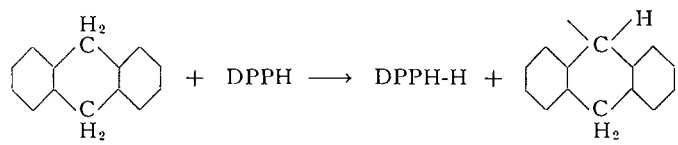
TABLE I

Rate constants (k_1) for the reaction of DPPH with 9,10-dihydroanthracene

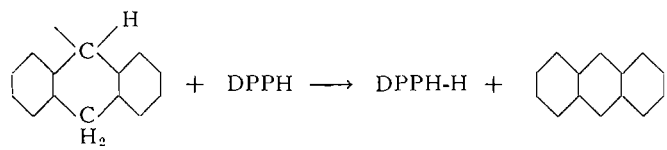
DPPH, mole/l.	Dihydroanthracene, mole/l.	Solvent	Temp., °C	k_1, cc/mole sec
0.1	0.25	Benzene	50	0.37
0.025	0.25	"	50	0.38
0.025	0.0625	"	50	0.35
0.018	0.20	"	50	0.36*
0.025	0.25	"	30	0.124
0.025	0.25	"	40	0.20
0.025	0.25	"	60	0.60
0.0125	0.125	Carbon tetrachloride	30	0.26
0.0166	0.166	"	50	0.68
0.025	0.25	Dioxan	50	0.22
0.025	0.25	"	70	0.68

**In vacuo.*

9,10-Dihydroanthracene was prepared by the reduction of anthracene in boiling ethanol with sodium amalgam. Its reaction with DPPH in benzene solution obeys simple second-order kinetics as illustrated by the data in Table I, and the rate of reaction is not significantly affected by the presence of air or by the addition of diphenylpicrylhydrazine. High yields of anthracene and diphenylpicrylhydrazine (DPPH-H) are obtained (4) and the main reaction presumably involves the following steps.



[1]



[2]

Reaction [1] is rate determining, and reaction [2] is rapid compared with the reverse of reaction [1].

Rate constants at different temperatures lead to an activation energy of 10.4 ± 0.5 kcal/mole and an Arrhenius A factor of 4.0×10^6 cc/mole sec for reactions in benzene

Can. J. Chem. Downloaded from www.nrcresearchpress.com by 210.87.254.40 on 09/05/12
For personal use only.

solution. The activation energy is within the range 4–16 kcal/mole observed in other hydrogen-abstraction reactions involving DPPH, but the A factor is low compared with values of the order of 10^{10} cc/mole sec normally observed. The low value is not surprising in view of the high probability of steric hindrance to reaction [1]; a comparable A factor is observed in the reaction of DPPH with 2,6-di-*t*-butylphenol (8). For carbon tetrachloride as solvent the activation energy is 9.2 ± 1 kcal/mole and the A factor is 1.1×10^{6} cc/mole sec, and for dioxan as solvent the corresponding values are 12.4 ± 1 kcal/mole and 5.4×10^{7} cc/mole sec.

When 1,4-dihydronaphthalene (9) is used as the hydrogen donor, the kinetic results do not follow the expected pattern. In individual reactions the rate of disappearance of DPPH in solutions containing a large excess of 1,4-dihydronaphthalene falls off only to a small extent in the first 75% of reaction, in contrast to the first-order dependence observed with 9,10-dihydroanthracene as donor. Rates of reaction are higher in air than in degassed systems and the reproducibility is poor. Some typical results are given in Table II for the rates of disappearance of DPPH at 30° in carefully degassed benzene

TABLE II

Rates of reaction of DPPH with 1,4-dihydronaphthalene

DPPH, mole/l.	Dihydronaphthalene, mole/l.	Rate$\times10^{10}$, mole/cc sec
0.0226	0.1	8.3
0.0113	0.1	6.3
0.0057	0.1	5.3
0.0113	0.025	1.3

solutions. They are approximately represented by the expression

$$-d[\text{DPPH}]/dt = k_2[\text{dihydronaphthalene}][\text{DPPH}]^{0.3}.$$

Diphenylpicrylhydrazine (0.0113 M) causes a reduction in rate of about 20% in reaction mixtures containing DPPH at a concentration of 0.0113 M. The activation energy of the over-all process is estimated to be 12.5 ± 1.5 kcal/mole from rate measurements at 20° C, 30° C, 40° C, and 50° C. Since high yields of both diphenylpicrylhydrazine and naphthalene are obtained (4), a mechanism similar to that suggested for the dihydroanthracene reaction may be put forward; the activation energy of the primary hydrogen abstraction process would then be 12.5 kcal/mole. However, the low order of reaction with respect to DPPH shows that the reaction mechanism may be complex. A similar low order was observed in the early stages of the reaction of DPPH with mercaptans (1), but in that case the order increased to one for the major part of the reaction.

ACKNOWLEDGMENTS

The authors are indebted to the National Research Council for a grant and to Queen's University for R. S. McLaughlin and Milton Hersey scholarships.

1. K. E. Russell. J. Phys. Chem. **58**, 437 (1954).
2. A. G. Brook, R. J. Anderson, and J. Tissot Van Patot. Can. J. Chem. **36**, 159 (1958).
3. A. H. Ewald. Trans. Faraday Soc. **55**, 792 (1959).
4. E. A. Braude, A. G. Brook, and R. P. Linstead. J. Chem. Soc. 3574 (1954).
5. A. S. Kuz'minskiĭ and L. G. Angert. Doklady Akad. Nauk S.S.S.R. **96**, 1187 (1954).

Can. J. Chem. Downloaded from www.nrcresearchpress.com by 210.87.254.40 on 09/05/12
For personal use only.

6. J. E. HAZELL and K. E. RUSSELL. Can. J. Chem. **36**, 1729 (1958).
7. J. C. MCGOWAN, T. POWELL, and R. RAW. J. Chem. Soc. 3103 (1959).
8. J. S. HOGG, D. H. LOHMANN, and K. E. RUSSELL. To be published.
9. E. S. COOK and A. J. HILL. J. Am. Chem. Soc. **62**, 1995 (1940).

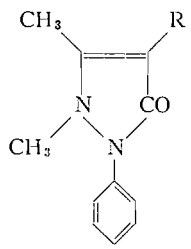
RECEIVED JANUARY 17, 1961.
DEPARTMENT OF CHEMISTRY,
QUEEN'S UNIVERSITY,
KINGSTON, ONTARIO.

Can. J. Chem. Downloaded from www.nrcresearchpress.com by 210.87.254.40 on 09/05/12
For personal use only.

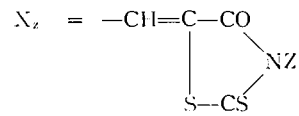
THE CONDENSATION OF RHODANINE AND DERIVATIVES WITH 4-ANTIPYRINALDEHYDE

FREDERICK J. ALLAN[1] AND G. GRAHAM ALLAN[2]

More than three-quarters of a century has elapsed since antipyrine (I*a*) was introduced into medicine by Knorr as an antipyretic and analgesic (1). Although pyrazolone analgesics have now virtually vanished from the scene in North America and the Scandinavian countries (2), they are still widely used in other areas and considerable efforts have been expended to improve their pharmacological properties (3, 4). In recent years some of this effort has been focused on 4-antipyrinaldehyde (I*b*)[3] and its derivatives (5–14), principally in connection with antineuralgic and febrifugal effects. While insecticidal pyrazolones have been described (15–17), other nonanalgesic applications of 4-antipyrinaldehyde or its derivatives have received little attention other than brief reports of tuberculostatic (18) and bacteriostatic activity (19).



(I)



a. R = H
b. R = CHO
c. R = X_H
d. R = X_{Et}
e. R = X_{All}
f. R = X_{Ph}
g. R = X_{Cm}

in X_H (Z = H)
X_{Et} (Z = ethyl)
X_{All} (Z = allyl)
X_{Ph} (Z = phenyl)
X_{Cm} (Z = carboxymethyl)

As part of a study of potential bacteriostats (20, 21), rhodanine has been condensed with a variety of carbonyl-containing compounds (22–29), including the highly effective monoheterocyclic furan and thiophen aldehydes (30). However, no rhodanine condensation products have been prepared which contain a carbonyl-derived moiety comprising a five-membered ring with two heteroatoms. The pyrazolone aldehyde (I*b*) was

[1]*To whom enquiries should be addressed.*
[2]*Present address: Electrochemicals Department, E. I. du Pont de Nemours & Co., Inc., Wilmington, Del., U.S.A.*
[3]*In the early literature this aldehydic structure was erroneously assigned to an isomeric ketone (6).*

6. J. E. HAZELL and K. E. RUSSELL. Can. J. Chem. **36**, 1729 (1958).
7. J. C. MCGOWAN, T. POWELL, and R. RAW. J. Chem. Soc. 3103 (1959).
8. J. S. HOGG, D. H. LOHMANN, and K. E. RUSSELL. To be published.
9. E. S. COOK and A. J. HILL. J. Am. Chem. Soc. **62**, 1995 (1940).

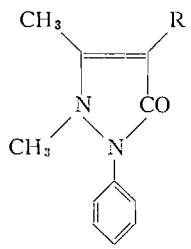
RECEIVED JANUARY 17, 1961.
DEPARTMENT OF CHEMISTRY,
QUEEN'S UNIVERSITY,
KINGSTON, ONTARIO.

Can. J. Chem. Downloaded from www.nrcresearchpress.com by 210.87.254.5 on 09/05/12
For personal use only.

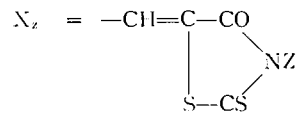
THE CONDENSATION OF RHODANINE AND DERIVATIVES WITH 4-ANTIPYRINALDEHYDE

FREDERICK J. ALLAN[1] AND G. GRAHAM ALLAN[2]

More than three-quarters of a century has elapsed since antipyrine (I*a*) was introduced into medicine by Knorr as an antipyretic and analgesic (1). Although pyrazolone analgesics have now virtually vanished from the scene in North America and the Scandinavian countries (2), they are still widely used in other areas and considerable efforts have been expended to improve their pharmacological properties (3, 4). In recent years some of this effort has been focused on 4-antipyrinaldehyde (I*b*)[3] and its derivatives (5–14), principally in connection with antineuralgic and febrifugal effects. While insecticidal pyrazolones have been described (15–17), other nonanalgesic applications of 4-antipyrinaldehyde or its derivatives have received little attention other than brief reports of tuberculostatic (18) and bacteriostatic activity (19).



(I)



a. R = H
b. R = CHO
c. R = X_H
d. R = X_{Et}
e. R = X_{All}
f. R = X_{Ph}
g. R = X_{Cm}

in X_H (Z = H)
X_{Et} (Z = ethyl)
X_{All} (Z = allyl)
X_{Ph} (Z = phenyl)
X_{Cm} (Z = carboxymethyl)

As part of a study of potential bacteriostats (20, 21), rhodanine has been condensed with a variety of carbonyl-containing compounds (22–29), including the highly effective monoheterocyclic furan and thiophen aldehydes (30). However, no rhodanine condensation products have been prepared which contain a carbonyl-derived moiety comprising a five-membered ring with two heteroatoms. The pyrazolone aldehyde (I*b*) was

[1]*To whom enquiries should be addressed.*
[2]*Present address: Electrochemicals Department, E. I. du Pont de Nemours & Co., Inc., Wilmington, Del., U.S.A.*
[3]*In the early literature this aldehydic structure was erroneously assigned to an isomeric ketone (6).*

therefore condensed with rhodanine, and its 3-ethyl, -allyl, -phenyl, and -carboxymethyl relatives, using sodium acetate in a mixture of acetic acid and anhydride as the condensing medium (24). The products,[4] (I*c*) to (I*g*), separated from the reaction mixture in an almost pure state.

EXPERIMENTAL[5]

5-[4-(1-Phenyl-2,3-dimethylpyrazol-5-onyl)methylene]rhodanine (Ic)

A mixture of 4-antipyrinaldehyde (216 mg, 0.001 mole) and rhodanine (133 mg, 0.001 mole) in acetic acid (1 ml) to which sodium acetate (200 mg) and acetic anhydride (0.1 ml) had been added, was refluxed for 30 minutes. The reaction mixture was allowed to cool when crystals separated. Recrystallization from dimethylformamide–ethanol gave (I*c*) as small golden yellow needles (102 mg, yield 31%) m.p. 325–327° with decomposition. Calc. for $C_{15}H_{13}N_3O_2S_2$ (331.402): C, 54.36; H, 3.95. Found: C, 54.21; H, 3.76%. The following compounds were similarly prepared.

3-Ethyl-5-[4-(1-phenyl-2,3-dimethylpyrazol-5-onyl)methylene]rhodanine (Id)

Orange plates (300 mg, yield 33%) m.p. 265–267°, crystallized from ethanol–benzene–dimethylformamide. Calc. for $C_{17}H_{17}N_3O_2S_2$ (359.462): C, 56.79; H, 4.77. Found: C, 56.48; H, 5.08%.

3-Allyl-5-[4-(1-phenyl-2,3-dimethylpyrazol-5-onyl)methylene]rhodanine (Ie)

Golden yellow blades (425 mg, yield 57%) m.p. 203–204°, crystallized from acetic acid. Calc. for $C_{18}H_{17}N_3O_2S_2$ (371.472): C, 58.18; H, 4.61. Found: C, 58.32; H, 4.72%.

3-Phenyl-5-[4-(1-phenyl-2,3-dimethylpyrazol-5-onyl)methylene]rhodanine (If)

Bright orange plates (435 mg, yield 54%) m.p. 266–268° with darkening, crystallized from ethanol–dimethylformamide. Calc. for $C_{21}H_{17}N_3O_2S_2$ (407.502): C, 61.9; H, 4.17. Found: C, 61.62; H, 4.03%.

3-Carboxymethyl-5-[4-(1-phenyl-2,3-dimethylpyrazol-5-onyl)methylene]rhodanine (Ig)

Orange-yellow needles (200 mg, yield 26%) m.p. 260–262°, crystallized from ethanol–dimethylformamide. Calc. for $C_{17}H_{15}N_3O_4S_2$ (389.442): C, 52.44; H, 3.88. Found: C, 52.65; H, 3.72%.

1. L. KNORR. Ber. **17**, 546, 2032 (1884).
2. T. L. JACOBS. *In* Heterocyclic compounds. Vol. 5. *Edited by* R. C. Elderfield. John Wiley & Sons, Inc., New York. 1957. p. 153.
3. L. GOODMAN and A. GILMAN. The pharmacological basis of therapeutics. 2nd ed. The Macmillan Co., New York. 1955. pp. 318–323.
4. L. A. GREENBERG. Antipyrine. Hillhouse Press, New Haven. 1950.
5. K. BODENDORF, J. MILDNER, and T. LEHMAN. Ann. **563**, 1 (1949).
6. K. BODENDORF and A. POPELAK. Ann. **566**, 84 (1950).
7. K. BODENDORF and H. RAAF. Ann. **592**, 26 (1955).
8. M. RIDI. Gazz. chim. ital. **71**, 95, 100, 106 (1941); **77**, 3 (1947).
9. M. RIDI and S. CHECCHI. Ann. chim. (Rome), **43**, 816 (1953).
10. M. PASSERINI, M. RIDI, and G. LOSCO. Gazz. chim. ital. **80**, 803 (1950).
11. J. LEDRUT and G. COMBES. Bull. soc. chim. France, 127, 786 (1950).
12. J. LEDRUT, G. COMBES, and H. SWIERKOT. Bull. soc. chim. France, 185 (1952).
13. A. WINTERNITZ, J. LEDRUT, and G. COMBES. Bull. soc. chim. France, 398 (1952).
14. G. COMBES, M. F. HEBBELYNCK, and J. LEDRUT. Bull. soc. chim. France, 315 (1953).
15. R. GASSER. Ber. schweiz. botan. Ges. **62**, 66 (1952).
16. G. R. FERGUSON and C. C. ALEXANDER. J. Agr. Food Chem. **1**, 888 (1953).
17. H. GYSIN. Chimia Switz. **8**, 205, 221 (1954).
18. J. KLOSA. Arch. Pharm. **288**, 217 (1955); **288**, 545 (1955).

[4] *Fungicidal and bacteriostatic evaluation of which we hope to publish later elsewhere.*
[5] *Melting points are uncorrected.*

Can. J. Chem. Downloaded from www.nrcresearchpress.com by 210.87.254.5 on 09/05/12
For personal use only.

19. J. H. T. LEDRUT, *to* Luxema S. A., U.S. Patent No. 2,650,219 (August 25, 1953). Equivalent Brit. Patent No. 688,225 (March 4, 1953).
20. F. J. ALLAN and G. G. ALLAN. Rec. trav. chim. In press.
21. F. J. ALLAN and G. G. ALLAN. J. Org. Chem. **23**, 639 (1958).
22. G. G. ALLAN, D. MACLEAN, and G. T. NEWBOLD. J. Chem. Soc. 5053 (1952).
23. F. J. ALLAN, G. G. ALLAN, and J. B. THOMSON. J. Org. Chem. **23**, 112 (1958).
24. F. J. ALLAN, G. G. ALLAN, and J. B. THOMSON. Can. J. Chem. **36**, 1579 (1958).
25. F. J. ALLAN and G. G. ALLAN. Rec. trav. chim. **78**, 67 (1959).
26. F. J. ALLAN, G. G. ALLAN, and C. M'F. M'NEIL. Nature, **184**, 1637 (1959).
27. F. J. ALLAN and G. G. ALLAN. Rec. trav. chim. **78**, 375 (1959).
28. F. J. ALLAN, G. G. ALLAN, G. CRANK, and J. JACK. Rec. trav. chim. **79**, 247 (1960).
29. F. J. ALLAN, G. G. ALLAN, and G. CRANK. J. Appl. Chem. **11**, 68 (1961).
30. F. C. BROWN, C. K. BRADSHER, and E. N. LAWTON. Ind. Eng. Chem. **45**, 1027 (1953).

RECEIVED JANUARY 23, 1961.
DEPARTMENT OF CHEMISTRY,
PAISLEY TECHNICAL COLLEGE,
PAISLEY, SCOTLAND.

Can. J. Chem. Downloaded from www.nrcresearchpress.com by 210.87.254.5 on 09/05/12
For personal use only.

Can. J. Chem. Downloaded from www.nrcresearchpress.com by 210.87.254.5 on 09/05/12
For personal use only.

Canadian Journal of Chemistry

Issued by THE NATIONAL RESEARCH COUNCIL OF CANADA

VOLUME 39 JULY 1961 NUMBER 7

THE HYDROGEN ISOTOPE EFFECT IN THE PYROLYSIS OF CYCLOPROPANE[1]

ARTHUR T. BLADES

ABSTRACT

The hydrogen isotope effect in the thermal rearrangement of cyclopropane has been determined by the copyrolysis of cyclopropane and cyclopropane-d_6. The isotope effect in the temperature range 407–514° C and at pressures of about 60 cm Hg may be expressed by

$$k_H/k_D = 0.82 \exp(1300/RT).$$

The isotope effect is pressure dependent, decreasing from 1.98 at 76 cm Hg to 1.35 at 0.0178 cm Hg at 482° C.

The isotope effect and its temperature and pressure dependence are discussed in relation to the mechanism. The conclusion is reached that though trimethylene may be formed as an intermediate, the isotope effect is consistent only with an activated complex where a hydrogen atom is weakly bonded both to its original and ultimate carbon atoms, a situation which might also lead directly to propylene. A similar argument is presented to account for the previously described isotope effect in the decomposition of cyclobutane.

INTRODUCTION

The thermal rearrangement of cyclopropane to propylene is an unusually interesting reaction for a number of reasons. It is a unimolecular reaction wherein chain processes and heterogeneous behavior are readily eliminated, and it is the simplest of a group of cycloalkane reactions which exhibit a quasi-unimolecular behavior at relatively high pressures. Two completely different mechanisms have been proposed (1) for the reaction, one involving the intermediate formation of trimethylene diradical, and the other, formation of a transition state wherein one hydrogen atom is in the act of transferring from one carbon atom to another as the carbon–carbon bond breaks. While both mechanisms have some merit in explaining the accumulated experimental data, the latter is greatly favored on the basis of the theoretical treatment of the reaction by Slater (2).

A study of the hydrogen isotope effect in this reaction provides an important clue to the sequence of events which ultimately leads to reaction. The effect of pressure on the isotope effect may contribute to the understanding of the quasi-unimolecular behavior of unimolecular reactions at low pressures.

The tritium isotope effect in this reaction has been examined by Weston (3) and by Lindquist and Rollefson (4) by comparing the tritium content of a mixture of cyclopropane and cyclopropane-t_1 with that of propylenes produced by its isomerization. Lindquist and Rollefson found a relative rate constant expression $k/k_1 = 0.63 \exp(825/RT)$ at a pressure of 200 mm Hg in the temperature range 447–555° C, the isotope effect being 6–27%. Weston reports $k/k_1 = 0.86 \exp(385/RT)$ at the same pressure in the temperature range 406–492° C with an isotope effect up to only 17% despite the lower temperatures used. Weston also measured the isotope effect down to 0.4 mm Hg where it had decreased to approximately zero. While both of these studies suffer from

[1]*Manuscript received February 3, 1961.*
Contribution No. 147 from the Research Council of Alberta, Edmonton, Alberta.

the difficulty of tritium analysis, most uncertainty arises in the interpretation of the experimental results, i.e. the conversion of k/k_1 values to true isotope effects. Here the analysis by Weston seems preferable, but the temperature coefficients so obtained (5900±2000 and 8300 cal/mole) are impossibly high, as he states. In his appraisal of the pressure effect, Weston attempted to fit the data to two simple models. Both assumed that the isotope effect had fallen to its low-pressure limit at zero effect and the data fit both equally well. He pointed out that the zero effect at low pressure as found was coincidental since the isotope effect at low pressure is expected to be temperature dependent.

More recently, Schlag and Rabinovitch (5) have reported an isotope effect of 1.22 from a comparison of the rates of isomerization of cyclopropane and cyclopropane-d_2 at 718° K. Using Weston's conversion technique, this gives ($k_H/k_D = 2.18$) but this value did not decrease appreciably with pressure.

The present paper reports a study of the isotope effect in cyclopropane-d_6 as a function of temperature and pressure.

EXPERIMENTAL

The cyclopropane was Ohio Chemical Anesthetic grade and the cyclopropane-d_6 was supplied by Merck & Co. Both contained small amounts of impurities, especially propylene, which were removed by vapor phase chromatography. The deuterated compound was 93% d_6, the remainder being mainly d_5 and d_4.

The two cylindrical aluminum (2S) pyrolysis furnaces, accommodating 18- and 875-cc Pyrex reaction cells, were heated by directly applied asbestos-insulated Chromel "A" resistance wire and were lagged with 1.5-in. Marinite asbestos board with additional thicknesses at the ends. In each furnace, the reaction cell was surrounded on the sides by 1 in. of aluminum and on the ends by 1.5 in. The temperature of the small reactor was taken from the surrounding aluminum and of the large reactor from an axial thermocouple well extending to the center of the reactor. Temperatures were measured on a calibrated Pt: Pt – 10% Rh thermocouple.

The vacuum system utilized silicone-greased stopcocks throughout. No correction was attempted for reactor dead space as this was an insignificant percentage of the reactor volumes.

If two molecular species are copyrolyzed so that both have the same time and temperature history and if both exhibit first-order kinetics, then

$$k_1/k_2 = f_1/f_2 \cdot \frac{1 + 1/2f_1 + 1/3f_1^2 \ldots}{1 + 1/2f_2 + 1/3f_2^2 \ldots}$$

where f_1 and f_2 are the fractional conversions, i.e. the ratio of rate constants is the ratio of the fractional conversions modified by a correction term. If the conversions are kept below 0.1, the correction term remains small and great precision is not required in the individual conversions; the ratio of the two may be accurately determined from the ratios of the reactants and of the products. For present purposes a stock mixture of the normal and deuterated cyclopropanes was prepared and used in all subsequent experiments.

Separations of the two propylene products from reactants were carried out on a 15-ft dodecyl phthalate vapor phase chromatographic column at room temperature with hydrogen as carrier gas. The propylenes were collected in liquid-air traps, measured, and examined on a mass spectrometer. Isotope analysis of the first part of a vapor phase

Can. J. Chem. Downloaded from www.nrcresearchpress.com by 210.87.254.5 on 09/05/12
For personal use only.

chromatographic peak of a propylene sample indicated some fractionation; care was subsequently taken to collect the total chromatographic "peak".

In the mass spectrometric analysis of the propylene, the parent ions at mass 48 ($C_3D_6^+$) and 42 ($C_3H_6^+$) were taken as indicative of the relative proportions of the two isotopic species. Since the ion $C_3D_3^+$ makes a significant contribution at mass 42 at 50 v, a correction factor was determined from a sample of propylene-d_6 produced by the rearrangement of 10% of a sample of the deuterated cyclopropane. This procedure was also carried out at an ionization potential of 12 v where these corrections are considerably reduced but no significant or systematic difference was noted between the two analyses.

A similar procedure was followed in the analysis of the stock mixture of cyclopropane and cyclopropane-d_6.

In the study of the temperature coefficient, the small reactor was used throughout, conventional techniques being employed for introducing and retrieving the reactants. In the study of the pressure effect, the small reactor was used down to 50 mm Hg and the large reactor for lower pressures. In the very low pressure range, the pressure was calculated from the quantity of reactants introduced to the reactor. In experiments below 1 mm Hg, several successive runs were combined to provide sufficient sample for isotope-ratio analysis of the products.

RESULTS

The effect of pressure on the isotope effect is shown in Fig. 1 where k_H/k_D at 482° C

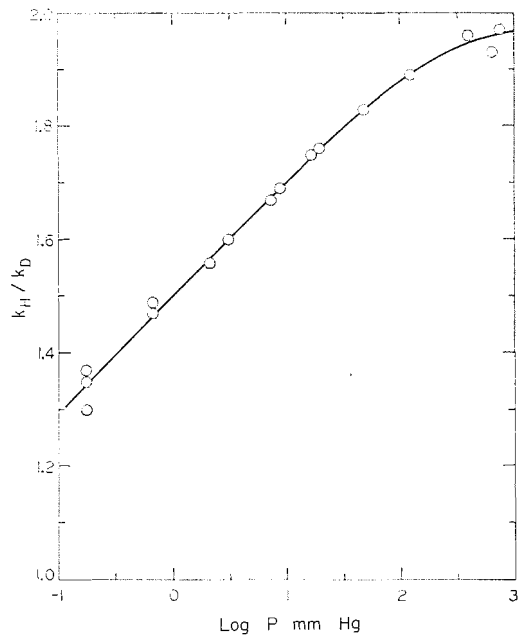


FIG. 1. The effect of pressure on the isotope effect at 482° C.

is plotted against the logarithm of pressure for comparison with the similar plot by Weston (3). To determine the isotope effect at infinite pressure, the best plot was that suggested by Schlag and Rabinovitch (5), k_D/k_H vs. $p^{-1/2}$; the value so obtained at 482° C is 1.96.

Can. J. Chem. Downloaded from www.nrcresearchpress.com by 210.87.254.5 on 09/05/12
For personal use only.

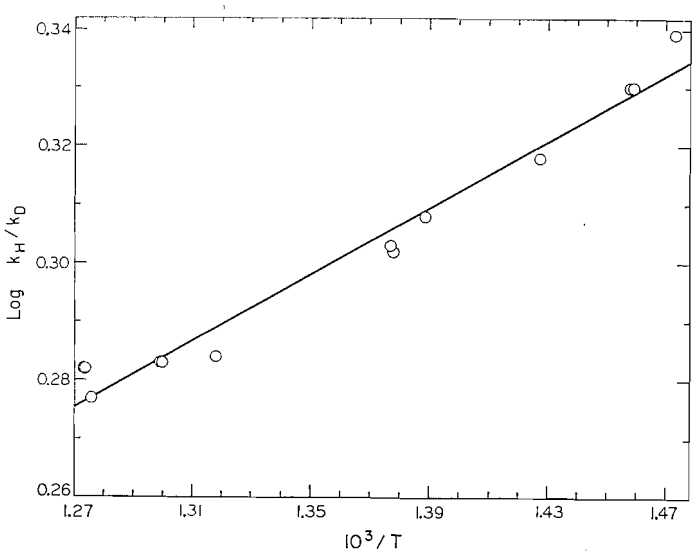


FIG. 2. The temperature dependence of the isotope effect.

The effect of temperature on the isotope effect is illustrated in Fig. 2 and the pertinent data are presented in Table I. A least-squares treatment of these data gives an isotope effect expression.

$$k_H/k_D = 0.82 \exp (1300 \pm 150/RT)$$

TABLE I
Data for the relative rate constants at high pressure

Expt. No.	Pressure, cm Hg	Temperature, °K	Conversion correction	k_H/k_D
16	67.6	720.0	1.026	2.03
17	66.8	700.4	1.017	2.08
18	64.4	783.3	1.032	1.89
25	63.6	758.6	1.027	1.92
27	62.2	725.7	1.034	2.00
28	62.1	726.1	1.037	2.01
30	59.6	678.6	1.006	2.18
31	58.7	785.1	1.034	1.91
32	58.1	785.4	1.034	1.91
33	58.3	769.4	1.037	1.92
34	57.5	769.6	1.037	1.92
35	56.6	685.8	1.009	2.12
36	56.4	685.3	1.009	2.12

Since these data were obtained in the pressure range 56–68 cm Hg, it would be expected that the pre-exponential term for the isotope effect at infinite pressure would be slightly higher.

DISCUSSION

The high-pressure hydrogen isotope effect reported here (2.04 at 445° C) compares favorably with effects observed in other gas phase reactions at the same temperature, for example the ethyl–ethyl-d_5 acetate decomposition (2.23) (6) and the abstraction

Can. J. Chem. Downloaded from www.nrcresearchpress.com by 210.87.254.5 on 09/05/12
For personal use only.

reaction of CD_3 with acetone and acetone-d_6 (2.5) (7). The activation energy difference of 1300 cal/mole is slightly less than the values of 1515 cal/mole and 1670 cal/mole respectively for these two reactions but is still substantially above the maximum value of about 1150 cal/mole derivable from a single C—H stretching frequency being converted to a very weak vibration in the activated complex. It is therefore obvious that the hydrogen isotope effect in this reaction is a primary effect and that considerable carbon–hydrogen bond relaxation occurs during activation.

The decrease in the isotope effect with decreasing pressure confirms the observation of this same effect with cyclopropane-t_1 (3). Unlike that effect, which decreased to zero at 0.4 mm Hg, the present effect has not decreased to nearly the same extent at this pressure, nor is there any suggestion of its reaching a limiting value. Since this would happen only when the reaction has become truly second order, the present data must be considered as a more reliable measure of the variation of the effect with pressure.

Two quite distinct mechanisms have been proposed for the rearrangement of cyclopropane: the first, a mechanism wherein a hydrogen atom transfers from one carbon atom to another with the simultaneous breaking of the carbon ring; the second, involving the intermediate formation of a trimethylene diradical by the simple scission of the carbon ring, the propylene being subsequently formed by the transfer of a hydrogen atom from the middle carbon to a terminal one. This latter mechanism has recently been supported by the re-examination of data on the iodination of cyclopropane and on the rearrangement of cyclopropane-d_2 by Benson (8). Following the notation of Benson, the mechanism is given as

$$\triangle \underset{b}{\overset{a}{\rightleftharpoons}} \mathrm{T}: \overset{c}{\rightarrow} \mathrm{P}$$

and applying the steady-state treatment, the rate of formation of propylene becomes

$$\frac{d\mathrm{P}}{dt} = \frac{k_a k_c}{k_b} \triangle \Big/ \left(1 + \frac{k_c}{k_b}\right).$$

If the ratio k_c/k_b is small, then the over-all rate constant for the reaction becomes $k_a k_c/k_b$. Hence the hydrogen isotope effect observed must arise in one of these constants, and, since reaction (*c*) involves the transfer of a hydrogen atom, it must be assumed that k_c is the source of the primary effect, k_a and k_b probably having little, if any, isotope dependence.

The rate constant expressions derived by Benson for k_b and k_c indicate that at 444° C the reactions of trimethylene are so rapid that virtually no opportunity exists for collisions even at one atmosphere pressure. If true, this can only mean that the pressure effect in the isomerization occurs in the reaction (*a*), and, because the isotope effect is postulated to occur in (*c*) and not (*a*), then the isotope effect should not be pressure dependent. Since this is contrary to the experimental results, the mechanism must be incorrect unless either the instability of the trimethylene has been exaggerated, or the isotope effect in reaction (*a*) is of primary importance. Some assurance that the former is not the case may be gained from the results of Flowers and Frey (9), who found that at 100° C, trimethylene from the photolysis of cyclobutanone reacted with ethylene, but no such reaction occurred when cyclopropane was rearranged in the presence of excess ethylene. Both of these results are to be expected on the basis of half lives of the trimethylene radical at the two temperatures as calculated from Benson's rate-constant equations.

Can. J. Chem. Downloaded from www.nrcresearchpress.com by 210.87.254.5 on 09/05/12
For personal use only.

Can. J. Chem. Downloaded from www.nrcresearchpress.com by 210.87.254.5 on 09/05/12
For personal use only.

Two alternate interpretations may be put on a major isotope effect occurring in the reaction (*a*). It may be assumed that a transition state exists for the formation of trimethylene which involves a largely broken C—H bond, the hydrogen being in such a position as to considerably influence the carbon–carbon bond break. This would require that reactions (*b*) and (*c*) also have isotope effects and that they be of about the same magnitude. Since the geometric isomerization can be explained by the rotation in the trimethylene radical, it is unnecessary that the configuration of the activated complex allow for this alternate reaction. Secondly, it may be assumed that this transition state is such as to allow for geometric isomerism if it reverts to cyclopropane, and that it may go over directly to propylene. This would suggest an activated complex of the structure suggested by Smith (10) in which two hydrogens and the three carbon atoms are coplanar, with one of the hydrogens weakly bonded to its original carbon atom and to its ultimate acceptor. The postulate of a trimethylene intermediate from such a complex is unnecessary in explaining the experimental facts. The hydrogen isotope effect data does not conclusively decide between these two reaction schemes. It seems most reasonable to accept the latter, however, purely on the basis that, if the hydrogen does become bridged from one carbon to the next, as it must if it is to be of any assistance in the rupture of the carbon–carbon bond, then it will be most advantageous for it to continue on its path toward that carbon atom.

It is interesting to compare the isotope effect in this reaction with that observed for the decomposition of cyclobutane (11) to ethylene where the effect is 1.37 at 449° C, and the activation energy difference, 1400 cal/mole. The existence of this effect, despite the fact that the hydrogens do not transfer during the reaction, suggests that there is some similarity between the cyclopropane rearrangement and this decomposition. The similarity of the activation energy differences (1400 and 1300 cal/mole) suggests that the critical processes involved in reaching the activated complex are the same for each. If then, for the sake of argument, one proposes a mechanism for cyclobutane involving the tetramethylene diradical as an intermediate in the path to ethylene, and applies

$$\square \underset{b}{\overset{a}{\rightleftharpoons}} \mathrm{T} \xrightarrow{c} 2\mathrm{E}$$

the same steady-state treatment as for cyclopropane, it must be true that reaction (*a*) is the isotope-dependent step since the effect is again pressure dependent. The reaction (*c*) in cyclobutane does not involve a hydrogen transfer and would not be expected to involve a hydrogen isotope effect. In reaction (*b*), however, the activated complex is the same as for the forward reaction, and a roughly equivalent C—H bond weakening must occur as in reaction (*a*); hence a fairly large activation energy difference would be expected. Since this would tend to cancel the energy difference in (*a*), a relatively small temperature coefficient would have been expected in the isotope effect. The experimental value does not support this thesis, and it therefore seems reasonable to suggest that the decomposition of cyclobutane involves a transition state in which the carbon–carbon bond split is assisted by the partial bonding of one hydrogen to its neighboring carbon atom.

If this is a reasonable description of the mechanism of the reaction, some correlation must exist between the critical difference between the cyclopropane and cyclobutane mechanisms, i.e. the transfer and non-transfer of hydrogen atoms, and the considerable difference in the isotope effects, i.e. 2.04 vs. 1.37. The fact that the ratio of these two numbers is about 1.5 suggests that this difference arises from that part of the isotope

effect which is due to the relative reduced mass ratio in the reaction co-ordinate in the region of the transition state, which, for hydrogen isotope effects, is about 1.4. This implies that the difference in these isotope effects arises not in the mode of formation of the activated complex nor of its geometry, but rather in the unique way in which the hydrogen atom is concerned in that degree of freedom of the complex which results in reaction.

ACKNOWLEDGMENTS

The author wishes to thank Dr. B. S. Rabinovitch for his manuscript prior to publication and Dr. M. G. H. Wallbridge and P. W. Gilderson for fruitful discussions. Assistance in the form of a grant for fundamental research from the National Research Council is also gratefully acknowledged.

REFERENCES

1. T. S. CHAMBERS and G. B. KISTIAKOWSKY. J. Am. Chem. Soc. **56**, 399 (1934).
2. N. B. SLATER. Proc. Roy. Soc. A, **218**, 224 (1953).
3. P. E. WESTON, JR. J. Chem. Phys. **26**, 975 (1957).
4. R. H. LINDQUIST and G. K. ROLLEFSON. J. Chem. Phys. **24**, 725 (1956).
5. E. W. SCHLAG and B. S. RABINOVITCH. J. Am. Chem. Soc. **82**, 5996 (1960).
6. A. T. BLADES and P. W. GILDERSON. Can. J. Chem. **38**, 1407 (1960).
7. J. R. MCNESBY, T. W. DAVIS, and A. S. GORDON. J. Am. Chem. Soc. **76**, 823 (1954).
8. S. W. BENSON. J. Chem. Phys. **34**, 521 (1961).
9. M. C. FLOWERS and H. M. FREY. J. Chem. Soc. 2758 (1960).
10. F. T. SMITH. J. Chem. Phys. **29**, 235 (1958).
11. J. LANGRISH and H. O. PRITCHARD. J. Phys. Chem. **62**, 761 (1958).

Can. J. Chem. Downloaded from www.nrcresearchpress.com by 210.87.254.5 on 09/05/12
For personal use only.

Can. J. Chem. Downloaded from www.nrcresearchpress.com by 210.87.254.105 on 09/05/12
For personal use only.

CONSTITUTION OF THE GALACTOMANNAN FROM THE KERNEL OF GREEN PALMYRA PALM NUT (BORASSUS FLABELLIFER LINN.)[1]

A. K. MUKHERJEE, D. CHOUDHURY, AND P. BAGCHI

ABSTRACT

The water-soluble polysaccharide extracted from the kernel of green palmyra palm nut (*Borassus flabellifer* Linn.) was shown to be composed of D-galactose and D-mannose in the proportion of 1:2.4. Hydrolysis of the fully methylated galactomannan yielded 2,3,4,6-tetra-*O*-methyl-D-galactose, 2,3,6-tri-*O*-methyl-D-mannose, and 2,3-di-*O*-methyl-D-mannose in the molar ratio of 1:1.4:0.95. Partial hydrolysis of the galactomannan afforded 4-*O*-β-D-mannopyranosyl-D-mannose, 6-*O*-α-D-galactopyranosyl-D-mannose, and two trisaccharides. Based on these results a structural formula for the galactomannan has been proposed, additional evidence for which was adduced from periodate-oxidation studies.

In 1956 Subrahmanyan *et al.* (1) reported the isolation of a polysaccharide from the kernel by extraction with 10% sodium hydroxide which gave, on hydrolysis, D-galactose and D-mannose in the ratio of 1:2.9 approximately. However, no detailed investigations seem to have been carried out on its structure.

This paper reports the structural studies on the polysaccharide obtained by precipitating the aqueous extract of the soft kernel with ethanol. Hydrolysis of the polysaccharide, $[\alpha]_D^{30}$ +8.5° (in 4% sodium hydroxide solution) gave D-galactose and D-mannose in the molar proportion of 1:2.4 as estimated by the periodate method (2).

The galactomannan was methylated first by repeated treatment with methyl sulphate and alkali (3) and then by Purdie's method (4). The resulting methylated galactomannan, which showed no hydroxyl absorption band in the I.R. spectrum, was a glassy solid —OCH_3 43.25%, $[\alpha]_D^{29}$ +29° (in chloroform). After methanolysis of the methylated polysaccharide and hydrolysis of the resulting mixture of methyl glycosides the mixture of methyl sugars, so obtained, on paper chromatographic examination using solvents B and D showed the presence of three methylated sugars together with a trace amount of another. The mixture of methylated sugars was separated on a cellulose column (5) using butanone–water azeotrope (6) as eluent.

Identification of the various methylated sugars obtained by column chromatography showed them to be 2,3,4,6-tetra-*O*-methyl-D-galactose (1 mole), 2,3,6-tri-*O*-methyl-D-mannose (1.35 moles), 2,3,6-tri-*O*-methyl-D-galactose (0.035 mole), and 2,3-di-*O*-methyl-D-mannose (1.03 moles).

The relative proportion of 2,3,4,6-tetra-*O*-methyl-D-galactose, 2,3,6-tri-*O*-methyl-D-mannose, and 2,3-di-*O*-methyl-D-mannose was estimated by hypoiodite titration (7) after separation on paper using solvent B and was found to be 1:1.4:0.95. This ratio is in good agreement with that obtained by weighing the different fractions obtained during column chromatographic examination of the mixture.

The tetra-*O*-methyl sugar fraction, $[\alpha]_D^{30}$ +109° (in water) obtained as a sirup, gave on demethylation (8) D-galactose only along with some partially demethylated sugars and was characterized to be 2,3,4,6-tetra-*O*-methyl-D-galactose through its anilide (9).

The tri-*O*-methyl-D-mannose $[\alpha]_D^{30}$ −9° (in water) was characterized as 2,3,6-tri-*O*-methyl-D-mannose through the crystalline 2,3,6-tri-*O*-methyl-D-mannose, 1,4-di-*p*-nitrobenzoate (10).

[1]*Manuscript received January 24, 1961.*
Contribution from the Department of Macromolecules, Indian Association for the Cultivation of Science, Calcutta 32, India.

Can. J. Chem. Downloaded from www.nrcresearchpress.com by 210.87.254.105 on 09/05/12
For personal use only.

The fraction containing the trace quantity of the tri-*O*-methyl sugar gave D-galactose and D-mannose on demethylation and on paper chromatography using solvent B gave two spots corresponding to those of 2,3,6-tri-*O*-methyl-D-galactose and 2,3,6-tri-*O*-methyl-D-mannose the relative proportions of which were calculated from the observed specific rotation.

The dimethyl sugar fraction having $[\alpha]_D^{30}$ $-16.4°$ (in water) was chromatographically pure and was characterized to be 2,3-di-*O*-methyl-D-mannose by conversion to 2,3-di-*O*-methyl-D-mannonic acid phenyl hydrazide (11).

From the above results it is possible to assign a structure to the galactomannan. Demonstration of the existence of 2,3,4,6-tetra-*O*-methyl-D-galactose alone in the tetramethyl fraction of the hydrolyzate of the methylated polysaccharide shows that D-galactose in the pyranose form constitutes the non-reducing ends of the molecule.

That the backbone of the molecule is made up of $1 \rightarrow 4$-linked mannopyranose residues is proved by the characterization of 2,3,6-tri-*O*-methyl-D-mannose in the hydrolyzate of the methylated galactomannan.

The fact that 2,3-di-*O*-methyl-D-mannose is present in the hydrolyzate indicates that the polysaccharide is branched and that at branch points the mannose residues are linked through C_1, C_4, and C_6.

The trace amount of the tri-*O*-methyl-D-galactose might have originated from partial demethylation of the tetra-*O*-methyl-D-galactose fraction during methanolysis and hydrolysis of the methylated galactomannan (12) and is considered to have no structural significance.

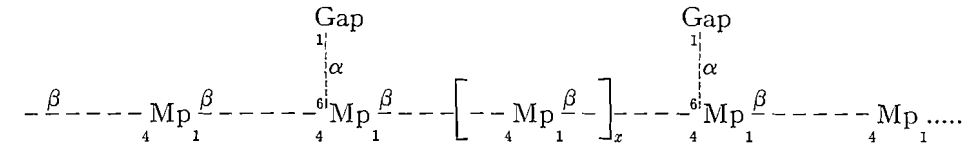
Further support for the proposed structure for the galactomannan was obtained from the periodate oxidation of the galactomannan. It was found that one molar proportion of formic acid was liberated for every 3.7 hexose units in 25 hours and that 1.30 moles of periodate were consumed per hexose unit in 30 hours. If one galactopyranose residue is present as non-reducing terminal group for every 2.4 units of mannopyranose residues, on the average, in the chain, then theoretically the consumption of periodate works out to be 1.30 moles per hexose residue. The results of periodate uptake are thus in good agreement with the theoretically expected results.

When the periodate-oxidized polysaccharide was reduced with sodium borohydride and hydrolyzed, glycerol and erythritol were obtained from the non-reducing units and $1 \rightarrow 4$-linked mannose residues respectively in the molar proportion of 1:2.45. The linkages at the branch points through C_1, C_4, and C_6 as mentioned above were confirmed by the absence of mannose in this hydrolyzate. The length of the repeating unit (3.45) calculated from the amounts of glycerol and erythritol obtained is in good agreement with those obtained from methylation and periodate-oxidation studies.

In order to establish the stereochemistry of the linkages between the sugar units the galactomannan was subjected to graded hydrolysis. After separation by column and paper chromatography, two disaccharides, viz. 4-*O*-β-D-mannopyranosyl-D-mannose and 6-*O*-α-D-galactopyranosyl-D-mannose, and two trisaccharides, *O*-β-D-mannopyranosyl $(1 \rightarrow 4)$-*O*-β-D-mannopyranosyl$(1 \rightarrow 4)$-*O*-β-D-mannose and another triose having one galactose residue and two mannose residues with mannose residue at the reducing end, were isolated and, in pure form, studied.

The presence of mannobiose and mannotriose in comparatively larger amounts clearly shows a $1 \rightarrow 4$ β-linked mannose chain in the molecule. The existence of α-linked galactopyranose residues as non-reducing terminal units is confirmed by the isolation and characterization of 6-*O*-α-D-galactopyranosyl-D-mannose.

Based on the above results it can be concluded that the galactomannan has a structure of the following type:



where x has the value of 1 in one segment and 2 in the next, Gap = galactopyranose residue, Mp = mannopyranose residue.

The low specific rotation (+8.5° in 4% sodium hydroxide) of the galactomannan indicates the presence of both α and β linkages in the molecule.

During purification of the galactomannan through copper complex (13*a*, 13*b*) it was observed that the proportion of galactose gradually decreased. The ratio of galactose to mannose was found to change from 1:2.4 to 1:3.4 during five treatments with Fehling's solution. It was also noticed that only galactose residues were released when the galactomannan was hydrolyzed under very mild condition employing 0.02 *N* oxalic acid. The resulting galactomannan after 4 hours had galactose-to-mannose ratio of 1:3.7. Hence the increase in the mannose content during purification through copper complex may be attributed to the fact that some of the α-linked galactose residues, which are more labile, were removed during the acid treatment employed for destruction of the copper complex.

The galactomannan was acetylated in the usual way (14, 15). The triacetate, which showed an increased mannose content, was fractionally precipitated from a solution of the substance in a solvent containing *s*-tetrachloroethane and 95% ethanol in the ratio of 9:1, by gradual addition of methanol. The different fractions after deacetylation and hydrolysis were found to have galactose-to-mannose ratios between 1:2.4 to 1:3.2. It is significant to note that none of the fractions had the ratio of galactose to mannose more than 1:2.4. One of these fractions (fraction 5) having galactose-to-mannose ratio 1:3.2 was methylated directly (14) first by treating a solution of the triacetate in dry tetrahydrofuran with solid sodium hydroxide and methyl sulphate and then by Purdie's method. The resulting fully methylated polysaccharide, $-OCH_3$, 43.05%, $[\alpha]_D^{25}$ +24° (in chloroform) was subjected to methanolysis and hydrolysis. The mixture of the methyl sugars obtained, on paper chromatography, showed the presence of 2,3,4,6-tetra-*O*-methyl-D-galactose, 2,3,6-tri-*O*-methyl-D-mannose, and 2,3-di-*O*-methyl-D-mannose in the ratio of 1:2.11:1.08 as estimated by alkaline hypoiodite method. The mixture (ca. 200 mg) was separated on Whatman No. 3MM papers and the individual sugars were identified as above.

The isolation and characterization of the same methylated sugars from this fraction show that the original material was essentially homogeneous and that during acetylation some of the labile α-linked galactose units were eliminated.

The molecular weight of the methylated galactomannan as determined by light-scattering method was found to be 1.39×10^5.

The galactomannan obtained from palm kernel is similar in the essential structure to those obtained from fenugreek seed (16), carob seed (11, 17), and guar seed (18, 19, 20) but differs from that obtained from the kernel of coconut (*Cocos nucifera*) (paper in press).

Can. J. Chem. Downloaded from www.nrcresearchpress.com by 210.87.254.105 on 09/05/12
For personal use only.

Can. J. Chem. Downloaded from www.nrcresearchpress.com by 210.87.254.105 on 09/05/12
For personal use only.

EXPERIMENTAL

All specific rotations are equilibrium values. Unless otherwise stated, all evaporations were carried out *in vacuo* at 30°–40° C. The solvent mixtures (v/v) used for partition chromatography of sugars and their derivatives were:

(A) ethyl acetate:pyridine:water (8:2:1);
(B) methyl ethyl ketone – water azeotrope;
(C) butanol:acetic acid:water (4:1:5) upper layer;
(D) butanol:ethanol:water (40:11:19);
(E) butanol:ethanol:water (4:1:5) upper layer;
(F) ethyl acetate:acetic acid:water (9:2:2).

Whatman No. 1 filter papers were used for paper partition chromatography. The spray reagents used were:

(*a*) aniline hydrogen oxalate (saturated aqueous solution);
(*b*) *p*-anisidine hydrochloride (3% solution in butanol);
(*c*) ammoniacal silver nitrate solution.

Isolation and Purification of the Galactomannan

The kernel obtained from the market was peeled and the soft fleshy material was macerated in a high-speed "Kenmix 55" blender for 2 minutes in the presence of ethanol. The resulting slurry was kept overnight under ethanol and then was filtered through cloth. The residue was freed from ethanol by squeezing and then dried in air. The material (50 g) so obtained was allowed to swell with water (1500 ml) for some time and heated, while being stirred, on a boiling-water bath for 5 hours. After being kept overnight in a refrigerator the slurry was diluted with water (1500 ml) and the coarse suspended material was removed by filtration through cloth. The filtrate was passed through Cepa supercentrifuge at 25,000–30,000 r.p.m. for further clarification. The clear liquid was slowly added, with stirring, to acidified (pH 4–5) 95% ethanol when a white fibrous precipitate appeared. This was separated by centrifuge and triturated five times with absolute ethanol and finally with ether. The product was dried in air and then *in vacuo*. It was a white amorphous powder, yield: 12 g, moisture 10.9%, ash 0.36%, $[\alpha]_D^{30}$ +8.5° (in 4% aqueous sodium hydroxide solution, *c*, 0.5), intrinsic viscosity 1.25 dl/g (in 4% sodium hydroxide solution), pentosan (21) 0.5%, methoxyl group (22) 0.3%, nitrogen 0.7%, uronic acid (23) negligible. D-Galactose and D-mannose were detected by paper chromatography in the hydrolyzate of the polysaccharide using solvent A. A small portion of the hydrolyzate was separated quantitatively by paper chromatography using solvent A. The zones corresponding to each sugar were eluted in the usual way and estimated by the periodate method (2). D-Galactose and D-mannose were found in the ratio of 1:2.4.

The galactomannan was purified by complexing (13*a*, 13*b*) with Fehling's solution. The galactomannan (10 g) was dissolved in 4% sodium hydroxide solution (1 l.) in an atmosphere of nitrogen, and freshly prepared Fehling's solution (500 ml) was added to it while it was stirred in a cold bath (10° C). The flocculent blue precipitate so obtained was filtered through a piece of fine nylon cloth and washed with water till the filtrate was colorless. The precipitate was suspended in water (500 ml) in a cold bath (10° C) and 2 *N* HCl was added dropwise with stirring till the mixture was just acidic. The stirring was continued for 2 hours more when a homogeneous dispersion was obtained. This was then added slowly, with stirring, to ethanol (800 ml) when a white fibrous

precipitate separated out. This was centrifuged, washed with a mixture of 80% ethanol: HCl (100:1), and triturated with ethanol till free from acid and finally with ether. Yield 8.75 g, $[\alpha]_D^{30}$ +9° (in 4% sodium hydroxide solution, *c*, 0.5). On hydrolysis of the purified polysaccharide D-galactose and D-mannose were obtained in the ratio of 1:2.6.

Each repetition of the process led to a product showing higher mannose content. After five precipitations the ratio of galactose to mannose was found to be 1:3.4.

Mild Hydrolysis of the Galactomannan with Oxalic Acid

The galactomannan (1 g) was dispersed in water (50 ml) to which 0.04 *N* oxalic acid (50 ml) had been added and was heated on a water bath (90°–95° C). At intervals of 1 hour aliquots (25 ml) were withdrawn and precipitated with ethanol (30 ml). The supernatant liquids were concentrated to sirups. Each of these on paper chromatographic examination using solvent A indicated the presence of D-galactose only. The precipitated polysaccharide from the fourth stage was washed with alcohol and then hydrolyzed with 2 *N* sulphuric acid. The hydrolyzate was treated in the usual manner and the resulting sirup had D-galactose and D-mannose in the ratio of 1:3.7.

Hydrolysis and Identification of D-*Galactose and* D-*Mannose*

The galactomannan (0.5 g) was kept with 72% sulphuric acid (24) at room temperature overnight and diluted with water to give normal acid solution. The solution was heated for 8 hours on a boiling-water bath when the hydrolysis, followed iodometrically (25), was complete. The solution obtained after neutralization with barium carbonate and filtration, was deionized by passage through Amberlite I.R. 120(H)* and Amberlite I.R. 45(OH)* and was concentrated to a sirup. A portion of this sirup (200 mg) was separated on a Whatman No. 3MM filter paper using solvent A. The strips corresponding to D-galactose and D-mannose were each eluted with water (20 ml) and evaporated to give sirups, D-galactose, $[\alpha]_D^{30}$ +79° (in water, *c*, 1) and D-mannose, $[\alpha]_D^{30}$ +14° (in water, *c*, 1). Each of these components were refluxed with *p*-nitroaniline in methanol acidified with hydrochloride acid (26). The galactose component gave *p*-nitro-*N*-phenyl-D-galactosyl amine, m.p. and mixed m.p. 217°–218° C, $[\alpha]_D^{30}$ −245° (in dry pyridine, *c*, 0.5), lit. (26) −248°. D-Mannose component gave *p*-nitro-*N*-phenyl-D-mannosyl amine, m.p. and mixed m.p. 217°–218°, $[\alpha]_D^{30}$ −325° (in dry pyridine, *c*, 0.5) lit. (26) −325°.

Methylation of the Galactomannan

The galactomannan (10 g) was methylated by treatment first with methyl sulphate and alkali and then with methyl iodide and silver oxide according to the method of Falconer and Adams (27*a*, 27*b*) to yield a methylated derivative (3.22 g) showing no hydroxyl absorption band in the infrared spectrum. It had intrinsic viscosity 0.267 dl/g in chloroform and $[\alpha]_D^{29}$ +28.7° (in chloroform, *c*, 1). (Anal. Calc. for $C_9H_{16}O_5$, —OCH_3 44.7; found —OCH_3 43.25%.)

Molecular-Weight Determination of the Methylated Galactomannan

All measurements of the intensity of scattered light for molecular-weight determination of the methylated galactomannan were carried out with a Brice Phoenix light-scattering photometer (Model OM 1000A) using semioctagonal cells. Intensities of scattered light at four angles (viz. 0°, 45°, 90°, and 135°) over a concentration range of 0.5 to 4.5×10^{-3} g/ml were measured and working standard method was used to calculate turbidity (τ). The solutions used for the measurement were taken from a stock solution of known

**A product of Rohm & Hass Company, Pennsylvania, U.S.A.*

Can. J. Chem. Downloaded from www.nrcresearchpress.com by 210.87.254.105 on 09/05/12
For personal use only.

concentration in redistilled chloroform and diluted to a definite volume in a calibrated volumetric flask with the same solvent. Special precaution was taken to avoid dust and suspended particles by filtering the stock solution and solvent through sintered glass (G 4) and (G 5) respectively. The concentration of each solution was determined by dry-weight method. The refractive indices of the solutions were determined with Brice Phoenix differential refractometer at the same wave length and temperature. The turbidities and dissymmetries obtained by the above procedure were reproducible indicating absence of anomalous aggregation. The molecular weight of the methylated galactomannan was found to be 1.39×10^5 calculated by dissymmetry method (28*a*) assuming particle-scattering factor (P 90°) (28*b*, 28*c*) for random coil.

Methanolysis and Hydrolysis of the Methylated Galactomannan

The methylated galactomannan (1 g) was refluxed with 4% methanolic hydrogen chloride (100 ml) till the rotation reached a constant value (15 hours). The solution was evaporated to a sirup and the resulting mixture of methyl glycosides was hydrolyzed with N hydrochloric acid (75 ml) till the rotation reached constant value (14 hours). The hydrolyzate was neutralized (silver carbonate), filtered, and the resulting solution deionized by passage through Amberlite I.R. 120(H) and Amberlite I.R. 45(OH). The mixture of methylated sugars was evaporated to a sirup (0.85 g).

A preliminary analysis was made by paper partition chromatography using solvents B and D and spray reagent *a*. The following spots were identified.

Spot No.	R_f Solv. B	R_G* Solv. D	Sugars
1	0.69	0.91	2,3,4,6-Tetra-*O*-methyl-D-galactose
2	0.51	0.82	2,3,6-Tri-*O*-methyl-D-mannose
3	0.47	—	2,3,6-Tri-*O*-methyl-D-galactose (trace)
4	0.24	0.61	2,3-Di-*O*-methyl-D-mannose

*R_G values are with respect to *n*-tetra-*O*-methyl-D-glucose.

Separation of the Mixture of Methylated Sugars by Column Chromatography

The mixture of methylated sugars (825 mg) was separated on a cellulose column (5) (60×2.5 cm) using solvent B (6) on an automatic fraction collector. The total eluent was then divided into the following five fractions guided by the difference in the refractive indices of the solvent and solution in each test tube using a Brice Phoenix differential refractometer and also by examination by paper chromatography.

Fraction	Tube No.	Sugars	Molar ratio
A	21–25	2,3,4,6-Tetra-*O*-methyl-D-galactose	1
B	26	2,3,4,6-Tetra-*O*-methyl-D-galactose and 2,3,6-tri-*O*-methyl-D-mannose	
C	27–29	2,3,6-Tri-*O*-methyl-D-mannose	1.25
D	30–31	2,3,6-Tri-*O*-methyl-D-mannose and 2,3,6-tri-*O*-methyl-D-galactose	
E	35–44	2,3-Di-*O*-methyl-D-mannose	1.03

Identification of 2,3,4,6-Tetra-O-methyl-D-galactose

Fraction A on evaporation gave a sirup (245.7 mg) having $[\alpha]_D^{30}$ +109° (in water, *c*, 1) lit. (29) +109.5°. The sirup (5 mg) was demethylated (8) by heating for 5 minutes on a

Can. J. Chem. Downloaded from www.nrcresearchpress.com by 210.87.254.105 on 09/05/12
For personal use only.

boiling-water bath with 48% hydrobromic acid (2 ml) in a sealed tube in an atmosphere of nitrogen. The resulting solution after usual treatment gave a sirup, which on paper chromatographic analysis using solvent A, indicated the presence of D-galactose only along with some partially demethylated sugars. The identity of 2,3,4,6-tetra-*O*-methyl sugar was confirmed by preparing the *N*-phenyl-2,3,4,6-tetra-*O*-methyl-D-galactosyl amine in the usual way, m.p. and mixed m.p. 187° C, lit. 188°–190° C (8), 186°–188° (30); $[\alpha]_D^{30}$ +38° (in acetone), lit. +39° (8), +40.7° (31).

Examination of Fraction B

This fraction on evaporation yielded a sirup (53.3 mg) having $[\alpha]_D^{30}$ +5° (in water). Demethylation of a small portion of this fraction gave D-galactose and D-mannose along with partially demethylated sugars. Paper partition chromatography using solvent D with authentic samples indicated that the mixture contained 2,3,4,6-tetra-*O*-methyl-D-galactose and 2,3,6-tri-*O*-methyl-D-mannose by comparison with authentic samples. Specific rotation value showed that the tetramethyl galactose and the trimethyl mannose were present in the proportion of 1:7 approximately.

Identification of 2,3,6-Tri-O-methyl-D-mannose

The fraction C on evaporation gave a sirup (277 mg). This was chromatographically homogeneous and had $[\alpha]_D^{30}$ −9° (in water, *c*, 1) lit. −13° (9), −10° (11). It gave D-mannose along with some partially demethylated sugars on demethylation of a portion of it. The 2,3,6-tri-*O*-methyl-D-mannose was characterized through its crystalline 2,3,6-tri-*O*-methyl-D-mannose, 1,4-di-*p*-nitrobenzoate (10), m.p. and mixed m.p. 189°–190° C, lit. (9) 190°–191° C; $[\alpha]_D^{30}$ +32° (in chloroform), lit. (10) +33°.

Examination of Fraction D

This fraction yielded a sirup (33 mg) having $[\alpha]_D^{30}$ +13.5° (in water). Demethylation of a part of it yielded D-galactose and D-mannose along with other partially demethylated sugars. Examination of this sirup using solvent D with authentic samples indicated that it contained a mixture of 2,3,6-tri-*O*-methyl-D-galactose and 2,3,6-tri-*O*-methyl-D-mannose. Optical rotation value indicated that they were present in the ratio of 1:3 approximately.

Identification of 2,3-Di-O-methyl-D-mannose

Fraction E on evaporation gave a sirup (212.9 mg) having $[\alpha]_D^{30}$ −16° (in water) lit. (32) −15.8°. This fraction was chromatographically pure and gave D-mannose only along with partially demethylated sugars on demethylation of a part of it. The sirup (25 mg) was oxidized with bromine water at room temperature (10) for 68 hours. The bromine was removed by aeration and the solution after usual treatment yielded a thick sirup containing the lactone $[\alpha]_D^{29}$ +58° (in water, after 24 hours), which could not be induced to crystallization. This was converted to the phenylhydrazide by heating it with phenylhydrazine in ethanol on a boiling-water bath. The 2,3-di-*O*-methyl-D-mannonic acid phenylhydrazide was crystallized from methanol–ether (11), m.p. 158° C, lit. 156° (18), 168° C (10); $[\alpha]_D^{29}$ −24° (in water), lit. −24.2° (18), −25° (10).

Estimation of the Methyl Sugars

A small quantity of the mixture of methylated sugars (5 mg) was separated by paper chromatography using solvent B. Each sugar was eluted in the usual way and estimated by alkaline hypoiodite (7) method. The molar ratio of the different sugars found

Can. J. Chem. Downloaded from www.nrcresearchpress.com by 210.87.254.105 on 09/05/12
For personal use only.

were as follows: 2,3,4,6-tetra-*O*-methyl-D-galactose:2,3,6-tri-*O*-methyl-D-mannose:2,3-di-*O*-methyl-D-mannose as 1:1.4:0.95. The 2,3,6-tri-*O*-methyl-D-galactose was obtained in negligible amount.

Periodate Oxidation of the Galactomannan

The galactomannan (84.2 mg) was dispersed in water (50 ml) and oxidized by shaking with 0.1 *M* sodium metaperiodate (50 ml) in the dark at 15° C. The liberated formic acid and the amount of periodate consumed during the reaction were estimated in the usual way (33) at regular intervals of time. The liberation of formic acid became constant in 25 hours, 3.7 hexose residues liberating 1 mole of formic acid. The periodate uptake became constant after 30 hours corresponding to 1.30 moles of the oxidant per hexose residue.

Reduction of the Periodate-oxidized Galactomannan

The periodate-oxidized product (140 mg) was neutralized with barium hydroxide and filtered, and to the clear solution sodium borohydride (200 mg) was added. The reduction was allowed to proceed for 4 hours at room temperature. The resulting solution after usual treatment (34) yielded a sirup which, on paper chromatographic examination using solvent E and spray reagent *c*, indicated the presence of erythritol and glycerol.

The above sirup was separated on Whatman No. 3MM filter paper using solvent E. The zones corresponding to erythritol and glycerol were eluted and evaporated to sirups. They were characterized through their crystalline tetra- and tri-tosyl derivatives respectively. The tetratosyl erythritol had m.p. and mixed m.p. 163°–165° C, lit. (35) 165°–166°. The tritosyl glycerol had m.p. and mixed m.p. 102°–103° C, lit. (35) 103°–104° C.

Quantitative Estimation of the Polyhydric Alcohols

A small portion of the mixture was separated quantitatively by paper chromatography using solvent E, and the polyhydric alcohols were estimated by the method of Lambert and Neish (36). The ratio of glycerol to erythritol was found to be 1:2.45.

Acetylation of the Galactomannan

The galactomannan (8 g) was dispersed by stirring for 5 hours in formamide (100 ml). To this dispersion pyridine (150 ml) was added followed by the dropwise addition, with stirring, of acetic anhydride (120 ml) for a period of 4 hours at 20°. The stirring was continued for 3 days at room temperature and the galactomannan acetate was precipitated by pouring the dark viscous material into ice-cold water. The precipitate was washed first with water, then with methanol, and finally with ether. Completely dried material was once again acetylated by dissolving it in pyridine (150 ml) and adding acetic anhydride (120 ml) in a dropwise manner and then proceeding as above. Yield 6.8 g, $[\alpha]_D^{30}$ +11° (in chloroform, *c*, 1), intrinsic viscosity 5.65 dl/g (in chloroform), acetyl content (37) 43.07%. On deacetylation (38) and hydrolysis D-galactose and D-mannose were obtained in the ratio of 1:2.6.

Fractionation of the Acetylated Galactomannan

The acetylated galactomannan was fractionated according to the method of Hamilton and Kircher (14). The material (5.95 g) was dissolved in a solvent containing *s*-tetrachloroethane:95% ethanol in the ratio of 9:1 and fractionally precipitated by the gradual addition of methanol. Seven fractions could be collected in this way. The last two fractions

Can. J. Chem. Downloaded from www.nrcresearchpress.com by 210.87.254.105 on 09/05/12
For personal use only.

were obtained on concentration of the solution after the fifth precipitation and after addition of petroleum ether. The results of studies on each of these fractions are shown in the following table.

Sample		Wt. (g)	$[\alpha]_D^{30°}$ in $CHCl_3$	I.V. (dl/g) in $CHCl_3$	Acetyl content (%)	Gal:Man
Original galactomannan acetate		5.95	+11°	5.65	43.07	1:2.6
Fraction	1	0.345	+11°	3.4	39.1	1:2.4
"	2	0.136	+11°	4.7	39.7	1:2.5
"	3	0.988	+11°	7.2	42.2	1:2.5
"	4	1.460	+11°	7.8	43.5	1:2.6
"	5	2.240	+12°	6.3	44.2	1:3.2
"	6	0.233	+11.5°	2.1	42.3	1:3
"	7	0.081	+11.5°	1.0	42.8	1:3

Methylation of the Acetylated Galactomannan (Fraction 5)

The fraction 5 (2 g) of the galactomannan triacetate was dissolved in dry tetrahydrofuran (40 ml) and methylated directly with methyl sulphate (35 ml) and solid sodium hydroxide (30 g) according to the method of Hamilton and Kircher (14). The product was methylated twice by Purdie's method. Yield 0.85 g, $-OCH_3$, 43.05%, $[\alpha]_D^{20}$ +24° (in chloroform).

Methanolysis and Hydrolysis of the Methylated Galactomannan

The methylated galactomannan was methanolyzed and the mixture of methyl glycosides was hydrolyzed as described earlier. On paper partition chromatography using solvent B the mixture of methyl sugars gave only three spots corresponding to 2,3,4,6-tetra-*O*-methyl-D-galactose, 2,3,6-tri-*O*-methyl-D-mannose, and 2,3-di-*O*-methyl-D-mannose. They were isolated and characterized as described earlier.

A portion of this mixture was quantitatively separated by paper chromatography using solvent B and each component estimated by the alkaline hypoiodite method (7). The 2,3,4,6-tetra-*O*-methyl-D-galactose, 2,3,6-tri-*O*-methyl-D-mannose, and 2,3-di-*O*-methyl-D-mannose were found in the molar ratio of 1:2.11:1.08.

Graded Hydrolysis of the Galactomannan

The galactomannan (15 mg) was dispersed in water (750 ml), 0.4 *N* sulphuric acid (750 ml) was added and the mixture was heated on a boiling-water bath for 2 hours. The solution was filtered and the residue was again hydrolyzed with 0.2 *N* sulphuric acid for 2 hours. The two solutions were combined and neutralized, filtered, and passed through ion exchange resins I.R. 120(H) and I.R. 45(OH). The resulting mixture of sugars was concentrated to 50 ml. Paper partition chromatography using solvent F indicated the presence of D-galactose, D-mannose, two disaccharides, and two trisaccharides.

Spot	R_{Gal} (in solvent F)	Sugars
1	0.62	4-*O*-β-D-Mannopyranosyl-D-mannose
2	0.54	6-*O*-α-D-Galactopyranosyl-D-mannose
3	0.34	A triose
4	0.30	*O*-β-D-Mannopyranosyl-(1 → 4) *O*-β-D-Mannopyranosyl-(1 → 4) *O*-β-D-Mannose

Can. J. Chem. Downloaded from www.nrcresearchpress.com by 210.87.254.105 on 09/05/12
For personal use only.

Separation of the Oligosaccharides by Column Chromatography

The sugar mixture was allowed to soak into the top of a cellulose–charcoal (60–80 mesh) (39) column (35×4.2 cm). The column was first eluted with water and then subjected to stepwise elution (40) using 2.5%, 5%, 7.5%, and 10% aqueous ethanolic solutions successively. Eight liters of each fraction was collected and each was concentrated to small volume. The monosaccharides were eluted with water and the di- and oligo-saccharides with aqueous ethanol. All the alcoholic eluates were found to contain mixtures.

The mixture was separated on Whatman No. 3MM filter papers using solvent F into chromatographically pure fractions and the corresponding di- and tri-saccharide fractions were combined and evaporated to sirups. Thus two disaccharides and two trisaccharides were collected.

*Identification of 4-O-β-*D*-Mannopyranosyl-*D*-mannose*

The sirup (243.7 mg) having $[\alpha]_D^{30}$ −8° → −7° (in water), lit. $[\alpha]_D^{23}$ −7.7 → 2.2 (19), $[\alpha]_D^{25}$ −8.13° → −7.4° (14), −4.4° (41), gave on hydrolysis D-mannose only. The molecular weight determined by the alkaline hypoiodite method was found to be 329 (calc. for $C_{12}H_{22}O_{11}$, 342). The oxidation of mannobiose (65 mg) with 0.3 *M* sodium metaperiodate (10 ml) made up to 50 ml with water was followed by determining the formic acid liberated and uptake of periodate at various intervals of time. The corresponding values are 1.35 moles (10 hours), 2.45 moles (20 hours), and 2.90 moles (30 hours) and 2.40 moles (10 hours), 3.90 moles (20 hours), and 4.91 moles (35 hours). But when the same oxidation was carried out in acetate buffer (pH 3.7) the disaccharide (50 mg) consumed 4.06 moles of the oxidant per mole of the disaccharide in 3 hours (constant value). The periodate-oxidized product was freed from the oxidant in the usual way and reduced with sodium borohydride. After hydrolysis and usual treatments the mixture was found to contain glycerol and erythritol on paper chromatographic examination using spray reagent *c*.

A small portion of the disaccharide (30 mg) was converted to the phenylhydrazone in the usual way to give yellow crystals having m.p. 198°–199° C, lit. (42) 200°–201° C.

*Identification of 6-O-α-*D*-Galactopyranosyl-*D*-mannose*

The fraction 2 on evaporation gave a sirup (114.7 mg) having $[\alpha]_D^{30}$ +124° (in water), lit. (41) +123°. On hydrolysis it afforded D-galactose and D-mannose in equal proportion and the hydrolyzed sirup had $[\alpha]_D^{30}$ +49° (in water, *c*, 1). Hydrolysis of a portion after reduction with sodium borohydride indicated the presence of only D-galactose. The disaccharide (36 mg) was oxidized with sodium metaperiodate and the liberation of formic acid and consumption of periodate were recorded at various intervals of time. The corresponding values per mole of the disaccharide are, 1.95 moles (10 hours), 4.0 moles (20 hours), and 4.93 moles (30 hours) and 3.05 moles (10 hours), 4.75 moles (20 hours), and 5.95 moles (30 hours) respectively. On oxidation in the presence of acetate buffer (pH 3.7), however, the disaccharide (25 mg) consumed 5.14 moles of the oxidant per mole of the disaccharide in 2.5 hours (constant value). The oxidized product was reduced and hydrolyzed as before and the mixture was found to contain only glycerol. The 6-*O*-α-D-galactopyranosyl-D-mannose was characterized by preparing its phenylhydrazone, m.p. 168°–169° C, lit. (41) 170° C.

Examination of Fraction 3

This fraction on evaporation gave a sirup (48.3 mg) having $[\alpha]_D^{30}$ +33° (in water, *c*, 1).

Can. J. Chem. Downloaded from www.nrcresearchpress.com by 210.87.254.105 on 09/05/12
For personal use only.

On hydrolysis it afforded D-galactose and D-mannose in the proportion of 1:2. On reduction and hydrolysis it indicated the presence of D-galactose and D-mannose on a paper chromatogram using spray reagent *a* indicating the presence of mannose residue at the reducing end. A portion (25 mg) was oxidized with sodium metaperiodate in acetate buffer (pH 3.7) and was found to consume 6.12 moles of the oxidant per mole of the sugar. The sugar thus seems to be a trisaccharide containing 1 mole of D-galactose residue and 2 moles of D-mannose residues.

Identification of the Mannotriose

This fraction yielded a sirup (82.6 mg) having $[\alpha]_D^{30}$ −15° (in water, *c*, 1), lit. −16° and −22° (41), −15° (19), −24.7° → −23.3 (43), −15.7° → −20.2° (42). On hydrolysis it afforded only D-mannose. The molecular weight of this sugar was determined by the alkaline hypoiodite method and was found to be 488 (calc. for $C_{18}H_{32}O_{16}$, 504). A portion of this fraction (30 mg) was oxidized with sodium metaperiodate in acetate buffer (pH 3.7). One mole of the trisaccharide was found to consume 5.08 moles of the periodate.

REFERENCES

1. V. SUBRAHMANYAN, G. S. BAINS, C. P. NATARAJAN, and D. S. BHATIA. Arch. Biochem. Biophys. **60**, 27 (1956).
2. E. L. HIRST and J. K. N. JONES. J. Chem. Soc. 1659 (1949).
3. W. N. HAWORTH. J. Chem. Soc. **107**, 8 (1915).
4. T. PURDIE and J. C. IRVINE. J. Chem. Soc. **83**, 1021 (1903).
5. L. HOUGH, J. K. N. JONES, and W. H. WADMAN. J. Chem. Soc. 2511 (1949).
6. L. BOGGS, L. S. CUENDET, I. EHRENTHAL, R. KOCH, and F. SMITH. Nature, **166**, 520 (1950).
7. E. L. HIRST, L. HOUGH, and J. K. N. JONES. J. Chem. Soc. 928 (1949).
8. L. HOUGH, J. K. N. JONES, and W. H. WADMAN. J. Chem. Soc. 1702 (1950).
9. N. PRENTICE, L. S. CUENDET, W. F. GEDDES, and F. SMITH. J. Am. Chem. Soc. **81**, 684 (1959).
10. P. A. REBERS and F. SMITH. J. Am. Chem. Soc. **76**, 6097 (1954).
11. E. L. HIRST and J. K. N. JONES. J. Chem. Soc. 1278 (1948).
12. K. FREUDENBERG and H. BOPPEL. Ber. **73**, 609 (1940).
13*a*. S. K. CHANDA, E. L. HIRST, J. K. N. JONES, and E. G. V. PERCIVAL. J. Chem. Soc. 1289 (1950).
13*b*. C. P. J. GLAUDEMANS and T. E. TIMELL. J. Am. Chem. Soc. **80**, 1209 (1958).
14. J. K. HAMILTON and H. W. KIRCHER. J. Am. Chem. Soc. **80**, 4703 (1958).
15. J. F. CARSON and W. D. MACLAY. J. Am. Chem. Soc. **68**, 1015 (1946).
16. P. ANDREWS, L. HOUGH, and J. K. N. JONES. J. Chem. Soc. 2744 (1952).
17. F. SMITH. J. Am. Chem. Soc. **70**, 3249 (1948).
18. C. M. RAFIQUE and F. SMITH. J. Am. Chem. Soc. **72**, 4634 (1950).
19. R. L. WHISTLER and J. Z. STEIN. J. Am. Chem. Soc. **73**, 4187 (1951).
20. Z. F. AHMED and R. L. WHISTLER. J. Am. Chem. Soc. **72**, 2524 (1950).
21. C. DOREE. The methods of cellulose chemistry. 2nd ed. Chapman & Hall Ltd., London. 1947. p. 381.
22. E. P. CLARK. Semimicro quantitative organic analysis. Academic Press, Inc., New York. 1943. p. 68.
23. C. DOREE. The methods of cellulose chemistry. 2nd ed. Chapman & Hall Ltd., London. 1947. p. 391.
24. J. K. HAMILTON and E. V. PARTLOW. J. Am. Chem. Soc. **80**, 4880 (1958).
25. F. L. BAKER and H. F. E. HALTON. Biochem. J. **14**, 754 (1920).
26. F. WEYGAND, W. PERKOW, and P. KUHNER. Chem. Ber. **84**, 594 (1951).
27*a*. E. L. FALCONER and G. A. ADAMS. Can. J. Chem. **34**, 338 (1956).
27*b*. G. A. ADAMS. Can. J. Chem. **36**, 755 (1958).
28*a*. P. DEBYE. J. Phys. Chem. **51**, 18 (1947).
28*b*. G. OSTER. Chem. Revs. **43**, 352 (1948).
28*c*. P. DOTY and R. F. STEINER. J. Chem. Phys. **28**, 1211 (1950).
29. J. C. IRVINE and A. CAMERON. J. Chem. Soc. **85**, 1071 (1904).
30. R. JOHNSTON and E. G. V. PERCIVAL. J. Chem. Soc. 1994 (1950).
31. W. N. HAWORTH and G. C. LEITCH. J. Chem. Soc. **113**, 188 (1918).
32. G. J. ROBERTSON. J. Chem. Soc. 330 (1934).
33. P. FLEURY and J. LUNGE. J. pharm. chim. **17**(8), 107 (1933).
34. F. SMITH and H. C. SRIVASTAVA. J. Am. Chem. Soc. **81**, 1715 (1959).
35. J. K. HAMILTON and F. SMITH. J. Am. Chem. Soc. **78**, 5907 (1956).
36. M. LAMBERT and A. C. NEISH. Can. J. Research, B, **28**, 83 (1950).
37. J. B. NIEDERL and V. NIEDERL. Methods of quantitative organic analysis. 2nd ed. John Wiley & Sons, Inc., New York. 1948. p. 252.
38. F. C. PETERSON, A. J. BARRY, H. UNKAUF, and L. E. WISE. J. Am. Chem. Soc. **62**, 2361 (1940).
39. R. L. WHISTLER. Science, **26**, 899 (1954).
40. A. TISELIUS. Endeavour, **11**(41), 5 (1952).
41. M. F. HENDERSON, L. HOUGH, and T. J. PAINTER. J. Chem. Soc. 3519 (1958).
42. G. O. ASPINALL, R. B. RASHBROOK, and G. KESSLER. J. Chem. Soc. 215 (1958).
43. R. L. WHISTLER and C. G. SMITH. J. Am. Chem. Soc. **74**, 3795 (1952).

Can. J. Chem. Downloaded from www.nrcresearchpress.com by 210.87.254.105 on 09/05/12
For personal use only.

Can. J. Chem. Downloaded from www.nrcresearchpress.com by 210.87.254.105 on 09/05/12
For personal use only.

THE MERCURY-PHOTOSENSITIZED OXIDATIONS OF HYDROCARBONS

PART I. INTERACTION OF MERCURY WITH PRODUCTS FORMED IN THE REACTING MIXTURE[1]

K. M. BELL[2] AND C. A. MCDOWELL

ABSTRACT

The interaction of mercury with two hydrocarbon oxidation systems, namely those of oxygen and cyclohexene, and oxygen and isobutane, has been studied at 30° C in a conventional static photochemical apparatus. The removal of mercury from the gas phase in the mercury-photosensitized oxidation of isobutane is attributed to a reaction with ozone,

$$Hg + O_3 \rightarrow HgO + O_2,$$

whilst interaction with an intermediate of the oxidation chain is responsible for mercury removal in the cyclohexane oxidation reaction:

$$Hg + RO_2 \rightarrow HgO + RO.$$

INTRODUCTION

Several workers have observed the interaction of mercury with oxidation chain systems. Marshall (1), while studying the mercury-photosensitized hydrogen and oxygen reaction, found that HgO was deposited simultaneously on the vessel walls with the formation of water and hydrogen peroxide. Later Small and Ubbelohde (2) found the yield of peroxides in the thermal oxidation of *n*-hexane to be greatly reduced by the addition of small amounts of mercury vapor. Mercuric oxide was observed by Gray (3) to be deposited on the vessel walls during a study of the mercury-photosensitized oxidation of ethane, in a flow system at 25° C. Studying the same reaction in a similar manner Watson and Darwent (4) found that mercuric oxide was formed at 25° C, but that none was detected when the temperature was raised to between 40 and 45° C. Callear, Patrick, and Robb (5) have recently reported the removal of mercury as mercuric oxide from $Hg–O_2$ mixtures on illumination with 2537-Å radiation at 25° C.

In any mercury-photosensitized hydrocarbon oxidation system there are clearly two main possibilities for interaction of mercury with the products formed in the reacting mixture. It may react (i) with the products from the excited oxygen molecule reactions, or (ii) with the intermediates or final products of the hydrocarbon oxidation chain.

Two systems, isobutane–oxygen–mercury and cyclohexene–oxygen–mercury have been studied and found to illustrate these two types of interaction.

EXPERIMENTAL

A conventional static photochemical apparatus was used. A Cintel QVA 39 phototube, with a quartz envelope, was used in conjunction with a potentiometer circuit to give relative intensity variations in the parallel beam of radiation, transmitted through the reaction mixture. The reactions were carried out in a cylindrical quartz cell of 2-cm light path and 4-cm diameter. The light source was a water- and air-cooled Hanovia low-pressure mercury arc lamp, emitting 85–90% of its radiation at 2537 Å as determined by filters and the known spectral response characteristics of the phototube. Phillips

[1]*Manuscript received December 12, 1960.*
Contribution from the Department of Chemistry, University of British Columbia, Vancouver 8, B.C., Canada. This paper was presented at the 43rd annual conference of the Chemical Institute of Canada at Ottawa, June 15, 1960.
[2]*Postdoctoral Fellow, 1958–60.*

Petroleum Company cyclohexene of 99.98% purity was freed from peroxide by refluxing with copper stearate and subsequent distillation under nitrogen. The same firm also supplied Research Grade isobutane. Oxygen was piped from a cylinder to a storage bulb through a spiral cooled to −78° C.

Mercury vapor was introduced into a selected hydrocarbon–oxygen mixture by alternately raising and lowering the level of mercury in a premixing vessel several times. The reactants were passed into the evacuated cell through two U tubes, packed with small glass helices, surrounded by ice. The procedure of mixing and admittance to the cell was standardized, and reproducible light absorptions could be obtained. Results using greater than 24 mm Hg pressure of cyclohexene were obtained by dispensing with the traps cooled to 0° C.

PHOTOMETRY

The intensities of light transmitted through the reaction cell were related to the resistance needed to balance a potentiometer circuit, and calibrated by comparison with the potassium ferrioxalate actinometer of Hatchard and Parker (6).

If

I_t = intensity of transmitted radiation
I_o = intensity of incident radiation
I_a = intensity of radiation absorbed by reactants in the cell,

then

$$I_t/I_o = \exp\{-\epsilon[\mathrm{Hg}]l\}$$

and by differentiation

$$-d[\mathrm{Hg}]/dt = \frac{1}{\epsilon l}\frac{d\{\log (I_t/I_o)\}}{dt},$$

where ϵ = extinction coefficient and l = light path. If the quantum yield of mercury removal is Φ, then we have

$$\Phi = -\frac{\Delta[\overline{\mathrm{Hg}}]}{\Delta t}\cdot\frac{1}{I_a}$$

that is

$$\Phi = \frac{1}{\epsilon l}\frac{\Delta \log (I_t/I_o)}{\Delta t}\cdot\frac{1}{I_a}.$$

I_t and I_o were measured at the beginning of each experiment. As the concentration of mercury vapor [Hg] was known, it was possible to calculate the value of the extinction coefficient ϵ. Since Δt and I_a were known for each kinetic run, it was possible to calculate Φ. It was found that Φ was a useful parameter to give a measure of the interaction of mercury with the reactive species in the system, having a constant value (±5%), while more than 50% of the mercury vapor reacted. The measurable range of values for using the full intensity of the lamp ($\sim 3\times10^{14}$ quanta/sec) was from 1×10^{-4} to 9×10^{-3}.

RESULTS

The results of typical experiments are presented in Fig. 1. In the series of experiments using C_4H_{10}–O_2–Hg, Φ decreases from 7×10^{-3} to 9×10^{-4} in the isobutane pressure range 0–25 mm Hg (Fig. 2). The relative quenching cross sections of isobutane and oxygen are such that oxygen quenches more than 90% of the 6^3P_1 excited mercury atoms for partial pressures of isobutane of less than 25 mm Hg with P_{O_2} = 100 mm Hg.

Can. J. Chem. Downloaded from www.nrcresearchpress.com by 210.87.254.105 on 09/05/12
For personal use only.

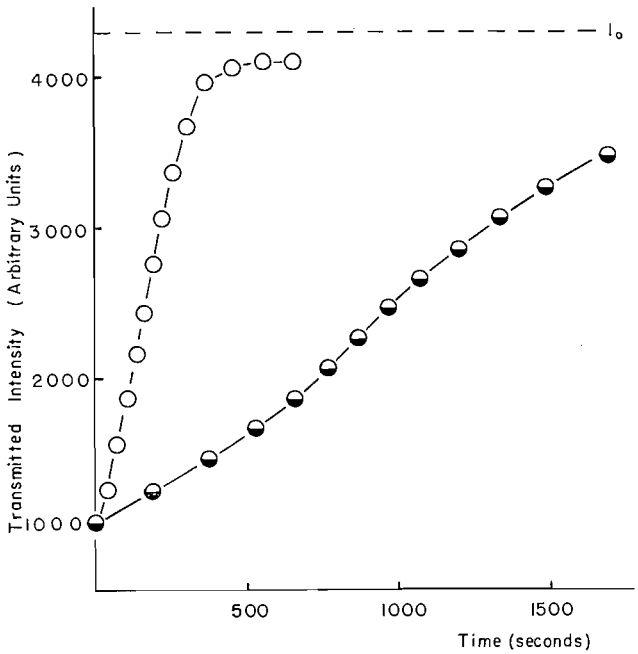


FIG. 1. Typical experiments showing variation in rate of removal of excited 6^3P_1 mercury atoms in the isobutane/oxygen and cyclohexene/oxygen systems at 30° C. ○ $p_{C_6H_{10}}$ = 24 mm Hg; p_{O_2} = 200 mm Hg. ◒ $p_{C_4H_{10}}$ = 50 mm Hg; p_{O_2} = 100 mm Hg. Arbitrary intensity units = potentiometer ohms.

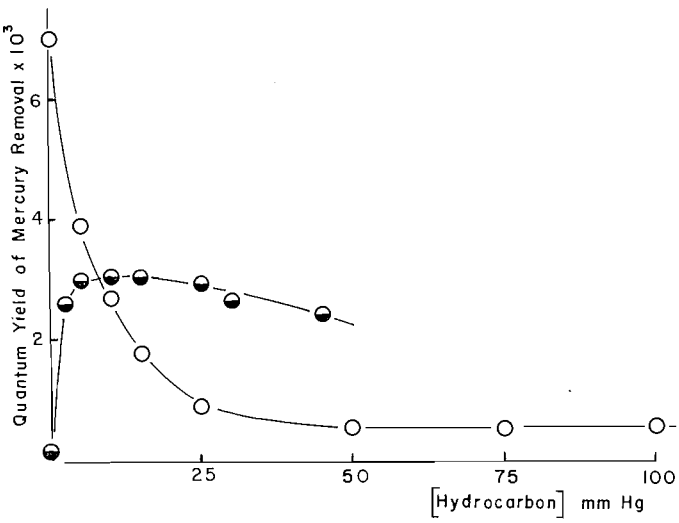


FIG. 2. Quantum yield of mercury removal as a function of partial pressure of hydrocarbon at constant oxygen pressure at 30° C. ○ Isobutane series p_{O_2} = 100 mm Hg. ◒ Cyclohexene series p_{O_2} = 200 mm Hg.

Mercury and oxygen react rapidly in a clean reaction vessel ($\Phi = 7\text{–}10\times10^{-3}$), but if an experiment using oxygen and mercury alone is performed after several using cyclohexene, oxygen, and mercury, the mercury–oxygen reaction is inhibited ($\Phi \sim 2\times10^{-4}$) presumably by involatile products having been deposited on the walls. In the presence of an increasing concentration of cyclohexene, Φ rapidly increases to a maximum value of 3×10^{-3} (Fig. 2).

Can. J. Chem. Downloaded from www.nrcresearchpress.com by 210.87.254.105 on 09/05/12
For personal use only.

DISCUSSION

The interaction of oxygen and mercury on illumination with 2537-Å radiation has recently been interpreted by Callear, Patrick, and Robb (5) in terms of the following series of equations [1]–[5]:

$$O_2 + Hg(6^3P_1) \rightarrow O_2^* + Hg(6^1S_0) \quad [1]$$

$$O_2 + O_2^* \rightarrow O_3 + O \quad [2]$$

$$O_2 + O_2^* \rightarrow O_2 + O_2 \quad [2']$$

$$O + O_2 + M \rightarrow O_3 + M \quad [3]$$

$$O_3 + Hg \rightarrow HgO + O_2 \quad [4]$$

$$O + O_3 \rightarrow O_2 + O_2. \quad [5]$$

In the presence of hydrocarbon, the products formed by the reactions indicated by equations [2] and [3] will react rapidly with the hydrocarbon, presumably by the following processes:

$$RH + O_3 \rightarrow RO + HO_2 \quad [6]$$

$$RH + O \rightarrow R + OH. \quad [7]$$

There will thus be a competition between the hydrocarbon molecules and mercury atoms for reaction with ozone. This will result in the observed decrease in Φ for increasing partial pressure of isobutane, since the rate of ozone production will not be appreciably altered on using a large excess of oxygen. Under the conditions of a large excess of isobutane ($p_{C_4H_{10}}/p_{O_2} = 600/30$), $\Phi < 2\times10^{-4}$, whilst the peroxide quantum yields were about 0.85, indicating a negligible interaction between mercury and the intermediates or final products of the reaction.

As mentioned earlier the mercury–oxygen reaction, i.e. reaction [4], seems to be inhibited in a vessel which has been used for several experiments with cyclohexene. This is illustrated in Fig. 2 from which we see that, under the circumstances mentioned, the quantum yield for the disappearance of mercury vapor in the presence of 200 mm Hg of oxygen has an initial value of about 2×10^{-4}. On adding cyclohexene the value of Φ increases until it reaches a maximum of about 3×10^{-3}. This maximum occurs when the pressure of cyclohexene is approximately 10 mm Hg. The reasons for the initial inhibition of the mercury–oxygen reaction are not clear. Reaction [4] would be expected to take place to some extent, but apparently the HgO is not stabilized on the walls of the reaction vessel after these have been exposed to the products from the cyclohexene reaction. Were this the case then it would, of course, be easy to understand the initial low value observed for Φ. The addition of increasing amounts of cyclohexene would reduce the rate of diffusion of the HgO to the walls of the vessel, and so we thus have some of the features of a wall-inhibited reaction. In this type of kinetic system, i.e. one with a step which is wall-inhibited, the rate of the over-all process studied increases with pressure because at the higher pressures the inhibiting influence of the walls becomes less important owing to the rate of diffusion of the active species being smaller at the higher pressures. The shape of the curve in Fig. 2 showing the variation of Φ with increasing cyclohexene pressure is in agreement with these requirements and so the suggested explanation would appear to be a reasonable one.

Since mercury does not react with cyclohexene in the absence of oxygen, our results suggest that the mercury vapor is removed by reaction with some product, or intermediate, of the oxidation. If the lamp was shielded midway through a run, the light

Can. J. Chem. Downloaded from www.nrcresearchpress.com by 210.87.254.105 on 09/05/12
For personal use only.

absorption was the same on reillumination as it was immediately prior to shielding, indicating that the mercury reacts with an active intermediate rather than a final product. Radicals produced in reaction [7], or by direct cleavage of the R—H bond in the hydrocarbon, will react rapidly with oxygen according to equation [8].

$$R\cdot + O_2 \rightarrow RO_2\cdot \qquad [8]$$

The subsequent reaction of the peroxy radical with mercury as indicated in equation [9]

$$RO_2 + Hg \rightarrow HgO + RO\cdot \qquad [9]$$

seems reasonable. This reaction was postulated by Small and Ubbelohde (2) as being responsible for the reduction of peroxide yield in the presence of mercury for the oxidation of *n*-hexane. Reaction [9] does not, however, necessarily lead to removal of $RO_2\cdot$ from the system if $RO\cdot$ reacts by the following scheme.

$$RO\cdot + RH \rightarrow ROH + R\cdot \qquad [10]$$

$$R\cdot + O_2 \rightarrow RO_2\cdot \qquad [8]$$

In the cyclohexene oxidation, low quantum yields of peroxide were obtained (< 0.08). The final amounts of products were very low owing to the limited period of initiation resulting from the rapid removal of mercury, the original concentration of which was about 5×10^{-10} g-mole liter^{-1}. As the quantities of products produced were extremely small the only analysis done was for peroxide. A modification of the sensitive ferrous thiocyanate method of Young *et al.* (8) was used. Cyclohexene will probably have a higher quenching cross section for excited 6^3P_1 mercury atoms than oxygen, and the decrease in Φ towards higher cyclohexene values where the cyclohexane is quenching an appreciable fraction of the excited mercury, suggests that each C_6H_{10}–Hg* quenching process has a lower radical-producing efficiency than the corresponding O_2–Hg* quenching process. The final radical yield would then be expected to be low since the yield of ozone in the O_2–Hg reaction was determined by Callear, Patrick, and Robb to be 0.14 (5). The final peroxide yield will also be low since the work of Burgess and Robb (7) indicates that it is unlikely that a hydrocarbon peroxide chain will be operative at 30° C.

ACKNOWLEDGMENT

We wish to thank the National Research Council of Canada for generous grants in aid of this work.

REFERENCES

1. A. L. MARSHALL. J. Phys. Chem. **30**, 34 (1926).
2. N. J. H. SMALL and A. R. UBBELOHDE. J. Chem. Soc. 4619 (1952).
3. J. A. GRAY. J. Chem. Soc. 3150 (1952).
4. J. S. WATSON and B. de B. DARWENT. J. Phys. Chem. **61**, 577 (1957).
5. A. B. CALLEAR, C. R. PATRICK, and J. C. ROBB. Trans. Faraday Soc. **55**, 280 (1959).
6. C. G. HATCHARD and C. A. PARKER. Proc. Roy. Soc. (London), A, **235**, 518 (1956).
7. R. H. BURGESS and J. C. ROBB. Trans. Faraday Soc. **54**, 1015 (1958).
8. C. A. YOUNG, R. R. VOIGT, and J. A. NIEULAND. Ind. Eng. Chem. Anal. Ed. **8**, 198 (1936).

Can. J. Chem. Downloaded from www.nrcresearchpress.com by 210.87.254.105 on 09/05/12
For personal use only.

Can. J. Chem. Downloaded from www.nrcresearchpress.com by 210.87.254.6 on 09/05/12
For personal use only.

MERCURY-PHOTOSENSITIZED OXIDATIONS OF HYDROCARBONS

PART II. THE MERCURY-PHOTOSENSITIZED OXIDATION OF ISOBUTANE[1]

K. M. BELL[2] AND C. A. MCDOWELL

ABSTRACT

The mercury-photosensitized oxidation of isobutane has been studied over a wide range of pressures of the hydrocarbon and oxygen, in a conventional static photochemical apparatus at the temperatures of 30° C and 100° C. The main products of the reaction are tertiary butyl hydroperoxide, together with tertiary butyl alcohol, acetone, and corresponding small quantities of formaldehyde and methyl alcohol. Isobutyraldehyde was also detected; ditertiary butyl peroxide being notably absent. Peroxide yields suggest that a reaction between an excited isobutane molecule and oxygen is important in the initiation processes and that peroxide is formed in the reaction

$$RO_2 + HO_2 \rightarrow ROOH + O_2.$$

INTRODUCTION

The mercury-photosensitized oxidations of methane, ethane, and propane have previously been studied in flow systems (1, 2, 3). The original classical concept of the peroxide chain reaction

$$RO_2\cdot + RH \rightarrow ROOH + R \qquad [19]$$

occurring at 25° C was modified in the most recently published work of this type by Watson and Darwent (4), who explained the low yields of peroxide obtained in the ethane oxidation by suggesting the following reaction

$$RO_2\cdot + HO_2 \rightarrow ROOH + O_2 \qquad [3]$$

as the source of hydroperoxide rather than reaction [19]. These workers found that the yields of peroxide decreased on raising the reaction temperature or on lowering the flow rate. They attributed these effects to thermal and photochemical decomposition of the peroxide. The hydroperoxide was characterized as ethyl hydroperoxide by Gray (1), and so this work provides no evidence on the nature of the mutual interaction of HO_2 radicals.

In an effort to elucidate further the nature of certain aspects of hydrocarbon oxidation mechanisms we have studied the mercury-photosensitized oxidation of isobutane in a static photochemical apparatus employing low light intensities.

EXPERIMENTAL

The apparatus and photochemical techniques employed were the same as those described in Part I (K. M. Bell and C. A. McDowell. Can. J. Chem. This issue). Using a modification of the ferrous thiocyanate method of Young, Voigt, and Nieuland (5), 5×10^{-9} mole of peroxides could be determined. The method is non-stoichiometric, and a calibration curve was prepared using purified solutions of tertiary butyl hydroperoxide. The hydroperoxide was also determined gas chromatographically, dinonyl phthalate on chromosorb being used as the column material. The other products were determined and identified by their characteristic elution times on different columns. Formaldehyde

[1]*Manuscript received December 12, 1960.*
Contribution from the Department of Chemistry, University of British Columbia, Vancouver 8, B.C., Canada. This paper was presented at the 43rd Annual Conference of the Chemical Institute of Canada at Ottawa, June 15, 1960.
[2]*Postdoctoral Fellow, 1958–60.*

was estimated by the method of Bricker and Johnson (6). In all cases the final yield of product was limited by the slow removal of the mercury vapor (see Part I). The rate of removal was greater at 30° C than 100° C. For a mixture of 50 mm Hg of isobutane and 100 mm Hg of oxygen, Φ (the quantum yield of *removal* of excited 6^3P_1 Hg atoms) was 6×10^{-4} at 30° C and 2×10^{-4} at 100° C.

RESULTS

The main product of the oxidation was tertiary butyl hydroperoxide, together with smaller yields of tertiary butyl alcohol, acetone, methyl alcohol, formaldehyde, and isobutyraldehyde. Evidence was also obtained for a trace of isobutyl alcohol. Tests were specifically made for ditertiary butyl peroxide but none could be detected under conditions where the lower limit of detection corresponded to a quantum yield of 0.02. It is also to be noted that we were unable to detect isobutylene oxide despite several attempts using our gas chromatographic apparatus. Close agreement was obtained between the total peroxide determined colorimetrically, and tertiary butyl hydroperoxide determined gas chromatographically.

The yield of peroxide was directly proportional to the integrated absorbed light intensity (Fig. 1) for constant incident intensity, and also to the average absorbed

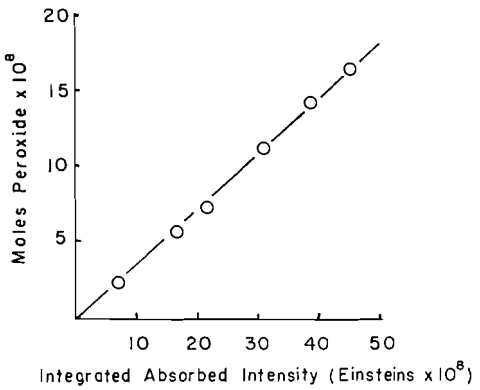


FIG. 1. Yield of peroxide as a function of the integrated absorbed intensity, for constant incident intensity, in the mercury-photosensitized oxidation of isobutane at 30° C, $p_{O_2} = p_{C_4H_{10}} = 100$ mm Hg.

intensity when a given isobutane–oxygen mixture was illuminated for a given time (500 seconds) at varying light intensities (Fig. 2). The integrated absorbed light intensity was obtained from the sum of the average numbers of quanta absorbed between determined short time intervals during the course of the reaction (see Part I). The time of illumination (500 seconds) for the intensity variation was the minimum required to obtain an accurately determinable quantity of peroxide at the lowest intensity, so minimizing the change in absorbed intensity, which in no case was greater than 15% of the total.

The quantum yield of peroxide was constant for a given isobutane–oxygen ratio for oxygen pressures in excess of 30 mm Hg, but increased as the fraction of isobutane in the mixture increased (Fig. 3). The yield of tertiary butyl alcohol underwent the same variation with varying light intensity as the peroxide (Fig. 4), and was constant in the region of constant peroxide (Fig. 5). The total yield of (tertiary butyl alcohol + acetone) was approximately proportional to the corresponding yield of peroxide (Fig. 6).

Can. J. Chem. Downloaded from www.nrcresearchpress.com by 210.87.254.6 on 09/05/12
For personal use only.

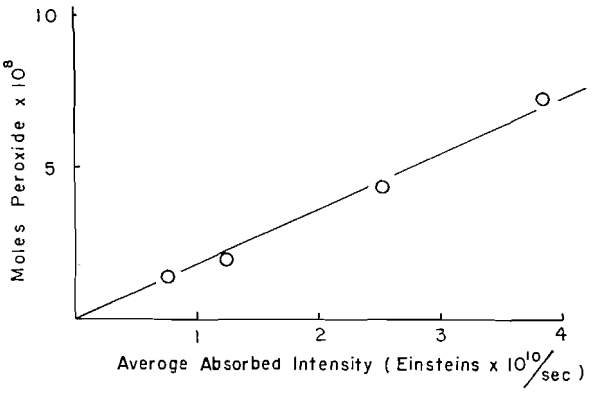


FIG. 2. Yield of peroxide as a function of the average absorbed intensity, varying the incident intensity and illuminating for constant time (500 seconds), in the mercury-photosensitized oxidation of isobutane at 30° C, $p_{O_2} = p_{C_4H_{10}} = 100$ mm Hg.

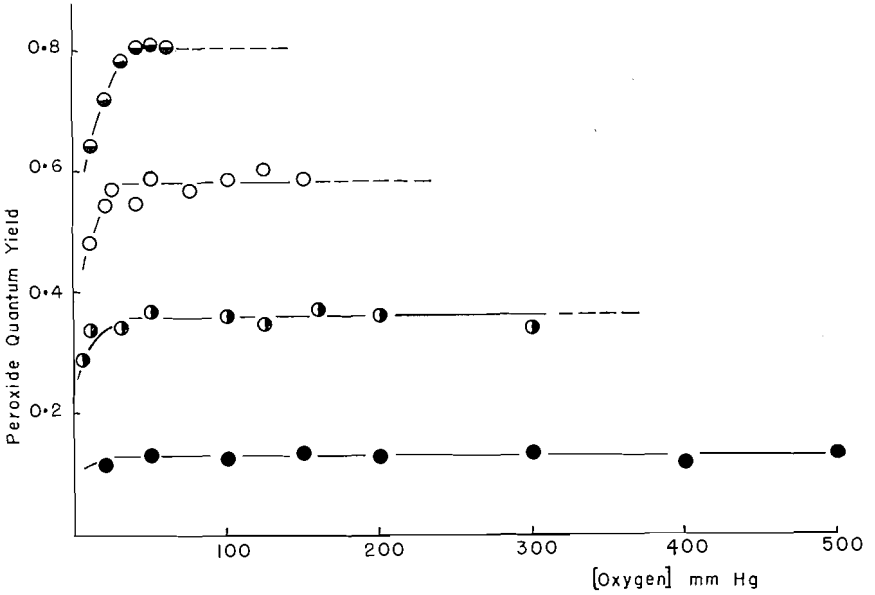


FIG. 3. Peroxide quantum yield as a function of the concentration of reactants at fixed hydrocarbon–oxygen ratios, in the mercury photosensitized oxidation of isobutane at 30° C. ◒ $p_{C_4H_{10}}:p_{O_2} = 10:1$; ○ $p_{C_4H_{10}}:p_{O_2} = 3:1$; ◑ $p_{C_4H_{10}}:p_{O_2} = 1:1$; ● $p_{C_4H_1}:p_{O_2} = 1:10$.

At 100° C an almost identical set of results was obtained (Tables I and II), modified

TABLE I

Quantum yields of products in the isobutane mercury-photosensitized oxidation at 30° C

$p_{C_4H_{10}}/p_{O_2}$ (ratio)	$p_{C_4H_{10}}/p_{O_2}$ (mm Hg)	% Hg(6^3P_1) quenched by C_4H_{10}	Total perioxide	*t*-BuOOH	*t*-BuOH	Acetone	Isobutyraldehyde
1/10	40/400	3	0.13	N.D.	0.065	N.D.	0.08
1/1	220/220	24	0.36	0.33	0.12	0.02	0.12
3/1	330/110	48	0.58	0.55	0.23	0.03	0.09
10/1	400/40	76	0.80	0.76	0.36	0.06	0.05

Can. J. Chem. Downloaded from www.nrcresearchpress.com by 210.87.254.6 on 09/05/12
For personal use only.

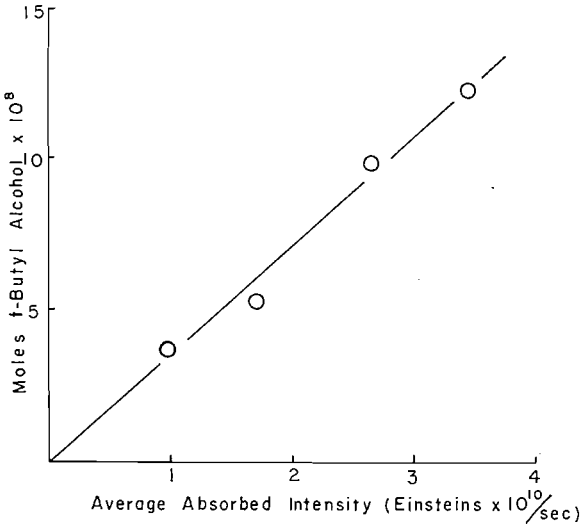


FIG. 4. Tertiary butyl alcohol as a function of the average absorbed intensity, varying the incident intensity and illuminating for constant time (1000 seconds), in the mercury-photosensitized oxidation of isobutane at 30° C, $p_{C_4H_{10}}$ = 400 mm Hg; p_{O_2} = 40 mm Hg.

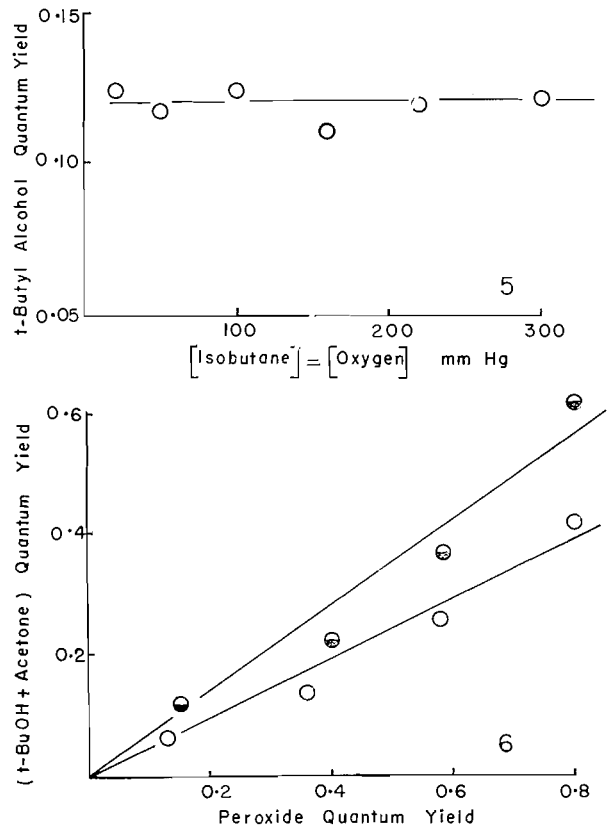


FIG. 5. Tertiary butyl alcohol quantum yield as a function of the concentration of reactants at fixed hydrocarbon–oxygen ratio = 1:1 in the mercury-photosensitized oxidation of isobutane at 30° C.

FIG. 6. Quantum yields of (*t*-butyl alcohol + acetone) as a function of tertiary butyl hydroperoxide quantum yield in the mercury-photosensitized oxidation of isobutane. ○ 30° C; ◒ 100° C.

Can. J. Chem. Downloaded from www.nrcresearchpress.com by 210.87.254.6 on 09/05/12
For personal use only.

TABLE II

Quantum yields of products in the isobutane mercury-photosensitized oxidation at 100° C

$p_{C_4H_{10}}/p_{O_2}$ (ratio)	$p_{C_4H_{10}}/p_{O_2}$ (mm Hg)	% $Hg(6^3P_1)$ quenched by C_4H_{10}	Total peroxide	*t*-BuOOH	*t*-BuOH	Acetone	CH_3OH	CH_2O	Isobutyraldehyde
1/10	40/400	3	0.15	0.12	0.04	0.08	N.D.	0.07	0.06
1/1	220/220	24	0.40	0.38	0.08	0.14	N.D.	0.12	0.09
3/1	330/110	48	0.58	0.55	0.13	0.24	N.D.	0.16	0.07
10/1	400/40	76	0.80	0.75	0.20	0.42	0.17	0.23	0.035

only by an increased yield of acetone relative to tertiary butyl alcohol, and an increased total yield of (tertiary butyl alcohol + acetone). With the increase in acetone, methanol and formaldehyde were detected. The variation with conditions for all products was the same at 100° C as at 30° C. Small quantum yields of isobutyl alcohol verging on the lower limit of detection ($\phi \simeq 0.02$–0.03) were observed at the higher isobutane–oxygen ratios.

Results showing the thermal stability of the peroxide to both homogeneous and heterogeneous decomposition during the course of an experiment, are given in Table III, the

TABLE III

Thermal stability of peroxide at 30° C and 100° C
($p_{O_2} = p_{C_4H_{10}} = 100$ mm Hg)

Period of illumination (seconds)	Period of shielding (seconds)	Peroxide	Temp. (°C)
500	—	0.36	30
500	1000	0.35	30
500	—	0.40	100
500	1000	0.39	100

products being left in the reaction cell for 1000 seconds, with the lamp shielded, after a 500-second period of illumination. The hydrocarbon conversion was never greater than 1%, and in the case of the colorimetric peroxide determination often less than 0.1%, thus minimizing photochemical decomposition with subsequent reaction of intermediate and final products.

DISCUSSION

Variation of the concentrations of the reactants in a mercury-photosensitized oxidation will possibly have an effect on the initiation reactions. The rate of initiation will depend upon the relative quenching cross sections of the two gases and also upon the numbers of radicals produced as a result of each quenching process. Values of the quenching cross section of oxygen have been variously reported in the literature lying in the range 13.2–19.9 Å² (7, 8). Burgess and Robb in a recent paper (9) adopted a value for $\sigma^2_{O_2,Hg(6^3P_1)}$ of 17.2 Å² and for $\sigma^2_{C_4H_{10},Hg(6^3P_1)}$ of 6.9 Å², both determined in the same way. Using these values the number of excited mercury atoms quenched by each gas is given by

Can. J. Chem. Downloaded from www.nrcresearchpress.com by 210.87.254.6 on 09/05/12
For personal use only.

$$\frac{Z_{O_2,Hg(6^3P_1)}}{Z_{C_4H_{10},Hg(6^3P_1)}} = 3.2\,\frac{n}{(1-n)}$$

where n is the mole fraction of oxygen in the mixture (see Table I).

Radicals are produced from the hydrocarbon quenching reaction [*a*],

$$Hg(6^3P_1) + RH \rightarrow Hg(6^1S_0) + R + H. \qquad [a]$$

Radical yields in mercury-photosensitized decompositions are usually below unity. For isobutane a yield of 0.2 radicals has been determined by Darwent and Winkler (10), indicating that reaction [*b*] must occur.

$$RH^* + M \rightarrow RH + M \qquad [b]$$

In this equation RH* represents an excited RH molecule.

In the presence of oxygen it is possible that reaction [*c*] will occur.

$$RH^* + O_2 \rightarrow R + HO_2 \qquad [c]$$

Burgess and Robb (9) postulated that each O_2–Hg quenching collision led to three radicals in the sequence of reaction [*d*] to [*i*] since reaction [*e*] was stated to have an efficiency close to unity.

$$Hg(6^3P_1) + O_2 \rightarrow O_2^* + Hg(6^1S_0) \qquad [d]$$

$$O_2^* + O_2 \rightarrow O_3 + O \qquad [e]$$

$$RH + O_3 \rightarrow RO + HO_2 \qquad [f]$$

$$RO + RH \rightarrow ROH + R \qquad [g]$$

$$RH + O \rightarrow R + OH \qquad [h]$$

$$RH + OH \rightarrow R + H_2O \qquad [i]$$

In a subsequent paper Callear, Patrick, and Robb (11) while studying the O_2–$Hg(6^3P_1)$ reaction found the net efficiency of process [*e*] including reaction [*j*]

$$O + O_2 + M \rightarrow O_3 + M \qquad [j]$$

to be 0.14, due to deactivation of the active species in reaction [*k*]

$$O_2^* + O_2 \rightarrow O_2 + O_2. \qquad [k]$$

This seems to contradict the value adopted in their earlier paper. In hydrocarbon–oxygen mixtures the reactions [*l*] and [*m*]

$$RH + O_2^* \rightarrow R + HO_2 \qquad [l]$$

and

$$RH + O_2^* \rightarrow RO + OH \qquad [m]$$

are also possibilities.

The situation is obviously complex since efficiencies cannot be accurately assigned to all the above reactions. One simplification which can be made is to operate at a constant ratio of hydrocarbon to oxygen. Under these conditions the rate of initiation should not vary, provided the over-all gas pressures are adequate to provide complete quenching of all the excited mercury atoms. Using different ratios it is possible to assign efficiencies to some of the above reactions.

The fact that the quantum yields of peroxide were below unity and independent of

Can. J. Chem. Downloaded from www.nrcresearchpress.com by 210.87.254.6 on 09/05/12
For personal use only.

the hydrocarbon-concentration variation in a mixture containing a fixed hydrocarbon–oxygen ratio (Fig. 3) indicates the absence of a peroxide chain reaction at the temperatures studied. The operation of the simple mechanism below:

$$RH \xrightarrow{R_i} R + H \qquad [1]$$

$$R + O_2 \xrightarrow{k_2} RO_2 \qquad [2]$$

$$H + O_2 \xrightarrow{k_{2'}} HO_2 \qquad [2']$$

$$RO_2 + HO_2 \xrightarrow{k_3} ROOH + O_2 \qquad [3]$$

leads, on applying the stationary state hypothesis, to the kinetic equation

$$d[\mathrm{ROOH}]/dt = R_i = \phi I_a$$

where ϕ is the effective primary radical yield in all initiation processes.

For a given hydrocarbon–oxygen ratio the total yield of peroxide should be proportional to the absorbed light intensity as observed (Fig. 2). Yields of tertiary butyl alcohol vary in a manner parallel to those of the hydroperoxide (Figs. 4 and 5) suggesting that the tertiary butoxy radical, which must be the immediate precursor of the alcohol, in the absence of ditertiary butyl peroxide, originates in reaction [4]

$$RO_2 + RO_2 \rightarrow 2RO\cdot + O_2 \qquad [4]$$

with subsequent hydrogen abstraction from the parent hydrocarbon as follows,

$$RO + RH \rightarrow ROH + R. \qquad [5]$$

Reaction [4] is not a terminating step and, therefore, does not affect the rate equation for peroxide production. In addition to reaction [5] a similar type of process, namely [3′], merits some consideration.

$$RO + HO_2 \rightarrow ROH + O_2 \qquad [3']$$

It is difficult to decide definitively between the two reactions [3′] and [5]. If [3′] is assumed to be the process leading to the production of tertiary butyl alcohol this would imply a primary radical yield of greater than unity for those mixtures with an isobutane–oxygen ratio of 10:1, since [3′] is a terminating reaction. The value of 0.8 found for the quantum yield of tertiary butyl hydroperoxide suggests that [3] alone is the main terminating reaction. For these reasons, reaction [5] would seem to be a better suggestion for the production of tertiary butyl alcohol. Figure 5, however, shows that the quantum yield of tertiary butyl alcohol is constant and independent of pressure for a fixed ratio of isobutane–oxygen and this is predicted by equation [3′]. The inclusion of equation [5] and omission of [3′] would lead to a decrease in alcohol and an increase in acetone production for lower values of isobutane in the fixed isobutane–oxygen ratio. Either equation [5] or [3′] leads to the same expected change in the rate of formation of alcohol and acetone with variation in light intensity. The kinetic data we have obtained is in favor of reaction [3′] as being the process responsible for the formation of the tertiary butyl alcohol. It would, however, also be reasonable to include reaction [5] on the basis of the values and trends observed for the quantum yields of tertiary butyl alcohol. It must, however, be pointed out that the constant value found for the ratio tertiary butyl alcohol – acetone for varying values of the ratio [isobutane]–[oxygen] (see Table II) is predicted

Can. J. Chem. Downloaded from www.nrcresearchpress.com by 210.87.254.6 on 09/05/12
For personal use only.

by neither [3′] nor [5] if either is in competition with equation [6], which is obviously the source of the acetone found.

$$(CH_3)_3CO \rightarrow CH_3COCH_3 + CH_3 \quad [6]$$

However, the process represented by equation [6] may not necessarily be so simple as there indicated. Should equation [6] be more complex than indicated it is possible that the inclusion of equation [5] may give the correct form of the variation of the quantum yields of tertiary butyl alcohol with hydrocarbon concentration.

The decomposition of the tertiary butoxy radical indicated in equation [6] is almost complete at temperatures about 190° C, even in the presence of an excess of a hydrocarbon containing a weak R—H bond (13, 14, 15, 16). At room temperature, it appears that the abstraction predominates because it requires a much lower activation than the decomposition. At 100° C the increasing yields of acetone are a measure of increasing extent to which the decomposition reaction [6] occurs. There is much uncertainty regarding the reaction of the resulting methyl radicals with oxygen to form methyl alcohol and formaldehyde (1, 16, 17, 18, 19, 20, 21). Below are listed some of the reactions considered possible at 100° C in the absence of significant yields of methyl hydroperoxide.

$$CH_3 + O_2 \rightarrow CH_3O_2 \quad [7]$$

$$CH_3O_2\cdot + HO_2 \rightarrow CH_3OOH + O_2 \quad [8]$$

$$CH_3O_2\cdot \rightarrow CH_2O + OH \quad [9]$$

$$CH_3OOH \xrightarrow{\text{surface}} CH_3O\cdot + OH \quad [10]$$

$$CH_3O_2\cdot + RO_2\cdot \rightarrow \underset{(R = CH_3 \text{ or } (CH_3)_3C)}{CH_3O\cdot + RO + O_2} \quad [11]$$

$$CH_3O\cdot + (CH_3)_3CH \rightarrow CH_3OH + (CH_3)_3C \quad [12]$$

$$CH_3O + O_2 \rightarrow CH_2O + HO_2 \quad [13]$$

It is not, of course, possible to assign individual efficiencies to reactions [7]–[13] given above. Tables I and II show that the peroxide yields and the variations of these with the composition of the reactants are about the same at 30° and 100°. Similar reactions as indicated in [7]–[13] must have about the same efficiencies at both these temperatures.

Close agreement between the total peroxide and tertiary butyl hydroperoxide indicates that neither the mutual interaction of hydroperoxy radicals nor abstraction from the parent hydrocarbon to form hydrogen peroxide occurs to any appreciable extent. The exothermicity for abstraction by the tertiary butyl peroxy radical from the isobutane molecule, equation [5′]

$$RO_2 + RH \rightarrow RO_2H + R, \quad [5']$$

is about 1.5 kcal mole^{-1}, and the activation energy has been determined by Burgess and Robb (9) to be 16 kcal mole^{-1}, thus accounting for the radical–radical reaction at 30° C. Abstraction from the isobutane molecule by the tertiary butoxy radical, equation [5], is exothermic by about 16 kcal mole^{-1}, and the activation energy is presumably less than for the peroxy abstraction, equation [5′], being sufficiently low to exclude the occurrence of the radical–radical reaction at 30° C.

The above isobutane–oxygen reaction scheme predicts that, providing $[HO_2] = [RO_2]$, the quantum yield of peroxide should be proportional to the sum of the reactions involving the RO· radical, i.e. tertiary butyl alcohol + acetone. Figure 6 shows that this is what our experimental results indicate.

Can. J. Chem. Downloaded from www.nrcresearchpress.com by 210.87.254.6 on 09/05/12
For personal use only.

The yields of peroxide which are formed in the main terminating reaction [3] increase with the increasing role of hydrocarbon in the excited mercury quenching processes (Tables I and II) and suggest that reaction [*c*] in the initiation processes has an efficiency close to unity. Low peroxide yields ($\phi < 0.15$) for the oxygen–isobutane = 10:1 mixtures are attributed to a low efficiency of reaction [*e*]. The value for ϕ in this case is close to that determined by Callear, Patrick, and Robb (11) for the oxygen–mercury reaction.

The detection of small yields of isobutyraldehyde was surprising. This is regarded as being formed from the isobutoxy radical according to equation [14]

$$(CH_3)_2CHCH_2O + O_2 \rightarrow (CH_3)_2CHCHO + HO_2. \qquad [14]$$

In the absence of significant quantities of the corresponding hydroperoxide the isobutoxy radicals will probably be formed as primary products without going through the isobutyl peroxy stage, where the opportunity for formation of the hydroperoxide exists. The data in Table II show that the ratio isobutyraldehyde – tertiary butyl peroxide increases with the increase in the percentage of the excited mercury atoms quenched by molecular oxygen. This suggests that the reactions [15] and [16] may be of some importance:

$$(CH_3)_2CHCH_3 + O_3 \rightarrow (CH_3)_2CHCH_2O + HO_2 \qquad [15]$$

$$(CH_3)_2CHCH_3 + O_2^* \rightarrow (CH_3)_2CHCH_2O + OH. \qquad [16]$$

Both of these are very exothermic.

The occurrence of [14] and [15] maintains the balance of hydroperoxy radicals at high oxygen–hydrocarbon ratios where each effective oxygen quenching process has the potentiality of producing three $RO_2\cdot$ radicals and only one HO_2 radical (reactions [*c*] to [*i*]).

Hydrogen abstraction by oxygen from the isobutoxy radical must have a lower activation energy than abstraction by the isobutoxy radical from the parent hydrocarbon, in view of the low yields of isobutyl alcohol found. Hydrogen abstraction from the tertiary butoxy radical by oxygen does not occur to any extent because the product of this reaction, namely isobutylene oxide, was not detected. A small fraction of the formaldehyde yields is attributable to decomposition of the isobutoxy radical occurring at 100° C where the quantum yields of the aldehyde are lower. The over-all increase in the yield of (acetone + *t*-butyl alcohol) at 100° C suggests reaction [4] may have a small activation energy. The slight increase in peroxide at 100° C for oxygen-rich mixtures is explained if the efficiency of [*e*] increases with increasing temperature.

A pressure of $\sim$ 3 mm Hg of oxygen will give complete quenching in a system containing mercury vapor at its room temperature equilibrium vapor pressure. The tail-off in peroxide yield at oxygen pressures below 30 mm Hg may be attributable to a competition between deactivation processes and reaction with oxygen for removal of active isobutane molecules as portrayed by equations [17] and [18]

$$C_4H_{10}^* \rightarrow C_4H_{10} \qquad [17]$$

$$C_4H_{10}^* + O_2 \rightarrow C_4H_9 + HO_2. \qquad [18]$$

The slow, absolute rate of reaction of mercury with the isobutane oxidation system will not be significant in reducing the rate of production of radicals in the initiation processes (see Part I).

Can. J. Chem. Downloaded from www.nrcresearchpress.com by 210.87.254.6 on 09/05/12
For personal use only.

ACKNOWLEDGMENTS

We wish to thank the National Research Council of Canada for generous grants in aid of this work. We are also indebted to Dr. G. B. Porter for several discussions on aspects of this research.

REFERENCES

1. J. A. GRAY. J. Chem. Soc. 3150 (1952).
2. A. B. NALBANDYAN. Doklady Akad. Nauk, S.S.S.R. **66**, 413 (1949).
3. A. B. NALBANDYAN and N. V. FOK. Doklady Akad. Nauk, S.S.S.R. **86**, 589 (1952).
4. J. S. WATSON and B. de B. DARWENT. J. Phys. Chem. **61**, 577 (1957).
5. C. A. YOUNG, R. R. VOIGT, and J. A. NIEULAND. Ind. Eng. Chem. Anal. Ed. **8**, 198 (1936).
6. C. E. BRICKER and H. R. JOHNSON. Anal. Chem. **17**, 400 (1945).
7. W. A. NOYES, JR. and P. A. LEIGHTON. Photochemistry of gases. Reinhold. 1941. p. 221.
8. A. C. G. MITCHELL and M. W. ZEMANSKY. Resonance radiation and excited atoms. Cambridge. 1934. p. 204.
9. R. H. BURGESS and J. C. ROBB. Trans. Faraday Soc. **54**, 1015 (1958).
10. B. de B. DARWENT and C. A. WINKLER. J. Phys. Chem. **49**, 150 (1945).
11. A. B. CALLEAR, C. R. PATRICK, and J. C. ROBB. Trans. Faraday Soc. **55**, 280 (1959).
12. N. A. MILAS and D. M. SURGENOR. J. Am. Chem. Soc. **68**, 205 (1946).
13. L. M. DORFMAN and Z. W. SALSBURG. J. Am. Chem. Soc. **73**, 255 (1951).
14. J. MURAWSKI, J. S. ROBERTS, and M. SZWARC. J. Chem. Phys. **19**, 698 (1951).
15. G. McMILLAN and M. J. H. WIJEN. Can. J. Chem. **36**, 1227 (1958).
16. E. R. BELL, J. H. RALEY, F. F. RUST, F. H. SEUBOLD, and W. E. VAUGHAN. Discussions Faraday Soc. **10**, 242 (1951).
17. J. R. BATES and R. SPENCE. J. Am. Chem. Soc. **53**, 381, 1689 (1931).
18. W. J. BLAEDEL, R. A. OGG, JR., and P. A. LEIGHTON. J. Am. Chem. Soc. **64**, 2500 (1942).
19. D. E. HOARE and A. D. WALSH. Trans. Faraday Soc. **53**, 1102 (1957).
20. F. B. MARCOTTE and W. A. NOYES, JR. Discussions Faraday Soc. **10**, 236 (1951).
21. P. L. HANST and J. G. CALVERT. J. Phys. Chem. **63**, 71, 104 (1959).

Can. J. Chem. Downloaded from www.nrcresearchpress.com by 210.87.254.6 on 09/05/12
For personal use only.

Can. J. Chem. Downloaded from www.nrcresearchpress.com by 210.87.254.6 on 09/05/12
For personal use only.

METAL OXIDE ALKOXIDE POLYMERS

PART I. THE HYDROLYSIS OF SOME PRIMARY ALKOXIDES OF ZIRCONIUM[1]

D. C. BRADLEY[2] AND D. G. CARTER[3]

ABSTRACT

Ebulliometric studies have been made on the hydrolysis of some zirconium alkoxides, $Zr(OR)_4$ where R = Et, Pr^n, Bu^i, and Bu^n. The variation of the degree of polymerization of the zirconium oxide alkoxides so produced was determined as a function of the degree of hydrolysis. The results are interpreted in terms of structural models based on octahedrally 6-co-ordinated zirconium.

INTRODUCTION

It is well established (1) that zirconium alkoxides $Zr(OR)_4$ are polymeric compounds involving metal–oxygen co-ordinate bonds. Although these alkoxides hydrolyze with great facility it is possible under rigorously controlled conditions to isolate the intermediate oxide alkoxides $ZrO_x(OR)_{4-2x}$. These products are of particular interest from the structural viewpoint because they may involve both condensation polymerization (giving ZrOZr systems) and co-ordination polymerization. In addition they are of interest as inorganic polymers which are intermediate between the relatively small polymers of the tetraalkoxide and the macromolecular metal oxide. Studies on the hydrolysis of titanium alkoxides (2, 3, 4) led to the suggestion of structural models for the titanium oxide ethoxides based on octahedrally 6-co-ordinated titanium. Since titanium exhibits a maximum co-ordination number of 6 but zirconium may expand its co-ordination to 7 or 8 it was important to determine whether or not the zirconium oxide alkoxides conformed to the same structural models as the corresponding titanium compounds. We now report the results of an ebulliometric study of the hydrolysis of four primary alkoxides of zirconium in which the degree of polymerization was determined as a function of the degree of hydrolysis.

EXPERIMENTAL AND RESULTS

Zirconium Alkoxides

These were prepared and analyzed using previously described (1) methods. The compounds were distilled at 0.1 mm pressure prior to the hydrolysis experiments.

Zirconium isobutoxide had not previously been described and it was prepared as follows. Freshly distilled zirconium tetraisopropoxide (9 g) was caused to react with isobutanol (125 cc), and the liberated isopropanol removed by fractional distillation. The solution was concentrated to ca. 30 cc and a mass (9 g) of crystals of the *solvate* $Zr(OBu^i)_4,Bu^iOH$ was deposited on cooling. At 100° C at 0.1 mm the crystals softened and lost isobutanol, and the tetraisobutoxide was distilled at 213° C at 0.3 mm. The gummy solid (found: Zr, 24.5; $Zr(OBu^i)_4$ requires: Zr, 23.8%) was recrystallized from isobutanol to reform the *solvate*. Found: Zr, 20.2. $Zr(OBu^i)_4,Bu^iOH$ requires: Zr, 19.9%. Heated under atmospheric pressure the *solvate* softened at 146° C and melted with dissociation at 154° C.

[1]*Manuscript received March 6, 1961.*
Contribution from the Department of Chemistry, Birkbeck College, London, W.C.1, England.
[2]*Present address: Department of Chemistry, The University of Western Ontario, London, Ontario.*
[3]*Present address: Department of Chemistry, Norwood Technical College, London, England.*

Can. J. Chem. Downloaded from www.nrcresearchpress.com by 210.87.254.6 on 09/05/12
For personal use only.

Ebulliometry

An all-glass ebulliometer, similar to that already described (5) and incorporating a differential water thermometer, was used. About 20 cc of dry alcohol was distilled into the ebulliometer in each experiment, the exact amount being determined by weighing to 0.01 g. The water levels in the differential thermometer were read to 0.01 mm using a travelling microscope. About 20 minutes were required after each addition of solute for thermal equilibrium to be re-established.

The following procedure was adopted for the ebulliometric hydrolysis studies. First a series of additions of weighed amounts (Δm) of zirconium alkoxide was made and the corresponding elevations of the boiling point (ΔT) were recorded. The slope of the linear plot of ΔT versus Δm was then found graphically. Next, several weighed amounts of the pure standard (either fluorene or azobenzene) were added and the ΔT's again plotted against weight of solute. The molecular weight of the zirconium compound was then calculated from a knowledge of the two slopes and the molecular weight of the standard. Finally, a series of additions of known aqueous alcohol were made. These solutions contained less than 10% w/w of water and were made up gravimetrically. The addition of aqueous alcohol caused an immediate decrease in the boiling point elevation due to the increase in molecular weight caused by hydrolysis of the zirconium compound. To obtain the correct degree of polymerization of the hydrolysis product an allowance was made for the additional solvent added, and for the amount of alcohol liberated by hydrolysis. These experiments were of several hours' duration and the ebulliometer was weighed at the end of the experiment to determine whether solvent had been lost by evaporation. The process being studied may be depicted by the following equation:

$$[ZrO_{x_1}(OR)_{4-2x_1}]n_1 + (n_2x_2 - n_1x_1)H_2O \rightarrow n_1/n_2[ZrO_{x_2}(OR)_{4-2x_2}]n_2 + 2(n_2x_2 - n_1x_1)ROH$$

where $n_2 > n_1$ and $x_2 > x_1$. In fact the system may contain a distribution of polymer sizes and the values of n determined are number-average degrees of polymerization. The degree of hydrolysis, namely the ratio of gram-molecules of water added per gram-atom of zirconium, is designated by h. In principle h may be varied from 0 to 2 but some experiments were terminated when insoluble products appeared in the ebulliometer.

Zirconium Ethoxide

Experiments were made at three initial concentrations of zirconium ethoxide. The results are given in the following tables.

(*a*) Initial concentration of $Zr(OEt)_4$: 0.186 g-mol./kg ethanol.

TABLE I

h	0.00	0.01	0.10	0.22	0.38	0.52	0.69	0.92	1.16	1.49	1.63	(1.87)
n	2.10	2.15	2.42	2.70	3.18	3.68	4.53	6.55	9.39	9.97	11.4	(10.9)

Precipitation of a white solid occurred 5 minutes after the addition corresponding to $h = 1.87$.

(*b*) Initial concentration of $Zr(OEt)_4$: 0.409 g-mol./kg ethanol.

TABLE II

h	0.000	0.060	0.148	0.273	0.422	0.630	0.825	1.027	(1.229)
n	2.17	2.47	2.83	3.12	3.60	4.81	6.65	10.3	(13.3)

Opalescence in the solution was just perceptible at $h = 0.630$ and became appreciable

at $h = 1.229$. The hydrolysis was continued to $h = 1.433$ before allowing the system to cool when about 0.1 g solid was deposited.

(*c*) Initial concentration of $Zr(OEt)_4$: 0.723 g-mol./kg ethanol.

TABLE III

h	0.000	0.037	0.080	0.121	0.182	0.248	0.344	0.463	0.612	0.766
n	2.24	2.42	2.61	2.81	3.01	3.22	3.54	3.94	4.66	5.79

Opalescence was first detected at $h = 0.612$ and became appreciable at $h = 0.888$.

Zirconium n-Propoxide

The concentration of $Zr(OPr^n)_4$ was 0.147 g-mol./kg *n*-propanol.

TABLE IV

h	0.000	0.159	0.400	0.711	1.118	1.469
n	2.44	2.79	3.30	4.21	7.27	13.9

The experiment was terminated at $h = 1.814$ because the thermometer reading was unsteady. This behavior is believed to indicate the presence of water in the system.

Zirconium n-Butoxide

The concentration of $Zr(OBu^n)_4$ was 0.0707 g-mol./kg *n*-butanol.

TABLE V

h	0.000	0.483	0.953	1.671
n	1.77	2.46	3.81	9.39

The experiment was terminated by fluctuations in the thermometer reading at $h = 2.606$.

Zirconium Isobutoxide

The concentration of $Zr(OBu^t)_4$ was 0.0766 g-mol./kg isobutanol.

TABLE VI

h	0.000	0.223	0.506	0.882	1.403	1.845
n	1.52	1.61	1.71	2.03	2.50	3.31

DISCUSSION

Before discussing the structural implications of the results on zirconium oxide alkoxides it is necessary to recapitulate briefly the structural models considered by Bradley, Gaze, and Wardlaw (3, 4) to explain the behavior of titanium oxide alkoxides. Three structural models were proposed, each involving 6-co-ordinated titanium. Model I was based on the unsolvated trimeric alkoxide $Ti_3(OR)_{12}$ (Fig. 1) and gave a series of trilinear polymers, e.g. $Ti_6O_4(OR)_{16}$ (Fig. 2) and the infinite polymer $[Ti_3O_4(OR)_4]_\infty$ (Fig. 3). These structures all fitted the general relationship $n = 12/(4-3h)$, where $h = 0$ to 1.333. A feature of the system is the fact that the number-average degree of polymerization n is uniquely determined by h and is thus independent of the distribution of polymer sizes. Model II was based on a solvated dimeric species $Ti_2(OR)_8,2ROH$ (Fig. 4) and gave bilinear

Can. J. Chem. Downloaded from www.nrcresearchpress.com by 210.87.254.6 on 09/05/12
For personal use only.

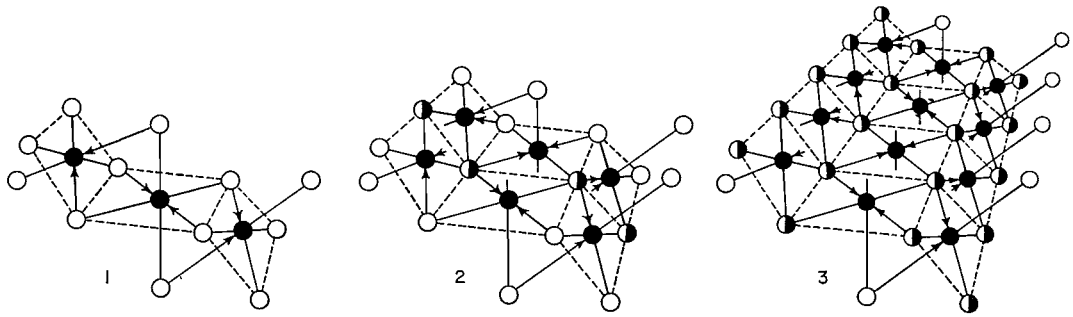


FIG. 1. $Ti_3(OR)_{12}$. ● = Ti; ○ = oxygen in OR groups; R groups omitted.
FIG. 2. $Ti_6O_4(OR)_{16}$. ● = Ti; ◑ = oxygen in Ti.O.Ti; ○ = oxygen in OR (some OR groups omitted for clarity); R groups omitted.
FIG. 3. Section of infinite trilinear polymer $Ti_{3(x+1)}O_{4x}(OR)_{4(x+3)}$. ● = Ti; ◑ = oxygen in Ti.O.Ti; ○ = oxygen in OR (some OR groups omitted for clarity); R groups omitted.

polymers (Fig. 5) corresponding to $n = 6/(3-2h)$, $h = 0$ to 1.5. A third model was based on a monomeric solvated species $Ti(OR)_4$,2ROH. This gave rise to the relation $n = 3/(3-h)$.

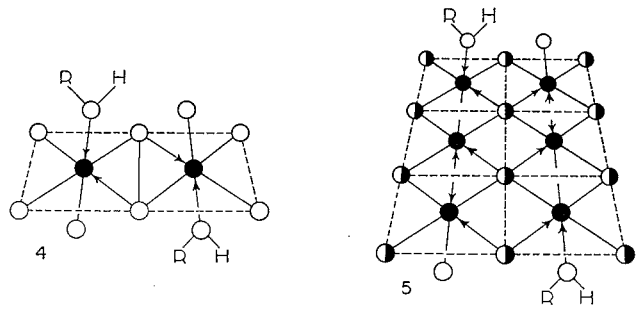


FIG. 4. Solvated dimer $Ti_2(OR)_8$,2ROH. ● = Ti; ○ = oxygen in OR.
FIG. 5. Section of infinite bilinear solvated polymer $Ti_2O_3(OR)_2$,2ROH. ● = Ti; ◑ = oxygen in Ti.O.Ti; ○ = oxygen in OR (some OR and R omitted for clarity); some ROH molecules omitted for clarity.

Accordingly, if the oxide alkoxides of zirconium conform to the same structural series, based on octahedrally 6-co-ordinated zirconium, then we should expect the variation of n with h to resemble one of the predicted relationships. For example, if the original alkoxide is trimeric in its boiling alcohol it should follow the requirements of model I and so forth.

Zirconium Oxide Ethoxides

In Fig. 6 we show a comparison between the experimental data for $Zr(OEt)_4$ and the predicted curves for models I and II. Two features are immediately apparent. Firstly it is noteworthy that practically all of the experimental points lie between the predicted curves for models I and II. Secondly it is clear that in the initial stages experimental points drift closer to the curve I, then remain fairly constant in distance from the curve before deviating towards curve II at h values >1.0. This general behavior is reminiscent of that shown by the hydrolysis products of $Ti(OEt)_4$ (3) and it seems reasonable to apply the principles developed by Bradley, Gaze, and Wardlaw. For a system containing species belonging to models I and II, if the degree of hydrolysis h is

Can. J. Chem. Downloaded from www.nrcresearchpress.com by 210.87.254.6 on 09/05/12
For personal use only.

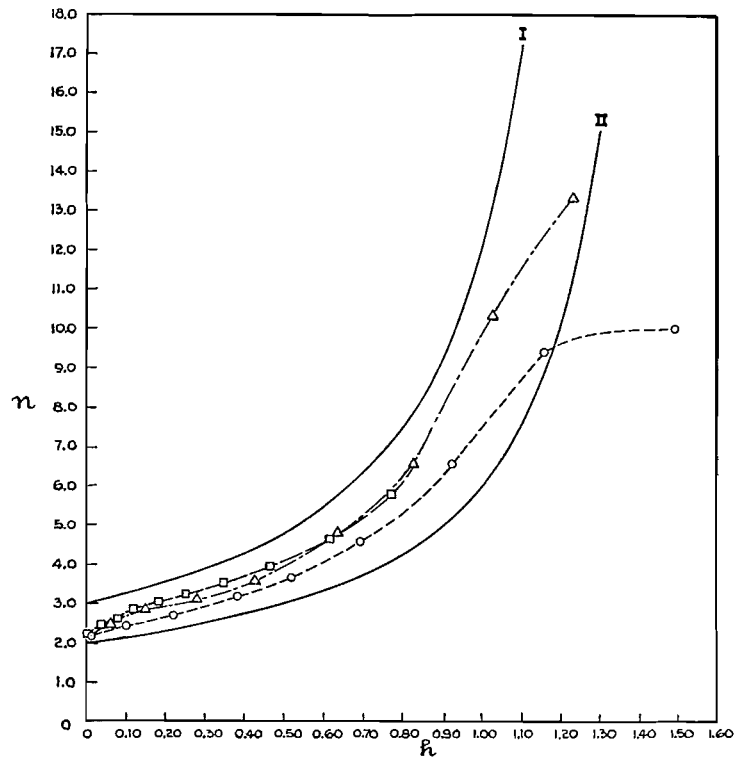


FIG. 6. The hydrolysis of $Zr(OEt)_4$ in boiling ethanol. □ = initial concentration 0.723 g-mol. $Zr(OEt)_4$/kg EtOH; △ = initial concentration 0.409 g-mol. $Zr(OEt)_4$/kg EtOH; ○ = initial concentration 0.186 g-mol. $Zr(OEt)_4$/kg EtOH.

the same for each model, it is readily deduced that the fraction of zirconium atoms in model I is α_I, where $\alpha_I = n_I(n - n_{II})/n(n_I - n_{II})$. In this expression n_I is the degree of polymerization if all the zirconium were in model I and n_{II} if all were in model II. In Fig. 7 is shown the variation of α_I with h for each experiment. Bearing in mind the sensitivity of α_I to experimental error the data still show clearly the rapid initial rise in α_I with increase in h followed by the attainment of a fairly constant value over a range of h and finally a decrease near the completion of the experiment. The latter phenomenon is probably the result of increasing solvation (model II) as the molar concentration of the polymeric species becomes low. This is a consequence of the experimental method since the mass of zirconium is constant throughout the experiment whereas the average molecular size of the zirconium oxide ethoxide species increases steadily with increasing degree of hydrolysis. The striking increase in α_I in the early stages of hydrolysis is more difficult to explain. Thus it is tempting to suggest that the original zirconium ethoxide ($h = 0$) exhibits a low value of n due to the steric effect of the ethyl groups opposing co-ordination polymerization. Then as hydrolysis proceeds and ethoxide groups are removed, co-ordination polymerization develops more fully. However, studies in the alkoxide field have shown (1) that n-alkyl groups exert relatively small steric effects in metal tetraalkoxides and it is surprising that such a large change could be due to this effect. Another puzzling feature is that zirconium ethoxide exhibits a slightly lower degree of polymerization in boiling ethanol than titanium ethoxide but a higher value in boiling benzene. In other words, in boiling ethanol, zirconium apparently has a greater

Can. J. Chem. Downloaded from www.nrcresearchpress.com by 210.87.254.6 on 09/05/12
For personal use only.

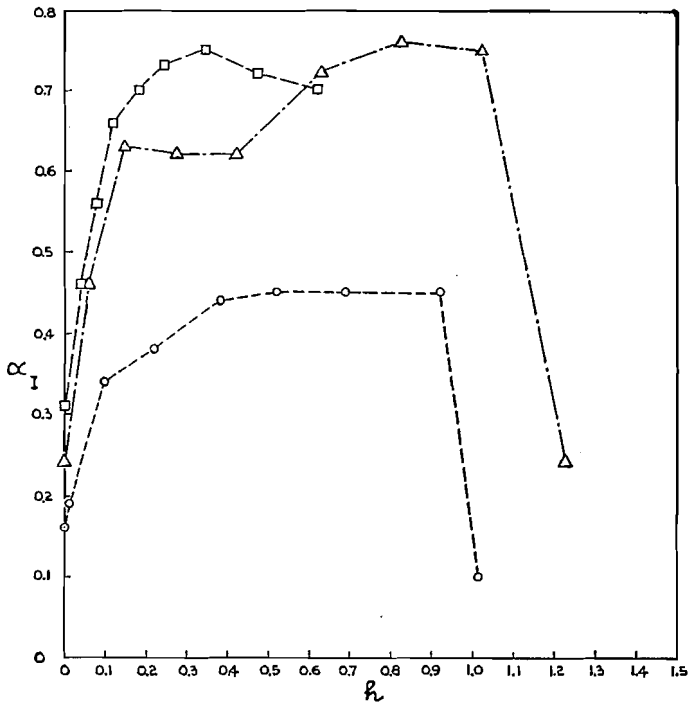


FIG. 7. The variation of α_I with h for zirconium oxide ethoxides. □ = initial concentration 0.723 g-mol. $Zr(OEt)_4$/kg EtOH; △ = initial concentration 0.409 g-mol. $Zr(OEt)_4$/kg EtOH; ○ = initial concentration 0.186 g-mol. $Zr(OEt)_4$/kg EtOH.

tendency to obtain 6-co-ordination by co-ordination with alcohol rather than by polymerization of the ethoxide. The electronic factors involved in bonding in these polymers must also be considered. For example, we should expect that the electron density on the oxygen will be greater for the oxygen in a ZrOZr system than in ZrOEt or EtOH because zirconium is more electropositive than hydrogen or carbon. Therefore the ZrOZr oxygen should be a stronger donor than ZrOEt or EtOH oxygens. Hence as hydrolysis is increased and the proportion of ZrOZr groups becomes significant this may lead to the favoring of polymerization at the expense of solvation and thus a change from model II to model I. The alternative polymers for $h = 1.0$ illustrate this point. In the molecule $Zr_{12}O_{12}(OEt)_{24}$ (model I) one half of the ZrOZr oxygens are utilized in co-ordination polymerization but in $Zr_6O_6(OEt)_{12}$,6EtOH (model II) only one third of the ZrOZr oxygens are so used. These proportions remain constant throughout the oxide ethoxide series and accordingly it would be expected that the values of α_I would rise rapidly at the initial stages of hydrolysis and then remain sensibly constant over a range of h values. Nevertheless, calculations show that this suggestion does not fully account for the rise in α_I with increase in h from 0.0 to 0.5. We are forced to conclude that zirconium tetraethoxide in boiling ethanol is not in true equilibrium with regard to trimer (unsolvated) and dimer (solvated) species but that the oxide ethoxide molecules act as catalysts in bringing the system nearer to equilibrium. There is other evidence which points to the suggestion that solutions of $Zr(OEt)_4$ in boiling ethanol are not in true equilibrium. For example in determining the molecular weight of $Zr(OEt)_4$ a number of additions of solute are made over a range in concentration yet the plot of ΔT (elevation of boiling point) vs. concentration of solute is linear, although a non-integral value for n suggests that more than one

Can. J. Chem. Downloaded from www.nrcresearchpress.com by 210.87.254.6 on 09/05/12
For personal use only.

polymer species is present and hence the molecular weight should be concentration dependent. On the other hand we find that the elevation of boiling point at a given concentration remains constant over a period of hours suggesting that a pseudo equilibrium is set up. The sudden decline in α_I at $h > 1.0$ may be a dilution effect (decrease in polymer concentration) which favors solvation or alternatively it could be caused by the presence of ZrOH groups.

The structural model I reaches a limiting, infinite trilinear polymer at $h = 1.333$ and it would be expected that such a polymer would be insoluble. Our ebulliometric experiments were in fact limited by the onset of turbidity in the system. In the case of the experiment at the intermediate concentration of $Zr(OEt)_4$ a slight opalescence was detected at $h = 0.63$ and the experiment was terminated when precipitation occurred at $h = 1.43$. The precipitate was isolated and analysis showed that its composition was near to that for the infinite polymer $[Zr_3O_4(OEt)_4]_\infty$. Found: Zr, 51.2; EtO, 36.3. $Zr_3O_4(OEt)_4$ requires: Zr, 52.8; EtO, 35.0%. The degree of hydrolysis in the solid product corresponded to $h = 1.28$ and this would give a polymer with a number-average degree of polymerization of ~90. It is not surprising that such a large molecular species was sparingly soluble. However, it is interesting that it corresponded to a slightly lower degree of hydrolysis than that calculated from the known addition of water. This lends further support to the suggestion that hydrolysis may not be quantitative in the later stages of the experiment.

Zirconium Oxide n-Propoxides

The variation of n with h in this system is shown in Fig. 8. No precipitation occurred up to $h = 1.469$ but following the next addition of water (to $h = 1.814$) the behavior of the water thermometer suggested that hydrolysis was no longer quantitative. The shape of the hydrolysis curve suggests that polymers of the models I and II are present in the early stages of hydrolysis but for $h > 1.0$ solvation becomes more effective as the molar concentration of polymers decreases and hence the polymers are based on models II and III. In Table VII we report the values for α_I, $1 - \alpha_I$, α_{II}, and $1 - \alpha_{II}$ as a

TABLE VII

h	α_I	$1 - \alpha_I$	α_{II}	$1 - \alpha_{II}$	c
0.000	0.54	0.46	—	—	0.0602
0.159	0.72	0.28	—	—	0.0532
0.400	0.48	0.52	—	—	0.0445
0.711	0.24	0.76	—	—	0.0349
1.118	—	—	0.98	0.02	0.0197
1.469	—	—	0.88	0.12	0.0101

function of h and the average molar concentration of polymers c (g-mol./kg). α_{II} is defined by $\alpha_{II} = n_{II}(n - n_{III})/n(n_{II} - n_{III})$ where n_{II} and n_{III} are the calculated degrees of polymerization for models II and III respectively.

The interesting point about these data is the small rise in α_I in the early stages (compared with the zirconium oxide ethoxide system) and thereafter the steady increase in proportion of the more solvated species of models II and III. The relatively small rise in α_I at first suggests that the initial solution of $Zr(OPr^n)_4$ in boiling n-propanol is nearer to the true equilibrium between polymer species than was the solution of $Zr(OEt)_4$ and this may be due to the higher boiling point of n-propanol. The higher boiling point of the alcohol is probably responsible for the more rapid onset of solvation in the zirconium

Can. J. Chem. Downloaded from www.nrcresearchpress.com by 210.87.254.6 on 09/05/12
For personal use only.

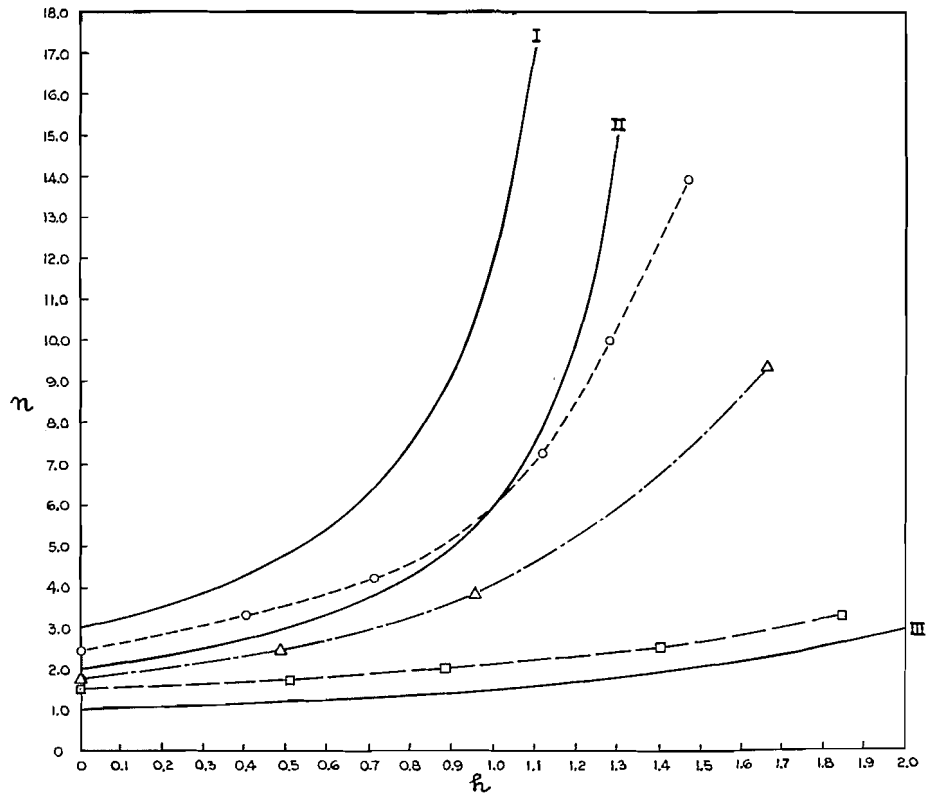


FIG. 8. The hydrolyses of $Zr(OPr^n)_4$, $Zr(OBu^n)_4$, and $Zr(OBu^i)_4$ in their respective alcohols. ○ = $Zr(OPr^n)_4$, initial concentration 0.147 g-mol./kg ROH; △ = $Zr(OBu^n)_4$, initial concentration 0.0707 g-mol./kg ROH; □ = $Zr(OBu^i)_4$, initial concentration 0.0766 g-mol./kg ROH.

oxide *n*-propoxide system. Thus Bradley, Gaze, and Wardlaw (4) suggested that solvation of the polymeric species would be promoted both by a decrease in molar concentration of polymer species and by increase in temperature. The data in Table VII suggest that the presence of polymers based on model III becomes increasingly significant with increase in h for $h > 1.0$. It is especially noteworthy that according to model III the highest polymer (at $h = 2.0$) possible is the trimer, whereas models I and II predict infinite linear polymers at $h = 1.33_4$ and 1.50 respectively. In our experiment no precipitation was observed although the reaction was terminated at $h = 1.814$ due to the presence of residual water in the system. The absence of a precipitate is thus in agreement with the presence of polymers based on model III in the final stages of hydrolysis. However, the presence of water at $h = 1.814$ also suggests that hydrolysis may be reversible at this stage due to the presence of Zr—OH groups and this offers an alternative means of producing low polymers.

Zirconium Oxide n-Butoxides

The high boiling point of *n*-butanol should promote the solvation process even more than *n*-propanol. The variation of n with h for the $Zr(OBu^n)_4$ system, shown in Fig. 8, agrees with this supposition. It appears that the polymeric species involve models II and III (with II predominating) and the dependence of α_{II} on h is shown in Fig. 9. It is extremely interesting to note that there is only a small initial rise in α_{II} at the early stages of

Can. J. Chem. Downloaded from www.nrcresearchpress.com by 210.87.254.6 on 09/05/12
For personal use only.

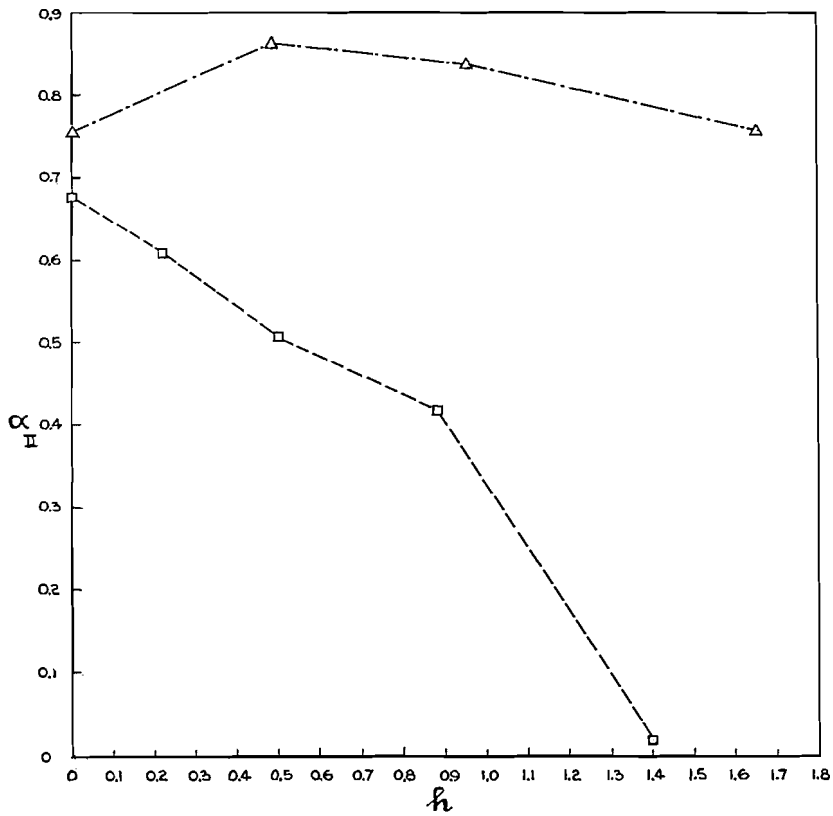


FIG. 9. The variation of α_{II} with h for zirconium oxide *n*-butoxides and zirconium oxide isobutoxides. △ = $Zr(OBu^n)_4$, initial concentration 0.0707 g-mol./kg ROH; □ = $Zr(OBu^i)_4$, initial concentration 0.0766 g-mol./kg ROH.

hydrolysis, followed by a steady decline in α_{II} as the decrease in polymer concentration with increase in n favors the model III species. No precipitation was observed and this suggests the predominance of model III in the final stages of hydrolysis. However, the detection of residual water at $h > 1.671$ means that hydrolysis may be reversible and incomplete in this region.

Zirconium Oxide Isobutoxides

The interesting feature of this system is that in spite of the lower boiling point of isobutanol compared with *n*-butanol, the solvation of $Zr(OBu^i)_4$ appears to be greater than for $Zr(OBu^n)_4$. This may well be due to the greater steric effect of the isobutoxide groups. It is well established (1) that branching of the alkyl groups in zirconium alkoxides opposes the formation of Zr—O intermolecular bonds and thus prevents co-ordination polymerization. The zirconium is thus forced to achieve its higher co-ordination by the process of solvation. Striking evidence in support of the preferential solvation of $Zr(OBu^i)_4$ was the isolation of the relatively stable solvate $Zr(OBu^i)_4,Bu^iOH$, in contrast to $Zr(OBu^n)_4$, which does not form a solvate. The variation of n with h for $Zr(OBu^i)_4$ is shown in Fig. 8. In Fig. 9 we show the steady decrease of α_{II} with increase in h, which suggests that model III species become favored as hydrolysis becomes extensive. No precipitation occurred up to $h = 1.845$ and this is in agreement with the predominance of model III species. Above $h = 1.845$ residual water was detected and this suggests that hydrolysis is reversible in this region.

Can. J. Chem. Downloaded from www.nrcresearchpress.com by 210.87.254.6 on 09/05/12
For personal use only.

CONCLUSIONS

The zirconium oxide alkoxides $ZrO_x(OR)_{4-2x}$, where R = Et, Pr^n, Bu^t, and Bu^n, exhibit low number-average molecular weights in solution in their progenitive alcohols at the boiling point. The variation of degree of polymerization with degree of hydrolysis is reasonably explained in terms of structural models based on 6-co-ordinated zirconium. With the exception of the ethoxides the zirconium compounds exhibited a greater degree of co-ordination polymerization than the corresponding titanium compounds.

REFERENCES

1. D. C. Bradley, R. C. Mehrotra, J. D. Swanwick, and W. Wardlaw. J. Chem. Soc. 2025 (1953).
2. D. C. Bradley, R. Gaze, and W. Wardlaw. J. Chem. Soc. 721 (1955).
3. D. C. Bradley, R. Gaze, and W. Wardlaw. J. Chem. Soc. 3977 (1955).
4. D. C. Bradley, R. Gaze, and W. Wardlaw. J. Chem. Soc. 469 (1957).
5. D. C. Bradley, W. Wardlaw, and A. Whitley. J. Chem. Soc. 5 (1956).

Can. J. Chem. Downloaded from www.nrcresearchpress.com by 210.87.254.6 on 09/05/12
For personal use only.

THE INFLUENCE OF HYDROGEN ION CONCENTRATION ON THE MYOSIN-CATALYZED HYDROLYSIS OF ADENOSINE TRIPHOSPHATE[1]

GÉRARD E. PELLETIER[2] AND LUDOVIC OUELLET

ABSTRACT

The Michaelis constants for the system myosin–ATP have been measured at 5° C and 15° C from pH 7.0 to pH 10.5, in the presence of 0.4 *M* potassium chloride and 0.005 *M* calcium chloride. The experimental data point to the presence, in the active center, of two ionizable groups, with experimental acid p*K* of 7.35 and 8.6 respectively at 15° C. The apparent heats of ionization of these groups are about 9 kcal/mole for the first one and close to zero for the second. These data are interpreted as indication of the presence in the active center of myosin of a histidyl and a sulphydryl residue. A mechanism is proposed for the hydrolysis of ATP in the presence of myosin.

The kinetics of hydrolysis of adenosine triphosphate (ATP) in the presence of myosin has been described under several of its aspects. The reaction follows the Michaelis–Menten law. The influence of concentration of substrate, activator ions, ionic strength, and dielectric constants have been reported and have been summarized by Laidler (1). Recently Nihei and Tonomura (2) have observed an increase in the Michaelis constant at pH around 6.8. Blum (3) has also mentioned the variation of the Michaelis constant with the concentration of *p*-chloromercuribenzoate, an inhibitor probably reacting with sulphydryl residues.

The present paper describes the variation of the Michaelis constant of myosin as a function of the pH at two temperatures. The data so obtained will be used as information on the nature of the active groups of myosin.

DESCRIPTION OF THE DATA

The data reported in this paper were collected in terms of the usual system describing the influence of hydrogen ions on the rate of an enzymatic reaction. As the work progressed, however, it became evident that the simple usual scheme had to be modified to describe the experimental results.

The fundamental scheme is represented in Fig. 1. The enzyme is assumed to exist in

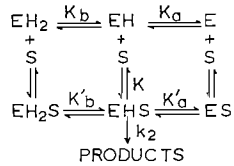


FIG. 1. Scheme representing the ionization states of an enzyme E and the enzyme substrate complex when the active center includes two acid groups.

three different ionic states EH_2, EH, E, in equilibria one with the other. The ionization constants K_b and K_a describe the ionization equilibrium. The charges and the hydrogen ions participating in the equilibrium have been left out. In the general case, these three

[1]*Manuscript received February 14, 1961.*
Contribution from the Department of Chemistry, Laval University, Quebec, Que.
[2]*Present address: Research Division, Imperial Oil Ltd., Sarnia, Ont.*

enzymic forms react with a substrate molecule S to give the complexes EH_2S, EHS, and ES. The complex EHS is usually assumed to give products.

Assuming the above system to be in equilibrium, the rate of hydrolysis V is given by the Michaelis–Menten equation:

$$V = \bar{V}_m[S]/(\bar{K}_m + [S]) \quad [1]$$

where $\bar{V}_m$, the rate at very high substrate concentration, assuming no substrate inhibition, is given by:

$$\bar{V}_m = V_m \Big/ \left(1+\frac{[H^+]}{K_b'}+\frac{K_a'}{[H^+]}\right) \quad [2]$$

and $\bar{K}_m$, the Michaelis constant, is:

$$\bar{K}_m = K_m\left(1+\frac{K_a}{[H^+]}+\frac{[H^+]}{K_b}\right) \Big/ \left(1+\frac{K_a'}{[H^+]}+\frac{[H^+]}{K_b'}\right). \quad [3]$$

The variation of $\bar{V}_m$ and $\bar{K}_m$ with pH provides information on the values of K_a, K_b, K_a', and K_b'. The techniques suggested by Dixon (5) and Massey and Alberty (6) have been used to estimate the ionization constants from the experimental data.

For a discussion of the various hypotheses involved in this representation, one is referred to Laidler (4).

EXPERIMENTAL PART

Myosin of the Weber–Edsall type (7) was used. Adenosine triphosphate (ATP) was the crystalline sodium salt purchased from Pabst Laboratories. All the other reagents were reagent grade.

In the determination of the Michaelis constants, all rates were measured by an electrometric titration method, as the hydrolysis of ATP liberates phosphoric acid according to the following equation.

$$ATP^{-4} + H_2O \rightarrow HPO_4^{=} + ADP^{-3} + H^+ \quad [4]$$

By continuously titrating standard alkali into the reaction mixture to maintain the pH constant, it is possible to follow the rate of formation of the acid.

The apparatus used consisted of a titrator (type TTT 1b) equipped with glass and calomel electrodes, a titrigraph (type SBR2b), and syringe microscrew burette (type SBU1a), from Radiometer (Copenhagen).

Nineteen milliliters of a 0.4 M solution of potassium chloride containing the required amount of ATP and calcium chloride (0.005 M) was pipetted into a double-jacketed reaction vessel. Circulation of water from a constant-temperature bath maintained the temperature within 0.1° C. Stirring was provided magnetically.

To minimize absorption of carbon dioxide from the atmosphere, air which had been twice washed in 30% potassium hydroxide solutions, followed by washing in water at the experimental temperature, was circulated over the surface of the reaction mixture. This proved effective up to pH 10, where a small blank correction was applied. One milliliter of the enzyme solution was injected to the above reaction mixture. The amount of alkali added was recorded as a function of time by the titrigraph. The total volume of sodium hydroxide added never exceeded 2% and was usually less than 1% of the reaction volume.

The rate at high substrate concentration was obtained from a series of runs, made in

1 day at one enzyme concentration. The results so obtained were then multiplied by $(\bar{K}_m + [S])/[S]$. At pH lower than 8, the rate at high concentration of substrate was obtained from analyses for orthophosphate by a colorimetric method (8).

RESULTS

Influence of pH on $\bar{V}_m$

Figure 2 shows the results obtained when the logarithm of the apparent maximum

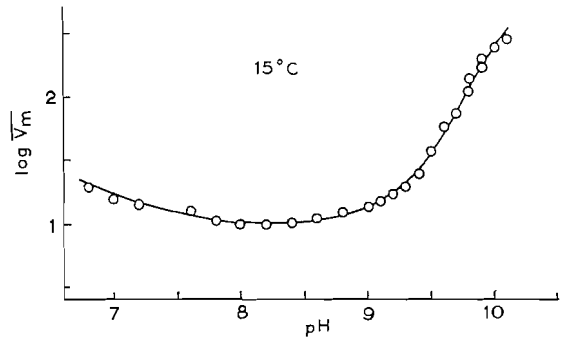


FIG. 2. Plot of the logarithm of the rate of hydrolysis of ATP at high concentration of substrate, $\bar{V}_m$, as a function of pH, at 15.1° C. The rates are in arbitrary units.

rate $\bar{V}_m$ was plotted against the pH at 15.1° C. The curve passes through a minimum in the neighborhood of pH 8.2. No true maxima could be obtained on the alkaline side of these curves, due in part to precipitation in the system and myosin inactivation (9). At 5.2° C, the alkaline branch of the curve was displaced toward higher pH values. Those results are consistent with observations reported by other investigators. Mommaerts and co-workers (10) as well as Tonomura and co-workers (11) have traced $\bar{V}_m$-vs.-pH curves under different conditions of temperature and ionic strength. In general, the curves passed through a minimum at low pH and reached a maximum in the vicinity of pH 9–10, after which a sharp drop resulted. By light-scattering experiments Blum (12) showed that this last phenomenon was due to an irreversible inactivation of the enzyme. Morales (13) has further shown that the concentration of calcium ions affects the position of the alkaline part of the curve, the curve shifting to lower pH values as the concentration of calcium ions is increased.

As no true maximum can be observed under our conditions, these curves cannot be used to estimate the pK of ionization of the myosin–ATP complex. All the experimental data pertaining to the ionization have perforce been obtained from a study of the variation of the Michaelis constant with pH.

The experimental Michaelis constants $\bar{K}_m$ were determined at two different temperatures over a range extending from pH 6.7 to 10.0 at 15.1° C and pH 7.0 to 10.4 at 5.2° C. Figure 3 represents examples of Lineweaver–Burk (14) plots of the reciprocal of the rate against the reciprocal of the ATP concentration. Each Michaelis constant was determined on the same day to eliminate errors due to possible loss in enzyme activity. The Michaelis–Menten law was found to hold under all the conditions studied. The usual determinations of $\bar{K}_m$ covered a ratio of 20 to 50 in concentrations of substrate.

Influence of pH on $\bar{K}_m$

For purposes of interpretation, the influence of pH on the apparent Michaelis constant is usually represented in the form of plots of p$\bar{K}_m$ ($-\log \bar{K}_m$) against pH. Figure 4

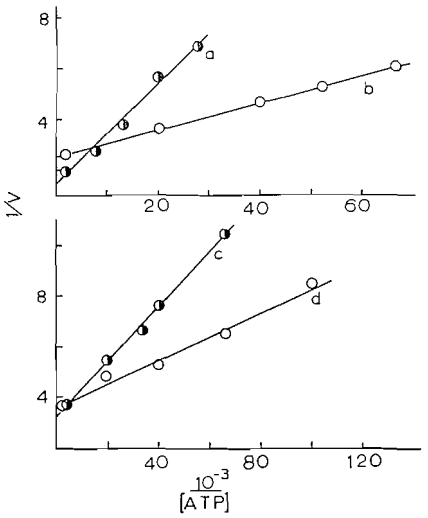


FIG. 3. Lineweaver–Burk plots of the reciprocal of the rate of hydrolysis in arbitrary units as a function of the reciprocal of the ATP concentration at 15.1° C. pH: a = 9.8; b = 7.2; c = 7.0; d = 8.0.

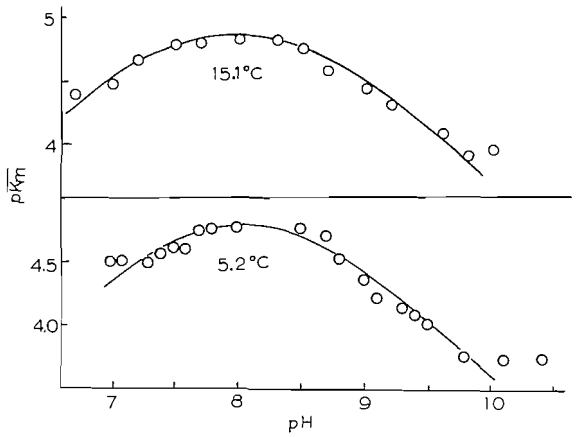


FIG. 4. Plots of $p\bar{K}_m$ ($-\log \bar{K}_m$) as a function of pH. The curves are theoretical curves drawn assuming $K_b' \gg K_b$ and $K_a' \ll K_a$ in equation [3] and pK_a = 8.6, pK_b = 7.34 at 15.1° C and pK_a = 8.6, pK_b = 7.6 at 5° C.

represents such plots at 15.1 and 5.2° C. Classical bell-shaped curves were obtained in both cases. These results are consistent with the observations of Nihei and Tonomura (2), who found that in buffered solutions containing 0.08 M THAM–maleate under two different ionic strength conditions, $\bar{K}_m$ hardly changed in the range of pH between pH 6.7 and 8.0 but increased with decreasing pH below 6.7. The ionization constants were calculated from these data by the method developed by Massey and Alberty (6). One assumes that the top part of the curve down to a point 0.3 $p\bar{K}_m$ units below the maximum is unaffected by any complication, and can be described by two ionization constants. Plots of $\bar{K}_m$ as a function of hydrogen ion concentrations or reciprocal of hydrogen ion concentrations, Figs. 5 and 6, gave approximately the same results, which have been tabulated in Table I.

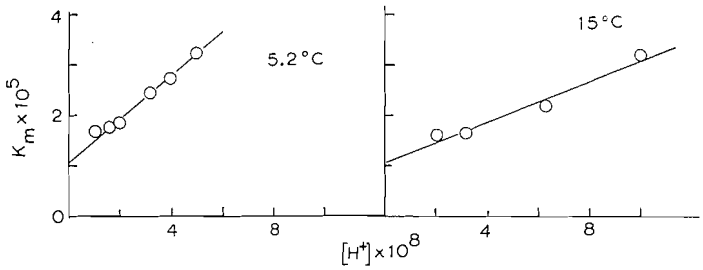


FIG. 5. Plots of $\bar{K}_m$ as a function of the hydrogen ion concentration.

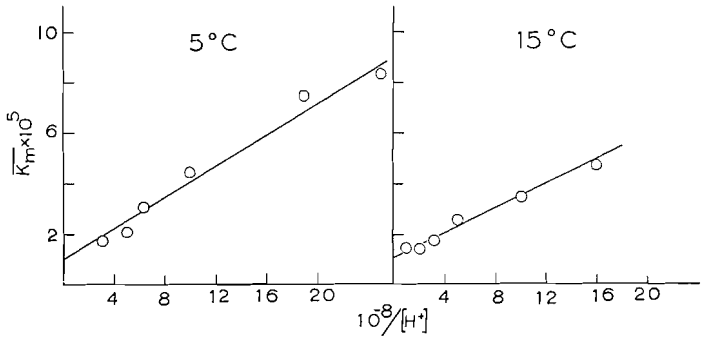


FIG. 6. Plots of K_m as a function of the reciprocal of hydrogen ion concentration.

TABLE I

pK_a and pK_b values for the active center of myosin at 15.1 and 5.2° C

	Temperature	pK_a	pK_b
Alberty and Massey's equation	5.2	8.60	7.60
	15.1	8.60	7.34
$\bar{K}_m$ vs. $[H^+]$ or $1/[H^+]$	5.2	8.53	7.60
	15.1	8.62	7.34

The two methods give similar values and an inspection of Fig. 4 indicates that these pK's correspond to pH where there are definite changes in direction in the $p\bar{K}_m$–pH curves (5).

The apparent heat of ionization of the group identified by pK_b is about 9 kcal/mole while that of the group identified by pK_a is close to zero with an indication that it might be an exothermic quantity.

The data represented in Figs. 5 and 6 show that the value of the pH-independent Michaelis constant is the same at 5.2 and 15.1° C at 1.05×10^{-5} mole/liter. This would suggest that the formation of the myosin–ATP complex is athermic, and is accompanied by an increase in entropy of about 23 e.u.

At high pH, the curves of $p\bar{K}_m$ vs. pH level off. Normally, this would be interpreted as a contribution of an ionizable group in the complex to the function representing $\bar{K}_m$. Such a function does not appear in the rate at high substrate concentration (Fig. 2), as there is no indication of a leveling of the curve. The experiments could not be carried to higher pH because of myosin inactivation (9).

DISCUSSION

The data presented in this paper do not follow the pattern expected from a simple system like the one suggested in the description of the data. No really satisfactory explanation has been given for the minimum in the rate-vs.-pH curve (Fig. 2). Two possibilities will be mentioned here.

The description of the rate as a function of pH can be handled by assuming several complexes like EH_2S, EHS, ES, all yielding products. From a purely formal point of view, one can easily show that $\bar{K}_m$ is still described by equation [3]. On the other hand $\bar{V}_m$ can be described accurately, if one uses three complexes. One can criticize that hypothesis from two different points of view. First, it is evident that the inclusion of a sufficient number of constants will allow a good description of the data. The constants used, in our opinion, cannot be interpreted to give any information on the process. Second, the hypothesis implies several mechanisms in parallel for the transformation of one substrate into given products by one enzyme. So the hypothesis should not be considered, except as an explanation available if no other one is justified.

One may rather assume that the active complex is unique (e.g. EHS) and that the odd behavior of $\bar{V}_m$ as a function of pH is due to the influence of other factors, probably the electrostatic charge. It can certainly be argued that the presence of a negative ion such as ATP in the active center can reduce considerably the tendency of hydrogen ion to leave the protein molecule. This could move pK_B from about 7.3 in the enzyme, to values higher than 10 in the enzyme–substrate complex and inactivation becomes important before it can be determined. The fact that the rate of the hydrolytic reaction does not vary with the pH could then be explained by the variation of the ionization constant K_B with pH. As will be seen later, such an explanation assumes that the charge of the complex varies with pH. No data are available on that particular point.

Other hypotheses, such as acid–base catalysis of the hydrolysis of the complex, have been considered. In all cases it appeared impossible to obtain information on the ionizing groups in the active center from the rate at high substrate concentration.

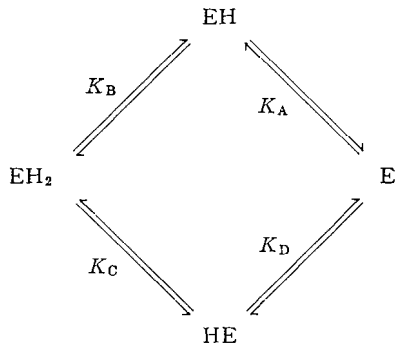
According to Dixon (5), concave bends in the $p\bar{K}_m$-vs.-pH plots are due to ionizing groups of either the enzyme or the free substrate. Investigations on the calcium activation of ATPase (15) suggest that the substrate of ATPase is the calcium salt of adenosine triphosphate, $ATPCa^{-2}$, for which Smith and Alberty (16) have reported a pK_a value of 5.3 at 0.2 ionic strength at 25° C. In the present experiments the pK appearing in the maxima of the $p\bar{K}_m$-vs.-pH graphs are all above 7 and are therefore too high to be due to the substrate in the form of $ATPCa^{-2}$. Nihei and Tonomura (2) have, however, interpreted their results on the pH-dependence of $\bar{K}_m$, which indicated a pK in the neighborhood of 6.8 at 25° C, by assuming that the "true" substrate is ATP^{-4} since, according to Smith and Alberty (16), this substance has a pK of 6.95 at 25° C and 0.2 ionic strength. The pK of ionization which we have estimated from Nihei and Tonomura's data at 25° C is not inconsistent with our data at 5 and 15° C, although using it in the calculations would give a heat of ionization of about 12 kcal/mole. However, Alberty *et al.* (17) report pK values for ATP^{-4} of 6.48 at 25° C and 6.50 at 38° C in 0.15 *M* sodium chloride, giving a negligible heat of ionization. It therefore seems that the interpretation given by Nihei and Tonomura is incorrect and that the substrate of ATPase is the calcium salt form of ATP. On this basis, we can conclude that the dissociation constants appearing in the maxima in the $p\bar{K}_m$-vs.-pH curves refer to the enzyme and not to the substrate.

The simplest description of the curve of $p\bar{K}_m$ vs. pH (Fig. 4) involves two ionization constants, K_a and K_b. As equation [3] contains ionization constants of the enzyme in the

numerator and ionization constants of the enzyme–substrate complex in the denominator, the possibility of a third group of the active center ionizing within the pH area considered is not eliminated. In order to describe the experimental data, with three groups, the third one with a pK around 9, one has only to assume that pK_b' is also about 9. This type of evidence cannot be used to show the existence of three ionizable groups in the active center, but it shows that our data are not sufficient to eliminate the possibility that three, maybe more, acid groups participate in the catalyzed reaction.

Alternate Dissociation Paths

In the presence of two acid groups, there are two ionization paths, as suggested by Alberty (18).



If K_a and K_b are experimental constants, they are related to the true constants by:

$$1/K_a = 1/K_A + 1/K_D \quad [5]$$

$$K_b = K_B + K_C. \quad [6]$$

In the simplest case of no interaction between the acid groups, i.e. if $K_A = K_C$ and $K_B = K_D$

$$K_{A \text{ or } B} = \frac{K_b \pm \sqrt{(K_b^2 - 4K_bK_a)}}{2}. \quad [7]$$

This equation imposes a minimum value of 4 to the ratio K_b/K_a, giving identical true ionization constants, $K_A = K_B$. This case has been reported by Alberty (18) in the fumarase case where, in acetate buffer, pK's of 5.9 and 6.5 are found.

If the ionization of one group does not affect the ionization of the other group, equation [7] gives at 5.2° C pK_B = 7.65 and pK_A = 8.55, while at 15° C pK_B = 7.37 and pK_A = 8.57. The correction on the pK is, however, within the limits of the experimental error and the hypothesis of no interaction possibly renders it insignificant. The important conclusion to be drawn from consideration of the alternate paths is that the actual nature of the ionized group is not known, that is, the one with a low pK could be unionized and the one with a high pK ionized in the most "stable" complex.

Electrostatic Effects

The influence of the electric charge of the molecule on the ionization process is much more important than the effects discussed above.

The two groups ionizing in the active center could be identical, if they are close so that the electrostatic charge developed on the ionized group reduces the tendency of the

second one to lose a proton. Differences of 1 and 1.3 are observed between the pK of symmetric dicarboxylic acids such as glutaric and succinic acids (19). In the case of myosin, it could be argued that a distance of about 7 Å between protons, based on the distance calculated from electrostatic effects in glutaric acid (19), is a reasonable quantity. However, the fact that the two groups have different heats of ionization, or that the difference between the pK of ionization varies with temperature, would suggest that the groups are of a different nature.

In order to estimate the influence of the electrostatic charge the following data on myosin are to be considered. According to Mihalyi (20), myosin has an isoionic point of about 5.75 in potassium chloride. At 15° C the molecule has lost 33 hydrogen ions on the average at pH 8.6 while at 5° C it has lost 30.5 hydrogen ions at the same pH. At pH 7.6, at 5° C, it has lost 25.2 protons and 24.5 at pH 7.35 at 15° C. All these data are reported to a weight of 10^5 grams of protein.

On the other hand, Lewis and Saroff (21) have found that most of the hydrogen ions are replaced by potassium ions at concentrations higher than 0.1 M of potassium chloride. The protein is, under these conditions, negatively charged if the pH is higher than about 5.8 (19, 21). In the presence of calcium chloride, electrophoresis experiments show that the protein is positively charged at pH 8.7 in 0.06 M calcium chloride (22). Under our conditions 0.01 M calcium chloride, 0.4 M potassium chloride, the charge on myosin is probably small, although it could be either positive or negative.

A semiquantitative treatment of the influence of the electrostatic charge Z on the ionization constant of an acid group on a protein is given by Scatchard (23).

[8] $$pK = pK_0 - 2wZ/2.3,$$

where w is given by

$$w = \frac{e^2}{2DkT}\left(\frac{1}{b} - \frac{\kappa}{1+\kappa a}\right).$$

The expression for w involves e the electronic charge, D the dielectric constant of the medium, k the Boltzman constant, T the absolute temperature, b the radius of the protein molecule assumed to be a sphere, and $\kappa/(1 + \kappa a)$ is a Debye–Hückel term including ionic strength effects. The quantity pK_0 is the pK at charge zero.

In the case of myosin, the correction is probably small, as the charge is small.

However, this effect explains the low value of the apparent heat of ionization for the group with a pK of 8.6. Myosin has a large number of ϵ amino residues with a heat of ionization of about 11 kcal/mole, and a pK around 10 at 25° C (24). At pH 8.6 these groups contribute to the charge of the proteins. If the temperature is raised 10° C the pK of a lysyl ϵ amino group is lowered by about 0.3 pK units, making the protein molecule more negative, at pH 8.6. If a group in the active center, with a pK at 8.6, has a heat of ionization of 6 to 7 kcal/mole, its pK is displaced by 0.15 to 0.18 pK unit for the same rise in temperature. But at the pH equal to the new pK, the charge of the protein is more negative, increasing the pK of ionization, following equation [8]. In the case of myosin, it appears that the lowering of the pK of ionization due to rise in temperature from 5 to 15° C is compensated by an increase in negative charge (or decrease in positive charge) due to ionization of ϵ amino groups.

The above interpretation requires that the heat of ionization of the group with a pK at 8.6 be smaller than that of ϵ amino groups. A value of 6 to 7 kcal/mole would be reasonable. The fact that the mobility of the protein is small in electrophoresis experiments would indicate a small charge on the enzyme and, probably, a small variation of

Z with pH in the region of pH 8.6. At pH 10, the increase in negative charge could be sufficient to eliminate the influence of pH on $p\bar{K}_m$, as the pK of ionization could well increase as fast as the pH. Erdös (24) has reported that in the presence of 0.1 M calcium chloride the electrophoretic mobility of myosin becomes suddenly negative as the pH is increased above 9.3 at an unspecified temperature.

Around pH 7.3, at 15° C, carboxylate groups affect the charge and the same effect probably contributes a rise in the heat of ionization. According to Mihalyi (20), the average heat of ionization of groups in myosin at pH 7.5 at 10° C, is very slightly above 5 kcal/mole, that is, lower than the value for histidyl (24) or sulphydryl (26) residues. Then, as the temperature is increased, the charge would have a tendency to become more positive as the pK is lowered, increasing the apparent temperature effect. This would lead to a true heat of ionization somewhat smaller than 9 kcal/mole for the group with a pK of 7.34 at 15° C.

Group in the Active Center

The suggestions on the nature of the groups in the active center of myosin will use the following conclusions. The first ionizable group has a pK of 7.34 at 15° C (7.1 at 25° C) and a heat of ionization smaller than 9 kcal/mole. As the charge on the protein is probably small, this value would be close to pK_0. Such values could well be attributed to the imidazole group of histidine, which has a pK_0 of ionization of 7.0 and a heat of ionization of 7 kcal/mole at 25° C (23).

The second group, with a pK of 8.6 and a heat of ionization significantly lower than 11 kcal/mole, would be attributed to a sulphydryl residue of cysteine. In cysteine itself, the pK of ionization of the —SH group is 8.5 for the species carrying no net charge (26). The heat of ionization of the —SH group of thioglycolic acid has been given as 7 kcal/mole (26). This identification would take into account the fact that *p*-chloromercuribenzoate, one of the best —SH inhibitors, inhibits myosin ATPase activity (27, 3) and that cysteine has been separated recently from the active center of myosin (28).

Suggestion of a Mechanism

Taking into account the fact that the substrate at very high concentration inhibits myosin, the above two groups, and a mechanism recently proposed by Krupka and Laidler (29) for the action of cholinesterase, we would like to suggest the following mechanism. ATP is bound in a regular Michaelis complex to an imidazole group and an unionized sulphydryl group of myosin. In the following step, the unionized SH group of myosin is phosphorylated to give enzyme $-S-PO_3^=$. This intermediate is then hydrolyzed with the participation of the imidazole group. This step is required to take substrate inhibition into account together with the large increase in pK_b observed when the substrate is attached to the enzyme. The hydrolysis of enzyme $-S-PO_3^=$ intermediate would be rate limiting.

CONCLUSION

The influence of hydrogen ion concentration on the rate of hydrolysis of ATP in the presence of myosin suggests that the active center of the enzyme is made of at least one imidazole and one sulphydryl group. A two-step mechanism similar to that proposed for the enzyme cholinesterase would explain the experimental results presented.

ACKNOWLEDGMENTS

The authors are grateful to the National Research Council for financial assistance.

One of us (G. E. P.) wishes to acknowledge the award of a Cominco and a Shell Oil Co. scholarship during the time this work was carried out.

REFERENCES

1. K. J. LAIDLER. The chemical kinetics of the enzyme action. Oxford, 1958. p. 280.
2. T. NIHEI and Y. TONOMURA. J. Biochem. (Tokyo), **46**, 305 (1959).
3. J. J. BLUM. Arch. Biochem. Biophys. **87**, 104 (1960).
4. K. J. LAIDLER. The chemical kinetics of enzyme action. Oxford, 1958. p. 117.
5. M. DIXON. Biochem. J. **55**, 161 (1953).
6. R. A. ALBERTY and V. MASSEY. Biochem. et Biophys. Acta, **12**, 347 (1954).
7. J. BOTTS and M. F. MORALES. J. Cellular Comp. Physiol. **37**, 27 (1951).
8. C. H. FISKE and J. SUBBAROW. J. Biol. Chem. **81**, 629 (1929).
9. G. E. PELLETIER and L. OUELLET. Can. J. Chem. **39**, 265 (1961).
10. F. W. H. M. MOMMAERTS and I. GREEN. J. Biol. Chem. **208**, 833 (1954).
11. Y. TONOMURA, S. WATANABE, and K. YAGI. J. Biochem. (Tokyo), **40**, 27 (1953).
12. J. J. BLUM. Arch. Biochem. Biophys. **43**, 176 (1953).
13. M. L. MORALES, A. J. OSBAHR, H. L. MARTIN, and R. W. CHAMBERS. Arch. Biochem. Biophys. **72**, 54 (1957).
14. H. LINEWEAVER and D. BURK. J. Am. Chem. Soc. **56**, 658 (1934).
15. G. E. PELLETIER and L. OUELLET. Can. J. Chem. **36**, 896 (1958).
16. R. M. SMITH and R. A. ALBERTY. J. Am. Chem. Soc. **78**, 2376 (1956).
17. R. A. WEBER, R. M. SMITH, and R. M. BOCK. J. Biol. Chem. **193**, 425 (1951).
18. R. A. ALBERTY. J. Cellular and Comp. Physiol. **47**, 245 (1956).
19. E. H. WESTHEIMER and M. W. SHOOKHOFF. J. Am. Chem. Soc. **61**, 555 (1939).
20. E. MIHALYI. Enzymologia, **14**, 224 (1950).
21. M. W. LEWIS and H. A. SAROFF. J. Am. Chem. Soc. **79**, 2112 (1957).
22. T. ERDÖS and O. SNELLMAN. Biochim. et Biophys. Acta, **2**, 672 (1948).
23. G. SCATCHARD. Ann. N.Y. Acad. Sci. **51**, 660 (1949).
24. E. J. COHN and J. T. EDSALL. Proteins, amino acids and peptides. Reinhold Publishing Corp., New York. 1943. p. 445.
25. T. ERDÖS. Acta Physiol. Acad. Sci. Hung. **7**, 1 (1955).
26. R. E. BENESCH and R. BENESCH. J. Am. Chem. Soc. **77**, 5877 (1955).
27. E. S. G. BARRON and T. P. SINGER. J. Biol. Chem. **157**, 221 (1945).
28. O. SNELLMAN. Acta Chem. Scand. **12**, 503 (1958).
29. R. M. KRUPKA and K. J. LAIDLER. Trans. Faraday Soc. **56**, 1467 (1960).

Can. J. Chem. Downloaded from www.nrcresearchpress.com by 210.87.254.105 on 09/05/12
For personal use only.

THE EFFECT OF INITIAL ACID CONCENTRATION ON THE LIGNIN ISOLATED BY THE ACIDOLYSIS OF ASPEN WOOD[1]

J. M. Pepper and M. Siddiqueullah[2]

ABSTRACT

A further study has been made of the isolation, by acidolysis, of lignin from aspen wood meal (*Populus tremuloides* Michx.) using a dioxane–water (9:1) solvent medium containing hydrogen chloride and a low extraction temperature of 87±2° for a short extraction time of 0.5 hour. Lignins so isolated included those: (*a*) under different initial acid concentrations of 0.0, 0.05, 0.1, 0.2, 0.3, 0.4, 0.5, 0.6, 0.8, and 1.7 equivalents of HCl/liter of solvent medium; (*b*) from successive extractions under increasing initial acid concentrations of 0.2, 0.4, 0.8, and 1.6 equivalents/liter; and (*c*) from successive extractions under constant initial acid concentrations of 0.2 equivalent/liter.

All the lignin fractions so isolated were studied with respect to their yield, methoxyl content, infrared absorption spectra, and the yields of vanillin and syringaldehyde obtained from them by oxidation using alkaline nitrobenzene.

Evidence is presented in support of the non-homogeneity of the whole protolignin. This may be the result of the presence of possibly two basic types. One fraction, comprising around 70–85%, is most readily extracted, has a consistently high methoxyl content (ca. 21%), and is capable of being oxidized to give high yields of syringaldehyde and vanillin in a ratio close to 2.5:1. The second fraction is characterized by a greater difficulty of extraction, lower methoxyl content, and significantly lower yields of the aldehydes in a ratio closer to 1:1.

In a previous communication, Pepper, Baylis, and Adler (1) reported a study of the effect of extraction time on the isolation and properties of the lignin fraction obtained by the acidolysis of spruce and aspen wood meals. The extractions were carried out under reflux for periods ranging from 0.5 to 48 hours using a constant initial hydrochloric acid concentration, namely 0.2 *N* with respect to the dioxane–water (9:1) solvent medium. As the time of extraction was increased, the yields of the isolated lignin fractions also increased, but the yields of phenolic aldehydes (vanillin from spruce or a mixture of vanillin and syringaldehyde from aspen) obtained from them by alkaline nitrobenzene oxidation gradually decreased. It was also shown that with increasing time of acidolysis of the aspen wood, a rise in the carbon-methyl to methoxyl ratio was observed for the isolated lignins. A similar finding had been made earlier for spruce lignin isolated under the same conditions (2). As a result of these studies, it was suggested that such a lignin fraction isolated under conditions of 1-hour extraction with the 0.2 *N* acid solvent may be only mildly modified during extraction and hence suitable for subsequent chemical investigation.

This report deals with a study of the effect of the initial acid concentration on the yield and nature of the lignin isolated by a similar acidolysis of aspen wood.

An extraction time of 0.5 hour was chosen and all extractions were effected at 87±2°, which represented a simmering state for all media. The lignin fractions so isolated are named by means of their association with the initial acid strengths of the solvent media, which were 0.0 *N*, 0.05 *N*, 0.1 *N*, 0.2 *N*, 0.4 *N*, 0.5 *N*, 0.6 *N*, 0.8 *N*, and 1.7 *N* expressed as equivalents of dry hydrogen chloride per liter of solvent medium. The yields of the lignins so isolated by this acidolysis procedure are given in Table I.

[1]*Manuscript received February 9, 1961.*
Contribution from the Department of Chemistry, University of Saskatchewan, Saskatoon, Saskatchewan. This paper constitutes part of the thesis submitted by M. Siddiqueullah in partial fulfillment of the requirements for the Ph.D. degree, September, 1960.
[2]*Colombo Plan student in Canada at the University of Saskatchewan, 1957–60.*

TABLE I

Effect of initial acid concentration on the isolation of aspen lignin*

Initial HCl (N)	Lignin recovery†	Initial HCl (N)	Lignin recovery†
0.0	1.6	0.4‡	63.0
0.05	17.1	0.5	69.4
0.1	22.2	0.6	72.9
0.2	44.0	0.8	74.8
		1.7	89.6

*Pre-extracted wood meal (25 g); dioxane–water (9:1) (500 ml); temperature, 87±2°; time, 0.5 hour, under nitrogen.
†Expressed as percentage of Klason lignin.
‡Media of concentrations of 0.4 and higher were two-phase systems at room temperature.

These results indicate that approximately 70–75% of the lignin is comparatively easily recoverable at lower acid concentrations, but that the isolation of the remainder requires higher initial acid concentrations. To study further the behavior of isolation of the lignin, extraction experiments were carried out along the following two lines: (1) lignin was isolated from the same wood meal by successive extractions under increasing initial acid concentrations (see Table II), and (2) lignin was isolated from the same wood meal by successive extractions under constant initial acid concentrations (see Table III).

TABLE II

Lignin isolation by successive extractions under increasing initial acid concentrations*

Initial HCl (N)	Isolated lignin	Recovery† (%)	Combined recovery† (%)
0.2	Lignin A	45.7	45.7
0.4	Lignin B	43.2	88.9
0.8	Lignin C	6.9	95.8
1.6	Lignin D	1.2	97.0

*Pre-extracted aspen wood meal (25 g) was successively extracted with increased normality of HCl in dioxane–water (9:1) (500 ml), at 87±2°, each extraction for 0.5 hour.
†Expressed as percentage of Klason lignin.

TABLE III

Lignin isolation by successive extractions under constant initial acid concentrations*

Isolated lignin	Recovery (%)†	Total combined recovery (%)†
Lignin A_1	43.2	43.2
Lignin A_2	12.1	55.3
Lignin A_3	4.4	59.7
Lignin A_4	1.2	60.9

*Pre-extracted wood meal (25 g) was successively extracted with 0.2 N HCl in dioxane–water (9:1) (500 ml), at 87±2°, each extraction for 0.5 hour.
†Expressed as a percentage of original Klason lignin.

General Description of Isolated Lignins

It was quite evident that as the conditions of isolation became more drastic the isolated lignin fractions showed progressive deterioration of color, ranging from a light tan-colored, 0.2 N lignin to a dark brown, 1.7 N lignin. The explanation of this change is not clear, but there is good evidence that under increasing initial conditions of acidity

Can. J. Chem. Downloaded from www.nrcresearchpress.com by 210.87.254.105 on 09/05/12
For personal use only.

a dark-colored material is isolated, in increasing amounts, which may be of rather different chemical composition* to the major lignin fraction (3). It is very probable that this change is caused by increasing condensation of the lignin.

A similar color change had been noted in the lignins isolated under similar acidolysis conditions with increasing time of extraction, and also in those lignin samples which were isolated originally by a 1-hour extraction and subsequently treated under similar conditions for varying times (1). This color change is not associated with any significant loss of methoxyl, but the conclusion that either some structural change is occurring or that lignin fractions having different structures are being isolated is borne out by the steadily decreasing yields of vanillin and syringaldehyde that are obtained by the alkaline nitrobenzene oxidation of these lignins.

Using approximately two milligrams of sample per 4 milliliters of solvent as a criterion of solubility, all the isolated lignins were found to be soluble in dioxane, glacial acetic acid, 80% ethanol, 80% methanol, and 80% acetone but insoluble in carbon tetrachloride, chloroform, acetone, ethanol, methanol, carbon disulphide, acetonitrile, and nitromethane. The various lignin samples were tested using the color reaction reported by Gierer (4) involving the coupling with quinone monochloroimide. An intense green-blue coloration, indicative of the presence of the *p*-hydroxybenzyl alcohol grouping, was obtained in all cases except for the 1.7 *N* lignin, lignin C, and lignin D. For these samples the test was very weak, or, if positive, was masked by the reddish-brown coloration of the original solution.

From the results of these isolation studies some conclusions may be drawn regarding the nature of the protolignin in the wood. From Table III, it is apparent that with successive extractions of wood meal using constant initial acid concentrations, the yields of recovered lignin decreased until on the fourth extraction only 1.2% of the original lignin was so recovered. It may be argued that if the protolignin were homogeneous, both with respect to its chemical structure and linkage to other cell components, and if no change were being effected under the conditions of isolation, a much more equal recovery by each extraction would have been expected. For aspen wood it may be that about seventy-five per cent of the total lignin is comparatively easily recoverable (see Tables I and III) but that the remaining part requires more drastic conditions for isolation. It is known that lignin is located both in the middle lamella and in other layers of the cell wall. According to Ritter (5) about seventy-five per cent is associated with the middle lamella and twenty-five per cent elsewhere. Even though this latter figure may be appreciably high, it is quite reasonable that the more easily isolated part, as obtained in these extraction experiments, may be the middle lamella lignin whilst the cell-wall lignins, if they are more intimately linked with carbohydrate, require the more drastic conditions for isolation.

All the isolated lignins described in Tables I, II, and III were analyzed for their methoxyl content and some representative samples were analyzed for carbon and hydrogen. These results are given in Table IV.

These few carbon and hydrogen analyses are sufficient to indicate that as the conditions of isolation become increasingly more drastic, the isolated lignins have increasing percentages of carbon and lower percentages of hydrogen. This is most simply explained by an increasing extent of an inter- or intra-molecular dehydration, but may in part

**It may be significant that these products had a methoxyl content ranging from 9.7 to 10.6%, which is half of that reported for the isolated lignins.*

Can. J. Chem. Downloaded from www.nrcresearchpress.com by 210.87.254.105 on 09/05/12
For personal use only.

TABLE IV

Analyses of isolated lignins

Isolated lignin	Methoxyl (%)	Isolated lignin	Methoxyl (%)
0.05 *N* lignin	20.3	Lignin A (0.2 *N*)§	21.2
0.2 *N**	20.7	B (0.4 *N*)‖	21.2
0.4 *N*	20.7	C (0.8 *N*)	18.5
0.5 *N*	20.5	D (1.6 *N*)	16.6
0.6 *N*	20.5	Lignin A_1	21.2
0.8 *N*†	20.5	A_2	20.9
1.7 *N*‡	19.1	A_3	20.7
		A_4	20.1

*C, 57.9; H, 6.31; ash, ca. 1%. †C, 59.9; H, 5.71; ash, ca. 1%. ‡C, 60.2; H, 5.58%. §C, 58.9; H, 6.02%. ‖C, 59.7; H, 5.96; ash, ca. 0.5%.

be due to the extraction of increasing amounts of a second lignin-like component having a higher carbon percentage.

The consistently high methoxyl content (av. 20.7%) obtained for all lignins except 1.7 *N* lignin, lignin C, and lignin D is in general agreement with the values of 19.8 and 21.5% methoxyl reported for native aspen lignin (6) and milled wood aspen lignin (7) respectively, both of which are considered to be representative lignins. It must be realized that the methoxyl content alone serves only to show that other non-lignin components are absent and is not necessarily a good criterion of the unchanged quality of the lignin. For example Klason aspen lignin, although drastically modified chemically as shown by the only trace amounts of vanillin and syringaldehyde obtainable by alkaline nitrobenzene oxidation, has a methoxyl content of 21.4%. The significantly lower methoxyl content of the 1.7 *N* lignin and lignins C and D may best be explained by the presence of either non-lignin (carbohydrate) residues carried by the lignin through chemical bondage or lower methoxyl-containing lignins such as those mentioned earlier. If this is so then the ability to isolate at least seventy-five per cent of the protolignin with a constant methoxyl content supports the belief that the major part of the lignin is of a higher methoxyl content than the remainder. This distinction may be related to the observation discussed earlier concerning the ease of isolation from which a similar conclusion was drawn.

From a survey of recent studies (8, 9, 10) it would appear that the major infrared investigations on lignin have been carried out to evaluate lignins obtained from the same species by different processes or from different species by the same process. No detailed spectroscopic investigation has been conducted for a study of the lignin fractions obtained from a particular species using the same general extraction procedure but under a variety of conditions. This would permit of a better understanding of the changes taking place in the same lignin substance as a result of the controlled changes in reaction conditions. Once the nature of the major functional groups present and the changes undergone by them are known, a clearer interpretation with respect to the structure of the lignin molecule may be made.

With this general objective, the infrared absorption spectra were determined on all the isolated lignins described in Tables I, II, and III, as well as those described previously (1), which had been isolated from aspen wood at constant initial acid concentrations (0.2 *N*) under increasing times of reactions from 0.5 hour through 48 hours. For purposes of comparison, spectra were also obtained on both aspen and spruce Klason lignins. Since

Can. J. Chem. Downloaded from www.nrcresearchpress.com by 210.87.254.105 on 09/05/12
For personal use only.

the spectra were determined on a qualitative basis only, minor variations, slight lessening or strengthening in the intensity of peaks, were not considered since they could arise due to the variation in the concentration of the sample. In their general nature all spectra for the hardwood (aspen) lignins were basically similar but were distinctly different from the spectrum of a typical softwood (spruce) lignin. This is in agreement with their known chemical differences and therefore adds support to the belief that an interpretation of such spectra may reveal chemical changes taking place in the lignin substance as a result of any series of studies on the effect of various chemical treatments such as those described in this investigation.

The sharpness of the strong, characteristic, aromatic ring vibrations absorption bands near 1600 cm^{-1} and 1500 cm^{-1} progressively decreased as the conditions of lignin isolation became more severe, until for the 48-hour lignin and for the aspen Klason lignin the bands had become distinctly broad. This indicates that a significant change is occurring involving the substitution pattern associated with the aromatic nuclei and is in agreement with the analytical data already discussed and with the decreasing yields of phenolic aldehydes obtained by alkaline nitrobenzene oxidation to be discussed later. A similar conclusion could be drawn regarding the observed progressive lessening in intensity of the 1225–1235 cm^{-1} band attributed to the aryl C—O (phenolic) stretching mode (10), indicative of some condensation involving phenolic hydroxyl groups.

The significant differences between the aspen and spruce infrared spectra are associated principally with the carbonyl band and the aromatic substitution pattern. For the spruce lignin a weak, broad band at 1660–1670 cm^{-1} was present but absent in all the aspen lignins, whilst the 1710–1725 cm^{-1} band was distinctly stronger for spruce than for aspen. These two bands have been associated with carbonyl groupings, the first according to Herger (10) being, "a ketone carbonyl alpha to an aromatic ring, with the *para*-position etherified and with an oxygen atom (as a hydroxyl group or etherified) in the two-position" and the second, a non-conjugated carbonyl group. Distinct, weak bands occurred in the spruce lignin spectrum at 855 cm^{-1} and 810–820 cm^{-1} and are characteristic of the guaiacyl nucleus and due to the monohydrogen and two adjacent ring hydrogen out-of-plane deformations respectively. For the aspen lignin, which contains both the syringyl (with only a monohydrogen deformation possible) and the guaiacyl nuclei, it is not surprising that only a weak, broad band at 830–850 cm^{-1} appeared as a result of a combination of the two types of nuclei.

All the isolated lignins recorded in Tables I, II, and III were oxidized using alkaline nitrobenzene and the yields of vanillin and syringaldehyde are recorded in Table V. The quantitative analytical procedure of Stone and Blundell (11) was used. It has been reported previously that the possible interference of acetovanillone and acetosyringone in the chromatographic procedure did not exist due to the absence of these compounds in the products obtained at 180° (12). No *p*-hydroxybenzaldehyde was detected in the lignin oxidation products.

Further evidence is hereby presented for the marked decrease in the percentage recoveries of both vanillin and syringaldehyde obtained by the oxidation of wood meal and calculated on the basis of the Klason lignin content. Some possible explanations of this observation have been discussed (13) but none is entirely satisfactory. Experimental evidence does support the belief that protolignin itself, or that lignin substance formed at the moment of liberation from its close association, either physical or chemical, with other cell-wall constituents, is very reactive and rapidly undergoes side-chain rearrangements and/or intramolecular condensations. The ease of such rearrangements in isolated

Can. J. Chem. Downloaded from www.nrcresearchpress.com by 210.87.254.105 on 09/05/12
For personal use only.

TABLE V

Alkaline nitrobenzene oxidation of isolated lignins

Lignin substance	Yield of oxidation products*†		
	Vanillin (V) (%)	Syringaldehyde (S) (%)	Molar ratio (S/V)
0.1 *N* lignin	8.0	19.7	2.1
0.2 *N*	6.7	19.3	2.4
0.4 *N*	6.7	19.9	2.5
0.5 *N*	6.3	19.4	2.6
0.6 *N*	5.7	17.3	2.5
0.8 *N*	5.6	16.4	2.4
1.7 *N*	5.3	14.8	2.3
Lignin A	6.7	21.7	2.7
Lignin B	6.7	17.5	2.2
Lignin C	5.3	7.3	1.1
Lignin D	4.8	5.8	1.0
Pre-extracted aspen wood‡	11.5	29.1	2.1

*Reported values are means of two separate analyses.
†Percentage yields calculated on a weight basis.
‡Percentage yields calculated on the basis of the Klason lignin content.

lignins whereby C-methyl groups are produced has been reported (1, 2). Such changes can be envisioned to destroy, at least in part, the linkages which give rise to the aldehydic group on oxidation. On the other hand, the rather consistent yields of both vanillin and syringaldehyde (Table V) obtained from those lignins isolated under increasing strengths of initial acid concentrations, at least up to until about seventy per cent of the lignin has been removed, suggest that, in the protolignin, two different structural units are present. Both such linkages may be cleaved to yield the phenolic aldehydes under the conditions of alkaline nitrobenzene oxidation but only one is destroyed by the more common processes of lignin isolation. Support for this suggestion is found in the decreasing yields of the phenolic aldehydes obtained from the 0.6 *N*, 0.8 *N*, and 1.7 *N* lignins and even more definitely in the yields obtained from lignins B, C, and D isolated by successive extractions under increasing initial acid concentrations (Table II).

Of equal interest and structural significance are the molar ratios of syringaldehyde to vanillin reported in Table V. For those fractions representing a total recovery of lignin of 80–85% (previously suggested as the middle lamella lignin) an average molar ratio of about 2.5 (2.1–2.7) is found; whereas for the remainder (previously suggested as cell-wall lignin) an average ratio of close to 1 is found. In a previous communication (1) the ratio of the yields of the phenolic aldehydes obtained by the oxidation of lignin samples isolated under increasing times of reaction using an initial acid concentration of 0.2 *N* have been reported. If these yields are calculated on a molar basis, similar ratios (2.0–2.6) to those found in this investigation are obtained. It was therein pointed out that it is difficult to correlate the average methoxyl content of approximately twenty-one per cent of at least the major part of the isolated lignin with this molar ratio of syringaldehyde to vanillin obtained by oxidation of these same lignins. On the basis of the widely believed assumption that hardwood lignin is of a complex polyconiferyl alcohol – polysinapyl alcohol nature, a molar ratio of these two different nuclei of from 2:1 to 1:1, depending on the extent of side-chain oxidation, would be required to analyze for about twenty-one per cent methoxyl. This is in direct contrast to the actual ratio of the phenolic aldehydes produced by oxidation. It may be that as a result of the chemical reactions occurring

Can. J. Chem. Downloaded from www.nrcresearchpress.com by 210.87.254.105 on 09/05/12
For personal use only.

during isolation, a greater proportion of vanillin-yielding nuclei than syringaldehyde-yielding nuclei are destroyed. However, the consistency of these experimental observations suggests that these ratios are of real structural significance. An attempt to correlate some of these data will be made in a forthcoming publication.

EXPERIMENTAL

Pre-extracted (alcohol–benzene) aspen sapwood meal (*Populus tremuloides* Michx.) similar to that in the work reported by Pepper, Baylis, and Adler (1) was used. It was dried to constant weight over P_2O_5. Anal: Klason lignin, 18.2%; methoxyl, 5.13%.

All dioxane was purified according to Fieser (14). All water was purified and carefully freed of oxygen prior to use. Gaseous hydrogen chloride was used to prepare the extraction solvents, the strength of the acidic media being obtained by titration against standard carbonate-free sodium hydroxide. All dioxane–water systems were prepared on a 9:1 v/v basis.

Lignin Isolation under Different Initial Acid Concentrations

Pre-extracted, vacuum-dried aspen wood meal (25 g) was placed in a 1-liter, four-necked, round bottom Pyrex flask, fitted with a reflux condenser, nitrogen inlet, dropping funnel, thermometer, and a three-way stopcock to a water pump. The flask was then evacuated. A pressure of 10–15 mm of mercury was maintained in the flask for 15–20 minutes. Then the stopcock leading to the pump was closed and the solvent (500 ml) was added from the dropping funnel slowly with caution so that no air entered the flask. When about half of the solvent had been added, the pressure was restored by slowly introducing nitrogen. The remaining half of the solvent was added. The contents of the flask were gradually heated over a period of 15–20 minutes with stirring to 87±2°. This temperature was maintained for 30 minutes. A slow stream of nitrogen, at the rate of 80–100 bubbles/minute was maintained throughout the period of heating and subsequent cooling.

After the reaction mixture had cooled down to 35–40°, it was filtered under a stream of nitrogen. The wood residue was washed with neutral dioxane–water (9:1) until the washings were colorless. The filtrate and washings were combined.

This red-brown filtrate was neutralized with solid sodium bicarbonate with stirring. It was then concentrated to 30–40 ml by distillation under reduced pressure (10–15 cm) to yield a dark syrupy liquid. The concentrate containing the bicarbonate sludge was transferred to a separatory funnel fitted to a 1-liter suction flask containing 500 ml of a 1% Na_2SO_4 solution in oxygen-free water.

By applying suction to the flask a partial vacuum was maintained inside it. The concentrate along with the sludge was then allowed to drop slowly into the sodium sulphate solution which was kept vigorously stirred. After the whole concentrate had been added, the precipitated lignin was recovered by centrifugation. It was then washed several times with a large excess of oxygen-free water until the washings were free from inorganic salts. Finally it was dried, while still lying in the centrifuge tubes, under vacuum over phosphorus pentoxide. It was then transferred to a weighing bottle and weighed.

Following this general procedure, lignin was isolated at the different initial acid concentrations of the solvent of 0.0 *N*, 0.05 *N*, 0.1 *N*, 0.2 *N*, 0.4 *N*, 0.5 *N*, 0.6 *N*, 0.8 *N*, 1.7 *N*.

Can. J. Chem. Downloaded from www.nrcresearchpress.com by 210.87.254.105 on 09/05/12
For personal use only.

Lignin Isolated by Successive Extractions under Increasing Initial Acid Concentrations

Pre-extracted wood meal (25 g) was first extracted with 0.2 *N* solvent and the lignin was recovered according to the procedure described above. The wood residue left after the precipitated lignin had been washed with neutral dioxane–water (9:1) was transferred to the previously used reaction flask. Again suction was applied for about thirty minutes and then the 0.4 *N* solvent was added and the extraction of the lignin and its recovery was carried out as usual. The wood residues were successively extracted in a similar fashion with the 0.8 *N* solvent and the 1.6 *N* solvent.

Lignin Isolation by Successive Extractions under Constant Initial Acid Concentrations

Pre-extracted wood meal (25 g) was successively extracted four times in a fashion similar to that described immediately above. In this case the initial concentration of the solvent for each extraction was the same (0.2 *N*).

Analytical Procedures

The methoxyl analyses were determined using the procedure of Gran (15). The infrared spectra were obtained using a Perkin–Elmer Model 21 spectrophotometer with sodium chloride optics and Nujol mulls. The alkaline nitrobenzene oxidations and quantitative estimations of the phenolic aldehydes were conducted according to the procedure of Stone and Blundell (11) with the recent modifications of Pepper and Siddiqueullah (12).

ACKNOWLEDGMENTS

We wish to express our thanks for the assistance given to one of us (M.S.) by the Pakistan Council of Scientific and Industrial Research during the tenure of a Colombo Plan Scholarship at the University of Saskatchewan. We also gratefully acknowledge the support of the National Research Council.

REFERENCES

1. J. M. PEPPER, P. E. T. BAYLIS, and E. ADLER. Can. J. Chem. **37**, 1241 (1959).
2. E. ADLER, J. M. PEPPER, and E. ERIKSOO. Ind. Eng. Chem. **49**, 1391 (1957).
3. J. M. PEPPER and M. SIDDIQUEULLAH. Unpublished results.
4. J. GIERER. Acta Chem. Scand. **8**, 1319 (1954).
5. G. J. RITTER. Ind. Eng. Chem. **17**, 1194 (1925).
6. M. A. BUCHANAN, F. E. BRAUNS, and R. L. LEAF. J. Am. Chem. Soc. **71**, 1297 (1949).
7. A. BJÖRKMAN. Ind. Eng. Chem. **49**, 1395 (1957).
8. F. F. NORD and W. J. SCHUBERT. Tappi, **40**, 285 (1957).
9. R. A. DURIE, B. M. LYNCH, and S. STERNHILL. Australian J. Chem. **13**, 156 (1960).
10. H. L. HERGERT. J. Org. Chem. **25**, 405 (1960).
11. J. E. STONE and N. J. BLUNDELL. Anal. Chem. **23**, 771 (1951).
12. J. M. PEPPER and M. SIDDIQUEULLAH. Can. J. Chem. **38**, 2324 (1961).
13. J. M. PEPPER. Tappi, **42**, 793 (1959).
14. L. F. FIESER. Experiments in organic chemistry. 3rd ed. D. C. Heath & Co. 1955.
15. G. GRAN. Svensk Papperstidn. **55**, 255 (1952).

Can. J. Chem. Downloaded from www.nrcresearchpress.com by 210.87.254.105 on 09/05/12
For personal use only.

Can. J. Chem. Downloaded from www.nrcresearchpress.com by 210.87.254.42 on 09/05/12
For personal use only.

THE FIVE-COMPONENT SYSTEM: LITHIUM–SODIUM–POTASSIUM–SULPHATE–CHLORIDE–WATER, AT 25° C[1]

A. N. CAMPBELL, E. M. KARTZMARK, AND H. M. HUTTON[2]

ABSTRACT

The system consisting of the ions Li_2^{++}, Na_2^{++}, K_2^{++}, $Cl_2^{=}$, $SO_4^{=}$, and water at 25° C has been investigated by the chemical analysis of the solutions and of the wet residues. In the solid model eight volumes were found where the following solid phases were in equilibrium with solution: $Li_2SO_4.H_2O$, K_2SO_4, $Na_2SO_4.10H_2O$, $K_3Na(SO_4)_2$, $KLiSO_4$, solid solution of Na_2SO_4 and Li_2SO_4, KCl, and NaCl. Anhydrous Na_2SO_4 was found to exist only as a surface in the solid diagram. Another volume, $LiCl.H_2O$, was not obtained experimentally owing to its close proximity to the LiCl corner of the diagram.

Five invariant points were discovered. No ternary salt was found to exist in the interior of the phase model at the temperature of this study, 25° C.

This paper marks the completion of a study of Campbell, Kartzmark, and their associates of the five-component system named in the title. Hitherto no such complete study has existed. Earlier papers (1) have dealt with the subsystems which had not previously been studied. All the component binary, ternary, and quaternary systems, including the reciprocal salt pairs, are now known at 25° C. There remained only the five-component system proper, represented graphically by the interior of the solid model.

EXPERIMENTAL PROCEDURE

Since the five quaternary subsystems were now completed and represented as the five surfaces (two triangular and three rectangular) of the Jänecke prism, the procedure adopted was to trace the paths of univariant curves from the corresponding quaternary invariant points on the outside surfaces till they met in quinquenary invariant points in the body of the diagram. This was accomplished experimentally by saturating with the phases of the quaternary invariant equilibrium, then adding increasing quantities of ions not participating in the quaternary equilibrium, and thus delineating the space curves. Since quinquenary invariant points mark the intersection of four curves (four solid phases), it was possible to check all these invariant points by approaching them along independent curves and this was always done. The experimental test for invariance was found in the sudden occurrence of a new ion in the solid phase, which was, of course, analyzed every time. The occurrence in large amount of a fresh ion is definitive, except for the change of sodium sulphate decahydrate to anhydrous sulphate, but here the change of water content was conclusive.

As an aid to clear thinking we constructed, while the experimental work was in progress, a solid model of stout wire, and suspended our analyzed points in the body of the model at the appropriate distances from the ends of the prism. In this way the direction of a line in space could be visualized.

As to the technique of solubility work, this has been too frequently described for mention here. Chloride ion was determined gravimetrically as silver chloride but the direct determination of sulphate ion as barium sulphate was avoided since we have found this to be completely inaccurate in the presence of alkali metal ions. Sulphate ion was determined solely by difference. Flame photometry was used to determine the alkali metal cations: our instrument was the Perkin–Elmer flame photometer. The accuracy of cation estimation was about two per cent but this is much better than can be attained by any other method of alkali determination in mixtures of alkali cations.

[1]*Manuscript received February 23, 1961.*
Contribution from the Chemistry Department, University of Manitoba, Winnipeg, Manitoba.
[2]*Holder of Cominco Fellowship, 1959–60.*

Can. J. Chem. Downloaded from www.nrcresearchpress.com by 210.87.254.42 on 09/05/12
For personal use only.

Since it is important to know the nature of the solid phases in contact with saturated solutions, it would be very desirable to have unequivocal methods of doing this but the usual methods, viz. X-ray powder photography or measurement of optical properties could not be applied because of the necessity of keeping the solid phase wet with equilibrium solution. If the solid phases are allowed to dry, phase change may occur, even at room temperature. Furthermore, the strongest X-ray reflections of sodium chloride and of sodium sulphate happen to be very close together, so that the X-ray method is less sensitive than usual. Consequently, we were forced to rest our determinations of the nature of solid phases entirely on the identification of the new phase which appeared at an invariant point. When a new ion suddenly appears, in quantity, in the solid phase, there is usually no question regarding the nature of the new phase. Moreover, the intersection of two or more solubility curves left little doubt about the nature of the four solid phases present at the invariant point.

EXPERIMENTAL RESULTS

The experimental results are given in Table I, which gives the mole% of each of Li_2^{++}, Na_2^{++}, K_2^{++}, $Cl_2^{=}$, and $SO_4^{=}$ in both the solid phase and the liquid phase, as well as m, the number of moles of water per "mole" of salt, and the nature of the solid phase.

Pictures of the equilibrium diagrams are shown in Fig. 1, with the invariant points marked as outlined in the caption. These are the solids in equilibrium with solution at 25° C. The photographs in Fig. 1 show the approximate positions of the quinquenary invariant points. To help differentiate the various lines in the prism, the quaternary lines on the surface are grey, while the quinquenary lines inside the prism are black. Picture (*a*) is shown with the K_2SO_4 corner nearest the right front; in picture (*b*) the NaCl corner is forward, presenting a view diagonally opposite to the first picture. Due to the difficulties in assembling this solder-and-wire diagram, the lines and invariant points are positioned only approximately. With the experimental data obtained, the invariants marked 2 and 4 in the photographs, Fig. 1, should be closer than indicated, actually almost touching.

One other invariant point, $LiCl.H_2O$, $Li_2SO_4.H_2O$, NaCl, KCl, in equilibrium with solution, exists in this system, but could not be obtained experimentally or even represented on this diagram. It is situated in the LiCl corner of the prism and theoretically is represented by the expanded diagram, Fig. 2.

The small volume which the lithium chloride salt occupies is the result of the powerful action of this chloride in displacing other salts from solution. This was expected from the data of the quaternary systems.

To illustrate the existence of the volumes indicating solution saturated with one salt, approximate cross sections at constant anion composition were drawn, using the three-dimensional wire model as a guide. The 16 diagrams are represented in Figs. 3–18.

Figure 3 is the sulphate end of the prism. In this system all the sulphates, $Li_2SO_4.H_2O$, K_2SO_4, and $Na_2SO_4.10H_2O$, are present with Na_2SO_4 anhydrous represented by the lines *ab*, and *ab'*. Only two addition compounds, $KLiSO_4$ and $K_3Na(SO_4)_2$, exist; at this temperature solid solution occurs between the lithium and sodium sulphates. Figures 4 and 5 show the change of the $Li_2SO_4.H_2O$, solid solution, and $Na_2SO_4.10H_2O$ areas. In Fig. 6, at the quinquenary invariant point (No. 5), where $K_3Na(SO_4)_2$, $KLiSO_4$, Na_2SO_4, $Na_2SO_4.10H_2O$ are the solids in excess in solution, another small wedge of solid solution appears: Na_2SO_4 anhydrous is still represented on the surface of the solid solution, that is *ab*, *ab'*, and *ab''*. Past this quinquenary invariant, in Fig. 7, $Na_2SO_4.10H_2O$

Can. J. Chem. Downloaded from www.nrcresearchpress.com by 210.87.254.42 on 09/05/12
For personal use only.

TABLE I

	Mole per cent solid phase					Mole per cent liquid phase						
No.	Li_2^{++}	Na_2^{++}	K_2^{++}	Cl_2^{--}	SO_4^{--}	Li_2^{++}	Na_2^{++}	K_2^{++}	Cl_2^{--}	SO_4^{--}	Water content*	Nature of solid phase
1	5.0	10.6	33.7	0.7	50.0	23.3	8.7	17.3	9.8	40.9	24.2	K_2SO_4, $K_3Na(SO_4)_2$, $KLiSO_4$
2	24.1	6.9	17.4	10.8	40.8	22.1	8.8	19.8	21.7	27.6	20.0	K_2SO_4, $K_3Na(SO_4)_2$, $KLiSO_4$
3	16.4	4.9	27.6	4.6	46.5	16.0	13.3	20.0	45.7	5.0	17.3	K_2SO_4, $K_3Na(SO_4)_2$, $KLiSO_4$, KCl
4	14.5	0.2	35.6	22.6	27.1	21.6	4.3	24.3	45.7	4.1	18.4	K_2SO_4, $KLiSO_4$, KCl
5	19.1	3.7	26.7	3.4	47.1	18.0	14.6	21.4	41.9	4.2	18.2	K_2SO_4, $K_3Na(SO_4)_2$, $KLiSO_4$, KCl
6	28.8	11.3	11.0	13.7	35.2	3.2	15.3	31.4	48.1	2.0		K_2SO_4, $K_3Na(SO_4)_2$, KCl
7	1.2	10.5	39.9	12.3	36.1	7.5	14.2	29.7	45.7	2.9	18.5	K_2SO_4, $K_3Na(SO_4)_2$, KCl
8	1.0	7.8	43.6	23.2	24.4	12.0	11.0	27.3	45.7	4.0	18.4	K_2SO_4, $K_3Na(SO_4)_2$, KCl
9	1.0	11.6	40.3	14.3	32.8	14.3	12.5	24.0	45.3	3.9	17.7	K_2SO_4, $K_3Na(SO_4)_2$, KCl
10	6.2	1.9	43.9	37.1	11.0	16.3	13.1	21.8	45.1	3.7	17.0	K_2SO_4, $K_3Na(SO_4)_2$, KCl
	Average invariant point #1					17.0	13.9	20.7	43.8	4.6	17.8	K_2SO_4, $K_3Na(SO_4)_2$, $KLiSO_4$, KCl
11	0.4	36.1	14.9	40.0	8.6	5.8	31.0	14.4	45.9	2.9	14.4	$K_3Na(SO_4)_2$, KCl, NaCl
12	9.5	31.7	9.6	33.2	16.0	18.1	21.5	11.9	46.5	2.0	14.4	$K_3Na(SO_4)_2$, KCl, NaCl
13	11.2	29.1	9.1	33.9	16.7	23.7	16.4	10.1	47.7	2.2	14.3	$K_3Na(SO_4)_2$, KCl, NaCl
14	20.7	9.8	19.2	26.7	23.6	25.9	14.9	10.2	47.4	1.6	14.3	$K_3Na(SO_4)_2$, KCl, NaCl
15	10.7	30.8	9.9	32.7	15.9	37.5	6.8	6.2	48.1	1.4	13.0	$KLiSO_4$, NaCl, KCl
16	9.6	31.0	9.1	36.3	14.0	36.1	7.3	6.9	48.5	1.2	13.4	$KLiSO_4$, NaCl, KCl
17	26.2	11.2	10.7	24.4	27.5	33.5	9.9	6.2	47.2	3.2	15.6	$KLiSO_4$, NaCl, KCl
18	6.9	34.2	9.1	38.7	11.1	30.8	11.6	7.5	47.7	2.4	22.5	$KLiSO_4$, NaCl, KCl
19	9.5	34.4	8.6	32.4	15.1	28.4	12.3	8.0	48.9	2.4	14.1	$KLiSO_4$, $K_3Na(SO_4)_2$, KCl, NaCl
20	11.0	0.9	37.1	26.9	24.1	21.0	12.5	16.4	46.1	4.0	16.5	$KLiSO_4$, $K_3Na(SO_4)_2$, KCl
21	24.9	0.9	24.7	3.3	6.2	25.3	12.9	12.5	46.5	2.8	16.1	$KLiSO_4$, $K_3Na(SO_4)_2$, KCl
22	18.4	7.5	20.1	31.2	22.8	28.2	12.5	8.4	48.5	2.4	14.0	$KLiSO_4$, $K_3Na(SO_4)_2$, KCl, NaCl
	Average invariant point #2					28.3	12.4	8.2	48.7	2.4	14.1	$KLiSO_4$, $K_3Na(SO_4)_2$, KCl, NaCl
23	28.8	0.2	21.2	23.9	25.9	40.9	3.0	6.1	48.5	1.5	25.6	$KLiSO_4$, $Li_2SO_4.H_2O$, KCl
24	25.0	7.3	17.4	27.4	22.9	39.5	4.3	5.1	49.9	1.2	12.5	$KLiSO_4$, $Li_2SO_4.H_2O$, KCl
25	20.2	18.9	9.5	32.8	18.6	38.4	5.2	5.6	49.1	1.7	12.9	$KLiSO_4$, $Li_2SO_4.H_2O$, KCl
26	22.5	10.0	17.3	21.6	28.6	38.6	5.6	5.9	48.7	1.2	12.8	$KLiSO_4$, $Li_2SO_4.H_2O$, KCl, NaCl
27	20.7	19.4	10.2	27.9	21.8	38.7	6.8	5.4	47.7	1.4	12.8	$KLiSO_4$, $Li_2SO_4.H_2O$, KCl, NaCl
28	38.4	6.4	5.5	2.6	47.1	43.5	6.3	1.1	12.8	36.3	16.9	$KLiSO_4$, $Li_2SO_4.H_2O$, solid solution
29	32.9	8.9	8.2	6.3	43.7	41.2	7.3	1.3	30.2	20.0	18.0	$KLiSO_4$, $Li_2SO_4.H_2O$, solid solution
30	31.4	10.4	8.9	11.9	37.4	41.2	7.0	1.8	37.2	12.8	17.8	$KLiSO_4$, $Li_2SO_4.H_2O$, solid solution
31	32.3	10.0	8.0	17.0	32.7	39.6	7.8	2.4	43.3	6.9	16.8	$KLiSO_4$, $Li_2SO_4.H_2O$, solid solution
32	27.8	13.3	11.8	12.0	35.1	40.2	4.8	5.3	47.3	2.4	14.6	$KLiSO_4$, $Li_2SO_4.H_2O$, solid solution
33	13.2	28.1	8.4	38.8	11.5	39.4	5.1	5.5	48.6	1.4	12.7	$KLiSO_4$, $Li_2SO_4.H_2O$, NaCl, KCl
	Average invariant point #3					38.9	5.8	5.6	48.3	1.4	12.8	$KLiSO_4$, $Li_2SO_4.H_2O$, NaCl, KCl

Can. J. Chem. Downloaded from www.nrcresearchpress.com by 210.87.254.42 on 09/05/12
For personal use only.

TABLE I (*Concluded*)

	Mole per cent solid phase					Mole per cent liquid phase						
No.	Li_2^{++}	Na_2^{++}	K_2^{++}	Cl_2^{--}	SO_4^{--}	Li_2^{++}	Na_2^{++}	K_2^{++}	Cl_2^{--}	SO_4^{--}	Water content*	Nature of solid phase
34	16.8	25.6	7.9	36.6	13.1	42.3	2.8	3.9	50.2	0.8	11.9	$Li_2SO_4.H_2O$, NaCl, KCl
35	15.7	23.9	8.7	39.7	12.0	46.1	0.9	2.5	50.1	0.4	10.0	$Li_2SO_4.H_2O$, NaCl, KCl
36	1.5	33.7	13.7	26.7	24.4	6.5	36.4	5.7	37.8	13.6	14.3	$K_3Na(SO_4)_2$, NaCl, solid solution
37	13.7	28.7	7.8	23.9	25.9	13.1	30.2	6.9	43.4	6.4	15.3	$K_3Na(SO_4)_2$, NaCl, solid solution
38	14.0	30.4	6.2	28.4	21.0	21.5	23.4	5.1	46.1	3.9	15.4	$K_3Na(SO_4)_2$, NaCl, solid solution
39	16.0	27.2	5.9	30.2	20.7	30.6	14.3	5.2	47.5	2.4	14.8	$K_3Na(SO_4)_2$, $Li_2SO_4.H_2O$, $KLiSO_4$, NaCl
40	23.9	24.1	2.0	25.5	24.5	34.4	15.1	1.0	44.7	4.9	15.0	$Li_2SO_4.H_2O$, NaCl, solid solution
41	25.4	20.5	4.7	23.9	25.5	35.1	15.5	1.0	44.4	4.0	14.9	$Li_2SO_4.H_2O$, NaCl, solid solution
42	27.9	14.5	9.6	14.6	33.4	31.5	15.9	3.4	45.5	3.7	15.8	$Li_2SO_4.H_2O$, NaCl, solid solution
43	22.8	14.1	10.4	14.7	38.0	29.8	15.3	4.3	47.7	2.9	15.2	$Li_2SO_4.H_2O$, $K_3Na(SO_4)_2$, $KLiSO_4$, NaCl
	Average invariant point #4					30.2	14.8	4.8	47.6	2.6	15.0	$Li_2SO_4.H_2O$, $K_3Na(SO_4)_2$, $KLiSO_4$, NaCl
44	26.1	12.5	10.7	10.6	40.1	29.9	13.1	6.2	46.1	4.7	16.4	$K_3Na(SO_4)_2$, $KLiSO_4$, solid solution
45	24.8	13.7	10.5	11.8	39.2	29.8	16.6	4.0	44.1	5.5	17.0	$K_3Na(SO_4)_2$, $KLiSO_4$, solid solution
46	26.2	13.0	10.9	6.4	43.5	29.7	14.7	6.5	38.0	11.1	19.1	$K_3Na(SO_4)_2$, $KLiSO_4$, solid solution
47	25.5	15.3	10.6	4.6	44.0	22.7	24.0	3.6	26.3	23.4	18.4	$K_3Na(SO_4)_2$, $KLiSO_4$, solid solution
48	17.2	22.7	10.2	3.1	46.8	10.2	33.4	6.9	29.1	20.4	15.9	$K_3Na(SO_4)_2$, $KLiSO_4$, solid solution
49	5.9	42.3	2.1	1.1	48.6	4.3	41.6	5.1	17.7	31.3	15.1	$K_3Na(SO_4)_2$, Na_2SO_4, $Na_2SO_4.10H_2O$
50	5.9	33.7	8.9	1.7	49.8	4.2	40.3	5.1	18.5	31.9	15.3	$K_3Na(SO_4)_2$, Na_2SO_4, $Na_2SO_4.10H_2O$
51	12.3	38.5	1.6	0.9	46.7	8.2	35.1	6.3	17.5	32.9	16.1	$K_3Na(SO_4)_2$, Na_2SO_4, $Na_2SO_4.10H_2O$
52	9.6	32.6	8.6	1.7	47.5	9.5	34.5	6.5	16.9	32.6	16.6	$K_3Na(SO_4)_2$, Na_2SO_4, $Na_2SO_4.10H_2O$, $KLiSO_4$
53	0.8	41.5	8.8	0.4	48.5	7.9	35.1	6.4	4.6	46.0	15.8	$K_3Na(SO_4)_2$, Na_2SO_4, $Na_2SO_4.10H_2O$
54	1.4	21.2	29.3	0.6	47.5	8.1	37.1	5.6	6.6	42.6	15.1	$K_3Na(SO_4)_2$, Na_2SO_4, $Na_2SO_4.10H_2O$
55	7.8	31.1	10.5	0.6	50.0	8.1	35.7	6.1	9.3	40.8	15.6	$K_3Na(SO_4)_2$, Na_2SO_4, $Na_2SO_4.10H_2O$
56	8.6	34.7	6.5	1.5	48.7	9.6	34.0	6.4	18.2	31.8	16.3	$K_3Na(SO_4)_2$, $KLiSO_4$, Na_2SO_4, $Na_2SO_4.10H_2O$
57	22.8	15.0	12.2	0.6	49.4	20.5	24.5	4.6	4.9	45.5	16.5	$K_3Na(SO_4)_2$, $KLiSO_4$, Na_2SO_4
58	24.4	16.0	10.4	2.0	47.2	19.5	27.3	3.5	9.4	40.3	17.2	$K_3Na(SO_4)_2$, $KLiSO_4$, Na_2SO_4
59	19.3	15.5	14.8	1.8	48.6	10.3	34.5	5.8	17.3	32.1	16.2	$K_3Na(SO_4)_2$, $KLiSO_4$, Na_2SO_4, $Na_2SO_4.10H_2O$
	Average invariant point #5					9.8	34.3	6.2	17.5	32.2	16.4	$K_3Na(SO_4)_2$, $KLiSO_4$, Na_2SO_4, $Na_2SO_4.10H_2O$

*Moles of water per mole of salt.

Can. J. Chem. Downloaded from www.nrcresearchpress.com by 210.87.254.42 on 09/05/12
For personal use only.

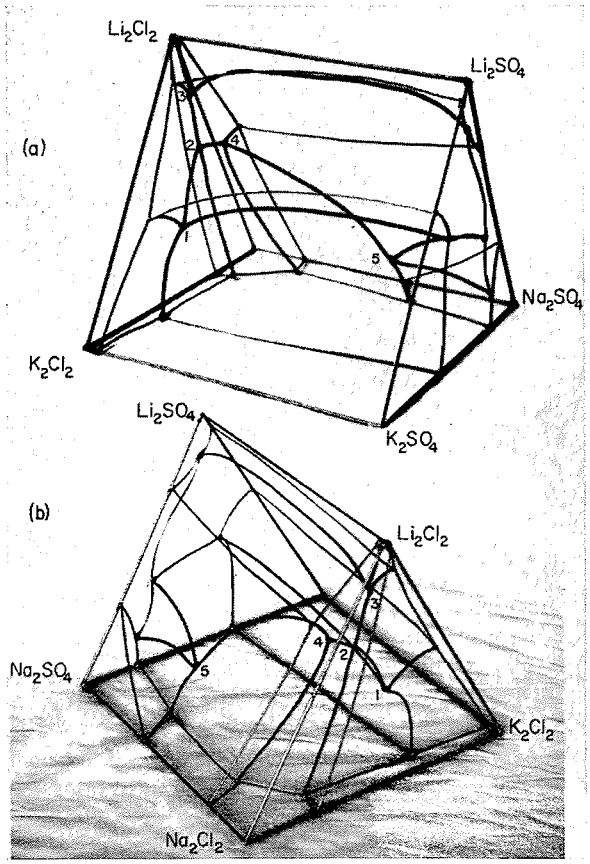


FIG. 1. 1. K_2SO_4, $K_3Na(SO_4)_2$, $KLiSO_4$, KCl
2. $KLiSO_4$, $K_3Na(SO_4)_2$, KCl, NaCl
3. $KLiSO_4$, $Li_2SO_4.H_2O$, NaCl, KCl
4. $Li_2SO_4.H_2O$, $K_3Na(SO_4)_2$, $KLiSO_4$, NaCl
5. $K_3Na(SO_4)_2$, $KLiSO_4$, Na_2SO_4, $Na_2SO_4.10H_2O$

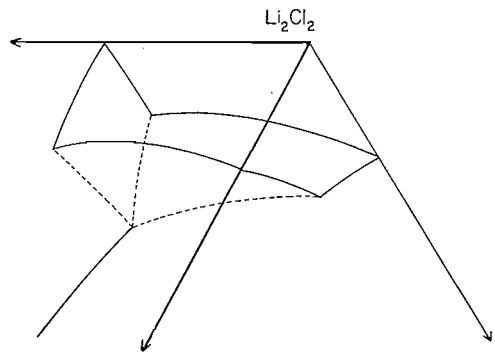
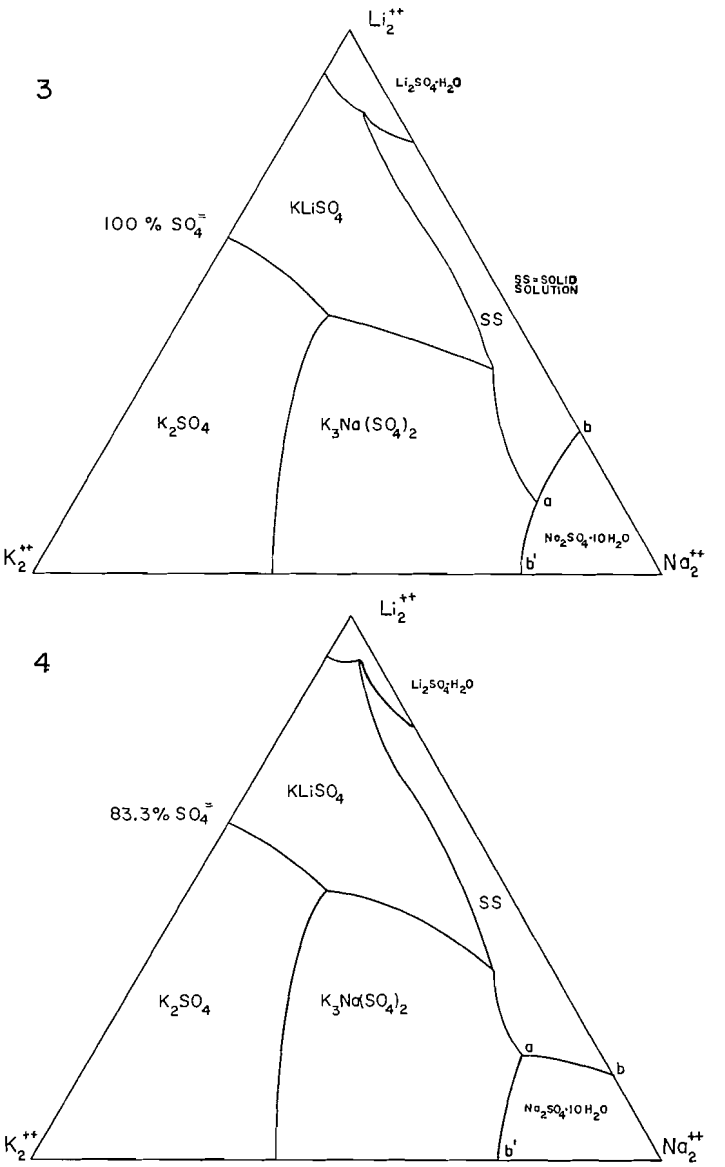


FIG. 2.

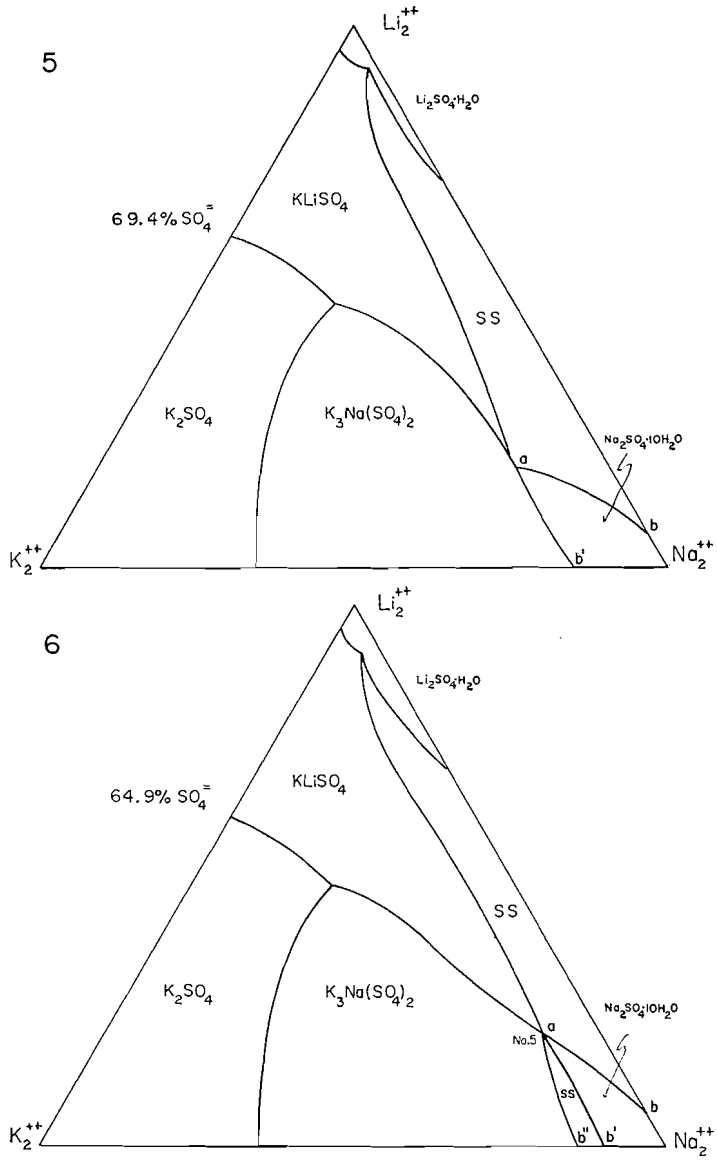
Can. J. Chem. Downloaded from www.nrcresearchpress.com by 210.87.254.42 on 09/05/12
For personal use only.



FIGS. 3 AND 4.

is still evident, with the anhydrous form existing on the base below the solid solution. Finally in Fig. 8 the decahydrate volume has vanished. In this interval the $KLiSO_4$–$K_3Na(SO_4)_2$ surface has been tilted upward at the $KLiSO_4 - K_3Na(SO_4)_2$ – solid solution line, as evident in Fig. 9. The first appearance of a chloride, NaCl, is observed in Fig. 10, its area increasing in Figs. 11 and 12, at the expense of the solid solution region. Figure 13

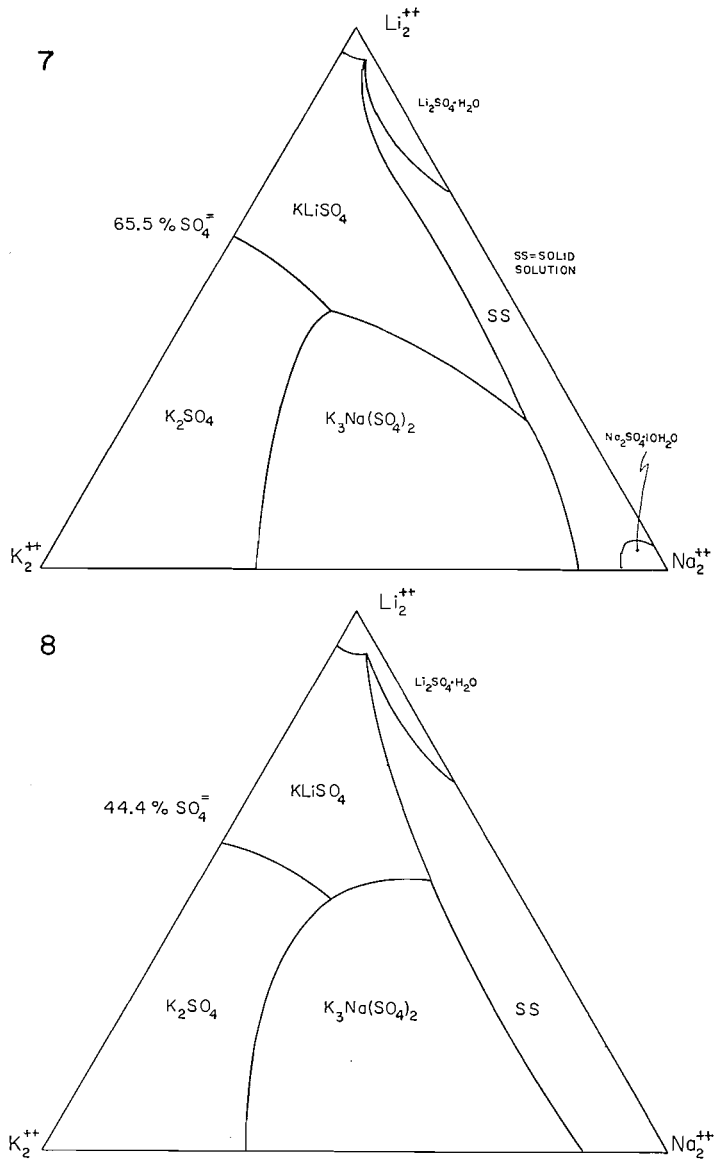
Can. J. Chem. Downloaded from www.nrcresearchpress.com by 210.87.254.42 on 09/05/12
For personal use only.



FIGS. 5 AND 6.

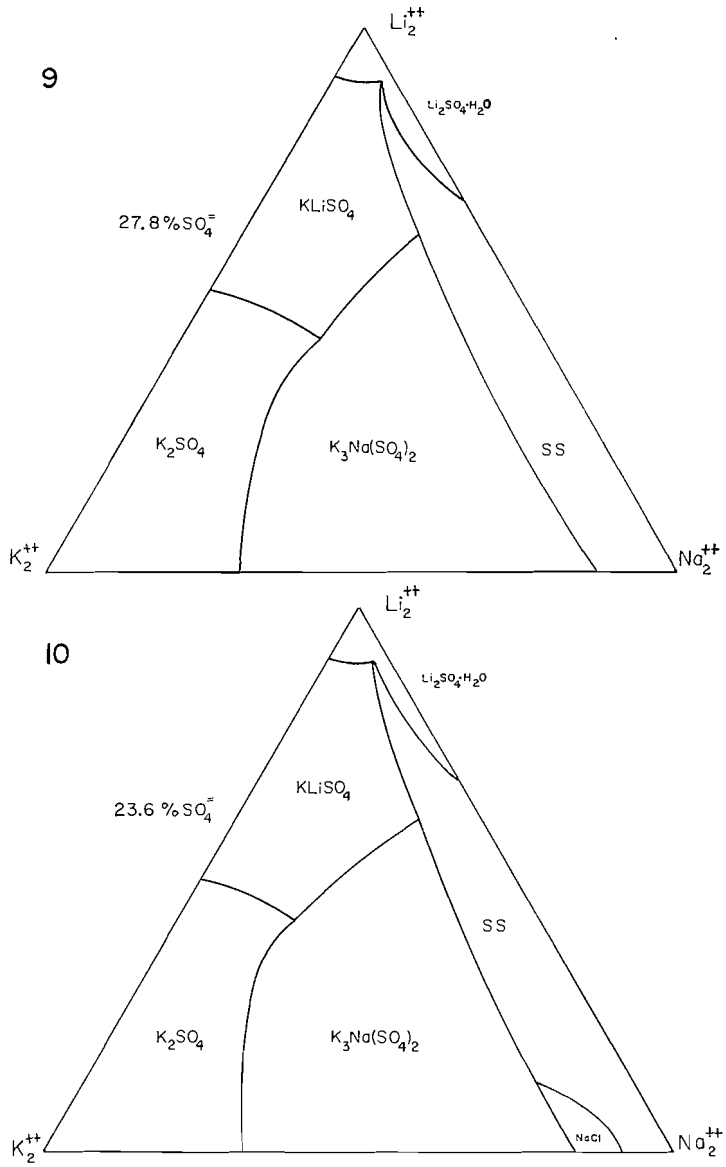
is drawn through the quaternary invariant point $Li_2SO_4.H_2O$, solid solution, NaCl in the lithium–sodium–chloride–sulphate–water system. Solid solution here is completely in the body of the diagram and in Fig. 14 it is quickly disappearing as another quinquenary invariant is approaching. Figure 14 also represents the quinquenary invariant (No. 1) $KLiSO_4$, $K_3Na(SO_4)_2$, K_2SO_4, KCl; KCl appears for the first time, but cannot

Can. J. Chem. Downloaded from www.nrcresearchpress.com by 210.87.254.42 on 09/05/12
For personal use only.



FIGS. 7 AND 8.

be represented since it is on the plane immediately behind Fig. 14. In Fig. 15, the invariant $K_3Na(SO_4)_2$, $KLiSO_4$, Li_2SO_4, $Li_2SO_4.H_2O$, NaCl (No. 4) has been reached, this being one extremity of solid solution, that is, lithium sulphate; K_2SO_4 has all but disappeared. This surface represents the last plane of existence of the double salts $KLiSO_4$ and $Na_3K(SO_4)_2$. Between Figs. 15 and 16, the $Li_2SO_4.H_2O$ – NaCl line has moved rapidly

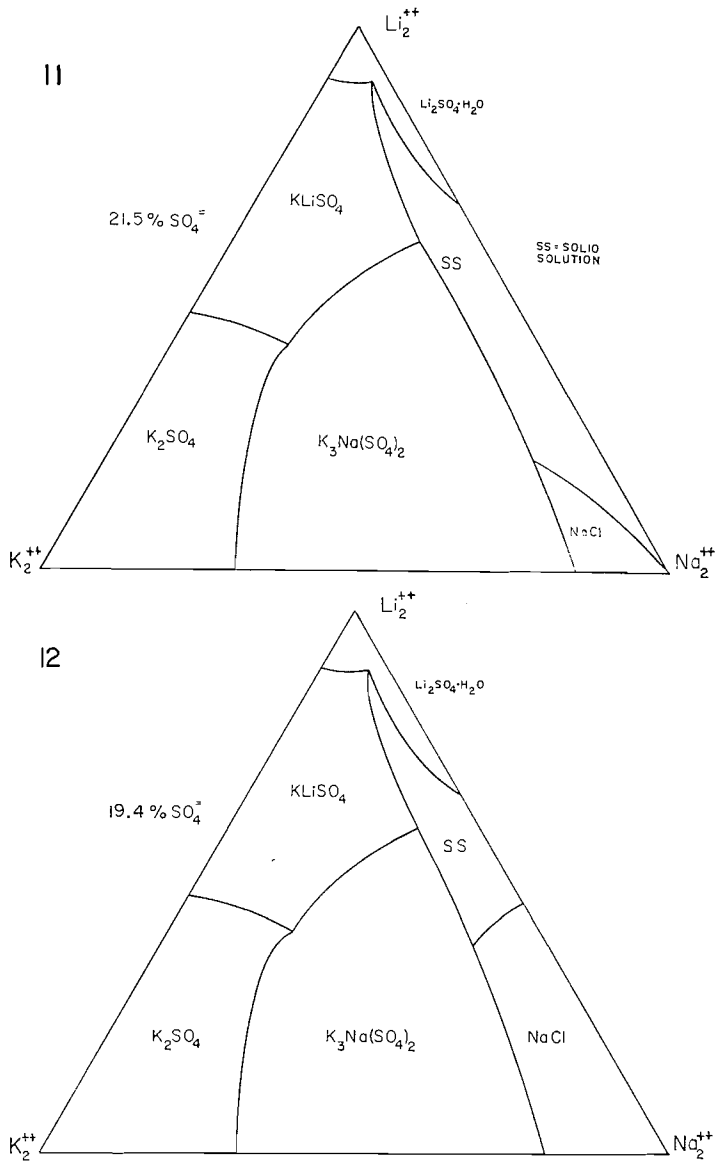


FIGS. 9 AND 10.

upward. Two quinquenary invariants are evident in Fig. 16: the $Li_2SO_4.H_2O$, $KLiSO_4$, NaCl, KCl (No. 3) and $Na_3K(SO_4)_2$, $KLiSO_4$, NaCl, KCl (No. 2) invariants, although not all the salts can be represented. Figure 17 shows the existence of the chlorides of sodium and potassium and the sulphate of lithium. The last, Fig. 18, where only the chlorides are present, represents only the sodium and potassium chlorides. Lithium

Can. J. Chem. Downloaded from www.nrcresearchpress.com by 210.87.254.42 on 09/05/12
For personal use only.

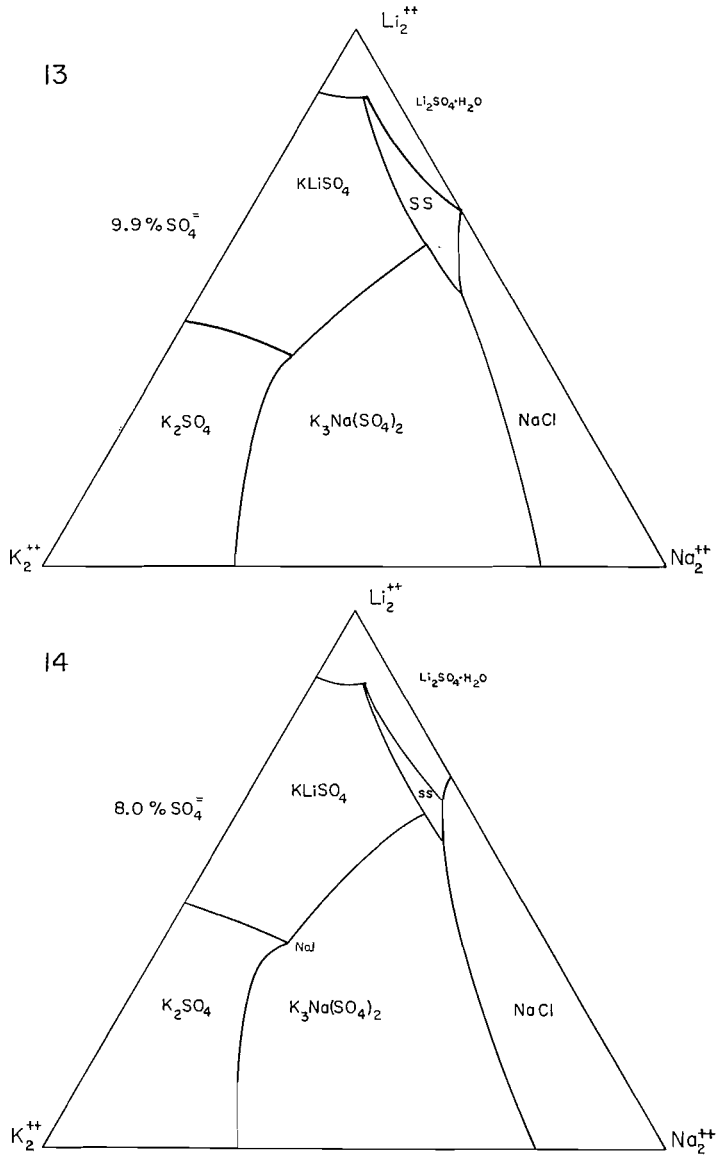
Can. J. Chem. Downloaded from www.nrcresearchpress.com by 210.87.254.42 on 09/05/12
For personal use only.



FIGS. 11 AND 12.

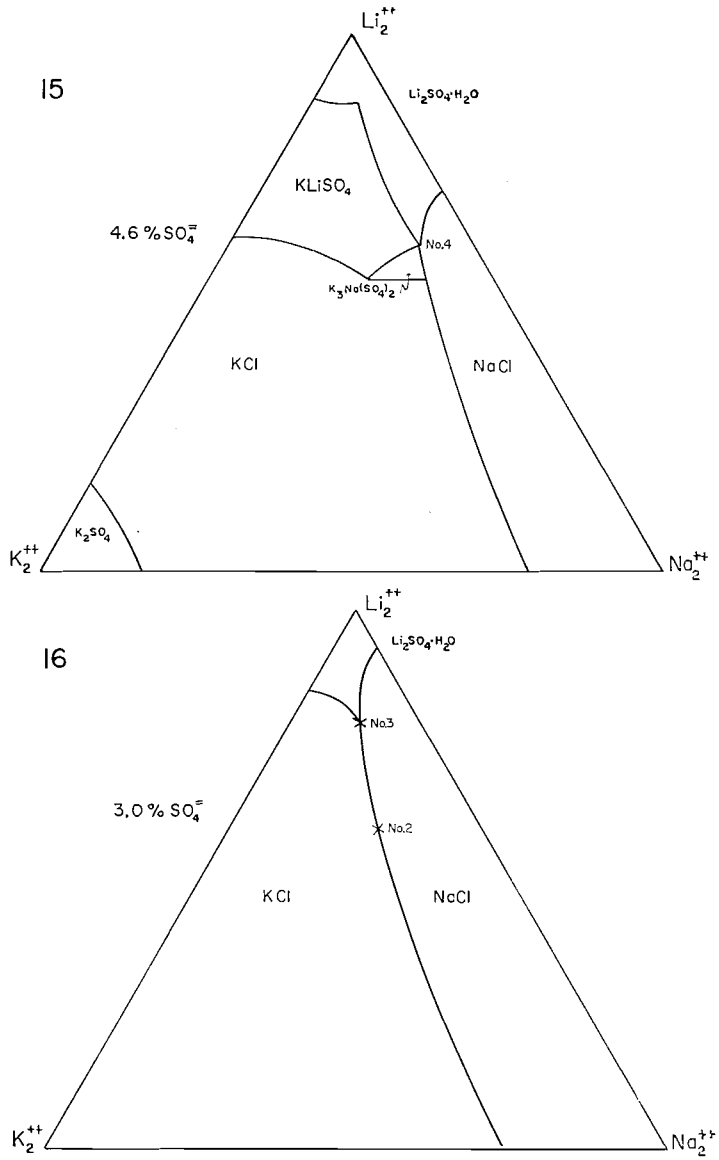
chloride so strongly displaces other salts from solution that its area of existence cannot be indicated on the diagram with the scale used. The other quinquenary invariant point $Li_2SO_4 . H_2O$, $LiCl . H_2O$, NaCl, KCl was not represented due to its position extremely close to the LiCl corner of the prism.

Can. J. Chem. Downloaded from www.nrcresearchpress.com by 210.87.254.42 on 09/05/12
For personal use only.

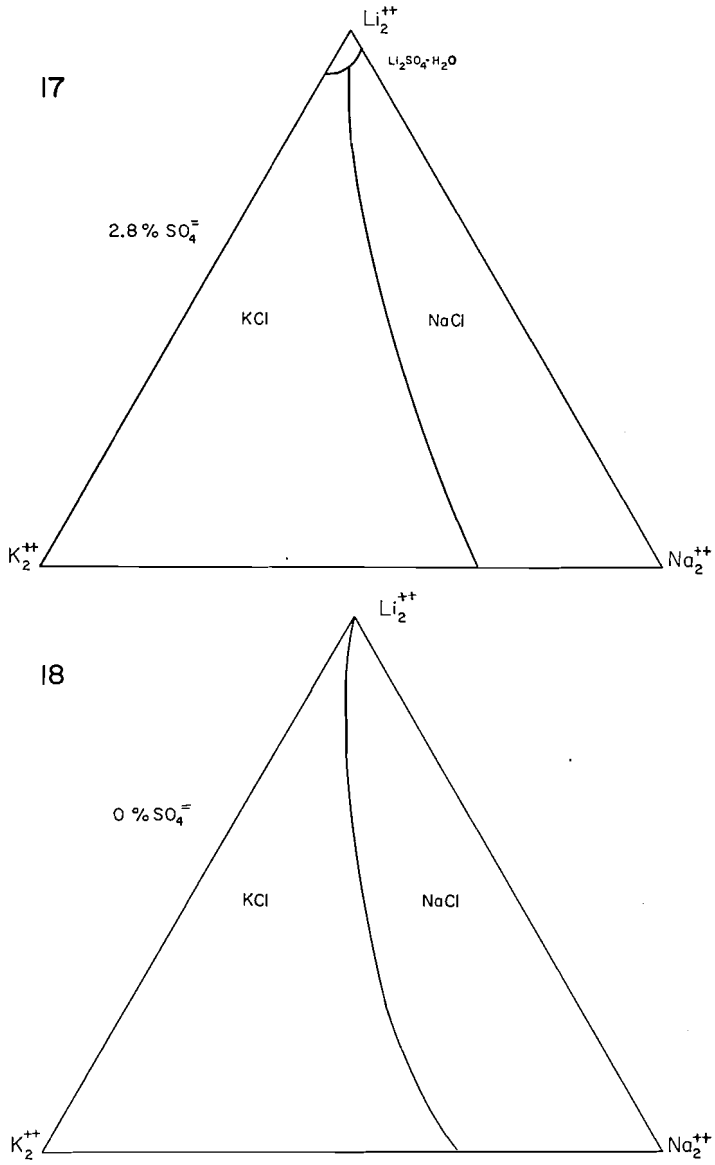


FIGS. 13 AND 14.

Can. J. Chem. Downloaded from www.nrcresearchpress.com by 210.87.254.42 on 09/05/12
For personal use only.



FIGS. 1 AND 16



FIGS. 17 AND 18.

REFERENCES

1. A. N. CAMPBELL and E. M. KARTZMARK. Can. J. Chem. **34**, 672 (1956); **36**, 171 (1958); **37**, 1409 (1959). A. N. CAMPBELL, E. M. KARTZMARK, and E. LOVERING. Can. J. Chem. **36**, 1511 (1958).

Can. J. Chem. Downloaded from www.nrcresearchpress.com by 210.87.254.42 on 09/05/12
For personal use only.

Can. J. Chem. Downloaded from www.nrcresearchpress.com by 210.87.254.40 on 09/05/12
For personal use only.

EFFECT OF AMBIENT OXYGEN ON THE SEMICONDUCTIVITIES OF EVAPORATED FILMS OF MESONAPHTHODIANTHRENE AND MESONAPHTHODIANTHRONE[1]

H. KURODA[2] AND E. A. FLOOD

ABSTRACT

The electrical conductivity of an "evaporated" film of mesonaphthodianthrene increases when the film is exposed to oxygen. The increase in conductivity is associated with changes in the semiconductivity activation energies. The activation energy for the oxygen-free anthrene (bulk conduction) is 0.74 ev while that associated with oxygen adsorption (surface conduction) is 0.40 ev. In marked contrast, the conductivity of an evaporated film of mesonaphthodianthrone decreases when exposed to oxygen. An oxygen-free film of the anthrone has different activation energies in different temperature regions, the activation energies being 0.73 ev and 0.43 ev in the higher and lower temperature regions, respectively. The conduction associated with the lower activation energy decreases when the film is exposed to oxygen.

The effect of oxygen on the semiconductivities of mesonaphthodianthrene and mesonaphthodianthrone are compared with the effect of oxygen on their electron spin resonance spectra.

INTRODUCTION

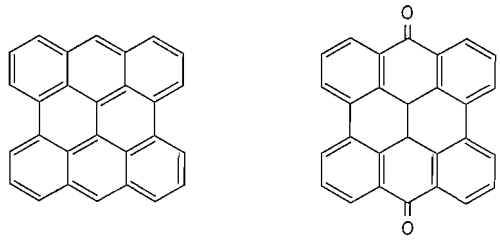
The adsorption of gas molecules on the surface of metals and semiconductors modifies the electrical properties associated with the surface (e.g. work function, contact potential, surface conductance, etc.) especially when the surface reaction involves an electron-transfer mechanism. While in the case of inorganic semiconductors there is a large body of scientific literature dealing with such effects, in the case of organic semiconductors comparatively few papers exist, in spite of the fact that adsorption on organic crystal surfaces can also involve electron-transfer mechanisms. Pick and Wissman observed that the electrical conductivity of a napthalene single crystal was affected markedly by ambient oxygen (1). The influence of ambient oxygen on the photoconductivity of the anthracene crystal has been studied by many investigators (2, 3, 4). The effect of oxygen on the photoconductivity of phthalocyanine is also known (5).

Recently Matsunaga found that a sharp absorption peak appeared in the electron spin resonance spectrum of mesonaphthodianthrene powder when it was exposed to air (6). This suggests that some kind of electron transfer is taking place between the hydrocarbon crystal and oxygen molecules adsorbed on the surface. It seemed, therefore, interesting to investigate the influence of ambient oxygen on the electrical conductivities of thin films formed by evaporation (evaporated films) of these compounds. A brief account of our findings on this subject has been presented in a previous note wherein it was pointed out that ambient oxygen does indeed exert an influence on the electrical conductivities of such films (7).

EXPERIMENTAL

Mesonaphthodianthrene (I) and mesonaphthodianthrone (II) were both purified by repeated sublimation in a high vacuum. Immediately after the final sublimation, a small amount of the powder of the sample was sealed in the conductivity apparatus,

[1]*Manuscript received March 22, 1961.*
Contribution from the Division of Pure Chemistry, National Research Council, Ottawa, Canada.
Issued as N.R.C. No. 6336.
[2]*National Research Council of Canada Postdoctorate Fellow. Present address: Department of Chemistry, Faculty of Science, University of Tokyo, Tokyo, Japan.*



I II

which is schematically shown in Fig. 1. The powder of the sample was placed at the bottom of the small tube A. The cell was evacuated by means of a two-stage mercury diffusion pump together with two liquid nitrogen traps. The whole vacuum system except the region containing the sample was baked during the evacuation. The final vacuum attained after a long evacuation was 10^{-6} mm Hg. The sample was first evaporated to the upper part of the tube A and then re-evaporated from there to the flat surface B, which was equipped with two electrodes of platinum foil embedded in the glass as shown in Fig. 1. It was found necessary to carry out the sublimation rather

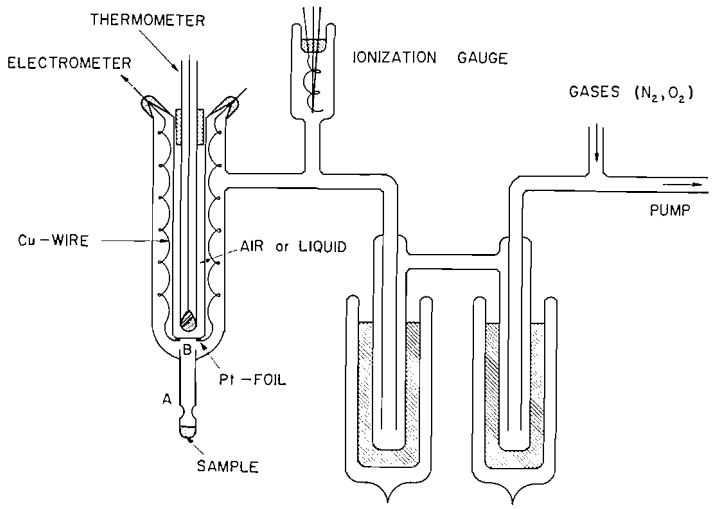


FIG. 1. The apparatus for the measurement of the conductivity.

slowly, in order to obtain a coherent film. The films so obtained were transparent and the order of 1 μ in thickness. The electrical conductivities of the oxygen-free films were studied immediately after the preparation of the films, without breaking the high vacuum.

Conductivity measurements were made using a d-c. method. Direct-current voltage of 135 v was applied between the two electrodes by means of dry cells. The distance between the two electrodes was 1–3 mm. The current through the film was measured with a Hewlett and Packerd DC Micro-volt-ammeter Model 425. The output of the electrometer was connected to a Varian G-10 recorder. The conductivity change was followed by the change in current.

Can. J. Chem. Downloaded from www.nrcresearchpress.com by 210.87.254.40 on 09/05/12
For personal use only.

RESULTS

(a) Mesonaphthodianthrene Film

The temperature dependence of the conductivity of a film of mesonaphthodianthrene is shown in Fig. 2. The current, i, through the film is plotted in logarithmic scale against $(1/T)$. In order to avoid any permanent change due to the evaporation of the compound from the film, the temperature of the measurement was not raised to more than 150° C when the measurement was made in vacuum. With an oxygen-free film a linear relation is obtained between log i and $(1/T)$. There is no appreciable deviation between the curve for the heating process and that for the cooling process.

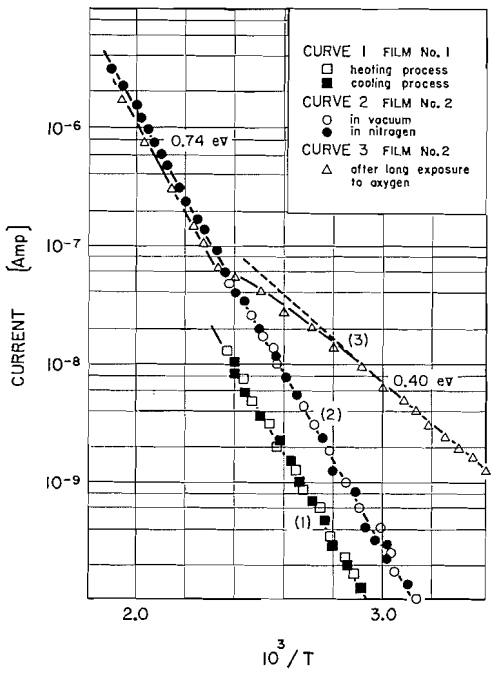


FIG. 2. Temperature dependence of the current through mesonaphthodianthrene films.

The temperature dependence of the conductivity in nitrogen was measured using the same film as that used previously for measurements in vacuum. The results are shown in Fig. 2, curve 2. The temperature range of the measurement was extended up to 250° C. The plot of log i vs. $(1/T)$ gives again a straight line, which coincides with the results measured in vacuum at temperatures below 150° C. This indicates that nitrogen does not influence the electrical conductivity of the film appreciably. The temperature dependence described above can be expressed by an exponential function as is usually found with semiconductors,

$$i = i_0 \exp(-E/kT) \quad [1]$$

where E is the activation energy for the semiconductivity. The value of E determined from the experimental results is 0.74 ev.

If an evaporated film of mesonaphthodianthrene is kept in oxygen or air for a long period, it shows quite a different behavior in respect to the temperature dependence of the electrical conductivity (cf. curve 3 of Fig. 2). In this case the slope of the log i vs. $(1/T)$ curve in the lower-temperature region differs distinctly from that in the higher-temperature region. The latter coincides exactly with the curve obtained in nitrogen.

Can. J. Chem. Downloaded from www.nrcresearchpress.com by 210.87.254.40 on 09/05/12
For personal use only.

The slope of the curve in the lower-temperature region corresponds to a smaller activation energy, 0.40 ev. At lower oxygen pressures the semiconductivity of the "anthrene" as a function of temperature shows considerable hysteresis due to adsorption–desorption effects.

If the evaporated film is placed in contact with oxygen at room temperature the conductivity increases gradually with time. The conductivity change at 24° C is shown in Fig. 3. This is a very slow process. The rate of the conductivity change is dependent upon

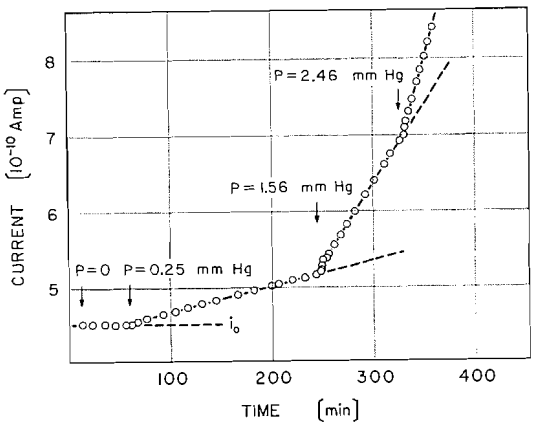


FIG. 3. Variation of the current through a mesonaphthodianthrene film in lower pressures of oxygen at 24° C.

the pressure of the ambient oxygen, being nearly proportional to the pressure when it is less than a few millimeters of mercury. This is illustrated in Fig. 4. If the pressure is high, the conductivity increases rapidly during a short initial period, after which the rate of increase falls off and the conductivity approaches constant values.

At a pressure about 100 mm Hg, the change in the conductivity practically ceases after a few days. When oxygen is pumped off, the conductivity of the film decreases slowly. This again is a very slow process. The change described above is evidently associated with the adsorption of oxygen molecules, and is reversible to a large extent.

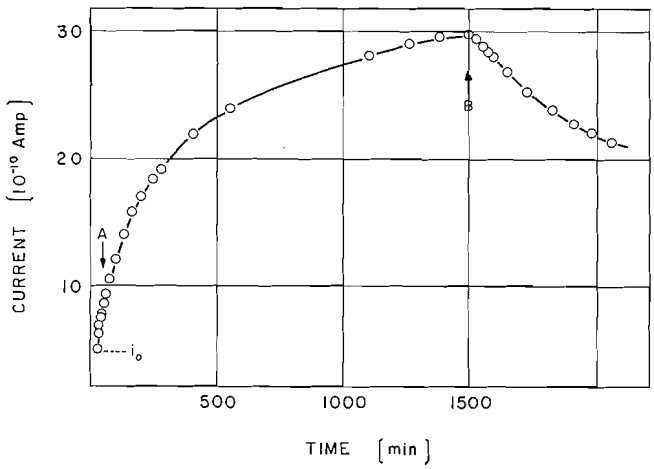


FIG. 4. Variation of the current through a mesonaphthodianthrene film in oxygen (10 mm Hg) at 24° C. The ambient oxygen is introduced into the cell at point A and pumped off at point B.

Can. J. Chem. Downloaded from www.nrcresearchpress.com by 210.87.254.40 on 09/05/12
For personal use only.

The temperature dependence of the electrical conductivity was measured at different stages of the oxygen adsorption although some difficulties due to temperature adsorption–desorption effects were encountered. It was found that the rate of the conductivity increase associated with the oxygen adsorption, as well as that of the reverse change, is faster at higher temperatures. Accordingly, the measurements were made as quickly as possible at temperatures below 40° C, and reproducible results were obtained. The results are shown in Fig. 5 and indicate clearly that the conduction mechanism associated with the lower activation energy is the one which is created by oxygen adsorption. The log i vs. $(1/T)$ curve is not a straight line when the amount of adsorbed oxygen is small. The slope of the curve at the high-temperature end is almost equal to that of the oxygen-free film, and the slope at the low-temperature end corresponds to the activation energy of 0.40 ev. As the amount of oxygen adsorption increases, the region in which the activation energy is 0.40 ev becomes predominant at temperatures below 40° C.

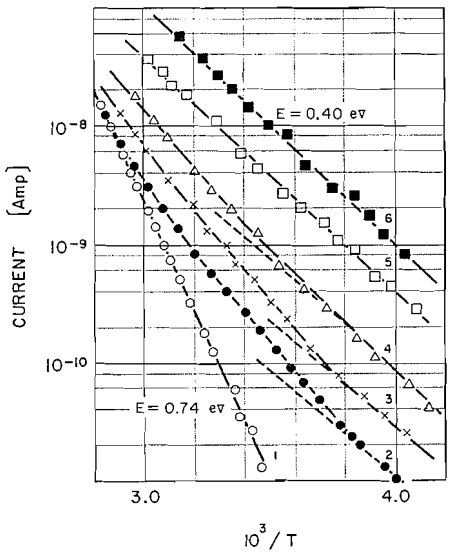


FIG. 5. Temperature dependence of the current through a mesonaphthodianthrene film which has been exposed to oxygen at various pressures for different lengths of time. (1) Oxygen-free state; (2) 1 mm Hg, ½ hr; (3) 3 mm Hg, ½ hr; (4) 10 mm Hg, ½ hr; (5) 50 mm Hg, 1 hr; (6) 300 mm Hg, 2 hr.

(b) Mesonaphthodianthrone Film

The temperature dependence of the conductivity of a mesonaphthodianthrone film is shown in Fig. 6. In marked contrast to the behavior of the mesonaphthodianthrene film, the activation energy of the oxygen-free film of mesonaphthodianthrone in the higher-temperature region differs distinctly from that in the lower-temperature region. In the latter region the activation energy is 0.43 ev while in the former it is 0.73 ev. Further if the film is exposed to air or oxygen the low-temperature activation energy of 0.43 ev disappears from the log i vs. $(1/T)$ curve, the activation energy becoming the same as at the higher temperature, i.e. it becomes 0.73 ev over the whole range thus resembling the oxygen-free anthrene.

The conductivity change due to ambient oxygen at 24° C is shown in Fig. 7 in which i_0 denotes the current in high vacuum; oxygen is introduced into the cell at point A and pumped off at point B. The conductivity of a mesonaphthodianthrone film decreases

Can. J. Chem. Downloaded from www.nrcresearchpress.com by 210.87.254.40 on 09/05/12
For personal use only.

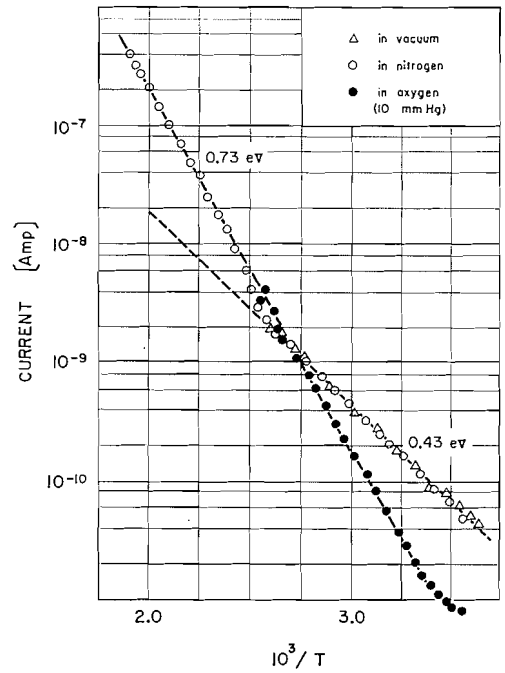


FIG. 6. Temperature dependence of the current through a mesonaphthodianthrone film.

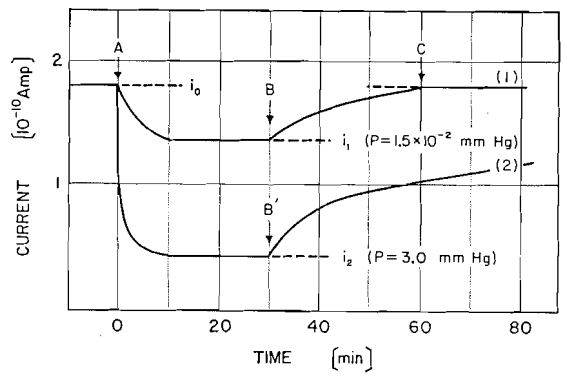


FIG. 7. Variation of the current through a mesonaphthodianthrone film caused by exposure to oxygen. Oxygen is introduced into the cell at point A and pumped off at point B (240° C).

rather rapidly when the film is exposed to oxygen, usually becoming constant within 10 minutes. As oxygen is pumped off the conductivity increases gradually with time, and goes back to the original value after evacuation during a long period. The magnitude of the conductivity at the equilibrium state is dependent upon the pressure of the ambient oxygen, as illustrated in Fig. 8 in which the current through a film with a constant applied potential difference is plotted against the pressure of oxygen.

Can. J. Chem. Downloaded from www.nrcresearchpress.com by 210.87.254.40 on 09/05/12
For personal use only.

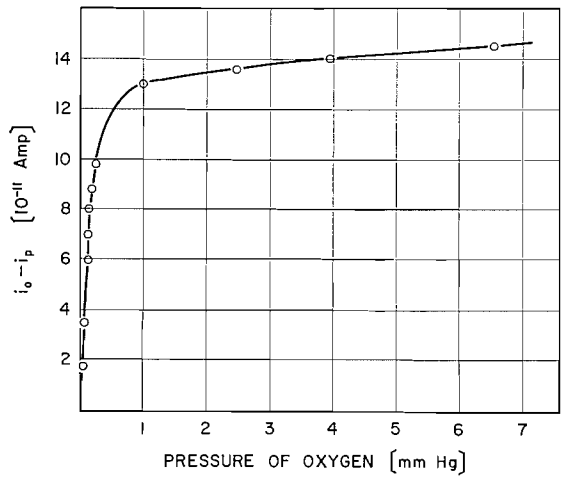


FIG. 8. Current through a mesonaphthodianthrone film at the equilibrium state in oxygen as a function of the oxygen pressure (24° C).

DISCUSSION

From the results described above it is evident that there are at least two mechanisms involved in the electrical conduction of mesonaphthodianthrene films as well as in the conduction of mesonaphthodianthrone films. One of them, in each case, is dependent upon the ambient oxygen while the other is independent. The oxygen-sensitive conduction is associated with a lower activation energy. It is known that the conductivity of the intrinsic semiconductor can be described by the following equation,

$$\sigma = \sigma_0 \exp(-\epsilon/2kT), \quad [2]$$

where σ_0 is a constant dependent upon the concentration of the electronic states and the mobility of the carrier, and ϵ is the energy gap in the band structure of the semiconductor. The semiconductivities of these compounds have been studied by Inokuchi using compressed-powder specimens (8). The energy gaps were estimated from the equation given above as 1.2 ev and 1.3 ev for mesonaphthodianthrene and mesonaphthodianthrone, respectively. Applying the same equation to our results the energy gaps corresponding to the two activation energies of the semiconductivity of mesonaphthodianthrene film are estimated as 1.48 ev and 0.80 ev, while those of the mesonaphthodianthrone film are 1.46 ev and 0.86 ev.

It is difficult to distinguish between bulk and surface conductivities where data refer to net conductivities of either compressed powders or to evaporated films, both of which may have fairly large surfaces. Surface effects might be expected to be particularly significant in the case of very thin evaporated films; of course surface states can control the semiconductivity. However, our results suggest that the activation energy, which is independent of the ambient oxygen, the higher activation energy, is associated with bulk conduction, i.e. independent of the surface.

The data given in Fig. 5, the temperature dependence of the electrical conductivity of mesonaphthodianthrene film in oxygen, can be described quite well by the following equation,

$$\sigma = \sigma_1 \exp(-E_1/kT) + \sigma_2 \exp(-E_2/kT), \quad [3]$$

Can. J. Chem. Downloaded from www.nrcresearchpress.com by 210.87.254.40 on 09/05/12
For personal use only.

where E_1 is 0.74 ev and E_2 is 0.40 ev. The value of σ_1 remains constant for all curves while σ_2 increases as the amount of oxygen adsorbed increases. The values of σ_1 and σ_2 are dependent upon the mobility of the charge carrier and the concentration of the electronic states, i.e. the concentration of the impurity levels in the case of extrinsic semiconduction. As is well known, the surface state can contribute to the electrical conductivity either by forming a surface band through which charge carriers can move, or by behaving as an impurity level which provides the charge carriers to the bulk conduction. It seems probable in the present case that the electron-acceptor levels are created by oxygen adsorption on the surface and that the increase in the magnitude of σ_2 is due to the increase in the concentration of such acceptor levels. According to this model, 0.80 ev is the energy gap between the acceptor level and the lower band.

According to Matsunaga (6), mesonaphthodianthrene powder shows an electron spin resonance spectrum with a fine structure consisting of at least seven peaks separated by 4.4 oersted when it is detected in vacuum. The spin concentration corresponding to this electron spin resonance is 3×10^{21} per mole, g-value being 2.0024. If the powder is exposed to air the central peak of the electron spin resonance spectrum grows slowly reaching the maximum intensity after a few days. The spin concentration corresponding to this sharp absorption is about one tenth of that of the broad absorption mentioned above. The intensity of the sharp absorption decreases with time when air is pumped off. This change is evidently due to the interaction between oxygen and mesonaphthodianthrene crystals. Matsunaga also studied the electron spin resonance of mesonaphthodianthrone powder. It gives an electron spin resonance spectrum similar to that of the hydrocarbon, its spin concentration being about one third of that of the latter. In this case, however, the oxygen effect was not detected.

It is interesting to compare the effect of oxygen on the electrical conductivity with that on the electron spin resonance. In the first place, both effects take place very slowly at room temperature, taking a few days to reach the equilibrium state in air, and both are reversible. In the second place, the creation of the acceptor level and that of the spin center are caused by the ambient oxygen only in the case of the hydrocarbon. These facts suggest that the impurity level created as a result of oxygen adsorption is associated with the formation of a free radical on the surface of the hydrocarbon crystal.

The change in the electrical conductivity of mesonaphthodianthrene film in oxygen is accelerated if the film is illuminated with visible light. Photooxidation is known to occur with anthracene, tetracene, and some other hydrocarbons when oxygen-containing solutions of these hydrocarbons are illuminated with ultraviolet light (9). The molecular structures of these photooxides are known, an oxygen molecule "bridging" two active positions of each hydrocarbon molecule. Since molecules are closely packed in the crystals of these hydrocarbons, it is hard for an oxygen molecule to penetrate into the crystal to form a photooxide. Thus photooxidation can not take place in the bulk of the crystal, as it is illuminated in the ambient oxygen. On the surface of the crystal, however, photooxidation can occur much more easily. The photoconductivity of anthracene increases remarkably in the presence of oxygen, and has been attributed to the formation of a peroxide layer on the surface of the anthracene crystal (2, 3, 4). A similar effect is expected with crystals of various aromatic hydrocarbons which have reactive positions for oxygen in the molecular structure. The two meso positions of the mesonaphthodianthrene molecule are generally considered to be strongly reactive toward oxygen. The photooxide of this hydrocarbon, however, has not been isolated from the solution illuminated with light (10). This might be due to the fact that the two reactive positions are too far apart

Can. J. Chem. Downloaded from www.nrcresearchpress.com by 210.87.254.40 on 09/05/12
For personal use only.

from each other for an oxygen molecule to "bridge" them without considerable strain, thus leading to a "photooxide" so unstable that it can not be isolated. However, this does not exclude the possibility of considerable photooxidation on the surface of the crystal since the photooxide could be stabilized by surface forces. It thus seems that the acceleration of the change in the electrical conductivity in oxygen, caused by the illumination with light, is due to photooxidation. We are not sure if this reaction product is a peroxide or not. Whatever the structure of the reaction product may be, the bond between the oxygen molecule and hydrocarbon molecule must be a loose one, since oxygen molecules can be liberated rather easily. Thus it seems probable that the reaction product is a molecular complex formed between an excited hydrocarbon molecule and an oxygen molecule.

A mesonaphthodianthrone molecule is not markedly reactive to oxygen, no oxygen effect having been detected by electron spin resonance. The presence of the oxygen-sensitive mechanism of conduction in the oxygen-free film of this quinone indicates that the surface state of the crystal of the quinone itself is making an important contribution to the electrical conduction. An oxygen molecule behaves generally as an electron acceptor. Thus, if the semiconductor is *p*-type, the conductivity would be expected to increase in oxygen. While we do not know the nature of the charge carrier in the semiconduction of this quinone, it appears possible that the conduction associated with the activation energy of 0.43 ev is due to a surface conduction in which the majority of carriers are electrons. While this would be consistent with our experimental results, evidently a good deal more experimental data are needed concerning the very interesting reaction of oxygen with the surfaces of quinones. Some interesting recent papers germane to these problems are listed in References (11, 12, 13, 14).

ACKNOWLEDGMENT

The authors wish to express their thanks to Dr. Y. Matsunaga for his valuable advice and discussion.

REFERENCES

1. H. PICK and W. WISSMAN. Z. physik. Chem. **138**, 436 (1954).
2. A. G. CHYNOWETH. J. Chem. Phys. **22**, 1029 (1957).
3. A. BREE, D. J. CARSWELL, and L. E. LYONS. J. Chem. Soc. 1728 (1955).
4. T. C. WADDINGTON and W. G. SCHNEIDER. Can. J. Chem. **36**, 789 (1958).
5. A. T. VARTANYAN. J. Phys. Chem. (U.S.S.R.), **22**, 769 (1948).
6. Y. MATSUNAGA. Can. J. Chem. **38**, 323 (1960).
7. H. KURODA and E. A. FLOOD. J. Chem. Phys. **33**, 952 (1960).
8. H. INOKUCHI. Bull. Chem. Soc. Japan, **24**, 222 (1951).
9. CH. DUFRAISSE and I. GILLET. Compt. rend. **225**, 191 (1947).
10. M. G. SAUVAGE. Compt. rend. **225**, 247 (1947).
11. D. BIJL, H. KAINER, and A. C. ROSE-INNES. J. Chem. Phys. **30**, 765 (1959).
12. M. M. LABES, R. SEHR, and M. BOSE. J. Chem. Phys. **33**, 868 (1960).
13. J. KOMMANDEUR and F. R. HALL. J. Chem. Phys. **34**, 129 (1961).
14. L. S. SINGER and J. KOMMANDEUR. J. Chem. Phys. **34**, 133 (1961).

Can. J. Chem. Downloaded from www.nrcresearchpress.com by 210.87.254.40 on 09/05/12
For personal use only.

Can. J. Chem. Downloaded from www.nrcresearchpress.com by 210.87.254.42 on 09/05/12
For personal use only.

RADIOIODINE EXCHANGE BETWEEN IODOSTEARIC ACID MONOLAYERS AND SUBSTRATE IODIDE. III[1]

J. M. RAMARADHYA[2] AND R. F. ROBERTSON[3]

ABSTRACT

Further studies have been made of the isotopic exchange reaction between monolayers at the air/water interface of I^{131}-α-iodostearic acid and KI substrates. The dependence of the exchange velocity on substrate iodide ion concentration has been examined by employing KCl–KI mixtures of constant over-all molarity to minimize possible variations in film characteristics with substrate salt concentration. The order in substrate I^- ion concentration was found to be fractional at pH 2 and indeterminate at pH 3. The velocity of exchange at all KI concentrations was increased when KCl was added to the substrate. Surface potential measurements showed α-iodostearic acid to have a negative surface potential at high molecular areas which decreased to zero as the film was compressed. The apparent negativity of the surface potential increased as salt was added to the substrate. The surface potential was found to vary with the substrate pH, passing through a maximum between pH 2 and 3. The isotopic exchange velocity and the surface potential were found to be closely related. The variation of the surface potential with time during isotopic exchange has been examined both for monolayers and for collapsed films.

INTRODUCTION

The present investigation is an extension of earlier studies (1, 2) of the homogeneous isotopic exchange reaction

$$CH_3(CH_2)_{15}CHI^*COOH + KI \rightarrow CH_3(CH_2)_{15}CHICOOH + KI^*$$

occurring between I^{131}-labeled α-iodostearic acid, spread as a monolayer at the air/water interface, and iodide ion in the substrate.

In the earlier papers the temperature dependence of the reaction and the possible influence of film characteristics on the exchange rate were reported. The reaction was found to be first-order in surface concentration of film molecules but of indeterminate order in concentration of substrate KI. The impossibility of establishing the order of the exchange reaction in substrate concentration was attributed to changes in the film characteristics of α-iodostearic acid as the concentration of KI in the substrate was varied (1). The influence of pH on the exchange rate was also studied in detail (2). The rate was found to decrease almost 20-fold as the pH of the substrate was varied from 1 to 10 pH units. Between pH 2 and 3 the rate plot passed through a maximum.

In the present paper, further studies are reported on the influence of substrate iodide ion concentration on the exchange reaction, under conditions of constant film characteristics. The surface potential technique of Schulman and Rideal (3) has been employed to study α-iodostearic acid films on various substrates and I^{131}-α-iodostearic acid films during exchange.

EXPERIMENTAL PART

The trough, barriers, and radiochemical counting equipment employed have been described elsewhere (1, 2). The surface balance was the automatic, self-compensating, self-recording, vertical pull instrument described in another paper (4). The experimental

[1]*Manuscript received March 13, 1961.*
Contribution from the Department of Chemistry, McGill University, Montreal, Que.
[2]*Present address: Department of Chemistry, University of Alberta, Edmonton, Alberta.*
[3]*The Department of Chemistry, McGill University, Montreal, Que.*

techniques employed were essentially the same as in these earlier publications. However, the following changes in equipment and materials should be noted.

(1) The surface potential measuring equipment.—The air electrode was a 5 mc Po^{210}-plated source obtained from the Commercial Products Division, Atomic Energy of Canada. This electrode was used in conjunction with a standard calomel half-cell (Beckman) dipping into the film-free substrate solution behind a stationary barrier on the trough. The air electrode, when in use, was positioned approximately $\frac{1}{4}$ inch above the film surface. The potential was measured by a Beckman Model G pH meter connected to the electrodes by shielded and grounded leads. The trough was insulated from the supporting stand by a teflon sheet. The outer aluminum casing of the air bath served, when electrically grounded, as a most satisfactory Faraday screen.

(2) Radiochemically tagged I^{131}-α-iodostearic acid.—Some minor modifications in the preparation of I^{131}-α-iodostearic acid resulted in samples of consistently higher specific activity than obtained previously. A solution of 0.02 g of stock α-iodostearic acid in 5 ml of absolute ethanol was placed in the reaction flask described earlier (1), and 10 mc of carrier-free NaI^{131} in 1 ml of water was added to the solution with 2 drops of constant-boiling HCl. This solution was refluxed for $1\frac{1}{2}$–2 hours, allowed to cool, and 50–75 ml of 0.01 *M* HCl was added. The mixture was left for 10 to 12 hours to permit good crystal growth, filtered on a sintered glass filter, washed with 25 to 50 ml of 0.01 *M* HCl, and dried by suction for a further 12 hours. The spreading solution was prepared in a 10 ml volumetric flask by dissolving the acid from the filter with warm reagent grade benzene.

(3) Other materials.—The benzene, KCl, and KI employed were of reagent grade. Tests for surface-active contamination by the usual compression and surface pressure technique indicated these chemicals to be suitable for use without further purification. A trace of sodium bisulphite was added in the trough to all KI substrate solutions to remove any iodine formed by air oxidation.

RESULTS

1. *The Effect of Substrate KI Concentration on the Isotopic Exchange Rate*

Studies of the π–A isotherms of α-iodostearic acid on KI substrates (2) and on KCl substrates indicated that the curves were identical for the two salts at the same substrate concentration. Substrates of KCl–KI mixtures should then give isotherms characteristic of the total substrate molarity and independent of the relative amounts of the two salts present. Isotopic halogen exchange reactions examined on such substrates could be assumed to be studied under conditions of constant film characteristics for any given total substrate molarity.

Solutions were prepared by the addition of the appropriate amounts of dry KI and KCl to distilled water to give two series of substrate solutions. One series was of unit over-all molarity in KCl and KI but 0.25, 0.5, 0.75, and 1.0 *M* in KI alone and the other, 2 *M* in over-all molarity but 0.25, 0.5, 0.75, 1.0, 1.5, and 2 *M* in KI. Exchange reactions were studied on these substrate solutions at 25° C and at pH 2 and 3. The film of α-iodostearic acid was maintained at a constant surface pressure of 4 dynes/cm during the exchange. After the appropriate background corrections were made, the ratio of the initial count rate at time $t = 0$, $C(0)$, to the count rate at time $t = t$, $C(t)$, was determined from the paper trace of the surface count rate against time. A plot of log $C(0)/C(t)$ vs. time was made for each exchange experiment. The typical linear semilogarithmic plots obtained in all these experiments are illustrated in Fig. 1 for the 2 *M* KI–KCl mixture at

Can. J. Chem. Downloaded from www.nrcresearchpress.com by 210.87.254.42 on 09/05/12
For personal use only.

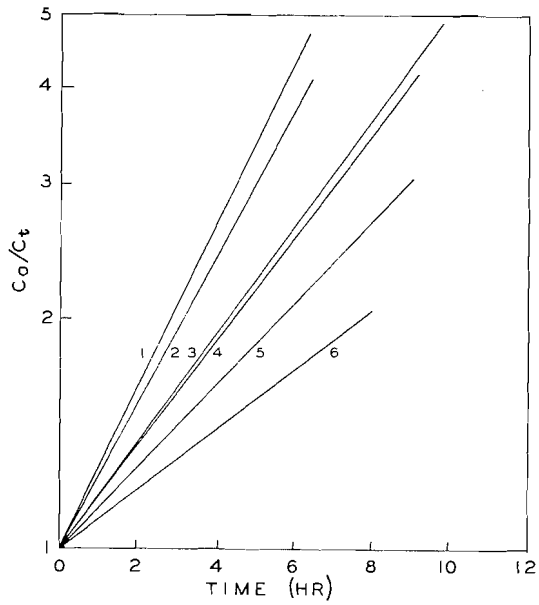


FIG. 1. Semilogarithmic plot of relative count rate against time at 25° C and pH 2 for substrates of variable composition. Curve (1) 2.0 *M* KI; (2) 1.5 *M* KI, 0.5 *M* KCl; (3) 1.0 *M* KI, 1.0 *M* KCl; (4) 0.75 *M* KI, 1.25 *M* KCl; (5) 0.5 *M* KI, 1.5 *M* KCl; (6) 0.25 *M* KI, 1.75 *M* KCl.

pH 2. The pseudo-first-order isotopic exchange rate constant, k', as defined previously (1) by the equation

$$k' = \frac{2 \cdot 303}{t(\text{min})} \log \frac{C(0)}{C(t)}$$

was calculated from the slope of each rate plot. The values of k' so obtained are collected in Table I for 1.0 *M* and 2.0 *M* substrates respectively.

TABLE I

Variation of the first-order isotopic exchange rate constant with substrate composition
(Temp. 25° C, π = 4 dynes/cm)

Substrate composition, moles/liter			$10^4\,k'$, min^{-1}	$10^4\,k'$, min^{-1}
KI	KCl	Total	pH 2	pH 3
0.25	0.75	1	11.21	10.62
0.50	0.50	,,	17.70	13.00
0.75	0.25	,,	23.10	19.60
1.00	0.00	,,	24.00	23.90
0.25	1.75	2	15.15	10.25
0.50	1.50	,,	20.50	16.30
0.75	1.25	,,	26.30	25.22
1.0	1.00	,,	27.10	25.60
1.5	1.50	,,	37.18	25.60
2.0	0.00	,,	40.80	34.34

Can. J. Chem. Downloaded from www.nrcresearchpress.com by 210.87.254.42 on 09/05/12
For personal use only.

The equation for the specific rate constant, k_s, of the exchange reaction was given in the original paper (1) by the equation

$$V = k_s n\, m^y$$

where n is the surface concentration of monolayer; m, the concentration of I^- in the substrate; and y, the order of the reaction in substrate iodide ion. A plot of log k' vs. log m should be a straight line of slope y. Figure 2 gives these plots for 1 and 2 M sub-

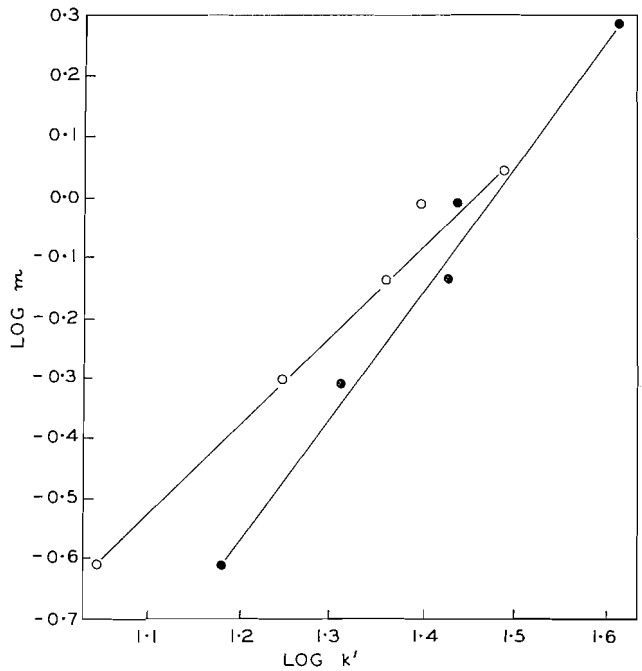


FIG. 2. Plot of logarithm of substrate KI concentration against logarithm of isotopic exchange rate constant. Temperature 25° C, substrate pH 2. Total molarity of substrate in KI and KCl: 1 M, open circles; 2 M, closed circles.

strates at pH 2. A value of y of 0.67 for 1.0 M and 0.48 for 2 M solution is calculated from these slopes. At pH 3 marked deviations from linearity appeared in the plot and calculations of the order could not be made (Table I).

2. The Surface Potential and the Isotopic Exchange Reaction

In an earlier publication (2) it was noted that in the range of pH 2 to pH 5 for 1 M KI substrates, the π–A isotherms of α-iodostearic acid remained essentially constant but the isotopic exchange rate varied markedly. Films of α-iodostearic acid were examined by the surface potential technique in this pH range to elucidate any relation between the surface potential (ΔV) and the rate constant for exchange.

The π–A–ΔV plots for 0.01 M HCl substrates are given in Fig. 3 and the corresponding plots for 1.0 M KI substrates at different values of the pH are given in Fig. 4. At both 17.5° C and 25° C the surface potential of the α-iodostearic acid monolayers on 0.01 M HCl was negative at high molecular areas and approached zero as the film was compressed to smaller areas per molecule. In the range 75 to 80 sq. Å/molecule the plot of ΔV vs. area showed a sudden increase in slope at both temperatures although no change in the

Can. J. Chem. Downloaded from www.nrcresearchpress.com by 210.87.254.42 on 09/05/12
For personal use only.

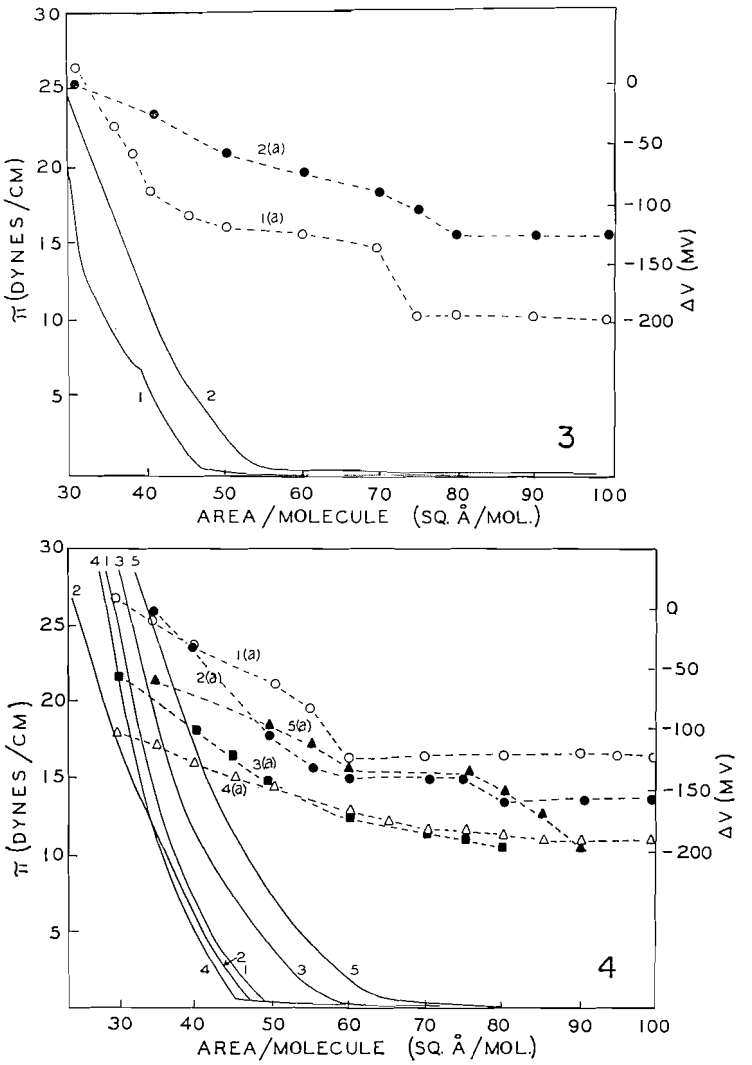


FIG. 3. Pressure–area isotherms and surface potential – area plots for α-iodostearic acid on 0.01 *M* HCl substrates. Curve (1) π–A isotherm 17.5° C; (2) π–A isotherm 25° C. Curves 1*a*, 2*a*, corresponding ΔV–A plots.

FIG. 4. Pressure–area isotherms and surface potential – area plots for α-iodostearic acid on 1.0 *M* KI substrates at 25° C. Curve (1) π–A, pH 1.2; (2) π–A, pH 2.0; (3) π–A, pH 2.8; (4) π–A, pH 3.2; (5) π–A, pH 3.8. Curves 1*a*, 2*a*, 3*a*, 4*a*, 5*a*, corresponding ΔV–A plots.

slope of the π–A isotherms could be detected in this region of molecular area. The transition to a liquid condensed film at 40 sq. Å/molecule in the 17.5° isotherm on 0.01 *M* HCl was markedly reflected in the ΔV-vs.-area plot. The surface potential approached zero very rapidly during compression once the transition point was crossed. The surface potentials of monolayers spread on 1.0 *M* KI substrates (Fig. 4) were decidedly more negative than for 0.01 *M* HCl at all values of the pH above 1.2. The same discontinuous change in slope of the ΔV-vs.-area plot was observed for all the isotherms on KI as on 0.01 *M* HCl except at pH 2.8 and 3.2. The range of area/molecule at which this discontinuity in slope appeared was considerably wider on KI substrates.

Can. J. Chem. Downloaded from www.nrcresearchpress.com by 210.87.254.42 on 09/05/12
For personal use only.

The variations of ΔV with pH are given in Fig. 5 for constant molecular areas of 100, 75, 50, and 35 sq. Å/molecule. Surface potential measurements made on I^{131}-α-iodostearic acid monolayers during exchange are given in Fig. 6 for a substrate pH of 2 and at 25 and 17.5° C with the corresponding semilogarithmic plots for the exchange reaction. The surface potential and semilogarithmic plots of an exchange reaction at 25° C in a collapsed film are also included in this figure.

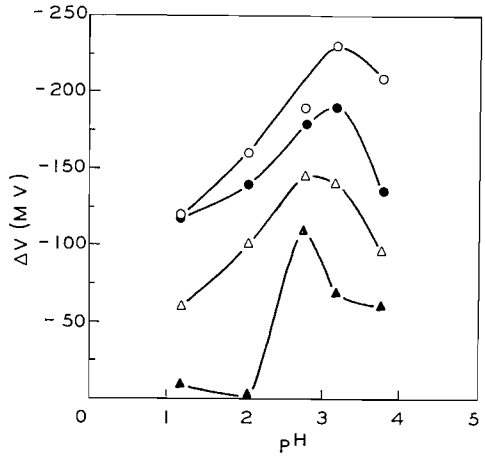


FIG. 5. Surface potential of α-iodostearic acid monolayer on 1 M KI at 25° C as a function of substrate pH at 35 sq. Å/molecule (▲); 50 sq. Å/molecule (Δ); 75 sq. Å/molecule (●); 100 sq. Å/molecule (○).

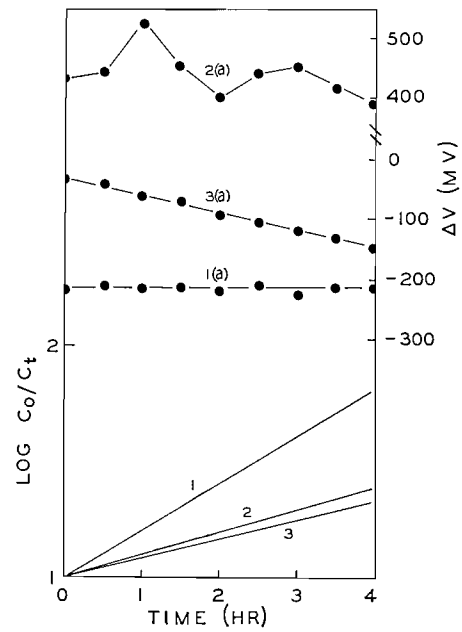


FIG. 6. Semilogarithmic plot of relative surface count rate against time and ΔV–time plot for I^{131}-α-odostearic acid during exchange on 1 M KI at pH 3. Curve (1), π = 4 dynes/cm, 25° C; (2) collapsed film 25° C; (3) π = 4 dynes/cm, 17.3° C. Curves 1a, 2a, 3a, corresponding ΔV– time plots.

Can. J. Chem. Downloaded from www.nrcresearchpress.com by 210.87.254.42 on 09/05/12
For personal use only.

Can. J. Chem. Downloaded from www.nrcresearchpress.com by 210.87.254.42 on 09/05/12
For personal use only.

DISCUSSION

The pseudo-first-order rate constants obtained in the presence of KCl at KI concentrations of 1.0 *M* or less were consistently higher than those obtained in KI substrates of the same molarity but with no KCl present (1). Since no exchange occurred on KCl substrates alone, the increase in the isotopic exchange rate in the presence of KCl is difficult to explain. Kinetic salt effects which have been reported for other monolayer reactions (5) seem hardly to be applicable to an exchange reaction of the type being studied. The kinetic accessibility of the I^- in the substrate to the I^{131} atom in the α-iodostearic acid monolayer can be assumed to remain constant on substrate solutions of constant total molarity in KCl and KI. No changes occur in the π–A isotherms for such substrates and consequently no reorientation of the film molecules would be expected which could change the accessibility and hence the rate of exchange. Possibly the addition of KCl to the substrate may increase the effective concentration of I^- in the surface region below the monolayer. The more rapid exchange on substrates 2 *M* in total salt concentration for all KI concentrations would tend to support this view.

The failure to determine the order in substrate I^- concentration at pH 3 might be related to the apparent discontinuity found in the Arrhenius plot for the activation energy at this same pH (2). Both the apparent discontinuity in the activation energy and the apparent deviations from linearity at pH 3 in the plots for the reaction order in substrate I^- may have a common origin in undetected minor variations of the pH, since close control of this factor in the monolayer trough is most difficult. It has been shown (2) that the isotopic halogen exchange rate constant becomes markedly sensitive to pH near the maximum of the pH-vs.-k' plot. Since this maximum occurs near pH 3, small changes in the pH could lead to significant variations in the reaction velocity and thus to the results observed in the activation energy and substrate I^- order plots.

The negative value of the surface potential obtained for α-iodostearic acid monolayers on HCl substrates is similar to that obtained by Frumkin (6) with monolayers of ω-bromohexadecanoic acid. This negative surface potential suggests that the negative end of the vertical component of the dipole moment of the molecule is uppermost. The iodine atom is then above the carboxyl group in the monolayer surface. On compressing the iodostearic acid monolayers the relative planes of the iodine atom and carboxyl group, parallel to the water surface, must approach one another on compression as the surface potential approaches zero. At higher molecular areas, the increased negativity of the surface potential as the temperature is lowered from 25° C to 17.5° C (−130 mv to −190 mv at 90 sq. Å/molecule) may be related to a decrease in the relative solubility of the film molecules in the substrate. This effect would tend to force the α-iodine atom to a position in the surface above the carboxyl group.

The surface potential of films on 1.0 *M* KI substrates at pH 2 (25° C) is more negative at all higher molecular areas than the corresponding curve on HCl substrates but the two curves approach one another as the area per molecule is decreased. The greater degree of negativity on KI substrates might be related to salting out of the film molecules on the addition of electrolyte to the substrate.

The variation of the surface potential with pH on 1.0 *M* KI substrates would be expected to be associated with the variation in the degree of dissociation of the carboxyl group of the monolayer acid as the acidity of the substrate is decreased. The surface potential would presumably increase as the degree of dissociation increased with numerically increasing pH. In the range of pH studied (1–5 pH units) the change in the

film characteristics of α-iodostearic acid is small, only a slight expansion being detectable (2). Consequently, in the absence of the characteristic marked expansion to a gaseous film which occurs as a monolayer acid approaches complete dissociation, only a small increase in the degree of dissociation must have occurred in traversing this pH range. Since the degree of dissociation can only increase with increasing pH, the maximum of Fig. 5, detectable over a wide range of molecular areas, cannot be accounted for on the basis of the degree of dissociation alone. It must be concluded that the variation of surface potential with pH must arise from other unknown factors as well as the degree of dissociation. That the maximum of Fig. 5 is real seems to be established when the rate constants for isotopic halogen exchange (2) and the present surface potential data are plotted against substrate pH as in Fig. 7. The similarity between the two curves is

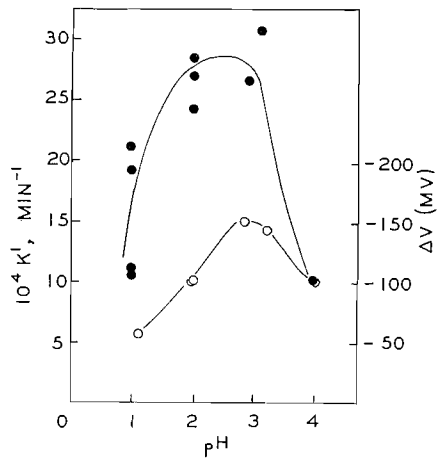


FIG. 7. Plot of isotopic exchange rate constant k' (closed circles) and ΔV (open circles) against substrate pH. Temperature 25° C, molecular area 35 sq. Å.

immediately evident, both the surface potential and the rate constant k' pass through a maximum near pH 3 for the same area/molecule in the monolayer. It seems reasonable to conclude that the variations in surface potential and k' with pH on 1.0 M KI substrates are closely related and are the result of changes in the degree of ionization of the stearic acid derivative and unknown changes, probably of both steric and electrical nature, occurring in the surface region.

The curves of the simultaneous relative surface count rate decrease and surface potential variations with time, taken during the course of an exchange reaction (Fig. 6) with I^{131}-α-iodostearic acid, indicate that at 25° C, pH 3, for a surface pressure of 4 dynes/cm, the surface potential remains essentially constant during the reaction and shows the same value of ΔV as obtained for the inactive films. When the temperature of exchange was lowered to 17.5° C, however, the surface potential was more erratic and slowly increased with time. At this temperature the apparent discontinuities appeared in the Arrhenius plot in earlier experiments and the liquid-intermediate monolayer was present in the π–A isotherms (1, 2). A progressive, slow change in the film characteristics of the monolayer itself might explain the variable surface potential and exchange rate constants in this region of temperature. The surface potential of the collapsed film changed from the negative or zero values found for homogeneous films to large positive

Can. J. Chem. Downloaded from www.nrcresearchpress.com by 210.87.254.42 on 09/05/12
For personal use only.

values. This probably indicates the formation of at least one layer of inverted α-iodostearic acid molecules above the original monolayer, out of the surface and, as indicated by the markedly reduced exchange rate, no longer available for exchange.

ACKNOWLEDGMENTS

The authors are indebted to Dr. L. Yaffe for advice and assistance in the radiochemical procedures. Grateful acknowledgment is also made to the National Research Council for financial support under grant A605.

REFERENCES

1. R. F. ROBERTSON, C. A. WINKLER, and S. G. MASON. Can. J. Chem. **34**, 716 (1956).
2. W. RABINOVITCH, R. F. ROBERTSON, and S. G. MASON. J. Colloid Sci. **13**, 600 (1958).
3. J. H. SCHULMAN and E. K. RIDEAL. Proc. Roy. Soc. (London), A, **130**, 259 (1931).
4. W. RABINOVITCH, R. F. ROBERTSON, and S. G. MASON. Can. J. Chem. **38**, 1881 (1960).
5. J. T. DAVIES and E. K. RIDEAL. Proc. Roy. Soc. (London), A, **194**, 417 (1948).
6. A. FRUMKIN. J. Chem. Phys. **4**, 624 (1936).

Can. J. Chem. Downloaded from www.nrcresearchpress.com by 210.87.254.42 on 09/05/12
For personal use only.

Can. J. Chem. Downloaded from www.nrcresearchpress.com by 210.87.254.5 on 09/05/12
For personal use only.

BACTERIOSTATS

V. THE PREPARATION AND BACTERIOSTATIC PROPERTIES OF AMIDINE DERIVATIVES[1]

D. L. GARMAISE,[2] R. W. KAY,[2] R. GAUDRY,[3] H. A. BAKER,[3] AND A. F. MCKAY[2]

ABSTRACT

A number of polyamidines, N-substituted amidines, and diamidines were prepared for evaluation as bacteriostats. N,N′-Bis-(3,4-dichlorobenzyl)-sebacamidine dihydrochloride was the most active compound prepared in this investigation.

Compounds with unsubstituted amidine groups have been employed as chemotherapeutic agents (1) but there have been relatively few investigations of N-substituted amidines. Some bacteriostatically active N-substituted monoamidines were found (2) to be too toxic for use in guinea pig infections. A series of N,N′-bis-(alkyl)-adipamidines and -sebacamidines has been patented (3) for use in disinfectant compositions, and high bacteriostatic activity has been claimed (4) for a number of polymeric amidines which were obtained by the reaction of diiminoethers with diamines. These polymers were highly toxic (5). The preparation and bacteriostatic evaluation of a number of N-substituted amidines, alkylenediamidines, arylenediacetamidines, and some new polyamidine hydrochlorides are described in the present paper.

The monosubstituted monoamidines (Table I) were prepared by reaction of amines with iminoether hydrochlorides, while the condensation of amines with imidic chlorides was the most convenient method for the preparation of N,N′-disubstituted monoamidines (Table I) and N,N′,N″,N‴-tetrasubstituted diamidines. The N,N′-bis-(aryl)-adipamidines (Table II) were readily prepared by condensation of adiponitrile with substituted aniline hydrochlorides, but no crystalline products could be obtained from the similar reaction of dinitriles with substituted benzylamine hydrochlorides.

The N,N′-bis-(benzyl)-diamidines (Table II) were prepared by heating dinitriles with benzylamine benzenesulphonic acid salts according to the general procedure described by Oxley and Short (6, 7). Conversion of the diamidine dibenzenesulphonates to the corresponding dihydrochlorides was accomplished by passing the dibenzenesulphonate in methanol through a column of Amberlite IRA-400 resin in the chloride form.

Three polyamidine salts (Table III) were prepared by the self-condensation of ω-aminonitrile hydrochlorides. The polymerization was effected by heating the molten hydrochloride in a nitrogen atmosphere until threads could be drawn from the melt. The polyamidine salts listed in Table IV were prepared in the same manner by heating hexamethylenediamine dihydrochloride with dinitriles. These polyamidine hydrochlorides with the exception of the polymer from 4-cyanobenzylamine hydrochloride, are water-soluble, hygroscopic solids with low melting points. The free polymeric bases could be precipitated from aqueous solutions of the hydrochlorides by addition of alkali.

The minimal growth inhibitory concentrations listed in Table V show that all the amidine derivatives are more effective against gram-positive than gram-negative organisms. In the polymeric series, the polymer derived from 10-cyanodecylamine hydrochloride was the most active. The β-(3,4-dichlorophenyl)-ethyl substituent was somewhat more effective than the 3,4-dichlorobenzyl group in the monoamidine derivatives.

[1]*Manuscript received March 24, 1961.*
Contribution No. 32 from the L. G. Ryan Research Laboratories of Monsanto Canada Limited, LaSalle, Que., and the Research Laboratories of Ayerst, McKenna and Harrison Limited, Montreal, Que.
[2]*Monsanto Canada Limited.*
[3]*Ayerst, McKenna and Harrison Limited.*

Can. J. Chem. Downloaded from www.nrcresearchpress.com by 210.87.254.5 on 09/05/12
For personal use only.

TABLE I

N-Substituted amidines, $3,4\text{-}Cl_2C_6H_3(CH_2)_nC(NR')NHR$

R	R′	*n*	M.p. (°C)	Yield (%)	Formula	C		H		Cl		N	
						Calc.	Found	Calc.	Found	Calc.	Found	Calc.	Found
3,4-Dichloro-benzyl	H	1	96–98[a]	59	$C_{15}H_{12}Cl_4N_2$	49.75	49.85	3.34	3.33	39.17	39.16	7.74	7.54
			184–185[b]	100[c]	$C_{21}H_{15}Cl_4N_5O_7$	42.66	42.32	2.56	2.80	23.99	23.81	11.85	11.76
β-(3,4-Dichloro-phenyl)-ethyl	H	1	78–80[a]	45.6	$C_{16}H_{14}Cl_4N_2$	51.09	51.32	3.75	3.87	37.71	37.16	7.45	7.18
4-Chlorobenzyl	3,4-Dichloro-benzyl	0	121–123[a]	32.2	$C_{21}H_{15}Cl_5N_2$	53.37	52.98	3.20	3.34	37.52	37.64	5.93	5.91
3,4-Dichloro-benzyl	3,4-Dichloro-benzyl	0	117–118[a]	10.1	$C_{21}H_{14}Cl_6N_2$	49.74	49.54	2.78	2.87	41.95	42.25	5.53	5.59

[a]Crystallized from ether – petroleum ether.
[b]From aqueous ethanol.
[c]Picrate.

Can. J. Chem. Downloaded from www.nrcresearchpress.com by 210.87.254.5 on 09/05/12
For personal use only.

TABLE II

N,N′-Disubstituted alkylenediamidines, $RNHC(NH)(CH_2)_nC(NH)NHR$

R	n	M.p. (°C)	Yield (%)	Formula	C		H		Cl		N	
					Calc.	Found	Calc.	Found	Calc.	Found	Calc.	Found
4-Chlorophenyl	4	247.5–248 (decomp.)[a]	17.4[k]	$C_{18}H_{22}Cl_4N_4.H_2O$	47.60	47.80	5.33	5.37	31.23	31.47	12.34	12.49
		179.5–180.5[b]	92.5[l]	$C_{30}H_{26}Cl_2N_{10}O_{14}$	43.86	44.17	3.19	3.31	8.63	8.77	17.08	17.02
3,4-Dichlorophenyl	4	243–244[a] (decomp.)	38.0[k]	$C_{18}H_{20}Cl_6N_4$	42.81	43.06	3.99	4.14	42.11	41.71	11.09	11.50
		181–182[b]	97.7[l]	$C_{30}H_{24}Cl_4N_{10}O_{14}$	40.47	40.80	2.72	2.72	15.93	15.57	15.73	16.05
4-Chlorobenzyl	4	194–196[c]	10.9[m]	$C_{32}H_{36}Cl_2N_4O_6S_2$[n]	54.30	54.34	5.13	5.24	10.03	9.63	7.92	7.83
		204–205[d]	42.0[k]	$C_{20}H_{26}Cl_4N_4.H_2O$	49.80	50.26	5.85	5.60	29.42	29.31	11.62	11.70
2,4-Dichlorobenzyl	4	197–198[e]	20.9[m]	$C_{32}H_{34}Cl_4N_4O_6S_2$[o]	49.50	49.55	4.41	4.40	18.26	18.45	7.22	7.48
		224–226[f]	89.8[k]	$C_{20}H_{24}Cl_6N_4$	45.06	45.07	4.54	4.41	39.89	39.84	10.51	10.23
3,4-Dichlorobenzyl	4	213.5–215.5[f]	11.4[m]	$C_{32}H_{34}Cl_4N_4O_6S_2$[p]	49.50	49.60	4.41	4.40	18.26	18.44	7.22	7.47
		242–244[f]	85.4[k]	$C_{20}H_{24}Cl_6N_4$	45.06	45.07	4.54	4.40	39.89	39.66	10.51	10.18
3,4-Dichlorobenzyl	6	197.5–198.5[a]	17.9[m]	$C_{34}H_{38}Cl_4N_4O_6S_2$[q]	50.75	50.73	4.76	4.50	17.63	17.59	6.96	7.13
		187–188[f]	88.4[k]	$C_{22}H_{28}Cl_6N_4$	47.09	47.38	5.03	5.15	37.90	37.64	9.98	10.02
3,4-Dichlorobenzyl	8	—[g, h]	68.0[k]	$C_{24}H_{32}Cl_6N_4$	48.92	49.41	5.47	5.73	36.11	35.44	9.50	9.23
3,4-Dichlorobenzyl	10	—[g, i]	54.0[k]	$C_{26}H_{36}Cl_6N_4$	50.58	50.99	5.88	6.07	34.47	34.31	9.07	9.52
3,4-Dichlorobenzyl	12	—[g, j]	61.5[k]	$C_{28}H_{40}Cl_6N_4$	52.11	52.43	6.25	6.57	32.96	32.45	8.68	8.93

[a]Crystallized from methanol–ether.
[b]From ethanol.
[c]From methanol.
[d]From ethanol – ethyl acetate.
[e]From water.
[f]From ethanol–ether.
[g]Non-crystalline solid.
[h]R_f 0.883 using butanol:acetic acid:water (50:40:10) on Whatman No. 1 filter paper.
[i]R_f 0.832.
[j]R_f 0.887.
[k]Dihydrochloride.
[l]Dipicrate.
[m]Dibenzenesulphonate.
[n]Calc.: S, 9.06%; found: S, 8.86%.
[o]Calc.: S, 8.25%; found: S, 7.92%.
[p]Calc.: S, 8.25%; found: S, 8.02%.
[q]Calc.: S, 7.97%; found: S, 7.88%.

TABLE III

Polymers from ω-aminonitrile hydrochlorides

Monomer	M.p. (°C)	Bath temp. (°C)	Time (hr)	Properties of polymer
6-Cyanohexylamine hydrochloride	—	215	1	Water-soluble sticky brown wax
10-Cyanodecylamine hydrochloride	55	223	13	Water-soluble yellow glass
4-Cyanobenzylamine hydrochloride	240–275	270–280	1	Water-soluble red-brown glass

TABLE IV

Polymers from dinitriles and hexamethylenediamine dihydrochloride

Dinitrile	M.p. (°C)	Bath temp. (°C)	Time (hr)	Properties of polymer
Succinonitrile	45–55	190	11	Water-soluble brown glass
Adiponitrile	50[a]	240–260	8	Water-soluble brown glass
Sebaconitrile	70	270	7	Brown glass, forms gel in water
p-Xylylenedicyanide	140	240–260	3	Water-soluble yellow-brown glass
N,N′-Di-(4-cyanobutyl-carbamyl)-hexamethylenediamine	65	223	9	Water-soluble yellow glass
N,N′-Di-(10-cyanodecyl-carbamyl)-hexamethylenediamine	90–100	223	9	Pale yellow glass, partially soluble in water

[a]Prepared by Hunt and Kirby (4).

In the alkylenediamidine series, N-aryl substituents were considerably less effective than N-benzyl groups. The 3,4-dichlorobenzyl derivative possessed the highest activity. A similar observation has been made in several other series of compounds (8). The most effective of the alkylenediamidines was N,N′-bis-(3,4-dichlorobenzyl)-sebacamidine dihydrochloride with a minimal growth inhibitory concentration of 1:5,120,000 for *Micrococcus pyogenes* var. *aureus* (penicillin resistant) and 1:10,240,000 for *Sarcina lutea*. Compounds possessing shorter or longer alkylene chains were less active. The introduction of additional 3,4-dichlorobenzyl substituents, as in N,N′,N″,N‴-tetrakis-(3,4-dichlorobenzyl)-sebacamidine dihydrochloride, caused a reduction in activity. In the related series of arylenediacetamidines, N,N′-bis-(3,4-dichlorobenzyl)-toluene-2,4-diacetamidine dihydrochloride was found to be highly active.

In general, the diamidines retained a fair degree of their bacteriostatic effectiveness in the presence of 10% serum. The arylenediacetamidine derivative was more sensitive to deactivation by serum protein than the alkylenediamidines. Among the latter, serum deactivation had a leveling effect on the activity of members of the homologous series, and the relationship between chain length and optimum bacteriostatic activity, which was observed in the absence of serum, was no longer apparent.

EXPERIMENTAL[4]

N-(3,4-Dichlorobenzyl)-3,4-dichlorophenylacetamidine

A solution of 3,4-dichlorobenzyl cyanide (20.67 g, 0.11 mole) and anhydrous methanol (3.56 g, 0.11 mole) in anhydrous ether (250 ml) was saturated with hydrogen chloride at 0°. The solution was allowed to stand at 5° for 4 days. Methyl 3,4-dichlorophenylacetimidate hydrochloride, m.p. 105° (decomp.), was recovered by filtration, yield 18.0 g (63.6%).

[4]*All melting points are uncorrected. Microanalyses were performed by Micro-Tech Laboratories, Skokie, Ill.*

Can. J. Chem. Downloaded from www.nrcresearchpress.com by 210.87.254.5 on 09/05/12
For personal use only.

Can. J. Chem. Downloaded from www.nrcresearchpress.com by 210.87.254.5 on 09/05/12
For personal use only.

TABLE V

Bacteriostatic activities (M.I.C., $1/x.10^{-3}$)[a] of amidine derivatives

Product	*M. pyogenes* var. *aureus* (S)	*M. pyogenes* var. *aureus* (R)	*Sarcina lutea*	*Streptococcus faecalis*	*Escherichia coli* No. 198	*Aerobacter aerogenes*	*Salmonella pullorum*	*Pseudomonas aeruginosa*	*Proteus mirabilis*	*Proteus vulgaris*
Polymeric hexamethylenesuccinamidine dihydrochloride	1,280	160	160	80	160	20	40	10	20	10
Polymeric hexamethyleneadipamidine dihydrochloride[b]	160	160	1,280	40	160	160	160	80	160	80
Polymeric hexamethylenesebacamidine dihydrochloride	320	640	640	1,280	160	40	80	20	20	20
Polymeric hexamethylene *p*-phenylenediacetamidine dihydrochloride	160	80	80	40	320	80	80	80	160	80
Polymeric 10-cyanodecylamine hydrochloride	1,280	1,280	2,560	1,280	640	80	80	80	40	80
N-(4-Chlorobenzyl)-N′-(3,4-dichlorobenzyl)-3,4-dichlorobenzamidine	160	320	320	160	80	10	10	10	20	10
N,N′-Bis-(3,4-dichlorobenzyl)-3,4-dichlorobenzamidine	160	320	1,280	640	20	10	10	10	20	20
N-(3,4-Dichlorobenzyl)-3,4-dichlorophenylacetamidine	320	320	640	320	320	160	160	20	80	80
N-(β-(3,4-Dichlorophenyl)-ethyl)-3,4-dichlorophenylacetamidine	640	1,280	1,280	320	640	80	80	20	40	40
N,N′-Bis-(4-chlorophenyl)-adipamidine dihydrochloride	10	10	10	10	10	10	10	10	10	10
N,N′-Bis-(3,4-dichlorophenyl)-adipamidine dihydrochloride	80	80	80	40	80	20	40	20	10	20
N,N′-Bis-(4-chlorobenzyl)-adipamidine dihydrochloride	80	40	640	20	80	20	10	10	40	40
N,N′-Bis-(2,4-dichlorobenzyl)-adipamidine dihydrochloride	160	160	1,280	40	80	20	20	10	40	20
N,N′-Bis-(3,4-dichlorobenzyl)-adipamidine dihydrochloride	640	320	5,120	160	320	80	40	20	80	80
N,N′-Bis-(3,4-dichlorobenzyl)-suberamidine dihydrochloride	320	640	5,120	320	160	40	40	20	40	20
In presence of 10% serum	160	160	5,120	40	160	40	40	20	40	20
N,N′-Bis-(3,4-dichlorobenzyl)-sebacamidine dihydrochloride	2,560	5,120	10,240	640	640	80	160	40	40	40
In presence of 10% serum	160	160	640	80	160	40	40	10	20	20
N,N′-Bis-(3,4-dichlorobenzyl)-dodecanediamidine dihydrochloride	2,560	2,560	5,120	2,560	640	40	160	40	80	80
In presence of 10% serum	320	320	1,280	640	160	40	40	40	40	20
N,N′-Bis-(3,4-dichlorobenzyl)-tetradecanediamidine dihydrochloride	2,560	640	2,560	2,560	320	160	160	20	40	40
In presence of 10% serum	320	160	1,280	160	80	40	20	10	20	20
N,N′,N″,N‴-Tetrakis-(3,4-dichlorobenzyl)-sebacamidine dihydrochloride	320	160	1,280	1,280	160	40	20	10	20	40
N,N′-Bis-(3,4-dichlorobenzyl)-*p*-phenylenediacetamidine dihydrochloride	320	320	320	40	160	10	20	10	20	10
N,N′-Bis-(3,4-dichlorobenzyl)-toluene-2,4-diacetamidine dihydrochloride	2,560	1,280	5,120	640	640	80	160	80	80	40
In presence of 10% serum	80	80	640	20	20	20	20	10	10	10

[a]Minimal inhibitory concentration determined by serial dilution tube technique, e.g., the value of 1,280 is equivalent to a concentration of 1 part in 1,280,000.
[b]Prepared by Hunt and Kirby (4).

The iminoether hydrochloride (3.40 g, 0.00134 mole) and 3,4-dichlorobenzylamine (2.34 g, 0.00134 mole) were dissolved in anhydrous methanol (30 ml) and the solution was allowed to stand at room temperature for 4 days. The residue from evaporation of the solution was added to 0.1 *N* sodium hydroxide solution (147.4 ml) and ether (100 ml). The dried ether extract was concentrated to a small volume and diluted with petroleum ether to give N-(3,4-dichlorobenzyl)-3,4-dichlorophenylacetamidine, m.p. 94–97°, yield 2.86 g (59%). Recrystallization from ether – petroleum ether raised the melting point to 96–98°.

The iminoether hydrochloride on treatment with 2-(3,4-dichlorophenyl)-ethylamine (9) by the above procedure gave N-(β-(3,4-dichlorophenyl)-ethyl)-3,4-dichlorophenylacetamidine (Table I).

N-(3,4-Dichlorobenzyl)-3,4-dichlorobenzamide

Sodium hydroxide (8.0 g, 0.20 mole) in water (100 ml) was added dropwise to a stirred mixture of 3,4-dichlorobenzylamine hydrochloride (21.25 g, 0.10 mole) and 3,4-dichlorobenzoyl chloride (20.9 g, 0.10 mole) in water (250 ml) at 25°. After the addition period of 2 hours, the mixture was stirred for 6 hours. The crude product (m.p. 118–123°) was recovered by filtration, yield 28.6 g (82.0%). Crystallization from ethanol raised the melting point to 131–132.5°, yield 21.5 g (61.6%). Anal. Calc. for $C_{14}H_9Cl_4NO$: C, 48.18; H, 2.60; Cl, 40.64; N, 4.01%. Found: C, 48.36; H, 2.65; Cl, 40.65; N, 3.89%.

N,N′-Di-(3,4-dichlorobenzyl)-3,4-dichlorobenzamidine

A solution of N-(3,4-dichlorobenzyl)-3,4-dichlorobenzamide (10.4 g, 0.03 mole) and phosphorus pentachloride (6.24 g, 0.03 mole) in benzene (60 ml) was refluxed for 3 hours. Evaporation of the solvent yielded N-(3,4-dichlorobenzyl)-3,4-dichlorobenzimidic chloride as an oil which gradually solidified, m.p. 83–86°. 3,4-Dichlorobenzylamine (5.3 g, 0.03 mole) in ether (25 ml) was added, and the solution was allowed to stand for 3 days. The precipitate (2.8 g, m.p. 200–220°) was filtered, and the filtrate was shaken with 2 *N* hydrochloric acid (100 ml), giving an additional precipitate of 4.8 g, m.p. 210–230°. The combined solids were extracted with boiling water (25 ml) and the residue was recrystallized from dimethylformamide (30 ml). N,N′-Di-(3,4-dichlorobenzyl)-3,4-dichlorobenzamidine hydrochloride, m.p. 243–244.5°, was recovered in 15.1% yield (2.3 g).

A sample of the hydrochloride (1.6 g, 0.0032 mole) in dimethylformamide (15 ml) was added to 5% sodium hydroxide solution (100 ml) and chloroform (50 ml). The aqueous layer was extracted with chloroform (2×50 ml) and the combined chloroform extracts were washed with water, dried, and evaporated. The residue (1.3 g), m.p. 92–97°, was crystallized from ether – petroleum ether, giving the free base melting at 117–118°, yield 1.0 g (10.1% based on the amide).

Reaction between the imidic chloride and 4-chlorobenzylamine gave N-(4-chlorobenzyl)-N′-(3,4-dichlorobenzyl)-3,4-dichlorobenzamidine (Table I).

Preparation of Dinitriles

p-Xylylenedicyanide (m.p. 95–97°) was prepared in 60% yield from *p*-xylylenedibromide by the method of Titley (10).

Toluene-2,4-diacetonitrile

2,4-Di-(chloromethyl)-toluene (150 g, 0.79 mole) in ethanol (200 ml) was added, with stirring, to sodium cyanide (100 g, 2.04 moles) in water (90 ml) at 76–80° during a period of 30 minutes. The mixture was refluxed for 2 hours, and then cooled and filtered. Most

Can. J. Chem. Downloaded from www.nrcresearchpress.com by 210.87.254.5 on 09/05/12
For personal use only.

of the ethanol was removed by concentration of the filtrate at reduced pressure, and the oily residue was extracted with benzene (200 ml). The benzene layer was dried and evaporated, and the residue was distilled, giving the crude product, b.p. 162–170° at 0.1 mm, yield 91 g (68%).

The distillate was shaken with 50% sulphuric acid (100 ml) for 5 minutes, and the resulting emulsion was extracted with benzene (100 ml). The benzene layer was washed with sodium bicarbonate solution and water, dried, and evaporated. Distillation of the residue yielded the pure product, b.p. 182° at 0.7 mm, m.p. 38–42.5°, yield 64.8 g (49%). Anal. Calc. for $C_{11}H_{10}N_2$: C, 77.65; H, 5.88; N, 16.47%. Found: C, 77.73; H, 6.30; N, 16.43%.

1,12-Dicyanododecane

1,12-Dodecanedicarboxylic acid (20.7 g, 0.08 mole) was added to thionyl chloride (28.6 g, 0.24 mole) in benzene (100 ml) at room temperature. After being allowed to stand for 90 minutes, the solution was refluxed for 3 hours. The solvent and excess thionyl chloride were removed by concentration *in vacuo*, and the dark-brown residue was added dropwise to concentrated aqueous ammonia (67 ml) at 15°. The precipitated 1,12-dodecanedicarboxamide was recovered by filtration, m.p. 182–187°, yield 19.3 g (94.2%). After recrystallization from dimethylformamide, the diamide melted at 186–187°, resolidified, and remelted at 194–197°. Anal. Calc. for $C_{14}H_{28}N_2O_2$: C, 65.58; H, 11.01; N, 10.93%. Found: C, 65.44; H, 10.80; N, 10.79%.

The diamide (15.7 g, 0.061 mole) was refluxed with thionyl chloride (16.0 g, 0.134 mole) in benzene (100 ml) for 7 hours. The solution was evaporated and the residue was distilled, giving 1,12-dicyanododecane, b.p. 151–153° at 0.04 mm, m.p. 35.5–36°, yield 8.5 g (63.3%). Anal. Calc. for $C_{14}H_{24}N_2$: C, 76.31; H, 10.98; N, 12.71%. Found: C, 76.15; H, 10.83; N, 12.52%.

N,N′-Bis-(3,4-dichlorophenyl)-adipamidine Dihydrochloride

A mixture of 3,4-dichloroaniline hydrochloride (9.93 g, 0.05 mole) and adiponitrile 2.71 g, 0.025 mole) was heated to 210°. After 20 minutes at 205–210°, the melt solidified. Crystallization of the solid from hot water yielded material melting at 226–232° (decomp.), yield 8.62 g (68.2%). The pure dihydrochloride melting at 243–244° (decomp.) was obtained by recrystallization from methanol–ether solution, yield 4.82 g (38.0%).

N,N′-Bis-(4-chlorophenyl)-adipamidine dihydrochloride (Table II) was prepared by the same procedure.

N,N′-Bis-(3,4-dichlorobenzyl)-adipamidine

3,4-Dichlorobenzylamine (35.2 g, 0.20 mole) was added to a solution of benzenesulphonic acid (35.2 g, 0.22 mole) in methanol (600 ml). The solution was concentrated to 250 ml. 3,4-Dichlorobenzylamine benzenesulphonate (m.p. 244–248°) crystallized out on standing, yield 50.7 g (75.9%).

3,4-Dichlorobenzylamine benzenesulphonate (47.0 g, 0.141 mole) was stirred with adiponitrile (7.62 g, 0.0705 mole) at 235° for 35 minutes. The mixture was crystallized from methanol (150 ml) yielding some unchanged starting material (15.7 g, m.p. 206–235°). Concentration of the mother liquors yielded the crude product (14.7 g, m.p. 170–199°), which on recrystallization from water (600 ml), gave N,N′-bis-(3,4-dichlorobenzyl)-adipamidine dibenzenesulphonate (6.0 g, 11.4%), m.p. 210–213°. The analytical sample melted at 213.5–215° after recrystallization from methanol–ether solution.

A solution of the dibenzenesulphonate (3.83 g, 0.00493 mole) in methanol (80 ml) was passed through a column of Amberlite IRA-400 resin (50 ml), which had previously

Can. J. Chem. Downloaded from www.nrcresearchpress.com by 210.87.254.5 on 09/05/12
For personal use only.

been saturated with chloride ion. The column was washed with methanol (100 ml) and the combined eluates were evaporated, giving N,N′-bis-(3,4-dichlorobenzyl)-adipamidine dihydrochloride, m.p. 241–244°, yield 2.38 g (85.4%). Recrystallization from methanol–ether raised the melting point to 242–244°.

The other N,N′-diaralkyldiamidines described in Table II were prepared by the same method.

N,N′-Bis-(3,4-dichlorobenzyl)-p-phenylenediacetamidine

A mixture of *p*-xylylenedicyanide (14.3 g, 0.0915 mole) and 3,4-dichlorobenzylamine benzenesulphonate (61.3 g, 0.183 mole) was stirred in a nitrogen atmosphere at 230° for 90 minutes. The cooled reaction mixture was extracted successively with dimethylformamide (50 ml) and boiling methanol (100 ml), giving the product as the dibenzenesulphonic acid salt, m.p. 311–312°, yield 31 g (41%). The analytical sample melted at 313–314° after crystallization from dimethylformamide. Anal. Calc. for $C_{36}H_{34}Cl_4N_4O_6S_2$: C, 52.44; H, 4.16; Cl, 17.20; N, 6.74; S, 7.78%. Found: C, 52.30; H, 4.23; Cl, 17.45; N, 6.98; S, 7.88%.

The dibenzenesulphonate (30.0 g, 0.0364 mole) was dissolved in dimethylformamide (430 ml), and a solution of potassium hydroxide (30 g) in methanol (100 ml) was added. Dilution with water precipitated the product as the free base, m.p. 164–165°, yield 17.2 g (93%). The melting point was raised to 168–169° by recrystallization from dilute ethanol. Anal. Calc. for $C_{24}H_{22}Cl_4N_4$: C, 56.71; H, 4.36; Cl, 27.91; N, 11.02%. Found: C, 56.64; H, 4.68; Cl, 27.70; N, 10.77%.

N,N′-Bis-(3,4-dichlorobenzyl)-toluene-2,4-diacetamidine

Toluene-2,4-diacetonitrile (6.8 g, 0.04 mole) and 3,4-dichlorobenzylamine benzenesulphonate (26.8 g, 0.08 mole) were heated at 210–230° for 3 hours. The cooled mixture on crystallization from methanol and ether gave 8.4 g (31.4%) of unreacted 3,4-dichlorobenzylamine benzenesulphonate. Evaporation of the mother liquors yielded the product as an amorphous solid (yield 22 g, 66%) which gave a single spot, R_f 0.85, when chromatographed with butanol:acetic acid:water (50:40:10). A methanolic solution (200 ml) of the product was passed through a column of Amberlite IRA-400 resin (150 ml) in the chloride form, and the column was washed with methanol (200 ml). Evaporation of the eluate gave the product as the amorphous dihydrochloride (yield 14.7 g, 62%).

A sample of the dihydrochloride (4.5 g, 0.0086 mole) was added to fumaric acid (1.0 g, 0.0086 mole) in ethanol (30 ml). Addition of ether (20 ml) yielded the crystalline fumarate salt, m.p. 170–190°, which was recrystallized from dimethylformamide to a constant melting point of 190.5–193°, yield 1.95 g (35%). Anal. Calc. for $C_{29}H_{28}Cl_4N_4O_4.H_2O$: C, 53.06; H, 4.61; Cl, 21.61%. Found: C, 53.38; H, 5.13; Cl, 21.04%.

N,N′-Bis-(3,4-dichlorobenzyl)-sebacamide

Sebacyl chloride (23.9 g, 0.10 mole) in benzene (50 ml) was added dropwise to a solution of 3,4-dichlorobenzylamine (35.2 g, 0.20 mole) and pyridine (15.8 g, 0.20 mole) in dry benzene (300 ml) at 15–20° C. The solution was allowed to stand overnight and the precipitate was filtered and washed with water. Recrystallization from methanol gave the pure diamide, melting at 123–124°, resolidifying, and remelting at 135–136°, yield 38.0 g (69.5%). Anal. Calc. for $C_{24}H_{28}Cl_4N_2O_2$: C, 55.62; H, 5.44; Cl, 27.37; N, 5.41%. Found: C, 55.43; H, 5.50; Cl, 27.41; N, 5.37%.

N,N′,N″,N‴-Tetrakis-(3,4-dichlorobenzyl)-sebacamidine

N,N′-Bis-(3,4-dichlorobenzyl)-sebacamide (5.18 g, 0.010 mole) was refluxed with phosphorus pentachloride (4.20 g, 0.020 mole) in dry benzene (70 ml) for 3.5 hours. The

Can. J. Chem. Downloaded from www.nrcresearchpress.com by 210.87.254.5 on 09/05/12
For personal use only.

benzene solution, after being decanted from the resinous by-products, was added to 3,4-dichlorobenzylamine (6.02 g, 0.040 mole), and the solution was allowed to stand for 2 hours.

The residue obtained on evaporation of the benzene was partitioned between ether (100 ml) and 2 *N* sodium hydroxide (100 ml). The ether solution was dried and evaporated, and the residue was extracted repeatedly with petroleum ether. The residual oil gave a single spot, R_f 0.93, in a paper chromatogram with the solvent system butanol:acetic acid:water (50:40:10).

The product was dissolved in ethanol (50 ml) and acidified with aqueous hydrochloric acid. Evaporation of the solution yielded the dihydrochloride as an amorphous solid which resisted all attempts at crystallization, yield 3.8 g (42%). Anal. Calc. for $C_{38}H_{40}Cl_{10}N_4$: C, 50.31; H, 4.44; N, 6.18%. Found: C, 49.54; H, 4.75; N, 5.58%.

Polyamidines

A mixture of succinonitrile (3.06 g, 0.382 mole) and hexamethylenediamine dihydrochloride (7.23 g, 0.382 mole) was heated, with stirring, in a nitrogen atmosphere until a homogeneous melt was obtained. Immersion in a bath at 245° for 15 minutes was required to melt the mixture. The bath temperature was lowered to 190° and the heating was continued for 10 hours. The pressure was reduced to 10 mm and the heating was continued for 1 hour. On cooling, the viscous mass solidified to a brown hygroscopic glass melting at 45–55°.

The other polymers described in Tables II and III were prepared in the same manner. In each case the mixture or the aminonitrile hydrochloride was first melted and then heated at the bath temperature noted in the tables until threads could be drawn from the polymeric mass. The pressure was reduced toward the end of the reaction to remove volatile impurities.

REFERENCES

1. H. GILMAN (*Editor*). Organic chemistry. An advanced treatise. Vol. III. John Wiley & Sons, Inc., New York. 1953. p. 486.
2. G. NEWBERRY and W. WEBSTER. J. Chem. Soc. 738 (1947).
3. M. HUNT and J. E. KIRBY. U.S. Patent No. 2,364,074 (1944).
4. M. HUNT and J. E. KIRBY. U.S. Patent No. 2,310,789 (1943).
5. J. F. LONTZ. U.S. Patent No. 2,310,799 (1943).
6. P. OXLEY and W. F. SHORT. J. Chem. Soc. 147 (1946).
7. W. F. SHORT and P. OXLEY. U.S. Patent No. 2,433,489 (1947).
8. A. F. MCKAY, D. L. GARMAISE, R. GAUDRY, H. A. BAKER, G. Y. PARIS, R. W. KAY, G. E. JUST, and R. SCHWARTZ. J. Am. Chem. Soc. **81**, 4328 (1959).
9. A. F. MCKAY, D. L. GARMAISE, G. Y. PARIS, S. GELBLUM, and R. RANZ. Can. J. Chem. **38**, 2042 (1960).
10. A. F. TITLEY. J. Chem. Soc. 508 (1926).

Can. J. Chem. Downloaded from www.nrcresearchpress.com by 210.87.254.5 on 09/05/12
For personal use only.

Can. J. Chem. Downloaded from www.nrcresearchpress.com by 210.87.254.40 on 09/05/12
For personal use only.

INORGANIC SALTS DISSOLVED IN NON-AQUEOUS OR IN MIXED SOLVENTS

XIII. VISCOSITY STUDIES OF $SnCl_4.5H_2O$ AND $SnCl_2.2H_2O$ DISSOLVED SEPARATELY AND TOGETHER IN METHANOL – CARBON TETRACHLORIDE[1]

P. A. D. DE MAINE AND E. R. RUSSELL

ABSTRACT

Here is reported evidence from viscosity data for competitive, reversible complex formation between species of Sn(IV) or Sn(II) and Sn(IV) or methanol in methanol – carbon tetrachloride solutions of $SnCl_4.5H_2O$ and $SnCl_2.2H_2O$. Empirical relations between the viscosity parameter and the salt or methanol concentrations are also reported.

INTRODUCTION

Spectrophotometric and conductance data for $SnCl_4.5H_2O$ and $SnCl_2.2H_2O$ dissolved separately (1, 2, 3, 4, 5) and together (6, 7) in methanol or in methanol – carbon tetrachloride have shown that there is competitive, reversible complex formation between Sn(IV) and Sn(II) species, between two Sn(IV) species, between Sn(IV) species and methanol, and between Sn(II) species and methanol. The ratio, R (molar conductance at 45° C/molar conductance at 20° C), is independent of salt concentration for each solvent composition. Interactions between Sn(IV) species and Sn(II) or Sn(IV) species are favored by desolvation of methanolated Sn(IV) and Sn(II) (through elevation of the temperature or increase of the carbon tetrachloride concentration).

Here we report viscosity data for $SnCl_4.5H_2O$ and $SnCl_2.2H_2O$ dissolved separately and together in methanol – carbon tetrachloride at 25° and 45° C. These new data can be interpreted in terms of the four competitive, reversible complex formation modes noted in the preceding paragraph. Thus the spectral, conductance, and viscosity data all lead to the same interpretation.

EXPERIMENTAL

Fisher Spectrograde methanol and carbon tetrachloride were dispensed under an atmosphere of dry nitrogen (dew point less than −60° C). Fisher Certified Reagent Grade $SnCl_4.5H_2O$ and $SnCl_2.2H_2O$ were used without further purification. However analyses for tin and chlorine (4) showed that the actual composition of each salt is within 1% of the theoretical composition.

The techniques for preparation of solutions have been described (1, 6). Viscosities were measured with calibrated Ostwald–Fenske viscometers in thermostated baths at 25° and 45° C. Densities for each solution were calculated from density data for the pure solvents (8) and for tin chloride solutions of the highest concentrations, at both temperatures. In separate experiments we have shown that for methanol and methanol – carbon tetrachloride solutions of tin chlorides, densities calculated on the assumption of additive volumes agree to within 0.35% of actually measured densities over the range of concentrations used in this study.

Duplicated experiments showed that all measurements can be reproduced to better

[1]*Manuscript received December 15, 1960.*
Contribution from the Department of Chemistry, University of Mississippi, University, Mississippi.

Can. J. Chem. Downloaded from www.nrcresearchpress.com by 210.87.254.40 on 09/05/12
For personal use only.

TABLE I

Salt concentration ranges and composition of the methanol – carbon tetrachloride solvent for which viscosity data were recorded at 25 and 45° C
(All concentrations are moles/liter; in parentheses are the number of different salt concentrations for each range)

	CCl_4 concentration									
	0.000	1.029	2.058	3.087	4.116	5.145	6.174	7.203	8.235	9.261
	Salt concentration range									
$SnCl_2.2H_2O$	0.080–1.000 (13)	0.080–0.880 (11)	0.080–0.800 (10)	0.080–0.640 (8)	0.080–0.560 (7)	0.080–0.480 (6)	0.080–0.400 (5)	0.080–0.240 (3)	0.080–0.160 (2)	0.080 (1)
$SnCl_4.5H_2O$	0.100–1.000 (10)	0.100–0.900 (9)	0.100–0.800 (8)	0.100–0.500 (5)(*a*)	0.100–0.400 (4)(*a*)	0.100–0.200 (2)(*a*)	0.100 (1)(*a*)	0.100 (1)(*a*)	(*a*)	(*a*)
$SnCl_2.2H_2O$ $+SnCl_4.5H_2O$	0.180–0.900 (5)	0.180–0.900 (5)	0.180–0.720 (4)	0.180–0.540 (3)	0.180–0.540 (3)	0.180–0.360 (2)	0.180–0.360 (2)	0.180 (1)(*a*)	(*a*)	(*a*)

NOTE: *a* denotes concentrations where systems formed two layers. Reference 4 is a study of these two-layer systems.

than 0.30% with another set of solutions. Table I indicates the ranges of solvent composition and salt concentration over which viscosity data was collected.

RESULTS

In this work we define salt molar viscosity (η_{salt}) thus:

$$\eta_{salt} = (\eta_s - \eta_o)/c = \eta_{sp}\eta_o/c$$

where η_s and η_o are the measured viscosity coefficients of the solution and solvent respectively, η_{sp} is the specific viscosity coefficient, and c is the salt concentration in moles/liter.

Systems with $SnCl_4.5H_2O$ as Solute

For all salt concentrations and both temperatures, plots of viscosity coefficient versus carbon tetrachloride concentration, for solutions with fixed $SnCl_4.5H_2O$ concentration, are linear (Fig. 1).

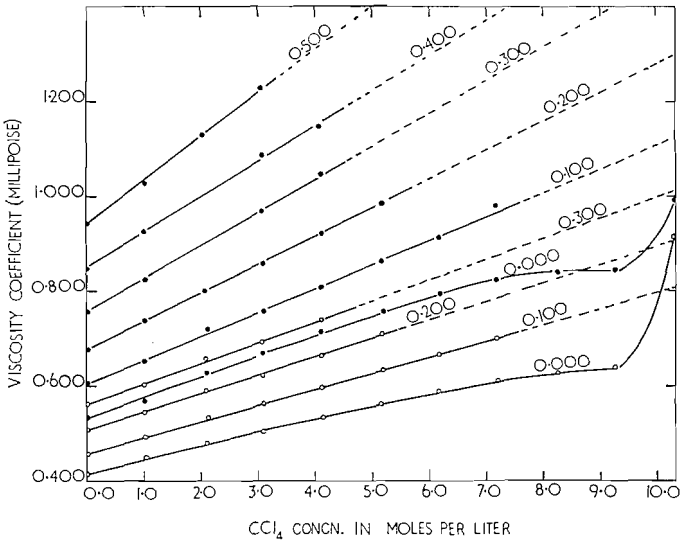


FIG. 1. Viscosity coefficient for $SnCl_4.5H_2O$ – methanol – carbon tetrachloride solutions versus carbon tetrachloride concentration (moles/liter) at the indicated temperatures and molar salt concentrations. ● 25° C; ○ 45° C.

Plots of $SnCl_4.5H_2O$ molar viscosity (η_{IV}) versus salt concentration for solutions with fixed solvent composition and temperature are linear with positive slope (Fig. 2). The ratio B (η_{IV} at 25°/η_{IV} at 45° C) appears to be independent of the salt concentration. Average B values and the square-root-mean-square deviations are given in Table II.

Systems with $SnCl_2.2H_2O$ as Solute

Plots of viscosity coefficient for solutions with fixed $SnCl_2.2H_2O$ concentration versus carbon tetrachloride concentration are illustrated in Fig. 3. Here linearity in the plots was observed only for the higher salt concentrations at both temperatures. The $SnCl_2.2H_2O$ molar viscosity (η_{II}) appears to be independent of salt concentration at each temperature and solvent composition. The average η_{II} values do increase on addition of carbon tetrachloride (Table III, data for 25° C).

Can. J. Chem. Downloaded from www.nrcresearchpress.com by 210.87.254.40 on 09/05/12
For personal use only.

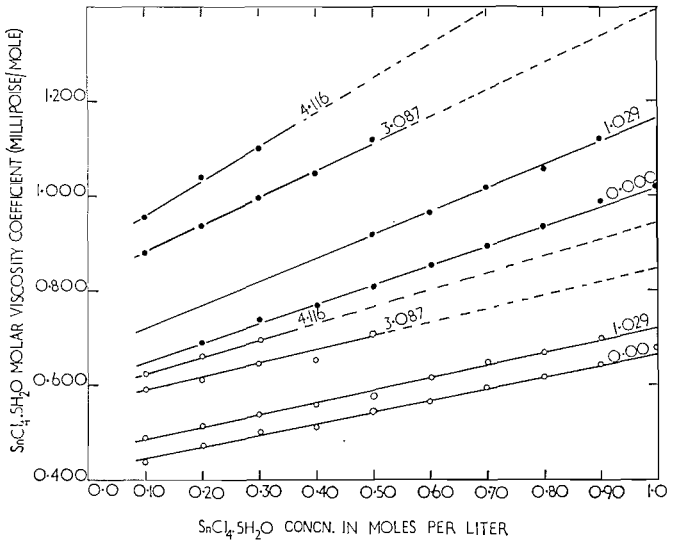


FIG. 2. $SnCl_4.5H_2O$ molar viscosity versus salt concentration at the indicated concentrations of carbon tetrachloride in moles/liter. ● 25° C; ○ 45° C.

TABLE II

Average values for B, B', and B'' (η_{salt} at 25°/η_{salt} at 45° C) for the indicated salts dissolved in methanol – carbon tetrachloride at the indicated concentration
(Below each ratio is given the square-root-mean-square deviation (SRMS) and in parentheses the number of averaged values)

		CCl_4 concentration (M)							
		0	1.029	2.058	3.087	4.116	5.145	6.174	7.203
$SnCl_4.5H_2O$	B	1.492	1.595	1.534	1.567	1.560	1.535		
	SRMS	0.024	0.019	0.024	0.031	0.022	—		
		(7)	(8)	(4)	(4)	(3)	(1)		
$SnCl_2.2H_2O$	B'	1.460	1.582	1.556	1.493	1.519	1.514	1.389	1.450
	SRMS	0.022	0.046	0.023	0.026	0.016	0.019	0.024	0.022
		(12)	(8)	(7)	(5)	(4)	(4)	(3)	(2)
$SnCl_4.5H_2O$	B''	1.496	1.581	1.563	1.545	1.555	1.538	1.586	
$+SnCl_2.2H_2O$	SRMS	0.015	0.026	0.036	0.006	0.022	0.011	—	
		(4)	(4)	(4)	(2)	(3)	(2)	(1)	

The ratio B' (η_{II} at 25°/η_{II} at 45° C) is independent of salt concentration for each solvent composition. B' does depend on solvent composition. Table II lists average B' values together with square-root-mean-square deviations and the number of values averaged.

Systems with $SnCl_4.5H_2O$ and $SnCl_2.2H_2O$ as Solute

For solutions with a constant total salt concentration, plots of viscosity coefficient versus carbon tetrachloride concentration are similar in form to the plots in Fig. 3. The increase in measured viscosity coefficient ($\eta_s - \eta_o$) on addition of the mixed salts to solvents of fixed composition and temperature is noted in Table IV. Also given are the sums of increments of viscosity for separate solutions of each salt at the concentrations and temperature of the corresponding mixed-salt system in the same solvent.

Can. J. Chem. Downloaded from www.nrcresearchpress.com by 210.87.254.40 on 09/05/12
For personal use only.

Can. J. Chem. Downloaded from www.nrcresearchpress.com by 210.87.254.40 on 09/05/12
For personal use only.

TABLE III

Salt molar viscosity values at 25° C for $SnCl_2.2H_2O$ dissolved in methanol – carbon tetrachloride at the indicated carbon tetrachloride concentrations (Average values and the square-root-mean-square deviations are given. Values not included in the average are denoted with a prime)

$SnCl_2.2H_2O$ concn. (M)	CCl_4 concentration (M)									
	0	1.029	2.058	3.087	4.116	5.145	6.174	7.203	8.235	9.261
0.080	0.263′	—	—	0.375	0.400	—	0.463	0.425′	0.580	0.625
0.160	0.294	0.388′	—	0.363	0.388	0.431	0.406′	0.506	0.581	
0.240	0.283	0.362	—	0.354	0.396	0.421	0.462	0.500		
0.320	0.284	0.347	0.319	0.372	0.394	—	0.447			
0.400	0.283	0.343	0.333	0.373	0.422	0.447	0.490			
0.480	0.281	0.340	0.335	0.373	0.414	0.445				
0.560	0.286	0.344	0.334	0.386	0.411					
0.640	0.292	0.344	0.347	0.387						
0.720	0.294	0.340	0.348							
0.800	0.293	0.345	0.354							
0.880	0.300	0.353								
0.960	0.303′									
1.000	0.308′									
Average value	0.287	0.346	0.342	0.373	0.404	0.436	0.465	0.503	0.581	0.625
SRMS	0.005	0.007	0.008	0.010	0.014	0.011	0.015	0.003	—	—

Can. J. Chem. Downloaded from www.nrcresearchpress.com by 210.87.254.40 on 09/05/12
For personal use only.

TABLE IV

Increase in measured viscosity coefficient, $(\eta_s-\eta_o)_M$, and increase in calculated viscosity coefficient, $(\eta_s-\eta_o)_C$, for systems containing both $SnCl_4.5H_2O$ and $SnCl_2.2H_2O$ dissolved in methanol – carbon tetrachloride

(Carbon tetrachloride and salt concentrations are indicated as moles/liter values. The calculated value is underlined in cases where it is larger than the measured value)

			Carbon tetrachloride concentration													
			0.000		1.029		2.058		3.087		4.116		5.145		6.174	
			Temperature													
Sn(IV) concn.	Sn(II) concn.		25° C	45° C	25° C	45° C	25° C	45° C	25° C	45° C	25° C	45° C	25° C	45° C	25° C	45° C
0.100	0.080	$(\eta_s-\eta_o)_M$	0.089	0.065	0.114	0.066	0.103	0.067	0.123	0.085	0.131	0.086	0.145	0.095	0.166	0.105
		$(\eta_s-\eta_o)_C$	0.089	0.059	0.120	0.066	0.114	0.069	0.118	0.084	0.127	0.084	0.144	0.098	0.157	0.098
0.200	0.160	$(\eta_s-\eta_o)_M$	0.190	0.129	0.221	0.140	0.229	0.142	0.257	0.167	0.281	0.178	0.321	0.208		
		$(\eta_s-\eta_o)_C$	0.185	0.125	0.230	0.134	0.216	0.144	0.245	0.162	0.270	0.175	0.299	0.192		
0.300	0.240	$(\eta_s-\eta_o)_M$	0.302	0.201	0.353	0.229	0.360	0.230	0.408	0.263	0.408	0.291				
		$(\eta_s-\eta_o)_C$	0.290	0.196	0.342	0.208	0.400	0.229	0.384	0.251	0.425	0.274				
0.400	0.320	$(\eta_s-\eta_o)_M$	0.417	0.279	0.486	0.305	0.496	0.327								
		$(\eta_s-\eta_o)_C$	0.399	0.268	0.469	0.293	—	0.307								
0.500	0.400	$(\eta_s-\eta_o)_M$	0.561	0.370	0.642	0.399										
		$(\eta_s-\eta_o)_C$	0.517	0.349	0.597	0.364										

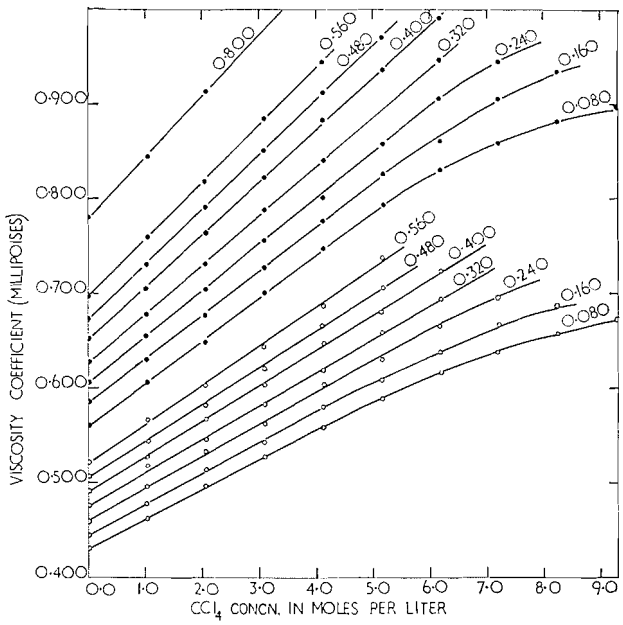


FIG. 3. Viscosity coefficient for $SnCl_2.2H_2O$ – methanol – carbon tetrachloride systems versus concentration of carbon tetrachloride at the indicated temperatures and salt concentrations (moles/liter). ● 25° C; ○ 45° C.

DISCUSSION

Acceptance of the hypothesis that partial reversible association of either covalent or ionic species will lead to a corresponding increase in the molar viscosity of the salt permits an analysis of the new viscosity data which are consistent with earlier conclusions from spectrophotometric and conductance data for the separate and mixed $SnCl_4.5H_2O$ and $SnCl_2.2H_2O$ – methanol – carbon tetrachloride systems. The hypothesis can be justified upon careful consideration of the Stokes' viscosity equation.

Systems with $SnCl_4.5H_2O$ as Solute

The linear dependence of the $SnCl_4.5H_2O$ molar viscosity on salt concentration for solutions with fixed solvent composition and temperature (Fig. 2) may be explained with the supposition that partial reversible dimerization of covalent tin(IV) species occur together with reversible methanolysis of monomeric tin(IV) species. Addition of carbon tetrachloride leads to partial demethanolysis of the monomeric species and a consequent increase in the concentration of the dimeric form. Thus the salt molar viscosity coefficient increases. The increase in positive slope of the straight-line plots in Fig. 2 on addition of carbon tetrachloride supports the competitive dimerization–methanolysis reaction invoked to explain spectrophotometric (1) and conductance (3, 5) data for this system.

Systems with $SnCl_2.2H_2O$ as Solute

As $SnCl_2.2H_2O$ molar viscosity (Table III) is independent of salt concentration for solutions of fixed solvent composition and temperature, partial reversible polymerization of Sn(II) species cannot be significant. There is reversible methanolysis of Sn(II) species. These same conclusions were obtained from spectral (1) and conductance data (3, 5). The gradual increase in the $SnCl_2.2H_2O$ molar viscosity on addition of carbon tetrachloride (Table III) indicates that ion-pair formation and demethanolation may both contribute to the salt molar viscosity.

Can. J. Chem. Downloaded from www.nrcresearchpress.com by 210.87.254.40 on 09/05/12
For personal use only.

Systems with $SnCl_4.5H_2O$ and $SnCl_2.2H_2O$ as Solute

If the interaction between tin(IV) and tin(II) species occurs only after demethanolation of the species, the measured $(\eta_s - \eta_o)$ should be greater than the corresponding value calculated with values for the salts in separate solutions. The difference should increase with increased total salt or carbon tetrachloride concentration. Data in Table IV confirm these predictions. Experiments for which the situation is reversed occur because of the relatively small salt molar concentrations and consequent greater experimental error.

Temperature Dependence of Salt Molar Viscosity

As the ratios B and B' are independent of salt concentration for fixed solvent composition for each salt system (Table II) it seems that the salt species in solution behave as Arrhenius–Guzman liquids (9).

ACKNOWLEDGMENT

Financial support of this work by the donors of the Petroleum Research Fund, administered by the American Chemical Society, is gratefully acknowledged.

REFERENCES

1. M. M. DE MAINE and P. A. D. DE MAINE. J. Inorg. & Nuclear Chem. **11**, 13 (1959).
2. P. A. D. DE MAINE. J. Inorg. & Nuclear Chem. **14**, 262 (1960).
3. P. A. D. DE MAINE, M. M. DE MAINE, and G. E. MCALONIE. J. Inorg. & Nuclear Chem. **14**, 268 (1960).
4. P. A. D. DE MAINE and M. M. DE MAINE. J. Inorg. & Nuclear Chem. **14**, 142 (1960).
5. P. A. D. DE MAINE and E. J. WALSH. J. Inorg. & Nuclear Chem. In press.
6. P. A. D. DE MAINE and M. M. DE MAINE. J. Inorg. & Nuclear Chem. **11**, 144 (1959).
7. P. A. D. DE MAINE, G. E. MCALONIE, and M. M. DE MAINE. J. Inorg. & Nuclear Chem. **14**, 273 (1960).
8. INTERNATIONAL CRITICAL TABLES. McGraw-Hill Book Co., Inc., New York. 1926.
9. S. GLASSTONE. Textbook of physical chemistry. 2nd ed. D. Van Nostrand Company, Inc., New York. 1946.

Can. J. Chem. Downloaded from www.nrcresearchpress.com by 210.87.254.40 on 09/05/12
For personal use only.

Can. J. Chem. Downloaded from www.nrcresearchpress.com by 210.87.254.6 on 09/05/12
For personal use only.

REARRANGEMENT STUDIES WITH C^{14}

XI. THE FORMOLYSIS OF 2-PHENYLETHYL-1-C^{14} *p*-TOLUENESULPHONATE WITH OR WITHOUT ADDED SODIUM *p*-TOLUENESULPHONATE-S^{35} [1]

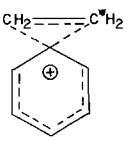
J. W. CLAYTON[2] AND C. C. LEE

ABSTRACT

The formolysis of 0.350 *M* 2-phenylethyl-1-C^{14} *p*-toluenesulphonate (I) was carried out at 74±0.2° C with or without the presence of an equimolar amount of sodium *p*-toluenesulphonate-S^{35} (III). The over-all first-order rate constant, k_1, was found to be 2.6×10^{-5} sec^{-1} and 3.0×10^{-5} sec^{-1}, respectively, for the reaction with and without added III. The determination of the degrees of rearrangement of the C^{14}-labeled atoms from the C-1 to the C-2 positions in the 2-phenylethyl *p*-toluenesulphonate (I_r) recovered from the reaction mixture at various reaction times permitted the evaluation of k^{14}, the rate of return from ionic intermediates to covalent bonding. Using the experimental data, it was possible to calculate k_s and k_Δ, the rates, respectively, for the anchimerically unassisted and assisted solvolysis. As expected, formolysis of I proceeded principally by the anchimerically assisted process. Calculations also showed that the fraction of the anchimerically assisted ionization returning to covalent bonding was about 15% for the reaction in the presence of III, while in the absence of III, the return was about 9%. For the formolysis of I in the presence of III, the extents of incorporation of S^{35} in the recovered sulphonate I_r were also determined. The S^{35} incorporation in I_r, when considered in conjunction with the C^{14} rearrangement in I_r, led to the conclusion that the return from ionic intermediates to covalent bonding during the formolysis of I included both internal and external returns, the extent of external return being the greater of the two.

INTRODUCTION

In earlier publications (1, 2), isotope position rearrangements observed in the solvolysis of 2-phenylethyl-1-C^{14} *p*-toluenesulphonate (I) under various conditions were reported. When acetolysis and formolysis of I were interrupted at about 50% completion, the rearrangement of C^{14}-labeled atoms from the C-1 to C-2 positions in the recovered 2-phenylethyl-*x*-C^{14} *p*-toluenesulphonate (I_r) indicated some return to covalent bonding through the intermediate ethylphenonium ion (II) or its equivalent. Solvolysis of I



(II)

in the presence of sodium *p*-toluenesulphonate-S^{35} (III) made possible the simultaneous determinations of C^{14} rearrangement and S^{35} incorporation in the sulphonate I_r recovered from the partially solvolyzed mixture. The data obtained for formolysis (2) indicated that some of the *p*-toluenesulphonate anions involved in the return to give the isotopically rearranged 2-phenylethyl-2-C^{14} *p*-toluenesulphonate were derived from an intramolecular process, thus pointing to the occurrence of some internal return from an intimate ion pair (3–6) during the formolysis of I.

[1]*Manuscript received March 16, 1961.*
Contribution from the Department of Chemistry, University of Saskatchewan, Saskatoon, Saskatchewan.
[2]*Holder of a Canadian Industries Limited Fellowship, 1959–60, and a National Research Council of Canada Studentship, 1960–61.*

Can. J. Chem. Downloaded from www.nrcresearchpress.com by 210.87.254.6 on 09/05/12
For personal use only.

A drawback in the earlier work (1, 2) has been a lack of any concurrent kinetic data for consideration in conjunction with the observed C^{14} rearrangement and S^{35} exchange. In the present study, the formolysis of I was carried out at 74° C with or without the presence of an equimolar amount of III. At various stages of reaction, the rearrangements of the C^{14}-labeled atoms from the C-1 to C-2 positions were determined in the product, 2-phenylethyl-*x*-C^{14} formate (IV), and in the 2-phenylethyl-*x*-C^{14} *p*-toluenesulphonate (I_r) recovered from the reaction mixture. For the formolysis in the presence of III, the incorporations of S^{35} in I_r were also measured. Concurrent kinetic studies were made by potentiometric titration of the *p*-toluenesulphonic acid liberated, by isotope dilution of the product, IV, that was formed, and by isotope dilution of the reactant, I_r, that remained.

METHODS AND RESULTS

Formolysis of 2-Phenylethyl-1-C^{14} p-Toluenesulphonate (I) without Added Sodium p-Toluenesulphonate-S^{35} (III)

The reaction was carried out in an all-glass apparatus. The reaction vessel of about 75-ml capacity was provided with a cold-finger condenser at the top and a drain with stopcock at the bottom. The vessel was enclosed in a pyrex jacket which was fitted with a reflux condenser and connected to a pot of boiling liquid. The vapor from the boiling liquid heated the reaction mixture and maintained a constant temperature. The boiling liquid used in the present work was ethyl acetate, giving a jacket temperature of 74±0.2° C for all experiments.

Fifty-milliliter portions of 0.350 *M* solution of I in anhydrous formic acid were heated in the reaction vessel at 74±0.2° C for various lengths of time. Each experiment was stopped by draining the reaction mixture into an ice-cooled receiver. A 2-ml aliquot was pipetted into dry acetic acid for potentiometric titration of the liberated *p*-toluenesulphonic acid (7). A larger aliquot (40 ml) was added to ice water. Known weights of ordinary 2-phenylethyl formate and 2-phenylethyl *p*-toluenesulphonate were added as carriers. The diluted reaction product (IV) and remaining reactant (I_r) were isolated as

TABLE I

Date from the formolysis of 0.350 *M* 2-phenylethyl-1-C^{14} *p*-toluenesulphonate (I) at 74±0.2° C with no added salt

Reaction time (min)	Observed concn. (mole/l.) From titration HOTs	From isotope dilution: IV*	From isotope dilution: I_r†	Corrected‡ initial concn. *a* (mole/l.)	Mean value of $(a-x)$ (mole/l.)	% C^{14} rearrangement from C-1 to C-2: In IV*	% C^{14} rearrangement from C-1 to C-2: In I_r†
51	0.035	0.034	—	0.350	0.315	45.9	0.17
167	0.103	0.104	—	0.351	0.247	45.0	0.76
275	—	0.149	0.199	0.352	0.201	43.9	1.83
600	0.245	0.236	0.131	0.354	0.119	46.0	3.37
600	0.244	0.235	0.136	0.354	0.122	46.1	3.30
900	0.293	0.275	0.073	0.355	0.071	—	5.78
1155	0.320	0.327	0.043	0.357	0.036	44.8	8.60
1200	0.317	—	0.043	0.357	0.041	45.0	8.88
						45.2§	

*IV is the formolysis product, 2-phenylethyl-*x*-C^{14} formate.
†I_r is the recovered reactant, 2-phenylethyl-*x*-C^{14} *p*-toluenesulphonate.
‡Corrected for decrease in volume due to decomposition of HCOOH.
§Mean value.

described previously (2). By isotope dilution calculations, the concentrations of IV and I_r were then ascertained. The results are tabulated in Table I.

Let a be the initial concentration of I, x the concentration at time t of the products, p-toluenesulphonic acid and IV, then $(a-x)$ would be the concentration of the recovered reactant I_r. From the titration and isotope dilution data, three separate values of $(a-x)$ could be calculated. In these calculations, a small correction on a was made because prolonged heating caused slight decreases in volume due to decomposition of the formic acid. For example, one of the reactions, stopped at a reaction time of 600 minutes, showed, by titration, a p-toluenesulphonic acid concentration of 0.245 M. From an independent trial, heating of the formolysis mixture at 74±0.2° C for 600 minutes caused a decrease in volume from 500 to 494 ml. The effective value of a for the aliquot titrated at 600 minutes of reaction time would be $(500/494)\times0.350 = 0.354$ M. Hence $(a-x)$ from potentiometric titration was $0.354-0.245 = 0.109$ M. Similarly, isotope dilution calculations showed that the concentration of IV was 0.236 M. Thus $(a-x)$ would be $0.354-0.236 = 0.118$ M. Again from isotope dilution, the concentration of I_r was 0.131 M. Correcting for the decrease in volume, $(a-x)$ would be $(0.350/0.354)\times0.131 = 0.129$ M. The mean value for $(a-x)$ is therefore $(0.109+0.118+0.129)/3 = 0.119$ M. Such mean values of $(a-x)$ corresponding to various reaction times are also given in Table I. From a semilogarithmic plot of the mean $(a-x)$ values vs. t (Fig. 1), a straight line was obtained

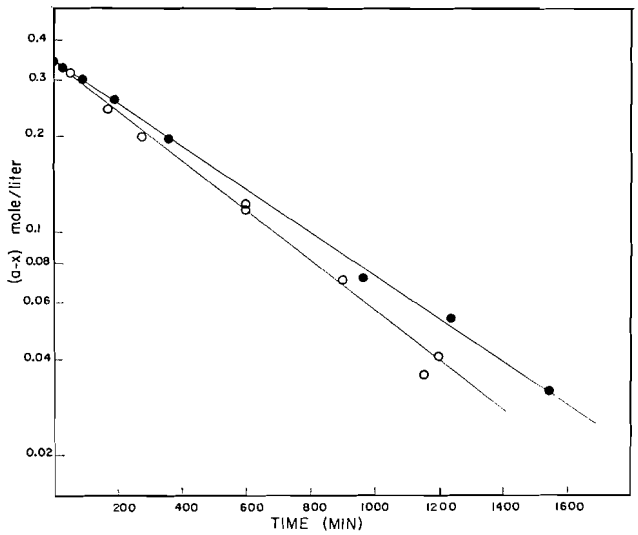


FIG. 1. Rate of formolysis of 2-phenylethyl-1-C^{14} p-toluenesulphonate. Open and closed circles, respectively, represent reaction without and with added sodium p-toluenesulphonate-S^{35}.

indicating a first-order reaction. The first-order specific rate constant, k_1, derived from Fig. 1 is 3.0×10^{-5} sec^{-1}.*

Besides the isotope dilution studies, the rearrangements of the C^{14} label from C-1 to C-2 were determined in the recovered reactant I_r, and in the product IV (2). Treatment of I_r with sodium iodide in acetone gave 2-phenylethyl-x-C^{14} iodide which was oxidized

**Winstein and co-workers (8) reported a k_1 of 3.59×10^{-5} sec^{-1} at 74.62° C for 0.074 M initial concentration of the sulphonate. The agreement appears satisfactory since other data given by these authors (8) showed that at a given temperature, an increase in initial concentration decreased k_1.*

Can. J. Chem. Downloaded from www.nrcresearchpress.com by 210.87.254.6 on 09/05/12
For personal use only.

with potassium permanganate (1) to yield benzoic acid whose activity gave a measure of the C^{14} content in the C-2 position of I_r. For the reaction product IV, alkaline permanganate oxidation also yielded benzoic acid whose activity showed the degree of rearrangement of C^{14} to the C-2 position of IV. The C^{14} rearrangements in I_r and IV corresponding to various reaction times are included in Table I.

Formolysis of 2-Phenylethyl-1-C^{14} p-Toluenesulphonate (I) with Added Sodium p-Toluenesulphonate-S^{35} (III)

p-Toluenesulphonic acid-S^{35} was prepared by sulphonation of toluene with concentrated sulphuric acid containing S^{35} (2). Instead of a simple neutralization as a means of obtaining the sodium salt (2), the following series of reactions was used to synthesize III so as to eliminate any possible presence of impurities. *p*-Toluenesulphonic acid was converted to the sulphonyl chloride. Reaction of the latter with ethanol in pyridine (9) gave ethyl *p*-toluenesulphonate-S^{35}, which, in turn, was treated with sodium iodide in acetone to give the desired sodium salt, III.

The formolysis was carried out in a reaction vessel of about 600-ml capacity enclosed in a pyrex jacket as described earlier. Five hundred milliliters of anhydrous formic acid solution, 0.350 *M* in I and in III, was heated in the reaction vessel by the vapor of refluxing ethyl acetate. At zero time, when the jacket temperature first reached 74±0.2° C, and at various time intervals thereafter, aliquots of the reaction mixture were withdrawn for potentiometric titrations of *p*-toluenesulphonic acid, for isotope dilution determinations of the concentrations of I_r and IV, and for the measurements of C^{14} rearrangement in I_r and IV as outlined in the previous section. In addition, the degrees of incorporation of S^{35} in the various samples of recovered reactant I_r were measured. The procedure (2) was based on the treatment of I_r with sodium iodide in acetone, which gave, besides 2-phenylethyl-*x*-C^{14} iodide, sodium *p*-toluenesulphonate whose S^{35} content represented the amount of S^{35} incorporated in I_r. The results obtained from formolysis of I in the presence of an equimolar amount of III are summarized in Table II. A semilogarithmic

TABLE II

Data from formolysis of 0.350 *M* 2-phenylethyl-1-C^{14} *p*-toluenesulphonate (I) at 74±0.2° C with the presence of 0.350 *M* sodium *p*-toluenesulphonate-S^{35} (III)

Reaction time (min)	Mean value of $(a-x)$* (mole/l.)	Extent of reaction (%)	% C^{14} rearrangement from C-1 to C-2		% S^{35} incorporated in I_r‖	Calc. % S^{35} in I_r for external return
			In IV†	In I_r‡		
0	0.347	0.9	—	0.16	—	—
31	0.329	6.0	—	0.47	0.78	0.91
92	0.301	14.0	42.8	1.20	2.22	2.24
186	0.260	25.8	48.2	2.52	4.28	4.46
357	0.197	43.8	48.2	4.15	6.79	6.81
965	0.072	79.4	48.4	10.3	14.3	14.7
1238	0.054	84.6	46.8	13.6	15.3	19.1
1543	0.032	90.8	46.8	16.8	18.6	23.1
			46.9§			

*Mean of two or three values calculated from the concentration of *p*-toluenesulphonic acid determined by titration; the concentration 2-phenylethyl-*x*-C^{14} formate and the concentration 2-phenylethyl-*x*-C^{14} *p*-toluenesulphonate determined by isotope dilution.
†IV is the formolysis product, 2-phenylethyl-*x*-C^{14} formate.
‡I_r is the recovered reactant, 2-phenylethyl-*x*-C^{14} *p*-toluenesulphonate.
§Mean value.
‖(Specific activity of sodium *p*-toluenesulphonate-S^{35} derived from I_r/specific activity of sodium *p*-toluenesulphonate-S^{35} added to the reaction mixture)×100. The specific activity of the added sodium *p*-toluenesulphonate-S^{35} is about 4000 c.p.m. per infinitely thick sample counted.

Can. J. Chem. Downloaded from www.nrcresearchpress.com by 210.87.254.6 on 09/05/12
For personal use only.

plot of $(a-x)$ vs. t (Fig. 1) also gave a straight line from which k_1 was calculated to be 2.6×10^{-5} sec^{-1}.

DISCUSSION

With reference to the results tabulated in Tables I and II, the fact that there was rearrangement of the C^{14}-labeled atoms from the C-1 to C-2 positions in every sample of 2-phenylethyl-x-C^{14} p-toluenesulphonate (I_r) recovered from partially solvolyzed reaction mixtures definitely confirmed the earlier conclusion (2) that there was some return to covalent bonding involving an intermediate ethylphenonium ion (II) or its equivalent. The C^{14} rearrangement in I_r could be regarded as a simple isotopic exchange reaction, the rate of exchange being proportional to $Y_\infty - Y$, where Y is the fraction exchanged at time t, and Y_∞ the fraction exchanged at infinite time. This treatment has been applied by Jenny and Winstein (6) in the consideration of data from the solvolysis of 2-p-methoxyphenylethyl-1-C^{14} p-toluenesulphonate.

Thus

$$[1] \qquad \frac{d(\%\ C_2^{14})}{dt} = k^{14}(\%\ C_{2\infty}{}^{14} - \%\ C_2^{14})$$

where $\%\ C_2^{14}$ and $\%\ C_{2\infty}{}^{14}$ are, respectively, percentage rearrangement of C^{14} to C-2 at time t and at infinite time. Using the maximum rearrangement of 50% as $\%\ C_{2\infty}{}^{14}$, integration gave

$$[2] \qquad k^{14}t = 2.303 \log \frac{50}{50 - \%\ C_2^{14}}.$$

From semilogarithmic plots of $50 - \%\ C_2^{14}$ vs. t (Fig. 2), k^{14} could be evaluated. Values

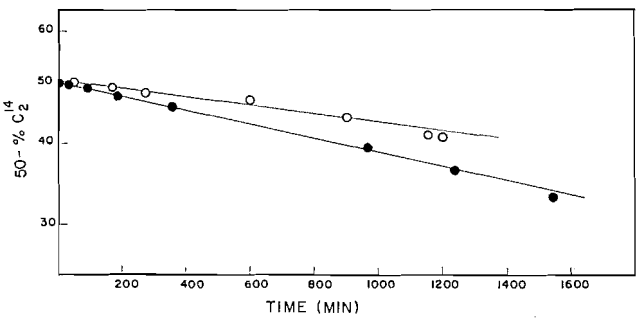
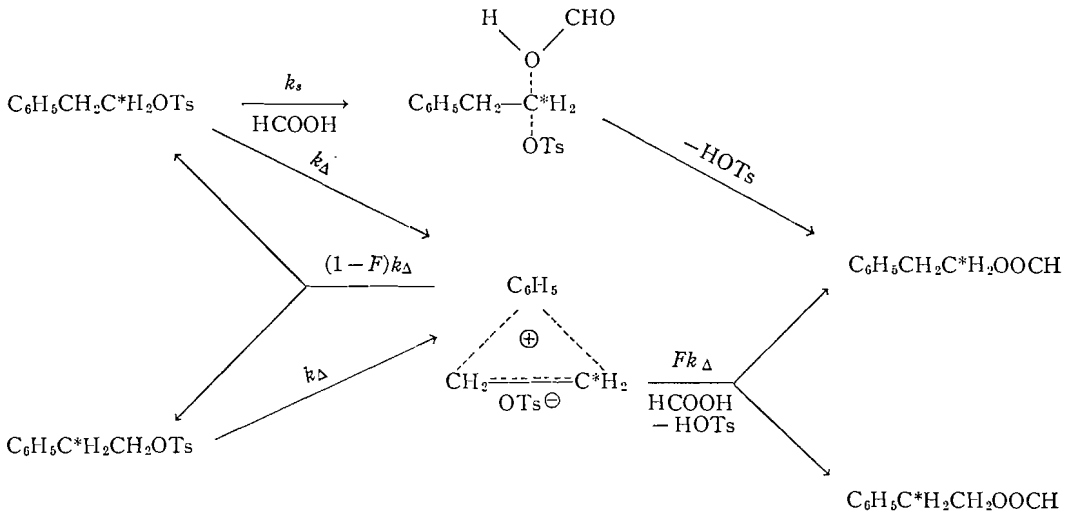


FIG. 2. Rate of C^{14} rearrangement in 2-phenylethyl p-toluenesulphonate recovered from partially solvolyzed mixtures. Open and closed circles, respectively, represent formolysis without and with added sodium p-toluenesulphonate-S^{35}.

of 4.2×10^{-6} sec^{-1} and 2.5×10^{-6} sec^{-1} were obtained, respectively, for k^{14} for formolysis of I with and without the presence of an equimolar quantity of III.

Using the symbolism of Winstein, with k_s and k_Δ designating, respectively, the anchimerically unassisted and assisted solvolysis, the following scheme may be written:

Can. J. Chem. Downloaded from www.nrcresearchpress.com by 210.87.254.6 on 09/05/12
For personal use only.



In this scheme, F is that fraction of the anchimerically assisted ionization which leads to solvolysis products, and $(1-F)$ is that fraction which returns to covalent bonding. With the aid of equations [3], [4], and [5], k_s, k_Δ, and F can be calculated (6). The results, together with values of k_1 and k^{14} derived from Figs. 1 and 2, are summarized in Table III.

[3] $$k_1 = Fk_\Delta + k_s$$

[4] $$k^{14} = (1-F)k_\Delta$$

[5] $$\frac{k_\Delta}{k_s} = \frac{\text{mean \% rearrangement in formate IV}}{50 - \text{mean \% rearrangement in formate IV}}$$

TABLE III

Summary of rate data for the formolysis of 2-phenylethyl-1-C^{14} *p*-toluenesulphonate (I) with or without the presence of an equimolar amount of sodium *p*-toluenesulphonate-S^{35} (III)

$NaOTs\text{-}S^{35}$	10^5k_1 (sec^{-1})	10^5k^{14} (sec^{-1})	10^5k_s (sec^{-1})	10^5k_Δ (sec^{-1})	F
None	3.0	0.25	0.4	2.9	0.91
Equimolar	2.6	0.42	0.2	2.8	0.85

From Table III, it may be noted that the relative values of k_s and k_Δ showed that the reaction proceeded chiefly by anchimerically assisted ionization as one would expect for solvolysis in formic acid, a highly ionizing solvent. The over-all formolysis rate, k_1, was some 13% slower when the reaction was carried out with added III. This could be explained on the basis of the so-called mass-law effect (10) with the common *p*-toluenesulphonate ion causing a rate depression. The data also demonstrated that this rate depression was attributable to a greater degree of return to covalent bonding when an excess of *p*-toluenesulphonate ion was present during the formolysis. This was indicated by a greater k^{14} for the formolysis in the presence of III. From the calculated F values, it can also be seen that the fraction of the anchimerically assisted ionization returning to

Can. J. Chem. Downloaded from www.nrcresearchpress.com by 210.87.254.6 on 09/05/12
For personal use only.

covalent bonding was some 15% for the reaction in the presence of III as compared with a return of only 9% when III was absent.

In connection with returns to covalent bonding, it may also be of interest to point out that in a study of the rates of solvolysis of 2-phenylethyl-1,1-d_2 and 2-phenylethyl-2,2-d_2 *p*-toluenesulphonates (I_b and I_c), Saunders and co-workers (11) noted the absence of any drift of the rate constants toward a common value and concluded that "internal return from a phenonium–tosylate ion pair cannot be appreciable, since in its presence I_b and I_c would be interconverted and their rate constants would drift toward a common value as the reaction proceeded". This conclusion would be valid only if the rate of the return process were great enough to cause an almost complete scrambling of the C-1 and C-2 positions in I_r before the product-forming reaction proceeded to completion. Inspection of the data in Table I shows that after a reaction time of 1200 minutes (about 88% completion), the C^{14} rearrangement in I_r was 8.88%, far from a 50% rearrangement expected for a complete scrambling of the C-1 and C-2 positions. Thus the interconversion of I_b and I_c was not great enough during the formolysis of these compounds to cause an observable drift towards a common rate constant. The fraction $(1-F)$ from the present data indicated that a return to covalent bonding did occur to the extent of about 9% of the anchimerically assisted ionization.

The processes of return from ionic intermediates to covalent bonding may be differentiated as internal and external returns, with internal return designating return from the "intimate ion pair" and external return designating return from the "solvent-separated ion pair" or dissociated ions (4, 5). In such a differentiation, internal return would be pictured as an intramolecular process. It was hoped that the inclusion of S^{35}-labeled sodium *p*-toluenesulphonate (III) in the formolysis studies might provide data which could shed some light on the extent, if any, of the intramolecular return.

The degrees of incorporation of S^{35} in the various samples of I_r are given in Table II. These results could not be treated kinetically as data for a simple exchange reaction between 2-phenylethyl *p*-toluenesulphonate (I) and sodium *p*-toluenesulphonate-S^{35} (III) because one of the reactants, I, was being continually converted to 2-phenylethyl formate (IV). Moreover, the S^{35} incorporated in I_r, besides arising from external return, might have resulted also from a direct displacement reaction between I and the added *p*-toluenesulphonate-S^{35} anion, and (or) by exchange between the labeled *p*-toluenesulphonate anion and the *p*-toluenesulphonate anion of the intimate ion pair. However, a qualitative consideration of the S^{35} incorporation in I_r in conjunction with the C^{14} rearrangement in I_r can be made (2). If the C^{14} rearrangement in I_r were to arise entirely from reaction between ethylphenonium ions (II) and the added *p*-toluenesulphonate-S^{35} anions, in other words entirely from external return, the percentage of S^{35} incorporated in I_r would be twice the percentage of C^{14} rearrangement in I_r. A correction should be made because the added *p*-toluenesulphonate-S^{35} anions would be progressively diluted by the *p*-toluenesulphonic acid liberated from I during the course of the reaction. The S^{35} in I_r would be decreased by this dilution effect. For example, for a reaction stopped at 10% completion, on the average, the incorporation of S^{35} would be decreased by a factor of $100/(100+10/2)$. The values obtained from [100/(100+% reaction/2)] ($2\times$% C^{14} rearrangement in I_r) would be the calculated percentage of S^{35} in I_r if the return process were only external or intermolecular. These calculated values are given in column 7 of Table II. Compared with the observed percentage of S^{35} in I_r (column 6, Table II), it can be seen that during the earlier stages of the reaction, the observed S^{35} in I_r were slightly lower than the calculated S^{35} for pure external return, while at the later stages

Can. J. Chem. Downloaded from www.nrcresearchpress.com by 210.87.254.6 on 09/05/12
For personal use only.

of reaction, the observed S^{35} in I_r were considerably lower than the calculated values. Since the observed S^{35} in I_r should be the sum of the S^{35} incorporated via external return, via direct displacement between I and the added *p*-toluenesulphonate-S^{35}, and possibly even via return from an intimate ion pair containing some exchanged *p*-toluenesulphonate-S^{35} anions, if the return process were only intermolecular between II and *p*-toluenesulphonate-S^{35}, one would expect the observed S^{35} in I_r to be at least equal to, or possibly greater than the calculated % S^{35} in I_r for pure external return. The fact that the observed percentage of S^{35} in I_r were smaller than the calculated values, even though only slightly smaller, indicated that very probably some intramolecular return also took place. It may, therefore, be concluded that the return from ionic intermediates to covalent bonding during the formolysis of I included both internal and external returns, with external return accounting for the major portion of the return processes.

ACKNOWLEDGMENTS

The financial support given by the National Research Council of Canada is gratefully acknowledged.

REFERENCES

1. C. C. Lee, G. P. Slater, and J. W. T. Spinks. Can. J. Chem. **35**, 1417 (1957).
2. C. C. Lee, R. Tkachuk, and G. P. Slater. Tetrahedron, **7**, 206 (1959).
3. W. G. Yound, S. Winstein, and H. L. Goering. J. Am. Chem. Soc. **73**, 1958 (1951).
4. S. Winstein, E. Clippinger, A. H. Fainberg, R. Heck, and G. C. Robinson. J. Am. Chem. Soc. **78**, 328 (1956).
5. S. Winstein and G. C. Robinson. J. Am. Chem. Soc. **80**, 169 (1958).
6. E. F. Jenny and S. Winstein. Helv. Chim. Acta, **41**, 807 (1958).
7. S. Winstein and H. Marshall. J. Am. Chem. Soc. **74**, 1120 (1952).
8. S. Winstein, C. R. Lindegren, H. Marshall, and L. L. Ingraham. J. Am. Chem. Soc. **75**, 147 (1953).
9. R. S. Tipson. J. Org. Chem. **9**, 235 (1944).
10. C. K. Ingold. Structure and mechanism in organic chemistry. G. Bell & Sons Ltd., London. 1953. pp. 360–370.
11. W. H. Saunders, Jr., S. Asperger, and D. H. Edison. J. Am. Chem. Soc. **80**, 2421 (1958).

Can. J. Chem. Downloaded from www.nrcresearchpress.com by 210.87.254.6 on 09/05/12
For personal use only.

Can. J. Chem. Downloaded from www.nrcresearchpress.com by 210.87.254.40 on 09/05/12
For personal use only.

CONDENSATION OF SPRUCE PERIODATE LIGNIN WITH FORMALDEHYDE[1]

EDGAR EISENBRAUN[2] AND C. B. PURVES

ABSTRACT

The use of 73% sulphuric acid at 41° for 1 hour or less caused the periodate lignin to condense with 32% by weight of formaldehyde, as shown by direct measurement and by employing C^{14}-formaldehyde. Analyses of the product, however, suggested that the elements of water had been expelled during the condensation and that the true yield was about 120%. Up to 106% was recovered as material insoluble in dilute sulphuric acid (Ross–Potter lignin), and about 9% as a more soluble form. The approximate equivalence in weight of the Ross–Potter lignin to the original periodate (or Klason) lignin thus originated in the cancellation of three large errors. Formaldehyde periodate lignin failed to yield vanillin when oxidized in alkali with nitrobenzene or cupric hydroxide. Oxidation with alkaline potassium permanganate, or with iodic acid at not more than 200°, yielded benzenepentacarboxylic acid and perhaps mellitic acid (total, 3.9%) but none of the 1,2,4,5-tetracarboxylic acid recovered (together with the pentacarboxylic acid) from similar oxidations of periodate lignin. Convenient semimicro-scale oxidations with cupric hydroxide and with iodic acid, and the chromatography of the benzene-penta- and -tetra-carboxylic acids on paper, were described.

INTRODUCTION

It is well known that the treatment of wood meal with 72% sulphuric acid near 20°, as in the Klason determination of lignin, soon degrades and dissolves all of the carbohydrates but leaves the lignin as a dark brown, amorphous powder insoluble in all liquids. In 1929, however, Ross and Hill (1) observed that when the wood meal was first soaked in formalin all dissolved in the sulphuric acid, and this solution had to be diluted with water in order to precipitate "formaldehyde lignin". The yield appeared to be quantitative from softwoods, but not from hardwoods, and the products were soluble in alcohol, acetone, or acetic acid containing a little water. Ross and Potter (2) modified the procedure to determine lignin in paper pulps, but the Klason method proved to be more reproducible (3). Since formaldehyde could be expected to condense freely with lignin (a phenolic material) it seemed anomalous that the yield of Ross–Potter lignin was not substantially greater than that of the Klason lignin. The solubility of formaldehyde lignin suggested (2) that the formaldehyde had substituted active centers in the lignin, which normally condensed with each other to form the insoluble Klason lignin. The present research was planned to gain information on these possibilities.

Borisek and Polcin (4) determined the amount of formaldehyde that condensed with sulphite waste liquor solids under various conditions. No condensation occurred in neutral solution, and in alkali the formaldehyde underwent the Cannizzaro reaction. In sulphuric acid, the amount condensed increased as the concentration of the acid was increased to 27%, and 2 hours were sufficient for the reaction. Samples pretreated with sulphurous or sulphuric acid failed to react under the conditions tried. The lignin used on the present occasion was isolated by alternately oxidizing spruce wood meal with sodium periodate near pH 4, and extracting the oxidized polysaccharides with cold, dilute alkali. Although free of carbohydrates and dissolving at almost the normal rate during a calcium bisulphite cook of the type used in pulping wood, the periodate lignin was somewhat oxidized. Nevertheless, it served as a good model substance for lignin

[1]*Manuscript received March 13, 1961.*
Contribution from the Wood Chemistry Division, Pulp and Paper Research Institute of Canada, and from the Division of Industrial and Cellulose Chemistry, McGill University, Montreal, Quebec. Abstracted from a Ph.D. thesis submitted to the University by E.E. in April 1959.
[2]*Present address: Arnold Hoffman Corporation, Providence, Rhode Island, U.S.A.*

Can. J. Chem. Downloaded from www.nrcresearchpress.com by 210.87.254.40 on 09/05/12
For personal use only.

in situ. Periodate lignin, when saturated with formalin, proved to be completely soluble at 41° in sulphuric acid provided the concentration of acid in the final mixture was at least 69% by weight.

The simplest way of isolating the main product (method (*a*)) was to pour this solution into a large volume of cold water, which was kept near neutrality by the simultaneous addition of sodium hydroxide, and to purify the precipitated formaldehyde periodate lignin by dialysis. The yield was 104% by weight. To recover the soluble products, dialysis was avoided in method (*b*), in which the neutralized, concentrated liquors were freed of sodium sulphate by dilution with ethanol and acetone. Evaporation of the mother liquor gave a yellow glass highly contaminated with inorganic material and formaldehyde polymer, but extraction with organic solvents recovered 9% of product, which with 106% for the main fraction raised the total yield to 115%, free of ash and moisture. This figure was accepted as being close to the yield actually formed in the condensation. Both the major and the minor fractions retained ultraviolet absorption spectra in 0.1% solution of the type characteristic of most lignins, with a broad, prominent maximum near wave length 280 mμ. A third attempt at isolation (method (*c*)) involved pouring the original sulphuric acid solution into an excess of acetic anhydride and anhydrous sodium acetate more than sufficient to combine with all the water and acid present. After isolation by precipitation into water followed by dialysis, the acetylated periodate formaldehyde lignin was recovered in 92% yield as a dark, hard resin.

The consumption of formaldehyde in the condensation was estimated, by difference, from the initial and final amounts. The results showed that 100 g of the lignin condensed with 32 g of formaldehyde, but the true amount might be as high as 35 g, since Freudenberg and Sohns (5) obtained 2 to 3% of formaldehyde by distilling various lignins with sulphuric acid. Thus the expected yield of formaldehyde periodate lignin was at least 132% by weight, whereas 115% was the most that was ever recovered. According to the book by Walker (6), the strongly acidic conditions necessary to cause the condensation of formaldehyde with simple phenolic ethers or with ethylenic compounds were usually, although not always, sufficient to condense the hydroxymethyl derivatives initially formed to cyclic acetals, to ethers, or to derivatives of diphenylmethane. The above discrepancy in the yield of formaldehyde periodate lignin might thus originate in the condensation of hydroxymethyl groups with loss of the elements of water.

To investigate this possibility, the composition of an adduct from 100 parts by weight of periodate lignin and 32 parts of formaldehyde was calculated as shown in Table I, line C. A loss in weight of this adduct in the ratio 132:120 (instead of the observed ratio, 132:115) would result in the calculated composition given in line D, although the figures were no longer percentages. Comparison of line D with line E, the observed percentage composition of formaldehyde periodate lignin, showed that the latter retained all of the original carbon atoms and methoxyl groups but had lost hydrogen and oxygen in the ratio 1:8 characteristic of the composition of water. These calculations were approximate, because they were based on the major Ross–Potter fraction of the formaldehyde periodate lignin rather than on the entire amount, and ignored a sulphur content of 1% derived from the sulphuric acid used in the condensation.

Comparison of columns 4 and 5 in Table I showed that periodate lignin failed to respond to a methylation attempted with diazomethane, and therefore contained no hydroxyl groups of a phenolic nature; the increase of 1.8% observed in a similar methylation of the formaldehyde periodate lignin (line E) suggested that a few phenolic groups had been formed in the condensation, probably by the hydrolytic action of the 73% sulphuric

TABLE I

Composition of spruce periodate lignin and of its formaldehyde derivative

	% C	% H	% O[a]	% OCH_3	Methylated % OCH_3[b] CH_2N_2	Methylated % OCH_3[b] Me_2SO_4	Acetylated % acetyl
A. Periodate lignin (obs.)	62.2	5.6	32.2	12.2	—	17.6	—
				12.5[c]	13.1[c]	17.8[c]	5.0[c]
				11.5[d]	11.2[d]	—	—
B. Formaldehyde (obs.)	40.0	6.7	53.3	0	0	0	0
C. Adduct, 100 g A:32 g B[e]	56.8	5.9	37.3	9.2	(~10.0)	(13.3)	(3.8)
D. Adduct C condensed 132 g to 120 g[f]	62.5	6.5	41.0	10.1	(~11.0)	(14.8)	(4.2)
E. Formaldehyde periodate lignin (obs.)[g]	62.4	5.4	32.2	9.9	11.7	15.2	3.9[h]

[a]By difference. All analyses corrected for ash and moisture.
[b]Diazomethane in dry ether; dimethyl sulphate in 30% sodium hydroxide.
[c]Data from Wieckowski (ref. 7); acetylation in pyridine.
[d]Data from Cabott and Purves (ref. 8).
[e]Calculated from A and B by method of mixtures. Formaldehyde contributed 17.2% of the carbon content.
[f]Calculated, but not as percentage composition.
[g]Major fraction, 105% by weight, uncorrected for 1% of sulphur.
[h]Acetylated with anhydrous sodium acetate.

acid. Methylation with dimethyl sulphate caused practically the same increase (17.6–12.2%) and (15.2–9.9%) in the methoxyl contents of the two lignins (columns 4 and 6), and thus both had the same total number of phenolic and aliphatic hydroxyl groups. Since the formaldehyde periodate lignin seemed to contain a few phenolic groups, its content of aliphatic hydroxyl groups was probably less than that of the periodate lignin. The acetyl contents of the two acetylated lignins (column 7, lines A and E) also suggested that aliphatic hydroxyl groups had been diminished, rather than increased, by the condensation with formaldehyde.

Two small-scale condensations were carried out with radioactive C^{14}-formaldehyde to determine, by an independent method, the proportion of carbon in formaldehyde periodate lignin which was contributed by the formaldehyde. The procedure of Das Gupta and Nair (9) was adapted to oxidize the various samples quantitatively by combustion to carbon dioxide, the activity of which was measured after conversion to barium carbonate. The count rates given by layers of the carbonate varying in thickness were plotted in Fig. 1 to eliminate the self-absorption factor, and to give comparison for samples of identical superficial density. Individual measurements deviated from the plots by not more than 10%. The open and filled circles (upper plot, left-hand ordinates) represented duplicate combustions of the original C^{14}-formaldehyde, and yielded a single smooth plot. When the ordinate scale shown at the right of Fig. 1 was chosen, the data from duplicate combustions of one C^{14}-formaldehyde periodate lignin sample fitted the same plot (open and filled triangles). It followed that 900/6000, or 15% of the carbon in this sample was derived from the formaldehyde. The values obtained for the second preparation of C^{14}-formaldehyde periodate lignin (crosses) corresponded to 16% of C^{14}.

Downes (16), however, found that C^{14}-formaldehyde condensed with dimedon to form the insoluble bismenthone, $C_{17}H_{24}O_4$, at only 0.93 times the rate displayed by the C^{12} isotope; if a similar effect occurred in the condensation with lignin, the above results would become 16% and 17%, respectively. In the present experiments, some of the C^{14}-formaldehyde was converted quantitatively to the bismenthone to eliminate the isotope effect, and the carbon in the product was recovered as barium carbonate before being counted. The results (Fig. 1, lower plot, open and half-filled circles) showed that 5.0 to

Can. J. Chem. Downloaded from www.nrcresearchpress.com by 210.87.254.40 on 09/05/12
For personal use only.

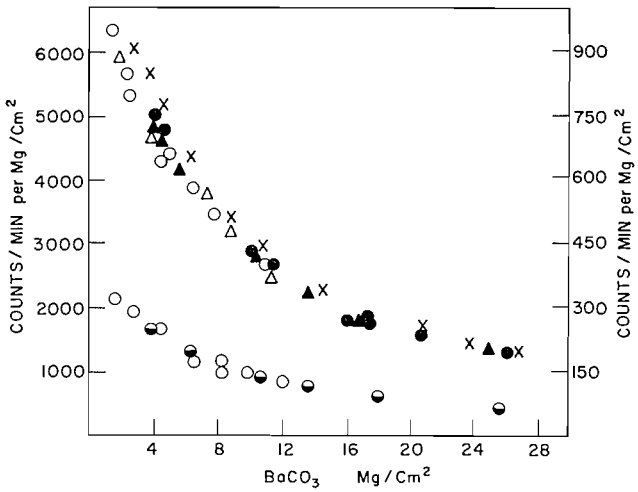


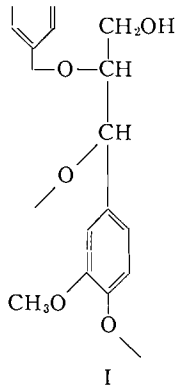
FIG. 1. Activity of C^{14}-compounds as mg barium carbonate per sq. cm. Left-hand ordinates, upper plots, open and filled circles, formaldehyde. Right-hand ordinates, open and filled triangles, formaldehyde periodate lignin; crosses, a duplicate preparation of the lignin; lower plot, open and half-filled circles, duplicate preparations of formaldehyde bismenthone.

5.4% of the carbon was derived from the C^{14}-formaldehyde, whereas the value calculated for the bismenthone, 5.9%, was higher by about one-tenth. The cause of this discrepancy was not determined. Whether the C^{14}-formaldehyde count or that of its bismenthone derivative was accepted as the primary standard, the amount of C^{14} in the C^{14}-formaldehyde periodate lignin appeared to be between 15% and 18% of the total carbon content. This result agreed well with the value of 17.2% assumed in Table I.

Since the detailed structure of the lignin macromolecule remained unknown, that of the formaldehyde derivative could only be surmised. The greater part of the macromolecule, however, is currently supposed to resemble structure I, in which the ether links in the phenylpropane side chains were assigned to arbitrary positions (11, 12). Cross links rendered the lignin insoluble in all chemically indifferent liquids, but were not numerous enough to prohibit swelling. The action of sulphuric acid by itself would be to cleave some of the ether bonds, but autocondensation would simultaneously yield the insoluble, and presumably more highly cross-linked, Klason lignin. A loss of the elements of water probably occurred in such condensations (13). Perhaps the alpha positions in the side chains and the sixth positions in the nucleii were among those involved in condensation, because the former were probably sulphonated when lignin was heated in aqueous sodium bisulphite (12) and the latter could be chlorinated. A preferential condensation of each of these reactive sites with 1 mole of formaldehyde would increase the base molecular weight of the lignin from about 187 to about 247, or in the ratio 100:132 by weight, and the formaldehyde would contribute 16.7% of the carbon in the adduct. The loss of a molecule of water would lead to a new ether link (structure II) and reduce the yield by weight in the ratio 132:122. These figures were close to those observed. Carbon atoms originating as formaldehyde were denoted by asterisks in this and subsequent structures.

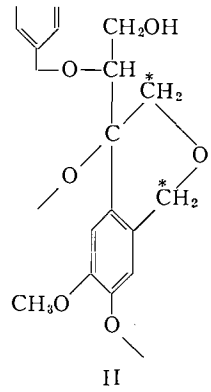
The ready solubility of formaldehyde lignin in several liquids suggested that condensation with formaldehyde did not bring about cross linking, and an intramolecular arrangement of the new ether group was chosen for structure II. Wherever this group was located, its existence reduced the number of the free hydroxyl groups to the original number, as

Can. J. Chem. Downloaded from www.nrcresearchpress.com by 210.87.254.40 on 09/05/12
For personal use only.



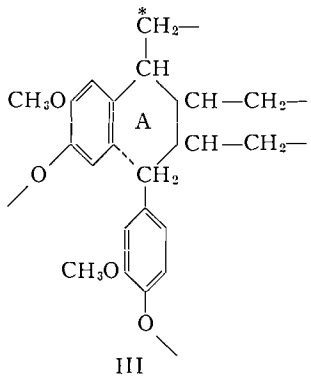
I

Base molecular weight ~187

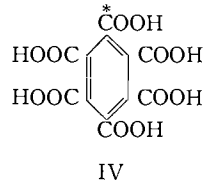


II

Base molecular weight ~229



III



IV

Mellitic acid

was found. Most lignins, including Klason lignin (14) and periodate lignin (15), when heated with nitrobenzene and alkali yielded vanillin, presumably by oxidative cleavage at the alpha carbon atom in structure I. The nitrobenzene could be replaced with cuprous hydroxide (16), whose use was adapted to a convenient semimicro scale. Neither oxidant produced a trace of vanillin from the Ross–Potter fraction, or the acid-soluble fraction, of formaldehyde periodate lignin, and attempts to isolate a carboxyvanillin from the oxidation liquor also failed. These failures were not inconsistent with structure II, since substitution of the alpha positions by formaldehyde might render the molecule more resistant at this point to oxidative cleavage.

Samples of the Ross–Potter fraction were then thoroughly oxidized with potassium permanganate in hot aqueous alkali to carbon dioxide, acetic acid, oxalic acid, and a mixture of benzenepolycarboxylic acids (17). Since the oxalic acid was radioactive when C^{14}-formaldehyde periodate lignin was used, the formaldehyde had formed a C—C bond, rather than a C—O—C bond, with the lignin, as shown in structure II. All aromatic rings directly substituted with oxygen, however, were known to be destroyed in this oxidation, and structure II would yield no benzenecarboxylic acids. As previously discussed (17), the production of these acids suggested that a minor part of the lignin macromolecule consisted of lignan elements in which the β-carbon atoms of the phenylpropane units were directly joined. Substitution of a hydroxymethyl group in the α-position of the lignan, followed by cyclization as shown by the broken line (structure

Can. J. Chem. Downloaded from www.nrcresearchpress.com by 210.87.254.40 on 09/05/12
For personal use only.

III), would yield a cyclohexene ring (A) entirely substituted by carbon atoms. Benzenehexacarboxylic (mellitic) acid (IV) would result when this ring was oxidized, and also benzenepentacarboxylic acid by partial decarboxylation. A new paper chromatographic technique was used to isolate the benzenepentacarboxylic acid in a pure condition, but the mellitic acid, if present, stayed on the starting line, and no benzenetetracarboxylic acids were present. When C^{14}-formaldehyde periodate lignin was oxidized, the supposed mellitic acid had some activity, but the pentacarboxylic acid had none.

Although parallel oxidations of spruce Klason lignin yielded about the same amount, 4%, of benzenepolycarboxylic acids as did the formaldehyde periodate lignin, the mixture consisted exclusively of benzenepentacarboxylic acid and the 1,2,4,5-tetracarboxylic acid, and mellitic acid was absent (17). This sharp difference between the two lignins strongly supported the view that some of the formaldehyde substituted the alpha positions of the phenylpropane units of structure III, as well as those in structure I. Mellitic acid, benzene-penta-, -1,2,4,5-tetra-, and -1,2,3,5-tetra-carboxylic acid were oxidized to the extent of only 0.7, 2.2, 1.9, and 5.0%, respectively, by iodic acid in concentrated sulphuric acid at 180° to 190°, although Kleinert and Dlouhy (18) recently showed that these acids were quantitatively oxidized at 220° to carbon dioxide. Oxidation at the lower temperature proved to be a simple method of recovering the benzenepolycarboxylic acids from periodate and formaldehyde periodate lignin.

Another aldehyde capable of condensing with lignin was chloral hydrate in the presence of a little hydrochloric acid. Ogait (19) extracted most of the lignin from spruce wood meal with this reagent, and recovered about half as a thermoplastic "chloral lignin" soluble in chloroform and containing about 15% of chlorine. A repetition of this work with spruce periodate lignin yielded a "chloral periodate lignin" with only 9.2% of chlorine and soluble in acetone, but the results were otherwise too similar to those of Ogait to justify detailed reproduction here. They served to show, however, that the cleavage of lignin–carbohydrate bonds was not an essential step in the production of chloral lignin (19), since the periodate lignin was free of carbohydrates.

EXPERIMENTAL

Materials and Methods

Woodmeal of 20–30 mesh fineness was prepared from a log of black spruce which was free of bark and about 30 years old. The oxidation of a 2160-g batch with 660 g of sodium paraperiodate in 18 liters of water adjusted to pH 3.6–4.0 with acetic acid, and the subsequent extraction of the oxidized carbohydrates with cold 0.1 *N* sodium hydroxide, were as previously described (15, 20). After four or five oxidation–extraction cycles, the water-wet, gelatinous periodate lignin was solvent-exchanged first into acetone, which yielded a free-flowing, easily filterable suspension, and then through methyl ethyl ketone into ligroin, b.p. 30°–60°. Final drying, *in vacuo* over phosphorus pentoxide and solid paraffin, had to be thorough. Found: C (21), 60.1; H (21), 5.4; OCH_3 (22), 11.9; ash (21), 2.5; Klason lignin (23), 87%; holocellulose (24), trace. The product, and also samples isolated by freeze-drying the water-wet mass, were light-colored powders of low density, whereas samples dried directly from water were hard, darker resins. Periodate lignin had a low but noticeable cation-exchange capacity, and the acid form acquired sodium ion from aqueous sodium chloride.

Distilled water and organic liquids of C.P. or equivalent grade were used throughout

Can. J. Chem. Downloaded from www.nrcresearchpress.com by 210.87.254.40 on 09/05/12
For personal use only.

the work. Evaporations were performed at not more than 45° in a rotary evaporator under vacuum; often the solutions or suspensions, especially when neutral, produced much froth initially and the pressure had to be reduced gradually. Unless stated otherwise, final drying was *in vacuo* over phosphorus pentoxide, and analyses were in duplicate, the averages of concordant determinations being quoted. Seamless cellulose dialyzer tubing, 0.00072 inch thick, was used in dialyses, which were against large volumes of water. Phenolic compounds were chromatographed on paper with *n*-butanol saturated with 2% aqueous ammonia (16) (solvent A) or with ligroin–dioxane–water in the ratio 4:2:1 by volume (solvent B) as eluents. The spray described by Barton, Evans, and Gardner (25) was made more sensitive by the use of a mixture of 1% ferric chloride, 10 ml; 1% potassium ferricyanide, 6 ml; saturated boric acid solution, 10 ml; and water, 20 ml. The eluent for organic acids was a 10:1:1 mixture of methyl isobutyl ketone, water, and formic acid (solvent C) with bromphenol blue as the spray. Prior to spraying, the paper was dried at 130° *in vacuo* to eliminate formic acid. Yields and analyses were quoted on a moisture- and ash-free basis.

Condensations with Formaldehyde (1, 2)

Many preliminary experiments showed the necessity of immersing the lignin in formalin *before* adding the sulphuric acid, which had to attain at least 69% concentration by weight in the mixture. The required concentration was reached by adding 88.5% sulphuric acid, since the use of the concentrated acid yielded a more highly sulphonated product.

In a typical experiment, 50 g of periodate lignin (47.1 g on a moisture- and ash-free basis) was soaked for 2 hours in changes of commercial 37% formalin, 224 g of which was retained when the swollen mass was recovered on a filter. The moist lignin was mixed in a 1.5-liter beaker with 250 g of solid carbon dioxide, and ice-cold 88.5% sulphuric acid (about 700 g) was slowly added with stirring until the final concentration was 73±1%, the composition being: lignin, 47.1 g; formaldehyde, 83 g; sulphuric acid, 620 g; and water, 227 g. The gummy mixture was then maintained near 41° and was worked with a glass rod until a uniform, dark red-brown solution was obtained. No more solid particles could be detected after 30 to 50 minutes; the solution was then cooled and the product isolated in one of the following ways.

Method (a)

The reaction mixture and about 8 liters of cold, 10% aqueous sodium hydroxide were simultaneously poured into 15 liters of cold water so that the pH remained between 5 and 9, the final value being 3.5. The precipitate was separated on a centrifuge and the liquors were extracted at pH 2 with methyl ethyl ketone, which removed 0.3 g of a dark, non-volatile, brittle solid. This solid was extracted from the ketone by 5% sodium hydroxide. The major product, 74 g including 30% of sodium sulphate, was mixed with 250 ml of water and was dialyzed for 3 days. Acidification of the dialyzate to pH 1.8 and extraction with methyl ethyl ketone removed 1.8% of a gum which was soluble in water and dilute alkali. Found: OCH_3, 9.2; sulphated ash, 3.9%. This gum remained partly on the starting line, and partly in the solvent front, when chromatographed on paper with solvents A or B.

The contents of the dialysis sac, when evaporated at pH 6, yielded 52.5 g of formaldehyde periodate lignin as dark brown lumps which were powdered in a mortar. Found: C, 59.3; H, 5.1; OCH_3, 9.4; S, 1.0; ash, 4.6%. The yield, ash-free, was 104% of the periodate lignin, and the two minor fractions increased this figure to 107.4%.

Can. J. Chem. Downloaded from www.nrcresearchpress.com by 210.87.254.40 on 09/05/12
For personal use only.

Can. J. Chem. Downloaded from www.nrcresearchpress.com by 210.87.254.40 on 09/05/12
For personal use only.

Method (b)

A solution of formaldehyde periodate lignin in 73% sulphuric acid, made from 9.7 g of periodate lignin, was poured into 400 ml of water at 0°, and the precipitated Ross–Potter lignin was washed on the centrifuge with four 250-ml volumes of water; a little sulphuric acid had to be added in the last washing to obtain a good separation. The liquors were neutralized with sodium carbonate and were evaporated at pH 8 to 700 ml, when crystalline sodium sulphate was removed at 4°. After acidification to pH 0.5 with sulphuric acid, the liquor was alternately concentrated to 50 ml and diluted with water several times to decompose and eliminate most of the formaldehyde polymers. The neutralized liquor, 40 ml, was highly diluted with acetone to precipitate inorganic material, and the portion soluble in dry acetone was recovered as a near-white, dry gum. Yield: 6.53 g. Found: ash, 27.1; loss in weight on heating in air for 70 minutes at 105°, 45.3%.

This loss of weight represented the decomposition of formaldehyde polymer. A suspension of the gum in 80 ml of water was continuously extracted first with ether and then with methyl ethyl ketone at 240 mm pressure. The ether extract yielded 0.57 g of material of which 0.17 g was non-volatile at 105°, while 0.72 g of the 0.76 g recovered from the ketone was non-volatile. Samples of both extracts were hydrolyzed in boiling 16% sulphuric acid and the formaldehyde liberated from the polymer was determined by the sodium sulphite method (4, 26). The aqueous residue from the extractions contained 2.7 g of a white, amorphous solid. Found: OCH_3, 20.5; S, 21.3; ash, 54.6%. Calc. for $H_2C(OCH_3)OSO_3Na$: OCH_3, 18.9; S, 19.5; ash as Na_2SO_4, 43.3%. The substance failed to give a positive test for sulphate ion with aqueous barium chloride, but the ash did so.

The Ross–Potter fraction was dissolved in dilute sodium hydroxide except for an 0.28-g residue with 45% of ash. Acidification of the brown filtrate reprecipitated the main product, which was washed with water and redissolved while still wet in much acetone. A residue separated on the centrifuge yielded 0.17 g of material insoluble in water (ash, 13.7%), and 0.29 g soluble in water (ash, 30.3%). The acetone solution was diluted with water, adjusted to pH 5.7, concentrated, and the product was isolated as a friable, brown powder by freeze-drying. Yield: 10.43 g: ash, 6.1%. The total recovery of organic material, excluding formaldehyde polymer, was (0.17+0.72+0.14+0.15+0.2 +9.8 g) 11.2 g, or 115% by weight.

Method (c)

A solution of formaldehyde periodate lignin, prepared in 73% sulphuric acid from 3.2 g of periodate lignin, was mechanically stirred into a mixture of glacial acetic acid, 81 ml; acetic anhydride, 540 ml; and anhydrous sodium acetate, 105 g. Although the flask was cooled externally with solid carbon dioxide, the temperature rose to 51°. The resulting slurry was kept near 2° for 18 hours, when the excess acetic anhydride was cautiously hydrolyzed with water and the liquor was thoroughly dialyzed against water. The non-dialyzed portion was isolated by evaporation at pH 6.5 followed by drying to constant weight. The dark brown resin weighed 3.21 g. Found: OCH_3, 7.8; acetyl (27), 4.2; ash, 13.4%.

Methylations of Ross–Potter Fraction

A portion of the product isolated by method (*a*) was suspended in dry tetrahydrofuran and an excess of dry diazomethane was added. Twelve hours later, the liquor was evaporated and the residue dried *in vacuo* over phosphorus pentoxide and solid sodium hydroxide. Found: OCH_3, 11.2; ash, 4.5%.

Another portion of the same Ross–Potter fraction was methylated with dimethyl sulphate and 30% sodium hydroxide in aqueous tetrahydrofuran, the atmosphere being oxygen-free nitrogen. Both the acetone-soluble and acetone-insoluble fractions of the product (yields 37% and 46%, respectively) had the same methoxyl content, not increased by remethylation. Found for the acetone-soluble fraction: OCH_3, 15.0; S, 0.44; ash, 2.0%. A sample of periodate lignin was completely methylated in the same way. Found: OCH_3, 17.5; ash, 1.2%.

Consumption of Formaldehyde

The apparatus consisted of a stout-walled glass bomb of 100-ml capacity with a side-arm dipping into water to trap any formaldehyde expelled when pressure increased. The top of the bomb was connected by a short piece of rubber hose to an air-tight, mercury-sealed stirrer consisting of a stout glass rod reaching almost to the bottom. The flexible connection made it possible to work the particles of lignin into solution. Paraformaldehyde, 42 g, and 68 ml of 0.05 *N* hydrochloric acid were boiled under reflux and the almost clear solution, when analyzed by the steam distillation – sodium sulphite method (4, 26), contained 36.2, 36.1% formaldehyde by weight. Three grams (2.86 g ash-free) of periodate lignin and 15 g of the formaldehyde solution were weighed into the apparatus; next day 44.8 g of 88% sulphuric acid was added and the condensation completed as previously described.

The resulting solution was cooled, diluted with water, and quantitatively transferred to a 1-liter flask arranged for steam distillation. The suspension, 400 ml, was kept just below the boiling point for 50 minutes to hydrolyze formaldehyde polymers, and was then steam-distilled for 3 to 4 hours, the distillate being exactly 1 liter. Aliquots, 100 ml, of the distillate were then analyzed by the sodium sulphite method, which employed *N* hydrochloric acid and a thymolphthalein indicator in the final titration (26). Found: CH_2O, 4.30, 4.26 g, whereas a blank containing no lignin yielded 5.28, 5.27 g. The difference, 0.99 g, had therefore condensed with 2.86 g of periodate lignin, or in the proportion of 34.5:100. Since any trace of sulphuric acid carried into the distillate would have registered as formaldehyde, independent experiments were carried out in which the distillates were neutralized to thymolphthalein before the determination of formaldehyde. Found: CH_2O, 4.38, 4.32 g, and 5.29, 5.26 g in the blank. In this case, 32 g of formaldehyde condensed with 100 g of the lignin. The still residues yielded 3.07, 3.09 g of the Ross–Potter fraction, or 104, 105%, and a further 0.22 g or 7.8% of formaldehyde periodate lignin was recovered from the mother liquors after removal of sulphate ion as the barium salt. The removal of sulphate ion by the cation-exchange resin "Amberlite IR-120" reduced the recovery of the acid-soluble lignin to 5.7% in the duplicate experiment.

C^{14}-Formaldehyde Periodate Lignin (Fig. 1)

A solution of radioactive formaldehyde was made by heating 18 mg of C^{14}-paraformaldehyde (obtained from Merck Company of Canada, Limited) and 5 g of inert paraformaldehyde with 8.5 ml of 0.05 *N* hydrochloric acid in a sealed glass bomb at 100° for several hours. Found for the clear solution by the bisulphite (4, 26) method: H_2CO, 35.8, 35.8, 36.2%. This result was checked by precipitating the formaldehyde in 0.5-g samples with 2 g of dimedon in 300 ml of water at pH 4.6. One gram of the bismenthone was equivalent to 0.1027 g of formaldehyde (26). Found: H_2CO, 35.7, 36.25%. Two batches of C^{14}-formaldehyde periodate lignin were prepared as described in method

Can. J. Chem. Downloaded from www.nrcresearchpress.com by 210.87.254.40 on 09/05/12
For personal use only.

(*a*), each from 2.5 g of the above solution, 0.5 g of periodate lignin, and 8.5 g of 88.5% sulphuric acid. After the dialysis, solutions of the Ross–Potter fractions in dilute sodium hydroxide were filtered through sintered glass to remove insoluble but active material (15 mg or less), thoroughly dialyzed again, and freeze-dried. Yield: 470, 488 mg.

To determine C^{14}-carbon, 50-mg samples were burned to carbon dioxide in a conventional microcombustion furnace (28), those of the original formaldehyde solution being introduced in a fine glass tube sealed at one end. The carrier gas was purified oxygen, and the carbon dioxide was absorbed by passage through each of two 250-ml centrifuge tubes one-third filled with aqueous barium hydroxide free of carbonate. Each tube contained a small magnetic stirrer to make sure that the distribution of C^{14}-carbon in the precipitated barium carbonate would be uniform (29), and some samples were mixed with pulverized potassium dichromate to prevent any loss of carbon dioxide as sodium carbonate during the combustion. The precipitated barium carbonate was recovered by centrifugation and was magnetically stirred with changes of wash water (free of carbon dioxide) and finally exchanged into acetone, giving a fine-grained product suitable for counting.

A suspension of this precipitate in acetone was deposited in varying amounts on tared aluminum pans 3 cm in diameter; drying was under an infrared lamp and all samples were measured over the same area. A gas-flow proportional counter was used whose efficiency, compared with a 2π gas-flow windowless counter, was checked at 13% on several samples. Each measurement for formaldehyde and the Ross–Potter fraction totalled at least 30,000 and, with two exceptions, at least 11,000 for formaldehyde bismenthone. Each measurement was corrected for background, and the sensitivity and window position of the instrument were kept constant throughout.

Oxidations with Nitrobenzene and Cuprous Hydroxide

One gram of the lignin, 2.3 ml of pure benzaldehyde, and 20 ml of 4 *N* sodium hydroxide were heated together in a stainless steel bomb at 175° for 3 hours (30, 31). The contents were distilled in steam, the still residue was extracted with benzene, acidified to pH 3, and continuously extracted with ether. Portions of the residue from the ether extract were then chromatographed on paper with solvent A.

In the oxidations with cuprous hydroxide (16), 2 g of the lignin, 42 ml of 3 *N* sodium hydroxide, and 12 g of finely divided cuprous hydroxide were heated at 175° for 3 hours. The suspension was then filtered, and filtrate plus washings were acidified to pH 2 and continuously extracted with ether. When the extract from an oxidation of periodate lignin was re-extracted with saturated aqueous sodium bisulphite, a 20% yield of vanillin was recovered, some of which was isolated with the correct melting point and mixed melting point. Products from formaldehyde periodate lignin yielded ether extracts which deposited insoluble material continuously during extractions with aqueous sodium bisulphite, bicarbonate, or hydroxide. Every attempt to isolate vanillin, a carboxyvanillin, or vanillic acid failed.

The above oxidation was reduced to the semimicro scale previously described for oxidations with nitrobenzene (30), the 5-ml steel bombs being charged with lignin, 50 mg; cuprous hydroxide, 300 mg; and 2 ml of 2 *N* sodium hydroxide. During the heating in an air oven at 175° for 2.5 hours, the bomb was twice shaken vigorously by hand. The liquor could then be directly spotted on chromatograph paper; when the spots had been dried, they were exposed for a minute to the vapor of acetic acid to neutralize any free alkali and were then developed with solvent A.

Can. J. Chem. Downloaded from www.nrcresearchpress.com by 210.87.254.40 on 09/05/12
For personal use only.

Chromatography of Some Benzenepolycarboxylic Acids

Samples, 15 μg, of the authentic, pure acids were spotted on chromatograph paper, and were subsequently developed with solvent C for 4 hours, the spray being bromphenol blue. The R_F values observed were as follows: mellitic acid, 0.0; benzenepentacarboxylic, 0.035; benzene-1,2,3,4-tetracarboxylic acid, 0.12; the 1,2,4,5-isomer, 0.22; and the 1,2,3,5-isomer, 0.24. A mixture of the five acids in equal amount when chromatographed yielded the first three in a pure state, but the separation between the last two was unsatisfactory.

Oxidations with Potassium Permanganate

A suspension of 10 g of the formaldehyde periodate lignin in 1.6 liters of 1% potassium hydroxide was thoroughly oxidized near 97° by a total of 90 g of potassium permanganate added during 4 days. After the product had been isolated, first as barium salts and then as an aqueous solution of the free acids, in the way described (17), crystalline oxalic acid dihydrate was separated. The residual material after reoxidation with boiling, concentrated nitric acid yielded 0.39 g or 3.9% of a pale yellow solid shown by chromatography to contain benzenepentacarboxylic acid but none of the benzenetetracarboxylic acids.

The above oxidation was repeated with 0.8 g of C^{14} formaldehyde periodate lignin, but when the alkaline oxidation liquor was acidified the carbon dioxide was expelled and recovered as barium carbonate. This carbonate was radioactive, and so was the crystalline oxalic acid dihydrate, which had the correct melting point of 101°. Yield 0.14 g or 17.5%. After the final product had been chromatographed on paper, the spot containing the benzenepentacarboxylic acid was excised and placed in a counter, but no activity was observed. Some activity remained at the starting line of the chromatogram.

Oxidations with Iodic Acid (13, 18)

One gram of the lignin was mixed in an open 50-ml flask with 10 ml of a saturated solution of potassium iodate in concentrated sulphuric acid. When the initial violent reaction subsided, 10 g of powdered potassium iodate was cautiously added in small portions, more heat and iodine being evolved. Nitrogen was then bubbled through the solution, which was kept at 180° to 200°, for 40 minutes. An additional 10 ml of concentrated sulphuric acid was added, and 10 minutes later, 50 mg of paraformaldehyde, to reduce any remaining iodic acid. The solution was cooled 20 minutes later, cautiously diluted with 25 ml of water, and then boiled to expel free iodine. A second dilution with water brought the volume to 60 ml, and the solution was extracted continuously with ether. This extract was evaporated with water several times to expel free iodine that formed, and the final liquor, 8 ml, was ready for paper chromatography. Spots of R_F 0.14 and 0.23 to 0.24 indicated the presence of benzenepentacarboxylic acid and benzene-1,2,4,5-tetracarboxylic acid in the product from periodate lignin, but there was no trace of the latter spot in the products from various fractions of formaldehyde periodate lignin.

ACKNOWLEDGMENTS

The authors thank the National Research Council of Canada for the Research Grant that defrayed part of the costs, Dr. Leo Yaffe for great assistance in the work with radioactive carbon, and Dr. T. N. Kleinert for helpful discussions. One author (E.E.) gratefully acknowledges the award of a Union Carbide (Visking Division) Corporation Fellowship and of Summer Stipends from the Pulp and Paper Research Institute of Canada.

Can. J. Chem. Downloaded from www.nrcresearchpress.com by 210.87.254.40 on 09/05/12
For personal use only.

REFERENCES

1. J. H. Ross and A. C. Hill. Pulp Paper Mag. Can. **27**, 541 (1929).
2. J. H. Ross and J. C. Potter. Pulp Paper Mag. Can. **29**, 569 (1930).
3. P. S. Billington, F. A. Simmons, and P. K. Baird. Paper Trade J. **96**(4), Tappi Section, 258 (1933).
4. R. Borisek and J. Polcin. Chem. zvesti (Chem. News), **5**, 322 (1951); Chem. Abstr. **46**, 4223 (1952).
5. K. Freudenberg and F. Sohns. Ber. **66**, 262 (1936).
6. J. F. Walker. Formaldehyde. 2nd ed. Reinhold Publishing Corporation, New York, N.Y. 1953. pp. 235–270.
7. E. Wieckowski. Ph.D. Thesis, McGill University, Montreal, Que. 1957.
8. I. M. Cabott and C. B. Purves. Pulp Paper Mag. Can. **56**(5), 151 (1956).
9. A. K. Das Gupta and C. K. N. Nair. J. Sci. Ind. Research (India), **15B**, 1 (1956).
10. A. M. Downes. Australian J. Sci. Research, Ser. A, **5**, 521 (1952).
11. F. Brauns and H. Hibbert. J. Am. Chem. Soc. **55**, 4720 (1933).
12. B. Leopold. Pulp Paper Mag. Can. **55**(3), 184 (1954).
13. T. N. Kleinert and E. J. Dostal. Tappi, **41**, 689 (1958).
14. K. Iwadare. J. Chem. Soc. Japan, **62**, 1095 (1941); Chem. Abstr. **41**, 3291 (1947).
15. P. F. Ritchie and C. B. Purves. Pulp Paper Mag. Can. **48**, 74 (1947).
16. I. A. Pearl and D. L. Beyer. Tappi, **33**, 544 (1950); J. Am. Chem. Soc. **76**, 6106 (1954).
17. D. E. Read and C. B. Purves. J. Am. Chem. Soc. **74**, 120 (1952).
18. R-M. Dlouhy and T. N. Kleinert. Holzforschung, **13**(1), 13 (1959).
19. A. Ogait. Cellulosechemie, **22**, 15 (1944).
20. D. M. Smith and C. B. Purves. J. Am. Chem. Soc. **81**, 2405 (1959).
21. Schwartzkopf Microanalytical Laboratory. Woodside, N.Y. U.S.A.
22. F. Vieböck and A. Schwappach. Ber. **63**, 2818 (1930).
23. Tappi Standards, T 13m-54, Technical Association of the Pulp and Paper Industry, New York. 1950.
24. E. F. Kurth and G. J. Ritter. J. Am. Chem. Soc. **56**, 2720 (1934).
25. G. M. Barton, R. S. Evans, and J. A. F. Gardner. Nature, **170**, 249 (1952).
26. J. F. Walker. Formaldehyde. 2nd ed. Reinhold Publishing Corporation, New York, N.Y. 1953. pp. 382, 390.
27. E. P. Clark. Ind. Eng. Chem. Anal. Ed. **8**, 487 (1936); **9**, 539 (1937).
28. W. W. Scott. Standard methods of chemical analysis. 5th ed. Vol. 2. D. van Nostrand Co., Inc., New York. 1939. p. 2475.
29. W. D. Armstrong, L. Singer, S. H. Zbarsky, and B. Dunshee. Science, **112**, 531 (1950).
30. J. E. Stone and M. J. Blundell. Anal. Chem. **23**, 771 (1951).
31. K. R. Kavanagh and J. M. Pepper. Can. J. Chem. **33**, 24 (1955).

Can. J. Chem. Downloaded from www.nrcresearchpress.com by 210.87.254.40 on 09/05/12
For personal use only.

Can. J. Chem. Downloaded from www.nrcresearchpress.com by 210.87.254.42 on 09/05/12
For personal use only.

CYCLOHEXANE COMPOUNDS

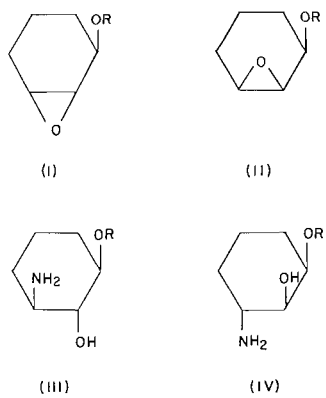
III. THE 1-METHOXY- AND 1-ETHOXY-2-HYDROXY-3-BROMOCYCLOHEXANES[1, 2]

R. A. B. Bannard and L. R. Hawkins

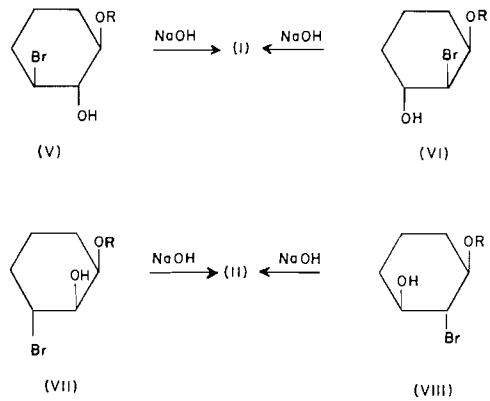
ABSTRACT

1α-Methoxy-2β-hydroxy-3α-bromocyclohexane and 1α-methoxy-2α-hydroxy-3β-bromocyclohexane have been prepared by the action of hydrobromic acid on 1β-methoxy-2α,3α-epoxycyclohexane and 1α-methoxy-2α,3α-epoxycyclohexane respectively. Assignment of stereochemical configuration to 1α-methoxy-2β-hydroxy-3α-bromocyclohexane was made by catalytic debromination of the phenyl- and 1-naphthyl-urethanes to derivatives of 2β-methoxy-1α-cyclohexanol. An alternative proof of structure was obtained by de-etherification of the bromohydrin to 3α-bromo-1α,2β-cyclohexanediol, which was catalytically debrominated to 1α,2β-cyclohexanediol and oxidized via periodate to 2-bromoadipaldehyde, isolated as the bis-2,4-dinitrophenylhydrazone. The structure of 1α-methoxy-2α-hydroxy-3β-bromocyclohexane was established by de-etherification to 3β-bromo-1α,2α-cyclohexanediol, which was oxidized by periodate 10 times more rapidly than its isomer. The corresponding ethoxy compounds were prepared and their structures were elucidated in a completely analogous manner.

In an earlier paper (1) the mixtures of bromohydrins resulting from the action of aqueous N-bromosuccinimide on 1-methoxy- and 1-ethoxy-cyclohexene-2 were utilized for synthesis of the stereoisomeric 1-methoxy- and 1-ethoxy-2,3-epoxycyclohexanes I and II (R = CH_3 or C_2H_5) and led ultimately by ammonolysis of the latter to the 1-methoxy- and 1-ethoxy-2-hydroxy-3-aminocyclohexanes III and IV (R = CH_3 or C_2H_5). The formation of two oxides by the action of aqueous sodium hydroxide on each 1-alkoxy-cyclohexene-2 bromohydrin demonstrated the presence in each of at least two trans-oriented bromohydrins (2, 3), but the possibility existed that all four bromohydrins V–VIII were present. Attempts to separate the bromohydrin mixtures by fractionation *in vacuo* were unsuccessful, and attention was, therefore, directed toward preparation of pure bromohydrins from the pure oxides by the action of hydrobromic acid, since it was anticipated that knowledge gained concerning the physical and chemical characteristics of any of the possible components of the mixtures would facilitate the development of a method for separation and identification of all the components.



[1]*Manuscript received February 23, 1961.*
Contribution from Defence Research Chemical Laboratories, Ottawa, Canada. Presented in part at the 42nd Annual Conference of the Chemical Institute of Canada, Halifax, N.S., May 25–27, 1959.
Issued as D.R.C.L. Report No. 312.
[2]*For Part II of this series see reference 1.*



Theoretically, two bromohydrins can be formed from each oxide if ring scission occurs in both possible directions (4). However, our previous experience with ammonolysis of the oxides, in which derivatives of 3-amino-1,2-cyclohexanediol were formed exclusively (1), together with the results obtained by Lemieux, Kullnig, and Moir (5) on methanolysis of the oxides, suggested that 1-alkoxy-2-hydroxy-3-bromocyclohexanes would probably be the only bromohydrins formed. The work now to be described is concerned only with the synthesis and proof of structure of the 1-methoxy- and 1-ethoxy-2-hydroxy-3-bromocyclohexanes. Application of the information gained therefrom to solution of the problem of the composition of the bromohydrin mixtures referred to above is reserved for a subsequent communication.

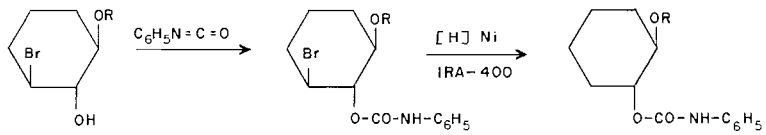
1β-Methoxy-2α,3α-epoxycyclohexane (I, R = CH_3) on treatment with hydrobromic acid gave a solid bromohydrin, m.p. 68.5–69°, in 63% yield. The liquid fraction isolated from the reaction was shown to consist of 27% bromohydrin (by isolation of the 1-naphthylurethane, m.p. 185–186°) and 19% of a 1-methoxy-2,3-cyclohexanediol (identified by periodate cleavage followed by isolation of the bis-2,4-dinitrophenylhydrazone of 2-methoxyadipaldehyde, m.p. 192–193.5°, and by isolation of a 1-methoxy-2,3-cyclohexanediol bis-1-naphthylurethane, m.p. 224–226°) leaving approximately 50% of the oil unidentified. No further attempt was made to characterize this portion of the product but the suggestion is offered that it could well be a 2-methoxy-3-bromocyclohexanol formed by methoxyl migration (6). In support of this suggestion is the observation (see below) that the action of hydrobromic acid on the cis oxide II produces the corresponding bromohydrin in 93% yield with formation of only a very minor quantity of methoxydiol. The absence of a large fraction of unknown structure is to be expected in this instance because facile migration of the methoxyl group is hindered by virtue of the cis relationship of the methoxyl and its neighboring hydroxyl group.

The bromohydrin was characterized by preparation of its phenylurethane, m.p. 133–134° (86%), 1-naphthylurethane, m.p. 185–186° (94%), and its acetyl derivative, m.p. 56–56.5° (90%), and its structure was established as 1α-methoxy-2β-hydroxy-3α-bromocyclohexane (V, R = CH_3) by the following methods.

The phenylurethane of the bromohydrin (IX, R = CH_3) was debrominated according to the method of McCasland and Horswill (7) using hydrogen, Raney nickel, and an anion exchange resin, producing 2β-methoxy-1α-cyclohexanol phenylurethane (X, R = CH_3), m.p. 66–67.5°, in 78% yield. The identity of the latter compound was established by comparison with an authentic specimen obtained from 2β-methoxy-1α-cyclohexanol (8).

Can. J. Chem. Downloaded from www.nrcresearchpress.com by 210.87.254.42 on 09/05/12
For personal use only.

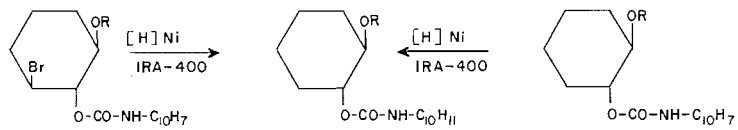
Prior to use of the debromination method it was shown that no concomitant reduction of the benzene or urethane groups occurred under the conditions employed, since debromination of 2β-bromo-1α-cyclohexanol phenylurethane, m.p. 85–87° (9) gave cyclohexanol phenylurethane, m.p. 83–84.5° (10), in 86.5% yield. The bromine atom must have occupied a position trans to the hydroxyl group in the original bromohydrin since the latter yields the oxide I (R = CH_3) on treatment with alkali (2, 3) and it therefore follows that the bromohydrin must be 1α-methoxy-2β-hydroxy-3α-bromocyclohexane (V, R = CH_3).



(V) (IX) (X)

R = CH_3, m.p. 68.5–69° R = CH_3, m.p. 133–134° R = CH_3, m.p. 66–67.5°
R = C_2H_5, m.p. 46–47.5° R = C_2H_5, m.p. 132–133.5°

A similar proof of structure was obtained using the 1-naphthylurethane (XI, R = CH_3) rather than the phenylurethane. During debromination, however, simultaneous reduction of one of the benzenoid rings occurred, leading to the tetralin derivative (XII, R = CH_3). The latter substance was identified by comparison with an authentic specimen prepared by reduction of 2β-methoxy-1α-cyclohexanol 1-naphthylurethane (XIII, R = CH_3) under the same conditions as used for debromination.



(XI) (XII) (XIII)

R = CH_3, m.p. 185–186° R = CH_3, m.p. 89.5–91° R = CH_3, m.p. 111–112°
R = C_2H_5, m.p. 196–197° R = C_2H_5, m.p. 71–72.5° R = C_2H_5, m.p. 131–132°

It was also shown that debromination of 2β-bromo-1α-cyclohexanol 1-naphthylurethane by the hydrogen – Raney nickel method leads to a cyclohexanol tetrahydro-1-naphthylurethane identical with that obtained by reduction of cyclohexanol 1-naphthylurethane under the same conditions. These experiments did not establish which benzenoid ring was reduced. However, by analogy with work reported by Papa and Schwenk (11) it seems probable that reduction occurred in the unsubstituted ring.

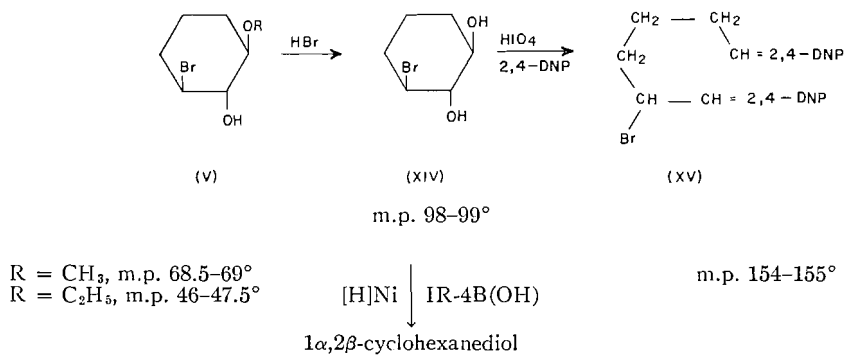
The urethanes were used rather than the bromohydrin V (R = CH_3) itself to avoid the possibility of intermediate oxide formation, which would invalidate any structural assignment based on the debromination experiments since the oxide I (R = CH_3) could result just as readily from VI as from V (R = CH_3). It will be demonstrated in the sequel, however, that the use of derivatives is unnecessary because oxide formation is readily preventable and, moreover, if it is forced to occur the oxide is not reduced under the conditions of debromination.

De-etherification of the bromohydrin with fuming hydrobromic acid gave a bromodiol, m.p. 98–99°, in 89% yield, which was further characterized via its bis-1-naphthylurethane, m.p. 210–210.5°, and diacetate, m.p. 65.5–66.5°, and was shown to be a

Can. J. Chem. Downloaded from www.nrcresearchpress.com by 210.87.254.42 on 09/05/12
For personal use only.

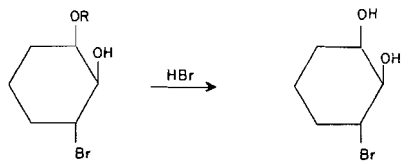
Can. J. Chem. Downloaded from www.nrcresearchpress.com by 210.87.254.42 on 09/05/12
For personal use only.

derivative of 1,2-cyclohexanediol, since periodate oxidation followed by treatment with 2,4-dinitrophenylhydrazine gave a 97% yield of the bis-2,4-dinitrophenylhydrazone of 2-bromoadipaldehyde (XV). The steric orientation of the 1,2-diol group was shown to be trans since debromination in the presence of Amberlite IR-4B (OH) resin gave *dl*-1α,2β-cyclohexanediol in 91% yield. Since the bromine and its adjacent hydroxyl group in the original bromohydrin are in a trans orientation, it follows that the bromodiol must be *dl*-3α-bromo-1α,2β-cyclohexanediol (XIV) and the bromohydrin must be *dl*-1α-methoxy-2β-hydroxy-3α-bromocyclohexane (V, R = CH_3) in agreement with the structural assignment reached on the basis of debromination of the urethanes. This proof of structure is based on two assumptions. First, that no inversion of configuration occurs during de-etherification and second, that elimination of bromine is not assisted by intermediate oxide formation. The first assumption was shown to be valid by de-etherification of 2β-methoxy-1α-cyclohexanol under conditions identical with those used for the bromohydrin, when 1α,2β-cyclohexanediol was obtained in 92% yield. It was also shown that the oxide cannot be an intermediate in the debromination reaction since 1β-methoxy-2α,3α-epoxycyclohexane and other oxides are not reduced by Raney nickel and hydrogen under the conditions used. In complete agreement with this result is the observation that debromination of the bromodiol XIV does not proceed in the presence of Amberlite IRA-400 (OH) resin, whereas the use of identical conditions with the phenyl- and 1-naphthyl-urethanes IX and XI (R = CH_3) had furnished high yields of the debrominated compounds X and XII (R = CH_3). Debromination of XIV is readily achieved, however, in the presence of Amberlite IR-4B (OH). This behavior was explained when the action of the two anion exchange resins on 1α-methoxy-2β-hydroxy-3α-bromocyclohexane (V, R = CH_3) was examined. In the presence of the weakly basic resin, IR-4B, the bromohydrin remains unchanged, but in the presence of the strongly basic resin it is converted to the oxide I (R = CH_3), which does not undergo reduction to a diol under the conditions used. These results underline the efficacy of the protection afforded against intermediate oxide formation by the presence of urethane groups in the earlier debromination experiments in which the strongly basic resin was used.



1α-Methoxy-2α,3α-epoxycyclohexane II (R = CH_3) on treatment with hydrobromic acid gave a 93% yield of a liquid bromohydrin VII (R = CH_3) b.p. 62–63° at 0.01 mm. This substance was quite different from the solid bromohydrin V (R = CH_3) obtained from the isomeric oxide, as demonstrated by comparison of their derivatives and infrared spectra. Conversion of the liquid bromohydrin to a 1-naphthylurethane, m.p. 122–124°, in 86% yield and to a liquid acetyl derivative, b.p. 63–65° at 0.01 mm in 95% yield

suggested that the compound was sterically pure. The proof of structure of this bromohydrin was not as exhaustively pursued as that of its stereoisomer and the simplicity of the de-etherification approach led us to follow this method. Ether cleavage of the bromohydrin gave a bromodiol, m.p. 70.5–71°, in 74% yield together with 8% of unchanged starting material. The new compound gave a liquid diacetyl derivative, b.p. 85–86° at 0.1 mm, in 95% yield and a bis-1-naphthylurethane, m.p. 176–178°, in 95% yield. The bromodiol was shown to be a 3-bromo-1,2-cyclohexanediol since periodate oxidation followed by treatment with 2,4-dinitrophenylhydrazine gave the bis-2,4-dinitrophenylhydrazone of 2-bromoadipaldehyde (XV) which had been obtained earlier from similar treatment of its isomer XIV. The orientation of the hydroxyl groups in the lower-melting bromodiol was shown to be cis since its rate of oxidation by periodate at 20° was 10 times more rapid than that of its isomer. Since the liquid bromohydrin yields the oxide II (R = CH_3) on treatment with alkali, it follows (2, 3) that the structure of the bromohydrin must be *dl*-1α-methoxy-2α-hydroxy-3β-bromocyclohexane (VII, R = CH_3) and the corresponding bromodiol must be *dl*-3β-bromo-1α,2α-cyclohexanediol (XVI).



(VII) (XVI)

A solid bromohydrin, m.p. 46–47.5°, was obtained in 61% yield by the action of hydrobromic acid on the trans oxide I (R = C_2H_5) and was further characterized by preparation of the phenylurethane, m.p. 132.5–133.5° (75%), 1-naphthylurethane, m.p. 196–197° (97%), and acetyl derivative, m.p. 29.5–30.5° (92%). Its structure was established as *dl*-1α-ethoxy-2β-hydroxy-3α-bromocyclohexane (V, R = C_2H_5) by debromination of the 1-naphthylurethane XI (R = C_2H_5) to the tetrahydronaphthylurethane of *dl*-2β-ethoxy-1α-cyclohexanol XII (R = C_2H_5) in 88% yield and by de-etherification of the bromohydrin to the bromodiol XIV in 86% yield.

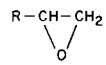
As in the case of the cis methoxy oxide II (R = CH_3), the action of hydrobromic acid on the ethyl homologue produced a liquid bromohydrin, b.p. 71–72° at 0.01 mm, in 82% yield. This bromohydrin failed to yield a solid 1-naphthylurethane and gave a liquid acetyl derivative, b.p. 72–74° at 0.05 mm, in 90% yield. The substance was assigned the structure 1α-ethoxy-2α-hydroxy-3β-bromocyclohexane VII (R = C_2H_5) since de-etherification with hydrogen bromide gave the bromodiol XVI in 51% yield together with 26% of unreacted bromohydrin.

The n.m.r. spectra of the bromohydrin acetates and bromodiol diacetates were measured by Dr. R. R. Fraser of Ottawa University. Interpretation of these spectra according to the principles elaborated by Lemieux, Kullnig, Bernstein, and Schneider (12) fully confirmed the structural assignments made above on the basis of chemical evidence. An additional check on the purity of the two liquid bromohydrins (VII, R = CH_3 and C_2H_5) and their corresponding liquid acetyl derivatives was thereby provided, since there were no abnormalities in the spectra indicative of contamination of any of these substances with positional isomers or stereoisomers.

In recent years considerable attention has been focused upon mechanisms of oxide

Can. J. Chem. Downloaded from www.nrcresearchpress.com by 210.87.254.42 on 09/05/12
For personal use only.

ring scissions and the mode of addition of nucleophiles to unsymmetrically substituted oxides. The results of these investigations have been summarized by Winstein and Henderson (4) and Parker and Isaacs (13) in extensive review articles, but no unifying theory capable of accurately predicting the products of such reactions has emerged. The stereoisomeric 1-alkoxy-2,3-epoxycyclohexanes I and II (R = CH_3 or C_2H_5), which were first prepared by McRae, Moir, and co-workers (14, 15, 16), provided, during and after elucidation of their structures (5, 1), useful models for examination of certain aspects of the mechanisms of oxide ring cleavages by careful product analysis. Investigations by McRae *et al.* (14), Lemieux, Kullnig, and Moir (5), and Bannard and Hawkins (1) made it evident that under alkaline conditions these oxides are attacked by nucleophiles such as methanol, water, and ammonia predominantly at position 3 (yields in excess of 70%). Although some work on the opening of the oxides under acidic conditions by water (17) and *p*-toluenesulphonic acid (5) was also reported earlier, yields of isolated products were not sufficiently high to permit a definite conclusion to be drawn regarding the preferred position of attack. The results of the present work make it quite clear, however, that position 3 is still the preferred point of attack under acidic conditions and that there is apparently no tendency toward reversal of the mode of opening of the oxide ring in 1-alkoxy-2,3-epoxycyclohexanes as has frequently been observed for unsymmetrical oxides of the type XVII (18, 13, 15, 21).



(XVII)

In the reactions cited above, opening of the oxide ring was attended by Walden inversion at position 3, which is suggestive that an S_N2 mechanism is operating (19). This result agrees with the majority of evidence in the literature (13, 15, 20, 21), which supports the S_N2 mechanism for oxide scissions. No indication of the presence of products formed by ring opening with retention of configuration was obtained in any of the work summarized above. This observation makes improbable the intervention of an S_N1 process as a major feature of the mechanism (see references 18, 4, 13, 20, 21) since under such circumstances at least some cis-2,3-oriented products would be expected (13, 19, 20, 21). The latter mechanism may occur to a minor extent, however, because in none of the reactions under consideration was a total material balance of completely characterized products obtained. The results of Lemieux, Kullnig, and Moir (5), obtained when the ring was opened with water under alkaline conditions and arrived at by a method of product analysis which was sensitive enough to reveal minor products formed by attack at position 2, suggests that further careful product analysis is required in all these reactions before intervention of the S_N1 mechanism to a minor extent can be ruled out. No clear picture of the role of polar and steric effects in determining the point of attack of nucleophiles on the 1-alkoxy-2,3-epoxycyclohexanes has resulted. On the basis of simple polar effects and the view that the important feature in S_N2 processes is the facilitation of reagent approach (18, 19, 20) (which is adequate for explanation of the mode of addition to oxides of type XVII), it would be predicted that attack should occur at position 2, which is not the case. Lemieux, Kullnig, and Moir (5) have pointed out however, that the observed result is in agreement with prediction if the governing factor in S_N2 mechanisms is ease of development of carbonium ion character in the transition state (22, 13, 20). Also, there is no uniformity in prediction of the position

Can. J. Chem. Downloaded from www.nrcresearchpress.com by 210.87.254.42 on 09/05/12
For personal use only.

of attack by the nucleophile on the basis of Angyal's (23) extension of the Fürst–Plattner rule (24) which visualizes the more stable conformer undergoing reaction to produce a chair form by diaxial ring opening. This theory predicts the observed result for the cis oxides but not for the trans oxides. If the view is taken that steric ease of approach of the nucleophile determines the point of attack, the observed products are predicted for the trans oxides because attack at position 2 is inhibited by the presence of the methoxyl group at position 1 in a cis relationship to the entering nucleophile, as indicated by Lemieux, Kullnig, and Moir (5). However, such an effect would be absent from reactions involving the cis oxides and it might have been expected that attack would occur at positions 2 and 3 with equal facility. It seems evident from these observations that much work still remains to be done before the mechanisms of oxide ring openings can be placed on a firm basis.

EXPERIMENTAL*†

dl-1α-Methoxy-2β-hydroxy-3α-bromocyclohexane (V, R = CH_3)

dl-1β-Methoxy-2α,3α-epoxycyclohexane (42.5 g, 0.332 mole) was dissolved in acetone (100 ml) and the solution was cooled with mechanical stirring to −10°. Hydrobromic acid (48%, 56.0 g, 0.332 mole) was added dropwise at −10° to 0°, the solution was allowed to come to room temperature, the excess acid was neutralized by addition of sodium carbonate, the precipitated salt was removed by filtration, and the solution was evaporated to dryness *in vacuo*. The residue was recrystallized from ether, yielding 43.9 g (63.3%) of *dl*-1α-methoxy-2β-hydroxy-3α-bromocyclohexane, as colorless needles, m.p. 68.5–69°. Calc. for $C_7H_{13}O_2Br$: C, 40.22; H, 6.27; Br, 38.22%. Found: C, 40.10; H, 6.25; Br, 38.10%. A liquid fraction (13.1 g), b.p. 65–67° at 0.03 mm, was also obtained which was shown to contain more of the bromohydrin V (R = CH_3) and a 1-methoxy-2,3-dihydroxycyclohexane (see below).

Derivatives of dl-1α-Methoxy-2β-hydroxy-3α-bromocyclohexane

The phenylurethane (IX, R = CH_3) was obtained in 86.1% yield, m.p. 133–134°, after recrystallization from 95% ethanol. Calc. for $C_{14}H_{18}O_3NBr$: C, 51.23; H, 5.53; N, 4.27; Br, 24.35%. Found: C, 51.13; H, 5.35; N, 4.21; Br, 24.72%.

The 1-naphthylurethane (XI, R = CH_3) was obtained in 94.4% yield, m.p. 185–186°, after recrystallization from ether. Calc. for $C_{18}H_{20}O_3NBr$: C, 57.15; H, 5.33; N, 3.70; Br, 21.13%. Found: C, 57.16; H, 5.28; N, 3.91; Br, 21.12%.

The acetyl derivative was obtained in 90.0% yield as colorless needles, m.p. 56–56.5°, after recrystallization from ether–heptane. Calc. for $C_9H_{15}O_3Br$: C, 43.04; H, 6.02; Br, 31.82%. Found: C, 42.99; H, 6.13; Br, 32.08%.

dl-1α-Methoxy-2β,3α-cyclohexanediol Bis-1-naphthylurethane

A sample (1.00 g) of the liquid fraction from preparation of 1α-methoxy-2β-hydroxy-3α-bromocyclohexane was treated with 1-naphthylisocyanate (2.00 g) at 70°. The crude mixture of resultant 1-naphthylurethanes was washed with petroleum ether, then fractionally crystallized from ether, yielding 0.43 g (27%) of *dl*-1α-methoxy-2β-hydroxy-3α-bromocyclohexane 1-naphthylurethane, m.p. 185–186°—identified by mixed melting point and infrared spectrum, and 0.41 g (13%) of *dl*-1α-methoxy-2β,3α-cyclohexanediol bis-1-naphthylurethane, m.p. 224–226°. Calc. for $C_{29}H_{28}O_5N_2$: C, 71.88; H, 5.82; N, 5.78%. Found: C, 71.72; H, 5.84; N, 5.94%.

**All melting points are uncorrected.*
†Microanalyses by J. G. Helie of these laboratories.

Can. J. Chem. Downloaded from www.nrcresearchpress.com by 210.87.254.42 on 09/05/12
For personal use only.

Can. J. Chem. Downloaded from www.nrcresearchpress.com by 210.87.254.42 on 09/05/12
For personal use only.

2-Methoxyadipaldehyde Bis-2,4-dinitrophenylhydrazone

A second portion (1.00 g) of the above-mentioned liquid fraction was dissolved in ethanol (20 ml) and treated with sodium metaperiodate (3 g in 50 ml water). The solution was kept for 4 hours at room temperature, evaporated to dryness *in vacuo*, and extracted with ether. After evaporation, the residue from the ether extract was treated with 2,4-dinitrophenylhydrazine reagent (25). The bis-2,4-dinitrophenylhydrazone of 2-methoxyadipaldehyde separated as a yellow solid and after recrystallization from ethyl acetate had m.p. 192–193.5°. Yield, 0.64 g (19%). Calc. for $C_{19}H_{20}O_9N_8$: C, 45.24; H, 4.00; N, 22.22%. Found: C, 45.31; H, 4.17; N, 21.80%.

Debromination of dl-2β-Bromo-1α-cyclohexanol Phenylurethane

dl-2β-Bromo-1α-cyclohexanol phenylurethane (cf. Bedos (9)), m.p. 85–87° (0.900 g, 3.02×10^{-3} mole), was debrominated by the same method as described below for *dl*-1α-methoxy-2β-hydroxy-3α-bromocyclohexane phenylurethane. The crude product after recrystallization from ethanol–heptane furnished 0.57 g (86.5%) of cyclohexanol phenylurethane, m.p. 83–84.5°, alone and in admixture with an authentic sample (cf. Stengl *et al.* (10)).

dl-2β-Methoxy-1α-cyclohexanol Derivatives

dl-2β-Methoxy-1α-cyclohexanol was prepared by the method of Winstein and Henderson (8) and converted to the phenylurethane in 82% yield, m.p. 66–67.5°, after recrystallization from aqueous ethanol. Calc. for $C_{14}H_{19}O_3N$: C, 67.45; H, 7.68; N, 5.62%. Found: C, 67.40; H, 7.54; N, 5.70%. The 1-naphthylurethane was obtained in 77% yield, m.p. 111–112°, after recrystallization from ether–heptane. Calc. for $C_{18}H_{21}O_3N$: C, 72.22; H, 7.07; N, 4.69%. Found: C, 72.31; H, 7.09; N, 4.74%.

Debromination of dl-1α-Methoxy-2β-hydroxy-3α-bromocyclohexane Phenylurethane

dl-1α-Methoxy-2β-hydroxy-3α-bromocyclohexane phenylurethane (0.900 g, 2.74×10^{-3} mole) was dissolved in ethanol (50 ml), Raney Nickel W-7 (26) catalyst (10 g) and Amberlite IRA-400 (OH) resin (2 ml) were added, and the mixture was shaken for 24 hours at room temperature at 40 p.s.i. hydrogen pressure. The mixture was filtered and the filtrate was evaporated to dryness *in vacuo* yielding a crystalline residue, which, after recrystallization from ether–heptane, furnished 0.53 g (78%) of *dl*-2β-methoxy-1α-cyclohexanol phenylurethane (X, R = CH_3), m.p. 66–67.5°, alone and in admixture with an authentic specimen. The infrared spectra of the two samples (KBr pellet) were also identical.

dl-2β-Methoxy-1α-cyclohexanol Tetrahydro-1-naphthylurethane (XII, R = CH_3)

dl-2β-Methoxy-1α-cyclohexanol 1-naphthylurethane (0.200 g, 6.7×10^{-4} mole) was reduced by the same method as described for *dl*-1α-methoxy-2β-hydroxy-3α-bromocyclohexane phenylurethane except that ethanol–benzene (2:1, v/v; 30 ml) was used as solvent. Recrystallization of the crude product from aqueous ethanol gave 0.199 g (98.5%) of fine colorless needles, m.p. 89.5–91°. Calc. for $C_{18}H_{25}O_3N$: C, 71.25; H, 8.31; N, 4.62%. Found: C, 71.26; H, 8.27; N, 4.67%.

Debromination of dl-1α-Methoxy-2β-hydroxy-3α-bromocyclohexane 1-Naphthylurethane

dl-1α-Methoxy-2β-hydroxy-3α-bromocyclohexane 1-naphthylurethane (1.00 g, 2.65×10^{-3} mole) was debrominated by the same method as given for *dl*-2β-methoxy-1α-cyclohexanol 1-naphthylurethane. The crude product was recrystallized from aqueous ethanol yielding 0.690 g (86%) of *dl*-2β-methoxy-1α-cyclohexanol tetrahydro-1-naphthylurethane,

m.p. 89.5–91°, alone and in admixture with an authentic specimen. The infrared spectra (KBr pellet) of the two substances were also identical.

dl-2β-Bromo-1α-cyclohexanol 1-Naphthylurethane

This compound was obtained in 75% yield from *dl*-2β-bromo-1α-cyclohexanol (27) after recrystallization from ether, m.p. 177–177.5°. Calc. for $C_{17}H_{18}O_2NBr$: C, 58.63; H, 5.21; N, 4.03; Br, 22.95%. Found: C, 58.54; H, 5.19; N, 4.19; Br, 22.74%.

Cyclohexanol Tetrahydro-1-naphthylurethane

Cyclohexanol 1-naphthylurethane (cf. Bickel and French (28)), m.p. 131–132.5° (1.10 g, 4.07×10^{-3} mole), was reduced by the same method as described for 2β-methoxy-1α-cyclohexanol 1-naphthylurethane. Recrystallization of the crude product from aqueous ethanol gave 1.01 g (90.2%) of cyclohexanol tetrahydro-1-naphthylurethane as fine colorless needles, m.p. 105–106.5°. Calc. for $C_{17}H_{23}O_2N$: C, 74.69; H, 8.48; N, 5.12%. Found: C, 74.77; H, 8.48; N, 5.15%.

Debromination of dl-2β-Bromo-1α-cyclohexanol 1-Naphthylurethane

dl-2β-Bromo-1α-cyclohexanol 1-naphthylurethane (0.340 g, 9.77×10^{-4} mole) was debrominated by the same procedure as described for *dl*-2β-methoxy-1α-cyclohexanol 1-naphthylurethane. Recrystallization of the crude product from aqueous ethanol gave 0.250 g (93.7%) of cyclohexanol tetrahydro-1-naphthylurethane as colorless needles, m.p. 105–106.5°, alone and in admixture with an authentic specimen. The infrared spectra (KBr pellet) of the two samples were also identical.

Conversion of dl-1α-Methoxy-2β-hydroxy-3α-bromocyclohexane to dl-1β-Methoxy-2α,3α-epoxycyclohexane via Amberlite IRA-400 (OH) Resin

dl-1α-Methoxy-2β-hydroxy-3α-bromocyclohexane (4.18 g, 0.02 mole) was placed in a 500-ml pressure bottle together with Amberlite IRA-400 (OH) resin (40 ml) and ether (200 ml) and the mixture was shaken for 24 hours at atmospheric pressure. The resin was collected, washed with ether (100 ml), and the filtrate and washings dried over anhydrous sodium sulphate. The ether was removed by distillation at atmospheric pressure, after which the residue was fractionated *in vacuo* yielding 2.18 g (85.1%) of *dl*-1β-methoxy-2α,3α-epoxycyclohexane as a colorless oil, b.p. 60–61° at 12 mm, n_D^{25} 1.4511. The substance was identified by its infrared spectrum (1).

Attempted Reduction of dl-1β-Methoxy-2α,3α-epoxycyclohexane with Raney Nickel and Hydrogen

dl-1β-Methoxy-2α,3α-epoxycyclohexane (6.00 g, 4.68×10^{-2} mole), dissolved in ether (100 ml), was shaken with Raney nickel catalyst (10 ml) at room temperature under 40 p.s.i. hydrogen pressure for 24 hours. The mixture was filtered, the filtrate was concentrated by removal of the ether at atmospheric pressure, and the residue was distilled *in vacuo* yielding 5.60 g (93.4%) of unchanged starting material, b.p. 54–55° at 10 mm, which was identified via its infrared spectrum (1).

Action of Amberlite IR-4B (OH) Resin on dl-1α-Methoxy-2β-hydroxy-3α-bromocyclohexane (V, R = CH_3)

dl-1α-Methoxy-2β-hydroxy-3α-bromocyclohexane (1.00 g, 4.78×10^{-3} mole), dissolved in 95% ethanol (100 ml), was shaken for 24 hours with Amberlite IR-4B (OH) resin. The mixture was filtered, and the filtrate was allowed to evaporate to dryness at room temperature in an evaporating dish. The residual crystals were collected, recrystallized from ether, and identified as *dl*-1α-methoxy-2β-hydroxy-3α-bromocyclohexane by their melting

Can. J. Chem. Downloaded from www.nrcresearchpress.com by 210.87.254.42 on 09/05/12
For personal use only.

point of 68–69°, alone and in admixture with an authentic specimen. Recovery, 0.925 g (92.5%).

De-etherification of dl-1α-Methoxy-2β-hydroxy-3α-bromocyclohexane (V, R = CH_3) to dl-3α-Bromo-1α,2β-cyclohexanediol (XIV)

dl-1α-Methoxy-2β-hydroxy-3α-bromocyclohexane (1.05 g, 5.0×10^{-3} mole) was finely ground and heated for 1.5 hours in a sealed tube at 65° with fuming hydrobromic acid (1.0 ml, 68%, 1.57×10^{-2} mole). The pale yellow solution was transferred quantitatively to a 250-ml, round-bottomed flask (in ca. 50 ml of water), the excess acid was neutralized by addition of solid sodium bicarbonate, and the solution was evaporated to dryness *in vacuo*. The residue was transferred to a Soxhlet extractor, extracted for 4 hours with anhydrous ether, and the extract evaporated to dryness. Crystallization of the product from ether gave 0.861 g (88.8%) of *dl*-3α-bromo-1α,2β-cyclohexanediol as colorless prisms, m.p. 98–99°. Calc. for $C_6H_{11}O_2Br$: C, 36.94; H, 5.68; Br, 40.97%. Found: C, 36.96; H, 5.64; Br, 41.07%.

Derivatives of dl-3α-Bromo-1α,2β-cyclohexanediol (XIV)

The bis-1-naphthylurethane was obtained in 84.5% yield as fine colorless needles, m.p. 210–210.5°, after recrystallization from acetone. Calc. for $C_{28}H_{25}O_4N_2Br$: C, 63.04; H, 4.72; N, 5.25; Br, 14.98%. Found: C, 62.89; H, 4.93; N, 5.49; Br, 14.68%.

The diacetate was obtained in 95.1% yield as fine colorless needles, m.p. 65.5–66.5°, after recrystallization from ether–heptane. Calc. for $C_{10}H_{15}O_4Br$: C, 43.03; H, 5.42; Br, 28.63%. Found: C, 43.17; H, 5.62; Br, 28.73%.

dl-1α,2β-Cyclohexanediol from dl-2β-Methoxy-1α-cyclohexanol

dl-2β-Methoxy-1α-cyclohexanol (0.650 g, 5.0×10^{-3} mole) was heated for 1 hour at 75° with fuming hydrobromic acid (3.0 ml, 68%, 4.70×10^{-2} mole) in a sealed tube. The product was isolated by the same procedure as described for the de-etherification of *dl*-1α-methoxy-2β-hydroxy-3α-bromocyclohexane, except that final purification was effected by sublimation *in vacuo*. In this manner, 0.533 g (92.0%) of colorless crystals, m.p. 104.5–105.5°, alone and in admixture with an authentic specimen of *dl*-1α,2β-cyclohexanediol, were obtained.

Debromination of dl-3α-Bromo-1α,2β-cyclohexanediol (XIV)

dl-3α-Bromo-1α,2β-cyclohexanediol (0.400 g, 2.05×10^{-3} mole) was placed in a 500-ml pressure bottle together with ethanol (100 ml), Amberlite IR-4B (OH) resin (3 g), and Raney nickel catalyst and shaken for 24 hours under 40 p.s.i. hydrogen pressure at room temperature. The mixture was filtered and the crystalline residue, which resulted from evaporation to dryness of the filtrate, was sublimed *in vacuo*, yielding 213 mg (90.3%) of colorless crystals, m.p. 104.5–105.5°, alone and in admixture with an authentic specimen of *dl*-1α,2β-cyclohexanediol. The infrared spectra of the two specimens (KBr pellet) were also identical.

2-Bromoadipaldehyde Bis-2,4-dinitrophenylhydrazone (XV) from dl-3α-Bromo-1α,2β-cyclohexanediol (XIV)

dl-3α-Bromo-1α,2β-cyclohexanediol (1.00 g, 5.12×10^{-3} mole) and sodium metaperiodate (4.18 g, 2×10^{-2} mole) were dissolved in water and the solution was kept overnight at 25°, then evaporated to dryness *in vacuo* at room temperature. The residue was extracted with ether and the latter was removed *in vacuo*. The product was dissolved in ethanol and treated with 2,4-dinitrophenylhydrazine reagent (25). The yellow precipitate

Can. J. Chem. Downloaded from www.nrcresearchpress.com by 210.87.254.42 on 09/05/12
For personal use only.

was collected and washed three times with hot ethanol yielding 2.75 g (96.8%) of 2-bromoadipaldehyde bis-2,4-dinitrophenylhydrazone, m.p. 154–155° (with decomposition). Calc. for $C_{18}H_{17}O_8N_8Br$: C, 39.07; H, 3.10; N, 20.25; Br, 14.44%. Found: C, 39.35; H, 3.09; N, 19.90; Br, 14.41%.

dl-1α-Methoxy-2α-hydroxy-3β-bromocyclohexane (VII, R = CH_3)

The procedure was identical with that used for the preparation of *dl*-1α-methoxy-2β-hydroxy-3α-bromocyclohexane (V, R = CH_3) except that the cis oxide II (R = CH_3) (12.0 g, 9.37×10^{-2} mole) was employed as starting material. The crude liquid product was fractionated *in vacuo* yielding 18.3 g (93.3%) of a colorless viscous oil, b.p. 62–63° at 0.01 mm; n_D^{25} 1.5080. Calc. for $C_7H_{13}O_2Br$: C, 40.22; H, 6.27; Br, 38.22%. Found: C, 40.01; H, 6.17; Br, 38.27%.

Derivatives of dl-1α-Methoxy-2α-hydroxy-3β-bromocyclohexane

The 1-naphthylurethane was obtained in 86.5% yield, m.p. 122–124°, after recrystallization from acetone – petroleum ether (65–110°). Calc. for $C_{18}H_{20}O_3NBr$: C, 57.15; H, 5.33; N, 3.70; Br, 21.13%. Found: C, 57.27; H, 5.16; N, 3.80; Br, 20.83%.

The acetyl derivative was obtained in 95.5% yield as a colorless liquid, b.p. 63–65° at 0.01 mm; n_D^{25} 1.4828. Calc. for $C_9H_{15}O_3Br$: C, 43.04; H, 6.02; Br, 31.82%. Found: C, 43.00; H, 5.94; Br, 32.07%.

De-etherification of dl-1α-Methoxy-2α-hydroxy-3β-bromocyclohexane to dl-3β-Bromo-1α,2α-cyclohexanediol (XVI)

dl-1α-Methoxy-2α-hydroxy-3β-bromocyclohexane (2.09 g, 1.0×10^{-2} mole) was subjected to ether cleavage under conditions identical with those used for its stereoisomer. The resultant mixture of oil and crystals (1.82 g) was washed with anhydrous ether to dissolve the oil, and recrystallization of the residue from anhydrous ether gave 1.44 g (73.8%) of *dl*-3β-bromo-1α,2α-cyclohexanediol as colorless prisms, m.p. 70.5–71°. This substance was shown to be quite different from its stereoisomer, by comparison of their infrared spectra (KBr pellet). Calc. for $C_6H_{11}O_2Br$: C, 36.94; H, 5.68; Br, 40.97%. Found: C, 37.11; H, 5.43; Br, 40.78%. The oil fraction from this preparation was distilled in an air bath at 25–30° at 0.001 mm pressure yielding 170 mg (8.1%) of colorless oil, n_D^{25} 1.5085, identified via its infrared spectrum as *dl*-1α-methoxy-2α-hydroxy-3β-bromocyclohexane (VII, R = CH_3).

Derivatives of dl-3β-Bromo-1α,2α-cyclohexanediol

The bis-1-naphthylurethane was obtained in 95.3% yield as colorless crystals, m.p. 176–178°, after recrystallization from ethyl acetate. Calc. for $C_{28}H_{25}O_4N_2Br$: C, 63.04; H, 4.72; N, 5.25; Br, 14.98%. Found: C, 63.20; H, 4.73; N, 5.15; Br, 15.14%.

The diacetyl derivative was obtained in 95.0% yield as a colorless viscous oil, b.p. 85–86° at 0.1 mm pressure; n_D^{25} 1.4810. Calc. for $C_{10}H_{15}O_4Br$: C, 43.03; H, 5.42; Br, 28.63%. Found: C, 43.02; H, 5.20; Br, 28.93%.

2-Bromoadipaldehyde Bis-2,4-dinitrophenylhydrazone (XV) from dl-3β-Bromo-1α,2α-cyclohexanediol (XVI)

The procedure used was identical with that given for the periodate oxidation and subsequent 2,4-dinitrophenylhydrazone formation from *dl*-3α-bromo-1α,2β-cyclohexanediol (XIV). The bis-2,4-dinitrophenylhydrazone was obtained in 95% yield, m.p. 154–155°, and had an infrared spectrum (KBr pellet) identical with that of an authentic specimen of XV.

Can. J. Chem. Downloaded from www.nrcresearchpress.com by 210.87.254.42 on 09/05/12
For personal use only.

Periodate Oxidation of dl-3α-Bromo-1α,2β-cyclohexanediol (XIV) and dl-3β-Bromo-1α,2α-cyclohexanediol (XVI)

The experimental procedure used for periodate oxidation of the bromodiols XIV and XVI was identical with that described earlier for oxidation of the *p*-nitrobenzoyl derivatives of the 3-amino-1,2-cyclohexanediols (1), except that the determinations were performed at 20° and 14-mg samples of the bromodiols were used. The results showed uptake of 1 mole of periodate by the cis diol in 15 minutes and by the trans diol in 180 minutes. Comparison of the $t_{\frac{1}{4}}$ values (1.75 minutes for XVI and 18.0 for XIV) indicated that the rate of oxidation of the cis diol is approximately 10 times that of the trans diol.

dl-1α-Ethoxy-2β-hydroxy-3α-bromocyclohexane (V, R = C_2H_5)

dl-1β-Ethoxy-2α,3α-epoxycyclohexane (I, R = C_2H_5) (14.2 g, 0.100 mole) on treatment with hydrobromic acid in the same manner as described for its lower homologue gave 13.6 g (61.0%) of *dl*-1α-ethoxy-2β-hydroxy-3α-bromocyclohexane as colorless needles, m.p. 46–47.5°, after recrystallization from ether. Calc. for $C_8H_{15}O_2Br$: C, 43.07; H, 6.78; Br, 35.82%. Found: C, 42.91; H, 6.58; Br, 35.61%.

Derivatives of dl-1α-Ethoxy-2β-hydroxy-3α-bromocyclohexane

The phenylurethane (IX, R = C_2H_5) was obtained as fine needles in 75.3% yield, m.p. 132.5–133.5°, after recrystallization from ether–heptane. Calc. for $C_{15}H_{20}O_3NBr$: C, 52.64; H, 5.89; N, 4.09; Br, 23.35%. Found: C, 52.68; H, 5.84; N, 4.16; Br, 23.38%.

The 1-naphthylurethane (XI, R = C_2H_5) was obtained in 96.6% yield as fine needles, m.p. 196–197°, after recrystallization from ethyl acetate. Calc. for $C_{19}H_{22}O_3NBr$: C, 58.17; H, 5.65; N, 3.57; Br, 20.37%. Found: C, 58.32; H, 5.46; N, 3.88; Br, 20.04%.

The acetate was obtained as fine colorless needles in 92.4% yield, m.p. 29.5–30.5°, after recrystallization from *n*-hexane. Calc. for $C_{10}H_{17}O_3Br$: C, 45.29; H, 6.46; Br, 30.14%. Found: C, 45.28; H, 6.28; Br, 30.31%.

dl-2β-Ethoxy-1α-cyclohexanol 1-Naphthylurethane (XIII, R = C_2H_5)

dl-2β-Ethoxy-1α-cyclohexanol (b.p. 75–77° at 11 mm; n_D^{25} 1.4538) was prepared in 73% yield by the same method (8) as used for the corresponding methoxy compound (cf. Mousseron *et al.* (29)) and was converted in 94.2% yield to the 1-naphthylurethane, which was obtained as fine needles, m.p. 131–132°, after recrystallization from ethyl acetate. Calc. for $C_{19}H_{23}O_3N$: C, 72.81; H, 7.40; N, 4.47%. Found: C, 73.08; H, 7.39; N, 4.67%.

dl-2β-Ethoxy-1α-cyclohexanol Tetrahydro-1-naphthylurethane (XII, R = C_2H_5)

dl-2β-Ethoxy-1α-cyclohexanol 1-naphthylurethane (0.830 g, 2.66×10^{-3} mole) was reduced by the same method as described for *dl*-2β-methoxy-1α-cyclohexanol 1-naphthylurethane. Recrystallization of the crude product from aqueous ethanol gave 0.760 g (90.3%) of fine colorless needles, m.p. 71–72.5°, of the tetrahydro-1-naphthylurethane. Calc. for $C_{19}H_{27}O_3N$: C, 71.88; H, 8.57; N, 4.41%. Found: C, 71.80; H, 8.67; N, 4.58%.

Debromination of dl-1α-Ethoxy-2β-hydroxy-3α-bromocyclohexane 1-Naphthylurethane (XI, R = C_2H_5)

dl-1α-Ethoxy-2β-hydroxy-3α-bromocyclohexane 1-naphthylurethane (0.900 g, 2.88×10^{-3} mole) was debrominated by the same method as described for *dl*-2β-methoxy-1α-cyclohexanol 1-naphthylurethane. The crude product was recrystallized from aqueous ethanol yielding 0.640 g (87.9%) of *dl*-2β-ethoxy-1α-cyclohexanol tetrahydro-1-naphthylurethane as colorless needles, m.p. 71–72.5°, alone and in admixture with an authentic sample. The infrared spectra (5% in carbon tetrachloride) were also identical.

Can. J. Chem. Downloaded from www.nrcresearchpress.com by 210.87.254.42 on 09/05/12
For personal use only.

dl-3α-Bromo-1α,2β-cyclohexanediol (XIV) from dl-1α-Ethoxy-2β-hydroxy-3α-bromocyclohexane (V, R = C_2H_5)

dl-1α-Ethoxy-2β-hydroxy-3α-bromocyclohexane (1.12 g, 5.0×10^{-3} mole) was subjected to ether cleavage under conditions identical with those described for the lower homologue. The crude product was recrystallized from ether yielding 831 mg (85.7%) of colorless prisms, m.p. 98–99°, alone and in admixture with an authentic specimen of *dl*-3α-bromo-1α,2β-cyclohexanediol.

dl-1α-Ethoxy-2α-hydroxy-3β-bromocyclohexane (VII, R = C_2H_5)

dl-1α-Ethoxy-2α,3α-epoxycyclohexane (II, R = C_2H_5) (14.2 g, 0.100 mole) was treated with hydrobromic acid in the same manner as described for *dl*-1β-methoxy-2α,3α-epoxycyclohexane. The crude liquid product was fractionated *in vacuo* yielding 18.3 g (82.0%) of *dl*-1α-ethoxy-2α-hydroxy-3β-bromocyclohexane, b.p. 70–71° at 0.01 mm; n_D^{25} 1.4971. Calc. for $C_8H_{15}O_2Br$: C, 43.07; H, 6.78; Br, 35.82%. Found: C, 43.11; H, 6.85; Br, 35.69%.

dl-1α-Ethoxy-2α-acetoxy-3β-bromocyclohexane

dl-1α-Ethoxy-2α-hydroxy-3β-bromocyclohexane (2.23 g, 1.00×10^{-2} mole) was heated under reflux for 1 hour with acetic anhydride (10 ml). The excess anhydride was removed by distillation *in vacuo* and the residue was distilled *in vacuo* yielding 2.39 g (90.2%) of colorless mobile oil, b.p. 64–64.5° at 0.01 mm; n_D^{25} 1.4760. Calc. for $C_{10}H_{17}O_3Br$: C, 45.29; H, 6.46; Br, 30.14%. Found: C, 45.13; H, 6.13; Br, 30.25%.

De-etherification of dl-1α-Ethoxy-2α-hydroxy-3β-bromocyclohexane to dl-3β-Bromo-1α,2α-cyclohexanediol (XVI)

dl-1α-Ethoxy-2α-hydroxy-3β-bromocyclohexane (2.23 g, 1.0×10^{-2} mole) was subjected to ether cleavage under conditions identical with those described for its homologue, yielding a mixture of oil and crystals (1.67 g) which, after recrystallization from anhydrous ether, gave 988 mg (50.6%) of colorless prisms, m.p. 70.5–71°, alone and in admixture with an authentic sample of *dl*-3β-bromo-1α,2α-cyclohexanediol (XVI). The residual oil was distilled in an air bath at 28–33° at 0.001 mm pressure yielding 588 mg (26.4%) of colorless oil, n_D^{25} 1.4981, which was identified as *dl*-1α-ethoxy-2α-hydroxy-3β-bromocyclohexane (VII, R = C_2H_5) via its infrared spectrum.

ACKNOWLEDGMENTS

We are indebted to Prof. R. U. Lemieux and Dr. R. R. Fraser for measurement and interpretation of the n.m.r. spectra of the bromohydrin acetates and bromodiol diacetates, to Dr. R. Y. Moir for a helpful discussion, to Mr. A. A. Casselman for preparation of quantities of the ethoxybromohydrins, to Dr. G. M. Brown for assistance, and to Mr. R. Gravelle for measurement of infrared spectra.

REFERENCES

1. R. A. B. Bannard and L. R. Hawkins. Can. J. Chem. **36**, 1241 (1958).
2. P. D. Bartlett. J. Am. Chem. Soc. **57**, 224 (1935).
3. D. H. R. Barton, D. A. Lewis, and J. F. McGhie. J. Chem. Soc. 2907 (1957).
4. S. Winstein and R. B. Henderson. *In* Heterocyclic compounds. Vol. 1. John Wiley & Sons, Inc., New York. 1950. p. 29.
5. R. U. Lemieux, R. K. Kullnig, and R. Y. Moir. J. Am. Chem. Soc. **80**, 2237 (1958).
6. S. Winstein and L. L. Ingraham. J. Am. Chem. Soc. **74**, 1160 (1952).
7. G. E. McCasland and E. C. Horswill. J. Am. Chem. Soc. **75**, 4020 (1953).
8. S. Winstein and R. B. Henderson. J. Am. Chem. Soc. **65**, 2196 (1943).
9. P. Bedos. Bull. soc. chim. France, **39**, 252 (1926).
10. H. Stengl, F. Fichter, and H. Arni. Helv. Chim. Acta, **19**, 392 (1936).
11. E. Schwenk and D. Papa. U.S. Patent No. 2,475,718 (July 12, 1949); Chem. Abstr. **43**, 7510*i* (1949).

Can. J. Chem. Downloaded from www.nrcresearchpress.com by 210.87.254.42 on 09/05/12
For personal use only.

12. R. U. LEMIEUX, R. K. KULLNIG, H. J. BERNSTEIN, and W. G. SCHNEIDER. J. Am. Chem. Soc. **80**, 6098 (1958).
13. R. E. PARKER and N. S. ISAACS. Chem. Revs. **59**, 737 (1959).
14. J. A. MCRAE, R. Y. MOIR, J. W. HAYNES, and L. G. RIPLEY. J. Org. Chem. **17**, 1621 (1952).
15. R. Y. MOIR. M.A. Thesis, Queen's University, Kingston, Ont. 1942.
16. S. W. FENTON. M.Sc. Thesis, Queen's University, Kingston, Ont. 1946.
17. R. Y. MOIR. Ph.D. Thesis, McGill University, Montreal, Que. 1948.
18. R. G. KADESCH. J. Am. Chem. Soc. **68**, 41 (1946).
19. C. K. INGOLD. Structure and mechanism in organic chemistry. Cornell University Press, Ithaca, New York. 1953.
20. E. S. GOULD. Mechanism and structure in organic chemistry. Henry Holt & Co., New York. 1959. Chap. 8.
21. A. A. FROST and R. G. PEARSON. Kinetics and mechanism. John Wiley & Sons, Inc., New York. 1953. Chap. 11.
22. A. STREITWEISER. Chem. Revs. **56**, 571 (1956).
23. S. J. ANGYAL. Chem. & Ind. (London), 1230 (1954).
24. A. FÜRST and PL. A. PLATTNER. Abstracts of Papers, 12th International Congress of Pure and Applied Chemistry, New York. 1951. p. 405.
25. R. L. SHRINER, R. C. FUSON, and D. Y. CURTIN. *In* The systematic identification of organic compounds. 4th ed. John Wiley & Sons, Inc., New York. 1956. p. 111.
26. H. ADKINS and H. R. BILLICA. J. Am. Chem. Soc. **70**, 695 (1948).
27. C. O. GUSS and R. ROSENTHAL. J. Am. Chem. Soc. **77**, 2549 (1955).
28. V. T. BICKEL and H. E. FRENCH. J. Am. Chem. Soc. **48**, 747 (1926).
29. M. MOUSSERON, R. GRANGER, and A. MERLE. Bull. soc. chim. France, 459 (1947).

Can. J. Chem. Downloaded from www.nrcresearchpress.com by 210.87.254.42 on 09/05/12
For personal use only.

Can. J. Chem. Downloaded from www.nrcresearchpress.com by 210.87.254.5 on 09/05/12
For personal use only.

NOTES

DIFFUSION OF Zn IN ZnO

E. A. Secco

INTRODUCTION

The experimental results reported in the literature on the diffusion of Zn in ZnO appear conflicting and cannot be fitted to a single conventional defect model. There is also a discrepancy between the parabolic rate constant for zinc oxidation and the diffusion of Zn in ZnO if the Wagner equation (3, 17)

$$K = \int_{a_1}^{a_2} D \, d \ln a$$

relating the parabolic rate constant K and the diffusion coefficient D of the zinc metal is accepted. The diffusion of zinc has been suggested to occur via the interstitial sites. However, the apparent disagreement among the experimental results obtained to date, reviewed elsewhere (1, 2, 3), and reproduced in Table I in simple equation form, has led

TABLE I

		Temp., ° K	Ref.
Oxidation	Parabolic rate equation		
	$K = 3.3\times10^{-7} \exp(-29.0 \text{ kcal}/RT)$ cm² sec⁻¹	648–673	Moore and Lee (4)
	$K = 1.1\times10^{-5} \exp(-35.0 \text{ kcal}/RT)$ cm² sec⁻¹	873–973	Krupkowski and Balicki (5)
	$K = 2.5\times10^{-7} \exp(-25.0 \text{ kcal}/RT)$ cm² sec⁻¹	703–752	Gebhardt (6)
Exchange	Diffusion equation		
	$D = 4.8 \exp(-73 \text{ kcal}/RT)$ cm² sec⁻¹	1183–1300	Secco and Moore (7)
	$D = 1.8\times10^{5} \exp(-89 \text{ kcal}/RT)$ cm² sec⁻¹	1189–1540	Spicar (8)
	$D^* = 30 \exp(-75 \text{ kcal}/RT)$ cm² sec⁻¹	1189–1540	Moore (3)
	$D = 1.7\times10^{2} \exp(-76 \text{ kcal}/RT)$ cm² sec⁻¹	1073–1463	Lamatsch (9)
	$k_e = 4.0\times10^{5} \exp(-40 \text{ kcal}/RT)$ sec⁻¹	993–1113	Secco (14)
	$D = 10 \exp(73.0 \text{ kcal}/RT)$ cm² sec⁻¹	993–1113	Secco (14)
Tracer	Diffusion equation		
	$D = 1.3 \exp(-74 \text{ kcal}/RT)$ cm² sec⁻¹	1073–1600	Lindner (10)
	$D = 1.3\times10^{-5} \exp(-44 \text{ kcal}/RT)$ cm² sec⁻¹	1273–1463	Moore and Williams (11)
Conductivity	Diffusion equation		
	$D = 1.6\times10^{-2} \exp(-39 \text{ kcal}/RT)$ cm² sec⁻¹	973–1603	Pohl (12)
	$D = 1.5\times10^{-2} \exp(-39 \text{ kcal}/RT)$ cm² sec⁻¹	1100–1370	Arneth (13)

*This diffusion coefficient is obtained from the one above it by correcting to constant zinc pressure on the basis of $D \propto P_{Zn}^{1/2}$.

to the speculation of other structural defects, such as oxide vacancies and Frenkel defects.

Recently, the exchange of zinc vapor with polycrystalline zinc oxide has been studied in a static system under different conditions of temperature and pressure (14). Plots of $\log_{10}\alpha^*$ (exchange fraction) versus time revealed two processes at the temperatures studied, 720°–840° C. The initial process was a rapid simple exchange whose data were fitted to a first-order rate law with the Arrhenius expression given by

$$k_e = 4.0\times10^{5} \exp(-40 \text{ kcal}/RT) \text{ sec}^{-1}.$$

This first-order rate law was found to persist to a depth of 20–25 molecular thicknesses

at 720° C, i.e. one half of particle radius, and to increasing depths at the higher temperatures. A second, slower process, which appeared to be diffusion-controlled, with the diffusion equation expressed by $D = 10 \exp (73.0 \text{ kcal}/RT)$ cm^2 sec^{-1}, followed the initial process. This diffusion equation is in agreement with diffusion equations obtained in other exchange studies using single crystals.

Close examination of the above data reveals that the diffusion coefficient as obtained from the exchange studies is equal to, within the limits of experimental uncertainty, the product of the parabolic rate constant or the diffusion coefficient from conductivity studies and the exchange constant k_e from polycrystalline studies. That is, the diffusion coefficient in the exchange work appears to be a composite quantity consisting of a mobility term and an exchange term, $D_e = D_i k_e$, namely, an interstitialcy type of diffusion mechanism.

Let us consider an interstitial particle of the non-Frenkel type (interstice occupied by a particle without the existence of a corresponding vacancy) diffusing through a lattice. From Fick's law the diffusion coefficient for the interstitial atom D_i is $D_i = \nu_i \lambda^2 \exp(-E_i/RT)$ cm^2 sec^{-1} where λ is the distance between the adjacent interstitial positions, and ν_i is the frequency of vibration or the number of attempts per second made by the interstitial atom to cross the energy barrier E_i. For diffusion of this type the over-all diffusion coefficient may be expressed as $D = D_i f_i$ where f_i = fraction of interstices available for occupancy by a mobile interstitial atom, i.e. $f_i = (N_i - n_i)/N_i$ where N_i = number of *effectively* available interstices and n_i = number of interstices occupied by atoms. The diffusion coefficient becomes $D = ((N_i - n_i)/N_i)D_i$. Under conditions of unsaturation, it is assumed that $n_i \ll N_i$, the diffusion coefficient becomes identical with the interstitial mobility, $D = D_i$. Whereas under equilibrium conditions, when $n_i \approx N_i$, the diffusion coefficient becomes zero, $D = 0$, which means that the simple interstitial mechanism of diffusion is impossible when all available interstices are occupied. Essentially, this condition is visualized when the direct interstice-to-interstice movement becomes energetically unfeasible because of the narrowing in the constriction separating the interstices at saturation caused by the large difference in radii, 1.4 Å for Zn atom and 0.7 Å for the octahedral interstice. Provided the latter condition obtains, the only other alternative would be a diffusion mechanism of the coupled, interstitial-lattice type.

An inspection of the ZnO lattice shows that an interstitial zinc has the same energy barrier E_i, judging solely from lattice dimensions, by the direct interstice path or via a vacant lattice site. In each case the interstitial atom must move through a similar constriction of the atoms constituting the host lattice. In the case of the interstitialcy mechanism the interstitial must possess an additional energy E_e if the lattice site is occupied. That is, the over-all energy required would be $E_e + E_i$. Now, if the rate of exchange of lattice atoms is given by $k_e = \nu_e \exp(-E_e/RT)$, and the interstitial mobility by $D_i = \nu_i \lambda^2 \exp(-E_i/RT)$, then the interstitialcy diffusion coefficient would be expected to be $D = \nu_i \nu_e \lambda^2 \exp((E_i + E_e)/RT) = D_i k_e$, where $\nu_i \nu_e$ represents the frequencies of vibration of the interstitial and lattice atoms. Thus diffusion occurs when the normal modes of vibration, with adequate energy, of the interstitial and lattice atoms come sufficiently into phase to give the vital configuration for its critical push. The diffusion equation would be $D = \nu_o \lambda^2 \exp(-(E_e + E_i)/RT)$ where ν_o is the over-all frequency of the linked process. Thus, the interstitialcy diffusion coefficient becomes $D = 10^{-2} - 10^{-1} \exp(-(E_e + E_i)/RT)$ cm^2 sec^{-1} for $\nu_o = 3 \times 10^{13}$ sec^{-1} and $\lambda = 3 \times 10^{-8}$ cm for the case of ZnO.

Can. J. Chem. Downloaded from www.nrcresearchpress.com by 210.87.254.5 on 09/05/12
For personal use only.

On the basis of the above discussion the interpretation to be given to the two processes observed in the exchange studies on polycrystalline zinc oxide is that the exchange reaction and zinc diffusion via interstices occur simultaneously. But if the interstitial mobility of the zinc is more rapid the exchange process predominates. As soon as the *effectively* available interstices become filled the transport or diffusion step becomes rate-controlling and supersedes the simple exchange process. The critical experiment to check the above hypothesis and empirical relationship is evidently the exchange reaction between zinc oxide, previously saturated with inactive zinc, and active Zn^{65} vapor.

EXPERIMENTAL

The polycrystalline ZnO used in this work was from the batch previously reported (14). The zinc oxide was exposed to excess inactive zinc vapor, ca. 0.15 atm, at 760° C for 5 hours. The exchange runs using this saturated zinc oxide were carried out in a static system which has already been described.

RESULTS

In Fig. 1 is given a plot of the logarithm of the exchange reaction against time for

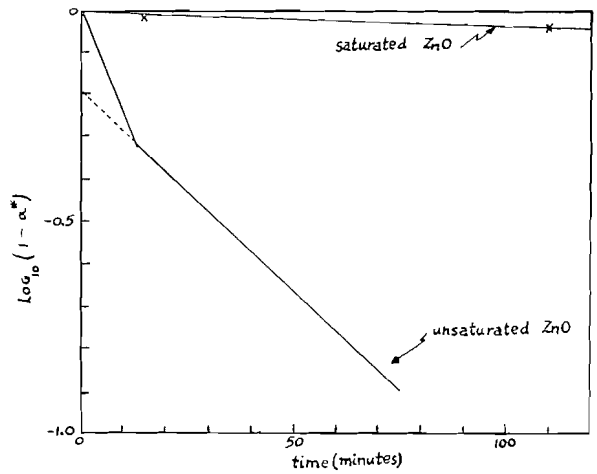


FIG. 1. Plot of logarithm of the unexchanged-fraction versus time at 760° C; saturated ZnO curve from present work, unsaturated ZnO from work already reported (14).

Zn^{65} exchange with the saturated ZnO and for Zn^{65} exchange with untreated ZnO, at 760° C. Figure 2 shows the plot of the non-dimensional (Dt/a^2) as a function of time for Zn^{65} exchange with the pretreated ZnO at temperatures 760° and 800° C. The values of Dt/a^2 were taken from Crank (16). The diffusion coefficients were evaluated as the product of the slope of the straight line in Fig. 2 and the square of the particle radius, a^2. The diffusion equation as obtained from these two temperatures is $D = 0.40 \exp(-76.5 \text{ kcal}/RT)$ $\text{cm}^2 \text{ sec}^{-1}$, which is in agreement with existing exchange data on zinc oxide.

It was thought in the pretreatment of ZnO with zinc vapor that sintering could have occurred resulting in a diminution of the surface area and hence increased particle size. The surface area of the oxide used could not be measured but another sample of oxide from the same batch heated in air at 760° C for 2 hours was found to drop from an original

Can. J. Chem. Downloaded from www.nrcresearchpress.com by 210.87.254.5 on 09/05/12
For personal use only.

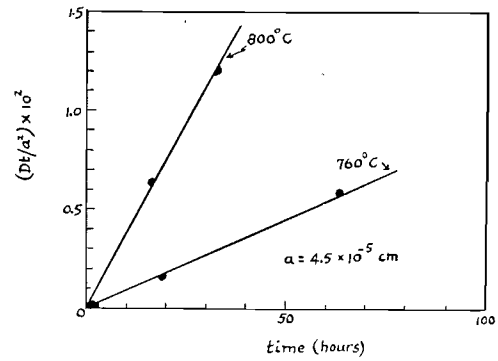


FIG. 2. Plot of non-dimensional (Dt/a^2) versus time at 760° and 800° C.

value of 3.50 m^2/g to 1.20 m^2/g. The change in surface area is negligible compared to the decrease observed in the exchange reaction rate.

DISCUSSION

It can be concluded that the hypothesis set forth in the introduction of this paper has been verified. The results, therefore, give strong support to the empirical relationship, $D_e = D_i \cdot k_e$, obtained from the reported data in Table I and the interstitialcy model of diffusion described above. The pre-exponential term for $D_e = D_i \cdot k_e$, using the mobility term from conductivity measurements, is at variance with the theoretical model by a factor of 10^3. D_i as calculated from the conductivity data is based on the assumption that the decay in conductivity was due solely to diffusion of interstitial zinc. The latter assumption may or may not be valid. A better fit to the theoretical interstitialcy model is obtained with the mobility term from the parabolic oxidation data.

If the sequence of rate-controlling steps as postulated for the observed processes in the exchange reaction on polycrystalline oxide were correct, then it is possible to calculate the diffusion coefficient of zinc via interstices if the time required for saturation of the oxide with interstitial zinc is taken as that time up to the onset of the interstitialcy diffusion (14). For temperatures 720°, 740°, 760°, and 780° C and using the simple relationship of $a^2 = 2Dt$, where a is the radius of the particle, the diffusion equation $D_i = 3 \times 10^{-7} \exp(-25 \text{ kcal}/RT)$ $cm^2\ sec^{-1}$ was obtained. This equation is concordant with the parabolic rate data, hence the mobility term.

An alternative interpretation of the data in Table I and the results reported herein could be given in terms of zinc vacancies. The existence of zinc vacancies would fit the theoretical model presented, where the mobility term would be diffusion via zinc vacancies under unsaturated conditions, while the exchange reaction under saturated conditions (no Zn vacancies) would consist of an interstitialcy mechanism. This interpretation would demand zinc oxide to be p-type instead of n-type semiconductor as observed. Furthermore, the diffusion constant would show an inverse dependence on zinc pressure, which is not the case.

The parabolic rate and diffusion equations as observed in the oxidation and conductivity studies are explained on the basis of a simple interstitial mechanism. Here, it is assumed that the diffusion coefficient was measured or determined while the excess zinc was diffusing through an unsaturated oxide lattice (oxidation) or out of a saturated oxide (conductivity). In the exchange experiments the diffusion coefficient on the other

Can. J. Chem. Downloaded from www.nrcresearchpress.com by 210.87.254.5 on 09/05/12
For personal use only.

hand was determined while the zinc was diffusing through a saturated oxide lattice. The widely divergent results of Lindner on compressed sintered polycrystalline pellets of zinc oxide and of Moore and Williams on single crystals of zinc oxide are explained in a similar manner. That is, the drastic preannealing in the sintering stages of Lindner's experiments permitted saturation of the oxide powder by decomposition of the oxide as already reported (15), while the very moderate preannealing procedure by Moore and Williams produced only a very small concentration of interstitial zinc.

The author is grateful to Mr. J. A. Hackett, J. Bradley Streit Company Ltd., and Mr. Louis Chesler, all of Toronto, Ontario, and a benefactor who wishes to remain anonymous.

1. G. Heiland, E. Mollwo, and F. Stockmann. Solid State Phys. **8**, 191 (1959).
2. G. Heiland and E. Mollwo. Discussions Faraday Soc. **28**, 123 (1959).
3. W. J. Moore. Progress Report U.S. Atomic Energy Commission. Indiana University, Bloomington, Indiana. August 1, 1958.
4. W. J. Moore and J. K. Lee. Trans. Faraday Soc. **47**, 501 (1951).
5. A. Krupkowski and S. Balicki. Métaux & corrosion, **12**, 89 (1937).
6. E. Gebhardt. Z. Metallk. **37**, 87 (1946).
7. E. A. Secco and W. J. Moore. J. Chem. Phys. **26**, 942 (1957).
8. E. G. Spicar. Dissertation, University of Stuttgart, Germany. 1956.
9. H. Lamatsch. Diplomarbeit, University of Erlangen, Germany. 1958.
10. R. Lindner. Acta Chem. Scand. **6**, 457 (1952).
11. W. J. Moore and E. L. Williams. Discussions Faraday Soc. **28**, 86 (1959).
12. R. Pohl. Z. Physik, **155**, 120 (1959).
13. R. Arneth. Diplomarbeit, University of Erlangen, Germany. 1955.
14. E. A. Secco. Discussions Faraday Soc. **28**, 94 (1959); Fourth International Symposium on the reactivity of solids, Amsterdam, 1960. In press.
15. E. A. Secco. Can. J. Chem. **38**, 596 (1960).
16. J. Crank. The mathematics of diffusion. Clarendon Press, Oxford, 1956. p. 90.
17. C. Wagner. Atom movements. Am. Soc. Metals, Cleveland, 1953. p. 153.

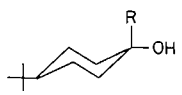
Received January 20, 1961.
Chemistry Department,
St. Francis Xavier University,
Antigonish, Nova Scotia.

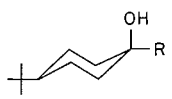
Can. J. Chem. Downloaded from www.nrcresearchpress.com by 210.87.254.5 on 09/05/12
For personal use only.

CONNAISSANCE DES *tert*-BUTYL-4 NITROMÉTHYL-1 CYCLOHEXANOLS-1 *cis* ET *trans*

H. Favre et D. Gravel

L'étude de la désamination nitreuse d'α-aminoalcools et plus particulièrement celle de la réaction de Tiffeneau (1) nous ont amenés à préparer les *tert*-butyl-4 nitrométhyl-1 cyclohexanols-1 *cis* (I*a*) et *trans* (II*a*) et à déterminer leurs configurations respectives. Nous posons que le groupe *tert*-butyle adoptera la conformation équatoriale (2, 3) dans les molécules étudiées.







I*a* R = CH_2NO_2 II*a* III
I*b* R = CH_2NH_2
I*c* R = $CH_2NC_5H_{10}$
I*d* R = CH_3 II*d*

hand was determined while the zinc was diffusing through a saturated oxide lattice. The widely divergent results of Lindner on compressed sintered polycrystalline pellets of zinc oxide and of Moore and Williams on single crystals of zinc oxide are explained in a similar manner. That is, the drastic preannealing in the sintering stages of Lindner's experiments permitted saturation of the oxide powder by decomposition of the oxide as already reported (15), while the very moderate preannealing procedure by Moore and Williams produced only a very small concentration of interstitial zinc.

The author is grateful to Mr. J. A. Hackett, J. Bradley Streit Company Ltd., and Mr. Louis Chesler, all of Toronto, Ontario, and a benefactor who wishes to remain anonymous.

1. G. Heiland, E. Mollwo, and F. Stockmann. Solid State Phys. **8**, 191 (1959).
2. G. Heiland and E. Mollwo. Discussions Faraday Soc. **28**, 123 (1959).
3. W. J. Moore. Progress Report U.S. Atomic Energy Commission. Indiana University, Bloomington, Indiana. August 1, 1958.
4. W. J. Moore and J. K. Lee. Trans. Faraday Soc. **47**, 501 (1951).
5. A. Krupkowski and S. Balicki. Métaux & corrosion, **12**, 89 (1937).
6. E. Gebhardt. Z. Metallk. **37**, 87 (1946).
7. E. A. Secco and W. J. Moore. J. Chem. Phys. **26**, 942 (1957).
8. E. G. Spicar. Dissertation, University of Stuttgart, Germany. 1956.
9. H. Lamatsch. Diplomarbeit, University of Erlangen, Germany. 1958.
10. R. Lindner. Acta Chem. Scand. **6**, 457 (1952).
11. W. J. Moore and E. L. Williams. Discussions Faraday Soc. **28**, 86 (1959).
12. R. Pohl. Z. Physik, **155**, 120 (1959).
13. R. Arneth. Diplomarbeit, University of Erlangen, Germany. 1955.
14. E. A. Secco. Discussions Faraday Soc. **28**, 94 (1959); Fourth International Symposium on the reactivity of solids, Amsterdam, 1960. In press.
15. E. A. Secco. Can. J. Chem. **38**, 596 (1960).
16. J. Crank. The mathematics of diffusion. Clarendon Press, Oxford, 1956. p. 90.
17. C. Wagner. Atom movements. Am. Soc. Metals, Cleveland, 1953. p. 153.

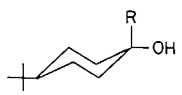
Received January 20, 1961.
Chemistry Department,
St. Francis Xavier University,
Antigonish, Nova Scotia.

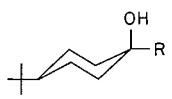
Can. J. Chem. Downloaded from www.nrcresearchpress.com by 210.87.254.5 on 09/05/12
For personal use only.

CONNAISSANCE DES *tert*-BUTYL-4 NITROMÉTHYL-1 CYCLOHEXANOLS-1 *cis* ET *trans*

H. Favre et D. Gravel

L'étude de la désamination nitreuse d'α-aminoalcools et plus particulièrement celle de la réaction de Tiffeneau (1) nous ont amenés à préparer les *tert*-butyl-4 nitrométhyl-1 cyclohexanols-1 *cis* (I*a*) et *trans* (II*a*) et à déterminer leurs configurations respectives. Nous posons que le groupe *tert*-butyle adoptera la conformation équatoriale (2, 3) dans les molécules étudiées.







I*a* R = CH_2NO_2 II*a* III
I*b* R = CH_2NH_2
I*c* R = $CH_2NC_5H_{10}$
I*d* R = CH_3 II*d*

L'action du nitrométhane sur la *tert*-butyl-4 cyclohexanone, en présence d'éthylate de sodium (4), conduit aux deux nitroalcools isomères I*a* et II*a*. Nous avons pu séparer facilement du mélange, par crystallisation fractionnée, l'isomère prédominant p.f. 86–87° et, plus difficilement, l'isomère p.f. 56–57°, qui ne représente que quelques pour-cents du mélange.

Nous attribuons la configuration cis au nitroalcool p.f. 86–87° après l'avoir transformé en méthyl-1 *tert*-butyl-4 cyclohexanol-1 *cis* (I*d*), p.f. 93–95°, en passant par l'α-aminoalcool I*b* et l'époxyde III. Cross et Whitham (5) viennent de décrire l'action de l'iodure de méthylmagnésium sur la *tert*-butyl-4 cyclohexanone et d'attribuer la configuration cis à leur isomère p.f. 89–90° et la configuration trans à l'isomère p.f. 70°; ils signalent toutefois que l'isomère cis n'est pas très pur. Dans nos mains les deux isomères purs fondent à 97–98° et 69–70°; nous leur attribuons les configurations cis et trans respectivement, après avoir mesuré les vitesses de saponification de leurs *p*-nitrobenzoates, à la manière de Hennion et O'Shea (3).

Le passage du nitroalcool I*a* à l'alcool I*d* s'est fait de la manière suivante. L'aminoalcool I*b*, obtenu de I*a* par réduction par le nickel de Raney (4), a été désaminé par l'acide nitreux; le produit brut de désamination a été réduit par l'hydrure de lithium et d'aluminium, puis oxydé par l'acide chromique et chromatographié: on isole la *tert*-butyl-4 cycloheptanone et l'alcool I*d*. Ces résultats font du produit de désamination de l'aminoalcool I*b* un mélange de *tert*-butyl-4 cycloheptanone et de l'époxyde III.[1] Cet époxyde n'a pas été isolé; outre sa transformation en alcool tertiaire I*d*, qui prouve son existence dans les produits de la désamination de I*b*, il a été caractérisé par un pipéridinoalcool (6) dont la formule probable est I*c*, à l'image de l'ouverture des époxydes dissymétriques par les amines (7, 8). La *tert*-butyl-4 cycloheptanone,[2] produit majeur de la désamination, a été caractérisée par sa dinitro-2,4 phénylhydrazone.

Pour que la preuve de configuration avancée ici soit valable il faut qu'il n'y ait aucune inversion de configuration en passant de I*a* à I*b* à III à I*d*. Les étapes I*a* $\rightarrow$ I*b* et III $\rightarrow$ I*d* n'offrent pas de difficultés d'interprétation; elles se font avec rétention de configuration; pour le passage de I*b* à III, nous avançons un mécanisme retenant la configuration, à l'image de la formation des époxydes dans l'agrandissement de cycle des cyclanones par le diazométhane (11) et dans la désamination nitreuse d'aminoalcools axiaux chez les stéroïdes (12, 13, 14).

PARTIE EXPÉRIMENTALE[3]

1. tert-Butyl-4 nitrométhyl-1 cyclohexanols-1 cis et trans (Ia et Ib)

En suivant fidèlement les indications opératoires de Dauben *et al.* (4) 25 g de *tert*-butyl-4 cyclohexanone conduisent à 25.8 g (74%) du mélange des deux nitroalcools, I*a* et I*b*, p.f. brut 65–75°. Après une recristallisation dans de l'éther de pétrole on isole 20 g de *tert*-butyl-4 nitrométhyl-1 cyclohexanol-1 *cis* (I*a*) (prismes incolores), p.f. 86–87°. Calculé pour $C_{11}H_{21}O_3N$: C, 61.37; H, 9.83; N, 6.51. Trouvé: C, 61.29; H, 9.91; N, 6.46%. L'isomère trans (II*a*) (paillettes incolores, 400 mg) p.f. 56–57°, s'obtient par 10 recristallisations fractionnées du résidu. Trouvé: C, 61.39; H, 9.84; N, 6.49%.

[1]*Il est bien connu que la cétone agrandie est le produit majeur de la désamination des aminométhyl-1 cyclanols-1 (1). Overberger et Katchman (9) ont signalé la formation d'époxydes dans la série hétérocyclique.*

[2]*Nozoe et ses collaborateurs (10) ont obtenu cette cétone en agrandissant la tert-butyl-4 cyclohexanone par le diazométhane.*

[3]*Les points de fusion (p.f.) ont été déterminés en tubes capillaires, avec un thermomètre étalonné avec des substances pures de p.f. connu, en provenance du Bureau des Standards de Washington.*

Can. J. Chem. Downloaded from www.nrcresearchpress.com by 210.87.254.5 on 09/05/12
For personal use only.

2. tert-Butyl-4 aminométhyl-1 cyclohexanol-1 cis (Ib)

En suivant fidèlement le mode opératoire de Dauben *et al.* (4) 25 g du nitroalcool I*a*, p.f. 86–87°, conduisent à 21.6 g (84%) du chlorhydrate du *tert*-butyl-4 aminométhyl-1 cyclohexanol-1 *cis* (I*b*), p.f. 235–236°. Calculé pour $C_{11}H_{24}ONCl$: C, 59.57; H, 10.91; N, 6.32. Trouvé: C, 59.40; H, 10.91; N, 6.37%.

3. Désamination du tert-butyl-4 aminométhyl-1 cyclohexanol-1 cis

À 1.2 g de chlorhydrate de *tert*-butyl-4 aminométhyl-1 cyclohexanol-1 *cis* dans 20 ml d'eau on ajoute 5.5 ml de soude 0.1 *N* pour libérer l'amine de son sel et 9.3 ml d'acide acétique glacial. La petite quantité de chlorure de sodium ne nuit pas à la réaction.

Le mélange est refroidi à 0° et une solution de 1.12 g de nitrite de sodium dans 4.5 ml d'eau est ajoutée goutte à goutte, en 45 minutes. Le mélange est ensuite agité à 0° pendant 2 heures, puis neutralisé par addition d'une solution de soude à 20%, sans que la température ne s'élève au dessus de 0°. On doit cesser l'addition de la soude au moment où l'aminoalcool non-réagi commence à se séparer sous forme de précipité blanc. On ajoute assez d'acide acétique glacial pour redissoudre le précipité, puis 15 gouttes en excès.

La solution acide est extraite à l'éther. Les solutions éthérées sont lavées au bicarbonate de sodium à 5%, à l'eau saturée de chlorure de sodium puis réunies, séchées et évaporées. On obtient une huile jaune pesant 795 mg. Des eaux acides on retire, à la manière habituelle l'aminoalcool qui n'a pas réagi (70 mg). Le produit brut de la réaction (795 mg) est repris par 10 ml de méthanol et 1 ml de pipéridine, puis chauffé à reflux pendant 2 heures. Le solvant est évaporé sous vide à 50°. Le résidu est repris par 100 ml d'éther anhydre; cette solution éthérée est lavée par de l'eau jusqu'à neutralité puis extraite par trois portions de 10 ml d'acide chlorhydrique aqueux 10%.

On examine (A) les solutions aqueuses et (B) la solution éthérée.

(A) Les solutions aqueuses acides sont réunies et évaporées sous vide. On obtient ainsi 82 mg de chlorhydrate de *tert*-butyl-4 pipéridinométhyl-1 cyclohexanol-1 *cis*, p.f. 242–243°. Calculé pour $C_{16}H_{32}ONCl$: C, 66.29; H, 11.13; N, 4.83. Trouvé: C, 66.18; H, 10.92; N, 4.87%.

(B) La solution éthérée est lavée au bicarbonate de sodium à 10%, à l'eau saturée de chlorure de sodium puis séchée et évaporée. On obtient ainsi 768 mg de *tert*-butyl-4 cycloheptanone sous forme d'huile jaune que l'on caractérise par sa dinitro-2,4 phénylhydrazone p.f. 146–147°. Calculé pour $C_{17}H_{24}O_4N_4$: C, 58.61; H, 6.94; N, 16.08. Trouvé: C, 58.58; H, 6.92; N, 16.19%.

4. Méthyl-1 tert-butyl-4 cyclohexanols-1 cis et trans (Id et IId)

Une solution de 10 g de *tert*-butyl-4 cyclohexanone dans 50 ml d'éther anhydre est traitée à 0° par de l'iodure de méthylmagnésium (préparé à partir de 2.37 g de magnésium et de 23.9 g d'iodure de méthyle dans 160 ml d'éther anhydre) à la façon habituelle. Le mélange des alcools tertiaires est un solide blanc (10.9 g) p.f. 40 à 58°.

Une partie du produit (9.7 g) est mise en solution dans 100 ml d'éther de pétrole (p. éb. 30–43°) et chromatographiée sur 388 g d'alumine Merck pour chromatographie.

L'élution de la colonne donne: (*a*) par de l'éther anhydre, une trace de cétone non réagie, identifiée par son spectre infrarouge; (*b*) par un mélange éther 95% – chloroforme 5%, 4.06 g de méthyl-1 *tert*-butyl-4 cyclohexanol-1 *trans* p.f. 69–70° (après sublimation); Cross et Whitham donnent (5) p.f. 70°; (*c*) par un mélange chloroforme 90% – méthanol 10%, 4.16 g de méthyl-1 *tert*-butyl-4 cyclohexanol-1 *cis* p.f. 97–98° (recristallisation dans l'éther de pétrole). Calculé pour $C_{11}H_{22}O$: C, 77.58; H, 13.02. Trouvé: 77.47; H, 13.20%.

Can. J. Chem. Downloaded from www.nrcresearchpress.com by 210.87.254.5 on 09/05/12
For personal use only.

Les résultats de cette chromatographie montrent que l'isomère cis et l'isomère trans se sont formés dans un rapport de 1:1.

p-Nitrobenzoates des méthyl-1 tert-butyl-4 cyclohexanols-1 cis et trans

Préparation selon Hennion et Barrett (15).

Cis: p.f. 128–129° (EtOH–eau). Trouvé: C, 67.72; H, 7.94; N, 4.50%.

Trans: p.f. 115–116° (EtOH–eau). Trouvé: C, 67.66; H, 7.91; N, 4.48%. Calculé pour $C_{18}H_{25}O_4N$: C, 67.69; H, 7.89; N, 4.39%.

5. Preuve de configuration du nitroalcool Ia

Le produit brut (1.9 g) obtenu à la suite de la désamination nitreuse de 2.5 g de chlorhydrate du *tert*-butyl-4 aminométhyl-1 cyclohexanol-1 p.f. 235–236° (voir section 3) est immédiatement réduit par 1.9 g d'hydrure de lithium et d'aluminium dans 50 ml d'éther. Le produit de réaction est une huile incolore.

Une solution de 1.0 g de cette huile dans 25 ml d'acide acétique glacial est traitée, à 15°, par 500 mg d'anhydride chromique, ajoutée par petites portions. Le mélange est agité à la température de la pièce pendant 48 heures, puis versé dans 300 ml d'eau glacée et extrait par de l'éther de pétrole (p. éb. 30–43°). La couche organique est lavée par $NaHCO_3$ 10% et à l'eau, puis séchée et évaporée. Le produit brut de la réaction (600 mg) est chromatographié sur 15 g d'alumine Merck pour chromatographie. L'élution de la colonne par un mélange éther de pétrole – éther, donne la *tert*-butyl-4 cycloheptanone, identifiée par son spectre infrarouge et l'élution par de l'éther anhydre donne un solide blanc, p.f. 93–95°, dont le spectre infrarouge est identique à celui du méthyl-1 *tert*-butyl-4 cyclohexanol-1 *cis*, p.f. 97–98°. Point de fusion mixte avec un échantillon authentique: 95–96°.

6. Configuration des alcools tertiaires Id et IId

La configuration des alcools tertiaires est déterminée par l'étude des taux de saponification des *p*-nitrobenzoates à 24.8° dans le mélange acétone–eau, 4–1. La méthode employée est celle utilisée par Hennion et O'Shea (3).

Le *p*-nitrobenzoate de méthyl-1 *tert*-butyl-4 cyclohexanol-1 *trans*, p.f. 115–116°, a donné (deux essais): $k_2 = 4.9\times10^{-4}$ et 4.6×10^{-4}, moyenne: 4.75×10^{-4} litre mole^{-1} sec^{-1}. L'isomère cis, p.f. 128–129°, a donné (deux essais): $k_2 = 20.8\times10^{-4}$ et 19.5×10^{-4}; moyenne 20.2×10^{-4} litre mole^{-1} sec^{-1}.

Nous exprimons nos remerciements au Conseil National des Recherches du Canada, pour une bourse (D.G.) et un octroi de recherches (H.F.), ainsi qu'aux Établissements Dow Chemical of Canada Ltd., Montréal, pour la quantité généreuse de *tert*-butyl-4 cyclohexanols-1 mise à notre disposition.

1. P. A. S. Smith et D. R. Baer. Organic reactions. Vol. XI. John Wiley & Sons, Inc., New York 1960. p. 157.
2. S. Winstein et N. J. Holness. J. Am. Chem. Soc. **77**, 5562 (1955).
3. G. F. Hennion et F. X. O'Shea. J. Am. Chem. Soc. **80**, 614 (1958).
4. H. J. Dauben, Jr., H. J. Ringold, R. H. Wade et A. G. Anderson, Jr. J. Am. Chem. Soc. **73**, 2359. (1951).
5. B. Cross et G. H. Whitham. J. Chem. Soc. 3892 (1960).
6. E. Mosettig et A. Burger. J. Am. Chem. Soc. **52**, 3456 (1930).
7. S. Winstein et R. B. Henderson. Heterocyclic compounds. Vol. 1. John Wiley & Sons, Inc., New York. 1950. p. 33.
8. M. Tiffeneau, P. Weill et B. Tchoubar. Compt. rend. **205**, 54 (1937).
9. C. G. Overberger et A. Katchman. J. Am. Chem. Soc. **78**, 1965 (1956).
10. T. Nozoe, H. Kishi et A. Yoshikoshi. Proc. Japan Acad. **27**, 149 (1951).

Can. J. Chem. Downloaded from www.nrcresearchpress.com by 210.87.254.5 on 09/05/12
For personal use only.

11. R. ROBINSON et L. H. SMITH. J. Chem. Soc. 371 (1937).
12. M. MOUSSERON. Bull. soc. chim. France, 1008 (1956).
13. R. J. W. CREMLYN, D. L. GARMAISE et C. W. SHOPPEE. J. Chem. Soc. 1847 (1953).
14. F. WINTERNITZ et S. LADABAUM. Bull. soc. chim. France, 597 (1960).
15. G. F. HENNION et S. O. BARRETT. J. Am. Chem. Soc. **79**, 2148 (1957).

REÇU LE 4 AVRIL 1961.
DÉPARTEMENT DE CHIMIE,
UNIVERSITÉ DE MONTRÉAL,
MONTRÉAL, QUÉ.

Can. J. Chem. Downloaded from www.nrcresearchpress.com by 210.87.254.5 on 09/05/12
For personal use only.

A CHEMILUMINESCENT REACTION*

H. W. HOLDEN† AND K. O. KUTSCHKE

Recently, Vasil'ev *et al.* (1) observed weak chemiluminescence during the thermal decomposition of certain compounds. Several hydroperoxides were decomposed in their preparative solutions; benzoyl peroxide and azobisisobutyronitrile were studied in chlorobenzene solution. The temperature dependence of the luminescent intensity led the authors to suggest that the emission arose as a rare event which occurred during the combination of radicals. While the evidence for this interpretation is not yet conclusive, it has the corollary that stabilization by emission should be a more probable event in the gas phase where deactivating collisions occur less frequently.

We wish to report here the observation of luminescence in a system containing gaseous ethyl hyponitrite, undergoing thermal decomposition, upon the addition of acetaldehyde. The light was observed with a 1P21 photomultiplier tube in an Eldorado PH200 photometer at signal-to-noise ratios as high as 20 to 1 under some experimental conditions. The system was chosen since it was anticipated that it would contain large concentrations of acetyl radicals produced by the thermal reactions

$$C_2H_5ONNOC_2H_5 \rightarrow 2C_2H_5O + N_2, \qquad [1]$$

$$C_2H_5O + CH_3CHO \rightarrow C_2H_5OH + CH_3CO. \qquad [2]$$

In general terms it was hoped to produce the low-lying triplet state of biacetyl, which possesses a high phosphorescent efficiency (2), by the combination of acetyl radicals formed in [2]. The triplet state is well known in the photochemistry of biacetyl; details of the latter have been reviewed in considerable detail (3).

Ethyl hyponitrite was prepared by Partington and Shah (4) by the esterification of silver hyponitrite with ethyl iodide; they reported a rapid decomposition at 70° C. In our preparation a liberal excess (25–30 mole%) of the silver salt was used (we are indebted to Dr. L. C. Leitch for a supply of silver hyponitrite); this was required because of difficulties encountered in removing ethyl iodide from earlier preparations. The ester, dried over $CaCl_2$, was introduced into the vacuum system along with a small residue of ether solvent. While the ester was being outgassed at −85° C, it was observed to solidify gradually as the ether was removed. The ester was distilled at −10° C to a storage tube held at −85° C and was stored behind a mercury cutoff. It was crystalline in appearance and melted at a temperature slightly above the −85° C storage temperature.

The cell system consisted of a Pyrex vessel of 8-cm³ capacity having a thinned window. It was contained in an oven and connected by 6 mm i.d. tubing to a magnetically

*Issued as N.R.C. No. 6330.
†*N.R.C. Postdoctoral Fellow 1958–60. Present address: Central Research Laboratory, Canadian Industries Limited, McMasterville, Quebec.*

11. R. ROBINSON et L. H. SMITH. J. Chem. Soc. 371 (1937).
12. M. MOUSSERON. Bull. soc. chim. France, 1008 (1956).
13. R. J. W. CREMLYN, D. L. GARMAISE et C. W. SHOPPEE. J. Chem. Soc. 1847 (1953).
14. F. WINTERNITZ et S. LADABAUM. Bull. soc. chim. France, 597 (1960).
15. G. F. HENNION et S. O. BARRETT. J. Am. Chem. Soc. **79**, 2148 (1957).

REÇU LE 4 AVRIL 1961.
DÉPARTEMENT DE CHIMIE,
UNIVERSITÉ DE MONTRÉAL,
MONTRÉAL, QUÉ.

A CHEMILUMINESCENT REACTION*

H. W. HOLDEN† AND K. O. KUTSCHKE

Recently, Vasil'ev *et al.* (1) observed weak chemiluminescence during the thermal decomposition of certain compounds. Several hydroperoxides were decomposed in their preparative solutions; benzoyl peroxide and azobisisobutyronitrile were studied in chlorobenzene solution. The temperature dependence of the luminescent intensity led the authors to suggest that the emission arose as a rare event which occurred during the combination of radicals. While the evidence for this interpretation is not yet conclusive, it has the corollary that stabilization by emission should be a more probable event in the gas phase where deactivating collisions occur less frequently.

We wish to report here the observation of luminescence in a system containing gaseous ethyl hyponitrite, undergoing thermal decomposition, upon the addition of acetaldehyde. The light was observed with a 1P21 photomultiplier tube in an Eldorado PH200 photometer at signal-to-noise ratios as high as 20 to 1 under some experimental conditions. The system was chosen since it was anticipated that it would contain large concentrations of acetyl radicals produced by the thermal reactions

$$C_2H_5ONNOC_2H_5 \rightarrow 2C_2H_5O + N_2, \qquad [1]$$

$$C_2H_5O + CH_3CHO \rightarrow C_2H_5OH + CH_3CO. \qquad [2]$$

In general terms it was hoped to produce the low-lying triplet state of biacetyl, which possesses a high phosphorescent efficiency (2), by the combination of acetyl radicals formed in [2]. The triplet state is well known in the photochemistry of biacetyl; details of the latter have been reviewed in considerable detail (3).

Ethyl hyponitrite was prepared by Partington and Shah (4) by the esterification of silver hyponitrite with ethyl iodide; they reported a rapid decomposition at 70° C. In our preparation a liberal excess (25–30 mole%) of the silver salt was used (we are indebted to Dr. L. C. Leitch for a supply of silver hyponitrite); this was required because of difficulties encountered in removing ethyl iodide from earlier preparations. The ester, dried over $CaCl_2$, was introduced into the vacuum system along with a small residue of ether solvent. While the ester was being outgassed at −85° C, it was observed to solidify gradually as the ether was removed. The ester was distilled at −10° C to a storage tube held at −85° C and was stored behind a mercury cutoff. It was crystalline in appearance and melted at a temperature slightly above the −85° C storage temperature.

The cell system consisted of a Pyrex vessel of 8-cm³ capacity having a thinned window. It was contained in an oven and connected by 6 mm i.d. tubing to a magnetically

*Issued as N.R.C. No. 6330.
†*N.R.C. Postdoctoral Fellow 1958–60. Present address: Central Research Laboratory, Canadian Industries Limited, McMasterville, Quebec.*

operated glass circulation pump, a manometer, and a mercury cutoff. Earlier attempts were made to observe the luminescence in a cell designed for measurements of the photo-excited fluorescence. These attempts consumed reagent wastefully since about 75% of the cell system was heated to the decomposition temperature whereas only a small volume could be observed by the photocell.

Measurements of the luminescent intensity were made at several temperatures in the range 56 to 72° C; these yield an apparent activation energy of about 30 kcal/mole. This may be interpreted, following Vasil'ev *et al.* (1), as the activation energy for the decomposition of the ester. At least one alternative explanation involving the reactions

$$R + R \rightarrow R_2^*$$
$$R_2^* + B \rightarrow B^*$$
$$B^* \rightarrow B + h\nu$$

cannot be eliminated on the basis of measurements made thus far. Here R_2^* represents the initially excited dimer of the radicals R (which might be acetyl), and B and B^*, the unexcited and excited states of the product biacetyl. Much more intensive study is required, including identification of the emitting species, before a mechanism can be considered seriously.

The hyponitrite is a difficult compound with which to work and very little is known of the mechanism of its decomposition. The kinetics of the pyrolysis of ditertiarybutyl peroxide are well known. First trials with this initiator were unsuccessful, however, presumably because of the instability of acetyl radicals at the temperature necessary for its rapid decomposition (above 150° C), or because of the instability of the triplet state of biacetyl at that temperature (3).

It is hoped to follow this preliminary investigation with a more complete study in an attempt to determine the mechanism of the phenomenon.

1. R. F. Vasil'ev, O. N. Karpukhin, and V. Ya. Shlyapintokh. Doklady Akad. Nauk S.S.S.R. **125**, 106 (1959).
2. J. W. Sidman and D. S. McClure. J. Am. Chem. Soc. **77**, 6461 (1955). G. M. Almy and P. R. Gillette. J. Chem. Phys. **11**, 188 (1943).
3. W. A. Noyes, Jr., G. B. Porter, and J. E. Jolley. Chem. Revs. **56**, 49 (1956). J. Heicklen. J. Am. Chem. Soc. **81**, 3863 (1959). R. M. Hochstrasser and G. B. Porter. Quart. Revs. (London), **14**, 146 (1960).
4. J. F. Partington and C. C. Shah. J. Chem. Soc. 2589 (1932).

Received April 13, 1961.
Division of Pure Chemistry,
National Research Council,
Ottawa, Canada.

THE SYNTHESIS OF 17α-FLUOROPROGESTERONE

R. Deghenghi and R. Gaudry

The biological activity of progesterone can be enhanced by the presence of appropriate substituents in positions α to the 20-carbonyl group. Thus 21-fluoro- and 17α-bromo-progesterone were shown to be twice as active as the natural hormone (1, 2). It was of interest therefore to prepare 17α-fluoroprogesterone and to compare its activity with that of the chloro and bromo analogues.

operated glass circulation pump, a manometer, and a mercury cutoff. Earlier attempts were made to observe the luminescence in a cell designed for measurements of the photo-excited fluorescence. These attempts consumed reagent wastefully since about 75% of the cell system was heated to the decomposition temperature whereas only a small volume could be observed by the photocell.

Measurements of the luminescent intensity were made at several temperatures in the range 56 to 72° C; these yield an apparent activation energy of about 30 kcal/mole. This may be interpreted, following Vasil'ev *et al.* (1), as the activation energy for the decomposition of the ester. At least one alternative explanation involving the reactions

$$R + R \rightarrow R_2^*$$
$$R_2^* + B \rightarrow B^*$$
$$B^* \rightarrow B + h\nu$$

cannot be eliminated on the basis of measurements made thus far. Here R_2^* represents the initially excited dimer of the radicals R (which might be acetyl), and B and B*, the unexcited and excited states of the product biacetyl. Much more intensive study is required, including identification of the emitting species, before a mechanism can be considered seriously.

The hyponitrite is a difficult compound with which to work and very little is known of the mechanism of its decomposition. The kinetics of the pyrolysis of ditertiarybutyl peroxide are well known. First trials with this initiator were unsuccessful, however, presumably because of the instability of acetyl radicals at the temperature necessary for its rapid decomposition (above 150° C), or because of the instability of the triplet state of biacetyl at that temperature (3).

It is hoped to follow this preliminary investigation with a more complete study in an attempt to determine the mechanism of the phenomenon.

1. R. F. Vasil'ev, O. N. Karpukhin, and V. Ya. Shlyapintokh. Doklady Akad. Nauk S.S.S.R. **125**, 106 (1959).
2. J. W. Sidman and D. S. McClure. J. Am. Chem. Soc. **77**, 6461 (1955). G. M. Almy and P. R. Gillette. J. Chem. Phys. **11**, 188 (1943).
3. W. A. Noyes, Jr., G. B. Porter, and J. E. Jolley. Chem. Revs. **56**, 49 (1956). J. Heicklen. J. Am. Chem. Soc. **81**, 3863 (1959). R. M. Hochstrasser and G. B. Porter. Quart. Revs. (London), **14**, 146 (1960).
4. J. F. Partington and C. C. Shah. J. Chem. Soc. 2589 (1932).

Received April 13, 1961.
Division of Pure Chemistry,
National Research Council,
Ottawa, Canada.

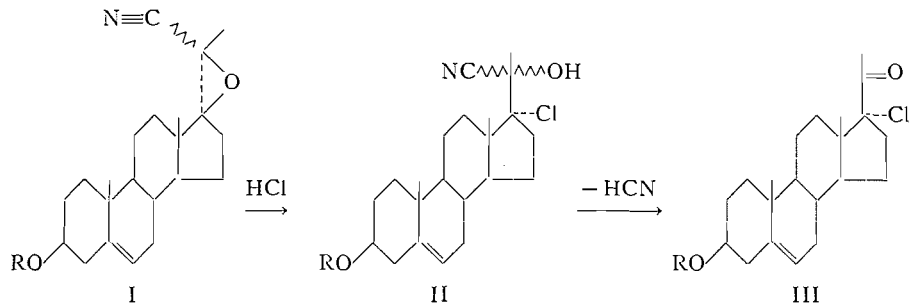
THE SYNTHESIS OF 17α-FLUOROPROGESTERONE

R. Deghenghi and R. Gaudry

The biological activity of progesterone can be enhanced by the presence of appropriate substituents in positions α to the 20-carbonyl group. Thus 21-fluoro- and 17α-bromo-progesterone were shown to be twice as active as the natural hormone (1, 2). It was of interest therefore to prepare 17α-fluoroprogesterone and to compare its activity with that of the chloro and bromo analogues.

Can. J. Chem. Downloaded from www.nrcresearchpress.com by 210.87.254.40 on 09/05/12
For personal use only.

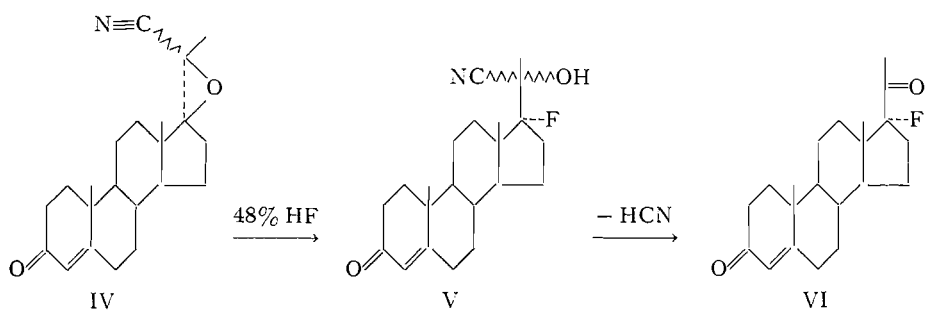
A previous attempt to introduce a fluorine in position 17 by opening a suitable 16,17-epoxypregnane with hydrogen fluoride, was reported to be unsuccessful (3); we chose, therefore, to investigate the reaction of a 20-cyano-17,20-epoxypregnane (I) with hydrogen halides. The latter pathway was recently used for the preparation of 17α-fluoro-11-dehydrocorticosterone acetate (4). Starting from 17α-bromopregnenolone we prepared readily the corresponding cyanoepoxide (I, R = H) by the action of alcoholic potassium cyanide at room temperature (5, 6). A proof of structure of (I) was obtained by its conversion to the known (7) 17α-chloropregnenolone acetate (III, R = Ac).



I II III

When 17α-bromoprogesterone was similarly allowed to react with potassium cyanide, a crystalline cyanoepoxide was obtained in high yield, the α,β-unsaturated 3-ketone being inert under our reaction conditions. This cyanoepoxide (IV), however, proved to be remarkably stable towards the action of anhydrous HF under the reaction conditions previously described in the 11-oxygenated series (4). It would seem that an 11-oxygen function facilitates the acid-catalyzed opening of the epoxide ring in 17,20 by anhydrous HF. In our case we found that treatment of IV with aqueous HF in a heterogeneous system resulted in the formation of the desired 17α-fluoro-20-cyanohydrin (V), smoothly and in good yield.

The resulting cyanohydrin (V) was found to be stable in non-hydroxylated solvents like ether, but it readily lost the elements of hydrogen cyanide when dissolved in an aqueous alcohol. Alternatively the regeneration of the 20-ketone function was effected by heating the cyanohydrin in organic bases, such as collidine, in a more conventional but less satisfactory manner. A proof of structure for the resulting 17α-fluoroprogesterone was obtained by removal of hydrogen fluoride upon prolonged treatment with refluxing dimethylformamide in the presence of LiBr and Li_2CO_3 (8), providing the known 16-dehydroprogesterone.



IV V VI

Can. J. Chem. Downloaded from www.nrcresearchpress.com by 210.87.254.40 on 09/05/12
For personal use only.

It was interesting to note that a substitution of fluorine at position 17α causes a positive increment in the rotation[1] (see Table I), contrary to the effect of a chlorine or bromine substituent. A hypsochromic displacement of the 20-ketone frequency in the infrared was observed due to the axial fluorine atom. There is only a slight shift with a 17α-chloro substituent, and no effect at all with a 17α-bromine atom. These shifts parallel those observed for an 11-ketone in the 9α-halogenated series (9). 17α-Fluoroprogesterone is slightly less active, in the Clauberg subcutaneous test, than the parent natural hormone.

TABLE I

	$[\alpha]_D$ $CHCl_3$	M_D	ΔM_D	$\Delta\nu$ 20-C=O $CHCl_3$ (cm^{-1})
Progesterone	+202°	+635	—	—
17α-Br-progesterone (2)	+ 20°	+ 80	−555	—
17α-Cl-progesterone (7)	+ 51°	+180	−455	+ 5
17α-F-progesterone	+196°	+650	+ 15	+20

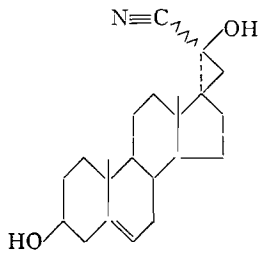
EXPERIMENTAL[2]

Reaction between 17α-Bromopregnenolone and KCN

17α-Bromopregnenolone (5.00 g) (m.p. 158–159° C) was dissolved in 310 ml of 95% ethanol. A solution of 1.50 g of KCN and 2.20 g potassium acetate in 40 ml water was added and the resulting clear solution was stirred at room temperature for 19 hours. The product (4.0 g) was isolated by pouring the solution into 2 l. of ice water and filtering.

A 2-g portion of the crude bromine-free precipitate was suspended in benzene and chromatographed over 100 g of silica gel. Ethyl acetate – benzene 10:90 eluted 1 g of amorphous material, the infrared spectrum of which was consistent with the *cyanoepoxide* structure I (R = H): ν_{nujol} 3350 cm^{-1} (OH), 2240 cm^{-1} (—CN).

Increasing quantities of EtOAc in benzene eluted crystalline substances whose infrared spectra indicated the presence of a cyanohydrin group, m.p. 250–255° decomp., raised by crystallization from ethanol to 267–298° decomp. A sample was crystallized for analysis, m.p. 290° decomp. According to Barton's suggestions in the corresponding 11-oxygenated series (4) we assign to this substance the structure of a cyclopropanone cyanohydrin VII (or its epimer), intermediate in a Favorski rearrangement. Calc. for



VII

$C_{22}H_{31}O_2N$: C, 77.37; H, 9.15; N, 4.10%. Found: C, 77.67; H, 8.98; N, 3.91%. ν_{nujol} 3440 and 3240 cm^{-1} (OH), 2240 cm^{-1} (C≡N), 1053 cm^{-1} (C—O). Both hydroxyl groups were acetylated by acetic anhydride in pyridine at room temperature.

[1]*Professor Carl Djerassi kindly informed us that he observed a positive Cotton effect for 17α-fluoropregnenolone, prepared independently by Dr. Jensen of the University of Chicago.*

[2]*Melting points were determined in evacuated capillaries and corrected.*

Can. J. Chem. Downloaded from www.nrcresearchpress.com by 210.87.254.40 on 09/05/12
For personal use only.

17α-Chloropregnenolone Acetate (III, R = Ac)—Proof of Structure I

The amorphous cyanoepoxide I (0.500 g) was dissolved in 10 ml acetic acid. Anhydrous HCl was bubbled through the solution at room temperature for 30 minutes. A reddish-brown color developed. Ice water was added and the precipitate was collected on a filter and air-dried to give 0.514 g of a solid with a positive Beilstein test. One-half gram of this precipitate (II, R = Ac) was refluxed for 1 hour with 10 ml of toluene and 1 ml of a toluene solution containing 2.3% of collidine. The cooled solution was extracted with CH_2Cl_2, washed with iced dilute HCl, $NaHCO_3$ solution, and water, dried, and the solvent removed to give 0.495 g of a yellow oil which was reacetylated overnight at room temperature with 10 ml of pyridine and 2 ml of acetic anhydride. The usual working up gave 0.472 g of a crude product which was chromatographed on silica gel. EtOAc–benzene 3:97 eluted crystalline fractions (300 mg) which were recrystallized from ether–methanol for analysis, m.p. 142–144° C (III, R = Ac). Calc. for $C_{23}H_{33}ClO_3$: C, 70.30; H, 8.46; Cl, 9.02%. Found: C, 70.52; H, 8.01; Cl, 9.54%. This substance did not depress the melting point of an authentic sample of 17α-chloropregnenolone acetate (7). The infrared spectra were identical.

20-Cyano-17β,20-epoxy-4-pregnene-3-one (IV)

To 17α-bromoprogesterone (20.0 g) in 1200 ml commercial ethanol, there was added a mixture of 5.8 g KCN and 8.5 g CH_3COOK in 150 ml of water. The resulting solution was stirred at room temperature for 24 hours. At the end of this time 3.0 g of 20-cyano-17β,20-epoxy-4-pregnene-3-one crystallized out and was collected on a filter. The alcoholic filtrate was poured into ice water and the precipitate collected on a filter and washed with water. The combined dried precipitate weighed 17.0 g representing crude cyanoepoxide IV, m.p. 230–240° C. A sample was crystallized three times for analysis, m.p. 246–250° C (methanol). $[\alpha]_D^{25}$ +21.3 ($CHCl_3$ 1%); λ_{max} 241 mμ, ε 17,400. Calc. for $C_{22}H_{29}O_2N$: C, 77.84; H, 8.61; N, 4.13%. Found: C, 77.81; H, 8.46; N, 4.06%. ν_{CHCl_3} 2250 cm^{-1} (C≡N), 1665 and 1620 cm^{-1} (3-ketone-Δ^4). The structure of this substance was proved by conversion to the known 17α-chloroprogesterone (7), m.p. 165–167° C. The infrared spectra were identical and no depression of the melting point with an authentic sample was observed.

17α-Fluoroprogesterone (VI)

20-Cyano-17β,20-epoxy-4-pregnene-3-one (IV), 2.4 g, was slurried with 30 g of 48% aqueous HF at room temperature for 1 hour. The resulting oily substance was taken up in ether and washed to neutrality with $NaHCO_3$ solution and water. Evaporation of the solvent gave 2.45 g of a white solid, which crystallized from ether, m.p. 210–211° decomp. ν_{CHCl_3} 3360 cm^{-1} (OH), 2240 cm^{-1} (C≡N), 1663 and 1619 cm^{-1} (3-keto-Δ^4). When this substance, representing crude 17α-fluoro-4-pregnene-3-one-20-cyanohydrin, was refluxed in aqueous methanol overnight, HCN gas was evolved and crude 17α-fluoroprogesterone was recovered by evaporation of the solvent. Alternatively the cyanohydrin, 1.0 g, was refluxed for 1 hour in 5 ml of collidine. After the usual working up, 0.98 g of a yellow oil was obtained which was chromatographed on neutral alumina (Woelm III). The petroleum ether – benzene eluates contained 0.450 g of 17α-fluoroprogesterone, m.p. 170–174° C. A sample was recrystallized from acetone–hexane for analysis, m.p. 177–179° C, $[\alpha]_D$ +195.7° ($CHCl_3$). Calc. for $C_{21}H_{29}O_2F$: C, 75.87; H, 8.79; F, 5.71%. Found: C, 76.08; H, 8.85; F, 5.90%. ν_{CHCl_3} 1718 cm^{-1} (20-ketone, 17α-fluoro), 1665 and 1620 cm^{-1} (3-ketone-Δ^4).

Can. J. Chem. Downloaded from www.nrcresearchpress.com by 210.87.254.40 on 09/05/12
For personal use only.

Dehydrofluorination

To 17α-fluoroprogesterone, 130 mg, dissolved in 10 ml of dimethylformamide, there was added 130 mg of LiBr and 130 mg Li_2CO_3. The mixture was refluxed under N_2 for 24 hours. Usual working up gave 80 mg of a yellow oil which crystallized from acetone. The melting point did not depress upon admixture with an authentic sample of 16-dehydroprogesterone, m.p. 184–186° C. The infrared spectrum showed the characteristic Δ^{16} band at 1591 cm^{-1}.

Attempted Reaction of IV with Anhydrous HF

The cyanoepoxide IV, 5.0 g, was dissolved in 100 ml of dry tetrahydrofuran. To this solution, cooled into a dry ice – acetone bath, there was added 20 g of anhydrous HF. The resulting solution was stirred at room temperature for 18 hours. The usual working up (4) gave 5.0 g of a solid which crystallized from ether, m.p. 225–236° decomp. The infrared spectrum was identical with that of IV.

ACKNOWLEDGMENTS

We are indebted to Drs. C. Revesz and C. I. Chappel for the biological data, to Mr. M. Boulerice for the ultraviolet determinations, and to Dr. G. Papineau-Couture for the infrared spectra.

1. P. Tannhauser and E. V. Jensen. J. Am. Chem. Soc. **78**, 2658 (1956).
2. Ch. R. Engel and H. Jahnke. Can. J. Biochem. Physiol. **35**, 1047 (1957).
3. E. L. Shapiro, M. Steinberg, D. Gould, M. J. Gentles, H. L. Herzog, M. Gilmore, W. Charney, E. B. Hershberg, and L. Mandell. J. Am. Chem. Soc. **81**, 6483 (1959).
4. H. L. Herzog, M. J. Gentles, H. M. Marshall, and E. B. Hershberg. J. Am. Chem. Soc. **82**, 3691 (1960).
5. R. Justoni and M. Terruzzi. Gazz. chim. ital. **78**, 155 (1948).
6. R. Gerbaux. Bull. acad. roy. Belg. (V) **24**, 88 (1938).
7. D. J. Marshall and R. Gaudry. Can. J. Chem. **38**, 1495 (1960).
8. R. Joly and J. Warnant. Bull. soc. chim. France, 367 (1958).
9. A. H. Nathan, B. J. Magerlein, and J. A. Hogg. J. Org. Chem. **24**, 1517 (1959).

Received April 13, 1961.
Ayerst, McKenna & Harrison Limited,
P.O. Box 6115,
Montreal, Que.

SOME REMARKS ON AGGREGATION OF POLYTHENE IN SOLUTION

H. P. Schreiber

INTRODUCTION

In a recent article Trementozzi (1) noted serious differences in the weight-average molecular weights, $\overline{M_w}$, obtained for high- and low-pressure polythene samples from light scattering in α-chloronaphthalene (α-CN) and tetralin solutions. He suggested that these differences were due to association of polythene molecules in α-CN solutions at the temperatures in question (~100–140° C). Thus, the α-CN data presumably gave the dimension of aggregates of polythene chains, rather than that of the average molecular chain. The suggested association was supported by data showing a decrease in $\overline{M_w}$ values obtained for one high-pressure polythene as the temperature of the α-CN solutions rose from 95–141° C. Subsequently Tung (2) noted similar differences in $\overline{M_w}$ values

Can. J. Chem. Downloaded from www.nrcresearchpress.com by 210.87.254.40 on 09/05/12
For personal use only.

Dehydrofluorination

To 17α-fluoroprogesterone, 130 mg, dissolved in 10 ml of dimethylformamide, there was added 130 mg of LiBr and 130 mg Li_2CO_3. The mixture was refluxed under N_2 for 24 hours. Usual working up gave 80 mg of a yellow oil which crystallized from acetone. The melting point did not depress upon admixture with an authentic sample of 16-dehydroprogesterone, m.p. 184–186° C. The infrared spectrum showed the characteristic Δ^{16} band at 1591 cm^{-1}.

Attempted Reaction of IV with Anhydrous HF

The cyanoepoxide IV, 5.0 g, was dissolved in 100 ml of dry tetrahydrofuran. To this solution, cooled into a dry ice – acetone bath, there was added 20 g of anhydrous HF. The resulting solution was stirred at room temperature for 18 hours. The usual working up (4) gave 5.0 g of a solid which crystallized from ether, m.p. 225–236° decomp. The infrared spectrum was identical with that of IV.

ACKNOWLEDGMENTS

We are indebted to Drs. C. Revesz and C. I. Chappel for the biological data, to Mr. M. Boulerice for the ultraviolet determinations, and to Dr. G. Papineau-Couture for the infrared spectra.

1. P. Tannhauser and E. V. Jensen. J. Am. Chem. Soc. **78**, 2658 (1956).
2. Ch. R. Engel and H. Jahnke. Can. J. Biochem. Physiol. **35**, 1047 (1957).
3. E. L. Shapiro, M. Steinberg, D. Gould, M. J. Gentles, H. L. Herzog, M. Gilmore, W. Charney, E. B. Hershberg, and L. Mandell. J. Am. Chem. Soc. **81**, 6483 (1959).
4. H. L. Herzog, M. J. Gentles, H. M. Marshall, and E. B. Hershberg. J. Am. Chem. Soc. **82**, 3691 (1960).
5. R. Justoni and M. Terruzzi. Gazz. chim. ital. **78**, 155 (1948).
6. R. Gerbaux. Bull. acad. roy. Belg. (V) **24**, 88 (1938).
7. D. J. Marshall and R. Gaudry. Can. J. Chem. **38**, 1495 (1960).
8. R. Joly and J. Warnant. Bull. soc. chim. France, 367 (1958).
9. A. H. Nathan, B. J. Magerlein, and J. A. Hogg. J. Org. Chem. **24**, 1517 (1959).

Received April 13, 1961.
Ayerst, McKenna & Harrison Limited,
P.O. Box 6115,
Montreal, Que.

SOME REMARKS ON AGGREGATION OF POLYTHENE IN SOLUTION

H. P. Schreiber

INTRODUCTION

In a recent article Trementozzi (1) noted serious differences in the weight-average molecular weights, $\overline{M_w}$, obtained for high- and low-pressure polythene samples from light scattering in α-chloronaphthalene (α-CN) and tetralin solutions. He suggested that these differences were due to association of polythene molecules in α-CN solutions at the temperatures in question (~100–140° C). Thus, the α-CN data presumably gave the dimension of aggregates of polythene chains, rather than that of the average molecular chain. The suggested association was supported by data showing a decrease in $\overline{M_w}$ values obtained for one high-pressure polythene as the temperature of the α-CN solutions rose from 95–141° C. Subsequently Tung (2) noted similar differences in $\overline{M_w}$ values

Can. J. Chem. Downloaded from www.nrcresearchpress.com by 210.87.254.105 on 09/05/12
For personal use only.

obtained for low-pressure polythenes from light scattering in α-CN solution and from calculations involving their intrinsic viscosities, $[\eta]$, in tetralin solution. Tung postulated the existence of long-chain branches in the supposedly linear polythenes used in his work. Long branching would reduce values of the intrinsic viscosity of the polymers (3) and result in calculations of erroneously low $\overline{M}_w$ values from an equation established on the basis of calibration data obtained for linear polythenes. This postulate gives internal consistency to the results, but does not explain the results of the earlier work (1), in which light scattering in α-CN and tetralin solutions of high-pressure polythenes (which are generally assumed to contain long-chain branches) also resulted in large $\overline{M}_w$ differences.

The possible aggregation of polythene in α-CN solution would cast doubt on a considerable body of published molecular weight data. Consequently comparisons of the temperature coefficients of intrinsic viscosity of two polythenes in α-CN and tetralin solutions were carried out to test further the possibility of association. This article reports the results of these comparisons.

THEORETICAL

The well-known theoretical treatment of Flory and Fox (4) gives the intrinsic viscosity $[\eta]$ of a polymer solution as

$$[\eta] = KM^{\frac{1}{2}}\alpha^3 \qquad [1]$$

where M is the molecular weight of the polymer, K is a temperature-dependent parameter, and α is the linear expansion coefficient which depends on the configuration of the polymer molecule in a specified solution.

The temperature dependence of $[\eta]$, discussed in detail by Flory (5) and more recently by Kawai and Ueyama (6), is due to the temperature coefficients of K and α in equation [1]. In general, K tends to decrease as the temperature rises, but its temperature dependence is generally small compared with that of α. The temperature dependence of α may be shown (5, 6) to reflect the solvent–polymer interaction in any system, the sign being settled by the heat of dilution in the pertinent system. As a rule, for nonpolar polymer–solvent systems this is positive (5). Thus in polythene solutions, α may be expected to increase with increasing temperature, especially in the vicinity of θ, the critical temperature for miscibility of the infinite polymer homologue in a given solvent.

If, in the investigated temperature range 100–150° C, appreciable association between polythene molecules occurs in α-CN solutions as compared with tetralin solutions, then the degree of solvent–solute interaction in α-CN is appreciably less than in tetralin solutions. The α-CN solutions are consequently closer to their characteristic θ temperatures and the temperature coefficient of $[\eta]$ in α-CN should be positive and significantly greater than that in tetralin. Further, if the assumption of aggregation is true, the greater tendency for expansion of the polythene molecules in tetralin solutions must result in $[\eta]_t > [\eta]_{\alpha\text{-CN}}$ at comparable temperatures (the subscript t is used to denote tetralin solution). These experimental consequences seem necessary to support the contention of association, although they are not sufficient to establish this behavior unequivocally.

EXPERIMENTAL

Materials

Two unfractionated polythenes were used in this work. One was a low-pressure linear polythene L, the other a high-pressure branched polythene B. Some of their physical properties are summarized below. Methyl group contents for the two samples were

Can. J. Chem. Downloaded from www.nrcresearchpress.com by 210.87.254.105 on 09/05/12
For personal use only.

	Density (g/cc)	CH_3/1000 carbons	$\overline{M_w}$
Polythene L	0.960	1.1	13.5×10^4
Polythene B	0.920	22.7	12.8×10^4

obtained from infrared spectrophotometry and attest to the essential linearity of sample L, and the presence of branches in B. The $\overline{M_w}$ values were obtained from light-scattering measurements in α-CN solution at 120° C using a modified Bryce-Pheonix apparatus. In view of the uncertainty of the meaning of the values, however, the quoted molecular weights are not considered to be absolute. The two samples were in fact chosen because of similarities in their melt viscosities over an appreciable shear-stress range, which suggested that their molecular weights were not greatly different.

Viscosity Measurements

Solution viscosity measurements were carried out in modified Ubbelohde viscometers described by Schulken and Sparks (7), and no kinetic energy or shear corrections were applied. In the investigated range, 100–150° C, temperatures were controlled to about ±0.05° C. Polythene samples used to make up appropriate solutions were stabilized against oxidation by incorporating 0.1% by weight of a commercial antioxidant on a two-roll mill. Viscosity measurements on the redistilled solvents showed these to be thermally stable over periods which were long compared with the working life of a given solution. Minimum exposure of solutions to air was ensured by carrying out all viscosity determinations in a nitrogen atmosphere. Intrinsic viscosities were obtained from extrapolation to zero concentration (c) of plots of η_{sp}/c vs. c and $\ln \eta_r/c$ vs. c, where η_{sp} is the specific viscosity and η_r the relative viscosity of the solution. These plots were found to be linear in the range $0.1 < c < 0.6$ g/100 ml. Values of $[\eta]$ so obtained had a high degree of internal consistency, the precision being not less than ±2%.

RESULTS

The pertinent intrinsic viscosity data are given in Table I. The temperature coefficient

TABLE I

Intrinsic viscosities of polythene solutions at various temperatures

Temp. (°C)	$[\eta]$ (dl g^{-1})			
	Polymer L		Polymer B	
	Tetralin	α-CN	Tetralin	α-CN
100	1.91		1.21	
110		1.43		1.00
120	1.94	1.47	1.23	1.02
140	1.94	1.56	1.21	1.05
150	1.92	1.60	1.19	1.07

of $[\eta]$ in α-CN is positive and substantially greater for both polythenes than the corresponding coefficients in tetralin solutions. Further, the $[\eta]$ values in tetralin for both polymers are significantly greater than the corresponding α-CN values. This indicates a greater tendency for polymer expansion in tetralin, which is therefore thermodynamically the better solvent. The results are in keeping with the theoretical development outlined above; consequently they are consistent with the supposition of solute aggregation in α-CN solutions of polythene (1).

Can. J. Chem. Downloaded from www.nrcresearchpress.com by 210.87.254.105 on 09/05/12
For personal use only.

DISCUSSION

Differences between the $[\eta]$–temperature relationships of polythenes L and B are more readily seen from a plot of $[\eta]$ versus T, such as given in Fig. 1. The temperature

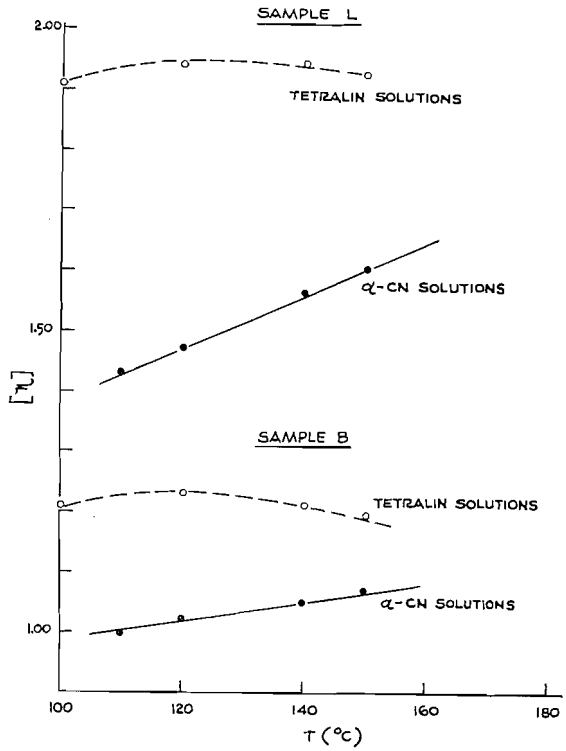


FIG. 1. Temperature dependence of intrinsic viscosity in polythene solutions.

coefficient of $[\eta]_{\alpha\text{-CN}}$ for polythene L is substantially greater than for polythene B, the respective slopes of the linear plots being 2.1×10^{-3} and 1.2×10^{-3}. Since the apparent $\overline{M}_w$ of these samples is roughly equivalent, it is suggested that the polymer L – α-CN pair may be closer to its characteristic θ temperature than the pair polymer B – α-CN at the temperatures involved in these experiments. In terms of a solute-association hypothesis, the molecules of polymer L thus have a greater tendency for aggregation than do those of polymer B. In view of the generally held opinion that linear polymers are more subject to segmental entanglements (8) than are branched polymers, an aggregation in α-CN solution could result simply from the inability of the weak solvent to disrupt these entanglements. The aggregation should therefore be increasingly evident with rising molecular weight, lowered temperature (in line with the findings of Trementozzi (1) and Tung (2)), and increasing linearity of the polythene, but should be partially reduced or eliminated in thermodynamically better solvents such as tetralin.

The $[\eta]_t$ values appear to attain a maximum near 120° C, more noticeably so for polythene B. Kawai and Ueyama (6) have recently suggested such a maximum to be generally expected in high-polymer systems and have noted its occurrence in polythene–xylene. The temperature at which this maximum occurs increases with the flexibility

Can. J. Chem. Downloaded from www.nrcresearchpress.com by 210.87.254.105 on 09/05/12
For personal use only.

of the polymer chain (6); since the maximum for sample L should then occur at a somewhat higher temperature than that of sample B, its more pronounced manifestation in polythene B may be understood. The weak temperature coefficient of $[\eta]_t$ indicates a general balance of thermal effects due to changes in K and α of equation [1] and, as previously noted, suggests an appreciably stronger solvent–solute interaction than in the α-CN solution systems.

The temperature at which the solute molecule appears to expand to the same extent in α-CN as it does in a corresponding tetralin solution may be estimated from the $[\eta]$–T relationships in Fig. 1. Thus, if $[\eta]_t$ is assumed to attain a maximum near 120° C for both polythenes, then the linear $[\eta]_{\alpha\text{-CN}}$–$T$ plots may be extrapolated to the appropriate maximum value of $[\eta]_t$. For polythene L the temperature for "solvent equivalence" appears to be about 230° C; for B about 270° C. This admittedly gross procedure suggests that light-scattering experiments using α-CN solutions of polymers L and B at the above temperatures, and tetralin solutions at 120° C, should yield equal values of $\overline{M}_w$ for each of the two resins. Both of the suggested temperatures for α-CN experimentation would, of course, be well beyond limits of practicability.

CONCLUSIONS

Tetralin is thermodynamically a superior solvent for polythene than α-CN. At the temperatures normally utilized for light-scattering measurements of $\overline{M}_w$, α-CN solutions of polythene seem closer to their characteristic θ temperatures, and would therefore be the preferred solution systems for such measurements, provided no solute aggregation occurred. The present results, however, are fully consistent with the suggestion of polythene aggregation in α-CN solutions (1), although they do not unequivocally establish its existence. In view of this, further critical experimentation into the state of the polymer molecule in α-CN solution would appear to be called for.

ACKNOWLEDGMENTS

I am indebted to Messrs. R. Baxter and P. Kruus for much of the viscosity work, to Mr. A. W. Pross for infrared determinations, and to Dr. M. H. Waldman for light-scattering data.

1. Q. A. Trementozzi. J. Polymer Sci. **36**, 113 (1959).
2. L. H. Tung. J. Polymer Sci. **46**, 409 (1960).
3. B. H. Zimm and R. W. Kilb. J. Polymer Sci. **37**, 19 (1959).
4. P. J. Flory and T. G. Fox, Jr. J. Am. Chem. Soc. **73**, 1904 (1951).
5. P. J. Flory. Principles of polymer chemistry. Cornell University Press, Ithaca, New York. 1953. Chap. XIV.
6. T. Kawai and T. Ueyama. J. Appl. Polymer Sci. **3**, 227 (1960).
7. R. M. Schulken and M. L. Sparks. J. Polymer Sci. **26**, 227 (1957).
8. F. Bueche. J. Chem. Phys. **20**, 1959 (1952).

Received November 9, 1960.
Canadian Industries Limited,
Central Research Laboratory,
McMasterville, Quebec.

Can. J. Chem. Downloaded from www.nrcresearchpress.com by 210.87.254.105 on 09/05/12
For personal use only.

Can. J. Chem. Downloaded from www.nrcresearchpress.com by 210.87.254.5 on 09/05/12
For personal use only.

Canadian Journal of Chemistry

Issued by THE NATIONAL RESEARCH COUNCIL OF CANADA

VOLUME 39 AUGUST 1961 NUMBER 8

STRUCTURE OF AN ARABINOGALACTAN FROM TAMARACK (LARIX LARICINA)[1]

S. HAQ[2] AND G. A. ADAMS

ABSTRACT

Partial acid hydrolysis of an arabinogalactan from tamarack wood yielded:
(I) L-arabinose,
(II) D-galactose,
(III) 3-*O*-β-L-arabinopyranosyl-L-arabinose,
(IV) 6-*O*-β-D-galactopyranosyl-D-galactose,
(V) 3-*O*-β-D-galactopyranosyl-D-galactose,
(VI) *O*-D-galactopyranosyl(1 → 6)-*O*-D-galactopyranosyl(1 → 6)-D-galactose,
(VII) 3,6-di-*O*-(galactopyranosyl)-D-galactopyranose,
(VIII) *O*-D-galactopyranosyl(1 → 3)-*O*-D-galactopyranosyl(1 → 3)-D-galactose,
(IX) *O*-D-galactopyranosyl(1 → 6)-*O*-D-galactopyranosyl(1 → 3)-D-galactose,
(X) *O*-D-galactopyranosyl(1 → 6)-*O*-D-galactopyranosyl(1 → 6)-*O*-D-galactopyranosyl (1 → 3)-D-galactose,
(XI) *O*-D-galactopyranosyl(1 → 6)-*O*-D-galactopyranosyl(1 → 3)-*O*-D-galactopyranosyl (1 → 3)-D-galactose.

A previously published structure for the tamarack polysaccharide was revised to show that not more than two consecutive 1 → 3 or 1 → 6 linkages respectively were present in the main core of the repeating unit. Some of the 6-*O*-β-D-galactopyranosyl-D-galactose units occurred as side chains as well as in the main body of the molecule.

It has been shown previously that the water-soluble polysaccharide of tamarack (*Larix laricina*) is a highly branched arabinogalactan composed of L-arabinose and D-galactose in the ratio of 1:3.8 (1). Evidence was presented to indicate that the galactose residues were joined predominantly by 1 → 3 and 1 → 6 glycosidic linkages. The original view (2) that arabinose was attached as a single molecule in the furanose form in ε-galactan polysaccharides was made untenable by the isolation of β-3-*O*-L-arabinopyranosyl-L-arabinose from a mild hydrolysis of both a larch ε-galactan (3) and an arabinogalactan from western larch (*Larix occidentalis*) (4). The present work which describes the fragmentation analysis of arabinogalactan from tamarack was undertaken to provide additional information on the fine structure of the polysaccharide.

The polysaccharide was subjected to a progressive, mild acidic hydrolysis, as it was observed previously (1) that such treatment released arabinose units almost completely from the main body of the polysaccharide, resulting in a degraded galactan. The chromatographic picture of the hydrolyzate (0.01 *N* H_2SO_4 for 3 hours and .02 *N* H_2SO_4 for 4 hours) revealed as the main components, L-arabinose, D-galactose, a disaccharide of arabinose, and a disaccharide of galactose. In addition, there were several minor spots of sugars giving pink or reddish-brown colors with *p*-anisidine hydrochloride spray reagent. Two of these moved on paper chromatograms faster than arabinose and two moved

[1]*Manuscript received April 6, 1961.*
Contribution from the Division of Applied Biology, National Research Council, Ottawa, Canada. Issued as N.R.C. No. 6350.
[2]*N.R.C. Postdoctorate Fellow, 1959–1961.*

between galactobiose and arabinobiose and gave a reddish-brown color with *p*-anisidine hydrochloride. One of the faster-moving components had the same R_F value as L-rhamnose but it was not sufficient in amount to permit further characterization. The components moving between galactobiose and arabinobiose were probably the products of resynthesis because heating of a mixture of arabinose and galactose under the same conditions showed very faint spots having the same flow rates on the chromatogram.

After the foregoing mild hydrolysis, the degraded galactan was subjected to a more rigorous hydrolysis. From the hydrolyzates the various sugars were isolated through a combination of cellulose and charcoal–celite column chromatography. The results are shown in Table I. The preliminary hydrolysis released the monosaccharides, the disaccharides of arabinose, and galactobiose (IV). The more rigorous hydrolysis released D-galactose (II), additional galactobiose (IV), and all other oligosaccharides. L-Arabinose and D-galactose were crystallized and identified by their physical properties.

TABLE I

Sugars recovered from partial acid hydrolysis of arabinogalactan of tamarack

	Name	Yield (mg)
(I)	L-Arabinose	Not determined
(II)	D-Galactose	Not determined
(III)	3-*O*-β-L-Arabinopyranosyl-L-arabinose	500
(IV)	6-*O*-β-D-Galactopyranosyl-D-galactose	850
(V)	3-*O*-β-D-Galactopyranosyl-D-galactose	390
(VI)	*O*-D-Galactopyranosyl(1 → 6)-*O*-D-galactopyranosyl(1 → 6)-D-galactose	17
(VII)	3,6-Di-*O*-(galactopyranosyl)-D-galactopyranose	32
(VIII)	*O*-D-Galactopyranosyl(1 → 3)-*O*-D-galactopyranosyl(1 → 3)-D-galactose	106
(IX)	*O*-D-Galactopyranosyl(1 → 6)-*O*-D-galactopyranosyl(1 → 3)-D-galactose	93
(X)	*O*-D-Galactopyranosyl(1 → 6)-*O*-D-galactopyranosyl(1 → 6)-*O*-D-galactopyranosyl (1 → 3)-D-galactose	35
(XI)	*O*-D-Galactopyranosyl(1 → 6)-*O*-D-galactopyranosyl(1 → 3)-*O*-D-galactopyranosyl (1 → 3)-D-galactose	94

The disaccharide of arabinose on complete acidic hydrolysis and chromatographic examination gave arabinose as the only monosaccharide. On complete methylation and hydrolysis, the disaccharide gave (i) 2,3,4-tri-*O*-methyl-L-arabinose, (ii) 2,4-di-*O*-methyl-L-arabinose, and (iii) 2,5-di-*O*-methyl-L-arabinose. These sugars were characterized through their respective crystalline derivatives.

The presence of 2,4- and 2,5-di-*O*-methyl-L-arabinose in the hydrolyzate of the methylated disaccharide indicated that the disaccharide was a mixture of β-3-*O*-L-arabinopyranosyl-L-arabinopyranose and β-3-*O*-L-arabinopyranosyl-L-arabinofuranose. From the amount of 2,4-di-*O*-methyl-L-arabinose (93 mg) and 2,5-di-*O*-methyl-L-arabinose (14.2 mg) it was concluded that the two forms of the disaccharide were present in the mixture in the ratio of 6.5:1. Approximately the same ratio was found between the 2,4- and 2,5-di-*O*-methyl arabinoses by gas–liquid chromatography (5, 6). The lower specific rotation of the disaccharide and that of its methylated derivative compared to those reported by previous workers (3, 4) also indicated the possibility of a disaccharide present in furanose form. The 2,5-di-*O*-methyl-L-arabinose could not have arisen from incomplete methylation of the disaccharide because the methoxyl content of the methylated derivative agreed with the theoretical value and no adsorption corresponding to $(OH)^-$ group could be detected in the infrared spectrum.

The disaccharide of galactose, which was obtained by mild acid hydrolysis, was crystallized and identified as β-6-*O*-D-galactopyranosyl-D-galactose and was identical with

Can. J. Chem. Downloaded from www.nrcresearchpress.com by 210.87.254.5 on 09/05/12
For personal use only.

Can. J. Chem. Downloaded from www.nrcresearchpress.com by 210.87.254.5 on 09/05/12
For personal use only.

galactobiose (IV) described below. The amount released in the preliminary hydrolysis was approximately one quarter of the total amount that was recovered from all hydrolyses. Galactobiose (IV) was obtained in crystalline form and its specific rotation indicated a β-linkage. The mode of linkage in the disaccharide was established by the isolation of 2,3,4,6-tetra-*O*-methyl-D-galactose and 2,3,4-tri-*O*-methyl-D-galactose from the hydrolyzate of fully methylated disaccharide. Thus the structure of galactobiose (IV) was confirmed as β-6-*O*-D-galactopyranosyl-D-galactose.

Galactobiose (V) on complete acidic hydrolysis gave only galactose and its flow rate on a chromatogram indicated that it was a disaccharide. On complete methylation and hydrolysis, the disaccharide gave 2,3,4,6-tetra-*O*-methyl-D-galactose and 2,4,6-tri-*O*-methyl-D-galactose, and its structure was established as 3-*O*-D-galactopyranosyl-D-galactose.

Galactotriose (VI) and galactotriose (VII) were isolated in very small amounts and complete structural studies by methylation were not possible. However, some preliminary experiments revealed their probable structure. Galactotriose (VI) on partial hydrolysis gave galactose, galactobiose (IV), and the original sugar. On reduction and partial hydrolysis of the reduced product, galactose and galactobiose (IV) were obtained as reducing sugars. Therefore galactotriose (VI) is probably *O*-D-galactopyranosyl (1 → 6)-*O*-D-galactopyranosyl(1 → 6)-D-galactose. Galactotriose (VII) on partial acidic hydrolysis gave galactose, galactobiose (IV), galactobiose (V), and the original sugar. After reduction and partial hydrolysis of the derived glycitol, galactose was obtained as the only reducing sugar. Therefore the evidence suggests that galactobiose (VII) is probably a branched trisaccharide having the tentative structure 3,6-digalactopyranosyl-D-galactose.

Galactotriose (IX) on complete methylation and hydrolysis of the methylated product gave 2,3,4,6-tetra-*O*-methyl-D-galactose; 2,3,4-tri-*O*-methyl-D-galactose; and 2,4,6-tri-*O*-methyl-D-galactose in equimolar proportion. These results indicated that the trisaccharide was a straight chain containing 1 → 6 and 1 → 3 glycosidic linkages. The trisaccharide on partial acidic hydrolysis gave galactobiose (IV) and galactobiose (V). The sequence of glycosidic linkages was established by the reduction of the trisaccharide and partial hydrolysis of the derived glycitol. On reduction and hydrolysis the trisaccharide gave galactose and galactobiose (IV) as reducing sugars. This finding confirmed that the 1 → 3 linkage was at the reducing end of the molecule while the 1 → 6 linkage was penultimate to the reducing end. Therefore the structure of galactotriose (IX) was established as *O*-D-galactopyranosyl(1 → 6)-*O*-D-galactopyranosyl(1 → 3)-D-galactose.

Galactotriose (VIII) was obtained in crystalline form for the first time. The sugar, after partial acidic hydrolysis, gave galactose, galactobiose (V), and the original trisaccharide. After reduction and partial hydrolysis it gave galactose and galactobiose (V) as reducing sugars. Therefore it was probably a straight-chain trisaccharide containing 1 → 3 glycosidic linkages. On methylation and hydrolysis of the methylated product, the trisaccharide gave 2,3,4,6-tetra-*O*-methyl-D-galactose (1 mole) and 2,4,6-tri-*O*-methyl-D-galactose (2 moles). Therefore the structure of galactotriose (VIII) was established as *O*-D-galactopyranosyl(1 → 3)-*O*-D-galactopyranosyl(1 → 3)-D-galactose.

Galactotetraose (X) on partial acidic hydrolysis produced galactose, galactobiose (IV), galactobiose (V), galactotriose (VI), galactotriose (IX), and the original sugar. On reduction and hydrolysis it gave galactose, galactobiose (IV), and galactotriose (VI). Therefore the structure of galactotetraose (X) was proposed as *O*-D-galactopyranosyl (1 → 6)-*O*-D-galactopyranosyl(1 → 6)-*O*-D-galactopyranosyl(1 → 3)-D-galactose. Similarly,

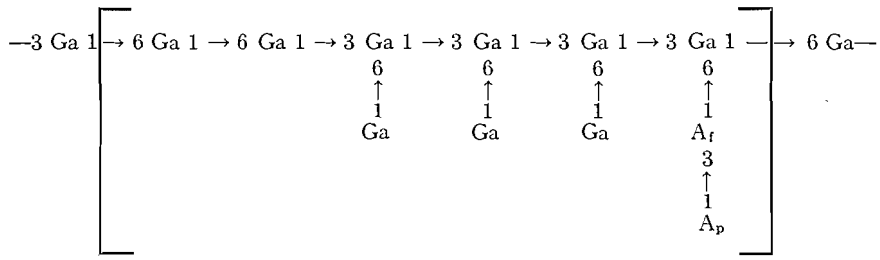
on the basis of the products of partial hydrolysis of the sugar and its reduced product, the structure of galactotetraose (XI) was proposed as *O*-D-galactopyranosyl(1 → 6)-*O*-D-galactopyranosyl(1 → 3)-*O*-D-galactopyranosyl(1 → 3)-D-galactose. No other galactotetraoses were found. Figure 1 shows a diagrammatic representation of the oligosaccharide

$O_1 \rightarrow {}_6\emptyset$ galactobiose (IV)	$O_1 \rightarrow {}_3\emptyset$ galactobiose (V)
$O_1 \rightarrow {}_6O_1 \rightarrow {}_6\emptyset$ galactotriose (VI)	$O_1 \rightarrow {}_6\emptyset_3$ $\uparrow$ O_1 galactotriose (VII)
$O_1 \rightarrow {}_6O_1 \rightarrow {}_3\emptyset$ galactotriose (IX)	$O_1 \rightarrow {}_3O_1 \rightarrow {}_3\emptyset$ galactotriose (VIII)
$O_1 \rightarrow {}_6O_1 \rightarrow {}_6O_1 \rightarrow {}_3\emptyset$ galactotetraose (X)	$O_1 \rightarrow {}_6O_1 \rightarrow {}_3O_1 \rightarrow {}_3\emptyset$ galactotetraose (XI)

FIG. 1. Diagrammatic representation of D-galactose oligosaccharides from tamarack arabinogalactan: O, galactose; Ø, galactose (reducing unit).

structures of the various sugars isolated from tamarack in the present study. Of these, (IV), (V), (VI), (VII), and (VIII) have been previously reported as products of partial hydrolysis of European larch galactan (8).

A possible structure for the tamarack arabinogalactan (Fig. 2) was proposed earlier



Structure I

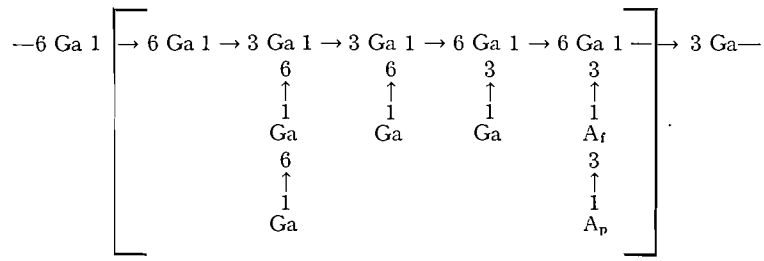
FIG. 2. Structure originally proposed for repeating unit of tamarack arabinogalactan.

(1) and was based on methylation and periodate oxidation evidence. The isolation and identification of the oligosaccharides obtained in the present study confirm, in general, most of the main features of this structure. Some revisions, as will be pointed out below, are required. The occurrence of 1 → 3 and 1 → 6 linked galactopyranose units in the core of the molecule was proved by the isolation of galactobiose (IV) and (V). Two galactose trisaccharides (VIII) and (VI) joined by 1,3- and by 1,6-linkages respectively were isolated and have established that two consecutive 1 → 3 and 1 → 6 linkages exist in the polysaccharide. In addition, two trisaccharides containing both 1,3- and 1,6-linkages were found. In these, galactotrioses (IX) and (VII), the galactose units constituting the reducing end of the chains were linked to the remainder of the molecule through C_3; in addition, the reducing terminal unit of galactotriose (VII) was branched through C_6. From the structure of galactotetraoses (X) and (XI), it appears that not more than two 1 → 3 or two 1 → 6 linkages occur consecutively in the polysaccharide.

Partial hydrolysis using very dilute acid yielded 1 → 6 linked galactobiose but no

Can. J. Chem. Downloaded from www.nrcresearchpress.com by 210.87.254.5 on 09/05/12
For personal use only.

$1 \rightarrow 3$ linked galactobiose. Approximately one quarter of the $1 \rightarrow 6$ linked disaccharide was released by this treatment, the remainder being formed by more rigorous hydrolysis. The $1 \rightarrow 6$ and the $1 \rightarrow 3$ linkages are present in approximately equal proportions (1) and the preferential release of the $1 \rightarrow 6$ linked galactobiose units indicated that some of them were in side chains. This observation was further substantiated by recovery of most of the intact polysaccharide after the preliminary mild acid hydrolysis. The attachment of $1 \rightarrow 6$ linked galactose units as side chains has been proposed also for the ϵ-galactan of European larch (8). These findings have necessitated changes from structure I (Fig. 2) to structure II (Fig. 3). This latter structure accounts for the formation of all



Structure II

FIG. 3. Modified structure proposed for repeating unit of tamarack arabinogalactan.

the oligosaccharides shown in Fig. 1. In addition, the methylation and periodate oxidation found in a previous study (1) support this structure.

The structure as originally proposed for the tamarack arabinogalactan (1) and shown in Fig. 2 predicted that some of the L-arabinose units were attached in such a way as to yield 3-*O*-L-arabinopyranosyl-L-arabinofuranose on partial hydrolysis. This disaccharide has now been isolated and identified and found to be identical with that previously isolated from larch ϵ-galactans (3, 4). In addition, a much larger amount of arabinose occurred as 3-*O*-L-arabinopyranosyl-L-arabinopyranose. It is presumed that the disaccharide of arabinose existed in the original polysaccharide with its reducing unit in the furanose form and was attached directly to the D-galactose units in the main structure but no positive proof is presently available.

Possible structures for repeating units in galactans from other larch species have been proposed by White (7) and Aspinall (8). The structure proposed by White is characterized by a main chain of 1,6-linked galactose units substituted in position 3 by a secondary chain of three $1 \rightarrow 3$ linked D-galactose residues, the structure proposed by Aspinall consists of a $1 \rightarrow 3$ linked D-galactose main core with two $1 \rightarrow 6$ linked D-galactose units attached to it through position 6. Neither of these formulations would explain the formation of all the oligosaccharides isolated from tamarack arabinogalactan; nor could the proportion of methylated sugars obtained from fully methylated tamarack arabinogalactan be produced from these structures. Assuming the validity of these different proposed structures, it is apparent that some species differences in these polysaccharides must exist.

Further studies of the structural relationships of L-arabinose in the tamarack arabinogalactan are being undertaken through enzymic degradation.

Can. J. Chem. Downloaded from www.nrcresearchpress.com by 210.87.254.5 on 09/05/12
For personal use only.

Can. J. Chem. Downloaded from www.nrcresearchpress.com by 210.87.254.5 on 09/05/12
For personal use only.

EXPERIMENTAL

The organic phase of the following solvent systems (v/v) was used for chromatography:

(A) ethyl acetate – pyridine – water (2.5:1:2.5),
(B) butan-1-ol–ethanol–water (5:1:4),
(C) benzene–ethanol–water–ammonia (200:47:14:1),
(D) ethyl acetate – acetic acid – water (9:2:2).

Paper chromatography was carried out on Whatman No. 1 and No. 3MM papers for qualitative and quantitative separations respectively.

A 3% ethanolic solution of *p*-anisidine hydrochloride was used for detecting reducing sugars (9). All specific rotations were measured in water and at 25° C unless otherwise stated. Evaporations were done under reduced pressure at 32–34° C.

Hydrolysis of the Polysaccharide

Arabinogalactan (20 g) as previously prepared (1) was heated on a boiling-water bath with 0.01 *N* H_2SO_4 (500 ml) for 3 hours. After the solution had cooled, it was neutralized with barium carbonate, filtered, and concentrated to a small volume (100 ml). The concentrated solution was poured dropwise into 95% ethanol (2 l.), which was rapidly stirred. The precipitated polysaccharide was removed by filtration and the filtrate was evaporated to dryness (1.1 g). The precipitated polysaccharide was hydrolyzed twice more with 0.02 *N* H_2SO_4 (500 ml) for 2 hours and recovered as above. Chromatograms of all the hydrolyzates showed L-arabinose, D-galactose, a disaccharide of L-arabinose, a disaccharide of D-galactose, and traces of other sugars running faster on paper than L-arabinose.

The sugars (3 g) were separated on a cellulose column (40×6 cm) and eluted with a mixture of butanol–ethanol–water (40:11:19) at a rate of 7 ml per 18 min. The following fractions were collected.

A. (Tube 61–109).—This fraction gave a syrup (30 mg) which contained traces of arabinose and two other sugars, (i) R_{arab} 1.56, (ii) R_{arab} 2.32 in solvent A. L-Rhamnose has R_{arab} 1.56 in solvent A.

B. (Tube 110–114).—This fraction gave a syrup (777 mg) containing mainly arabinose and traces of galactose. The mixture crystallized from aqueous ethanol giving pure L-arabinose which, after three recrystallizations from the same solvent, had m.p. 159–160° C, $[\alpha]_D$ +105° (*c*, 1.74).

C. (Tube 145–275).—This fraction gave a mixture of sugars (1.63 g) containing L-arabinose, D-galactose, and a disaccharide of L-arabinose. The mixture was separated on a charcoal–celite (1:1) column (27×4.5 cm). The column was washed first with water (2 l.) to remove monosaccharides, and the disaccharide was removed by gradient elution (20% ethanol run into 1.5 l. of water). All the fractions (8–11) showing a single spot on paper chromatogram were combined and evaporated to dryness. A chromatographically pure disaccharide of L-arabinose (500 mg) was obtained.

D. (Tube 293–416).—This fraction on evaporation gave a sugar (220 mg) which contained mainly a galactobiose, R_{gal} 0.32 in solvent A with traces of galactose, a trisaccharide, and another sugar giving a reddish-brown color with *p*-anisidine reagent and moving on paper slightly faster than galactobiose. A crystalline sugar was obtained by keeping a methanolic solution of the syrup in the cold for 10 days. After recrystallization from methanol, the crystals had m.p. 168–170° C with swelling at 98–100° C and sintering at 120° C. The crystalline sugar was identical with β-6-*O*-galactopyranosyl-D-galactose (see later).

Identification of Arabinobiose

The syrup (500 mg) had $[\alpha]_D$ +193° (*c*, 3.77) and R_{arab} 0.74 in solvent A. It gave a characteristic pink color with *p*-anisidine hydrochloride spray reagent and on complete hydrolysis yielded L-arabinose.

The disaccharide (290 mg) dissolved in water (5 ml), was cooled in an ice bath, and dimethyl sulphate (1 ml) was added. The solution was stirred vigorously and 30% sodium hydroxide solution (2 ml) was added dropwise during 7 hours and the reaction mixture was further stirred for 5 hours. Then 30% sodium hydroxide solution was added 5 ml at a time and dimethyl sulphate (3 ml) was allowed to run in dropwise and the reaction mixture was further stirred for 14 hours. The solution was heated at 60° C for 1 hour to decompose any unreacted dimethyl sulphate, and then the partially methylated sugar was continuously extracted with chloroform for 4 days. After removal of the chloroform the sugar was once again methylated as above except that the sodium hydroxide solution was added first to keep the reaction mixture alkaline. The partially methylated products were then methylated twice with Purdie's reagent. The methylated disaccharide (300 mg) had $[\alpha]_D$ +160° (*c*, 0.76 in chloroform). (Found: MeO, 50.3%. $C_{16}H_{30}O_9$ requires: OMe, 50.6%.)

The methylated disaccharide (260 mg) was hydrolyzed by heating on a water bath at 100° C for 7 hours with 0.5 *N* HCl (20 ml). The solution was neutralized with silver carbonate, filtered, and the filtrate was evaporated to dryness. The syrup (240 mg), on examination by paper chromatography in solvent B, showed two spots with R_G 0.81 and R_G 0.63. The sugars were separated on paper in the same solvent.

Fraction I

This fraction proved to be 2,4-di-*O*-methyl-L-arabinose (93 mg), $[\alpha]_D$ +118° (*c*, 0.9). (Found: OMe, 33.3. $C_7H_{14}O_5$ requires: OMe, 34.8%.) A portion (32 mg) of the sugar was heated on a water bath with freshly distilled aniline (17 mg) in ethanol (2 ml) for 3 hours. The solvent was removed and the syrup was dissolved in hot butanol, and on cooling, crystals (plates) were formed. After recrystallization from the same solvent the crystals had m.p. and mixed m.p. 135–136° C. (On an uncovered glass plate the crystals melted at 145–147° C; the same behavior was observed with authentic samples of 2,4-di-*O*-methyl-*N*-phenyl-L-arabinosylamine.)

Another portion (40 mg) was oxidized with 2 drops of bromine in water (0.5 ml). Barium carbonate (20 mg) was added to the reaction mixture, which was stored in the dark for 72 hours. Bromine was removed by aeration and the acidified solution was extracted with chloroform. After removal of the chloroform the residual syrup was distilled (bath temperature 120–145° C at 0.02 mm). The distillate was dissolved in methanol (10 ml), saturated with ammonia, and kept in the cold overnight. On evaporation of methanol, the amide crystallized and after recrystallization from methanol in the cold the crystals had m.p. 158–159° C (reported m.p. of 2,4-di-*O*-methyl-L-arabonamide is 160–161° C) (4). (Found: MeO, 32.0%. $C_7H_{14}O_5N$ requires: MeO, 32.3%).

Fraction II (120.4 mg)

When this fraction was examined by paper chromatography in solvent C it was found to consist of two sugars. This observation was also confirmed when the sugar (2 mg) was refluxed with methanolic hydrogen chloride (2%), and examined by gas–liquid chromatography (5, 6). The sugars were separated on paper in solvent C.

(*a*) 2,5-Di-*O*-methyl-L-arabinose (14.2 mg), $[\alpha]_D$ −19.7° (*c*, 0.71). The sugar was oxidized as above with bromine and the corresponding arabonic acid was distilled (bath temperature 120–140° C at 0.02 mm). The lactone was dissolved in ammoniacal methanol and

Can. J. Chem. Downloaded from www.nrcresearchpress.com by 210.87.254.5 on 09/05/12
For personal use only.

kept overnight in the cold. On evaporation of methanol the product crystallized and after recrystallization from ethanol the crystals had m.p. 130–131° C, undepressed on admixture with an authentic specimen of 2,5-di-*O*-methyl-L-arabonamide.

(*b*) 2,3,4-Tri-*O*-methyl-L-arabinose (42 mg) (there was some accidental loss of material). The sugar was oxidized with bromine as above and the resulting product was distilled (bath temperature 105–120° C at 0.02 mm). The lactone was heated with phenylhydrazine in methanol (3 ml) for 3 hours. Methanol was removed and the syrup crystallized on seeding. After recrystallization from ethyl acetate the phenylhydrazide of 2,3,4-tri-*O*-methyl-L-arabonolactone had m.p. and mixed m.p. 156–158° C.

Hydrolysis of the Degraded Polysaccharide

The degraded galactan (20 g) recovered from previous hydrolysis with dilute H_2SO_4 was further hydrolyzed on a boiling-water bath with 0.1 *N* H_2SO_4 (500 ml) for a total of 6 hours. Three hydrolysis periods of 2 hours each were used, with recovery of polysaccharide after each hydrolysis by precipitation with 92% ethanol. The hydrolysis procedure was again repeated with 0.2 *N* H_2SO_4 for 2 hours and with 0.5 *N* H_2SO_4 for 3 hours. The chromatographic picture of all hydrolyzates was similar, showing galactose and oligosaccharides of galactose.

The sugars (12 g) from the combined hydrolyzates were fractionated on a charcoal–celite (1:1) column (48×6.5 cm). The column was first washed with water (3 l.) to remove monosaccharides. Then gradient elution technique was applied in which 10% ethanol was allowed to run into water (4 l.) to elute the oligosaccharides. After 185 fractions had been collected (80–100 ml each), 10% ethanol was replaced by 20% ethanol.

The water eluate on evaporation gave mainly D-galactose (8.1 g) and traces of L-arabinose. D-Galactose was crystallized from aqueous ethanol and after recrystallization had m.p. 165–166° C, $[\alpha]_D$ +80.6° (*c*, 2.02).

The individual sugars were further purified by paper chromatography in solvent A. Galactotriose (VI) gave a single spot in all solvent systems, but when examined by paper electrophoresis in borate buffer at pH 10 it showed two sugars, galactotriose (VI) (M_G 0.81) and galactotriose (VII) (M_G 0.69). These sugars were separated on paper electrophoresis in borate buffer.

Identification of the Oligosaccharides

Galactobiose (IV)

The sugar (650 mg) crystallized from methanol with 2 moles of methanol as solvent of crystallization, m.p. 168–170° C with swelling at 98–100° C and softening at 120° C, $[\alpha]_D$ 28° (*c*, 1.43). (Found: C, 41.39; H, 7.57. $C_{12}H_{22}O_{11}$,$2CH_3OH$ requires: C, 41.30; H, 7.38.) After removal of the solvent of crystallization at 100° C *in vacuo* over P_2O_5, the disaccharide had m.p. 168–170° C with softening at 120° C, $[\alpha]_D$ 34.2° (*c*, 1.52). (Found: C, 41.94; H, 6.54. $C_{12}H_{22}O_{11}$ requires: C, 42.1; H, 6.48.) On complete hydrolysis it gave D-galactose.

The disaccharide (306 mg) was methylated initially with dimethyl sulphate (13 ml) and 30% sodium hydroxide solution (24 ml) as described above for arabinobiose, and subsequently by two methylations with Purdie's reagent. The methylated product (303 mg) crystallized from the syrup as needles but could not be crystallized from any solvent. It had m.p. 68–70° C, $[\alpha]_D$ −5.7° (*c*, 2.4 in methanol). (Found: C, 51.96; H, 8.28; MeO, 52.4%. $C_{20}H_{38}O_{11}$ requires: C, 52.42; H, 8.12; MeO, 54.6%.)

Can. J. Chem. Downloaded from www.nrcresearchpress.com by 210.87.254.5 on 09/05/12
For personal use only.

Can. J. Chem. Downloaded from www.nrcresearchpress.com by 210.87.254.5 on 09/05/12
For personal use only.

The methylated disaccharide (250 mg) was hydrolyzed with *N* HCl at 100° C for 5 hours. The solution was neutralized with silver carbonate, filtered, and evaporated to dryness. The individual methylated sugars were separated on paper in solvent C and two fractions were obtained.

*(a) 2,3,4,6-Tetra-O-methyl-*D*-galactose (86.7 mg).*—The sugar (40 mg) was heated with freshly distilled aniline (25 mg) in ethanol (3 ml) for 3 hours. When the solution was concentrated and cooled, crystals of 2,3,4,6-tetra-*O*-methyl-*N*-phenyl-D-galactosylamine separated which, after recrystallization from ethanol, had m.p. and mixed m.p. 194–196° C.

*(b) 2,3,4-Tri-O-methyl-*D*-galactose (80.3 mg).*—A portion of the sugar (20 mg) was heated with freshly distilled aniline (15 mg) for 3 hours in ethanol (3 ml). Ethanol was removed by distillation and the residual syrup was extracted with hot ethyl acetate. After removal of the ethyl acetate the syrup was crystallized from acetone. On recrystallization from the same solvent the crystals (plates) had m.p. 165–167° C, undepressed on admixture with an authentic specimen of 2,3,4-tri-*O*-methyl-*N*-phenyl-D-galactosylamine. Another portion of the trimethyl galactose (22 mg) was oxidized with bromine for 48 hours. Bromine was removed by aeration and the acidified solution extracted with chloroform. After removal of the chloroform, the acid was distilled (bath temperature 150–160° C at 0.02–0.01 mm). The distillate was dissolved in methanol (10 ml), saturated with ammonia, and kept at +4° C overnight. After removal of methanol the product crystallized and on recrystallization from ethanol the 2,3,4-tri-*O*-methyl-D-galactonamide had a m.p. and mixed m.p. 166–167° C.

Galactobiose (V)

This fraction, $[\alpha]_D$ +60.3° (*c*, 2.1), was a chromatographically pure sugar (390 mg) but it could not be induced to crystallize even by seeding with authentic samples of 3-*O*-*β*-D-galactopyranosyl-D-galactose. On complete hydrolysis it gave D-galactose as the only monosaccharide.

The sugar (175 mg), on methylation as described above, gave a methylated product (145 mg). (Found: MeO, 52.37%. $C_{20}H_{38}O_{11}$ requires: MeO, 54.6%.) The methylated sugar (140 mg) was hydrolyzed by being heated on a boiling-water bath with *N* HCl (15 ml) for 7 hours. The acid was neutralized with silver carbonate, the precipitate was filtered off, and the filtrate was evaporated to dryness. The methylated sugars were separated on paper in solvent B and two fractions were obtained.

*(a) 2,3,4,6-Tetra-O-methyl-*D*-galactose (56.6 mg).*—The sugar was converted into its anilide derivative which, after crystallization, had m.p. 195–197° C, undepressed on admixture with an authentic specimen.

*(b) 2,4,6-Tri-O-methyl-*D*-galactose (51.7 mg).*—The sugar, on being heated with freshly distilled aniline (30 mg) in ethanol (3 ml) for 3 hours, gave a product which crystallized from acetone on cooling. After recrystallization, the crystals (needles) had m.p. 177–179° C, undepressed on admixture with an authentic sample of 2,4,6-tri-*O*-methyl-*N*-phenyl-D-galactosylamine, m.p. 176° C. On the basis of these findings the disaccharide was identified as 3-*O*-*β*-D-galactopyranosyl-D-galactose.

Galactotriose (VI) (17 mg)

Galactotriose (VI) was chromatographically pure sugar which had the same R_{gal} value (0.10) as galactotriose (VII) (0.10) in solvent A but which differed in M_G values in borate buffer. The sugar on partial acidic hydrolysis gave galactose, galactobiose (IV), and the original sugar. After reduction (potassium borohydride) and partial acidic

hydrolysis it gave galactose and galactobiose (IV) as reducing sugars. This trisaccharide is probably *O*-D-galactopyranosyl(1→ 6)-*O*-D-galactopyranosyl(1 → 6)-D-galactose.

Galactotriose (VII) (31.6 mg)

The sugar on partial acidic hydrolysis gave galactose, galactobiose (IV), and galactobiose (V). On reduction (potassium borohydride) and partial hydrolysis it gave galactose as the only reducing sugar.

Galactotriose (IX) (93 mg)

This was a chromatographically pure sugar, $[\alpha]_D$ +20.5° (*c*, 4.0). On partial acidic hydrolysis it gave galactose, galactobiose (IV), galactobiose (V), and the original sugar. On reduction of the trisaccharide (potassium borohydride) and partial acidic hydrolysis of the glycitol only galactose and galactobiose (IV) were found as reducing sugars.

The trisaccharide (80 mg) was methylated twice as described above with dimethyl sulphate (2.5 ml) and 30% sodium hydroxide solution (5 ml). After two further methylations with Purdie's reagent the methylated trisaccharide (66.5 mg) had MeO content 49.37%; $C_{29}H_{54}O_{16}$ requires: MeO, 51.8%. The methylated product was hydrolyzed with *N* HCl (10 ml) by being heated on a boiling-water bath for 5 hours. The acidic solution was neutralized with silver carbonate, filtered, and evaporated to a syrup (50 mg). The hydrolyzed product on a paper chromatogram in solvent B showed two sugars: (*a*) the faster-moving, corresponding to tetra-*O*-methyl-D-galactose, and (*b*) a slow-moving elongated spot. The mixture was separated on paper in solvent B.

(a) 2,3,4,6-Tetra-O-methyl-D-galactose (18.5 mg).—The sugar gave a crystalline anilide derivative, m.p. and mixed m.p. 195–197° C, when heated with aniline (10 mg).

(b) 2,3,4- and 2,4,6-Tri-O-methyl-D-galactose (29 mg).—Chromatographic separation was done using solvent C. The paper was irrigated and when the solvent front was near the bottom of the paper, the paper was dried and again irrigated. This operation was repeated four times but still gave an imperfect separation. However, about $\frac{3}{4}$ in. of the paper in the middle of the band of sugars was discarded and the top portion of the band was extracted with water to give a sugar (9.2 mg). When heated with a drop of aniline in ethanol the sugar gave a product which crystallized from acetone. After recrystallization, the crystals (plates) melted at 165° C, undepressed on admixture with an authentic specimen of 2,3,4-tri-*O*-methyl-*N*-phenyl galactosylamine. The lower portion of the paper gave a sugar (7.9 mg) which gave a crystalline (needles) anilide derivative, m.p. 176–178° C, undepressed on admixture with an authentic specimen of 2,4,6-tri-*O*-methyl-*N*-phenyl galactosylamine.

Galactotriose (VIII) (106 mg)

The sugar crystallized from aqueous ethanol, m.p. 240–245° C (decomposed), $[\alpha]_D$ +51° (*c*, 0.87). (Found: C, 42.00; H, 6.31. $C_{18}H_{32}O_{16}$ requires: C, 42.10; H, 6.34.) The trisaccharide after partial acidic hydrolysis gave galactose, galactobiose (V), and the original sugar. After reduction (potassium borohydride) and partial acidic hydrolysis it gave galactose and galactobiose (V) as reducing sugars.

The trisaccharide (75 mg) was methylated as above. The methylated product (75.6 mg) crystallized from ethanol on slow evaporation of the solvent at room temperature, m.p. 158–160° C, $[\alpha]_D$ −10.0° (*c*, 1.45 in methanol). (Found: MeO, 50.6%. $C_{29}H_{54}O_{16}$ requires: MeO, 51.8%).

The methylated trisaccharide (60 mg) was hydrolyzed in *N* HCl (10 ml) by being heated on a boiling-water bath for 5 hours. The acid was neutralized with silver carbonate, the precipitate was filtered, and the filtrate evaporated to dryness. The syrup on separation on paper in solvent B gave two fractions.

Can. J. Chem. Downloaded from www.nrcresearchpress.com by 210.87.254.5 on 09/05/12
For personal use only.

*(a) 2,3,4,6-Tetra-O-methyl-*D*-galactose (17.2 mg).*—On being heated with aniline (10 mg) in ethanol (2 ml) for 3 hours the product crystallized from ethanol. After recrystallization from the same solvent it had m.p. and mixed m.p. 195–197° C.

*(b) 2,4,6-Tri-O-methyl-*D*-galactose (28.6 mg).*—The syrup was heated with aniline (16 mg) in ethanol (3 ml) for 3 hours. The solvent was removed and the product was crystallized from acetone. After recrystallization, the crystals (needles) had m.p. and mixed m.p. 177–178° C. On the basis of above findings this sugar was identified as *O*-D-galactopyranosyl(1 → 3)-*O*-D-galactopyranosyl(1 → 3)-D-galactose.

Galactotetraose (X) (35 mg)

On partial acidic hydrolysis with 0.1 *N* H_2SO_4 for 1 hour the sugar gave galactose, galactobiose (IV), galactobiose (V), galactotriose (VI), galactotriose (IX), and the original sugar. On reduction and hydrolysis it gave galactose, galactobiose (IV), and galactotriose (VI) as reducing sugars.

Galactotetraose (XI) (94 mg)

On partial acidic hydrolysis the sugar gave galactose, galactobiose (IV), galactobiose (V), galactotriose (IX), galactotriose (VIII), and the original sugar. After reduction of the tetrasaccharide, followed by partial acid hydrolysis, the derived glycitol gave galactose, galactobiose (IV), galactobiose (VI), and galactotriose (IX) as reducing sugars.

ACKNOWLEDGMENTS

The authors wish to thank Professor J. K. N. Jones, Queen's University, Kingston, and Dr. Hans O. Bouveng, Swedish Forest Products Research Laboratory, Stockholm, Sweden, for gifts of 2,4-di-*O*-methyl-*N*-phenyl-L-arabinosylamine. Thanks are also due Dr. G. O. Aspinall, Edinburgh University, and Dr. A. S. Perlin, National Research Council, Saskatoon, for crystalline specimens of 3-*O*-β-D-galactopyranosyl-D-galactose. Carbon, hydrogen, and methoxyl analyses were done by Mr. A. E. Castagne.

REFERENCES

1. G. A. Adams. Can. J. Chem. **38**, 280 (1960).
2. E. V. White. J. Am. Chem. Soc. **64**, 507 (1942).
3. J. K. N. Jones. J. Chem. Soc. 1672 (1953).
4. H. Bouveng and B. Lindberg. Acta Chem. Scand. **10**, 1515 (1956).
5. A. G. McInnes, D. H. Ball, F. P. Cooper, and C. T. Bishop. J. Chromatog. **1**, 556 (1958).
6. C. T. Bishop and F. P. Cooper. Can. J. Chem. **38**, 388 (1960).
7. E. V. White. J. Am. Chem. Soc. **64**, 2838 (1942).
8. G. O. Aspinall, E. H. Hirst, and Else Ramstad. J. Chem. Soc. 593 (1958).
9. L. Hough, J. K. N. Jones, and W. H. Wadman. J. Chem. Soc. 1702 (1950).

Can. J. Chem. Downloaded from www.nrcresearchpress.com by 210.87.254.5 on 09/05/12
For personal use only.

Can. J. Chem. Downloaded from www.nrcresearchpress.com by 210.87.254.5 on 09/05/12
For personal use only.

THE CRYSTAL STRUCTURE OF 1,4-DIBROMONAPHTHALENE[1]

J. TROTTER

ABSTRACT

Crystals of 1,4-dibromonaphthalene are monoclinic with eight molecules in a unit cell of dimensions $a = 27.45$, $b = 16.62$, $c = 4.09$ Å; $\beta = 91.9°$; space group $P2_1/a$. The high proportion of bromine in the crystal probably precludes location of the carbon atoms with sufficient precision to give accurate molecular dimensions, and it has therefore not been considered worth while proceeding beyond the detailed examination of the projection along the short c-axis. There are two molecules in the asymmetric unit, and the solution of the structure from $hk0$ Patterson and Fourier projections has indicated that these two molecules are related, at least in projection, by a pseudo center of symmetry. The projected bond distances indicate significant deviations of the bromine atoms from the aromatic plane. Approximate values of the bond lengths in the molecule have been deduced from the projected distances and estimated orientation angles.

INTRODUCTION

The crystal structure of 1,4-dibromonaphthalene has been determined as part of a series of investigations of derivatives of naphthalene (1).

EXPERIMENTAL

Crystals of 1,4-dibromonaphthalene, obtained by crystallization from aqueous ethanol, consist of colorless plates elongated along the c-axis with the (010) face developed. The approximate density was determined by flotation in standard heavy liquids. The unit-cell dimensions and space group were determined from rotation and oscillation photographs of a crystal rotating about the c-axis, $hk0$ and $hk1$ Weissenberg films, and an $h0l$ precession film.

Crystal Data

1,4-Dibromonaphthalene, $C_{10}H_6Br_2$; molecular weight = 286.0; m.p. = 83° C.

Monoclinic, $a = 27.45 \pm 0.08$, $b = 16.62 \pm 0.04$, $c = 4.09 \pm 0.01$ Å; $\beta = 91°55' \pm 10'$.

Volume of the unit cell = 1864.9 Å^3.

Density, calculated (with $Z = 8$) = 2.037 g cm^{-3}, measured ~2.0 g cm^{-3}.

Absorption coefficient for X-rays, $\lambda = 1.542$ Å, $\mu = 105.4$ cm^{-1}; $\lambda = 0.7107$ Å, $\mu = 94.2$ cm^{-1}.

Total number of electrons per unit cell = $F(000) = 1088$.

Absent spectra: $h0l$ when h is odd, $0k0$ when k is odd.

Space group is $P2_1/a$—C_{2h}^5.

The intensities of the $hk0$ reflections* were recorded on Weissenberg exposures for a crystal rotating about the c-axis, using Cu $K\alpha$ radiation, with multiple-film technique to correlate strong and weak reflections. The $h0l$ reflections were recorded on precession films with Mo $K\alpha$ radiation. All the intensities were estimated visually, the range being about 2000 to 1. The cross section of the crystal normal to the c-axis was 0.08×0.02 mm, so that absorption is negligible, and no corrections were applied. The structure amplitudes were derived by the usual formulae for a mosaic crystal, the absolute scale being established later by correlation with the calculated structure factors. Three hundred and sixty-eight independent $hk0$ reflections were observed, representing about 62% of the possible number observable with Cu $K\alpha$ radiation.

[1]*Manuscript received April 7, 1961.*
Contribution from the Department of Chemistry, University of British Columbia, Vancouver 8, B.C.
**The 200, 110, and 210 reflections were cut off by the beam stop.*

STRUCTURE ANALYSIS

The best approach to determining the complete structure was obviously by examination of the *c*-axis Patterson projection. The *hk*0 Patterson map is shown in Fig. 1. There are

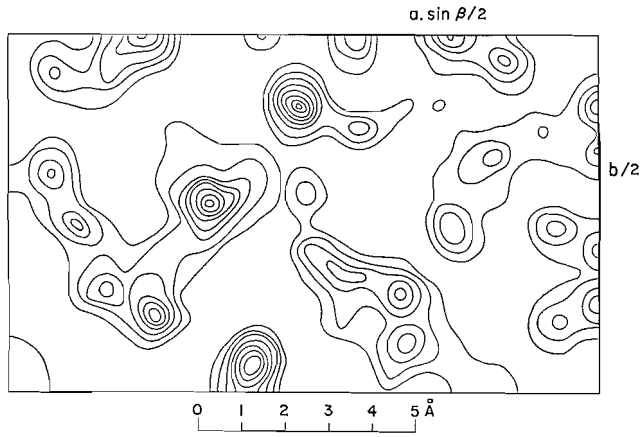


FIG. 1. *c*-Axis Patterson projection; contours at arbitrary intervals.

two molecules and hence four bromine atoms in the asymmetric unit and the plane group for this projection is *pgg*, so that the vector distribution is complex, with many multiple peaks. However, the four Harker peaks on each of the lines $x = \frac{1}{2}$ and $y = \frac{1}{2}$ were easily distinguished, and 16 possible positions (x_j, y_j, z_j) for the four bromine atoms readily deduced. A search was then made for single bromine–bromine vectors at positions $(2x_j, 2y_j, 2z_j)$; this eliminated several of the 16 possibilities but ambiguities still remained. However, it was possible to determine the most probable position for one of the bromine atoms, and a minimum function was then constructed by placing the origin of the Patterson function, in turn, at this bromine position and at the three symmetry-related positions. There were only four significant independent peaks on the resulting map, all of about the same height, and these were taken as corresponding to the four bromine atoms. It was noted that they were related in pairs by a pseudo center of symmetry, so that the larger peaks on the Patterson map correspond to fourfold coincidences of Br–Br vectors.

Structure factors were calculated for all the observed *hk*0 reflections using the scattering factor for bromine of the *Internationale Tabellen* (2) with $B = 3.8$ Å^2, and the discrepancy factor was 44.6%. A Fourier series was then summed, using as coefficients the measured structure amplitudes together with the calculated signs. On the resulting electron-density map all the bromine and carbon atoms were well-resolved, although the carbon contours were considerably distorted, as might be expected in the presence of the much heavier bromine atoms. New positions were chosen for the bromine atoms, and co-ordinates also obtained for all 20 carbon atoms in the asymmetric unit. Structure factors were recalculated using the scattering curve for carbon of Berghuis *et al.* (3) with $B = 3.8$ Å^2; the R value was 24.3%. A second Fourier synthesis was then computed, and on the resulting electron-density map (Fig. 2), the resolution of the carbon atoms was much improved. No changes were suggested in the positional parameters of the bromine atoms, but improved co-ordinates were obtained for the carbons. Since it was not considered worth

Can. J. Chem. Downloaded from www.nrcresearchpress.com by 210.87.254.5 on 09/05/12
For personal use only.

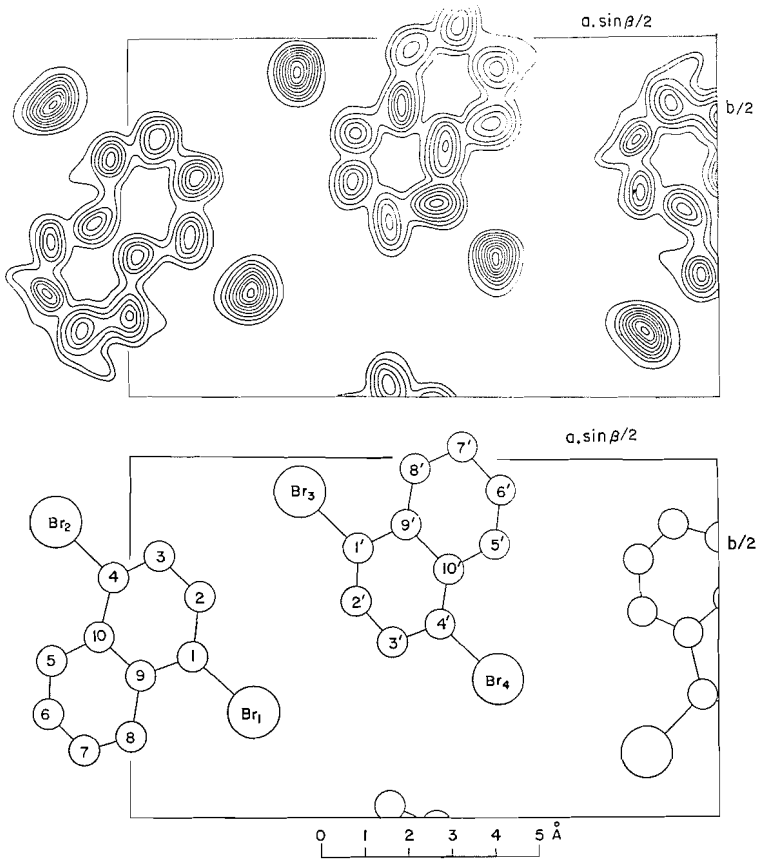


FIG. 2. Electron-density projection along [001] (contours on the carbon atoms at intervals of 1 e Å^{-2}, starting at 2 e Å^{-2}, and on the bromine atoms at intervals of 5 e Å^{-2}, starting at 5 e Å^{-2}), and projection of the structure along [001].

while carrying out further intensive refinement, structure factors were not recalculated; the values at the penultimate stage ($R = 24.3\%$) are not included here, to save space, but are available from the author.

It was apparent that no resolution of the individual atoms could be expected in the projections down the long *a*- and *b*-axes, so that three-dimensional methods would be required to determine the *z*-co-ordinates. It was not considered that the results which could be obtained from such an analysis would be sufficiently accurate, nor that the problem was sufficiently important, to justify the great amount of work involved, and so no effort has been made to determine the *z*-co-ordinates of the atoms.

Co-ordinates and Bond Distances

The final positional parameters are listed in Table I, referred to the crystal axes and expressed as fractions of the unit-cell edges. There is a pseudo center of symmetry at about (0.124, 0.300). The projected bond distances calculated from these co-ordinates are given in the first column of Table II. In order to deduce true bond lengths from these

Can. J. Chem. Downloaded from www.nrcresearchpress.com by 210.87.254.5 on 09/05/12
For personal use only.

TABLE I

Final positional parameters

Atom	x	y	Atom	x	y
Br_1	.1037	.1471	Br_3	.1437	.4510
Br_2	−.0620	.4115	Br_4	.3115	.1908
C1	.0525	.2204	C1′	.1931	.3725
2	.0594	.3025	2′	.1918	.2996
3	.0247	.3597	3′	.2214	.2398
4	−.0146	.3295	4′	.2633	.2693
5	−.0658	.2126	5′	.3090	.3799
6	−.0707	.1393	6′	.3146	.4573
7	−.0384	.0893	7′	.2813	.5175
8	.0012	.1098	8′	.2419	.4879
9	.0091	.1906	9′	.2333	.4070
10	−.0260	.2461	10′	.2625	.3458

TABLE II

Bond distances (Å) and orientation angles (θ)

Bond	Projected bond distances, d_{proj}	θ	Bond distances, $d = \frac{d_{proj}}{\cos\theta}$	Mean bond lengths	Naphthalene bond lengths
1—2	1.378	19°	1.459		
1′—2′	1.212		1.283		
5—6	1.225		1.297		
5′—6′	1.295		1.371		
				1.35	1.36
3—4	1.189	27°	1.336		
3′—4′	1.250		1.405		
7—8	1.138		1.279		
7′—8′	1.188		1.335		
4—10	1.421	19°	1.504		
4′—10′	1.271		1.345		
8—9	1.360		1.440		
8′—9′	1.366		1.446		
				1.44	1.43
5—10	1.226	27°	1.378		
5′—10′	1.396		1.569		
1—9	1.289		1.448		
1′—9′	1.242		1.396		
2—3	1.344	23°	1.461		
2′—3′	1.283		1.394	1.41	1.42
6—7	1.215		1.321		
6′—7′	1.355		1.473		
9—10	1.333	23°	1.449	1.43	1.41
9′—10′	1.294		1.406		
Br_1—1	1.859	12°	1.898		
Br_3—1′	1.881		1.921	1.91	—
Br_2—4	1.884		1.924		
Br_4—4′	1.858		1.897		

projected distances the following assumptions were made:

(i) that the C—Br distances are equal to the normal single bond length (1.91 Å),

(ii) that the naphthalene skeletons are planar and have symmetry *mmm*,

(iii) that the average bond length for each of the three groups of parallel C—C bonds is equal to the corresponding average length in naphthalene (4, 5).

Can. J. Chem. Downloaded from www.nrcresearchpress.com by 210.87.254.5 on 09/05/12
For personal use only.

The inclinations of the various bonds from the plane of projection, derived from these assumptions, are listed in the second column of Table II, and the true bond distances in the third column. Although there are some large deviations from *mmm* symmetry, these cannot be considered as significant, and the mean bond lengths are given in the fourth column of the table.

Although it has been assumed, in deriving the true bond distances, that the average distances in the various directions are equal to the corresponding average distances in naphthalene, this does not imply that the individual distances must be equal, and so it is permissible to compare the mean bond lengths in 1,4-dibromonaphthalene with the distances in naphthalene. This comparison is included in Table II; the agreement is extremely good, suggesting, as we might expect, that the mean distances are more accurate than the individual values, and also that the assumptions made are plausible.

Comparison of the inclination angles for the C—Br bonds (12°) and for bonds such as 9—10 (23°) indicates that the bromine atoms are displaced from the naphthalene plane, the two bromine atoms in the molecule being displaced in opposite directions from the aromatic plane by about 0.4 Å. If it had been assumed that the bromine atoms were situated on the naphthalene plane, the true C—Br distances would have been 2.03 Å, considerably longer than the normal single bond length, so that the bromine atom displacements are probably real. The deviations are possibly the result of small steric interactions with the *peri* hydrogen atoms.

Projected distances indicate that all the intermolecular contacts correspond to normal van der Waal's interactions.

The author thanks the National Research Council for grants-in-aid for this work.

REFERENCES

1. J. TROTTER. Acta Cryst. **13**, 276 (1960).
2. INTERNATIONALE TABELLEN ZUR BESTIMMUNG VON KRISTALLSTRUKTUREN. Vol. 2. Borntraeger, Berlin. 1935.
3. J. BERGHUIS, IJ. M. HAANAPPEL, M. POTTERS, B. O. LOOPSTRA, C. H. MACGILLAVRY, and A. L. VEENENDAAL. Acta Cryst. **8**, 478 (1955).
4. S. C. ABRAHAMS, J. M. ROBERTSON, and J. G. WHITE. Acta Cryst. **2**, 238 (1949).
5. D. W. J. CRUICKSHANK. Acta Cryst. **10**, 504 (1957).

Can. J. Chem. Downloaded from www.nrcresearchpress.com by 210.87.254.5 on 09/05/12
For personal use only.

Can. J. Chem. Downloaded from www.nrcresearchpress.com by 210.87.254.40 on 09/05/12
For personal use only.

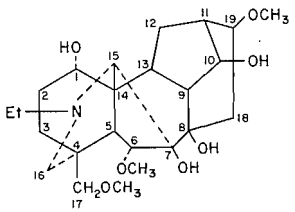
THE EPIMERIZATION OF DELCOSINE[1]

VINKO SKARIĆ[2] AND LÉO MARION

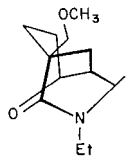
ABSTRACT

Delcosine has been assigned tentatively the same C—N skeleton as lycoctonine. In lycoctonine, ring A carries at C-1 a methoxyl group which is directed away from the nitrogen ring. In delcosine, C-1 carries a hydroxyl group which has the opposite configuration and is directed towards the nitrogen. An attempt to correlate the two structures first involves epimerization at C-1 in delcosine. This has been carried out by oxidation of desethyldelcosine to an azomethine, the ethiodide of which, by the action of methanolic potassium hydroxide, is converted to oxo-1-epidelcosine in two steps. Oxo-1-epidelcosine in an acid-catalyzed rearrangement is transformed to a pinacone which, after methylation, gives O,O-dimethyl-anhydro-oxo-1-epidelcosine. This compound was compared with O-methyl-anhydro-oxolycoctonine, prepared from oxolycoctonine, but was not identical. Removal of a methoxyl, which in each compound is ortho to a carbonyl, by the action of sodium amalgam, produced O,O-dimethyl-6-desmethoxy-anhydro-oxo-1-epidelcosine and O-methyl-6-desmethoxy-anhydro-oxolycoctonine, which are not identical, but show in their infrared spectra much less dissimilarity than the spectra of the pair of compounds from which they were derived. These results are discussed in terms of the structure of delcosine.

As a working hypothesis, the alkaloid delcosine ($C_{24}H_{39}O_7N$) has been assumed to possess the same C—N skeleton as lycoctonine ($C_{25}H_{41}O_7N$). All the chemical reactions of delcosine studied so far are in agreement with such an assignment. In order to prove or disprove that delcosine has the previously assigned (1, 2, 3) structure I, it has been



I



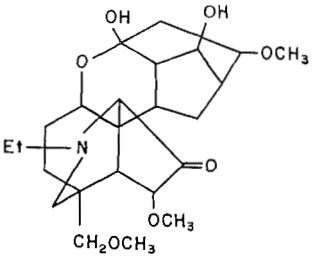
II

attempted in the work now reported to correlate it with lycoctonine. Although we have failed in our main objective, the results obtained firmly establish the position of all but two of the substituents on the C—N skeleton.

It has been shown earlier (2, 3) that delcosine contains a secondary hydroxyl substituted on the six-membered ring A. Oxidation of delcosine with either silver oxide or N-bromosuccinimide gives rise to a carbinolamine ether, anhydrohydroxydelcosine II (1, 3), the formation of which involves this secondary hydroxyl, which was assumed to occupy position C-1 by analogy with lycoctonine. This conclusion is also supported by the results of the oxidation of oxodelcosine with lead tetraacetate (3). Although the product of this reaction should contain a five-membered and a six-membered cyclic ketone, actually it is a ketohemiketal III in which cyclization has occurred between the secondary hydroxyl of ring A and the carbonyl of the six-membered cyclic ketone (3, 4). Position C-1 for the secondary hydroxyl of ring A is the only one that allows the formation

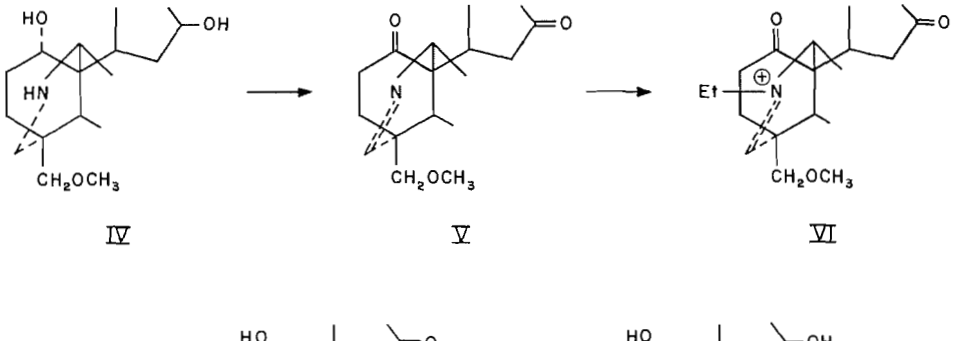
[1]*Manuscript received April 7, 1961.*
Contribution from the Division of Pure Chemistry, National Research Council, Ottawa, Canada.
Issued as N.R.C. No. 6358.
[2]*National Research Council of Canada Postdoctorate Fellow, 1957–1959.*

of a six-membered cyclic hemiketal and appears to be the only one where the formation of a ring is geometrically possible. To account for the formation of the carbinolamine ether it is further necessary that the C-1 hydroxyl be directed on the same side of ring A as the nitrogen ring (3). This configuration is different from that of the methoxyl at C-1 in lycoctonine (5).

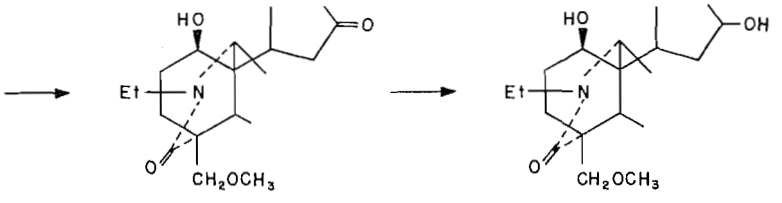


III

Hence, any attempt to correlate delcosine with lycoctonine would initially involve epimerization at C-1. Sparatore, Greenhalgh, and Marion (6) have attempted this epimerization in delsoline, which is a monomethyldelcosine (2), but their reported result is in error, and the compound that they have described is not epidelsoline but Δ′-anhydrodelsoline ($C_{25}H_{39}O_6N$). Dvornik and Edwards (7) reported the epimerization of a hydroxyl in ajaconine, and Dr. Dvornik suggested to us an adaptation of the method by which it has now proved possible to prepare epidelcosine from N-desethyldelcosine, a previously described oxidation product of the base (1). N-Desethyldelcosine (IV) was oxidized by Sarett's reagent to a mixture of N-desethyl-1,10-didehydrodelcosine-azomethine (V) and the neutral N-desethyl-1,10-didehydro-oxodelcosine. The former was converted to the ethiodide (VI), which on being refluxed with 10% methanolic potassium hydroxide, yielded 10-dehydro-oxo-1-epidelcosine (VII). Reduction of VII with sodium boro-



IV V VI

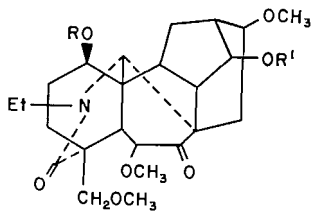


VII VIII

Can. J. Chem. Downloaded from www.nrcresearchpress.com by 210.87.254.40 on 09/05/12
For personal use only.

hydride gave oxo-1-epidelcosine (VIII), m.p. 128–130°, $[\alpha]_D^{25}$ +19.8°, and this on treatment with lithium aluminum hydride produced 1-epidelcosine, m.p. 177–178°, $[\alpha]_D^{26}$ +38.9°, which formed a perchlorate, m.p. 199–201°.

For the purpose of correlating epidelcosine with lycoctonine it was necessary to methylate the primary hydroxyl group in the latter. Although this could be achieved, the yield was poor and it was more usual to obtain a dimethylated product in which one of the two vicinal tertiary hydroxyls had reacted. This complication made it necessary to use derivatives of the two alkaloids in which the tertiary hydroxyls were no longer present. Such derivatives are accessible via the pinacolic rearrangement which these alkaloids undergo readily (8, 9). Oxo-1-epidelcosine was, therefore, heated with acetic acid containing sulphuric acid according to the method described earlier (8, 9), and thus converted to the pinacone, anhydro-oxo-1-epidelcosine (IX, R = R′ = H), which was methylated to O,O-dimethyl-anhydro-oxo-1-epidelcosine (IX, R = R′ = CH_3), $C_{26}H_{39}O_7N$, m.p. 178–180°, $[\alpha]_D^{22}$ −56.3°, showing in the ultraviolet a maximum at 303 and a minimum at 263 mμ. In the infrared it showed no absorption in the hydroxyl region, but produced a band at 1727 cm^{-1} due to a six-membered cyclic ketone and a band at 1648 cm^{-1} attributable to the lactam carbonyl.



IX

By acid-catalyzed pinacolic rearrangement, oxolycoctonine (previously designated lycoctonam) was converted to anhydro-oxolycoctonine (9), which was methylated to O-methyl-anhydro-oxolycoctonine, $C_{26}H_{39}O_7N$, m.p. 126–128°, $[\alpha]_D^{25}$ +9.2°. In the ultraviolet it showed a maximum at 302 and a minimum at 267 mμ while in the infrared the spectrum contained bands at 1725 and 1642 cm^{-1}. The melting point and optical rotation of this compound are quite different from those of IX (R = R′ = CH_3), and, also, both compounds contain the same functional groups as shown by both the ultraviolet and infrared spectra; the fingerprint region of their I.R. spectra showed marked differences.

It has been shown by X-ray crystallography that the methoxyl at C-6 in lycoctonine is equatorial whereas in aconitine the methoxyl in the same position is axial (5). The non-identity of the two pinacones (IX (R = R′ = CH_3) and O-methyl-anhydro-oxolycoctonine) could be due to a similar difference between lycoctonine and delcosine. Since in the two pinacones the methoxyl at C-6 is vicinal, or α, to the carbonyl, it is removable by the action of sodium amalgam (10, 11). Both O,O-dimethyl-anhydro-oxoepidelcosine and O-methyl-anhydro-oxolycoctonine were, therefore, dissolved in absolute ethanol and demethoxylated at C-6 by treatment with sodium amalgam. O,O-Dimethyl-6-desmethoxy-anhydro-oxoepidelcosine thus produced, m.p. 152.5–154°, $[\alpha]_D^{25}$ −35.2°, showed a maximum at 282 mμ and a minimum at 262 mμ in the ultraviolet. Its infrared spectrum contained an absorption band at 1715 cm^{-1} due to the six-membered cyclic ketone and one at 1645 cm^{-1} due to the lactam carbonyl. The O-methyl-6-desmethoxy-anhydro-oxolycoctonine, m.p. 161–163°, $[\alpha]_D^{26}$ +3.4°, showed in the ultraviolet a maximum

Can. J. Chem. Downloaded from www.nrcresearchpress.com by 210.87.254.40 on 09/05/12
For personal use only.

at 282 mμ and a minimum at 262 mμ; and in the infrared, a band at 1716 cm^{-1} and one at 1638 cm^{-1}. The two desmethoxy compounds are not identical, but the fingerprint region of their infrared spectra are much more closely alike than the spectra of the preceding pair of compounds in the same region, which may indicate that the C-6 methoxyl in delcosine is axial.

The demethoxylating action of sodium amalgam establishes the location of the methoxyl at C-6. The presence of the two tertiary hydroxyls at C_7 and C_8 is firmly established by the formation of secodiketones from anhydrohydroxydelcosine (5), from oxodelcosine (3), and from the related oxodelsoline (6). The presence of a methoxyl at C-19 is indicated by the elimination of methanol and the formation of $\alpha\beta$-unsaturated ketones from the secodiketones derived from anhydrohydroxydelcosine (5) and oxodelsoline (6). It has not been established, however, whether the stereochemistry at C-19 is the same as in lycoctonine. None of the many oxidation reactions of delcosine that have been studied has yielded an acid product, thus indicating the absence of a primary alcoholic group. Since, however, according to the N.M.R. spectrum, no methyl group attached to carbon is present besides that of the N-ethyl group, it becomes highly probable that the third methoxyl in the molecule is present in a methoxy-methyl group at C-17. Delcosine contains a secondary hydroxyl attached to a five-membered ring (1, 3). This hydroxyl has been located at C-10 by analogy with lycoctonine, which contains a methoxyl at that position, but besides the fact that it must be a substituent on ring D, there is no proof of its exact location. It could be at C-10 and have a configuration different from that of the C-10 methoxyl in lycoctonine, or it could be at C-12. Although the derivatives of delcosine and lycoctonine that have been compared did not prove to be identical, it still remains that the chemical reactions of delcosine and its transformations all point to the alkaloid possessing the same carbon–nitrogen skeleton as lycoctonine. It is hoped, with work presently underway, to locate the position of the secondary hydroxyl on ring D, and to complete the correlation of delcosine with lycoctonine.

EXPERIMENTAL

Ultraviolet spectra were determined in 95% ethanol and recorded with a Beckman DU instrument. The infrared absorption spectra were recorded with a Perkin–Elmer double-beam model 21 spectrophotometer, and unless it is otherwise mentioned, the samples were suspended in nujol. Melting points were determined on a Kofler hot stage and were uncorrected. Optical rotations were determined in a dm microbore tube and, unless otherwise stated, in chloroform solution. The neutral alumina used for chromatography was standardized according to Brockmann, and the eluants were collected in fractions of 20 ml.

Δ′-Anhydrodelsoline

To a solution of delsoline (220 mg) in dried, chilled pyridine (5.5 ml), *p*-toluenesulphonyl chloride (440 mg) dissolved in pyridine (5.5 ml) was added, and the mixture allowed to stand at room temperature for 54 hours. It was then concentrated under reduced pressure at room temperature to a syrup which was dissolved in chloroform and extracted with 4% aqueous sodium carbonate. The chloroform solution was dried and evaporated to dryness. The residue was triturated in ether, and the ether-soluble fraction (176 mg) was crystallized from hexane, yield 84 mg, m.p. 135–140°. It was dissolved in benzene and chromatographed on alumina (activity II to III, 1.4 g). Elution with chloroform gave a product which, after crystallization from hexane, melted at 139–141°. For analysis

Can. J. Chem. Downloaded from www.nrcresearchpress.com by 210.87.254.40 on 09/05/12
For personal use only.

this sample was sublimed at 145° at 5×10^{-4} mm. $[\alpha]_D^{24}$ +27.7±0.7° (*c*, 1.37). Found: C, 66.62; H, 8.81. Calc. for $C_{25}H_{39}O_6N$: C, 66.79; H, 8.75%. Ultraviolet: end absorption. IR: 3470 and 3390 cm^{-1} (hydroxyl).

Hydrogenation of 1-Dehydro-oxodelcosine

1-Dehydro-oxodelcosine (35 mg obtained by oxidation of monoacetyldelcosine, followed by hydrolysis (3)) in glacial acetic acid (5 ml) was hydrogenated over Adams' catalyst (17 mg) for 1 hour at 3.9 atm. The catalyst was filtered off and the filtrate evaporated to dryness; the residue was dissolved in chloroform and the solution extracted with 4% aqueous sodium carbonate; the chloroform layer was evaporated to dryness and the residue (35 mg) was crystallized from ether from which it separated as colorless prisms, 31 mg, m.p. 241–243.5° undepressed on admixture with authentic oxodelcosine. $[\alpha]_D^{24}$ +42.2±1.1° (*c*, 0.9). The infrared spectrum of the product and that of oxodelcosine were superimposable.

Oxidation of N-Desethyldelcosine

(a) N-Desethyl-didehydrodelcosine-azomethine (V).—To freshly distilled pyridine (10 ml) cooled to 0°, chromic anhydride (1.0 g) was added portionwise with stirring. To the precipitated yellow complex a solution of N-desethyldelcosine (1) (500 mg) in pyridine (18 ml) was added and the mixture allowed to stand at room temperature for 12 hours in a stoppered flask. Subsequently sulphur dioxide was bubbled into the reaction mixture and the solvent evaporated under diminished pressure. Ice and 3 *N* sulphuric acid were added to the residue, and the resulting green solution was extracted with chloroform. The chloroform extract containing the neutral component was set aside. The aqueous acid layer was neutralized by the gradual addition of powdered sodium carbonate and made alkaline by the further addition of 10% aqueous sodium hydroxide. It was then extracted with chloroform, the extract washed with water, dried, and evaporated to dryness. The residue (270 mg) was redissolved in dry, pure, chloroform, chromatographed on alumina grade III (6.0 g), and eluted with chloroform. The eluate, on evaporation, yielded 248 mg of the azomethine which was crystallized twice from acetone–ether from which it separated as rhombohedral prisms, m.p. 219–220°, $[\alpha]_D^{25}$ +257.5±1.3° (*c*, 0.8). Found: C, 63.15; H, 6.81. Calc. for $C_{22}H_{29}O_7N$: C, 62.99; H, 6.97%. Ultraviolet: λ_{max} 269 mμ, log ε 2.105; λ_{max} 290 mμ, log ε 2.123; λ_{min} 281 mμ, log ε 2.098. Infrared: 3420 cm^{-1} (hydroxyl), 1745 cm^{-1} (five-membered cyclic ketone), 1702 cm^{-1} (six-membered cyclic ketone), 1633 cm^{-1} (—CH=N—); in chloroform: 3520, 3470, 1753, 1715, 1635 cm^{-1}.

(b) N-Desethyl-1,10-didehydro-oxodelcosine.—The chloroform solution containing the neutral fraction of the product (mentioned above) was washed with 4% aqueous sodium carbonate, dried, and evaporated to dryness. The residue (114 mg) was triturated with ether and the material recrystallized from acetone–hexane from which it separated as colorless prisms, m.p. 274–275.5°, $[\alpha]_D^{28}$ +139±0.9° (*c*, 1.12). Found: C, 60.63; H, 6.53. Calc. for $C_{22}H_{29}O_8N$: C, 60.68; H, 6.71%. Ultraviolet: λ_{max} 300 mμ, log ε 2.039; λ_{min} 262 mμ, log ε 1.312. Infrared: 3430 cm^{-1} (hydroxyl), 3350 cm^{-1} (imine), 1740 cm^{-1} (five-membered cyclic ketone), 1703 cm^{-1} (six-membered cyclic ketone), 1665 cm^{-1} (lactamic carbonyl); in chloroform: 3460, 3380 cm^{-1} (hydroxyl), 3280 cm^{-1} (imino group).

Ethiodide of N-Desethyl-1,10-didehydrodelcosine-azomethine (VI)

Desethyldidehydrodelcosine-azomethine (290 mg) was dissolved in acetone (30 ml), and ethyl iodide (6 ml) was added to the solution. The mixture was left at room temperature for 24 hours in the dark, after which it was evaporated to dryness under

Can. J. Chem. Downloaded from www.nrcresearchpress.com by 210.87.254.40 on 09/05/12
For personal use only.

reduced pressure. The crystalline residue (414 mg) was recrystallized repeatedly from acetone–hexane from which it separated as pale-yellow microcrystals, m.p. 168–171°, $[\alpha]_D^{28}$ +132.4±1.0° (*c*, 1.02 in methanol). Found: C, 50.27; H, 6.13. Calc. for $C_{24}H_{34}O_7NI$: C, 50.09; H, 5.96%. Ultraviolet: shoulders at λ_{max} 258 mμ, log ε 2.918 and λ_{max} 350 mμ, log ε 1.851; λ_{max} 300 mμ, log ε 2.498; λ_{min} 292 mμ, log ε 2.484. Infrared: 3440, 3220 cm^{-1} (hydroxyls), 1755 cm^{-1} (five-membered cyclic ketone), 1713 cm^{-1} (six-membered cyclic carbonyl), 1652 cm^{-1} (—C=N$^+$).

10-Dehydro-oxo-1-epidelcosine (VII)

The ethiodide of desethyldidehydrodelcosine-azomethine (85 mg) was dissolved in 10% methanolic potassium hydroxide (5 ml), and the mixture was refluxed for 90 minutes and evaporated to dryness under reduced pressure. The residue was dissolved in water, and the solution extracted with chloroform. The chloroform extract was washed first with 3 *N* sulphuric acid, then with water, dried, and evaporated to dryness. The residue (62 mg), which failed to crystallize, was dissolved in chloroform, chromatographed on alumina (activity III), and eluted with chloroform. The product obtained from the eluate could not be induced to crystallize, $[\alpha]_D^{27}$ +10.4±0.8° (*c*, 1.25). Ultraviolet: λ_{max} 295 mμ, log ε 1.456; λ_{min} 265 mμ, log ε 0.736. Infrared in chloroform: 3575, 3500, 3420 cm^{-1} (hydroxyls), 1750 cm^{-1} (five-membered cyclic ketone), 1640 cm^{-1} (lactamic carbonyl).

Oxo-1-epidelcosine (VIII)

(a) Sodium borohydride (300 mg) was added to a solution of 10-dehydro-oxo-1-epidelcosine (230 mg) in 80% methanol (20 ml), and the mixture allowed to stand at room temperature for 2 hours and then evaporated to dryness. The residue was dissolved in water and the solution extracted with chloroform. The chloroform extract was washed with 3 *N* sulphuric acid, with water, dried, and evaporated to dryness. There was left a residue (208 mg) which crystallized from ether, wt. 161 mg, m.p. 124–126°. The crystalline product was dissolved in benzene, chromatographed on alumina (5.0 g, activity III), and eluted with chloroform. From the eluate there was obtained a fraction, m.p. 126–130°, which was recrystallized from acetone–hexane. The colorless hexagonal prisms thus obtained, after being dried at 100° at 5×10^{-4} mm, melted at 128–130°, $[\alpha]_D^{25}$ +19.8±0.9° (*c*, 1.16). Found: C, 61.39; H, 8.14. Calc. for $C_{24}H_{37}O_8N$: C, 61.65; H, 7.98%. Infrared in chloroform: 3640, 3570, 3490 cm^{-1} (hydroxyls), 1638, 1628 cm^{-1} (double peak due to lactam carbonyl).

(b) The above product was also obtained as follows. 10-Dehydro-oxo-1-epidelcosine (65 mg), dissolved in glacial acetic acid (6.5 ml), was shaken under hydrogen with Adams' catalyst (50 mg) at 3.9 atm for 1 hour. The catalyst was filtered off and the filtrate evaporated to a syrup which was dissolved in chloroform and washed with 4% aqueous sodium carbonate. The dried chloroform solution was evaporated to dryness and the residue (60 mg) crystallized from acetone–ether–hexane, m.p. 126–128°, undepressed by admixture with the sample of oxo-1-epidelcosine obtained above. The infrared spectra of both samples were superimposable.

Didehydro-oxodelcosine from Oxo-1-epidelcosine

To a solution of oxo-1-epidelcosine (69 mg) in glacial acetic acid (5 ml), a solution of sodium dichromate (35 mg) in glacial acetic acid (5 ml) was added dropwise, and the reaction mixture set aside for 1 hour at room temperature. Sulphur dioxide was bubbled in to reduce the excess reagent and the solvent removed under reduced pressure. The

Can. J. Chem. Downloaded from www.nrcresearchpress.com by 210.87.254.40 on 09/05/12
For personal use only.

residue was dissolved in chloroform and the solution washed first with 3 *N* sulphuric acid, then with 4% aqueous sodium carbonate, dried, and evaporated under reduced pressure. It left a residue (63 mg) which crystallized from ether. Recrystallization from acetone–ether–hexane yielded 44 mg, m.p. 208–209° undepressed by mixture with an authentic sample of didehydro-oxodelcosine, $[\alpha]_D^{25}$ +128.0±1.0° (*c*, 1.0). The infrared spectra of both samples were superimposable.

Epi-1-delcosine

To a solution of oxo-1-epidelcosine (50 mg) in pure dioxane (5 ml), powdered lithium aluminum hydride (60 mg) was added in small portions under a nitrogen atmosphere. The suspension was refluxed and stirred for 1 hour. The excess of reagent was decomposed with methanol, water was added, the precipitated aluminum hydroxide was filtered with suction and washed with acetone and with methanol. The combined filtrate and washings was evaporated to dryness under reduced pressure and the residue dissolved in chloroform. The chloroform solution was washed with several portions of 3 *N* sulphuric acid, the acid solution made basic with sodium hydroxide and extracted with chloroform. This last chloroform solution when evaporated to dryness left a residue (40 mg) which crystallized from water (2 drops). The product was recrystallized twice from benzene–hexane, from which it separated as colorless prisms, m.p. 177–178°, $[\alpha]_D^{26}$ +38.9±1.0° (*c*, 0.95). Found: C, 63.69; H, 8.66. Calc. for $C_{24}H_{39}O_7N$: C, 63.55; H, 8.67%. Infrared: 3590, 3504, 3410, 3364 cm^{-1} (hydroxyls).

1-Epidelcosine (30 mg) dissolved in methanol (2 ml) was made just acid to Congo red by the dropwise addition of perchloric acid. The solution was evaporated to dryness under reduced pressure and the crystalline residue recrystallized from methanol–ether from which it separated as colorless hexagonal prisms, m.p. 197–200°. After several recrystallizations the salt melted at 199–201° when immersed in a bath at 193°, $[\alpha]_D^{28}$ +26.8±1.8° (*c*, 0.56 in methanol). Found: C, 52.15; H, 7.40. Calc. for $C_{24}H_{39}O_7N.HClO_4$: C, 52.03; H, 7.27%.

Anhydro-oxo-1-epidelcosine (IX, R = R′ = H)

Oxo-1-epidelcosine (150 mg) in glacial acetic acid (5 ml, containing 0.1% by volume of sulphuric acid) was heated at 75–80° for 70 minutes. The warm solution was poured onto crushed ice, neutralized with ice-cold 20% aqueous potassium hydroxide, and extracted with chloroform. The chloroform layer was evaporated to dryness and the residue refluxed for 1 hour with 10% methanolic potassium hydroxide (10 ml) and water (1.0 ml). The solution was evaporated to dryness, and the residue dissolved in water and extracted with chloroform. The extract was washed with 3 *N* sulphuric acid, with water, dried, and evaporated to dryness under reduced pressure. The residue (144 mg) was dissolved in benzene containing 15% of chloroform and chromatographed on alumina, activity III (2.7 g). Chloroform was used to elute the column, and the eluate yielded the pinacone which crystallized from ether, m.p. 225–229°. Recrystallization from acetone–ether–hexane raised the melting point to 227–231°, wt. 86 mg. For analysis the product was recrystallized once more and obtained as colorless long needles, m.p. 230–232°, $[\alpha]_D^{23}$ −23.8±2° (*c*, 0.55). Found: C, 64.13; H, 7.80; OMe, 20.53. Calc. for $C_{24}H_{35}O_7N$: C, 64.12; H, 7.85; 3OMe, 20.71%. Ultraviolet: λ_{max} 302 mμ, log ε 1.810; λ_{min} 265 mμ, log ε 0.993. Infrared: 3360 cm^{-1} (hydroxyl), 1725 cm^{-1} (six-membered cyclic ketone), 1625 cm^{-1} (lactam carbonyl); in chloroform: 3578, 3440 cm^{-1} (hydroxyls), 1727 and 1642 cm^{-1} (carbonyls).

Can. J. Chem. Downloaded from www.nrcresearchpress.com by 210.87.254.40 on 09/05/12
For personal use only.

O,O-Dimethyl-anhydro-oxo-1-epidelcosine (IX, R = R′ = CH_3)

The pinacone described above (93 mg) was dissolved in dioxane (9 ml) and a slight excess of sodium hydride was added to the solution, which was brought to a boil and, after the addition of excess methyl iodide, was refluxed, with stirring, in a hydrogen atmosphere for 10 hours. The reaction product was filtered through a Hyflo-Supercel column, the filtrate evaporated to dryness, and the residue dissolved in water and extracted with chloroform. The chloroform solution was washed with 3 *N* sulphuric acid, with water, dried, and evaporated to dryness. The residue (quantitative yield) was dissolved in benzene containing 20% hexane and chromatographed on alumina (2.9 g, activity III). Elution of the column was done first with benzene and then with a benzene–chloroform (3:1) mixture. Both eluates yielded the same product, which crystallized from ether, m.p. 177–180°, wt. 71.5 mg. A sample for analysis was recrystallized from ether, m.p. 178–180°, $[\alpha]_D^{22}$ −56.3±1.3° (*c*, 0.80), and sublimed at 145° at 5×10^{-4} mm. Found: C, 65.64; H, 8.40; OMe, 32.41. Calc. for $C_{26}H_{39}O_7N$: C, 65.39; H, 8.23; 5OMe, 32.49%. Ultraviolet: λ_{max} 303 mμ, log ε 1.897; λ_{min} 263 mμ, log ε 1.423. Infrared: 1727 cm^{-1} (six-membered cyclic ketone), 1648 cm^{-1} (lactam carbonyl).

O,O-Dimethyl-6-desmethoxy-anhydro-oxo-1-epidelcosine

Sodium amalgam (5%, 680 mg) was added to a solution of the methylated pinacone, O,O-Dimethyl-anhydro-oxo-1-epidelcosine (74 mg), in absolute ethanol (1.6 ml). The mixture was shaken for 90 minutes, filtered through a Hyflo-Supercel column, and the filtrate diluted with water and extracted with chloroform. Evaporation of the chloroform extract left a residue (67 mg) which was dissolved in benzene–hexane (1:1) and chromatographed on alumina (2.4 g, activity III). From benzene and benzene containing 30% chloroform eluates, there was isolated a middle fraction (36 mg) which crystallized from ether, m.p. 149–154°. Recrystallized from ether–pentane, the product consisted of colorless prisms, m.p. 152.5–154°, $[\alpha]_D^{25}$ −35.2±1.8° (*c*, 0.54). Found: C, 67.26; H, 8.29. Calc. for $C_{25}H_{37}O_6N$: C, 67.09; H, 8.33%. Ultraviolet: λ_{max} 282 mμ, log ε 1.744; λ_{min} 261 mμ, log ε 1.533. Infrared: 1715 cm^{-1} (six-membered cyclic ketone), 1645 cm^{-1} (lactam carbonyl).

O-Methyl-anhydro-oxolycoctonine

Anhydro-oxolycoctonine was prepared from acetyl-oxolycoctonine by acid-catalyzed rearrangement followed by hydrolysis as described above for the corresponding oxoepidelcosine derivative. The pinacone (155 mg) was dissolved in dioxane (9 ml) and excess sodium hydride was added to the solution which was brought to a boil and, after the addition of excess methyl iodide, was refluxed, with stirring, for 7 hours under a hydrogen atmosphere. The reaction mixture was filtered through a Hyflo-Supercel column and the product worked up exactly as described above for the corresponding delcosine derivative. The crude product was dissolved in benzene–hexane (4:1), chromatographed on alumina (4 g, activity III), and eluted (*a*) with benzene, (*b*) with benzene–chloroform (4:1), and (*c*) with benzene–chloroform (1:1). The first two eluates (*a* and *b*) together yielded a fraction (104 mg) which crystallized from ether and after recrystallization from the same solvent consisted of colorless needles, m.p. 126–128°, $[\alpha]_D^{25}$ +9.2±0.8° (*c*, 1.2). Found: C, 65.57; H, 8.09; OMe, 32.40. Calc. for $C_{26}H_{39}O_7N$: C, 63.59; H, 8.23; 5OMe, 32.49%. Ultraviolet: λ_{max} 302 mμ, log ε 1.856; λ_{min} 267 mμ, log ε 1.471. Infrared: 1725 cm^{-1} (six-membered cyclic ketone), 1642 cm^{-1} (lactam carbonyl).

The third eluate (*c*) from the chromatogram yielded a by-product (20 mg) which crystallized from ether, m.p. 185–201°, $[\alpha]_D^{26}$ +85.9±1.6° (*c*, 0.63). Infrared: 1728 cm^{-1} (six-membered cyclic ketone), 1650 cm^{-1} and 1643 cm^{-1} (lactam carbonyl).

Can. J. Chem. Downloaded from www.nrcresearchpress.com by 210.87.254.40 on 09/05/12
For personal use only.

O-Methyl-6-desmethoxy-anhydro-oxolycoctonine

Sodium amalgam (5%, 610 mg) was added to a solution of the above methylated oxolycoctonine pinacone (67 mg) in absolute ethanol (1.8 ml) and the mixture shaken for 2 hours. It was afterwards filtered through a Hyflo-Supercel column and the filtrate diluted with water and extracted with chloroform. The extract was evaporated and the residue (quantitative yield) crystallized from ether, wt. 52 mg, m.p. 159–163°. After recrystallization from ether it consisted of colorless needles, m.p. 161–163°, $[\alpha]_D^{26}$ $+3.4\pm1.1°$ (*c*, 0.89). Found: C, 67.26; H, 8.30; OMe, 27.60. Calc. for $C_{25}H_{37}O_6N$: C, 67.09; H, 8.33; 4OMe, 27.73%. Ultraviolet: λ_{max} 282 mμ, log ϵ 1.643; λ_{min} 262 mμ, log ϵ 1.410. Infrared: 1716 cm^{-1} (six-membered cyclic ketone), 1638 cm^{-1} (lactam carbonyl).

ACKNOWLEDGMENTS

The authors wish to express their indebtedness to Dr. R. Norman Jones and Mr. R. Lauzon of these laboratories for the determination of the infrared absorption spectra and to Mr. H. Seguin for the microanalyses.

REFERENCES

1. R. ANET, D. W. CLAYTON, and L. MARION. Can. J. Chem. **35**, 397 (1957).
2. V. SKARIĆ and L. MARION. J. Am. Chem. Soc. **80**, 4434 (1958).
3. V. SKARIĆ and L. MARION. Can. J. Chem. **38**, 2433 (1960).
4. R. ANET and L. MARION. Can. J. Chem. **36**, 766 (1958).
5. M. PRZYBYLSKA and L. MARION. Can. J. Chem. **37**, 1843 (1959).
6. F. SPARATORE, R. GREENHALGH, and L. MARION. Tetrahedron, **4**, 157 (1958).
7. D. DVORNIK and O. E. EDWARDS. Proc. Chem. Soc. 280 (1958).
8. R. C. COOKSON and M. E. TREVETT. Chem. & Ind. (London), 1324 (1954); J. Chem. Soc. 3864 (1956).
9. O. E. EDWARDS, L. MARION, and D. K. R. STEWART. Can. J. Chem. **34**, 1315 (1956).
10. H. KONDO and E. OCHIAI. Ann. **470**, 224 (1929).
11. O. E. EDWARDS, L. MARION, and K. H. PALMER. Can. J. Chem. **36**, 1097 (1958).

Can. J. Chem. Downloaded from www.nrcresearchpress.com by 210.87.254.40 on 09/05/12
For personal use only.

Can. J. Chem. Downloaded from www.nrcresearchpress.com by 210.87.254.6 on 09/05/12
For personal use only.

THE KINETICS OF REACTION OF 2,2-DIPHENYL-1-PICRYLHYDRAZYL WITH PHENOLS[1]

J. S. Hogg, D. H. Lohmann, and K. E. Russell

ABSTRACT

The kinetics of reaction between 2,2-diphenyl-1-picrylhydrazyl (DPPH) and a wide variety of phenols have been studied. The rate of disappearance of DPPH is of first order with respect to both the DPPH and the reacting phenol. The rates of reaction can be roughly correlated with the Hammett σ value of the phenol substituent in the range $-0.4 < \sigma < 0.2$, a ρ value of -6 being obtained. *t*-Butyl groups in both ortho positions of the phenol give rise to steric hindrance, the reduction in rate being largely due to a reduction in the A factor. Hydrogen abstraction from the less reactive phenols is strongly retarded by the product, 2,2-diphenyl-1-picrylhydrazine.

The rate-determining step probably involves the abstraction of a hydrogen atom from the phenol by the DPPH to give diphenylpicrylhydrazine and a phenoxy radical. The retardation by diphenylpicrylhydrazine is readily explained if this primary step is reversible.

Hydrogen-abstraction reactions involving 2,2-diphenyl-1-picrylhydrazyl (DPPH) as the acceptor molecule are relatively easily studied and a number of recent publications have been concerned with the rates of reaction of this radical with hydrogen donors. Information has been obtained concerning the reactivities of restricted ranges of donors containing C—H (1), N—H (2, 3), O—H (4, 5, 6), and S—H (7, 8) bonds. Phenols are well suited to an investigation of hydrogen abstraction from O—H-containing compounds (3). A wide range of phenols is available and a detailed study of the effect of substituents is possible.

During the course of the work, a paper by McGowan, Powell, and Raw was published (4) giving rate constants for the second-order reactions of DPPH with a large number of phenols, showing that substituents may exert considerable polar and steric influences on the reaction. Their measurements were normally made at room temperature using carbon tetrachloride as solvent, but with three phenols, measurements were made over a temperature range. In the work described here benzene was used as solvent, activation energies and A factors were obtained for all the phenols studied, and the effect of the product 2,2-diphenyl-1-picrylhydrazine on the rate of reaction was determined. Some additional evidence was obtained that the primary reaction involves the hydrogen atom of the O—H group, and the stoichiometry of the process was investigated.

EXPERIMENTAL

Materials

2,2-Diphenyl-1-picrylhydrazine was prepared by the reaction of picryl chloride and 1,1-diphenylhydrazine (9, 10). DPPH was prepared by the oxidation of diphenylpicrylhydrazine with lead dioxide (9). Complexed solvent was removed by heating *in vacuo* at 60° for several hours.

2-Methylanisole and 1- and 2-methoxynaphthalene (Eastman Kodak) were used without further purification.

Phenols were obtained from the Aldrich Chemical Company or from the Eastman Kodak Company. The liquids were distilled and the solids were either sublimed at reduced pressure or recrystallized; 2,6-di-*t*-butylphenol was used without further purification.

[1]*Manuscript received February 16, 1961.*
Contribution from the Department of Chemistry, Queen's University, Kingston, Ontario.

Procedure

The experimental method has been described elsewhere (3). The rates of disappearance of DPPH were normally followed in the presence of air. With phenol, experiments were performed at various concentrations using degassed solutions and a comparison of rates was made at corresponding extents of reaction. Initial DPPH concentrations were in the range $4–20\times10^{-5}$ *M*. Phenol concentration ranges were chosen to give convenient rates of reaction; a minimum value of 2×10^{-5} *M* was used with the very reactive 2,4-dichloro-1-naphthol and a maximum value of 2×10^{-2} *M* with 4-acetylphenol. Measurements were normally performed at 30° C and activation energies were derived from measurements taken over a temperature range of at least 20 degrees.

The stoichiometry of the reaction was investigated by making up solutions containing ratios of DPPH to phenol between 2.5:1 and 1:1 and determining the optical densities of the solutions diluted 10-fold with benzene after appropriate times. If optical density is plotted against DPPH-to-phenol ratio, a break in the curve is observed which gives the stoichiometry applying under the particular experimental conditions. The break is sharp for the more reactive phenols; Fig. 1 shows the results obtained with 1-naphthol

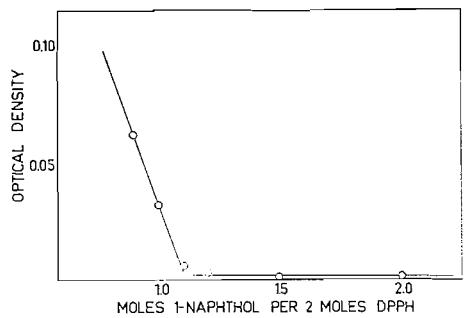


FIG. 1. Stoichiometry of the reaction of DPPH with 1-naphthol.

after 85 minutes at 50° C and an initial DPPH concentration of 2.5×10^{-3} *M*. With phenols whose reaction with DPPH is strongly retarded by diphenylpicrylhydrazine, the break in the curve is less sharp and the stoichiometric ratios are probably not known to better than 10% of their value.

Retardation by diphenylpicrylhydrazine was investigated by determining initial rates of reaction for solutions to which the hydrazine had been added at a concentration twice that of the initial DPPH concentration. With the very reactive phenols 4-methoxyphenol, 1-naphthol, and 2,4-dichloro-1-naphthol, the concentration of diphenylpicrylhydrazine was 8×10^{-5} *M* and with all other phenols it was 2×10^{-4} *M*.

The yield of diphenylpicrylhydrazine was determined for the reactions between DPPH and phenol and 1-naphthol. Reaction mixtures containing a slight excess of phenol were allowed to react until more than 99% of the DPPH had disappeared, and the products were separated on a column of alumina deactivated by the addition of 4% water. The diphenylpicrylhydrazine, identified by melting point and mixed melting point, was obtained in greater than 80% yield when phenol was the donor and in a yield of 90% to 95% when 1-naphthol was the donor.

Infrared spectra of mixtures obtained by the reaction of DPPH with various phenols in chloroform solution were examined. The high yields of diphenylpicrylhydrazine were confirmed but little information was obtained concerning the structures of the other products.

Can. J. Chem. Downloaded from www.nrcresearchpress.com by 210.87.254.6 on 09/05/12
For personal use only.

Can. J. Chem. Downloaded from www.nrcresearchpress.com by 210.87.254.6 on 09/05/12
For personal use only.

RESULTS AND DISCUSSION

Diphenylpicrylhydrazine (DPPH—H) is a major product of the reaction of DPPH with phenols, confirming that the main reaction is a hydrogen-abstraction process. The very low rates of reaction observed with the methylated phenols 1-methoxynaphthalene, 2-methoxynaphthalene, and 2-methylanisole indicate that the hydrogen of the O—H is attacked in the rate-determining step.

$$\text{DPPH} + \text{XOH} \rightarrow \text{DPPH—H} + \text{XO}\cdot \qquad [1]$$

The change in substituent from O—H to O—Me might affect the rate of hydrogen abstraction from C—H but relative rates greater than a thousand would not be expected. Further support is given by the observation that pentachlorophenol, which contains no C—H bonds, reacts with DPPH to give diphenylpicrylhydrazine as a major product, and the rate of reaction is approximately that predicted from reactions involving monochlorophenols. In addition, Bickel and Kooyman (6) observed a deuterium isotope effect in the second-order reaction of DPPH with 4-methyl-2,6-di-*t*-butylphenol and concluded that the rate-determining step involved the simple attack of DPPH on the O—H group. It is probable that a similar conclusion applies in the reactions of DPPH with all phenols.

In this study the rates of disappearance of DPPH were usually found to be of first order with respect to both the DPPH and the phenol. The only exceptions were the reactions involving phenol, pentachlorophenol, and 2,6-di-*t*-butylphenol where the order was slightly less than one with respect to the phenol. The reactions were normally studied in the presence of air and it is possible that oxygen has some effect on the rate of reaction and on the nature of the products. The effect on the rate of reaction of DPPH with phenol is small, for when degassed solutions are used a reduction in rate of a few per cent is observed.

The kinetic results are summarized in Table I. The rate constants (k) for the hydrogen-abstraction process of reaction [1] have been calculated from the observed initial rates of disappearance of DPPH at 30° C and the stoichiometry of the reaction. The activation energies (E) are probably correct to better than ± 1.0 kcal/mole with phenols which have very high rate constants or which undergo reactions which are strongly retarded by diphenylpicrylhydrazine; with other phenols the activation energies are probably correct to ± 0.5 kcal/mole. The uncertainty in the A factors is determined largely by the uncertainty in the corresponding activation energy.

The rate constant for hydrogen abstraction varies considerably with the nature of the substituent. 4-Methoxyphenol, for example, gives a rate constant some 20,000 times that given by 4-nitrophenol. In Fig. 2 values of $\log_{10}(k/k_0)$, where k is the second-order rate constant for the substituted phenol and k_0 is the rate constant for phenol at 30° C, are plotted against the Hammett σ value (11). For σ values less than 0.2 the relationship

$$\log_{10}(k/k_0) = -6$$

is very roughly obeyed but for values of σ greater than 0.2 the slope is much lower. The high negative value of the slope in the range $-0.4 < \sigma < 0.2$ has been compared with the smaller slopes of -3.7 for hydrogen-abstraction reactions involving phenols and alkylperoxy radicals (12) and of -2.5 for phenols and polystyryl radicals and is interpreted as evidence for the great importance of polar factors in the free-radical reactions between DPPH and phenols (5). However, the referee has pointed out that recent discussions of substituent effects (13, 14) indicate that the substituents from which the

TABLE I

The reaction of DPPH with phenols and methylated phenols

	k at 30° (cc/mole sec)	E (kcal/mole)	A (cc/mole sec)	Stoichiometry	Retardation
Phenol	22.4	10.4	7.1×10^{8}	1.1	0.14
4-Methyl-	377	9.0	1.2×10^{9}	1.1	0.72
3-Methyl-	68	10.2	1.6×19^{9}	1.25	0.29
2-Methyl-	180	9.1	6.6×10^{8}	1.2	0.68
4-*t*-Butyl-	337	9.5	2.4×10^{9}	1.2	0.082
4-Phenyl-	936	8.7	1.8×10^{9}	1.2	0.12
2-Phenyl-	96	9.7	9.5×10^{8}	1.25	0.22
4-Chloro-	40	10.5	1.5×10^{9}	1.1	0.23
3-Chloro-	5.0	12.4	4.4×10^{9}	1.3	0.078
2-Chloro-	10.6	10.6	4.7×10^{8}	1.2	0.24
4-Fluoro-	92	9.6	7.8×10^{8}	1.3	0.22
4-Nitro-	1.5	14.6	5.1×10^{10}	1.1	0.11
3-Nitro-	1.0	14.1	1.5×10^{10}	1.2	0.099
4-Methoxy-	29,100	4.8	8.4×10^{7}	1.1	0.53
3-Methoxy-	134	11.1	1.4×10^{10}	1.2	0.14
4-Acetyl-	3.5	16.1	1.4×10^{12}	1.2	0.051
2,6-Dimethyl-	585	6.1	1.5×10^{7}	1.1	0.78
2,6-Diisopropyl-	425	6.4	1.8×10^{7}	1.0	0.95
2,6-Di-*t*-butyl-	18	6.0	3.8×10^{5}	1.0	0.87
2,6-Di-*t*-butyl-4-methyl-	126	6.1	3.2×10^{6}	1.0	0.96
Pentachloro-	6.1	10.5	2.3×10^{8}	1.7	0.16
1-Naphthol	33,600	4.9	1.1×10^{8}	1.1	0.93
2-Naphthol	2,150	6.6	1.2×10^{8}	1.1	0.24
2,4-Dichloro-1-naphthol	49,800	4.5	8.8×10^{7}	1.9	0.75
1-Methoxynaphthalene	40	—	—	—	—
2-Methoxynaphthalene	0.01	—	—	—	—
2-Methylanisole	0.01	—	—	—	—

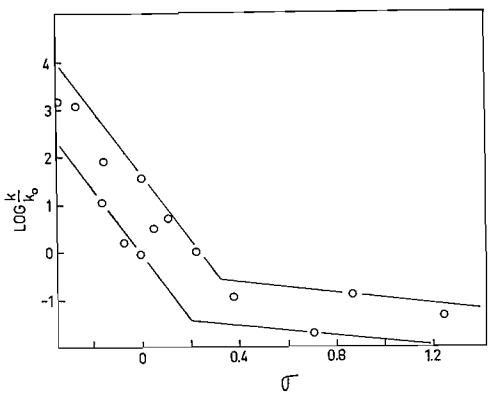


FIG. 2. Variation of rate constant with Hammett σ value of phenol substituent.

value of $\rho = -6$ is deduced are ones for which the unmodified Hammett equation is not valid. Taft (14) has shown that a meaningful measure of the inductive contribution of a substituent to the reactivity of a benzene derivative is the ρ_I value obtained from a Hammett σ plot using only selected meta substituents. The value of ρ_I for the DPPH–phenol reaction obtained from rate constants for phenol, *m*-chlorophenol, *m*-cresol, and *m*-nitrophenol is -2.1. Assuming that the inductive effect is the same for meta and para substituents, it is possible to estimate the resonance contributions of substituents to the reactivities of benzene derivatives. Taft defines a specific resonance parameter $\bar{\sigma}_R$ and

Can. J. Chem. Downloaded from www.nrcresearchpress.com by 210.87.254.6 on 09/05/12
For personal use only.

shows that deviations from the Hammett equation which result from a specific dependence of resonance effects on reaction type can usually be detected by deviation of the specific resonance parameter from its "normal" value. In the reaction of DPPH with phenols, considerably enhanced values of $\bar{\sigma}_R$ are observed for *p*-methoxy, *p*-methyl, and *p*-phenyl substituents. Both electrophilic and free-radical reactivities (14) give enhanced values of $\bar{\sigma}_R$ for these substituents and at this stage it is not possible to use $\bar{\sigma}_R$ values to place the DPPH–phenol reaction in one of these classes. More data for the present reaction, and for free-radical reactions generally, would be helpful, but the difficulty largely stems from our use of a highly polar free radical as a hydrogen acceptor. McGowan, Powell, and Raw (4) prefer an ionic mechanism for the DPPH–phenol reaction and suggest that the DPPH abstracts a hydride ion from the phenol. The main evidence for this suggestion is that the relative rates of hydrogen abstraction from phenols by DPPH are remarkably close to those for the solvolysis of dimethylbenzyl chlorides. We believe, however, that the rate-determining step of the reaction of DPPH with phenols is not significantly different from that generally put forward for the reaction of alkylperoxy radicals (12) and polystyryl radicals (5) with phenols and for the reaction of DPPH with hydroaromatic compounds (1), aromatic amines (4), and mercaptans (7).

The rate constants for the reaction of DPPH with phenols in carbon tetrachloride solution (4) are greater than those obtained using benzene as solvent under similar conditions; the ratio is of the order of three but varies with the phenol. The dielectric constant of the medium has been shown to be important in determining the rate of reaction of DPPH with mercaptans (8) but the similar values for carbon tetrachloride and benzene make it unlikely that the difference in rates can be accounted for in terms of dielectric constant alone. With mercaptans as hydrogen donors it was found that the reactions were approximately twice as fast in cyclohexane as in benzene (7) and it was suggested that the loose complex formed between benzene and DPPH could account for the slower reaction in benzene. This explanation may apply to the reaction of DPPH with phenols since carbon tetrachloride does not complex with DPPH to any great extent.

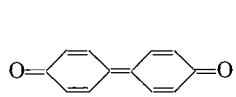
McGowan, Powell, and Raw have pointed out that alkyl substituents in the two ortho positions of the phenol can cause steric hindrance to the hydrogen-abstraction reaction (4). The effect is small for two methyl groups but the rate of reaction drops to approximately one hundredth of the expected rate when there are *t*-butyl groups in both ortho positions. The present work shows that the reduction in rate is caused largely by a reduction in the A factor rather than an increase in activation energy. The A factors are normally of the order of 10^9 cc/mole sec but higher values are usually observed in reactions of comparatively high activation energy and lower values in reactions of low activation energy. The expected values for the 2,6-disubstituted phenols would be of the order of 10^8 cc/mole sec and the lower values observed for 2,6-dimethylphenol and 2,6-diisopropylphenol may indicate that some steric hindrance is occurring in these cases. The value of 3.8×10^5 cc/mole sec observed for 2,6-di-*t*-butylphenol is much lower than the expected value and there is little doubt that steric hindrance is the main factor involved. Some caution must be exercised in arguments of this type as the A factor found for the reaction involving 2,6-di-*t*-butyl-4-methylphenol is considerably larger (3.2×10^6 cc/mole sec), yet it is not significantly different from that found for di-*t*-butylphenol because of the wide limits of experimental uncertainty.

The effect of the product 2,2-diphenyl-1-picrylhydrazine on the rate of reaction is shown in Table I. The values recorded are the ratios of the rate constants k_1/k where k

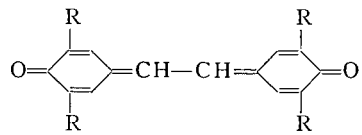
Can. J. Chem. Downloaded from www.nrcresearchpress.com by 210.87.254.6 on 09/05/12
For personal use only.

applies to the normal reaction and k_1 to the reaction retarded by the addition of diphenylpicrylhydrazine at a concentration twice that of the initial DPPH concentration. For the less reactive phenols the values of k_1/k are generally small and in these cases the accumulation of diphenylpicrylhydrazine as the product of a normal reaction will cause a considerable decrease in rate. It is clear that accurate kinetic analyses can only be made using initial rates of reaction where the concentration of retarding product is low. The retardation can be simply explained if reaction [1] is reversible; the rate of production of dehydrogenation products of the phenols is determined by the concentration of XO· radicals and any lowering of this concentration by a reversal of reaction [1] results in a decreased rate of production of dehydrogenation products and a decreased rate of disappearance of DPPH. The quantitative effect of the diphenylpicrylhydrazine on the rate of reaction depends on the reactivity of XO· towards diphenylpicrylhydrazine and also on the further reactions of XO· radicals with themselves, and with DPPH. In many cases these further reactions become rate controlling even at low concentrations of diphenylpicrylhydrazine, and detailed kinetic studies of the retarded reactions may be useful in distinguishing between the alternative secondary processes.

Some indication of the nature of the secondary reactions is given by the stoichiometric results; these are recorded in Table I as the number of moles of phenol reacting with 2 moles of DPPH. In most cases the ratio of DPPH to phenol consumed is approximately 2:1.1 and since the yields of diphenylpicrylhydrazine are high, an average of almost two hydrogen atoms is abstracted from each phenol molecule. The second hydrogen atom is probably in the ortho or para position because if these positions are blocked as in 2,4-dichloro-1-naphthol the DPPH-to-phenol ratio is closer to 1:1. Products of the type I and II are suggested by the stoichiometry and by previous work on the oxidation of



I



II

phenols (15, 16). The infrared spectra of the product mixtures do not show a strong absorption in the carbonyl stretching region, however, and there is no direct evidence for the formation of quinonoid compounds. With all phenols examined the OH stretching absorption of the reacting phenol decreases in intensity as the reaction proceeds, but in the case of 1-naphthol a new absorption at a frequency some 40 cm^{-1} below that of the 1-naphthol is observed in the products. It appears that the paths followed in the further reactions of the phenoxy radicals may vary with the phenol.

ACKNOWLEDGMENTS

The authors are indebted to the National Research Council for a grant and to Queen's University for R. S. McLaughlin and Milton Hersey fellowships.

REFERENCES

1. E. A. Braude, A. G. Brook, and R. P. Linstead. J. Chem. Soc. 3574 (1954).
2. A. S. Kuz'minskiĭ and L. G. Angert. Doklady Akad. Nauk S.S.S.R. **96**, 1187 (1954).
3. J. E. Hazell and K. E. Russell. Can. J. Chem. **36**, 1729 (1958).

Can. J. Chem. Downloaded from www.nrcresearchpress.com by 210.87.254.6 on 09/05/12
For personal use only.

4. J. C. McGowan, T. Powell, and R. Raw. J. Chem. Soc. 3103 (1959).
5. M. P. Godsay, D. H. Lohmann, and K. E. Russell. Chem. & Ind. (London), 1603 (1959).
6. A. F. Bickel and E. C. Kooyman. J. Chem. Soc. 2415 (1957).
7. K. E. Russell. J. Phys. Chem. **58**, 437 (1954).
8. A. H. Ewald. Trans. Faraday Soc. **55**, 792 (1959).
9. S. Goldschmidt and K. Renn. Ber. **55**, 628 (1922).
10. R. H. Poirier, E. J. Kahler, and F. Benington. J. Org. Chem. **17**, 1439 (1952).
11. H. H. Jaffé. Chem. Revs. **53**, 191 (1953).
12. C. E. Boozer, G. S. Hammond, C. E. Hamilton, and J. N. Sen. J. Am. Chem. Soc. **77**, 3238 (1955).
13. H. Van Bekkum, P. E. Verkade, and B. M. Wepster. Rec. trav. chim. **78**, 815 (1959).
14. R. W. Taft, Jr. and I. C. Lewis. J. Am. Chem. Soc. **81**, 5343 (1959); R. W. Taft, Jr. J. Phys. Chem. **64**, 1805 (1960).
15. S. L. Cosgrove and W. A. Waters. J. Chem. Soc. 388 (1951).
16. A. F. Bickel and E. C. Kooyman. J. Chem. Soc. 3211 (1953).

Can. J. Chem. Downloaded from www.nrcresearchpress.com by 210.87.254.6 on 09/05/12
For personal use only.

Can. J. Chem. Downloaded from www.nrcresearchpress.com by 210.87.254.105 on 09/05/12
For personal use only.

AN ALTERNATIVE SYNTHESIS OF 5-*O*-METHYL-L-ARABINOSE[1]

I. R. SIDDIQUI,[2] C. T. BISHOP, AND G. A. ADAMS

ABSTRACT

5-*O*-Methyl-L-arabinose has been synthesized by an unambiguous route in which *O*-benzyl groups were used to block positions 2 and 3 in the L-arabinose molecule. In addition to the usual indirect proofs of structure, a direct proof is described involving isolation of the product from periodate oxidation of the 5-*O*-methyl-L-arabinose. Two new derivatives, the phenylhydrazide and amide of 5-*O*-methyl-L-arabonic acid, were prepared.

The probable occurrence of 5-*O*-methyl-L-arabinose among the hydrolysis products of methylated wheat bran hemicellulose (1) prompted the synthesis of this compound by Dutton *et al.* (2). These authors used *O*-acetyl groups to block positions 2 and 3 in ethyl α-L-arabinofuranoside during methylation by Purdie's reagents and stated that "although sugar acetates may undergo acetyl migration even in the presence of such a weak base as silver oxide there was no indication of such migration in the preparation described here" (2). This result indicated that *O*-acetyl migrations, which are known to occur in the hexopyranoside series (3–6) and in D-glucose diethyl thioacetal tetracetate (7), may not happen in the pentofuranoside series.

Authentic samples of mono- and di-*O*-methyl ethers of L-arabinose were required in connection with another problem (8) and were obtained from various laboratories. Examination of the methyl glycosides of these compounds by gas–liquid partition chromatography (9, 10) revealed that all of the samples that were syrups contained more than one component. These samples had been obtained by chromatography on cellulose and the results showed that pure methyl ethers of arabinose may be difficult to isolate by that method.

Because of the unexpected absence of *O*-acetyl migration in the synthesis of Dutton *et al.* (2), the apparent difficulties in purification of these compounds by cellulose chromatography, and the urgent need for an authentic sample of this important reference sugar, an alternative synthesis of 5-*O*-methyl-L-arabinose seemed desirable. The present paper reports such a synthesis together with a proof of structure and two new derivatives of this sugar, namely the phenylhydrazide and the amide of 5-*O*-methyl-L-arabonic acid.

The route followed in this synthesis was similar to that used by Dutton *et al.* (2) except that *O*-benzyl rather than *O*-acetyl groups were used to block positions 2 and 3 in the L-arabinose molecule. The sequence of reactions was as follows. Ethyl α-L-arabinofuranoside was tritylated and the product was benzylated to yield ethyl 2,3-di-*O*-benzyl-5-*O*-trityl-α-L-arabinoside. This compound was successively detritylated, methylated, debenzylated, and hydrolyzed to yield 5-*O*-methyl-L-arabinose. Purities of the compounds obtained in each step of the synthesis were checked by analysis and, where possible, by gas–liquid partition chromatography and paper chromatography.

Confirmation that the syrupy mono-*O*-methyl-L-arabinose from the above synthesis was 5-*O*-methyl-L-arabinose was obtained from the following evidence. Complete methylation of the methyl glycosides, prepared by refluxing the mono-*O*-methyl-L-arabinose in methanolic hydrogen chloride, yielded methyl 2,3,5-tri-*O*-methyl α- and β-L-arabinosides,

[1]*Manuscript received February 23, 1961.*
Contribution from the Division of Applied Biology, National Research Council, Ottawa 2, Canada.
Issued as N.R.C. No. 6357.
[2]*N.R.C. Postdoctorate Fellow, 1958–1960.*

readily distinguished from the methyl glycosides of 2,3,4-tri-*O*-methyl-L-arabinose by gas–liquid partition chromatography (8). Oxidation of the mono-*O*-methyl-L-arabinose by bromide yielded a lactone that crystallized from the chloroform extract of the reaction mixture. This lactone showed a very slow change in rotation in aqueous solution and had carbonyl absorption at 1773 cm^{-1} in the C=O stretching frequency of its infrared spectrum. Barker *et al.* (11) have shown that γ-lactones of aldonic acids have their carbonyl absorption bands in the range 1765–1790 cm^{-1} while those of δ-lactones are between 1726 and 1760 cm^{-1}. This was confirmed here by observation of the infrared spectra of the following lactones, which showed carbonyl absorption as indicated: D-gluconic acid δ-lactone (1720 cm^{-1}); 2,5-di-*O*-methyl-L-arabonic acid-γ-lactone (1777 cm^{-1}); and 3,5-di-*O*-methyl-D-galactonic acid-γ-lactone (12) (1786 cm^{-1}). The results of methylation and the isolation of the γ-lactone showed that the parent mono-*O*-methyl-L-arabinose was capable of existing in the furanose form and therefore that the *O*-methyl group could not be located at C_4.

The mono-*O*-methyl-L-arabonic acid-γ-lactone provided a crystalline phenylhydrazide and a crystalline amide on reaction with phenylhydrazine and ammonia respectively. The amide gave a positive Weerman (13) reaction showing the presence of a free hydroxyl at C_2. This conclusion was supported by isolation of an osazone from the mono-*O*-methyl-L-arabinose without loss of methoxyl and by the large M_G value of the parent sugar on paper electrophoresis in borate buffer (14).

On oxidation by periodate the methyl glycosides of the mono-*O*-methyl-L-arabinose consumed one molar proportion of oxidant and released neither formic acid nor formaldehyde. This result could not have been obtained from methyl 3-*O*-methyl-L-arabinoside, which would not be oxidized in either the furanoside or pyranoside form, and showed that C_3 in the mono-*O*-methyl-L-arabinose must carry a free hydroxyl.

The foregoing evidence showed that free hydroxyls existed on C_2, C_3, and C_4 of the mono-*O*-methyl-L-arabinose and constituted indirect proof that the *O*-methyl group was located on C_5. On periodate oxidation the mono-*O*-methyl-L-arabinose yielded methoxyacetaldehyde, isolated by azeotropic distillation with water and identified as its *p*-nitrophenylhydrazone (15, 16). The isolation of this product, which could have arisen only from the 5-*O*-methyl isomer, constituted a direct proof of structure.

The physical constants of the 5-*O*-methyl-L-arabinose, 5-*O*-methyl-L-arabonolactone, and 5-*O*-methyl arabinosazone isolated in the present study are in reasonable agreement with the values reported for these derivatives by Dutton *et al.* (2) except for the specific rotations of the free sugar and of its osazone. Although certain partially methylated reducing sugars are known to give anomalous results when oxidized by periodate (17, 18), Dutton *et al.* (2) have shown that 5-*O*-methyl-L-arabinose behaves normally under these conditions, a conclusion supported by the present work.

EXPERIMENTAL

Paper chromatograms were run by the descending method on Whatman No. 1 paper using the organic phase of butanone saturated with water containing 2% of concentrated ammonium hydroxide. Paper electrophoresis was done on Whatman 3MM paper at 700–800 v for 2 hours using 0.2 *M* borate buffer, pH 10. Sugars were detected on the papers by the *p*-anisidine hydrochloride spray reagent (19). Infrared spectra were measured in the frequency range 3800–699 cm^{-1} either on chloroform solutions or by the Nujol mull technique. Gas–liquid partition ch romatograms were done on a Pye Argon

Can. J. Chem. Downloaded from www.nrcresearchpress.com by 210.87.254.105 on 09/05/12
For personal use only.

Chromatograph using straight, 4-ft columns with the following packings:

(*a*) butanediol succinate polyester on Chromosorb W, 60–80 mesh (1:9 w/w),

(*b*) polyphenyl ether, *m*-bis(*m*-phenoxyphenoxy)-benzene, on Celite 545, 80–100 mesh (1:6 w/w).

Flow rates and temperatures were as cited for individual analyses. Evaporations were carried out at 35° C under diminished pressure unless otherwise stated and melting points are corrected.

Ethyl 5-O-Trityl-α-L-arabinoside

Ethyl α-L-arabinofuranoside (10.8 g, m.p. 48–49° C, $[\alpha]_D^{26}$ −117°±1.5° (*c*, 1.7% in water) (20)) was dissolved in dry pyridine (100 ml) and triphenylchloromethane (16.85 g) was added. After the solution had been kept at room temperature (25–26° C) for 41 hours isolation of the product (21) yielded ethyl 5-*O*-trityl-α-L-arabinoside as a syrup (yield 25.0 g or 98%), $[\alpha]_D^{22}$ −51.4° (*c*, 3.1% in methanol). Anal: Calc. for $C_{26}H_{28}O_5$: trityl, 59.8%; C, 74.26%; H, 6.71%. Found: trityl (22), 59.67%; C, 74.99%; H, 6.92%.

Ethyl 2,3-Di-O-benzyl-5-O-trityl-α-L-arabinoside

Ethyl 5-*O*-trityl-α-L-arabinoside (23 g) was benzylated according to the procedure of Dennison and McGilvray (23). The syrupy product showed very weak hydroxyl absorption in its infrared spectrum but the high yield (35.0 g, 106%) indicated incomplete removal of benzyl chloride or benzyl alcohol from the reaction mixture. $[\alpha]_D^{22}$ −40.5° ±1° (*c*, 1.7% in chloroform). Anal: Calc. for $C_{40}H_{40}O_5$: C, 80.0%; H, 6.71%. Found: C, 81.1%; H, 6.71%.

Ethyl 2,3-Di-O-benzyl-α-L-arabinofuranoside

Ethyl 2,3-di-*O*-benzyl-5-*O*-trityl-α-L-arabinoside (34.8 g) was dissolved in dry chloroform (100 ml) and the solution was saturated at 0° C with dry hydrogen chloride. After 1 hour, the solution was neutralized with silver carbonate, silver salts were filtered, and the filtrate was evaporated to a syrup. A methanolic solution of this syrup yielded crystals of triphenylcarbinol when kept at 0° C. The crystals (4.0 g) were removed and the filtrate was evaporated to dryness. The residue, slurried in petroleum ether (65–110° C), was added to a column of alumina (3.5×28 cm) which was then eluted with petroleum ether (700 ml) to remove triphenylmethane (10 g, m.p. 93° C). Elution of the column with methanol (500 ml) and evaporation of the eluate then yielded the syrupy product (14.66 g, 74.5%), $[\alpha]_D^{24}$ −28.5°±0.5° (*c*, 2.4% in chloroform). Anal: Calc. for $C_{21}H_{26}O_5$: C, 70.37%; H, 7.31%. Found: C, 70.53%; H, 7.10%.

Ethyl 2,3-Di-O-benzyl-5-O-methyl-α-L-arabinoside

Ethyl 2,3-di-*O*-benzyl-α-L-arabinofuranoside (14 g) was methylated with methyl iodide (125 ml) and silver oxide (19 g). Filtration and evaporation of the filtrate yielded a product which still had hydroxyl absorption in its infrared spectrum. One more methylation yielded a product (14.1 g, 96%) with no hydroxyl absorption in the infrared and having $[\alpha]_D^{24}$ −22.3°±0.5° (*c*, 2.0% in chloroform). Anal: Calc. for $C_{22}H_{28}O_5$: C, 70.94%; H, 7.58%. Found: C, 71.58%; H, 7.08%.

Ethyl 5-O-Methyl-α-L-arabinoside

Ethyl 2,3-di-*O*-benzyl-5-*O*-methyl-α-L-arabinoside (13.0 g) was debenzylated by reduction with sodium in alcohol (24) to yield a syrupy product (4.66 g, 78.5%). Analysis of this product by gas–liquid partition chromatography, column A, 170° C, 300 ml argon/min, showed the presence of one major component (68.9%) and four minor

Can. J. Chem. Downloaded from www.nrcresearchpress.com by 210.87.254.105 on 09/05/12
For personal use only.

components. The minor components were undoubtedly partially benzylated products that were soluble in water. Because of this evidence of a mixture, no analyses or measurement of specific rotation were done.

Hydrolysis of Ethyl 5-O-Methyl-α-L-arabinoside

The syrupy glycoside obtained above (2.5 g) was heated with 0.05 *N* sulphuric acid (50 ml) at 100° C and the hydrolysis was followed by gas–liquid partition chromatography using the conditions just described for examination of the products from debenzylation. The glycosides gradually disappeared and none could be detected after 2 hours of hydrolysis. The hydrolyzate was neutralized with barium carbonate, filtered, and the filtrate was evaporated to dryness yielding a syrup (1.9 g, 91.2%). Paper chromatography of this material showed the presence of a major component of R_G 0.39 and minor components of R_G values 1.1, 1.0, 0.77, 0.22, and 0.12 (R_G = movement relative to 2,3,4,6-tetra-*O*-methyl-D-glucose).

Isolation of 5-O-Methyl-L-arabinose

The syrupy mixture from the hydrolysis (1.9 g) was resolved by chromatography on 22 sheets of Whatman No. 3MM paper (46×57 cm) and elution of the appropriate areas yielded the major component (R_G 0.39), which was recovered as a syrup (0.90 g, 47.4%). The yield was corrected for material lost on the guide strips used to locate the sugars.

Dutton *et al.* (2) reported $[\alpha]_D^{25}$ −32.0° (*c*, 0.484% in water) for 5-*O*-methyl-L-arabinose. The sugar isolated in the present work had $[\alpha]_D^{25}$ −25.3°±1.5° (*c*, 1.0% in water) and a methoxyl content of 18.7%; a mono-*O*-methyl pentose requires a methoxyl content of 18.9%. On paper chromatography and paper electrophoresis this sugar gave R_G, R_F, and M_G values of 0.39, 0.32, and 0.74 respectively. Gas–liquid partition chromatography of a methanolyzate of this compound on column B showed only two peaks, which corresponded to the anomeric glycosides of 5-*O*-methyl-L-arabinose. These results show that 5-*O*-methyl-L-arabinose is readily purified by chromatography on cellulose despite the apparent difficulties, referred to in the discussion, in obtaining pure samples of arabinose methyl ethers by that procedure.

Methylation of 5-O-Methyl-L-arabinose

The mono-*O*-methyl pentose (ca. 2 mg) was heated at 100° C in a sealed tube with 2% methanolic hydrogen chloride (1.0 ml) for 12 hours. Acid was neutralized with silver carbonate, and the filtrate from removal of silver salts was evaporated to a syrup which was shaken overnight with silver oxide (20 mg), methyl iodide (0.2 ml), and dimethyl formamide (0.2 ml) (25). The reaction mixture was examined by gas–liquid partition chromatography using column B, 200° C, 85 ml argon/min. Two components were found, in the methylation reaction, with retention volumes (V_R), which were made relative to methyl 2,3,5-tri-*O*-methyl-α-L-arabinoside, of 1.00 and 1.28 corresponding to the α- and β-methyl glycosides respectively of 2,3,5-tri-*O*-methyl-L-arabinose. Under the conditions used, the α- and β-methyl glycosides of 2,3,4-tri-*O*-methyl-L-arabinose ran as one component with V_R = 1.75 and none was found in the methylated product.

5-O-Methyl-L-arabonolactone

A mixture of 5-*O*-methyl-L-arabinose (300 mg), water (3 ml), barium carbonate (300 mg), and bromine (30 drops) was kept in the dark at room temperature for 70 hours. Bromine was removed by aeration and the aqueous solution was extracted continuously with chloroform for 5 days. The lactone crystallized from the chloroform solution and

Can. J. Chem. Downloaded from www.nrcresearchpress.com by 210.87.254.105 on 09/05/12
For personal use only.

evaporation of the solution left more of the lactone as a crystalline residue. Recrystallization from ethanol – petroleum ether (30–60° C) yielded 5-*O*-methyl-L-arabonolactone (170 mg), m.p. 137–138° C; $[\alpha]_D^{25}$ $-79.1°\pm1° \rightarrow -71.3°\pm1°$, 6 days incomplete (*c*, 1.0% in water); ν_{max}^{Nujol} 1773 cm^{-1}. Reported (2) values are m.p. 135° C, $[\alpha]_D^{25}$ $-76.2°$ (*c*, 0.22% in water). Anal: Calc. for $C_6H_{10}O_5$: C, 44.44%; H, 6.22%; OCH_3, 19.3%. Found: C, 44.12%; H, 5.99%; OCH_3, 19.1%.

5-O-Methyl-L-arabonamide

5-*O*-Methyl-L-arabonolactone (50 mg) was dissolved in saturated methanolic ammonia and stored at 5° C for 20 hours. Evaporation of the solution and recrystallization from ethanol–ether yielded the amide, m.p. 141–143° C, $[\alpha]_D^{25}$ $+40.7°\pm2°$ (*c*, 0.8% in methanol). Anal: Calc. for $C_6H_{13}O_5N$: C, 40.22%; H, 7.31%; N, 7.82%. Found: C, 39.98%; H, 7.09%; N, 7.76%.

A portion of the amide (ca. 5 mg) was oxidized with sodium hypochlorite and on addition of semicarbazide hydrochloride (13) gave a white precipitate of hydrazodicarbonamide.

5-O-Methyl-L-arabonic Acid Phenylhydrazide

5-*O*-Methyl-L-arabonolactone (40 mg) was dissolved in methanol (3 ml), and freshly distilled phenylhydrazine (30 mg) was added. The solution was refluxed for 3 hours and then evaporated to a syrup which crystallized from ethanol–ether to give the phenylhydrazide, m.p. 176.5–178° C, $[\alpha]_D^{25}$ $+23.6°\pm3°$ (*c*, 0.38% in methanol). Anal: Calc. for $C_{12}H_{18}O_5N_2$: N, 10.37%. Found: N, 10.58%.

5-O-Methyl-L-arabinose Phenylosazone

A mixture of 5-*O*-methyl-L-arabinose (50 mg), 20% acetic acid (3 ml), sodium bisulphite (50 mg), and phenylhydrazine (0.5 ml) was heated for 1 hour at 80° C and was then left for 24 hours at room temperature. The yellow, crystalline precipitate (25 mg) was recrystallized from aqueous acetone to give 5-*O*-methyl-L-arabinose phenylosazone, m.p. 153–155° C, $[\alpha]_D^{25}$ $+3°\pm1°$ (*c*, 0.97% in methanol). Reported (2) values are m.p. 154.5° C, $[\alpha]_D^{25}$ $-16.6°$ (*c*, 0.4% in methanol). Anal: Calc. for $C_{18}H_{22}O_3N_4$: C, 63.14%; H, 6.48%; N, 16.4%; OCH_3, 9.05%. Found: C, 63.08%; H, 6.51%; N, 16.57%; OCH_3, 9.11%.

Periodate Oxidation of 5-O-Methyl-L-arabinose

5-*O*-Methyl-L-arabinose (90 mg) was dissolved in 0.10 *M* sodium metaperiodate (20 ml) and the solution was stored in the dark at room temperature for 24 hours. The solution was then distilled and to the distillate was added an aliquot (4 ml) of a solution of *p*-nitrophenylhydrazine (0.4 g) in water (25 ml) and concentrated hydrochloric acid (0.4 ml) (15). The dense yellow precipitate was filtered after 5 minutes and recrystallized from ethanol:water (2:3) to yield methoxyacetaldehyde-*p*-nitrophenylhydrazone, m.p. 114–116° C. Reported (15, 16) values are m.p. 116° C and 115–115.5° C. Anal: Calc. for $C_9H_{11}O_3N_3$: C, 51.67%; H, 5.30%; N, 20.09%. Found: C, 51.30%; H, 5.39%; N, 19.95%.

Periodate Oxidation of Methyl 5-O-Methyl-(α,β)-L-arabinoside

5-*O*-Methyl-L-arabinose (40 mg) was refluxed with 2% methanolic hydrogen chloride (3 ml) for 6 hours. The solution was neutralized with silver carbonate, filtered, and the filtrate was evaporated to a syrup. The syrup (33.7 mg) was oxidized in aqueous solution (25 ml) containing 0.3 *M* sodium metaperiodate (10 ml); a blank was run concurrently. The consumption of periodate, estimated by the arsenite method (26), was 0.96 mole

Can. J. Chem. Downloaded from www.nrcresearchpress.com by 210.87.254.105 on 09/05/12
For personal use only.

per mole of glycoside, constant after 24 hours. No formic acid or formaldehyde could be detected.

ACKNOWLEDGMENTS

The technical assistance of Mr. F. P. Cooper with the gas–liquid partition chromatograms is gratefully acknowledged. Analyses were performed by Mr. A. E. Castagne.

REFERENCES

1. G. A. ADAMS. Can. J. Chem. **33**, 56 (1955).
2. G. G. S. DUTTON, Y. TANAKA, and K. YATES. Can. J. Chem. **37**, 1955 (1959).
3. A. P. DOERSCHUK. J. Am. Chem. Soc. **74**, 4202 (1952).
4. W. N. HAWORTH, E. L. HIRST, and E. G. TEECE. J. Chem. Soc. 2858 (1931).
5. R. L. WHISTLER and S. J. KAZENIAC. J. Am. Chem. Soc. **76**, 5812 (1954).
6. H. O. BOUVENG, B. LINDBERG, and O. THEANDER. Acta Chem. Scand. **11**, 1788 (1957).
7. R. U. LEMIEUX and H. F. BAUER. Can. J. Chem. **32**, 362 (1954).
8. G. A. ADAMS and C. T. BISHOP. Can. J. Chem. **38**, 2380 (1960).
9. A. G. MCINNES, D. H. BALL, F. P. COOPER, and C. T. BISHOP. J. Chromatog. **1**, 556 (1958).
10. C. T. BISHOP and F. P. COOPER. Can. J. Chem. **38**, 388 (1960).
11. S. A. BARKER, E. J. BOURNE, R. M. PINHARD, and D. H. WHIFFEN. Chem. & Ind. (London), 658 (1958).
12. I. R. SIDDIQUI and G. A. ADAMS. Can. J. Chem. **38**, 2029 (1960).
13. R. A. WEERMAN. Rec. trav. chim. **37**, 16 (1917).
14. A. B. FOSTER. Advances in Carbohydrate Chem. **12**, 81 (1957).
15. J. K. HAMILTON, G. W. HUFFMAN, and F. SMITH. J. Am. Chem. Soc. **81**, 2173 (1959).
16. N. L. DRAKE, H. M. DUVALL, T. L. JACOBS, H. T. THOMPSON, and H. M. SONNICHSEN. J. Am. Chem. Soc. **60**, 73 (1938).
17. E. L. HIRST and J. K. N. JONES. J. Chem. Soc. 1659 (1949).
18. J. M. BOBBITT. Advances in Carbohydrate Chem. **11**, 1 (1956).
19. L. HOUGH, J. K. N. JONES, and W. H. WADMAN. J. Chem. Soc. 1702 (1950).
20. J. W. GREEN and E. PACSU. J. Am. Chem. Soc. **60**, 2056 (1938).
21. B. HELFERICH and J. BECKER. Ann. **440**, 1 (1924).
22. F. J. BATES and ASSOCIATES. Polarimetry, saccharimetry and the sugars. Circ. Natl. Bur. Standards C440, U.S. Govt. Printing Office, Washington. 1942. p. 512.
23. J. C. DENNISON and D. I. MCGILVRAY. J. Chem. Soc. 1616 (1951).
24. K. FREUDENBERG and E. PLANKENHORN. Ann. **536**, 257 (1938).
25. R. KUHN, H. TRISCHMANN, and I. LÖW. Angew. Chem. **67**, 32 (1955).
26. P. P. FLEURY and J. LANGE. J. pharm. chim. **17**, 107 (1933).

Can. J. Chem. Downloaded from www.nrcresearchpress.com by 210.87.254.105 on 09/05/12
For personal use only.

Can. J. Chem. Downloaded from www.nrcresearchpress.com by 210.87.254.105 on 09/05/12
For personal use only.

THE REACTION OF NITROGEN ATOMS WITH OXYGEN ATOMS IN THE ABSENCE OF OXYGEN MOLECULES[1]

C. MAVROYANNIS[2] AND C. A. WINKLER

ABSTRACT

The reaction has been studied in a fast-flow system by introducing nitric oxide in the gas stream with excess active nitrogen. The nitrogen atom consumption was determined by titrating active nitrogen with nitric oxide at different positions along the reaction tube. The rate constant is found to be $k_1 = 1.83\ (\pm 0.2) \times 10^{15}$ cc^2 mole^{-2} sec^{-1} at pressures of 3, 3.5, and 4 mm, and with an unheated reaction tube.

The homogeneous and surface decay of nitrogen atoms involved in the above system were studied using the nitric oxide titration method, and the rate constants were found to be $k_3 = 1.04 \pm 0.17 \times 10^{16}$ cc^2 mole^{-2} sec^{-1}, and $k_4 = 2.5 \pm 0.2$ sec^{-1} ($\gamma = 7.5 \pm 0.6 \times 10^{-5}$), respectively, over the range of pressures from 0.5 to 4 mm with an unheated reaction tube.

INTRODUCTION

The emission spectrum of the blue nitric oxide afterglow has been studied recently by Kaplan and his associates (1). From the sensitivity of its vibrational intensity distribution to the addition of helium, it has been postulated that the spectrum arises from the three-body recombination of a ground-state oxygen atom and a ground-state nitrogen atom, by way of some intermediate state, into the excited upper states of the beta, gamma, and infrared bands,

$$N(^4S) + O(^3P) + He \rightarrow NO\ (\text{intermediate}) + He \rightarrow NO(A^2\Sigma, B^2\Pi) + He.$$

The lifetime of the intermediate, relative to the duration of the collision, is not known. Kaufman and Kelso (2) have obtained support for the above mechanism.

In the present paper, the kinetic characteristics of the reaction between nitrogen atoms and oxygen atoms have been studied, using a fast-flowing system.

EXPERIMENTAL

Active nitrogen was produced by a microwave generator. A quartz tube of 12-mm i.d., and 10 cm long, was used as a discharge tube, and the reaction vessel consisted of a pyrex tube of 20-mm i.d., and 30 cm long. Nitrogen (>99.9% pure) was passed into the discharge tube through a liquid-air trap to remove water, while purified nitric oxide was passed into the reaction tube through small jets, located at four different points along the reaction tube.

Oxygen atoms were produced by addition of nitric oxide at the first jet, to an excess of active nitrogen, at pressures of 3, 3.5, and 4 mm and with an unheated reaction tube. The nitrogen atom consumption, after the first jet, was determined by titrating active nitrogen with nitric oxide (2, 3) at subsequent jet positions along the reaction tube.

The same procedure was used to study the homogeneous and surface decay of nitrogen atoms, that is, the disappearance of nitrogen atoms along the reaction tube was determined by titration with nitric oxide at the different jet positions.

[1]*Manuscript received April 11, 1961.*
Contribution from the Upper Atmosphere Chemistry Research Group, McGill University, with financial assistance from Contract AF19(604)4104, the Geophysics Research Directorate, Air Force Research Division, from the Defence Research Board of Canada, and from the National Research Council of Canada.
[2]*Holder of a Cominco Fellowship, 1959–60, and a National Research Council Studentship, 1960–61.*

RESULTS AND DISCUSSION

The following reactions may be involved:

$$N + O + M \xrightarrow{k_1} NO + M \quad [1]$$

$$NO + N \xrightarrow{k_2} N_2 + O \quad [2]$$

$$N + N + M \xrightarrow{k_3} N_2 + M \quad [3]$$

$$N + \text{wall} \xrightarrow{k_4} \tfrac{1}{2}N_2 + \text{wall} \quad [4]$$

$$O + O + M \xrightarrow{k_5} O_2 + M \quad [5]$$

$$O + \text{wall} \xrightarrow{k_6} \tfrac{1}{2}O_2 + \text{wall}. \quad [6]$$

The reaction

$$NO + O + M \rightarrow NO_2 + M \quad [7]$$

was not taken into account, since NO_2 would react rapidly with oxygen atoms to produce NO (4) and, moreover, reaction [2] is very fast (5) in comparison with reaction [7]. Since the system was free from O_2, except for small amounts formed by reactions [5] and [6], it was assumed that there would be negligible influence from the reactions

$$O + O_2 + M \rightarrow O_3 + M \quad [8]$$

$$O + O_3 \rightarrow 2O_2 \quad [9]$$

$$N + O_2 \rightarrow NO + O. \quad [10]$$

The disappearance of nitrogen atoms in reactions [1] to [4] is given by

$$\frac{-d(N)}{dt} = 2k_1(N)(O)(M) + k_3(N)^2(M) + k_4(N)$$

and

$$k_1 = k_5 \frac{\log \dfrac{(N)_{t_1}}{(N)_{t_2}} - \dfrac{k_4 \Delta t}{2.303} - \log\left[1 + \dfrac{k_3(M)(N)_{t_1}}{k_4}(1 - e^{-k_4 \Delta t})\right]}{\log\left[1 + \dfrac{2k_5(M)(O)_{t_1}}{k_6}(1 - e^{-k_6 \Delta t})\right]}.$$

The rate constant for reaction [5] was assumed to be $k_5 = 1.6 \times 10^{15}$ cc^2 mole^{-2} sec^{-1}, with $\gamma = 1.65 \times 10^{-5}$ (6) which, for the conditions used, corresponds to a value of $k_6 = 0.516$ sec^{-1}. Several values of k_3 and k_4 have been reported; the value of k_4 in particular presumably depends on the condition of the wall of the reaction vessel used. Reinvestigation of reactions [3] and [4], with the procedure described above, gave the results shown in Fig. 1, on the assumption that only homogeneous decay of nitrogen atoms occurred, i.e. that the rate constant, over the pressure range 0.5 to 4 mm, is given by

$$k_3 = \frac{1}{(M)\Delta t}\left[\frac{1}{(N)_{t_2}} - \frac{1}{(N)_{t_1}}\right]. \quad [11]$$

The data indicate that the value of k_3 decreases as the pressure is increased up to about 2.5 mm, then remains essentially constant with further increase of pressure. Hence, the

Can. J. Chem. Downloaded from www.nrcresearchpress.com by 210.87.254.105 on 09/05/12
For personal use only.

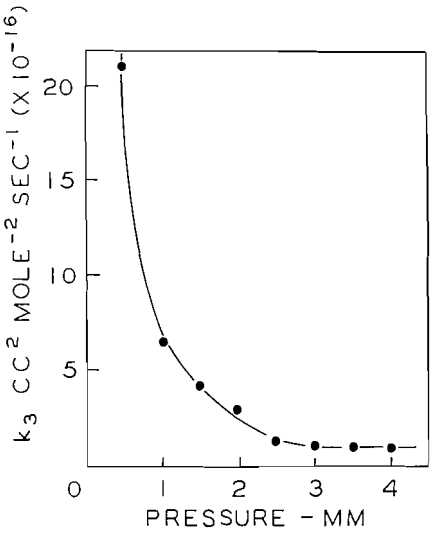


FIG. 1.

surface decay of nitrogen atoms is practically negligible at pressures above about 2.5 mm. A typical plot of $1/((N)_t(M))$ against reaction time at 2.5 mm pressure yields a straight line (Fig. 2).

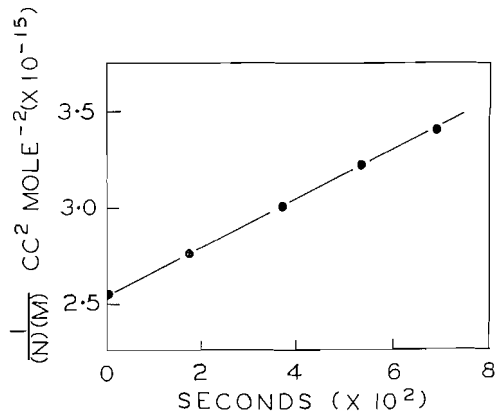


FIG. 2.

To separate the homogeneous and surface decay of nitrogen atoms, plots were made of ln (N) against time. Approximately straight lines were obtained, the slopes of which depended, of course, on (M). The average slopes of these lines are plotted against (M) in Fig. 3. For pressures of 2.5 mm and above, an extrapolation of the line passes through zero, indicating the small effect of the surface decay at these pressures. For pressures lower than 2.5 mm, an extrapolation gives an intersection corresponding to $k_4 = 2.5 \pm 0.2$ sec^{-1}. The recombination coefficient is given (7) by $\gamma = (2rk_4)/\bar{c}$, where r is the radius of the reaction vessel and $\bar{c}$ is the root mean square atomic velocity, and is found to be $\gamma = (7.5 \pm 0.6) \times 10^{-5}$. The value of γ, and that of k_3 (Table I), are in good agreement

Can. J. Chem. Downloaded from www.nrcresearchpress.com by 210.87.254.105 on 09/05/12
For personal use only.

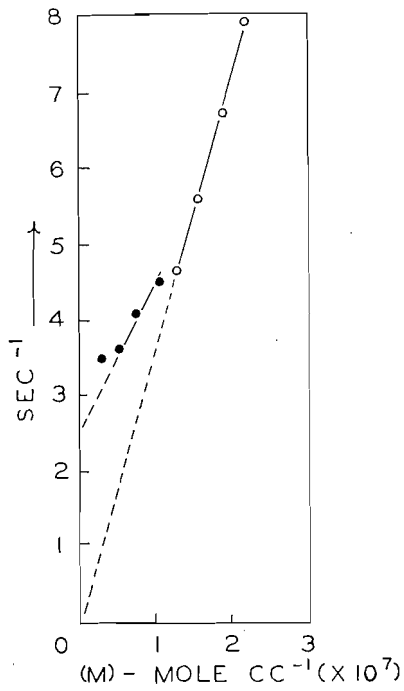


FIG. 3.

TABLE I

Variation of k_3 (from equation [11]) as a function of pressure, reaction time, and initial reactant concentrations with unheated reaction tube

Total pressure (mm)	(M) (mole/cc) $\times 10^7$	$(N)_{t_1}$ (mole/cc) $\times 10^9$	$(N)_{t_2}$ (mole/cc) $\times 10^9$	t (sec) $\times 10^2$	k_3 ($cc^2\ mole^{-2}\ sec^{-1}$) $\times 10^{-16}$
2.5	1.34	2.95	2.70	1.80	1.25
"	"	2.70	2.50	1.90	1.29
"	"	2.95	2.50	3.70	1.20
"	"	2.95	2.32	5.35	1.26
"	"	2.95	2.20	6.90	1.24
					Average 1.25
3.0	1.6	3.10	2.85	1.50	1.24
"	"	3.40	3.10	1.60	1.00
"	"	3.74	3.40	1.82	0.93
"	"	3.74	3.10	3.42	0.95
"	"	3.74	2.85	4.92	1.05
					Average 1.00
3.5	1.87	3.38	3.05	1.48	1.12
"	"	3.72	3.38	1.57	0.94
"	"	4.25	3.72	1.82	1.00
"	"	4.25	3.38	3.39	0.96
"	"	4.25	3.05	4.87	1.00
					Average 1.00
4.0	2.15	3.95	3.50	1.50	0.94
"	"	4.48	3.95	1.60	0.88
"	"	5.20	4.48	1.80	0.86
"	"	4.48	3.50	3.10	0.90
"	"	5.20	3.95	3.40	0.86
"	"	5.20	3.50	4.90	0.87
					Average 0.90

NOTE: Average $k_3 = 1.04\ (\pm 0.17) \times 10^{16}\ cc^2\ mole^{-2}\ sec^{-1}$ (this value is for the disappearance of *two* N atoms). t_1 refers to zero time.

Can. J. Chem. Downloaded from www.nrcresearchpress.com by 210.87.254.105 on 09/05/12
For personal use only.

with those of other investigators (8, 9, 10, 11) but not with those previously reported from this laboratory (12, 13).

Since the reaction of nitrogen atoms with oxygen atoms was studied at pressures of 3, 3.5, and 4 mm, the effect of reaction [4] is very small, and has been neglected. The integrated equation for k_1, with $k_4 = 0$, is given by

$$k_1 = k_5 \frac{\log \frac{(N)_{t_1}}{(N)_{t_2}} - \log\,(1+k_3(M)(N)_{t_1}\Delta t)}{\log\left[1+\frac{2k_5(M)(O)_{t_1}}{k_6}\,(1-e^{-k_6\Delta t})\right]}. \qquad [12]$$

The results are shown in Table II, with an average value of $k_1 = 1.83(\pm 0.2)\times 10^{15}$ cc^2 mole^{-2} sec^{-1}.

TABLE II

Rate constants for the reaction of nitrogen atoms with oxygen atoms at various pressures with unheated reaction tube

Total pressure (mm)	$(N)_{t_1}$ (mole/cc) $\times 10^9$	$(O)_t$ (mole/cc) $\times 10^9$	$\log \frac{(N)_{t_1}}{(N)_{t_2}}$	t (sec) $\times 10^2$	k_1 (cc^2 mole^{-2} sec^{-1}) $\times 10^{-15}$
3.0	1.47	2.30	0.0701	4.35	1.80
"	"	"	0.0962	6.30	1.75
"	1.22	2.56	0.0375	2.10	1.85
"	"	"	0.0632	4.35	1.65
"	"	"	0.1239	8.12	2.00
"	1.15	2.63	0.0555	4.35	1.70
"	"	"	0.0767	6.30	1.60
"	"	"	0.0989	8.12	1.52
3.5	1.58	2.67	0.0457	2.15	1.92
"	"	"	0.0937	4.40	2.03
"	"	"	0.1335	6.40	2.00
"	"	"	0.1659	8.24	1.95
4.0	2.60	2.60	0.0681	2.15	1.70
"	2.46	2.74	0.0708	2.15	2.15
"	"	"	0.1326	4.40	1.80
"	"	"	0.1844	6.40	1.75
"	"	"	0.2459	8.25	2.05
"	0.86	4.34	0.1645	8.25	1.70

NOTE: Average $k_1 = 1.83\ (\pm 0.2) \times 10^{15}$ cc^2 mole^{-2} sec^{-1}.

COMPARISON WITH THEORY

Using the hard sphere collision model, and assuming the reaction scheme to be

$$N + O \underset{k_{-1}'}{\overset{k_1'}{\rightleftarrows}} NO^*$$

$$NO^* + M \xrightarrow{k_2'} NO + M,$$

the stationary concentration of the binary complex NO* may be taken approximately as $(NO)^* = Z_{N.O}\tau_{NO}(N)(O)$, where $Z_{N.O}$ is the collision frequency of N and O, and τ_{NO} is the mean lifetime of the complex NO*.

Can. J. Chem. Downloaded from www.nrcresearchpress.com by 210.87.254.105 on 09/05/12
For personal use only.

The over-all rate is

$$\frac{d(\text{products})}{dt} = k_1(\text{N})(\text{O})(\text{M}) = k_2'(\text{M})(\text{NO}^*)$$
$$= k_2'(\text{M})(\text{N})(\text{O})Z_{\text{N.O}}\tau_{\text{NO}}$$

from which, by substituting $k_2' = PZ_{\text{NO}^*.\text{M}}e^{-E_2/RT}$, the experimental specific rate constant may be written as $k_{\text{exp}} = PZ_{\text{NO}^*.\text{M}}\tau_{\text{NO}}e^{-E_2/RT}$; τ_{NO} is the reciprocal of a unimolecular rate constant, and it should be about 10^{-13} sec, if we neglect activation energy. If there is any activation energy, it may be absorbed in the exponential term, thus, $Z_{\text{ter}} = Z_{\text{NO}^*.\text{M}}Z_{\text{N.O}}\tau_{\text{NO}}$. The collision frequencies can be calculated, assuming collision diameters of 3.5, 3.75, 2.95, and 1.8×10^{-8} cm for NO, (M) = N_2, N, and O respectively. For $T = 300°$ K, $Z_{\text{ter}} = 1.65\times10^{15}$ cc^2 mole^{-2} sec^{-1}.

The calculated value of Z_{ter} is in good agreement with that given experimentally by $k_1 = 1.83\ (\pm0.2)\times10^{15}$ cc^2 mole^{-2} sec^{-1}.

Wigner (14) has developed an expression which gives an upper limit for the rate of association reactions, by determining the probability of decrease of the relative energy of the two atoms below zero, under the influence of a third body. For the atomic reaction $A_1 + A_2 + A_3 \rightarrow A_1A_2 + A_3$ the rate constant is given by

$$k' = -2\pi\frac{g_{12}}{g_1g_2}\left(\frac{2\pi m_r}{kT}\right)^{1/2}\int_{V_0<0}V_0q_{12}\,[(a_{13}^2-a_{23}^2)(a_{13}/m_1-a_{23}/m_2) \qquad [13]$$
$$+2(a_{13}^2/m_1+a_{23}^2/m_2)q_{12}+(a_{13}/m_1+a_{23}/m_2)q_{12}^2]dq_{12}$$

where k' is the rate constant, k the Boltzmann constant; V_0 is the relative potential energy of the atoms A_1 and A_2 for infinite separation of A_3; m_r, m_1, m_2 are the reduced mass and the masses of A_1 and A_2; g_{12}, g_1, and g_2 are the statistical weight factors of A_1A_2, A_1, and A_2; q_{12} is the separation of the atoms A_1 and A_2; a_{13} and a_{23} are the sum of the collision radii of A_1A_3, and A_2A_3 respectively. The term $T^{-\frac{1}{2}}$ will cause a small fall-off in rate with increasing temperature.

For V_0, the Hulburt–Hirschfelder (15) potential energy curve was used, given by the equation

$$V(r) = 6.609[(1-e^{-x})^2+0.0678x^3(1+2.663x)e^{-2x}-1]\text{ ev},$$

where $x = 3.1579\ (r-r_e)/r_e$, $V(\infty) = 0$, and $r_e = 1.1508$ Å, which, according to Vanderslice (16), fits better than a Morse curve for the $X^2\Pi$ state of NO. The adopted radii were 0.89 (17), 1.49, and 1.875 Å (derived from viscocity data) for O, N, and N_2 respectively. The ratio of the statistical weights may be taken as

$$\frac{g_{\text{NO}}}{g_{\text{N}}g_{\text{O}}} = \frac{3.1}{4\times8.7},$$

taking into account the separation of the levels. The final result, for $T = 300°$ K, is $k' = 3.4\times10^{16}$ cc^2 mole^{-2} sec^{-1}. The agreement between the observed and calculated value might be taken as satisfactory, since equation [13] gives an upper limit for the reaction rate, when only atoms are involved.

Can. J. Chem. Downloaded from www.nrcresearchpress.com by 210.87.254.105 on 09/05/12
For personal use only.

REFERENCES

1. C. A. BARTH, W. J. SCHADE, and J. KAPLAN. J. Chem. Phys. **30**, 347 (1959).
2. F. KAUFMAN and J. R. KELSO. J. Chem. Phys. **27**, 1209 (1957).
3. G. B. KISTIAKOWSKY and G. G. VOLPI. J. Chem. Phys. **27**, 1141 (1957).
4. H. W. FORD and N. ENDOW. J. Chem. Phys. **27**, 1156 (1957).
5. G. B. KISTIAKOWSKY and G. C. VOLPI. J. Chem. Phys. **28**, 665 (1958).
6. J. E. MORGAN, L. ELIAS, and H. I. SCHIFF. J. Phys. Chem. **33**, 930 (1960).
7. K. E. SCHULER and K. J. LAIDLER. J. Chem. Phys. **17**, 1212 (1949).
8. G. G. MANELLA, R. R. REAVES, and P. HARTECK. J. Chem. Phys. **29**, 608 (1958).
9. J. HERRON, J. L. FRANKLIN, P. BRADT, and V. H. DIBELER. J. Chem. Phys. **29**, 230 (1958).
10. T. WENTINK, JR., J. O. SULLIVAN, and K. L. WRAY. J. Chem. Phys. **29**, 231 (1958).
11. J. HERRON, S. L. FRANKLIN, P. BRADT, and V. H. DIBELER. J. Chem. Phys. **30**, 879 (1959).
12. R. KELLY and C. A. WINKLER. Can. J. Chem. **37**, 62 (1959).
13. R. BACK, W. DUTTON, and C. A. WINKLER. Can. J. Chem. **37**, 2059 (1959).
14. E. WIGNER. J. Chem. Phys. **5**, 720 (1937); Trans. Faraday Soc. **34**, 29 (1938); J. Chem. Phys. **7**, 646 (1939).
15. H. M. HULBURT and J. O. HIRSCHFELDER. J. Chem. Phys. **9**, 61 (1941).
16. J. T. VANDERSLICE, E. A. MASON, and W. G. MAISCH. J. Chem. Phys. **31**, 738 (1959).
17. LANDOLT-BORNSTEINS TABLES. 1st Erganzungsband. p. 69.

Can. J. Chem. Downloaded from www.nrcresearchpress.com by 210.87.254.105 on 09/05/12
For personal use only.

Can. J. Chem. Downloaded from www.nrcresearchpress.com by 210.87.254.40 on 09/05/12
For personal use only.

HELMINTHOSPORAL, THE TOXIN FROM HELMINTHOSPORIUM SATIVUM

I. ISOLATION AND CHARACTERIZATION[1]

P. DE MAYO,[2] E. Y. SPENCER,[3] AND ROBERT W. WHITE[3]

ABSTRACT

The toxin produced by *Helminthosporium sativum* P.K. and B.[4] has been isolated in crystalline form. It has the formula $C_{15}H_{22}O_2$ and has been shown to contain one saturated aldehyde function, one α,β-unsaturated aldehyde, and two carbocyclic rings.

The significance of toxins as agents in plant pathology is now generally recognized, and these substances may be of considerable economic significance. *Helminthosporium sativum*[4] is a fungus which produces a seedling blight, foot and root rot, head blight, and leaf spot of cereals and grasses. The disease is widespread in North America and elsewhere and in particular affects wheat and barley crops. It has been estimated that the loss of the wheat crops in Western Canada caused by the action of this fungus has ranged from 3 to 13% during the past 25 years (2); an estimated loss of the order of $50,000,000.00.

Recently Ludwig (3) has demonstrated that the action of the fungus is dependent on the presence of a toxin produced by the fungus. Means were found for the artificial growth of the fungus, and the cell-free culture filtrates were able to produce many of the general symptoms characteristic of seedling blight, the degree of damage being related directly to the dosage. However, the combined action of spore suspensions, themselves reported innocuous (3), and culture filtrate resulted in the plants becoming diseased and the plants generally died. Ludwig concluded that the nonspecific toxin predisposed the plants to invasion of the organism.

For the preparation of the toxin on a large scale, the fungus was grown (see Experimental) in a 25-gal jacketed fermenter on sucrose–potato infusion. The culture filtrate was then stirred with charcoal upon which the active principle was absorbed. It was eluted with chloroform, and after filtration through alumina it was then distilled at low pressure. The distillate crystallized, and was purified by recrystallization.

The substance so obtained, helminthosporal, showed characteristic absorptions in the ultraviolet (λ_{max} 266 mμ) and infrared (ν_{max} 1715 and 1685 cm^{-1}). The original crude toxin concentrate before heat treatment either did not show these bands or (in certain batches where perhaps inadvertent heating had occurred) they were present but very weak, but, weight for weight, showed essentially the same biological activity. It would seem, therefore, that helminthosporal exists in the fungus as a precursor, from which it is formed by the fungus. This change can also be effected by heat, acid or base.

Helminthosporal analyzed in accordance with the empirical formula $C_{15}H_{22}O_2$. It is unstable to air, even at low temperature, and at room temperature takes up oxygen in a quantity equivalent to half an atom in 5 days. The presence of two bands in the carbonyl region of the infrared at 1715 and 1685 cm^{-1} suggested that these accounted for both oxygen atoms. This was supported indirectly by the absence of any bands in the infrared attributable to hydroxyl or ether groupings. It was demonstrated directly by the preparation of a bis oxime.

[1]*Manuscript received April 10, 1961.*
Joint contribution from Pesticide Research Institute, Canada Department of Agriculture, University Sub Post Office, London, Ontario, and the Department of Chemistry, University of Western Ontario, London, Ontario.
[2]*Department of Chemistry, University of Western Ontario.*
[3]*Pesticide Research Institute.*
[4]*The fungus has recently (1) been reclassified as Bipolaris sorokiniana (Sacc. in Sorok) Shoemaker. The older nomenclature is retained in this communication for consistency with earlier publications on this subject.*

Can. J. Chem. Downloaded from www.nrcresearchpress.com by 210.87.254.40 on 09/05/12
For personal use only.

The ultraviolet absorption spectrum indicated the presence of conjugation of some sort. That this was due to conjugation of a double bond with one or both of the carbonyl functions and was not to be attributed to a diene system was shown by reduction of helminthosporal with lithium aluminum hydride to the glycol, the latter being characterized as the crystalline bis-3,5-dinitrobenzoate. The glycol showed no high-intensity absorption in the ultraviolet above 210 mμ.

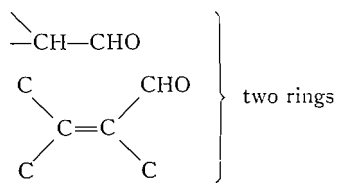
A band in the infrared at 2720 cm^{-1} was suggestive of the presence of an aldehyde. That this was so was shown directly by oxidation of helminthosporal with alkaline silver oxide in good yield to the corresponding monoacid, further characterized as the acid oxime. The acid showed bands in the infrared at 1705 and 1670 cm^{-1}, indicating that the conjugated carbonyl had not been affected. This was confirmed by the fact that the ultraviolet absorption (λ_{max} 265 mμ) was also essentially unchanged.

Attempts at further oxidation, of the remaining carbonyl group, led to intractable material, and a decision between an (second) aldehyde and a ketone function was arrived at by two methods. First, although the presence of a carboxyl group obscured the 2750 cm^{-1} region and rendered the C—H aldehyde stretch undetectable, there was present in the near infrared a band at 4480 cm^{-1} characteristic of aldehydes and very strongly suggestive of a conjugated aldehyde (4).

Secondly, the proton resonance spectrum of helminthosporal (in CCl_4) showed a singlet equivalent to one hydrogen at $\tau = 0.1$ and a doublet, also equivalent to one hydrogen at $\tau = 0.5$ ($J \sim 4$ c.p.s.). In the corresponding monoacid the doublet was replaced by a singlet at $\tau = 1.48$ (carboxyl hydrogen), the singlet being unaffected. This provided strong evidence that the remaining carbonyl was aldehydic, and this was confirmed by the spectrum of the derived oxime in which the singlet at $\tau = 0.1$ had been replaced by a singlet at $\tau = 1.93$ in accord with expectance for the grouping —CH=N·OH (5).

Of the five double-bond equivalents indicated by the empirical formula of helminthosporal and its derivatives, three have been accounted for as two carbonyl groups and a double bond. The latter is required to be tetrasubstituted since no bands attributable to vinyl hydrogen appear in the N.M.R. spectrum of helminthosporal or any of its simple derivatives. This was confirmed by the fact that the bis-3,5-dinitrobenzoate already referred to reacted with one molecule of osmium tetroxide to give a tetraol bis-3,5-dinitrobenzoate which was recovered unchanged on attempted acetylation.

That no other tetrasubstituted double bond was present was shown as follows. Reduction of the aldehyde acid with sodium borohydride gave, directly, a lactone. This reacted with one molecule of osmium tetroxide to give a diol which was optically transparent in the ultraviolet above 200 mμ. It must therefore be concluded that helminthosporal contains two carbocyclic rings. This, together with the observation that the band at $\tau = 0.5$ in helminthosporal is a doublet, allow the functions of this substance to be expressed as in I.



I

The results of the further work in progress will be reported in due course.

Can. J. Chem. Downloaded from www.nrcresearchpress.com by 210.87.254.40 on 09/05/12
For personal use only.

EXPERIMENTAL

Infrared spectra and nuclear magnetic resonance spectra were determined in carbon tetrachloride solution, ultraviolet spectra in ethanol, and optical rotations in chloroform unless otherwise stated. Light petroleum refers to the fraction of b.p. 35–60°. Melting points were taken on the Köfler hot stage.

The N.M.R. spectra were determined in ca. 10% w/v solution with 1% tetramethylsilane using a Varian V-4302 spectrometer. The peak positions were determined using an audio oscillator calibrated with a Hewlett Packard 522-B frequency counter.

Isolation

The same strain of *H. sativum* as used earlier (3) was employed in the production of toxin for isolation and characterization studies. Inoculum for the fermenter tank was prepared by inoculating four 500-ml Erlenmeyer flasks, each containing 150 ml of medium (prepared from 100 ml infusion of 100 g potatoes and 10 g sucrose) with 5 ml of spore suspensions from agar slants of the fungus and incubating the cultures at 27° C on a shaker for 3 to 5 days. The inoculum was then transferred aseptically to 8 l. of sterilized medium similar to the above. The suspension was aerated at room temperature for 3 to $3\frac{1}{2}$ days. This was then used to inoculate 100 l. of a sterilized infusion from 5000 g potatoes and 1500 g sucrose in a 35-gal jacketed fermenter. Aeration with stirring was continued for $3\frac{1}{2}$ days followed by separation of the mycelium from the culture filtrate in a Tolhurst basket centrifuge. The filtrate was adjusted to pH 2 and activated charcoal (Nuchar C 145-A; 400 g) was added and stirred. The charcoal with the absorbed toxin was separated from the liquid in a Tolhurst centrifuge and suspended in ethanol (1500 ml). After filtering on a Buchner funnel the charcoal cake was suspended in chloroform (1200 ml), stirred, and filtered. This process was repeated three times. The chloroform extracts were combined and the solvent removed *in vacuo* to yield between 25 and 35 g of crude extract.

The oil (58 g) was heated under nitrogen at 120° for 12 hours. During this time small amounts of water, ethanol, and chloroform were lost, leaving a residue of 47 g which was dissolved in light petroleum (b.p. 60–80°, 150 ml) and applied to a column of alumina (Merck, acid-washed; 400 g). Elution with the same solvent (4 l.) gave a trace (100 mg) of oil. Elution with ether (8 l.) gave, after evaporation, a brown oil (38 g). Distillation of this oil (b.p. 115–120/0.015 mm) afforded a yellow oil (18 g) which slowly set. A portion was crystallized twice from light petroleum to give helminthosporal, m.p. 56–59°; $[\alpha]_D$ −49° (*c*, 1.18); λ_{max} 266 mμ (ϵ 11,000); ν_{max} 1715, 1685, and 1618 (C=C) cm^{-1}. Calc. for $C_{15}H_{22}O_2$: C, 76.88; H, 9.46; C—Me (2), 12.83%; M.W. 234. Found: C, 76.72; H, 9.27; C—Me, 12.56%; M.W. (isopiestic, av.) 232, (Rast, av.) 247. Biological tests showed little difference in activity between the crude distillate and the recrystallized material.

The bis-*oxime* (hydroxylamine hydrochloride – pyridine at room temperature) had m.p. 177–182° (from aq. EtOH). Calc. for $C_{15}H_{24}O_2N_2$: C, 68.15; H, 9.15; N, 10.60%. Found: C, 68.0; H, 8.87; N, 10.69%.

Reduction of Helminthosporal with Lithium Aluminum Hydride

To lithium aluminum hydride (50 mg) in ether (50 ml) was added slowly with stirring a solution of the aldehyde (50 mg) in ether (100 ml) over 30 minutes. The mixture was refluxed for 30 minutes, after which the excess hydride was decomposed with ice water, and the product isolated in the usual way. The glycol was obtained as a colorless oil showing no high-intensity absorption in the ultraviolet above 210 mμ.

The glycol (40 mg) in pyridine (1 ml) containing 3,5-dinitrobenzoyl chloride (230 mg) was allowed to stand for 24 hours. Isolation of the neutral material with ether, followed by washing the ether with 0.5 *N* HCl, aqueous $NaHCO_3$ and water, successively, gave, after evaporation of the solvent, a yellow semisolid (78 mg). This was percolated in ethyl acetate solution through a short column of alumina, and the solvent evaporated. The product was crystallized from ethanol to give the bis-3,5-dinitrobenzoate (69 mg), m.p. 151–152.5°. Calc. for $C_{29}H_{30}O_{12}N_4$: C, 55.59; H, 4.83%. Found: C, 55.41, 55.66; H, 4.79, 4.72%.

The glycol diester (39 mg) in dioxan (3 ml) solution with osmium tetroxide (38.5 mg) was allowed to stand 5 days. Pyridine (1 ml) was then added and the mixture allowed to stand a further 5 days. Decomposition of the osmic ester with hydrogen sulphide, filtration, followed by concentration gave the tetraol diester as an amorphous powder. Calc. for $C_{29}H_{32}O_{14}N_4$: C, 52.73; H, 4.73%. Found: C, 52.68; H, 4.96%. Attempted acetylation (acetic anhydride – pyridine) gave back material, the infrared spectrum of which was superposable on that of the diester.

Oxidation with Silver Oxide

To the aldehyde (200 mg) in ethanol (8 ml) was added in one portion, a solution of silver nitrate (320 mg) in water (4 ml). The mixture was stirred while sodium hydroxide (113 mg) in water (2 ml) was added dropwise. After completion of the addition the stirring was continued for 2 hours.

After removal of the silver oxide by filtration the solution was diluted with water and neutral material removed by extraction with ether previously used to wash the silver oxide residue. The aqueous phase was then acidified with sulphuric acid (6 *N*; 5 ml) and the acidic material isolated with ether. Evaporation of the solvent gave a partly solidified oil (203 mg). This was chromatographed on silica gel (6 g). The material eluted with ether:benzene (1:19) was crystallized from light petroleum (b.p. 60–80°) to give the acid, m.p. 127–128°; λ_{max} 265 mμ (ϵ 7000); ν_{max} 1705, 1670 cm^{-1}; $[\alpha]_D$ −64° (*c*, 1.07). Calc. for $C_{15}H_{22}O_3$: C, 71.97; H, 8.86%. Found: C, 72.05; H, 8.98%.

The acid (50 mg) was converted into the oxime (hydroxylamine hydrochloride – pyridine). Crystallized from light petroleum (b.p. 60–80°) it had m.p. 142–143°. Calc. for $C_{15}H_{23}O_3N$: C, 67.89; H, 8.74; N, 5.28%. Found: C, 68.11; H, 8.63; N, 5.47%.

Reduction of the Aldehyde-Acid with Sodium Borohydride

To the monoacid (695 mg) in aqueous ethanol (50%; 200 ml) was added, in portions, sodium borohydride (1.0 g). The mixture was allowed to stand at room temperature with occasional swirling for 2 hours, after which it was acidified with H_2SO_4 (6 *N*), allowed to stand 30 minutes, diluted with water (500 ml), and extracted with ether. The ether extracts were then extracted with 5% sodium carbonate solution. This alkaline solution was then acidified with dilute H_2SO_4, allowed to stand 30 minutes, and again extracted with ether.

This process was repeated four times and the combined neutral material washed with water, dried, and evaporated to dryness. The product thus obtained (539 mg) was crystallized from light petroleum to yield the lactone (459 mg), m.p. 133.5–135°; ϵ_{200} 6000; ν_{max} 3080, 1780, 1615, 905 cm^{-1}; $[\alpha]_D$ +136° (*c*, 1.14). Calc. for $C_{15}H_{22}O_2$: C, 76.88; H, 9.46%. Found: C, 77.00; H, 9.46%. The compound showed bands at τ = 4.74 and 5.03 (doublets, $J \sim 5$ c.p.s.) (exomethylene group).

Ozonolysis in carbon tetrachloride solution at −15° gave formaldehyde, characterized as the dimedone derivative, in 25% yield.

Can. J. Chem. Downloaded from www.nrcresearchpress.com by 210.87.254.40 on 09/05/12
For personal use only.

Reaction of the Lactone with Osmium Tetroxide

To the lactone (320 mg), dissolved in ether (2 ml) was added pyridine (0.5 ml) and osmium tetroxide (383 mg). This mixture was kept in the dark at room temperature for 23 days when it was diluted with ethanol and the osmic ester decomposed with hydrogen sulphide. The precipitate was filtered off on Celite and washed thoroughly with ethanol. The combined filtrate and washings were evaporated to dryness to leave an oil which solidified on standing. Chromatography on silica gel (20 g) gave, on elution with ether–benzene (1:19), unchanged lactone (70 mg). Elution with ether–benzene (1:1) gave a product (250 mg) which on crystallization from ether – light petroleum gave the lactone diol (190 mg), m.p. 159–164°; ϵ_{190} <200; ν_{max} 3600, 3500, and 1785 cm^{-1}; $[\alpha]_D$ +64° (*c*, 1.01). Calc. for $C_{15}H_{24}O_4$: C, 67.13; H, 9.02%. Found: C, 66.97; H, 8.59%.

ACKNOWLEDGMENTS

The authors would like to thank Mr. L. G. Crawford for able assistance, and Dr. R. A. Ludwig for advice, in growing the toxin. They would also like to express their appreciation to Dr. J. B. Stothers for the determination of the N.M.R. spectra.

REFERENCES

1. R. A. SHOEMAKER. Can. J. Botany, **37**, 879 (1959); R. H. BURRAGE and R. D. TINLINE. Can. J. Plant Sci. **40**, 672 (1960).
2. B. J. SALLANS. Can. Plant Disease Survey, **38**, 11 (1958).
3. R. A. LUDWIG. Can. J. Botany, **35**, 291 (1957).
4. J. F. KING, P. DE MAYO, and B. VIG. In preparation.
5. J. B. STOTHERS. Personal communication.

Can. J. Chem. Downloaded from www.nrcresearchpress.com by 210.87.254.40 on 09/05/12
For personal use only.

Can. J. Chem. Downloaded from www.nrcresearchpress.com by 210.87.254.5 on 09/05/12
For personal use only.

THE REACTION OF BENZOYL CHLORIDE AND ETHYL BENZOATE WITH SOME ALKALI METAL SALTS OF FLUORENE[1]

G. W. H. Scherf and R. K. Brown

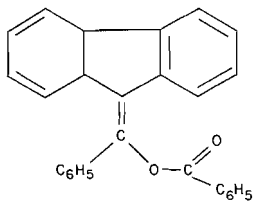
ABSTRACT

In hydrocarbon or ether solvents, the sodium or potassium salt of fluorene or of 9-benzoylfluorene reacts with an equimolar amount of benzoyl chloride to form 9,1′-benzoyloxybenzylidenefluorene (I). The reaction of equimolar quantities of the lithium salt of fluorene or of 9-benzoylfluorene and benzoyl chloride in ether solvents gives rise to a mixture of 9,9-dibenzoylfluorene (II) and 9,1′-benzoyloxybenzylidenefluorene (I), but in hydrocarbon solvents produces only 9,9-dibenzoylfluorene (II).

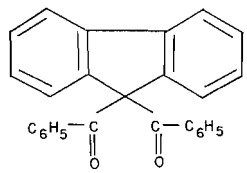
Only 9-benzoylfluorene is isolated from the reactions of the monometal salts of fluorene or of 9-benzoylfluorene with ethyl benzoate.

INTRODUCTION

The dibenzoylation of fluorene at carbon 9 gives rise to two products, the enol ester (I) and the β-diketone (II). The first recorded synthesis of 9,9-dibenzoylfluorene (II) was



(I)



(II)

that of Schlenk and Bergmann (1, 2), who, from the reaction between 9-fluorenyllithium and benzoyl chloride in benzene, isolated di-(9-fluorenyl)-phenylcarbinol along with a small amount of a compound, m.p. 180°, of unknown structure. This compound, obtained only by painstaking effort, was later identified by Kliegl *et al.* as the β-diketone (II) (3). Subsequent preparations of II have followed this (4) or similar procedures (5). The enol ester (m.p. 189.5–190°) was first obtained by Kliegl and co-workers (3) from the reaction of benzoyl chloride with 9-fluorenylsodium in ether. The only other product reported from this reaction was unchanged fluorene. No mention was made that 9-benzoylfluorene was obtained as one of the products from the reaction of benzoyl chloride with either 9-fluorenyllithium (1, 2) or 9-fluorenylsodium (3). However, recent work (5) shows that 9-propionylfluorene can be prepared in 10% yield by the reaction of 9-fluorenyllithium with propionyl chloride in ether if the reaction is carried out at reflux temperature, whereas at room temperature 9,9-dipropionylfluorene is obtained. The 9-benzoylfluorene can be synthesized quite conveniently by the reaction of fluorene with potassium metal and ethyl benzoate (6, 7).

In view of the finding that the relative amount of mono- and di-alkylation at C_9 of fluorene obtained from the reaction of equimolar quantities of alkyl halide and monometalated fluorene depended upon the metal and solvent employed (8), a study was undertaken of the reaction of benzoyl chloride with some of the alkali metal salts of fluorene in ether and in hydrocarbon solvents.

[1]*Manuscript received February 10, 1961.*
Contribution from the Department of Chemistry, University of Alberta, Edmonton, Alberta. Taken from the thesis of G. W. H. Scherf to be submitted to the Graduate School of the University of Alberta as part of the requirements for the degree of Doctor of Philosophy.

Can. J. Chem. Downloaded from www.nrcresearchpress.com by 210.87.254.5 on 09/05/12
For personal use only.

RESULTS

Unless otherwise stated, all experiments involved equimolar proportions of fluorene, metal, and benzoyl chloride or ethyl benzoate in hydrocarbon or ether solvent.

The Reaction of Benzoyl Chloride with 9-Fluorenyl-lithium, -sodium, or -potassium

When 9-fluorenylpotassium (9) was treated at room temperature with benzoyl chloride in either dioxane or diethyl ether, wherein the salt is only partly soluble, the major product consisted of 9,1′-benzoyloxybenzylidenefluorene, I. The expected 9-benzoylfluorene was obtained only as a minor product and could be removed quite readily, along with much unreacted fluorene, by boiling the solid reaction product with ethyl alcohol, in which the enol ester is insoluble. The same results were obtained when the solid 9-fluorenylpotassium, freed from dioxane (9), was suspended in pentane and treated with benzoyl chloride. Similar results were obtained when 9-fluorenylpotassium, completely dissolved in dimethoxyethane, or 9-fluorenylsodium dissolved in dimethoxyethane or diethoxyethane (8, 10) was allowed to react with benzoyl chloride.

On the other hand, the reaction of 9-fluorenyllithium and benzoyl chloride gave results quite different from those obtained with the sodium or potassium analogues. Under the heterogeneous conditions obtained in the suspension of the lithium salt in pentane, 9,9-dibenzoylfluorene was produced in 28% yield, uncontaminated by the enol ester (I). The unreacted fluorene, along with a small amount of monobenzoylfluorene, was easily removed by extraction from the insoluble β-diketone (II) with hot ethanol. However, equimolar amounts of 9-fluorenyllithium and the acid halide in diethoxyethane or dimethoxyethane yielded, after removal of unchanged fluorene and some monobenzoylfluorene, a mixture of 9,9-dibenzoylfluorene and 9,1′-benzoyloxybenzylidenefluorene. Efforts to separate this mixture were unsuccessful. The infrared spectra obtained for both I and II showed clearly the presence of this mixture.

The infrared spectrum of the enol ester, I, in carbon disulphide showed a strong band at 1738 cm^{-1}, typical of a conjugated ester carbonyl group and a band of medium strength at 1650 cm^{-1} due to the enol double bond (11). The enol ester showed no absorption at 1688 cm^{-1}. The spectrum of the diketone, II, exhibited a strong doublet at 1688 cm^{-1} and 1660 cm^{-1}, but no absorption at 1738 cm^{-1}. The presence of one isomer as an impurity in the other was thus easily detected by the bands at 1738 cm^{-1} and 1688 cm^{-1}. A further distinct difference occurred in the region of aromatic C—H out-of-plane bending frequencies. The β-diketone showed one sharp band of medium intensity at 762 cm^{-1} whereas the enol ester gave two sharp bands, one at 762 cm^{-1}, the other at 775 cm^{-1}.

The spectrum of 9-benzoylfluorene also showed a doublet at 1670 cm^{-1} and 1688 cm^{-1}, though it was not as well resolved as that found for the diketone. In addition, a strong band at 1273 cm^{-1} and a weak band at 1723 cm^{-1} occurred in the spectrum of the monobenzoylfluorene but not in that of the diketone. The 9-benzoylfluorene is considered to exist in the more stable keto form (12). The double carbonyl band of the keto form of 9-benzoylfluorene is not unusual since this phenomenon has been observed in a number of compounds containing only one carbonyl group (13).

The Reaction of Ethyl Benzoate with 9-Fluorenyl-lithium, -sodium, and -potassium

The reaction of 9-fluorenylpotassium, either in dioxane or in pentane, with ethyl benzoate gave a 40% yield of 9-benzoylfluorene. This is considerably better than the yield of 28% of the monobenzoylated fluorene obtained by Wislicenus and Fehrle (7) from the reaction of fluorene, potassium, and ethyl benzoate mixed in the ratio 1:1:1. The reaction of 9-fluorenyllithium, either partly dissolved in dimethoxyethane or as an

insoluble suspension in pentane, when treated with ethyl benzoate, gave 40–45% of 9-benzoylfluorene. In all cases much fluorene was isolated, but no evidence was found for the formation of the enol ester, I, or the diketone, II.

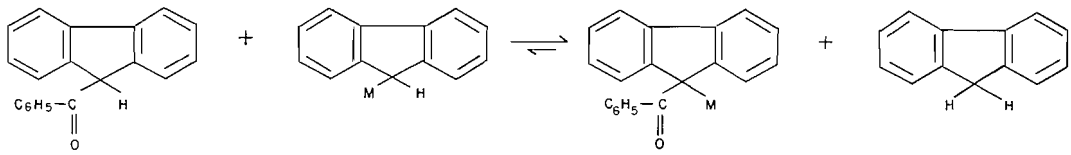
The Reaction of 9-Benzoyl-9-fluorenyl-lithium, -sodium, or -potassium with Benzoyl Chloride or Ethyl Benzoate

The compound 9-benzoylfluorene was converted readily to the lithium, sodium, or potassium salt, and then brought into reaction with benzoyl chloride or ethyl benzoate. In the ether solvents, dimethoxyethane or diethoxyethane, 9-benzoyl-9-fluorenyllithium and benzoyl chloride produced 55–65% of an inseparable mixture of enol ester and diketone. But when pentane was the solvent, a 54% yield of diketone was obtained, uncontaminated by enol ester. The sodium salt in dimethoxyethane or diethoxyethane, and the potassium salt in dimethoxyethane gave a 50–60% yield of the enol ester uncontaminated by the diketone.

The potassium or sodium salt of 9-benzoylfluorene in dimethoxyethane, reacting with ethyl benzoate, produced only unchanged 9-benzoylfluorene.

DISCUSSION

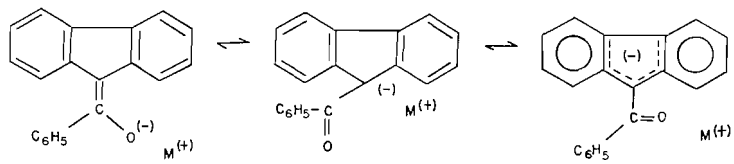
The results obtained clearly indicate that the following equilibrium occurs in the reaction of 9-fluorenyl-lithium, -sodium, or -potassium with benzoyl chloride in ether or in hydrocarbon solvents and under homogeneous or heterogenous conditions.



M = Li, Na, K

The enhanced acidic character of the remaining hydrogen at C_9 causes 9-benzoylfluorene to react with the remaining monometalated fluorene much more readily than the latter does with the benzoyl chloride.

The sodium and potassium salts of 9-benzoylfluorene will be largely, if not completely, ionic and stabilized by contributing structures A, B, and C. When the reaction with



A B C

benzoyl chloride occurs, the carbon–metal bond, highly ionic in both hydrocarbon and ether solvents, permits the accumulation of negative charge preferentially on the oxygen atom, the most electronegative atom in the anion. Reaction thus produces the enol ester, I, exclusively.

On the other hand, the carbon–*lithium* bond has considerable covalent character,

Can. J. Chem. Downloaded from www.nrcresearchpress.com by 210.87.254.5 on 09/05/12
For personal use only.

especially so in hydrocarbon solvents (14–16). In pentane the attack of benzoyl chloride therefore occurs at the carbon–metal bond directly, yielding only the diketone, II. However, in ether solvents, particularly dimethoxyethane and diethoxyethane, some association occurs between the metal and the unshared electron pairs of the oxygen atoms of the ethers (8), enhancing the ionic character of the carbon–lithium bond. Benzoyl chloride will then have two alternative competitive courses of reaction. Approach to the carbonyl oxygen atom produces the enol ester, with the assistance of the ether associated with the metal. Approach to the carbon–lithium bond results in facile displacement of the ether with consequent reaction directly at the carbon–lithium bond, thus yielding the diketone. The infrared spectra of the inseparable mixture of these two products obtained from the reaction of 9-benzoyl-9-fluorenyllithium and benzoyl chloride in the ethers mentioned indicate that the enol ester and the diketone are formed in the ratio of nearly 1:2.

The formation of only 9-benzoylfluorene along with unchanged fluorene from the reaction of ethyl benzoate and 9-fluorenyl-lithium, -sodium, or -potassium in ether or hydrocarbon solvents is no doubt due to the lower nucleophilic character of the resonance-stabilized anion ABC as compared with that of the ethoxide ion. The ethoxide ion, which must be formed if this anion reacts with ethyl benzoate, readily reacts with the enol ester or β-diketone to reconvert it to the more stable monobenzoylfluorenyl anion ABC. Such a decomposition of an enol ester or diketone by a strong base has been shown previously (4, 7). The failure of the Grignard reagent to form the expected tertiary alcohol from 9-methyl-9-benzoylfluorene also demonstrates the labile nature of 9-benzoylfluorene under basic conditions (17). A similar explanation has been offered for the failure of metalated diphenylmethane to react with more than one equivalent of ester (18).

EXPERIMENTAL

The experimental procedure is generally quite similar in all the reactions performed. A typical experiment for the reactions carried out in ether solvent and one for the reaction conducted with pentane as solvent are shown below. The essential details for the remainder of the experiments carried out are shown in the accompanying table.

All preparations involving organometallic compounds were carried out under nitrogen. Products were identified by mixed melting points with authentic specimens and (or) by comparison of the infrared spectra.

The Reaction of 9-Fluorenylpotassium with Benzoyl Chloride

(1) In dioxane.—Fluorene (16.6 g, 0.1 mole) and potassium (3.9 g, 0.1 mole) were kept for 4 hours in 160 ml of pure, dry, refluxing dioxane. Under these conditions all the potassium was consumed. The mixture was allowed to cool to room temperature and then benzoyl chloride (14 g, 0.1 mole), dissolved in 50 ml of dioxane, was slowly added. The dark red color of the original solution turned to light orange and a viscous solution was formed. Addition of ether and water followed by several washings of the ether layer with water permitted removal of the inorganic salts and the dioxane. At room temperature the ether layer contained yellow crystals which were separated. A second crop of crystals was obtained when the mother liquor was reduced in volume. The yield of crude material was 11.7 g (31%). After unreacted fluorene and 9-benzoylfluorene were removed by trituration with hot ethyl alcohol, pure 9,1′-benzoyloxybenzylidenefluorene, m.p. 189°, was obtained.

(2) In pentane.—Fluorene (8.3 g, 0.05 mole) and potassium metal (1.95 g, 0.05 mole)

Can. J. Chem. Downloaded from www.nrcresearchpress.com by 210.87.254.5 on 09/05/12
For personal use only.

TABLE I

Original compound	Metal	Metalation medium[a]	Solvent medium for benzoylation	Benzoylating agent[b]	Product[c]; yield
Fluorene	K	Dioxane	Dioxane	Ethyl benzoate	39% 9-benzoylfluorene + unchanged fluorene
Fluorene	K	Dioxane	Pentane	Ethyl benzoate	42% 9-benzoylfluorene + unchanged fluorene
Fluorene	Li	DEE (10)	DEE	Benzoyl chloride	31% of a mixture of I and II + unchanged fluorene
Fluorene	Li	DEE (10)	Pentane	Benzoyl chloride	28% of II + unchanged fluorene
Fluorene	Li	DEE (10)	DEE	Ethyl benzoate	45% of 9-benzoylfluorene + unchanged fluorene
Fluorene	Li	DEE (10)	Pentane	Ethyl benzoate	41% of 9-benzoylfluorene + unchanged fluorene
9-Benzoylfluorene	Li	DEE (10)	DEE	Benzoyl chloride	67% of a mixture of I and II + unchanged 9-benzoylfluorene
9-Benzoylfluorene	Li	DME	DME	Benzoyl chloride	56% of a mixture of I and II + unchanged 9-benzoylfluorene
9-Benzoylfluorene	Li	DEE	Pentane	Benzoyl chloride	54% of II + unchanged 9-benzoylfluorene
9-Benzoylfluorene	Li	DEE	DEE	Ethyl benzoate	Only unchanged 9-benzoylfluorene
9-Benzoylfluorene	Li	DEE	Pentane	Ethyl benzoate	Only unchanged 9-benzoylfluorene
9-Benzoylfluorene	Na	DME	DME	Benzoyl chloride	60% of I + unreacted 9-benzoylfluorene
9-Benzoylfluorene	Na	DEE	DEE	Benzoyl chloride	Only I (amount undetermined) + unreacted 9-benzoylfluorene
9-Benzoylfluorene	Na	DME	DME	Ethyl benzoate	Only unchanged 9-benzoylfluorene
9-Benzoylfluorene	K	DME	DME	Benzoyl chloride	48% of I + unchanged 9-benzoylfluorene
9-Benzoylfluorene	K	DME	DME	Ethyl benzoate	Only unchanged 9-benzoylfluorene

[a]Metalation was complete in all cases, although the time varied between 0.5 and 2 hours for complete reaction with 9-benzoylfluorene and 4 to 5 hours for the metalation of fluorene. DEE = diethoxyethane. DME = dimethoxyethane.
[b]The slower reaction with ethyl benzoate was allowed to continue overnight, with stirring, to ensure complete reaction. Benzoyl chloride reacted more rapidly but was given a 1- to 3-hour reaction time to ensure completeness.
[c]The 9-benzoylfluorene was freed from fluorene by crystallization from ethanol. Hot ethanol removed fluorene and 9-benzoylfluorene from the alcohol-insoluble enol ester and/or diketone.

were kept for 4 hours in 40 ml of pure, refluxing dioxane. The cooled solution, containing no unreacted potassium, was poured into 500 ml of dry pentane, whereupon the 9-fluorenylpotassium precipitated. The liquid was decanted and the precipitate washed by decantation using pentane, and then suspended in 100 ml of pentane. To this was added slowly a solution of 7 g (0.05 mole) of benzoyl chloride in 50 ml of dry pentane. Reaction occurred immediately but was allowed to continue for 3 hours, with stirring, to assure maximum reaction of the suspended solid. After removal of inorganic substances by water washes, there remained a solid material suspended in the pentane layer. When this was removed and dried it weighed 9.9 g. Contaminating fluorene and 9-benzoylfluorene were removed by extraction of the crude material with hot ethanol, in which both the 9,1′-benzoyloxybenzylidenefluorene and 9,9-dibenzoylfluorene are insoluble. There was obtained 5.1 g (27%) of material analyzing correctly for the enol ester and melting at 189°.

The pentane mother liquor, upon evaporation, yielded a small amount of 9-benzoylfluorene and a considerable quantity of unreacted fluorene.

Can. J. Chem. Downloaded from www.nrcresearchpress.com by 210.87.254.5 on 09/05/12
For personal use only.

ACKNOWLEDGMENT

The authors wish to express their appreciation for the financial assistance so generously given by the National Research Council of Canada.

REFERENCES

1. W. SCHLENK and E. BERGMANN. Ann. **463**, 125 (1928).
2. W. SCHLENK and E. BERGMANN. Ber. **62**, 748 (1929).
3. A. KLIEGL, F. WENG, and G. WIEST. Ber. **63**, 1262 (1930).
4. P. PFEIFFER and E. LUBBE. Ber. **63**, 762 (1930).
5. J. A. KING, R. J. MELTZER, and J. DOCZI. J. Am. Chem. Soc. **77**, 2217 (1955).
6. A. WERNER and G. SCHOLER. Ber. **39**, 1287 (1906).
7. W. WISLICENUS and A. FEHRLE. Ber. **48**, 1320 (1915).
8. G. W. H. SCHERF and R. K. BROWN. Can. J. Chem. **39**, 799 (1961).
9. G. W. H. SCHERF and R. K. BROWN. Can. J. Chem. **38**, 697 (1960).
10. G. W. H. SCHERF and R. K. BROWN. Can. J. Chem. **38**, 2450 (1960).
11. L. J. BELLAMY. The infrared spectra of complex molecules. 2nd ed. John Wiley & Sons, Inc., New York. 1958.
12. K. H. MEYER and H. GOTTLIEB BILLROTH. Ber. **54**, 575 (1921).
13. R. N. JONES, C. L. ANGELL, T. ITO, and R. J. D. SMITH. Can. J. Chem. **37**, 2007 (1959).
14. J. HINE. Physical organic chemistry. McGraw-Hill Book Co., Inc., Toronto. 1956.
15. R. L. LETSINGER. J. Am. Chem. Soc. **72**, 4842 (1950).
16. D. Y. CURTIN and E. E. HARRIS. J. Am. Chem. Soc. **73**, 2716 (1951).
17. P. M. G. BAVIN. Can. J. Chem. **37**, 2023 (1959).
18. R. S. YOST and C. R. HAUSER. J. Am. Chem. Soc. **69**, 2325 (1947).

Can. J. Chem. Downloaded from www.nrcresearchpress.com by 210.87.254.5 on 09/05/12
For personal use only.

Can. J. Chem. Downloaded from www.nrcresearchpress.com by 210.87.254.40 on 09/05/12
For personal use only.

INTERMOLECULAR FORCES AND LIQUID STRUCTURE IN SOME METAL ALKOXIDES[1]

D. C. BRADLEY,[2] CALLIOPE C. A. PREVEDOROU,[2] AND W. WARDLAW[3]

ABSTRACT

The viscosities of some alkoxides of titanium, zirconium, cerium (IV), thorium, and tin (IV) have been measured in the temperature range 25–40° C. The liquid structure in these compounds is discussed in terms of the activation energy, free energy, and entropy of activation for viscous flow, and the energies of cohesion and vaporization.

INTRODUCTION

Previously (1) we investigated the liquid-state properties of a number of germanium tetraalkoxides (alkyl orthogermanates) in order to establish a basis for comparison with similar properties of a number of metal alkoxides. The germanium alkoxides are monomeric whereas some of the metal alkoxides studied in this research are known to be polymeric. It was of interest, in connection with the theory of intermolecular forces in the liquid state, to study the behavior of both monomeric and polymeric metal alkoxides since these large molecules are believed to have globular or quasi-spherical structures. We now report some results on the viscosities of a number of alkoxides of the group IV metals and discuss these in conjunction with related properties of the liquid state.

EXPERIMENTAL

Preparation of the Alkoxides

The alkoxides of titanium (2), zirconium (2), cerium (3), thorium (4), and tin (5) were prepared, purified, and analyzed by the previously described methods. Titanium tetraethoxide is a supercooled liquid at room temperature but it did not change in viscosity when kept in the apparatus over 8 hours.

Viscosity Measurements

All-glass Ostwald viscometers were calibrated using pure benzene at 25, 30, 35, and 40° C. The sample of alkoxide was distilled into the rigorously dried viscometer at 0.1 mm pressure and dry nitrogen was then admitted at atmospheric pressure. The temperature of the viscometer was controlled to ±0.01° C and three separate determinations were carried out on each compound. The reproducibility was of the order of ±0.0001 poises for the least viscous and ±0.01–0.02 poises for the most viscous compounds. The results (viscosity in poises) are presented in Table I.

The activation energies of viscosity E_{visc} (kcal/mole) were evaluated graphically from the plot of $\log \eta$ versus $1/T°$ K. The free energies of activation of viscous flow $\Delta F^{\ddagger}$ (kcal/mole) were calculated from Eyring's (6) equation:

$$\eta = (hN/V) \cdot e^{(\Delta F^{\ddagger}/RT)}.$$

The molar volumes were taken from our previous work (8) and the molar heats of vaporization from the results of vapor pressure studies (2).

[1]*Manuscript received February 3, 1961.*
Contribution from the Department of Chemistry, Birkbeck College, London, W.C. 1, England.
[2]*Present address: Department of Chemistry, the University of Western Ontario, London, Ontario.*
[3]*Deceased December 18, 1958.*

TABLE I

Viscosities (poises) of metal alkoxides

Compound	25° C	30° C	35° C	40° C
$Ti(OEt)_4$	0.447	0.357	0.285	0.236
$Ti(OPr^n)_4$	1.749	1.306	1.070	0.851
$Ti(OBu^n)_4$	0.692	0.579_5	0.483	0.406_5
$Ti(OBu^t)_4$	0.0352	0.0315	0.0285	0.0258
$Zr(OBu^t)_4$	0.0317	0.0278	0.0246	0.0224
$Ti(OCMe_2Et)_4$	0.0808	0.0714	0.0626	0.0537
$Zr(OCMe_2Et)_4$	0.0759	0.0673	0.0589	0.0518
$Sn(OCMe_2Et)_4$	0.166_5	0.143	0.120_5	0.102
$Ti(OCMe_2Pr^n)_4$	0.0479	0.0434	0.0395	0.0362
$Zr(OCMe_2Pr^n)_4$	0.0464	0.0419	0.0379	0.0346
$Sn(OCMe_2Pr^n)_4$	0.0986	0.0840	0.0716	0.0644
$Ce(OCMe_2Pr^n)_4$	8.13	5.89	4.28	3.16
$Ti(OCMeEt_2)_4$	0.345	0.299_5	0.260	0.220_5
$Zr(OCMeEt_2)_4$	0.281	0.236_5	0.200	0.170_5
$Sn(OCMeEt_2)_4$	0.413	0.339	0.265_5	0.225
$Ce(OCMeEt_2)_4$	0.216	0.169_5	0.141	0.119
$Ce(OCEt_3)_4$	0.526	0.451_5	0.387_5	0.332_5
$Th(OCEt_3)_4$	0.492	0.387	0.322	0.269

DISCUSSION

The data on E_{visc}, $\Delta F^{\ddagger}$, and $\Delta S^{\ddagger}$ (cal/deg mole), at 25° C, are presented in Table II.

TABLE II

Compound	E_{visc} (kcal/mole)	$\Delta F^{\ddagger}$ (kcal/mole)	$\Delta S^{\ddagger}$ (cal/°C mole)
$Ti(OEt)_4$	7.9	5.9	+6.7
$Ti(OPr^n)_4$	8.4	6.9	+5.3
$Ti(OBu^n)_4$	7.1	6.5	+2.0
$Ti(OBu^t)_4$	4.1	4.8	−2.4
$Zr(OBu^t)_4$	4.4	4.8	−1.4
$Ti(OCMe_2Et)_4$	5.2	5.4	−0.7
$Zr(OCMe_2Et)_4$	5.4	5.4	0
$Sn(OCMe_2Et)_4$	6.4	5.8	+2.0
$Ti(OCMeEt_2)_4$	6.1	6.3	−0.7
$Zr(OCMeEt_2)_4$	6.6	6.2	+1.3
$Ce(OCMeEt_2)_4$	7.0	6.1	+3.5
$Sn(OCMeEt_2)_4$	8.2	6.7	+5.0
$Ti(OCMe_2Pr^n)_4$	3.8	5.2	−5.0
$Zr(OCMe_2Pr^n)_4$	4.0	5.2	−4.0
$Ce(OCMe_2Pr^n)_4$	12.6	8.1	+15.1
$Sn(OCMe_2Pr^n)_4$	5.6	5.6	0
$Ce(OCEt_3)_4$	6.3	6.6	−1.3
$Th(OCEt_3)_4$	7.6	6.6	+3.5

The errors in E_{visc} and $\Delta F^{\ddagger}$ were of the order of ± 0.5–1.0%, whilst for $\Delta S^{\ddagger}$ the errors probably range from about $\pm 5\%$ for values around 5 cal/deg mole to about $\pm 15\%$ for values around 1 cal/deg mole.

Considering first the *n*-alkoxides of titanium, $Ti(OR)_4$, where R = Et, Pr^n, and Bu^n, it is noteworthy that for both η and E_{visc} there is a maximum value at the *n*-propoxide. This is in marked contrast to the behavior of the corresponding germanium *n*-alkoxides where E_{visc} increases steadily with molecular size (1). Moreover, the values of E_{visc} for the titanium derivatives are two to three times greater than for the corresponding germanium derivatives. There is little doubt that this "anomalous" behavior of the titanium compounds is a consequence of their polymeric nature. For example, Caughlan *et al.* (7)

Can. J. Chem. Downloaded from www.nrcresearchpress.com by 210.87.254.40 on 09/05/12
For personal use only.

showed cryoscopically that the number-average degree of polymerization of titanium *n*-alkoxides in benzene increased with increasing concentration to a limiting value of three. They suggested that the trimer was of structural significance and deduced two possible structures based on octahedral titanium atoms in which 6-co-ordination was attained by intermolecular bonds from oxygen to titanium. It seems reasonable to assume that these alkoxides would also be trimeric in the pure liquid state. Concerning the mechanism of viscous flow, there seem to be two alternatives for the polymeric derivatives. Either the trimers migrate individually or they may dissociate into more mobile monomer units which then migrate. We have already observed that for the germanium *n*-alkoxides, which are monomeric, E_{visc} increases steadily with increase in molecular size. It is also clear from the data in Table II that for the monomeric tertiary alkoxides of titanium (and zirconium) E_{visc} again increases steadily with molecular size. Hence it might reasonably be expected that E_{visc} for the trimer $Ti_3(OR)_{12}$ would be almost triple that for the monomer $Ti(OR)_4$ if the trimer migrates as a whole. We have estimated, by extrapolation from the values of E_{visc} for the monomeric tertiary alkoxides, that the values of $(E_{visc})_{mon}$ for "monomeric" normal alkoxides of titanium should be approximately: $Ti(OEt)_4$, 2.2; $Ti(OPr^n)_4$, 3.2; $Ti(OBu^n)_4$, 4.1 kcal/mole. These figures are reasonably close to the corresponding values for the work of cohesion W_c (see later) and W_c should be $\simeq E_{visc}$ for simple molecules (9). The ratios $E_{visc}/(E_{visc})_{mon}$ are as follows: $Ti(OEt)_4$, 3.6; $Ti(OPr^n)_4$, 2.6; $Ti(OBu^n)_4$, 1.7. Bearing in mind the approximations involved, it might be agreed that the figures for $Ti(OEt)_4$ and $Ti(OPr^n)_4$ are consistent with these compounds exhibiting flow by migration of trimeric molecules, but such is not the case for $Ti(OBu^n)_4$. Moreover, the alternative mechanism of flow involving depolymerization of the trimers and migration of monomers would also require anomalously high values of E_{visc} because the activation energy for viscous flow would include the energy of depolymerization ΔE. Assuming that $E_{visc} = (E_{visc})_{mon} + \Delta E$, the following values for ΔE are derived: $Ti(OEt)_4$, 5.7; $Ti(OPr^n)_4$, 5.2; $Ti(OBu^n)_4$, 3.0 kcal/mole. The observed order of E_{visc} would then be a consequence of the decrease in depolymerization energy (ΔE) with increase in length of the alkyl chains. We are inclined to the view that the second mechanism, i.e. depolymerization followed by migration of monomers, is the correct one because of the entropies of activation $\Delta S^{\ddagger}$ shown in Table II. Thus the monomeric germanium *n*-alkoxides had negative entropies of activation and the monomeric titanium tertiary alkoxides also have negative entropies of activation. Hence we should expect the migration of trimeric molecules to involve a similar negative entropy of activation. However, the titanium *n*-alkoxides have relatively large positive entropies of activation and this is consistent with the proposition that depolymerization is involved in the mechanism of flow since such a process should cause a considerable degree of disorder in attaining the activated configuration. It is noteworthy that the positive $\Delta S^{\ddagger}$ values decrease in the same order as the values of ΔE.

Turning now to the monomeric alkoxides of titanium and zirconium, we note that η and E_{visc} increase with molecular size from $M(OCMe_3)_4$ to $M(OCMe_2Et)_4$ to $M(OCMeEt_2)_4$, with the titanium derivative having a slightly higher viscosity but slightly lower E_{visc} than the corresponding zirconium derivative. The $\Delta S^{\ddagger}$ values are slightly more positive for the zirconium compounds. However, the E_{visc} values for the $M(OCMe_2Pr^n)_4$ derivatives of Ti and Zr are remarkably low and suggest that the mechanism of flow must differ in these molecules from the mechanism of "molecular jumps" which probably occurs in the other tertiary alkoxides. This is reflected in the large negative $\Delta S^{\ddagger}$ values for the $M(OCMe_2Pr^n)_4$ molecules. The behavior of the stannic

Can. J. Chem. Downloaded from www.nrcresearchpress.com by 210.87.254.40 on 09/05/12
For personal use only.

alkoxides is surprising since the values for η and E_{visc} are higher and $\Delta S^{\ddagger}$ more positive than in the corresponding titanium and zirconium derivatives. Previous work (8) showed that the stannic compounds also had anomalously low parachors compared with the Ti and Zr compounds. The reason for this is still not clear. The effect of polymerization is strikingly revealed in the viscosity data for the cerium derivatives of dimethyl *n*-propyl carbinol and methyl diethyl carbinol. On the other hand the triethyl carbinol derivatives of cerium and thorium, which are monomeric, seem to have η and E_{visc} values of the correct order of magnitude.

Grunberg and Nissan (9) have shown that important structural information on liquids may be deduced from a comparison of the internal energy of vaporization $E_v(\Delta H_v - RT)$, the work of cohesion W_c ($2\gamma N^{1/3} V_l^{2/3}$, where γ is the surface tension and V_l the molar volume of the liquid), and the activation energy of viscosity E_{visc}. Eyring (6) has shown that for many liquids, $E_v/\Delta F^{\ddagger} \simeq 2.5$ and E_v/E_{visc} is 3–4, and has interpreted deviations from these values in terms of structural abnormalities. We have calculated the values for W_c (kcal/mole) (8) and the ratios E_v/E_{visc} etc. for some liquid metal alkoxides and the data are given in Table III.

TABLE III

Compound	E_v (kcal/mole)	W_c (kcal/mole)	$E_v/\Delta F^{\ddagger}$	E_v/E_{visc}	E_v/W_c	E_{visc}/W_c
$Ti(OEt)_4$	21.0	2.84	3.55	2.50	7.39	2.95
$Ti(OPr^n)_4$	15.1	3.78	2.18	1.71	3.99	2.33
$Ti(OBu^n)_4$	19.5	4.39	3.00	2.71	4.44	1.63
$Ti(OBu^t)_4$	14.0	4.92	2.91	3.41	3.00	0.83
$Zr(OBu^t)_4$	14.6	4.47	3.04	3.32	3.27	0.98
$Ti(OCMe_2Et)_4$	16.1	6.03	2.98	3.10	2.67	0.86
$Zr(OCMe_2Et)_4$	15.7	5.46	2.90	2.91	2.88	0.98
$Ti(OCMeEt_2)_4$	18.4	6.92	2.92	3.01	2.66	0.88
$Zr(OCMeEt_2)_4$	18.4	6.30	2.96	2.80	2.92	1.05
$Ti(OCMe_2Pr^n)_4$	18.9	6.75	3.63	4.97	2.73	0.57
$Zr(OCMe_2Pr^n)_4$	18.4	6.28	3.54	4.60	2.93	0.64

In addition, the values of W_c and the ratio E_{visc}/W_c have been calculated for some alkoxides whose latent heats of vaporization are not known: $Sn(OCMe_2Et)_4$: W_c 4.96, E_{visc}/W_c 1.31; $Sn(OCMe_2Pr^n)_4$: 4.99, 1.13; $Ce(OCMeEt_2)_4$: 6.23, 1.12; $Ce(OCEt_3)_4$: 7.03, 0.90; $Th(OCEt_2)_4$: 6.09, 1.25.

Grunberg and Nissan (9) showed that for various monomeric liquids, $E_{visc} = W_c$, and it is clear that in these cases the energy requirements for translating a molecule from one equilibrium position to another in viscous flow are the same as in displacing a molecule to expose fresh surface of the liquid. They also noted that for "associated" liquids, $E_{visc} > W_c$, and suggested that the difference $E_{visc} - W_c$ could be attributed to the energy of dissociation of the associated molecules since W_c does not contain the dissociation energy but E_{visc} does. This difference presumably arises because E_{visc} is determined from a rate process whereas the determination of W_c involves an equilibrium system. In principle, a higher value of W_c including the energy of dissociation might be obtained by using a dynamic method in which the surface tension was measured during a time interval which was short compared with the lifetime of a "dissociated" molecule. The results for the monomeric tertiary alkoxides $M(OCMe_nEt_{3-n})_4$, where M = Ti or Zr and n = 3, 2, or 1, and also for some of the tertiary alkoxides of tin, cerium, and thorium, show that the ratio E_{visc}/W_c is indeed close to unity. Evidently these large

Can. J. Chem. Downloaded from www.nrcresearchpress.com by 210.87.254.40 on 09/05/12
For personal use only.

Can. J. Chem. Downloaded from www.nrcresearchpress.com by 210.87.254.40 on 09/05/12
For personal use only.

globular molecules behave similarly to simple molecules in the processes of viscous flow and surface formation. No doubt this is because the intermolecular forces between the monomeric tertiary alkoxides are mainly determined by the peripheral alkyl groups and these forces will be of the dispersion type. It is quite clear that the central metal atom has little influence on the magnitude of these forces and this is in accordance with the earlier theory of Bradley *et al.* (2, 3, 4, 5) that the highly branched tertiary alkoxide groups effectively screen the metal and prevent intermolecular bonding involving the metal. The behavior of the monomeric alkoxides $Ti(OCMe_2Pr^n)_4$ and $Zr(OCMe_2Pr^n)_4$ is extremely interesting. In both cases the ratio E_{visc}/W_c is considerably less than unity and it appears, from a comparison with the data for the other monomeric titanium and zirconium alkoxides, that for $M(OCMe_2Pr^n)_4$ the values of W_c are normal but values of E_{visc} are abnormally low. This suggests that the mechanism of flow for $M(OCMe_2Pr^n)_4$ liquids does not involve the discrete movement of the whole molecule but, more probably, migration occurs by a "molecular wriggle" mechanism. It is noteworthy that these compounds also have fairly large negative entropies of activation for viscous flow and this recalls the mechanism of flow postulated by Moore, Gibbs, and Eyring (10) for straight-chain hydrocarbons. They noted that these compounds had low values of E_{visc} in the low-temperature region and gave negative $\Delta S^{\ddagger}$'s. It was suggested that these liquids had a quasi-crystalline structure and that viscous flow involved a co-operative movement analogous to the movement of dislocations in the lattice of a metal.

It is extremely interesting to note that for the polymeric *n*-alkoxides of titanium, the values of E_{visc}/W_c are much greater than unity due to the abnormally high values for E_{visc}. In fact, the values of W_c for the *n*-alkoxides are remarkably close to the values calculated for hypothetical "monomeric" derivatives by extrapolation from the data on the monomeric tertiary alkoxides. From this we deduce that the intermolecular forces which are overcome in the creation of fresh surface are the same in nature for both the polymeric and the monomeric alkoxides and hence must involve predominantly the dispersion forces between the peripheral alkyl groups. Hence the values of W_c for the polymeric alkoxides do not involve the dissociation energy of the polymers whereas we have argued earlier that E_{visc} does include the dissociation energy. Therefore, the difference $E_{visc} - W_c \simeq \Delta E$ and provides an alternative measure for ΔE. The values of ΔE so calculated are: $Ti(OEt)_4$, 5.1 (5.7); $Ti(OPr^n)_4$, 4.6 (5.2); $Ti(OBu^n)_4$, 2.7 (3.0); the values in parentheses are the ones deduced earlier in the paper by the other method.

For the monomeric tertiary alkoxides which exhibit the "molecular jump" mechanism of flow it appears that $E_v/\Delta F^{\ddagger}$ is 3.0 rather than 2.5 as found by Eyring (6) for "normal" liquids. This discrepancy may well be due to the fact that Eyring's values of E_v were calculated from heats of vaporization at the normal boiling point whereas in the metal alkoxides our values of E_v are derived from vapor pressure results at lower pressures (where ΔH_v will be larger). For the same compounds E_v/E_{visc} is around 3.0 whereas for the "abnormal" polymeric alkoxides E_v/E_{visc} is low and for $M(OCMe_2Pr^n)_4$ (M = Ti, Zr) the values are rather high.

Finally, it is interesting to explore the application of Grunberg and Nissan's (9) ideas on the structure of liquids to our data. For liquids composed of simple molecules they suggested that there is a statistical structure in which each molecule is surrounded by *n* nearest neighbors and that intermolecular forces may be considered as localized in "bonds" between nearest neighbors. In the process of vaporization all of these "bonds" must be disrupted before a molecule is free to escape into the vapor. However, in surface formation the number of "bonds" which need to be disrupted in order to expose a

"central" molecule depends on the quasi structure in the liquid and this is why $E_v > W_c$. They deduced that the ratio $E_v > W_c$ would be determined by the co-ordination number and the structure of the liquid as follows: for hexagonal (c.p.), cubic (c.p.), and cubic (b.c.) packing, $E_v/W_c = 4$; for octahedral packing, $E_v/W_c = 3$; and for tetrahedral packing, $E_v/W_c = 2$. For the monomeric tertiary alkoxides the data in Table III show that the zirconium compounds have E_v/W_c values about 10% greater than the corresponding titanium derivatives. This is a reflection of the fact that the zirconium compounds have lower values of W_c but about the same values of E_v as the titanium compounds. Nevertheless, the value of E_v/W_c for all of these compounds is around 3.0 and suggests that the molecules have an average co-ordination number of 6. This figure must be treated with caution since the molecules under consideration are large and complicated in structure and hence may not conform to the requirements of the theory.

CONCLUSIONS

1. From considerations of the energies of intermolecular attraction as deduced from the processes of vaporization, viscous flow, and surface formation, it appears that the monomeric tertiary alkoxides behave rather like simple covalent molecules which are bound by dispersion forces in the liquid state. This agrees with the conclusions from other work that the steric effect of the branched alkoxide groups largely precludes the central metal atom from being involved in intermolecular interaction.

2. In the *n*-alkoxides of titanium, which are polymeric due to intermolecular bonding between titanium and oxygen, it appears that the mechanism of viscous flow involves dissociation of the polymers with consequent abnormally high activation energy. On the other hand the process of surface formation appears to involve only the relatively weak dispersion forces between the molecules.

REFERENCES

1. D. C. Bradley, L. J. Kay, J. D. Swanwick, and W. Wardlaw. J. Chem. Soc. 3656 (1958).
2. D. C. Bradley, R. C. Mehrotra, J. D. Swanwick, and W. Wardlaw. J. Chem. Soc. 2025 (1953); D. C. Bradley, R. C. Mehrotra, and W. Wardlaw. J. Chem. Soc. 4204 (1952).
3. D. C. Bradley, A. K. Chatterjee, and W. Wardlaw. J. Chem. Soc. 2600 (1957).
4. D. C. Bradley, M. A. Saad, and W. Wardlaw. J. Chem. Soc. 3488 (1954).
5. D. C. Bradley, E. V. Caldwell, and W. Wardlaw. J. Chem. Soc. 4775 (1957).
6. H. Eyring. J. Chem. Phys. **4**, 283 (1936).
7. C. N. Caughland, H. S. Smith, W. Katz, W. Hodgson, and R. W. Crowe. J. Am. Chem. Soc. **73**, 5652 (1951).
8. D. C. Bradley, C. C. A. Prevedorou, J. D. Swanwick, and W. Wardlaw. J. Chem. Soc. 1010 (1958).
9. L. Grunberg and A. H. Nissan. Trans. Faraday Soc. **45**, 125 (1949).
10. R. J. Moore, P. Gibbs, and H. Eyring. J. Phys. Chem. **57**, 172 (1953).

Can. J. Chem. Downloaded from www.nrcresearchpress.com by 210.87.254.40 on 09/05/12
For personal use only.

Can. J. Chem. Downloaded from www.nrcresearchpress.com by 210.87.254.105 on 09/05/12
For personal use only.

MOLECULAR INTERACTIONS

I. INFRARED SPECTRA OF SOME CARBOXYLIC ACIDS IN CARBON TETRACHLORIDE AND BENZENE SOLUTIONS[1]

F. E. MURRAY[2] AND S. SUNDARAM

ABSTRACT

Infrared spectra of benzoic, *o*-chlorobenzoic, and salicylic acids in the range 700 to 3800 cm^{-1} have been studied. Measurements have been made on the three acids in carbon tetrachloride and benzene solutions, at a number of concentrations in each case. The results are interpreted in terms of the molecular species present in each solution and the effect of the solvents on these species. Assignments have been made of the observed bands to the various vibrational modes characteristic of the COOH group.

INTRODUCTION

Dimeric carboxylic acids have been the subject of study by a number of investigators in the past. The infrared and Raman spectra have been used to show the presence of strong hydrogen bridges between the carbonyl and the hydroxyl groups of the two molecules. Even in dilute solutions in certain solvents, the association between the molecules persists.

The abnormally strong hydrogen bonds in these acids is an advantage in correlating the characteristic distortions of the O—H stretching modes with the association. There are also other regions of the spectra that are equally important. The C=O region (1700 cm^{-1}) gives indications of the immediate environment of the COOH group. The other regions that provide additional useful data are 1300–1400 cm^{-1}, corresponding to C—O stretching and O—H in-plane deformation, and near 950 cm^{-1}, attributed to the O—H out-of-plane mode.

The infrared spectra of benzoic acid in solution in carbon tetrachloride have been studied by Davies and Sutherland (1), Harris and Hobbs (2), and Bratoz *et al.* (3). Hadzi and Sheppard (4) have also observed the infrared spectrum of solid benzoic acid below 1500 cm^{-1}. Among others, Murty and Seshadri (5) have reported the Raman spectrum of benzoic acid in solution in benzene and indicated the presence of ring dimers. Brooks *et al.* (6, 7) have recently investigated the C=O and O—H frequencies in the infrared spectra of benzoic and *o*-chlorobenzoic acid in ether–CCl_4 and CCl_4 solutions respectively and of substituted salicylic acids and their esters in CCl_4 solutions. The Raman spectrum of salicylic acid in benzene solution has been studied by Murty and Seshadri (8). They concluded that some chelate monomer is present in benzene solution but the major molecular species is a polymer, the structure of which was not clear.

The present study was begun to obtain information on the effect of the ortho substituents in benzoic acid on the tendency of this compound to form dimers in solution. The presence of an ortho substituent in benzoic acid makes possible the formation of chelate monomers. This tendency for chelation depends on the donor or acceptor strength of the ortho substituent group. Thus, for these compounds there are two competing processes for the formation of donor–acceptor bonds leading to the production of chelate monomers or to associated polymers. The effect of the solvent on the type of the molecular species present in solution has also been investigated.

[1]*Manuscript received April 7, 1961.*
Contribution from the British Columbia Research Council, University of British Columbia, Vancouver 8, B.C.
[2]*Present address: Research Department, Consolidated Paper Corporation, Grand'Mere, Que.*

Three acids, benzoic, *o*-chlorobenzoic, and salicylic were chosen for study. The spectra for these three compounds were obtained at various concentrations in solution in carbon tetrachloride and in benzene.

EXPERIMENTAL

All the spectra were recorded using a Perkin–Elmer Model 21 double-beam spectrometer equipped with sodium chloride optics. The instrument was calibrated against atmospheric absorption bands and a polystyrene film. The accuracy in the O—H stretching band region is estimated at ± 10 cm^{-1}. Measurements were made using 5-mm matched cells. The solvents used, carbon tetrachloride and benzene, were spectrograde and the acids used were analytical reagent grade. All of the above compounds were used without any attempts at further purification.

RESULTS

(*a*) Infrared spectral data for benzoic acid in carbon tetrachloride solution at a concentration of 8.2 millimoles per liter.—Principal absorption bands (cm^{-1}): 3650, 3545, 3060, 3020, 3005, 2875, 2658, 2590, 2540, 2080, 1970, 1927, 1912, 1815, 1780, 1737, 1692, 1620, 1455, 1420, 1352, 1320, 1287, 1177, 1125, 1090, 1065, 1025, 935.

(*b*) Infrared spectral data for benzoic acid in benzene solution at a concentration of 17.2 millimoles per liter.—Principal absorption bands (cm^{-1}): 3660, 3630, 3470, 3220, 3000, 2780, 2665, 2630, 2540, 2345, 2300, 2197, 2080, 1902, 1725, 1690, 1650, 1640, 1355, 1290, 1272.

(*c*) Infrared spectral data for salicylic acid in carbon tetrachloride solution at a concentration of 6.58 millimoles per liter.—Principal absorption bands (cm^{-1}): 3535, 3060, 2918, 2870, 2590, 2530, 1690, 1660, 1612, 1482, 1462, 1442, 1382, 1297, 1180, 1162, 1152, 1135, 1072, 1033, 903.

(*d*) Infrared spectral data for salicylic acid in benzene solution at a concentration of 4.4 millimoles per liter.—Principal absorption bands (cm^{-1}): 3655, 3450, 3240, 3000, 2820, 2635, 2570, 2540, 1787, 1687, 1655, 1642, 1417, 1342, 1330, 1290, 1265.

(*e*) Infrared spectral data for *o*-chlorobenzoic acid in carbon tetrachloride solution at a concentration of 12.8 millimoles per liter.—Principal absorption bands (cm^{-1}): 3585, 3080, 3030, 3000, 2910, 2655, 2555, 1977, 1947, 1755, 1700, 1565, 1480, 1442, 1410, 1297, 1180, 1165, 1145, 1130, 1100, 1050, 1042, 925.

(*f*) Infrared spectral data of *o*-chlorobenzoic acid in benzene solution at a concentration of 12.8 millimoles per liter.—Principal absorption bands (cm^{-1}): 3655, 3460, 3210, 2775, 2670, 2530, 1717, 1690, 1332, 1270.

DISCUSSION

In the following discussion of the spectra observed, the absorption bands in the various regions are assigned to the molecular species which appear to exist for each of the acids in the two solvents. The assignments are based on the position of the band and on the behavior of the intensity of the band with changing concentration of the solute. In some cases, the positions of the bands change significantly as the concentration of the solute is changed. This effect, which must be caused by an interaction between solvent molecules and the functional group which gives rise to the vibrational band, has not been considered in any detail.

1. Region of the O—H Stretching Fundamental

The results obtained in the region of the O—H stretching vibrational frequency are shown in Fig. 1. The acids in solution in carbon tetrachloride show sharp monomer

Can. J. Chem. Downloaded from www.nrcresearchpress.com by 210.87.254.105 on 09/05/12
For personal use only.

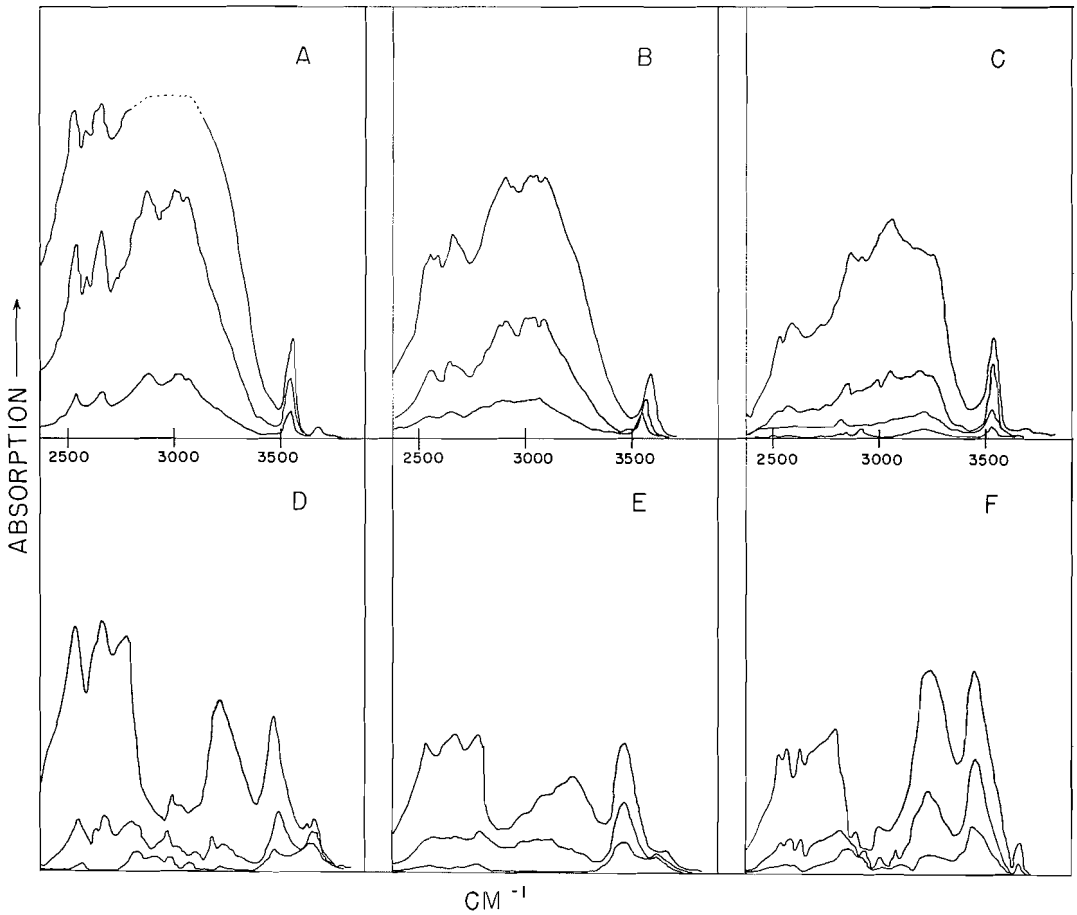


FIG. 1. Region of the O—H stretching fundamental bands: A, benzoic acid in carbon tetrachloride at concentrations 32, 8.2, and 1.3 millimoles per liter; B, orthochlorobenzoic acid in carbon tetrachloride at concentrations 12.8, 3.84, and 1.15 millimoles per liter; C, salicylic acid in carbon tetrachloride at concentrations 6.58, 1.98, 0.59, and 0.18 millimoles per liter; D, benzoic acid in benzene at concentrations 17.2, 3.4, and 0.68 millimoles per liter; E, orthochlorobenzoic acid in benzene at concentrations 12.8, 3.84, and 1.15 millimoles per liter; F, salicylic acid in benzene at concentrations 14.5, 4.4, and 1.32 millimoles per liter.

O—H bands at 3545, 3585, and 3535 cm^{-1} for benzoic, *o*-chlorobenzoic, and salicylic acids, respectively. In this solvent, the band of the associated form is strong and broad with the actual position of the peaks obscured by the overlapping C—H bands.

In benzene solution, the monomeric bands appear at lower frequencies than the bands for the same acids in carbon tetrachloride solution. The monomer bands are at 3470, 3460, and 3450 cm^{-1} respectively for the benzoic, *o*-chlorobenzoic, and salicylic acids. The bands for the associated species are clearly defined for each acid and appear at 3220, 3210, and 3240 cm^{-1} for the benzoic, *o*-chlorobenzoic, and salicylic acids.

Subsidiary maxima, with somewhat narrower half-band widths, have been observed in all the solutions in the region 2500–3000 cm^{-1}. These bands have been very satisfactorily accounted for by a summation-band hypothesis by Hadzi and Sheppard (4).

2. Region of the C=O Stretching Fundamental

The spectra obtained for the three acids in both the solvents, in the region of the C=O stretch, are shown in Fig. 2. The effect of the solvent change on the C=O stretching

Can. J. Chem. Downloaded from www.nrcresearchpress.com by 210.87.254.105 on 09/05/12
For personal use only.

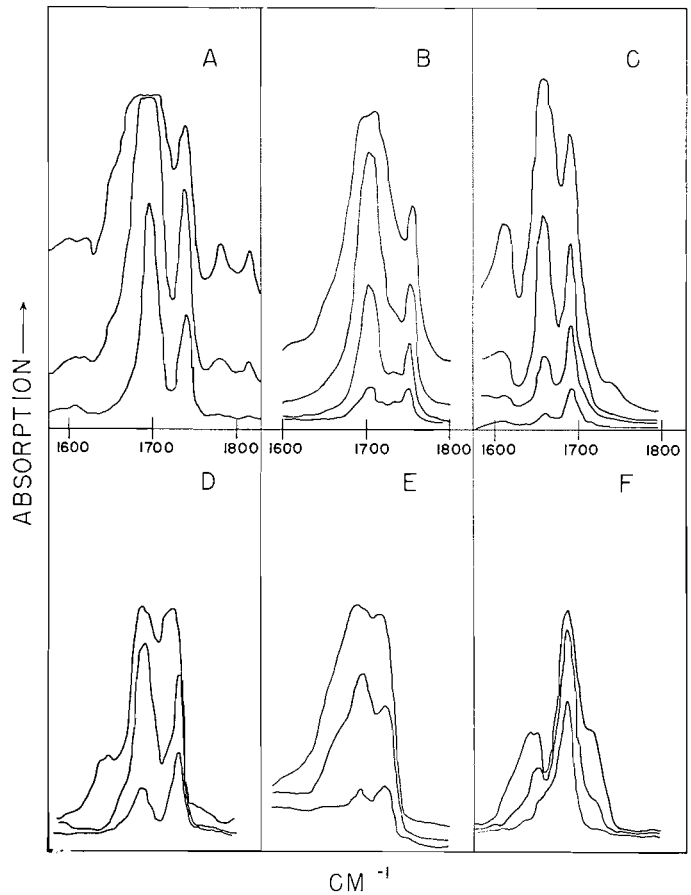


FIG. 2. Region of the C=O stretching fundamental bands: A, benzoic acid in carbon tetrachloride at concentrations 32, 8.2, and 1.3 millimoles per liter; B, orthochlorobenzoic acid in carbon tetrachloride at concentrations 12.8, 3.84, 1.15, and 0.35 millimoles per liter; C, salicylic acid in carbon tetrachloride at concentrations 6.58, 1.98, 0.59, and 0.18 millimoles per liter; D, benzoic acid in benzene at concentrations 17.2, 3.4, and 0.68 millimoles per liter; E, orthochlorobenzoic acid in benzene at concentrations 12.8, 3.84, and 1.15 millimoles per liter; F, salicylic acid in benzene at concentrations 14.5, 4.4, and 1.32 millimoles per liter.

vibration is not nearly as great as it is on the O—H stretching vibration. Thus, the C=O bands are shifted only slightly in changing from the solvent carbon tetrachloride to benzene. This region yields considerable information regarding the molecular species present in each case.

Monomer bands for the benzoic, *o*-chlorobenzoic, and salicylic acids in carbon tetrachloride appear at 1737, 1755, and 1690 cm^{-1} respectively. In the case of the salicylic acid, the peak at 1690 cm^{-1} is characteristic of the chelated form of the acid as shown in Figs. 5*e* and 5*f*, and the small shoulder at 1730 cm^{-1} arises from the presence of some unchelated monomer. The peaks for the associated forms of the benzoic, *o*-chlorobenzoic, and salicylic acids in carbon tetrachloride solution appear at 1692, 1700, and 1660 cm^{-1} respectively.

In benzene solution, the benzoic acid shows a monomer band at 1725 cm^{-1} and the bands for the associated forms of the acid at 1690 and 1650 cm^{-1}. The monomer peak for the *o*-chlorobenzoic acid in benzene solution appears at 1717 cm^{-1} with the peak for the associated species at 1690 cm^{-1}.

Can. J. Chem. Downloaded from www.nrcresearchpress.com by 210.87.254.105 on 09/05/12
For personal use only.

The chelated form of salicylic acid in benzene solution shows an absorption band at 1687 cm^{-1} with a shoulder arising from the unchelated monomer at 1710 cm^{-1}. The band for the associated species appears at 1655 cm^{-1}.

3. Region of the O—H In-plane Bending and the C—O Stretching Vibrations

Figure 3 shows the spectra observed in the region 1250 to 1500 cm^{-1} for the three acids

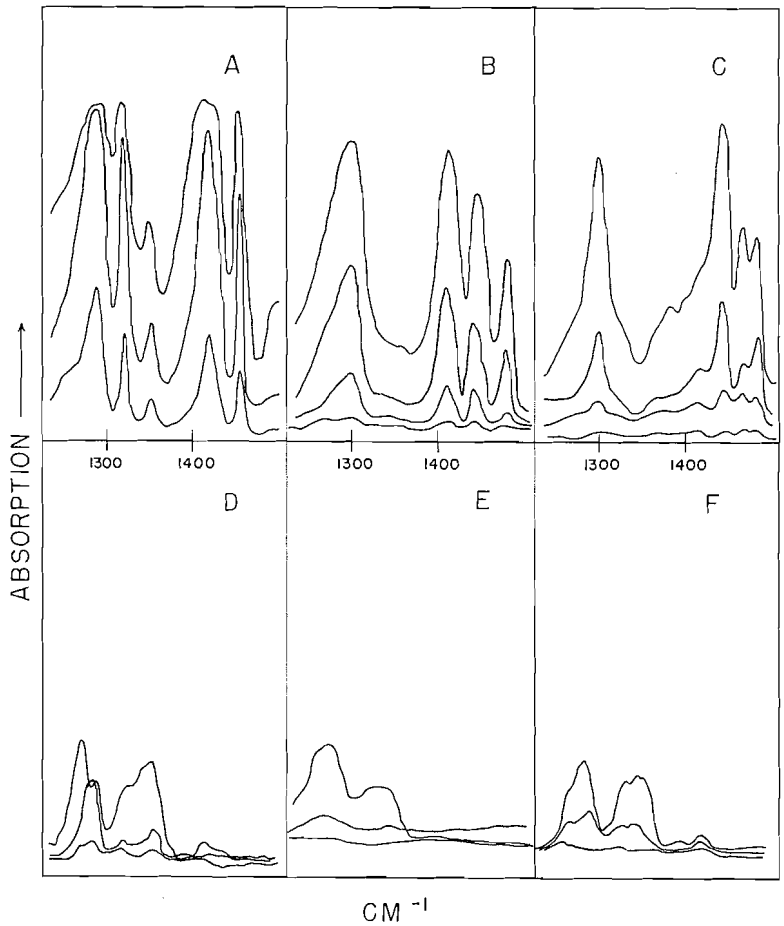


FIG. 3. Region of the O—H in-plane bending and C—O stretching: A, benzoic acid in carbon tetrachloride at concentrations 32, 8.2, and 1.3 millimoles per liter; B, orthochlorobenzoic acid in carbon tetrachloride at concentrations 12.8, 3.84, 1.15, and 0.35 millimoles per liter; C, salicylic acid in carbon tetrachloride at concentrations 6.58, 1.98, 0.59, and 0.18 millimoles per liter; D, benzoic acid in benzene at concentrations 17.2, 3.4, and 0.68 millimoles per liter; E, orthochlorobenzoic acid in benzene at 12.8, 3.84, and 1.15 millimoles per liter; F, salicylic acid in benzene at concentrations 14.5, 4.4, and 1.32 millimoles per liter.

in both the solvents. The spectra in benzene are rather poorly defined in this region as a result of the solvent absorption. It is noteworthy, however, that the bands appearing between 1400 and 1500 cm^{-1} in carbon tetrachloride solution are essentially absent for the acids in benzene solution. Hadzi and Sheppard (4) have reported 1420 and 1287 cm^{-1} in this region for the characteristic frequencies of the COOH group of solid benzoic acid.

The internal co-ordinates of the COOH group which might account for the frequencies in the region between 1500 and 800 cm^{-1} are the C—O stretching, O—H motion perpendicular to the plane of the dimer, or the torsional motion of the O—H band about the

Can. J. Chem. Downloaded from www.nrcresearchpress.com by 210.87.254.105 on 09/05/12
For personal use only.

C—O linkage for the monomeric molecule. The assignment of these modes to this frequency range has been confirmed by Hadzi and Sheppard (4), who observed the behavior of the two bands corresponding to the in-plane and the out-of-plane O—H bending on deuteration. One is, however, left with the ambiguity with regard to distinguishing the C—O stretching and the O—H in-plane bending frequencies in the region of 1450–1300 cm^{-1}. They both belong to the same symmetry species and might be expected to interact appreciably. While there is a marked disagreement in the literature concerning their precise assignments, and Hadzi and Sheppard (4) have also concluded that a clear-cut assignment in terms of the C—O stretching and O—H in-plane bending vibrations is not possible, the present results, as discussed below, favor the assignment of the band $\backsim$1400 cm^{-1} to the O—H in-plane bending mode. This is also compatible with the unambiguous assignment, by Hadzi and Sheppard (4), of the band at 1050 cm^{-1} in the COOD group to the O—D in-plane bending.

4. Region of the O—H Out-of-plane Bending Vibration

Figure 4 shows the region of the O—H out-of-plane bending vibration for the three

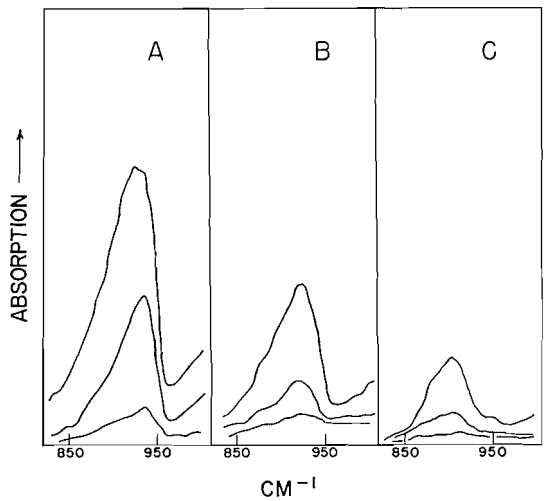


FIG. 4. Region of the O—H out-of-plane bending: A, benzoic acid in carbon tetrachloride at concentrations 32, 8.2, and 1.3 millimoles per liter; B, orthochlorobenzoic acid in carbon tetrachloride at concentrations 12.8, 3.84, and 1.15 millimoles per liter; C, salicylic acid in carbon tetrachloride at concentrations 6.58, 1.98, and 0.59 millimoles per liter.

acids in carbon tetrachloride solution. That this region is definitely that of the O—H out-of-plane bending has been suggested on less direct experimental evidence by Davies and Sutherland (1) and confirmed by Hadzi and Sheppard (4). The changes in this band caused by dilution in carbon tetrachloride solutions are as spectacular as those occurring for the O—H stretching frequencies. The interest in the study of this band also stems from the energy change implied by the deviation from a linear hydrogen bond configuration. This band was absent in benzene solution.

The absence of these bands in the benzene solution may be caused by the relatively strong absorption of the solvent in this region. However, data from the region of the O—H stretching vibration indicate that benzene interacts with the O—H sufficiently to shift the monomer O—H bands by about 100 cm^{-1} on changing from carbon tetrachloride to benzene solution. This interaction may also act to suppress the O—H bending vibrations in both the in-plane and the out-of-plane modes. This possible explanation for the

Can. J. Chem. Downloaded from www.nrcresearchpress.com by 210.87.254.105 on 09/05/12
For personal use only.

absence of appreciable bands for all the three acids in benzene solution at about 900 cm^{-1} and at 1400 cm^{-1} requires further study but appears reasonable.

On the basis of the above explanation for the absence of the O—H in-plane and out-of-plane bending modes in benzene solution, it appears that the absorption peaks appearing in the region of 1400 to 1500 cm^{-1} (Fig. 3A, B, and C) in carbon tetrachloride solutions arise from the O—H in-plane bending modes for the various molecular species. The bands at $\backsim$1300 cm^{-1} therefore can be reasonably assigned to the C—O stretching mode.

CONCLUSIONS

The data presented in Figs. 1 to 4 cannot be considered accurate enough to yield quantitative intensity values. However, the results are semiquantitative and conclusions may be drawn on the basis of the intensity changes with concentration.

An examination of Figs. 1 and 2 indicates that the ratio of associated to monomer form is appreciably higher for all the three acids in carbon tetrachloride than in benzene solutions. Thus, it appears that benzene interacts more strongly with the solute molecules in every case and suppresses to some extent the tendency of the acids to form associated species.

It has been established by cryoscopic methods (9) that benzoic acid exists primarily as a dimer (Fig. 5*b*) in benzene solution. The peaks appearing at 1692 cm^{-1} in carbon

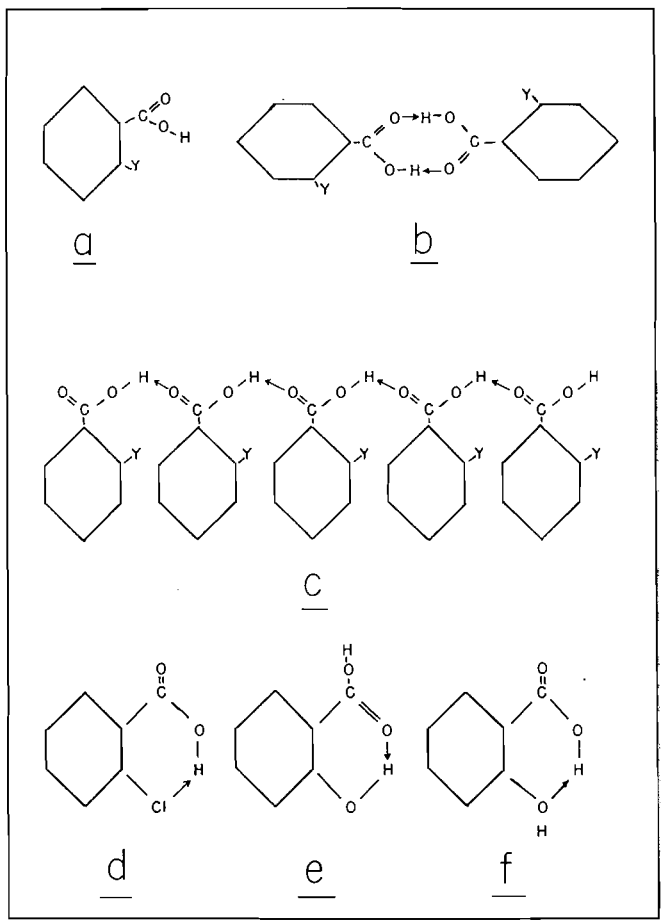


FIG. 5. Various molecular species which may be present in the ortho-substituted benzoic acids.

Can. J. Chem. Downloaded from www.nrcresearchpress.com by 210.87.254.105 on 09/05/12
For personal use only.

tetrachloride solution (Fig. 2A), and at 1690 cm^{-1} in benzene solution (Fig. 2D), appear to be the dimer peaks. The results shown in Figs. 1D and 2D indicate that appreciable amounts of the monomer are also present in benzene solution and the C=O peak at 1650 cm^{-1} (Fig. 2D) indicates that some polymer (Fig. 5*c*) or open dimer is also present.

Only two molecular species are present in the *o*-chlorobenzoic acid solution in carbon tetrachloride or benzene. The associated form is most probably a dimer. The results obtained in carbon tetrachloride solution are in agreement with those of Brooks *et al.* (6).

It is noteworthy that the position of the monomer band for the *o*-chlorobenzoic acid in benzene solution is lower by about 40 cm^{-1} than the corresponding band in carbon tetrachloride solution. This large decrease in frequency that occurs on changing the solvent is not apparent in the case of the benzoic or the salicylic acids and may well indicate that the monomer of *o*-chlorobenzoic acid in benzene solution is a chelate form such as that shown in Fig. 5*d*.

The results shown in Fig. 2F indicate that the most stable form of salicylic acid at low concentrations in benzene is the chelate form (Fig. 5*e* or *f*). As the acid concentration is increased, the appearance of the peak at 1655 cm^{-1} indicates the formation of some polymer and the appearance of the shoulder at 1710 cm^{-1} indicates the presence of some unchelated monomer. This unchelated monomer would be expected as an intermediate species arising from the equilibrium

$$\text{chelated monomer} \leftrightharpoons \text{unchelated monomer} \leftrightharpoons \text{polymer.}$$

The strong band at 1660 cm^{-1} for the salicylic acid in carbon tetrachloride solution indicates the presence of large amounts of polymer in this solvent. The presence of unchelated monomer is shown by the shoulder at 1730 cm^{-1}.

As pointed out by Murty and Seshadri (7), the peaks for the associated form of the salicylic acid (Figs. 2C and F) occur at appreciably lower frequency than the dimer peaks for the benzoic acid or for the *o*-chlorobenzoic acid. This raises some question of whether these peaks at about 1655 cm^{-1} arise from dimers or polymers. The occurrence of a polymer peak in the case of the benzoic acid in benzene solution (Fig. 2D) at 1650 cm^{-1} seems to favor the conclusion that the associated species in salicylic acid solution is a polymer form probably of the type shown in Fig. 5*c*.

ACKNOWLEDGMENT

This research has been aided by a grant from the National Research Council, Ottawa, and the authors are thankful for this assistance.

REFERENCES

1. M. M. Davies and G. B. B. M. Sutherland. J. Chem. Phys. **6**, 755 (1938).
2. J. T. Harris and M. E. Hobbs. J. Am. Chem. Soc. **76**, 1419 (1954).
3. S. Bratoz, D. Hadzi, and N. Sheppard. Spectrochim. Acta, **8**, 249 (1956).
4. D. Hadzi and N. Sheppard. Proc. Roy. Soc. (London), A, **216**, 247 (1953).
5. G. V. L. N. Murty and T. R. Seshadri. Proc. Indian Acad. Sci. A, **16**, 264 (1942).
6. C. J. W. Brooks, G. Eglinton, and J. F. Morman. J. Chem. Soc. 106 (1961).
7. C. J. W. Brooks, G. Eglinton, and J. F. Morman. J. Chem. Soc. 661 (1961).
8. G. V. L. N. Murty and T. R. Seshadri. Proc. Indian Acad. Sci. A, **19**, 17 (1944).
9. B. C. Barton and C. A. Kraus. J. Am. Chem. Soc. **73**, 4561 (1951).

Can. J. Chem. Downloaded from www.nrcresearchpress.com by 210.87.254.105 on 09/05/12
For personal use only.

Can. J. Chem. Downloaded from www.nrcresearchpress.com by 210.87.254.105 on 09/05/12
For personal use only.

INFRARED SPECTRA AND THE STRUCTURES OF XANTHATES AND DIXANTHOGENS[1]

M. L. SHANKARANARAYANA AND C. C. PATEL[2]

ABSTRACT

The infrared spectra of representative dialkyl dixanthogens and a few xanthates have been examined. All these compounds have two strong absorption bands in the regions 1140–1265 and 1010–1080 cm^{-1}. On the basis of the shift of the bands with the changes in the substituents in the xanthic acid, the former band is assigned to the C═S group, while the latter to the CO group. Except in the ionic compounds, the canonical structure $-\bar{S}_2C{=}\dot{O}R$ contributes very little to the structures of dixanthogens and covalent metal complexes.

Although infrared spectra of some of the xanthates and dixanthogens have been reported (1–5), an interpretation of the vibration frequencies of C═S and C—O groups of these compounds has not been attempted. The assignment of these group frequencies is somewhat difficult since both of them lie in the same region 1000 to 1275 cm^{-1}. Further, the absorption bands of both these groups are intense and very susceptible to the environmental changes in the molecules. In fact, Bellamy (6, p. 355) has pointed out that the location of the C═S absorption frequency has been a matter of some difficulty in organic thio compounds. Bak (7) *et al.* have assigned the band close to 1200 cm^{-1} to the C═S stretching mode of vibration in dithioesters, while Bellamy and Rogasch (8) have assigned the frequencies between 1000 and 1200 cm^{-1} for different types of thio compounds. These examples point out that the CO and C═S group frequencies fall in the same region. The CO symmetrical stretching vibration takes place around 1030 cm^{-1} in alkyl esters, alcohols, and silicon ethers and around 1200 cm^{-1} in aryl esters (9). In the present paper, it is assumed that the higher frequency around 1200 cm^{-1} is due to the C═S group, while the lower one around 1030 cm^{-1} is due to the CO group. The validity of this assumption is considered later.

Felumb (1) reported the infrared spectra of dimethyl, diethyl, and di-*n*-propyl dixanthogens and arbitrarily located the C═S frequency in the region 1210–1230 cm^{-1}. Little and Leja (2) gave the spectra of diethyl dixanthogen and some xanthates but could not make assignments to the frequencies because of the lack of information of infrared data. The infrared spectrum of potassium ethyl xanthate has been lately reported by several investigators (3–5) but they have not located the group frequencies for C═S and CO groups.

Gordy's Relation and C═S and CO Group Frequencies

Gordy's relation (10), in combination with the equation for the simple harmonic oscillator, has been helpful in assigning the P—S and PO frequencies (11). The same relations have been tried here to get the probable spectral regions for the C═S and CO vibrations. Gordy's relation [1] (10) gives the bond-stretching force constant, $k \times 10^{-5}$ in dynes/cm, as follows:

$$[1] \qquad k = 1.67N\left(\frac{\chi_A \cdot \chi_B}{d^2}\right)^{3/4} + 0.30,$$

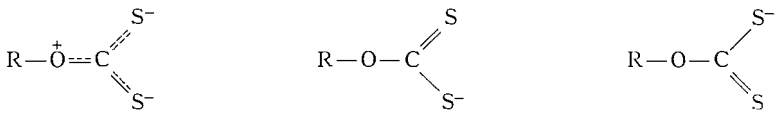
where χ_A and χ_B are respectively the electronegativities (in Pauling's scale) of the atoms

[1]*Manuscript received March 6, 1961.*
Contribution from the Department of Inorganic and Physical Chemistry, Indian Institute of Science, Bangalore 12, India.
[2]*To whom the correspondence may be addressed.*

involved, d is the internuclear distance between the atoms in Å, and N is the bond order. The values of $k\times10^{-5}$ for C═S and CO are 6.88 and 5.26 dynes/cm respectively (d for C═S is 1.6 Å) (12). By substituting these values in the equation for the simple harmonic oscillator, the frequencies for C═S and CO are 1161 and 1147 cm^{-1} respectively. In the above calculation for CO, d is taken as 1.43 Å, as given by Pauling (12). If, however, the average value of d for CO (1.38 Å) is taken, as deduced by Carrai and Gottardi (13), the ν_{CO} falls at 1170 cm^{-1}. These values of $\nu_{C=S}$ and ν_{CO} are so close to each other, and overlapping, that it is difficult to make assignments to C═S and CO groups when they occur in the same molecule, as in the derivatives of xanthic acids. In the following discussion, an alternative approach is, therefore, made to assign the frequencies on the basis of the effect of the substituents in xanthic acid.

Assignment of C═S and CO Frequencies of Xanthates

The xanthate ion can be represented in the following three forms.



(I) (II) (III)

Dithiocarbamate ion, which is similar to the xanthate ion, is also represented in the same way (14). Analogous to the structure of ionic salts of carboxylic acids, investigated in detail by Lecomte and co-workers (15) from the infrared studies, the structure of xanthate ion in ionic compounds can mainly be represented as a canonical structure (I). In such a case, the π-bond character of C═S will be lowered while the σ bond of CO will acquire a partial π-bond character. This is expected to result in the lowering of the C═S frequency and the enhancing of the CO frequency. This expectation has come true when the corresponding absorption frequencies of sodium ethyl xanthate are compared with those of the symmetrical compound di-*n*-butyl dixanthogen (Table I). The C═S frequency in sodium xanthate is lowered to 1179 cm^{-1}, while that of CO is raised to 1040

TABLE I

Characteristic frequencies of C═S and CO groups of the derivatives of xanthic acid

Substance	Medium	C═S frequency (cm^{-1})	CO frequency (cm^{-1})
Sodium ethyl xanthate (2)	Nujol mull	1179	1040
Potassium ethyl xanthate (3–5)	KCl disk (3) / KBr disk (4)	1143	1055
Potassium *n*-butyl xanthate (2)	Nujol mull	1153	1077
Cuprous ethyl xanthate (2)	"	1200	1037
Zinc ethyl xanthate (2)	"	1212	1035
Lead ethyl xanthate (2)	"	1220	1020
Diethyl dixanthogen	CCl_4 solution	1242 / 1262 (split band)	1026
Diisopropyl dixanthogen	"	1258	1010
Di-*n*-butyl dixanthogen	"	1258	1026
Diisoamyl dixanthogen	"	1258	1024
Ethyl xanthic S-ethyl ester (5)	—	1190	1053–1000 (triply split band)

Can. J. Chem. Downloaded from www.nrcresearchpress.com by 210.87.254.105 on 09/05/12
For personal use only.

Can. J. Chem. Downloaded from www.nrcresearchpress.com by 210.87.254.105 on 09/05/12
For personal use only.

cm^{-1}, as compared to the respective frequencies of the dixanthogen at 1258 and 1026 cm^{-1}. Now, if sodium is replaced by potassium in the ethyl compound, the ionic character of the xanthate ion will increase according to the Fajan's rule and also according to the lower electronegativity of the bigger potassium ion. We thus expect the π-bond character of C═S to decrease further while that of CO to increase, resulting in further lowering of the C═S frequency and enhancement of the CO frequency. This expectation has also been realized, which is evident from the comparison of the C═S and CO frequencies of the sodium and potassium ethyl xanthates (Table I). The frequency for C═S in the potassium salt is lowered to 1143 cm^{-1} while that for CO is raised to 1055 cm^{-1}. When the ethyl group is replaced by the *n*-butyl group in the potassium xanthate both the C═S and CO bands move to higher frequencies (Table I), probably due to the greater electron-releasing tendency of the *n*-butyl group.

In a covalent compound such as cuprous ethyl xanthate, resonating structures (II) and (III) predominate. No bonding is expected between the covalent copper and π-bonded sulphur. This non-bonding is similar to the behaviors of arsenic (III) (13) and lead (II) (16) in their xanthates, studied by X-ray and electron diffraction respectively. Under such circumstances, the π-bond character of C═S and σ-bond character of CO are greatly enhanced in cuprous xanthate, as compared to those in the alkali metal xanthates. A shift of the C═S to the higher frequency and of the CO to the lower one could be expected for cuprous xanthate. A comparison of the C═S and CO frequencies of cuprous xanthate and of alkali metal xanthates confirms the above reasoning. It is seen from the above discussion that as the metal–sulphur bond strengthens, the CO vibration frequency and its bond order are lowered.

Much experimental data are not available on the spectra of the divalent metal xanthates. The relative shifts of C═S and CO frequencies of zinc and lead ethyl xanthates (Table I) are not in accordance with the electronegativities of their metal atoms. It is possible that other considerations such as the thermodynamic stability and the stereochemistry of the metal xanthates may also be contributory factors in determining the shifts of the C═S and CO frequencies in such compounds.

Apart from the discrepancy encountered in the divalent metal xanthates, the results of the alkali metal and cuprous xanthates are sufficient to indicate that the strong band around 1200 cm^{-1} is due to C═S and the band around 1030 cm^{-1} is due to CO absorption.

C═S and CO Group Frequencies of Dixanthogens

The dixanthogen absorption spectra (Table I and Fig. 1) do not show any appreciable change in the C═S and CO frequencies, even though the alkyl groups of different dixanthogens vary. The C═S group frequency is practically constant at 1258 cm^{-1} while that of CO, at 1025 cm^{-1}. A small shift of CO frequency to 1010 cm^{-1} in the case of diisopropyl dixanthogen is probably due to the vibrational coupling of the CO group with the C—C skeletal stretching vibration. Diisoamyl dixanthogen has also a similar branched alkyl group, but its remoteness from the CO group probably prevents the analogous interaction. The constancy of the C═S group frequency at 1258 cm^{-1} in the dixanthogens is due to the symmetry of the groups in either parts of the molecules. It is interesting to note that the asymmetric ethyl xanthic S-ethyl ester gives the C═S frequency at 1190 cm^{-1}. The splitting of the C═S band of diethyl dixanthogen (Fig. 1) is interesting and peculiar to this dixanthogen. Such a splitting has been observed with this compound both in the solid state (2) and in the carbon tetrachloride solution.

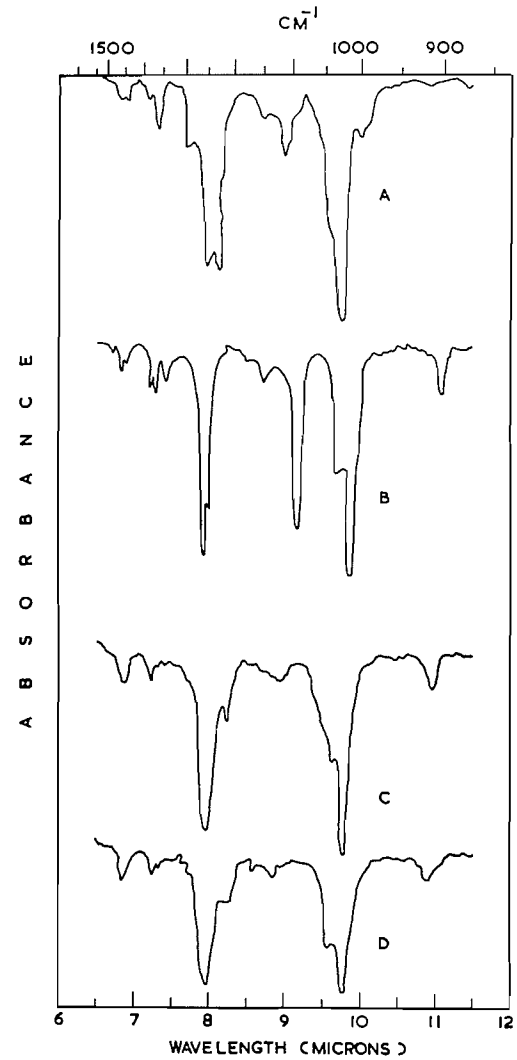


FIG. 1. Infrared spectra of dialkyl dixanthogens. A, diethyl dixanthogen; B, diisopropyl dixanthogen; C, di-*n*-butyl dixanthogen; D, diisoamyl dixanthogen.

EXPERIMENTAL

Dixanthogens

Diethyl, diisopropyl, di-*n*-butyl, and diisoamyl dixanthogens were prepared by oxidation of the respective high-purity potassium alkyl xanthates by iodine and were purified by extraction with petroleum ether (b.p. 40–60° C). The purity of the dixanthogens was over 99.7% as analyzed by the method developed in this laboratory (17).

Spectra

The spectra of the dixanthogens in the region 700–4000 cm^{-1} were obtained in carbon tetrachloride solution (0.1 *M*), with a Perkin–Elmer double-beam recording Infracord spectrophotometer, Model 137. The spectra in the range 850–1500 cm^{-1} with NaCl prism are reproduced in Fig. 1. The infrared spectrum of diethyl dixanthogen in carbon

Can. J. Chem. Downloaded from www.nrcresearchpress.com by 210.87.254.105 on 09/05/12
For personal use only.

tetrachloride solution agrees well with that of the solid substance given by Little and Leja (2).

Diisopropyl dixanthogen gives rise to a characteristic intense band at 1087 cm^{-1}. This band is peculiar to this dixanthogen and may be due to the rocking mode of vibration of methyl groups, coupled strongly with the skeletal vibration of isopropyl group. A similar band is found around 1100 cm^{-1} in the derivatives of isopropyl alcohol as in isopropyl nitrate (6, p. 368) and diisopropyl ether (18). In the spectrum of the diethyl dixanthogen alone a medium band occurs at 1105 cm^{-1} owing to the rocking mode of vibration of C—CH_3.

ACKNOWLEDGMENT

The authors thank Prof. M. R. A. Rao for his keen interest in this work.

REFERENCES

1. R. FELUMB. Bull. soc. chim. France, 890 (1957).
2. L. H. LITTLE and J. LEJA. Proceedings of the second international congress of surface activity. Vol. III. Butterworths Scientific Publications, London. 1957. p. 261.
3. J. I. JONES, W. KYNASTON, and J. W. HALES. J. Chem. Soc. 614 (1957).
4. D. A. ANDREWS, F. G. HURTUBISE, and H. KRASSIG. Can. J. Chem. **38**, 1381 (1960).
5. E. KLEIN, J. K. BOSARGE, and I. NORMAN. J. Phys. Chem. **64**, 1666 (1960).
6. L. J. BELLAMY. The infra-red spectra of complex molecules. 2nd ed. Methuen & Co. Ltd., London. 1958.
7. B. BAK, L. H. NYGAARD, and C. PEDERSEN. Acta Chem. Scand. **12**, 1451 (1958).
8. L. J. BELLAMY and P. E. ROGASCH. J. Chem. Soc. 2121 (1960).
9. V. A. A. STUART, C. L. LAU, and H. BREEDERVELD. Rec. trav. chim. **74**, 747 (1955).
10. W. GORDY. J. Chem. Phys. **14**, 305 (1946).
11. R. C. GORE. Discussions Faraday Soc. **9**, 138 (1950).
12. L. PAULING. The nature of the chemical bond. Cornell Univ. Press, Ithaca. 1960. p. 224.
13. G. CARRAI and G. GOTTARDI. Z. Krist. **113**, 373 (1960).
14. J. CHATT, L. A. DUNCANSON, and L. M. VENANZI. Suomen Kemistilehti, B, **29**, 75 (1956).
15. J. LECOMTE. Discussions Faraday Soc. **9**, 125 (1950).
16. H. HAGIHARA, H. UCHIKOSHI, and H. YAMASHITA. Proceedings of the second international congress of surface activity. Vol. III. Butterworths Scientific Publications, London. 1957. p. 343.
17. M. L. SHANKARANARAYANA and C. C. PATEL. Analyst, **86**, 98 (1961).
18. R. B. BARNES, U. LIDDEL, and V. Z. WILLIAMS. Ind. Eng. Chem. Anal. Ed. **15**, 659 (1943).

Can. J. Chem. Downloaded from www.nrcresearchpress.com by 210.87.254.105 on 09/05/12
For personal use only.

Can. J. Chem. Downloaded from www.nrcresearchpress.com by 210.87.254.105 on 09/05/12
For personal use only.

THE CRYSTAL AND MOLECULAR STRUCTURES OF *m*-DINITROBENZENE AND *p*-DINITROBENZENE[1]

J. TROTTER

ABSTRACT

The structures of *m*-dinitrobenzene and *p*-dinitrobenzene have been refined by three-dimensional (F_o—F_c) syntheses. The results indicate that both nitro groups in each molecule are twisted 11° out of the aromatic plane, about the C—N bonds, in contrast to nitrobenzene, where the whole molecule is completely planar. These molecular configurations are shown to be in accord with those which might be expected from intramolecular steric effects. The dimensions of the three molecules have also been compared.

INTRODUCTION

The crystal structure of *m*-dinitrobenzene has recently been reinvestigated using new three-dimensional data, the refinement of positional and anisotropic temperature parameters proceeding by use of the block diagonal least-squares method (1). This analysis yielded a reasonably precise account of the geometry of the molecule: all the carbon and nitrogen atoms are situated on one plane, but each of the oxygen atoms is displaced from this plane by about 0.2 Å, the deviations being in such a sense that the molecular symmetry is *m* within the limits of experimental error. The nitro groups are thus rotated about the C—N bonds out of a completely planar configuration, the angles of rotation being about 11°.

The results of this least-squares refinement are, however, unsatisfactory in several respects. Firstly, there was a large increase (of about 20%) in the over-all scale factor during the three cycles of refinement. Secondly, the final anisotropic temperature parameters vary widely, haphazardly, and do not appear to correspond to any physically reasonable rigid-body vibrations of the molecule. Thirdly, although the deviations of the oxygen atoms from coplanarity suggest that the molecule has symmetry *m*, detailed study of the bond lengths and valency angles indicates that this is very far from being so, the measured values of two chemically identical bonds, for example, differing by 0.12 Å. It seems unlikely that these large bond length differences and large temperature factor variations can be real, and probably they result from some inadequacy of the refinement process. One possible source of error is unsuitability of the weighting system, but the weights used were those normally adopted, and there would appear to be no reason for supposing that they are unsuitable in this case. A second source of error is termination of the refinement process before shifts become negligible, but again the positional and temperature parameter changes in the final cycle were very small, and were not generally in directions which indicated that continued refinement would make the final results more reasonable. Thirdly, introduction of anisotropic thermal parameters at too early a stage in the refinement might introduce errors in positional parameters, but it is difficult to comment on this possible source of inaccuracy; the DEUCE least-squares program used automatically produces anisotropic temperature parameters, although it is, of course, possible to reinsert isotropic ones manually. Another obvious source of error might be inaccuracies in the measured structure factor data, but it is considered that this can be completely discounted, as the photographic records were

[1]*Manuscript received April 7, 1961.*
Contribution from the Department of Chemistry, University of British Columbia, Vancouver 8, British Columbia.

all very good, and inaccuracies in visual intensity estimation are unlikely to produce such wide variations in molecular dimensions and temperature factors as are observed.

In view of all these uncertainties it seemed that some useful information might be obtained by repeating the whole refinement process, using a different method. In order that the results might be comparable with those obtained for nitrobenzene (2), it seemed that differential syntheses would be most convenient, but since no program was available for computing these, it was decided to proceed, instead, by calculating three-dimensional $(F_o—F_c)$ syntheses. The final results should then be equivalent to those which would be obtained from differential syntheses with backshift corrections.

It also seemed that some useful information might be derived from a similar refinement of the crystal structure of *p*-dinitrobenzene. This structure had been investigated previously (3) and the molecular geometry had been established with considerable precision (4), but it was decided that it would be useful to refine it further so that the results would be directly comparable with those obtained for nitrobenzene and *m*-dinitrobenzene.

REFINEMENT OF THE STRUCTURES

m-Dinitrobenzene

Structure factors were calculated for all the observed reflections from the previous final positional parameters of the carbon, nitrogen, and oxygen atoms, but using an isotopic temperature factor $B = 4.5$ Å^2 for all the atoms. The discrepancy factor R was 22%, and the over-all scale factor had returned to the value prior to the anisotropic least-squares refinement. Further refinement proceeded by computing successive $(F_o—F_c)$ syntheses and altering the positional and isotropic temperature parameters to minimize the difference–density slopes and magnitudes at the atomic centers. After two cycles, R had been reduced to 19% and no further significant changes in atomic co-ordinates or temperature factors were indicated. Refinement was terminated at this point so that the results would be directly comparable with those for nitrobenzene. Any further work would require introduction of a contribution from the hydrogen atoms and of anisotropic thermal parameters for the heavier atoms, and in view of the unsatisfactory results which had already been obtained with the only program available to us for carrying out the refinement of anisotropic temperature factors, it was not considered worth while proceeding any further with the refinement. The measured structure factor data previously listed (1) should be multiplied by a scale factor 0.822 to convert them to an absolute scale.

p-Dinitrobenzene

No new structure factor data were collected for *p*-dinitrobenzene, but structure factors were calculated for all the reflections measured by Llewellyn (3), using the positional parameters of the carbon, nitrogen, and oxygen atoms listed by Abrahams (4), with $B = 4.6$ Å^2 for all the atoms. R was 25%. Refinement proceeded as for *m*-dinitrobenzene, and after two cycles of three-dimensional $(F_o—F_c)$ syntheses, R had been reduced to 19% and no further changes were indicated in any of the parameters.

CO-ORDINATES AND MOLECULAR DIMENSIONS

m-Dinitrobenzene

The positional and temperature parameters of the carbon, nitrogen, and oxygen atoms are listed in Table I. The atomic co-ordinates are referred to the principal crystallographic

Can. J. Chem. Downloaded from www.nrcresearchpress.com by 210.87.254.105 on 09/05/12
For personal use only.

TABLE I

Final positional and temperature parameters for *m*-dinitrobenzene (and deviations, Δ, from the aromatic plane)

Atom	x	y	z	B (Å²)	Δ (Å)
C_1	.1416	.3667	−.0055	3.5	−0.02
C_2	.1788	.4513	−.1408	3.5	+0.02
C_3	.2795	.4568	−.1093	3.5	−0.01
C_4	.3478	.3884	.0226	4.0	−0.01
C_5	.2999	.3032	.1363	4.0	+0.01
C_6	.1956	.2929	.1187	4.0	+0.01
N_1	.0297	.3535	−.0197	5.2	−0.02
N_2	.3282	.5479	−.2419	5.2	+0.01
O_1	−.0065	.2857	.1424	7.0	−0.25
O_2	−.0189	.4109	−.1945	7.0	+0.21
O_3	.2759	.6021	−.4038	7.0	+0.21
O_4	.4152	.5609	−.1900	7.0	−0.15

axes, x, y, z being expressed as fractions of the unit-cell edges.

The equation of the best plane through the carbon atoms is

$$0.0836X - 0.3945\,Y - 0.9151Z + 1.8230 = 0,$$

where X, Y, Z are expressed in Å units; the deviations of the atoms from this plane are listed in the final column of Table I. The equations of the planes of the nitro groups are

$$N_1O_1O_2\text{: } 0.1098X - 0.5803\,Y - 0.8070Z + 2.7621 = 0,$$

$$N_2O_3O_4\text{: } 0.2218X - 0.4850\,Y - 0.8459Z + 1.9737 = 0.$$

The angle between the plane of the carbon atoms and the $N_1O_1O_2$ plane is 12.4°, and between the carbon atom plane and the $N_2O_3O_4$ plane, 10.3°.

The bond distances and valency angles in the *m*-dinitrobenzene molecule, calculated from the co-ordinates of Table I, are shown in Fig. 1*a*. The estimated standard deviations of the atomic positions (5) are $\sigma(x) = \sigma(y) = \sigma(z) = 0.02$ Å for all the atoms.

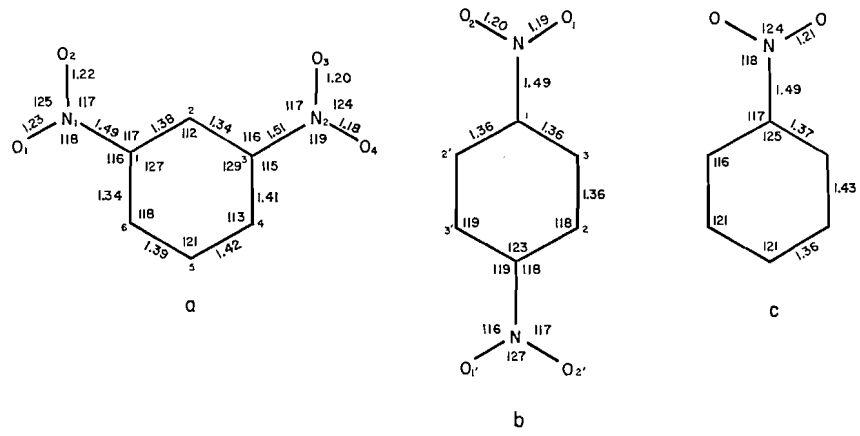


FIG. 1. Measured bond lengths (Å) and valency angles (deg) in (*a*) *m*-dinitrobenzene, (*b*) *p*-dinitrobenzene, and (*c*) nitrobenzene.

Can. J. Chem. Downloaded from www.nrcresearchpress.com by 210.87.254.105 on 09/05/12
For personal use only.

p-Dinitrobenzene

The final positional and thermal parameters are listed in Table II, x, y, z being

TABLE II

Final positional and temperature parameters for *p*-dinitrobenzene (and deviations, Δ, from the aromatic plane)

Atom	x	y	z	B (Å²)	Δ (Å)
C_1	.0688	.1819	.0885	3.6	+0.01
C_2	.0317	−.1177	−.2042	4.2	+0.01
C_3	.1006	.0725	−.1165	4.2	−0.01
N	.1440	.3903	.1858	3.6	−0.01
O_1	.2171	.4719	.0587	5.5	−0.24
O_2	.1231	.4624	.3811	4.9	+0.18

co-ordinates referred to the principal crystallographic axes and expressed as fractions of the unit-cell edges.

The equation of the plane through the six carbon atoms of the aromatic ring is

$$0.5285X' - 0.6577\,Y + 0.5367Z' = 0,$$

where X', Y, Z' are co-ordinates expressed in Å units and referred to orthogonal axes a, b, and c'; the deviations of the atoms from this plane are given in the last column of Table II. The equation of the nitro group plane is

$$0.6697X' - 0.6313\,Y + 0.3911Z' = 0.1123,$$

and the angle between this plane and the plane of the aromatic ring is 11.8°.

The bond lengths and valency angles in the molecule were calculated from the co-ordinates of Table II, and are shown in Fig. 1*b*. The standard deviations of the atomic positions are about 0.02 Å for all the atoms.

DISCUSSION

The molecule of nitrobenzene in the crystalline state is completely planar within the limits of experimental error, the maximum deviation from the mean molecular plane being 0.03 Å, and the root mean square deviation, 0.016 Å (in comparison with an e.s.d. in atomic position of 0.014 Å). This suggests that the most stable configuration of a typical aromatic nitro compound, with only hydrogen atoms ortho to the nitro group, is a completely planar one. This is, of course, the configuration required by resonance theory, since maximum resonance interaction between the aromatic π-electrons and the substituent nitro group is obtained when the nitro group is coplanar with the aromatic ring. This situation may be contrasted with that in a molecule which has bulky substituents ortho to the nitro group; in a molecule of this type the steric effects of the bulky ortho groups cause the nitro group to be twisted markedly out of the aromatic plane, about the C—N bond. In nitromesitylene, for example, the angle of twist is 66° and the oxygen atoms lie one above and one below the aromatic plane at perpendicular distances of 0.95 Å from it.

The six-membered ring of carbon atoms in the *m*-dinitrobenzene molecule is completely planar within the limits of experimental error, the maximum deviation from the mean plane (Table I) being 0.02 Å and the root mean square deviation, 0.015 Å (e.s.d. of atomic position 0.02 Å). The nitrogen atoms also lie on this aromatic plane (deviations only

Can. J. Chem. Downloaded from www.nrcresearchpress.com by 210.87.254.105 on 09/05/12
For personal use only.

Can. J. Chem. Downloaded from www.nrcresearchpress.com by 210.87.254.105 on 09/05/12
For personal use only.

-0.02 Å for N_1 and $+0.01$ Å for N_2), but the oxygen atoms of each nitro group lie one above and one below the plane, so that each group is twisted about the C—N bond, out of the plane of the carbon and nitrogen atoms, the angles of twist being 12.4° for $N_1O_1O_2$ and 10.3° for $N_2O_3O_4$. The small difference between these two angles is probably not significant, so that each nitro group may be considered to be rotated out of the aromatic plane by 11.4°. The mean oxygen atom displacement from this plane is 0.21 Å, and these displacements are in directions such that the symmetry $mm—C_{2v}$ which would pertain in a completely planar model is reduced to $m—C_h$ (neglecting, for the moment, variations in bond distances and valency angles).

In the *p*-dinitrobenzene molecule all the carbon atoms lie in one plane, within experimental error, the maximum and root mean square deviations being 0.01 Å (Table II). The nitrogen atoms also lie on this aromatic plane, but the oxygen atoms of a nitro group are displaced one above and one below the plane, so that the group is rotated about the C—N bond 11.8°, out of the plane of the carbon and nitrogen atoms. The differences between the oxygen atom displacements are probably not significant, the mean value being 0.21 Å. The displacements are in directions such that the symmetry $mmm—D_{2h}$ possessed by a planar model is reduced to $2/m—C_{2h}$ (only a center of symmetry being required from space group considerations).

We see then that while the nitrobenzene molecule is completely planar, in *m*-dinitrobenzene and *p*-dinitrobenzene the groups are all twisted out of the aromatic planes by about 11°. Since the most stable configuration for the nitrobenzene molecule is apparently a completely planar one, and since the steric considerations in all three molecules are very similar, the author has previously considered that the deviations from planarity in *m*-dinitrobenzene and *p*-dinitrobenzene are probably the result of intermolecular forces (1, 2). However, it is now evident that all the nitro groups in *m*- and *p*-dinitrobenzenes are twisted out of the aromatic planes by about the same amount, although their environments in the crystals are not similar, and this suggests that perhaps some intramolecular steric effects, which are similar for both these molecules but absent in nitrobenzene, are operative.

In order to investigate intramolecular steric effects, planar models were constructed for all three molecules, using for the values of the van der Waal's radii: 1.40 Å for the oxygen atoms and 1.20 Å for hydrogen (Fig. 2). In all three molecules there is apparently

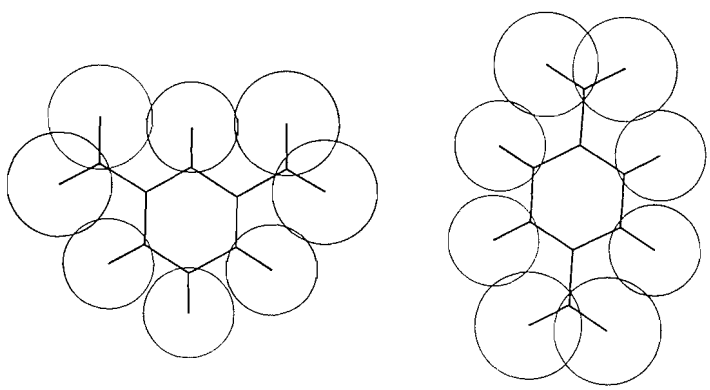


FIG. 2. Coplanar configurations of *m*-dinitrobenzene and *p*-dinitrobenzene, drawn to scale with van der Waals radii: oxygen = 1.40 Å, hydrogen = 1.20 Å.

a small steric interference between the oxygen atoms and the neighboring ortho hydrogen atoms. For nitrobenzene, however (the model is similar to that for *p*-dinitrobenzene, but with one nitro group replaced, of course, by a much smaller hydrogen atom), this steric repulsion can be relieved by small in-plane displacements of the hydrogen atoms, and no displacements of the oxygen atoms from the aromatic plane are necessary. In-plane displacements would clearly be inadequate in the *m*-dinitrobenzene molecule (Fig. 2), where relief of steric repulsions between the oxygen atoms and that hydrogen atom which is ortho to both nitro groups can be accomplished only by out-of-plane displacements. The steric effects in *p*-dinitrobenzene are apparently very similar to those in nitrobenzene, but closer examination of Fig. 2 indicates that any in-plane displacements of the hydrogen atoms would result in steric interferences between these atoms, so that relief of oxygen–hydrogen steric effects would again have to involve deviations of the oxygen atoms from the aromatic plane. These simple considerations of the steric effects are certainly in accord with the experimentally determined molecular configurations.

The variations in the measured bond lengths for *m*-dinitrobenzene (Fig. 1*a*) are smaller than those previously noted in the least-squares refinement, but there is still quite a large difference between the values for two chemically identical bonds. However, a χ^2 test of the differences between the chemically equivalent bonds (Table III) shows

TABLE III

χ^2 test

	Least-squares refinement	Fourier refinement
$\Sigma\,[\Delta(l)]^2$	0.0219 Å^2	0.0107 Å^2
$\sigma^2(l) = [\sqrt{2}\sigma(x)]^2$	<0.0004 Å^2	0.0008 Å^2
$\chi^2 = \Sigma\,\Delta^2/\sigma^2$	>55	13.4
Degrees of freedom	6	6
Probability P	$0.001 > P$	$0.05 > P > 0.01$
Significance level	Highly significant	Possibly significant

clearly that these differences were in the highly significant range in the least-squares refinement, but have now been reduced to the possibly significant range. This improvement is still evident even if $\sigma(x)$ is taken as 0.02 Å for both sets of results. For *p*-dinitrobenzene the measured molecular dimensions (Fig. 1*b*) suggest that the molecule does not deviate from symmetry $2/m$. When the mean bond distances in nitrobenzene (Fig. 1*c*), *m*-dinitrobenzene, and *p*-dinitrobenzene are compared, the most significant feature is that all the C—N distances are greater than the value usually quoted for the C(sp^3)—N single-bond length (1.475 Å). The measured molecular configurations indicate that some force, possibly resonance interaction, is tending to keep the molecules planar, or as nearly planar as steric effects will allow, so that the non-observance of any reduction of the C—N bond distances below the single-bond lengths might be due to the fact that any such reduction would further increase the steric repulsions.

ACKNOWLEDGMENTS

The author is indebted to the University of Glasgow for an I.C.I. Research Fellowship, during the tenure of which some of this work was carried out, and to the National Research Council for grants-in-aid for the work.

Can. J. Chem. Downloaded from www.nrcresearchpress.com by 210.87.254.105 on 09/05/12
For personal use only.

REFERENCES

1. J. TROTTER. Acta Cryst. **14**, 244 (1961).
2. J. TROTTER. Acta Cryst. **12**, 884 (1959).
3. F. J. LLEWELLYN. J. Chem. Soc. 884 (1947).
4. S. C. ABRAHAMS. Acta Cryst. **3**, 194 (1950).
5. D. W. J. CRUICKSHANK. Acta Cryst. **2**, 65 (1949).

Can. J. Chem. Downloaded from www.nrcresearchpress.com by 210.87.254.105 on 09/05/12
For personal use only.

Can. J. Chem. Downloaded from www.nrcresearchpress.com by 210.87.254.5 on 09/05/12
For personal use only.

THE OXIDATION OF NITRITE AND IODATE IONS BY HYPOCHLORITE IONS[1]

M. W. Lister and P. Rosenblum

ABSTRACT

The oxidation of nitrite ions and of iodate ions by hypochlorite ions in aqueous solution has been examined. The oxidation of nitrite is really a reaction of hypochlorous acid, with the slow stage $HOCl + NO_2^- + H_2O \rightarrow H_3O^+ + Cl^- + NO_3^-$. The rate constant is given by $\log k = 7.36 - 6450/RT$ (time in minutes, and the activation energy in calories). The oxidation of iodate is chiefly a reaction of hypochlorite ions, probably $ClO^- + IO_3^- \rightarrow Cl^- + IO_4^-$, although the rate is somewhat increased by a higher concentration of hydroxide ions. The rate constant is given by $\log k = 16.15 - 26{,}100/RT$. These results are compared with other oxidations by hypochlorite ions, to see if any general trends are apparent.

Sodium hypochlorite solution will oxidize many substances, and the mechanisms of these oxidations have been the subject of considerable investigation, e.g. ref. 1–4. Some of these reactions have, in fact, turned out to be reactions of free hypochlorous acid, but at present it does not seem possible to predict whether any particular reaction will go through hypochlorite ions or the free acid. On the other hand, there does seem to be a rough correlation between the heats of these reactions and their rates; for instance, the very exothermic oxidation of sulphite ions is very fast, while the slightly endothermic oxidation of iodate ions is slow. This is certainly what might be expected; however, there are one or two notable exceptions, and this matter will be briefly discussed later. The present work was undertaken in order to increase the information on which any generalizations about the reactions of hypochlorites could be based.

1. REACTION OF NITRITE AND HYPOCHLORITE IONS

This reaction has been known in relatively acid solution for a long time, and is the basis of one method for estimating nitrites. Some measurements on the reaction under these conditions have been made by Shilov (5), who found a considerable dependence of the rate on pH over the range 5 to 8. However, he gives very little detail about his results.

The present work was on the reaction in alkaline solution, where it was thought that a reaction of two ions might occur. As will be seen in what follows, this also proved to be a reaction of hypochlorous acid.

Experimental Method

Mixtures in solution of sodium hypochlorite, sodium nitrite, and sodium hydroxide of various concentrations were made up; these were then kept at constant temperature, and analyzed at intervals as described below.

The sodium hypochlorite was made in the usual way from sodium hydroxide and chlorine. The solutions consequently contained sodium chloride in amounts at least equimolar to the sodium hypochlorite. Sodium nitrite and hydroxide stock solutions were made from reagent grades of these chemicals. Reagent grade sodium chloride was added to control the ionic strength.

The solutions were kept stirred in a water thermostat, and, at intervals, 10-ml samples were pipetted out and analyzed as follows. The cooled sample was diluted to a known

[1]*Manuscript received April 13, 1961.*
Contribution from the Department of Chemistry, University of Toronto, Toronto, Ontario.

volume in a volumetric flask, and the optical density of the diluted solution was measured at 292 mμ, where there is a maximum in the absorption spectrum of hypochlorite ions, and at 360 mμ, which is close to the maximum in the absorption spectrum of nitrite ions. A Beckmann DU spectrophotometer was used. The known extinction coefficients for the various ions at these wave lengths were checked on separate samples, and the following values were used in the calculations:

Ion	λ = 292	360 mμ
OCl^-	345	10.2
NO_2^-	8.8	21.8
NO_3^-	6.4	0.01

It was assumed that all nitrogen was present either as nitrite or nitrate; hence, if the original concentration of nitrite is known, measurements at these two wave lengths suffice to determine the concentrations of hypochlorite, nitrite, and nitrate ions. This assumption was justified by the consistency of the results. Most of the disappearance of hypochlorite ions is due to reaction with nitrite, but a small part (between 0.1 and 0.5%) is due to their decomposition to chlorate and chloride ions. This is shown by the slow increase of the difference, $[NO_2^-]-[OCl^-]$. Results from a typical run are given in Table I. The

TABLE I

(Run 1; at 60° C; ionic strength 1.46; [NaOH] = 0.3901 *M*)

Time, min	$[OCl^-]$, *M*	$[NO_2^-]$, *M*	Difference, *M*	$\log [OCl^-]/[NO_2^-]$
0	0.0951	0.3255	0.2304	$\bar{1}.466$
60.4	0.0834	0.3139	0.2305	$\bar{1}.424$
120.2	0.0745	0.3050	0.2305	$\bar{1}.388$
210.7	0.0622	0.2927	0.2305	$\bar{1}.327$
331.0	0.0505	0.2811	0.2306	$\bar{1}.254$
481.2	0.0392	0.2698	0.2306	$\bar{1}.162$
692.2	0.0281	0.2587	0.2306	$\bar{1}.036$
1411.6	0.0100	0.2407	0.2307	$\bar{2}.619$

last column gives $\log [OCl^-]/[NO_2^-]$, which should give a straight line when plotted against time if the reaction is first order in hypochlorite and in nitrite ions. This was found to be the case for all runs.

The evaluation of the rate constants was done as follows. Two reactions are occurring simultaneously in the mixture:

$$NO_2^- + OCl^- \rightarrow NO_3^- + Cl^-, \quad k_1,$$

$$2OCl^- \rightarrow ClO_2^- + Cl^-, \quad k_2,$$

where the rate constants are respectively k_1 and k_2. The second reaction is followed by further oxidation of chlorite to chlorate ions. Then if $[OCl^-] = x$, and $[NO_2^-] = y$, these equations require that

$$\frac{dx}{dt} = -k_1xy - \frac{3}{2}k_2x^2,$$

$$\frac{dy}{dt} = -k_1xy.$$

Can. J. Chem. Downloaded from www.nrcresearchpress.com by 210.87.254.5 on 09/05/12
For personal use only.

The rigorous solution of these equations is difficult; but since k_2 is small, an approximate solution can be obtained as follows.

If $k_2 = 0$, it is easily shown that the solution is

$$\ln \frac{x_0 y}{y_0 x} = -k_1(x_0 - y_0)t,$$

where x_0 and y_0 are the initial concentrations. Under these conditions a plot of $\ln(x/y)$ against time would give a straight line of slope $k_1(x_0 - y_0)$.

If k_2 is not zero, the equations above give

$$\frac{d \ln(x/y)}{dt} = k_1(x-y) - \frac{3}{2} k_2 x,$$

and since $(x-y)$ is very nearly constant and k_2 is small, in practice a plot of $\ln(x/y)$ against time does in fact give a virtually straight line. Table I, for instance, shows that in run 1, $(x-y)$ varied by only 0.13%; and the slope of the graph is such that k_1 is of the order of 100 times as large as k_2. If s is the slope of the graph of $\ln(x/y)$ against time, then approximately

$$s = k_1(\overline{x-y}) - \frac{3}{2} k_2 \bar{x},$$

where the bar over the symbols indicates the average value during a run. The rate constant k_1 was calculated from this equation, with the results given in Table II; k_2 was

TABLE II

Run	Temp., °C	Ionic strength	Initial concentrations, g-mol./l. [OCl^-]	[NO_3^-]	[OH^-]	$k_1 \times 10^3$, (g-mol./l.)$^{-1}$ min^{-1}
1	60.0	1.46	0.0978	0.3283	0.390	6.18
2	"	1.46	0.0978	0.3283	0.390	6.12
3	"	1.53	0.2942	0.1028	0.391	5.98
4	"	1.53	0.2942	0.1028	0.391	5.94
5	"	1.43	0.0966	0.3283	0.196	15.93
6	"	1.42	0.0966	0.3283	0.196	15.89
7	"	1.50	0.0963	0.2462	0.117	26.59
8	"	1.50	0.0963	0.2462	0.117	26.48
9	"	2.65	0.0957	0.3283	0.390	7.28
10	"	2.65	0.0957	0.3283	0.390	7.28
11	70.0	1.45	0.0949	0.3265	0.388	13.17
12	"	1.45	0.0949	0.3265	0.388	13.15
13	50.0	1.47	0.1215	0.3299	0.397	2.645
14	"	1.47	0.1215	0.3299	0.397	2.674

taken from reference 1, the following values being used:

T, °C	50	60	70
$k_2 \times 10^5$, (g-mol./l.)$^{-1}$ min^{-1}	1.5	5.0	15.5

The values in Table II show that the rate is dependent on the hydroxide concentration; and, in fact, [OH^-].k_1 is approximately constant, as shown by the following values, all for 60° C:

Runs	1, 2	5, 6	7, 8
[OH^-].$k_1 \times 10^3$	2.40	3.11	3.11

Can. J. Chem. Downloaded from www.nrcresearchpress.com by 210.87.254.5 on 09/05/12
For personal use only.

This is equivalent to saying that the rate is proportional to the hydrogen ion concentration, and the most probable explanation is that this is really a reaction of hypochlorous acid, with

$$\text{rate} = k[\text{HOCl}].[\text{NO}_2^-].$$

Nitrous acid is a much stronger acid than hypochlorous, so it is much more likely that the H^+ is attached to the hypochlorite. On this assumption, the true rate constant, k, is given by

$$k = \frac{k_1[\text{OH}^-]}{K_h},$$

where K_h is the equilibrium constant for the hydrolysis of hypochlorite ions:

$$\text{OCl}^- + \text{H}_2\text{O} \rightleftharpoons \text{HOCl} + \text{OH}^-.$$

The ionization constant of hypochlorous acid is 3.8×10^{-8} at 27° C (6), and combining this with the ionization constant of water, K_h is 3.1×10^{-7} at 27° C. At 25° C, ΔH for this hydrolysis is 11.0 kcal; if we assume that this value holds up to 60° C, then K_h is 1.92×10^{-6} at 60° C. This value cannot be claimed to be very accurate, but is the best available on the present data. Hence $k = 1.61\times10^3$ (g-mol./l.)$^{-1}$ min^{-1} at 60° C.

The data in Table II make the apparent activation energy 17.4 kcal/g-mol. However, since the heat of hydrolysis of hypochlorite ions is 11.0 kcal, the true activation energy is 6.4 kcal. If k is given by the usual formula $k = Ae^{-E/RT}$, then $\log A = 7.41$. This is a rather small value, but there are others as small (see e.g. ref. 7).

Runs 7 and 8, in conjunction with the others, show that the rate constant increases with ionic strength, though the change is fairly small.

2. REACTION OF HYPOCHLORITE AND IODATE IONS

The total reaction here is

$$\text{NaOCl} + \text{NaIO}_3 + 2\text{NaOH} \rightarrow \text{NaCl} + \text{Na}_3\text{H}_2\text{IO}_6.$$

It was checked, by analytical methods given below, that the number of gram-molecules of periodate formed was within 1/2% of the number of gram-molecules of iodate disappearing. This confirms the stoichiometry of the reaction, and also checks the analytical methods. In alkaline solution a precipitate of sodium periodate forms. This was analyzed and found to be $Na_3H_2IO_6$, in agreement with the phase diagram for the system sodium hydroxide, periodic acid, water, as found by Hill (8).

The reaction was followed by mixing solutions of sodium hypochlorite and reagent grade sodium iodate and sodium hydroxide, with sodium chloride added to keep the ionic strength constant. The mixture was kept at constant temperature, and samples for analysis were taken at intervals. It was found that both hypochlorite and periodate ions absorb light strongly at about 300 mμ, so spectrophotometric analysis was not possible. The following titrations were therefore used.

Methods of Analysis

A sample was taken, cooled in ice for a short time, and any sodium periodate was filtered off. The solution was then allowed to warm up to room temperature, and aliquots were pipetted out for analysis. This procedure was necessary, as, otherwise, sodium periodate crystallized from the solution after pipetting. The aliquots were analyzed by the following methods.

Can. J. Chem. Downloaded from www.nrcresearchpress.com by 210.87.254.5 on 09/05/12
For personal use only.

(*a*) The aliquot was diluted and mixed with a known volume of standardized arsenious oxide solution and a large excess of sodium bicarbonate. Then 3 g of potassium iodide was added, and the excess arsenious oxide was titrated with standard iodine solution. In this titration the hypochlorite first oxidizes the arsenite to arsenate; and then, on adding potassium iodide, the periodate liberates iodine (which reacts with the arsenite):

$$Na_3H_2IO_6 + 2KI + H_2O \rightarrow NaIO_3 + 2KOH + 2NaOH + I_2.$$

Hence this titration measures hypochlorite plus periodate. It is essential to allow the sodium hypochlorite to react before adding potassium iodide.

(*b*) The aliquot was mixed with excess dilute (about 0.7 *N*) sulphuric acid and boiled for 10 minutes. This treatment destroys hypochlorite, but did not affect the iodate and periodate present. The solution was then cooled, excess potassium iodide was added, and the liberated iodine was titrated with sodium thiosulphate. This titration measures iodate plus periodate.

(*c*) The aliquot was boiled with dilute sulphuric acid as in (*b*). Borax was added in considerable excess (the pH being about 8); then potassium iodide was added and the liberated iodine was titrated with arsenious oxide. This measures the periodate alone.

From these titrations the concentrations of hypochlorite and iodate ions in the solution could be calculated. The constancy found for the difference, $[OCl^-]-[IO_3^-]$, besides being evidence of the stoichiometry of the reaction, is a check on the reliability of the analytical methods. In this reaction, chlorate formation accounted for less than 0.1% of the total decomposition.

The results show that the reaction is first order in hypochlorite and iodate ions; hence the equations that governed the reaction with nitrite apply here also. The results of a typical run are given in Table III.

TABLE III

(Run at 60.0° C; ionic strength 1.23; [NaOH] = 0.4328 *M*)

Time, min	$[OCl^-]$, *M*	$[IO_3^-]$, *M*	Difference	$\log [OCl^-]/[IO_3^-]$
0	0.1798	0.06009	0.1197	1.0826
34.0	0.1630	0.04321	0.1198	1.3277
68.5	0.1511	0.03233	0.1188	1.5423
107.8	0.1430	0.02295	0.1200	1.8300
151.5	0.1359	0.01732	0.1186	2.0605
196.5	0.1319	0.01246	0.1194	2.3603
241.0	0.1284	0.00901	0.1194	2.6572
291.0	0.1260	0.00657	0.1194	2.9547

The values of the rate constant, k_1, are given in Table IV. Inspection of these values shows that there is little change of the rate constant with hydroxide concentration. Apart from a degree of scattering in the constants, there seems to be a definite upward drift of the rate constant with hydroxide concentration. Roughly the constants at 60° C obey the equation

$$k_1 = 5.08\times10^{-2}(1+0.195[NaOH]_0).$$

The main reaction is therefore one of hypochlorite ions, presumably

$$OCl^- + IO_3^- \rightarrow Cl^- + IO_4^-,$$

but there is some third-order reaction with hydroxide ions as well.

Can. J. Chem. Downloaded from www.nrcresearchpress.com by 210.87.254.5 on 09/05/12
For personal use only.

TABLE IV

Run	Temp., °C	Initial: Ionic strength	Initial: [OCl^-]	Initial: [IO_3^-]	Initial: [OH^-]	Final [OH^-]	$k_1 \times 10^2$, (g-mol./l.)$^{-1}$ min^{-1}
15	60.0	1.40	0.1798	0.06009	0.433	0.325	5.35
16	"	1.41	0.1913	0.07688	0.418	0.309	5.39
17	"	1.35	0.0690	0.1887	0.392	0.299	5.48
18	"	1.36	0.0656	0.1864	0.406	0.315	5.57
19	"	1.31	0.0667	0.1916	0.574	0.495	5.67
20	"	1.34	0.0683	0.1885	0.582	0.511	5.91
21	"	1.31	0.0648	0.1887	0.190	0.110	5.13
22	"	1.31	0.0649	0.1884	0.190	0.110	5.36
23	50.0	1.36	0.0597	0.2043	0.383	0.305	1.64
24	"	1.36	0.0598	0.2037	0.384	0.305	1.60
25	40.0	1.38	0.0606	0.2042	0.389	0.299	0.441
26	"	1.36	0.0602	0.1958	0.386	0.299	0.450
27	60.0	1.36	0.0627	0.1608	1.014	0.929	6.02
28	"	1.36	0.0627	0.1608	1.014	0.929	6.11

The dependence on temperature corresponds to an activation energy of 26.1 kcal/g-mol. Expressing k_1 as $Ae^{-E/RT}$, $\log A = 15.83$. This is a relatively high value, though not unprecedentedly high.

3. DISCUSSION OF RESULTS

A number of oxidations by hypochlorite have now been examined by various workers, and it is of interest to see whether any generalizations can be made. Table V gives a

TABLE V

Reaction	log A*	Activation energy, kcal	ΔH^0, kcal	Ref.
$OCl^- + IO_3^-$	16.15	26.1	2.8	—
$HOCl + NO_2^-$	7.36	6.45	−36.2	—
$OCl^- + OCl^-$	12.03	24.8	− 5.7	1
$OCl^- + ClO_2^-$	11.52	20.8	−21.6	1
$HOCl + OCN^-$	12.30	15.1	—	9
$HOCl + Br^-$	8.55	4.5	− 7.5	3
$OCl^- + MnO_4^{-3}$ †	13.96	14.1	—	4
$HOCl + HC_2O_4^-$	15.76	15.0	−82.5	10
$OCl^- + ClO_3^-$	Very slow		−22.5	—
$OCl^- + SO_3^{--}$	Very fast		−82.1	—
$OCl^- + CN^-$	"	"	−84.0	—
$OCl^- + I^-$	"	"	−28.4/OCl^-	—

*Time in minutes.
†This rate is proportional to $[H_3O^+]^2$.

summary of these reactions. The first column gives the reagents indicating whether hypochlorous acid or hypochlorite ions are involved. The activation energies and log A values refer to the reactions as written, allowing for hydrolysis to HOCl where necessary. The ΔH^0 values also refer to the reactions as written, and assume that the reagents and products are all in aqueous solution. The last four entries are for reactions producing, respectively, perchlorate, sulphate, cyanate, and iodate ions. Here only qualitative observations on the rates are available, but the rates are either very fast or very slow.

Can. J. Chem. Downloaded from www.nrcresearchpress.com by 210.87.254.5 on 09/05/12
For personal use only.

Table V perhaps chiefly emphasizes our limited knowledge of the reactions of hypochlorites, but slight indications of trends are apparent. In the first place, log A generally falls when E does, so the actual rate constants are not as different as the activation energies would suggest. The fall in log A is not great enough to offset the change in activation energy; in fact it is about half as large as would be necessary for this. At present no general explanation is suggested.

There is some indication that, if the reaction is relatively exothermic, the activation energy is lower. This is perhaps to be expected, since if the new bond to oxygen is strong, this would tend to lower the energy of the activated complex as it is formed. However, this trend is not universal; for instance, the very exothermic oxidation of oxalate has quite a high activation energy. This particular reaction may be a little different from the others, since it is apparently not an oxygen transfer but an electron transfer; although it could be formulated either way. A more puzzling case is the reluctance of hypochlorite ions to oxidize chlorate ions to perchlorate, although this would be a fairly exothermic process. Some of these reactions involve hypochlorous acid, and some hypochlorite ions, but at present no general explanation can be offered for this distinction.

REFERENCES

1. M. W. LISTER. Can. J. Chem. **34**, 465 (1956).
2. F. FOERSTER and P. DOLCH. Z. Elektrochem. **23**, 127 (1917).
3. L. FARKAS, M. LEWIN, and R. BLOCH. J. Am. Chem. Soc. **71**, 1988 (1949).
4. M. W. LISTER and Y. YOSHINO. Can. J. Chem. **39**, 96 (1961).
5. E. A. SHILOV. J. Appl. Chem. (U.S.S.R.), **17**, 354 (1944).
6. M. W. LISTER. Can. J. Chem. **30**, 879 (1952).
7. E. A. MOELWYN-HUGHES. The kinetics of reactions in solution. 2nd ed. Oxford University Press. p. 76.
8. A. E. HILL. J. Am. Chem. Soc. **50**, 2678 (1928).
9. M. W. LISTER. Can. J. Chem. **34**, 489 (1956).
10. R. O. GRIFFITH and A. MCKEOWN. Trans. Faraday Soc. **28**, 518 (1932).

Can. J. Chem. Downloaded from www.nrcresearchpress.com by 210.87.254.5 on 09/05/12
For personal use only.

Can. J. Chem. Downloaded from www.nrcresearchpress.com by 210.87.254.6 on 09/05/12
For personal use only.

THE ELECTRONIC STATES OF LINEAR METHYLENE[1]

G. W. KING AND G. L. MALLI[2]

ABSTRACT

The electronic energy levels of the linear methylene radical, with r(C—H) = 1.0295 Å, have been calculated by the LCAO/MO/CI procedure. The state of lowest energy has $^3\Sigma_g^-$ symmetry, and is accompanied by low-lying $^1\Delta_g$ and $^1\Sigma_g^+$ states. Allowed intravalence shell transitions from the ground state ($^3\Pi_u$–$^3\Sigma_g^-$, $^3\Sigma_u^-$–$^3\Sigma_g^-$) are too high in energy to account for the observed transition at 8.6 ev, indicating that the latter is of Rydberg type if it is between linear combining states.

INTRODUCTION

A spectroscopic transition in absorption at 8.6 ev, obtained during the flash photolysis of diazomethane, has been assigned to the elusory methylene radical by Herzberg and Shoosmith (1), who showed that the lower combining state has a bond angle between 140° and 180° and is non-totally symmetrical. Although experimental data did not permit a complete analysis, it appeared very likely (2) that the spectrum arises from a $^3\Sigma_g^-$ linear ground state, with r''(C—H) in the range 1.029–1.034 Å. Photolysis of diazomethane in solid inert gas matrices at low temperatures has also yielded a product, tentatively identified as methylene, with absorption bands in the near ultraviolet (3, 4). More recently, further flash photolysis work on diazomethane vapor has revealed an extensive absorption spectrum between 6000 and 9000 Å, which may also be due to methylene (2). This spectrum resembles the α-band system of NH_2 (5) and is probably due to an analogous transition ($^1B_1$–$^1A_1$) between states differing in geometry, but with the $^1A_1$ state lying above the triplet ground state.

Theoretical predictions of the shape and electronic structure of methylene present a divergence of views (6, 7, 8). Apart from these and other qualitative discussions on the nature of the ground state (9, 10), quantitative LCAO/MO/SCF calculations by Padgett and Krauss (11) indicated a $^3B_1$ ground state with an equilibrium bond angle of 120°, while more extensive calculations by Foster and Boys (12) gave the same ground state with an angle of 129°; but in the latter work, the calculated energy of the corresponding $^3\Sigma_g^-$ linear state was greater by only 0.3 ev, a difference that is not significant when compared with the accuracy of the calculation. In both these papers, electronic energy was determined as a function of bond angle, the results confirming Walsh's prediction (13) that if the ground state is a triplet it has linear, or nearly linear, geometry. Walsh also concluded that for such a ground state, the allowed transition at longest wavelengths would occur in the far ultraviolet, but could be either intra- or extra-valence shell in character. However, Padgett and Krauss predicted a low-energy $^3\Pi_u$ state permitting a non-Rydberg ($^3\Pi_u$–$^3\Sigma_g^-$) allowed transition at 1.5 ev; for slightly bent states, the corresponding ($^3B_1$–$^3A_1$) transition would also be expected to lie at fairly long wavelengths.

It is clear that further theoretical work on methylene is desirable. Padgett and Krauss and Foster and Boys have both calculated the energies of a few excited states. We report here the values of a much larger number of these for the linear molecule, obtained by procedures which, on the basis of previous work, give useful semiquantitative results.

[1]*Manuscript received February 21, 1961.*
Contribution from the Burke Chemical Laboratories, Hamilton College, McMaster University, Hamilton, Ontario.
[2]*Holder of Shell Oil Company Scholarship, 1959–1960. Present address: Department of Physics, University of Chicago, Chicago, Illinois.*

By the Franck–Condon principle, calculated energies for transition in absorption should give the positions of vibrational bands of maximum intensity in such excited states as may prove to be bent.

THEORETICAL

The LCAO/MO/CI method is outlined in previous papers (14, 15), whose notation is followed here. Accurate wave functions $\Psi'_k(q_{O\ldots N})$ for the stationary states of a molecular system can be constructed as sums of Slater determinants Φ_p only if a complete set of basic single-electron molecular spin orbitals $\phi_{iv}(\mathbf{r}_v)$ are available. In practice it is necessary to use a restricted number of MSO's as the basic set for approximating to the wave functions of a system. Foster and Boys (12) used exponential functions expanded into a limited number of configurational determinants. On the other hand, in the SCF calculations of Padgett and Krauss (11), Ψ_k was approximated by a single Slater determinant or by a small number of these in linear combination, a modified Hartree–Fock procedure being used to obtain the best MSO's. In general, minimization of the expectation values E_k and E_l for the energies of two states Ψ_k and Ψ_l (necessarily obeying the orthogonality restriction $\int \Psi^*_k \Psi_l d\tau = \delta_{kl}$) will lead to different values of parameters and scaling factors within a restricted set of MSO's from which wave functions are constructed, and energy minimization for each separate state presents a formidable problem in computation. Best SCF ground-state orbitals cannot be assumed suitable for calculating excited-state energies; Padgett and Krauss made this assumption, although they introduced a limited perturbation treatment to compensate for errors.

In the calculation reported here, the basic MSO's were symmetry orbitals constructed from Slater AO's with fixed parameters, and had the same form for all the electronic states considered. This relatively crude approximation simplifies the orthogonalization of wave functions and reduces computation for a large number of electronic states to manageable proportions: errors are reduced by allowing for the interactions between large numbers of configurations. In view of the difficulty of evaluating multicenter integrals over AO's that occur in the calculation, a more sophisticated procedure does not seem justified at present.

Application to Methylene

A linear centrosymmetric geometry was assumed for the radical, with r(C—H) = 1.0295 Å. With Cartesian axes centered on the carbon atom and hydrogen atoms H′ and H″ on the positive and negative z-axis respectively, the basic Slater AO's have the following form:

$$\begin{aligned}
h' \equiv \mathrm{H}'(1s) &= (\delta_{\mathrm{H}}/\pi)^{1/2} \exp(-\delta_{\mathrm{H}} r') \\
h'' \equiv \mathrm{H}''(1s) &= (\delta_{\mathrm{H}}/\pi)^{1/2} \exp(-\delta_{\mathrm{H}} r'') \\
1s \equiv \mathrm{C}(1s) &= (\delta'_c/\pi)^{1/2} \exp(-\delta'_c r_c) \\
s \equiv \mathrm{C}(2s) &= (\delta_c^{5/3}\pi)^{1/2} r_c \exp(-\delta_c r_c) \\
\left.\begin{aligned} \pi \equiv \mathrm{C}(2p_x) &= \\ \bar{\pi} \equiv \mathrm{C}(2p_y) &= \\ \sigma \equiv \mathrm{C}(2p_z) &= \end{aligned}\right\} &\quad (\delta_c^5/\pi)^{1/2} r_c \exp(-\delta_c r_c) \left\{\begin{aligned} x_c \\ y_c \\ z_c \end{aligned}\right.
\end{aligned}$$

with $\delta_{\mathrm{H}} = 1$, $\delta'_c = 5.70$, $\delta_c = 1.57$. The latter value and that for r(C—H) were chosen together to facilitate interpolation in tables of molecular integrals (16); the internuclear separation is itself only defined approximately by experiment. The carbon $2s$ orbital was used in the orthogonalized form,

$$s^0 = (s - 0.20848.1s)/0.97803,$$

Can. J. Chem. Downloaded from www.nrcresearchpress.com by 210.87.254.6 on 09/05/12
For personal use only.

in evaluating all carbon mononuclear integrals (14). The AO's h', h'', s, π, $\bar{\pi}$, and σ form a reducible representation of the $D_{\infty h}$ point group for the linear molecule

$$\Gamma = 2\Sigma_g^+ + 2\Sigma_u^+ + 2\Pi_u,$$

and the set of orthogonal LCAO/MO's, which form bases for the irreducible representations and were used in the calculation, are given in Table I.

TABLE I

LCAO/MO's for linear methylene

	Symmetry	Analytical form
ϕ_0	σ_g^+	$0.5280s+0.3400(h'+h'')$
ϕ_1	σ_u^+	$0.5300\sigma+0.4200(h'-h'')$
$\phi_2 = \phi_3^*$	π_u	$2^{-\frac{1}{2}}(\pi+i\bar{\pi})$
$\phi_3 = \phi_2^*$	π_u	$2^{-\frac{1}{2}}(\pi-i\bar{\pi})$
ϕ_4	σ_g^+	$1.5500s-0.9995(h'+h'')$
ϕ_5	σ_u^+	$1.4990\sigma-1.1875(h'-h'')$

The carbon 1s electrons were taken as screening the nucleus, leaving a total of 924 different ways of distributing the remaining six electrons among the MSO's ϕ_i to satisfy the Pauli principle. Since each way of doing this gives one determinantal function Φ_p, a very large secular equation would have to be solved for the energy, but the order can be reduced in various ways. A somewhat similar procedure to that used here has been outlined by Slater (17) for the diatomic oxygen molecule. We need only select in the first place those determinantal functions Φ_k with eigenvalue $M_S = 0$ (three α and three β spins for the electrons) of S_z, the z-component of the spin operator, since every electronic state has a component with this eigenvalue. The MSO's ϕ_i and the determinants Φ_k constructed from them are eigenfunctions of the symmetry operators i and C_ϕ of the $D_{\infty h}$ point group, which commute with the Hamiltonian for the system and each other, thus factorizing the secular determinant. Further factorization is achieved by recombining the Φ_k as eigenfunctions of S^2; suitable linear combinations Ω^S are readily found for states with up to four singly occupied MO's, but the 20 states with six singly occupied orbitals were not included owing to the complexity of the wave functions resulting from their spin degeneracy. These states, energetically high in LCAO/MO approximation, should only contribute negligibly to the wave functions $\Psi_k{}^S$ of the states considered below. Finally, for configurations containing partly filled orbitals ϕ_2 and ϕ_3, the Ω^S are not eigenfunctions of the operator σ_v (reflection in a plane through the nuclei), and fresh linear combinations are taken to remedy this. Thus the original secular determinant can be factored into blocks, each referring to one particular symmetry class and multiplicity. These reduced equations were rigorously solved on a Bendix D-15G computer to obtain their lowest roots.

Evaluation of Matrix Elements

The elements of the secular determinants expand into sums of integrals over the AO's, on either one, two, or three nuclear centers. Mononuclear and two-center integrals were obtained from analytic expressions (18, 19) and tables (16, 20), each integral being calculated by more than one method where possible, to minimize errors.

Of the various approximations available, the Ruedenberg–Mulliken method (21) was used for evaluating three-center integrals, by which the latter are expanded as sums of

Can. J. Chem. Downloaded from www.nrcresearchpress.com by 210.87.254.6 on 09/05/12
For personal use only.

one- and two-center integrals. The nuclear attraction integrals $(\sigma:h'h'')$ and $(H'':h'\sigma)$, of form

$$(A:\chi_b\chi_c) = \int \chi_b^*(1)\ |Z_a/r_a|\ \chi_c(1)d\tau_1,$$

were evaluated by the method of Barker and Eyring (22). The Ruedenberg–Mulliken approximation for the integral

$$(h'\pi:h''\pi) = \iint h'(1)\pi(1)\ |1/r_{12}|\ h''(2)\pi(2)d\tau_1 d\tau_2$$

fails here, giving the value zero. Gray, Ross, and Yates (23) found an analogous situation in their work on benzene, and give an approximate formula for the integral which was used in this calculation.

RESULTS

The relative energies of all the states considered are given in Table II. These include: the three states $^3\Sigma_g^-$, $^1\Delta_g$, and $^1\Sigma_g^+$ of lowest energy; the $^3\Pi_u$ and $^3\Sigma_u^-$ states, which can

TABLE II

Calculated energy levels

Symmetry	Calculated energy (ev)		
	This work	Padgett and Krauss	Foster and Boys
$^3\Sigma_g^-$	0.00	0.00	0.00 ev
$^1\Delta_g$	2.17	2.0	2.6
$^1\Sigma_g^+$	3.30	3.7	
$^5\Sigma_g^-$	15.94		
$^3\Delta_g$	19.99		
$^3\Pi_u$	20.35	1.5	
$^3\Sigma_g^+$	21.60		
$^1\Pi_u$	25.56		
$^1\Sigma_g^-$	27.17		
$^3\Sigma_u^-$	27.65		
$^1\Sigma_u^-$	34.46		

spectroscopically combine with the ground $^3\Sigma_g^-$ state; and a number of other states differing in multiplicity from these, whose calculation used many of the same basic integrals. Detailed energy calculations were not carried out for the Π_g states, which cannot combine with any of the three low-lying states, or for the Σ_u^+ states, which cannot combine with the ground state and which, preliminary LCAO/MO calculations showed, were some 40 ev higher in energy.

The low-lying group of states $^3\Sigma_g^-$, $^1\Delta_g$, and $^1\Sigma_g^+$ all arise, in LCAO/MO approximation, from the configuration $(\sigma_g^2\sigma_u^2\pi_u^2)$; similar states occur in the oxygen and boron molecules which also have two electrons in degenerate π-orbitals. The calculated energies agree well with those found by Padgett and Krauss (11) and by Foster and Boys (12), which are also shown in Table II. However, the $^3\Pi_u$ state is found to be 20 ev above the ground state, much higher energetically than in the former authors' calculations, and in accordance with Walsh's predictions (13).

In calculations such as these, the basic set of MSO's does not include extravalence shell orbitals, formed from AO's with quantum number $n > 2$, since values for all the necessary integrals are not readily available. Experimentally it is known that many simple organic molecules have Rydberg states some 10 ev above the ground state, leading

Can. J. Chem. Downloaded from www.nrcresearchpress.com by 210.87.254.6 on 09/05/12
For personal use only.

to ionization potentials in the 10–15 ev region. These Rydberg states should properly be included in a configuration interaction scheme. In the methylene radical, there are no low-lying excited states which can combine with the ground state; and since the ionization potential is 11.7 ev (24), it must be concluded that the lowest excited states of many species shown at high energy in Table II are in fact largely Rydberg in character, and occur at lower energies. In particular the observed transition at 8.6 ev, if it indeed arises from the $^3\Sigma_g^-$ linear ground state, must be of Rydberg type, as has been suggested (2).

If the absorption spectrum of methylene in the visible region is similar to that of NH_2, then it may well be between the two components ($^1A_1$ and $^1B_1$) into which the $^1\Delta_g$ state transforms on bending. If, as in NH_2, the upper state is linear, the electronic origin of the transition cannot be at energies greater than 2.2 ev, else the actual ground state of the molecule will be bent ($^1A_1$). Both CH_2 and NH_2 show this type of transition in the same spectral region, and detailed analysis for the latter molecule gives the origin at 1.24 ev (5). An origin of similar value for the methylene spectrum is therefore consistent with a linear ground state.

REFERENCES

1. G. HERZBERG and J. SHOOSMITH. Nature, **183**, 1801 (1959).
2. G. HERZBERG. Robert A. Welsh Foundation Symposium, Texas, November 1959. Personal communication.
3. G. W. ROBINSON and M. MCCARTY. J. Am. Chem. Soc. **82**, 1859 (1960).
4. T. D. GOLDFARB and G. C. PIMENTEL. J. Am. Chem. Soc. **82**, 1865 (1960).
5. D. A. RAMSAY. Advances in spectroscopy. Vol. I. Interscience Publishers Inc., New York. 1959.
6. G. A. GALLUP. J. Chem. Phys. **26**, 716 (1957).
7. B. F. GRAY. J. Chem. Phys. **28**, 1252 (1958).
8. G. A. GALLUP. J. Chem. Phys. **28**, 1252 (1958).
9. J. LENNARD-JONES. Trans. Faraday Soc. **30**, 70 (1934).
10. K. J. LAIDLER and E. J. CASEY. J. Chem. Phys. **17**, 213 (1949).
11. A. PADGETT and M. KRAUSS. J. Chem. Phys. **32**, 189 (1960).
12. J. M. FOSTER and S. F. BOYS. Revs. Mod. Phys. **32**, 305 (1960).
13. A. D. WALSH. J. Chem. Soc. 2260 (1953).
14. H. HOWARD and G. W. KING. Can. J. Chem. **37**, 700 (1959).
15. G. W. KING. Can. J. Chem. **38**, 365 (1960).
16. M. KOTANI, A. AMENIYA, E. ISHIGURO, and T. KIMURA. Tables of molecular integrals. Maruzen Company, Ltd., Tokyo. 1955.
17. J. C. SLATER. Solid-state and molecular theory group. Technical Report No. 3. Massachusetts Institute of Technology, Cambridge, Massachusetts. 1953.
18. C. C. J. ROOTHAN. J. Chem. Phys. **19**, 1445 (1951).
19. M. P. BARNETT and C. A. COULSON. Trans. Roy. Soc. A, **243**, 221 (1951).
20. J. O. HIRSCHFELDER and J. W. LINNETT. J. Chem. Phys. **18**, 130 (1950).
21. K. RUEDENBERG. J. Chem. Phys. **19**, 1433 (1951).
22. R. S. BARKER and H. EYRING. J. Chem. Phys. **21**, 912 (1953); **22**, 1177 (1954).
23. F. A. GRAY, I. G. ROSS, and J. YATES. Australian J. Chem. **12**, 347 (1959).
24. A. LANGER, J. A. HIPPLE, and D. P. STEVENSON. J. Chem. Phys. **22**, 1836 (1954).

Can. J. Chem. Downloaded from www.nrcresearchpress.com by 210.87.254.6 on 09/05/12
For personal use only.

Can. J. Chem. Downloaded from www.nrcresearchpress.com by 210.87.254.5 on 09/05/12
For personal use only.

SULPHONIUM SALT SOLVOLYSIS

PART II. COMMON-ION EFFECT AND THE ION-PAIR MECHANISM IN THE SOLVOLYSIS OF DIMETHYL-*t*-BUTYL SULPHONIUM SALTS[1]

J. B. HYNE and J. W. ABRELL[2]

ABSTRACT

The kinetic effect of added common anion in the solvolysis of dimethyl-*t*-butyl sulphonium halides in ethanol–water mixtures is analyzed in terms of a mechanism involving solvolysis through an ion-pair intermediate. The simple ion-pair role, however, does not account for the kinetic behavior at higher added common-anion concentrations. A normal salt effect and further involvement of the ion pair in S_N2 attack by common anion are compared as possible explanations for the observed kinetic behavior.

INTRODUCTION

Evidence presented in the previous paper of this series (1) was interpreted as indicative of the increasing role of an ion-pair mechanism in the solvolysis of dimethyl-*t*-butyl sulphonium salts as the dielectric constant of the medium is reduced. Further experimental

[1] $$\begin{array}{ccc} R_3S^+ + X^- & \overset{K_A}{\rightleftharpoons} & R_3S^+X^- \\ \downarrow k_+ & & \downarrow k_{ip} \end{array}$$

evidence in support of this proposed mechanism is presented in this paper. It is clear from equation [1] that such a mechanism should be affected by the concentration of common anion X^-. Higher concentrations should favor ion-pair formation and a higher proportion of the over-all solvolysis should proceed through the ion-pair intermediate. The over-all rate of solvolysis (k_{obs}) of dimethyl-*t*-butyl sulphonium iodide and chloride has therefore been measured as a function of both added common anion and solvent composition.

In the previous paper of this series it was shown that if the ion-pair mechanism is correct, $k_{ip} > k_+$. Consequently, added common anion should increase the over-all rate of solvolysis (k_{obs}) since a greater proportion of the solvolytic process will proceed through the faster ion-pair pathway. As the dielectric constant of the solvolytic medium is reduced, the ion-pair association constant (K_A) will increase and together with increasing concentration of common anion these factors will result in virtually complete conversion of the sulphonium ion to the ion-pair state. The over-all rate of solvolysis should therefore increase with added common anion and lower dielectric constant but should approach an upper limiting value as the degree of ion pairing approaches 100%.

EXPERIMENTAL METHOD AND RESULTS

All rates were measured by the radiochemical flow counting technique of Hyne and Wolfgang (2). C^{14}-labelled dimethyl-*t*-butyl sulphonium iodide was prepared as described previously (2) and converted to the chloride by metathesis with freshly prepared silver chloride. Solvent mixtures were prepared by weight from doubly distilled water (10^{-7} mhos) and redistilled absolute ethanol. Reagent grades of lithium chloride and iodide

[1]*Manuscript received January 13, 1961.*
Contribution from the Department of Chemistry, University of Alberta in Calgary, Calgary, Alberta. Work done partly at Dartmouth College, Hanover, New Hampshire. Presented in part before The Organic Chemistry Division, 138th Meeting of the American Chemical Society, New York, September 1960.
[2]*Present address: Department of Chemistry, Washington University, St. Louis, Missouri.*

TABLE I

Rates of solvolysis of dimethyl-*t*-butyl sulphonium iodide, at 75.75° C, as a function of added common anion and solvent mole fraction composition
(Letters on each column refer to data-fit plots in Fig. 1)

(*a*) 0.954 EtOH				(*b*) 0.845 EtOH				(*c*) 0.713 EtOH				(*d*) 0.550 EtOH				(*e*) 0.000 EtOH			
Sulphonium salt, $M\times10^3$	Added LiI, $M\times10^3$	Corrected I^-, $M\times10^3$	$k^{75.75}_{obs}$ $\times10^4$, sec^{-1}	Sulphonium salt, $M\times10^3$	Added LiI, $M\times10^3$	Corrected I^-, $M\times10^3$	$k^{75.75}_{obs}$ $\times10^4$, sec^{-1}	Sulphonium salt, $M\times10^3$	Added LiI, $M\times10^3$	Corrected I^-, $M\times10^3$	$k^{75.75}_{obs}$ $\times10^4$, sec^{-1}	Sulphonium salt, $M\times10^3$	Added LiI, $M\times10^3$	Corrected I^-, $M\times10^3$	$k^{75.75}_{obs}$ $\times10^4$, sec^{-1}	Sulphonium salt, $M\times10^3$	Added LiI, $M\times10^3$	Corrected I^-, $M\times10^3$	$k^{75.75}_{obs}$ $\times10^4$, sec^{-1}
0.16	0.00	0.14	4.35	0.08	0.00	0.07	4.15	0.16	0.00	0.14	4.03	1.00	0.00	0.88	3.75	1.00	0.00	0.88	2.52
0.32	0.00	0.28	4.46	0.16	0.00	0.14	4.24	1.00	0.00	0.88	4.12	1.00	10.2	11.1	3.88	1.00	15.0	15.9	2.53
1.00	0.00	0.88	4.74	0.32	0.00	0.28	4.37	1.00	0.00	0.88	4.07		19.8	20.7	3.98		35.0	35.9	2.50
1.00	0.00	0.88	4.72	1.00	0.00	0.88	4.51	1.00	1.01	1.89	4.18		30.1	31.0	4.14				
1.00	0.50	1.40	4.75	1.00	1.05	1.93	4.58		4.07	4.95	4.33		40.4	41.3	4.15				
	0.58	1.46	4.85		1.96	2.84	4.66		4.13	5.01	4.34								
	1.03	1.91	5.09		2.47	3.35	4.69		4.37	5.25	4.39								
	1.04	1.92	5.03		3.98	4.86	4.87		7.04	7.92	4.41								
	2.69	3.57	5.28		5.98	6.86	5.06		9.97	10.8	4.54								
	5.00	5.88	5.40		9.25	10.3	5.30		19.7	20.6	4.70								
	5.50	6.38	5.42		15.9	16.8	5.51		30.1	31.0	4.74								
	8.64	9.52	5.72		21.0	21.9	5.45		40.7	41.6	4.95								
	13.0	13.88	5.82		30.3	31.2	5.82												
	15.7	16.6	6.07		42.2	43.1	6.11												
	16.2	17.1	5.99																
	18.3	19.2	6.18																
	22.9	23.8	6.33																
	23.9	24.8	6.49																
	26.9	27.8	6.69																
	38.9	39.8	7.25																
	46.0	46.9	7.58																

Can. J. Chem. Downloaded from www.nrcresearchpress.com by 210.87.254.5 on 09/05/12
For personal use only.

were used as sources of the common anion. The concentration of sulphonium salt used throughout was 1×10^{-3} M except in a few cases noted where rates at concentrations of anion less than 10^{-3} M were required. Observed rates as a function of concentration of added anion and solvent composition are shown in Tables I (a)–(e) for the sulphonium iodide and II (a)–(c) for the sulphonium chloride. All rates were measured at 75.75° C.

TABLE II

Rates of solvolysis of dimethyl-*t*-butyl sulphonium chloride, at 75.75° C, as a function of added common anion and solvent mole fraction composition

(Letters on each column refer to data-fit plots in Fig. 2)

(a) 0.973 EtOH				(b) 0.800 EtOH				(c) 0.550 EtOH			
Sulphonium salt, $M\times10^3$	Added LiCl, $M\times10^3$	Corrected Cl^-, $M\times10^3$	$k^{75.75}_{obs}$ $\times10^4$, sec^{-1}	Sulphonium salt, $M\times10^3$	Added LiCl, $M\times10^3$	Corrected Cl^-, $M\times10^3$	$k^{75.75}_{obs}$ $\times10^4$, sec^{-1}	Sulphonium salt, $M\times10^3$	Added LiCl, $M\times10^3$	Corrected Cl^-, $M\times10^3$	$k^{75.75}_{obs}$ $\times10^4$, sec^{-1}
0.50	0.00	0.45	4.27	1.00	0.00	0.88	4.09	1.00	0.00	0.88	3.64
1.00	0.00	0.88	4.47	1.00	0.00	0.88	4.19	1.00	7.45	8.33	3.73
1.00	0.80	1.68	4.79	1.00	2.80	3.68	4.36	1.00	18.7	19.5	3.83
1.00	1.40	2.28	4.90	1.00	5.70	6.58	4.57	1.00	29.6	30.4	3.99
1.00	2.90	3.78	4.98	1.00	10.1	11.0	4.61	1.00	50.5	51.4	4.24
1.00	5.70	6.58	5.27	1.00	20.0	20.9	4.75				
1.00	19.7	20.5	5.59	1.00	32.4	33.3	5.01				
1.00	26.9	27.8	5.76	1.00	40.4	41.3	5.23				
1.00	35.0	35.9	6.05								

The rate data plotted in Figs. 1 and 2 show the predicted increase in rate as common anion is added. The observed initial increase, furthermore, becomes more pronounced as the dielectric constant of the solvent decreases. These phenomena are in keeping with the mechanism proposed in equation [1] since the ion-pair association constant increases as the dielectric constant decreases and consequently the effect of added common anion in displacing the equilibrium to the ion pair will also be greater. However, it is seen from these plots that the k_{obs} does not approach a limiting value as the added anion concentration is increased but becomes linearly dependent upon the anion concentration. Two possible explanations of this effect are offered and the relative merits of each considered in the subsequent sections of this paper. Both interpretations involve the equilibrium between free sulphonium ions and sulphonium ion pairs with the anion as postulated in equation [1]. The values of the ion-pair association constant K_A, obtained by analysis of the kinetic data, are both similar in magnitude and in variation with solvent composition to those obtained conductimetrically for similar sulphonium salt systems. There appears to be little doubt, therefore, that such an ion-pair equilibrium is involved in the solvolysis.

MECHANISM INVOLVING S_N2 ATTACK BY THE ANION ON THE ION PAIR

In this interpretation of the observed kinetic behavior the following extended form of equation [1] is proposed.

[2] $$\begin{array}{ccccc} R_3S^+ + X^- & \overset{K_A}{\rightleftharpoons} & R_3S^+X^- & \xrightarrow[k_{ip}']{+X^-} & \text{products} \\ \downarrow k_+ & & \downarrow k_{ip} & & \\ \text{products} & & \text{products} & & \end{array}$$

Can. J. Chem. Downloaded from www.nrcresearchpress.com by 210.87.254.5 on 09/05/12
For personal use only.

Can. J. Chem. Downloaded from www.nrcresearchpress.com by 210.87.254.5 on 09/05/12
For personal use only.

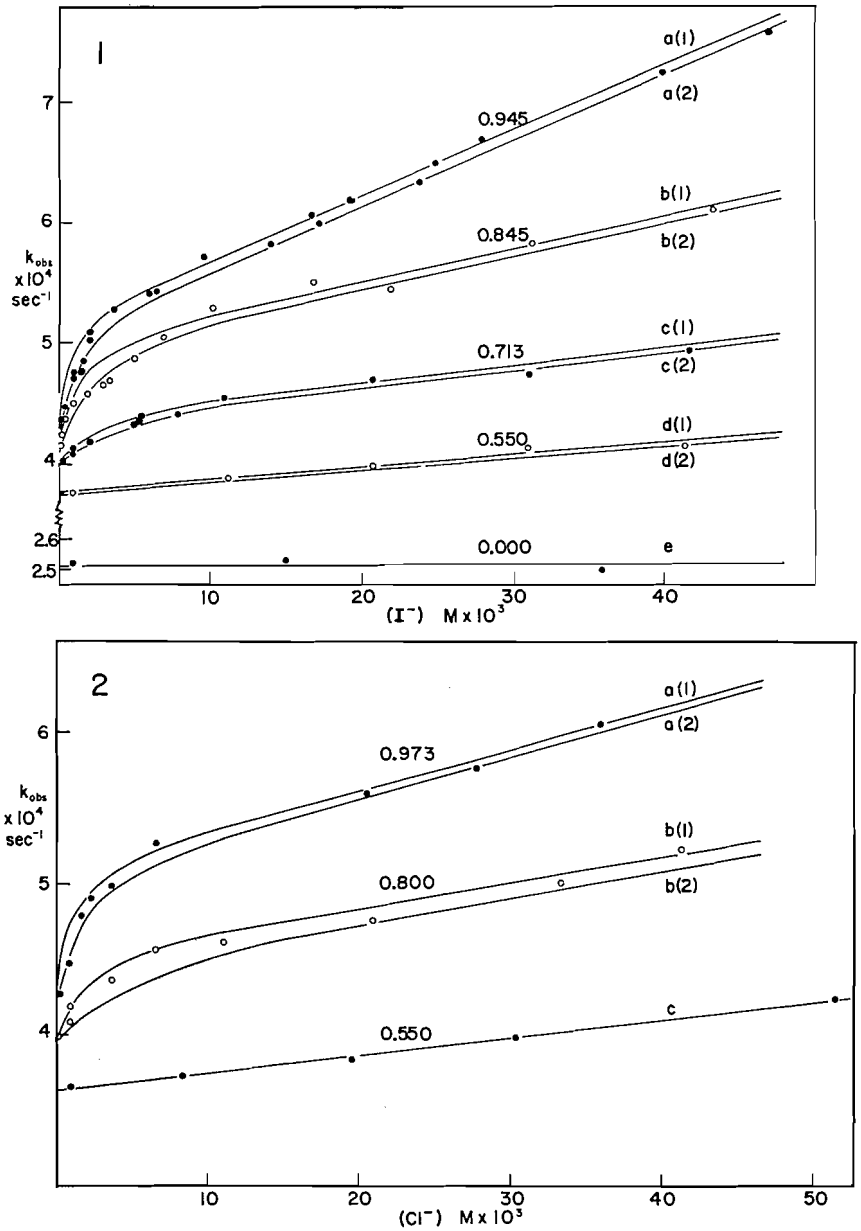


FIG. 1. Fit of experimentally determined k_{obs} (Table I) for dimethyl-*t*-butyl sulphonium iodide solvolysis to calculated curves from kinetic-expression equations [10] or [17]. (See Table III for values of constants for each calculated line.)

FIG. 2. Fit of experimentally determined k_{obs} (Table II) for dimethyl-*t*-butyl sulphonium chloride solvolysis to calculated curves from equations [10] or [17]. (See Table III for values of constants for each calculated line.)

This mechanism differs from that proposed in equation [1] in that a third rate-determining step, k_{ip}', has been added, which is a bimolecular attack of a free halide ion on the ion pair.

Derivation of Rate Equation

Assuming the mechanism proposed in equation [2] above, a rate expression for k_{obs} can be derived. Consider the three paths available for the reaction of the sulphonium salt to dimethyl sulphide and other products; in each case the only assumption made is that dimethyl sulphide is produced in the rate-determining step of each path. From equation [2] the observed rate of production of dimethyl sulphide is

$$r = k_+[R_3S^+]+k_{ip}[R_3S^+X^-]+k_{ip}'[R_3S^+X^-][X^-]. \quad [3]$$

However,

$$[R_3S^+X^-] = K_A[R_3S^+][X^-], \quad [4]$$

and substituting [4] in [3],

$$r = k_+[R_3S^+]+k_{ip}K_A[R_3S^+][X^-]+k_{ip}'K_A[R_3S^+][X^-]^2. \quad [5]$$

The observed pseudo first-order over-all rate of production of dimethyl sulphide, r, must be equal to the rate of removal of the salt (total) if dimethyl sulphide is produced in the rate-determining step of all paths, hence

$$r = k_{obs}[R_3SX]_T. \quad [6]$$

Substituting [6] in [5] and rearranging,

$$k_{obs} = \{[R_3S^+]/[R_3SX]_T\}\{k_+ + k_{ip}'K_A[X^-]+k_{ip}K_A[X^-]^2\}. \quad [7]$$

But at all times,

$$[R_3SX]_T = [R_3S^+]+[R_3S^+X^-] \quad [8]$$

$$= [R_3S^+]+K_A[R_3S^+][X^-]. \quad [9]$$

Substitution of [9] for $[R_3SX]_T$ in [7] and rearranging,

$$k_{obs} = \frac{k_+ + k_{ip}K_A[X^-]+k_{ip}'K_A[X^-]^2}{1+K_A[X^-]}. \quad [10]$$

Equation [10] requires that k_{obs} increases as $[X^-]$ increases due to the k_{ip} and k_{ip}' terms. However, it does not predict a leveling off of the rate at high $[X^-]$ as in equation [1] since when $K_A[X^-]$ becomes large compared with unity and k_+, equation [10] reduces to

$$k_{obs} \doteq k_{ip}+k_{ip}'[X^-], \quad [11]$$

showing a continued linear dependence of k_{obs} on $[X^-]$.

Analysis of Data by Equation [10]

Equation [10] may be rearranged to

$$k_{obs} = k_+ + K_A\{k_{ip}[X^-]-k_{obs}[X^-]+k_{ip}'[X^-]^2\}, \quad [12]$$

which has the general form of a straight line with slope K_A and intercept k_+.

From equation [12] it is seen that k_{obs} is a linear function of a complex term involving $[X^-]$. Thus in order for k_{obs} to follow first-order kinetics, as indeed it does, the $[X^-]$ must be assumed to be constant throughout a given run (i.e. a given determination of k_{obs}). It is now necessary to examine the validity of this assumption for, during the course of a given run, the amount of halide involved in ion pairing will change. On solvolysis

Can. J. Chem. Downloaded from www.nrcresearchpress.com by 210.87.254.5 on 09/05/12
For personal use only.

the sulphonium salt liberates halide, previously tied up in ion pairs, as HX; as a result the free [X^-] does not remain constant over the entire run. However, inspection of the plots of the basic experimental data (see e.g. ref. 2) shows that first-order behavior of the rate is not observed until some three half lives of reaction have elapsed. This is due to an artifact of the method and not a fundamental change in reaction order (2). Consequently, some 88% of the sulphonium salt has reacted by this point, freeing the halide from ion pairs, and the following half lives over which the rate is determined liberate such a small amount of X^- that the concentration change cannot be detected as affecting the rate of reaction. This concentration effect was corrected for by assuming the total halide concentration present in a given run to be the amount of added lithium halide *plus* 88% of the initial concentration of the sulphonium salt. This corrected halide ion concentration is shown in Tables I and II. It is obvious that this correction is most important at low concentrations of added halide.

An additional complication arises in the computation of the anion concentration, due to the incomplete dissociation of the lithium halide in low dielectric media. Data of sufficient detail is not available to enable precise corrections to be made for this effect. However, the dissociation of lithium chloride in ethanol has been studied (3) and these results show that the salt is still 90% dissociated at 10^{-2} M. Although the neglect of this effect will introduce errors in the analysis presented here these errors will not affect the internal consistency of the treatment although they will be reflected in the absolute values of the constants computed.

The values for k_{ip} and k_{ip}' must be known if K_A and k_+ are to be found graphically. Upon inspection of the data given in Tables I and II and plotted in Figs. 1 and 2, it is noted that after an initial steep rise in k_{obs} with added X^- the relationship approximates linearity. After addition of a sufficient amount of common ion (LiX) the sulphonium ion is present almost entirely in the form of an ion pair, especially in the lower dielectric media where K_A is large. At this point equation [11] should hold. Thus, upon back extrapolation of the linear sections of the plot to zero [X^-], the intercept gives an approximate value for k_{ip} and the slope yields a value for k_{ip}'. Approximate values for k_+ were obtained by back extrapolation of the initial steep section of the plots to zero X^- concentration. As noted in Tables I and II several rate determinations were made at salt concentrations less than 10^{-3} M in order to permit more accurate back extrapolations. Using the approximate values of k_+, k_{ip}, and k_{ip}' so obtained, and arbitrarily chosen values of K_A, best-fit curves, as shown in Figs. 1 and 2, were calculated by successive approximation. In some cases the values of k_{ip} and k_{ip}' had to be altered slightly to obtain better fits. It should be noted that k_+ and K_A are theoretically obtainable from a plot of the experimentally determined values of k_{obs}, [X^-], k_{ip}, and k_{ip}' according to equation [12]. It was found, however, that a plot of this type is extremely sensitive to [X^-] and that the value of the bracketed term in equation [12] is a very small difference between very large numbers. The experimental errors in k_{obs} and [X^-] are therefore too great to permit analysis on the basis of a plot of the function as described in equation [12]. Consequently, resort to the technique of successive approximation to a best fit was necessary.

Figure 1 is a composite of the experimental data for the sulphonium iodide (Table I) and the upper and lower limiting theoretical curves for each set of points computed from equation [10] using the values for the constants shown in Table III. Figure 2 is a similar composite for the sulphonium chloride data (Table II), the values for the constants being shown in Table III.

Can. J. Chem. Downloaded from www.nrcresearchpress.com by 210.87.254.5 on 09/05/12
For personal use only.

TABLE III

Values of constants in theoretical kinetic expressions (equations [10] and [17]) for solvolysis of dimethyl-*t*-butyl sulphonium salts

Mole fraction ethanol	D (75.75°) (12)	Curve No. (Figs. 1 and 2)	K_A, l./mole	k_+ (or k_+^0) $\times 10^4$, sec^{-1}	k_{ip} (or k_{ip}^0) $\times 10^4$, sec^{-1}	$k_{ip}' \times 10^3$, l./mole sec	b
Iodide							
0.945	17.5	*a* (1)	3500	4.15	5.15	5.40	1.05
		a (2)	1500				
0.845	19.3	*b* (1)	900	4.10	5.10	2.46	0.48
		b (2)	500				
0.713	22.0	*c* (1)	340	4.00	4.51	1.20	0.27
		c (2)	250				
0.550	25.7	*d* (1)	180	3.75	3.85	0.929	0.24
		d (2)	120				
0.000	62.0	*e*	<20	2.51	—	—	—
Chloride							
0.973	16.8	*a* (1)	2000	4.15	5.08	2.65	0.52
		a (2)	1000				
0.800	20.3	*b* (1)	600	3.95	4.60	1.53	0.34
		b (2)	200				
0.550	25.7	*c*	~100	3.63	3.70	1.30	0.35

Discussion of Analysis by Equation [10]

The fit of experimental data to curves calculated from equation [10], as shown in Figs. 1 and 2, supports the kinetic model for the solvolysis from which equation [10] was derived. The formal similarity of the rate behavior in this case to that observed by Fainberg and Winstein (4) for the special salt effect in alkyl halide and benzene sulphonate solvolysis is immediately obvious. The similarity arises from the fact that in this case an initial-state ion can solvolyze by ion-pair formation whereas in the alkyl halide and benzene sulphonates a covalent initial state can solvolyze by passing to the ion-pair intermediate.

The ion-pair association constants (K_A) obtained from the kinetic analysis and shown in Table III exhibit the same form of dependence on solvent dielectric as those reported from conductance measurements on the trimethyl sulphonium iodide system (5, 6). The orders of magnitude are also comparable. This observation can be interpreted as further support for the proposed mechanism. It is also noted that K_A (I^-) > K_A (Cl^-) in a given solvent medium, which is in keeping with the observed order of ion-pair association constants for lead (7) and lithium halides (8). The probable error associated with the K_A values determined by the kinetic analysis is large compared with the accuracy attainable in modern conductimetric methods. It should be noted, however, that in cases such as the sulphonium salt under study here the kinetic method is the only available technique for K_A determination since the salt reacts with the solvent.

In Table IV the percentages of the sulphonium salt (10^{-3} M) present as ion pairs in various solvents with 10^{-2} M added common anion are shown. These values are calculated

Can. J. Chem. Downloaded from www.nrcresearchpress.com by 210.87.254.5 on 09/05/12
For personal use only.

TABLE IV

Percentage association to ion pairs for 10^{-3} M sulphonium salt with 10^{-2} M added common anion as a function of K_A (iodide)

Mole fraction ethanol	K_A (median)	% association
0.945	2.5×10^3	96
0.845	7×10^2	88
0.713	3×10^2	75
0.550	1.5×10^2	60
0.000	~20	~25

from the median values of K_A for each solvent composition shown in Table III for the iodide case. A similar table may be constructed for the chloride system but the iodide case suffices for illustration. The concentration of added common anion of 10^{-2} M was chosen since inspection of Fig. 1 will show that in all solvent compositions the dependence of k_{obs} on added common anion has become linear at this point. It is seen from Table IV that in all solvent compositions above 0.550 mole fraction ethanol more than half of the sulphonium salt is present as ion pairs at this concentration of added common anion. It is beyond this concentration of added anion that the S_N2 attack of the anion on the ion pair is postulated to be important. The fact that most of the sulphonium salt is present as the ion pair and that there is at least a 10-fold excess of anion over sulphonium salt establishes that the necessary species for such a mechanism are present in abundance.

The early interest in the solvolysis of sulphonium salts was primarily due to the fact that such systems represent the case where charge is dispersed on passing to the transition state and the rate would be expected to increase with decreasing dielectric constant. It is clear from the data presented here, however, that the observed rate (k_{obs}) is not the rate of solvolysis of the ion in lower dielectric media. Hence previous attempts to correlate the observed rate with dielectric constant have been unsuccessful. In this analysis, however, values for k_+ are obtained (as shown in Table III) over the whole solvent composition range. These values are plotted versus dielectric constant in Fig. 3 and describe a linear relationship. The additional points in Fig. 3 at $D = 37$ (0.324 mole

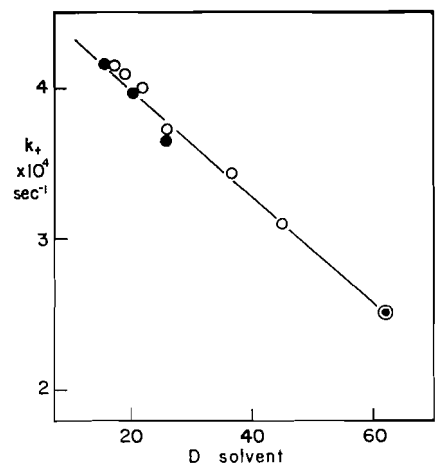


FIG. 3. k_+ versus dielectric constant of solvent: ○, iodide; ●, chloride.

Can. J. Chem. Downloaded from www.nrcresearchpress.com by 210.87.254.5 on 09/05/12
For personal use only.

fraction ethanol) and $D = 45$ (0.203 mole fraction ethanol) are computed from rates for the solvolysis of dimethyl-*t*-butyl sulphonium iodide at 50.3° and 78.4° (9). Figure 3 also shows that the k_+ values for both the chloride and iodide salts lie on the same line, an observation consistent with the kinetic model proposed, since k_+ is a measure of the rate of solvolysis of the free sulphonium ion and does not involve the anion in the rate-determining step.

The dependence of k_{ip} and k_{ip}' on dielectric constant of the solvent is shown in Fig. 4(*a*

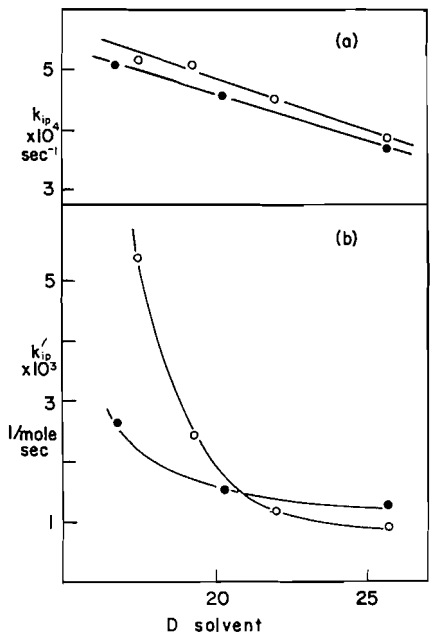


FIG. 4. (*a*) k_{ip}, (*b*) k_{ip}' versus dielectric constant of solvent: ○, iodide; ●, chloride.

and *b*). According to the kinetic model presented previously, both rates should show a dependence on the nature of the anion since this species is involved in the rate-determining step. Such a dependence is noted in both cases but is considerably greater in the k_{ip}' than in the k_{ip} rate. Furthermore the dielectric-constant dependence of k_{ip}' is larger than that of k_{ip}. The mechanism proposed to account for these observations together with the other features of the over-all solvolytic process are summarized in Fig. 5.

The S_Ni-type mechanism proposed for the rate process k_{ip} is in keeping with the first-order character of the rate constant. Formal charge is presumably partially dispersed in the initial ion-pair state so that little change in charge character results on passing to a transition state involving intramolecular nucleophilic attack of the halide component of the ion pair on the adjacent *t*-butyl carbon atom; hence the relative insensitivity of k_{ip} to solvent dielectric constant changes. Dimethyl sulphide is liberated in the rate-determining step as assumed in the kinetic analysis and *t*-butyl halide is also formed. Subsequent solvolysis or elimination of the *t*-butyl halide to yield alcohol or olefin will not be rate determining since the rates of such reactions under the experimental conditions used in this work are considerably greater than those of the sulphonium salt rates (10, 11). It is perhaps a little surprising that the rate differences between the iodide and chloride

Can. J. Chem. Downloaded from www.nrcresearchpress.com by 210.87.254.5 on 09/05/12
For personal use only.

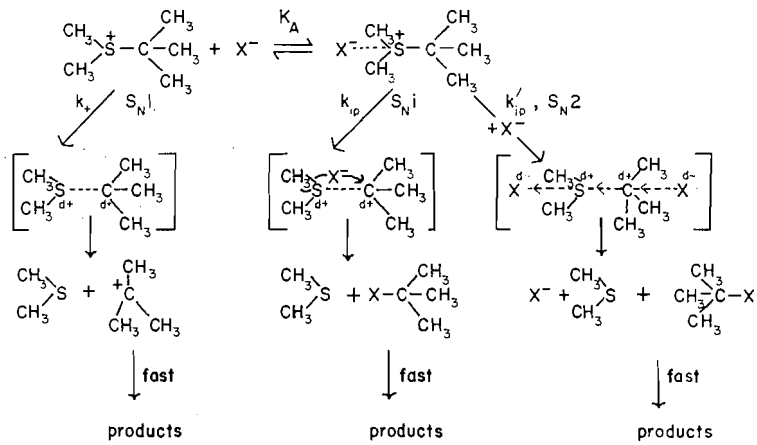


FIG. 5.

salts are not greater than those observed in Fig. 4(*a*). The small differences, however, are in the expected order since the iodide ion is more nucleophilic than the chloride ion and should react somewhat more readily in the S_Ni mechanism.

The bimolecular mechanism proposed for the rate process k_{ip}' is in accord with the second-order form of this constant. In low-dielectric media the bulk of the sulphonium ions are readily converted to ion pairs by initial addition of small amounts of common anion (see Table IV) so that further additions provide halide ions which participate in S_N2-type attack on the ion pair. The marked dependence of k_{ip}' on dielectric constant (Fig. 4(*b*)) is characteristic of reactions involving the dispersal of ionic charge in the formation of the transition state. Such would be the case in the mechanism proposed here where a halide ion and an ion pair form a charge-dispersed transition state. The greater nucleophilicity of the iodide ion is also reflected in the relative magnitudes of k_{ip}' for the two salts. It is questionable whether the apparent crossover in Fig. 4(*b*) is real, due to the accuracy with which k_{ip}' can be determined from the best-fit analysis. Dimethyl sulphide is again liberated in the rate-determining step and the subsequent *t*-butyl halide solvolysis is fast.

MECHANISM INVOLVING NORMAL SALT EFFECT

The alternative explanation for the linear dependence of k_{obs} on added common anion at higher concentrations is based on the possible role of normal salt effects. The derivation of the rate expression in this case is exactly similar to that shown previously in equations [3] through [10] except for the omission of the additional k_{ip}' term. The resulting rate equation obtained is

$$k_{obs} = \frac{k_+ + k_{ip} K_A[X^-]}{1 + K_A[X^-]}. \qquad [13]$$

If a normal salt effect is considered, however, k_+ and k_{ip} are not constants independent of $[X^-]$. Using the approximation favored by Fainberg and Winstein (13) for salt effects in other than pure aqueous media these effects can be expressed as a linear function of anion concentration, i.e.

$$k_+ = k_+^0 (1 + a[X^-]) \qquad [14]$$

$$k_{ip} = k_{ip}^0 (1 + b[X^-]). \qquad [15]$$

Can. J. Chem. Downloaded from www.nrcresearchpress.com by 210.87.254.5 on 09/05/12
For personal use only.

Hence

$$[16] \qquad k_{obs} = \frac{k_+^0 + k_{ip}^0 K_A[X^-] + k_+^0 a[X^-] + k_{ip}^0 b K_A[X^-]^2}{1 + K_A[X^-]}.$$

In the derivation of this equation we have made no simplifying assumptions regarding the nature of the normal salt effect. It would be unjustifiable to assume that the constants a and b are equal since they represent the salt effect on two different processes: one, the solvolysis of an ion and the other, of an ion pair. However, from the experimental data plotted in Fig. 1 it is seen that in the more aqueous media, where the bulk of the solvolysis proceeds via the ion (k_+), the slope of the linear section is very small and in pure water virtually zero. This is the region of solvent composition where the salt effect is largely determined by the term $k_+^0 a[X^-]$ in equation [16]. Consequently it seems reasonable to assume that a is small compared with b since in more ethanolic solvents, where the proportion of the solvolysis proceeding through the ion (k_+) is small compared with that through the ion pair (k_{ip}), the salt effect is much greater and is determined by the term $k_{ip}^0 b K_A[X^-]^2$ in equation [16]. As a first approximation, therefore, equation [16] may be written as

$$[17] \qquad k_{obs} = \frac{k_+^0 + k_{ip}^0 K_A[X^-] + k_{ip}^0 b K_A[X^-]^2}{1 + K_A[X^-]}.$$

This approximation is tantamount to the assumption that the normal salt effect on the free sulphonium ion reaction may be neglected (equation [14]) due to the smaller magnitude of this effect compared with that on the ion pair and the diminishing role of the free-ion reaction in lower dielectric media. It should be noted that a simplifying assumption of this kind is necessary at this stage since equation [16] has more unknowns than can be evaluated from the data presently available. The possible errors inherent in this assumption are considered in the discussion of the b values in a subsequent section.

It is seen immediately that equation [17] has the same form as equation [10] derived for the alternative S_N2-type mechanism explanation for the non-limiting rate behavior. Consequently $k_{ip}' = k_{ip}^0 b$, and since $k_{ip}^0 = k_{ip}$ of equation [10], $b = k_{ip}'/k_{ip}$. Values of b so calculated are shown in Table III.

Discussion of Analysis by Equation [17]

The normal salt effect b values obtained from analysis of the experimental data by equation [17] and shown in Table III indicate that a normal salt effect would be one of acceleration since all values are positive. It is further seen that the b values decrease as the dielectric constant of the medium increases. It should be noted, however, that at mole fractions of ethanol of 0.550 and lower, the first-order approximation made in order to simplify equation [16] may become invalid since the $k_+^0 a[X^-]$ term may now be significant compared with the $k_{ip}^0 b K_A[X^-]^2$ term. This suspicion is warranted since in the more aqueous media a larger contribution to the over-all k_{obs} is made by the k_+ term and furthermore, we have no knowledge of how the normal salt effect constant, a, varies with solvent composition. Consequently, while the contribution to k_{obs} from the free-ion pathway (k_+) is still significant, the assumption that the salt effect on this pathway (viz. a) is negligible is a dubious one. This error may be the reason for the apparent similarity of the b values at 0.713 and 0.550 mole fraction ethanol in the iodide case and at 0.800 and 0.550 mole fraction in the chloride case. In both systems the b values at 0.550 mole fraction may be in error due to the increasing significance of the a value.

Can. J. Chem. Downloaded from www.nrcresearchpress.com by 210.87.254.5 on 09/05/12
For personal use only.

There can be no doubt, however, that if a normal salt effect is responsible for the linear dependence of k_{obs} on added anion concentration then this effect is one of acceleration, i.e. a positive salt effect. The prediction of the sign of normal salt effects depends upon a knowledge of the relative charge character of the initial and transition states in the rate-determining step. It is known, however, that for reactions in aqueous media, positive salt effects are observed for reactions between two ions of like sign where the transition state has a higher charge density than the initial state while negative salt effects are noted for reactions between oppositely charged ions where the transition state has a lower charge density due to partial neutralization of the two charges. Since all kinetic evidence indicates that the solvolysis of sulphonium salts involves charge delocalization in going to the transition state, it therefore seems reasonable to expect a *negative* normal salt effect and not a positive one. The validity of extension of these principles to systems in non-aqueous media is supported in the work of Fainberg and Winstein on the solvolysis of toluenesulphonates (4) in ethanol and acetic acid, which demonstrated a positive salt effect, in keeping with the fact that charge is created in moving from the polar initial state to a more ion-like transition state. The b values obtained here refer to the salt effect on a reaction proceeding from an ion-pair initial state to a charge-dispersed transition state. Here the difference in charge character between the two states is presumably even smaller than that between a free sulphonium ion initial state and a charge-dispersed transition state. Yet the b value for the ion-pair process appears to be greater than the a value for the solvolysis from the free ion, as indicated by the virtual independence of k_{obs} on anion concentration in water. There is every indication, therefore, that if our interpretation of the charge character of the sulphonium salt solvolysis is correct, then the observed linear dependence of the rate on salt concentration has the wrong sign for an explanation based on a normal salt effect. Regarding the observed increase in b with lowering of dielectric constant, it is clearly impossible to offer an explanation for this behavior until the more fundamental question of the sign of the effect can be answered.

CONCLUSIONS

There seems little doubt that in the solvolysis of sulphonium salts in media of dielectric constant less than 25, a reaction pathway involving ion pairs plays a significant role. The correspondence between ion-pair association constants obtained from the kinetic analysis and those for similar systems determined conductimetrically appears to be too close to be fortuitous. There still remains considerable doubt, however, about the explanation for the observed linear dependence of the over-all rate of solvolysis on added salt at higher concentrations when the sulphonium salt is largely in the form of ion pairs. The evidence at the moment would appear to favor an explanation based upon the onset of a third S_N2-type attack by anion on the ion pair but there is as yet insufficient evidence to exclude conclusively an explanation based on a normal salt effect. Further work on the effect of added non-common ions and investigation of the stereochemistry of the solvolysis of salts with optically active alkyl groups should provide the necessary information to enable a distinction or an assignment of relative roles of the two phenomena to be made.

ACKNOWLEDGMENTS

The authors wish to acknowledge financial support for this work from Research Corporation and the U.S. Atomic Energy Commission.

Can. J. Chem. Downloaded from www.nrcresearchpress.com by 210.87.254.5 on 09/05/12
For personal use only.

REFERENCES

1. J. B. HYNE. Can. J. Chem. **39**, 1207 (1961).
2. J. B. HYNE and R. WOLFGANG. J. Phys. Chem. **64**, 699 (1960).
3. J. R. GRAHAM, G. S. KELL, and A. R. GORDON. J. Am. Chem. Soc. **79**, 2352 (1957).
4. A. H. FAINBERG and S. WINSTEIN. J. Am. Chem. Soc. **78**, 2767 (1956).
5. E. D. HUGHES, C. K. INGOLD, R. MOK, and Y. POCKER. J. Chem. Soc. 1238 (1957).
6. A. L. JACOBSON and J. B. HYNE. J. Am. Chem. Soc. **82**, 2418 (1960).
7. A. I. BIGGS, M. H. PANCKHURST, and H. N. PARTON. Trans. Faraday Soc. **51**, 802, 806 (1955).
8. J. KENTTAMMA. Suomen Kemistilehti, B, **32**, 9 (1959).
9. J. B. HYNE and R. E. WONKKA. To be published.
10. S. WINSTEIN and A. H. FAINBERG. J. Am. Chem. Soc. **79**, 5937 (1957).
11. A. H. FAINBERG and S. WINSTEIN. J. Am. Chem. Soc. **79**, 1602 (1957).
12. G. AKERLOF. J. Am. Chem. Soc. **54**, 4125 (1932).
13. A. H. FAINBERG and S. WINSTEIN. J. Am. Chem. Soc. **78**, 2763 (1956).

Can. J. Chem. Downloaded from www.nrcresearchpress.com by 210.87.254.5 on 09/05/12
For personal use only.

Can. J. Chem. Downloaded from www.nrcresearchpress.com by 210.87.254.105 on 09/05/12
For personal use only.

THE VELOCITY OF RATE-CONTROLLING SURFACE DIFFUSION REACTIONS IN THE ELECTRODEPOSITION OF METALS AS A FUNCTION OF DISLOCATION DENSITY[1]

H. KITA, M. ENYO, AND J. O'M. BOCKRIS

ABSTRACT

The rate constant for the surface diffusion velocity of Cu adions in the deposition of Cu appears to depend on the current density of measurement. An interpretation is suggested in which it is proposed that the number of growth sites during the deposition of Cu under "monolayer" conditions depends upon potential, owing to the dependence of the critical radius for growth upon supersaturation. Calculations based upon this hypothesis are compared with experiment. The dependence of the shape of the Tafel relation in metal deposition (transient conditions) is related to the effect of changing the number of "active" growth sites.

1. INTRODUCTION

It has been recently suggested (1, 2) that in the buildup of the first few layers of a metal surface at low current densities in electrodeposition, the surface diffusion of adions (2), from the sites at which they land on the metal from the solution to growth steps on the metal surface, is the rate-determining step in the over-all reaction $M^{z+}+ze_0^- = M$. Evidence for a similar rate-determining step in dissolution is available (1). The velocity of surface diffusion may be expressed approximately by

$$V_{\text{diff}} = v_0\left(\frac{c_x - c_0}{c_0}\right) \qquad [1]$$

where $v_0^* = D(c_0/x_0^2)$, c_x is the concentration of adions at distance x from a growth step, c_0 is their concentration at $x = 0$ or the concentration at equilibrium, D is the surface diffusion coefficient, and x_0 is the half distance between growth steps. If the concentration of growth steps is independent of the current density, i, of deposition and dissolution, x_0 and hence v_0 should be independent of i, and this was the approximation made in the first quantitative theory of surface diffusion control for metal deposition or dissolution (1).

Evidence is now available (3, 4) which shows that on Cu and Ag, v_0 increases with i; at low current densities, there is a rough proportionality between v_0 and i. It will be shown here that this result is consistent with the model of rate-controlling surface diffusion already discussed, if the dependence on potential of the number of dislocations which may form growth steps is taken into account.

The assumption of the independence of dc/dx with x, implicit in [1], may be dropped (4); whereupon $\partial^2 c_x/\partial x^2 \neq 0$, so that, during steady-state deposition at a constant overpotential, and assuming a surface far from saturation in respect to adion concentration,

$$D\left(\frac{\partial^2 c_x}{\partial x^2}\right) + \frac{i_0}{ZF}\exp(-\alpha_c F\eta/RT) - \frac{i_0}{ZF}\exp(\alpha_a F\eta/RT) = 0, \qquad [2]$$

[1]*Manuscript received March 27, 1961.*
Contribution from the John Harrison Laboratory of Chemistry, University of Pennsylvania, Philadelphia 4, Pa.

**In moles cm^{-2} sec^{-1}. It is the rate of the surface diffusion when the surface adion concentration is that at equilibrium.*

where i_0 is the exchange current density, α_c and α_a the transfer coefficients for the electrochemical reaction, and η the overpotential; F, R, and T have their usual meaning and x is counted from the growth step.

The rate of surface diffusion at $x = 0$ is also equal to the rate of the over-all reaction of deposition and dissolution. In mass per unit area per unit time it is given by

[3] $$V_{x=0} = \frac{D}{x_0}\left(\frac{\partial c}{\partial x}\right)_{x=0}.$$

2. DEPENDENCE OF "EQUILIBRIUM SURFACE DIFFUSION FLUX" UPON CURRENT DENSITY

The critical diameter (5), l_c, which must be exceeded before a nucleus can grow on a surface, is related to the surface free energy of the edge, γ, and the degree of supersaturation, $RT \ln c/c_0$, by (6)

[4] $$l_c = \frac{2A\gamma}{\rho RT \ln \frac{c}{c_0}}$$

where A is the atomic weight, ρ the density, c the concentration of surface adions at the condition considered, and c_0 that at equilibrium. The surface of a real crystal contains a certain concentration of screw dislocations, which constitute surface steps. All steps of length l, the distance between pairs of dislocations, which provide steps having $l > l_c$, will grow when they receive material by means of surface diffusion. Assuming a random distribution of steps of various lengths, it may be shown that (6)

[5] $$\frac{dN_l}{N_0} = 2\frac{l}{\bar{l}^2}\exp\left[-\left(\frac{l}{\bar{l}}\right)^2\right]dl$$

where dN_l is the number of steps of length between l and $l+dl$, $\bar{l}$ is the average length of a step, and N_0 is the total number of steps per unit area. Further, on the assumption of a random distribution, one has that

$$\left(\frac{1}{N_{\text{dls}}}\right)^{1/2} = \bar{l}$$

where N_{dls} = mean number of dislocations cm^{-2}. Hence $\bar{l}^2 N_{\text{dls}} = 1$. But $2N_0 = N_{\text{dls}}$ and hence $\bar{l}^2 2N_0 = 1$, or

[6] $$\bar{l}^2 N_0 = \tfrac{1}{2}.$$

Thus, the number of steps which are active in crystal growth is

$$N_{l>l_c} = \int_{l=l_c}^{l=\infty} 2N_0 \frac{l}{\bar{l}^2}\exp\left[-\left(\frac{l}{\bar{l}}\right)^2\right]dl = N_0 \exp\left[-\left(\frac{l_c}{\bar{l}}\right)^2\right].$$

Using [4] and [6],

[7] $$N_{l>l_c} = N_0 \exp\left[-\left(\frac{2\sqrt{2}A\gamma N_0^{1/2}}{\rho RT \ln \frac{c}{c_0}}\right)^2\right].$$

This number, $N_{l>l_c}$, of steps which will take part in lattice growth influences the rate

Can. J. Chem. Downloaded from www.nrcresearchpress.com by 210.87.254.105 on 09/05/12
For personal use only.

of surface diffusion because increase of $N_{\iota>\iota_c}$ decreases x_0 and hence increases v_0 (cf. equation [1]).* A relation between i and v_0 arises because, in steady-state metal deposition or dissolution,

$$V_{\text{diff}} = \frac{i}{ZF}. \qquad [8]$$

Or, using [1],

$$\ln \frac{c}{c_0} = \ln\left(1+\frac{i}{ZFv_0}\right). \qquad [9]$$

Further,

$$v_0 = \frac{Dc_0}{x_0^2} = 8Dc_0N_{\iota>\iota_c} \qquad [10]$$

$$= 8Dc_0N_0 \exp\left[-\left\{\frac{2\sqrt{2}A\gamma N_0^{1/2}}{\rho RT \ln\left(1+\frac{i}{8ZFDC_0N_{\iota>\iota_c}}\right)}\right\}^2\right] \qquad [11]$$

from which v_0 can be determined for a given N_0, $N_{\iota>\iota_c}$ being determined graphically from [7], [9], and [10].

3. THE TAFEL RELATION AS A FUNCTION OF DISLOCATION DENSITY

It has been shown (Mehl and Bockris (1)) that the i–η relation for a metal exchange reaction (adion coverage far from saturation) is

$$i = \frac{i_0[\exp(-\alpha_c F\eta/RT)-\exp(\alpha_a F\eta/RT)]}{1+\frac{i_0}{ZFv_0}\exp(\alpha_a F\eta/RT)}. \qquad [12]$$

Correspondingly, the expression for the concentration of adions as a function of x can be found from [2] for certain boundary conditions. Thus, if

$$c = c_0, \qquad x = 0$$

$$\partial c/\partial x = 0, \qquad x = x_0$$

then (4)

$$\frac{c_x}{c_0} = \exp[-(\alpha_a+\alpha_c)F\eta/RT] + \frac{1-\exp[-(\alpha_a+\alpha_c)F\eta/RT]}{1+\exp[-2X]}\left[\exp(-2X)\exp\left(X\frac{x}{x_0}\right)+\exp\left(-X\frac{x}{x_0}\right)\right], \qquad [13]$$

where

$$X = \left(\frac{i_0}{ZFv_0}\right)^{1/2}\exp(\alpha_a F\eta/2RT). \qquad [14]$$

Hence, from [3] and [13],

$$\frac{i}{ZF} = V_{x=0} = \frac{Dc_0}{x_0^2}\cdot X\cdot[1-\exp(-2F\eta/RT)]\left[1-\frac{2}{1+\exp(-2X)}\right]. \qquad [15]$$

Equation [15] reduces to the normal Butler–Volmer equation for transfer control if $v_0 \gg i_0$, i.e. the rate-controlling reaction is transfer. Hence, qualitatively, it is clear

**The model is applicable only under the condition total quantity of electricity passed ≡ less than one monolayer under which the measurements recorded here were taken.*

Can. J. Chem. Downloaded from www.nrcresearchpress.com by 210.87.254.105 on 09/05/12
For personal use only.

from [11] and [15] that if surface diffusion is the rate-controlling reaction at low current densities, transfer control will tend to be rate determining at some higher current density,* as has indeed been experimentally found (1, 4). (It is assumed that the experimental conditions are such that diffusion in solution is always "fast".)

4. COMPARISON WITH EXPERIMENT

Comparison will be made for experimental material on Cu (3). Thus, $A = 63$, $z = 2$, $\rho = 8.9$ g cc^{-1}. Values of c_0D, γ, and N_0 require discussion and no measured values of D for surface diffusion on metals in contact with aqueous solutions exist at room temperature.

One can take the value of c_0, in order of magnitude terms, to be 10^{-10} mole cm^{-2}. The value depends sensitively on surface conditions: an intermediate value of those known experimentally (3, 7) was taken here.

D may be roughly estimated by extrapolation from high-temperature values obtained in the gas phase on Cu (8) by using an activation energy† of the order of 1/20th of the heat of sublimation (6). By this method, one obtains $10^{-6} \sim 10^{-7}$ cm^2/sec. The values thus calculated are, however, concerned with *adatom* movement whilst in the electrodeposition case one is concerned with the movement of adions which have a fractional charge (2). The activation energy for the adions is expected to be higher than that of adatoms, and from considerations of an energy cycle, similar to that described by Conway and Bockris (2); the value of D is found to be reduced by about 10^{-1} from the adatoms to the adion case.

Values of the number of dislocations per square centimeter of metal surface recorded in the literature vary from about 10^8–10^{12} dislocation lines cm^{-2}, the upper limit being for cold-worked material (9). The value of N_0 on a quenched surface would be likely to be some 100 less than that on a cold-worked surface. On the latter type of surface, for Cu, the mean number of dislocation from two methods (energy and density measurements) is about 4×10^{11} cm^{-2} (10). Hence it sounds reasonable to accept 4×10^9 cm^{-2}. In the present calculation, 10^{10} cm^{-2} for N_0 was taken. This higher value seems possible to accept for the following reasons. (i) The basis of the estimate of 4×10^9 cm^{-2} is very approximate (i.e., it is the generally observed order of magnitude for the ratio of the number of dislocations for a quenched, compared with a cold-worked, material). (ii) In the preparation of the specimens, SiO_2 or SiO may evaporate from the Vycor tube or diffuse from the glass sheath of the electrode and introduce increased dislocations into the surface. (iii) According to Hirsch and Silcox (11), 10^{10} dislocations cm^{-2} was observed on the rapidly quenched Al.

γ for Cu has been determined by Udin *et al.* (12), who found 1800 ergs cm^{-2} for a Cu surface at 1100° K. The value for Cu at 300° K can be approximately estimated by use of the Ramsey-Shields equation, using $T_C = 0.6\times T_B$ (cf. *Textbook of physical chemistry* by Glasstone). The value is 2250 ergs cm^{-2}. However, this value refers to surface atoms and it is necessary to have a value of γ corresponding to atoms in the edges to which the surface adions diffuse. The value of γ for a site at which the co-ordination number

**An earlier explanation of the change in the rate-controlling step at higher current densities (1) involved a qualitative interpretation in terms of potential-dependent* nucleation. *This process does not seem a likely path in metal deposition or dissolution on surfaces such as those discussed here until current densities are much higher than those used (except on metals, e.g. vapor-phase dendrites, in which the dislocation density is particularly low).*

†Obtained from calculation of the intersection points of potential energy – distance curves using both a Lennard Jones potential (Burton and Cabrera (6)) or a Morse function (Conway and Bockris (2)).

Can. J. Chem. Downloaded from www.nrcresearchpress.com by 210.87.254.105 on 09/05/12
For personal use only.

is $c_{S,1}$ may be related to that of a surface atom through Stefan's relation, according to which one finds

$$\frac{\gamma_{S,1}}{\gamma_{S,2}} = \frac{1-\frac{c_{S,1}}{c_B}}{1-\frac{c_{S,2}}{c_B}},$$

where $c_{S,2}$ is the co-ordination of the surface atoms and c_B is that of the bulk liquid. Taking $c_{S,1} = 7$, $c_{S,2} = 9$, and $c_B = 12$, one obtains $\gamma_{S,1} = 3750$ ergs cm^{-2}.

Comparison with experiment is shown in Fig. 1. It is seen that, having the above deduced parameters, we can achieve a moderate agreement with experiment.

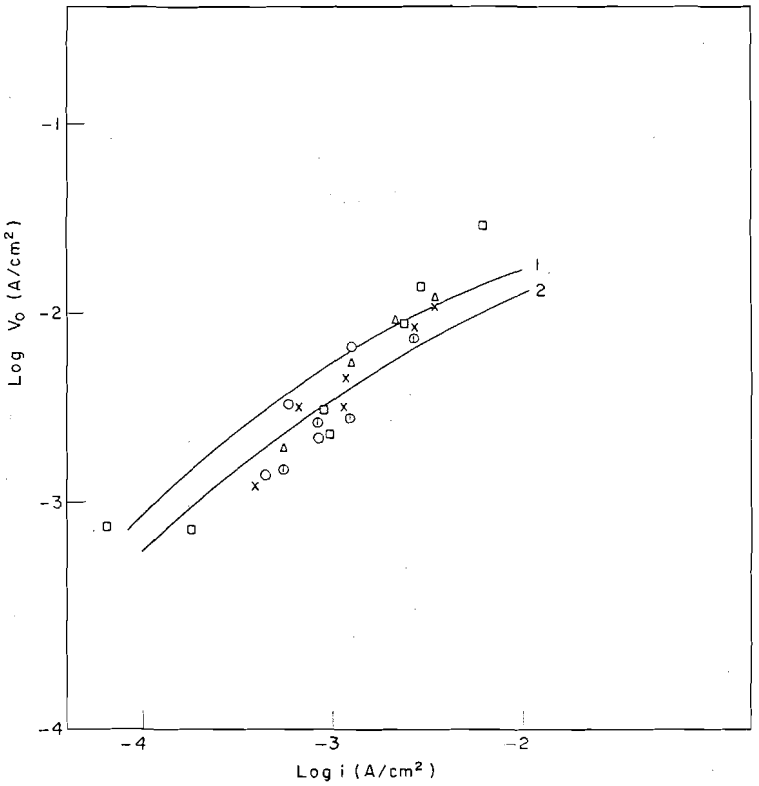


FIG. 1. Change of observed (3) and calculated v_0 with i.
Electrode: quenched electrode in He.
Solution: 0.5±0.1 mole/l. H_2SO_4 and ×, 0.46; ○, 0.30; □, 0.096; △, 0.073; ⊙, 0.012 mole/l. $CuSO_4$.
——: Calculated v_0 using numerical values of $N_0 = 10^{10}$/cm^2, $DC_0 = 10^{-18}$ mole/sec; (1) $\gamma = 2250$ ergs/cm^2, (2) $\gamma = 3750$ ergs/cm^2.

The existence of deviations from the Butler–Volmer equation at low current densities that are due to rate-determining surface diffusion is also well rendered (Fig. 2). With an increasing number of dislocations, the Tafel lines at a given current density (Fig. 2) become increasingly coincident with those for the Tafel equation expected from transfer control. The disappearance of diffusion control with increase of current density, previously reported (1, 7), is thus satisfactorily described.

Can. J. Chem. Downloaded from www.nrcresearchpress.com by 210.87.254.105 on 09/05/12
For personal use only.

Can. J. Chem. Downloaded from www.nrcresearchpress.com by 210.87.254.105 on 09/05/12
For personal use only.

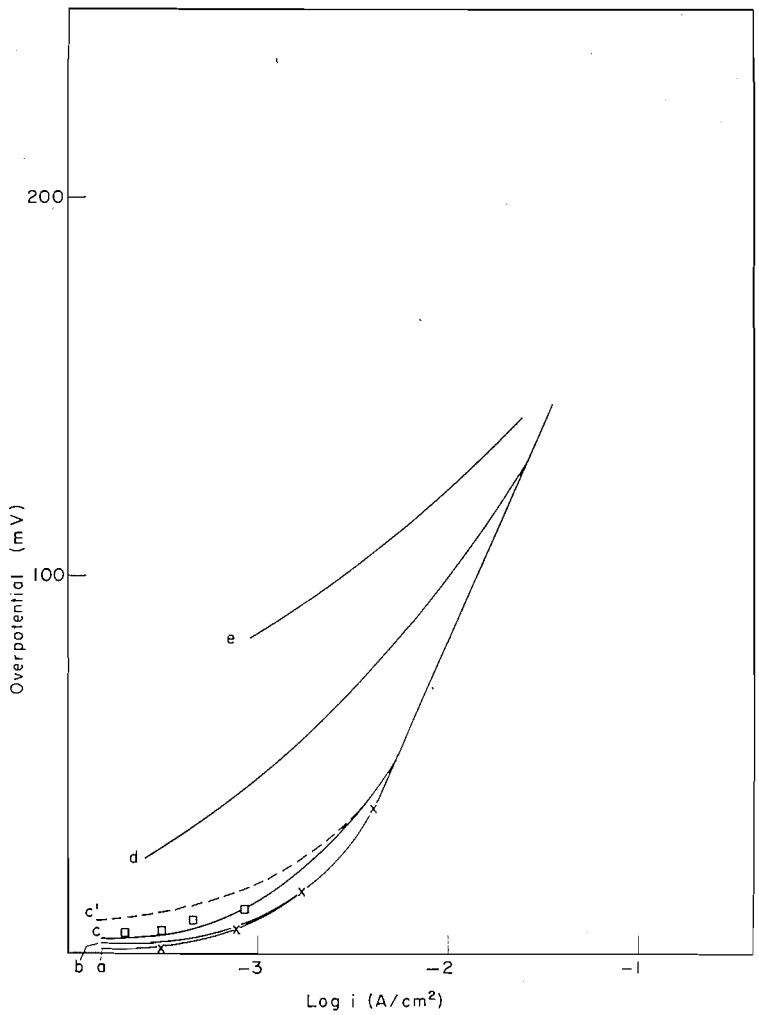


FIG. 2. Deviation from Tafel line due to "surface diffusion". *a*, Tafel line (transfer rate-controlling); *b*, $N = 10^{10}/cm^2$, $D = 10^{-8}$ cm²/sec; *c*, $N = 10^8/cm$, $D = 10^{-8}$ cm²/sec; *d*, $N = 10^6/cm$, $D = 10^{-8}$ cm²/sec; *e*, $N = 10^8/cm$, $D = 10^{-9}$ cm²/sec; *c'*, the case where N changes with applied current; ×, experimental results on electrodeposited electrode; □, experimental results on quenched electrode.

ACKNOWLEDGMENTS

The authors wish to thank the American Electroplater's Society and the U.S. Steel Company for financial support of the present work.

REFERENCES

1. H. GERISCHER and W. VIELSTICH. Z. Elektrochem. **56**, 380 (1952). H. GERISCHER. Z. physik. Chem. **201**, 55 (1952). W. LORENZ. Z. physik. Chem. **202**, 275 (1953). W. MEHL and J. O'M. BOCKRIS. J. Chem. Phys. **27**, 818 (1957); Can. J. Chem. **37**, 190 (1959).
2. B. E. CONWAY and J. O'M. BOCKRIS. Proc. Roy. Soc. (London), A, **248**, 394 (1958); H. GERISCHER. Z. Elektrochem. **62**, 256 (1958).
3. J. O'M. BOCKRIS and M. ENYO. J. Chem. Phys. In press.
4. A. R. DESPIC and J. O'M. BOCKRIS. J. Chem. Phys. **32**, 389 (1960).
5. M. VOLMER and A. WEBER. Z. physik. Chem. **119**, 277 (1926).

6. W. K. BURTON, N. CABRERA, and F. C. FRANK. Phil. Trans. Roy. Soc. London, A, **263**, 299 (1951). N. CABRERA and W. K. BURTON. Discussions Faraday Soc. **5**, 40 (1949). F. C. FRANK. Discussions Faraday Soc. **5**, 48 (1949).
7. E. MATTSON and J. O'M. BOCKRIS. Trans. Faraday Soc. **55**, 1586 (1959). W. LORENZ. Z. physik. Chem. **19**, 377 (1959). H. GERISCHER. Z. Elektrochem. **62**, 256 (1958).
8. N. HACKERMAN and N. H. SIMPSON. Trans. Faraday Soc. **52**, 628 (1956).
9. IMPURITIES AND IMPERFECTIONS. Am. Soc. for Metals, Cleveland, Ohio. 1955. p. 162.
10. M. LLAREBROUGH, M. E. HARGEAVES, and G. W. WEST. Acta Met. **5**, 783 (1957).
11. P. B. HIRSCH and J. SILCOX. Growth and perfection of crystals. John Wiley & Sons, Inc., New York. 1958. p. 262.
12. H. UDIN, A. J. SHALER, and J. WULF. J. Metals, Trans. AIME, **1**, 186 (1949).

Can. J. Chem. Downloaded from www.nrcresearchpress.com by 210.87.254.105 on 09/05/12
For personal use only.

Can. J. Chem. Downloaded from www.nrcresearchpress.com by 210.87.254.40 on 09/05/12
For personal use only.

THE PROTON RESONANCE SPECTRA OF THE 2,5-DIMETHYL-2,5-DIMETHOXY-3,4-DIPHENYLHEXANES[1]

S. BROWNSTEIN

ABSTRACT

The relative free energies of the various conformations for the diastereomeric 2,5-dimethyl-2,5-dimethoxy-3,4-diphenylhexanes have been determined. Hindered and free rotation about the various bonds has been observed and assignments of the proton resonance signals to specific conformations have been made.

Proton resonance spectroscopy has been found well suited to the study of hindered rotation in substituted ethanes (1, 2). Hindered rotation in the 2,5-dimethyl-2,5-dimethoxy-3,4-diphenylhexanes has been demonstrated by dipole moment studies (3). The present investigation extends the previous work and provides some quantitative data.

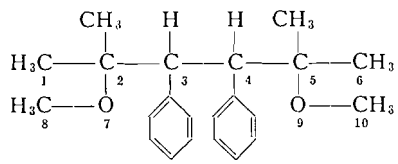
For a substituted ethane with the symmetry CHXY—CHXY there are two non-equivalent conformations for the meso diastereomer and three non-equivalent conformations for the *d,l* diastereomer. In one of the conformations of the meso diastereomer the two hydrogens will be non-equivalent. In the other they will both be equivalent, but will not be in the same environment as either of the hydrogens which are non-equivalent. Therefore if rotation about the central carbon–carbon bond is sufficiently hindered one could theoretically observe one signal from one conformation and a pair of peaks from the other conformation. This assumes that there is a sufficient population of molecules in each of the conformations. However, with rapid rotation, only a single signal will be observed, whose position is the weighted average of the individual signals. All three conformations of the *d,l* diastereomer have the hydrogens of a given conformation equivalent; but each conformation has them in a unique environment. Therefore with hindered rotation one signal should be observed for each conformation. The same conclusions apply to the groups X and Y if they also contain protons.

The relative populations in any two conformations of a given diastereomer will be given by

$$\frac{P1}{P2} = e^{-\frac{\Delta E}{RT}}$$

where ΔE is the free energy difference between the two conformations. Therefore if rotation is sufficiently hindered so that proton resonance signals are observed for the individual conformations, but sufficiently rapid so that thermal equilibrium of the populations is obtained in a reasonable time, then the variation in relative intensities of the signals as the temperature is varied will yield the free energy differences between the conformations.

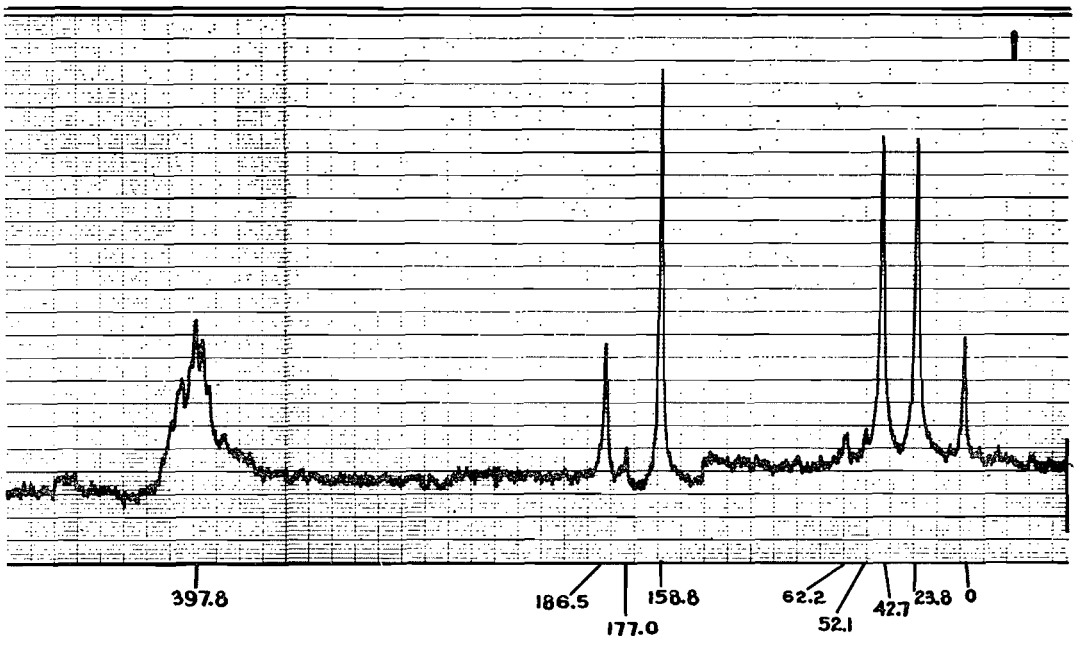
The rotations and conformations will be discussed with respect to the numbering shown in the following formula.



[1]*Manuscript received April 26, 1961.*
Contribution from the Division of Applied Chemistry, National Research Council, Ottawa, Canada. Issued as N.R.C. No. 6388.

The methyl groups attached to carbon atoms 2 and 5 may be considered as part of a system of symmetry CX_2Y—CPQR. It has been shown that regardless of the rate of rotation about the central carbon–carbon bond the two groups X will always be magnetically non-equivalent (4). However, if rotation is hindered it may be possible to observe two peaks for each conformation.

The spectra of the meso and *d,l* isomers at 296° K are shown in Figs. 1 and 2. Some of the peaks of the less abundant conformations are too weak to be observed at this temperature but become apparent in spectra obtained at higher temperatures. The chemical



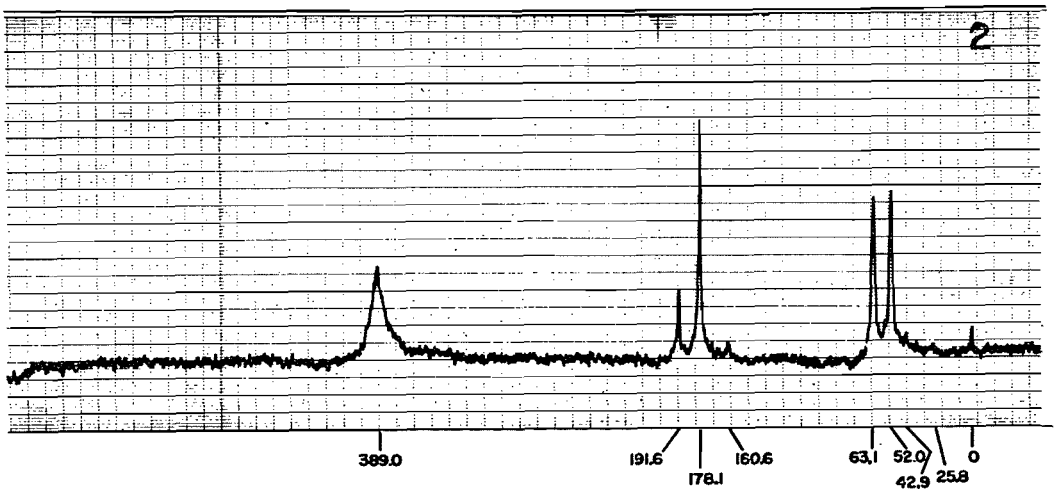


FIG. 1. meso-2,5-Dimethyl-2,5-dimethoxy-3,4-diphenylhexane.
FIG. 2. *d,l*-2,5-Dimethyl-2,5-dimethoxy-3,4-diphenylhexane.

Can. J. Chem. Downloaded from www.nrcresearchpress.com by 210.87.254.40 on 09/05/12
For personal use only.

shifts which may be assigned to definite conformations are listed in Table I. The conformations are designated as shown in Fig. 3.

TABLE I

Peak positions of the 2,5-dimethyl-2,5-dimethoxy-3,4-diphenylhexanes

Assignment	meso		Conformation	*d,l*		Conformation
Intense CH_3	23.8	42.7	A	52.0	63.1	D
Weak CH_3	52.1	62.2	B	25.8	42.9	C
Intense OCH_3	158.8		A	178.1		D
Weak OCH_3	177.0		B	160.6		C
Intense CH	186.5		A	191.6		D
Weak CH	179.9	188.9*	B	188.5*		C

*Position likely due to a hydrogen which is between the dimethylmethoxy group and the hydrogen attached to the opposite carbon atom of the central carbon–carbon bond.

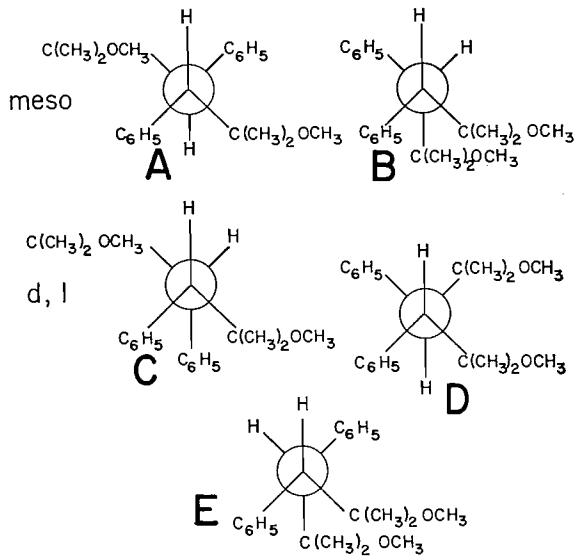


FIG. 3. Conformations of the diastereomeric 2,5-dimethyl-2,5-dimethoxy-3,4-diphenylhexanes.

The assignment to the individual conformations was done according to the following reasoning. Conformation B is the only one with non-equivalent hydrogens on the central carbon atoms; therefore the weak CH peaks must arise from this conformation. The assignment of the other peaks of the meso isomer necessarily follows. The positions reported for the weak CH peaks are those they would have in the absence of spin coupling. Actually, a four-line *AB*-type spectrum is obtained. Analysis yields the peak positions shown and a spin coupling constant of 1.55±0.2 cycles/sec (5). The dihedral angle between these protons in conformation B is 60°. For this angle the Karplus theory of spin coupling predicts a coupling constant of 1.7 cycles/sec, which agrees nicely with this observation (6).

For the *d,l* isomer, the dimethylmethoxy group in conformation C is located between the phenyl and the hydrogen attached to the opposite carbon atom of the central carbon–carbon bond. It is in a similar environment for conformation A of the meso isomer.

Can. J. Chem. Downloaded from www.nrcresearchpress.com by 210.87.254.40 on 09/05/12
For personal use only.

Therefore the peaks in the *d,l* isomer which occur in the same position as those of conformation A may be assigned to conformation C. In conformation D the dimethylmethoxy group is located between the hydrogen and the dimethylmethoxy group attached to the opposite carbon atom of the central carbon–carbon bond. It is in a similar environment for conformation B of the meso isomer. Therefore the remaining methyl and methoxyl peaks of the *d,l* isomer are in good agreement with an assignment to conformation D.

Because it is impossible to assign the C—H peaks of conformation B to a given hydrogen of that conformation, one cannot compare the agreement with the position for the C—H peak of conformation C. However, because of the close similarity in chemical shifts it seems likely that the positions marked with an asterisk in Table I are both due to a hydrogen which is between the dimethylmethoxy group and the hydrogen attached to the opposite carbon atom of the central carbon–carbon bond. In both conformations A and D the C—H is located between the phenyl group and the dimethylmethoxy group attached to the opposite carbon atom of the central carbon–carbon bond. In this case there is not very good agreement between the chemical shifts in the two isomers. The assignment of the peaks to conformations C and D cannot be considered as proved; however, excellent agreement in the positions of 14 of the 16 peaks makes the assignment quite probable. No peaks were observed which could be attributed to conformation E.

So far one can say that there is strongly hindered rotation about the 3—4 bond and free rotation about the 1—2, 5—6, 7—8, and 9—10 bonds. There could be either free or hindered rotation about the 2—3, 2—7, 4—5, or 5—9 bonds. However, if rotation is hindered, only one conformation about the bond in question can be present in any appreciable amount. As the temperature is raised it is observed that the peaks due to the methyl groups in conformation B are not of equal intensity. Above 345° K another peak appears at 56.0 cycles/sec. These results may be explained on the basis of strongly hindered rotation about the 2—7 and 5—9 bonds with conformation F of Fig. 4 as the most stable. As the population of conformation G increases with temperature, the relative intensity of the peak at 52.1 decreases and that at 62.2 increases. Eventually the peak at 56.0 is observed. Therefore the peaks at 52.1 and 62.2 may be assigned to conformation F of conformation B, and the peaks at 56.0 and 62.2 to conformation G of conformation B.

These conclusions about free and hindered rotation agree with the results obtained by dipole moment studies (3). Although it is not possible to determine the freedom of rotation about the 2—3 and 4—5 bonds, examination of Fisher–Hirschfelder models indicates that free rotation is likely.

The variation in the relative intensities of the peaks with temperature is shown in Table II. From this, one can calculate that conformation A is more stable than conformation B by 1.72±0.11 kcal/mole. Similarly conformation D is more stable than

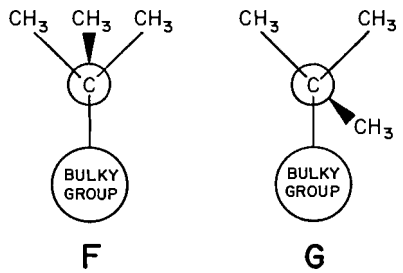


FIG. 4. Conformations about the carbon–oxygen bonds 2—7 and 5—9.

Can. J. Chem. Downloaded from www.nrcresearchpress.com by 210.87.254.40 on 09/05/12
For personal use only.

TABLE II

Temperature variation of the relative peak intensities

Isomer	T, °K	Protons measured	$P1/P2$	ΔE, kcal/mole
d,l	296	—O—CH_3 —C—CH_3 —C—H	.050	1.76
d,l	302	—O—CH_3 —C—CH_3 —C—H	.056	1.72
d,l	321	—O—CH_3 —C—CH_3 —C—H	.053	1.87
d,l	345	—O—CH_3 —C—CH_3 —C—H	.056	1.97
d,l	371	—O—CH_3 —C—CH_3 —C—H	.067	1.99
d,l	390	—O—CH_3 —C—CH_3 —C—H	.059	2.18
meso	296	—O—CH_3	.067	1.58
meso	302	—O—CH_3	.071	1.58
meso	321	—O—CH_3	.071	1.68
meso	345	—O—CH_3	.083	1.70
meso	371	—O—CH_3	.074	1.91
meso	389	—O—CH_3	.091	1.85

conformation C by 1.92 ± 0.13 kcal/mole. It is also possible to say that conformation F is more stable than conformation G. Because of the low intensities involved it was not possible to get quantitative information. However, it is possible to state that the energy difference between these two conformations, F and G, is much greater for conformation A than for conformation B. No contribution from conformation G was detected in the spectra attributed to conformations C and D. However, it is very likely that the energy difference between F and G in conformation D is also greater than for conformation B since no lines due to G are observed even though the lines from conformation D are quite intense. Because of the greater energy difference of the *d,l* conformations compared to those of the meso diastereomer it is impossible to extend this comparison to conformations B and C.

Only a single signal was seen for the C—H protons in both meso- and *d,l*-1,2-dibromo-1,2-diphenylethane. Their limited solubility did not allow observations below 350° K for the meso isomer and 225° K for the *d,l* isomer. Replacement of the dimethylmethoxy group by bromine, or other less bulky groups, would lower the energy of the barrier to rotation, but would not be likely to decrease the energy difference between conformations. At a temperature low enough for hindered rotation it is quite possible that the more stable conformation would predominate to such an extent that no signals could be observed for the other conformation. Therefore this system does not seem to be a suitable one for determining the relative sizes of groupings by determining the change in the barrier to rotation as these groupings replace dimethylmethoxy.

EXPERIMENTAL

The proton resonance spectra were obtained on a Varian Associates high-resolution nuclear magnetic resonance spectrometer Model V4300C operating at 56.4 Mc/sec. The spectra were calibrated using side-band modulation (7) counted with a Hewlett Packard

Can. J. Chem. Downloaded from www.nrcresearchpress.com by 210.87.254.40 on 09/05/12
For personal use only.

Model 521C frequency counter. The thermostated probe assembly has been described previously (8). The chemical shifts are listed in cycles per second to low field from tetramethylsilane as an internal reference. Solutions in carbon tetrachloride, saturated at room temperature, were used throughout, except for meso-1,2-dibromo-1,2-diphenylethane which was dissolved in bromoform. Since comparisons of intensity were only made for the same grouping in a somewhat different environment, peak heights rather than peak areas were used to determine intensities. For a given grouping the line width at half height was the same in both conformations. The line width for the C-methyl group was significantly greater than for the O-methyl group. This is unlikely to arise from hindrance to rotation about the 1—2 and 5—6 bonds since the line width did not decrease significantly at the higher temperatures. Both diastereomers of 1,2-dibromo-1,2-diphenylethane were prepared as reported in the literature (9).

ACKNOWLEDGMENT

The compounds which made this investigation possible were kindly donated by Prof. G. F Wright.

REFERENCES

1. J. J. DRYSDALE and W. D. PHILLIPS. J. Am. Chem. Soc. **79**, 319 (1957).
2. J. A. POPLE. Mol. Phys. **1**, 3 (1958).
3. H. SAWATZKY, G. K. WHITE, and G. F WRIGHT. Can. J. Chem. **37**, 1132 (1959).
4. P. M. NAIR and J. D. ROBERTS. J. Am. Chem. Soc. **79**, 4565 (1957).
5. J. A. POPLE, W. G. SCHNEIDER, and H. J. BERNSTEIN. High-resolution nuclear magnetic resonance. McGraw-Hill Book Co., New York. 1959.
6. M. KARPLUS. J. Chem. Phys. **30**, 11 (1959).
7. J. T. ARNOLD and M. E. PACKARD. J. Chem. Phys. **19**, 1608 (1951).
8. S. BROWNSTEIN. Can. J. Chem. **37**, 1119 (1959).
9. J. WISLICENUS and F. SEELER. Ber. **28**, 2693 (1895).

Can. J. Chem. Downloaded from www.nrcresearchpress.com by 210.87.254.40 on 09/05/12
For personal use only.

Can. J. Chem. Downloaded from www.nrcresearchpress.com by 210.87.254.6 on 09/05/12
For personal use only.

AN EXTRACELLULAR POLYSACCHARIDE FROM GIBBERELLA FUJIKUROI (FUSARIUM MONILIFORME)[1]

I. R. SIDDIQUI[2] AND G. A. ADAMS

ABSTRACT

Growth of *Gibberella fujikuroi* (*Fusarium moniliforme*) on a glucose medium produced an extracellular polysaccharide containing D-glucose, D-mannose, D-galactose, D-glucuronic acid (molar ratio 1.0:1.1:1.3:0.6), and possibly D-mannuronic acid. Protein was retained tenaciously by the polysaccharide and several deproteinization methods reduced the nitrogen content only slightly. Methylation studies showed that the polysaccharide was highly branched with D-glucose and D-mannose forming the non-reducing ends in the molecule. Most of the D-mannose and D-galactose units were joined by $1 \rightarrow 2$ and $1 \rightarrow 6$ linkages with some branching also at C_2 and C_6 positions; D-galactose occurred exclusively in the furanose form. D-Glucose units were joined by $1 \rightarrow 2$ and $1 \rightarrow 3$ linkages. The D-glucuronic acid residues were mainly non-terminal and were attached to both D-galactose and D-mannose units. Periodate oxidation studies supported the foregoing conclusions.

Although there are many reports in the literature dealing with the isolation of polysaccharides from a variety of fungi (1–4), few investigations of the structural features of fungal polysaccharides have been made. Galactocarolose, a polysaccharide elaborated by *Penicillium charlesii*, has been shown to contain 9–10 β-galactofuranose units linked through the $1 \rightarrow 5$ position (5). A polysaccharide (varianose) containing $1 \rightarrow 4$ linked galactose units terminated by glucose and idose or altrose has been isolated from *Penicillium varians* (6). Barker *et al.* (7) have shown that an extracellular polyglucosan isolated from *Aspergillus niger* consisted of D-glucose units linked α $1 \rightarrow 4$ and α $1 \rightarrow 3$. A recent survey by Martin and Adams (8) of the polysaccharides produced by 31 species of fungi showed a wide variation in sugar components in both the intracellular and extracellular polysaccharides. In this laboratory, four strains of *Fusarium* (*Fusarium lini* NRC 666, 9593; *Fusarium moniliforme* NRC F73; *Fusarium* species NRC 68) and one strain of *Trichoderma viride* NRC v139 were examined for polysaccharide production, using procedures described by Martin and Adams (8). Following this preliminary study, a more intensive investigation was made of the preparation, isolation, and structural features of the polysaccharide from *Gibberella fujikuroi* (*Fusarium moniliforme*) NRC F73, ATCC 10052. The results of this investigation form the basis for the present communication.

G. fujikuroi was grown on buffered enriched salts medium with glucose as the carbon source. The crude polysaccharide was precipitated from the concentrated culture medium by ethanol after the removal of the cells and salts. Addition of 'Cetavlon' (9) to an aqueous solution of the acidic polysaccharide gave a small oily precipitate, an acid hydrolyzate of which showed equal amounts of the same sugar components as were in an acid hydrolyzate of the Cetavlon-soluble fraction. Since no amino sugars were detectable in an acid hydrolyzate of the polysaccharide, it was assumed that the nitrogen content (3.96%) represented mainly protein contaminants. This observation was confirmed by the presence of amino acids (ninhydrin test) in the acid hydrolyzates. Attempts to remove or reduce the protein content of the crude polysaccharide material by the Sevag method (10) were not practicable since considerable quantities of the polysaccharide were removed

[1]*Manuscript received May 4, 1961.*
Contribution from the Division of Applied Biology, National Research Council, Ottawa 2, Canada.
Issued as N.R.C. No. 6394.
[2]*National Research Council Postdoctorate Fellow, 1958–60. Present address: Pulp and Paper Institute of Canada, McGill University, Montreal, Quebec.*

along with the denatured protein. The conclusion that the protein was firmly bound to the polysaccharide was substantiated by the failure of prolonged tryptic digestion (11) to remove it. The use of phenol–water partition (12), however, produced some purification as shown by the lower nitrogen content of the water-soluble fraction (2.9%) as compared with that of the phenol-soluble fraction (3.8%).

The sugar components of the partially purified acidic polysaccharides were glucose, mannose, galactose, and hexuronic acid (1.0:1.1:1.3:0.6). This sugar ratio was determined in an acid hydrolyzate of the polysaccharide obtained by heating the mixture at 100° C for 3 hours with 2 *N* sulphuric acid, and does not take into account the sugars bound in the uronic acid complexes. Boundary electrophoresis (13) of the polysaccharide in borate buffer showed one major peak along with a smaller stationary peak (Fig. 1) which was

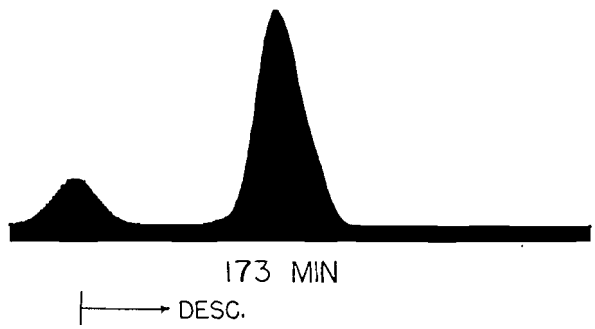


FIG. 1. Electrophoretic pattern of polysaccharide in acetate buffer (pH 5).

presumably a boundary anomaly. The major peak, however, was not symmetrical and hence the polysaccharide may not be homogeneous. The infrared spectrum confirmed the presence of carboxylic acid groupings. The spectrum of the sodium salt showed absorption at 1615 cm^{-1} and 1405 cm^{-1}, which is characteristic of the carboxylate ion. Amide bands (C=O, 1650 cm^{-1}; and —N—H, 1520 cm^{-1}), such as those given by proteins, were also detected. The absence of absorption at 1735 cm^{-1} in the spectrum of the sodium salt of the acidic polysaccharide precluded the existence of *O*-acetyl groups. The ultraviolet absorption spectrum showed an absorption peak at 275 mμ which is characteristic of proteins containing aromatic amino acids (14).

The mixture of sugars produced by heating the polysaccharide with 2 *N* sulphuric acid at 100° C for 3 hours was fractionated first on an anion exchange resin and subsequently on paper chromatograms. From the hydrolysis products, D-glucose, D-mannose, and D-galactose were recovered and characterized either in crystalline form or as crystalline derivatives. The acidic components were identified as D-glucuronic acid, and an aldobiouronic acid which was a glucuronosyl-galactofuranose as established by reduction, methylation, and hydrolysis. Two aldotriouronic acids were isolated in amounts too small to establish their structure; one contained galactose, mannose, and glucuronic acid, the other, galactose, mannose, and a hexuronic acid, which appeared to be mannuronic acid.

The polysaccharide was methylated and the hydrolysis products were separated by chromatography on an anion exchange column and then on paper chromatograms. The weights of the fractions finally isolated, together with that of the di-*O*-methyl uronic acid, corresponded to the following approximate molar ratios: tetra-*O*-methyl hexose, 3;

Can. J. Chem. Downloaded from www.nrcresearchpress.com by 210.87.254.6 on 09/05/12
For personal use only.

tri-*O*-methyl hexose, 2; di-*O*-methyl hexose, 2. The components of each of the above fractions along with their relative ratios are listed in Table I. All of these sugars, with the

TABLE I

Yield of methylated sugars

Fraction	Weight (mg)	Components	Molar ratio
Tetra-*O*-methyl hexose	680	2,3,4,6-Tetra-*O*-methyl-D-glucose 2,3,4,6-Tetra-*O*-methyl-D-mannose	3
Tri-*O*-methyl hexose	390	2,4,6-Tri-*O*-methyl-D-glucose 3,4,6-Tri-*O*-methyl-D-glucose 3,5,6-Tri-*O*-methyl-D-galactose 2,3,5-Tri-*O*-methyl-D-galactose 2,3,4-Tri-*O*-methyl-D-mannose 3,4,6-Tri-*O*-methyl-D-mannose	2
Di-*O*-methyl hexose	380	3,5-Di-*O*-methyl-D-galactose 3,4-Di-*O*-methyl-D-mannose 3,6-Di-*O*-methyl-D-mannose	2

exception of 3,5,6-tri-*O*-methyl-D-galactose and 3,6-di-*O*-methyl-D-mannose, were obtained either in crystalline form or were characterized by the isolation of crystalline derivatives.

The ratio of glucose:mannose:galactose, calculated from the weights of the methylated sugars, was 1.0:1.4:1.1, in reasonable agreement with that found for the original polysaccharide (1.0:1.1:1.3).

The number and proportion of methylated sugars indicated, in general, that the molecule was highly branched. The relatively large amount of tetra-*O*-methyl sugars represented a high proportion of non-reducing terminal units in the molecule. Of these, there was a predominance of glucose over mannose end groups; galactose units were apparently not present on the periphery of the molecule.

A considerable proportion of the main body of the molecule was made up of D-mannose units linked $1 \rightarrow 2$ and $1 \rightarrow 6$ as shown by the occurrence of 3,4,6-tri-*O*-methyl-D-mannose and 2,3,4-tri-*O*-methyl-D-mannose. Lesser amounts of glucose were linked $1 \rightarrow 2$ and $1 \rightarrow 3$. Galactose was recovered as 2,3,5-tri-*O*-methyl-D-galactose and 3,5,6-tri-*O*-methyl-D-galactose on hydrolysis and showed that the D-galactofuranose units were linked glycosidically $1 \rightarrow 6$ and $1 \rightarrow 2$. The presence of 3,5-di-*O*-methyl-D-galactose showed that some of the galactofuranose units formed branch points through C_2 and C_6. Smaller amounts of 3,4-di-*O*-methyl-D-mannose likewise showed that some of the mannopyranose units formed branch points through C_2 and C_6. The tentative identification of 3,6-di-*O*-methyl-D-mannopyranose indicated that some D-mannose units had some minor branching through C_2 and C_4.

Mild acid hydrolysis of the polysaccharide as provided by heating in 0.01 *N* sulphuric acid at 100° C for periods as long as 6 hours did not release any sugars, showing that no more than two furanoside units were contiguous and that no terminal furanoside ring forms were present. This latter observation was further substantiated by the fact that no 2,3,5,6-tetra-*O*-methyl-D-galactose was detected in the cleavage products of the methylated polysaccharide.

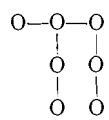
Evidence that the major portion of the D-glucuronic acid residues were non-terminal was provided by the identification of 2,3-di-*O*-methyl-D-glucose as a hydrolysis product of the reduced methylated uronic acid isolated from the fully methylated polysaccharide. A small amount of D-glucuronic acid was identified also as 2,3,4-tri-*O*-methyl-D-glucose

Can. J. Chem. Downloaded from www.nrcresearchpress.com by 210.87.254.6 on 09/05/12
For personal use only.

after separation, reduction, and hydrolysis of the methylated uronic acid components of the fully methylated polysaccharide. The conclusion that some of the uronic acid was attached to the galactose unit was provided by the isolation of a glucuronosyl galactose by partial hydrolysis of the polysaccharide. Hydrolysis of a methylated aldobiouronic acid fraction yielded 3,4-di-*O*-methyl-D-mannose and a methylated uronic acid, showing that some of the uronic acid was attached to D-mannose through C_2 or C_6. Following methanolysis, reduction, and hydrolysis, the uronic acid portion appeared as 2,3-di-*O*-methyl-D-glucose. Hydrolysis of a methylated aldotriouronic acid yielded 3,4-di-*O*-methyl-D-mannose, 3,5-di-*O*-methyl-D-galactofuranose, and 2,3,4-tri-*O*-methyl-D-glucuronic acid. This observation showed that some D-glucuronic units were attached terminally to either unit of contiguous D-galactose and D-mannose residues.

On periodate oxidation, the acidic polysaccharide consumed 1.3 moles of periodate and produced 0.5 mole of formic acid. Acid hydrolysis of the periodate-oxidized polysaccharide gave large amounts of galactose and small amounts of acidic components. Examination of the oxidized polysaccharide by the procedure of Smith *et al.* (15) showed, in addition to the components detected in the acid hydrolyzate, small amounts of arabinose, traces of two components ($R_{glucose}$ 1.01 and 1.23), glycerol, but no erythritol. The absence of erythritol precluded 1,4 linkages in the polysaccharide but the presence of arabinose clearly indicated that at least some of the galactose residues were in the furanose form with C_5 and C_6 unsubstituted. This is in accord with the isolation of 3,5,6-tri-*O*-methyl-D-galactose from the methylated polysaccharide. Galactose units in the furanose form that were not oxidized by periodate were linked through C_2 and C_6 and gave rise to 3,5-di-*O*-methyl-D-galactofuranose as a product of methylation and hydrolysis. The yield of 0.5 mole of formic acid indicated that 50% of the sugar units (pyranose form) were either linked $1 \rightarrow 6$ or were present in non-reducing end groups. Approximately 30% of the residues consumed periodate but did not produce formic acid; such units could be either in the pyranose or furanose form and could be linked $1 \rightarrow 2$. The remainder of the sugar residues did not consume periodate; of these, the pyranose sugars must be linked $1 \rightarrow 3$ or be branched, and the furanose forms must be attached through C_2 and C_6. Such an attachment of the galactofuranose units would account for the relatively high yield of 3,5-di-*O*-methyl-D-galactofuranose obtained on hydrolysis of the fully methylated polysaccharide.

Present data do not permit formulation of a unique structure for the polysaccharide, although certain structural features have been established. However, no certainty exists that the polysaccharide examined was a homogeneous molecule. Electrophoretic examination indicated that minor amounts of other materials were present. On the basis of methylation and periodate oxidation results, it is suggested that an average general repeating unit consisted of seven sugar units arranged in the following pattern.



Such a formulation would not only account for the molar ratio (3:2:2) obtained for the tetra-, tri-, and di-*O*-methyl ethers but would also yield the periodate oxidation result of 1.3 moles periodate consumed, and 0.5 mole formic acid produced. It is suggested that the polysaccharide may consist of repeating units conforming to the general pattern

Can. J. Chem. Downloaded from www.nrcresearchpress.com by 210.87.254.6 on 09/05/12
For personal use only.

shown above and containing various sugars. Fragmentation studies now being planned are necessary to reveal further fine features of this polysaccharide.

EXPERIMENTAL

The following solvents (v/v ratios) were used for chromatographic separations: (A) *n*-butanol:ethanol:water (5:1:4); (B) butanone saturated with water containing 2% ammonia; (C) benzene:ethanol:water:ammonia (200:47:14:1); (D) *n*-butanol:acetic acid:water (40:1:5); (E) pyridine:ethyl acetate:water (1:2.5:2.5); (F) *n*-butanol:ethanol:water (40:11:19). Sugars, as their borate complexes, were separated by electrophoresis in 0.2 *M* borate buffer (pH 10) and uronic acids were analyzed in acetate buffer (pH 5) (17). All electrophoretic examinations were made on Whatman No. 3MM paper at 700–800 v. Uronic acid content was determined by the method of Barker *et al.* (17). Reducing sugars were detected on paper chromatograms or electrophoretograms with *p*-anisidine hydrochloride spray (18); non-reducing sugars were detected by alkaline silver nitrate (19). Evaporations were carried out at 35° C on a rotary film evaporator. Melting points are corrected and rotations are equilibrium values unless otherwise stated.

Cultural Conditions

The organism *G. fujikuroi* was grown on a culture medium as described by Martin and Adams (8), the glucose solution (20 l.) and the other nutrients were sterilized separately and then mixed aseptically in a bottle of 40-l. capacity. The culture was grown on a malt–agar slant and the spores were used to prepare successively larger batches of inoculum. The final inoculated medium was grown at 29° on a rotary shaker with aeration provided by an air stream of about 1 l. per minute passing over the surface of the solution. The cultures were harvested when 80–85% of the sugar had been consumed.

Isolation of the Polysaccharide

The mycelium was removed by filtration through paper and the filtrate was concentrated about 10-fold at 30° C in a Majonnier evaporator and then dialyzed against cold water (2° C) for 2 days. The non-dialyzable material was poured into 3 volumes of ethanol with vigorous stirring. The precipitate was removed by centrifugation, washed with ethanol and ether, and dried *in vacuo* over phosphorus pentoxide (yield 300 mg/l., 7% based on glucose consumed).

The crude polysaccharide (12 g) was extracted with water to yield a water-soluble fraction (6.4 g) and a water-insoluble residue (5.6 g). Chromatographic and electrophoretic examination of hydrolyzates of each fraction showed that the water-soluble material contained glucose, galactose, mannose, and uronic acid components; the residue contained only traces of glucose and mannose, and was discarded.

Attempted Removal of Protein from the Polysaccharide

The crude, water-soluble polysaccharide had a nitrogen content of 3.96%. Since its acid hydrolyzate gave a negative test for amino sugars (20) and a positive test (ninhydrin) for amino acids, it was concluded that the contaminant was protein.

Fractionation by Cetavlon (9) gave a small oily precipitate which on electrophoretic examination in borate buffer gave the same pattern as the unprecipitated material. Examination, by chromatography, of hydrolyzates of the two materials showed that the same sugars were present in each.

Fractionation by phenol (12) gave a water-soluble fraction having a nitrogen content

Can. J. Chem. Downloaded from www.nrcresearchpress.com by 210.87.254.6 on 09/05/12
For personal use only.

of 2.9% while that of the phenol-soluble material was 3.8%, but the two fractions had identical sugar components.

Digestion with trypsin (11) for 5 days at 35° C did not lower the nitrogen content of the polysaccharide preparation significantly.

Analysis of Acidic Polysaccharide

The polysaccharide ($[\alpha]_D^{28}$ $+12.7\pm1°$ (*c*, 1.02 in water)) on analysis gave the following: N, 2.9%; ash, 3.9%; P, nil; and uronic acid, 15%. Electrophoretic examination in a Spinco apparatus model H in 0.5 *M* borate buffer (pH 9.2) showed a single asymmetric peak (Fig. 1). The polysaccharide (10 mg) was hydrolyzed with 2 *N* sulphuric acid for 4 hours at 100° C. The sugars were recovered and determined quantitatively according to Nelson (21), giving a ratio of glucose:mannose:galactose of 1.0:1.1:1.3.

Acid Hydrolysis of the Polysaccharide

Polysaccharide (1.5 g) was hydrolyzed with 2 *N* sulphuric acid (30 ml) for 3 hours at 100° C. After neutralization ($BaCO_3$) and filtration, the filtrate was slurried with ion exchange resin Dowex 1 (carbonate form, 35 g) for 24 hours. The resin was then washed with water (1 l.) in a column to remove the neutral sugars (0.95 g). The uronic acid fraction was eluted with *N* ammonium carbonate (500 ml) and recovered (0.250 g) by removing excess ammonium carbonate by distillation *in vacuo* at 65–70° C and the remainder with Amberlite IR-120 (H) resin.

A. Neutral Sugars

A portion of the neutral sugars was separated on Whatman 3MM paper using solvent E. Elution with water yielded glucose, mannose, and galactose as syrups.

(i) D-*Glucose*

The syrup was refluxed for 15 minutes with an aliquot (1 ml) of a solution containing *p*-nitroaniline (9 g), methanol (200 ml), and concentrated hydrochloric acid (0.14 ml). The mixture was filtered while hot and after it had cooled, crystallization occurred. Two recrystallizations from methanol gave *N*-*p*-nitrophenyl-D-glucopyranosylamine dihydrate having m.p. and mixed m.p. 184° C. Reported (22): m.p. 184° C.

(ii) D-*Mannose*

The syrup was similarly characterized as *N*-*p*-nitrophenyl-β-D-mannopyranosylamine dihydrate having m.p. 219° C and $[\alpha]_D^{26}$ $-330°$ (*c*, 0.112 in dry pyridine). Reported (22): m.p. 219° C.

(iii) D-*Galactose*

The sugar crystallized from methanol to give m.p. 164–167° C and $[\alpha]_D^{26}$ $+80.2\pm1°$ (*c*, 0.445 in water), and was therefore D-galactose.

B. Uronic Acid Fraction

The acidic sugars (0.25 g) were separated on Whatman No. 1 paper with solvent A. Three main components were recovered corresponding to hexuronic (A), aldobiouronic (B), and aldotriouronic acid (C) respectively. Two very minor components, one (D) near the starting line and another (E) which moved ahead of (A), were recovered in trace amounts.

(i) Hexuronic Fraction (A)

This fraction (20 mg) was converted to its methyl ester glycoside form by refluxing with methanolic hydrogen chloride (2%) for 6 hours. Reduction with lithium aluminum hydride (23) (80 mg) in tetrahydrofuran:ethyl ether solution (4:1) yielded the corresponding methyl hexoside. Acid hydrolysis and paper chromatography showed glucose

Can. J. Chem. Downloaded from www.nrcresearchpress.com by 210.87.254.6 on 09/05/12
For personal use only.

with traces of mannose and galactose. The main hexuronic acid was therefore glucuronic acid.

(ii) Aldobiouronic Acid Fraction (B)

A portion of this fraction (7.5 mg) was hydrolyzed with 2 *N* sulphuric acid for 3 hours at 100° C. Paper chromatography in solvent A showed glucuronic acid, galactose, and some original material. A portion of the acid (70 mg) was converted to its methyl glycoside methyl ester and reduced with lithium aluminum hydride as described above. Examination of the acid hydrolyzate (solvent E) showed glucose and galactose. The methyl bioside (43 mg) was dissolved in tetrahydrofuran (5 ml) and methylated by the Falconer and Adams procedure (24). The product was recovered by extraction with chloroform. Three methylations by this method followed by one methylation by Purdie's method (methyl iodide, 10 ml; silver oxide, 1 g) gave a fully methylated product, as indicated by its infrared spectrum. Hydrolysis of the methylated disaccharide and separation of the sugars by paper chromatography (solvent B) yielded 2,3,4,6-tetra-*O*-methyl-D-glucose and a tri-*O*-methyl galactose (R_g 0.86).

(iii) Aldotriouronic Acid Fraction (C)

Paper chromatography of this fraction in solvent A for 4 days showed the presence of two components C_I ($R_{glucose}$ 0.23) and C_{II} ($R_{glucose}$ 0.17). Acid hydrolysis (2 *N* sulphuric at 100° C for 3 hours) and chromatographic examination of the hydrolyzates (solvents A and E) showed the components of C_I to be galactose, mannose, and hexuronic acid (which appeared to be mannuronic acid); the components of C_{II} were galactose, mannose, and glucuronic acid.

Spectra of the Polysaccharide

The ultraviolet absorption spectrum of an aqueous solution (0.5%) of the polysaccharide showed a peak at 275 mμ. The infrared spectrum was determined in potassium chloride disks on the free acid form and also the sodium salt of the polysaccharide. The main characteristics of the spectra of both forms were bands ν_{max} 1615, 1405, 1520, and 1650 cm^{-1}; the free acid had an additional band at 1735 cm^{-1}.

Periodate Oxidation

The polysaccharide was oxidized according to the method of Jeanes and Wilham (25). The number of moles of periodate consumed and formic acid produced per 162 g of polysaccharide are given in the following table:

Time (hours)	24	48	72	96	112
Periodate consumption	0.93	1.00	1.20	1.33	1.36
Formic acid production	0.36	0.47	0.54	0.58	0.60

Extrapolation of these values to 0 time showed a ratio of periodate consumed:formic acid produced of 1.3:0.5 mole per 162 g of polysaccharide.

The remaining solution of oxidized polysaccharide was treated with ethylene glycol, dialyzed against tap water, and the product recovered by freeze-drying. A portion was hydrolyzed and on paper chromatographic examination showed large amounts of galactose and small amounts of uronic acid. The remainder of the periodate-oxidized material (40 mg) was dissolved in water (4 ml) and after deionization with Amberlite ion exchange resins IR-45 and IR-120, a solution of potassium borohydride (150 mg in 1 ml of water) was added. After 24 hours, the solution was neutralized with acetic acid, dialyzed for

Can. J. Chem. Downloaded from www.nrcresearchpress.com by 210.87.254.6 on 09/05/12
For personal use only.

24 hours, and the reduced product was recovered by freeze-drying. A small amount was hydrolyzed with 2 *N* sulphuric acid for 3 hours at 100° C. After neutralization, the hydrolyzate was examined by paper chromatography in solvent E and contained galactose, arabinose, and two spots ($R_{glucose}$ 1.01 and 1.23) which gave a light green color with *p*-anisidine spray reagent. A chromatogram of the same hydrolyzate in solvent F and sprayed with silver nitrate reagent (19) showed glycerol but no erythritol.

Methylation

The polysaccharide (3.0 g), dissolved in water (30 ml), was methylated by the dropwise addition of 30% sodium hydroxide (160 ml) and dimethyl sulphate (60 ml) and was stirred for 24 hours. The reagents were added at such a rate that the reaction mixture was always alkaline. The addition of the methylating agents was repeated twice. The methylation mixture was heated for 75 minutes at 80° C, then cooled, and finally neutralized with sulphuric acid. The precipitated salts were dissolved in water, and the partly methylated polysaccharide was extracted with chloroform. The recovered methylated polysaccharide (2.78 g) showed a definite hydroxyl band at 3500–3600 cm^{-1} in its infrared spectrum. The partially methylated polysaccharide was dissolved in tetrahydrofuran (150 ml) containing pulverized sodium hydroxide (15 g), and dimethyl sulphate (18 ml) was added dropwise over 6 hours with constant stirring. The mixture was stirred for 18 hours, and then sufficient water was added to dissolve the solids. The pH was adjusted to 9.0 and the solution was extracted with chloroform. The recovered methylated polysaccharide still contained free hydroxyl groups as shown by its infrared spectrum: consequently, the previous methylation was repeated twice more. The methylated product still showed a small hydroxyl group in the infrared spectrum and was methylated further by Purdie's method (methyl iodide, 100 ml; silver oxide, 20 g). After two Purdie methylations there were no free hydroxyl groups shown in the infrared spectrum. Yield 3.1 g, methoxyl content 39.0%.

Hydrolysis of Methylated Polysaccharide

The methylated polysaccharide (3.1 g) was refluxed with 4% methanolic hydrogen chloride (100 ml) for 24 hours. The solution was neutralized with silver carbonate, filtered, and evaporated *in vacuo* to a syrup, which was hydrolyzed with *N* sulphuric acid for 30 hours at 100° C. Periodic analysis of aliquots of the hydrolyzate by gas–liquid partition chromatography (26) showed that the prolonged hydrolysis period was necessary to hydrolyze the glycosides completely. The hydrolyzate was neutralized with barium carbonate, filtered, and concentrated to about 100 ml.

Separation of Acidic and Neutral Sugars

The above hydrolyzate (100 ml) was stirred for 30 hours with Dowex 1 (carbonate form) (35 g). The resin was then poured into a column and washed with water (1.5 l.) to elute neutral methyl sugars (1.99 g) and with *N* ammonium carbonate (700 ml) to elute the methylated uronic acid fraction (0.34 g). The latter was recovered by removing most of the ammonium carbonate by sublimation *in vacuo* at 65–70° C and the remainder by passing the solution over Amberlite resin IR-120.

A. Separation of Tetra-, Tri-, and Di-O-methyl Sugars

The mixture of neutral methyl sugars (1.6 g) was separated on large sheets of Whatman No. 3 MM papers using solvent A. The three bands located on the papers corresponded to tetra-*O*-methyl, tri-*O*-methyl, and di-*O*-methyl sugars having R_g values of 1.0, 0.84,

Can. J. Chem. Downloaded from www.nrcresearchpress.com by 210.87.254.6 on 09/05/12
For personal use only.

Can. J. Chem. Downloaded from www.nrcresearchpress.com by 210.87.254.6 on 09/05/12
For personal use only.

and 0.64 respectively. The weights were: tetra-*O*-methyl, 680 mg; tri-*O*-methyl, 390 mg; and di-*O*-methyl, 380 mg, which corresponds to an approximate molar ratio of 3:2:2.

B. Examination and Identification of Tetra-O-methyl Fraction

The syrupy tetra-*O*-methyl fraction had $[\alpha]_D^{25}$ +48.8° (*c*, 2.06% in water) and a methoxyl content 50.8% (theoretical value for $C_{10}H_{20}O_6$, 52.5%). Demethylation with boron trichloride (27) gave glucose and mannose as the parent sugars. The tetra-*O*-methyl fraction (2–3 mg) was heated in a sealed tube with 2% methanolic hydrogen chloride for 12 hours and neutralized with silver carbonate. The mixture of glycosides was examined by gas–liquid partition chromatography (26) using a 4-ft column of 20% Apiezon M on Celite 545 at 150° C and an argon flow rate of 150 ml/min. The examination showed the presence of the methyl glycosides of 2,3,4,6-tetra-*O*-methyl-D-glucose and 2,3,4,6-tetra-*O*-methyl-D-mannose in a ratio of 58.9:41.1. Optical rotation measurements of the original mixture indicated a ratio of 2,3,4,6-tetra-*O*-methyl-D-glucose:2,3,4,6-tetra-*O*-methyl-D-mannose of 57.3:42.7.

(i) 2,3,4,6-Tetra-O-methyl-D-glucose

The foregoing tetra-*O*-methyl fraction (550 mg) was dissolved in ethyl ether, small amounts of impurities were centrifuged off, and petroleum ether was added drop by drop. On being cooled, the solution deposited crystals (70 mg) which, after several recrystallizations from ether – petroleum ether (1:1), gave 2,3,4,6-tetra-*O*-methyl-D-glucose, m.p. 95–96° C; $[\alpha]_D^{25}$ +82.6±2° (*c*, 0.605% in water). An aliquot of the mother liquor (27 mg) was heated with aniline (15 mg) in methanol (2 ml) and the solution refluxed for 2 hours. The anilide crystallized on partial removal of the solvent and on recrystallization from ethanol gave 2,3,4,6-tetra-*O*-methyl-*N*-phenyl-D-glucosylamine, m.p. 134–137° C. Reported value: 137–138° C (28).

(ii) 2,3,4,6-Tetra-O-methyl-D-mannose

A portion of the original tetra-*O*-methyl hexose mixture was run on sheets of Whatman No. 1 paper using solvent B until the solvent front reached the bottom of the papers. The sugars were located on the papers, the appropriate strips cut out and attached to the top of new sheets of paper, and the chromatograms again run with solvent B. The sugar band was located and the slower-moving fourth of the area was cut out and eluted with water. The syrupy product (20 mg) in methanol (2 ml) was refluxed with aniline (10 mg) to yield crystalline 2,3,4,6-tetra-*O*-methyl-*N*-phenyl-D-mannosylamine, which was recrystallized from ethyl ether to give a melting point of 144–146° C, undepressed on admixture with an authentic specimen. Reported (29): m.p. 142–143° C. The X-ray diffraction pattern of the crystals was identical with that of the authentic specimen of 2,3,4,6-tetra-*O*-methyl-*N*-phenyl-D-mannosylamine.

C. Examination and Identification of Tri-O-methyl Fraction

The tri-*O*-methyl fraction (390 mg) ($[\alpha]_D^{26}$ +12.6° (*c*, 2.53 in water)) yielded galactose, mannose, and a minor amount of glucose on demethylation by boron trichloride (26). Paper electrophoresis (17) (borate buffer, pH 10) separated the sugars into two borate-complexing fractions (0.154 g and 0.0125 g respectively) and a non-complexing fraction (0.126 g).

(i) Borate Non-complexing Fraction

This fraction, when demethylated as before, showed the presence of galactose, mannose, and a small amount of glucose. Paper chromatography in solvent B separated three components, two of which had the same R_g values (0.57 and 0.65) and color reactions with

p-anisidine hydrochloride as 2,4,6-tri-*O*-methyl-D-glucose and 2,3,4-tri-*O*-methyl-D-mannose respectively. The third component had an R_g of 0.74.

2,4,6-Tri-O-methyl-D-glucose.—The syrup (5 mg) was refluxed with aniline (3 mg) in methanol (1 ml) for 3 hours. The product crystallized on partial evaporation of the solvent and on recrystallization from ether gave 2,4,6-tri-*O*-methyl-*N*-phenyl-D-glucosylamine, m.p. 159–162° C. Reported value: 162–166° C (30).

2,3,4-Tri-O-methyl-D-mannose.—The syrup (33.5 mg) was oxidized with bromine (0.1 ml) in the presence of barium carbonate (30 mg) for 70 hours. Bromine was removed by aeration and the acidified solution was extracted with chloroform for 2 days. The chloroform extract was dried with anhydrous sodium sulphate and concentrated to a syrup, which was distilled (bath temperature 130–160° C at 0.01 mm). The distilled syrup was dissolved in methanol saturated with ammonia (5 ml) and allowed to stand for 24 hours at 5° C. Removal of the solvent gave a syrup which crystallized from ethanol:ethyl ether solution giving 2,3,4-tri-*O*-methyl-D-mannosamide, m.p. and mixed m.p. 143° C. Reported (31): m.p. 143° C.

2,3,5-Tri-O-methyl-D-galactose.—The syrup (33 mg) (R_g 0.74, solvent B) was oxidized by bromine as described above. The syrupy lactone showed a strong C=O stretching peak at 1786 cm^{-1} in its infrared spectrum and was therefore a γ lactone. Treatment with methanolic ammonia gave a crystalline amide, m.p. 145–146° C; $[\alpha]_D^{26}$ $-5.1\pm1.5°$ (*c*, 0.72 in methanol). Anal. Calc. for $C_9H_{19}O_6N$: C, 45.5%; H, 8.02%; N, 5.9%; OMe, 39.2%. Found: C, 45.15%; H, 8.3%; N, 6.04%; OMe, 38.9%. Since the galactose was in the furanose form this sugar was either 2,3,5- or 2,5,6-tri-*O*-methyl-D-galactose. Periodate oxidation of its amide by the method of Baddiley *et al.* (32) showed a negative test, thus eliminating 2,5,6-tri-*O*-methyl-D-galactofuranose, and hence the sugar was tentatively identified as 2,3,5-tri-*O*-methyl-D-galactofuranose.

(ii) Borate-complexing Fraction I

This fraction on demethylation gave mannose and glucose as the parent sugars. Paper chromatography in solvent C separated two components having R_t values and color reactions with *p*-anisidine spray reagent (18) identical with 3,4,6-tri-*O*-methyl-D-mannose (75 mg) and 3,4,6-tri-*O*-methyl-D-glucose (10 mg).

3,4,6-Tri-O-methyl-D-mannose.—The syrup (75 mg) crystallized on seeding with an authentic specimen of 3,4,6-tri-*O*-methyl-α-D-mannose. On recrystallization from ether: hexane the sugar had a melting point of 102–103° C (undepressed on admixture with an authentic sample) and $[\alpha]_D^{25}$ $+32\pm2°$ (*c*, 0.875 in methanol). Reported values (33): m.p. 101–102° C; $[\alpha]_D$ +36° (methanol).

3,4,6-Tri-O-methyl-D-glucose.—On seeding with an authentic specimen of 3,4,6-tri-*O*-methyl-D-glucose, the syrup (10 mg) crystallized. Recrystallization from ether:hexane at 0° C gave 3,4,6-tri-*O*-methyl-α-D-glucose, m.p. 76–77°. Reported value (34): m.p. 76–77° C.

(iii) Borate-complexing Fraction II (12 mg)

3,5,6-Tri-O-methyl-D-galactose.—The syrup had $[\alpha]_D^{25}$ $-16.2\pm1.5°$ (*c*, 1.23 in water). Demethylation by boron trichloride showed galactose as the only parent sugar. Movement on electrophoresis in borate buffer showed that C_2 was unsubstituted and the sugar was tentatively identified as 3,5,6-tri-*O*-methyl glucose. An aliquot (2 mg) was converted to the methyl glycoside by heating in 2% methanolic hydrogen chloride. The glycoside was methylated by the Kuhn procedure (35), and examination of the product by gas–liquid chromatography yielded the glycoside of 2,3,5,6-tetra-*O*-methyl-D-galactose.

Can. J. Chem. Downloaded from www.nrcresearchpress.com by 210.87.254.6 on 09/05/12
For personal use only.

D. Examination and Identification of Di-O-methyl Sugars

The fraction had $[\alpha]_D^{20}$ −12.5° (*c*, 1.35 in water); OMe, 28.7%. Calculated for $C_8H_{16}O_6$: OMe, 29.8%. Demethylation by boron trichloride (26) and examination of the sugars showed mainly galactose with small amounts of mannose. Paper electrophoresis in borate buffer showed the presence of two components (M_G values, 0.66, 0.52). Paper chromatography in solvent B showed three components (R_g values, 0.28, 0.33, and 0.41). The syrup (0.35 g) was separated on Whatman No. 1 paper using solvent B to give the three fractions (R_g 0.28, 14 mg; R_g 0.33, 28 mg; and R_g 0.41, 242 mg).

*(i) 3,5-Di-O-methyl-*D*-galactose*

This new sugar (R_g 0.41) was characterized, and the results have been published previously (36).

*(ii) 3,4-Di-O-methyl-*D*-mannose*

The syrup (R_g 0.33) (28 mg) crystallized from ethyl acetate, giving 3,4-di-*O*-methyl-D-mannose, m.p. and mixed m.p. 70–73° C. Reported (37): m.p. 70–73° C.

*(iii) 3,6-Di-O-methyl-*D*-mannose*

Demethylation of a portion of the sugar (R_g 0.28) and examination of the products showed mannose as the parent sugar. Paper electrophoresis in borate buffer showed three components; two of these were in trace amounts and had the same M_g values as 2,3- and 2,4-di-*O*-methyl-D-mannose. The main component was assumed to be 3,6-di-*O*-methyl-D-mannose since its M_g value did not correspond to that of either 2,6- or 4,6-di-*O*-methyl-D-mannose. A small sample (1–2 mg) was converted to its methyl glycoside by heating for 12 hours in 2% methanolic hydrogen chloride. The glycoside was methylated by Purdie's reagents (methyl iodide, 2 ml, and silver oxide, 20 mg). Examination of the fully methylated sugar by gas–liquid partition chromatography (26) showed the glycosides of 2,3,4,6-tetra-*O*-methyl-D-mannose. On the basis of the foregoing evidence, the sugar was tentatively identified as 3,6-di-*O*-methyl-D-mannose. Scarcity of material precluded further identification.

E. Examination of Methylated Uronic Acid Fractions

The methylated uronic fraction, separated from the neutral sugars, weighed 300 mg. Separation on filter paper using solvent D gave three fractions (R_g 0.85, 0.61, and 0.50).

(i) Fraction 1

Yield 30 mg, R_g value 0.85. A small portion (2 mg) was hydrolyzed with *N* sulphuric acid (0.5 ml) for 8 hours at 100° C. Chromatographic examination of the hydrolyzate in solvent B failed to show the presence of any neutral sugars. The remainder of the fraction was then converted to its methyl ester methyl glycoside by being heated in 2% methanolic hydrogen chloride in a sealed tube for 12 hours. After reduction with lithium aluminum hydride in ether solution, the disaccharide was recovered and hydrolyzed with *N* sulphuric acid. Paper chromatography (solvent B) and paper electrophoresis (borate buffer) showed one spot having R_g and M_g values of 0.30 and 0.13 respectively. These values corresponded to those of 2,3-di-*O*-methyl glucose. Demethylation of the sugar yielded glucose. The methylated uronic acid was therefore 2,3-di-*O*-methyl-glucuronic acid.

(ii) Fraction 2

Yield 22 mg, R_g value 0.61. Paper chromatography and paper electrophoresis (solvent B and borate buffer, pH 10) of an acid hydrolyzate of this material showed the presence of 3,4-di-*O*-methyl mannose as the only neutral sugar. As described above, the sugar acid was converted into the methyl ester methyl glycoside, reduced with lithium aluminum

Can. J. Chem. Downloaded from www.nrcresearchpress.com by 210.87.254.6 on 09/05/12
For personal use only.

hydride, and hydrolyzed with acid. The sugars, identified by chromatography and electrophoresis, were 2,3-di-*O*-methyl-D-glucose and 3,4-di-*O*-methyl mannose with traces of 2,3,4-tri-*O*-methyl-D-glucose. Demethylation of the reduced sugar produced glucose and mannose.

(iii) Fraction 3

Yield 28 mg, R_g 0.50. Acid hydrolysis and chromatographic examination of the sugars showed 3,4-di-*O*-methyl mannose, 3,5-di-*O*-methyl galactose, and trimethyl glucuronic acid. Methanolysis, reduction, and hydrolysis as described for earlier fractions produced 2,3,4-tri-*O*-methyl-D-glucose, 3,4-di-*O*-methyl mannose, and 3,5-di-*O*-methyl galactose. Demethylation of the reduced trisaccharide yielded glucose, mannose, and galactose.

ACKNOWLEDGMENTS

The authors wish to thank Mr. F. P. Cooper for assistance with the gas–liquid chromatography, Mr. A. E. Castagne for performing the microchemical analyses, and Miss M. T. Clement for preparing the cultures of the organisms.

REFERENCES

1. A. W. Dox and R. E. Niedig. J. Biol. Chem. **19**, 235 (1914).
2. P. W. Clutterbuck, W. N. Haworth, H. Raistrick, G. Smith, and M. Stacey. Biochem. J. **28**, 94 (1934).
3. P. W. Clutterbuck. J. Soc. Chem. Ind. (London), **55**, 551 (1936).
4. L. Hough and M. B. Perry. Biochem. J. **61**, 8 (1955).
5. W. N. Haworth, H. Raistrick, and M. Stacey. Biochem. J. **31**, 640 (1937).
6. W. N. Haworth, H. Raistrick, and M. Stacey. Biochem. J. **29**, 2668 (1935).
7. S. A. Barker, E. J. Bourne, and M. Stacey. J. Chem. Soc. 3084 (1953).
8. S. M. Martin and G. A. Adams. Can. J. Microbiol. **2**, 715 (1956).
9. A. S. Jones. Biochim. et Biophys. Acta, **10**, 607 (1953).
10. H. G. Sevag. Biochem. Z. **273**, 419 (1934).
11. G. S. Berenson. Biochim. et Biophys. Acta, **28**, 176 (1958).
12. O. Westphal, O. Luderitz, and F. Bister. Z. Naturforsch. Pt. b, **7**, 148 (1952).
13. D. H. Northcote. Biochem. J. **58**, 353 (1954).
14. G. H. Beavan and E. R. Holliday. Advances in Protein Chem. **7**, 320 (1952).
15. M. Abdel-Akher, J. K. Hamilton, R. Montgomery, and F. Smith. J. Am. Chem. Soc. **74**, 4970 (1952).
16. A. B. Foster. J. Chem. Soc. 982 (1953).
17. S. A. Barker, A. B. Foster, I. R. Siddiqui, and M. Stacey. Talanta, **1**, 216 (1958).
18. L. Hough, J. K. N. Jones, and W. H. Wadman. J. Chem. Soc. 1702 (1950).
19. W. E. Trevelyan, D. P. Procter, and J. S. Harrison. Nature, **166**, 444 (1950).
20. S. M. Partridge. Biochem. J. **42**, 240 (1948).
21. N. Nelson. J. Biol. Chem. **153**, 375 (1944).
22. F. Weygard, W. Perkow, and P. Kuhner. Chem. Ber. **84**, 594 (1951).
23. M. A. Abdel-Akher and F. Smith. Nature, **166**, 1037 (1950).
24. E. L. Falconer and G. A. Adams. Can. J. Chem. **34**, 338 (1956).
25. A. Jeanes and C. A. Wilham. J. Am. Chem. Soc. **72**, 2655 (1950).
26. A. G. McInnes, D. H. Ball, F. P. Cooper, and C. T. Bishop. J. Chromatog. **1**, 556 (1958).
27. S. Allen, T. G. Bonner, E. J. Bourne, and N. M. Saville. Chem. & Ind. (London), 630 (1958).
28. J. C. Irvine and A. M. Moodie. J. Chem. Soc. **93**, 95 (1908).
29. J. C. Irvine and D. McNicoll. J. Chem. Soc. **97**, 1449 (1910).
30. H. Granichstädten and E. G. V. Percival. J. Chem. Soc. 54 (1943).
31. W. N. Haworth, E. L. Hirst, F. A. Isherwood, and J. K. N. Jones. J. Chem. Soc. 1878 (1939).
32. J. Baddiley, J. G. Buchanan, R. E. Hanschumacher, and J. F. Prescott. J. Chem. Soc. 2818 (1956).
33. H. G. Bott, W. N. Haworth, and E. L. Hirst. J. Chem. Soc. 1395 (1930).
34. R. L. Sundberg, C. M. McCloskey, D. E. Rees, and G. H. Coleman. J. Am. Chem. Soc. **67**, 1080 (1945).
35. R. Kuhn, H. Trischmann, and I. Low. Angew. Chem. **67**, 32 (1955).
36. I. R. Siddiqui and G. A. Adams. Can. J. Chem. **38**, 2029 (1960).
37. P. A. J. Gorin and A. S. Perlin. Can. J. Chem. **34**, 1796 (1956).

Can. J. Chem. Downloaded from www.nrcresearchpress.com by 210.87.254.6 on 09/05/12
For personal use only.

Can. J. Chem. Downloaded from www.nrcresearchpress.com by 210.87.254.6 on 09/05/12
For personal use only.

THE REDUCTION OF NITROBENZENE BY SODIUM SULPHIDE IN AQUEOUS ETHANOL[1]

O. J. Cope and R. K. Brown

ABSTRACT

The reduction of nitrobenzene by sodium sulphide in aqueous ethanol has been examined. Hydrosulphide and hydrodisulphide ions give rise to quite similar, though slow, rates of reduction. Sulphide ion appears to be two to three times as effective as the hydrosulphide ion. Both the sulphide and hydrosulphide species are considered to be responsible for the initial, very slow reduction with possibly some contribution from traces of polysulphide ions. The reduction is markedly accelerated by the addition of elemental sulphur to form di- and polysulphide, a much more reactive reducing species. The formation of "active" elemental sulphur during the course of the reduction produces disulphide and thus gives rise to an autocatalytic reaction. Some of this elemental sulphur is lost as thiosulphate by reaction with hydroxyl ions produced by the reduction itself, and by hydrolysis of sulphide and disulphide ions. The addition of base increases the rate of reduction due to a shift in the equilibria $S^{=} + H_2O \leftrightharpoons HS^- + OH^-$ and $S_2^{=} + H_2O \leftrightharpoons HS_2^- + OH^-$, but this is offset somewhat by greater loss of the active elemental sulphur as thiosulphate, thus decreasing the autocatalytic acceleration of rate.

Although, from its absorption at 265 mμ, nitrobenzene concentration could be accurately measured, no satisfactory method was found for estimating the concentration of disulphide ions during the course of the reduction.

INTRODUCTION

In order to understand the variable results obtained in this laboratory in the alkaline sulphide reduction of nitro compounds and to rationalize the well-known selectivity observed in the sulphide reduction of mono- and poly-nitro compounds (1–4), a detailed study of the sulphide reduction of nitrobenzene was undertaken.

Reduction of aromatic nitro compounds by such reagents as titanous chloride or stannous chloride under acidic conditions has been followed by measurement of the consumption of reducing agent (5–7). Since the disappearance of the nitro compounds was not followed directly, one must either determine or assume that certain definite changes occur in the reducible substance and that all the reducing agent has been consumed by this process and no other. This approach has revealed that the reaction is first order with respect to both nitro compound and reducing agent, and agrees with the generally accepted course of the reaction suggested by Haber (8) and shown as follows.

$$RNO_2 \xrightarrow{\text{slow}} RNO \xrightarrow{\text{fast}} RNH(OH) \xrightarrow{\text{fast}} RNH_2 \qquad (a)$$

There is a considerably greater difficulty in following the reduction by measuring change in concentration of reducing agent when sulphide ions are employed, since the composition of the reduction mixture is more complex than it is in the case of stannous chloride. It is known that a solution of sodium sulphide contains a number of species including sulphide, hydrosulphide, disulphide, hydrodisulphide, and thiosulphate ions, the relative composition of which depends upon the source of the sodium sulphide used for its preparation and the conditions under which the solution is made. The particular species responsible for the reduction, as well as its concentration, must be determined.

Since a method which measured the disappearance of nitrobenzene directly would

[1]*Manuscript received February 9, 1961.*
Contribution from the Department of Chemistry, University of Alberta, Edmonton, Alberta. Taken from the thesis of O. J. Cope to be submitted to the Graduate School of the University of Alberta in partial fulfillment of the requirements for the degree of Doctor of Philosophy.

possess obvious advantages, attention was directed to the development of a spectrophotometric method which followed the change in extent of absorption at λ_{max} 265 mμ with change in nitro concentration. Such a method was indeed obtained. However, during the course of our experiments, Ogata *et al.* (9) reported an investigation of the kinetics of the reduction of aromatic nitro compounds by sodium disulphide in aqueous methanol (40% volume methanol:water). The choice of sodium disulphide stemmed from their observations that reduction with the monosulphide was too slow for satisfactory kinetic study. These authors followed the course of the reaction by measurement of the changes in the absorption of nitrobenzene at λ_{max} 270 mμ, although in cases where a large excess of nitrobenzene was employed, the spectrophotometric method was checked by an electrometric titration of the sodium disulphide with silver ion. Their results showed that the reduction was first order in nitrobenzene. A second-order dependence upon disulphide ion was found also, but when allowance was made for hydrolysis, the reaction was reported to be first order with respect to disulphide ion as well.

Bullock and Forbes (10) have also studied the reduction of certain nitrobenzene sulphonates in aqueous solution by sulphide, disulphide, and polysulphide ions. From their measurements of polysulphide concentration by iodometric titration, they concluded that the reduction was first order in both nitro compound and polysulphide, although no allowance for the extent of hydrolysis of the polysulphide appeared to have been made.

The present work describes the results of a study of the reduction of nitrobenzene with sodium sulphide in aqueous ethanol by following the change in absorption of the nitrobenzene at λ_{max} 265 mμ.

EXPERIMENTAL

Chemicals and Solvents

Sodium sulphide ($Na_2S.9H_2O$), obtained from the Nichols Chemical Company, was of reagent grade. It was colorless and apparently free from the yellowish polysulphide impurities found in sodium sulphide obtained from some other sources.

Nitrobenzene was Fisher certified reagent grade material. This was distilled, before use, at 85–86° C at 10 mm.

Sulphur was Merck sublimed material, used without further purification.

Aqueous ethanol (40%) was prepared by addition of the requisite amount of distilled water to 95% ethanol. This solution was deaerated before use by gentle reflux and subsequent cooling under an atmosphere of oxygen-free nitrogen.

Solutions

The stock solution of sodium sulphide was prepared by the addition of sufficient $Na_2S.9H_2O$ (neglecting the change in the water concentration due to the water of hydration) to the 40% aqueous ethanol to make the solution 0.960 molar with respect to the Na_2S. This stock solution was then diluted appropriately with the 40% aqueous ethanol in the preparation of a 0.160 *M* solution of sodium sulphide. A 0.160 *M* solution of sodium sulphide made in this manner contained 61.2% of water and 38.8% of ethanol.

Apparatus

A Beckman Model DU spectrophotometer, equipped with a power pack, was used to make the absorption measurements. Matched, glass-stoppered quartz cells of 10-mm light path were used for all measurements.

The pH determinations were made with a Beckman Zeromatic meter equipped with

Can. J. Chem. Downloaded from www.nrcresearchpress.com by 210.87.254.6 on 09/05/12
For personal use only.

a high pH electrode. The standardization was made with a saturated solution of pure calcium hydroxide which has a pH of 12.45 at 25° C (11), and also with standard buffers at lower pH.

The reaction was carried out in a 500-ml, four-necked flask fitted with an efficient, water-cooled reflux condenser, a stirrer, an inlet for the addition of sodium sulphide solutions, and an inlet for a nitrogen bleed. In addition, a tube dipping below the surface of the solutions held a 1-ml pipette and thus permitted sampling so that there was a minimum of exposure of the solution surface to air. The apparatus was thermostatted at 50.0° C.

A calibrated dropping funnel was used to introduce the solution of sodium sulphide into the reaction vessel.

Procedure

The reaction vessel was first flushed with nitrogen and subsequently a slight positive pressure of nitrogen was maintained in the apparatus above the solution throughout the entire reaction period.

About 50 ml of the stock solution (0.960 *M* sodium sulphide in aqueous ethanol) was added to the reaction vessel, followed by a sufficient volume of the mixed solvent to give a final concentration of 0.160 *M* sodium sulphide. For the cases which required the addition of sodium hydroxide or elemental sulphur, the necessary quantity of the reagent was added before the diluting solvent had been completely added, followed by the remainder of the solvent needed to make up the required volume. The solutions made by the addition of sodium hydroxide or sulphur were allowed to stand for $\frac{1}{2}$ hour to ensure equilibration of the species in the solution. No change in absorption was noted in such an equilibrated solution, even upon prolonged standing. Finally the nitrobenzene was introduced by means of a Victor Meyer bottle into the rapidly stirred solution.

For following the change in absorption at 450 mμ, the Beckman DU cell container was thermostatted at 50.0° C. The glass-stoppered cell was completely filled with freshly prepared initial reaction solution obtained from the reaction flask and the change in absorbance was measured continuously and directly. This eliminated errors due to cooling and air oxidation which would occur if fresh samples were taken periodically from the reaction flask.

To follow the change in nitrobenzene concentration, 1-ml samples were withdrawn from time to time and immediately diluted to 100 ml with a standard mixture of 40% aqueous ethanol containing four times the calculated amount of hydrochloric acid required to convert all the sodium sulphide to H_2S and the amine to the hydrochloride. These solutions, properly protected and capped, were allowed to stand for the duration of the experiment (2–4 hours) before measurements were made, and then the absorbances were obtained at 25° C at 265 mμ. The period of standing produced no alteration in absorption and thus permitted the choice of a more convenient time for the absorption measurements. Interfering absorption at 265 mμ due to polysulphide was subtracted from the total absorption at this wave length to give a measure of the nitrobenzene concentration. The magnitude of this interfering absorption due to polysulphide was evaluated by measurement of the polysulphide concentration from its absorbance at 450 mμ at 50° C and conversion of this reading to the corresponding (and lower) one at 25° C using calibration plots of concentration of polysulphide versus absorbance at 450 mμ at these two temperatures. From this value of absorption at 450 mμ, the corresponding interfering absorption

Can. J. Chem. Downloaded from www.nrcresearchpress.com by 210.87.254.6 on 09/05/12
For personal use only.

at 265 mμ was obtained from a plot relating absorption at 450 mμ to absorption of the same solution at 265 mμ after having been diluted 100-fold and acidified with the standard aqueous ethanolic solution of hydrochloric acid. These measurements were all made at 25° C.

The solutions required for the comparative absorption of disulphide and hydrodisulphide ions were made up as follows. All preparations were carried out in an atmosphere of nitrogen. To the stock solution of 0.960 *M* sodium sulphide was added the requisite amount of elemental sulphur. Ten-milliliter aliquots of the resulting solution were then separately treated with base, acid, or bicarbonate as required and then diluted to 60 ml with the 40% aqueous ethanol. The aliquot which was to supply the solution of disulphide was first basified by addition of the necessary amount of solid sodium hydroxide to give a concentration of added base equal to 4 *M* and then the volume made up to 60 ml. One of the aliquots which was to supply the solution of hydrodisulphide was acidified by careful addition of the requisite quantity of constant-boiling hydrochloric acid to the rapidly stirred solution. The pH of the solution was followed during this addition and found to be 10.7 when all the necessary hydrochloric acid had been added. To the other aliquot was added sufficient solid sodium bicarbonate to convert all the sodium sulphide and sodium disulphide to the corresponding hydrosulphide and hydrodisulphide (12) and then the volume made up to 60 ml. This solution was cooled to 0° C and the sodium carbonate allowed to precipitate. The supernatant solution of sodium hydrosulphide and sodium hydrodisulphide (pH = 10.7) was removed from the flask, under nitrogen pressure, through a porous plate.

The solutions of sodium hydrosulphide, and sodium hydrosulphide containing hydrodisulphide, were prepared from the 0.960 *M* sodium sulphide stock solution, by appropriate addition of elemental sulphur in the latter case, and then suitable acidification with hydrochloric acid during the dilution, to give the final concentration of 0.160 mole per liter.

Iodometric titrations were carried out by standard procedures.

RESULTS AND DISCUSSION

A method similar to that devised by Ogata *et al.* (9) was used to follow the reduction of nitrobenzene.

The absorption of nitrobenzene in aqueous ethanol was found to follow Beer's law over the concentration ranges studied.

Although reduction of nitrobenzene in alkaline media is known to yield bimolecular reduction products (azoxybenzene and azobenzene), a careful examination of a typical reaction at the λ_{max} at which these compounds absorb showed conclusively that bimolecular reduction products were not present nor were they involved in the reaction. Azoxybenzene has been converted to azobenzene by sulphide (13, 14). We have found that a 0.005 *M* solution of azoxybenzene in aqueous ethanol made 0.150 *M* in sodium sulphide gave approximately 1% conversion to azobenzene in 200 minutes, but only when elemental sulphur was added to form the more actively reducing polysulphide species. Hence, had such bimolecular reductions been involved in our sulphide reductions, azobenzene would surely have accumulated and been detected. Thus the only organic products found at any time during the reaction were nitrobenzene and aniline, in agreement with the observations of previous investigators (9, 10) and with the scheme of reduction given by Haber (8).

Can. J. Chem. Downloaded from www.nrcresearchpress.com by 210.87.254.6 on 09/05/12
For personal use only.

Bullock and Forbes (10) have suggested that the over-all reaction for the reduction of nitrobenzene as expressed by equation (*b*):

$$RNO_2 + S_2^{=} + H_2O \rightarrow RNH_2 + S_2O_3^{=}, \qquad (b)$$

can be broken into three separate reactions as follows:

$$RNO_2 + 3S_x^{=} + 4H_2O \rightarrow RNH_2 + 3S_x^{0} + 6OH^{-} \qquad (c)$$

$$S^0 + S^{=} \rightarrow S_2^{=} \qquad (d)$$

$$4S^0 + 6OH^{-} \rightarrow S_2O_3^{=} + 2S^{=} + 3H_2O. \qquad (e)$$

Of these products, only polysulphide interfered at 265 mμ. However, this could be estimated from suitable Beer's law plots (see Experimental).

Ogata's method (9) of allowance for polysulphide absorption was considered unsatisfactory for our work since polysulphide does not absorb to the same extent at 265 mμ and 240 mμ. This is illustrated in the following table for different concentrations of sodium disulphide.

Absorption at 265 mμ	Absorption at 240 mμ
0.098	0.125
0.213	0.260
0.361	0.412
0.510	0.580

Hence for the present work the actual absorption of the disulphide at 265 mμ was determined in each case.

On the assumption that a 10-fold excess of sodium sulphide over nitrobenzene would give a pseudo-first-order reaction, data for the disappearance of nitrobenzene with time were obtained for the reaction of 0.015 *M* nitrobenzene with 0.160 *M* sodium sulphide in aqueous ethanol (approximately 61:39 water:alcohol, by weight) at 50° C, carefully protected by an atmosphere of nitrogen. The data is shown conveniently in Fig. 1, plot I, and in Fig. 2. The existence of an induction period and an autocatalytic reaction, clearly shown here, has been observed previously by Bullock and Forbes (10) in their experiments on sulphide reduction of nitro compounds in aqueous solution. They discovered that, of the products obtained from these reactions (equations (*c–e*)), only polysulphide was responsible for the autocatalytic reaction. This has been supported by our observation that replacement of some of the sodium sulphide by disulphide shortened or practically eliminated the induction time (Fig. 1, plots II–IV). When 2% of the sodium sulphide was present as disulphide, the induction period was reduced to about 25 minutes, while a molarity of added elemental sulphur greater than 0.0075 (4.7%) gave a reaction practically devoid of an induction period.

Corroboration that the reactive species is, in fact, an increasing quantity of polysulphide was found by simultaneously following the change in polysulphide concentration during the course of the reduction. Polysulphide absorbs quite strongly over a broad region but is quite measurable at 450 mμ. In a plot of concentration of sulphur as polysulphide in 0.160 *M* sodium sulphide in aqueous ethanol versus absorption at 450 mμ at 25° and at 50° C, it was found that Beer's law held remarkably well even up to a molarity of 0.08 for elemental sulphur.

The exact composition of a combination of elemental sulphur with sodium sulphide,

Can. J. Chem. Downloaded from www.nrcresearchpress.com by 210.87.254.6 on 09/05/12
For personal use only.

Can. J. Chem. Downloaded from www.nrcresearchpress.com by 210.87.254.6 on 09/05/12
For personal use only.

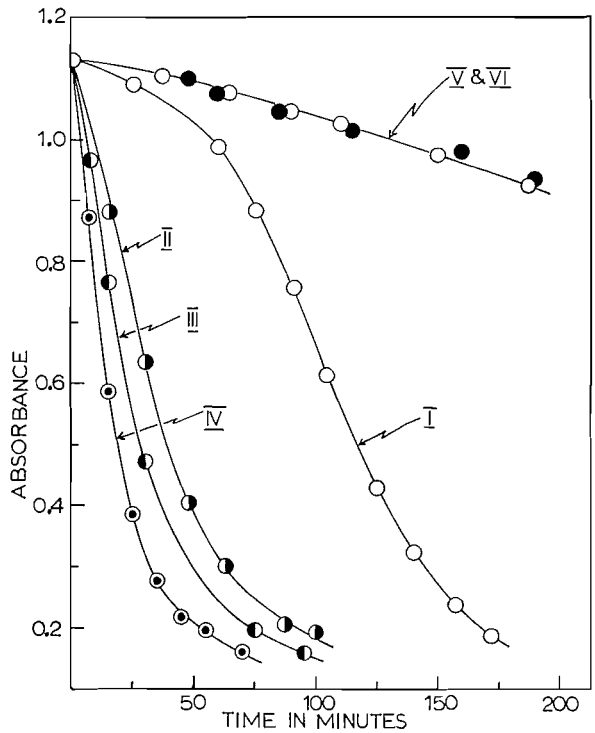


FIG. 1. The change in absorbance of nitrobenzene at 265 mμ with time during the reduction at 50° C of 0.015 *M* nitrobenzene by aqueous ethanolic sodium sulphide. I to IV have a Na_2S concentration of 0.160 *M*; II, III, and IV are 0.0075 *M*, 0.015 *M*, and 0.030 *M* respectively in dissolved sulphur; V and VI plots both contain 0.160 *M* NaHS, VI (●) being also 0.015 *M* in sulphur.

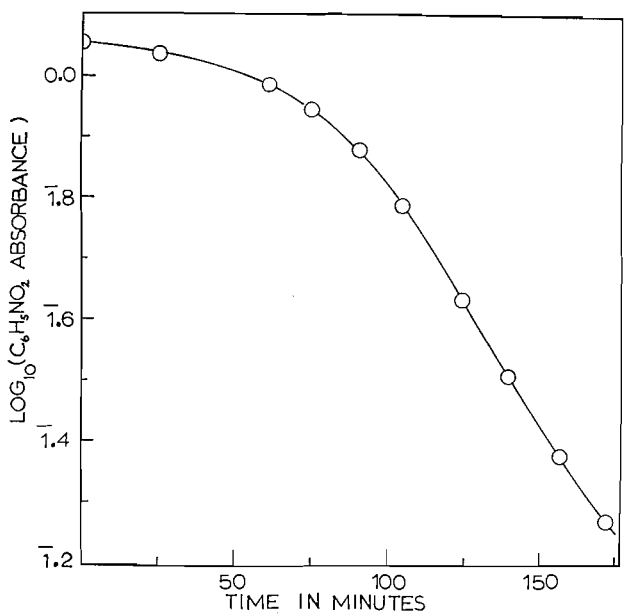


FIG. 2. A plot of $\log_{10}$ of the nitrobenzene absorbance at 265 mμ vs. time for the reduction of 0.150 *M* nitrobenzene by 0.160 *M* Na_2S in aqueous ethanol at 50° C.

and hence the nature of the absorbing species, is uncertain (15–18). The adherence to Beer's law noted above, and our finding that the intensity of absorption of Na_2S_3 in the aqueous ethanol employed is nearly *three* times that of Na_2S_2 under the same conditions, favors the view that $S_2^=$ is essentially the species present when the concentration of sulphur is considerably less than that of the sodium sulphide. However, in view of the uncertainty of the composition of our polysulphide, for convenience the term *disulphide* will be used.

From Fig. 3, plot I, it is seen that in the initial stage of the reaction between sodium

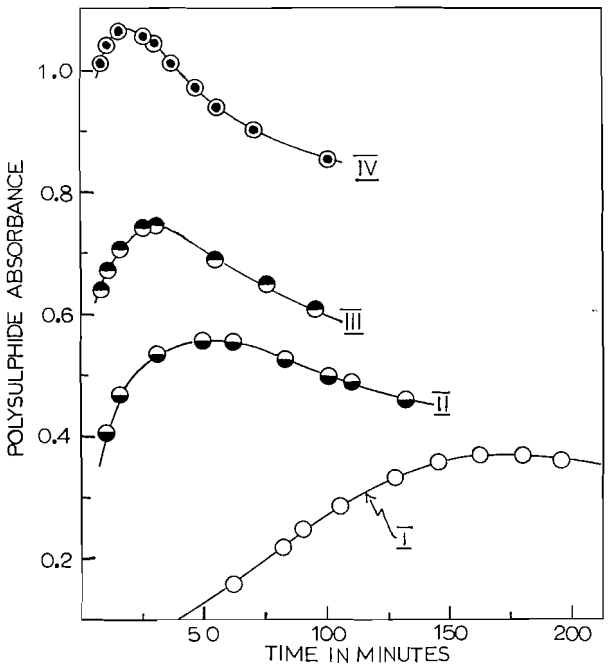


FIG. 3. The change in absorbance at 450 mμ with time during the reduction at 50° C of 0.015 *M* nitrobenzene in aqueous ethanolic sodium sulphide. I to IV have a Na_2S concentration of 0.160 *M*; in addition II, III, and IV are 0.0075 *M*, 0.015 *M*, and 0.030 *M* respectively in dissolved sulphur.

sulphide and nitrobenzene, the disulphide concentration was indeed quite small, but increased to a maximum at about 175 minutes of reaction, slowly decreasing thereafter. This value became constant when the reduction had been completed, a fact not shown in the plot but actually determined in two separate cases. When sulphur was added initially, not only was the rate of increase of disulphide greater with larger initial concentration of disulphide, but so was the rate of loss of disulphide. Furthermore, from the pseudo-first-order logarithmic plot (Fig. 2) it is seen that no truly linear section occurred.

In an attempt to rationalize these findings the following aspects of the reaction were considered.

The Probable Extent of Hydrolysis of Sodium Sulphide in Aqueous Ethanol

An aqueous solution of sodium sulphide is considered to be extensively hydrolyzed (17). Kuster and Heberlein (19, compare also 17) indicate that a 1 *M* solution of sodium sulphide is hydrolyzed to about 50%. Ogata (9) has used a figure of 10 for the hydrolysis constant for a solution of sodium sulphide in aqueous media. However, disagreement

Can. J. Chem. Downloaded from www.nrcresearchpress.com by 210.87.254.6 on 09/05/12
For personal use only.

concerning the value of the second ionization constant of hydrogen sulphide (20, 21) makes the value of the concentration of sulphide and hydrosulphide ions, calculated by the use of the value 10, somewhat uncertain.

Little is known about the extent of hydrolysis of sodium sulphide in aqueous ethanol. The reasoning presented by Ogata *et al.* (9) indicates that the hydrolysis constant of sodium sulphide in aqueous methanol at room temperature is somewhat less than the value of 10.[2] It is reasonable that a similar decrease in magnitude of the hydrolysis constant applies to the aqueous ethanol employed in our work. But, in view of the lack of more precise knowledge of the hydrolysis constant of sodium sulphide in aqueous ethanol, particularly at 50° C, an estimation of the extent of hydrolysis was made by pH measurements according to the following procedure.

In a comparison of pH readings obtained from equimolar solutions (at 50° C) of sodium hydroxide in water and in the stock aqueous ethanol, ranging from 0.050 to 0.500 M in sodium hydroxide, it was found that an apparent constant difference of 0.60 pH units occurred, and could be expressed as

$$pH_{H_2O} = pH_{H_2O-alc} - 0.60.$$

This "alcohol effect" on pH readings obtained for solutions in aqueous alcohol has been recorded previously (22). It is seen that a knowledge of the concentration of sodium hydroxide in water and the pH to which it corresponds can be used to estimate the concentration of sodium hydroxide in an alcohol–water mixture by measurement of the pH of the latter solution. In this manner, advantage can be taken of the known values of pK_w in water for conversion of pH to pOH and hence to hydroxyl ion concentration. For example, a pH of 12.60 found for a certain amount of sodium hydroxide dissolved in aqueous ethanol at 50° C corresponded to an equivalent pH of 12.00 in water. Using $pK_w = 13.26$, the value reported for a temperature of 50° (23), one obtained the hydroxyl ion concentration of 5.5×10^{-2} M. The pH readings were considered to be accurate to ± 0.02 units, hence the hydroxyl ion concentration was expressed as 0.055 ± 0.002 M.

A further complication arose from the fact that the pH measures *activity* of the hydrogen ion and not the actual hydrogen ion concentration directly. A knowledge of the activity values would permit calculation of the hydrogen ion, and hence hydroxyl ion, concentration. The lack of such data led to the following evaluation.

A 0.050 M solution of sodium hydroxide in *water* at 50° C gave a pH reading of 11.90 whereas the calculated figure, using pK_w at 50° C = 13.26, was 11.96—a difference of 0.06 units. Sodium hydroxide solutions, 0.1 and 0.5 M in strength, showed respectively the difference of 0.160 and 0.260 between calculated and observed values of pH. Thus the pH value found for aqueous alcoholic solutions of sodium hydroxide, even though corrected for the alcohol effect, gave an apparent hydroxyl ion concentration which was, in the region of 0.050 molarity, about 0.06 pH units lower than that actually present.

The foregoing considerations and observations were then applied to the problem of determining the sulphide ion concentration of a 0.160 M sodium sulphide solution in aqueous ethanol at 50° C. The pH of this solution was found to be 12.60 ± 0.02. When corrected for the alcohol effect, the value was 12.00 ± 0.02. This was identical with the pH found for a 0.160 M solution of the same concentration of sodium sulphide in water

[2]*These authors show a ratio of hydrolysis constants in aqueous media of* $K_{S^-}/K_{S_2^-} = 4$. *Since* S_2^- *should hydrolyze less than does* S^-, *either in water or in aqueous ethanol, and since Ogata obtained a value of 1.4 for the hydrolysis constant,* K_h, *of* S_2^- *in aqueous methanol, the* K_h *of sodium sulphide in aqueous methanol may also be approximately four times this figure, i.e. 5.6. If aqueous ethanol and aqueous methanol are comparable, the* K_h *of* Na_2S *in aqueous ethanol then might be about 5.*

Can. J. Chem. Downloaded from www.nrcresearchpress.com by 210.87.254.6 on 09/05/12
For personal use only.

at 50° C. Using the pK_w value of 13.26, the hydroxyl ion concentration was estimated at 0.055 ± 0.002 *M*. Allowing for the "activity measurements" indicated above, the hydroxyl ion concentration was estimated to be 0.063 ± 0.002 *M*.

On the basis of the above calculations of the hydroxyl ion concentration, the extent of hydrolysis of a 0.160 *M* solution of sodium sulphide in the aqueous ethanol at 50° C was $39 \pm 2\%$. The sulphide ion concentration was therefore 0.097 ± 0.002 *M*. From these figures a value of 4.1×10^{-2} was obtained for the hydrolysis constant of sodium sulphide in the aqueous ethanol at 50° C. It is realized that these calculations are approximations. However, they do supply us with a rough estimate of the sulphide ion concentration.

The Initial Slow Reduction

The initially slow reaction between sodium sulphide and nitrobenzene (Figs. 1 and 2, plot I) might be attributed to one or a combination of the species present as a result of hydrolysis of sodium sulphide. These are principally the sulphide and hydrosulphide ions with possibly small concentrations of disulphide and hydrodisulphide ions as contaminants. It was originally thought that the slow reaction was due largely, if not completely, to the small concentration of contaminating disulphide ion. Support for this view was obtained by the observation that this initial rate was found occasionally to be considerably greater than that usually observed, depending upon the source (and hence extent of contamination by $S_2^=$) of the sodium sulphide. This apparent doubling of the initial rate could hardly be attributed to significant change in the monosulphide ion concentration due to hydrolysis, since the concentration of 0.160 *M* in sodium sulphide was adhered to as closely as possible. The species which could change sufficiently in concentration to effect this twofold increase in initial rate was more reasonably the contaminating disulphide ions. However, because of the reasons indicated below, the view is now held that the initial slow reduction is at least to a large extent due to sulphide and hydrosulphide species.

The extent of hydrolysis, obtained from pH measurements, gives for a 0.160 *M* solution of sodium sulphide, at the beginning of the reduction, a concentration of sulphide and hydrosulphide ions of 0.097 ± 0.002 *M* and 0.063 ± 0.002 *M* respectively. It is reasonable to assume that of these two ions, the sulphide ion should possess the greater capability for reduction. But the fact that the initial reduction rate by a solution which contains only hydrosulphide ions (Fig. 1, plot V) is not much different from that found when more than half of the hydrosulphide is converted to sulphide ion (Fig. 1, plot I) indicates that the sulphide and hydrosulphide (and also hydrodisulphide, Fig. 1, plot VI) ions are all of the same order of reducing power.

The extremely slow reduction by the sulphide ion might be due to the fact that it is much more strongly hydrated than is the hydrosulphide ion (23). The displacement of the water to allow association of the sulphide ion with the nitro group for the subsequent electron transfer occurs with difficulty. In contrast, disulphide and polysulphide ions reduce nitrobenzene much more rapidly, no doubt due in part to the lower degree of hydration of these ions (18). Furthermore, it is not unreasonable to assume that the conversion $:\dot{\underset{\cdot\cdot}{\overset{\cdot\cdot}{S}}}:\dot{\underset{\cdot\cdot}{\overset{\cdot\cdot}{S}}}:^{=} \rightarrow 2e + \dot{\underset{\cdot\cdot}{\overset{\cdot\cdot}{S}}}:\,:\dot{\underset{\cdot\cdot}{\overset{\cdot\cdot}{S}}}$ is more facile than is the analogous change of $:\dot{\underset{\cdot\cdot}{\overset{\cdot\cdot}{S}}}:^{=} \rightarrow 2e + \dot{\underset{\cdot\cdot}{\overset{\cdot\cdot}{S}}}:$ on the basis that the combination of the two sulphur atoms yields a more stable product.

In this connection it is of interest to record the observation that the rate of reduction of nitrobenzene by a dilute, aqueous ethanolic solution of sodium *tri*sulphide was

Can. J. Chem. Downloaded from www.nrcresearchpress.com by 210.87.254.6 on 09/05/12
For personal use only.

approximately the same as, although constantly slightly lower than, that found for an equal concentration of sodium *di*sulphide under otherwise identical conditions. This agrees with the view expressed by Ogata (9) that attack by disulphide ion is on the nitrogen atom of the nitro group. The bulkier trisulphide ion would find such an approach somewhat more difficult.

The Autocatalytic Reaction

Since the effective reducing species is the disulphide ion, and this is present in a concentration less than or comparable with that of the nitrobenzene, although increasing as the reaction progresses, it is obvious that a pseudo-first-order reaction cannot be obtained. The data shown in Figs. 1 and 3 indicate an autocatalytic reaction; hence it might be possible to apply the equation for such a reaction (24) and thus evaluate the rate constant, providing the concentrations of both reactants are known or can be measured.

The concentration of one reactant, nitrobenzene, is easily and accurately determined by absorption measurements, and is found to decrease continually with time. However, the concentration of disulphide ion is governed by several factors. The process of reduction itself (equation (*c*)) with simultaneous production and reaction of elemental sulphur (equations (*d*) and (*e*)) is one factor which must be considered. When this is coupled with the unknown extent of hydrolysis of the disulphide ion, which, in turn, is affected by the change in hydroxyl ion concentration,[3] the task of measuring the disulphide ion concentration is indeed quite formidable. Since, to our knowledge, the hydrolysis constant of the disulphide ion is unknown either in aqueous media or in aqueous ethanolic solution at 50° C, the determination of the disulphide ion concentration by this route is not feasible.

The Relative Absorbances of Disulphide and Hydrodisulphide Species and the Attempt at Estimation of Disulphide Ion Concentration by Absorption Measurements

During the course of these experiments it was also shown that the absorption of "disulphide ion" at 450 mμ does not give a direct measure of the disulphide ion concentration since both disulphide and hydrodisulphide species contribute to this absorption, although to different extents.

An attempt was made to convert a solution of sodium disulphide, on the one hand, to one containing entirely unhydrolyzed disulphide ion (and sulphide ion), and, on the other hand, to a solution containing only hydrodisulphide ion (and hydrosulphide ion). Measurement of the absorption would then provide a means of estimating the extent of hydrolysis of sodium disulphide in our reduction mixture.

A series of aqueous ethanolic solutions, 0.160 *M* in sodium sulphide, containing 21.4% of sulphur as disulphide, were made up to contain progressively greater concentrations of sodium hydroxide. The results of absorbance measurements, made at 25° C at 450 mμ, are shown in Fig. 4. The absorbance rose from 1.013 units for the unbasified equilibrium mixture to a maximum of 1.820 units when the molarity of added base reached 4.0. Further addition of base produced no change in absorbance. The most reasonable explanation of these results is that of repression of hydrolysis by the added base to produce essentially disulphide ion, which must then absorb to a greater degree than does an equal amount of hydrodisulphide ion.

When the aqueous ethanolic solution, 0.160 *M* in sodium sulphide and containing

[3]*In one experiment involving the reduction of nitrobenzene by sodium sulphide at 50° C, the changes in* pH *were found to be: initial* pH, *12.60; after 45 minutes of reaction, a maximum* pH *of 12.95; and after 130 minutes, well beyond one half life, a* pH *of 12.50.*

Can. J. Chem. Downloaded from www.nrcresearchpress.com by 210.87.254.6 on 09/05/12
For personal use only.

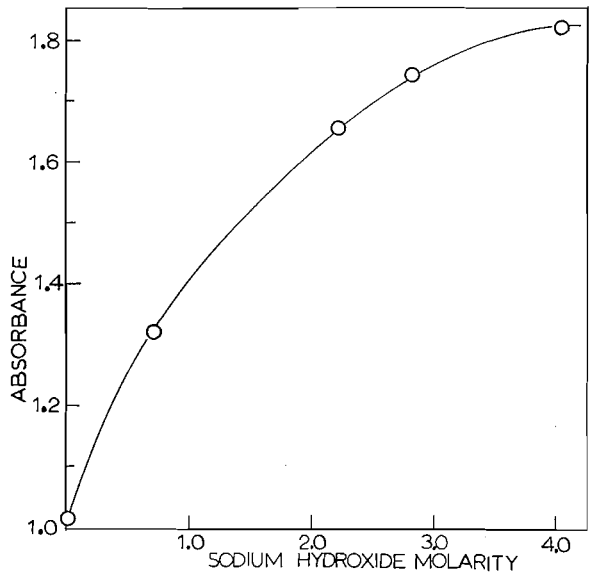


FIG. 4. The effect of the addition of NaOH on the absorbance at 450 mμ of a solution of sulphur in 0.160 *M* Na_2S (in aqueous ethanol).

elemental sulphur as disulphide, was treated so as to convert sulphide and disulphide ions to hydrosulphide and hydrodisulphide ions (see Experimental) the absorption *increased* rather than decreased as would be expected from the results of the work involving basified solutions. No constant value for absorption was obtained since the extent of absorption increased with increasing amounts of hydrochloric acid added. No explanation could be found for this phenomenon.

From these experiments, it is obvious that the ratio $HS_2^-/S_2^=$ could not be calculated from absorbance measurements. Hence the concentration of disulphide ion could not be found, thus making a satisfactory kinetic study of the reduction of nitrobenzene by sodium sulphide under our conditions quite difficult.

The Effect of Addition of Base on the Reduction of Nitrobenzene by Sodium Sulphide

The addition of sodium hydroxide increased the rate of reduction of nitrobenzene by sulphide (Fig. 5, plots I–IV), but not in proportion to the amount of base added. Eventually a state was reached where further addition of base actually had the reverse effect (Fig. 5, plot V). The increased rate was no doubt due to the conversion of the relatively unreactive HS_2^- to the much more reactive species, $S_2^=$. A large concentration of base would convert essentially all the polysulphide to the unhydrolyzed state and result in a maximum rate of reduction. However, the increased concentration of base caused greater reaction between hydroxyl ion and the "active sulphur" (10), hence less disulphide was formed, thus leading to a lower acceleration of rate. With sufficiently high concentration of base it is expected that most if not all of the active sulphur would be lost as thiosulphate and no autocatalysis would be observed. This could not be tested in our solutions since a concentration of base significantly greater than 4 *M* resulted in a salting out of the ethanol.

The changes in "polysulphide concentration" accompanying the reductions in each of these cases are shown in Fig. 6. It has been shown that this absorption is due to both

Can. J. Chem. Downloaded from www.nrcresearchpress.com by 210.87.254.6 on 09/05/12
For personal use only.

Can. J. Chem. Downloaded from www.nrcresearchpress.com by 210.87.254.6 on 09/05/12
For personal use only.

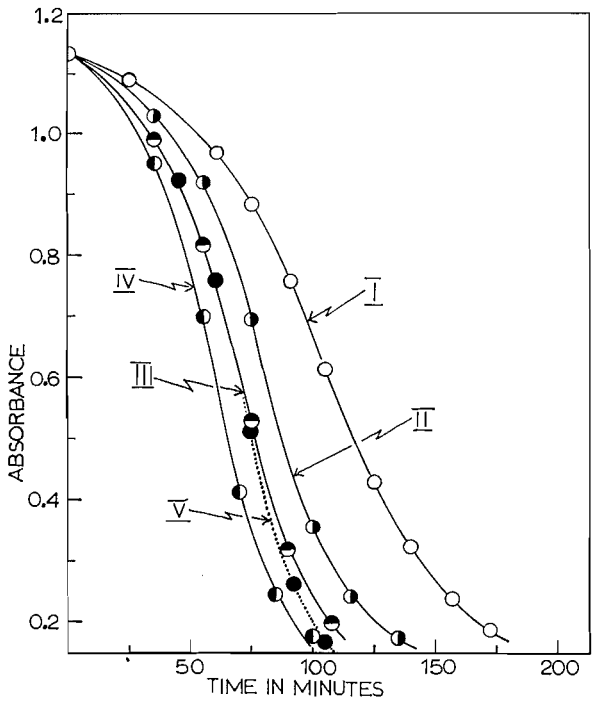


FIG. 5. Absorbance at 265 mμ vs. time during the reduction of 0.015 *M* nitrobenzene in aqueous ethanol at 50° C by 0.160 *M* Na_2S. I contains no added NaOH; II, III, IV, and V are 0.160 *M*, 0.320 *M*, 0.800 *M*, and 1.600 *M* in NaOH respectively.

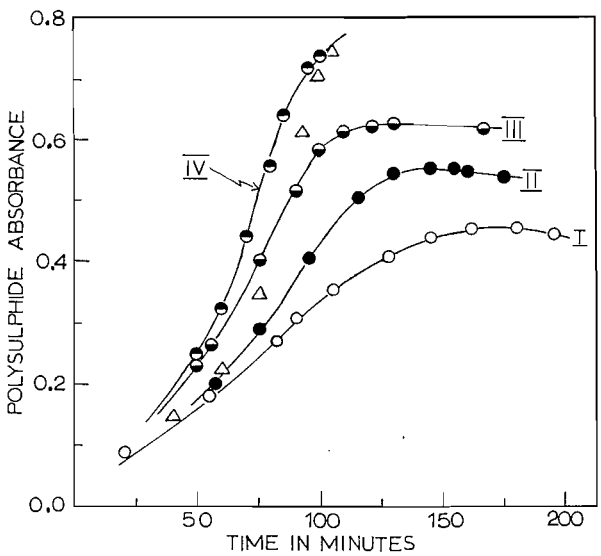


FIG. 6. The absorbance at 450 mμ vs. time during the reduction of 0.015 *M* nitrobenzene in aqueous ethanol at 50° C by 0.160 *M* Na_2S. I contains no added NaOH; II, III, IV, and V (△) are 0.160 *M*, 0.320 *M*, 0.800 *M*, and 1.600 *M* in NaOH respectively.

hydrodisulphide and disulphide species, and that addition of base changes their relative proportion and hence the total absorption (Fig. 4). In the preparation of solutions of sulphur in 0.160 *M* sodium sulphide, containing up to 0.160 *M* sulphur, it was found that the pH changed negligibly,[4] hence it was concluded that the ratio of disulphide ion to hydrodisulphide ion remained essentially constant in these solutions. Absorption of the 0.160 *M* sodium sulphide solutions containing various amounts of sulphur as polysulphide then reflected reasonably well the *concentration* of elemental sulphur, although not the *ratio* of disulphide ion to hydrodisulphide ion. This is embodied in the linear relation between absorbance and elemental sulphur found in the calibration plot which followed Beer's law.

The absorption shown in Fig. 6 must then be a composite of increased polysulphide concentration as result of reduction, and a larger ratio of disulphide to hydrodisulphide ion, the magnitude of which depends upon the hydroxyl ion concentration. Hence, calculation of the polysulphide sulphur from these absorption measurements, using the calibration data from the Beer's law plot would give erroneous results. With the aid of Fig. 4, the absorbances at various base concentrations have been converted to those where no base was added and thus it was possible to show the real increase of polysulphide sulphur which occurred during these reductions in basified solutions. Figure 7 shows more

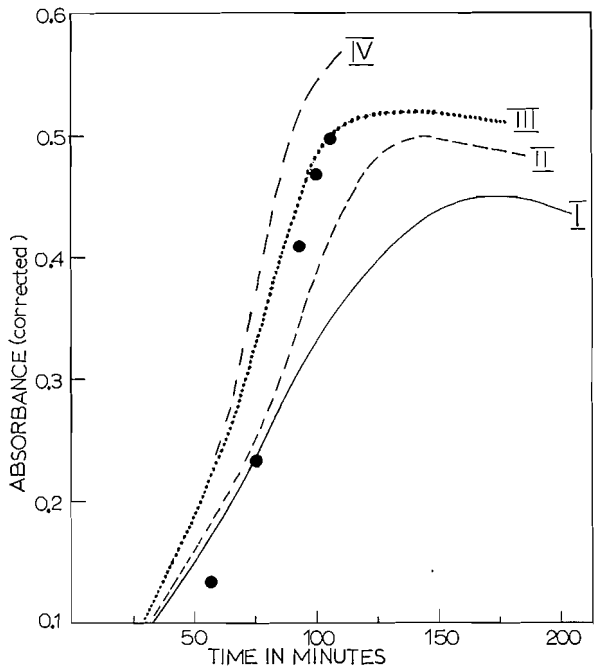


FIG. 7. The corresponding absorbances at 450 mμ from Fig. 6 corrected for the effect of increased OH ion concentration on the absorbance at 450 mμ (here ● represents 1.600 *M* NaOH).

clearly the diminishing increase of polysulphide sulphur as the initial concentration of base is increased and thus the greater extent of loss of sulphur by reaction with base.

Figure 4 was obtained by progressive basification of a sodium sulphide solution

[4]*A decrease in* pH *was expected since the disulphide ion should hydrolyze to a lower extent than does the sulphide ion (9). However, these results were repeatable using several different electrodes to avoid the chance that an electrode might have become contaminated or unreliable.*

Can. J. Chem. Downloaded from www.nrcresearchpress.com by 210.87.254.6 on 09/05/12
For personal use only.

containing *one* specific concentration of polysulphide, and gave a figure of 1.80 for the ratio of absorbance of basified (4 *M*) solution to that of the unbasified solution. The same figure of 1.80 was obtained when a number of solutions were prepared, differing only in concentration of polysulphide, and made 4 *M* in sodium hydroxide. Hence the use of Fig. 4 and the ratio 1.80 for conversion of absorbances of the basified polysulphide solutions shown in Fig. 6 is justified.

The Formation of Thiosulphate during the Course of the Reduction

The possibility of air oxidation of sulphide to thiosulphate was avoided by careful deaeration of all solutions and by use of a nitrogen atmosphere. Iodometric titration of thiosulphate (25) requires preliminary removal of both sulphide and hydroxide ions. The addition of cadmium sulphate, rather than cadmium carbonate (10), accomplished this satisfactorily. However, it was found that the precipitated cadmium sulphide adsorbed some of the thiosulphate, thus giving low results in spite of attempts at recovery of adsorbed thiosulphate by extractions. Hence small changes in thiosulphate concentration during a reaction might easily be missed.

There existed the possibility of thiosulphate formation in our solutions due to the interaction of polysulphide sulphur with hydroxyl ions formed as a result of hydrolysis, especially since the pH of the solutions were well above 8 (10). This could not be determined satisfactorily by iodometric titrations for the reason cited above. However, an oxygen-free solution of 0.160 *M* sodium sulphide, containing 10% of sulphur as polysulphide, when kept at room temperature or at 50° C under nitrogen for 12 hours, showed no change in absorption or in pH. This is consistent with the view that little or no formation of thiosulphate occurred via reaction (*e*) by interaction of polysulphide sulphur and hydroxyl ion.

However, in contrast, much thiosulphate was formed *during* the reduction of nitrobenzene by sulphide solutions, in agreement with the observation of Bullock and Forbes (10). Iodometric titrations, after removal of hydroxyl and sulphide ions with cadmium sulphate, in spite of the loss due to adsorption, showed at least a ninefold increase of thiosulphate during the first 70 minutes of a typical reaction. That the base should react with sulphur formed *during* the reduction but not with the sulphur in polysulphide when nitrobenzene is absent can be reasonably explained. The negative charge on both hydroxyl and polysulphide ions prohibits their mutual interaction. On the other hand, the sulphur released during nitrobenzene reduction is uncharged and therefore can react readily with hydroxyl ions or with sulphide ions according to equations (*e*) and (*d*). This form of sulphur has been termed "active sulphur" by Bullock and Forbes and appears to be much more readily soluble in the sulphide solution than is elemental sulphur, ordinarily used for the preparation of polysulphide solutions.

Reduction of Nitrobenzene with Sodium Hydrosulphide and Sodium Hydrodisulphide

Reduction of nitrobenzene (0.015 *M*) by solutions of sodium hydrosulphide and sodium hydrodisulphide were carried out at 50° C. The results, shown in Fig. 1, plot V, indicate that during the initial stage of the reduction by hydrosulphide the rate was only $\frac{1}{2}$ to $\frac{1}{3}$ that found for the reduction with sodium sulphide. The marked autocatalytic effect observed in the latter case did not occur in hydrosulphide reduction of nitrobenzene. The addition of enough sulphur to convert about 10% of the sodium hydrosulphide to the hydrodisulphide gave no apparent increase in initial rate of this slow reaction and thus shows that sodium sulphide, sodium hydrosulphide, and the hydrodisulphide have

Can. J. Chem. Downloaded from www.nrcresearchpress.com by 210.87.254.6 on 09/05/12
For personal use only.

apparently the same order of reducing capacity. The slow increase in rate shown in Fig. 1, plot V, could be ascribed to a gradual shift in the equilibrium $S_2^= + H_2O \leftrightarrows HS_2^- + OH^-$ to the left due to the increase in hydroxyl ion concentration resulting from the slow reduction. The observation that the pH rose from 10.0 to 10.9 over a period of 630 minutes of reaction supports this point of view. This is further supported by the observation of a greater rate of reaction in one preparation of hydrosulphide wherein only enough hydrochloric acid had been added to reduce the pH of the solution to 12.1 rather than the usual 10.0 to 10.2.

Summary of the Course of Reduction of Nitrobenzene by Sodium Sulphide in Aqueous Ethanol

The studies described in the preceding sections assist in clarifying the course of the reduction of nitrobenzene by sodium sulphide solution.

As the reaction progresses, to the initial, slow reduction by sulphide and hydrosulphide ions is added the much faster reduction due to polysulphide formed by the sulphur produced during the reduction. Since the conversion of *one* molecule of nitrobenzene to aniline forms *three* atoms of sulphur, which then rapidly react preferentially with sulphide or hydrosulphide ions present, an exponential increase of polysulphide occurs, accounting for the rapid autocatalysis. At the same time some of this active sulphur reacts with the hydroxyl ions to form thiosulphate. This reaction must be considerably slower than is the combination of sulphur with sulphide ions, otherwise the autocatalytic effect would be less pronounced. The increase in absorption at 450 mμ reflects an increase in polysulphide species. Eventually a state is reached where the rate of reduction appears to be constant, as a result of a balance between the increasing concentration of active polysulphide ions, the drop in nitrobenzene concentration, and the removal of some of the active sulphur as thiosulphate by the increasing concentration of hydroxyl ions. Following this, the reduction rate decreases as expected.

After the peak of the reduction rate has passed, the loss of polysulphide as thiosulphate, through preliminary reaction with nitrobenzene to produce active sulphur and its subsequent combination with base, becomes more competitive. This is no doubt due to the fact that only a 10-fold excess of sodium sulphide over nitrobenzene was employed as well as the fact that three sulphide (or polysulphide) ions are necessary to reduce one molecule of nitrobenzene to aniline. Thus, as reaction proceeds, there is a rapid decrease in the concentration of the charged sulphide species, which will react with the active sulphur formed by the reduction, to such a low level that the competitive reaction of sulphur with the hydroxyl ions becomes more important.

When the nitrobenzene has been practically completely reduced, the formation of thiosulphate and polysulphide ceases, as indicated by the constancy of the absorption of the polysulphide solution noted in at least two instances where such measurements were made over a period of 24 hours.

ACKNOWLEDGMENTS

The authors wish to express their appreciation to the National Research Council of Canada for financial assistance throughout the course of this work.

Grateful acknowledgment is also made to Dr. W. Wallace, Dr. G. Freeman, and Dr. W. E. Harris of the Department of Chemistry of the University of Alberta for helpful discussions.

Can. J. Chem. Downloaded from www.nrcresearchpress.com by 210.87.254.6 on 09/05/12
For personal use only.

REFERENCES

1. R. ANSCHUTZ and F. HEUSLER. Ber. **19**, 2161 (1886).
2. H. H. HODGSON. J. Soc. Dyers Colourists, **62**, 114 (1946).
3. H. H. HODGSON. J. Chem. Soc. 242 (1948).
4. H. H. HODGSON. J. Chem. Soc. 2017 (1948).
5. S. A. NEWTON, F. J. STUBBS, and SIR C. HINSHELWOOD. J. Chem. Soc. 3384 (1953).
6. M. J. STEPHEN and SIR C. HINSHELWOOD. J. Chem. Soc. 1393 (1955).
7. Y. OGATA and I. SUGIYAMA. Science (Tokyo), **19**, 232 (1949). Chem. Abstr. **45**, 5116 (1951).
8. F. HABER. Z. physik. Chem. **32**, 193 (1900).
9. M. HOJO, Y. TAKAGI, and Y. OGATA. J. Am. Chem. Soc. **82**, 2459 (1960).
10. J. L. BULLOCK and G. S. FORBES. J. Am. Chem. Soc. **55**, 232 (1933).
11. R. G. BATES, V. E. BOWER, and R. E. SMITH. J. Research Natl. Bur. Standards, **56**, 305 (1956).
12. H. H. HODGSON and E. R. WARD. J. Chem. Soc. 242 (1948).
13. S. GABRIEL. Ber. **9**, 1406 (1876).
14. H. H. HODGSON, W. H. NORRIS, and G. R. WOOD. J. Soc. Dyers Colourists, **66**, 473 (1950).
15. F. FEHRER. Angew. Chem. **67**, 337 (1955).
16. D. PESCHANSKI. Compt. rend. **227**, 770 (1948).
17. G. SATYANARAYANA RAO and G. GORIN. J. Org. Chem. **24**, 749 (1959).
18. H. GERISCHER. Z. anorg. Chem. **259**, 220 (1949).
19. F. W. KUSTER and E. HEBERLEIN. Z. anorg. u. allgem. Chem. **43**, 53 (1905).
20. H. KUBLI. Helv. Chim. Acta, **29**, 1962 (1946).
21. P. SOUCHEY and R. SCHAAL. Bull. soc. chim. France, 819 (1950).
22. I. M. KOLTHOFF and C. ROSENBLUM. Acid base indicators. The MacMillan Co., New York. 1937. p. 356.
23. HANDBOOK OF CHEMISTRY AND PHYSICS. 37th ed. Chemical Rubber Publishing Co., Cleveland, Ohio. 1955–56.
24. A. A. FROST and R. G. PEARSON. Kinetics and mechanism. John Wiley & Sons, Inc., New York. 1956.
25. W. W. SCOTT. Standard methods of chemical analysis. D. Van Nostrand & Co., New York. 1917. p. 408.

Can. J. Chem. Downloaded from www.nrcresearchpress.com by 210.87.254.6 on 09/05/12
For personal use only.

HYDROGEN BONDING IN SOLUTIONS OF SUBSTITUTED ACETIC ACIDS[1]

LEONARD W. REEVES

ABSTRACT

The changes in chemical shift of the acid proton in some simple carboxylic acids on dilution in four solvents has been studied. The existence of chainlike hydrogen-bonded polymers in solution is suggested by the results. The association of the monomer molecules in dilute solution with donor centers in the solvent molecules is suggested from a study of the —O—H monomer stretching bond in the vapor and in two solvents. There is a difference in the behavior of acetic and trifluoroacetic acid in N-methyl and N,N-dimethyl formamide, which has been explained in terms of protonation of the amides in trifluoroacetic acid solutions.

INTRODUCTION

The proton resonance technique has been a useful tool in measuring changes in the amount of hydrogen bonding in fluid systems (1, 2, 3, 4). The changes in chemical shift with the amount of hydrogen bonding are often very large. Recent improvements in standardization of chemical shifts and their measurement and the introduction of 60 Mc/s as a proton high-resolution frequency have made the sensitivity for detection of very weak interactions of the hydrogen-bonding type superior to any other technique (5, 6). The short lifetime of the hydrogen bond association compared to the inverse frequency shift due to various environments results in an averaging of the varying proton-shielding parameter, and one signal is observed (1, 7). The position of this signal corresponds to the average environment of the various equilibrium processes involved in the hydrogen bonding. This is a particular disadvantage in a system in which polymeric association via hydrogen bonds occurs, since the variation of averaged nuclear-shielding parameter with concentration or temperature does not provide enough information for the obtaining of a true association chemical shift, or equilibrium constants (8, 9). Some attempt has been made to calculate equilibrium constants for the monomer–dimer equilibrium in dilute alcohol solutions in CCl_4 using a region of concentration known to involve only monomers and dimers (10, 11).

The study of strong dimer associations such as carboxylic acids or intramolecular hydrogen bonds has been pursued in an attempt to avoid some of the above difficulties (12, 13, 14, 15). It has been suggested that acetic acid forms polymeric hydrogen-bonded associations in concentrated nonpolar solutions (15) while longer-chain acids show only dimer associations in the same concentration regions (13). The present study of substituted acetic acids was undertaken to investigate possible polymeric hydrogen bonding and to try to provide an explanation for the difference in behavior of acetic acid (15).

EXPERIMENTAL

Dichloroacetic acid, trifluoroacetic acid, and α-bromo- and α-chloro-proprionic acid were purified by fractional distillation in a dry atmosphere. A small middle cut was taken in each case. Monochloroacetic, trichloroacetic, trimethyl acetic, phenyl acetic, bromoacetic, and β-bromoproprionic acids were either recrystallized from chloroform or taken as reagent grade chemicals. The acids which are deliquescent were handled in a dry box.

The solvents used, carbon tetrachloride and 1,2-dichloroethane, were fractionally distilled in a dry atmosphere. The dilution chemical shift studies were made using 0.5

[1]*Manuscript received November 25, 1960.*
Contribution from the Chemistry Department, University of British Columbia, Vancouver 8, B.C.

Can. J. Chem. Downloaded from www.nrcresearchpress.com by 210.87.254.40 on 09/05/12
For personal use only.

mole% cyclohexane in each solvent as an internal reference signal. The mole fraction of solute was computed using the total moles of solvent, solute, and internal standard.

The measurements were made with a V-4300 Varian 40-Mc spectrometer with field stabilizer V.K. 3506. An audio-oscillator was calibrated using Lisajoux figures at multiples of 60 c.p.s. mains frequency and the later measurements of audio frequencies were calibrated by a Hewlitt Packard Electronic Counter. The side-band technique of measurement was used in all cases. Chemical shifts are accurate to ± 1.5 c.p.s. in this work. Solutions were made up by weighing the liquids in capped vials.

RESULTS

Chemical shift measurements of the carboxyl proton resonance, using an internal cyclohexane reference, are plotted in Fig. 1 for various concentrations of acid in carbon tetrachloride. The acids measured were mono-, di- and tri-chloroacetic, α-chloro- and α-bromo-proprionic, trifluoroacetic, and trimethyl acetic acid. As the solid acids were not completely soluble at 28° C, the dilution shift curves are not complete for these acids. Monochloroacetic acid is soluble to about 10 mole% and the dilution shift curve is coincident as far as it goes with dichloroacetic acid. Trichloroacetic acid shows distinct behavior (see curve 2) in dilute solution but, between 8 mole% acid and the solubility limit, 20 mole%, the dilution shift curve is the same as that for the other chloroacetic acids. All dilution chemical shifts except that for trimethyl acetic acid showed a low-field movement with decreasing acid concentration. The change in chemical shift to low-field ranges from 19 cycles in dichloroacetic to 9 cycles in trifluoroacetic. Figure 1 also shows the carboxyl proton resonance in trifluoroacetic acid as a function of concentration in *n*-methyl formamide (curve 7), and the dilute regions are continued and shown as curve 7 in Fig. 2. In even more dilute solutions, the carboxyl proton in this system is found at -170 c.p.s. in 3.00 mole% solution compared to the proton resonance in cycloC_6H_{12}. This constitutes a shift of 320 c.p.s. (8 p.p.m.) from the chemical shift of the same proton in a 50:50 mole mixture with N-methyl formamide (Fig. 1). The N-methyl peak is a doublet in the amide because of indirect spin–spin coupling with the N-proton; and the other peak in the spectra of these mixtures corresponded to the aldehyde proton (16). Significant changes in chemical shift were obtained in the chemical shift of these protons; this is shown in an inset of Fig. 2(*b* and *c*). The chemical shift scale is the same but the concentration axis is halved in length for the same concentration change. Figure 2 also shows the dilution chemical shifts for three acids in 1,2-dichloroethane. Figure 3 shows a comparison of the dilution chemical shifts for the acid proton in acetic and trifluoroacetic acid dissolved in N-methyl and N,N-dimethyl formamide.

The infrared spectra of the —OH stretching region was investigated for CCl_3COOH and CF_3COOH in various solvents and in the vapor phase. The spectra for CCl_3COOH are shown in Fig. 4(*a*) and those for CF_3COOH are shown in Fig. 4(*b*). The frequency shifts from the vapor phase monomer frequency are shown in Table I together with values of the half widths of the single peak and details of concentration. In addition to these, reliable values for the vapor phase frequency from the literature (25, 26) for the —OH stretching in monomeric acetic and formic acid are shown, and the value for this frequency for iodoacetic acid in CCl_4 is also measured and quoted in this work. Spectra were recorded on a Perkin–Elmer 21 double-beam spectrometer with sodium chloride optics on the normal automatic 927 program. The wavelength calibration was carefully performed with the water vapor spectrum in this same region. Wave numbers quoted are accurate to ± 2 cm^{-1}. Solution spectra were taken using balanced 0.1-mm cells or a

Can. J. Chem. Downloaded from www.nrcresearchpress.com by 210.87.254.40 on 09/05/12
For personal use only.

Can. J. Chem. Downloaded from www.nrcresearchpress.com by 210.87.254.40 on 09/05/12
For personal use only.

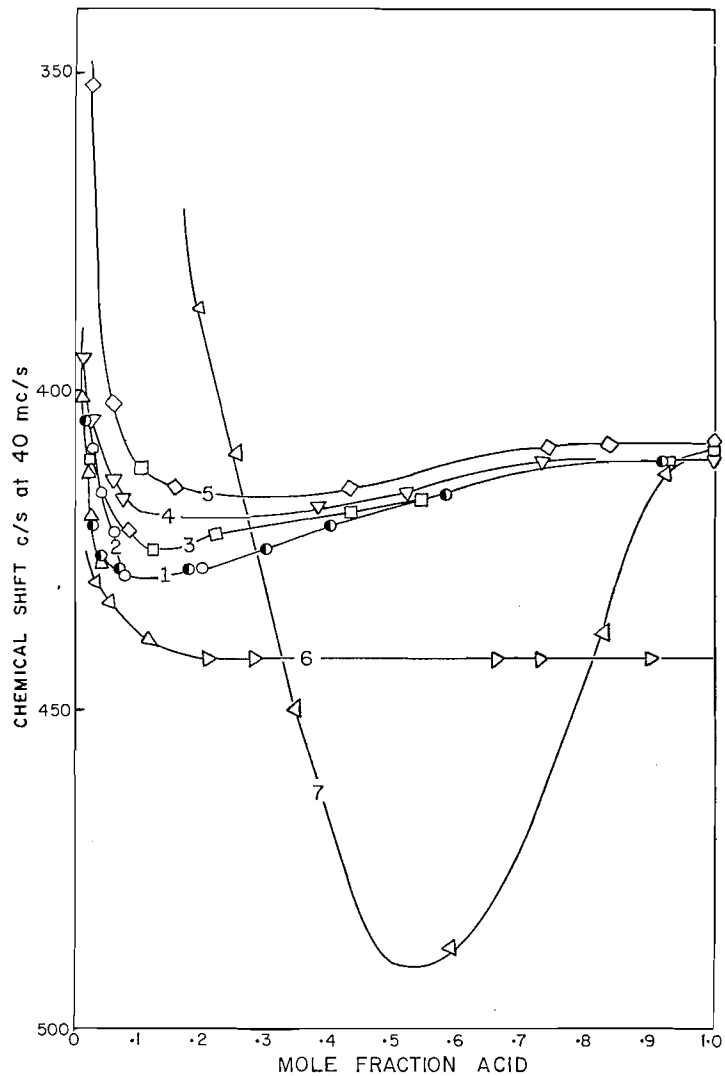


FIG. 1. Dilution chemical shifts of acids in 99.5 mole% CCl_4 and 0.5 mole% cycloC_6H_{12} as solvent: ○ CCl_3COOH (curve 2); ◐ $CHCl_2CO.OH$ (curve 1); △ $CH_2ClCO.OH$ (curve 1); □ $CH_3.CH.Cl.CO.OH$ (curve 3); ▽ $CH_3CHBr.CO.OH$ (curve 4); ◇ CF_3COOH (curve 5); ▷ $C.(CH_3)_3.CO.OH$ (curve 6). Curve 7 shows changes in chemical shift of the carboxyl proton of $CF_3.CO.OH$ as a function of concentration in N-methyl formamide. In all cases, chemical shifts are referred to an internal cyclohexane reference.

3-mm cell with a variable-length cell for balancing solvent absorptions. No solvent had a seriously large absorption at exactly the region required for accurate wave-number measurements on the acids. The vapor spectrum of CF_3COOH was obtained by using a 10-cm gas cell which was equilibrated with liquid CF_3COOH under vacuum conditions at 25° C, and the vapor obtained in the cell was expanded into a volume about 3 times the volume of the cell. The cell was closed off and spectra run using two blank sodium chloride windows of the same thickness as those in the gas cell in the compensating beam. The spectrum of CCl_3COOH vapor at 25° C was obtained using a 5-meter compensated gas

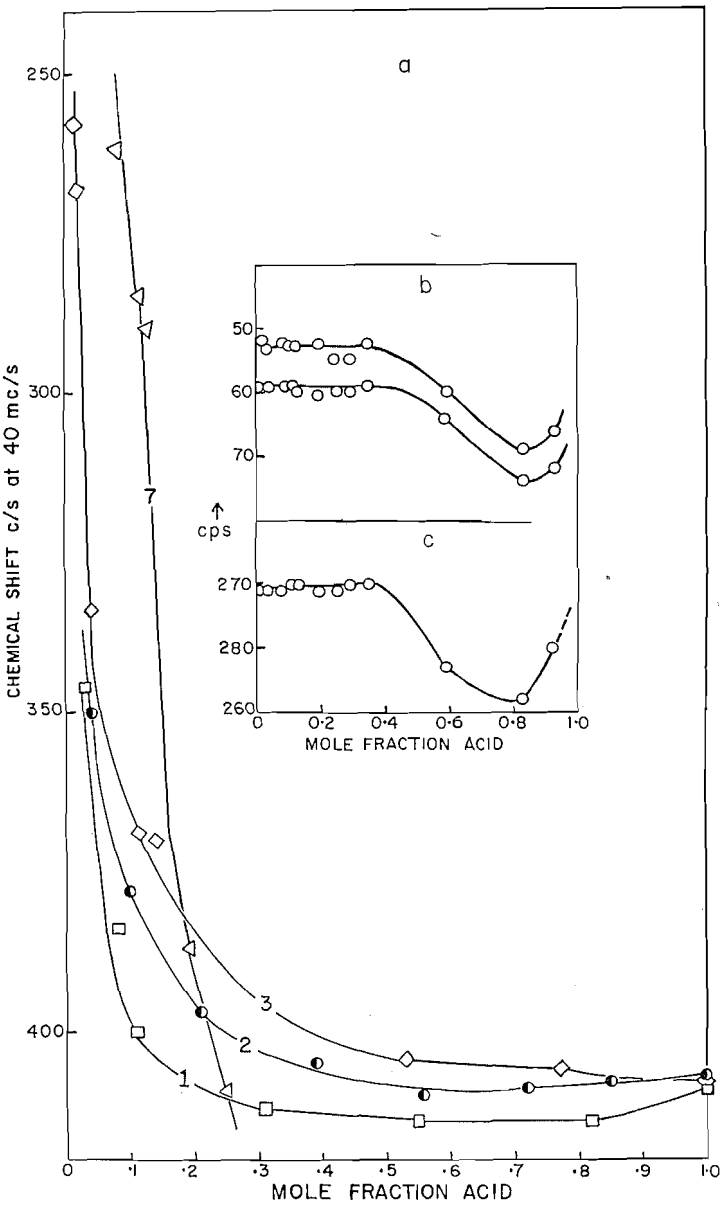


FIG. 2. (*a*) Dilution chemical shifts of acids in 1,2-dichloroethane: ◐ $CHCl_2CO.OH$ (curve 2); □ $CH_3CHClCO.OH$ (curve 1); ◇ $CF_3CO.OH$ (curve 3). The dilute region for carboxyl protons in the $CF_3CO.OH$ – N-methyl formamide system appears as curve 7, a continuation of the same curve in Fig. 1.
(*b*) Dilution shifts of methyl doublet of N-methyl formamide in $CF_3CO.OH$ system.
(*c*) Dilution shifts of aldehyde proton in N-methyl formamide in $CF_3CO.OH$ system.

cell. Dry nitrogen flowed through CCl_3COOH which had been recrystallized from chloroform in a dry atmosphere and stored in a desiccator; the vapor of the acid was carried through a Perkin–Elmer 5-meter gas cell and recorded with the Perkin–Elmer 21 spectrometer.*

**The author is greatly indebted to Dr. R. H. Wright of the B.C. Research Council for performing this experiment, using the 5-meter gas cell.*

Can. J. Chem. Downloaded from www.nrcresearchpress.com by 210.87.254.40 on 09/05/12
For personal use only.

Can. J. Chem. Downloaded from www.nrcresearchpress.com by 210.87.254.40 on 09/05/12
For personal use only.

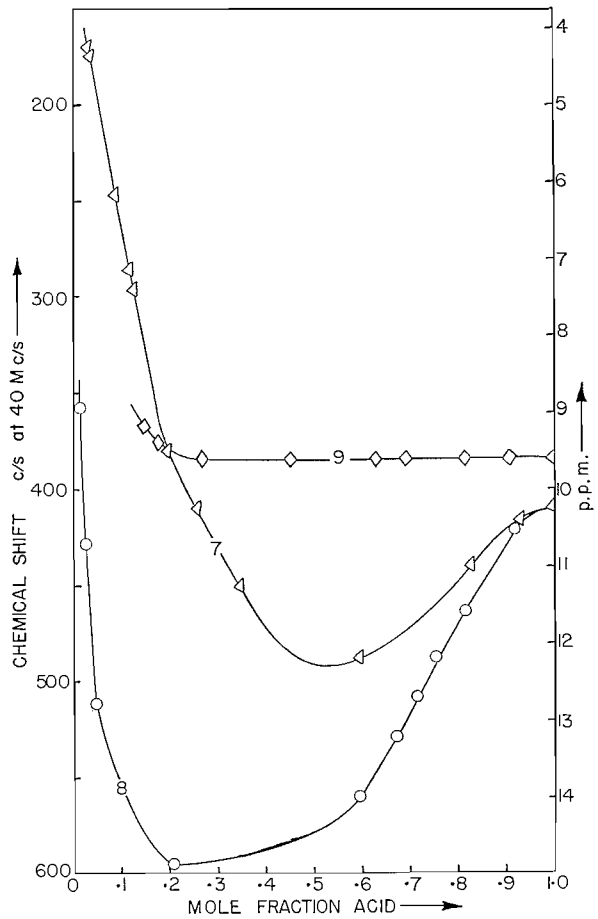


FIG. 3. Dilution chemical shifts for the acid proton in $CH_3CO.OH$ and $CF_3CO.OH$ in amide solvents: CF_3COOH in N-methyl formamide (curve 7); CF_3COOH in N,N-dimethyl formamide (curve 8); $CH_3CO.OH$ in N,N-dimethyl formamide (curve 9).

TABLE I

Hydroxyl stretching frequencies in simple carboxylic acids for the monomer molecules

Mole fraction concentration	Solvent	Acid	Hydroxyl stretching frequencies (cm^{-1})		
			$\Delta\nu_{\frac{1}{2}}$*	ν_{OH}	$\Delta\nu_{vap}$†
4.2×10^{-3}	CCl_4	$CCl_3CO.OH$	6	3490	90
6.4×10^{-4}	CCl_4	$CCl_3CO.OH$	6	3490	90
1.6×10^{-3}	$C_2H_4Cl_2$	$CCl_3CO.OH$	21	3378	202
Vapor	—	$CCl_3CO.OH$	3.5	3580	0
1.7×10^{-2}	$C_2H_4Cl_2$	CF_3COOH	18	3390	180
1.9×10^{-3}	CCl_4	CF_3COOH	6.5	3485	85
2.6×10^{-3}	CCl_4	$CF_3CO.OH$	7.0	3485	85
Vapor spectrum		CF_3COOH	4	3570	0
Vapor	—	CH_3COOH (21)	—	3577	
Vapor	—	HCOOH (22)	—	3567	
Vapor	—	DCOOH (22)	—	3567	
10^{-2}	CCl_4	CH_2ICOOH	—	3505	

*Half width of monomer O—H absorption.
†Difference between values of OH in the vapor and in the solvent under study for the particular acid.
NOTE: Other work is referred to the tabulation of literature at the end of the paper.

Can. J. Chem. Downloaded from www.nrcresearchpress.com by 210.87.254.40 on 09/05/12
For personal use only.

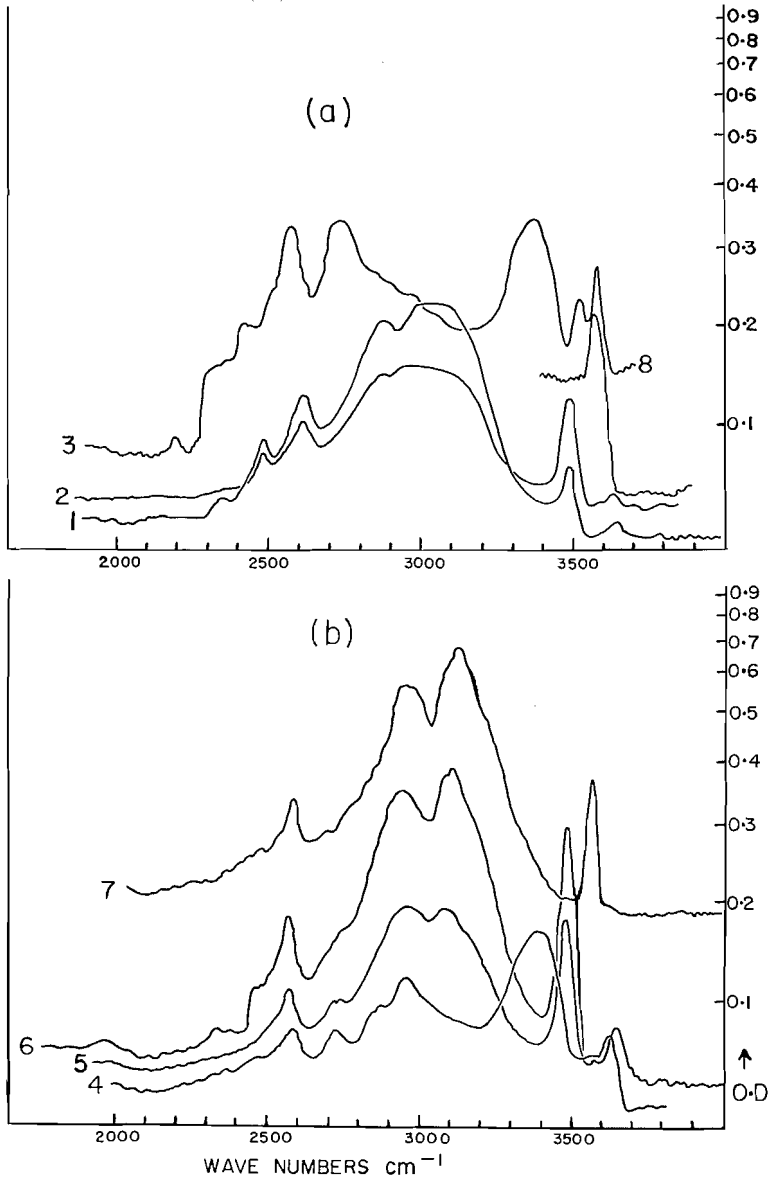


FIG. 4. (*a*) Infrared spectra of the —O—H stretching region for CCl_3COOH. Curves are identified by numbers: (1) 4.2×10^{-3} mole fraction in CCl_4, 0.1-mm cell; (2) 6.4×10^{-4} mole fraction in CCl_4, 3.0-mm cell; (3) 1.4×10^{-3} mole fraction in 1,2-dichloroethane, 3-mm cell; (8) vapor spectrum CCl_3COOH at 35° C, 5-m gas cell.

(*b*) Infrared spectra of —O—H stretching region for $CF_3CO.OH$. Curves are identified by numbers: (4) 1.7×10^{-2} mole fraction in 1,2-dichloroethane, 0.1-mm, cell; (5) 1.904×10^{-3} mole fraction in CCl_4, 3.0-mm cell; (6) 2.9×10^{-3} mole fraction in CCl_4, 3.0-mm cell; (7) vapor spectrum of CF_3COOH at 25° C, 10-cm gas cell.

The —OH monomer stretching frequency occurs in the vapor phase for all acids measured at 3574 ± 6.5 cm^{-1}. The frequency difference from acid to acid is significant but quite small compared to a shift of 85–90 cm^{-1} to the monomer absorption in CCl_4

solution for all acids. An even larger shift of 180–202 cm^{-1} occurs when the acid monomer absorbs in $CH_2Cl—CH_2Cl$ solution. Each of these solvent shifts is accompanied by large changes in the absorption half widths, $\Delta\nu_{\frac{1}{2}}$.

DISCUSSION

Consideration of the Case for Open-chain Hydrogen-bonded Polymers

In Fig. 1, the low-field dilution shift obtained for the acid proton resonance in the following acids: trifluoroacetic, trichloroacetic, dichloroacetic, monochloroacetic, and α-bromo- and α-chloro-proprionic acids, will be interpreted as resulting from the occurrence of open- and polymeric-chain association in equilibrium with the cyclic dimer form of these acids in concentrated solution. The result is similar to that obtained by Reeves and Schneider (15) with acetic acid solutions although not similar to the curves obtained for the acids C_3 to C_{17} (13).

The polymeric hydrogen-bonded form of acetic acid in solution suggested by dielectric measurements (23, 28), Raman spectra (19), and nuclear magnetic resonance (15) is probably related to the polymeric form in the crystal of acetic acid (18). The order introduced by cyclic or chainlike polymers in solution as opposed to cyclic dimer formation must be compensated by an increased strength of the individual hydrogen bonds. The occurrence of proton resonance at higher field for the carboxyl proton and the fact that the hydrogen bonds are individually stronger can only be reconciled by chainlike polymerization as opposed to a cyclic structure.

The proton resonance occurs at higher field because a chainlike structure involves one terminal acetic acid molecule which has one non-hydrogen-bonded proton. It is possible that the rapid averaging of the proton shielding gives rise to a net displacement to high field for the acid proton. In Table II, the chemical shifts relative to water of various O—H - - - O hydrogen bonds is given together with the O—H - - - O distance where data is available. It can be seen from this table that there is good correlation between the

TABLE II

Comparison of chemical shifts in O—H - - - O hydrogen-bonding systems and bond distances when available

Compound	Concentration dependent?	Chemical shift, H_2O, p.p.m.	O—H - - - O distance in crystal, Å	Reference to chemical shifts
Pure acetic acid	Yes	−6.8	—	15
Pure substituted acetic acids	Yes	−6.9	—	Present work
Pure C_3–C_{10} acids	No	−7.2	—	13
Pure trimethyl acetic acid	No	−7.5	—	Present work
$CF_3CO.OH$ – N-methyl formamide 1:1 complex	Yes	−8.7	—	Present work
Calculated acetic acid dimer shift from K_{dimer}	No	−9.7	2.76+	24
Acetylacetone-enol form	No	−10.0	—	12
Calculated benzoic acid dimer shift	No	−10.25	2.64+	24
$CF_3CO.OH$–N,N-dimethyl formamide, lowest field position acid proton	Yes	−12.0	—	Present work
Triacetylmethane-enol form	No	−12.6	—	25
Potassium hydrogen maleate	No	−15.4		26
Sodium hydrogen maleate	No	−15.03	2.41+ to 2.43	26
Potassium hydrogen phthalate	No	−15.15		26

NOTE: Uncertainties of ±0.2 p.p.m. exist in any given chemical shift due to varying referencing procedures. "+" bond distances obtained from reference 20.

Can. J. Chem. Downloaded from www.nrcresearchpress.com by 210.87.254.40 on 09/05/12
For personal use only.

hydrogen-bond strength and the paramagnetic chemical shift of the hydrogen-bonded proton. This supports the suggestions of Pople and Marshall (31) that the strongest hydrogen bonds have the largest negative chemical shifts, and the experimental measurements of Reeves, Allan, and Strømme (14, 27).

The suggestions of Pitzer and Davis (24) that the reduction of the O—O distance across the hydrogen bond eventually causes increased shielding due to electrons of the noncovalently bonded oxygen is not experimentally proved. The only explanation therefore of the low-field shift on dilution of some carboxylic acids is the occurrence of chainlike polymers.

The careful experimental work of Pitzer and Davis (24) warrants some discussion since the calculated dimer chemical shift in their work lies considerably to low field with respect to the dimer shifts assumed in the work of Reeves and Schneider (15) and, later, Reeves (13). The occurrence of abnormally large variations of monomer chemical shift with temperature (24) using equilibrium constants obtained from infrared measurements and the extremely large absolute magnitude of the monomer–dimer chemical shifts must reflect some uncertainty in either the equilibrium constants used or the basic assumptions that only monomers and cyclic dimers exist at the concentrations studied. A variation of 400 cycles in chemical shift due to a neighboring ring current effect (24) over an 80° C range is almost one order of magnitude too large (5). Even when the equilibrium constants are adjusted so as to obtain constant values of δ_{monomer} and δ_{dimer} with temperature, the uncertainty about the existence of open dimers, trimers, or higher polymers renders this adjustment of the value of δ_{monomer} somewhat artificial. Recent dielectric measurements (28) suggest the existence of polymers of the open-chain type in concentrated solutions of *n*-caproic and cyclohexane carboxylic acid in nonpolar solvents. The complicated question of species present in nonpolar solutions of long-chain acids is not resolved but in acetic acid and the substituted acetic acids measured here, the occurrence of open-chain polymers is indicated.

Association of the Monomer Form of Carboxylic Acids with Solvents

A weak hydrogen-bond acceptor such as chloroform forms hydrogen-bonded complexes with donor solvents such as acetone (4) and even with weak donor systems such as benzene or olefins (5). It is to be expected that a much stronger acceptor such as the acid proton of the monomer form of carboxylic acids will form a stronger hydrogen-bond association than chloroform, with the same donor solvents. The position of the monomer acid proton chemical shift is shown to be strongly temperature dependent in the work of Pitzer and Davis (24) but the calculated position of the signal is subject to large systematic errors. The interpretation suggested by several workers (13, 15, 17) that the monomer form appears in solutions of higher dielectric constant merely because of the higher dipole moment of the monomer is not entirely true. Recent work on the infrared spectra of solute molecules has shown conclusively that spectral shifts can be associated with specific association with a solvent molecule through a hydrogen bond (30, 29). The figures in Table I are evidence for the specific association of the acid monomers with solvent molecules on this basis. The frequency shift of the monomer —O—H stretching frequency between the vapor phase and essentially infinite dilution in CCl_4 is about 80–90 cm^{-1}. This is too large to be accounted for on the basis of dispersion forces alone. At the same time the half width of the single line observed increases markedly between the vapor and the solution as seen from Table I. The frequency shift and increase in

Can. J. Chem. Downloaded from www.nrcresearchpress.com by 210.87.254.40 on 09/05/12
For personal use only.

half width of the monomer —O—H absorption is much more marked in 1,2-dichloroethane (Fig. 4 and Table I), indicating a stronger hydrogen-bonded complex with the monomer in this case. The frequency shift of the monomer absorption in the vapor phase amongst a series of acids is quite small, ± 6.5 cm^{-1}, compared with the change between vapor and solvent. The variation of monomer absorption frequency in CCl_4 amongst three acids measured (Table I) is also quite small. The weak hydrogen-bond association of carbon tetrachloride with carboxylic acid monomers is to be expected since this molecule is a very weak donor.

The dimer band is considerably more intense than the monomer even at the concentrations studied, but an intensification factor of 37× on dimer formation suggested by Pimentel and McClellan (32, Table 3-VIII) indicates that little dimer is present.

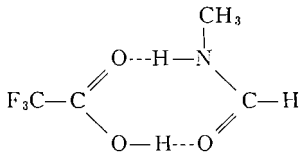
The Chemical Shift Changes in 1,2-Dichloroethane

The dilution chemical shifts of three acids in 1,2-dichloromethane indicate that the polymeric hydrogen-bonded forms and the dimer form are dissociated appreciably at much higher acid concentrations. The situation at infinite dilution of acid will correspond to some kind of hydrogen-bonded complex between the acid monomer and dichloromethane. The behavior of the substituted acids in this solvent is very similar to that reported previously for other carboxylic acids in dichloroethane, acetone, and acetonitrile. The dissociation at higher concentrations of acid is encouraged in a solvent of higher dielectric constant.

The Behavior of Carboxylic Acids in Basic Solvents

The changes in chemical shift of the acid proton of trifluoroacetic acid in N-methyl and N,N-dimethyl formamide (Figs. 1, 2, and 3) are of some interest since the low-field extremes of these shifts are quite remarkable. Such a low-field shift is consistent only with the formation of a very strong hydrogen bond. There is considerable heat evolution on making up the solutions, which is not usually detectable when there is a change in the strength and number of hydrogen bonds formed.

The formation of a stronger hydrogen bond in a 1:1 complex could conceivably occur between trifluoroacetic acid and N-methyl formamide in a configuration similar to an acid dimer, as shown below.



This particular form of a 1:1 complex depends on the existence of both donor and acceptor ends of the hydrogen bond in the correct spatial arrangement on the amide molecule. This is excluded in N,N-dimethyl formamide but the extreme low-field chemical shift of the acid proton becomes greater in these solutions as shown in Fig. 3. The form of the 1:1 complex above is not therefore the cause of this extreme low-field shift.

The form of these dilution chemical shift curves are explicable in terms of proton transfer to the amide.

$$CF_3CO.OH + NMe_2CHO \rightleftharpoons CF_3COO^- + NMe_2CH_2O^+$$

The strength of trifluoroacetic acid is sufficient to cause proton transfer to the amide,

Can. J. Chem. Downloaded from www.nrcresearchpress.com by 210.87.254.40 on 09/05/12
For personal use only.

although in such concentrated solutions the medium effects prohibit quantitative prediction of the extent of protonation. The addition of amide to the acid causes the chemical shift of the acid proton to move to low field. This can be explained in terms of the protonation of almost all amide molecules and the formation of a very strong hydrogen bond between the conjugate acid of the amide and the trifluoroacetate anion. This is equivalent to the formation of ion pairs in moderately concentrated solution. The chemical shift of the acid proton observed is an average of the various environments since rapid proton exchange is evident from the single sharp line observed. In a 1:1 mole ratio of acid to amide it is expected that almost all the molecules present are involved in ion-pair formation. Addition of further amide will raise the dielectric constant of the solution and cause dissociation of the ion pairs. The breaking of the strong hydrogen bond in the ion pairs in dilute solution causes the very large chemical shift change in the high-field direction. The nature of the amide conjugate acid is not indicated by these results.

The dilution chemical shift of acetic acid in the N,N-dimethyl formamide is quite small and not detectable until dilute acid solutions. The strength of acetic acid is much smaller so it is expected that protonation of the amide is inappreciable.

The chemical shift in dilute solutions of acetic acid in N,N-dimethyl formamide is not measurable (~15 mole% acid) because of broadening of the acid proton resonance below noise level. This is indicative of proton exchange in the critical region for n.m.r. measurements (7). Further studies of these processes are being made.

ACKNOWLEDGMENTS

The author is indebted to Dr. Ross Stewart for discussions, Dr. W. G. Schneider in correspondence, and the Petroleum Research Fund of the American Chemical Society and the Research Corporation for financial support of this research.

REFERENCES

1. J. T. Arnold and H. G. Packard. J. Chem. Phys. **19**, 1608 (1951).
2. U. Liddel and N. F. Ramsey. J. Chem. Phys. **19**, 1601 (1951).
3. W. G. Schneider, H. J. Bernstein, and J. A. Pople. J. Chem. Phys. **28**, 601 (1958).
4. G. Korinek and W. G. Schneider. Can. J. Chem. **35**, 1157 (1957).
5. L. W. Reeves and W. G. Schneider. Can. J. Chem. **35**, 251 (1957).
6. T. Schaefer and W. G. Schneider. J. Chem. Phys. **32**, 1218, 1224 (1960).
7. H. S. Gutowsky and A. Saika. J. Chem. Phys. **21**, 1688 (1956).
8. E. D. Becker, U. Liddel, and J. N. Shoolery. J. Mol. Spectroscopy, **2**, 1 (1958).
9. E. D. Becker. J. Chem. Phys. **31**, 269 (1959).
10. M. Saunders and J. B. Hyne. J. Chem. Phys. **31**, 270 (1959).
11. C. Reid and T. M. Connor. Private communication.
12. L. W. Reeves. Can. J. Chem. **35**, 1351 (1957).
13. L. W. Reeves. Trans. Faraday Soc. **55**, 1684 (1959).
14. L. W. Reeves. Can. J. Chem. **38**, 748 (1960).
15. L. W. Reeves and W. G. Schneider. Trans. Faraday Soc. **54**, 314 (1958).
16. A. Berger, A. Loewenstein, and S. Meiboom. J. Am. Chem. Soc. **81**, 62 (1959).
17. G. Allen and E. F. Caldin. Quart. Revs. (London), **7**, 255 (1953).
18. R. E. Jones and D. H. Templeton. Acta Cryst. **11**, 484 (1958).
19. M. I. Batueev. Compt. rend. acad. sci. U.R.S.S. **52**, 401 (1946).
20. Interatomic Distances. Chem. Soc. (London), Spec. Publ. No. 11 (1958).
21. J. K. Wilmshurst. J. Chem. Phys. **25**, 1171 (1956).
22. J. K. Wilmshurst. J. Chem. Phys. **25**, 478 (1958).
23. R. J. W. Le Fevre and H. Vine. J. Chem. Soc. 1795 (1938).
24. J. C. Davis and K. S. Pitzer. J. Phys. Chem. **61**, 886 (1960).
25. S. Forsen and M. Nilsonn. Acta Chem. Scand. **13**, 1383 (1959).
26. S. Forsen. J. Chem. Phys. **31**, 852 (1959).
27. L. W. Reeves, E. A. Allan, and K. O. Strømme. Can. J. Chem. **38**, 748 (1960).
28. G. Loveluck. J. Phys. Chem. **64**, 385 (1960).
29. L. J. Bellamy, H. E. Hallam, and R. L. Williams. Trans. Faraday Soc. **54**, 1120 (1958).
30. G. L. Caldow and R. W. Thompson. Proc. Roy. Soc. (London), A, **254**, 1 (1960).
31. J. A. Pople and T. W. Marshall. Mol. Phys. **1**, 199 (1958).
32. G. C. Pimentel and A. L. McClellan. The hydrogen bond. W. H. Freeman Co. 1960. p. 102.

Can. J. Chem. Downloaded from www.nrcresearchpress.com by 210.87.254.40 on 09/05/12
For personal use only.

Can. J. Chem. Downloaded from www.nrcresearchpress.com by 210.87.254.105 on 09/05/12
For personal use only.

NOTES

SAPONINS AND SAPOGENINS

XI. ON THE PRESENCE OF ECHINOCYSTIC ACID AND QUERCETIN IN FLOWERS OF ALBIZZIA LEBBEK BENTH.*

I. P. VARSHNEY AND MOHD. S. Y. KHAN

Seeds of *Albizzia lebbek* Benth. from Utter Pradesh have previously been reported to yield saponin from which oleanolic acid and echinocystic acid have been obtained (1), while the complete beans of *A. lebbek* Benth. from Bengal yield, in addition to these two acids, another isomer of echinocystic acid named albigenic acid (2). Another species, *Albizzia anthelmintica* (3), yields echinocystic acid alone. *Albizzia procera* from Madhya Pradesh (4) and *Albizzia odoratissima* seeds from Maharashtra (5) yield machaerinic acid.

Although much work has been done on the seeds from various species, no work seems to have been done on the flowers of any of the species of *Albizzia* and therefore the work on the flowers of *A. lebbek* Benth. was undertaken.

The flowers of *A. lebbek* Benth., collected locally from the university campus, yielded, by alcoholic extraction and subsequent treatment, a colorless hygroscopic powder giving all the tests for saponins. The sulphuric acid hydrolysis of the saponin gave the sapogenin (acid), m.p. 297–301°. It gave a diacetate, m.p. 257–262°, and diacetyl methyl ester, m.p. 201–202°. It is a pentacyclic triterpenic acid belonging to the β-amyrin group and has been identified as echinocystic acid ($3\beta,16\alpha$-dihydroxy-Δ^{12}-oleanene-28-oic acid) by mixed melting point with authentic samples of echinocystic acid and derivatives (c.f. echinocystic acid, m.p. 305–312°; acetate, m.p. 272–275°; acetyl methyl ester, m.p. 200–201° (1, 6)). The infrared spectra of the acetyl methyl ester, which is superimposable with that of an authentic sample, confirmed its identity as echinocystic acid.

The flowers also yield an anthoxanthin glycosidic fraction. The product did not crystallize and therefore was hydrolyzed. The aglycone obtained was then chromatographed on filter paper. The chromatogram showed the presence of at least three components quite different from each other. One of the components was identified as quercetin by chromatography with an authentic sample of quercetin.

EXPERIMENTAL

All the melting points recorded have been taken on a Kofler hot microscopical stage and are corrected. The infrared spectra have been taken in these laboratories by one of the authors (I. P. V.) using a Perkin–Elmer spectrometer model 137 (Infracord) in nujol mull.

Saponin and sapogenin.—The flowers (200 g), after being exhausted with light petroleum ether, were extracted with 95% alcohol and the saponin (10.5 g) was obtained as a colorless hygroscopic powder in the usual manner (4). It gave all the tests for saponin, i.e. it foams copiously when shaken with water, is toxic to fishes in dilute concentrations, and haemolyzes red blood corpuscles in dilute solutions (7). The saponin (5 g) was hydrolyzed with sulphuric acid (7%) (4) and the genin obtained (1.5 g) was then transformed into the potassium salt by being refluxed with methyl alcoholic potassium

**Part X. Arch. Pharm. In press.*

hydroxide. The solution of the potassium salt was extracted with ether to remove any neutral sapogenin present. Hydrochloric acid, added to the alkaline solution remaining after ether extraction, precipitated the acid sapogenin, which was filtered, washed free of the acid, and dried.

Acetate.—The genin (200 mg) was acetylated hot, in the usual manner, with pyridine and acetic anhydride. The acetate obtained was crystallized from methyl alcohol as colorless needles, m.p. 257–262° (cf. diacetyl echinocystic acid, m.p. 272–275° (6); 248–249° (1)). The melting point was not depressed when a mixed melting point was taken with an authentic sample of diacetyl echinocystic acid. I.R. spectra: λ_{max}^{nujol} 5.81, 5.90, 8.09 μ.

Genin.—The acetate (100 mg) was deacetylated with methyl alcoholic potassium hydroxide (10%) and the free genin (80 mg) obtained was crystallized from isopropyl alcohol as colorless crystals, m.p. 297–301° (cf. echinocystic acid, m.p. 305–312° (6); 291–293° (1)). No depression was noted when a mixed melting point was taken with an authentic sample of echinocystic acid. I.R. spectra: λ_{max}^{nujol} 2.87, 5.97 μ.

Acetyl methyl ester.—The acetate (100 mg) was methylated with diazomethane and the methyl ester obtained was crystallized from methyl alcohol as colorless fine needles (90 mg) melting at 201–202°. It was found to be identical with acetyl methyl echinocystate as no depression was observed in the mixed melting point with an authentic sample of diacetyl methyl echinocystate and the infrared spectra were identical (cf. echinocystic acid diacetyl methyl ester, m.p. 200–201° (1, 6); I.R. spectra: λ_{max}^{nujol} 5.75, 8.09 μ). I.R. spectra: λ_{max}^{nujol} 5.75, 8.09 μ.

Anthoxanthin glycosides.—The residue obtained after the evaporation of the alcoholic extract was dissolved in water and the solution extracted with *n*-butyl alcohol. The recovery of the butyl alcohol gave a mixture of the saponin and the glycoside. It was dissolved in alcohol, filtered, and then added dropwise into a large volume of acetone to precipitate the saponin. The saponin was filtered off and the acetone solution was evaporated to dryness and then again dissolved in alcohol and reprecipitated with acetone. This operation was repeated twice to remove the saponin completely. The acetone, after the removal of the saponin, was evaporated to dryness and the product obtained gave a salmon-pink coloration with magnesium and hydrochloric acid (8). All attempts to crystallize the glycoside were fruitless.

Aglycone.—The aqueous solution of the glycoside containing a little alcohol was hydrolyzed by refluxing with sulphuric acid (10%) for 3 hours. The aglycone obtained was filtered and washed free of acid. It was dissolved in alcohol and two drops of dilute lead acetate solution added to it precipitated the impurities. It was then filtered and the filtrate was treated with hydrogen sulphide to remove any lead which might have passed into the filtrate. The solution thus obtained was evaporated to dryness under reduced pressure. The product (aglycone) obtained gave acidic cyanidin and Wilson's boric acid tests (8, 9).

Paper chromatography.—The aglycone dissolved in a few drops of alcohol was deposited on Whatman filter paper No. 1 and chromatographed beside an authentic sample of quercetin (L. Light & Co. Ltd., England). An acetic acid:water (60:40) (10) solvent mixture and the ascending technique were used. The chromatogram was run for 16 hours and then dried and sprayed with sodium carbonate solution, ferric chloride solution, or examined under ultraviolet light and ultraviolet light and ammonia (10, 11) vapors. It showed three clear spots, one of which was found to be identical with quercetin. All attempts to crystallize the aglycone failed.

Can. J. Chem. Downloaded from www.nrcresearchpress.com by 210.87.254.105 on 09/05/12
For personal use only.

The authors are thankful to the Council of Scientific and Industrial Research, New Delhi, for the award of a junior research fellowship to one of them (M. S. Y. K.).

1. I. P. VARSHNEY. D.Sc. Thesis, Université de Paris, Paris, France. 1956. CH. SANNIÉ, H. LAPIN, and I. P. VARSHNEY. Bull. soc. chim. France, 1440 (1957).
2. A. K. BARUA and S. P. RAMAN. Tetrahedron, **7**, 19 (1959).
3. R. TSCHESCHE and D. FORSTMANN. Ber. **90**, 2383 (1957).
4. M. O. FAROOQ, I. P. VARSHNEY, and H. HASAN. Arch. Pharm. **292**, 57 (1959); Compt. rend. **246**, 3261 (1958); Current Sci. (India), **27**, 489 (1958).
5. I. P. VARSHNEY and MOHD. S. Y. KHAN. J. Pharm. Sci. In press.
6. I. BERGSTEINSSON and C. R. NOLLER. J. Am. Chem. Soc. **56**, 1403 (1934).
7. CH. SANNIÉ. Exposés ann. biochim. méd. **9**, 175 (1948).
8. Y. ASAHINA and M. INUBUSE. Ber. B, **61**, 1646 (1928).
9. C. W. WILSON. J. Am. Chem. Soc. **61**, 2303 (1939).
10. T. B. GAGE, C. D. DOUGLASS, and S. H. WENDER. Anal. Chem. **23**, 1582 (1951).
11. E. C. BATE-SMITH and R. G. WESTALL. Biochim. et Biophys. Acta, **4**, 427 (1950).

RECEIVED MARCH 6, 1961.
DEPARTMENT OF CHEMISTRY,
MUSLIM UNIVERSITY,
ALIGARH, INDIA.

PREPARATION OF UNDECENOL AND UNDECENYL BROMIDE

D. G. M. DIAPER

Although complex hydrides have revolutionized the preparation of primary alcohols from acids and esters, the Bouveault–Blanc procedure may still be preferable for preparative work on the grounds of expense, especially when catalytic hydrogenation cannot be employed. To prepare undecenol (undec-10-en-1-ol) in quantity (1), sodium–ethanol reduction of ethyl undecylenate (undec-10-enoate) was used. Yields previously reported for this and other Bouveault–Blanc reductions vary widely, and rarely exceed 80%. Smith (2) obtained undecenol in 76% yield by sodium and ethanol reduction and only 30% was obtained (3) in butanol. Poor yields have been attributed to the presence of water, which gives sodium hydroxide, destroying the ester by conversion to the sodium salt, which is not attacked by the reagent. In long-chain ester reductions this concurrent production of the sodium salt of the acid is doubly serious since it not only reduces the yield but complicates isolation of the alcohol which is entrained in the soapy aqueous layer. Intensive drying of the ethanol is the customary solution of this problem—a tedious affair which must be repeated at intervals if the stock of ethanol is exposed to air in intermittent use. Even so, Darzens (4) contends that reaction of the ester with sodium thus,

$$R.COOEt + 2H_2 \rightarrow RCH_2OEt + H_2O, \qquad [1]$$

inevitably produces some water and thus sodium salt. This interpretation implies a stoichiometric equivalence of ethyl ether production, water formation, and ester destruction.

In an attempt to assess the effects of traces of water (such as are removed in an intensive drying operation) upon the reaction, progressive amounts were added to the solvent in successive reductions under standard conditions. The saponification yield was found by titration and the results are represented in Fig. 1, curve A. The first part of the curve is steep, demonstrating that the effect of water upon the saponification reaction is catalytic

Can. J. Chem. Downloaded from www.nrcresearchpress.com by 210.87.254.105 on 09/05/12
For personal use only.

The authors are thankful to the Council of Scientific and Industrial Research, New Delhi, for the award of a junior research fellowship to one of them (M. S. Y. K.).

1. I. P. VARSHNEY. D.Sc. Thesis, Université de Paris, Paris, France. 1956. CH. SANNIÉ, H. LAPIN, and I. P. VARSHNEY. Bull. soc. chim. France, 1440 (1957).
2. A. K. BARUA and S. P. RAMAN. Tetrahedron, **7**, 19 (1959).
3. R. TSCHESCHE and D. FORSTMANN. Ber. **90**, 2383 (1957).
4. M. O. FAROOQ, I. P. VARSHNEY, and H. HASAN. Arch. Pharm. **292**, 57 (1959); Compt. rend. **246**, 3261 (1958); Current Sci. (India), **27**, 489 (1958).
5. I. P. VARSHNEY and MOHD. S. Y. KHAN. J. Pharm. Sci. In press.
6. I. BERGSTEINSSON and C. R. NOLLER. J. Am. Chem. Soc. **56**, 1403 (1934).
7. CH. SANNIÉ. Exposés ann. biochim. méd. **9**, 175 (1948).
8. Y. ASAHINA and M. INUBUSE. Ber. B, **61**, 1646 (1928).
9. C. W. WILSON. J. Am. Chem. Soc. **61**, 2303 (1939).
10. T. B. GAGE, C. D. DOUGLASS, and S. H. WENDER. Anal. Chem. **23**, 1582 (1951).
11. E. C. BATE-SMITH and R. G. WESTALL. Biochim. et Biophys. Acta, **4**, 427 (1950).

RECEIVED MARCH 6, 1961.
DEPARTMENT OF CHEMISTRY,
MUSLIM UNIVERSITY,
ALIGARH, INDIA.

PREPARATION OF UNDECENOL AND UNDECENYL BROMIDE

D. G. M. DIAPER

Although complex hydrides have revolutionized the preparation of primary alcohols from acids and esters, the Bouveault–Blanc procedure may still be preferable for preparative work on the grounds of expense, especially when catalytic hydrogenation cannot be employed. To prepare undecenol (undec-10-en-1-ol) in quantity (1), sodium–ethanol reduction of ethyl undecylenate (undec-10-enoate) was used. Yields previously reported for this and other Bouveault–Blanc reductions vary widely, and rarely exceed 80%. Smith (2) obtained undecenol in 76% yield by sodium and ethanol reduction and only 30% was obtained (3) in butanol. Poor yields have been attributed to the presence of water, which gives sodium hydroxide, destroying the ester by conversion to the sodium salt, which is not attacked by the reagent. In long-chain ester reductions this concurrent production of the sodium salt of the acid is doubly serious since it not only reduces the yield but complicates isolation of the alcohol which is entrained in the soapy aqueous layer. Intensive drying of the ethanol is the customary solution of this problem—a tedious affair which must be repeated at intervals if the stock of ethanol is exposed to air in intermittent use. Even so, Darzens (4) contends that reaction of the ester with sodium thus,

$$R.COOEt + 2H_2 \rightarrow RCH_2OEt + H_2O, \qquad [1]$$

inevitably produces some water and thus sodium salt. This interpretation implies a stoichiometric equivalence of ethyl ether production, water formation, and ester destruction.

In an attempt to assess the effects of traces of water (such as are removed in an intensive drying operation) upon the reaction, progressive amounts were added to the solvent in successive reductions under standard conditions. The saponification yield was found by titration and the results are represented in Fig. 1, curve A. The first part of the curve is steep, demonstrating that the effect of water upon the saponification reaction is catalytic

Can. J. Chem. Downloaded from www.nrcresearchpress.com by 210.87.254.105 on 09/05/12
For personal use only.

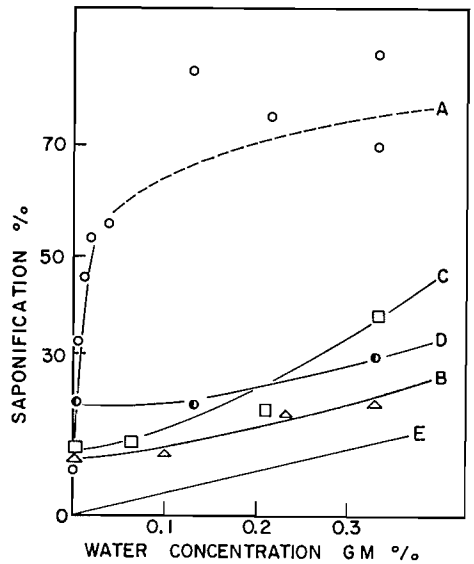


FIG. 1. Saponification of ethyl undecylenate during Bouveault–Blanc reduction as a function of water concentration. Curve A (open circles), ethanol alone; curve B (triangles), ethanol (30 ml) and acetic anhydride (1 ml); curve C (squares), ethanol (30 ml) and acetic acid (0.5 ml); curve D (half-filled circles), ethanol (30 ml) and acetic acid (1 ml); curve E, theoretical saponification yield.

and not stoichiometric. Curve E represents stoichiometric utilization of water in saponification (by calculation). It is suggested that the latter part of curve A (dotted) is indefinite for the following reason. The Bouveault–Blanc reaction is performed extremely rapidly and there must be a competition between two rapid reactions. Reduction probably occurs principally at or near the sodium surface; saponification, in all regions of the ethanol phase. The competition will therefore be controlled by the effective surface area of the molten metal and therefore by the degree of turbulence of the mixture during a brief critical period of time. This condition is hard to control or reproduce.

The use of ammonium chloride (5) and trialkyl borates (6) as additives to suppress saponification in sodium reductions has been advocated. We find that acetic anhydride (curve B, Fig. 1) and acetic acid (curves C and D) have similar effects. Such a result for acetic anhydride is not unexpected, for this reagent can effectively diminish water concentration by conversion to acetic acid. The product, acetate ion in this case, would attack the ester starting material much more slowly than the hydroxide ion. The acetic acid result is more surprising, for it must react with hydroxide ion as follows:

$$OH^- + CH_3.COOH \rightarrow H_2O + CH_3.COO^-. \qquad [2]$$

On this basis, a mole of water is regenerated for a mole of hydroxide ion destroyed. This can react further with sodium giving a mole of hydroxide back again, so the effect of acetic acid is not expected to destroy water or hydroxide but to keep the amounts of these constant in a cyclic process. Possibly the acetic acid functions, with its ion, as a buffer, diminishing hydroxide concentration during the early critical part of the reaction. An increased acetic acid concentration (curve D, compare C) actually leads to a poorer result with traces of water. This is attributed to precipitation of sodium salts on the sodium surface, hindering migration of ester to the site of reduction and exposing it for a relatively longer time to saponification.

Can. J. Chem. Downloaded from www.nrcresearchpress.com by 210.87.254.105 on 09/05/12
For personal use only.

The Darzens hypothesis (equation [1]) would require that the crude undecenol should contain some of its ethyl ether as an impurity. It was found that a single peak was obtained in gas chromatographic analysis and it was shown that an authentic sample of 1-ethoxy-10-undecene can be separated from undecenol under the conditions employed. To prepare the ether, undecenyl bromide was made by an improved method which incorporates removal of starting material (which boils close to the product) as acidic phosphate esters.

While the evidence now available confirms catalytic rather than stoichiometric participation of water and rules out significant formation of ethyl ether as a side reaction, it sheds little light on the mechanism of the reduction process. It is demonstrated, however, that the necessity for "super-dry" ethanol as a solvent in this instance may be avoided.

EXPERIMENTAL

Undecenol—Preparative Method

Ethyl undecylenate (46 g, 0.22 mole, n_D^{20} 1.4390) was mixed with ethanol (200 ml) which had been drawn from the stock of absolute ethanol without special drying. Acetic acid (3 ml) was added. The solution was poured, as rapidly as possible without loss, down an inclined condenser attached to a flask containing sodium (40 g, 1.7 moles, cut in several large pieces under xylene and melted under nitrogen) and heated in a salt bath at 160°. After the reaction had moderated, the solution was boiled under reflux for 5 minutes in a dry nitrogen atmosphere. A steam inlet was then quickly attached and the bulk of the ethanol was removed by steam distillation while the unreacted sodium was simultaneously destroyed. It is important that air is not allowed to enter the system until all the sodium has been destroyed. The residual liquid was extracted with ether, washed once with water, and dried. Upon distillation, undecenol was obtained in three runs of similar scale in yields of 78, 84, and 82%, b.p. 134–139° at 12 mm. Scale-up to 100 g of ester diminished this to 74%. The discrepancy between these yields and those indicated in Fig. 1, curve C, may be due to scale-up or distillation loss. The undecenol in each case gave a single peak in gas chromatographic analysis as described below.

Undecenol—Estimation of Concurrent Saponification

A 500-ml three-necked flask was fitted with an inlet tube for dry nitrogen, a large-liquid-capacity Allihn condenser, arranged for reflux somewhat inclined from the vertical, and a stopper. The condenser was capped with a drying tube. All apparatus was standard taper glassware, oven dried at 120° and quickly filled with nitrogen after assembly, while still hot. Sodium metal (approximately 9 g, 0.39 mole) was cut in a single lump, under xylene, with a knife and a large, warm, lightly greased cork borer. It was pressed out of the cork borer directly into the flask while a vigorous stream of nitrogen emerged. The flask was then immersed in a salt bath at 170°. The sodium should melt to give a bright globule with a thin broken black film. There should be no visible pieces of white crust. Dry ethyl undecylenate (10 g, 0.047 mole) was quickly weighed into a flamed flask while still hot, and dry ethanol (30 ml) was siphoned in. The ethanol stock had been dried by the magnesium ethoxide method; it was then collected in hot glassware previously filled with dry nitrogen, and stored in a ground-joint apparatus fitted with a siphon and drying tube. Immediately before being poured onto the sodium, the required additives (acetic acid, water, or acetic anhydride (see Fig. 1)) were added by pipette in the form of freshly prepared ethanol or benzene solutions of accurately known concentration in the

Can. J. Chem. Downloaded from www.nrcresearchpress.com by 210.87.254.105 on 09/05/12
For personal use only.

1–10% range. The nitrogen stream was interrupted while the solution was poured down the condenser and restarted immediately after. A few minutes were allowed to elapse after the reaction subsided and the apparatus was then quickly fitted with a steam inlet, care being taken to avoid ingress of air. When all the sodium had been destroyed, the solution was acidified with sulphuric acid and ice, and continuously extracted with ether. The ether extract was made up to 100 ml with ethanol and an aliquot was neutralized to bromcresol green. Sodium hydroxide (0.0486 *N* in ethanol) was added from a burette in excess, and, after it had been allowed to stand several hours under nitrogen to ensure saponification of ester, the alkali was back-titrated with standard acid. Solvent blank reactions were performed (ethanol, sodium, acetic acid or anhydride, but no ethyl undecylenate), giving titration values within 0.2 ml of the theoretical figures. Curves B, C, and D were plotted using titration values corrected for acetic acid content. All points represent single determinations, except the first point (water concentration = 0) on curve A, which was the mean of a triplicate determination (7.0, 7.6, and 8.3%).

Undecenyl Bromide (11-Bromo-1-undecene)

Conversion of undecenol to the bromide (6) is complicated by the fact that starting material and product boil at nearly the same temperature. The following modification ensures freedom from undecenol. After undecenol (86 g, 0.51 mole) was treated with phosphorus tribromide (50 g, 0.18 mole) in toluene (250 ml) at −5° and then at 90° for 3 hours, toluene was removed under reduced pressure and the solution was diluted with dry ether (150 ml). It was treated with phosphorus pentoxide (two 20-g portions) and next day decanted into 250 ml of 50% aqueous methanol. Ammonia was quickly added until the mixture was alkaline to phenolphthalein and, after it was washed with a similar portion of aqueous methanolic ammonia and with water, the ether solution was dried and distilled, giving 57 g (48%) of undecenyl bromide, b.p. 136–141° at 15 mm, n_D^{20} 1.4638. By vapor phase chromatography in hydrogen at 160 ml/minute and 183° on an Apiezon grease column the bromide came through as a single peak with a retention time of 15.6 minutes. Under similar conditions undecenol had a retention time of 8.4 minutes and a sample of undecenyl bromide, prepared as above but omitting the phosphoric anhydride – ammonia purification, showed two peaks. The infrared absorption spectrum of this sample had a peak in the O—H region, absent from the purified sample.

1-Ethoxy-10-undecene

By condensation of undecenyl bromide with one equivalent of sodium ethoxide in dry ethanol or by condensation of ethyl bromide with one equivalent of sodium undecenoxide in dry benzene, a liquid product was obtained, boiling at 114–115° at 4 mm, n_D^{21} 1.4344. Although it analyzed correctly for $C_{13}H_{26}O$ (found: C 79.1, H 12.9; calc: C 78.8, H 13.1%), the vapor chromatogram (in hydrogen at 160 ml/minute over Apiezon at 220°) showed two peaks at 3.25 and 4.0 minutes. The latter was identified as undecenol by admixture with an authentic sample and accounted for about 5% of the product. The fact that both methods of preparation gave a similar proportion after distillation indicates that an azeotropic mixture is formed. Separation was achieved by column chromatography over alumina and the purified ethoxy undecene gave a single vapor phase chromatograph peak. After distillation it had n_D^{21} 1.4336.

Support for this research was received from Defence Research Board under Grant No. 9530-17 and is gratefully acknowledged.

Can. J. Chem. Downloaded from www.nrcresearchpress.com by 210.87.254.105 on 09/05/12
For personal use only.

1. D. G. M. DIAPER and D. L. MITCHELL. Can. J. Chem. **38**, 1976 (1960).
2. R. ASHTON and J. C. SMITH. J. Chem. Soc. 1308 (1934).
3. T. F. DANKOVA, E. I. GENKIN, and N. A. PREOBRAZHENSKII. J. Gen. Chem. (U.S.S.R.), **15**, 189 (1945).
4. G. DARZENS. Compt. rend. **224**, 570 (1947).
5. P. ANGLARET and L. PALFRAY. Compt. rend. **223**, 205 (1946).
6. C. G. TOMECKO and R. ADAMS. J. Am. Chem. Soc. **49**, 527 (1927).

RECEIVED DECEMBER 5, 1960.
DEPARTMENT OF CHEMISTRY,
ROYAL MILITARY COLLEGE,
KINGSTON, ONTARIO.

Can. J. Chem. Downloaded from www.nrcresearchpress.com by 210.87.254.105 on 09/05/12
For personal use only.

THE CRYSTALLIZATION OF POLYAMINO POLYACETIC ACIDS IN AN ION EXCHANGE MEMBRANE CHAMBER

R. A. KUNTZE

Ethylenediamine tetraacetic acid (EDTA) as represented by the formula $(HOOCCH_2)_2N(CH_2)_nN(CH_2COOH)_2$, where $n = 2$, has received considerable attention because of its ability to form highly stable chelates with a variety of metal ions. It is generally synthesized by condensation of sodium chloracetate and ethylenediamine (1) or by modifications of the Strecker-type synthesis (2). The free acid can be crystallized from the alkaline reaction mixtures by acidification to pH 1.5–2 with a mineral acid.

In the course of an investigation of the properties of polyamino polyacetic acids as inhibitors of the precipitation of calcium salts, the methods of synthesis and crystallization of several acids similar to EDTA were examined. It was found that diethylenetriamine pentaacetic acid (DTPA), with the formula $(HOOCCH_2)_2N(CH_2)_2NCH_2COOH(CH_2)_2$-$N(CH_2COOH)_2$, can be synthesized by both the Strecker-type synthesis and the chloracetate method, although it has been claimed that the latter method cannot be used for this purpose (3). The chloracetate method is preferred since the accompanying impurities are well known, whereas those of the Strecker-type synthesis have not been determined (4).

Attempts to obtain the free acid of DTPA by crystallization from the reaction mixture on acidification with a mineral acid were unsuccessful. Similarly, no success was encountered with crystallization methods used for other polyamino polyacetic acids (5). It is apparently necessary to remove the majority of the sodium ions from the reaction mixture before crystallization can take place.

Subsequently, an ion exchange membrane method was developed which permits crystallization in a simple and efficient manner. The apparatus employed (Fig. 1) was

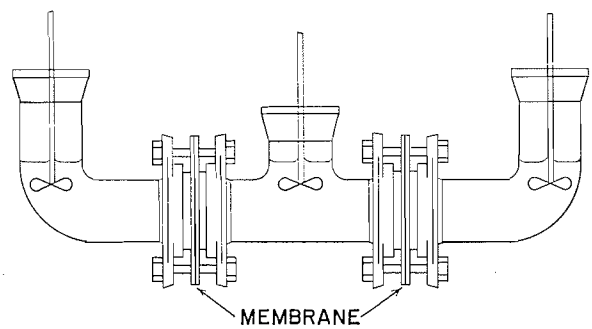


FIG. 1. Ion exchange membrane vessel.

1. D. G. M. DIAPER and D. L. MITCHELL. Can. J. Chem. **38**, 1976 (1960).
2. R. ASHTON and J. C. SMITH. J. Chem. Soc. 1308 (1934).
3. T. F. DANKOVA, E. I. GENKIN, and N. A. PREOBRAZHENSKII. J. Gen. Chem. (U.S.S.R.), **15**, 189 (1945).
4. G. DARZENS. Compt. rend. **224**, 570 (1947).
5. P. ANGLARET and L. PALFRAY. Compt. rend. **223**, 205 (1946).
6. C. G. TOMECKO and R. ADAMS. J. Am. Chem. Soc. **49**, 527 (1927).

RECEIVED DECEMBER 5, 1960.
DEPARTMENT OF CHEMISTRY,
ROYAL MILITARY COLLEGE,
KINGSTON, ONTARIO.

Can. J. Chem. Downloaded from www.nrcresearchpress.com by 210.87.254.42 on 09/05/12
For personal use only.

THE CRYSTALLIZATION OF POLYAMINO POLYACETIC ACIDS IN AN ION EXCHANGE MEMBRANE CHAMBER

R. A. KUNTZE

Ethylenediamine tetraacetic acid (EDTA) as represented by the formula $(HOOCCH_2)_2N(CH_2)_nN(CH_2COOH)_2$, where $n = 2$, has received considerable attention because of its ability to form highly stable chelates with a variety of metal ions. It is generally synthesized by condensation of sodium chloracetate and ethylenediamine (1) or by modifications of the Strecker-type synthesis (2). The free acid can be crystallized from the alkaline reaction mixtures by acidification to pH 1.5–2 with a mineral acid.

In the course of an investigation of the properties of polyamino polyacetic acids as inhibitors of the precipitation of calcium salts, the methods of synthesis and crystallization of several acids similar to EDTA were examined. It was found that diethylenetriamine pentaacetic acid (DTPA), with the formula $(HOOCCH_2)_2N(CH_2)_2NCH_2COOH(CH_2)_2$-$N(CH_2COOH)_2$, can be synthesized by both the Strecker-type synthesis and the chloracetate method, although it has been claimed that the latter method cannot be used for this purpose (3). The chloracetate method is preferred since the accompanying impurities are well known, whereas those of the Strecker-type synthesis have not been determined (4).

Attempts to obtain the free acid of DTPA by crystallization from the reaction mixture on acidification with a mineral acid were unsuccessful. Similarly, no success was encountered with crystallization methods used for other polyamino polyacetic acids (5). It is apparently necessary to remove the majority of the sodium ions from the reaction mixture before crystallization can take place.

Subsequently, an ion exchange membrane method was developed which permits crystallization in a simple and efficient manner. The apparatus employed (Fig. 1) was

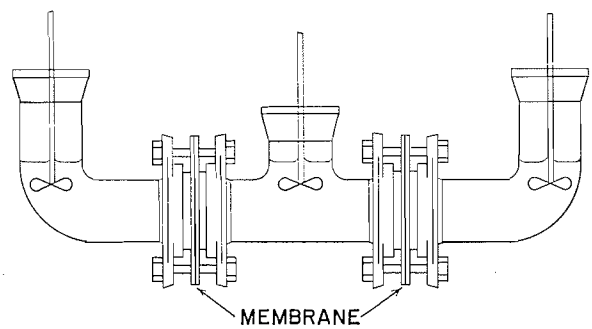


FIG. 1. Ion exchange membrane vessel.

assembled from standard 3-in. glass pipe using two 90° elbows and one T piece. This results in a W-shaped vessel whereby each of the two elbows are on the outside separated from the T piece in the center by a No. 3142 Permutit cation exchange membrane inserted between two polyethylene gaskets. Thus, three compartments in series are formed, the outer two containing dilute hydrochloric acid and the center compartment containing the alkaline reaction mixture. The membranes permit the passage of sodium ions from the center compartments into the outer compartments but prevent migration of chloride, chloracetate, or polyamino polyacetate ions from one compartment into the other. In this way, sodium ions are gradually removed from the reaction mixture, the speed of which depends upon the amount of sodium ions and the strength of the hydrochloric acid solution. For example, if 0.75 liter $N/5$ hydrochloric acid is used in each outer compartment (renewed every 4 hours), and if the concentration of the reaction mixture is adjusted to contain 2.5 mole NaOH, the crystallization of DTPA can be expected to occur within 24 hours. The DTPA obtained in this manner melted with decomposition at 224° C. Calculated for $C_{14}H_{23}O_{10}N_3$: C, 42.75; H, 5.89; N, 10.68%. Found: C, 42.81; H, 5.93; N, 10.63; Cl, <0.05; Na, <0.05%. This crystallization is quantitative, as shown by control experiments, and can be accelerated by renewing the hydrochloric acid solution at shorter intervals and by applying a potential across the compartments.

The higher homologues of EDTA such as trimethylenediamine to hexamethylenediamine tetraacetic acids (n = 3–6) were also prepared by the chloracetate method and crystallized in the ion exchange vessel.

1. F. MÜNZ. U.S. Patent No. 2,130,505 (September 20, 1938).
2. R. SMITH *et al.* J. Org. Chem. **14**, 355 (1949).
3. F. C. BERSWORTH. U.S. Patent No. 2,407,645 (September 17, 1946).
4. R. SMITH. Master's Thesis, Clark University, Worcester, Mass. 1942.
5. G. SCHWARZENBACH *et al.* Helv. Chim. Acta, **31**, 1029 (1948).

RECEIVED APRIL 25, 1961.
DEPARTMENT OF CHEMISTRY,
ONTARIO RESEARCH FOUNDATION,
TORONTO, ONT.

A RECORDING GLASS SPIRAL MANOMETER

F. H. C. EDGECOMBE AND D. A. JARDINE

INTRODUCTION

In a study of the kinetics of a reaction in which a pressure change occurred, it was found necessary to devise a pressure-measuring device which could be used in an atmosphere corrosive to mercury and which would be robust and accurate and able to provide a continuous record of the changing pressure.

METHOD

The glass spoon gauge (1) and its recording counterpart devised by Hooley (2) were not sufficiently robust, when designed, to be sensitive, and hence the stronger glass spiral manometer described by Johnson and McIntosh (3) was modified to make a recording instrument.

In Fig. 1, a schematic representation of the manometer, B and C form the plates of a

Can. J. Chem. Downloaded from www.nrcresearchpress.com by 210.87.254.42 on 09/05/12
For personal use only.

assembled from standard 3-in. glass pipe using two 90° elbows and one T piece. This results in a W-shaped vessel whereby each of the two elbows are on the outside separated from the T piece in the center by a No. 3142 Permutit cation exchange membrane inserted between two polyethylene gaskets. Thus, three compartments in series are formed, the outer two containing dilute hydrochloric acid and the center compartment containing the alkaline reaction mixture. The membranes permit the passage of sodium ions from the center compartments into the outer compartments but prevent migration of chloride, chloracetate, or polyamino polyacetate ions from one compartment into the other. In this way, sodium ions are gradually removed from the reaction mixture, the speed of which depends upon the amount of sodium ions and the strength of the hydrochloric acid solution. For example, if 0.75 liter $N/5$ hydrochloric acid is used in each outer compartment (renewed every 4 hours), and if the concentration of the reaction mixture is adjusted to contain 2.5 mole NaOH, the crystallization of DTPA can be expected to occur within 24 hours. The DTPA obtained in this manner melted with decomposition at 224° C. Calculated for $C_{14}H_{23}O_{10}N_3$: C, 42.75; H, 5.89; N, 10.68%. Found: C, 42.81; H, 5.93; N, 10.63; Cl, <0.05; Na, <0.05%. This crystallization is quantitative, as shown by control experiments, and can be accelerated by renewing the hydrochloric acid solution at shorter intervals and by applying a potential across the compartments.

The higher homologues of EDTA such as trimethylenediamine to hexamethylenediamine tetraacetic acids (n = 3–6) were also prepared by the chloracetate method and crystallized in the ion exchange vessel.

1. F. Münz. U.S. Patent No. 2,130,505 (September 20, 1938).
2. R. Smith *et al.* J. Org. Chem. **14**, 355 (1949).
3. F. C. Bersworth. U.S. Patent No. 2,407,645 (September 17, 1946).
4. R. Smith. Master's Thesis, Clark University, Worcester, Mass. 1942.
5. G. Schwarzenbach *et al.* Helv. Chim. Acta, **31**, 1029 (1948).

Received April 25, 1961.
Department of Chemistry,
Ontario Research Foundation,
Toronto, Ont.

A RECORDING GLASS SPIRAL MANOMETER

F. H. C. Edgecombe and D. A. Jardine

INTRODUCTION

In a study of the kinetics of a reaction in which a pressure change occurred, it was found necessary to devise a pressure-measuring device which could be used in an atmosphere corrosive to mercury and which would be robust and accurate and able to provide a continuous record of the changing pressure.

METHOD

The glass spoon gauge (1) and its recording counterpart devised by Hooley (2) were not sufficiently robust, when designed, to be sensitive, and hence the stronger glass spiral manometer described by Johnson and McIntosh (3) was modified to make a recording instrument.

In Fig. 1, a schematic representation of the manometer, B and C form the plates of a

Can. J. Chem. Downloaded from www.nrcresearchpress.com by 210.87.254.105 on 09/05/12
For personal use only.

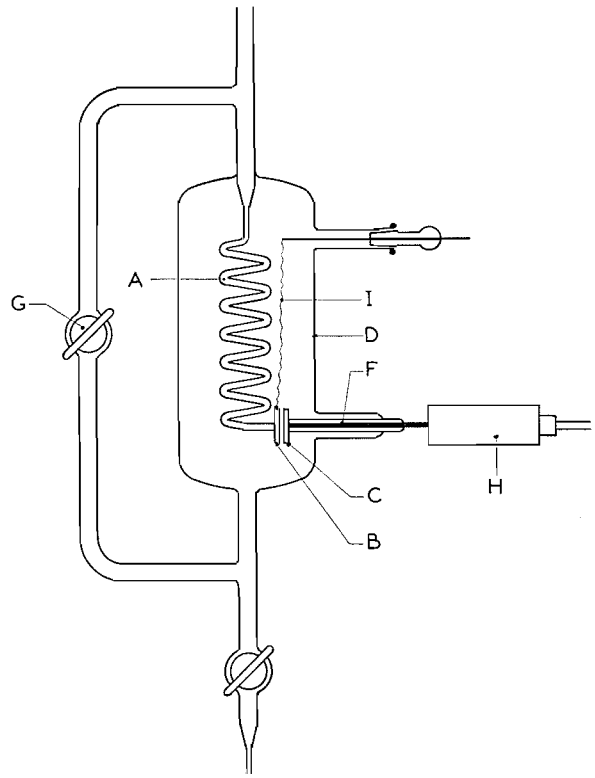


FIG. 1. Schematic diagram of the recording glass spiral manometer.

simple parallel condenser; B, a thin brass plate attached to the glass spiral, is grounded through a wire I. I should be preferably very flexible, e.g. Litz wire, in order to eliminate, so far as possible, drag on the spiral. C is another brass plate attached to a metal rod which, in turn, is sealed in wax to permit adjustment of the distance between the plates. Connected to C through the metal rod is H, the capacitance transducer, obtained from the Decker Corporation of Bala-Cynwyd, Pennsylvania. D is a vacuum-tight glass envelope and G a shorting stopcock through which the envelope may be evacuated when the gauge is used as a differential manometer. The transducer probe, H, is described in detail by Lion (4). Every variation of the gauge capacitor causes a corresponding change in the output voltage of the transducer. In our application of the system the plates C and B of Fig. 1 form the variable capacitance. The voltage output of the transducer is fed through an attenuator to a continuously operating recorder.

The spiral is calibrated by referring the voltage applied to the recorder to the pressure on the spiral, as measured on a mercury manometer by a cathetometer.

PERFORMANCE

The glass spiral used is capable of withstanding the sudden application of a differential pressure of one atmosphere. The sensitivity of such a manometer when used in the system described is very high. By fabrication of thinner spirals, increased sensitivity may be obtained but only at the expense of increasing the "noise level" caused by vibration of the building, which is transmitted to the spiral.

Can. J. Chem. Downloaded from www.nrcresearchpress.com by 210.87.254.105 on 09/05/12
For personal use only.

Over small pressure ranges there exists a linear relationship between pressure applied and output voltage. As the applied pressure increases, the calibration curve becomes hyperbolic in form since the plates no longer approximate a parallel relationship due to increased angular displacement of the spiral. This fact cannot be counted as too great a disadvantage, since once an accurate calibration curve has been obtained it remains valid for a considerable period of time.

The zero drift of the instrument is less than 1% over a period of 24 hours and its stability to ambient temperature changes is sufficient not to require any thermostatic control.

Over a pressure range from 0 to 10 cm of mercury the average voltage output from the transducer is 0.2 v per cm of mercury pressure. When this voltage is applied through an attenuator to a 10-mv, full-scale recorder it is evident that very high sensitivities can be obtained. The usable sensitivity is limited by the noise produced by vibration of the spiral. The maximum noise level is equivalent to 0.05 cm of mercury, and by suitable location and mounting of equipment could be reduced to less than that equivalent to 0.01 cm. The experiments in which we used the spiral manometer did not require pressure measurements of precision greater than 0.05 cm and hence no special mounting of the gauge was necessitated although, on occasion, when heavy motors were operating in the vicinity of the gauge, the noise brought about by building vibration was troublesome.

1. R. G. W. Norrish. J. Chem. Soc. **127**, 2316 (1925).
2. J. G. Hooley. Can. J. Chem. **35**, 1414 (1957).
3. F. M. Johnson and D. McIntosh. J. Am. Chem. Soc. **31**, 1138 (1909).
4. K. S. Lion. Rev. Sci. Instr. **27**, 222 (1956).

Received April 10, 1961.
Du Pont of Canada Limited,
Research Centre,
Kingston, Ontario.

APPLICATION OF THE VARRENTRAPP REACTION TO THE PREPARATION OF LONG-CHAIN DICARBOXYLIC ACIDS

R. G. Ackman, M. A. Bannerman, M. E. Retson, and F. A. Vandenheuvel

Aliphatic dicarboxylic acids with 11 or more carbon atoms were required for gas–liquid chromatographic identification of similar materials produced by ozonolysis of marine-oil fatty acids. Aside from brassylic acid, prepared by oxidative fission of erucic acid, these acids are not conveniently available. As an alternative to individual syntheses, modification of the Varrentrapp reaction (1–4) by limiting it to redistribution of the 13:14 double bond in erucic acid into adjacent positions, followed by oxidative fission and recovery of the dicarboxylic acids, offered a means of obtaining a number of these acids in one preparation.

The product of alkali fusion at 320° C was selected for oxidative fission as the iodine value of 60 indicated that the Varrentrapp reaction proper, production of the saturated acid two carbon atoms shorter than the original monounsaturated acid, had proceeded only to a limited extent. Since double bonds migrating to the 6:7 or 7:8 positions rapidly participate in the final stages of this reaction (2), it was expected that the residual double bonds in the fusion product would be in positions more remote from the carboxyl group.

Can. J. Chem. Downloaded from www.nrcresearchpress.com by 210.87.254.105 on 09/05/12
For personal use only.

Over small pressure ranges there exists a linear relationship between pressure applied and output voltage. As the applied pressure increases, the calibration curve becomes hyperbolic in form since the plates no longer approximate a parallel relationship due to increased angular displacement of the spiral. This fact cannot be counted as too great a disadvantage, since once an accurate calibration curve has been obtained it remains valid for a considerable period of time.

The zero drift of the instrument is less than 1% over a period of 24 hours and its stability to ambient temperature changes is sufficient not to require any thermostatic control.

Over a pressure range from 0 to 10 cm of mercury the average voltage output from the transducer is 0.2 v per cm of mercury pressure. When this voltage is applied through an attenuator to a 10-mv, full-scale recorder it is evident that very high sensitivities can be obtained. The usable sensitivity is limited by the noise produced by vibration of the spiral. The maximum noise level is equivalent to 0.05 cm of mercury, and by suitable location and mounting of equipment could be reduced to less than that equivalent to 0.01 cm. The experiments in which we used the spiral manometer did not require pressure measurements of precision greater than 0.05 cm and hence no special mounting of the gauge was necessitated although, on occasion, when heavy motors were operating in the vicinity of the gauge, the noise brought about by building vibration was troublesome.

1. R. G. W. Norrish. J. Chem. Soc. **127**, 2316 (1925).
2. J. G. Hooley. Can. J. Chem. **35**, 1414 (1957).
3. F. M. Johnson and D. McIntosh. J. Am. Chem. Soc. **31**, 1138 (1909).
4. K. S. Lion. Rev. Sci. Instr. **27**, 222 (1956).

Received April 10, 1961.
Du Pont of Canada Limited,
Research Centre,
Kingston, Ontario.

APPLICATION OF THE VARRENTRAPP REACTION TO THE PREPARATION OF LONG-CHAIN DICARBOXYLIC ACIDS

R. G. Ackman, M. A. Bannerman, M. E. Retson, and F. A. Vandenheuvel

Aliphatic dicarboxylic acids with 11 or more carbon atoms were required for gas–liquid chromatographic identification of similar materials produced by ozonolysis of marine-oil fatty acids. Aside from brassylic acid, prepared by oxidative fission of erucic acid, these acids are not conveniently available. As an alternative to individual syntheses, modification of the Varrentrapp reaction (1–4) by limiting it to redistribution of the 13:14 double bond in erucic acid into adjacent positions, followed by oxidative fission and recovery of the dicarboxylic acids, offered a means of obtaining a number of these acids in one preparation.

The product of alkali fusion at 320° C was selected for oxidative fission as the iodine value of 60 indicated that the Varrentrapp reaction proper, production of the saturated acid two carbon atoms shorter than the original monounsaturated acid, had proceeded only to a limited extent. Since double bonds migrating to the 6:7 or 7:8 positions rapidly participate in the final stages of this reaction (2), it was expected that the residual double bonds in the fusion product would be in positions more remote from the carboxyl group.

Can. J. Chem. Downloaded from www.nrcresearchpress.com by 210.87.254.5 on 09/05/12
For personal use only.

The petroleum-ether-soluble ozonolysis product contained chiefly monocarboxylic acids such as palmitic, stearic, and arachidic, with appreciable amounts of odd-numbered monocarboxylic acids of 11 or fewer carbon atoms. The methanol-soluble ozonolysis product contained approximately 60% of roughly equal amounts of the dicarboxylic acids with 7 to 16 and 17 carbon atoms and 40% of monocarboxylic acids with 7 to 16 carbon atoms (Fig. 1).

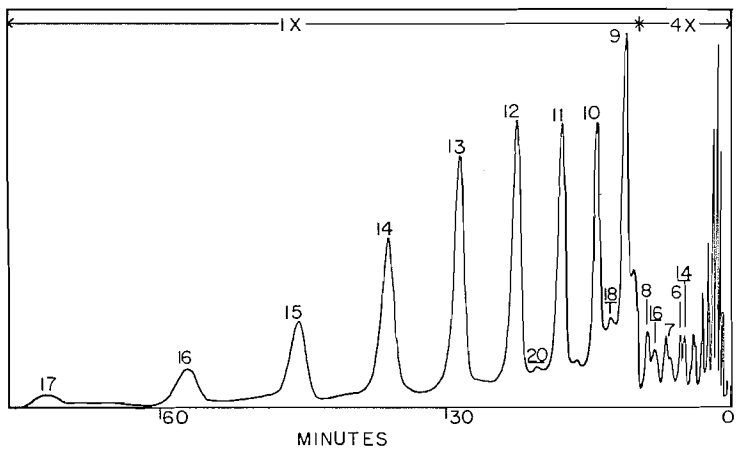


FIG. 1. Gas–liquid chromatogram of methyl esters of dicarboxylic acids. Column, 10 ft×¼ in., packed with 25% LAC-3R-728 on 60–80 mesh Chromosorb. Analysis of 0.005 ml at 200° C with hydrogen carrier gas flowing at 80 ml/minute. Numerals indicate the number of carbon atoms in the acid chains, monocarboxylic acids being underlined.

Since double bonds are increasingly less susceptible to the Varrentrapp reaction when more remote from the carboxyl group, a higher proportion of long-chain dicarboxylic acids with 15 or more carbon atoms could be obtained by prolonged fusion at lower temperatures. The over-all dicarboxylic acid yield would, however, be diminished as a consequence of further completion of the Varrentrapp reaction.

EXPERIMENTAL

A technical erucic acid, iodine value 85, was employed in this reaction. Gas–liquid chromatography indicated a composition of 72.8% erucic acid, 12.4% eicosenoic acid, 6.7% oleic acid, and minor amounts of palmitic, stearic, linoleic, and arachidic acids. Alkali fusions were carried out in a covered iron vessel fitted with a nitrogen inlet and a stirrer of iron pipe. Equal weights of erucic acid, sodium hydroxide, and potassium hydroxide were placed in this vessel, and it was then placed in a Wood's metal bath preheated 40° C above the reaction temperature. The mixture was stirred continuously for ½ hour and intermittently for a further half hour. The cooled reaction mass was dissolved in water, acidified, and the fatty acids extracted with petroleum ether. Weight recoveries were approximately 80%, with iodine values of 38, 60, and 69 from fusions at, respectively, 360, 320, and 300° C for 1 hour. Gas–liquid chromatography indicated almost complete destruction of the oleic, linoleic, and eicosenoic acids, the products thus consisting chiefly of saturated acids and docosenoic acids.

The alkali fusion product of iodine value 60 (5 g) was ozonized in glacial acetic acid and the ozonide decomposed with hydrogen peroxide (2). The final solution was diluted

Can. J. Chem. Downloaded from www.nrcresearchpress.com by 210.87.254.5 on 09/05/12
For personal use only.

to 400 ml with water and extracted with diethyl ether (400 ml). The ether solution was washed with water (50 ml), and the aqueous phases discarded. The ether was removed and the product (5.7 g) was dissolved in 90% methanol (200 ml) and extracted with petroleum ether (b. p. 40–60° C, 200 ml). The petroleum-ether-soluble material (0.9 g) and the methanol-soluble material (4.8 g) were converted to methyl esters with diazomethane. Identification of certain components was effected through mixed gas–liquid chromatograms with authentic materials employing both silicone grease and polyester substrates. The identification of the remainder was confirmed by plots of logarithm retention time vs. number of carbon atoms.

1. F. VARRENTRAPP. Ann. **35**, 196 (1840).
2. R. G. ACKMAN, SIR PATRICK LINSTEAD, B. J. WAKEFIELD, B. C. L. WEEDON, and R. A. DYTHAM. Tetrahedron, **8**, 221 (1960).
3. A. LUTTRINGHAUS and W. REIF. Ann. **618**, 221 (1958).
4. A. V. RONCERO, F. R. AYERBE, and M. A. A. ROMERO. Fette, Seifen, Anstrichmittel, **61**, 900 (1959).

RECEIVED APRIL 21, 1961.
FISHERIES RESEARCH BOARD OF CANADA,
TECHNOLOGICAL STATION,
HALIFAX, NOVA SCOTIA.

Can. J. Chem. Downloaded from www.nrcresearchpress.com by 210.87.254.5 on 09/05/12
For personal use only.

AMINO ACID DISTRIBUTION IN BIOLOGICALLY ACTIVE PEPTIDES
II. DIPEPTIDES HAVING LOW STATISTICAL SIGNIFICANCE

SAUL B. NEEDLEMAN

In the previous publication of this series (1), the amino acid sequences of a number of biologically active proteins were examined for the occurrence of relative chain position preferences of the individual constituent amino acids and for statistically significant repeating amino acid sequences comprising dipeptidic couplet units. Thirty-five dipeptide structures were found for which the chi-square values exceeded the 90% confidence limits for one degree of freedom (2.706). The study is now extended to dipeptide sequences which occur at a very low level of statistical significance.

A total of 10 couplets, listed in Table I, occurred only once in the proteins included in

TABLE I

Dipeptide couplets having low chi-square values

Dipeptide couplet	χ^2 *	Dipeptide couplet	χ^2 *
Ala–Phe	0.000	Cys–Lys	0.013
Asp–Gly	0.003	Cys–Pro	0.013
Asp–Lys	0.000	Gly–Phe	0.015
Cys–Ser	0.001	Leu–Cys	0.013
Glu–Gly	0.002	Lys–Cys	0.013
Glu–Thr	0.000	Lys–Thr	0.016
Leu–Asp	0.000	Phe–Asp	0.023
Pro–Asp	0.000	Phe–Tyr	0.023
Pro–Tyr	0.000	Ser–Asp	0.019
Tyr–Val	0.003	Ser–Gly	0.013
		Ser–Val	0.015
Asp–Ser	0.023	Thr–Lys	0.019
Asp–Phe	0.023	Tyr–Phe	0.023
Cys–Leu	0.013	Val–Ala	0.015

*The chi-square value is calculated from the formula, $\chi^2 = \Sigma (A - C)^2/C$, where A is the "actual" occurrence of a particular dipeptide unit and C is the "chance" occurrence of that couplet.

to 400 ml with water and extracted with diethyl ether (400 ml). The ether solution was washed with water (50 ml), and the aqueous phases discarded. The ether was removed and the product (5.7 g) was dissolved in 90% methanol (200 ml) and extracted with petroleum ether (b. p. 40–60° C, 200 ml). The petroleum-ether-soluble material (0.9 g) and the methanol-soluble material (4.8 g) were converted to methyl esters with diazomethane. Identification of certain components was effected through mixed gas–liquid chromatograms with authentic materials employing both silicone grease and polyester substrates. The identification of the remainder was confirmed by plots of logarithm retention time vs. number of carbon atoms.

1. F. VARRENTRAPP. Ann. **35**, 196 (1840).
2. R. G. ACKMAN, SIR PATRICK LINSTEAD, B. J. WAKEFIELD, B. C. L. WEEDON, and R. A. DYTHAM. Tetrahedron, **8**, 221 (1960).
3. A. LUTTRINGHAUS and W. REIF. Ann. **618**, 221 (1958).
4. A. V. RONCERO, F. R. AYERBE, and M. A. A. ROMERO. Fette, Seifen, Anstrichmittel, **61**, 900 (1959).

RECEIVED APRIL 21, 1961.
FISHERIES RESEARCH BOARD OF CANADA,
TECHNOLOGICAL STATION,
HALIFAX, NOVA SCOTIA.

Can. J. Chem. Downloaded from www.nrcresearchpress.com by 210.87.254.105 on 09/05/12
For personal use only.

AMINO ACID DISTRIBUTION IN BIOLOGICALLY ACTIVE PEPTIDES
II. DIPEPTIDES HAVING LOW STATISTICAL SIGNIFICANCE

SAUL B. NEEDLEMAN

In the previous publication of this series (1), the amino acid sequences of a number of biologically active proteins were examined for the occurrence of relative chain position preferences of the individual constituent amino acids and for statistically significant repeating amino acid sequences comprising dipeptidic couplet units. Thirty-five dipeptide structures were found for which the chi-square values exceeded the 90% confidence limits for one degree of freedom (2.706). The study is now extended to dipeptide sequences which occur at a very low level of statistical significance.

A total of 10 couplets, listed in Table I, occurred only once in the proteins included in

TABLE I

Dipeptide couplets having low chi-square values

Dipeptide couplet	χ^2 *	Dipeptide couplet	χ^2 *
Ala–Phe	0.000	Cys–Lys	0.013
Asp–Gly	0.003	Cys–Pro	0.013
Asp–Lys	0.000	Gly–Phe	0.015
Cys–Ser	0.001	Leu–Cys	0.013
Glu–Gly	0.002	Lys–Cys	0.013
Glu–Thr	0.000	Lys–Thr	0.016
Leu–Asp	0.000	Phe–Asp	0.023
Pro–Asp	0.000	Phe–Tyr	0.023
Pro–Tyr	0.000	Ser–Asp	0.019
Tyr–Val	0.003	Ser–Gly	0.013
		Ser–Val	0.015
Asp–Ser	0.023	Thr–Lys	0.019
Asp–Phe	0.023	Tyr–Phe	0.023
Cys–Leu	0.013	Val–Ala	0.015

*The chi-square value is calculated from the formula, $\chi^2 = \Sigma (A - C)^2/C$, where A is the "actual" occurrence of a particular dipeptide unit and C is the "chance" occurrence of that couplet.

this study. All had chi-square values of less than 0.00393 at the 0.95 probability level and for one degree of freedom.

If the data are randomly or normally distributed and agree with the null hypothesis, one should expect to get χ^2 values greater than 0.00393 95% of the time. Since these values are much lower, it is possible that the data for these couplets, as well as for the 106 dipeptide combinations (of 400 possible combinations for 20 amino acids) which did not appear at all, are not random, or, that the couplets, somehow, have been preselectively avoided in the natural synthesis of these biologically active proteins.

An additional 18 dipeptide couplets had chi-square values of less than 0.025.

1. S. B. NEEDLEMAN, R. Q. BLACKWELL, and L. S. FOSDICK. Can. J. Chem. **38**, 477 (1960).

RECEIVED MARCH 17, 1961.
RESEARCH LABORATORIES,
NALCO CHEMICAL COMPANY,
6216 W. 16TH PLACE,
CHICAGO, ILL.
AND
DEPARTMENT OF CHEMISTRY,
NORTHWESTERN UNIVERSITY,
CHICAGO, ILL.

SOME NEUTRAL AND ACIDIC EXTRACTIVES FROM CEANOTHUS AMERICANUS L.

R. A. ABRAMOVITCH AND G. TERTZAKIAN

The extractives from *Ceanothus americanus*, also known as New Jersey tea, have been the subject of many investigations (for a survey of the literature on this subject see ref. 1). A number of alkaloidal and acidic constituents have been isolated from the root bark, and some of the fatty and dicarboxylic acids have been identified (2). Bertho and Liang (3) reported the isolation of an alkaloid, ceanothin, for which they gave the molecular formula $C_{29}H_{36}N_4O_4$. On the other hand, Julian, Pikl, and Dawson isolated a high-melting monohydroxydicarboxylic acid which they called ceanothic acid and to which they assigned the molecular formula $C_{29}H_{44}O_5$ (4). The fact that both this acid and the above alkaloid were reported to be C_{29} compounds might indicate a possible structural relationship between them and it was thought to be of interest to examine systematically the composition of the neutral and acidic extractives from *Ceanothus americanus* root bark.

When the ground root bark (kindly supplied by Flint, Eaton and Co., Decatur, Illinois) was percolated and worked up as described by Julian, Pikl, and Dawson (4) no ceanothic acid could be isolated. A crude acid mixture was in fact isolated from which betulic acid was obtained as the main component (the fatty acids and simple dicarboxylic acids being eliminated in the work-up procedure). The same mixture of acids could be obtained by ether extraction. Betulic acid was characterized further as the methyl ester, the methyl ester acetate, and the acetate. A red pigment, believed to be a tannin, can also be isolated in relatively large quantities (11.5% based on dry root bark). Chromatography of the crude high-melting acids on silica gel gave betulic acid as well as a yellow amorphous acid, m.p. 250–260° (decomp.), which could not be purified but whose infrared spectrum indicated the presence of a $\diagdown\!\!\diagup C{=}CH_2$ group.

Can. J. Chem. Downloaded from www.nrcresearchpress.com by 210.87.254.105 on 09/05/12
For personal use only.

this study. All had chi-square values of less than 0.00393 at the 0.95 probability level and for one degree of freedom.

If the data are randomly or normally distributed and agree with the null hypothesis, one should expect to get χ^2 values greater than 0.00393 95% of the time. Since these values are much lower, it is possible that the data for these couplets, as well as for the 106 dipeptide combinations (of 400 possible combinations for 20 amino acids) which did not appear at all, are not random, or, that the couplets, somehow, have been preselectively avoided in the natural synthesis of these biologically active proteins.

An additional 18 dipeptide couplets had chi-square values of less than 0.025.

1. S. B. NEEDLEMAN, R. Q. BLACKWELL, and L. S. FOSDICK. Can. J. Chem. **38**, 477 (1960).

RECEIVED MARCH 17, 1961.
RESEARCH LABORATORIES,
NALCO CHEMICAL COMPANY,
6216 W. 16TH PLACE,
CHICAGO, ILL.
AND
DEPARTMENT OF CHEMISTRY,
NORTHWESTERN UNIVERSITY,
CHICAGO, ILL.

SOME NEUTRAL AND ACIDIC EXTRACTIVES FROM CEANOTHUS AMERICANUS L.

R. A. ABRAMOVITCH AND G. TERTZAKIAN

The extractives from *Ceanothus americanus*, also known as New Jersey tea, have been the subject of many investigations (for a survey of the literature on this subject see ref. 1). A number of alkaloidal and acidic constituents have been isolated from the root bark, and some of the fatty and dicarboxylic acids have been identified (2). Bertho and Liang (3) reported the isolation of an alkaloid, ceanothin, for which they gave the molecular formula $C_{29}H_{36}N_4O_4$. On the other hand, Julian, Pikl, and Dawson isolated a high-melting monohydroxydicarboxylic acid which they called ceanothic acid and to which they assigned the molecular formula $C_{29}H_{44}O_5$ (4). The fact that both this acid and the above alkaloid were reported to be C_{29} compounds might indicate a possible structural relationship between them and it was thought to be of interest to examine systematically the composition of the neutral and acidic extractives from *Ceanothus americanus* root bark.

When the ground root bark (kindly supplied by Flint, Eaton and Co., Decatur, Illinois) was percolated and worked up as described by Julian, Pikl, and Dawson (4) no ceanothic acid could be isolated. A crude acid mixture was in fact isolated from which betulic acid was obtained as the main component (the fatty acids and simple dicarboxylic acids being eliminated in the work-up procedure). The same mixture of acids could be obtained by ether extraction. Betulic acid was characterized further as the methyl ester, the methyl ester acetate, and the acetate. A red pigment, believed to be a tannin, can also be isolated in relatively large quantities (11.5% based on dry root bark). Chromatography of the crude high-melting acids on silica gel gave betulic acid as well as a yellow amorphous acid, m.p. 250–260° (decomp.), which could not be purified but whose infrared spectrum indicated the presence of a $\diagdown\!\!\diagup C{=}CH_2$ group.

Can. J. Chem. Downloaded from www.nrcresearchpress.com by 210.87.254.40 on 09/05/12
For personal use only.

The root bark was continuously extracted with ether and the brown oil obtained was saponified with aqueous ethanolic potassium hydroxide (ammonia was evolved during the saponification and identified as ammonium picrate). Steam distillation gave a very small quantity of a saturated aliphatic alcohol which has been tentatively identified as 2-nonanol by comparison of its relative retention time (relative to ethanol) on vapor phase chromatography on two different columns (silicone on firebrick and Apiezon "N" on firebrick) with that of an authentic sample, as well as by a comparison of their infrared spectra. From the steam distillation residue a small amount of β-sitosterol glucoside could be extracted out. Working up the non-saponifiable fraction led to the isolation of (*a*) β-sitosterol, characterized as its acetate and its benzoate, and (*b*) lupeol, characterized further as lupeol acetate and dihydrolupeol acetate. A mixture of saturated hydrocarbons was also isolated chromatographically but not characterized further as were also a number of minor compounds.

EXPERIMENTAL

Melting points are uncorrected. Petroleum ether refers to the fraction, b.p. 40–50°, which had been freed of unsaturation. All yields are given as a per cent of dry root bark.

Isolation of the Acidic Components

Dry root bark (2.25 kg) was continuously extracted with ether (8 l.) in a Soxhlet extractor for 3 days. The solution was concentrated to 1 l. and kept in the refrigerator for a few days. The white, oily solid which separated was filtered and extracted exhaustively with petroleum ether. The residue was a tan-colored powder (A). This was dissolved in ether (250 ml), extracted with 10% sodium carbonate solution, and the ether layer dried (Na_2SO_4) and evaporated to give whitish crystals (15.3 g; 0.69%), which after numerous recrystallizations from methanol yielded betulic acid,* m.p. 312°, $[\alpha]_D^{25}$ +6.04° (pyridine). Found: C, 78.71; H, 10.85. Calc. for $C_{30}H_{48}O_3$: C, 78.89; H, 10.59. Robertson, Soliman, and Owen give m.p. 317°, $[\alpha]_D$ +7.8° (pyridine) for betulic acid (5). The melting point was undepressed on admixture with an authentic sample of betulic acid. This acid gave the acetate, m.p. 290° (reported (5) m.p. 289–291°); the methyl ester with diazomethane, m.p. 222–223°, $[\alpha]_D^{25}$ +3.5° (pyridine) (reported (5) m.p. 223–224°, $[\alpha]_D$ +8.01° (pyridine)) (found: C, 78.88; H, 10.68; calc. for $C_{31}H_{50}O_3$: C, 79.10; H, 10.71); and the methyl ester acetate, m.p. 203° (reported (5) m.p. 201–202°).

The crude mixture of acids (A) (2.55 g) was chromatographed on a column of silica gel (70 g). Elution with petroleum ether–benzene (1:2) (3900 ml) gave betulic acid (1.078 g), m.p. 295–300° after recrystallization from aqueous acetone. The infrared spectrum of this acid was identical with that of authentic betulic acid. Elution with benzene–ether (1:1) (2500 ml) gave an amorphous yellow powder (369 mg) m.p. 250–260° (decomp.). Infrared spectrum (main peaks): 3400 (br)(m), 1680 (s), 1635 (m), 1603 (w), 1508 (w), 1280 (br)(m), 1230 (br)(s), 1190 (br), 1105 (m), 1030 (m), and 880 (m) cm^{-1}. This product could not be purified by recrystallization and was not examined further at this stage.

Saponification of the Ether Extractives—The Non-saponifiable Fraction

The viscous, brown ether extractives after removal of betulic acid (16.81 g) were boiled under reflux with 7% aqueous ethanolic (2:3) potassium hydroxide solution (250 ml) for 24 hours. The solution was concentrated at atmospheric pressure at 80° and water was then added and the mixture steam distilled. The distillate was saturated with salt,

**Betulic acid is insoluble in sodium carbonate solution.*

Can. J. Chem. Downloaded from www.nrcresearchpress.com by 210.87.254.40 on 09/05/12
For personal use only.

extracted with ether, and the dried ether layer evaporated. Distillation of the residue gave 2-nonanol, b.p. 82° at 12 mm, $[\alpha]_D^{25}$ +0.74° (methanol), n_D^{21} 1.4320. Vapor phase chromatography on 6-ft columns of silicone on firebrick and Apiezon "N" on firebrick respectively indicated that this product had the same relative retention times as authentic 2-nonanol. The infrared spectra of the two samples were identical. The reported (6) boiling point of 2-nonanol is 81–83° at 15 mm.

The residue from the steam distillation was continuously extracted with ether. White, needle-like crystals (40 mg), m.p. 310°, separated in the extraction flask and were shown to be identical with β-sitosterol glucoside by comparison of the infrared spectrum with that of an authentic specimen and by a mixed melting point determination. Evaporation of the ethereal extract gave a yellow wax (1.75 g, 0.13%) which crystallized from methanol to give β-sitosterol, m.p. 133.5–135.5°, $[\alpha]_D^{25}$ −31.2° (chloroform). The melting point was undepressed on admixture with an authentic specimen of β-sitosterol. Found: C, 83.55; H, 12.16. Calc. for $C_{29}H_{50}O$: C, 83.99; H, 12.15. The sterol gave the acetate, m.p. 123.5–124.5°, $[\alpha]_D^{26}$ −39.2° (chloroform) (found: C, 81.72; H, 11.07; calc. for $C_{31}H_{52}O_2$: C, 81.52; H, 11.48) (lit. (7) m.p. 126.5–127.5°, $[\alpha]_D$ −36.56°) and the benzoate, m.p. 142–143°.

The crude, non-saponifiable, non-steam-volatile fraction (5 g) after extraction with ether was chromatographed on a column of alumina (28 cm × 2.2 cm). Elution with petroleum ether gave a colorless oil (309 mg), b.p. 200–240° at 0.5 mm (with darkening), n_D^{25} 1.4795, $[\alpha]_D^{26}$ +1.16° (chloroform). Found: C, 86.82, 86.12; H, 13.11, 13.77; mol. wt. (ebullioscopic), 226. Calc. for $C_{20}H_{36}$: C, 86.86; H, 13.14; mol. wt., 276. Calc. for $C_{18}H_{34}$: C, 86.32; H, 13.68; mol. wt., 250. Infrared spectrum (liquid film): 2900 (s), 2860 (s), 1462 (m), and 1371 (m) cm^{-1}. This oil did not take up hydrogen on shaking in the presence of Adams' catalyst even in dioxane – glacial acetic acid solution (20:1) at 2 atm. It did not consume any peracid on treatment with monopherphthalic acid but did decolorize bromine water. In view of the inconsistent analyses this product was not examined further at this stage.

Elution with petroleum ether – benzene (1:2) gave at first a mixture (587 mg) of a ketonic and a non-ketonic compound. The ketonic portion was removed with Girard's reagent "T" giving the non-ketonic portion (493 mg) as a yellow solid which, on recrystallization from methanol, gave lupeol, m.p. 203–204°, $[\alpha]_D^{26}$ +29.5° (chloroform). Found: C, 84.66; H, 12.06; mol. wt. (Rast), 437. Calc. for $C_{30}H_{50}O$: C, 84.44; H, 11.81; mol. wt., 427. The melting point was undepressed on admixture with an authentic specimen of lupeol kindly supplied by Dr. T. R. Govindachari. It formed an acetate, m.p. 204–205°. Found: C, 82.03; H, 11.07. Calc. for $C_{32}H_{52}O_2$: C, 81.99; H, 11.18. Heilbron, Kennedy, and Spring (8) give m.p. 214–215° for lupeol acetate. This acetate was hydrogenated over Adams' catalyst to give dihydrolupeol acetate, m.p. 241–242° (lit. (8) m.p. 245–246°).

Further elution with petroleum ether – benzene (1:2) gave β-sitosterol (980 mg). Elution with somewhat more polar solvents gave intractable materials. Finally, methanol (6750 ml) eluted a brown solid (1.063 g), m.p. 250° (decomp.), which could not be recrystallized.

ACKNOWLEDGMENTS

This work was carried out during the tenure (by G. T.) of a University Research Demonstratorship and with the financial assistance of the National Research Council. The authors wish to express their gratitude to Flint, Eaton and Co. for a generous

Can. J. Chem. Downloaded from www.nrcresearchpress.com by 210.87.254.40 on 09/05/12
For personal use only.

supply of plant material, to Dr. T. R. Govindachari (Madras) for a sample of lupeol, and to Dr. R. E. Corbett for an authentic sample of betulic acid.

1. G. TERTZAKIAN. M.Sc. Thesis, Saskatchewan. 1960.
2. C. W. ROSCOE and N. A. HALL. J. Am. Pharm. Assoc. **49**, 108 (1960).
3. A. BERTHO and W. S. LIANG. Arch. Pharm. **271**, 273 (1933).
4. P. L. JULIAN, J. PIKL, and R. DAWSON. J. Am. Chem. Soc. **60**, 77 (1938).
5. A. ROBERTSON. G. SOLIMAN, and E. C. OWEN. J. Chem. Soc. 1267 (1939).
6. G. V. NAIR and E. VON RUDLOFF. Can. J. Chem. **38**, 177 (1960).
7. J. W. COOK and M. F. C. PAIGE. J. Chem. Soc. 336 (1944).
8. I. M. HEILBRON, T. KENNEDY, and F. S. SPRING. J. Chem. Soc. 329 (1938).

RECEIVED APRIL 10, 1961.
DEPARTMENT OF CHEMISTRY,
UNIVERSITY OF SASKATCHEWAN,
SASKATOON, SASKATCHEWAN.

Can. J. Chem. Downloaded from www.nrcresearchpress.com by 210.87.254.40 on 09/05/12
For personal use only.

DECARBOXYLATION OF AROMATIC CARBOXYLIC ACIDS IN ISOTOPIC STUDIES

F. B. FISHER AND A. N. BOURNS[1]

It is occasionally necessary in C^{13}-isotopic studies to isolate in a form suitable for mass spectrometric analysis a carbon atom attached directly to an aromatic nucleus. This may be accomplished by oxidation of the compound in question to an aryl carboxylic acid which, on decarboxylation, furnishes carbon dioxide derived exclusively from the carbon whose isotopic abundance is to be determined. When precise isotopic ratios are required, as in kinetic isotope effect studies, it is essential that these degradative reactions proceed with high conversion, otherwise they may give rise to isotopic fractionation which could introduce a serious error in the results.

The two principal decarboxylation methods used in isotopic studies are the copper chromite – quinoline reaction and the Schmidt reaction. The former has given variable yields (1) and, in our hands, contamination from extraneous carbon has been difficult to avoid. The Schmidt reaction has been reported (2) to give carbon dioxide in 55% yield from benzoic acid. By making certain modifications in the original procedure, we have been able to increase the yield to 95% for benzoic and *p*-anisic acid. When, however, the method was applied to aromatic acids containing electronegative substituents the yield of carbon dioxide fell drastically.

A further method of decarboxylation of value in preparative organic chemistry is the Hunsdecker reaction involving the action of bromine on the silver salt of a carboxylic acid. The higher yields of aryl halide reported for the nitrobenzoic acids compared to benzoic acid (3, 4, 5) suggested that this reaction might be satisfactorily applied to the production of carbon dioxide from aromatic carboxylic acids containing electron-withdrawing groups. This has indeed proved to be the case, yields of over 90% having been obtained from *m*-nitrobenzoic acid and *p*-trifluoromethylbenzoic acid. The two reactions, therefore, provide complementary methods for the decarboxylation of aromatic carboxylic acids in isotopic investigations.

[1]*To whom all correspondence should be addressed.*

supply of plant material, to Dr. T. R. Govindachari (Madras) for a sample of lupeol, and to Dr. R. E. Corbett for an authentic sample of betulic acid.

1. G. TERTZAKIAN. M.Sc. Thesis, Saskatchewan. 1960.
2. C. W. ROSCOE and N. A. HALL. J. Am. Pharm. Assoc. **49**, 108 (1960).
3. A. BERTHO and W. S. LIANG. Arch. Pharm. **271**, 273 (1933).
4. P. L. JULIAN, J. PIKL, and R. DAWSON. J. Am. Chem. Soc. **60**, 77 (1938).
5. A. ROBERTSON. G. SOLIMAN, and E. C. OWEN. J. Chem. Soc. 1267 (1939).
6. G. V. NAIR and E. VON RUDLOFF. Can. J. Chem. **38**, 177 (1960).
7. J. W. COOK and M. F. C. PAIGE. J. Chem. Soc. 336 (1944).
8. I. M. HEILBRON, T. KENNEDY, and F. S. SPRING. J. Chem. Soc. 329 (1938).

RECEIVED APRIL 10, 1961.
DEPARTMENT OF CHEMISTRY,
UNIVERSITY OF SASKATCHEWAN,
SASKATOON, SASKATCHEWAN.

Can. J. Chem. Downloaded from www.nrcresearchpress.com by 210.87.254.5 on 09/05/12
For personal use only.

DECARBOXYLATION OF AROMATIC CARBOXYLIC ACIDS IN ISOTOPIC STUDIES

F. B. FISHER AND A. N. BOURNS[1]

It is occasionally necessary in C^{13}-isotopic studies to isolate in a form suitable for mass spectrometric analysis a carbon atom attached directly to an aromatic nucleus. This may be accomplished by oxidation of the compound in question to an aryl carboxylic acid which, on decarboxylation, furnishes carbon dioxide derived exclusively from the carbon whose isotopic abundance is to be determined. When precise isotopic ratios are required, as in kinetic isotope effect studies, it is essential that these degradative reactions proceed with high conversion, otherwise they may give rise to isotopic fractionation which could introduce a serious error in the results.

The two principal decarboxylation methods used in isotopic studies are the copper chromite – quinoline reaction and the Schmidt reaction. The former has given variable yields (1) and, in our hands, contamination from extraneous carbon has been difficult to avoid. The Schmidt reaction has been reported (2) to give carbon dioxide in 55% yield from benzoic acid. By making certain modifications in the original procedure, we have been able to increase the yield to 95% for benzoic and *p*-anisic acid. When, however, the method was applied to aromatic acids containing electronegative substituents the yield of carbon dioxide fell drastically.

A further method of decarboxylation of value in preparative organic chemistry is the Hunsdecker reaction involving the action of bromine on the silver salt of a carboxylic acid. The higher yields of aryl halide reported for the nitrobenzoic acids compared to benzoic acid (3, 4, 5) suggested that this reaction might be satisfactorily applied to the production of carbon dioxide from aromatic carboxylic acids containing electron-withdrawing groups. This has indeed proved to be the case, yields of over 90% having been obtained from *m*-nitrobenzoic acid and *p*-trifluoromethylbenzoic acid. The two reactions, therefore, provide complementary methods for the decarboxylation of aromatic carboxylic acids in isotopic investigations.

[1]*To whom all correspondence should be addressed.*

Can. J. Chem. Downloaded from www.nrcresearchpress.com by 210.87.254.5 on 09/05/12
For personal use only.

EXPERIMENTAL

Hunsdecker Reaction

The silver salts were prepared by the method outlined by Cason and Rapoport (6), collected on a sintered-glass funnel, and dried in a vacuum desiccator. Yields were 90% for benzoic acid and better than 95% for the substituted benzoic acids.

The apparatus for the decarboxylation consisted of a 200-ml three-necked flask fitted with a dropping funnel, nitrogen-inlet tube, and a reflux condenser. Nitrogen gas, used to sweep carbon dioxide from the reaction mixture, was purified by passing through Fieser's solution and concentrated sulphuric acid and was led to the top of the dropping funnel as well as to the inlet tube. The condenser was connected to a CO_2-absorption train consisting of a dry ice – acetone trap and a CO_2 absorber described by Calvin *et al.* (7).

Silver salt, sufficient to produce approximately 100 mg of barium carbonate, and 60–80 ml of dry carbon tetrachloride were placed in the reaction flask, which was fitted temporarily with a downward distillation assembly in place of the reflux condenser and CO_2-absorption train. The system was flushed with nitrogen and about one third of the carbon tetrachloride removed by distillation. The condenser and absorption train were quickly replaced and, with a slow stream of nitrogen passing through the apparatus, the suspension was heated to the boiling point and stirred magnetically. Bromine (10% in carbon tetrachloride) was added a few drops at a time to the reaction mixture, with time being allowed between successive additions for the solution to decolorize. When the reaction was essentially complete, as usually indicated by the flocculation of silver bromide, a further three to five drops of bromine solution were added and heating continued for an additional 20–30 minutes. Barium carbonate was precipitated by the usual procedure (7). Blank experiments carried out in the absence of silver salt gave less than one milligram of precipitate.

Schmidt Reaction

The procedure described by Doering *et al.* (2) was used with minor modification. Ethylene dichloride was used as solvent instead of chloroform and the effluent carbon dioxide was passed through a dry ice – acetone trap and 5% permanganate in 1 *N* sulphuric acid (8) and absorbed in sodium hydroxide (7). Sodium azide was added over a period of 40 minutes at 40° C, and stirring and heating were continued an additional 50 minutes. Contamination with extraneous carbon dioxide was found in blank experiments to be less than one per cent.

RESULTS

The per cent yields of barium carbonate from each of four acids using the two methods of decarboxylation are shown in the following table:

	Per cent yield of $BaCO_3$	
Acid	Hunsdecker*	Schmidt
p-Anisic	61	95
Benzoic	90	95
p-Trifluoromethylbenzoic	93	28†
m-Nitrobenzoic	98	9

*Based on silver salt.
†Reaction temperature of 56–60° C.

ACKNOWLEDGMENT

The support of the National Research Council is gratefully acknowledged.

1. W. G. DAUBEN, J. C. REID, P. E. YANKWICH, and M. CALVIN. J. Am. Chem. Soc. **72**, 121 (1950).
2. W. v. E. DOERING, T. I. TAYLOR, and E. F. SCHOENEWALDT. J. Am. Chem. Soc. **70**, 455 (1948).
3. W. G. DAUBEN and H. TILLES. J. Am. Chem. Soc. **72**, 3185 (1950).
4. R. A. BARNES and R. J. PROCHASKA. J. Am. Chem. Soc. **72**, 3188 (1950).
5. J. W. H. OLDHAM. J. Chem. Soc. 100 (1950).
6. J. CASON and H. RAPOPORT. Laboratory text in organic chemistry. Prentice-Hall, Inc., New York. 1950. p. 271.
7. M. CALVIN, C. HEIDELBERGER, J. C. REID, B. M. TOLBERT, and P. E. YANKWICH. Isotopic carbon. John Wiley & Sons, Inc., New York. 1949. p. 83.
8. E. F. PHARES. Arch. Biochem. Biophys. **33**, 173 (1951).

RECEIVED APRIL 25, 1961.
BURKE CHEMICAL LABORATORIES,
HAMILTON COLLEGE,
MCMASTER UNIVERSITY,
HAMILTON, ONTARIO.

HELVETICA CHIMICA ACTA

SCHWEIZERISCHE CHEMISCHE GESELLSCHAFT
Verlag Helvetica Chimica Acta
Basel 7 (Schweiz)

Seit 1918 43 Jahre

Abonnemente: Jahrgang 1961, Vol. XLIV $31.50 incl. Porto

Es sind noch lieferbar:

Neudruck ab Lager
Vol. I–XXVII (1918–1944)

Originalausgaben, druckfrisch und antiquarisch.
Vol. XXVIII–XLIII (1945–1960)

Diverse Einzelhefte ab Vol. XX
Preise auf Anfrage. Nur solange Vorrat.

Das wissenschaftliche Organ der SCHWEIZERISCHEN CHEMISCHEN GESELLSCHAFT

Can. J. Chem. Downloaded from www.nrcresearchpress.com by 210.87.254.5 on 09/05/12
For personal use only.

Can. J. Chem. Downloaded from www.nrcresearchpress.com by 210.87.254.5 on 09/05/12
For personal use only.

Canadian Journal of Chemistry

Issued by THE NATIONAL RESEARCH COUNCIL OF CANADA

VOLUME 39 SEPTEMBER 1961 NUMBER 9

THE POTASSIUM SALTS OF FUMARIC ACID: PREPARATION, UNIT CELL CONSTANTS, SPACE GROUPS, AND X-RAY DIFFRACTION POWDER IDENTIFICATION DATA[1]

M. P. GUPTA[2] AND W. H. BARNES

ABSTRACT

The preparation of the three crystalline potassium salts of fumaric acid, "acid" potassium hydrogen fumarate ($2KHC_4H_2O_4.H_2C_4H_2O_4$), potassium hydrogen fumarate ($KHC_4H_2O_4$), and dipotassium fumarate dihydrate ($K_2C_4H_2O_4.2H_2O$), is discussed, and suitable pH values for the growth of single crystals of each are given. Unit cell, space group, and X-ray diffraction powder identification data for the three salts are presented.

INTRODUCTION

There are three crystalline potassium salts of fumaric acid, $K_2C_4H_2O_4.2H_2O$, $KHC_4H_2O_4$, and $2KHC_4H_2O_4.H_2C_4H_2O_4$. The first two were prepared by Rieckher in 1844 (1), and all three were obtained by Carius in 1867 (2). Rieckher (1) saturated fumaric acid in water with potassium carbonate and allowed the aqueous solution to evaporate, thus obtaining the normal salt which he found to be a dihydrate from the loss in weight at 100° C; by incineration to potassium carbonate he determined the formula as "KO,C_4HO_3+2Aq" (i.e., $K_2C_4H_2O_4.2H_2O$). Potassium hydrogen fumarate was prepared from the neutral salt and acetic acid, from fumaric acid and potassium carbonate followed by the addition of more fumaric acid, and from the neutral salt and fumaric acid. Rieckher showed that crystals of potassium hydrogen fumarate are anhydrous, and, by conversion to potassium sulphate, he established the formula as "$KO,C_4HO_3+C_4HO_3,HO$" (i.e., $KHC_4H_2O_4$). Carius (2), apparently unaware of Rieckher's work, treated solutions of barium fumarate with potassium sulphate and various concentrations of sulphuric acid, and thus obtained not only the two salts to be expected of a dibasic acid but, in addition, an "acid" potassium hydrogen fumarate, $2KHC_4H_2O_4.H_2C_4H_2O_4$, which he first considered to be a monohydrate (2) but later (3) decided was anhydrous. His analysis of dipotassium fumarate was carried out after the compound was dried at 100° C so that his formula corresponds to that of the anhydrous salt and not to that of the dihydrate. Carius also observed, like Rieckher, that $KHC_4H_2O_4$ could be crystallized from a solution of $K_2C_4H_2O_4$ and fumaric acid, but he also reports (3) that it is not obtained from a solution of the former and "acid" potassium hydrogen fumarate, which recrystallize separately.

Dehn and Merling (4) prepared $K_2C_4H_2O_4$ (presumably anhydrous) from fumaric acid and potassium hydroxide in anhydrous ether. Zechmeister and Szécsi (5) obtained "acid" potassium hydrogen fumarate from an alcohol extract of *Capsella bursa-pastoris*, and also from the appropriate molar proportions of fumaric acid and potassium hydroxide.

[1]*Manuscript received May 11, 1961.*
Contribution from the Division of Pure Physics, National Research Council, Ottawa, Canada.
Issued as N.R.C. No. 6403.
[2]*National Research Council Postdoctorate Fellow, now with the University Department of Physics, Ranchi University, Ranchi, Bihar, India.*

Finally, Sabalitschka and Kubisch (6) prepared potassium hydrogen fumarate from fumaric acid and $N/2$ KOH solution. All three salts are included in the 1893 and 1942 editions of Beilstein's *Handbuch* (although the latter gives the normal salt in its anhydrous form) but $2KHC_4H_2O_4.H_2C_4H_2O_4$ does not appear in the edition of 1920 (7).

Crystals of $K_2C_4H_2O_4.2H_2O$ are described by Rieckher (1) as "brilliant, short, striated prisms" and by Carius (3) as "bright, monoclinic prisms and plates". Rieckher (1) refers to crystals of $KHC_4H_2O_4$ variously as "clear and regular", and as "irregular needles", while Carius (3) describes them as "thick, monoclinic (?) plates". Crystals of $2KHC_4H_2O_4.H_2C_4H_2O_4$ are said by Carius (3) to be "needle-like prisms" and are referred to as "elongated and tapering" by Zechmeister and Szécsi (5). Optical crystallographic data are given by Repossi (8) (see also Groth (9)) for crystals of $KHC_4H_2O_4$ said to have been obtained from aqueous solution. Stafford (10) reports refractive indices for dipotassium fumarate but fails to indicate whether they are for the anhydrous salt or the dihydrate. Gupta (11) describes a preliminary investigation of the crystal structures of "acid" potassium hydrogen fumarate and of "acid" rubidium hydrogen fumarate which were prepared by the addition of fumaric acid to aqueous solutions of the appropriate hydroxides; the composition of the potassium salt was verified by an analysis for carbon and hydrogen. As Gupta points out, the composition of the potassium salt may be expressed as $2KC_4H_3O_4+C_4H_4O_4$ or as $K_2C_4H_2O_4+2C_4H_4O_4$ but the two-dimensional structure analysis did not enable a choice to be made between the two formulations, if indeed there is any real difference between them. In the present paper the "acid" potassium hydrogen fumarate is designated by the first formula, namely $2KHC_4H_2O_4.H_2C_4H_2O_4$.

In anticipation of crystal structure investigations of $KHC_4H_2O_4$ and $K_2C_4H_2O_4.2H_2O$, crystals of all three salts have been grown from aqueous solutions of KOH or K_2CO_3 and fumaric acid, but it immediately became apparent that the particular salt obtained was dependent on the pH of the solution. An extensive series of crystallization experiments, therefore, have been carried out to establish suitable pH ranges within which satisfactory crystals of the various salts may be grown. Unit cell and space group data for $KHC_4H_2O_4$ and $K_2C_4H_2O_4.2H_2O$ have been collected, and indexed X-ray diffraction powder data for all three salts have been obtained.

PREPARATION

The potassium salts first were prepared by the addition of weighed amounts of pure fumaric acid to solutions containing previously weighed amounts of KOH or K_2CO_3. The potassium fumarate solutions were boiled, filtered, and set aside to crystallize spontaneously and slowly in an air-conditioned room at 19 to 21° C and $<50\%$ relative humidity. The uncertain proportion of carbonate in solid KOH, and a significant proportion of hydrate (shown by X-ray powder photographs) even in fresh, unopened bottles of the highest grade of "anhydrous" K_2CO_3, made it preferable to add measured volumes of a standardized solution of KOH (free from carbonate) to weighed samples of the fumaric acid; KOH is more satisfactory than K_2CO_3 because there is a tendency for $KHCO_3$ to crystallize first from the more strongly acid solutions. As soon as the approximate range of pH appropriate for the appearance of each fumarate had been determined, solutions were prepared by dissolving fumaric acid in $N/10$ KOH solution (carbonate free) and adjusting the pH to within the range desired. Universal indicator papers (such as Cenco pHydrion) are adequate for following the changes in pH although a Beckman pH meter with external electrodes is more satisfactory.

When crystals appeared, the solutions were tested for pH and the crystals were removed with tweezers, rolled gently on absorbent (bibulous) paper, and allowed to air-dry.

400107

Can. J. Chem. Downloaded from www.nrcresearchpress.com by 210.87.254.5 on 09/05/12
For personal use only.

Can. J. Chem. Downloaded from www.nrcresearchpress.com by 210.87.254.5 on 09/05/12
For personal use only.

Distilled water was added to the solution, which was warmed to accelerate solution of unremoved crystals, and the beaker was set aside until the next small crop of crystals was obtained. This procedure was repeated until the volume had been reduced usually to a few drops. The solution was then allowed to evaporate to dryness and the solid residue was ground and mixed thoroughly. Representative crystals from each crop, and samples of the final residues, were identified by X-ray powder photographs.

The standard powder patterns employed for identification purposes were authenticated as follows: $2KHC_4H_2O_4.H_2C_4H_2O_4$, from data given by Gupta (11) for material analyzed for carbon and hydrogen; $KHC_4H_2O_4$, material analyzed for carbon and hydrogen; $K_2C_4H_2O_4.2H_2O$, crystallized from solution containing excess KOH, 4 g (air-dried at 19° C and 60% relative humidity) showed a loss in weight of 15.80% after heating to constant weight at 150° C (calculated for conversion of dihydrate to anhydrous salt, 15.78%). The authenticity of the standard patterns for $KHC_4H_2O_4$ and $K_2C_4H_2O_4.2H_2O$ later was confirmed by successful indexing on the basis of the unit cell and space group data.

No difficulty was experienced in the preparation of $K_2C_4H_2O_4.2H_2O$. The solubility was determined gravimetrically as approximately 62.4 g *anhydrous* $K_2C_4H_2O_4$ per 100 ml H_2O at 21° C; the pH of a saturated solution at this temperature is about 10. Because of the high solubility, several recrystallizations under conditions of greatly reduced evaporation at room temperature were frequently necessary to obtain well-formed single crystals of reasonably small dimensions.

"Acid" potassium hydrogen fumarate is much less soluble in water (approximately 2.01 g $2KHC_4H_2O_4.H_2C_4H_2O_4$ per 100 ml H_2O at 21° C), and the pH of a saturated solution at 21° C is about 3.2_3. If the appropriate volume of standard KOH added to a weighed amount of fumaric acid is not sufficient for complete solution of the fumarate, water may be introduced until all solid has dissolved. Spontaneous crystallization by slow evaporation at room temperature usually gave good acicular single crystals. An annoying feature of solutions of this salt, however, was a propensity for nurturing the growth of mold over the sometimes long periods of evaporation necessary for the growth of the best crystals; this can be prevented by the addition of one or two drops of dilute formaldehyde solution. On a few occasions, crystals of fumaric acid (easily recognizable as opaque, feathery clusters) preceded the appearance of the first crystals of "acid" potassium hydrogen fumarate, particularly when the initial pH of the solutions was less than 3.0. The solubility of fumaric acid was determined gravimetrically as approximately 0.51 g $H_2C_4H_2O_4$ per 100 ml H_2O at 21° C; the pH of a saturated solution at this temperature is about 2.2_2.

On the evaporation of a solution containing the proper proportions of fumaric acid and KOH (or K_2CO_3) to give $KHC_4H_2O_4$, the first crystals to appear are those of $2KHC_4H_2O_4.H_2C_4H_2O_4$. As crystallization of this salt proceeds, the pH of the solution rises until it approaches about 3.7_5 when crystallization of "acid" potassium hydrogen fumarate is replaced by that of $KHC_4H_2O_4$, which continues until the pH has risen to about 5. As evaporation proceeds to dryness, and the pH continues to rise, crystals of $K_2C_4H_2O_4.2H_2O$ appear. Similarly, when crystals of $KHC_4H_2O_4$ are dissolved in water, and the solution is allowed to evaporate, the same sequence of crystal identities and increasing pH is observed. Mold growth was troublesome in the acidic stages of these tests also until a drop or two of dilute formaldehyde was added to the initial solutions.

For the preparation of the potassium salts of fumaric acid, therefore, it is recommended that pure fumaric acid be dissolved in measured volumes of a standard KOH solution (free from carbonate) and that the pH of the solutions be adjusted to, and maintained at,

about 3.3 for $2KHC_4H_2O_4.H_2C_4H_2O_4$, about 4 for $KHC_4H_2O_4$, and about 8 for $K_2C_4H_2O_4.2H_2O$. The first and last may be recrystallized directly from water, but, after dissolving $KHC_4H_2O_4$ in water, the pH must be increased to about 4 in order to suppress crystallization of "acid" potassium hydrogen fumarate. The great difference in the solubilities of "acid" potassium hydrogen fumarate and dipotassium fumarate dihydrate should be kept in mind when one is selecting the initial volume of KOH solution for a

TABLE I

Single-crystal data for (A) $2KHC_4H_2O_4.H_2C_4H_2O_4$, (B) $KHC_4H_2O_4$, (C) $K_2C_4H_2O_4.2H_2O$

	A	B	C
a (Å)	7.48	6.95_2	6.35_4
b (Å)	8.73	7.48_3	18.22_8
c (Å)	6.96	6.24_6	7.27_2
α	114° 18′	107° 05′	90° 00′
β	101° 54′	117° 00′	98° 20′
γ	98° 00′	96° 04′	90° 00′
Space group	$P1$	$P\bar{1}$ (probable)	$P2_1/c$
Z (molecules per cell)	1	2	4
ρ_{calc} (g/ml)	1.796	1.927	1.819
ρ_{obs} (g/ml)	1.785	1.936	1.817

TABLE II

X-Ray diffraction powder data for $2KHC_4H_2O_4.H_2C_4H_2O_4$ (indexed for $d > 2.30$ Å)

	d (Å)				d (Å)				d (Å)	
I/I_1	Obs.	Calc.	hkl	I/I_1	Obs.	Calc.	hkl	I/I_1	Obs.
20	7.76	7.70	100			2.83	$11\bar{2}$	10	1.90
20	7.14	7.08	010	20	2.82	2.82	$1\bar{2}1$	5	1.88
18	6.40	6.38	001			2.81	$2\bar{1}1, 01\bar{2}$	8B	1.84
	*	6.06	$10\bar{1}$			2.77	$\bar{1}2\bar{2}$	10B	1.81
		6.02	$\bar{1}10$	1B	2.76	2.74	$30\bar{1}$	10	1.78
30	5.46	5.46	$\bar{1}11$			2.73	$\bar{2}22, 12\bar{1}$	10	1.74
1	5.02	4.99	011	15	2.65	2.64	$102, \bar{3}10$	[8	1.70] †
—	—	4.66	110			2.62	121	10	1.68
—	—	4.52	$01\bar{1}$		*	2.60	$\bar{3}12$	1	1.64
	*	4.24	101			2.59	$\bar{3}21$	1	1.62
	*	4.06	$\bar{2}1\underline{1}, 11\bar{1}$	45	2.56	2.57	300	1	1.60
20	3.98	3.97	$20\bar{1}$			2.54	$21\underline{1}$	1	1.58
55	3.87	3.85	200	—	—	2.53	$21\bar{2}$	10	1.46
—	—	3.81	$\bar{2}10$			2.50	$0\underline{22}$	1	1.43
	*	3.76	$1\bar{1}1$			2.48	$1\bar{1}2$	1	1.41
		3.58	$\bar{1}20$	10B	2.48	2.47	$11\underline{2}$	1	1.38
100B	3.56	3.54	$\bar{1}21, 020$			2.46	$30\bar{2}, \bar{1}31$	2	1.36
		3.53	$11\underline{1}$	10	2.44	2.44	$\bar{1}30$	1	1.34
75	3.41	3.40	$10\bar{2}$	5	2.41	2.42	$\bar{3}22$	2	1.32
5	3.35	3.36	$\bar{1}12$			2.41	$2\bar{2}1$	1	1.27
	*	3.24	$0\underline{21}$	60	2.39	2.40	$\bar{2}31$	2B	1.25
15	3.20	3.20	$\bar{2}21$			2.38	$\bar{3}20$	5	1.22
		3.19	$00\underline{2}$		*	2.36	030	8	1.20
15	3.14	3.14	$\bar{2}12$	1	2.34	2.33	$22\underline{0}$	2	1.14
20	3.09	3.07	$21\underline{0}, 21\bar{1}$	1	2.32	2.32	$31\bar{1}$	2	1.12
		3.03	$20\bar{2}$	20B	2.28			1	1.08
45	3.04	3.02	$01\underline{2}$	20	2.16			2	1.06
		3.01	$\bar{2}2\underline{0}$	15	2.13			2	1.05
	*	2.97	$02\bar{1}$	15	2.06			1	1.03
		2.95	$12\underline{0}$	10	2.02				
2	2.89	2.88	$\underline{201}$	25	1.99				
		2.87	$\bar{3}11$	2	1.97				

*Reflection probably present but with $I/I_1 < 1$.

†Broad band; I/I_1 varies from 8 at edge corresponding to $d = 1.70$ Å to 10 at edge corresponding to $d = 1.68$ Å.

Can. J. Chem. Downloaded from www.nrcresearchpress.com by 210.87.254.5 on 09/05/12
For personal use only.

given preparation. Adjustment of pH upwards may be effected by the addition of KOH solution; if the solutions are not to be evaporated to dryness, dilute acetic acid may be employed for lowering the pH. In all cases, a few representative crystals from each crop should be ground and an X-ray powder photograph taken, for identification purposes, and to confirm that crystals of one salt only are present.

The foregoing notes throw light on some of the statements appearing in the early literature. Thus when Carius (3) recrystallized mixed solutions of $K_2C_4H_2O_4.2H_2O$ and $2KHC_4H_2O_4.H_2C_4H_2O_4$, he must have recovered not only these two salts separately as he reports, but crystals of $KHC_4H_2O_4$ must also have been present. Rieckher's description (1) of crystals of the normal salt actually suggests $KHC_4H_2O_4$, while his varied comments on crystals of the latter sometimes suggest $2KHC_4H_2O_4.H_2C_4H_2O_4$. If the crystals which Repossi (8) employed for his optical crystallographic study of $KHC_4H_2O_4$ were recrystallized from water, without any adjustment of the pH of the solution, they may actually have been those of $2KHC_4H_2O_4.H_2C_4H_2O_4$.

UNIT CELL AND SPACE GROUP DATA

The unit cell constants and the space group of $KHC_4H_2O_4$ and of $K_2C_4H_2O_4.2H_2O$ were determined by the Buerger precession method using Mo $K\alpha$ (λ = 0.7107 Å) radiation for the first and Cu $K\alpha$ (λ = 1.5418 Å) radiation for the second. Film shrinkage corrections were applied to all film measurements. Corresponding data for $2KHC_4H_2O_4.H_2C_4H_2O_4$ have been reported by Gupta (11) and, therefore, were not redetermined in the present

TABLE III

X-Ray diffraction powder data for $KHC_4H_2O_4$ (indexed for $d > 2.20$ Å)

	d (Å)				d (Å)				d (Å)
I/I_1	Obs.	Calc.	hkl	I/I_1	Obs.	Calc.	hkl	I/I_1	Obs.
13	6.866	6.866	010	—	—	2.666	120	2	1.915
10	5.940	5.945	100	—	—	2.644	$\bar{2}20$	8BB	1.854
1	5.541	5.523	$10\bar{1}$	15	2.585	2.590	$0\bar{2}2$	15	1.786
15	5.272	5.288	$\bar{1}10$	—	—	2.568	002	1	1.759
—	—	5.181	$0\bar{1}1$	25	2.524	2.528	111	10	1.739
		5.135	001			2.517	$\bar{2}21$	8	1.703
—	—	4.669	$11\bar{1}$			2.485	210	8	1.671
20	3.991	4.012	$\bar{1}11$	15	2.470	2.475	$0\bar{3}1$	1	1.626
		3.976	110			2.467	$\bar{1}12$	15B	1.577
75	3.550	3.557	$0\bar{2}1$	—	—	2.450	021	1	1.536
35	3.507	3.513	011	15	2.431	2.435	$\bar{2}12$	1	1.516
		3.445	$20\bar{1}$	—	—	2.370	$\bar{1}30$	2BB	1.489
25	3.432	3.433	020	1	2.354	2.355	$22\bar{1}$	1	1.444
		3.425	$1\bar{1}1$	55	2.327	2.334	$2\bar{2}2$	10	1.425
		3.417	$\bar{1}20$			2.333	$1\bar{3}1$	1	1.393
		3.168	101			2.295	$2\bar{1}1$	1	1.364
60	3.158	3.165	$\bar{2}11$	—	—	2.288	030	1	1.350
		3.140	$12\bar{1}$			2.280	$30\bar{1}$	1BB	1.324
—	—	3.096	$11\bar{2}$	1	2.272	2.270	$\bar{3}11$	2	1.283
—	—	3.059	$\bar{2}10$	45	2.240	2.240	$13\bar{1}$	1	1.262
		3.000	$21\bar{1}$	8	2.205	2.214	$2\bar{2}1$	2	1.238
100	2.965	2.973	$10\bar{2}$			2.204	$30\bar{2}$	5	1.210
		2.972	$200, 1\bar{2}1$	5	2.144			5	1.194
		2.783	$0\bar{1}2$	1	2.116			2	1.184
20	2.774	2.761	$20\bar{2}$	5	2.084			1	1.164
—	—	2.733	$\bar{1}21$	1	2.048			1BB	1.142
		2.710	$21\bar{2}$	40	2.000			1BB	1.104
15B	2.698	2.692	$12\bar{2}$	15B	1.961				

Can. J. Chem. Downloaded from www.nrcresearchpress.com by 210.87.254.5 on 09/05/12
For personal use only.

investigation. Densities (at about 20° C) were measured by flotation in binary solutions of toluene and ethylene dibromide in the case of "acid" potassium hydrogen fumarate, and toluene and methylene iodide in the other two cases. Data for the three salts are summarized in Table I.

The unit cell of $2KHC_4H_2O_4.H_2C_4H_2O_4$ represented in Table I(A) was derived by Delaunay reduction from that of Gupta (11), $a = 8.64$ Å, $b = 7.48$ Å, $c = 6.96$ Å, $\alpha = 78.1°, \beta = 112.9°, \gamma = 107.9°$, although the latter is the more convenient structurally. The transformation matrix from the original cell (1) to the reduced cell (Table I) is $010/101/00\bar{1}$.

In the case of $KHC_4H_2O_4$ the reciprocal lattice elements of two different cells were measured and both were reduced to that represented in Table I(B). The direct cell elements of the first were $a = 6.92_2$ Å, $b = 6.95_2$ Å, $c = 17.95_7$ Å, $\alpha = 36° 44'$, $\beta = 32° 11'$, $\gamma = 53° 31'$; transformation matrix to give the reduced cell of Table I(B),

TABLE IV

X-Ray diffraction powder data for $K_2C_4H_2O_4.2H_2O$ (indexed for $d > 2.24$ Å)

	d (Å)				d (Å)				d (Å)	
I/I_1	Obs.	Calc.	hkl	I/I_1	Obs.	Calc.	hkl	I/I_1	Obs.
30	9.152	9.114	020			2.824	042	20	2.088
—	—	6.693	011			2.814	151	25	2.047
40	6.295	6.287	100	100BB	2.810	2.801	122	1	2.028
5	5.952	5.943	110			2.799	061	1	2.004
40	5.636	5.647	021			2.792	230	75	1.982
15	5.180	5.175	120	—	—	2.735	160	1	1.956
2	4.929	4.926	$11\bar{1}$			2.724	$23\bar{1}$	2	1.929
—	—	4.642	031	75B	2.706	2.708	$21\bar{1}$	1	1.903
30	4.558	4.557	040			2.693	$14\bar{2}$	20B	1.890
1	4.461	4.461	$12\bar{1}$	—	—	2.649	132	1	1.864
—	—	4.369	130	1B	2.617	2.623	221	1	1.848
—	—	4.302	111			2.612	$16\bar{1}$	15	1.822
35	3.987	3.982	121	—	—	2.588	240	25	1.798
25	3.905	3.913	$13\bar{1}$	—	—	2.561	$05\bar{2}$	1	1.781
—	—	3.850	041			2.558	$20\bar{2}$	10	1.752
1	3.684	3.690	140	5	2.532	2.533	$21\bar{2}, 24\bar{1}$	10B	1.636
30	3.581	3.598	002	35	2.505	2.505	161	8B	1.576
		3.578	131			2.497	231	8B	1.552
	*	3.530	$01\bar{2}$			2.473	$14\bar{2}$	1B	1.523
—	—	3.403	$14\bar{1}$	30	2.471	2.463	$22\bar{2}$	1	1.487
80	3.342	3.346	$02\bar{2}$			2.462	$15\bar{2}$	20	1.474
		3.338	$10\bar{2}$	—	—	2.448	071	1B	1.440
80	3.285	3.283	$11\bar{2}$	—	—	2.406	170	10	1.411
—	—	3.252	051	2	2.382	2.381	250	10	1.400
		3.175	141			2.378	013	2	1.384
20B	3.156	3.154	150	—	—	2.358	$23\bar{2}$	2	1.368
		3.143	200	—	—	2.347	$24\bar{1}$	2	1.353
		3.134	$12\bar{2}$	—	—	2.338	$11\bar{3}, 25\bar{1}$	8	1.303
25	3.099	3.098	210	45	2.323	2.321	$06\bar{2}, 17\bar{1}$	8	1.296
		3.096	032			2.319	023	15	1.282
	*	3.038	$06\bar{0}$			2.290	$15\bar{2}$	2	1.262
30	3.012	3.005	$21\bar{1}$	45	2.281	2.282	$12\bar{3}$	2	1.250
		2.972	220			2.278	080	2	1.224
45B	2.950	2.969	$15\bar{1}$	10	2.244	2.247	$16\bar{2}$	2B	1.202
		2.944	$10\bar{2}$			2.244	171	1	1.176
		2.926	$13\bar{2}$	15	2.198			1	1.130
5	2.900	2.906	$11\bar{2}$	1	2.150				
		2.890	$22\bar{1}$	1	2.120				

*Reflection probably present but with $I/I_1 < 1$.

Can. J. Chem. Downloaded from www.nrcresearchpress.com by 210.87.254.5 on 09/05/12
For personal use only.

$010/\bar{2}\bar{1}1/1\bar{1}0$. The direct cell elements of the second were $a = 12.70_9$ Å, $b = 13.13_7$ Å, $c = 18.03_0$ Å, $\alpha = 161° 33'$, $\beta = 163° 07'$, $\gamma = 27° 56'$; transformation matrix to give the reduced cell of Table I(B), $110/\bar{1}\bar{2}\bar{2}/\bar{1}01$. Numerical values for corresponding reduced-cell constants agreed to better than 0.01_5 Å in linear dimensions, and 20′ in the angles; the values selected for Table I(B) are those for the first cell because they gave slightly better agreement with the powder data.

POWDER IDENTIFICATION DATA

The powdered samples were taken up in thin-walled glass capillary tubes as described elsewhere (12), and cylindrical cameras of 114.6-mm diameter were employed. The photographs were taken with Co $K\alpha$ radiation ($\lambda = 1.790$ Å), Straumanis film mounting, and the apparatus "cut-off" was about 20 Å. Film shrinkage corrections were $<1/1000$, and were not applied to the measurements. Intensities were estimated visually with the aid of a calibrated strip. The patterns were indexed on the basis of the unit cell and space group data of Table I, with the exception of $2KHC_4H_2O_4.H_2C_4H_2O_4$ for which the constants of the unreduced cell (11) were employed. The results are given in Tables II, III, and IV, where B and BB in the columns of I/I_1 indicate lines which were broader and much broader, respectively, than the general average for a given pattern, and an asterisk in the columns of d (obs.) indicates that the reflection probably was present but with $I/I_1 < 1$, thus making a reasonably accurate measurement of 2θ impractical.

REFERENCES

1. T. Rieckher. Liebigs Ann. Chem. **49**, 31 (1844).
2. L. Carius. Ann. Chem. Pharm. **142**, 129 (1867).
3. L. Carius. Ber. deut. chem. Ges. **4**, 928 (1871).
4. W. M. Dehn and R. E. Merling. J. Am. Chem. Soc. **39**, 2646 (1917).
5. L. Zechmeister and P. Szécsi. Ber. deut. chem. Ges. **54**, 172 (1921).
6. Th. Sabalitschka and G. Kubisch. Z. anorg. u. allgem. Chem. **134**, 79 (1924).
7. F. Beilstein. Handbuch der organischen Chemie. Vol. 1. Voss, Hamburg and Leipzig. 1893. p. 698; Vol. 2. Springer, Berlin. 1920. p. 740; Vol. 2. Springer, Berlin. 1942. p. 637.
8. E. Repossi. Atti reale accad. Lincei, Ser. 5, Part 2, **13**, 468 (1904).
9. P. Groth. Chemische Krystallographie. Vol. 3. Engelman, Leipzig. 1910. p. 284.
10. R. W. Stafford. Ind. Eng. Chem. Anal. Ed. **14**, 694 (1942).
11. M. P. Gupta. Acta Cryst. **9**, 263 (1956).
12. W. H. Barnes and H. M. Sheppard. Bull. Narcotics, U.N. Dept. Social Affairs, **6**(2), 27 (1954).

Can. J. Chem. Downloaded from www.nrcresearchpress.com by 210.87.254.5 on 09/05/12
For personal use only.

Can. J. Chem. Downloaded from www.nrcresearchpress.com by 210.87.254.40 on 09/05/12
For personal use only.

ON THE SOLUBILITY OF ANHYDROUS CALCIUM SULPHATE AND OF GYPSUM IN CONCENTRATED SOLUTIONS OF SODIUM CHLORIDE AT 25° C, 30° C, 40° C, AND 50° C[1]

E. Bock

ABSTRACT

The solubilities of anhydrous $CaSO_4$ and $CaSO_4.2H_2O$ in concentrated aqueous solutions of NaCl at a series of temperatures—25° C, 30° C, 40° C, and 50° C, have been determined. It was found that the transition temperature for the reaction

$$CaSO_4.2H_2O \rightarrow CaSO_4 + 2H_2O,$$

which in pure water has a value of 42° C, is shifted progressively to lower temperatures with increasing NaCl concentration. It was also found that the variation of the transition temperature with NaCl concentration could be adequately represented by the equation

$$\Delta G = \Delta H - T\Delta S + 2RT \ln P/P_0,$$

where ΔG, ΔH, and ΔS are the Gibbs free energy, enthalpy, and entropy of the reaction and P_0 and P are the vapor pressures of pure water and the solution respectively at the absolute temperature T.

INTRODUCTION

It has long been known that the gypsum–anhydrite transition point is depressed by addition of strong electrolytes. However, it appears that no systematic study of this aspect of this system has ever been made, and only isolated experiments are reported in the literature (1).

Since many naturally occurring gypsum deposits which are used as raw material for the commercial production of plaster of paris and building plaster are contaminated with various amounts of sodium chloride, it was decided to carry out a systematic study of the behavior of the system gypsum–anhydrite in the presence of varying amounts of sodium chloride. The results of such a study should afford a clearer understanding of the factors that govern the deposition of anhydrite or gypsum, as the case may be, from a slurry of hemihydrate ($CaSO_4.\frac{1}{2}H_2O$) and water, contaminated with NaCl.

EXPERIMENTAL

The salts used in this research, i.e. $CaSO_4$ anhyd., $CaSO_4.2H_2O$, and NaCl, were all Fisher certified reagents of high purity. No recrystallization of the salts was attempted since it was felt that nothing would be gained by it in view of the high initial purity of the materials. An ignition analysis of $CaSO_4.2H_2O$ showed a loss in weight equal to the theoretically expected value of 20.8%. The anhydrous $CaSO_4$ was heated at 900° C for 1 hour and subsequently kept in a desiccator at a temperature of 60° C.

Saturated solutions of gypsum and anhydrite were obtained as follows. Excess solid was added to an aqueous solution of sodium chloride of known composition. The latter was contained in an all-hard-pyrex-glass solubility cell (Fig. 1). The cell and contents were then immersed in a water bath the temperature of which was controlled by an electronic relay and was constant to within 0.05° C. The temperature of the water bath was read by means of a Beckmann thermometer. The latter was calibrated against a standard platinum resistance thermometer. The solutions were agitated for at least 48 hours by means of a pyrex-glass stirrer. This time interval was found to be quite

[1]*Manuscript received April 17, 1961.*
Contribution from the Department of Chemistry, University of Manitoba, Winnipeg, Manitoba.

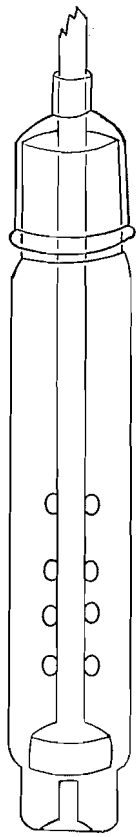


FIG. 1. Solubility cell.

satisfactory in the case of the more stable solid phase. Thus periodic checks in which the solution was stirred for 48 hours, 72 hours, and 96 hours showed no difference in the solubility, i.e. the solubility was identical within the limits of experimental error of $\frac{1}{2}\%$. In the case of the less stable solid phase some difficulties were encountered. It was found that the solubility decreased with longer periods of stirring. It was necessary to make several solubility determinations for different durations of stirring. The maximum solubility value was taken as the "true" solubility of the phase.

After it was deemed that the solution had been stirred for a sufficient length of time, the excess solid was separated from the liquid phase by quickly emptying the contents of the solubility cell into a large sintered-glass filter and applying suction to the suction flask by means of a water aspirator. The act of filtration never lasted longer than 1 minute, thus making any possible loss of water due to evaporation from the saturated solution negligible.

The analysis of the saturated solution was carried out as follows. Two 50-ml samples of the solution were put into two previously weighed Erlenmeyer flasks. The latter were immediately stoppered with rubber stoppers. The flasks and contents were weighed on an analytical balance. Next, the calcium ion concentration was determined by titration with standard E.D.T.A. using "Calred" as indicator. The sodium chloride content was similarly determined on two different samples by titration with standard $AgNO_3$ solution following Mohr's method. Blanks were run in each case.

Can. J. Chem. Downloaded from www.nrcresearchpress.com by 210.87.254.40 on 09/05/12
For personal use only.

EXPERIMENTAL RESULTS

The experimental results are summarized in Table I. In this table is recorded the solubilities of gypsum and anhydrite at various temperatures and sodium chloride concentrations. In Figs. 3 and 4 the solubilities are represented in a graphical manner. Figure 3 shows the solubilities of the two salts in pure water. Lastly, Fig. 2 shows the variation of the transition-point temperature with sodium chloride content of the solution.

TABLE I

Solubility of $CaSO_4$ and $CaSO_4.2H_2O$ in sodium chloride solutions

Moles of NaCl in 1000 g water	Solubility, g $CaSO_4$/100 g water		Moles of NaCl in 1000 g water	Solubility, g $CaSO_4$/100 g water	
	$CaSO_4$	$CaSO_4.2H_2O$		$CaSO_4$	$CaSO_4.2H_2O$
25° C			40° C		
—	0.275	0.207	—	0.225	0.218
1.00	0.751	0.614	0.94	0.630	0.607
1.59	0.816	0.709	1.77	0.691	0.720
2.58	0.831	0.773	2.90	0.697	0.760
3.70	0.770	0.741	3.70	0.640	0.736
4.67	0.664	0.698	4.70	0.572	0.690
5.24	0.631	0.647	5.60	0.508	0.632
30° C			50° C		
—	0.262	0.222	—	0.190	0.212
0.92	0.688	0.600	0.93	0.522	0.599
1.72	0.764	0.713	1.80	0.611	0.722
2.85	0.768	0.755	2.88	0.619	0.775
3.70	0.720	0.726	3.70	0.590	0.752
4.64	0.635	0.658	4.71	0.521	0.700
5.55	0.564	0.616	6.30	0.486	
			5.87		0.638

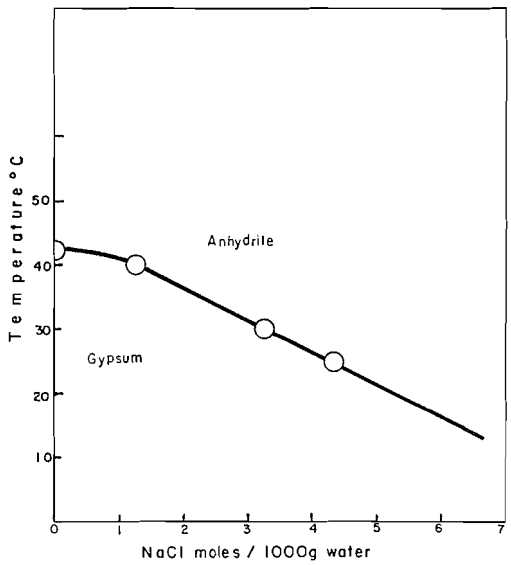


FIG. 2. Variation of transition point with temperature.

Can. J. Chem. Downloaded from www.nrcresearchpress.com by 210.87.254.40 on 09/05/12
For personal use only.

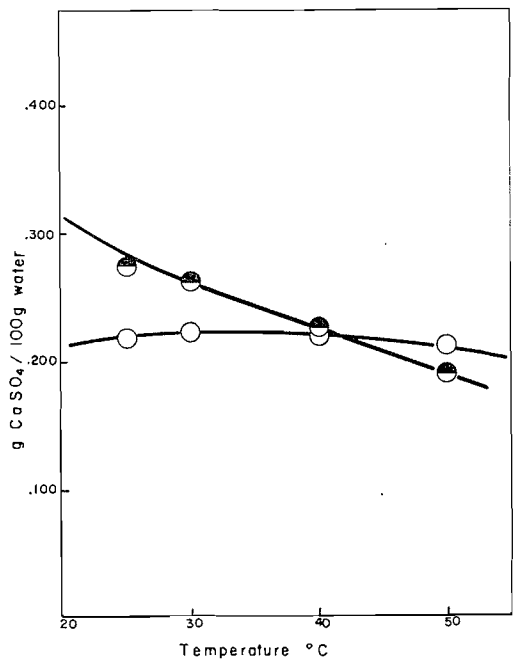


FIG. 3. Solubility in pure water: ◓ $CaSO_4$ anhyd., ○ $CaSO_4.2H_2O$.

DISCUSSION OF RESULTS

From the phase rule it is known that the number of degrees of freedom F, i.e. the number of undetermined variables of a system consisting of C components which are in mutual equilibrium and exist in P phases, is given by the expression

$$F = C - P + 2. \qquad [1]$$

An aqueous solution of gypsum or anhydrite, containing, in addition, dissolved sodium chloride, constitutes a system of three components: $CaSO_4$, NaCl, and H_2O. If the temperature and pressure are fixed at some arbitrary value, the vapor phase may be disregarded. Hence if all sodium chloride is in solution there are only two phases present: the liquid phase—solution, and the solid phase—$CaSO_4$ anhyd. or $CaSO_4.2H_2O$. From eq. [1] it is apparent that F, the number of degrees of freedom, is unity. However, as soon as a second solid phase appears, the system will become invariant, i.e. $F = 0$. It is clear that when $F = 0$ the solution must be saturated with respect to both solid phases, $CaSO_4$ anhyd. and $CaSO_4.2H_2O$. In other words, the two solids will be in equilibrium with one another. By determining the solubility of both salts separately and constructing a plot of solubility versus sodium chloride content of solution, it is possible from the intersection of the two corresponding isotherms to obtain the transition-point temperature of the two salts. That is, the point of intersection of the two curves represents that state of affairs in which both salts have the same solubility and this, as has been shown above, is just the condition for equilibrium. Hence the temperature of the isotherm is the transition temperature for the system in the presence of a certain definite quantity of sodium chloride, the actual quantity of which is defined by the intersection of the two isotherms. By plotting the temperature of the isotherms versus the sodium chloride

Can. J. Chem. Downloaded from www.nrcresearchpress.com by 210.87.254.40 on 09/05/12
For personal use only.

Can. J. Chem. Downloaded from www.nrcresearchpress.com by 210.87.254.40 on 09/05/12
For personal use only.

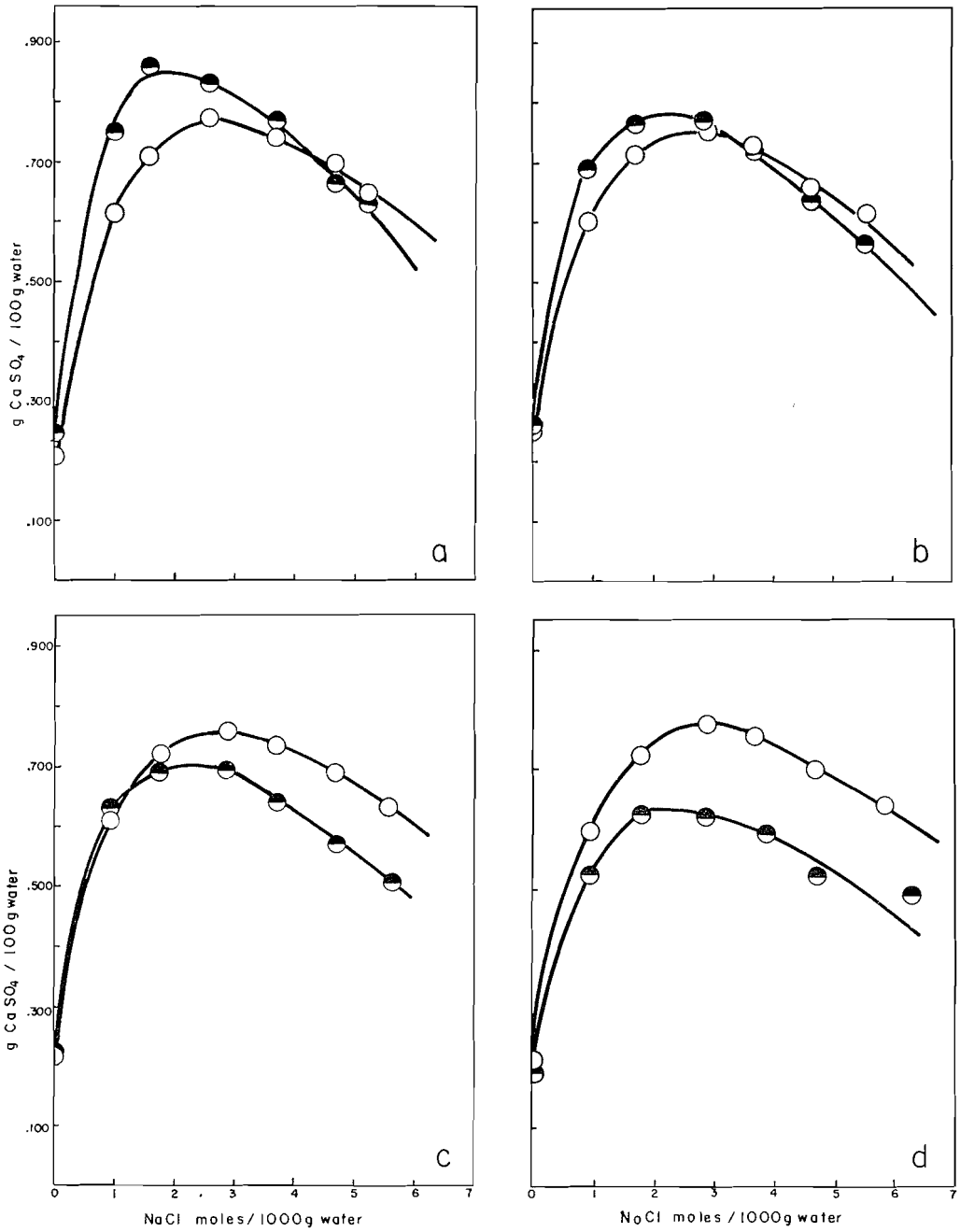


Fig. 4. Isotherms: (*a*) 25° C, (*b*) 30° C, (*c*) 40° C, (*d*) 50° C; ◓ $CaSO_4$ anhyd., ○ $CaSO_4.2H_2O$.

content of the solutions corresponding to the intersection points a graph is obtained which represents the variation of the transition-point temperature with sodium chloride content of solution. By means of this graph (Fig. 2) one can predict the nature of the precipitate that will result from an evaporation of a solution of $CaSO_4$ containing a known quantity of sodium chloride. Thus, for all solutions of a given sodium chloride content, $CaSO_4$

anhyd. will be deposited provided the temperature is above the curve in Fig. 2 or, alternatively, gypsum will be the solid thrown out if the temperature is below the curve.

The variation of the transition-point temperature with sodium chloride content may be also derived from theoretical considerations. The problem is to derive an expression for the variation of the equilibrium constant with temperature for the reaction

$$CaSO_4.2H_2O \rightarrow CaSO_4 + 2H_2O. \quad [2]$$

Employing the known relationships

$$\Delta G^0 = -RT \ln K, \quad [3]$$

$$\Delta G^0 = \Delta H^0 - T\Delta S^0, \quad [4]$$

where ΔG^0, ΔH^0, and ΔS^0 are the standard Gibbs free energy, enthalpy, and entropy and K the equilibrium constant for the reaction, it is possible to arrive at a value of K for any temperature T provided the other quantities involved are known. This procedure was employed by Macdonald (2) in the calculation of the transition point for the above system. A few words should be said concerning the water term on the right-hand side of eq. [2]. This term refers to pure water. But in presence of NaCl the water is no longer pure; its activity is said to be depressed by the presence of NaCl. The extent of this depression may be calculated approximately from vapor pressure values of aqueous sodium chloride solution. These are extensively recorded in the *International Critical Tables* (3). Inserting the numerical values for ΔH, ΔS, and R the gas constant (4), and recognizing that at equilibrium, $\Delta G = 0$, one obtains

$$\Delta G = 163.89T + 0.0215T^2 - 65.17 \log_{10} T - 2495 + 2RT \times 2.303 \log_{10} (P/P_0). \quad [5]$$

Table II shows a number of calculated transition-point temperatures along with those

TABLE II

Variation of transition point with temperature

Moles of NaCl in 1000 g water	Temperature, °C	
	Experimental	Calculated
5.30	20.0*	19.0
4.30	25.0	25.2
3.28	30.0	31.0
2.30	35.0	32.5
0.00	42.0	40.0

*Extrapolated.

experimentally determined. The agreement is quite satisfactory if one takes into account the approximations involved in arriving at eq. [5].

ACKNOWLEDGMENT

The author is indebted to Western Gypsum Products Co. Ltd. of Winnipeg, Manitoba, for a generous grant.

REFERENCES

1. E. Posnjak. Am. J. Sci. A, **35**, 247 (1938). W. M. Madgin and D. A. Swails. J. Appl. Chem. (London), **6**, 482 (1956).
2. J. F. Macdonald. Am. J. Sci. **251**, 884 (1953).
3. International Critical Tables. McGraw-Hill Book Co., New York. 1933.
4. K. K. Kelly, J. C. Southard, and C. T. Anderson. U.S. Bur. Mines, Tech. Papers. 625. 1941.

Can. J. Chem. Downloaded from www.nrcresearchpress.com by 210.87.254.40 on 09/05/12
For personal use only.

Can. J. Chem. Downloaded from www.nrcresearchpress.com by 210.87.254.40 on 09/05/12
For personal use only.

THE RELATIVE BASICITIES OF WATER, METHANOL, AND ETHANOL[1]

C. E. NEWALL AND A. M. EASTHAM

ABSTRACT

From the kinetics of the reaction of ethylene oxide with aqueous ethanol and methanol, catalyzed by perchloric acid, the relative basicities of water, methanol, and ethanol have been determined. The value of K_1 in the expression

$$K_1 = \frac{[H_3O^+][ROH]}{[H_2O][ROH_2^+]}$$

has been found to be 1.2×10^2 for methanol and 2.1×10^2 for ethanol, in good agreement with previous values.

In alcohol solution a number of acid-catalyzed reactions are known to be strongly retarded by traces of water (1, 2, 3). The generally accepted explanation of this effect, first put forward by Goldschmidt about 1900 (2), attributes the decrease in rate to the great affinity of water for protons, with a resulting conversion of the acid ROH_2^+ to the weaker H_3O^+. This view has received strong support in recent years from measurements of the relative basicity of water with respect to alcohols, notably by Braude and Stern (4), Koskikallio (5), and others (6). The results indicate that K_1, where

$$K_1 = \frac{[H_3O^+][ROH]}{[ROH_2^+][H_2O]},$$

has a value of about 100 for methanol and 200 for ethanol at ordinary temperatures.

Our studies of the acid-catalyzed reaction of ethylene oxide with alcohols have prompted us to attempt an estimation of K_1 for methanol and ethanol from kinetic data. This reaction seems particularly well suited to the purpose not only because it shows a large and easily measured retardation by water, but because the uncatalyzed reaction is negligibly slow, and because it now seems quite certain that the reaction mechanism involves a preliminary rapid proton transfer to equilibrium, followed by a slow reaction of the protonated epoxide with the solvent.

$$HA + \underset{\diagdown O \diagup}{CH_2{-}CH_2} \rightleftharpoons \underset{\diagdown OH^+ \diagup}{CH_2{-}CH_2} + A^- \qquad \text{rapid} \qquad [1]$$

$$\underset{\diagdown OH^+ \diagup}{CH_2{-}CH_2} + \begin{matrix}ROH\\ \text{or}\\ H_2O\end{matrix} \xrightarrow{k_1} \begin{matrix}ROCH_2CH_2OH\\ \text{or}\\ HOCH_2CH_2OH\end{matrix} \qquad \text{slow} \qquad [2]$$

Furthermore, water and alcohols react at rather similar rates with the protonated epoxide so at low water concentrations the value of k_1 can be assumed to be independent of the solvent over a workable range of solvent compositions.

From the equilibrium expressions

$$K_2 = \frac{[\text{oxide.H}^+][ROH]}{[\text{oxide}][ROH_2^+]} \quad \text{and} \quad K_3 = \frac{[\text{oxide.H}^+][H_2O]}{[\text{oxide}][H_3O^+]} = K_2/K_1$$

and from the reasonable approximations: (*a*) that the sum of the concentrations of ROH_2^+ and H_3O^+ equals the concentration of added acid (i.e. that ionization is complete and the concentration of protonated epoxide very small), and (*b*) that $[H_3O^+]$ is small

[1]*Manuscript received May 10, 1961.*
Contribution from the Division of Applied Chemistry, National Research Council, Ottawa, Canada.
Issued as N.R.C. No. 6406.

compared to $[H_2O]$, one can derive, as the rate expression for the reaction at low water concentrations, the equation

$$-d(\text{oxide})/dt = k_1K_2[\text{HA}][\text{oxide}]\left\{\frac{[\text{ROH}]}{K_1[H_2O]+[\text{ROH}]}\right\} \quad [3]$$

which in anhydrous solution reduces to the usual rate expression

$$-d(\text{oxide})/dt = k_1K_2\,[\text{HA}][\text{oxide}].$$

K_1 can then be estimated either by measuring k_1K_2 in anhydrous alcohol and solving equation [3] at various water concentrations or by plotting $1/k_{sp}$ against $[H_2O]$, where

$$k_{sp} = \frac{-d(\text{oxide})/dt}{[\text{HA}][\text{oxide}]} = \frac{k_1K_2[\text{ROH}]}{K_1[H_2O]+[\text{ROH}]}, \quad [4]$$

$$1/k_{sp} = \frac{K_1[H_2O]}{k_1K_2[\text{ROH}]}+\frac{1}{k_1K_2}.$$

Since, at low water concentrations, [ROH] is approximately constant, the plot is a straight line of slope $K_1/k_1K_2[\text{ROH}]$ and intercept $1/k_1K_2$.

EXPERIMENTAL

Rate measurements were made dilatometrically, evaluated by the Guggenheim method (7), and expressed in terms of moles per liter per minute at 25° C, essentially as previously described (3). Ethylene oxide was measured out as the vapor in a vacuum system and sealed into ampoules which were then broken into the reaction mixture. Methanol was dried with magnesium turnings in the usual way and used to dilute a stock solution of perchloric acid in dry methanol. The stock solution was prepared from the commercial 70% acid ($HClO_4.2H_2O$). For a few experiments in which an attempt was made to reduce the water content below the 0.01 *M* limit imposed by the 70% acid, anhydrous perchloric acid was prepared in the vacuum apparatus as described elsewhere (8) and diluted at low temperature with dry methanol.

Data for ethanol were taken from the previous paper (3).

RESULTS

The average values of k_{sp} for a series of mixtures of methanol and water are shown in Table I.

TABLE I

$[H_2O]$	$[CH_3OH]$	k_{sp} (av.) (l. mole^{-1} min^{-1})	Glycol in product (mole%)	H_2O in solvent (mole%)
55.6	—	0.58	101	100
50	2.5	0.61	92	95
40	6.5	0.51	77.5	86
30	11	0.48	63	73
20	15	0.345	50	57
12	19	0.35	34	39
8	20	0.39	26	29
4	22	0.73	17	15
2	24	1.35	10	7.7
1	24	2.3	(5)	4
0.50	24.5	4.1	(4)	2
0.25	24.5	5.7		
0.10	24.5	10.4		
0.02	24.5	13.7		
0.01	24.5	12.5		
0.0	24.5	14.1		

Can. J. Chem. Downloaded from www.nrcresearchpress.com by 210.87.254.40 on 09/05/12
For personal use only.

It is apparent from the product analysis that, over most of the range of solvent mixtures, methanol is somewhat more reactive than water. The deviations at low water concentrations are believed to be due to experimental errors in determining the small amounts of glycol present, errors resulting from some oxidation of the methanol. Certainly there is no indication in the analyses that k_1 cannot be considered constant over small changes in solvent composition.

Attempts to determine k_1K_2 by direct measurement of the rate in anhydrous methanol were not very successful, apparently because the reaction is so sensitive to traces of water. Improved techniques could doubtless reduce the error but as the final results show that an error of 1% in the rate corresponds to an error of less than 0.002 M in the concentration of water, this approach does not appear very promising. The best values of k_1K_2 appear to be those obtained by extrapolating the plot of $1/k_{sp}$ against $[H_2O]$ to zero water concentration (Fig. 1). The plots are linear up to 1–2 M water and yield the following constants:

	Methanol	Ethanol
k_1K_2	13.7	6.7
K_1	1.2×10^2	2.1×10^2

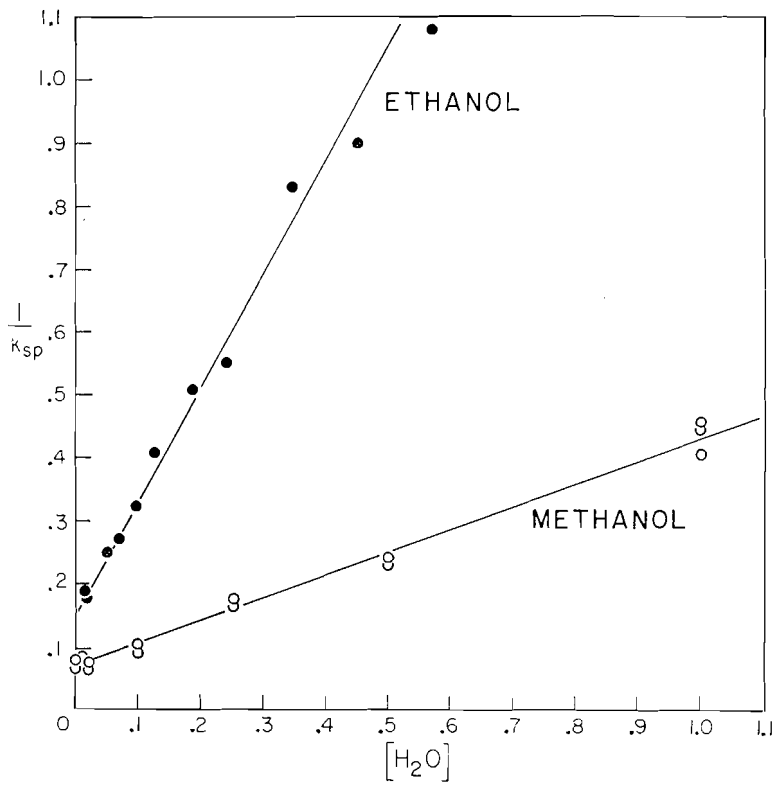


FIG. 1. Plots of $1/k_{sp}$ against water concentration: ● in ethanol (data of Brown and Eastham (3)); ○ in methanol.

The value of K_1 for ethanol is in good agreement with the value of 220 obtained by Braude and Stern (4) from indicator measurements, presumably at about 20° C, while the value for methanol is consistent with values from 110 to 140 obtained by various workers and by a variety of methods, at 25° (5).

Can. J. Chem. Downloaded from www.nrcresearchpress.com by 210.87.254.40 on 09/05/12
For personal use only.

Can. J. Chem. Downloaded from www.nrcresearchpress.com by 210.87.254.40 on 09/05/12
For personal use only.

While the agreement of the present values of K_1 with other work seems good, inspection of the data suggests that the probable error in our values may be as high as $\pm 10\%$. The error lies largely in the value for k_1K_2 since the extrapolation is by no means precise. There is, however, one rather disturbing feature of the results, namely the relative values of k_1K_2 for the two alcohols. If K_1 is twice as large for ethanol as for methanol then one might expect the same to be true for K_2, and it follows that k_1 should be about four times as large for methanol as for ethanol. The glycol analyses, however, suggest that k_1 cannot be more than twice as large for methanol as for ethanol. A comparison of this kind is perhaps dangerous since the two sets of constants were obtained in different solvents (methanol and ethanol) but does suggest that the results should be treated with caution.

In Fig. 2, values of k_{sp} calculated from the above constants have been plotted, along

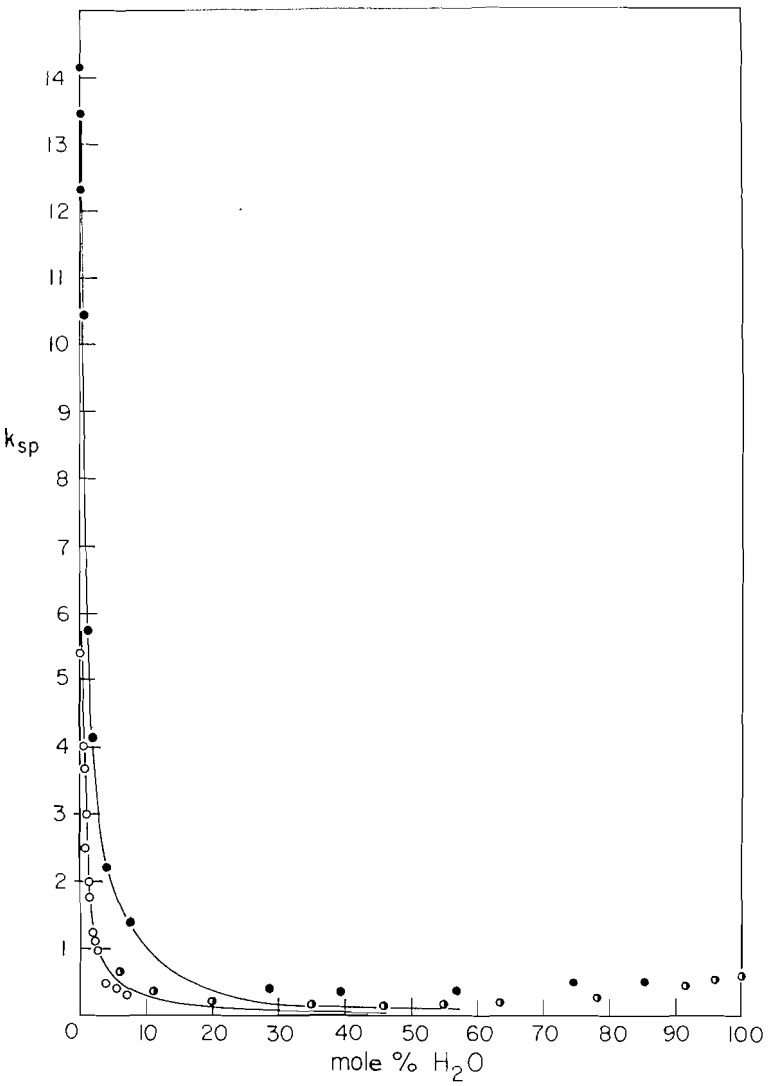


FIG. 2. Plots of k_{sp} against solvent composition. Solid lines are rates calculated for methanol and ethanol from the values of k_1K_2 and K_1 obtained in this work. Circles are experimental values: ● methanol–water; ○ ethanol–water; ◑ ethanol–water at constant ionic strength (ClO_4^- = 0.055 M).

with the experimental data, against the solvent composition. As the proportion of water in the solvent increases, deviations from the calculated rates become severe at about 10–15 mole% water, while at about 50 mole% water the rate starts to increase again. These changes may be due in part to general medium effects such as changes in the dielectric constant but there are also a number of specific causes which have not been taken into account here. In particular we may note (*a*) that salt effects are about five times larger in ethanol than in water so a small rate decrease should occur with increasing water, (*b*) that equation [3] treats the solvent as pure alcohol and does not allow for an increase in molarity (from 17 to 55 in the case of ethanol–water) as the water concentration increases, and (*c*) over a wide range of concentrations the value of k_1 will not be constant in methanol–water mixtures because of the lower reactivity of water.

REFERENCES

1. A. J. DEYRUP. J. Am. Chem. Soc. **56**, 60 (1934).
2. H. GOLDSCHMIDT and E. SUNDE. Ber. **39**, 711 (1906). H. GOLDSCHMIDT and O. UDBY. Z. physik. Chem. **60**, 728 (1907).
3. R. K. BROWN and A. M. EASTHAM. Can. J. Chem. **38**, 2039 (1960).
4. E. A. BRAUDE and E. S. STERN. J. Chem. Soc. 1976 (1948).
5. J. KOSKIKALLIO. Acta Chem. Scand. **13**, 671 (1959).
6. H. A. SMITH and C. H. REICHARDT. J. Am. Chem. Soc. **63**, 605 (1941).
7. E. A. GUGGENHEIM. Phil. Mag. **2**, 538 (1926).
8. S. J. TAUBER and A. M. EASTHAM. J. Am. Chem. Soc. **82**, 4888 (1960).

Can. J. Chem. Downloaded from www.nrcresearchpress.com by 210.87.254.40 on 09/05/12
For personal use only.

Can. J. Chem. Downloaded from www.nrcresearchpress.com by 210.87.254.5 on 09/05/12
For personal use only.

CORRELATIONS OF INFRARED GROUP FREQUENCIES AND BAND INTENSITIES IN ORGANIC MOLECULES WITH SUBSTITUENT CONSTANTS: A STATISTICAL EVALUATION[1]

C. N. R. RAO[2] AND R. VENKATARAGHAVAN[3]

ABSTRACT

A statistical evaluation of the empirical linear correlations of infrared group frequencies and band intensities in aliphatic and benzene derivatives with substituent constants has been carried out. The correlations of frequencies with substituent constants generally give low standard deviations and acceptable correlation coefficients, and may thus be employed for the estimation of substituent constants. The correlations of band intensities with substituent constants show an interesting trend of the sign and magnitude of the slopes (ρ values) with the electrical property of the bond or group involved in the vibration. The ρ value decreases with the increasing electron-withdrawing power of the group.

INTRODUCTION

Although the various substituent constants were devised to correlate the structure of organic molecules with their chemical reactivity, many physical properties of the molecules may also be correlated with these constants (1, 2). Such empirical or semiempirical relations give a better insight into the structure and behavior of organic molecules, particularly when the chemist cannot yet disentangle the various structural factors into finer and more fundamental contributions. Considerable interest has been exhibited, in recent years, in correlating the infrared group frequencies and band intensities of related groups of organic molecules with substituent constants (3–9). The infrared frequencies and intensities are controlled by different factors. While the frequency is mainly determined by the bond force constants, the intensity is controlled by dipole derivatives with respect to bond length, $(\delta\mu/\delta r_{ij})$. Change of substituent group may affect the force constants, static dipole moments, or $(\delta\mu/\delta r_{ij})$, through inductive or (and) resonance effects. Substituent groups generally affect both the frequency and the intensity, though not always in the same direction. Sometimes the frequency shift is very small and the change in band intensity is large or vice versa. It is therefore important to correlate the frequencies and intensities of groups with substituent constants to understand the mechanism(s) involved. Although there have been several reports of such correlations with substituent constants in the literature (3–9), there has been no systematic evaluation of these correlations. We have now carried out a statistical evaluation (10) of the correlations of group frequencies and band intensities of aliphatic and benzene derivatives, in order to test the validity and utility of the correlations. Such an evaluation is justified by the high precision and accuracy of the recent infrared data on related groups of organic molecules, used in these correlations.

[1]*Manuscript received March 10, 1961.*
Joint contribution from the Department of Organic Chemistry and the Department of Inorganic and Physical Chemistry, Indian Institute of Science, Bangalore-12, India.
[2]*To whom all the correspondence should be addressed at the Department of Inorganic and Physical Chemistry, Indian Institute of Science, Bangalore-12, India.*
[3]*Indian Institute of Science Research Scholar in the Department of Organic Chemistry.*

Can. J. Chem. Downloaded from www.nrcresearchpress.com by 210.87.254.5 on 09/05/12
For personal use only.

RESULTS AND DISCUSSION

A linear relation of the infrared group frequencies in meta- and para-disubstituted benzene derivatives with the Hammett σ constants (11) has been suggested by several workers (3, 8, 12). The relation may be expressed by a Hammett-type equation,

$$\nu = \nu_0 + \rho\sigma, \quad [1]$$

where ν is the observed group frequency in the meta- or para-disubstituted benzene, ν_0 is the group frequency in the monosubstituted derivative, and σ and ρ have their usual significance. Thompson *et al.* (3) have expressed doubt about the roughly linear plots of ν against σ having much significance and have considered the possibility of plotting ν^2 versus σ. A linear relationship of the group frequencies in the meta- and para-benzene derivatives has also been proposed (4) with the electrophilic substituent constants, σ^+ (13, 14).

$$\nu = \nu_0^+ + \rho^+\sigma^+ \quad [2]$$

The σ^+ values differ from the σ values by an extra resonance factor resulting from greater opportunity for resonance in electrophilic reactions. The results of the statistical treatment of the correlations of the available data on the infrared group frequencies of benzene derivatives, with the σ and σ^+ constants, have been summarized in Table I. The σ constants were taken from the recent compilation by McDaniel and Brown (27) and σ^+ constants from the compilations by Brown and Okamoto (14). For the 18 sets of frequencies of meta- and para-substituted benzene derivatives correlated with the σ and σ^+ constants, the average standard deviations for the $\nu-\sigma$ and $\nu-\sigma^+$ correlations are 3.3 and 3.3 cm^{-1} respectively, while the correlation coefficients are 0.938 and 0.924 respectively. It may be concluded that both the substituent constants correlate the frequencies equally well. This is not completely unexpected, because the vibrational frequencies, being associated with mechanical properties of bonds, may not show any preference between σ and σ^+ constants.

A linear relationship of the infrared group frequencies in aliphatic derivatives with the σ^* constants of Taft (28) has been proposed.

$$\nu = \nu_0^* + \rho^*\sigma^* \quad [3]$$

The results of the statistical evaluation of the correlations of the available data with the σ^* constants have been summarized in Table II. The average standard deviation is rather high (14.1 cm^{-1}), compared to the value of 3 cm^{-1} in the case of benzene derivatives (Table I).

Several possible correlations of infrared band intensities in meta- and para-substituted benzene derivatives with σ and σ^+ constants have been suggested (3, 4, 5, 9, 36). The best correlation is probably between the logarithm of the vibrational band intensities, $\log A$, and the substituent constants. Thompson and co-workers (3, 8) have correlated $\log A$ with Hammett σ constants:

$$\log A = \log A_0 + \rho\sigma. \quad [4]$$

Rao (4, 9, 22) has suggested a similar linear relation with the σ^+ constants:

$$\log A = \log A_0^+ + \rho^+\sigma^+. \quad [5]$$

Can. J. Chem. Downloaded from www.nrcresearchpress.com by 210.87.254.5 on 09/05/12
For personal use only.

TABLE 1

Correlation of infrared group frequencies in *p*- and *m*-substituted benzene derivatives with σ and σ^+ substituent constants

Series	Solvent	Frequency	ν_0 [b] (cm^{-1})	ρ [c]	s [d]	r [e]	ν_0^+ [b] (cm^{-1})	ρ^+ [c]	s [d]	r [e]	n [f]
Phenols (15)[a]	C	ν_{OH}	3610	−13.4	5.3	0.958	3608	− 9.51	3.3	0.924	15, 14
Benzoic acids (16)	C	ν_{OH}	3553	−10.1	3.4	0.793	3552	−10.6	2.4	0.956	6
Benzoyl peroxides (17)	D	$\nu_{C=O}$	1776	18.3	3.3	0.978	1779	12.5	4.1	0.898	10
Benzophenones (12)	C	$\nu_{C=O}$	1663	13.9	1.5	0.946	1664	6.9	3.6	0.831	9
Acetophenones (18)	C	$\nu_{C=O}$	1690	15.9	1.6	0.975	1692	10.6	3.3	0.974	14
Benzaldehydes (3)	C	$\nu_{C=O}$	1704	10.9	2.8	0.872	1707	9.1	3.1	0.989	7, 6
Benzoic acids (16)	C	$\nu_{C=O}$ (monomer)	1742	12.9	1.5	0.962	1743	9.1	2.0	0.961	6
Benzoic acids (16)	C	$\nu_{C=O}$(dimer)	1695	14.2	3.1	0.994	1697	9.9	1.4	0.976	6
Ethyl benzoates (3)	C	$\nu_{C=O}$	1717	14.9	2.9	0.959	1719	9.9	1.7	0.977	6
Acetanilides (8)	CH	$\nu_{C=O}$	1691	21.1	3.3	0.940	1694	13.9	1.3	0.904	8
Acetanilides (19)	C	$\nu_{NH(trans)}$	3437	−3.0	2.8	0.835	3436	−1.8	2.3	0.783	10, 9
Anilines (20)[a]	C	$\nu_{NH(asym)}$	3476	30.5	3.8	0.979	3482	21.3	4.0	0.864	16
Anilines (21)[a]	C	$\nu_{NH(sym\ overtone)}$	—	—	—	—	6697	41.3	2.9	0.992	19
Anisoles (22)	C	ν_{C-O-C}	1243	14.6	5.1	0.868	1246	14.5	5.7	0.782	10
Nitrobenzenes (23)	B	$\nu_{NO_2(asym)}$	1523	30.5	3.6	0.961	1528	19.2	5.6	0.934	9
Benzonitriles (24)	C	$\nu_{C\equiv N}$	2232	7.4	1.4	0.965	2233	5.3	3.6	0.954	9
Isothiocyanates (25)	C	$\nu_{N=C=S}$	2048	−48.2	6.0	0.987	2042	−30.0	5.9	0.981	7, 6
Thiocyanates (26)	CH	$\nu_{S-C\equiv N}$	2167	8.3	5.1	0.977	2169	5.1	2.9	0.949	7
					Av. 3.3	0.938			Av. 3.3	0.924	

NOTE: solvents: C, carbon tetrachloride; D, dichloroethane; CH, chloroform; B, bromoform.

[a]In these systems σ^- values ("dual" values) were used for some of the electron-withdrawing groups.

[b]Intercept (value for the unsubstituted compound).

[c]Slope.

[d]Standard deviation in cm^{-1}.

[e]Correlation coefficient.

[f]Number of compounds in the correlation.

A statistical evaluation of the correlations of log A with σ and σ^+ constants (Table III) seems to indicate that σ^+ constants are probably better suited for the correlations. In some cases, like benzonitriles and anilines, the correlations with σ^+ constants are far superior. Such a preference to σ^+ constants is understandable, since band intensities are related to electrical properties of bonds. Excellent linear correlations have also been

TABLE II

Correlation of infrared group frequencies in aliphatic derivatives with Taft σ^* constants

Series	Solvent	Frequency	$\nu_0{}^{*a}$	ρ^{*b}	s^c	r^d	n^e
Simple aliphatic ketones (29)	C	$\nu_{C=O}$	1714	19.6	9.9	0.906	9
Hetero-atom conjugated ketones (30)	P	$\nu_{C=O}$	1654	53.8	17.3	0.954	6
Amides (31)	CH	$\nu_{C=O}$	1685	19.9	12.1	0.901	7
Acids (32)	C	ν_{OH}	3530	−9.4	0.5	0.995	11
Nitro compounds (33, 34)	C	$\nu_{NO_2(asym)}$	1557	25.1	5.7	0.989	7
Simple and β-substituted nitriles (35)	CH	$\nu_{C\equiv N}$	2253	14.7	38.8	0.889	8
					Av. 14.1	0.939	

NOTE: solvents: C, carbon tetrachloride; P, condensed phase; CH, chloroform.
[a]Intercept (value for the unsubstituted compound).
[b]Slope.
[c]Standard deviation in cm^{-1}.
[d]Correlation coefficient.
[e]Number of compounds used in the correlation.

found between the logarithms of molar extinction coefficients, log ϵ, and σ^+ constants in the case of C—O—C stretching vibrations of anisoles (22) and NH stretching overtones of anilines (21).

The infrared band intensities in aliphatic derivatives may be correlated with σ^* constants:

$$\log A = \log A_0{}^* + \rho^*\sigma^*, \quad [6]$$

but the correlations are not satisfactory (Table IV).

GENERALIZATIONS

In the correlations of group frequencies with substituent constants, there is no particular relation between the sign and the magnitude of ρ and the nature of the bond or group involved in the vibration as might be expected. However, in the correlations of band intensities, there is a systematic variation of the sign of ρ with the nature of the bond involved. A negative slope of the log $A-\sigma$, log $A-\sigma^+$, or log $A-\sigma^*$ plot is always found when the bond or the group involved is electron-withdrawing in nature, as in carbonyl derivatives and nitriles. A positive slope is found when the bond or group involved is electron-donating in character. The magnitude of ρ seems to vary in proportion to the extent to which the groups can withdraw or donate electrons. The slope of the log $A-\sigma$ or log $A-\sigma^+$ plot decreases with the increasing electron-withdrawing power of the group. These generalizations may be clearly seen from Table V.

This relation of the sign of ρ in the log $A-\sigma$, log $A-\sigma^+$, or log $A-\sigma^*$ plot to the electrical property of the bond or group is found because the band intensity is itself dependent

Can. J. Chem. Downloaded from www.nrcresearchpress.com by 210.87.254.5 on 09/05/12
For personal use only.

Can. J. Chem. Downloaded from www.nrcresearchpress.com by 210.87.254.5 on 09/05/12
For personal use only.

TABLE III

Correlation of infrared band intensities in *m*- and *p*-substituted benzene derivatives with σ and σ^+ constants

Series	Solvent	Frequency	log A_0 [a]	ρ [b]	s [c]	r [d]	log A_0^+ [a]	ρ^+ [b]	s [c]	r [d]	n [e]
Benzaldehydes (3)	C	$\nu_{C=O}$	1.044	−0.089	0.021	0.916	1.040	−0.067	−0.068	0.986	5
Ethyl benzoates (3)	C	$\nu_{C=O}$	1.193	−0.080	0.023	0.945	1.205	−0.055	0.062	0.955	6
Acetanilides (8)	C	$\nu_{C=O}$	1.195	−0.145	0.033	0.979	1.173	−0.099	0.020	0.969	8
Phenols[f] (15)	C	ν_{OH}	0.790	0.137	0.040	0.879	0.813	0.106	0.040	0.875	14
Anilines[f] (20)	C	$\nu_{NH(asym)}$	1.188	0.166	0.053	0.889	1.217	0.130	0.044	0.923	16
Benzonitriles (36)	C	$\nu_{C\equiv N}$	0.356	−0.787	0.088	0.930	0.299	−0.461	0.033	0.982	7
					Av. 0.043	0.923			Av. 0.044	0.948	

NOTE: solvent: C, carbon tetrachloride.

[a] Intercept (value for the unsubstituted compound).

[b] Slope.

[c] Standard deviation in cm^{-1}.

[d] Correlation coefficient.

[e] Number of compounds in the correlation.

[f] In these systems $\sigma-$ values ("dual" values) wese used for some of the electron-withdrawing groups.

TABLE IV

Correlation of infrared band intensities in aliphatic derivatives with Taft σ^* constants

Series	Solvent	Frequency	log $A_0{}^{*a}$	ρ^{*b}	s^c	r^d	n^e
Amides (31)	CH	$\nu_{C=O}$	0.613	−0.017	0.030	0.593	7
Alcohols (37)	C	ν_{OH}	0.681	0.397	0.082	0.881	12
Nitriles (35)	CH	$\nu_{C\equiv N}$	0.736	−0.491	0.087	0.792	8
				Av.	0.066	0.755	

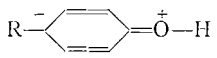
NOTE: solvents: C, carbon tetrachloride; CH, chloroform.
[a]Intercept (value for the unsubstituted compound).
[b]Slope.
[c]Standard deviation in cm^{-1}.
[d]Correlation coefficient.
[e]Number of compounds in the correlation.

TABLE V

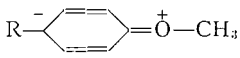
Generalizations regarding the correlation of infrared spectra of organic molecules with substituent constants

Series	Frequency	Group	para-σ of the group	$\frac{\log A - \sigma}{\rho}$	$\frac{\log A - \sigma^+}{\rho^+}$
Anilines (20)	ν_{NH}	$-NH_2$	−0.66	0.166	0.130
Phenols (15)	ν_{OH}	—OH	−0.37	0.137	0.106
Ethyl benzoates (3)	$\nu_{C=O}$	$-COOC_2H_5$	0.45	−0.08	−0.055
Nitriles (24)	$\nu_{C\equiv N}$	—CN	0.66	−0.26	−0.509

on $(\delta\mu/\delta r_{ij})$. Substituents favoring a dipole of a bond always increase its band intensity. Thus, the OH band intensity in phenols increases with electron-withdrawing ability of the group in the para or meta position (positive slope), while the C≡N band intensity in benzonitriles increases with the increasing electron-donating ability of the para or meta substituent (negative slope). This type of generalization is extremely useful in identifying the prominent resonance forms in aromatic systems. For example, the most prominent resonance structures in phenols (I) and anisoles (II) should be similar since

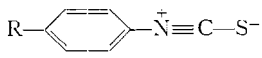


I

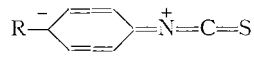


II

the slopes of the log $A - \sigma$ plots are positive in both cases (22). The most prominent resonance structure of the organic isothiocyanates has been proposed to be III (38) or IV (39). This proposal may now be supported by the band intensity measurements of Caldow



III



IV

and Thompson (26) in para- and meta-substituted phenyl isothiocyanates. The —NCS band intensity increases with the electron-withdrawing power of the substituents.

Can. J. Chem. Downloaded from www.nrcresearchpress.com by 210.87.254.5 on 09/05/12
For personal use only.

Can. J. Chem. Downloaded from www.nrcresearchpress.com by 210.87.254.5 on 09/05/12
For personal use only.

UTILITY OF THE CORRELATIONS IN ESTIMATING REACTIVITIES OF GROUPS

An obvious application of these different linear relations would be in the estimation of substituent constants of groups. The frequency correlation would be more useful for this purpose because frequencies can be measured very easily with high precision and accuracy. The measurement of band intensities, on the other hand, is rather tedious. One could, however, make use of extinction coefficient data, to a certain extent. If one were to employ the frequency correlations (Tables I and II) for estimating the substituent constant for a group, one has to determine the characteristic frequency of a functional group in the unsubstituted and substituted derivatives and then calculate the substituent constant by making use of the ρ values given in the tables (employing the same solvent). One should choose a functional group which has the most structure-sensitive frequency. Carbonyl stretching vibration is probably best for the purpose.

NOTE ADDED IN PROOF: Brown (40) has recently suggested that the substituent constants should be linearly related to the square roots of the infrared absorption intensities in substituted benzene derivatives. We have now carried out the statistical evaluation of the linear relations of $A^{\frac{1}{2}}$ with σ and σ^+ constants and have found that the $A^{\frac{1}{2}}$–σ^+ correlations are as good as the log A – σ^+ correlations. The average standard deviation and correlation coefficient of $A^{\frac{1}{2}}$–σ^+ correlations for the six series of benzene derivatives (Table III) are found to be 0.081 and 0.957 respectively.

ACKNOWLEDGMENTS

The authors are highly thankful to Professor D. K. Banerjee and Professor M. R. A. Rao for their keen interest in the work.

REFERENCES

1. C. N. R. RAO. J. Sci. Ind. Research (India), **20A**, 24 (1961).
2. R. W. TAFT, JR., P. S. SKELL, and N. C. DENO. Ann. Rev. Phys. Chem. **9** (1958).
3. H. W. THOMPSON, R. W. NEEDHAM, and D. JAMESON. Spectrochim. Acta, **9**, 208 (1957).
4. C. N. R. RAO and G. B. SILVERMAN. Current Sci. (India), **26**, 375 (1957).
5. T. L. BROWN. Chem. Revs. **58**, 581 (1958).
6. P. J. KRUEGER and H. W. THOMPSON. Proc. Roy. Soc. (London), A, **250**, 22 (1959).
7. H. W. THOMPSON. Spectrochim. Acta, **14**, 145 (1959).
8. H. W. THOMPSON and D. A. JAMESON. Spectrochim. Acta, **13**, 236 (1958).
9. C. N. R. RAO. Chem. & Ind. (London), 891 (1958).
10. H. H. JAFFE. Chem. Revs. **53**, 191 (1953).
11. L. P. HAMMETT. Physical organic chemistry. McGraw-Hill Book Co. Inc., New York. 1940. Chap. VII.
12. N. FUSON, M. L. JOSIEN, and E. M. SHELTON. J. Am. Chem. Soc. **76**, 2526 (1954).
13. Y. OKAMOTO and H. C. BROWN. J. Org. Chem. **22**, 485 (1957).
14. H. C. BROWN and Y. OKAMOTO. J. Am. Chem. Soc. **80**, 4979 (1958).
15. P. J. STONE and H. W. THOMPSON. Spectrochim. Acta, **10**, 17 (1957).
16. M. ST. C. FLETT. Trans. Faraday Soc. **44**, 767 (1948).
17. W. H. T. DAVISON. J. Chem. Soc. 2456 (1951).
18. R. N. JONES, W. F. FORBES, and W. A. MUELLER. Can. J. Chem. **35**, 504 (1957).
19. R. MOCCIA and H. W. THOMPSON. Spectrochim. Acta, **10**, 240 (1957).
20. P. J. KRUEGER and H. W. THOMPSON. Proc. Roy. Soc. (London), A, **243**, 143 (1957).
21. K. B. WHETSEL, W. E. ROBERSON, and M. W. KRELL. Anal. Chem. **30**, 1598 (1958).
22. G. K. GOLDMAN, H. LEHMAN, and C. N. R. RAO. Can. J. Chem. **38**, 171 (1960).
23. R. D. KROSS and V. A. FASSEL. J. Am. Chem. Soc. **78**, 4225 (1956).
24. M. R. MANDER and H. W. THOMPSON. Trans. Faraday Soc. **53**, 1402 (1957).
25. C. N. R. RAO, J. RAMACHANDRAN, and S. SOMASEKHARA. Current Sci. (India), **27**, 474 (1958).
26. G. L. CALDOW and H. W. THOMPSON. Spectrochim. Acta, **13**, 212 (1958).
27. D. H. MCDANIEL and H. C. BROWN. J. Org. Chem. **23**, 420 (1958).
28. R. W. TAFT, JR. *In* Steric effects in organic chemistry. *Edited by* M. S. Newman. John Wiley & Sons, Inc., New York. 1956. Chap. 13.
29. C. N. R. RAO, G. K. GOLDMAN, and C. LURIE. J. Phys. Chem. **63**, 1311 (1959).

30. D. G. O'SULLIVAN and P. W. SADLER. J. Chem. Soc. 4144 (1957).
31. T. L. BROWN, J. F. REGAN, R. D. SCHULTZ, and J. C. STEENBERG. J. Phys. Chem. **63**, 1324 (1959).
32. J. D. S. GOULDEN. Spectrochim. Acta, **6**, 129 (1954).
33. R. N. HASZELDINE. J. Chem. Soc. 2525 (1953).
34. J. MASON and J. DUNDERDALE. J. Chem. Soc. 759 (1956).
35. J. P. JESSON and H. W. THOMPSON. Spectrochim. Acta, **13**, 217 (1958).
36. T. L. BROWN. J. Am. Chem. Soc. **80**, 794 (1958).
37. T. L. BROWN. J. Am. Chem. Soc. **80**, 6490 (1958).
38. E. LIEBER, C. N. R. RAO, and J. RAMACHANDRAN. Spectrochim. Acta, **13**, 296 (1959).
39. C. N. R. RAO and R. VENKATARAGHAVAN. Unpublished results.
40. T. L. BROWN. J. Phys. Chem. **64**, 1798 (1960).

Can. J. Chem. Downloaded from www.nrcresearchpress.com by 210.87.254.5 on 09/05/12
For personal use only.

Can. J. Chem. Downloaded from www.nrcresearchpress.com by 210.87.254.5 on 09/05/12
For personal use only.

THE PREPARATION OF SOME MERCAPTO MONOSACCHARIDES[1]

N. C. JAMIESON AND R. K. BROWN

ABSTRACT

Methyl 4,6-O-benzylidene-2-benzylthio-2-deoxy-α-D-altropyranoside and methyl 4,6-O-benzylidene-3-benzylthio-3-deoxy-α-D-altropyranoside have been prepared by the reaction of sodium benzylmercaptide with methyl 2,3-anhydro-4,6-O-benzylidene-α-D-allopyranoside and methyl 2,3-anhydro-4,6-O-benzylidene-α-D-mannopyranoside respectively.

These two thio ethers were successfully reduced by sodium in liquid ammonia to methyl 2-deoxy-2-mercapto-α-D-altropyranoside and methyl 3-deoxy-3-mercapto-α-D-altropyranoside. An attempted replacement of the tosyl group in 1,2;5,6-di-O-isopropylidene-3-O-tosyl-α-D-glucofuranose by benzyl mercaptan was unsuccessful.

INTRODUCTION

The preparation of monosaccharides in which an oxygen atom has been replaced by a sulphur atom has received renewed attention in recent years, primarily due to the fact that these compounds provide a route to the synthesis of deoxy sugars. A review by Raymond covering the literature on thio sugars to 1944 (1) refers to the preparation of a number of thioglycosides and ω-deoxy-ω-alkylthio-hexoses and -pentoses. The only monosaccharide mentioned which contained a free mercapto group on a carbon atom other than the anomeric carbon (2–4) was a substance described as "3-deoxy-3-mercapto-D-glucose" obtained by Freudenberg and Wolf (5) in their attempt to apply the Tschugaeff reaction (6) to the preparation of an unsaturated monosaccharide.

Since 1944, a considerable amount of work has appeared in this area, but primarily concerning the preparation of the thioglycosides and thio ethers of monosaccharides (7–12). A few reports have been made of the preparation of monosaccharides with a free mercapto group. An improved synthesis of 1-thio-D-glucose by the reaction of hydrogen sulphide with 1,2-anhydro-D-glucose and its 3,4,6-tri-O-acetate in dimethylformamide has been described (13). The reduction with lithium aluminum hydride of 5,6-dideoxy-5,6-epithio-1,2-O-isopropylidene-β-L-idose has yielded 5,6-dideoxy-5-mercapto-L-idose (14). There has also been reported the preparation of 5,6-dideoxy-1,2-O-isopropylidene-5,6-(thiocarbonyldithio)-β-L-idose, a compound which, no doubt, can be reduced readily to 5,6-dideoxy-1,2-O-isopropylidene-5,6-dimercapto-β-L-idose with lithium aluminum hydride in accordance with similar reductions carried out on the trithiocarbonates of some hexitols (14, 15).

Since a number of mercapto monosaccharides were required in this laboratory, a program for their preparation was begun. This paper presents some results obtained in this direction.

RESULTS AND DISCUSSION

The debenzylation of S-benzylcysteine has been accomplished by the use of sodium in liquid ammonia (16) and this technique has been successfully applied in this laboratory to the preparation of mercaptoindoles (17). These results suggested that mercapto monosaccharides might be prepared by the reaction of benzyl mercaptan with suitable anhydro monosaccharides followed by the reductive cleavage of the resulting benzylthio ethers with sodium in liquid ammonia. This did indeed prove to be the case.

[1]*Manuscript received May 19, 1961.*
Contribution from the Department of Chemistry, University of Alberta, Edmonton, Alberta. Taken from the thesis of N. C. Jamieson to be submitted to the Graduate School of the University of Alberta in partial fulfillment of the requirements for the degree of Master of Science.

Can. J. Chem. Downloaded from www.nrcresearchpress.com by 210.87.254.5 on 09/05/12
For personal use only.

When methyl 2,3-anhydro-4,6-O-benzylidene-α-D-allopyranoside (18, 19) was treated with sodium benzylmercaptide in methanol as solvent an almost quantitive yield of crystalline methyl 4,6-O-benzylidene-2-benzylthio-2-deoxy-α-D-altropyranoside was obtained. Similarly, methyl 2,3-anhydro-4,6-O-benzylidene-α-D-mannopyranoside (19), when treated with sodium benzylmercaptide, gave crystalline methyl 4,6-O-benzylidene-3-benzylthio-3-deoxy-α-D-altropyranoside. The direction of opening of the anhydro ring agreed with observations recorded in the literature (7–9) and with the requirement that ring opening proceed preferentially via the more stable trans diaxial transition state according to Furst and Plattner's rule (20, 21). The position of the benzylthio group was verified by desulphurization of the benzylthio ethers with Raney nickel (9, 22) to produce the corresponding deoxy monosaccharides. These were compared with authentic specimens prepared by the reduction with lithium aluminum hydride of methyl 2,3-anhydro-4,6-O-benzylidene-α-D-mannopyranoside and methyl 2,3-anhydro-4,6-O-benzylidene-α-D-allopyranoside (23).

When treated with sodium in liquid ammonia, methyl 4,6-O-benzylidene-2-benzylthio-2-deoxy-α-D-altropyranoside gave a good yield of solid methyl 2-deoxy-2-mercapto-α-D-altropyranoside which readily crystallized from alcohol. Reduction of methyl 4,6-O-benzylidene-3-benzylthio-3-deoxy-α-D-altropyranoside under the same conditions gave a colorless syrup which solidified on trituration with water. Attempts at purification by direct crystallization from a wide variety of solvents and solvent pairs were abortive. However, chromatography of the crude mercapto sugar on neutral alumina yielded bibenzyl in the initial fractions followed by a viscous colorless syrup which again readily solidified on trituration with water. Crystallization of this solid from ethyl propionate was slow, but large prismatic crystals were produced whose analysis agreed with the formulation of this substance as methyl 3-deoxy-3-mercapto-α-D-altropyranoside. It is thus seen that sodium in liquid ammonia removes not only the benzyl group from the sulphur atom but also provides a convenient route for the removal of the benzylidene group without affecting the glycosidic linkage. Simultaneous cleavage of the benzylidene group and desulphurization have been obtained by the use of a large excess of Raney nickel (8, 9). However, when no more than a fourfold excess of Raney nickel was employed, reductive desulphurization occurred unaccompanied by removal of the benzylidene group (9). Since 1,2;5,6-di-O-isopropylidene-α-D-glucofuranose (24) was quite unaffected by sodium in liquid ammonia, this reductive cleavage may be specific for the benzylidene group.

Hydrolysis of methyl 2-deoxy-2-mercapto-α-D-altropyranoside and the 3-mercapto isomer with *N* sulphuric acid gave yellow solids which charred on heating but would not melt. Infrared spectra showed the substances to be quite impure and afforded no information as to their structures. Neither they, nor the products obtained from attempts to prepare their acetyl, benzoyl, or 3,5-dinitrobenzoyl derivatives, could be obtained in crystalline form.

Freudenberg and Brauns (25) reported that treatment of 1,2;5,6-di-O-isopropylidene-3-O-tosyl-α-D-glucofuranose with hydrazine replaced the 3-tosyloxy group by the hydrazine moiety. The resulting compound has recently been shown unequivocally to have the allo configuration (26). Although Reichstein *et al.* (9, 27) have shown that both sodium methoxide and sodium methylmercaptide did not replace the tosyloxy group but merely caused detosylation, it was thought that the greater nucleophilic character of the benzylmercaptide might induce a reaction analogous to that obtained by Freudenberg and Brauns and thus lead to the formation of 3-deoxy-3-mercapto-D-allose. However, here again, reaction of sodium benzylmercaptide with 1,2;5,6-di-O-isopropylidene-3-O-tosyl-α-D-glucofuranose resulted only in detosylation with retention of configuration about C_3.

Can. J. Chem. Downloaded from www.nrcresearchpress.com by 210.87.254.5 on 09/05/12
For personal use only.

EXPERIMENTAL

All melting points are uncorrected.

Methyl 4,6-O-Benzylidene-2-benzylthio-2-deoxy-α-D-altropyranoside

Sodium (2 g) was dissolved in methanol (40 ml) containing benzyl mercaptan (2.6 g, 0.022 mole) (28). Methyl 2,3-anhydro-4,6-O-benzylidene-α-D-allopyranoside (5 g, 0.019 mole) (18, 19) was added and the mixture then refluxed under nitrogen for 2 hours. The solution, left standing overnight at room temperature, deposited crystalline material which was removed and recrystallized from ethanol. The methanolic mother liquor was diluted with water and extracted with chloroform. The chloroform extract was washed with water until neutral and dried with sodium sulphate. Elimination of the solvent gave a further quantity of crystalline material. Total yield of methyl 4,6-O-benzylidene-2-benzylthio-2-deoxy-α-D-altropyranoside was 7 g (95%). M.p., 136–137° C; $[\alpha]_D^{CHCl_3}$ at 22°, +90.6° (c = 1.668). Anal. Calc. for $C_{21}H_{24}O_5S$: C, 64.93; H, 6.23; S, 8.25. Found: C, 64.97; H, 6.22; S, 8.30.

Methyl 4,6-O-Benzylidene-3-benzylthio-3-deoxy-α-D-altropyranoside

Methyl 2,3-anhydro-4,6-O-benzylidene-α-D-mannopyranoside (19) was treated in a manner similar to that given the allo isomer with the exception that the reaction time was extended to 15 hours. Crystallization did not occur when the solution stood at room temperature overnight; therefore the reaction mixture was diluted with water and extracted with chloroform. The chloroform solution was washed until neutral and then dried with sodium sulphate. Removal of the solvent left a viscous syrup which solidified after trituration with ether. Recrystallization from methanol afforded colorless crystals. M.p., 105–106° C; yield, 88%; $[\alpha]_D^{CHCl_3}$ at 22°, −112°. (c = 1.436). Anal. Calc. for $C_{21}H_{24}O_5S$: C, 64.93; H, 6.23; S, 8.25. Found: C, 64.90; H, 6.44; S, 8.18.

Methyl 2-Deoxy-2-mercapto-α-D-altropyranoside

Finely powdered methyl 4,6-O-benzylidene-2-benzylthio-2-deoxy-α-D-altropyranoside (5 g) was added to liquid ammonia (150 ml) in an Erlenmeyer flask cooled in dry ice. Small pieces of sodium metal were added to the solution, constantly stirred by a magnetic stirrer, until the blue color persisted for 10 minutes. At the end of this time, ammonium chloride was added until the blue color was discharged, whereupon the ammonia was allowed to evaporate, under a blanket of nitrogen to prevent oxidation of the mercaptan. The residue was extracted with chloroform (N_2) which, upon evaporation, left a colorless solid possessing a sweetish odor. Yield of crude product, 90%; m.p., 140–145° C. Recrystallization from ethanol, in which the compound was found to be quite soluble, yielded small colorless needles, m.p., 145–146° C; $[\alpha]_D^{CHCl_3}$, +95.2° (c = 0.9352). Anal. Calc. for $C_7H_{14}O_5S$: C, 39.99; H, 6.71; S, 15.25. Found: C, 39.95; H, 6.71; S, 15.14.

Methyl 3-Deoxy-3-mercapto-α-D-altropyranoside

Finely powdered methyl 4,6-O-benzylidene-3-benzylthio-3-deoxy-α-D-altropyranoside was subjected to a sodium-in-liquid-ammonia reduction under the same conditions as outlined above for the 2-isomer. On removal of the solvent from the chloroform extract, a colorless viscous syrup remained which solidified on trituration with water. A solution of this material in a benzene–methanol mixture (5:1) was passed through a column of neutral alumina prepared in benzene. The initial fractions contained bibenzyl and were discarded. Subsequent fractions yielded a colorless viscous syrup which solidified when triturated with water.

Several recrystallizations from ethyl propionate gave pure methyl 3-deoxy-3-mercapto-α-D-altropyranoside as large prismatic crystals. M.p., 85–87° C; $[\alpha]_D^{H_2O}$, +68.6°

(c = 1.428). Anal. Calc. for $C_7H_{14}O_5S$: C, 39.99; H, 6.71; S, 15.25. Found: C, 40.08; H, 6.80; S, 15.44.

ACKNOWLEDGMENT

The authors wish to thank the National Research Council of Canada for its generous financial support throughout the course of this work.

REFERENCES

1. A. L. RAYMOND. Advances in carbohydrate chemistry. Vol. 1. Academic Press Inc., New York 10, N.Y. 1945. p. 129.
2. W. SCHNEIDER, R. GILLE, and K. EISFELD. Ber. **61**, 1244 (1928).
3. F. WREDE. Z. physiol. Chem. **119**, 46 (1922).
4. N. K. RICHTMYER, C. J. CARR, and C. S. HUDSON. J. Am. Chem. Soc. **65**, 1477 (1943).
5. K. FREUDENBERG and A. WOLF. Ber. **60**, 232 (1927).
6. L. TSCHUGAEFF. Ber. **32**, 3332 (1899).
7. R. JEANLOZ, D. A. PRINS, and T. REICHSTEIN. Helv. Chim. Acta, **29**, 371 (1946).
8. H. R. BOLLINGER and D. A. PRINS. Helv. Chim. Acta, **29**, 1061 (1946).
9. A. C. MAEHLY and T. REICHSTEIN. Helv. Chim. Acta, **30**, 496 (1947).
10. J. DAVOLL, B. LYTHGOE, and S. TRIPPETT. J. Chem. Soc. 2230 (1951).
11. S. MUKHERJEE and A. R. TODD. J. Chem. Soc. 969 (1947).
12. C. D. ANDERSON, L. GOODMAN, and B. R. BAKER. J. Am. Chem. Soc. **81**, 898 (1959).
13. V. PREY and F. GRUNDSCHOBER. Monatsh. Chem. **91**, 358 (1960).
14. A. M. CREIGHTON and L. N. OWEN. J. Chem. Soc. 1024 (1960).
15. S. M. IQBAL and L. N. OWEN. J. Chem. Soc. 1030 (1960).
16. R. H. SIFFERD and V. DU VIGNEAUD. J. Biol. Chem. **108**, 753 (1935).
17. E. PIERS, V. B. HAARSTAD, R. J. CUSHLEY, and R. K. BROWN. In preparation.
18. N. K. RICHTMYER and C. S. HUDSON. J. Am. Chem. Soc. **63**, 1727 (1941).
19. G. J. ROBERTSON and C. F. GRIFFITH. J. Chem. Soc. 1193 (1935).
20. F. H. NEWTH. Quart. Revs. (London), **13**, 30 (1959).
21. R. E. PARKER and N. S. ISAACS. Chem. Revs. **59**, 737 (1959).
22. R. MOZINGO, D. E. WOLF, S. A. HARRIS, and K. FOLKERS. J. Am. Chem. Soc. **65**, 1013 (1943).
23. D. A. PRINS. J. Am. Chem. Soc. **70**, 3955 (1948).
24. H. VAN GRUNENBERG, C. BREDT, and W. FREUDENBERG. J. Am. Chem. Soc. **60**, 1507 (1938).
25. K. FREUDENBERG and F. BRAUNS. Ber. **55**, 3233 (1922).
26. R. U. LEMIEUX. J. Am. Chem. Soc. **80**, 4745 (1958).
27. B. ISELIN and T. REICHSTEIN. Helv. Chim. Acta, **29**, 508 (1946).
28. G. G. URQUHART, J. W. GATES, JR., and R. CONNOR. Organic syntheses. Vol. 21. John Wiley & Sons, Inc., New York. 1941. p. 36.

Can. J. Chem. Downloaded from www.nrcresearchpress.com by 210.87.254.5 on 09/05/12
For personal use only.

Can. J. Chem. Downloaded from www.nrcresearchpress.com by 210.87.254.5 on 09/05/12
For personal use only.

THE RADIOLYSIS OF CYCLOHEXANE

IV. BINARY MIXTURES IN THE VAPOR PHASE[1]

J. M. RAMARADHYA[2] AND G. R. FREEMAN

ABSTRACT

The variation of the hydrogen yield with the composition of binary gaseous mixtures containing cyclohexane and benzene, cyclohexene, or propylene is qualitatively similar to that in the liquid phase.

The quantitative experimental data were tested against several possible reaction mechanisms and two mechanisms gave straight-line plots.

One mechanism involved scavenging of hydrogen atoms. The values of the kinetic parameters derived from this mechanism might not be unreasonable in the mixtures of cyclohexane with cyclohexene or propylene. The values for benzene, however, seem less likely.

The second mechanism involved the transfer of energy (excitation or ionization) from cyclohexane to the second substance. The values of the ratio of the rate constants, k_7/k_6, of the reactions

$$C_6H_{12}^{**} \rightarrow H_2 + \text{products}, \qquad [6]$$

$$C_6H_{12}^{**} + P \rightarrow C_6H_{12} + P^* \qquad [7]$$

is about 10^3 times greater in the gas than in the liquid phase. Consideration of possible detailed mechanisms of reactions [6] and [7] indicates that this difference is reasonable if $C_6H_{12}^{**}$ is a positive ion rather than an excited molecule.

INTRODUCTION

The study of binary systems has helped considerably in the investigation of the primary chemical processes involved in radiation chemistry. When a solute is dissolved in a solvent and the solution irradiated, the yields of the products are frequently quite different than they would have been if the substances had been irradiated separately. If the solvent product yields are lowered, the solute is said to "protect" the solvent. Thus the amount of hydrogen from cyclohexane radiolysis is considerably lowered by the presence of benzene.

Such a protective action of the solute might be caused either by trapping the free radicals produced from the primarily excited and ionized molecules or by trapping the energy from these molecules.

Our aim was to study the protection role played by benzene, cyclohexene, and propylene in the decomposition of cyclohexane during irradiation in the vapor phase.

EXPERIMENTAL

Cyclohexane and benzene were Eastman-Kodak spectrograde. Cyclohexene was obtained from Matheson, Coleman and Bell. Propylene was Phillips Research Grade material. All the materials were used as obtained.

The apparatus and techniques employed in this investigation were the same as those previously described (1). Binary mixtures of cyclohexane with benzene, cyclohexene, or propylene were irradiated at 108° C with Po^{210} α-particles. The concentration of these protectors ranged from 0.8 to 100 mole% in each case.

The mixtures of cyclohexane with benzene or cyclohexene were prepared as follows. Liquid solutions of various concentrations of protector in cyclohexane were made. Two milliliters of a given solution was thoroughly degassed and then volatilized into a liter bulb, heated electrically to 108° C.

[1]*Manuscript received April 14, 1961.*
Contribution from the Department of Chemistry, University of Alberta, Edmonton, Alberta. Paper presented at the 138th Meeting of the American Chemical Society, New York, September, 1960.
[2]*Present address: Consolidated Mining and Smelting Company, Trail, B.C.*

The mixtures of cyclohexane with propylene were prepared by volatilizing the appropriate amount of cyclohexane into the liter bulb and then injecting the required amount of propylene, such that the total pressure in the bulb was about the same as in the preceding mixtures (ca. 360 mm).

The liter bulb contained a calibrated Po^{210}-plated source (nominally 100 mc). The source was calibrated by Fricke dosimetry, using $G(Fe^{+++}) = 5.5$ (1). The irradiation time was 2 hours. Approximately 0.01% of the sample was decomposed. The pressure of the vapors in the bulb was such that all the energy was absorbed from the α-particles (1).

The products were analyzed by a Toepler pump – McLeod gauge combination and by gas chromatography.

The major product was hydrogen, with smaller amounts of ethylene, ethane, acetylene, propylene, propane, a C_4 hydrocarbon, cyclohexene, and dicyclohexyl. Under the conditions used, only the hydrogen could be measured accurately as a function of protector concentration. The precision of the measurements was 3% or better.

RESULTS

The results are presented in Fig. 1. In these plots, the observed values of $G(H_2)$, the number of molecules of hydrogen produced per 100 ev absorbed, are plotted against the "electron fraction" of the protector. The broken lines in the plots indicate the hydrogen

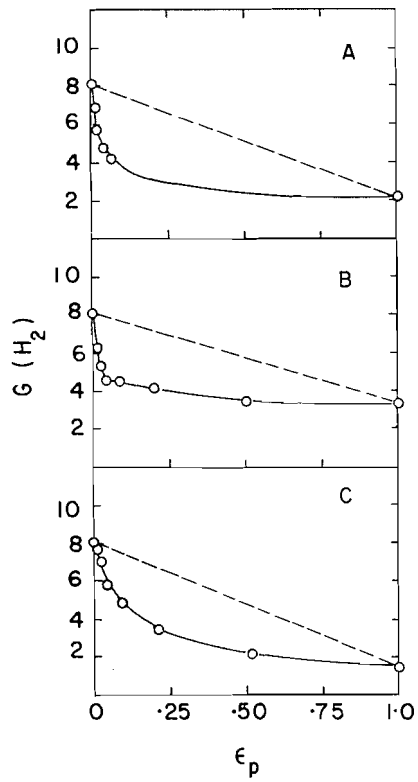


FIG. 1. Hydrogen yield as a function of protector concentration. ϵ_P = electron fraction of protector, P; (A) P = propylene; (B) P = cyclohexene; (C) P = benzene.

Can. J. Chem. Downloaded from www.nrcresearchpress.com by 210.87.254.5 on 09/05/12
For personal use only.

yield that might have been expected if there had been no interaction between the components and if the energy absorption were directly proportional to the electron fraction of the component (2, 3).

The variation of the hydrogen yield with the composition of the binary gaseous mixtures is qualitatively similar to that observed in the liquid phase (2, 3, 4). The hydrogen yield decreases quite rapidly with increasing protector concentration.

DISCUSSION

The experimental results were tested against several reaction mechanisms and two mechanisms were found to give straight-line plots. One mechanism involved scavenging of hydrogen atoms and the other involved energy transfer from cyclohexane to the protector. The two mechanisms will be treated separately.

I. Scavenging Mechanism

$$C_6H_{12} \xrightarrow{I} C_6H_{12}^* \quad [1]$$

$$C_6H_{12}^* \rightarrow H + C_6H_{11} \quad [2]$$

$$H + C_6H_{12} \rightarrow H_2 + C_6H_{11} \quad [3]$$

$$H + P \rightarrow PH \quad [4]$$

$$H + P \rightarrow H_2 + P- \quad [5]$$

In the above equations, I represents the rate of formation of $C_6H_{12}^*$, which subsequently decomposes to produce a hydrogen atom; P represents the protector; and PH and P− represent the corresponding radicals. Since the kinetic treatment is based on the hydrogen yield and since the formation of other products does not appreciably affect the hydrogen yield under the present conditions, the steps for the formation of other products have not been included. It may, however, be mentioned that a more complete mechanism involving some of the other products has been suggested by Freeman for the liquid-phase γ-radiolysis of cyclohexane–benzene (3) and cyclohexane–cyclohexene (4) systems.

By steady-state treatment of the above mechanism, it can be shown that

$$\frac{d(H_2)}{dt} = I\left\{\frac{1+k_5(P)/k_3(C_6H_{12})}{1+(k_4+k_5)(P)/k_3(C_6H_{12})}\right\}, \quad [i]$$

which may be rearranged to

$$\left\{1+w\frac{(P)}{(C_6H_{12})}\right\}\frac{I}{d(H_2)/dt} = 1+v\frac{(P)}{(C_6H_{12})} = \rho, \quad [ii]$$

where $w = k_5/k_3$, $v = (k_4+k_5)/k_3$, and ρ represents the left-hand side of equation [ii].

The numerical values of $I/[d(H_2)/dt]$ can be determined from the experimental data (3). The experimental G values were corrected for the hydrogen produced by direct excitation of the protector (3).

By giving arbitrary values to w, sets of values of ρ can be calculated. A wide range of these sets of values were plotted against the ratio $(P)/(C_6H_{12})$ to see if a straight line with an intercept of unity could be obtained for each of benzene, cyclohexene, and propylene. Such a line was obtained in each case (see Fig. 2). The values of the various ratios of rate constants derived from these plots are shown in Table I.

Can. J. Chem. Downloaded from www.nrcresearchpress.com by 210.87.254.5 on 09/05/12
For personal use only.

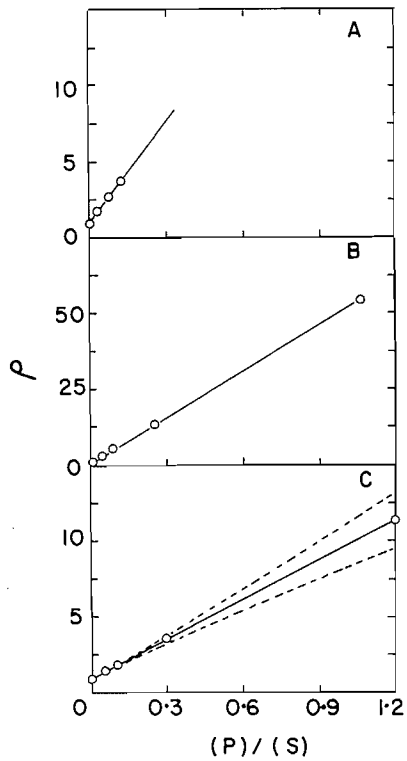


FIG. 2. Kinetic plots of mechanism I. $\rho = \{1 + w[(P)/(C_6H_{12})]\}I/[d(H_2)/dt]$; (A) P = propylene; (B) P = cyclohexene; (C) P = benzene (the upper and lower broken lines correspond to values of w of 3.0 and 2.0 respectively).

TABLE I

Values of rate-constant ratios obtained from mechanism I

P	k_5/k_3	k_4/k_3	k_4/k_5
C_6H_6	2.5±0.2	5.9±0.5	2.4
C_6H_{10}	25±10	31±19	1.2
C_3H_6	>10	>105	11

These values of the rate-constant ratios might not be unreasonable in the cases of cyclohexene and propylene. The value of k_5/k_3 obtained for benzene, however, is surprisingly high, even if the hydrogen atoms were epithermal. It implies that abstraction of hydrogen from benzene is 2.5 times faster than from cyclohexane. The smaller amount of hydrogen in benzene, and the stronger C—H bond in benzene than in cyclohexane, make this seem unlikely. It thus appears doubtful that the scavenging mechanism alone can account for the observed results.

Now let us consider the energy-transfer mechanism.

II. Energy-Transfer Mechanism

$$C_6H_{12} \xrightarrow{I'} C_6H_{12}^{**} \qquad [1']$$

$$C_6H_{12}^{**} \rightarrow H_2 + \text{products} \qquad [6]$$

$$C_6H_{12}^{**} + P \rightarrow C_6H_{12} + P^* \qquad [7]$$

$$P^* \rightarrow xH_2 + \text{products}, \quad 0 \leqslant x \leqslant 1. \qquad [8]$$

Can. J. Chem. Downloaded from www.nrcresearchpress.com by 210.87.254.5 on 09/05/12
For personal use only.

The x signifies that perhaps not every P* results in the formation of an H_2. Reactions [6] and [8] represent over-all processes and might comprise several steps each. Steady-state treatment of this mechanism yields

$$\{1+y(\mathrm{P})\}I'/[d(\mathrm{H_2})/dt] = 1+z(\mathrm{P}) \qquad [iii]$$
$$= \rho',$$

where $y = xk_7/k_6$, $z = k_7/k_6$, and ρ' represents the left-hand side of equation [iii]. Assuming arbitrary values for y, sets of values of ρ' were calculated and plotted against the protector concentration, (P), in an attempt to obtain a straight line with an intercept of unity (Fig. 3). The value of y that gave the desired line in each system, along with the slope of the line, z, and corresponding value of x, is presented in Table II.

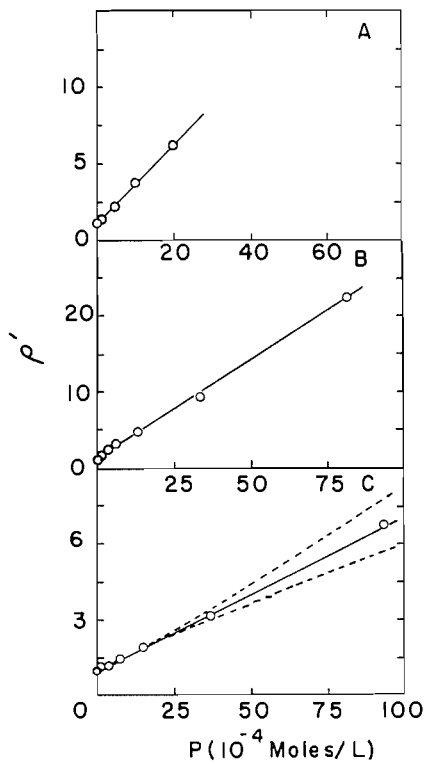


FIG. 3. Kinetic plots of mechanism II. $\rho' = \{1+y(\mathrm{P})\}I/[d(\mathrm{H_2})/dt]$; (A) P = propylene; (B) P = cyclohexene; (C) P = benzene (the upper and lower broken lines correspond to values of y of 180 and 120 liter/mole respectively).

TABLE II

Values of kinetic parameters obtained from mechanism II

P	y (liter/mole)	x	z (k_7/k_6, liter/mole)
C_6H_6	150±18	0.25±0.01	610±25
C_6H_{10}	1200±420	0.44±0.01	2700±800
C_3H_6	>1200	0.47±0.01	>2570

The value of the ratio k_7/k_6 gives an indication of the ratio of the rate of energy transfer to the rate of decomposition of the excited cyclohexane species. The value of the ratio

Can. J. Chem. Downloaded from www.nrcresearchpress.com by 210.87.254.5 on 09/05/12
For personal use only.

k_7/k_6 in liquid cyclohexane + benzene was 0.78 liter/mole (3) and in liquid cyclohexane + cyclohexene, 0.54 liter/mole (4). Thus the value of this ratio in the gas phase is of the order of 10^3 greater than that in the liquid phase. This has three possible causes: (*a*) k_6 is much smaller in the gas than in the liquid phase; (*b*) k_7 is much larger in the gas than in the liquid phase; or (*c*) both.

Assuming that mechanism II is the correct one, the exact nature of $C_6H_{12}^{**}$ is not known. It is probably a positive ion or an electronically excited molecule.

Consider the possibility that $C_6H_{12}^{**}$ is a positive ion. If reaction [6] corresponds to the dissociative recombination of the ion and electron, k_6 would be several orders of magnitude smaller in the gas than in the liquid phase. It is believed that the lifetime of a positive ion in an irradiated liquid is of the order of 10^{-13} sec (5). However, under the present conditions of gas-phase irradiation (10^{13} ev absorbed/ml sec, k (ion–electron recombination) $\approx 10^{-6}$ ml/ion sec (6)), the lifetime of the positive ion is about 10^{-3} sec. Thus k_6 might be smaller by a factor of the order of 10^{-10} in the gas phase than in the liquid phase. It also seems likely that k_7 would be much smaller in the gas phase than in the liquid phase (reference 7 combined with reference 8). Thus it is possible that the value of the ratio k_7/k_6 in the gas phase would be several orders of magnitude larger than in the liquid phase (about 10^{10} divided by the appropriate ratio of k_7 values in the two phases).

If $C_6H_{12}^{**}$ were an electronically excited molecule, the rate of its decomposition might be the same in both the liquid and gaseous states. This would be especially true if the internal conversion of some of the electronic energy into vibrational energy occurs as rapidly as it is presently thought to occur (in the order of 10^{-13} sec (9)). Thus k_6 might be expected to be of the same order of magnitude in the gas and liquid phases. Most theories of electronic excitation transfer imply that the value of k_7 in the gas phase would be similar to or much smaller than the value in the liquid phase. The exciton theory (10) and the sensitized fluorescence theory (11) imply much smaller rate constants in the gas phase. If $C_6H_{12}^{**}$ were an electronically excited molecule, it appears that the value of the ratio k_7/k_6 in the gas phase should have been the same as or smaller than that in the liquid phase.

If the second mechanism applies, the observed increase in the value of k_7/k_6 by a factor of about 10^3, when the phase is changed from liquid to gas, may be taken as an indication that $C_6H_{12}^{**}$ is a positive ion.

In the liquid-phase cyclohexane–benzene system, two 'protection' processes occur to comparable extents (3). The lack of resolution between the two gas-phase mechanisms in the present paper might be due to the occurrence of both. It is possible that the rate constants and concentrations are such that the two mechanisms cannot be resolved in the gas phase by the present technique. However, the apparent value of k_5/k_3 in the benzene–cyclohexane system is so high that the occurrence of only the scavenging mechanism is doubtful. Even if the energy-transfer mechanism contributed only a portion, say one half, of the over-all protection, the calculated values of k_7/k_6 would be of the same order of magnitude as those in Table II. The conclusion that the activated species taking part in the energy-transfer mechanism is probably a positive ion would still hold.

ACKNOWLEDGMENT

The authors are grateful to the National Research Council of Canada for financial support.

Can. J. Chem. Downloaded from www.nrcresearchpress.com by 210.87.254.5 on 09/05/12
For personal use only.

REFERENCES

1. J. M. RAMARADHYA and G. R. FREEMAN. J. Chem. Phys. **34**, 1726 (1961).
2. J. P. MANION and M. BURTON. J. Phys. Chem. **56**, 560 (1952).
3. G. R. FREEMAN. J. Chem. Phys. **33**, 71 (1960).
4. G. R. FREEMAN. Can. J. Chem. **38**, 1043 (1960).
5. A. H. SAMUEL and J. H. MAGEE. J. Chem. Phys. **21**, 1085 (1953).
6. M. A. BIONDI and S. C. BROWN. Phys. Rev. **76**, 1697 (1949).
7. D. R. BATES and N. LYNN. Proc. Roy. Soc. (London), A, **253**, 141 (1959).
8. G. R. FREEMAN. J. Chem. Phys. **33**, 957 (1960).
9. M. BURTON. J. Chem. Educ. **36**, 273 (1959).
10. J. FRENKEL. Phys. Rev. **37**, 17, 1276 (1931).
11. TH. FÖRSTER. Ann. Physik, **2**, 55 (1948).

Can. J. Chem. Downloaded from www.nrcresearchpress.com by 210.87.254.5 on 09/05/12
For personal use only.

Can. J. Chem. Downloaded from www.nrcresearchpress.com by 210.87.254.40 on 09/05/12
For personal use only.

THE LUMINESCENCE OF COMPLEX MOLECULES IN RELATION TO THE INTERNAL CONVERSION OF EXCITATION ENERGY

PART III. THE TOTAL EMISSION SPECTRA OF 1-NAPHTHOIC ACID[1]

ROBIN M. HOCHSTRASSER

ABSTRACT

After excitation by 3130-Å light the anion of 1-naphthoic acid in ethanol solution internally converts to the triplet form of the acid. The excited-state equilibrium can be shifted by the addition of a base or an acid. Numerous total emission spectra of 1-naphthoic acid in various solvents can be understood in terms of some well-established principles governing non-radiative energy transfer processes within and between complex molecules.

No quantitative equilibrium studies are presented. The results indicate that the lowest excited states of the acid, singlet and triplet, are of π,π^* character. The lowest excited singlet state of the anionic form is most probably n,π^*, while the lowest triplet level is π,π^*.

INTRODUCTION

Parts I and II of this series were concerned with the influence of the excitation energy on the luminescence of complex molecules (1, 2). In this part the technique of total emission spectroscopy, i.e. the simultaneous measurement of fluorescence and phosphorescence and the relative yields of these processes, is applied to 1-naphthoic acid. In a previous paper (3) the emission spectra of 1,1-binaphthyl were examined in various media as a function of temperature. If the electronic levels of 1-naphthoic acid are considered to be weakly perturbed versions of the levels of naphthalene, then the acid dimer structure is analogous to 1,1′-binaphthyl with the naphthalene rings about three times farther apart. The total emission spectra of the acid resemble, in their spectral location, the spectra of both naphthalene and the binaphthyls but the phosphorescence and fluorescence efficiencies are found to be quite different and strongly solvent dependent. Changes of this type must be related to variations of the non-radiative processes which occur after light absorption in the complex molecule.

The fluorescence and absorption spectra of 1-naphthoic acid and the 1-naphthoate ion have been used by Weller (4) to measure the pK of the acid and of the protonated acid. El-Bayoumi and Kasha (5) have measured solvent spectral shifts for the monomer and dimer acid. Preliminary observations of the emission spectrum of the dimer and monomer indicated that the exiton model of Kasha and McRae (6) could not explain satisfactorily the spectra of 1-naphthoic acid in various solvent systems. Both the ground state and excited molecules can undergo solvolysis reactions, the products of which have considerably modified electronic structures.

This part is a study of the photochemical processes which occur during the electronic excitation lifetime of an organic acid, and provides an interesting example of how the established principles of molecular spectroscopy may be employed to deduce the detailed mechanism of a photochemical reaction.

EXPERIMENTAL

The experimental details have been published previously (3). A monochromatic source was used to excite the luminescence. All the spectra were recorded spectrophotometrically on a modified Hilger E2 spectrograph. The solvents had optical densities of less than

[1]*Manuscript received May 25, 1961.*
Contribution from the Chemistry Department, the University of British Columbia, Vancouver 8, B.C. This research was financially supported by the National Research Council of Canada.

0.01/cm, and no emission was detectable from the pure solvents, on excitation with 3130-Å light. The coolant was ice-free liquid nitrogen. The spectra are not corrected for the response of the 1P28(RCA) photomultiplier. In order to estimate absolute phosphorescence–fluorescence yield ratios from the figures, the phosphorescence curves should be magnified by about 1.5 times.

Table I shows the estimated probable 0–0 transition energies for 1-naphthoic acid and its conjugate base in various media. The phosphorescence to fluorescence yields in the last column of Table I are corrected for photomultiplier response.

TABLE I

Solvent	Temp., °K	Origin of emission, cm^{-1} ±40		ϕ_P/ϕ_F*
		Fluorescence	Phosphorescence	
Methylcyclohexane	300	28,330	—	—
Methylcyclohexane	77	29,680	19,880	0.10
Ethanol	300	26,950	—	—
Ethanol	77	30,340	19,830	1.36
Ethanol – KOH (0.05 *M*)	77		20,540	20

*ϕ_P/ϕ_F is the *intersystem crossing ratio*, being the ratio of the fluorescence and phosphorescence quantum yields. The values in the table were obtained by comparing the areas of the corrected emission spectra.

Luminescence of Alkaline Solutions

The pK_a of 1-naphthoic acid is 3.7 units at 290° K. The ΔH of ionization in protic solvents for acids of this strength is usually very small (~1000 cal); therefore, pK_a may increase by about 1 unit when the temperature is reduced to 77° K. The acid should therefore be 50% ionized in a rigid ethanol glass at a concentration of about 2×10^{-4} mole/liter. In 0.05 *M* KOH – ethyl alcohol the acid is completely ionized at 77° K.

The pK_S (K_S, acid dissociation constant of the lowest singlet excited level) is 2–4 units higher than pK at 300° K (7). At 77° K, pK_S should be at least 7.8; therefore the acid is completely ionized in 0.05 *M* KOH at this temperature.

Figure 1 therefore represents the total emission spectrum of the acid anion. The

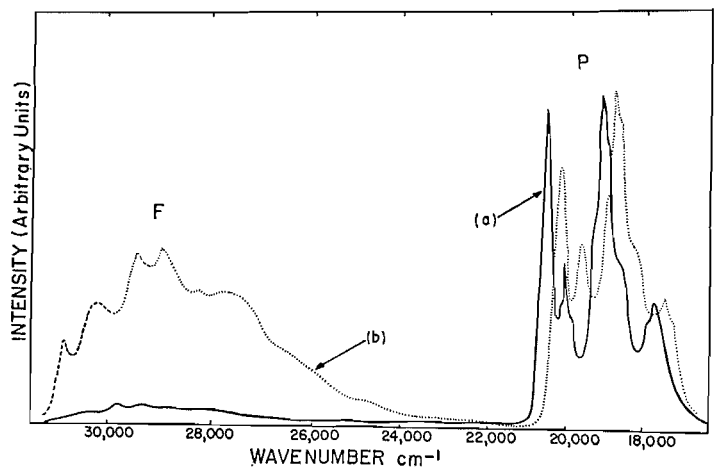


FIG. 1. Total emission spectrum of 1-naphthoic acid at 77° K. F and P indicate the fluorescence and phosphorescence regions.
(*a*) 1.1×10^{-5} mole/liter; solvent, ethanolic KOH (0.05 *M*).
(*b*) 2.0×10^{-4} mole/liter; solvent, ethanol.

Can. J. Chem. Downloaded from www.nrcresearchpress.com by 210.87.254.40 on 09/05/12
For personal use only.

outstanding feature of this spectrum is the extremely high ratio of phosphorescence to fluorescence yield. This is typical of the class of molecules whose lowest excited singlet levels are reached by $n \rightarrow \pi^*$ promotional transitions. For molecules with singlet ground states, fluorescence from $^1(n,\pi^*)$ levels is always weak because of the forbidden character of the transition. Non-radiative intercombinations with upper triplet levels of the molecule can proceed at the usual rate for polyatomic molecules (10^{+7} sec^{-1}) so that the phosphorescent level is populated in favor of fluorescence (8). The spectrum of 1-naphthoic acid in ethanol is shown in Fig. 1 for comparison.

In view of the large gap between the origins of fluorescence and phosphorescence (10,000 cm^{-1}), it is probable that the lowest triplet level of the anion is of $^3(\pi,\pi^*)$ character. Such a gap would be much larger than any previously measured splitting between an n,π^* singlet and triplet state. Further, qualitative estimates have proved that the half-life of phosphorescence for the acid and the anion are about equal. Thus there is good indication that states of the same nature are involved.

Luminescence of Ethanolic Solutions

As mentioned previously there are two absorbing species in solutions of the acid at low concentrations in ethanol. Absorption by the anion and the acid will give rise to two different emissions so the systems will be treated independently.

Primary Light Absorption by the Anion

The excited singlet (n,π^*) anion can undergo two reactions in solution at 77° K. Firstly, intersystem crossing to the triplet anion may occur; the half-life for this process is about 10^{-7} sec. The newly formed triplet is rapidly thermally equilibrated and the reverse reaction has a vanishing probability at 77° K. The singlet anion is also involved in the solvolysis reaction

$$R^*COOH \underset{^1k_2}{\overset{^1k_1}{\rightleftharpoons}} R^*COO^- + H^+_{solv.} \qquad (A)$$

The equilibrium constant for this dissociation is at most 1.3×10^{-8} (see previous section) and the hydrogen ion concentration is 2×10^{-4} mole/liter at 50% ionization in the ground state. The rate constant $^1k_2$ for the proton recombination reaction is diffusion controlled and should be within an order of magnitude of 10^{10} liters mole^{-1} sec^{-1}. Thus the half-life of recombination is about 5×10^{-7} sec. Once reformed, the acid could not ionize again within times comparable to its half-life of fluorescence. The anion may therefore form the excited acid by proton recombination *or* it may form the triplet anion; for the example chosen, these processes have about equal probability although at lower acid concentrations the latter alternative will be strongly favored.

The triplet anion may now undergo one of two courses: either radiative intercombination with the ground state (phosphorescence), with a half-life of close to 1 sec, *or* the proton recombination

$$^3(R^*COOH) \underset{^3k_2}{\overset{^3k_1}{\rightleftharpoons}} {}^3(R^*COO^-) + H^+_{solv.} \qquad (B)$$

The phosphorescence 0–0 transition of the ion is shifted by 1.8 kcal/mole to higher energy than the corresponding transition of the acid at 77° K. The value of pK_T (acid dissociation of the triplet) at 77° K is therefore 5.1 units.

Can. J. Chem. Downloaded from www.nrcresearchpress.com by 210.87.254.40 on 09/05/12
For personal use only.

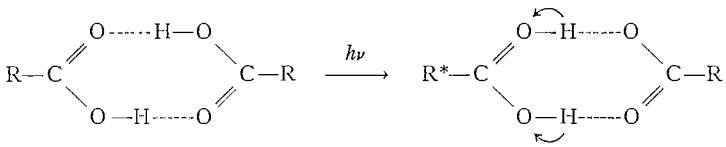
As for $^1k_2$, the value of $^3k_2$ is about 10^{10} liters mole^{-1} sec^{-1} and therefore the half-life of recombination is 5×10^{-7} sec; $^3k_1$ is therefore 8.7×10^4 sec^{-1}. The half-life of emission for each of the triplet molecules in (B) is 1 sec, which means that less than 1.0% of the phosphorescence observed in ethanol solution is from the triplet anion. Figure 1(*b*) shows the total emission spectra from ethanolic solutions of 1-naphthoic acid. The fluorescence is from the acid singlet level and the phosphorescence is from the acid triplet level, both attained after primary light absorption by the anion, as described above. Some of the fluorescence may have originated from directly excited acid but under the present experimental conditions these could not be separated.

The phosphorescence–fluorescence yield ratio in ethanolic solution is high and could be altered by adding acid (e.g. H_2SO_4) in accordance with the above scheme.

The Luminescence of 1-Naphthoic Acid in Methylcyclohexane

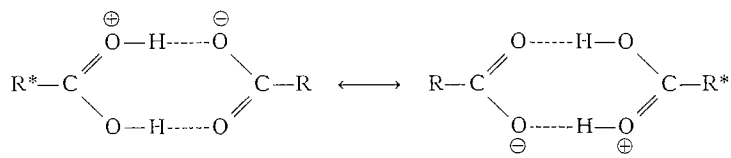
In this solvent the acid is dimerized completely at 10^{-3} mole/liter at 300° K (9). The heat of dimerization of carboxylic acids is usually around 10 kcal/mole so at concentrations as low as 10^{-6} mole/liter the acid will be completely dimeric at 77° K. It was not possible to glassify solutions more concentrated than 10^{-6} *M* without forming microcrystals which themselves have an intense emission in the blue region of the spectrum.

Weller has shown that the carbonyl oxygen becomes more basic in the lowest excited singlet state of the acid (10). The acidic oxygen also becomes more basic in this excited state, i.e., the acid is weaker. The protons in the hydrogen bridges of the dimer must therefore both be attracted towards the half of the dimer in which the excitation energy is localized.



It is unlikely that the protonated acid (excited) and the anion (unexcited) will separate completely as the former is still a very strong acid and the latter a very strong base.

Strictly, the excitation energy is not initially localized in one of the naphthalene rings. The electronic states of the separated conjugated systems are weakly coupled in the dimer and the excitation energy may be transferred non-radiatively between the two configurations. The half-life of transfer may be about 10^{-11} sec for weak coupling situations of this type. In the excited state the dimer is therefore stabilized by a resonance force interaction which may be represented as follows.



The total emission in Fig. 2(*b*) is interpreted as dimer emission. Owing to the very weak coupling between the rings, the emission spectra in Fig. 2 should not differ appreciably from the pure monomer emission. The phosphorescence to fluorescence yield ratio is very low for the dimer (1:10) and is similar to the value for unsubstituted naphthalene.

Can. J. Chem. Downloaded from www.nrcresearchpress.com by 210.87.254.40 on 09/05/12
For personal use only.

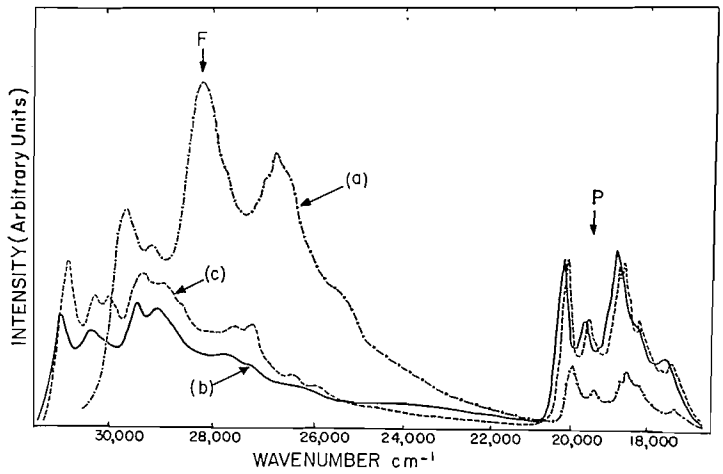


FIG. 2. Total emission spectrum of 1-naphthoic acid at 77° K. F and P indicate the fluorescence and phosphorescence regions.
(*a*) 4.6×10^{-6} mole/liter; solvent, methylcyclohexane.
(*b*) 4.6×10^{-6} mole/liter; solvent, methylcyclohexane – ether (0.25 *M*).
(*c*) 4.6×10^{-6} mole/liter; solvent, methylcyclohexane – ethanol (0.026 *M*).

Low values for the phosphorescence yield are characteristic of molecules with lowest excited singlet states of π,π^* character. The transition moment for the singlet–singlet emission of 1-naphthoic acid is known to lie in the plane of the molecule (11). Thus the fluorescence observed from the dimer is $^1(\pi,\pi^*) \rightarrow {}^1$(ground state) emission.

An enhancement of phosphorescence was expected on dimerization. The lowest excited electronic state of the dimeric acid has zero combination probability with the ground state of the dimer—if the structure of the planar dimer is the same as that in the crystal (12). The low probability of fluorescence should cause increased probability of non-radiative processes such as intersystem crossing and hence an increase in the ratio of phosphorescence to fluorescence yields compared to the monomer (6). However, this would not arise if *either* the dimer were twisted *or* if the dimer splittings were of the order of kT. Both of these conditions are possibly upheld in the present case (11).

Emission in Mixed Solvents

(I) The addition of a small amount of ethanol (0.5 *M*) to the dimeric solution in methylcyclohexane caused a marked increase in phosphorescence yield. This is shown in Fig. 2(*c*). The ethanol presumably breaks up the dimer and the previously discussed sequence of reactions in the excited state may occur.

(II) Figure 2(*b*) shows the effect of diethyl ether (0.5 *M*) on the dimer emission spectrum. As in (I) the fluorescence is decreased and the phosphorescence is increased. This experiment indicates that a hydrogen bond to the acid oxygen of naphthoic acid is the sole requirement for the establishment of ionization in the ground state, and suggests that the electronic environment of the carboxylic oxygen does not seriously affect the acid–base reaction in the neighborhood of the acidic oxygen.

(III) Figure 3(*b*) shows the effect of adding a small quantity of acetic acid (0.04 *M*) to the dimeric methylcyclohexane solution. The spectrum is broadened but the phosphorescence to fluorescence yield ratio is hardly altered from the dimer value. The acetic acid

Can. J. Chem. Downloaded from www.nrcresearchpress.com by 210.87.254.40 on 09/05/12
For personal use only.

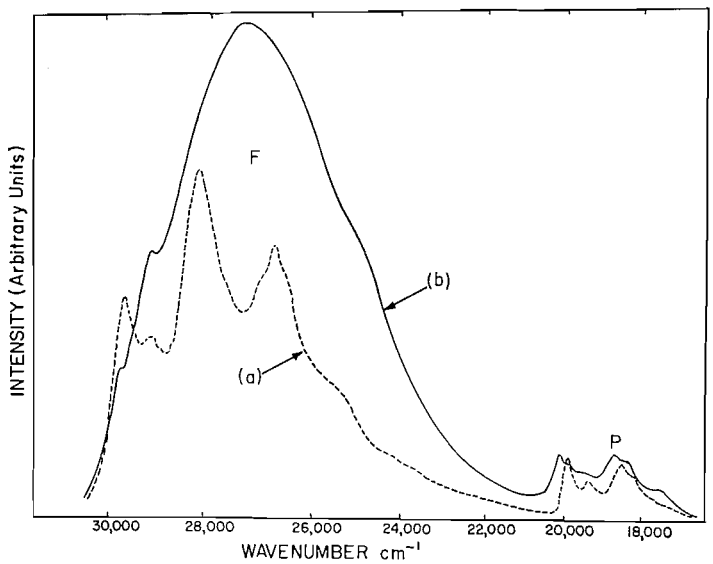
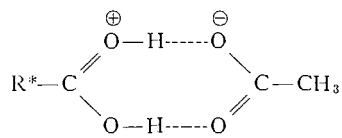


FIG. 3. Total emission spectrum of 1-naphthoic acid at 77° K. F and P indicate the fluorescence and phosphorescence regions.
(*a*) 4.6×10^{-6} mole/liter; solvent, methylcyclohexane.
(*b*) 4.6×10^{-6} mole/liter; solvent, methylcyclohexane – acetic acid (0.04 *M*).

is likely to be strongly hydrogen bonded to the naphthoic acid and the resulting species is a mixed dimer which is mainly undissociated in the ground state. In the excited state



the bridged protons would shift toward the basic and acidic sites of the naphthoic acid. It is unlikely that the mixed dimer would actually split into an excited protonated acid and an acetate ion, although the effect of excitation would be the reduction of the energy of dimerization. The influence of acetic acid on the emission spectrum is exactly what is expected on the basis of the explanations given in previous sections. Very similar results have been obtained for β-naphthoic acid. However, it was possible to obtain more concentrated solutions of the β-isomer in methylcyclohexane as no precipitation occurred in this case. The phosphorescence–fluorescence yield ratios were slightly lower than those for 1-naphthoic acid.

ACKNOWLEDGMENT

The author would like to thank Professor Jack Halpern for some stimulating discussions.

REFERENCES

1. R. M. HOCHSTRASSER. Can. J. Chem. **37**, 1367 (1959).
2. R. M. HOCHSTRASSER. Can. J. Chem. **38**, 233 (1960).

Can. J. Chem. Downloaded from www.nrcresearchpress.com by 210.87.254.40 on 09/05/12
For personal use only.

3. R. M. HOCHSTRASSER. Can. J. Chem. **39**, 459 (1961).
4. A. WELLER. Z. Elektrochem. **60**, 1146 (1956); **61**, 957 (1957).
5. M. A. EL-BAYOUMI and M. KASHA. H-bonded complexes. In preparation.
6. E. G. MCRAE and M. KASHA. J. Chem. Phys. **28**, 721 (1958).
7. A. WELLER. Private communication.
8. E. CLEMENTI and M. KASHA. J. Mol. Spectroscopy, **2**, 297 (1958).
9. W. G. WRIGHT. J. Chem. Soc. 683 (1949).
10. A. WELLER and W. URBAN. Angew. Chem. **66**, 336 (1954).
11. R. M. HOCHSTRASSER. Can. J. Chem. This issue.
12. J. TROTTER. Acta Cryst. **13**, 732 (1960).

Can. J. Chem. Downloaded from www.nrcresearchpress.com by 210.87.254.40 on 09/05/12
For personal use only.

Can. J. Chem. Downloaded from www.nrcresearchpress.com by 210.87.254.42 on 09/05/12
For personal use only.

INFRARED SPECTRA OF XANTHATE COMPOUNDS

III. ORGANIC SOLVENT EFFECT ON THE C=S FREQUENCY[1]

L. H. LITTLE,[2] G. W. POLING, AND J. LEJA

ABSTRACT

The previously made absorption-band assignment (1) for the C=S stretching mode in xanthate-type compounds, 1020–1070 cm^{-1}, has been confirmed by the characteristic behavior of the C=S dipole in a range of different solvents (Bellamy and Rogasch (2)).

Assignments for the C=S stretching mode in xanthates, proposed by various investigators, cover the frequency range from 1000–1400 cm^{-1} and conflict with the assignments for the stretching vibrations of the C—O groups. It was felt necessary, therefore, to seek additional evidence to confirm our recent C=S band assignment (1) by solvent effects. Bellamy and Rogasch (2) found that a linear relationship exists between the frequency displacements ($\nu_{vapor} - \nu_{solution}$) of the C=S stretching vibrations in cyclic trithiocarbonates (dithioesters and some thioamides) and the frequency displacements of the C=O band in acetophenone, when studied in a particular sequence of solvents.

The same solvent sequence as that employed by Bellamy and Rogasch was used in the study of xanthate-type compounds. However, owing to the very low vapor pressures of solid xanthate compounds, their vapor-state spectra could not be obtained and the band displacements in the various solvents had to be represented relative to the frequency in cyclohexane. In the work of Bellamy and Rogasch cyclohexane solutions gave band frequencies close to those of the respective vapors. The behaviors of the two strong "xanthate bands", 1020–1070 cm^{-1} and 1200–1280 cm^{-1}, both of which had been assigned by various investigators (1, 3) to the C=S stretching mode, were contrasted; the shift of the 1020–1070 cm^{-1} band to lower frequencies (positive shift) in the solvent sequence from cyclohexane to tetrabromoethane confirms the fact that this band had been correctly assigned to the C=S stretching vibration.

EXPERIMENTAL

Materials.—Zinc *n*-butyl xanthate, *n*-butyl dixanthogen, and O-octadecyl,S-octadecyl dithiocarbonate were the same reagents which were previously used for the assignment of frequencies (1) and all analyzed 99%+ in purity. Solvents used were Eastman Kodak Company materials, designated "Specially pure for infrared spectroscopy", with the exception of dioxane, which was a C.P. grade reagent.

Procedure.—The spectra were recorded differentially (relative to pure solvent in the reference beam) on a Perkin–Elmer 221G spectrophotometer. The rotational lines of the ammonia-gas spectrum were used for frequency calibration (accuracy ±1 cm^{-1}). Due to the intense absorption bands of many solvents in the spectral region of interest and due to the asymmetrical nature of the xanthate bands themselves, the accuracy of the frequencies determined in some solvents was probably of the order of ±3 cm^{-1}.

RESULTS

Table I lists the frequencies and the relative displacements, $\Delta\nu = (\nu_{cyclohexane} - \nu_{solvent})$ cm^{-1}, of the two characteristic intense absorption bands, 1020–1070 and 1200–1280 cm^{-1},

[1]*Manuscript received April 24, 1961.*
Contribution from the Department of Mining and Metallurgy, University of Alberta, Edmonton, Alberta.
[2]*Present address: Department of Chemistry, University of Western Australia, Perth, Western Australia.*

Can. J. Chem. Downloaded from www.nrcresearchpress.com by 210.87.254.42 on 09/05/12
For personal use only.

TABLE I

Absorption-band frequencies* and frequency shifts*

	1020–1070 cm^{-1} band						1200–1280 cm^{-1} band						Bellamy and Rogasch (2)	
	Zn *n*-butyl xanthate		*n*-Butyl dixanthogen		O-Octadecyl, S-octadecyl xanthate		Zn *n*-butyl xanthate		*n*-Butyl dixanthogen		O-Octadecyl, S-octadecyl xanthate		Ethylene trithiocarbonate	
	ν	$\Delta\nu$	ν	$\Delta\nu$	ν	$\Delta\nu$	ν	$\Delta\nu$	ν	$\Delta\nu$	ν	$\Delta\nu$	ν	$\Delta\nu$
Cyclohexane	1046	0	1028	0	1061	0	1238	0	1264	0	1214	0	1086	0
Diethyl ether	~1050	—	~1030	—	Insoluble		1203	35	1266	−2	~1218	−4	—	—
Carbon tetrachloride	1044	2	1027	1	1060	1	1244	−6	1266	−2	1218	−4	1083	3
Benzene	1062, 1030	—	1023	5	1060	1	1241	−3	1268	−4	1221	−7	1078	8
Dioxane	Solvent absorption		1022	6	Insoluble		1208	30	1269	−5	Insoluble		—	—
Acetonitrile	1060, 1037	—	1021	7	Insoluble		1235, 1200, 1180	—	1273	−9	Insoluble		1075	11
Nitromethane	Insoluble		1023	5	Insoluble		Insoluble		1274	−10	Insoluble		—	—
Methylene chloride	1039	7	1024	4	1057	4	1242	−4	1280, 1248	—	1220	−6	1074	12
Chloroform	1040	6	1026	2	1058	3	1245	−7	1273	−9	Solvent absorption		1075	11
Bromoform	1038	8	1020	8	1054	7	1247	−9	1267	−3	1224	−10	1070	16
1,1,2,2-Tetrabromoethane	1037	9	1020	8	1056	5	1255, 1213	—	1267	−3	Solvent absorption		1069	17
Solid or liquid	1045_s	1	1022_{liq}	6	1062_s	−1	1209_s	29	1264_{liq}	0	1219_s	5	—	—

*In cm^{-1}.

for the three compounds Zn *n*-butyl xanthate, *n*-butyl dixanthogen, and O,S-dioctadecyl dithiocarbonate, in different organic solvents arranged in the same sequence as that used by Bellamy and Rogasch (2). For comparison, data given by Bellamy and Rogasch for ethylene trithiocarbonate are presented in the last column with the frequency displacements recalculated relative to the frequency in cyclohexane (instead of that of the vapor). Figure 1(A, B) shows selected spectra of two of the above-mentioned compounds in various solvents and in the 900–1300 cm^{-1} region.

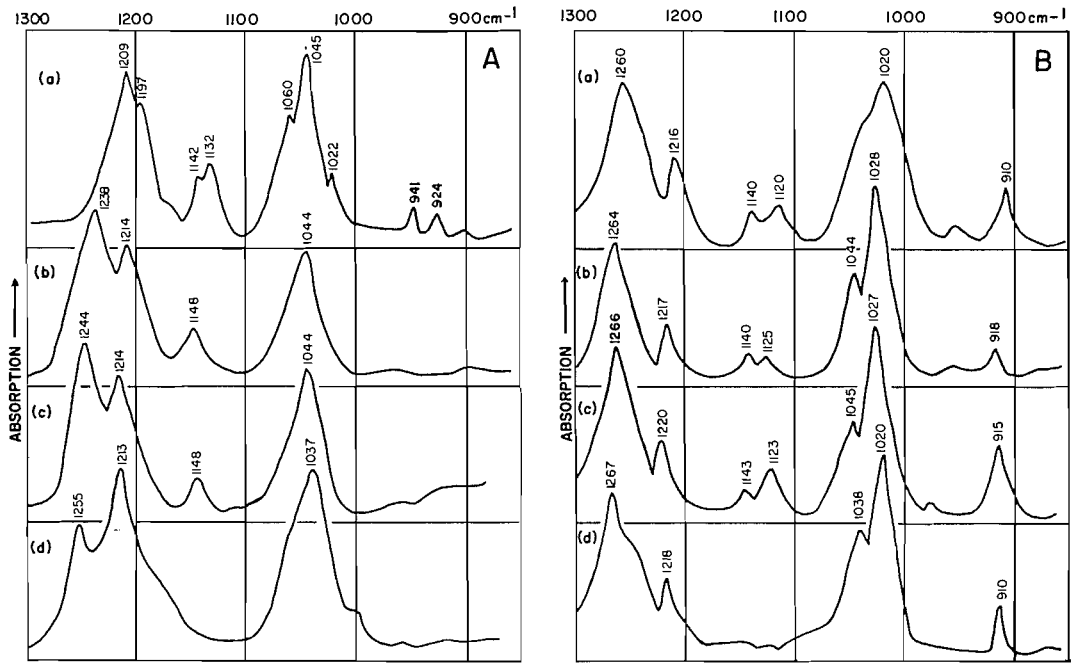


FIG. 1. Typical solvent spectra of Zn *n*-butyl xanthate and *n*-butyl dixanthogen.
A. Zn *n*-butyl xanthate in: (*a*) nujol mull, (*b*) cyclohexane, (*c*) carbon tetrachloride, (*d*) tetrabromoethane.
B. *n*-Butyl dixanthogen in: (*a*) capillary film, (*b*) cyclohexane, (*c*) carbon tetrachloride, (*d*) tetrabromoethane.

DISCUSSION

The frequency shifts ($\Delta\nu$) of the 1020–1070 cm^{-1} bands, reported in Table I, are all positive and of the order of 0–9 cm^{-1}. The corresponding data of Bellamy and Rogasch, recalculated relative to cyclohexane, give a progressive change of $\Delta\nu$ from 0 to 7 cm^{-1} for dithioacetates and $\Delta\nu$ = 0–17 cm^{-1} for ethylene trithiocarbonate. The frequency displacements of *n*-butyl dixanthogen and O,S-dioctadecyl dithiocarbonate exhibit more scatter (i.e. deviate more from linearity) than do those reported for dithioacetates and ethylene trithiocarbonates by Bellamy and Rogasch. However, since the general shifts of the 1200–1280 cm^{-1} band are toward higher frequencies (negative) in the same solvent sequence, the evidence clearly indicates that the 1020–1070 cm^{-1} band follows the typical C=S behavior while the 1200–1280 cm^{-1} band does not. This evidence confirms the assignment of the 1020–1070 cm^{-1} band to the C=S stretching mode in xanthate-type compounds and not the 1210–1230 cm^{-1} band as assigned by Felumb (3).

Can. J. Chem. Downloaded from www.nrcresearchpress.com by 210.87.254.42 on 09/05/12
For personal use only.

ACKNOWLEDGMENTS

We acknowledge the support of this work by the National Research Council of Canada under grants A699 and E140.

REFERENCES

1. L. H. LITTLE, G. W. POLING, and J. LEJA. Can. J. Chem. **39**, 745 (1961).
2. L. J. BELLAMY and P. E. ROGASCH. J. Chem. Soc. 2218 (1960).
3. R. FELUMB. Bull. soc. chim. France, Ser. 5, **24**, 890 (1957).

Can. J. Chem. Downloaded from www.nrcresearchpress.com by 210.87.254.42 on 09/05/12
For personal use only.

Can. J. Chem. Downloaded from www.nrcresearchpress.com by 210.87.254.105 on 09/05/12
For personal use only.

THE ACIDITY OF NITROGUANIDINE AND ITS HOMOLOGUES[1]

A. A. Amos, P. D. Cooper, E. Nishizawa, and George F Wright

ABSTRACT

It has been shown that nitroguanidine, nitriminoimidazolidine, and 1-benzyl-2-nitriminoimidazolidine behave like urea by formation of potassium salts which completely hydrolyze in water. By contrast to true primary nitramines with which they might be considered to be tautomeric, the nitrimines are classed like urea as practically neutral compounds. Despite this ostensible tautomerism which was formerly evoked to explain the survival of nitroguanidine and nitriminoimidazolidine in alkaline solution it is now believed that the salts of nitroguanidine and nitraminoimidazolidine, from which the original nitrimines are regenerated upon acidification, are not intermediates, but rather end products, in the slow reaction with alkali. The intermediate is now postulated as an hydroxyisonitraminate anion from which the several products of the reaction are formed by appropriate fission. Presumably this anionic intermediate also is operative when tetraethylnitroguanidine or 1,3-dibenzyl-2-nitriminoimidazolidine is converted by alkali into tetraethylurea and 1,3-dibenzyl-2-imidazolidine respectively.

The chemistry of nitroguanidine and its homologues with alkalies seems to have been left in a state of confusion which may in part be due to an error appearing in one of our publications. In this paper we shall correct this error and shall suggest instead a more consistent explanation for the reaction with alkalies.

It is now recognized that nitroguanidine exists commonly as the nitrimine, $H_2NC(NNO_2)NH_2$, rather than as the tautomeric primary nitramine. Nitroguanidine does not react appreciably with alkali in aqueous solution in contrast to primary nitramines for which $K_a \simeq 10^{-5}$ to 10^{-6} (1). Its electric moment is much lower (μ = 6.95 D) than would be expected (2) if the substance were a nitramine, especially since the latter would be expected to have zwitterion characteristics. Also the ultraviolet absorption spectrum does not resemble those of known nitramines (2, 3) (which absorb at 225–240 mμ) but its strong absorption at 265 mμ is near the 268 mμ absorption found to be characteristic of *sym*-tetraethylnitroguanidine (4) which certainly is a nitrimine. Essentially by the same criteria, the studies with 2-nitriminoimidazolidine (1), 1-nitro-2-nitriminoimidazolidine (5), and azobisnitroformamidine (6, 7) have shown that with few exceptions (8) most of the homologues of nitroguanidine have nitrimino structures.

Nitrimines like these are formally analogous with urea and, indeed, there are similarities. Like urea, the acidity of nitrimines in water, as shown by potentiometric (2) and spectroscopic (9) examination, is negligible (pK 12–14). The basicity of nitroguanidine has been reported as $pK_b = 14.5$ (10). Indeed the existence of salts such as the hydrochloride (11) in media minimal in content of water would indicate that the basicity is comparable with that of urea (K_b at 25°, 1.5×10^{-14}).

With bases, in nonaqueous media (potassium amide in liquid ammonia), urea will form a potassium salt. Under the same conditions potassium nitroguanidine (m.p. 155–156° C) is obtained in 49% yield. A salt of lesser purity (m.p. 149° C) is obtained in lower yield from molar potassium methoxide in methanol. These salts regenerate nitroguanidine when they are dissolved in water, but they can be crystallized satisfactorily from methanol containing potassium methoxide. The potassium nitroguanidine is recovered unchanged after a few hours in boiling dimethylformamide or acetonitrile, but alone it decomposes at 100° C (0.3 mm Hg pressure); cyanamide and dicyanamide have been found in the strongly basic residue.

[1]*Manuscript received March 20, 1961.*
Contribution from the Department of Chemistry, University of Toronto, Toronto, Ontario.

The potassium nitroguanidine has been characterized, like its urea analogue, by reaction with benzyl chloride in absolute ethanol or in dimethylformamide. The yields of benzylnitroguanidine are 39% and 43% respectively, the remainder of the product being nitroguanidine. No trace of a benzylisonitramine, a characteristic product of primary nitramines, has been detected.

The acidimetric titration of benzylnitroguanidine in 50% aqueous ethanol (curve I, Fig. 1) shows that it is a nitrimine, since it does not react with 1 equivalent of alkali

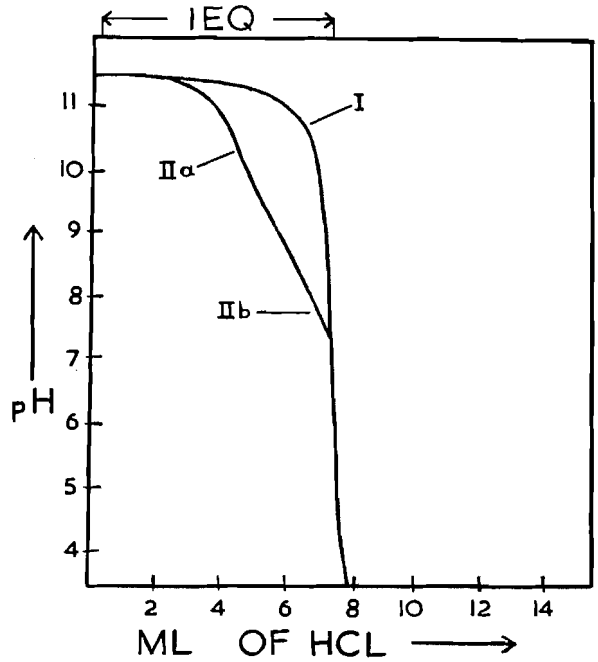


FIG. 1.

immediately after addition. However, when such a solution is aged for 62 hours its properties are altered according to titration curve II of Fig. 1. This curve shows two inflections: II*b* is indicative of about 10% decomposition to an amine, while II*a* shows that about 50% of the nitrimine has been converted to an acidic substance. Since 78% of benzylnitroguanidine is recoverable from the system, compared with 90% recovery from a freshly prepared solution, it is evident that the acidic substance must be present as the salt of isomeric benzylnitroguanidine.

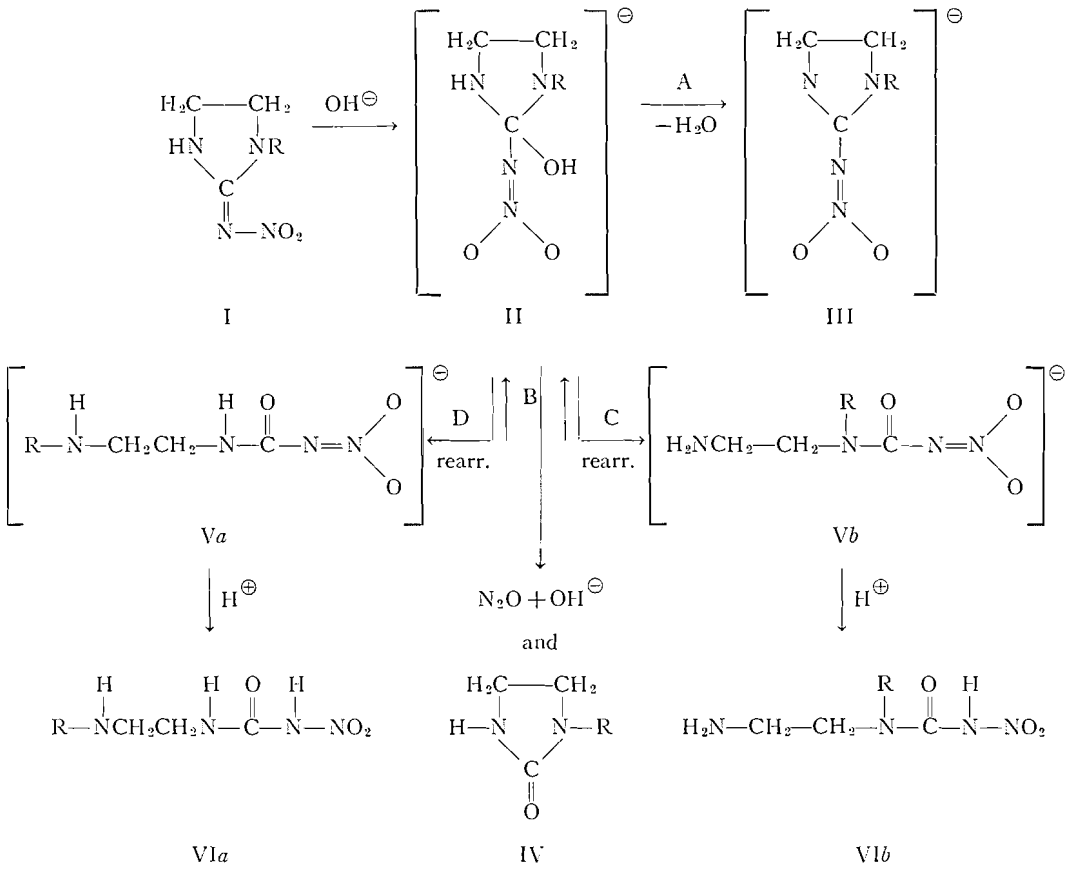
In a former publication (1) from this laboratory, the isomer of non-salt-forming nitroguanidine (which isomer must have been present as the sodium salt in an aged alkaline solution) was designated as the nitramino form, $NH_2C(NH)NHNO_2$. Likewise the sodium salt of nitraminoimidazoline had to be present, together with the sodium salt of 3-β-aminoethylnitrourea, after neutral nitriminoimidazolidine was aged in alkaline solution. From this experimental evidence it was postulated that nitraminoimidazoline was intermediate in the formation of 3-β-aminoethylnitrourea or its cyclic isomer, 2-hydroxy-2-nitraminoimidazoline.

This postulation is absurd. Nitraminoimidazoline cannot be an intermediate in the formation of 3-β-aminoethylnitrourea and, in the same system, be the source of recovered

Can. J. Chem. Downloaded from www.nrcresearchpress.com by 210.87.254.105 on 09/05/12
For personal use only.

starting material when the components of that system have neutralized an entire equivalent of alkali, since it has been shown that 3-β-aminoethylnitrourea in alkali does not yield any nitriminoimidazolidine when the latter system is acidified. Although the recovery of nitriminoimidazolidine by acidification of its aged alkaline solution definitely indicates that the salt of the nitramino tautomer is present, the latter cannot be an intermediate.

We suggest that the intermediate is the anion 2-hydroxy-2-imidazolidinylisonitraminate, II. The alkaline aging reaction may therefore be formulated as shown in the accompanying scheme (where R = H). After the isonitraminate ion, II, is formed



slowly from nitriminoimidazolidine, I, it may react by paths A, B, C, or D. Loss of water (path A) leads to the salt of the nitramine, III, from which I may be regenerated by acidification. Or the ion may decompose along path B, losing nitrous oxide and hydroxyl ion, to give the imidazolidone, IV (R = H). Finally the anion II (R = H) may rearrange by either path C or D to give the anions V*a* or V*b* of 3-β-aminoethylnitrourea, VI*a* or VI*b*. When R = H, paths C and D are identical.

The same four paths will be involved in the alkaline reactions of nitroguanidines. Although all three products (urea, nitrourea, and nitroguanidine) have been detected from nitroguanidine, path A seems to be predominant. The large recovery of benzylnitroguanidine likewise indicates that path A is followed. On the other hand alkaline

Can. J. Chem. Downloaded from www.nrcresearchpress.com by 210.87.254.105 on 09/05/12
For personal use only.

Can. J. Chem. Downloaded from www.nrcresearchpress.com by 210.87.254.105 on 09/05/12
For personal use only.

treatment of nitriminoimidazolidine seems to follow chiefly path C, less along path A, and negligibly along path B.

It would seem then that the course of reaction is determined by the substituent groups. In conformity with this expectation we have now found that only paths B and D are followed when 1-benzyl-2-nitriminoimidazolidine (I, R = benzyl) is aged with alkali.

This substance may be prepared by treatment with benzyl chloride in hot ethanol of potassium nitriminoimidazolidine which is obtained in 47% yield by the method of Franklin and Stafford. The remainder of the reaction system is accounted as 2-nitriminoimidazolidine, and no trace of benzyl imidazolinylnitraminate or isonitraminate can be detected.

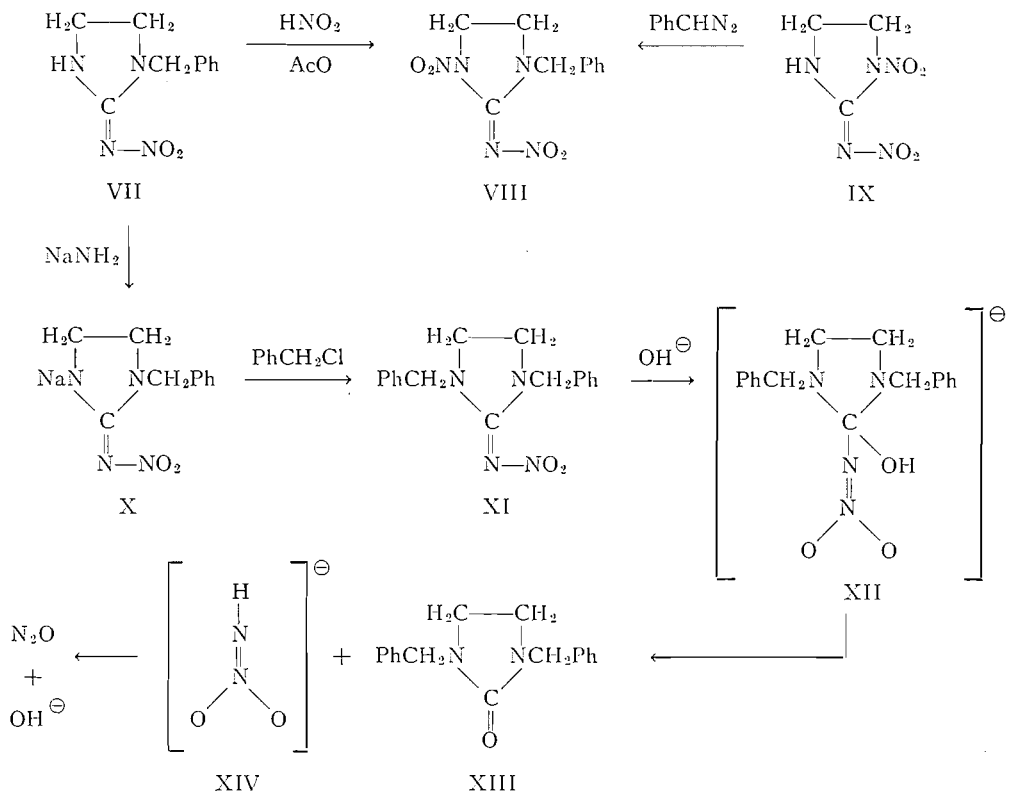
A 0.1 *N* solution of sodium hydroxide in water does not dissolve 1-benzyl-2-nitriminoimidazolidine (I, R = benzyl), but the solution may be made homogeneous by addition of ethanol. When the system is acidified within an hour, the starting material is recovered quantitatively. On the other hand, when the system is aged for 72 hours, a mixture is obtained in which none of the starting material is present. The mixture is comprised of 1-benzylimidazolidone (IV, R = benzyl) and a substance, the hydrochloride of which has been isolated, which we consider to be 3-β-benzylaminoethyl-1-nitrourea, VI*a* (R = benzyl). This latter assignment has been made because nitrous acid reacts to give the dinitrosamine $PhN(NO)CH_2CH_2N(NO)CONHNO_2$ but no nitrogen. Since the alternative VI*b* contains a primary amino group it is excluded by this test.

In previous publications (12, 13, 14) we have avoided a specific designation of structure for substances such as 3-β-benzylaminoethyl-1-nitrourea because of evidence showing that tautomeric forms (so-called ring-chain isomers typified in the present instance as 1-benzyl-2-hydroxy-2-nitriminoimidazolidine) are operative in this chemistry. Essentially the same reservation is implied in the formulations of equilibria between VI*a*, VI*b*, and II (R = benzyl); indeed this implication is supported by the instability of the substance designated as VI*a*. In 10% alkali this substance is slowly converted to 1-benzylimidazolidone, presumably via the anion II. The conversion of a nitriminoimidazolidine to an imidazolidone (IV) may thus lead to a somewhat complicated rate expression in which IV is formed both directly and indirectly from II. It is possible that difficulties of this sort have been encountered previously (15).

It may be true that I and VI*b* are present in quantities too small to be detected by our methods of isolation. Within the limits of these methods, paths A and C are excluded in favor of paths B and D, and this direction may be attributed to the substituent benzyl group in the intermediate anion II. However, it would be surprising if variations in ionic strength of the system did not divert the reaction into the other paths. Insufficient work has been done to make an assessment of this possibility.

The chemical reactions of 1-benzyl-2-nitriminoimidazolidine VII conform with those of analogous nitrimines. Thus it may be nitrated to 1-benzyl-2-nitrimino-3-nitroimidazolidine, VIII, which has also been prepared by treatment of 1-nitro-2-nitriminoimidazolidine (IX) with phenyldiazomethane. As has been shown above, benzylnitriminoimidazolidine (VII) does not itself form a stable alkali salt in aqueous solution. However, in nonaqueous media it reacts with sodamide to give a sodium salt, X, which, with benzyl chloride in ethanol, gives 1,3-dibenzyl-2-nitriminoimidazolidine, XI.

When this unquestionable nitrimine, XI, is treated with aqueous alkali the substance loses the elements of nitramide and becomes 1,3-dibenzyl-2-imidazolidone, XIII. It is



reasonable to postulate that the isonitraminate ion, XII, is intermediate in this conversion to the ketone and the anion, XIV, corresponding to nitramide. This ion, XIV, is known to decompose to nitrous oxide and hydroxyl ion. But this reaction series is only a special case of the alkaline aging reaction described over the formulation series I → VI inclusive which is shown above. In this special instance substituent groups on nitrogen prevent reaction along paths A, C, and D, leaving only path C available. The same explanation applies to the alkaline conversion of *sym*-tetraethylnitroguanidine to *sym*-tetraethylurea (4).

Probably the two errors in our original publication on the acidity of nitroguanidines have by inadvertence led to criticism which has tended to obscure rather than clarify the chemistry of these substances. It is of interest that neither of these errors was actually detected by the critics.

The first error was quickly detected by us and it was reported shortly (6, 13) that, although neutral substances of appropriate constitution must be classified as nitrimines, it does not follow that the isomeric nitramino structure is applicable if the substance is moderately acidic. Such acidity may be induced by electron-withdrawing groups (such as the 1-nitro group in 1-nitro-2-nitriminoimidazolidine) without the occurrence of any atomic shift of a tautomeric nature.

Unfortunately the correction outlined above was not generally acknowledged (9). The evaluation of very weak acidities by spectroscopic means has obscured our definition of neutrality. In the sense that we used it, neutrality applies to the practical basis whereby a substance like nitroguanidine or nitriminoimidazolidine can be separated from an

Can. J. Chem. Downloaded from www.nrcresearchpress.com by 210.87.254.105 on 09/05/12
For personal use only.

aqueous alkaline solution without any evidence of sodium salt formation. Such compounds may be called neutral in the same sense that Hantzch called the pseudo acid nitromethane a neutral form in order to contrast it to the *aci* form of this substance. Such a classification does not eliminate the pseudo acid nitromethane from its proper place in the pK_a scale. One can also write a resonance hybrid structure for ordinary nitromethane, but it has no direct relationship to the pseudo-*aci* behavior of this substance.

The situation is now unambiguous if in the publication by De Vries and Gantz (9) the term "nitramine" is read as "nitrimine" and all of the substances listed in their Table I are considered to be nitrimines. Also it should be realized that these valuable data by De Vries and Gantz do not contribute to the question of slow tautomerism because their analyses were not carried out under conditions which would reveal the isomeric process.

Our second error in stipulation of a tautomeric shift of nitrimine to nitramine as the first step in the reaction with alkali has now been corrected in terms of the initial formation of hydroxyaminate ion from which the sodium salt of the nitramine is formed subsequently. Therefore the slow tautomerism is an over-all experimental observation of a process in which the intermediate steps can lead to products additional to the nitrimine that is recoverable by acidification from the sodium salt of the nitramine. It is to be hoped that this clarification will eliminate the confusion about the reactions of nitroguanidine and its homologues with alkali.

EXPERIMENTAL

Melting points have been corrected against reliable standards.

Potassium Nitroguanidine

A solution was prepared of potassium metal (1.95 g, 0.05 g-atom) in 80 ml of anhydrous ammonia. Formation of potassium amide was allowed to proceed spontaneously. When the solution was colorless, 5.20 g (0.05 mole) of nitroguanidine was added, and the system was stirred while the substance dissolved. During the next 2 hours the white potassium salt precipitated. It was filtered off, m.p. 153.5–154° C, and then washed thrice with liquid ammonia, m.p. 155.5–156° C, 3.46 g (49.5%). Anal. Calc. for $CH_3KN_4O_2$: N, 39.4; K, 27.5. Found: N, 38.5; K, 27.1.

When the salt was heated for 1 hour at 65° C in 20 ml of anhydrous dimethylformamide and cooled, 75% (m.p. 145–146° C) was filtered off. The filtrate, after vacuum evaporation to half volume and dilution with diethyl ether, yielded 23% more, m.p. 133–137° C. Crystallization of the whole from 5 *M* methanolic potassium hydroxide gave a total yield of 98%, m.p. 152–153° C, not lowered by admixture with the original salt.

When the potassium salt was heated during 20 hours at 100° C (0.3 mm), gas was continually evolved. The residue in aqueous 10% nitric acid was filtered to remove nitroguanidine. Subsequent treatment of the filtrate with silver nitrate yielded yellow silver cyanamide.

Potassium 2-Nitriminoimidazolidine

This salt was prepared in 47% yield as described above. Admixture of the salt, m.p. 215–216° C, with 2-nitriminoimidazolidine gave a melting point depression. The salt was hydrolyzed by water to yield nitriminoimidazolidine. Anal. Calc. for $C_3H_5KN_4O_2$: K, 23.2. Found: K, 23.2.

Can. J. Chem. Downloaded from www.nrcresearchpress.com by 210.87.254.105 on 09/05/12
For personal use only.

Potassium 1-Benzyl-2-nitriminoimidazolidine

The reagent was not very soluble in liquid ammonia, but an 85% yield of salt was obtained, m.p. 226–227° C. Its hydrolyzate with water yielded 112% of the expected potassium content according to titration with acid.

1-Benzyl-2-nitroguanidine

To 0.57 g (0.004 mole) of potassium nitroguanidine in 20 ml of anhydrous dimethylformamide was added 0.75 ml (0.005 mole) of benzyl chloride. After 12 hours at 80° C this stirred system was filtered hot to remove sodium chloride. The vacuum-evaporated filtrate left a sticky solid which, extracted with diethyl ether and then water, left 0.365 g (43%), m.p. 170–172° C. Three crystallizations from absolute ethanol raised this melting point to 182–183° C, not lowered by admixture with authentic material (16).

A solution of 0.116 g (0.0006 mole) of this substance in 15 ml of hot absolute ethanol was cooled to 25° C, and 10 ml each of water and 0.1340 *N* sodium hydroxide were added. Back-titration with 0.1010 *N* hydrochloric acid showed exact equivalence with the alkali. When the system was evaporated to a 1-ml volume it yielded 0.104 g (90%) of benzylnitroguanidine, m.p. 178–179° C.

A similar solution was aged for 62 hours. Potentiometric titration with 0.1010 *N* hydrochloric acid showed, by the inflection on the curve, that ½ equivalent of free alkali had been consumed in neutralization of a weak acid. From this system 78% of benzylnitroguanidine, m.p. 178° C, was recovered.

1-Benzyl-2-nitriminoimidazolidine

To 35 ml of dry benzene was added 5.2 g (0.04 mole) of 2-nitriminoimidazolidine and 2.0 g (0.051 mole) of sodium amide. The system was stirred for 8 hours at 70° C. The excess of amide was then destroyed carefully with absolute ethanol and then treated with 5.0 ml (0.044 mole) of benzyl chloride. After 8 hours of further stirring the system was cooled and the solvent was vacuum-evaporated. The residue was eluted with absolute ethanol and filtered to remove salts. The filtrate was decolorized with Darco and then evaporated to a 20-ml volume. The benzylnitriminoimidazolidine which precipitated was crystallized from ethanol, 3.6 g (41%), m.p. 148–149° C, not depressed by admixture with an authentic sample (17).

1-Benzyl-2-nitrimino-3-nitroimidazolidine

(a) From Benzylnitriminoimidazolidine

To a mixture of 7 ml (0.073 mole) of acetic anhydride, 7 ml of acetic acid, and 1 ml (0.024 mole) of 99% nitric acid stirred at 5° C was added slowly 0.5 g (0.0023 mole) of 1-benzyl-2-nitriminoimidazolidine. After an additional hour at 5° C the system was filtered to remove 0.5 g (88%), m.p. 150–152° C, decomp. After three crystallizations from 95% ethanol the melting point was raised to 154–154.5° C, decomp.

(b) From 1-Nitro-2-nitriminoimidazolidine

To a methanolic solution containing 0.003 mole of phenyldiazomethane (17) was added 0.5 g (0.0027 mole) of 1-nitro-2-nitriminoimidazolidine (III), and the system was warmed slightly to complete the evolution of nitrogen. Upon cooling to 4° C, 0.35 g of III precipitated. Upon evaporation to half volume, 0.15 g (72% of III consumed), m.p. 150–153° C, was obtained. Three crystallizations from ethanol raised this melting point to 154–155° C, not depressed by admixture with product from procedure (*a*). Anal. Calc. for $C_9H_{11}N_4O_4$: C, 45.2; H, 4.63. Found: C, 45.0; H, 4.41.

Can. J. Chem. Downloaded from www.nrcresearchpress.com by 210.87.254.105 on 09/05/12
For personal use only.

1,3-Dibenzyl-2-nitriminoimidazolidine

The treatment with benzyl chloride of the potassium salt from 8.8 g (0.04 mole) of 1-benzyl-2-nitriminoimidazolidine was carried out exactly in the manner of the benzylation of nitriminoimidazolidine. The product, 5.2 g (42%), m.p. 120–121° C, was thrice crystallized from chloroform (1.5 ml per g, +20° C to −75° C), m.p. 125–125.5° C. Some dibenzylimidazolidone, in one instance as much as 44%, was found in the crystallization mother liquors. Anal. Calc. for $C_{17}H_{18}N_4O_2$: C, 65.8; H, 5.81. Found: C, 65.5; H, 5.82. The five strongest spacings, in Angstroms, by X-ray diffraction using Cu K_α radiation (Ni-filtered) are expressed as intensities: $[I/I_1]$ as [10] 2.79 [8] 5.04 [7] 4.11 [6] 2.10 [5] 2.29.

1,3-Dibenzyl-2-imidazolidone

To 0.176 g of 1,3-dibenzyl-2-nitriminoimidazolidine was added 7 ml of 20% aqueous sodium hydroxide. The solution was refluxed for 10 minutes, then chilled and extracted with 40 ml of diethyl ether. The extract, dried with magnesium sulphate, was evaporated, leaving 0.14 g, m.p. 85–90° C. Three crystallizations from absolute ethanol (4 ml per g) raised the melting point to 93–93.5° C, not depressed by admixture with the compound prepared by the method of Lob (19), yield 94%.

1-Benzyl-2-nitriminoimidazolidine (I, R = Benzyl) with Alkali

(a) Recovery of I (R = Benzyl)

To a cooled solution of 1.16 g (0.0053 mole) of 1-benzyl-2-nitriminoimidazolidine in 150 ml of absolute ethanol was added 187 ml of water containing 5.33 ml (0.012 mole) of 2.5 *N* aqueous sodium hydroxide solution. A 25-ml portion of this well-mixed system was extracted with three 20-ml portions of chloroform. The extract was dried by use of sodium sulphate and then was vacuum-evaporated to leave 0.089 g (100%) of I (R = benzyl), m.p. 146–148° C, authenticated by mixture melting point.

After several intervals of time, 25-ml portions were extracted and otherwise treated identically with that described above. The chloroform-extracted aqueous solution was acidified and again extracted with chloroform. The melting points of the evaporated extracts are recorded in the table below.

Reaction time (hr)	Recovered from alkaline solution		Recovered from acid solution	
	Wt. (g)	M.p. (°C)	Wt. (g)	M.p. (°C)
0	0.089	146–148	Omitted	
24	0.056	145–148	0.056	136–143
72	0.051	115–125	0.049 (gum)	

(b) Isolation of 1-Benzyl-2-imidazolidone and 3-β-Benzylaminoethyl-1-nitrourea

A well-mixed system was prepared identical with that of procedure (*a*). The system was allowed to age for 62 hours at 25° C. After evaporation at 40° C (15 mm) to a volume of 30 ml the crystals were filtered off, twice washed with 2-ml portions of water, and dried at 40° C (15 mm), giving 0.432 g of 1-benzylimidazolidone, m.p. 126.5–128° C. The aqueous filtrate and washings were combined and extracted with 30 ml of chloroform. Evaporation of the extract left 1.60 g of the same substance, m.p. 126–128° C. The total yield, 64%, was identified by mixture melting point with an authentic sample (17).

The extracted aqueous filtrate was then acidified with 3 ml of 20% hydrochloric acid

Can. J. Chem. Downloaded from www.nrcresearchpress.com by 210.87.254.105 on 09/05/12
For personal use only.

and then was extracted with 20 ml of chloroform. The extract (containing 0.007 g of gum) was discarded while the aqueous phase was evaporated at 35° C (15 mm) to a 5-ml volume. The crystals were filtered off, 0.363 g (24%), m.p. 155–182° C. This 3-β-benzylaminoethyl-1-nitrourea hydrochloride was crystallized from methanol – methyl acetate and then from cold methanol–acetone mixture, m.p. 192–194° C (decomp.). The substance gave a strong Franchimont (20) and a positive Beilstein test. Anal. Calc. for $C_{10}H_{15}N_4O_3.HCl$: C, 43.7; H, 5.50; N, 20.5. Found: C, 43.9; H, 5.54; N, 20.5.

The pH of the filtrate from which this hydrochloride was removed was adjusted to 5.5 and some silica was filtered off. After 17 hours at 25° C stubby needles separated, which were filtered off and washed with 1 ml of ethanol to leave 0.075 g (6%), m.p. 170–171° C. This 3-β-benzylaminoethyl-1-nitrourea was recrystallized twice from hot water, m.p. 175–175.5° C. Anal. Calc. for $C_{10}H_{15}N_4O_3$: C, 50.4; H, 5.93; N, 23.6. Found: C, 50.7; H, 6.01; N, 23.1.

1-Benzylimidazolidone

A solution of 0.10 g (0.00036 mole) of 3-β-benzylaminoethyl-1-nitrourea hydrochloride in 10 ml (0.025 mole) of 10% aqueous sodium hydroxide solution was thrice extracted with 15-ml portions of diethyl ether. The ethereal extract contained about 10 mg of brown gum. After 2 days the aqueous phase deposited stubby needles which were filtered off and washed with 5 ml of water to leave 20 mg, m.p. 126–128° C, mixture melting point with authentic material not lowered.

When this 1-benzylimidazolidone was boiled 5 minutes with 2.5 *N* sodium hydroxide it was recovered unchanged. Also, when its solution in 6% hydrochloric acid was allowed to age at 25° C for 12 hours, and then evaporated at 40° C (15 mm) to a volume of 0.5 ml and neutralized with aqueous sodium bicarbonate, the substance was quantitatively recovered unchanged, m.p. and mixture m.p. 126–128° C.

3-β-N-Benzyl-N-nitrosaminoethyl-3-nitroso-1-nitrourea

To a solution of 0.274 g (0.001 mole) of 3-β-benzylaminoethyl-1-nitrourea (VI*a*, R = benzyl) in 8 ml (0.004 mole) of 1.8% aqueous hydrochloric acid at 0° C and under nitrogen was slowly added 0.276 g (0.004 mole) of sodium nitrite in 2 ml of water. This nitrite solution was added during 200 minutes from a mechanically driven hypodermic syringe. No gas was evolved and the solution remained clear and colorless until the last 30 minutes of the addition period.

When addition was complete a solid was filtered off and methanol-washed (0.083 g, 35%); it was unchanged starting material, m.p. 174–176° C, mixture m.p. not lowered. The filtrate was evaporated at 35° C (15 mm) to dryness and the residue was extracted with 5 ml of hot acetone. This extract was evaporated to a 2-ml volume and then was chilled to −80° C to precipitate 0.06 g (cold-acetone-washed), m.p. 172–175° C (decomp.). This 21% yield of dinitroso derivative was crystallized from absolute methanol, m.p. 184.5–185° C. The substance gave a strong Liebermann nitroso test (while the Liebermann test for the starting material was negative) and a positive Franchimont nitramine test. Anal. Calc. for $C_{10}H_{12}N_6O_5$: C, 40.6; H, 4.08. Found: C, 40.6; H, 4.05.

REFERENCES

1. S. S. BARTON, R. H. HALL, and G. F WRIGHT. J. Am. Chem. Soc. **73**, 2201 (1951).
2. W. D. KUMLER and P. P. T. SAH. J. Org. Chem. **18**, 669 (1953).
3. R. N. JONES and G. D. THORN. Can. J. Research, B, **27**, 828 (1949).
4. M. W. KIRKWOOD and G. F WRIGHT. Can. J. Chem. **35**, 527 (1957).

Can. J. Chem. Downloaded from www.nrcresearchpress.com by 210.87.254.105 on 09/05/12
For personal use only.

5. M. W. KIRKWOOD and G. F WRIGHT. J. Org. Chem. **18**, 159 (1953).
6. G. F WRIGHT. Can. J. Chem. **30**, 62 (1952).
7. W. D. KUMLER. J. Am. Chem. Soc. **75**, 3092 (1953).
8. R. H. MEEN and G. F WRIGHT. J. Am. Chem. Soc. **74**, 2077 (1952).
9. J. E. DE VRIES and E. S. GANTZ. J. Am. Chem. Soc. **76**, 1008 (1954).
10. L. M. HALL, J. E. DE VRIES, and E. S. GANTZ. J. Am. Chem. Soc. **77**, 6507 (1955).
11. J. THIELE. Ann. **270**, 1 (1892).
12. R. H. HALL, A. F. MCKAY, and G. F WRIGHT. J. Am. Chem. Soc. **73**, 2205 (1951).
13. M. W. KIRKWOOD and G. F WRIGHT. J. Org. Chem. **18**, 629 (1953).
14. M. W. KIRKWOOD and G. F WRIGHT. J. Am. Chem. Soc. **76**, 1836 (1954).
15. M. A. WEINBERGER and A. F. MCKAY. J. Am. Chem. Soc. **77**, 1321 (1955).
16. A. F. MCKAY. J. Am. Chem. Soc. **71**, 1968 (1949).
17. A. F. MCKAY. J. Org. Chem. **16**, 1395 (1951).
18. T. L. DAVIS and I. ABRAMS. Proc. Am. Acad. Arts Sci. **61**, 437 (1923).
19. J. LOB. Rec. trav. chim. **55**, 866 (1936).
20. A. P. N. FRANCHIMONT. Rec. trav. chim. **16**, 226 (1897).

Can. J. Chem. Downloaded from www.nrcresearchpress.com by 210.87.254.105 on 09/05/12
For personal use only.

Can. J. Chem. Downloaded from www.nrcresearchpress.com by 210.87.254.40 on 09/05/12
For personal use only.

METHYLATION OF SUGAR MERCAPTALS

II. L-ARABINOSE DIETHYL MERCAPTAL[1]

G. G. S. Dutton and Y. Tanaka

ABSTRACT

Methylation of L-arabinose diethyl mercaptal in tetrahydrofuran with methyl iodide and silver oxide yielded mainly 2-*O*-methyl-L-arabinose and a trace of 5-*O*-methyl-L-arabinose. The identity of the major component was inferred by its behavior on electrophoresis and confirmed by the preparation of the crystalline amide. The polymethylated components were not examined. 2-*O*-Methyl-L-arabono-γ-lactone, previously known as a sirup, has now been obtained crystalline.

In Part I it was reported (1) that in the Purdie methylation of D-glucose diethyl mercaptal the 2-position was methylated exclusively but no methylation took place with other sugar mercaptals. This was attributed to the insolubility of the other mercaptals in methyl iodide. When the methylation was carried out in tetrahydrofuran not only D-glucose mercaptal but also other sugar mercaptals were found to be reactive towards Purdie's reagents; the qualitative investigation of these mercaptals has been described previously (1).

The present paper is the second in a series on the relative reactivities of hydroxyl groups in sugar mercaptals and describes the methylation of L-arabinose diethyl mercaptal in tetrahydrofuran. As with D-glucose diethyl mercaptal, the hydroxyl on C_2 of L-arabinose diethyl mercaptal is the most reactive to methylation in tetrahydrofuran. The primary C_5-hydroxyl group is also reactive but to a much lesser extent. No monomethylarabinoses were found other than the 2-*O*- and 5-*O*-methyl isomers, and a colorimetric estimation showed these to be present in the approximate ratio of 30:1.

L-Arabinose diethyl mercaptal was shaken at room temperature in tetrahydrofuran in the presence of silver oxide and drierite, in a quantity of methyl iodide adjusted so that a reasonable amount of monomethylarabinoses was obtained. Acid hydrolysis of the methylation mixture gave a mixture of methylated L-arabinoses which was shown by paper chromatography to contain, *inter alia*, two mono-*O*-methyl isomers. These two components were isolated by paper chromatography using butanone–water azeotrope as the developing solvent.

The fast-running component (R_f 0.30 in butanone–water azeotrope) was assumed first to be 5-*O*-methyl-L-arabinose (2), since it ran at the same rate as the latter on paper chromatography in butanone–water azeotrope. However, paper electrophoresis of this component showed that it was a mixture of 5-*O*-methyl-L-arabinose (M_g 0.80, faint) and a polymethylated arabinose (M_g 0.00, strong), the structure of which was not investigated. Since the amount of 5-*O*-methyl-L-arabinose produced in this methylation was very small, as shown by a faint spot on electrophoresis, it was not possible to isolate it and identify it by the preparation of a crystalline derivative.

The slow-running component (R_f 0.15 in butanone–water azeotrope) was shown to be electrophoretically homogeneous (M_g 0.33), and the crystalline amide was prepared (m.p. 131–132° C) from the sirup by oxidation with bromine followed by treatment with methanolic ammonia. Both 2- and 3-*O*-methyl-L-arabonamides have been reported

[1]*Manuscript received June 27, 1960.*
Contribution from the Department of Chemistry, University of British Columbia, Vancouver 8, B.C. Presented at the 138th American Chemical Society meeting in New York, September, 1960.

(m.p. 131° C and 132° C, respectively (3)), but our amide was assumed to be the 2-*O*-methyl derivative from the fact that substitution of the 2-hydroxyl with a methyl group results in retardation of migration in electrophoresis (4). Admixture of our amide with an authentic sample prepared by the method of Jones, Kent, and Stacey (5) and of Hirst and Jones (6) showed no depression of the melting point.

Confirmation of the identity of the slow-moving component as 2-*O*-methyl-L-arabinose was obtained by showing that (*a*) the derived amide gave a negative Weerman test (7), (*b*) the infrared spectra of the amide of the unknown sugar and of the synthetic 2-*O*-methyl-L-arabonamide were superimposable, and (*c*) a mixed melting point of the unknown amide with an authentic sample of 3-*O*-methyl-L-arabonamide (m.p. 131–132° C) was 80–105° C. During the preparation of the authentic 2-*O*-methyl-L-arabonamide the 2-*O*-methyl-L-arabono-γ-lactone was obtained in crystalline form, m.p. 88° C.

In addition to these two monomethylarabinoses, a number of polymethylarabinoses and unreacted arabinose were also detected on paper chromatography, but they were not investigated further.

EXPERIMENTAL

Methylation of L-*Arabinose Diethyl Mercaptal*

L-Arabinose diethyl mercaptal (500 mg) was dissolved in 50 ml of dry tetrahydrofuran, and 500 mg of silver oxide and 3 g of drierite were added to the solution. Methyl iodide (10 ml) was added to the mixture which was then shaken at room temperature for 20 hours, during which time 30 ml of methyl iodide were added in aliquots of 10 ml at 5-hour intervals. The reaction mixture was filtered and evaporated *in vacuo* to a sirup which was then dissolved in 30 ml of chloroform, and a small amount of inorganic impurities was removed by filtration. The chloroform solution was evaporated *in vacuo*, and the sirup (564.3 mg) thus obtained was dissolved in a mixture of ethanol (10 ml) and concentrated hydrochloric acid (2.5 ml) and refluxed in boiling water for 5 hours. After neutralization with Duolite A-4 resin, the solution was evaporated *in vacuo* to give a light brown sirup (290.8 mg).

Chromatographic Separation of the Methylated L-*Arabinoses*

The sirup showed the following spots by paper chromatography: R_f 0.91 to 0.75 (two (?) components); 0.59, 0.47, 0.36, 0.30, 0.15, and 0.05 (butanone–water azeotrope); R_f 0.84 to 0.77 (two (?) components); 0.66, 0.57, 0.52, 0.45, 0.37, and 0.18 (ethyl acetate – formic acid – acetic acid – water, 18–1–3–4).

The sirup was chromatographed using butanone–water azeotrope for about 13 hours on Whatman No. 3MM paper previously washed with the same solvent. The components which corresponded to R_f 0.30 and R_f 0.15 (butanone–water azeotrope) were detected on both edges of the chromatogram, and the strips containing these components were extracted with boiling methanol. After three extractions the extract gave a very faint Molisch test. Yields of the fast- and slow-running compounds were 7.0 mg and 32.6 mg respectively. These two components were examined by electrophoresis (750–1000 v, 1.5 hours, 0.05 *M* sodium borate solution) and showed the following M_g values: slow-running component (R_f 0.15), M_g 0.33; fast-running component (R_f 0.30), M_g 0.80 (faint) and 0.00 (strong); synthetic 5-*O*-methyl-L-arabinose, M_g 0.80; (D-glucose, M_g 1.00).

A quantitative analysis of the fast-running component by the phenol – sulphuric acid

Can. J. Chem. Downloaded from www.nrcresearchpress.com by 210.87.254.40 on 09/05/12
For personal use only.

method (11) showed a ratio of 6:1 for the components with M_g 0.00 and 0.80. This gives approximately 30:1 for the ratio of 2-*O*-methyl-L-arabinose to the 5-*O*-methyl isomer.

Identification of the Slow-running Component as 2-O-Methyl-L-arabinose

The sirup (20.7 mg) was oxidized with bromine for 24 hours according to the ordinary procedure and the lactone (11.0 mg) was dissolved in 10 ml of ethanol (absolute), saturated with dry ammonia, and kept overnight at room temperature. Evaporation of the solvent gave 9.0 mg of sirup which was crystallized from ethanol – light petroleum ether. Yield: 45%, based on the monomethylarabinose. M.p. and mixed m.p. 131–132° C. Mixed m.p. with 3-*O*-methyl-L-arabonamide 80–105° C.

Synthesis of 2-O-Methyl-L-arabinose

This was prepared by the published method (6) from methyl β-L-arabopyranoside (m.p. 168° C, 4 g), anhydrous copper sulphate (50 g), and acetone (200 ml). The sirupy isopropylidene derivative (3.29 g) was methylated three times by Purdie's method and the product (2.45 g) hydrolyzed with *N* sulphuric acid for 4 hours on the steam bath. Neutralization (Duolite A-4 resin) and evaporation gave a sirup (1.67 g) which on chromatographic examination showed two strong spots (R_{arab} 3.76 and 10.7) and one weak spot (R_{arab} 1.0, butanone–water). Separation of the sirup on a cellulose–hydrocellulose column (9) using butanone–water yielded 691 mg of chromatographically pure 2-*O*-methyl-L-arabinose (R_{arab} 3.76, $[\alpha]_D^{22}$ 94.0° (*c*, 0.26 in water)).

When the preparation of this compound was attempted by refluxing for 24 hours a mixture of the sirupy glycosides (10 g) with anhydrous copper sulphate (50 g) and acetone (250 ml), the yield of chromatographically pure 2-*O*-methyl-L-arabinose was only 438 mg.

2-O-Methyl-L-arabono-γ-lactone

Synthetic 2-*O*-methyl-L-arabinose (173.2 mg) was oxidized with bromine, and the lactone (153.0 mg, 89.5%), obtained initially as a sirup, was crystallized from acetone or ethyl acetate as needles, m.p. 88° C; $[\alpha]_D^{20}$ −49.1° → −46.3° (24 hours, *c*, 0.128 in water); λ_{max}^{nujol} 5.73 μ (8). Anal. Calc. for $C_6H_{10}O_5$: OMe, 19.2%. Found: OMe, 19.2, 19.5%. The lactone (111 mg) was converted to the amide (92 mg, 76%), which was recrystallized from ethyl acetate – acetone or ethyl acetate – methanol as fine needles; m.p. 131° C, lit. (6) m.p. 131° C. The infrared spectra of this amide and that obtained from the slow-running component were identical.

3-O-Methyl-L-arabinose

This was prepared by the courtesy of Mr. A. E. Barlay according to the method of Hirst, Jones, and Williams (10). The sugar had $[\alpha]_D^{22}$ 107° (*c*, 1.4 in water), and the derived 3-*O*-methyl-L-arabonamide, after recrystallization from ethyl acetate – petroleum ether, had m.p. 131–132° C.

ACKNOWLEDGMENTS

We are grateful to the Research Corporation for financial support and one of us (Y. T.) thanks the National Research Council for the award of a studentship.

REFERENCES

1. G. G. S. DUTTON and K. YATES. Can. J. Chem. **36**, 550 (1958).
2. G. G. S. DUTTON, Y. TANAKA, and K. YATES. Can. J. Chem. **37**, 1955 (1959).
3. G. G. MAHER. *In* Advances in Carbohydrate Chemistry. Vol. 10. Academic Press, New York. 1955. p. 257.

Can. J. Chem. Downloaded from www.nrcresearchpress.com by 210.87.254.40 on 09/05/12
For personal use only.

4. A. B. FOSTER. *In* Advances in Carbohydrate Chemistry. Vol. 12. Academic Press, New York. 1957. p. 81.
5. J. K. N. JONES, P. W. KENT, and M. STACEY. J. Chem. Soc. 1341 (1947).
6. E. L. HIRST and J. K. N. JONES. J. Chem. Soc. 1221 (1947).
7. M. R. A. WEERMAN. Rec. trav. chim. **37**, 16 (1918).
8. S. A. BARKER, E. J. BOURNE, R. M. PINKARD, and D. H. WHIFFEN. Chem. & Ind. (London), 658 (1958).
9. J. D. GEERDES, B. A. LEWIS, R. MONTGOMERY, and F. SMITH. Anal. Chem. **26**, 264 (1954).
10. E. L. HIRST, J. K. N. JONES, and E. M. L. WILLIAMS. J. Chem. Soc. 1062 (1947).
11. M. DUBOIS, K. A. GILLES, J. K. HAMILTON, P. A. REBERS, and F. SMITH. Anal. Chem. **28**, 350 (1956).

Can. J. Chem. Downloaded from www.nrcresearchpress.com by 210.87.254.40 on 09/05/12
For personal use only.

Can. J. Chem. Downloaded from www.nrcresearchpress.com by 210.87.254.5 on 09/05/12
For personal use only.

THE ALKALOIDS OF CORYDALIS GOVANIANA[1]

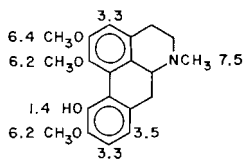
O. E. Edwards and K. L. Handa[2]

ABSTRACT

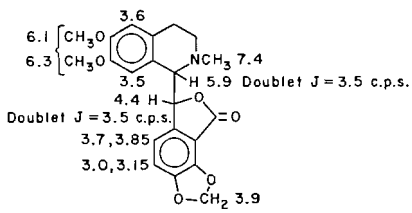
The Himalayan plant *Corydalis govaniana* (Wall. Tent.) has been shown to contain the alkaloids protopine, corlumine, bicuculline, and isocorydine, as well as fumaric acid and choline.

The alkaloids of the genus *Corydalis* have been the subject of intensive investigation (1). The species *govaniana* (Wall. Tent.), however, appears to have escaped chemical examination until the present work. It is native to the western Himalayas, where the inhabitants use the roots in treating skin diseases.

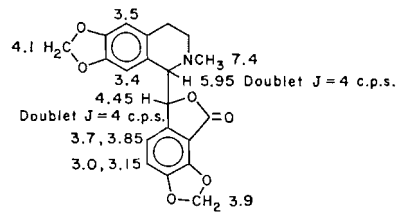
An alcohol extract of the dried ground root was concentrated to a syrup under reduced pressure, and the alkaloids extracted into dilute sulphuric acid. They were then separated using the general procedure devised by Manske (2) (see Flow Sheet I). Only known alkaloids were encountered: protopine, isocorydine (I), corlumine (II), and bicuculline (III) in the approximate ratio of 1:1:8:3. The latter two ran together with several solvent systems on paper, were not separated by chromatography on alumina, but could be partially separated by fractional crystallization. However, countercurrent distribution between benzene and buffer of pH 3 effected a clean separation of the two bases.



I



II



III

We were surprised to find the phthalide isoquinoline base corlumine (II) appearing, in part, among the phenolic bases. The lactone rings in it and bicuculline are hence readily opened by alkali, a fact supported by the fairly rapid shift of their ultraviolet absorption spectra in alkaline ethanol. The identity of the bases was surmised after study of their ultraviolet, infrared, and N.M.R. spectra and comparison of empirical formula and melting point with literature values. Finally, comparison was made with authentic samples kindly supplied by Dr. Léo Marion and Dr. R. H. F. Manske. The ultraviolet spectra and description of new salts of the alkaloids are documented in the experimental part. Our assignment of the main bands of the N.M.R. spectra have been indicated on the formula in τ ($CDCl_3$ solutions) (3). The infrared spectra of the alkaloids are reproduced in Fig. 1. Two features of the spectra of general interest are the N—CH_3 bands near 2800 cm^{-1} and the OCH_3 bands near 2850 cm^{-1}. These supplement the sometimes

[1]*Manuscript received June 1, 1961.*
Contribution from the Division of Pure Chemistry, National Research Council, Ottawa, Canada.
Issued as N.R.C. No. 6443.
[2]*Colombo Plan Research Fellow, 1961.*

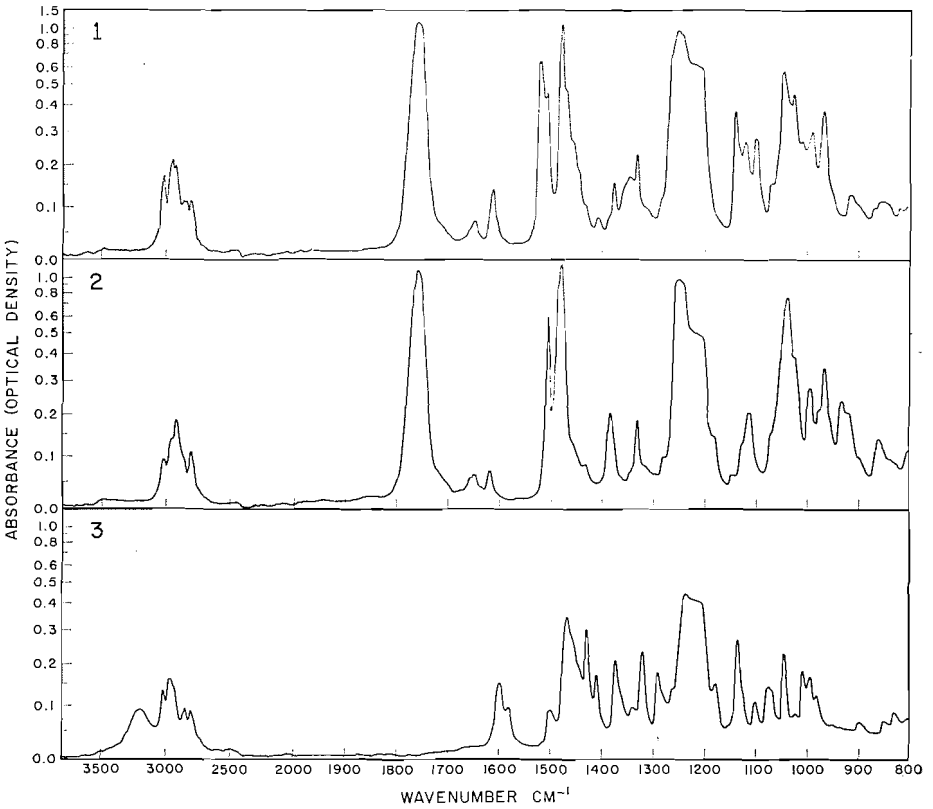


FIG. 1. Infrared spectra in chloroform in a 0.1-mm cell: 1, corlumine; 2, bicuculline; 3, isocorydine.

ambiguous evidence from analyses and N.M.R. spectra. The acidic material from the plant yielded fumaric acid, while the water-soluble part of the ethanol extract gave choline reineckate when treated with ammonium reineckate.

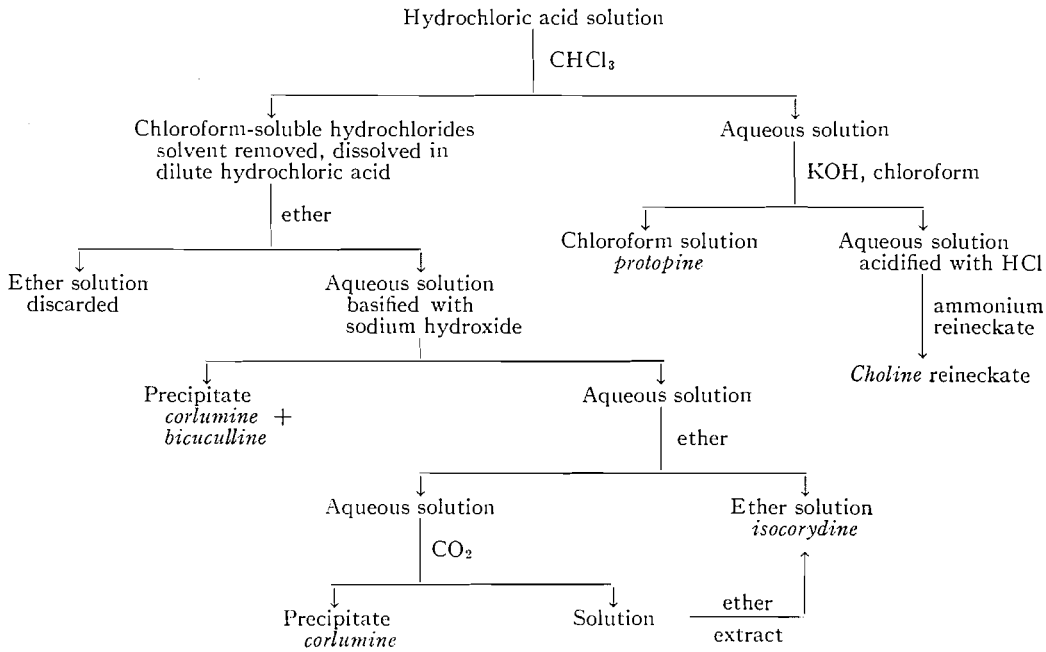
EXPERIMENTAL

Ultraviolet spectra were determined in 95% ethanol (intensities in ϵ are cited in parentheses), rotations in chloroform, and N.M.R. spectra in deuterochloroform with tetramethylsilane as internal standard. The pK_a' values were determined in the aqueous alcohol mixtures specified, by titration with *p*-toluenesulphonic acid in the same solvent. Melting points were determined on a Kofler hot stage.

Extraction and Separation

Roots of *Corydalis govaniana* (Wall. Tent.) were collected in September 1960, air-dried, and ground. An exhaustive ethanol extraction of 5 kg of this material was made at room temperature. The extract was concentrated to a syrup under reduced pressure. The alkaloids were extracted from the syrup into dilute sulphuric acid. The acid solution was basified with ammonia and the alkaloids recovered by extraction into chloroform. After removal of the chloroform the residue was dissolved in 300 ml of 10% hydrochloric acid. After standing overnight, this solution was extracted six times with 200-ml portions of chloroform. The subsequent operations are shown on Flow Sheet I.

Can. J. Chem. Downloaded from www.nrcresearchpress.com by 210.87.254.5 on 09/05/12
For personal use only.



FLOW SHEET I

The corlumine–bicuculline mixture was not separated by chromatography on 20 times its weight of alumina, activity III. Five grams of the mixture was loaded in five Craig tubes (capacity, 10 ml of each phase) in benzene. It was then subjected to 100 transfers past phosphate–citrate buffer of pH 3. Tubes 15–45 contained one substance with peak concentration in tube 30. The contents of tubes 20 to 40 were combined and 3.6 g alkaloid recovered. After one recrystallization from methanol it melted at 160–161° and proved to be corlumine. Tubes 55–75 were mainly one alkaloid (peak concentration at tube 65) but a tailing out toward higher tube number suggested the presence of another. The contents of tubes 60 to 75 were combined. The alkaloid from these (1.3 g) melted at 197–198° after one recrystallization from methanol, and proved to be bicuculline. No pure alkaloids were obtained from the remaining tubes.

Corlumine

Yield, 17.2 g (0.36%). After four recrystallizations from methanol it melted at 162°; $[\alpha]_D^{25}$ 77° (*c*, 1.0); pK_a' (50% aqueous methanol) 6.3. Ultraviolet spectrum: λ_{max} 222 (30,640), 287 (3980), and 326 (5260) mμ, unchanged on addition of acid. In alkaline ethanol it had λ_{max} 219 (53,600) and 287 (7280) mμ. It did not depress the melting point of an authentic sample with m.p. 160°. The base formed a crystalline picrate, m.p. 204°. Found: C, 52.32; H, 3.71; N, 10.09. Calc. for $C_{27}H_{24}O_{13}N_4$: C, 52.92; H, 3.90; N, 9.14. Its perchlorate melted at 180–181° C. Found: C, 51.70; H, 4.70. Calc. for $C_{21}H_{21}O_6N.HClO_4$: C, 52.11; H, 4.56. Its picrolonate melted at 225°.

Bicuculline

Yield, 5.3 g (0.106%). After five recrystallizations from methanol this base melted at 199° and had $[\alpha]_D^{25}$ 131° (*c*, 1.6) and pK_a' (50% aqueous methanol) 6.2. It did not depress the melting point of an authentic sample of bicuculline, m.p. 198°. It had λ_{max} 225 (36,700),

Can. J. Chem. Downloaded from www.nrcresearchpress.com by 210.87.254.5 on 09/05/12
For personal use only.

296 (6390), and 324 (5870) mμ, unchanged in acidified ethanol. In alkaline ethanol it had λ_{max} 222 (48,440) and 293 (9540) mμ. Its picrate melted at 202°. Found: C, 52.40; H, 3.31. Calc. for $C_{26}H_{20}N_4O_{13}$: C, 52.35; H, 3.35. Its picrolonate melted at 195°.

Isocorydine

Yield, 2.1 g (0.04%). After recrystallization from methanol this base melted at 186° and had $[\alpha]_D$ 195° (*c*, 1.0) and pK_a' (80% methanol) 6.3. It did not depress the melting point of an authentic sample of isocorydine, m.p. 185°. It had λ_{max} 220 (51,500), 266 (18,760), and 304 (6650) mμ. In alkaline ethanol it had λ_{max} 342 (19,440) mμ. Its methiodide melted at 224° (lit. 224 (4)).

Protopine

Yield, 3.4 g (0.068%). After recrystallization from methanol this melted at 210° and showed no mixed melting point depression with authentic protopine, m.p. 211°. Its pK_a' was 8.2 in 90% methanol. It had λ_{max} 290 (10,170) mμ unchanged on addition of alkali. In a 1 *N* solution of hydrogen chloride in 95% ethanol it had λ_{max} 290 (9180) and 240 (9880) mμ.

Choline

The reineckate was converted to the chloroaurate (0.215 g), m.p. 242°, undepressed when mixed with choline chloroaurate, m.p. 244°.

Fumaric Acid

The acid-insoluble part of the ethanol extract was extracted with hot water. On being cooled the solution deposited crystals of fumaric acid which sublimed above 200° and melted at 297° (sealed capillary); mixed m.p. with authentic fumaric acid, 297°.

ACKNOWLEDGMENTS

We thank Mr. H. Seguin for the microanalysis, Mr. R. Lauzon for the infrared spectra, and Mr. J. Nicholson for the N.M.R. spectra. One of us (K. L. H.) is grateful to the Canadian Colombo Plan authorities for financial assistance.

REFERENCES

1. R. H. F. MANSKE and H. L. HOLMES (*Editors*). The alkaloids. Vol. IV. Academic Press, New York. 1954. Chap. 28–32 and 34.
2. R. H. F. MANSKE. Can. J. Research, B, **8**, 210 (1933).
3. G. V. TIERS. J. Phys. Chem. **62**, 1151 (1958).
4. E. SCHLITTLER and H. U. HUBER. Helv. Chim. Acta, **35**, 111 (1952).

Can. J. Chem. Downloaded from www.nrcresearchpress.com by 210.87.254.5 on 09/05/12
For personal use only.

Can. J. Chem. Downloaded from www.nrcresearchpress.com by 210.87.254.5 on 09/05/12
For personal use only.

STEROIDS AND RELATED PRODUCTS

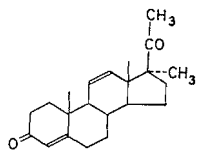
XVI. AN IMPROVED SYNTHESIS OF 11-DEHYDRO-17α-METHYLPROGESTERONE[1,2]

CH. R. ENGEL,[3] G. JUST, AND R. BUTTERY

ABSTRACT

An improved synthesis of 11-dehydro-17α-methylprogesterone, previously synthesized by this group, has been devised. The new hormone analogue has the same luteoid activity as 17α-methylprogesterone; in this case, the 11,12-unsaturation has no potentiating effect on the progestational activity. Some stereochemical aspects of the Faworsky rearrangement of 17α-halo-20-keto steroids are discussed in a preliminary fashion.

In a recent paper (2) this group reported the synthesis of a new progestational agent, 11-dehydro-17α-methylprogesterone (I), in which were combined two chemical features

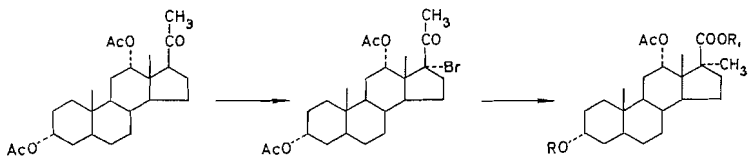


I

that independently increase the luteoid activity of the natural hormone, i.e. an 11,12-double bond and a 17α-methyl group. While we had established that the new hormone analogue possessed marked activity, more material was needed for a quantitative biological evaluation.

Since the yields of two reaction sequences of the previously reported synthesis (2) had proved unsatisfactory, we devised an improved pathway for the preparation of the desired progestin.

One of these unsatisfactory sets of reactions had been the transformation of the starting material, 3α,12α-diacetoxypregnane-20-one (II), to the 17α-bromo derivative III and thence, by a Faworsky rearrangement, to ester derivatives of the 17α-methyl etianic acid IV. Since it is known (compare ref. 3) that a Faworsky rearrangement of impure



II III

IV, R = H, R₁ = H
IVa, R = H, R₁ = CH_3
IVb, R = Ac, R₁ = CH_3

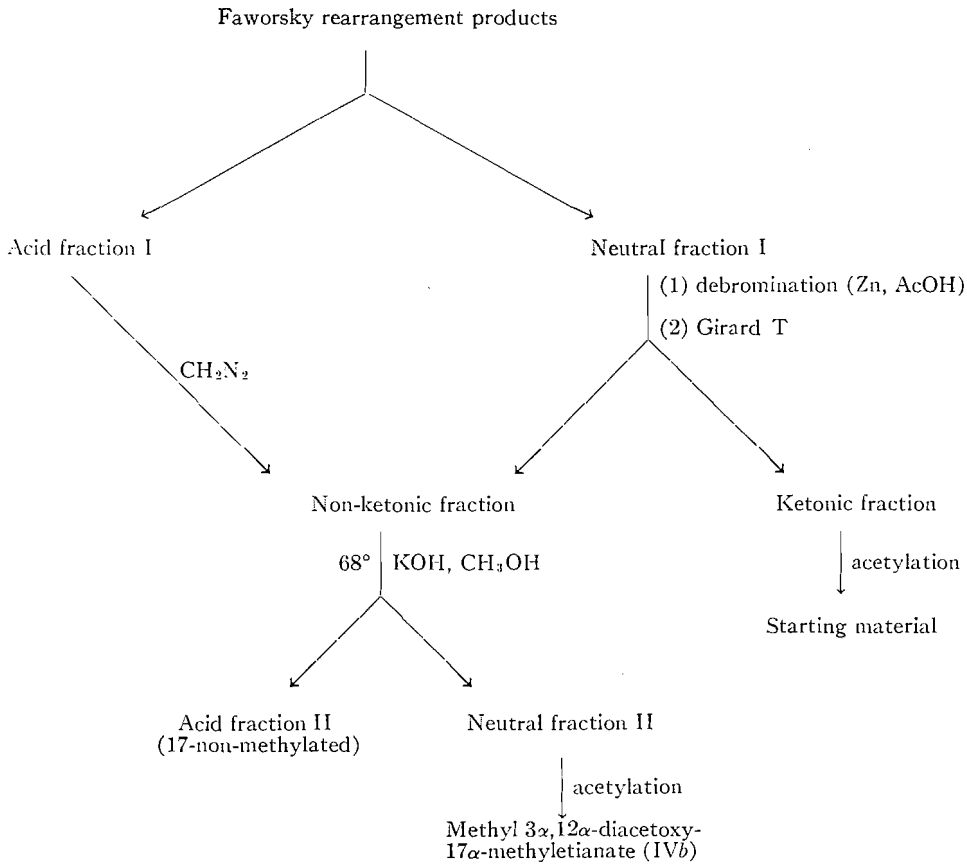
17α-bromo-20-ketones gives a poor yield of 17α-methylated etianic acid derivatives, we considered that at least part of our difficulties stemmed from the fact that the amorphous

[1]*Manuscript received June 15, 1961.*
Contribution from the Departments of Medical Research and Chemistry of the University of Western Ontario, London, Ontario, and the Department of Chemistry, Laval University, Quebec, Que. Some of the results reported in this paper were included in a communication presented at the 41st Annual Conference of the Chemical Institute of Canada, Toronto, Ontario, June, 1958.
[2]*For paper XV of this series see reference 1.*
[3]*Correspondence should be addressed to this author at the Faculty of Science, Laval University.*

17α-bromide III could not be isolated in the pure state. We were able to improve the yield of this reaction sequence by replacing the acid-catalyzed bromination of II with molecular bromine by a free-radical bromination with N-bromosuccinimide, using the procedure of Schock and Karpel (4). Furthermore, we simplified and improved the method of isolation of the desired rearrangement product by using a series of operations schematized in Flowsheet I and described in detail below under *Experimental*. Thus it was possible to raise the yield of the transformation of II to IV*b* by almost 50%, namely from 30–35% to 45–50%.

FLOWSHEET I

Isolation of methyl 3α,12α-diacetoxy-17α-methyletianate (IV*b*)

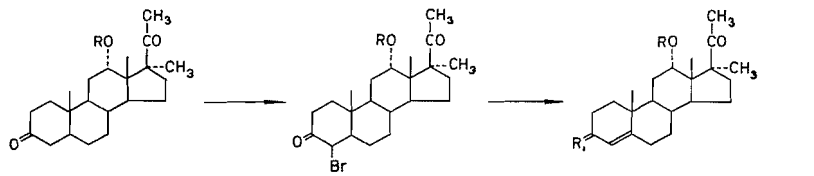


It is noteworthy that, as in the case of the previously reported Faworsky rearrangement of crude bromide III, we were not able to isolate any 17-epimeric rearrangement products, in spite of the fact that large amounts of material were used and carefully worked up. This is in accord with the results obtained when 17α-bromopregnenolone acetate is treated with bicarbonate (3), and in contrast to those of the rearrangement with bicarbonate of 17α-bromo-3α-acetoxypregnane-11,20-dione (5) (compare also the rearrangement of this compound with sodium ethylate, reported by Wendler *et al.* (6)). In the case of Faworsky rearrangements of 17α-bromo-20-keto steroids without carbonyl functions

Can. J. Chem. Downloaded from www.nrcresearchpress.com by 210.87.254.5 on 09/05/12
For personal use only.

in ring C, by the action of bicarbonate, the mechanism proposed by Loftfield (7) seems unacceptable. Indeed, this mechanism consists in the concerted formation of a cyclopropanone intermediate which is opened by base; hence the reaction should proceed with inversion in 17 and result, in the case of a 17α-bromo-20-ketone, in a 17β-methyl-17-isoetianic acid derivative. A synionic transfer of bromine from position 17 to 21, prior to the formation of the cyclopropanone intermediate, as postulated by Wendler *et al.* (6) (compare also an earlier proposal by Richard (8)), seems likewise improbable, at least in this instance, since the rearrangement of 21-halogenated 20-ketones gives a mixture of 17-epimeric etianic acid derivatives (compare ref. 9). A detailed discussion of this problem, together with new experimental data, will be reported in a forthcoming paper of this series.

A second unsatisfactory set of transformations in our previous synthesis of 11-dehydro-17α-methylprogesterone was the penultimate sequence of reactions, consisting in the introduction of the Δ^4-double bond into 12α-tosyloxy-17α-methylpregnane-3,20-dione (compare V*a* $\rightarrow$ VI*a* $\rightarrow$ VII*c* $\rightarrow$ VII*b* (2)). The introduction of this double bond into the corresponding free 12α-hydroxy derivative V (compare the transformations V $\rightarrow$ VI $\rightarrow$ VII*a* $\rightarrow$ VII) had also proved unsatisfactory. Since the analogous sequence of reactions



V , R = H
Va , R = Ts

VI , R = H
VIa , R = Ts

VII ,R = H , R1 = O
VIIa,R = H , R1 = N-NH-CO-NH2
VIIb,R = Ts , R1 = O
VIIc,R = Ts , R1 = N-NH-CO-NH2

proceeded in much better yields in the case of methyl 12α-tosyloxy-3-oxo-17α-methyletianate (2), we decided to introduce the Δ^4-double bond at an early stage of our new synthesis, prior to the elaboration of the methyl ketone side chain.

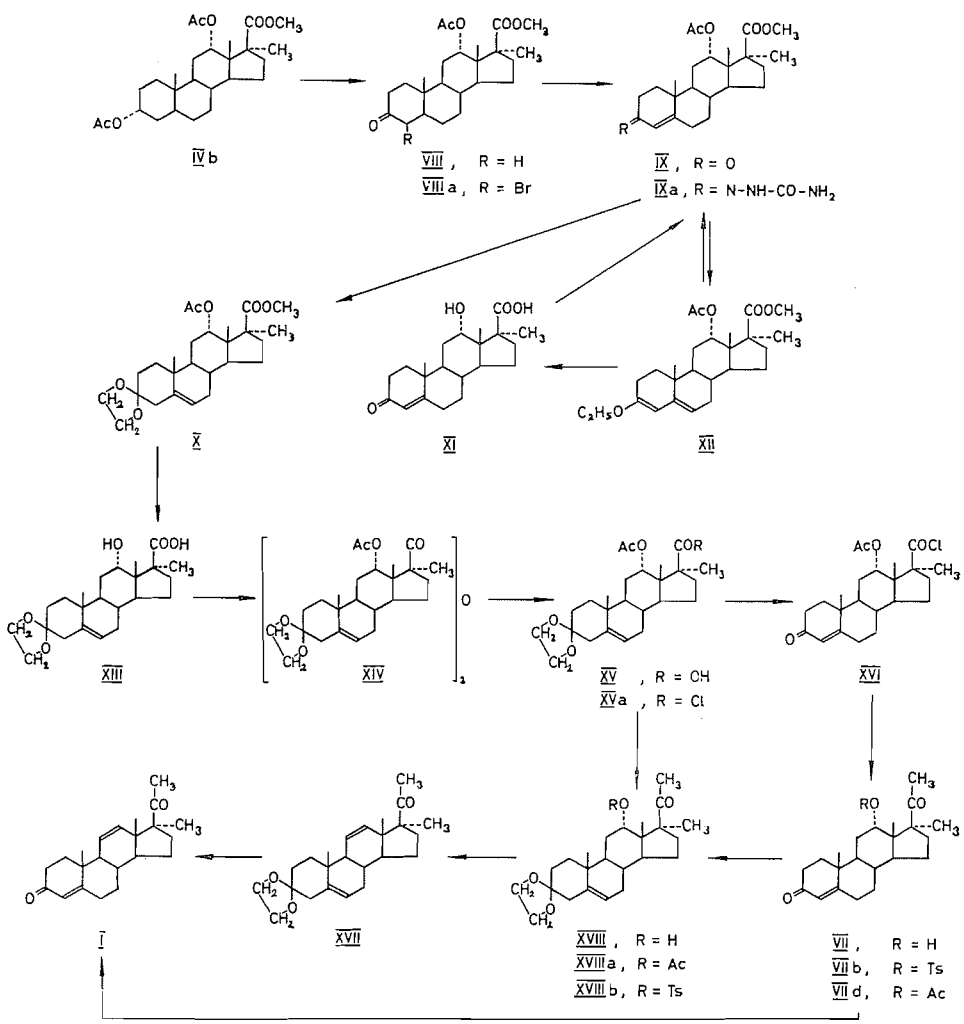
We transformed methyl 3α,12α-diacetoxy-17α-methyletianate (IV*b*) to methyl 12α-acetoxy-3-oxo-17α-methyletianate (VIII), as previously described (2). The 3-keto ester VIII was converted in high yield to the 4-bromide VIII*a* by bromination with bromine in acetic acid, and the Δ^4-double bond was introduced by McGuckin and Kendall's method (10), via the 4-unsaturated 3-semicarbazone IX*a*, in almost quantitative yield.

The Δ^4-3-keto moiety of the resulting methyl Δ^4-12α-acetoxy-3-oxo-17α-methyletienate (IX) was protected against the vigorous alkaline treatment necessary for the saponification of 17-methylated etianic esters, by formation of an ethylene ketal (X). Prolonged treatment of ester X with methanolic potassium hydroxide under pressure and at elevated temperature led, in 90% yield, to the 3-ethylenedioxy acid XIII.

Protection of the α,β-unsaturated ketone by the formation of an enol ether, which had proved satisfactory in previous experiments of this series (11, 12), gave somewhat disappointing results: the yield of the formation of enol ether XII was lower than anticipated and its conversion to the Δ^4-3-keto etienic acid XI was not as simple as in the analogous cases which we described previously.

The 12α-hydroxy-3-ethylenedioxy acid XIII was transformed to its acetate XV by

Can. J. Chem. Downloaded from www.nrcresearchpress.com by 210.87.254.5 on 09/05/12
For personal use only.



treatment with acetic anhydride in pyridine at reflux temperature and by hydrolysis with potassium carbonate of the 12α-acetoxy anhydride XIV thus formed.

Whereas the carbonyl function of acid XV reacts readily with oxalyl chloride and whereas the acid chloride formed gives an excellent yield of a 17α,21-dimethyl-20-ketone upon treatment with dimethyl cadmium, the protecting ketal function in position 3 tends to be removed during this sequence of reactions, particularly in the course of the preparation of the acid chloride. Thus, the acetoxy ketal acid XV can be transformed in 87% yield to crystalline 12α-acetoxy-17α-methylprogesterone (VII*d*) without a separate hydrolysis step. If every trace of moisture is excluded during the preparation of the acid chloride, it is possible to obtain the 3-ethylenedioxy-20-ketone XVIII*a* as the main reaction product (approximately 70% yield of crude and 45% yield of purified product), from which the concomitantly formed Δ^4-3,20-diketone VII*d* can be separated in the pure state in an approximate yield of 10% by crystallization and chromatography. This unsaturated diketone VII*d* can in turn be converted in over 50% yield to the monoketal

Can. J. Chem. Downloaded from www.nrcresearchpress.com by 210.87.254.5 on 09/05/12
For personal use only.

XVIII*a* by the usual treatment with ethylene glycol and *p*-toluenesulphonic acid in boiling benzene. The retention of the ketal group in position 3 is desirable because alkaline hydrolysis of the 12α-acetate requires, in the presence of a 17-methyl group, relatively drastic conditions (compare ref. 2) to which a free Δ^4-3-ketone should not be exposed.[4]

The hydrolysis of acetate XVIII*a* with methanolic potassium hydroxide proceeded in almost quantitative yield. Tosylation of the resulting hydroxy adduct XVIII was slow, but the desired 12α-tosylate XVIII*b* was obtained in 78% yield when care was taken to avoid hydrolysis of the ketal function during the working up. Dehydrotosylation was achieved in good yield by chromatography on activated aluminum oxide at elevated temperature, as described in the previous paper of this series (1) (compare also ref. 13), and the Δ^4-3-keto moiety was set free by an exchange reaction with acetone in the presence of *p*-toluenesulphonic acid at room temperature (compare ref. 14). The resulting product was identical with authentic 11-dehydro-17α-methylprogesterone (I), previously prepared by our group (2).

Doctors P. Perlman and M. Eisler of the Schering Corporation, Bloomfield, N.J., kindly tested the new hormone analogue I for progestational activity, in the Clauberg assay. They found that the product was, upon parenteral administration, two to three times as active as progesterone, hence of the same activity as 17α-methylprogesterone (3). Evidently, the additional presence of the Δ^{11}-double bond, which raises the progestational activity of progesterone by a factor of 3 (15), had in this instance no potentiating effect. This is interesting because it is well established that in the majority of cases the inclusion in one molecule of more than one chemical feature which independently raises the same hormonal activity leads to potentiation of the biological effect. However, the finding is not entirely unexpected since Meystre and Wettstein (16) reported that 11-unsaturation of 17α-ethinyltestosterone even lowered the progestational activity. It may be tempting to speculate that the enhancement of progestational activity brought about by an 11-double bond is confined to progesterone itself, or possibly to progestins with an unmodified methyl ketone side chain; that is to say, that this activity-enhancing effect of the 11-double bond could be due to an indirect effect on the interaction of the side chain with the receptor. However, more experimental data on 11-unsaturated progestins are needed before any valid conclusion can be reached concerning the mechanism by which this double bond exerts its effects on progestational activity, in the case of 11-dehydroprogesterone.

EXPERIMENTAL[5, 6, 7]

17α-Bromo-3α,12α-diacetoxypregnane-20-one (III)

To a hot solution of 49.872 g of 3α,12α-diacetoxypregnane-20-one (II) in 500 cc of dry carbon tetrachloride, 35.8 g of N-bromosuccinimide was added. The mixture was stirred, and irradiated for 9 minutes with a 660-watt photo flood lamp at reflux temperature. The product was cooled and filtered over sodium sulphate and the filtrate was washed

[4]*It is possible to transform the Δ^4-3-keto-hydroxy acid XI without protection of the alcohol function directly to Δ^4-12α-hydroxy-17α-methylpregnene-3,20-dione (VII), which in turn can be converted to the tosylate VIIb and thence to 11-dehydro-17α-methylprogesterone; however, as one would expect, the yield of this transformation is low.*

[5]*The melting points were taken in evacuated capillaries and the temperatures were corrected.*

[6]*The microanalytical work was performed by Mr. J. F. Alicino, Metuchen, N.J., and Drs. F. and O. Schwarzkopf, Woodside, N.Y.; we wish to express our sincere appreciation to them.*

[7]*For chromatography, Merck aluminum oxide was treated as described in footnote 18 of reference 13; cf. also footnote 18 of reference 11. We sincerely thank Merck and Company, Montreal, for the generous gift of aluminum oxide.*

Can. J. Chem. Downloaded from www.nrcresearchpress.com by 210.87.254.5 on 09/05/12
For personal use only.

with cold 10% sodium bisulphite solution and with water. After having been dried over sodium sulphate, the solvent was removed *in vacuo*. The remaining crude amorphous bromide III (73 g) was used without further purification in the following reaction.

Methyl 3α,12α-Diacetoxy-17α-methyletianate (IVb)[8]

To a solution of the above-mentioned crude bromide III (73 g) in 2.47 l. of methanol, a solution of 138 g of potassium bicarbonate in 480 cc of water was added. The mixture was refluxed for 4 hours and its volume was reduced *in vacuo* to 600 cc. The product was poured into 6 l. of water and the precipitate was extracted with ether. The ethereal solution was washed with water, dried over sodium sulphate, and taken to dryness, thus affording 47.46 g of "*neutral fraction I*". The aqueous alkaline phase remaining after the extraction was acidified with sulphuric acid to a congo blue reaction and the resulting mixture was extracted with chloroform. The organic solution was washed with water, dried over sodium sulphate, and the solvent was removed. Thus 5 g of "*acid fraction I*" was isolated.

"Neutral fraction I" was dissolved in 750 cc of acetic acid and 75 cc of water. Then, at 60°, 75 g of zinc powder was added, portionwise and with repeated shaking, and the mixture was subsequently heated to 85° for 45 minutes with repeated shaking. The product was cooled and filtered and the filtrate was extracted with ether; the ethereal solution was washed repeatedly with dilute hydrochloric acid, with sodium carbonate and sodium bicarbonate solutions, and with water, and was then dried over sodium sulphate. Evaporation of the solvent afforded 46.06 g of a light yellow oil.

To a solution of this product in 460 cc of absolute ethanol and 46 cc of acetic acid, 51.5 g of freshly recrystallized Girard T reagent was added. The mixture was refluxed for 45 minutes, allowed to cool, and subsequently poured into 4.22 l. of an iced 0.15 *N* sodium hydroxide solution. The product was extracted with ether, the ethereal solution was washed with water and dried over sodium sulphate, and the solvent was removed. Thus there was obtained 28.16 g of the "*non-ketonic fraction*". The alkaline solution was acidified with sulphuric acid and the resulting product was extracted with ether. The ethereal solution was washed with iced sodium bicarbonate solution and with water and was dried over sodium sulphate. Evaporation of the solvent gave 23.87 g of the "*ketonic fraction*".

A solution of the "ketonic fraction" (23.87 g) in 82 cc of pyridine was refluxed for 90 minutes with 41 cc of acetic anhydride with the exclusion of moisture. The usual working up gave 24.1 g of an amorphous product. Chromatographic purification on aluminum oxide afforded 16.234 g of authentic starting material, *3α,12α-diacetoxypregnane-20-one* (II), m.p. 117–120°.

"Acid fraction I" (5.0 g) was dissolved in 80 cc of absolute methanol and 119 cc of absolute ether. To this solution was added, at 0°, 130 cc of a 2% ethereal diazomethane solution. The mixture was allowed to stand overnight at room temperature. The excess diazomethane was neutralized with acetic acid and the solvents were removed. The resulting methylated product (5.7 g) was combined with the "non-ketonic fraction". This mixture was refluxed for 4 hours in 570 cc of a 6.8% methanolic potassium hydroxide solution. After addition of 140 cc of water, the volume was reduced *in vacuo* to 200 cc and another 70 cc of water was added. The solution was now reduced *in vacuo* to 170 cc and then poured into 2.6 l. of distilled water. The mixture was extracted with ether and the ethereal solution was washed with water, treated with sodium sulphate, and taken to dryness. Thus 20.2 g of "*neutral fraction II*" was obtained. The aqueous alkaline residue

[8]*Compare Flowsheet I.*

Can. J. Chem. Downloaded from www.nrcresearchpress.com by 210.87.254.5 on 09/05/12
For personal use only.

Can. J. Chem. Downloaded from www.nrcresearchpress.com by 210.87.254.5 on 09/05/12
For personal use only.

of the ether extraction was acidified with sulphuric acid to a congo blue reaction and was extracted with chloroform. The organic solution was washed with water and dried over sodium sulphate. Evaporation of the solvent afforded 10.1 g of "*acid fraction II*", containing 17-non-methylated acids.

A solution of "neutral fraction *II*" (20.2 g) in 65 cc of pyridine was refluxed for 90 minutes with 33 cc of acetic anhydride with the exclusion of moisture. The usual working up gave 25.35 g of a partly crystalline product. Recrystallization from methanol gave 11.987 g of *methyl 3α,12α-diacetoxy-17α-methyletianate* (IV*b*), m.p. 159–161°. Chromatographic purification of the mother liquors on aluminum oxide gave another 5.126 g of IV*b*, m.p. 158–160°. The identity of this product was established by mixed melting point with an authentic sample and by comparison of the infrared spectra. In consideration of the recovery of starting material, the yield of methyl 3α,12α-diacetoxy-17α-methyletianate (IV*b*) from 3α,12α-diacetoxypregnane-20-one (II) amounted to 47.5%. No 17β-methyl-17-isoetianate could be obtained.

Methyl Δ⁴-12α-Acetoxy-3-oxo-17α-methyletienate (IX)

(*a*) Methyl 3α,12α-diacetoxy-17α-methyletianate (IV*b*) was transformed to methyl 12α-acetoxy-3-oxo-17α-methyletianate (VIII) as previously described (2). To a solution of 2 g of this keto ester VIII, m.p. 149–150°, in 40 cc of acetic acid were added a drop of hydrogen bromide solution in acetic acid and subsequently, dropwise and with stirring, over a period of 30 minutes, 5.9 cc of a 0.845 *M* bromine solution in acetic acid. The mixture was stirred for another 10 minutes and then poured into 500 cc of ice water. The precipitate was extracted with ether and the ethereal solution was washed with iced potassium bicarbonate solution and with water and was dried over sodium sulphate. Removal of the solvent *in vacuo* gave 2.56 g of crude crystalline methyl *4β-bromo-12α-acetoxy-3-oxo-17α-methyletianate* (VIII*a*). Recrystallization from methanol–ether yielded 1.463 g of bromide VIII*a*, melting between 177.5 and 179.5°, and 169 mg of slightly less pure bromide VIII*a*, melting at 172–175°.

The mother liquors (900 mg) were debrominated in the usual fashion (see above) with 2 g of zinc dust in 22 cc of 90% acetic acid. Thus 636 mg of crude saturated 3-keto ester VIII, m.p. 115–125°, was recovered; recrystallization from ether–hexane gave 330 mg of pure ester VIII, m.p. 142.5–144.5°. In consideration of this recovery of pure starting material, the yield of bromide VIII*a* amounted to 81.8%.

A solution of 1.369 g of bromide VIII*a*, m.p. 177.5–179.5°, in 43 cc of absolute chloroform and 71 cc of *t*-butyl alcohol was flushed with carbon dioxide. Freshly recrystallized semicarbazide (434 mg) was added and the reaction mixture was again flushed with carbon dioxide and the flask was sealed. The mixture was occasionally shaken during 150 minutes. The usual color changes (compare ref. 10) were observed. After filtration, the solvents were removed *in vacuo* at 40° and the solid residue was taken up in a mixture of 60 cc of ethanol and 3.5 cc of water. This solution was concentrated *in vacuo* to 30 cc and then poured into 280 cc of cold water. The mixture was stored for 2 hours at −10° and the crystalline precipitate was filtered and dried. The *methyl Δ⁴-12α-acetoxy-3-oxo-17α-methyletienate-3-semicarbazone* (IX*a*) thus obtained (1.227 g) melted with decomposition at 193–196°; λ_{max}^{EtOH} 270 mμ (log ε 4.7).

To a solution of the semicarbazone IX*a* (1.227 g) in 37 cc of acetic acid and 13.3 cc of water, 3.3 cc of a 1.64 *N* aqueous pyruvic acid solution was added. The mixture was flushed with carbon dioxide and the flask was sealed. After 19 hours the product was poured into 300 cc of ice water and the precipitate was extracted with ether. The organic

solution was washed with cold sodium carbonate solution, with iced dilute hydrochloric acid, with bicarbonate solution, and with water, and was then dried over sodium sulphate. Removal of the solvent afforded 1.104 g (96.9% yield from VIII*a*) of *methyl* Δ^4-*12α-acetoxy-3-oxo-17α-methyletienate* (IX), m.p. 164–167.5°. A sample was recrystallized twice from ether–hexane for analysis; colorless needles, m.p. 165.5–167.5°, $[\alpha]_D^{22}$ 242.5° (*c*, 0.756 in $CHCl_3$), λ_{max}^{EtOH} 239 mμ (log ε 4.46). Anal. Calc. for $C_{24}H_{34}O_5$: C, 71.61; H, 8.51. Found: C, 71.56; H, 8.42.

(*b*) In another series of experiments, 3.59 g of the acetoxy keto ester VIII was transformed in a similar manner to 4.457 g of crude bromide VIII*a* which afforded, upon crystallization from ether–methanol, 2.41 g of pure bromo ketone VIII*a*, m.p. 181–183°. This bromide was transformed, as described above, to 2.424 g of semicarbazone IX*a*, m.p. 186–194° decomp., which gave upon hydrolysis with aqueous acetic acid and pyruvic acid (compare above) 1.934 g of the 4-unsaturated ester IX, m.p. 164–166°. The mother liquors from the crystallization of the crude bromide (2.043 g) were treated in the same way as the pure bromide. Purification by chromatography and recrystallization of the resulting Δ^4-3-ketonic material gave 1.106 g of slightly less pure ester IX, m.p. 157–163°. In this run the total yield of the transformation of the saturated ester VIII to the unsaturated ester IX amounted to 85.1%.

Methyl $\Delta^{3,5}$*-3-Ethoxy-12α-acetoxy-17α-methyletiadienate (XII)*

By the procedure described by Julian and co-workers (17), 1.934 g of the Δ^4-3-keto ester IX was transformed to the enol ether XII. Recrystallization of the crude crystalline reaction product from acetone–methanol in the presence of traces of pyridine gave 1.428 g (69%) of beautiful needles, m.p. 180.5–182°. From the mother liquors, 119 mg (5.8%) of a product of lesser purity, m.p. 169–173°, was isolated. A sample was recrystallized four times for analysis; m.p. 183–184.5°, $[\alpha]_D^{24}$ −12.2° (*c*, 1.04 in pyridine), λ_{max}^{EtOH} 240 mμ (log ε 4.4). Anal. Calc. for $C_{26}H_{38}O_5$: C, 72.52; H, 8.90. Found: C, 72.71; H, 9.03.

Hydrolysis

A sample of 65 mg of enol ether XII was dissolved in 5 cc of acetone and treated for 12 hours, at room temperature, with 1 cc of 2 *N* hydrochloric acid. Ether extraction gave an amorphous product which yielded, after crystallization from ether–hexane, 32 mg of the Δ^4-3-keto ester IX, m.p. 166.5–168.5°, not depressed upon admixture of an authentic sample.

Δ^4*-12α-Hydroxy-3-oxo-17α-methyletienic Acid (XI)*

(*a*) In a sealed tube, 1.428 g of enol ether XII was heated for 48 hours to 169° with 60 cc of a 6.9% methanolic potassium hydroxide solution. The product was cooled, diluted with 400 cc of water, and acidified with 40 cc of 2 *N* sulphuric acid. Filtration of the precipitate afforded 1.063 g of a crude product which melted between 192.5 and 196.5°. Repeated crystallization from acetone afforded 808 mg (70.3% yield) of Δ^4-3-keto acid XI, m.p. 274–280°. The product was recrystallized for analysis; short, fine needles, m.p. 277–280°, $[\alpha]_D^{25}$ 123° (*c*, 0.934 in methyl cellosolve). Anal. Calc. for $C_{21}H_{30}O_4$: C, 72.80; H, 8.73. Found: C, 72.70; H, 8.67.

(*b*) In another run, 705 mg of enol ether XII was saponified as described under (*a*). The reaction product was acidified with concentrated hydrochloric acid and the mixture was diluted with chloroform. The product was kept for 30 minutes at room temperature, with repeated shaking. Subsequently, the organic solution was washed until neutral and the solvent was removed. Thus 520 mg (91.7% yield) of acid XI, m.p. 272.5–276°, was obtained.

Can. J. Chem. Downloaded from www.nrcresearchpress.com by 210.87.254.5 on 09/05/12
For personal use only.

Can. J. Chem. Downloaded from www.nrcresearchpress.com by 210.87.254.5 on 09/05/12
For personal use only.

Remethylation and Reacetylation

A solution of 60 mg of the hydroxy keto acid XI, m.p. 275–277°, in 10 cc of absolute methanol was treated at 0° with 15 cc of a 2% ethereal diazomethane solution. The mixture was stored for 8 hours at 0° and the solvents were removed *in vacuo*. The crude reaction product was dissolved in 5 cc of pyridine and refluxed for 90 minutes with 2.5 cc of acetic anhydride. The usual working up gave 96 mg of an oil which was chromatographed on 2.5 g of aluminum oxide. Petroleum ether – benzene (1:1, 1:4), benzene, and benzene–ether (4:1) eluted 71 mg of acetoxy keto ester IX, m.p. 155–162°. Recrystallization raised the melting point to 163–166°; the melting point was not depressed upon admixture of authentic ester IX.

Methyl Δ^5-3-Ethylenedioxy-12α-acetoxy-17α-methyletienate (X)

A solution of 2.759 g of methyl Δ^4-12α-acetoxy-3-oxo-17α-methyletienate (IX), m.p. 162.5–165°, in 206 cc of absolute benzene was reduced to 150 cc. Freshly distilled ethylene glycol (40.6 cc) and *p*-toluenesulphonic acid (112 mg) were added. The mixture was refluxed for 13.5 hours, with exclusion of moisture and with repeated removal of moist benzene. The reaction product was cooled and poured into an iced, saturated sodium bicarbonate solution, and the precipitate was extracted with ether. The organic solution was washed with iced 1% sodium carbonate solution and with water and was dried over sodium sulphate. Upon removal of the solvent, 3.02 g (98.7% yield) of ketal ester X, m.p. 176–180°, was obtained. The product was recrystallized twice from ether–hexane for analysis; colorless needles, m.p. 181.5–183°, $[\alpha]_D^{23}$ 51.9° (*c*, 0.847 in $CHCl_3$). Anal. Calc. for $C_{26}H_{38}O_6$: C, 69.92; H, 8.58. Found: C, 69.92; H, 8.66.

Δ^5-12α-Hydroxy-3-ethylenedioxy-17α-methyletienic Acid (XIII)

In a sealed tube, 4.984 g of acetoxy ketal ester X, m.p. 177–180°, was treated for 48 hours with 102 cc of a 6.8% methanolic potassium hydroxide solution at 170°. The reaction product was poured into 1 l. of water and the mixture was extracted with ether. The usual working up of the ethereal solution gave 7 mg of an amorphous product. The aqueous alkaline solution was carefully acidified with 1 *N* sulphuric acid to the congo blue reaction, and the mixture was extracted with chloroform. The organic solution was washed until neutral and then dried over sodium sulphate. Removal of the solvent afforded 4.49 g of a crystalline residue which gave, upon recrystallization from ether–methanol, 3.572 g of acid XIII, m.p. 125–130°/209–212°, and a second crop of 471 mg, m.p. 125–130°/207–209° (yield of recrystallized product 93%). A sample was recrystallized four times from ether–methanol for analysis; plates, m.p. 211–214°, $[\alpha]_D^{26}$ −10° (*c*, 0.700 in $CHCl_3$). Anal. Calc. for $C_{23}H_{34}O_5$: C, 70.74; H, 8.78. Found: C, 70.82; H, 8.59.

Δ^5-12α-Acetoxy-3-ethylenedioxy-17α-methyletienic Acid (XV)

A solution of 513 mg of the hydroxy ketal acid XIII, in 9 cc of pyridine and 4.5 cc of acetic anhydride, was refluxed for 1.5 hours. After the solution had been cooled, 30 cc of ice water was added and the mixture was allowed to stand for 30 minutes. Subsequently, it was diluted with another 200 cc of ice water and shaken repeatedly during 15 minutes. Extraction with ether afforded 566 mg of crude crystalline *Δ^5-12α-acetoxy-3-ethylenedioxy-17α-methyletienic acid anhydride* (XIV), which was dissolved in 30 cc of methanol and 7 cc of benzene. A solution of 750 mg of potassium carbonate in 5 cc of water was added and the mixture was refluxed for 1 hour. After dilution with 300 cc of ice water and extraction with ether, the remaining aqueous alkaline solution was carefully acidified in the cold with 0.5 *N* sulphuric acid to give a congo blue reaction. The mixture was extracted

with ether and the organic solution was washed until neutral and dried over sodium sulphate. Removal of the solvent gave 558 mg (98.2% yield) of crystalline Δ^5-*12α-acetoxy-3-ethylenedioxy-17α-methyletienic acid* (XV), m.p. 223–224.5°. A sample was recrystallized four times from methylene chloride – hexane for analysis; very fine, short needles, m.p. 231.5–233.5°, $[\alpha]_D^{25}$ 39.8° (*c*, 0.775 in $CHCl_3$). Anal. Calc. for $C_{25}H_{36}O_6$: C, 69.42; H, 8.39. Found: C, 69.70; H, 8.44.

Δ^4-12α-Acetoxy-17α-methylpregnene-3,20-dione (VIId)

At 0°, a solution of 4.05 cc of oxalyl chloride in 19.3 cc of absolute benzene was added dropwise to a suspension of 513 mg of well-dried Δ^5-12α-acetoxy-3-ethylenedioxy-17α-methyletienic acid (XV) in 23 cc of absolute benzene. During the addition, which took 5 minutes, the flask was shaken vigorously. The agitation was continued for another 30 minutes at room temperature, and subsequently the solvent was removed *in vacuo* at 20–30°. The residue was redissolved in absolute benzene and taken to dryness *in vacuo*; this operation was repeated twice in order to rid the compound completely of oxalyl chloride. The product showed a strong absorption at 240 mμ and represented crude *Δ^4-12α-acetoxy-3-oxo-17α-methyletienic acid chloride* (XVI). A solution of this chloride in 25 cc of absolute ether and 5 cc of absolute benzene was added, with stirring, to an ethereal solution of dimethyl cadmium prepared, as previously described (2), from 1.29 g of magnesium, 5.3 g of cadmium chloride, and the amounts of methyl bromide and ether equivalent to those used in previous experiments (2). The mixture was refluxed for 1 hour and the excess dimethyl cadmium was destroyed by careful addition of a 10% acetic acid solution. The product was extracted with ether and the ethereal solution was washed with cold, dilute sulphuric acid, with cold sodium bicarbonate solution, and with water, and was then dried over sodium sulphate. Removal of the solvent afforded 397 mg (86.6%) of crude crystalline *Δ^4-12α-acetoxy-17α-methylpregnene-3,20-dione* (VII*d*), m.p. 162–171°, λ_{max}^{EtOH} 239 mμ (log ε 4). Recrystallization from ether–hexane raised the melting point to 177.5–183.5°. The analytical sample was prepared by three further recrystallizations from methylene chloride – hexane, from ether–methanol, and finally from pure methanol; colorless prisms, m.p. 189–190°, $[\alpha]_D^{23}$ 165° (*c*, 0.809 in $CHCl_3$), λ_{max}^{EtOH} 240 mμ (log ε 4.2); ν_{max}^{KBr} 1722 and 1248 cm^{-1} (12α-acetate), 1690 cm^{-1} (17-methyl-20-ketone), 1667 and 1616 cm^{-1} (Δ^4-3-keto doublet). Anal. Calc. for $C_{24}H_{34}O_4$: C, 74.58; H, 8.87. Found: C, 74.55; H, 8.92.

Δ^5-12α-Acetoxy-3-ethylenedioxy-17α-methylpregnene-20-one (XVIIIa)

(a) From Δ^5-12α-Acetoxy-3-ethylenedioxy-17α-methyletienic Acid (XV)

A quantity of Δ^5-12α-acetoxy-3-ethylenedioxy-17α-methyletienic acid (XV) was dried by repeated evaporation of its benzene solution and by subsequent prolonged heating to 130° in high vacuum. A portion of 2.73 g of this product was suspended in 124 cc of absolute benzene. A solution of 21.6 cc of oxalyl chloride in 103 cc of absolute benzene was added dropwise and with agitation, at 0°, within 5 minutes. The agitation was continued for another 25 minutes. Subsequently, the resulting clear solution was allowed to stand for 30 minutes at room temperature and the product was taken to dryness *in vacuo* at 20–30°. The residue was further dried by repeated evaporation *in vacuo* of its benzene solution and by being kept for 18 hours in high vacuum. The resulting product, which was practically transparent to ultraviolet light in the region of 240 mμ, and which represented *Δ^5-12α-acetoxy-3-ethylenedioxy-17α-methyletienic acid chloride* (XV*a*), was dissolved in 134 cc of absolute ether. This solution was added, as described above for the preparation of the diketone VII*d*, to an ethereal dimethyl cadmium solution prepared from 6.96 g

Can. J. Chem. Downloaded from www.nrcresearchpress.com by 210.87.254.5 on 09/05/12
For personal use only.

Can. J. Chem. Downloaded from www.nrcresearchpress.com by 210.87.254.5 on 09/05/12
For personal use only.

of magnesium, 29 g of cadmium chloride, and the quantities of methyl bromide and ether equivalent to those used in previous experiments (2). The mixture was refluxed for 1 hour and worked up in the usual way. Thus 2.762 g of a crystalline solid, melting between 115 and 140°, was obtained. The product was filtered over aluminum oxide. The crystalline fractions eluted with ether (2.174 g) were recrystallized from ether–hexane to give 822 mg of a substance melting between 137 and 147°. Further recrystallization from ether–hexane gave 254 mg (10.4%) of pure *Δ^4-12α-acetoxy-17α-methylpregnene-3,20-dione* (VII*d*), m.p. 184–188°, identified by mixed melting point and infrared analysis.

The mother liquors of the first crystallization of this product weighed 1.312 g (48.3%) and crystallized readily from methanol; after one recrystallization they melted at 163–166° and showed, in the ultraviolet, no absorption maximum typical of an α,β-unsaturated ketone.

The methanol fraction of the aluminum oxide filtration (849 mg) was filtered again over aluminum oxide. The resulting crystalline fraction eluted with ether was combined with the crystalline mother liquors of the diketone VII*d*, showing no ultraviolet absorption in the 240 mμ region (see above), and with mother liquors of further recrystallizations of the unsaturated diketone VII*d*. This product (1.8 g, 73.8%), representing crude ketal XVIII*a* contaminated with some Δ^4-3-keto derivative VII*d*, was chromatographed on 54 g of aluminum oxide (pH 8.5). Petroleum ether – benzene mixtures, benzene, and benzene–ether mixtures eluted 1.104 g (45.3%) of purified *Δ^5-12α-acetoxy-3-ethylenedioxy-17α-methylpregnene-20-one* (XVIII*a*), melting between 159 and 170°. The majority of the fractions melted between 168 and 171°. A sample was recrystallized four times from ether–hexane for analysis; small, fine needles, m.p. 171–172°, $[\alpha]_D^{23}$ 36° (*c*, 1.055 in $CHCl_3$). Anal. Calc. for $C_{26}H_{38}O_5$: C, 72.52; H, 8.90. Found: C, 72.40; H, 8.92.

(b) From Δ^4-12α-Acetoxy-17α-methylpregnene-3,20-dione (VIId)

A solution of 254 mg of the Δ^4-3,20-diketo acetate VII*d* in 310 cc of absolute benzene was refluxed for 3 hours with 8 cc of ethylene glycol and 22 mg of *p*-toluenesulphonic acid. During this period the mixture was stirred vigorously and the moist benzene was removed periodically by the use of a water trap. The usual working up afforded 294 mg of a product which crystallized upon trituration with methanol; m.p. 132–140°. Recrystallization from ether–hexane gave 94 mg (33.1%) of monoketal XVIII*a*, m.p. 164–166°, not depressed upon admixture of authentic 3-monoketal XVIII*a*. The mother liquors were chromatographed on aluminum oxide. Petroleum ether – benzene (1:1) eluted 11 mg of a product (m.p. 168–170°) which showed no ketonic absorption in the infrared and to which the structure of *Δ^4-12α-acetoxy-3,20-bisethylenedioxy-17α-methylpregnene* is tentatively assigned. Further elutions with petroleum ether – benzene gave 54 mg of authentic monoketal XVIII*a*, m.p. 158–161° (total yield of monoketal XVIII*a* from diketone VII*d*: 52.4%).

Δ^5-12α-Hydroxy-3-ethylenedioxy-17α-methylpregnene-20-one (XVIII)

A solution of 239 mg of the 12α-acetoxy monoketal XVIII*a*, m.p. 164–167°, in 15 cc of 6.6% methanolic potassium hydroxide was refluxed for 4 hours. The product was cooled and poured into cold water, the precipitate was extracted with ether, and the ethereal solution was washed until neutral and dried over sodium sulphate. Evaporation of the solvent afforded 215 mg (99.7%) of a product which crystallized upon addition of a drop of hexane; m.p. 172.5–173.5°. A sample was recrystallized three times from ether–hexane for analysis; colorless prisms, m.p. 174.5–175.5°, $[\alpha]_D^{23}$ −23.8°, (*c*, 0.875 in $CHCl_3$); ν_{max}^{KBr} 3525 cm^{-1} (12-hydroxy), 1684 cm^{-1} (17-methyl-20-ketone)

1102 cm^{-1} (ketal). Anal. Calc. for $C_{24}H_{36}O_4$: C, 74.20; H, 9.34. Found: C, 74.31; H, 9.19.

Δ^5-12α-Tosyloxy-3-ethylenedioxy-17α-methylpregnene-20-one (XVIIIb)

To a solution of 221 mg of hydroxy ketal XVIII, m.p. 164–167°, in 2.6 cc of absolute pyridine, 332 mg of *p*-toluenesulphonyl chloride, m.p. 67–69°, was added. The flask was flushed with nitrogen and sealed, and the mixture was heated for 14 days to 55°. The product was cooled and poured into 100 cc of an ice-cold, saturated sodium bicarbonate solution containing 10 cc of pyridine. This mixture was shaken for 1 hour at room temperature. Subsequently, the product was extracted with ether. The ethereal solution was washed with cold sodium bicarbonate solution and with water and was dried over sodium sulphate. Removal of the solvent *in vacuo* gave 242 mg (78.4%) of a product which crystallized upon addition of a drop of methanol; m.p. 129–131°, λ_{max}^{EtOH} 225 mμ (log ε 4.1). One recrystallization from methylene chloride – methanol raised the melting point to 135–137°, a second recrystallization, to 140–141°; $[\alpha]_D^{25}$ −10.1° (*c*, 0.957 in $CHCl_3$). For the subsequent experiment crude crystalline tosylate XVIII*b* was used.

$\Delta^{4,11}$-17α-Methylpregnadiene-3,20-dione (11-Dehydro-17α-methylprogesterone) (I)

A quantity of 198 mg of crude tosyloxy ketal XVIII*b* was dissolved in a small quantity of benzene and absorbed on 40 g of aluminum oxide (activity 1, pH 8). The column was drained and then heated for 6 hours to 45°. The column was allowed to cool, and elutions with benzene – petroleum ether (4:1) were made; they afforded 100 mg of crude crystalline *$\Delta^{5,11}$-3-ethylenedioxy-17α-methylpregnadiene-20-one* (XVII), m.p. 167–174°, giving a positive tetranitromethane test. Chromatography of the non-crystalline fractions, under similar conditions, yielded another 13 mg of the same product (total yield: 83.6%). Purification afforded 69 mg (60% yield) of purified ketal XVII, m.p. 171–174°. A solution of this product (69 mg) and of 22 mg of *p*-toluenesulphonic acid in 17 cc of absolute acetone was allowed to stand for 42 hours in a carbon dioxide atmosphere. Ice and aqueous potassium bicarbonate solution were added and the precipitate was extracted with ether. The ethereal solution was washed with potassium bicarbonate and sodium carbonate solutions and with water, was dried over sodium sulphate, and was taken to dryness. The resulting crude crystalline *$\Delta^{4,11}$-17α-methylpregnadiene-3,20-dione (11-dehydro-17α-methylprogesterone)* (I) weighed 58 mg and was purified by chromatography on aluminum oxide. Thus 37 mg of pure, authentic 11-dehydro-17α-methylprogesterone (I), m.p. 125–139°, was obtained. One further chromatographic purification gave a product melting at 137–138°.

ACKNOWLEDGMENTS

We express warm thanks to Mrs. J. Capitaine for her devoted assistance in these experiments, to Mr. R. W. White, Science Service Laboratory, London, Ontario, for the infrared analyses, and to Drs. P. Perlman and M. Eisler, Schering Corporation, Bloomfield, N.J., for the biological tests. We are indebted to the Federal–Provincial Departments of National Health and Welfare, Ottawa and Toronto, the Ciba Ltd., Montreal, the Schering Corporation, Bloomfield, N.J., the Schering Corporation Ltd., Montreal, and the Canadian Life Insurance Officers Association, for financial support; and to Canada Packers Ltd., Toronto, for a gift of starting material. Sincere thanks are expressed to Dean J. B. Collip for his constant encouragement and for financial assistance extended to one of us (G. J.), and to Dr. J. A. Gunton for his kind interest. We are greatly indebted to the authorities of Laval University, in particular to Professors P. A. Giguère and J. Risi, for their generous help during the installation of our new laboratory.

Can. J. Chem. Downloaded from www.nrcresearchpress.com by 210.87.254.5 on 09/05/12
For personal use only.

REFERENCES

1. CH. R. ENGEL and S. PAPADOPOULOS. J. Org. Chem. In press.
2. CH. R. ENGEL, K. F. JENNINGS, and G. JUST. J. Am. Chem. Soc. **78**, 6153 (1956).
3. H. HEUSSER, CH. R. ENGEL, P. TH. HERZIG, and PL. A. PLATTNER. Helv. Chim. Acta, **33**, 2229 (1950).
4. R. U. SCHOCK and W. J. KARPEL. U. S. Patent No. 2,684,963 (1954).
5. CH. R. ENGEL. J. Am. Chem. Soc. **77**, 1064 (1955); **78**, 4727 (1956).
6. N. L. WENDLER, R. P. GRABER, and G. G. HAZEN. Chem. & Ind. (London), 847 (1956); Tetrahedron, **3**, 144 (1958).
7. R. B. LOFTFIELD. J. Am. Chem. Soc. **73**, 4707 (1951).
8. G. RICHARD. Compt. rend. **200**, 1944 (1935).
9. H. HEUSSER, CH. R. ENGEL, and PL. A. PLATTNER. Helv. Chim. Acta, **33**, 2237 (1950).
10. W. F. MCGUCKIN and E. C. KENDALL. J. Am. Chem. Soc. **74**, 5811 (1952).
11. CH. R. ENGEL and G. JUST. J. Am. Chem. Soc. **76**, 4909 (1954).
12. CH. R. ENGEL and G. JUST. Can. J. Chem. **33**, 1515 (1955).
13. G. JUST and CH. R. ENGEL. J. Org. Chem. **23**, 12 (1958).
14. H. SCHINZ and G. SHÄPPI. Helv. Chim. Acta, **30**, 1483 (1947).
15. CH. MEYSTRE, E. TSCHOPP, and A. WETTSTEIN. Helv. Chim. Acta, **31**, 1463 (1948).
16. CH. MEYSTRE and A. WETTSTEIN. Helv. Chim. Acta, **32**, 1978 (1949).
17. P. L. JULIAN, E. W. MEYER, W. J. KARPEL, and W. COLE. J. Am. Chem. Soc. **73**, 1982 (1951).

Can. J. Chem. Downloaded from www.nrcresearchpress.com by 210.87.254.5 on 09/05/12
For personal use only.

Can. J. Chem. Downloaded from www.nrcresearchpress.com by 210.87.254.105 on 09/05/12
For personal use only.

METAL OXIDE ALKOXIDE POLYMERS

PART II. THE HYDROLYSIS OF TANTALUM PENTAETHOXIDE[1,2]

D. C. BRADLEY[3] AND H. HOLLOWAY[4]

ABSTRACT

The hydrolysis of tantalum pentaethoxide has been studied in boiling benzene and in boiling ethanol. Soluble tantalum oxide ethoxides were obtained over a considerable range of hydrolysis. Infrared studies suggest that Ta—OH groups are absent in these products. Ebulliometric studies have shown that the number-average degree of polymerization varies with the degree of hydrolysis in a characteristic manner and this has been quantitatively explained in terms of fundamental structural models based on octahedrally 6-co-ordinated tantalum.

INTRODUCTION

Recent work on the hydrolysis of titanium (1, 2) and zirconium (3) alkoxides has revealed that some of the metal oxide alkoxide polymers conform reasonably well to structural models based on the 6-co-ordinated metal. In these inorganic macromolecules, polymerization is based on two fundamental processes, namely "condensation" involving M·O·M bridges and co-ordination involving intermolecular metal–oxygen bonds. The previous work in this field (1, 2, 3) has involved the quadrivalent states of titanium and zirconium but the fundamental principles mentioned above should make the structural theory applicable to metals in other valence states. Tantalum forms a pentaethoxide which is essentially dimeric $Ta_2(OEt)_{10}$ (4) and is believed to involve 6-co-ordinated tantalum. Assuming this to be true it seemed that the polymeric tantalum oxide ethoxides $TaO_x(OEt)_{5-2x}$ should provide a good test for the aforementioned structural theory. In particular the system should be considerably simpler from the structural point of view than the titanium and zirconium compounds because the number of possible solvated species is fewer and there should be less possibility of ambiguity in the interpretation of the results. Accordingly, we have made a detailed investigation, mainly by the ebulliometric technique, of the hydrolysis of tantalum pentaethoxide under rigorously controlled conditions.

EXPERIMENTAL AND RESULTS

Tantalum Pentaethoxide

The compound was prepared by the previously described method (4) involving the reaction of $TaCl_5$ with ethanol and anhydrous ammonia in benzene. The $TaCl_5$ was prepared by chlorination of tantalum (99.9% purity metal) at about 400° C. The pentaethoxide (found: Ta, 44.6%; $Ta(OEt)_5$ requires: Ta, 44.6%) was distilled under reduced pressure immediately prior to an experiment and was obtained as a colorless distillate (b.p. 147° C at 0.2 mm).

Ebulliometric Measurements

The technique adopted in this work was similar to that described in our earlier studies (1, 3) and an all-glass ebulliometer involving a differential water thermometer was used.

[1]*Manuscript received March 10, 1961.*
Contribution from the Department of Chemistry, Birkbeck College, London, W.C.1, England.
[2]*Part I (see ref. 3).*
[3]*Present address: Department of Chemistry, The University of Western Ontario, London, Ontario.*
[4]*Present address: Post Office Research Station, Dollis Hill, London, N.W.2, England.*

Two refinements were developed. One was the use of a silicone-fluid heating bath instead of the flame of a microburner. The heating bath gave steadier ebullition. It was also found that the slight loss of solvent during a long experiment could be obviated by greasing the standard joints of the ebulliometer with a fluorocarbon grease.

Molecular Weight of Tantalum Pentaethoxide in Boiling Ethanol

An accurate knowledge of the degree of polymerization of tantalum pentaethoxide in boiling ethanol was essential for the accurate determination of the degree of polymerization of the tantalum oxide ethoxide produced by hydrolysis in the ebulliometer. Bradley, Wardlaw, and Whitley (4) reported a value of 1.78 compared with 1.98 in boiling benzene. The lower value in boiling ethanol was believed to be due to the presence of a solvated monomeric species, $Ta(OEt)_5$,EtOH, which still involved 6-co-ordinated tantalum. It was important therefore to investigate the degree of polymerization of the pentaethoxide in boiling ethanol over a wide range in concentration since a simple dimer–monomer equilibrium should show a concentration dependence of molecular weight. Five separate determinations were made, each involving several additions of freshly distilled pentaethoxide over the concentration range of approximately 0.01–0.25 g-mol. (dimer)/1000 g solvent. The method of "internal calibration" (5) using fluorene as standard substance was used. In each experiment there was a linear dependence of the elevation of boiling point with concentration within the probable experimental error of the measurements, and the following values for the degree of polymerization were obtained: 1.85, 1.83, 1.87, 1.81, and 1.88. The mean value of 1.85 was therefore adopted for the degree of polymerization of tantalum pentaethoxide in boiling ethanol. An interesting and puzzling point is the absence of the expected concentration dependence of the molecular weight. The method was quite sensitive enough for detection of a change in degree of polymerization with concentration of the order required by a dimer–monomer equilibrium. It is possible that the system is not in true equilibrium. However, the values obtained in several experiments were quite consistent and it appears that over 90% of the tantalum is present in the dimeric state.

Hydrolysis in Boiling Ethanol

The addition of known quantities of aqueous ethanol (3.70% H_2O, w/w) to boiling ethanolic solutions of tantalum pentaethoxide caused immediate decreases in the elevation of the boiling point due to the increase in degree of polymerization which resulted from the hydrolysis. The correct degree of polymerization of the tantalum oxide ethoxide species was deduced by applying the small correction for the ethanol added with the water. The results of four separate experiments involving different initial concentrations of tantalum ethoxide are recorded in Tables I–IV. The number-average degree of polymerization is denoted by n and the degree of hydrolysis (ratio of moles H_2O added/g-atom of Ta) by h.

TABLE I

(Expt. 1: initial concn. of $Ta_2(OEt)_{10}$ = 0.064 g-mol./kg)

h	0.110	0.214	0.321	0.444	0.540	0.634	0.733	0.808	
n	1.94	2.10	2.31	2.58	2.84	3.21	3.50	3.87	
h	0.905	0.992	1.085	1.175	1.27	1.35	1.44	1.55	1.69
n	4.44	5.22	6.08	7.65	8.76	9.21	9.62	9.62	9.94

Can. J. Chem. Downloaded from www.nrcresearchpress.com by 210.87.254.105 on 09/05/12
For personal use only.

TABLE II

(Expt. 2: initial concn. of $Ta_2(OEt)_{10}$ = 0.132 g-mol./kg)

h	0.157	0.355	0.547	0.663	0.702	0.824	0.943	0.996
n	2.02	2.37	2.82	3.14	3.27	3.84	4.51	4.87
h	1.043	1.113	1.17	1.23	1.31	1.37	1.52	1.60
n	5.39	6.00	6.72	7.64	8.59	8.70	9.23	Precipitation

TABLE III

(Expt. 3: initial concn. of $Ta_2(OEt)_{10}$ = 0.1525 g-mol./kg)

h	0.101	0.249	0.354	0.451	0.602	0.750	0.910
n	1.94	2.13	2.28	2.49	2.90	3.37	4.01
h	1.02	1.14	1.24	1.35	1.45	1.56	
n	4.66	5.73	7.01	8.30	8.70	Precipitation	

TABLE IV

(Expt. 4: initial concn. of $Ta_2(OEt)_{10}$ = 0.2455 g-mol./kg)

h	0.059	0.214	0.294	0.420	0.510	0.576	0.646	0.728
n	1.89	2.07	2.20	2.41	2.62	2.80	2.99	3.29
h	0.822	0.973	1.10	1.24	1.34	1.46	1.59	
n	3.66	4.53	5.41	7.44	9.14	10.2	Precipitation	

Hydrolysis in Benzene

In an attempt to avoid the complications of solvation we determined the degree of polymerization of some tantalum oxide ethoxides in boiling benzene in which tantalum pentaethoxide is dimeric within probable experimental error. The main problem in this aspect of the work is the complete removal of ethanol from the hydrolysis product. The following procedure was believed to be reliable. A known amount of water (as 5% aqueous ethanol) was slowly added with stirring to a known amount (ca. 5 g) of $Ta_2(OEt)_{10}$ in benzene (ca. 100 cc) at room temperature. The solution was then refluxed for $\frac{1}{2}$ hour, allowed to cool under dry nitrogen, and then evaporated at room temperature and 0.1 mm pressure to remove benzene and ethanol. To ensure removal of ethanol the product was redissolved in dry benzene (ca. 50 cc) and the solution again evaporated. This procedure was repeated twice and finally the product was maintained under 0.1 mm at room temperature for about 16 hours. The product was then analyzed for tantalum and ethoxide and its molecular weight was determined ebullioscopically in benzene using the "internal calibration" method involving fluorene. The results are presented in Table V where n_{calc} is obtained by substituting the appropriate value of h in the theoretical equation $n = 6/(3-2h)$ and M is the molecular weight.

TABLE V

	Found, %		Calc., %				
h	Ta	OEt	Ta	OEt	*M*	*n*	n_{calc}
0.000	44.6	55.2	44.6	55.4	810	2.00	2.00
0.271	46.8	51.5	46.9	52.1	889, 830	2.27, 2.22	2.44
0.300	47.4	50.5	47.1	51.6	885	2.32	2.50
0.390	47.8	50.0	48.1	50.5	1050, 935	2.77, 2.55	2.70
0.551	49.4	47.5	49.6	48.0	1180	3.22	3.17
0.750	51.8	41.9	52.5	43.7	1510	4.32	4.00

Can. J. Chem. Downloaded from www.nrcresearchpress.com by 210.87.254.105 on 09/05/12
For personal use only.

Disproportionation of a Tantalum Oxide Ethoxide

Tantalum ethoxide in benzene, when hydrolyzed to $h = 1.20$ as in the aforementioned manner, gave a gummy oxide ethoxide. (Found: Ta, 57.3; OEt, 36.2. $TaO_{1.2}(OEt)_{2.6}$ requires: Ta, 57.1; OEt, 37.0%.) This was heated at 290–300° C at 0.01 mm for 3 hours during which time a volatile liquid distilled over and a light brown solid residue remained. (Found: Ta, 78.4%.) The liquid proved to be tantalum pentaethoxide. (Found: Ta, 44.9. $Ta(OEt)_5$ requires: Ta, 44.6%.) This experiment demonstrated that tantalum oxide ethoxides undergo disproportionation when heated *in vacuo*.

Infrared Spectra of Tantalum Oxide Ethoxides

The absorption spectra of the oxide ethoxides corresponding to $h = 0.55$ and 1.20 were measured in CS_2 solution and compared with the spectrum for tantalum ethoxide. The spectra are too complex to permit a complete interpretation at this stage but it was interesting to find no evidence for hydroxyl bands in the hydrolysis products. Another feature was the steady decrease in intensity of the bands around 3.5 μ, 7 μ, and 18 μ with increase in degree of hydrolysis and these bands presumably involve the ethoxide groups. Simultaneously there was a strengthening of the broad bands in the 19–22 μ region and the appearance of broad, ill-defined bands in the 12–14 μ region. These bands presumably involve the Ta·O·Ta groups. (We are indebted to C. G. Barraclough of University College, London, England, for measuring these spectra.)

DISCUSSION

The hydrolysis of tantalum ethoxide in ethanol was shown by the ebulliometric studies to be an extremely rapid process. The analyses of the products of the hydrolyses carried out in benzene (Table V) and the infrared spectra show that tantalum oxide ethoxides $TaO_x(OEt)_{5-2x}$ are produced and not tantalum hydroxide ethoxides. Our experiments, under rigorously controlled conditions, have shown that a continuous series of tantalum oxide ethoxides may be produced and that the number-average degree of polymerization increases steadily with the degree of hydrolysis (Tables I–V). Let us now examine these results in the light of the structural theory developed by Bradley, Gaze, and Wardlaw (1, 2) to explain the behavior of titanium oxide alkoxides.

Polymeric Species in Boiling Ethanol

Assuming that tantalum attains octahedral 6-co-ordination in the pentaethoxide, then there are two probable structures, the dimeric unsolvated species (Fig. 1) and the solvated monomer (Fig. 2). These are clearly related to model II (based on $Ti_2(OR)_8,2ROH$)

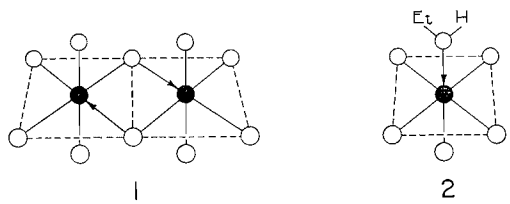
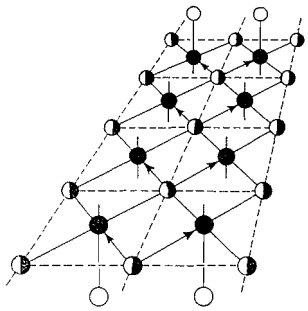


FIG. 1. The dimer $Ta_2(OEt)_{10}$. ● = Ta, ○ = oxygen in OEt (Et groups omitted).
FIG. 2. The solvated monomer $Ta(OEt)_5,EtOH$. ● = Ta, ○ = oxygen in OEt (Et groups omitted).

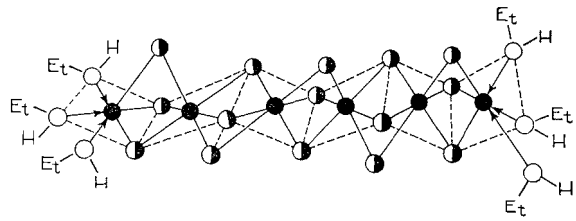
and model III (based on $Ti(OR)_4,2ROH$) respectively in the titanium tetraalkoxide structures. If the tantalum pentaethoxide were entirely dimeric in boiling ethanol we should predict that the tantalum oxide ethoxides would conform to a structural series

Can. J. Chem. Downloaded from www.nrcresearchpress.com by 210.87.254.105 on 09/05/12
For personal use only.

based on model II for which $n = 6/(3-2h)$ but which have the general formula $Ta_{2(x+1)}O_{3x}(OEt)_{2(2x+5)}$, where $x = 0, 1, 2, 3 \ldots \infty$. The limiting bilinear polymer would thus be $[Ta_2O_3(OEt)_4]_\infty$ (Fig. 3) corresponding to $h = 1.5$. If the pentaethoxide were entirely monomeric its hydrolysis products might be expected to conform to the analogue of model III for which $n = 3/(3-h)$, and whose formulae would be given by $Ta_{(x+1)}O_{3x}(OEt)_{(5-x)},(EtOH)_{(x+1)}$. We note that the ultimate polymer in this series ($x = 5$, Fig. 4) corresponds to a hypothetical solvated form of tantalum pentoxide. The



3



4

FIG. 3. The infinite polymer $[Ta_2O_3(OEt)_4]_\infty$. ● = Ta, ○ = oxygen in OEt (Et groups and some OEt groups omitted), ◑ = oxygen in Ta·O·Ta groups.
FIG. 4. The hexamer $Ta_6O_{15},(EtOH)_6$. ● = Ta, ◑ = oxygen in Ta·O·Ta groups.

molecular-weight studies in boiling ethanol showed that the number-average degree of polymerization of tantalum pentaethoxide was 1.85 ± 0.035 and it is thus reasonable to propose that the tantalum oxide ethoxides should exhibit a dependence of number-average degree of polymerization on degree of hydrolysis rather close to the predictions of model II. In Fig. 5 is shown the variation of n with h for all the data included in Tables I–IV in comparison with the theoretical curves for the model II and model III systems. The experimental points are close to the theoretical curve II for $h = 0$–1.3 but deviate at $h > 1.3$ towards curve III. It must be remembered that for the relation $n = 6/(3 - h)$ the value of n becomes very sensitive to errors in h at values of $h > 1.0$. For example, at $h = 0.5$ an error of 10% in h would result in an error of only 5% in n, but at $h = 1.0$ a 10% error in h causes a 25% error in n, whilst at $h = 1.25$ a 10% error in h causes a 100% error in n. Hence it is not surprising to find greater scatter in the experimental points at the higher values of h. There is the added factor that the probable experimental error in measuring n is greater at the higher values of n. If we rearrange the expression $n = 6/(3-2h)$ to $1/n = 0.5000-0.3333_4h$, it follows that a plot of $1/n$ versus h should be linear. Similarly the equation representing the theoretical curve III may be transformed to $1/n = 1.0000-0.3333_4h$. It is easily shown that in any system involving, simultaneously, models II and III with a constant value for α_{II} (the proportion of metal atoms in model II), then an equation of the form $1/n = 1.0000-0.5\alpha_{II}-0.3333_4h$ should be obeyed. We have taken all of the experimental data for $h = 0$–1.270 and determined by the method of least squares the best straight line for the plot of $1/n$ versus h. The results are shown in Fig. 6 where the straight line represents the least-squares equation $1/n = 0.5458-0.3389h$. Assuming that values of h are correct, the coefficient of variation for errors in n is ±4.5% and there are 30 changes in sign in the errors when the 52 results are arranged in ascending order of h. The errors are, of course,

Can. J. Chem. Downloaded from www.nrcresearchpress.com by 210.87.254.105 on 09/05/12
For personal use only.

Can. J. Chem. Downloaded from www.nrcresearchpress.com by 210.87.254.105 on 09/05/12
For personal use only.

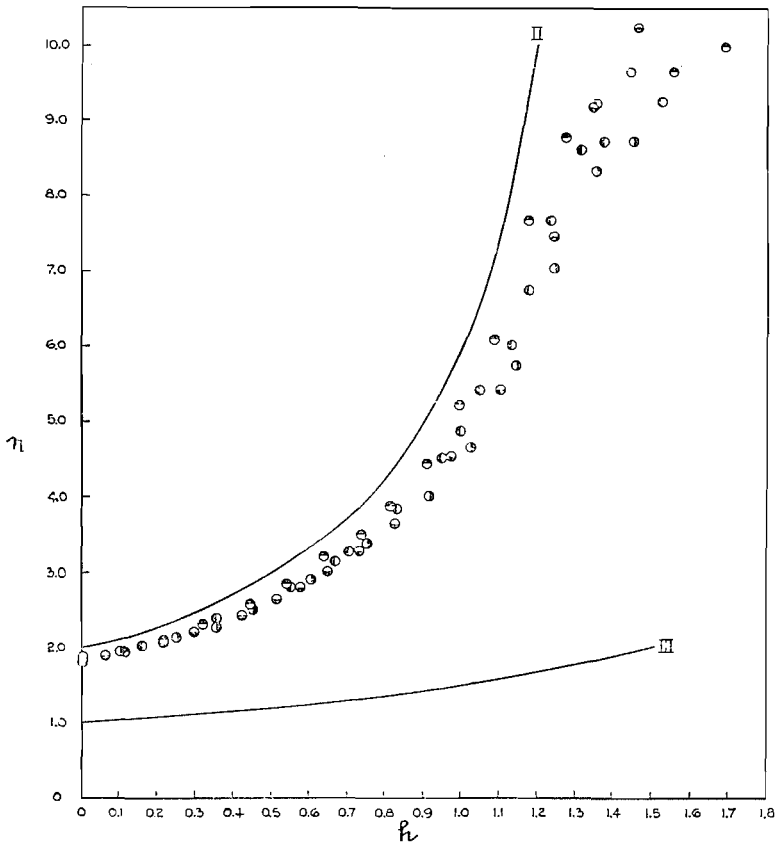


FIG. 5. The variation of n with h for tantalum oxide ethoxides in boiling ethanol. ◓ = data from expt. 1, ◐ = data from expt. 2, ◑ = data from expt. 3, ◒ = data from expt. 4.

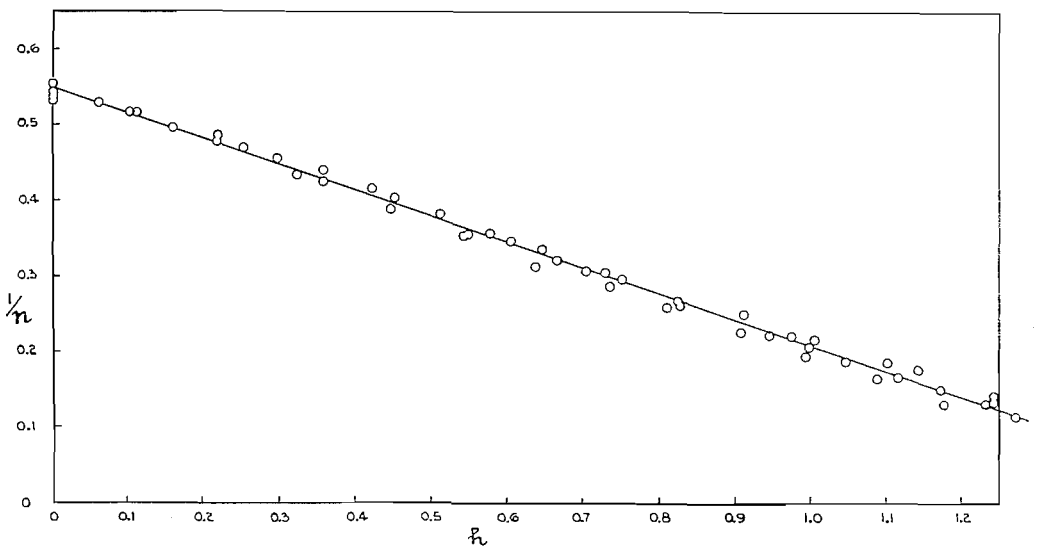
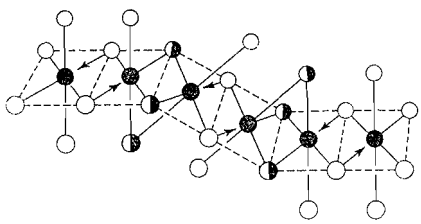
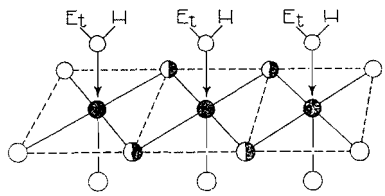


FIG. 6. The plot of $1/n$ versus h for tantalum oxide ethoxides in boiling ethanol.

higher at the higher values of h and the coefficient of variation for the first 24 points (h = 0–0.602) is only $\pm 1.76\%$ and this is slightly less than the percentage deviation in determining the degree of polymerization of tantalum pentaethoxide. It is interesting to note that the value of α_{II} derived from our least-squares equation is 0.908 and corresponds to a value of n = 1.83 for the pentaethoxide compared with the value n = 1.85 ± 0.035 obtained from the five experiments on the pentaethoxide alone. In addition, the least-squares slope of 0.339 is quite close to the "theoretical" value of 0.333. The experimental values of n for $h > 1.3$ show increasing deviations from n_{calc} with increase in h. This may correspond to a decrease in α_{II} as solvation becomes more developed at the lower molar concentrations of polymers, although we cannot rule out the alternative possibility that hydrolysis is incomplete at high values of h due to the presence of relatively stable Ta—OH groups in solution. Before leaving the ebulliometric studies, mention must be made of some alternative structural models which have been considered for the tantalum oxide ethoxide polymers. In model II the repeating units in the bilinear polymer (Fig. 3) involve three oxygen atoms bridging four tantalum atoms along the common edge of four octahedra. This results in the unusual example of a quaternary oxygen bonded to four tantalums in a plane. However, by allowing dimer units to be joined by three oxygens between two tantalums sharing a common face of two octahedra we arrive at another structural model having exactly the same variation of n with h as model II. The alternative model is illustrated by the structure for $Ta_6O_6(OEt)_{18}$ shown in Fig. 7. A zigzag arrangement of the dimers would result in the formation of an infinite linear polymer $[Ta_2O_3(OEt)_4]_\infty$ containing no quaternary oxygens. Our present technique cannot distinguish between these two alternatives. We have also considered an alternative to structural model III. The latter may be criticized in having, in some of its species, tantalum atoms which are formally exhibiting oxidation numbers higher or lower than five although the average valency is always five. This problem may be averted by causing the octahedra to share edges as illustrated by the trimer $Ta_3O_4(OEt)_7,(EtOH)_3$ (Fig. 8).



7



8

FIG. 7. The hexamer $Ta_6O_6(OEt)_{18}$. ● = Ta, ○ = oxygen in OEt (Et groups omitted), ◑ = oxygen in Ta·O·Ta groups.
FIG. 8. The trimer $Ta_3O_4(OEt)_7,(EtOH)_3$. ● = Ta, ○ = oxygen in OEt (Et groups omitted), ◑ = oxygen in Ta·O·Ta groups.

The general formula for this series, which we term model IV, is $Ta_{(x+1)}O_{2x}(OEt)_{5+x}$, $(EtOH)_{x+1}$ and this leads to a new equation: $n = 2/(2-h)$, and an infinite linear polymer; $[TaO_2(OEt),EtOH]_\infty$. If the tantalum oxide ethoxides involve models II and IV it is readily shown that a linear equation $1/n = 1.000 - 0.500\alpha_{II} - (0.5000 - 0.1667\alpha_{II})h$ should obtain. This gives exactly the same intercept for $1/n$ at $h = 0$ as the equation given by the combination of models II and III. However, the two equations differ in slope. Using the least-squares value for $\alpha_{II} = 0.908$, a slope of -0.349 is predicted for

Can. J. Chem. Downloaded from www.nrcresearchpress.com by 210.87.254.105 on 09/05/12
For personal use only.

the model II – model IV combination compared with the value of -0.333 required by the model II – model III combination. The least-squares value of the slope is -0.339 and this evidently favors the model II – model III system, although the result is hardly decisive.

Insoluble Tantalum Oxide Ethoxides

According to the model II series $n = 6/(3-2h)$, infinite polymers should form as $h \rightarrow 1.5$, whereas for model III the highest possible polymer is the hexamer Ta_6O_{15}, 6EtOH, and model IV predicts an infinite polymer at $h = 2.0$. Therefore, insoluble products would be expected somewhere in the region $h = 1.5$–2.5. In fact, solution of the least-squares equation $1/n = 0.5458-0.3389h$, which satisfactorily described the results up to $h = 1.3$, suggests that n will be infinite at $h = 1.61$. In our ebulliometric experiments we obtained precipitates at $h = 1.60$; at the three higher concentrations of tantalum pentaethoxide, 1.56 and 1.59, whilst at the lowest concentration no precipitate was formed up to $h = 1.69$. The formation of precipitates in the region of $h \sim 1.6$ is thus reasonable but the presence of species for $h > 1.5$ where model II predicts an infinite polymer requires some comment. If the polymers, even in this region, do conform to models II and III, then soluble species for $h > 1.5$ could obtain if the degree of hydrolysis in model II were less than in model III. This may be illustrated by the following example. Let us imagine that at an over-all average value of $h = 1.55$ the value of α_{II} is 0.8. Then the polymer equation will be $1/n = 0.6-h/3$ and for $h = 1.55$ we find $n_{calc} = 12.0$. Now, let us further assume that the average value of h_{II} for the species adopting model II is 1.45; this would correspond to $n_{II} = 60$ and these polymers could well be soluble. It follows that if the over-all average h for both species is 1.55 then the average h_{III} for the species in model III must be 1.95, for which $n_{III} = 2.85$. Finally, it is easily shown that if 80% of the tantalum has an average degree of polymerization $n_{II} = 60$ while the remaining 20% has $n_{III} = 2.85$, then the over-all average value of n is 12, which is the value predicted from the original equation. Therefore it follows that for all the polymer species to remain soluble at $h > 1.5$, $\alpha_{II} < 1$ and $h_{III} > h_{II}$.

The Molecular Weights of Tantalum Oxide Ethoxides in Benzene

If the tantalum pentaethoxide were not solvated it would be expected to conform exclusively to model II based on the dimer, and the number-average degree of polymerization of the oxide ethoxides would follow the requirements of the equation $1/n = 0.5000-0.3333h$. In boiling benzene, tantalum pentaethoxide is dimeric and hence it was important to determine molecular weights of the oxide ethoxides in benzene. Some results at five values of h between 0 and 0.750 are reported in Table V. It is clear that the observed values of n are reasonably close to n_{calc} evaluated from the theoretical equation. The coefficient of variation in n (assuming h is correct) is $\pm 5.5\%$ and this is a satisfactory value, bearing in mind the difficulties mentioned in the experimental section.

CONCLUSIONS

1. The hydrolysis of tantalum pentaethoxide in either ethanol or benzene solution under controlled conditions leads to the formation of polymeric oxide ethoxides.

2. The number-average degree of polymerization of these polymers can be accounted for with the assumption that these compounds are condensation – co-ordination polymers in which the tantalum achieves the co-ordination number of 6 in an octahedral configuration.

3. These octahedral structures are of fundamental significance since they are applicable to either titanium (IV) oxide ethoxides or tantalum (V) oxide ethoxides.

Can. J. Chem. Downloaded from www.nrcresearchpress.com by 210.87.254.105 on 09/05/12
For personal use only.

ACKNOWLEDGMENT

We gratefully acknowledge the support of the Department of Scientific and Industrial Research through a Maintenance Grant (to H. H.).

REFERENCES

1. D. C. BRADLEY, R. GAZE, and W. WARDLAW. J. Chem. Soc. 3977 (1955).
2. D. C. BRADLEY, R. GAZE, and W. WARDLAW. J. Chem. Soc. 469 (1957).
3. D. C. BRADLEY and D. G. CARTER. Can. J. Chem. **39**, 1434 (1961).
4. D. C. BRADLEY, W. WARDLAW, and A. WHITLEY. J. Chem. Soc. 726 (1955).
5. D. C. BRADLEY, W. WARDLAW, and A. WHITLEY. J. Chem. Soc. 5 (1956).

Can. J. Chem. Downloaded from www.nrcresearchpress.com by 210.87.254.105 on 09/05/12
For personal use only.

Can. J. Chem. Downloaded from www.nrcresearchpress.com by 210.87.254.105 on 09/05/12
For personal use only.

THE REVERSIBILITY OF AROMATIC MERCURATION[1]

M. Malaiyandi, H. Sawatzky, and G. F Wright

ABSTRACT

The ratio of isomeric bisperchloratomercuribenzenes obtained from the monomercurial and mercuric perchlorate in perchloric acid varies slightly with concentration of the acid, but is preponderantly meta. However, more para than meta isomer is obtained under conditions where the para isomer is insoluble in the system. This indicates a mobile equilibrium among the isomers, which is found to extend to all of the polymercuration products. The postulated intermediate for the equilibration, which is 1,2,4-trichloratomercuribenzene, is indicated by the isolation of the similarly oriented 1,2,4,5-perchloratomercuritetrakisbenzene. Although none of the ortho-diperchloratomercuribenzene can be found from this reaction in perchloric acid, it is the principal isomer when phenylmercuric acetate is acetoxymercurated neat.

The literature of aromatic mercuration is marked by many inconsistencies. Thus, although Dimroth (1) at 170° C converted mercuric benzoate to anhydro-*o*-hydroxybenzoic acid, an equivalent mixture of benzoic acid and mercuric acetate at 130° C was found to yield the *o*-, *m*-, and *p*-mercurated benzoic acids in the ratio 25:57:18 (2). On the other hand, the same equivalence in acetic acid (2.5 hours at 110° C) gave a ratio of 80:20:0 (3).

Several workers have suggested that the discrepancies are due to isomerization. The various results of Table I have in part been explained by Jackson and Frant (2) by the

TABLE I
Mercuration of nitrobenzene

Mercurating agent	Medium	Conditions of reaction	Product ratio *o*	*p*	*m*	Ref.
$Hg(OAc)_2$	Nitrobenzene	1:5 by wt. at 150° C until Hg^{++} test is neg.	58		42	4
		1:5 by wt. at 150° C for 3.5 hr	53	9	38	5
		1:5 by wt. at 95° C for 2.5 hr	57		43	6
		1:5 by wt. at 150° C for 2.5 hr	52		48	6
		1:5 by wt. at 150° C for 2.5 hr	53	15	32	2
		1:2.7 by wt. at 155° C for 2.5 hr	27	6	67	3
$Hg(NO_3)_2$	110 ml 68% HNO_3	1:2.7 by wt. at 99° C for 7 hr	37	6	56	3
$Hg(ClO_4)_2$	250 ml 60% $HClO_4$	1:1.2 by wt. at 23° C for 10 days	11		89	6
	40% $HClO_4$, 250 ml 60% $HClO_4$	1:1.2 by wt. at 95° C for 11 hr	37		63	6

possibility that equilibrium is not always attained at once in systems where the mercurated nitrobenzenes are not equally stable. Likewise, as is shown for toluene mercuration in Table II, Brown and McGary (9) have suggested that isomerization of the initially

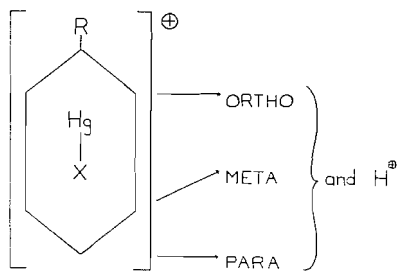
[1]*Manuscript received February 20, 1961.*
Contribution from the Department of Chemistry, University of Toronto, Toronto, Ontario.

TABLE II

Mercuration of toluene

Reagents			Conditions of reaction		Product ratio			
$Hg(OAc)_2$, mole	Toluene, mole	Medium, ml	Time, hr	Temp., °C	*o*	*p*	*m*	Ref.
0.1	0.1	Neat	5.6	40	43	44	13	7
			5.6	110	43	44	13	6
0.1	0.1	Toluene, 150	1.5	110	41	37	21	6
0.1	0.1	HOAc, 200 $HClO_4$, 10	6.5	30	17	77	6	6
0.1	0.1	"	6.5	25	21	67	12	8
0.1	0.1	"	1	25	95	69	21	9
0.1	0.1	"	2	25	40	20	40	9
0.1	0.3	HOAc, 300	ca. 4	50	31	56	13	10
0.1	0.6	"	ca. 4	70	32	53.5	14.5	10
			ca. 4	90	32.5	51.8	15.7	10

formed mercurials seems to be occurring, and that mercuration, like sulphonation (11), is reversible. A similar opinion (12) had been affirmed earlier.



I

The ionization of mercuric salts is sufficiently incomplete that one may presume aromatic mercuration to involve initially a cationic transition state of appreciable stability. If the decomposition of the intermediate cation is fast, first order, and rate independent of the reaction system, the occurrence of monomercurial isomerization is unexpected, whether or not the reaction is reversible. The intermediate, I, may be expected to be deprotonated along paths related directly with the free energy of the products in the system. Either the activation energy for this final step of mercuration is greater than seems to prevail for other aromatic substitutions or else the isomerization must be related to another mechanism.

Reversible polymercuration provides an alternative path leading to isomerization. Indeed, the substitution of more than one anionomercuri group is so likely that most workers have been troubled by it. Attempts to avoid it (9) are understandable since aromatic polymercurials are difficult to manipulate because of low solubility. Nevertheless, we have deliberately chosen polymercuration of benzene in order to clarify the quandary of variable isomer ratios. By this expedient the directing and the entering group are identical.

Can. J. Chem. Downloaded from www.nrcresearchpress.com by 210.87.254.105 on 09/05/12
For personal use only.

At first we started with benzene in aqueous perchloric acid containing mercuric perchlorate. However, we were unable to get consistent results, despite the success of others (13), with this two-phase system. Subsequently we have obtained results that are reproducible by mercuration of mercuric perchlorate with mercuric perchlorate (prepared *in situ* from mercuric oxide) in perchloric acid. The results of a series of experiments in which the water – perchloric acid ratio has been varied are shown in Table III.

TABLE III

Mercuration of 0.0017 mole of phenylmercuric perchlorate with 0.0017 mole of mercuric perchlorate in perchloric acid for 2.5 hours at 25° C

Expt. No.	Perchloric acid		Recovered phenylmercuric perchlorate, %	Yield polymercurated benzenes, %	Isomer, % in polymercurated benzenes		
	Wt.% $HClO_4$	Wt. used, g			1,4	1,3	1,3,5
1	50	26	47	46	18	82	Trace
2	50	417	49	10			
3	55	417	60	28	18	82	Trace
4	60	417	17	64	19	81	Trace
5	65	417	12	74	34	62	5
6	70	417	12	77	57	39	3
7	70	670	16	75	28	69	3

The analyses of the products have been accomplished, after solvent-extractive separation of phenylmercuric chloride from the physically intractable benzenepolymercuric chlorides, by quantitative conversion to the polybromobenzenes. The methods used previously (14, 15) have been modified slightly. The distillable dibromobenzenes have been identified by infrared absorption using the intense bands relating to out-of-plane wagging modes. The results have been checked by thermal analyses and by isolation of *m*-dibromophenylchlorophenylsulphonamide when the ortho isomer is absent.

The series of experiments which are outlined in Table III show that in perchloric acid none of the ortho isomer can be detected with certainty. In the more dilute perchloric acid (expts. 1–4 inclusive) the meta isomer is preponderant; there are lesser amounts of para isomer and of symmetrical trimercurated benzene. Since the sum of these polymercurated products together with unchanged phenylmercuric perchlorate does not constitute a quantitative yield one may expect that other polymercurated benzenes, in small amount, have been missed. Also some benzene must have been formed, and lost, if aromatic mercuration is reversible. This reversibility is apparent when 50% perchloric acid is used in large excess as the reaction medium (expt. 2, Table III). The low yield of polymercurials may be contrasted to 4.6 times as much as that obtained from expt. 1. Since separate experiments show that these are equilibrium states which were attained after 150 minutes, and the amount of recovered monomercurial is essentially the same for expts. 1 and 2, the difference must be attributed to the formation of benzene.

In this connection it is of interest that at 25° C the solubility in 50% aqueous perchloric acid of phenylmercuric hydroxide (20 g/l.) is 10 times as great as in 70% perchloric acid. Thus it would appear that the phenylmercuric salt was more highly ionized or hydrated (or both) in the more aqueous medium.

Addition of sodium perchlorate to the reaction systems described in Table III does not alter appreciably either the yields or the isomer ratio of substitution products. Neither does the acid concentration (see expts. 1, 3, and 4) up to a level of 61%, but in the same

Can. J. Chem. Downloaded from www.nrcresearchpress.com by 210.87.254.105 on 09/05/12
For personal use only.

amount of more concentrated perchloric acid (expts. 5 and 6) the relative yield of meta isomer decreases. The reason is quite apparent: after 20 minutes from 65% or after 4 minutes from 70% perchloric acid a precipitate appears which is nearly pure 1,4-diperchloratomercuribenzene. The amount of this precipitate increases when the total volume of 70% perchloric acid is decreased, or (expt. 7) much less of the precipitate appears when the volume of the system is greater.

Inspection of Table III shows that when this precipitation occurs (expts. 5 and 6) the meta isomer decreases in quantity and only slightly in favor of some 1,3,5-trimercurial which appears. It would seem that this meta isomer, which may be the initial polymercuration product, is converted to para isomer which then can precipitate. Indeed, when a system identical with that of expt. 6 is quenched after 4 minutes of reaction time (and before precipitation has commenced), the product contains only 25% of 1,4-bismercurial instead of the 57% obtained after the 150-minute reaction period of expt. 6 during which precipitation occurs. Moreover, the initial formation of the meta isomer must be rapid, because the polymercurial yield after 4 minutes is 60% of that obtained after 150 minutes of reaction time.

In order to test further the possibility that the meta isomer is the initial perchloratomercuration product we have prepared 1,3-hydroxymercuribisbenzene from 1,3-benzenedisulphinic acid and have dissolved it in 70% perchloric acid. After 2 hours the reaction system is drowned with aqueous sodium chloride. Besides a 20% yield of phenylmercuric chloride the mixture has been shown to contain 1,4-chloromercuribisbenzene as well as a small amount of 1,3,5-trismercurial. Thus a profound disproportionation of 1,3-bismercurial has occurred, undoubtedly to give benzene as well.

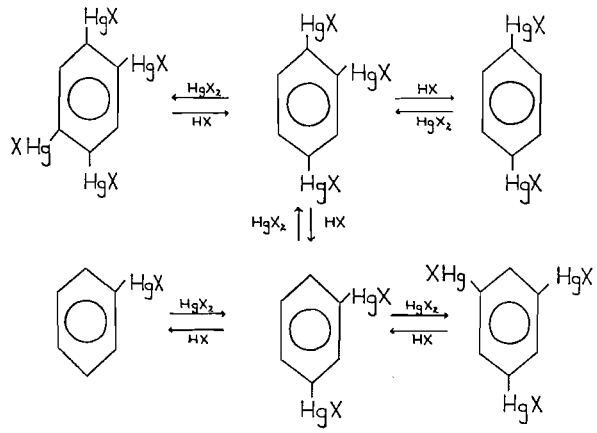
Except when it precipitates from solution, the 1,4-perchloratomercuribisbenzene is not inert toward the reaction system. When it is treated with a 12 molar excess of mercuric perchlorate in 70% perchloric acid for 2 hours the yield of mono- and di-mercurials is very small. Bromination of the remainder shows that *sym*-trismercurial is the principal product although a 5% yield of 1,2,4,5-tetrabromobenzene indicates the presence of this tetramercurial.

The perchloratomercuritrisbenzene also must not be considered to be an ultimate end product. When it is treated with monoperchloratomercuribenzene in 70% perchloric acid the system, after 2 hours, contains only 40% of the trismercurial while 40% of the two dimercurials has appeared.

On the basis of these findings the mode of reaction given below has been drawn up (X = ClO_4), although one important piece of evidence is lacking. In all of the systems which have been analyzed, the key substance, 1,2,4-tribromobenzene, indicative of the analogous trismercurial, has been sought assiduously, but never found. Despite the fact that the low melting point (44°) of 1,2,4-tribromobenzene makes isolation difficult, we are inclined to attribute the apparent absence of 1,2,4-triperchloratomercuribenzene to its high reactivity. Certainly it cannot be excluded because ortho perchloratomercuration is involved since the isolation of 1,2,4,5-tetrabromobenzene shows that ortho substitution can occur. Therefore, the transition to and from meta and para dimercurated benzenes seems to be explicable better by postulation of the 1,2,4-trisubstituted intermediate than by simple "isomerization".

The absence of evidence for initial ortho mercuration in the studies with perchloric acid should not be construed as proof that it does not occur. The perchloratomercuration of 1,2-perchloratomercuribisbenzene and the alternative reversal from the 1,2,4-trismercurial to 1,3-perchloratomercuribisbenzene may be so rapid that only the appearance

Can. J. Chem. Downloaded from www.nrcresearchpress.com by 210.87.254.105 on 09/05/12
For personal use only.



of the latter substance is first observed. However, initial ortho mercuration need not be a necessary condition of the reaction. Meta substitution may be a very rapid reaction, as is observed when phenyltrimethylammonium salts are nitrated to give exclusively the meta nitro compound in high yield (16, 17). No postulation of prior ortho–para substitution can be made in this event since nitration is essentially irreversible.

Actually a preponderance of ortho substitution is observed when phenylmercuric acetate is fused with mercuric acetate at 145–150° C. The reaction does not seem to be amenable to detailed study because of the complication that the acetato group also is mercurated (18) even though a reasonable separation of the mercurated acetic acid can be made (19). Although the yields vary unaccountably between 35 and 50% the ratio of bismercurials, *o*:*m*:*p*, is consistent at 65–66:23.5–24.5:11. An otherwise comparable experiment, in which mercuric acetamide replaces the acetate, yields 43% of bismercurials in *o*:*m*:*p* ratio of 69:18:12.

EXPERIMENTAL

Mercuration of Phenylmercuric Perchlorate

This procedure was used when various concentrations of perchloric acid were compared in mercuration. A sample of phenylmercuric hydroxide (m.p. 226–228° C) (20) weighing 0.50 g (0.0017 mole) was dissolved in perchloric acid (usually 417 ml) of the desired concentration. To this stirred solution at 25° was added 0.37 g (0.0017 mole) of mercuric oxide. The closed system was stirred only gently (to minimize loss of benzene) for 150 minutes.

Subsequently the system was poured into 1 liter of crushed ice, and 20% aqueous sodium hydroxide was added until the mixture was slightly basic. Then 1 g of sodium bromide was added. Acidification with acetic acid produced a precipitate which was allowed to settle while the remainder of the ice was melting. The precipitate was filtered off and washed thoroughly with water to remove soluble salts. Then it was washed with boiling ethanol and boiling benzene to remove phenylmercuric bromide, leaving the insoluble polymercurated benzenes.

p-Chloromercuribisbenzene

Following the procedure outlined above with 70% perchloric acid (d_{20} 1.67, 417 ml) the original system was stirred for 20 minutes. Then 0.05 g (0.00017 mole) of phenylmercuric

Can. J. Chem. Downloaded from www.nrcresearchpress.com by 210.87.254.105 on 09/05/12
For personal use only.

hydroxide and 0.037 g (0.00017 mole) of mercuric oxide were added. Subsequently, nine more such additions were made every 20 minutes with continued stirring. Twenty minutes after the last addition the solid was filtered off and dissolved in water, then treated with sodium chloride. The purity of the infusible *p*-chloromercuribisbenzene (0.65 g, 32%) is indicated by the melting point (74–82°) of the *p*-dibromobenzene, which may be prepared from it quantitatively (21).

Treatment of the remainder of the reaction system (the filtrate) with ice and then with sodium bromide yielded 0.56 g of polymercurated benzenes which contained 22% of 1,4-bromomercuribisbenzene according to the prescribed bromination analysis described below.

Isomerization of p-Dimercurated Benzene

The 1,4-perchloratomercuribisbenzene was filtered from a reaction system such as has just been described; it was washed thoroughly with ethanol and then was dried *in vacuo* at 25° C. A mixture of 0.50 g (0.00074 mole) of 1,4-perchloratomercuribisbenzene in 200 ml of 70% perchloric acid containing 0.238 g (0.0011 mole) of mercuric oxide was stirred at 25° C. After 180 minutes the clear solution was drowned and treated as described above to give 0.04 g (17%) of phenylmercuric bromide and 0.40 g (25%) of polymercurated benzenes. Analytical bromination showed that this mixture contained 10% of the *p*-isomer, 57% of the *m*-isomer, and 24% of the 1,3,5-perchloratomercuritrisbenzene.

In a variation of this procedure 0.25 g (0.00037 mole) of 1,4-perchloratomercuribisbenzene in 50 ml or 70% perchloric acid containing 1.00 g (0.0046 mole) of mercuric oxide was stirred at 25° C for 2 hours and then was processed according to the earlier description to remove *p*-isomer (filtration) and then phenylmercuric salt (benzene–ethanol extraction). The remainder (0.31 g) when treated with bromine gave 0.09 g of solid polybromobenzenes. A hot ethanol (2.5 ml) solution, upon cooling, yielded 0.004 g (5%) of 1,2,4,5-tetrabromobenzene, m.p. 165–173° C. After crystallization from ethanol (m.p. 179–180° C) a mixture melting point with an authentic sample (22) was not depressed.

The ethanolic mother liquors were concentrated to yield 0.07 g, m.p. 65–92° C. Crystallization from petroleum ether (b.p. 40–60° C) showed that this material was largely 1,3,5-tribromobenzene, m.p. 118–119° C.

1,3-Chloromercuribisbenzene

A suspension of 4.70 g (0.0238 mole) of *m*-benzenedisulphinic (23) acid in 10 ml of water was made alkaline by addition of 50% aqueous sodium hydroxide and the whole was added to a boiling solution of 16.35 g (0.06 mole) of mercuric chloride in 50 ml of water. A curd appeared after 30 seconds and the system thickened to a paste on the steam bath. After 20 minutes the strongly acidic system was diluted with 50 ml of water and was maintained on the steam bath for 6 hours. The precipitate was filtered off and washed with hot water until free from mercuric salts (of which 0.015 mole was washed out), and then with boiling ethanol and boiling benzene. The remainder weighed 70.7 g or 82% of theoretical. Anal. Calc. for $C_6H_4Hg_2Cl_2$: C, 13.15; H, 0.73. Found: C, 13.0; H, 1.2. Upon treatment with bromine in excess the *m*-dibromobenzene, b.p. 85–90° C (15 mm), which was obtained in 65% yield, was converted to 2,4-dibromobenzenesulphonyl chloride, m.p. 75–78° C, mixed m.p. not depressed.

1,3-Hydroxymercuribisbenzene

A suspension of 10.7 g (0.0196 mole) of 1,3-chloromercuribisbenzene in 2 liters of 0.65%

Can. J. Chem. Downloaded from www.nrcresearchpress.com by 210.87.254.105 on 09/05/12
For personal use only.

aqueous sodium hydroxide was heated to boiling and filtered hot. The filtrate was evaporated to a 200-ml volume and cooled, precipitating 3.76 g (38%) of chlorine-free product. Treatment with bromine according to the procedure described below gave a quantitative yield of pure 1,3-dibromobenzene, b.p. 86–90° C (15 mm), according to freezing point (−2° C) and to the 2,4-dibromobenzenesulphonyl chloride, m.p. 77–78° C, which was derived from it.

Isomerization of 1,3-Perchloratomercuribisbenzene

Some heat is evolved when 0.50 g (0.00096 mole) of 1,3-hydroxymercuribisbenzene is dissolved in 150 ml of 70% perchloric acid. The solution was cooled to 25° C and let stand for 2 hours and then was drowned in ice, neutralized with alkali, and treated with sodium chloride. Extraction with hot benzene–ethanol removed 0.06 g of phenylmercuric chloride, m.p. 248° C. The alcohol- and benzene-insoluble part (0.36 g) was found by the analytical bromine technique to contain 25% of the *p*-isomer and less than 1% of bromotrisbenzene.

1,3,5-Chloratomercuritrisbenzene

A solution of 0.20 g (0.00068 mole) of phenylmercuric hydroxide in 100 ml of 70% perchloric acid was treated at 25° C with 1.70 g (0.00785 mole) of mercuric oxide. The system became and remained clear, unlike systems without excess of mercuric perchlorate. After 2 hours the system was poured into 2 kg of ice, and 20% aqueous sodium hydroxide was added to slight basicity. Then 1 g of sodium bromide was added, together with sufficient acetic acid for slight acidity. The precipitate, essentially bromomercuritrisbenzene, weighed 0.62 g (100%) and when brominated gave 0.21 g, m.p. 97° C. Crystallization from petroleum ether raised this melting point to 118–119° C; mixed m.p. not lowered.

Demercuration of Chloratomercuritrisbenzene

A quantity of material which was chiefly chloromercuritrisbenzene according to the bromination method of analysis was converted to the hydroxymercurial by washing it exhaustively with alkali. A suspension of 0.49 g (0.00067 mole) of this hydroxymercurial with 0.16 g (0.00054 mole) of phenylmercuric hydroxide was stirred with 150 ml of 70% perchloric acid for 3 minutes until the system was homogeneous. After 2 hours the system was drowned and processed as is outlined above. The recovered phenylmercuric chloride and the polymercurial portion weighed 0.07 g and 0.41 g respectively. Analysis of the latter by the bromination technique showed that 48% was dimercurated benzenes while 52% was trimercurated. This amount of trismercurial is 42% of that originally used, so that at least 58% has been demercurated. Likewise, the recovery of monomercurial is 44% of that first introduced to the system.

Acetoxymercuration of Phenylmercuric Acetate

A finely ground mixture of 10.0 g (0.03 mole) of phenylmercuric acetate and 12.78 g (0.047 mole) of purified mercuric acetate was heated in a large test tube and was immersed in a sulphuric acid bath at 150° C during 30 minutes. The clear melt became quite viscous. The system was allowed to cool gradually, then was finely ground and exhaustively washed with boiling ethanol and benzene to remove 1.2 g of unchanged phenylmercuric acetate. The remainder was washed five times with 200-ml portions of 5% aqueous sodium hydroxide containing 10% sodium bromide. After each washing the material was dried and reground. Finally it was washed with dilute acetic acid and with water. There remained after drying 9.5 g (58%) of infusible solid. Analysis by

Can. J. Chem. Downloaded from www.nrcresearchpress.com by 210.87.254.105 on 09/05/12
For personal use only.

the bromination method (spectral analysis) showed that it contained 64.8% ortho, 24.4% meta, and 10.8% para isomer. Duplication gave 65.8% ortho, 23.3 meta, and 10.8 para.

An otherwise identical experiment with mercuric acetamide gave a product with an *o*:*m*:*p* ratio of 69.3:18.4:12.3.

Identifications and Analyses

Because of the large atomic weight of mercury, an elemental analysis for carbon is chiefly, and for hydrogen or mercury entirely, meaningless. For this reason the mercurials and mixtures of them that are described in this report have largely been characterized by conversion to brominated benzenes. For a quantity of mercurial not to exceed 0.70 g the following procedure is used.

Bromination of Mercurials

The sample is added to a stirred two-phase system comprised of 5.0 ml of carbon tetrachloride with a solution of 3.0 g of potassium bromide in 15 ml of water. Bromine is added at such a rate that its color is just maintained. When the solid has disappeared the brominated benzenes are in the non-aqueous phase and the mercuric salts are in the aqueous phase.

The non-aqueous phase is vacuum-evaporated and the residue is distilled under 13 mm. The dibromobenzenes distill at 85–87° C while the residue consists of polybromobenzenes, 96–108° C. A single crystallization from 95% ethanol raises this melting point to 118–119° C, not depressed by admixture with 1,3,5-tribromobenzene. Since the weight of the distillation residue is 5% higher than the known amount from a calculated mixture of dibromobenzenes and 1,3,5-tribromobenzene, this residue weight less 5% is taken as presumptive for anionomercuritrisbenzene.

The method of Ferguson and Levant (24) for infrared spectral analysis of chlorobromobenzenes was simplified by use of the same cell for all determinations of 7–10% solutions in carbon disulphide so that optical density instead of extinction coefficient could be employed. The wag frequencies chosen include the three corresponding (but at lower frequencies) to those chosen by Whiffen *et al.* in their analysis of cresols (25) although the number has been extended (607 and 742 cm^{-1} for ortho; 664, 723, and 765 cm^{-1} for meta; 805 cm^{-1} for para). The optical densities of 12 known mixtures over the entire range of concentrations have been plotted for each frequency. Since these plots are practically linear and there is little overlap of the key frequencies, the percentages of isomer are read directly and (in the case of ortho and meta) averaged for the several frequencies used for these isomers. Although part of the *p*-dibromobenzene may be separated as such (m.p. 85–86° C) by chilling the distilled mixture of dibromobenzenes they are usually analyzed *in toto*.

When the ortho isomer is practically absent a two-component thermal analysis may be made for percentages of the meta and para dibromobenzenes. The hot oil is transferred by means of small capillaries to melting-point tubes about 1 mm in diameter. The disappearance of the last crystal is recorded while the sample is stirred by reciprocal motion of the capillary. The rate of heating is about 1° C per 5 minutes in a thaw-point apparatus (26). The diagram is shown in Fig. 1.

Meta–para mixtures of dibromobenzene also may be analyzed by the method of Huntress and Carten (27) because 1,4-dibromobenzene does not react with chlorosulphonic acid. For example, 0.30 g (0.0012 mole) of dibromobenzenes (from which part of the para isomer had been removed by filtration at 4° C) was treated at 0° C with 2.50 g (0.0215 mole) of chlorosulphonic acid (distilled at 147–149° C in a stream of

Can. J. Chem. Downloaded from www.nrcresearchpress.com by 210.87.254.105 on 09/05/12
For personal use only.

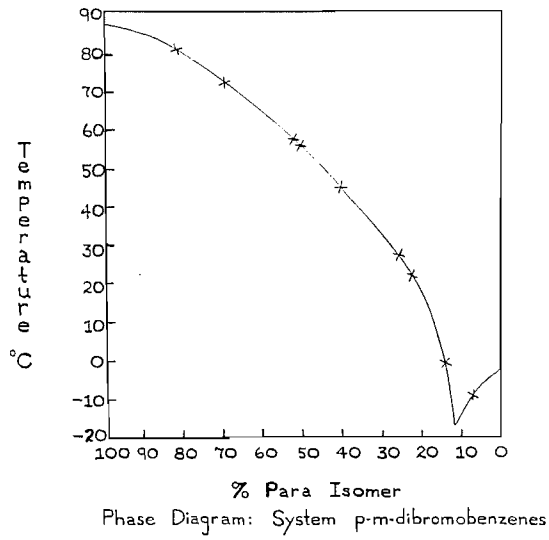


FIG. 1.

hydrogen chloride). After the reaction had subsided the system was warmed and held for 20 minutes at 20–25° C and then was drowned in ice. The white solid, 0.36 g, m.p. 57–73° C, was crystallized from 4 ml of petroleum ether (b.p. 40–60° C), yielding 0.33 g, m.p. 80–82° C, not depressed by admixture with authentic 2,4-dibromobenzenesulphonyl chloride. Refluxing with concentrated ammonia converts this product to 2,4-dibromobenzenesulphonamide, m.p. 189–190° C.

REFERENCES

1. O. DIMROTH. Ber. **35**, 2852 (1902).
2. G. R. JACKSON, JR. and M. S. FRANT. J. Am. Chem. Soc. **77**, 5625 (1955).
3. Y. OGATA and M. TSUCHIDA. J. Org. Chem. **20**, 1637 (1955).
4. O. DIMROTH. Ann. **446**, 148 (1925).
5. J. JURGENS. Rec. trav. chim. **45**, 61 (1926).
6. W. KLAPPROTH and F. H. WESTHEIMER. J. Am. Chem. Soc. **72**, 4461 (1950).
7. S. COFFEY. J. Chem. Soc. **127**, 1029 (1925).
8. H. C. BROWN and K. L. NELSON. J. Am. Chem. Soc. **75**, 6292 (1953).
9. H. C. BROWN and C. W. MCGARY, JR. J. Am. Chem. Soc. **77**, 2300 (1955).
10. H. C. BROWN and C. W. MCGARY, JR. J. Am. Chem. Soc. **77**, 2306 (1955).
11. A. F. HOLLEMAN and P. CALAND. Ber. **44**, 2519 (1911).
12. F. WESTHEIMER, E. SEGEL, and R. SCHRAMM. J. Am. Chem. Soc. **69**, 773 (1947).
13. R. M. SCHRAMM, W. KLAPPROTH, and F. H. WESTHEIMER. J. Phys. & Colloid Chem. **55**, 803 (1951).
14. O. DIMROTH. Ber. **35**, 2870 (1900).
15. M. S. KHARASCH and L. CHALKLEY, JR. J. Am. Chem. Soc. **43**, 607 (1921).
16. T. G. BONNER, M. E. JAMES, A. M. LOWEN, and G. WILLIAMS. Nature, **163**, 955 (1949).
17. G. WILLIAMS and A. M. LOWEN. J. Chem. Soc. 3312 (1950).
18. J. E. MARCH and R. J. F. STRUTHERS. J. Chem. Soc. 2685 (1927).
19. K. S. MCMAHON and K. E. KOBE. Ind. Eng. Chem. **49**, 42 (1957).
20. R. M. SCHRAMM. J. Am. Chem. Soc. **69**, 1831 (1947).
21. H. SAWATZKY and G. F WRIGHT. Can. J. Chem. **36**, 1555 (1958).
22. A. RICHE and P. BÉRARD. Ann. **133**, 51 (1865).
23. W. AUTENRIETH and R. HENNING. Ber. **35**, 1398 (1902).
24. L. N. FERGUSON and A. J. LEVANT. Ind. Eng. Chem. Anal. Ed. **23**, 1510 (1951).
25. D. H. WHIFFEN, P. TARKINGTON, and H. W. THOMPSON. Trans. Faraday Soc. **41**, 200 (1945).
26. H. RHEINBOLDT and M. KIRCHEISEN. J. prakt. Chem. **113**, 348 (1926).
27. E. H. HUNTRESS and F. H. CARTEN. J. Am. Chem. Soc. **62**, 511 (1940).

Can. J. Chem. Downloaded from www.nrcresearchpress.com by 210.87.254.105 on 09/05/12
For personal use only.

Can. J. Chem. Downloaded from www.nrcresearchpress.com by 210.87.254.5 on 09/05/12
For personal use only.

THE RADIOLYSIS OF ETHANOL

I. VAPOR PHASE[1]

J. M. RAMARADHYA[2] AND G. R. FREEMAN

ABSTRACT

The alpha radiolysis of ethanol vapor at 108° C produced hydrogen as the major single product, with smaller amounts of methane, carbon monoxide, ethylene, ethane, acetaldehyde, formaldehyde, water, 2,3-butanediol, 1,2-propanediol, propanol, and butanol. The initial yield of hydrogen was $G(H_2) = 8.9 \pm 0.4$, which is much higher than the values reported for the liquid phase ($G(H_2) \approx 4$).

A mechanism is proposed to account for the formation of the products. However, the observed value of $G(H_2O) = 5.4$ is over four times larger than can be explained by the mechanism.

There is a good material balance in the observed reaction products, which indicates that little polymerization occurred during the radiolysis. This is in marked contrast with the vapor phase radiolysis of cyclohexane.

INTRODUCTION

Although the radiolysis of liquid ethanol has been studied using helium ions (1, 2) and Co^{60} gamma rays (3), very little attention has been paid to the vapor phase radiolysis of ethanol. In the liquid phase radiolysis of ethanol, the gaseous products were hydrogen, carbon monoxide, methane, ethylene, and ethane and the liquid products were formaldehyde, acetaldehyde, and vicinal glycols.

One previous study of ethanol vapor by cathode-ray bombardment has been reported by McLennan and Patrick (4). The products reported were hydrogen, carbon monoxide, carbon dioxide, methane, ethane, formaldehyde, and acetaldehyde. In this paper, an investigation of the radiolysis of ethanol vapor by Po^{210} alpha particles is described.

EXPERIMENTAL

The apparatus and the general experimental technique used in this investigation are similar to those described in an earlier paper (5).

The ethanol was from Reliance Chemical Ltd., containing about 0.11 mole% water. Three and one-half grams of sodium was dissolved in 500 ml of ethanol and 14 g of diethyl phthalate was added to the solution (6). This solution was refluxed for 2 hours and was distilled in a system protected from moist air by passing dry hydrogen through it. The hydrogen was dried by passing it through a trap containing silica gel, immersed in liquid nitrogen. Only the middle one-third of the distillate was retained. After the purification the ethanol contained only 0.005 mole% water.

The purified ethanol was degassed and stored under vacuum in a reservoir. Prior to irradiation, 1.6 ml of the ethanol was distilled into a calibrated tube, where its volume was accurately measured at 0° C, and then volatilized into the reaction chamber.

The reaction chamber was a 1-liter bulb, heated to 108° C, containing a nominally 100-mc Po^{210} source (5). The polonium source was calibrated by Fricke dosimetry, using $G(Fe^{+++}) = 5.5$ (5). All the energy of the alpha particles was absorbed by the ethanol vapor during an experiment.

The products of the ethanol vapor radiolysis were analyzed by low-temperature distillation and by gas chromatography. The fraction of gaseous products that was volatile

[1]*Manuscript received May 23, 1961.*
Contribution from the Department of Chemistry, University of Alberta, Edmonton, Alberta.
[2]*Present address: Consolidated Mining and Smelting Co., Trail, B.C.*

at −196° C consisted of hydrogen, carbon monoxide, and methane. It was collected and measured in a McLeod–Toepler apparatus and then analyzed on a 1-m activated charcoal column. Another gaseous fraction, noncondensable at −112° C and consisting of residual methane and C_2, C_3, and trace amounts of C_4 hydrocarbons, was analyzed using a 2.5-m silica gel column. The analyses of the various liquid products were performed using 2.5-m carbowax 1500, 2.5-m didecyl phthalate, and 1-m ucon columns.

Anhydrous ethanol is very hygroscopic. Water was also a reaction product. When the yield of water was being determined, samples of unirradiated ethanol were put through the entire analytical procedure and then analyzed for water on a 2.5-m carbowax 1500 column. The differences between the blanks and the irradiated samples were used to calculate the G of water.

The acetaldehyde yield was determined polarographically (7).

The amount of formaldehyde was measured by the chromotropic acid method. Analyses were done in triplicate and three standard samples and a blank were done concurrently with the unknowns. The procedure for an individual analysis was as follows. Chromotropic acid (110±1 mg) was weighed into each of seven 10-ml Erlenmeyer flasks and 0.80 ml of distilled water was added to each. Only a small portion of the chromotropic acid dissolved. Then 0.20 ml of irradiated ethanol, or of pure ethanol or standard ethanolic solution of formaldehyde, was added to the various flasks. Three different standard concentrations of formaldehyde were used to bracket the concentration in the unknowns. The solutions were then evaporated to dryness by suspending the flasks for 25 minutes in an oil bath at 110±2° C. The oil was stirred to obtain a uniform temperature for all the flasks in the bath. The flasks were then removed from the bath and allowed to cool for 3 or 4 minutes. Five milliliters of concentrated sulphuric acid was pipetted into each flask and they were then heated for 30 minutes in an oil bath at 130±2° C. After the flasks were removed from the bath and cooled, the acid solutions were transferred into 50-ml, glass-stoppered flasks. The solutions were diluted with 15.0 ml of distilled water, cooled, and their optical densities measured at 570 mμ. The temperatures and times in the analytical procedure should be kept as constant as possible and the diluted solution should not stand more than 1 hour before being measured in a spectrophotometer (the color fades). The sensitivity of the method decreases markedly if the water/ethanol ratio in the initial chromotropic acid solution decreases below 4/1. Acetaldehyde does not interfere with the analysis.

RESULTS

Pure ethanol was subjected to alpha radiation and the gaseous-product yield distribution was studied as a function of dose over the range 0.50×10^{19} ev to 3.77×10^{19} ev. The total yield of gases noncondensable at −196° C, $G(-196)$, appears to be constant at 10.1±0.4 over this dose range, while that of gases volatile at −112° C, $G(-112)$, decreases with increasing dose.

The products that constituted the fractions volatile at −196° C and −112° C were measured and their G values are presented as a function of dose in Fig. 1.

The yields of methane are the combined yields obtained from the two gas fractions. The portion of the total methane, derived from the −112° C fraction, increased from 21% at the lowest dose to 58% at the highest dose. However, the methane yield obtained from the gases volatile at −196° C remained approximately constant with a G of 1.1±0.1 except for the lowest-dose experiment.

Can. J. Chem. Downloaded from www.nrcresearchpress.com by 210.87.254.5 on 09/05/12
For personal use only.

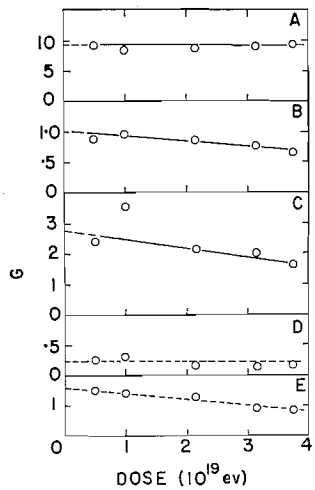


FIG. 1. G values of products volatile at −196° C and −112° C, as a function of dose: (A) hydrogen, (B) carbon monoxide, (C) methane, (D) ethane, (E) ethylene. The sample was 1.6 ml liquid ethanol volatilized into a 1-l. bulb at 108° C.

Since the amounts of liquid products were too small to be measured in these dose-function experiments, appreciably higher doses, about 8×10^{20} ev, were given to three ethanol samples and the liquid products were measured. The average yields are given in Table I along with the yields of the gaseous products obtained at the same dose. Comparison of the gaseous product yields in Table I and Fig. 1 indicates little change in the dose region from about 4 to 80 $\times10^{19}$ ev.

TABLE I

G values of products obtained by irradiating ethanol vapor
(Irradiation temperature 108° C, dose ≈ 8×10^{20} ev)

Product	G	Product	G
Hydrogen	7.6	Formaldehyde	0.9
Carbon monoxide	1.1	Acetaldehyde	4.5
Methane	1.66	Propanol	0.6
Ethane	0.23	Butanol	0.19
Ethylene	0.72	1,2-Propanediol	0.15
Acetylene	0.03	2,3-Butanediol	1.2
C_3 and C_4 hydrocarbons	Trace	Total glycols	1.6
Water	5.4		

There is fair agreement between the total glycols (ucon column) and the sum of the vicinal glycols (carbowax column). Ethylene glycol, 1,3-butanediol, and 1,4-butanediol were not present in detectable amounts.

DISCUSSION

The values of $G(H_2)$ obtained in the previous investigations of liquid ethanol (1–3) are around 4. The present vapor phase radiolysis of ethanol has yielded an average value of $G(H_2) = 8.9\pm0.4$ in the dose region from 0.5 to 3 $\times10^{19}$ ev/g. In hydrocarbon

Can. J. Chem. Downloaded from www.nrcresearchpress.com by 210.87.254.5 on 09/05/12
For personal use only.

radiolyses, the 100-ev hydrogen yields are also larger in the gas phase reactions than in the liquid phase reactions (5).

The following mechanism is suggested to account for the observed reaction products:

$$CH_3CH_2OH \sim\sim\rightarrow CH_3CH_2OH^* \quad [1a]$$

$$\sim\sim\rightarrow CH_3CH_2OH^+ + e \quad [1b]$$

$$CH_3CH_2OH^* \rightarrow CH_3CHOH + H \quad [2a]$$

$$\rightarrow CH_3 + CH_2OH \quad [2b]$$

$$CH_3CH_2OH^* \rightarrow CH_3CHO + H_2 \quad [3a]$$

$$\rightarrow CH_2O + CH_4 \quad [3b]$$

$$\rightarrow C_2H_4 + H_2O \quad [3c]$$

$$CH_3CH_2OH^+ + CH_3CH_2OH \rightarrow CH_3CH_2OH_2^+ + CH_3CHOH \quad [4]$$

$$CH_3CH_2OH_2^+ + e \rightarrow CH_3CH_2 + H_2O \quad [5a]$$

$$\rightarrow CH_3CH_2O + H_2 \quad [5b]$$

$$H + CH_3CH_2OH \rightarrow H_2 + CH_3CHOH \quad [6]$$

$$CH_3 + CH_3CH_2OH \rightarrow CH_4 + CH_3CHOH \quad [7]$$

$$C_2H_5 + CH_3CH_2OH \rightarrow C_2H_6 + CH_3CHOH \quad [8]$$

$$CH_3CH_2O + CH_3CH_2OH \rightarrow CH_3CH_2OH + CH_3CHOH \quad [9]$$

$$C_2H_4 + H \rightarrow C_2H_5 \quad [10]$$

$$CH_3 + CH_3CHOH \rightarrow \begin{matrix} CH_3CHOH \\ | \\ CH_3 \end{matrix} \quad [11a]$$

$$\rightarrow CH_4 + CH_3CHO \quad [11b]$$

$$C_2H_5 + CH_3CHOH \rightarrow \begin{matrix} CH_3CHOH \\ | \\ C_2H_5 \end{matrix} \quad [12a]$$

$$\rightarrow C_2H_6 + CH_3CHO \quad [12b]$$

$$\rightarrow C_2H_4 + C_2H_5OH \quad [12c]$$

$$2CH_3CHOH \rightarrow CH_3CHOHCHOHCH_3 \quad [13a]$$

$$\rightarrow CH_3CH_2OH + CH_3CHO \quad [13b]$$

$$CH_3CHOH + CH_2OH \rightarrow CH_3CHOHCH_2OH \quad [14a]$$

$$\rightarrow CH_3CH_2OH + CH_2O \quad [14b]$$

$$\rightarrow CH_3CHO + CH_3OH \quad [14c]$$

$$CH_3CHOH + CH_3CH_2O \rightarrow CH_3CHO + C_2H_5OH \quad [15a]$$

$$\rightarrow \begin{matrix} CH_3CHOH \\ | \\ OC_2H_5 \end{matrix} \rightarrow CH_3CHO + C_2H_5OH. \quad [15b]$$

Reactions [4] and [5*a*, *b*] are quite speculative but they are being considered in an investigation of the radiolysis of liquid ethanol in this laboratory. It is assumed that the positive charge on the species in reactions [4] and [5*a*, *b*] is localized on the oxygen atom.

Can. J. Chem. Downloaded from www.nrcresearchpress.com by 210.87.254.5 on 09/05/12
For personal use only.

Can. J. Chem. Downloaded from www.nrcresearchpress.com by 210.87.254.5 on 09/05/12
For personal use only.

Acetaldehyde may be formed by reactions [3*a*], [11*b*], [12*b*], [13*b*], [14*c*], and [15*a*, *b*]. The radicals involved in these reactions are CH_3, C_2H_5, CH_3CH_2O, CH_3CHOH, and CH_2OH. From the *G* values of products which require these radicals for their formation, the amounts of CH_3, C_2H_5, ($CH_3CHOH + CH_3CH_2O$), and CH_2OH radicals can be calculated to be respectively 1.1–2.3 (depending on the mechanism of formation of CO), 0.43, 12.35, and 1.05 *G* units. Since the amount, and therefore the concentration, of ($CH_3CHOH + CH_3CH_2O$) radicals is much greater than that of any other radical, the disproportionation reaction of these radicals (reactions [13*b*] and [15]) might be considered as a major source of acetaldehyde. The steady-state concentration of CH_3CH_2O will probably be much smaller than that of CH_3CHOH because of reaction [9] and because the latter radicals can be generated in many more reactions than can the former radicals (see the above mechanism).

Since the C—C bond is the weakest bond in the ethanol molecule, one might have expected a large yield of products resulting from CH_3 and CH_2OH radicals in the gas phase. In the liquid phase, there may be recombination of the CH_3 and CH_2OH radicals in the Franck–Rabinowitch cages and hence the yields of the corresponding products would be low. Low yields of methane (0.43) and formaldehyde (0.3) were experimentally observed by McDonell and Newton (1). In the gas phase, where the cage effect is not operative, larger yields of methane (1.7) and formaldehyde (0.9) were observed in the present work.

Carbon monoxide might be formed by decomposition of formaldehyde and acetaldehyde.

Propanol and butanol are probably formed by the addition of methyl and ethyl radicals to CH_3CHOH radicals (reactions [11*a*] and [12*a*]).

The vicinal glycols (2,3-butanediol and 1,2-propanediol) that were measured in the present investigation were probably formed by combination of CH_3CHOH radicals with themselves and with CH_2OH radicals (reactions [13*a*] and [14*a*]). From the relative yields of these two glycols it may readily be calculated that the yield of ethylene glycol would be negligible. If CH_2CH_2OH radicals were present in appreciable concentration during the decomposition of ethanol, the combination of CH_2CH_2OH radicals with each other and with CH_3CHOH would have led to the formation of 1,4-butanediol and 1,3-butanediol. Since these products were not produced to a measurable extent, the concentration of CH_2CH_2OH radicals was negligible in the present system.

The ethyl radicals produced by reactions [5*a*] and [10] might abstract (reaction [8]) or disproportionate to give ethane.

$$2C_2H_5 \rightarrow C_4H_{10} \qquad [16a]$$

$$\rightarrow C_2H_4 + C_2H_6 \qquad [16b]$$

Since the value of the ratio of disproportionation to combination of ethyl radicals is about 0.12 (9), the amount of ethane from reaction [16*b*] would be about one-eighth of the amount of butane. The yield of butane in the present work was only a trace, and thus a negligible amount of ethane originates from the disproportionation reaction. Therefore the major source of ethane is probably reaction [8].

Ethylene, which has an appreciable yield, is assumed to be formed by reactions [3*c*], [12*c*], and [16*b*]. Since [16*b*] was precluded as a significant source of ethane, it may also be neglected as a source of ethylene.

It is not known whether the acetylene is a primary or a secondary product but it will be assumed to be mechanistically as well as stoichiometrically equivalent to ($C_2H_4 - H_2$).

The preceding mechanism can be reduced to the following stoichiometric equations:

$$\begin{aligned} n\mathrm{C_2H_5OH} &= \mathrm{H_2} + \mathrm{CH_3CHO} \\ &= \mathrm{H_2} + \mathrm{CH_4} + \mathrm{CO} \\ &= \mathrm{H_2} + (\mathrm{CH_3CHOH})_2 \\ &= \mathrm{H_2} + \mathrm{C_2H_2} + \mathrm{H_2O} \\ &= \mathrm{H_2} + \mathrm{C_3H_7OH} + \mathrm{CH_2O} \\ &= \mathrm{C_2H_4} + \mathrm{H_2O} \\ &= \mathrm{C_3H_7OH} + \mathrm{CH_3OH} \\ &= \mathrm{CH_4} + \mathrm{CH_3CHO} + \mathrm{CH_3OH} \\ &= \mathrm{CH_4} + \mathrm{CH_3CHOHCH_2OH} \\ &= \mathrm{CH_4} + \mathrm{CH_2O} \\ &= \mathrm{C_4H_9OH} + \mathrm{H_2O} \\ &= \mathrm{C_2H_6} + \mathrm{CH_3CHO} + \mathrm{H_2O} \\ &= \mathrm{C_2H_6} + (\mathrm{CH_3CHOH})_2 + \mathrm{H_2O}, \end{aligned}$$

where $n = 1$, 2, or 3. The products can be written in several equivalent combinations. Equations such as

$$3\mathrm{C_2H_5OH} = \mathrm{CH_4} + (\mathrm{CH_3CHOH})_2 + \mathrm{CH_3OH}$$

can be included without altering the over-all picture or the calculations that follow.

From the above equations, the yields of hydrogen, water, and methane were correlated to the yields of other products.

$$G(\mathrm{H_2}) = G(\mathrm{CH_3CHO}+\mathrm{CO}+(\mathrm{CH_3CHOH})_2+\mathrm{C_2H_2}+\mathrm{C_3H_7OH}-\mathrm{CH_3OH}-\mathrm{C_2H_6})$$

Using Table I, the sum of the G values of the products on the right-hand side of this equation is equal to $7.2-G(\mathrm{CH_3OH})$.

Similarly

$$\begin{aligned} G(\mathrm{H_2O}) &= G(\mathrm{C_2H_2}+\mathrm{C_2H_4}+\mathrm{C_4H_9OH}+\mathrm{C_2H_6}) \\ &= 1.2, \\ G(\mathrm{CH_4}) &= G(\mathrm{CO}+\mathrm{CH_3OH}+\mathrm{CH_3CHOHCH_2OH}+\mathrm{CH_2O}-\mathrm{C_3H_7OH}) \\ &= 1.55+G(\mathrm{CH_3OH}). \end{aligned}$$

The values of $G(\mathrm{H_2}) = 7.2-G(\mathrm{CH_3OH})$ and $G(\mathrm{CH_4}) = 1.55+G(\mathrm{CH_3OH})$ are in approximate agreement with the observed values, $G(\mathrm{H_2}) = 7.6$ and $G(\mathrm{CH_4}) = 1.66$, if $G(\mathrm{CH_3OH})$ is small.

From the above, an approximate expected yield of methanol would be $G(\mathrm{CH_4})-1.55 \approx 0.1$. In the liquid phase radiolysis of ethanol (1), the value of the ratio of the yields of formaldehyde to methanol is 0.2. If this ratio had the same value in the vapor phase, the expected yield of methanol would be about 0.2. Thus the methanol yield is probably quite small, although methanol could not be measured by the present analytical system.

The predicted value of $G(\mathrm{H_2O}) = 1.2$ is much lower than the observed value of 5.4. The source of this excess water is not obvious. It might have been formed by reactions not considered in the mechanism, or the sample might have absorbed water from the atmosphere during the analytical procedure. However, the analysis of the blank samples should have compensated for the latter possibility. An unaccountable excess of water was also observed by McDonell and Newton (1) in the liquid phase radiolysis of ethanol.

Can. J. Chem. Downloaded from www.nrcresearchpress.com by 210.87.254.5 on 09/05/12
For personal use only.

A mass balance for carbon, hydrogen, and oxygen has been worked out from the products and is presented in Table II. This mass balance corresponds to an empirical

TABLE II

Mass balance of carbon, hydrogen, and oxygen in the products obtained in the radiolysis of ethanol vapor

Product	G	Mass balance C	H	O
Hydrogen	7.6	—	15.2	—
Carbon monoxide	1.1	1.1	—	1.1
Methane	1.66	1.7	6.6	—
Ethylene	0.72	1.4	2.9	—
Ethane	0.23	0.5	1.4	—
Acetylene	0.03	0.1	0.1	—
Water	5.4	—	10.8	5.4
Formaldehyde	0.9	0.9	1.8	0.9
Acetaldehyde	4.5	9.0	18.0	4.5
Propanol	0.6	1.8	4.8	0.6
Butanol	0.19	0.8	1.9	0.2
1,2-Propanediol	0.15	0.5	1.2	0.3
2,3-Butanediol	1.2	4.8	12.0	2.4
	Total	22.2	76.7	15.4

NOTE: The numbers under C, H, and O in the table were obtained by multiplying the G value of the product by the respective number of atoms of C, H, or O in that product.

formula $C_{2.00}H_{6.76}O_{1.36}$, which has slightly more hydrogen and oxygen in it than does ethanol, C_2H_6O.

If water is generated only by reactions [3*c*] and [5*a*], then $G(H_2O)$ should be equal to 1.2. The excess water in G units is $(5.4-1.2) = 4.2$. If the corresponding amounts of H (8.4) and O (4.2) are subtracted from the mass balance in Table II, the empirical formula of the total products becomes $C_{2.00}H_{6.02}O_{0.99}$.

This good mass balance indicates that little or no polymer was formed during irradiation, unless polymer was a coproduct of the observed excess of water. It was also observed that the Po^{210}-alpha-particle source intensity showed no decrease during the ethanol irradiations. In the radiolysis of hydrocarbons (5, 8), there was a poor mass balance and a decrease in source intensity due to the deposition of polymer on the surface of the source. The lack of decrease in source intensity and a good mass balance in the ethanol products corroborate little or no polymer formation during the radiolysis of ethanol.

It might be mentioned that the decrease in the yields of CO, CH_4, and C_2H_4 between 0.5 and 4×10^{19} ev does not appear to be accompanied by a comparable decrease in the hydrogen yield (Fig. 1). Thus the decrease does not appear to be entirely a scavenging effect.

REFERENCES

1. W. R. McDONELL and A. S. NEWTON. J. Am. Chem. Soc. **76**, 4651 (1954).
2. A. S. NEWTON and W. R. McDONELL. J. Am. Chem. Soc. **78**, 4554 (1956).
3. J. G. BURR. J. Phys. Chem. **61**, 1477 (1957).
4. J. C. McLENNON and W. L. PATRICK. Can. J. Research, **5**, 470 (1931).
5. J. M. RAMARADHYA and G. R. FREEMAN. J. Chem. Phys. **34**, 1726 (1961).
6. L. F. FIESER. Experiments in organic chemistry. 3rd ed. D. C. Heath and Co., New York. 1955. p. 286.
7. G. W. C. MILNER. The principles and applications of polarography. Longmans Green and Co., New York. 1957.
8. J. M. RAMARADHYA and G. R. FREEMAN. To be published.
9. S. J. LAPPORTE. Angew. Chem. **72**, 759 (1960).

Can. J. Chem. Downloaded from www.nrcresearchpress.com by 210.87.254.5 on 09/05/12
For personal use only.

Can. J. Chem. Downloaded from www.nrcresearchpress.com by 210.87.254.40 on 09/05/12
For personal use only.

THE RADIOLYSIS OF ETHANOL

II. BINARY VAPOR MIXTURES[1]

J. M. RAMARADHYA[2] AND G. R. FREEMAN

ABSTRACT

Benzene and cyclohexene cause a marked decrease in the hydrogen yield from the vapor phase radiolysis of ethanol.

The experimental data were tested against the two reaction mechanisms that gave straight-line plots for the corresponding cyclohexane–protector systems. Both of these mechanisms also gave straight-line plots for the ethanol–protector systems.

One mechanism involved scavenging of hydrogen atoms. The values of the kinetic parameters derived from this mechanism are quite similar in the cyclohexane and ethanol systems.

The second mechanism involved the transfer of energy (excitation or ionization) from ethanol to the protector. The values of the kinetic parameters derived from this mechanism showed some differences between the ethanol and cyclohexane systems.

One possible reason for the lack of resolution between the two reaction mechanisms might be that they both occur to comparable extents. Two mechanisms appear to occur to comparable extents in the liquid cyclohexane system.

INTRODUCTION

In the isolation of steps in radiolytic mechanisms, the study of binary systems should be very helpful. In that connection, the radiolyses of mixtures of hydrocarbons have been frequently investigated (1–5). However, the radiolyses of organic compounds with functional groups and of their mixtures with other compounds are less common. As a part of a general program, we have investigated the vapor phase radiolysis of ethanol by Po^{210} alpha particles (6). Newton and McDonell (7) were the first to report the protection of liquid ethanol by acetaldehyde and by hexene. The present paper reports the results of a study of the protective effect of benzene and of cyclohexene on ethanol during radiolysis in the vapor phase.

EXPERIMENTAL

The ethanol used in these investigations was obtained from Reliance Chemical Ltd. and contained about 0.11 mole% water. The benzene was Eastman Kodak spectrograde and cyclohexene was from Matheson, Coleman and Bell. All the compounds were used without any further purification.

The apparatus used was a conventional vacuum manifold and the general techniques used in this investigation have been previously described (8, 9).

Binary vapor mixtures of ethanol and benzene or cyclohexene were irradiated at 108° C with Po^{210} alpha particles. The Po^{210} source (nominally 100 mc) was calibrated by Fricke dosimetry, using $G(Fe^{+++}) = 5.5$. The concentration of the protector in the vapor mixtures ranged from 2 to 100 mole% in each case. A quantity (1.6 ml) of well-degassed liquid solution was volatilized into a heated 1-liter reaction vessel that contained the Po^{210} source. The irradiation time was 2 hours. Approximately 0.01% of the sample was decomposed.

[1]*Manuscript received May 23, 1961.*
Contribution from the Department of Chemistry, University of Alberta, Edmonton, Alberta. Presented at the 139th American Chemical Society Meeting, St. Louis, Missouri, March 1961.
[2]*Present address: Consolidated Mining and Smelting Co., Trail, B.C.*

Can. J. Chem. Downloaded from www.nrcresearchpress.com by 210.87.254.40 on 09/05/12
For personal use only.

RESULTS

The radiolysis of pure ethanol vapor has been studied as a function of dose (6). The major single product was hydrogen, with smaller amounts of carbon monoxide, methane, ethane, ethylene, acetaldehyde, formaldehyde, vicinal glycols, and water. Under the conditions of the present work, only the total fraction volatile at −196° C (comprised of about 80% H_2, 10% CO, and 10% CH_4) could be measured accurately as a function of protector concentration.

The results are presented in Fig. 1. In these plots, the observed values of $G(-196)$,

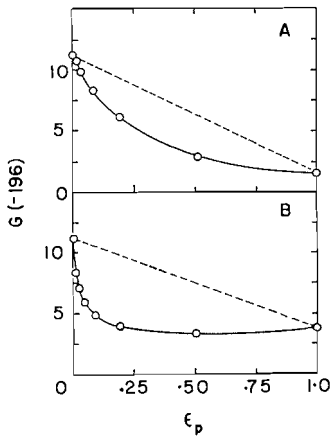


FIG. 1. G(−196), gas fraction volatile at −196° C, as a function of protector concentration: ϵ_p = electron fraction of protector P; (A) P = benzene; (B) P = cyclohexene.

the 100-ev yield of the gas fraction volatile at −196° C, are plotted against the "electron fraction" of the protector, ϵ_p. The value of $G(-196)$ decreases with increasing inhibitor concentration in both the systems. It is clear from Fig. 1 that cyclohexene reduces the yield of the −196° C fraction more rapidly than does benzene. The broken lines in the plots indicate the yield that might have been expected if there had been no interaction between the components and if the energy absorption were directly proportioned to the electron fraction of the compounds.

DISCUSSION

The experimental data were tested against the two reaction mechanisms that gave straight-line plots for the binary vapor mixtures of cyclohexane and benzene, cyclohexene, or propylene (9). The two mechanisms will be treated separately, making the simplifying assumption that the variation of the total gas fraction volatile at −196° C is a measure of the variation of the hydrogen yield.

I. Scavenging Mechanism

$$C_2H_5OH \xrightarrow{I} C_2H_5OH^* \quad [1]$$

$$C_2H_5OH^* \rightarrow H + C_2H_5O \text{ or } C_2H_4OH \quad [2]$$

$$H + C_2H_5OH \rightarrow H_2 + C_2H_4OH \quad [3]$$

$$H + P \rightarrow PH \quad [4]$$

$$H + P \rightarrow H_2 + P- \quad [5]$$

In the above, I represents the rate of formation of $C_2H_5OH^*$, P represents the protector, and PH and P— represent the corresponding radicals. The following equation can be derived by steady-state treatment of the above mechanism:

$$\left\{1+w\frac{(P)}{(C_2H_5OH)}\right\}\frac{I}{d(H_2)/dt} = 1+v\frac{(P)}{(C_2H_5OH)} = \rho,$$

where $w = k_5/k_3$, $v = (k_4+k_5)/k_3$, and ρ represents the left-hand side of the equation. The numerical values of $I/[d(H_2)/dt]$ were determined from the experimental data (4). By giving arbitrary values to w, sets of values of ρ were calculated. These sets of values were plotted against the ratio $(P)/(C_2H_5OH)$ to see whether a straight line with an intercept of unity could be obtained for each of benzene and cyclohexene. Such a line was obtained in each case (see Fig. 2). The values of the various ratios of rate con-

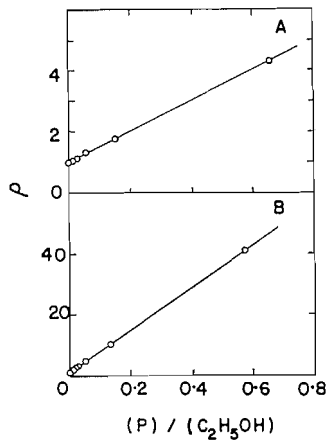


FIG. 2. Kinetic plots of mechanism I: $\rho = \{1+w[(P)/(C_2H_5OH)]\}I/[d(H_2)/dt]$; (A) P = benzene; (B) P = cyclohexene.

stants derived from these plots are shown in Table I. The corresponding values obtained in the cyclohexane systems (9) are given in parentheses.

TABLE I

Values of rate-constant ratios obtained from mechanism I

P	k_5/k_3	k_4/k_3	k_4/k_5
C_6H_6	0.9±0.3 (2.5±0.2)[a]	4.2±0.5 (5.9±0.5)	4.7 (2.4)
C_6H_{10}	20±5 (25±10)	50±10 (31±19)	2.5 (1.2)

[a]Corresponding cyclohexane system values given in parentheses.

It is apparent that the values obtained for the rate-constant ratios are rather similar in the cyclohexane and ethanol systems. While this similarity between the reactivities of ethanol and cyclohexane is not surprising (the rates of reaction of methyl radicals with cyclohexane and ethanol are approximately equal at 182° C and their activation energies are similar (10)), the same comments that were made in the earlier paper (9) can be

Can. J. Chem. Downloaded from www.nrcresearchpress.com by 210.87.254.40 on 09/05/12
For personal use only.

repeated here. The values of the rate-constant ratios obtained with cyclohexene might not be unreasonable. However, the value of k_5/k_3 obtained from benzene is surprisingly high, even if the hydrogen atoms are epithermal. It implies that abstraction of hydrogen atoms from benzene is as easy as from ethanol. The much stronger C—H bonds in benzene than in ethanol make this seem unlikely.

Now consider the second mechanism.

II. Energy (Ionization or Excitation) Transfer Mechanism

$$C_2H_5OH \xrightarrow{I'} C_2H_5OH^{**} \quad [1]$$

$$C_2H_5OH^{**} \rightarrow H_2 + \text{products} \quad [6]$$

$$C_2H_5OH^{**} + P \rightarrow C_2H_5OH + P^* \quad [7]$$

$$P^* \rightarrow xH_2 + \text{products}, \ 0 \leqslant x \leqslant 1 \quad [8]$$

The x signifies that perhaps not every P* results in the formation of a hydrogen molecule. Reactions [6] and [8] represent over-all processes and might comprise several steps each. Steady-state treatment of this mechanism yields

$$\{1+y(P)\}I'/d(H_2)/dt = 1+z(P) = \rho'$$

where $y = xk_7/k_6$, $z = k_7/k_6$, and ρ' represents the left-hand side of the equation. Assuming arbitrary values for y, sets of values of ρ' were calculated and plotted against the protector concentration (P), in an attempt to obtain a straight line with an intercept of unity. Figure 3 shows the lines that were obtained. The value of y that gave the desired

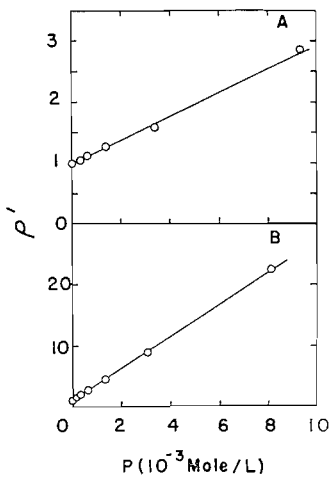


FIG. 3. Kinetic plots of mechanism II: $\rho' = \{1+y(P)\}I'/d(H_2)/dt$; (A) P = benzene; (B) P = cyclohexene.

line in each system, along with the slope of the line, z, and the corresponding value of x, are presented in Table II. The values obtained in the corresponding cyclohexane systems (9) are given in parentheses.

Can. J. Chem. Downloaded from www.nrcresearchpress.com by 210.87.254.40 on 09/05/12
For personal use only.

TABLE II

Values of kinetic parameters obtained from mechanism II

P	y (liter/mole)	x	z (k_7/k_6 (liter/mole))
C_6H_6	6±6 (150±18)[a]	0.03±0.03 (0.25±0.01)	190±20 (610±25)
C_6H_{10}	720±180 (1200±420)	0.28±0.01 (0.46±0.01)	2600±600 (2700±800)

[a]Corresponding cyclohexane system values given in parentheses.

Table II shows certain differences between the cyclohexane and ethanol systems. The apparent value of x (the fraction of the P*, activated by energy transfer from the substrate, that decomposes to yield H_2) is smaller in the ethanol systems than in the cyclohexane systems. Also, the apparent value of the ratio k_7/k_6 (the ratio of the rate of energy transfer to the rate of decomposition of the activated substrate species) is smaller in ethanol–benzene than in cyclohexane–benzene, while it is the same in the two systems containing cyclohexene.

It does not seem useful to speculate here upon the possible reasons for these similarities and differences. Further work, especially using compounds with widely differing ionization potentials and hydrogen-atom activities, is required.

It may be remarked, however, that one possible reason for the present lack of resolution between the scavenging and energy-transfer mechanisms might be that they both occur to comparable extents. Two mechanisms appear to occur to comparable extents in the liquid cyclohexane systems (4). It is possible that the rate constants and concentrations are such in the gas phase that the two mechanisms will be difficult to resolve.

REFERENCES

1. C. S. SCHOEPFLE and C. H. FELLOWS. Ind. Eng. Chem. **23**, 1396 (1931).
2. J. P. MANION and M. BURTON. J. Phys. Chem. **56**, 560 (1952).
3. M. BURTON and W. M. PATRICK. J. Phys. Chem. **58**, 424 (1954).
4. G. R. FREEMAN. J. Chem. Phys. **33**, 71 (1960).
5. G. R. FREEMAN. Can. J. Chem. **38**, 1043 (1960).
6. J. M. RAMARADHYA and G. R. FREEMAN. Can. J. Chem. This issue. p. 1836.
7. A. S. NEWTON and W. R. MCDONELL. J. Am. Chem. Soc. **78**, 4554 (1956).
8. J. M. RAMARADHYA and G. R. FREEMAN. J. Chem. Phys. **34**, 1726 (1961).
9. J. M. RAMARADHYA and G. R. FREEMAN. Can. J. Chem. This issue. p. 1769.
10. A. F. TROTMAN-DICKENSON. Gas kinetics. Butterworth's Scientific Publications, London. 1955. pp. 200–201.

Can. J. Chem. Downloaded from www.nrcresearchpress.com by 210.87.254.40 on 09/05/12
For personal use only.

Can. J. Chem. Downloaded from www.nrcresearchpress.com by 210.87.254.5 on 09/05/12
For personal use only.

NOTES

β,β,β-TRIFLUOROLACTIC ACID[1]

SUMNER H. BURSTEIN AND H. J. RINGOLD

In a search for inhibitors of lactic acid dehydrogenase it was of interest to prepare and evaluate the hitherto unknown β,β,β-trifluorolactic acid. Our synthesis was effected by a straightforward route patterned after the preparation of α-methyl-β,β,β-trifluorolactic acid (1). Trifluoroacetaldehyde (2) was treated with hydrogen cyanide and the intermediate cyanohydrin was hydrolyzed by vigorous treatment with sulphuric acid to yield the desired *dl*-acid as a crystalline solid.

Trifluorolactic acid and its sodium salt were not oxidized by a crystalline rabbit muscle lactic dehydrogenase in the presence of DPN nor did they inhibit the enzymatic oxidation of sodium lactate or the reduction of sodium pyruvate. The procedure used was similar to that described by Busch and Nair (3) and by Baker and co-workers (4).

EXPERIMENTAL

The infrared spectrum was determined with a Beckman model IR4 instrument, while ultraviolet determinations were made with a Carey model 14 recording spectrophotometer.

β,β,β-Trifluorolactic Acid

Cold 16 *N* sulphuric acid (108 ml) was added dropwise over a period of 1 hour to a solution of trifluoroacetaldehyde hydrate (2) (39.2 g), potassium cyanide (21.6 g), and water (83 ml), held at 0–5°. The mixture was then allowed to come to room temperature and stand for 16 hours. Extraction with ether (4×125 ml), removal of solvent after sodium sulphate drying, and distillation of the residue at reduced pressure gave 33.3 g of intermediate cyanohydrin,[2] b.p. 75–76° (45 mm). The cyanohydrin (30 g) was added dropwise over a 10-minute period to concentrated sulphuric acid (29 ml) with a considerable evolution of heat ensuing as well as the appearance of a thick precipitate. The temperature was slowly raised to 120° and held there for 15 minutes before the mixture was cooled and cautiously diluted with ice water (150 ml). The resulting solution was boiled for 10 hours under reflux and then cooled, saturated at room temperature with sodium sulphate, and extracted with ether (4×125 ml). The ether extract was washed once with saturated sodium sulphate and then dried, and the solvent removed at atmospheric pressure. The residue was distilled at 60–95° (1–2 mm) through a short-path condenser and yielded 23.6 g of β,β,β-trifluorolactic acid as a solid, m.p. 64–67°. An analytical specimen was obtained by recrystallization from methylene chloride – pentane, m.p. 68–69°. Infrared: λ_{max}^{KBr} 5.69 μ. Anal. Calc. for $C_3H_3F_3O_3$: C, 25.01; H, 2.10; F, 39.57. Found: C, 25.42; H, 2.28; F, 39.35.

Attempted Enzymatic Oxidation of Trifluorolactic Acid and Inhibition Studies

The following solutions were added successively to a cuvette: 0.1 *M* phosphate buffer, pH 8.5 (2.7 ml), lactic dehydrogenase[3] (5γ in 0.1 ml of buffer), DPN (1.2 mg in 0.1 ml

[1]*This work was aided by grant No. T-185 from the American Cancer Society.*
[2]*A sample of cyanohydrin allowed to stand for 1 week at room temperature polymerized.*
[3]*Purchased from Worthington Biochemical Corporation.*

of water), and trifluorolactic acid or sodium trifluorolactate (1–40 mg in 0.1 ml phosphate buffer). Readings were taken at 15-second intervals in the spectrophotometer at 340 mμ to follow the appearance of DPNH but no oxidation of substrate occurred over a 30-minute period. When sodium *dl*-lactate (2.2 mg in 0.1 ml of phosphate buffer) was substituted for trifluorolactate, DPNH appeared at an initial rate of 0.05 optical density units per 15 seconds and the addition of varying amounts of trifluorolactate (1–40 mg) did not influence the rate of oxidation.

The reduction of pyruvate to lactate was carried out by the addition to a cuvette of 0.1 *M* phosphate buffer, pH 7.4 (2.7 ml), lactic dehydrogenase (5γ in 0.1 ml of buffer), DPNH (0.3 mg in 0.1 ml of water), and sodium pyruvate (0.55 mg in 0.1 ml of buffer). Readings at 340 mμ showed an initial decrease of 0.2 optical density units per 15 seconds. The addition of up to 10 mg of sodium trifluorolactate in buffer solution, previous to the addition of sodium pyruvate, did not inhibit the reduction of pyruvate.

1. R. A. Darral, F. Smith, M. Stacey, and J. C. Tatlow. J. Chem. Soc. 2329 (1959).
2. M. Braid, H. Iserson, and F. E. Lawlor. J. Am. Chem. Soc. **76**, 4027 (1954).
3. H. Busch and P. V. Nair. J. Biol. Chem. **229**, 377 (1957).
4. B. R. Baker, W. W. Lee, W. A. Skinner, A. P. Martinez, and E. Tong. J. Med. Pharm. Chem. **2**, 633 (1960).

Received May 26, 1961.
Worcester Foundation for
Experimental Biology,
Shrewsbury, Massachusetts.

CARBONIUM PERCHLORATES IN CHLOROFORM SOLUTION

A. L. Gatzke and Ross Stewart

In connection with other work on the spectra of carbonium ions, we have examined the behavior of triarylmethyl perchlorates in chloroform solution. The lowering in the apparent degree of ionization (1–12) of triarylmethyl salts dissolved in organic solvents has been the subject of some speculation. Several reactions might occur, including: (*a*) repression of the ionization of carbonium salts in the organic medium (1) (eq. [1]); (*b*) co-ordination of the carbonium ion with a solvent molecule, for example ether (4, 12) or acetone (7) (eq. [2]); and (*c*) solvolysis reactions (10) which would include both the reaction of the carbonium ion with an organic solvent molecule, for example nitromethane (9) (eq. [3]), and hydrolysis to the carbinol by traces of water remaining in the imperfectly dried solvents (11) (eq. [4]).

$$Ar_3C^+Y^- \rightleftharpoons Ar_3C{-}Y \qquad [1]$$

$$Ar_3C^+Y^- + (CH_3)_2CO \rightleftharpoons Ar_3C{-}\overset{+}{O}{=}C(CH_3)_2 \; Y^- \qquad [2]$$

$$Ar_3C^+Y^- + CH_3NO_2 \rightarrow Ar_3CCH_2NO_2 + HY \qquad [3]$$

$$Ar_3C^+Y^- + H_2O \rightleftharpoons Ar_3C{-}OH_2^+Y^- \rightleftharpoons Ar_3COH + HY \qquad [4]$$

Can. J. Chem. Downloaded from www.nrcresearchpress.com by 210.87.254.5 on 09/05/12
For personal use only.

of water), and trifluorolactic acid or sodium trifluorolactate (1–40 mg in 0.1 ml phosphate buffer). Readings were taken at 15-second intervals in the spectrophotometer at 340 mμ to follow the appearance of DPNH but no oxidation of substrate occurred over a 30-minute period. When sodium *dl*-lactate (2.2 mg in 0.1 ml of phosphate buffer) was substituted for trifluorolactate, DPNH appeared at an initial rate of 0.05 optical density units per 15 seconds and the addition of varying amounts of trifluorolactate (1–40 mg) did not influence the rate of oxidation.

The reduction of pyruvate to lactate was carried out by the addition to a cuvette of 0.1 *M* phosphate buffer, pH 7.4 (2.7 ml), lactic dehydrogenase (5γ in 0.1 ml of buffer), DPNH (0.3 mg in 0.1 ml of water), and sodium pyruvate (0.55 mg in 0.1 ml of buffer). Readings at 340 mμ showed an initial decrease of 0.2 optical density units per 15 seconds. The addition of up to 10 mg of sodium trifluorolactate in buffer solution, previous to the addition of sodium pyruvate, did not inhibit the reduction of pyruvate.

1. R. A. Darral, F. Smith, M. Stacey, and J. C. Tatlow. J. Chem. Soc. 2329 (1959).
2. M. Braid, H. Iserson, and F. E. Lawlor. J. Am. Chem. Soc. **76**, 4027 (1954).
3. H. Busch and P. V. Nair. J. Biol. Chem. **229**, 377 (1957).
4. B. R. Baker, W. W. Lee, W. A. Skinner, A. P. Martinez, and E. Tong. J. Med. Pharm. Chem. **2**, 633 (1960).

Received May 26, 1961.
Worcester Foundation for
Experimental Biology,
Shrewsbury, Massachusetts.

CARBONIUM PERCHLORATES IN CHLOROFORM SOLUTION

A. L. Gatzke and Ross Stewart

In connection with other work on the spectra of carbonium ions, we have examined the behavior of triarylmethyl perchlorates in chloroform solution. The lowering in the apparent degree of ionization (1–12) of triarylmethyl salts dissolved in organic solvents has been the subject of some speculation. Several reactions might occur, including: (*a*) repression of the ionization of carbonium salts in the organic medium (1) (eq. [1]); (*b*) co-ordination of the carbonium ion with a solvent molecule, for example ether (4, 12) or acetone (7) (eq. [2]); and (*c*) solvolysis reactions (10) which would include both the reaction of the carbonium ion with an organic solvent molecule, for example nitromethane (9) (eq. [3]), and hydrolysis to the carbinol by traces of water remaining in the imperfectly dried solvents (11) (eq. [4]).

$$Ar_3C^+Y^- \rightleftharpoons Ar_3C{-}Y \qquad [1]$$

$$Ar_3C^+Y^- + (CH_3)_2CO \rightleftharpoons Ar_3C{-}\overset{+}{O}{=}C(CH_3)_2 \; Y^- \qquad [2]$$

$$Ar_3C^+Y^- + CH_3NO_2 \rightarrow Ar_3CCH_2NO_2 + HY \qquad [3]$$

$$Ar_3C^+Y^- + H_2O \rightleftharpoons Ar_3C{-}OH_2^+Y^- \rightleftharpoons Ar_3COH + HY \qquad [4]$$

Can. J. Chem. Downloaded from www.nrcresearchpress.com by 210.87.254.5 on 09/05/12
For personal use only.

We have examined chloroform as a solvent since it is unlikely to co-ordinate with carbonium ions. Unlike carbon tetrachloride, however, it will dissolve reasonable amounts of carbonium salts.

EXPERIMENTAL

Solvents

Reagent grade chloroform was washed with 95% sulphuric acid followed by repeated washings with distilled water and was then dried over $CaCl_2$ and P_2O_5. Distillation under nitrogen from Drierite through a 30-cm fractionating column yielded a fraction which was stored in a dark bottle under nitrogen over anhydrous potassium carbonate. The bottle was equipped with a drying tube and a siphoning arrangement. Partially dried solvents were prepared in the same manner but were dried for shorter periods. "Wet" chloroform was prepared by saturating this material with water at 10°. Its water content was estimated from solubility data to be 3.5×10^{-2} *M*.

Reagents

Triphenylmethyl perchlorate and tris-*p*-methoxyphenylmethyl perchlorate were prepared essentially as described by Hofmann and Kirmreuther (13). Tri-*p*-tolylmethyl perchlorate was prepared by the addition of perchloric acid and dry ether to an acetic anhydride solution of the carbinol. The product was recrystallized from acetic anhydride – ether and freed from solvent under vacuum. Titration with standard potassium hydroxide gave a molecular weight of 389; calculated, 384. Tri-*p*-tolylcarbinol was prepared by the Grignard reaction of *p*-tolylmagnesium bromide on di-*p*-tolyl ketone. The crude product was purified through the chloride which was then hydrolyzed by sulphuric acid to the carbinol. Recrystallization from petroleum ether gave the product, m.p. 94–96°.

Measurements

A sample of the perchlorate (5–15 mg) was weighed into a dry volumetric flask and dissolved in acetic anhydride. Aliquots (0.05–0.5 ml) of this solution were transferred to 5-ml volumetric flasks and evaporated to dryness under vacuum. Dry air was then admitted to the flask. The succeeding operations of filling the flask with solvent and then filling the glass-stoppered absorption cells with solvent were carried out in a dry box. Light absorption measurements were made on a Beckman DU or a Cary, Model 14 spectrophotometer. Since the color intensities in the chloroform were temperature dependent (except for the *p*-methoxy compound) the cell compartment was kept at 25.0±0.2°. Optical densities of more-concentrated solutions were measured using 0.1-cm cells. A very rapid initial partial fading, which could not be followed, occurred with the tri-*p*-tolyl and triphenyl compounds. This was followed by a slow fading reaction which obeyed exact second-order kinetics. This was corrected for by extrapolation to zero time.

RESULTS

The absorption spectra of the triarylmethyl perchlorates in chloroform in the visible region were very similar to those obtained in 50–70% sulphuric acid* except that the absorption maxima were shifted from 2–8 mμ to the red. The quantity $D_{\lambda_{max}}/\int Dd_\lambda$, the

**We have observed that the carbonium ion spectrum for each of these compounds is altered in more-concentrated sulphuric acid. These changes, which are still being investigated, become marked in regions above 80%, 100%, and 102% sulphuric acid for tris-p-methoxyphenylmethyl, tri-p-tolylmethyl, and triphenylmethyl cations, respectively, and may account for some of the discrepancies in carbonium ion spectra reported in the literature.*

Can. J. Chem. Downloaded from www.nrcresearchpress.com by 210.87.254.5 on 09/05/12
For personal use only.

optical density at the wavelength maxima divided by the area under the curve, was identical to within 2% in sulphuric acid and chloroform.

The variation of optical density with concentration of dissolved salt is shown in Fig. 1

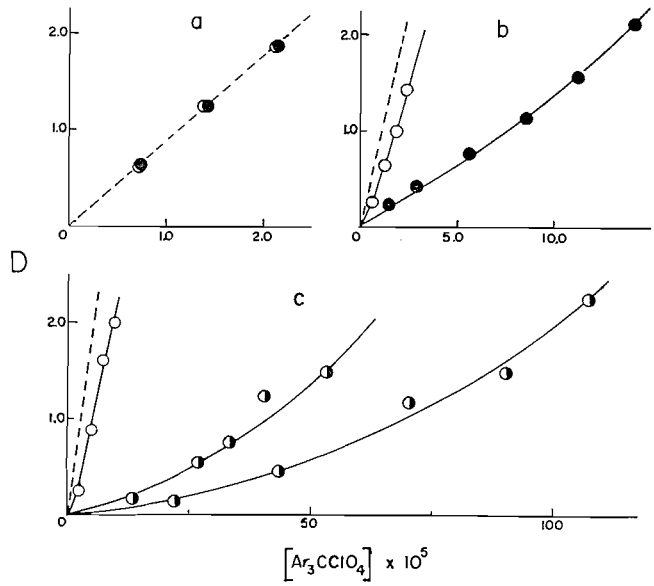


FIG. 1. Variation of optical density with molarity of dissolved triarylmethyl perchlorate. (*a*) $(p\text{-}CH_3OC_6H_4)_3C^+ClO_4^-$, (*b*) $(p\text{-}CH_3C_6H_4)_3C^+ClO_4^-$, (*c*) $(C_6H_5)_3C^+ClO_4^-$; ○ dry $CHCl_3$, ◑ partially dried $CHCl_3$, ● wet $CHCl_3$; the broken line corresponds to the extinction coefficient found for the carbonium ions in H_2SO_4 (Table I).

TABLE I

Spectral data for carbonium perchlorates

Tris-*p*-methoxyphenol			Tri-*p*-tolyl			Triphenyl		
Solvent	λ_{max} (mμ)	$\epsilon \times 10^{-4}$	Solvent	λ_{max} (mμ)	$\epsilon \times 10^{-4}$	Solvent	λ_{max} (mμ)	$\epsilon \times 10^{-4}$
56.8% H_2SO_4	484	8.8	83.0% H_2SO_4	452	9.0	96.0% H_2SO_4	433	3.8
$CHCl_3$	492		$CHCl_3$	454		$CHCl_3$	435	

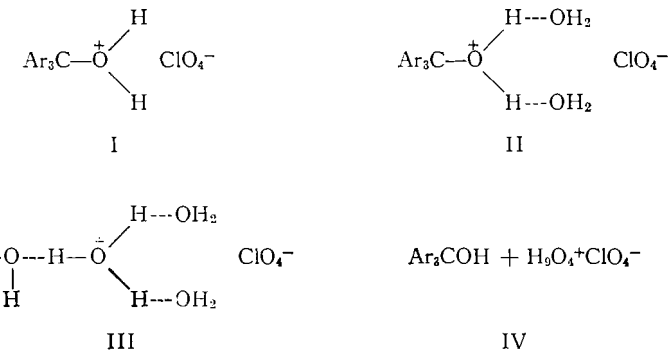
for the three carbonium perchlorates dissolved in both "dry" and "wet" chloroform. It can be seen that the ionization of tris-*p*-methoxyphenylmethyl perchlorate is complete in both wet and dry chloroform and that hydrolysis of this highly resonance stabilized carbonium ion does not proceed to a measurable extent. (The excellent agreement in Fig. 1*a* between the experimental points for chloroform solution and the line for 56.8% sulphuric acid may be fortuitous since a somewhat *higher* extinction coefficient has been reported for this ion in nitrobenzene (3).)

Tri-*p*-tolylmethyl perchlorate and triphenylmethyl perchlorate both show a reduction in the concentration of carbonium ion, particularly the triphenyl compound in the partially dried solvent (Fig. 1*c*). A wet chloroform solution of the latter could not be studied since a turbid solution resulted when sufficient perchlorate was used to produce a measurable color. The difficulty in obtaining reproducibly "dry" samples of chloroform precludes any exact comparison between the three perchlorates in the dried and partially dried solvents.

Can. J. Chem. Downloaded from www.nrcresearchpress.com by 210.87.254.5 on 09/05/12
For personal use only.

Since all the triarylmethyl perchlorates are highly colored in the solid state, it is generally believed that covalent forms of these compounds are unimportant. The approach, in the present cases, to complete ionization, which accompanies rigorous drying of the solvent is in accord with this. The slow fading of the carbonium ion color may be due to a solvolysis reaction corresponding to eq. [3] or to ether formation, but it seems unlikely that the very fast initial decrease in color could be due to this. We believe, in fact, that the latter effect is due to the rapid hydrolysis of the carbonium perchlorate ion pair by the small amount of water present and that the curves in Fig. 1 are explained by the equilibria shown in eq. [4]. (Traces of acid present in the chloroform would reverse these reactions but we believe that acids are absent since prolonged treatment with anhydrous potassium carbonate always *increased* the apparent extinction coefficient.)

There are several possible structures for the colorless hydrolysis product, and their relative concentrations should depend on the amount of water present.



Specific solvation effects such as those shown above involving hydrogen bonding (14, 15) will be most important in the low dielectric solvent chloroform. With a limited amount of water it seems likely that I would be formed whereas in the wetter solutions the carbinol would be expected to become less and less important in the dispersal of the positive charge. That is, the ion pairs II, III, and eventually IV, the carbinol plus the normal hydrated form of perchloric acid (16, 17), should become the principal cations in solution.

ACKNOWLEDGMENT

The financial support of the Research Corporation is gratefully acknowledged.

1. A. HANTZSCH. Ber. **54**, 2573 (1921).
2. A. G. EVANS, A. PRICE, and J. H. THOMAS. J. Chem. Soc. 52, 332 (1956).
3. E. PRICE and N. N. LICHTIN. Tetrahedron Letters, **18**, 10 (1960).
4. J. E. LEFFLER. The reactive intermediates of organic chemistry. Interscience Publishers, New York. 1956. pp. 96–98.
5. K. ZIEGLER and H. WOLLSCHITT. Ann. **479**, 90 (1930).
6. N. N. LICHTIN and N. P. LEFTIN. J. Phys. Chem. **60**, 164 (1956).
7. I. LIFSHITZ and G. GIRBES. Ber. **61**, 1463 (1928).
8. D. W. A. SHARP and N. SHEPPARD. J. Chem. Soc. 674 (1957).
9. H. BURTON and G. W. H. CHEESEMAN. J. Chem. Soc. 832 (1953).
10. A. HANTZSCH and A. BURAWOY. Ber. **63**, 1181 (1930).
11. N. DILTHEY and W. AUFLAUS. Ber. **62**, 2078 (1929).
12. W. B. SMITH and P. S. RAO. J. Org. Chem. **26**, 254 (1961).
13. K. A. HOFMANN and H. KIRMREUTHER. Ber. **43**, 185 (1910). H. J. DAUBEN, Jr., L. R. HONNEN, and K. M. HARMON. J. Org. Chem. **25**, 1442 (1960).

Can. J. Chem. Downloaded from www.nrcresearchpress.com by 210.87.254.5 on 09/05/12
For personal use only.

14. R. W. TAFT, Jr. J. Am. Chem. Soc. **82**, 2965 (1960).
15. H. J. CAMPBELL and J. T. EDWARD. Can. J. Chem. **38**, 2109 (1960).
16. D. G. TUCK and R. W. DIAMOND. Proc. Roy. Soc. (London), A, **228**, 322 (1955).
17. R. P. BELL. The proton in chemistry. Cornell University Press, Ithaca, N.Y. 1959. p. 83.

RECEIVED MAY 11, 1961.
DEPARTMENT OF CHEMISTRY,
UNIVERSITY OF BRITISH COLUMBIA,
VANCOUVER, B.C.

Can. J. Chem. Downloaded from www.nrcresearchpress.com by 210.87.254.5 on 09/05/12
For personal use only.

THE POLARIZATION OF THE FLUORESCENCE OF 1- AND 2-NAPHTHOIC ACID[1]

ROBIN M. HOCHSTRASSER

The naphthoic acids have received considerable spectroscopic attention within recent years. Weller (1) and, more recently, Porter and Jackson (2) have determined pK values for the lowest excited states of the molecule. Kasha and El Bayoumi (3) have measured solvent spectral shifts in solution. Hochstrasser examined the fluorescence and phosphorescence spectra in various solvents (10).

Porter and Jackson concluded that excitation to the lowest excited singlet level of the acids involves an orbital promotion of the type $n \rightarrow \pi^*$. This conclusion was based on the vastly different pK values for the molecule in its ground and first excited singlet state. The large difference in pK (pK^* − pK = 8 units) quoted by these authors applies to the protonated acid − acid equilibrium and not, as stated, to the acid–anion equilibrium (1). The value of ΔpK for the anionic system is about 2–4 units (5). Therefore the conclusions regarding the orbital nature of the lowest excited singlet level are not convincing.

On the basis of absorption intensity and solvent effects, El Bayoumi and Kasha assumed that the first excited singlet state is of π,π^* character, for which only slight changes of acid strength would be predicted.

Absorption spectra need not always provide proof of the character of the *lowest excited level* of a molecule. If absorption to this state is very weak, as for example would be the case for an $n \rightarrow \pi^*$ transition, a nearby strong transition, e.g. $\pi \rightarrow \pi^*$, could mask the weak transition. This is especially true for organic acids since the absorption spectra are characteristically diffuse.

Fluorescence originates from the lowest excited singlet level for essentially all common polyatomic molecules. Thus only by means of emission studies of diffuse spectra can conclusive date be obtained for extremely weak bands which lie very close to stronger bands. In this note some results on the polarized emission spectra of thin crystals of 1- and 2-naphthoic acid are presented in order to determine the direction of the transition moment connecting the ground and emitting levels.

The crystal structures of 1-naphthoic acid (6) and of 2-naphthoic acid (7) are known and these provide the exact orientations of the molecules in the unit cell. For both acids the crystal is composed of planar dimeric units and for 1-naphthoic acid the normal to the dimer plane is nearly coincident with the crystallographic b-axis. Very thin ($\sim$30 μ), microscopically perfect plates were prepared by sublimation. The crystals were mounted on quartz disks with the b-axis vertical and the blue fluorescence (excited by Hg 3130 Å) was observed normal to the *100* face. The emission was analyzed by a polaroid sheet

[1]*This work was supported by a grant from the National Research Council of Canada.*

14. R. W. TAFT, Jr. J. Am. Chem. Soc. **82**, 2965 (1960).
15. H. J. CAMPBELL and J. T. EDWARD. Can. J. Chem. **38**, 2109 (1960).
16. D. G. TUCK and R. W. DIAMOND. Proc. Roy. Soc. (London), A, **228**, 322 (1955).
17. R. P. BELL. The proton in chemistry. Cornell University Press, Ithaca, N.Y. 1959. p. 83.

RECEIVED MAY 11, 1961.
DEPARTMENT OF CHEMISTRY,
UNIVERSITY OF BRITISH COLUMBIA,
VANCOUVER, B.C.

Can. J. Chem. Downloaded from www.nrcresearchpress.com by 210.87.254.6 on 09/05/12
For personal use only.

THE POLARIZATION OF THE FLUORESCENCE OF 1- AND 2-NAPHTHOIC ACID[1]

ROBIN M. HOCHSTRASSER

The naphthoic acids have received considerable spectroscopic attention within recent years. Weller (1) and, more recently, Porter and Jackson (2) have determined pK values for the lowest excited states of the molecule. Kasha and El Bayoumi (3) have measured solvent spectral shifts in solution. Hochstrasser examined the fluorescence and phosphorescence spectra in various solvents (10).

Porter and Jackson concluded that excitation to the lowest excited singlet level of the acids involves an orbital promotion of the type $n \rightarrow \pi^*$. This conclusion was based on the vastly different pK values for the molecule in its ground and first excited singlet state. The large difference in pK (pK^* − pK = 8 units) quoted by these authors applies to the protonated acid − acid equilibrium and not, as stated, to the acid–anion equilibrium (1). The value of ΔpK for the anionic system is about 2–4 units (5). Therefore the conclusions regarding the orbital nature of the lowest excited singlet level are not convincing.

On the basis of absorption intensity and solvent effects, El Bayoumi and Kasha assumed that the first excited singlet state is of π,π^* character, for which only slight changes of acid strength would be predicted.

Absorption spectra need not always provide proof of the character of the *lowest excited level* of a molecule. If absorption to this state is very weak, as for example would be the case for an $n \rightarrow \pi^*$ transition, a nearby strong transition, e.g. $\pi \rightarrow \pi^*$, could mask the weak transition. This is especially true for organic acids since the absorption spectra are characteristically diffuse.

Fluorescence originates from the lowest excited singlet level for essentially all common polyatomic molecules. Thus only by means of emission studies of diffuse spectra can conclusive date be obtained for extremely weak bands which lie very close to stronger bands. In this note some results on the polarized emission spectra of thin crystals of 1- and 2-naphthoic acid are presented in order to determine the direction of the transition moment connecting the ground and emitting levels.

The crystal structures of 1-naphthoic acid (6) and of 2-naphthoic acid (7) are known and these provide the exact orientations of the molecules in the unit cell. For both acids the crystal is composed of planar dimeric units and for 1-naphthoic acid the normal to the dimer plane is nearly coincident with the crystallographic b-axis. Very thin ($\sim$30 μ), microscopically perfect plates were prepared by sublimation. The crystals were mounted on quartz disks with the b-axis vertical and the blue fluorescence (excited by Hg 3130 Å) was observed normal to the *100* face. The emission was analyzed by a polaroid sheet

[1]*This work was supported by a grant from the National Research Council of Canada.*

and detected by our modified Hilger E2 spectrograph (4). The emitted intensities polarized parallel to the crystallographic axes were either maximal or minimal. The spectra was measured with the crystals at 300° K.

Crystallographic Data

The data of Trotter (6, 7) were used for the descriptions that follow. 'Oriented gas' intensity ratios were calculated from known atomic co-ordinates.

1-Naphthoic acid.—The crystal is monoclinic (space group $P2_1/a$) with $\beta = 92.2°$. The unit-cell dimensions are $a = 31.12$, $b = 3.87$, $c = 6.92$ Å. The acid crystallizes, either from solution or after sublimation, in prisms which are elongated along the b-axis with (*100*) developed. The aromatic rings of the centrosymmetric dimer and the carboxyl (hydrogen-bonded) ring are not in the same plane. The deviation from coplanarity amounts to approximately 11°. The 'oriented gas' intensity ratio for a transition polarized perpendicular to the carboxyl plane is $I_b/I_c = 2.6$ while the value of this ratio for moments perpendicular to the aromatic ring planes is 4.2. The molecules are so arranged in the crystal that a line with any direction, but lying on the molecular plane (aromatic *or* carboxyl), always has a larger projection on the c than on the b crystallographic axis. This line need only deviate by a small angle from the plane for I_b/I_c to exceed unity. For example, the values of I_c/I_b (in parenthesis) for the lines joining certain carbon atoms of the 1-naphthyl group are as follows: 1,4 (4.5); 2,7 (6.9); 1,5 (1.4); 2,6 (6.3). Thus, for this crystal, a measurement of the dichroic ratio in absorption or the intensity ratio in emission normal to the (*100*) face should indicate unambiguously whether or not the electronic transition is polarized in or out of plane.

2-Naphthoic acid.—The crystal is monoclinic ($P2_1/a$) with $\beta = 92.6°$; $a = 30.59$, $b = 5.00$, $c = 5.63$ Å. The acid crystallizes as prisms elongated along the b-axis and sublimation flakes are developed on (*100*). The aromatic and carboxyl planes are parallel within experimental limits. The intensity ratio normal to (*100*) cannot give nearly so much information in this case. Both in-plane and out-of-plane transitions may be b-polarized. Values of I_b/I_c are as follows: 1.43 (normal to the plane of the dimer); 4.0 (longest axis of naphthyl); 3.6 (shortest axis of naphthyl). If the measured value is greater than 1.43 yet less than 3.6 there is good indication that the transition moment lies in the molecular plane.

The Fluorescence of 1-Naphthoic Acid

The emission spectrum is a broad band with a peak intensity at 4415 Å. The intensity ratio I_c/I_b was 1.8:1. The polarization ratio is consistent with a transition moment in the molecular plane, directed along a line which joins the bisectors of 1—2 and 5—6 bonds of a naphthalene ring. However, this conclusion neglects crystal-induced mixing of oppositely polarized states which could considerably modify the presently assumed 'oriented gas' model.

The Fluorescence of 2-Naphthoic Acid

The fluorescence was broad and structureless with an intensity maximum at 4565 Å. The polarization ratio was $I_b/I_c = 1.7$, which suggests a transition moment in the plane of the molecule.

The Assignment of the Nature of the Transitions

$n \rightarrow \pi^*$ promotional transitions correspond to the promotion of an electron from the lone-pair orbital of the carbonyl oxygen (or the acidic oxygen) into an antibonding π-orbital which is mainly localized on the carbonyl group. Such transitions between

Can. J. Chem. Downloaded from www.nrcresearchpress.com by 210.87.254.6 on 09/05/12
For personal use only.

orbitals which are respectively symmetric and antisymmetric to reflection in the molecular plane are necessarily polarized perpendicular to the molecular plane. $\pi \rightarrow \pi^*$ transitions are polarized in the molecular plane. The allowed levels in the C_{2h} symmetry of the dimer are B_u (x- and y-polarized) and A_u (z or $\perp$ polarization). Therefore the vibronic symmetry of the emitting level is B_u and the nature of the transition from this level to the ground state is $B_u \rightarrow A_g$ ($n^2\pi\pi^* \rightarrow n^2\pi^2$).

The excited states of the monomer are probably split by exciton interaction (8) in the dimer. If the monomeric lowest excited level is considered to lie in the plane and along the long axis of the aromatic ring, the resulting dimer states are A_g and B_u in order of increasing energy. Fluorescence from a dimer of this type would be an electronically forbidden transition. The order of dimer states is inverted for short-axis transition moments in the monomer. It is very likely that the lowest transition of the monomer involves contributions from both polarizations as in the case of unsubstituted naphthalene (9).

The transition-moment direction calculated from the observed polarization ratio for 1-naphthoic acid should correspond to the resultant of the monomeric moments. A theoretical computation (dipole–dipole approximation) of the dimer levels which arise from the interaction of two monomeric states of this nature yields the result that the lowest excited dimer level has B_u symmetry. This is consistent with the notion that the observed emission involves an allowed electronic transition $B_u \rightarrow A_g$ and is not mainly a vibronically allowed combination as would have to be the case if the lowest dimer excited state had the symmetry A_g.

Further results of the 1-naphthoic acid crystal are in preparation.

1. A. Weller and W. Urban. Angew. Chem. **66**, 637 (1954).
2. G. Porter and G. Jackson. Proc. Roy. Soc. (London), **260**, 13 (1961).
3. M. Ashraf El Bayoumi and M. Kasha. Molecular exciton interaction in H-bonded complexes. In preparation.
4. R. M. Hochstrasser. Can. J. Chem. **39**, 459 (1961).
5. A. Weller. Private communication.
6. J. Trotter. Acta Cryst. **13**, 732 (1960).
7. J. Trotter. Acta Cryst. **14**, 101 (1961).
8. M. Kasha and E. G. McRae. J. Chem. Phys. **28**, 721 (1958).
9. D. P. Craig, L. E. Lyons, S. H. Walmsley, and J. R. Walsh. Proc. Chem. Soc. 389 (1959).
10. R. M. Hochstrasser. Can. J. Chem. This issue.

Received May 25, 1961.
Chemistry Department,
University of British Columbia,
Vancouver 8, B.C.

IMPROVED PREPARATION OF BISTRIFLUOROMETHYLARSINE*

W. R. Cullen

Bistrifluoromethylarsine was first prepared by reducing iodobistrifluoromethylarsine with either lithium aluminum hydride (16% yield) or zinc and hydrochloric acid (43% yield) (1). The reduction of chlorobistrifluoromethylarsine with lithium aluminum hydride has been reported to proceed smoothly at ca. −25°, giving a higher yield of bistrifluoromethylarsine (70%) (2). It has now been found that this method is unreliable

*This research was supported by a grant from the National Research Council of Canada.

Can. J. Chem. Downloaded from www.nrcresearchpress.com by 210.87.254.6 on 09/05/12
For personal use only.

orbitals which are respectively symmetric and antisymmetric to reflection in the molecular plane are necessarily polarized perpendicular to the molecular plane. $\pi \rightarrow \pi^*$ transitions are polarized in the molecular plane. The allowed levels in the C_{2h} symmetry of the dimer are B_u (x- and y-polarized) and A_u (z or $\perp$ polarization). Therefore the vibronic symmetry of the emitting level is B_u and the nature of the transition from this level to the ground state is $B_u \rightarrow A_g$ ($n^2\pi\pi^* \rightarrow n^2\pi^2$).

The excited states of the monomer are probably split by exciton interaction (8) in the dimer. If the monomeric lowest excited level is considered to lie in the plane and along the long axis of the aromatic ring, the resulting dimer states are A_g and B_u in order of increasing energy. Fluorescence from a dimer of this type would be an electronically forbidden transition. The order of dimer states is inverted for short-axis transition moments in the monomer. It is very likely that the lowest transition of the monomer involves contributions from both polarizations as in the case of unsubstituted naphthalene (9).

The transition-moment direction calculated from the observed polarization ratio for 1-naphthoic acid should correspond to the resultant of the monomeric moments. A theoretical computation (dipole–dipole approximation) of the dimer levels which arise from the interaction of two monomeric states of this nature yields the result that the lowest excited dimer level has B_u symmetry. This is consistent with the notion that the observed emission involves an allowed electronic transition $B_u \rightarrow A_g$ and is not mainly a vibronically allowed combination as would have to be the case if the lowest dimer excited state had the symmetry A_g.

Further results of the 1-naphthoic acid crystal are in preparation.

1. A. Weller and W. Urban. Angew. Chem. **66**, 637 (1954).
2. G. Porter and G. Jackson. Proc. Roy. Soc. (London), **260**, 13 (1961).
3. M. Ashraf El Bayoumi and M. Kasha. Molecular exciton interaction in H-bonded complexes. In preparation.
4. R. M. Hochstrasser. Can. J. Chem. **39**, 459 (1961).
5. A. Weller. Private communication.
6. J. Trotter. Acta Cryst. **13**, 732 (1960).
7. J. Trotter. Acta Cryst. **14**, 101 (1961).
8. M. Kasha and E. G. McRae. J. Chem. Phys. **28**, 721 (1958).
9. D. P. Craig, L. E. Lyons, S. H. Walmsley, and J. R. Walsh. Proc. Chem. Soc. 389 (1959).
10. R. M. Hochstrasser. Can. J. Chem. This issue.

Received May 25, 1961.
Chemistry Department,
University of British Columbia,
Vancouver 8, B.C.

IMPROVED PREPARATION OF BISTRIFLUOROMETHYLARSINE*

W. R. Cullen

Bistrifluoromethylarsine was first prepared by reducing iodobistrifluoromethylarsine with either lithium aluminum hydride (16% yield) or zinc and hydrochloric acid (43% yield) (1). The reduction of chlorobistrifluoromethylarsine with lithium aluminum hydride has been reported to proceed smoothly at ca. −25°, giving a higher yield of bistrifluoromethylarsine (70%) (2). It has now been found that this method is unreliable

*This research was supported by a grant from the National Research Council of Canada.

Can. J. Chem. Downloaded from www.nrcresearchpress.com by 210.87.254.40 on 09/05/12
For personal use only.

and can result in complete failure. However, bistrifluoromethylarsine can be prepared by the reaction of chlorobistrifluoromethylarsine with excess hydrogen chloride, in the presence of mercury. The yield is high and the arsine can be easily separated from unreacted hydrogen chloride and the only other volatile reaction product, tetrakistrifluoromethyldiarsine.

Analogous reactions have been used to prepare alkyl- and aryl-trifluoromethylarsines (3, 4):

$$R_2AsI + Hg + CF_3I \rightarrow R_2AsCF_3.$$

Burg and Mahler (5) have reported that bistrifluoromethylphosphine can be prepared in 35% yield from the reaction of iodobistrifluoromethylphosphine with hydrogen chloride in the presence of mercury: other protic acids such as trifluoroacetic acid and phosphoric acid can be used. However, no bistrifluoromethylarsine is obtained when trifluoroacetic acid is used instead of hydrogen chloride. Burg and Mahler have suggested that the phosphine is formed through the following sequence:

$$(CF_3)_2PI + 2Hg \rightarrow (CF_3)_2PHg_2I \xrightarrow{HCl} (CF_3)_2PH,$$

but this does not easily account for the low yield of bistrifluoromethylphosphine or for the formation of chlorobistrifluoromethylphosphine. This scheme could apply to the present reaction though an alternative seems as likely:

$$(CF_3)_2AsCl + Hg \rightarrow (CF_3)_2As{-}As(CF_3)_2 \xrightarrow{HCl} (CF_3)_2AsH + ClAs(CF_3)_2.$$

Both these steps are possible since the reaction of chlorobistrifluoromethylarsine with mercury produces the diarsine quantitatively (2), and shaking the diarsine with excess hydrogen chloride and mercury produces bistrifluoromethylarsine in high yield. Such a mechanism, if it were the only one operating, would limit the yield of bistrifluoromethylphosphine to a maximum of 50% since chlorobistrifluoromethylphosphine does not react with mercury (6).

EXPERIMENTAL

Volatile reactants and products were manipulated in a glass vacuum system out of contact with oxygen and moisture. Chlorobistrifluoromethylarsine was prepared by reacting the corresponding iodoarsine with silver chloride (1). The product was distilled in a nitrogen atmosphere and boiled at 47° (lit. value, 46° (by extrapolation) (7)). Tetrakistrifluoromethyldiarsine was prepared by reducing chlorobistrifluoromethylarsine with mercury (2).

Reaction of Chlorobistrifluoromethylarsine with Hydrogen Chloride in the Presence of Mercury

The arsine (0.673 g), dry hydrogen chloride (0.729 g), and mercury (82 g), in a sealed tube (50 ml), were shaken at 23° for 17 hours. Trap-to-trap distillation gave only three fractions: tetrakistrifluoromethyldiarsine (0.067 g), which condensed at −78° and which was identified by its low vapor pressure (<20 mm at 23°) and by its infrared spectrum (1); bistrifluoromethylarsine (0.505 g, 86% yield), which condensed at −130° and which was identified by its molecular weight (found: 214, calc: 214) and by its infrared spectrum (1); hydrogen chloride (0.614 g), which condensed at −196°. No permanent gas was produced.

Can. J. Chem. Downloaded from www.nrcresearchpress.com by 210.87.254.40 on 09/05/12
For personal use only.

Reaction of Chlorobistrifluoromethylarsine with Trifluoroacetic Acid in the Presence of Mercury

The arsine (0.713 g), trifluoroacetic acid (7.6 g), and mercury (60.5 g), in a sealed tube (50 ml), were shaken at 23° for 40 hours. A slow reaction took place and eventually a considerable amount of white solid was deposited. Trap-to-trap distillation and infrared examination of the fractions isolated showed that no bistrifluoromethylarsine had been produced.

Reaction of Tetrakistrifluoromethyldiarsine with Hydrogen Chloride in the Presence of Mercury

The diarsine (1.128 g), hydrogen chloride (0.614 g), and mercury (63 g), in a sealed tube (50 ml), were shaken at 23° for 22 hours. Trap-to-trap distillation gave only three fractions: unreacted tetrakistrifluoromethyldiarsine (0.149 g), which condensed at −78°; bistrifluoromethylarsine (0.943 g, 84% yield), which condensed at −132°; and hydrogen chloride, which condensed at −196°. The fractions were identified as above. No permanent gas was produced.

1. H. J. Emeléus, R. N. Haszeldine, and E. G. Walachewski. J. Chem. Soc. 1552 (1953).
2. W. R. Cullen. Ph.D. Dissertation, Cambridge. 1958.
3. W. R. Cullen. Can. J. Chem. **38**, 439 (1960).
4. W. R. Cullen. Can. J. Chem. **38**, 445 (1960).
5. A. B. Burg and W. Mahler. J. Am. Chem. Soc. **79**, 4242 (1957).
6. F. W. Bennett, H. J. Emeléus, and R. N. Haszeldine. J. Chem. Soc. 1565 (1953).
7. E. G. Walachewski. Ber. **86**, 272 (1953).

Received May 1, 1961.
Chemistry Department,
University of British Columbia,
Vancouver, B.C.

INTEGRAL HEATS OF MIXING OF C_6-ALKANES IN PERFLUOROTRIBUTYLAMINE AND IN PERFLUOROCYCLIC OXIDE ($C_8F_{16}O$) AT 60° C

Dan E. Nicholson

In connection with studies of the thermodynamic properties of solutions of isomeric C_6-hydrocarbons, the integral heats of mixing of these compounds have been determined in a perfluoroamine and a perfluoroether. The calorimeter and accessory apparatus were described previously (1). Provision was made in the calorimeter design for investigations of energy changes at elevated pressures and temperatures. Earlier studies of the experimental and theoretical heat effects involved in other fluorocarbon–hydrocarbon systems have been reported (2, 3, 4). Spectroscopic grade hydrocarbons obtained from the American Petroleum Institute were used without further purification. Perfluorocyclic oxide and perfluorotributylamine were purchased from the Minnesota Mining and Manufacturing Company under the designation FC-75 and FC-43, respectively. Both samples were purified by distillation in a 50-plate column so that the initial 20% and the final 20% portions were discarded.

Eight calorimetric experiments for each of the 10 binary solutions of the five hydrocarbons in the two solvents were performed covering the concentration range from 0.1

Can. J. Chem. Downloaded from www.nrcresearchpress.com by 210.87.254.40 on 09/05/12
For personal use only.

Reaction of Chlorobistrifluoromethylarsine with Trifluoroacetic Acid in the Presence of Mercury

The arsine (0.713 g), trifluoroacetic acid (7.6 g), and mercury (60.5 g), in a sealed tube (50 ml), were shaken at 23° for 40 hours. A slow reaction took place and eventually a considerable amount of white solid was deposited. Trap-to-trap distillation and infrared examination of the fractions isolated showed that no bistrifluoromethylarsine had been produced.

Reaction of Tetrakistrifluoromethyldiarsine with Hydrogen Chloride in the Presence of Mercury

The diarsine (1.128 g), hydrogen chloride (0.614 g), and mercury (63 g), in a sealed tube (50 ml), were shaken at 23° for 22 hours. Trap-to-trap distillation gave only three fractions: unreacted tetrakistrifluoromethyldiarsine (0.149 g), which condensed at −78°; bistrifluoromethylarsine (0.943 g, 84% yield), which condensed at −132°; and hydrogen chloride, which condensed at −196°. The fractions were identified as above. No permanent gas was produced.

1. H. J. Emeléus, R. N. Haszeldine, and E. G. Walachewski. J. Chem. Soc. 1552 (1953).
2. W. R. Cullen. Ph.D. Dissertation, Cambridge. 1958.
3. W. R. Cullen. Can. J. Chem. **38**, 439 (1960).
4. W. R. Cullen. Can. J. Chem. **38**, 445 (1960).
5. A. B. Burg and W. Mahler. J. Am. Chem. Soc. **79**, 4242 (1957).
6. F. W. Bennett, H. J. Emeléus, and R. N. Haszeldine. J. Chem. Soc. 1565 (1953).
7. E. G. Walachewski. Ber. **86**, 272 (1953).

Received May 1, 1961.
Chemistry Department,
University of British Columbia,
Vancouver, B.C.

INTEGRAL HEATS OF MIXING OF C_6-ALKANES IN PERFLUOROTRIBUTYLAMINE AND IN PERFLUOROCYCLIC OXIDE ($C_8F_{16}O$) AT 60° C

Dan E. Nicholson

In connection with studies of the thermodynamic properties of solutions of isomeric C_6-hydrocarbons, the integral heats of mixing of these compounds have been determined in a perfluoroamine and a perfluoroether. The calorimeter and accessory apparatus were described previously (1). Provision was made in the calorimeter design for investigations of energy changes at elevated pressures and temperatures. Earlier studies of the experimental and theoretical heat effects involved in other fluorocarbon–hydrocarbon systems have been reported (2, 3, 4). Spectroscopic grade hydrocarbons obtained from the American Petroleum Institute were used without further purification. Perfluorocyclic oxide and perfluorotributylamine were purchased from the Minnesota Mining and Manufacturing Company under the designation FC-75 and FC-43, respectively. Both samples were purified by distillation in a 50-plate column so that the initial 20% and the final 20% portions were discarded.

Eight calorimetric experiments for each of the 10 binary solutions of the five hydrocarbons in the two solvents were performed covering the concentration range from 0.1

Can. J. Chem. Downloaded from www.nrcresearchpress.com by 210.87.254.105 on 09/05/12
For personal use only.

to 0.9 volume fractions. The integral heat of mixing data could be represented by an equation of the form

$$\Delta H = x_1x_2[-c_1+c_2(x_1-x_2)+c_3(x_1-x_2)^2],$$

where

x = mole fraction of a component,

c = constant,

ΔH = endothermic integral heat of mixing, cal per mole of mixture, and subscript 1 refers to the hydrocarbon.

A summary of the experimental data is given in Table I. The constants shown will

TABLE I

	c_1	c_2	c_3
n-Hexane–$(C_4F_9)_3N$	2182	349	2322
2-Methylpentane–$(C_4F_9)_3N$	−2106	196	2444
3-Methylpentane–$(C_4F_9)_3N$	−2170	66.8	2204
2,2-Dimethylbutane–$(C_4F_9)_3N$	−2271	777	610
2,3-Dimethylbutane–$(C_4F_9)_3N$	−2251	561	1538
n-Hexane–$C_8F_{16}O$	−2212	357	555
2-Methylpentane–$C_8F_{16}O$	−2274	614	191
3-Methylpentane–$C_8F_{16}O$	−2174	501	542
2,2-Dimethylbutane–$C_8F_{16}O$	−1967	607	508
2,3-Dimethylbutane–$C_8F_{16}O$	−2133	285	701

reproduce the calorimetric measurements within about ±1%. The maximum endothermic integral heat of mixing calculated from the equation above is approximately 550 cal per mole of mixture in solutions equimolar in *n*-hexane and perfluorotributylamine.

One of the objectives of the present investigation was to determine whether or not useful empirical relationships involving the group-equivalent concept could be formulated to correlate the heats of mixing. For example, one may consider the heat of mixing of 2,3-dimethylbutane with a solvent to arise from contributions of two isopropyl groups. Likewise, for 2-methylpentane the observed heat effects could be attributable to isopropyl and *n*-propyl groups. An internally consistent set of relationships based upon this approach could not be developed. As an illustration of the application of the group-equivalent concept the values shown in Table II were estimated for the $C_8F_{16}O$–C_6H_{14}

TABLE II

Structural unit	Contribution to the heat of mixing in $C_8F_{16}O$ as solvent at infinite dilution, cal/mole
$H_3C—CH_2—CH_2---$	1055
$H_3C—\underset{\displaystyle H}{\overset{\displaystyle CH_3}{\overset{\vert}{\underset{\vert}{C}}}}---$	930
$H_3C—CH_2---$	703
$H_3C—CH_2—CH_2—CH_2---$	1406
$H_3C—CH_2—\overset{\displaystyle CH_3}{\overset{\vert}{CH}}---$	1295
$H_3C—\underset{\displaystyle CH_3}{\overset{\displaystyle CH_3}{\overset{\vert}{\underset{\vert}{C}}}}---$	1087

Can. J. Chem. Downloaded from www.nrcresearchpress.com by 210.87.254.105 on 09/05/12
For personal use only.

systems. The heats of mixing at infinite dilution were obtained by means of large-scale plots. The group-equivalent quantities for propyl, ethyl, and *n*-butyl structures were assigned from the heats of mixing of *n*-hexane. The value for the isopropyl group was derived from the appropriate quantities for 2-methylpentane and the propyl group. Similarly, for the *sec*-butyl structure, the group-equivalent value was obtained from 3-methylpentane while the *tert*-butyl structure was estimated from heats of mixing for 2,2-dimethylbutane. For 2,3-dimethylbutane the calculated heat of mixing is, therefore, 2×930 or 1860 cal/mole of hydrocarbon. The observed value for the heat of mixing is 2040 cal/mole.

Some comparisons between the experimental heat changes from the current work and those from regular solution theory (equation 17, p. 124, reference 5) have also been made. From solubility parameters and the appropriate molar volumes (3, 6) the values given in Table III are found for solutions in $C_8F_{16}O$ (solubility parameter = 5.9).

TABLE III

Mole fraction of *n*-hexane	ΔH (experimental), cal/mole of mixture	ΔE, cal/mole of mixture
0.2	350	48
0.4	515	78
0.6	560	84
0.8	450	61

Sufficient data are not available to test the more refined versions of the theoretical equations for predicting heats of mixing.

ACKNOWLEDGMENT

The writer is indebted to Mr. Theo Hines for assistance with experimental work.

1. D. E. Nicholson. J. Chem. Eng. Data, **5**, 35 (1960).
2. T. M. Reed, III. J. Phys. Chem. **59**, 425 (1955).
3. B. G. Kyle and T. M. Reed, III. J. Am. Chem. Soc. **80**, 6170 (1958).
4. R. L. Scott. J. Phys. Chem. **62**, 136 (1958).
5. J. H. Hildebrand and R. L. Scott. The solubility of nonelectrolytes. Reinhold Publishing Corp., New York. 1950.
6. American Petroleum Institute Research Project 44. Selected values of properties of hydrocarbons. Natl. Bur. Standards, Washington, D.C. 1950.

Received January 9, 1961.
Research and Development Division,
Humble Oil and Refining Company,
Baytown, Texas.

MOLECULAR ADDITION COMPOUNDS OF TRIOXAN

Douglas Hamer and James Leslie[1]

Trioxan, the cyclic trimer of formaldehyde, is generally unreactive, but in the presence of acids, it is depolymerized to formaldehyde (1). For this reason trioxan is used in many organic reactions as an *in situ* source of formaldehyde, the formaldehyde being liberated by the addition of acid. No other chemical reactions of trioxan have been reported. This note describes the preparation of molecular addition compounds of this cyclic ether with

[1]*Present address: Department of Chemistry, Oklahoma State University, Stillwater, Oklahoma, U.S.A.*

Can. J. Chem. Downloaded from www.nrcresearchpress.com by 210.87.254.105 on 09/05/12
For personal use only.

systems. The heats of mixing at infinite dilution were obtained by means of large-scale plots. The group-equivalent quantities for propyl, ethyl, and *n*-butyl structures were assigned from the heats of mixing of *n*-hexane. The value for the isopropyl group was derived from the appropriate quantities for 2-methylpentane and the propyl group. Similarly, for the *sec*-butyl structure, the group-equivalent value was obtained from 3-methylpentane while the *tert*-butyl structure was estimated from heats of mixing for 2,2-dimethylbutane. For 2,3-dimethylbutane the calculated heat of mixing is, therefore, 2×930 or 1860 cal/mole of hydrocarbon. The observed value for the heat of mixing is 2040 cal/mole.

Some comparisons between the experimental heat changes from the current work and those from regular solution theory (equation 17, p. 124, reference 5) have also been made. From solubility parameters and the appropriate molar volumes (3, 6) the values given in Table III are found for solutions in $C_8F_{16}O$ (solubility parameter = 5.9).

TABLE III

Mole fraction of *n*-hexane	ΔH (experimental), cal/mole of mixture	ΔE, cal/mole of mixture
0.2	350	48
0.4	515	78
0.6	560	84
0.8	450	61

Sufficient data are not available to test the more refined versions of the theoretical equations for predicting heats of mixing.

ACKNOWLEDGMENT

The writer is indebted to Mr. Theo Hines for assistance with experimental work.

1. D. E. Nicholson. J. Chem. Eng. Data, **5**, 35 (1960).
2. T. M. Reed, III. J. Phys. Chem. **59**, 425 (1955).
3. B. G. Kyle and T. M. Reed, III. J. Am. Chem. Soc. **80**, 6170 (1958).
4. R. L. Scott. J. Phys. Chem. **62**, 136 (1958).
5. J. H. Hildebrand and R. L. Scott. The solubility of nonelectrolytes. Reinhold Publishing Corp., New York. 1950.
6. American Petroleum Institute Research Project 44. Selected values of properties of hydrocarbons. Natl. Bur. Standards, Washington, D.C. 1950.

Received January 9, 1961.
Research and Development Division,
Humble Oil and Refining Company,
Baytown, Texas.

MOLECULAR ADDITION COMPOUNDS OF TRIOXAN

Douglas Hamer and James Leslie[1]

Trioxan, the cyclic trimer of formaldehyde, is generally unreactive, but in the presence of acids, it is depolymerized to formaldehyde (1). For this reason trioxan is used in many organic reactions as an *in situ* source of formaldehyde, the formaldehyde being liberated by the addition of acid. No other chemical reactions of trioxan have been reported. This note describes the preparation of molecular addition compounds of this cyclic ether with

[1]*Present address: Department of Chemistry, Oklahoma State University, Stillwater, Oklahoma, U.S.A.*

Can. J. Chem. Downloaded from www.nrcresearchpress.com by 210.87.254.5 on 09/05/12
For personal use only.

picric acid and 1,3,5-trinitrobenzene. The derivative with 1,3,5-trinitrobenzene is a well-defined crystalline compound with a sharp melting point and may be of use in the classification and identification of trioxan. Trioxan did not form addition compounds with picrolonic acid or 1,2,7-trinitrofluorenone. Other cyclic ethers, e.g., dioxan and paraldehyde, did not form compounds with 1,3,5-trinitrobenzene or picric acid.

EXPERIMENTAL

Reaction of Trioxan with 1,3,5-Trinitrobenzene

Two grams of 1,3,5-trinitrobenzene was dissolved in slightly over the minimum quantity of boiling ethanol and 1.75 g of trioxan was added. Cooling of the solution caused the separation of pale yellow crystalline needles (2.6 g) which, on recrystallization from ethanol, yielded a compound of m.p. 94–97°. It was necessary to add a small amount of trioxan during the recrystallization; otherwise crystals of 1,3,5-trinitrobenzene separated. The addition compound could be similarly obtained in carbon tetrachloride, chloroform, or benzene. The derivative, however, did not readily precipitate from these solvents, but an apparently purer compound was obtained from carbon tetrachloride as pure white needles, m.p. 97°. Analysis: Found: C, 35.74; H, 2.92; N, 14.20; CH_2O, 30.16. $(CH_2O)_3.C_6H_3(NO_2)_3$ requires: C, 35.65; H, 2.99; N, 13.86; CH_2O, 29.70. The analysis indicates a 1:1 molecular compound of trioxan and 1,3,5-trinitrobenzene.

Reaction of Trioxan with Picric Acid

A hot saturated solution of picric acid in ethanol was added to an almost saturated solution of trioxan in boiling ethanol. When the mixture was cooled, a bulky yellow mass which consisted mainly of trioxan, separated. The trioxan was removed by evaporation in air at room temperature, leaving a pale yellow residue, presumably a picrate of trioxan. This derivative decomposed on attempted recrystallization so no analysis was made. The melting point was 58°, and mixtures with trioxan and with picric acid melted at 40–60° and 60–90° respectively, suggesting that the derivative was indeed a compound of trioxan and picric acid.

All melting points are uncorrected.

ACKNOWLEDGMENT

The authors wish to thank the Ministry of Education for Northern Ireland for a Postgraduate Studentship to J. Leslie.

1. J. F. WALKER. Formaldehyde. American Chemical Society Monograph. Reinhold, New York. 1953.

RECEIVED MAY 23, 1961.
CHEMISTRY DEPARTMENT,
COLLEGE OF TECHNOLOGY,
BELFAST 1, NORTHERN IRELAND.

Can. J. Chem. Downloaded from www.nrcresearchpress.com by 210.87.254.5 on 09/05/12
For personal use only.

A SIMPLE REAGENT FOR THE SPECIFIC DEHYDRATION OF TERPENE ALCOHOLS*

E. VON RUDLOFF

The dehydration of terpene alcohols in the liquid phase with the common acidic reagents usually results in the formation of several isomeric olefins. This is undesirable both for structure determination and for preparative purposes. The dehydration of sesquiterpene alcohols with a weakly basic reagent, viz. thionyl chloride in the presence

*Issued as N.R.C. No. 6408.

picric acid and 1,3,5-trinitrobenzene. The derivative with 1,3,5-trinitrobenzene is a well-defined crystalline compound with a sharp melting point and may be of use in the classification and identification of trioxan. Trioxan did not form addition compounds with picrolonic acid or 1,2,7-trinitrofluorenone. Other cyclic ethers, e.g., dioxan and paraldehyde, did not form compounds with 1,3,5-trinitrobenzene or picric acid.

EXPERIMENTAL

Reaction of Trioxan with 1,3,5-Trinitrobenzene

Two grams of 1,3,5-trinitrobenzene was dissolved in slightly over the minimum quantity of boiling ethanol and 1.75 g of trioxan was added. Cooling of the solution caused the separation of pale yellow crystalline needles (2.6 g) which, on recrystallization from ethanol, yielded a compound of m.p. 94–97°. It was necessary to add a small amount of trioxan during the recrystallization; otherwise crystals of 1,3,5-trinitrobenzene separated. The addition compound could be similarly obtained in carbon tetrachloride, chloroform, or benzene. The derivative, however, did not readily precipitate from these solvents, but an apparently purer compound was obtained from carbon tetrachloride as pure white needles, m.p. 97°. Analysis: Found: C, 35.74; H, 2.92; N, 14.20; CH_2O, 30.16. $(CH_2O)_3.C_6H_3(NO_2)_3$ requires: C, 35.65; H, 2.99; N, 13.86; CH_2O, 29.70. The analysis indicates a 1:1 molecular compound of trioxan and 1,3,5-trinitrobenzene.

Reaction of Trioxan with Picric Acid

A hot saturated solution of picric acid in ethanol was added to an almost saturated solution of trioxan in boiling ethanol. When the mixture was cooled, a bulky yellow mass which consisted mainly of trioxan, separated. The trioxan was removed by evaporation in air at room temperature, leaving a pale yellow residue, presumably a picrate of trioxan. This derivative decomposed on attempted recrystallization so no analysis was made. The melting point was 58°, and mixtures with trioxan and with picric acid melted at 40–60° and 60–90° respectively, suggesting that the derivative was indeed a compound of trioxan and picric acid.

All melting points are uncorrected.

ACKNOWLEDGMENT

The authors wish to thank the Ministry of Education for Northern Ireland for a Postgraduate Studentship to J. Leslie.

1. J. F. WALKER. Formaldehyde. American Chemical Society Monograph. Reinhold, New York. 1953.

RECEIVED MAY 23, 1961.
CHEMISTRY DEPARTMENT,
COLLEGE OF TECHNOLOGY,
BELFAST 1, NORTHERN IRELAND.

A SIMPLE REAGENT FOR THE SPECIFIC DEHYDRATION OF TERPENE ALCOHOLS*

E. VON RUDLOFF

The dehydration of terpene alcohols in the liquid phase with the common acidic reagents usually results in the formation of several isomeric olefins. This is undesirable both for structure determination and for preparative purposes. The dehydration of sesquiterpene alcohols with a weakly basic reagent, viz. thionyl chloride in the presence

*Issued as N.R.C. No. 6408.

Can. J. Chem. Downloaded from www.nrcresearchpress.com by 210.87.254.105 on 09/05/12
For personal use only.

of excess pyridine, has been described recently by Motl *et al.* (1, 2), who obtained a mixture of isomeric hydrocarbons from both selin-4-ol and dihydro-α-cadinol. When this reagent was used in the current study with α-terpineol, dipentene (70%) and terpinolene (21%) were obtained and no other isomeric hydrocarbon was detected by gas–liquid chromatography (GLC). This is a considerable reduction in the number of isomers formed over that obtained when acidic reagents were used (3). However, because of the large excess of pyridine used with this reagent, the reaction is cumbersome. A much more convenient, and in some instances more specific, dehydration has now been obtained by heating the alcohol under reflux at 200 to 230° from 1 to 6 hours in the presence of twice its weight of neutral alumina (Woelm, activity grade I) to which 1 to 2% of pyridine or quinoline had been added. This reagent gave highly satisfactory results with α-terpineol, dihydro-α-terpineol, menthol, borneol, cedrol, and dihydroeudesmol, although the products obtained from linalool and isopulegol were more complex.

The amount of α-terpineol which had reacted with the reagent during 1 hour at 180°, 200°, and 220° C was 10%, 40%, and 82% respectively. The dehydration was virtually complete after 6 hours at 220° C, when dipentene (83%) and terpinolene (6%) were the only compounds detected by GLC. When α-terpineol was heated under reflux with neutral alumina alone, the steam-volatile product was found to be composed of α-terpinene (13%), dipentene (31%), *p*-cymene (16%), γ-terpinene (9%), terpinolene (26%), and *p*-mentha-2,4(8)-diene (5%), a composition very similar to that obtained with aqueous acidic reagents (2).

With dihydro-α-terpineol this base-modified alumina gave *trans*- (47%) and *cis*- (44%) *p*-menth-8-ene and *p*-menth-4(8)-ene (7%) after 1 hour reaction time. Since the ratio of cis to trans isomers in the starting material was 1:1 there appears to be no preferential reaction of either of the two isomers. Using the reagent of Motl *et al.* (1) the same mixture of hydrocarbons was obtained, but the yield of the *p*-menth-8-ene isomers was only 70%. Menthol, when treated with the new reagent for 1 hour, gave *p*-menth-2-ene (40%) and *p*-menth-3-ene (6%), whereas borneol was dehydrated to a mixture of camphene (68%) and tricyclene (16%). These results are very similar to those described by Pines and Pillai (4), who carried out the dehydration reaction of menthol, borneol, and neopentyl alcohol over ammonia-modified alumina in the gas phase. These authors propose that the dehydration takes place by a concerted mechanism involving both acidic and basic sites on the catalyst, whereas isomerization is suppressed by the preferential poisoning of the "strong acid sites" (5). Neutralization of acidic sites was confirmed in this study by evacuating the pyridine-treated alumina for 6 hours, when about 0.8% base was retained and no change in the reaction with α-terpineol was observed. Recently, Beranek *et al.* (6) have studied the dehydration of 4-methylcyclohexanol in the gas phase with a pyridine-modified alumina and have demonstrated that the active centers of the catalyst responsible for dehydration differ from those causing olefin isomerization. These authors also showed that, with unmodified alumina, isomerization is extensive and subsequent to dehydration. Thus there appears to be no difference in the reaction of tertiary or secondary alcohols over alumina catalysts in either the gas or liquid phase. The main feature of the base-modified alumina catalyst is the suppression of isomerization of the primary dehydration products by inhibiting carbonium-ion formation.

Dehydration of sesquiterpene alcohols with the new dehydrating agent also proceeds smoothly. Cedrol was converted to α-cedrene (85%) in 1 hour at 230° with only traces of an isomeric hydrocarbon being detected by GLC. When cedrol was treated with the thionyl chloride – pyridine reagent these two isomers were obtained in the ratio of 5:3. Dihydroeudesmol was similarly converted in high yield to a single hydrocarbon. Its

Can. J. Chem. Downloaded from www.nrcresearchpress.com by 210.87.254.105 on 09/05/12
For personal use only.

infrared spectrum had strong bands at 1645 and 880 cm^{-1}, showing it to be the isomer with the isopropenyl group. The dehydration of dihydroeudesmol with other reagents, as studied by Ruzicka *et al.* (7), produced invariably a mixture of dihydroeudesmene isomers. Thus it appears that the new reagent inhibits the formation of an exocyclic double bond, and it forms, therefore, an excellent complement to the common acidic reagents, which produce the exocyclic double bond preferentially in the early stages of the reaction.

The simplicity of the reaction with base-modified aluminas, however, does not seem to be general. Whereas the major reaction product with linalool was myrcene, four other hydrocarbons were detected in the reaction product. With isopulegol an even more complex mixture was obtained, nine hydrocarbon peaks and five peaks in the oxygenated terpene range being recorded by GLC. Since both of these alcohols are unstable at their boiling points, the formation of a complex mixture may be due to thermal decomposition or rearrangement rather than to the dehydration reaction itself. The reaction is being studied in more detail and the results obtained will be reported elsewhere.

EXPERIMENTAL

The gas chromatographic analyses were carried out with a modified Beckman GC-2 chromatograph. Quantitative data were obtained on the 12 ft$\times\frac{1}{4}$ in. (O.D.) rapeseed oil and 6 ft$\times\frac{1}{4}$ in. adipate and azelate polyester and polyethylene glycol columns described previously (2, 8, 9). The percentage composition was obtained by the triangulation method ($\pm 3\%$) and the average values are reported. The retention times of the sesquiterpenes and the *p*-menthenes are shown in Tables I and II. Those of the other compounds

TABLE I

Retention times* (in minutes) of sesquiterpenes at 180° C

Compound	Column:	Adipate polyester	Azelate polyester
	Flow rate (ml He/min):	58	43
α-Cedrene		3.6	5.8
Cedrene isomer		4.1	6.8
α-Cedrol		19.8	31.0
Dihydroeudesmene		3.5	5.6
Dihydroeudesmol		23.9	40.4
Eudesmol		27.6	46.0

*Measured at the initial emergence of the peaks.

TABLE II

Retention times* (in minutes) of *p*-menthenes at 80° C

Compound	Column:	Adipate polyester	Azelate polyester	Polyethylene glycol	Rapeseed oil
	Flow rate (ml He/min):	78	103	91	75
p-Menth-2-ene		3.1	4.5	4.8	60.0
p-Menth-3-ene		3.5	4.8	5.5	64.2
p-Menth-4(8)-ene		5.6	7.3	8.7	85.7
p-Menth-8-ene (trans)		3.9	5.2	6.4	67.2
p-Menth-8-ene (cis)		5.0	6.3	7.3	76.3
Limonene		8.2	12.1	13.3	99.6

*Measured at the initial emergence of the peaks.

Can. J. Chem. Downloaded from www.nrcresearchpress.com by 210.87.254.105 on 09/05/12
For personal use only.

have been reported earlier (9). Preparative runs were carried out as before on a 10- to 20-mg scale (2). The infrared spectra were recorded with a Perkin–Elmer model 21 double-beam spectrophotometer. Borneol, menthol, linalool, and isopulegol were commercial products, whereas dihydro-α-terpineol (50% trans and 50% cis) was prepared by hydrogenation of redistilled α-terpineol (99% pure), using platinum oxide as catalyst and methanol as solvent. Dihydroeudesmol, m.p. 85–86° C, $[\alpha]_D^{25}$ +18.0° ($CHCl_3$), was obtained by a similar hydrogenation of eudesmol.

A typical dehydration experiment was carried out as follows. Neutral alumina (Woelm, activity grade I) (2.0 g) was placed into a 25-ml flask having two necks with ground-glass joints. To this was added pyridine (0.02 to 0.04 g) and α-terpineol (1.00 g) and the mixture was heated under reflux at 220° C (oil bath) for 6 hours. The mixture was then steam-distilled and the volatile product was taken up in a small volume of ether. After the ethereal solution had been dried over anhydrous sodium sulphate, it was transferred quantitatively to a flask having a long neck (2) and the ether was evaporated on a steam bath. The residue (0.79 g, 89% of theory) was analyzed by GLC. The composition of the hydrocarbons obtained was determined on the different columns at 80° C, and the amount of unreacted α-terpineol (in relation to the amount of hydrocarbons formed), at 110° or 130° C. The data obtained showed less than 1% unreacted alcohol, 93% dipentene, and 7% terpinolene. When quinolene was used as base instead of pyridine the respective yields of hydrocarbons were 92 and 6%.

In another experiment, neutral alumina (100.0 g) was thoroughly mixed with pyridine (2.0 g) and the mixture was evacuated to 0.5 mm Hg at room temperature for 6 hours. The residue (100.8 g) was used as such in the dehydration of α-terpineol, when practically identical results were obtained.

All other alcohols mentioned, except dihydroeudesmol, were dehydrated in the manner described in the first instance. Dihydroeudesmol (0.05 g) was weighed into a 10 cm × 5 mm glass tube. To this was added pyridine-modified alumina (0.20 g) and the lower end of the tube was immersed into an oil bath at 230° C in such a manner that the upper half of the tube acted as an air condenser. After 1 hour the tube was cooled and the mixture was extracted with ether. The residue (0.03 g), after evaporation of the ether, was analyzed on the polyester columns at 160° and 180° C, when only a single hydrocarbon peak was recorded. The infrared spectrum was, therefore, recorded directly without further purification.

The dehydrations with thionyl chloride were carried out as follows. To the alcohol (1.00 g) was added dry pyridine (40 ml) and the solution was cooled to about 5° C. Thionyl chloride (3.0 g) was then added dropwise with shaking. After the mixture had been shaken for another 5 minutes, sodium carbonate (3 g) in water (15 ml) was added slowly. The mixture was extracted thrice with ether and the ethereal solution was washed with a saturated tartaric acid solution until all pyridine had been removed; pyridine was found to interfere with the GLC analysis. It was then washed with water and worked up as described above.

The author is grateful to Mr. M. Granat for technical assistance and to Miss I. M. Gaffney for recording the infrared spectra.

1. O. Motl, V. Herout, and F. Sorm. Collection Czechoslov. Chem. Communs. **23**, 1293 (1958).
2. O. Motl, V. Sykora, V. Herout, and F. Sorm. Collection Czechoslov. Chem. Communs. **23**, 1297 (1958).

Can. J. Chem. Downloaded from www.nrcresearchpress.com by 210.87.254.105 on 09/05/12
For personal use only.

3. E. VON RUDLOFF. Can. J. Chem. **39**, 1 (1961).
4. H. PINES and C. N. PILLAI. J. Am. Chem. Soc. **82**, 2401 (1960).
5. H. PINES and W. HAAG. J. Am. Chem. Soc. **82**, 2471 (1960).
6. L. BERANEK, M. KRAUS, K. KOCHLOEFL, and V. BAZANT. Collection Czechoslov. Chem. Communs. **25**, 2513 (1960).
7. L. RUZICKA, A. L. WIND, and D. R. KOOLHAAS. Helv. Chim. Acta, **14**, 1132 (1931).
8. E. VON RUDLOFF. Can. J. Chem. **38**, 631 (1960).
9. E. VON RUDLOFF. Can. J. Chem. **39**, 1190 (1961).

RECEIVED MAY 12, 1961.
NATIONAL RESEARCH COUNCIL OF CANADA,
PRAIRIE REGIONAL LABORATORY,
SASKATOON, SASKATCHEWAN.

Can. J. Chem. Downloaded from www.nrcresearchpress.com by 210.87.254.105 on 09/05/12
For personal use only.

SOLVENT EFFECTS ON THE RING PROTON MAGNETIC RESONANCE SPECTRA OF SOME SUBSTITUTED QUINOLINES

T. SCHAEFER

Proton resonance spectra of unsaturated ring compounds are strongly solvent dependent. The spectra of substituted benzenes and heterocyclic compounds are affected both by the nature of the solvent and the degree of dilution (1, 2). The variation of the "internal" chemical shifts in these compounds in different solvents is surprisingly large since these systems are not generally regarded as involving either hydrogen bonding or other specific molecular association. Comparison of the shifts of the ring protons in these aromatic compounds in *n*-hexane, acetone, and benzene solvents leads to the conclusion that highly specific solute–solvent interactions are involved, at least in the benzene solutions. This note extends the experimental results to some substituted quinolines.

EXPERIMENTAL AND RESULTS

Dilute solutions of the compounds were made up to a uniform concentration of 5 mole% in *n*-hexane, benzene, and acetone. All measurements were made at 60 Mc/sec and peak positions were measured relative to an external chloroform reference.* Bulk susceptibility corrections were applied.

In Table I the shifts of the ring protons, corrected for bulk susceptibility differences, are tabulated relative to an external chloroform reference. The shifts are given only to the nearest cycles/sec because in many cases the analysis of the complex spectra did not allow a closer estimation. In some cases the benzene solvent peak obscured a few solute peaks but sometimes the preferential shifts caused by benzene allowed analysis of the spectra in benzene but not in *n*-hexane or acetone. An aid in the assignment of peaks was the fact that the ring protons ortho to a methyl or methylene group couple weakly to the latter protons. However, this also decreased the accuracy with which shifts and coupling constants could be extracted.

In Fig. 1 the proton shifts in *n*-hexane are taken as a reference point and the alterations of the shifts in the acetone and benzene solutions are plotted for all compounds. In Table II are given the coupling constants which could be obtained from the spectra. The estimated errors are relatively large because of the effects mentioned above.

**The calibrated spectra of the pure compounds and of the solutions are available upon request.*

3. E. VON RUDLOFF. Can. J. Chem. **39**, 1 (1961).
4. H. PINES and C. N. PILLAI. J. Am. Chem. Soc. **82**, 2401 (1960).
5. H. PINES and W. HAAG. J. Am. Chem. Soc. **82**, 2471 (1960).
6. L. BERANEK, M. KRAUS, K. KOCHLOEFL, and V. BAZANT. Collection Czechoslov. Chem. Communs. **25**, 2513 (1960).
7. L. RUZICKA, A. L. WIND, and D. R. KOOLHAAS. Helv. Chim. Acta, **14**, 1132 (1931).
8. E. VON RUDLOFF. Can. J. Chem. **38**, 631 (1960).
9. E. VON RUDLOFF. Can. J. Chem. **39**, 1190 (1961).

RECEIVED MAY 12, 1961.
NATIONAL RESEARCH COUNCIL OF CANADA,
PRAIRIE REGIONAL LABORATORY,
SASKATOON, SASKATCHEWAN.

Can. J. Chem. Downloaded from www.nrcresearchpress.com by 210.87.254.105 on 09/05/12
For personal use only.

SOLVENT EFFECTS ON THE RING PROTON MAGNETIC RESONANCE SPECTRA OF SOME SUBSTITUTED QUINOLINES

T. SCHAEFER

Proton resonance spectra of unsaturated ring compounds are strongly solvent dependent. The spectra of substituted benzenes and heterocyclic compounds are affected both by the nature of the solvent and the degree of dilution (1, 2). The variation of the "internal" chemical shifts in these compounds in different solvents is surprisingly large since these systems are not generally regarded as involving either hydrogen bonding or other specific molecular association. Comparison of the shifts of the ring protons in these aromatic compounds in *n*-hexane, acetone, and benzene solvents leads to the conclusion that highly specific solute–solvent interactions are involved, at least in the benzene solutions. This note extends the experimental results to some substituted quinolines.

EXPERIMENTAL AND RESULTS

Dilute solutions of the compounds were made up to a uniform concentration of 5 mole% in *n*-hexane, benzene, and acetone. All measurements were made at 60 Mc/sec and peak positions were measured relative to an external chloroform reference.* Bulk susceptibility corrections were applied.

In Table I the shifts of the ring protons, corrected for bulk susceptibility differences, are tabulated relative to an external chloroform reference. The shifts are given only to the nearest cycles/sec because in many cases the analysis of the complex spectra did not allow a closer estimation. In some cases the benzene solvent peak obscured a few solute peaks but sometimes the preferential shifts caused by benzene allowed analysis of the spectra in benzene but not in *n*-hexane or acetone. An aid in the assignment of peaks was the fact that the ring protons ortho to a methyl or methylene group couple weakly to the latter protons. However, this also decreased the accuracy with which shifts and coupling constants could be extracted.

In Fig. 1 the proton shifts in *n*-hexane are taken as a reference point and the alterations of the shifts in the acetone and benzene solutions are plotted for all compounds. In Table II are given the coupling constants which could be obtained from the spectra. The estimated errors are relatively large because of the effects mentioned above.

**The calibrated spectra of the pure compounds and of the solutions are available upon request.*

TABLE I

Shifts in cycles/sec at 60 Mc/sec from an external $CHCl_3$ reference (corrected for bulk susceptibility)
(Increasing shifts correspond to a higher magnetic field)

Compound	Solvent, 5 mole% solution in:	H_2	H_3	H_4	H_5	H_6	H_7	H_8
Quinoline	*n*-Hexane	−79	20	−27	—	—	—	−36
	Acetone	−85	1.3	−37	—	—	—	−48
	Benzene	−53	66	21	—	—	—	−25
7-Ethylquinoline	*n*-Hexane	−78	23	−24	−4	13	—	−26
	Acetone	−85	4	−46	−22	0	—	−26
	Benzene	−59	61	13	25	—	—	−21
6,8-Dimethyl-quinoline	*n*-Hexane	−77	20	−20	12	—	12	—
	Acetone	−81	6	−37	4	—	4	—
	Benzene	−57	59	15	—	—	—	—
5,8-Dimethyl-quinoline	*n*-Hexane	−79	19	−36	—	23	11	—
	Acetone	−86	1	−51	—	13	2	—
	Benzene	−61	58	3	—	—	—	—
5,7-Dimethyl-quinoline	*n*-Hexane	−76	22	−34	—	26	—	−15
	Acetone	−83	5	−51	—	15	—	−14
	Benzene	−59	57	3	—	56	—	−12
4,6-Dimethyl-quinoline	*n*-Hexane	−66	31	—	−8	—	7	−30
	Acetone	−71	15	—	−20	—	−3	−27
	Benzene	−53	68	—	22	—	37	−27
3,8-Dimethyl-quinoline	*n*-Hexane	−72	—	−10	—	—	—	—
	Acetone	−78	—	−29	—	—	—	—
	Benzene	−58	—	28	—	—	—	—
2,8-Dimethyl-quinoline	*n*-Hexane	—	23	−19	—	—	—	—
	Acetone	—	8	−37	—	—	—	—
	Benzene	—	6	16	—	—	—	—

DISCUSSION

The preferential shifts of the ring protons at various positions relative to the polar group still await a satisfactory explanation. It is clear that a specific solute–solvent interaction is present, at least in benzene. In contrast to the substituted toluenes (1), however, we can observe the solution shifts of protons in both the meta (β) and para (γ) position (protons 3 and 4) to the nitrogen. From Table I and Fig. 1 it is clear that although proton 4 occurs to a much lower field than proton 3 in *n*-hexane solutions (resonance effect) its behavior in benzene and acetone solution parallels that of proton 3. Hence there is no simple relationship between charge density at the carbon to which the proton is bonded and the magnitude of the solvent shift for the proton. Qualitatively it is clear that the solvent effects increase as the distance between the negative nitrogen atom and the protons increases, but again there is no simple relationship since protons 5, 6, 7 are shifted less than protons 3 and 4 in benzene solutions. The shifts to high field of protons 5, 6, 7 are about 30 cycles/sec and this is about the value expected for the ordinary dilution shift in benzene due to the ring current effect (see reference 1). It follows that the higher shift for protons 3 and 4 must somehow be connected with the presence of the polar nitrogen although this connection is obscure. Since the π electrons of the benzene molecules are repelled by the negative nitrogen, it may be that the planar benzene molecules pack about the planar quinoline molecules in such a way as to avoid the nitrogen. This would explain why protons 2 and 8 are shifted to high field by a lesser amount than would be expected on the ring current effect of about 25–30 cycles/sec.

With one exception, the coupling constants in Table II have the values expected for ring protons. J_{23} is found to have a value of 4.0 ± 0.2 cycles/sec for all compounds, about half the value for a normal coupling constant between protons in the ortho position. This

Can. J. Chem. Downloaded from www.nrcresearchpress.com by 210.87.254.105 on 09/05/12
For personal use only.

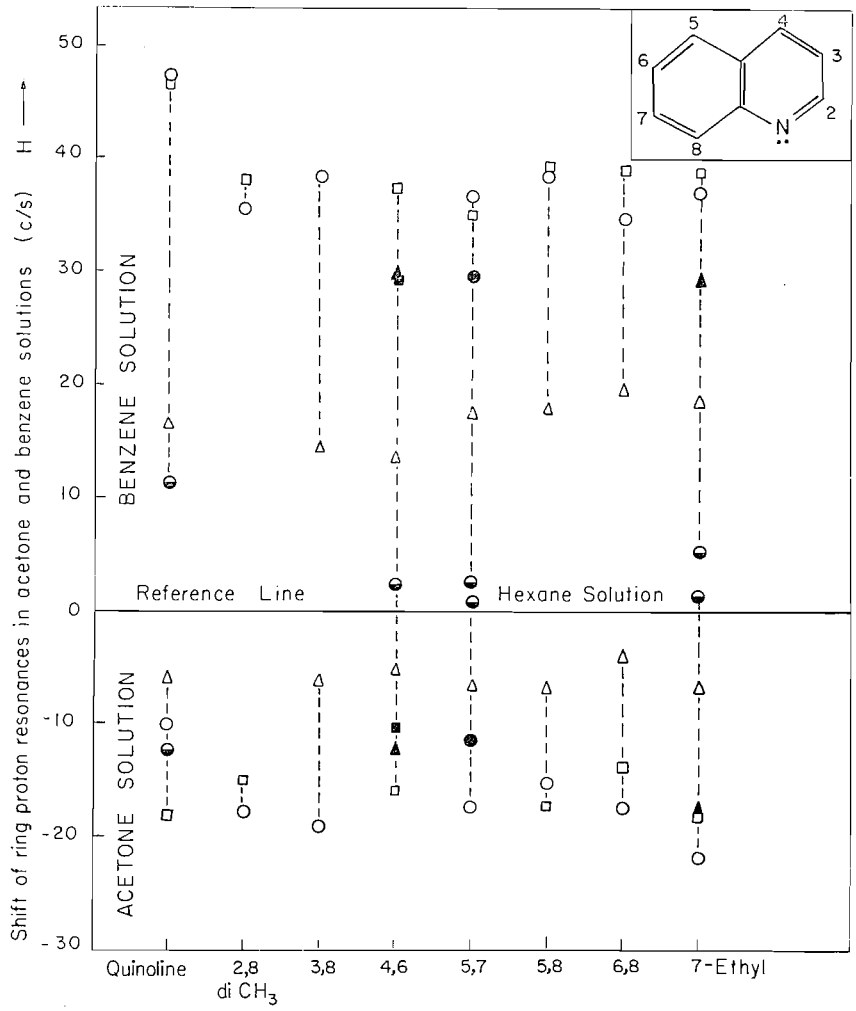


FIG. 1. Shifts of the ring protons of substituted quinolines in dilute acetone and benzene solutions relative to their position in the field for a dilute *n*-hexane solution. The shifts are given in cycles/sec for a measuring frequency of 60 Mc/sec. △, 2; □, 3; ○, 4; ▲, 5; ●, 6; ■, 7; ◒, 8.

value can be compared with one of 5.0 cycles/sec obtained from a spectrum of quinoline at 40 Mc/sec under somewhat lower resolution than was available in these experiments at 60 Mc/sec (3). Coupling of protons across the ring at positions 4 and 8 was found to be about 1 cycle/sec. Valence-bond calculations indicate coupling due to π electrons of less than 0.1 cycle/sec for the similar protons in naphthalene (4). Similar values have been found by Anet in 5,7-dimethylquinoline and 5,7-dichloroquinoline. As noted by Anet, such long-range coupling is limited to the 4- and 8-hydrogens and is comparable to coupling between hydrogen separated by five bonds in some olefins (5).

Finally, one might point out that in spectra as complex as these, preferential solvent shifts are extremely helpful in assignment of peaks as well as in the detailed analysis of groups of strongly coupled nuclei.

Can. J. Chem. Downloaded from www.nrcresearchpress.com by 210.87.254.105 on 09/05/12
For personal use only.

Can. J. Chem. Downloaded from www.nrcresearchpress.com by 210.87.254.105 on 09/05/12
For personal use only.

TABLE II

Coupling constants between ring protons in cycles/sec

Compound	J_{23}	J_{24}	J_{34}	J_{48}	J_{56}	J_{57}	J_{67}	J_{78}	J_{68}
Quinoline	4.1±0.2	1.8±0.2	8.5±0.3	1.0±0.2	—	—	—	8.2±0.3	2.1±0.2
2,8-Dimethylquinoline	4.2±0.2	2.2±0.2	—	—	—	—	—	—	—
4,6-Dimethylquinoline	—	—	—	—	—	1.8±0.2	—	8.5±0.2	—
5,7-Dimethylquinoline	4.0±0.1	1.6±0.1	8.4±0.1	0.5	—	—	—	—	—
5,8-Dimethylquinoline	4.1±0.1	1.7±0.1	8.4±0.2	—	—	—	7.2±0.3	—	—
6,8-Dimethylquinoline	4.1±0.1	1.8±0.1	8.2±0.2	—	—	—	—	—	—
7-Ethylquinoline	4.1±0.1	1.8±0.1	8.3±0.2	0.8±0.2	8.4±0.1	—	—	—	—

ACKNOWLEDGMENTS

The measurements were done on the spectrometer in the Pure Chemistry Division at the National Research Council. I would like to thank Dr. W. G. Schneider for permission to work in his laboratory and the many informative discussions which took place. I thank Mr. Yves Lupien for preparing the solutions.

1. T. SCHAEFER and W. G. SCHNEIDER. J. Chem. Phys. **32**, 1218 (1960).
2. T. SCHAEFER and W. G. SCHNEIDER. J. Chem. Phys. **32**, 1224 (1960).
3. J. A. POPLE, W. G. SCHNEIDER, and H. J. BERNSTEIN. High resolution nuclear magnetic resonance. McGraw-Hill Book Company, Inc., New York. 1959. p. 269.
4. H. M. MCCONNELL. J. Chem. Phys. **30**, 126 (1959).
5. F. A. L. ANET. J. Chem. Phys. **32**, 1274 (1960).

RECEIVED MAY 11, 1961.
DEPARTMENT OF CHEMISTRY,
UNIVERSITY OF MANITOBA,
WINNIPEG, MANITOBA.

Can. J. Chem. Downloaded from www.nrcresearchpress.com by 210.87.254.105 on 09/05/12
For personal use only.

Can. J. Chem. Downloaded from www.nrcresearchpress.com by 210.87.254.5 on 09/05/12
For personal use only.

Canadian Journal of Chemistry

Issued by THE NATIONAL RESEARCH COUNCIL OF CANADA

VOLUME 39 OCTOBER 1961 NUMBER 10

SURFACE EXCHANGE REACTIONS OF SILVER AND ITS IONS[1]

J. E. SANDOR[2]

ABSTRACT

The exchange reactions between silver and its ions in solution have been investigated by the use of radioactive tracers. Silver of highest purity was cleaned carefully and immersed into a radioactive silver nitrate solution. The course of the early absorption process and subsequent diffusion of the ions into the interior of the metal was followed in detail, and the diffusion coefficient at room temperature was calculated. The penetration depth was determined by controlled electropolishing of the metal, and the reverse movement of active ions from the metal into inactive solutions was also observed.

INTRODUCTION

The exchange reaction between metallic silver and its ions in solution has been investigated by several authors. This metal is of particular interest because it is available in high purity, is chemically inert, and has a convenient radioactive isotope with a half-life of 270 days.

Rollin (1) found that metallic silver, shaken with a silver nitrate solution containing radioactive silver, acquired an activity corresponding to more than 100 apparent atomic layers of silver. Baerg and Winkler (2) found that "abraded" and etched foil exchanged to different depths. They measured the "true" area by the Bowden–Rideal method (3) and tried to correlate surface area and exchange, but concluded that "the metal surfaces were poorly reproducible in respect to both exchange and area". Gerischer and Vielstich (4) observed that after a rapid initial exchange, which depended on the surface treatment, a second, slower increase in observed activity took place, and they attributed this increase to solid-state diffusion.

Tingley, Henderson, and Coffin (5) concluded from their work that generally there are two mechanisms acting in silver exchange reactions, one "kinetic" and the other a "true exchange"; which one of these was acting depended on the state of the surface.

King and McKinney (6) recently also found evidence that solid-state diffusion occurs in silver, accompanying the exchange reaction. A theoretical study of the heterogeneous reaction was done by Zimens (7). He devised equations relating the progress of the solid–liquid exchange with time, assuming that one of the following processes is the rate-determining one: (1) diffusion across the interface, (2) chemical reaction at the phase boundary, and (3) diffusion of the exchanging atoms into the interior of the solid. The rate laws for these processes are formally similar and are usually of an exponential nature.

It was the purpose of the present experiments to study the exchange between silver and its ions, following Zimens' model.

[1]*Manuscript received November 10, 1960.*
Contribution from the Mineral Sciences Division, Mines Branch, Department of Mines and Technical Surveys, Ottawa, Canada.
[2]*National Research Council Postdoctorate Fellow 1958–1960. Present address: Semiconductor Products Department, General Electric Company, Syracuse, N.Y.*

The main questions to be solved were: (1) the probable mechanism for a fast exchange to a depth of more than 100 atom layers, (2) the cause of the slow increase in observed activity after the initial exchange, and (3) a decision as to which of the three processes in Zimens' model were the rate-controlling ones. Gerischer and Vielstich (4) assumed that self-diffusion is the controlling step in the exchange; King and McKinney found some penetration of the radioisotope after the exchange. To confirm or deny these authors' findings and assumptions, an electropolishing technique was developed to measure the penetration of the radioisotope inside the solid.

Three major practical factors were considered essential to the success of the experiments: (1) use of high purity materials, (2) avoidance of oxidation and corrosion, and (3) careful preparation of the surfaces.

It should be stressed that small variations in technique can affect markedly the results of all such exchange experiments.

EXPERIMENTAL DETAILS

The radioisotope utilized for all the experiments was silver-110, obtained from Atomic Energy of Canada Ltd. It has a half-life of 270 days, and a complex beta- and gamma-ray spectrum with a maximum beta energy of 2.8 Mev and a maximum gamma-ray energy of 1.516 Mev.

All the activity measurements were done with a well-type NaI(Tl) scintillation counter. A statistical analysis of the counting assembly was done using a known source of Ag-110; the test indicated a satisfactory operation of the unit.

A 10^{-2} M silver nitrate solution was prepared with a specific activity of 6.5 μc/cc and a pH of 6.6. Metal foils were prepared from Johnson-Matthey 99.999% silver. Rods of 1.9-cm diameter and 2.5-cm length were alternately cold-rolled to 50% reduction and annealed 15 minutes at 500° C, to a final thickness of 0.0025 cm.

From these foils, samples of 1.5 cm^2 area were cut in such a way as to leave a short tip on one of the sides to use as a holder during the handling of the samples. (Silver-plated tweezers were used during all the experiments.)

These foils were cleaned in boiling ethanol for 1 hour, electropolished in a cyanide bath for 10 minutes, annealed for 20 minutes at 400° C, and finally electropolished again for 10 minutes. Samples prepared in this way showed no surface deformation when X-ray diffraction pictures were taken. These samples also stayed bright and untarnished when stored for considerable periods.

It was found that high annealing temperatures or long annealing periods produced some thermal etching, and that the pits were noticeably broadened during electropolishing.

EXPERIMENTS ON EXCHANGE AS A FUNCTION OF TIME

To find out if there was a continuous increase in activity after long periods of immersion,* 12 samples were left in a 100-cc Petri dish containing 50 ml of radioactive solution. The Petri dish was kept, for the duration of the experiments, in a well-shielded lead castle.

To simplify the handling of the specimens, they were attached by their tips to a ring of Lucite with a drop of paraffin. In this way some samples were immersed for as long as 37 days. This arrangement was adopted to avoid concentration changes in the solution

*By "long" is understood more than 1 day.

Can. J. Chem. Downloaded from www.nrcresearchpress.com by 210.87.254.5 on 09/05/12
For personal use only.

by evaporation, and at the same time to make it possible to subject at least 12 samples simultaneously to exchange processes.

The solution was not stirred; it was assumed that even without agitation the diffusion through the diffusion layer in the liquid was much faster than the solid-state diffusion in the metal and so this factor would not influence the final results. (The ratio $D_l/D_s = 10^{12}$.)

The samples were taken out at regular intervals, rinsed carefully with cold water and alcohol, dried, and counted in the scintillation counter. The first counting was done after 9 days of immersion. No counting was done at the beginning of the exchange, because previous experiments had established a very rapid increase in activity during the first few minutes of the exchange. In the work described here the emphasis was on the longer-term exchange, particularly to show whether there is a continuous increase in activity in the samples, and whether this slow increase is due to solid-state diffusion.

A small correction had to be made to take into account the decay of the radioisotope.

EXPERIMENTAL RESULTS

Activity Increase as a Function of Time

The results of the long-term immersion tests are plotted in Fig. 1 in terms of apparent

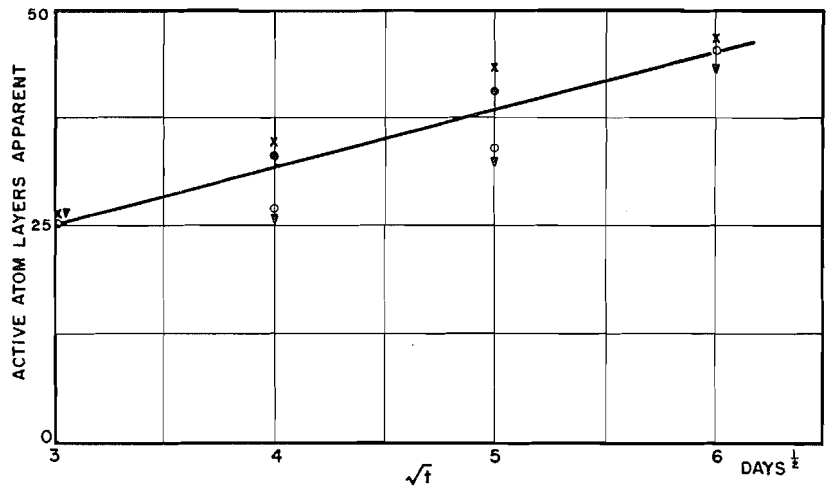


FIG. 1. Exchange as a function of time of immersion: ×, ●, ▼, ○ represent different samples.

layers of exchanged atoms as a function of time of immersion. The relation between adsorbed activity and equivalent atom layers had been established in an auxiliary electropolishing experiment. The first count was obtained after 9 days of immersion, and subsequent ones at intervals of 3 or 4 days.

The points correspond to different samples, but it seemed better to plot the average curve of the different samples than to draw a curve for each sample. There is some scatter in the points, but this was not the case when each sample was counted individually.

From this curve it can be seen that the activity increases approximately as a function of the square root of time, as expected if a diffusion process is the rate-determining process.

Can. J. Chem. Downloaded from www.nrcresearchpress.com by 210.87.254.5 on 09/05/12
For personal use only.

In the case of three samples the activity pickup was much higher than for the others. The reason for this divergence is not clear, but it may have been caused by some disturbance of the adsorption equilibrium, or by a deformation of the surfaces during the handling, which interfered with the reaction exchange – solid-state diffusion. This curve does not fit the equation $A_t = f(\sqrt{t})$.

Measurement of Penetration Depths

To find out if there was a measurable penetration of the radioactive isotope, and to calculate a self-diffusion coefficient for silver, the "exchanged" specimens were electropolished under reproducible conditions. It was ascertained that the same period of electropolishing removed the same weight of silver each time. In addition to this, before electropolishing, the samples were immersed in the electrolyte for short periods of time—ranging from 1 second to 1 minute—without applying electrical current, to see which portion of the activity was "re-exchangeable". The remaining activity in the samples was then counted.

In Table I are summarized the results of the immersion of the samples in the electrolyte

TABLE I

Exchanged samples immersed in the electropolishing solution without applying current

Sample No.	History	Time of immersion in electrolyte, sec	Initial activity, c.p.m.	Remaining activity, c.p.m.	Loss of activity, %
1	Exchanged 34 days, stored 60 days	1	14,000	8,900	36
		60		7,000	50
2	Exchanged 34 days, stored 30 days	1	12,000	7,700	36
		60		6,100	49
4	Exchanged 37 days, stored 60 days	1	25,000	18,000	28
		60		14,300	43
6	Exchanged 31 days, stored 60 days	1	13,600	7,700	43
		60		6,800	50
8	Exchanged 25 days, immediately after	1	25,000	19,200	23
		60		14,600	42
9	Exchanged 25 days, immediately after	1	24,600	18,000	27
		60		10,600	57

without applying current. It is evident that more than 40% of the activity is "exchangeable", and that between 20 and 45% of the activity is lost after the first second of immersion; in addition to this, the samples that picked up higher activity have a higher fraction of "exchangeable" atoms.

The results of the experiments done by progressively electropolishing the exchanged samples show that there is a measurable penetration of the radioactive tracer.

In Fig. 2*a* are plotted the penetration curves of some of the samples listed in Table I. The logarithm of the activity in c.p.m. is plotted as a function of the time of electropolishing. It was established by previous experiments that, under the operating conditions used, in the exchanged samples 1 minute of electropolishing was equivalent to removing an amount of silver equivalent to a thickness of 1μ.

It was observed that there was a large decrease of activity after removing the first 0.13 to 0.25 μ, and then a much smaller decrease in activity when a subsequent comparable thickness was removed.

It can be seen in Fig. 2*b* that the penetration curves are clearly the combination of two

Can. J. Chem. Downloaded from www.nrcresearchpress.com by 210.87.254.5 on 09/05/12
For personal use only.

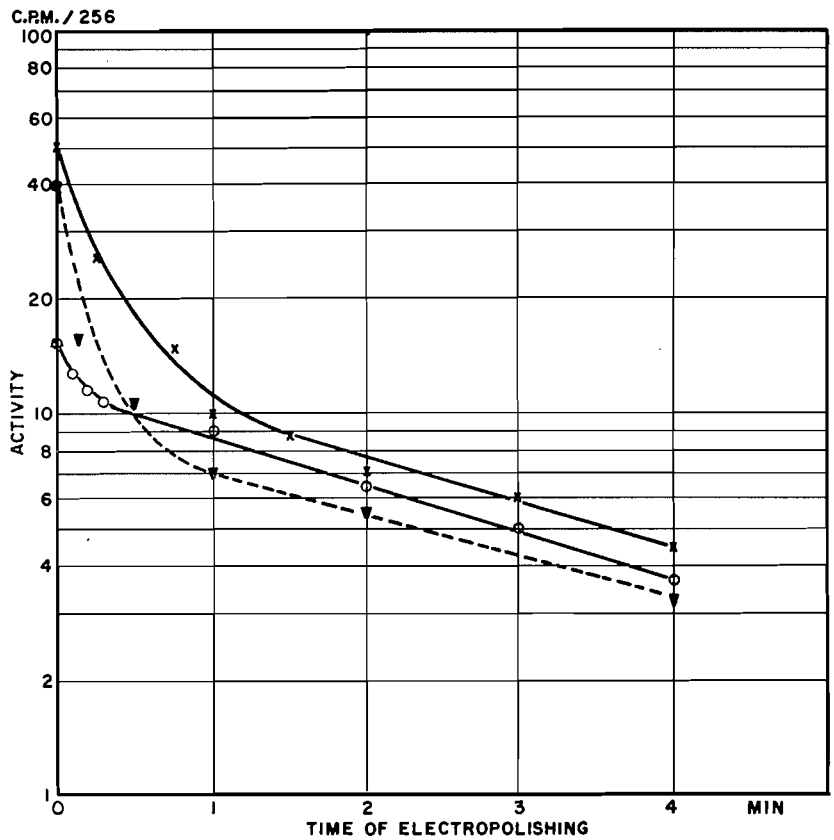


FIG. 2*a*. Penetration curves for fresh samples: ○, sample No. 2; ×, sample No. 8; ▼, sample No. 9.

independent exponential functions representing two processes proceeding at different rates.

It was observed that long storage of the foils after the exchange process affected the slope of the second part of the curves, and it made some difference in their initial slope. This effect is shown in Fig. 3. Longer storage times tended to flatten this first part.

CALCULATION OF DIFFUSION COEFFICIENT

From the data of the penetration curves the self-diffusion coefficient of silver at room temperature was calculated.

Fisher (8) made a mathematical analysis of the relation between grain boundary diffusion D_b and volume diffusion D_v by assuming that grain boundary diffusion is analogous to the diffusion of heat along a thin copper foil embedded in cork. He arrived at an expression

$$D_b = 2D_v^{1/2}(\log e)^2 \Big/ \delta\left(\frac{d\log a_x}{dx}\right)^2 (\pi t)^{1/2},$$

where e is the logarithm base and δ the grain boundary thickness. The same author

Can. J. Chem. Downloaded from www.nrcresearchpress.com by 210.87.254.5 on 09/05/12
For personal use only.

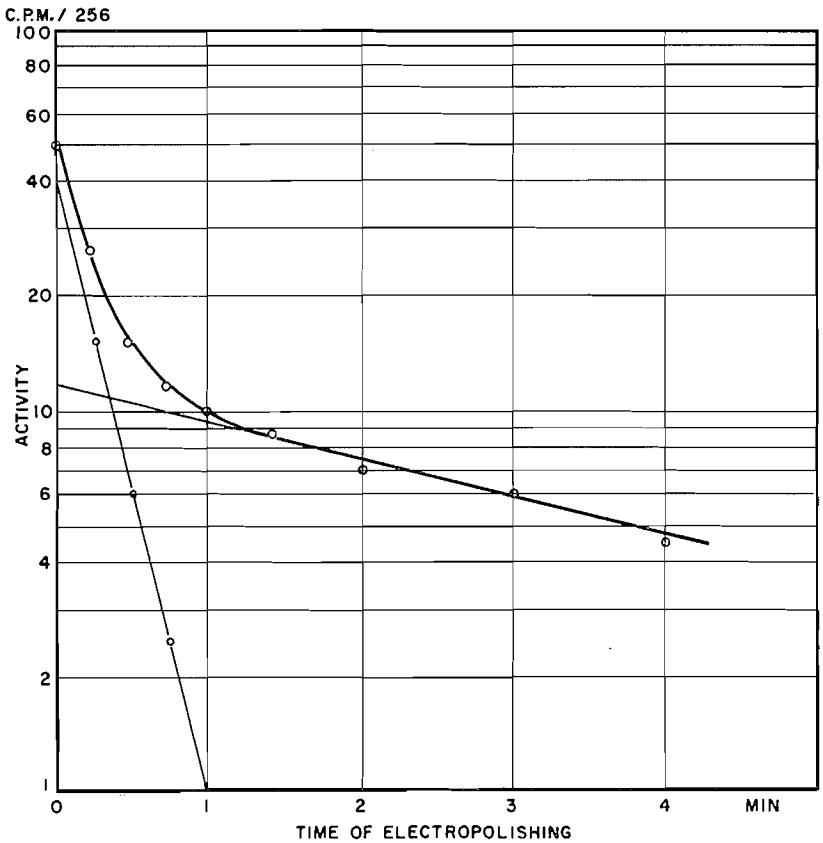


FIG. 2*b*. Penetration curves: analysis of typical curve.

assumed for δ a value of 5×10^{-8} cm that has since been criticized (9) because it is very hard to establish a uniform thickness for the grain boundaries of metals, but it can be used as an approximation. D_v can be calculated from the formula of Hoffman and Turnbull (10):

$$D_v = 0.895\exp(-49{,}500/RT)\ \text{cm}^2/\text{sec};$$

the value at 25° C is $D_v = 9.8\times10^{-38}$ cm²/sec. Inserting this value into the equation for D_b gives

$$D_b = 6\times10^{-11} \Big/ \left(\frac{d\log a_x}{dx}\right)^2 t^{1/2}$$

$$= 1.37\times10^{-20}\ \text{cm}^2/\text{sec},$$

where a_x = activity, x = penetration, and t = time of exchange. The slope of the straight part of the curves of Fig. 2*a* and a value of t = 34 days were used for the calculation.

Can. J. Chem. Downloaded from www.nrcresearchpress.com by 210.87.254.5 on 09/05/12
For personal use only.

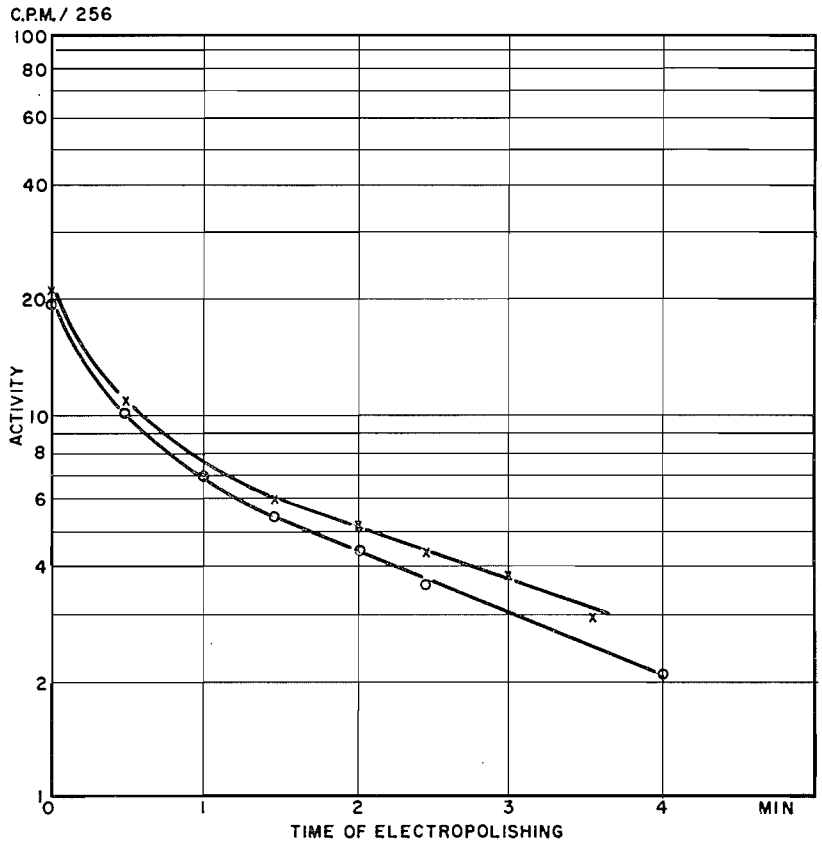


FIG. 3. Penetration curves for aged samples: ×, sample No. 11; ○, sample No. 12.

DISCUSSION AND CONCLUSIONS

The results of this work confirm the conclusions from previous work that self-diffusion of silver is the rate-controlling step in the exchange reaction, and show clearly that there is fast diffusion in the uppermost atomic layers (approximately 300 layers). In the absence of corrosion, oxidation, or local cell action, in the case of silver a rapid exchange takes place between the surface atoms of the metal and the ions in the liquid on immersing the electropolished foils in the exchange solution. At the same time, some local cell action due to the presence of different crystal faces may take place, but in a polycrystalline material the electromotive force resulting from this difference must be negligible.

To measure the extent of reversibility of this exchange reaction, the reverse experiment was carried out. It was found that close to 50% of the activity of the samples was lost after a few seconds of immersion in an inactive silver nitrate solution. This would indicate that the adsorbed (chemisorbed and ionic double-layer) atoms re-exchange readily with the solution; the results are plotted in Fig. 4.

The results of the long-term experiments on the increase of activity with time gave a clear indication that a diffusion process was involved. The penetration curves confirmed this supposition. It was found that fast exchange at the surface is followed by diffusion of the atoms inside the solid.

Can. J. Chem. Downloaded from www.nrcresearchpress.com by 210.87.254.5 on 09/05/12
For personal use only.

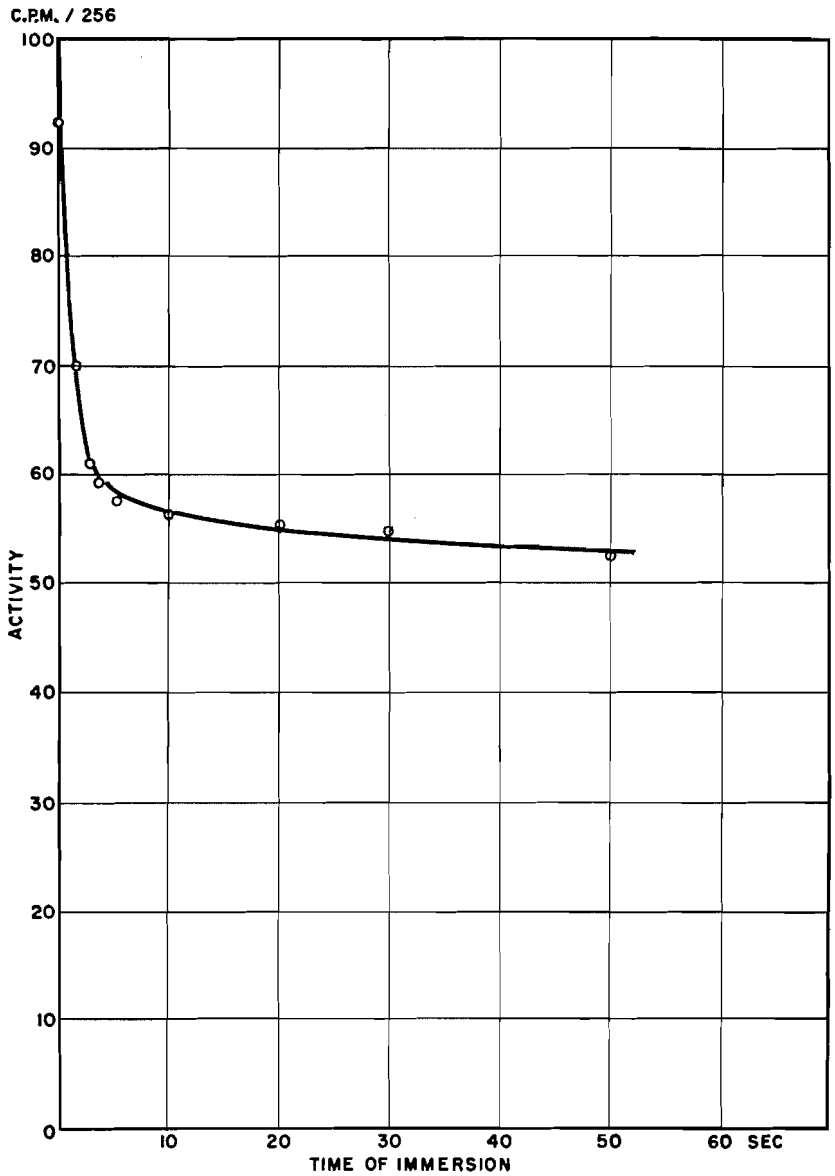


FIG. 4. Reverse exchange, active metal immersed in inactive solution.

It follows that two different mechanisms are acting, a fast diffusion process down to a depth of 300 atomic layers, followed by a much slower one at greater depth.

The diffusion coefficient found in the present study for this second process is $D_b = 1.37 \times 10^{-20}$ cm^2/sec. This compares with a value of $D_b = 6.14 \times 10^{-22}$ cm^2/sec, using Hoffman and Turnbull's formula and calculating for 25° C of temperature.

The difference of two orders of magnitude can be explained either as a result of extrapolation, because the work of Hoffman and Turnbull was done at high temperatures, or

Can. J. Chem. Downloaded from www.nrcresearchpress.com by 210.87.254.5 on 09/05/12
For personal use only.

because there is a difference in the activation energy, indicating that another mechanism is acting at low temperatures.

Other authors found a difference of 4 or 5 orders of magnitude; this can be attributed to less-pure samples, or to less-well-polished surfaces.

It is an accepted theory that self-diffusion in face-centered cubic metals takes place by a lattice-vacancy mechanism. It has already been shown that in diffusion curves for polycrystals unusually high activity was noted at small penetration depths (11). The same result is found in the present study, so it is probable that there is a much more disordered and loose structure of atoms close to the surface exposed to the solution.

This would explain the high rate of adsorption at the beginning of the exchange reaction. It also accounts for the fact that in cold-rolled samples there is a faster diffusion than in annealed specimens, and for the observation that pretreating the surfaces in inactive silver before the exchange experiments tends to decrease the exchange rate.

The whole process can be pictured as in Fig. 5, i.e., similar to the interdiffusion of two solids.

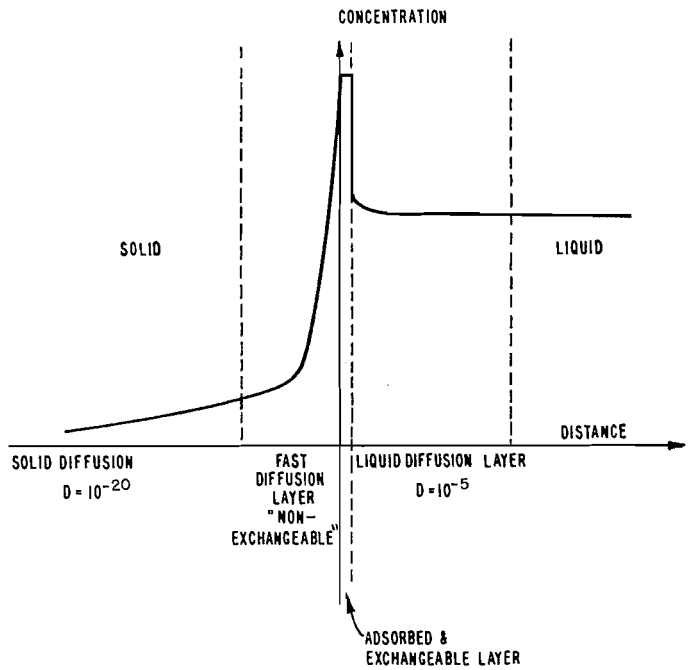


FIG. 5. Diagram of exchange layers.

The smallest diffusion coefficient is in the solid phase and it is the rate-determining factor in the whole exchange process under near-equilibrium conditions at the surface.

The atoms move from a solid lattice structure through a "fast diffusion" layer, through a phase boundary, through the liquid diffusion layer, and finally to the bulk of the liquid.

Summary

(1) A continuous increase in activity was found by immersing electropolished and annealed silver foils in a silver nitrate solution containing radioactive silver, for periods of 9 to 37 days. The adsorption process was a square root function of time.

Can. J. Chem. Downloaded from www.nrcresearchpress.com by 210.87.254.5 on 09/05/12
For personal use only.

(2) Close to 50% of the activity was lost by reverse exchange when the exchanged samples were immersed in inactive silver nitrate solution; the remainder was removed from the contact area by diffusion into the interior of the metal.

(3) The measurement of the penetration of the radioactive isotope after exchange was carried out using an electropolishing technique and showed an exponential distribution with depth.

It is concluded that a fast diffusion occurs close to the surface, followed by a slower one inside the metal. The calculated diffusion coefficient in the bulk of the solid does not differ much from the one calculated from Hoffman and Turnbull's results.

(4) A model of the whole exchange process is proposed, assuming that self-diffusion in the solid is the rate-determining process.

ACKNOWLEDGMENTS

The author wishes to express his appreciation to Dr. G. G. Eichholz for his help during all this work, to Dr. J. D. Keys for many helpful discussions, and to many members of the Physics and Radiotracer Section of the Mineral Sciences Division, Mines Branch, for their advice and assistance. This work was done during the tenure of a National Research Council of Canada Postdoctorate Fellowship at the Mines Branch of the Department of Mines and Technical Surveys, Ottawa, which is gratefully acknowledged. This paper is published by permission of the Director of the Mines Branch, Department of Mines and Technical Surveys, Ottawa.

REFERENCES

1. B. V. ROLLIN. J. Am. Chem. Soc. **62**, 86 (1940).
2. A. BAERG and C. A. WINKLER. Can. J. Chem. **31**, 319 , 521 (1953).
3. A. E. HUTCHEON and C. A. WINKLER. Can. J. Research, B, **27**, 353 (1949).
4. H. GERISCHER and W. VIELSTICH. Z. Elektrochem. **56**, 380 (1952); **58**, 919 (1954).
5. I. I. TINGLEY, I. H. S. HENDERSON, and C. C. COFFIN. Can. J. Chem. **34**, 14 (1956).
6. C. V. KING and N. E. MCKINNEY. Can. J. Chem. **37**, 205 (1959).
7. K. E. ZIMENS. Arkiv Kemi, **20**, 10 (1945).
8. J. C. FISHER. J. Appl. Phys. **22**, 74 (1951).
9. P. LACOMBE. Private communication.
10. R. E. HOFFMAN and D. TURNBULL. J. Appl. Phys. **22**, 634 (1951).
11. P. J. FENSHAW. Australian J. Sci. Research, Ser. A, **3**, 91 (1950).

Can. J. Chem. Downloaded from www.nrcresearchpress.com by 210.87.254.5 on 09/05/12
For personal use only.

Can. J. Chem. Downloaded from www.nrcresearchpress.com by 210.87.254.40 on 09/05/12
For personal use only.

CLAM POISON

II. PURIFICATION OF CLAM POISON RESIDUES OF LOW TOXICITY BY A HEAVY-PAPER TECHNIQUE[1]

R. A. B. Bannard and A. A. Casselman

ABSTRACT

The usefulness of Whatman seed-test and No. 17 papers has been examined for purification and recovery on a preparative scale of the toxin present in residues of low toxicity from the Schantz alumina chromatographic method for purification of clam poison. A method was developed to minimize introduction of impurities from the papers into fractions recovered after chromatography when *t*-butanol:acetic acid:water (2:1:1) was used as developer. Seed-test paper gave better separation of the toxin from other components of the residues than did No. 17 paper. Residues of bio-assay as low as 300 MU/mg were found to be capable of enrichment by the method. On a scale of 500 mg per 18×22-in. sheet of pretreated seed-test paper, using residues of toxicity 1400 MU/mg, a 67% recovery of toxin enriched fourfold to 5800 MU/mg was achieved in four passes. Increased loading of the paper led to a decrease in both enrichment per pass and over-all recovery of toxin. The paper chromatographic properties, toxicity, and infrared spectrum of the recovered poison agree with those reported by Schantz and co-workers for pure clam poison dihydrochloride, but the specific rotation is lower by 25%. Four possible alternative explanations for the observed anomalous rotation are discussed.

INTRODUCTION

In the method devised by Schantz and co-workers (1) for purification of clam poison, the final step involves chromatography of clam poison dihydrochloride of 55–70% purity on acid-washed alumina, employing absolute and aqueous ethanol as eluants. In this step, 25–45% of the toxin applied is recovered in pure form and an over-all recovery of 70–90% is achieved, but some of the toxin remains on the column and must be removed by elution with water. Some of the fractions resulting from the process proved capable of further enrichment by recycling in the same manner, but it was not found profitable to attempt enrichment of samples of purity less than 30–50% in this way (2). In recent years, considerable quantities of clam poison residues of low toxicity from this process (hereinafter referred to as clam poison tailings) have accumulated, and it has been estimated (3) that as much as 25 g of toxin could be made available for study if a suitable method of purification could be devised. Several attempts were made to enrich clam poison tailings by chromatography on paper, cellulose columns, cation exchange resins, and acid-washed alumina, but these proved fruitless (4). The successful application of paper chromatography to this problem on a semimicro scale, which we recently reported (5), led us to attempt extension of the method to a preparative scale by the use of heavy paper. The present communication describes a method whereby clam poison tailings of toxicity 1400 MU/mg can be enriched to toxicity 5800 MU/mg in 67% yield on a scale of 500 mg.

RESULTS AND DISCUSSION

The purification of clam poison dihydrochloride and clam poison tailings by chromatography on a semimicro scale on Whatman No. 1 paper using *t*-butanol:acetic acid:water (2:1:1) as developer has recently been described (5). In this work extensive pretreatment of the paper was necessary to minimize the introduction of impurities into the recovered toxin. Brownell, Hamilton, and Casselman (6) previously established the usefulness of

[1]*Manuscript received May 18, 1961.*
Contribution from Defence Research Chemical Laboratories, Ottawa, Canada.
Issued as D.R.C.L. Report No. 346A.

chromatography on Whatman seed-test paper for the purification of amino acids and pyrophosphate esters on a preparative scale and found extensive pretreatment of the paper unnecessary since no appreciable quantities of impurities were introduced into the recovered substances by the neutral solvent systems which they employed. We were committed to use of the acidic solvent system mentioned above because of its ability to separate the components present in clam poison tailings and it seemed to us that the effectiveness of the heavy-paper technique would depend largely on the quantities of impurities introduced into the various fractions during chromatography. The other factor upon which the usefulness of the method would primarily depend is the degree of resolution of components attainable relative to the loading of the paper.

Attention was first directed to the question of impurities introduced during chromatography and the steps required to minimize them. Untreated Whatman No. 17 and seed-test papers were developed in *t*-butanol:acetic acid:water (2:1:1) by the descending method and air-dried; rectangular strips corresponding to preselected R_F ranges were removed and eluted with water; and the quantities of extractable impurities were determined by weighing, after lyophilization. Papers were then pretreated by the chromatographic washing procedure which had proved to be most effective for the removal of impurities from Whatman No. 1 paper (5) and the quantities of residues recovered by aqueous elution were determined as described above. Finally, the residues thus obtained were taken up in water and the quantities of impurities remaining after (*a*) filtration through a fritted glass filter and (*b*) elution through Amberlite IRA-400 (Cl) resin were determined.

It is evident from Table I that, as anticipated, unwashed seed-test paper yields much

TABLE I

Impurity recovered from Whatman seed-test and No. 17 papers

R_F range of band	Weight recovered by simple elution (mg/in²)		Weight after filtration (mg/in²)		Weight after resin treatment (mg/in²)	
	Unwashed	Pretreated	Unwashed	Pretreated	Unwashed	Pretreated
Whatman seed-test						
0–10	0.317	0.054	0.285	0.038	0.223	0.024
14–25	0.563	0.061	0.535	0.040	0.438	0.026
29–39	1.151	0.061	1.097	0.035	0.984	0.025
40–51	2.010	0.061	1.946	0.043	1.791	0.026
55–65	2.960	0.058	2.899	0.040	2.760	0.027
79–90	3.363	0.076	3.256	0.058	3.085	0.035
Whatman No. 17						
0–10	0.086	0.057	0.079	0.037	0.041	0.028
14–25	0.092	0.038	0.072	0.031	0.047	0.022
29–39	0.143	0.041	0.132	0.029	0.084	0.016
40–51	0.175	0.050	0.162	0.026	0.089	0.017
55–65	0.645	0.059	0.605	0.028	0.234	0.017
79–90	0.736	0.058	0.734	0.036	0.353	0.021

larger quantities of impurities than does No. 17 paper. The quantity of impurity in both unwashed papers increases rapidly with increasing R_F, in agreement with results obtained earlier with unwashed Whatman No. 1 paper. Pretreatment reduces the quantities of impurities extracted from both papers to the same order of magnitude and leads to greater uniformity in the weight of impurity as the R_F is increased. In the R_F range 0.14–0.39, which is the region in which clam poison was expected to be located in actual

Can. J. Chem. Downloaded from www.nrcresearchpress.com by 210.87.254.40 on 09/05/12
For personal use only.

Can. J. Chem. Downloaded from www.nrcresearchpress.com by 210.87.254.40 on 09/05/12
For personal use only.

chromatograms, pretreated No. 17 and seed-test paper gave quantities of impurities which were respectively three and four times as large as those found for Whatman No. 1 paper by simple elution. Portions of these impurities can be eliminated from the reconstituted aqueous eluates by filtration through a fritted disk. The relative improvement thereby produced is in the following order: pretreated No. 17 ≈ pretreated seed-test > unwashed No. 17 ≈ unwashed seed-test. These results indicate that pretreatment produces a relatively larger quantity of insoluble fibrous debris than was present in the unwashed paper, but effectively removes the majority of the impurity initially present, which was mainly soluble rather than fibrous. More impurities can be eliminated from the reconstituted aqueous eluates from the filtration treatment by passing the solution through Amberlite IRA-400 (Cl) resin. The relative improvement was approximately identical for all but unwashed seed-test paper. These results suggest that the type of anionic impurity which is being removed from all but unwashed seed-test paper is uniform and this impurity could well be acetate ion which had been introduced by the pretreatment. The type of anionic impurity present in unwashed seed-test paper would be expected to be less uniform since the paper received no pretreatment.

By combined pretreatment, filtration, and elution through resin, the impurities in the R_F range 0.14–0.39 for No. 17 and seed-test papers were reduced respectively to one and one-half and twice the quantities obtained from pretreated Whatman No. 1 paper. Attempts were made to reduce the quantities of impurities still further by the use of millipore filters but no improvement resulted. Huffman and co-workers (7) found during alternate successive aqueous extraction and drying of Whatman No. 1 paper that no further reduction in the water-soluble carbohydrate impurities recovered occurred after the third extraction. This phenomenon was considered (7) to be related to the deterioration of cellulose caused by alternate wetting and drying of the paper and by the action of ozone at high moisture levels. Since the pretreatment method which was used for the purification of Whatman No. 1 paper (5) and the papers in the present investigation involved air-drying prior to water-washing after treatment with each irrigant, it seemed worth while to investigate the effect of eliminating the drying steps by using a continuous washing procedure. The quantities of residues found by this method after subsequent filtration and resin treatment were approximately one-third larger than given by the intermittent washing procedure and therefore no improvement resulted. Continuous washing did have the advantage, however, of reducing the time required for washing the papers from 39 to 30 days.

As a result of the purification of the heavy papers it was estimated that if a toxin fraction as large as 100 mg could be confined to a rectangular band 1×18 in., only 0.3 to 0.4% of impurity would be introduced by the paper, and this level of impurity was considered to be quite acceptable for our purposes.

Preliminary chromatograms were performed on Whatman No. 1, No. 17, and seed-test papers using clam poison tailings of toxicity 1400 MU/mg (25%) and $[\alpha]_D^{25}$ +26.3°. The results given in Table II indicate the presence of six components, only three of which are Weber-positive (8). The atypical Sakaguchi (9) and ninhydrin reactions shown by component 2 were observed earlier (5) to be characteristic of clam poison and it was concluded that this was the desired material. The components were sufficiently well separated in these chromatograms to suggest that successful separations could be achieved at considerably heavier loading.

A sample of clam poison tailings (100 mg, toxicity 1400 MU/mg, $[\alpha]_D^{25}$ +26.3°) was applied to a $4\frac{3}{4}$×22-in. sheet of specially pretreated Whatman seed-test paper and

TABLE II

Qualitative paper chromatography of clam poison tailings

Component number	R_F on Whatman			Color with chromogenic agent			
	No. 1	No. 17	Seed-test	Weber	Sakaguchi	Ninhydrin	Ultraviolet
1	0.26	0.28	0.19	Pink	Red	Purple	Blue (f)
2	0.32	0.34	0.23	Pink	Yellowish green	Yellow	Blue (s)
3	0.38	0.38	0.29	Pink	Red	Purple	Blue (f)
4	0.40	0.44	0.34				Blue (f)
5	0.53	0.58	0.40				Blue (f)
6	0.64	0.74	0.53				Blue (f)

NOTE: (s) = strong, (f) = faint.

developed with *t*-butanol:acetic acid:water (2:1:1). The components were located on the air-dried chromatogram by their fluorescence under ultraviolet irradiation and were recovered by elution with water, and the eluates lyophilized, weighed, and bio-assayed as described in the experimental section. In this manner, fractions 1–6, given in Table III, were obtained. All the toxic material was confined to fractions 1, 2, and 3 and although

TABLE III

Quantitative paper chromatography of clam poison tailings*

Pass No.	Fraction No.	R_F	Corrected weight (mg)	Toxicity (MU/mg)	Total MU		% recovery
					Interim	Final	
1	1	0.18	17.40	800	13,900		
	2	0.23	23.30	4,400	103,000		
	3	0.27	35.37	800	28,400		
	4	0.34	24.00	Nil			
	5	0.42	1.21	Nil			
	6	0.50	0.69	Nil			
2	7	0.19	12.55	400		5,020	3.6
	8	0.24	12.20	2,900	35,400		
	9	0.30	28.10	100		2,810	2.0
3	10	0.19	3.71	1,000		3,710	2.7
	11	0.25	3.44	4,800	16,500		
	12	0.31	5.29	400		2,120	1.5
4	13	0.19	7.32	1,100		8,050	5.8
	14	0.25	16.10	5,800		93,400	66.9
	15	0.31	3.49	200		700	0.5
						116,000	83.0

*100 mg tailings (1400 MU/mg) applied (total MU = 140,000).

the percentage recovery on both a weight (102%) and toxicity (104%) basis was slightly greater than theoretical, the values found are within the experimental error of the method. The procedure is clearly capable of effecting a significant enrichment of clam poison present in the tailings since, judging from its toxicity, fraction 2 has been enriched threefold and contains 73% of the toxin originally applied to the paper. Fractions 1 and 3, on the other hand, are less pure than the original tailings and provided suitable material for examination of the effectiveness of the procedure for enrichment of tailings containing toxin approximately half as pure as that in the original sample. Fractions 1 and 3, after repurification as described above, gave fractions 7, 8, and 9. As before, the majority of

Can. J. Chem. Downloaded from www.nrcresearchpress.com by 210.87.254.40 on 09/05/12
For personal use only.

the toxicity (80%) was confined to the fraction of R_F 0.24, which had been enriched 3.5-fold to a toxicity of 2900 MU/mg. Although the degree of enrichment was slightly greater than that obtained in the first pass, the purity of fraction 8 is considerably less than that of fraction 2 because of the differential in purity of the two samples employed. Fractions 7 and 9 contain only 8000 MU of poison, which is little more than 1 mg of pure toxin (assuming the toxicity of pure clam poison to be 5500 MU/mg), and these fractions were discarded. In a subsequent experiment, however, in which 166 mg of tailings of bio-assay 300 MU/mg was purified by the same method, a 70% recovery of poison enriched approximately sevenfold to 2000 MU/mg was obtained, indicating that the procedure is effective even for concentration of tailings which contain as little as 5% of the poison. Fraction 8 was repurified in the same manner, yielding fractions 10, 11, and 12. In this pass, only an approximately twofold enrichment resulted and both the over-all recovery (64%) and percentage recovery in the most toxic band (47%) decreased sharply. By means of passes 2 and 3, however, the over-all recovery of poison of toxicity 4400 MU/mg or greater was increased to 85% from 73%. Fractions 2 and 11 were combined for a final purification to determine whether poison of toxicity identical with that reported by Schantz *et al.* (1) for pure clam poison dihydrochloride could be obtained by the method. The results given for fractions 14, 15, and 16 demonstrate that this objective was achieved.

In four treatments on seed-test paper it was thus possible to effect a fourfold enrichment of the toxin in 67% yield and to recover a further 17% of the poison in a less pure condition. Translating these results from $4\frac{3}{4}\times22$-in. strips to 18×22-in. sheets indicated that the method should be capable of treating 500 mg of tailings per sheet. In a subsequent experiment 500 mg of tailings was purified in the same manner as described above and produced identical results.

In another experiment the loading was increased to 200 mg per $4\frac{3}{4}\times22$-in. strip (i.e. 1.0 g per 18×22-in. sheet). In the first pass, 87% of the toxicity was recovered in the band of R_F 0.24, but the enrichment achieved was only 1.9-fold from 1400 MU/mg to 2600 MU/mg. After the fourth pass, 56% of the toxin applied in the first step was recovered, enriched 3.6-fold to 5000 MU/mg, and an additional 25% of the poison was recovered at lower enrichment levels. Thus, the lighter loading (500 mg per 18×22-in. sheet) is capable of producing more efficient enrichment than the heavier loading.

The usefulness of pretreated Whatman No. 17 paper in this method of purification was also examined, but was found less satisfactory than seed-test paper on the basis of both degree of enrichment and over-all recovery of toxin.

Previously, it was shown that clam poison dihydrochloride which had been purified by the semimicro paper chromatographic method (5) possesses a toxicity and rotation within the range of values reported by Schantz and co-workers (1, 10, 13) (5500 ± 500 MU/mg, $[\alpha]_D^{25}$ $+130°\pm5°$) for the pure material. Also the infrared spectrum (KBr pellet) of toxin purified by the paper chromatographic method (5) was indistinguishable from that found by Schantz and co-workers. Samples of clam poison which bio-assayed at 5000–5800 MU/mg after purification by the heavy-paper technique described above were also found to exhibit an infrared spectrum indistinguishable from that previously reported for clam poison dihydrochloride (5) and we were therefore surprised to find that the specific rotations of these samples fell within the range 94–101°, which is well below the limit accepted for pure clam poison. Rechromatography of these samples on pretreated Whatman No. 1 paper gave only one Weber-positive spot, R_F 0.32 (cf. Table II). When ninhydrin was used as the chromogenic agent, however, very faint purple spots, R_F 0.26 and 0.38, were also revealed and very faint red spots with the same R_F's

Can. J. Chem. Downloaded from www.nrcresearchpress.com by 210.87.254.40 on 09/05/12
For personal use only.

Can. J. Chem. Downloaded from www.nrcresearchpress.com by 210.87.254.40 on 09/05/12
For personal use only.

were observed with Sakaguchi reagent. It thus appears that traces of components 1 and 3 (Table II) still remain in toxin (component 2) purified by the heavy-paper technique even when the bio-assay exceeds 5000 MU/mg. The intensities of the spots revealed by ninhydrin and Sakaguchi reagents were very weak, however, and it was considered unlikely that sufficient of these materials were present to markedly depress the rotation of the samples unless these components possess a high negative rotation. That such is not the case was determined by examination of side bands from the purification which are rich in the ninhydrin-positive components 1 or 3 and also contain a small amount of the Weber-positive toxin (component 2). The first fraction examined had toxicity 600 MU/mg and $[\alpha]_D^{25}$ +18.5°. On rechromatography on Whatman No. 1 paper it gave a strong ninhydrin-positive spot at R_F 0.26, and a faint Weber-positive toxin spot at R_F 0.32, indicating the majority of this band to be component 1. The second fraction examined had toxicity 600 MU/mg and $[\alpha]_D^{25}$ +14.5°. On rechromatography on Whatman No. 1 paper it gave a faint Weber-positive toxin spot at R_F 0.32 and a strong ninhydrin-positive spot at R_F 0.38, indicating the majority of this band to be component 3. Judging from the toxicity assays on the two fractions, not more than 10% of each can be toxin. It was therefore concluded that the minor amounts of components 1 and 3 which are present in highly toxic samples recovered from the tailings are not responsible for the low optical rotations observed. It was also established that the low rotations do not owe their origin to an impurity extracted from the paper during recovery of the toxin. Measurements on 1% aqueous solutions of the impurity recovered from seed-test paper in the R_F range 0.14–0.25 exhibited negligible optical activity and in the actual purification of tailings the concentration of the impurity in the recovered toxin is approximately 100-fold more dilute.

Four alternative explanations for the observed rotations are possible. (*a*) Paper chromatography has eliminated some impurity with a rotation higher than +100° which was not removed from clam poison by the methods of Schantz *et al.* (*b*) The toxin present in the tailings is not clam poison but another toxin of closely related structure which has a lower positive rotation. (*c*) The tailings contain two toxins, clam poison and another toxin of lower positive rotation, which are not separated by paper chromatography. (*d*) The tailings contain a non-toxic impurity with a high negative rotation which is not separated from clam poison by paper chromatography.

Alternative (*a*) appears unlikely because Schantz *et al.* (1, 10) obtained clam poison of identical toxicity and rotation (5500±500 MU/mg and $[\alpha]_D^{25}$ +130°±5°) by three different methods of purification, viz. by chromatography on alumina, by chromatography on Norit A followed by crystallization as the helianthate, and by countercurrent distribution. Also, we have observed the same physical constants for clam poison purified by semimicro quantitative paper chromatography (5). It should be emphasized, however, that the chromatographic properties of the clam poison sample purified earlier (5) by the semimicro method and the clam poison tailings purified by the macro method reported herein do not correspond in all respects. It seems reasonable, therefore, to assume that the abnormal optical rotations encountered in the present work owe their origin to some material in the tailings which was absent from the sample purified earlier by the semimicro method and that the nature of the unknown material is explicable by one of the alternatives (*b*), (*c*), or (*d*) mentioned above. Alternative (*b*) at first appears unlikely because of the infrared spectral data. However, the infrared spectrum of clam poison contains little fine structure and may be relatively insensitive to minor structural changes involving, for example, stereoisomerism or tautomerism. In this connection it has been

Can. J. Chem. Downloaded from www.nrcresearchpress.com by 210.87.254.40 on 09/05/12
For personal use only.

shown by Schantz *et al.* (10, 13) that little change in the spectrum results from conversion of clam poison to dihydro clam poison by catalytic hydrogenation, even though all the toxicity is lost in the process and the chromatographic properties change markedly (10). Mold *et al.* have obtained evidence from countercurrent distribution studies at pH 8 that clam poison can exist in two tautomeric forms, both of which are highly toxic (10). It may therefore be that the reason for retention of the tailings toxin by the alumina during the original purification is that its structure differs in some subtle manner from clam poison. That minor structural changes can cause significant differences in ease or order of elution of compounds in adsorption chromatography is well known (11). The possibility should also not be overlooked that the toxin recovered from the tailings is a partially degraded clam poison. Dr. E. J. Schantz has recently informed us in a private communication that studies in his laboratory have shown that the optical rotation of clam poison decreases to +50° without concomitant reduction in toxicity by treatment with aqueous alkali under anaerobic conditions. Also, evidence has been obtained by Dr. Schantz and his co-workers that the portion of the molecule responsible for toxicity is not responsible for the optical activity.

If the tailings toxin does differ from clam poison it is possible that the toxicity of the former could be significantly greater than the limits observed by Schantz *et al.* (1) for pure clam poison. Samples of tailings toxin of toxicity 5400±400 MU/mg and $[\alpha]_D^{25}$ +98°±4° were repurified repeatedly by the heavy-paper technique but neither the toxicity nor the specific rotation was significantly increased. It was therefore concluded that either the maximum purity for the material had been attained or that paper chromatography was incapable of effecting further purification. These results make it impossible to differentiate among alternatives (*b*), (*c*), and (*d*) at the present time and an answer to these questions must await further examination of the homogeneity of the tailings toxin by development of other methods of purification.

This work has established the feasibility of enriching and recovering by preparative paper chromatography on seed-test paper a toxin from hitherto intractable residues of low toxicity from the Schantz alumina chromatographic method for purification of clam poison. Residues of bio-assay as low as 300 MU/mg can be enriched by multiple batch treatments. On a 500-mg scale, tailings of toxicity 1400 MU/mg and $[\alpha]_D^{25}$ +26° can be enriched fourfold to 5400±400 MU/mg and $[\alpha]_D^{25}$ +98°±4° in 67% yield by four passes. Further work is required to elaborate the identity of the recovered toxin.

EXPERIMENTAL

Pretreatment of Papers

Whatman No. 17 and seed-test papers were trimmed to 18×22 in. and ½-in. serrations were cut along one 18-in. edge. To the other 18-in. edge was attached a stirrup and two wicks of Whatman 3MM paper (6). Eight such sheets supported by glass rods in a Model A 300 Chromatocab equipped with solvent troughs and reservoirs (6) were washed chromatographically by the procedure described earlier (5) for Whatman No. 1 paper.

Blank Runs on Pretreated Paper

After removal of one wick, the pretreated paper was developed by the descending method with *t*-butanol:acetic acid:water (2:1:1) until the solvent front was 1 to 1½ in. from the serrated edge. This operation required 16 hours for No. 17 paper and 40 hours for seed-test paper. The paper was air-dried at room temperature and rectangular strips were cut from the papers at the R_F ranges specified in Table I. To each strip a stirrup and two wicks of pretreated Whatman No. 1 paper were attached, after which the strips

were eluted with water (20 ml). The eluates were concentrated *in vacuo*, then lyophilized and weighed (5). To determine the quantity of particulate impurity in the residues, the latter were reconstituted in water (3 ml), filtered through a fine-porosity fritted-glass funnel, and the combined filtrate and washings (8 ml) were concentrated, lyophilized, and weighed. To determine the anionic impurity removable from the latter residues, they were reconstituted in water (3 ml) and eluted through Amberlite IRA-400 (Cl) resin (3 ml). The combined eluate and washings (15 ml) were concentrated, lyophilized, and weighed.

Preliminary Purification and Chromatography of Clam Poison Tailings

A sample of clam poison hydrochloride tailings approximately 25% pure was kindly provided for study by the U.S. Army Chemical Research and Development Laboratories. When samples of the aqueous alcoholic solution (14 mg/ml total solids, 18,700 MU/ml, specified by sender) were lyophilized, the total solids found was 14.7 mg/ml and the presence of oily droplets in the lyophilizates, which were water insoluble, was observed. Accordingly, the entire aqueous alcoholic solution was lyophilized and the mixture of oil and solid extracted with 5×2 ml of water to separate the water-soluble material from the oil. The oil and water-soluble fractions were lyophilized after filtration, and bio-assay confirmed that all the toxicity was confined to the water-soluble fraction, which weighed 2.02 g, and had toxicity 1400 MU/mg and $[\alpha]_D^{25}$ +26.3° (1% aqueous solution). Solutions used for chromatography were prepared directly from this material. For chromatograms on pretreated Whatman No. 1 paper, 20 λ of a 1% aqueous solution (200 γ), and on the pretreated heavy papers, 10 λ of a 30% aqueous solution (3 mg), were applied and developed in glass chromatographic tanks by the descending method. The air-dried chromatograms were examined under ultraviolet light and sprayed with Weber reagent (8), Sakaguchi reagent (9), or ninhydrin for location of the components.

Purification of Clam Poison Tailings on Seed-test Paper

A sample of clam poison tailings solution was lyophilized, weighed, and made up to exactly 2 ml in a volumetric flask. Aliquots (0.2 ml) of this solution were applied as a streak $3\frac{1}{2}$ in. long to a strip of pretreated seed-test paper $4\frac{3}{4}$×22 in., air-drying between each application until the desired quantity of tailings had been applied. The paper was developed by the descending method in a glass chromatographic tank (or in a Model A 300 Chromatocab when 18×22-in. sheets were used) containing *t*-butanol:acetic acid:water (2:1:1) for 40 hours, using a single wick of Whatman 3MM paper. The chromatogram was air-dried and examined under ultraviolet light for location of the components. The bands containing the fluorescent materials were cut from the paper and a stirrup and single wick of pretreated Whatman No. 1 paper was attached to each strip. The strips were eluted with water (20 ml) and the eluates were concentrated *in vacuo* to a volume of 3–5 ml. The concentrates were passed through Amberlite IRA-400 (Cl) resin (3–4 ml), filtered through a fine-porosity fritted-glass disk, concentrated *in vacuo* to a volume of ca. 1 ml, lyophilized, and weighed on the microbalance. From the weights of fractions thus obtained the weights of impurities known to be introduced as a result of blank runs on the same batch of pretreated paper were subtracted to give the corrected weight of each fraction. When side bands from purifications (e.g. fractions 1 and 3, Table III) were reprocessed, the size of the strip of paper to which such material was applied was decreased so that a loading equivalent to 500 mg per 18×22-in. sheet was employed. For bio-assay, solutions of concentration 20 γ/ml were prepared using water of pH 3.00 (hydrochloric acid). Rotations were measured on 1% aqueous solutions.

Can. J. Chem. Downloaded from www.nrcresearchpress.com by 210.87.254.40 on 09/05/12
For personal use only.

Bio-assay

Bio-assays were performed on male mice weighing 19–21 g by the method of Schantz *et al.* (12), using ten mice per assay. The conversion factor (C.F. value) for the strain of mice used in these experiments was determined using a standard sample of clam poison provided by Dr. Schantz and was found to be 0.160 γ per MU.

ACKNOWLEDGMENTS

We wish to thank the U.S. Army Chemical Research and Development Laboratories for providing the clam poison tailings used in these studies and Dr. E. J. Schantz of the U.S. Army Biological Laboratories for supplying a sample of pure clam poison for standardization of the bio-assay results.

We are greatly indebted to Dr. A. D. Tennant and Mr. R. Tuszynski of the Laboratory of Hygiene, Department of National Health and Welfare, Ottawa, for performing the bio-assays and to Dr. R. N. Jones and Mr. R. Lauzon, Division of Pure Chemistry, National Research Council, Ottawa, for measurement of infrared spectra.

REFERENCES

1. E. J. SCHANTZ, J. D. MOLD, D. W. STANGER, J. SHAVEL, F. J. RIEL, J. P. BOWDEN, J. M. LYNCH, R. S. WYLER, B. RIEGEL, and H. SOMMER. J. Am. Chem. Soc. **79**, 5320 (1957).
2. E. J. SCHANTZ. Private communication.
3. T. C. SIMMONS. Private communication.
4. E. A. METCALF. Private communication.
5. A. A. CASSELMAN, R. GREENHALGH, H. H. BROWNELL, and R. A. B. BANNARD. Can. J. Chem. **38**, 1277 (1960).
6. H. H. BROWNELL, J. G. HAMILTON, and A. A. CASSELMAN. Anal. Chem. **29**, 550 (1957).
7. G. W. HUFFMAN, P. A. REBERS, D. R. SPRIESTERBACH, and F. SMITH. Nature, **175**, 990 (1955).
8. C. J. WEBER. J. Biol. Chem. **78**, 465 (1948).
9. S. SAKAGUCHI. J. Biochem. (Tokyo), **5**, 13, 25 (1925).
10. J. D. MOLD, J. P. BOWDEN, W. D. STANGER, J. E. MAURER, J. M. LYNCH, R. S. WYLER, E. J. SCHANTZ, and B. RIEGEL. J. Am. Chem. Soc. **79**, 5235 (1957).
11. D. H. R. BARTON and R. S. COOKSON. Quart. Revs. (London), **10**, 44 (1956).
12. E. J. SCHANTZ, E. F. MCFARREN, M. L. SCHAFER, and K. H. LEWIS. J. Assoc. Offic. Agr. Chemists, **41**, 160 (1958).
13. E. J. SCHANTZ. Ann. N.Y. Acad. Sci. **90**, 843 (1960).

Can. J. Chem. Downloaded from www.nrcresearchpress.com by 210.87.254.40 on 09/05/12
For personal use only.

Can. J. Chem. Downloaded from www.nrcresearchpress.com by 210.87.254.105 on 09/05/12
For personal use only.

THE FRACTIONATION OF POLYTHENE[1]

W. R. BLACKMORE[2] AND W. ALEXANDER[3]

ABSTRACT

An apparatus is described for fractionating large quantities (400 g) of polythene into five roughly equal fractions using a fractional precipitation technique. Application of this method of fractionation to a linear polythene has shown that the width of the molecular-weight distribution of the successive fractions decreases as the fractionation proceeds. Consequently, the initial high-molecular-weight fractions require refractionation to produce equally narrow distributions in them as are found in later fractions. Good agreement is obtained with the experimentally determined values of the number-average and weight-average molecular weight for the parent polymer when the measured values of M_n and M_w for each fraction are used to calculate the values for the parent. The differential molecular-weight distribution function of the parent polymer was calculated on a Bendix G-15 computer from the data for the fractions by using the weight, number-average and weight-average molecular weight, measured for each fraction in conjunction with an assumed log-normal or negative binomial molecular-weight distribution function in each fraction.

INTRODUCTION

The preparation of polythene samples with narrow molecular-weight distributions is more conveniently done by fractionation than by synthesis. Two techniques are most commonly used, fractional solution and fractional precipitation. Both methods appear to be equally efficient when used in dilute solution at or above the melting point of the polymer (1). The present study used a precipitation technique in which the polymer was dissolved in a suitable solvent (*p*-xylene) and then partially precipitated by adding a non-solvent (triethylene glycol) (2). In this way, a large-scale fractionator was used to divide a 400-g polymer charge into five 80-g fractions. The fractions were then stored until enough material had been collected in each fraction to warrant refractionation.

EXPERIMENTAL

Apparatus

The large-scale fractionator consisted of an upper borosilicate glass separator vessel of 50-liter capacity and a lower 40-liter metal storage tank, both immersed in a 200-gal, totally enclosed oil bath maintained at an operating temperature of 130° C by six thermistor-controlled 1000-w electric heaters. The temperature of the bath was measured by means of six precision thermometers placed at different locations in the bath. Temperature fluctuations were held to within ±0.05° C of the operating temperature throughout the entire bath by employing a highly efficient stirring arrangement and by using two specially designed ultrasensitive thermistor controllers (3) to control the temperature. The bath fluid, a water-white mineral oil maintained under an atmosphere of CO_2 to prevent oxidation, could be used for 2 months before it darkened and had to be discarded. Phase boundaries in the separator vessel were illuminated by means of three strategically placed, sealed-beam automobile head lamps submerged in the oil bath, and could be viewed through several glass observation ports in the side of the bath. The solvent, *p*-xylene, and the non-solvent, triethylene glycol, were separately preheated to 130° C in steam-jacketed, glass-lined kettles which were connected by steam-traced lines to the separator vessel. A specially designed burette was used to determine the quantities of hot triethylene glycol added to the separator. The layout of the apparatus is shown in Fig. 1. The selection

[1]*Manuscript received May 29, 1961.*
Contribution from the Central Research Laboratory, Canadian Industries Limited, McMasterville, Que.
[2]*Present address: Canadian Industries Limited, Management Services Department, 1253 McGill College Avenue, Montreal, Que.*
[3]*Present address: Canadian Industries Limited, Textile Fibres Division, Technical Department, Millhaven, Ont.*

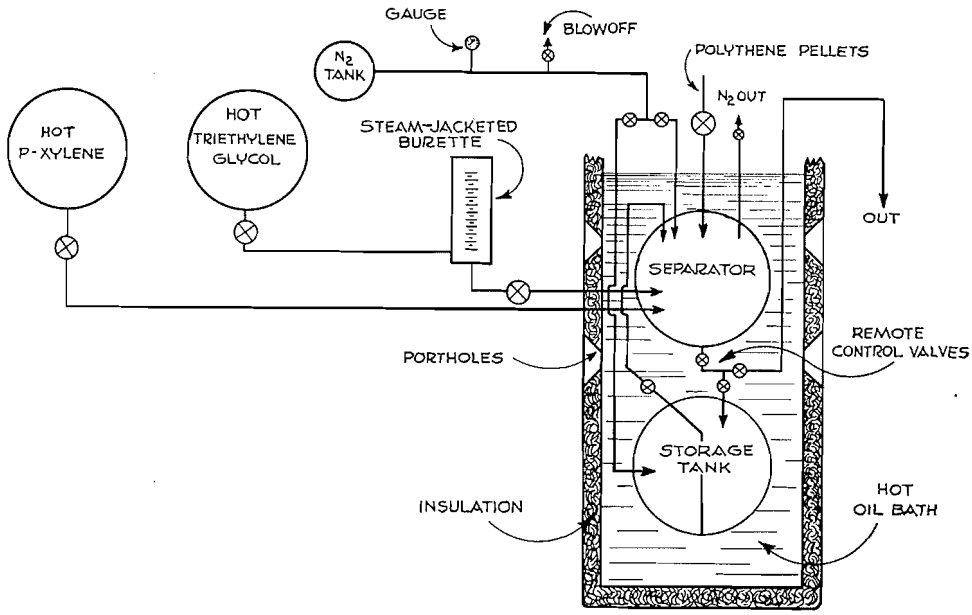


FIG. 1. Apparatus for large-scale fractionation of polythene.

of the operating temperature was determined by the melting point of the polymer and was chosen so that the precipitated material would be liquid and crystallization would not interfere with the equilibrium distribution of polymer between the two phases.

Procedure

The polymer was fractionated by partial precipitation in a manner similar to that described by Tung (2). A 1.6% solution (w/v) of the polythene in *p*-xylene (containing 0.1% w/v 2,6-ditertiary-butyl-*p*-cresol as antioxidant) was vigorously stirred under dry nitrogen in the separator and the non-solvent, triethylene glycol, slowly added until the first signs of opacity appeared in the solution. Sufficient non-solvent (determined by trial and error) was then added to precipitate out approximately 20% (80 g) of the total charge of polythene in the solution. After a period of vigorous agitation followed by a settling period, the upper gel phase was separated from the lower solution in the following manner: the lower solution was drained into the storage tank, then enough fresh *p*-xylene was added to form a clear solution of the gel phase, finally the gel was redissolved, and the fresh solution was siphoned out of the separator and into 10 gal of vigorously stirred cold methanol.

The solution in the storage tank was then transferred to the separator vessel by applying nitrogen pressure to the storage tank. Subsequent fractions were then precipitated by following the same procedure. In general the first fraction required 3 hours to settle; however, later fractions required longer settling times, fraction 4 requiring at least 12 hours. The fifth fraction was obtained by siphoning off the solution from the gel phase of fraction 4 and adding it directly to cold methanol. Each 80-g fraction was filtered off and then washed five times with cold methanol before being transferred to a special washing vessel in which the filtrate was stirred in contact with cold methanol (containing 0.05% antioxidant) for at least 24 hours before being filtered off and dried to constant weight in a vacuum oven. The yield efficiency of these partial precipitations was found

Can. J. Chem. Downloaded from www.nrcresearchpress.com by 210.87.254.105 on 09/05/12
For personal use only.

to be about 95%. Studies indicated that polymer losses in filtration and washing amounted to 2.5%, leaving a further 2.5%, or 10 g, of polymer unaccounted for. This loss may have been due to low-molecular-weight material present in the polythene dissolving in the cold methanol/xylene mixture. However, cooling the methanol/xylene mixture to −72° C and allowing the material to warm up slowly until the xylene crystals melted failed to yield any precipitate.

DISCUSSION

Results

As an indication of the extent of fractionation actually achieved with the above system, measurements on fractions obtained from a linear polythene are given in Table I.

TABLE I

Typical fractionation results with a linear polythene

Run	Fraction	Cumulative wt. (g)	Cumulative % recovered	M_n (Me/1000)	M_n (vinyl)	η (120° C, tetralin)	Calc. M_w	M_w/M_n (vinyl)
4	1	63.4	15.8	33,300	29,700	3.70	240,000	8.1
	2	138.4	34.6	24,900	33,200	2.27	128,000	3.9
	3	237.4	59.3	30,800	29,200	1.22	58,000	2.0
	4	319.5	79.8	14,600	16,900	0.70	28,500	1.7
	5	382.0	95.5	2,400	3,800	0.28	8,800	2.3
Parent polymer as measured:				12,900	11,000	1.71	90,000	8.2
Calculated for the parent from the measured values for the fractions:					13,100		87,600	8.2

Columns 5 and 6 list number-average weights (M_n) for each fraction, based on the assumption that each polymer molecule is terminated by a methyl group at one end and a vinyl group at the other. Both groups were measured by infrared spectroscopy, to within an accuracy of 20% in the methyl group determination (4) and 5% in the case of the vinyl group determination. Vinyl group measurements were based on the change in intensity of the 908 cm^{-1} band which arises when the sample is brominated (5). The weight-average molecular weights (M_w) were calculated from the intrinsic viscosities (η) for each fraction using the Duch and Kuchler relationship (7). The intrinsic viscosities were measured at 120° C in tetralin solutions using Schulken and Sparks (6) viscometers. The good agreement between (M_n) values determined by the two methods verifies the assumption that the molecule is terminated by a methyl and a vinyl group. The decreasing values of the ratios of the molecular weights, M_w/M_n, indicate that the width of the distribution in each consecutive fraction decreases and that refractionation is necessary if fractions of equally narrow molecular-weight distribution are required. Cragg and Hammerschlag (1) have pointed out that refractionation more than thrice is inefficient and this number of refractionations has been accepted as the limit. The value of the number-average molecular weight for the parent polymer was calculated using the measured number-average molecular weights of the fractions and the formula $M_n = \sum n_i m_i / \sum n_i$ and showed good agreement with the experimentally determined value for the unfractionated polymer (Table I). Likewise, the weight-average molecular weight of the parent polymer calculated from the expression $M_w = \sum m_i w_i / \sum w_i$ also showed good agreement with the value calculated from the measured intrinsic viscosity of the

Can. J. Chem. Downloaded from www.nrcresearchpress.com by 210.87.254.105 on 09/05/12
For personal use only.

unfractionated polymer. This agreement suggests that the parent polymer had not been chemically changed by the fractionation procedure.

Calculation of the Molecular-Weight-Distribution Curves

Pre-1939 molecular-weight-distribution curves were obtained by making some estimate of the molecular weight of each fraction and then plotting the cumulative weight of the first n fractions against the estimated molecular weight of the nth fraction to yield the integral weight-distribution curve. This procedure assumed incorrectly that there was no overlap between fractions and also that every species present in the nth fraction had a molecular weight between the average measured for the $(n-1)$th and nth fractions. A somewhat more realistic approach was made by Schulz (8), who assumed the fraction to be symmetrically distributed about its average molecular weight. In this calculation, the total weight of the first $(n-1)$ fractions plus half the weight of the nth fraction is plotted against the molecular weight of the nth fraction; however, this still neglects the overlapping between fractions.

In the last decade, serious attempts have been made to allow for the overlap of the fractions by assuming a differential distribution function for each fraction, summing these functions to obtain the differential distribution curve for the parent polymer, and then forming the integral distribution curve (9, 10, 11). More recently two independent studies (12, 13) have suggested that the most satisfactory results are obtained when the amount of each fraction and the number- and weight-average molecular weight are also known. The differential distribution function for the parent polymer may then be calculated using these three parameters and assuming a relatively simple form for the distribution functions of the fractions. A program for the calculation of the molecular-weight distribution of the parent polymer was written for the Bendix G-15 computer, given the three parameters and assuming either a log-normal or a negative binomial distribution for the fractions. Results are given in Table I.

ACKNOWLEDGMENTS

The authors wish to acknowledge discussions of this work with Mr. A. M. Birks; to thank Dr. D. C. West for having programed the calculation of the polymer molecular-weight-distribution function on the Bendix computer; and to thank Mr. T. Finn, who performed most of the experimental work. The authors also wish to thank Mr. A. W. Pross for the infrared measurements and Dr. H. P. Schreiber for the intrinsic viscosity results.

REFERENCES

1. L. H. Cragg and H. Hammerschlag. Chem. Revs. **39**, 79 (1946).
2. L. H. Tung. J. Polymer Sci. **20**, 495 (1956).
3. H. H. Wood. Unpublished work.
4. A. H. Willbourn. J. Polymer Sci. **34**, 569 (1959).
5. R. G. J. Miller and M. Willis. Personal communication to A. W. Pross, Central Research Laboratory, Canadian Industries, McMasterville, Que.
6. R. M. Schulken and M. L. Sparks. J. Polymer Sci. **26**, 227 (1957).
7. E. Duch and L. Kuchler. Z. Electrochem. **60**, 218 (1956).
8. G. V. Schulz and A. Dinglinger. Z. physik. Chem. B, **43**, 47 (1939).
9. G. Beall. J. Polymer Sci. **4**, 483 (1949).
10. D. Cleverdon, D. Laker, and P. G. Smith. Trans. Faraday Soc. **47**, 908 (1951).
11. G. M. Guzman. J. Polymer Sci. **19**, 519 (1956).
12. R. Koningsveld and C. A. F. Tuijnman. J. Polymer Sci. **39**, 445 (1959).
13. C. Booth and L. R. Beason. J. Polymer Sci. **42**, 81, 93 (1960).

Can. J. Chem. Downloaded from www.nrcresearchpress.com by 210.87.254.105 on 09/05/12
For personal use only.

Can. J. Chem. Downloaded from www.nrcresearchpress.com by 210.87.254.40 on 09/05/12
For personal use only.

THE GAS–LIQUID PARTITION CHROMATOGRAPHY OF CARBOHYDRATE DERIVATIVES

PART I. THE SEPARATION OF GLYCITOL AND GLYCOSE ACETATES[1]

S. W. GUNNER, J. K. N. JONES, AND M. B. PERRY

ABSTRACT

Gas–liquid partition chromatography has been used to separate the fully acetylated derivatives of tetritols, pentitols, hexitols, heptitols, octitols, and anomeric glycoses.

DISCUSSION

Gas–liquid partition chromatography (G.L.P.C.) has already been shown to be a powerful technique for the preparative separation and for the qualitative and quantitative analysis of carbohydrate derivatives. Bishop and his co-workers (1, 2) were the first to report the separation of methyl *O*-methyl glycosides by G.L.P.C. and have since demonstrated the use of such separations in the analysis of these derivatives obtained from the fission of methylated polysaccharides (3, 4, 5). Kircher (6) has also described the G.L.P.C. separation of methylated methyl glycosides employing other types of liquid phases. *O*-Methyl aldonolactones (7), *O*-methyl-*O*-acetyl glycitols (8), *O*-acetyl glycitols (9), and other carbohydrate derivatives (10) have also been successfully resolved using the G.L.P.C. technique.

In view of its potential use in the field of carbohydrate chemistry, a systematic program was undertaken in this laboratory to explore the conditions under which favorable separations of a variety of carbohydrate derivatives might be undertaken using G.L.P.C. This paper records the results obtained in investigations into the separation of glycitol and glycose acetates. Until recently the methods available for the separation of acetylated glycitols and glycoses involved column chromatography on a Magnesol–Celite or Silene EF – Celite (11*a*) mixture using benzene – *tert*-butyl alcohol as the mobile phase, cellulose column chromatography, or paper chromatography (11*b*). It is considered that the G.L.P.C. method of separation will provide a more rapid and refined procedure.

The recorded separations were carried out using samples of the acetate derivatives (2–5 γ) developed on a Pye Gas Argon Chromatograph fitted with an ionization detector (12), and in cases where larger amounts of material (20–200 mg) were used for preparative work, the Burrell Kromo-Tog, Model K-2 apparatus was used. Experience with other types of chromatographic equipment showed that it was necessary for the sample to be injected directly onto the column packing material in order to prevent the decomposition of the samples, which was observed when a dead space existed between the injection site and the beginning of the column packing material. In this connection it is important to note that small gaps in the packing material itself should be avoided and that the detector should be placed as close as possible to the end of column packing for satisfactory results.

Acid-washed Chromosorb W or silver-coated Chromosorb W proved to be a suitable inert support which did not show excessive adsorption of the acetate derivatives. The non-polar liquid phases chosen were Apiezon M vacuum grease or Dow Corning stopcock grease, and the polar phase selected was butanediol succinate polyester. Columns prepared containing 20% w/w of the non-polar liquid phases gave fair separations of the

[1]*Manuscript received June 8, 1961.*
Contribution from the Department of Organic Chemistry, Queen's University, Kingston, Ontario. Abstracted in part from the M.Sc. Thesis of S. W. Gunner, Queen's University, 1961.

Can. J. Chem. Downloaded from www.nrcresearchpress.com by 210.87.254.40 on 09/05/12
For personal use only.

acetate derivatives with only slight adsorption-tailing effects. Columns prepared using 20% w/w of the polar phase on Chromosorb W gave increased resolution of the derivatives but had the disadvantage of markedly increasing their retention times. It was considered that mixtures of the packing materials made up of a non-polar and polar liquid phase component might combine the advantages of each individual liquid phase to give a column packing which would have a high resolving power and would give reasonable retention times for the glycitol and glycose acetates. In practice it was found that the ideal combinations were (*a*) a 1:1 w/w mixture of 20% w/w Apiezon M grease on silver-coated Chromosorb W and 20% w/w butanediol succinate polyester on Chromosorb W (column packing A) and (*b*) a 1:1 w/w mixture of 20% w/w Dow Corning grease on Chromosorb W and 20% w/w butanediol succinate polyester on Chromosorb W (column packing B).

In attempts to find a column packing material suitable for the separation of oligosaccharide acetates (13), H. G. Jones, in this laboratory, developed a packing material of 0.1 to 0.3% Apiezon M vacuum grease on silver-coated glass beads (column packing D). It was found that the retention times for monosaccharide acetates on this column were extremely short. The previously mentioned mixed column packings (A and B) gave satisfactory separations for the glycitol and glycose acetates up to those derived from the C_6 compounds but those derivatives of higher molecular weight showed considerable broadening of the peaks with increasing retention times. This latter difficulty was overcome by using a column made from a 1:1 v/v mixture of column packings A and D (column packing C), which gave satisfactory separations of the acetates derived from the C_7 and C_8 glycitols and glycoses, as well as retaining the ability to resolve the lower molecular weight derivatives. The glass bead column (column packing D) provided a rapid separation of the acetates derived from C_4 to C_8 glycitols in order of their increasing molecular weights, but under the conditions used it did not separate the individual glycitol acetates having the same molecular weights.

Typical separations of the glycitol acetates on column packing A are shown in Fig. 1, on column packing C in Fig. 2, and on column packing D in Fig. 3. Typical separations of anomeric glycose acetates on column packing A are shown in Fig. 4.

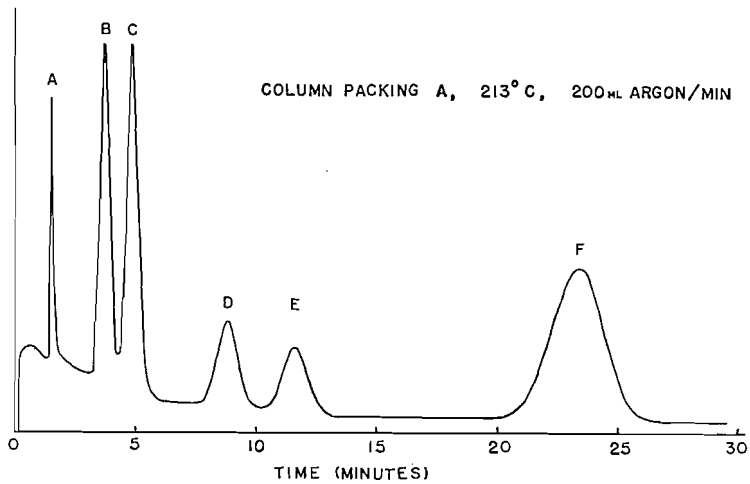


FIG. 1. Separation of glycitol acetates: (A) tetra-*O*-acetylerythritol, (B) penta-*O*-acetylribitol, (C) penta-*O*-acetylxylitol, (D) hexa-*O*-acetylallitol, (E) hexa-*O*-acetyl-D-iditol, and (F) hepta-*O*-acetyl-D-*glycero*-D-galactoheptitol.

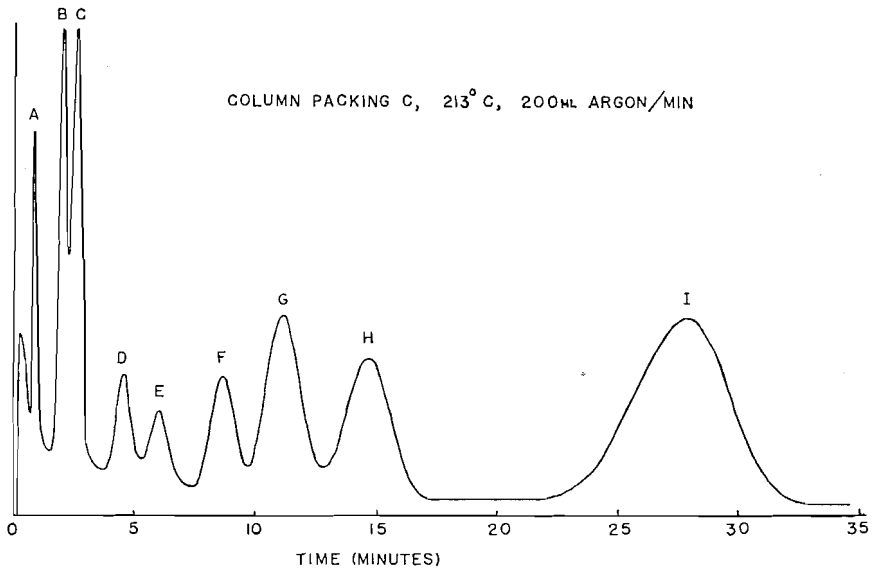


FIG. 2. Separation of glycitol acetates: (A) tetra-*O*-acetylerythritol, (B) penta-*O*-acetylribitol, (C) penta-*O*-acetylxylitol, (D) hexa-*O*-acetylallitol, (E) hexa-*O*-acetyl-D-iditol, (F) hepta-*O*-acetyl-meso-*glycero*-alloheptitol, (G) hepta-*O*-acetyl-D-*glycero*-D-mannoheptitol, (H) hepta-*O*-acetyl-L-*glycero*-D-glucoheptitol, and (I) octa-*O*-acetyl-D-*erythro*-L-galactooctitol.

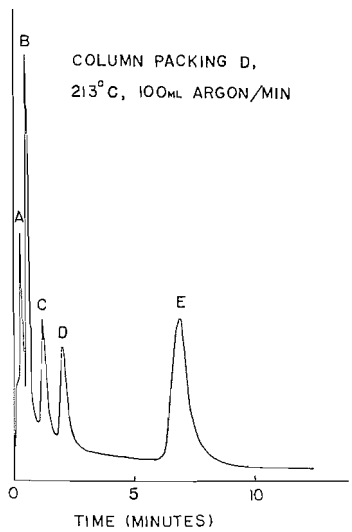


FIG. 3. Separation of glycitol acetates: (A) penta-*O*-acetyl-L-arabitol, (B) hexa-*O*-acetyl-D-glucitol, (C) hepta-*O*-acetyl-D-*glycero*-D-galactoheptitol, (D) octa-*O*-acetyl-D-*threo*-L-galactooctitol, and (E) hepta-*O*-acetyl 5-*O*-β-D-xylopyranosyl-L-arabitol.

Table I records the retention times of the glycitol acetates relative to penta-*O*-acetyl-L-arabitol (= 1.00) on all four column packing materials. Table II records the retention times of glycose acetates relative to penta-*O*-acetyl-L-arabitol (= 1.00) on column packing materials A, B, and C.

Can. J. Chem. Downloaded from www.nrcresearchpress.com by 210.87.254.40 on 09/05/12
For personal use only.

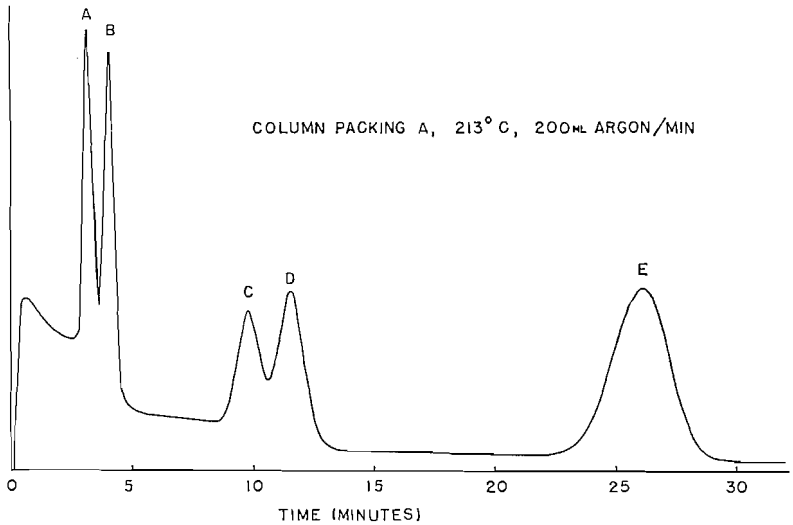


FIG. 4. Separation of anomeric glycose acetates: (A) tetra-*O*-acetyl-α-D-xylopyranose, (B) tetra-*O*-acetyl-β-D-xylopyranose, (C) penta-*O*-acetyl-α-D-glucopyranose, (D) penta-*O*-acetyl-β-D-glucopyranose, and (E) hexa-*O*-acetyl-D-*glycero*-α-D-glucoheptopyranose.

TABLE I

Retention times of fully acetylated glycitols relative to penta-*O*-acetyl-L-arabitol at 213° C

Glycitol acetate	Column packing material			
	A	B	C	D
Glycerol	0.120	0.118	0.122	—
Erythritol	0.378	0.358	0.393	—
D-Threitol	0.403	0.429	0.433	—
Ribitol	0.918	0.895	0.944	—
L-Arabitol	1.000	1.000	1.000	1.000
Xylitol	1.18	1.18	1.20	—
Allitol	1.78	1.89	1.90	—
D-Talitol	2.07	2.16	2.03	—
D-Mannitol	2.13	2.25	2.16	—
D-Glucitol	2.39	2.59	2.73	1.85
Galactitol	2.42	2.59	2.75	—
D-Iditol	2.74	2.97	2.85	—
6-Deoxy-L-talitol	0.707	0.712	0.698	—
L-Rhamnitol	0.715	0.733	0.730	—
D-Fucitol	0.750	0.778	0.750	—
Pentaerythritol	0.807	0.798	0.790	—
meso-*Glycero*-alloheptitol	—	—	3.56	—
D-*Glycero*-D-altroheptitol	—	—	4.06	—
D-*Glycero*-D-mannoheptitol	—	—	4.73	—
meso-*Glycero*-guloheptitol	—	—	4.90	—
D-*Glycero*-D-galactoheptitol	5.60	—	5.05	3.92
D-*Glycero*-D-glucoheptitol	—	—	5.10	—
L-*Glycero*-D-glucoheptitol	—	—	6.11	—
meso-*Glycero*-idoheptitol	—	—	6.60	—
D-*Erythro*-L-galactooctitol	—	—	11.50	—
D-*Threo*-L-galactooctitol	—	—	12.61	6.52
5-*O*-β-D-Xylopyranosyl-L-arabitol	—	—	—	22.3

These results show that by using column packings A, B, and C, well-defined separations of the two tetritol derivatives, tetra-*O*-acetylerythritol and tetra-*O*-acetyl-D-threitol, and

Can. J. Chem. Downloaded from www.nrcresearchpress.com by 210.87.254.40 on 09/05/12
For personal use only.

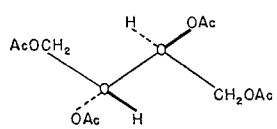
TABLE II

Retention times of glycose acetates and acetylated methyl glycosides relative to penta-*O*-acetyl-L-arabitol at 213° C

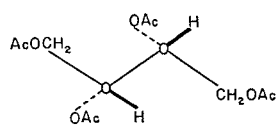
	Column packing material		
	A	B	C
Glycose acetates			
Tetra-*O*-acetyl-α-D-xylopyranose	0.715	0.700	0.605
Tetra-*O*-acetyl-β-D-xylopyranose	0.910	0.891	0.778
Penta-*O*-acetyl-α-D-galactopyranose	2.04	2.05	1.92
Penta-*O*-acetyl-β-D-galactopyranose	2.70	2.258	2.55
Penta-*O*-acetyl-α-D-glucopyranose	2.14	2.25	2.21
Penta-*O*-acetyl-β-D-glucopyranose	2.57	2.57	2.41
Penta-*O*-acetyl-α-D-mannopyranose	2.22	2.35	2.26
Penta-*O*-acetyl-β-D-mannopyranose	2.74	2.73	2.64
Tetra-*O*-acetyl-α-D-ribopyranose	1.00	1.07	0.988
Tetra-*O*-acetyl-α-D-ribofuranose	1.12	1.21	1.13
Penta-*O*-acetyl-α-D-altropyranose	2.52	2.69	2.50
Penta-*O*-acetyl-α-L-lyxose	0.842	0.802	0.800
Hexa-*O*-acetyl-D-*glycero*-α-D-mannoheptopyranose	4.96	4.93	4.93
Hexa-*O*-acetyl-D-*glycero*-α-D-glucoheptopyranose	5.60	5.63	5.60
Acetylated methyl glycosides			
Methyl tri-*O*-acetyl-α-L-rhamnopyranoside	0.291	0.293	0.310
Methyl tetra-*O*-acetyl-β-D-glucopyranoside	1.48	1.45	1.40

the three pentitol derivatives, penta-*O*-acetylribitol, penta-*O*-acetyl-L-arabitol, and penta-*O*-acetylxylitol, were obtained. All the hexitol acetate derivatives, with the exception of hexa-*O*-acetyl-D-glucitol and hexa-*O*-acetylgalactitol could be separated from each other. All the heptitol acetate derivatives could be separated from each other as well as the two octitol acetate derivatives which were examined. The order of emergence of the glycitol acetates was found to be independent of the nature of the column packing materials used, although some differences in the relative retention times for the compounds were observed. It was also found that the same order of emergence of the compounds was retained using column temperatures ranging from 200° to 250° C. At 250° the retention times for the glycitol acetates were very much decreased, and sharper peaks than those recorded in Figs. 1, 2, and 3 were obtained. No decomposition of the derivatives was detected using column temperatures up to 250° and the derivatives were recovered unchanged from preparative-scale separations.

The results collected so far indicate that a relationship exists between the retention times of the glycitol acetates and their stereochemical structure described in the conventional zig-zag conformations. The retention times of the glycitol acetates having the same molecular weight depends on the arrangement of acetoxy groups attached to the non-terminal carbon atoms. The greater the number of these acetoxy groups which are arranged on one side of the molecule, the greater is the affinity of the compound for the liquid phase and hence the greater its retention time. Thus, tetra-*O*-acetylerythritol (I) has a shorter retention time than tetra-*O*-acetyl-D-threitol (II), which has the two acetoxy groups attached to the non-terminal carbon atoms arranged on one side of the molecule.



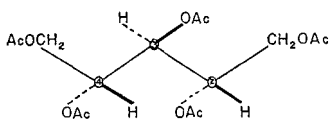
(I)



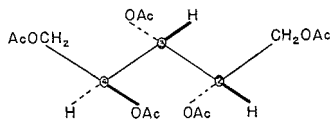
(II)

Can. J. Chem. Downloaded from www.nrcresearchpress.com by 210.87.254.40 on 09/05/12
For personal use only.

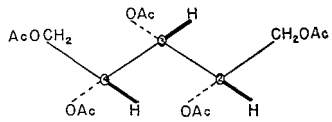
In the case of the three pentitol acetate derivatives, both penta-*O*-acetylribitol (III) and penta-*O*-acetyl-L-arabitol (IV) have a maximum of two acetoxy groups attached to non-terminal carbon atoms arranged on one side of the molecule. It would appear that in this case as well as the case of hexitol acetate and heptitol acetate derivatives, where there are two or more glycitol acetates of the same molecular weight and having the same maximum number of acetoxy groups arranged on one side of the molecule, the closer these acetoxy groups are to each other the greater is the affinity of the compound for the liquid phase and hence the greater its retention time. Thus, penta-*O*-acetylribitol (III) has a lower retention time than penta-*O*-acetyl-L-arabitol (IV). Penta-*O*-acetylxylitol (V), with the maximum of three acetoxy groups attached to non-terminal carbon atoms arranged on one side of the molecule, has the longest retention time of the three pentitol acetate derivatives.



(III)

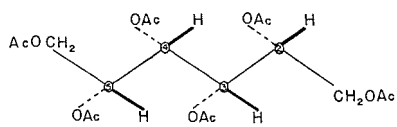


(IV)

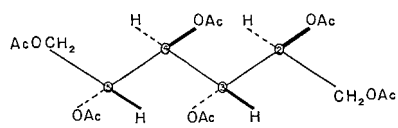


(V)

On the basis of the empirical rules set out above it would be predicted that hexa-*O*-acetyl-D-iditol (VI), which has all four of its acetoxy groups attached to non-terminal carbon atoms arranged on one side of the molecule, should be the hexitol acetate derivative having the longest retention time, and hexa-*O*-acetylallitol (VII), which has a maximum of two acetoxy groups attached to non-terminal carbon atoms arranged on one side of the molecule, and having the maximum possible separation, should be the hexitol acetate derivative having the shortest retention time. This prediction has proved correct in practice.

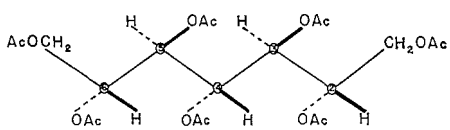


(VI)

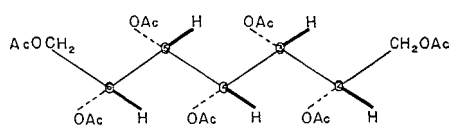


(VII)

In agreement with the above statements, it was found that hepta-*O*-acetyl meso-*glycero*-alloheptitol (VIII), which has a maximum of three acetoxy groups attached to non-terminal carbon atoms arranged on one side of the molecule and having the maximum possible separation, has the shortest retention time of all the heptitol acetate derivatives, whereas hepta-*O*-acetyl-meso-*glycero*-idoheptitol (IX), which has all the acetoxy groups attached to the non-terminal carbon atoms arranged on one side of the molecule, has the longest retention time. The chromatographic behavior of the glycitol acetate derivatives having relative retention times between the extremes cited above is in agreement with



(VIII)



(IX)

Can. J. Chem. Downloaded from www.nrcresearchpress.com by 210.87.254.40 on 09/05/12
For personal use only.

that predicted from a consideration of the spatial distribution of the acetoxy groups attached to the non-terminal carbon atoms.

The acetate derivatives of the deoxyglycitols, 6-deoxy-L-talitol, L-rhamnitol, and D-fucitol, can be separated by G.L.P.C., and their order of elution from the columns used is the same as those of their parent hexitol derivatives (L-talitol, L-mannitol, and galactitol).

The anomeric acetates of D-xylopyranose, D-galactopyranose, D-glucopyranose, and D-mannopyranose were separated by G.L.P.C. as were the tetra-*O*-acetyl derivatives of α-D-ribopyranose and α-D-ribofuranose. It is probable that the retention times for these derivatives depend upon the relative positions of the axial and equatorial *O*-acetyl groups but with the limited results available at this time it is not possible to rationalize their chromatographic behavior.

G.L.P.C. has also been shown to afford a method for the separation of acetylated glycosides.

EXPERIMENTAL

Apparatus

The recorded separations were carried out using a Pye Argon Chromatograph fitted with an ionization detector (80 μc radium D) and employing straight glass columns (120×0.5-cm I.D.) packed with the appropriate support enclosed at each end by small glass wool plugs. The samples (2–5 γ) in dry chloroform solution were placed on the top of the column packing using a micropipette and development was made using dry argon as the carrier gas.

Preparative-scale separations (20–200 mg) were made on U-shaped glass columns (255×1.3-cm I.D.) filled with the support material, using the Burrell Kromo-Tog, Model K-2 apparatus fitted with a thermal detector and employing helium as the carrier gas.

Column Packing

Chromosorb W (Johns-Manville), 60–80 mesh, was washed with 2 *N* hydrochloric acid and then with distilled water until the washings were neutral, was dried at 110°, and was then screened to remove fines. Silver-coated Chromosorb W was prepared by treating acid-washed Chromosorb W (60–80 mesh) (10 g) with 120 ml each of two solutions A and B. Solution A was prepared by just adding sufficient dilute ammonium hydroxide solution to a solution of silver nitrate (15.8 g) in water (300 ml) to produce a clear solution. Solution B was prepared by adding a solution of Rochelle salt ($NaKC_4H_4O_6$, 2.5 g) in water (25 ml) to a boiling solution of silver nitrate (3 g) in distilled water (350 ml) and, after filtration, the volume of the solution was adjusted to 350 ml. After treatment of the stirred Chromosorb W with the first two portions of solutions A and B the supernatant was removed after 10 minutes, and the residue was further treated with the same amounts of these two solutions. The resulting silver-coated Chromosorb was filtered off, washed with distilled water followed by acetone, and finally dried in an oven at 140°. The weight of silver deposited was 3 g.

Silver-coated glass beads were prepared in a manner similar to that used in the preparation of silver-coated Chromosorb by treating glass beads (60 plus mesh; MS-H; Microbeads Inc., Jackson, Mississippi) (500 g), previously washed with dilute nitric acid and distilled water, with the same quantities of solutions A and B.

The following liquid phases were used: (*a*) Apiezon M vacuum grease (Fisher Scientific Company), (*b*) Dow Corning stopcock grease (Fisher Scientific Company), and (*c*)

Can. J. Chem. Downloaded from www.nrcresearchpress.com by 210.87.254.40 on 09/05/12
For personal use only.

butanediol succinate polyester (Craig) prepared according to the directions of Bishop *et al.* (2). The packing materials were prepared by stirring a slurry of a weighed amount of the liquid phase dissolved in chloroform with a weighed amount of the inert support in an open beaker at room temperature while the bulk of the solvent was removed by aeration. The last traces of the solvent were removed by heating the material *in vacuo* at 140°.

The packing materials prepared are described below.

(1) Column packing A.—1:1 w/w mixture of (*a*) 20% w/w butanediol succinate polyester on 60–80 mesh Chromosorb W and (*b*) 20% w/w Apiezon M grease on 60–80 mesh silver-coated Chromosorb W.

(2) Column packing B.—1:1 w/w mixture of 20% w/w butanediol succinate polyester on 60–80 mesh Chromosorb W and (*b*) 20% w/w Dow Corning grease on 60–80 mesh Chromosorb W.

(3) Column packing C.—1:1 v/v mixture of (*a*) column packing A and (*b*) column packing D.

(4) Column packing D.—0.3% w/w Apiezon M grease on 60 plus mesh silver-coated glass beads.

The dried column packing materials were run into the glass columns under gravity with gentle tapping to ensure even packing and the absence of any cavities. The packed columns were purged for 3 hours at 240° with dry nitrogen gas before use. It was found that the columns could be used for several hundred analyses at 213° C before any significant deterioration in their resolving power became apparent.

ACKNOWLEDGMENTS

We wish to thank Dr. Nelson K. Richtmyer, National Institutes of Arthritis and Metabolic Diseases, National Institutes of Health, Bethesda, for the gift of the parent heptitols and octitols. We also wish to thank the National Research Council of Canada for financial assistance (Grants No. NRC 706 and T 39) and for the award of a scholarship to one of us (S. W. G.).

REFERENCES

1. A. G. McINNES, D. H. BALL, F. P. COOPER, and C. T. BISHOP. J. Chromatog. **1**, 556 (1958).
2. C. T. BISHOP and F. P. COOPER. Can. J. Chem. **38**, 388 (1960).
3. C. T. BISHOP and F. P. COOPER. Can. J. Chem. **38**, 793 (1960).
4. C. T. BISHOP, F. BLANK, and P. E. GARDNER. Can. J. Chem. **38**, 869 (1960).
5. G. A. ADAMS and C. T. BISHOP. Can. J. Chem. **38**, 2380 (1960).
6. H. W. KIRCHER. Anal. Chem. **32**, 1103 (1960).
7. J. K. N. JONES. Paper presented at the Chemical Society Symposium on Physical, Chemical and Biological Methods in the Study of Carbohydrates of High Molecular Weight, Edinburgh, July, 1960.
8. C. T. BISHOP. Can. J. Chem. **38**, 1636 (1960).
9*a*. S. W. GUNNER, J. K. N. JONES, and M. B. PERRY. Chem. & Ind. (London), 255 (1961).
9*b*. W. J. A. VANDEN HEUVEL and E. C. HORNING. Biochem. Biophys. Research Commun. **4**, No. 6 (1961).
10. E. J. HEDGLEY, O. MERESZ, W. G. OVEREND, and R. RENNIE. Chem. & Ind. (London), 938 (1960). E. J. HEDGLEY and W. G. OVEREND. Chem. & Ind. (London), 378 (1960).
11*a*. W. W. BINKLEY. Advances in Carbohydrate Chem. **10**, 83 (1955).
11*b*. B. WICKBERG. Acta Chem. Scand. **12**, 615 (1958).
12. J. E. LOVELOCK. J. Chromatog. **1**, 35 (1958).
13. H. G. JONES, J. K. N. JONES, and M. B. PERRY. In preparation.

Can. J. Chem. Downloaded from www.nrcresearchpress.com by 210.87.254.40 on 09/05/12
For personal use only.

Can. J. Chem. Downloaded from www.nrcresearchpress.com by 210.87.254.105 on 09/05/12
For personal use only.

FREE RADICALS BY MASS SPECTROMETRY

XXVI. PRIMARY STEPS IN THE MERCURY-PHOTOSENSITIZED DECOMPOSITION OF METHYL ACETATE[1]

R. F. POTTIE[2] AND F. P. LOSSING

ABSTRACT

The Hg($^3P_1$)-photosensitized reaction of methyl acetate at micron pressures in the presence of 8 mm of helium has been examined in a flow system by mass spectrometry. At 55° C the primary dissociation is mainly into acetyl and methoxy radicals. An alternative dissociation into CO_2 and two CH_3 radicals occurs with a frequency of about one fifth of the principal reaction. A small amount of $COOCH_3$ radical is also formed. No CH_3CO_2 radicals could be found. Since the yield of H_2 is less than 2% of the methyl acetate decomposed, a primary dissociation to give H atoms and CH_3COOCH_2 or CH_2COOCH_3 radicals is quite small.

INTRODUCTION

The photolysis of methyl acetate in the wavelength region 2200–2600 Å was investigated some years ago by Roth and Rollefson (1). From the products of the photolysis at 20° C and 14 mm pressure they concluded that a primary dissociation into acetyl and methoxy radicals accounted for about 95% of the total reaction. A dissociation into CO_2 and, presumably, two methyl radicals accounted for the remainder. They also examined the Hg($^3P_1$)-photosensitized decomposition under similar conditions and found that the decomposition proceeded by essentially the same paths. The direct photolysis has been investigated in further detail by Wijnen (2, 3, 4), and briefly by Ausloos (5). Wijnen found, in agreement with the earlier work, that the main primary dissociation was to form acetyl and methoxy radicals. A dissociation to give CO_2 also occurred, but to a larger extent than found by Roth and Rollefson. As will be discussed below, Wijnen's data lead to a ratio of about 4:1 for the two modes of dissociation at 30° C.

In the present work, the relative importance of the primary dissociation steps in the mercury-photosensitized decomposition has been reinvestigated.

EXPERIMENTAL

The Hg($^3P_1$)-photosensitized reactions were carried out using a fast-flow system coupled to a mass spectrometer. This apparatus and its characteristics have been described in earlier publications in this series (6, 7, 8). The reactant and mercury vapor at partial pressures of a few microns were carried in a stream of helium at 8 mm through a tubular fused-silica reaction cell strongly illuminated by a low-pressure mercury lamp of high intensity. A representative portion of the stream entered the ionization chamber of a mass spectrometer through a small orifice at the end of the illuminated zone. The temperature of the cell was maintained at 55° C by circulation of water from a thermostatted bath. The contact time in the illuminated zone was about 0.001 second. The intensity of 2537-Å radiation absorbed was sufficient to decompose acetone, for example, to the extent of about 22% in this period. In effect, the reaction conditions resemble those of flash photolysis, since radical–radical reactions greatly predominate over radical–substrate reactions (8).

[1]*Manuscript received May 5, 1961.*
Contribution from the Division of Pure Chemistry, National Research Council, Ottawa, Canada.
Issued as N.R.C. No. 6461.
[2]*National Research Council Postdoctorate Fellow 1958–60.*

Can. J. Chem. Downloaded from www.nrcresearchpress.com by 210.87.254.105 on 09/05/12
For personal use only.

RESULTS AND DISCUSSION

The yields of products in the mercury-photosensitized decomposition of methyl acetate are given in Table I. The yield of H_2 was less than 2% of the methyl acetate decomposed.

TABLE I

Hg-Photosensitized decomposition of methyl acetate at 55° in 8 mm of helium (partial pressure in microns)

	Run No.			
	1	2	3	4
CH_3COOCH_3				
Lamp off	5.64	5.56	10.27	10.82
Lamp on	4.78	4.54	9.08	9.30
Decomposed	0.86	1.03	1.19	1.51
% decomposed	15.2	18.5	11.6	14.0
$(CH_3CO)_2$	0.030	0.038	0.057	0.078
CH_3COCH_3	0.073	0.093	0.092	0.148
CH_3CHO	0.041	0.061	0.075	0.102
$CH_2{=}CO$	0.131	0.127	0.157	0.177
$(CH_3O)_2CH_2$	0.006	0.005	0.015	0.015
$HCOOCH_3$	0.008	0.017	0.017	0.017
CH_3OCH_3	0.047	0.061	0.064	0.091
CH_3OH	0.189	0.231	0.262	0.326
CH_2O	0.198	0.244	0.279	0.369
C_2H_6	0.073	0.086	0.093	0.144
CH_4	0.074	0.095	0.097	0.138
CH_3	0.171	0.116	0.140	0.122
CO_2	0.122	0.125	0.131	0.154
CO	0.258	0.327	0.303	0.367
C bal., %	73	74	72	73
O bal., %	74	74	70	70
H bal., %	74	71	71	74
R_{CH_3O}, %	50	53	53	54
R_{CH_3CO}, %	34	35	37	39
Total reaction [1], %	59	60	58	58
Total reactions [2] to [4], %	15	14	12	11

In addition to the products listed, a considerable amount of a polymeric substance was formed, which deposited on the walls of the reactor as a yellowish-brown stain. The formation of this material is presumably responsible for the low carbon, oxygen, and hydrogen balances. The low mass balances cannot be attributed to the formation of polymers of formaldehyde. In the photosensitized decomposition of dimethyl ether the carbon and oxygen balances were 95%, although large amounts of formaldehyde were formed (9). Moreover, the near equality of the carbon, oxygen, and hydrogen balances in Table I indicates that the material unaccounted for must have a C:O:H ratio essentially the same as in methyl acetate itself. Since some 25% of the methyl acetate disappears to form an unidentified and presumably non-volatile product, the conclusions reached as to the relative importance of various primary modes of dissociation are necessarily approximate.

The variations in the percentage of methyl acetate decomposed in the four runs in Table I result from the difficulties encountered in keeping the reactor walls reasonably free from opaque deposits.

The presence of substantial yields of products such as $(CH_3CO)_2$, CH_3COCH_3, and CH_3CHO indicates that acetyl radicals are formed in abundance in the decomposition. The corresponding fragment, CH_3O, is clearly the precursor of such products as CH_3OCH_3,

CH_3OH, and CH_2O. The formation of CO_2 and $HCOOCH_3$, on the other hand, must result from an alternative primary step in which a CH_3 radical or possibly two CH_3 radicals are lost from the methyl acetate molecule. Evidently two, and possibly four, primary decomposition steps must be taken into account:

$$CH_3\overset{\overset{O}{\|}}{C}OCH_3 + Hg^* \rightarrow CH_3CO + OCH_3 + Hg \quad [1]$$

$$CH_3\overset{\overset{O}{\|}}{C}OCH_3 + Hg^* \rightarrow CH_3 + \overset{\overset{O}{\|}}{C}OCH_3 + Hg \quad [2]$$

$$CH_3\overset{\overset{O}{\|}}{C}OCH_3 + Hg^* \rightarrow CH_3\overset{\overset{O}{\|}}{C}O + CH_3 + Hg. \quad [3]$$

If the CH_3CO_2 or $COOCH_3$ radicals decompose almost immediately, reactions [2] and [3] will be equivalent to the following reaction:

$$CH_3\overset{\overset{O}{\|}}{C}OCH_3 + Hg^* \rightarrow 2CH_3 + CO_2 + Hg. \quad [4]$$

The secondary reactions of radicals formed in these steps will be (*a*) from reaction [1]:

$$2CH_3CO \rightarrow (CH_3CO)_2 \quad [5]$$

$$2CH_3CO \rightarrow CH_3CHO + CH_2{=}CO \quad [6]$$

$$CH_3CO \rightarrow CH_3 + CO \quad [7]$$

$$CH_3CO + Hg^* \rightarrow CH_2{=}CO + H + Hg \quad [8]$$

$$CH_3CO + CH_3 \rightarrow CH_3COCH_3 \quad [9]$$

$$CH_3CO + CH_3 \rightarrow CH_2{=}CO + CH_4 \quad [10]$$

$$2CH_3O \rightarrow CH_3OH + CH_2O \quad [11]$$

$$CH_3O + CH_3 \rightarrow CH_3OCH_3 \quad [12]$$

$$CH_3O + CH_3 \rightarrow CH_2O + CH_4 \quad [13]$$

$$CH_3O + CH_3CO \rightarrow CH_3OH + CH_2{=}CO \quad [14]$$

$$CH_3O + CH_3CO \rightarrow CH_2O + CH_3CHO \quad [15]$$

$$CH_3COCH_3 + Hg^* \rightarrow CH_3CO + CH_3 + Hg \quad [16]$$

$$CH_3OCH_3 + Hg^* \rightarrow CH_3O + CH_3 + Hg \quad [17]$$

$$CH_3OCH_3 + Hg^* \rightarrow CH_3OCH_2 + H + Hg \quad [18]$$

$$CH_3OCH_2 + OCH_3 \rightarrow CH_3OCH_2OCH_3, \quad [19]$$

and (*b*) from reactions [2]–[4]:

$$2CH_3 \rightarrow C_2H_6 \quad [20]$$

$$CH_3\overset{\overset{O}{\|}}{C}O \rightarrow CH_3 + CO_2 \quad [21]$$

$$\overset{\overset{O}{\|}}{C}OCH_3 \rightarrow CH_3 + CO_2 \quad [22]$$

$$\overset{\overset{O}{\|}}{C}OCH_3 + CH_3O \text{ (or } CH_3CO) \rightarrow H\overset{\overset{O}{\|}}{C}OCH_3 + CH_2O \text{ (or } CH_2{=}CO). \quad [23]$$

Can. J. Chem. Downloaded from www.nrcresearchpress.com by 210.87.254.105 on 09/05/12
For personal use only.

Can. J. Chem. Downloaded from www.nrcresearchpress.com by 210.87.254.105 on 09/05/12
For personal use only.

Since many of these products can be formed in several ways it is not possible to establish the relative importance of these secondary reactions. The reactions of radicals such as CH_3CO and CH_3O with a second excited mercury atom under conditions of intense illumination in the present apparatus cannot be entirely neglected (7). The reaction of secondary products such as CH_3OCH_3 with excited mercury must also occur. For example, $CH_3OCH_2OCH_3$ is most probably formed by the sequence of reactions [12], [18], and [19].

The relative importance of the primary step [1] can be estimated from the amount of products derived from CH_3O and from CH_3CO radicals according to the following relations:

$$R_{CH_3O} = 2R_{(CH_3O)_2CH_2} + R_{CH_3OCH_3} + R_{CH_2O} + R_{CH_3OH} \quad [24]$$

$$R_{CH_3CO} = 2R_{(CH_3CO)_2} + R_{CH_3CHO} + R_{CH_2=CO} + R_{CH_3COCH_3}. \quad [25]$$

The yield of CO cannot be included in either of these relations, since CH_3O and CH_3CO radicals may both give CO by reaction with Hg^*. As shown in Table I, the yield of CH_3O amounts to 50–53% of the methyl acetate decomposed. The yield of CH_3CO is, however, only 34–38%. The difference presumably results from CH_3CO radicals which have disappeared to form products other than those listed in equation [25], that is, by reaction [7]. Since CH_3CO radicals would be thermally stable at 55° C, it is possible that some of the acetyl radicals carry over from the primary step sufficient energy to cause them to dissociate. Alternatively, reaction [7], like reaction [8], may be brought about by collision with an excited Hg atom.

An attempt was made to obtain an upper limit to acetyl production by introducing CH_3 radicals into the reaction stream and measuring the limiting yield of CH_3COCD_3. In this experiment, $Hg(CD_3)_2$ was added to the carrier gas as described in earlier publications (9, 10). The mercury-photosensitized decomposition of the $Hg(CD_3)_2$ then provided a large concentration of CD_3 radicals. According to Wijnen (2), the ratio of disproportionation to combination for $CH_3 + CH_3CO$ is about 0.06, and for the present purposes reaction [10] can be neglected compared to reaction [9]. The limiting yield of CH_3COCD_3 formed in the presence of a large excess of CD_3 should then provide an indication of the number of CH_3CO radicals which survive the primary step long enough to react with CD_3 radicals. The yields of CH_3COCD_3 obtained in this way are given in Table II. A plot of CH_3COCD_3 against added $Hg(CD_3)_2$ is given in Fig. 1. Although the yield is

TABLE II

CH_3COCD_3 formed by addition of CD_3 radicals to methyl acetate decomposition at 55° C
(Helium pressure 8 mm; methyl acetate partial pressure 10.34;
$Hg(CD_3)_2$ partial pressure in arbitrary units)

$Hg(CD_3)_2$ added	CH_3COOCH_3 decomposed (μ)	CH_3COCD_3 formed (μ)	CH_3COCD_3/CH_3COOCH_3 (decomp.)
15.0	1.24	0.115	0.093
29.0	1.21	0.172	0.142
42.5	1.24	0.237	0.191
59.5	1.24	0.287	0.231
93.0	1.22	0.322	0.264
113.0	1.22	0.344	0.282
140.5	1.10	0.347	0.315
192.0	1.08	0.364	0.337
273.0	0.96	0.357	0.372

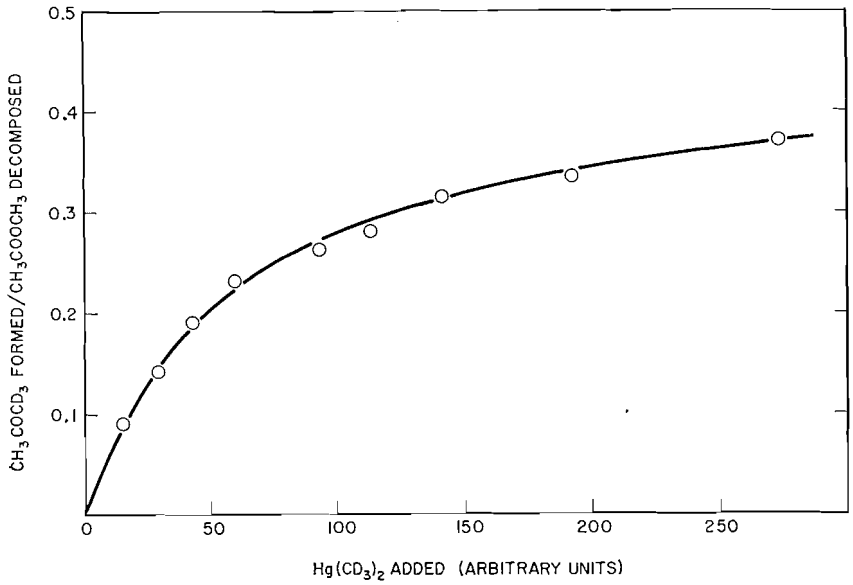


FIG. 1. Yield of CH_3CO radicals as shown by addition of CD_3 radicals to reaction stream.

still rising slowly even with the largest amount of added $Hg(CD_3)_2$, it is apparent that the limiting yield of CH_3CO is appreciably less than the 53% yield obtained for CH_3O. It is, in fact, not much higher than the CH_3CO yield in Table I as obtained from equation [28]. The difference between the values of 53% and of about 40% suggests that an appreciable fraction, possibly about one fifth, of the CH_3CO radicals formed in [1] decomposes to CH_3 and CO before the CH_3CO radicals have time to react with the other radicals present.

A slightly higher limit for the occurrence of reaction [1] can be obtained on the basis that

$$\text{total reaction [1]} = \tfrac{1}{2}(R_{CH_3O} + R_{CH_3CO} + R_{CO}). \qquad [26]$$

As shown in Table I, reaction [1] on this basis accounts for about 58% of the methyl acetate disappearing or about 82% of the total oxygen recovered.

The relative importance of the primary steps [2] and [4] can also be estimated from the yields in Table I. The only product other than CO_2 which could be formed only by reactions [2] and [4] was a small amount of methyl formate. In a separate experiment, a sample of reaction products was condensed from the gas stream in a liquid-nitrogen trap. G.L.P.C. fractionation of this sample yielded a fraction which by the retention time and by the mass spectrum was shown to be methyl formate and not the isomeric acetic acid. This points to the presence of $COOCH_3$ radicals resulting from reaction [2]. Confirmation of the presence of this radical was provided by the addition of CD_3 radicals to the reaction stream by means of $Hg(CD_3)_2$. The formation of a small peak at mass 77 (CD_3COOCH_3) supports the view that methyl formate was formed from $COOCH_3$ radical by reaction [23] rather than by combination of HCO and CH_3O radicals. The $COOCH_3$ radical was found in earlier work (8) to be reasonably stable at 55° C. The CH_3CO_2 radical, on the other hand, if formed at all, must dissociate immediately. The

Can. J. Chem. Downloaded from www.nrcresearchpress.com by 210.87.254.105 on 09/05/12
For personal use only.

extent of the primary steps [2] and [4], then, can be estimated from the sum of the yields of CO_2 and methyl formate in Table I to be 13% of the methyl acetate decomposed. This is 18% of the total oxygen recovered.

A search was made for the CH_2COOCH_3 and CH_3COOCH_2 radicals which would result from removal of a hydrogen atom in a primary step. In the presence of a large excess of added CH_3 radicals no ethyl acetate or methyl propionate could be detected. The CH_2COOCH_3 radical, if present, should have been detected in this experiment, since it must have an appreciable lifetime at 55° C. Wijnen found $CH_3OCH_2COOCH_3$ from the combination of CH_2O and CH_2COOCH_3 to be a product of the photolysis even at 217° C (2). In this case the CH_2COOCH_3 radical was formed by a hydrogen-atom abstraction by CH_3 or CH_3O. The absence of these radicals in the present experiments, together with the low yield of H_2 mentioned above, indicates that the amount of decomposition proceeding by removal of a hydrogen atom was quite small.

In view of the 25% of methyl acetate which disappears to form unidentified products, any conclusions as to the ratios of various primary modes of dissociation are rather unreliable. It appears, however, that of that fraction which does give identifiable products, about 82% decomposes by reaction [1] and the remainder by reactions [2] and [4]. The ratio $R_1/(R_2+R_4)$ is about 4.4:1. This is not greatly different from the ratio observed by Wijnen (2) in the direct photolysis using a S-500 Hanovia arc. Using the data in Wijnen's Table 1 (excepting runs No. 13, 14, and 20 for which the CO_2 yield is anomalously low), one obtains values for the ratio of CH_3CO production to CO_2 production ($2R_{(CH_3CO)_2}+R_{CH_3COCH_3}+R_{CO}/R_{CO_2}$) ranging from 3.6 to 5.1. Ausloos (5) also found that CO production predominated in the photolysis of esters with unfiltered light, but that the formation of CO_2 became equally important at longer wavelengths.

REFERENCES

1. W. L. Roth and G. K. Rollefson. J. Am. Chem. Soc. **64**, 490 (1942).
2. M. H. J. Wijnen. J. Chem. Phys. **27**, 710 (1957).
3. M. H. J. Wijnen. J. Chem. Phys. **28**, 271 (1958).
4. M. H. J. Wijnen. J. Chem. Phys. **28**, 939 (1958).
5. P. Ausloos. Can. J. Chem. **36**, 383 (1958).
6. F. P. Lossing, D. G. H. Marsden, and J. B. Farmer. Can. J. Chem. **34**, 701 (1956).
7. F. P. Lossing. Can. J. Chem. **35**, 305 (1957).
8. P. Kebarle and F. P. Lossing. Can. J. Chem. **37**, 389 (1959).
9. R. F. Pottie, A. G. Harrison, and F. P. Lossing. Can. J. Chem. **39**, 102 (1961).
10. J. Collin and F. P. Lossing. Can. J. Chem. **35**, 778 (1957).

Can. J. Chem. Downloaded from www.nrcresearchpress.com by 210.87.254.105 on 09/05/12
For personal use only.

Can. J. Chem. Downloaded from www.nrcresearchpress.com by 210.87.254.5 on 09/05/12
For personal use only.

FURTHER EVIDENCE FOR CYCLIC MONOMERS IN HEATED LINSEED OIL[1]

A. G. McInnes,[2] F. P. Cooper, and J. A. MacDonald[3]

ABSTRACT

The distillable esters of heated linseed oil contain a fraction, designated NAFD, which fails to form an adduct with urea. NAFD itself has now been separated into three fractions by gas–liquid partition chromatography. The chemical structure of these component esters was investigated by means of their infrared spectra and by analysis of the products obtained on oxidation of the esters with periodate–permanganate. It is concluded that all the components have the same carbon skeleton, namely, 1-propyl-2-alkenecarboxycyclohexene, but differ in the position of the double bond in the side chain.

INTRODUCTION

Wells and Common (1) have shown that the distillable (monomeric) ethyl esters obtained by ethanolysis of heated linseed oil contain a fraction, designated NAFD, that fails to form an adduct with urea. These authors suggested that NAFD contains a non-terminal ring structure preventing urea-adduct formation. Subsequently, MacDonald (2) obtained evidence for the presence of a six-membered non-terminal ring structure when he isolated phthalic anhydride following aromatization and oxidation of NAFD. MacDonald (2) also established that NAFD consisted of ethyl esters of C_{18} monocarboxylic acids containing an average of two double bonds per molecule. The double bonds did not contribute to the failure of NAFD to form a urea adduct because hydrogenated NAFD also failed to form an adduct (2). However, the low yield (about 1% of theory) of phthalic anhydride obtained (2) indicated that further investigation was necessary in order to determine the positions of the ring and the double bonds in the NAFD carbon chain.

In the present work, oxidation of NAFD by the periodate–permanganate oxidative procedure of Lemieux and von Rudloff (3) yielded a complex mixture of products, suggesting that NAFD was itself a mixture of C_{18} esters differing in the positions of the double bonds, of the ring, or both. On subjecting the methyl esters of NAFD acids to gas–liquid partition chromatography (G.L.P.C.), at least three components were detected. Two of the components were collected from the effluent gas stream and their structures were investigated separately by the periodate–permanganate oxidative procedure (3).

EXPERIMENTAL

Preparation of NAFD

NAFD was prepared from two distillation fractions of ethyl esters of heated linseed oil collected at 60° and 70°, respectively (2). The oxidation experiments were carried out with NAFD prepared from the fraction collected at 60° (NAFD 60°). Since this material was used up in these experiments, subsequent studies, e.g., fractionation of NAFD by G.L.P.C., were carried out with NAFD prepared from the fraction collected at 70° (NAFD 70°). The use of NAFD 70° was justified by the fact that (*a*) its refractive index (n_D^{20}, 1.47200) differed only slightly from the value (n_D^{20}, 1.47195) reported for NADF

[1]*Manuscript received June 9, 1961.*
Contribution from the Division of Applied Biology, National Research Council, Ottawa, Canada.
Issued as N.R.C. No. 6453.
[2]*N.R.C. Postdoctorate Fellow 1956–58. Present address: Department of Chemistry, University of Ottawa, Ottawa, Canada.*
[3]*Deceased March 1, 1957.*

60° (2); (*b*) both preparations contained the same component esters (Fig. 1, Table I); and (*c*) their infrared spectra were identical (Fig. 2).

Oxidation of NAFD

Total NAFD (ethyl esters) or NAFD fractions (methyl esters) obtained by G.L.P.C. were converted to free acids by saponification with ethanolic 0.5 *N* potassium hydroxide, followed by removal of the ethanol *in vacuo*, acidification, and extraction with ethyl ether. The free acids were dissolved in sodium bicarbonate solution at pH 7.6 (prior conversion to soaps by titration with 1 *N* sodium hydroxide hastened solution of the acids) and were oxidized with periodate–permanganate according to the procedure of Lemieux and von Rudloff (3). In a typical experiment, 1.03 g (3.69 mmoles) of NAFD acids consumed 17.0 mmoles of periodate (115% of theory for oxidation of two double bonds) after 30 hours, and yielded 1.22 g (theory 1.50 g) of oxidation products containing 3.12 equivalents (theory 5.0 equivalents) of acid per mole of NAFD oxidized.

A portion of the oxidation products of NAFD 60° was methylated with diazomethane in ethyl ether, and the resulting methyl esters were partially fractionated by distillation at 0.05 mm Hg; 75% of the products was collected up to 134° and this fraction is designated as "volatile" products; the remaining material is designated as "non-volatile" products.

Analysis of Oxidation Products

(a) Gas–Liquid Partition Chromatography (G.L.P.C.)

G.L.P.C. was carried out by the method of James and Martin (4) using a Podbielniak "Chromacon" (series 947-3V) which was modified to take glass chromatographic columns and to improve the pressure regulator, temperature control, and injection and collection systems. Helium was used as carrier gas, and a katharometer was used as detector.

Analyses of the methyl esters of oxidation products were made at 197° on a 4-ft column of Apiezon M – Celite 545 (1:4, w/w) (5). Separation of the methyl esters of NAFD was carried out at 240° on an 8-ft column of the same stationary phase.

(*b*) *Paper Chromatography*

Oxidation products were chromatographed as free acids by the method of Kolbe (6) for the separation of dicarboxylic acids, on Schleicher and Schuell 2043B paper using ethanol – 6 *N* ammonia – 3 *N* ammonium carbonate (6:1:1, v/v) as solvent. The chromatograms were developed for 20 hours at room temperature, dried, and sprayed with a solution of methyl red in borate buffer (6) to detect the acids. To isolate the separated acids, the mixture was applied as a band to sheets of Schleicher and Schuell paper (ca. 43 mg/sheet) and chromatographed as described above. The separated components were located on a guide strip cut from the middle of the sheet, and were eluted from the remaining paper with 3 *N* ammonia solution. The acids were isolated by acidifying the concentrated eluates with 0.1 *N* HCl and extracting with ethyl ether.

It is important to note that paper chromatography will analyze the total oxidation products, whereas G.L.P.C. will analyze only the volatile products.

RESULTS

Fractionation of NAFD by G.L.P.C.

The methyl esters of NAFD 60° or NAFD 70° were resolved by G.L.P.C. at 240° into three fractions (Fig. 1), the concentrations and relative retentions of which are given in Table I. The three fractions from both preparations of NAFD had the same relative retentions but differed in their relative proportions. As might be expected, NAFD 70°

Can. J. Chem. Downloaded from www.nrcresearchpress.com by 210.87.254.5 on 09/05/12
For personal use only.

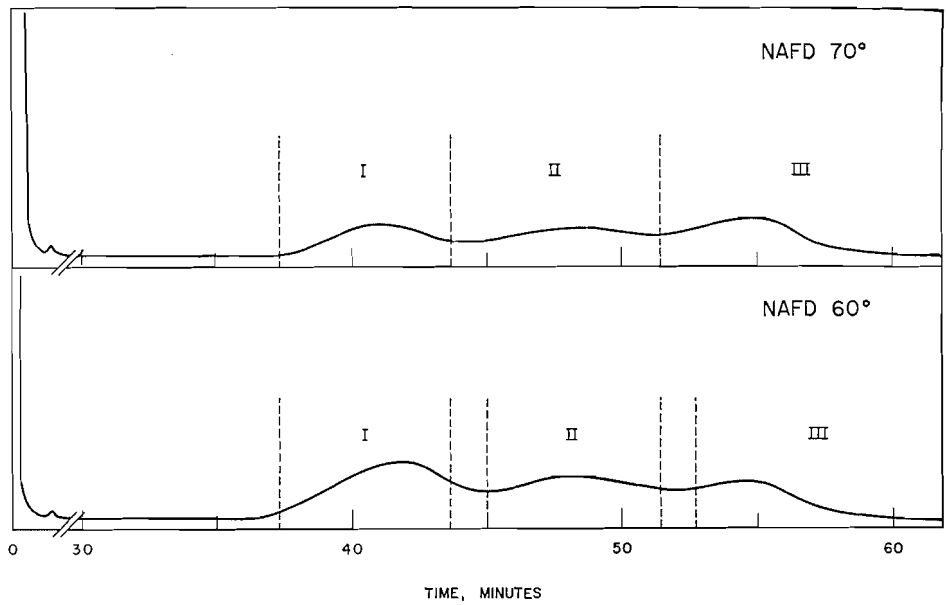


FIG. 1. Fractionation of NAFD 60° and NAFD 70° by G.L.P.C. on Apiezon M at 240°. Broken lines indicate collected fractions.

TABLE I

Components of NAFD methyl esters separated by G.L.P.C.

NAFD analyzed	Fraction	Relative retention*	Weight distribution, % of total
NAFD 60°	I	3.55	42
	II	4.05	31
	III	4.48	27
NAFD 70°	I	3.55	36
	II	4.05	25
	III	4.48	39

*Values are relative to that of methyl myristate on Apiezon M at 240°; relative retentions of standard methyl esters: palmitate, 2.21 and stearate, 4.67.

contained a higher proportion of fraction III and a lower proportion of fraction I than did NAFD 60°. Samples of each of the fractions (from NAFD 70°) were collected from the effluent gas stream for further investigation.

Examination of the infrared spectra of the fractions (Fig. 2) showed that the band at 660 cm^{-1}, considered characteristic of NAFD (2), was completely absent in the spectrum of fraction I, moderately intense in fraction II, and greatest in fraction III. Since fraction II appeared to be contaminated with both fractions I and III, only the latter fractions were subjected to further analysis. Anal. Calc. for methyl octadecadienate: iodine value, 173; C—CH_3, 9.20%. Found for fraction I: iodine value (7), 154; C—CH_3 (11), 9.13%. Found for fraction III: iodine value (7), 160; C—CH_3 (11), 8.20%.

Can. J. Chem. Downloaded from www.nrcresearchpress.com by 210.87.254.5 on 09/05/12
For personal use only.

Can. J. Chem. Downloaded from www.nrcresearchpress.com by 210.87.254.5 on 09/05/12
For personal use only.

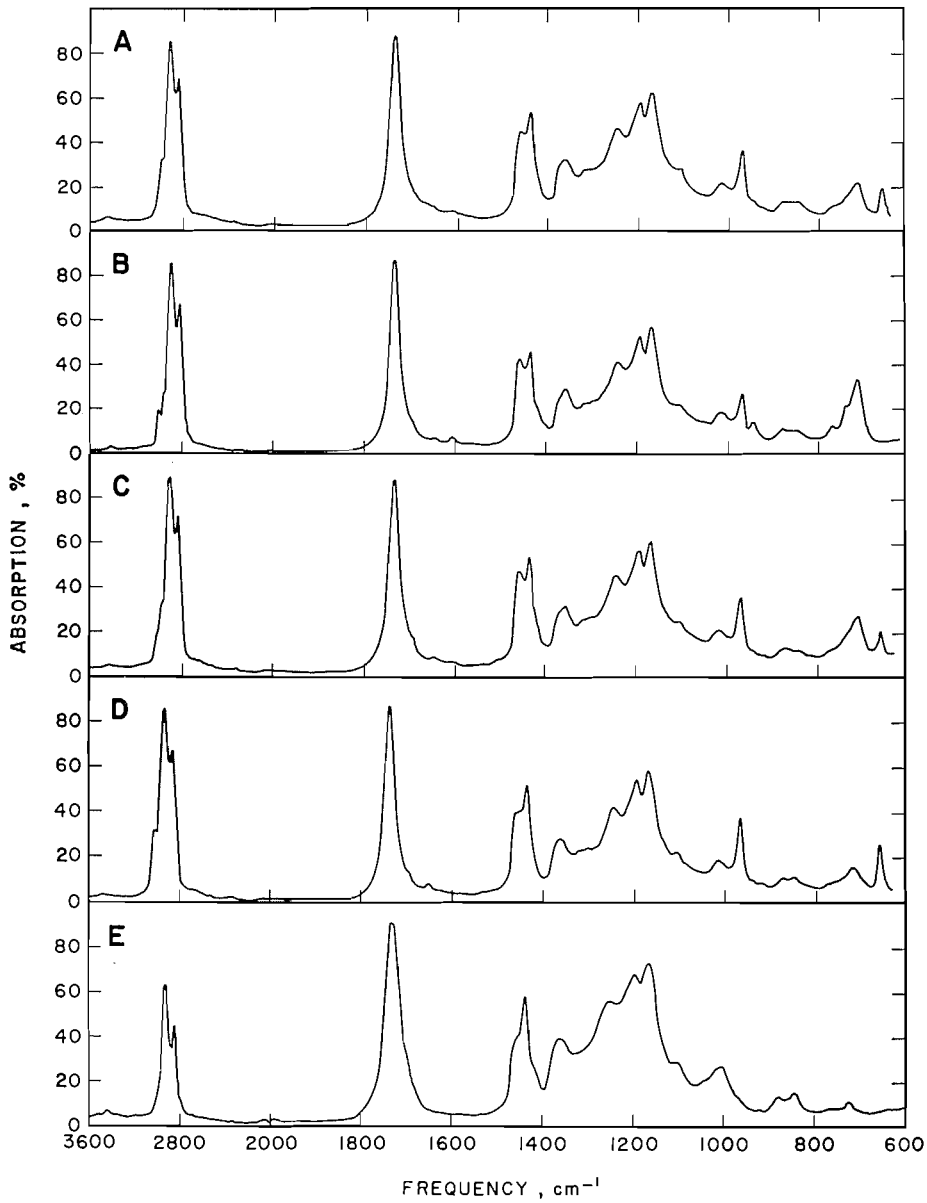


FIG. 2. Infrared spectra. A, NAFD 60° or 70°; B, fraction I; C, fraction II; D, fraction III; E, methyl ester of polycarboxylic acid from fraction III (purified by chromatography on silicic acid). Spectra were run on the undiluted oils.

Oxidation Products

Results of typical analyses of the oxidation products of total NAFD 60° and of fractions I and III by G.L.P.C. and by paper chromatography are presented in Tables II and III, respectively. NAFD 60° and fraction I yielded five major products, some of which

TABLE II

Analysis of oxidation products (as methyl esters) by G.L.P.C.

Identity of products	Retention relative to methyl myristate at 197°*	Relative molar concentration of oxidation products from:		
		NAFD 60°	Fraction I	Fraction III
Unidentified	0.0155	—	—	0.24
n-Hexanoate	0.0244	0.03	0.03	0.06
Succinate	0.0301	0.01	—	—
Unidentified	0.0320	—	—	0.04
n-Heptanoate	0.0378	0.01	—	—
Glutarate	0.0503	0.02	0.04	0.19
n-Propyl succinate	0.0746	0.75	0.65	—
Adipate	0.0820	Trace	—	0.53
Pimelate	0.131	0.13	0.10	0.37
Suberate	0.212	0.64	0.31	1.54
Unidentified	0.287	0.14	—	—
Azelate	0.342	1.00	1.00	1.00
Unidentified	0.455	0.21	—	—
Unidentified	0.506	0.44	—	0.80
Unidentified	0.532	—	0.31	—

*Values for standard methyl esters: valerate, 0.0142; *n*-hexanoate, 0.0245; succinate, 0.0292; *n*-heptanoate, 0.0377; glutarate, 0.0500; *n*-octanoate, 0.0623; *n*-propyl succinate, 0.0746; adipate, 0.0822; *n*-nonanoate, 0.098; pimelate, 0.132; *n*-decanoate, 0.156; suberate, 0.214; azelate, 0.344; sebacate, 0.562.

TABLE III

Analysis of oxidation products (as free acids) by paper chromatography*

Identity of acids	R_F value relative to sebacic acid‡	Relative concentration of acids from:†				
		NAFD 60°				
		Total products	"Non-volatile" products	"Volatile" products	Fraction I	Fraction III
Unidentified§	0.204	+	+	−	+	+
Unidentified§	0.298	+++	+++	−	−	+++++
Unidentified	0.560	+	−	+	+	−
Adipic	0.611	−	−	−	−	++
Pimelic	0.721	−	−	−	−	+
n-Propyl-succinic	0.755	++	−	++	++	−
Suberic	0.820	++	−	++	++	+++
Azelaic	0.915	+++	−	+++	+++	++

*The system used (6) does not separate monocarboxylic acids, which move with solvent front.
†Relative concentration indicated by number of +'s; − indicates component not detected; only major components are revealed by the spray reagent (6).
‡Relative R_F of standard acids: oxalic, 0.095; malonic, 0.211; succinic, 0.424; glutaric, 0.516; adipic, 0.611; pimelic, 0.721; *n*-propyl-succinic, 0.755; suberic, 0.820; azelaic, 0.915; sebacic, 1.00.
§Probably tricarboxylic acids.

were identified as azelaic, *n*-propyl-succinic, suberic, and pimelic acids (in decreasing concentration). The products from fraction III consisted mostly of a tricarboxylic acid together with small amounts of dicarboxylic acids, some of which were identified as suberic, azelaic, adipic, pimelic, and glutaric acids (in decreasing concentration). The major dicarboxylic acid methyl esters from total NAFD 60°, after separation by G.L.P.C., were collected from the effluent gas stream, converted to free acids, and characterized by analysis and melting point.

n-Propyl-succinic acid.—This component, after recrystallization from benzene–petroleum ether (b.p. 40–60°), had m.p. 90–91°, alone or when admixed with authentic

Can. J. Chem. Downloaded from www.nrcresearchpress.com by 210.87.254.5 on 09/05/12
For personal use only.

n-propyl-succinic acid (m.p. 92–93°). Anal. Calc. for $C_7H_{12}O_4$: C, 52.49%; H, 7.55%; neutral equiv., 80.0. Found: C, 52.41%; H, 7.68%; neutral equiv., 79.8.

Suberic acid.—This component was recrystallized from water and had m.p. 139.5°, alone or when admixed with authentic suberic acid (m.p. 140–141°). Anal. Calc. for $C_8H_{14}O_4$: C, 55.16%; H, 8.10%; neutral equiv., 87.4. Found: C, 55.40%; H, 8.38%; neutral equiv., 87.4.

Azelaic acid.—This component, after recrystallization from benzene, had m.p. 104.5–105°, alone or in admixture with authentic azelaic acid (m.p. 106.5°). Anal. Calc. for $C_9H_{16}O_4$: C, 57.43%; H, 8.57%; neutral equiv., 94.0. Found: C, 57.67%; H, 8.42%; neutral equiv., 93.6.

The "volatile" fraction of the oxidation products of NAFD 60° on analysis by G.L.P.C. showed the same components as the total oxidation products of NAFD 60° given in Table II. The "non-volatile" products showed no peaks up to methyl sebacate under the same conditions, but on paper chromatography showed two components with R_F values (relative to sebacic acid) of 0.204 and 0.298 (Table III). These acids were almost completely absent from the oxidation products of fraction I, but were the predominating products from fraction III (Table III). Since these "non-volatile" products had low R_F values on paper chromatography, and had longer retention times than methyl sebacate on G.L.P.C., it was tentatively concluded that they were tricarboxylic acids of molecular weight greater than sebacic acid.

The tricarboxylic acid components were isolated by large-scale paper chromatography of 435 mg of the "non-volatile" fraction of total NAFD 60°; 32.9 mg of the acid with R_F 0.204 and 402.0 mg of the acid with R_F 0.298 were obtained as oily residues which failed to crystallize. Only the component with R_F 0.298 was investigated further. Its methyl ester showed strong ester absorption in the infrared at 1730 cm^{-1}, as well as a weak lactone band at 1775 cm^{-1}. Chromatography of the methyl ester on silicic acid with chloroform as eluant yielded a fraction (170 mg), the infrared spectrum of which showed only the ester band at 1730 cm^{-1}. The ester gave only one peak, with retention relative to methyl myristate of 3.09, when analyzed by G.L.P.C. on Apiezon M at 240°. The relative retention of the ester indicated that it had a molecular weight not less than that of methyl heptadecanoate (M.W., 284; relative retention, 3.20). Anal. Found: C, 61.55%; H, 8.89%; C—CH_3 (11), 7.20%; OCH_3, 24.1%; saponification equivalent, 117. Calc. for $C_{16}H_{19}(COOCH_3)_3$: C, 60.7%; H, 8.92%; C—CH_3, 8.55%; OCH_3, 29.4%; saponification equiv., 105.4. Calc. for $C_{11}H_{21}(COOCH_3)_3$: C, 61.8%; H, 9.14%; C—CH_3, 8.18%; OCH_3, 28.1%; saponification equiv. 110.0.

The analytical and chromatographic data suggest that the ester is a trimethyl ester of a C_{13} or C_{14} tricarboxylic acid with one terminal methyl group.

DISCUSSION

The analysis of NAFD by G.L.P.C. showed that it contained at least three components (Fig. 1, Table I), the relative retentions and analyses of which were consistent with those of methyl esters of diunsaturated C_{18} fatty acids (5). These esters cannot be simple open-chain diunsaturated compounds since it has already been shown that NAFD (1) and hydrogenated NAFD (2) fail to form an adduct with urea. The failure of NAFD to form a urea adduct might be due either to the presence of a non-terminal ring (1, 2) or to the presence of branching in the fatty-acid chain. However, the oxidation products of NAFD or of fractions I and III contained only traces of lower fatty acids (propionic through caproic, Table II) and failed to form oximes or hydrazones, indicative of the absence of

Can. J. Chem. Downloaded from www.nrcresearchpress.com by 210.87.254.5 on 09/05/12
For personal use only.

ketones. Furthermore, terminal methyl values for fractions I and III indicated the presence of only one C—CH_3 group per molecule. Since a branched-chain unsaturated fatty acid would yield either a ketone or a monocarboxylic acid on oxidation, and would have more than one terminal methyl group per molecule, it follows that none of the NAFD components can be branched, and therefore, that they contain a non-terminal ring.

Examination of the infrared spectra of the components of NAFD (fractions I, II, and III; see Fig. 2) revealed that the band at 660 cm^{-1}, attributed to the C—H out-of-plane deformation of a cis-disubstituted double bond in a six-membered ring (2), was present in III (and to a lesser extent in II) but not in I. Furthermore, the intensity of the band at 970 cm^{-1}, attributed to a trans-disubstituted double bond (8, 9), increased in the order I < II < III, and the weak absorption at 1650 cm^{-1}, due to the C=C double-bond stretching vibration (9), also increased in the same order. Finally the absorption at 715 cm^{-1}, characteristic of the methylene rocking vibration (9), decreased in intensity in the order I > II > III.

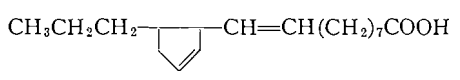
These data suggest that fraction III contains one trans-disubstituted double bond, one cis-disubstituted double bond (probably in a six-membered ring), and short methylene chains, whereas fraction I contains no trans-disubstituted double bonds and longer methylene chains. The weak absorption at 970 cm^{-1} (trans double bond) in fraction I is probably due to the presence of a small amount of fraction II.

Separation of the components of NAFD by G.L.P.C. on Apiezon M may be attributed largely to differences in stereochemistry at the unsaturated centers, since compounds with trans double bonds have longer retention times than the cis isomers (see James (10)). The operation of other factors, such as the position of the ring and the lengths of the methylene chains, may be responsible for the incomplete separation and overlapping of the components, as evidenced by the complexity of the mixtures of oxidation products obtained from fractions I and III (Tables II and III). Nevertheless, the data in Tables II and III show that the major oxidation products of fraction I are azelaic and *n*-propyl-succinic acids, together with smaller amounts of suberic, pimelic, and an unknown acid, and those of fraction III are the tricarboxylic acid, suberic acid, and azelaic acid, together with smaller amounts of adipic, pimelic, and an unidentified acid. On the basis of the formation of these major oxidation products, one can suggest possible structures which would at least account for a major part of the material in fractions I and III.

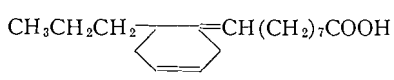
Thus the formation of *n*-propyl-succinic and azelaic acids from fraction I indicates that the latter contains the two fragments

$$CH_3CH_2CH_2—\underset{\displaystyle CH_2—C=}{\overset{\displaystyle |}{CH}}—C= \quad \text{and} \quad =CH(CH_2)_7COOH.$$

These fragments account for 16 carbon atoms and 3 double bonds, whereas fraction I contains 18 carbon atoms and only 2 double bonds. Formation of azelaic acid fixes the carboxyl end of the structure and also the position of one double bond, while the *n*-propyl-succinic acid fixes the methyl end of the structure. Two possible structures, A or B, could account for these products.



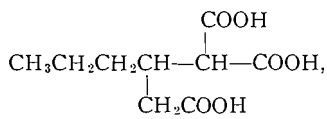
A



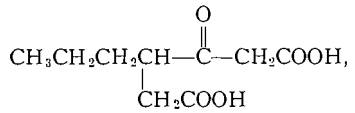
B

Can. J. Chem. Downloaded from www.nrcresearchpress.com by 210.87.254.5 on 09/05/12
For personal use only.

Structure A, on oxidation, would give rise to azelaic acid and an acid,

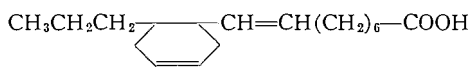


which would be oxidatively decarboxylated to *n*-propyl-succinic acid. Structure B would yield azelaic and a β-keto acid,

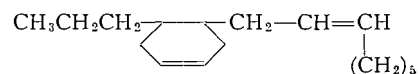


which would also be oxidatively decarboxylated to *n*-propyl-succinic acid. However, structure B fits the infrared data better than A, since B would not be expected to absorb strongly at 970 cm^{-1} (characteristic of a trans-disubstituted double bond) whereas the double bond in the side chain of A would be in the more thermodynamically stable trans conformation, as a result of the conditions of formation (2), and would thus absorb strongly at 970 cm^{-1}.

Formation of suberic acid and pimelic acid from fraction I might be accounted for by the presence of compounds (C and D) with a modified structure B, in which the exocyclic double bond is displaced by one or two carbon atoms towards the carboxyl group.



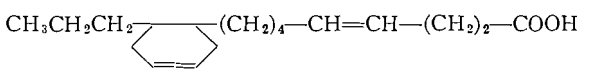
C



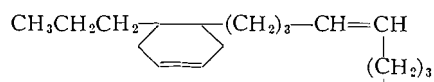
D

Oxidation of C and D would yield, in addition to suberic and pimelic acids, C_{10} and C_{11} tricarboxylic acids, respectively, possibly accounting for the small amount of tricarboxylic acids detected on paper chromatograms of the oxidation products of fraction I (Table III). It is quite likely that the bulk of fraction II consists of these two acids (C and D), incompletely resolved from the component with structure B present in fraction I.

To account for the formation of large amounts of C_{13} or C_{14} tricarboxylic acid from fraction III, structures E and F are postulated.



E



F

Oxidation of structures E and F would yield a C_{14} tricarboxylic acid and succinic acid, and a C_{13} tricarboxylic acid and glutaric acid, respectively. The presence of glutaric acid in the oxidation products of fraction III (Table II) adds additional support for structure F. Suberic and pimelic acids in the oxidation products of fraction III probably arise from structures C and D, which were not completely separated from fraction III.

The proposed structures should account for the fact that fraction I does not absorb at 660 cm^{-1}, the region attributed to C—H out-of-plane deformation of a cis double bond in a six-membered ring. All the structures proposed (B, C, D, E, and F) contain a cis double bond in a six-membered ring, but in structure B (the major component of

Can. J. Chem. Downloaded from www.nrcresearchpress.com by 210.87.254.5 on 09/05/12
For personal use only.

fraction I), the second double bond is attached directly to the ring. It is possible that this double bond hinders the C—H out-of-plane deformation of the ring double bond to the extent that no absorption at 660 cm^{-1} occurs, whereas the exocyclic double bonds in structures C, D, E, and F, being further removed, offer no such hindrance.

Finally, the proposed structures should be consistent with the finding (2) that NAFD gave low yields of phthalic anhydride after allylic bromination, dehydrohalogenation, and oxidation of the side chains. The steric requirement for dehydrohalogenation in a six-membered ring is that the halogen and hydrogen atoms must be trans-diaxially oriented in the transition state (12). This requirement could not easily be fulfilled by an unsaturated six-membered ring such as in the proposed structures (particularly structure B), and therefore low yields of phthalic anhydride would be expected from any of these structures.

ACKNOWLEDGMENTS

The infrared spectra were taken by Mr. C. F. Rollin, and the microanalyses were carried out by Mr. A. E. Castagne. The generous help of Dr. M. Kates in preparation of the manuscript is acknowledged.

REFERENCES

1. A. F. Wells and R. H. Common. J. Sci. Food Agr. **4**, 233 (1953).
2. J. A. MacDonald. J. Am. Oil Chemists' Soc. **33**, 394 (1956).
3. R. U. Lemieux and E. von Rudloff. Can. J. Chem. **33**, 1701 (1955).
4. A. T. James and A. J. P. Martin. Biochem. J. **50**, 679 (1952).
5. A. T. James and A. J. P. Martin. Biochem. J. **63**, 144 (1956).
6. H. Kolbe. Z. physiol. Chem. Hoppe-Seyler's, **297**, 32 (1954).
7. L. Klee and G. H. Benham. J. Am. Oil Chemists' Soc. **27**, 130 (1950).
8. O. D. Shreve, M. R. Heether, H. B. Knight, and D. Swern. Anal. Chem. **22**, 1261 (1950).
9. L. V. Bellamy. The infrared spectra of complex molecules. Methuen and Co. Ltd., London. 1954. Chap. 3.
10. A. T. James. J. Chromatog. **2**, 552 (1959).
11. W. F. Bartel and F. B. LaForge. Ind. Eng. Chem. Anal. Ed. **16**, 434 (1944).
12. S. J. Cristol and N. L. Hause. J. Am. Chem. Soc. **74**, 2193 (1952).

Can. J. Chem. Downloaded from www.nrcresearchpress.com by 210.87.254.5 on 09/05/12
For personal use only.

Can. J. Chem. Downloaded from www.nrcresearchpress.com by 210.87.254.105 on 09/05/12
For personal use only.

THE DIFFERENTIAL THERMAL ANALYSIS OF WOOD[1]

D. F. ARSENEAU

ABSTRACT

Differential thermal analysis was used to study the thermal breakdown of balsam fir and its components in air from 50° to 420° C. In this range, the thermogram of balsam fir is simply a composite of the individual thermograms of the components of the wood, with little, if any, interaction between the components.

INTRODUCTION

Wood is a multicomponent, molecularly non-homogeneous material in which part of the components exist in continuous separate intermingling structures. Balsam fir is reported (1) to contain about 27.7% lignin, 49.4% alpha-cellulose, 15.4% hemicelluloses, 1.5% acetyl, 0.5% ash, and 4.6% extractives. These extractives comprise an extraordinary diversity of substances and could include fats, fatty acids, resin acids, resins, waxes, tannins, phlobaphenes, coloring matters, gums, starches, and many others. All of these components contribute certain physical and chemical properties to the wood substance. Differential thermal analysis (D.T.A.) is able to determine to some degree what contributions some of these components make to the thermal decomposition characteristics of the wood.

Previous workers have used D.T.A. to study lignin (2), cellulose (3), and the carbonation of wood (2, 4). One study (2) indicated that the pyrolysis of birchwood was accompanied by considerable interaction between its components. Since preliminary work on balsam fir did not indicate this same interaction, a further study was undertaken.

EXPERIMENTAL

Apparatus

The apparatus for this study consisted of a vertical-type brass furnace (Fig. 1) in which three identical holes were drilled to a depth of $2\frac{3}{4}$ inches. Great care was taken to see that these were equidistant from the perimeter of the furnace. Two of these holes were to receive the sample holders, the third was to receive the thermocouple that feeds a signal to the temperature controller. The furnace was wound with 20 ft of 24 gauge Chromel 'A' wire, wrapped in asbestos, and placed in a metal container 5 in. in diameter. Glass wool between the furnace and the container provided further heat insulation. The sample holders were brass tubes fitted with iron–constantan thermocouples and had a capacity of 0.7 ml, although their total capacity was not always utilized. These holders were inserted vertically through the bottom of the furnace.

The temperature of the furnace was regulated using an F and M Model 40 Linear Temperature Programmer with an iron–constantan thermocouple. A heating rate of 5.8° C per min was used in all determinations in this study. The signal from the differential thermocouples was preamplified by a Leeds and Northrup Model 9835-B Stabilized D-C Microvolt Indicating Amplifier and was recorded with a Varian Graphic Recorder Model G-10 with a span of 10 mv. Stable, reproducible results were obtained using this arrangement.

[1]*Manuscript received June 26, 1961.*
Contribution from the Department of Chemistry, Xavier Junior College, Sydney, Nova Scotia.

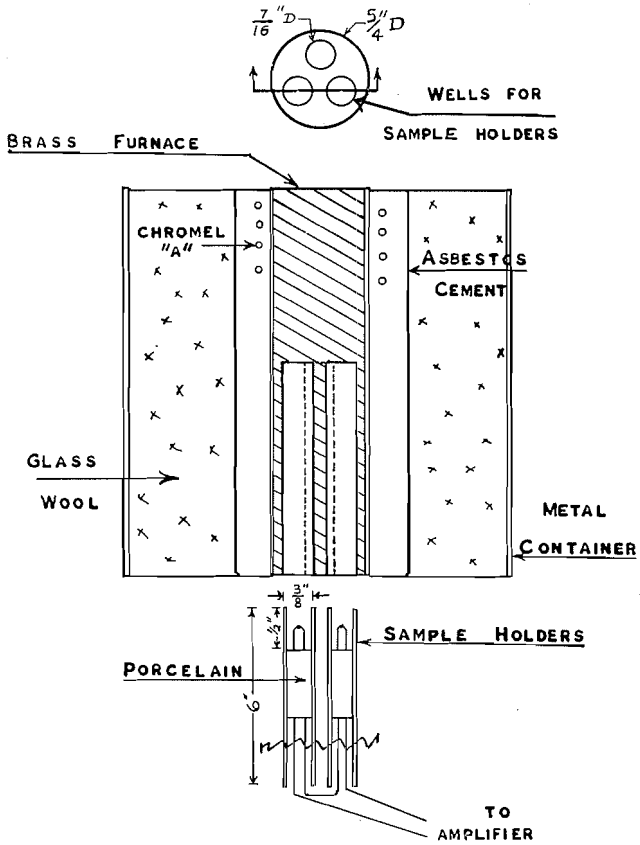


FIG. 1. Essentials of furnace and sample holders.

Wood Preparation

Air-dry balsam fir (*Abies balsamea* (L.) Mill.) was powdered using a metal file and then screened. That fraction passing mesh No. 70 but retained by mesh No. 200 was used in this work.

Removal of Extractives

Wood powder was extracted for 8 hours at room temperature with a mixture of 65 parts benzene, 35 parts ethanol, and 15 parts water. This mixture resulted in two layers. Upon evaporation, the benzene–alcohol layer yielded a brown, tarry material which was believed to contain resins. The alcohol–water layer was allowed to evaporate to near dryness at room temperature and was then further dried at 110° C. It yielded a gray material which was easily powdered. Some of the mixture appeared crystalline, and was very hygroscopic. A water solution of this material, acidified with acetic acid, gave a white precipitate with a solution of lead acetate, indicating the presence of tannins.

After the benzene–alcohol–water extraction, the wood powder was dried, and further extracted with 65 parts benzene and 35 parts ethanol. No extract was obtained. The wood was washed with water at 60° C and vacuum-dried at 100° C for 48 hours. This wood was designated as "free of extractives".

Can. J. Chem. Downloaded from www.nrcresearchpress.com by 210.87.254.105 on 09/05/12
For personal use only.

Isolation of Lignin

Two grams of wood free of extractives was added to 25 ml of 72% sulphuric acid at 10° C and stirred for 1 minute. The temperature was allowed to rise to 21° C. This mixture was allowed to stand for 2 hours with frequent stirring. The mixture was then diluted to 3% acid concentration, and boiled for 4 hours. The lignin residue was then filtered off using a fritted-glass crucible and washed with a liter of hot water until acid free. The lignin was dried at 110° C under vacuum for 24 hours.

Isolation of Some Hemicelluloses

One gram of wood powder free of extractives was treated with 50 ml of 20% potassium hydroxide for 18 hours under an inert atmosphere. Sufficient water was added to reduce the concentration of the potassium hydroxide to 3%, and the mixture was allowed to stand at 65 to 70° C for 2 hours before filtration. Excess acetic acid was added to neutralize the potassium hydroxide, and the hemicelluloses precipitated, twice the volume of methanol being used. After settling for about 2 hours, the precipitate was filtered off using a fritted-glass crucible, washed free of acid, washed with acetone, and vacuum-dried in a desiccator at room temperature.

Preparation for an Analysis

Calcined alumina, kept at 400° C until needed, was placed in both holders, the inert-sample holder being completely filled, the active-sample holder being filled to about $\frac{1}{8}$ of an inch of the thermocouple junction. Five milligrams of the active sample mixed with an equal volume of alumina was packed around the junction. Alumina was used to complete the filling of the sample holder. The two sample holders were inserted vertically into the furnace and a very slow current of air was circulated around the sample.

RESULTS AND DISCUSSION

Figure 2 shows eight thermograms over a range of 50° to 420° C. The interesting portions of the thermogram for air-dry wood powder have been lettered. Although some are very minor endotherms or exotherms, they reoccurred in all of the thermal analysis runs on the air-dry wood. As shown in Table I, all of the inflections except C can

TABLE I

Summary of peaks and their causes

Peak from air-dry wood	Fraction
A, endotherm at 145° C	Alcohol–water extract
B, endotherm at 163° C	Alcohol–water extract
C, 210° C	Unaccounted
D, 265° C	Possibly acid lignin
E, exotherm at 285° C	Benzene–alcohol extract
F, exotherm at 300° C	Sum of benzene–alcohol extract and acid lignin
G, exotherm at 330° C	Cellulose
H, exotherm at 360° C	Same as F

be attributed to reactions in the various fractions that go to make up the wood substance.

Thermogram II of the alcohol–water extract of wood discloses two endotherms at 144° and 163° C which could account for endotherms A and B. The extract melts at the former temperature and decomposes into a gas and a white powder at the latter.

Can. J. Chem. Downloaded from www.nrcresearchpress.com by 210.87.254.105 on 09/05/12
For personal use only.

Can. J. Chem. Downloaded from www.nrcresearchpress.com by 210.87.254.105 on 09/05/12
For personal use only.

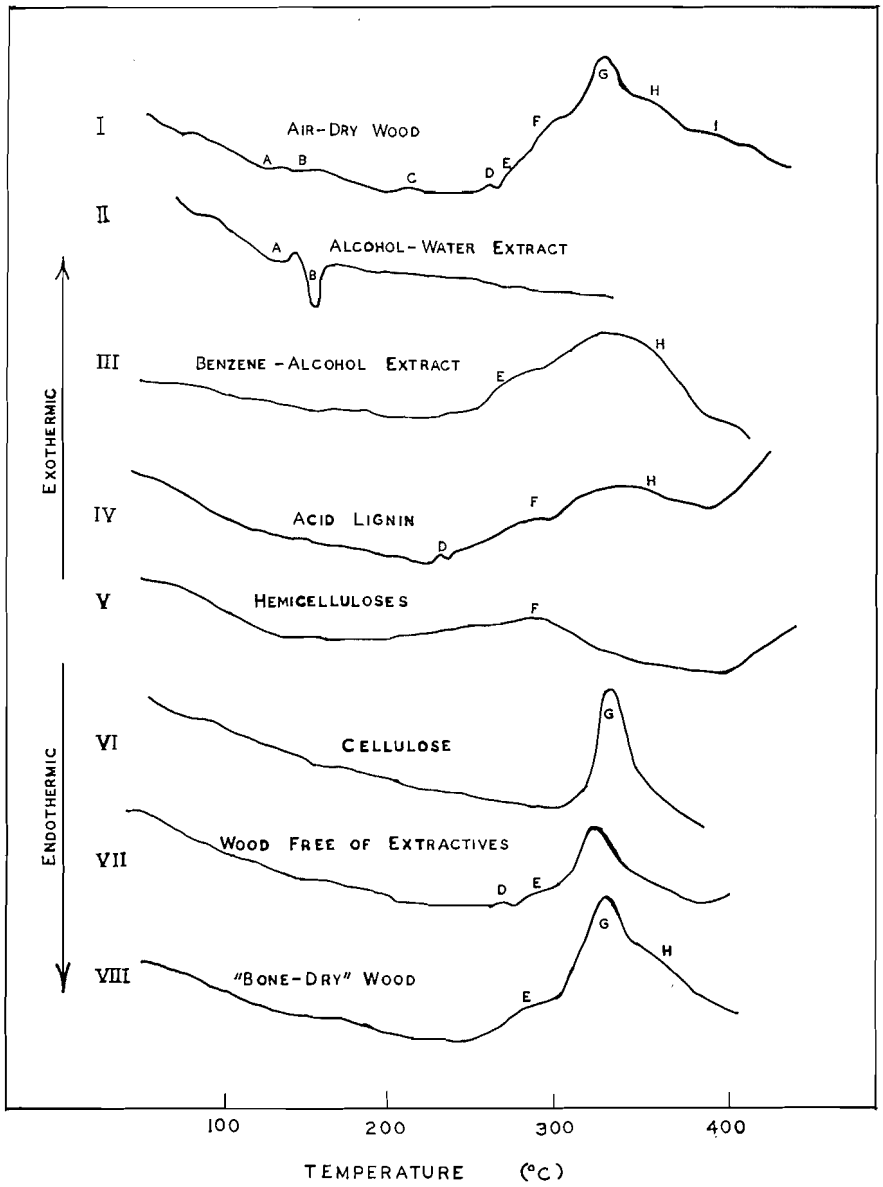


FIG. 2. Thermograms of balsam fir and its components.

The isolated acid lignin (IV) shows activity around 230° C quite similar to the variations D at 265° C in the thermogram for wood. This displacement could result from physical or chemical changes occurring in the lignin during the isolation procedure.

The main system of exothermic peaks from 270° to 400° C is actually a composite of several exothermic reactions. The shoulder E can be traced to the first portion of the main exothermic reaction of the benzene–alcohol extract (III). Section F is the sum of the tailing portion of the foregoing exotherm plus the 290° C exotherm of the acid lignin (IV).

Peak G is quite clearly the cellulose exotherm (VI) superimposed on the less intense exotherms of the lignin and the benzene–alcohol extract.

The hemicelluloses isolated by the procedure outlined above gave an exothermic peak which gradually reached a maximum at 285° C.

Morita and Rice (3) report that cellulose is characterized by an endotherm at 340° C when heated in an atmosphere of nitrogen. This present work shows that in air the endotherm becomes an exotherm at 330° C. The minor temperature shift can be attributed to the slower heating rate used here.

It is interesting to compare the thermograms of acid lignin and of the benzene–alcohol extract. Their marked similarity would suggest the presence of native lignin in the extract. In fact, a small amount (8 to 10%) of the protolignin in wood can be extracted in an unchanged form using indifferent solvents. Such lignin is termed "native" lignin. An acetone extract of wood, which would contain mainly resins, gave a thermogram identical with that of the benzene–alcohol extract. This similarity between the thermograms of lignin and resins could be expected because of a similarity in their basic structures.

These two thermograms do differ above 400° C, however. The acid lignin indicates the beginning of an intense exotherm, while the benzene–alcohol extract does not, nor does the unextracted wood powder show an exotherm in this range. Obviously the lignin has undergone some changes upon its isolation.

For thermogram VIII the original wood powder was vacuum-dried over drierite at 80° C for 48 hours. It was then left over drierite for 3 months at room temperature. Five milligrams of it was mixed with an equal volume of alumina and thermogramed. Many of the previously mentioned peaks were missing or decreased in intensity. It is difficult to account for these differences unless adsorbed water assists the breakdown of wood in a hydrolytic manner.

As would be expected, the thermogram of wood powder free of extractives (VII) displays the characteristic exotherm of cellulose at 330° C, and to a lesser extent, the exotherm of lignin, but not the peaks characteristic of the extractives.

It would appear, therefore, that over the range from 50° to 420° C the differential thermogram for balsam fir when heated in air is simply a composite of the individual thermograms of the various components of the wood, with little, if any, interaction between these components.

ACKNOWLEDGMENTS

The author wishes gratefully to acknowledge equipment grants from the Nova Scotia Research Foundation and from the National Research Council of Canada.

REFERENCES

1. L. P. CLERMONT and H. SCHWARTZ. Pulp Paper Mag. Can. **52**, No. 13, 103 (1951).
2. V. N. SERGEEVA and A. VAIVADS. Latvijas PSR Zinātņu Akad. Vēstis, No. 9 (whole No. 86), 103 (1954).
3. H. MORITA and H. M. RICE. Anal. Chem. **27**, 336 (1955).
4. T. WIDELL. Acta Polytech., Chem. Met. Ser. **1**, No. 6, 35 (1949).

Can. J. Chem. Downloaded from www.nrcresearchpress.com by 210.87.254.105 on 09/05/12
For personal use only.

Can. J. Chem. Downloaded from www.nrcresearchpress.com by 210.87.254.42 on 09/05/12
For personal use only.

THE REACTION BETWEEN METHYL RADICALS AND ISOBUTANE[1]

A. R. BLAKE,[2] J. F. HENDERSON,[3] AND K. O. KUTSCHKE

ABSTRACT

It has been confirmed that the apparent rate constant for the reaction between methyl radicals, produced by the photolysis of deuterated acetone, and isobutane increases with decreasing isobutane pressure. An explanation is proposed to account for this observation suggesting that the production of methane by disproportionation between methyl and *t*-butyl radicals was not negligible as has been assumed previously.

INTRODUCTION

Observations made recently in this laboratory indicated that values of the apparent rate constants for the abstraction of hydrogen by methyl radicals, calculated using conventional methods, depended on the pressure of the added hydrogen donor. The reaction of methyl radicals with isobutane using the pyrolysis of di-*t*-butyl peroxide as a source of methyl radicals is an example of such a system (1). When mixtures of deuterated acetone and hydrogen were photolyzed, the rate constant for the reaction of methyl radicals with hydrogen was found to be a function of the hydrogen pressure (2). In view of the apparent similarities between the two systems, an investigation of the photolysis of deuterated acetone – isobutane mixtures was made.

EXPERIMENTAL

The apparatus and methods of analysis were similar to those employed in the photolysis of the deuterated acetone – hydrogen mixtures (2, 3). The deuterated acetone consisted of 98.2% acetone-d_6 and 1.8% acetone-d_5. Phillips Research Grade isobutane was outgassed by bulb-to-bulb distillations at $-160°$ C. The temperature of the reaction cell was $471 \pm 0.5°$ K for all experiments.

RESULTS AND DISCUSSION

In the photolysis of mixtures of deuterated acetone and isobutane, it is usually assumed that methane and ethane are formed by the following reactions:

$$CD_3 + CD_3 \rightarrow C_2D_6 \qquad [a]$$

$$CD_3 + CD_3COCD_3 \rightarrow CD_4 + CD_2COCD_3 \qquad [b]$$

$$CD_3 + i\text{-}C_4H_{10} \rightarrow CD_3H + t\text{-}C_4H_9. \qquad [c]$$

When the deuterated acetone was photolyzed alone (2), small amounts of CD_3H were formed due to the presence of acetone-d_5 in the sample, and its yield was given by

$$R_{CD_3H}/R_{C_2D_6}^{1/2} = 0.014[A] \times 10^{-12} \text{ (molecules/cc sec)}^{1/2}, \qquad [1]$$

where $[A]$ is the acetone concentration in molecules/cc. Allowance for this CD_3H was made when calculating values of $k_c/k_a^{1/2}$.

$$\rho = (k_c/k_a^{1/2})_{app} = R_{CD_3H}/R_{C_2D_6}^{1/2}[i\text{-}C_4H_{10}] \qquad [2]$$

Values of ρ are shown in Table I and it is evident that the apparent rate constant

[1]*Manuscript received July 20, 1960.*
Contribution from the Division of Pure Chemistry, National Research Council, Ottawa, Canada.
Issued as N.R.C. No. 6462.
[2]*National Research Council Postdoctorate Fellow, 1957–59. Present address: The Chemistry Department, University of Bristol, Bristol, England.*
[3]*National Research Council Postdoctorate Fellow, 1957–59. Present address: Polymer Corporation Limited, Sarnia, Ontario.*

Can. J. Chem. Downloaded from www.nrcresearchpress.com by 210.87.254.42 on 09/05/12
For personal use only.

TABLE I

Products of the reaction at 471° K

Run	Time, sec	Concn., 10^{18} molecules/cc			Rate, 10^{12} molecules/cc sec					Ratio of rate constants, 10^{-13} (molecules/ml)$^{-1/2}$ sec$^{-1/2}$	
		d-Acetone	*i*-C_4H_{10}	*n*-C_4F_{10}	CO	Methane	Ethane	% CD_4	% C_2D_6	$k_b/k_a^{1/2}$	ρ
163	3,600	2.17	0.118		6.01	4.06	2.92	62.3	98.2	6.88	74.0
162	3,600	2.15	0.324		7.63	6.61	2.96	39.1	98.1	7.05	72.2
172	3,600	2.15	0.328		5.80	5.36	2.06	38.9	98.2	6.79	69.5
168	3,600	2.15	0.311	3.24	5.91	5.23	2.13	39.7	98.1	6.66	67.8
178	4,500	2.16	0.299	3.29	5.99	5.25	2.13	39.7	98.2	6.64	69.4
161	7,200	2.17	0.645		7.60	8.44	1.94	25.3	97.9	7.12	70.6
176	7,260	2.16	0.676		5.41	6.51	1.14	24.3	98.0	6.90	68.3
160	5,400	2.17	1.08		7.54	9.92	1.30	17.0	98.0	6.91	67.3
164	9,000	2.17	2.19		7.04	11.1	0.525	9.64	97.7	6.89	63.7
166	18,000	0.652	1.09		2.22	3.39	0.204	5.91	97.6	6.88	65.5
165	10,800	1.09	1.08		3.50	5.06	0.434	9.63	97.8	6.85	64.7
171	10,830	1.09	1.07	1.06	3.22	4.80	0.390	9.55	97.8	6.81	65.2
169	7,241	1.09	1.08	3.22	3.76	5.30	0.495	9.60	97.7	6.73	63.2
173	6,300	3.23	1.07		7.52	10.1	1.22	23.3	98.1	6.69	65.3

determined by equation [2] varies with the isobutane pressure, which confirms the earlier observation (1). Unlike the addition of hydrogen (2), however, the addition of isobutane to acetone-d_6 did not affect the ratio $R_{CD_4}/R^{1/2}_{C_2D_6}[A]$ in any way. Finally, ρ did not appear to be influenced by the addition of perfluoro-*n*-butane which indicates the absence of excited species in the system.

To account for these observations, it is proposed that the disproportionation reaction between methyl and *t*-butyl radicals was important in the systems discussed here, and that the observed variation of ρ with isobutane pressure is due to the assumption that this reaction was negligible. By inclusion of the following radical–radical reactions in the mechanism, allowance for this additional source of CD_3H can be made in the following manner:

$$CD_3 + t\text{-}C_4H_9 \rightarrow CD_3H + i\text{-}C_4H_8 \qquad [d]$$

$$\rightarrow CD_3C_4H_9 \qquad [e]$$

$$t\text{-}C_4H_9 + t\text{-}C_4H_9 \rightarrow i\text{-}C_4H_{10} + i\text{-}C_4H_8 \qquad [f]$$

$$\rightarrow C_8H_{18} \qquad [g]$$

$$CD_3 + CD_2COCD_3 \rightarrow C_2D_5COCD_3 \qquad [h]$$

$$t\text{-}C_4H_9 + CD_2COCD_3 \rightarrow (CH_3)_3CCD_2COCD_3 \qquad [i]$$

$$CD_2COCD_3 + CD_2COCD_3 \rightarrow CD_3COCD_2CD_2COCD_3. \qquad [j]$$

The abstraction of deuterium from acetone-d_6 by t-C_4H_9 radicals is neglected on thermochemical grounds. On the basis of statistics, it is assumed that

$$2k_a = (2k_f + k_g) = 2k_j = k_d + k_e = k_h = k_i = k. \qquad [3]$$

Although this expression is not entirely correct due to differences in masses and entropies of the collision complexes, the error will be small (see Appendix I).

By the use of [3] and the mass balances in CD_3, t-C_4H_9, and CD_3COCD_2 radicals, the following expressions for m were derived (see Appendix II):

$$m_{\mathrm{I}} = 1 - [\beta\lambda_E^{1/2}(1 - \lambda_D - \lambda_E^{1/2})/\lambda_H] \qquad [4]$$

$$m_{\mathrm{II}} = ([1 + \beta(1 - \lambda_D)]/2\beta\lambda_H)\{1 - [1 - (4\beta\lambda_H)/(1 + \beta(1 - \lambda_D))^2]^{1/2}\} \qquad [5]$$

$$m_{\mathrm{III}} = (1 - \lambda_D - \lambda_E^{1/2})/\lambda_H \qquad [6]$$

$$m_{\mathrm{IV}} = 1/(1 + \beta\lambda_E^{1/2}), \qquad [7]$$

where $\beta = k_d/(k_d + k_e)$, $\lambda_D = R_{CD_4}/2R_{CO}$, $\lambda_H = R_{CD_3H}/2R_{CO}$, $\lambda_E = R_{C_2D_6}/R_{CO}$, and m is the yield of CD_3H from [*c*] relative to the total yield of CD_3H (i.e., $m = k_c[CD_3][i\text{-}C_4H_{10}]/R_{CD_3H}$).

Values of m were calculated for $\beta = 0.446$ corresponding to $k_d/k_e = 0.806$. This was calculated from the data of Kerr and Trotman-Dickenson (4) using [3] rather than [3*a*] (Appendix I), which was employed by the original authors. This procedure is logically more consistent with the present work than the use, directly, of the value $k_d/k_e = 0.699$ as reported by the original authors. In the recalculation, k_f/k_g was taken as 4.44, being the average of the values reported by Kraus and Calvert (5). It is interesting to note that the recalculated value is in better agreement than the original with the less precisely but more directly determined value $k_d/k_e = 0.9$ found by McMillan (6) using a method which did not require the assumption of either [3] or [3*a*]. Frey's value (7) is also based on the assumption of [3*a*] but no data are given to permit recalculation.

It was assumed throughout that CH_3 and CD_3 behave identically in respect to their reactions with t-C_4H_9 radicals.

Can. J. Chem. Downloaded from www.nrcresearchpress.com by 210.87.254.42 on 09/05/12
For personal use only.

The agreement among the numerical values of m_{I}, m_{II}, m_{III}, and m_{IV}, Table II, while

TABLE II

Correction factors and corrected constants

Run	m_{I}	m_{II}	m_{III}	m_{IV}	λ_{E}	$10^{13}\,\rho m_{IV} = 10^{13} k_c/k_a^{1/2}$	β
163	0.752	0.737	0.805	0.765	0.477	56.8	0.353
162	0.773	0.783	0.828	0.785	0.378	56.8	0.338
172	0.782	0.788	0.831	0.792	0.347	54.9	0.346
168	0.770	0.786	0.867	0.790	0.355	54.5	0.257
178	0.764	0.781	0.893	0.791	0.352	57.1	0.203
161	0.806	0.808	0.871	0.818	0.250	57.5	0.294
176	0.821	0.824	0.879	0.831	0.208	56.9	0.304
160	0.839	0.838	0.877	0.845	0.169	56.8	0.342
164	0.889	0.884	0.920	0.893	0.0720	57.0	0.322
166	0.878	0.873	0.914	0.883	0.0894	57.9	0.316
165	0.861	0.857	0.896	0.866	0.120	56.2	0.337
171	0.867	0.869	0.872	0.867	0.118	56.9	0.428
169	0.856	0.852	0.901	0.862	0.129	54.8	0.306
173	0.845	0.843	0.863	0.848	0.162	55.5	0.393
					Mean	56.4	0.324
					Standard deviation	0.3	0.015

not surprising in view of the algebraic identity which can be shown to exist (Appendix II), is, nevertheless, very gratifying when the algebraic complexity of some of the expressions is considered. Values of $k_c/k_a^{1/2}$ were determined using m_{IV} and equation [8]; they are independent of the pressure of isobutane (Table II and Fig. 1).

$$k_c/k_a^{1/2} = \rho m_{IV} \qquad [8]$$

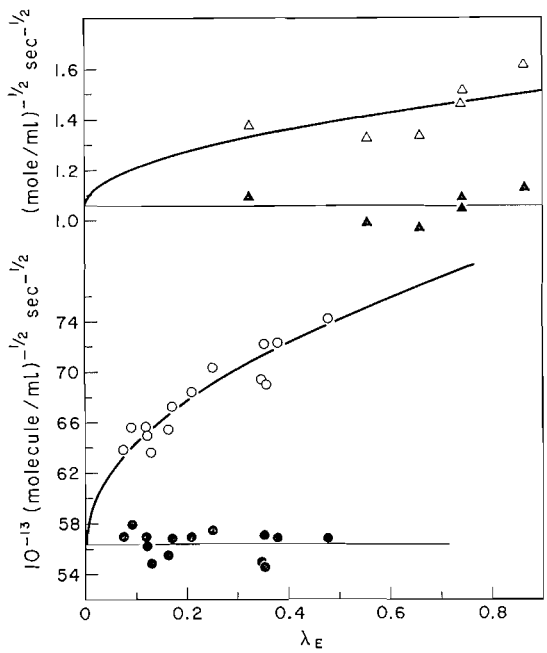


FIG. 1. Variation of apparent and corrected rate constants. *d*-Acetone, *i*-C_4H_{10} system (471° K): ○ ρ; ● $k_c/k_a^{1/2}$. DTBP, *i*-C_4H_{10} system (411° K): △ $R_{CH_4}/R_{C_2D_6}^{1/2}[i\text{-}C_4H_{10}]$; ▲ $k_c/k_a^{1/2}$. In both cases the curve is drawn from equation [8].

Can. J. Chem. Downloaded from www.nrcresearchpress.com by 210.87.254.42 on 09/05/12
For personal use only.

By equating any two of the expressions [4], [5], [6], and [7] it is found that β is given by the relation

$$\beta = [\lambda_H - (1 - \lambda_D - \lambda_E^{1/2})]/\lambda_E^{1/2}(1 - \lambda_D - \lambda_E^{1/2}). \quad [9]$$

Because of the many subtractions involved, measurements of β made in this way cannot be regarded as highly precise; this is shown by the considerable scatter of its values (Table II).

Inspection of equation [7] indicates that m decreases with increasing λ_E, i.e. with increasing light intensity or decreasing isobutane pressure, and tends to $1/(\beta+1)$ in the limit. In Fig. 2, m_{IV} is plotted against the logarithm of λ_E (equation [7]) and approaches

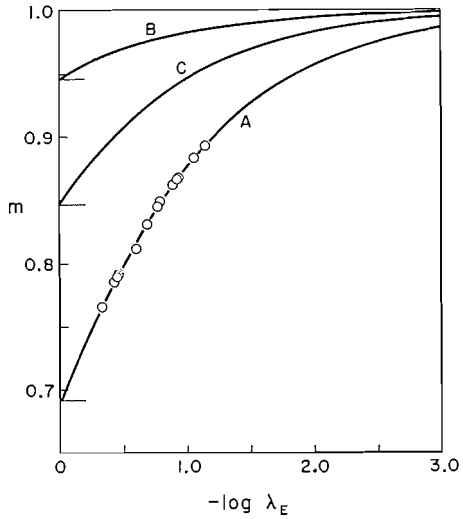


FIG. 2. Variation of m_{IV} with λ_E. A: m_{IV}, $\beta = 0.446$; B: m_{IV}, $\beta = 0.057$; C: m_{IV}, $\beta = 0.18$. The points on A are taken from Table II.

unity only when λ_E becomes exceedingly small; e.g. $m = 0.95$, 0.98, and 0.99 when $\lambda_E =$ 0.0139, 0.0021, and 0.0005 respectively. Consequently, to carry out experiments under conditions where the disproportionation reaction [*d*] would be negligible, the formation of ethane would have to be virtually completely suppressed.

If the earlier data, obtained by the pyrolysis of di-tertiary-butyl peroxide in the presence of isobutane (1), can be represented by a mechanism composed of reactions [*l*] and [*m*],

$$\text{DTBP} \rightarrow 2(CH_3)_3CO \quad [l]$$

$$(CH_3)_3CO \rightarrow CH_3 + CH_3COCH_3, \quad [m]$$

along with [*a*], [*c*], [*d*], [*e*], [*f*], and [*g*], an expression may be obtained which is identical in form with m_{IV}. However, in this application $\lambda_E = 2R_{C_2H_6}/R_{CH_3COCH_3}$. Acetone was not determined in those experiments but its rate of formation may be calculated with sufficient accuracy from the Arrhenius equation for the decomposition of the peroxide. Figure 1 also shows these data, in the original units, and indicates that application of the extended mechanism, with $\beta = 0.446$, gives essentially constant values of $k_c/k_a^{1/2}$. This is in contrast to the curvature observed in $R_{CH_4}/R_{C_2D_6}^{1/2}[i\text{-}C_4H_{10}]$ also shown in Fig. 1.

It is useful to note how the systematic error which arises from the neglect of reactions

Can. J. Chem. Downloaded from www.nrcresearchpress.com by 210.87.254.42 on 09/05/12
For personal use only.

of the type [*d*] varies, through the value of β, with various hydrocarbons. Values of m_{IV} were calculated for $\beta = 0.057$ ($k_d/k_e = 0.06$ as found (7) for $CH_3 + C_2H_5$) and $\beta = 0.18$ ($k_d/k_e = 0.22$ as found (4) for $CH_3 + sec\text{-}C_3H_7$), and are shown in Fig. 2 as curves B and C respectively. The very much lower values of β encountered in these systems allow the taking of data without significant error at considerably larger values of λ_E.

The question also arises as to what effect neglect of the disproportionation reaction [*d*] has on the activation energy of the hydrogen-transfer reaction [*c*] when $m < 1.0$. It becomes immediately obvious when equation [2] is rewritten as follows that, provided m is kept independent of the temperature, the apparent and true activation energies will be identical.

$$\rho = m^{-1}(R_{CD_3H})_c/R^{1/2}_{C_2D_6}[i\text{-}C_4H_{10}] = (k_c/k_a^{1/2})_{app} \qquad [10]$$

If, owing to a decrease in λ_E, m increases with increasing temperature, the apparent value will be less than the true value, but the difference will be small in most instances. For example, it will be approximately 0.5 kcal mole^{-1} if m increases by 0.20 between 100° C and 250° C; this is comparable to the uncertainty often quoted in determinations of activation energy.

In conclusion, the variation with isobutane pressure of ρ (or $R_{CH_4}/R^{1/2}_{C_2D_6}[i\text{-}C_4H_{10}]$ in the DTBP system) can be accounted for by assuming the disproportionation reaction [*d*] to be a significant source of methane in these systems under some conditions. It is possible to relate the contribution of [*d*] to the known or measurable quantities β, λ_H, λ_D, and λ_E and thus to correct the data for that contribution. Some assumptions were necessary in the development of the relevant expressions but it is doubtful that the quantitative conclusions are seriously in error.

ACKNOWLEDGMENTS

We wish to thank Dr. E. W. R. Steacie for his interest in this work, Dr. R. J. Cvetanovic for some useful discussion of its interpretation, and Mrs. Bernice Riem for mass spectrometric analyses.

REFERENCES

1. A. R. Blake and K. O. Kutschke. Can. J. Chem. **37**, 1462 (1959).
2. J. F. Henderson and E. W. R. Steacie. Can. J. Chem. **38**, 2161 (1960).
3. E. Whittle and E. W. R. Steacie. J. Chem. Phys. **21**, 993 (1956).
4. J. A. Kerr and A. F. Trotman-Dickenson. J. Chem. Soc. 1609 (1960).
5. J. W. Kraus and J. G. Calvert. J. Am. Chem. Soc. **79**, 5921 (1957).
6. G. R. McMillan. J. Am. Chem. Soc. **82**, 2422 (1960).
7. H. M. Frey. Proc. Chem. Soc. 385 (1959).
8. C. A. Heller. J. Chem. Phys. **28**, 1255 (1958).
9. J. A. Kerr and A. F. Trotman-Dickenson. Chem. & Ind. (London), 125 (1959).
10. A. F. Trotman-Dickenson. Ann. Repts. on Progr. Chem. (Chem. Soc. London), **55**, 36 (1959).
11. A. Shepp. J. Chem. Phys. **24**, 939 (1956).
12. P. J. Boddy and J. C. Robb. Proc. Roy. Soc. (London), A, **249**, 547 (1959).

APPENDIX I

The referee of the present paper has asked us to comment on our use of [3] rather than [3*a*], the analogue of which occurs frequently in the literature.

$$k_e/k_a^{1/2}k_g^{1/2} = 2 \qquad [3a]$$

Kerr and Trotman-Dickenson (4, 9) and Trotman-Dickenson (10) have cited several systems in which [3*a*] appears to be verified experimentally.

Can. J. Chem. Downloaded from www.nrcresearchpress.com by 210.87.254.42 on 09/05/12
For personal use only.

Perhaps the simplest discussion can be given if the more general case is considered.

$$R_1 + R_1 \rightarrow \text{alkane}_1 + \text{alkene}_1 \quad [A]$$
$$\rightarrow R_1R_1 \quad [B]$$
$$R_1 + R_2 \rightarrow \text{alkane}_1 + \text{alkene}_2 \quad [C]$$
$$\rightarrow \text{alkene}_1 + \text{alkane}_2 \quad [D]$$
$$\rightarrow R_1R_2 \quad [E]$$
$$R_2 + R_2 \rightarrow \text{alkane}_2 + \text{alkene}_2 \quad [F]$$
$$\rightarrow R_2R_2 \quad [G]$$

The formulations corresponding to [3] and [3*a*] are, respectively,

$$(k_C+k_D+k_E)/(k_A+k_B)^{1/2}(k_F+k_G)^{1/2} = 2, \quad [i]$$

and

$$k_E/k_B^{1/2}k_G^{1/2} = 2. \quad [ii]$$

[A] and [D] are not observed when R_1 is a methyl radical.

It should be emphasized that [i], and thus [3], is the correct statistical formulation provided that each collision results in either disproportionation or combination of the colliding pair of radicals. The latter assumption, of course, underlies all the development in the body of this paper. If the steric factor is much less than unity for the sum of mutual disproportionation plus combination for some radical species, no theoretical relationship exists when a methyl radical is taken with that radical in a cross combination; this follows from the fact that the steric factor for the combination of methyl radicals is very close to unity (11). In that case, then, there is no a priori reason to expect either [i] or [ii] to hold.

If [i] is a correct formulation and the experimental data lead to [ii], it follows that the right side of [iii] must very nearly be unity.

$$(1/2)k_E/k_B^{1/2}k_G^{1/2} = [1+(k_B/k_A)]^{1/2}[1+(k_F/k_G)]^{1/2}/[1+(k_C/k_E)+(k_D/k_E)] \quad [iii]$$

Data are available to check [iii] for the systems tabulated.

R_1	R_2	k_A/k_B	k_F/k_G	k_C/k_E	k_D/k_E	[iii]
CH_3	C_2H_5	0	0.12*	0	0.06†	1.0
CH_3	n-C_3H_7	0	0.16‡	0	0.14§	0.94
CH_3	n-C_4H_9	0	0.94‖	0	0.15‖	1.21
C_2H_5	i-C_3H_7	0.12*	0.60¶	0.43§	0.06**	0.90

*K. O. KUTSCHKE, M. H. J. WIJNEN, and E. W. R. STEACIE. J. Am. Chem. Soc. **74**, 714 (1952).
†Reference 8.
‡J. A. KERR and A. F. TROTMAN-DICKENSON. Trans. Faraday Soc. **55**, 572 (1959).
§J. C. J. THYNNE. Proc. Chem. Soc. 68 (1961).
‖J. C. J. THYNNE. Proc. Chem. Soc. 18 (1961).
¶R. H. RIEM and K. O. KUTSCHKE. Can. J. Chem. **38**, 2332 (1960). J. A. KERR and A. F. TROTMAN-DICKENSON. Trans. Faraday Soc. **55**, 921 (1959). C. A. HELLER and A. S. GORDON. J. Phys. Chem. **60**, 1315 (1956).
**Calculated from $k_D/k_C = 0.15$ and $k_C/k_E = 0.43$ given in footnote §.

Thus, within some 20%, the cancellation to unity is observed. This uncertainty is not much greater than that of the experimental values reported for $R_1R_2/(R_1R_1)^{1/2}(R_2R_2)^{1/2}$ used to support the use of [ii] and [3*a*].

It should be noted that the values of k_C/k_E reported in reference 4 for the systems CH_3, i-C_3H_7 and CH_3, t-C_4H_9 cannot be used to check [iii], since those values were obtained indirectly in that the equivalent of [ii] was used to calculate unmeasured products. The

Can. J. Chem. Downloaded from www.nrcresearchpress.com by 210.87.254.42 on 09/05/12
For personal use only.

ratios of rate constants reported by Boddy and Robb (12) were not considered here; reasons for questioning the reliability of those data have been advanced elsewhere (4, 10).

APPENDIX II

A brief description is given of the derivation of the expressions for m which appear in the text as equations [4], [5], [6], and [7]. To simplify the nomenclature, the following abbreviations are used: $[CD_3COCD_3] = a$, $[i\text{-}C_4H_{10}] = b$, $[CD_3] = v$, $[t\text{-}C_4H_9] = u$, $[CD_3COCD_2] = w$, and $\sigma = v+u+w$.

The balances for v, w, and u respectively are:

$$2R_{CO} = 2k_a v^2+k_b av+k_c bv+(k_d+k_e)uv+k_h wv \quad [i]$$

$$R_{CD_4} = k_b av = k_h vw+k_i uw+2k_j w^2 \quad [ii]$$

$$mR_{CD_3H} = k_c bv = (k_d+k_e)uv+2(k_f+k_g)u^2+k_i uw. \quad [iii]$$

If it is assumed that

$$2k_a = 2(k_f+k_g) = 2k_j = (k_d+k_e) = k_h = k_i = k, \quad [3]$$

the addition of [i], [ii], and [iii] and substitution of [3] yields [iv].

$$\sigma = (2R_{CO}/k)^{1/2} \quad [iv]$$

Combination of equations [ii] and [iv] gives

$$w = \sigma R_{CD_4}/2R_{CO} = \sigma\lambda_D. \quad [v]$$

Similarly, from equations [iii] and [iv],

$$u = m\sigma R_{CD_3H}/2R_{CO} = m\sigma\lambda_H. \quad [vi]$$

Because $(2R_{C_2D_6})^{1/2} = k^{1/2}v$, [iv] may be used to show that

$$v = \sigma(R_{C_2D_6}/R_{CO})^{1/2} = \sigma\lambda_E{}^{1/2}. \quad [vii]$$

Rearrangement of the relation

$$R_{CD_3H} = k_c bv+k_d uv = mR_{CD_3H}+k_d uv$$

and application of equation [iv] yields the following expression for m:

$$m = 1-(\beta uv/\sigma^2\lambda_H), \quad [viii]$$

where

$$\beta = k_d/(k_d+k_e). \quad [ix]$$

However,

$$u = \sigma-v-w = \sigma(1-\lambda_D-\lambda_E{}^{1/2}), \quad [x]$$

and the expression for m_I is obtained by substitution of [x] into [viii]. Similarly,

$$v = \sigma(1-\lambda_D-m\lambda_H), \quad [xi]$$

and, substituting in [viii], the expression for m_{II} is obtained. Substitution of uv in [viii] by

$$uv = m\sigma^2\lambda_H\lambda_E{}^{1/2} \quad [xii]$$

Can. J. Chem. Downloaded from www.nrcresearchpress.com by 210.87.254.42 on 09/05/12
For personal use only.

gives the relation for m_{IV}. In addition, [iii] can be rewritten using [x] as

$$mR_{CD_3H} = k\sigma u = k\sigma^2(1-\lambda_D-\lambda_E^{1/2}).$$

The expression for m_{III} follows after substitution of [iv].

If any pair of the relations for m are equated, the same expression for β is obtained. The manipulation is easy except when m_{II} is one of the expressions in the pair taken. Furthermore, substitution of this expression for β into the relations for m_I, m_{II}, or m_{IV} yields that for m_{III}. This provides good evidence for the existence of the algebraic identity $m_I = m_{II} = m_{III} = m_{IV}$. Consequently, when calculating values of m the relation which gives the most precise result can be used.

Finally, because λ_E tends to unity as light intensity is increased and isobutane pressure is decreased, it can be shown that m will tend to $1/(1+\beta)$ at high light intensity and low isobutane pressure and that m will tend to unity under the opposite conditions, i.e. $\lambda_E \rightarrow 0$ (equation [7]).

Can. J. Chem. Downloaded from www.nrcresearchpress.com by 210.87.254.42 on 09/05/12
For personal use only.

Can. J. Chem. Downloaded from www.nrcresearchpress.com by 210.87.254.6 on 09/05/12
For personal use only.

DESIGN AND CALIBRATION OF AN INEXPENSIVE FREE-FLOW ELECTROVISCOMETER[1]

P. A. D. DE MAINE AND E. R. RUSSELL

ABSTRACT

Here are reported the design and calibration of a new inexpensive free-flow electroviscometer for rapid and accurate measurement of the viscosity coefficients for conducting and non-conducting solutions. Flow times of 30 seconds are easily reproduced to within 0.02 second.

INTRODUCTION

In the past, several comprehensive review articles about viscometers have been published (1–5). An automatic viscometer designed to measure flow times accurately without constant attention by the operator has been reported by Goldfinger and Greatbatch (6). This viscometer used a photoelectrically triggered timing device to measure flow times to within 1 part in 10,000. Stock (7) has designed an electric resistance stream gauge type viscometer.

Measurements with free-flow type viscometers are limited in accuracy by the response time of the observer and the flow time of the viscometer. Rotary cone and the Goldfinger–Greatbatch types are relatively expensive and create problems where temperature control is desired.

Here is described a new modification of the Ostwald–Fenske viscometer which can be immersed in the usual thermostated bath. Even the low flow times, less than 30 seconds, are measured electronically to better than 1 part in 1000.

DESCRIPTION OF APPARATUS

Electrodes of No. 24 gauge platinum were sealed into an Ostwald–Fenske viscometer at the locations shown in Fig. 1. Platinum-to-glass or Hysol cement seals are satisfactory. Special care should be taken to locate the lowest electrode (No. 3) away from the capillary entrance. The top two electrodes (Nos. 1 and 2) are located centrally to minimize holdback of the solution. Lead wires are soldered to the three electrodes and then are coated with Dupont Duco cement for electrical insulation. Cover assemblies were cut from solid Plexiglass and were cemented directly onto the viscometer with Dupont Duco cement. These cover assemblies fit into openings in the lid of the Precision Temp-trol kinematic viscosity bath (Precision Scientific Company, Chicago, Illinois), and thus correct positioning of the viscometer is assured at all times.

Two Model 30 Fisher transistor relays (Fisher Scientific Company, New York, N.Y.) were connected to the platinum electrodes on the viscometer (Fig. 2) through variable resistances (0 to 0.50 meg) and to a Precision Time-it timer (Precision Scientific Company, Chicago, Illinois) graduated in 1/10 seconds. Viscosity measurements at constant, desired temperatures were achieved by placing the viscometers in the Temp-trol kinematic viscosity bath or in a similar laboratory-constructed unit.

OPERATION AND CALIBRATION

Methanol – carbon tetrachloride solutions of $SnCl_4.5H_2O$ and methanol solutions of iron group metal chlorides were used in the calibration of the modified Ostwald–Fenske

[1]*Manuscript received April 10, 1961.*
Contribution from the Department of Chemistry, University of Mississippi, University, Miss., U.S.A.

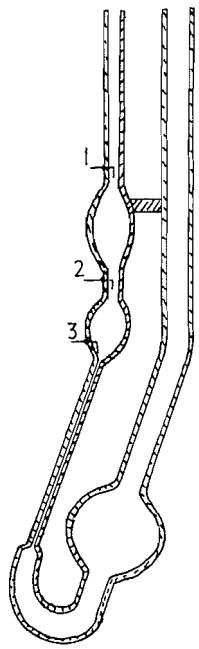


FIG. 1. Diagram of the modified Ostwald–Fenske viscometer showing location of the No. 24 gauge platinum electrodes.

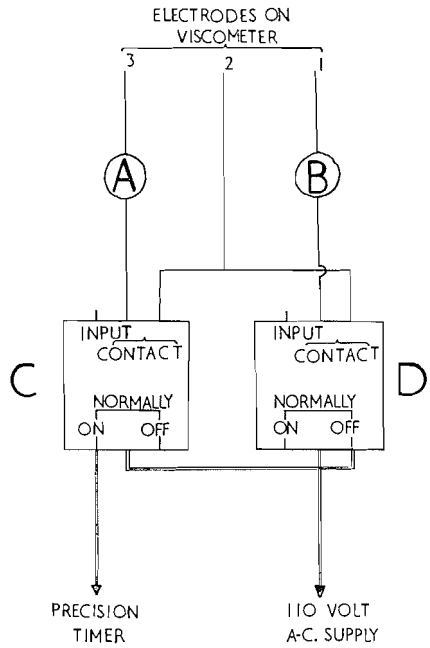


FIG. 2. Electrical circuit diagram for the electroviscometer. A and B: variable resistances (0 to 0.5 meg), graduated in 10,000-ohm units; C and D: Fisher transistor relays with switches in "delay off" and "NC" positions.

Can. J. Chem. Downloaded from www.nrcresearchpress.com by 210.87.254.6 on 09/05/12
For personal use only.

viscometers. $CaCl_2$, $CrCl_3.6H_2O$, $MnCl_2.4H_2O$, $CoCl_2.6H_2O$, $CoCl_2.2H_2O$, $NiCl_2.6H_2O$, $NiCl_2.2H_2O$, $CuCl_2.2H_2O$, and $ZnCl_2$ were used. Accurate viscosity data for these solutions as measured with normal Ostwald–Fenske viscometers at 20° C or 25° C and 45° C have been reported (8, 9). It has also been shown that molar conductance values for these solutions are in the range 0.80 to near 160 (10, 11, 12). Densities accurate to four decimal places have also been reported (8, 12).

Ten milliliters of solution was pipetted into the electroviscometer. The resistance (R) between electrodes 1 and 2 or between 2 and 3 (Fig. 1) with the viscometer immersed in the thermostated bath, and the immediate change in resistance (ΔR) as the solutions flowed past the two top electrodes, were measured directly with a Simpson Avometer. The maximum resistance ($\bar{R}$) required to operate the contact circuits for each of the two relays, C and D (Fig. 2), was determined by varying resistances A and B respectively. For the four relays used in this work, $\bar{R}$ lies between 200,000 and 310,000 ohms. The variable resistances A and B were set at a value $\mathring{R}$ so that $\mathring{R}+\Delta R = \bar{R}+10{,}000$. Experiments have shown that for all the conducting solutions studied, $\mathring{R}$ can be set at any value between 50,000 and $(\bar{R}-20{,}000)$ ohms. $\bar{R}$ usually lies between 200,000 and 310,000 ohms. Values for $\mathring{R}$ between these limits do not give any change in flow-time values.

The solution was drawn up in the viscometer so as to cover electrodes 1, 2, and 3. As the falling solution passed the top electrode the timer was switched on automatically and then the timer was switched off as the liquid passed the second electrode. Typical data collected for solutions of $SnCl_4.5H_2O$ are given in Table I. The factor limiting the accuracy appears to be the 0.1-second units (readable to 0.05 second) on the timer.

TABLE I

Flow rates for solutions of composition indicated, at 25° C, as measured with the electroviscometer

$SnCl_4.5H_2O$ (concn., M)	CCl_4 (concn., M)	Time (sec.)	No of trials	SRMS
0.100	0.000	40.17	7	0.02
0.200	0.000	43.37	7	0.02
0.300	0.000	46.81	7	0.03
0.400	0.000	50.55	10	0.03
0.500	0.000	54.88	7	0.03
0.600	0.000	59.07	8	0.04
0.700	0.000	63.63	9	0.03
0.800	0.000	68.71	7	0.02
0.900	0.000	74.11	7	0.02
1.000	0.000	79.97	6	0.03
0.100	1.029	39.72	7	0.02
0.100	2.057	39.23	6	0.03
0.100	3.086	39.01	8	0.03
0.100	4.114	38.84	7	0.02
0.100	5.143	38.49	8	0.02
0.100	6.171	38.27	9	0.02
0.100	7.200	38.57	7	0.03
0.100 / 0.100	Two-layer formation*			

NOTE: Average times listed are for the solution to flow from the first electrode to the second electrode. Square root mean square (SRMS) deviations and the number of independent measurements made are also given. For each solution the maximum deviation did not exceed 0.05 second.

*P. A. D. de Maine and M. M. de Maine. J. Inorg. & Nuclear Chem. **14**, 142 (1960).

Can. J. Chem. Downloaded from www.nrcresearchpress.com by 210.87.254.6 on 09/05/12
For personal use only.

In Figs. 3 and 4 are plotted viscosity coefficients, determined with the usual Ostwald–Fenske viscometer (flow time 400 to 1100 seconds), versus the product of density (8, 12)

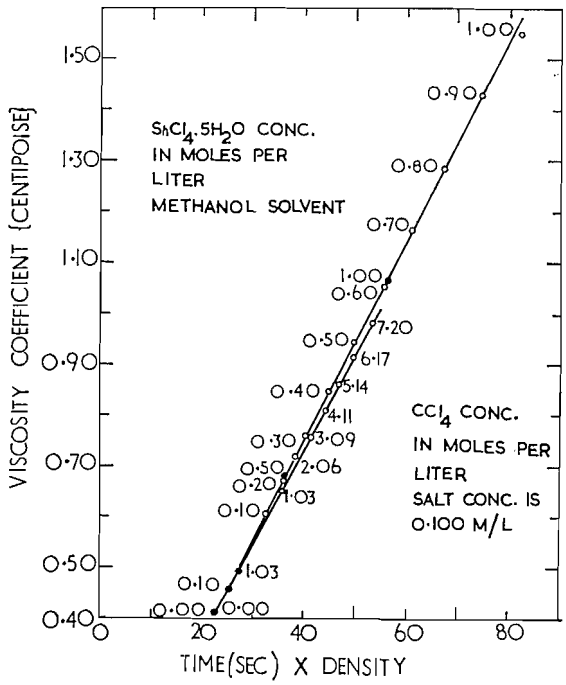


FIG. 3. Plots of viscosity coefficient, determined with normal Ostwald–Fenske viscometers, versus the product of density×time, measured with the electroviscometer, for $SnCl_4.5H_2O$ dissolved in pure methanol or in methanol – carbon tetrachloride: ○ 25° C; ● 45° C. (Except for the 1.000 *M* $SnCl_4.5H_2O$ solution, the maximum deviation from each straight line is near 1 part in 1000.)

and flow time (in seconds) measured with the new electroviscometer. The linear relations (maximum deviation 0.10%) found for the methanol solutions (Figs. 3 and 4) indicate that the flow characteristics of the modified Ostwald–Fenske viscometer do not change significantly with temperature or with the viscosity of the solution. For $SnCl_4.5H_2O$ solutions, similar linear relations exist for each solvent composition studied. The deviation for the plot for systems of high carbon tetrachloride concentration is just 1% from the plot for solutions with pure methanol as solvent (Fig. 3). This deviation probably arises from the gross changes in the surface tension and density as one passes from pure methanol to methanol – carbon tetrachloride, with the latter of high concentration.

Thus with calibration plots for each solvent and a modified Ostwald–Fenske viscometer, the viscosity coefficient of conducting solutions can be rapidly and accurately determined at any temperature. In our laboratory 200 measurements for 20 different solutions at two temperatures were made in less than 6 hours. Moreover, this inexpensive electroviscometer has been adapted to measure flow times for non-conducting liquids by addition of small amounts of a conducting compound, by use of higher resistances in parallel, or by different spacing of the electrodes.

Can. J. Chem. Downloaded from www.nrcresearchpress.com by 210.87.254.6 on 09/05/12
For personal use only.

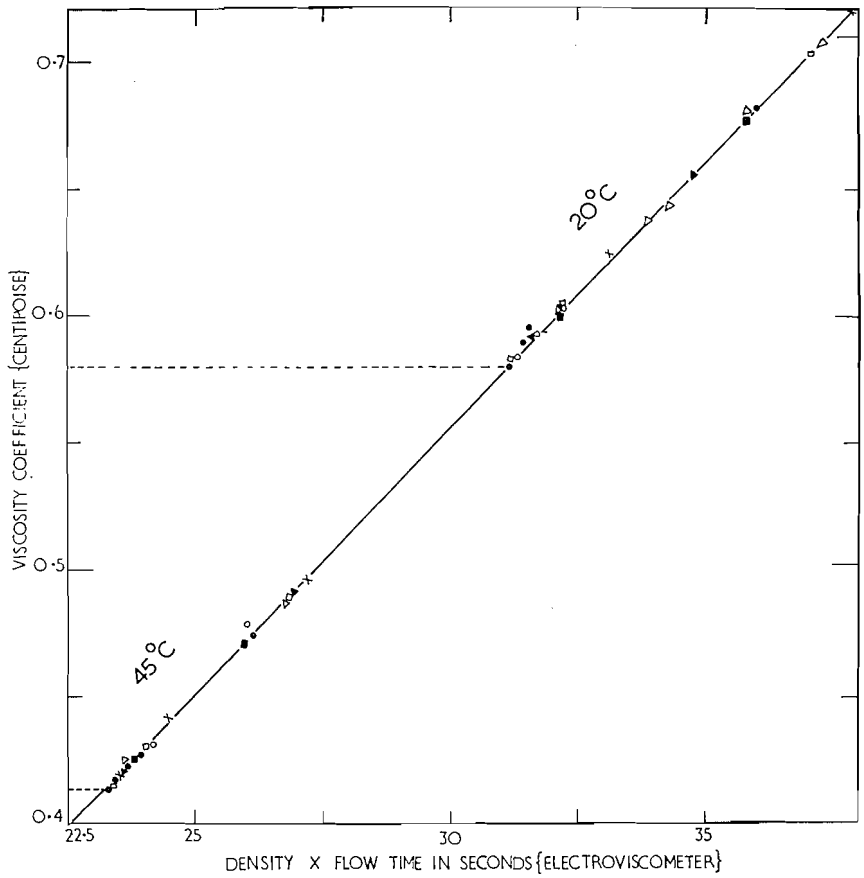


FIG. 4. Plots of viscosity coefficient, determined with normal Ostwald–Fenske viscometers, versus the product of density×time, measured with the electroviscometer, for salts dissolved in pure methanol: ○ $CaCl_2$; □ $CuCl_2.2H_2O$; × $NiCl_2.6H_2O$; ● $NiCl_2.2H_2O$; ■ $CoCl_2.6H_2O$; △ $CoCl_2.2H_2O$; ▲ $CrCl_3.6H_2O$; – – – viscosity coefficient for pure methanol. (Only 36 of the 66 points falling on the straight line are shown.)

ACKNOWLEDGMENT

Financial support from Research Corporation is gratefully acknowledged.

REFERENCES

1. H. UMSTATTER. Dechema Monograph. **14**, 72 (1950).
2. W. H. MARKWOOD, JR. Am. Soc. Testing Materials, Proc. **51**, 441 (1951).
3. F. WILOTH. Gummi u Asbest, **6**, 426, 471 (1953).
4. P. A. IVANOV. Zavodskaya Lab. **23**, 457 (1957).
5. W. B. ASBECK. J. Soc. Cosmetic Chemists, **8**, 282 (1957).
6. G. GOLDFINGER and W. GREATBATCH. Instr. and Automation, **30**, 88 (1957).
7. C. R. STOCK. U.S. Patent No. 2,484,761. 1949.
8. P. A. D. DE MAINE and E. R. RUSSELL. Can. J. Chem. **39**, 1502 (1961).
9. E. R. RUSSELL and P. A. D. DE MAINE. Unpublished.
10. P. A. D. DE MAINE, M. M. DE MAINE, and G. E. MCALONIE. J. Inorg. & Nuclear Chem. **14**, 268 (1960).
11. P. A. D. DE MAINE and E. J. WALSH. J. Inorg. & Nuclear Chem. In press.
12. P. A. D. DE MAINE and G. E. MCALONIE. J. Inorg. & Nuclear Chem. **18**, 286 (1961).

Can. J. Chem. Downloaded from www.nrcresearchpress.com by 210.87.254.6 on 09/05/12
For personal use only.

Can. J. Chem. Downloaded from www.nrcresearchpress.com by 210.87.254.40 on 09/05/12
For personal use only.

HYDROGEN EXCHANGE BETWEEN CELLULOSE AND WATER

I. MEASUREMENT OF ACCESSIBILITY[1]

O. SEPALL[2] AND S. G. MASON

ABSTRACT

Estimates of the extent of the hydrogen exchange reaction between cellulose and water vapor determined by an improved method using tritiated water and by the use of heavy water were usually in good agreement. With certain samples, surface roughness had a small effect upon the measurement of tritium radioactivity in cellulose.

The accessibility or limiting extent of the exchange increased slightly with relative humidity in the range 20 to 100% and was attributed to the reduction of crystalline order reported recently in similar experiments.

In contrast to cellulose whose accessibility corresponds approximately to the amorphous fraction, a partially crystalline amylose was 100% accessible while an amorphous xylan was 52% accessible, indicating that in these substances the accessibility and the fraction of amorphous material are not identical.

INTRODUCTION

Although valuable contributions to the knowledge of the fine structure of cellulose have been made by studies of the hydrogen exchange reaction with water (1, 2, 3), work based on this technique has not been extensive because the experimental methods are time consuming and of limited applicability. This paper describes measurements of exchange using tritiated water (HTO) by an improved method which permits greater scope in studies of the reaction.

In most investigations, the exchange of deuterium with D_2O has been measured either by determining isotopic dilution (3) or the infrared absorption of deuterated and unreacted hydroxyl groups (1). The present results were obtained by the tritium exchange method devised by Lang and Mason (2) but using an improved apparatus (4) which is simpler and gives a more precise measurement. To calibrate the method and corroborate the results, the exchange of deuterium with pure D_2O was also determined by infrared (1) and gravimetric (5) techniques.

The accessibility, A^0, defined as the limiting extent of the exchange, was determined for various cellulose samples, starch, and xylan. The influence upon A^0 of the crystallinity of the sample and relative humidity was also investigated in a preliminary study of the factors governing hydrogen exchange in cellulose and similar polymers.

EXPERIMENTAL PART

Materials

The samples listed below were used.

1. Amylopectin: commercial grade, manufactured from potato starch from Stein Hall and Co.

2. Amylose: as for sample 1.

3. Cellophane: air-dried viscose film without additives, supplied by Dupont of Canada Ltd.

4. Wood cellulose: softwood, acetate grade wood pulp; 96% alpha cellulose (TAPPI method).

[1]*Manuscript received June 14, 1961.*
Contribution from the Physical Chemistry Division, Pulp and Paper Research Institute of Canada, and the Department of Chemistry, McGill University, Montreal, Que.
[2]*Holder of a Canadian Industries Limited Fellowship, 1960–61.*

5. Bacterial cellulose: kindly supplied by Dr. J. R. Colvin of the National Research Council, Ottawa.

6. Cotton linters: dewaxed by alcohol–benzene extraction.

7. Commercial paper grade woodpulps by Anglo Paper Products Ltd., Quebec, Que.

8. Xylan: birch (*Betula papyrifera*) xylan prepared by the method of Glaudemans and Timell (6).

9. Milled wood cellulose: sample 4 milled in an Intermediate Model Wiley Cutting Mill using three passes with a 150-mesh screen.

Methods

1. Deuterium Exchange: Gravimetric (A_1)

The method is based on that of Morrison (5) and involves determining the increase in mass of the sample following exchange with pure D_2O.

The apparatus used (Fig. 1) consisted of a 100-ml Pyrex flask (G) with two outlets

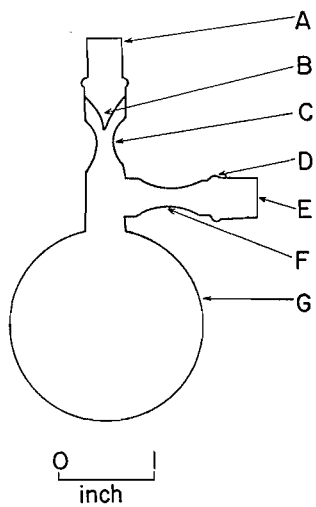


FIG. 1. Cell for gravimetric measurement of deuterium exchange. A, outlet to fit Veeco Quick Vacuum Coupling (No. C-50); B, break-seal; C and F, constrictions for sealing; D, expanded section for vacuum seal with O-ring; G, 100-ml flask.

(A and E) of suitable diameter to fit a Veeco Quick Vacuum Coupling on a vacuum system. The expanded section in the outlet as at D helped to form the vacuum seal created by an O-ring. The vessel could be sealed by fusing at the constrictions C and F. The break-seal (B) eliminated the need for a stopcock.

About 6 g of sample was placed in the flask of tared weight W_1 and dried by evacuating through outlet E for 48 hours at 75° C and at 1 μ Hg vacuum. The flask was sealed and weighed (W_2). The break-seal was opened by inserting a steel rod in A, and the apparatus shown in Fig. 2 was used to react the sample with pure D_2O. Dry air, obtained from the evaporation of liquid air in a Dewar flask shown at H in Fig. 2, was bubbled through liquid D_2O in J at constant temperature and then conducted into the sample in flask L (immersed in a thermostat) by a stainless steel tube (K). After the desired reaction time, the sample was dried by evacuating the flask for 48 hours at 75° C and at 1 μ Hg vacuum.

The flask was weighed (W_3) and the difference in weight ($W_3 - W_2$) was corrected for

Can. J. Chem. Downloaded from www.nrcresearchpress.com by 210.87.254.40 on 09/05/12
For personal use only.

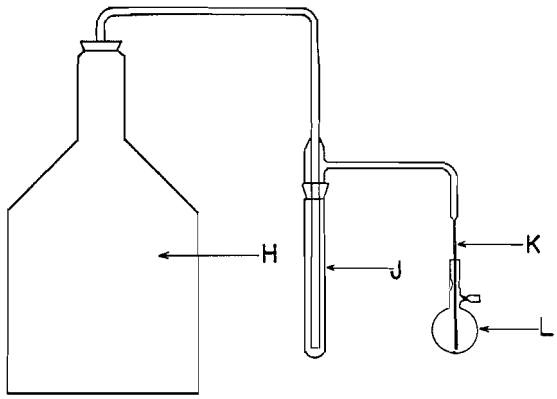


FIG. 2. Apparatus for conducting exchange with D_2O. H, Dewar flask with liquid air; J, vessel containing D_2O liquid; K, stainless steel tube; L, vessel shown in Fig. 1.

changes in air buoyancy to give the increase of mass ΔW corresponding to exchange of hydrogen by deuterium. The mass S of the sample was determined similarly from $(W_2 - W_1)$. The percentage of accessibility A_1 was calculated from

$$[1] \qquad A_1 = 100(\Delta W)/F \times S.$$

The factor F is the fractional increase in mass of the same substance after the hydroxyl hydrogens have been completely exchanged by deuterium. For cellulose and starch, $F = 0.0185$; for birch xylan, F was calculated to be 0.0140, assuming a linear chain of β-D-xylopyranose residues, linked by 1,4-glycosidic bonds and having a single terminal side chain of the potassium salt of 4-O-methyl-α-D-glucuronic acid attached glycosidically to C_2 of every 11th xylose residue (7).

No correction for the isotopic purity of the D_2O (99.7%) was necessary.

In contrast to Morrison's experiments (5), the exchange was conducted at constant relative humidity. This was done to avoid the partial reaction with inaccessible hydroxyl groups, shown to occur if the sample moisture was varied during the exchange (8).

The results reported are for single measurements only and were reproducible to 1%.

2. Tritium Exchange: Radioactivity (A_2)

The method used for measuring tritium exchange between cellulose and tritiated water (HTO) vapor has already been described (4), and consisted of (*a*) exposing the sample to tritiated water vapor, (*b*) drying, and (*c*) determining tritium radioactivity in the sample using a methane-filled, windowless proportional counter of special design in which all three operations were carried out.

During the treatment with tritiated water vapor, the relative humidity (RH) was kept constant to ±3% by suitably controlling the temperature of the liquid-HTO reservoir, and the sample temperature, to ±0.5° C. The samples were dried at 75° C in a vacuum of 1 μ Hg for 15 hours to remove sorbed water (2).

The samples were used in sheet form of superficial density of about 3 mg/cm².

Amylose was dissolved in water at 160° C and a film was deposited from the solution on a polished, chromium-plated surface by drying at room temperature. An aqueous amylopectin solution was prepared at room temperature, and, since the unsupported film tended to crack during drying, it was deposited onto a cellophane supporting film. Handsheets were prepared from fibrous materials such as wood cellulose by the TAPPI

Can. J. Chem. Downloaded from www.nrcresearchpress.com by 210.87.254.40 on 09/05/12
For personal use only.

procedure which consisted of (*a*) depositing the wet sheet of fibers from a water suspension on a fine screen, (*b*) pressing to remove moisture, and (*c*) drying the sheet at room temperature in contact with a polished, chromium-plated surface. The cotton linters required a preliminary beating before a satisfactory handsheet could be formed; this was done in a PFI Laboratory mill. Cellophane film was used as received.

The accessibility A_2 was determined from the relation

$$[2] \qquad A_2 = \frac{Rf}{c}\left(\frac{c_0}{R_0 f_0}\right) A_{1,0},$$

where R is the sample count rate; c, the activity of the tritiated water (about 1.5 μc/mg in these experiments); and f, the vapor/liquid partition ratio of tritium at the temperature of the liquid-HTO reservoir. The factor f is a known correction factor for the principal isotope effect (9). Quantities with the subscripts "0" are those of a standard sample whose accessibility $A_{1,0}$ was determined by the gravimetric D_2O exchange method under the identical conditions of temperature and relative humidity used in measuring R_0. Cellophane at 75% relative humidity and at 25° C was used as the standard sample.

The results are averages of four determinations on cellophane, and of two on wood cellulose and other materials; they were reproducible to 1%.

The principal difference between A_2 and the quantity A_s measured by Lang and Mason (2) was that the samples were dried rigorously after the exchange reaction by thoroughly evacuating at 75° C instead of room temperature. In addition, the precision of R was greater.

3. Deuterium Exchange: Infrared (A_3)

The accessibility of amylose and amylopectin was estimated by the infrared absorption method used by Marrinan and Mann for deuterated cellulose (1). An infrared cell (Fig. 3) suitable for investigating evacuated samples was constructed for use with the

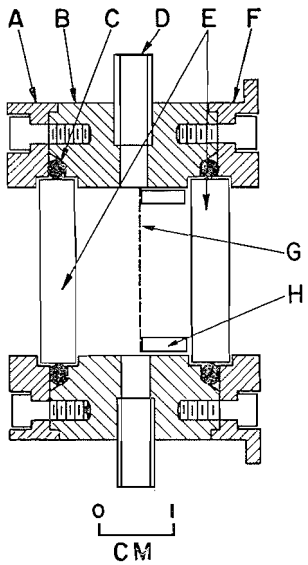


FIG. 3. Vacuum infrared absorption cell. A, front cover (stainless steel); B, cell body (stainless steel); C, O-ring; D, D_2O vapor circulation line; E, calcium fluoride windows; F, back cover to fit mounting on Perkin–Elmer model 21; G, sample film; H, annular sample holder.

Can. J. Chem. Downloaded from www.nrcresearchpress.com by 210.87.254.40 on 09/05/12
For personal use only.

Perkin–Elmer model 21 spectrometer. Samples were inserted by removing cover plate A, which was sealed by O-rings to the standard calcium fluoride windows and to the body (B) of the cell. D_2O vapor was circulated through tube D, which was sealed by vacuum valves (not shown).

Sample films having a superficial density of 0.8 mg/cm^2 were prepared by evaporating aqueous solutions of amylose and amylopectin on a mercury surface. The film (G in Fig. 3) was attached to the annular sample holder (H) by a small amount of vacuum grease.

The sample film was reacted with D_2O vapor while in the absorption cell. A stream of air containing the vapor was produced with the arrangement shown in Fig. 2 and was circulated through the cell for 8 hours. The cell was evacuated for an hour to remove most of the sorbed water and sealed.

The absorbance was measured at $\nu_1 = 2530$ cm^{-1}, corresponding to an absorption peak for the OD group, and at $\nu_2 = 3360$ cm^{-1}, for OH (1). Assuming Beer's law to apply

$$[3] \qquad \frac{\log (I_0/I)\nu_1}{\log (I_0/I)\nu_2} = \frac{k_{OD}\, c_{OD}}{k_{OH}\, c_{OH}} = 1.11 \frac{c_{OD}}{(1-c_{OD})}$$

$$[4] \qquad = 1.11 \frac{A_3}{1-A_3}.$$

I_0 and I are the intensities of the incident and transmitted radiation; c is the mole fraction of absorbing groups and k the extinction coefficient; A_3 ($= c_{OD}$) is the corresponding accessibility. It was assumed that in starch $k_{OD}/k_{OH} = 1.11$, the same value used for cellulose (1), so that A_3 could be evaluated by equation [4].

As in the gravimetric measurement, the correction for isotopic purity of the heavy water was neglected.

RESULTS

Reaction Time

The time required to achieve limiting values of A_1 and A_2 was investigated at 75% RH and 25° C for cellophane and wood cellulose. The results given in Table I show that A_1

TABLE I

Effect of reaction time upon A_1 and A_2 (75% RH, 25° C)

Sample	Reaction time (days)	A_1 (%)	Sample	Reaction time (hours)	A_2 (%)
Cellophane	2	60.5	Wood cellulose	1	50.8
,,	4	78.5	,,	2	54.6
,,	4	79.0	,,	4	57.0
,,	6	78.0	,,	8	58.0
			,,	32	58.3

was approximately constant after 4 days and A_2, after about 8 hours. The long time required for deuterium exchange was undoubtedly due to the low rate of transfer of D_2O to the sample in the presence of air.

The influence of relative humidity in the range 20 to 75% RH upon the time required for A_2 to approach a limit A_2^0 was investigated for cellophane. Values of A_2 for different reaction times are plotted in Fig. 4 and show that after the initial rapid reaction reported

Can. J. Chem. Downloaded from www.nrcresearchpress.com by 210.87.254.40 on 09/05/12
For personal use only.

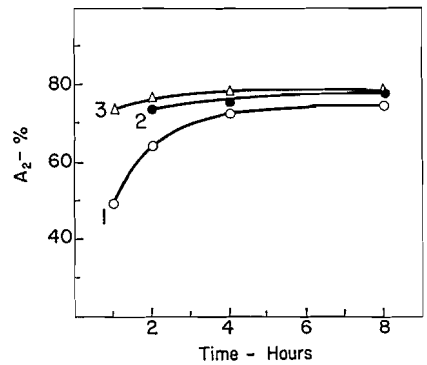


FIG. 4. Tritium exchange versus time for cellophane in HTO vapor. Curves 1, 2, and 3 correspond to relative humidities of 20, 50, and 75% respectively at 25° C.

earlier (1), the extent of the exchange tended to an asymptotic limit after about 8 hours. The reaction was slower at lower relative humidity and A_2 approached a smaller value. The decreased rate of reaction was probably due to slower diffusion of water vapor in cellulose at the lower moisture content (10). The lower limiting exchange, indicating that fewer reactive hydroxyls were available, is discussed later.

For amylopectin, a limiting value of $A_2^0 = 98\%$ at 75% RH and 25° C was also found after 8 hours. It was assumed that the rate of exchange with the other cellulose samples was similar to that with cellophane and wood cellulose.

For measurements of the limiting extent of the exchange denoted by the superscript "0", at least 4 days' exposure to D_2O was allowed in measuring A_1^0 and at least 8 hours' exposure, in measuring A_2^0. For A_3^0, an exposure of 8 hours was used, although it has been shown that little further reaction is detected in cellulose film after 1 hour in D_2O vapor (1).

Comparison of A_1^0, A_2^0, and A_3^0 for Different Samples

Values of A^0 were measured by the different methods for a number of samples at 75% RH and 25° C (Table II). The differences between A_2^0 and measurements of A_3 on

TABLE II

Comparison of methods of measuring A (75% RH, 25° C)

Sample	A_1^0 (%)	A_2^0 (%)	A_3^0 (%)
Cellophane	79	(79)*	
Amylopectin	96	98	97
Amylose	99	95–98	98
Wood cellulose	58	58	
Bacterial cellulose	42	39	
Cotton linters	40	44	
Birch xylan	52		
Milled wood cellulose	76		

*Assumed for purposes of calibration.

similar samples of Lang and Mason (2) ranged from 2 to 8% and were probably due to the slightly different experimental conditions employed.

In most cases, A_1^0 and A_2^0 were in good agreement (Fig. 5), except for +4% difference

Can. J. Chem. Downloaded from www.nrcresearchpress.com by 210.87.254.40 on 09/05/12
For personal use only.

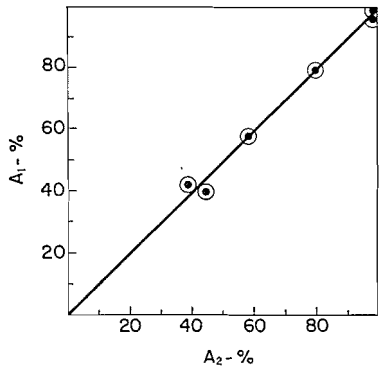


FIG. 5. Comparison of deuterium exchange (gravimetric) and tritium exchange methods of measuring A^0 (75% RH, 25° C).

for cotton linters and -3% for bacterial cellulose. It is believed that these discrepancies arose from surface roughness of the samples. The influence of surface roughness upon the measurement of tritium in tritiated cellulose, considered by calculating counting rates for simple models for the samples listed in Table II, is discussed elsewhere (11). It was concluded that the shape of surface irregularities influenced the measurement while the bulk density had negligible effect; the analysis made it possible to account for the differences observed here. The error can be avoided by using smooth samples or by independently calibrating the tritiation method for each material.

The high accessibility of amylose and amlyopectin was confirmed by the three methods. It is possible that here $A^0 = 100\%$, but that the measured values were influenced by factors such as (*a*) impurities in the samples, (*b*) deviations from Beer's law, and (*c*) contamination of D_2O by atmospheric moisture during the exchange reaction. Limited exchange in fully deuterated amylose and amylopectin from potato starch has recently been reported from infrared absorption measurements (12). The extent of the reaction was measured by the ratio (area of OD absorption band)/(area of OH absorption band), which was about 2.6 for both deuterated samples (12), while in the present measurements, the ratio was 55 for deuterated amylose. The reason for the difference is not clear; possibly the method of isolation can affect the properties.

Only A_1^0 was measured for xylan and milled wood cellulose because contact with water, as during preparation of sheet samples, has been found to produce recrystallization in similar materials (13). Milling increased A_1^0 as expected since a similar treatment has been shown to increase the amorphous fraction in cellulose determined by X-ray diffraction (13). The crystallinity parameter K_{002} (13) was found to be 1.25 for the original material and 1.13 for the milled samples, indicating some destruction of crystalline regions. The radial photometer traces for the samples showed that the crystallinity was not entirely destroyed by milling; this is presumably the reason for A_1^0 being less than 100%.

X-ray diagrams of amylose exhibited distinct diffraction rings while those of birch gave a diffuse halo, indicating that the former was partially crystalline and the latter wholly amorphous. The results were unexpected because complete accessibility of amylose, by analogy with cellulose, implied the absence of crystallinity. Evidently the analogy is not necessarily valid and other factors which are presently unknown determine the accessibility of amylose and xylan.

Can. J. Chem. Downloaded from www.nrcresearchpress.com by 210.87.254.40 on 09/05/12
For personal use only.

Relative Humidity

Values of A_2^0 were measured for wood cellulose and cellophane from 0.6 to 100% RH and at 25, 50, and 100° C. The results, summarized in Table III, indicate that A_2^0, at

TABLE III

Effect of relative humidity upon the accessibility of cellulose

Sample	Temp. (°C)	RH (%)	A_1^0 (%)	A_2^0 (%)
Cellophane	25	20		76
,,		50		79
,,		75	79	(79)*
,,		95		80
,,		100		80
Wood cellulose	25	20	56	55
,,		50		57
,,		75	58	58
,,		85		60
,,		95		61
,,		100		62
,,	50	25		58
,,		75		57
,,	100	0.6		67
,,		3		66
,,		10		68
,,		25		64

*Assumed value for purposes of calibration (eq. [2]).

25° C, of wood cellulose, and to a lesser extent of cellophane, increased slightly with increasing relative humidity. At 50 and 100° C the results appeared to be unaffected by relative humidity. It is not known whether the higher values at 100° C indicate a higher accessibility or a temperature-dependent isotope effect in the partition of tritium between HTO vapor and the hydroxyl groups in cellulose. Attempts to measure A_1^0 at 100° C were unsuccessful mainly because no satisfactory correction could be made for the loss in mass of cellulose occurring during contact with air under these conditions. The decrease in mass may have resulted from chemical degradation which has been observed in cotton linters as a reduction of degree of polymerization and of carboxyl groups after only 20 minutes in air at 100° C (14).

There is a possible error in the measurements of tritium exchange at different relative humidities because the tritium is concentrated in the residue during evaporation as in drying the sample. However, the effect was probably small because drying was rapid and the equilibrium separation would not have occurred. The higher values of A_2^0 with increasing relative humidity are therefore believed to indicate a greater number of reactive hydroxyls. The significance of the result is discussed below.

Comparison of Commercial Woodpulps

Values of A_2^0 were measured for commercial woodpulps prepared by alkaline (kraft and soda) and sulphite processes from Canadian softwoods and hardwoods. Since the samples also contained lignin and hemicelluloses in addition to cellulose, the values of A_2^0 are not necessarily the percentage of hydroxyl groups reacted. The results indicate only the relative abundance of reactive hydroxyls in the different samples compared with cellulose.

The results (Table IV) show only small differences between the samples. Wood fibers

Can. J. Chem. Downloaded from www.nrcresearchpress.com by 210.87.254.40 on 09/05/12
For personal use only.

TABLE IV

Comparison of commercial woodpulps

Sample	A_2^0 (%)
Bleached softwood sulphite	59.0
Bleached softwood kraft	60.0
Bleached hardwood kraft	57.5
Bleached hardwood soda	57.5
Unbleached softwood sulphite (Permanganate No. 10)*	58.0
Unbleached softwood sulphite (Permanganate No. 20)	57.5
Unbleached softwood sulphite (Permanganate No. 30)	55.5

*TAPPI method. (The permanganate number is a measure of lignin content and is approximately zero in bleached pulps.)

with higher lignin content appeared to have fewer accessible hydroxyls, as would be expected, since the hydroxyl content of lignin is lower than that of cellulose. The slightly lower values for hardwood fibers may have similarly indicated a higher content of xylan.

DISCUSSION

The results demonstrate the validity, versatility, and convenience of the tritium exchange method of measuring A, particularly for sheet cellulose samples.

The results for amylose and amylopectin differ from those of Ceh and Hadzi (12), and suggest the interesting possibility that starch can exist in stable forms which are either completely or only partially accessible. The xylan from birch wood is a linear polysaccharide like cellulose and similarly was only partially accessible. The differences between commercial wood fibers were small, suggesting that pulping processes have little effect upon the properties of cellulose.

It was surprising that A^0 did not increase to a greater extent with increasing relative humidity since reactive hydroxyl groups are believed to be formed as a result of disrupting hydrogen bonds by water (15). However, X-ray diffraction studies have indicated that the fraction of crystalline material is the same in wet and dry cellulose (16), although recently it was reported that a small reduction of the molecular order in crystalline regions occurred with increasing relative humidity (17). The similarity of the effect of relative humidity upon the crystalline and inaccessible portion supports the concept of stable, discrete crystallites which largely do not participate in the swelling or in many chemical reactions of cellulose. There is evidence, however, that crystallites tend to migrate in the structure during changes of relative humidity (2) as described further in the following paper (8).

The most interesting results were the apparently anomalous properties of amylose and birch xylan which implied that accessibility was not necessarily dependent upon the crystallinity. It is likely that steric effects dominate the extent of exchange of hydrogen in cellulose as found with other reactions (18), and that the conditions which preclude exchange can exist independently of crystallinity. The extent of exchange may therefore be expected to vary in different crystals.

REFERENCES

1. J. MANN and H. J. MARRINAN. Trans. Faraday Soc. **52**, 481, 487, 492 (1956).
2. A. R. G. LANG and S. G. MASON. Can. J. Chem. **38**, 373 (1960).
3. V. J. FRILETTE, J. HANLE, and H. MARK. J. Am. Chem. Soc. **70**, 1107 (1948).

Can. J. Chem. Downloaded from www.nrcresearchpress.com by 210.87.254.40 on 09/05/12
For personal use only.

4. O. SEPALL, A. R. G. LANG, and S. G. MASON. Can. J. Chem. **39**, 827 (1961).
5. J. L. MORRISON. Nature, **185**, 160 (1960).
6. C. P. J. GLAUDEMANS and T. E. TIMELL. Svensk Papperstidn. **61**, 1 (1958).
7. C. P. J. GLAUDEMANS and T. E. TIMELL. J. Am. Chem. Soc. **80**, 1209 (1958).
8. O. SEPALL and S. G. MASON. Can. J. Chem. This issue.
9. O. SEPALL and S. G. MASON. Can. J. Chem. **38**, 2024 (1960).
10. P. H. HERMANS and D. VERMAAS. J. Polymer Sci. **1**, 149 (1946).
11. O. SEPALL and S. G. MASON. Tappi. In press.
12. M. CEH and D. HADZI. Starke, **10**, 99 (1958).
13. M. KOURIS, H. RUCK, and S. G. MASON. Can. J. Chem. **36**, 931 (1958).
14. L. E. HESSLER and H. WORKMAN. Textile Research J. **29**, 487 (1959).
15. B. OTT and H. M. SPURLIN. Cellulose and cellulose derivatives. 2nd ed. Interscience Publishers Inc., New York. 1954.
16. P. H. HERMANS and A. WEIDINGER. Makromol. Chem. **18/19**, 75 (1956).
17. O. ANT-WUORINEN and A. VISAPÄÄ. Paperi ja Puu, **10**, 515 (1960).
18. A. G. ASSAF, R. H. HAAS, and C. B. PURVES. J. Am. Chem. Soc. **66**, 59 (1944).

Can. J. Chem. Downloaded from www.nrcresearchpress.com by 210.87.254.40 on 09/05/12
For personal use only.

Can. J. Chem. Downloaded from www.nrcresearchpress.com by 210.87.254.6 on 09/05/12
For personal use only.

HYDROGEN EXCHANGE BETWEEN CELLULOSE AND WATER

II. INTERCONVERSION OF ACCESSIBLE AND INACCESSIBLE REGIONS[1]

O. SEPALL[2] AND S. G. MASON

ABSTRACT

Exchange of hydrogen between water and some of the inaccessible hydroxyl groups in cellulose resulted from changes in the relative humidity and was most pronounced near 0 and 100% RH. A similar exchange occurred during prolonged immersion in liquid water. The extent of the reaction varied in different samples, increased with temperature, and was reproducible. By repeatedly wetting and drying cellophane, the exchange was cumulative and all the hydroxyl groups became exchanged after up to 100 cycles. The accessibility decreased slightly after repeated drying. The measurements were made by exchange with deuterated and tritiated water.

The behavior was interpreted as an interchange of ordered and disordered regions resulting from molecular rearrangement caused by interaction between cellulose and water.

INTRODUCTION

When cellulose is dried from heavy water (D_2O) (1) or tritiated water (HTO) (2), some of the hydrogen isotope becomes incorporated in inaccessible hydroxyl groups, i.e., hydroxyls which will not exchange hydrogen when the cellulose is re-exposed to water. Mann and Marrinan (1) suggested that the phenomenon was partly due to a reduction in the number of reactive hydroxyls by drying. However, Lang and Mason (2) showed by repeatedly wetting and drying cellophane in HTO that inaccessible hydroxyl groups were progressively exchanged with little change in the accessibility. The theory was proposed that during wetting and drying, a rearrangement of molecules occurs in cellulose and results in a partial interchange of accessible and inaccessible regions (2).

The present investigation was undertaken to study the causes of the changes in molecular order. It was also of interest to determine if all crystallites could be disrupted by repeatedly wetting and drying cellulose a sufficient number of times as appeared likely from the previous studies (2). The work included a study of the influence of temperature, relative humidity, and the number of cycles upon the irreversible exchange during drying.

The quantities measured were similar to those investigated by Lang and Mason (2) and are defined as follows. The accessibility A_n is the extent of the exchange reaction with water at 75% relative humidity (RH) and 25° C after n drying cycles. The quantity $\delta\omega_n$ represents the inaccessible hydroxyl groups reacted with water during the nth cycle while W_n is the net inaccessible hydroxyl groups reacted during n cycles. The three quantities were expressed as percentage of the total hydroxyls. Measurements were made by both tritium and deuterium exchange.

EXPERIMENTAL PART

Methods

1. Measurement of Accessibility

The accessibility (A_n) was determined by the HTO exchange method described previously (3). The measurement was calibrated for each material by determining the exchange of deuterium with D_2O by the gravimetric method (3); this was done to eliminate

[1]*Manuscript received June 14, 1961.*
Contribution from the Physical Chemistry Division, Pulp and Paper Research Institute of Canada, and the Department of Chemistry, McGill University, Montreal, Que.
[2]*Holder of a Canadian Industries Limited Fellowship, 1960–61.*

the small error resulting from the effect of surface roughness upon the measurement of tritium radioactivity (3). The results were averages for two determinations and were reproducible to $\pm 1\%$.

Since it was known (3) that A_n varies slightly with relative humidity (RH), standard conditions for the measurement were arbitrarily selected as 75% RH and 25° C.

2. Drying Cycles Using HTO

Three types of cycles, designated as D_1, D_2, and D_3 and representing regions of intermediate, low, and high RH respectively, were employed to study limited ranges of RH. Shorter drying times than required for equilibrium conditions (e.g., 23 hours to achieve moisture equilibrium in cellophane (4)) were used to permit the study of the effects of large numbers of cycles within a reasonable time.

The procedure for each type of cycle is outlined below.

Cycle D_1 (partial drying).—The treatment consisted of exposing the sample to HTO vapor during a cyclic change of RH and was conducted in a special counter designed for use of tritiated sheets (5). Only single cycles were studied. The initial exposure was to H_2O followed by HTO at the same RH. The vapor pressure of the HTO was then altered by changing the temperature of the HTO liquid reservoir. The duration of each exposure was 4 hours.

Cycle D_2 (rigorous drying).—The cycle consisted of exposing the sample, as in D_1, to HTO vapor and then vacuum-drying for 15 hours at 1 μ Hg and various temperatures. The exposure to HTO was usually for 8 hours at 75% RH and 25° C. For repeated treatments, one cycle, including the determination of tritium in the sample after drying, was performed each day.

Cycle D_3 (immersion and partial drying).—The sample was immersed in HTO liquid and partially dried at different temperatures kept constant during the experiment. The procedure devised by Lang and Mason (2) was used. The sample and a quantity of HTO liquid (30:1), large enough so that dilution effects could be neglected, were sealed in an evacuated, inverted U tube with the sample held at one end. During drying, the HTO arm was placed in an ice-water bath and the other in a water thermostat at the desired temperature. The wetting step was performed by tilting the U tube and allowing the HTO to flow to the sample end. Two hours were usually allowed for each step; preliminary experiments with cellophane showed that the exchange was over 80% completed during this period. For repeated treatments, three cycles were performed each day; one wetting step (conducted overnight) took 14 hours.

3. Reacted Inaccessible Hydroxyls by HTO Exchange

During each of the drying cycles, tritium became incorporated in both inaccessible and accessible hydroxyl groups. For example, after n successive D_2 cycles, the total tritium activity corresponded to (A_n+W_n). By exposing the sample to H_2O and thus removing the labile tritium (A_n), W_n alone was determined by the following procedure. The treated sample was placed in a 2-cm glass tube through which air at 75% RH and 25° C was circulated for 8 hours; 16 hours gave the same result. The residual tritium activity in the sample was measured in a counter (5) identical with that used for accessibility measurements but without the accessories for conducting the exchange reaction. The fraction of tritiated hydroxyl groups (W_n), corrected for isotope effects, was calculated from the measured counting rate as previously described for A_n (3).

It would have been desirable to end all drying cycles at 75% RH to avoid further change of sample moisture content during removal of labile tritium. Although this was done only in certain cases, the cycles were always terminated at a RH $< 95\%$ and, as will be shown later, the difference in RH during the final drying had little effect.

Can. J. Chem. Downloaded from www.nrcresearchpress.com by 210.87.254.6 on 09/05/12
For personal use only.

For the measurement of $\delta\omega_n$ a similar procedure was used. The $(n-1)$ cycles were performed in H_2O and the nth cycle in HTO. The labile tritium was removed as described above and the residual tritium activity corresponded to $\delta\omega_n$. It should be noted that, by definition, $\delta\omega_1 = W_1$.

The results were usually reproducible to $\pm 5\%$ or less. In cellophane, however, differences were as large as 50% and may have been due to a lack of uniformity in the properties as a result of manufacturing conditions.

The quantities $\delta\omega_n$ and W_n defined by Lang and Mason (2) were determined after immersing the sample in H_2O liquid and air-drying, and are therefore lower than the present values because, as will be shown, a large fraction of the inaccessible hydroxyl is reacted during drying.

4. Reacted Inaccessible Hydroxyls by D_2O Exchange

To corroborate the experiments using HTO, a method of measuring (A_n+W_n) for cycle D_3 was devised based on the gravimetric measurement of A using D_2O (3). The method has the advantage that the samples are not required in sheet form. The apparatus is shown in Fig. 1 and served the same purpose as the U tube described above in the

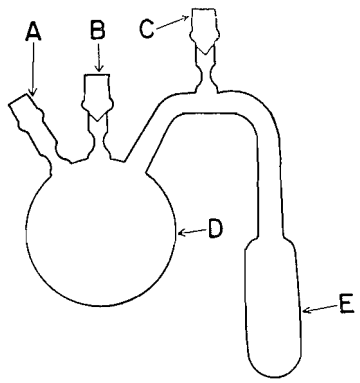


FIG. 1. Cell for measuring A_n+W_n by D_2O exchange. A, outlet; B and C, outlet with break-seals; D, 50-ml glass flask; E, 20-ml receiver.

corresponding experiment with HTO. It consisted of a 50-ml glass flask (D) connected by an inverted U tube to the 20-ml vessel (E). The three outlets (A, B, and C) were of suitable diameter to fit a Veeco Quick Vacuum Coupling on a vacuum manifold and B and C contained break-seals. The expanded sections in the outlets helped to form the vacuum seal created by an O-ring. The vessel could be sealed by fusing at the constrictions.

To correct for air buoyancy during weighings, the volume of the apparatus was determined by weighing the flask empty (M_0), and filled with water. A 3-g sample of cellulose was placed in the flask and dried rigorously by evacuating through outlet A for 48 hours at 75° C and 1 μ Hg (6). The flask was sealed by fusing at the constriction and weighed (M_1). The break-seal in B was opened by thrusting a steel rod in the outlet. To reduce subsequent dilution effects, the sample was exchanged with pure (99.7%) D_2O vapor by circulating a mixture of D_2O and air, at 75% RH, through the vessel for 4 days. The procedure resulted in a limiting exchange corresponding to the accessibility A_0*. A quantity (15.0 ml) of D_2O liquid was then added to the flask, which was sealed after evacuation,

**The limiting or equilibrium accessibility was previously (3) denoted by A^0. In this paper it is more convenient to designate this quantity as A_0 since it corresponds to A_n when $n = 0$.*

Can. J. Chem. Downloaded from www.nrcresearchpress.com by 210.87.254.6 on 09/05/12
For personal use only.

with the flask immersed in liquid air to prevent loss of D_2O. The sample was subjected to the desired number of D_3 cycles as in the corresponding HTO experiment. The break-seal in outlet C was opened and the flask evacuated to dry the sample, then sealed under vacuum, and weighed (M_2).

The increase of mass ΔM, corresponding to exchange of H atoms on hydroxyl groups by D atoms, was determined from the difference of the weight (M_2-M_1) corrected for changes in air buoyancy. The mass M of the sample was determined similarly from (M_1-M_0).

To determine (A_n+W_n) it was necessary to correct for the dilution of D_2O resulting from exchange with ($A_n+W_n-A_0$) of the hydroxyl groups which did not react during the exposure to D_2O vapor. For a sample of mass M the dilution effect corresponded to ($0.167W_nM$) g H_2O; it was reasonable to assume that ($A_n+W_n-A_0$) = W_n because the correction was small and, as will be shown, $A_n = A_0$ (approx.). The final purity P of D_2O was therefore given by

$$P = 99.7 - \frac{100(0.167W_nM)}{(15.0\times.997)+(0.185A_0M)}.$$

In this relation, 99.7% is the initial purity; the second term represents the percentage dilution by H_2O.

The quantity (A_n+W_n) was then calculated from the relation

$$A_n+W_n = \frac{100}{P} \times \frac{100(\Delta M+\Delta M_B)}{0.0185M}$$

where 0.0185 represents the fractional increase in mass for cellulose after all hydroxyl groups have been exchanged by deuterium and ΔM_B is the change in mass in the same experiment but conducted in H_2O. ΔM_B was a correction for a loss in mass probably due to degradation of the cellulose.

The value of (A_n+W_n) was estimated first by assuming no dilution of D_2O (P = 99.7%). P was then calculated and a second approximation of (A_n+W_n) gave the desired accuracy.

Materials

The samples listed below were used.

1. Cellophane (supplied by Dupont of Canada Limited) was air-dried viscose film containing no additives.
2. Wood cellulose was a softwood acetate grade woodpulp with 96% alpha cellulose (TAPPI method).
3. Cotton linters were dewaxed by alcohol–benzene extraction.
4. Bacterial cellulose was kindly supplied by Dr. R. J. Colvin of the National Research Council, Ottawa.
5. Amylose was the commercial grade supplied by Stein Hall and Co. The samples were prepared as before (3).

RESULTS

Comparison of Cycles

Various modifications of the three drying cycles were tried to establish the conditions under which the interconversion of accessible and inaccessible hydroxyls occurred most readily. The experimental conditions and results for wood cellulose are listed in Table I;

Can. J. Chem. Downloaded from www.nrcresearchpress.com by 210.87.254.6 on 09/05/12
For personal use only.

TABLE I

W_1 for various drying cycles for wood cellulose

Expt. No.	Cycle	Temp. (°C)	Conditions	W_1 (%)
1	Control	30	(1) Conditioned in H_2O, 8 hr at 65% RH (2) Exposed to HTO, 8 hr at 65% RH (3) Exposed to H_2O, 8 hr at 65% RH (as for measurement of W_1)	0.6
2	Control	100	(1) Conditioned in liquid H_2O, 4 hr (2) Immersed in liquid HTO, 4 hr (3) Immersed in liquid H_2O, 8 hr (4) Air-dried	0.9
3	D_1	30	(1) Conditioned in H_2O, 4 hr at 60% RH (2) Exposed to HTO, 4 hr at 60% RH (3) RH changed to 14% for 2 hr (4) RH returned to 50% for 2 hr (5) Exposed to H_2O, 8 hr at 60% RH (as for measurement of W_1)	1.7
4	D_1	30	(1) Same as No. 3 except in step (3) RH changed to 90% for 2 hr	1.
5	D_2	25	(1) Exposed to HTO, 4 hr at 75% RH (2) Dried 15 hr at 1 μ Hg (3) Exposed to H_2O, 8 hr at 75% RH (as for measurement of W_1)	2.
6	D_2	25	(1) Dried 15 hr at 1 μ Hg (2) Exposed to HTO, 8 hr at 75% RH (3) Exposed to H_2O, 8 hr at 75% RH (as for measurement of W_1)	2.7
7	D_2	See conditions	(1) Dried 15 hr at 1 μ Hg, 75° C (2) Exposed to HTO, 8 hr at 75% RH, 25° C (3) Exposed to H_2O, 8 hr at 75% RH, 25° C, as for measurement of W_1	4.1
8	D_3	25	(1) Immersed in liquid HTO, 2 hr (2) Dried 2 hr at 20% RH (3) Exposed to H_2O, 8 hr at 75% RH (as for measurement of W_1)	5.0

two control experiments in which the sample was exposed to HTO and subsequently to H_2O without changing the RH are included.

In both control experiments (Nos. 1 and 2), W_1 was small but significant. Experiment 2 was similar to one described by Mann and Marrinan (1), who found that cellophane retained small quantities of deuterium after immersion in liquid D_2O followed by H_2O. The same experiment performed by Lang and Mason (2) in HTO liquid at 25° C gave values of 0 and 0.2% for W_1.

In expts. 3 and 4, cyclic changes of RH in a range from 15 to 95% yielded larger values of W_1 than expt. 1 although the time of exposure to HTO vapor was the same.

In expt. 5 (cycle D_2) the sample was exposed to HTO vapor only during desorption and in 6, only during adsorption; the values of W_1 were larger than in Nos. 3 and 4, presumably because of the lower RH during drying, and were approximately equal, showing that the change occurred with both increasing and decreasing moisture content.

Experiment 7 (cycle D_2) was similar to No. 6 with the exception that the sample was dried at 75° C to remove strongly bound moisture (6). A pronounced increase in W_1 occurred which was undoubtedly associated with adsorption of HTO at zero regain. The corresponding desorption experiment, in which the sample was dried from HTO to zero regain at 25° C, could not be studied because all the sorbed water could not be removed at this temperature under the conditions of evacuation used.

The greatest W_1 was formed in No. 8 in which the sample was immersed in HTO liquid and dried in contact with HTO vapor at 20% RH; the large effect apparently occurred in the range of relative humidity from 95 to 100%.

It was concluded from the experiments that (*a*) tritiated inaccessible hydroxyls were formed on changing the RH up or down and (*b*) the effect was most pronounced at the

Can. J. Chem. Downloaded from www.nrcresearchpress.com by 210.87.254.6 on 09/05/12
For personal use only.

extreme ends of the drying cycle, i.e., at 0 and 100% RH. As found earlier (1, 2), a smaller but significant amount of reacted inaccessible cellulose resulted from exposure at constant RH.

The influence of other variables was studied with cycles D_2 and D_3 because they incorporated the two extreme conditions which produced the greatest changes.

Effect of Temperature

The influence of temperature upon W_1 in wood cellulose and cellophane was investigated between 25 and 100° C for cycles D_2 and D_3. The specified temperature for cycle D_2 was for the vacuum-drying only, whereas in cycle D_3, it was for both immersion and partial drying.

The results (Fig. 2) show that W_1 increased with temperature in both cycles.

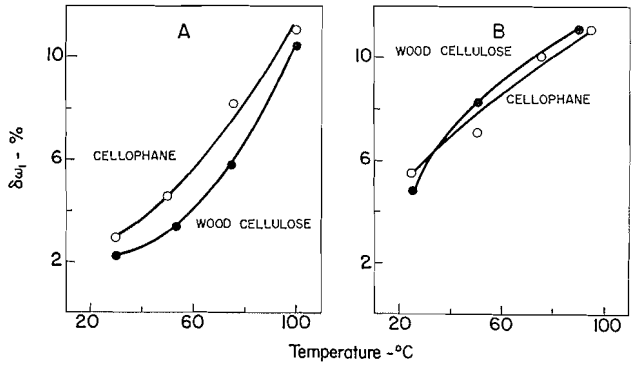


FIG. 2. Effect of temperature upon W_1. A, cycle D_1; B, cycle D_3.

Apart from the temperature during drying, two secondary factors may have contributed to the increase of W_1 with temperature, namely, heating the sample from 25° C to the higher temperature in cycle D_2 and the lower RH when drying at higher temperature in cycle D_3. To determine if the temperature of drying was of importance, the modified cycles described in Table II were conducted on wood cellulose.

TABLE II

W_1 for modifications of cycles D_2 and D_3 on wood cellulose

Expt. No.	Cycle	Conditions	W_1* (%)
9	D_2	(1) Exposed to HTO, 8 hr at 75% RH, 25° C (2) Dried 15 hr at 1 μ Hg, 75° C	5.8
10	D_2	(1) Exposed to HTO, 2 hr at 2.3% RH, 75° C (2) Dried 15 hr at 1 μ Hg, 75° C	6.6
11	D_2	As for expt. 9 with drying at 100° C	12.1
12	D_2	As for expt. 9 with drying at 100° C for 40 hr	11.7
13	D_3	(1) Immersed in liquid HTO, 2 hr, 50° C (2) Dried 12 hr at 95% RH, 50° C	8.3
14	D_3	As for expt. 13 with drying for 2 hr at 15% RH	8.5
15	D_3	As for expt. 13 with drying for 2 hr at 1 μ Hg	8.5

*In each experiment, W_1 was measured after the sample was exposed to H_2O for 8 hours at 75% RH and 25° C, as described in the text.

Cycle D_2 at 75° C, as described above, is presented for comparison as expt. 9. In expt. 10 (cycle D_2), the temperature (75° C) was constant throughout and the RH was

Can. J. Chem. Downloaded from www.nrcresearchpress.com by 210.87.254.6 on 09/05/12
For personal use only.

lower (2.3%) during exposure to HTO. The comparable values for W_1 in Nos. 9 and 10 show that the temperature during drying at low RH determined the value of W_1 in cycle D_2. Continued heating of the dried sample produced no additional change (expts. 11 and 12).

In expts. 13 to 15 (cycle D_3) the RH during drying ranged from 10^{-3} to 95% and similar values of W_1 were found. Therefore the temperature during soaking, or drying, from 100 to 95% RH determined the magnitude of W_1 in cycle D_3.

Comparison of Samples

Values of W_1 for cycles D_2 and D_3 are listed in Table III for different types of cellulose

TABLE III

W_1 for different samples

Sample	A_0* (%)	W_1 (%)	
		Cycle D_2 at 75° C	Cycle D_3 at 50° C
Cellophane	79	8.3	7.1
Wood cellulose	58	5.8	8.5
Cotton linters	40	4.3	9.1
Bacterial cellulose	42	2.6	8.5
Amylose	98	<0.1	<0.1

*From ref. 3.

and amylose. With cycle D_2, W_1 for cellulose increased with increasing A_0 whereas with cycle D_3 there appeared to be no correlation. With amylose, $W_1 = 0$ in both cycles as would be expected if the substance were completely accessible. Although the measured accessibility of amylose was consistently a little lower than 100% the difference probably did not indicate the presence of unreactive hydroxyls but an impurity in the sample, as discussed previously (3).

Repeated Cycles (HTO)

(a) Effect upon A_n and $\delta\omega_n$

Table IV lists values of A_n and $\delta\omega_n$ for samples which have undergone $(n-1)$ drying cycles (D_2 and D_3) in H_2O.

TABLE IV

Effect of repeated drying upon A_n and $\delta\omega_{n+1}$ by HTO exchange

Sample	Drying history*			A_n (%)	$\delta\omega_{n+1}$	
	Cycle	n	Temp. (°C)		Cycle D_2 at 75° C	Cycle D_3 at 50° C
Wood cellulose		0		58	5.8	8.5
,,	D_2	2	100	58	6.4	
,,	D_2	10	75	57	6.5	7.8
,,	D_3	10	95	56	6.0	7.5
,,	D_3	50	50	55	6.2	7.0
Cellophane		0		79	8.3	7.1
,,	D_2	10	75	76	10.7	6.8
,,	D_3	50	50	76	9.5	4.9
Bacterial cellulose		0		42		
,,	D_2	8	75	41		

*Before the present experiments, cellophane and bacterial cellulose had been air-dried while wood cellulose had probably been dried at >100° C during manufacturing.

Can. J. Chem. Downloaded from www.nrcresearchpress.com by 210.87.254.6 on 09/05/12
For personal use only.

The accessibility was decreased slightly by drying, e.g., from 58 to 55% for wood cellulose after 50 D_3 cycles at 50° C, but the change in A_n during the first few cycles was negligible. Values of $\delta\omega_n$ for cycle D_2 increased with n, while for cycle D_3 the value decreased. The greatest change (from $\delta\omega_1 = 7.1\%$ to $\delta\omega_{51} = 4.9\%$ after 50 D_3 cycles at 50° C) occurred in cellophane and was similar to the earlier result (2).

(b) Effect upon W_n

The previously reported (2) increase of W_n with n was investigated under various conditions to determine if exchange with all hydroxyl groups, corresponding to $(A_n+W_n) = 100\%$, would occur when n was made large. Figures 3 and 4 show the results for cycles

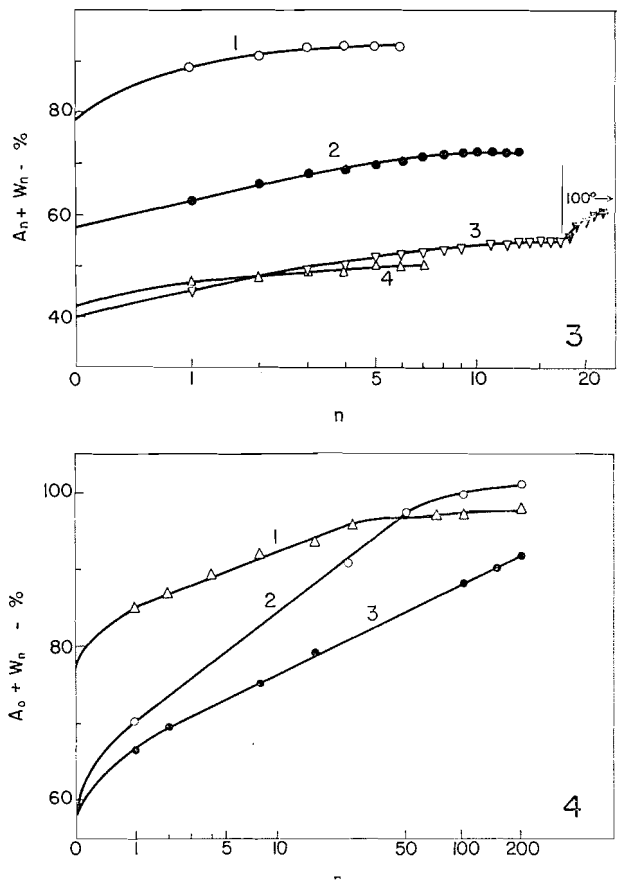


FIG. 3. A_n+W_n for cycle D_2 at 75° C. Curve 1, cellophane; 2, wood cellulose; 3, cotton linters; 4, bacterial cellulose.

FIG. 4. A_0+W_n for cycle D_3. Curve 1, cellophane at 50° C; 2, wood cellulose at 100° C; 3, wood cellulose at 50° C.

D_2 and D_3. In the latter experiments W_n was determined, and the data are shown as (A_0+W_n); this procedure is reasonable since A_0 and A_n are approximately equal. In both figures, log $(n+1)$ is plotted to include results for large n's while still showing the large changes occurring in the early cycles.

For cycle D_2 at 75° C, (A_n+W_n) was found to increase to a characteristic limiting value (Fig. 3) which remained constant to $\pm 0.1\%$ after several further cycles. By

Can. J. Chem. Downloaded from www.nrcresearchpress.com by 210.87.254.6 on 09/05/12
For personal use only.

increasing the drying temperature, as shown with cotton linters, a higher value was obtained. However, complete exchange was not achieved and higher temperatures than 100° C could not be studied with the present apparatus.

Using cycle D_3, (A_0+W_n) for wood cellulose and cellophane increased linearly with log $(n+1)$ until approximately 100% and then leveled off, indicating that complete exchange had occurred. The further increase in (A_0+W_n) above 100% was undoubtedly due to the continued increase of W_n as A_n decreased slowly with n (see Table IV). The quantity (A_n+W_n) would have been expected to remain constant at 100%.

The rate of increase of (A_0+W_n) with n was greater at higher temperature; it appeared that more than 20 times as many cycles would have been required at 50° C than at 100° C to reach $(A_0+W_n) = 100\%$.

(c) Effect of Prolonged Soaking in HTO upon W_n

Each of the D_3 cycles involved a period of immersion in liquid HTO. At large n the total immersion period, although not continuous, became large and, on the basis of the control experiment (No. 2, Table I), may have accounted for some of the increase in W_n reported above. The magnitude of the effect was estimated by measuring the variation of W_1 for cycle D_3 using soaking times from 2 hours to 135 days and the usual drying time of 2 hours.

Results for wood cellulose are given in Table V for temperatures from 25 to 100° C.

TABLE V

Effect of prolonged soaking upon W_1 in cycle D_3 for wood cellulose

Soaking time	Temperature (°C)	W_1 (%)
2 hours	25	5.0
64 days	,,	8.9
135 days	,,	10.2
2 hours	50	8.5
64 days	,,	16.4
135 days	,,	17.8
2 hours	100	12.2
15 days	,,	26.6
64 days	,,	28.9

The value of W_1 increased with soaking time and temperature. For large numbers of D_3 cycles, the exchange due to soaking undoubtedly constituted a large part of W_n. For example, the increase in W_1 due to the first 15 days of soaking at 100° C was 14.4% (Table V) while $(W_{50}-W_1)$ for 49 D_3 cycles, which included a total of 17 days' soaking, was 27.2%. The experiments with D_3 cycles thus measured the combined effects of repeated drying and of soaking.

Repeated Cycles (D_2O)

Two values of (A_n+W_n) were measured for cycle D_3 using D_2O with cellophane and wood cellulose to check the above results with HTO.

The results listed in Table VI are in satisfactory agreement with cellophane but not with wood cellulose. The error is believed to be in the measurement of deuterium exchange and in the correction term ΔW_B (see Experimental Part) which represents the loss in mass of cellulose probably due to chemical degradation. Since the degradation could be estimated only in H_2O and would be expected to be different in D_2O, the correction was

Can. J. Chem. Downloaded from www.nrcresearchpress.com by 210.87.254.6 on 09/05/12
For personal use only.

TABLE VI
Comparison of results for cycle D_3 by exchange with D_2O and HTO

Sample	n	ΔM (%)	ΔM_B (%)	(A_n+W_n) (%), D_2O exchange	(A_0+W_n) (%), HTO exchange
Cellophane	50	1.57	−0.15	94	97
Wood cellulose	185	1.09	−0.31	76	90

probably invalid. Evidence of chemical reaction in cellulose after the cyclic drying was the distinct yellowing of the sample which had occurred, particularly where it was in contact with glass.

The gravimetric measurement of deuterium exchange with D_2O has, however, been used with excellent results for the measurement of accessibility (3). It appears that the degradative processes in cellulose have a significant effect upon the mass of cellulose only at high temperature (3) and during prolonged exposure to water.

DISCUSSION

The results may be summarized as follows:

1. exchange with the inaccessible hydroxyl groups in cellulose accompanied a change of relative humidity, either up or down;
2. the effect was most pronounced near 0 and 100% RH and increased with temperature;
3. the magnitude of the exchange was characteristic for different forms of cellulose;
4. when cellulose was wetted and dried repeatedly, the exchange increased until, as previously predicted, all hydroxyl groups had reacted;
5. the accessibility A of cellulose decreased slowly with large numbers of drying cycles; and
6. reaction with inaccessible hydroxyls also occurred during prolonged soaking and increased with temperature.

The formation of reacted inaccessible hydroxyls is assumed to result from the conversion of accessible regions to the inaccessible form, and thus implies localized changes in the degrees of molecular order. According to more recent concepts (7), the fine structure of cellulose can be described by a distribution of lateral order, the highly ordered regions corresponding to crystallites and the low-ordered, representing amorphous cellulose. Some evidence suggests that the inaccessible regions are highly ordered cellulose such as the interiors of crystallites, and perhaps also strongly hydrogen-bonded amorphous regions. For example, samples are graded in the same order by measurements of both accessibility and amorphous fraction by X-ray diffraction (7). Furthermore, the inaccessible hydroxyls in cellulose and crystalline cellopentaose give similar infrared absorption bands (1). It was also found that the change in accessibility with relative humidity is small (3) and similar to the effect upon the amorphous fraction determined by X-ray diffraction (8, 9). However, recent studies suggest that the accessibility of regenerated cellulose and of single crystals (10) of cellulose II may be similar (11). Anomalous behavior is also shown by substances other than cellulose. For example, a partially crystalline amylose was completely accessible while an amorphous xylan was only 52% accessible (3). It is evident, therefore, that one cannot unequivocally assume that inaccessible cellulose corresponds to the crystalline part although the two properties appear to

Can. J. Chem. Downloaded from www.nrcresearchpress.com by 210.87.254.6 on 09/05/12
For personal use only.

be related in some way. In the present discussion it will be assumed for simplicity that the disruption of inaccessible regions represents destruction of crystallites.

To explain the accessible–inaccessible transformations during drying it was suggested previously that a molecular rearrangement occurred at an intermediate moisture content favorable for the formation of hydrogen bonds and for mobility of molecular chains (2). Under these conditions a dynamic equilibrium was believed to exist between accessible and inaccessible cellulose. It was assumed that at lower moisture content the cellulose chains became immobilized by interchain hydrogen bonding, while the swelling in the wet state prevented the formation of hydrogen bonds between cellulose molecules. Since the present results show that transformations occurred in cellulose over a wide range of moisture contents corresponding to relative humidities from 0 to 100%, this hypothesis does not appear to be valid. Furthermore, the changes were greatest at very low and high relative humidity when conditions were least favorable for the proposed equilibrium. The slight decrease of accessibility with decreasing relative humidity (3) may partly account for the formation of inaccessible cellulose during drying. However, the same effects were observed during sorption of water and have not been fully explained.

It is now proposed that molecular rearrangements, which have previously been assumed to occur only in the amorphous regions, with changes in the quantity of sorbed water (12), are also responsible for disrupting and reforming ordered regions. The destruction of the crystallite can be attributed to molecular stresses created in amorphous regions by the swelling action of sorbed water or by hydrogen bonds tending to draw cellulose molecules together when water is removed. Since the molecules extend through many regions of different order, the stresses, which on a molecular scale must become exceedingly high, are transmitted throughout the structure. The pronounced changes occurring in W_1 near 0 and 100% RH can be associated with characteristic interactions of cellulose and water at these relative humidities. At zero regain, water is very strongly bonded to cellulose, and Urquhart (13) has suggested that each H_2O molecule is bound to two hydroxyl groups. The resultant linking by the sorbed water can be conceived as drawing cellulose molecules together and causing a rearrangement. At the other extreme, the pronounced swelling near 100% RH could have the same result. The increasing transformation with temperature may be attributed to greater mobility of cellulose molecules; the reduction of sorption hysteresis with temperature has been ascribed to the same effect (14).

With the present rudimentary concepts it is not possible to consider the significance of the magnitude of the changes under various conditions. Presumably the results reflect the interplay between the network geometry of the molecular chains and the drying treatment. It is possible that the magnitude of these effects may characterize the fine structure and indicate, for example, the ease of molecular rearrangements in different samples.

The disruption of crystallites by molecular stresses suggests that similar effects may arise by mechanical deformation. It is known that by stretching cellulose, an orientation is created in the structure. However, little change in crystallinity was noted; cellulose acetate filaments, however, stretched up to 20 times their original length and when saponified underwent an increase in crystallinity (15). Whether crystallites were disrupted during the stressing was not known. With wool fibers, stretching was found to increase the reactivity of the disulphide bonds and was interpreted as a configurational change influencing the extent of the reaction (16). This effect appears to be somewhat analogous to the exchange with inaccessible hydroxyl groups in cellulose during drying.

Can. J. Chem. Downloaded from www.nrcresearchpress.com by 210.87.254.6 on 09/05/12
For personal use only.

The small effect of drying upon the accessibility and upon the values of $\delta\omega_n$ suggests that there is little permanent change in the cellulose. Other investigators have similarly reported only small changes in cellulose reactivity to nitration (17), hydrolysis (18), and exchange with D_2O (19) by repeated wetting and drying. The effects are not always the same; for example, accessibility to iodine absorption increased after drying (20) while accessibility to thallation decreased (19). It is therefore not clear whether the degree of molecular order is affected by drying, but in any event the change cannot be large. The reduction of accessibility after large numbers of drying cycles in the present work indicated an increase of the crystalline fraction. Recrystallization may have resulted from hydrolysis, since the DP of cellulose has been found to decrease in similar experiments (21).

A result of interest was the increasing exchange in the inaccessible regions with higher temperature during prolonged immersion in water. It appeared that at some temperature greater than 100° C, the cellulose may be completely accessible for the usual reaction time of several hours allowed in the measurement. The result suggests that crystallites may be continuously being disrupted and reformed by the thermal energies of the molecules. The effect may be greater in the presence of liquid water because, like other plasticizers (22), it would be expected to lower the second-order transition temperature and thereby permit the molecular rearrangement to occur more readily.

The transient existence of crystallites, as suggested by the present results, would also be expected to play a role in other chemical and physical changes in cellulose.

REFERENCES

1. J. Mann and H. J. Marrinan. Trans. Faraday Soc. **52**, 481, 487, 492 (1956).
2. A. R. G. Lang and S. G. Mason. Can. J. Chem. **38**, 373 (1960).
3. O. Sepall and S. G. Mason. Can. J. Chem. This issue.
4. J. M. Kuzmak. Ph.D. Thesis, McGill University, Montreal, Que. 1953.
5. O. Sepall, A. R. G. Lang, and S. G. Mason. Can. J. Chem. **39**, 827 (1961).
6. A. R. G. Lang and S. G. Mason. Can. J. Chem. **37**, 1829 (1959).
7. B. Ott and H. M. Spurlin. Cellulose and cellulose derivatives. 2nd ed. Interscience Publishers, Inc., New York. 1954.
8. P. H. Hermans and A. Weidinger. Makromol. Chem. **18/19**, 75 (1956).
9. O. Ant-Wuorinen and A. Visapää. Paperi ja Puu, **10**, 515 (1960).
10. R. St. J. Manley. Nature, **189**, 391 (1961).
11. R. St. J. Manley. Private communication.
12. P. H. Hermans. Physics and chemistry of cellulose fibers. Elsevier Publishing Company, Inc., Amsterdam. 1949.
13. J. Honeyman. Recent advances in the chemistry of cellulose and starch. Heywood and Company Ltd., London. 1959.
14. A. R. Urquhart and A. M. Williams. J. Textile Inst. **15**, T559 (1924).
15. B. S. Sprague and H. D. Noether. To be published.
16. J. P. E. Human and H. Lindley. Textile Research J. **27**, 917 (1957).
17. T. P. Yin and R. J. Brown. Can. J. Chem. **37**, 444 (1959).
18. B. G. Ranby. Fundamentals of papermaking fibers. Technical Section of the British Paper and Board Makers Association Inc. 1958.
19. W. J. Brickman, N. B. Dunford, E. M. Tory, J. L. Morrision, and R. E. Brown. Can. J. Chem. **31**, 550 (1953).
20. I. Slavik and M. Mahdalik. Papír a celulosa, **12**, 73 (1957).
21. W. von Koblitz and H. Kiessig. Das Papier, **14**, 179 (1960).
22. V. A. Kargin, P. V. Kozlov, and W. Mai Ch'ang. Doklady Akad. Nauk S.S.S.R. **130**, 356 (1960).

Can. J. Chem. Downloaded from www.nrcresearchpress.com by 210.87.254.6 on 09/05/12
For personal use only.

Can. J. Chem. Downloaded from www.nrcresearchpress.com by 210.87.254.42 on 09/05/12
For personal use only.

OZONOLYSIS OF UNSATURATED FATTY ACIDS

I. OZONOLYSIS OF OLEIC ACID[1]

R. G. ACKMAN, M. E. RETSON, L. R. GALLAY, AND F. A. VANDENHEUVEL[2]

ABSTRACT

Ozonolysis of oleic acid in methanol, a reacting solvent, with subsequent decomposition of the ozonide products by hydrogen peroxide in formic acid, gives yields of principal dicarboxylic acid fission products exceeding 95% with a minimum of secondary acidic products. The method is highly reproducible and offers unique advantages in the total recovery of the dicarboxylic acids and the elimination of peroxidic materials. The principal non-acidic by-products were tentatively identified as the C_8 alcohols and their formyl esters.

INTRODUCTION

The study of the position of the ethylenic double bonds in long-chain fatty acids is important in connection with the isolation of various naturally occurring fatty acids, and even more important in fields where the chemical treatment of the fatty acid by partial hydrogenation, alkali fusion, or other prototropic reactions leads to the formation of positional isomers. In the former instance, any reasonable yield of principal fission products resulting from the scission of the double bond is satisfactory for bond location, particularly as naturally occurring fatty acids are usually homogeneous in bond position and impurities will differ enough structurally to be recognized as such. In the case of mixtures of positional isomers, the over-all yield is less important than two other factors which must be considered. Firstly, the occurrence of abnormal fission products such as lower homologues of the principal fission products must be reduced to a minimum, and secondly, the method of recovery and analysis of the products must be such that the analysis reflects the true proportions of these products.

Scission of the double bonds is usually achieved by oxidative fission. Some work has been done to give aldehydes as primary products (1–9), but the more extensive application of this technique has always been in the direction of obtaining the more tractable acidic fission products. Ozonolysis is an attractive technique owing to the complete reaction of ozone with the starting material (8) and the simplicity of the reagents and procedures generally adopted. The chief disadvantages, other than the necessity of an ozone generator, have always been the nominal yields (70–85%) (10–16) of primary acidic fission products, the associated formation of carbonyl, peroxidic, and polymeric materials (1, 7, 17), and the presence of one or more secondary acidic oxidation products. The latter can cause considerable uncertainty where minor amounts of positional isomers are being determined, while by-products hinder both separation and analysis of the products (10, 18). Certain procedures do give high yields of products, but the silver oxide oxidation method of Asinger (3, 12, 19) and the procedure of Klenk and Bongard (20) are somewhat complex, while that of Pryde *et al.* (8) yields aldehydes as principal products.

The most common alternatively employed oxidizing agent, potassium permanganate, also gives only moderate yields of acidic products and considerable secondary oxidation (11, 12, 18, 21–24). The recently introduced permanganate-catalyzed periodate method of von Rudloff (3, 25–28) is much more attractive owing to the simplicity of the method

[1]*Manuscript received March 20, 1961.*
Contribution from the Fisheries Research Board of Canada, Technological Station, Halifax, Nova Scotia.
[2]*Present address: Department of Agriculture, Research Branch, Animal Research Institute, Ottawa, Canada.*

Can. J. Chem. Downloaded from www.nrcresearchpress.com by 210.87.254.42 on 09/05/12
For personal use only.

and the very high yields of primary products. These techniques do suffer from a disadvantage in that recovery of the primary products, in particular the dicarboxylic acids, must be made by extraction from a highly mineralized aqueous solution, with consequent risk of losses of the more soluble lower dicarboxylic acids. In the past this factor has led to erroneous results in determining the relative proportions of positionally isomeric double bonds (13, 24, 29, 30).

If ozonolysis is to be considered as a useful method for the sensitive determination of double-bond position in long-chain fatty acids it must satisfy the following requirements:

1. the method should have a high yield of primary products and should give rise to the least possible amounts and variety of "abnormal" products;
2. the procedure of working-up should give the highest possible recoveries of related products even when these have differing physical properties;
3. the method should be simple and reproducible;
4. the method of analysis should be sensitive and accurate.

It was deemed desirable that the principal products should be acidic in order to capitalize on the stability and low volatility of the desirable dicarboxylic acids. The method outlined below, based on ozonolysis in methanol, a reacting solvent, with decomposition of the ozonide product with hydrogen peroxide in formic acid, satisfies the above requirements. The yield of principal dicarboxylic acid product averages 95%, accompanied by only 2–4% lower homologous dicarboxylic acids and 2–4% other materials. The principal non-dicarboxylic acid by-product has been tentatively identified as the alcohol formed from the principal acidic product through the loss of one carbon atom, occurring both as the alcohol and as its formyl ester. Since only volatile solvents and reagents are employed, and the monocarboxylic acids are removed by steam distillation, total recovery of the dicarboxylic acids present is possible. The method is relatively simple and while some variation is found in the proportion of non-dicarboxylic products to dicarboxylic acids, the ratio of total secondary dicarboxylic acid products to principal dicarboxylic acid product is remarkably stable. The mixture of products is readily analyzed with a high degree of accuracy by gas–liquid chromatography. The methanol – formic acid procedure is derived from that employed by Bailey (31, 32) for the production of adipic acid by ozonolysis of cyclohexene, by Perry (33) in the ozonolysis of norbornylene, and by Pryde *et al.* (8) in the ozonolysis of methyl oleate to give carbonyl products. Methanol has also been employed recently by other workers in the ozonolysis field (34–37), although not necessarily in exploitation of the same type of reaction.

EXPERIMENTAL

Pure oleic acid was prepared from filbert oil (38) via the methyl esters by established procedures (39, 40). The following properties were determined: iodine value 91.2 (Wijs), 89.1 (by precision semimicro hydrogenation (41)) (calc. 89.9); n_D^{25} 1.45785 (cf. n_D^{25} 1.45792 (42)). Ultraviolet spectrophotometry showed no diene or triene content prior to alkali isomerization* and the latter procedure showed a diene content of 0.1% or less. Gas–liquid chromatography of the methyl ester showed only an oleate peak.

It has been reported that an oleic acid prepared from olive oil by standard methods contained appreciable amounts of positional isomers (29). The present and other studies (13, 14) have confirmed that oleic acid homogeneous in bond position can be readily

**Modification of the method of Vandenheuvel and Richardson (43); 21% KOH in ethylene glycol, effective heating time 15 minutes.*

prepared. The ultimate criterion of purity in all cases must be the analysis of both mono- and di-carboxylic acid fission products. Thus the presence of small amounts of suberic acid in the dicarboxylic acid product does not signify the presence of octadec-8-enoic acid unless decanoic acid can be found in the complementary monocarboxylic acids. In the present studies the occurrence of both mono- and di-carboxylic acid products containing 10 carbon atoms has been noted in amounts of $\leqslant 0.1\%$. Thus the amounts of octadec-8- and octadec-10-enoic acids cannot have exceeded this level.

Ozone was furnished by a pyrex corona discharge tube (4). At an oxygen flow rate of 1.1 l./hr, the ozone content was determined as 2.2% (w/w) by decomposition of potassium iodide (44). A dry-ice trap supplemented chemical drying of the oxygen.

1. Ozonolysis in Methanol

Pure oleic acid (ca. 1 g) was weighed in a long-necked, 100-ml standard taper flask. Absolute methanol (Fisher Spectrophotometric Grade, 40 ml) was added and the solution was chilled to $-30°$ C and treated with ozone-containing oxygen until complete absorption ceased. The flask was fitted with a distilling head in order to admit a capillary tube (nitrogen) and was connected through a dry-ice trap to a mechanical vacuum pump system. The flask was immersed in water at room temperature and vacuum applied in stages until all the methanol was removed and the pressure was less than 1 mm. Formic acid (98%, 25 ml) was added to dissolve the syrupy residue and hydrogen peroxide (30 or 50% aqueous solution, 10 mole-equivalents) added. A reflux condenser was immediately fitted to the flask and gentle warming induced an exothermic reaction, on completion of which the mixture was heated for 1 hour on a steam bath. The peroxide and peracid content fell rapidly below measurable limits.

Water (20 ml) was added and the solution transferred to a continuous steam-distillation unit, a few drops of acetone serving as rinse. In this case, 200 ml of distillate was collected for recovery of the nonanoic and associated monocarboxylic acid products. The dicarboxylic acid solution was transferred to a distillation unit and evaporated nearly to dryness under aspirator vacuum. Toluene was added in small lots (ca. 10 ml) and removed under reduced pressure until the distillate was free of water and formic acid (45). Further vacuum treatment eliminated residual toluene. The product was dissolved in acetone (100 ml) and aliquots were taken for determination of yield by weight and titration. The balance of the material was freed of solvent and esterified with distilled diazomethane (18) in ether solution. The ether was removed and the product examined by gas–liquid chromatography. The results are presented in Table I.

The steam distillate was extracted with hexane (100 ml). The hexane solution was dried over sodium sulphate, and after removal of solvent the monocarboxylic acids were converted to methyl esters with diazomethane. Analysis of these methyl esters is presented in Table II.

The methanol in the cold trap was diluted with water and extracted with hexane. The bulk of the solvent was removed and the remaining solution examined by gas–liquid chromatography. Only traces of nonaldehyde were observed.

2. Ozonolysis in Acetic Acid and Other Solvents

Ozonolyses were carried out as described above employing 40 ml of a mixture of acetic acid and methyl formate (3:1), acetone, or methyl formate, with cooling in an ice-water bath. After complete ozone absorption had ceased, aqueous hydrogen peroxide (30%, 5 ml) was added and the flask was fitted with a reflux condenser. After standing overnight at room temperature, the mixtures were heated on a steam bath for 1 hour.

Can. J. Chem. Downloaded from www.nrcresearchpress.com by 210.87.254.42 on 09/05/12
For personal use only.

TABLE I

Dicarboxylic acids obtained from ozonolysis of oleic acid and control oxidations

Experiment			% yield		Weight% dicarboxylic acid composition*							% other material‡
Run	Material	Solvent	Weight†	Titration†	C_9	C_8	C_7	C_6	C_5	C_4	C_3	
1-A	Oleic	CH_3CO_2H	96.2	77.5	70.6	7.1	6.1	3.8	4.7	6.9	0.8	24.1‖
1-B	Oleic	$(CH_3)_2CO$	83	73	86.8	8.2	1.2	1.1	1.1	1.6	—	20.7§
2-A	Oleic	MeOH	100	93.5	97.2	1.9	0.4	0.2	0.2	0.1	—	5.6‖
2-B	Oleic	MeOH	100	93.1	97.5	2.2	0.1	0.1	0.1	—	—	3.1‖
2-C	Oleic	MeOH	100	95.5	98.7	0.9	0.1	0.1	0.1	0.1	—	1.8‖
2-D	Oleic	MeOH	106	100	97.6	1.9	0.1	0.1	0.1	0.1	—	3.9‖
2-A	Oleic	MeOH			96.0	2.5	0.6	0.3	0.3	0.3	—	5.4§
2-B	Oleic	MeOH			95.4	2.9	0.7	0.4	0.2	0.4	—	4.2§
2-C	Oleic	MeOH			97.9	1.5	0.1	0.1	0.2	0.2	—	0.7§
2-D	Oleic	MeOH			97.8	1.5	0.2	0.2	0.2	0.1	—	1.5§
3-A	Azelaic	HCO_2H	97.7	98.2	98.9	1.0	—	—	0.1	—	—	1.1‖
3-A	Azelaic	HCO_2H			98.5	1.2	0.1	—	0.1	0.1	—	1.1§
3-B	Azelaic	HCO_2H	98.6	100.3	99.1	0.6	0.1	—	0.1	0.1	—	0.6§

*% of total dicarboxylic acids indicated by gas–liquid chromatography.
†Calculated as azelaic acid.
‡% of total volatile materials indicated by gas–liquid chromatography.
§Polyester substrate.
‖Silicone grease substrate.

TABLE II

Monocarboxylic acids from ozonolysis of oleic acid

Run†	% monocarboxylic acids	Weight% monocarboxylic acid composition*			% other material‡
		C_9	C_8	C_7	
2-D	95.8§	98.1	1.6	0.3	4.2
	95.7‖	98.4	1.2	0.4	4.3

*% of total monocarboxylic acids indicated by gas–liquid chromatography.
†Details set forth in Table I.
‡% of total volatile materials indicated by gas–liquid chromatography.
§Silicone grease substrate.
‖Polyester substrate.

Monocarboxylic acids were removed by extraction with hexane (100 ml) after addition of water (100 ml). The aqueous solution containing the dicarboxylic acids was freed of solvents and volatile acids as described above, yields were determined, and the product was converted to methyl esters. Gas–liquid chromatographic analyses of the products are presented in Table I for the acetic acid and acetone products. The methyl formate product did not differ appreciably from the acetone product.

3. Control Oxidation of Azelaic Acid

Pure azelaic acid (100% by gas–liquid chromatography of the dimethyl ester) was refluxed for $1\frac{1}{2}$ hours with hydrogen peroxide solution in formic acid in the proportions used in the ozonolysis procedure. After removal of the solvent the recovery was 97.7% by weight. The esters were examined by gas–liquid chromatography and gave dicarboxylic acid chromatograms almost identical with those obtained from ozonolysis (Table I). The only significant feature appears to be the lower amounts of pimelic and adipic acids formed and the absence of the alcohol by-product.

4. Control Oxidation of Azelaic Acid Methyl Ester Semialdehyde Acetal

Azelaic acid methyl ester semialdehyde was prepared from methyl oleate by ozonolysis in acetic acid and reduction with zinc (8, 9). After a preliminary distillation, a concentrate

Can. J. Chem. Downloaded from www.nrcresearchpress.com by 210.87.254.42 on 09/05/12
For personal use only.

was converted to the acetal by refluxing with methanolic HCl (46). The acetal methyl ester was treated with sodium bisulphite solution and after removal of solvent was purified by preparative gas–liquid chromatography (47). The product was not completely pure (cf. ref. 8), but on treatment with hydrogen peroxide in formic acid, a vigorous exothermic reaction took place, and working-up of the products, as in section 2 above, gave a product the gas–liquid chromatogram of which was virtually identical with that obtained by oxidation of azelaic acid.

5. Determination of Peroxidic Materials

An aqueous solution of hydrogen peroxide (30%, 5 ml) was added to the solvent under consideration (40 ml) in a round-bottomed standard taper flask fitted with a reflux condenser. The solution was heated on a steam bath, aliquots being withdrawn at intervals for analysis. Determination of hydrogen peroxide was made with ceric sulphate, and of peracids, with potassium iodide and sodium thiosulphate (48). Only formic acid showed an appreciable peracid content at any time, and only with formic acid or mixtures containing formic acid was rapid destruction of all active oxygen evident.

6. Gas–Liquid Chromatography

The apparatus employed was a Podbielniak Chromacon. Columns were 10 ft in length and $\frac{1}{4}$ in. in diameter, packed with 30% of either high-vacuum silicone grease (Dow Corning), especially treated (49), or diethylene glycol – adipic acid polyester (LAC-2-R-446), on 60–80 mesh Chromosorb. Analyses of monocarboxylic esters were carried out at 100° C with hydrogen flow rates of 55 ml/min for the polyester column and 100 ml/min for the silicone column. Dicarboxylic esters were analyzed at 160° with hydrogen flow rates of 85 ml/min for the polyester column and 38 ml/min for the silicone column. Areas were determined by a ball-and-disk-type integrator. The errors associated with the small peaks ($\sim$0.1%) may be $\pm$30% owing to the few counts available (50).

The monocarboxylic acid chromatograms showed, in addition to minor amounts of octanoic and heptanoic methyl esters, three other components. The minor one was identified as nonanal and the others as octanol and octyl formate, the latter predominating. These identifications are assigned on the basis of complete coincidence of small additions of authentic materials added to the ozonolysis product, carried out on both polyester and silicone substrates.

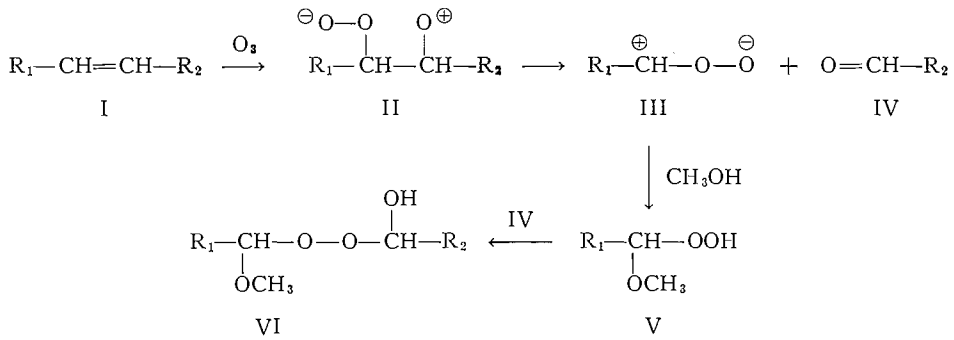
In addition to a large number of very minor peaks, the dicarboxylic acid ester chromatograms showed one major non-dicarboxylic acid by-product. Methyl 8-hydroxyoctanoate was not available, but methyl 9-hydroxynonanoate was prepared by the method of Diaper and Mitchell (51). Calculations of the equivalent chain lengths (52) of methyl 8-hydroxyoctanoate were made from the retention times of methyl 9-hydroxynonanoate. These indicated that the retention times, relative to dimethyl azelate, would be 0.605 on the silicone column and 1.16 on the polyester column. Minor peaks were in fact observed at 0.610 and 1.20 respectively. The formyl ester of the alcohol methyl ester could be similarly shown to have relative retention times, calculated from those of the formyl ester of methyl 9-hydroxynonanoate, of 0.680 on the silicone grease column and 0.905 on the polyester column. These values correlate with the relative retention times of the major non-dicarboxylic acid product, 0.706 and 0.902 respectively. The value of the relative retention time for the by-product peak on the silicone grease column could not be accurately determined as it was overlapped by the dimethyl suberate peak. Mixed runs with small amounts of methyl azelaaldehyde (9) did not coincide with any component on either silicone or polyester analyses.

Can. J. Chem. Downloaded from www.nrcresearchpress.com by 210.87.254.42 on 09/05/12
For personal use only.

Can. J. Chem. Downloaded from www.nrcresearchpress.com by 210.87.254.42 on 09/05/12
For personal use only.

DISCUSSION

The Criegee ozonolysis mechanism (1, 53, 54) suggests that the zwitterion (III) in the presence of a reacting solvent, in this case methanol, leads to a methoxy hydroperoxide (V). There is a possibility that this may then react with the aldehyde (IV) to give a hemiperacetal (VI). If the latter step were not complete (cf. ref. 33), some loss of volatile aldehyde would be expected when the methanol is removed under vacuum, whereas only a trace of free aldehyde (nonaldehyde) has been observed in this step. Reaction of the aldehydes with methanol to give hemiacetals or acetals is also a possibility (37).



The decomposition of the hydroperoxides, hemiperacetals, hemiacetals etc. is readily accomplished by treatment with hydrogen peroxide and formic acid, the active agent probably being performic acid (55) formed *in situ*. Peracetic acid has been employed in similar cases (15, 16, 37). Performic acid decomposes readily on heating, ensuring the rapid destruction (31, 32) of all peroxidic materials, to leave inert products. Regardless of the nature of the material being oxidized, less than 1% nonaldehyde and only traces of azelaic semialdehyde are found in all cases. This can be taken as a reliable indication that oxidation is virtually complete.

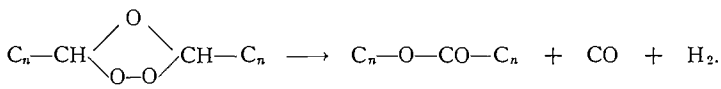
The quality of the reagents is significant. Thus results 2-A and 2-B, Table I, where ordinary reagent grade methanol was employed, show slightly higher amounts of both dicarboxylic acid and non-dicarboxylic acid by-products than results 2-C and 2-D where spectrophotometric grade methanol was used.

The acidic composition of the monocarboxylic acid fraction (Table II) parallels, in certain respects, that of the dicarboxylic acid product. However, since the recovery is only about 90% and losses of lower materials are high, the results are less significant.

The close duplication of the ozonolysis results by the control oxidations of azelaic acid and azelaic acid methyl ester semialdehyde acetal (see Table I, also above), not only in terms of secondary dicarboxylic by-products, but also partly in the miscellaneous by-products, indicates that these materials result from true secondary oxidation by the hydrogen peroxide in formic acid, and do not form during the ozonolysis step.

The occurrence of the presumed alcohol by-products in both the monocarboxylic and dicarboxylic acid products suggests a symmetrical reaction characteristic of isolated double bonds, and since they are not found in the control oxidation reactions (see above), their formation must take place during the ozonolysis or decomposition of the ozonide. Two possible mechanisms may be considered. In the first instance Pasero *et al.* (56–58)

have observed the formation of appreciable amounts of esters during the ozonolysis of monoethylenic acids, and ascribe this to simple decomposition of the ozonide:



Thus monooctyl azelate is one of the two potential products in the ozonolysis of oleic acid, and in the presence of formic acid and water, might be expected to hydrolyze or transesterify to give both octanol and octyl formate, together with azelaic acid.

Lefort *et al.* (59, 60) have observed the formation of similar esters (C_n—O—CO—C_n) when aliphatic peracids are heated, although under anhydrous conditions, suggesting a complex reaction of peracids during the ozonide decomposition with hydrogen peroxide in formic acid. On the present evidence either mechanism might be applicable.

Complete elimination of by-products is a highly desirable but rarely attained end in all oxidative fission procedures. The methanol – formic acid procedure reduces the by-product level to a point where gas–liquid chromatography is greatly facilitated, while at the same time retaining the advantage of total recovery of the dicarboxylic acids. The by-products do not, therefore, detract from the advantages of this technique, combined with gas–liquid chromatography, as a quantitative means of analysis of the position of ethylenic double bonds in long-chain monounsaturated fatty acids.

ACKNOWLEDGMENTS

The authors are indebted to Mrs. M. Bannerman for carrying out gas–liquid chromatographic analyses and to Mr. P. M. Jangaard for the ultraviolet and alkali isomerization studies.

REFERENCES

1. P. S. Bailey. Chem. Revs. **58**, 925 (1958).
2. A. B. Brown and J. W. Sparks. U.S. Patent No. 2,819,279 (1958).
3. J. Cason and P. Tavs. J. Biol. Chem. **234**, 1401 (1959).
4. A. L. Henne and W. L. Perilstein. J. Am. Chem. Soc. **65**, 2183 (1943).
5. G. Izumi. J. Chem. Soc. Japan Ind. Chem. Sect. **59**, 1129 (1956).
6. W. Stoffel and E. H. Ahrens, Jr. J. Am. Chem. Soc. **80**, 6604 (1958).
7. M. Stoll and A. Rouvé. Helv. Chim. Acta, **27**, 950 (1944).
8. E. H. Pryde, D. E. Anders, H. M. Teeter, and J. C. Cowan. J. Org. Chem. **25**, 618 (1960).
9. C. R. Noller and R. Adams. J. Am. Chem. Soc. **48**, 1074 (1926).
10. F. L. Benton, Arthur A. Kiess, and H. J. Harwood. J. Am. Oil Chemists' Soc. **36**, 457 (1959).
11. R. H. Backderf and J. B. Brown. Arch. Biochem. Biophys. **76**, 15 (1958).
12. J. G. Keppler. Rec. trav. chim. **76**, 49 (1957).
13. R. G. Ackman. Ph.D. Thesis, University of London, England. 1956.
14. R. G. Ackman, Sir Patrick Linstead, B. J. Wakefield, B. C. L. Weedon, and R. A. Dytham. Tetrahedron, **8**, 221 (1960).
15. H. Wilms. Ann. **567**, 96 (1950).
16. K. Ziegler, W. Hechelhammer, H. D. Wagner, and H. Wilms. Ann. **567**, 99 (1950).
17. A. Rieche, R. Meister, H. Sauthoff, and H. Pfeiffer. Ann. **553**, 187 (1942).
18. A. T. James and J. Webb. Biochem. J. **66**, 515 (1957).
19. F. Asinger. Ber. **75**, 656 (1942).
20. E. Klenk and W. Bongard. Z. physiol. Chem. Hoppe-Seyler's, **290**, 181 (1952).
21. P. Haverkamp Begemann, J. G. Keppler, and H. A. Boekenoogen. Rec. trav. chim. **69**, 439 (1950).
22. K. S. Markley. Fatty acids, their chemistry and physical properties. Interscience Publishers, Inc., New York. 1947. p. 387.
23. E. F. Armstrong and T. P. Hilditch. J. Soc. Chem. Ind. (London), **44**, 43T (1925).
24. Armand J. Fulco and James F. Mead. J. Biol. Chem. **234**, 1411 (1959).
25. R. U. Lemieux and E. von Rudloff. Can. J. Chem. **33**, 1701 (1955).
26. E. von Rudloff. Can. J. Chem. **34**, 1413 (1956).
27. E. von Rudloff. J. Am. Oil Chemists' Soc. **33**, 126 (1956).
28. E. P. Jones and J. A. Stolp. J. Am. Oil Chemists' Soc. **35**, 71 (1958).

Can. J. Chem. Downloaded from www.nrcresearchpress.com by 210.87.254.42 on 09/05/12
For personal use only.

29. R. R. ALLEN and A. A. KIESS. J. Am. Oil Chemists' Soc. **32**, 400 (1955).
30. J. T. KNEGTEL, C. BOELHOUWER, M. TELS, and H. I. WATERMAN. J. Am. Oil Chemists' Soc. **34**, 336 (1957).
31. PHILIP S. BAILEY. J. Org. Chem. **22**, 1548 (1957).
32. PHILIP S. BAILEY. Ind. Eng. Chem. **50**, 993 (1958).
33. ROBERT H. PERRY, JR. J. Org. Chem. **24**, 829 (1959).
34. D. G. DIAPER and D. L. MITCHELL. Can. J. Chem. **38**, 1976 (1960).
35. S. P. FORE, R. L. HOLMES, and W. G. BICKFORD. J. Am. Oil Chemists' Soc. **37**, 490 (1960).
36. N. A. MILAS, J. T. NOLAN, and P. PH. H. L. OTTO. J. Org. Chem. **23**, 624 (1958).
37. R. H. CALLIGHAN, M. F. TARKER, JR., and M. H. WILT. J. Org. Chem. **25**, 820 (1960).
38. M. J. CHISHOLM and C. Y. HOPKINS. Can. J. Chem. **31**, 1131 (1953).
39. H. A. SCHUETTE and S. DAL NOGARE. J. Am. Oil Chemists' Soc. **28**, 229 (1951).
40. D. H. WHEELER and R. W. RIEMENSCHNEIDER. Oil & Soap, **16**, 207 (1939).
41. F. A. VANDENHEUVEL. Anal. Chem. **24**, 847 (1952).
42. B. M. CRAIG. Can. J. Chem. **31**, 499 (1953).
43. F. A. VANDENHEUVEL and G. H. RICHARDSON. J. Am. Oil Chemists' Soc. **30**, 104 (1953).
44. GEORGE SLOMP, JR. J. Org. Chem. **22**, 1277 (1957).
45. L. H. HORSLEY. Anal. Chem. **19**, 508 (1947).
46. G. M. GRAY. J. Chromatog. **4**, 52 (1960).
47. R. G. ACKMAN, M. BANNERMAN, and F. A. VANDENHEUVEL. Unpublished work.
48. F. P. GREENSPAN and D. G. MACKELLAR. Anal. Chem. **20**, 1061 (1948).
49. F. R. CROPPER and A. HEYWOOD. Nature, **174**, 1063 (1954).
50. J. JANAK. J. Chromatog. **3**, 308 (1960).
51. D. G. M. DIAPER and D. L. MITCHELL. Can. J. Chem. **38**, 1976 (1960).
52. T. K. MIWA, K. L. MIKOLAJCZAK, F. EARLE, and I. A. WOLFF. Anal. Chem. **32**, 1739 (1960).
53. R. CRIEGEE. Ann. **560**, 127 (1948).
54. R. CRIEGEE. Record Chem. Progr. (Kresge-Hooker Sci. Lib.), **18**, 111 (1957).
55. E. BRINER and E. DALLWIGK. Compt. rend. **244**, 1695 (1957).
56. J. PASERO and M. NAUDET. Rev. franç. corps gras, **7**, 189 (1960).
57. J. PASERO, J. CHOUTEAU, and M. NAUDET. Bull. soc. chim. France, 1717 (1960).
58. M. NAUDET and J. PASERO. Fette Seifen Anstrichmittel, **62**, 1110 (1960).
59. D. LEFORT, C. PAQUOT, and J. SORBA. Bull. soc. chim. Belges, **9**, 1385 (1959).
60. D. LEFORT, D. TEMPIER, and J. SORBA. Bull. soc. chim. France, 442 (1960).

Can. J. Chem. Downloaded from www.nrcresearchpress.com by 210.87.254.42 on 09/05/12
For personal use only.

Can. J. Chem. Downloaded from www.nrcresearchpress.com by 210.87.254.105 on 09/05/12
For personal use only.

THE CRYSTAL STRUCTURE OF 1,3-DICHLORONAPHTHALENE[1]

J. TROTTER

ABSTRACT

Crystals of 1,3-dichloronaphthalene are monoclinic with four molecules in a unit cell of dimensions $a = 15.11$, $b = 3.92$, $c = 14.86$ Å; $\beta = 96.0°$; space group $P2_1/n$. The x and z parameters of the chlorine and carbon atoms have been determined from Patterson and Fourier projections along the b-axis. The bond distances in the molecule, determined from the lengths projected on (010) together with estimated orientation angles, are very similar to the corresponding distances in naphthalene.

INTRODUCTION

One of the molecules being studied during investigations of the crystal structures of some naphthalene derivatives was previously reported as 1,2-dichloronaphthalene (1). During the course of the analysis, however, it became evident that the b-axis Patterson projection corresponded not to 1,2-dichloronaphthalene, but to the 1,3-derivative, and melting-point studies revealed that, while the main bulk of the sample was rather impure 1,2-dichloronaphthalene, the well-formed sublimed crystals used in recording the X-ray data were pure 1,3-dichloronaphthalene (2). The present communication gives details and results of the analysis of these sublimed crystals.

EXPERIMENTAL

Crystals of 1,3-dichloronaphthalene, which were formed by sublimation over a period of several months, consist of colorless prisms elongated along the b-axis. The density was measured by flotation in aqueous potassium iodide solution. The unit-cell dimensions and space group were determined from rotation and oscillation photographs of a crystal rotating about the b-axis, $h0l$ and $h1l$ Weissenberg films, and $hk0$ and $0kl$ precession films.

Crystal Data

1,3-Dichloronaphthalene: $C_{10}H_6Cl_2$; molecular weight = 197.1; melting point = 61° C.

Monoclinic; $a = 15.11 \pm 0.04$, $b = 3.92 \pm 0.01$, $c = 14.86 \pm 0.04$ Å; $\beta = 96°00' \pm 10'$.

Volume of the unit cell = 875.4 Å^3.

Density: calculated (with $Z = 4$) = 1.495 g cm^{-3}, measured = 1.494 g cm^{-3}.

Absorption coefficient for X rays: $\lambda = 1.542$ Å, $\mu = 60.6$ cm^{-1}.

Total number of electrons per unit cell = $F(000) = 400$.

Absent spectra: $h0l$ when $(h+l)$ is odd, $0k0$ when k is odd. Space group is $P2_1/n$—C_{2h}^5.

The intensities of the $h0l$ reflections[2] were recorded on Weissenberg exposures for a crystal rotating about the b-axis, using Cu $K\alpha$ radiation, with multiple-film technique to correlate strong and weak reflections. The intensities were estimated visually, the range being about 1500 to 1. The crystal cross section normal to the b-axis was fairly uniform, and no absorption corrections were applied. The structure amplitudes were derived by

[1]*Manuscript received June 12, 1961.*
Contribution from the Department of Chemistry, University of British Columbia, Vancouver 8, B.C.

[2]*The $\bar{1}01$ reflection was cut off by the beam stop.*

the usual formulae for a mosaic crystal, the absolute scale being established later by correlation with the calculated structure factors. Two hundred and twenty-nine independent $h0l$ reflections were observed, representing about 78% of the possible number observable with Cu $K\alpha$ radiation.

STRUCTURE ANALYSIS

The b-axis Patterson projection exhibited no peak corresponding to the Cl–Cl vector in a 1,2-derivative. Taking the two largest peaks on the map as corresponding to Cl–Cl interactions, positions were derived for the two chlorine atoms in the asymmetric unit, and by setting the origin of the Patterson function in turn at these two positions and at the positions related to them by the center of symmetry at the origin of the cell, a vector convergence (minimum) function was plotted. This map indicated quite clearly that the molecule was 1,3-dichloronaphthalene, all 10 carbon atoms being well-resolved, and co-ordinates were obtained for all the chlorine and carbon atoms. Structure factors were calculated for all the observed $h0l$ reflections, using the scattering factor for chlorine of Tomiie and Stam (3) with $B = 4.8$ Å^2, and the curve of Berghuis *et al.* (4) for carbon with $B = 4.8$ Å^2. The discrepancy factor was 28.2%.

Refinement proceeded by computing successive $(F_o—F_c)$ syntheses, and by altering the positional and temperature parameters to minimize the slopes and difference electron densities at the atomic centers. After two cycles the R value had been reduced to 15.5%; observed and calculated structure factors are not listed, but are available from the author. The final F_o synthesis, computed with measured structure amplitudes and calculated signs, is shown in Fig. 1.

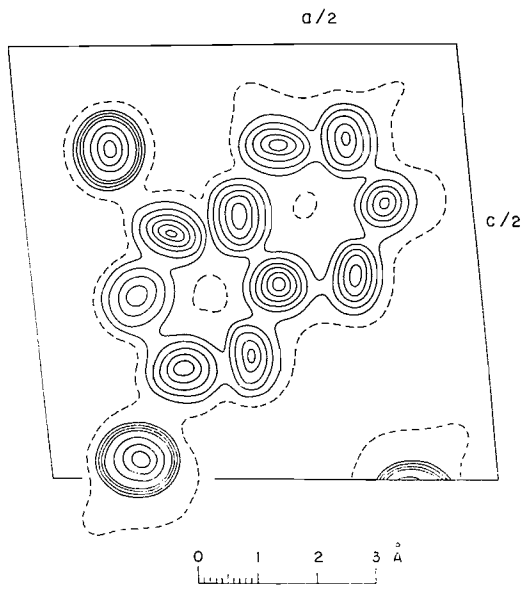


FIG. 1. Electron-density projection along the b-axis. Contours at intervals of 1 e Å^{-2} except at the chlorine atoms, where contours above 5 e Å^{-2} are at intervals of 5 e Å^{-2}; the one-electron line is broken.

No effort has been made to determine the y co-ordinates, since three-dimensional methods would be required, and it is not considered that the problem is sufficiently important to justify the great amount of work which would be involved.

Can. J. Chem. Downloaded from www.nrcresearchpress.com by 210.87.254.105 on 09/05/12
For personal use only.

Co-ordinates and Bond Distances

The final positional parameters are listed in Table I, referred to the crystal axes and

TABLE I

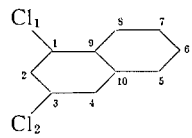
Final positional parameters

Atom	x	z
Cl_1	.1016	.1308
Cl_2	.0991	−.2315
C1	.159	.037
2	.119	−.045
3	.159	−.126
4	.241	−.111
5	.369	−.018
6	.409	.069
7	.371	.145
8	.289	.137
9	.246	.052
10	.281	−.025

expressed as fractions of the unit-cell edges. The projected bond distances calculated from these co-ordinates are given in the second column of Table II. The inclinations of

TABLE II

Bond distances (Å) and orientation angles (θ)



Bond	Projected bond distances, d_{proj}	θ	Bond distances, $d = \frac{d_{proj}}{\cos\theta}$	Mean bond lengths	Naphthalene bond lengths
1—2	1.299	15°	1.342	1.36	1.36
5—6	1.375		1.421		
3—4	1.234	23°	1.342		
7—8	1.238		1.346		
4—10	1.362	15°	1.407	1.42	1.43
8—9	1.357		1.402		
5—10	1.331	23°	1.447		
1—9	1.321		1.436		
2—3	(1.401)	22°	(1.513)	1.42	1.42
6—7	1.313		1.418		
9—10	1.308	22°	1.413	1.41	1.41
Cl_1—1	1.716	13°	1.76	1.76	—
Cl_2—3	1.722	12°	1.76		

the various sets of parallel bonds to the plane of projection, the true bond lengths, and the mean distances were derived as for 1,4-dibromonaphthalene (5), and the values are included in Table II. The agreement between the mean lengths and those in naphthalene (6, 7), which are listed in the final column of the table, is extremely good, indicating that the mean distances are more accurate than the individual values.

Comparison of the inclination angles for the C—Cl bonds and for parallel C—C bonds indicates that Cl_1 is displaced from the naphthalene plane by 0.28 Å. This displacement

Can. J. Chem. Downloaded from www.nrcresearchpress.com by 210.87.254.105 on 09/05/12
For personal use only.

is probably real, and is a result of steric interaction with the *peri* hydrogen atom. The deviation of Cl_2 from the aromatic plane is smaller (0.09 Å) and probably not significant.

Projected distances indicate that all the intermolecular contacts correspond to normal van der Waals interactions.

ACKNOWLEDGMENT

The author thanks the National Research Council for financial support.

REFERENCES

1. J. TROTTER. Acta Cryst. **13**, 276 (1960).
2. J. TROTTER. Proc. Chem. Soc. 78 (1961).
3. Y. TOMIIE and C. H. STAM. Acta Cryst. **11**, 126 (1958).
4. J. BERGHUIS, IJ. M. HAANAPPEL, M. POTTERS, B. O. LOOPSTRA, C. H. MACGILLAVRY, and A. L. VEENENDAAL. Acta Cryst. **8**, 478 (1955).
5. J. TROTTER. Can. J. Chem. **39**, 1574 (1961).
6. S. C. ABRAHAMS, J. M. ROBERTSON, and J. G. WHITE. Acta Cryst. **2**, 238 (1949).
7. D. W. J. CRUICKSHANK. Acta Cryst. **10**, 504 (1957).

Can. J. Chem. Downloaded from www.nrcresearchpress.com by 210.87.254.105 on 09/05/12
For personal use only.

Can. J. Chem. Downloaded from www.nrcresearchpress.com by 210.87.254.5 on 09/05/12
For personal use only.

RADICAL RECOMBINATION REACTIONS

PART II. TRIFLUOROMETHYL AND HEPTAFLUORO-*n*-PROPYL RADICALS[1,2]

G. O. PRITCHARD,[3] G. H. MILLER,[3] AND J. R. DACEY[4]

ABSTRACT

Mixtures of hexafluoroacetone and perfluoro-di-*n*-propyl ketone were photolyzed, and the ratio of the rates of formation of the three fluorocarbons, $R_{C_4F_{10}}/R^{1/2}_{C_2F_6}R^{1/2}_{C_6F_{14}}$, was found to equal 1.77 ± 0.10 over a 107° temperature range.

INTRODUCTION

In this paper we are concerned with the photolytic cogeneration of $CF_3\cdot$ and $C_3F_7\cdot$ radicals in a gas-phase system, and the temperature dependence, if any, of the three recombination reactions:

$$CF_3\cdot + CF_3\cdot \xrightarrow{k_{1-1}} C_2F_6, \qquad [1\text{-}1]$$

$$CF_3\cdot + C_3F_7\cdot \xrightarrow{k_{1-2}} C_4F_{10}, \qquad [1\text{-}2]$$

$$C_3F_7\cdot + C_3F_7\cdot \xrightarrow{k_{2-2}} C_6F_{14}, \qquad [2\text{-}2]$$

with respect to each other.

In a steady-state condition we have

$$k_{1\text{-}2}/k^{1/2}_{1\text{-}1}\,k^{1/2}_{2\text{-}2} = R_{C_4F_{10}}/R^{1/2}_{C_2F_6}R^{1/2}_{C_6F_{14}}, \qquad [I]$$

provided these reactions are the only sources of the three fluorocarbons.

At the pressures used there are no third-body restrictions affecting the recombinations, and the small temperature dependence associated with the collision number will cancel out in expression [I]. Thus any temperature variation of this ratio must be due to differing activation energies for one or all of the processes.

EXPERIMENTAL

The apparatus has essentially been described previously (1). The 3130-Å radiation was collimated by a single quartz lens and a stop, passed through a blue glass (Corning 9863), and into a 157-ml, cylindrical, 10-cm-long quartz reaction cell, fully illuminating it. The cell was surrounded by an outer steam jacket. Refluxing liquids used to attain temperatures other than 100° were xylene, 140°; *o*-dichlorobenzene, 180°; and tetralin, 207°.

The radical sources were the two ketones, $(CF_3)_2CO$ and $(C_3F_7)_2CO$, purified as described previously (2, 3). No detectable impurities were found in the mass spectra. Photolysis of the ketones individually in the temperature range of our experiments yields CO and the corresponding fluorocarbon in a 1:1 ratio via a free-radical mechanism (2, 3).

[1]*Manuscript received June 23, 1961.*
[†]*Contribution from the Chemistry Department, University of California, at Santa Barbara, Goleta, California, and the Chemistry Department, Royal Military College, Kingston, Ontario.*
[2]*For Part I of this series see reference 1.*
[3]*University of California.*
[4]*Royal Military College.*

A Toepler pump was attached to the reaction cell to ensure complete mixing of the ketones before irradiation. After photolysis, the CO was separated at −195° and measured in a gas burette. The remainder of the reaction mixture was condensed into a tube containing thoroughly outgassed distilled water. After the contents had warmed up, the tube was shaken vigorously and reattached to the vacuum system. Blank experiments showed that this procedure removed all of the $(CF_3)_2CO$ and most of the $(C_3F_7)_2CO$ as hydrates. C_2F_6 was then separated on Ward – Le Roy stills at −160°, and C_4F_{10} at −120°. The purity of all the products was checked mass spectrometrically. A fraction collected at −80° was slightly larger than that required by radical balance and contained C_6F_{14} and some unreacted $(C_3F_7)_2CO$. Perfluorohexane was identified unambiguously from the relative peak heights at masses 119 ($C_2F_5^+$), 131 ($C_3F_5^+$), and 169 ($C_3F_7^+$) in the mass spectrum (4).

The ultraviolet spectrum of the heavier ketone was taken on a Cary Model 14 recording spectrophotometer. There is strong absorbance between 2500 and 3600 Å, with structure between 3000 and 3500 Å. The absorbance maximum is at 3130 Å; molar extinction coefficient 32.0 l. mole^{-1} cm^{-1}. This is about four times as large as that for $(CF_3)_2CO$ at 3130 Å (2). Mixtures of the ketones gave additive spectra.

RESULTS

The data are collected in Table I. Due to the clear-cut nature of the photolysis mechanisms, C_6F_{14} has been calculated from CO − $(C_2F_6 + C_4F_{10})$. Consideration of runs 4 to 10 indicates the constancy of the ratio $k_{1\text{-}2}/k_{1\text{-}1}^{1/2}k_{2\text{-}2}^{1/2}$ over 107°, so that further experimentation did not appear worth while.

No experiments below 100° were envisaged due to the temperature and pressure dependence of the quantum yields, especially for $(CF_3)_2CO$, in this range. However, even at 100° in the early experiments (run 3 is given as an example), a suppression of $CF_3\cdot$ products was found. Ratios deduced from them were not considered reliable due to the small amounts of C_2F_6 obtained. Runs 1 and 2 give data for the ketones when they were photolyzed separately. The percentage decompositions are in accord with the high-pressure quantum yields, 0.6 for $(CF_3)_2CO$ and 1.0 for $(C_3F_7)_2CO$ at 100°, and the enhanced absorbance of the heavier over the lighter ketone at 3130 Å. Examination of runs 3, 4, and 5 shows suppression of the $(CF_3)_2CO$ photodecomposition with increasing $(C_3F_7)_2CO$ concentration. This can only be due to the very efficient deactivation of the excited species $(CF_3)_2CO^*$ by the heavier ketone. As expected, this effect lessens with rising temperature.[5] Decrease in the initial $(C_3F_7)_2CO$ concentrations enabled us to approximate to the ideal fluorocarbon product ratio of 1:2:1.

Percentage decompositions were calculated from the ratios $(C_2F_6 + \frac{1}{2}C_4F_{10})/(CF_3)_2CO$ and $[CO - (C_2F_6 + \frac{1}{2}C_4F_{10})]/(C_3F_7)_2CO$. On a time basis the latter are not entirely self-consistent as the voltage to the lamp was not stabilized. For the short period of a particular experiment constant light intensity can be assumed. In any case small sporadic intensity fluctuations are of no consequence. Expression [I] is not subject to stationary-state limitations, and will remain constant until either ketone is completely consumed. We conclude that expression [I] = 1.77±0.10.

[5]*The other possibility of losing* $CF_3\cdot$ *products,*

$$CF_3\cdot + (C_3F_7)_2CO \rightarrow [CF_3(C_3F_7)_2CO\cdot] \rightarrow C_3F_7\cdot + CF_3COC_3F_7,$$

would lead to excess $C_3F_7\cdot$ *products, which was not observed, and contrary to the experimental findings, the effect would increase with temperature as such reactions require an activation energy of about 6–7 kcal/mole (see reference 10).*

Can. J. Chem. Downloaded from www.nrcresearchpress.com by 210.87.254.5 on 09/05/12
For personal use only.

Can. J. Chem. Downloaded from www.nrcresearchpress.com by 210.87.254.5 on 09/05/12
For personal use only.

TABLE I

Run	Temp. (°C)	Time (sec)	Reactants (mole $cc^{-1} \times 10^6$)		Products (mole $\times 10^6$)				k_{1-2}	% decomposition	
			$(CF_3)_2CO$	$(C_3F_7)_2CO$	CO	C_2F_6	C_4F_{10}	C_6F_{14}	$k_{1-1}^{1/2}\ k_{2-2}^{1/2}$	$(CF_3)_2CO$	$(C_3F_7)_2CO$
1	100	600	2.24	—	20.1	20.0	—	—	—	5.72	—
2	100	300	—	1.38	46.7	—	—	—	—	—	21.6
3	100	150	4.30	1.89	32.9	0.64	4.90	27.4	1.17	0.47	10.0
4	100	150	4.81	0.687	19.7	6.10	9.16	4.44	1.76	1.41	8.36
5	100	150	4.38	0.860	26.3	1.95	9.26	15.1	1.71	0.96	14.6
6	100	600	2.06	0.430	58.6	5.85	24.1	28.7	1.86	5.54	60.3
7	140	300	3.65	0.543	38.1	6.57	17.5	14.0	1.82	2.67	26.7
8	180	150	2.15	1.29	25.9	1.24	8.05	16.6	1.78	1.56	10.2
9	180	300	4.81	0.637	50.1	13.3	23.2	13.6	1.73	3.30	25.2
10	207	300	3.61	0.668	46.6	11.7	21.6	13.2	1.74	3.97	23.0

Can. J. Chem. Downloaded from www.nrcresearchpress.com by 210.87.254.5 on 09/05/12
For personal use only.

DISCUSSION

(a) Pre-exponential Ratios

Assuming identical activation energies and steric factors for radical recombination reactions we have $k_{1\text{-}2}/k_{1\text{-}1}^{1/2}k_{2\text{-}2}^{1/2} = Z_{1\text{-}2}/Z_{1\text{-}1}^{1/2}Z_{2\text{-}2}^{1/2}$. By simple collision theory this reduces to approximately 2 in radical–radical systems. (The picture is somewhat more complicated if disproportionation reactions occur.) Using $\sigma CF_3\cdot = 4.0$ Å and $\sigma C_3F_7\cdot = 6.5$ Å, we obtain 2.2.

Kerr and Trotman-Dickenson (5) have shown that the experimental values for the combination of unlike radicals, in many cases, lie close to 2, and are independent of temperature, indicating that combination occurs on every collision. Calvert (6) has pointed out while this may be so for simple alkyl radicals, it is not true where one of the radicals is highly polar as a potential barrier to recombination exists. In the $CH_3\cdot + CF_3\cdot$ system (1) we noted a decrease from 3.0 to 1.8 over 140°, which was attributed to the polarity of the $CF_3\cdot$ radical, leading to a value of $E_{1\text{-}1} = 2$ kcal/mole. It has been pointed out (6, 7) that radicals formed in photolytic systems may not be thermally equilibrated, as evidenced in some cases by increasing disproportionation/recombination ratios with rising temperatures and falling pressure. If the disproportionation,

$$CF_3\cdot + CH_3\cdot \rightarrow CF_3H + CH_2\cdot,$$

occurred to a large extent, increasing with temperature, it could account for the observed decrease in $k_{1\text{-}2}/k_{1\text{-}1}^{1/2}k_{2\text{-}2}^{1/2}$. There was no positive evidence for it (1); also, the reaction has not been suggested in other $CH_3\cdot + CF_3\cdot$ systems (8, 9). The polar effect appears to be real.

Data from other similar systems are scant, as the determination of expression [I] was not the objective of the experiments. For $C_2H_5\cdot + C_3F_7\cdot$, it is 3.0, and admittedly scattered (5), and 2 ± 1 for $CH_3\cdot + C_2F_5\cdot$ (10), both ratios being temperature independent. Other gas-phase values at room temperature are 2.2 for $CF_2Cl\cdot + CF_2ClCF_2\cdot$ (11) and 1.9 for $CF_2Cl\cdot + CFCl_2\cdot$ (12).

Polar effects are being further studied by the cophotolysis of $(CH_3)_2CO$ and $(C_3F_7)_2CO$; the results will be presented in a later publication.

(b) Activation Energies

In the present system we have $E_{1\text{-}2} - \frac{1}{2}E_{1\text{-}1} - \frac{1}{2}E_{2\text{-}2} = 0$. The only reasonable assumption is that all three activation energies are equal. We may infer that there is a barrier to recombination of about 2 kcal/mole for all simple perfluoroalkyl radicals.

If we consider the system

$$X\cdot + R\text{—}H \rightarrow X\text{—}H + R\cdot$$
$$X\cdot + X\cdot \rightarrow X_2,$$

where $X\cdot$ is $CF_3\cdot$, $C_2F_5\cdot$, or $C_3F_7\cdot$, the activation energy of the first reaction will be determined mainly by the R—H and X—H bond strengths, and the repulsive forces between $X\cdot$ and R—H, and X—H and R. (13). As the activation energy for the second reaction remains constant, we may assume that the repulsive forces in the first do not vary significantly with $X\cdot$. If D(X—H) is constant, the activation energy should not vary with $X\cdot$.

Price and Kutschke (10) have summarized the available data for $CF_3\cdot$, $C_2F_5\cdot$, and $C_3F_7\cdot$ radicals. For CH_4 we have the following $E - \frac{1}{2}E$ values (±0.5 kcal): 10.3, 10.6, and 9.5 kcal, and for H_2: 8.8, 11.9, and 12.3 kcal. For $CF_3\cdot$ and $C_3F_7\cdot$ radicals only, we

have for D_2: 9.7 and 13.8 kcal, and for C_2H_6: 7.5 and 9.2 kcal. However, the last figure may be high by 1–2 kcal (14). Some correlation does exist, although $CF_3\cdot + H_2$ and $CF_3\cdot + D_2$ are exceptions.

ACKNOWLEDGMENTS

We wish to thank Mr. K. R. Chang for performing some of the photolyses, and Mr. J. K. Foote for taking the ultraviolet spectra and for helpful discussions. Our thanks are due to the National Science Foundation for a grant-in-aid (G.O.P. and G.H.M.), and to the Defence Research Board of Canada, under Grant 9530/13, for financial assistance (J.R.D.).

REFERENCES

1. G. O. Pritchard and J. R. Dacey. Can. J. Chem. **38**, 182 (1960).
2. P. B. Ayscough and E. W. R. Steacie. Proc. Roy. Soc. A, **234**, 476 (1956).
3. G. H. Miller, G. O. Pritchard, and E. W. R. Steacie. Z. physik. Chem. **15**, 262 (1958).
4. F. L. Mohler, V. H. Dibeler, and R. M. Reese. J. Research Natl. Bur. Standards, **49**, 343 (1952).
5. J. A. Kerr and A. F. Trotman-Dickenson. Chem. & Ind. (London), 125 (1959).
6. J. G. Calvert. Ann. Rev. Phys. Chem. **11**, 41 (1960).
7. J. C. J. Thynne. Proc. Chem. Soc. (London), 18 and 68 (1961).
8. R. A. Sieger and J. G. Calvert. J. Am. Chem. Soc. **76**, 5197 (1954).
9. R. M. Smith and J. G. Calvert. J. Am. Chem. Soc. **78**, 2345 (1956).
10. S. J. W. Price and K. O. Kutschke. Can. J. Chem. **38**, 2138 (1960).
11. R. Bowles, H. Derbyshire, J. R. Majer, and C. R. Patrick. Nature, **185**, 683 (1960).
12. R. Bowles, J. R. Majer, and J. C. Robb. Nature, **187**, 314 (1960).
13. J. M. Tedder. Quart. Revs. (London), **14**, 336 (1960).
14. G. O. Pritchard and G. H. Miller. J. Phys. Chem. **63**, 2074 (1959).

Can. J. Chem. Downloaded from www.nrcresearchpress.com by 210.87.254.5 on 09/05/12
For personal use only.

Can. J. Chem. Downloaded from www.nrcresearchpress.com by 210.87.254.42 on 09/05/12
For personal use only.

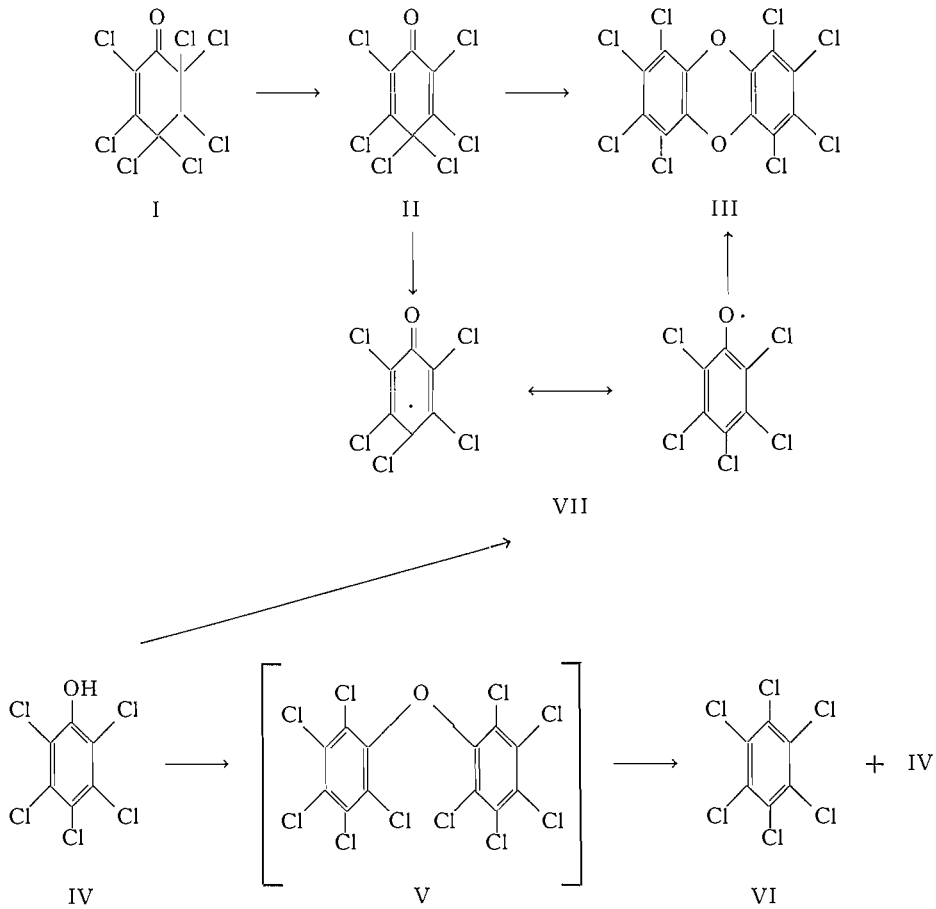
OCTAHALOGENODIBENZO-*p*-DIOXINS[1]

MARSHALL KULKA

ABSTRACT

Pentahalogenophenols have been converted to 1,2,3,4,6,7,8,9-octahalogenodibenzo-*p*-dioxins in almost quantitative yields using the halogens or halogen-producing compounds as initiators of the reaction. It is suggested that an intermediate in this reaction is the pentahalogenophenoxy radical.

In 1872, Merz and Weith (1) heated the potassium salt of pentachlorophenol and obtained a high-melting compound which they called perchlorophenylenoxyd. This compound was also obtained when pentachloroanisole was treated with concentrated sulphuric acid (2). A few years later it was shown that when "α-heptachloroketotetrahydrobenzol" (I) was heated at 180°, it yielded 2,3,4,4,5,6-hexachloro-2,5-cyclohexadienone (II) and when the temperature was raised over 200° the product was the "perchlorophenylenoxyd" (3, 4). Although the formula $(C_6Cl_4O)_x$ was assigned to "perchlorophenylenoxyd" there is little doubt that it was 1,2,3,4,6,7,8,9-octachlorodibenzo-*p*-dioxin (III).



I II III VII IV V VI + IV

[1]*Manuscript received July 7, 1961.*
Contribution from the Research Laboratories, Dominion Rubber Company Limited, Guelph, Ontario.

Can. J. Chem. Vol. 39 (1961)

About fifty years later, Denivelle and his co-workers (5) condensed a salt of pentachlorophenol with 2,3,4,4,5,6-hexachloro-2,5-cyclohexadienone (II) in an inert solvent to form 4-*p*-chlorophenoxy-2,3,4,5,6-pentachloro-2,5-cyclohexadienone. This compound then underwent a number of reactions, including cyclization, to form 1,2,3,4,6,7,8,9-octachlorodibenzo-*p*-dioxin (III).

Finally Sandermann, Stockmann, and Casten (6) were able to prepare III in poor yield directly from pentachlorophenol (IV) by heating it at 300°. The yield was poor because two simultaneous reactions occurred and the main product was hexachlorobenzene (VI). The formation of VI was explained in the following manner. Dehydration of two molecules of pentachlorophenol (IV) yielded the intermediate decachlorodiphenyl ether (V), which underwent cleavage in the presence of hydrogen chloride to form hexachlorobenzene (VI) and pentachlorophenol (IV). In the second reaction, two molecules of pentachlorophenol (IV) formed III with the elimination of two molecules of hydrogen chloride.

The writer has now developed a method for the conversion of pentachlorophenol (IV) to 1,2,3,4,6,7,8,9-octachlorodibenzo-*p*-dioxin (III) in almost quantitative yield by heating the phenol in the presence of an initiator. First of all, the work of Biltz (4) was repeated and it was found that when 2,3,4,4,5,6-hexachloro-2,5-cyclohexadienone (II) was heated over 200°, chlorine gas was liberated and the octachlorodibenzo-*p*-dioxin (III) was formed in high yield. From this observation the following mechanism of the reaction II → III became evident. Under the influence of heat, II dissociates to chlorine and the pentachlorophenoxy radical VII. Two of the radicals then associate, eliminate two chlorine atoms, and form III.

In view of the fact that hindered phenols can be oxidized to the corresponding phenoxy radicals (7, 8) it was decided to search for an oxidant which would convert pentachlorophenol (IV) to the pentachlorophenoxy radical VII and thus provide a method of preparing III from pentachlorophenol. 2,3,4,4,5,6-Hexachloro-2,5-cyclohexadienone (II) filled the requirements of such an oxidant because it not only liberated an oxidizing agent (chlorine) on being heated but also was converted to III. When an equimolecular mixture of pentachlorophenol (IV) and 2,3,4,4,5,6-hexachloro-2,5-cyclohexadienone (II) was heated under reflux for 16 hours in 1,2,4-trichlorobenzene as solvent, or at 250–300° for 15 minutes without solvent, octachlorodibenzo-*p*-dioxin (III) was formed in 85% yield. Furthermore, the amount of II could be decreased to the point where almost catalytic quantities were sufficient to initiate the reaction of IV → VII → III. The reason for this becomes evident when one realizes that the chlorine liberated in the reaction VII → III can be used in the oxidation of IV to VII. An outside source of chlorine is necessary only to initiate the reaction and to replenish undue losses from the internal source. It is interesting to note that in the reaction VII → III, the ortho chlorines are eliminated, and little, if any, para elimination occurs. No poly(1,4-phenylene oxide) of the type described by Price (8) could be detected.

Although 2,3,4,4,5,6-hexachloro-2,5-cyclohexadienone (II) is a very convenient initiator of the reaction IV → VII → III, it can be replaced by elementary halogens. When chlorine gas was bubbled slowly into a boiling solution of pentachlorophenol (IV) in 1,2,4-trichlorobenzene, the octachlorodibenzo-*p*-dioxin (III) was formed in 82% yield. Bromine and iodine were not as effective initiators as chlorine.

1,2,3,4,6,7,8,9-Octabromodibenzo-*p*-dioxin and 1,2,4,6,7,9-hexabromo-3,8-dichlorodibenzo-*p*-dioxin were prepared similarly from the corresponding phenols, showing that the method may have general application.

Can. J. Chem. Downloaded from www.nrcresearchpress.com by 210.87.254.42 on 09/05/12
For personal use only.

Can. J. Chem. Downloaded from www.nrcresearchpress.com by 210.87.254.42 on 09/05/12
For personal use only.

EXPERIMENTAL

2,3,4,4,5,6-Hexachloro-2,5-cyclohexadienone (II)

A reaction mixture of pentachlorophenol (500 g), *sym*-tetrachloroethane (400 ml), and iron powder (0.5 g) was stirred and heated at 90–100° while a slow stream of chlorine gas was passed in. When the weight increased by 80 g (12 hours) the dark reaction mixture was filtered and the filtrate concentrated *in vacuo* and allowed to cool overnight. The heavy, yellow crystals were filtered, washed with petroleum ether and with methanol, and dried. The yield from three successive crops was 444 g or 79%, and the product melted at 105–106°. The reported melting point is 106–107° (9).

1,2,3,4,6,7,8,9-Octachlorodibenzo-p-dioxin (III)

(a) From 2,3,4,4,5,6-Hexachloro-2,5-cyclohexadienone (II)

The hexachlorocyclohexadienone (II) (20 g) was heated at 270–280° in an atmosphere of carbon dioxide for ½ hour. The resulting cake was crystallized twice from 1,2,4-trichlorobenzene, yielding white needles (11 g or 73%) melting at 330–332°. Anal. Calc. for $C_{12}Cl_8O_2$: C, 31.30; Cl, 61.75. Found: C, 31.74, 31.61; Cl, 62.26, 61.74. This compound sublimed readily *in vacuo* (12 mm pressure). It was very stable and crystallized from hot, concentrated sulphuric acid without charring.

(b) From Pentachlorophenol Using II as Initiator

A solution of pentachlorophenol (IV) (40 g), 2,3,4,4,5,6-hexachloro-2,5-cyclohexadienone (II) (2 g), and 1,2,4-trichlorobenzene (80 ml) was heated under reflux for 16 hours. Hydrogen chloride and chlorine were evolved. The solution was allowed to cool and the white crystalline precipitate was filtered, washed with methanol, and dried. The product weighed 30 g (86%) and melted at 330°.

In another experiment an equimolecular mixture of pentachlorophenol (IV) and II was treated as above. The yield of III, based on the combined weights of II and IV, was 85%.

(c) From Pentachlorophenol Using Chlorine as Initiator

A solution of pentachlorophenol (IV) (25 g) in 1,2,4-trichlorobenzene (75 ml) was heated under reflux for 6 hours while chlorine gas was bubbled slowly into the reaction mixture. Then the refluxing was continued for another 10 hours without the introduction of chlorine. The resulting solution was allowed to cool, the white crystals were filtered, washed with methanol, and dried, m.p. 325–328°. The yield was 18 g or 83%.

(d) From Pentachlorophenol Using Bromine as Initiator

The experiment was carried out as in (*c*) but instead of the chlorine, 2 drops of bromine were added every 2 hours for the first 6 hours. The yield of III was 52%.

(e) From Pentachlorophenol Using Iodine as Initiator

The experiment was carried out as in (*c*) but instead of the chlorine, solid iodine (0.2 g) was added to the reaction mixture. Iodine vapors were visible in the reaction flask throughout the whole reaction time of 16 hours. The yield of III was 23%.

1,2,3,4,6,7,8,9-Hexabromodibenzo-p-dioxin

A mixture of pentabromophenol (35 g) and 2,3,4,4,5,6-hexachloro-2,5-cyclohexadienone (II) (0.2 g) was heated at 310–320° for ½ hour and then at 360° for a few minutes. Hydrogen bromide and bromine were evolved. The cooled product, on crystallization from 1,2,4-trichlorobenzene, yielded white plates (15 g or 52%) melting at 403–406°. Anal. Calc. for $C_{12}Br_8O_2$: Br, 78.43. Found: Br, 78.95, 79.02.

2,3,5,6-Tetrabromo-4-chlorophenol

Bromine (320 g) was added dropwise over 6 hours to a stirred solution of *p*-chlorophenol (64 g) in *sym*-tetrachloroethane (200 ml) and iron powder (0.2 g), in a reaction flask fitted with a condenser, stirrer, and dropping funnel. The temperature was kept at 90–100° by heating the mixture. Then the dark reaction mixture was heated at 100–120° for 15 hours and allowed to cool. The white precipitate was filtered and crystallized from benzene. The product (135 g) melted at 210–212°. A small portion, when crystallized from benzene–methanol, melted at 213–214° (lit. (10) m.p. 215°). Anal. Calc. for C_6HClBr_4O: C, 16.20; H, 0.23. Found: C, 16.12, 16.79; H, 0.70, 0.80.

1,2,4,6,7,9-Hexabromo-3,8-dichlorodibenzo-p-dioxin

A mixture of 2,3,5,6-tetrabromo-4-chlorophenol (30 g) and 2,3,4,4,5,6-hexachloro-2,5-cyclohexadienone (II) (0.2 g) was heated at 300–310° for 15 minutes and then at 350° for 15 minutes. The cooled product was crystallized from 1,2,4-trichlorobenzene, yielding 15 g (62%) of almost white crystals melting at 385–388°. Anal. Calc. for $C_{12}Cl_2Br_6O_2$: C, 19.5. Found: C, 19.84, 19.75.

In another experiment, 1,2,4-trichlorobenzene was used as solvent. After the solution had been heated for 16 hours the reaction was not complete because a considerable amount of the starting 2,3,5,6-tetrabromo-4-chlorophenol was recovered, and the yield of the product melting at 385–388° was only 36%.

REFERENCES

1. V. Merz and W. Weith. Ber. **5**, 460 (1872).
2. L. Hugounenq. Ann. chim. phys. **20** [6], 546 (1890).
3. Th. Zinke. Ber. **27**, 550 (1894).
4. H. Biltz. Ber. **37**, 4009 (1904).
5. L. Denivelle, R. Fort, and V. Pham. Compt. rend. **248**, 2766 (1959); Chem. Abstr. **54**, 6612 (1960).
6. W. Sandermann, H. Stockmann, and R. Casten. Ber. **90**, 690 (1957).
7. H. S. Banchard. J. Org. Chem. **25**, 264 (1960).
8. G. D. Staffin and C. C. Price. J. Am. Chem. Soc. **82**, 3632 (1960).
9. R. Fort. Ann. chim. (Paris), **4** [13], 203 (1959); Chem. Abstr. **54**, 19533 (1960).
10. M. Kohn and G. Domotor. Monatsh. **47**, 207 (1926); Chem. Abstr. **21**, 574 (1927).

Can. J. Chem. Downloaded from www.nrcresearchpress.com by 210.87.254.42 on 09/05/12
For personal use only.

Can. J. Chem. Downloaded from www.nrcresearchpress.com by 210.87.254.5 on 09/05/12
For personal use only.

α-KETOETHERS

II. INFRARED SPECTRA AND ROTATIONAL ISOMERISM OF PHENACYL ETHERS[1,2]

PETER YATES,[3] SHERRY LIPINSKY, AND DOROTHEA VOSSIUS

ABSTRACT

Bifurcation of the carbonyl-stretching bands in the infrared spectra of several phenacyl ethers has been observed and is interpreted in terms of rotational isomerism.

The infrared spectra of α-haloketones have been the subject of intensive study during the past decade. As a result of the work of Jones, Corey, Brutcher, and others, the dependence of the carbonyl-stretching frequency of cyclic α-haloketones on their geometry has been elucidated (2). Recently Bellamy and his collaborators (3) have studied the infrared spectra of acyclic α-chloroketones and have observed that these frequently show the presence of two carbonyl-stretching bands. Jones and Spinner (4) have also observed such bifurcation in the spectra of certain other types of α-substituted ketones. We report here a cognate phenomenon in the case of several α-ketoethers.

The positions of the carbonyl-stretching bands of these compounds in carbon disulphide solution are shown in Table I, together with those of the parent ketones and of two

TABLE I

Carbonyl-stretching bands of ketoethers and their parent ketones

Compound						
No.	Formula	R	Source	$\lambda_{max}^{CS_2}$ (μ)[a]	Δλ (μ)	ϵ_1/ϵ_2[b]
1	$C_6H_5COCH_2R$	H	[c]	5.92		
2	,,	OCH_3	[d]	5.86, 5.93	0.07	1.3
3	,,	OC_2H_5	[d]	5.86, 5.93	0.07	1.2
4	,,	OC_4H_9-n	[d]	5.86, 5.93	0.07	1.2
5	,,	$OC_{10}H_{21}$-n	[e]	5.86, 5.93	0.07	1.2
6	,,	OC_6H_5	[f]	5.85, 5.93	0.08	1.4
7	,,	CH_2OCH_3	[g]	5.93		
8	,,	$CH_2OC_2H_5$	[g]	5.92		
9	,,	C_6H_5	[h]	5.91,[i] 5.94	0.03	0.77
10	$C_6H_5COCHC_6H_5$ | OCH_3		[j]	5.89, 5.94	0.05	0.62
11	$C_6H_5CH_2COCH_3$		[c]	5.78,[i] 5.82	0.04	0.73
12	$C_6H_5CH_2COCH_2OCH_3$		[k]	5.78,[i] 5.80	0.02	1.1

[a] Concentration: ca. 2%.
[b] Ratio of apparent extinction coefficients of lower and higher wave-length bands.
[c] Commercial.
[d] See Experimental section.
[e] Prepared by Dr. T. J. Clark by the method of Newman and Beal (6).
[f] Ref. 1.
[g] Prepared by the method of F. Straus and A. Berkow. Ann. **401**, 121 (1913).
[h] Prepared by Dr. D. R. Moore by the method of D. A. Ballard and W. M. Dehn. J. Am. Chem. Soc. **54**, 3970 (1952).
[i] This band often appeared as a shoulder.
[j] Prepared by Dr. B. L. Shapiro by the method of E. Fischer. Ber. **26**, 2412 (1893).
[k] Cf. R. B. Moffett and R. L. Shriner. Org. syntheses, Coll. Vol. III, 562 (1955).

[1] *Manuscript received June 8, 1961.*
Contribution from the Department of Chemistry, Harvard University, Cambridge, Massachusetts.
[2] *For Part I of this series see reference 1.*
[3] *Present address: Department of Chemistry, University of Toronto, Toronto, Ontario.*

Can. J. Chem. Downloaded from www.nrcresearchpress.com by 210.87.254.5 on 09/05/12
For personal use only.

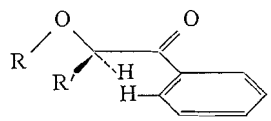
β-ketoethers. Several features of these data may be noted.

(i) The α-ketoethers of type $C_6H_5COCH_2OR$ (compounds 2–6) show a band close in position to the single band of acetophenone, together with a second band at lower wave length; the band separation of 0.07–0.08 μ is identical to that observed by Bellamy for compounds of type $ArCOCH_2Cl$ in solution in carbon tetrachloride.

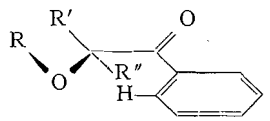
(ii) The two β-ketoethers of type $C_6H_5COCH_2CH_2OR$ (compounds 7 and 8) each show a single band close in position to that of acetophenone.

(iii) The remaining α-ketoethers (compounds 10 and 12) show splitting of the carbonyl band; the splitting is smaller, however, than that observed for the compounds of type $C_6H_5COCH_2OR$, and the parent ketones (compounds 9 and 11) also show a small splitting of their carbonyl bands.

The splitting of the carbonyl bands of the ketoethers of type $C_6H_5COCH_2OR$ can best be interpreted in terms similar to those suggested by Bellamy in the case of the phenacyl halides. The band at lower wave length is assigned to a rotational isomer in which the dipole associated with the CH_2—O—R group is in the same plane as that of the carbonyl group and acts in approximately the same direction, while the other band is assigned to a rotational isomer in which the CH_2—O—R dipole lies appreciably out of this plane. Although detailed interpretation in the present case is made more difficult by the greater multiplicity of rotational isomers, examination of scale molecular models indicates that the two types of rotational isomers most likely to be present are I and II. The isomer



I, R′ = H, R = alkyl or C_6H_5
VIII, R′ = C_6H_5, R = CH_3

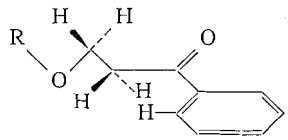


II, R′ = R″ = H, R = alkyl or C_6H_5
VI, R′ = C_6H_5, R″ = H, R = CH_3
VII, R′ = H, R″ = C_6H_5, R = CH_3

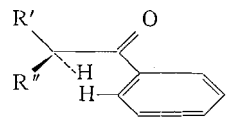
I in which the CH_2—O bond is cis to the C=O bond is considered to give rise to the carbonyl band at lower wave length because of dipole interaction, while the gauche isomer II is assigned the higher wave-length band, which is close in position to the band of acetophenone.* It was found that the spectra of these ketoethers in solvents of increased polarity show an increase in the relative intensity of the lower wave-length band, as would be predicted on the basis of these assignments, and as observed previously in the case of the phenacyl halides (3).

The occurrence of a single carbonyl-stretching band in the spectra of the two β-ketoethers, $C_6H_5COCH_2CH_2OR$, may be attributed both to the attenuation of the field effect of the CH_2—O—R dipole upon the C=O dipole with increasing separation and to the probable large preponderance of the single type of rotational isomer III. It is of interest that the CH_2—O—R dipole in this species is directed approximately in the trans sense relative to the C=O dipole and thus any residual field effect would tend to increase the wave length of its carbonyl-stretching band relative to that of acetophenone. The fact that the single band of these two β-ketoethers falls very close to that of acetophenone implies that either this residual effect is negligible or that it is compensated by an inductive effect, which would operate in the opposite sense (cf. refs. 3 and 4).

House and Blaker (5) have interpreted the presence of two carbonyl bands in the infrared spectra of glycidic esters in related terms.



III



IV, R′ = C_6H_5, R″ = H
V, R′ = H, R″ = C_6H_5

The splitting of the carbonyl band of the parent ketone, deoxybenzoin (compound 9), is again most probably due to the presence of two types of rotational isomers,* i.e. IV and V. The fact that the related α-ketoether (compound 10) shows two bands in closely similar positions to those of the parent suggests that it exists in carbon disulphide solution mainly as rotational isomers of types VI and VII, but not VIII, which is analogous to I and would be expected to give rise to a band at a significantly lower wave length.† Similar considerations apply to the cases of phenylacetone (compound 11) and the related α-ketoether, compound 12; here, the increased number of possible types of rotational isomers prohibits detailed discussion, but again the close similarity of the positions of the bands of the ketoether to those of the parent ketone suggests that rotational isomers in which the C—O—CH_3 group is disposed with respect to the C=O group, as in I and VIII, do not make a major contribution to the rotational isomer mixture.

EXPERIMENTAL

Sources and Purification of Compounds

The sources of the compounds, other than the α-alkoxyacetophenones, are given in Table I. The α-alkoxyacetophenones were prepared by the acid-catalyzed decomposition of α-diazoacetophenone in alcoholic solutions by a method exemplified by the case of α-butoxyacetophenone below. The compounds were purified by distillation, molecular distillation, or crystallization, and their physical properties were checked with those reported in the literature or with those of samples prepared by standard methods in our laboratory.

α-Butoxyacetophenone‡

α-Diazoacetophenone (0.500 g) was added to a solution of *p*-toluenesulphonic acid monohydrate (0.045 g) in butanol (10 ml) maintained under a nitrogen atmosphere. Gas evolution began immediately. The mixture was heated under reflux at 98° for 2.75 hours. The excess of 1-butanol was removed under reduced pressure and the residue was subjected to molecular distillation at 78° (2 mm). The product was obtained as a pale yellow liquid in 70% yield. A second molecular distillation provided a colorless sample whose infrared spectrum was indistinguishable from that of the once-distilled product. This was characterized as its 2,4-dinitrophenylhydrazone which was recrystallized from methanol and had m.p. 136–137°.

Anal. Calc. for $C_{18}H_{20}N_4O_5$: C, 58.06; H, 5.41; N, 15.05. Found: C, 58.33; H, 5.49; N, 15.02.

**Jones and Spinner (4) have previously reported the splitting of the carbonyl-stretching band of deoxybenzoin in carbon tetrachloride solution and attributed it to rotational isomerism.*

†Examination of scale molecular models suggests that steric factors might well favor the preponderance of isomers of type VI and VII over those of type VIII.

‡This method is a modification of that of Newman and Beal (6).

Can. J. Chem. Downloaded from www.nrcresearchpress.com by 210.87.254.5 on 09/05/12
For personal use only.

Infrared Spectra

The spectra were recorded with a Perkin–Elmer Model 21 spectrophotometer with NaCl prism and were calibrated against the atmospheric band at 5.88 μ.

REFERENCES

1. P. YATES, D. G. FARNUM, and G. H. STOUT. J. Am. Chem. Soc. **80**, 196 (1958).
2. E. A. BRAUDE and E. S. WAIGHT. *In* Progress in stereochemistry. Vol. I. *Edited by* W. Klyne. Butterworths Scientific Publications, London. 1954. p. 169. R. N. JONES and C. SANDORFY. *In* Chemical applications of spectroscopy. *Edited by* W. West. Interscience, New York. 1956. p. 477. L. J. BELLAMY. The infra-red spectra of complex molecules. 2nd ed. Methuen, London. 1958. p. 400.
3. L. J. BELLAMY, R. C. THOMAS, and R. L. WILLIAMS. J. Chem. Soc. 3704 (1956). L. J. BELLAMY and R. L. WILLIAMS. J. Chem. Soc. 4294 (1957). L. J. BELLAMY. The infra-red spectra of complex molecules. 2nd ed. Methuen, London. 1958. p. 400.
4. R. N. JONES and E. SPINNER. Can. J. Chem. **36**, 1020 (1958).
5. H. O. HOUSE and J. W. BLAKER. J. Am. Chem. Soc. **80**, 6389 (1958).
6. M. S. NEWMAN and P. F. BEAL. J. Am. Chem. Soc. **72**, 5161 (1950).

Can. J. Chem. Downloaded from www.nrcresearchpress.com by 210.87.254.5 on 09/05/12
For personal use only.

Can. J. Chem. Downloaded from www.nrcresearchpress.com by 210.87.254.5 on 09/05/12
For personal use only.

THE EFFECT OF THE AMBIENT OXYGEN ON THE ELECTRICAL PROPERTIES OF AN EVAPORATED FILM OF PENTACENE[1]

HARUO KURODA[2] AND E. A. FLOOD

ABSTRACT

The "oxygen effect" on the dark current as well as that on the photocurrent was investigated using thin evaporated films of pentacene, 1,2-benzpentacene, 1,2,8,9-dibenzpentacene, 6,13-diphenylpentacene, and 5,7,12,14-tetraphenylpentacene. No oxygen effect could be detected in the dark current.

From the photocurrent dependence on oxygen pressure and from the rate of photocurrent decay, it is concluded that additional charge carriers are produced on illumination by photo-excitation of a surface complex.

INTRODUCTION

Ambient gases exert a considerable influence on the surface photoconductivities and semiconductivities of a number of organic crystals. In the case of anthracene crystals, the electron "acceptor" type gases O_2, NO, SO_2, HCl, BF_3, etc. increase the photoconductivity while the donor gases NH_3, $(CH_3)_2O$, $(CH_3)N$, etc., which are usually less strongly adsorbed, decrease the photoconductivity (1).

Chynoweth has suggested that ambient oxygen forms a surface peroxide with anthracene which decreases the rate of recombination of the charge carriers (2). Bree and Lyons (3) have adduced evidence that unstable surface peroxides are formed on exposure of anthracene to oxygen and they have suggested that an "anthracene peroxide biradical" is largely responsible for the increased conductivity.

In previous papers we have shown that the semiconductivities of films of mesonaphthodianthrene formed by sublimation are increased markedly by exposure to oxygen (4, 5). It was further shown that oxygen produces a new conduction mechanism with a lower activation energy, and we have attributed the effect to the formation of a complex between oxygen and the surface molecules. A similar oxygen effect might be expected in the case of crystals of other aromatic molecules which are reactive to oxygen. However, although pentacene is relatively highly reactive towards oxygen and readily forms an addition compound when solutions of pentacene are exposed to air, oxygen has but little effect on the dark-current semiconductivity of pentacene films.

In what follows we present the results of some exploratory experiments on the effect of ambient oxygen on the electrical properties of "evaporated films" of pentacene and of some pentacene derivatives. As will be seen, the effect of oxygen on these films is quite different from its effect on the mesonaphthodianthrene film.

EXPERIMENTAL

The experimental procedures and the equipment used were essentially the same as described previously (5), except for the addition of the photoconductivity cell which is shown in Fig. 1. The evaporated films were prepared by high-vacuum sublimation onto a teflon substrate carrying two carbon electrodes which had been painted on previously using a water suspension of graphite (Aquadag). The evaporated films of hydrocarbon

[1]*Manuscript received July 11, 1961.*
Contribution from the Division of Pure Chemistry, National Research Council, Ottawa, Canada.
Issued as N.R.C. No. 6490.
[2]*National Research Council Postdoctorate Fellow. Present address: Department of Chemistry, Faculty of Science, University of Tokyo, Hongo, Tokyo, Japan.*

were of the order of a few microns in thickness. A tungsten-filament lamp was used as a light source. Direct-current voltage was applied between the two electrodes and the current through the film was measured by means of a Hewlett and Packard d-c. microvoltammeter model 425, together with a suitable recorder.

Pentacene, 1,2-benzpentacene,[3] and 1,2,8,9-dibenzpentacene[3] were obtained from L. Light and Company. 6,13-Diphenylpentacene and 5,6,12,14-tetraphenylpentacene were kindly supplied by Dr. R. N. Jones of the National Research Council, Ottawa.

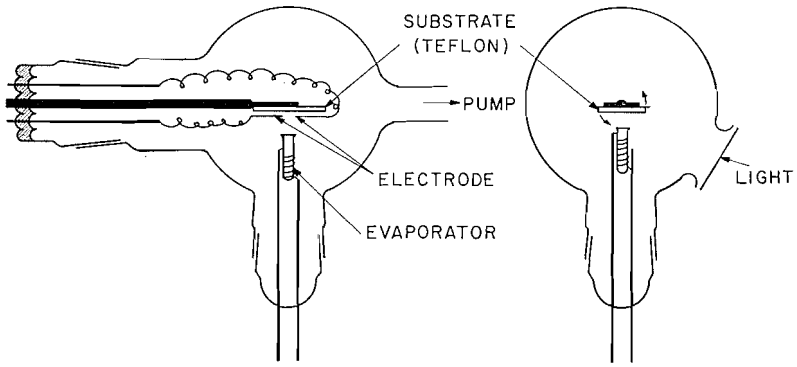


FIG. 1. Cell for the measurement of the oxygen effect on photoconduction.

RESULTS AND DISCUSSIONS

A. Dark Current

The temperature dependence of the dark current was determined, in nitrogen, with each film immediately after its preparation. In the temperature range 0° C to 150° C, the temperature dependence of the dark current was found to obey the exponential law

$$[1] \qquad i_{\text{dark}} = i_0 \exp(-E/kT),$$

where E is the activation energy for the semiconduction. No break was found in the $\log i$ vs. $(1/T)$ curves corresponding to any of the films of pentacene and pentacene derivatives studied. The values of the activation energies determined from experimental results are listed in Table I.

TABLE I

Activation energy of semiconduction

Compound	E (ev)
Pentacene	0.81
Diphenylpentacene	0.80
Tetraphenylpentacene	0.81
Dibenzpentacene	0.75
Benzpentacene	0.86

Although the reactivity of pentacene toward oxygen is as high as that of mesonaphthodianthrene, no appreciable change in either the dark current or the dark-current temperature dependence could be detected on exposure of pentacene films to oxygen. This

[3]*According to A. M. Patterson, L. T. Capell, and D. F. Walker ("The ring index". 2nd ed. American Chemical Society. 1960) the preferred names of these compounds are benzo[a]pentacene for 1,2-benzpentacene and dibenzo[a,l]pentacene for 1,2,8,9-dibenzpentacene.*

Can. J. Chem. Downloaded from www.nrcresearchpress.com by 210.87.254.5 on 09/05/12
For personal use only.

behavior is in marked contrast to the effect of oxygen adsorption on the dark current observed with mesonaphthodianthrene. Films of the other pentacene derivatives studied in this work behaved in a manner similar to that of pentacene films.

Of course we cannot conclude from this behavior that the surface reactions between these organic crystals and oxygen are purely physical adsorption or Van der Waals interactions, since the activation energy required to liberate a charge carrier from the surface complex could be higher than that of the semiconduction process in the bulk of the crystal or in the bulk of the microcrystalline mass. This seems not improbable in view of the reactivities of these pentacenes toward oxygen.

B. Change in Photocurrent on Exposure to Oxygen

The change in photocurrent of a freshly deposited pentacene film on exposure to oxygen is shown in Fig. 2. On exposure of the film to oxygen under 200 mm Hg pressure,

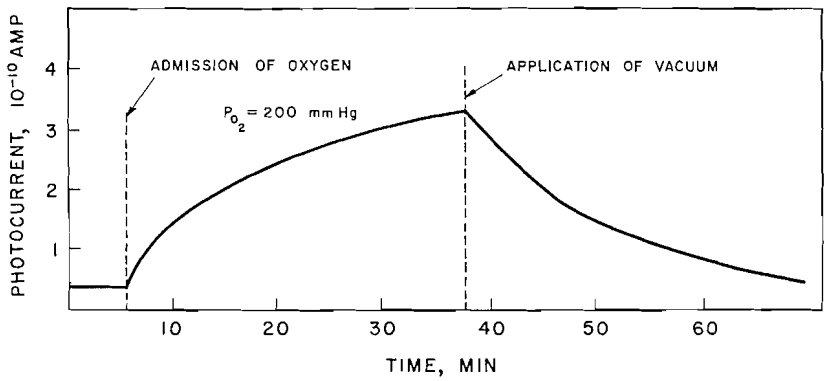


FIG. 2. Change in photocurrent through a pentacene film on exposure to oxygen.

the photocurrent rises slowly from the high-vacuum value and reaches a considerably higher stationary value in something over an hour. On evacuation, the photocurrent decreases, gradually approaching the original high-vacuum photocurrent.

Evidently the oxygen effect is reversible and the interaction between the surface and the oxygen molecule is not very strong. These rates of change are temperature dependent, the rates being higher at the higher temperatures.

Oxygen adsorption influences not only the magnitude of the photocurrent but also the rate of response to illumination. In the absence of oxygen the current through a pentacene film rises rapidly on exposure to light, taking less than a minute to reach its stationary value. In the presence of oxygen, however, the behavior is quite different. On exposure to light, the current rises rapidly to about the same value as in the case of the oxygen-free film, but the current continues to rise slowly until a considerably higher stationary value is obtained. When the light is extinguished, a rapid decrease in photocurrent is shown, the magnitude of its decrease being equal to that of the initial rapid rise; the photocurrent then decays slowly. The behavior is illustrated in Fig. 3. The rates of rise and fall of the current are temperature dependent, being higher at the higher temperatures.

If the photocurrent is observed with a light pulse of short duration (5–6 seconds) in place of the long continuous illumination, the height of the photocurrent pulse is not changed appreciably by exposure to oxygen. These facts suggest that two distinct

Can. J. Chem. Downloaded from www.nrcresearchpress.com by 210.87.254.5 on 09/05/12
For personal use only.

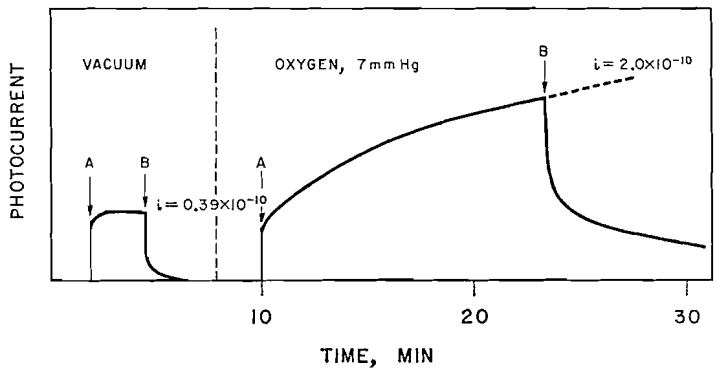


FIG. 3. Response of photocurrent to illumination. Light is admitted at A and shut off at B.

mechanisms are involved in the photoconduction process. In order to illustrate this situation more clearly, the following experiment was carried out. A pentacene film was exposed to oxygen for a long enough period for adsorption equilibrium to be attained. The film with ambient oxygen was then illuminated continuously until the stationary photocurrent was reached. At this point the continuous illumination was shut off and the sample subjected to short light pulses at 1-minute intervals. The photocurrent responses corresponding to the above experiment are shown in Fig. 4.

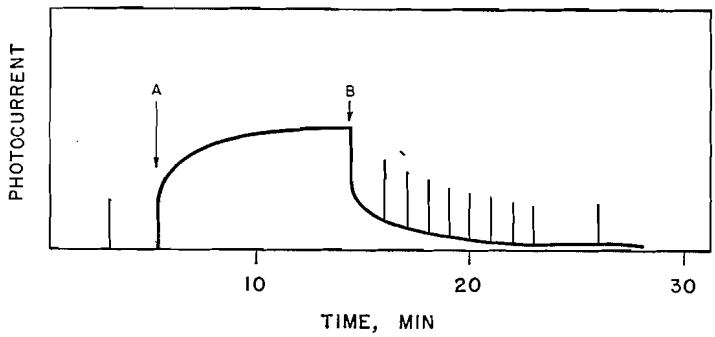


FIG. 4. Response of photocurrent to illumination in ambient oxygen. Continuous illumination is given between A and B.

It is interesting to note that the "heights" of the photocurrent pulses observed during the slow decay process are of almost the same magnitude as that of the pulse observed either for an oxygen-free film or for a film in oxygen before continuous illumination. This strongly suggests that the photocurrent observed in ambient oxygen consists of two more or less independent components, one of which has a short lifetime and is not sensitive to ambient oxygen while the other component has a relatively long lifetime and is oxygen sensitive. We shall represent the first of these photocurrent components by i_1 and the second, oxygen-sensitive component by $i_2(p)$, and write for the total photocurrent[4]

$$i = i_1 + i_2(p). \qquad [2]$$

[4]*Under our experimental conditions i_1 corresponds very approximately to an apparent conductivity of the order of 10^{-11} to 10^{-12}. The intrinsic conductivity of pentacene (30°) is of the order of 10^{-14}; anthracene, 10^{-18}; carbons, 10^{-7} to 1; graphite, $\geqslant 10^{3}$.*

Can. J. Chem. Downloaded from www.nrcresearchpress.com by 210.87.254.5 on 09/05/12
For personal use only.

Can. J. Chem. Downloaded from www.nrcresearchpress.com by 210.87.254.5 on 09/05/12
For personal use only.

Films of 1,2-benzpentacene, 1,2,8,9-dibenzpentacene, and 6,13-diphenylpentacene exhibit oxygen-sensitive photoconductivities which are quite similar to those of the pentacene films.

Molecules in the pentacene crystal are closely packed as they are in crystals of anthracene and tetracene; hence, it is unlikely that the oxygen molecule can penetrate deeply into these crystals. In the case of aromatic molecules having substituent groups as large as rubrene (6,5,11,12-tetraphenylnaphthacene) we might expect a somewhat different situation, and, in fact, it is known that photooxidation can take place in the bulk of the rubrene crystal (6). Although the phenyl groups in 5,7,12,14-tetraphenylpentacene are not adjacent, as they are in rubrene, we might expect the crystals of the tetraphenylpentacene to be also rather loosely packed and that a transannular peroxide could be formed either by direct oxidation or by photooxidation. On this basis one might expect the "oxygen effect" on the photoconductivities of tetraphenylpentacene films to be larger than those on films of the other pentacenes. However, surprisingly enough, no oxygen effect could be detected at all, either in the photocurrent or in the dark current when films of 5,7,12,14-tetraphenylpentacene were examined experimentally.

While in solution, pentacene can be oxidized by exposure to oxygen, forming a transannular peroxide; in the case of the solid, the oxygen molecule cannot penetrate the closely packed crystal and appreciable oxidation of the solid does not normally occur on exposure to oxygen. It seems, therefore, safe to assume that under our experimental conditions, "oxide" formation is limited to the surface of the pentacene crystal. Thus in equation [2], i_1 is considered to be bulk photoconductivity while $i_2(p)$ is considered to be associated with surface states and hence sensitive to surface "oxide" formation.

C. Stationary Photocurrent and Oxygen Pressure

The stationary photocurrent determined after a long, continuous illumination is dependent on the oxygen pressure, as shown in Fig. 5.

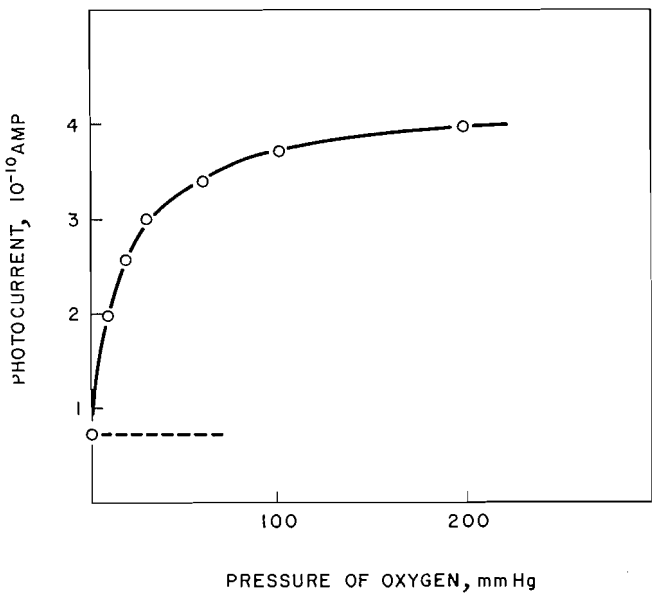


FIG. 5. Dependence of photocurrent on oxygen pressure.

Assuming that the adsorption of oxygen can be expressed by means of a Langmuir-type equation, we can write,

$$\frac{\theta}{1-\theta} = k_1 p, \quad [3]$$

where θ is the fractional surface area covered with oxygen at the pressure p, and k_1 the appropriate proportionality constant. When it is assumed that

$$i_2(p) = k_2\theta, \quad [4]$$

then

$$\frac{k_2}{i_2(p)} = (1/k_1)(1/p)+1 \quad [5]$$

and

$$i_2(p) = \Delta i(p) = i_{\text{photo}}(p) - i_{\text{photo}}(0). \quad [6]$$

Thus equation [5] can be expressed as

$$(1/\Delta i) = (1/k_1k_2)(1/p) + (1/k_2), \quad [7]$$

i.e., $1/\Delta i(p)$ is a linear function of the reciprocal of the oxygen pressure. In Fig. 6 the

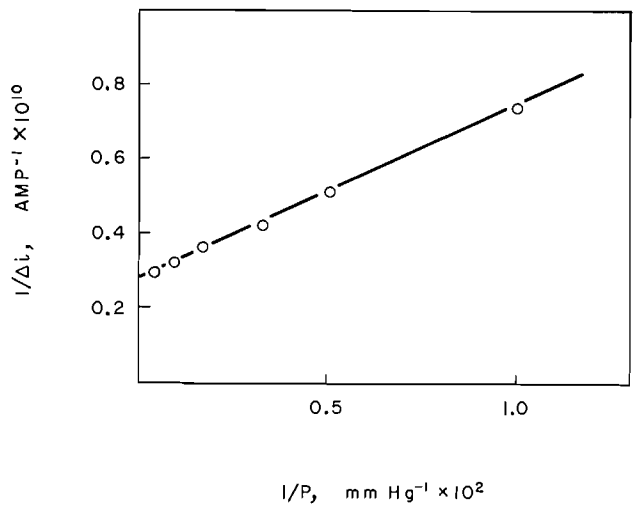


FIG. 6. Plot of reciprocal of photocurrent against reciprocal pressure.

reciprocals of the observed values of $\Delta i(p)$ are plotted against the reciprocals of the oxygen pressures and, as will be seen, $1/\Delta i(p)$ is indeed a linear function of $1/p$. Thus the evidence seems to indicate the validity of equation [4].

A relation similar to that of equation [7] has been reported for the effect of ambient gases on the photoconductivity of the anthracene crystal and has been attributed to the change in surface mobility of the charge carriers caused by adsorption (1). Recently Rosenberg (7) has also attributed the effect of oxygen on the photoconductivity of β-carotene to increased mobilities of charge carriers. While an increase in photocurrent caused by adsorption can be attributed either to an effective increase in the number of

Can. J. Chem. Downloaded from www.nrcresearchpress.com by 210.87.254.5 on 09/05/12
For personal use only.

charge carriers, or to an increase in their mobilities, or to a combination of both these mechanisms, the proportionality between $i_2(p)$ and θ can be explained much more directly if we assume the photoinjection of additional charge carriers from the surface complex. Further, this latter mechanism leads quite naturally to an explanation of the influence of ambient oxygen on the rates of the photocurrent responses.

D. Mechanism of Slow Photocurrent Decay

A photoconductive response of the type shown in Fig. 4 is usually associated with traps. As is well known, the decay of the photocurrent response in many cases can be described by an exponential decay law. The slow decay of Fig. 4, however, does not obey an exponential law.

If we assume that the photocurrent consists of two more or less independent components, namely bulk photocurrent and surface photocurrent, the decay will occur through the fast recombination in the bulk of the crystal, presumably according to an exponential decay law and this will be followed by the slower surface decay.

The oxygen molecule usually behaves as an electron acceptor toward the surface of a number of semiconductors and usually increases the electrical conductivity of p-type semiconductors, presumably by injection of additional p-type charge carriers. If the increase in the photocurrent of the pentacene films on exposure to oxygen is also due to the injection of additional p-carriers, as a result of photoinduced electron transfer to surface oxygen atoms, negatively charged surface complexes must remain on the surface and they will behave as traps for p-type carriers in the surface recombination process. This behavior would be consistent with the known chemistry of pentacene. On this basis, the decay of the photocurrent, after cessation of illumination, will take place by fast recombination in the bulk of the crystal and also by the relatively slow trapping of the injected p-type carriers by the negatively charged surface complexes, the two mechanisms being more or less independent.[5]

According to the model given above, the carriers at the tail of the photocurrent decay must be p-type carriers in the surface region and the number of these carriers must be equal to the net number of negatively charged traps on the surface. Thus for this part of the decay we can write

$$-\frac{dn}{dt} = Kn(N_t - n_t), \tag{8}$$

where N_t is the total number of negatively charged surface traps formed initially and n_t the number of trapped carriers. Hence $n = N_t - n_t$ and equation [8] becomes a second-order reaction equation, namely

$$-\frac{dn}{dt} = Kn^2 \tag{9}$$

or

$$1/n - 1/n_0 = Kt. \tag{10}$$

Since $i(t)$ is proportional to n, equation [10] can be written as

$$1/i(t) - 1/i(0) = K't,$$

[5]*If the bulk decay is truly exponential and very rapid, it suggests that the recombination is essentially a "trapping" mechanism in which the number of "traps" is relatively large and independent of the number of carriers. If this is indeed the case, these bulk recombination "traps" must be ineffective in trapping the additional p-type carriers.*

Can. J. Chem. Downloaded from www.nrcresearchpress.com by 210.87.254.5 on 09/05/12
For personal use only.

that is, $1/i(t)$ becomes a linear function of time. That this is actually the case may be seen from Fig. 7.

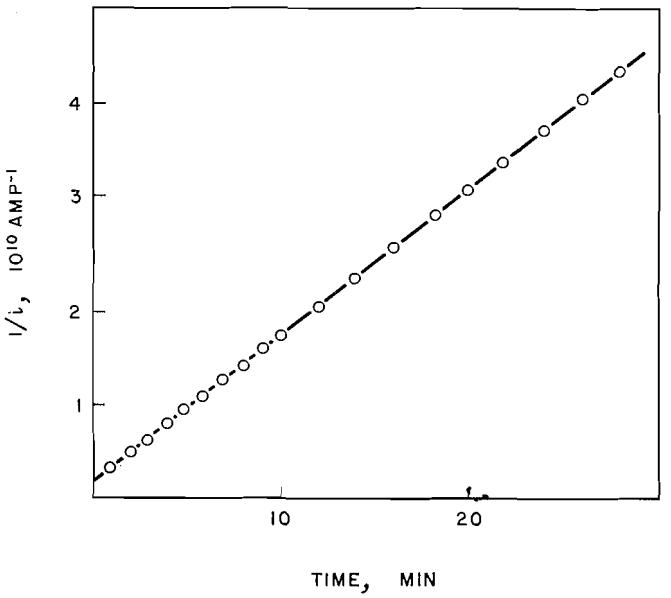


FIG. 7. Photocurrent decay in ambient oxygen (200 mm Hg).

While the above is a very unsophisticated description of the effect of oxygen on the photoconductivity of films of pentacene and some of its derivatives, both the dependence of the stationary photocurrent on the oxygen pressure as well as the decay of the photocurrent have been explained in terms of a very simple, plausible model, namely the formation of a surface "oxide" capable of providing additional *p*-type charge carriers on illumination. This model is reasonably consistent with the known tendency of some of these complex hydrocarbons to form biradical addition complexes and is reasonably consistent with the effect of oxygen on their absorption spectra. While, in the case of pentacene, the nature of the surface oxide is not known, the reversibility of the "oxygen effect" suggests that comparatively weak bonds are involved. Presumably the surface "oxide" is a "molecular" compound involving some resonance with a transient ionic form or biradical. On illumination, electrons are transferred and localized on the relatively immobile oxygen atoms, leaving unlocalized positive holes capable of acting as charge carriers.

ACKNOWLEDGMENTS

The authors would like to express their gratitude to Dr. W. G. Schneider for helpful suggestions and discussions, and to Dr. R. N. Jones for his kindness in supplying some of the pentacenes.

REFERENCES

1. W. G. SCHNEIDER and T. C. WADDINGTON. J. Chem. Phys. **25**, 358 (1956).
2. A. G. CHYNOWETH. J. Chem. Phys. **22**, 1029 (1954).
3. A. BREE and L. E. LYONS. J. Chem. Phys. **25**, 1284 (1956).
4. H. KURODA and E. A. FLOOD. J. Chem. Phys. **33**, 952 (1960).
5. H. KURODA and E. A. FLOOD. Can. J. Chem. **39**, 1475 (1961).
6. R. M. HOCHSTRASSER and M. RITCHIE. Trans. Faraday Soc. **52**, 1363 (1956).
7. B. ROSENBERG. J. Chem. Phys. **34**, 812 (1961).

Can. J. Chem. Downloaded from www.nrcresearchpress.com by 210.87.254.5 on 09/05/12
For personal use only.

Can. J. Chem. Downloaded from www.nrcresearchpress.com by 210.87.254.5 on 09/05/12
For personal use only.

DEUTERIUM KINETIC ISOTOPE EFFECTS

V. TEMPERATURE DEPENDENCE OF β-DEUTERIUM EFFECTS IN WATER SOLVOLYSIS OF ISOPROPYL COMPOUNDS[1]

K. T. LEFFEK,[2] R. E. ROBERTSON, AND S. E. SUGAMORI

ABSTRACT

The secondary β-deuterium isotope effect (k_H/k_D) has been measured over a range of temperature for the water solvolysis reactions of isopropyl methanesulphonate, *p*-toluenesulphonate, and bromide. In these cases the isotope effect is due to a difference in entropies of activation of the isotopic analogues rather than a difference in the enthalpies of activation. It is suggested that the observed isotope effect is due to internal rotational effects of the methyl groups in the isopropyl radical, and the lack of an isotope effect on the enthalpy of activation is accounted for by a cancellation of an effect from this source and one from zero-point energy.

Secondary β-deuterium isotope effects in solvolytic reactions have been studied by several groups of workers (1–12). In all cases, replacement of hydrogen on β-carbon atoms of the alkyl radical by deuterium led to a reduction in the rate of solvolysis. The rate ratio (k_H/k_D) was found to vary from close to unity, for primary compounds (11, 12), to about 2.5, for tertiary compounds (1, 11). The source of this reduction in rate with deuterium substitution has usually been discussed in terms of the effect of changes in hyperconjugation associated with the activation process. The resulting weakening of C—H and C—D bonds implies a corresponding change in the difference in the zero-point energies. If this is the main source of the observed isotope effect, then an analysis of the temperature dependence of this effect should show a difference in the corresponding enthalpies of activation and any difference in the entropies and heat capacities of activation should be small. This explanation is in accord with the results reported by Shiner and Verbanic (2, 13) and by Lewis and Coppinger (5), who found in three solvolytic reactions that deuteration led to a change in both enthalpy and entropy of activation, the former being the major factor.

As a continuation of our general survey of β-deuterium isotope effects in the water solvolysis of alkyl halides and sulphonates (11), we have examined to what extent the above assumption is valid for the isopropyl system.

RESULTS AND DISCUSSION

Rate data over a range of temperature are given in Table I for the hydrolysis of isopropyl methanesulphonate, *p*-toluenesulphonate, and bromide, and their fully β-deuterated analogues. The rate data for the normal compounds were calculated from the three constant rate – temperature relationships previously determined in this laboratory (14). These relationships have been shown to reproduce the rate constants to better than the experimental error, and agreement between the rates so derived and experimentally determined for the protium compound was demonstrated for each of the above compounds, immediately prior to rate determinations on the deuterated

[1]*Manuscript received June 1, 1961.*
Contribution from the Division of Pure Chemistry, National Research Council, Ottawa, Canada. First presented at the 139th Meeting of the American Chemical Society, St. Louis, Missouri, March 1961.
Issued as N.R.C. No. 6492.
[2]*National Research Council Postdoctorate Fellow 1961.*

TABLE I

Temperature dependence of the β-deuterium isotope effect for the solvolysis of isopropyl compounds in water

Compound	$10^4 k_H$ (sec^{-1})	$10^4 k_D$ (sec^{-1})	Temp. (°C)	k_H/k_D (±0.006)
Isopropyl methanesulphonate	3.691	2.386	30.001	1.54_7
	1.965	1.267	25.000	1.55_1
	1.019	0.6570	20.002	1.55_1
	0.3619	0.2340	12.514	1.54_7
	0.3612	0.2345	12.501	1.54_0
	0.1197	0.07698	5.000	1.55_5
Isopropyl *p*-toluenesulphonate	7.664	4.960	30.017	1.54_5
	7.650	4.942	30.001	1.54_8
	4.085	2.655	25.005	1.53_9
	4.082	2.648	24.999	1.54_2
	2.122	1.375	20.005	1.54_3
	1.071	0.6933	15.003	1.54_5
	0.5248	0.3415	10.003	1.53_7
	0.2900	0.1881	6.008	1.54_2
Isopropyl bromide	10.11	7.638	69.994	1.32_4
	10.10	7.670	69.993	1.31_7
	6.004	4.542	65.002	1.32_2
	3.486	2.645	60.000	1.31_8
	3.461	2.631	59.933	1.31_5
	1.981	1.509	55.005	1.31_3
	0.3123	0.2381	40.005	1.31_2
	0.3123	0.2371	40.005	1.31_7

compound. The rate ratios (k_H/k_D), given in the final column, are seen to be almost independent of temperature. The results were fitted to the transition-state relationship

$$[1] \qquad \log_{10}(k_H/k_D) = \frac{(\Delta H_D^{\ddagger} - \Delta H_H^{\ddagger})}{2.303RT} - \frac{(\Delta S_D^{\ddagger} - \Delta S_H^{\ddagger})}{2.303R}$$

by the method of least squares, and the resulting enthalpy and entropy differences are given in Table II. Thus the rate decrease resulting from β-deuteration in this system is

TABLE II

Changes in enthalpy and entropy of activation produced by β-deuteration in the solvolysis of isopropyl compounds in water

Compound	$(\Delta H_D^{\ddagger} - \Delta H_H^{\ddagger})$ ±std. error (cal mole^{-1})	$(\Delta S_D^{\ddagger} - \Delta S_H^{\ddagger})$ ±std. error (cal mole^{-1} deg^{-1})
Isopropyl methanesulphonate	7±28	−0.84±0.1
Isopropyl *p*-toluenesulphonate	−21±14	−0.93±0.05
Isopropyl bromide	−35±15	−0.65±0.05

due almost entirely to a difference between the entropies of activation of the isotopic analogues. This is in marked contrast to the earlier work and cannot be explained in terms of zero-point energy effects alone.

When equation [1] is used, it is assumed that the heat capacities of activation ($\Delta C_p^{\ddagger}$) for the protium and deuterium compounds are the same. Since it has been observed that $\Delta C_p^{\ddagger}$ is much more sensitive to changes in the anionic group than to changes in the alkyl radical (15), this assumption probably would not introduce a significant error in the general case. If such an error were detectable it would appear as a curvature in

Can. J. Chem. Downloaded from www.nrcresearchpress.com by 210.87.254.5 on 09/05/12
For personal use only.

a plot of $\log_{10}(k_H/k_D)$ versus T^{-1}. For the present case of the isopropyl compounds, $(\Delta H_D^{\ddagger} - \Delta H_H^{\ddagger})$ is approximately zero and, therefore, $(\Delta C_{p,D}^{\ddagger} - \Delta C_{p,H}^{\ddagger})$ must also be very close to zero (less than -0.5 cal mole^{-1} deg^{-1}).

Any explanation of the results in Table II must be capable of producing the entropy of activation difference and at the same time account for the lack of an enthalpy of activation difference. The probable sources of secondary deuterium isotope effects will be examined in the light of these requirements.

Zero-Point Energy Effects

It has been generally claimed that the formation of a positive charge in the transition state of a solvolytic reaction proceeding via a carbonium ion brings about an increase in hyperconjugation in the activation process. The vibrational frequencies of the β-C—H (or β-C—D) bonds are, therefore, reduced in the transition state relative to the initial state. As a result, the difference between the zero-point energies of the β-C—D bonds and the β-C—H bonds is less in the transition state than in the initial state, leading to a higher enthalpy of activation for the deuterated compound. This argument is well established (1–12) and was applied in an earlier paper (11) to isopropyl compounds solvolyzing in water. Our present results show that if such an effect is present in the isopropyl case, it must be cancelled by another enthalpy effect of the opposite sign. The earlier work of Shiner *et al.* (2, 13) and Lewis *et al.* (5) on the temperature dependence of the secondary deuterium isotope effect seems to indicate that, in general, enthalpy of activation differences do occur. It is concluded, therefore, that the lack of an enthalpy difference in our system is probably due to a fortuitous cancellation of two (or more) effects.

Solvation Effects

Specific solvation effects as a source of secondary β-deuterium isotope effects in solvolytic reactions were considered by Shiner (1, 2), although Lewis and Coppinger (5) and later Streitwieser *et al.* (7) produced evidence against such an explanation.

Indirect evidence against solvation effects as a major contributor to the isotope effect is also available from the derived kinetic parameters for hydrolysis reactions. Briefly, a consideration of the changes in the entropy of activation ($\delta_R \Delta S^{\ddagger}$) accompanying the structural change ethyl to isopropyl for a series of halides and sulphonates leads to the conclusion that no appreciable solvent reorganization has taken place about the alkyl group at the transition state (14). Even stronger evidence is the lack of significant differences in the solvent isotope effect (15). The lack of correlation between $\delta_R \Delta S^{\ddagger}$ and $\delta_R \Delta C_p^{\ddagger}$ is also consistent with this conclusion.

Finally, there is the evidence from the work of Maccoll *et al.* (17) that an isotopic effect very similar to those reported here has been observed in the absence of solvent. In the gas-phase pyrolysis of normal and β-deuterated isopropyl bromide, a reaction which is postulated to have a quasi-carbonium-ion transition state, an isotope effect $(k_H/k_D) = 2.5$ was obtained. This rate ratio was also not greatly dependent on temperature. The result, by its marked similarity to those results given in Table I, supports the conclusion that solvation effects are not an important source of the isotope effect in this system, although the evidence is not strong enough to rule them out entirely.

Internal Effects

Isotope effects from this source arise as a result of differences between the partition functions of the normal and deuterated molecules in the initial and transition states

Can. J. Chem. Downloaded from www.nrcresearchpress.com by 210.87.254.5 on 09/05/12
For personal use only.

(equation [2]). The partition function Q may be factorized into $Q_{trans} \times Q_{rot} \times Q_{vib} \times Q_{int\ rot}$.

$$[2] \qquad (k_H/k_D)_{int} = \frac{Q_H^{\ddagger}}{Q_H} \cdot \frac{Q_D}{Q_D^{\ddagger}}.$$

The maximum rate ratios which could arise from the translational and rotational partition function differences would occur if the initial state were unsolvated and the transition state highly solvated (11). For this extreme case the rate ratios are given by the equations

$$[3] \qquad (k_H/k_D)_{trans} = \left(\frac{M_D}{M_H}\right)^{3/2},$$

$$[4] \qquad (k_H/k_D)_{rot} = \left(\frac{\Pi I_D}{\Pi I_H}\right)^{1/2}.$$

In practice neither of these contributions to the isotope effect can be expected to exceed a few per cent. The contribution from the vibrational partition function is also small at the ordinary temperatures used in this study (18, 19).

The theory regarding internal rotation in molecules has remained less than adequate despite the considerable amount of research into the subject (20). Nevertheless, it has been recognized that changes in barriers to internal rotation during chemical reactions must be important in determining the thermodynamic reaction parameters (20). The isotope effects observed during this study can be accounted for semiquantitatively on the basis of the following two postulates concerning the barriers to internal rotation of the methyl groups in isopropyl compounds for the water solvolysis reaction. It is postulated: (*a*) that there is a considerable decrease in the barrier to rotation of the CH_3 (or CD_3) groups on going from the initial to the transition state and (*b*) that the barrier to rotation of the methyl groups is higher in the protium compound than in the deuterium compound in the initial state.

The justification of the first postulate is the empirical rule that sixfold barriers to rotation are considerably smaller than threefold barriers (20, 21). Examples can be found in methyl derivatives of benzene where the barriers to rotation of the methyl groups are about 0.5 kcal per mole (21). If it is accepted that the transition state in the water solvolysis of isopropyl sulphonates and halides approximates a planar carbonium ion, then the barrier will become sixfold during the activation process and hence will be greatly reduced in the transition state. The entropy of activation for the water solvolysis reaction becomes increasingly more positive along the series ethyl halide, isopropyl halide, tertiary butyl halide (16), a variation which is also in qualitative agreement with postulate (*a*).

Postulate (*b*) is based on a limited number of microwave spectroscopic measurements. Swalen and Costain (22) found that the barrier to internal rotation for the CH_3 group in acetone is approximately 6% higher than that for the CD_3 groups in acetone-d_6. In nitromethane, the barrier to internal rotation of the methyl group is 16% greater in the normal compound that in the deuterated compound (23). On the other hand, recent work on the barrier in deuterated ethanes, using infrared data, gives no clear indication that CH_3 groups have a higher barrier than CD_3 groups (24). Theoretical support for postulate (*b*) is not easily found since barriers to internal rotation are not well understood. Bartell (25) has recently drawn attention to the size effects among isotopic molecules as a possible explanation for secondary deuterium isotope effects. Since

Can. J. Chem. Downloaded from www.nrcresearchpress.com by 210.87.254.5 on 09/05/12
For personal use only.

hydrogen–carbon bonds are slightly longer and have slightly larger amplitudes of vibration than deuterium–carbon bonds, it might be expected that normal methyl groups will have higher barriers to rotation than deuteromethyl groups, in consideration of the calculations made by Kreevoy and Mason (26) on steric effects and barriers to rotation. Libby suggests (27) "that a further investigation of the dependence of barrier height on isotopic substitution might settle the question as to whether repulsion between hydrogen atoms is the cause of the barrier in ethane". While it is admitted that steric considerations alone certainly grossly oversimplify the problem of barriers to internal rotation, further experimental measurements may well prove postulate (*b*) correct.

On the basis of the two postulates, approximate calculations have been made for a molecule $(CH_3)_2CHX$, where X is a heavy group. For several assumed barrier heights, the contributions to the enthalpy and entropy of activation from the restricted rotation of methyl groups were determined using Pitzer's Tables (28). The use of these tables introduces the additional assumption that the two methyl groups in the isopropyl radical are non-interacting, an assumption which is probably incorrect. However, since the values of the moments of inertia and barrier heights used in the calculation are only approximate, the results contain inherent uncertainties large enough to justify the neglect of any methyl–methyl interaction.

Some results of these calculations are shown in Table III. The top half of this table

TABLE III

Contributions to the secondary β-deuterium isotope effects for the solvolysis of isopropyl compounds in water from internal rotation effects

Barrier to methyl rotation (cal mole^{-1})				
Initial state		Transition state	$(\Delta H_D^{\neq} - \Delta H_H^{\neq})_{int\ rot}$ per methyl group (cal mole^{-1})	$(\Delta S_D^{\neq} - \Delta S_H^{\neq})_{int\ rot}$ per methyl group (cal mole^{-1} deg^{-1})
H cpd.	D cpd.	Both cpds.		
3000	3000	0	−65	0.06
3000	3000	600	−29	0.05
3000	3000	1200	−15	0.04
3000	2400	0	−93	−0.26
3000	2400	600	−31	−0.26
3000	2400	1200	−44	−0.26

shows results obtained by the application of postulate (*a*) alone. The entropy of activation difference here is due to the difference in mass between hydrogen and deuterium and is seen to be small and in the direction opposite to that observed in Table II. The bottom half of Table III shows the results obtained by application of both postulates, assuming a 20% difference between the barriers to internal rotation of the normal methyl and deuteromethyl groups. When the figures in the right-hand column, for the entropy of activation difference per methyl group, are multiplied by 2, quite a large part of the observed entropy difference can be explained. At the same time an enthalpy of activation difference is obtained opposite in sign to that springing from a zero-point energy effect.

It is therefore suggested that the major part of the observed isotope effect for the water solvolysis of isopropyl compounds is due to internal rotational effects, and that the most probable cause of the lack of an isotope effect on the enthalpy of activation is a fortuitous cancellation between enthalpy effects arising from zero-point energy sources and internal rotational effects.

Can. J. Chem. Downloaded from www.nrcresearchpress.com by 210.87.254.5 on 09/05/12
For personal use only.

EXPERIMENTAL

Isopropyl-β-d_6 alcohol was obtained by the reduction of acetone-d_6 with lithium aluminum hydride using the procedure described by Shiner (29). The crude product was redistilled, boiling point range 83.5–84.5° C. Yields up to 99% were obtained using this procedure. The N.M.R. spectrum of this compound showed that the β-carbon atom was fully deuterated. Treatment of the alcohol with "constant boiling" hydrobromic acid yielded the bromide, boiling point range 60–61° C, in 55% yield after purification.

Isopropyl-β-d_6 methanesulphonate and p-toluenesulphonate were prepared by reaction of the bromide with the appropriate silver sulphonate as previously described for ethyl compounds (30). The sulphonates were purified by distillation under a vacuum.

The protium analogues of the above compounds were prepared by parallel reactions and were used to check the rate constants which had been previously determined in this laboratory (14).

The rate measurements were made conductometrically as described in detail in Part III of this series (31).

ACKNOWLEDGMENTS

Among those with whom we have discussed the above results, we would like to mention, in particular, Professor E. S. Lewis and Dr. J. M. W. Scott.

REFERENCES

1. V. J. Shiner. J. Am. Chem. Soc. **75**, 2925 (1953).
2. V. J. Shiner. J. Am. Chem. Soc. **76**, 1603 (1954).
3. V. J. Shiner. J. Am. Chem. Soc. **78**, 2653 (1956).
4. E. S. Lewis and C. E. Boozer. J. Am. Chem. Soc. **76**, 791 (1954).
5. E. S. Lewis and G. M. Coppinger. J. Am. Chem. Soc. **76**, 4495 (1954).
6. E. S. Lewis, R. R. Johnson, and G. M. Coppinger. J. Am. Chem. Soc. **81**, 3140 (1959).
7. A. Streitwieser, R. H. Jagow, R. C. Fahey, and S. Suzuki. J. Am. Chem. Soc. **80**, 2326 (1958).
8. S. Winstein and J. Takahashi. Tetrahedron, **2**, 316 (1958).
9. M. L. Bender, M. S. Feng, and J. M. Jones. Chem. & Ind. 1350 (1959).
10. W. H. Saunders, S. Asperger, and D. H. Edison. Chem. & Ind. 1417 (1957).
11. K. T. Leffek, J. A. Llewellyn, and R. E. Robertson. Can. J. Chem. **38**, 2171 (1960).
12. E. S. Lewis, J. C. Brown, and W. C. Herndon. Can. J. Chem. **39**, 954 (1961).
13. V. J. Shiner and C. J. Verbanic. J. Am. Chem. Soc. **79**, 373 (1957).
14. R. L. Heppolette, R. E. Robertson, and J. M. W. Scott. Forthcoming publication.
15. R. L. Heppolette and R. E. Robertson. J. Am. Chem. Soc. **83**, 1834 (1961).
16. E. A. Halevi. Intern. J. Appl. Radiation and Isotopes, **7**, 192 (1960).
17. A. Maccoll. Theoretical organic chemistry (The Kekule Symposium). Butterworths Scientific Publications, London. 1959. p. 238.
18. K. Wiberg. Chem. Revs. **55**, 713 (1955).
19. L. Melander. Isotope effects on reaction rates. The Ronald Press Co., New York. 1960. p. 19.
20. E. B. Wilson. Adv. in Chem. Physics. Vol. II. *Edited by* I. Prigogine. Interscience Publications, Inc., New York. 1959. p. 367.
21. K. S. Pitzer and D. W. Scott. J. Am. Chem. Soc. **65**, 803 (1943).
22. J. D. Swalen and C. C. Costain. J. Chem. Phys. **31**, 1562 (1959).
23. E. Tannenbaum, R. J. Myers, and W. D. Gwinn. J. Chem. Phys. **25**, 42 (1956).
24. D. R. Lide. J. Chem. Phys. **29**, 1426 (1958).
25. L. S. Bartell. Tetrahedron Letters, **6**, 13 (1960).
26. E. A. Mason and M. M. Kreevoy. J. Am. Chem. Soc. **77**, 5808 (1955).
27. W. F. Libby. Private communication.
28. K. S. Pitzer and W. D. Gwinn. J. Chem. Phys. **10**, 428 (1942).
29. V. J. Shiner. J. Am. Chem. Soc. **74**, 5285 (1952).
30. K. T. Leffek, J. A. Llewellyn, and R. E. Robertson. Can. J. Chem. **38**, 1505 (1960).
31. K. T. Leffek, J. A. Llewellyn, and R. E. Robertson. J. Am. Chem. Soc. **82**, 6315 (1960).

Can. J. Chem. Downloaded from www.nrcresearchpress.com by 210.87.254.5 on 09/05/12
For personal use only.

Can. J. Chem. Downloaded from www.nrcresearchpress.com by 210.87.254.6 on 09/05/12
For personal use only.

THE CONSTITUTION OF THE HEMICELLULOSE OF APPLE WOOD (MALUS PUMILA L. VAR. GOLDEN TRANSPARENT)[1]

G. G. S. DUTTON AND T. G. MURATA

ABSTRACT

The hemicellulose isolated by direct alkaline extraction of the wood has been shown to be a 4-*O*-methylglucuronoxylan. Methylation data indicate a backbone of approximately 120 D-xylopyranose units linked by β, 1—4 bonds with single units of 4-*O*-methyl-D-glucuronic acid linked by α, 1—2 bonds. The proportion of acid units to xylose is approximately 1:6. Two artifacts were isolated from the hydrolysis products of the methylated polysaccharide: 4-*O*-(2,3-di-*O*-methyl-α-D-xylopyranosyl)-2,3-di-*O*-methyl-D-xylose and 2,3-di-*O*-methyl-D-lyxose.

Hemicelluloses from many deciduous and coniferous trees have been isolated and studied, and these results have been reviewed (1). The majority of the trees so far investigated have been those of commercial importance for pulping, such as birch, beech, hemlock, and spruce, etc. Certain generalizations on the structure of hemicelluloses have emerged as a result of these studies, the most notable being that the hemicelluloses from coniferous trees have a high mannose content whereas those from deciduous trees are very low in this sugar (1). It was of interest to include other species in these structural investigations and accordingly the hemicelluloses from two members of the Rosaceae family have been studied. The present paper reports the results on *Malus pumila* Mill. (var. Golden Transparent), and the results on *Prunus avium* L. (var. Bing) will be reported later (2).

Finely ground apple wood was extracted with hot alcohol:benzene (1:2) and the air-dried residue was shaken with 0.1 *N* sodium hydroxide. The highly colored extract was discarded and the residue re-extracted with 1 *N* sodium hydroxide according to the method of McDonald (3). The hemicellulose was isolated by pouring the alkaline extract into acidified ethanol and, after being dried by solvent exchange, amounted to 8–12% of the dry wood.

The hydrolysis products of the hemicellulose were resolved on ion exchange resins into a neutral and an acidic fraction. Chromatographic analysis of the former showed it to contain predominantly D-xylose which was characterized as the crystalline sugar. There were also trace amounts of arabinose, galactose, and rhamnose, together with two components having a greater mobility than rhamnose. The identities of these two sugars have not yet been determined. The acidic fraction contained appreciable amounts of an aldobiouronic acid, characterized by conversion to the crystalline methyl 2-*O*-(2,3-di-*O*-acetyl-4-*O*-methyl-α-D-glucopyranosyl)uronate 3,4-di-*O*-acetyl-D-xylopyranoside (4), together with smaller amounts of materials assumed to be free uronic acid and an aldotriouronic acid.

The hemicellulose was methylated, fractionated, and cleaved by methanolysis. After the methyl esters of the acidic components had been saponified with barium hydroxide the mixture of glycosides was resolved into neutral and acidic portions. The acidic fraction was re-esterified with diazomethane and reduced with lithium aluminum hydride with the expectation that the crystalline methyl 2-*O*-(2,3,4-tri-*O*-methyl-D-glucopyranosyl)-3-*O*-methyl-D-xyloside would be obtained. The sirup did not crystallize, even on

[1]*Manuscript received July 10, 1961.*
Contribution from the Department of Chemistry, University of British Columbia, Vancouver, B.C. Presented at the 43rd C.I.C. Conference, Ottawa, June 1960.

seeding, although on hydrolysis, 3-*O*-methyl-D-xylose and 2,3,4-tri-*O*-methyl-D-glucose were obtained and characterized as their crystalline anilides. Later work (5) has suggested that not all the uronic acid units are terminal and hence the aldobiouronic acid fraction, and thus the derived disaccharide fraction, would not be a single component. This was not apparent in the methylation study reported here.

The neutral sugar glycosides were hydrolyzed and resolved on a cellulose–hydrocellulose column (6). The principal component was 2,3-di-*O*-methyl-D-xylose, with small amounts of 2,3,4-tri-*O*-methyl-D-xylose and 2-*O*- and 3-*O*-methyl-D-xylose. There was also a very small amount of a material judged to be a tri-*O*-methylrhamnose from its chromatographic behavior. Other components isolated were 4-*O*-(2,3-di-*O*-methyl-α-D-xylopyranosyl)-2,3-di-*O*-methyl-D-xylose, i.e. a methylated xylobiose, and 2,3-di-*O*-methyl-D-lyxose. The former compound has an R_F value of about 0.70 (butanone–water), $[\alpha]_D$ 112° (*c*, 3 in methanol) and a melting point of 83.0–83.5° C. It appears to be identical with the sirupy compound isolated by Geerdes and Smith from methylated flax hemicellulose (7). Since the disaccharide D-xylose-$\beta(1 \rightarrow 4)$-D-xylose is well known and has a negative rotation (8) it may be assumed that its methylated derivative would also be negative. For this reason and also because it has been shown that the acid reversion of D-xylose produces α-linked disaccharides (9) it is assumed that the methylated disaccharide isolated in the present case has the alpha configuration and that it arises by acid reversion from 2,3-di-*O*-methyl-D-xylose. There is, however, the possibility that the native xylan contains a few alpha linkages and that these disaccharides accumulate in the hydrolysis products by analogy with the known greater stability of methyl α-D-glycopyranosides (10). On the other hand, maltose is known to be hydrolyzed faster than cellobiose (10). Until such time as mild hydrolysis of a xylan demonstrates the existence, in nature, of xylose units joined by alpha linkages the reversion theory seems more acceptable. The acid reversion of 2,3-di-*O*-methyl-D-xylose is now being studied.

The second artifact, 2,3-di-*O*-methyl-D-lyxose, caused some trouble. In the column separation of the methylated sugars there was isolated a small amount of a component having an R_F value of 0.40 (butanone–water) and $[\alpha]_D$ −26° in methanol. A compound which was chromatographically identical was also isolated in larger amounts from methylated cherry wood hemicellulose (2). A negative rotation is not recorded for any methyl ethers of D-xylose and two attempts to carry out a hydrobromic acid demethylation (11) led to complete disintegration of the compound. Fortunately the elegant boron trichloride method of demethylation (12) yielded a clean product which was readily identified by chromatography as D-lyxose. The compound 2,3-di-*O*-methyl-D-lyxose has been reported crystalline (13) and has been so obtained by us in another instance (2) but the material isolated here did not crystallize and was too small in amount to convert into a crystalline derivative. The presence of the 2,3-di-*O*-methyl-D-lyxose must be due to a facile epimerization of the D-xylose derivative caused by the alkali present in the barium carbonate used for neutralizing sulphuric acid hydrolyzates. Further work has shown that 2,3-di-*O*-methyl-D-xylose is very readily epimerized by base and these results will be reported later. A recheck of the hydrolyzate of the original polysaccharide failed to show the presence of any lyxose. Epimerization of methylated sugars from polysaccharides has not previously been recorded, although it is well known in the case of monosaccharides and has also been described in the case of aldobiouronic acids (14, 15).

A sample of the neutral methylated sugars was chromatographed, and their ratio estimated by the phenol – sulphuric acid method (16). These values together with that

Can. J. Chem. Downloaded from www.nrcresearchpress.com by 210.87.254.6 on 09/05/12
For personal use only.

obtained gravimetrically for the aldobiouronic acid gave a mole ratio of 1:97:21:19 for tri-, di-, mono-*O*-methyl pentoses, and uronic acid respectively. The slight excess of mono-*O*-methyl pentose over that required by the uronic acid might indicate a small degree of branching, but in view of the observations of Croon and Timell this seems unlikely (17). These results therefore indicate that apple wood hemicellulose has a chain length of approximately 120 D-xylose units and a xylose:uronic acid ratio of 6:1. It would thus appear that this hemicellulose is similar in structure to other wood hemicelluloses except that the proportion of uronic acid is higher than has been found for the majority of deciduous trees so far examined. This ratio is usually about 10 or 11 to 1 (1) although white elm has been found to have a ratio of 7:1 (18). In general it is characteristic of coniferous woods to have a high uronic acid content, i.e. 5 or 6 to 1.

EXPERIMENTAL

The following solvent systems (v/v) were used: (A) ethyl acetate:acetic acid:formic acid:water, 18:3:1:4; (B) 1-butanol:ethanol:water:ammonia, 40:11:19:1; (C) butanone–water azeotrope; (D) 1-butanol:acetone:water, 5:4:1. With solvent system D, phosphate-impregnated papers, which were prepared by dipping papers into a disodium hydrogen phosphate and potassium dihydrogen phosphate buffer (pH 5), were used (19). Electrophoresis was carried out using 0.05 *M* sodium borate (20). Evaporations were carried out *in vacuo* at 40° C and rotations were recorded at 22±2° C.

Isolation of Apple Wood Hemicellulose

Sawdust (200 g) was extracted with hot alcohol–benzene (1:2) for 4 hours and air dried. The sawdust was suspended in sodium hydroxide (0.1 *N*, 1.8 l.) for 24 hours at room temperature, after which the mixture was filtered and the filtrate discarded. The residue was washed with water and then extracted with sodium hydroxide (1 *N*, 1.8 l.) with shaking, for 48 hours, at room temperature. The suspension was filtered and the residue washed with water to give a total volume of 2 l. The hemicellulose was isolated by pouring the extract into cold ethanol containing acetic acid. The material thus obtained was dried by solvent exchange and a typical preparation had $[\alpha]_D$ −62° (*c*, 1.2 in 8% NaOH) and an ash content of 4.7%. The yield was 10–12 g of hemicellulose per 100 g of sawdust.

Hydrolysis of the Hemicellulose

Hemicellulose (214 mg) in sulphuric acid (1 *N*) was heated on a steam bath for 9 hours during which time the rotation changed from $[\alpha]_D$ −62° to +41°. Sulphuric acid was neutralized with barium carbonate and the solution was passed through Amberlite IR 120 and Duolite A4 resins. Evaporation of the neutral eluate yielded a sirup (144 mg), which was examined in solvents A, B, C, and D. In each system a large spot corresponding to xylose was observed, in solvent D traces of arabinose, rhamnose, and galactose were observed, and in solvent C two additional components with R_F 0.17 and 0.30 were detected.

The acidic components were eluted from the anion resin with sodium hydroxide (2 *N*, 5 ml), and the free acids were liberated by passage through fresh cation resin. Evaporation yielded a sirup (24.5 mg) which, in solvent A, showed three components having R_{xylose} 1.2, 1.0, and 0.69. These correspond to uronic acid, aldobiouronic acid, and aldotriouronic acid (21).

In a similar way, approximately 30 g of hemicellulose was hydrolyzed to yield 22.14 g of neutral sugars and 5.84 g of acids. The sirup containing the neutral sugars crystallized

Can. J. Chem. Downloaded from www.nrcresearchpress.com by 210.87.254.6 on 09/05/12
For personal use only.

spontaneously, and the D-xylose after recrystallization from methanol–water had m.p. and mixed m.p. 143–145° C and $[\alpha]_D$ 17.7° (*c*, 1.69 in water, equil.). The mother liquor contained a component chromatographically and electrophoretically indistinguishable from rhamnose and also two compounds with R_F values 0.17 and 0.30 in solvent C.

A portion of the acid sirup was streaked on Whatman 3MM paper and irrigated with solvent A for 16 hours. The section containing the component with R_x 1.0 was eluted with methanol and this component was characterized as methyl 2-*O*-methyl(2,3-di-*O*-acetyl-4-*O*-methyl-α-D-glucopyranosyl)uronate 3,4-di-*O*-acetyl-D-xylopyranoside according to the method of Timell (4); m.p. 191–193° C, undepressed by an authentic sample.

Methylation and Methanolysis of the Hemicellulose

The hemicellulose was methylated with methyl sulphate and sodium hydroxide five times and then three times with methyl iodide and silver oxide. After these treatments there was no hydroxyl band in the I.R. spectrum and the methoxyl content was 38.7%. Fractional precipitation of a chloroform solution with petroleum ether (30–60°) gave a fraction having $[\alpha]_D$ −57.8° (chloroform) and methoxyl 39.1%. A portion of this material (2.02 g) was refluxed for 7 hours in 3% methanolic hydrogen chloride, and after neutralization (Ag_2CO_3) and evaporation there was obtained a dark sirup of the methyl glycosides (2.13 g). This sirup was dissolved in saturated barium hydroxide (25 ml) and heated at 60° for 2 hours. The aqueous solution was continuously extracted with petroleum ether (30–60°) for 20 hours and was then resolved into neutral and acidic fractions by Amberlite IR 120 and Duolite A4 resins in the usual way. The petroleum ether extract was added to the sirup from the neutral eluate and re-evaporation gave the methyl glycosides (1.52 g). The acidic component amounted to 475 mg.

Identification of the Acidic Component

The acidic component was dissolved in methanol and treated with diazomethane. The resulting ester was dissolved in dry tetrahydrofuran (75 ml), and a solution of lithium aluminum hydride (500 mg) in the same solvent (20 ml) was slowly added, with stirring, at room temperature. Reduction was completed by refluxing for 1 hour, and the product was isolated by acetylation as previously described (22). The colorless sirup (344 mg) failed to crystallize even on seeding. Accordingly a portion of the disaccharide (186 mg) was dissolved in methanol (10 ml) containing acetyl chloride (0.5 ml) and refluxed for 5 hours. The mixture was neutralized (Ag_2CO_3), filtered, and evaporated to give a mixture of glycosides (202 mg) which were then hydrolyzed by sulphuric acid (1 *N*, 5 ml) on the steam bath for 7 hours. The solution was deionized with Duolite A4 and after concentration, chromatographic and electrophoretic examination revealed components identical with 2,3,4,-tri-*O*-methyl-D-glucose, 3-*O*-methyl-D-xylose, and a trace of what was assumed to be incompletely hydrolyzed material.

The mixture of sugars (126 mg) was separated on a cellulose–hydrocellulose column (6) using butanone–water azeotrope (36 ml per hour) and fractions were collected at 20-minute intervals. Concentration of the contents of tubes 11–17 gave a sirup (37 mg), $[\alpha]_D$ 73° (*c*, 0.7 in ethyl acetate), chromatographically identical with 2,3,4-tri-*O*-methyl-D-glucose. This was confirmed by the preparation of 2,3,4-tri-*O*-methyl-*N*-phenyl-D-glucosylamine, which had m.p. 141–143° C on recrystallization from ethyl acetate – petroleum ether (lit. value 145–146° C (23)).

Concentration of the contents of tubes 60–80 gave a sirup (24 mg) electrophoretically identical with 3-*O*-methyl-D-xylose. The derived 3-*O*-methyl-*N*-phenyl-D-xylosylamine had m.p. 133–134° C (lit. value m.p. 137° C (24)).

Can. J. Chem. Downloaded from www.nrcresearchpress.com by 210.87.254.6 on 09/05/12
For personal use only.

Can. J. Chem. Downloaded from www.nrcresearchpress.com by 210.87.254.6 on 09/05/12
For personal use only.

Identification of the Neutral Sugars

The methyl glycosides (1.36 g) were hydrolyzed with sulphuric acid (1 *N*, 60 ml) by heating the mixture on the steam bath for 8 hours. Neutralization ($BaCO_3$) and evaporation yielded a sirup (1.16 g), part of which (1.04 g) was separated on a cellulose–hydrocellulose column as before. One hundred fractions were collected at 10-minute intervals and a further 100 fractions at 30-minute intervals. The results are shown in Table I.

TABLE I

Separation of methylated sugars of apple wood hemicellulose

Component	Tube number	Weight, mg	Identity
1	6–9	17.0	Tri-*O*-methylrhamnose
	10		1+2
2	11–13	21.9	2,3,4-Tri-*O*-methyl-D-xylose
	14–15	14.7	2+3
3	16–22	56.0	Methylated xylobiose
	23–31	32.6	3+4
4	32–53	637.6	2,3-Di-*O*-methyl-D-xylose
	54–59	22.0	4+5
5	60–75	23.0	2,3-Di-*O*-methyl-D-lyxose
6	109–113	15.6	2- and 3-*O*-Methyl-D-xylose
7	160–185	8.6	D-Xylose
		849	

NOTE: Recovery 82%.

Component 1.—This had R_F 0.86 and gave a characteristic pale yellow color with the *p*-anisidine spray. It was thus tentatively identified as a tri-*O*-methylrhamnose.

Component 2.—This was chromatographically identical with 2,3,4-tri-*O*-methyl-D-xylose. The rotation of the sirup, $[\alpha]_D$ ca. 6° (*c*, 0.4 in methanol), indicated that it was not pure and attempts to crystallize the sirup and prepare the crystalline *N*-phenylglycosylamine both failed.

Component 3.—This fraction had R_F 0.71 and $[\alpha]_D$ 112° (*c*, 3 in methanol). On evaporation of the solvent it readily crystallized to long, feathery needles. All attempts to recrystallize the solid failed but it was readily recovered in crystalline form by allowing the solvent to evaporate; m.p. 83.0–83.5° C. Hydrolysis with hot sulphuric acid (1 *N*) gave a compound chromatographically identical with 2,3-di-*O*-methyl-D-xylose.

Component 4.—This material had R_F 0.50 and was the major component. It was identified as 2,3-di-*O*-methyl-*N*-phenyl-D-xylosylamine, m.p. 122–123° C, on recrystallization from ethyl acetate – petroleum ether (lit. m.p. 121–123° C (25)).

Component 5.—This fraction had R_F 0.40 and was present in only small amount. It had $[\alpha]_D$ ca. −26° in methanol and was chromatographically identical with the material characterized as 2,3-di-*O*-methyl-D-lyxose isolated from cherry wood hemicellulose (2). This was confirmed as follows. A portion of the unknown sugar (10 mg) was dissolved in dry dichloromethane (3 ml) and the solution cooled to −78°. Boron trichloride (1–2 g) was distilled into this solution and the temperature maintained at −78° for 30 minutes. The solution was allowed to come to room temperature and to evaporate overnight. Electrophoresis and chromatography (solvent D) of the residue dissolved in aqueous methanol indicated the presence of lyxose.

Component 6.—This was readily shown by electrophoresis to be a mixture of 2-*O*- and 3-*O*-methyl-D-xylose.

Component 7.—This was chromatographically identical with xylose.

Quantitative Analysis of Neutral Sugars

A portion of the neutral sugars was separated on Whatman No. 1 paper using butanone–water azeotrope. The zones corresponding to tri-, di-, and mono-*O*-methylpentoses were separately eluted with water and the concentration of the sugars determined by the phenol – sulphuric acid method (16). The ratios thus determined were 1:97:2. Standard curves were prepared from 2,3,4-tri-*O*-methyl-D-xylose, 2,3-di-*O*-methyl-D-xylose, and 2-*O*-methyl-D-xylose.

ACKNOWLEDGMENTS

We are grateful to Dr. T. E. Timell for the gift of authentic samples, and to the National Research Council for generous financial support.

We are also indebted to Dr. C. T. Bishop for kindly presenting this material at the 43rd Conference of the Chemical Institute of Canada.

REFERENCES

1. G. O. Aspinall. Advances in Carbohydrate Chem. **14**, 429 (1959).
2. S. A. McKelvey. M.Sc. Thesis. University of British Columbia, Vancouver, B.C. 1960.
3. I. R. C. McDonald. J. Chem. Soc. 3183 (1952).
4. T. E. Timell. Can. J. Chem. **37**, 827 (1959).
5. G. G. S. Dutton and A. M. Unrau. Unpublished results.
6. J. D. Geerdes, B. A. Lewis, R. Montgomery, and F. Smith. Anal. Chem. **26**, 264 (1954).
7. J. D. Geerdes and F. Smith. J. Am. Chem. Soc. **77**, 3572 (1955).
8. R. L. Whistler and C. C. Tu. J. Am. Chem. Soc. **73**, 1389 (1951).
9. D. H. Ball, J. K. N. Jones, W. N. Nicholson, and T. J. Painter. Tappi, **39**, 438 (1955).
10. F. Shafizadeh and A. Thompson. J. Org. Chem. **21**, 1059 (1956).
11. L. Hough, J. K. N. Jones, and W. H. Wadman. J. Chem. Soc. 1702 (1950).
12. T. G. Bonner, E. J. Bourne, and S. McNally. J. Chem. Soc. 2929 (1960).
13. J. P. Verheijden and P. J. Stoffyn. Tetrahedron, **1**, 253 (1957).
14. A. Roudier and L. Eberhard. Mém. serv. chim. état (Paris), **40**, 285 (1955); Chem. Abstr. **52**, 720 (1958).
15. A. Roudier and L. Eberhard. Compt. rend. **247**, 1505 (1958).
16. M. Dubois, K. A. Gilles, J. K. Hamilton, P. A. Rebers, and F. Smith. Anal. Chem. **28**, 350 (1956).
17. I. Croon and T. E. Timell. Can. J. Chem. **38**, 720 (1960).
18. J. K. Gillham and T. E. Timell. Can. J. Chem. **36**, 1467 (1958).
19. M. Meier and K. C. D. Wilkie. Holzforschung, **13**, 177 (1959).
20. J. L. Frahn and J. A. Mills. Australian J. Chem. **12**, 65 (1959).
21. H. C. Srivastava and G. A. Adams. J. Am. Chem. Soc. **81**, 2409 (1959).
22. G. G. S. Dutton and F. Smith. J. Am. Chem. Soc. **78**, 3744 (1956).
23. S. Peat, E. Schluchterer, and M. Stacey. J. Chem. Soc. 581 (1939).
24. R. A. Laidlaw and E. G. V. Percival. J. Chem. Soc. 528 (1950).
25. I. Ehrenthal, M. C. Rafique, and F. Smith. J. Am. Chem. Soc. **74**, 1341 (1952).

Can. J. Chem. Downloaded from www.nrcresearchpress.com by 210.87.254.6 on 09/05/12
For personal use only.

Can. J. Chem. Downloaded from www.nrcresearchpress.com by 210.87.254.5 on 09/05/12
For personal use only.

THE CHEMISTRY OF ALUMINUM–NITROGEN COMPOUNDS

I. REACTIONS OF TRIMETHYLALUMINUM AND TRIMETHYLALUMINUM TRIMETHYLAMINE WITH SEVERAL METHYLHYDRAZINES[1]

NEIL R. FETTER AND BODO BARTOCHA

ABSTRACT

The reactions of trimethylaluminum and trimethylaluminum trimethylamine with various methylhydrazines have produced a number of complexes and polymers: with methylhydrazine, both Me_3Al and $Me_3Al{:}NMe_3$ produce the polymer $[—MeAlNHNMe—]_n$; with 1,2-dimethylhydrazine, both produce the polymer $[—Al(MeNNMe)_{1.5}—]_n$; with 1,1-dimethylhydrazine, Me_3Al produces $[Me_2Al—NHNMe_2]_2$ and $Me_3Al{:}NMe_3$ produces the unusual complex $Me_2Al(NHNMe_2)(NH_2NMe_2)$; with trimethylhydrazine, Me_3Al produces $[Me_2Al—NMeNMe_2]_2$ and $Me_3Al{:}NMe_3$ produces an isomer with the same formula but an as-yet-uncharacterized structure. In addition, the intermediate $Me_3Al{:}NHMeNMe_2$ has been isolated from the reaction of either Me_3Al or $Me_3Al{:}NMe_3$ with trimethylhydrazine. With tetramethylhydrazine, Me_3Al produces $Me_3Al{:}NMe_2NMe_2$. The formation of the complexes with covalent aluminum–nitrogen bonds is specific and methane is the only gas eliminated during these reactions.

INTRODUCTION

Until recently, only a few molecular addition compounds of aluminum with ligands of group V had been reported (1). In some of the earliest work, Brown and Davidson (2) described methylaluminum–methylamine complexes. Later, Wiberg and May (3) reported some reactions of aluminum hydride with amines and ammonia, an area of interest recently extended by studies of Ruff and Hawthorne (4, 5). Bonitz (6) isolated a triethylaluminum isoquinoline complex, and Ziegler, Gellert, and Neumann (7) base some analytical procedures on the reaction of alkylaluminum hydrides with amines. The compound $Et_2Al—NMe_2$ was reported in the patent literature (8), and a note on a new aluminum hydride adduct appeared in print (9).

Most of the compounds described in these previous publications contain a covalent aluminum–nitrogen bond which is formed by one of two general reactions:

(1) elimination of a hydrocarbon when an aluminum trialkyl reacts with a secondary or primary amine:

$$R_3Al + NHR_2' \rightarrow [R_3Al{:}NHR_2'] \rightarrow R_2Al—NR_2' + RH;$$

(2) elimination of hydrogen when an alkylaluminum hydride or aluminum hydride reacts with ammonia or a primary or secondary amine:

$$R_2AlH + NH_3 \rightarrow [R_2AlH{:}NH_3] \overset{\Delta}{\rightarrow} R_2Al—NH_2 + H_2,$$

$$R_2AlH + NHR_2' \rightarrow [R_2AlH{:}NHR_2'] \overset{\Delta}{\rightarrow} R_2Al—NR_2' + H_2.$$

In both cases a stable covalent bond is formed via an intermediate with a dative bond, and in several instances the materials seem to react further to form polymeric substances (10).

We were interested in the interactions of hydrazines with aluminum alkyls or aluminum hydride, and, in particular, of those hydrazines which carry both functional groups, namely, the N—H and N—C bonds. In this paper we report the reactions of trimethylaluminum and trimethylaluminum trimethylamine with methylhydrazines. Several new compounds with covalent or dative Al—N bonds were synthesized, and their physical constants determined.

[1]*Manuscript received April 7, 1961.*
Contribution from U.S. Naval Ordnance Laboratory, Corona, Calif., U.S.A.

Can. J. Chem. Downloaded from www.nrcresearchpress.com by 210.87.254.5 on 09/05/12
For personal use only.

EXPERIMENTAL

Apparatus

Most of the reactions were carried out in a conventional high-vacuum system. The hydrazine was transferred *in vacuo* to a cold trap (−196° C) containing the Me_3Al or $Me_3Al{:}NMe_3$ and any necessary solvent, such as pentane. After the mixtures had reached room temperature or had been heated so that the reaction would be completed, the solvent was pumped off and, if possible, the product was purified by sublimation.

In a few cases, use of the vacuum technique resulted in explosions, and the reactions were therefore carried out at atmospheric pressure under a nitrogen atmosphere. The hydrazine was added slowly to a cooled (−10° C) pentane solution of Me_3Al or $Me_3Al{:}NMe_3$. After the addition had been completed and the reaction mixture had reached room temperature, the solvent was removed in vacuum.

Molecular Weights

Molecular-weight determinations were conducted in a conventional freezing-point apparatus with cyclohexane as the solvent. The inner vessel was designed so that samples and solvent could be weighed in a dry box.

Reagents

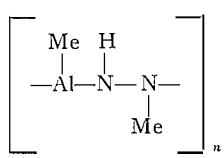
Methylhydrazine (Commercial Solvents Corporation), 1,1-dimethylhydrazine (Olin Mathieson Corporation), 1,2-dimethylhydrazine (Metalectro Corporation), and tetramethylhydrazine (Metalectro Corporation) were distilled over calcium hydride before use. The trimethylhydrazine was prepared by the method of Class, Aston, and Oakwood (11). Trimethylaluminum was purchased from the Ethyl Corporation of Baton Rouge, Louisiana, and vacuum-distilled before use. The preparation of trimethylaluminum trimethylamine was based on a procedure described by Brown and Davidson (2). All solvents were reagent grade, and all were distilled over calcium hydride before use.

Analysis

The evolved gases were measured by fractionating the mixtures through a series of traps into a calibrated volume and removing the uncondensable material with a Toepler pump. Aluminum was determined as Al_2O_3 after the sample had been decomposed with methanol and ashed. Elemental analyses were performed by the Schwarzkopf Microanalytical Laboratory, Woodside 77, New York.

Reaction of Trimethylaluminum Trimethylamine with Methylhydrazine

The atmospheric method was used for the reaction of $Me_3Al{:}NMe_3$ with H_2NNHMe. After 1.53 g (11.7 mmoles) of $Me_3Al{:}NMe_3$ and 0.602 g (13.1 mmoles) of H_2NNHMe had reacted and the solvent had been removed, a powdery white solid remained. This material could not be sublimed and was insoluble in hydrocarbons. It did not have a sharp melting point but decomposed slowly when heated to 200° C. Elemental analysis gave results which agree with the empirical formula $C_2H_7N_2Al$. Calc.: Al, 31.34%; C, 27.90%; H, 8.20%; N, 32.55%. Found: Al, 30.40%; C, 28.18%; H, 8.05%; N, 30.37%. From this formula, the following structure may be written:



Can. J. Chem. Downloaded from www.nrcresearchpress.com by 210.87.254.5 on 09/05/12
For personal use only.

The equation for the reaction is

$$n\mathrm{Me_3Al{:}NMe_3} + n\mathrm{H_2NNHMe} \rightarrow [\text{—MeAlNHNMe—}]_n + 2n\mathrm{CH_4} + n\mathrm{NMe_3}.$$

Hydrolysis of 0.243 g (2.83 mmoles) of the product yielded 0.0338 g (2.11 mmoles) of methane. The molar ratio of CH_4 to $[\text{—MeAlNHNMe—}]_n$ is 0.775.

Reaction of Trimethylaluminum with Methylhydrazine

By the procedure described above, the reaction of Me_3Al with methylhydrazine produces a material whose physical properties are the same as those of the $Me_3Al{:}NMe_3$–methylhydrazine polymer. An aluminum assay gave 30.55% Al (calc.: 31.34%), and the infrared spectra of the two materials were identical. The reaction may thus be written:

$$n\mathrm{Me_3Al} + n\mathrm{H_2NNHMe} \rightarrow [\text{—MeAlNHNMe—}]_n + 2n\mathrm{CH_4}.$$

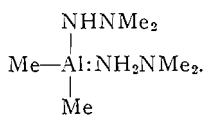
Reaction of Trimethylaluminum with 1,1-Dimethylhydrazine

By the vacuum method, the direct reaction of 0.680 g (9.45 mmoles) of Me_3Al with 0.632 g (10.5 mmoles) of H_2NNMe_2 gave a crystalline solid (m.p. 77–78.5° C)* and 0.143 g (8.45 mmoles) of methane. The molar ratio of CH_4 to Me_3Al is 0.945. Sublimed once, at 60° and 0.005 mm Hg, the reaction product was analyzed, and the results were found to agree with the empirical formula $C_4H_{13}N_2Al$. Calc.: Al, 23.23%; C, 41.36%; H, 11.28%; N, 24.13%. Found: Al, 23.82%; C, 41.12%; H, 11.04%; N, 24.21%. Two molecular-weight values of 238 and 240 indicate that this compound is dimeric (calc.: 230.2). The equation for the reaction is

$$2\mathrm{Me_3Al} + 2\mathrm{H_2NNMe_2} \rightarrow [\mathrm{Me_2Al—NHNMe_2}]_2 + 2\mathrm{CH_4}.$$

Reaction of Trimethylaluminum Trimethylamine with 1,1-Dimethylhydrazine

Again by the vacuum method, direct reaction of 1.63 g (10.4 mmoles) of $Me_3Al{:}NMe_3$ with 1.62 g (27.1 mmoles) of H_2NNMe_2 yielded a white crystalline solid (m.p. 81–82.0° C), 0.141 g (8.86 mmoles) of methane, and 0.451 g (7.65 mmoles) of trimethylamine. The molar ratio of CH_4 to $Me_3Al{:}NMe_3$ is 0.852, and the molar ratio of NMe_3 to $Me_3Al{:}NMe_3$ is 0.746. Elemental analysis of the product, which had been purified by sublimation at 30° C and 0.005 mm Hg, gave results which correspond to the percentages calculated for the empirical formula $C_6H_{21}N_4Al$. Calc.: Al, 15.30%; C, 40.89%; H, 12.01%; N, 31.78%. Found: Al, 15.95%; C, 40.60%; H, 11.77%; N, 31.58%. These data and a molecular-weight determination of 179 (calc.: 176.1) suggest the structural formula



Hydrolysis of 0.275 g (2.08 mmoles) of the complex produced 0.0685 g (4.28 mmoles) of methane; thus, the expected 2:1 molar ratio of methane to complex was obtained. The reactions of Me_3Al and $Me_3Al{:}NMe_3$ with 1,1-dimethylhydrazine are not influenced by the ratios of starting materials. An experiment with a molar ratio of 1:1 for H_2NNMe_2 and $Me_3Al{:}NMe_3$ yielded only $Me_2Al(NHNMe_2)(H_2NNMe_2)$ and an experiment with a starting molar ratio of 1.5:1 for H_2NNMe_2 and Me_3Al produced only $[Me_2Al—NHNMe_2]_2$.

Reaction of Trimethylaluminum Trimethylamine with 1,2-Dimethylhydrazine

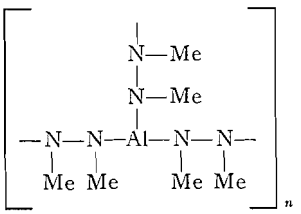
By the vacuum method, 0.812 g (6.20 mmoles) of $Me_3Al{:}NMe_3$ was treated with 0.530 g (8.83 mmoles) of NHMeNHMe at room temperature for 18 hours. At the end of this

**All melting points reported are uncorrected.*

period a white precipitate had formed, and 0.293 g (18.3 mmoles) of methane and 0.427 g (5.77 mmoles) of NMe_3 had been recovered. The molar ratio of recovered CH_4 to starting $Me_3Al{:}NMe_3$ is 2.96, and the molar ratio of NMe_3 to $Me_3Al{:}NMe_3$ is 0.932. The product was insoluble in hydrocarbons, did not have a sharp melting point, and could not be sublimed; however, on elemental analysis, the crude product gave results which agree with the formula $C_3H_9N_3Al$. Calc.: Al, 23.65%; C, 31.58%; H, 7.94%. Found: Al, 24.09%; C, 30.34%; H, 7.94%. From these data, the following reaction may be formulated:

$$n\text{Me}_3\text{Al:NMe}_3 + 1.5n\text{NHMeNHMe} \rightarrow [\text{—Al(MeNNMe)}_{1.5}\text{—}]_n + 3n\text{CH}_4 + n\text{NMe}_3.$$

The reaction product probably is a completely cross-linked polymer, with each aluminum atom incorporating one half of three [—MeNNMe—] units; hence the structural formula may be written as follows:



Hydrolysis of this material produces no methane, as expected, and the infrared spectrum shows no N—H bond in the 3.05-μ region.

Trimethylaluminum reacts with 1,2-dimethylhydrazine to produce the same polymer.

Reaction of Trimethylaluminum with Trimethylhydrazine

In all the reactions discussed above, the elimination of methane accompanied the complex formation. However, in the reaction of Me_3Al with $HNMeNMe_2$, the adduct intermediate was isolated and then converted into the covalent structure with elimination of methane. The intermediate was fairly stable; in fact, heating the reaction mixture for 20 hours at 60° C was required to effect the conversion.

By the vacuum procedure, 3.53 g (49.1 mmoles) of Me_3Al was treated with 9.61 g (130 mmoles) of $HNMeNMe_2$ at room temperature. From the liquid residue remaining after removal of the excess trimethylamine, a volatile, white crystalline solid (m.p. 80.0–83.0° C) was isolated by evaporation at 25° C onto a cold finger maintained at −15° C. The elemental analysis corresponds to the values for the formula $C_6H_{19}N_2Al$. Calc.: Al, 18.45%; C, 49.29%; H, 13.10%; N, 19.16%. Found: Al, 18.58%; C, 50.14%; H, 12.60%; N, 18.92%. A molecular-weight measurement gave the value 142.0 (calc.: 146.2). The initial reaction may thus be written:

$$\text{Me}_3\text{Al} + \text{HNMeNMe}_2 \rightarrow \text{Me}_3\text{Al:NHMeNMe}_2.$$

I

Compound I was then heated for 20 hours at 60° C and resublimed. A white crystalline solid (m.p. 125.0–126.5° C) was obtained and analyzed. Calc. for $C_5H_{15}N_2Al$: Al, 20.73%; C, 46.13%; H, 11.61%; N, 21.52%. Found: Al, 20.34%; C, 44.82%; H, 11.77%; N, 22.82%. A molecular-weight determination gave the value 258.0 (calc.: 260.4). The elimination reaction may then be written as follows:

$$2\text{Me}_3\text{Al:NHMeNMe}_2 \xrightarrow{60^\circ\text{ C}} [\text{Me}_2\text{Al—NMeNMe}_2]_2 + 2\text{CH}_4.$$

II

Can. J. Chem. Downloaded from www.nrcresearchpress.com by 210.87.254.5 on 09/05/12
For personal use only.

Compound II was also synthesized directly from Me_3Al and trimethylhydrazine by heating together 1.24 g (17.3 mmoles) of Me_3Al and 1.26 g (17.1 mmoles) of $HNMeNMe_2$ to 55° C for 20 hours. A crystalline solid (m.p. 125.0–126.5° C) and 0.270 g (16.8 mmoles) of methane were produced. Calc.: Al, 20.73%; C, 46.13%; H, 11.61%; N, 21.52%. Found: Al, 20.42%; C, 45.59%; H, 11.52%; N, 23.49%.

Reaction of Trimethylaluminum Trimethylamine with Trimethylhydrazine

In its initial step, this reaction is similar to that between Me_3Al and $HNMeNMe_2$ except that NMe_3 is displaced during the formation of the intermediate:

$$Me_3Al{:}NMe_3 + HNMeNMe_2 \rightarrow Me_3Al{:}NHMeNMe_2 + NMe_3.$$

In vacuo, 1.34 g (10.2 mmoles) of $Me_3Al{:}NMe_3$ was heated at 60° C with 0.813 g (11.0 mmoles) $HNMeNMe_2$ until NMe_3 evolution ceased (20 hours). Elemental analysis of this sublimed complex (m.p. 80.0–83.0° C) agreed with the formula for I. Calc.: Al, 18.45%; C, 49.29%; H, 13.10%; N, 19.16%. Found: Al, 18.27%; C, 50.99%; H, 13.33%; N, 18.57%.

However, in another experiment 1.96 g (14.9 mmoles) of $Me_3Al{:}NMe_3$ and 2.31 g (31.1 mmoles) of $HNMeNMe_2$ were heated at 75° C for 2 days. When gas evolution ceased, a clear liquid remained, and 0.192 g (12.0 mmoles) of CH_4 and 0.576 g (9.77 mmoles) of NMe_3 had been recovered. The liquid was vacuum-distilled at 25° C into a −30° C trap, and elemental analysis of the distillate (m.p. 13.5–15.0° C) gave results that correspond to the values for II. Calc.: Al, 20.73%; C, 46.13%; H, 11.61%; N, 21.52%. Found: Al, 21.94%; C, 44.09%; H, 11.63%; N, 23.11%. The reaction may be written as follows:

$$Me_3Al{:}NMe_3 + HNMeNMe_2 \xrightarrow[\text{excess } HNMeNMe_2]{75^\circ\ C} C_5H_{15}N_2Al + CH_4 + NMe_3.$$

Two molecular-weight measurements gave the values 189 and 195 (calc. for the monomer: 130.2; for the dimer: 260.4). Hydrolysis of 0.229 g (17.6 mmoles) produced 0.0483 g (30.2 mmoles) of methane; hence, the molar ratio of CH_4 to $C_5H_{15}N_2Al$ is 1.72. These data indicate that this complex is not compound II, but that it does contain an Me_2Al group and its empirical formula is the same as that for II. The molcular-weight data suggest a complex which is only partially associated in cyclohexane; however, the data are insufficient to indicate structural formula at this time.

Two attempts were made to convert compound II to the liquid complex described above. In the first attempt, 0.5 g of compound II was heated at 75° C for 48 hours followed by 120° C for 2 hours. The material remained unchanged. In the second attempt, 0.5 g of II was heated at 75° C for 48 hours with 1.0 g of trimethylhydrazine. After removal of the trimethylhydrazine an attempt to vacuum-distill the liquid residue at 90° C under 0.001 mm Hg pressure failed. The compound would not distill. The infrared spectrum of the liquid indicated it was neither II nor the material obtained above.

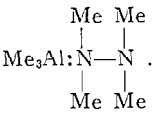
It should be noted that the temperature employed to prepare $Me_3Al{:}HNMeNMe_2$ from $Me_3Al{:}NMe_3$ and trimethylhydrazine (60° C) is also that used to convert $Me_3Al{:}HNMeNMe_2$ into $Me_2Al—NMeNMe_2$ when the former complex is prepared from Me_3Al and trimethylhydrazine. The authors have no explanation for this anomaly, but it must be presented as the condition under which these reactions occurred.

Reaction of Trimethylaluminum with Tetramethylhydrazine

By the vacuum method, 1.10 g (15.3 mmoles) of Me_3Al was treated with 1.50 g (17.0 mmoles) of Me_2NNMe_2 for 2 hours at room temperature. No gas evolution was observed

Can. J. Chem. Downloaded from www.nrcresearchpress.com by 210.87.254.5 on 09/05/12
For personal use only.

during this period, and a white crystalline solid formed in the reaction vessel. The material was sublimed at 60° C (m.p. 65.5–66.0° C), and elemental analysis of the sublimate agreed with the values calculated for the 1:1 complex:



Calc.: Al, 16.84%; C, 52.47%; H, 13.21%; N, 17.48%. Found: Al, 16.87%; C, 52.48%; H, 13.03%; N, 17.04%. A molecular-weight measurement gave the value 164 (calc.: 160.3); hence, the following reaction may be written:

$$Me_3Al + Me_2NNMe_2 \xrightarrow{25^\circ C} Me_3Al{:}NMe_2NMe_2.$$

All of the compounds described above hydrolyze rapidly in methanol, ethanol, and 1,4-dioxane and react vigorously with water. They decompose in air without inflaming and they react slowly with dry air. The polymeric compounds are somewhat less sensitive to moisture and oxygen. Yields of purified products were approximately 65–70 mole% of the initial quantity of Me_3Al or $Me_3Al{:}NMe_3$.

DISCUSSION

The reactions described above occur by two sequential steps. The first is the formation of a dative-bonded complex of trimethylaluminum and the hydrazine:

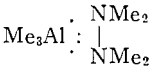
$$Me_3Al + R_2NNR_2 \rightarrow Me_3Al{:}R_2NNR_2. \qquad [1]$$

The second is the elimination of methane to form a complex with a covalent aluminum–nitrogen bond:

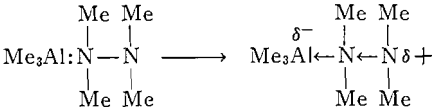
$$Me_3Al{:}RHNNR_2 \rightarrow Me_2Al{-}NRNR_2 + CH_4. \qquad [2]$$

The structure of the dative-bonded complexes cannot be determined from the data available, but it should be noted that in the two cases wherein the complexes could be isolated, i.e., the reactions of trimethylhydrazine and tetramethylhydrazine with trimethylaluminum, only 1:1 adducts are formed. This fact suggests a structure which prohibits further complexing of another Me_3Al molecule to the other nitrogen atom of the hydrazine.

A complex involving a pentaco-ordinated aluminum atom:



or the charge distribution on the structure with a tetraco-ordinated aluminum atom:



would inhibit further addition; hence one of these two formulas may represent the configuration of the dative-bonded adducts.

The elimination of methane during the formation of the covalent-bonded complexes

Can. J. Chem. Downloaded from www.nrcresearchpress.com by 210.87.254.5 on 09/05/12
For personal use only.

is a striking feature of *all* the reactions in which such elimination occurs. The absence of ethane which would be liberated if the following mechanism:

$$Me_3Al + H_2NNMe_2 \rightarrow Me_2AlNMeNH_2 + C_2H_6, \qquad [3]$$

was followed indicates that in unsymmetrical hydrazines, the nitrogen atom with the largest number of N—H bonds forms the covalent bond with aluminum:

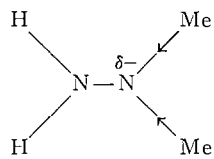
$$Me_3Al{:}MeHNNMe_2 \rightarrow Me_2Al{-}NMeNMe_2 + CH_4.$$

The specificity of this reaction may be the combined effect of steric and electronic factors. For example, with unsymmetrical hydrazines, if one assumes the formation of a tetraco-ordinated intermediate, the Me_3Al may bond with the least sterically hindered nitrogen atom, namely, the one with the greatest number of N—H bonds and the subsequent methane elimination occurs from these adjacent aluminum and nitrogen atoms. If one postulates the pentaco-ordinated aluminum complex:

$$Me_3Al{:}\begin{array}{l}NHMe\\|\\NMe_2\end{array},$$

the aluminum atom may be forced into closer proximity to the nitrogen atom with N—H bonds, and covalent bonding with aluminum would tend to occur here.

The classical theory of inductive effect would assign to the nitrogen atom of an unsymmetrical hydrazine with the greatest number of methyl groups the greater negative charge:



One would thus expect a Lewis acid such as Me_3Al to form a dative bond with this nitrogen atom. The formation of the covalent bond should produce ethane, however (eq. [3]). Since none is observed, this hypothesis is not tenable. If electronic effects influence the formation of the covalent Al—N bond, then they are of an order that cannot be inferred from the available data.

Analysis of the reaction products obtained from trimethylaluminum and either methylhydrazine (eq. [4]) or 1,2-dimethylhydrazine (eq. [5]) shows that both nitrogen atoms react with equal probability. It has been observed from the evidence available (7, 8)

$$Me_3Al + NHMeNHMe \longrightarrow \left[\begin{array}{l}\quad\quad Me\ Me\\|\quad\ |\quad\ |\\-Al-N-N-\end{array}\right]_n \qquad [4]$$

$$Me_3Al + H_2NNHMe \longrightarrow \left[\begin{array}{l}\quad Me\ H\ \ Me\\|\quad\ |\ \ |\\-Al-N-N-\end{array}\right]_n \qquad [5]$$

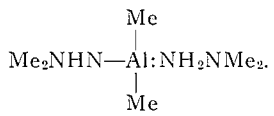
that no more than one aluminum trialkyl molecule will add to the nitrogen atom of H_2NMe; hence, the alternative structural formula:

$$\left[\begin{array}{l}Me\\|\\-Al-N-\\\quad\ |\\Me-N-H\end{array}\right]_n$$

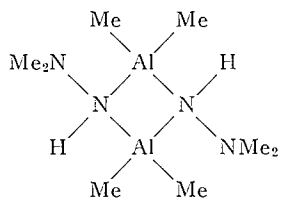
Can. J. Chem. Downloaded from www.nrcresearchpress.com by 210.87.254.5 on 09/05/12
For personal use only.

for the product of reaction [4] seems unlikely. Even when a large excess of trimethylaluminum is present and even under vigorous reaction conditions (i.e., heating for a prolonged period of time), we also found no indication that an $—NH_2$ group would react more than once with the trimethylaluminum.

A very interesting compound is formed in the reaction between 1,1-dimethylhydrazine with trimethylaluminum trimethylamine. Brown and Davidson (2) report that $Me_2Al—NMe_2$ does not react further with diethyl ether or trimethylamine to form a dative-bonded complex; however, in the case of the hydrazine reaction, a compound was isolated which appeared to contain both covalent and dative Al—N bonds:



Our molecular-weight determinations have shown that at least two of the compounds are dimeric: $[Me_2Al—NHNMe_2]_2$ and $[Me_2Al—NMeNMe_2]_2$. It has been shown (12, 13) that similar boron compounds associate through nitrogen bridges; hence, it is reasonable to assume that the dimeric compounds which we prepared also associate through Al—N bridges:



In conclusion, it can be said that, in general, hydrazines react with trimethylaluminum in the same manner as do primary or secondary amines, but the reactions of methylhydrazines and trimethylaluminum trimethylamine have produced, in some cases, compounds of unusual character. We believe that additional insight into the nature of these and similar reactions will be provided by work currently in progress at this laboratory.

ACKNOWLEDGMENTS

This work was supported by the Advanced Research Projects Agency through the Bureau of Naval Weapons, Department of the Navy. The authors wish to thank Dr. Charles P. Haber and Dr. Frederick E. Brinckman, Jr., for their assistance during the course of this work.

REFERENCES

1. F. G. A. Stone. Chem. Revs. **58**, 101 (1958).
2. H. C. Brown and N. Davidson. J. Am. Chem. Soc. **64**, 316 (1942).
3. E. Wiberg and A. May. Z. Naturforsch. **b**, **10**, 232 (1955) and Z. Naturforsch. **b**, **10**, 234 (1955).
4. J. K. Ruff and M. F. Hawthorne. J. Am. Chem. Soc. **82**, 2141 (1960).
5. J. K. Ruff and M. F. Hawthorne. J. Am. Chem. Soc. **83**, 535 (1961).
6. E. Bonitz. Ber. **88**, 742 (1955).
7. K. Ziegler and H. G. Gellert. Ann. **629**, 20 (1960). W. P. Neumann. Ann. **629**, 23 (1960).
8. K. Ziegler. Brit. Patent No. 799,823 (August 13, 1958).
9. J. M. Davidson and T. Wartik. J. Am. Chem. Soc. **82**, 5506 (1960).
10. A. W. Laubengayer, J. D. Smith, and G. G. Ehrlich. J. Am. Chem. Soc. **83**, 542 (1961).
11. J. B. Class, J. G. Aston, and T. S. Oakwood. J. Am. Chem. Soc. **75**, 2937 (1953).
12. K. Hedberg and A. J. Stosick. J. Am. Chem. Soc. **74**, 954 (1952).
13. L. M. Trefonas and W. N. Lipscomb. J. Am. Chem. Soc. **81**, 4435 (1959).

Can. J. Chem. Downloaded from www.nrcresearchpress.com by 210.87.254.5 on 09/05/12
For personal use only.

Can. J. Chem. Downloaded from www.nrcresearchpress.com by 210.87.254.5 on 09/05/12
For personal use only.

VIBRATIONAL SPECTRA OF PYRIDINIUM SALTS[1]

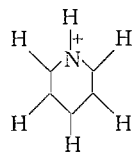
DENYS COOK

ABSTRACT

The vibrational spectrum of the pyridinium ion, $C_5H_5NH^+$, and the N-deuterated species has been studied in several pyridinium salts. By comparison with benzene and deuterobenzene (with which the pyridinium ion is isoelectronic) a fairly complete assignment has been made. The N—H bonds, which are hydrogen bonded to the anions, have stretching vibrations which show systematic variations depending on the nature of the anion. The N—H in-plane deformation vibrations show little variation while the out-of-plane deformation vibrations, some of which do vary, are probably affected, in addition, by other factors.

INTRODUCTION

Pyridine forms salts with many strong mineral and organic acids. In these salts it is assumed that complete proton transfer takes place between the acid and the pyridine molecule, giving the pyridinium ion I and an anion.



I

Little spectroscopic data on such salts is available in the published literature.* Greenwood and Wade (1) assigned a few bands from their published spectra of $C_5H_5NH^+Cl^-$ and $C_5H_5NH^+BCl_4^-$, while Kynaston and co-workers (2) listed all the bands in the latter salt. Spinner published a list of frequencies in the infrared and Raman spectrum (aqueous solution) of $C_5H_5NH^+Cl^-$ (3) and made a few assignments.

In these papers emphasis was placed on similarities between these salts and C_5H_5N. It is believed that a more pertinent and helpful comparison is between the pyridinium ion and C_6H_6. These molecules contain the same number of atoms, are isoelectronic, and, apart from the mass and electronegativity of the nitrogen atom, would be identical. This physical similarity breaks down, however, when the symmetry of the two molecules is compared. C_6H_6 has D_{6h}, and $C_5H_5NH^+$ is expected to have C_{2v} symmetry. Thus C_6H_6 has only four (strictly) infrared-active fundamentals and seven Raman fundamentals. $C_5H_5NH^+$ will have 30 Raman-active fundamentals and 27 infrared-active fundamentals. (The selection rules are shown in Table I.) The comparison between C_6H_5D and $C_5H_5ND^+$, however, reveals a much closer similarity, since both molecules now have C_{2v} symmetry, with identical selection rules.

[1]*Manuscript received May 26, 1961.*
Contribution No. 39 from the Exploratory Research Laboratory, Dow Chemical of Canada, Limited, Sarnia, Ontario. This work was presented, in part, at the Seventh Ottawa Symposium on Applied Spectroscopy, October 5, 1960.

**As this paper was being prepared, a partial listing of the frequencies in some pyridinium salts was published (R. H. Nuttall, D. W. A. Sharpe, and T. C. Waddington. J. Chem. Soc. 4965 (1960)), but not in a complete enough state to warrant comparison at this time.*

TABLE I

Selection rules for the pyridinium ion (symmetry C_{2v})

Class	Symmetry elements			Raman	I.R.	Vibrations		
	C_2 (z)	σ_v (xz)	σ_v (yz)			Ring	H	Total
A_1	*s*	*s*	*s*	*p*	*a*	5	6	11
A_2	*s*	*as*	*as*	*dp*	*ia*	1	2	3
B_1	*as*	*s*	*as*	*dp*	*a*	4	6	10
B_2	*as*	*as*	*s*	*dp*	*a*	2	4	6

Accordingly, many pyridinium salts have been prepared, together with their N-deuterated analogues,* and their infrared spectra in the solid state have been recorded with the high precision of a prism-grating spectrophotometer. The Raman shifts (of the HCl salt in aqueous solution), together with polarization measurements, were obtained through the courtesy of Dr. J. C. Evans, Chemical Physics Research Laboratory, the Dow Chemical Company, Midland, Michigan, U.S.A. (4). The spectra have been compared with those of C_6H_6 and C_6H_5D for which the assignments are known with precision and confidence (5–11).

EXPERIMENTAL

The Spectra

The spectra were recorded on a Perkin–Elmer model 221 spectrometer equipped with a sodium chloride prism-grating combination.

All the spectra were of the solid state as emulsions in nujol or fluorolube. Some of the salts which were hygroscopic, and all the deuterium salts, were handled in a dry box.

Preparation of the Compounds

$C_5H_5NH^+Cl^-$.—Anhydrous HCl was passed through an ethereal solution of pyridine. The resulting precipitate was recrystallized from a methanol–acetone mixture. M.p. 140–142° C; HCl: found: 31.5%, calc.: 31.6%.

$C_5H_5NH^+Br^-$.—An ether solution of pyridine was treated with anhydrous HBr to give a white solid which was recrystallized from a methanol–acetone mixture. M.p. 213–214° C; HBr: found: 51.7%, calc.: 50.5%.

$C_5H_5NH^+I^-$.—Aqueous HI was added to an ethereal solution of pyridine. The white precipitate so formed was recrystallized from methanol. M.p. 214° C (decomp.); HI: found: 63.0%, calc.: 61.8%.

$(C_5H_5NH^+)_2ZnCl_4^=$.—Acetone solutions of $C_5H_5NH^+Cl^-$ and $ZnCl_2$ were mixed and poured into ether; a white solid separated. This was identical with that formed when the pyridine:$ZnCl_2$ complex in warm acetone was treated with HCl. M.p. 179–182° C.

$(C_5H_5NH^+)_2SnBr_6^=$.—Chloroform solutions of $C_5H_5NH^+Br^-$ and $SnBr_4$ were mixed, and the resulting pale yellow precipitate was recrystallized from water. M.p. 280° C; Sn: found: 13.8%, calc.: 15.7%.

$(C_5H_5NH^+)_2SnCl_6^=$.—Chloroform solutions of $C_5H_5NH^+Cl^-$ and $SnCl_4$ were mixed, and the resulting white precipitate was recrystallized from water. M.p. 280° C; Sn: found: 26.0%, calc.: 24.0%; Cl: found: 45.0%, calc.: 43.7%.

$C_5H_5NH^+ClO_4^-$.—Perchloric acid (70%) was added slowly to liquid pyridine. The

**For the sake of brevity, the terms* H *salt and* D *salt may be employed in what follows. It is to be understood that* D *salt means* D *substitution for* H *only at the nitrogen atom.*

Can. J. Chem. Downloaded from www.nrcresearchpress.com by 210.87.254.5 on 09/05/12
For personal use only.

white precipitate so formed was recrystallized from 95% ethanol. M.p. 280–283° C; $HClO_4$: found: 56.9%, calc.: 56.0%.

$C_5H_5NH^+BF_4^-$.—Aqueous 50% HBF_4 added to pyridine gave a white solid, which was taken up in acetone and recrystallized by the addition of ether. M.p. 208–210° C.

$C_5H_5NH^+SbCl_6^-$.—Chloroform solutions of $C_5H_5NH^+Cl^-$ and $SbCl_5$, on being mixed, gave a white precipitate which was used without further treatment after washing with ether. M.p. 215–218° C; Sb: found: 29.1%, calc.: 29.5%; Cl: found: 53.0%, calc.: 51.3%.

Pyridinium reineckate.—Aqueous solutions of $C_5H_5NH^+Cl^-$ and reinecke salt were mixed. Removal of solvent gave a purple solid, which was recrystallized from ethanol. M.p. 205–209° C.

Deuterated salts.—Deuterated salts were prepared by twice exchanging with D_2O, the excess being pumped off *in vacuo* with a mercury diffusion pump.

RESULTS

The spectrum of one of the salts is shown in Fig. 1. It is actually as recorded on blank paper, after first recording on grid paper. The broken lines are drawn in by hand from the recorded spectrum of the deuterated compound, occasionally with slight alteration of background for the sake of clarity. Table II shows the bands in these spectra, while Table III shows a comparison of the assigned fundamentals with those of C_6H_6 and C_6H_5D. Bands due to polyatomic anions have been omitted since their locations are known and no new factors are involved.

DISCUSSION

It will be convenient to accept I as a model for the assignments of the cation. This has C_{2v} symmetry, requiring 30 fundamentals of which 3 would be inactive in the infrared; all of them would be Raman active. Table I shows the selection rules for the various vibrations, and Table IV describes their approximate character. The notation is that of Wilson (5), which has been followed by many authors. The use, in parentheses, of a capital *A* or *B* with subscript 1 or 2 obviously refers to the species of a vibration. When confusion would otherwise result, the frequency designation may be followed by H or D, in parentheses, to distinguish between the H salt and the D salt.

For the purpose of discussion, the frequencies of the salt $(C_5H_5NH^+)_2SnBr_6^=$ and its deuterated analogue will be used. Certain bands show trends depending on the anion. The $SnBr_6^=$ salt is approximately median with respect to these trends. It will be convenient to divide the spectra into four regions.

The 3500 to 1650 cm^{-1} Region

All the C—H and N—H stretching bands will occur in this region. The various spectra are characterized by large variations in frequency and intensity. Certain medium-intensity bands do show a consistent pattern and are to be identified as the C—H stretching modes above 3000 cm^{-1}. Of greater interest is the band which can be described as a N—H stretching vibration: this is ν_{7a}. It shows a large variation in intensity, band width, and frequency—from a very broad, intense band at 2439 cm^{-1} in $C_5H_5NH^+Cl^-$ to a sharp, medium intensity band at 3300 cm^{-1} in $C_5H_5NH^+SbCl_6^-$. In the median compound chosen, it is at 3236 cm^{-1} (with two submaxima) and in the deuterated salt it is at 2392 cm^{-1}, a ratio of 1.35. This band could then be properly designated as due mainly

Can. J. Chem. Downloaded from www.nrcresearchpress.com by 210.87.254.5 on 09/05/12
For personal use only.

Can. J. Chem. Downloaded from www.nrcresearchpress.com by 210.87.254.5 on 09/05/12
For personal use only.

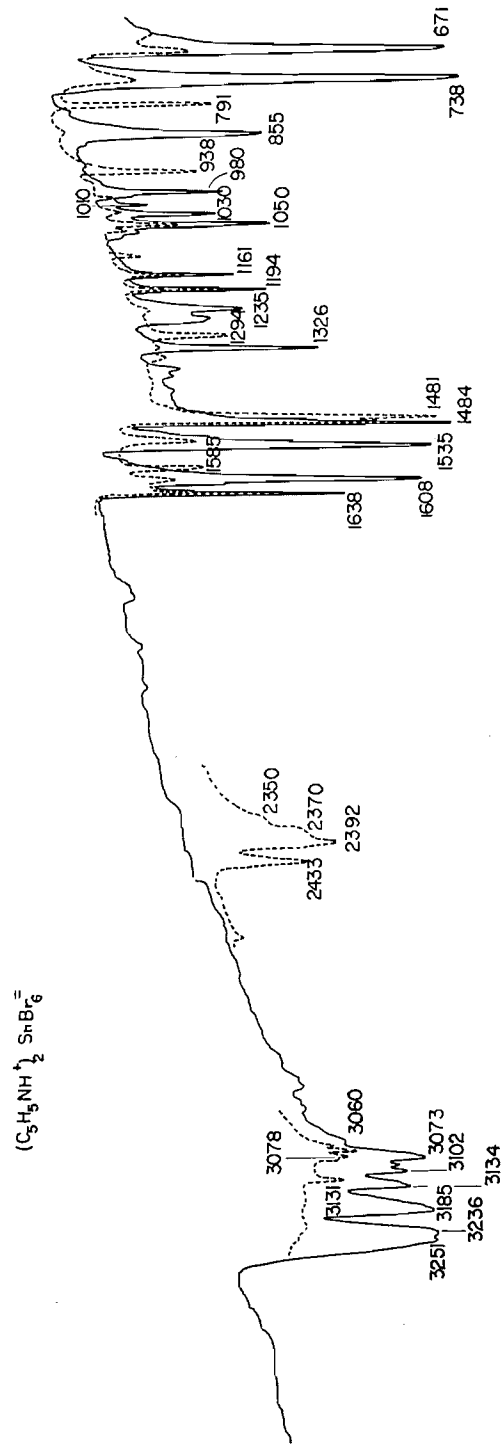


FIG. 1. Spectrum of $(C_5H_5NH^+)_2SnBr_6^=$.

to the hydrogen motion. Further discussion on the shape, intensity, and position of this band will be reserved for a later section.

The 1650 to 1400 cm^{-1} Region

All the spectra show a striking similarity in this region for all the compounds studied. Four bands of a remarkable constancy in frequency and intensity ratio are located near 1635, 1610, 1535, and 1485 cm^{-1}. This constancy in position and intensity indicates that they arise from motions unlikely to be affected by peripheral interaction, and suggests that they are due to nuclear vibrations. They have been assigned to the following vibrations respectively: ν_{8a} (A_1), ν_{8b} (B_1), ν_{19b} (B_1), ν_{19a} (A_1). The motions involved in these vibrations are visualized approximately in Fig. 2, which shows a set of normal co-ordinate

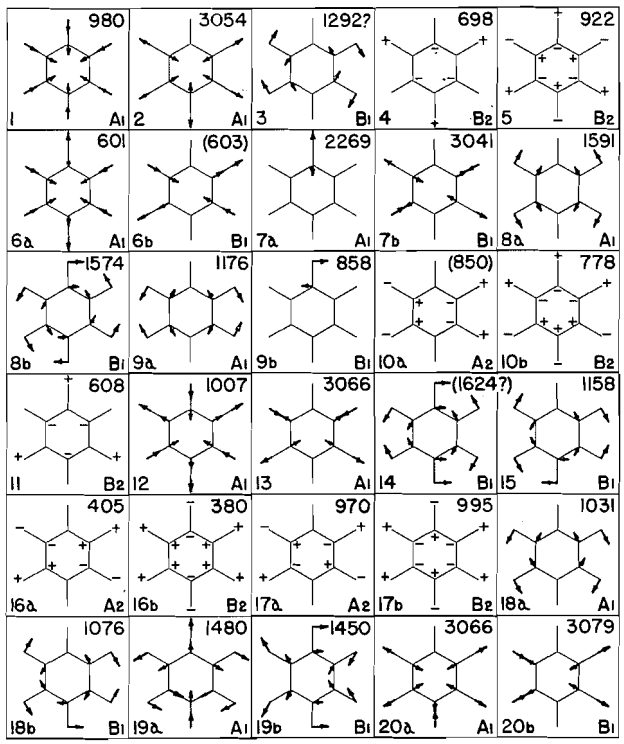


FIG. 2. Normal co-ordinate displacements for C_6H_5D.

displacements for C_6H_5D, collected from several of Ingold's papers (7). The displacements are not intended to be strictly accurate.

The Raman spectrum shows the 1635 and 1610 cm^{-1} bands to be depolarized and the 1485 cm^{-1} band probably polarized. The 1635 cm^{-1} band would be expected to be polarized completely, but even a slight polarization is consistent with a vibration of A_1 species.

The changes noticed in the N-deuterated analogue are those expected for vibrations having little or no movement of the H or D atom. The 1610 and 1535 cm^{-1} bands disappear, to be replaced by two bands at 1585 and 1475 cm^{-1}, the latter being often very close to ν_{9a} at 1485 cm^{-1}. The ratios ν_H/ν_D for ν_{8b} and ν_{19b} are 1.02 and 1.04, respectively, which are very close to those of C_6H_6 and C_6H_5D as shown in Table III.

Can. J. Chem. Downloaded from www.nrcresearchpress.com by 210.87.254.5 on 09/05/12
For personal use only.

Can. J. Chem. Downloaded from www.nrcresearchpress.com by 210.87.254.5 on 09/05/12
For personal use only.

TABLE II

Frequencies of the pyridinium ion in various salts

	Cl^-		Br^-		I^-		$ZnCl_4^=$		$SnBr_6^=$	
	H	D	H	D	H	D	H	D	H	D
	3130w	3118m	3128m	3120w	3140m	3118m	3130m 3105m	3130m	3134s	3131m
			3095m,sh					3090s	3088s	3088m
			3075m,sh	3070w					3073s	3078m
		3068m,sh				3065m	3070s	3070m	3060m	3061m
	3042s	3040s	3054s	3040m	3045m	3040m	3052m,sh	3055m	3045w	3052w
						2412m,b	3213vs	2420m	3251s	2433s
ν_{7a}	2439vs,b	1985vs,b	2591s,b	2120s,b	2833s,b	2300s,b	3155vs	2340vs,b	3236s	2392s
	2375vs,b	1915vs,b		2050s,b		2235m,b	3105vs	2315s	3185s	2370s
								2228m	3102s	2350m
ν_{8a}	1634m	1633m	1634m	1631m	1631s 1610m	1631s	1639s 1616m	1639m	1638s	1635m
ν_{8b}	1610vs	1588m	1604s	1582m	1600vs	1582m	1610s	1590m	1608vs	1585m
ν_{9b}	1532vs	1476vs	1525vs	1485vs	1525vs	1472vs	1530vs	1476vs	1535vs	1481vs
$2\ \nu_4$			1515w,sh				1513w,sh			
ν_{19a}	1488vs	1488vs	1478s	1474vs	1478vs	1478vs	1484vs	1484vs	1484vs	1486vs
$2\ \nu_{11}$	1377w		1358w		1360w		1366w			
	1342w									
ν_3	1318m	1300m	1330w	1300m	1322m	1300m	1326m	1300m	1326m	1294m
$\nu_{6a} + \nu_{6b}$			1245m		1245w		1247w,sh		1246w	
ν_{9b}	1244m	928m	1238m	927m	1235m	924m	1235m	932m	1235m	938m
ν_{9a}	1200w	1196m	1180w	1180w	1184m	1185m	1188m	1188m	1194m	1192m
ν_{15}	1162w	1160m	1150w	1150w	1148m	1150m			1161m	1160m
$\nu_{11} + \nu_{16b}$							1080w	1070w		
ν_{18b}	1060m	1058m	1052m	1055m	1050m	1050m	1050m	1050m	1050m	1050m
ν_{18a}	1030w	1030w	1029w	1025w	1029m	1025m	1028m	1025m	1030m	1025w
ν_5	1005m	812m	994m	804m	992m	793m	991m	800m	980m	791m
ν_1	995m,sh	992m	985m,sh	990m	985m,sh	989m	1007w	1008w	1010w	1008w
							910m,sh	914m,sh		
ν_{10b}	945m	720m	910w	685m	870m	685m	891m	680m	855m	680m
ν_4	750vs		750vs		741vs		750vs		738vs	
ν_{11}	680vs		678vs		671vs		675vs		671vs	

Can. J. Chem. Downloaded from www.nrcresearchpress.com by 210.87.254.5 on 09/05/12
For personal use only.

TABLE II (*Concluded*)

Frequencies of the pyridinium ion in various salts (*Concluded*)

	$SnCl_6^=$		ClO_4^-		BF_4^-		$SbCl_6^-$		$Rein^-$	
	H	D	H	D	H	D	H	D	H	D
	3140s	3139m	3148m	3140m	3148s	3148s	3151s	3140m		
	3110s				3100m	3104m	3110m	3100m		
			3090s	3096m		3090m	3095m	3090m		
	3075s	3080m		3072m			3078m,sh	3078m		
		3068m				3068w		3066w		
	3042w	3042w	3050m							
	3260s	2438s							3335s,sh	2470m,sh
	3240s	2398s	3268s	2446m	3290vs	2454s	3300s	2460s	3302s	2440s
ν_{7a}	3188s		3195s	2375s,b	3205s	2412 s	3252s	2435m		2400m
			3118m	2335m,sh	3122m	2365m	3209s	2418s		
ν_{8a}	1640s	1635m	1637m	1636m	1640s	1639m	1640m	1638m	1640m	1634m
ν_{8b}	1612vs	1586m	1610vs	1589m	1612vs	1590m	1613s	1588m	1608s	1585w
ν_{9b}	1531vs	1482vs	1538vs	1484vs	1542vs	1488vs	1541s	1492s	1538s	1478s
2 ν_4										
ν_{19a}	1482vs	1486vs	1488vs	1488vs	1490vs	1490vs	1490s	1485s	1482s	1486s
2 ν_{11}	1368w		1370w		1376w		1377w			
ν_3	1322m	1292m	1330m	1304m	1332m	1305m	1326m	1301m	1320w	1297w
$\nu_{6a} + \nu_{6b}$	1261w						1259w			
ν_{9b}	1239m	938m	1250m	930m	1255m	930m	1245w	946m	1245s	930w
ν_{9a}	1195m	1190m	1202m	1200w	1207w	1205w	1200m	1200m	1193w	1190w
ν_{15}	1164m	1159m	1170s	1170m	1174m	1172m	1168m	1164m	1161w	1160w
$\nu_{11} + \nu_{16b}$	1060w,sh						1065w	1065w	1060w	
ν_{18b}	1053m	1050m	1050vs	1050s			1050w	1050w	1048m	
	1035w									
ν_{18a}	1030m	1020w	1028vs	1028s			1030w	1025w	1029w	1025w
ν_5	982m	792m	997s	794m	990vs	797m	976m	782m	968m	780m
ν_1	1010w	1012w							1010w	1010w
ν_{10b}	862m	672m	895m,b	680m	900m,b		848m	680m	840m	680m
ν_4	740vs		748s		755s		731vs		730s	
ν_{11}	675vs		675s		681s		664vs		662s	

Can. J. Chem. Downloaded from www.nrcresearchpress.com by 210.87.254.5 on 09/05/12
For personal use only.

TABLE III

Fundamentals of benzene,* pyridinium ion, and monodeuterated* derivatives

C_6H_6					C_6H_5D				$C_5H_5NH^+$		
Raman and I.R. (gas)					Raman (liq.)	I.R. (gas)			H^+ (solid)	D^+ (solid)	
ν_{C-H}	ν_{20a}	E_{1u}	3080	I.R.	A_1	3060					
ν_{C-H}	ν_{20b}				B_1	3077	3079				
ν_{C-H}	ν_2	A_{1g}	3062	R	A_1	3055					
ν_{C-H}	ν_{13}	B_{1u}	3060	F	A_1	3060	3066		3060	3061	
ν_{C-H}	ν_{7a}	E_{2g}	3047	R	A_1	2269	2267	(1.35)	3236	2392	(1.35)
ν_{C-D}	ν_{7b}				B_1	3041			3045	3052	
ν_{C-C}	ν_{14}	B_{2u}	1309	F	B_1	1617?	1624?				
ν_{C-C}	ν_{8a}	E_{2g}	1596	R	A_1	1591			1638	1635	
ν_{C-C}	ν_{8b}				B_1	1574		(1.02)	1608	1585	(1.02)
ν_{C-C}	ν_{19a}	E_{1u}	1485	I.R.	A_1	1479	1481		1484	1486	
ν_{C-C}	ν_{19b}				B_1	1449	1452	(1.02)	1535	1481	(1.04)
δ_{C-H}	ν_3	A_{2g}	1326	F	B_1	1292			1326	1294	
δ_{C-H}	ν_{9a}	E_{2g}	1178	R	A_1	1176			1194	1192	
δ_{N-H}	ν_{9b}				B_1	857	859	(1.37)	1235	938	(1.32)
δ_{C-H}	ν_{15}	B_{2u}	1147	F	B_1	1158	1161		1161	1160	
δ_{C-H}	ν_{18a}	E_{1u}	1037	I.R.	A_1	1031	1030		1030	1023	
δ_{C-H}	ν_{18b}				B_1	1075	1078		1050	1050	
δ_{C-C}	ν_{12}	B_{1u}	1010	F	A_1	1007					
ν_{C-C}	ν_1	A_{1g}	992	R	A_1	980			1010	1008	
γ_{C-H}	ν_5	B_{2g}	985	F	B_2	922	922	(1.07)	980	791	(1.24)
γ_{C-H}	ν_{17a}	E_{2u}	970	F	A_2	970	*ia*		*ia*	*ia*	
γ_{C-H}	ν_{17b}				B_2	990	995				
γ_{C-H}	ν_{10a}	E_{1g}	849	R	A_2	850	*ia*		*ia*	*ia*	
γ_{C-H}	ν_{10b}				B_2	779	775	(1.09)	855	680	(1.26)
γ_{C-C}	ν_4	B_{2g}	703	F	B_2		698		738	620?	
γ_{C-H}	ν_{11}	A_{2u}	671	I.R.	B_2		608	(1.10)	671		
δ_{C-C}	ν_{6a}	E_{2g}	606	R	A_1	602					
δ_{C-C}	ν_{6b}				B_1	603					
γ_{C-C}	ν_{16a}	E_{2u}	405	F	A_2		*ia*		*ia*	*ia*	
γ_{C-C}	ν_{16b}				B_2	380	380	(1.06)			

*The data and assignments are those of Ingold and colleagues (7) except for ν_{14} and ν_{15} (8, 9, 11), which have been reassigned.

TABLE IV
Description of vibrations in different species

	A_1	A_2	B_1	B_2
C—H stretch	2, 13, 20*a*		7*b*, 20*b*	
N—H stretch	7*a*			
C—C (N) stretch	1, 8*a*, 19*a*		8*b*, 14, 19*b*	
C—H ∥ bend	9*a*, 18*a*		3, 15, 18*b*	
N—H ∥ bend			9*b*	
C—H ⊥ bend		10*a*, 17*a*		5, 11, 17*b*
N—H ⊥ bend				10*b*
C—C—C (N) ∥ bend	6*a*, 12			16*b*
C—C—C (N) ⊥ bend		16*a*		4

Although the frequency ratios between the H and D salts just mentioned seem satisfactory, the intensity changes on deuteration are not as clear. The 1610 cm^{-1} band, a strong band in the H salt, seems on occasion to be quite weak in some of the D salts. While changes like this are often real, it may be that the situation is complicated further by Fermi resonance between some overtone, or combination tone, and ν_{8b}. This would have an effect on the intensity of the band in the H salt but not in the D salt because of its new position. In the D salts some bands are seen near 1615 and 1610 cm^{-1}, which are thought to be real overtones or combination bands, not simply residual bands.

The 1400 to 1020 cm^{-1} Region

In this region there should be six in-plane hydrogen-deformation frequencies. In C_6H_6 and C_6H_5D, they are weak in the infrared. The same is true of the pyridinium ion. They have been identified and assigned as ν_3, 1320 cm^{-1}; ν_{9a}, 1194 cm^{-1}; ν_{9b}, 1235 cm^{-1}; ν_{15}, 1161 cm^{-1}; ν_{18a}, 1030 cm^{-1}; ν_{18b}, 1050 cm^{-1}. The changes that occur on deuteration are a shift of the 1320 cm^{-1} band to 1294 cm^{-1}, and a more pronounced shift of ν_{9b} from 1235 to 938 cm^{-1}. The ratio of these last two frequencies is 1.32, again identifying this vibration as predominantly an in-plane deformation of the hydrogen attached to the nitrogen atom. In C_6H_6 this band is at 1178 cm^{-1}, shifting to 859 cm^{-1} in C_6H_5D, a ratio of 1.37. The vibration ν_{9b} occurs at a very constant frequency in a large number of compounds. The corresponding band in pyrrole is at 1146 cm^{-1}, moving to 915 cm^{-1} in pyrrole-N-*d* (12). Here the ratio is 1.25, indicating the vibration to be a slightly mixed one.

The marked similarity in frequency of the in-plane hydrogen-deformation bands between C_6H_6 and $C_5H_5NH^+$ and their deuterated analogues is noteworthy. With the exception of ν_{9b}, the largest difference is 28 cm^{-1}, and the next largest is 16 cm^{-1}. This is to be expected if the proposed similarity between the two compounds exists. The largest difference between them is at the nitrogen atom. Thus the N—H motions would be expected to show the largest difference, with the other four C—H bonds being little different from C_6H_6.

There should also be in this region an in-plane carbon–carbon bending mode, ν_{12} (A_1). This is doubtless the Raman shift at 1050 cm^{-1} which is polarized and, therefore, belongs to the A_1 species. This band is unlikely to be strong in the infrared (it was not listed in the infrared spectrum of C_6H_5D vapor by Ingold); therefore, it seems preferable to retain the 1050 cm^{-1} band for ν_{18b} and regard ν_{12} as unidentified.

The 1020 to 640 cm^{-1} Region

This region will contain the ring-breathing and -bending modes as well as the characteristic out-of-plane hydrogen-deformation vibrations. The higher-frequency area in this

Can. J. Chem. Downloaded from www.nrcresearchpress.com by 210.87.254.5 on 09/05/12
For personal use only.

region is, unfortunately, not too well defined. The bands are weak, and their intensity ratios are variable in different salts. Neither is there any well-defined consistency in frequency such as that shown by the bands in the first two regions. These variations, however, though making the assignments a little more time consuming, eventually reveal trends which are important in determining intermolecular effects, which will be treated later.

A weak band in the infrared spectrum at 1010 cm^{-1} (998 cm^{-1} in the deuterium analogue) and at 1009 cm^{-1} in the Raman spectrum (the strongest band in the spectrum) can be confidently assigned to ν_1 (A_1), the totally symmetric ring-breathing mode.

Of the six out-of-plane hydrogen-bending frequencies, two belonging to the A_2 species are inactive in the infrared; these are ν_{17a} and ν_{10a}. A band at 980 cm^{-1} in $C_5H_5NH^+$, moving to 791 cm^{-1} (a ratio of 1.24) in $C_5H_5ND^+$, has been assigned to ν_5, by analogy with the 985 and 922 cm^{-1} bands in C_6H_6 and C_6H_5D. This band shows certain trends in different compounds, which will be discussed later, as does a band at 855 cm^{-1}, which has been assigned to ν_{10b}. This band disappears in the deuterated compound but a band at 680 cm^{-1} has been tentatively assigned to this vibration. Its precise identification hinges on the location of ν_4. The 738 cm^{-1} band fits this assignment reasonably well but it disappears on deuteration. The corresponding bands in C_6H_6 and C_6H_5D at 703 (forbidden) and 698 cm^{-1}, respectively, show virtually no shift on deuteration. The assignments in this region are hampered by the lack of knowledge of data below 640 cm^{-1}.

The ratios for the H and D species of ν_5 and ν_{10b} are 1.24 and 1.26 respectively, for the pyridinium ion; for C_6H_6 and C_6H_5D, they are 1.07 and 1.09. These are rather large differences but seem to be the most plausible assignments, though possible alternative ones are discussed in the next section.

This completes the assignments as far as possible at this stage. The assignments of the C—C (C—N) stretching modes and the C—H and N—H stretching modes, as well as the in-plane bending modes seem reasonably satisfactory, although the out-of-plane hydrogen-deformation vibrations and C—C (C—N) bending modes are rather more difficult to assign. One factor contributing is the absence of band shapes to assist vapor-phase assignments. This situation may be insuperable since experimental difficulties involved in recording a vapor-state spectrum seem formidable.

Alternative Assignments

Although the assignments in Table III seem satisfactory, some of the H/D ratios are a little different from the C_6H_6/C_6H_5D ratios, so that alternative assignments were considered in order to see if a more consistent set of values could be achieved. These are shown in Table V for the bands involving a shift on deuteration.

TABLE V

Alternative assignments of fundamentals

	C_6H_6	C_6H_5D	Ratio	$C_5H_5NH^+$	$C_5H_5ND^+$	Ratio
ν_{8b} (B_1)	1596	1574	1.02	1608	1585	1.02
ν_{19b} (B_1)	1485	1449	1.02	1535	1481	1.04
ν_{9b} (B_1)	1178	857	1.37	1235	(953)	(1.37)
ν_5 (B_2)				980	938	1.04
ν_{10b} (B_2)	849	775	1.09	855	791	1.08
ν_{11} (B_2)	671	608	1.10	671	(608)	(1.10)

The assignments of the 1610 and 1535 cm^{-1} bands to ν_{8b} and ν_{19b} seem unquestionably

Can. J. Chem. Downloaded from www.nrcresearchpress.com by 210.87.254.5 on 09/05/12
For personal use only.

correct. However, by displacing the other bands progressively to the next lower assignment, such that the 938 cm^{-1} band is allotted to ν_5, etc., an impressive agreement between the ratios is noticed. The figures in parentheses in Table V are calculated assuming the same ratio for the pyridinium series as for the benzene series.

The test of this set of assignments seems to be in the fate of the vibration ν_{9b} (D). If the 938 cm^{-1} band is allocated to ν_5 (D), then it is difficult to find a suitable band for ν_{9b} (D). Its calculated value would be about 953 cm^{-1}. No band near this frequency has been seen, unless it is obscured by the band at 938 cm^{-1}. (It will be recalled that ν_5 is a band which shows a trend depending on the anion.) This is unlikely since ν_5 is generally weak, and no structure can be observed in it. Moreover, it becomes even more unlikely to have to assume that ν_{9b} (D) is always hidden by ν_5 (D).

Another assumption, which begs the question, and is equally unpalatable, is that ν_{9b} (D) is so weak that it is unobservable even in thick films (or with electronic ordinate expansion). ν_{9b} for C_6H_5D is actually a medium strong band and is easily observable. It seems, therefore, that this assumption is unlikely to be valid for the pyridinium ion.

The alternative assignments quoted in Table V seem to require too many coincidences to appear plausible. They are considered simply because the other assignments seem to give H/D ratios which are not consistent between the benzene and pyridinium series. There may be good reasons why these ratios should not be so similar in the two compounds. The vibrations considered involve the nitrogen atom and the hydrogen atom attached to it. There is no doubt that this is a highly polar link, much more so than the C—H link in C_6H_6. It is, perhaps, therefore, not too unreasonable to expect different H/D ratios between the two compounds.

Comparison with Other Studies

Two previous papers have considered assignments of the pyridinium ion. Greenwood and Wade (1) made assignments after studying the hydrochloride and the tetrachloroborate; Spinner (3) published the Raman spectrum of an aqueous solution of the hydrochloride. Their results are shown in Table VI and compared with the present infrared data, and the Raman shifts measured by Evans (4).

All authors agree on the assignment of the 1634 and 1610 cm^{-1} bands to ν_{8a} and ν_{8b}. Greenwood and Wade reverse ν_{19a} and ν_{19b}, while Spinner does not record the 1535 cm^{-1} band. The presence of the almost certainly polarized band at 1490 cm^{-1}, although weak, justifies designation of this band as ν_{19a} of A_1 species rather than ν_{19b} of B_1 species. The absence of the 1532 cm^{-1} band in both Raman spectra can be taken as strong evidence that it is extraordinarily weak and, therefore, not an A_1 band.

Of the two bands at 1200 and 1244 cm^{-1}, the latter, because of its disappearance on N-deuteration, must be associated with the nitrogen—hydrogen atom. The analogy with the benzene spectrum, and the lower intensity of the Raman shift compared with the 1200 cm^{-1} band, establish the 1244 cm^{-1} band as ν_{9b} (B_1). The 1200 cm^{-1} band must then be ν_{9a} (A_1), though it is not polarized.

The Raman studies show the 1162 cm^{-1} band as depolarized and quite weak. This is in keeping with the species and assignment of ν_{15} (B_1).

The assignment of the 1030 and 1060 cm^{-1} infrared bands to ν_{18a} (A_1) and ν_{18b} (B_1) is firmly supported by the Raman shift at 1025 cm^{-1}, which is polarized and intense. The 1060 cm^{-1} band has been assigned to ν_{18b}, more by analogy with benzene than by regard to the Raman data. ν_{18b} in benzene was at 1075 cm^{-1}, but ν_{12} was not observed in the infrared vapor spectrum. It is, therefore, not inconsistent to assign the infrared 1060 cm^{-1}

Can. J. Chem. Downloaded from www.nrcresearchpress.com by 210.87.254.5 on 09/05/12
For personal use only.

TABLE VI

Fundamentals of $C_5H_5NH^+Cl^-$ by various authors

			I.R.*	I.R.†	I.R.‡	Raman‡	Raman§
ν_{N-H}	ν_{7a}	A_1	2840	2439			
			2740	2375			
ν_{C-C}	ν_{8a}	A_1	1631	1634	1630	1635 (12)‖	1636 (19) D¶
ν_{C-C}	ν_{8b}	B_1	1603	1610	1604	1615 (4)	1613 (12) D
ν_{C-C}	ν_{19a}	A_1	1530	1488	1479		1490 (2) ?
ν_{C-C}	ν_{19b}	B_1	1481	1532	1428		
δ_{C-H}	ν_3	B_1	1252	1318	1332	1334 (2)	
δ_{C-H}	ν_{9a}	A_1		1200	1189	1201 (10)	1200 (16) D
δ_{N-H}	ν_{9b}	B_1		1244	1245	1245 (3)	1254 (9) D
δ_{C-H}	ν_{15}	B_1	1198	1162	1155	1162 (2)	1163 (4) D
δ_{C-H}	ν_{18a}	A_1	1168	1030	1027	1027 (22)	1025 (50) P
δ_{C-H}	ν_{18b}	B_1		1060	1053	1060 (5)	
δ_{C-C}	ν_{12}	A_1	1059				1060 (11) P
ν_{C-C}	ν_1	A_1	1003	995	997	1010 (75)	1009 (100) P
γ_{C-H}	ν_5	B_2	940	1005	1012		
γ_{C-H}	ν_{10b}	B_2		945		952 (4)	
γ_{C-C}	ν_4	B_2	759	750	749		
γ_{C-H}	ν_{11}	B_2	684	680	682		
δ_{C-C}	ν_{6a}	A_1				639 (11)	637 (16) D
δ_{C-C}	ν_{6b}	B_1				611 (7)	611 (7) D
γ_{C-C}	ν_{16b}	B_2				393 (2)	396 (4) P

*Greenwood and Wade (1).
†This work.
‡Spinner (3).
§Evans (4).
‖Figures in parentheses refer to relative intensities.
¶Bands marked P are definitely polarized; those marked D appear to be depolarized but may be slightly polarized.

band to ν_{18b} while assigning the polarized 1060 cm^{-1} Raman shift to ν_{12} (A_1). Greenwood and Wade have ν_{12} (A_1) at 1059 cm^{-1} and this may indeed be so.

No exception is taken to the universal assignment of the band near 995 cm^{-1} to the totally symmetric ring-breathing mode, ν_1. It is the strongest band in the Raman spectrum and is polarized although it is weak in the infrared.

The out-of-plane hydrogen deformations ν_5 and ν_{10b} are assigned chiefly on their movement upon N-deuteration. No help can be gleaned from the Raman data since no bands were observed in this region. The 952 cm^{-1} band quoted by Spinner is said by Evans to be the 1009 cm^{-1} band excited by the 4348-Å Hg line.

The intense bands at 754 and 682 cm^{-1} are unequivocally assigned to ν_4, the ring-bending mode, and ν_{11}, the out-of-plane hydrogen deformation, respectively. Although these bands are not visible in the Raman shifts, their characteristic intensity and position in the infrared spectrum are unmistakable.

The assignments of the bands having been considered, it is now convenient to examine the variations or trends in certain bands that have been briefly noted previously.

Variation of ν_{7a}

Table VII shows the variation in frequency of ν_{7a}. Some of these bands are not single bands, but have two, three, or occasionally four components. The second column in the table is the one of strongest intensity.

This band varies in frequency from 2439 cm^{-1} in $C_5H_5NH^+Cl^-$ to 3302 cm^{-1} in pyridinium reineckate. As noted earlier, it is broad and strong at low frequencies, but becomes sharper and less intense as it moves towards higher frequencies. Half widths for some of the bands at higher frequency are: $SnBr_6^=$, 68 cm^{-1}; $SnCl_6^=$, 76; ClO_4^-, 93; BF_4^-, 95; $SbCl_6^-$, 76. Undoubtedly the breadth, intensity, and low frequency are due to a strong

Can. J. Chem. Downloaded from www.nrcresearchpress.com by 210.87.254.5 on 09/05/12
For personal use only.

TABLE VII

Pyridinium ion frequencies: nitrogen—hydrogen stretching frequencies, ν_{7a}

	H	D	H	D	H	D	H	D
Cl^-			2439 (1.23)	1985	2375 (1.24)	1915		
Br^-			2591 (1.22)	2120		2050		
I^-		2412	2833 (1.23)	2300		2225		
$ZnCl_4^=$	3213 (1.33)	2420	3155 (1.35)	2340	3105 (1.34)	2315		2228
$SnBr_6^=$	3251 (1.34)	2433	3236 (1.35)	2392	3185 (1.34)	2370	3102 (1.32)	2350
$SnCl_6^=$	3260 (1.33)	2438	3240 (1.35)	2398	3188			
ClO_4^-			3268 (1.34)	2446	3195 (1.35)	2375	3118 (1.34)	2335
BF_4^-			3290 (1.34)	2454	3205 (1.33)	2412	3122 (1.33)	2365
$SbCl_6^-$			3300 (1.34)	2460	3252 (1.33)	2435	3209 (1.33)	2418
$Rein^-$	3335 (1.35)	2470	3302 (1.35)	2440	3238 (1.35)	2400		

interaction between the nitrogen hydrogen and a small anion associated with an intense force field. In the series Cl^-, Br^-, I^-, as the anion gets larger and the force field weakens as the effect of the anionic charge is diminished by more and more completed electron shells, the band is found at 2439, 2591, and 2833 cm^{-1}, respectively. For the compounds containing polyatomic anions associated with weak peripheral force fields, the frequency rises to higher values, till, with anions such as the hexachloroantimonate, it is questionable whether there is any significant interaction, and the N—H stretching frequency might be termed free.

This behavior has been noted and discussed by Chenon and Sandorfy (various amine salts) (13), Ebsworth and Sheppard (trimethylamine salts) (14), Nakanishi, Goto, and Ohashi (various amine salts) (15), and, most recently, by Mathieu and Poulet (ammonium salts) (16), who also have the most extensive list of anions. Nakanishi *et al.* were of the opinion that the tetraphenyl boron anion represented a case of a free N—H stretching frequency. Mathieu and Poulet question this, however, and quote higher frequencies than that in the $B(C_6H_5)_4^-$ salt, and consider that there may be some interaction between the nitrogen hydrogen and the π electrons of the aromatic rings. Such phenomena have been considered previously by several authors (17–19). Be this as it may, $C_5H_5NH^+B(C_6H_5)_4^-$ certainly does have a lower frequency than pyridinium reineckate, or $C_5H_5NH^+SbCl_6^-$: it absorbs at 3215 cm^{-1}.

The presence of multiple N—H stretching bands is an interesting and controversial aspect of hydrogen bonding in amine salts. It has been suggested (20) that they are due to a double minimum in the potential surface of the vibrating species, though this is unlikely to be so in the present cases. One consideration to be borne in mind is that there may be different N—H---X distances within the structure, giving rise to different frequencies. This is certainly so in the one structure that is known. In pyridinium reineckate, $C_5H_5NH^+[Cr(NCS)_4(NH_3)_2]^-$, the organic ion is surrounded by 12 sulphur atoms belonging to N≡C—S^- groups (21). Nearest to the nitrogen—hydrogen atom, are two sulphur atoms at 3.36 Å and two at 3.60 Å. These are large distances but may be construed as very weak hydrogen bonds, giving rise to the two bands at 3238 and 3302 cm^{-1}. Preliminary data, supplied through the courtesy of Dr. C. Rérat, Bellevue, Paris, indicate a short hydrogen bond of 2.95 Å for the N—H---Cl bond in pyridine hydrochloride (22). At present it is not known whether there are other hydrogen bonds of different length in the structure.

Associated with this possibility, however, is the view that the satellites to the intense N—H stretching vibration are due to combination and difference bands between the

Can. J. Chem. Downloaded from www.nrcresearchpress.com by 210.87.254.5 on 09/05/12
For personal use only.

main fundamental and a low-frequency vibration associated with the N---X vibration in a hydrogen bond N—H---X (20).

Variation of ν_{9b}

It is rather surprising to find very little variation throughout the salts studied in the value of ν_{9b}, since it has been suggested that as a hydrogen bond is formed the stretching-vibration frequency is lowered, but the bending-vibration frequency is raised (23). The largest and smallest values are 1255 and 1230 cm^{-1}, and in the deuterated salt, 946 and 927 cm^{-1}. There is no smooth relation between ν_{9b} and ν_{7a} as the values in Tables VII and VIII show.

TABLE VIII

Pyridinium ion frequencies: in-plane and out-of-plane hydrogen-deformation frequencies

	ν_{9b}		ν_5		ν_{10b}		ν_{11}
	H	D	H	D	H	D	H
Cl^-	1244 (1.34)	928	1005 (1.24)	812	945 (1.31)	720	680
Br^-	1238 (1.33)	927	994 (1.22)	804	900 (1.31)	685	678
I^-	1235 (1.34)	924	992 (1.25)	793	870 (1.28)	685	671
$ZnCl_4^=$	1235 (1.33)	932	991 (1.24)	800	891 (1.31)	680	675
$SnBr_6^=$	1235 (1.32)	938	980 (1.24)	791	855 (1.26)	680	671
$SnCl_6^=$	1239 (1.32)	938	982 (1.24)	792	862 (1.28)	672	675
ClO_4^-	1250 (1.34)	930	997 (1.26)	794	895 (1.32)	680	675
BF_4^-	1255 (1.35)	930	990 (1.24)	797	900		681
$SbCl_6^-$	1245 (1.32)	946	976 (1.25)	782	848 (1.25)	680	664
$Rein^-$	1245 (1.34)	930	968 (1.24)	780	840 (1.24)	680	662

A study of the hydrogen-bending mode in trimethylamine-N-oxide salts has revealed (24) a difference of 15 cm^{-1} between the hydrochloride (1525 cm^{-1}) and the hydrobromide (1510 cm^{-1}), though four other salts ($B(C_6H_5)_4^-$, BF_4^-, ClO_4^-, and I^-) were reasonably constant around ~1500 cm^{-1}. There is a difference of ~700 cm^{-1} in the stretching vibration. Again it should be noted that the hydrofluoride has not been studied yet, and there may be a large difference between this and other salts. The situation is very similar in the trimethylamine salts as Table IX shows. The ammonium salts show

TABLE IX

Hydrogen-bending frequencies in some amine salts

	Me_3NOH^+	Me_3NH^+	NH_4^+	$C_5H_5NH^+$
F^-			1485	
Cl^-	1525	1482	1393	1245
Br^-	1510	1476	1385	1230
I^-	1498	1474	1388	1235
ClO_4^-	1505			1250
BF_4^-	1507			1255
BPh_4^-	1490	1478		

quite clearly a large difference between the fluoride and the other halides, which has been discussed by Plumb and Hornig (25).

Thus is would seem that while the hydrofluorides and hydrochlorides of these bases may have higher bending frequencies, salts with other anions show no systematic variations but minor differences due to coupling or mechanical interaction. Not enough types of

Can. J. Chem. Downloaded from www.nrcresearchpress.com by 210.87.254.5 on 09/05/12
For personal use only.

salts have been studied to see whether this behavior is the exception rather than the rule. Mathieu and Poulet's paper unfortunately gave no data on the bending modes. Miller and Wilkins (26), however, showed that for about 15 ammonium salts there was only a small variation of about ± 15 cm^{-1} in the bending frequency.

Variation of ν_5, ν_{10b}, and ν_{11}

ν_5, ν_{10b}, and ν_{11} are out-of-plane hydrogen-deformation vibrations (see Table VIII). They all show variations with the nature of the anion, that of ν_5 being the most convincing. A smooth relation between ν_5 and ν_{7a} suggests a connection between them. This is in line with the expectation that deformation frequencies get smaller, as stretching frequencies get larger, as hydrogen bonds get weaker. The total variation in ν_5 is really quite small, about 35 cm^{-1}, though most of this occurs in the last two salts, the hexachloroantimonate and the reineckate.

The case of ν_{10b} is a little more difficult. A total variation of about 105 cm^{-1} is observed, but much of the variation is random, without the fairly smooth relation that ν_5 exhibits. ν_{11} shows quite a small variation, only 20 cm^{-1}, again mostly to be seen in the last two compounds in the list, the hexachloroantimonate and the reineckate. Neglecting these two, the variation is 11 cm^{-1}, which cannot be called significant.

These variations in the bands just considered, at first sight seem to support the view that deformation frequencies rise as hydrogen bonds get stronger. However, because of the large deviations from a linear relationship between the stretching frequency, ν_{7a}, and the deformation frequency, this view must be taken as tentative at this stage. The near constancy of ν_{9b} and ν_{11} also does not support this view. There may be mechanical factors involved, too, which could complicate the matter.

ACKNOWLEDGMENTS

I am greatly indebted to Dr. J. C. Evans for his measurements of the Raman shifts in pyridine hydrochloride and for helpful discussion, and to Dr. C. Rérat for information on the structure of pyridine hydrochloride, before publication. The assistance of Miss C. D. Anderson in preparing some of the compounds and recording their spectra, and of Mr. D. G. Barnes for some of the analyses, is gratefully acknowledged.

REFERENCES

1. N. N. Greenwood and K. Wade. J. Chem. Soc. 1130 (1960).
2. W. Kynaston, B. E. Larcombe, and H. S. Turner. J. Chem. Soc. 1772 (1960).
3. E. Spinner. J. Chem. Soc. 1226 (1960).
4. J. C. Evans. Private communication.
5. E. B. Wilson, Jr. Phys. Rev. **45**, 706 (1934).
6. A. Langseth and R. C. Lord. Danske Videnskab. Selskab, Mat.-fys. Medd. **16**, 6 (1938).
7. C. R. Bailey, R. R. Gordon, J. B. Hale, N. Herzfeld, C. K. Ingold, and H. G. Poole. J. Chem. Soc. 299 (1946).
8. R. D. Mair and D. F. Hornig. J. Chem. Phys. **17**, 236 (1949).
9. F. A. Miller. J. Chem. Phys. **24**, 996 (1956).
10. S. Califano and B. Crawford, Jr. Spectrochim. Acta, **16**, 889 (1960).
11. J. R. Scherer and J. Overend. Spectrochim. Acta, **17**, 719 (1961).
12. R. C. Lord and F. A. Miller. J. Chem. Phys. **10**, 328 (1942).
13. B. Chenon and C. Sandorfy. Can. J. Chem. **36**, 1181 (1958).
14. E. A. V. Ebsworth and N. Sheppard. Spectrochim. Acta, **13**, 261 (1959).
15. K. Nakanishi, T. Goto, and M. Ohashi. Bull. Chem. Soc. Japan, **30**, 403 (1957).
16. J. P. Mathieu and H. Poulet. Spectrochim. Acta. **16**, 696 (1960).
17. M. L. Josien and N. Fuson. J. Chem. Phys. **22**, 1169 (1954).
18. D. Cook. J. Chem. Phys. **25**, 788 (1956).
19. D. S. Trifan, J. L. Weinmann, and L. P. Kuhn. J. Am. Chem. Soc. **79**, 6566 (1957).

Can. J. Chem. Downloaded from www.nrcresearchpress.com by 210.87.254.5 on 09/05/12
For personal use only.

20. N. SHEPPARD. *In* Hydrogen bonding. *Edited by* D. Hadzi. The Pergamon Press Ltd., London. 1959. p. 85. Review (with references) of the present position.
21. Y. TAKEUCHI and Y. SAITO. Bull. Chem. Soc. Japan, **30**, 319 (1957).
22. C. RÉRAT. Private communication.
23. G. C. PIMENTEL and A. L. MCCLELLAN. The hydrogen bond. W. H. Freeman and Co., San Francisco. 1960. p. 118.
24. D. COOK. In preparation.
25. R. C. PLUMB and D. F. HORNIG. J. Chem. Phys. **23**, 947 (1955).
26. F. A. MILLER and C. H. WILKINS. Anal. Chem. **24**, 1254 (1952).

Can. J. Chem. Downloaded from www.nrcresearchpress.com by 210.87.254.5 on 09/05/12
For personal use only.

Can. J. Chem. Downloaded from www.nrcresearchpress.com by 210.87.254.5 on 09/05/12
For personal use only.

SOME FACTORS AFFECTING THE KÖNIGS–KNORR SYNTHESIS OF GLYCOSIDES[1]

H. R. GOLDSCHMID[2] AND A. S. PERLIN

ABSTRACT

Glycosyl halides decompose readily in the presence of silver oxide under conditions generally used for the Königs–Knorr synthesis of glycosides. This "side reaction" probably accounts for the low yields commonly obtained in the synthesis of oligosaccharides, particularly those involving the formation of a glycosidic union through an unreactive secondary position. The rate of the side reaction, as well as that of the normal condensation reaction, is dependent on the condition of the silver oxide, and is retarded markedly by elemental iodine. This latter effect appears to be related to the improved yield obtained in Königs–Knorr syntheses when iodine is used. Among the products formed in the decomposition of 2,3,4,6-tetra-*O*-acetyl-α-D-mannopyranosyl bromide are 2,3,4,6-tetra-*O*-acetyl-D-mannose, a heptaacetyl 1,2,1′-linked dimeric orthoacetate, and a second high-molecular-weight compound that also shows ortho ester properties.

The Königs–Knorr reaction (1)—the condensation of a glycosyl halide with a hydroxylic compound in the presence of a catalyst or acid acceptor—constitutes a method of high stereochemical selectivity for the synthesis of glycosides. Several detailed reviews and articles deal with the mechanism of this reaction and its many applications (2–9). Although glycosides of simple alcohols and phenols may usually be prepared in high yield, the method is less generally effective for oligosaccharides. This is true particularly when the hydroxylic component is relatively unreactive. Yields of disaccharides thus are optimal (60–75%) when the glycosyl unit is coupled with a primary hydroxyl group (5, 10, 11), and much lower (frequently less than 10%) when the condensation involves an anomeric or a secondary hydroxyl group (5, 12, 13).

Generally, the synthesis of oligosaccharides involves the use of an "inert" solvent (e.g., chloroform or benzene), a desiccant to minimize hydrolysis of the glycosyl halide, and a condensing agent. Most commonly, the condensing agent is silver oxide or carbonate. Using these normal Königs–Knorr conditions for preparing certain disaccharides we have found that a reaction occurs readily between the acetohalogen sugar and the condensing agent *even in the absence of an added hydroxylic component.* Thus, addition of silver oxide to a solution of tetra-*O*-acetyl- (or *O*-benzoyl-) α-D-mannopyranosyl or D-glucopyranosyl bromide in dry benzene or chloroform resulted in a rapid drop in the optical rotation of the solution (Table I). Chromatographic examination of the reaction mixture at intervals (after prior treatment with sodium methoxide) showed that this drop was caused by decomposition of the halide and that derivatives of the parent hexose (i.e., D-mannose or D-glucose) were being formed.* The amount of rotatory change, to a maximum value, depended on the proportion of silver oxide used (Table I), and when this maximum change had occurred, little, or none, of the glycosyl halide remained intact. However, there was a wide variation in the activity of oxide samples from different

[1]*Manuscript received June 12, 1961.*
Contribution from the National Research Council of Canada, Prairie Regional Laboratory, Saskatoon, Saskatchewan.
Issued as N.R.C. No. 6512.
[2]*National Research Council of Canada Postdoctorate Fellow, 1958–60.*
**The glycosyl halides themselves are converted by excess sodium methoxide to the methyl glycosides. Hence, both the parent sugar and glycoside were detected in varying proportions at intermediate stages of the reaction between the halides and silver oxide (see footnotes, Table I).*

TABLE I

Rotatory changes on treatment of tetra-*O*-acetyl-α-D-glycosyl bromides with silver oxide

Halide	Solvent	Ag_2O/halide, equivalents	Observed rotation* in deg (and time in hr)					
D-Mannose	Benzene	1.4	5.50	(0)†	4.78	(1.5)	4.69	(18)
		4.0	"		2.38	(0.8)	2.27	(18)†
		8.0	"		0.43	(0.5)	−0.03	(18)§
		16.0	"		—		−0.17	(18)
		4.0‖	3.98	(0)	0.42	(7)	0.10	(18)
D-Mannose	Benzene–pyridine (75:25)	—	4.48	(0)	4.40	(6)	3.94	(18)
D-Mannose	Chloroform	4.0	3.33	(0)	1.56	(2.5)	−0.05	(10)
		8.0	"		0.64	(2.5)	−0.04	(10)
		4.0‖	3.28	(0)	0.94	(1)	0.06	(12)
D-Mannose	Tetrahydrofuran	4.0	3.14	(0)	2.18	(0.5)	0.28	(3)
		8.0	"		0.74	(1.0)	−0.08	(3)
		4.0‖	"		1.14	(1.0)	−0.40	(10)
D-Mannose (benzoate)	Benzene	8.0	1.56	(0)	−3.80	(5)		
D-Glucose	Benzene	8.0	5.70	(0)†	1.20	(1)§		
		8.0‖	"		1.95	(1)		

*α_D (1 dm); the concentration was generally 5–10%.
†Paper chromatographic examination of the deacetylated (with sodium methoxide) material showed methyl glycoside, no hexose.
‡Paper chromatographic examination of the deacetylated (with sodium methoxide) material showed methyl glycoside *plus* hexose.
§Paper chromatographic examination of the deacetylated (with sodium methoxide) material showed hexose, no methyl glycoside.
‖Silver carbonate.

sources, as shown by the varied amount of rotatory change produced* (Table II). The glycosyl halides were vigorously decomposed also with silver carbonate as well as in other solvents (e.g., tetrahydrofuran), but were much more stable in the presence of a soluble base, pyridine. These effects suggested that the metallic oxides serve as catalysts of the observed "side reaction", possibly as in the solvolysis of alkyl halides (16, 17).

TABLE II

Variation in activity of silver oxide (tetra-*O*-acetyl-α-D-mannosyl bromide (50 mg) in benzene (2 ml) containing Drierite (0.7 g) and silver oxide (25 mg); initial α_D 1.95° (0.5 dm))

Silver oxide	α_D° (5 hours)*
Prepared according to ref. 14	−0.26†
Prepared according to ref. 28	0.65
Commercial sample 1	0.69
Commercial sample 2	0.90
Commercial sample 3	1.43‡

*At 18 hours the rotational values were virtually unchanged.
†Paper chromatographic examination of the deacetylated (with sodium methoxide) material showed mannose, no methyl mannoside.
‡Paper chromatographic examination of the deacetylated (with sodium methoxide) material showed mannose *plus* methyl mannoside.

The reaction products isolated after treatment of the acetylated glycosyl halides with silver oxide in benzene were amorphous solids essentially free from halogen. They did

**Helferich and Klein (14) have noted that the effectiveness of silver oxide in disaccharide syntheses varies with the method of preparation of the oxide. The age of the oxide may also be important, and hence the literature contains frequent references to the use of a "freshly-prepared" sample. Two of the samples tested in the current study were found to be stable over a period of 1 year whereas the activity of a third sample decreased slowly. The importance of using properly prepared silver chloride for converting an α-D-glycosyl bromide to the β-D-chloride (15) is perhaps a related example of how the condition of a silver salt may affect the reactions of glycosyl halides.*

Can. J. Chem. Downloaded from www.nrcresearchpress.com by 210.87.254.5 on 09/05/12
For personal use only.

Can. J. Chem. Downloaded from www.nrcresearchpress.com by 210.87.254.5 on 09/05/12
For personal use only.

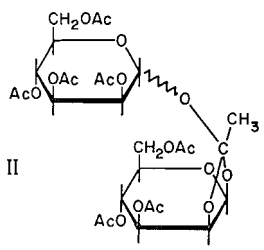
not exhibit unsaturated properties and absorbed weakly in the infrared region characteristic of hydroxyl groups. Elemental analysis data suggested that formation of these products involved the introduction of one oxygen atom per two tetraacetyl hexosyl residues (R), as represented by the reaction

$$2RBr + Ag_2O \rightarrow ROR + 2AgBr.$$

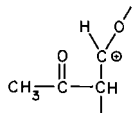
Consistent with this possibility was the finding that the reaction products contained a high proportion of dimeric (and possibly trimeric) components. These components were readily detected chromatographically, after deacetylation with sodium or barium methoxide, as material travelling at the rate of disaccharides and higher oligosaccharides. However, the free hexose was the major product found on the chromatograms.

By column chromatography on silicic acid, several fractions were obtained from each reaction product. Those fractions derived from the D-glucosyl bromide were syrups, but in the D-mannose series three crystalline compounds were isolated. Of these, the major identifiable product was 2,3,4,6-tetra-*O*-acetyl-D-mannose (I) (isolated as the α-anomer), accounting for about 25% of the total. The two other products (II and V) each amounted to about 10% of the mixture and, on deacetylation, were found to correspond chromatographically to two of the slow-moving materials referred to in the preceding paragraph.

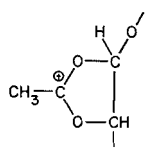
The total acetyl content (C-methyl groups) of compound II was greater than the *O*-acetyl content, the ratio of the two values being 8 to 7. When deacetylated with sodium methoxide, II afforded a crystalline material (III) which was reconverted to II by acetylation. Compound III was easily hydrolyzed by cold dilute acid to mannose and a syrupy product (IV) which, chromatographically and from a comparison of infrared absorption spectra, was indistinguishable from 2-*O*-acetyl-D-mannose (18, 19). These properties, together with the C-methyl content of III, suggested that III is composed of two D-mannose units linked by an orthoacetate structure, and that II is the corresponding heptaacetate. Further evidence for the presence of an ortho ester grouping in II was the rapid rotatory change produced by treatment with dilute methanolic hydrogen chloride, which closely paralleled that observed for other *O*-acetyl orthoacetates of D-mannose (19, 20, 21). As with tri-*O*-acetyl-D-mannose methyl 1,2-orthoacetate, the methanolysis yielded a product which appears to be 3,4,6-tri-*O*-acetyl-D-mannose (20, 22). Methylation of III via the liquid-ammonia procedure (23) afforded a crystalline ether which on hydrolysis yielded a tri- and a tetra-methyl derivative. From these data the structure of II is tentatively assigned a 1,2,1′-orthoacetyl linkage, as in formula II (Ac = CH_3CO).



II



VII



VIII

The molecular weight of V suggested that this product also is dimeric, and with methanolic hydrogen chloride the compound showed properties closely similar to those observed with II. On deacetylation with sodium methoxide, V yielded the crystalline

compound VI, which on a paper chromatogram was much slower than III and contained slightly less than one C-methyl group per two hexose units. Gentle acid hydrolysis of VI afforded mannose and a syrupy reducing ester which, however, was not 2-*O*-acetyl-D-mannose. This ester, on deacetylation with sodium methoxide, yielded non-reducing components as well as mannose. Hence V is not an isomer of II, although it also shows ortho ester properties. A more complete characterization of these new ortho esters and their various degradation products is being carried out. For the present purposes, however, it is clear that at least two types of high-molecular-weight ortho esters are produced during the decomposition of tetra-*O*-acetyl-α-D-mannosyl bromide in the presence of silver oxide.

The high-molecular-weight products formed in the decomposition of the D-glucosyl bromide also appear to be ortho esters since, as noted earlier, they are stable to methoxide ion, but were found to be hydrolyzed easily by acid. It is presumed, therefore, that the compounds are structurally akin to the D-mannose derivatives II and V.

Water appears to play a role in the formation of these products. Thus, tetra-*O*-acetyl-D-mannose may be derived from the bromide by hydrolysis. In the presence of silver ion this would be expected to involve dissociation of the bromide to yield a carbonium ion (e.g., partial structures VII and/or VIII) (6, 7, 8). Reaction, in turn, of the tetraacetate with VIII could yield an orthoacetate, such as II, but the formation of V appears to involve additional pathways. The practical difficulty of achieving completely anhydrous conditions (24),* together with the high efficiency of water in solvating carbonium ions, makes it possible that the water required for such reactions could be derived from sources such as the solvent, silver oxide,† or atmosphere. Since much of the reaction product is unaccounted for, there is the possibility also that water is produced by reaction of the silver oxide with hydrogen bromide, the elements of which come from the glycosyl halide. Alternatively, in view of the catalytic aspects of the reaction, it is not inconceivable that compounds such as II and V are produced on the surface of the silver oxide without the involvement of D-mannose tetraacetate, and that the latter is formed, at least partially, by hydrolysis of labile intermediates during processing of the reaction products. In any event, all attempts made in the present study to exclude and remove moisture from the reaction mixtures, including the precautions generally employed in Königs–Knorr syntheses (5), were ineffective in preventing the side reactions.

That side reactions of the same type occur during Königs–Knorr syntheses was shown by condensing the aforementioned glycosyl halides with 1,2,3,4-tetra-*O*-acetyl-β-D-glucose under conditions similar to those recommended by Reynolds and Evans (11). When the reaction mixtures were examined chromatographically at intervals, after prior treatment with sodium methoxide, it was found that a high proportion of the acetohalogen sugar present initially could not be accounted for either as synthesized gentiobiose or as unchanged material (i.e., as the methyl glycoside). With the D-mannosyl bromides the effect was more clearly evident from the appearance of an increasing proportion of free mannose.

Since water is a by-product of these syntheses, i.e.,

$$2RX + 2R'OH + Ag_2O \rightarrow 2ROR' + 2AgX + H_2O,$$

side reactions may be expected to occur even more readily when the hydroxylic component

*It is possible that the reaction of these glycosyl halides with silver oxide is related to the rotational changes exhibited by solutions of glycosyl chlorides of the "unstable" series, i.e., by 1,2-trans-(e,e)-chloride-acetates (see ref. 6). Recent evidence (24) shows that these changes are due not to anomerization but to hydrolysis by traces of moisture present in nominally "dry" solvents. Hydrolysis of the more stable halides used in the current study may occur in the same media only when catalytic agents, such as silver oxide, are present.

†Silver oxide is reported to adsorb hydroxyl ions strongly during preparation (25).

Can. J. Chem. Downloaded from www.nrcresearchpress.com by 210.87.254.5 on 09/05/12
For personal use only.

Can. J. Chem. Downloaded from www.nrcresearchpress.com by 210.87.254.5 on 09/05/12
For personal use only.

is present than when it is absent. To keep the concentration of liberated water to a minimum, Reynolds and Evans' procedure calls for slow addition of the glycosyl halide to the alcohol component in the presence of the condensing agent and a highly efficient desiccant. In this way the alcohol component is present in large excess (particularly at the outset) as for the preparation of simpler glycosides. Isbell and Frush (3) showed that when the method of addition is reversed, the yield of the normal condensation product is lowered, and suggested that interference by water then becomes marked. Thus, when methanol was added slowly to a solution of acetobromo-α-D-mannose or -glucose in the presence of silver carbonate (but not a desiccant) a high yield of the respective hexose tetraacetate was obtained (3). However, since the glycosyl halide and condensing agent were brought together in the absence of a large proportion of the hydroxylic component, the observed effects were probably caused, partly at least, by side reactions such as described above. *Hence, the practice of adding the glycosyl halide slowly to excess of the alcohol appears to be advantageous for minimizing side reactions having different origins.* The situation should be more difficult when the hydroxylic component is unreactive. Side reactions then may occur preferentially irrespective of whether or not water has been formed through glycoside synthesis, leaving little glycosyl halide for the desired condensation. This effect probably accounts for the poor yields of disaccharides obtained, as noted earlier, particularly in attempts to form a glycosidic union through a hindered secondary position.*

A preparation of silver oxide that promotes rapid decomposition of a glycosyl halide is also a vigorous Königs–Knorr condensing agent. Thus, by using one silver oxide sample (commercial sample 1, Table II) for the above synthesis of gentiobiose a reaction period of 2 hours was sufficient, as shown by the fact that only a trace of the D-glucosyl halide remained after that time, whereas the reaction period had to be extended to 70 hours for a less active silver oxide (sample 3). Therefore, the optimum duration of a Königs–Knorr reaction, or the optimum proportion of oxide to be used, may vary greatly, and experimental details of various recorded syntheses should not be regarded as universally applicable. According to the present data (Table II), however, the effectiveness of a given sample of silver oxide may be appraised in advance by polarimetric measurement of its reaction with the glycosyl halide to be used.

The use, as described by Helferich, Bohm, and Winkler (27), of elemental iodine as a catalyst in Königs–Knorr reaction mixtures is often followed, and makes for substantially increased yields (5, 11, 12, 21, 27). Since glycosyl halides may well react in these syntheses by an S_N1 mechanism (7, 8, 19), it has been suggested (7) that the effect of iodine is to increase the polarity of the solvent and hence the reaction rate. Although iodine is highly beneficial in the synthesis of gentiobiose (11), it was found during the experiments reported above that the disaccharide actually is formed more *slowly* in the presence of iodine than in its absence. However, iodine also suppresses the side reaction between glycosyl halides and silver oxide (Table III), a highly active sample of the oxide decolorizing the iodine solution more rapidly than a less active sample. Possibly, the side reaction is hindered more effectively in this way than is the condensation step, thereby leading to an enhanced yield of the desired product. When the proportion of iodine is low, the side reaction should be prominent (Table III), but there may be insufficient silver oxide for complete condensation if the ratio is too high. It follows that there should be an optimum proportion of iodine for Königs–Knorr syntheses, which may

**As shown by Curtis and Jones (26), it may be advantageous to use as the hydroxylic components, acyclic derivatives, the secondary hydroxyl groups of which are usually more reactive than those of related cyclic derivatives.*

TABLE III

Effect of iodine on the decomposition of tetra-*O*-acetyl-α-D-glycosyl halides in the presence of silver oxide*

Halide	Iodine	α_D in deg (and time in hr)		
D-Mannose	—	1.93 (0)†	0.18 (1)	−0.09 (18)‡
	+(25 mg)	"	0.90 (1)	0.10 (18)
	+(50 mg)	"	1.40 (1)	0.71 (18)§
D-Glucose	—	2.70 (0)†	0.70 (4)	0.69 (18)‡
	+(50 mg)	"	1.91 (4)	1.04 (18)§

*Glycosyl halide (50 mg) in benzene (2 ml) containing silver oxide (100 mg).
†Paper chromatographic examination of the deacetylated (with sodium methoxide) material showed methyl glycoside, no hexose.
‡Paper chromatographic examination of the deacetylated (with sodium methoxide) material showed hexose, no methyl glycoside.
§Paper chromatographic examination of the deacetylated (with sodium methoxide) material showed methyl glycoside *plus* hexose.

not coincide with the proportion generally used on the assumption that the iodine functions as a catalyst. Further, if iodine does in fact competitively inhibit the side reaction, there remains the possibility that more efficient inhibitors will be found.

EXPERIMENTAL

Solvents were purified and dried by standard methods. Silver oxide was prepared according to Young (28) and Helferich and Klein (14), or obtained commercially, and was dried in a high vacuum at 80° C. 2,3,4,6-Tetra-*O*-acetyl-α-D-mannopyranosyl bromide was prepared by the procedure of Talley, Reynolds, and Evans (21), and the corresponding benzoyl derivative according to Ness, Fletcher, and Hudson (29).

Paper chromatography was carried out with Whatman No. 1 paper using (A) butanol–ethanol–water (40:11:19) and (B) ethyl acetate – pyridine – water (10:4:3) as solvents, and *p*-anisidine hydrochloride (30) or ammoniacal silver nitrate (31) as spray reagents.

Silicic acid used for column chromatography was washed with water, then acetone, and dried at 110° C.

O-Acetyl was determined by a semimicro adaptation of the procedure of Kunz (32).

Optical rotations were measured at 25°±2°. Melting points are corrected.

Evaporations were carried out *in vacuo* at 40° C.

Treatment of 2,3,4,6-Tetra-O-acetyl-α-D-mannopyranosyl Bromide with Silver Oxide

A suspension of silver oxide (4.0 g) and Drierite (6.0 g) in benzene (15 ml) was shaken for 2 hours, the D-mannosyl bromide (1.5 g) was added, and the mixture was shaken for 18 hours; α_D −0.97° (0.5 dm). The solids were filtered off and washed well with benzene and the filtrate was concentrated. An amorphous solid was obtained and dried *in vacuo*, first at 80° for 2 hours and then at room temperature for 18 hours. Yield, 1.0 g. Calculated for $(C_{14}H_{19}O_9)_2O$: C, 49.56%; H, 5.65%. Found: C, 49.72%; H, 5.66%; bromine, 0.30%.

Chromatographic examination of the material after deacetylation with sodium methoxide showed (*p*-anisidine spray) the presence of mannose, two lesser components at $R_{mannose}$ 0.72 and 0.42, and a trace component at $R_{mannose}$ 0.79. No other products were detected with the silver nitrate spray.

Ortho Ester Acetate II

The amorphous product (19.7 g) obtained by treating the D-mannosyl bromide (24.0 g) with silver oxide in benzene,* as above, was dissolved in chloroform (25 ml) and trans-

**Compound II was also obtained (6% yield) when chloroform was used as the solvent.*

Can. J. Chem. Downloaded from www.nrcresearchpress.com by 210.87.254.5 on 09/05/12
For personal use only.

ferred to a silicic acid column (6×50 cm), and the column was washed with chloroform. The first major fraction eluted (1.5 g) crystallized from alcohol and after recrystallization had m.p. 152–154°; $[\alpha]_D$ −23.6° (*c*, 1.2, $CHCl_3$). Calculated for $C_{28}H_{38}O_{19}$: C, 49.56%; H, 5.65%; C-methyl (8 groups), 31.7%; *O*-acetyl (7 groups), 44.4%. Found: C, 49.53%; H, 5.78%; C-methyl, 30.52%; *O*-acetyl, 44.78%.

Methanolysis of II

The ortho ester acetate (16.7 mg) was dissolved in chloroform–methanol (0.8 ml, 1:1); α_D −0.16° (1 dm). Methanolic hydrogen chloride (0.1 ml, 1.5%) was added and the rotation of the solution was then α_D 0.28° (3 min), 0.33° (5 min), 0.34° (15 min). Excess of ethereal diazomethane was added and the solution was found chromatographically (solvent A) to contain a major component corresponding to 3,4,6-tri-*O*-acetyl-D-mannose (20, 22). Evaporation of the solution and treatment of the residual syrup with excess lead tetraacetate in acetic acid showed this component to be oxidized readily to yield a product which travelled more rapidly on a paper chromatogram and gave a typical pentose color with the *p*-anisidine spray, showing that the cleavage had occurred between carbons-1 and -2.

Ortho Ester III

Compound II (370 mg) was suspended in methanol (3 ml) and treated under reflux for 10 minutes with a slight excess of sodium methoxide. During this period the compound dissolved, and when the solution was cooled, a precipitate (170 mg) was obtained, which was crystallized from water–methanol; m.p. 120°; $R_{mannose}$ 0.72. Calculated for $C_{14}H_{24}O_{12}.CH_3OH$: C, 43.27%; H, 6.78%; C-methyl (1 group), 6.5%; methoxyl, 7.5%. Found: C, 43.43%; H, 6.73%; C-methyl, 7.34%; methoxyl, 8.23%.

Ortho ester III (138 mg) in pyridine (5 ml) was treated with acetic anhydride (3 ml) for 5 hours, the reaction mixture was decomposed with ice water, and the solid product was collected. Yield, 159 mg. After recrystallization from ethanol, the product had m.p. 152–154° C, $[\alpha]_D$ −25.9° (*c*, 1.1, $CHCl_3$).

Hydrolysis of III

The ortho ester (III) (200 mg) was dissolved in 0.1 *N* sulphuric acid (4 ml), and after 2 hours the solution was neutralized with Dowex-1 resin (bicarbonate form) and concentrated. The residual syrup was found to contain approximately equal proportions of mannose and a second component which travelled at the rate of 2-*O*-acetyl-D-mannose. By chromatography on sheets of Whatman 3 MM paper, using solvent A, the mixture was separated, and the unknown syrupy component was found by infrared spectroscopy (potassium bromide disk) to be indistinguishable from the known syrupy D-mannose monoacetate. The latter was prepared from 3,4,6-tri-*O*-acetyl-D-mannose-1,2-orthoacetate by the procedure used for conversion of the corresponding L-rhamnose ortho ester to 2-*O*-acetyl-L-rhamnose (18).

Methylation of III

The deacetylated ortho ester (III) (342 mg) in liquid ammonia (15 ml) was treated with a slight excess of potassium (23), the ammonia was evaporated off, and the residue was heated under reflux in methyl iodide (5 ml) for 3 hours. After evaporation of the methyl iodide, the methylation procedure was repeated twice. The final product (348 mg) was crystallized from *n*-hexane; m.p. 142–144° C, $[\alpha]_D$ −36.5° (*c*, 1.0, $CHCl_3$). Calculated for $C_{21}H_{38}O_{12}$: C, 52.27%; H, 7.94%; methoxyl, 45.0%. Found: C, 52.21%; H, 7.93%; methoxyl, 44.1%.

Can. J. Chem. Downloaded from www.nrcresearchpress.com by 210.87.254.5 on 09/05/12
For personal use only.

The methylation product (4.8 mg) in methanol (0.5 ml) (α_D −0.10°, 0.5 dm) was treated with methanolic hydrogen chloride (0.05 ml, 6%), which caused a change in rotation to α_D 0.35° (2 min), 0.40° (5 min). After neutralization with ethereal diazomethane, the solution was found by paper chromatography to contain two components corresponding to 3,4,6-tri- and 2,3,4,6-tetra-*O*-methyl-D-mannose, respectively. Assignment of a 3,4,6-structure to the former was supported by the fact that this component was readily oxidized by lead tetraacetate in acetic acid, yielding a faster-moving product (presumably trimethyl arabinose); the tetramethyl derivative was unaffected by this treatment. When the methylation product was treated under reflux with 1% methanolic hydrogen chloride, the two products formed corresponded, as indicated by gas–liquid chromatography, to a tri- and a tetra-*O*-methyl methyl glycoside, respectively.

2,3,4,6-Tetra-O-acetyl-α-D-mannose (I)

By continued washing of the silicic acid column (above) with chloroform, a second major fraction was obtained (5.4 g), which was crystallized from a highly concentrated solution in ether; m.p. 91–92° C, $[\alpha]_D$ 25.2° (*c*, 1.4, $CHCl_3$) (lit. (33) m.p. 93°, $[\alpha]_D$ 26.3°). Calculated for $C_{14}H_{20}O_{10}$: C, 48.27%; H, 4.79%; acetyl, 49.5%. Found: C, 48.53%; H, 5.83%; acetyl, 49.23%.

On acetylation with acetic anhydride – sodium acetate the compound afforded 1,2,3,4,6-penta-*O*-acetyl-β-D-mannose; m.p. 116–118°, $[\alpha]_D$ −24.5° (*c*, 1.2, $CHCl_3$).

Ortho Ester Acetate V

When the silicic acid column was washed with chloroform–ether (3:1) a fraction (2.1 g) was eluted, which crystallized, and was recrystallized from ethanol; m.p. 216–219°, $[\alpha]_D$ −26.5° (*c*, 1.1, $CHCl_3$). Found: C, 50.00%; H, 5.66%; acetyl, 42.77%; molecular weight (Rast), 753.

In another experiment, this ortho ester also was isolated directly from the reaction mixture. Silver oxide (20 g) in benzene (100 ml) was heated under reflux for 1 hour and then approximately 50 ml of the benzene was distilled off. Drierite (30 g) was added to the cooled suspension, followed by acetobromo-α-D-mannose (7.5 g) in benzene (50 ml). After being shaken for 10 hours, the reaction mixture (α_D −0.30°) was filtered, and the solution concentrated, affording an amorphous solid (5.0 g). The latter, on being dissolved in warm ethanol, yielded crystalline material (0.58 g), m.p. 206–208° C. Recrystallization from ethanol gave a melting point of 208–211°, undepressed by admixture with the ortho ester described in the preceding paragraph. Found: C, 50.11%; H, 5.69%; C-methyl, 27.51%; molecular weight (Rast), 705; (isothermal distillation (34), acetone), 690.

The ortho ester (22.6 mg) was dissolved in chloroform–methanol (1.0 ml, 1:1); α_D −0.51° (1 dm). On addition of methanolic hydrogen chloride (0.5 ml, 1%) to the solution, the observed rotation was α_D 0.20 (2 min), 0.38 (5 min), 0.43 (25 min). Neutralization of the solution with silver carbonate, followed by paper chromatographic examination, showed the presence of a major component corresponding to 3,4,6-tri-*O*-acetyl-D-mannose, this component being readily oxidized by lead tetraacetate in acetic acid.

Ortho Ester VI

Ortho ester acetate V (500 mg) was suspended in methanol (8 ml) and treated under reflux for 10 minutes with a slight excess of sodium methoxide. The clear solution, on being cooled, deposited a precipitate which was crystallized from water–ethanol; m.p.

Can. J. Chem. Downloaded from www.nrcresearchpress.com by 210.87.254.5 on 09/05/12
For personal use only.

156–157° C, $R_{mannose}$ 0.41, $[\alpha]_D$ −5.4° (*c*, 1.1, H_2O). Found: C, 45.15%; H, 6.42%; C-methyl, 5.85%.*

The deacetylation product (V) (194 mg) was treated with 0.1 *N* sulphuric acid (4 ml) for 3 hours at room temperature, and the solution was neutralized with Dowex-1 (bicarbonate form) and evaporated. Paper chromatographic examination of the product showed the presence of mannose and an equally prominent second component, $R_{mannose}$ 0.7 (solvent A) or $R_{mannose}$ 1.2 (solvent B). This mixture was separated on Whatman 3 MM paper affording the unknown component as a syrup (86 mg). The latter absorbed strongly in the infrared regions characteristic of acyl groups and, on treatment with excess sodium methoxide, yielded mannose and two non-reducing products having $R_{mannose}$ 2.5 and 2.8, respectively (solvent A).

Treatment of 2,3,4,6-Tetra-O-acetyl-α-D-glucopyranosyl Bromide with Silver Oxide

To a solution of the bromide (0.6 g) in benzene (7 ml) was added Drierite (3.0 g) and silver oxide (2.0 g), and the mixture was shaken for 16 hours; during this period the observed rotation changed from α_D 20.2° to 1.75° (1 dm). The solids were filtered off and washed with benzene, the filtrate was evaporated, and the amorphous solid obtained was dried in a high vacuum. Yield, 0.4 g. Calculated for $(C_{14}H_{19}O_9)_2O$: C, 49.56%; H, 5.65%. Found: C, 50.15%; H, 5.67%; bromine, 0.28%. On deacetylation with barium methoxide the product yielded glucose and two lesser-reducing components (*p*-anisidine spray) having $R_{glucose}$ 0.7 and 0.1, respectively. The latter two were hydrolyzed when the deacetylation mixture, acidified with acetic acid, was heated briefly.

The product was chromatographed on a column of silicic acid, using chloroform and chloroform–ether (varying proportions) as the eluting solvents. Several syrupy fractions were obtained, none of which, however, afforded crystalline material.

ACKNOWLEDGMENTS

The authors thank Dr. G. L. Mattock for helpful discussion, and Mr. J. W. L. C. Christ and Mrs. J. Nuttall for technical assistance. Microanalyses were performed by Mr. M. Mazurek, and infrared absorption spectra were prepared by Miss Inez Gaffney.

REFERENCES

1. W. Königs and E. Knorr. Ber. **34**, 957 (1901).
2. H. L. Frush and H. S. Isbell. J. Research Natl. Bur. Standards, **27**, 413 (1941).
3. H. S. Isbell and H. L. Frush. J. Research Natl. Bur. Standards, **43**, 161 (1949).
4. R. K. Ness, H. G. Fletcher, Jr., and C. S. Hudson. J. Am. Chem. Soc. **73**, 959 (1951).
5. W. L. Evans, D. D. Reynolds, and E. A. Talley. Advances in Carbohydrate Chem. **6**, 27 (1951).
6. R. U. Lemieux. Advances in Carbohydrate Chem. **9**, 1 (1954).
7. L. J. Haynes and F. H. Newth. Advances in Carbohydrate Chem. **10**, 207 (1955).
8. G. L. Mattock and G. O. Phillips. J. Chem. Soc. 1836 (1956).
9. J. Conchie, G. A. Levvy, and C .A. Marsh. Advances in Carbohydrate Chem. **12**, 157 (1957).
10. B. Helferich and K. F. Wedemeyer. Ann. **563**, 139 (1949).
11. D. D. Reynolds and W. L. Evans. J. Am. Chem. Soc. **60**, 2559 (1938).
12. C. M. McCloskY, R. E. Pyle, and G. H. Coleman. J. Am. Chem. Soc. **66**, 349 (1944).
13. P. Bachli and E. G. V. Percival. J. Chem. Soc. 1243 (1952).
14. B. Helferich and W. Klein. Ann. **450**, 219 (1926).
15. H. H. Schlubach. Ber. **59**, 840 (1926).
16. E. D. Hughes, C. K. Ingold, and S. Masterman. J. Chem. Soc. 1236 (1937).
17. E. D. Hughes. Quart. Revs. (London), **5**, 245 (1951).
18. W. N. Haworth, E. L. Hirst, and H. Samuels. J. Chem. Soc. 2861 (1931).
19. E. Pascu. Advances in Carbohydrate Chem. **1**, 77 (1945).

**In another experiment the product obtained was highly hygroscopic; m.p. 180°. Found:* C, *43.68%;* H, *6.42%;* C-*methyl*, *6.45%*.

Can. J. Chem. Downloaded from www.nrcresearchpress.com by 210.87.254.5 on 09/05/12
For personal use only.

20. H. S. ISBELL. J. Research Natl. Bur. Standards, **7**, 1115 (1931).
21. E. A. TALLEY, D. D. REYNOLDS, and W. L. EVANS. J. Am. Chem. Soc. **65**, 575 (1943).
22. A. S. PERLIN. Unpublished.
23. I. E. MUSKAT. J. Am. Chem. Soc. **56**, 693 (1934).
24. W. KORYTNYK and J. A. MILLS. J. Chem. Soc. 636 (1959).
25. W. A. COWDREY, E. D. HUGHES, and C. K. INGOLD. J. Chem. Soc. 1243 (1937).
26. E. J. C. CURTIS and J. K. N. JONES. Can. J. Chem. **37**, 358 (1959).
27. B. HELFERICH, E. BOHM, and S. WINKLER. Ber. **63**, 989 (1930).
28. C. B. YOUNG. *In* Polarimetry, saccharimetry and the sugars. U.S. Govt. Printing Office, Washington. 1942. p. 507.
29. R. K. NESS, H. G. FLETCHER, JR., and C. S. HUDSON. J. Am. Chem. Soc. **72**, 2200 (1950).
30. L. HOUGH, J. K. N. JONES, and W. H. WADMAN. J. Chem. Soc. 1702 (1950).
31. S. M. PARTRIDGE. Nature, **158**, 270 (1946).
32. A. KUNZ. J. Am. Chem. Soc. **48**, 1982 (1926).
33. P. A. LEVENE and R. S. TIPSON. J. Biol. Chem. **90**, 89 (1931).
34. C. E. CHILDS. Anal. Chem. **26**, 1963 (1954).

Can. J. Chem. Downloaded from www.nrcresearchpress.com by 210.87.254.5 on 09/05/12
For personal use only.

ALIPHATIC CHEMISTRY OF FLUORENE

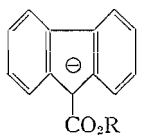
PART VII. SPIROLACTONES[1]

P. M. G. BAVIN[2]

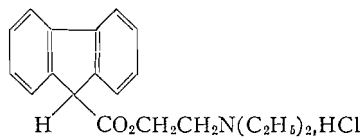
ABSTRACT

A number of spirolactones have been prepared from fluorene-9-carboxylic acid, either by the halolactonization reaction or by alkylation of the methyl ester with hydroxyalkyl halides.

The ease with which methyl fluorene-9-carboxylate anion (I*a*) reacts with a wide range of alkyl halides (1, 2, 3) prompted attempts to prepare 9-alkyl derivatives of the ester-hydrochloride (II), which has found use as an anti-spasmolytic agent (4) under the name Pavatrine (5, pp. 259–261). Attempts to alkylate the anion I*b* or to effect trans esterification of methyl 9-alkylfluorene-9-carboxylates with sodium 2-diethylaminoethoxide gave only traces of the desired products, but led indirectly to the preparation of some spirolactones.



I*a*, R = CH_3
I*b*, R = $CH_2CH_2N(C_2H_5)_2$



II

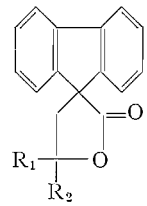
The reaction between 2,3-dihydroxypropyl chloride and either of the anions I*a* or *b* gave the hydroxy-γ-lactone III*b* in good yield. The unsubstituted γ (III*a*) and δ (IV*a*) lactones were prepared similarly, by alkylating I*a* with 2-bromoethanol and 3-chloropropanol,* respectively. The phenyl γ-lactone (III*c*) was obtained by reducing methyl 9-ω-phenacylfluorene-9-carboxylate (6) with sodium borohydride. The carbonyl stretching frequencies of chloroform solutions of these lactones and the related compound V*a* (7), isomeric with III*a*, agree well with the generally accepted values (8, pp. 159–160).

The hydroxylactone (III*b*) was first reported (3) as having the isomeric δ-structure (IV*b*), on the basis of the carbonyl stretching frequency of a sample prepared as a pressed potassium bromide disk. However, the infrared spectrum of a chloroform solution indicated the γ-lactone structure (III*b*), and this has been confirmed by reaction with thionyl chloride to give the chloro-γ-lactone (III*d*) (cf. reactions of the hydroxylactones derived from stilbene-2-carboxylic acids (9)). The chlorolactone has also been prepared from 9-allylfluorene-9-carboxylic acid (below). Structure III*b* for the hydroxylactone is in accord with the preferred formation of γ- over δ-lactones in the sugar series (10, pp. 33–34) and the hydroxylactones of stilbene-2-carboxylic acids (11).

The abnormal differences in the carbonyl stretching frequencies of samples of III*b* prepared as a potassium bromide disk and as a solution in chloroform may be due to

[1]*Manuscript received June 7, 1961.*
Contribution from the Chemistry Department, The University, Hull, East Yorkshire, England.
[2]*I.C.I. Fellow, 1958–60. Present address: Smith Kline & French Laboratories Ltd., Welwyn Garden City, Herts., England.*

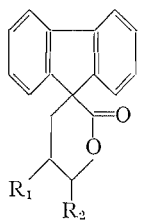
**Commercial 3-chloropropanol contained approximately 20% of an isomeric chlorohydrin which was eliminated by careful fractional distillation.*



III

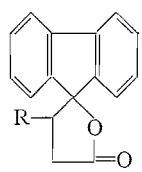
			$\nu_{C=O}$, cm^{-1}		
III	R_1	R_2	$CHCl_3$	KBr	Δ
a	H	H	1773	1765	8
b	H	CH_2OH	1767	1735	32
c	H	C_6H_5	1772		
d	H	CH_2Cl	1788 (1770*)		
e	H	CH_2Br	1787		
f	H	CH_2I	1793		
g	H	$CHBrCH_3$	1778		
h	Br	$CHBr_2$	1805		

*Shoulder.

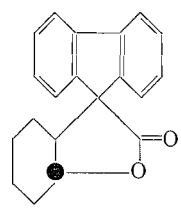


IV

			$\nu_{C=O}$, cm^{-1}		
IV	R_1	R_2	$CHCl_3$	KBr	Δ
a	H	H	1730	1730	0
b	OH	H	—	—	
c	Br	CH_3		1732	
d	Br	C_6H_5	1748		



Va, R = H, $\nu_{C=O}$ (mull) = 1772 cm^{-1}
Vb, R = Br, $\nu_{C=O}$ (mull) = 1795 cm^{-1}



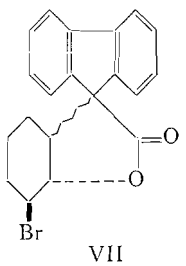
VI, $\nu_{C=O}$ ($CHCl_3$) = 1777 cm^{-1}

isomerization brought about by the high pressures required for disk formation (12, pp. 297–298; for another example of an abnormally low carbonyl frequency in a KBr disk, see ref. 13). Consequently, the infrared data discussed later in this paper refer to solutions in chloroform.

Reaction of the anion I*a* with *trans*-2-bromocyclohexanol, *cis*-2-chlorocyclohexanol, or cyclohexene oxide gave the same lactone (VI). Since cyclohexene oxide is known to react with nucleophiles with inversion at one carbon atom (14, 15), the lactone must have the trans structure. The lactone is formed from *trans*-2-bromocyclohexanol by prior formation of cyclohexene oxide (15) and from *cis*-2-chlorocyclohexanol by displacement with inversion (cf. the acetates of the 2-chlorocyclohexanols (16)). The reaction between I*a* and 2-chlorocyclohexanone failed, thwarting attempts to prepare the cis isomer of VI. Notwithstanding Westheimer's successful preparation of a hydroxy diester from cyclopentene oxide and diethyl malonate (14), the reaction between I*a* and *trans*-2-bromocyclopentanol failed to give the desired product.

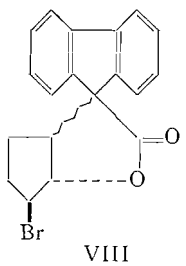
The halolactonization and related reactions have recently aroused considerable interest. Van Tamelen and Shamma (17) have suggested that the formation of iodolactones is of diagnostic value in determining the position of unsaturation in olefinic acids, and this technique has been found to be of some use (18, 19). The formation of halolactones has proved particularly useful in the bicyclo[221]heptene series (e.g. ref. 20). The mechanism has been examined by Bartlett (21), Craig (22, 23), Arnold and co-workers (24, 25, 26, 27), and, in some detail, by Berti (9, 11, 28, 29, 30, 31). It has been shown to be stereospecific (9) and much evidence suggests that a carbonium ion or related species is the essential intermediate. Since α,α-disubstituted allylacetic acids form halolactones particularly readily (9), the opportunity has been taken to examine some 9-alkenylfluorene-9-carboxylic acids. (For the method of preparation of the acids, see ref. 3.)

9-Allylfluorene-9-carboxylic acid has now been shown to form a chloro-γ-lactone (III*d*) as well as the corresponding bromo (25) and iodo (24) compounds (III*e* and *f*, respectively). 9-Crotylfluorene-9-carboxylic acid* has been found to yield mainly the bromo-γ-lactone (III*g*) together with a trace of the isomeric δ-lactone (IV*c*), not obtained pure. 9-Cinnamylfluorene-9-carboxylic acid gave only the bromo-δ-lactone (IV*d*), which decomposed surprisingly readily to 9-cinnamylidenefluorene. The reactions of the crotyl and cinnamyl acids, like those of *cis*- and *trans*-stilbene-2-carboxylic acids (9), are best interpreted as proceeding by way of the more stable carbonium ion. It had been the intention to test this conclusion by examining the reactions of para-substituted cinnamyl derivatives but insufficient time has curtailed the project. 9-Propargylfluorene-9-carboxylic acid gave the heavily substituted tribromo-γ-lactone (III*h*), which decomposed at its melting point with evolution of bromine.



VII

$\nu_{C=O}$ ($CHCl_3$) = 1777 cm^{-1}



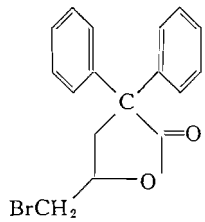
VIII

$\nu_{C=O}$ ($CHCl_3$) = 1777 cm^{-1}

**The structure of this acid was proved by hydrogenation of the methyl ester to the known (2) methyl 9-butylfluorene-9-carboxylate. This confirmation was necessary since crotyl bromide exists as an equilibrium mixture under normal conditions (32) and can give rise to 'abnormal products' by the S_N2 mechanism (33).*

9-3′-Cyclohexenylfluorene-9-carboxylic acid gave a good yield of the bromo-γ-lactone (VII). The homologous 3′-cyclopentenyl acid gave only a moderate yield of the lactone (VIII) but, nevertheless, afforded an example of the formation of a derivative of bicyclo-[330]octane under mild conditions. By analogy with Berti's studies (9), the lactones must have the partial stereochemistry shown. The preparation of VIII can be compared with the formation of the highly strained halo-β-lactones from dimethylmaleic and fumaric acids (21).

The carbonyl stretching frequency of the bromolactone prepared from allyldiphenylacetic acid (22) is 1783 cm^{-1}, showing it to be the γ-lactone IX.



IX

The infrared data in this paper show that introduction of halogen γ or δ to the carbonyl group of δ- and γ-lactones results in a shift of the carbonyl stretching frequency to higher frequencies, by 15–20 cm^{-1}. Similar results have only been reported previously for α-halo esters and α-halo ketones (12, pp. 443–509). The shift is shown by α-halo alicyclic ketones only when the halogen is equatorial and approximately coplanar with the carbonyl group. The larger shift of 32 cm^{-1} shown by the tribromolactone (III*h*) may be compared with the very exceptional shifts shown by esters of perfluoroalkyl carboxylic acids (34).

EXPERIMENTAL

Methyl fluorene-9-carboxylate was prepared and alkylated as described elsewhere (2, 3).

Lactone of 9-(2′-Hydroxyethyl)-fluorene-9-carboxylic acid (IIIa)

Methyl fluorene-9-carboxylate (0.7 g) and 2-bromoethanol gave the lactone, which crystallized from benzene as long white needles (0.5 g), m.p. 184–185°. Found: C, 82.56; H, 5.47%. Calculated for $C_{16}H_{12}O_2$: C, 82.73; H, 5.21%.

Reduction with ethereal lithium aluminum hydride gave an almost quantitative yield of 9-(2′-hydroxyethyl)-9-fluorenylmethanol, crystallizing from benzene–hexane as small colorless needles, m.p. 94–95°. Found: C, 80.0; H, 6.59%. Calculated for $C_{16}H_{16}O_2$: C, 79.97; H, 6.71%.

Methyl fluorene-9-carboxylate and methyl bromoacetate gave methyl 9-carbomethoxymethylfluorene-9-carboxylate (88%), which formed colorless prisms from methanol, m.p. 91–92°. Found: C, 72.84; H, 5.60%. Calculated for $C_{18}H_{16}O_4$: C, 72.96; H, 5.44%. Reduction with ethereal lithium aluminum hydride gave the diol described above, identity being established by mixed melting point determination and by comparison of infrared spectra.

Lactone of 9-(3′-Hydroxypropyl)-fluorene-9-carboxylic acid (IVa)

Methyl fluorene-9-carboxylate (0.7 g) and pure 3-chloropropanol (b.p. 69.5–70.0° at 19 mm; n_D^{24} 1.4487) gave the lactone, which formed colorless, well-defined prisms

(0.64 g) from benzene–hexane, m.p. 232–234°. Found: C, 81.69; H, 5.62%. Calculated for $C_{17}H_{14}O_2$: C, 81.58; H, 5.64%.

γ-Lactone of 9-(2′,3′-Dihydroxypropyl)-fluorene-9-carboxylic acid (IIIb)

Methyl fluorene-9-carboxylate and pure 2,3-dihydroxypropyl chloride gave the γ-lactone, which crystallized from chloroform–hexane as small colorless prisms (65–78%), m.p. 180–181°. Found: C, 76.85; H, 5.54%. Calculated for $C_{17}H_{14}O_3$: C, 76.67; H, 5.30%.

The infrared spectrum of a chloroform solution of the material retained in the mother liquors suggested the presence of methyl fluorene-9-carboxylate ($\nu_{C=O}$ 1760 cm^{-1}), further amounts of the γ-lactone (1770 cm^{-1}), and traces of the isomeric δ-lactone (1730 cm^{-1}).

Lactone of 9-(2′-Hydroxy-2′-phenylethyl)-fluorene-9-carboxylic acid (IIIc)

Methyl 9-ω-phenacylfluorene-9-carboxylate (6) (0.8 g) was reduced with a solution of sodium borohydride (0.5 g) in methanol (20 ml). The lactone separated from benzene–hexane as radiating clusters of elongated prisms (0.65 g), m.p. 180–181°, depressed to 165–171° by addition of the starting keto ester (m.p. 184–185°). Found: C, 84.49; H, 5.05%. Calculated for $C_{22}H_{16}O_2$: C, 84.59; H, 5.16%.

Trans Lactone of 9-(2′-Hydroxycyclohexyl)-fluorene-9-carboxylic acid (VI)

Methyl fluorene-9-carboxylate and cyclohexene oxide gave the lactone, which separated from benzene–hexane as small, well-defined rhombs (88%), m.p. 272–273°. Found: C, 82.74; H, 6.21%. Calculated for $C_{20}H_{18}O_2$: C, 82.73; H, 6.28%.

Alkylation with *cis*-2-chlorocyclohexanol (15) or *trans*-2-bromocyclohexanol (prepared by a general method (35)) gave the same lactone, identified by mixed melting point determinations and by careful comparison of the infrared spectra of chloroform solutions. To obtain good yields of lactone from the bromohydrin it was found necessary to employ 2 moles of methoxide, indicating that the reaction proceeded by prior formation of cyclohexene oxide.

Several attempts to alkylate methyl fluorene-9-carboxylate with *trans*-2-bromocyclopentanol (prepared as for the cyclohexane homologue (35)) were unsuccessful. Occasionally traces of methyl 9-hydroxyfluorene-9-carboxylate were obtained as long white needles from cyclohexane, m.p. 160–161°, identified by comparison with an authentic specimen ((36), m.p. 158–159°).

Halolactones

The 9-alkenylfluorene-9-carboxylic acids were prepared by a general method (3). Methyl esters were characterized only when obtained crystalline. Bromolactones were prepared by adding a slight excess of a solution of bromine in chloroform to the appropriate acid.

9-Allylfluorene-9-carboxylic acid (37), most easily prepared according to reference 2, and the lactone of 9-(3′-bromo-2′-hydroxypropyl)-fluorene-9-carboxylic acid (25) have been described elsewhere. The lactone of 9-(3′-iodo-2′-hydroxypropyl)-fluorene-9-carboxylic acid (24) was more conveniently prepared by Van Tamelen's procedure (17).

The lactone of 9-(3′-chloro-2′-hydroxypropyl)-fluorene-9-carboxylic acid (III*d*), prepared by reaction of the acid with a solution of chlorine in chloroform (9), crystallized as needles from heptane (76%), m.p. 166–167°. Found: C, 71.76; H, 4.65%. Calculated for $C_{17}H_{13}O_2Cl$: C, 71.71; H, 4.60%. The same lactone was obtained in 64% yield from the reaction between thionyl chloride and the hydroxylactone (III*b*), using the conditions described by Berti (9).

The Lactone of 9-(3′-Bromo-2′-hydroxybutyl)-fluorene-9-carboxylic acid (IIIg)

9-Crotylfluorene-9-carboxylic acid was obtained as small colorless prisms (65%), m.p. 120–122°, after three crystallizations from benzene–hexane. Found: C, 81.99; H, 6.04%. Calculated for $C_{18}H_{16}O_2$: C, 81.79; H, 6.10%. Esterification of the pure acid with diazomethane and hydrogenation of the oily methyl ester in methanol over 5% palladized charcoal gave methyl 9-butylfluorene-9-carboxylate, identical with an authentic specimen ((2), m.p. 34.0–34.5°). Saponification gave 9-butylfluorene-9-carboxylic acid, which crystallized as irregular rhombs from benzene, m.p. 115–116°. Found: C, 81.17; H, 6.81%. The identical acid was obtained by saponification of the authentic ester. The alternative product of hydrogenation, methyl 9-*s*-butylfluorene-9-carboxylate, has m.p. 70–71° (2).

The bromolactone separated from benzene–hexane as colorless needles (86%), m.p. 149–150°. Found: C, 63.06; H, 4.41%. Calculated for $C_{18}H_{15}O_2Br$: C, 63.00; H, 4.41%. Fractional crystallization of the mother liquors, using infrared spectra as a guide, gave a few milligrams of white needles, m.p. 112–116°, strongly depressed by the above lactone. The infrared spectra suggested that the minor product was the δ-lactone (IV*c*), originally present in approximately 1–4%.

The Lactone of 9-(2′,3′,3′-Tribromo-2′-hydroxypropyl)-fluorene-9-carboxylic acid (IIIh)

9-Propargylfluorene-9-carboxylic acid separated from benzene–hexane as colorless needles or prisms (72% based on methyl fluorene-9-carboxylate), m.p. 182–184° with decomposition. Found: C, 82.17; H, 4.85%. Calculated for $C_{17}H_{12}O_2$: C, 82.24; H, 4.87%. The methyl ester crystallized as colorless prisms from methanol, m.p. 117–119° (not analyzed). The infrared spectra of solutions of the acid and ester in chloroform showed the characteristic acetylenic C—H stretching band at 3300 cm^{-1} (8, p. 49).

The tribromolactone formed clusters of prisms (77%) from benzene–hexane, m.p. 155–156° with decomposition and evolution of bromine. Found: C, 42.05; H, 2.56%. Calculated for $C_{17}H_{11}O_2Br_3$: C, 41.92; H, 2.28%.

The Lactone of 9-(2′-Bromo-3′-hydroxy-3′-phenylpropyl)-fluorene-9-carboxylic acid (IVd)

9-Cinnamylfluorene-9-carboxylic acid crystallized from chloroform as well-defined prisms (71%), m.p. 162–163°. Found: C, 84.81; H, 5.72%. Calculated for $C_{23}H_{18}O_2$: C, 84.64; H, 5.56%. Hydrogenation in acetic acid over 10% palladium-on-charcoal gave 9-(3′-phenylpropyl)-fluorene-9-carboxylic acid, m.p. 124–126°, identical with an authentic specimen (38).

The crude bromolactone (1 g) was dissolved in cold chloroform (5 ml) and diluted with hot heptane (10 ml); pure lactone separated as small colorless prisms (0.6 g), m.p. 195–197° with decomposition to 9-cinnamylidenefluorene (below). Found: C, 68.24; H, 4.44; Br, 19.94%. Calculated for $C_{23}H_{17}O_2Br$: C, 68.16; H, 4.23; Br, 19.72%. The crude lactone was very unstable but samples of the pure substance have remained unchanged for 2 years.

The lactone (0.1 g) was boiled for 10 minutes with glacial acetic acid (2 ml). When the solution was cooled, 9-cinnamylidenefluorene separated as bright yellow needles (45 mg), m.p. 152–153° (lit. m.p. 150.5–151.0° for the all-trans isomer (39)).

The Lactone of 9-(3′-Bromo-2′-hydroxycyclohexyl)-fluorene-9-carboxylic acid (VII)

9-(3′-Cyclohexenyl)-fluorene-9-carboxylic acid, prepared from 3-bromocyclohexene (40), formed large, colorless prisms (73%) from benzene–hexane, m.p. 168–170° with decomposition. Found for a sample dried 12 hours at 80° and 1 mm; C, 82.52; H, 6.35%. Calculated for $C_{20}H_{18}O_2$: C, 82.73; H, 6.25%.

The bromolactone crystallized from benzene–hexane as colorless needles (89%), m.p. 186–187°. Found: C, 64.92; H, 4.70%. Calculated for $C_{20}H_{17}O_2Br$: C, 65.05; H, 4.64%.

The Lactone of 9-(3′-Bromo-2′-hydroxycyclopentyl)-fluorene-9-carboxylic acid (VIII)

Methyl 9-(3′-Cyclopentenyl)-fluorene-9-carboxylate

Alkylation of methyl fluorene-9-carboxylate with 3-chlorocyclopentene (41) gave a brown resin. Extraction with boiling heptane and passage of the resulting solution through a short column of activated alumina gave the pure ester, crystallizing from heptane as small colorless needles (67%), m.p. 93–94°. Found: C, 82.56; H, 6.32%. Calculated for $C_{20}H_{18}O_2$: C, 82.73; H, 6.25%. Hydrogenation in methanol over 5% palladized charcoal gave methyl 9-cyclopentylfluorene-9-carboxylate as elongated prisms from methanol or hexane, m.p. 83.0–84.5°. Found: C, 82.06; H, 6.78%. Calculated for $C_{20}H_{20}O_2$: C, 82.15; H, 6.89%. The same ester was obtained by alkylating fluorene ester with cyclopentyl bromide.

9-(3′-Cyclopentenyl)-fluorene-9-carboxylic acid separated from benzene–hexane as prismatic needles, m.p. 184–186°, after a change of crystalline form at 160–161°. Found: C, 83.12; H, 5.30%. Calculated for $C_{19}H_{16}O_2$: C, 82.78; H, 5.54%.

The bromolactone formed small prisms (45%) from benzene–hexane, m.p. 208–210°. Found: C, 64.17; H, 4.10%. Calculated for $C_{19}H_{15}O_2Br$: C, 64.24; H, 4.26%.

The Lactone of 5-Bromo-4-hydroxy-2,2-diphenylpentanoic acid (IX)

Allyldiphenylacetic acid was prepared as described (42) for methyldiphenylacetic acid. It formed rosettes of prisms (77%) from benzene–hexane, m.p. 143–144° (lit. m.p. 142–143° (43)). The lactone of 5-bromo-4-hydroxy-2,2-diphenylpentanoic acid (IX) crystallized as large prisms from benzene–hexane, m.p. 88–89° (lit. m.p. 87–88° (22)). Found: C, 62.03; H, 4.39%. Calculated for $C_{17}H_{15}O_2Br$: C, 61.64; H, 4.57%.

ACKNOWLEDGMENTS

The author is particularly indebted to Dr. G. W. Gray and Miss A. Stephenson for carefully recording the infrared spectra with a Unicam S.P.100 double beam instrument equipped with rock salt optics.

A gift of chemicals by G. D. Searle and Company is gratefully acknowledged.

REFERENCES

1. W. Wislicenus and W. Mocker. Ber. **46**, 2772 (1913).
2. F. A. L. Anet and P. M. G. Bavin. Can. J. Chem. **34**, 991 (1956).
3. P. M. G. Bavin. Anal. Chem. **32**, 554 (1960).
4. G. Lehmann and P. K. Knoefel. J. Pharmacol. **74**, 217, 274 (1942).
5. G. M. Dyson and P. May. May's chemistry of synthetic drugs. Longman's, London. 1959.
6. W. D. Garden and F. D. Gunstone. J. Chem. Soc. 2650 (1952).
7. D. M. W. Anderson, N. Campbell, J. T. Craig, and D. A. Crombir. J. Chem. Soc. 781 (1960).
8. L. J. Bellamy. The infra-red spectra of complex molecules. Methuen and Co., London. 1954.
9. G. Berti. Tetrahedron, 4, 393 (1958).
10. E. G. V. Percival. Structural carbohydrate chemistry. J. Garnet Miller Ltd., London. 1950.
11. G. Berti. J. Org. Chem. **24**, 934 (1959).
12. R. N. Jones and C .Sandorfy. Chemical applications of spectroscopy. Vol. IX. Techniques of organic chemistry. *Edited by* A. Weissburger. Interscience Publishers, Inc., New York. 1956.
13. C. Gual, R. I. Dorfman, and H. Rosenkranty. Spectrochim. Acta, **13**, 248 (1958).
14. W. E. Grigsby, J. Hind, J. Chanley, and F. H. Westheimer. J. Am. Chem. Soc. **64**, 2606 (1942).
15. P. D. Bartlett. J. Am. Chem. Soc. **57**, 224 (1935).
16. S. Winstein and R. E. Buckles. J. Am. Chem. Soc. **64**, 2782 (1942).
17. E. E. Van Tamelen and M. Shamma. J. Am. Chem. Soc. **76**, 2315 (1954).
18. R. Tschesche and A. K. Sen. Chem. Ber. **93**, 1903 (1960).
19. A. W. Burgstahler and I. C. Nordin. J. Am. Chem. Soc. **83**, 198 (1961).
20. R. B. Woodward and H. Baer. J. Am. Chem. Soc. **70**, 1161 (1948).
21. D. S. Tarbell and P. D. Bartlett. J. Am. Chem. Soc. **59**, 407 (1937).

22. P. N. CRAIG and I. H. WITT. J. Am. Chem. Soc. **72**, 4925 (1950).
23. P. N. CRAIG. J. Am. Chem. Soc. **74**, 129 (1952).
24. R. T. ARNOLD and K. L. LINDSAY. J. Am. Chem. Soc. **75**, 1048 (1953).
25. R. T. ARNOLD, M. DE MOURA CAMPOS, and K. L. LINDSAY. J. Am. Chem. Soc. **75**, 1044 (1953).
26. M. DE MOURA CAMPOS. J. Am. Chem. Soc. **76**, 4480 (1954).
27. M. DE MOURA CAMPOS. Chem. Ber. **93**, 317, 1075 (1960).
28. G. BERTI. Ann. chim. (Rome), **50**, 669 (1960).
29. G. BERTI and F. BOTTANI. J. Org. Chem. **25**, 1286 (1960).
30. G. BERTI. Gazz. chim. ital. **81**, 305 (1951).
31. G. BERTI. Gazz. chim. ital. **86**, 883 (1956).
32. S. WINSTEIN and W. G. YOUNG. J. Am. Chem. Soc. **58**, 104 (1936).
33. R. E. KEPNER, S. WINSTEIN, and W. G. YOUNG. J. Am. Chem. Soc. **71**, 115 (1949).
34. M. HAMPTSCHEIN, C. S. STOKES, and E. A. NODIFF. J. Am. Chem. Soc. **74**, 4005 (1952).
35. J. READ and W. G. REID. J. Chem. Soc. 1487 (1928).
36. P. A. PETYUNIN and I. S. BERDINOKIĬ. Zhur. Obscheĭ Khim. **27**, 2999 (1957); Chem. Abstr. **52**, 8111^{d} (1958).
37. R. T. ARNOLD, R. M. DODSON, and W. E. PARHAM. J. Am. Chem. Soc. **71**, 2439 (1949).
38. P. M. G. BAVIN. Can. J. Chem. **38**, 1099 (1960).
39. E. F. MAGOON and L. ZECHMEISTER. J. Am. Chem. Soc. **77**, 5642 (1955).
40. E. H. FARMER and F. W. SHIPLEY. J. Chem. Soc. 1519 (1947).
41. R. B. MOFFETT. Org. Syntheses, **32**, 41 (1952).
42. F. A. L. ANET and P. M. G. BAVIN. Can. J. Chem. **35**, 1084 (1957).
43. A. A. LARSEN, A. W. RUDDY, B. ELPERN, and M. MCMULLIN. J. Am. Chem. Soc. **71**, 532 (1949).

Can. J. Chem. Downloaded from www.nrcresearchpress.com by 210.87.254.40 on 09/05/12
For personal use only.

PYRROLES RELATED TO PORPHOBILINOGEN[1]

G. P. ARSENAULT[2] AND S. F. MACDONALD

ABSTRACT

A study of the decarboxylation of pyrroles related to 5-carboxyporphobilinogen has led to an improved synthesis of porphobilinogen, to isoporphobilinogen, and to other pyrroles required for the preparation of possible intermediates in the biosynthesis of porphyrins.

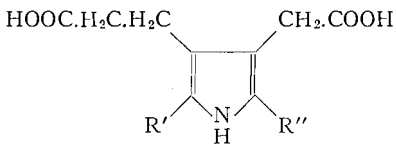
Among the porphobilinogen derivatives which have been considered as possible intermediates in the biosynthesis of uroporphinogens from porphobilinogen are isoporphobilinogen, 5-aminomethylporphobilinogen (2), the carbinols analogous to these and to porphobilinogen, and polypyrranes. The behavior of synthetic specimens of these with enzymes is pertinent to the biogenetic problem. Also, a study of isoporphobilinogen under conditions which convert porphobilinogen to uroporphinogens might clarify ill-defined assumptions relating the mechanisms of the enzymic and non-enzymic conversions of porphobilinogen.

Many projected syntheses of these postulated intermediates required pyrroles with one α-position free and the other bearing a potential aminomethyl group, carbinol group, or bridge. We had found only one route to such intermediates in the decarboxylation of 5-carboxyporphobilinogen lactam in boiling water, a method too dependent on structure for its applicability in analogous cases to be assessed other than empirically. Consequently, other methods were studied for decarboxylating 5-carboxypyrroles with appropriate substituents in the remaining positions.

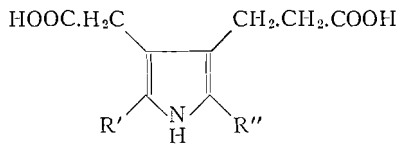
The triethyl ester of I*a* had been converted into the ester of I*c* and thence into I*c* itself (3). This last was treated with iodine in bicarbonate to yield the iodo-aldehyde I*f*. Although this product was obtained only once analytically pure, the other specimens were otherwise undistinguished and were quite satisfactory as intermediates. The analytical difficulties could not be ascribed to an iodine–pyrrole complex (4). The iodo-aldehyde I*f* was reduced catalytically to the α-free aldehyde I*h*. The carbinol (I, R′ = H, R″ = CH_2OH) would be expected to be very unstable (5) and has not yet been isolated as a reduction product of I*h*. The oxime, I*i*, was obtained from I*h* but more conveniently by two unexpected routes. An attempt to prepare the oxime of I*f* led directly to I*i*, iodine being lost; the ready dehalogenation of some iodopyrroles has been reported (4). This dehalogenation with hydroxylamine is of limited applicability as the triethyl ester of I*g* survived the same treatment unchanged. An attempt to improve the conversion of the aldehyde I*c* into its oxime I*d* (3) led to the third and best preparation of I*i*: longer heating resulted in the expected oxime I*d* being decarboxylated to I*i*. The ease of this decarboxylation may be unrelated to that of 5-carboxy-alkylpyrroles and of 5-carboxy-porphobilinogen lactam; some 5-carboxypyrromethenes also decarboxylate readily (6).

Under carefully chosen conditions (see below and Experimental) the catalytic reduction of I*i* gave as the sole product porphobilinogen I*j*, identified by comparison with natural material as such, as the hydrochloride, and as the lactam. The yield of porphobilinogen from the triethyl ester of I*a* in four steps was 29%. On a much smaller scale our previous synthesis (7) had given 5% in seven steps after extensive purification.

[1]*Manuscript received May 18, 1961.*
Contribution from the Division of Pure Chemistry, National Research Council, Ottawa, Canada. This work was reported at meetings of the Chemical Institute of Canada (1).
Issued as N.R.C. No. 6321.
[2]*National Research Council of Canada Postdoctorate Fellow, 1958–60.*

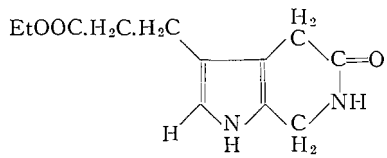


I

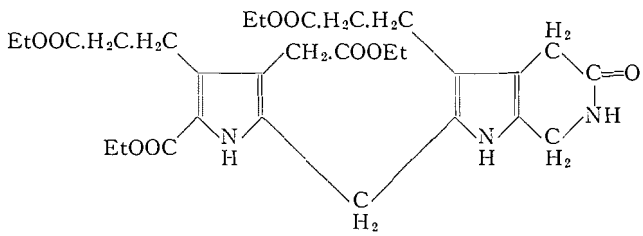


II

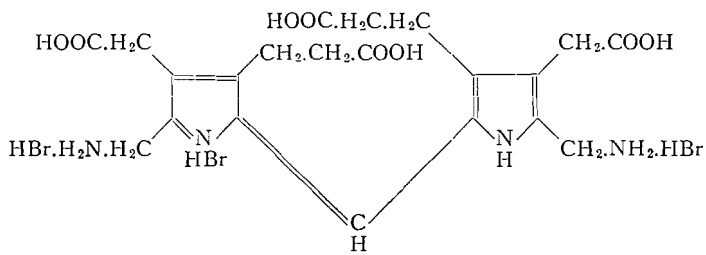
(*a*) R′ = COOH, R″ = CH_3
(*b*) R′ = COOH, R″ = CH_2Br
(*c*) R′ = COOH, R″ = CHO
(*d*) R′ = COOH, R″ = CH=N.OH
(*e*) R′ = COOH, R″ = $CH_2.NH_2$
(*f*) R′ = I, R″ = CHO
(*g*) R′ = I, R″ = COOH
(*h*) R′ = H, R″ = CHO
(*i*) R′ = H, R″ = CH=N.OH
(*j*) R′ = H, R″ = $CH_2.NH_2$
(*k*) R′ = H, R″ = CN
(*l*) R′ = COOH, R″ = H
(*m*) R′ = H, R″ = CH=C(CN)COOEt
(*n*) R′ = CHO, R″ = CN
(*o*) R′ = CHO, R″ = CH=C(CN)COOEt



III



IV



V

The carbinol (I, R′ = H, R″ = CH_2OH) was mentioned above, and routes to aminomethyl-porphobilinogen (I, R′ = R″ = CH_2NH_2) are also being explored. When the aldehyde group of I*h* was protected by condensation with cyanoacetic ester (8), the product, I*m*, could not be esterified. However, the aldehyde group of the ethyl ester of I*h* was similarly

Can. J. Chem. Downloaded from www.nrcresearchpress.com by 210.87.254.40 on 09/05/12
For personal use only.

protected and the resulting ester of I*m* was formylated to the ethyl ester of I*o* using dimethyl formamide and phosphorus oxychloride. The methyl ester of the oxime I*i*, which formed a stable hydrochloride, was converted into the methyl ester of the nitrile I*k* by dimethyl formamide and phosphorus oxychloride under mild conditions. Under more vigorous conditions the same reagents formylated the nitrile ester I*k* to the ester of the aldehyde-nitrile I*n*.

The structures of I*k* and I*n* were confirmed by conversion into known derivatives of II*a*: I*k* into II*l* and its ethyl ester, I*n* into II*c*. The sequence implies a formally general solution to the problem of interconverting isomeric 3,4-dialkylpyrroles such as I*a* and II*a*. Only particular solutions had been found to this problem which was once of some practical significance (9).

Both porphobilinogen and isoporphobilinogen (I*j* and II*j*) had been identified by paper chromatography among the products obtained by heating their 5-carboxy derivatives (I*e* and II*e*) with copper acetate in aqueous pyridine (10). However, neither had been isolated and in the case of porphobilinogen, our own experience with this synthesis had been discouraging (7). Accordingly, the synthesis of isoporphobilinogen originally projected depended on the decarboxylation of II*e* after acylating the primary amino group, a closer analogue of the easily decarboxylated 5-carboxyporphobilinogen lactam being hardly to be expected. To this end the ethyl ester of the aldehyde II*c*, obtained from II*a*, was converted to the ester of the oxime II*d* and thence to the ethyl ester hydrochloride of II*e*. We then turned to the following more attractive route analogous to the new synthesis of porphobilinogen. The aldehyde II*c*, obtained from its ester, was converted into isoporphobilinogen through II*f* and II*i*. We also converted II*f* into the α'-free aldehyde II*h*.

The reduction of the oxime I*i* to porphobilinogen, I*j*, had been carried out in relatively dilute solution to completely suppress the formation of a by-product of unknown structure and higher R_f (see Experimental). Although both products showed some reactions expected of porphobilinogen and gave similar analytical figures, the required product was identified through derivatives as a monohydrate corresponding to the structure I*j*, and through comparison with natural material, as porphobilinogen.

The reduction of the oxime II*i* to isoporphobilinogen, II*j*, had to be carried out at greater dilution than was that of I*i*, to completely suppress the formation of small amounts of an analogous by-product which again had a higher R_f. Isoporphobilinogen could be identified because it analyzed for anhydrous II*j*, had an R_f identical with that of porphobilinogen, and gave a well-characterized diethyl ester hydrochloride.

Of the pyrromethanes related to porphobilinogen, only the 5,5′-free compounds are known (11). In two approaches to others, the ethyl ester of porphobilinogen lactam, III, was condensed with the ester of I*b*, and 5-carboxyporphobilinogen, I*e*, was condensed with formic acid and hydrogen bromide to give compounds which may be provisionally formulated as IV and V, although we have not yet developed methods for checking the homogeneity of such pyrromethanes and pyrromethenes by paper chromatography. The methene V was reduced to a colorless substance which did not analyze well for the corresponding pyrromethane and which was not converted into uroporphyrins enzymically (12).

EXPERIMENTAL

The melting points are uncorrected as taken in capillaries. The infrared spectra in Nujol mull and X-ray powder photographs are by Dr. R. N. Jones and Mr. R. Lauzon,

Can. J. Chem. Downloaded from www.nrcresearchpress.com by 210.87.254.40 on 09/05/12
For personal use only.

and by Dr. Maria Przybylska. Paper chromatograms were ascending overnight runs in ethanol – concentrated ammonia – water (7:1:2), using an acidic permanganate spray (13) or, in the upper layer of *n*-butanol – glacial acetic acid – water (4:1:5), using an Ehrlich's spray. Such runs determining R_f's designated by "in ammonia" and "in acetic acid" respectively showed one spot only. Darco refers to Darco G-60 charcoal and ether, to anhydrous ether. The analyses on specimens dried to constant weight were by Mr. J. R. H. Séguin.

2-Formyl-5-carboxy-pyrrole-3-acetic acid-4-propionic acid (Ic)

The following method has given more consistent yields than did the earlier method (3). The triethyl ester of I*c* (16 g) (3) and 360 ml of absolute ethanol were added to 24 g of sodium hydroxide in 600 ml of water. Nitrogen was passed through while the mixture was warmed to solution and then kept at 50° for 1 hour. The orange solution was then concentrated to 100 ml in a rotary evaporator at <40°. The red concentrate was maintained below 10° while it was acidified to Congo red with 52 ml of concentrated hydrochloric acid. The temperature was then raised to 25°. The product crystallized as brownish-pink microneedles (12 g) which were filtered off after ¼ hour and washed with water, then with ether. It was purified by extracting into 800 ml of acetone (Soxhlet, 5 hours, 200 mg insoluble). The cooled acetone solution was forced by air pressure through a column (35 mm diam. × 60 mm of Darco/Celite 535 (1:1 by vol.) supported on a 15-mm bed of Celite 535) which was then thoroughly washed with acetone. When the pale yellow eluate was concentrated to 75 ml and cooled to 0°, 9.9 g (81%) of colorless needles separated; m.p. 241–243° (decomp., inserting at 235°), Ehrlich test dark red on heating; R_f "in ammonia": 0.19.

For analysis the product was recrystallized from acetone (Soxhlet) and dried at 56° and 5×10^{-2} mm. Calc. for $C_{11}H_{11}O_7N$: C, 49.07; H, 4.12; N, 5.20. Found: C, 49.33; H, 4.24; N, 5.32.

2-Formyl-5-iodopyrrole-3-acetic acid-4-propionic acid (If)

A suspension of 4.0 g of I*c* in 60 ml of water and 3.0 g of $KHCO_3$ was added to a solution of 9.0 g KI and 3.8 g of iodine in 60 ml of water. After the mixture was shaken to solution on the steam bath, heating was continued for 1 hour while carbon dioxide was evolved and the color lightened considerably. A cold finger, occasionally washed down with a few drops of absolute ethanol, prevented the loss of iodine. The solution was cooled to 20° and scratched. After ¼ hour the crude product (2.9 g, m.p. 196–197° decomp.) was filtered off and washed with water. After two recrystallizations from 65 ml of water, flesh-colored needles resulted (2.6 g, 50%); m.p. 199–200° (decomp., iodine evolved, inserted at 185°); Ehrlich test slowly positive cold; R_f "in ammonia": 0.40.

For analysis it was dried (60°, 1×10^{-4} mm). Calc. for $C_{10}H_{10}O_5NI$: C, 34.21; H, 2.87; N, 3.99; I, 36.15. Found: C, 34.28; H, 2.94; N, 4.17; I, 36.47, 36.04 (Schöniger), 35.97 (Carius).

2-Formylpyrrole-3-acetic acid-4-propionic acid (Ih)

The iodopyrrole I*f* (2.0 g) in 60 ml of absolute ethanol was added to 25 ml of water containing 776 mg of sodium acetate trihydrate and 250 mg of palladium black. The mixture was shaken under hydrogen (20°, 1 atm) until absorption ceased after the uptake of 1 mole during 1 hour. The filtrate and aqueous washings were taken to dryness in a rotary evaporator (bath at 50°) and 20 ml of water was twice added and removed in the same way. The residue was extracted with 5 ml of water and the insoluble product

Can. J. Chem. Downloaded from www.nrcresearchpress.com by 210.87.254.40 on 09/05/12
For personal use only.

filtered off and then washed (2×1 ml). This product was dried and then extracted into 200 ml of ether (Soxhlet, 6 hours). After the ether solution had been concentrated to 50 ml, yellow needles separated (970 mg, 76%); m.p. 176–180° (decomp., inserting at 160°); Beilstein test for halogen negative; Ehrlich test (magenta) fast in the cold; R_f "in ammonia": 0.33; in ethanol, λ_{max} 302 mμ ($\epsilon = 16\times10^3$). The aldehyde CH and the pyrrole ring CH were both confirmed by the N.M.R. spectrum.*

For analysis the product in acetone was decolorized by passage through a small column of Darco. The precipitate obtained from the eluate by adding ether was recrystallized three times from acetone–ether: colorless, flat needles, m.p. unchanged. Calc. for $C_{10}H_{11}O_5N$: C, 53.33; H, 4.92; N, 6.22. Found: C, 53.61; H, 4.94; N, 6.12.

2-Formylpyrrole-3-acetic acid-4-propionic acid Diethyl Ester

The aldehyde I*h* (351 mg) was warmed to solution in 5 ml of absolute ethanol, and diazoethane (from 3 g of nitrosoethylurea) in 75 ml of ether was added to the cooled solution. Evaporation left an oil which was dried *in vacuo* overnight and then crystallized by rubbing with ether. After sublimation (135°, 5×10^{-4} mm) it was obtained as pale yellow crystals (353 mg, 79%); m.p. 47–52°, softening from 37°; Ehrlich test red in the cold. The product of only one run crystallized and was not analyzed.

2-Formylpyrrole-3-acetic acid-4-propionic acid Oxime (Ii)

Method (a)

Hydroxylamine hydrochloride (500 mg) was dissolved in 3 ml of water, and 2 ml of 10% sodium hydroxide was added. The aldehyde I*h* (128 mg) and 1.4 ml of this solution were heated on the steam bath for ½ hour. The cooled solution was acidified to Congo red with 2 drops of concentrated hydrochloric acid and cooled at 0° for ½ hour; then the product (128 mg, 94%) was separated and washed successively with water, ethanol, and ether. It formed colorless microcrystals; m.p. 210–212° (decomp., inserted at 200°); Ehrlich test slowly violet cold. The R_f "in ammonia" (0.29) and the X-ray powder photograph were identical with those of the products of methods (*b*) and (*c*) below.

For analysis it was recrystallized four times (70% recovery) from 0.01 *N* NaOH/0.01 *N* HCl and dried at 60°, 0.02 mm. Calc. for $C_{10}H_{12}O_5N_2$: C, 50.00; H, 5.04; N, 11.66. Found: C, 49.82; H, 5.11; N, 11.55.

Method (b)

The iodopyrrole I*f* (3 g), 6 g of hydroxylamine hydrochloride, 36 ml of water, and 24 ml of 10% sodium hydroxide were heated for 1 hour on the steam bath (gases evolved). The cooled solution was passed through a column of Darco (22 mm diam.×10 mm), the column being washed with 15 ml of water. The yellow filtrate and washings were made acid to Congo red with ca. 18 ml of 2 *N* HCl, then cooled to 0° for 1 hour. The product (1.7 g, 81%) was separated and washed successively with water, ethanol, and ether to give cream-colored crystals; m.p. 212–213.5° (decomp., inserted at 200°); Beilstein halogen test negative, Ehrlich test slowly violet cold; in ethanol, λ_{max} 287 mμ ($\epsilon = 19\times10^3$).

For analysis it was recrystallized from acetone (Soxhlet) and dried (60°, 0.1 mm), giving cream-colored needles, m.p. 211–212° (decomp., inserted at 200°). Found: C, 49.89; H, 5.05; N, 11.51.

Preparative Method (c)

Hydroxylamine hydrochloride (24 g) in 144 ml of water was brought to pH 6–7 with

*We are grateful to Dr. H. J. Bernstein for this interpretation.

Can. J. Chem. Downloaded from www.nrcresearchpress.com by 210.87.254.40 on 09/05/12
For personal use only.

96 ml of 10% NaOH. The 5-carboxylpyrrole I*c* (9 g) was added and the solution was refluxed (mantle) under nitrogen for 7 hours in the dark. After being left at 20° in the dark overnight (important), the solution was filtered through a column of Darco (18 mm diam. × 40 mm, prewashed with water) and the column washed with water until the eluate was colorless. The purple eluate was acidified to Congo red with ca. 95 ml of 2 *N* HCl, scratched, and left at 0° for 1½ hours. The nearly colorless diamond-shaped crystals (6.02 g) were separated and washed successively with water, ethanol, and ether. A colorless product (5.29 g, 66%) was obtained after two recrystallizations from 0.1 *N* NaOH/2 *N* HCl (to pH 3); m.p. 210–211° (decomp., inserted at 200°); R_f "in acetic acid": 0.67.

For analysis it was recrystallized twice more in the same way and dried (60°, 0.01 mm). Found: C, 49.85; H, 5.33; N, 11.80.

2-Formylpyrrole-3-acetic acid-4-propionic acid Dimethyl Ester Oxime

A solution of 2 g of the oxime I*i* in 60 ml of 5% hydrogen chloride in methanol was kept at 0° overnight and then taken to dryness *in vacuo* below 20° in a rotary evaporator. To the residue dissolved in 100 ml of water, 4 ml of 2 *N* NaOH was added. After ½ hour the red-brown precipitate was separated, washed with water, dried (weight: 2 g), and extracted into 750 ml of ether (Soxhlet, 2 hours). The light brown extract was filtered through a column of Darco (18 mm diam. × 16 mm). The colorless eluate and ether wash were concentrated to 15 ml, and 50 ml of *n*-pentane was added with scratching. The colorless needles which separated (1.86 g, 83%) were washed with pentane; m.p. 130–133°; Beilstein halogen test negative; Ehrlich test slowly red cold; in ethanol, λ_{max} 285 mμ ($\epsilon = 20\times10^3$).

For analysis it was recrystallized twice from methanol–water (65% recovery) and dried (20°, 0.01 mm), m.p. 131–135°. Calc. for $C_{12}H_{16}O_5N_2$: C, 53.72; H, 6.01; N, 10.44; OMe, 23.14. Found: C, 53.86; H, 5.84; N, 10.53; OMe, 22.88.

2-Formylpyrrole-3-acetic acid-4-propionic acid Dimethyl Ester Oxime Hydrochloride

A solution of 201 mg of the oxime I*i* in 6 ml of 5% hydrogen chloride in methanol was kept at 0° for 3 hours and then taken to dryness at 20°; 6 ml of methanol was thrice added and removed in the same way. The residue was slurried with 10 ml of chloroform and the pink crystals (181 mg, 71%) filtered off, m.p. 160–164° (decomp., inserted at 150°); Beilstein halogen test positive; Ehrlich test very slowly violet cold.

For analysis it was twice precipitated from methanol by ether at 20° and dried (25°, 1×10^{-4} mm), giving colorless needles (35% recovery), m.p. 162–164° (decomp., inserted at 150°). Calc. for $C_{12}H_{16}O_5N_2.HCl$: C, 47.29; H, 5.62; N, 9.19; Cl, 11.64; OMe, 20.37. Found: C, 47.43; H, 5.65; N, 9.05; Cl, 11.44; OMe, 20.22.

2-Aminomethylpyrrole-3-acetic acid-4-propionic acid (Porphobilinogen, Ij)

A suspension of 5 g of the oxime I*i* and 2 g of palladium black in 100 ml of water was shaken under hydrogen at room temperature and pressure until absorption ceased after the uptake of 2 moles in about 2 hours. After the addition of 5 ml of concentrated ammonia to dissolve the product, filtration through paper (Whatman No. 5) gave a yellow solution. After bringing its pH to 7 with glacial acetic acid this solution was filtered through a column of alumina (Woelm, neutral, prewashed with water, 18 mm diam. × 50 mm) and the column washed with water until the Ehrlich reaction of the eluate was faint. The eluate (400 ml) was concentrated to 100 ml in a rotary evaporator (oil pump, baths 25–30° and ice–salt). The concentrate was acidified to pH 4.5 with glacial acetic acid with scratching, quickly cooled, and kept at 0° for 4 hours. The product, after being washed successively with water, ethanol, and ether, formed buff-colored, barrel-shaped

Can. J. Chem. Downloaded from www.nrcresearchpress.com by 210.87.254.40 on 09/05/12
For personal use only.

plates (3.2 g, 63% as the monohydrate); m.p. 174–177° (decomp., inserting at 167°); Ehrlich reaction rapidly positive cold. Its R_f "in acetic acid" (0.49) and its infrared mull spectrum were identical with those of natural porphobilinogen.

The X-ray powder photograph was identical with that of porphobilinogen synthesized over the lactam (7). Between these photographs and that of natural material there were differences in the relative intensities of 3 lines among 30. These differences are not considered significant because the natural porphobilinogen was photographed only as received, when its infrared mull spectrum showed a gross anomaly, unlike the spectrum of the same material after recrystallization as the hydrochloride and then as the base.

The synthetic porphobilinogen also agreed with natural material in the following respects:* (1) the quantitative Ehrlich reaction; (2) paper electrophoresis at pH 2.4, 4.4, 6.6, and 10.4; (3) the uroporphyrin mixtures (examined by paper chromatography after conversion to coproporphyrins) formed by the self-condensation of the porphobilinogen at various pH's; (4) the enzymic conversion to uroporphyrin.

For analysis it was recrystallized from 0.7 *N* ammonia – glacial acetic acid and dried (20°, 0.01 mm). Calc. for $C_{10}H_{14}O_4N_2.H_2O$: C, 49.17; H, 6.60; N, 11.47. Found: C, 48.88; H, 6.87; N, 11.41.

Porphobilinogen Lactam

This synthetic porphobilinogen was converted into the lactam (52%) by the method of Cookson and Rimington (14) as colorless hexagonal plates, Ehrlich test fast cold.

For analysis it was recrystallized from water (Soxhlet) and dried (20°, 0.01 mm), m.p. 281–283° (decomp., inserted at 270°). It was identical with the lactam from natural porphobilinogen by the following criteria: infrared mull spectrum, X-ray powder photograph, and R_f (0.63 "in acetic acid"). Calc. for $C_{10}H_{12}O_3N_2$: C, 57.68; H, 5.81; N, 13.46. Found: C, 57.43; H, 5.77; N, 13.35.

Porphobilinogen Hydrochloride

This synthetic porphobilinogen was converted into the monohydrate of the hydrochloride (59%) by the method of Cookson and Rimington (14).

For analysis it was recrystallized from 2 *N* hydrochloric acid, dried (2 hours, 20°, 0.01 mm), and then exposed to air overnight to give faintly pink microneedles giving an I.R. mull spectrum and X-ray powder photograph identical with those of the natural hydrochloride. Calc. for $C_{10}H_{14}O_4N_2.HCl.H_2O$: C, 42.78; H, 6.10; N, 9.98; Cl, 12.63. Found: C, 43.01; H, 5.98; N, 9.89; Cl, 12.44.

A *by-product* of the reduction of the oxime Ii to porphobilinogen was initially very troublesome. The formation of this by-product, like that of porphobilinogen, was accompanied by the uptake of 2 moles of hydrogen. The ratio of the two products was independent of the hydrogen pressure but the by-product was favored by higher oxime concentrations and by reduction in dilute ammonia rather than in water. For example, 100 mg of the oxime with the catalyst in 1 ml of 1.5 *N* ammonia (1 atm of hydrogen) gave the by-product and a trace of porphobilinogen; in 25 ml of 0.7 *N* ammonia (1 atm or 120 atm of hydrogen) or in 1 ml of 0.7 *N* acetic acid (1 atm of hydrogen), porphobilinogen and a trace of by-product resulted.

The by-product analyzed much like the porphobilinogen monohydrate, gave a positive Ehrlich test cold, gave uroporphyrins with hot 2 *N* hydrochloric acid, and formed a hydrochloride. However, it gave no lactam by the method of Cookson and Rimington (14)

*We are indebted to Dr. J. J. Scott and to Professor L. Bogorad for the tests with enzymes, and to Dr. D. Mauzerall for the other tests.

Can. J. Chem. Downloaded from www.nrcresearchpress.com by 210.87.254.40 on 09/05/12
For personal use only.

and it differed from porphobilinogen in its R_f (0.66 "in acetic acid"), in its X-ray powder photograph, and in the infrared mull spectra of both the base and hydrochloride.

For analysis it was recrystallized from 1.5 *N* ammonia – acetic acid and dried (20°, 1×10^{-4} mm) to give colorless hair-like microcrystals, m.p. 178–181° (decomp., inserted at 166°). Calc. for $C_{10}H_{14}O_5N_2$: C, 49.58; H, 5.83; N, 11.57. Found: C, 49.68; H. 6.31; N, 11.05.

2-(ω-Cyano-ω-carbethoxy-vinyl)-pyrrole-3-acetic acid-4-propionic acid Diethyl Ester (Ethyl Ester of Im)

The ethyl ester of the aldehyde I*h* (the crude oily product from 351 mg of I*h* and ethereal diazoethane) was heated for ½ hour on the steam bath with 200 mg of ethyl cyanoacetate, 5 ml of absolute ethanol, and 2 drops of 25% aqueous methylamine. The crude product, which separated on cooling and scratching, was recrystallized from ethanol, giving 297 mg (51%), m.p. 108–110°.

For analysis it was recrystallized four times from ethanol (80% recovery) and dried (60°, 0.01 mm), giving yellow microneedles; m.p. 111–112° (softening from 105°); Ehrlich's test blue hot; insoluble in cold ethanol. Calc. for $C_{19}H_{24}O_6N_2$: C, 60.62; H, 6.43; N, 7.44. Found: C, 60.91; H, 6.50; N, 7.34.

The acid I*m* was prepared analogously from I*h* using aniline as the catalyst. It formed yellow crystals from ethanol; m.p. 191–194° (decomp., inserted at 180°); soluble in hot acetone; insoluble in refluxing ether. Attempts to esterify it with 5% ethanolic hydrogen chloride and with ethereal diazoethane failed.

2-(ω-Cyano-ω-carbethoxy-vinyl)-5-formylpyrrole-3-acetic acid-4-propionic acid Diethyl Ester (Ethyl Ester of Io)

The ethyl ester of I*m* (247 mg), suspended in 0.428 ml of dimethyl formamide, was treated with 0.070 ml of phosphorous oxychloride (10% excess) and heated to solution on the steam bath, then for 10 minutes longer. Water (15 ml) containing 573 mg of sodium acetate trihydrate was added to the cooled solution. After the mixture was scratched and allowed to stand ½ hour, the brownish-yellow product separated. Its solution in 10 ml of chloroform was filtered through a column of alumina (Woelm neutral grade IV, 8 mm diam. × 20 mm). The residue left on evaporating the eluate was recrystallized from ether – *n*-pentane and then from ethanol–water, giving yellow needles (137 mg, 52%), m.p. 107–109°.

For analysis it was twice recrystallized from ethanol–water (65% recovery) and dried (56°, 5×10^{-4} mm), m.p. 110–111°. Calc. for $C_{20}H_{24}O_7N_2$: C, 59.40; H, 5.98; N, 6.93. Found: C, 59.35; H, 5.79; N, 6.99.

2-Cyanopyrrole-3-acetic acid-4-propionic acid Dimethyl Ester (Methyl Ester of Ik)

The dimethyl ester of I*i* (500 mg, 1.87 mmoles) was warmed to solution in 0.67 ml of dimethyl formamide (previously distilled over phosphorus pentoxide). This solution was shaken vigorously at −15° while 0.19 ml (2.06 mmoles) of phosphorus oxychloride was added slowly, then left at 20° for ¼ hour. The mixture was treated with 1.125 g (8.3 mmoles) of sodium acetate trihydrate in 5 ml of water, diluted to 25 ml with water, and scratched; light brown crystals (394 mg) then separated. These were extracted into 200 ml of ether (Soxhlet, 1 hour), the solution was filtered through a column of Darco (8 mm diam. × 15 mm), and the column was washed with ether. The colorless eluate was concentrated to 10 ml. Crystallization was induced by scratching and completed by evaporating more ether while adding *n*-pentane. The product (344 mg, 74%) formed colorless

Can. J. Chem. Downloaded from www.nrcresearchpress.com by 210.87.254.40 on 09/05/12
For personal use only.

glittering crystals, Ehrlich test faintly rose hot. It exists in two forms, m.p. 81–83° and 103–106°, either of which might separate from solution or melt and which gave identical infrared mull spectra (nitrile band at 2240 cm^{-1}). The U.V. spectrum in ethanol, λ_{max} at 256 mμ ($\epsilon = 12\times10^3$) and 235 mμ ($\epsilon = 8\times10^3$), with no absorption at 280–290 mμ, showed that the oxime was absent.

For analysis it was twice recrystallized from ether – *n*-pentane (74% recovery) and dried (20°, 0.01 mm), m.p. 80–82° (softening from 75°). Calc. for $C_{12}H_{14}O_4N_2$: C, 57.59; H, 5.64; N, 11.20; OMe, 24.80. Found: C, 57.40; H, 5.62; N, 11.35; OMe, 24.64.

2-Carboxypyrrole-3-acetic acid-4-propionic acid (IIl)

The dimethyl ester of the nitrile I*k* (102 mg) in 4 ml of 10% sodium hydroxide and enough ethanol (about 2 ml) to effect solution was heated on the steam bath for 6 hours while nitrogen was bubbled through it and its volume maintained at 4 ml by the occasional addition of water. The cooled solution was passed through a column of Amberlite IR-120 (wet hydrogen form, 16 g) and the column was washed with water until the eluate gave a negative Ehrlich test cold. The residue left on taking the eluate to dryness in a rotary evaporator (bath at 45°) was extracted by 5×15-ml portions of boiling acetone. The extract was filtered and concentrated to 5 ml, 20 ml of ether was added, and amorphous mauve-colored impurities were filtered off at once. When the filtrate was scratched, the product (55 mg, 56%) crystallized as nearly colorless rectangular plates; m.p. 183–184° (decomp., inserted at 165°), undepressed by authentic material derived from the ester of II*a* (lit. 178° (3)); Ehrlich test quickly bluish-red cold. The R_f "in ammonia" (0.16) was identical with that of authentic material.

2-Carboxypyrrole-3-acetic acid-4-propionic acid Triethyl Ester

The acid (from the ester of I*k*) with diazoethane in ether gave the product as colorless needles; Ehrlich test slowly bluish-red cold; m.p. 51–52.5°, undepressed by authentic material (lit. 51–52° (3)). The two specimens also gave identical infrared mull spectra and X-ray powder photographs.

2-Cyano-5-formylpyrrole-3-acetic acid-4-propionic acid Dimethyl Ester (Ester of In)

The ester of the nitrile I*k* (200 mg, 0.8 mmole) was dissolved in 0.4 ml of dimethyl formamide (previously distilled over phosphorus pentoxide), and 0.1 ml (1.1 mmole) of phosphorus oxychloride was added. The solution was heated for 25 minutes on the steam bath in an open vessel and cooled to 20°, and 592 mg (4.4 mmoles) of sodium acetate trihydrate in 2.5 ml of water was added. The suspended oil crystallized after the solution was scratched. After the volume of the mixture was made up to 8 ml with water, the buff-colored precipitate was filtered off and washed with water. The dried precipitate (134 mg) was dissolved in 125 ml of boiling ether and the cooled solution filtered through a column of Darco (8 mm diam. × 10 mm). The colorless eluate was concentrated to 2 ml, crystallization was induced by scratching, and the product (112 mg, 50%) was filtered off and washed with 1 ml of ether and then with *n*-pentane. It formed colorless plates; m.p. 113–116° (softening from 90°); Ehrlich test slowly brown hot; infrared band at 2255 cm^{-1} in Nujol mull; in ethanol, λ_{max} 294 mμ ($\epsilon = 19\times10^3$). It can be distilled at 160°, 1×10^{-5} mm.

For analysis it was recrystallized from ether and twice dried (20° and 1×10^{-2} mm, then 100° and 1×10^{-3} mm), giving colorless plates, m.p. 113–115°. Calc. for $C_{13}H_{14}O_5N_2$: C, 56.11; H, 5.07; N, 10.07. Found: C, 55.87; H, 4.98; N, 9.99. Specimens dried at 20°, softened from about 100°, and analyzed as a hydrate containing $\frac{1}{3}H_2O$.

Can. J. Chem. Downloaded from www.nrcresearchpress.com by 210.87.254.40 on 09/05/12
For personal use only.

2-Carboxy-5-formylpyrrole-3-acetic acid-4-propionic acid (IIc)

(a) From the Triethyl Ester of Ia via the Dimethyl Ester of In

This was carried out before the ester of I*n* had been obtained crystalline. The crude oily ester of I*n* (obtained as above by adding aqueous sodium acetate after reacting the ester of I*k* with dimethyl formamide and phosphorus oxychloride) was hydrolyzed for 6 hours on the steam bath in 10% sodium hydroxide. After passage through Amberlite IR-120 (hydrogen form), the solution was evaporated to dryness. The solution of the residue in acetone was decolorized by filtration through a column of Darco and was then taken to dryness. Adding ether to the residue induced the product to crystallize. This showed a single spot on paper chromatography and gave an infrared mull spectrum, X-ray powder photograph, and R_f ("in ammonia" but descending for 70 hours to ensure the absence of II*l*) identical with those of authentic material obtained ultimately from the ester of II*a* by method (*b*) below.

(b) Preparative Method (from the Triethyl Ester of IIa via the Triethyl Ester of IIc)

The triethyl ester of II*c* (3) (16 g) was hydrolyzed to II*c* just as the ester of I*c* was to I*c*. The crude product (red crystals, 9.36 g) was extracted into acetone and passed through Darco to give 7.34 g (60%) of cream-colored crystals; m.p. 234–238° (decomp., inserted at 225°); Ehrlich test slowly brownish-red cold; R_f "in ammonia" identical with that of I*c*.

For analysis it was recrystallized from acetone (Soxhlet) and then at <50° from water and then dried at 25° and 1×10^{-2} mm to give pink radiating needles. Calc. for $C_{11}H_{11}O_7N$: C, 49.07; H, 4.12; N, 5.20. Found: C, 48.97; H, 4.38; N, 5.14.

2-Formyl-5-iodopyrrole-3-propionic acid-4-acetic acid (IIf)

The preparation of II*f* from 4 g of II*c* followed that of I*f* from I*c*. The buff-colored crystalline crude product (1.89 g), m.p. 221–222° (decomp., introduced at 200°), was twice recrystallized from 110 ml of water. The product (1.46 g, 28%) formed yellow needles; m.p. 221–224° (decomp., iodine evolved, introduced at 200°); Ehrlich test slowly positive cold; R_f "in ammonia" identical with that of I*f*.

For analysis an acetone solution was decolorized by filtration through a small column of Darco. The precipitate, obtained from the eluate by adding hexane, was recrystallized four times from water and dried (56°, 1×10^{-4} mm), giving colorless needles, m.p. 215–220° (decomp., iodine evolved, introduced at 200°). Calc. for $C_{10}H_{10}O_5NI$: C, 34.21; H, 2.87; N, 3.99; I, 36.15. Found: C, 34.35; H, 3.12; N, 3.99; I, 36.24.

2-Formylpyrrole-3-propionic acid-4-acetic acid (IIh)

The iodopyrrole II*f* (500 mg) in 24 ml absolute ethanol was added to 194 mg sodium acetate trihydrate in 16 ml of water, and the solution was shaken for 1 hour under hydrogen (20°, 1 atm) with 125 mg of palladium black. The filtrate and aqueous washings from the catalyst were taken to dryness in a rotary evaporator (bath temp. 45°), then 5 ml of water was twice added and removed in the same way. The residue was extracted into 75 ml of ether (Soxhlet, 6 hours). The residue left on evaporating the ether was dissolved in 15 ml of boiling acetone. This solution was filtered through a column of Darco, the eluate concentrated to 5 ml, and the colorless product (175 mg, 55%) precipitated by the addition of 20 ml of ether.

For analysis it was recrystallized twice from water (56% recovery) and dried (56°, 1×10^{-4} mm) to give colorless needles; m.p. 178–182° (decomp., inserted at 160°); Beilstein test for halogen negative, Ehrlich test rapidly red cold; R_f "in ammonia" identical with that of its isomer I*h*. Calc. for $C_{10}H_{11}O_5N$: C, 53.33; H, 4.92; N, 6.22. Found: C, 53.50; H, 4.82; N, 6.25.

Can. J. Chem. Downloaded from www.nrcresearchpress.com by 210.87.254.40 on 09/05/12
For personal use only.

This preparation could presumably be improved by using the method later developed for I*h*, that is, by washing the crude product with water before extracting into ether.

*2-Formylpyrrole-3-propionic acid-4-acetic acid Oxime (II*i*)*

Hydroxylamine hydrochloride (2 g) was dissolved in 12 ml of water and 8 ml of 10% NaOH added (pH 6–7), then 1 g of the iodopyrrole II*f*. The solution was heated on the steam bath for $1\frac{1}{2}$ hours (gas evolved), cooled to 20°, brought to pH 3 with concentrated hydrochloric acid, and then left overnight at 0°. The precipitate (403 mg) was separated, washed with a little water, then pentane, and dissolved in 4 ml of boiling water. Left at 20° overnight, the solution deposited buff-colored crystals (366 mg, 54%); m.p. 178–180° (decomp., inserted at 160°); Ehrlich test very slowly blue cold; Beilstein halogen test negative. The R_f "in ammonia" (0.33) was exceptional in that it differed from that of the isomeric I*i* (0.29).

For analysis it was recrystallized from water and dried, giving buff-colored crystals, m.p. unchanged. Calc. for $C_{10}H_{12}O_5N_2$: C, 50.00; H, 5.04; N, 11.66. Found: C, 49.76; H, 4.89; N, 11.56.

This product appears to remain in supersaturated aqueous solutions more than does its isomer I*i* and to be more strongly retained on Darco. Paper chromatography indicated that it was the sole product when II*c* was treated as in the conversion of I*c* to I*i* by method (*c*), but the isolation of the II*i* resulting by this method has not been worked out.

*2-Aminomethylpyrrole-3-propionic acid-4-acetic acid (isoporphobilinogen, II*j*)*

The oxime II*i* (125 mg) and 250 mg of palladium black were shaken under hydrogen (20°, 1 atm) with 250 ml of redistilled water until absorption ceased after the uptake of 2 moles in 2 hours. The catalyst was filtered off (Whatman No. 1 paper) and the filtrate concentrated to 20 ml in a rotary evaporator (baths at 30° and 0°). The pink solution, after the pH was brought to 7, was filtered through an alumina column (Woelm, neutral, 8 mm diam. × 20 mm, prewashed with water), which was then washed with water until the eluate gave a very faint Ehrlich test in the cold. The eluate (50 ml) was concentrated in a rotary evaporator (baths at 30° and 0°) to about 0.5 ml. After the addition of 0.7 *N* ammonia, the pH was brought to 4–5 with glacial acetic acid (volume of solution now <2 ml). After the solution was scratched, it was left at 0° for 3 hours. The product (83 mg, 70%) was separated and washed with a little water to give colorless needles; m.p. 192–195° (decomp., inserted at 180°); Ehrlich test rapidly red cold; R_f "in acetic acid" identical with that of porphobilinogen. It was also characterized by its X-ray powder photograph and infrared mull spectrum.

For analysis it was recrystallized from 0.7 *N* ammonia – glacial acetic acid and dried (20°, 0.01 mm). Calc. for $C_{10}H_{14}O_4N_2$: C, 53.09; H, 6.24; N, 12.38. Found: C, 52.92; H, 6.29; N, 11.96.

Isoporphobilinogen Diethyl Ester Hydrochloride

A solution of 51 mg of isoporphobilinogen, II*j*, in 2 ml of 5% hydrogen chloride in ethanol was left at 0° overnight. The colorless solution was taken to dryness *in vacuo* below 20° and 1 ml of ethanol was three times added and removed as above. The product crystallized on adding ether and seeding, giving 66 mg (92%) of colorless needles; m.p. 97–98.5°; Ehrlich test rapidly red cold; soluble in water and in ethanol. It was also characterized by its X-ray powder photograph and infrared mull spectrum.

For analysis it was recrystallized from ethanol–ether (recovery 88%) and dried (20°, 0.01 mm), m.p. 99–100°. Calc. for $C_{14}H_{23}O_4N_2Cl$: C, 52.74; H, 7.27; N, 8.79; Cl, 11.12. Found: C, 52.68; H, 7.24; N, 8.63; Cl, 11.03.

Can. J. Chem. Downloaded from www.nrcresearchpress.com by 210.87.254.40 on 09/05/12
For personal use only.

2-Formyl-5-carboxypyrrole-3-propionic acid-4-acetic acid Triethyl Ester Oxime (Ethyl Ester of IId)

Hydroxylamine hydrochloride (122 mg) in 0.6 ml of water was added to 42 mg of sodium in 10 ml of ethanol and the precipitate was filtered off and washed with ethanol. The filtrate and 500 mg of the ester of II*c* (3) were refluxed for $\frac{3}{4}$ hour. The cooled solution was poured into 175 ml of ice water. After being left overnight at 0°, the product (435 mg, 83%) was filtered off and washed with water, leaving colorless needles, m.p. 104–109°.

For analysis it was twice recrystallized from aqueous ethanol (65% recovery) and dried (57°, 1×10^{-4} mm), m.p. 107–112° softening from 103° (lit. (10), 88°). Calc. for $C_{17}H_{24}O_7N_2$: C, 55.43; H, 6.56; N, 7.61. Found: C, 55.31; H, 6.38; N, 7.79.

2-Aminomethyl-5-carboxypyrrole-3-propionic acid-4-acetic acid Triethyl Ester Hydrochloride (Ester Hydrochloride of IIe)

The ethyl ester of II*d* (476 mg) was shaken under hydrogen (20°, 1 atm) with 100 mg of palladium black, 50 ml of absolute ethanol, and 0.25 ml of concentrated hydrochloric acid until the uptake of hydrogen ceased ($3\frac{1}{2}$ hours, 2 moles taken up). The filtered solution was concentrated to 5 ml *in vacuo*, and 50 ml of ether was added. Scratching induced the separation of the product (386 mg, 76%) as colorless crystals; m.p. 147.5–149°; soluble in 2 *N* HCl; Ehrlich reaction positive hot.

For analysis it was recrystallized from ethanol–ether (recovery 93%) and dried *in vacuo* at 90°, m.p. 147.5–149.5°. Calc. for $C_{17}H_{27}O_6N_2Cl$: C, 52.33; H, 6.96; N, 7.17; Cl, 9.07. Found: C, 52.44; H, 6.93; N, 6.99; Cl, 8.73. The m.p. of the free ester has been reported as 185° (10).

Porphobilinogen Lactam Ethyl Ester (III)

Porphobilinogen lactam (100 mg) (7) was left for 5 hours in 8% ethanolic hydrogen chloride at 20°. The solvent was removed *in vacuo*, then more ethanol was added and removed in the same way. When the residue was crystallized from 3 ml of hot ethanol, two crops of the product were obtained as tan irregular plates (66 mg, 58%), m.p. 239–244° (decomp., inserting at 230°). Calc. for $C_{12}H_{16}N_2O_3$: C, 61.00; H, 6.83; N, 11.86. Found: C, 60.99; H, 7.23; N, 12.01. The ester was also prepared from the lactam with diazoethane in ether–ethanol.

5-Aminomethyl-5′-carboxypyrromethane-4,3′-diacetic acid-3,4′-dipropionic acid Lactam Tetraethyl Ester (IV)

The ethyl ester of porphobilinogen lactam (III, 47.6 mg) and the ethyl ester of I*b* (83.7 mg) (15) were heated for 40 minutes on the steam bath with 1.7 ml of anhydrous sodium acetate in acetic acid (100 mg in 10 ml). Water (4 ml) was added slowly and the mixture heated nearly to a clear solution, then cooled slowly. When a few crystals had separated, the volume was brought to 20 ml with hot water. The nearly colorless amorphous product (81 mg, 70%) was separated from the cooled solution. At about 170° it either melted or changed to crystals, m.p. 181–186°.

For analysis it was extracted by ether (thimble) in which it is very slightly soluble, giving colorless microprisms which at 170° sintered and changed to needles, m.p. 185–189° (hot stage). Calc. for $C_{29}H_{39}N_3O_9$: C, 60.72; H, 6.85; N, 7.33; Found: C, 60.93; H, 6.85; N, 7.21.

The assigned structure is consistent with its U.V. spectrum in ethanol: minimum at 254 mμ and $\epsilon = 15.5\times10^3$ at the 281 mμ maximum. Compare the spectrum of the hexaethyl ester of 5,5′-dicarboxypyrromethane-3,3′-diacetic acid-4,4′-dipropionic acid

Can. J. Chem. Downloaded from www.nrcresearchpress.com by 210.87.254.40 on 09/05/12
For personal use only.

($\epsilon = 30.8 \times 10^3$ at 283 mμ (maximum); no minimum) and of the ethyl ester of porphobilinogen lactam (no maximum but a rise toward 210 mμ).

Condensation of 5-Carboxyporphobilinogen with Formic Acid

5-Carboxyporphobilinogen (7) (500 mg), Ie, was heated on the steam bath for $\frac{1}{2}$ hour with 5 ml of 98% formic acid and 2.5 ml of hydrogen bromide (30% in acetic acid). The cooled solution was scratched after the addition of 10 ml of acetic acid then kept at 0° for 1 hour. The crystalline product, formulated as V (472 mg, 72%), was washed with acetic acid, then ether, and twice recrystallized from formic acid – acetic acid (1:4). After being dried overnight at 20° *in vacuo* over sodium hydroxide, the product (57% recovery) formed orange microneedles, decomposing on heating. Calc. for $C_{21}H_{29}O_8N_4Br_3$: C, 35.76; H, 4.14; N, 7.95; Br, 34.00. Found: C, 36.07; H, 3.94; N, 7.49; Br, 33.08.

Adding three equivalents of sodium hydroxide to a solution of the hydrobromide in water precipitated yellow plates, which did not analyze for the free base of the pyrromethene; m.p. about 275° (decomp.); Beilstein halogen test negative. Calc. for $C_{21}H_{26}O_8N_4$: C, 54.54; H, 5.67; N, 12.12. Found: C, 52.08; H, 6.26; N, 14.68.

After the hydrobromide was reduced in dilute sodium hydroxide with sodium amalgam, acetic acid precipitated initially colorless crystals which, after recrystallization, did not analyze well for the pyrromethane. Calc. for $C_{21}H_{28}O_8N_4$: C, 54.30; H, 6.08; N, 12.06. For $C_{21}H_{28}O_8N_4.C_2H_4O_2$: C, 52.67; H, 6.15; N, 10.68. Found: C, 52.84; H, 6.30; N, 10.33.

REFERENCES

1. G. P. ARSENAULT and S. F. MACDONALD. Chem. in Can. **11**, 43 (1959); **12**, 68 (1960).
2. A. T. CARPENTER and J. J. SCOTT. Biochem. J. **71**, 325 (1959).
3. D. M. MACDONALD and S. F. MACDONALD. Can. J. Chem. **33**, 573 (1955).
4. W. TREIBS and H. J. KOLM. Ann. **614**, 176 (1958).
5. H. FISCHER and H. ORTH. Die Chemie des Pyrrols. Vol. I. Akademische, Leipzig. 1934. p. 138.
6. H. FISCHER and H. ORTH. Die Chemie des Pyrrols. Vol. II, Part 1. Akademische, Leipzig. 1937. pp. 54 ff.
7. A. H. JACKSON and S. F. MACDONALD. Can. J. Chem. **35**, 715 (1957).
8. H. FISCHER and H. WASENEGGER. Ann. **461**, 277 (1928).
9. S. F. MACDONALD. J. Chem. Soc. 4176 (1952).
10. K. S. N. PRASAD and R. RAPER, also C. RIMINGTON and S. KROL. Nature, **175**, 629 (1955).
11. G. P. ARSENAULT, E. BULLOCK, and S. F. MACDONALD. J. Am. Chem. Soc. **82**, 4384 (1960).
12. D. S. HOARE and H. HEATH. Biochim. et Biophys. Acta, **39**, 167 (1960).
13. Ž. PROCHÁZKA. Chem. listy, **44**, 43 (1950); Chem. Abstr. **45**, 5561 (1951).
14. G. H. COOKSON and C. RIMINGTON. Biochem. J. **57**, 476 (1954).
15. E. J. TARLTON, S. F. MACDONALD, and E. BALTAZZI. J. Am. Chem. Soc. **82**, 4389 (1960).

Can. J. Chem. Downloaded from www.nrcresearchpress.com by 210.87.254.40 on 09/05/12
For personal use only.

Can. J. Chem. Downloaded from www.nrcresearchpress.com by 210.87.254.42 on 09/05/12
For personal use only.

PHOTOLYSIS OF POLYACRYLONITRILE[1]

H. H. G. Jellinek and I. J. Bastien[2]

ABSTRACT

The photolysis of polyacrylonitrile has been investigated in solution (80:20 by weight of ethylene carbonate to propylene carbonate), in powder form, and as a film. Experiments have been carried out in vacuum and in the presence of oxygen. All polymer samples were exposed to ultraviolet light of wavelength 2537 Å. In solution a random chain-scission reaction with a small quantum yield (ca. 10^{-4} main chain bonds broken/quantum absorbed) takes place; at the same time, photochemical reactions occur involving side groups of the polymer chains, as evidenced by the change in the ultraviolet spectra of the polymer solutions. It seems likely that double-bond formation, both conjugated and isolated, and cyclization are responsible for the change in spectra. Infrared spectra do not show any change. Exposed polymer films become cross-linked and exposed powder also cross-links and evolves small molecules, such as nitriles, particularly HCN. Degradation in oxygen suppresses what is believed to be double-bond formation as evidenced by ultraviolet absorption spectra. The photolysis of glutaronitrile as a model substance has also been studied.

INTRODUCTION

Experiments on the photodegradation *in vacuo* of polyacrylonitrile dissolved in a mixture of ethylene carbonate and propylene carbonate (88:20 by weight) and exposed to light of wavelength 2537 Å were presented by Jellinek and Schlueter in a previous paper (1). It was shown that the experimental data could be represented with fair approximation by a random chain-scission process. The small quantum yield which was obtained for the photodegradation is in accord with such a random breakdown process. The rate constants derived on the basis of random degradation were found to be linearly dependent on the incident light intensity.

The present work deals with an extension of the investigation to the photodegradation as a function of polymer concentration, chain length, and history of the polymer samples. In addition, ultraviolet and infrared absorption spectra at various stages of the degradation process have been investigated in detail. The previous results of Jellinek and Schlueter (1) have been re-evaluated by the use of a more appropriate intrinsic viscosity – number-average molecular weight relationship. Further, experiments on the photodegradation of polyacrylonitrile in the form of films and powder and on the production of small molecules during degradation are presented. A model substance, glutaronitrile, has also been investigated.

EXPERIMENTAL

(a) Apparatus

The apparatus was similar to that used previously (1) with only some minor modifications. The irradiations were carried out with a stronger mercury lamp of the same type as employed before. It operated at not more than 600 R.M.S. volts and carried 60 ma instead of 30 ma. Not less than 95% of its light output occurred at 2537 Å. The light source was placed near the reaction vessel, which was located in a thermostat at $25\pm0.05°$ C. The light intensities were appreciably greater than those in the previous experiments and a higher experimental accuracy resulted. The lamp was stabilized by a

[1]*Manuscript received June 7, 1961.*
Contribution from the Department of Chemistry, Essex College, Assumption University of Windsor, Windsor, Ontario.
[2]*National Research Council of Canada Scholarship.*

constant-voltage transformer. The 30-ma lamp used previously was also employed for rate measurements as a function of light intensity.

Ultraviolet absorption spectra were measured on a Beckman spectrophotometer (Model DU) and on a Bausch and Lomb Spectronic 505. Infrared spectra were obtained with a Beckman IR-5.

All polymer solutions were irradiated in cylindrical Ultrasil quartz cells with plane, parallel, polished windows. The solutions were evacuated to 10^{-5} mm Hg or better and sealed off before exposure.

Intrinsic viscosities of the polymer samples were determined in Ostwald–Fenske viscometers. The measurements were carried out at 25±0.05° C. All intrinsic viscosities are expressed in $(g/100\ ml)^{-1}$.

(b) Materials

Polyacrylonitrile samples of number-average molecular weights 99,100, 54,590, and 26,320 were obtained from the Chemstrand Corporation. Their intrinsic viscosities in dimethylformamide and ethylene carbonate – propylene carbonate (80:20 by weight) respectively were $[\eta]_{DMF}$: 2.19, 1.40, 0.81, and $[\eta]_{EPC}$: 1.65, 1.21, 0.78.

The number-average molecular weights were derived from an equation by Cleland and Stockmayer (2) for dimethylformamide solutions: $[\eta]_{DMF} = 0.392\times10^{-3}\ M_n^{0.75}$.

A polymer sample was also prepared in the authors' laboratory. The procedure was as follows.* Acrylonitrile supplied by Eastman Kodak was washed successively with 3 *N* sulphuric acid, 3 *N* sodium carbonate, and water. It was dried with calcium chloride and distilled twice under atmospheric pressure. Ethylene carbonate was used as a solvent for the polymerization and Eastman Kodak azobisisobutyronitrile served as a catalyst. The solution was 0.058 *M* and 0.0135 *M* with respect to monomer and catalyst respectively. The polymerization was carried out under vacuum at a temperature of 60 to 65° C. After 45 minutes, the reaction mixture was poured into well-stirred methanol; the precipitated polymer was filtered off and washed thoroughly with methanol. Subsequently, it was first refluxed with ether (BDH Analar) for about 1 hour and then refluxed, filtered, and washed with methanol. The refluxing with methanol was repeated to ensure that the polymer was properly purified. The polymer sample was then dried to constant weight in a vacuum oven at 40° C. Its intrinsic viscosity in dimethylformamide and the solvent mixture was respectively 0.50 and 0.54, corresponding to a number-average molecular weight of 13,800.

The solvent mixture for the irradiation experiments was the same as that used previously (1): 80:20 by weight of ethylene carbonate to propanediol cyclic carbonate. The purification methods for these compounds were similar to those employed before.

Ethylene carbonate was accepted to be of sufficient purity when an 80:20 mixture by weight of the carbonate with optically pure methanol gave an optical density (1 cm) of less than 0.06 at 2537 Å, measured against distilled water. The melting point of the carbonate after purification was 34–35° C.

The 1,2 propanediol cyclic carbonate was purified by passage through columns of activated charcoal (BDH Norit) mixed with small amounts of adsorption alumina (Fisher).

The resultant 80:20 mixture by weight of the carbonates was dried in vacuum and had an optical density (1 cm) of 0.05 at 2537 Å.

All other materials used in this work were of Analar grade.

**The procedure was supplied by L. H. Peebles, Jr., of the Chemstrand Corporation.*

Can. J. Chem. Downloaded from www.nrcresearchpress.com by 210.87.254.42 on 09/05/12
For personal use only.

(c) Re-evaluation of Previous Experimental Results (1)

In the previous work all number-average chain lengths were evaluated by means of an equation obtained by Onyon (4) for dimethylformamide solutions:

$$[\eta]_{DMF} = 1.97\times10^{-3}\, M_n^{0.625}.$$

By measuring also intrinsic viscosities in the ethylene carbonate – propylene carbonate mixture, the following equation could be derived:

$$[\eta]_{EPC} = 8.9\times10^{-3}\, M_n^{0.47}.$$

All number-average chain lengths of the previous work were recalculated using the Cleland–Stockmayer (2) equation:

$$[\eta]_{DMF} = 0.392\times10^{-3}\, M_n^{0.75}.$$

Here again an equation was derived for the solvent mixture based on the above equation:

[1] $$[\eta]_{EPC} = 2.65\times10^{-3}\, M_n^{0.56}.$$

This equation was used for the recalculation of all the chain lengths. This resulted in different degradation rate constants k_{exp} derived from the equation

[2] $$\frac{1}{P_t} - \frac{1}{P_0} = k_{exp}t,$$

which is valid for a random chain-scission (3) process. P_0 and P_t are the number-average chain lengths at the beginning and at time t of the irradiation process, respectively. All subsequent calculations in this work were carried out using equation [1].

The new rate constants, derived from Jellinek and Schlueter's work, plotted against the relative light intensities give now a straight line passing through the origin of the co-ordinate system, as Fig. 1 shows. Previously, the straight line did not pass through the origin of the co-ordinate system. This could not be explained at the time.

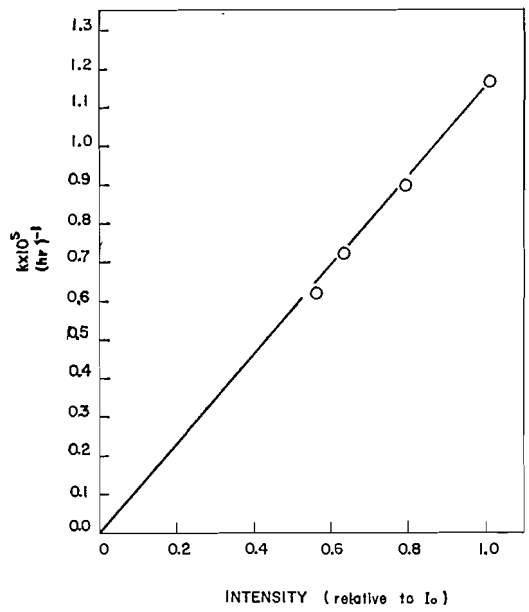


FIG. 1. Experimental rate constants as a function of relative light intensity (re-evaluated data from Jellinek and Schlueter (1)).

Can. J. Chem. Downloaded from www.nrcresearchpress.com by 210.87.254.42 on 09/05/12
For personal use only.

(d) Photodegradation as a Function of Polymer Concentration

Figure 2 shows intrinsic viscosities plotted as a function of time of irradiation for all

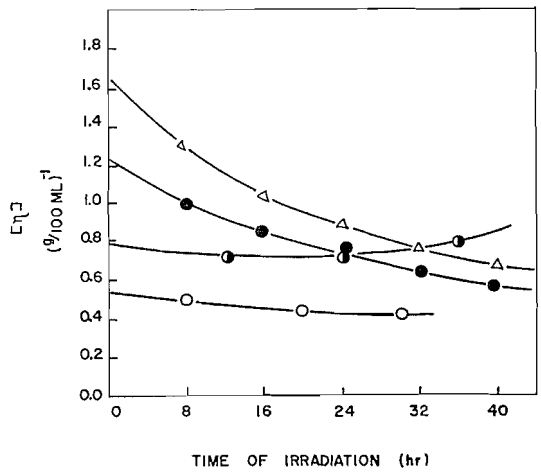


FIG. 2. Intrinsic viscosity as a function of irradiation time. Solutions (0.1% w/v) of PAN in ethylene carbonate – propylene carbonate (80:20 by weight): △ $[\eta]_{EPC,\,0} = 1.65$; ● $[\eta]_{EPC,\,0} = 1.21$; ◑ $[\eta]_{EPC,\,0} = 0.78$; ○ $[\eta]_{EPC,\,0} = 0.54$, homemade sample.

the samples. One sample of intrinsic viscosity $[\eta]_{EPC} = 0.78$ is quite abnormal. Its ultraviolet spectrum also does not agree with those of the other samples. In contrast to the other solutions, solutions of this sample turned distinctly yellow during degradation and showed appreciable fluorescence. This sample apparently cross-links, probably due to impurities. This was not further investigated.

The effect of polymer concentration on degradation was studied with the sample of $[\eta]_{EPC} = 1.21$ over a range of concentrations (0.1%, 0.2%, and 0.4%, w/v). The results are shown in Figs. 3 and 4, where $1/[\eta]_{EPC}$ and $1/P_t - 1/P_0$ respectively are plotted against the time of irradiation. Apparently, the rate is independent of the polymer concentration. The rate constant k_{exp} for equation [2], derived by the least-squares method, is 6.57×10^{-5} hr^{-1}. The number of quanta incident on the reaction vessel for these experiments was 2.58×10^{17} quanta/sec. The reaction vessel had a cross section of 11 cm^2.

(e) Photodegradation as a Function of Initial Polymer Chain Length

Figures 5 and 6 show plots of $1/[\eta]$ and $1/P_t - 1/P_0$ against irradiation time for 0.1% w/v polymer solutions. The rate constants for the two Chemstrand samples, which have similar histories, are quite close, whereas the homemade sample has an appreciably greater rate constant. It is also noteworthy that the $1/[\eta]$ versus t plots are straight lines with identical slopes for all samples. This is not the case when plotting $1/P_t - 1/P_0$ against time. The rate constants are given below.

P_0	$[\eta]_{EPC,\,0}$ ((g/100 ml)$^{-1}$)	$k_{exp} \times 10^5$ (hr^{-1})	$k' \times 10^2$ (100 ml hr^{-1} g^{-1})
1886	1.65	6.05	2.25
1030	1.21	6.57	2.25
252	0.54	9.60	2.25

Can. J. Chem. Downloaded from www.nrcresearchpress.com by 210.87.254.42 on 09/05/12
For personal use only.

Can. J. Chem. Downloaded from www.nrcresearchpress.com by 210.87.254.42 on 09/05/12
For personal use only.

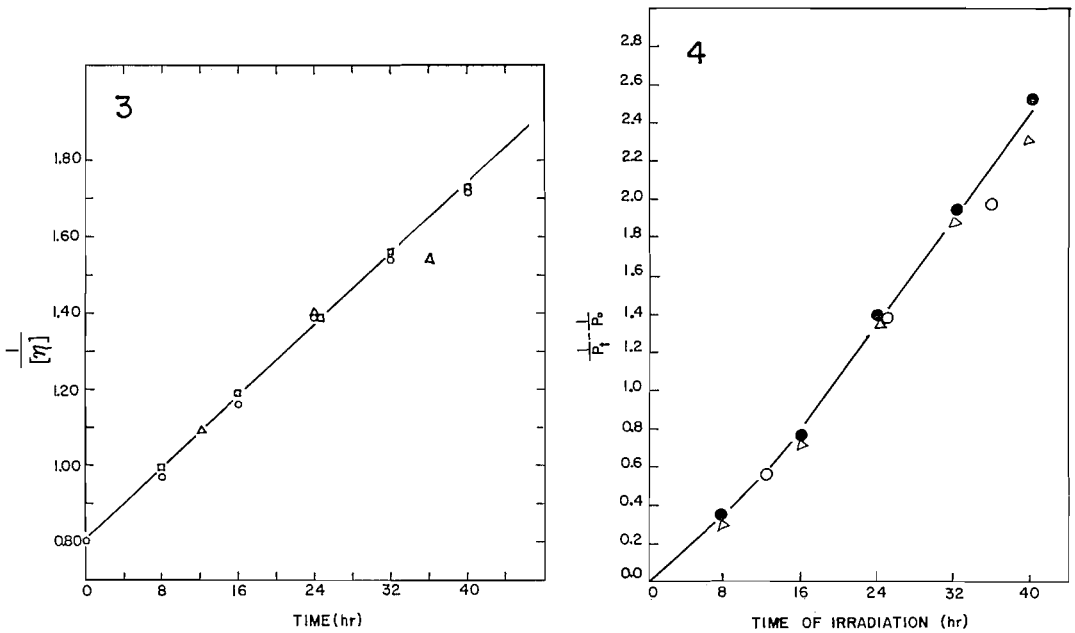


FIG. 3. $1/[\eta]$ as a function of irradiation time for different polymer concentrations (sample of $[\eta]_{EPC,\,0} = 1.21$): ○ 0.1% w/v; □ 0.2% w/v; △ 0.4% w/v in ethylene carbonate – propylene carbonate.

FIG. 4. $1/P_t - 1/P_0$ as a function of polymer concentration (sample of $[\eta]_{EPC,\,0} = 1.21$): △ 0.1% w/v; ● 0.2% w/v; ○ 0.4% w/v in ethylene carbonate – propylene carbonate.

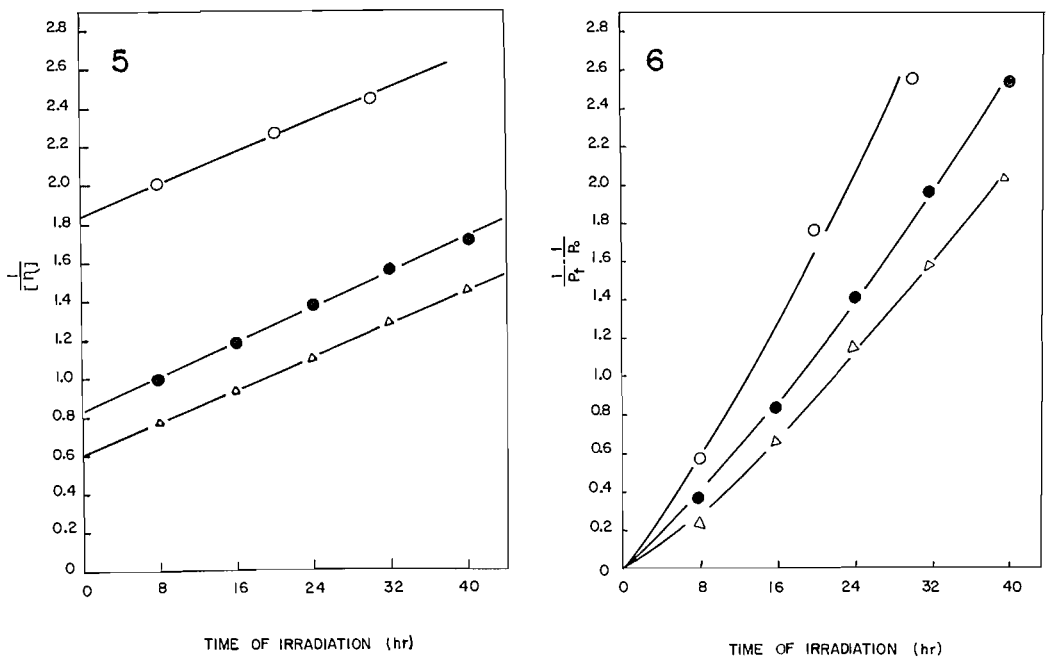


FIG. 5. $1/[\eta]$ as a function of irradiation time for different initial polymer chain lengths (0.1% w/v in ethylene carbonate – propylene carbonate): ○ $[\eta]_{EPC,\,0} = 0.54$, homemade sample; ● $[\eta]_{EPC,0} = 1.21$; △ $[\eta]_{EPC,\,0} = 1.65$.

FIG. 6. $1/P_t - 1/P_0$ as a function of irradiation time for different initial chain lengths (0.1% w/v in ethylene carbonate – propylene carbonate): ○ $[\eta]_{EPC,\,0} = 0.54$, homemade sample; ● $[\eta]_{EPC,\,0} = 1.21$; △ $[\eta]_{EPC,\,0} = 1.65$.

(f) Photodegradation as a Function of Incident Light Intensity

Irradiations were carried out at three incident light intensities on 0.1% w/v solutions of the sample of $[\eta]_{EPC} = 1.21$ (g/100 ml)$^{-1}$. The light intensities were obtained by different positions of the 60-ma lamp and also by employing the 30-ma lamp. The incident intensities were determined in terms of quanta by means of the uranyl actinometer (5). The rate constants obtained at the various intensities were as given below.

Light intensity incident on the 11-cm^2 reaction cell window $\times 10^{-17}$ (quanta/second)	$k_{exp} \times 10^5$ (hr^{-1})
2.58	6.57
1.67	3.92
0.61	1.52

Figure 7 shows that the rate constants are proportional to the first power of the light intensity.

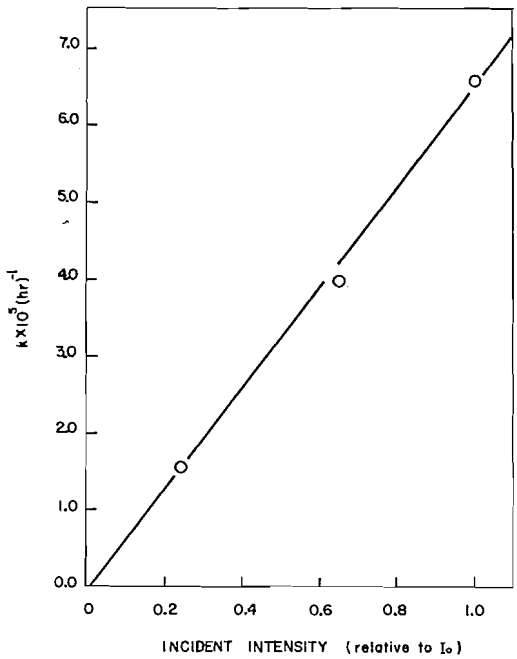


FIG. 7. Experimental rate constants as a function of relative light intensity (0.1% w/v of $[\eta]_{EPC, 0} = 1.21$).

(g) Ultraviolet Absorption Spectra

Figure 8 shows the ultraviolet absorption spectra of the polyacrylonitrile (PAN) sample of $[\eta]_{EPC} = 1.21$ exposed in 0.1% w/v solutions at different stages of the degradation. A pronounced absorption maximum develops at 2950 Å during the irradiation. In Figs. 9 and 10, optical densities at 2537 Å and 2950 Å respectively are given as a function of irradiation time.

Subsequently it was found, using the Bausch and Lomb Spectronic 505, that PAN also has an adsorption maximum at 2160 Å which changes during irradiation. This is shown in Fig. 11.

The homemade sample follows similar changes in its ultraviolet spectra as is the case with the two other samples, as Fig. 12 shows.

Can. J. Chem. Downloaded from www.nrcresearchpress.com by 210.87.254.42 on 09/05/12
For personal use only.

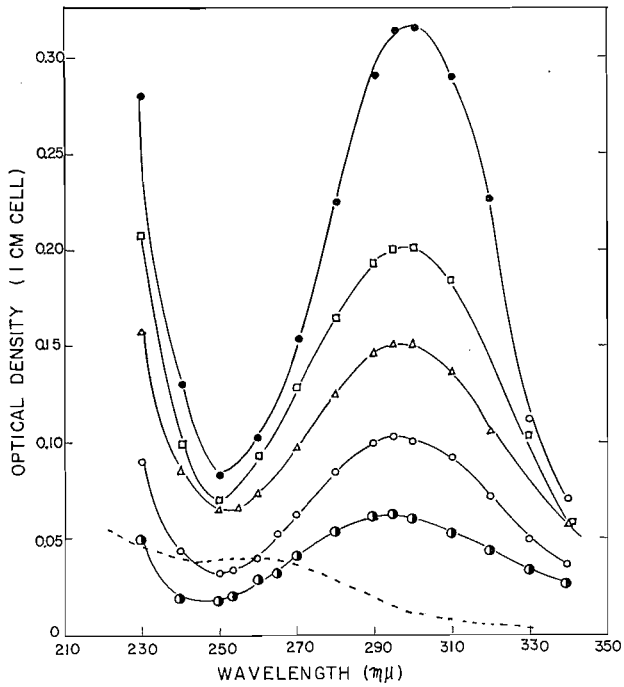


FIG. 8. Ultraviolet absorption spectra of sample of $[\eta]_{EPC,\,0} = 1.21$ as a function of irradiation time 0.1% w/v solutions): – – – unexposed; ◑ 8 hours; ○ 16 hours; △ 24 hours; □ 32 hours; ● 40 hours.

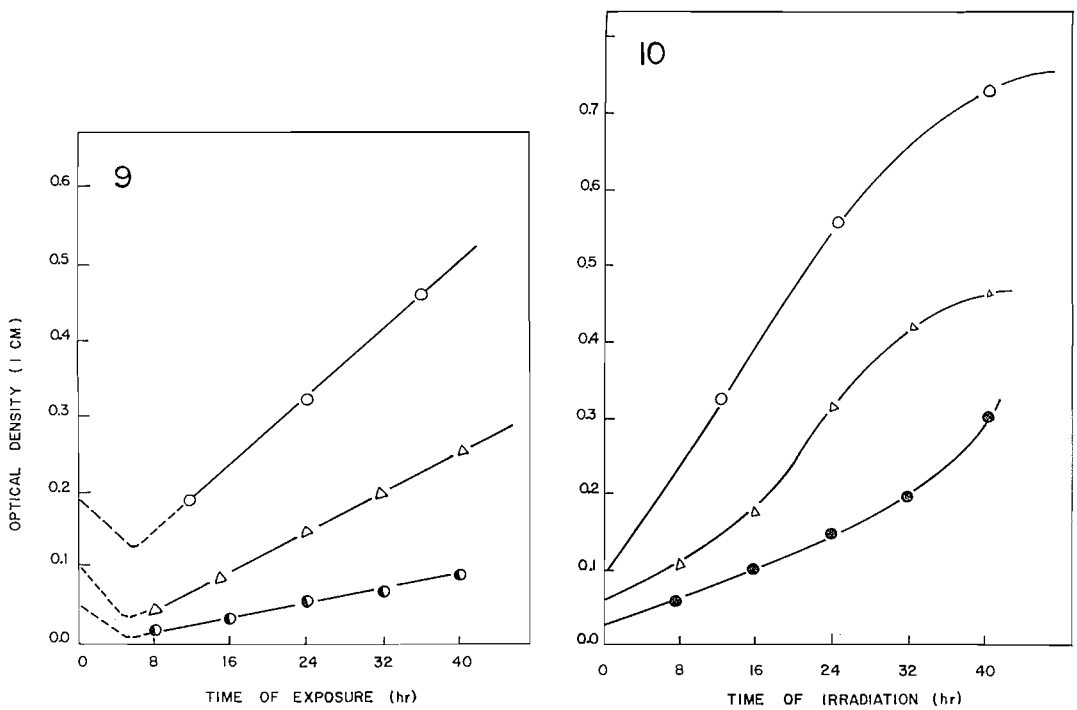


FIG. 9. Optical densities (1 cm) at 2537 Å as a function of irradiation time for sample of $[\eta]_{EPC,\,0} = 1.21$ at different concentrations: ◑ 0.1% w/v; △ 0.2% w/v; ○ 0.4% w/v.

FIG. 10. Optical densities (1 cm) at 2950 Å as a function of irradiation time for sample of $[\eta]_{EPC,\,0} = 1.21$ at different concentrations: ● 0.1% w/v; △ 0.2% w/v; ○ 0.4% w/v.

Can. J. Chem. Downloaded from www.nrcresearchpress.com by 210.87.254.42 on 09/05/12
For personal use only.

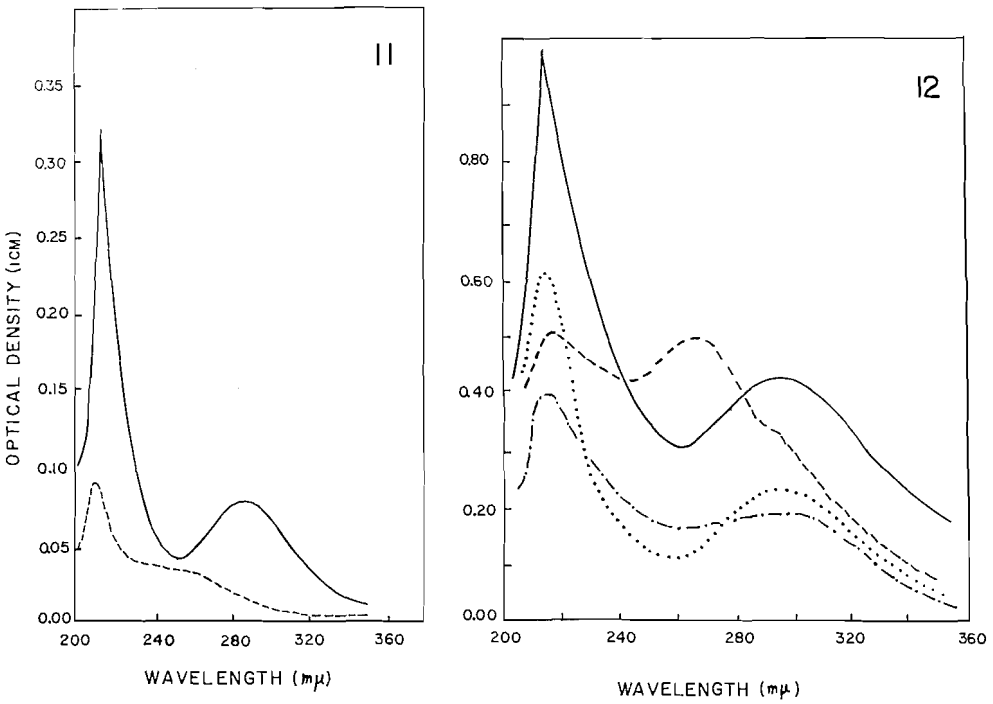


FIG. 11. Optical density (1 cm) of unexposed (– – –) and exposed for 4 hours (——) PAN, $[\eta]_{EPC,\,0} = 1.21$, 0.1% w/v, showing change in absorption at 2160 Å.

FIG. 12. Absorption spectra of 'homemade' PAN, $[\eta]_{EPC,\,0} = 0.54$, 0.1% w/v, as a function of irradiation time: – – – unexposed; –·– 8 hours; ... 20 hours; —— 30 hours.

(h) Infrared Absorption Spectra

One per cent w/v solutions of PAN of $[\eta]_{EPC} = 1.21$ (g/100 ml)$^{-1}$ were exposed under vacuum for 40 hours. Samples of unexposed and exposed polymer were precipitated from solution by distilled water; the precipitate was washed with water and dried under vacuum. A doublet appeared at 1770 to 1780 cm^{-1}, which could be shown to be due to residual solvent. No other significant changes could be detected.

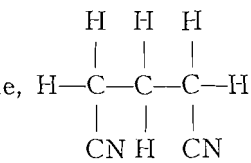
(i) Oxidative Photodegradation

A 1% w/v solution of PAN ($[\eta]_{EPC} = 1.21$ (g/100 ml)$^{-1}$) was irradiated under vacuum for 16 hours. The solution was diluted to 0.5% w/v, and its ultraviolet absorption spectrum determined. The solution was then saturated with oxygen and exposed again. The absorption spectra at various stages of the irradiation process are shown in Fig. 13.

It is apparent that on irradiation in the presence of oxygen, the maximum at 2950 Å is gradually eliminated, indicating that the group responsible for this maximum is subject to photooxidation.

(j) Photolysis of Glutaronitrile as a Model Substance

One per cent w/v solutions of glutaronitrile,



ture were exposed under vacuum to the ultraviolet light source. Ultraviolet absorption

Can. J. Chem. Downloaded from www.nrcresearchpress.com by 210.87.254.42 on 09/05/12
For personal use only.

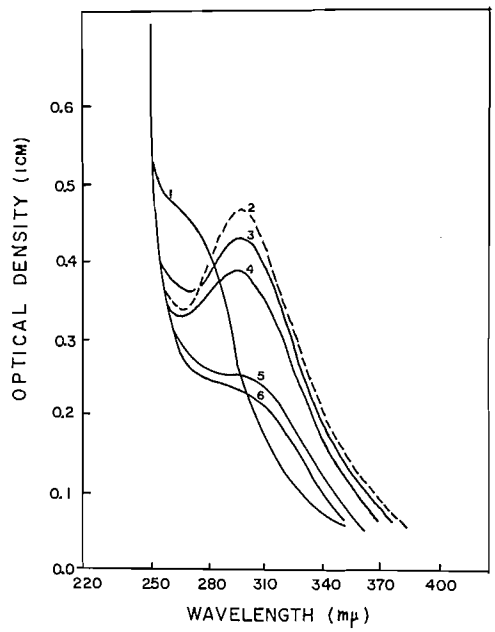


FIG. 13. Oxidative photodegradation of PAN ($[\eta]_{EPC,\,0} = 1.21$): (1) 1% w/v, unexposed; (2) 0.5% w/v, 16 hours in vacuum; (3) 0.5% w/v, 10 minutes in O_2; (4) 0.5% w/v, 20 minutes in O_2; (5) 0.5% w/v, 60 minutes in O_2; (6) 0.5% w/v, 120 minutes in O_2.

spectra of the unexposed and exposed solutions are shown in Fig. 14. It is seen that glutaronitrile shows characteristics very similar to those of PAN in the same solvent. The absorption maxima at 2160 Å increased and a new peak at 2950 Å appeared during

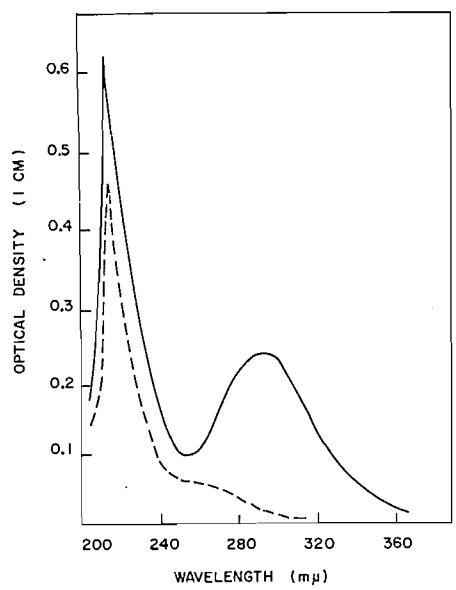


FIG. 14. Photolysis of glutaronitrile, 1% w/v in 80:20 by weight ethylene carbonate – propylene carbonate: – – – unexposed; —— 12 hours in vacuum (optical density (1 cm) of 0.33% w/v solution).

Can. J. Chem. Downloaded from www.nrcresearchpress.com by 210.87.254.42 on 09/05/12
For personal use only.

irradiation. This indicates that changes in the absorption spectra in PAN do not need to be directly related to the chain-scission reaction in the polymer.

(k) Photodegradation of PAN in Bulk and Production of Small Molecules During Irradiation

PAN ($[\eta]_{EPC} = 1.21$ (g/100 ml)$^{-1}$) was degraded in powder form and in the form of films. The powder was irradiated for 4 hours under vacuum; volatile products were collected in a trap cooled by liquid air. On removal of the liquid-air bath and addition of an alcoholic tincture of gum guaiac and 1:1000 $CuSO_4$ solution (6), a dark blue color appeared, indicating the presence of small molecules such as nitriles and ammonia. The product had a distinct smell of HCN. The exposed powder showed a light brown color and was insoluble in dimethylformamide; apparently cross linking had taken place.

PAN films ($[\eta]_{EPC} = 1.21$ (g/100 ml)$^{-1}$) were prepared by evaporating, under vacuum, dilute solutions of PAN in dimethylformamide. The films were dried under vacuum for at least 24 hours. Their thickness was approximately 30 μ. They were exposed to the ultraviolet light source both under vacuum and in the presence of air for about 6 hours. Loss of weight, either by weighing or with a quartz spring, could not be detected. However, for the same time of exposure, the films turned to a yellow color when exposed in air and to a dark brown color in vacuum. The exposed films were insoluble in dimethylformamide. Upon being heated on a steam bath, part of the films dissolved, leaving colored material in suspension.

One per cent w/v solutions exposed under vacuum gave positive tests for small molecules collected in a trap cooled by liquid air.

DISCUSSION

The experimental results agree quite satisfactorily with a random chain-scission process, although the rate constants depend to a certain extent on the history of the polymer. Also reactions other than chain scission take place simultaneously. In a recent note (7), the kinetics for a photodegradation process in solution leading to random chain scission was derived. The theory for films is considered in a different paper (8). It was assumed that the rate of breaking links is directly proportional to the absorbed light intensity, all main chain links being of equal strength. It is further required for a random chain-scission process that an appreciable decrease in the number-average chain length should take place and that the amounts of monomer produced should be negligible (3). Other assumptions made are as follows: (*a*) the absorbed light intensity remains constant during the degradation process, (*b*) Beer–Lambert's law is obeyed and, (*c*) the number of main chain scissions remains small. It was experimentally shown that the polymer solutions obey Beer–Lambert's law; also the number of chain scissions is small in all present experiments. Assumption (*a*) is not fulfilled; the absorption at 2537 Å first decreases and then increases linearly with the extent of degradation. However, this does not necessarily mean that the light absorption with respect to the main chain-scission process does not remain constant. According to the above assumption, the rate of breaking links is given by

$$-\frac{dn}{dt} = k_1 I_{abs}, \qquad [3]$$

where n is the concentration of C—C links in the chain of the polymer (number of links per unit volume) at time t of the irradiation process; k_1, a rate constant; and I_{abs}, the

Can. J. Chem. Downloaded from www.nrcresearchpress.com by 210.87.254.42 on 09/05/12
For personal use only.

absorbed light intensity (I_{abs} is the light absorbed per second over the length and 1 cm² of the cross section of the reaction cell). Equation [3] can also be written as

$$-\frac{dn}{dt} = \phi I'_{abs},$$

where ϕ is the quantum yield and I'_{abs} is the average number of quanta absorbed per cm³ per second. Equation [3] leads to (7)

$$[4] \qquad \frac{s}{P_0} = \frac{1}{P_t} - \frac{1}{P_0} = \frac{k_1(1-e^{-k_2 0 n l})I_0 t}{n_0},$$

where P_t and P_0 are the number-average chain lengths at time t and $t = 0$ respectively; I_0, the incident light intensity for each cm²; n_0, the concentration of main chain links at the beginning of the degradation process (as only a small number of links are broken during the degradation process, n_0 is practically constant); s, the average number of links broken in each original chain at time t; k_2, a constant; and l, the length of the reaction vessel. Further, $k_2 = 2.303E/(n_0 l)$, where $E = \log (I_0/I_t)$ is the optical density of the solution and I_t is the transmitted light intensity. For small light absorption, equation [4] reduces to

$$[5] \qquad \frac{s}{P_0} = \frac{1}{P_t} - \frac{1}{P_0} = k_1 k_2 l I_0 t = \phi k_2 I_0 t = \phi \frac{2.303E}{n_0 l} I_0 t,$$

where $\phi = k_1 l$ is the quantum yield given by

$$\phi = \frac{\text{number of main chain links broken in the system}}{\text{number of quanta absorbed by the system}}.$$

Equation [5] shows that for small light absorption, s/P_0 should be independent of initial chain length and polymer concentration and directly proportional to the incident light intensity. Hence $1/P_t$ plotted against time of irradiation should give straight lines, which is approximately the case (see Figs. 4 and 6). The rate constants $k_{exp} = k_1 k_2 l I_0$ should be independent of polymer concentration and initial chain length. This is true as far as the dependence on concentration is concerned (see Fig. 4); however, k_{exp} with respect to the initial polymer chain length seems also to be dependent on the history of the polymer. The condition that k_{exp} is directly proportional to the light intensity is very well fulfilled (see Fig. 7).

In the previous work (1), the quantum yield was found to be $\phi = 7.7 \times 10^{-4}$ main chain bonds broken for each quantum absorbed. In the present work, the quantum yield was calculated from equation [5] for one of the experiments (0.1% w/v of polymer of $[\eta]_{EPC} = 1.21$, $k_{exp} = 6.57 \times 10^{-5}$ hr^{-1}). The optical density was averaged for a 40-hour period of irradiation, assuming a straight-line relationship between the optical density at 2537 Å and the time of irradiation. The quantum yield in this case is 0.84×10^{-4} main chain bonds broken per quantum absorbed. This value is of the same magnitude as that obtained previously and is in accord with a random chain-scission process. Quantum yields for other polymers (9) are of similar magnitude except for polymethylmethacrylate which is known to follow a depolymerization process (10).

The small curvature in the $1/P_t$ versus time curves may be due to a number of reasons:

(*a*) The intrinsic viscosity – number-average molecular weight relationship may not

Can. J. Chem. Downloaded from www.nrcresearchpress.com by 210.87.254.42 on 09/05/12
For personal use only.

be quite correct; an increase in the exponent of M_n in the relationship would straighten the curves. This is indicated by the fact that straight lines are obtained when $1/[\eta]_{EPC}$ is plotted against the time of irradiation (see Figs. 3 and 5).

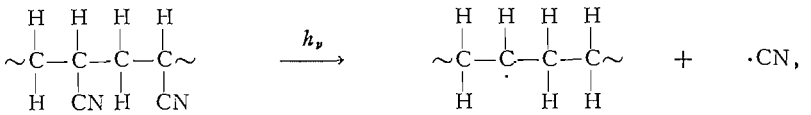
(*b*) The molecular-size distributions change during degradation, which may affect the parameters in the intrinsic viscosity – number-average molecular weight relationship.

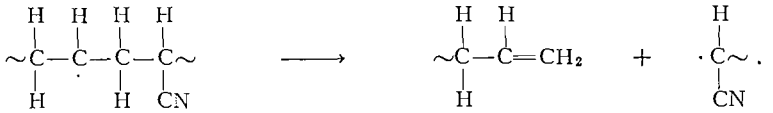
(*c*) The absorbed light intensity does not remain constant during irradiation.

It seems unlikely that the change in absorbed light intensity is the cause of the curvature in the $1/P_t$ versus time curves. Especially during the first 8 hours, a very pronounced change in absorption takes place at 2537 Å, which is not reflected in these curves (see Figs. 4 and 6). It is likely that the change in absorption spectra has nothing or very little to do with the chain-scission reaction. This is supported by the fact that the absorption spectrum for glutaronitrile changes in a way similar to that of the polymer during irradiation. Thus it is probable that this change in the spectra is mainly due to reactions at the nitrile groups leading to formation of other groups, which then cause the change in the absorption spectra. It appears, therefore, that the light absorption related to the chain-scission process remains reasonably constant, while absorption connected with other photochemical reactions changes appreciably. The most likely explanation for the curvature in the $1/P_t$ versus t curves seems, therefore, to be that the intrinsic viscosity – number-average molecular weight relationship is not quite appropriate for the samples employed in this work.

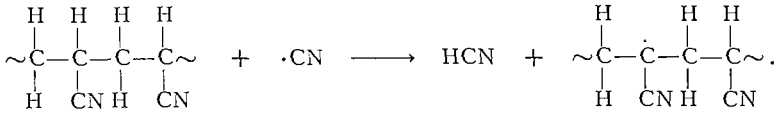
Tentative suggestions as to the reactions involved in the chain-scission process were presented in the previous paper. These reactions can now be elaborated in more detail on the basis of the additional information gained in this work. However, it must be kept in mind that any of the proposed reactions are speculative.

Chain scission may be brought about by the following reactions:

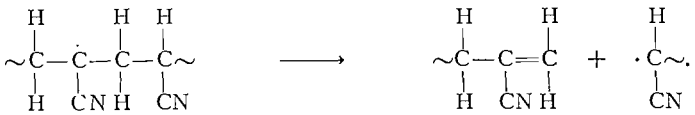
[1] 

[2] 

The ·CN radical could react with an α-hydrogen atom,

[3] 

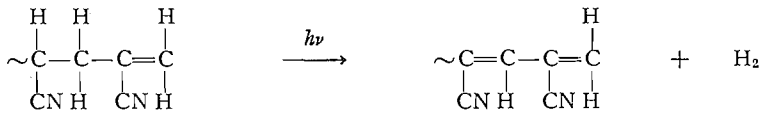
Reaction [3] may be followed by another chain scission,

[4] 

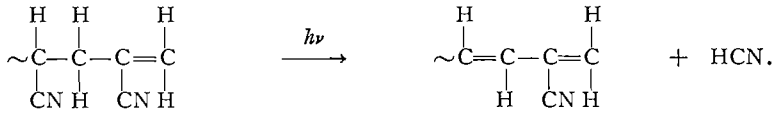
The terminal double bond may give rise to the increase of the absorption maximum at 2160 Å.

Can. J. Chem. Downloaded from www.nrcresearchpress.com by 210.87.254.42 on 09/05/12
For personal use only.

Two other reactions may take place, not leading to chain scission but producing small molecules:

[5] 

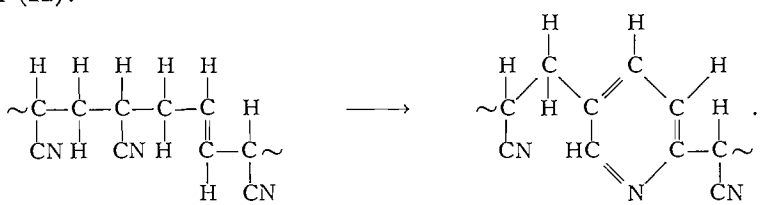
and

[6] 

Such conjugated systems may give rise to the absorption at 2950 Å.

A reaction in which HCN was produced was postulated by Straus and Madorsky (11) for the thermal degradation.

After removal of HCN, cyclization may also occur. This has been formulated by Kobayashi (12):

[7] 

Such substituted pyridines absorb in the 3000-Å region.

In summary, it may be stated that photodegradation of polyacrylonitrile in solution follows a random chain-scission process, although other photochemical reactions also occur at the same time. As a matter of fact, these side reactions are really more extensive than the chain-scission reaction from a chemical point of view, but the scission reaction is more prominent as it affects the molecular weight of the polymer so drastically. Exposure in bulk leads to cross linking and production of small molecules such as HCN.

ACKNOWLEDGMENTS

One of the authors (I. J. B.) wishes to thank the National Research Council of Canada for a studentship award. Thanks are also due to the Chemstrand Corporation for financial assistance.

REFERENCES

1. H. H. G. Jellinek and W. A. Schlueter. J. Appl. Polymer Sci. **3**, 206 (1960).
2. R. L. Cleland and W. H. Stockmayer. J. Polymer Sci. **17**, 473 (1955).
3. H. H. G. Jellinek. Degradation of vinyl polymers. Academic Press Inc., New York. 1955. p. 15.
4. P. F. Onyon. Trans. Faraday Soc. **52**, 80 (1956); J. Polymer Sci. **22**, 13 (1956).
5. G. S. Forbes and L. J. Heidt. J. Am. Chem. Soc. **56**, 2363 (1934). And W. G. Leighton and G. S. Forbes. J. Am. Chem. Soc. **52**, 3139 (1930).
6. Scott's Standard Methods of Chemical Analysis. Vol. 2. 5th ed. 1946. D. Van Nostrand Co., Inc., New York. 1939.
7. H. H. G. Jellinek. J. Appl. Polymer Sci. **4**, 253 (1960).
8. H. H. G. Jellinek. J. Polymer Sci. (1961). In press.
9. J. Jortner. J. Polymer Sci. **37**, 199 (1959). See also S. Stokes and R. B. Fox. U.S. Naval Research Laboratory, Report 5591. (1961).
10. P. R. E. J. Cowley and H. W. Melville. Proc. Roy. Soc. London, A, **210**, 461 (1952); A, **211**, 320 (1952).
11. S. Straus and S. L. Madorsky. J. Research Natl. Bur. Standards, **61**, 77 (1958).
12. H. Kobayashi. Kagaku (Tokyo), **23**, 366 (1953).

Can. J. Chem. Downloaded from www.nrcresearchpress.com by 210.87.254.42 on 09/05/12
For personal use only.

Can. J. Chem. Downloaded from www.nrcresearchpress.com by 210.87.254.6 on 09/05/12
For personal use only.

STEREOCHEMICAL STUDIES

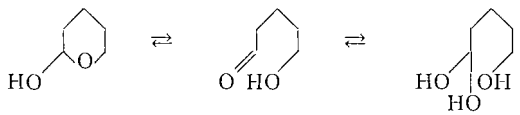
III. REACTIONS OF 4-OXA-5α-CHOLESTAN-3α-OL, A CARBOHYDRATE MODEL[1]

J. T. EDWARD, P. F. MORAND,[2] AND I. PUSKAS[2]

ABSTRACT

4-Oxa-5α-cholestan-3α-ol was prepared by reduction of 4-oxa-5α-cholestan-3-one with lithium aluminum hydride. It showed several typical carbohydrate reactions, such as mutarotation in aqueous tetrahydrofuran and condensation with alcohols in the presence of hydrogen chloride to give 3-alkoxy-4-oxa-5α-cholestanes. These compounds were also prepared by the reaction of alcohols with 3α-chloro-4-oxa-5α-cholestane in the presence of base. Factors governing the proportions of 3α and 3β isomers formed in these reactions are discussed.

The study of the pyranose ring system in simple compounds (e.g. I), devoid of the many hydroxyl groups and asymmetric carbon atoms of the common sugars, has attracted some interest (1, 2, 3, 4). Hurd and Saunders (5) showed that tetrahydropyran-2-ol (I) (6) in 75% aqueous dioxan had an ultraviolet absorption peak at 287 mμ, indicating the presence of the open-chain tautomer, 5-hydroxypentanal (II). From a comparison of the intensity of this peak with that of 5-methoxypentanal, they estimated that 5-hydroxypentanal made up 6% of the equilibrium mixture. They assumed the remaining 94% to be entirely in the lactol form I, but it is likely that about 2–3% is present as the hydrated aldehyde III (7, 8).



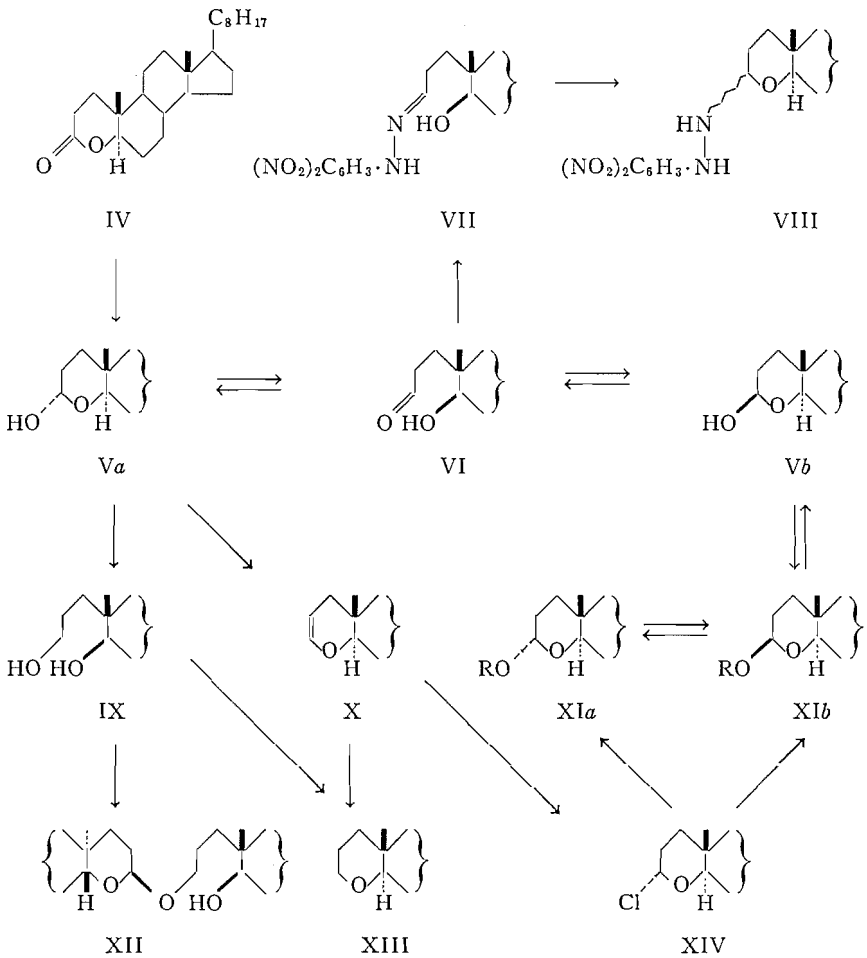
I II III

Substitution of the lactol stabilizes it with respect to the open-chain tautomer, which at equilibrium is present to only a very minor extent in solutions of the common pentoses and hexoses (9), perhaps because of conformational effects (10).

There appear to be advantages in studying the reactions of the lactol fused to a rigid polycyclic system, as in V. The use of optically active compounds makes it possible to determine the stereochemical course of reactions from the optical rotations of products, while the interpretation of results is simplified by the fact that the pyranose ring is locked into the C-1 conformation, the more stable conformation of glucose and many other pyranoses (11).

To obtain the desired lactol (V), 4-oxa-5α-cholestan-3-one (IV) (12, 13) in tetrahydrofuran was reduced with one-quarter of a mole of lithium aluminum hydride (14). A crystalline product, $C_{26}H_{46}O_2$, was obtained which possessed a potential carbonyl group, as shown by its reaction with 2,4-dinitrophenylhydrazine to form a derivative, $C_{32}H_{50}O_6N_4$. The infrared spectrum of this derivative had no hydroxyl peak, indicating that it had the cyclic structure VIII rather than the structure VII. Such cyclic structures have been postulated for the phenylhydrazones of some pyranoses, although the evidence for them is equivocal (15).

[1]*Manuscript received June 5, 1961.*
Contribution from the Department of Chemistry, McGill University, Montreal, Que.
[2]*Holders of N.R.C. Studentships, 1957–59 (P. F. M.), and 1959–61 (I. P.).*



The reduction product itself is also in a cyclic form (V), since no carbonyl peak characteristic of the hydroxyaldehyde VI could be detected in the ultraviolet absorption spectrum of the compound in 90% aqueous dioxan or 85–90% aqueous tetrahydrofuran, or in the infrared absorption spectrum of the compound as a solid or in solution in chloroform, carbon tetrachloride, or tetrahydrofuran. Evidently fusing the lactol I to the rigid BCD ring system of cholesterol stabilizes the cyclic form.

The α-configuration (V*a*) of the 3-hydroxyl group of the crystalline lactone V is shown by the molecular rotation of the lactol, given in Table I along with the values calculated for the 3α (V*a*) and 3β (V*b*) compounds (using the known value for the parent compound (XIII)) by the elegant and powerful method of Brewster (16). Calculation by Whiffen's method (17) gives almost the same values; however, Whiffen's parameters are considered to be slightly less reliable in the present application, since for the most part they are derived from rotations of compounds dissolved in water rather than in organic solvents. The effect of solvent on rotation, not taken in account in Whiffen's or Brewster's treatments, is appreciable for our compounds (cf. Table I), but not so large as to invalidate the use of these treatments for assigning configurations.

Can. J. Chem. Downloaded from www.nrcresearchpress.com by 210.87.254.6 on 09/05/12
For personal use only.

TABLE I

Molecular rotation $[M]_D$ values of 3-substituted 4-oxa-5α-cholestanes

3-Substituent	Compound	$[M]_{D,\ calc}$ (deg)	$[M]_{D,\ obs}$ (deg)	Solvent*
(Hydrogen)	XIII	(+186)	+180†	$CHCl_3$
			+189	CCl_4
			+190	THF
α-Hydroxy	V*a*	+286	+250	$CHCl_3$
			+256	CCl_4
			+344	THF
			+356	THF–H_2O (9:1, v/v)
β-Hydroxy	V*b*	+186	—	
α-Methoxy	XI*a*, R = Me	+391	+442	$CHCl_3$
			+410	CCl_4
			+460	THF–MeOH (1:1, v/v)
β-Methoxy	XI*b*, R = Me	+81	—	
α-Benzyloxy	XI*a*, R = CH_2Ph	+477‡	+466	$CHCl_3$
			+436	THF–$PhCH_2OH$ (2:3, v/v)
β-Benzyloxy	XI*b*, R = CH_2Ph	−5‡	−115	$CHCl_3$
			−19.2	THF–$PhCH_2OH$ (2:3, v/v)
α-Chloro	XIV	(ca. +686)	+672	$CHCl_3$
			+666	CCl_4
			+666	THF
β-Chloro		+186	—	

*THF = tetrahydrofuran.
†Fieser *et al.* (18) report the same value.
‡Calculated from the average increment in molecular rotation (+191° and −191°) in forming α- and β-benzyl-D-glycosides from the respective anomers (19).

While the optical rotation of the lactol V*a* dissolved in chloroform, carbon tetrachloride, or tetrahydrofuran showed no change on standing, it dropped rapidly for solutions in 85–90% aqueous tetrahydrofuran (Fig. 1), and with 1% hydrochloric acid

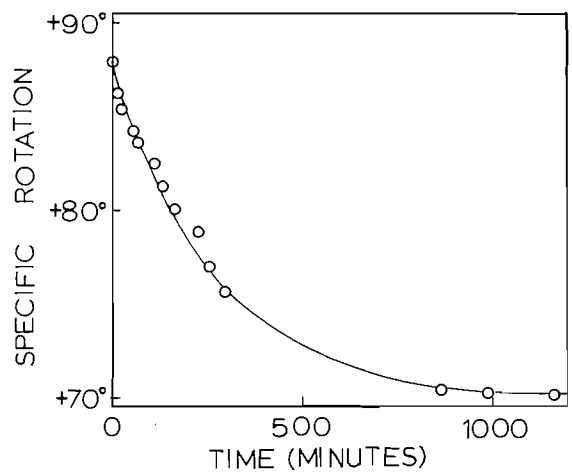


FIG. 1. Change in specific rotation of 4-oxa-5α-cholestan-3α-ol in 90% aqueous tetrahydrofuran (v/v) at 21° C. Theoretical curve for a first-order reaction having a rate constant of 0.0038 min^{-1} (natural logarithms).

Can. J. Chem. Downloaded from www.nrcresearchpress.com by 210.87.254.6 on 09/05/12
For personal use only.

in this solvent it had dropped to a steady value in less than 5 minutes. This change in rotation indicated the formation of the β isomer V*b*; such mutarotation is known to be catalyzed by acid (20). Assuming for the 3β isomer V*b* the molecular rotation shown in Table I, the lactol in 90% aqueous tetrahydrofuran is made up of 55% of the α isomer and 45% of the β isomer. However, all attempts to isolate the β isomer by crystallization from different solvents failed, only the α isomer being obtained.

Treatment of the lactol V*a* with hot acetic anhydride – sodium acetate gave 4-oxa-5α-cholest-2-ene (X), more conveniently prepared by the action of phosphorus oxychloride in pyridine. The acetate (XI, R = CH_3CO) could be prepared by the action of acetic anhydride in pyridine at 20° C, but proved reactive and difficult to purify; attempts to crystallize it from methanol afforded 3α-methoxy-4-oxa-5α-cholestane (XI*a*, R = Me), described below. Hydrogenation of the unsaturated ether X gave 4-oxa-5α-cholestane (XIII), previously obtained by dehydration of the diol IX (13).

Like dihydropyran (21), 4-oxa-5α-cholest-2-ene (X) in ether added hydrogen chloride to give a reactive chloro ether, which in the present instance must be 3α-chloro-4-oxa-5α-cholestane (XIV). This addition reaction may be reversible, like that of dihydropyran (21), because infrared studies showed the chloro ether always to be contaminated with small amounts of the unsaturated ether X, and attempts to purify it by crystallization from inert solvents always led to a drop in melting point. However, when a solution of the chloro ether in carbon tetrachloride ($[\alpha]_D$ +153°), shown by quantitative infrared measurements to contain 4% of the unsaturated ether, was saturated with hydrogen chloride, the specific rotation rose to +163° and the infrared peaks due to the unsaturated ether disappeared. The molecular rotations recorded in Table I for this compound are all for solutions saturated with hydrogen chloride.

The α-configuration at the 3-position of the chloro ether is probable from its molecular rotation (Table I). The molecular rotation of 3β-chloro-4-oxa-5α-cholestane should, according to the treatments of Whiffen and Brewster, be about the same as that of the parent compound (XIII); the molecular rotation of the 3α-chloro compound should be different, but the parameters which enable one to calculate it are not available. However, it is evident from Table II that the introduction of an α-chlorine atom at the 1-position

TABLE II

Molecular rotation values $[M]_D$ (deg) of sugar derivatives

Parent compound	Derivatives				
	1-Deoxy	1α-Chloro	$\Delta[M]_D$	1β-Chloro	$\Delta[M]_D$
3,4,6-Tri-*O*-acetyl-D-glucopyranose	+129 (22)	+608 (23)	+479	−48 (24)	−177
2,3,4,6-Tetra-*O*-acetyl-D-glucopyranose	+25 (25)	+600 (26)	+575	+62 (27)	+ 37
2,3,4,6-Tetra-*O*-acetyl-D-mannopyranose	−140 (28)	+331 (29)	+471		

of a pyranose ring in the C-1 conformation (11) causes a shift in molecular rotation of about +500°, the nature and configuration of the adjoining asymmetric center having a comparatively minor effect, so that the molecular rotation of 3α-chloro-4-oxa-5α-cholestane (XIV) should be about +686°, in good agreement with the values found for our chloro ether.

This argument by itself cannot be considered completely conclusive because the

Can. J. Chem. Downloaded from www.nrcresearchpress.com by 210.87.254.6 on 09/05/12
For personal use only.

Can. J. Chem. Downloaded from www.nrcresearchpress.com by 210.87.254.6 on 09/05/12
For personal use only.

evidence for the configurations assigned to the glycosyl halides is generally indirect and dependent on an interpretation of the stereochemical course of reactions (30). However, the configurations assigned to the stable glycosyl halides (30) and to 3α-chloro-4-oxa-5α-cholestane are those to be expected from the "anomeric effect" (31, 32, 33), discussed further below, which predicts that in dihydropyran rings a halogen atom on the carbon atom adjacent to the ring oxygen will be more stable in the axial orientation.

The lactol V*a* in methanol containing 3% hydrogen chloride gave an 88% yield of a crystalline methoxy derivative, shown by its rotation (Table I) to be 3α-methoxy-4-oxa-5α-cholestane (XI*a*, R = Me). This compound was stable in alkaline solution, but in aqueous acid was readily hydrolyzed to the lactol. Second crops from the preparation of the ether (XI*a*, R = Me), when obtained by rapid evaporation of the solvent at a low temperature (i.e. under non-equilibrating conditions (see below)), had a shoulder at 1068 cm^{-1}, absent in the infrared spectrum of the pure 3α isomer, which is probably due to the 3β isomer (XI*b*, R = Me). However, the latter could not be isolated in a pure state.

A solution of 3α-methoxy-4-oxa-5α-cholestane in methanol–tetrahydrofuran (1:1, v/v) having a low concentration (0.018 *M*) of hydrogen chloride showed a rapid drop in rotation (Fig. 2); with a 0.06 *M* concentration of hydrogen chloride the rotational drop

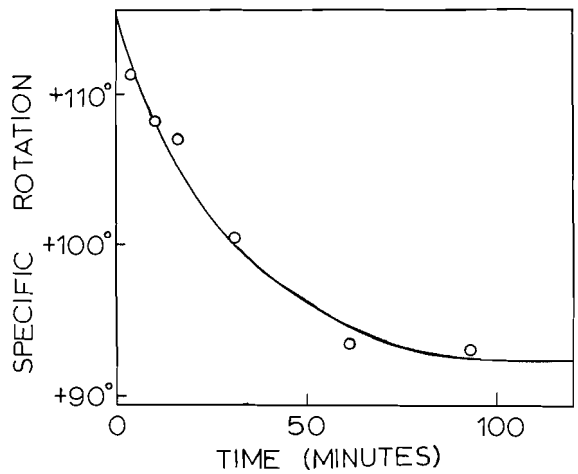
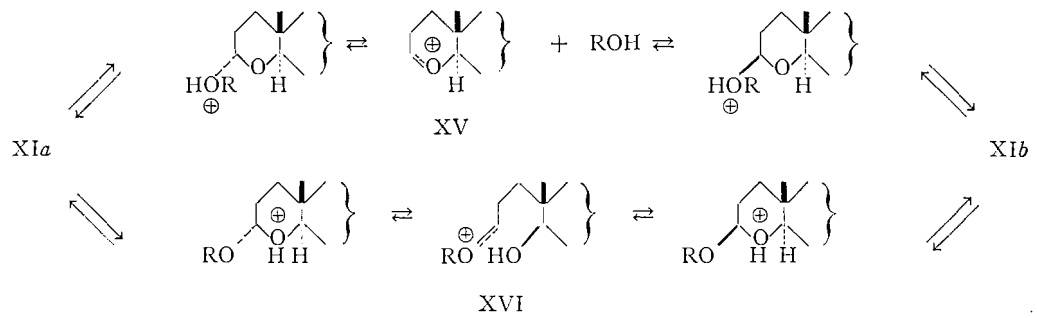


FIG. 2. Change in specific rotation of 3α-methoxy-4-oxa-5α-cholestane in tetrahydrofuran–methanol (1:1, v/v), 0.018 *M* with respect to hydrochloric acid, at 23° C. Theoretical curve for a first-order reaction having a rate constant of 0.040 min^{-1}.

was too fast to be measured. The solid recovered from the neutralized solution after equilibrium had been reached showed again a shoulder at 1068 cm^{-1}. These changes can be due only to the partial isomerization of the 3α (XI*a*, R = Me) to 3β (XI*b*, R = Me) compound. In methanol containing an acid these compounds would be expected to be in equilibrium via the intermediate cyclic (XV) (31) or acyclic carboxonium ion (XVI) (34).

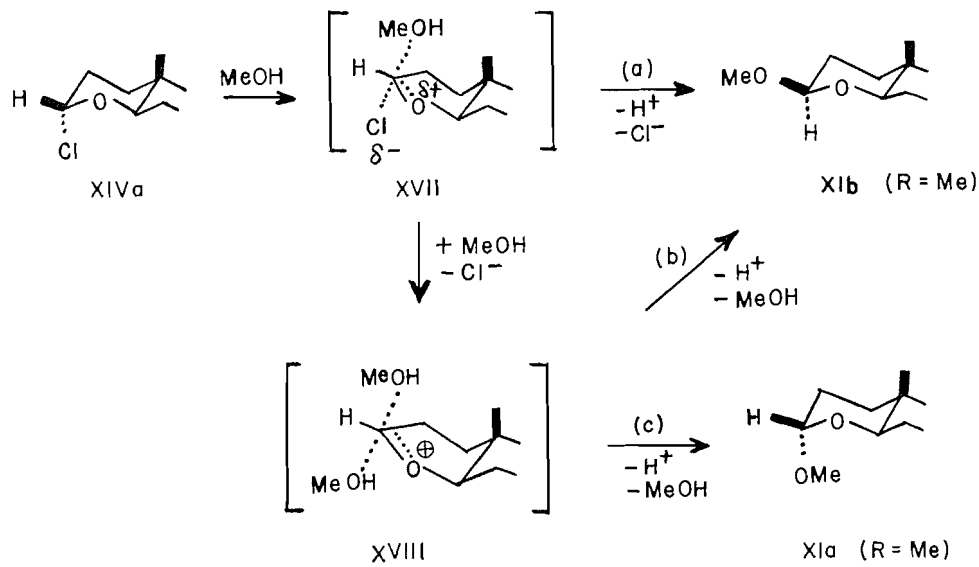
Accepting the calculated value (Table I) for the optical rotation of the 3β isomer, the change in rotation indicates a 24% conversion of the 3α to the 3β isomer.

The rate of this isomerization is considerably faster than that of α-methyl-2-deoxy-D-galactopyranoside (35), which in turn is faster than that of α-methyl-D-galactopyranoside (36). A progressive decrease in rate with the introduction of electron-attracting



groups is expected because of their effect in decreasing the basicity of the acetal oxygen, and hence the concentration of protonated intermediate, and also because of their effect in decreasing the stability, and hence probably the rate of formation, of the intermediate carboxonium ion (37, 38).

In an attempt to obtain a mixture rich in 3β-methoxy-4-oxa-5α-cholestane (XI*b*, R = Me), from which it might be isolated, the chloro ether XIV was solvolyzed in methanol containing methoxide ion or pyridine to neutralize the acid formed. With pyranosyl chlorides derived from methylated or acetylated sugars, such reactions take place with predominant inversion (30, 39, 40), provided that neighboring groups do not participate (41), and provided that steric hindrance to the entering group is not excessive (40). However, in the present instance the 3α-methoxy compound was the chief product, and no 3β-methoxy compound could be isolated, although its presence was indicated by a strong peak at 1068 cm^{-1}. The displacement of chlorine consequently takes place mainly with retention of configuration at the 3-position. The solvolysis of such a chloride in methanol is known to take place by an S_N1 mechanism (39, 40, 42, 43) and probably gives the solvated ion pair XVII (44). This ion pair would be more stable than the ion pairs formed from the chlorides of pyranose sugar derivatives because of the inductive effects of the many oxygen functions of the latter. Consequently, it would be relatively long lived, and not constrained to give an inverted product (XI*b*,



Can. J. Chem. Downloaded from www.nrcresearchpress.com by 210.87.254.6 on 09/05/12
For personal use only.

Can. J. Chem. Downloaded from www.nrcresearchpress.com by 210.87.254.6 on 09/05/12
For personal use only.

R = Me) by reacting with methanol before the chloride ion had diffused away (route (*a*)). The reaction of the symmetrically solvated carboxonium ion XVIII might seem equally likely to give the 3β (route (*b*)) and 3α product (route (*c*)); the preference for the latter probably arises from the steric effect of the angular methyl group at the 10-position, which generally favors the formation of α-substituted products in rings A and B of steroids (45). Very recently, Rhind-Tutt and Vernon (40) have observed a similar effect in the solvolysis of 2,3,4,6-tetra-*O*-methyl-α-D-mannopyranosyl chloride in methanol, which proceeded with 41–43% retention of configuration, while the corresponding glucose derivative gave almost complete inversion. This was attributed to steric hindrance in the mannopyranosyl chloride by the axial methoxyl group on the carbon adjacent to the reacting center, a far more severe hindrance than that offered by the angular methyl group of the chloro ether XIV. The fact that, even so, 57–59% inversion occurs in solvolysis of the mannopyranosyl chloride may be explained by the inductive effect mentioned above.*

Reaction of 3α-chloro-4-oxa-5α-cholestane with methanol in the presence of silver carbonate again gave mainly the 3α-methoxy compound, although under these conditions glycosyl halides generally give β-methoxy derivatives (46).

The reaction of 4-oxa-5α-cholestan-3α-ol with benzyl alcohol containing 3% hydrogen chloride gave a syrup from which was obtained, by chromatography on basic alumina (activity grade III), two compounds having the analysis and ultraviolet absorption spectra expected for the benzyl ethers (XI*a* and XI*b*, R = CH_2Ph). Their optical rotations (Table I) indicated one to be the 3α isomer (XI*a*, R = CH_2Ph) and the second to be the 3β isomer (XI*b*, R = CH_2Ph).

In a 0.005 *M* solution of hydrogen chloride in tetrahydrofuran – benzyl alcohol (2:3, v/v) both the 3α ($[\alpha]_D$ +91°) and 3β ($[\alpha]_D$ −4°) isomer underwent mutarotation to give a solution having $[\alpha]_D$ +66° (Fig. 3), and hence containing about 73% of the α and

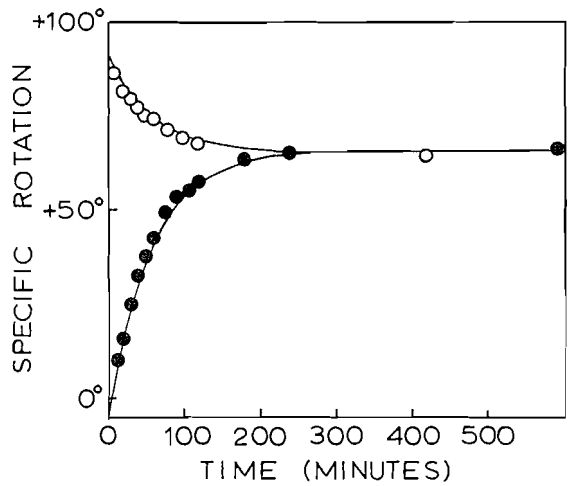


FIG. 3. Change in specific rotation of 3α- (○) and 3β-benzyloxy-4-oxa-5α-cholestane (●) in a 0.0032 *M* solution of hydrogen chloride in absolute tetrahydrofuran – benzyl alcohol (2:3, v/v) at 22.5° ± 0.5°C. Theoretical curves for first-order reactions having a rate constant of 0.0018 min^{-1}.

**Rhind-Tutt and Vernon (40) have claimed that the comparative unreactivity of pyranosyl chlorides derived from hexoses, as compared with simple α-chloro ethers, argues against a half-chair form of the carboxonium ion (31) being generated in solvolysis, with the positive charge localized chiefly on the oxygen. Such an argument ignores the inductive effects operating in derivatives of sugars.*

27% of the β isomer. This interpretation of the rotational changes was confirmed by starting with the pure 3α ether and isolating, after equilibration, 68% of the α and 12% of the β isomer. An attempt was made to catalyze this isomerization also by titanium tetrachloride in carbon tetrachloride, under conditions found successful for some carbohydrate derivatives (29). However, the only crystalline product to be isolated was 4-oxa-5α-cholestan-3α-ol (V*a*), probably formed from 3α-chloro-4-oxa-5α-cholestane when the mixture was treated with water at the end of the reaction.

Reaction of 3α-chloro-4-oxa-5α-cholestane (XIV) with benzyl alcohol in the presence of sodium acetate afforded the 3α and 3β benzyl ethers, isolated in 68% and 9% yields respectively. This is a further example of the solvolysis of the chloro ether proceeding mainly with retention of configuration at the 3-position.

While the benzyl ethers (XI*a* and XI*b*, R = CH_2Ph) would be expected to be fairly stable; in fact, on neutral and basic alumina of activity grade I, decomposition to 4-oxa-5α-cholest-2-ene (X) and 4-oxa-5α-cholestan-3α-ol (V*a*) took place. Consequently, all chromatographic separations were carried out with basic alumina, activity grade III, and even with this adsorbent there was evidence of slight decomposition.

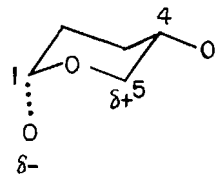
In Table III are summarized the results of the equilibrations of the 3-substituted

TABLE III

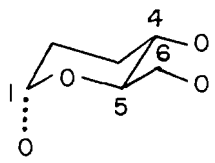
Thermodynamic constants for equilibrations of 3-substituted 4-oxa-5α-cholestanes at 22°±1° C

3-Substituent	Solvent	K	$-\Delta F_{obs}$ (cal/mole)	$-\Delta F_{calc}$ (cal/mole)
OH	Tetrahydrofuran–water (9:1, v/v)	1.2	110	170
OMe	Tetrahydrofuran–methanol (1:1, v/v)	3.1	670	710
OCH_2Ph	Tetrahydrofuran – benzyl alcohol (3:2, v/v)	2.7	590	710

4-oxa-5α-cholestanes expressed as equilibrium constants K (concentration of 3α isomer/concentration of 3β isomer). It is evident that in all cases the axial α isomer is more stable than the equatorial β isomer. This reversal of the usual order of stabilities found in cyclohexane derivatives is undoubtedly due to the ring oxygen, and has been variously explained (31, 32, 33). The most convincing explanation is due to Lemieux and Chu (32, 33), who showed that a consideration of bond lengths, bond angles, and dipoles in the structures XIX and XX indicated an attraction between C-5 and the anomeric oxygen (termed the "anomeric effect") large enough to overcome the steric repulsions from axial hydrogen atoms and hence to favor an axial orientation for the anomeric oxygen atom.



XIX



XX

Also shown in Table III are the free energy differences (ΔF_{obs}) between the 3α and 3β isomers given by the relation $\Delta F = -RT \ln K$. With some isomerizations and conformational changes such free energy differences have been successfully calculated by

Can. J. Chem. Downloaded from www.nrcresearchpress.com by 210.87.254.6 on 09/05/12
For personal use only.

Can. J. Chem. Downloaded from www.nrcresearchpress.com by 210.87.254.6 on 09/05/12
For personal use only.

additions of terms due to differences in non-bonded interactions in the two isomers (32, 33, 47) or conformers (48). In fact, the repulsion energies giving rise to these non-bonded interaction terms should affect only the enthalpy and not the entropy component of the free energy (49). However, Lemieux and Chu (32, 33) give reasons for believing that the entropy difference is negligible for the anomers of aldopentopyranose tetra-acetates and aldohexopyranose pentaacetates, and this may be true also for the isomeric forms of the ethers (XI, R = Me and CH_2Ph). It is less obviously true for the isomeric forms of the lactol V, as shown by the work of Kabayama, Patterson, and Piche (50) on the entropy differences between α and β forms of pyranose sugars in aqueous solution; however, their interpretation of these differences stresses the importance of the quasi-crystalline structure of water, and it is possible that the differences become less in organic solvents.

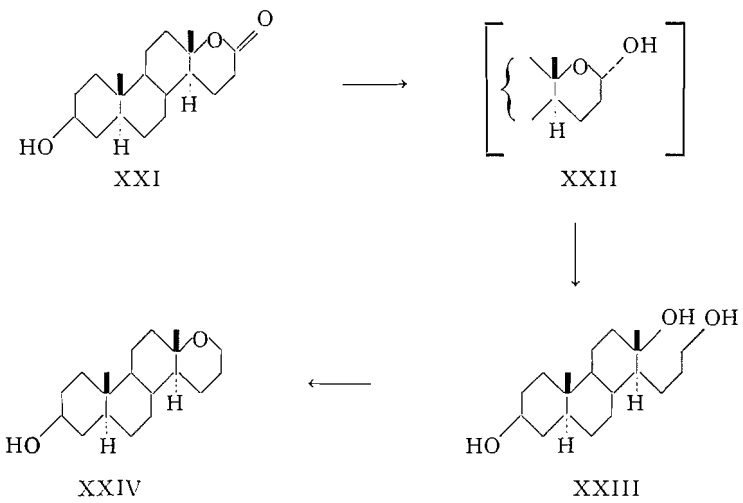
Lemieux and Chu (32, 33) found the free energies of sugar acetates to be additive functions of the following terms (among others): steric repulsion between axial hydrogen and axial oxygen, 180 cal/mole; anomeric effect for pentopyranose derivatives (XIX), 1290 cal/mole; anomeric effect for hexopyranose derivatives (XX), 1510 cal/mole. The first value seemed to be reasonably independent of the nature of the non-aqueous solvent (33), and is adopted here for the methyl and benzyl ethers (XI, R = Me and CH_2Ph), together with a value of 1070 cal/mole for the anomeric effect in these compounds. This latter value is derived on the assumption that the effect is due to the positive charge at C-5 caused by the ring oxygen atom. Addition of another oxygen atom at C-4 should increase the positive charge in the pentose derivatives XIX and give an anomeric effect of $1070+220 = 1290$ cal/mole, while addition of two oxygen atoms, at C-4 and C-6, should give an anomeric effect of $1070+2\times220 = 1510$ cal/mole in the hexose derivatives XX, on the assumption that the inductive effects of the C-4 and C-6 oxygens are the same, and that those of the C-2 and C-3 oxygens may be ignored. The free energy differences between α and β ethers (XI, R = Me and CH_2Ph) calculated using these terms are in reasonable agreement with the values found (Table III).

Chiurdoglu and Masschelein (51) have recently shown that the free energy of the axial hydroxyl – axial hydrogen interaction in cyclohexanol is 150–180 cal/mole, about the same as Lemieux and Chu's value for the axial acetoxyl – axial hydrogen interaction, and independent of the nature of the solvent. However, the most powerful hydrogen-donor solvent investigated by Chiurdoglu and Masschelein was chloroform. There is some evidence that the free energy of the axial hydroxyl – axial hydrogen interaction becomes considerably greater in aqueous or alcoholic solvents (33, 47), and Angyal and McHugh (48) calculated for it a value of 450 cal/mole from studies of the equilibria between cyclitols and their borate complexes in aqueous solution. The free energy difference between α and β forms of the lactol V calculated with this value and a value of 1070 cal/mole for the anomeric effect is again in reasonable agreement with the observed value (Table III), although this agreement may be fortuitous because of neglect of the entropy change.

While the reduction of the lactone IV with 0.25 mole of lithium aluminum hydride gave the lactol V*a*, with 1.2 mole of hydride it gave the diol IX (13), also obtained from the lactol V*a* by hydride reduction. In one experiment in which the lactone was reduced with 0.4 mole of hydride, a syrupy product was isolated, which, by chromatography on alumina, yielded 4-oxa-5α-cholest-2-ene, 4-oxa-5α-cholestan-3α-ol, a solid (product A), and 3,5-seco-A-norcholestan-3,5β-diol (IX). Product A was indicated by analysis to be composed of one molecule of 4-oxa-5α-cholestan-3α-ol and two molecules

of 3,5-seco-A-norcholestan-3,5β-diol, less one molecule of water; in agreement with this formulation, it gave, on treatment with methanolic hydrogen chloride, 3α-methoxy-4-oxa-5α-cholestane and the diol in about the expected proportions. It seems likely that it is a stable complex of one molecule of the structure XII with one molecule of diol, possibly formed when the eluent from the chromatogram containing the lactol V and diol was concentrated. The molecular rotation (+654°) supports this structure, being close to the value (+641°) calculated from the sum of the rotations of two molecules of diol and one molecule of 3α-alkoxy-4-oxa-5α-cholestane (assumed to have the same molecular rotation as the 3α-methoxy derivative). In camphor the complex is dissociated, a Rast determination of molecular weight indicating about half the theoretical value.

Attempts were made to prepare the lactol XXII, in which the steric repulsion of the angular methyl group would be expected to outweigh the anomeric effect, and which in consequence should have an equatorial hydroxyl group. However, reduction of the lactone XXI (52) with varying quantities of lithium aluminum hydride gave only starting material or the completely reduced diol XXIII. The latter was cyclized to 17α-oxa-D-homo-5α-androstan-3β-ol (XXIV) with benzenesulphonyl chloride in lutidine (cf. ref. 13).



EXPERIMENTAL

Where concentrations are not given, specific rotations are averages of 2–3 determinations using concentrations of 1.5–2.3 g/100 ml. Intensities of infrared absorption are indicated in parentheses after the frequencies either by the semiquantitative notation used previously (13), or as molecular extinction coefficients. Chromatography was on Woelm alumina; Brockmann activity grades shown.

4-Oxa-5α-cholestan-3α-ol (Va)

Lithium aluminum hydride (215 mg, 5.41 mmoles) in anhydrous, peroxide-free tetrahydrofuran (70 ml) was added under nitrogen to a stirred solution of 4-oxa-5α-cholestan-3-one (7.50 g, 19.33 mmoles) in the same solvent (75 ml), over a period of 10 minutes. During the addition, the reaction flask was cooled in an ice–salt bath; it was then allowed to warm up to room temperature while the stirring was continued for 1 hour. The reaction mixture was poured into cold 1 *N* sulphuric acid (150 ml). The white solid which precipitated was removed by filtration, washed with water, and dried. It was

Can. J. Chem. Downloaded from www.nrcresearchpress.com by 210.87.254.6 on 09/05/12
For personal use only.

taken up in anhydrous ethyl acetate and filtered through infusorial earth. Addition of petroleum ether to the filtrate resulted in the separation of colorless crystals (6.32 g, 84% yield), m.p. 184°–186° C. The melting point was raised, by recrystallization, to 188°–190° C (bath preheated to 180°, temperature rise 2° C per minute), but was dependent on the rate of heating. $[\alpha]_D^{25}$ +64° (in chloroform); $[\alpha]_D^{26}$ +88° (in tetrahydrofuran); $\nu_{max}^{CCl_4}$ in cm^{-1}: 3620 (55), 3385 (60), 2928 (495), 2853 (290), 1469 (152), 1449 (135), 1385 (115), 1368 (110), 1083 (285), 1045 (220), 947 (118). Calc. for $C_{26}H_{46}O_2$: C, 79.94; H, 11.87%. Found: C, 79.95; H, 12.02%.

3ξ-2′,4′-Dinitrophenylhydrazo-4-oxa-5α-cholestane (VIII)

A solution of 4-oxa-5α-cholestan-3α-ol (78 mg) in 96% ethanol (6 ml) was added to a solution of 2,4-dinitrophenylhydrazine (39.6 mg) in 96% ethanol (2 ml) containing concentrated hydrochloric acid (0.8 ml). The mixture was boiled for 10 minutes. When the solution was cooled, yellow crystals (71 mg) separated, which after two recrystallizations from ethanol–benzene (9:1, v/v) melted at 154.5°–155.5° C. $[\alpha]_D^{25}$ +3.2° (*c*, 2.36 in chloroform); $[\alpha]_D^{23}$ +7.6° (*c*, 1.58 in pyridine–methanol (1:1, v/v); $\lambda\lambda_{max}$ 262, 347 mμ, $\epsilon\epsilon_{max}$ 11,900, 22,800 (in chloroform); $\lambda\lambda_{max}$ 248–255 (flat peak), 328 mμ (shoulder at 367 mμ), $\epsilon\epsilon_{max}$ 10,900, 18,500 (in cyclohexane); $\nu_{max}^{CCl_4}$ in cm^{-1}: 3350 (95), 3092 (39), 2930 (370), 2850 (200), 1620 (510), 1470 (140), 1430 (195), 1338 (610), 1313 (340), 1280 (160), 1137 (180), 1072 (235), 1062 (220), 1050 (187), 926 (130). Calc. for $C_{32}H_{50}O_5N_4$: C, 67.34; H, 8.83; N, 9.82%. Found: C, 67.45; H, 8.75; N, 10.04%.

3,5-Seco-A-norcholestan-3,5β-diol (IX)

A solution of 4-oxa-5α-cholestan-3α-ol (200 mg) in tetrahydrofuran (5 ml) was added dropwise, with stirring, under nitrogen, to a solution of lithium aluminum hydride (13 mg) in tetrahydrofuran (3 ml). The mixture was stirred a further 1.5 hours, and then the excess hydride decomposed by slowly adding aqueous tetrahydrofuran. The reaction mixture was added to ice-cold 1 *N* sulphuric acid solution. An oil separated which soon solidified (176 mg, 86%), and was identified as 3,5-seco-A-norcholestan-3,5β-diol (IX) (13) by melting point, mixed melting point, and infrared spectrum.

Reduction Product A

4-Oxa–5α-cholestan-3-one (4.33 g) in diethyl ether (75 ml) was reduced with a slurry of lithium aluminum hydride (175 mg) in diethyl ether (30 ml), following the procedure described above for 4-oxa-5α-cholestan-3α-ol. Instead of a white solid, a syrup was obtained, which was chromatographed on alumina (Merck). Elution with the solvents indicated gave the following fractions: (1) a syrup (2.22 g), shown by infrared analysis to contain no hydroxyl group (ligroin); (2) 4-oxa-5α-cholest-2-ene (23 mg), identified by infrared spectrum (ligroin); (3) 4-oxa-5α-cholestan-3α-ol, isolated after several recrystallizations from ethyl acetate as needles (280 mg), m.p. 184–186°, and identified by mixed melting point and infrared spectrum (benzene–ether (1:1, v/v)); (4) product A (ether); (5) 3,5-seco-A-norcholestan-3,5β-diol, isolated after several recrystallizations from ethyl acetate as needles (65 mg), m.p. 133–134°, and identified by mixed melting point and infrared spectrum (ether–ethanol (1:1, v/v)).

Product A crystallized from anhydrous ethyl acetate as colorless needles (309 mg), m.p. 139.5°–140.5° C. $[\alpha]_D^{26}$ +56.5 (*c*, 2.66 in chloroform); $[\alpha]_D^{27}$ +54.9 (*c*, 1.98 in tetrahydrofuran); $\nu_{max}^{CCl_4}$ in cm^{-1}: 3580 (m), 3470 (m), 2960 (s), 2885 (s), 1473 (s), 1452 (s), 1387 (s), 1371 (m), 1347 (w), 1127 (m), 1036 (s), 933 (w). Calc. for $C_{78}H_{140}O_5$: C, 80.90; H, 12.18%; molecular weight, 1158. Found: C, 80.75; H, 12.17%; molecular weight (Rast, camphor), 590.

Can. J. Chem. Downloaded from www.nrcresearchpress.com by 210.87.254.6 on 09/05/12
For personal use only.

Reaction of Product A with Methanolic Hydrogen Chloride

Acetyl chloride (0.6 ml) was added to absolute methanol (15 ml) to give an approximately 3% solution of hydrogen chloride. Product A (150 mg) was dissolved in this solution, and the mixture refluxed for 1 hour and then concentrated by distillation to 7 ml. The solution, on cooling, deposited plates (44 mg), m.p. 86°–88° C, raised to 98°–99.5° by recrystallization from methanol, which were identified as 3α-methoxy-4-oxa-5α-cholestane (see below) by mixed melting point, specific rotation, and infrared spectrum.

The mother liquors from the first crystallization were taken to dryness *in vacuo*, and the solid thus obtained was washed with water and dried. The crude solid (97 mg, m.p. 115°–121° C), after recrystallization from ligroin, melted at 134°–134.5° C, and was identified as 3,5-seco-A-norcholestan-3,5β-diol (IX) (13) by mixed melting point and infrared spectrum.

4-Oxa-5α-cholest-2-ene (X)

(*a*) A solution of 4-oxa-5α-cholestan-3α-ol (900 mg) and phosphorus oxychloride (2.3 ml) in pyridine (7 ml) was refluxed for 1 hour. The cooled solution was diluted with water and extracted with ether. The ether solution was washed with aqueous bicarbonate, dried (sodium sulphate), concentrated, and diluted with methanol (10 ml). On standing, the solution deposited colorless prisms of 4-oxa-5α-cholest-2-ene (686 mg, 80% yield), m.p. 68–70° C, raised by recrystallization from ethanol to 70°–72° C. $[\alpha]_D^{25}$ +88.8° (chloroform); ϵ_{210} 5500 (in cyclohexane, end absorption only); $\nu_{max}^{CCl_4}$ in cm^{-1}: 3050 (40), 2930 (510), 1647 (133), 1470 (150), 1448 (120), 1386 (110), 1370 (79), 1243 (95), 1204 (82), 1080 (420), 945 (82), 914 (40). Calc. for $C_{26}H_{44}O$: C, 83.82; H, 11.91%. Found: C, 83.83; H, 12.00%.

(*b*) A solution of 4-oxa-5α-cholestan-3α-ol (300 mg) and fused sodium acetate (150 mg) in acetic anhydride (2.0 ml) was refluxed for 5 hours, and then poured into ice water. The brown oil separating slowly solidified, and was purified by several crystallizations from methanol, giving white plates, m.p. 67–68°, and shown by mixed melting point and infrared spectrum to be identical with 4-oxa-5α-cholest-2-ene obtained above.

4-Oxa-5α-cholestane (XIII)

4-Oxa-5α-cholest-2-ene (510 mg) in glacial acetic acid (20 ml) was hydrogenated over platinum oxide (140 mg). After 3 hours, 95% of the theoretical volume of hydrogen had been absorbed. The catalyst was removed by filtration, the solution diluted with ether and washed with water, aqueous bicarbonate, and water, and dried (sodium sulphate). Evaporation of the ether left a white solid (0.48 g), which after one crystallization from methanol had m.p. 89°–90° C, undepressed by admixture with 4-oxa-5α-cholestane prepared from 3,5-seco-A-norcholestan-3,5β-diol (13), and having the same infrared spectrum. Fieser *et al.* (18) have reported a melting point of 93°–94° C for this compound prepared by a different route.

3-Acetoxy-4-oxa-5α-cholestane (XI, R = MeCO)

4-Oxa-5α-cholestan-3α-ol (204 mg) was dissolved in pyridine (3 ml) with gentle warming, and acetic anhydride (0.3 ml) was added to the cooled solution. After 2 days, the solution was poured into ice water to give a solid which was washed free from acid with water and dried. The crude product (203 mg), m.p. 90°–101° C, was probably a mixture of the isomeric 3-acetoxy compounds (XI*a* and XI*b*, R = MeCO); $\nu_{max}^{CCl_4}$ in cm^{-1}: 2940 (s), 2860 (s), 1755 (s), 1473 (m), 1463 (sh), 1450 (m), 1385 (m), 1374 (m), 1222 (s), 1158 (m),

Can. J. Chem. Downloaded from www.nrcresearchpress.com by 210.87.254.6 on 09/05/12
For personal use only.

1142 (m), 1046 (s), 939 (m), 891 (m). Recrystallization from methanol afforded a mixture (164 mg), m.p. 65–80° C, as shown by chromatography on neutral alumina (5 g, grade III). The following fractions were eluted: (*a*) with hexane (30 ml), 3α-methoxy-4-oxa-5α-cholestane (72 mg), m.p. and mixed m.p. 93°–94° and 94°–95°; (*b*) with hexane–benzene, 1:1 (30 ml), a fraction (62 mg), m.p. 74°–85° C, having the same infrared spectrum as the crude acetate described above; (*c*) with ether (50 ml), 4-oxa-5α-cholestan-3α-ol (20 mg) identified by infrared spectrum. Attempts to recrystallize the acetate from anhydrous ether, tetrahydrofuran, benzene, or petroleum ether failed.

3α-Chloro-4-oxa-5α-cholestane (XIV)

A solution of 4-oxa-5α-cholest-2-ene (140 mg) in anhydrous ether (10 ml) saturated with hydrogen chloride was kept under nitrogen for 2 hours. Evaporation of the ether by a jet of dry nitrogen left crystals which sintered at 95° C, m.p. 104°–107° C. $[\alpha]_D^{20}$ +156° (*c*, 1.56 in absolute chloroform); $\nu_{max}^{CCl_4}$ in cm^{-1}: 2925 (585), 2855 (330), 1469 (150), 1448 (135), 1384 (110), 1367 (92), 1330 (47), 1155 (272), 1130 (292), 1119 (sh, 197), 1033 (258), 928 (82), 908 (56). Calc. for $C_{26}H_{45}OCl$: C, 76.34; H, 11.09%. Found: C, 76.16; H, 10.89%. Quantitative infrared measurements showed that this material, in different preparations, contained 3–6% of starting material; however, all attempts at recrystallization led to a lowering of the melting point.

3α-Methoxy-4-oxa-5α-cholestane (XI, R = Me)

(a) From 4-Oxa-5α-cholestan-3α-ol

Acetyl chloride (1.2 ml) was added to absolute methanol (30 ml) to give an approximately 3% solution of hydrogen chloride. A solution of 4-oxa-5α-cholestan-3α-ol (333 mg) in this solvent was refluxed for 30 minutes. When concentrated to 10 ml, the solution deposited glistening white plates (302 mg), m.p. 91–93° C. These were washed with water to remove traces of acid, dried, and recrystallized from methanol, giving crystals melting at 98°–99.5° C. $[\alpha]_D^{26}$ +109° (*c*, 1.43 in chloroform); $[\alpha]_D^{22}$ +113.5° (*c*, 1.49 in methanol–tetrahydrofuran (1:1, v/v)); $\nu_{max}^{CCl_4}$ in cm^{-1}: 2930 (580), 2860 (340), 1470 (170), 1457 (138), 1448 (148), 1382 (124), 1368 (134), 1132 (360), 1058 (360), 1039 (412), 934 (105), 893 (178). Calc. for $C_{27}H_{48}O_2$: C, 80.20; H, 11.95; OMe, 7.68%. Found: C, 80.25; H, 12.00; OMe, 7.92%.

Fieser *et al.* (18) have recently reported preparing, by a different route, a compound, m.p. 89°–92° C, having the structure of our compound but undefined stereochemistry; it is probably identical with our compound.

(b) From 3α-Chloro-4-oxa-5α-cholestane

Sodium (60 mg) was dissolved in absolute methanol (12 ml), followed by 3α-chloro-4-oxa-5α-cholestane (153 mg), dissolution of the latter requiring that the solution be warmed. The solution was refluxed for 40 minutes, and the solvent then removed under reduced pressure. The residue was treated with water (12 ml) and ether (12 ml), and the ether layer was washed, dried, and diluted with methanol (8 ml). On standing for 2 days, with partial evaporation of the ether, the solution deposited long plates of 3α-methoxy-4-oxa-5α-cholestane (110 mg), m.p. 98.5–99.5, undepressed by admixture with authentic material. Further concentration of the solution gave a brownish semisolid mass (48 mg), which in carbon tetrachloride solution had an infrared spectrum similar to that of pure 3α-methoxy-4-oxa-5α-cholestane, with the addition of a peak at 1068 cm^{-1} and a shoulder at 1126 cm^{-1}. This material resisted all attempts at purification.

Can. J. Chem. Downloaded from www.nrcresearchpress.com by 210.87.254.6 on 09/05/12
For personal use only.

(c) From 3α-Chloro-4-oxa-5α-cholestane in the Presence of Silver Carbonate

To a suspension of powdered calcium chloride (500 mg) and freshly prepared silver carbonate (53) (230 mg) in absolute chloroform (15 ml) was added a solution of 3α-chloro-4-oxa-5α-cholestane (287 mg) in absolute chloroform (15 ml), followed by the slow addition, with vigorous stirring, of methanol (0.12 ml) in absolute chloroform (3 ml). The mixture was stirred for 30 minutes at room temperature and 30 minutes at 50° C. Then water was added, the mixture was filtered through infusorial earth, and the organic layer was separated, washed with water, and dried. Concentration of this solution afforded a syrup which in contact with a little methanol solidified. The solid, crystallized from ether–methanol, gave a first crop (226 mg), m.p. 86°–94° C, $[\alpha]_D^{20}$ +110° (*c*, 1.15 in chloroform); second crop (15 mg), m.p. 79°–85° C, $[\alpha]_D^{20}$ +98.5° (*c*, 1.16 in chloroform); third crop (7 mg), m.p. 62°–68° C; and a brownish semisolid residue (28 mg). Infrared examination showed the first crop to be 3α-methoxy-4-oxa-5α-cholestane contaminated with a small amount of 4-oxa-5α-cholest-2-ene, and the third crop to have the spectrum of 3α-methoxy-4-oxa-5α-cholestane, with the addition of a weak shoulder at 1068 cm^{-1}.

Hydrolysis of 3α-Methoxy-4-oxa-5α-cholestane

A solution of 3α-methoxy-4-oxa-5α-cholestane (150 mg) in tetrahydrofuran (10 ml) – 15% aqueous hydrochloric acid (3.5 ml) was refluxed for 10 minutes, then poured into ice water. A solid was removed by filtration, washed with water, and dried; this crude product (125 mg), m.p. 154°–158° C, was recrystallized from methanol and identified as 4-oxa-5α-cholestan-3α-ol by melting point, mixed melting point, and infrared spectrum.

3α- and 3β-Benzyloxy-4-oxa-5α-cholestane (XIa and XIb, R = CH_2Ph)

(a) From 4-Oxa-5α-cholestan-3α-ol

Acetyl chloride (0.4 ml) was added to benzyl alcohol (10 ml), then 4-oxa-5α-cholestan-3α-ol (100 mg) was dissolved in this solution. The solution, after 24 hours at room temperature, was concentrated at 0.5 mm; removal of the dibenzyl ether formed in this reaction required that the flask be heated to 100°. The residual syrup, which partially crystallized, was chromatographed on basic alumina (25 g, grade III), and the fractions eluted from the column were examined by infrared spectroscopy. The fractions fell into the following groups: (*a*) with ligroin (b.p. 65–75°; 60 ml), 4-oxa-5α-cholest-2-ene, obtained as crystals (10 mg), m.p. 63–66°, having the characteristic infrared spectrum; (*b*) with more ligroin (110 ml), a syrup (65 mg) identified as 3α-benzyloxy-4-oxa-5α-cholestane (see below); (*c*) with ligroin–benzene (4:1, v/v) (30 ml), a syrup (25 mg) shown by infrared spectroscopy to be a slightly impure mixture of 3α- and 3β-benzyloxy-4-oxa-5α-cholestane; (*d*) with more ligroin–benzene (4:1, v/v) (50 ml), impure crystals of 3β-benzyloxy-4-oxa-5α-cholestane.

Fractions (*b*) were dissolved in hot methanol and filtered through charcoal–celite. The syrup (62 mg) which separated on being cooled was dried at 100° C at 0.5 mm. The syrup from some runs crystallized to a solid, m.p. 42–51° C, when cooled to 15° and rubbed; the syrup from other runs could not be crystallized, but was indistinguishable with respect to specific rotation and infrared spectrum. Attempts to recrystallize the solid at low temperatures with seeding afforded always a syrup without change in specific rotation or infrared spectrum: $[\alpha]_D^{26}$ +99° (*c*, 2.23 in chloroform); $[\alpha]_D^{22}$ +91° (*c*, 1.46 in 3:2 benzyl alcohol – tetrahydrofuran, v/v); $\lambda\lambda_{max}^{EtOH}$ 248, 252.5, 258, 264, 268 mμ; $\epsilon\epsilon_{max}$ 165, 234, 272, 217, 148; $\nu_{max}^{CCl_4}$ in cm^{-1}: 3060 (40), 3020 (55), 2920 (540), 2855 (355),

Can. J. Chem. Downloaded from www.nrcresearchpress.com by 210.87.254.6 on 09/05/12
For personal use only.

1470 (175), 1457 (175), 1382 (128), 1342 (88), 1164 (100), 1130 (250), 1052 (215), 1037 (380), 1027 (360), 945 (110), 935 (125), 889 (90), 696 (81). Calc. for $C_{33}H_{52}O_2$: C, 82.45; H, 10.91%. Found: C, 82.37; H, 10.84%.

Chromatographic fractions (*d*) were dissolved in ligroin and treated with charcoal. Evaporation of the solvent afforded well-formed prisms, which were washed on the filter with ligroin (cooled to −10° C) and then recrystallized from ligroin or methanol to give pure 3β-benzyloxy-4-oxa-5α-cholestane (12 mg), melting at 131°–132° C. $[\alpha]_D^{22}$ −22° (*c*, 2.02 in chloroform; $[\alpha]_D^{22}$ −3.8 (*c*, 1.46 in tetrahydrofuran – benzyl alcohol (2:3, v/v)); $\lambda\lambda_{max}$ 248, 252.5, 258.5, 264.5, 268 mμ; $\epsilon\epsilon_{max}$ 171, 218, 252, 210, 151 (in cyclohexane); $\nu_{max}^{CCl_4}$ in cm^{-1}: 3060 (40), 3028 (57), 2930 (575), 2850 (340), 1497 (40), 1469 (174), 1457 (180), 1450 (155), 1387 (134), 1370 (126), 1344 (102), 1166 (224), 1141 (210), 1120 (215), 1094 (190), 1070 (510), 1047 (335), 935 (122), 902 (66), 695 (88). Calc. for $C_{33}H_{52}O_2$: C, 82.45; H, 10.91%. Found: C, 82.38, H, 10.98%.

(b) From 3α-Chloro-4-oxa-5α-cholestane

A suspension of 3α-chloro-4-oxa-5α-cholestane (265 mg) and finely powdered anhydrous sodium acetate (150 mg) in anhydrous benzyl alcohol (5 ml) was heated on a steam bath for 1 hour. The solvent was then removed at reduced pressure, the residue dissolved in ether and water, and the ether layer dried and then taken to dryness. The residue was dissolved in hexane and chromatographed on basic alumina (grade III), as described above, to give slightly impure 3α-benzyloxy-4-oxa-5α-cholestane (239 mg, 76%) and 3β-benzyloxy-4-oxa-5α-cholestane (70 mg, 22%), identified by melting point and infrared spectra.

Isomerization of 3α-Benzyloxy-4-oxa-5α-cholestane (XIa, R = CH_2Ph)

Acetyl chloride (4 drops) was added to benzyl alcohol (0.4 ml) to generate hydrogen chloride, and the solution was diluted with anhydrous ether (3 ml). 3α-Benzyloxy-4-oxa-5α-cholestane (110 mg) was dissolved in this solution. After 4 hours at room temperature, the solvents were removed at reduced pressure (0.5 mm at 80° C) and the residual syrup was chromatographed on basic alumina (grade III) as described above to give starting material (71 mg) and 3β-benzyloxy-4-oxa-5α-cholestane (13 mg), identified by melting point, mixed melting point, and infrared spectrum.

For preparative purposes, the yield of β isomer was increased by allowing a syrupy mixture of isomers containing a trace of acid to stand for several weeks, after which time a certain amount of the β isomer had crystallized out. The whole mixture was then neutralized and chromatographed to give a 25% yield of β isomer.

Action of Titanium Tetrachloride on 3α-Benzyloxy-4-oxa-5α-cholestane

Titanium tetrachloride was purified by standard vacuum-line techniques, and an estimated 100–150 mg was distilled into a frozen solution of 3α-benzyloxy-4-oxa-5α-cholestane (120 mg) in carbon tetrachloride (5 ml). The mixture was allowed to melt under vacuum, refluxed for 5 hours with rigid exclusion of moisture, and then poured into ice water. More carbon tetrachloride was added and the organic layer was separated, washed with bicarbonate and water, and dried over magnesium sulphate. Removal of the solvent at reduced pressure left a yellowish solid (125 mg) which was treated with cold ligroin. The undissolved fraction (35 mg) proved by melting point and mixed melting point to be slightly impure 4-oxa-5α-cholestan-3α-ol. The ligroin solution, on chromatography on basic alumina (grade III), gave only glassy, unidentifiable materials, followed by a small quantity of impure 4-oxa-5α-cholestan-3α-ol (18 mg).

Can. J. Chem. Downloaded from www.nrcresearchpress.com by 210.87.254.6 on 09/05/12
For personal use only.

*17α-Oxa-*D*-homo-5α-androstan-3β-ol (XXIV) (40)*

13,17-Seco-5α-androstan-3β,13α-17-triol (54) (510 mg) was treated with benzenesulphonyl chloride in lutidine under conditions already described (13). The product, isolated in the usual way, was an oil (427 mg) which was chromatographed on alumina (activity II–III). Elution with ether–acetone, 9:1, gave 17α-oxa-D-homo-5α-androstan-3β-ol (114 mg), m.p. 171°–174° C, raised by one crystallization from methanol to 174°–175° C. $\nu_{max}^{CCl_4}$ in cm^{-1}: 3635 (m), 2940 (s), 2860 (sh), 2708 (w), 1462 (sh), 1451 (s), 1440 (sh), 1375 (s), 1282 (m), 1212 (w), 1155 (m), 1132 (sh), 1120 (s), 1080 (s), 1075 (sh), 1064 (sh), 1044 (s), 1032 (s), 973 (w), 955 (w), 945 (w), 935 (m), 923 (w), 895 (w), 877 (w), 848 (w), 840 (w). Calc. for $C_{19}H_{32}O_2$: C, 78.02; H, 11.03%. Found: C, 77.84; H, 10.79%.

ACKNOWLEDGMENTS

We are grateful to the National Research Council for generous financial support, Ayerst, McKenna and Harrison, Ltd., Montreal, for a gift of androsterone, Professor A. Taurins for help in obtaining infrared spectra, Professor M. Onyszchuk for collaboration in carrying out the experiment with titanium tetrachloride, and Professor R. U. Lemieux for helpful discussion.

REFERENCES

1. B. Helferich and T. Malkomes. Ber. **55**, 702 (1922). B. Helferich and R. Weidenhagen. Ber. **55**, 3348 (1922).
2. M. Bergmann and A. Miekeley. Ber. **55**, 1390 (1922). Ann. **432**, 319 (1923). M. Bergmann, A. Miekeley, and F. Stather. Ber. **56**, 2255 (1923).
3. C. D. Hurd and C. D. Kelso. J. Am. Chem. Soc. **70**, 1484 (1948). C. D. Hurd and O. E. Edwards. J. Org. Chem. **14**, 680 (1949). C. D. Hurd, J. Moffat, and L. Rosnati. J. Am. Chem. Soc. **77**, 2793 (1955).
4. R. Zelinski, A. Verbiscar, and H. J. Eichel. J. Org. Chem. **23**, 184 (1958).
5. C. D. Hurd and W. H. Saunders. J. Am. Chem. Soc. **74**, 5324 (1952).
6. L. E. Schniepp and H. H. Geller. J. Am. Chem. Soc. **68**, 1646 (1946).
7. W. Herold. Z. physik. Chem. B, **18**, 265 (1932).
8. R. P. Bell and J. C. Clunie. Trans. Faraday Soc. **48**, 439 (1952). R. P. Bell and A. O. McDougall. Trans. Faraday Soc. **56**, 1281 (1960).
9. S. M. Cantor and Q. P. Peniston. J. Am. Chem. Soc. **62**, 2113 (1940). J. M. Los and K. Wiesner. J. Am. Chem. Soc. **75**, 6346 (1953). J. M. Los, L. B. Simpson, and K. Wiesner. J. Am. Chem. Soc. **78**, 1564 (1956).
10. E. L. Eliel. *In* Steric effects in organic chemistry. *Edited by* M. S. Newman. John Wiley and Sons, Inc., New York. 1956.
11. R. E. Reeves. J. Am. Chem. Soc. **72**, 1499 (1950).
12. R. B. Turner. J. Am. Chem. Soc. **72**, 579 (1950).
13. J. T. Edward and P. F. Morand. Can. J. Chem. **38**, 1325 (1960).
14. G. E. Arth. J. Am. Chem. Soc. **75**, 2413 (1953).
15. E. G. V. Percival. Advances in Carbohydrate Chem. **3**, 23 (1948).
16. J. H. Brewster. J. Am. Chem. Soc. **81**, 5475, 5483 (1959).
17. D. H. Whiffen. Chem. & Ind. 964 (1956).
18. L. F. Fieser, T. Goto, and B. K. Bhattacharayya. J. Am. Chem. Soc. **82**, 1700 (1960).
19. L. J. Heidt. J. Franklin Inst. **234**, 473 (1942). B. Helferich and A. Porck. Ann. **586**, 239 (1954). H. G. Fletcher and R. K. Ness. J. Am. Chem. Soc. **76**, 760 (1954). H. Zinner and H. Brandner. Chem. Ber. **89**, 1507 (1956). C. L. Ballou, S. Roseman, and K. P. Link. J. Am. Chem. Soc. **73**, 1140 (1951).
20. C. G. Swain and J. F. Brown. J. Am. Chem. Soc. **74**, 2534 (1952).
21. D. G. Jones and A. W. G. Taylor. Quart. Revs. (London), 4, 195 (1950).
22. N. S. Richtmeyer, C. J. Carr, and C. S. Hudson. J. Am. Chem. Soc. **65**, 1477 (1943).
23. H. Skraup and R. Kremann. Monatsh. **22**, 375 (1901).
24. H. H. Schlubach. Ber. **59**, 840 (1926).
25. C. Tanaka. Bull. Chem. Soc. Japan, **5**, 214 (1930).
26. R. U. Lemieux and G. Huber. Can. J. Chem. **31**, 1040 (1953).
27. A. M. Gakhokidze. Zhur. Obshcheĭ Khim. **11**, 117 (1941).
28. H. G. Fletcher and H. W. Diehl. J. Am. Chem. Soc. **74**, 3175 (1952).
29. E. Pacsu. Ber. **61**, 1508 (1928).
30. L. J. Haynes and F. H. Newth. Advances in Carbohydrate Chem. **10**, 207 (1955).

Can. J. Chem. Downloaded from www.nrcresearchpress.com by 210.87.254.6 on 09/05/12
For personal use only.

31. J. T. EDWARD. Chem. & Ind. 1102 (1955).
32. R. U. LEMIEUX and P. CHU. Abstracts of Papers, 133rd Meeting of the American Chemical Society, San Francisco, Calif. April 13–18, 1958. 31 N.
33. N.-J. CHU. Ph.D. Thesis, University of Ottawa. 1959. p. 97.
34. B. LINDBERG. Acta Chem. Scand. **3**, 1153 (1949); **6**, 949 (1952).
35. W. G. OVEREND, F. SHAFIZADEH, and M. STACEY. J. Chem. Soc. 671 (1950).
36. C. L. JUNGIUS. Z. physik. Chem. **52**, 97 (1905).
37. M. M. KREEVOY and R. W. TAFT. J. Am. Chem. Soc. **77**, 3146, 5590 (1955).
38. F. SHAFIZADEH. Advances in Carbohydrate Chem. **13**, 9 (1958).
39. R. U. LEMIEUX and G. HUBER. Can. J. Chem. **31**, 1040 (1953); **33**, 128 (1955).
40. A. J. RHIND-TUTT and C. A. VERNON. J. Chem. Soc. 4637 (1960).
41. R. U. LEMIEUX and C. BRICE. Can. J. Chem. **30**, 295 (1952); **33**, 109 (1955); **34**, 1006 (1956).
42. F. H. NEWTH and G. O. PHILLIPS. J. Chem. Soc. 2896, 2900, 2904 (1953).
43. N. B. CHAPMAN and W. E. LAIRD. Chem. & Ind. 20 (1954).
44. A. STREITWEISER. Chem. Revs. **56**, 571 (1956).
45. L. F. FIESER and M. FIESER. Steroids. Reinhold Publishing Corp., New York. 1959. p. 14.
46. B. HELFERICH and H. RAUCH. Ber. **59**, 2655 (1926). B. HELFERICH and G. SPARMBERG. Ber. **66**, 806 (1933). G. ZEMPLEN. Fortschr. Chem. org. Naturstoffe, **1**, 1 (1938).
47. E. L. ELIEL. J. Chem. Educ. **37**, 126 (1960).
48. S. J. ANGYAL and D. J. MCHUGH. Chem. & Ind. 1147 (1956).
49. N. L. ALLINGER. J. Org. Chem. **21**, 915 (1956). R. M. GASCOIGNE. J. Chem. Soc. 876 (1958).
50. M. A. KABAYAMA, D. PATTERSON, and L. PICHE. Can. J. Chem. **36**, 557 (1958). M. A. KABAYAMA and D. PATTERSON. Can. J. Chem. **36**, 563 (1958).
51. G. CHIURDOGLU and W. MASSCHELEIN. Bull. soc. chim. Belges, **70**, 29 (1961).
52. H. LEVY and R. P. JACOBSEN. J. Biol. Chem. **171**, 71 (1947).
53. C. M. MCCLOSKEY and G. H. COLEMAN. *In* Organic syntheses. Vol. 25. *Edited by* W. E. Bachmann. John Wiley and Sons, New York. 1945. p. 53.
54. M. F. MURRAY, B. A. JOHNSON, R. L. PEDERSON, and A. C. OTT. J. Am. Chem. Soc. **78**, 981 (1956).

Can. J. Chem. Downloaded from www.nrcresearchpress.com by 210.87.254.6 on 09/05/12
For personal use only.

Can. J. Chem. Downloaded from www.nrcresearchpress.com by 210.87.254.40 on 09/05/12
For personal use only.

LYCOPODIUM ALKALOIDS

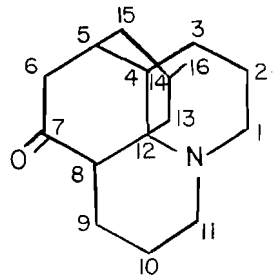
X. THE STRUCTURE OF LYCOPODINE[1]

W. A. HARRISON,[2] M. CURCUMELLI-RODOSTAMO, D. F. CARSON,[3]
L. R. C. BARCLAY, AND D. B. MACLEAN

ABSTRACT

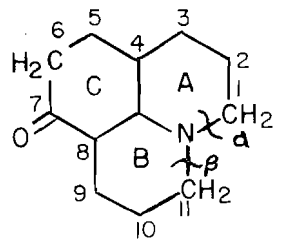
The reactions leading to the establishment of structure I for lycopodine are discussed. Structures are proposed for three cyclization products derived from lycopodine.

In a short communication (1) we proposed structure I for lycopodine. This structure has been confirmed by the work of Anet (2), who succeeded in interconverting several *Lycopodium* alkaloids, among which was lycopodine. In this paper we wish to give a full account of our work on the elucidation of the structure of the alkaloid and to discuss the structures of the tetracylic compounds obtained on elimination of hydrogen halide from lycopodine methiodide and α- and β-cyanobromolycopodine.



I

Partial structure A proposed in 1959 (3) is a convenient starting point for the ensuing discussion.



A

[1]*Manuscript received June 30, 1961.*
Contribution from the Department of Chemistry, McMaster University, Hamilton, Ontario.
[2]*Holder of a National Research Council Studentship, 1956–59.*
[3]*Holder of a National Research Council Bursary, 1958–59, and a National Research Council Studentship, 1959–60.*

Can. J. Chem. Downloaded from www.nrcresearchpress.com by 210.87.254.40 on 09/05/12
For personal use only.

In structure A the carbon atoms known with certainty at that time are designated, as are the bonds cleaved in the formation of α- and β-cyanobromolycopodine, II and III respectively (4, 5). The reasons for proposing structure A are reviewed briefly below. Entry had been gained to rings A and B by reaction with cyanogen bromide. The α-bromide II had been converted to the corresponding acid and thence to the ring-A lactam IV. The infrared spectrum of the latter indicated that ring A was six-membered or larger (3). The β-bromide III had been converted to the corresponding acid which, on reduction with sodium borohydride, readily formed a lactone (V). The infrared spectrum of the lactone indicated that it was either five- or six-membered (3). The carbonyl ring, C, was considered to be six-membered or larger because of the infrared absorption of the carbonyl group near 1700 cm^{-1} (4). The presence of the methylene group adjacent to the carbonyl had been established by conversion of α-cyanolycopodine (VI) to a benzylidene derivative (VII) and to an enolic α-diketone (VIII) (5). Finally, the hexahydrojulolidine system had been found in the alkaloid annotinine, then the only alkaloid of the *Lycopodium* group of known structure (6). No attempt was made at that time to locate the fourth ring of lycopodine.

Support for the proposal that ring B was six-membered came from the following sequence. The methyl ester, IX, of β-cyanolycopodine carboxylic acid (3) was converted by hydrolysis and subsequent treatment with diazomethane to the methyl ester of the corresponding amino acid. When the ester was heated under reflux in xylene it yielded the lactam X, $C_{16}H_{23}O_2N$, which showed absorption in the infrared at 1626 cm^{-1} indicative of a six-membered or larger lactam. Reduction of X with lithium aluminum hydride gave dihydrolycopodine XI (4). Thus no skeletal rearrangement had occurred in the reactions outlined.

The nature of four more carbon atoms in rings A and B was established by modified Kuhn–Roth oxidation of α- and β-cyanodihydrolycopodine, XII and XIII respectively (5, 7). The oxidations were performed according to the procedure of Lemieux and Purves (8). The volatile acids were recovered from the aqueous distillate as their sodium salts. The free acids were liberated with dry hydrogen chloride, distilled, and converted to their methyl esters with diazomethane. The esters were separated by liquid–vapor partition chromatography and identified by comparison of their retention times with values determined by running known mixtures under the same conditions.

Both XII and XIII yielded mixtures of acetic, propionic, and *n*-butyric acids, and it can be concluded that both compounds contain *n*-propyl groups attached to carbon. Oxidation of lycopodine under the same conditions yielded only acetic acid. Therefore, methylene groups can be written at C_2, C_3, C_9, and C_{10} in structure A. The relatively high proportion (24%) of butyric acid in the acid mixture derived from the oxidation of XII suggests that C_4 is not quaternary which implies that the carbon skeleton of lycopodine must differ from that of annotinine. These results establish the sequence $-(CH_2)_3-N-(CH_2)_3-$ in the lycopodine molecule and are consistent with structure A, but do not verify the proposed relationship between the carbonyl function and the nitrogen atom. However, the reactions of the carbonyl ring reported below have established that the proposed relationship is the correct one.

Partial structures for some of the above compounds are given in Chart I.

The benzylidene derivative, VII, of α-cyanolycopodine was the key compound in the investigation of ring C. Upon ozonolysis it yielded the enolic diketone VIII, which had been prepared previously by Barclay and MacLean (5) by bromination and hydrolysis

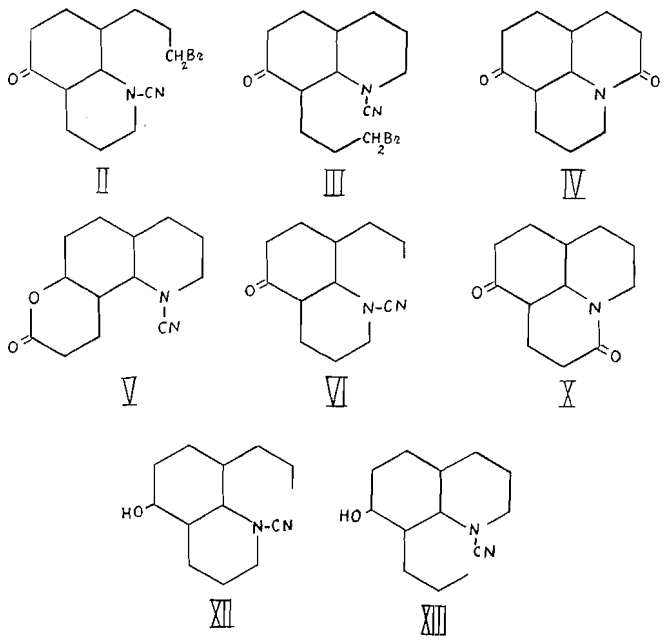
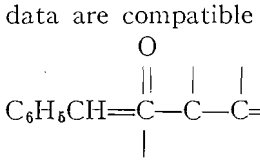


CHART I

of α-cyanolycopodine (VI). The enolic character of this α-diketone established that at least one enolizable hydrogen must be present on a carbon adjacent to one of its two carbonyl groups. The alternatives are represented in partial formulas VIII(*a*) and VIII(*b*).

Oxidation of VII with selenium dioxide yielded two products. One of these products was a compound (XIV), $C_{24}H_{30}O_2N_2$, which had hydroxyl absorption in its infrared spectrum at 3560 cm^{-1} and carbonyl absorption at 1692 cm^{-1} in chloroform solution. The carbonyl absorption of the starting material VII appeared at 1685 cm^{-1} in the same solvent. This shift in the carbonyl frequency implied that the hydroxyl group had entered alpha and axial to the carbonyl function. The second oxidation product (XV), $C_{24}H_{28}ON_2$, was a yellow compound formed from the starting material by loss of two hydrogens. The ultraviolet spectrum of XV differed markedly from that of both VII and XIV, in each of which a maximum occurred near 280 mμ. In XV the 280-mμ band of the starting material had shifted to 310 mμ. The infrared spectrum of XV was also very different from that of VII. There were three very sharp bands at 1677 cm^{-1}, 1626 cm^{-1}, and 1590 cm^{-1} when the spectrum was run in chloroform. The shift in the frequency of the carbonyl band from 1685 in VII to 1677 cm^{-1} in XV indicated that reaction had occurred adjacent to the carbonyl group. The band at 1626 cm^{-1} is assigned to olefin absorption and that at 1590 cm^{-1} to the conjugated phenyl group. The analysis and the spectral data are compatible with the presence, in the molecule, of the chromophoric system



. The spectrum of an analogous system has been studied in

Can. J. Chem. Downloaded from www.nrcresearchpress.com by 210.87.254.40 on 09/05/12
For personal use only.

the infrared (9) and in the ultraviolet region (10) and the results are similar to, although not identical with, the above. The formation of XV from VII occurred without alteration of the carbon skeleton since both VII and XV yielded the same product (XVI), $C_{24}H_{32}ON_2$, on treatment with hydrogen over a platinum catalyst.

Ozonolysis of XIV gave two products, a diketo alcohol (XVII), $C_{17}H_{24}O_3N_2$, and a lactone carboxylic acid (XVIII), $C_{17}H_{24}O_4N_2$. The former was a yellow compound with weak absorption in the ultraviolet at 420 mμ characteristic of an α-diketone. Treatment of XVII with H_2 and platinum yielded the enol VIII. However, unlike VIII, compound XVII had no enolic properties. One must therefore conclude that the hydroxyl group in XVII has replaced the only enolizable hydrogen in VIII and that the carbon adjacent to one of the two carbonyl groups is quaternary or at a bridgehead where enolization would be in violation of Bredt's rule.

Deuterium exchange of lycopodine (I) and α-cyanolycopodine (VI) established the presence of three enolizable hydrogens in each. Therefore, partial structure VIII(a) must represent enol VIII and partial structures XIV, XV, XVII, and XVIII, the hydroxybenzal compound, the olefinic benzal compound, the diketo alcohol, and the lactone carboxylic acid, respectively. Therefore, position 5 in partial structure A, must be quaternary or at a bridgehead. This represents again a departure from the annotinine skeleton. Partial structures for the compounds above are given in Chart II.

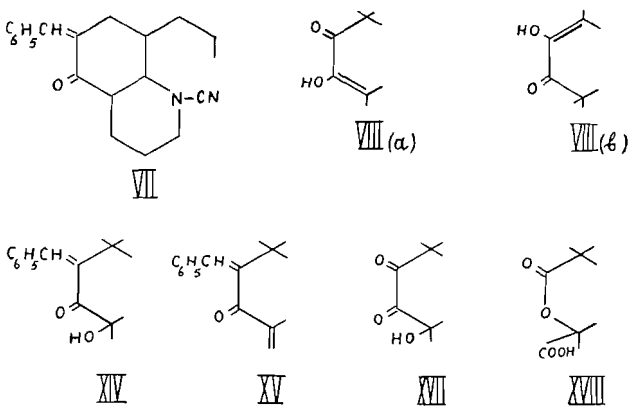
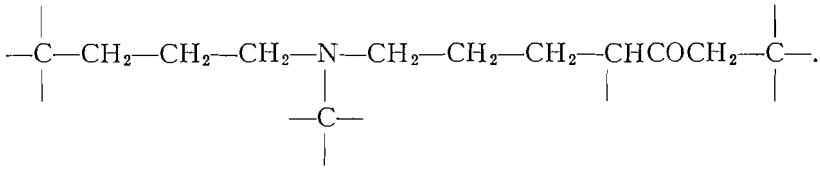


CHART II

The peripheral structure of the molecule can now be extended to



This is the only structure compatible with the formation of lactone V on borohydride reduction of the acid derived from ester IX, and with the above results.

This structure is in complete accord with partial structure A but, although the evidence

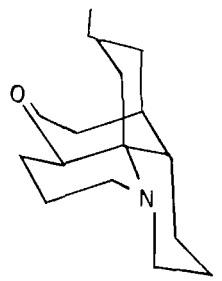
Can. J. Chem. Downloaded from www.nrcresearchpress.com by 210.87.254.40 on 09/05/12
For personal use only.

for structure A is substantial, it is not unequivocal. Rings A and B must make up a reduced quinolizine system if these rings are six-membered, as lactams IV and X suggest. There is evidence that rings B and C make up a reduced quinoline system, because dehydrogenation of XIX (a product formed by dehydration and hydride reduction of XII) yielded a base (XX), in small yield, with the properties of a quinoline. Although the structure of this base has not been proved, it may be 8-*n*-propyl-7-isobutylquinoline.

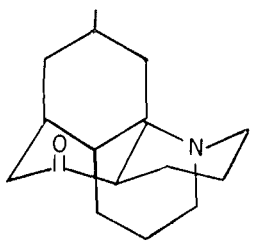
In partial structure A there are only three positions, C_4, C_5, and C_{12}, to which the fourth ring of the alkaloid, ring D, can be attached. Since it has been shown that C_5 is either quaternary or at a bridgehead and since there is evidence from chromic acid oxidation that C_4 is not quaternary, it appears that ring D is closed by a bridge between C_5 and C_{12}.

The structure of this bridge may be deduced from the dehydrogenation experiments of Marion and Manske (11). They found that lycopodine yielded five basic products on dehydrogenation, of which they were able to identify two: 7-methylquinoline and 5,7-dimethylquinoline. The tendency to form 7-methylquinoline was particularly strong. By bridging C_5 and C_{12} in structure A with the unit $-CH_2-\underset{\displaystyle CH_3}{\underset{|}{CH}}-CH_2-$, there is obtained structure I. This structure is completely consistent with the dehydrogenation results and is compatible with the rest of the chemical evidence. It is also in accord with the N.M.R. spectrum of lycopodine, which shows a single C-methyl group attached to a tertiary carbon.

The relative configuration of the asymmetric centers in lycopodine has been discussed by Anet (2). Except for the configuration at C_{14}, for which we had no experimental evidence, we had arrived at the same conclusion (12). The perspective formulas B and C give an idea of the spatial relationships which exist.



B



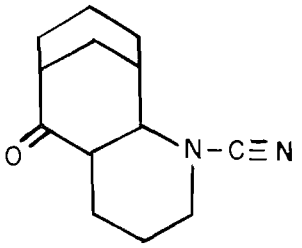
C

The elucidation of the structure of lycopodine has at the same time provided the structures of alkaloids L 2 and L 14. Douglas, Lewis, and Marion (13) have shown that L 2 is the acetyl derivative of dihydrolycopodine and that L 14 is anhydrodihydrolycopodine. The double bond in L 14 occupies the C_7—C_8 position, for Anet has shown, and we have confirmed, that its N.M.R. spectrum shows the presence of a single olefinic proton. We have also shown that alkaloid L 1, complanatine (14), is identical with dihydrolycopodine; its formula should be revised to $C_{16}H_{27}ON$. The formation of dihydrolycopodine from lycopodine by hydride reduction implies that the OH group

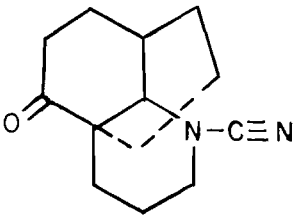
Can. J. Chem. Downloaded from www.nrcresearchpress.com by 210.87.254.40 on 09/05/12
For personal use only.

is axial in the chair conformation and cis to the C_5—C_{12} bridge since hydride reduction will occur from the less-hindered side of the system.

The structure of the cyclized product XXI, $C_{17}H_{24}ON_2$, formed from α-cyanobromolycopodine by treatment with alkali (4), has now been clarified. Recently (7) we proposed the alternative partial structures D and E for this compound. Deuterium exchange



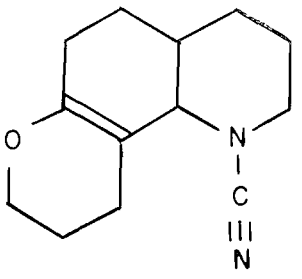
D



E

studies and infrared spectroscopy have allowed us to differentiate between the alternatives. It was found that XXI exchanged two hydrogens for deuterium and this is consistent with partial structure E. Such a result is possible but unlikely for the bicyclo-(3.3.1)nonane system present in D. In the infrared spectrum of XXI there is a band at 1413 cm^{-1} which is absent in deuterated XXI. This behavior is in keeping with ketones containing an α-methylene group (15, 16). Therefore partial structure E must pertain. It is the study of this cyclization reaction which has allowed an assignment of configuration to C_4 of the lycopodine molecule and the other alkaloids which Anet (2) has related to lycopodine.

An isomeric cyclized compound (XXII), $C_{17}H_{24}ON_2$, is obtained from the β-bromide III by treatment with base (4), and for this compound we proposed partial structure F (7).



F

This compound does not exchange hydrogen for deuterium, in keeping with the proposed structure. Its N.M.R. spectrum showed two groups of peaks which were distinctly separate from the bulk of the absorption. The areas under the curves corresponded in both cases to two protons. One group of peaks (δ = 2.36) was in the region characteristic of

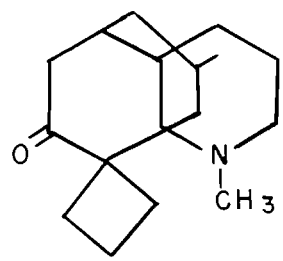
Can. J. Chem. Downloaded from www.nrcresearchpress.com by 210.87.254.40 on 09/05/12
For personal use only.

protons in a $—CH_2—O—$ group while the other (δ = 4.14) was probably associated with the hydrogens of C_1, which is adjacent to the cyanamide function. No band was observed which could be assigned to a $\diagdown C{=}C—H \diagup\diagdown$ group.* The N.M.R. spectrum of XXI was run for comparison, and it showed one unresolved band (δ = 4.09; area = two protons) slightly displaced from the rest of the spectrum. This band was attributed to the protons of C_{11}.

The reasons for the unusual stability of the enol ether function of XXII become clear when an examination is made of a molecular model. As can be seen from the perspective formulas of lycopodine, B and C, C_8 is particularly subject to steric hindrance. The approach of bulky reagents to the vicinity of C_8 will, therefore, be opposed. This will be generally true, not only of the alkaloid, but also of all the known derivatives. In addition, the nature of the structure is such that the $C_7—C_8$ position is a particularly favorable one for a double bond. The introduction of unsaturation at $C_7—C_8$ (or $C_8—C_9$) will relieve steric hindrance by eliminating the interaction of the C_8 hydrogen with the axial hydrogens of C_1 and C_3 as well as the interaction between the hydrogens of C_9 and C_{13}. It is to be expected that any attempt to destroy the planarity of C_8 by attack on the double bond will be resisted. Cyclized compound XXII is not the only known example of a lycopodine derivative with a very stable $C_7—C_8$ double bond. We have found that anhydrodihydrolycopodine is resistant to hydrogenation and ozonolysis.

A third cyclized compound (XXIII), $C_{17}H_{27}ON$, which has not been previously reported, has been derived from lycopodine methiodide by the action of potassium tertiary butoxide in tertiary butanol. This compound showed no double-bond absorption in its infrared and was inert to the action of ozone and hydrogen. Its N.M.R. spectrum was devoid of peaks in the region of olefinic protons. On treatment with cyanogen bromide it yielded a cyanamide (XXIV), $C_{17}H_{24}ON_2$, which was isomeric but not identical with either of the two cyclized compounds, XXI and XXII, discussed above. The oxygen function in XXIII was not affected by sodium borohydride in ethanol or by lithium aluminum hydride in ether or tetrahydrofuran. However, the infrared spectrum of XXIII showed a strong peak in the carbonyl region at 1695 cm^{-1} and there was also a peak at 1410 cm^{-1} characteristic of a $—CH_2—$ adjacent to a carbonyl function.

Deuterium exchange was carried out on this compound and it was found that two enolizable hydrogens were present. Furthermore, the absorption in the infrared at 1410 cm^{-1} was absent in the deuterated compound. The only structure consistent with these data is structure XXIII below.



XXIII

Displacements are recorded in parts per million from chloroform.

Can. J. Chem. Downloaded from www.nrcresearchpress.com by 210.87.254.40 on 09/05/12
For personal use only.

Can. J. Chem. Downloaded from www.nrcresearchpress.com by 210.87.254.40 on 09/05/12
For personal use only.

EXPERIMENTAL

Lycopodine

The alkaloid was isolated from *Lycopodium flabelliforme* by the procedure described by Barclay and MacLean (5). It melted at 116° after recrystallization from petroleum ether.

The nuclear magnetic resonance spectrum of the alkaloid showed a strong doublet, $\delta = 6.6$, whose area corresponded to three protons. This was attributed to the presence of a methyl group attached to a tertiary carbon.

Dihydrolycopodine

Dihydrolycopodine was prepared by the method of MacLean, Manske, and Marion (4). We have also isolated from *L. flabelliforme* an alkaloid identical with dihydrolycopodine. This alkaloid follows lycopodine in the chromatographic separation of the crude alkaloids (5), and appears to be the second most abundant alkaloid. We have also established (14) that complanatine, alkaloid L 1, is identical with dihydrolycopodine. Identity was established by a comparison of their infrared spectra and a mixed melting point determination. We are grateful to Dr. R. H. F. Manske for a sample of complanatine.

Reaction of Lycopodine with Cyanogen Bromide

The reaction was carried out and the bromocyanamides II and III isolated by the procedure described previously (4, 5).

Preparation of the β-Lactam

To a solution of 216 mg of ester IX* (m.p. 160–162°) (3) in *n*-propyl alcohol (2.5 ml) was added 15 ml of 2 *M* hydrochloric acid. After the mixture had been heated for 15 hours on a steam bath it was evaporated to dryness, and the residue was washed with ether to remove unhydrolyzed material. The residual crude amino acid hydrochloride was dissolved in methanol and the ice-cooled solution was treated with an excess of freshly prepared diazomethane solution. After 20 minutes the solution was evaporated and the residue worked up to give the basic product (150 mg). The infrared spectrum of the crude product showed strong ketone and ester carbonyl bands and weak absorption in the N—H region.

A solution of the crude amino ester (150 mg) in xylene (30 ml) was distilled very slowly at atmospheric pressure. After 10 hours, when the solution had been reduced to about one third of its original volume, the rest of the solvent was removed under reduced pressure. The infrared spectrum of the residual oil showed a strong band at 1625 cm^{-1} and weakened ester absorption. The oil was worked up to give basic and neutral fractions. Further purification of the neutral fraction was effected by chromatography on alumina with benzene–methanol as the eluant. A band, which passed down the column, yielded 58 mg of crystalline material. Recrystallization from ether – petroleum ether gave long, colorless needles which melted at 177–179°. Calc. for $C_{16}H_{23}O_2N$: C, 73.5; H, 8.87; N, 5.4%. Found: C, 73.5; H, 8.78; N, 5.5%.

The infrared spectrum of this compound, X, in nujol had strong maxima at 1700 cm^{-1} (ketone) and 1626 cm^{-1} (lactam carbonyl). When the spectrum was determined in chloroform solution, the bands appeared at 1709 and 1622 cm^{-1}. There was no absorption in the cyanamide and ester carbonyl regions.

A mixed melting point determination showed that lactams X and IV were not the same.

**This ester exists in two crystalline forms melting at 127–129° and 160–162°.*

Reduction of the β-Lactam with Lithium Aluminum Hydride

About 30 mg of lactam X was reduced for 20 hours with lithium aluminum hydride (0.1 g) in boiling tetrahydrofuran. The excess hydride was destroyed by the addition of wet tetrahydrofuran and the mixture evaporated. Sodium hydroxide solution was added to the residue and the organic material extracted with chloroform. Evaporation of the chloroform solution yielded an oil which partially crystallized, but attempts to obtain a sharp-melting product by recrystallization were unsuccessful. The crude product, was, therefore, dissolved in acetone and treated with methyl iodide. The crystalline methiodide which formed melted with decomposition at 287–289°. Its melting point was not depressed by the addition of dihydrolycopodine methiodide, m.p. 293–295° (decomp.). The infrared spectra of the methiodides were identical.

α-Cyanodihydrolycopodine XII

This compound was prepared by the method of Barclay and MacLean (5).

β-Cyanodihydrolycopodine XIII

This compound was prepared by the method of MacLean, Song, and Harrison (7).

Chromic Acid Oxidation of I, XII, and XIII

The oxidation procedure which was used was originally developed by Lemieux and Purves (8) for the quantitative estimation of acetyl, ethylidene, ethoxy, and α-hydroxyethyl groups. The distillate from the oxidation, which was pale yellow, was redistilled, and the colorless second distillate was titrated (pH meter) with 0.1 *N* sodium hydroxide. A small excess of alkali was added and the solution was evaporated to dryness.

Recovery of the acids was carried out by treating the residue of sodium salts with liquid hydrogen chloride. The excess hydrogen chloride was removed and the liberated acids distilled under high vacuum. The acids were recovered from their salts in about 90–95% yield by this procedure. The liberated acids contained a considerable amount of hydrogen chloride.

The recovered acids were treated with a slight excess of a freshly prepared solution of diazomethane in ether and the resulting solution of methyl esters was dried with a few crystals of anhydrous sodium sulphate. The solution was then separated into its components by gas chromatography. The methyl esters were identified by comparing the retention times of the bands with values obtained for known mixtures. The separation was carried out on a Perkin–Elmer column 'A' (didecyl phthalate on Celite) at 75° and at a flow rate of 150 ml/min. Under these conditions the following retention times (in minutes) were obtained:

Ether (used as reference)	0.00	Methyl butyrate	10.7
Methyl acetate	1.2	Methyl isovalerate	17.2
Methyl propionate	4.3	Methyl valerate	27
Methyl isobutyrate	6.8		

The actual retention time for ether was about 2 minutes. The relative yields of the acids formed in the oxidation were estimated by comparing the areas under the recorded ester peaks. The factors needed to correct the measured band areas for differences in the thermal conductivities of the esters were calculated from graphs obtained on chromatography of solutions of known composition. The over-all yield of acid was estimated from the amount of standard alkali which was required to neutralize the distillate from the oxidation. Since no titration blanks were run, however, the figures obtained for the over-all yields are not considered to be very reliable.

Can. J. Chem. Downloaded from www.nrcresearchpress.com by 210.87.254.40 on 09/05/12
For personal use only.

When oxidized by this procedure, both α- and β-cyanodihydrolycopodine, XII and XIII, gave a mixture of acetic, propionic, and butyric acid. Lycopodine gave only acetic acid. The yields of the acids were as follows:

	Relative yields (%)			Total yield of acid (%)
	Acetic	Propionic	Butyric	
I	100	—	—	(50)
XII	62	14	24	(50)
XIII	69	23	8	(70)

The yields listed in the table for I and XII were obtained by the oxidation of 100-mg samples with 10 ml of 30% aqueous chromium trioxide. Oxidation of this much material was found to be unnecessary and a sample size of 10–25 mg is now recommended.

Preparation of the Benzylidene Derivative VII

The benzylidene derivative was prepared by the procedure of Barclay and MacLean (5). The ultraviolet spectrum of this compound had two maxima, at 240 mμ, log ε = 4.3, and at 280 mμ, log ε = 4.14.

Preparation of the Enol VIII

A solution of VII (0.40 g) in 15 ml of glacial acetic acid and 15 ml of methanol was cooled to −40° in a dry ice – acetone bath. A stream of oxygen containing 5% ozone was passed through the solution for 15 minutes at a rate of 50 ml/min. The solution was then transferred to a hydrogenation bottle, platinum oxide catalyst was added, and the mixture was shaken for about 2 hours under hydrogen at a pressure of 30 p.s.i. The solution was then filtered and evaporated, dilute aqueous bicarbonate and ether were added to the residue, and the ether layer was separated. The ether solution was washed successively with dilute hydrochloric acid, sodium bicarbonate solution, and water, and then extracted with a solution of sodium hydroxide. The alkaline extract was acidified with hydrochloric acid and extracted with chloroform. Evaporation of the chloroform solution gave a crystalline product (0.25 g) which melted at 157–158° after recrystallization from ether – petroleum ether. The melting point is the same as that reported by Barclay and MacLean (4), and the melting point of a mixture of the two compounds was not depressed.

Treatment of the Benzylidene Compound VII with Selenium Dioxide

The benzylidene derivative VII (2.86 g) and selenium dioxide (1.09 g) were dissolved in 100 ml of dioxane and heated under reflux for 3 hours. The mixture was evaporated to dryness and the residue exhaustively extracted with ether. The ether extract was washed with water to remove excess selenium dioxide, dried, and concentrated. From the concentrated solution, 1.78 g of the hydroxy derivative XIV separated. This material, after recrystallization from ether, melted at 212–217° C. Calc. for $C_{24}H_{30}O_2N_2$: C, 76.1; H, 7.99; N, 7.4%. Found: C, 76.1; H, 7.90; N, 7.4%.

The infrared spectrum of this compound showed hydroxyl absorption at 3560 cm^{-1}, cyanamide absorption at 2210 cm^{-1}, and carbonyl absorption at 1692 cm^{-1}, in solution in chloroform. The ultraviolet spectrum showed a maximum at 285 mμ, log ε = 4.2.

The mother liquor from the separation of XIV above was treated with methanol. From the ether–methanol solution, 0.46 g of compound XV separated. After recrystallization from ether–methanol it melted at 199–202°. Calc. for $C_{24}H_{28}ON_2$: C, 79.9; H, 7.84; N, 7.8%. Found: C, 79.6; H, 7.84; N, 7.7%.

Can. J. Chem. Downloaded from www.nrcresearchpress.com by 210.87.254.40 on 09/05/12
For personal use only.

The infrared spectrum of this compound showed the usual cyanamide absorption at 2220 cm^{-1}, carbonyl absorption at 1677 cm^{-1}, a strong, sharp band at 1626 cm^{-1} attributed to double-bond absorption, and a band at 1590 cm^{-1} in the region of phenyl absorption.

The ultraviolet spectrum showed two maxima, at 310 mμ, log $\epsilon = 4.2$, and at 228 mμ, log $\epsilon = 3.0$.

Treatment of XIV with Ozone

Compound XIV (0.36 g) was dissolved in a mixture of 20 ml of methanol and 15 ml of glacial acetic acid. The solution was cooled to $-20°$ C and treated with a stream of 5% ozone in oxygen for a period of $\frac{1}{2}$ hour. The reaction mixture was then transferred to a flask fitted for steam distillation, and steam was passed through for 5–10 minutes. A yellow crystalline solid separated when the aqueous acetic acid mixture was cooled. The solid was collected and recrystallized from ether, and melted at 223–225° with decomposition. Calc. for $C_{17}H_{24}O_3N_2$: C, 67.1; H, 7.95; N, 9.2%. Found: C, 67.1; H, 7.99; N, 8.8%.

The infrared spectrum showed the usual cyanamide absorption at 2200 cm^{-1}, broad hydroxyl absorption and carbonyl absorption at 1724 cm^{-1}. The ultraviolet spectrum had a maximum at 420 mμ, log $\epsilon = 25$. There was no change in the ultraviolet spectrum when the solution was made alkaline.

The mother liquor from the separation of XVII above was extracted with chloroform. The chloroform extract was extracted with aqueous bicarbonate, and the bicarbonate extract was acidified and extracted again with chloroform. The latter chloroform extract was dried over sodium sulphate and evaporated to dryness. The residue was dissolved in a small volume of acetone from which it crystallized. After recrystallization from ether–acetone, compound XVIII melted at 206–208°. Calc. for $C_{17}H_{24}O_4N_2$: C, 63.7; H, 7.55; N, 8.7%. Found: C, 63.7; H, 7.71; N, 8.4%.

The infrared spectrum of this compound showed cyanamide absorption at 2210 cm^{-1}, a peak of 1735 cm^{-1} attributed to a six-membered lactone, and a peak at 1680 cm^{-1} attributed to a carboxyl group.

Conversion of XVII to VIII

The hydroxydione XVII (0.1 g) was dissolved in methanol and shaken with hydrogen at 35 p.s.i. over a platinum catalyst for 4 hours. The solution was filtered free of catalyst and evaporated to dryness, and the residue was crystallized from ether. The product melted at 157–158°, either alone or in admixture with the enol VIII.

Treatment of XV and VII with Hydrogen

Compound XV (0.15 g) was dissolved in methanol and shaken with hydrogen at 30 p.s.i. over a platinum catalyst for 11 hours. The solution was filtered free of catalyst and evaporated to dryness. Addition of ether gave a crystalline product which, after recrystallization from ether, melted at 206–208°. Calc. for $C_{24}H_{32}ON_2$: C, 79.1; H, 8.85; N, 7.7%. Found: C, 79.2; H, 8.85; N, 7.8%.

The infrared spectrum of XVI showed absorption in the carbonyl region in carbon tetrachloride solution at 1708 cm^{-1}. Its ultraviolet spectrum showed only non-conjugated phenyl absorption.

The same product was obtained on similar treatment of VII.

Deuterium Exchange and Deuterium Analysis

The compound (50 mg) was dissolved in deuteromethanol (CH_3OD), and 0.05 ml of

Can. J. Chem. Downloaded from www.nrcresearchpress.com by 210.87.254.40 on 09/05/12
For personal use only.

20% sodium deuteroxide was added. The reaction mixture was heated under reflux for ½ hour under an atmosphere of nitrogen and then taken to dryness. A total of four such exchanges was carried out on each sample. To the residue remaining after the last exchange there was added 0.5 ml of deuterium oxide, and the reaction mixture was extracted with ether. The ether extract was dried over anhydrous magnesium sulphate, and the ether was evaporated, leaving a residue, which was purified by sublimation or crystallization from a non-hydroxylic solvent.

The deuterated samples were analyzed for their deuterium content by the method of Jones and MacKenzie (17). Deuterobiphenyl, $C_{12}D_{10}$, was used as a standard to check the analytical method. The results are tabulated below.

Compound	Number of deuterium atoms per molecule
Biphenyl	10.1, 10.0, 10.3
Lycopodine	2.74, 2.78, 2.74
α-Cyanolycopodine, VI	2.51, 2.61
α-Cyclized compound, XXI	1.95, 1.93, 1.95
β-Cyclized compound, XXII	0.00, 0.00
Hofmann product, XXIII*	1.92, 1.89, 1.92

*In this case each exchange was carried out for a 12-hour period. Under the conditions stated above the following results were obtained: 1.69, 1.65, 1.69.

Cyclized Compound XXI

The compound was prepared by the method reported previously (4, 7).

Cyclized Compound XXII

The compound was prepared by the method reported previously (4, 7).

Preparation of XIX by Dehydration and Hydride Reduction of XII

Compound XII (1.0 g) was dissolved in xylene containing *p*-toluenesulphonic acid (0.15 g), and the mixture was refluxed for 4 hours. The reaction mixture was cooled, washed with dilute acid, dilute sodium bicarbonate, and water. On removal of the xylene under reduced pressure on the steam bath, there remained a mobile oil (0.75 g) which failed to crystallize even after chromatography on alumina.

The infrared absorption spectrum of a film of this compound showed weak absorption in the unsaturation region near 1650 cm^{-1} and lacked hydroxyl absorption. The cyanamide absorption appeared at 2210 cm^{-1}.

The anhydro compound (1.6 g), prepared as described above, was added to a solution of 1.0 g of lithium aluminum hydride in boiling ethyl ether. The mixture was refluxed in a nitrogen atmosphere overnight. The excess lithium aluminum hydride was decomposed with moist ether; water was added and the mixture extracted with chloroform. On distillation of the chloroform there remained 1.2 g of an oil. This crude material was dissolved in ether and the basic fraction extracted with dilute hydrochloric acid. The acid extract was made alkaline with ammonia and the free base removed by ether extraction. A sample of this amorphous base was dissolved in a small volume of acetone. Concentrated hydrochloric acid was added and crystals of the hydrochloride formed. Recrystallization from acetone produced colorless needles, m.p. 245–247° C. Calc. for $C_{16}H_{27}N.HCl$: C, 71.2; H, 10.10; N, 5.2%. Found: C, 71.5; H, 10.20; N, 5.0%.

In carbon tetrachloride, the free base XIX showed infrared absorption in the unsaturation region at 1655 cm^{-1} and lacked cyanamide absorption. The hydrochloride showed a strong band at 1585 cm^{-1} in nujol or in chloroform, attributed to the ionized salt of the secondary amine.

Can. J. Chem. Downloaded from www.nrcresearchpress.com by 210.87.254.40 on 09/05/12
For personal use only.

Can. J. Chem. Downloaded from www.nrcresearchpress.com by 210.87.254.40 on 09/05/12
For personal use only.

Dehydrogenation of XIX

The dehydrogenation was carried out in a 15-ml, round-bottomed flask sealed to a 15-cm tube which served as an air condenser for the refluxing mixture. The apparatus was constructed so that it could be evacuated, flushed with nitrogen, and the reaction carried out in a slow stream of purified nitrogen. A small thermometer was inserted into the reaction flask to permit direct reading of the temperature of the mixture.

Compound XIX (0.80 g) was mixed with 0.80 g of selenium powder in the dehydrogenation apparatus. The apparatus was flushed with nitrogen several times and then inserted into an electrically heated salt bath maintained initially at 250°. The temperature of the reaction mixture was raised to 295° in $\frac{1}{2}$ hour, at which time the decomposition appeared to be rapid. The dehydrogenation was allowed to continue overnight in a slow stream of nitrogen and at a temperature up to 300°. The residue was removed from the apparatus with boiling chloroform. The chloroform extract was evaporated to dryness and the residue treated with boiling ethyl ether. The ether-soluble material was extracted repeatedly with dilute hydrochloric acid, and the combined acid extract was basified and then extracted repeatedly with ether. The crude base isolated in this manner amounted to 0.37 g. This material was dissolved in a small volume of cyclohexane and chromatographed on alumina. The progress of the fractionation was followed by recording the ultraviolet spectra of the eluates. The first eluates showed identical spectra. These were combined, and the solvent was evaporated to yield 0.07 g of a clear oil. This material was dissolved in a small volume of ether and added to a solution of an equal weight of picric acid dissolved in refluxing ether. There was immediate separation of glistening, yellow plates which, after recrystallization from ether, melted at 160–162°. Calc. for $C_{22}H_{24}N_4O_7$: C, 58.0; H, 5.26; N, 12.3%. Found: C, 58.3; H, 5.27; N, 12.2%.

The free base recovered from the picrate was analyzed on a high-temperature mass spectrometer and found to have a parent mass of 227, corresponding to $C_{16}H_{21}N$. The ultraviolet spectrum of this compound was typical of alkyl quinolines and was remarkably similar to that of 7,8-dimethylquinoline.

Preparation of Cyclized Product XXIII

Lycopodine was dissolved in acetone, and methyl iodide added. The methiodide separated immediately and virtually quantitatively and was recrystallized from methanol–acetone.

Lycopodine methiodide (3.3 g) was added to a solution of potassium (1.5 g) in *t*-butyl alcohol (100 ml). The mixture was heated under reflux for 12 hours and then evaporated to dryness. Water was added to the residue and the aqueous mixture extracted with ether. The dried ether extract was evaporated to dryness and dissolved in acetone, and the base was precipitated as its hydrochloride by addition of concentrated hydrochloric acid. The hydrochloride was dissolved in water, and the solution was made basic with ammonia and then extracted with ether. Evaporation of the ether gave a crystalline residue which was recrystallized from petroleum ether to yield compound XXIII which melted at 82°. The crude yield was 86%. Calc. for $C_{17}H_{27}ON$: C, 78.2; H, 10.34; N, 5.4%. Found: C, 78.1; H, 10.21; N, 5.3%.

The compound showed a strong band at 1695 cm^{-1} in its infrared spectrum. There were no bands which might be attributed to an olefin or olefinic hydrogens. The N.M.R. spectrum showed the presence of $\diagdown\!\!\diagup N—CH_3$ and $\diagdown\!\!\diagup CHCH_3$ groups.

Treatment of XXIII with Cyanogen Bromide

A small sample of XXIII was dissolved in dry benzene and treated with an excess of cyanogen bromide in dry benzene, and the mixture was allowed to stand overnight in the refrigerator. The cyanogen bromide and benzene were removed under reduced pressure, and the residue was taken up in chloroform, washed with acid, alkali, and water, dried, and taken to dryness. The residue formed a crystalline solid which was recrystallized from ether and melted at 162° C. Calc. for $C_{17}H_{24}ON_2$: C, 75.0; H, 8.82; N, 10.3%. Found: C, 74.9; H, 8.71; N, 10.3%.

ACKNOWLEDGMENTS

The authors wish to express their thanks to the National Research Council of Canada, and to the Ontario Research Foundation, for financial assistance.

REFERENCES

1. W. A. HARRISON and D. B. MACLEAN. Chem. & Ind. (London), 261 (1960).
2. F. A. L. ANET. Tetrahedron Letters, **20**, 13 (1960).
3. D. B. MACLEAN and W. A. HARRISON. Can. J. Chem. **37**, 1757 (1959).
4. D. B. MACLEAN, R. H. F. MANSKE, and L. MARION. Can. J. Research, B, **28**, 460 (1950).
5. L. R. C. BARCLAY and D. B. MACLEAN. Can. J. Chem. **34**, 1519 (1956).
6. K. WIESNER, Z. VALENTA, W. A. AYER, L. R. FOWLER, and J. E. FRANCIS. Tetrahedron, 4, 87 (1958).
7. D. B. MACLEAN, W. SONG, and W. A. HARRISON. Can. J. Chem. **38**, 528 (1960).
8. R. U. LEMIEUX and C. B. PURVES. Can. J. Research, B, **25**, 485 (1947).
9. N. FUSON, M. L. JOSIEN, and E. M. SHELTEN. J. Am. Chem. Soc. **76**, 2526 (1954).
10. H. S. FRENCH. J. Am. Chem. Soc. **74**, 514 (1952).
11. L. MARION and R. H. F. MANSKE. Can. J. Research, B, **22**, 1 (1944).
12. W. A. HARRISON. Ph.D. Thesis, McMaster University, Hamilton, Ont. 1960.
13. B. DOUGLAS, D. G. LEWIS, and L. MARION. Can. J. Chem. **31**, 272 (1953).
14. R. H. F. MANSKE and L. MARION. Can. J. Research, B, **20**, 87 (1942).
15. B. NOLIN and R. N. JONES. J. Am. Chem. Soc. **75**, 5626 (1953).
16. R. N. JONES, A. R. H. COLE, and B. NOLIN. J. Am. Chem. Soc. **74**, 5662 (1952).
17. R. N. JONES and M. A. MACKENZIE. Talanta, **3**, 356 (1960).

Can. J. Chem. Downloaded from www.nrcresearchpress.com by 210.87.254.40 on 09/05/12
For personal use only.

Can. J. Chem. Downloaded from www.nrcresearchpress.com by 210.87.254.40 on 09/05/12
For personal use only.

LYCOPODIUM ALKALOIDS

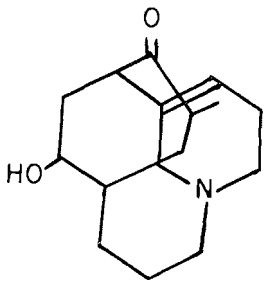
XI. THE STRUCTURE AND REACTIONS OF ACRIFOLINE[1]

W. N. FRENCH[2] AND D. B. MACLEAN

ABSTRACT

Structure A for acrifoline is proposed from a study of the products formed in the Hofmann degradation, von Braun degradation, and several oxidative degradations of the alkaloid. Structure C is proposed for a compound formed on treatment of dihydroacrifoline with copper sulphate in pyridine or with peroxytrifluoroacetic acid.

In a preliminary communication (1) we reported that acrifoline, $C_{16}H_{23}O_2N$, a minor alkaloid of *Lycopodium annotinum*, (2) had structure A. This structure has received support from the work of Anet (3), who has succeeded in interrelating acrifoline and several other *Lycopodium* alkaloids.

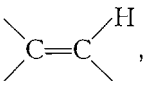
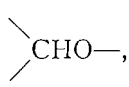
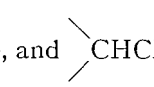


A

We now wish to report in greater detail the evidence in favor of this structure. Previously, Perry and MacLean (4) had established that acrifoline had a double bond, a hydroxyl group, a carbonyl group, and a tertiary nitrogen atom, and therefore was tetracyclic. The application of nuclear magnetic resonance spectroscopy has provided further information on the nature of these functional groups.

The N.M.R. spectrum of acrifoline showed absorptions of area 1 at displacements of 3.35 and 2.04 p.p.m.* attributed to $\diagdown$CHO— and $\diagdown$C=C$\diagup^{H}$ groups respectively. A doublet of area 3, occurring at a displacement of 6.20 p.p.m., established the presence of a $\diagdown$CHCH$_3$ group. The presence of one C-methyl group was also shown by Kuhn–Roth analysis of acrifoline (as its hydrobromide salt). An examination of the N.M.R. spectrum of acetylacrifoline (4) confirmed the above results. Its N.M.R. spectrum

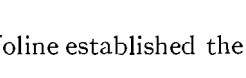
[1]*Manuscript received June 30, 1961.*
Contribution from the Department of Chemistry, McMaster University, Hamilton, Ontario.
[2]*Holder of a National Research Council Studentship, 1958–60.*
**Chemical shifts are given in parts per million (p.p.m.) from chloroform.*

showed absorptions attributed to  ,  , and  at displacements

of 1.97, 2.64, and 6.30 p.p.m. respectively. A sharp peak at a displacement of 5.50 p.p.m. was assigned to the $-COCH_3$ group. The absence of absorption at low field in both of the above N.M.R. spectra rules out the presence of an aldehyde group and therefore, the carbonyl group of acrifoline must be ketonic. The hydroxyl group is secondary since the signal area of the CHO group corresponded to one proton.

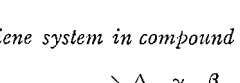
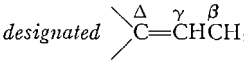
A clue to the spatial relationship of the carbonyl and hydroxyl groups came from infrared spectroscopy. The infrared spectrum of acrifoline in nujol showed hydroxyl absorption at 3310 cm^{-1}, but no carbonyl absorption, while in solution it exhibited strong carbonyl absorption at 1700 cm^{-1}, as well as the usual hydroxyl absorption. Both spectra showed ether absorption near 1100 cm^{-1}. The absence of carbonyl absorption in the solid state implies that acrifoline crystallizes as a hemiketal, whereas the presence of carbonyl absorption in solution indicates that an equilibrium exists between the hemiketal and the hydroxy-ketone forms. Since only five- and six-membered cyclic hemiketals form spontaneously, the carbonyl group and the carbon atom bearing the hydroxyl group must be separated by two or three atoms. The same phenomenon was also observed in many derivatives of acrifoline which contained the original carbonyl and hydroxyl groups.

A study of the products formed in the Hofmann degradation, in the von Braun degradation, and in several oxidative degradations led to the proposal of structure A for acrifoline. Each of these degradative approaches will be discussed in detail below.

The Hofmann degradation of acrifoline established the sequence  in

the molecule. Acrifoline readily formed a methiodide which, on treatment with potassium tertiary butoxide in boiling tertiary butanol, underwent Hofmann elimination to give a crystalline base (I), $C_{17}H_{25}O_2N$, in 70% yield. The infrared spectrum of I showed strong absorption at 900 cm^{-1} with an overtone at 1800 cm^{-1}, characteristic of a terminal methylene group. Strong absorption in the ultraviolet spectrum with a maximum at 2400 Å (ϵ = 24,000), along with an enhanced double-bond absorption in the infrared at 1625 cm^{-1}, showed that a conjugated diene system was present in compound I, and that the double bond introduced during the Hofmann reaction was in conjugation with the original double bond of acrifoline. Barring rearrangement, the original double bond in acrifoline must have occupied a γ,Δ position* relative to nitrogen. Ozonolysis of compound I, and subsequent isolation and identification of formaldehyde, confirmed the presence of a $=CH_2$ group. No other volatile carbonyl compound was isolated from the ozonolysis, nor were any non-volatile fragments characterized.

Catalytic reduction of the diene system in compound I led to the formation of a non-crystalline product which was probably a mixture of partially reduced and fully reduced compounds. A quantitative microhydrogenation of compound I showed the rapid uptake of one mole of hydrogen while the second mole was only partially consumed after several hours. However, chemical reduction of the diene system resulted in the formation of a

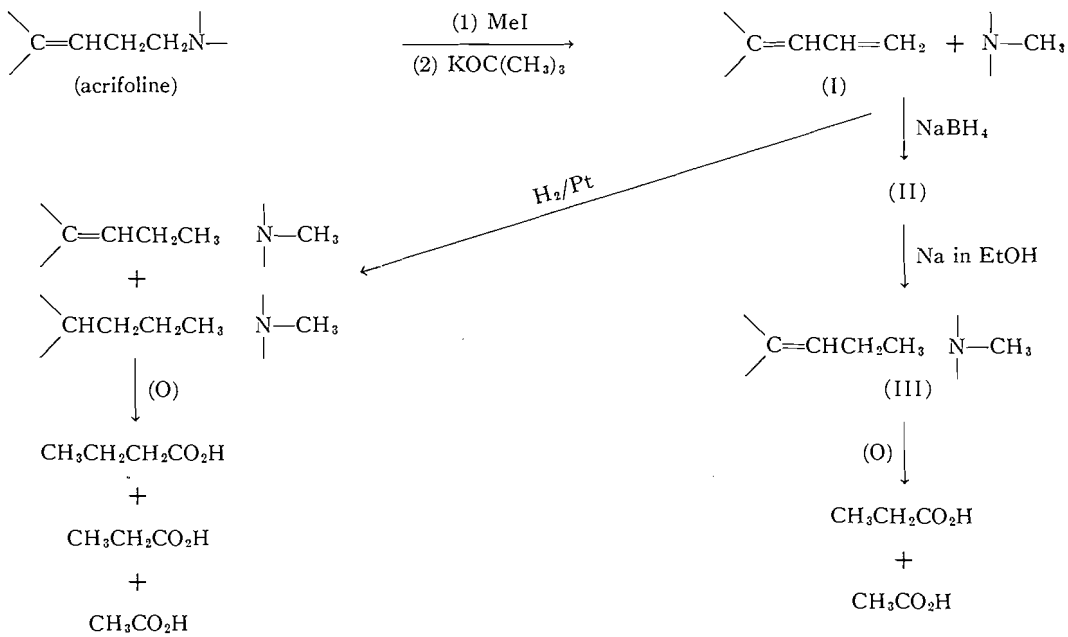
*The four carbon atoms in the conjugated diene system in compound I are designated  to facilitate the present discussion. Acrifoline is designated  .

Can. J. Chem. Downloaded from www.nrcresearchpress.com by 210.87.254.40 on 09/05/12
For personal use only.

1,2-reduced product. The carbonyl group in compound I was first reduced with sodium borohydride to give a diol (II), $C_{17}H_{27}O_2N$. Treatment of II with sodium in alcohol gave III, $C_{17}H_{29}O_2N$. Compound III was oxidized by a modified Kuhn–Roth method (5) and yielded acetic acid and propionic acid. The acids were identified by vapor-phase chromatography of their methyl esters. The isolation of propionic acid established the presence of an ethyl group in III and proved that a 1,2-reduction had occurred with sodium in alcohol. Acrifoline was subjected to the same treatment and yielded only acetic acid, as expected.

Modified Kuhn–Roth oxidation of the crude material obtained by hydrogenation of the Hofmann product, I, yielded butyric acid as well as propionic and acetic acids. Therefore, a *n*-propyl group was present in the product of complete hydrogenation of compound I.

The N.M.R. spectrum of acrifoline established that the double bond was trialkylated. The oxidation studies show that the double bond must occupy a γ,Δ-position relative to nitrogen with the Δ C-atom dialkylated. The preceding series of reactions is summarized in the chart below.



Products from Hofmann degradation

A study of the products of the von Braun reaction of acrifoline confirmed the results of the Hofmann degradation and, in addition, allowed an extension of the peripheral structure to $-CH_2CH_2CH_2-\underset{|}{N}-CH_2CH_2CH=C\diagup\diagdown$. Reaction of acrifoline with cyanogen bromide yielded two isomeric cleavage products, α- and β-cyanobromoacrifoline, IV and V, respectively. β-Cyanobromoacrifoline (V), $C_{17}H_{23}O_2N_2Br$, was isolated in 30% yield as a crystalline product and α-cyanobromoacrifoline (IV) was obtained in

Can. J. Chem. Downloaded from www.nrcresearchpress.com by 210.87.254.40 on 09/05/12
For personal use only.

22% yield as a crystalline quaternary ammonium bromide (VI), $C_{20}H_{32}O_2N_3Br$, on treatment of the mother liquor from the isolation of β-cyanobromoacrifoline (V) with trimethylamine. The quaternary ammonium bromide VI readily eliminated trimethylamine on treatment with potassium tertiary butoxide and formed a neutral product (VII), $C_{17}H_{22}O_2N_2$. The presence of a diene system in VII similar to that in I was established by an examination of its infrared and ultraviolet spectrum. One can conclude that the same ring cleavage occurred in the formation of both Hofmann product I, and α-cyanobromoacrifoline (IV).

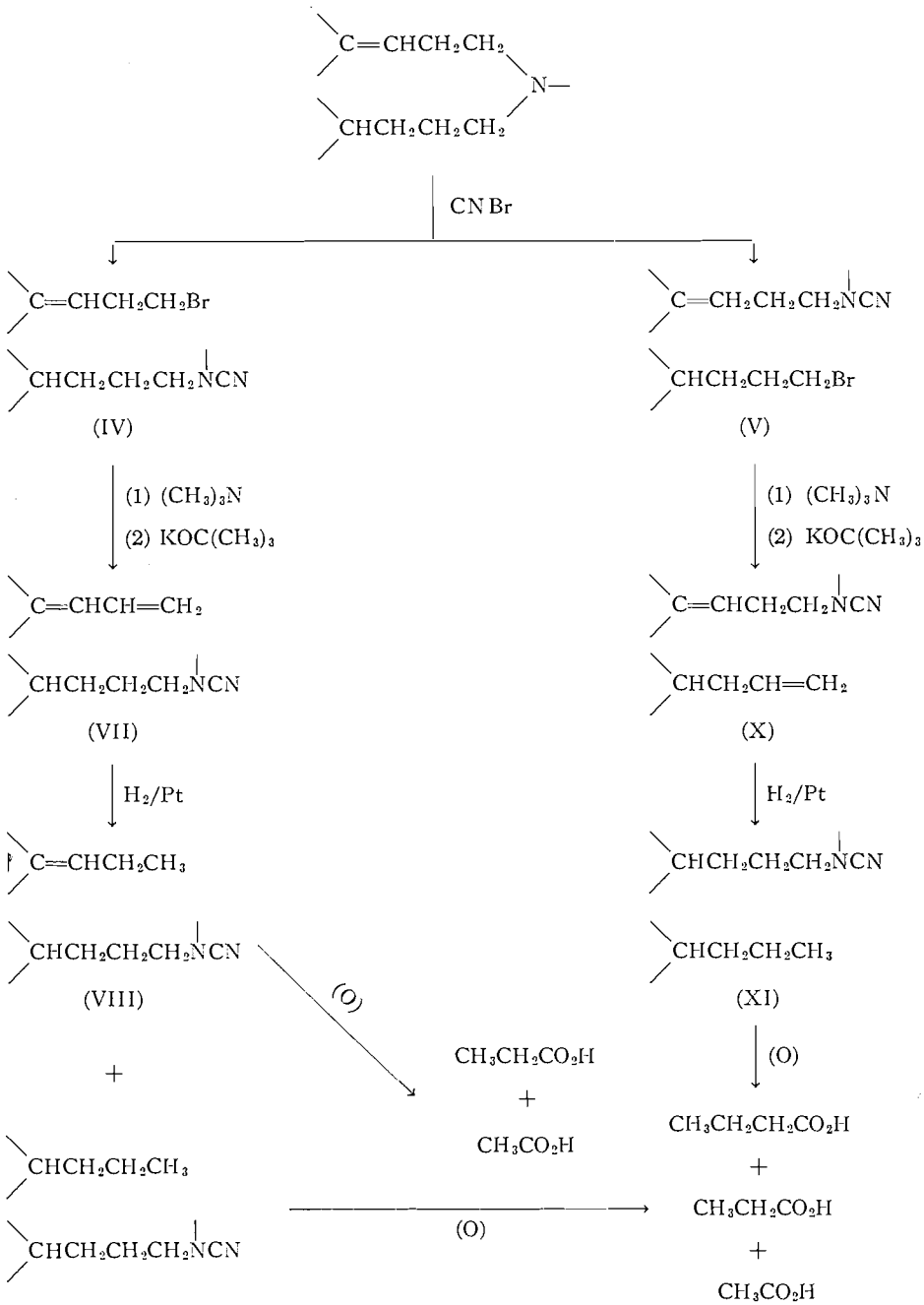
Treatment of compound VII with hydrogen and platinum resulted mainly in a 1,2-reduction of the conjugated diene system. The crystalline product VIII, $C_{17}H_{24}O_2N_2$, was isolated in 50% yield, and gave propionic and acetic acids on oxidation by the modified Kuhn–Roth procedure. Some fully saturated material containing a *n*-propyl side chain was also formed along with compound VIII since oxidation of the material in the mother liquor from the isolation of VIII yielded a small amount of butyric acid in addition to propionic and acetic acids. These results substantiate the presence of the sequence $\diagdown C{=}CHCH_2CH_2N \diagup\diagdown$, in acrifoline.

The reaction of crystalline β-cyanobromoacrifoline (V) with trimethylamine gave a non-crystalline, ether-insoluble quaternary ammonium bromide (IX). Other reactions carried out on compound V, including reduction of the carbonyl group with sodium borohydride and removal of the bromine atom with hydrogen and palladium at room temperature or dry-ice temperature, also gave non-crystalline products. Treatment of the quaternary bromide IX with potassium tertiary butoxide gave an oil (X) which contained a terminal methylene group, as indicated by its infrared spectrum, and confirmed by the formation of formaldehyde upon ozonolysis. The terminal double bond was not in conjugation with the original double bond since there was no intense absorption in the ultraviolet region. Hydrogenation of the diolefin X gave an oil that partially crystallized from ether. This crystalline product (XI), $C_{17}H_{26}O_2N_2$, gave butyric, propionic, and acetic acids in an over-all yield of 68%, in a molar ratio of approximately 44:14:42, on modified Kuhn–Roth oxidation. The presence of butyric acid among the oxidation products proved that compound XI had a *n*-propyl side chain, and therefore, that the sequence $-\overset{|}{\underset{|}{C}}CH_2CH_2CH_2N\diagup\diagdown$ was present in acrifoline. The relatively high yield of butyric acid indicated that the *n*-propyl group in compound XI was not joined to a quaternary center. The reactions are summarized in the chart below.

The sequence $-COCH(CH_3)CH_2-$ in acrifoline, as well as the relationship of this sequence to the $\diagdown CHOH \diagup$ function, was established by a study of the products of selenium dioxide oxidation of acrifoline. The major product XII, $C_{16}H_{21}O_2N$, of this reaction proved to be an α,β-unsaturated ketone. The infrared spectrum of its perchlorate showed carbonyl absorption at 1690 cm^{-1} and enhanced double-bond absorption at 1627 cm^{-1}, and the ultraviolet spectrum of its perchlorate exhibited a maximum at 2430 Å ($\epsilon = 5330$). The possibility of skeletal rearrangement during the formation of compound XII was excluded by hydrogenation of compound XII to dihydroacrifoline.

Can. J. Chem. Downloaded from www.nrcresearchpress.com by 210.87.254.40 on 09/05/12
For personal use only.

Can. J. Chem. Downloaded from www.nrcresearchpress.com by 210.87.254.40 on 09/05/12
For personal use only.



Products from von Braun degradation

The N.M.R. spectrum of compound XII had two peaks of area 1 at displacements of 1.96 and 3.37 p.p.m. representing the isolated double-bond proton and the $\diagdown$CHO

group respectively. A single, sharp peak at a displacement of 5.50 p.p.m. indicated that the methyl group was located on the double bond α,β to the carbonyl group. A single peak of area 1 occurring at a displacement of 0.23 p.p.m. was attributed to a proton on the β-carbon of the α,β-unsaturated ketone.

The minor product, XIII, isolated from the reaction of acrifoline with selenium dioxide had the same molecular formula, $C_{16}H_{21}O_2N$, as the major product XII. However, the ultraviolet spectrum of this material (as the perchlorate) showed no strong absorption while its infrared spectrum showed carbonyl absorption at 1725 cm^{-1}, but no hydroxyl absorption. Conversion of XII to XIII by treatment with base indicated that XIII was formed in the reaction medium by intramolecular addition of the hydroxyl group to the conjugated double-bond system. The ease of this addition implies that a five- or six-membered cyclic ether is formed, and that the carbon atom β to the carbonyl group and the carbon atom carrying the hydroxyl group are separated by two or three atoms. The N.M.R. spectrum of compound XIII had a doublet at a displacement of 6.22 p.p.m. representing the $\diagdown\!\!\diagup CHCH_3$ group, and a peak of area 1 at a displacement of 1.99 p.p.m. representing the single proton on the double bond. Two peaks, each of area 1, occurring at displacements of 3.19 and 3.54 p.p.m., were attributed to absorption by the two CHO groups, one group at either end of the ether linkage. The N.M.R. results on XII and XIII can only be explained if the sequence $-COC(CH_3)=CH-$ is present in the former and the sequence $-COCH(O\diagdown\!\!\diagup)CH-$ in the latter.

Oppenauer oxidation of dihydroacrifolinol* with aluminum tertiary butoxide and cyclohexanone in boiling toluene gave a crude product that showed two strong absorptions of equal magnitude at 1705 and 1735 cm^{-1} in the carbonyl region of the infrared spectrum, and hydroxyl absorption at 3500 cm^{-1}. Chromatography of the crude product led to the isolation of only one compound (XIV), $C_{16}H_{23}O_2N$, in 45% yield. The infrared spectrum of XIV showed a single, strong carbonyl absorption at 1705 cm^{-1} and no hydroxyl absorption. Compound XIV is probably a diketone with both carbonyl groups located in rings that are six-membered or larger. Absorption at 1420 cm^{-1} in the spectra of both the base XIV and its hydrobromide and none in this region in the spectrum of acrifoline (nujol, chloroform, or carbon tetrachloride) implies that a $-CH_2CO-$ group is present in compound XIV but is absent in acrifoline (6). Thus the $-CH_2CO-$ group in the diketone XIV must have arisen from a $-CH_2CHOH-$ group in acrifoline.

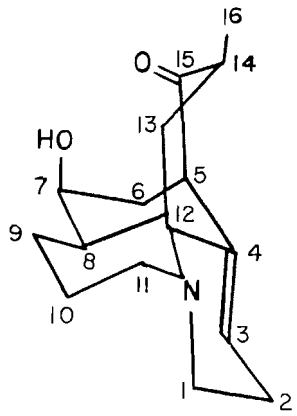
The occurrence of peaks at 1735 cm^{-1} and 3500 cm^{-1} in the infrared spectrum of crude compound XIV may be due to the presence of an aldol impurity containing a five-membered ketone ring.

**Previously, two dihydroacrifolinols were reported (4). α-Dihydroacrifolinol was reported to form by hydrogenation of acrifoline to dihydroacrifoline followed by reduction of the carbonyl group with lithium aluminum hydride. β-Dihydroacrifolinol was formed by initial reduction of the carbonyl group in acrifoline to give acrifolinol followed by hydrogenation. In the present investigation, the same product, melting at 192.5–193.0° and identical with α-dihydroacrifolinol, was formed by either of the above procedures.*

Can. J. Chem. Downloaded from www.nrcresearchpress.com by 210.87.254.40 on 09/05/12
For personal use only.

Structure A, which has been formulated for acrifoline, is in accord with the data presented above. It explains the existence of the hemiketal formed by interaction between the carbonyl and the hydroxyl functions. The facile conversion of the unsaturated compound XII to its saturated isomer XIII is readily accommodated by this structure. The separation of the double bond and the carbonyl group by a bridgehead carbon explains why an interaction between these two groups was never observed in acrifoline or its degradation products. The structure is biogenetically feasible and is compatible with the proposal recently put forward by Conroy (7). Furthermore, this structure is corroborated by the work, on annofoline, of Anet (8), who has also shown that annofoline is the C_4 epimer of dihydroacrifoline (4).

The stereochemistry of acrifoline has been discussed by Anet (3), who has proposed that it has the configuration shown in the perspective formula B below.



B

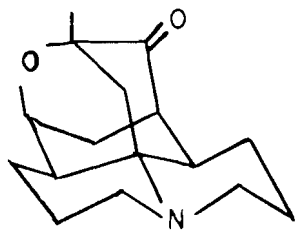
The only center where configuration might be in doubt is C_8, and the assignment shown is supported by the following experiments. Acrifoline underwent Wolff–Kishner reduction to XV, $C_{16}H_{25}ON$. The latter was converted by chromic acid oxidation to the ketone (XVI), $C_{16}H_{23}ON$, which was stable to the action of alkali.

Treatment of dihydroacrifoline, with copper sulphate in pyridine or with peroxytrifluoroacetic acid, resulted in the formation of a new compound (XVII), $C_{16}H_{23}O_2N$. The structure of this compound has been established and its formation involved an unexpected ether-bridging reaction.

Product XVII was formed in 78% yield on treatment of dihydroacrifoline with copper sulphate in pyridine. In its infrared spectrum there was a peak at 1725 cm^{-1} attributed to a carbonyl group, but no absorption which could be attributed to a hydroxyl group. The carbonyl peak was shifted by 25 cm^{-1} from its position in the starting material. The N.M.R. spectrum of XVII had absorption of area 1 at a displacement of 3.55 p.p.m. due to a $\diagdown\!\!\diagup$CHO— group, and a sharp, single peak at a displacement of 6.16 p.p.m. due to the methyl group on a carbon atom not carrying a proton. Compound XVII underwent reduction to a secondary alcohol (XVIII) with sodium borohydride and reacted with phenyllithium to form a phenylcarbinol (XIX). The alcohol XVIII yielded a monoacetate (XX) on treatment with a mixture of acetic acid and trifluoroacetic anhydride

Can. J. Chem. Downloaded from www.nrcresearchpress.com by 210.87.254.40 on 09/05/12
For personal use only.

and was converted with chromic acid to the ketone XVII. Compound XVII was, therefore, assigned structure C.



C

The over-all reaction closely resembles the oxidation of other aldehydes and ketones by various reagents (9, 10), in which oxidation occurs by a free radical process at the α-carbon atom after enolization has occurred.

The same product was obtained on attempted Baeyer–Villiger oxidation of dihydroacrifoline. The reaction was carried out under standard conditions (11, 12) using peroxytrifluoroacetic acid in methylene chloride in the presence of disodium phosphate.

EXPERIMENTAL

Acrifoline

Acrifoline was obtained from annotoxine according to the procedure of Perry and MacLean (4). Calc. for $C_{16}H_{23}O_2N.HBr$: one C-methyl, 4.39%. Found: C-methyl, 4.15%.

Acetyl Acrifoline

Acetyl acrifoline was prepared from acrifoline by the procedure of Perry and MacLean (4).

Preparation of Acrifoline Methiodide

A solution of acrifoline (1.0 g) in 15 ml of acetone and 3 ml of methyl iodide was heated under reflux and, within 2 minutes, a crystalline methiodide began to separate. The mixture was heated for 15 minutes longer, cooled, and allowed to stand at room temperature for 1 hour. Filtration gave 1.23 g (80%) of product melting at 278–279° (with decomposition). An additional 0.260 g (17%) of product was obtained from the filtrate on further treatment with methyl iodide in acetone. Recrystallization of the methiodide from methanol–acetone gave colorless needles melting at 280–281° (with darkening). Bertho and Stoll (13) report a melting point of 249–250°, and Achmatowicz and Rodewald (14), a melting point of 267–268° for this compound. Calc. for $C_{16}H_{23}O_2N.CH_3I$: C, 50.6; H, 6.49; N, 3.47%. Found: C, 50.5; H, 6.47; N, 3.12%.

Treatment of Acrifoline Methiodide with Potassium Tertiary Butoxide

A mixture of acrifoline methiodide (1.10 g) and potassium tertiary butoxide (1.50 g) in 60 ml of tertiary butanol and 2 ml of benzene was heated under reflux for 4 hours. The mixture was cooled, water was added, and the organic solvents were removed under reduced pressure. The resulting alkaline aqueous mixture was extracted several times

Can. J. Chem. Downloaded from www.nrcresearchpress.com by 210.87.254.40 on 09/05/12
For personal use only.

with chloroform. The chloroform extract was dried over anhydrous sodium sulphate and evaporated under reduced pressure. The residual oil was crystallized from petroleum ether to give 0.53 g (70%) of colorless needles melting at 158–159°. Recrystallization from petroleum ether gave compound I which melted sharply at 161°. Calc. for $C_{17}H_{25}O_2N$: C, 74.1; H, 9.15%. Found: C, 73.7; H, 9.02%.

The infrared spectrum of this material had hydroxyl absorption at 3500 cm^{-1}, carbonyl absorption at 1700 cm^{-1}, double-bond absorption at 1650 cm^{-1} (weak) and 1625 cm^{-1} (strong), and $=CH_2$ absorption at 900 cm^{-1} with an overtone at 1800 cm^{-1}. The ultraviolet spectrum had $\lambda_{max}^{C_2H_5OH}$ at 2400 Å, ϵ = 24,000.

Ozonolysis of the Hofmann Product I

A stream of ozone-enriched oxygen was passed through a solution of the Hofmann product (0.10 g) in 15 ml of glacial acetic acid until the uptake of ozone was complete (about 20 minutes), then zinc dust (0.50 g) was added and the mixture steam distilled.

Formaldehyde was isolated from the steam distillate as its 2,4-dinitrophenylhydrazone and as its dimedone derivative. The melting points of both derivatives agreed with recorded values, and showed no depression on admixture with authentic samples.

Reduction of I with Sodium Borohydride

A solution of compound I (0.20 g) and $NaBH_4$ (0.2 g) in 15 ml of absolute ethanol was allowed to stand at room temperature for 6 hours. The excess borohydride was destroyed with formaldehyde, water was added, and the organic solvent was removed under reduced pressure. The product was isolated by extraction of the aqueous alkaline mixture with chloroform, extraction of this chloroform solution with dilute aqueous acid, and extraction of the basified aqueous solution with chloroform. The latter chloroform solution was dried over anhydrous sodium sulphate and evaporated under reduced pressure, yielding 0.20 g of crystalline solid melting at 249–251°. An analytical sample of compound II, m.p. 251.5–252.0°, was obtained after two recrystallizations from methanol–acetone. Calc. for $C_{17}H_{27}O_2N$: C, 73.6; H, 9.81; N, 5.05; NCH_3, 10.5%. Found: C, 73.4; H, 9.83; N, 5.07; NCH_3, 10.8%.

The infrared spectrum had hydroxyl absorption in the 3000–3200 cm^{-1} region, no carbonyl absorption, double-bond absorption at 1625 and 1590 cm^{-1}, and $=CH_2$ absorption at 900 cm^{-1} with an overtone at 1800 cm^{-1}. The ultraviolet spectrum had $\lambda_{max}^{C_2H_5OH}$ at 2400 Å, ϵ = 28,000.

Sodium in Alcohol Reduction of the Diol II

A solution of compound II (0.30 g) in 75 ml of absolute ethanol was heated to boiling, and sodium was added in small pieces over a period of $3\frac{1}{2}$ hours at such a rate that metallic sodium was always present in the medium. The solution was cooled, ethanol and water were added, and the organic solvent was removed under reduced pressure. The resulting aqueous mixture was extracted several times with chloroform. The combined, pale yellow chloroform solution was extracted with dilute aqueous acid and the acid extract made alkaline with ammonia and extracted with chloroform. The latter chloroform solution was dried over anhydrous sodium sulphate and evaporated under reduced pressure. The residual colorless oil was crystallized from acetone–ether, yielding 0.264 g (88%) of compound III which melted at 191.5–192.5°. Recrystallization from acetone–ether raised the melting point to 194.5–195.0°. Calc. for $C_{17}H_{29}O_2N$: C, 73.0; H, 10.5%. Found: C, 72.8; H, 10.5%.

Can. J. Chem. Downloaded from www.nrcresearchpress.com by 210.87.254.40 on 09/05/12
For personal use only.

Neither the infrared nor ultraviolet spectrum of this compound showed absorption characteristic of a conjugated diene system.

Oxidative Determination of Alkyl Side Chains

The oxidations were carried out and the acids analyzed by the method described by Harrison (5).

Modified Kuhn–Roth Oxidation of Acrifoline

Oxidation of 0.025 g (0.096 millimole) of acrifoline yielded 0.082 milliequivalent (86%) of volatile carboxylic acid. Vapor-phase chromatography of its methyl ester indicated only the presence of methyl acetate.

Modified Kuhn–Roth Oxidation of the 1,2-Reduced Hofmann Product III

Oxidation of 0.030 g (0.108 millimole) of compound III yielded 0.183 milliequivalent (85%) of volatile carboxylic acids. Vapor-phase chromatography of their methyl esters revealed the presence of methyl acetate and methyl propionate in the molar ratio of 67:33 respectively.

Modified Kuhn–Roth Oxidation of Crude Hydrogenated Hofmann Product

The Hofmann product I (0.030 g, 0.109 millimole) was dissolved in methanol and treated with hydrogen (50 p.s.i.g.) and platinum (0.025 g PtO_2) for 15 hours. The catalyst was removed by filtration, and the solvent was evaporated under reduced pressure, leaving a colorless oil. Chromic acid oxidation of this crude product yielded 0.218 milliequivalent of volatile carboxylic acids. Vapor-phase chromatography of their methyl esters revealed the presence of methyl acetate, methyl propionate, and methyl butyrate in the molar ratio of 77:19:4 respectively.

Reaction of Acrifoline with Cyanogen Bromide

(a) Isolation of β-Cyanobromoacrifoline V

A solution of acrifoline (1.0 g) and cyanogen bromide (1.0 g) in 15 ml of anhydrous benzene was allowed to stand at room temperature for 40 hours. The solvent and excess cyanogen bromide were removed under reduced pressure and the residue taken up in chloroform, washed with dilute acid, water, and aqueous sodium bicarbonate. Acrifoline (0.13 g) was recovered from the acid extract. The chloroform solution was dried over anhydrous sodium sulphate and evaporated under reduced pressure leaving 1.0 g of a pale yellow oil, which was taken up in acetone–ether and placed in the refrigerator. After several hours, 0.41 g (30%) of colorless crystals, melting at 153–154°, were removed by filtration. Recrystallization from acetone–ether raised the melting point to 154.5°. Calc. for $C_{17}H_{23}O_2N_2Br$: C, 55.6; H, 6.31; N, 7.63%. Found: C, 56.0; H, 6.67; N, 7.92%.

The infrared spectrum of this material in nujol showed cyanamide absorption at 2200 cm^{-1} and hydroxyl absorption at 3300 cm^{-1}, but no absorption in the carbonyl region. The infrared spectrum in chloroform showed hydroxyl absorption at 3580 cm^{-1}, cyanamide absorption at 2205 cm^{-1}, weak carbonyl absorption at 1710 cm^{-1}, and double-bond absorption at 1670 cm^{-1}.

(b) Isolation of α-Cyanobromoacrifoline IV as its Quaternary Trimethylammonium Bromide VI

The filtrate from the separation of the crystalline bromide V was evaporated to dryness, yielding an oil, which was dissolved in 5 ml of absolute ethanol containing trimethylamine (0.00075 equiv. per ml). After the solution had remained for 24 hours at room temperature, the solvent and excess trimethylamine were removed under reduced pressure. The residue

Can. J. Chem. Downloaded from www.nrcresearchpress.com by 210.87.254.40 on 09/05/12
For personal use only.

partially crystallized on addition of acetone, and on filtration yielded 0.364 g (22%, based on the weight of acrifoline used) of colorless crystals melting at 276.0–276.5°. Recrystallization from methanol–acetone raised the melting point to 276.5–277.0°. Calc. for $C_{20}H_{32}O_2N_3Br$: C, 56.3; H, 7.57; N, 9.86%. Found: C, 56.5; H, 7.57; N, 9.66%.

The infrared spectrum showed hydroxyl absorption at 3300 cm^{-1}, cyanamide absorption at 2210 cm^{-1}, double-bond absorption at 1655 cm^{-1}, and weak carbonyl absorption at 1700 cm^{-1}.

Treatment of VI with Potassium Tertiary Butoxide

A mixture of the quaternary ammonium bromide VI (0.250 g) and potassium tertiary butoxide (0.50 g) in 25 ml of tertiary butanol and 1 ml of benzene was heated under reflux for 2 hours. The mixture was cooled, water was added, and the organic solvent was removed under reduced pressure. The resulting alkaline aqueous mixture was extracted several times with chloroform. The combined chloroform extract was dried over anhydrous sodium sulphate and evaporated under reduced pressure, yielding a colorless oil which crystallized from petroleum ether. The first crop of compound VII weighed 0.135 g (80%) and melted at 183.0–183.5°. Recrystallization from ether – petroleum ether did not raise the melting point. Calc. for $C_{17}H_{22}O_2N_2$: C, 71.3; H, 7.75; N, 9.78%. Found: C, 71.4; H, 7.67; N, 9.86%.

The infrared spectrum in nujol showed terminal methylene absorption at 900 cm^{-1} with an overtone at 1800 cm^{-1}, double bond absorption at 1640 cm^{-1} and 1590 cm^{-1}, cyanamide absorption at 2210 cm^{-1}, and hydroxyl absorption at 3300 cm^{-1}. The infrared spectrum in chloroform showed carbonyl absorption at 1705 cm^{-1} and hydroxyl absorption at 3480 cm^{-1} as well as the absorptions due to unsaturation and the cyanamide group. The ultraviolet spectrum had $\lambda_{max}^{95\%\ EtOH}$ at 2400 Å, $\epsilon = 24{,}800$.

Hydrogenation of VII

Compound VII (0.087 g) was dissolved in 20 ml of methanol and treated with hydrogen (50 p.s.i.g.) and platinum (0.050 g PtO_2) for 15 hours. The catalyst was removed by filtration, and the solvent was evaporated under reduced pressure. The colorless residue was dissolved in chloroform, and the chloroform solution was washed first with dilute hydrochloric acid and then with aqueous sodium bicarbonate, and dried over anhydrous sodium sulphate. Evaporation of the chloroform under reduced pressure left a colorless oil which partially crystallized from ether. A total of 0.045 g (50%) of crystalline product VIII, melting at 154–155°, was obtained. This material was sublimed at 0.001 mm and 140° for analysis. Calc. for $C_{17}H_{24}O_2N_2$: C, 70.8; H, 8.39%. Found: C, 70.3; H, 8.37%.

The infrared spectrum of this compound had broad hydroxyl absorption in the 3400 cm^{-1} region, weak carbonyl absorption at 1710 cm^{-1}, and cyanamide absorption at 2240 cm^{-1}. In chloroform solution, the infrared spectrum of VIII showed hydroxyl absorption at 3650 cm^{-1}, weak carbonyl absorption at 1710 cm^{-1}, cyanamide absorption at 2240 cm^{-1}, and strong ether absorption at 1100 cm^{-1}.

Modified Kuhn–Roth Oxidation of VIII

Oxidation of 0.0134 g (0.047 millimole) of VIII yielded 0.068 milliequivalent (73%) of volatile carboxylic acids. Vapor-phase chromatography of their methyl esters indicated the presence of methyl acetate and methyl propionate in the molar ratio of 69:31 respectively.

Modified Kuhn–Roth Oxidation of Crude Hydrogenated α-Cyano Compound VII

The filtrate obtained from the isolation of crystalline VIII was taken to dryness and

Can. J. Chem. Downloaded from www.nrcresearchpress.com by 210.87.254.40 on 09/05/12
For personal use only.

the residual oil distilled at 0.001 mm and 130–140°. Chromic acid oxidation of a portion of this material (0.012 g, 0.045 millimole) yielded 0.061 milliequivalent (68%) of volatile carboxylic acids. Vapor-phase chromatography of their methyl esters indicated the presence of methyl acetate, methyl propionate, and methyl butyrate in the molar ratios of 77:21:2 respectively.

Removal of Hydrogen Bromide from β-Cyanobromoacrifoline V

A solution of β-cyanobromoacrifoline (V) (0.20 g) in 7 ml of absolute ethanol containing trimethylamine (0.00075 equiv. per ml) was allowed to stand for 40 hours at room temperature. The solvent and excess trimethylamine were removed under reduced pressure, leaving an oil (IX) which could not be induced to crystallize.

A solution of the non-crystalline quaternary ammonium bromide IX in 20 ml of tertiary butanol and 1 ml of benzene was heated under reflux with potassium tertiary butoxide (0.60 g) for 3 hours. The mixture was cooled, water was added, and the organic solvents were removed under reduced pressure. The resulting aqueous mixture was extracted several times with chloroform. The combined chloroform extract was washed with dilute aqueous acid and aqueous sodium bicarbonate, dried over anhydrous sodium sulphate, and evaporated under reduced pressure. The residual colorless oil (X) (0.090 g, 58%) could not be induced to crystallize, even after purification by chromatography on alumina or by distillation *in vacuo*.

The infrared spectrum (film) of the oil X showed carbonyl absorption at 1705 cm^{-1}, double-bond absorption at 1635 cm^{-1}, terminal double-bond absorption at 910 cm^{-1} with an overtone at 1820 cm^{-1}, hydroxyl absorption at 3490 cm^{-1}, and cyanamide absorption at 2200 cm^{-1}. The crude oil showed no absorption in the ultraviolet region of the spectrum other than weak absorption owing to the carbonyl group.

Ozonolysis of Compound X

A solution of compound X (0.048 g) in 10 ml of glacial acetic acid was treated with an excess of ozone. Zinc dust (0.30 g) was added to the solution and the mixture steam distilled. The steam distillate (30 ml) was neutralized with sodium hydroxide, made slightly acid with acetic acid, and treated with 5 ml of dimedone solution. Five hours later, 0.044 g of needles, melting at 165–175°, was removed by filtration. Recrystallization gave 0.025 g of dimedone derivative with a sharp melting point of 190°. A mixture melting point with authentic formaldehyde dimedone derivative showed no depression.

Hydrogenation of X

Compound X, prepared as above from 0.205 g of V, was dissolved in methanol and treated with hydrogen (50 p.s.i.g.) and platinum (0.050 g of PtO_2) for 10 hours. The catalyst was removed by filtration and the solvent by evaporation under reduced pressure. The residual colorless oil was taken up in ether from which colorless crystals separated after several hours. The crystalline product XI amounted to 0.039 g (24%, based on the weight of β-cyanobromoacrifoline (V) used), and melted at 155.5–157.5°. This material was sublimed at 100–130° and 0.001 mm for analysis. Calc. for $C_{17}H_{26}O_2N_2$: C, 70.3; H, 9.03; N, 9.65%. Found: C, 70.4; H, 8.91; N, 9.43%.

The infrared spectrum of XI had a sharp absorption at 3370 cm^{-1} due to hydroxyl, strong absorption at 2200 cm^{-1} due to the cyanamide group, but no absorption in the 1600–1800 cm^{-1} region.

Modified Kuhn–Roth Oxidation of XI

Oxidation of 0.019 g (0.067 millimole) of dihydro-β-cyanoacrifoline (XI) yielded

Can. J. Chem. Downloaded from www.nrcresearchpress.com by 210.87.254.40 on 09/05/12
For personal use only.

0.086 milliequivalent (66%) of volatile carboxylic acids. Vapor-phase chromatography of their methyl esters revealed the presence of methyl acetate, methyl propionate, and methyl butyrate in the molar ratios of 42:14:44 respectively.

Selenium Dioxide Oxidation of Acrifoline

A stirred solution of 0.50 g of selenium dioxide and 0.50 g of acrifoline in 25 ml of aqueous dioxane (10% water) was heated under reflux under an atmosphere of nitrogen for 8 hours. During this period, black selenium metal precipitated and the solution became deep yellow in color. The solution was cooled, diluted with 50 ml of water, and excess selenium dioxide destroyed by reduction with sulphur dioxide. The precipitated metallic selenium was removed by filtration through a sintered glass funnel and the clear, yellow acidic filtrate was washed with chloroform, made alkaline with ammonia and extracted several times with chloroform. The latter chloroform extract was dried over anhydrous sodium sulphate and evaporated under reduced pressure. The residual yellow oil (0.415 g) was chromatographed on alumina with benzene. The first band, eluted with benzene, was a colorless oil (XIII) which formed 0.045 g (6.5%) of a crystalline perchlorate melting at 270–271° (with decomposition). Calc. for $C_{16}H_{21}O_2N.HClO_4$: C, 53.4; H, 6.16; N, 3.89%. Found: C, 53.4; H, 6.12; N, 4.05%.

The infrared spectrum of this compound had carbonyl absorption at 1725 cm^{-1}, double-bond absorption at 1680 cm^{-1}, but had no absorption in the hydroxyl region. The ultraviolet absorption spectrum showed only weak absorption at 2900 Å corresponding to a carbonyl group.

A second band was eluted from the column with chloroform. Evaporation of the solvent left a light yellow oil that partially formed a crystalline perchlorate from acetone–ether. The perchlorate (0.20 g) (30%) (m.p. 267–269°) was purified for analysis by two recrystallizations from methanol–acetone. It finally melted at 273.5–274.0°. Calc. for $C_{16}H_{21}O_2N.HClO_4$: C, 53.4; H, 6.16; N, 3.89%. Found: C, 53.6; H, 6.17; N, 3.97%.

The infrared spectrum of the perchlorate had hydroxyl absorption at 3530 cm^{-1}, carbonyl absorption at 1690 cm^{-1}, and conjugated double-bond absorption at 1627 cm^{-1}. The ultraviolet absorption spectrum had $\lambda_{max}^{C_2H_5OH}$ at 2430 Å, $\epsilon = 5330$.

The base recovered from the filtrate of the above perchlorate preparation weighed 0.150 g but was not characterized.

Conversion of the Unsaturated Compound XII to the Saturated Compound XIII

A solution of the perchlorate of the unsaturated carbonyl compound (0.020 g) in 6 ml of 95% ethanol containing sodium hydroxide (0.05 g) was allowed to stand at room temperature for 24 hours. The solution was diluted with water and extracted with chloroform. The chloroform extract was dried over anhydrous sodium sulphate and evaporated to dryness leaving a colorless oil which formed 0.015 g (75%) of crystalline perchlorate. The infrared spectrum of this salt was identical with that of the perchlorate of the saturated carbonyl compound XIII obtained from the selenium dioxide reaction.

Oppenauer Oxidation of Dihydroacrifolinol

A solution of 0.170 g of dihydroacrifolinol (4) and aluminum tertiary butoxide (0.50 g) in 2 ml of cyclohexanone and 25 ml of toluene was heated under reflux for 7 hours, then poured into cold dilute hydrochloric acid, and the organic layer extracted several times with dilute acid. The aqueous extract was made alkaline with sodium hydroxide solution and extracted with chloroform. The chloroform extract was dried over anhydrous sodium sulphate and evaporated under reduced pressure, leaving a pale yellow oil whose infrared

Can. J. Chem. Downloaded from www.nrcresearchpress.com by 210.87.254.40 on 09/05/12
For personal use only.

spectrum (film) showed two intense absorptions of equal magnitude at 1705 cm^{-1} and 1735 cm^{-1} in the carbonyl region, and absorption at 3500 cm^{-1} in the hydroxyl region.

The crude base obtained above was chromatographed on alumina with 25% chloroform in benzene, and yielded a colorless oil which crystallized in poor yield from ether – petroleum ether, giving 0.016 g of solid XIV which melted at 128–129°. The infrared spectrum of this solid XIV showed a single strong carbonyl absorption at 1705 cm^{-1} and no hydroxyl absorption. A sharp peak at 1420 cm^{-1} was indicative of a —CH_2— group adjacent to a carbonyl. The entire pure product obtained by chromatography was converted to the hydrobromide salt which was recrystallized twice from methanol–acetone for analysis. The total yield of salt (which melted above 315°) was 0.10 g (45%). Calc. for $C_{16}H_{23}O_2N$.HBr: C, 56.1; H, 7.07; N, 4.09%. Found: C, 56.2; H, 7.12; N, 4.11%.

The infrared spectrum of the hydrobromide showed a single, strong carbonyl absorption at 1700 cm^{-1}, but no hydroxyl absorption. A sharp peak at 1420 cm^{-1} was again indicative of a —CH_2— group adjacent to a carbonyl. There was no strong absorption in the ultraviolet spectrum.

A second product of the Oppenauer oxidation containing carbonyl absorption at 1735 cm^{-1} in the infrared spectrum was not isolated.

Wolff–Kishner Reduction of Acrifoline

A solution of acrifoline (0.75 g), potassium hydroxide (2.5 g), and 95% hydrazine hydrate (2 ml) in 25 ml of ethylene glycol was heated in a flask provided with a reflux condenser and a thermometer dipping into the liquid. The solution was heated under reflux for 4 hours (reaction medium at 155°), then the apparatus was arranged for distillation. Distillation was carried out until the flask contents reached a temperature of 185°. The solution was heated under reflux for 7 hours at this temperature, then cooled, diluted with water, and extracted with chloroform. The chloroform extract was washed with water, dried over anhydrous sodium sulphate, and evaporated to dryness under reduced pressure. The colorless residual oil readily crystallized and yielded 0.60 g (85%) of product which melted 122–123° on recrystallization from petroleum–ether. Calc. for $C_{16}H_{25}ON$: C, 77.7; H, 10.1; N, 5.7%. Found: C, 77.6; H, 10.3; N, 5.7%.

The infrared spectrum of this compound showed hydroxyl absorption at 3120 cm^{-1} and no carbonyl absorption. Carbonyl absorption was also absent when the spectrum was measured in chloroform.

Chromic Acid Oxidation of the Wolff–Kishner Product

A solution of 0.55 g of the Wolff–Kishner product in 20 ml of aqueous acetic acid (15% water) was cooled to −10° and treated with 1.0 g of chromic anhydride. The solution was stirred at this temperature for 1 hour, allowed to stand at 0° for 10 hours, and stirred at 0° for 4 hours. Ethanol was added to destroy excess oxidant, then water was added, and most of the acetic acid was removed by evaporation under reduced pressure. The resulting aqueous solution was made alkaline with ammonia and extracted with chloroform. The dried chloroform extract, on evaporation, yielded a colorless oil which readily crystallized without addition of solvent. Purification by sublimation at 80° and 0.001 mm gave 0.415 g (76%) of product melting at 73.5–75.0°.

The infrared spectrum showed strong carbonyl absorption at 1710 cm^{-1} and no hydroxyl absorption.

The perchlorate of this base melted at 246–247° and had strong carbonyl absorption at 1710 cm^{-1}.

Can. J. Chem. Downloaded from www.nrcresearchpress.com by 210.87.254.40 on 09/05/12
For personal use only.

Ketone XVI was recovered unchanged after treatment with sodium methoxide in methanol or potassium tertiary butoxide in tertiary butanol.

Oxidation of Dihydroacrifoline with Copper Sulphate

A solution of dihydroacrifoline (0.5 g), prepared by the method of Perry and MacLean (4), and $CuSO_4.5H_2O$ (1.2 g) in 12 ml of pyridine and 4 ml of water was heated on the steam bath for 24 hours. The deep blue solution was cooled, poured into water, and extracted several times with chloroform. The combined chloroform extract was dried over anhydrous sodium sulphate and evaporated under reduced pressure, leaving a yellow oil. Chromatography of this oil with chloroform on alumina yielded a colorless oil that readily formed 0.51 g (78%) of a crystalline hydrobromide (m.p. above 315°) from acetone. Calc. for $C_{16}H_{23}O_2N.HBr$: C, 56.1; H, 7.07; N, 4.09%. Found: C, 55.8; H, 6.87; N, 4.11%.

The infrared spectrum showed strong carbonyl absorption at 1720 cm^{-1} but no absorption in the hydroxyl region.

A sample of the hydrobromide of compound XVII was converted to the perchlorate salt which melted above 315°. Calc. for $C_{16}H_{23}O_2N.HClO_4$: C, 53.1; H, 6.68; N, 3.87%. Found: C, 53.4; H, 6.83; N, 3.99%.

The perchlorate showed strong absorption at 1720 cm^{-1} in the carbonyl region of the infrared spectrum, but no absorption in the hydroxyl region. Likewise, the infrared spectrum of the free base XXIV showed only carbonyl absorption and no hydroxyl absorption when measured either as a film or in chloroform solution.

Oxidation of Dihydroacrifoline with Peroxytrifluoroacetic Acid

A stock solution of peroxytrifluoroacetic acid in methylene chloride was prepared in the following manner. A solution of trifluoroacetic anhydride (6.3 ml) in 10 ml of methylene chloride was added to a cold, stirred suspension of 1 ml of 90% hydrogen peroxide in 10 ml of methylene chloride and the mixture was stirred until homogeneous and then diluted to 100 ml with methylene chloride. To 35 ml of this solution was added 0.10 g of dihydroacrifoline and 3.0 g of Na_2HPO_4. The mixture was heated under reflux for 16 hours, cooled, and poured into an aqueous solution of sulphur dioxide. After 30 minutes, the aqueous phase was made alkaline with ammonia and extracted several times with chloroform. The chloroform extract was dried over anhydrous sodium sulphate and evaporated under reduced pressure, leaving 0.050 g of colorless oil. This oil formed hydrobromide and perchlorate salts whose infrared spectra were identical with those of the corresponding salts of the product XVII isolated from the oxidation of dihydroacrifoline with copper sulphate.

Reduction of Compound XVII

A solution of the hydrobromide of XVII (0.20 g) and sodium borohydride (0.20 g) in 25 ml of absolute ethanol was heated under reflux for 1 hour. The mixture was cooled and acetone was added to destroy excess sodium borohydride. Water was then added, and the organic solvents removed under reduced pressure. The resulting aqueous mixture was extracted with chloroform, and the dried chloroform extract evaporated under reduced pressure. Crystallization of the residual oil from ether–petroleum ether gave 0.115 g (75%) of product XVIII which melted at 182–183°. This material was sublimed at 0.001 mm and 110° for analysis. It melted at 182–183°. Calc. for $C_{16}H_{25}O_2N$: C, 73.0; H, 9.56; N, 5.32%. Found: C, 73.1; H, 9.75; N, 4.65%.

The infrared spectrum of compound XVIII showed hydroxyl absorption at 3380 cm^{-1},

Can. J. Chem. Downloaded from www.nrcresearchpress.com by 210.87.254.40 on 09/05/12
For personal use only.

no carbonyl absorption, and peaks at 1070 cm^{-1} and 1100 cm^{-1} attributed to ether absorption.

The mother liquor from the separation of the crystalline base was acidified with hydrobromic acid, and yielded 0.040 g (20%) of hydrobromide salt of compound XVIII. The hydrobromide was crystallized twice from methanol–acetone for analysis. It melted above 310°. Calc. for $C_{16}H_{25}O_2N.HBr$: C, 55.8; H, 7.61; N, 4.07%. Found: C, 56.1; H, 7.45; N, 4.45%.

The infrared spectrum showed hydroxyl absorption at 3300 cm^{-1} and ether absorption at 1075 cm^{-1} and 1105 cm^{-1}.

Preparation of the Acetate of XVIII

A solution of 0.030 g of XVIII in the mixed anhydride of trifluoroacetic acid and acetic acid (prepared by mixing 0.10 ml of glacial acetic acid and 0.16 ml of trifluoroacetic anhydride) was allowed to stand overnight at room temperature. The solution was poured into a dilute aqueous ammonia solution, and then extracted with chloroform. The chloroform extract was dried over anhydrous sodium sulphate and evaporated under reduced pressure, leaving a colorless oil which slowly solidified. The solid, compound XX, was sublimed at 75° and 0.001 mm for analysis, and melted at 148–149°. Calc. for $C_{18}H_{27}O_3N$: C, 70.8; H, 8.91; N, 4.59%. Found: C, 71.1; H, 8.75; N, 4.88%.

The infrared spectrum of XX had no hydroxyl absorption but had strong acetate absorption at 1730 cm^{-1} and 1235 cm^{-1}. A strong peak at 1042 cm^{-1} was attributed to ether absorption.

Oxidation of Compound XVIII to XVII with Chromic Acid

A solution of 0.025 g of XVIII in 25 ml of 85% acetic acid–water was cooled to −15°, and treated with 0.10 g of chromic anhydride. The mixture was stirred at −15° for 2 hours, and then for 4 hours at −5°. Methanol was added to destroy excess chromic acid, and the solution allowed to stand overnight in the refrigerator. Water was added and the organic solvents removed under reduced pressure. The resulting aqueous solution was acidified with hydrochloric acid, extracted with ether, made alkaline with ammonia, and extracted with chloroform. The chloroform extract was dried over anhydrous sodium sulphate and evaporated under reduced pressure, leaving a colorless oil. The infrared spectrum of this oil (film) was identical with that of the XVII. The oil yielded 0.028 g (86%) of hydrobromide salt whose infrared spectrum was identical with that of the hydrobromide of the XVII.

Reaction of Compound XVII with Phenyllithium

To a solution of phenyllithium in ether (prepared from 0.10 g of lithium and 1.14 g of bromobenzene in 20 ml of ether) was added 0.202 g of the copper sulphate product XVII in 15 ml of ether. The solution was heated under reflux for 2 hours, allowed to stand overnight, and poured into cold dilute hydrochloric acid. The aqueous solution was extracted several times with ether, made alkaline with ammonia, and extracted with chloroform. The chloroform extract was dried over anhydrous sodium sulphate and evaporated under reduced pressure. The residual pale yellow oil partially solidified but a crystalline product was not obtained in good yield. The base was dissolved in acetone and treated with hydrobromic acid, yielding 0.289 g (89%) of colorless crystals melting above 315°. The salt was crystallized twice from methanol–acetone for analysis. Calc. for $C_{22}H_{29}O_2N.HBr$: C, 62.9; H, 7.19; N, 3.33%. Found: C, 62.9; H, 7.26; N, 3.32%.

The infrared spectrum of this compound had hydroxyl absorption at 3330 cm^{-1}, no

Can. J. Chem. Downloaded from www.nrcresearchpress.com by 210.87.254.40 on 09/05/12
For personal use only.

carbonyl absorption, and weak phenyl absorption at 1600 cm^{-1} and 1500 cm^{-1}. The ultraviolet spectrum showed benzenoid absorption with $\lambda_{max}^{95\%\ EtOH}$ at 2580 Å, $\epsilon = 237$.

ACKNOWLEDGMENTS

We wish to express our thanks to the National Research Council of Canada, and to the Ontario Research Foundation, for financial assistance.

REFERENCES

1. W. N. FRENCH and D. B. MACLEAN. Chem. & Ind. (London), 658 (1960).
2. R. H. F. MANSKE and L. MARION. J. Am. Chem. Soc. 69, 2126 (1947).
3. F. A. L. ANET. Tetrahedron Letters, **20**, 13 (1960).
4. G. S. PERRY and D. B. MACLEAN. Can. J. Chem. **34**, 1189 (1956).
5. W. A. HARRISON. Ph.D. Thesis, McMaster University, Hamilton, Ont. September, 1960.
6. R. N. JONES, A. R. H. COLE, and B. NOLIN. J. Am. Chem. Soc. **74**, 5662 (1952).
7. H. CONROY. Tetrahedron Letters, **10**, 31 (1960).
8. F. A. L. ANET and N. H. KHAN. Chem. & Ind. (London), 1238 (1960).
9. P. T. SPEAKMAN and W. A. WATERS. J. Chem. Soc. 40 (1955).
10. A. Y. DRUMMOND and W. A. WATERS. J. Chem. Soc. 497 (1955).
11. W. F. SAYER and A. DUCKWORTH. J. Am. Chem. Soc. **77**, 188 (1955).
12. W. D. EMMONS and G. B. LUCAS. J. Am. Chem. Soc. **77**, 2287 (1955).
13. A. BERTHO and A. STOLL. Ber. **85**, 663 (1952).
14. O. ACHMATOWICZ and W. RODEWALD. Roczniki Chem. **29**, 509 (1955).

Can. J. Chem. Downloaded from www.nrcresearchpress.com by 210.87.254.40 on 09/05/12
For personal use only.

Can. J. Chem. Downloaded from www.nrcresearchpress.com by 210.87.254.6 on 09/05/12
For personal use only.

PARALYTIC SHELLFISH POISON

VIII. SOME CHEMICAL AND PHYSICAL PROPERTIES OF PURIFIED CLAM AND MUSSEL POISONS[1]

EDWARD J. SCHANTZ, JAMES D. MOLD,[2] WILLIAM L. HOWARD,[3] JOHN P. BOWDEN, D. WARREN STANGER, JOSEPH M. LYNCH, OSKAR P. WINTERSTEINER, JAMES D. DUTCHER, DAVID R. WALTERS, AND BYRON RIEGEL[4]

ABSTRACT

Mild reduction of purified clam and mussel poisons with hydrogen yielded a nontoxic dihydro derivative. The poisons and the dihydro derivative showed no absorption in the ultraviolet but all absorbed in the infrared at 3, 6, and 9 μ. Mild oxidation of the poisons in alkaline solution produced nontoxic products with strong absorption in the ultraviolet. Preliminary studies on oxidation with permanganate or periodate and on hydrolysis with acid yielded only small fragments such as guanidopropionic acid, urea, guanidine, ammonia, and carbon dioxide. Titration of the poisons and the dihydro derivatives showed pK_a values at 8.1 and 11.5. The two poisons appear to be similar in their chemical and physical properties.

The purification of the paralytic poison found in toxic Alaska butter clams (*Saxidomus giganteus*) and in toxic mussels (*Mytilus californianus*), and some properties of these poisons, have been described in previous papers (1, 2, 3). The purified poisons[5] are white hygroscopic solids, very soluble in water and methanol, somewhat soluble in ethanol and glacial acetic acid, and insoluble in lipid solvents. They have a specific rotation of +130° and show no absorption in the ultraviolet above 220 mμ. The toxicity in white mice (Webster strain) is about 5.5×10^6 lethal doses per gram (4). The molecular formula is $C_{10}H_{17}N_7O_4.2HCl$ (molecular weight 372), and the molecule appears to exist in two tautomeric forms. A positive color test is given by both purified poisons with the Jaffe, Benedict–Behre, and Weber reagents, but the Sakaguchi test was negative. Additional physical and chemical properties are presented here to aid in the future elucidation of the structure of the poisons.

Both clam and mussel poisons were easily reduced with hydrogen to produce dihydro derivatives which were nontoxic (2). This reduction proceeded in aqueous neutral, acid, or alkaline solutions in the presence of a platinum catalyst, and under an atmosphere of hydrogen to a maximum uptake of 1 mole of hydrogen for each mole of poison. The loss of toxicity paralleled the hydrogen uptake and when 1 mole of hydrogen was consumed, 98% of the toxicity had disappeared. This relatively simple change in chemical structure resulting in almost complete loss of toxicity has been of considerable interest in studying many properties of the poison relating to structure and toxicity. The Benedict–Behre and Jaffe tests became negative upon reduction of the poisons whereas the Sakaguchi test remained negative and the Weber test remained positive. The application of these tests to the poison and the various derivatives has been described previously (2).

The infrared spectra of the poisons and the dihydro derivative are given in Fig. 1.

[1]*Manuscript received May 8, 1961.*
Contribution from the Chemical Corps Biological Laboratories, Fort Detrick, Md.; the Chemical Laboratory of Northwestern University, Evanston, Ill.; and the Squibb Institute for Medical Research, New Brunswick, N.J. The work performed in these laboratories was carried out under contract with the Chemical Corps.
[2]*Present address: Research Laboratory, Liggett and Myers Tobacco Co., Durham, North Carolina.*
[3]*Present address: 411 Poinsettia, Lake Jackson, Texas.*
[4]*Present address: G. D. Searle and Co., P.O. Box 5110, Chicago 80, Illinois.*
[5]*Countercurrent distribution studies have indicated that the preparations described as purified poison represent a single component to the extent of 95 to 98%.*

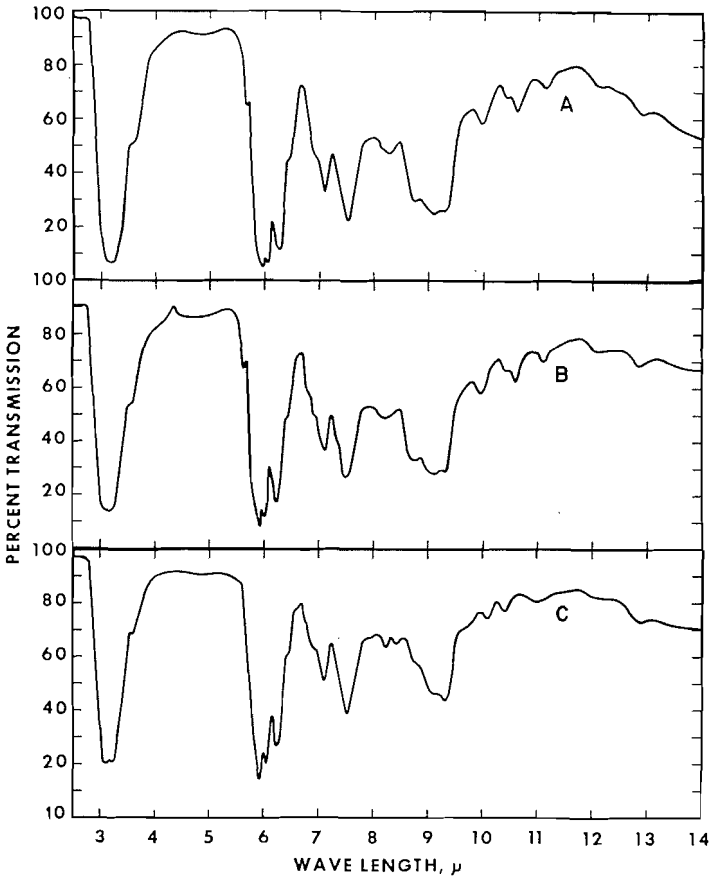


FIG. 1. Infrared spectra of (A) clam poison dihydrochloride, (B) mussel poison dihydrochloride, and (C) dihydro clam poison dihydrochloride.

The spectra for the two poisons are very similar and agree well with spectra obtained recently by Casselman *et al.* (3). The dihydro derivative showed some loss of absorption at 5.65 and 8.75 mμ.

No ultraviolet absorption above 220 mμ was observed for the poisons or for the dihydro derivatives. However, in alkaline solutions exposed to air, the poisons developed absorption maxima at 235 and 333 which reached maximum molecular extinctions of about 7000 at 235 mμ and about 5200 at 333 mμ. Under anaerobic conditions no maxima developed, which indicated that the absorption was brought about by an alkaline oxidation. Maximum extinction was reached and all toxicity disappeared when approximately 1 mole of oxygen was taken up per mole of poison (Fig. 2). The dihydro derivative did not take up oxygen in alkaline solution.

The specific rotation of both poisons (+130°) was affected by the presence of alkali, and under aerobic conditions there was a gradual decrease in the specific rotation to zero as the maximum extinctions at 235 and 333 were reached. Reduction of the poison with hydrogen did not change the rotation but eliminated the tautomeric forms.

Titration of the poisons in glacial acetic acid solution with perchloric acid and titration in aqueous solution with acid and alkali established that two base functions are present

Can. J. Chem. Downloaded from www.nrcresearchpress.com by 210.87.254.6 on 09/05/12
For personal use only.

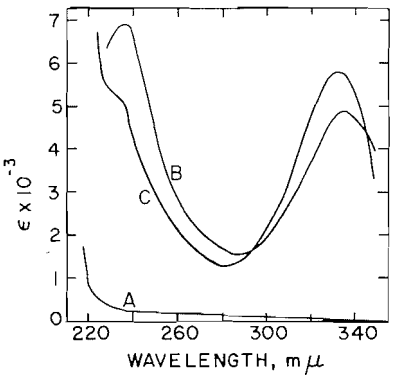


FIG. 2. Ultraviolet absorption spectra of (A) clam poison dihydrochloride, (B) alkaline oxidation product of clam poison in 0.25 *N* barium hydroxide, and (C) alkaline oxidation product of clam poison in acid solution, pH 1.

in equivalent amounts, pK_a 8.1 and ca. 11.5 (Fig. 3). No strong acidic group was found. Aqueous titration of the dihydro compounds from clam and mussel poisons gave results similar to those described for the poisons (pK_a 8.3 and ca. 11.5).

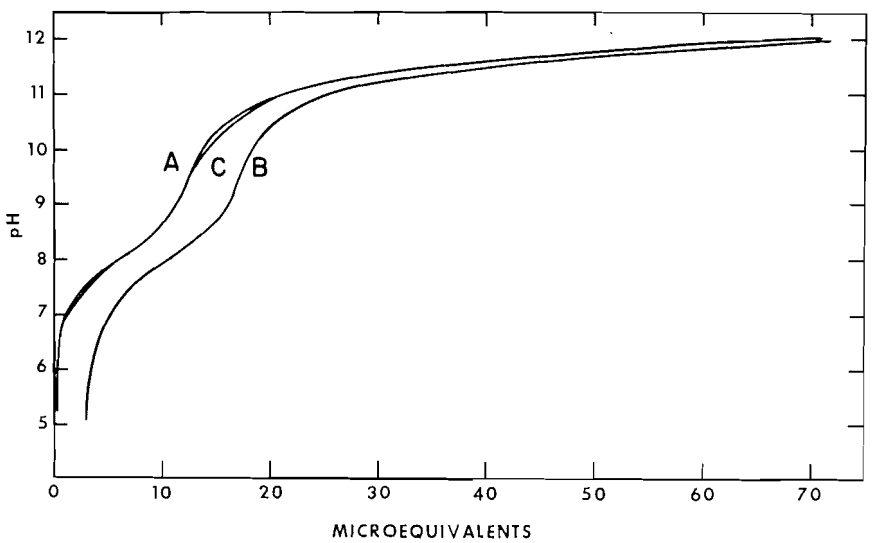


FIG. 3. Titration of clam poison dihydrochloride: (A) initial titration with 0.427 *N* barium hydroxide; (B) back-titration of (A) with 0.479 *N* sulphuric acid following aging at high pH; (C) second titration of (B) with 0.427 *N* barium hydroxide after evaporation from acid.

Preliminary studies on more drastic oxidation of the poisons with periodic acid or potassium permanganate have resulted in the isolation of guanidopropionic acid, urea, carbon dioxide, and ammonia, along with some unidentified products. No success was attained in isolating degradation products, from either the mild or strong oxidations, which represented a sufficiently large portion of the molecule to be of value in determining the chemical structure. Two moles of periodate were consumed very rapidly when the reaction was carried out at pH values between 5 and 13; a third mole was consumed within 24 hours and a fourth after 23 days. Each micromole of poison reduced

Can. J. Chem. Downloaded from www.nrcresearchpress.com by 210.87.254.6 on 09/05/12
For personal use only.

17 equivalents of permanganate in 5 minutes at 75° C. Hydrolysis of the dihydro poisons in 12 *N* hydrochloric acid yielded guanidine. Sakaguchi-positive substances were found among the products of oxidation and hydrolysis. The Benedict–Behre and Jaffe tests became negative.

In summary, it is apparent that both reduction with hydrogen or oxidation under aerobic conditions in alkaline solution resulted in the loss of an unsaturated bond essential for toxicity. In the first case it has been demonstrated by countercurrent studies (2) and by studies reported herein that a dihydro derivative of the poison was formed upon reduction. Secondly, no oxygen uptake was apparent for the dihydro derivative, under the conditions described for the mild oxidation of the poison. In addition, the Benedict–Behre and Jaffe tests, which are positive for the poison and negative for the dihydro derivative, were found to be negative for the oxidized poison. Both reduction and oxidation destroyed toxicity. Theoretically only $\frac{1}{2}$ mole of oxygen would be required to bridge a double bond. Because the complete destruction of toxicity required the uptake of 1 mole of oxygen per mole of poison and because the reduced poison took up no oxygen, it is assumed that the oxidation is initiated at the unsaturated bond and that other reactions concurrent with the loss of this bond are taking place. The fact that changes occurred in the ultraviolet absorption and in the optical rotation upon mild oxidation of the poison supports this assumption.

Because reduction of the poison did not change the optical rotation, it appears likely that this unsaturated bond, which is essential to the toxic structure, is not involved in the structure at the optical center.

The strongly basic group would indicate the possibility of an amine or a quaternary ammonium base. However, studies on the alkylation of the poisons gave no evidence for such structures. The absence of an acidic group precludes the existence of a betaine-type base.

The ultraviolet and infrared spectra indicate no aromatic structures, conjugate unsaturation, or isolated carbonyl groups but the elemental ratios require that ring structures be present. Analysis of mussel poison for alkoxyl, alkimide, and C-methyl groups showed the groups to be absent. The Kjeldahl procedure converts all nitrogen to ammonia, which indicates no nitrogen-to-nitrogen bonds. Some of the nitrogen atoms, therefore, must be in heterocyclic structures involving a guanidine group in the cycle to account for the strong basicity of the poison in conjunction with the negative Sakaguchi test. The fact that Sakaguchi-positive compounds are formed upon oxidation or hydrolysis of the poison supports the above indications.

EXPERIMENTAL

Catalytic Hydrogenation of Clam and Mussel Poisons

The catalytic hydrogenation of clam and mussel poisons was carried out in a Warburg respirometer by a procedure similar to that described by Umbreit (5). Platinum black, prepared from platinum dioxide, and platinum black absorbed on charcoal were both effective in catalyzing this reduction in neutral, acid, or alkaline aqueous solutions.

In a typical experiment, platinum black was suspended in 2.0 ml of 0.1 *M* hydrochloric acid in the annulus of a Warburg flask, and 0.40 ml of clam poison dihydrochloride solution (2.50 mg/ml) was placed in the side arm. After the apparatus was gassed with purified hydrogen, the flask was equilibrated at 30°, and the poison solution was tipped into the catalyst. After 440 minutes, the uptake of hydrogen had ceased at 2.65 μmoles, equivalent to 0.95 moles of hydrogen per mole of poison. Four samples of clam poison

Can. J. Chem. Downloaded from www.nrcresearchpress.com by 210.87.254.6 on 09/05/12
For personal use only.

had an average uptake of 1.03 moles of hydrogen per mole of poison (range, 0.95–1.16), and eleven samples of mussel poison gave an average of 1.02 moles (range, 0.88–1.25).

An aliquot of a solution of the reduction products from clam poison dihydrochloride (240 μg) was tested for ammonia with the Nessler reagent. A negative reaction was obtained, indicating less than 5 μg of ammonia nitrogen. Countercurrent distribution studies on the reduced poison showed that only one component was produced during the reduction (2). The diffusion coefficient determined in the Northrup diffusion cell was 4.6×10^{-6} cm^2 sec^{-1}, which is similar to that of the poison and therefore indicates a similar molecular weight. The neutralization equivalent was 188, and two titratable groups indicate a molecular weight of 376. Anal. Calc. for $C_{10}H_{21}N_7O_4Cl_2$: C, 32.06; H, 5.66; N, 26.2; O, 17.1; Cl, 18.95%. Found: C, 32.3; H, 5.4; N, 26.3; O (direct), 16.97%.

Infrared Absorption Spectra[6]

The infrared absorption spectra were determined for films, dried from aqueous solutions on polished plates of silver chloride, of the test substance. In order to obtain spectra with a minimum amount of material, the plates were masked with Parafilm (Menasha Products Co., Menasha, Wis.) to reduce the area over which the solution was deposited. Spectra were observed with a Perkin–Elmer Model 12 C spectrophotometer and the results are illustrated in Fig. 1. Comparable spectra were obtained for films of the poison on KRS-5 (potassium thallium bromide), for films deposited from ethyl alcohol solution on sodium chloride,[7] and for pellets with potassium bromide.[8]

Ultraviolet Absorption

All measurements of the ultraviolet spectrum were made in aqueous acid solution (pH 3 to 5) of the poisons in a Model DU Beckman spectrophotometer or a Cary Model 14 spectrophotometer. In special cases when the absorption spectra were measured during the process of alkaline oxidation, small samples were withdrawn from the alkaline reaction flask and measured at the pH of the reaction mixture. The spectra of the poison under various conditions are shown in Fig. 2.

Optical Rotation

Measurements of the optical rotation were made with a Rudolph and Sons No. 80 polarimeter and a sodium-vapor lamp. Normally the measurements were made on aqueous acid (pH 3 to 5) solutions of the poisons in 2-dm tubes. In cases where the rotation was measured during the process of alkaline oxidation, samples were withdrawn from the alkaline reaction flask for each measurement. Where measurements were made under anaerobic conditions the poison solution was kept in the tightly sealed polarimeter tube during the entire period of observation.

Alkaline Oxidation of the Clam Poison

A mixture of 0.5 ml of clam poison solution (4.31 mg/ml; 0.0132 *M*; pH 1.5) and 9.5 ml of 1 *N* sodium hydroxide was allowed to stand in a stoppered flask (no attempt was made initially to exclude oxygen) at room temperature. The solution slowly took on a yellow color, and the formation of the alkaline oxidation product was conveniently

[6]*The spectra were observed by Mr. Edward Weneck except where noted.*

[7]*These spectra were determined by Dr. Robert C. Gore, Stamford Research Laboratories, American Cyanamid Co.*

[8]*The spectra were observed with a Beckman IR2T recording spectrophotometer. U. Schiedt and H. Reinwein. Z. Naturforsch. Part b,* **7b**, *270 (1952); M. M. Stimson and M. J. O'Donnell. J. Am. Chem. Soc.* **74**, *1805 (1952); Perkin–Elmer Instrumental News,* **4**, *No. 3 (1953).*

Can. J. Chem. Downloaded from www.nrcresearchpress.com by 210.87.254.6 on 09/05/12
For personal use only.

followed by periodically determining the intensity of ultraviolet absorption at 333 mμ. Maximum absorption ($\epsilon = 5210$) was observed after 4 days. In 0.5 *N* or 0.25 *N* solutions of either sodium or barium hydroxide, 6 days were required for complete reaction, while in 7.5 *N* ammonium hydroxide, the molecular extinction at 333 mμ was only 1500 (30% of maximum) after the same period of time.

When carbon-dioxide-free air was bubbled through 4.0 ml of barium hydroxide solution containing 3.78 mg of clam poison the maximum extinction ($\epsilon = 5090$) was reached in only 9 hours.

The quantitative oxygen uptake involved in the alkaline oxidation reaction was determined by use of the Warburg apparatus. In the bottom of each Warburg flask was placed 0.8 ml of poison solution (4.85 mg/ml), and the side arm contained 0.8 ml of 0.5 *N* barium hydroxide. The center cup contained 0.2 ml of 0.2 *N* sulphuric acid to absorb any ammonia evolved during the reaction. After the flasks had been attached to the individual manometers, they were placed in a water bath maintained at 21°. When the flasks were fully equilibrated, the reaction was started by spilling the contents of the side arm into the bottom of each flask. As the flask was shaken the change in pressure was recorded periodically until the manometric readings remained constant. The results of 12 such determinations showed an average of 0.96 mole of oxygen consumed per mole of poison.

Potentiometric Titrations

Titrations of the poisons and their dihydro derivatives were performed with distilled-water solutions in a 10-ml beaker fitted with a cover provided with holes for the insertion of the glass electrode (No. 290) and calomel electrode (No. 270) of a Beckman pH meter (Model G), a microburette (Gilmont Combination Micro Pipet-Buret, Emil Greiner Co., New York, N.Y.), and a gas delivery tube. Dissolved carbon dioxide was removed from the titration solutions by thoroughly flushing with nitrogen prior to the insertion of the burette. The nitrogen was freed from acidic or basic contaminants by scrubbing with dilute alkali and acid. During the titration, the solution was magnetically stirred and maintained under a stream of the purified nitrogen. Increments of 0.4–0.5 *N* acid or base were added to produce changes in pH of about 0.1–0.2 units. No electrode corrections were applied to the readings taken at high pH because sodium and potassium ions were absent. The temperature of the room varied from 24–25° during the titrations, and no other temperature control was attempted. Values of pK_a were estimated from the data obtained after applying corrections for a distilled water blank.

Titration of Clam Poison Dihydrochloride

A 3.36-ml sample of an aqueous solution containing 4.79 mg of clam poison dihydrochloride was measured into the titration cell. Titration of the sample to pH 12.02 was completed in 24 minutes and required 0.170 ml of 0.427 *N* barium hydroxide. The burette was removed, and the solution was allowed to stand under nitrogen, without stirring, for 2 hours. There was no evidence of a precipitate, indicating that the exclusion of carbon dioxide was complete. A second burette was inserted and the solution was back-titrated with 0.479 *N* sulphuric acid. The final pH of 5.05 was attained in 26 minutes and required 0.145 ml of the reagent. After filtration and lyophilization, the product was dissolved in 5 ml of 0.01 *N* hydrochloric acid and slowly evaporated to dryness (24–48 hours) at room temperature in a vacuum desiccator over potassium hydroxide and phosphoric anhydride. This residue was redissolved in 3.36 ml of water and titrated with 0.168 ml of the standard barium hydroxide to pH 12.02 as described

Can. J. Chem. Downloaded from www.nrcresearchpress.com by 210.87.254.6 on 09/05/12
For personal use only.

above. The titration curves are shown in Fig. 3. After again being aged for $2\frac{1}{2}$ hours, the solution was back-titrated with 0.147 ml of the standard acid to pH 4.3. Bioassay of the final solution indicated that 74% of the original toxicity was still present.

Titration of Mussel Poison Dihydrochloride

A 3.27-ml sample of an aqueous solution containing 5.04 mg of mussel poison dihydrochloride was weighed into the titration cell and titrated in the same manner as above. The results were similar to those obtained for clam poison and are illustrated in Fig. 3.

Titration of Dihydro Mussel Poison Dihydrochloride

A sample of dihydro mussel poison dihydrochloride (5.1 mg) was dissolved in 2.0 ml of water and titrated as described above with 0.200 ml of 0.427 *N* barium hydroxide to pH 12.01. The results were similar to those for clam and mussel poisons.

Nonaqueous Titrations

These titrations were carried out with 5-mg samples of clam and mussel poisons according to the procedure given by Seaman and Allen (6) and by Pifer and Wollish (7).

ACKNOWLEDGMENTS

The authors wish to acknowledge the assistance of Dr. Herbert E. Carter and his co-workers, Drs. M. P. Gordon, W. H. Tallent, and G. Inglett, at the University of Illinois, Urbana, Illinois, and the assistance of Drs. R. K. Summerbell, A. S. Hussey, R. L. Letsinger, and H. W. Sause at Northwestern University, Evanston, Illinois.

REFERENCES

1. E. J. Schantz, J. D. Mold, D. W. Stanger, J. Shavel, F. J. Riel, J. P. Bowden, J. M. Lynch, R. S. Wyler, B. Riegel, and H. Sommer. J. Am. Chem. Soc. **79**, 5230 (1957).
2. J. D. Mold, J. P. Bowden, D. W. Stanger, J. E. Maurer, J. M. Lynch, R. S. Wyler, E. J. Schantz, and B. Riegel. J. Am. Chem. Soc. **79**, 5235 (1957).
3. A. A. Casselman, R. Greenhalgh, H. H. Brownell, and R. A. B. Bannard. Can. J. Chem. **38**, 1277 (1960).
4. E. J. Schantz, E. F. McFarren, M. L. Schafer, and K. H. Lewis. J. Assoc. Offic. Agr. Chemists, **41**, 160 (1958).
5. W. W. Umbreit, R. H. Burris, and J. F. Stauffer. Manometric techniques and tissue metabolism. Burgess Publishing Co., Minneapolis, Minn. 1949. p. 86.
6. W. Seaman and E. Allen. Anal. Chem. **23**, 592 (1951).
7. C. W. Pifer and E. G. Wollish. Anal. Chem. **24**, 300 (1952).

Can. J. Chem. Downloaded from www.nrcresearchpress.com by 210.87.254.6 on 09/05/12
For personal use only.

Can. J. Chem. Downloaded from www.nrcresearchpress.com by 210.87.254.5 on 09/05/12
For personal use only.

NOTES

THE MOLECULAR STRUCTURE OF (−)-N-METHYL-GELSEMICINE HYDRIODIDE, $C_{21}H_{29}O_4N_2I$*

MARIA PRZYBYLSKA AND LÉO MARION

Gelsemicine ($C_{20}H_{26}O_4N_2$), one of the minor alkaloids of *Gelsemium sempervirens* Ait., was discovered by Chou in 1931 (1). It is a monoacidic base which forms a non-basic monobenzoyl derivative so that its basic nitrogen is secondary, a conclusion confirmed by treatment of the base with methyl iodide which gives rise to N-methyl-gelsemicine hydriodide. On hydrogenation over Adams' catalyst, the alkaloid absorbs 3 moles of hydrogen (2) and a comparison of its infrared absorption spectrum with that of its reduction product shows that it must contain a benzene ring since the absorption bands characteristic of that group are no longer present in the spectrum of the reduction product (3). Furthermore, gelsemicine contains two methoxyl groups, and its infrared absorption spectrum contains an absorption band indicative of a carbonyl group (3). It carries a substituent on one of the nitrogens which has been assumed previously to be a methyl group. This sums up the chemical knowledge concerning the alkaloid.

There are two monoclinic forms of N-methyl-gelsemicine hydriodide, one of space group $P2_1$ with two molecules per asymmetric unit and another which crystallizes in space group $C2$ with one molecule per asymmetric unit. The latter compound was chosen for a detailed X-ray analysis. Its unit-cell dimensions are: $a = 16.75$, $b = 9.52$, $c = 14.06$ Å; $\beta = 90°13'$; and $z = 4$.

A total of 2800 reflections were measured and they amounted to 67% of those theoretically available with Cu radiation. The x and z co-ordinates of the iodine atom were derived from two-dimensional Patterson syntheses. After an assumption that the iodine atom lies at $y = \frac{1}{2}$ was made, a three-dimensional Fourier synthesis was evaluated using the phases based only on the iodine atom contributions. The electron-density maps had the symmetry of space group $C2/m$ and the real peaks of the structure were accompanied by mirror-image peaks related to them by planes of symmetry at $y = 0$ and $\frac{1}{2}$. In spite of this difficulty it was possible to locate 22 light atoms of the molecule. Several cycles of refinement using three-dimensional data led gradually to complete solution of the structure. Making use of the anomalous dispersion effects of Cu Kα radiation caused by the iodine atom, it was possible to determine the absolute configuration of this laevorotatory isomer. It is represented by the schematic drawing and the photograph of the molecular model (Fig. 1). The two nitrogen atoms were identified indirectly: that the methyl group is attached to one of them was taken into account, and the position of the second one was considered as established as soon as the oxindole nucleus was recognized (3).

The oxygen atoms were indicated by ρ_o and $(\rho_o - \rho_c)$ maps. Their location was further substantiated by the values of bond lengths, which are in good agreement with the nominal bond lengths.

The reliability factor, R, for all three-dimensional data is 0.16, whereas for the two zones ($h0l$) and ($0kl$), it is 0.16 and 0.10 respectively. The R factor for the centrosymmetric ($h0l$) zone is expected to be higher than for the non-centrosymmetric ($0kl$) data (4).

*Issued as N.R.C. No. 6470.

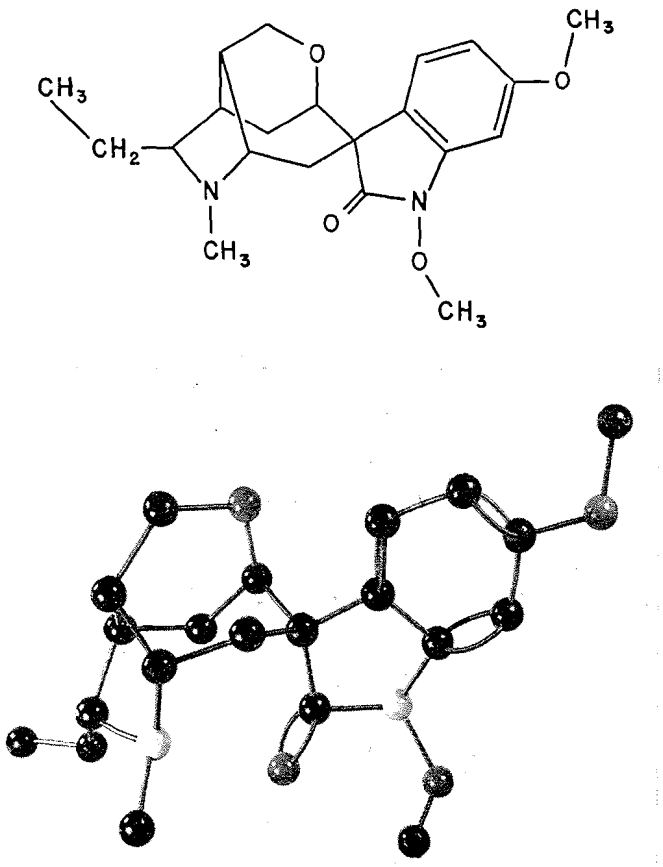


FIG. 1. Molecular model of (−)-N-methyl-gelsemicine.

A full account of this work will be published at a later date.

On comparison of the skeleton of N-methyl-gelsemicine and gelsemine (5) we find that they are very similar, but the skeleton of N-methyl-gelsemicine has one carbon atom less which leads to a somewhat simplified structure.

One unusual feature that deserves comment is the presence of a methoxyl group linked to the oxindole nitrogen. It has been shown chemically that the molecule of gelsemicine contains two methoxyl groups. The base forms salts which are normal and not of the anhydronium type as shown by their infrared spectra and by the recovery from these salts of the intact base still containing two methoxyl groups. Hence, the two-atom group attached to the carbon next to the basic nitrogen cannot be a methoxyl group.

The distance between the nitrogen ion $\begin{array}{l}\diagdown\\ \diagup\end{array}\!\!\overset{+}{\underset{|}{\text{N}}}\!\!-\text{H}$ (with CH_3 on the nitrogen) and the oxygen of the carbonyl group in N-methyl-gelsemicine hydriodide is 2.77 Å. Since the hydrogen atom attached to the nitrogen is directed towards the oxygen atom, an intramolecular hydrogen-bond formation is indicated. Additional evidence is supplied by the infrared absorption spectrum, Fig. 2,

Can. J. Chem. Downloaded from www.nrcresearchpress.com by 210.87.254.5 on 09/05/12
For personal use only.

Can. J. Chem. Downloaded from www.nrcresearchpress.com by 210.87.254.5 on 09/05/12
For personal use only.

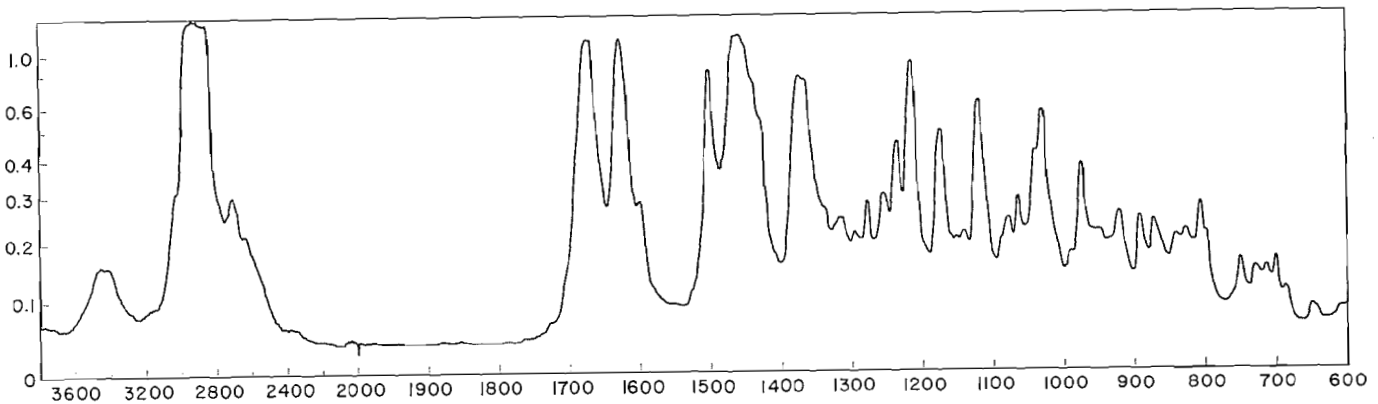


FIG. 2. Infrared absorption spectrum of N-methyl-gelsemicine hydriodide in Nujol mull.

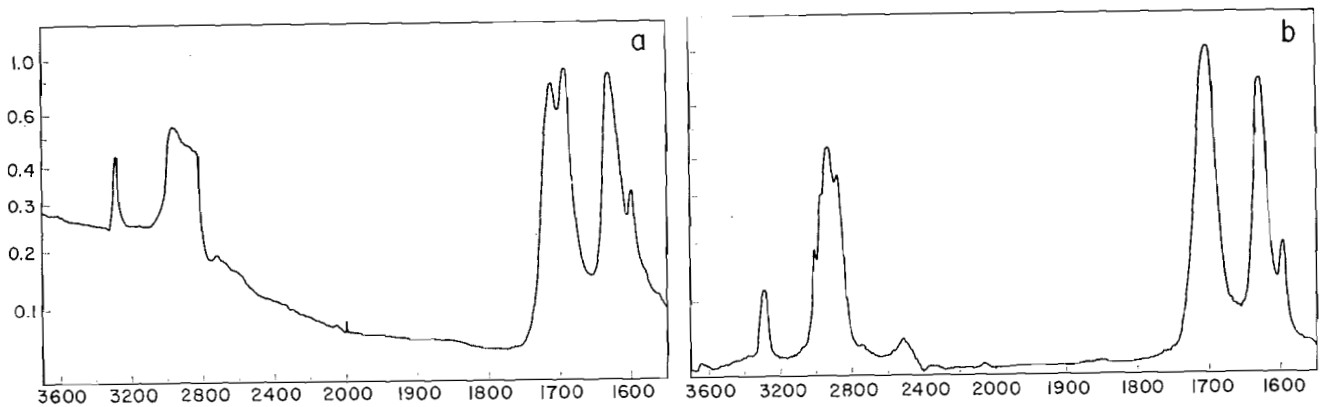


FIG. 3. Infrared spectra of gelsemicine: (*a*) in Nujol mull; (*b*) in chloroform solution.

which shows a markedly broadened band at ~3340 cm^{-1} and a considerable shift in the absorption of the carbonyl band, with a maximum at 1674 cm^{-1}.

It is of interest that the infrared spectrum of gelsemicine itself in Nujol mull shows a double peak in the carbonyl region, whereas a single maximum is obtained in chloroform solution (Fig. 3). It seems that the C=O group, only in some, but not all molecules of the crystalline gelsemicine, is involved in the hydrogen-bond formation. The C=O bond in the spectrum in chloroform solution lies between the position of the two peaks of the Nujol mull spectrum and this indicates that the C=O groups of all the molecules may be involved in H bonding with the C—H group of chloroform. Although crystalline gelsemicine itself has not been X-ray analyzed, some support to this explanation is given by the fact that in gelsemicine hydrobromide hemihydrate, N-methyl-gelsemicine hydrobromide tetrahydrate (6), and also in N-methyl-gelsemicine hydriodide of space group $P2_1$, the asymmetric unit was found to consist of two molecules which are, therefore, crystallographically not equivalent. This tendency of the compound to crystallize in pairs of molecules may well be due to the shape of its skeleton which contains a large planar oxindole group. In this connection, it is noteworthy that the infrared spectrum of dihydrogelsemine in chloroform also shows a single peak in the carbonyl region, although in a mull, a double peak is obtained.

ACKNOWLEDGMENTS

Grateful acknowledgment is made to Dr. F. R. Ahmed for computational assistance and invaluable discussions, and to Dr. S. McLean for the preparation of authenticated, pure crystals of the salt. Thanks are also due to Mrs. C. Mackey for her help in computing and preparing the X-ray data, and to Mr. R. Lauzon for the infrared absorption spectra.

1. T. Q. Chou. Chinese J. Physiol. **5**, 131 (1931); Chem. Abstr. **25**, 4085 (1931).
2. W. G. C. Forsyth, S. F. Marrian, and T. S. Stevens. J. Chem. Soc. 579 (1945).
3. H. Schwarz and L. Marion. Can. J. Chem. **31**, 958 (1953).
4. D. C. Phillips, D. Rogers, and A. J. C. Wilson. Acta Cryst. **3**, 398 (1950).
5. F. M. Lovell, R. Pepinsky, and A. J. C. Wilson. Tetrahedron Letters, 4, 1 (1959).
6. M. Przybylska. Acta Cryst. **14**, 694 (1961).

Received June 29, 1961.
Division of Pure Chemistry,
National Research Council,
Ottawa, Canada.

THE CLEAVAGE OF ETHERS BY *t*-BUTYLMAGNESIUM BROMIDE AND COBALTOUS CHLORIDE[1]

E. Eisenbraun[2] and C. B. Purves

In connection with attempts to break ether bonds in wood lignins by mild methods, the effect of the above Grignard – cobaltous chloride reagent on 2-methoxydiphenyl ether was briefly studied. Kharasch and Huang (1) discovered that the addition of anhydrous cobaltous chloride enabled a Grignard reagent to cleave many diaryl and benzyl aryl ethers to a mixture of the corresponding hydrocarbon and phenol in 3 to 4

[1]*Financed in part from a National Research Council of Canada grant.*
[2]*Holder of a Union Carbide Corporation (Visking Division) Fellowship in 1958–59. Present address: Arnold Hoffman and Company, Incorporated, Providence, Rhode Island, U.S.A.*

Can. J. Chem. Downloaded from www.nrcresearchpress.com by 210.87.254.5 on 09/05/12
For personal use only.

which shows a markedly broadened band at ~3340 cm^{-1} and a considerable shift in the absorption of the carbonyl band, with a maximum at 1674 cm^{-1}.

It is of interest that the infrared spectrum of gelsemicine itself in Nujol mull shows a double peak in the carbonyl region, whereas a single maximum is obtained in chloroform solution (Fig. 3). It seems that the C=O group, only in some, but not all molecules of the crystalline gelsemicine, is involved in the hydrogen-bond formation. The C=O bond in the spectrum in chloroform solution lies between the position of the two peaks of the Nujol mull spectrum and this indicates that the C=O groups of all the molecules may be involved in H bonding with the C—H group of chloroform. Although crystalline gelsemicine itself has not been X-ray analyzed, some support to this explanation is given by the fact that in gelsemicine hydrobromide hemihydrate, N-methyl-gelsemicine hydrobromide tetrahydrate (6), and also in N-methyl-gelsemicine hydriodide of space group $P2_1$, the asymmetric unit was found to consist of two molecules which are, therefore, crystallographically not equivalent. This tendency of the compound to crystallize in pairs of molecules may well be due to the shape of its skeleton which contains a large planar oxindole group. In this connection, it is noteworthy that the infrared spectrum of dihydrogelsemine in chloroform also shows a single peak in the carbonyl region, although in a mull, a double peak is obtained.

ACKNOWLEDGMENTS

Grateful acknowledgment is made to Dr. F. R. Ahmed for computational assistance and invaluable discussions, and to Dr. S. McLean for the preparation of authenticated, pure crystals of the salt. Thanks are also due to Mrs. C. Mackey for her help in computing and preparing the X-ray data, and to Mr. R. Lauzon for the infrared absorption spectra.

1. T. Q. Chou. Chinese J. Physiol. **5**, 131 (1931); Chem. Abstr. **25**, 4085 (1931).
2. W. G. C. Forsyth, S. F. Marrian, and T. S. Stevens. J. Chem. Soc. 579 (1945).
3. H. Schwarz and L. Marion. Can. J. Chem. **31**, 958 (1953).
4. D. C. Phillips, D. Rogers, and A. J. C. Wilson. Acta Cryst. **3**, 398 (1950).
5. F. M. Lovell, R. Pepinsky, and A. J. C. Wilson. Tetrahedron Letters, 4, 1 (1959).
6. M. Przybylska. Acta Cryst. **14**, 694 (1961).

Received June 29, 1961.
Division of Pure Chemistry,
National Research Council,
Ottawa, Canada.

THE CLEAVAGE OF ETHERS BY *t*-BUTYLMAGNESIUM BROMIDE AND COBALTOUS CHLORIDE[1]

E. Eisenbraun[2] and C. B. Purves

In connection with attempts to break ether bonds in wood lignins by mild methods, the effect of the above Grignard – cobaltous chloride reagent on 2-methoxydiphenyl ether was briefly studied. Kharasch and Huang (1) discovered that the addition of anhydrous cobaltous chloride enabled a Grignard reagent to cleave many diaryl and benzyl aryl ethers to a mixture of the corresponding hydrocarbon and phenol in 3 to 4

[1]*Financed in part from a National Research Council of Canada grant.*
[2]*Holder of a Union Carbide Corporation (Visking Division) Fellowship in 1958–59. Present address: Arnold Hoffman and Company, Incorporated, Providence, Rhode Island, U.S.A.*

Can. J. Chem. Downloaded from www.nrcresearchpress.com by 210.87.254.42 on 09/05/12
For personal use only.

hours at 36°, instead of in 15 to 18 hours at 180–200°. No scission of methyl phenyl and ethyl phenyl ethers was observed. *n*-Butylmagnesium bromide was effective (1, 2), but Tomita and Watanabe (3) found that the yield of cleavage products was somewhat greater when the tertiary isomer was used; the replacement of diethyl ether by tetrahydrofuran as the solvent increased the yield threefold.

On the present occasion, eight experiments with 2-methoxydiphenyl ether were carried out, the Grignard reagent being made from either *n*-butyl or *t*-butyl bromide, and the solvent being ether or tetrahydrofuran. The best result was obtained with *t*-butylmagnesium bromide in tetrahydrofuran. With a 30-fold molar excess, 36% of the original substance was recovered unchanged together with 35% of phenols, corresponding to a degree of cleavage of about 60%. This yield corresponded closely to the value of 62% obtained by Tomita and Watanabe (3) for the same compound. Both guaiacol and phenol were isolated as the pure, crystalline benzoates, and cleavage therefore occurred on both sides of the diphenyl ether oxygen atom, in agreement with the work of Kharasch and Huang (1). Tomita and Watanabe (3) thought that this ether oxygen atom was completely retained by the guaiacol (benzene presumably was the only other product), but an attempt to repeat their isolation of the guaiacol as the *p*-nitrobenzoate gave a crystalline product which probably contained some of the phenol derivative. Fruitless attempts were also made to detect catechol, by paper chromatography, among the products, and this negative result agreed with the claim that methyl phenyl ether groups were not affected by the reagent.

t-Butylmagnesium bromide – cobaltous chloride, when warmed with a suspension of fully methylated spruce formaldehyde periodate lignin (4) in tetrahydrofuran, produced 2% of phenolic material which resinified too rapidly to be examined in detail, together with a little neutral, high-boiling oil. There was no clear evidence that any cleavage of ether groups occurred in this lignin. When the experiment was repeated with fully methylated spruce periodate lignin, the resulting 4% of ether-soluble material probably contained guaiacol, and the 90% of residual lignin increased in methoxyl content from 17.2 to 18.5% on remethylation with diazomethane. In this case, about 0.7% of phenolic groups might have been liberated by cleavage.

EXPERIMENTAL

Materials

Tetrahydrofuran, boiling correctly at 76°, was used not more than 2 days after purification by distillation in succession from solid sodium hydroxide, metallic sodium, and lithium aluminum hydride. The Grignard reagent was made from pure *t*-butyl bromide and dry, polished magnesium ribbon (5, 6); the use of powdered crystals of sublimed magnesium, obtained through the courtesy of Dow Chemical Company of Canada, yielded a particularly clear, colorless reagent (7). Dilution of an aliquot with a known volume of standard acid, and a back titration with standard alkali to a phenolphthalein end point (8), established the molarity of the reagent. The yield amounted to 50% of the magnesium when tetrahydrofuran was the solvent, whereas the reported yield was 33% (6).

A published method (9) of preparing anhydrous cobaltous chloride was modified by heating the pure hexahydrate for 2 days at 45° and 20 mm pressure, and then gradually raising the temperature to 220° (1 mm). The light pink of the partly dehydrated product changed through dark blue to the pale blue color of the anhydrous salt, which was

Can. J. Chem. Downloaded from www.nrcresearchpress.com by 210.87.254.42 on 09/05/12
For personal use only.

extremely finely divided. Ullmann and Stein's method (10) was used to synthesize 2-methoxydiphenyl ether, which was recrystallized from hexane and redistilled under diminished pressure; m.p. 76°, the recorded value being 78°.

Cleavage of 2-Methoxydiphenyl Ether

The apparatus consisted of a three-necked flask equipped with ground-glass joints, a magnetic stirrer, a reflux condenser, leads for dry nitrogen gas, and an L-shaped tube, revolving in a ground-glass joint, for the addition of the anhydrous cobaltous chloride. This tube could be warmed externally to prevent the condensation of solvent, which made the finely divided chloride sticky. A solution of 0.098 mole of *t*-butylmagnesium bromide in tetrahydrofuran was filtered through dry glass wool into the flask, the volume plus rinsings being 80 ml. After 1.3 g (6.5 mmoles) of 2-methoxydiphenyl ether had been added, the apparatus was flushed with nitrogen, and solution was completed by gentle heating and stirring. The cobaltous chloride, 4.68 g (36 mmoles), was then added from the L tube in 12 successive portions at 15-minute intervals, after which the mixture was heated for 3 hours under reflux.

The mixture was acidified near 0° with 4 *N* hydrochloric acid and thoroughly extracted with ether, and the extract was re-extracted with 5% aqueous sodium hydroxide (1). A neutral fraction, 0.50 g, isolated from the ether, yielded 0.375 g (29%) of twice-recrystallized 2-methoxydiphenyl ether with the correct melting point and mixed melting point. Benzoylation (5) of the product extracted by the alkali, 0.50 g, yielded 0.72 g of crystals, m.p. 51–56°, which on recrystallization from ethanol produced 0.45 g of guaiacol benzoate, m.p. 57–58°, and mixed m.p. 56–58°. Evaporation of the ethanol mother liquors left a gum which on standing deposited 0.07 g (0.35 mmole) or 5% of crystals melting at 63–66°, increased to m.p. 69° by recrystallization. Authentic phenyl benzoate had this melting point, and a mixed melting point with the crystals was not depressed. A further 0.08 g of pure guaiacol benzoate, isolated from the final mother liquors, brought the total yield of this product to 2.3 mmoles or to 35% of theory. Since a control benzoylation of pure guaiacol gave only a 50% yield of the pure, recrystallized benzoate, the yield of guaiacol actually produced in the cleavage was probably near 70%.

In another experiment, a small portion of the alkali-soluble product from the scission of 1.04 g (5.2 mmoles) of 2-methoxydiphenyl ether was chromatographed on paper for 20 hours with butanol – 2% aqueous ammonia as the solvent and a ferric chloride mixture (4) as the spray. Only the spot characteristic of guaiacol, R_f 0.95, was present, and there was no spot in the catechol position, R_f 0.87. The remainder of the product, when esterified with *p*-nitrobenzoyl chloride in pyridine (5), yielded 0.47 g of material which was recrystallized once from ethanol. Although the crystals, 0.26 g, melted rather sharply at 96–97°, many recrystallizations from ethanol and methanol separated them into 0.15 g melting at 86–92°, and 0.03 g melting at 98–100°. Since the melting points of the *p*-nitrobenzoates of guaiacol and phenol were 97° and 102°, respectively, the above product was probably an incompletely resolved mixture of these two compounds.

Attempted Scission of Fully Methylated Lignins

A 1.4-g sample of dry, finely divided spruce formaldehyde periodate lignin, fully methylated to OCH_3, 15.0% (4), was suspended in 90 ml of tetrahydrofuran containing 80 mmoles of *t*-butylmagnesium chloride. Six grams of anhydrous cobaltous chloride was added in 12 portions during 3 hours, and the subsequent heating under reflux was for 3 hours. The cold, acidified suspension was then extracted with ether, and the aqueous

Can. J. Chem. Downloaded from www.nrcresearchpress.com by 210.87.254.42 on 09/05/12
For personal use only.

residue was dialyzed against distilled water. The non-dialyzed portion yielded 1.20 g of a precipitate. Found: ash, 0.7%; OCH_3, 12.5%, not altered by methylation with diazomethane. The ether extract contained 0.2 g of a neutral, high-boiling oil, and 0.03 g of alkali-soluble material with R_f 0.21 on paper chromatograms.

The experiment was repeated with 1.42 g of spruce periodate lignin fully methylated to OCH_3, 17.6; ash, 1.2% (4). Dialysis of the aqueous portion of the reaction mixture yielded 1.29 g of insoluble material. Found: ash, 0.2%; OCH_3, 17.2%, increased to 18.6% by remethylation with diazomethane. The neutral ether-soluble oil, 0.085 g, was volatile enough to leave only 0.02 g of residue when heated at 100° *in vacuo*. When the ether-soluble phenols, 0.06 g, were chromatographed on paper only the spot of R_f 0.95 pertaining to guaiacol was observed.

1. M. S. KHARASCH and R. L. HUANG. J. Org. Chem. **17**, 669 (1952).
2. R. L. HUANG. J. Chem. Soc. 3084 (1954).
3. M. TOMITA and Y. WATANABE. J. Pharm. Soc. Japan, **73**, 918 (1953).
4. E. EISENBRAUN and C. B. PURVES. Can. J. Chem. **39**, 1518 (1961).
5. A. I. VOGEL. A textbook of practical organic chemistry. 3rd ed. Longmans, Green and Co., Ltd., London. 1956.
6. H. GILMAN and E. A. ZOELLNER. J. Am. Chem. Soc. **50**, 425 (1928).
7. M. S. KHARASCH, S. C. KLEIGER, J. A. MARTIN, and F. R. MAYO. J. Am. Chem. Soc. **63**, 2305 (1941).
8. H. GILMAN, P. D. WILKINSON, W. P. FISHEL, and C. M. MEYERS. J. Am. Chem. Soc. **45**, 150 (1923).
9. G. L. CLARK, A. J. QUICK, and W. D. HARKINS. J. Am. Chem. Soc. **42**, 2483 (1920).
10. F. ULLMANN and A. STEIN. Ber. **39**, 622 (1906).

RECEIVED JUNE 12, 1961.
DIVISION OF INDUSTRIAL AND CELLULOSE CHEMISTRY,
MCGILL UNIVERSITY,
AND
DIVISION OF WOOD CHEMISTRY,
PULP AND PAPER RESEARCH INSTITUTE OF CANADA,
MONTREAL 2, QUEBEC.

THE DECOMPOSITION OF HYDROGEN PEROXIDE IN THE PRESENCE OF HYDROGEN

R. R. BALDWIN, D. BOOTH,* AND D. BRATTAN†

In a paper (1) presented at the Eighth International Combustion Symposium at Pasadena in September 1960, we reported a marked acceleration of the decomposition of H_2O_2 in the presence of H_2. The studies were carried out using a flow system at atmospheric pressure, the partial pressure of H_2O_2 varying from 0.2–1.0 mm Hg, and the partial pressure of H_2 varying from 10–760 mm Hg. In such a system, where the H_2/H_2O_2 ratios were relatively high, the experimental results are interpreted precisely by the following simple scheme:‡

$$H_2O_2 + M' = 2OH + M' \quad [7]$$

$$OH + H_2 = H_2O + H \quad [1]$$

$$H + H_2O_2 = H_2O + OH \quad [14]$$

$$H + H_2O_2 = H_2 + HO_2 \quad [14a]$$

$$OH + H_2O_2 = H_2O + HO_2 \quad [15]$$

$$2HO_2 = H_2O_2 + O_2. \quad [10]$$

*Now at Rutherford College of Technology, Newcastle, England.
†Now at Hull Technical College, Hull, England.
‡The numbering scheme is that used in earlier papers.

Can. J. Chem. Downloaded from www.nrcresearchpress.com by 210.87.254.42 on 09/05/12
For personal use only.

residue was dialyzed against distilled water. The non-dialyzed portion yielded 1.20 g of a precipitate. Found: ash, 0.7%; OCH_3, 12.5%, not altered by methylation with diazomethane. The ether extract contained 0.2 g of a neutral, high-boiling oil, and 0.03 g of alkali-soluble material with R_f 0.21 on paper chromatograms.

The experiment was repeated with 1.42 g of spruce periodate lignin fully methylated to OCH_3, 17.6; ash, 1.2% (4). Dialysis of the aqueous portion of the reaction mixture yielded 1.29 g of insoluble material. Found: ash, 0.2%; OCH_3, 17.2%, increased to 18.6% by remethylation with diazomethane. The neutral ether-soluble oil, 0.085 g, was volatile enough to leave only 0.02 g of residue when heated at 100° *in vacuo*. When the ether-soluble phenols, 0.06 g, were chromatographed on paper only the spot of R_f 0.95 pertaining to guaiacol was observed.

1. M. S. KHARASCH and R. L. HUANG. J. Org. Chem. **17**, 669 (1952).
2. R. L. HUANG. J. Chem. Soc. 3084 (1954).
3. M. TOMITA and Y. WATANABE. J. Pharm. Soc. Japan, **73**, 918 (1953).
4. E. EISENBRAUN and C. B. PURVES. Can. J. Chem. **39**, 1518 (1961).
5. A. I. VOGEL. A textbook of practical organic chemistry. 3rd ed. Longmans, Green and Co., Ltd., London. 1956.
6. H. GILMAN and E. A. ZOELLNER. J. Am. Chem. Soc. **50**, 425 (1928).
7. M. S. KHARASCH, S. C. KLEIGER, J. A. MARTIN, and F. R. MAYO. J. Am. Chem. Soc. **63**, 2305 (1941).
8. H. GILMAN, P. D. WILKINSON, W. P. FISHEL, and C. M. MEYERS. J. Am. Chem. Soc. **45**, 150 (1923).
9. G. L. CLARK, A. J. QUICK, and W. D. HARKINS. J. Am. Chem. Soc. **42**, 2483 (1920).
10. F. ULLMANN and A. STEIN. Ber. **39**, 622 (1906).

RECEIVED JUNE 12, 1961.
DIVISION OF INDUSTRIAL AND CELLULOSE CHEMISTRY,
MCGILL UNIVERSITY,
AND
DIVISION OF WOOD CHEMISTRY,
PULP AND PAPER RESEARCH INSTITUTE OF CANADA,
MONTREAL 2, QUEBEC.

THE DECOMPOSITION OF HYDROGEN PEROXIDE IN THE PRESENCE OF HYDROGEN

R. R. BALDWIN, D. BOOTH,* AND D. BRATTAN†

In a paper (1) presented at the Eighth International Combustion Symposium at Pasadena in September 1960, we reported a marked acceleration of the decomposition of H_2O_2 in the presence of H_2. The studies were carried out using a flow system at atmospheric pressure, the partial pressure of H_2O_2 varying from 0.2–1.0 mm Hg, and the partial pressure of H_2 varying from 10–760 mm Hg. In such a system, where the H_2/H_2O_2 ratios were relatively high, the experimental results are interpreted precisely by the following simple scheme:‡

$$H_2O_2 + M' = 2OH + M' \quad [7]$$

$$OH + H_2 = H_2O + H \quad [1]$$

$$H + H_2O_2 = H_2O + OH \quad [14]$$

$$H + H_2O_2 = H_2 + HO_2 \quad [14a]$$

$$OH + H_2O_2 = H_2O + HO_2 \quad [15]$$

$$2HO_2 = H_2O_2 + O_2. \quad [10]$$

*Now at Rutherford College of Technology, Newcastle, England.
†Now at Hull Technical College, Hull, England.
‡The numbering scheme is that used in earlier papers.

Can. J. Chem. Downloaded from www.nrcresearchpress.com by 210.87.254.42 on 09/05/12
For personal use only.

Reactions [15] and [14*a*] represent the termination reactions dominant at low and high H_2/H_2O_2 ratios respectively, and from the results, values for k_{15}/k_1 of 6.0 ± 0.5 and for k_{14a}/k_{14} of approximately 0.1 are obtained. In the presence of O_2, the termination reaction [4] also becomes important.

$$H + O_2 + M = HO_2 + M \qquad [4]$$

The results and discussion given by Forst (2) in a recent paper in this journal seem, at first sight, to be at variance with the simple mechanism given above, and we wish to show that Forst's results are, in fact, consistent with the above mechanism. Forst's results, all obtained at 431.5° C, fall into three sections, which are given below as points (*a*), (*b*), and (*c*).

(*a*) His Fig. 1 gives the pressure–time curve for the decomposition of H_2O_2 alone (9.6 mm Hg pressure) and in the presence of 19.2 and 96.2 mm Hg of H_2. With pure H_2O_2, the limiting pressure rise of 4.5 mm is close to the theoretical value (4.8 mm Hg), but the pressure rise decreases to 2.6 and 1.5 mm Hg respectively in the presence of H_2.

(*b*) Figure 2 gives the initial rate (mm Hg of O_2 per sec) of decomposition of 9.6 mm of H_2O_2 in the presence of 10–77.5 mm Hg of H_2.

(*c*) Figure 3 gives the initial rate of decomposition as a function of H_2O_2 concentration over the range 3–16 mm Hg, the pressure of H_2 being 57.9 mm Hg.

To allow for the different coefficients of H_2 and H_2O_2 in reaction [7], the rate of [7] may be written

$$R = k_{7P}[P]^2 + k_{7H_2}[H_2][P], \qquad [i]$$

where [P] is the concentration of H_2O_2. Forst* evaluated the ratio k_{7H_2}/k_{7P} as 0.18 by assuming that the ratio k_{7H_2}/k_{7He} is the ratio of the calculated collision frequencies (1.64), the ratio k_{7He}/k_{7P} having been determined as 0.11 (3). Use of this value for k_{7H_2}/k_{7P} gives the linear increase in rate with added H_2, as found experimentally, but the calculated rate increases slower than the experimental rate as H_2 is added. The same is found with the data of Fig. 3, and Forst concludes that some chemical effect of H_2 is also present. Since reactions [1], [14], and [14*a*] only increase the rate of H_2O_2 decomposition and do not affect the rate of O_2 formation, he concludes that other reactions must occur.

Studies of the H_2–O_2 reaction, however, indicate that the ratio k_{4H_2}/k_{4He} is almost twice the calculated collision frequency ratio and that the ratio of the values of k_4 is only equal to the collision frequency ratio if both gases are monatomic or if both gases are diatomic (4). A more likely estimate of the ratio of k_{7H_2}/k_{7P}, therefore, is obtained by assuming that the relative coefficients of H_2 and N_2 are the same in reactions [4] and [7]. Since $k_{4N_2}/k_{4H_2} = 0.43$ (4), and $k_{7P}/k_{7N_2} = 6$–7 (1, 5), k_{7H_2}/k_{7P} should be approximately 0.33–0.38.

A value in agreement with this estimate can be obtained from Forst's results if they are interpreted by the Baldwin–Brattan mechanism. This mechanism, which is also consistent with independent studies of the hydrogen–oxygen reaction (6, 7), gives the rate expressions

$$-\frac{d[P]}{dt} = \frac{2k_7[P][M']\{k_1[H_2]+k_{15}[P]\}}{\alpha k_1[H_2]+k_{15}[P]}, \qquad [ii]$$

$$\frac{d[O_2]}{dt} = k_7[P][M'], \qquad [iii]$$

**The authors are grateful to Dr. Forst for explaining the basis of this calculation.*

Can. J. Chem. Downloaded from www.nrcresearchpress.com by 210.87.254.42 on 09/05/12
For personal use only.

where $\alpha = k_{14a}/(k_{14}+k_{14a})$. Since Forst followed the decomposition by measurement of pressure change, his rate measurements are represented by [iii], which can be written in a similar manner to [i] and predicts the linear increase in rate with H_2 concentration shown in Fig. 2 of Forst's paper. From the gradient and intercept of this line, experimental values of k_{7H_2} and k_{7P} can be obtained, the ratio being 0.30. These experimental values can now be used to predict the variation of initial rate with H_2O_2 concentration at constant H_2 concentration. Figure 1 shows the experimental points taken from Forst's

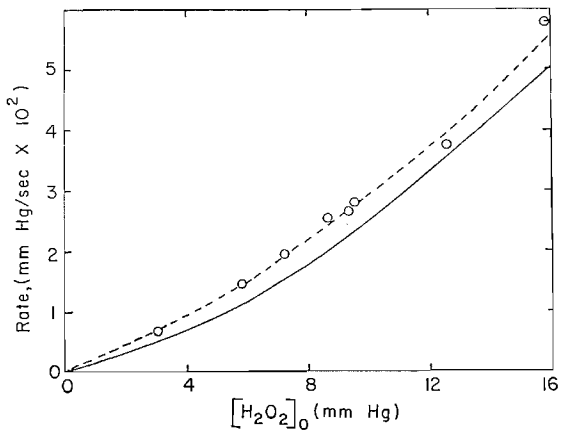


FIG. 1. Decomposition of H_2O_2 in the presence of hydrogen at 431.5° C (initial concentration H_2 = 57.9 mm Hg): O experimental points (Forst (2), Fig. 3); —— calculated curve (Forst (2), Fig. 3); – – – calculated curve (Baldwin–Brattan mechanism).

paper (Fig. 3), the calculated curve using Forst's ratio of 0.18, and the corresponding curve using a ratio of 0.30. This latter ratio thus accounts for both sets of experimental results obtained by Forst, and is in sufficiently close agreement with the estimate of 0.33–0.38 above, particularly since allowance for surface decomposition, admitted by Forst to be significant at this temperature, would increase the value of k_{7H_2}/k_{7P}.

From [ii] and [iii],

$$\frac{-d[P]}{d[O_2]} = \frac{2(k_1[H_2]+k_{15}[P])}{\alpha k_1[H_2]+k_{15}[P]}.$$

Integration* between the initial peroxide concentration $[P_0]$ and zero gives the total amount of O_2 formed as

$$2[O_2]_t = [P_0]-(1-\alpha)R[H_2]\log_e\frac{[P_0]+R[H_2]}{R[H_2]},$$

where $R = k_1/k_{15} = 1/6$ (1). Insertion of the values used in Fig. 1 of Forst's paper, $[H_2O_2]$ = 9.6 mm Hg, $[H_2]$ = 19.2 and 96.2 mm Hg, gives $[O_2]_t$ as 2.8 and 1.4 mm Hg, in close agreement with the experimental values of 2.6 and 1.5 mm Hg respectively.

It may thus be concluded that the Baldwin–Brattan mechanism gives a completely satisfactory account of Forst's observations without the necessity of postulating further reactions.

**This integration assumes that reaction [4] may be neglected and that* $[H_2]$ *is constant. From the known (1) values of* k_2/k_4 *and* k_{14}/k_2*, it can be shown that, under Forst's experimental conditions, reaction [4] will not compete with [14] until* $[H_2O_2] \approx 0.1$ *mm Hg. The error resulting from the assumption that* $[H_2]$ *is constant can also be neglected.*

Can. J. Chem. Downloaded from www.nrcresearchpress.com by 210.87.254.42 on 09/05/12
For personal use only.

Part of this work was carried out under contract AF 61 (052)-62 with the United States Air Force. A grant to D. Brattan from the Hull Education Committee is gratefully acknowledged.

1. R. R. BALDWIN and D. BRATTAN. Paper presented at Eighth International Combustion Symposium at Pasadena, 1960.
2. W. FORST. Can. J. Chem. **37**, 1616 (1959).
3. W. FORST. Can. J. Chem. **36**, 1308 (1958).
4. B. LEWIS and G. VON ELBE. J. Chem. Phys. **10**, 366 (1942).
5. D. E. HOARE, J. B. PROTHEROE, and A. D. WALSH. Trans. Faraday Soc. **55**, 548 (1959).
6. R. R. BALDWIN and L. MAYOR. Trans. Faraday Soc. **56**, 80, 103 (1960).
7. R. R. BALDWIN, P. DORAN, and L. MAYOR. Trans. Faraday Soc. **56**, 93 (1960).

RECEIVED MAY 5, 1961.
CHEMISTRY DEPARTMENT,
THE UNIVERSITY,
HULL, ENGLAND.

CRYSTALLOGRAPHIC DATA FOR ETHYL 3,5-DINITROBENZOATE

N. CAMERMAN AND J. TROTTER

An analysis of the crystal structure of ethyl 3,5-dinitrobenzoate was undertaken to investigate any deviations of the nitro groups from coplanarity with the aromatic ring. However, the structure has proved too complex for a complete determination of the molecular parameters, and since the crystallographic data might be useful, they are outlined in this note.

Crystals of ethyl 3,5-dinitrobenzoate, prepared by reaction of 3,5-dinitrobenzoyl chloride with ethanol, and recrystallized from ethanol, are pale yellow needles elongated along the *b*-axis, with the (001) plane developed and a smaller (100) face. The density was measured by flotation in aqueous potassium iodide solution, and the unit-cell dimensions and space group were determined from rotation and oscillation photographs of a crystal rotating about the *b*-axis, *h*0*l* and *h*1*l* Weissenberg films, and *hk*0 and 0*kl* precession films.

Crystal Data

Ethyl 3,5-dinitrobenzoate: $C_9H_8N_2O_6$; molecular weight = 240.2; melting point = 92–94° C.

Monoclinic; $a = 18.36 \pm 0.05$, $b = 4.78 \pm 0.01$, $c = 13.82 \pm 0.03$ Å; $\beta = 119.7° \pm 0.5°$.

Volume of the unit cell = 1054 Å^3.

Density: calculated (with $Z = 4$) = 1.505, measured = 1.511 g cm^{-3}.

Absorption coefficient for X rays, $\lambda = 1.542$ Å, $\mu = 12.9$ cm^{-1}.

Total number of electrons per unit cell = $F(000) = 496$.

Examination of the films revealed that *h*0*l* reflections are systematically absent when *h* is odd. Of the 0*k*0 reflections only 040 was observed, so that a screw axis parallel to *b* was indicated. Since only one 0*k*0 reflection was observable the presence of the 2_1 axis was not definitely established, but the $N(z)$ intensity distribution (1) for the *h*0*l* zone corresponded to a centrosymmetric projection. These facts, taken together, suggested that the space group was probably $P2_1/a$.

The intensities of the *h*0*l* reflections were measured by the Weissenberg multiple-film technique (2), with Cu $K\alpha$ radiation, and the values of the structure amplitudes were

Can. J. Chem. Downloaded from www.nrcresearchpress.com by 210.87.254.42 on 09/05/12
For personal use only.

Part of this work was carried out under contract AF 61 (052)-62 with the United States Air Force. A grant to D. Brattan from the Hull Education Committee is gratefully acknowledged.

1. R. R. BALDWIN and D. BRATTAN. Paper presented at Eighth International Combustion Symposium at Pasadena, 1960.
2. W. FORST. Can. J. Chem. **37**, 1616 (1959).
3. W. FORST. Can. J. Chem. **36**, 1308 (1958).
4. B. LEWIS and G. VON ELBE. J. Chem. Phys. **10**, 366 (1942).
5. D. E. HOARE, J. B. PROTHEROE, and A. D. WALSH. Trans. Faraday Soc. **55**, 548 (1959).
6. R. R. BALDWIN and L. MAYOR. Trans. Faraday Soc. **56**, 80, 103 (1960).
7. R. R. BALDWIN, P. DORAN, and L. MAYOR. Trans. Faraday Soc. **56**, 93 (1960).

RECEIVED MAY 5, 1961.
CHEMISTRY DEPARTMENT,
THE UNIVERSITY,
HULL, ENGLAND.

CRYSTALLOGRAPHIC DATA FOR ETHYL 3,5-DINITROBENZOATE

N. CAMERMAN AND J. TROTTER

An analysis of the crystal structure of ethyl 3,5-dinitrobenzoate was undertaken to investigate any deviations of the nitro groups from coplanarity with the aromatic ring. However, the structure has proved too complex for a complete determination of the molecular parameters, and since the crystallographic data might be useful, they are outlined in this note.

Crystals of ethyl 3,5-dinitrobenzoate, prepared by reaction of 3,5-dinitrobenzoyl chloride with ethanol, and recrystallized from ethanol, are pale yellow needles elongated along the *b*-axis, with the (001) plane developed and a smaller (100) face. The density was measured by flotation in aqueous potassium iodide solution, and the unit-cell dimensions and space group were determined from rotation and oscillation photographs of a crystal rotating about the *b*-axis, *h*0*l* and *h*1*l* Weissenberg films, and *hk*0 and 0*kl* precession films.

Crystal Data

Ethyl 3,5-dinitrobenzoate: $C_9H_8N_2O_6$; molecular weight = 240.2; melting point = 92–94° C.

Monoclinic; $a = 18.36 \pm 0.05$, $b = 4.78 \pm 0.01$, $c = 13.82 \pm 0.03$ Å; $\beta = 119.7° \pm 0.5°$.

Volume of the unit cell = 1054 Å^3.

Density: calculated (with $Z = 4$) = 1.505, measured = 1.511 g cm^{-3}.

Absorption coefficient for X rays, $\lambda = 1.542$ Å, $\mu = 12.9$ cm^{-1}.

Total number of electrons per unit cell = $F(000) = 496$.

Examination of the films revealed that *h*0*l* reflections are systematically absent when *h* is odd. Of the 0*k*0 reflections only 040 was observed, so that a screw axis parallel to *b* was indicated. Since only one 0*k*0 reflection was observable the presence of the 2_1 axis was not definitely established, but the $N(z)$ intensity distribution (1) for the *h*0*l* zone corresponded to a centrosymmetric projection. These facts, taken together, suggested that the space group was probably $P2_1/a$.

The intensities of the *h*0*l* reflections were measured by the Weissenberg multiple-film technique (2), with Cu $K\alpha$ radiation, and the values of the structure amplitudes were

Can. J. Chem. Downloaded from www.nrcresearchpress.com by 210.87.254.40 on 09/05/12
For personal use only.

derived by the usual formulae. One hundred and three reflections were recorded. In space group $P2_1/a$ there is one molecule in the asymmetric crystal unit, and the orientation of this molecule in the unit cell was deduced by Fourier-transform methods and from the intramolecular peaks in the Patterson projection. However, it was impossible to pack molecules in this orientation into the unit cell in space group $P2_1/a$, so that it seemed that there might be two molecules in the asymmetric unit arranged in space group Pa, the 010 and 030 reflections being by chance too weak to be observed, and the $N(z)$ test being misleading (a not uncommon occurrence). Alternatively there might be some type of disordered arrangement of molecules. The problem, therefore, seemed too complex for solution by the usual trial and error methods, and no further detailed structural analysis is proposed. The structure-factor data have been recorded (3).

We thank the National Research Council for financial support.

1. E. R. HOWELLS, D. C. PHILLIPS, and D. ROGERS. Acta Cryst. **3**, 210 (1950).
2. J. M. ROBERTSON. J. Sci. Instr. **20**, 175 (1943).
3. N. CAMERMAN. B.Sc. Thesis, University of British Columbia, Vancouver, B.C. 1961.

RECEIVED JUNE 12, 1961.
DEPARTMENT OF CHEMISTRY,
UNIVERSITY OF BRITISH COLUMBIA,
VANCOUVER 8, B.C.

Can. J. Chem. Downloaded from www.nrcresearchpress.com by 210.87.254.40 on 09/05/12
For personal use only.

A NEW METHOD FOR THE DEOXYGENATION OF AROMATIC *N*-OXIDES

R. A. ABRAMOVITCH AND K. A. H. ADAMS

In the course of a study of the cyclization of some nitrophenylpyridine derivatives with ferrous oxalate it was observed that when 2-*o*-nitrophenylpyridine-*N*-oxide was heated with this reagent the only product isolated was pyrido[1,2-*b*]indazole (1). It was also shown that the first stage in this reaction was probably the elimination of the *N*-oxide grouping; 2-phenylpyridine-*N*-oxide itself was deoxygenated under these conditions but was unaffected in the absence of the ferrous oxalate.

The scope of this deoxygenation has now been extended to a number of other pyridine-*N*-oxide derivatives and to *N*,*N*-dimethylaniline-*N*-oxide. The results are summarized in the table.

N-Oxide	Yield of tertiary amine, %
Pyridine-*N*-oxide	64
2-Picoline-*N*-oxide	62
3-Picoline-*N*-oxide	72
2-Aminopyridine-*N*-oxide	45
2-Phenylpyridine-*N*-oxide	63
N,*N*-Dimethylaniline-*N*-oxide	55 (crude)

This new procedure may well be of value, particularly in cases (e.g. when an amino group is present) where other methods currently in use (such as that involving phosphorus trichloride) may not be employed. Its limitations include applications to (*a*) those substances containing groupings, e.g. nitro, which are attacked by ferrous oxalate; and (*b*)

derived by the usual formulae. One hundred and three reflections were recorded. In space group $P2_1/a$ there is one molecule in the asymmetric crystal unit, and the orientation of this molecule in the unit cell was deduced by Fourier-transform methods and from the intramolecular peaks in the Patterson projection. However, it was impossible to pack molecules in this orientation into the unit cell in space group $P2_1/a$, so that it seemed that there might be two molecules in the asymmetric unit arranged in space group Pa, the 010 and 030 reflections being by chance too weak to be observed, and the $N(z)$ test being misleading (a not uncommon occurrence). Alternatively there might be some type of disordered arrangement of molecules. The problem, therefore, seemed too complex for solution by the usual trial and error methods, and no further detailed structural analysis is proposed. The structure-factor data have been recorded (3).

We thank the National Research Council for financial support.

1. E. R. HOWELLS, D. C. PHILLIPS, and D. ROGERS. Acta Cryst. **3**, 210 (1950).
2. J. M. ROBERTSON. J. Sci. Instr. **20**, 175 (1943).
3. N. CAMERMAN. B.Sc. Thesis, University of British Columbia, Vancouver, B.C. 1961.

RECEIVED JUNE 12, 1961.
DEPARTMENT OF CHEMISTRY,
UNIVERSITY OF BRITISH COLUMBIA,
VANCOUVER 8, B.C.

Can. J. Chem. Downloaded from www.nrcresearchpress.com by 210.87.254.42 on 09/05/12
For personal use only.

A NEW METHOD FOR THE DEOXYGENATION OF AROMATIC *N*-OXIDES

R. A. ABRAMOVITCH AND K. A. H. ADAMS

In the course of a study of the cyclization of some nitrophenylpyridine derivatives with ferrous oxalate it was observed that when 2-*o*-nitrophenylpyridine-*N*-oxide was heated with this reagent the only product isolated was pyrido[1,2-*b*]indazole (1). It was also shown that the first stage in this reaction was probably the elimination of the *N*-oxide grouping; 2-phenylpyridine-*N*-oxide itself was deoxygenated under these conditions but was unaffected in the absence of the ferrous oxalate.

The scope of this deoxygenation has now been extended to a number of other pyridine-*N*-oxide derivatives and to *N*,*N*-dimethylaniline-*N*-oxide. The results are summarized in the table.

N-Oxide	Yield of tertiary amine, %
Pyridine-*N*-oxide	64
2-Picoline-*N*-oxide	62
3-Picoline-*N*-oxide	72
2-Aminopyridine-*N*-oxide	45
2-Phenylpyridine-*N*-oxide	63
N,*N*-Dimethylaniline-*N*-oxide	55 (crude)

This new procedure may well be of value, particularly in cases (e.g. when an amino group is present) where other methods currently in use (such as that involving phosphorus trichloride) may not be employed. Its limitations include applications to (*a*) those substances containing groupings, e.g. nitro, which are attacked by ferrous oxalate; and (*b*)

probably aliphatic tertiary amine *N*-oxides, which are known (see ref. 2) to undergo elimination of the amine group by the action of heat and to give an olefin.

EXPERIMENTAL

The *N*-oxide was mixed with 4 molar equivalents of ferrous oxalate dihydrate and granulated lead (ca. 6 g/g of *N*-oxide), and the mixture ((*a*) in a flask arranged for distillation for *N*-oxides of liquid amines, or (*b*) in a flask fitted with a condenser for *N*-oxides of solid amines) was heated in a metal bath at 300° (bath temperature) for 30 minutes. The product isolated by distillation (in case (*a*)), or by ether extraction of the reaction mixture (in case (*b*)), was dried overnight over potassium hydroxide pellets. The identity of the products was established by comparison of their infrared spectra with those of authentic samples of the bases. The picrates of the products were prepared in the cases of pyridine-, 2-picoline-, 3-picoline-, and 2-phenylpyridine-*N*-oxides, and their identity confirmed by melting point and mixed melting point determinations. 2-Aminopyridine, as isolated from this reaction, was recrystallized from light petroleum (40–60°) and had m.p. 57–59°, which was not depressed on admixture with an authentic sample.

ACKNOWLEDGMENTS

This work was carried out during the tenure (by K. A. H. A.) of a C.I.L. Fellowship, and with the financial support of the National Research Council.

1. R. A. Abramovitch and K. A. H. Adams. Can. J. Chem. In press.
2. A. C. Cope, R. A. Pike, and C. S. Spencer. J. Am. Chem. Soc. **75**, 3212 (1953).

Received July 3, 1961.
Department of Chemistry,
University of Saskatchewan,
Saskatoon, Sask.

THE IRRADIATION OF β-IONONE

P. de Mayo, J. B. Stothers, and R. W. Yip

Study of the literature suggests that the irradiation of substances containing the system (I) where Y is carbon and (or) a hetero atom(s) leads to (reversible) hydrogen transfer and the formation of (II) which may then be further transformed. In those cases noted there is the possibility of $n \rightarrow \pi^*$ excitation, though this may not be a requirement. The irradiation of α,β-unsaturated ketones ((I), Y = C·CH_3) gives, for example, the β,γ-unsaturated isomer (1). All the requirements of the *o*-nitrobenzaldehyde ((I), Y = NO) – *o*-nitrosobenzoic acid conversion and related changes are met by the postulation of an intermediate ketene formed by hydrogen transfer (2). Recently it has been shown that substituted benzophenones ((I), Y = C·Ph) are enolized by irradiation (3).

β-Ionone (III) on irradiation has been shown (4) to give (reversibly) the pyran (IV) as main product, together with a by-product which was tentatively attributed the structure (V). The alternative (VI) was considered and rejected on reasonable but negative evidence. Since β-ionone falls into the class of substance under present consideration, by vinylogous extension, (VI) seemed mechanistically much more favored. We have repeated the preparation and determined the n.m.r. spectrum (Fig. 1), which was not available at the time of the earlier work.

Can. J. Chem. Downloaded from www.nrcresearchpress.com by 210.87.254.42 on 09/05/12
For personal use only.

probably aliphatic tertiary amine *N*-oxides, which are known (see ref. 2) to undergo elimination of the amine group by the action of heat and to give an olefin.

EXPERIMENTAL

The *N*-oxide was mixed with 4 molar equivalents of ferrous oxalate dihydrate and granulated lead (ca. 6 g/g of *N*-oxide), and the mixture ((*a*) in a flask arranged for distillation for *N*-oxides of liquid amines, or (*b*) in a flask fitted with a condenser for *N*-oxides of solid amines) was heated in a metal bath at 300° (bath temperature) for 30 minutes. The product isolated by distillation (in case (*a*)), or by ether extraction of the reaction mixture (in case (*b*)), was dried overnight over potassium hydroxide pellets. The identity of the products was established by comparison of their infrared spectra with those of authentic samples of the bases. The picrates of the products were prepared in the cases of pyridine-, 2-picoline-, 3-picoline-, and 2-phenylpyridine-*N*-oxides, and their identity confirmed by melting point and mixed melting point determinations. 2-Aminopyridine, as isolated from this reaction, was recrystallized from light petroleum (40–60°) and had m.p. 57–59°, which was not depressed on admixture with an authentic sample.

ACKNOWLEDGMENTS

This work was carried out during the tenure (by K. A. H. A.) of a C.I.L. Fellowship, and with the financial support of the National Research Council.

1. R. A. Abramovitch and K. A. H. Adams. Can. J. Chem. In press.
2. A. C. Cope, R. A. Pike, and C. S. Spencer. J. Am. Chem. Soc. **75**, 3212 (1953).

Received July 3, 1961.
Department of Chemistry,
University of Saskatchewan,
Saskatoon, Sask.

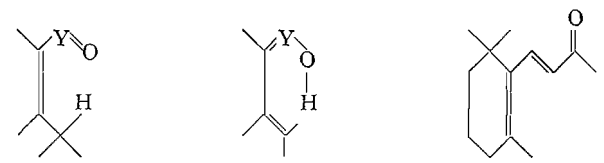
THE IRRADIATION OF β-IONONE

P. de Mayo, J. B. Stothers, and R. W. Yip

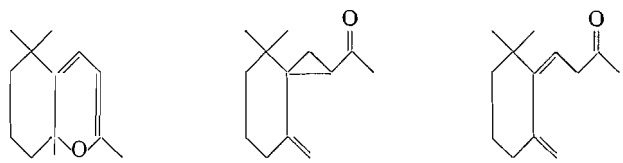
Study of the literature suggests that the irradiation of substances containing the system (I) where Y is carbon and (or) a hetero atom(s) leads to (reversible) hydrogen transfer and the formation of (II) which may then be further transformed. In those cases noted there is the possibility of $n \rightarrow \pi^*$ excitation, though this may not be a requirement. The irradiation of α,β-unsaturated ketones ((I), Y = C·CH_3) gives, for example, the β,γ-unsaturated isomer (1). All the requirements of the *o*-nitrobenzaldehyde ((I), Y = NO) – *o*-nitrosobenzoic acid conversion and related changes are met by the postulation of an intermediate ketene formed by hydrogen transfer (2). Recently it has been shown that substituted benzophenones ((I), Y = C·Ph) are enolized by irradiation (3).

β-Ionone (III) on irradiation has been shown (4) to give (reversibly) the pyran (IV) as main product, together with a by-product which was tentatively attributed the structure (V). The alternative (VI) was considered and rejected on reasonable but negative evidence. Since β-ionone falls into the class of substance under present consideration, by vinylogous extension, (VI) seemed mechanistically much more favored. We have repeated the preparation and determined the n.m.r. spectrum (Fig. 1), which was not available at the time of the earlier work.

Can. J. Chem. Downloaded from www.nrcresearchpress.com by 210.87.254.42 on 09/05/12
For personal use only.



(I) (II) (III)



(IV) (V) (VI)

At 60 Mc/sec in dilute carbon tetrachloride solution, the following peaks are found (in p.p.m. from internal tetramethylsilane): 1.06 (singlet), $(CH_3)_2C<$; 2.04 (singlet), $CH_3-\underset{|}{C}=O$: 3.16 (doublet, $J = 7.1$ cycles/sec), $=CH-\underline{CH_2}-C=O$; 5.33 (triplet, $J =$

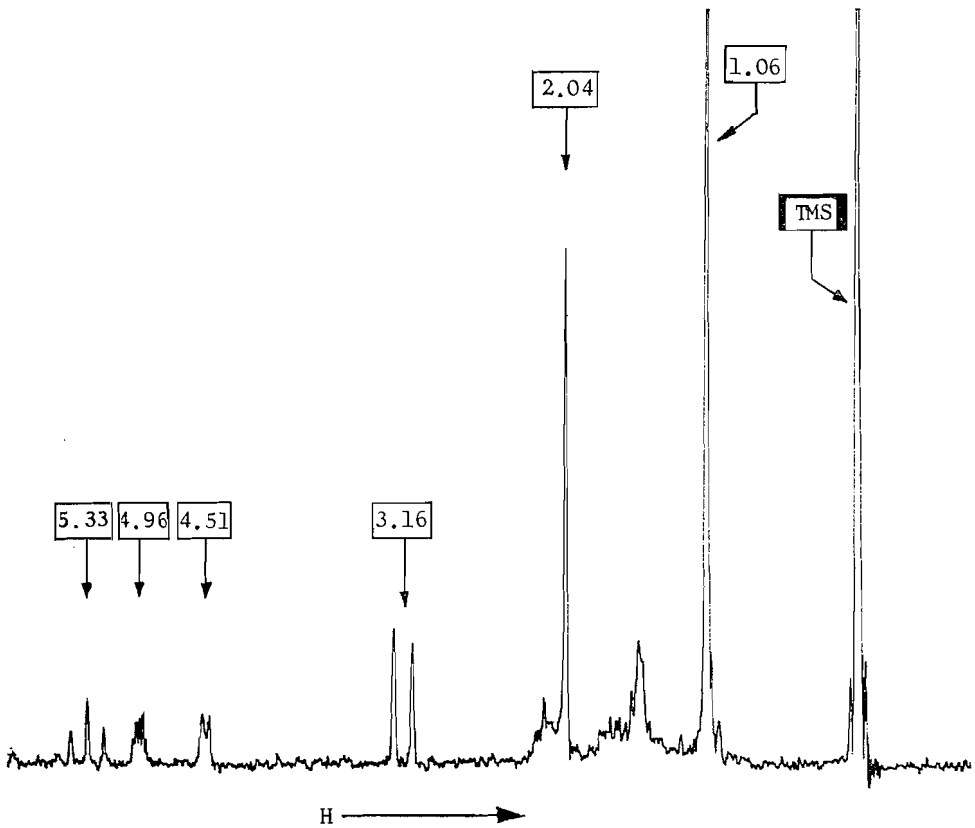


FIG. 1. 60 Mc/sec spectrum of the irradiation product (VI) of β-ionone.

Can. J. Chem. Downloaded from www.nrcresearchpress.com by 210.87.254.42 on 09/05/12
For personal use only.

7.1 cycles/sec), $=\underline{CH}-CH_2-C=O$; 4.51, 4.96 (multiplets), $=CH_2$. From the splitting observed in the latter two bands, it was found that $J = 2.6$ cycles/sec for the geminal coupling, while the lower band clearly showed a long-range interaction with $J = 1.3$ cycles/sec. It is to be noted that no absorption characteristic of the cyclopropane methylene group required by (V) is observed. These results conclusively establish the correctness of (VI).

1. R. Y. Levina, V. N. Kostin, and P. A. Gembitskii. J. Gen. Chem. U.S.S.R. **29**, 2421 (1959).
2. P. de Mayo and S. T. Reid. Quart. Revs. (London). In press.
3. N. C. Yang and C. Rivas. J. Am. Chem. Soc. **83**, 2213 (1961).
4. G. Büchi and N. C. Yang. J. Am. Chem. Soc. **79**, 2318 (1957).

Received July 3, 1961.
Department of Chemistry,
University of Western Ontario,
London, Ont.

Can. J. Chem. Downloaded from www.nrcresearchpress.com by 210.87.254.42 on 09/05/12
For personal use only.

Can. J. Chem. Downloaded from www.nrcresearchpress.com by 210.87.254.105 on 09/05/12
For personal use only.

Canadian Journal of Chemistry

Issued by THE NATIONAL RESEARCH COUNCIL OF CANADA

VOLUME 39 NOVEMBER 1961 NUMBER 11

DIELECTRIC RELAXATION IN LIQUIDS

II. ISOMERIC PENTANEDIOLS[1]

D. W. DAVIDSON

ABSTRACT

For five pentanediols the infrared spectra, the dipole moments, and the static dielectric constants show an increasing degree of internal hydrogen bonding with increasing proximity of the OH groups. The dielectric dispersion loci at low temperatures are skewed arcs over most of the dispersion range. Values of the parameter β decrease from ca. 1 to 0.55 in the series 1,5-, 1,4-, 1,2-, 2,4-, and 2,3-pentanediol, which is also the order of increasing relaxation time τ_0 at low temperatures. Increased τ_0 is associated with increased irregularity of intermolecular hydrogen bonding, an effect which supports the view that relaxation proceeds by a co-operative mechanism which is facilitated by regularity in the liquid structure. At temperatures of "structural relaxation", values of log τ_0 are linear in $(T-T_\infty)^{-1}$; the proportionality constants, but not the T_∞'s, are the same for all five diols.

The experimental behavior at relatively high frequencies departs from both the skewed-arc and Glarum equations, although less from the latter. These departures are compared with the high frequency dispersion regions in *n*-propanol.

In a previous paper (1) the ability of the skewed-arc expression to represent the results of dielectric relaxation measurements of liquids has been discussed. Most monohydroxyl alcohols exhibit a principal dispersion region which is, within the experimental errors, of the classical Debye type ($\beta = 1$ in the skewed-arc representation). This is in contrast to the relaxation behavior of such polyhydroxyl alcohols as have been studied, for which values of β considerably smaller than unity must be invoked. It is natural to attempt to relate this qualitative difference in the relaxation behavior to the absence in the polyhydroxyl liquids of the same degree of regularity in *inter*molecular hydrogen bonding that exists in the simple alcohols. In order to examine the role played by *intra*molecular hydrogen bonding and steric factors in the extent and regularity of the hydrogen bonding between polyhydroxyl molecules, we have studied the relaxation behavior of five isomeric pentanediols. With one exception, the pentanediols may be cooled sufficiently to bring the dispersion regions within the frequency range required for bridge measurements.

Information about the extent of *intra*molecular hydrogen bonding was provided by an examination of the hydroxyl-group stretching bands in the infrared spectra of dilute solutions of the pentanediols in carbon tetrachloride and by measurement of the dipole moments of the pentanediols in dioxane solution.

EXPERIMENTAL METHODS

1,2-Pentanediol was prepared by bromohydrination of pentene-1 with N-bromosuccinimide, conversion to the epoxide (b.p. 76–78°), and hydrolysis to the diol with Dowex 50 resin.

[1]*Manuscript received May 25, 1961.*
Contribution from the Division of Applied Chemistry, National Research Council, Ottawa, Canada. Issued as N.R.C. No. 6503.

The infrared spectrum of a commercial sample of 2,3-pentanediol showed a strong spurious band at 1733 cm^{-1}, which disappeared after saponification with sodium hydroxide. An authentic sample of the 2,3-diol was prepared from pentene-2 (which gas-chromatographic analysis showed to consist of roughly equal proportions of the trans and cis forms) by performic acid oxidation and hydrolysis. The product (*B*) consisted of approximately equal amounts of *threo* and *erythro* isomers. Its infrared spectrum was almost identical with that of the saponified commercial product (*A*).

The other pentanediols were commercial products.

All the pentanediols were fractionated in a Todd still. The boiling ranges and refractive indices are given in Table I.

TABLE I

Pentanediol		Boiling range (p, mm)	n_D
1,2		83–84° (3)	1.4387 (23°)
2,3	*A*	70–71° (3.5)	1.4404 (20°)
	B		1.4405 (20°)
1,4		221–222° (748)	
		103° (4)	1.4451 (25°)
2,4	*A*	199–200° (757)	1.4329 (25°)
	B	83° (5)	1.4329 (25°)
1,5		239° (759)	
		121° (6)	1.4495 (25°)

1,4-Dioxane was refluxed for several hours over calcium hydride and distilled.

The dielectric constant and loss measurements at frequencies up to 500 kc/sec and the temperature measurement and control were essentially as outlined previously (2). Less accurate measurements at higher frequencies were made in the case of 1,5-pentanediol with (*a*) a Model 260A Boonton Q-Meter and a cell consisting of two parallel-plate platinum electrodes mounted in a glass vessel, and (*b*) a Model 250A Boonton RX-Meter and a cell constructed of two coaxial stainless steel electrodes with Teflon insulation.

Measurements of the dipole moments of the pentanediols in dioxane were made by the method previously described (3). Infrared spectra of the carbon tetrachloride solutions were obtained with a Perkin–Elmer Model 112 infrared spectrometer equipped with sodium chloride and calcium fluoride optics.

RESULTS AND DISCUSSION

Intramolecular Hydrogen Bonding

(a) OH Stretching Vibrations

The fundamental OH stretching vibration region of the infrared spectra of solutions of the pentanediols in carbon tetrachloride is shown in Fig. 1. Following Kuhn (4) and others, one may associate the presence in this region of two bands of concentration-independent relative intensity at low concentrations (less than 0.1% or 0.015 molar) with the presence of both free and *intra*molecularly hydrogen-bonded OH groups. The frequencies of free OH groups and of those taking part in *intra*molecular and, at higher concentrations, in *inter*molecular hydrogen bonds are given in Table II. The latter are somewhat concentration dependent; the values given are for concentrations in the range 0.2 to 0.6%.

Can. J. Chem. Downloaded from www.nrcresearchpress.com by 210.87.254.105 on 09/05/12
For personal use only.

Can. J. Chem. Downloaded from www.nrcresearchpress.com by 210.87.254.105 on 09/05/12
For personal use only.

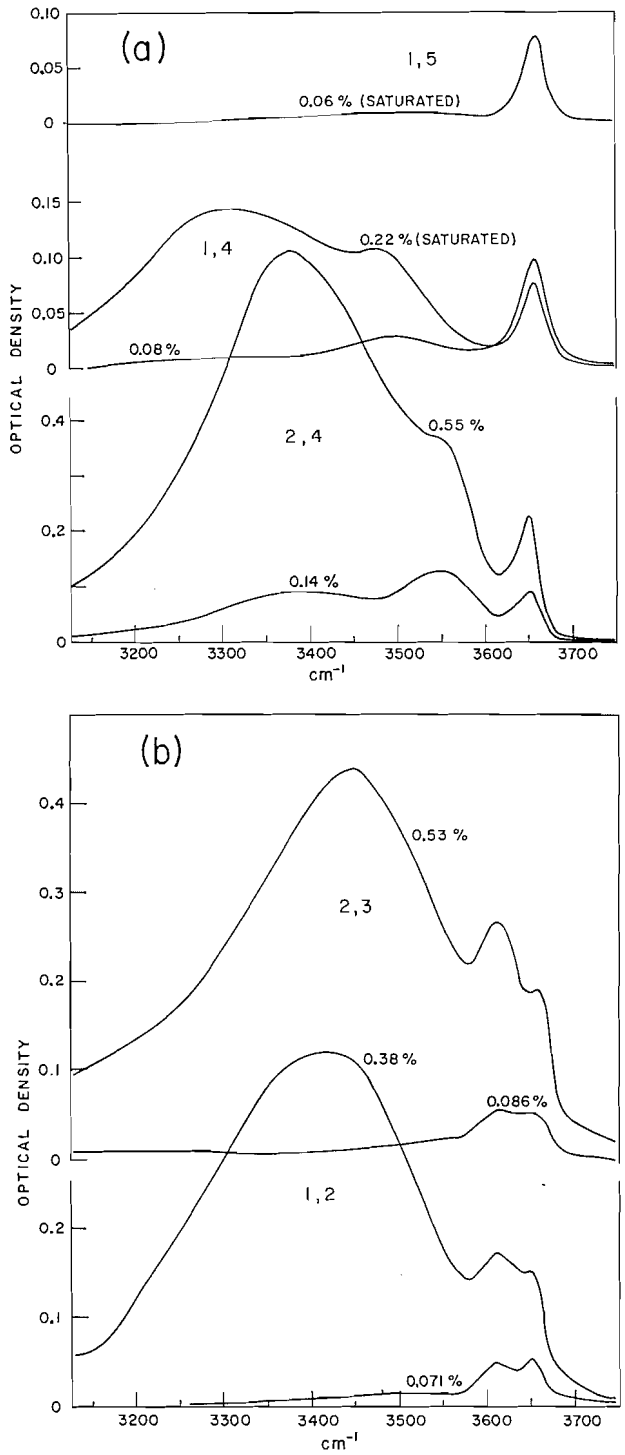


FIG. 1(*a*) and (*b*). OH stretching vibration region of the infrared spectra of the pentanediols in CCl_4.

TABLE II

OH stretching vibration bands of pentanediols in CCl_4

Diol	Frequencies (cm^{-1})			Approx. fraction of free OH groups*
	Free OH	*Intra*bonded OH	*Inter*bonded OH	
1,5	3639			1
1,4	3638	3464	3292	0.85
2,4	3639	3538	3369	0.65
1,2	3646	3604	3407	0.55
2,3	3646	3600	3437	0.50

*At low concentrations.

Like 1,6-hexanediol (4), 1,5-pentanediol shows no evidence of internal hydrogen bonding. A small degree of internal bonding takes place in 1,4-pentanediol, as shown by the presence of a weak band whose frequency shift from the free OH band ($\Delta\tilde{\nu} = 174$ cm^{-1}) is similar to that shown by 1,4-butanediol (156 cm^{-1} (4); 170 cm^{-1} (5)). More extensive *intra*molecular hydrogen bonding takes place in 2,4-pentanediol; the frequency difference (101 cm^{-1}) is somewhat larger than for 1,3-propanediol (78 cm^{-1} (4)) or 1,3-butanediol (80 cm^{-1} (5)). The bands arising from internally bonded OH groups in the vicinal pentanediols are about as strong as those arising from the free OH groups. The frequency shifts are similar to those found in other *vic*-diols.

In view of the well-known correlation between $\Delta\tilde{\nu}$ and hydrogen bond "strength", it is a fair inference that, although the number of molecules which are *intra*molecularly bonded *increases*, the strength of the bonds *decreases* in the sequence 1,4- to *vic*-diol. The frequencies associated with the broad bands due to *inter*molecular hydrogen bonding (Table II, column 4) likewise suggest that the bonds between molecules become somewhat weaker in the same sequence.

The estimates of the fraction of free OH groups given in the last column of Table II are based on the approximation that the extinction coefficient is the same for the free OH stretching band in all five pentanediols.

With increasing concentration the *intra*molecular hydrogen-bonding bands become obscured by the strong *inter*molecular ones. Solutions of the pentanediols in dioxane all show strong bands with peaks near 3480 cm^{-1} arising from association with the solvent.

(b) Dipole Moments

Because of the limited solubility of some of the pentanediols in CCl_4 and other inert solvents and the tendency of diol molecules in such solvents to associate even at low concentrations, the dipole moments were measured for solutions in dioxane. The results, based on measurements of 6 to 8 solutions in the weight fraction range between 0.005 and 0.08, are given in Table III. The dipole moments of some other diols are included for comparison.

Two primary solvent effects are to be expected: an enhanced moment for each OH group which is hydrogen bonded to the solvent, and a change (usually a reduction) in the molecular moment arising from the effect on the extent of *intra*molecular hydrogen bonding of the competition provided by bonding to dioxane. To get an indication of the magnitude of the first effect, the dipole moment of water in dioxane was measured with the same technique as was employed with the pentanediols. The resulting value of 1.91 debyes, like several earlier values (10), was only slightly greater than the vapor value of 1.85 debyes (11). The second effect is more difficult to gauge. The agreement

Can. J. Chem. Downloaded from www.nrcresearchpress.com by 210.87.254.105 on 09/05/12
For personal use only.

TABLE III

Dipole moments of diols (debyes) in dioxane

Diol	No. of C atoms between OH groups				Reference
	2	3	4	>4	
1,5-Pentane				2.37±0.03	This work
1,4-Pentane			2.51±0.03		
2,4-Pentane		2.71±0.03			
1,2-Pentane	2.24±0.02				
2,3-Pentane	2.13+0.05				
1,2-Ethane	2.27 (20°)				7
1,3-Propane		2.46 (20°)			7
1,2-Propane	2.25				8
1,4-Butane			2.47 (20°)		7
1,5-Pentane				2.39 (20°)	7
1,6-Hexane				2.48	8
2-Methyl-2,4-pentane		2.9			9
1,9-Nonane				2.45 (20°)	7
1,10-Decane				2.52	8

NOTE: Temperatures 25°, unless otherwise stated.

between the moment of 1,2-ethanediol in dioxane (2.29 debyes) and in the vapor (2.25 debyes) (12*a*) suggests that it is not great for the vicinal diols. The effect may well be greater for diols less completely internally hydrogen bonded than the vicinal ones.

The dipole moment of 1,5-pentanediol is very nearly $\sqrt{2}$ times as large as that typical of monohydroxyl alcohols (1.66 debyes). This suggests that there is, on the average, no net correlation between the directions of the two COH dipoles and that no appreciable internal hydrogen bonding exists. With increasing proximity of the OH groups in the pentanediols the moments increase, until, for the vicinal diols, they fall to their lowest values. As shown by the other moments in Table III, this trend is general for diols.

Calculation of the resultant moment of the internally hydrogen-bonded molecules is in general prevented by a lack of knowledge of the geometry of the rings formed. The presence of a linear hydrogen bond between two OH groups generally results in a higher moment than that to be expected for unbonded configurations, but the constraints imposed by the comparably inflexible valence-bond angles are likely to lead to considerable bending of the O—H- -O bond in small rings. A certain amount of bending increases the moment beyond its value for a linear bond and values of about 3 debyes are to be expected for angles of the order of 135°. This is consistent with the observed moments of 1,4- and 2,4-pentanediol if the extent of *intra*molecular hydrogen bonding is not greatly less in dioxane than in carbon tetrachloride (compare Table II).

For much larger angles of bend of the hydrogen bond a fall in the resultant moment is predicted. This is the case for the *vic*-diols, which, as considered in more detail in the Appendix, appear to consist substantially of internally hydrogen-bonded forms in which the two CO bonds are not far from gauche in their relative orientation about the connecting C—C bond. Part, at least, of the reduction in "strength" of the hydrogen bonds with decreasing separation of the OH groups in the molecule may be attributed to their increasing departure from linearity.

There is some evidence that the extent of internal hydrogen bonding increases with alkyl-group substitution on the carbon atoms bearing the OH groups, as is to be expected from steric considerations. Thus there is a pronounced increase of moment in the

Can. J. Chem. Downloaded from www.nrcresearchpress.com by 210.87.254.105 on 09/05/12
For personal use only.

series 1,3-propanediol, 2,4-pentanediol, 2-methyl-2,4-pentanediol (Table III). It appears possible for a highly substituted 1,5-pentanediol to be appreciably internally hydrogen bonded (13).

Static Dielectric Constants

Values of ϵ_0 for the pentanediols in the liquid state are plotted versus $1/T$ in Fig. 2.

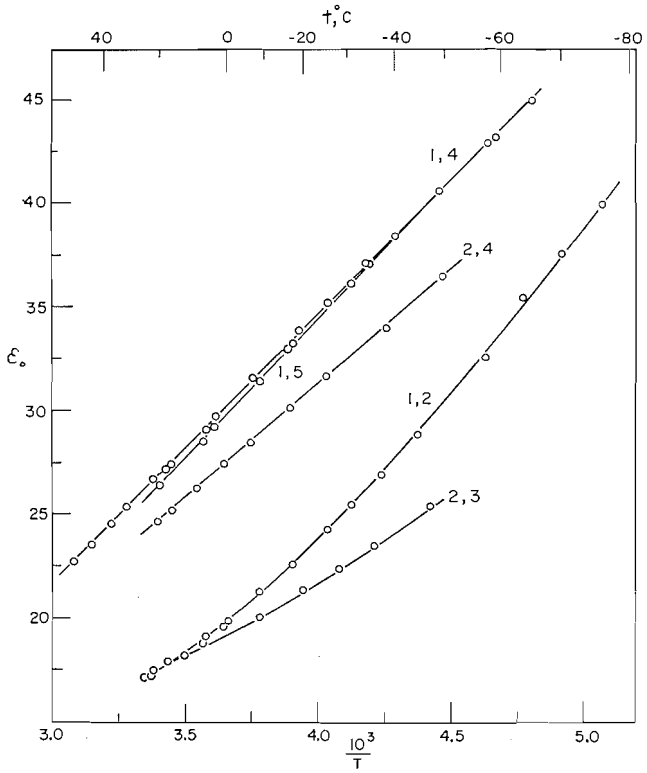


FIG. 2. Temperature dependence of the static dielectric constants of liquid pentanediols.

For three of the diols these values may be represented by a linear function of $1/T$ over the experimental temperature range. The static dielectric constants of the vicinal diols increase more rapidly at low temperatures and are given by

$$\epsilon_0 = a+b/(T-T_c)$$

for which the empirical constants have the values listed in Table IV.*

TABLE IV

Parameters for temperature dependence of ϵ_0

Pentanediol	Temp. range	a	$b\times10^{-3}$	T_c	Av. deviation (%)
1,5	−35 to 25°	−19.54	13.50	0	±0.2
1,4	−65 to 52°	−16.88$_5$	12.89	0	0.3
2,4	−50 to 25°	−12.51	10.96	0	0.2
1,2	−70 to 25°	− 1.13	3.244	120	0.6
2,3	−50 to 25°	+ 4.04	2.487	110	0.2

**Other reported dielectric constants of 1,5-pentanediol (with the values computed from the equation in parentheses) are: −20°, 33.5 (33.8); 0°, 30.0 (29.9); 25°, 26.3 (25.7) (14); and 20°, 26.2 (26.5) (7).*

Can. J. Chem. Downloaded from www.nrcresearchpress.com by 210.87.254.105 on 09/05/12
For personal use only.

Can. J. Chem. Downloaded from www.nrcresearchpress.com by 210.87.254.105 on 09/05/12
For personal use only.

The dielectric constants of 1,5- and 1,4-pentanediol suggest that the individual OH groups have almost as much freedom to associate with other molecules as has the single OH group in simple alcohols. Thus, each of these diols at 20° has a dielectric constant of which the part arising from the orientation of dipoles (ca. 27–3) is twice that of *n*-pentanol (15–3), a liquid with about half as many OH groups per unit volume. In the case of 1,4-pentanediol, it is likely that a reduced extent of *inter*molecular association is offset by the increased average moment resulting from some *intra*molecular hydrogen bonding. In 2,4-pentanediol the former effect predominates.

The lower dielectric constants of the vicinal diols reflect a high degree of internal hydrogen bonding. Formal calculation of the Kirkwood correlation factors from the observed dielectric constants give values somewhat greater than 2 at room temperature and progressively increasing values at lower temperatures. Although such values cannot be directly compared with those of simple alcohols, for which similar values are obtained (15), they are sufficiently high to suggest the presence of extensive hydrogen-bonded chains. The structure is complicated by the possibility of cross-linking of the chains of hydrogen bonds at some molecules which are not internally hydrogen bonded, a process which should result in higher dielectric constants and which may be responsible for the high values found, particularly for the 1,2-diol, at low temperatures.

Most of the pentanediols remained liquid at temperatures lower than those at which the dielectric dispersion–absorption effects (next section) occurred at audio frequencies.* However, the 1,5-diol froze rapidly when cooled below −30°, even when as much as 5% water was added. Examination of its dielectric constant in the solid revealed no anomalies at temperatures down to −190°. The dielectric constant remained almost invariant at about 2.7 as the sample was heated from this temperature until it started to rise a few degrees below the melting point (−16°).

Dielectric Relaxation

A typical absorption–dispersion locus for each pentanediol is illustrated in Fig. 3.

Since 1,5-pentanediol could not be sufficiently supercooled to bring the dispersion effects into the frequency range of bridge measurements, Q-meter and RX-meter measurements were made at higher frequencies. As shown in the plot of Fig. 3 for the 1,5-diol at −30°, the Q-meter results show considerable scatter, a large part of which may be attributed to changes in lead capacitance brought about by connecting and disconnecting the low potential lead to the cell. In the hope that these effects would show a random scatter, a large number of measurements were made. The RX-meter measurements, for which the height of the liquid between the coaxial electrodes was varied to eliminate fixed capacitance, were more reproducible, but were complicated by inductance effects at high frequencies. The data were not sufficiently accurate to distinguish between a semicircular locus with additional high-frequency dispersion regions, as in the simple alcohols, and a slightly skewed locus (with β of the order of 0.9). From measurements over a very extensive frequency range, Mme. Moriamez-Boullet reported (14) the presence of at least two distinct dispersion regions, of which the principal (low-frequency) one was semicircular. In view of the evidence already given for the ability of each OH group in 1,5-pentanediol to freely associate with other molecules, relaxation behavior similar to that of the simple monohydroxyl alcohols might well be expected.

For the other four pentanediols studied, as is evident from the extent of the agreement between the experimental and calculated points (Fig. 3), the skewed-arc locus provides

**One sample of 2,4-diol slowly froze after being maintained for several days at −45°.*

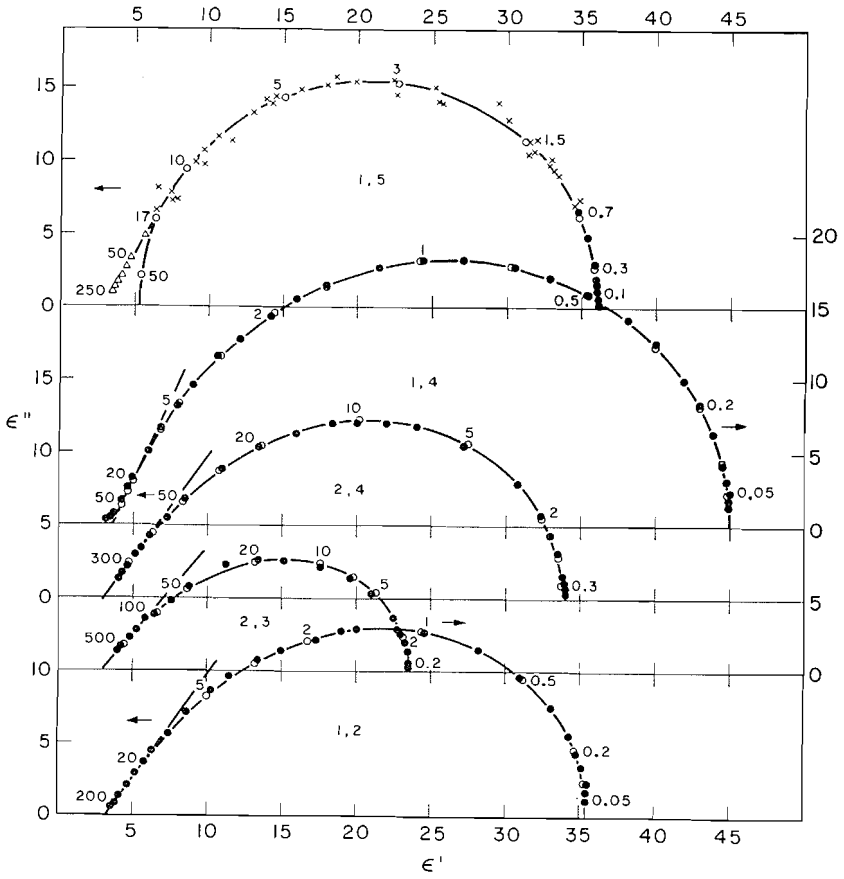


FIG. 3. Complex dielectric constant loci of the pentanediols: ● bridge, × Q-meter, and △ RX-meter measurements; O values calculated from the parameters starred in Table V. Numbers on loci are frequencies in Mc/sec for 1,5-pentanediol, in kc/sec for the others.

an accurate description of the dispersion effects (except at relatively high frequencies). Values of β tend to become smaller with the approach of the two OH groups to one another.

Values of the parameters used in the calculation of the absorption–dispersion loci of Fig. 3 are given in Table V, together with the corresponding skewed-arc parameters at several other temperatures.

Relaxation Times

The variation of the relaxation times with temperature is shown in Fig. 4.

The τ_0 values for 1,5-pentanediol are based on three types of measurement, as indicated in the caption of the figure. Debye behavior has been assumed. Bridge measurements of ϵ'' were made at frequencies on the low-frequency side of the absorption region and the relaxation times were calculated from the slope of a plot of ϵ'' vs. frequency, according to

$$\epsilon'' = 2\pi(\epsilon_0 - \epsilon_1)\beta\tau_0 f, \qquad [1]$$

with, in this case, $\beta = 1$. The experimental ϵ'' values were corrected for the contributions

Can. J. Chem. Downloaded from www.nrcresearchpress.com by 210.87.254.105 on 09/05/12
For personal use only.

TABLE V

Typical dispersion parameters of the pentanediols

Pentanediol	T (°K)	ϵ_0	ϵ_1	β	τ_0 (sec)
1,5	293.5	26.49		(1)	1.53×10^{-9}
	257.2	33.08		(1)	1.33×10^{-8}
	243.2	36.10*	(5.25)†	(1)	4.60×10^{-8}*
1,4	317.8	23.55			
	295.7	26.74			
	266.5	31.59	(3.48)	(0.77)	3.44×10^{-8}
	233.1	38.53	3.50	0.75	1.87×10^{-6}
	207.8	44.95*	3.64*	0.760*	2.23×10^{-4}*
	193.2	49.7	3.71	0.71	2.0×10^{-2}
1,2	296.8	17.31			
	264.5	21.32	(3.20)	(0.65)	1.70×10^{-8}
	228.5	28.86	3.25	0.64	2.27×10^{-6}
	209.5	35.51*	3.26*	0.629*	1.84×10^{-4}*
	197.2	40.0	3.30	0.63_5	1.07×10^{-2}
2,4	294.5	24.69			
	267.1	28.50	(3.00)	(0.68)	3.9×10^{-8}
	234.9	33.86*	3.08*	0.620*	2.49×10^{-5}*
	223.7	36.5	3.17	0.59	7.58×10^{-4}
2,3	296.9	17.37	(2.61)	(0.60)	4.0×10^{-9}
	253.8	21.39	(2.81)	(0.56)	5.0×10^{-7}
	237.8	23.52*	2.83*	0.545*	1.77×10^{-5}*

*Denotes values used for the computed loci of Fig. 3.
†Values in parentheses are values assumed in order to calculate τ_0.

from d-c. conductance. Relaxation times by this method were considered less accurate than those derived from the frequencies of maximum loss given by the Q-meter and RX-meter measurements, and were assigned half the weight in fitting the temperature dependence of the relaxation times by least squares.

Values of τ_0 of the other pentanediols were obtained from bridge measurements alone. Relaxation times of less than 3×10^{-7} second made use of values of β estimated by extrapolation from lower temperatures, and at the high end of the temperature range equation [1] was employed.

From Fig. 4 it is apparent that, with the possible exception of the 1,5-diol, the relaxation times do not follow an equation of the form

$$[2] \qquad \log_{10}\tau_0 = A'+B'/T.$$

They may, however, be represented over most of the temperature range of the measurements by

$$[3] \qquad \log_{10}\tau_0 = A+B/(T-T_\infty),$$

as in the case of a number of other alcohols (15, 16, 17) and alkyl halides (18). It was found that the values of B, as determined by least-squares best fit of equation [3] to the data, were very nearly the same for the four pentanediols. In fact, for the values of A and T_∞ of Table VI, a plot of the product $(\log_{10}\tau_0-A)(T-T_\infty) = B$ yields values of B which are, within experimental error, equal to 985 over most of the temperature range. (See inset of Fig. 5.) Moreover, the less accurate and extensive data for 1,5-pentanediol can be represented by the same B, with A and T_∞ given in Table VI, slightly better (average deviation between experimental and computed relaxation times of 6.7%) than by equation [2] with A' and B' evaluated by least squares (average deviation 7.7%). It is to be noted (Fig. 5) that, although the data for the 1,5- and 1,4-diols show no departures from equation [3] with $B = 985$ up to room temperature, those for the

Can. J. Chem. Downloaded from www.nrcresearchpress.com by 210.87.254.105 on 09/05/12
For personal use only.

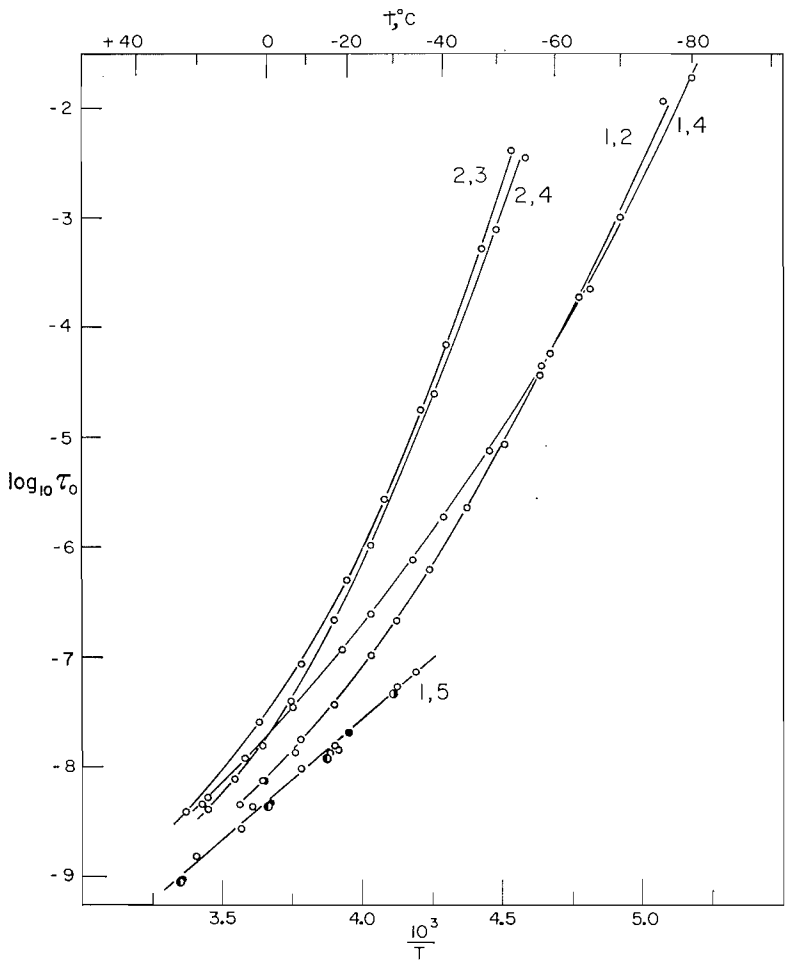


FIG. 4. Arrhenius plots of the relaxation times of the pentanediols: ○ bridge, ◑ Q-meter, ◐ RX-meter measurements; ● from reference 14.

TABLE VI

Parameters of equation [3] for the pentanediols. $B = 985$

Diol	T_∞ (°K)	A	Temp. range (°C)	No. of points	Av. deviation (%)
1,5	92	−13.814	−35, +25	13	6.7
1,4	111	−13.804	−80, +20	13	2.4
2,4	143	−15.327	−55, +3*	7	3.5
1,2	118.5	−14.595	−75, −15*	10	2.5
2,3	144	−15.279	−73, −10*	7	4.0

*Departures from equation [3] occur at higher temperatures.

2,4- and particularly for the vicinal diols show consistent departures at the high temperature end (Fig. 4) in the sense of greater relaxation times than predicted by equation [3]. It may be significant that the greater the degree of *inter*molecular hydrogen bonding the higher the upper temperature limit of validity of the equation.

Published values of the constant B of equation [3] as it has been applied to other

Can. J. Chem. Downloaded from www.nrcresearchpress.com by 210.87.254.105 on 09/05/12
For personal use only.

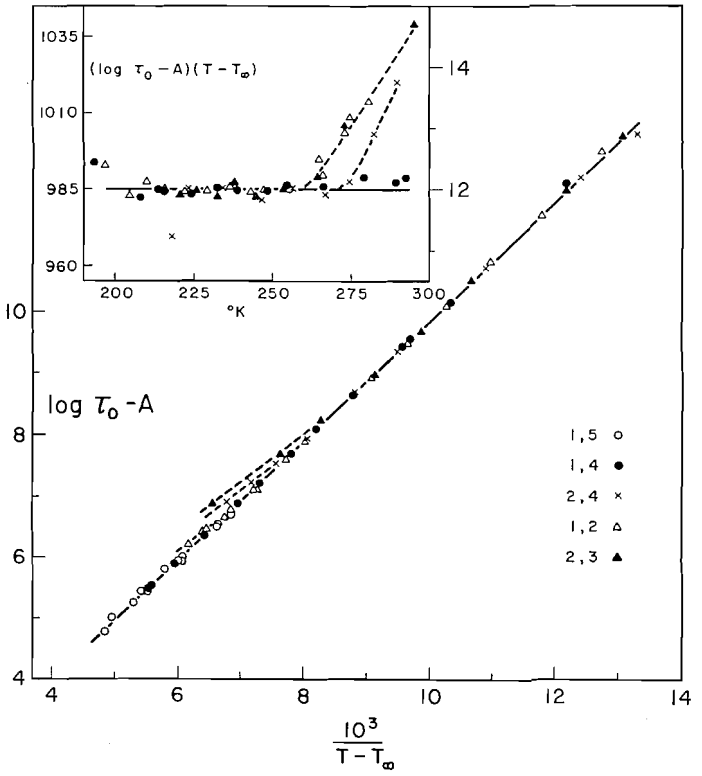


FIG. 5. Dependence of log $\tau_0 - A$ on $1/(T-T_\infty)$ for the values of A and T_∞ listed in Table VI. Inset: temperature variation of (log $\tau_0 - A)(T-T_\infty)$.

hydroxyl-containing liquids (16) are considerably smaller than 985, but this value is approached in the case of highly associated glycerol, for which $B = 957$ has been reported. It is now believed that the available data indicate a common value of B ($\simeq 985$) for liquids at low temperatures. The lower values of B that have been reported probably arise from the inclusion in the data treated of relaxation times obtained at temperatures beyond the range of the common low-temperature behavior.

The case of *n*-propanol may be particularly mentioned. By a combination of bridge and transient techniques, relaxation times between 10^{-8} and 10^{3} seconds have been measured for this liquid. Published (19) parameters for equation [3] (including $B = 477$) describe the experimental relaxation times between 210 and 130° K (that is, up to ca. 10^{-4} second) but not those obtained at lower temperatures. With $B = 985$, together with $A = -14.354$ and $T_\infty = 44°$, on the other hand, the relaxation times in the range 10^{-5} to 10^{3} seconds may be accurately described. Deviations similar to those shown by the vicinal pentanediols become evident at temperatures above 150° K.

The similarity between the temperature dependence of dielectric relaxation times, viscosities, and d-c. conductivities at low temperatures is a matter of common observation, as is also their tendency to depart from such common behavior as the temperature is raised (16, 20, 2). In the case of the pentanediols the conductivities (Fig. 6) vary with temperature very much as do the relaxation times. It was not possible to follow the temperature dependence of conductivity with the same accuracy as for the relaxation

Can. J. Chem. Downloaded from www.nrcresearchpress.com by 210.87.254.105 on 09/05/12
For personal use only.

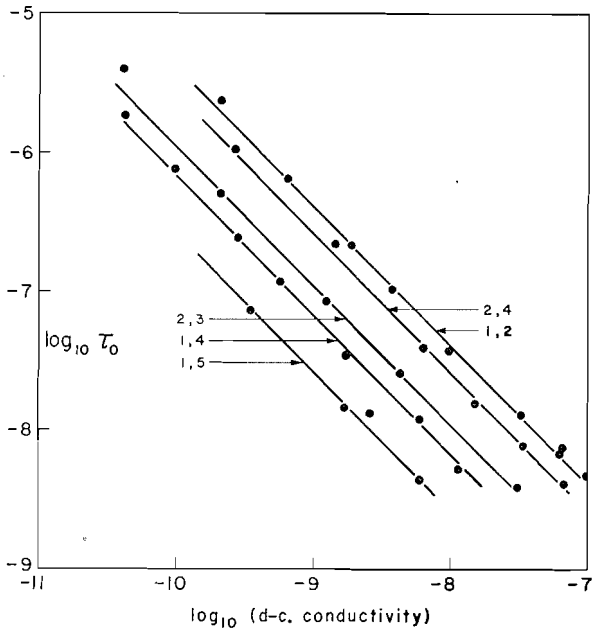


FIG. 6. Plot showing the proportionality between the relaxation times and d-c. conductivities of the pentanediols.

times, since it changed not only from sample to sample, but also slowly with time after the cell had been filled.

The evidence suggests that physical rate processes of many liquids at low temperatures may be represented by equation [3] with a common value of B and a value of T_∞ characteristic of the liquid. For a given liquid only A changes with the rate process being measured. It is planned to examine elsewhere the question of the general validity of equation [3] as a characteristic feature of what may be called "structural relaxation" of liquids.

It is apparent that the present representation of structural relaxation has much in common with Ferry's method of expressing mechanical relaxation times of polymers in terms of their values at an arbitrary standard temperature (21). When put into the form of equation [3], his expression corresponds to a value of B some 10% lower than the one employed here.

Dispersion at High Frequencies

If the principal dispersion region in 1,5-pentanediol is taken to be of the simple Debye type, our data (cf. Fig. 3) show the presence of an additional dispersion region at relatively high frequencies. They are consistent with the results of Mme Moriamez-Boullet (14), who reports at $-20°$ a second dispersion region which is a circular arc defined by $\epsilon_1 = 5.4 \pm 0.2$, $\epsilon_2 = 2.9 \pm 0.2$, $\alpha = 0.11 \pm 0.02$, and a most probable relaxation time some 80 times smaller than the single relaxation time of the primary dispersion.

The other pentanediols, like other liquids exhibiting skewed-arc behavior (1), show additional dispersion–absorption effects at frequencies of the order of several hundred times as great as that which corresponds to τ_0. The nature of these departures from the limiting straight line predicted by the skewed-arc locus for high frequencies is illustrated in the ϵ'' vs. ϵ' plots of Fig. 7.

Can. J. Chem. Downloaded from www.nrcresearchpress.com by 210.87.254.105 on 09/05/12
For personal use only.

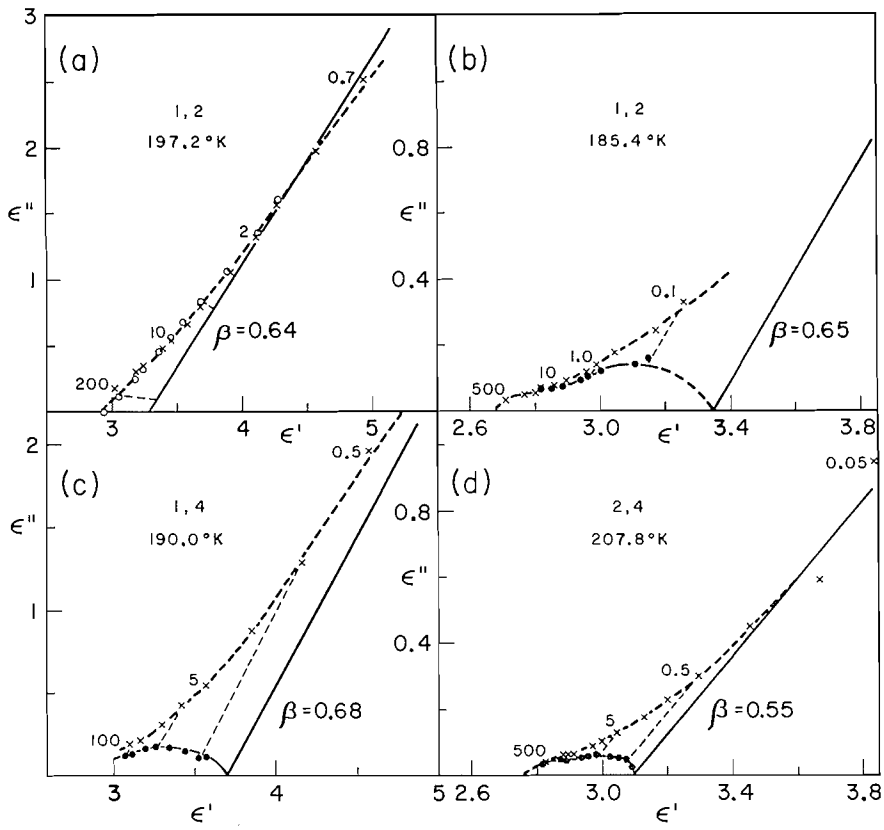


FIG. 7. Departures at relatively high frequencies of pentanediols from skewed-arc behavior: × experimental points; ○ Glarum locus with $a_0 = 4$, $\tau_0 = 1.07\times10^{-2}$ sec; ● points obtained by subtraction from experimental points of skewed-arc loci with values of τ_0 of (*b*) 6.4, (*c*) 3.2×10^{-2}, (*d*) 1.6 sec.

In order to explore the possibility that these effects may arise from the superposition of the skewed-arc locus and some physically distinct relaxation mechanism occurring at relatively high frequencies, attempts have been made to subtract the contribution of the skewed-arc locus to the experimental results. This procedure is more approximate than was the case of, for example, *n*-propanol (16, 19) since the skewed-arc locus makes much larger contributions at high frequencies and requires one more parameter (β) for its representation than does the Debye semicircle. As shown in Fig. 6(*b*, *c*, *d*), it is possible to obtain, by this somewhat laborious procedure, a residual absorption which resembles two overlapping circular arcs, much like those reported for *n*-propanol. It should be pointed out that the only justification for this arbitrary method of treating the data lies in the similarity between the resulting residues and those obtained for simple alcohols. Moreover, slight changes in the skewed-arc parameters lead to either overlap of the residual locus with the high-frequency end of the skewed-arc locus or to negative residual absorption at some frequencies. To get residues of the type shown, it is necessary to assign values of τ_0 which are somewhat larger than predicted by the linear relationship (see above) between $\log \tau_0$ and $1/(T-T_\infty)$.

The Glarum model (22) of relaxation leads to an expression which differs appreciably from that of the skewed arc only at high frequencies. The Glarum equation is capable

Can. J. Chem. Downloaded from www.nrcresearchpress.com by 210.87.254.105 on 09/05/12
For personal use only.

of representing the experimental results for the pentanediols to considerably higher frequencies than is the skewed-arc equation. This is illustrated for 1,2-pentanediol in Fig. 6(*a*). At still higher frequencies (or lower temperatures, Fig. 6(*b*)) the experimental absorption exceeds that of the Glarum locus which, in the limit of high frequencies, becomes a straight line which approaches the ϵ' axis at 45°. It is interesting to note that subtraction of the Glarum locus from the experimental one now leaves a single arc, which approximately corresponds to the higher-frequency arc of the pair that resulted from subtraction of the skewed arc.

In all events, there is an extremely broad loss spectrum at very high frequencies, which, if not completely accounted for by the diffusion-controlled relaxation process of Glarum, does appear to arise from a mechanism different from the co-operative orientation of locally ordered molecules responsible (1) for the behavior at lower frequencies.

The values of ϵ_1, whether determined by the high-frequency intercept of the skewed-arc or of the Glarum locus, decrease in the order 1,5-, 1,4-, 1,2-, 2,4-, and 2,3-pentanediol (see Table VII). This is roughly the order in which the relative number of weak and

TABLE VII

Variation of ϵ_1 and β with temperature (based on data between ca. −80 and −20° C)

	Skewed arc				Glarum,
Pentanediol	$\epsilon_1(-60°\text{ C})$	$d\epsilon_1/d(10^3/T)$	$\beta(-60°\text{ C})$	$d\beta/d(10^3/T)$	$\epsilon_1(-60°\text{ C})$
1,5	(5.2_5) (−30° C)		(1)		(5.2_5) (−30° C)
1,4	3.61	+0.020	0.73	−0.10	3.2_1
1,2	3.29	0.014	0.64	−0.03	2.9_8
2,4	3.17	0.012	0.55_5	−0.15	2.8_4
2,3	2.92	0.004	0.52_5	−0.03	2.6_9

broken hydrogen bonds increases, so that the magnitude of ϵ_1 cannot be directly related to the orientation of free or weakly hydrogen-bonded OH groups. At very high frequencies the absorption approaches zero at values of ϵ' of the order of 2.6 to 2.7, somewhat in excess of likely values of the square of the refractive indices, but similar to the dielectric constant observed for solid 1,5-pentanediol at comparable temperatures.

Temperature Dependence of the Dispersion

As may be seen from Table VII, the value of β in the skewed-arc representation tends to decrease with decreasing temperature. Although the values of $d\beta/d(1/T)$ tabulated are only approximate, they seem to show no systematic dependence on β. Moreover, the variation of β with temperature cannot be related to a model which assumes that the distribution of relaxation times arises from the presence of a temperature-independent distribution of barrier heights to rotation, such as may approximately account for the broadening of the dispersion exhibited by some solids with decreasing temperature (23).

In the Glarum representation (22), the shape of the dispersion–absorption locus depends on a_0 alone. As the temperature gets lower, the value of a_0 decreases, that is, the contribution of the diffusion-controlled relaxation becomes greater. Since $a_0 = l^2/D\tau_0$, this may be naively accounted for if the average defect diffusion relaxation time (l^2/D) increases less with decreasing temperature than does relaxation time for co-operative molecular rotation (τ_0) and the values of the two "relaxation times" therefore approach one another.

No extensive results are yet available for liquids at temperatures corresponding to β

Can. J. Chem. Downloaded from www.nrcresearchpress.com by 210.87.254.105 on 09/05/12
For personal use only.

less than 0.5 ($a_0 < 1$) where the Glarum theory makes the interesting prediction of behavior intermediate between that of the skewed arc and circular arc.

CONCLUSIONS

It may be concluded that departures of this type of asymmetric locus from the Debye semicircle arise from the presence of disordered regions in the liquid.

The increased asymmetry of the loss spectrum which results from increased interference with *inter*molecular hydrogen bonding as the OH groups move in from the ends of the pentane chain, in the sequence 1,5-, 1,4-, 1,2-, 2,4-, and 2,3-pentanediol, is accompanied at low temperatures by a large increase in the most probable relaxation time τ_0.* This type of relaxation is therefore not made easier by structural irregularity, within the present limits, but rather takes place most readily for liquids with the highest degree of local order. It is apparent that regularity of structure is somehow important in the activation process. This co-operative relaxation process may involve the sharing among many molecules of an accumulation of energy obtained at the expense of the vibrational energy of the quasi-crystalline lattice. The common nature of the variation of τ_0 with temperature is consistent with this picture.

REFERENCES

1. D. W. DAVIDSON. Can. J. Chem. **39**, 571 (1961).
2. D. W. DAVIDSON. Can. J. Chem. **35**, 458 (1957).
3. R. WALKER and D. W. DAVIDSON. Can. J. Chem. **37**, 492 (1959).
4. L. P. KUHN. J. Am. Chem. Soc. **74**, 2492 (1952).
5. V. I. MALYSHEV and V. N. MURZIN. Izvest. Akad. Nauk S.S.S.R. Ser. Fiz. **22**, 1107 (1958).
6. L. P. KUHN. J. Am. Chem. Soc. **80**, 5950 (1958).
7. J. A. A. KETELAAR and N. VAN NEURS. Rec. trav. chim. **76**, 437 (1957).
8. C. P. SMYTH and W. S. WALLS. J. Am. Chem. Soc. **53**, 2115 (1931).
9. A. H. WHITE and S. O. MORGAN. Physics, **2**, 313 (1932).
10. L. G. WESSON. Tables of electric dipole moments. The Technology Press, Cambridge, Mass. 1948.
11. A. A. MARYOTT and F. BUCKLEY. Tables of dielectric constants and electric dipole moments of substances in the gaseous state. Natl. Bur. Standards (U.S.) Circ. No. 537. 1953.
12. C. P. SMYTH. Dielectric behavior and structure. McGraw-Hill Book Co., Inc., New York. 1955. (*a*) p. 370; (*b*) p. 244.
13. K. KULKA, J. A. ROGERS, JR., O. HANSEN, and R. J. EISERLE. J. Org. Chem. In press.
14. C. MORIAMEZ-BOULLET. Compt. rend. **246**, 2364 (1958).
15. W. DANNHAUSER and R. H. COLE. J. Chem. Phys. **23**, 1762 (1955).
16. D. W. DAVIDSON and R. H. COLE. J. Chem. Phys. **19**, 1484 (1951).
17. F. X. HASSION and R. H. COLE. J. Chem. Phys. **23**, 1756 (1955).
18. R. H. COLE. Izvest. Akad. Nauk S.S.S.R. Ser. Fiz. **24**, 4 (1960).
19. D. W. DAVIDSON and J. WHEELER. J. Chem. Phys. **30**, 1357 (1959).
20. D. J. DENNEY. J. Chem. Phys. **30**, 159 (1959).
21. M. L. WILLIAMS, R. F. LANDEL, and J. D. FERRY. J. Am. Chem. Soc. **77**, 3701 (1955).
22. S. H. GLARUM. J. Chem. Phys. **33**, 639 (1960).
23. D. W. DAVIDSON. Can. J. Chem. **39**, 1321 (1961).
24. R. G. BENNETT. Compte rendu du 9e Colloque Ampere, Geneva, 1960. p. 62.

APPENDIX

Calculation of the Dipole Moment of Vicinal Diols

In Table VIII are listed values of dipole moments for assumed models of vicinal diols. The OH and OC bond moments have been taken to be 1.51 (12*b*) and 1.10 debyes, respectively, with all angles assumed, for simplicity, to be tetrahedral. Since the small CH moments have not been taken explicitly into account, their effects are approximately included in the value taken for the OC moment.

Forms (*c*) to (*g*) are internally hydrogen bonded. In (*d*) the free OH group is rotated

**A similar steric effect is noticed in the recent results of Bennett (24), who finds that 1-phenyl-propanol ($\beta = 0.7$) exhibits much higher relaxation times at low temperatures than do 3-phenyl-propanol and 2-phenyl-ethanol ($\beta = 1$).*

Can. J. Chem. Downloaded from www.nrcresearchpress.com by 210.87.254.105 on 09/05/12
For personal use only.

TABLE VIII

Calculated dipole moments of vicinal diols

Model	Dipole moment (debyes)
(*a*) Free rot. about all bonds	2.07
(*b*) Free rot. about trans CO bonds	2.01
(*c*) CO bonds cis, all atoms coplanar	2.91
(*d*) CO bonds cis, e.o. in plane	2.52
(*e*) CO bonds gauche, $r_{O\cdots H}$ min, $r_{H\cdots H}$ max	2.64
(*f*) CO bonds gauche, first e.o. in plane of CO, O- - -H	2.48
(*g*) CO bonds gauche, second e.o. in plane of CO, O- - -H	2.10

about its CO bond through 120° from the planar case (*c*) so as to bring the direction of maximum electron density of either of the lone pair electron orbitals (e.o.) into the plane of the rest of the molecule.

In the three gauche forms, (*e*) to (*g*), the length of the hydrogen bond is made a minimum by rotation of the bonded OH group about its CO bond. Form (*e*) results from rotation of the free OH group about the CO bond until its H atom is as far as possible from the H atom in the bond. In (*f*) and (*g*) one or the other of the e.o.'s on the O atom is brought by this rotation as near as possible to the H atom in the bond.

The O- - -H and O- - -O distances are 1.84 and 2.49 Å, respectively, for the cis forms, and 2.33 and 2.82 Å for the gauche forms, with the following bond lengths assumed: OH 0.97, OC 1.42, C—C 1.54 Å. The O—H- - -O angles, measured within the ring, are 122° (cis) and 111° (gauche).

Most of the calculated dipole moments of the internally hydrogen-bonded forms are higher than the experimental moments of Table III. Form (*g*) fits the data best, but, since there is no good reason for preferring it to (*f*), the r.m.s. value of the moments of these two forms should be taken. This value (2.31 debyes) is sufficiently close to the experimental moments to suggest that the predominant hydrogen-bonded species are approximately gauche forms in which the orbitals of the lone pair electrons of the O atom in the hydrogen bond tend to be oriented toward the H atom. It is likely that the energy of the hydrogen bond is too small to produce much of a rotation from the normal gauche toward the cis configuration. Although there is no evidence for an appreciable population of trans forms in CCl_4 (compare Table II), it is possible that such forms may be promoted in dioxane by hydrogen bonding to the solvent.

The approximate nature of the calculations should be borne in mind. Thus, the values of the OH and OC bond moments (1.55 and 1.30 debyes) required to give agreement with the experimental moment of 1.66 debyes for monohydroxyl alcohols are considerably larger than the ones assumed here, and result in calculated moments which are larger by some 0.2 debyes than those given in Table VIII. If the O angle is taken to be 105° instead of tetrahedral, the bond moments and the resultant moments are somewhat reduced.

Can. J. Chem. Downloaded from www.nrcresearchpress.com by 210.87.254.105 on 09/05/12
For personal use only.

Can. J. Chem. Downloaded from www.nrcresearchpress.com by 210.87.254.105 on 09/05/12
For personal use only.

SOLVOLYSIS IN HYDROGEN AND DEUTERIUM OXIDE

IV. HALIDES WITH NEIGHBORING GROUPS[1]

P. M. LAUGHTON[2] AND R. E. ROBERTSON

ABSTRACT

Rate data for the hydrolysis of a series of halohydrins and related compounds in light and heavy water are reported. The solvent isotope effects (k_{D_2O}/k_{H_2O}) from these measurements fall into three groups compared with those of simple halides. Thus the presence of a hydroxyl group in proximity to the seat of reaction may lead to increased, decreased, or normal solvent isotope ratios. The abnormal ratios can be interpreted in terms of the effect of anchimeric assistance on the solvation shell in the activation process.

In previous papers of this series, the solvent isotope effect (k_{D_2O}/k_{H_2O}) was shown to be remarkably insensitive to the structure of the alkyl group (1, 2, 3). This insensitivity appeared to rule out significant changing contributions from secondary isotope effects arising from variation in nucleophilic interaction (4, 5) and led to an explanation of the observed solvent isotope effect in terms of the relative stability of the initial state solvation shell. In the present paper we extend this hypothesis to include a series of compounds where apparent exceptions to the above generalization are found, and we are led to re-examine the hypothesis that transition state differences such as varying nucleophilic interaction may be neglected.

Specifically, we examine the solvent isotope effect for a series of halohydrins and analogous compounds substituted with alkoxyl or halide in positions where in certain cases other evidence leads to the expectation of anchimeric assistance in hydrolysis.

Rate data for the compounds studied in H_2O and D_2O were determined by a conductance method described in an earlier paper (6). It is generally recognized that this method gives the most accurate rate measurements available for this type of reaction, a fact of particular importance where questions relating to differences in rate ratios are involved. Since in this work we report a large number of kinetic data for a series of interesting compounds which, with few exceptions, had not previously been studied in water, it was considered desirable to publish now, even though only a qualitative interpretation is warranted at this time. Rate data for hydrolysis in D_2O and H_2O with corresponding temperatures are given in Table I. The sources of the compounds studied are included in the section on experimental detail, following the discussion.

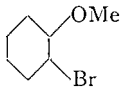
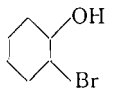
CORRELATION OF SOLVENT ISOTOPE EFFECTS

In earlier papers we showed that whereas there was a marked difference between the solvent isotope effect for sulphonates and halides, the differences between corresponding halides—chlorides, bromides, and iodides—were much smaller, and these could be further reduced if due allowance was made for the effect of temperature on this ratio (3). We

[1]*Manuscript received June 6, 1961.*
Contribution from the Division of Pure Chemistry, National Research Council, and the Department of Chemistry, Carleton University, Ottawa. Part of this work was assisted by a grant in aid of research from the National Research Council to one of us (P.M.L.). This work was presented in part at the Toronto Meeting of the Chemical Institute of Canada, May 27, 1958.
Issued as N.R.C. No. 6508.
[2]*Department of Chemistry, Carleton University, Ottawa.*

TABLE I

Solvolytic rate constants for the reaction in light and heavy water of some halides with neighboring groups

Code	Halide	Temp., °C	$k_{D_2O}, \times 10^5$ sec^{-1}	$k_{H_2O}, \times 10^5$ sec^{-1}	k_{D_2O}/k_{H_2O}
I	$HO\text{-}CH_2CH_2\text{-}Cl$	90.1_7	0.164 ± 0.0007	0.210 ± 0.0006	0.78
II	$HO\text{-}(CH_2)_3\text{-}Cl$	100.00	2.15 ± 0.03	2.66 ± 0.008	0.81
III	$HO\text{-}(CH_2)_4\text{-}Cl$	80.99	148.4 ± 0.2	171.0 ± 0.1	0.86
IV	$MeO\text{-}(CH_2)_4\text{-}Cl$	80.02	52.9 ± 0.1	59.5 ± 0.1	0.89
V	$HO\text{-}CH_2CH_2Br$	80.15	0.846 ± 0.009	1.082 ± 0.005	0.78
VI	$HO\text{-}(CH_2)_3\text{-}Br$	80.15	5.87 ± 0.01	7.03 ± 0.01	0.83_5
VII	$Br\text{-}(CH_2)_4\text{-}Br$	80.15	20.4 ± 0.02	24.9 ± 0.03	0.82
VIII	$MeO\text{-}(CH_2)_4\text{-}Br$	50.00	36.98 ± 0.04	44.09 ± 0.08	0.84
IX	$HO\text{-}CH_2CH_2\text{-}I$	80.15	0.325 ± 0.002	0.429 ± 0.003	0.76
X	$HO\text{-}(CH_2)_3\text{-}I$*	100.01	$12.1_5 \pm 0.1$	$15.9_5 \pm 0.07$	0.76
XI	$MeO\text{-}(CH_2)_3\text{-}I$*	100.01	$15.0_1 \pm 0.06$	$18.6_6 \pm 0.06$	0.80
XII	$HO\text{-}CMe_2CH_2\text{-}Cl$	90.00	0.940 ± 0.004	1.338 ± 0.009	0.70
XIII	$HO\text{-}CMe_2CH_2\text{-}Br$	80.15	6.30 ± 0.03	9.70 ± 0.01	0.65
XIV	$HO\text{-}CMe_2CHMe\text{-}Cl$	80.16	17.0 ± 0.1	23.4 ± 0.1	0.73
XV	$HO\text{-}CMe_2CHMe\text{-}Br$	51.10	16.3 ± 0.2	23.9 ± 0.2	0.68
XVI	$MeO\text{-}CMe_2CHMe\text{-}Br$*	70.01	$63.9_5 \pm 0.01$	74.6 ± 0.2	0.86
XVII	$HO\text{-}CMe_2CMe_2\text{-}Cl$	29.46	104.6 ± 0.0	141.4 ± 0.4	0.74
XVIII	$I\text{-}CH_2CMe_2\text{-}Cl$	5.09	50.5 ± 0.1	71.5 ± 0.3	0.71
XIX	$MeO\text{-}CH_2CMe_2\text{-}Cl$	40.00_5	$59.7_1 \pm 0.2$	$76.2_9 \pm 0.18$	0.78
XX	*trans* 	89.99	12.16 ± 0.04	14.62 ± 0.03	0.83
XXI	*trans* 	89.68	22.8 ± 0.1	31.1 ± 0.2	0.74
XXII	$MeO\text{-}CMe_2CH_2\text{-}Br$	100.01	$12.12 \pm .05$	13.64 ± 0.01	0.86
XXIII	$Br\text{-}CHMeCMe_2\text{-}Br$	70.00	$1.76_7 \pm 0.008$	1.400 ± 0.007	0.80

*Rates for these compounds were determined by L. E. Hakka, summer research assistant, 1961.

have recently shown (5) that the temperature dependence of the solvent isotope effect for isopropyl bromide can be expressed by the equation

$$[1] \qquad \log_{10} k_{D_2O}/k_{H_2O} = (-693.7073/T) - 4.4867 \log_{10} T + 13.2935$$

and from this we may determine average values of k_{D_2O}/k_{H_2O} to be expected for halides* over the experimental range.

The solid curve in Fig. 1 is a plot of log k_{D_2O}/k_{H_2O} versus $1/T$ for isopropyl bromide. This is shown to parallel the individual values for the k_{D_2O}/k_{H_2O} ratio for a wide range of halides supporting the above generalization.

It will be apparent from this plot that the ratios given in Table I for compounds having a hydroxyl or methoxyl so placed as to provide for a possibility of anchimeric assistance, may be divided with respect to this chosen norm into three groups. A number coincide within a few per cent with the reference curve based on equation [1]. These include the three ethylene halohydrins (I, V, and IX), pinacol chlorohydrin (XVII), and the strongly anchimeric tertiary chloride (XVIII) with a rate enhancement (in 80% ethanol) of 740 (7). Several other values of k_{D_2O}/k_{H_2O} from our earlier work are included in the plot as further evidence of the common trend with temperature in the value of the k_{D_2O}/k_{H_2O} ratio for the halides.

**Actually, because the value of k_{D_2O}/k_{H_2O} for isopropyl bromide is lower than for many halides, the true average would probably lie 1 to 2 per cent higher than given by equation [1].*

Can. J. Chem. Downloaded from www.nrcresearchpress.com by 210.87.254.105 on 09/05/12
For personal use only.

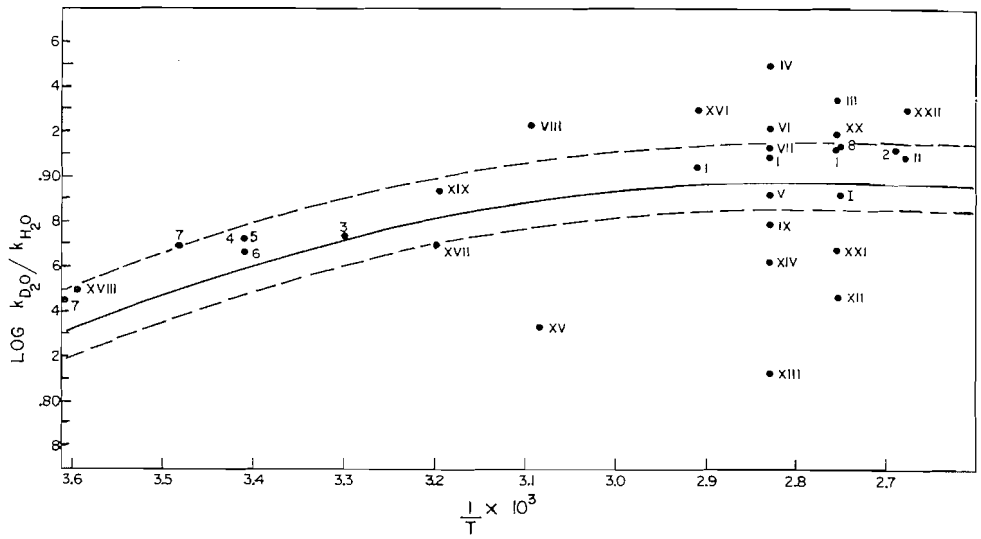
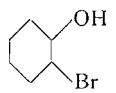


FIG. 1. The temperature dependence of solvent isotope effect for a series of halides, illustrating exceptional cases. Compounds from Table I are identified by Roman numerals. The remaining ratios are taken from paper III in this series (ref. 3): 1, MeBr; 2, EtBr; 3, *p*-$MeC_6H_4CH_2Cl$; 4, *p*-$MeC_6H_4CH_2Br$; 5, *o*-$MeC_6H_4CH_2Br$; 6, $PhCH_2Br$; 7, *t*-BuCl; 8, *t*-BuF. The solid line represents the data for *i*-PrBr from ref. 5.

The five compounds in the second group have ratios which lie below this arbitrary norm (Table II). These are the isobutylene and trimethylethylene halohydrins (XII, XIII, XIV, and XV) and the *trans*-cyclohexene bromohydrin (XXI). In the first four cases there appears to be anchimeric assistance, judging from the higher rates observed compared with the hydroxyl-free analogues and taking into consideration the fact that the normal inductive effect of β-hydroxyl would be reduction of the rate by a factor of 20 to 100 (8).

TABLE II

Rate ratios k_{D_2O}/k_{H_2O} for neighboring group halides showing lower than normal ratios

Code	Halide	k_{D_2O}/k_{H_2O} obs.	k_{D_2O}/k_{H_2O} normal*
XII	$HOCMe_2CH_2Cl$	0.70	0.789
XIII	$HOCMe_2CH_2Br$	0.65	0.788
XIV	$HOCMe_2CHMeCl$	0.73	0.788
XV	$HOCMe_2CHMeBr$	0.68	0.774
XXI	*trans* 	0.74	0.789

*Value calculated for *i*-PrBr at the same temperature.

The third group (Table III) displays somewhat higher values of the k_{D_2O}/k_{H_2O} ratio than normal and includes the three fast-reacting tetramethylene derivatives (III, IV, and VIII) and the isobutylene and trimethylethylene methoxybromides (XXII and XVI).

Can. J. Chem. Downloaded from www.nrcresearchpress.com by 210.87.254.105 on 09/05/12
For personal use only.

TABLE III

Rate ratios k_{D_2O}/k_{H_2O} for neighboring group halides showing higher than normal ratios

Code	Halide	k_{D_2O}/k_{H_2O} obs.	k_{D_2O}/k_{H_2O} normal*
III	$HO(CH_2)_4Cl$	0.86	0.789
IV	$MeO(CH_2)_4Cl$	0.89	0.789
VIII	$MeO(CH_2)_4Br$	0.84	0.772
XVI	$MeOCMe_2CHMeBr$	0.86	0.787
XXII	$MeOCMe_2CH_2Br$	0.86	0.786

*Value calculated for *i*-PrBr at the same temperature.

Thus it is apparent that an oxygen-containing β-substituent may raise, lower, or leave unchanged the solvent isotope effect. We now propose to show how these varying results can be fitted into the general explanation, based on the relative stability of the initial state solvation shell combined in certain cases (group 2, 3) with the influence of unusual reorganization arising in consequence of anchimeric assistance. It will be obvious that in the case of the halohydrins in D_2O, the OH will rapidly exchange with the medium to give OD, but it does not appear that secondary deuterium isotope effects from this source can provide a sufficient basis for the observed differences between the three groups. At any rate, another effect must dominate since this secondary isotope effect should result in shifting the ratios of all of the anchimerically assisted halohydrins in the same direction.

Evidence for Anchimeric Assistance in Hydrolysis

Because water is a fair nucleophile as well as a good ionizing medium, the probability of anchimeric interaction assisting solvolysis is less here than in the case with acetic acid as solvent (8), but it is not eliminated. With this reservation, evidence of such assistance follows the structural conditions noted in the less nucleophilic solvent. Thus ethylene halohydrins of Cl (I), Br (V), and I (IX) react at .043, .04, and .028 of the rate of the corresponding unsubstituted compounds, and a β-methoxyl introduces a rate reduction of 0.033 in the primary ethyl bromide (est. 5.1×10^{-5} sec^{-1} at 100°) (9), pointing to an absence of anchimeric effects. Methylation of the β- or hydroxyl-carbon leads to increased evidence for anchimeric assistance. For example, isobutylene chlorohydrin (XII) and bromohydrin (XIII) solvolyse more rapidly than ethylene chlorohydrin (I) and bromohydrin (V), as noted earlier by Nilsson and Smith (10) for reaction with alkali, thus differing sharply from the unsubstituted ethyl and isobutyl halides. Although the data are not available to calculate σ^* in the Taft equation ($\log k/k_0 = \rho\sigma^*$ (11)), for substrates isobutylene chlorohydrin (XII) and bromohydrin (XIII), it is plain that there must be substantial anchimeric assistance in these cases. Reasons for this substitution effect have been given by Thorpe *et al.* (12) and Schleyer (13). Tetramethylene chlorohydrin (III) reacts some 60 times more rapidly than *n*-propyl chloride, while trimethylene (II) and ethylene chlorohydrin (I) react successively more slowly. The difference in rate of hydrolysis between the tetramethylene methoxychloride (IV) and III is small. A similar trend is evident in the related bromides V, VI, VII, and VIII in Table I, the tetramethylene bromohydrin proving too reactive to obtain in a pure state. These data confirm the activating influence of a hydroxyl or other basic substituent in a 5-member ring-forming position, as noted by many workers, for example, Heine (14), and recently studied by Winstein *et al.* for solvolysis of methoxyalkyl brosylates (15).

Can. J. Chem. Downloaded from www.nrcresearchpress.com by 210.87.254.105 on 09/05/12
For personal use only.

Group 1. Normal k_{D_2O}/k_{H_2O} Values

These compounds in Table I which have normal values of k_{D_2O}/k_{H_2O} include without exception the halohydrins and corresponding methoxyhalides which give no evidence of anchimeric assistance. It would appear that the dihalides give "normal" values of k_{D_2O}/k_{H_2O} whether involving anchimeric assistance, XVIII, or not, XXIII. Tetramethylene dibromide (VII) is apparently a borderline case with the slightly higher than normal ratio of 0.818.

From our study of the temperature dependence of the solvent isotope effect for isopropyl bromide we concluded that the presence of the alkyl halide increased the structural stability of the initial state solvation shell relative to bulk water by about 20%. The very similar values of k_{D_2O}/k_{H_2O} found for the "normal" substrates in Table I suggest that the neighboring OH or MeO have not changed the degree of solvent reorganization about the anionic portion of the molecules in going from the initial to the transition state. Now it is very probable that the hydroxyl group is hydrogen bonded to the adjacent water structure, as is indicated by the large increase in solubility caused by its presence. In the absence of anchimeric assistance there is no reason to believe that this interaction is disturbed in the activation process, and hence there is no significant change in the energy required to reorganize the solvent in the activation process, from that required for the unsubstituted halide. It follows that normal k_{D_2O}/k_{H_2O} ratios are observed.

Group 2. Low k_{D_2O}/k_{H_2O} Values (Table II)

All of the compounds in this group are halohydrins; it is noteworthy that the corresponding methoxy compounds fall in group 3.

Following our earlier explanation of the solvent isotope effect, either the substrates with unusually low k_{D_2O}/k_{H_2O} ratios have a more stable solvent structure in the initial state or a more drastic reorganization occurs in the activation process. The first alternative is ruled out by the results of group 1 halohydrins, and since group 2 compounds all show anchimeric assistance, the second suggestion would seem more plausible. However, a further assumption is necessary since the third group with k_{D_2O}/k_{H_2O} values higher than "normal" also gives evidence of anchimeric assistance.

Judging from enhanced solubility compared with that of unsubstituted halides it may be inferred that the OH groups of those compounds giving abnormal k_{D_2O}/k_{H_2O} values must, like the normal compounds, interact, through hydrogen bonding, with the water in the initial state. It is noteworthy that the corresponding methoxy compounds fall into group 3.

Evidence of anchimeric assistance implies that, in contrast to group 1 compounds, this hydrogen bonding is more or less disrupted in the activation process. The phrase "more or less" is purposely vague for we do not yet possess sufficiently detailed knowledge to correlate the variation from the "normal" values of k_{D_2O}/k_{H_2O} with the degree of anchimeric assistance. To account for the abnormal k_{D_2O}/k_{H_2O} values it is sufficient to assume that the hydroxyl group will be pulled out of its initial state position in the water structure and bent laterally to form the transitory ethyleneoxonium ions. This more extensive rearrangement will, of course, accentuate the effects of structural differences between D_2O and H_2O as observed.

It is notable that as the seat of reaction changes successively from primary (XII, XIII) to secondary (XIV, XV) to tertiary (XVII) there is a trend toward more normal k_{D_2O}/k_{H_2O} ratios. This trend parallels the expected decrease in the importance of anchimeric assistance in these compounds.

Can. J. Chem. Downloaded from www.nrcresearchpress.com by 210.87.254.105 on 09/05/12
For personal use only.

While this rationalization is admittedly *ad hoc*, our proposed explanation has certain implications concerning accompanying changes in entropy, enthalpy, and heat capacity which are open to experimental verification and these are currently under investigation.

Group 3. High k_{D_2O}/k_{H_2O} Values (Table III)

There are a number of hydroxyl- and methoxyl-substituted halides which show varying degrees of anchimeric assistance and yet have solvent isotope ratios (k_{D_2O}/k_{H_2O}) closer to unity than "normal". These include the tetramethylene chlorohydrin (III), methoxychloride (IV), and methoxybromide (VIII); trimethylene bromohydrin (VI); and isobutylene (XXII), trimethylethylene (XVI), and *trans*-cyclohexene methoxybromides (XX), which are to be contrasted with the corresponding bromohydrins (XIII, XV, and XXI). To these may be added isobutyl and neopentyl bromide, which gave indications of "higher" than normal solvent isotope ratios (3). The solvent isotope effects here deviate less from the normal than those found for group 2, and it is by no means certain that these deviations arise from the same cause in every case.

In an earlier paper (1) we discounted the isotope effect arising from varying nucleophilic interaction, yet it was difficult to imagine that the degree of reorganization which occurs about the cation would have no solvent isotope effect at all. It was more reasonable to equate at least part of the scatter apparent among the unsubstituted halides (normal solvent isotope effect) to this source. Both when the substituent group in the initial state blocks the rear side of the carbon undergoing displacement, and particularly when, as in the anchimerically assisted cases, it also serves as the displacing nucleophile, a lesser degree than normal of solvent reorganization will take place. This should lead to ratios nearer unity.

While the differentiation between groups 2 and 3 has a strong *ad hoc* flavor, it does have the advantage of explaining the quite different behavior of the tetramethylene chlorides (III) and (IV), both of which are group 3 compounds, while the pairs of compounds (XIII) and (XXII), (XV) and (XVI), and (XX) and (XXI) split between groups 2 and 3. In the latter cases the lateral displacements of the intramolecular nucleophiles require, for (XIII), (XV), and (XXI), the removal of the hydroxyl group *from* the water shell, and for (XIII), (XVI), and (XX), the movement of methoxyl *within* the solvent shell. The former leads to extensive reorganization and lower isotopic ratios; the latter leads to higher ratios because the displacement leads to relatively less reorganization than the abstraction of one water molecule from the solvent shell to serve as nucleophilic reagent. In the case of (III) and (IV), on the other hand, the intramolecular nucleophile must lie properly oriented behind the carbon–halogen bond early in the activation process, hence little reorganization is required.

At first we found it troublesome to understand why the iodochloride (XVIII) did not have as high a ratio as the isobutylene methoxybromide (XXII). Inspection of models shows that the iodine atom is so large that it is already almost touching the backside of the tertiary carbon undergoing displacement in XVIII, while the methoxyl group in XXII has to move an appreciable distance. However, the iodine is not hydrogen bonded to water in the initial state but presumably interacts as an exposed iodonium ion in the transition state. The methoxyl oxygen, on the other hand, is protected from solvation in the transition state by the alkyl group.

The case of compounds (XX) and (XXI) is being further investigated because their thermodynamic parameters of activation (24) indicate no noticeable anchimeric rate enhancement, although they clearly split between groups 2 and 3. A more detailed

Can. J. Chem. Downloaded from www.nrcresearchpress.com by 210.87.254.105 on 09/05/12
For personal use only.

analysis may show whether an anchimeric reaction may be proceeding through an unfavorable diaxial conformation, thus offsetting the rate enhancement.

EXPERIMENTAL DETAIL

The sources of the compounds and the available physical constants are summarized in Table IV. Commercially available compounds were either recrystallized or fractionally distilled under reduced pressure. In all cases linear pseudo first-order plots were obtained and this was considered to be the best critique of purity for the present purpose. Those compounds not otherwise available were synthesized* by the methods referenced in Table IV.

TABLE IV

Summary of sources and characteristics of halides solvolysed

Code	Halide	Boiling point	n_D^{25}	Source
I	2-Chloroethanol	56° (40 mm)	1.4260	Comm.
II	3-Chloro-1-propanol	56° (10 mm)	1.4415	,,
III	4-Chloro-1-butanol	86° (20 mm)	1.4513 (23°)	,,
IV	4-Chloro-1-methoxybutane	48–53° (20 mm)	1.4290	*a*
V	2-Bromoethanol	51–52° (14 mm)	1.4880 (26°)	Comm.
VI	3-Bromo-1-propanol		1.4861 (26°)	,,
VII	1,4-Dibromobutane		1.5161	,,
VIII	4-Bromo-1-methoxybutane	46–49° (12 mm)	1.4479	16
IX	2-Iodoethanol	88° (30 mm)	1.5625	*b*
X	3-Iodo-1-propanol	88–90° (7 mm)	1.5768 (24°)	17
XI	3-Iodo-1-methoxypropane	155–158°	1.4873 (27°)	*c*
XII	1-Chloro-2-methyl-2-propanol	56° (40 mm)	1.4260	*d*
XIII	1-Bromo-2-methyl-2-propanol	45° (15 mm)	1.4704	19
XIV	3-Chloro-2-methyl-2-butanol		1.4415	18
XV	3-Bromo-2-methyl-2-butanol	48–49.5° (10 mm)	1.4719	19
XVI	3-Bromo-2-methoxy-2-methyl-butane	56–57° (24 mm)	1.4551	19
XVII	3-Chloro-2,3-dimethyl-2-butanol	45–50° (15 mm)	m. 63.5–64.5°	20
XVIII	2-Chloro-1-iodo-2-methylpropane	54.5–55.2° (25 mm)	(Colored)	8
XIX	2-Chloro-1-methoxy-2-methylpropane	88–90°	1.4039 (24°)	*e*
XX	*trans*-2-Bromo-1-methoxy-cyclohexane		1.4890	22
XXI	*trans*-2-Bromocyclohexanol	73–75° (5 mm)	1.5184	*f*
XXII	1-Bromo-2-methoxy-2-methylpropane		1.4575	*g*
XXIII	2,3-Dibromo-2-methyl-butane	45–49° (10 mm)	1.5030	23

a. Prepared by method of (16) applied to tetramethylene chloride. The material isolated by fractionation was further purified on a Perkin–Elmer V.P.C. column.

b. Finckelstein reaction on ethylene chlorohydrin.

c. Finckelstein reaction on 3-bromo-1-methoxypropane, b. 129°, n_D^{26} 1.4448, prepared as for compound VIII.

d. Method of Smith and Skyle (18) applied to isobutylene using a dry ice reflux condenser.

e. Prepared from the alcohol (21) by Dr. K. T. Leffek.

f. Kindly supplied by Dr. R. A. B. Bannard; m.p. 27°, but supercools readily.

g. Prepared by the method used for compound XVI, applied to isobutylene, and purified by fractional freezing.

ACKNOWLEDGMENT

We wish to acknowledge the assistance of Mr. S. Sugamori in determining many of the rate data on which this paper is based.

**The following Carleton University students contributed to these preparations: H. G. Dodds, L. E. Hakka, C. A. McDonell, W. J. Meath, A. D. Relf, R. D. Sully, and R. Wardle.*

Can. J. Chem. Downloaded from www.nrcresearchpress.com by 210.87.254.105 on 09/05/12
For personal use only.

REFERENCES

1. P. M. LAUGHTON and R. E. ROBERTSON. Can. J. Chem. **34**, 1714 (1956).
2. R. E. ROBERTSON and P. M. LAUGHTON. Can. J. Chem. **35**, 1319 (1957).
3. P. M. LAUGHTON and R. E. ROBERTSON. Can. J. Chem. **37**, 1491 (1959).
4. J. A. LLEWELLYN, R. E. ROBERTSON, and J. M. W. SCOTT. Can. J. Chem. **38**, 222 (1960).
5. R. L. HEPPOLETTE and R. E. ROBERTSON. J. Am. Chem. Soc. **83**, 1834 (1961).
6. R. E. ROBERTSON. Can. J. Chem. **33**, 1536 (1955).
7. A. STREITWIESER, JR. J. Am. Chem. Soc. **78**, 4935 (1956).
8. S. WINSTEIN and E. GRUNWALD. J. Am. Chem. Soc. **70**, 828 (1948).
9. M. J. BLANDAMER. Private communication.
10. H. NILSSON and L. SMITH. Z. physik. Chem. (Leipzig), A, **166**, 136 (1933).
11. R. W. TAFT, JR. J. Am. Chem. Soc. **75**, 4231 (1953).
12. R. M. BEESLEY, C. K. INGOLD, and J. F. THORPE. J. Chem. Soc. **107**, 1080 (1915).
13. P. VON R. SCHLEYER. J. Am. Chem. Soc. **83**, 1368 (1961).
14. H. W. HEINE, A. B. MILLER, W. H. BARTON, and R. W. GREINER. J. Am. Chem. Soc. **75**, 4778 (1953).
15. S. WINSTEIN, E. ALLRED, R. HECK, and R. GLICK. Tetrahedron, **3**, 1 (1958).
16. A. KIRRMANN and N. HAMAIDE. Bull. soc. chim. France, 789 (1957).
17. L. HENRY. Bull. classe sci. Acad. roy. Belg. **33** (3), 407 (1897).
18. L. SMITH and S. SKYLE. Acta Chem. Scand. **5**, 1415 (1951).
19. S. WINSTEIN and L. L. INGRAHAM. J. Am. Chem. Soc. **74**, 1163 (1952).
20. F. BÄYER AND CO. DRP 317, 635 (1916). Fortschritte der Teerfarben-fabrikation und Verwandter Industriezweige **13**, 73 (1916–21).
21. M. H. PALOMAA. Ann. Acad. Sci. Fennicae, Ser. A, **10**, No. 17 (1918).
22. S. WINSTEIN and R. R. HENDERSON. J. Am. Chem. Soc. **65**, 2196 (1943).
23. A. H. BLATT. Organic syntheses. Coll. Vol. II. John Wiley and Sons, Inc., New York. 1943. p. 408.
24. M. J. BLANDAMER and R. E. ROBERTSON. Unpublished data.

Can. J. Chem. Downloaded from www.nrcresearchpress.com by 210.87.254.105 on 09/05/12
For personal use only.

Can. J. Chem. Downloaded from www.nrcresearchpress.com by 210.87.254.42 on 09/05/12
For personal use only.

RADIATION CHEMISTRY OF CYCLOHEXANE

III. EFFECT OF BENZENE AND IODINE ON THE ISOTOPIC COMPOSITION OF RADIOLYTIC HYDROGEN FROM C_6D_{12}–C_6H_{12} MIXTURES[1]

P. J. Dyne and W. M. Jenkinson

ABSTRACT

The isotopic composition of hydrogen evolved in the radiolysis of C_6D_{12}–C_6H_{12} mixtures has been measured in the presence of various amounts of benzene and iodine. The yield of the unimolecular decomposition and the specific yield of the bimolecular reaction are reduced in approximately the same proportion as the yield of total hydrogen. It is concluded that (i) iodine and benzene interact to a comparable extent with both unimolecular and bimolecular decomposition modes, (ii) it is probable that neither of these additives act by scavenging, and (iii) it is probable that they act by quenching a common precursor of the two decomposition modes.

INTRODUCTION

We have shown from measurements of the isotopic composition of hydrogen produced in the radiolysis of C_6D_{12}–C_6H_{12} mixtures (1) that part of the hydrogen is formed in a bimolecular process

$$C_6H_{12} \text{ —}\sim\sim\rightarrow X_H + P \qquad \text{yield } G_2(H) \qquad [1]$$

$$X_H + C_6H_{12} \rightarrow H_2 + P \qquad [2]$$

where the atoms in the H_2 molecule come from two different cyclohexane molecules, and part is formed in a unimolecular process

$$C_6H_{12} \text{ —}\sim\sim\rightarrow H_2 + P \qquad \text{yield } G_1(H) \qquad [3]$$

where both hydrogen atoms come from the same cyclohexane molecule. The symbol P represents any product or residue and X_H is the reactive intermediate in the bimolecular process.

The specific yield of the decomposition

$$C_6D_{12} \text{ —}\sim\sim\rightarrow D_2 + P \qquad \text{yield } G_1(D) \qquad [4]$$

in a large excess of C_6H_{12} was shown to be 0.25 molecules/100 ev absorbed in the C_6D_{12}. However, the yield of reaction [3] in pure C_6H_{12} may amount to between 25% (2) and nearly 50% (3) of the total yield. It is conceivable that this large "isotope effect" expresses variations in $G_1(D)$ and $G_1(H)$ with the isotopic composition of the solvent due to some type of energy transfer or charge transfer effect. In the experiments described in this paper we used the yield of D_2 from C_6D_{12} as an "indicator" of the efficiency of unimolecular processes in benzene and iodine solutions in cyclohexane.

We also showed (1) that $G_1(D)$, the yield of reaction [4], was reduced by biphenyl, and slightly reduced by iodine. We concluded that biphenyl could act as a quenching agent[2] on the excited precursors involved in the unimolecular decomposition.

In this paper we describe a series of measurements of the isotopic composition of hydrogen evolved in the radiolysis of C_6D_{12}–C_6H_{12} mixtures in the presence of varying amounts of benzene and iodine. We find that, for both these substances, $G_1(D)$ is reduced in approximately the same proportion as the total hydrogen yield, and we infer that the unimolecular and bimolecular decompositions are quenched to approximately the same extent by these substances. Burton and Chang (4) have studied the change in isotopic

[1]*Manuscript received June 22, 1961.*
Contribution from the Research Chemistry Branch, Atomic Energy of Canada Limited, Chalk River, Ontario. Issued as A.E.C.L. No. 1340.

[2]*In this paper 'quenching' refers to any process (energy transfer, charge transfer), other than radical scavenging, which inhibits decomposition or reduces a yield.*

composition of hydrogen evolved from mixtures containing roughly equimolar amounts of C_6H_{12} and C_6D_{12} and have discussed their results in terms of the function

$$f = \frac{[HD]^2}{[H_2][D_2]}.$$

The addition of benzene, iodine, methyl iodide, and cyclohexene to a given mixture of C_6D_{12} and C_6H_{12} changes f very little, even though G(hydrogen) may be reduced by as much as 80%.

Our work is, in the main, in agreement with their results and conclusions.[3] It differs in the following respects: we studied solutions containing less than 10 mole% C_6D_{12}, and discuss our results in terms of changes in G_1(D) and G(HD) rather than in f. At these concentrations of C_6D_{12} we observed small changes in f on the addition of benzene and iodine to a C_6D_{12}–C_6H_{12} mixture.

EXPERIMENTAL

The salient experimental details have been given in ref. 1. In the present experiments, however, the 2-ml samples were irradiated for 2 hours at a dose rate of $\sim 2.2\times10^{22}$ ev/lt hr. The total dose is about one-third that given in the earlier experiments and the experimental values of G(hydrogen) are, consequently, higher.

Solutions of four concentrations of C_6D_{12}, viz. 2.43, 4.78, 6.98, and 9.09 mole% were studied at four concentrations of benzene and three of iodine. These results are shown in Table I.

TABLE I

Isotopic composition of radiolytic hydrogen evolved from C_6D_{12}–C_6H_{12} mixtures

Mole% C_6D_{12}	Concn. of additive	G(hydrogen)	% H_2	% HD	% D_2	$f = \frac{[HD]^2}{[H_2][D_2]}$
2.43 = *a*			98.01	1.84	0.15	0.230
4.78 = *b*	0	5.34	96.11	3.59	0.30	0.446
6.98 = *c*			94.33	5.21	0.46	0.625
9.09 = *d*			92.53	6.83	0.64	0.787
a			97.91	1.94	0.15	0.256
b	C_6H_6	4.80	95.92	3.75	0.33	0.444
c	0.25 mole%		93.93	5.58	0.49	0.676
d			92.03	7.27	0.70	0.820
a			97.86	1.99	0.15	0.269
b	C_6H_6	4.66	96.21	3.51	0.28	0.457
c	0.608 mole%		93.86	5.64	0.50	0.673
d			91.89	7.42	0.69	0.868
a			97.74	2.10	0.16	0.282
b	C_6H_6	4.03	95.61	4.06	0.33	0.522
c	1.22 mole%		93.67	5.83	0.50	0.722
d			91.62	7.67	0.71	0.903
a			97.50	2.31	0.19	0.288
b	C_6H_6	2.70	95.12	4.52	0.36	0.596
c	6.02 mole%		92.86	6.60	0.54	0.869
d			90.54	8.69	0.77	1.083
a			97.78	2.04	0.18	0.236
b	I_2	3.85	95.68	3.95	0.37	0.440
c	1×10^{-2} *M*		93.58	5.82	0.60	0.603
d			91.53	7.61	0.86	0.735
a			97.77	2.07	0.16	0.273
b	I_2	3.45	95.48	4.11	0.41	0.431
c	3×10^{-2} *M*		93.37	5.99	0.64	0.600
d			91.34	7.78	0.88	0.752
a			97.71	2.10	0.19	0.237
b	I_2	3.31	95.38	4.21	0.41	0.453
c	5×10^{-2} *M*		93.24	6.11	0.65	0.615
d			91.23	7.86	0.91	0.744

[3]*We are indebted to Professor Burton and Dr. Chang for their courtesy in sending us preprints of papers describing their work.*

Can. J. Chem. Downloaded from www.nrcresearchpress.com by 210.87.254.42 on 09/05/12
For personal use only.

Values of $G_1(D)$, the unimolecular yield, were obtained using the graphical extrapolation described in (1). Values of $g(HD)$,[4] the yield of HD per unit mole fraction of C_6D_{12}, were obtained from the slope of the linear plot of $G(HD)$ vs. mole fraction C_6D_{12}. These derived values, together with values normalized to the mixture containing neither benzene nor iodine, are given in Table II.

TABLE II
Values of absolute and normalized yields

Concn. of additive	G(hyd) ±0.08	Norm.	G_1(D) ±0.02	Norm.	g(HD) ±0.1	Norm.
None	5.34	1.00	0.32_2	1.00	3.59	1.00
0.25% C_6H_6	4.80	0.89_7	0.28	0.87_0	3.49	0.97_0
0.62% C_6H_6	4.66	0.87_1	0.25	0.77_7	3.27	0.90_9
1.22% C_6H_6	4.03	0.75_3	0.25	0.77_7	3.07	0.85_3
6.02% C_6H_6	2.70	0.50_4	0.19	0.59_0	2.37	0.65_8
1×10^{-2} M I_2	3.85	0.71_9	0.26	0.80_8	2.92	0.81_1
3×10^{-2} M I_2	3.45	0.64_5	0.25	0.77_7	2.68	0.74_5
5×10^{-2} M I_2	3.31	0.61_8	0.23	0.71_5	2.60	0.72_2

The error given in the value of G(hyd) in Table II covers the range of the experimental values. The errors in $G_1(D)$ and $g(HD)$ were obtained from the extreme values of the intercepts and slopes which could be derived from the experimental points and contain errors from both G(hydrogen) and from the isotopic analysis. Uncertainties in % D_2 at the lowest concentration of C_6D_{12} amount to ±10% and to ±2% at the highest.

The value of $G_1(D)$ in the absence of additives, 0.32±0.02, is greater than the value of 0.25 previously reported. This is because the present experiments were carried out at lower total doses. The newer value is more precise and compares well with the value of 0.35 obtained by Burton and Chang in similar experiments.

THE KINETIC ANALYSIS

The complete mechanism used for the interpretation of these results is:

$C_H \longrightarrow C_H^*$	yield $G_1(H)$
$C_H^* \rightarrow H_2 + P$	
$C_D \longrightarrow C_D^*$	yield $G_1(D)$
$C_D^* \rightarrow D_2 + P$	
$C_H \longrightarrow C_H^{**}$	yield $G_2(H)$
$C_H^{**} \rightarrow X_H + P$	
$C_D \longrightarrow C_D^{**}$	yield $G_2(D)$
$C_D^{**} \rightarrow X_D + P$	
$X_H + C_H \rightarrow H_2 + P$	rate constant k_1
$X_D + C_H \rightarrow HD + P$	k_2
$X_H + C_D \rightarrow HD + P$	k_3
$X_D + C_D \rightarrow D_2 + P$	k_4

where $C_H = C_6H_{12}$, $C_D = C_6D_{12}$. P and X_H have been defined in the introduction.

We have shown (1) that, in mixtures containing C_D moles of C_6D_{12} and C_H moles of C_6H_{12},

$$G(D_2) = G_2(D)\times k_4/k_2\times(C_D/C_H)^2+G_1(D)\times C_D/C_H \qquad [1]$$

when $CH \gg C_D$.

[4] *g*(HD) *is precisely defined in the discussion.*

Can. J. Chem. Downloaded from www.nrcresearchpress.com by 210.87.254.42 on 09/05/12
For personal use only.

A similar steady state argument gives

$$G(\mathrm{HD}) = \mathrm{C_D}/\mathrm{C_H}\,[(k_3/k_1)\times G_2(\mathrm{H})+G_2(\mathrm{D})] \qquad [2]$$

when $\mathrm{C_H} \gg \mathrm{C_D}$. We define $g(\mathrm{HD}) = (k_3/k_1)\times G_2(\mathrm{H})+G_2(\mathrm{D})$.

The above analysis identifies the unimolecular yield $G_1(\mathrm{D})$ as that fraction of the yield of $\mathrm{D_2}$ which is first order with respect to $\mathrm{C_D}$ and resolves the term $g(\mathrm{HD})$ into the sum of two terms, the weighted yields of the intermediates $\mathrm{X_H}$ and $\mathrm{X_D}$ in the bimolecular reactions. The terms $G_1(\mathrm{D})$, $G_2(\mathrm{D})$ and $G_1(\mathrm{H})$, $G_2(\mathrm{H})$ contribute to the total yields in proportion to the mole fractions of $\mathrm{C_6D_{12}}$ and $\mathrm{C_6H_{12}}$.

DISCUSSION: IMMEDIATE CONCLUSIONS

An additive may interfere with and reduce either or both of the two decomposition mechanisms. Consider an additive which quenches the unimolecular mechanism and leaves the bimolecular mechanism unchanged. The yield $G_1(\mathrm{D})$, measured in these experiments, will decrease, and should decrease more rapidly than the total yield of hydrogen if the effects on $G_1(\mathrm{D})$ and $G_1(\mathrm{H})$ are comparable. Further, in experiments where essentially all the observed $\mathrm{D_2}$ comes from the unimolecular decomposition (as in the present case), the percentage of $\mathrm{D_2}$ must decrease. Since, by hypothesis, $g(\mathrm{HD})$ is unchanged and $G(\mathrm{hydrogen})$ is reduced, then the % HD must increase.

The changes in % $\mathrm{D_2}$ and % HD will depend on the relative contributions of the unimolecular and bimolecular yields. If, for instance, the bimolecular yield is a large fraction of the total, then the change in % $\mathrm{D_2}$ will be of the same order as the percentage change in total hydrogen. If the bimolecular yield is small the change in % $\mathrm{D_2}$ will be large compared with the change in total hydrogen.

The possible changes in $G_1(\mathrm{D})$, $g(\mathrm{HD})$, and percentage composition are summarized below:

	$G_1(\mathrm{D})$	$g(\mathrm{HD})$	% $\mathrm{D_2}$	% HD
Unimolecular mechanism quenched	Decreased more rapidly than total hydrogen	Unchanged	Decreased	Increased
Bimolecular mechanism quenched or scavenged	Unchanged	Decreased more rapidly than total hydrogen	Increased	Decreased
Both mechanisms quenched/ scavenged	Decreased	Decreased	Small changes +ve or −ve	Small changes +ve or −ve

In the case where both mechanisms are quenched the magnitude of the decreases in $G_1(\mathrm{D})$ and $g(\mathrm{HD})$ relative to the decrease in $G(\mathrm{hydrogen})$ will depend on several factors: the relative yields of the two mechanisms, the sensitivity of the precursors $\mathrm{C_H}^*$, $\mathrm{C_H}^{**}$, or $\mathrm{X_H}$ to the additive, and isotope effects in the reactivity of $\mathrm{C_H}^*$ and $\mathrm{C_D}^*$ or $\mathrm{X_H}$ and $\mathrm{X_D}$ with the additive.

Qualitatively the results in Tables I and II and Fig. 1 fall into the third category, and it follows that both the unimolecular and bimolecular yields of hydrogen are quenched/ scavenged by benzene and by iodine to a comparable extent.

It can be argued, from these results, firstly, that the action of these additives is the quenching of both mechanisms, and secondly, that both mechanisms have a common precursor, i.e. $\mathrm{C_H}^* \equiv \mathrm{C_H}^{**}$. These arguments proceed as follows. If the bimolecular mechanism is reduced by scavenging then the scavenging reaction,

$$\mathrm{M} + \mathrm{X_H} \rightarrow \text{products}, \qquad [a]$$

has a comparable efficiency to the quenching of the unimolecular mechanism,

$$\mathrm{C_H}^* + \mathrm{M} \rightarrow \mathrm{C_H} + \mathrm{M}^*. \qquad [b]$$

Can. J. Chem. Downloaded from www.nrcresearchpress.com by 210.87.254.42 on 09/05/12
For personal use only.

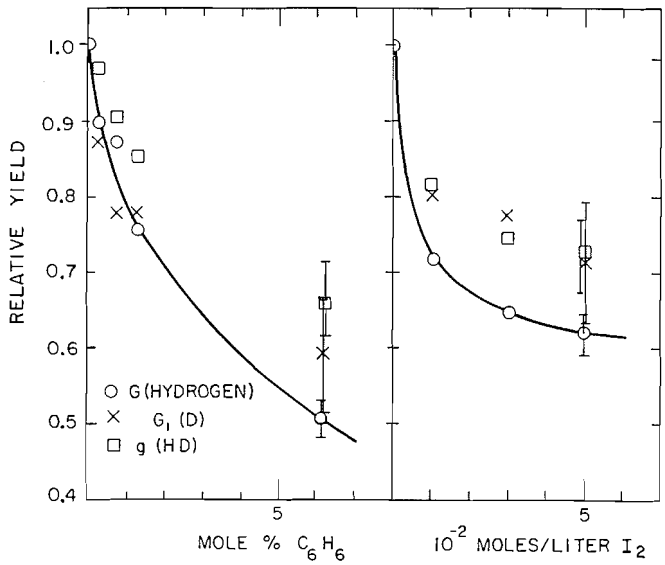


FIG. 1. Relative values of G(hydrogen), G_1(D), and g(HD) as a function of (*a*) benzene and (*b*) iodine concentrations. The precise numerical data may be found in Table II. The bars at the highest concentrations give the limits of error on the values.

These are different physical processes; one involves the rearrangement of chemical bonds, the other does not. It is consequently improbable that they would have rate constants which are within about 30% of one another, as implied by our data, and even more improbable that this would be so for both benzene and iodine. The mode of interaction is therefore *quenching* of both mechanisms, i.e. by [*b*] and

$$C_H^{**} + M \rightarrow C_H + M^*. \qquad [c]$$

It can also be argued that it is improbable that there are two quenching reactions [*b*] and [*c*] having comparable rates for both additives. The simplest explanation is that the precursors C_H^* and C_H^{**} are identical. The reaction scheme is therefore

$$C_H \rightsquigarrow C_H^*$$

$$C_H^* \begin{cases} \nearrow X_H + P \\ \searrow H_2 + P \end{cases}$$

$$C_H^* + M \rightarrow C_H + M^*.$$

This last conclusion would be inescapable if the isotopic composition were precisely unaltered by the addition of benzene or iodine.

However, as can be seen from an inspection of Table I, some changes in isotopic composition are observed. Further significant differences can be observed from the behavior of the function

$$f = [HD]^2/[H_2]\,[D_2].$$

If hydrogen were produced exclusively by a bimolecular mechanism which proceeded statistically with no isotopic discrimination, then $f = 4$.

From the kinetic scheme given above it can be shown that

$$f = 4\,\frac{k_2\,k_3}{k_1\,k_4}$$

Can. J. Chem. Downloaded from www.nrcresearchpress.com by 210.87.254.42 on 09/05/12
For personal use only.

and a consideration of the isotope effects in hydrogen and deuterium abstraction reactions shows that f will be always greater than 4.

As, experimentally, f is always less than 4 it follows that other processes forming H_2 and D_2 are operative: this is prima facie evidence that the contribution of the unimolecular processes is appreciable (2, 3) (or that the species X_H are not hydrogen atoms and the ratios k_1/k_2, k_3/k_4 are quite different from the estimates). In Fig. 2 we present a plot of f vs. mole% C_6D_{12}. The addition of benzene raises the value of f significantly; iodine lowers it slightly.

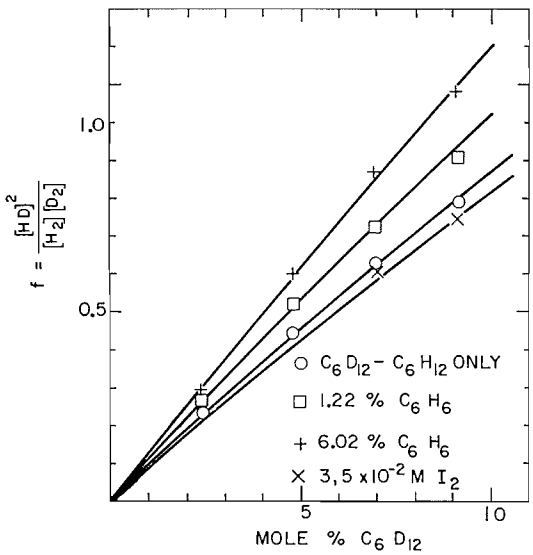


FIG. 2. Variation of f as a function of the concentrations of C_6D_{12} in the presence of varying amounts of benzene and iodine. The precise numerical data may be found in Table I.

These effects of benzene and iodine on f make it appear that, in effect, benzene quenches the unimolecular processes (giving H_2 and D_2) slightly more efficiently than the bimolecular processes. Iodine reacts conversely. The same conclusion can be reached from Fig. 1. For benzene, for instance, the curve for $G_1(D)$ lies below the curve for $g(HD)$. Such an effect could be produced by an isotopic effect in the efficiency of quenching C_H^* and C_D^*. If C_D^* were more efficiently quenched than C_H^*, then $G_1(D)$ would fall more rapidly than $g(HD)$, which is, in effect, the sum of the net yields of C_H^{**} and C_D^{**}.

In summary we conclude that (i) iodine and benzene interact to a comparable extent with both unimolecular and bimolecular decomposition modes, and (ii) it is probable that neither of these additives act by scavenging, and (iii) it is probable that they act by quenching a common precursor of the two decomposition modes. The first conclusion is clear; the second and third are debatable.

FURTHER IMPLICATIONS

The effects of benzene, iodine, and other additives on $G(H_2)$ from cyclohexane have been studied by many workers. (See, for instance, refs. 5–8.) In general the curve of $G(H_2)$ vs. additive concentration consists of two segments: an initial rapid decrease in

Can. J. Chem. Downloaded from www.nrcresearchpress.com by 210.87.254.42 on 09/05/12
For personal use only.

the concentration range 0–5% and a much slower decrease at higher concentrations. The yield curve cannot be described by simple kinetic schemes involving the quenching or scavenging of one precursor. The existence of two precursors is frequently postulated; one of these is readily quenched (or scavenged) at low concentrations, the other is only quenched (or scavenged) at high concentrations. As the additives are often supposed to be very reactive radical scavengers, the efficient reaction may be identified as radical scavenging and the less efficient reaction identified as the quenching of a non-scavengeable reaction, e.g. the unimolecular decomposition.

In this paper we have shown that benzene and iodine reduce the bimolecular (scavengeable) and unimolecular (unscavengeable) yields concurrently in the low concentration region, and it follows that the interpretations of the type outlined above are, at best, only partially true.

In the absence of chemical identification of the products of scavenging this discrepancy turns on two points, the validity of the kinetic analysis which distinguishes between the two processes and the assumption that the additive acts as a scavenger.

The kinetic analysis is generally performed on transformed versions of the yield curve involving functions of the reciprocal of the yield: these versions give linear plots. It should be noted that a reciprocal of a smooth curve (such as the yield curve) will always give an approximate straight line.[5] Consequently the linearity of these plots, if based on a limited region of the yield curve, is as significant or trivial as, for instance, the linearity of a logarithmic plot. (See for instance ref. 11.) A kinetic analysis which leads to the conclusion that two processes are occurring only demonstrates rigorously that one process in a simple scheme *cannot* account for the data.

It is well known that many reactive radical scavengers are potentially efficient energy sinks or charge acceptors. Our ignorance of the mechanism of energy and charge transfer in irradiated liquid systems is so profound that it is unwise to identify a substance, *a priori*, as a radical scavenger and assume that it cannot react otherwise.

For benzene there is chemical evidence that it does not act as a conventional scavenger, since G(-benzene) is small at these concentrations (9). This does not preclude the possibility (7, 10), that benzene acts as a "catalyst" by a series of reactions such as

$$C_6H_6 + H \rightarrow C_6H_7$$

$$C_6H_7 + C_6H_{11} \rightarrow C_6H_6 + C_6H_{12}.$$

For iodine it is known that HI is found in the initial stage of the radiolysis in an amount which is equivalent to the concurrent reduction in hydrogen yield, and which is also consistent with the 'hydrogen atom yield' derived from kinetic analysis. If the unimolecular decomposition of cyclohexane is a significant fraction of the total, then we would be forced to conclude, in spite of the strong arguments to the contrary advanced by Forrestal and Hamill (11), that HI is formed by some reaction other than hydrogen atom scavenging by molecular iodine.

ACKNOWLEDGMENTS

It is a pleasure to acknowledge both the detailed correspondence we have had with Professor Milton Burton and the helpful discussions we had with Dr. R. H. Betts.

[5]*The sceptical reader might test this with synthetic, freehand yield curves. We are obliged to Dr. J. W. Otvos for pointing out to us this property of numbers.*

Can. J. Chem. Downloaded from www.nrcresearchpress.com by 210.87.254.42 on 09/05/12
For personal use only.

REFERENCES

1. P. J. DYNE and W. M. JENKINSON. Can. J. Chem. **38**, 539 (1960).
2. T. D. NEVITT and L. P. REMSBERG. J. Phys. Chem. **64**, 969 (1960).
3. M. BURTON and J. CHANG. Private communication.
4. M. BURTON and J. CHANG. 137th Meeting of American Chemical Society, Cleveland, Ohio. 1960. Abstract 109, Section R.
5. M. BURTON, J. CHANG, S. LIPSKY, and M. P. REDDY. Radiation Research, **8**, 203 (1958).
6. G. E. ADAMS, J. H. BAXENDALE, and R. D. SEDGWICK. J. Phys. Chem. **63**, 854 (1959).
7. G. R. FREEMAN. J. Chem. Phys. **33**, 71 (1960).
8. T. J. HARDWICK. J. Phys. Chem. **65**, 101 (1961).
9. P. J. DYNE and J. A. STONE. Unpublished work.
10. P. J. DYNE, J. W. FLETCHER, and W. M. JENKINSON. A.E.C.L. Report CRC-941. July, 1960.
11. L. J. FORRESTAL and W. H. HAMILL. J. Am. Chem. Soc. **83**, 1535 (1961).

Can. J. Chem. Downloaded from www.nrcresearchpress.com by 210.87.254.42 on 09/05/12
For personal use only.

Can. J. Chem. Downloaded from www.nrcresearchpress.com by 210.87.254.40 on 09/05/12
For personal use only.

THE VIBRATIONAL SPECTRA OF SULPHURYL AND THIONYL HALIDES[1]

R. J. GILLESPIE AND E. A. ROBINSON[2]

ABSTRACT

New assignments are proposed for the fundamental frequencies of SOF_2, $SOCl_2$, SO_2Cl_2, SO_2F_2, and SO_2FBr, based on new measurements of the Raman spectrum of SO_2Cl_2 and previous measurements of the infrared and Raman spectra of these molecules. The fundamental frequencies of these molecules are found to be related to each other and to those of similar molecules when the normal modes are described in terms of characteristic vibrations of the SO, SO_2, S(Hal), and $S(Hal)_2$ groups.

INTRODUCTION

The purpose of this paper is to give a consistent assignment of the observed vibrational frequencies of the thionyl and sulphuryl halides to the various modes of vibration of these molecules. This work was undertaken as a necessary preliminary to the interpretation of the vibrational spectra of a number of more complicated polysulphuryl compounds (1). Although both the infrared and Raman spectra of several of these molecules have each been examined a number of times, no complete agreement has been reached concerning the assignments of the observed frequencies (e.g. references 2, 3, and 4). We have found, by comparing the spectra of these molecules and certain others containing SO, SO_2, S(Hal), and $S(Hal)_2$ groups, that a consistent and satisfactory set of assignments can be given for all the sulphuryl and thionyl halides that have been studied.

Of the spectra discussed, only the Raman spectrum of SO_2Cl_2 has been re-examined in the present work. The spectrum is shown in Fig. 1. The vibrational frequencies for

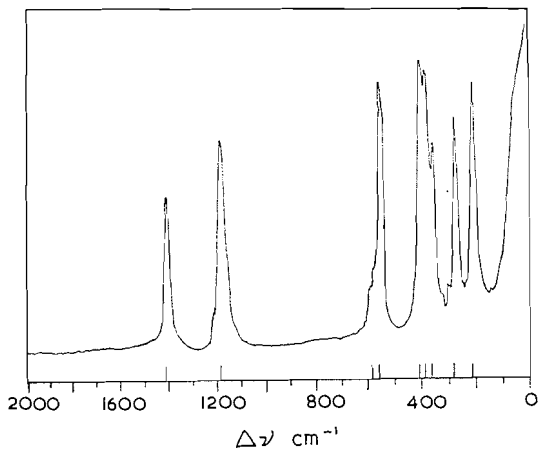


FIG. 1. The Raman spectrum of sulphuryl chloride.

sulphuryl chloride and for the other sulphuryl and thionyl halides obtained in the present and previous work are given in Tables I–V.

[1]*Manuscript received May 15, 1961.*
Contribution from the Department of Chemistry, McMaster University, Hamilton, Ontario.
[2]*Present address: Department of Chemistry, University of Toronto, Toronto, Ontario.*

TABLE I

Observed frequencies and assignments for SO_2F_2 (frequencies in cm^{-1})

Raman	Infrared	Assignment	
(*a*)	(*b*)	(*c*)	(*b*)
	274	Impurity	$\nu_4(a_1)$
388 dp	386	$\nu_9(b_2)$	$\nu_9(b_2)$
	539	$\nu_7(b_1)$	$\nu_7(b_1)$
547 dp	544	$\nu_4(a_1)$	$2\nu_4(A_1) = 548$
	553	$\nu_3(a_1)$	$\nu_3(a_1)$
	668	$\nu_6-\nu_2(B_1) = 656$	$\nu_4+\nu_9(B_2) = 660$
	720	$2\nu_5(A_1)$	$2\nu_5(A_1)$
	769	$2\nu_9(A_1) = 772$	$2\nu_9(A_1) = 772$
846 p	848	$\nu_2(a_1)$	$\nu_2(a_1)$
887	885	$\nu_8(b_2)$	$\nu_8(b_2)$
	925	$\nu_4+\nu_9(B_2) = 930$	$2\nu_4+\nu_9(B_2) = 930$
	954	$\nu_6-\nu_3(B_1) = 949$	$\nu_6-\nu_3(B_1) = 949$
	1077	$2\nu_7(A_1) = 1078$	$2\nu_7(A_1) = 1078$
	1092	$2\nu_4(A_1) = 1088$	$\nu_3+\nu_7(B_1) = 1092$
	1103	$\nu_3+\nu_4(A_1) = 1097$	$2\nu_3(A_1) = 1106$
	1118	$2\nu_3(A_1) = 1106$	$\nu_2+\nu_4(A_1) = 1122$
1270 p	1269	$\nu_1(a_1)$	$\nu_1(a_1)$
	1389	$\nu_2+\nu_7(B_1) = 1387$	$\nu_2+\nu_7(B_1) = 1387$
1502 dp	1502	$\nu_6(b_1)$	$\nu_6(b_1)$
	1698	$2\nu_2(A_1) = 1696$	$2\nu_2(A_1) = 1696$
	1772	$\nu_2+\nu_8(B_2) = 1733$	$\nu_2+\nu_8(B_2) = 1733$
	1820	$\nu_1+\nu_3(A_1) = 1822$	$\nu_1+\nu_3(A_1) = 1822$
	1889	?	?
	2052	$\nu_3+\nu_6(B_1) = 2055$	$\nu_3+\nu_6(B_1) = 2055$
	2115	$\nu_1+\nu_2(A_1) = 2117$	$\nu_1+\nu_2(A_1) = 2117$
	2355	$\nu_2+\nu_6(B_1) = 2350$	$\nu_2+\nu_6(B_1) = 2350$
	2536	$2\nu_1(A_1) = 2538$	$2\nu_1(A_1) = 2538$
	2760	$\nu_1+\nu_6(B_1) = 2771$	$\nu_1+\nu_6(B_1) = 2771$
	2995	$2\nu_6(A_1) = 3004$	$2\nu_6(A_1) = 3004$

NOTE: (*a*) Bender and Wood (21); (*b*) Hunt and Wilson (2); (*c*) this paper.

TABLE II

Observed frequencies and assignments for SO_2Cl_2 (frequencies in cm^{-1})

Raman		Infrared			Assignment	
(*a*)	(*b*)	(*c*)	(*d*)	(*e*)	(*f*)	(*d*)
218 p	209				$\nu_4(a_1)$	$\nu_4(a_1)$
282 dp	280				$\nu_7(b_1)$	$\nu_5(a_2)$
362 dp	363				$\nu_9(b_2)$	$\nu_7(b_1)$
388 dp	388				$\nu_5(a_2)$	$\nu_9(b_2)$
408 p	403				$\nu_8(a_1)$	$\nu_3(a_1)$
560 p	556		577	(557)	$\nu_2(a_1)$	$\nu_8(b_2)$
	563		586	(566)	$2\nu_7(B_1) = 564$	$\nu_2(a_1)$
580 dp	578		595	(575)	$\nu_8(b_1)$	$\nu_4+\nu_7(B_1) = 589$
			611	(591)	$\nu_4+\nu_9(B_2) = 580$	$\nu_4+\nu_9(B_2) = 606$
			619	(599)	$\nu_3+\nu_4(A_1) = 626$	$\nu_3+\nu_4(A_1) = 623$
			714	(694)	$\nu_3+\nu_7(B_1) = 690$	$2\nu_7(A_1) = 724$
			793	(773)	$\nu_2+\nu_4(A_1) = 778$	$\nu_2+\nu_4(A_1) = 784$;
						$\nu_4+\nu_8(B_1) = 775$
			946	(926)	$\nu_2+\nu_9(B_2) = 922$	$\nu_2+\nu_7(B_1) = 928$
			996	(976)	$\nu_3+\nu_8(B_2) = 988$	$\nu_3+\nu_8(B_2) = 962$;
						$\nu_2+\nu_3(A_1) = 971$
		1160	1171	(1151)	$2\nu_8(A_1) = 1160$	$2\nu_2(A_1) = 1132$;
						$\nu_2+\nu_8(B_1) = 1123$
1182 p	1186	1196	1205	(1185)	$\nu_1(a_1)$	$\nu_1(a_1)$
1414 dp	1411	1419	1434	(1414)	$\nu_6(b_1)$	$\nu_6(b_1)$
			2004	(1984)	$\nu_2+\nu_6(B_1) = 1974$	$\nu_2+\nu_6(B_1) = 1974$;
						$\nu_1+\nu_2+\nu_4(A_1) = 1961$
			2398	(2378)	$2\nu_1(A_1) = 2364$	$2\nu_1(A_1) = 2364$
			2632	(2612)	$\nu_1+\nu_6(B_1) = 2596$	$\nu_1+\nu_6(B_1) = 2596$
			2869	(2849)	$2\nu_6(A_1) = 2828$	$2\nu_6(A_1) = 2828$

NOTE: (*a*) Present work; (*b*) Vogel-Högler (19); (*c*) Schreiber (33); (*d*) Martz and Lagemann (18); (*e*) Infrared frequencies corrected to allow for discrepancy with Raman results (column (*d*) minus 20 cm^{-1}); (*f*) this paper.

Can. J. Chem. Downloaded from www.nrcresearchpress.com by 210.87.254.40 on 09/05/12
For personal use only.

TABLE III

Observed frequencies and assignments for SOF_2 (frequencies in cm^{-1})

Raman		Infrared	Assignment	
(*a*)	(*b*)	(*c*)	(*d*)	(*c*)
	326		$\nu_4(a')$	
393 dp	395	390	$\nu_6(a'')$	$\nu_6(a'')$
		(410)		$\nu_4(a')$
526 p	529	530	$\nu_3(a')$	$\nu_3(a')$
721 dp	720	748	$\nu_5(a'')$	$\nu_5(a'')$
801 p	795	806	$\nu_2(a')$	$\nu_2(a')$
		920	$\nu_3+\nu_6(A') = 920$	$\nu_3+\nu_6(A'') = 920$
		940	$\nu_1-\nu_6(A'') = 943$	$\nu_3+\nu_4(A') = 940$
		1136	$\nu_2+\nu_4(A') = 1132$	$\nu_5+\nu_6(A') = 1138$
				$\nu_5+\nu_4(A'') = 1158$
			$\nu_1(a')$	$\nu_1(a')$
1308 p	1312	1333	$\nu_2+\nu_3(A') = 1336$	$\nu_2+\nu_3(A') = 1336$
		1480	$2\nu_5(A') = 1496$	$2\nu_5(A') = 1496$
		1546	$\nu_2+\nu_5(A'') = 1554$	$\nu_2+\nu_5(A'') = 1554$
		1612	$2\nu_2(A') = 1612$	$2\nu_2(A') = 1612$
		1718	$\nu_1+\nu_6(A'') = 1723$	$\nu_1+\nu_6(A'') = 1723$
			$\nu_1+\nu_4(A') = 1743$	$\nu_1+\nu_4(A') = 1743$
		2144	$\nu_1+\nu_2(A') = 2139$	$\nu_1+\nu_2(A') = 2139$
		2652	$2\nu_1(A') = 2666$	$2\nu_1(A') = 2666$

NOTE: (*a*) Bender and Wood (21); (*b*) Yost (5); (*c*) O'Loane and Wilson (20); (*d*) this paper.

TABLE IV

Observed frequencies and assignments for $SOCl_2$ (frequencies in cm^{-1})

Raman	Infrared		Assignment
(*a*)	(*b*)	(*c*)	(*d*)
194 p			$\nu_4(a')$
284 dp			$\nu_6(a'')$
344 p			$\nu_3(a')$
443 dp		455	$\nu_5(a'')$
490 p		492	$\nu_2(a')$
		735	$\nu_5+\nu_6(A') = 739$
		778	$\nu_2+\nu_6(A'') = 776$
		800	$\nu_3+\nu_5(A'') = 799$
		833	$\nu_2+\nu_3(A') = 836$
		950	$\nu_2+\nu_5(A'') = 947$
	1140		
	1200		
	1238	1251	$\nu_1(a')$
	1350	1360	SO_2 impurity
		2506	$2\nu_1(a') = 2502$

NOTE: (*a*) Vogel-Högler (19), McDowell (34); (*b*) Schreiber (33); (*c*) Martz and Lagemann (18); (*d*) this paper and Martz and Lagemann (18).

The sulphuryl halides, SO_2X_2, have C_{2v} symmetry and they therefore have nine fundamental vibrations, four of which are totally symmetric. To a first approximation, at least, three of the vibrations can be associated with valency deformations of the SO_2 group (symmetric and asymmetric stretches and a bend) and three similar vibrations with the SX_2 group. The remaining normal modes can be described as a torsion (inactive in the infrared) and as SO_2 and SX_2 rocking modes.

The thionyl halides, SOX_2, have pyramidal structures with C_s symmetry and six fundamental vibrations which may be approximately described as an SX_2 symmetric and asymmetric stretch, an SX_2 rock, an SO stretch, and an SO wag (or OSX_2 deformation).

Can. J. Chem. Downloaded from www.nrcresearchpress.com by 210.87.254.40 on 09/05/12
For personal use only.

TABLE V

Observed frequencies and assignments for SO_2FBr
(frequencies in cm^{-1})

Infrared	Assignment	
(*a*)	(*b*)	(*a*)
270	$\nu_6(a')$	$\nu_6(a')$
320	$\nu_5(a')$	$\nu_9(a'')$
353	$2\nu_9(A')$	
450	$\nu_9+\nu_6(A'') = 446$	$\nu_5(A')$
461	$\nu_8(a'')$	$\nu_4(a')$
497	$\nu_4(a')$	$\nu_3(a')$
551	$2\nu_6(A') = 540$	
608	$\nu_3(a')$	$\nu_2(a')$
650	$2\nu_5(A') = 640$	
720	$2\nu_6+\nu_9(A'') = 716$	
728	$\nu_6+\nu_8(A'') = 731$	
814	$\nu_2(a')$	$\nu_8(a'')$
873	$\nu_3+\nu_6(A') = 878$	
930	$\nu_5+\nu_3(A') = 928$	
948	$\nu_4+\nu_8(A'') = 958$	
984	$\nu_2+\nu_9(A'') = 990$	
1069	$\nu_3+\nu_8(A'') = 1069$	
1080	$\nu_2+\nu_6(A') = 1084$	
1140	$\nu_7-\nu_6(A'') = 1140$	
1228	$\nu_1(a')$	$\nu_1(a')$
1305	$\nu_2+\nu_4(A') = 1311$	
1460	$\nu_7(a'')$	$\nu_7(a'')$
1511	$\nu_1+\nu_6(A') = 1498$	
1622	$2\nu_2(A') = 1624$	
1713	$\nu_7+\nu_6(A'') = 1730$	
1763	$\nu_5+\nu_7(A'') = 1780$	
2035	$\nu_1+\nu_2(A') = 2042$	
2265	$\nu_7+\nu_2(A'') = 2274$	
2440	$2\nu_1(A') = 2456$	
2650	$\nu_1+\nu_7(A'') = 2688$	
2890	$2\nu_7(A') = 2920$	

NOTE: (*a*) Crow and Lagemann (29); (*b*) this paper.

DISCUSSION

Thionyl Fluoride and Thionyl Chloride

All six normal vibrations have been observed for thionyl chloride, and, as expected, four of the lines in the Raman spectrum are polarized (Table IV). Only five fundamentals, three of which are polarized, have been observed with certainty for thionyl fluoride, although Yost (5) has claimed a line in the Raman spectrum at 326 cm^{-1}, in addition to the five lines reported by other workers.

Frequencies can readily be assigned to the SO stretch, the SX_2 stretches, and the SX_2 bend in both SOF_2 and $SOCl_2$ by comparison with the frequencies of these vibrations in similar molecules, as shown in Table VI. The polarized line at 344 cm^{-1} in the spectrum of $SOCl_2$ must then be assigned to the totally symmetric SO wag and the remaining line at 284 cm^{-1} (depolarized) to the SCl_2 rocking mode. Similarly in the spectrum of SO_2F_2 the depolarized line at 393 cm^{-1} must be assigned to the SF_2 rocking mode and the remaining line at 326 cm^{-1} to the SO wag. Although the degree of polarization of this line is not known, it seems reasonable to suppose that it is polarized, since only three of the other lines have been found to be polarized. Our assignment for $SOCl_2$ agrees with that given by Martz and Lagemann (18). Assignments for the spectra of selenium oxychloride (17) and selenium oxyfluoride (16) can readily be made by comparison with the

Can. J. Chem. Downloaded from www.nrcresearchpress.com by 210.87.254.40 on 09/05/12
For personal use only.

Can. J. Chem. Downloaded from www.nrcresearchpress.com by 210.87.254.40 on 09/05/12
For personal use only.

TABLE VI

Summary of assignments for the thionyl, sulphuryl, and selenyl halides (frequencies in cm^{-1})

	SOF_2	$SOCl_2$	SO_2F_2	SO_2Cl_2	SO_2FBr	Related molecules	$SeOF_2$	$SeOCl_2$
SO stretch*	1308	1229				SO, 1124 (6); R_2SO, 1040–1060 (7)	1012	955
SO_2 stretch, s			1269	1182	1228	R_2SO_2, 1130–1160, 1310–1335 (22, 23)		
SO_2 stretch, a			1502	1414	1460	CH_3SO_2Cl, 1175, 1370 (25); CH_3SO_2F, 1210, 1401 (26)		
SF_2 stretch, s	801		848			SF_6, 775, 644 (8); SF_4, 889, 867, 728 (9)	664	
SF_2 stretch, a	721		885			$XOSO_2F$, 820–850 (10, 11)	605	
SF stretch					814			
SCl_2 stretch, s		490		405		SCl_2, 514, 535 (12); S_2Cl_2, 447 (13)		388
SCl_2 stretch, a		443		362				347
SBr stretch					270			
SO_2 bend			545	560	608	SO_2, 525 (24); CH_3SO_2Cl, 538 (25); CH_3SO_2F, 531 (26)		
SF_2 bend	526		545			SF_6, 524 (8); SF_4, 557 (9); SOF_4, 567 (14); PF_3, 531, 486 (15)	373	
SCl_2 bend		194		218		SCl_2, 208 (12); PCl_3, 257, 190 (27)		279
SO_2 rock			545	580	497			
SF_2 rock	393		388				308	
SCl_2 rock		284		282				255
SO wag	326	344					278	279
SF wag					320			
SBr wag					176			
Torsion			360	388	461			

*Or SeO stretch etc., as appropriate.

spectra of the corresponding thionyl compounds. Our assignments for these molecules are given in Table VI.

Sulphuryl Chloride and Sulphuryl Fluoride

In the Raman spectrum of sulphuryl chloride eight of the expected nine lines are observed as distinctly resolved peaks. The ninth appears as a shoulder at approximately 580 cm^{-1} on the 560 cm^{-1} peak. Vogel-Högler (19) reported three lines at 556, 563, and 578 cm^{-1} in the infrared in this region. Martz and Lagemann (18) also reported three lines in the infrared, but at frequencies of 577, 586, and 595 cm^{-1}, of which the first two were intense and assigned as fundamentals while the third was rather weak and assigned as a combination band. We will assume that there are only two fundamentals in this region of the spectrum with frequencies of approximately 560 cm^{-1} and 580 cm^{-1}. Raman frequencies for the liquid appear to be consistently lower than the corresponding infrared frequencies for the gas. To facilitate comparison with the Raman data, infrared frequencies that have been reduced by 20 cm^{-1} are listed in addition to the observed values.

In the case of sulphuryl fluoride, three lines at 539, 544, and 553 cm^{-1} have been reported (2, 20) in the infrared spectrum but only one at 547 cm^{-1} in the Raman spectrum (4, 21). It seems likely that there are indeed three lines that are not resolved from each other in the Raman spectrum; accordingly three vibrations are each assigned a frequency of 545 cm^{-1}.

Frequencies can readily be assigned to the SO_2 stretches, the SO_2 bend, the SX_2 stretches, the SX_2 bends, and the SX_2 rocking mode by comparison with the frequencies of these vibrations in the thionyl halides or other similar molecules, as shown in Table VI. The only vibrations to which frequencies cannot be easily assigned in this way are the SO_2 rocking mode and the torsion, which is inactive in the infrared. In the spectrum of sulphuryl chloride we have unassigned lines at 388 cm^{-1} (R) and at 580 cm^{-1} (R and I.R.) and in the spectrum of sulphuryl fluoride at 274 cm^{-1} and at 545 cm^{-1} (the third of three lines with approximately this frequency). The torsion must therefore be assigned at 388 cm^{-1} in SO_2Cl_2. It is reasonable that no line of approximately this frequency is observed in the Raman spectrum of SO_2F_2, as it would probably not be resolved from the rather broad band at 388 cm^{-1}, which has been assigned as the SF_2 rocking mode. Hunt and Wilson (2) have indeed assigned this vibration at a frequency of 360 cm^{-1} in sulphuryl fluoride on the ground of the observation of a line at 720 cm^{-1} in the infrared, which they interpret as the first overtone of 360 cm^{-1}. This leaves a line at approximately 545 cm^{-1} in SO_2F_2 and the line at 580 cm^{-1} in SO_2Cl_2 to be attributed to the SO_2 rock in these molecules.

Hunt and Wilson (2) have assigned a frequency of 274 cm^{-1}, which they observed in the infrared spectrum of SO_2F_2, to the SF_2 bending mode by comparison with a frequency of 235 cm^{-1} in the spectrum of sulphur tetrafluoride, which has been assigned as an SF bending mode (9). It seems to us more probable that this low frequency of 235 cm^{-1} in the Raman spectrum of liquid SF_4 is due to some polymeric species formed by fluorine bridging between SF_4 molecules in the same way that antimony pentafluoride is associated by fluorine-bridge bonds (28). The line at 274 cm^{-1} reported by these authors is difficult to understand as its frequency seems to be too low for it to be due to any vibration of SO_2F_2. A possible explanation is that it is due to either SO_2Br_2 or SO_2FBr formed by attack on the bromide windows of the cell and, indeed, a frequency of 270 cm^{-1} has been observed in the spectrum of SO_2FBr (29). All the overtone bands that have been observed in the infrared spectra of SO_2F_2, SO_2Cl_2, $SOCl_2$, and SOF_2 can be satisfactorily accounted for as allowed combinations of the fundamentals, as shown in Tables I–IV.

Can. J. Chem. Downloaded from www.nrcresearchpress.com by 210.87.254.40 on 09/05/12
For personal use only.

Sulphuryl Bromofluoride

The infrared spectrum of sulphuryl bromofluoride, SO_2BrF, has been reported by Crow and Lagemann (29), who have given an assignment of the observed frequencies in terms of characteristic vibrations of the SO_2 and SFBr groups. We prefer, however, to treat the vibrations of the S—F and S—Br bonds separately and to describe the nine fundamental vibrations as an SO_2 symmetric and asymmetric stretch, an SO_2 bend and an SO_2 rock, an SF stretch and an SF wag, an SBr stretch and an SBr wag, and a torsion. On this basis we have been able to assign frequencies to all except one of the fundamental vibrations in a manner which is quite consistent with the assignments which have been proposed above for SO_2Cl_2 and SO_2F_2, as shown in Table VI. The justification for the majority of these assignments is obvious from the data given in this table. The frequency of the S—Br stretch would be expected to fall in the range 250–320 cm^{-1} from the following data for the P—Hal symmetric stretches: POF_3, 873 cm^{-1}; $POCl_3$, 486 cm^{-1}; $POBr_3$, 340 cm^{-1} (30, 31); and for the S—Hal stretches: SO_2F_2, 848 cm^{-1}; SO_2Cl_2, 405 cm^{-1}. Therefore, one of the frequencies 320 cm^{-1} or 270 cm^{-1} must be assigned to this vibration. The S—F wag might be expected to have a frequency somewhere near that of the S=O wag in SOF_2 (326 cm^{-1}), since the SF_2 bend and the SO_2 bend in SO_2F_2 have similar frequencies of approximately 545 cm^{-1}. Thus it seems reasonable to assign 320 cm^{-1} to this vibration, which leaves 270 cm^{-1} as the S—Br stretch. The S—Br wag would be expected to have a very low frequency, certainly lower than the S—Br stretch. P—Br bending modes have been assigned frequencies of 162 and 173 cm^{-1} in PBr_3 (32) and 173 cm^{-1} in $POBr_3$ (31), for which the stretching modes have been assigned at 380 and 340 cm^{-1}, respectively. We conclude therefore that the S—Br wag has a frequency less than 200 cm^{-1} and has not been observed. A detailed examination of the infrared spectrum leads to the conclusion that the infrared band at 353 cm^{-1} is best interpreted as the first overtone of the S—Br wag so that a frequency of 176 cm^{-1} can be assigned to this vibration. This assignment enables certain other overtone bands in the infrared to be assigned in a satisfactory manner (Table V). The remaining frequency of 461 cm^{-1} is assigned to the torsion. The complete infrared spectrum of SO_2BrF can be satisfactorily accounted for on the basis of the present assignment of the fundamental vibrations (Table V).

EXPERIMENTAL

Sulphuryl chloride was purified by double distillation of the commercial product, which had been dried over phosphoric oxide. The fraction boiling at 69° was collected. The Raman apparatus and the method used for obtaining depolarization factors are described in the following paper (1).

ACKNOWLEDGMENTS

The National Research Council and the Ontario Research Foundation are thanked for financial assistance.

REFERENCES

1. R. J. Gillespie and E. A. Robinson. Can. J. Chem. This issue. p. 2179.
2. E. R. Hunt and M. K. Wilson. Spectrochim. Acta, **16**, 570 (1960).
3. H. Stammreich, K. Kawai, and Y. Tavares. Spectrochim. Acta, **15**, 438 (1959).
4. H. Siebert. Z. anorg. Chem. **275**, 210 (1954).
5. D. M. Yost. Proc. Indian Acad. Sci. **8**, 333 (1938).
6. D. N. Read. Phys. Rev. **46**, 571 (1934).
7. L. J. Bellamy. The Infra-red Spectra of Complex Molecules. 2nd ed. Methuen, London. 1958. p. 350.
8. R. T. Lagemann and E. A. Jones. J. Phys. Chem. **19**, 534 (1951).
9. R. E. Dodd, L. A. Woodward, and H. L. Roberts. Trans. Faraday Soc. **52**, 1052 (1956).

Can. J. Chem. Downloaded from www.nrcresearchpress.com by 210.87.254.40 on 09/05/12
For personal use only.

10. F. B. DUDLEY, G. H. CADY, and D. F. EGGERS. J. Am. Chem. Soc. **78**, 290 (1956).
11. F. B. DUDLEY and G. H. CADY. J. Am. Chem. Soc. **79**, 513 (1957).
12. H. STAMMREICH, R. FORNERIS, and K. SORET. J. Chem. Phys. **23**, 972 (1955).
13. Y. MORINO and S. MIZUSHIMA. Sci. Papers Inst. Phys. Chem. Research (Tokyo), **32**, 220 (1937).
14. F. B. DUDLEY, G. H. CADY, and D. F. EGGERS. J. Am. Chem. Soc. **78**, 1553 (1956).
15. H. S. GUTOWSKY and A. D. LIEHR. J. Chem. Phys. **20**, 1653 (1952).
16. J. A. ROLFE and L. A. WOODWARD. Trans. Faraday Soc. **51**, 778 (1955).
17. H. GERDING, P. SMITS, and R. WESTRICK. Rec. trav. chim. **61**, 513 (1941).
18. D. E. MARTZ and R. T. LAGEMANN. J. Chem. Phys. **22**, 1193 (1954).
19. R. VOGEL-HÖGLER. Acta. Phys. Austriaca, **1**, 323 (1948).
20. J. K. O'LOANE and M. K. WILSON. J. Chem. Phys. **23**, 1313 (1955).
21. P. BENDER and J. M. WOOD. J. Chem. Phys. **23**, 1313 (1955).
22. E. A. ROBINSON. Can. J. Chem. **39**, 247 (1961).
23. L. J. BELLAMY and R. J. WILLIAMS. J. Chem. Soc. 863 (1957).
24. H. GERDING and W. J. NIJVOLD. Nature, **137**, 1070 (1936).
25. R. N. HASZELDINE and J. M. KIDD. J. Chem. Soc. 2901 (1955).
26. N. S. HAM and A. N. HAMBLY. Australian J. Chem. **6**, 33 (1953).
27. A. BRAUNE and G. ENGELBRECHT. Z. physik. Chem. (Leipzig), B, **19**, 303 (1932).
28. C. J. HOFFMAN, B. E. HOLDER, and W. L. JOLLY. J. Phys. Chem. **62**, 364 (1958).
29. T. T. CROW and R. T. LAGEMANN. Spectrochim Acta, **12**, 143 (1958).
30. M. L. DEWAULLE and M. F. FRANCOIS. Compt. rend. **226**, 894 (1948).
31. M. L. DEWAULLE and M. F. FRANÇOIS. Compt. rend. **220**, 817 (1945).
32. M. L. DEWAULLE. Compt. rend. **222**, 1391 (1946).
33. K. C. SCHREIBER. Anal. Chem. **21**, 1168 (1949).
34. C. A. MCDOWELL. Trans. Faraday Soc. **49**, 371 (1953).

Can. J. Chem. Downloaded from www.nrcresearchpress.com by 210.87.254.40 on 09/05/12
For personal use only.

THE RAMAN SPECTRA OF SOME POLYSULPHURYL CHLORIDES AND FLUORIDES[1]

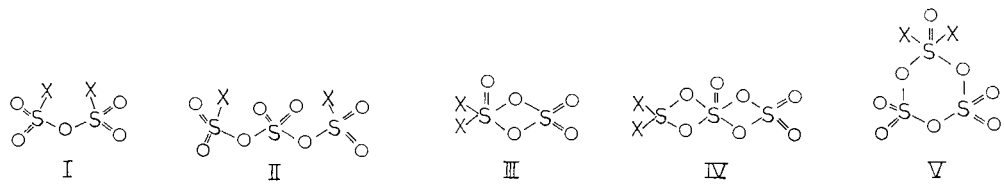
R. J. GILLESPIE AND E. A. ROBINSON[2]

ABSTRACT

The Raman spectrum of disulphuryl chloride, $S_2O_5Cl_2$, has been reinvestigated and the Raman spectra of $S_2O_5F_2$, S_2O_5ClF, $S_3O_8Cl_2$, $S_3O_8F_2$, and the new compound S_3O_8ClF are reported for the first time. The vibrational spectra of these polysulphuryl halides are interpreted in terms of characteristic group frequencies by comparison with the vibrational spectra of simple sulphuryl compounds. The spectra are consistent with acyclic structures for the polysulphuryl halides.

The Raman spectrum of disulphuryl chloride, $S_2O_5Cl_2$, has been investigated previously by Gerding and Linden (1), and the infrared spectrum of disulphuryl fluoride, $S_2O_5F_2$, has been obtained over a limited frequency range (2). We have measured the Raman spectra of both of these compounds and also of disulphuryl chlorofluoride, S_2O_5ClF; trisulphuryl chloride, $S_3O_8Cl_2$; trisulphuryl fluoride, $S_3O_8F_2$; and the new compound trisulphuryl chlorofluoride, S_3O_8ClF. The spectra are given in Tables I, II, and III and Fig. 1.

It has generally been assumed that these substances have the acyclic configurations I and II, although no direct experimental evidence for these structures has been obtained. The fluorine n.m.r. spectrum of $S_2O_5F_2$ has been found to consist of a single line (3), and in the present work we have found that the n.m.r. spectrum of $S_3O_8F_2$ also consists of



I II III IV V

a single line, showing that the fluorine atoms are structurally equivalent; this is consistent with structures I and II. Other formally possible formulations such as III, IV, and V contain improbable four-membered rings and five-co-ordinated sulphur. It has been shown, moreover, that $S_2O_5Cl_2$ is not just a molecular "addition compound" of SO_2Cl_2 and SO_3 since it is not formed in mixtures of these substances at room temperature or on being refluxed at 60°. Similarly $S_3O_8F_2$ is not formed from $S_2O_5F_2$ and SO_3 (4). Hydrolysis of $S_2O_5Cl_2$ and $S_2O_5F_2$ gives 2 moles of the corresponding halogenosulphuric acid and not sulphuric acid and the sulphuryl halide, as would be expected for structure III. Thus the acyclic structures I and II seem very probable, and it is shown in this paper that the Raman spectra are also consistent with these structures.

[1]*Manuscript received May 15, 1961.*
Contribution from the Department of Chemistry, McMaster University, Hamilton, Ontario. Presented in part at the 43rd Annual Conference of the Chemical Institute of Canada, Ottawa, Ontario, June 13–15, 1960.
[2]*Present address: Department of Chemistry, University of Toronto, Toronto, Ontario.*

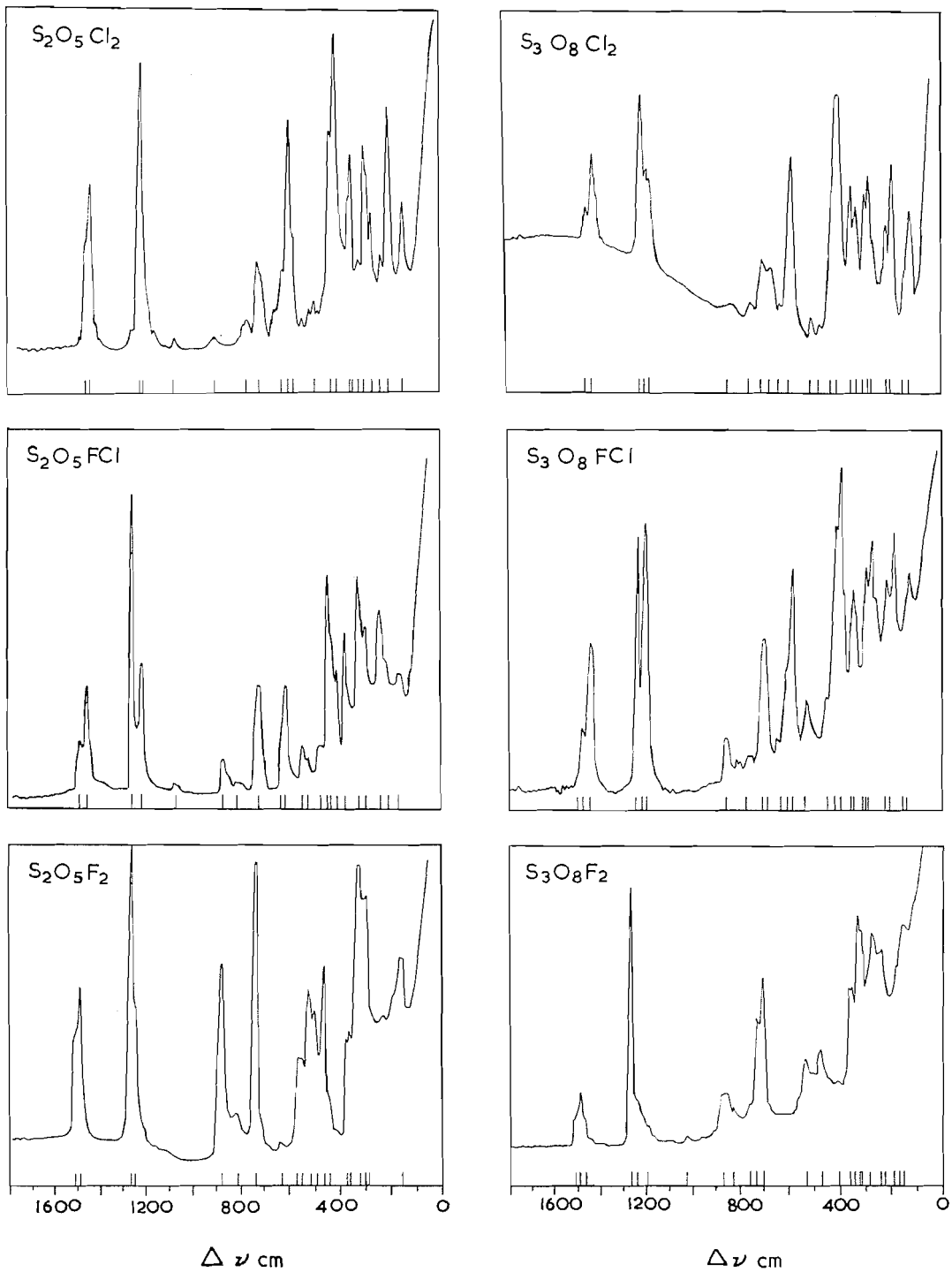
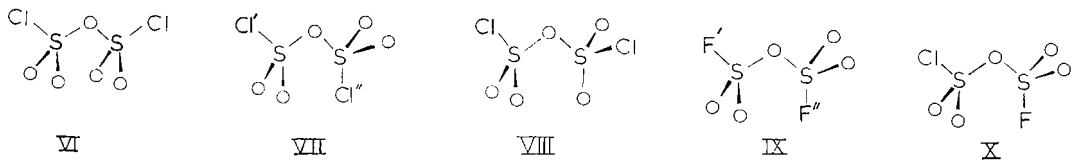


FIG. 1. Raman spectra.

DISULPHURYL HALIDES

If the disulphuryl halides have the acyclic structure I they should have 21 normal modes of vibration. Gerding and Linden (1) assumed that $S_2O_5Cl_2$ had the conformation VI and C_{2v} symmetry. In this case all 21 normal modes are active in the Raman effect



VI VII VIII IX X

and 7 of the Raman lines should be polarized. It seems more likely, however, that the molecule will have a staggered conformation, either VII, in which the halogen atoms are trans to each other (C_s symmetry), or VIII, in which the halogen atoms are in the "*gauche*" position and which has no symmetry elements. For VII, 13 of the 21 Raman lines should be polarized. We find at least nine of the Raman lines of $S_2O_5Cl_2$ to be polarized, which supports a staggered configuration such as VII or VIII rather than the cis conformation VI. Similarly $S_2O_5F_2$ and S_2O_5ClF would be expected to have the conformations IX and X respectively.

It is convenient to describe the normal modes of vibration in terms of the group frequencies that have been used previously for the simple sulphuryl compounds (5). This description can only be a rather crude approximation, but, as we shall show, it does enable a very reasonable assignment to be made for the majority of the Raman shifts of the polysulphuryl halides.

Seven vibrations may be ascribed to the SO_2X group: SO_2 symmetric and asymmetric stretches, an SO_2 bend, an SO_2 rock, an S—X stretch, an S—X wag, and a torsion. Each of these gives rise to two lines in the spectrum. These may be regarded as arising from coupling between the two halves of the molecule, and they may be conveniently described as in-phase and out-of-phase motions of the two SO_2X groups. In the staggered conformations VII and VIII the two SO_2X groups are not equivalent to each other, so slightly different frequencies for each group would be expected even if there were no coupling between them. In addition, the SO_2 rocking vibrations and the S—X wags can each occur parallel to, or perpendicular to, the plane containing the SOS group. Finally, three vibrations may be assigned to the SOS bridging group: a symmetric stretch, an asymmetric stretch, and a bend.

Frequencies can be readily assigned to the SO_2 stretches, the SO_2 bends, and the SF and SCl stretching modes, as shown in Tables I and II, by comparison with the frequencies observed for these vibrations in the simple sulphuryl halides (5). The SO_2 stretching frequencies are consistent with the linear relationship that has been shown to hold between the frequencies of the symmetric and asymmetric SO_2 stretches (6). The mean SO_2 symmetric and asymmetric frequencies in $S_2O_5F_2$ are both slightly lower than the corresponding frequencies in SO_2F_2, which is consistent with the replacement of fluorine by the slightly less electronegative SO_3F group. On the other hand, in $S_2O_5Cl_2$ these frequencies are both slightly higher than the corresponding frequencies in SO_2Cl_2; this is consistent with the replacement of chlorine by the more electronegative SO_3Cl group (6). In S_2O_5ClF, one of the SO_2 symmetric stretches, one of the asymmetric

TABLE I

Raman spectra of $S_2O_5Cl_2$

Present work			Gerding and Linden (1)		
Frequencies (cm^{-1})	Assignment	Species (C_s symmetry)	Frequencies (cm^{-1})	Assignment	Species (C_2 symmetry)
147 p	SOS bend	a'	143 p	SCl wag	a_1
200	SCl wag	a''	202	SCl wag	a_2, b_2
235	SCl wag	a'	234	SCl wag	
273	Torsion	a''	264 p	SCl wag	b_1
298 p	SOS stretch, s	a'	293	Torsion	a_2, b_2
326	SCl wag				
353 p	SCl wag	a'	350	SO_2 rock	a_2, b_2
370	Torsion	a''			
412 p	SCl stretch, i	a'	412 p	SCl stretch	a_1
427 p	SCl stretch, o	a'	434	SCl stretch	b_1
490	SO_2 rock, ∥, i	a'	486 p	SOS bend	a_1
560	SO_2 rock, ⊥, i	a''	545 p	SO_2 rock	a_1, b_1
593 p	SO_2 bend, i	a'	592 p	SO_2 bend	a_1, b_1
607 p	SO_2 bend, o	a'			
621	SO_2 rock, ⊥, o	a''			
716	SO_2 rock, ∥, o	a'	716 p	SOS stretch, s	a_1
760	SOS stretch, a	a''	773	SOS stretch, a	b_1
(885)	?				
(1090)	?				
1189	SO_2 stretch, s, o	a'			
1209 p	SO_2 stretch, s, i	a'	1221 p	SO_2 stretch, s	a_1
1442	SO_2 stretch, a, o	a''	1446	SO_2 stretch, a	a_1, b_2
1462	SO_2 stretch, a, i	a''			

NOTE: p, polarized line; s, symmetric vibration; a, asymmetric vibration; i, in-phase vibration; o, out-of-phase vibration; ∥, parallel to SOS plane; ⊥, perpendicular to SOS plane. Frequencies in parentheses indicate extremely weak lines.

TABLE II

Raman spectra of $S_2O_5F_2$ and S_2O_5ClF

$S_2O_5F_2$			S_2O_5ClF	
Frequencies (cm^{-1})				
Raman	I.R. (2)	Assignment	Frequencies (cm^{-1})	Assignment
157 p		SOS bend	154 p	SOS bend
290		Torsion	204	SCl wag
301		SF wag	231	SCl wag
323 p		SOS stretch, s	284	Torsion
350		SF wag	313 p	SOS stretch, s
366		Torsion	360	Torsion
435		SF wag	397 p	SF wag
455 p		SF wag	419	SF wag
487		SO_2 rock, ∥, i	432 p	SCl stretch
518 p		SO_2 bend, i	458	SO_2 rock, ∥, i
540		SO_2 bend, o	515	SO_2 bend
560		SO_2 rock, ⊥, i	535	SO_2 rock, ⊥, i
630		SO_2 rock, ⊥, o	602 p	SO_2 bend
733 p	735	SO_2 rock, ∥, o	616	SO_2 rock, ⊥, o
814	824	SOS stretch, a	715	SO_2 rock, ∥, o
872 p	872	SF stretch	802	SOS stretch, a
1249 p	1248	SO_2 stretch, s, o	860 p	SF stretch
1264 p		SO_2 stretch, s, i	(1068)	?
1490		SO_2 stretch, a, i	1205 p	SO_2 stretch, s, o
1511	1513	SO_2 stretch, a, i	1248 p	SO_2 stretch, s, i
			1453	SO_2 stretch, a, o
			1487	SO_2 stretch, a, i

NOTE: p, polarized line; s, symmetrical vibration; a, asymmetric vibration; i, in-phase vibration; o, out-of-phase vibration; ∥, parallel to SOS plane; ⊥, perpendicular to SOS plane. Frequencies in parentheses indicate extremely weak lines.

stretches, and one of the SO_2 bends have frequencies close to those in $S_2O_5F_2$, while the other frequencies for these vibrations are close to those in $S_2O_5Cl_2$.

SOS Skeletal Vibrations

An important feature of the spectra of $S_2O_5F_2$, S_2O_5ClF, and $S_2O_5Cl_2$ is the occurrence of rather broad, moderately strong, polarized lines at 157, 154, and 147 cm^{-1}, respectively. No lines at such a low frequency are observed in the spectra of the simple sulphuryl halides and they can therefore only be reasonably attributed to an SOS skeletal vibration; since the SOS bending mode would be expected to have the lowest frequency of the three skeletal vibrations, they are assigned to this vibration. The similar frequencies of this vibration in the three molecules suggest that the corresponding SOS symmetric stretches might also have rather similar frequencies. An examination of the frequency of the symmetric stretch in a number of simple nonlinear triatomic molecules shows that this is generally approximately twice that of the bend (7). Thus the relatively strong polarized lines at 323, 313, and 298 cm^{-1}, are assigned as the SOS symmetric stretch in $S_2O_5F_2$, S_2O_5ClF, and $S_2O_5Cl_2$, respectively. The asymmetric SOS stretch is more difficult to assign. It is expected to have a considerably higher frequency than the symmetric stretch since it is largely the vibration of an oxygen atom between the two relatively heavy SO_2X groups. A weak depolarized line, which cannot be attributed to any of the group vibrations which are observed in the simple sulphuryl halides, occurs in all three spectra at approximately 800 cm^{-1}. Therefore the lines at 814, 802, and 760 cm^{-1} in the spectra of $S_2O_5F_2$, S_2O_5ClF, and $S_2O_5Cl_2$, respectively, are assigned to the asymmetric SOS stretch.

Our assignment for these skeletal vibrations is consistent with the assignment recently given by Kriegsmann (8) for the Si—O—Si vibrations in some siloxanes. For example, for hexamethyldisiloxane he gives the Si—O—Si bend at 180 cm^{-1}, the symmetric Si—O—Si stretch at 519 cm^{-1}, and the asymmetric stretch at 1055 cm^{-1}.

SO_2 Rocking Modes

The SO_2 rock has been assigned frequencies of 580 and 545 cm^{-1} in SO_2Cl_2 and SO_2F_2 respectively (5). It is apparent from a model that for structure VII there is considerable interaction between one SO_2 group and the halogen atom on the other sulphur atom. This would be expected to lead to a considerable difference in the frequencies of the two SO_2 parallel rocking modes. The out-of-phase mode, in which the two SO_2 groups move towards each other, would be expected to have the higher frequency. A rather strong, polarized line is observed at 733, 715, and 716 cm^{-1} in the spectra of $S_2O_5F_2$, S_2O_5ClF, and $S_2O_5Cl_2$, respectively, and this is assigned to the out-of-phase SO_2 parallel rock. In the spectrum of $S_2O_5Cl_2$ there are three lines between 716 cm^{-1} and the lines due to the S—Cl stretching modes at 427 and 412 cm^{-1}. These lines, at 621, 560, and 490 cm^{-1}, are tentatively assigned to the three remaining SO_2 rocking modes, possibly the perpendicular out-of-phase, the perpendicular in-phase, and the parallel in-phase, respectively. Similarly in $S_2O_5F_2$ and in S_2O_5ClF these vibrations are assigned frequencies of 630, 560, and 487 cm^{-1} and of 616, 535, and 458 cm^{-1} respectively.

SX Wagging Modes

The SCl wag has been assigned a frequency of 200 cm^{-1} in chlorosulphuric acid and 220 cm^{-1} in the chlorosulphate ion (9), and it is a rather similar vibration to the SCl_2 bend, which is at 218 cm^{-1} in SO_2Cl_2 and 194 cm^{-1} in $SOCl_2$. Therefore the pair of frequencies at 200 and 235 cm^{-1} in the spectrum of $S_2O_5Cl_2$ can be reasonably assigned as the SCl′ wags. The higher frequencies of 326 and 353 cm^{-1} are assigned to the SCl″ wags,

as the motions of the Cl″ atom are restricted by the proximity of the SO_2 group to which it is not directly bonded. This assignment receives some confirmation from the fact that lines at 204 and 231 cm^{-1}, which must also presumably be assigned as SCl wags, are found in the spectrum of S_2O_5ClF.

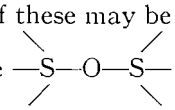
In SO_2FBr and CH_3SO_2F the SF wag has been assigned frequencies of 320 and 326 cm^{-1} respectively (5, 10); thus the two lines at 301 and 350 cm^{-1} in the spectrum of $S_2O_5F_2$ may be reasonably assigned as SF′ wagging modes and the pair of lines at 435 and 455 cm^{-1}, which are analogous to the pair at 326 and 353 cm^{-1} in the spectrum of $S_2O_5Cl_2$, are assigned to the SF″ wagging modes. The conformation of S_2O_5ClF is expected to be X in which the chlorine atom resembles the Cl′ in $S_2O_5Cl_2$ and the F atom resembles the F″ in $S_2O_5F_2$. Thus the S—Cl wags should correspond to the low-frequency pair in $S_2O_5Cl_2$ and the SF wags should correspond to the high-frequency pair in $S_2O_5F_2$. The latter may therefore be assigned to the pair of lines at 397 and 419 cm^{-1}.

Torsional Modes

In sulphuryl chloride and sulphuryl fluoride the torsional mode has a frequency of approximately 360 cm^{-1} (5). It seems reasonable, therefore, to attribute the as-yet-unassigned lines at 366 cm^{-1} for $S_2O_5F_2$, 370 cm^{-1} for $S_2O_5Cl_2$, and 360 cm^{-1} for S_2O_5ClF to one of the torsional modes in these molecules.

There is another moderately strong line, as yet unassigned, which occurs at a very similar frequency for each of the species, i.e. $S_2O_5F_2$, 290 cm^{-1}; S_2O_5ClF, 284 cm^{-1}; $S_2O_5Cl_2$, 273 cm^{-1}, in the spectrum of each of the disulphuryl halides. This line we also assign to a torsion on the grounds that the frequency is relatively independent of the nature of the halogen atoms involved, as is the case for the torsional modes in SO_2Cl_2 and SO_2F_2.

Although a number of the assignments made above are somewhat tentative, it is clear that others are quite certain, e.g. the SO_2 and S(Hal) stretching modes, and the SOS bend and symmetric stretch, which are characteristic of the disulphuryl group. The strong polarized line at approximately 700 cm^{-1}, which is very probably the SO_2 parallel rocking vibration, and the vibration in the region of 270 to 290 cm^{-1}, which we have assigned as a torsion, also appear to be diagnostic of the disulphuryl group. Use is made of these assignments in identifying disulphuryl compounds in other systems, e.g. disulphuric acid and fluoro- and chloro-disulphuric acids, as will be discussed in following papers.

A number of rather weak or ill-defined shoulders on various peaks in the spectra have not been assigned. It seems probable that at least some of these may be due to conformational isomers arising from hindered rotation around the  bonds.

Comparison with Previous Work

A number of our assignments for $S_2O_5Cl_2$ differ from those given previously by Gerding and Linden (1). For example, these authors assign the polarized line at 147 cm^{-1} as an S—Cl wag whereas we have assigned it as the SOS bend. The earlier assignment is not consistent with the fact that an obviously similar line is found at 157 cm^{-1} in the spectrum of $S_2O_5F_2$ since S—F wags are expected, and are generally found, to have appreciably higher frequencies than the corresponding S—Cl vibrations. Gerding and Linden assign to the SOS bend a frequency of 486 cm^{-1}: this is presumably the line we find at 490 cm^{-1}, which does not appear to be polarized and which we have assigned as an SO_2 rock. These authors assign to the SOS symmetric stretch the frequency of 716 cm^{-1}, which seems very

high in view of the total mass of the atoms attached to each sulphur atom, and which is, moreover, not consistent with our assignment for the SOS bend. For both of these reasons our assignment of the polarized line at 298 cm^{-1} to the SOS symmetric stretch seems more reasonable.

TRISULPHURYL HALIDES

The trisulphuryl halides presumably have one of several possible staggered conformations with C_s symmetry such as II. They have 33 normal modes of vibration, all of which should be active in the Raman effect. In terms of the description we have used for the disulphuryl halides there will be three symmetric and three asymmetric SO_2 stretching modes, three parallel and three perpendicular SO_2 rocking modes, three SO_2 bending

TABLE III

Raman spectra of $S_3O_8Cl_2$, $S_3O_8F_2$, and S_3O_8ClF

Frequency (cm^{-1})	Assignment	Frequency (cm^{-1})	Assignment
$S_3O_8Cl_2$			
136 p, 169 p	Skeletal bends	512	SO_2 rock
200	SCl wag	595 p	SO_2 bend
226	SCl wag	650	SO_2 rock
275	Torsion	686	SO_2 rock
291, 308	Skeletal stretches	723 p	SO_2 rock
342	SCl wag or torsion	770, 870	Skeletal stretches
362	Torsion	1193, 1208, 1220	SO_2 stretches, s
415 p	SCl stretch	1450, 1480	SO_2 stretches, a
440	SCl stretch		
485	SO_2 rock		
$S_3O_8F_2$			
145 p, 165, 195, 226, 245	Skeletal bends	699 p	SO_2 rock
288	Torsion	724 p	SO_2 rock
318, 324	Skeletal stretches	761, 835	Skeletal stretches
350, 359	SF wag and torsion	876 p	SF stretch
403	SF wag	(1029)	
468	SF wag	1198, 1198, 1241 p, 1268	SO_2 stretches, s
528	SO_2 bend	1468, 1490, 1515	SO_2 stretches, a
S_3O_8ClF			
150 p, 158 p	Skeletal bends	580	SO_2 bend
204	SCl wag	598 p	SO_2 bend
235	SCl wag	620	SO_2 rock
274	Skeletal bend	658	SO_2 rock
290	Torsion	700	SO_2 rock
301, 318	Skeletal stretches	715 p	SO_2 rock
353, 366	Torsion and/or SF wag	778	Skeletal stretch
398	SF wag	865 p	SF stretch and skeletal stretch
418 p	SCl stretch	1210 p, 1222 p, 1257 p	SO_2 stretches, s
435	SCl stretch	1453, 1462, 1499	SO_2 stretches, a
468	SO_2 rock		
549	SO_2 bend		

modes, and three torsions. In addition there will be two SX stretches and four SX wags for $S_2O_5X_2$ molecules, or an SX stretch, an SY stretch, two SX wags, and two SY wags for S_3O_8XY molecules, and nine skeletal, or SOSOS, vibrations.

By comparing the spectra of the trisulphuryl halides with each other and with the spectra of the disulphuryl halides it was possible to make reasonable assignments for all the observed lines, as shown in Table III. There are several features that distinguish the spectra of trisulphuryl compounds from those of disulphuryl compounds. An important characteristic of the spectra of the trisulphuryl halides is the occurrence of two high-frequency SO_2 rocks in the region of 700 cm^{-1}, as compared to the occurrence of a single line in this region in the spectra of disulphuryl compounds. A similar "splitting" of a frequency in this region of the spectra has been previously claimed as diagnostic of the change in structure in going from a diphosphate to a triphosphate (11). In the infrared spectra of diphosphates an absorption band near 730 cm^{-1} is replaced by two bands near 680 and 730 cm^{-1} in triphosphates. Another distinct difference between the spectra of disulphuryl and trisulphuryl compounds is that the symmetric stretch near 300 cm^{-1} in disulphuryl compounds is replaced by two skeletal stretches in the same region of the spectrum in trisulphuryl compounds and that the SOS asymmetric stretch, which occurs near 800 cm^{-1} in the spectrum of disulphuryl halides, is replaced by two skeletal stretches of similar frequencies in trisulphuryl compounds.

In addition to the four stretching modes the SOSOS skeleton also has five bending modes. These are thought to give rise to the low-frequency lines at 145, 165, 195, 226, and 241 cm^{-1} in the spectrum of $S_3O_8F_2$. Fewer than five lines that can be attributed to these bending modes are observed in the spectra of $S_3O_8Cl_2$ and S_3O_8ClF; this is probably because they coincide with the very strong lines due to the SCl wags which also occur in this region of the spectrum.

EXPERIMENTAL

Disulphuryl Fluoride

This compound was prepared by the reaction between antimony pentafluoride and liquid sulphur trioxide, according to the method of Hayek and Koller (12). The components were heated under gentle reflux for 2 hours and the resulting $S_2O_5F_2$ was distilled off. The product was washed with 100% sulphuric acid to remove sulphur trioxide and redistilled, b.p. 51–52°.

Disulphuryl Chloride

This compound was made by the reaction of 2 moles of sulphur trioxide and 1 mole of carbon tetrachloride at 40 to 45° for several hours. The mixture was then distilled and the fraction boiling above 140° collected. It was washed with 100% sulphuric acid and redistilled. The fraction boiling at 151 to 153° at atmospheric pressure was collected. Redetermination of the boiling point gave 152°.

Disulphuryl Chlorofluoride

This compound was prepared by fluorinating $S_2O_5Cl_2$ with AgF_2. Contrary to a previous report (13) this was found to be a satisfactory method. Disulphuryl chloride was added slowly from a dropping funnel to AgF_2 in a flask equipped with a reflux condenser. Two moles of $S_2O_5Cl_2$ were used per mole of AgF_2. After the vigorous reaction had subsided the product was distilled and the fraction boiling above 95° collected. Redistillation through an efficient column gave a fraction of b.p. 100–101°. The material had a fluorine n.m.r. spectrum consisting of a single peak. The % F was determined by comparing the

areas of the fluorine n.m.r. peaks in a mixture of the compound with $S_2O_5F_2$ (found, 9.5%; calculated for S_2O_5ClF, 9.57%).

Trisulphuryl Fluoride

This compound was prepared by the method of Lehmann and Kolditz (14) by bubbling BF_3 gas through liquid sulphur trioxide until a dense, solid white mass resulted. Sulphuric acid, previously cooled in ice, was then added to the mixture, and two liquid layers were obtained, a lower layer of sulphuric acid and an upper layer containing $S_3O_8F_2$. (It made little difference whether the decomposition was carried out with 70% sulphuric acid, as recommended by Lehmann, or with 100% acid.) The trisulphuryl fluoride layer was separated and washed several times with sulphuric acid to remove sulphur trioxide. It was then washed with water and dried over phosphoric oxide. The fraction of b.p. 29–31° at a pressure of 2 to 4 mm Hg was collected. Redetermination of the boiling point at atmospheric pressure gave a value of 121.5° (Lehmann and Kolditz reported a value of 120°), but slow decomposition takes place under these conditions. The material had a fluorine n.m.r. spectrum consisting of a single peak. The % F was determined by comparing the areas of the two fluorine n.m.r. peaks in a mixture of the compound with $S_2O_5F_2$ (found, 15.0%; calculated for $S_3O_8F_2$, 14.87%).

Trisulphuryl Chloride

This compound was prepared by the method of Lehmann and Ladwig (15) by heating 4 moles of sulphur trioxide and 1 mole of carbon tetrachloride under reflux for 4 hours during which time the temperature was raised to 85°:

$$CCl_4 + 3SO_3 = S_3O_8Cl_2 + COCl_2.$$

The mixture was distilled under reduced pressure and gave $S_3O_8Cl_2$, b.p. 55–65° at 2 to 3 mm Hg pressure, and a small amount of $S_2O_5Cl_2$. The product was washed with sulphuric acid and redistilled. The fraction b.p. 60–65° at 2.5 to 3 mm Hg was collected.

Trisulphuryl Chlorofluoride

This compound was prepared by fluorination of $S_3O_8Cl_2$ with AgF_2, using 2 moles of $S_3O_8Cl_2$ to 1 mole of AgF_2. In contrast to the violent reaction of $S_2O_5Cl_2$ with AgF_2 the reaction was slow, as indicated by the conversion of the fluoride to silver chloride, and it was necessary to heat the reaction mixture to 100° for 12 hours. The product was separated from silver chloride and distilled under reduced pressure. Redistillation at 15 to 20 mm of Hg pressure gave S_3O_8ClF, b.p. 40–45°. At atmospheric pressure the substance boils with decomposition at approximately 145°. The material had a fluorine n.m.r. spectrum consisting of a single peak. The % F was determined by comparing the areas of the two fluorine n.m.r. peaks in a mixture of the compound with $S_3O_8F_2$ (found, 6.8%; calculated for 6.82%).

Apparatus

The apparatus consisted of a Hilger E612 Raman spectrometer with glass prisms, used in conjunction with a water-cooled mercury-arc lamp. After the spiral of the lamp had been preheated with infrared lamps, and the mercury pool electrodes with nichrome heaters, the arc was easily struck by using the discharge from a "tesla" coil. The power supply was 250 volts d-c. and an operating current of 12 amp was used.

Liquid samples from 5 to 40 ml were contained in Pyrex glass cells mounted vertically and surrounded by a jacket containing saturated sodium nitrite solution as an optical filter. The filter solution was cooled and circulated through the jacket.

A prism was used to reflect the Raman radiation through 90° and a two-lens system ensured that most of the light scattered from the sample was collected. Spectra were recorded on Kodak 103*a*O, 2*a*O, or 3*a*O spectroscopic plates and the positions of the lines were measured by means of a Leeds and Northrup microphotometer, using an iron arc for calibration. Raman shifts could be measured to ± 3 cm^{-1} directly from the chart paper. When a qualitative comparison of the intensities of lines from different samples was required the spectra were compared on the same photographic plate. When fast plates (103*a*O or 2*a*O) were used, exposures of a few minutes gave excellent spectra with little background and tolerable broadening of the 4358 Å exciting line, so that Raman shifts as small as 150 cm^{-1} were easily resolved from the exciting line.

Polarization measurements were carried out using polaroid cylinders polarized parallel to and perpendicular to the plane of the incident light. A system of baffles was used to ensure that the incident light was perpendicular to the plane of the polaroid, which was situated inside the filter jacket surrounding the sample tube. Such polarization measurements are only qualitative.

CONCLUSIONS

Our Raman spectra provide strong support for the acyclic structures I and II for the di- and tri-sulphuryl halides.

The general consistency of the assignments of group vibrational frequencies for all the molecules we have discussed show that our approximate description of the normal modes is useful for at least some of the vibrations, and that characteristic spectral features due to —SO_2—, —S_2O_5—, and S_3O_8— groups can be recognized. Use is made of these conclusions in following papers to obtain structural information on some related compounds.

The close similarities between the spectra of S_3O_8ClF and those of $S_3O_8F_2$ and $S_3O_8Cl_2$, and also the expected relationship to the spectrum of S_2O_5ClF, appear to adequately establish its structure; additional evidence will be presented in a following paper.

ACKNOWLEDGMENTS

Mr. A. W. Richardson and Mr. R. C. Dixon are thanked for the preparation of disulphuryl chlorofluoride and for help with the measurement of its Raman spectrum.

Our thanks are also due to Professor H. L. Welsh of the Department of Physics, University of Toronto, for assistance with the construction of the "Toronto" mercury-arc lamp.

The National Research Council, the Defence Research Board, and the Allied Chemical Company are thanked for financial assistance.

REFERENCES

1. H. Gerding and A. C. Linden. Rec. trav. chim. **61**, 735 (1942).
2. H. C. Clark and H. J. Emeleus. J. Chem. Soc. 190 (1958).
3. E. L. Muetterties and D. D. Coffman. J. Am. Chem. Soc. **80**, 5914 (1958).
4. R. J. Gillespie and E. A. Robinson. Can. J. Chem. This issue. p. 2189.
5. R. J. Gillespie and E. A. Robinson. Can. J. Chem. This issue. p. 2171.
6. E. A. Robinson. Can. J. Chem. **39**, 247 (1961).
7. G. Herzberg. Molecular spectra and molecular structure. Vol. 2. D. van Nostrand Inc., New York. 1945. p. 167.
8. H. Kriegsmann. Z. Electrochem. **61**, 1088 (1957); Z. anorg. Chem. **299**, 78 (1959).
9. R. J. Gillespie and E. A. Robinson. To be published.
10. N. S. Ham, A. N. Hambly, and R. H. Laby. Australian J. Chem. **4**, 443 (1960).
11. D. E. C. Corbridge and E. J. Lowe. J. Chem. Soc. 493 (1954).
12. E. Hayek and W. Koller. Monatsh. **82**, 942 (1951).
13. A. Engelbrecht. Z. anorg. Chem. **273**, 269 (1953).
14. H. A. Lehmann and L. Kolditz. Z. anorg. Chem. **272**, 76 (1953).
15. H. A. Lehmann and G. Ladwig. Z. anorg. Chem. **284**, 1 (1956).

Can. J. Chem. Downloaded from www.nrcresearchpress.com by 210.87.254.42 on 09/05/12
For personal use only.

THE RAMAN SPECTRA OF LIQUID SULPHUR TRIOXIDE AND SOLUTIONS OF SULPHUR TRIOXIDE IN INERT SOLVENTS[1]

R. J. GILLESPIE AND E. A. ROBINSON[2]

ABSTRACT

The Raman spectra of liquid sulphur trioxide and of sulphur trioxide dissolved in a number of "inert" solvents have been investigated. A detailed analysis of the spectrum of liquid sulphur trioxide supports the earlier suggestion of Gerding and Nijveld that the main polymeric species in liquid sulphur trioxide is the cyclic trimer. Frequencies are assigned for all the Raman active vibrations of the cyclic trimer. These assignments differ substantially from those given previously by Gerding and Nijveld.

The spectra of dilute solutions of sulphur trioxide in sulphur dioxide, sulphuryl chloride, carbon tetrachloride, tetrachlorethylene, and trichlorfluormethane (Freon 11) show that the sulphur trioxide is present mainly in the monomeric form at low concentrations while at higher concentrations a polymeric form, which is very probably the trimer, is also present.

The chemistry of sulphur trioxide is complex due to the ease with which it polymerizes. In the solid state, three principal forms are recognized: the γ or ice-like form, the β or low-melting asbestos form, and the α or high-melting asbestos form. Liquid sulphur trioxide is stable under anhydrous conditions but in the presence of a trace of water, high-molecular-weight polymers are formed and a solid phase separates. The structures of the solid forms and of liquid sulphur trioxide have been examined previously by Raman spectroscopy and by X-ray diffraction (1, p. 351; 2–9).

Only one strong line at 1069 cm^{-1} has been found in the Raman spectrum of sulphur trioxide gas at a pressure of 11 atm (2). Vapor pressure measurements have shown (5) that sulphur trioxide is monomeric in the gas phase, so this line can be assigned to the monomer. Other vibration frequencies for the monomer have been obtained from the spectra of mixtures of sulphur trioxide and sulphur dioxide at 60° (7, 8). The SO_3 molecule is planar (10) and therefore has four fundamental vibrations one of which is inactive in the Raman and one inactive in the infrared (Table I). The present measurements on

TABLE I

The vibrational frequencies of sulphur trioxide monomer

Assignment	cm^{-1}	
ν_1'	1069*	Forbidden in infrared
ν_2'	652	Forbidden in Raman
ν_3'	1390	
ν_4'	532	

*Sharp, strong, and diagnostic.

liquid sulphur trioxide and on solutions of sulphur trioxide dissolved in various solvents support these assignments. The Raman spectrum of sulphur trioxide monomer is therefore well established and the strong, sharp line at 1069 cm^{-1} is diagnostic of this species.

LIQUID SULPHUR TRIOXIDE

The most extensive previous study of the Raman spectrum of liquid sulphur trioxide is due to Gerding and Nijveld (9), who also summarized the earlier work of Bhavagantam

[1]*Manuscript received May 15, 1961.*
Contribution from the Department of Chemistry, McMaster University, Hamilton, Ontario.
[2]*Present address: Department of Chemistry, University of Toronto, Toronto, Ontario.*

(3) and Venkateswaren (4). Gerding and Nijveld found 17 Raman lines, 5 of which were definitely polarized, in addition to those of the monomer. In the present work, 25 Raman shifts were observed, 5 of which were found to be definitely polarized and 1 possibly weakly polarized (Table II and Figs. 1 and 2). Liquid sulphur trioxide, obtained by

TABLE II

The Raman spectrum of sulphur trioxide (frequencies in cm^{-1})

	Liquid		Gas	Solid		
				γ-SO_3	β-SO_3	α-SO_3
(*a*)	(*b*)	(*c*)	(*d*)	(*e*)	(*f*)	(*g*)
147	166(1)					
(243)*		255			254(1/2)	
290	290(6)	289		292(1)	286(0)	
322	319(1)	319			328(1)	327(1/2)
(337)						
368 p†	370(7) p	369 p		371(1d)		
407	408(1)	408			425(0)?	
480	483(1)	483			458(0)	
534	531(3)	531 p	530	525(0)		
560					566(0)	
(600)	597(1/2)	597				
657 p	650(2) p	651 p		662(1/2)	652(1)	650(1/2)
665 p	668(3) p	664				
698 p	699(3) p	697 p		698(1/2)		689(0)
(773)	775(0)	775				
844	840(1)	840				
860	866(1/2)	866				
(1018)						
1073 p	1068(5) p	1068 p	1069	1074(1/2)		1076(0+)
(1162)						
1231	1229(1)	1231				
1270 p	1271(6) p	1271 p		1273(2)	1258(1−)	1260(1/2)
1390	1390(1)	1390	1390			
1489	1490(2)	1487				
1515	1516(1) p?	1515				

NOTE: (*a*) This investigation at approximately 25°; (*b*) collected results from Hibben (2); (*c*) Gerding and Nijveld (9); (*d*) Gerding, Nijveld, and Muller (6); (*e*), (*f*), and (*g*) Gerding and Moerman (7).
*Frequencies in brackets are lines of very weak intensity.
†p indicates a polarized line.

distillation from 65% oleum, and "Sulfan B" (stabilized liquid sulphur trioxide) gave exactly the same Raman lines although the relative intensity of the monomer lines was slightly greater in the "Sulfan B" than in the freshly distilled material.

Sulphur trioxide can presumably polymerize to give either rings or long chains, e.g. structures I, II, III, and IV. The dimer I, which involves a four-membered ring, and other possible higher polymers involving the same ring are rather improbable because of the high degree of strain that would be present, particularly at the oxygen atoms. The corresponding dimetaphosphate ion V, for example, is not known (11). In the trimer II, tetramer III, similar larger cyclic polymers, and long chains such as IV, the configuration around sulphur is tetrahedral and the structures are expected to be non-planar. Gerding and Nijveld (9) have calculated the number of fundamental vibrations of both the planar and the more probable non-planar forms of the dimer, trimer, and tetramer (Table III). Although their evidence was by no means conclusive these authors suggested that liquid sulphur trioxide consists mainly of a mixture of the cyclic trimer II and the monomer. When the temperature is raised extensive depolymerization apparently takes

Can. J. Chem. Downloaded from www.nrcresearchpress.com by 210.87.254.42 on 09/05/12
For personal use only.

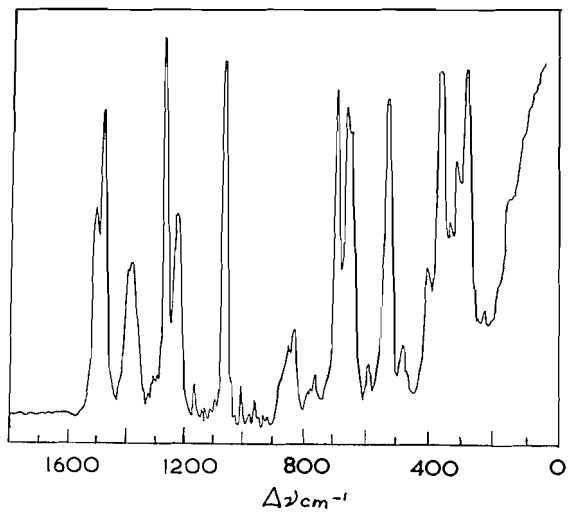


FIG. 1. The Raman spectrum of liquid sulphur trioxide.

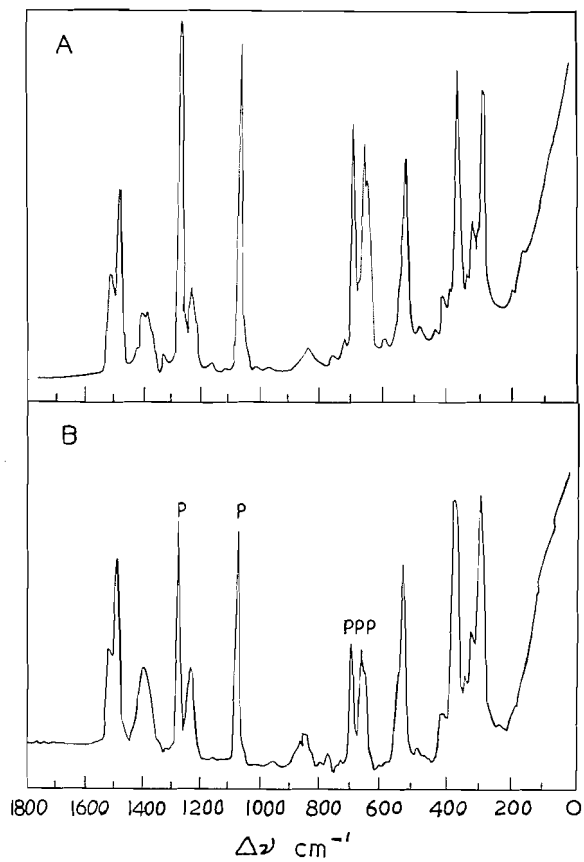


FIG. 2. Polarization measurements on liquid sulphur trioxide: (A) incident light polarized in a vertical plane; (B) incident light polarized in a horizontal plane (polarized lines denoted by P are of reduced intensity).

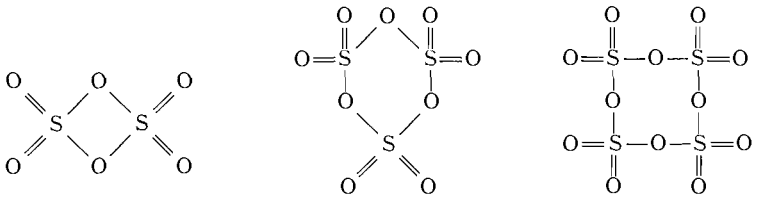
Can. J. Chem. Downloaded from www.nrcresearchpress.com by 210.87.254.42 on 09/05/12
For personal use only.

TABLE III

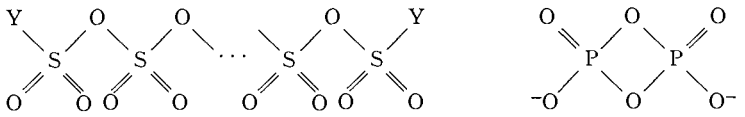
Raman active vibrations for sulphur trioxide polymers

Polymer	Symmetry	Number of vibrations
S_2O_6	D_{2h} (planar)	9 (4p, 5dp)
	C_{2v} (non-planar)	18 (7p, 11dp)
S_3O_9 ring	D_{3h} (planar)	14 (4p, 10dp)
	C_{3v} (non-planar), "chair form"	17 (7p, 10dp)
	C_s (non-planar), "boat form"	30 (17p, 13dp)
S_4O_{12} ring	D_{4h} (planar)	15 (4p, 11dp)
	C_{4v} (non-planar)	29 (7p, 22dp)

place, as the Raman spectrum of the liquid at 100° (7) shows only those vibration frequencies which have been assigned to the monomer. Open chains IV, of varying lengths, may also be present in the liquid at room temperature but presumably only in small amounts as they require end groups Y, which would have to originate from impurities.



I II III



IV V

Further support for the suggestion that liquid sulphur trioxide consists of the trimer in equilibrium with the monomer can be obtained by a comparison of the spectrum of the liquid with the spectra of the solid α, β, and γ forms. The lines of the γ form all occur quite strongly in the spectrum of the liquid, and this form has been shown by X-ray crystallography to have a structure consisting of trimeric rings (III) in the "chair" form with C_{3v} symmetry. The solid β form on the other hand consists of SO_4 tetrahedra linked together to form long spiral chains (12, 13).

If it is assumed that the trimer is the main species present in the liquid and that the trimer is, at least mainly, in the chair form, frequencies can be assigned to this molecule as shown in Table IV. There are 20 normal vibrations of which the three A_2 vibrations are inactive in the Raman. Seven of the vibrations, 3 of which are polarized, can be assigned to the ring and the other 10, 4 of which should be polarized, involve the atoms of the SO_2 groups (9) (Fig. 3).

Sulphuryl Group Vibrations

Sulphuryl group vibrations would be expected to have frequencies close to those observed in simple molecules such as sulphuric acid and sulphuryl fluoride and would be expected therefore to occur at approximately the following frequencies: symmetric

Can. J. Chem. Downloaded from www.nrcresearchpress.com by 210.87.254.42 on 09/05/12
For personal use only.

TABLE IV

Assignment of fundamental frequencies for the *chair* conformation of trimeric sulphur trioxide

Species	Vibration	Assignment (cm^{-1}) (*a*)	(*b*)	
A_1	ν_1	1270	1271	Polarized
	ν_2	534*	657	Polarized
	ν_3	368	664	Polarized
	ν_4	665 or 657	698	Polarized
	ν_5	1515	1489	Polarized
	ν_6	698	775	Polarized
	ν_7	665 or 657	369	Polarized
A_2	ν_8	—	597	Forbidden
	ν_9	—	319	Forbidden
	ν_{10}	—	1515	Forbidden
E	ν_{11}	1231	1271	
	ν_{12}	480	657	
	ν_{13}	560	319	
	ν_{14}	407	408	
	ν_{15}	860	1231	
	ν_{16}	840	840	
	ν_{17}	1489	1489	
	ν_{18}	680	775	
	ν_{19}	322	597	
	ν_{20}	290	289	

NOTE: (*a*) This investigation; (*b*) Gerding and Nijveld (9).
*Coincident with the analogous vibration of the monomer.

stretches, 1100–1300 cm^{-1}; asymmetric stretches, 1300–1500 cm^{-1}; symmetric deformations, 500–600 cm^{-1}; rocking and torsional vibrations, 300–600 cm^{-1} (14).

The five lines observed at frequencies greater than 1200 cm^{-1} can only be reasonably assigned as SO_2 stretching vibrations. One of these, at 1390 cm^{-1}, is due to the monomer and the other four may be assigned in pairs as the in-phase symmetric and asymmetric stretch ν_1 and ν_5 at 1270 cm^{-1} and 1515 cm^{-1}, respectively, and the out-of-phase symmetric and asymmetric stretch ν_{11} and ν_{17} at 1231 and 1489 cm^{-1}, respectively (Table II). The in-phase vibrations are of species A_1 and should therefore be polarized. The vibration at 1270 cm^{-1} is definitely polarized and that at 1515 cm^{-1} was reported to be weakly so by Venkateswaren (4). The frequencies of both pairs of lines are consistent with the linear relationship that has been found between the SO_2 symmetric and asymmetric stretching frequencies (15, 16). The relatively high values of the SO_2 vibrational frequencies imply that the S—O bonds exterior to the ring have substantial double-bond character. This is consistent with the bond length of 1.4 Å and the large OSO angle of 122° (17). It appears reasonable to assign the in-phase vibrations at higher frequencies than the out-of-phase vibrations since in the former, but not in the latter, distortion of the ring occurs. Gerding and Nijveld (9) assumed that coupling between the SO_2 groups is very weak and that the in-phase and out-of-phase vibrations of the SO_2 group are degenerate. They assigned the line at 1270 cm^{-1} to the symmetric stretch and the line at 1489 cm^{-1} to the asymmetric stretch. These authors attributed the 1515 cm^{-1} frequency to the forbidden ring vibration ν_{10} and the line at 1230 cm^{-1} to the ring vibration ν_{15}.

In simple sulphuryl compounds such as sulphuric acid, the SO_2 bend is in the range 500–600 cm^{-1}, and in the sulphur trioxide monomer the similar vibration is at 532 cm^{-1}. In liquid sulphur trioxide there is a line at 534 cm^{-1} which is relatively strong and is

Can. J. Chem. Downloaded from www.nrcresearchpress.com by 210.87.254.42 on 09/05/12
For personal use only.

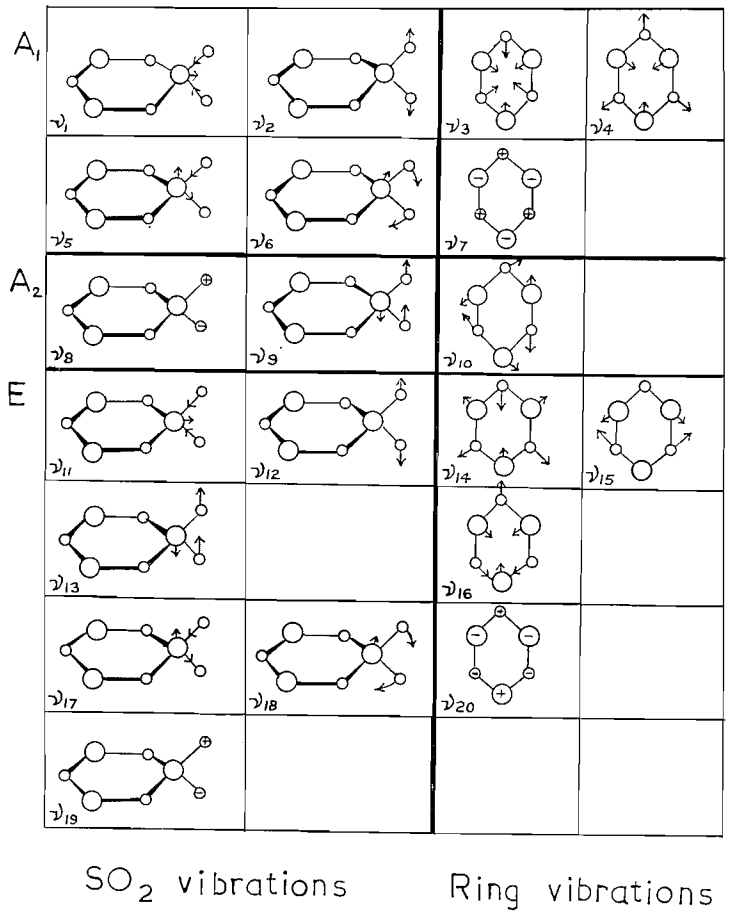


FIG. 3. Approximate atomic motions in the normal modes of S_3O_9. In the A_1 and A_2 vibrations the motions of the three SO_2 groups are in-phase while in the E vibrations the motions of the SO_2 groups are out-of-phase.

probably polarized and this we assign to the in-phase bend of the trimer ν_2, as well as to the monomer, since it is much stronger in the liquid than would be expected for the amount of monomer implied by the intensity of the 1070 cm^{-1} Raman shift in the liquid.

The out-of-phase SO_2 bend, ν_{12}, may be tentatively assigned as the rather weak line at 480 cm^{-1}. Gerding and Nijveld assigned the polarized line at 651 cm^{-1} to the SO_2 bend, but although a large number of compounds have been investigated the SO_2 bend has never been found at such a high frequency and it very rarely occurs at a frequency higher than 600 cm^{-1} (14).

Rocking and torsional modes of the sulphuryl group have frequencies in the range 300–600 cm^{-1} in simple sulphuryl compounds (14). In trimeric sulphur trioxide there is a total of six vibrations of these types: four rocking modes ν_6, ν_9, ν_{13}, and ν_{18} and two torsional modes ν_8 and ν_{19}, of which ν_8 and ν_9 are forbidden in the spectrum for a molecule with C_{3v} symmetry. Vibration ν_6 is of species A_1 and should therefore be polarized. There are four polarized lines as yet unassigned at 368, 657, 665, and 698 cm^{-1}. A model of the chair form of sulphur trioxide trimer shows that the axial oxygens of the SO_2 groups are close together and there will be considerable interaction between these oxygen atoms

Can. J. Chem. Downloaded from www.nrcresearchpress.com by 210.87.254.42 on 09/05/12
For personal use only.

Can. J. Chem. Downloaded from www.nrcresearchpress.com by 210.87.254.42 on 09/05/12
For personal use only.

in vibration ν_6; this would be expected to increase its frequency above the range of 500–600 cm^{-1} found for simple sulphuryl compounds, and therefore one of the lines at 657, 665, or 698 cm^{-1} must be assigned to this vibration. Tentatively we choose the 698 cm^{-1} line as it has been found in the di- and tri-sulphuryl halides, where similar interaction between an SO_2 group and a halogen occurs in an SO_2 rocking mode, that the frequency can be raised as high as 730 cm^{-1} (18). The frequency of ν_{18} would be expected to be fairly close to that of ν_6. There is no obvious depolarized line in this region of the spectrum and it must be assumed that it is of low intensity and is hidden under the broad, incompletely resolved band between 657 and 698 cm^{-1}. The remaining SO_2 rocking mode, ν_{13}, would be expected to be of lower frequency and the only possibility seems to be to assign it to the shoulder of the 534 cm^{-1} line at approximately 560 cm^{-1}. As ν_{13} would give a depolarized line, this provides an explanation for the difficulty of observing the expected polarization of the 534 cm^{-1} line. Torsional modes have frequencies in the range 270–370 cm^{-1} in mono-, di-, and tri-sulphuryl chlorides and fluorides (14, 18) and therefore it seems reasonable to assign the line observed at 322 cm^{-1} to ν_{19}. Gerding and Nijveld assigned the very weak line at 600 cm^{-1} to this vibration, but in none of the simple sulphuryl, or polysulphuryl, compounds has a torsional mode been found to have such a high frequency.

Ring Vibrations

The three vibrations ν_3, ν_4, and ν_7 should give rise to polarized lines; they must therefore be assigned to the three lines at 368, 657, and 665 cm^{-1}. The symmetric breathing vibration would be expected to have the lowest frequency and can therefore be assigned to the 368 cm^{-1} line. This vibration is, moreover, rather similar to the symmetric SOS skeletal stretch of the disulphuryl halides which have been assigned at 298, 313, and 323 cm^{-1} for $S_2O_5Cl_2$, S_2O_5ClF, and $S_2O_5F_2$ respectively.

The remaining unassigned lines, other than very weak lines and some very low frequency lines, are at 860, 840, 407, and 290 cm^{-1}. If we assume that the order of the frequencies of the ring vibrations of species E will be the same as for the analogous vibrations of the benzene ring, then these may be assigned as ν_{15}, ν_{16}, ν_{14}, and ν_{20} respectively. The analogous vibrations of the benzene molecule have frequencies of 1585, 1478, 606, and 404 cm^{-1} respectively (19). The assignment of these ring vibrations agrees with that given by Gerding and Nijveld except that they assigned ν_{15} to the 1231 cm^{-1} line which we have assigned as ν_{11}. Gerding and Nijveld did not assign the 860 cm^{-1} line and they assumed that ν_{11} had the same frequency as ν_1, i.e. 1270 cm^{-1}.

Weak Lines

Of the 25 lines observed with certainty in the Raman spectrum of liquid sulphur trioxide, 18 have been assigned to the chair form of the trimer together with the monomer, 16 to the trimer, and 3 to the monomer with one coincidence. This assignment accounts for all except seven very weak lines at 150, 243, 327, 600, 773, 1018, and 1162 cm^{-1} and some very indefinite shoulders on the side of the exciting line at frequencies of less than 150 cm^{-1}. Some of these lines could be overtone or combination bands but perhaps the most likely explanation for most of them is the presence of small amounts of the "boat" form of the trimer. Other possible species that may be present in small quantities are the tetramer and higher cyclic polymers, together with acyclic polymers, presumably of fairly high molecular weight. The line at 150 cm^{-1} could be due to acyclic polymers since the SOS skeletal bending mode has been assigned frequencies of approximately 150 cm^{-1} in the di- and tri-sulphuryl halides (18).

Conclusion

The Raman spectrum of liquid sulphur trioxide can be reasonably satisfactorily accounted for in terms of an equilibrium between the monomer and the "chair" form of the cyclic trimer. All except the very weakest lines in the spectrum can be accounted for in this way. The additional lines are probably due to small concentrations of the "boat" form of the trimer and higher cyclic or acyclic polymers.

SOLUTIONS OF SULPHUR TRIOXIDE

Solutions of sulphur trioxide in sulphur dioxide, sulphuryl chloride, disulphuryl chloride, disulphuryl fluoride, carbon tetrachloride, tetrachlorethylene, and trichlorfluormethane (Freon 11) were investigated. In most cases, the spectra show only lines due to sulphur trioxide and the solvent, although in a few cases there are additional lines which can be attributed to small amounts of polysulphuryl halides. An estimate of the proportions of monomeric and trimeric sulphur trioxide can be made from the relative intensities of the line at approximately 1069 cm^{-1}, characteristic of the monomer, and the strongest line of the trimer at 1270 cm^{-1}.

Solutions in Sulphur Dioxide

The spectra of three solutions of composition approximately 10, 20, and 40% sulphur trioxide by weight were investigated at approximately −10°. All the spectra (Fig. 3 and Table V) clearly show that sulphur trioxide in sulphur dioxide is present mainly

TABLE V

Raman spectra of solutions of sulphur trioxide in liquid sulphur dioxide (frequencies in cm^{-1})

Mole fraction of SO_3:			
0.088	0.170	0.370	Assignment
530 (mw)	530 (mw)	530 (mw)	ν_2'
1071 (s)	1071 (s)	1071 (s)	ν_1'
—	—	1270 (vw)	ν_1
1400 (vw)	1400 (w)	1390 (vw)	ν_3'
—	—	1405 (vw)	

Solvent: 530 (mw); 1139 (vs); 1330 (w).

as the monomer. Only in the 40% solution did the 1270 cm^{-1} line characteristic of S_3O_9 appear. The spectra of the solutions are just a superposition of the components and no new substances appear to be formed. Previous workers (1, p. 358) have claimed the occurrence of an unstable volatile liquid with the composition $2SO_3.SO_2$ but no evidence for such a compound is given by our Raman spectra.

Solutions in Sulphuryl Halides

The Raman spectra of these solutions show that there is no reaction between sulphur trioxide and sulphuryl chloride (Fig. 2) at room temperature, although higher polysulphuryl halides could, in principle, have been formed, e.g. $S_2O_5Cl_2 + SO_3 = S_3O_8Cl_2$. For solutions of sulphur trioxide in disulphuryl chloride and in disulphuryl fluoride similar results were obtained. In the case of sulphuryl chloride this conclusion has also been reached by other workers (20, 21), who refluxed sulphur trioxide with various proportions of sulphuryl chloride for periods up to 24 hours and obtained only the pure components on distillation. The compound $2SO_2Cl_2.SO_3$ has been claimed at low temperatures but is reported as being unstable above the melting point (22).

Can. J. Chem. Downloaded from www.nrcresearchpress.com by 210.87.254.42 on 09/05/12
For personal use only.

The Raman spectra show that at low concentrations, sulphur trioxide is almost entirely in the form of the monomer while solutions containing more sulphur trioxide than 0.2 mole fraction contain increasing concentrations of the trimer (Table VI).

TABLE VI
Raman spectra of solutions of sulphur trioxide in sulphuryl chloride (frequencies in cm^{-1})

Mole fraction of SO_3:				
0.106	0.309	0.420	0.549	Assignment
—	—	—	478 (vw)	ν_{14}
530 (w)	525 (w)	528 (w)	528 (m)	ν_2' and ν_2
—	—	—	650 (w)	ν_3
—	—	—	667 (w)	ν_7 or ν_{15}
—	—	—	694 (w)	ν_4 or ν_7
—	—	—	848 (vw)	ν_{16}
—	—	—	1009 (vw)	?
1073 (m)	1068 (s)	1073 (s)	1072 (vs)	ν_1'
—	—	—	1163 (w)	ν_{16}
—	—	—	1226 (w)	ν_{11}
1270 (vw)	1270 (w)	1265 (m)	1265 (s)	ν_1
—*	—*	1405 (m)	1375 (mw)	ν_3'
—	1485 (w)	1480 (w)	1488 (w)	ν_{13}
—	1515 (w)	1510 (w)	1510 (w)	ν_5

Solvent: 218 (s); 282 (s); 362 (s); 388 (vs); 408 (vs); 560 (vs); 600 (w); 1180 (s); 1414 (s).
*1390 cm^{-1} of monomeric sulphur trioxide obscured by solvent line at 1414 cm^{-1}.

Solutions in Halogen-substituted Hydrocarbons

The spectra of solutions of sulphur trioxide in carbon tetrachloride, tetrachlorethylene, and trichlorfluormethane are shown in Tables VII–IX and in Fig. 4. Except for the

TABLE VII
Raman spectra of solutions of sulphur trioxide in carbon tetrachloride (frequencies in cm^{-1})

Mole fraction of SO_3:			
0.129	0.306	0.461	Assignment
—	—	136 (w)	$S_2O_5Cl_2$
—	188 (vw)	188 (w)	$S_2O_5Cl_2$
256 (vw)	261 (vw)	257 (w)	?
—	286 (vw)	290 (s)	ν_{20}
—	345 (vw)	345 (m)	ν_9
358 (vw)	364 (w)	367 (m)	ν_6
—	—	388 (w)	$S_2O_5Cl_2$?
415 (vw)	408 (vw)	408 (w)	ν_{18}
528 (w)	530 (w)	528 (ms)	ν_2'
—	543 (vw)	543 (w)	ν_2
—	576 (vw)	573 (w)	$S_2O_5Cl_2$
605 (vw)	605 (w)	602 (m)	$S_2O_5Cl_2$
—	660 (vw)	665 (m)	ν_7 or ν_4
—	693 (w)	693 (m)	ν_4 or ν_7
—	—	717 (w)	$S_2O_5Cl_2$
—	833 (vw)	815 (w)	?
—	873 (w)	873 (w)	ν_{15}
1068 (m)	1068 (s)	1068 (s)	ν_1'
1200 (w)	1200 (w)	1197 (m)	$S_2O_5Cl_2$
1250 (vw)	1245 (w)	1245 (m)	ν_{11}
1267 (w)	1267 (m)	1267 (m)	ν_1
1380 (vw)	1380 (vw)	1394 (w)	ν_3'
—	1488 (vw)	1482 (w)	ν_{17}

Solvent: 217 (s); 315 (s); 459 (s); 760 (m); 790 (m); 1537 (w).

Can. J. Chem. Downloaded from www.nrcresearchpress.com by 210.87.254.42 on 09/05/12
For personal use only.

Can. J. Chem. Downloaded from www.nrcresearchpress.com by 210.87.254.42 on 09/05/12
For personal use only.

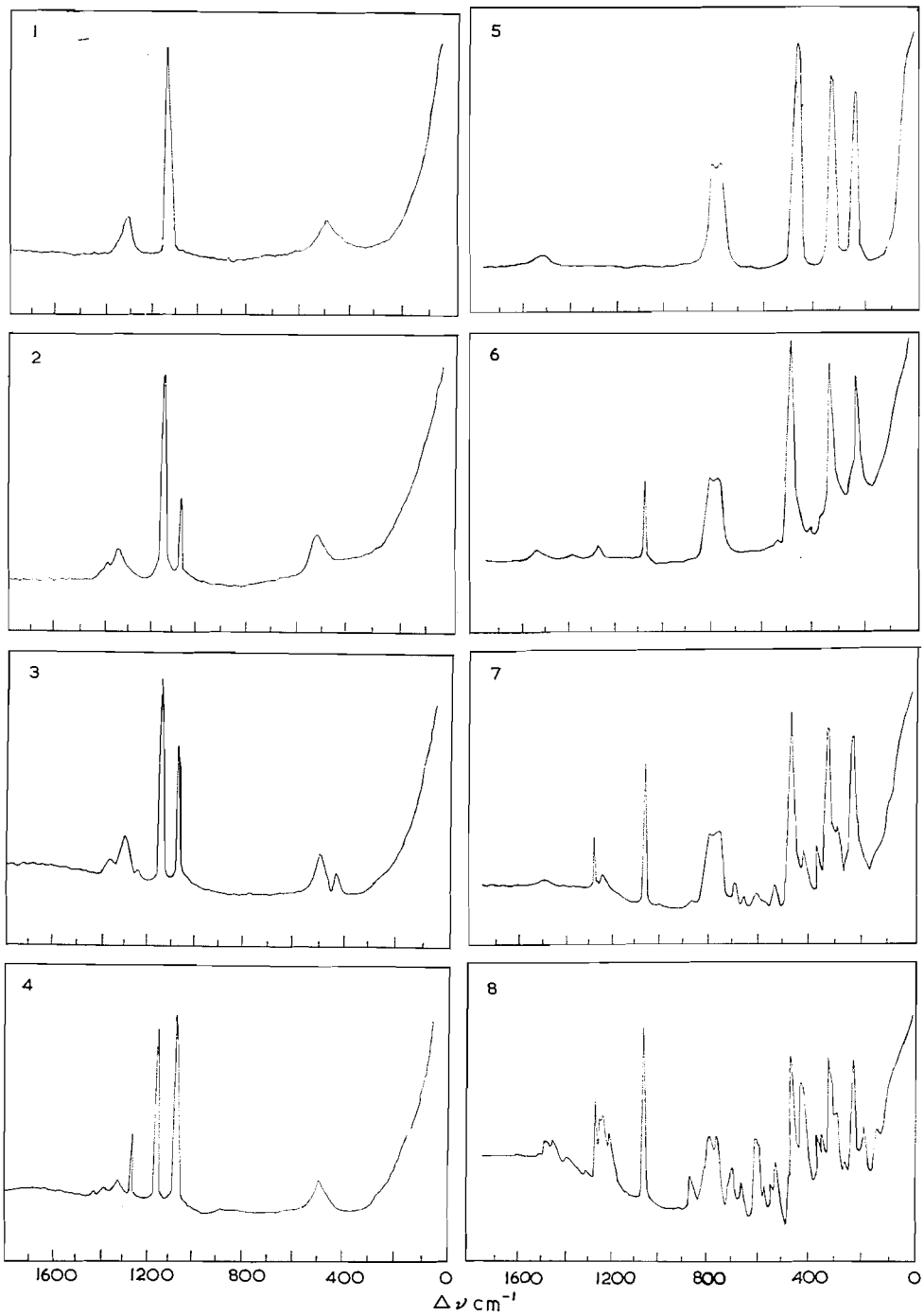


FIG. 4. Raman spectra of solutions of sulphur trioxide in liquid sulphur dioxide and in carbon tetrachloride: (1) liquid sulphur dioxide; (2, 3, 4) solutions of sulphur trioxide in liquid sulphur dioxide, N_{SO_3} = 0.088, 0.170, and 0.370; (5) carbon tetrachloride; (6, 7, 8) solutions of sulphur trioxide in carbon tetrachloride, N_{SO_3} = 0.129, 0.306, and 0.461.

Can. J. Chem. Downloaded from www.nrcresearchpress.com by 210.87.254.42 on 09/05/12
For personal use only.

TABLE VIII

Raman spectra of solutions of sulphur trioxide in tetrachlorethylene (frequencies in cm^{-1})

Mole fraction of SO_3:			
0.194	0.368	0.678	Assignment
290 (w)	290 (m)	281 (m)	ν_{20}
—	—	381 (w)	ν_{13}
—	369 (m)	370 (w)	ν_6
398 (w)	398 (w)	398 (w)	ν_{18}
530 (vw)	527 (w)	530 (mw)	ν_2' and ν_2
650 (vw)	646 (w)	650 (m)	ν_3
668 (vw)	662 (w)	665 (m)	ν_7 or ν_4
698 (vw)	698 (w)	698 (m)	ν_4 or ν_7
—	—	849 (w)	ν_{16}
1068 (m)	1068 (s)	1068 (vs)	ν_1'
—	—	1225 (w)	ν_{11}
—	—	1247 (w)	?
1270 (w)	1267 (m)	1270 (vs)	ν_1
—	1385 (vw)	1385 (w)	ν_3'
—	1488 (w)	1490 (m)	ν_{17}
—	1520 (vw)	1517 (w)	ν_5

Solvent: 133 (vw); 183 (w); 241 (s); 322 (w); 350 (m); 395 (w); 450 (vs); 466 (w); 515 (m); 580 (w); 725 (vw); 780 (vw); 1005 (vw); 1028 (w); 1572 (s); 1820 (w); 2000 (w); 2020 (vw).

TABLE IX

Raman spectra of solutions of sulphur trioxide in trichlorfluormethane (Freon 11) (frequencies in cm^{-1})

Mole fraction of SO_3:		
0.245	0.427	Assignment
—	322 (vw)	?
—	368 (m)	ν_6
369 (w)	375 (m)	ν_6
—	650 (w)	ν_3
668 (w)	666 (m)	ν_7 or ν_4
698 (w)	695 (m)	ν_4 or ν_7
—	865 (w)	ν_{15}
1072 (m)	1068 (s)*	ν_1'
—	1245 (vw)	ν_{11}
1270 (m)	1265 (s)	ν_1
1390 (vw)	1390 (w)	ν_3'
1485 (vw)	1491 (w)	ν_{17}
1520 (vw)	1520 (w)	ν_5

Solvent: 146 (vw); 192 (vw); 247 (s); 298 (w);† 355 (s); 402 (s); 478 (w); 540 (s);† 785 (w); 835 (s); 1073 (m broad);* 1660 (w); 1680 (vw).

*Coincidence between solvent line and the S—O symmetric stretch of monomeric SO_3 but latter is sharp and strong.

†Coincidence with SO_3 line.

carbon tetrachloride solutions the observed lines can be attributed to the solvent or to SO_3 monomer or trimer.

Sulphur trioxide is known to react with carbon tetrachloride under reflux (22) to give polysulphuryl halides according to the equation

$$CCl_4 + nSO_3 = SO_2(SO_3)_{n-1}Cl_2 + COCl_2.$$

The Raman spectra show that this reaction appears to proceed slowly even at room temperature, as additional lines, which can reasonably be attributed to $S_2O_5Cl_2$, appear

in the spectra of the carbon tetrachloride solutions. The amounts of polysulphuryl halides formed in a few hours are however quite small and carbon tetrachloride is for many purposes a useful solvent for sulphur trioxide.

In all the solutions studied, monomer and trimer are in equilibrium. At low concentrations the equilibrium favors the monomer but the actual position of the equilibrium for a given concentration of sulphur trioxide depends on the solvent. Thus in solutions of a given concentration in the following solvents, the monomer–trimer equilibrium shifts progressively in favor of the trimer in the order sulphur dioxide, sulphuryl chloride, halogenated hydrocarbons.

EXPERIMENTAL

The Raman spectrometer has been described previously (18). When necessary, for example for sulphur dioxide solutions, an additional jacket was provided between the sample tube and the filter jacket through which cold alcohol could be passed to cool the sample.

Sulphur trioxide was obtained by distillation from 65% oleum from which sulphur dioxide had been removed by oxidation with potassium persulphate. "Sulfan B" was obtained from the Allied Chemical Company. The solvents used were dried over phosphoric oxide and purified by distillation except for sulphur dioxide, which was obtained from a cylinder and purified by trap-to-trap distillation. Sulphuryl chloride was stored in the absence of light. The preparation of disulphuryl chloride and disulphuryl fluoride has been described previously (18, 23).

ACKNOWLEDGMENTS

We thank the National Research Council, the Ontario Research Foundation, and the Allied Chemical Company for financial assistance.

REFERENCES

1. GMELINS HANBUCH DER ANORGANISCHEN CHEMIE. No. 9, B1. Verlag Chemie, Weinheim. 1953.
2. J. H. HIBBEN. The Raman effect and its chemical applications. Reinhold, New York. 1939.
3. S. BHAVAGANTAM. Indian J. Phys. **5**, 1, 49 (1930).
4. S. VENKATESWAREN. Phil. Mag. **15**, 263 (1933).
5. A. SMITS and N. F. MOERMAN. Nature, **134**, 698 (1934).
6. H. GERDING, W. J. NIJVELD, and G. J. MULLER. Z. physik. Chem. B, **35**, 193 (1937); Nature, **137**, 1033 (1936).
7. H. GERDING and N. F. MOERMAN. Z. physik. Chem. B, **35**, 216 (1937).
8. H. GERDING and J. LECOMTE. Physica, **6**, 737 (1939).
9. H. GERDING and W. J. NIJVELD. Rec. trav. chim. **59**, 1209 (1940).
10. W. G. PALMER. J. Am. Chem. Soc. **60**, 2360 (1950).
11. J. R. VAN WAZER. Phosphorus and its compounds. Vol I. Chemistry. Interscience Publishers Inc., New York. 1958.
12. R. WESTRICK and C. H. MACGILLAVRAY. Rec. trav. chim. **60**, 794 (1941).
13. R. WESTRICK and C. H. MACGILLAVRAY. Acta Cryst. **7**, 764 (1954).
14. R. J. GILLESPIE and E. A. ROBINSON. Can. J. Chem. This issue. p. 2171.
15. L. J. BELLAMY and R. L. WILLIAMS. J. Chem. Soc. 863 (1957).
16. E. A. ROBINSON. Can. J. Chem. **39**, 247 (1961).
17. L. E. SUTTON (*Editor*). Tables of interatomic distances. Chem. Soc. (London), Spec. Publ. No. 11 (1958).
18. R. J. GILLESPIE and E. A. ROBINSON. Can. J. Chem. This issue. p. 2179.
19. G. HERZBERG. Infrared and Raman spectra of polyatomic molecules. D. van Nostrand Co., Inc., New York. 1945. p. 367.
20. A. PICTET and G. KARL. Bull. soc. chim. France, **3**, 1114 (1908).
21. E. HAYEK and K. HINTERAUER. Monatsh. **82**, 205 (1951).
22. G. P. LUCHINSKII and A. I. LIKHACHEVA. J. Gen. Chem. (U.S.S.R.), **7**, 405 (1937).
23. E. HAYEK and W. KOLLER. Monatsh. **82**, 942 (1951).

Can. J. Chem. Downloaded from www.nrcresearchpress.com by 210.87.254.42 on 09/05/12
For personal use only.

Can. J. Chem. Downloaded from www.nrcresearchpress.com by 210.87.254.42 on 09/05/12
For personal use only.

SOME STEREOCHEMICAL STUDIES ON α,β-UNSATURATED KETONES USING RAMAN SPECTROPHOTOMETRY[1]

K. NOACK[2] AND R. NORMAN JONES

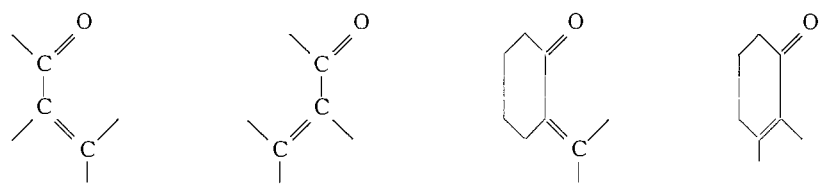
ABSTRACT

The Raman spectra of 12 α,β-unsaturated open-chain and cyclic ketones have been measured in the region of the C=O and C=C stretching vibrations, and the band positions and intensities have been compared with the corresponding bands in the infrared spectra. If due allowance is made for solvent effects, the infrared and Raman bands are observed at the same positions, but the relative intensities of the C=O and C=C bands are different; in particular, the Raman C=O stretching bands of the ketones in the *s*-trans configuration are from 5 to 10 times more intense than the Raman bands for the *s*-cis isomers. The cyclic *s*-trans ketones with a hydrogen atom on the α-carbon atom exhibit a solvent-sensitive doubling of the carbonyl maximum similar to that noted previously for certain α,β-unsaturated lactones, unsaturated acid anhydrides, and Δ^2-cyclopentenone derivatives. These doublet carbonyl maxima are observed also in the infrared spectra. The C=C frequency is not similarly perturbed and the effect is distinct from the doubling of both the C=O and the C=C bands exhibited by some open-chain α,β-unsaturated ketones that exist in the liquid phase as equilibrium mixtures of *s*-cis and *s*-trans isomers.

INTRODUCTION

The use of Raman spectroscopy by organic chemists for the characterization of natural products has been limited by the intrinsic weakness of the Raman effect and the need to employ large samples of material. Recent instrumental developments make it practical to record Raman spectra photoelectrically, using liquid samples excited in capillary tubes. Complete spectra can be measured over the range 150–4000 cm^{-1} using 25- to 200-mg samples, and the more intense bands, such as those associated with C=C and C≡C stretching modes, can be recorded with 10-mg samples in carbon disulphide solution.

In the absence of steric hindrance, a system of two conjugated double bonds will favor a planar conformation, for which *s*-cis (I) and *s*-trans (II) structures are possible. In cyclic ketones (III, IV) these configurations are fixed. In open-chain structures one



I II III IV

of the conformations will commonly be preferred to the virtual exclusion of the other; occasions do arise, however, where the energy differences are small and both forms are present in significant concentration in the liquid or vapor phase.

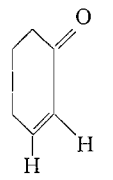
Mecke and Noack (1, 2) have shown that, for α,β-unsaturated ketones, such conformational isomers can be distinguished by the positions and intensities of the C=O and C=C stretching bands in the infrared spectrum, and additional examples have been cited by Erskine and Waight (3) and by Timmons (4). The Raman spectra of some of

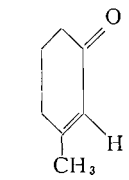
[1]*Manuscript received June 21, 1961.*
Contribution from the Division of Pure Chemistry, National Research Council of Canada, Ottawa, Canada. Issued as N.R.C. No. 6513.
[2]*National Research Council of Canada Postdoctorate Fellow.*

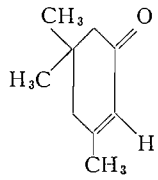
these compounds have now been measured. The Raman frequencies of the C=O and C=C stretching bands agree with the infrared frequencies if allowances are made for solvent effects; these effects are particularly significant for the C=O stretching band of the *s*-trans isomers. The relative intensities of the C=O and the C=C Raman and infrared bands differ, but the Raman spectra confirm the conformational assignments proposed by Noack and Mecke for the open-chain compounds on the basis of infrared measurements. Some of the cyclic *s*-trans ketones exhibit solvent-sensitive doublet carbonyl peaks in the Raman spectra, and on reinvestigation the same effects are noted in the infrared spectra. Doublet C=O and C=C bands also occur in some open-chain ketones, but, in these cases, conformational equilibria are involved. Ketones exhibiting conformational equilibria of this type are dealt with in a separate paper in which effects of temperature change are also examined (5).

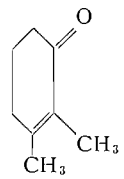
EXPERIMENTAL

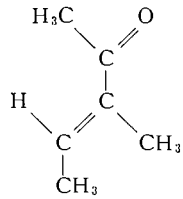
The ketones employed in this investigation (V–XVI) were obtained from a collection prepared by Mecke and Noack for the infrared studies, and their chemical characterization

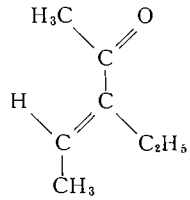

V

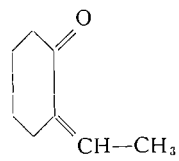

VI

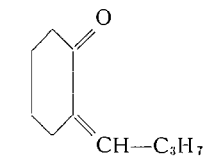

VII

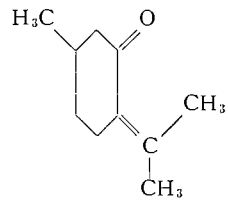

VIII

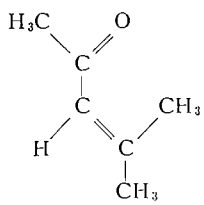

IX

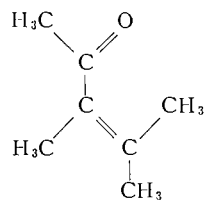

X

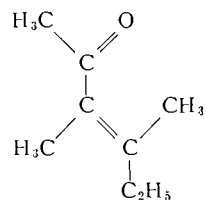

XI


XII


XIII


XIV


XV


XVI

Can. J. Chem. Downloaded from www.nrcresearchpress.com by 210.87.254.42 on 09/05/12
For personal use only.

has already been described (2). The Raman spectra were measured on a Cary Model 81 spectrophotometer using a micro sample tube of 2-mm external diameter and 200-microliter volume. After quantitative dilution with carbon tetrachloride, as described below, the freshly distilled ketone was introduced into the Raman tube by means of a narrow, flexible metal capillary tube attached to a hypodermic syringe mounted vertically on a stand. Ketone mole ratios of approximately 0.4 were normally employed, and 120–150 mg of the ketone was needed to fill the cell. The spectra were measured at a spectral slit width of 5 cm^{-1} and the estimated uncertainty in the positions of the band maxima is ± 2 cm^{-1}. A scanning rate of 15 cm^{-1} per minute was normally used.

The Toronto-type arc lamp was constructed of Corning 1720 glass, and the Hg 4358 Å exciting line was isolated with aqueous potassium nitrite and aqueous Rhodamine GDN extra filter solutions in separate annular jackets with a common dividing wall. The potassium nitrite solution in the outer jacket was circulated through a cooling system; the Rhodamine solution was not circulated and was stabilized by the addition of hydrochloric acid. A cylindrical Polaroid polarizer with the direction of polarization perpendicular to the axis of the Raman tube was inserted between the filter system and the Raman tube to eliminate effects of oblique illumination.

Intensity Measurements

The peak heights of the Raman bands were measured relative to the 459 cm^{-1} band of carbon tetrachloride, which was taken as 100 units. The accurate evaluation of this intensity involves several instrumental and theoretical factors (6–9). The unit employed here, and in other contemporary papers from this laboratory, does not take into account all the variables that may affect the accuracy of the measurements; it has been devised to meet immediate needs, and to cope with technical problems associated with the use of the capillary sample tube.

The determination of the Raman band intensities involves comparison with an internal or external standard (8). If an external standard is used the emission intensity of the measured Raman band is compared with the standard band as observed with a matched sample tube under the same experimental conditions. This assumes that the illumination of the Raman tube, and its alignment with respect to the spectrometer optics, are reproducible. These conditions are usually not critical, but the external-standard method also suffers from the serious defect that the sample spectrum and the standard spectrum are usually obtained from media of different refractive index. The refractive index influences the intrinsic intensity of the Raman radiation through a solvent field effect and it also determines the fraction of the total Raman radiation that enters the spectrometer. Using wide tubes, where wall effects can be neglected, Woodward and George (9) have shown that the instrumental effect is inversely proportional to the square of the refractive index of the medium. Rea (7) has analyzed the problem for narrower tubes where wall effects become significant, though his initial treatment was not complete, and the application of an additional empirical correction was later required (10). When the Raman radiation is generated within a capillary tube, the energy entering the spectrometer from a Pyrex capillary is found to increase by a factor of five with increase in the refractive index from 1.35 to 1.65. It would appear that under these conditions, the wall effect becomes dominant, the radiation probably suffering multiple reflection before reaching the entrance slit; a considerable proportion is accordingly lost through the walls of the tube en route.

The difficulties associated with the intensity measurement can be largely circumvented

Can. J. Chem. Downloaded from www.nrcresearchpress.com by 210.87.254.42 on 09/05/12
For personal use only.

by the addition of the standard calibrating liquid to the sample in known proportion. The standard band is then measured in a medium of the same refractive index as the sample band. The internal-standard technique can only be used where the overlap of the two spectra is not significant, but using the 459 cm^{-1} carbon tetrachloride band as standard, this problem caused no difficulty for the ketones considered in this paper. The use of the internal standard also avoids the need to determine the density of the liquid, which is otherwise required if the intensities are to be expressed on a molar basis. The intrinsic intensity of the standard may be modified by intermolecular interactions but this can be checked to some extent by use of a series of measurements at different concentrations, or by cross checking with different secondary standard bands; significant variations may be involved here (11) but more extensive experimental and theoretical study is needed if these effects are to be properly interpreted. In our investigations the concentrations were so adjusted that the peak height of the 459 cm^{-1} carbon tetrachloride band was comparable with the C=O and C=C bands, and, for this, mole fractions of about 0.4 ketone and 0.6 carbon tetrachloride were required.

On the basis of these considerations, the Raman intensity coefficient was expressed as

$$[1] \qquad k_A^{\nu} = \frac{I_A^{\nu}}{I_{CCl_4}^{459}} \cdot \frac{N_{CCl_4}}{N_A} \cdot 100,$$

where k_A^{ν} = the Raman intensity coefficient at ν cm^{-1} displacement from the exciting line for substance A;

I_A^{ν} = the emission intensity at ν cm^{-1} displacement from the exciting line, measured in arbitrary units;

$I_{CCl_4}^{459}$ = the emission intensity at the 459 cm^{-1} peak of carbon tetrachloride measured in the same units as I_A^{ν};

N_A = the mole fraction of A;

N_{CCl_4} = the mole fraction of carbon tetrachloride.

No correction was applied for the change in the spectral sensitivity of the spectrophotometer since this did not vary by more than 3% over the measured wavenumber range.

The insertion of the cyclindrical polarizer influences the intensity considerably, as the 459 cm^{-1} carbon tetrachloride band is highly polarized, and the convergence errors are large if the measured band has a different depolarization ratio from the standard band. Comparisons made with and without the Polaroid filter (oriented to transmit radiation with the electric vector perpendicular to the tube axis) consistently gave values for these ketones that were 30% lower when the polarizer was in place. The Raman C=O bands of compounds VII and XIV have also been measured by Michel and Duyckaerts (8) with no polarizer in their spectrometer. Their measurements were some 30% greater than the values we obtain when the polarizer is used. The constancy of this systematic intensity difference is attributed to the fact that all the C=O bands in these ketones have similar depolarization ratios close to 0.4.

The measurement of band height against a sloping background invariably introduces uncertainty in the location of the baseline. Where feasible, the line was drawn tangentially to the curve, usually at about three half band widths on either side of the band center. In some cases the location of the line was rather arbitrary; this accounts for the major uncertainty in the measured intensity coefficients and largely invalidates any attempts to apply corrections for smaller physical variables affecting the accuracy of the measurements.

Can. J. Chem. Downloaded from www.nrcresearchpress.com by 210.87.254.42 on 09/05/12
For personal use only.

Band Area Measurements

The area beneath the Raman band was not measured directly, but a quantity approximately proportional to it was calculated. This quantity, which we call the *band area coefficient* (L), is defined as

$$[2] \qquad L_A^{\nu_{max}} = k_A^{\nu_{max}} \cdot \frac{\Delta\nu_{\frac{1}{2}}^{A}}{\Delta\nu_{\frac{1}{2}}^{CCl_4}},$$

where $L_A^{\nu_{max}}$ = the band area coefficient for the band of substance A;
$\Delta\nu_{\frac{1}{2}}^{A}$ = the band width at half maximal intensity, measured on the spectral chart in arbitrary units;
$\Delta\nu_{\frac{1}{2}}^{CCl_4}$ = the band width at half maximal intensity of the 459 cm^{-1} band of carbon tetrachloride measured under the same conditions as $\Delta\nu_{\frac{1}{2}}^{A}$.

The band area coefficient is, therefore, equal to 100 times the ratio of the sample band area to that of the (internal) standard band. The ratio L can be derived directly from the measured spectrum without resort to arithmetical integration, and it is adequate for the comparison of gross differences between Raman bands of varying types. More refined measurements are not justified in view of the large errors associated with contemporary microtechniques.

RESULTS

The positions and intensities of the C=O and C=C stretching bands in the Raman and infrared spectra of ketones V–XVI are listed in Table I.

Band Positions

Though the two fundamental absorption bands of α,β-unsaturated ketones in the 1750–1600 cm^{-1} range are coupled, it is customary (and convenient) to identify the band at higher wavenumber with a localized "C=O stretching" vibration and the band at lower wavenumber with a "C=C stretching" mode.*

Comparison of ν_{max} for the infrared and Raman bands listed in Table I indicates that the bands fall into the same frequency ranges in both the infrared and the Raman spectra. The *s*-cis and *s*-trans structures can therefore be distinguished from the Raman band positions as well as from the infrared, and the conformational assignments for the open-chain ketones made by Mecke and Noack from the infrared data are confirmed by the Raman measurements. For both the cyclic and open-chain *s*-cis compounds the Raman and infrared C=O and C=C band frequencies agree within the precision of the experimental data (±3 cm^{-1}) and this holds also for the C=C bands of the cyclic and open-chain *s*-trans ketones. For the cyclic and open-chain *s*-trans ketones, however, the Raman C=O frequencies given in Table I are uniformly 4–8 cm^{-1} lower than the corresponding infrared values. Whereas the Raman spectra were measured at high concentrations in carbon tetrachloride, the infrared spectra were initially obtained at much lower concentrations in tetrachloroethylene. When the infrared spectra were remeasured on capillary films in carbon tetrachloride at the same concentrations as were used for the Raman spectra, the band positions listed in Table II were obtained. This table demonstrates clearly that the significant differences between the infrared and Raman C=O peak positions are due to solvent effects. The infrared band positions in dilute solutions of

**The tacit assumption that the "C=O" band invariably lies above the "C=C" band may not be justified, and Cook has recently suggested that the sequence may be inverted for 2,6-dimethyl-4-pyrone (12).*

Can. J. Chem. Downloaded from www.nrcresearchpress.com by 210.87.254.42 on 09/05/12
For personal use only.

Can. J. Chem. Downloaded from www.nrcresearchpress.com by 210.87.254.42 on 09/05/12
For personal use only.

TABLE I

Positions and intensities of the C=O and C=C stretching bands in the Raman and infrared spectra of α,β-unsaturated ketones*

	Raman spectrum* †						Infrared spectrum‡ §					
	ν_{C-O}			ν_{C-C}			ν_{C-O}			$\nu_{C=C}$		
Compound	ν_{max}	L	k	ν_{max}	L	k	ν_{max}	$E\times10^{-2}$		ν_{max}	$E\times10^{-2}$	
s-Trans configuration												
V. Δ^2-Cyclohexen-1-one	1686 1677	155	71	1617	51	81	1689 1675	110	(8.9)	1621	0.3	(0.03)
VI. 3-Methyl-Δ^2-cyclohexen-1-one	1664 (1676)	135	76	1632	81	67	1680 1672	117	(9.45)	1635	18	(1.53)
VII. 3,5,5-Trimethyl-Δ^2-cyclohexen-1-one	1668	165	120	1635	118	127	1674	110	(9.0)	1637	18	(1.52)
VIII. 2,3-Dimethyl-Δ^2-cyclohexen-1-one	1666	151	106	1635	167	155	1673	103	(8.5)	1635	22	(1.87)
IX. *trans*-3-Methyl-Δ^3-penten-2-one	1669	262	215	1646	290	309	1675	81	(6.64)	1646	17	(1.44)
X. *trans*-3-Ethyl-Δ^3-penten-2-one	1667	177	146	1640	223	258	1675	74	(6.06)	1642	16	(1.34)
s-Cis configuration												
XI. 2-Ethylidene cyclohexanone	1692	17	13	1621	148	103	1693	55	(4.4)	1622	46	(4.08)
XII. 2-(*n*-Butylidene) cyclohexanone	1690	21	21	1617	185	134	1692	56	(4.51)	1620	46	(4.04)
XIII. 5-Methyl-2-isopropylidene-cyclohexanone	1684	28	14	1610	223	50	1685	61	(4.98)	1611	40	(3.51)
XIV. 4-Methyl-Δ^3-penten-2-one	1692	22	19	(1630) 1623	261	127	1693	48	(3.88)	(1636) 1622	72	(6.28)
XV. 3,4-Dimethyl-Δ^3-penten-2-one	1686	38	22	1622	130	42	1689	61	(4.98)	1622	31	(2.66)
XVI. *trans*-3,4-Dimethyl-Δ^3-hexene-2-one	1686	46	11	1623	81	41	1690	60	(4.87)	1625	31	(2.65)

*Inflections are indicated in parentheses in the wavenumber columns.

†For a mole ratio of 0.4 ketone in carbon tetrachloride, approximately equivalent to 3 M.

‡For approximately 0.02 M solutions in tetrachloroethylene. These data are taken from the paper of Mecke and Noack (2).

§The infrared band intensities are recorded in the "practical unit" defined by the Commission on Molecular Structure and Spectroscopy of IUPAC (19). This unit is given by $E_{\nu_1}^{\nu_2} = \int_{\nu_1}^{\nu_2} \epsilon_\nu d\nu$, where $\epsilon_\nu = 1/bc \log_{10} (I_0/I)_\nu$ in which b is the cell length in cm, c is the concentration in moles per liter, and $\log_{10}(I_0/I)$ is the absorbance.

Mecke and Noack employed an intensity unit based on a wavelength abscissa, and their values ($A_{(M)}$) are given in parentheses in the infrared band intensity columns of the table. The IUPAC "practical unit" E and the Mecke unit $A_{(M)}$ are related, in close approximation, by the equation $E = 0.434 A_{(M)} \nu_{max}^2 .10^{-2}$.

TABLE II

Solvent effects on the C=O and C=C band positions for *s*-trans ketones*

	Concn. (*M*)	Solvent	Compound V	VI	VII	VIII
C=O band						
Raman	3	CCl_4	1686±2	1664±2	1668±2	1666±2
Infrared	3	CCl_4	1686±1	1666±1	1670±1	1665±1
Infrared	0.02	CCl_4	1689	1680 1672	1674	1670
Infrared	0.02	C_2Cl_4	1689	1680	1674	1673
Infrared	0.02	$CHCl_3$	1687 1669	1662	1665	1656
C=C band						
Raman	3	CCl_4	1617±2	1632±2	1635±2	1635±2
Infrared	3	CCl_4	1618±1	1634±1	1634±1	1633±1
Infrared	0.02	CCl_4	n.m.	1635	1634	1635
Infrared	0.02	C_2Cl_4	1621	1635	1637	1635
Infrared	0.02	$CHCl_3$	n.m.	1633	1635	1632

*Positions of band maxima in cm^{-1}.

NOTE: n.m. = weak band, position not measured.

carbon tetrachloride agree with the measurements on dilute solutions in tetrachloroethylene and the considerable displacements between the infrared and Raman C=O frequencies of the *s*-trans ketones are due more to the concentration difference than to the specific nature of the solvent.

The open-chain *s*-trans ketones IX and X, and 2,3-dimethyl-Δ^2-cyclohexen-1-one (VIII) give Raman C=O bands of normal contour. The C=O bands of the cyclic *s*-trans compounds V–VII, however, exhibit asymmetry of varying degree (Figs. 1–3). This is most apparent for the Raman spectrum of cyclohexenone (Fig. 1), which exhibits a main peak at 1686 cm^{-1} and a shoulder at 1677 cm^{-1} in carbon tetrachloride solution. In chloroform, the relative intensities of these peaks are reversed. On re-examination, the

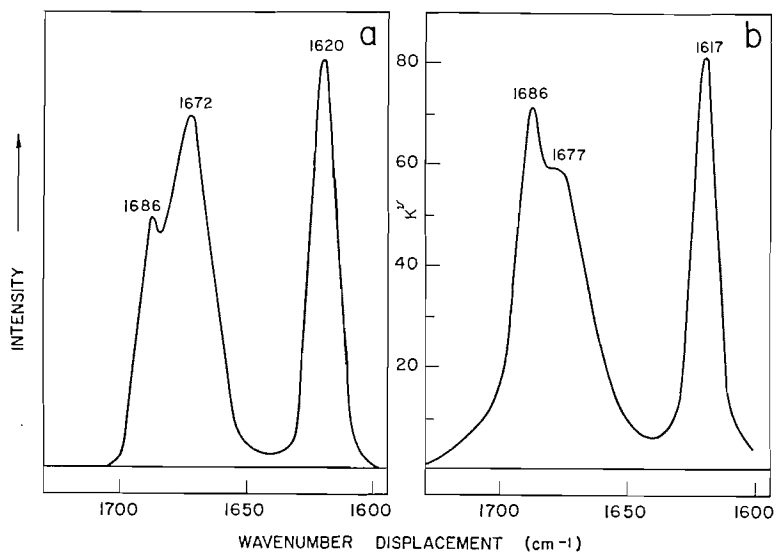


FIG. 1. Raman spectrum of Δ^2-cyclohexen-1-one (V): *a*, in chloroform; *b*, in carbon tetrachloride.

Can. J. Chem. Downloaded from www.nrcresearchpress.com by 210.87.254.42 on 09/05/12
For personal use only.

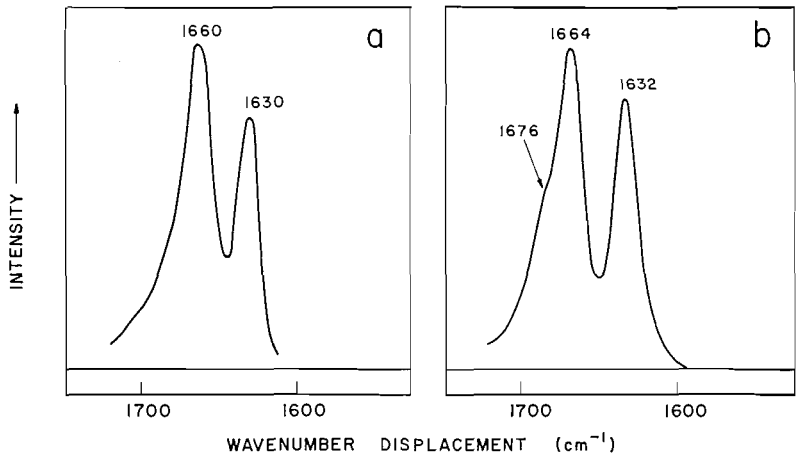


FIG. 2. Raman spectrum of 3-methyl-Δ^2-cyclohexen-1-one (VI): *a*, in chloroform; *b*, in carbon tetrachloride.

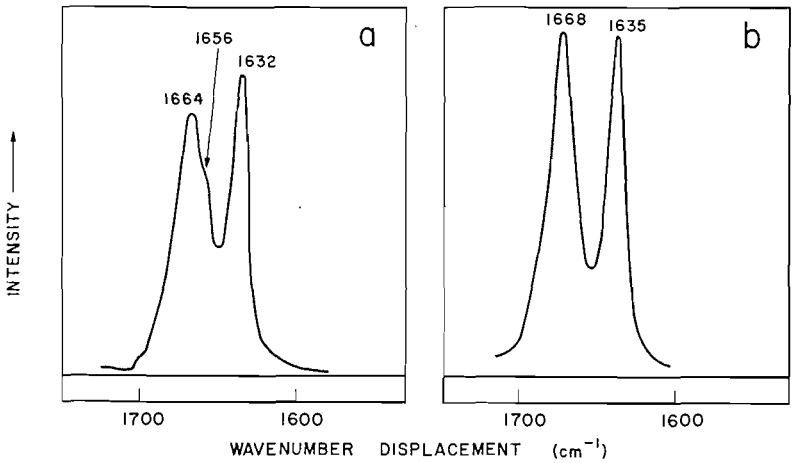


FIG. 3. Raman spectrum of 3,5,5-trimethyl-Δ^2-cyclohexen-1-one (VII): *a*, in chloroform; *b*, in carbon tetrachloride.

infrared spectra of the cyclic *s*-trans ketones demonstrated similar C=O band asymmetry in an enhanced degree (Figs. 4–6). These infrared spectra were measured on a Perkin–Elmer Model 112 spectrometer at a spectral slit width of 1.5 cm^{-1} and were subsequently checked on a nitrogen-purged Model 221 Perkin–Elmer spectrometer at a spectral slit width of 1 cm^{-1}. The purity of the ketones used for these measurements was established by vapor phase chromatography, and, for all four samples, over 99% of the material passed through the column in a single symmetrical peak. In both the Raman and infrared spectra of cyclohexenone the band component of higher frequency augments in intensity in carbon tetrachloride and the lower frequency band intensifies in chloroform solution. (Figs. 1 and 4). This resembles the behavior noted by Yates and collaborators (13, 14) for derivatives of Δ^2-cyclopentenone and by Jones and collaborators (15) for α,β-unsaturated lactones and cyclic unsaturated acid anhydrides. The asymmetry of VI follows

Can. J. Chem. Downloaded from www.nrcresearchpress.com by 210.87.254.42 on 09/05/12
For personal use only.

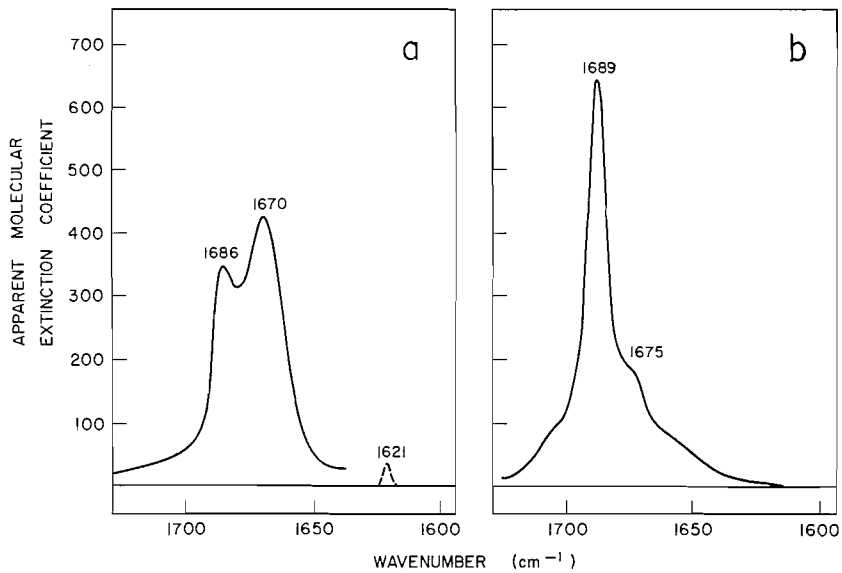


FIG. 4. Infrared spectrum of Δ^2-cyclohexen-1-one (V) (C=C band measured on liquid film): *a*, in chloroform; *b*, in carbon tetrachloride.

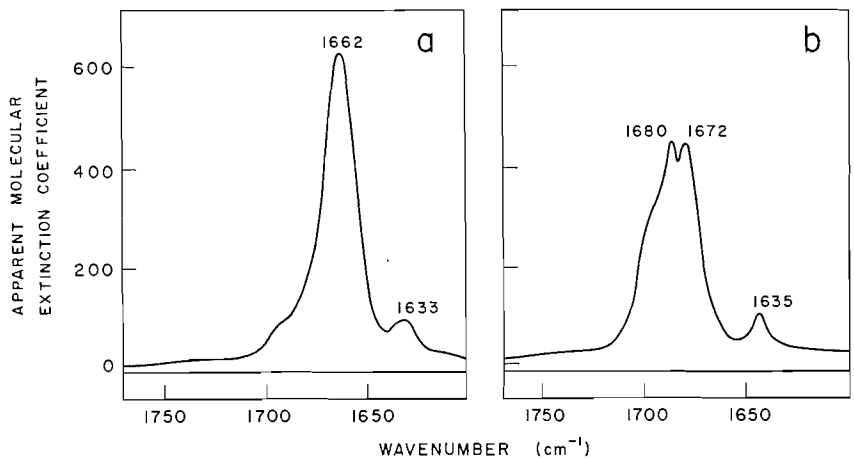


FIG. 5. Infrared spectrum of 3-methyl-Δ^2-cyclohexen-1-one (VI): *a*, in chloroform; *b*, in carbon tetrachloride.

the same pattern as V, though the high-frequency component is weaker. The spectra of VII differ in that the asymmetry is more pronounced in chloroform than in carbon tetrachloride.

The failure to observe any C=O band asymmetry for VIII supports the view that the partial structure XVII, with a free α-hydrogen atom, is required for this effect, and it is commonly presumed that this solvent-sensitive C=O band splitting is caused by a Fermi resonance with the overtone of the α-C—H out-of-plane deformation vibration.

Can. J. Chem. Downloaded from www.nrcresearchpress.com by 210.87.254.42 on 09/05/12
For personal use only.

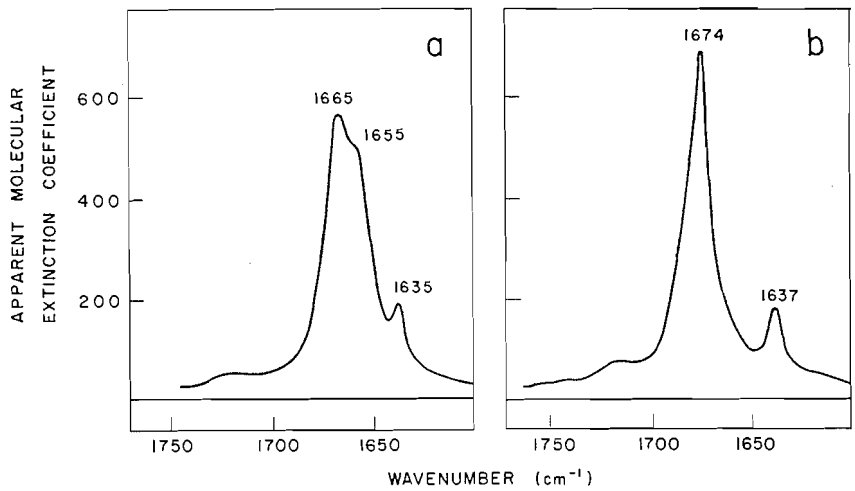
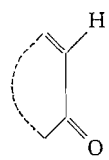
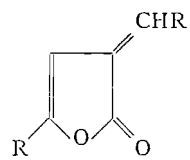


FIG. 6. Infrared spectrum of 3,5,5-trimethyl-Δ^2-cyclohexen-1-one (VII): *a*, in chloroform; *b*, in carbon tetrachloride.

The absence of the carbonyl doublet from the spectra of the *s*-cis cyclic ketones XI and XII is in conformity with the failure to observe it for exocyclic unsaturated lactones, such as XVIII, which have been studied in the infrared by Brügel (16).



XVII



XVIII

Band Intensities

The relationships between band intensity and steric configuration are different for the Raman and the infrared spectra. The intensities of the infrared C=O bands of all the conjugated ketones lie in a comparatively narrow range. The *s*-cis compounds have weaker infrared C=O bands than the *s*-trans compounds, but no significant differences are noted between cyclic *s*-cis and open-chain *s*-cis compounds. The cyclic *s*-trans ketones have more intense infrared C=O bands than the open-chain *s*-trans ketones but this may be associated with the doublet character of the bands of the cyclic compounds.

The intensities of the infrared C=C stretching bands are more variable and the bands for the *s*-cis compounds are significantly stronger than for the *s*-trans. The extreme weakness of the infrared C=C band in Δ^2-cyclohexenone is particularly remarkable.

In the Raman spectra the band area coefficients of the C=C bands vary from 51 units for V to 290 units for IX but the variations do not fall into any distinguishable classes in terms of conformation or cyclization. The Raman C=O band intensities, on the contrary, show marked stereochemical specificity, and the *s*-trans C=O bands (135–263 units) are from 5 to 10 times more intense than the *s*-cis bands (17.5–46 units). In terms of peak heights, the relationships are similar, though the band area measurements for the doublet carbonyl bands of V–VII group more closely with VIII–X than do the peak height measurements.

Can. J. Chem. Downloaded from www.nrcresearchpress.com by 210.87.254.42 on 09/05/12
For personal use only.

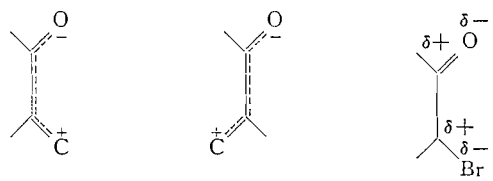
Can. J. Chem. Downloaded from www.nrcresearchpress.com by 210.87.254.42 on 09/05/12
For personal use only.

These Raman band intensities can be compared with data in the literature for C=O and C=C groups in non-conjugated systems. An extensive study of the Raman C=C stretching bands of mono-olefins by Rea (10) has shown that alkyl substitution has little effect and the integrated intensities fall in the range 30–50 when converted to units that are comparable with ours.* Conjugation with the ketone therefore raises the Raman C=C stretching band intensity by a factor of 5 to 10. According to Michel and Duyckaerts (8) the peak heights of the Raman C=O bands for saturated ketones fall in the range 10–13 in our units, reducing to approximately 8–10 units when corrected for polarization convergence effects. In the *s*-cis configuration, conjugation with the ethylene bond enhances the C=O band intensity slightly, and in the *s*-trans configuration it is raised by a factor of about 10. Mecke and Noack (2) have pointed out previously that for the infrared spectra the C=O intensity for *s*-cis ketones may actually be weaker than for comparable non-conjugated systems.

DISCUSSION

The four distinguishing features of the *s*-cis configuration are (*a*) greater frequency separation between the C=O and the C=C stretching bands in comparison with the *s*-trans; (*b*) the greatly diminished intensity of the Raman C=O band; (*c*) the lesser, but still significant diminution in the infrared C=O band intensity; (*d*) the increase in the infrared C=C band intensity. It is difficult to account for all these effects by any simple and self-consistent mechanism.

In both the *s*-cis and the *s*-trans configurations, the C=O and the C=C band frequencies are displaced downwards from their positions in non-conjugated systems carrying comparable substituents. Assuming, for the time being, that the two frequencies are not vibrationally coupled, it follows that both the C=O and the C=C bonds have reduced force constants in the conjugated system, presumably because of the mesomeric effect. This in turn must lead to charge displacements on the terminal atoms, and the polarized *s*-cis structure XIX will then be further stabilized by a direct field interaction between the ends of the conjugated system. This could lead to an additional lowering of both the C=O and the C=C frequencies in comparison with the *s*-trans frequencies. If it is assumed that change in bond polarization with bond length increases in systems where the bond is more highly polarized in the equilibrium position, both the *s*-cis C=O and the *s*-cis C=C infrared bands should be intensified by this field effect. This is consistent with the observed changes for the C=C band, but not for the C=O band.



XIX XX XXI

The closer proximity of the terminal charges for XIX in comparison with XX may also induce mutual perturbations of the C=O and C=C bond polarizations of a more direct type, and these are considered by Erskine and Waight (3) to have the major effect

**Rea's intensities are based on the use of an external standard and a wider Raman tube. One of his intensity units is approximately equivalent to one hundred of ours (10).*

in influencing the C=O and C=C band intensities. Such direct field effects can be quite large, as is well recognized in systems such as XXI where the C—Br dipole induces an upward displacement of 20 cm^{-1} in the C=O frequency, and also diminishes the intensity (17). Regarded from this point of view, the dipole interaction in XIX should produce an opposite effect on the C=O band than does the C—Br group, since the direction of the dipole is reversed. On this basis we would also expect both the C=O and the C=C infrared bands to be intensified and displaced to lower frequency in the *s*-cis configuration. It is therefore difficult in these terms to account for the diminished intensity and upward frequency displacement of the *s*-cis C=O infrared band.

The Raman band intensities, being dependent on the change in the bond polarizability during the vibration, might be expected to vary with the electron density in the bond and should, therefore, be increased by factors that increase the degree of double-bond character. The very low intensity of the Raman C=O band in the *s*-cis configuration would then indicate a high charge displacement at the equilibrium bond length. However, Michel and Duyckaerts (8) have shown that in general the Raman and infrared C=O band intensities vary in the same sense, and not inversely, and more extensive investigations are obviously needed to clarify the relationships between bond polarization and bond polarizability in conjugated systems.

These difficulties may in part be due to the fact that the C=O and C=C stretching bands should not be regarded as localized vibrations. Since the separation between the two bands is less in the *s*-trans than the *s*-cis form, the vibrational coupling will be greater for *s*-trans isomers. As the unperturbed C=O and C=C frequencies approach the same value, the character of the vibrations will change from localized double-bond stretching modes to in-phase and out-of-phase coupled modes extending through the conjugated system. In the limit the bands will become analogues of the doublet C=O band systems of acid anhydrides and peroxides. The over-all pseudosymmetry of the conjugated system may then become an important factor in determining the relative intensity of the two bands, as Bellamy and collaborators have suggested for the anhydride and peroxide systems (18). There may be a minimum separation distance between the observed "C=O" and "C=C" frequencies below which the coupling becomes strong enough to force the frequencies apart again. It is not suggested that these are the *dominant* factors in the conjugated systems considered here, and the fact that the band at higher frequency is much more sensitive to solvent effects (particularly in the trans configuration) is a good indication that this band is predominantly carbonylic while the band at lower frequency is predominantly ethylenic (Table II). Nevertheless, considerations of this kind must be kept in mind when one is dealing with vibrational modes of conjugated systems. Analogies with substitutional effects in non-conjugated carbonylic and olefinic systems, must be made with caution, particularly when attempts are made to consider the substitution effects quantitatively, as, for example, by correlating them with Taft or Hammett sigma parameters.

ACKNOWLEDGMENTS

We wish to thank the Cyanamid European Research Institute for providing facilities for vapor phase chromatography and for the use of the Model 221 spectrophotometer. We are also grateful to Mrs. M. A. MacKenzie and Dr. J. W. Elliott for measuring four Raman and infrared spectra at Ottawa.

Can. J. Chem. Downloaded from www.nrcresearchpress.com by 210.87.254.42 on 09/05/12
For personal use only.

REFERENCES

1. R. MECKE and K. NOACK. Spectrochim. Acta, **12**, 391 (1958).
2. R. MECKE and K. NOACK. Chem. Ber. **93**, 210 (1960).
3. R. L. ERSKINE and E. S. WAIGHT. J. Chem. Soc. 3425 (1960).
4. C. J. TIMMONS. Proceedings of the IVth International Meeting of the European Molecular Spectroscopy Group, Bologna, Italy. 1959. In press.
5. K. NOACK and R. N. JONES. Can. J. Chem. This issue. p. 2225.
6. H. J. BERNSTEIN and G. ALLEN. J. Opt. Soc. Am. **45**, 237 (1955).
7. D. G. REA. J. Opt. Soc. Am. **49**, 90 (1959).
8. G. MICHEL and G. DUYCKAERTS. Spectrochim. Acta, **10**, 259 (1958).
9. L. A. WOODWARD and J. H. B. GEORGE. Nature, **167**, 193 (1951).
10. D. G. REA. Anal. Chem. **32**, 1638 (1960).
11. D. G. REA. J. Mol. Spectroscopy, **4**, 507 (1960).
12. D. COOK. Can. J. Chem. **39**, 1184 (1961).
13. P. YATES, N. YODA, W. BROWN, and B. MANN. J. Am. Chem. Soc. **80**, 202 (1958).
14. P. YATES, and L. L. WILLIAMS. J. Am. Chem. Soc. **80**, 5896 (1958).
15. R. N. JONES, C. L. ANGELL, T. ITO, and R. J. D. SMITH. Can. J. Chem. **37**, 2007 (1959).
16. W. BRÜGEL, K. DURY, G. STENGEL, and H. SUTER. Angew. Chem. **68**, 440 (1956).
17. R. N. JONES, D. A. RAMSAY, F. HERLING, and K. DOBRINER. J. Am. Chem. Soc. **74**, 2828 (1952).
18. L. J. BELLAMY, B. R. CONNELLY, A. R. PHILPOTTS, and R. L. WILLIAMS. Z. Elektrochem. **64**, 563 (1960).
19. International Union of Pure and Applied Chemistry, Comptes Rendus de la Vingtième Conférence. Vol. 20. Butterworths Scientific Publications, London. 1959. p. 187.

Can. J. Chem. Downloaded from www.nrcresearchpress.com by 210.87.254.42 on 09/05/12
For personal use only.

Can. J. Chem. Downloaded from www.nrcresearchpress.com by 210.87.254.5 on 09/05/12
For personal use only.

CONFORMATIONAL EQUILIBRIA IN DIETHYL KETONE[1]

R. NORMAN JONES AND K. NOACK[2]

ABSTRACT

A variable-thickness, variable-temperature absorption cell, modified from the design of Holden, Taylor, and Johnston, has been used to compare the infrared spectrum of diethyl ketone at −75° and +25° C. The Raman spectrum of diethyl ketone has also been measured at +6°, +25°, and +85° C, and the proton magnetic resonance spectrum over the range −61° to 104° C.

Both the infrared and Raman spectra exhibit pronounced temperature sensitivity, which is attributed to the presence of at least two conformational isomers in the liquid phase. Possible structures for these isomers are considered. Small but significant chemical shifts are noted in the proton magnetic resonance spectrum.

The vibrational spectra of large molecules are particularly difficult to interpret when the substance exists as a mixture of conformational isomers in the liquid state; to analyze such spectra it is first necessary to recognize the presence of the equilibria and to sort out the bands belonging to the different forms. This may sometimes be done by comparison with the spectrum of the crystalline solid, since only one conformational form will normally be present in the crystal lattice. The solid phase spectra, however, may be perturbed by intermolecular force fields and hydrogen bonding. In the liquid phase the equilibrium between the conformational isomers is usually temperature sensitive and the spectra of the isomers can be differentiated by noting the relative changes in the band intensities with temperature.

Cells suitable for such measurements tend to become complicated, particularly if it is desired to control the temperature with some accuracy, and to make measurements at temperatures that depart appreciably from those obtainable with simple cryostatic systems. In this paper we describe a cell suitable for the measurement of infrared spectra over a wide range of temperature, and discuss its use to investigate conformational equilibria in diethyl ketone.

EXPERIMENTAL

The variable-temperature infrared absorption cell is illustrated in Figs. 1 and 2. It is based on the excellent design of Holden, Taylor, and Johnston (1), but is intended only for use above −190°; this permits a simplification of the cell proper and of the gear mechanism and controls for varying the sample thickness without breaking the vacuum. The apparatus is portable and the cell fits conveniently into the 14-cm working space of the Perkin–Elmer Model 21 and Model 112 spectrometers.

The cell proper consists of a pair of silver chloride windows (2.5-cm diameter) sealed by Teflon washers and separated by one convolution of a soft bronze bellows, which is soldered to fixed and moveable units of the cell body. Motion is provided by means of a worm drive attached through a universal joint to the control shaft, which passes out through the top of the vacuum chamber through a vacuum seal. The maximum cell window separation is about 1 mm. The cell assembly is held vacuum tight by a steel spring and three set screws, as shown in the exploded section of the diagram in Fig. 2. A copper–constantan thermocouple is inserted in a hole in one of the silver chloride

[1]*Manuscript received June 21, 1961.*
Contribution from the Division of Pure Chemistry, National Research Council, Ottawa, Canada.
Issued as N.R.C. No. 6514.
[2]*National Research Council of Canada Postdoctorate Fellow.*

Can. J. Chem. Downloaded from www.nrcresearchpress.com by 210.87.254.5 on 09/05/12
For personal use only.

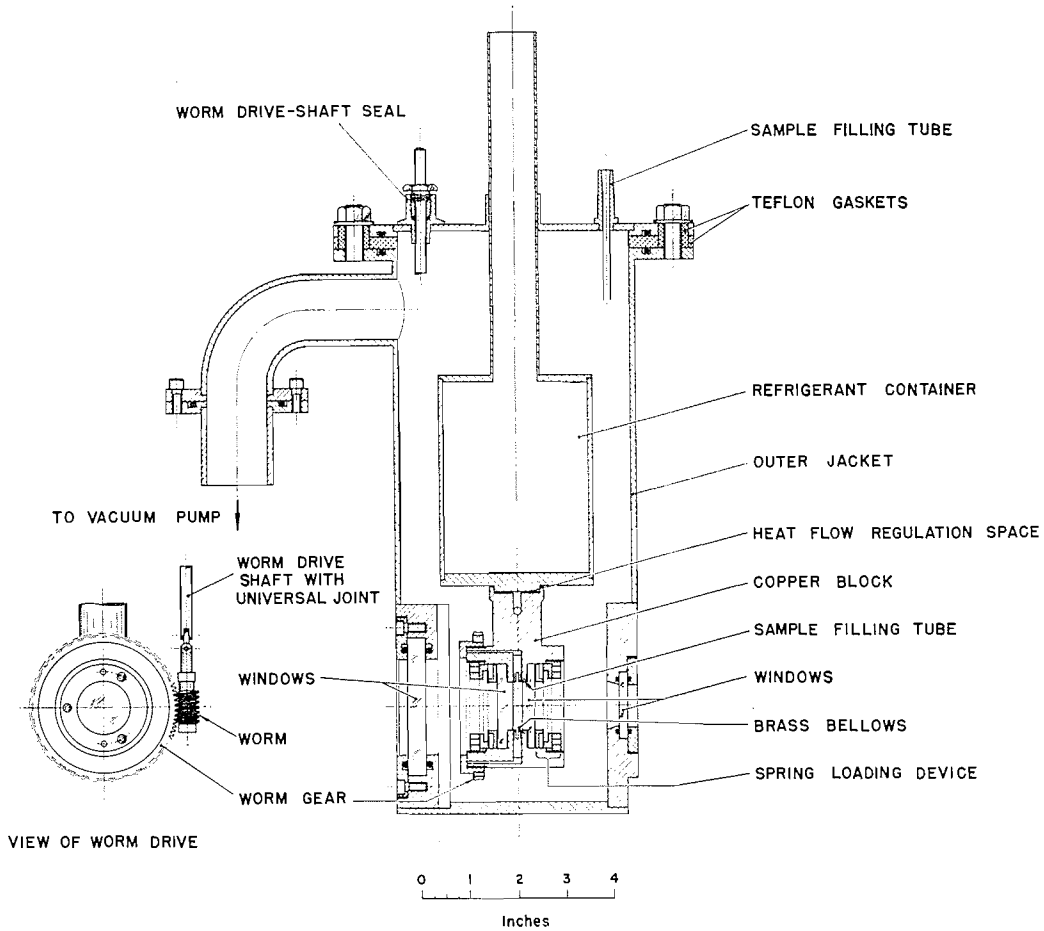


FIG. 1. Variable-temperature infrared cell. General diagram.

windows, with the leads passing out through the top of the cell. The cell unit is attached by a heavy copper bar to the coolant chamber. As in the design of Holden, Taylor, and Johnston, a transverse slot is milled into the neck of the copper bar, and provision is made for the slot to be filled with hydrogen to raise the heat conduction; alternatively the slot cavity can be evacuated for maximal thermal insulation of the cell unit. A 100-watt heating coil is wrapped around the cell proper so that temperatures above the cryostatic control temperature can be maintained.

The cell unit is mounted in an outer container which can be evacuated with an oil diffusion pump. This pump, not shown in the diagram, is welded directly to the wide vacuum connection tube of the lower component of the outer jacket. The apparatus is demountable, the inner cell unit being attached to the upper portion of the outer container through which pass all access tubes and controls except the evacuation outlet. The upper unit is bolted to the lower unit by a flange. The two sections of this flange are separated by a Teflon ring to improve the thermal insulation. The inner cell unit is constructed of copper and the outer vessel of brass, while stainless steel is used for all metal sections in which heat transfer is to be avoided. A mechanical backing pump, a

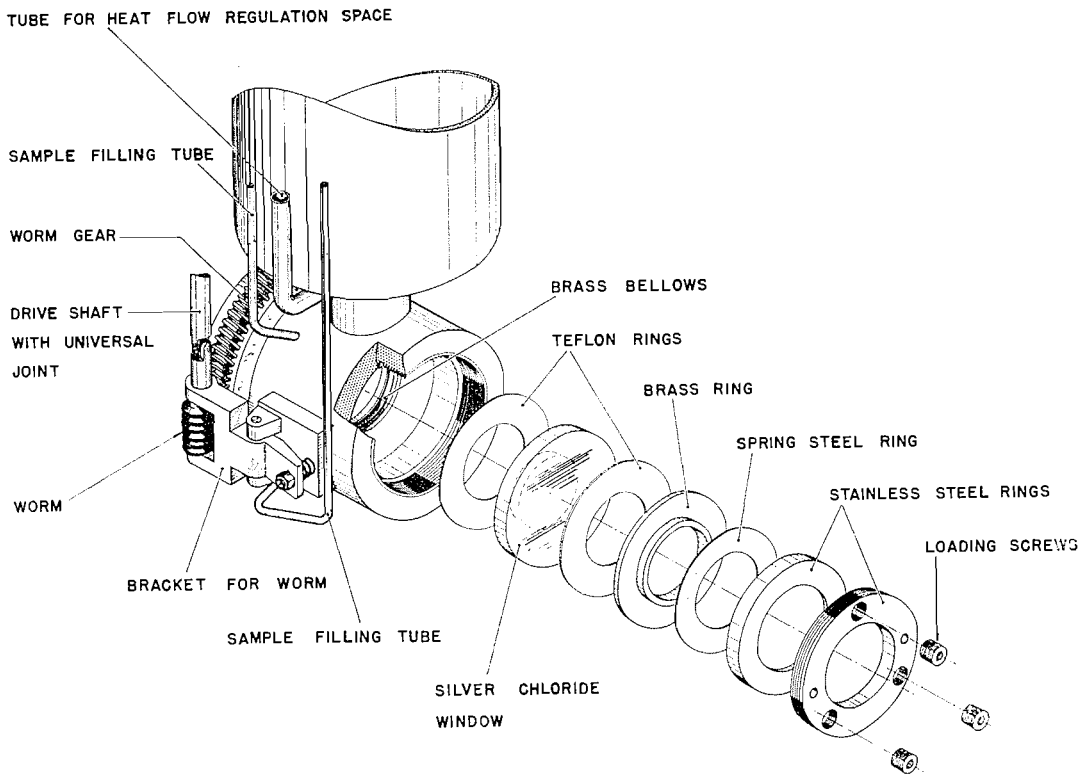


FIG. 2. Variable-temperature infrared cell. Details of inner cell structure.

Phillips vacuum gauge, a potentiometer, and a control Variac for adjusting and monitoring the temperature and pressure in the cell are mounted separately on a portable carriage which permits the cell to be used conveniently with different spectrometers.

For low-temperature measurements in solution, carbon disulphide can be used to $-100°$. For the range 1500–1300 cm^{-1}, where carbon disulphide is opaque, a ternary mixture of carbon tetrachloride, chloroform, and tetrachloroethylene in proportions of 58:36:6 by volume can be used to $-80°$, and a binary mixture of carbon tetrachloride and tetrachloroethylene (70:30), to $-58°$. The latter solvent mixture has superior transparency, particularly near 1450 cm^{-1}.

In precision low-temperature infrared spectrophotometry there are several sources of systematic error that need to be considered. Allowance must be made for the change in concentration due to the increase in the density of the cooled solution, and a small additional error, of opposite sign, may be introduced by the linear contraction of the cell thickness. In these investigations the density of the solvent was measured at $-75°$ and the extinction coefficients were adjusted proportionately; it was assumed that the densities of the solutions and the solvent did not differ significantly. No correction was applied for the cell-length contraction.

In the Perkin–Elmer Model 112 spectrometer, the beam chopper is located between the cell and the detector. Under these conditions rotation of the chopper may induce a

Can. J. Chem. Downloaded from www.nrcresearchpress.com by 210.87.254.5 on 09/05/12
For personal use only.

pulsed temperature change at the tuned amplifier frequency due to the fact that when the chopper interrupts the beam, the thermocouple "sees" black-body radiation at a temperature different from that radiated by the cooled cell. This would manifest itself as a displacement of the zero-transmission line. For the region between 1500 and 1350 cm^{-1} this source of error has been checked by observing the apparent transmission through a 1-mm path length of carbon disulphide at $+25°$ and $-75°$ C. In this wavenumber range carbon disulphide is almost totally absorbing and can be used as a temperature-variable shutter. The displacement of the zero-transmission curve with cooling did not exceed 2%, and the photometric errors due to this cause were considered negligible though they could become appreciable in other regions of the spectrum and at lower temperatures. It was also observed that with 1-mm path length of cooled carbon disulphide in the cell the zero-transmission line was not significantly displaced when an opaque shutter, at room temperature, was placed either between the cell and the entrance slit of the spectrometer, or between the source and the cell.* In the discussion of the infrared spectrum of diethyl ketone which follows we are concerned only with relative changes in the intensities of neighboring bands, but the factors considered above will have to be investigated more thoroughly before attempts are made to evaluate absolute infrared band intensities at depressed or elevated temperatures.

The Raman spectra were measured on a Cary Model 81 spectrophotometer. Room-temperature spectra were obtained with an internal carbon tetrachloride standard, using the technique described previously (2) except that a 5-ml Raman tube was used in place of the capillary tube and the convergent errors were not corrected with a polarizer. Depolarization ratios were measured by the method of Edsall and Wilson (3) and are also uncorrected for convergence. Raman spectra at $+6°$ and $+85°$ were obtained by surrounding the Raman tube with a jacket through which cooled or heated water was circulated.

RESULTS

The positions and intensities of both the infrared and Raman spectra, measured at room temperature, are summarized in Table I.

At room temperature, diethyl ketone exhibits a series of six infrared bands at 1461, 1454, 1414, 1379, 1355, and 1327 cm^{-1} (bands A–F of Fig. 3). These were investigated in carbon tetrachloride solution by Nolin and Jones (4), and from a comparative study of the spectra of selectively deuterated derivatives it was established that bands A, B, and D involve methyl group vibrations while C and E are associated with methylene groups. These investigators did not discuss the weak band F at 1320 cm^{-1} but it is evident from their published spectra that this also is a methylene band. The infrared spectrum of diethyl ketone in the ternary solvent mixture at $+25°$ and $-70°$ is shown in Fig. 3. The spectra of the pure liquid at room temperature and of the solid at $-75°$, measured under slightly lower resolution, are compared in Fig. 4, and the Raman spectrum in the presence of 9% by weight of carbon tetrachloride, measured at $+25°$, is shown in Fig. 5.

With falling temperature, most of the bands sharpen because of thermal solvent effects, and caution is necessary to distinguish this from the more fundamental effects of temperature on the molecular structure of the solute. Band C at 1414 cm^{-1} splits into a doublet in the cooled solution (Fig. 3) and it is clear from the shape of the band envelope that this is a real change and not merely a consequence of the band sharpening. The other

*We wish to thank Dr. R. Ripley for making these measurements.

Can. J. Chem. Downloaded from www.nrcresearchpress.com by 210.87.254.5 on 09/05/12
For personal use only.

TABLE I

Infrared and Raman spectra of diethyl ketone at room temperature

Infrared spectrum*		Raman spectrum†		
ν_{max} (cm^{-1})	ϵ_{max}*	ν_{max} (cm^{-1})	k_{max}	$\rho_{apparent}$
n.m.	—	216	0.3	0.65
310	12	307	0.3	0.75
408	2.8	406	8.2	0.44
—	—	468	0.2	—
525	2.4	526	0.4	0.5
—	—	580	0.1	—
620	3.5	621	0.5	0.74
—	—	748	4.3	0.27
784	4	784	5.1	0.31
810	21	(812)	0.4	—
939	20	944	1.2	0.87
955	31	960	1.5	0.90
1008	12	—	—	—
(1014)	—	1017	4.0	0.61
1094	19	1097	9.3	0.27
1120	63	(1121)	0.7	—
1167	18	1174	0.2	—
1240	4	1238	2.0	0.86
1327	3	1329	0.5	0.50
1358	60	—	—	—
1380	83	(1384)	0.7	—
1414	56	1421	8.8	0.83
1455	23	—	—	—
1461	109	1463	10.3	0.90
1718	206	1717	9.4	0.45
—	—	2788	2.7	—
(2883)	40	(2890)	18	—
2902	45	2908	47	0.33
2936	65	2945	65	0.29
2977	95	2984	30	0.72

NOTE: n.m. = region not measured.

*The infrared spectra were measured in carbon tetrachloride (3000–1300 cm^{-1}), carbon disulphide (1300–650 cm^{-1}), and *n*-hexane (650–300 cm^{-1}) using a Perkin–Elmer Model 112 single-beam spectrometer with CaF_2, NaCl, and CsBr prisms, under the standard operating conditions of the laboratory (9).

†See experimental section.

pair of methylene bands also shows significant changes. The peak at 1355 cm^{-1} shifts to 1362 cm^{-1} with a shoulder remaining at 1355 cm^{-1}, and the absorption at 1325 cm^{-1} intensifies. Comparison with the changes in the solid phase spectrum (Fig. 4) also suggests that real structural changes in the molecule are involved. The changes in the methyl bands are more difficult to assess. The intensification of band D without frequency displacement is probably only a thermal effect. Bands A and B are both more clearly resolved in the low-temperature spectrum, but the ratio of the peak intensities is not significantly altered. In the spectrum of the solid the most notable change is the complete disappearance of the 1355 cm^{-1} band, the development of the 1333 cm^{-1} maximum, and the profound change in the methyl absorption between 1475 and 1440 cm^{-1}.

The Raman spectrum, shown in Fig. 5, is less informative in the 1500–1300 cm^{-1} region, as the bands are less well resolved. The absence of the 1375 cm^{-1} band is in accord with the well-established fact that the symmetrical C—H bending mode of the methyl group is Raman inactive in aliphatic hydrocarbons.

Spectra in Other Regions

Apart from noting their complexity, Nolin and Jones did not discuss the spectra of the

Can. J. Chem. Downloaded from www.nrcresearchpress.com by 210.87.254.5 on 09/05/12
For personal use only.

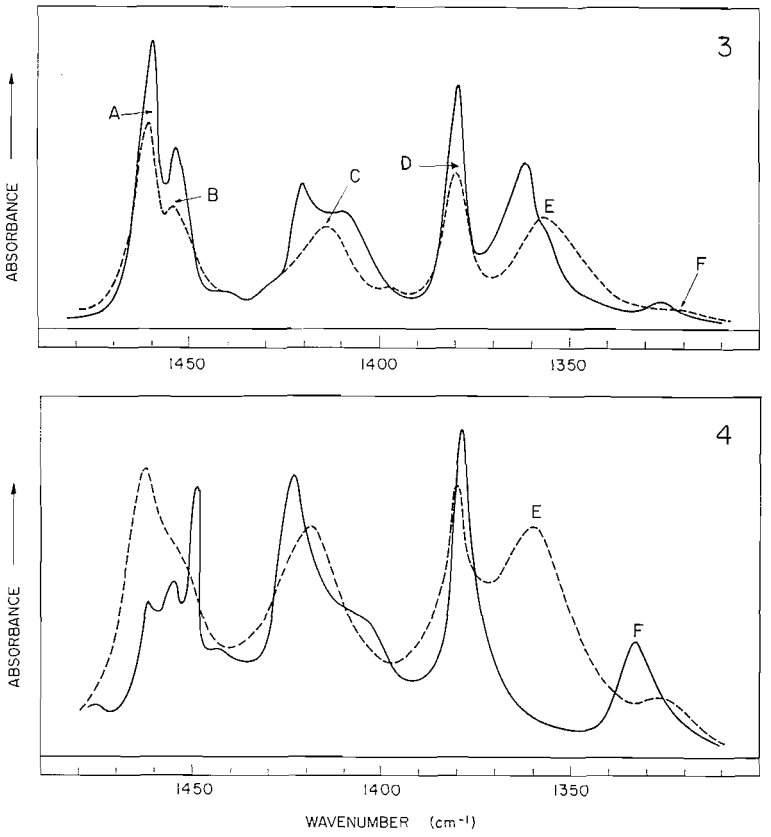


FIG. 3. Infrared spectrum of diethyl ketone. The effect of temperature on 1500–1300 cm^{-1} region in $CCl_4/C_2Cl_4/CHCl_3$ solution at 0.3 *M* concentration. —— −70° C; – – – +25° C.

FIG. 4. Infrared spectrum of diethyl ketone. Comparison of spectra in liquid and solid phases over the range 1500–1300 cm^{-1}. —— solid at −75° C; – – – liquid at +25° C.

deuterated diethyl ketones below 1300 cm^{-1}. The infrared and Raman spectra shown in Figs. 5–7 exhibit a number of temperature-sensitive bands; particularly notable is the highly polarized pair of Raman bands at 784 and 748 cm^{-1}, which reverse in relative intensity at +85°. The most significant temperature effect in the infrared spectrum is the weakening of the 1167 cm^{-1} and the 939 cm^{-1} bands in the cooled solution, and the disappearance of these bands from the spectrum of the solid.

The carbonyl stretching band, measured in the ternary solvent mixture at 0.3 *M* concentration, is symmetrical, with a maximum at 1761 cm^{-1} at 25° C. When the solution is cooled to −75° the maximum shifts to 1710 cm^{-1} with no significant change in the band shape. Such a solvent–temperature shift is normal to a monomolecular species and discounts dimolecular association as an explanation for the behavior of the other temperature-sensitive bands. The band is at 1710 cm^{-1} for the solid at room temperature. In the C—H stretching region both the infrared and the Raman spectra exhibit the four bands that have been discussed previously and none show significant temperature sensitivity.

Can. J. Chem. Downloaded from www.nrcresearchpress.com by 210.87.254.5 on 09/05/12
For personal use only.

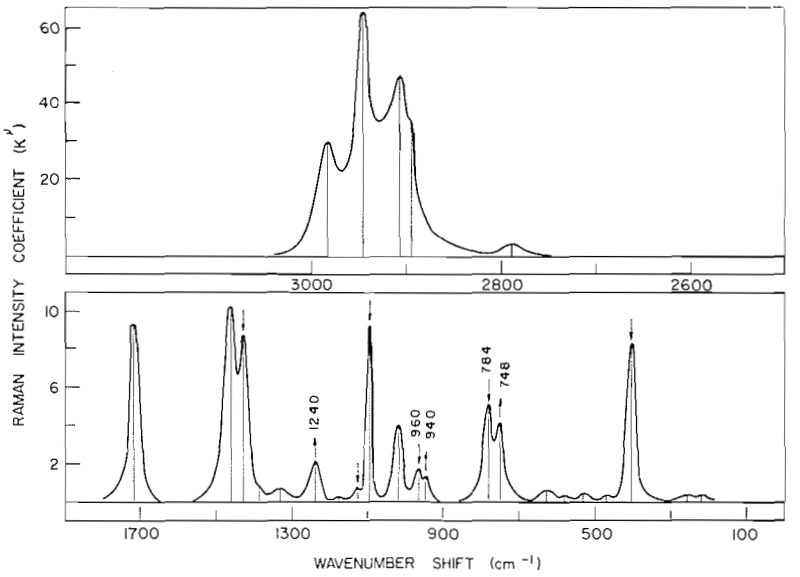


FIG. 5. Raman spectrum of diethyl ketone at room temperature (+25° C). The measured band positions and intensities are indicated by the vertical lines. The band contours are diagrammatic only. Bands which intensify on heating are indicated by upward pointing arrows.

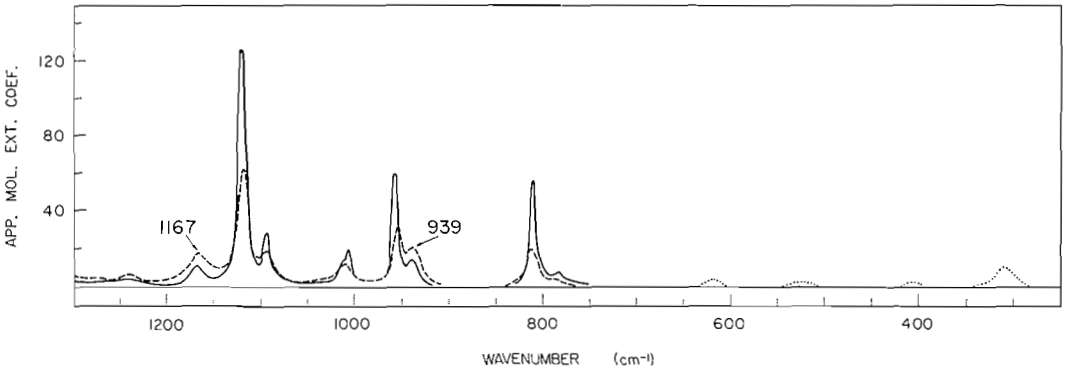


FIG. 6. Infrared spectrum of diethyl ketone in the range 1300–280 cm^{-1}. —— CS_2 solution, −75° C, 0.35 M; – – – CS_2 solution, +25° C, 0.35 M; . . . n-C_6H_{14} solution, +25° C, 0.78 M.

DISCUSSION

The flexibility of the diethyl ketone molecule permits great freedom for conformational variation, and any attempt to relate these spectral changes to the molecular structure must, of necessity, be speculative. Assuming restricted rotation about the CO—CH_2 bonds, but free rotation about the C—CH_3 bonds, the four conformational structures I–IV can be written for diethyl ketone. They all possess either a plane of symmetry, a twofold axis of symmetry, or both. There are, in addition, innumerable forms with C_s symmetry which may be visualized as derived from I by the synchronous rotation of the C—Et bonds in the same direction; after rotation through 180°, structure IV is

Can. J. Chem. Downloaded from www.nrcresearchpress.com by 210.87.254.5 on 09/05/12
For personal use only.

Can. J. Chem. Downloaded from www.nrcresearchpress.com by 210.87.254.5 on 09/05/12
For personal use only.

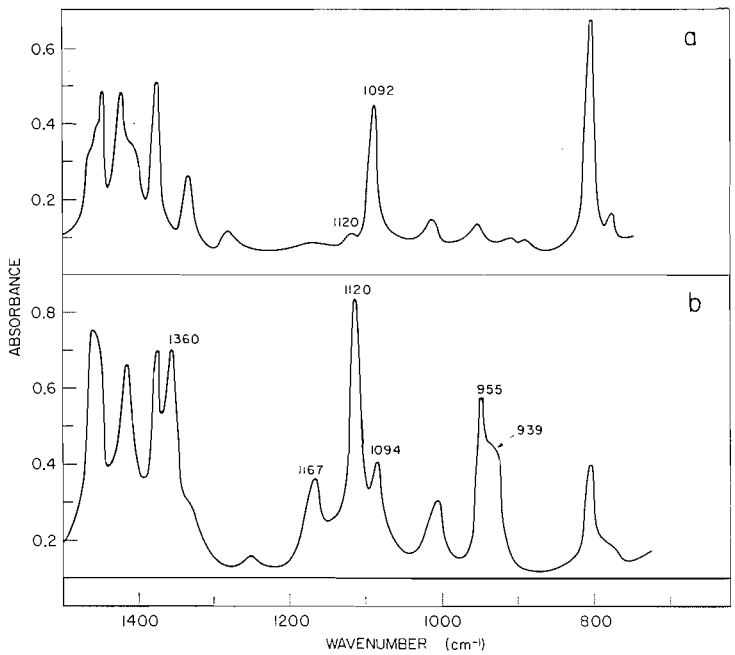
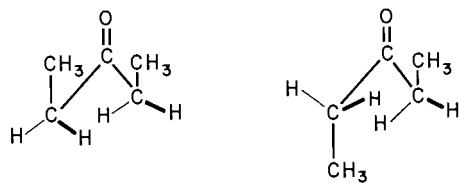
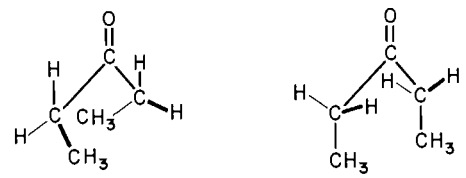


FIG. 7. Infrared spectrum of diethyl ketone. Comparison of the spectra in the solid (*a*, −75° C) and liquid (*b*, +25° C) phases over the range 1500–700 cm^{-1}.



I (C_{2V}) II (C_S)



III (C_2) IV (C_{2V})

reached. If the C—Et bonds of I are synchronously rotated in opposite directions an infinite set of C_2 structures is obtained; a 120° rotation corresponding to III while an 180° rotation again produces IV. Unequal rotation of the C—Et bonds in either direction will produce skew structures with no symmetry elements save identity.

Sirkar and Bishui (5) consider that the presence of a totally depolarized Raman

band with a depolarization ratio close to the theoretical maximum of 0.857 is acceptable as evidence for a plane or twofold axis of symmetry in a molecule. They noted such bands in the spectra of liquid acetone, methyl ethyl ketone, and di-*n*-propyl ketone, but not in diethyl ketone. We observed bands in the Raman spectrum of diethyl ketone at 1463, 1238, 960, and 944 cm^{-1} with measured depolarization ratios of 0.90, 0.86, 0.90, and 0.87 respectively, but the significance to be attached to these figures depends very critically on the magnitude of the convergence error. When this was evaluated by the method of Rank and Kagarise (6), our correction curve was found to slope much less steeply than that reported by the original authors, who used a lamp of different geometrical form. In particular, our correction was negligibly small for measured depolarization ratios above 0.8 and large (>0.2) for strongly polarized bands. Our measurements, therefore, lead us to conclude that at least four bands in the Raman spectrum of diethyl ketone are totally depolarized. Furthermore, it is difficult to believe that diethyl ketone would exist exclusively in skew conformations while such closely related molecules as methyl ethyl ketone and di-*n*-propyl ketone possess a plane of symmetry, or a twofold axis of symmetry, or both.

In the present state of our knowledge, caution must be exercised in attaching structural significance to "totally depolarized" bands. More accurate techniques for the absolute measurement of depolarization ratios are needed, and experience must be acquired in interpreting their significance in connection with the normal vibrations of large molecules.

This discussion will be developed in terms of the four structures illustrated above which, from symmetry considerations, must approximate closely to conformations of minimum or maximum energy. Displacements may occur to minimize the non-bonded hydrogen–hydrogen and hydrogen–oxygen interactions but unless the molecule is thermally excited these should be small; they are more likely to be symmetrical than skew.

The spectrographic data do not distinguish unequivocally among the structures I–IV, but there are no features of the liquid phase spectra that are inconsistent with a simple equilibrium between two of these species. Structure IV can be rejected on thermodynamic grounds, because of the close packing of the hydrogen atoms of the methyl groups. The non-bonded interaction energies will undoubtedly be minimal for III, in which the methyl groups project forward and backward from the plane of the C—CO—C skeletal unit. Structure III would accordingly seem strongly preferred in the liquid phase. Structural significance is undoubtedly associated with the splitting of the 1415 cm^{-1} band into the 1420, 1410 cm^{-1} doublet on cooling. The displacement of this α-methylene scissoring band from its unperturbed position near 1467 cm^{-1} in aliphatic hydrocarbons depends on its steric relation to the carbonyl group. The appearance of the two peaks at low temperature favors II for the form stabilized at low temperature in the liquid phase, as this is the only structure in which the steric environment of the two methylene groups differs. The 1410 cm^{-1} frequency approaches closely to the low α-methylene scissoring frequency of 1406 cm^{-1} in cyclopentanone, with which one of the α-methylene groups of II has configurational similarity. The increased complexity of the methylene wagging absorption at 1362, 1355, and 1327 cm^{-1} in the cooled solution is also consistent with this structure. Splitting of the α-methylene scissoring band could come about through an in-phase and out-of-phase coupling between the scissoring modes of the two methylene groups provided they are suitably located relative to one another. This might be realized in I, but this structure is not preferred in the liquid phase because there will be appreciable non-bonded repulsion between the eclipsed hydrogens of the two methylene groups which occupy

Can. J. Chem. Downloaded from www.nrcresearchpress.com by 210.87.254.5 on 09/05/12
For personal use only.

1,3 positions (7); there will also be repulsion between the methyl groups and the oxygen atom.

In so far as the solid is concerned, it is unfortunate that no X-ray diffraction measurements have yet been made, and recent attempts to prepare single crystals suitable for such analysis have been unsuccessful (8). The planar zig-zag structure (I) would pack more conveniently into a lattice and this entropy factor could favor I for the crystal in spite of the objections in the preceding paragraph. Its higher C_{2v} symmetry is also in accord with the much simpler infrared spectrum of the solid in comparison with the cooled liquid (Fig. 5).*

In summary, these spectrographic measurements indicate that diethyl ketone exists as an equilibrium mixture of at least two conformational forms in the liquid state. It is not possible to identify the particular structures involved, and the flexibility of the molecule would permit innumerable skew structures of low symmetry. Certain aspects of the spectra are most simply reconciled with the requirements of conformational stability by an equilibrium between structures II and III in which II predominates at low temperatures. The ketone may crystallize as II or possibly as I.

Proton Magnetic Resonance Spectrum

The n.m.r. spectrum of diethyl ketone has also been measured at a concentration of 5 mole% in cyclopentane over a temperature range from −61° to 104° C, using tetramethylsilane as an internal frequency standard. The spectrum exhibits the quartet and triplet band systems characteristic of the methylene and methyl groups. The band contours exhibit no significant changes with temperature but the centers of the band systems are displaced, the methylene signals moving to higher field and the methyl signals to lower field with increasing temperature (Table II). Though the shifts are not directly

TABLE II

Temperature effects on the proton magnetic resonance spectrum of diethyl ketone

Temperature (°C)	Proton chemical shift*		
	Methylene	Methyl	Difference
−61	139.5	57.0	82.5
+28	137.0	59.0	78.0
+60	138.0	60.0	78.0
+104	134.5	60.0	74.5

*Measured in cycles per second at 60 Mc/sec relative to tetramethylsilane at 5 mole% concentration in cyclopentane.

interpretable in terms of molecular structure, they are not inconsistent with the changes in the vibrational spectra.

ACKNOWLEDGMENTS

We wish to thank Mr. J. R. Nicholson for measuring the n.m.r. spectrum and to acknowledge our appreciation to Dr. W. G. Schneider and Dr. A. W. Hanson for helpful discussion in connection with n.m.r. and X-ray spectroscopy.

**The band at 1120 cm^{-1} calls for comment. This appears to intensify on cooling of the solution (Fig. 6) but virtually disappears from the infrared spectrum of the cooled solid (Fig. 7).*

Can. J. Chem. Downloaded from www.nrcresearchpress.com by 210.87.254.5 on 09/05/12
For personal use only.

REFERENCES

1. R. B. HOLDEN, W. J. TAYLOR, and H. L. JOHNSTON. J. Opt. Soc. Am. **40**, 757 (1950).
2. K. NOACK and R. N. JONES. Can. J. Chem. This issue. p. 2201.
3. J. T. EDSALL and E. B. WILSON. J. Chem. Phys. **6**, 124 (1938).
4. B. NOLIN and R. N. JONES. J. Am. Chem. Soc. **75**, 5626 (1953).
5. S. C. SIRKAR and B. M. BISHUI. Indian J. Phys. **20**, 35 (1946).
6. D. H. RANK and R. E. KAGARISE. J. Opt. Soc. Am. **40**, 89 (1950).
7. D. H. R. BARTON and R. C. COOKSON. Quart Revs. (London), **10**, 44 (1956).
8. A. W. HANSON. Personal communication.
9. R. N. JONES. Spectrochim. Acta, **9**, 235 (1957).

Can. J. Chem. Downloaded from www.nrcresearchpress.com by 210.87.254.5 on 09/05/12
For personal use only.

Can. J. Chem. Downloaded from www.nrcresearchpress.com by 210.87.254.40 on 09/05/12
For personal use only.

CONFORMATIONAL EQUILIBRIA IN OPEN-CHAIN α,β-UNSATURATED KETONES[1]

K. NOACK[2] AND R. NORMAN JONES

ABSTRACT

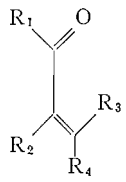
The infrared and Raman spectra of *trans*-Δ^3-penten-2-one have been measured over the temperature range +30° to −75° and +85° to +5° respectively. The temperature-dependent changes observed in the spectra indicate that this ketone exists as an equilibrium mixture of *s*-cis and *s*-trans conformational isomers in the liquid state. The *s*-trans form is the more stable and is present exclusively in the crystalline solid.

Similar measurements have been carried out on Δ^3-buten-2-one. The infrared and Raman spectra of this ketone also exhibit temperature effects that can be explained by a similar equilibrium, though the evidence is not as conclusive as for *trans*-Δ^3-penten-2-one.

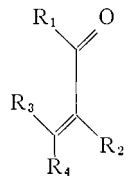
The influence of alkyl substitution at the α- and β-carbon atoms on the relative stability of the *s*-cis and *s*-trans forms of α,β-unsaturated ketones is discussed.

INTRODUCTION

The *s*-cis (I) and *s*-trans (II) conformations of open-chain α,β-unsaturated ketones can be distinguished from the positions and intensities of the C=O and C=C stretching

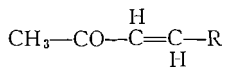


I



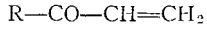
II

bands in the infrared (1–4) and Raman (5) spectra. In the liquid state most conjugated ketones exist predominantly or perhaps exclusively in one or other of the two conformations, but Mecke and Noack (2) have observed that the infrared spectrum of *trans*-Δ^3-penten-2-one (III*a*) and related compounds (III*b*–III*d*) exhibit two carbonyl bands near 1700 cm^{-1} and 1680 cm^{-1} in tetrachloroethylene solution. The positions of these bands



III

(*a*) R = —CH_3
(*b*) R = —CH_2—CH_3
(*c*) R = —CH_2—CH_2—CH_3
(*d*) R = —$CH(CH_3)_2$



IV

(*a*) R = —CH_3
(*b*) R = —CH_2—CH_3

suggested an equilibrium between the *s*-cis and *s*-trans isomers. Similar doublet carbonyl bands were noted by Mecke and Noack for ketones of structure IV*a*–IV*b*. Timmons and collaborators (4) have commented similarly on the spectrum of *trans*-Δ^3-penten-2-one, and other examples of this behavior have been cited by Erskine and Waight (3).

In the present investigation the effects of temperature on the infrared and Raman spectra of *trans*-Δ^3-penten-2-one and Δ^3-buten-2-one have been examined in an attempt to confirm the existence of these equilibrium systems.

[1]*Manuscript received June 21, 1961.*
Contribution from the Division of Pure Chemistry, National Research Council of Canada, Ottawa, Canada. Issued as N.R.C. No. 6515.
[2]*National Research Council of Canada Postdoctorate Fellow.*

Can. J. Chem. Downloaded from www.nrcresearchpress.com by 210.87.254.40 on 09/05/12
For personal use only.

EXPERIMENTAL METHODS AND RESULTS

The preparation and purification of the ketones have been described by Mecke and Noack (2). The infrared spectra were measured on Perkin–Elmer Model 21 and Model 112 spectrometers using the low-temperature technique described previously (6). The Raman spectra were obtained with a Cary Model 81 spectrometer (5). The spectra are illustrated in Figs. 1–8 and the numerical data are summarized in Tables I–III.

TABLE I

Band positions and intensities in the infrared and Raman spectra of trans-Δ^3-penten-2-one

Raman spectrum*		Infrared spectrum†		Raman spectrum*		Infrared spectrum†	
Wavenumber‡ (cm^{-1})	k^{max}	Wavenumber‡ (cm^{-1})	ϵ_{max}	Wavenumber‡ (cm^{-1})	k^{max}	Wavenumber‡ (cm^{-1})	ϵ_{max}
377§	4.5	381	4	1303	14.0	(1300)	—
—	—	418	4	—	—	1310	25
501	12.0	498	6	(1360)	—	1359	98
543	2.6	543	31	1377	14.9	1378	72
557	1.3	(560)	—	—	—	1425	52
603§	3.7	604	27	—	—	(1435)	—
620§	1.9	(622)	—	1443	26.4	1441	97
799	11.6	798	11	(1619)	30	(1615)	60
861	1.0	860‖¶	10	1631	59§	1630‖¶	196
943	2.5	943	35	1644	47	1645	72
(967)	—	971	146	1673	90	1674	400
992	12.7	(993)	—	(1697)	—	1693‖¶	144
—	—	1018	17	2856	10.5		—
1042	3.6	1040	6	2881	9.0		—
1065	2.4	—	—	2918	78		
1105	5.0	—	—	2944	26	n.m.	
1175	v.w.	1177‖¶	70	2974	18		
1252	17.7	1250	168	(3008)	—		
—	—	1270	46	3020	23		
(1291)§	4.9	1289‖¶	25				

NOTE: v.w. = resolved but very weak band; n.m. = region not measured.

*Intensities are measured relative to the 459 cm^{-1} band of CCl_4 ($k^{459}_{CCl_4} = 100$). Measured in the presence of 9% by weight of CCl_4 at +5° C.

†Measured at +30° C. For experimental details see references 6 and 9.

Wavenumber range (cm^{-1})	Solvent	Concentration (M)
1750–1320	$CHCl_3/CCl_4/C_2Cl_4$	0.24
1320–700	CS_2	0.36
700–300	n-C_6H_{14}	0.7

‡Inflections are indicated in parentheses.
§The Raman band intensifies at higher temperature.
‖The infrared band weakens at higher temperature.
¶The band is absent from the infrared spectrum of the solid.

Spectra of trans-Δ^3-Penten-2-one

The infrared spectrum of *trans*-Δ^3-penten-2-one, measured in a eutectic mixture of carbon tetrachloride, tetrachloroethylene, and chloroform (6) in the region of the C=O and C=C stretching bands is shown in Fig. 1. At room temperature, four well-resolved bands (A–D) are observed at 1693, 1674, 1645, and 1630 cm^{-1} with a weaker shoulder (E) at 1615 cm^{-1}. In the Raman spectrum, measured at +5° in the presence of 9% by weight of carbon tetrachloride, the bands occur near the same positions (Fig. 2), but the relative intensities are different; band A, in particular, is reduced to a weak inflection. From comparison with the spectra of other α,β-unsaturated ketones (2, 5), bands A and D can be assigned to the *s*-cis isomer and bands B and C to the *s*-trans form. The weak

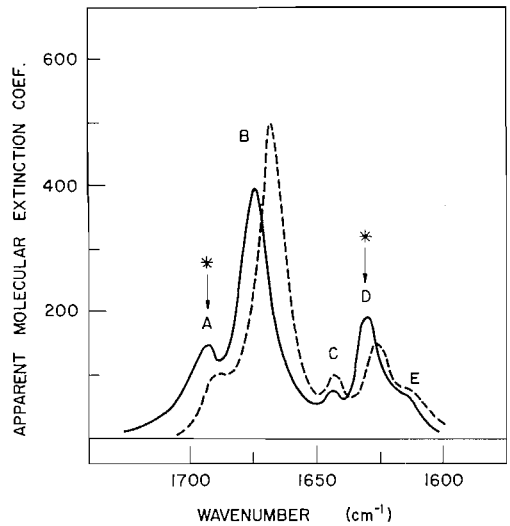


FIG. 1. Infrared spectrum of *trans*-Δ^3-penten-2-one in $CHCl_3/CCl_4/C_2Cl_4$ solvent. Bands indicated by arrows and asterisks weaken in the cooled solution and are absent from the spectrum of the solid. —— +30° C; - - - −75° C.

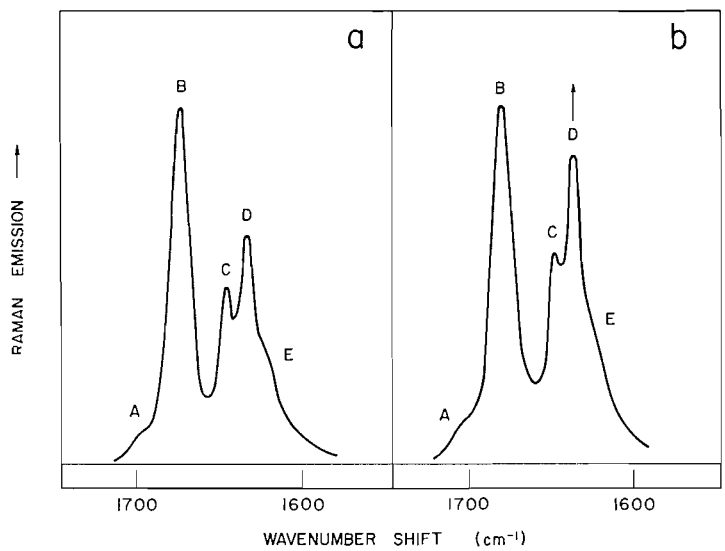


FIG. 2. Raman spectrum of *trans*-Δ^3-penten-2-one measured in the presence of 9% by weight of carbon tetrachloride: *a*, +6° C; *b*, +85° C. The intensity scale is arbitrarily adjusted so that band B is of equal height in both spectra.

band E is probably an overtone or combination band; its weakness in the Raman spectrum is an argument against attributing it to a C=C vibration of an impurity.

In the infrared spectrum at −75° (Fig. 1) bands B and C are more intense than at room temperature while bands A and D are weaker, indicating the greater thermodynamic stability of the *s*-trans form. Bands A and D are absent from the spectrum of the solid

Can. J. Chem. Downloaded from www.nrcresearchpress.com by 210.87.254.40 on 09/05/12
For personal use only.

at $-100°$, suggesting that the ketone crystallizes exclusively in the *s*-trans form. The Raman spectrum at $+85°$ shows a relative intensification of the *s*-cis bands. The intensity ratio k_B/k_D is 1.38 at $+5°$ and 1.17 at $+85°$ and the ratio k_D/k_C is 1.28 and 1.47 respectively at the lower and higher temperatures. While these figures indicate an intensification of the *s*-cis band relative to the *s*-trans with rising temperature, they are not necessarily proportional to the concentration changes, since the bands broaden with rising temperature. Unfortunately the band overlap is too great to permit evaluation of the areas beneath the component peaks from which the relative concentrations of the isomers might be derived.

The fact that both the C=O and the C=C bands are temperature sensitive indicates that the band splitting is not due to a Fermi resonance of the type associated with C=O band splitting in cyclic *s*-trans ketones (5). It is also significant in this connection that the room-temperature spectra for dilute solutions in carbon tetrachloride, chloroform, and tetrachloroethylene closely resemble the spectrum of the liquid ketone; only minor changes in band position and intensity are noted, such as would be expected from normal solvent effects.

Other regions of the infrared and Raman spectra of *trans*-Δ^3-penten-2-one are shown in Figs. 3 and 4. Infrared bands of liquids and solutions usually become narrower and sharper with diminishing temperature, and it is difficult to distinguish an increase in band height due to this solvent–solute effect from band intensification due to an increase in the relative concentration of a conformational isomer. The inverse effect, viz. the weakening of a band at lower temperature due to the fall in concentration of a less-stable isomer is more convincing as evidence for a change in isomer equilibrium, and in the infrared spectrum of *trans*-Δ^3-penten-2-one in carbon disulphide at $-65°$ the bands at 1289, 1177, and 860 cm^{-1} weaken in this fashion. Furthermore the bands at 1289 cm^{-1} and 860 cm^{-1} are absent from the spectrum of the solid ketone at $-100°$, while the band at 1177 cm^{-1} persists only as a broad residuum. These bands can all be attributed to the *s*-cis form. For the spectra at elevated temperatures, the converse argument applies, and the bands that intensify on heating are most plausibly indentified with a change in the equilibrium in favor of the *s*-cis form. In the Raman spectrum at $+85°$ this is observed for the bands at 1291, 620, 603, and 377 cm^{-1}.

Spectra of Δ^3-Buten-2-one

The infrared spectrum of Δ^3-buten-2-one, measured on a capillary film of the undiluted ketone, exhibits two bands in the C=O stretching region at 1701 and 1683 cm^{-1} (bands A and B of Fig. 5). Cooling the film to $-65°$ changes the relative intensities; the ratios of the maximal absorbances (B/A) are 1.64 at $+30°$ and 2.08 at $-65°$. The positions are consistent with the assignment of band A to the *s*-cis isomer and band B to the *s*-trans form. In the infrared spectrum of the solid at $-100°$ there is no band near 1700 cm^{-1} but there is a doublet at 1680 and 1673 cm^{-1} (Fig. 5). It seems reasonable to interpret this as a splitting of band B, and the disappearance of band A. The splitting introduces a complication in the interpretation of the structure of the solid; it could be due to combination with a lattice vibration or to the packing of two molecules in a slightly different environment in the unit cell. The latter explanation is supported by the similar close splitting of the C=C band, also shown in Fig. 5. In the Raman spectrum at $+5°$ the 1700 cm^{-1} component appears only as a weak inflection on the high-frequency side of the strong band at 1677 cm^{-1} and there is no measurable change at higher temperature. The weakness of this Raman band is consistent with the *s*-cis assignment (5).

Can. J. Chem. Downloaded from www.nrcresearchpress.com by 210.87.254.40 on 09/05/12
For personal use only.

Can. J. Chem. Downloaded from www.nrcresearchpress.com by 210.87.254.40 on 09/05/12
For personal use only.

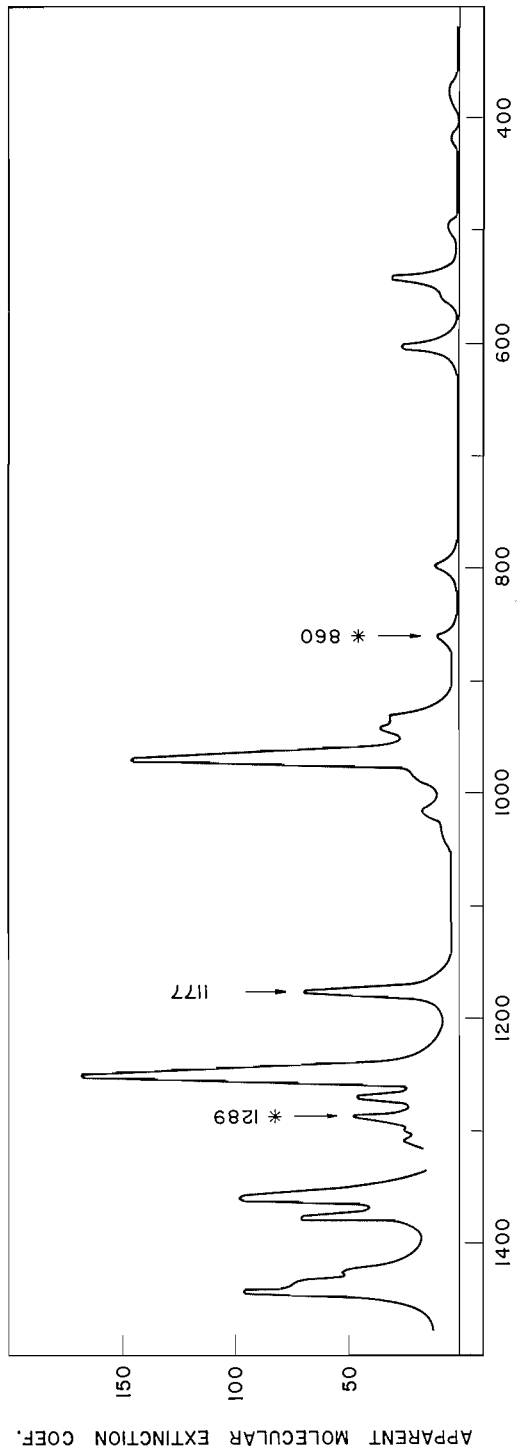


FIG. 3. Infrared spectrum of *trans*-Δ^3-penten-2-one. For conditions see footnote † of Table I and footnote to Fig. 1.

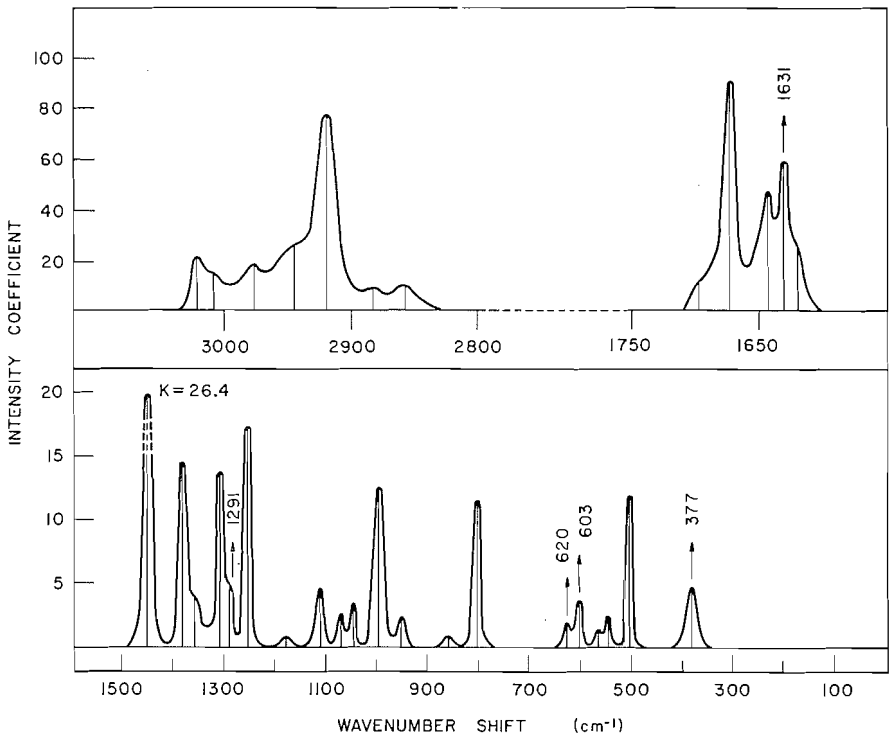


FIG. 4. Raman spectrum of *trans*-Δ^3-penten-2-one measured in the presence of 9% by weight of carbon tetrachloride. The carbon tetrachloride bands at 459, 314, and 218 cm^{-1} are omitted. The band contours are diagrammatic only. Upward pointing arrows designate bands that intensify on heating.

Δ^3-Buten-2-one exhibits only one C=C stretching maximum in both the infrared and the Raman spectra, and if the two carbonyl bands are to be attributed to a conformational equilibrium it is necessary to assume that the C=C stretching bands for both the *s*-cis and the *s*-trans forms overlap each other and are not resolved. In the case of *trans*-Δ^3-penten-2-one the parallel changes in the A/D and B/C band pairs are a strong argument in support of the equilibrium system, and the failure to observe similar behavior for Δ^3-buten-2-one adds considerably to the difficulty in interpreting the other temperature changes in this spectrum. In Table III the positions and intensities of the C=O and C=C bands of Δ^3-buten-2-one in carbon tetrachloride and chloroform are compared. The ratios of the C=O band intensities in the two solvents are not very different and do not suggest that we are dealing with a Fermi resonance type of carbonyl band splitting (5, 7). The change in the relative heights of several bands distributed through the 1400–900 cm^{-1} region of the spectrum are described below, and these also are inconsistent with the Fermi resonance explanation.

The infrared spectrum of Δ^3-buten-2-one from 1750 to 280 cm^{-1} is shown in Fig. 6, and the temperature-sensitive bands are illustrated in the three infrared spectra shown in Fig. 7, covering the 1400–900 cm^{-1} range at temperatures extending from -65 to $+85°$. Changes are particularly notable for the bands at 1360, 1248, 991, and 954 cm^{-1}, which intensify on cooling, and for the band at 1180 cm^{-1}, which weakens on cooling and is absent from the spectrum of the solid. These changes are most readily reconciled with

Can. J. Chem. Downloaded from www.nrcresearchpress.com by 210.87.254.40 on 09/05/12
For personal use only.

TABLE II

Band positions and intensities in the infrared and Raman spectra of Δ^3-buten-2-one

Raman spectrum*		Infrared spectrum†		Raman spectrum*		Infrared spectrum†	
Wavenumber‡ (cm^{-1})	k_{max}	Wavenumber‡ (cm^{-1})	ϵ_{max}	Wavenumber‡ (cm^{-1})	k_{max}	Wavenumber‡ (cm^{-1})	ϵ_{max}
278	4.6	—	—	—	—	1063	11
298	4.4	300	4	1183	0.8	1180§‖	73
426	1.6	427	4	—	—	1216	19
487	1.5	485	14	1247	7.0	1246	86.5
527	2.1	523	4	1280	15.6	1274	16
600	1.6	603	7	1293	10.4	—	—
—	—	669		1357	0.8	1360	88
686	1.0	685		—	—	1400	106
760	12.1	758	6	1408	16.8	—	—
773	7.3	773	4	—	—	1423	49
—	—	824	2	(1430)	—	—	—
—	—	(940)		1616	54	1616	65.5
946	6.1	951	103	1677	70	1687	376
963	4.7	(963)		(1700)	—	1706§‖	141
—	—	982	54	2926	53		
997	0.4	992	57	2987	25	n.m.	n.m.
—	—	1020	23	3026	72		
1054	10.9	—	—	3103	26.4		

NOTE: n.m. = region not measured.

*Intensities are measured relative to the 459 cm^{-1} band of CCl_4 ($k^{459}_{CCl_4} = 100$). Measured in the presence of 9% by weight of CCl_4 at +5° C.

†

Wavenumber range (cm^{-1})	Solvent	Concentration (M)
1750–1600	CCl_4	0.16
1500–1300	CCl_4	0.6
1300–650	CS_2	0.6
650–280	n-C_6H_{14}	0.7

‡Inflections are indicated in parentheses.

§The infrared band weakens at higher temperature.

‖The band is absent from the infrared spectrum of the solid.

TABLE III

Solvent effects of the C=O and C=C infrared bands of Δ^3-buten-2-one*

	A		B			C	
	Position (cm^{-1})	Intensity	Position (cm^{-1})	Intensity	B/A	Position (cm^{-1})	Intensity
Carbon tetrachloride	1700	(140)	1687	(375)	2.68	1616	(66)
Chloroform	1700	(115)	1680	(340)	2.94	1616	(75)

*Concentration, 0.02 M.

the *s*-cis ⇌ *s*-trans equilibrium though they mainly involve intensification on cooling. It may be significant that a band near 1180 cm^{-1} appears to be associated with the *s*-cis forms of both Δ^3-buten-2-one and *trans*-Δ^3-penten-2-one. The Raman spectrum of Δ^3-buten-2-one measured at +5° is shown in Fig. 8; raising of the temperature to +70° causes the bands at 1247, 1054, 686, and 527 cm^{-1} to diminish in peak height by about 30% while the remaining bands retain 90–100% of their intensity at +5°.

In summary we infer from these experiments that *trans*-Δ^3-penten-2-one exists as a mixture of *s*-cis and *s*-trans isomers. For Δ^3-buten-2-one, the failure to observe two C=C

Can. J. Chem. Downloaded from www.nrcresearchpress.com by 210.87.254.40 on 09/05/12
For personal use only.

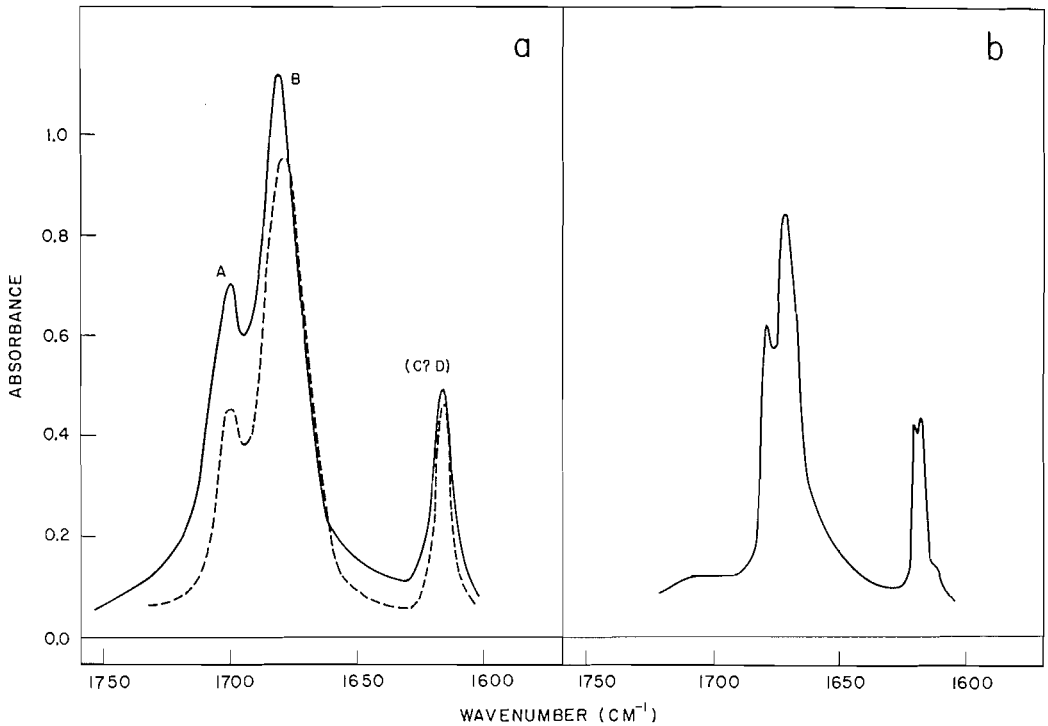


FIG. 5. Infrared spectrum of Δ^3-buten-2-one, measured on the undiluted liquid ketone: *a*, liquid film, —— +30° C, - - - - −65° C; *b*, solid film, −100° C.

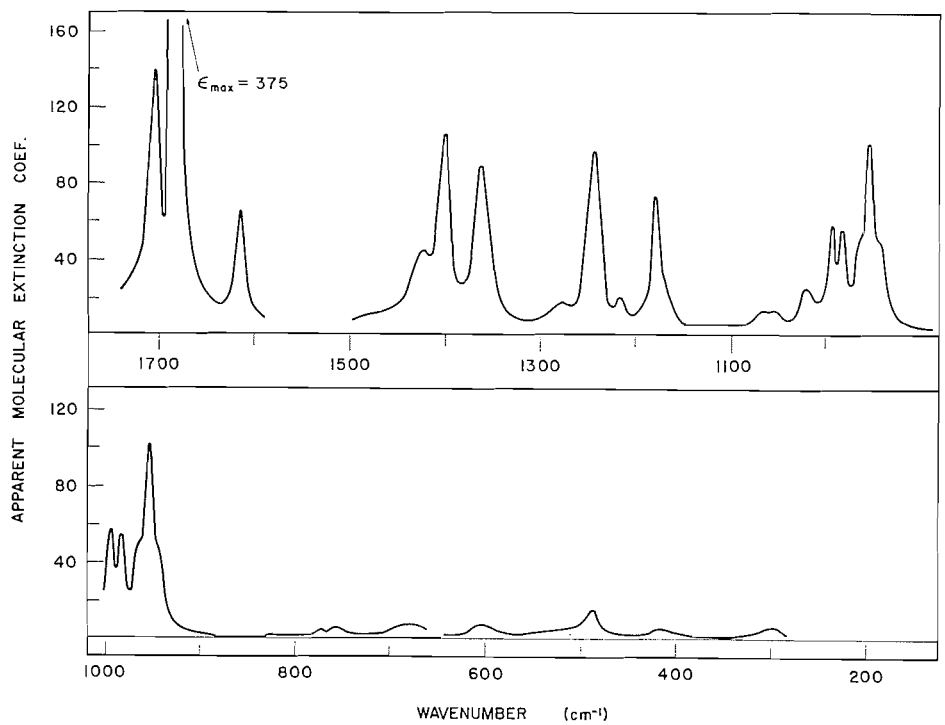


FIG. 6. Infrared spectrum of Δ^3-buten-2-one. For conditions see footnote † of Table II.

Can. J. Chem. Downloaded from www.nrcresearchpress.com by 210.87.254.40 on 09/05/12
For personal use only.

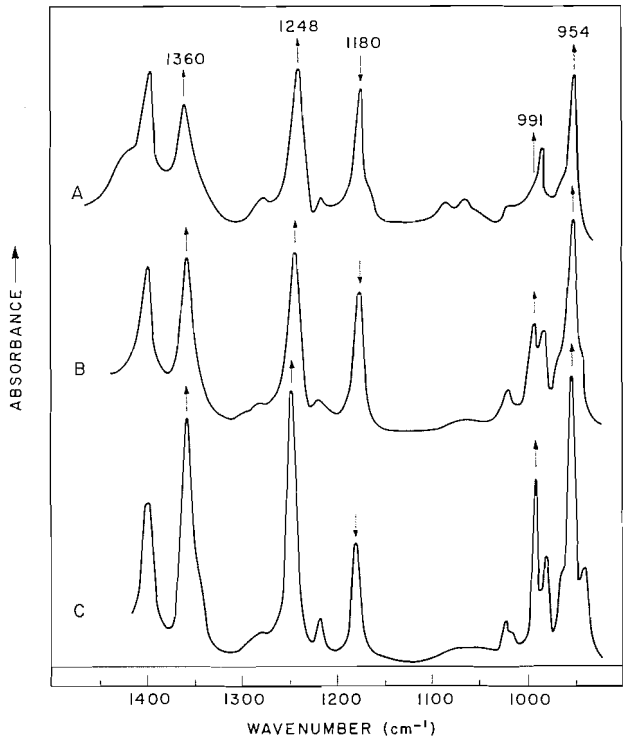


FIG. 7. Effects of temperature on the infrared spectrum of Δ³-buten-2-one. For curve A (+85° C) the solvent is tetrachloroethylene and for curves B (+30° C) and C (−65° C), carbon disulphide. Upward pointing arrows designate bands that intensify on cooling.

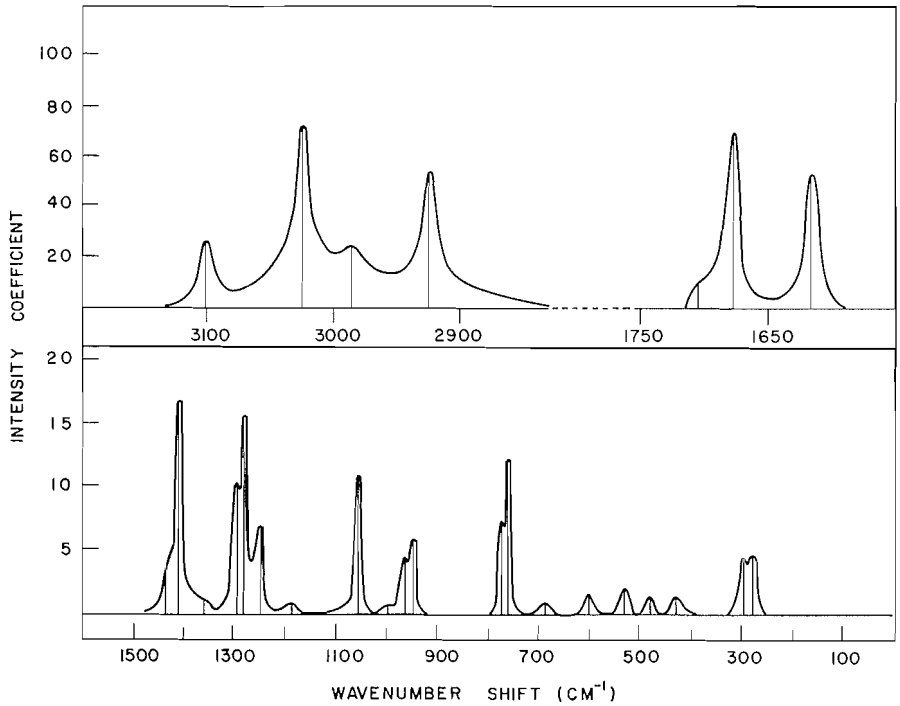


FIG. 8. Raman spectrum of Δ³-buten-2-one.

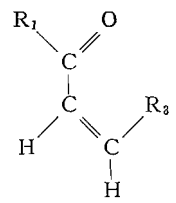
Can. J. Chem. Downloaded from www.nrcresearchpress.com by 210.87.254.40 on 09/05/12
For personal use only.

stretching bands makes it unwise to draw definite conclusions, though the temperature changes through the remainder of the spectrum are consistent with the presence of the equilibrium system.

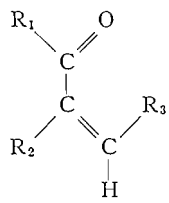
CONCLUDING REMARKS

The α,β-unsaturated ketones for which equilibria between *s*-cis and *s*-trans forms have been observed or postulated possess common structural features. It appears necessary that (*a*) the α-carbon atom carry a hydrogen atom, (*b*) the *s*-trans form be sterically unhindered (viz. R_2 and R_3 = H in I and II).

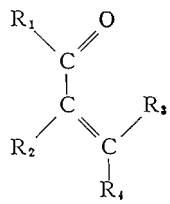
If the hydrogen at R_2 is replaced by alkyl, only the *s*-trans form is obtained, presumably because the *s*-cis structure is destabilized by repulsion between the non-bonded hydrogen atoms on R_1 and R_2.* If R_3 is alkyl there will be strong repulsion in the *s*-trans form between the hydrogen atoms on R_1 and R_3; ketones of structure V therefore exist exclusively in the *s*-cis form. This remains the preferred configuration even when alkyl groups are present at R_2 and R_4 (VI, VII), although, as noted above, there is some steric



V



VI



VII

strain between R_1 and R_2 in these structures. In VI and VII the conditions are favorable for non-planar forms, but the three ketones of these types included in these investigations show no abnormal displacements of the C=O and C=C frequencies. These would be expected if the molecules were significantly non-planar. It is notable that the infrared C=C stretching bands of ketones of structure VI and VII are very broad, their half band widths are 20.5, 36, and 17.5 cm^{-1} respectively in tetrachloroethylene solution, compared with normal values in the range 8.5–16.5 cm^{-1} for other types of open-chain α,β-unsaturated ketones;† the Raman spectra show similar behavior.‡ This band broadening is probably attributable to the destabilization of the planar structure, resulting in a shallow potential-energy well for rotation about the center C—C bond of the conjugated system. As a result, the torsionally excited energy levels will be more highly populated and these will be associated with decreased C=C stretching frequencies.

It is also to be noted that the ketones that exist predominantly or exclusively in the *s*-cis conformation readily undergo a partial isomerization to the β,γ-unsaturated ketones in the presence of iodine or other catalysts. Ketones with unhindered *s*-trans structures are much less reactive under these conditions and isomerize only to the (*s*-cis) cis α,β-unsaturated ketones without migration of the double bond.

**Equilibrium systems containing the s-cis isomer might be expected for the converse structure where* R_1 = H *and* R_2 = *alkyl, i.e. α-methylacrolein. The infrared spectrum of this aldehyde, measured on the pure liquid, shows no significant change on cooling from +30 to −65° (8); it has normal singlet* C=O *and* C=C *bands (2, 7) and is presumably entirely in the s-trans form.*

†See compounds 43–45 in the table in reference 2.

‡See compounds XV and XVI in Table I of reference 5. The half band widths are not reported in this paper but they are proportional to L/k.

Can. J. Chem. Downloaded from www.nrcresearchpress.com by 210.87.254.40 on 09/05/12
For personal use only.

REFERENCES

1. R. MECKE and K. NOACK. Spectrochim. Acta. **12**, 391 (1958).
2. R. MECKE and K. NOACK. Chem. Ber. **93**, 210 (1960).
3. R. L. ERSKINE and E. S. WAIGHT. J. Chem. Soc. 3425 (1960).
4. C. J. TIMMONS. Proceedings of the IVth International Meeting of the European Molecular Spectroscopy Group, Bologna, Italy. In press.
5. K. NOACK and R. N. JONES. Can. J. Chem. This issue. p. 2201.
6. R. N. JONES and K. NOACK. Can. J. Chem. This issue. p. 2214.
7. R. N. JONES, C. L. ANGELL, T. ITO, and R. J. D. SMITH. Can. J. Chem. **37**, 2007 (1959).
8. K. NOACK and R. N. JONES. Unpublished observation.
9. R. N. JONES. Spectrochim. Acta, **9**, 235 (1957).

Can. J. Chem. Downloaded from www.nrcresearchpress.com by 210.87.254.40 on 09/05/12
For personal use only.

Can. J. Chem. Downloaded from www.nrcresearchpress.com by 210.87.254.105 on 09/05/12
For personal use only.

POLAROGRAPHIC DETERMINATION OF THE DISSOCIATION CONSTANT OF THE SULPHYDRYL GROUP AND DIFFUSION COEFFICIENT MEASUREMENTS OF THIOMALIC ACID[1]

R. C. KAPOOR, O. P. AGRAWAL, AND T. D. SETH

ABSTRACT

Polarographic study of thiomalic acid has been made in the pH range 1–12.5 using Britton–Robinson buffer at 30°. The half-wave potential ($E_{\frac{1}{2}}$) values have been used to determine the pK_3 (SH) value of the acid (pK_3 = 10.55).

The diffusion current obtained in these experiments has been utilized to calculate the diffusion coefficients of the different charged species of thiomalic acid. The values thus obtained for the respective species are $H_3A = 1.20\times10^{-6}$ cm²/sec; $H_2A^- = 1.16\times10^{-5}$ cm²/sec; $HA^{--} = 1.08\times10^{-5}$ cm²/sec; and $A^{---} = 7.67\times10^{-6}$ cm²/sec.

The standard potential of the reaction

$$TSH + Hg = TSHg + H^+ + e^-$$

has been calculated as +0.266 volt vs. N.H.E.

Thiomalic acid or mercaptosuccinic acid has been recently used in a number of studies with metal complexes such as copper (1), zinc, cobalt, and nickel (2), and some other metals (3). Polarographic behavior of this compound has been systematically investigated (4, 5, 6) in these laboratories.

Cheney, Fernando, and Freiser (2) have reported the acid dissociation constants of thiomalic acid as calculated from potentiometric titration data.

Thiomalic acid has three replaceable hydrogen ions as indicated in the formula below.

$$\begin{array}{l} {}^{III}HSCHCOOH^{I} \\ \quad\quad\quad\quad | \\ \quad\quad\quad CH_2COOH^{II} \end{array}$$

If we represent the acid as H_3A the equilibria involved are

$$H_3A \rightleftharpoons H_2A^- + H^+, \quad [1]$$

$$H_2A^- \rightleftharpoons HA^{--} + H^+, \quad [2]$$

$$HA^{--} \rightleftharpoons A^{---} + H^+, \quad [3]$$

which correspond to the three dissociation constants K_1, K_2, and K_3. K_1 and K_2 correspond to the two carboxylic hydrogen atoms while K_3 corresponds to the hydrogen atom linked to the sulphur atom. The three values reported by Cheney *et al.* (2) at 25° are pK_1 = 3.30; pK_2 = 4.94; pK_3 (SH) = 10.64.

The authors have used polarographic data in calculating the pK_3 value of thiomalic acid. The different charged species of thiomalic acid have been shown to have different diffusion properties. The diffusion coefficient values of these species have also been calculated.

MATERIAL

Thiomalic acid was obtained as a gift from Evans Chemetics Incorporated, New York. The material was 99% pure and was used as such. Stock solutions were prepared in doubly distilled water, and only freshly prepared solutions were used. All other chemicals used were of AnalaR or chemically pure grade. The mercury used in the dropping mercury

[1]*Manuscript received June 19, 1961.*
Contribution from the Chemistry Department, University of Allahabad, Allahabad, Uttar Pradesh, India.

electrode was first purified chemically by treatment with nitric acid and subsequently distilled twice.

EXPERIMENTAL

Automatic polarograms were taken with a Leeds and Northrup Electro-Chemograph, Type E. Current–voltage curves in all cases were also taken manually with a circuit described by Lingane and Kolthoff (7).

Current–voltage curves were taken at 30°. All potentials were measured against the saturated calomel electrode (S.C.E.). An atmosphere of purified nitrogen was maintained throughout all investigations.

The characteristics of the capillary used are $m = 1.357$ mg/sec; $t = 3.37$ sec; $m^{2/3}/t^{1/6} = 1.501$ $mg^{2/3}sec^{-1/2}$.

The pH measurements were made with a Leeds and Northrup pH meter (Cat. 7666).

RESULTS AND DISCUSSION

Dissociation Constant of the Sulphydryl Group

Polarograms of 5×10^{-4} M thiomalic acid were taken at different pH values using Britton–Robinson buffer. Fig. 1 shows the current–voltage curves of 5×10^{-4} M thiomalic acid at different pH values.

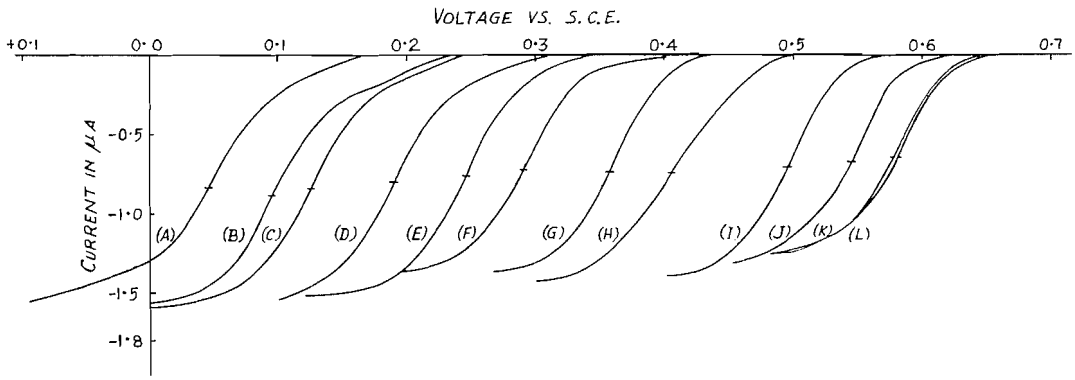


FIG. 1. Anodic waves of 5×10^{-4} M thiomalic acid in B-R buffer at different pH values. The pH and $E_{\frac{1}{2}}$ values are given respectively as (A) 1.15, −0.045 v; (B) 2.0, −0.095 v; (C) 2.5, 0.125 v; (D) 3.7, −0.190 v; (E) 4.6, −0.246 v; (F) 5.6, −0.291 v; (G) 6.6, -0.357_5 v; (H) 7.7, −0.405 v; (I) 9.0, −0.495 v; (J) 10.0, −0.545 v; (K) 11.35, -0.577_5 v; (L) 11.7, -0.582_5 v.

Thiomalic acid gives a prewave at low pH values up to 3.7. Such prewaves are often given by sulphur compounds such as glutathione, thioglycollic acid, and 2,3-dimercaptopropanol (8, p. 470). These prewaves have adsorption character and occur at more negative potential than the main anodic wave. The half-wave potentials of the main waves have been marked after separation of the prewaves. However, the total current is diffusion-controlled and corresponds to a one-electron change in all the polarograms.

The characteristics of the anodic wave of thiomalic acid have already been established (4, 5, 6). It has been shown that the anodic wave is not due to formation of a dimer but due to the formation of a mercury compound as indicated below:

$$TSH + Hg = TSHg + H^+ + e^-.$$

A plot of $E_{\frac{1}{2}}$ values against pH is given in Fig. 2. It can be easily seen that there are

Can. J. Chem. Downloaded from www.nrcresearchpress.com by 210.87.254.105 on 09/05/12
For personal use only.

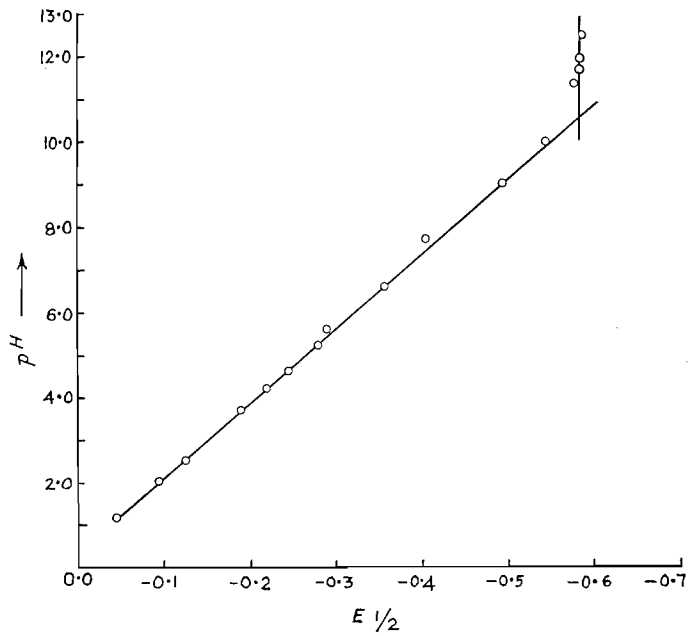


FIG. 2. Plot of $E_{\frac{1}{2}}$ and pH values.

two linear portions in the plot, whose intersection corresponds to the pH of 10.55. This indicates that under the conditions of the experiment the H^+ ion of the sulphydryl group has a pK of 10.55 (8, p. 472). This value agrees fairly well with that obtained by Cheney, Fernando, and Freiser (2) at 25°.

The change of $E_{\frac{1}{2}}$ per unit change of pH in the pH range 1–10 is 0.057 volt, which is sufficiently near the theoretical value of 0.060 volt at 30°.

The value of $E_{\frac{1}{2}}$, extrapolated to zero pH (hydrogen ion concentration = 1), is +0.02 volt, which corresponds to the standard potential of the reaction taking place at the electrode:

$$TSH + Hg = TSHg + H^+ + e^-.$$

The value thus calculated is +0.266 volt vs. N.H.E.

Diffusion Coefficients of Different Charged Species of Thiomalic Acid

Measurements of diffusion currents of thiomalic acid have been made in the pH range 1.15 to 12.50. Table I includes the values of the diffusion coefficient constants calculated according to the Ilkovič equation. The value of the diffusion current decreases on increasing the pH.

Thiomalic acid, as indicated earlier, exists in solution in four different species. The percentage of the different species can be calculated by the three pK values of this acid. The variation of the acid constants with temperature can be estimated from the apparent heats of ionization ($\Delta H'$) for the two carboxyl groups by applying the van't Hoff's equation and assuming that $\Delta H'$ is independent of temperature over the range of measurement.

The $\Delta H'$ for the two acid dissociation constants, K_1 and K_2, of succinic acid have been reported as +710 cal/mole and −340 cal/mole respectively (9). These same values of

Can. J. Chem. Downloaded from www.nrcresearchpress.com by 210.87.254.105 on 09/05/12
For personal use only.

TABLE I

pH	i_d (μa)	$D\times10^5$ (cm²/sec)	$E_{\frac{1}{2}}$ (v)
1.15	−1.48	1.20	−0.045
2.0	−1.38	1.20	−0.095
2.5	−1.50	1.23	−0.125
3.7	−1.43	1.13	−0.190
4.2	−1.545	1.15	−0.220
4.6	−1.55	1.16	−0.246
5.2	−1.505	1.09	−0.280
5.6	−1.45	1.01	−0.291
6.6	−1.455	1.03	-0.375_5
7.7	−1.50	1.08	−0.405
9.0	−1.43	0.980	−0.495
10.0	−1.365	0.894	−0.545
11.35	−1.30	0.810	-0.577_5
11.7	−1.285	0.795	-0.582_5
11.95	−1.29	0.801	-0.582_5
12.5	−1.26	0.767	-0.587_5

$\Delta H'$ were used for the two carboxyl groups of thiomalic acid to give calculated pK values at 30° of $pK_1 = 3.29$ and $pK_2 = 4.94$.

pK_3 as determined by our experiments from the $E_{\frac{1}{2}}$ values is 10.55 at 30°.

The percentage of different species of thiomalic acid can be calculated on the basis of the above pK values.

The concentration of different species have been calculated on such a basis that we see that at pH 1.15 practically all the acid exists in the form of uncharged H_3A species. At pH 7.7 almost all the acid is in the form of HA^{--}, while at pH 12.5 the only species present in the solution is the completely ionized form A^{---}.

Thus the diffusion currents at these three pH values can be used to calculate the diffusion coefficients of the above-mentioned three species. The diffusion coefficient of the remaining species, H_2A^-, can be calculated from the intermediate measurements in the pH range 3.70–5.60 using the already calculated D values of H_3A and HA^{--} species.

TABLE II
Diffusion coefficient values of different species of thiomalic acid at 30°

Species	$D\times10^5$ (cm²/sec)	pH
H_3A	1.20	1.15
HA^{--}	1.08	7.7
A^{---}	0.767	12.5
H_2A^-	1.16	4.2
H_2A^-	1.19	4.6
H_2A^-	1.14	5.2

The average value of the species H_2A has been taken as 1.16×10^{-5} cm²/sec.

REFERENCES

1. I. M. Klotz, G. H. Czerlinski, and H. A. Fiess. J. Am. Chem. Soc. **80**, 2920 (1958).
2. G. E. Cheney, Q. Fernando, and H. Freiser. J. Phys. Chem. **63**, 2055 (1959).
3. R. N. Sen Sarma. Science and Culture, **23**, 434 (1958).
4. R. C. Kapoor and S. K. Tiwari. Proc. Natl. Acad. Sci. (India), A, **28**, 52 (1959).
5. S. K. Tiwari and R. C. Kapoor. Proc. Natl. Acad. Sci. (India), A, **28**, 272 (1959).
6. S. K. Tiwari and R. C. Kapoor. Proc. Natl. Acad. Sci. (India), A, **28**, 278 (1959).
7. J. J. Lingane and I. M. Kolthoff. Chem. Revs. **24**, 1 (1939).
8. M. Brezina and P. Zuman. Polarography in medicine, biochemistry and pharmacy. Interscience Publishers, Inc., New York. 1958. p. 470.
9. E. J. Cohn and J. T. Edsall. Proteins, amino acids and peptides. Reinhold Publishing Corporation, New York. 1943. p. 82.

Can. J. Chem. Downloaded from www.nrcresearchpress.com by 210.87.254.105 on 09/05/12
For personal use only.

Can. J. Chem. Downloaded from www.nrcresearchpress.com by 210.87.254.6 on 09/05/12
For personal use only.

ASSOCIATION IN THE BINARY LIQUID SYSTEM DIMETHYL SULPHOXIDE – WATER[1]

J. M. G. Cowie and P. M. Toporowski

ABSTRACT

The viscosities and densities of several mixtures of dimethyl sulphoxide and water have been measured at 25°, 45°, and 65° C. Heats of mixing and refractive indices at 25° C are also reported. The results indicate there is strong association of the two liquids which may be attributed to hydrogen bonding.

INTRODUCTION

The widespread application of dimethyl sulphoxide (DMSO) as a solvent, plasticizer, and chemical intermediate has led to its large-scale production in recent years. In spite of the increased use of this compound its physical properties do not appear to have been studied extensively.

DMSO is a colorless, non-toxic liquid which boils at 189° C and freezes at 18.5° C. It is completely miscible with water and is strongly hygroscopic, but little has been reported about the behavior of DMSO–H_2O mixtures (1). During the course of a recent investigation on the solution properties of amylose dissolved in DMSO, it was found that water alters the viscosity of amylose–DMSO solutions in such a manner as to suggest a strong interaction between DMSO and H_2O.

Many binary liquid systems exhibit non-linear viscosity isotherms which pass through a minimum. However, a smaller group possess a maximum, indicating some form of liquid–liquid interaction, and the DMSO–H_2O system was found to belong to this latter class.

Viscosities and densities of 14 mixtures have been measured at 25°, 45°, and 65° C while refractive indices and heats of mixing have been determined at 25° C.

EXPERIMENTAL

Solvents

DMSO, supplied by Crown Zellerbach Corporation, was carefully dried by refluxing for 24 hours over CaO. It was left in contact with this drying agent for about 10 days with occasional shaking and then fractionally distilled under reduced pressure. The middle fraction, with boiling point approximately 68° C at 6–7 mm pressure, was collected and used in all physical measurements. The purity of this fraction was determined by analysis for water using two independent methods.

LeBel and Goring (1) have suggested a method using infrared spectroscopy in which the height of the OH absorption peak at 3500 cm^{-1} is measured and can be related to the water concentration in the sample. The method was calibrated using mixtures up to 0.5% water but no peak was detected in the distilled DMSO used in this investigation.

Analysis for water by the Karl Fischer (2) technique indicated that there was less than 0.01% water present in the DMSO.

Viscosity

The viscometer used was a Cannon-Ubbelohde model designed to have negligible

[1]*Manuscript received July 10, 1961.*
Contribution from the Division of Applied Chemistry, National Research Council, Ottawa, Canada.
Issued as N.R.C. No. 6510.

kinetic energy correction (3). Absolute viscosities, measured in centipoise, could be obtained from the flow time of the liquid, its density, and a calibration constant supplied by the manufacturer. The viscometer was reproducibly positioned in the thermostat baths by a three-point suspension system. Thermostat temperatures were maintained at 25°, 45°, and 65°±0.01° C.

Density

The liquid densities were determined at 25°, 45°, and 65° C using a Sprengel Ostwald pycnometer with a capacity of about 21 ml.

Refractive Index

Refractive indices were measured on an Abbé refractometer at 25° C using the sodium D line (λ = 5893 Å).

Calorimetry

The heats of mixing of several mixtures of water and DMSO were measured in a Dewar calorimeter similar to the one described by Vold (4). The liquids were kept separate in the calorimeter before being mixed by means of a hollow glass cylinder resting on a pool of mercury. Rapid mixing was obtained by raising the cylinder and stirring one liquid into the other. The final liquid volume was always about 150 ml, which kept the vapor space above the mixtures at a minimum. Recorded temperature rises varied from 7° to 25° C. The heat capacity of the calorimeter and its contents was determined after each measurement by passing a specific amount of electric current through the heater and measuring the temperature rise produced.

RESULTS

Table I lists the viscosities, densities, and refractive indices of several DMSO–H_2O mixtures. The results all show a positive deviation from ideality, which strongly suggests

TABLE I

Viscosity, density, and refractive index values for the system DMSO–H_2O

Mole fraction water	25° C			45° C		65° C	
	Viscosity (centipoise)	Density (g/ml)	Refractive index	Viscosity (centipoise)	Density (g/ml)	Viscosity (centipoise)	Density (g/ml)
0.000	2.003	1.0956	1.4765	1.394	1.0756	1.038	1.0556
0.047	2.054	1.0961	1.4754	1.423	1.0762	1.055	1.0564
0.089	2.118	1.0965	1.4741	1.457	1.0768	1.073	1.0570
0.186	2.298	1.0976	1.4710	1.553	1.0781	1.126	1.0582
0.335	2.708	1.0990	1.4648	1.758	1.0799	1.233	1.0604
0.522	3.449	1.0983	1.4525	2.083	1.0802	1.378	1.0612
0.590	3.676	1.0964	1.4460	2.164	1.0787	1.402	1.0603
0.651	3.764	1.0927	1.4385	2.172	1.0756	1.389	1.0574
0.702	3.674	1.0881	1.4308	2.102	1.0715	1.340	1.0538
0.743	3.467	1.0826	1.4232	1.985	1.0667	1.273	1.0495
0.812	2.854	1.0693	1.4075	1.672	1.0548	1.088	1.0391
0.867	2.232	1.0537	1.3911	1.346	1.0411	0.897	1.0268
0.910	1.748	1.0388	1.3757	1.086	1.0280	0.743	1.0150
0.945	1.382	1.0238	1.3607	0.880	1.0146	0.615	1.0032
0.975	1.110	1.0102	1.3461	0.724	1.0024	0.516	0.9920
1.000	0.898	0.9971	1.3330	0.599	0.9902	0.435	0.9806

that there is association of the liquids through hydrogen bonding. This is illustrated in Fig. 1, where the solution viscosity is plotted against the mole fraction of water. In the

Can. J. Chem. Downloaded from www.nrcresearchpress.com by 210.87.254.6 on 09/05/12
For personal use only.

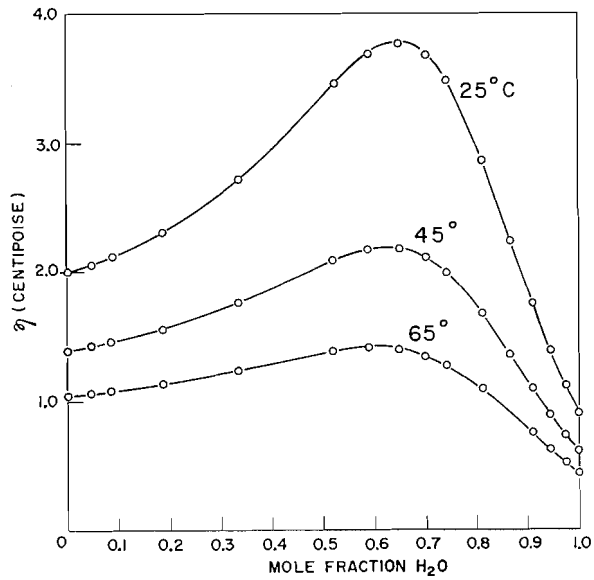


FIG. 1. The viscosities of DMSO–H_2O mixtures at 25°, 45°, and 65° C as a function of mole fraction of water.

region of 0.65 mole fraction of water, each isotherm exhibits a maximum which decreases with increase in temperature, and shifts slightly towards a lower water concentration. A maximum is also observed in the density measurements at 0.40 mole fraction of water which shifts towards higher water concentration with increase in temperature.

It has been suggested by Geddes (5) that such maxima have no real meaning and that it is the point of greatest deviation from linearity which is related to the composition of any complex formed on mixing. On this basis both viscosiy and density measurements have maximum deviations at a ratio of 2 moles water to 1 mole DMSO.

Heats of mixing are listed in Table II. These are negative over the whole range of compositions examined, which is again indicative of a strong interaction between the

TABLE II

Heats of mixing of DMSO and water

Mole fraction water	ΔH (calories per mole solution)	ΔH (calories per mole water)
0.183	−258	−1408
0.307	−412	−1338
0.436	−575	−1321
0.558	−604	−1083
0.675	−611	− 905
0.725	−600	− 828
0.792	−574	− 724
0.897	−348	− 388

two liquids. A graph of the heat of mixing expressed in calories/mole solution plotted against mole fraction water passes through a flat maximum at 0.63 mole fraction water and $\Delta H = -620$ calories.

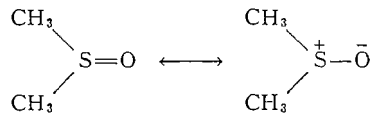
Can. J. Chem. Downloaded from www.nrcresearchpress.com by 210.87.254.6 on 09/05/12
For personal use only.

Can. J. Chem. Downloaded from www.nrcresearchpress.com by 210.87.254.6 on 09/05/12
For personal use only.

DISCUSSION

Aqueous solutions of non-electrolytes are the most difficult class of binary liquid systems to understand, and as a result no theory has been developed which can describe their thermodynamic properties adequately. An attempt has been made by Rowlinson (6) to classify these systems in terms of increasing numbers of solute–water hydrogen bonds, ranging from weakly interacting substances such as ketones to the strongly bonded hydrogen peroxide – water system.

The results obtained here indicate that there is a greater degree of association in water–DMSO mixtures than in water alone, which may be explained in terms of the polar sulphoxide group. The DMSO molecule can be represented (7) by the forms I and II,



I II

in which the negatively charged oxygen should form hydrogen bonds with the water molecules. This hypothesis is substantiated by the considerable volume contraction on mixing, the large negative heat of mixing, and the positive maxima in the viscosity isotherms.

Thus it is probable that a DMSO hydrate is formed, although it cannot be stated definitely from the above data that a stable compound exists at the temperatures investigated. The fact that the maximum in the viscosity isotherm decreases with increasing temperature suggests that any association complex formed is thermally labile and could only be expected to exist in a completely undissociated state at low temperatures. Further investigation would be necessary to establish its existence and composition.

CONCLUSIONS

The system DMSO–H_2O belongs to the class of solutions possessing numerous solute–water bonds which are stronger than the hydrogen bonds between water molecules. Evidence is presented for the existence of a 2:1 association complex between water and DMSO, but this cannot be proved on the basis of the data presented. Finally it should be stressed that DMSO must be carefully dried before being used as a solvent in physical measurements, especially viscosity determinations, if meaningful results are to be obtained.

ACKNOWLEDGMENTS

The authors wish to thank Dr. D. A. I. Goring for allowing them access to his manuscript prior to publication, Mr. R. Ironside for carrying out the water analyses, and Dr. S. Bywater for his interest in the work.

REFERENCES

1. R. G. LeBel and D. A. I. Goring. J. Chem. Eng. Data. In press.
2. J. Mitchell and D. M. Smith. Aquametry. Interscience Publishers Inc., 1948.
3. M. R. Cannon, R. E. Manning, and J. D. Bell. Anal. Chem. **32**, 355 (1960).
4. R. D. Vold. J. Am. Chem. Soc. **59**, 1515 (1937).
5. J. A. Geddes. J. Am. Chem. Soc. **55**, 4832 (1933).
6. J. S. Rowlinson. Hydrogen bonding. Proc. Conf. I.U.P.A.C. Ljubljana, Yugoslavia. 1957. p. 423.
7. W. A. Waters. Physical aspects of organic chemistry. Routledge and Kegan Paul Ltd., London. 1953.

Can. J. Chem. Downloaded from www.nrcresearchpress.com by 210.87.254.42 on 09/05/12
For personal use only.

THE DECOMPOSITION OF CARBON DIOXIDE BY Hg $6(^3P_1)$ AND Hg $6(^3P_0)$ ATOMS[1]

OTTO P. STRAUSZ AND HARRY E. GUNNING

ABSTRACT

Carbon dioxide has been shown to decompose into carbon monoxide and oxygen atoms, when exposed to radiation at 2537 Å, in the presence of mercury vapor. The rate rises steeply with decreasing substrate pressure, and varies directly with the 1.8 ± 0.1 power of the light intensity. The proposed mechanism attributes reaction to the collision of electronically excited CO_2 molecules with Hg $6(^3P_1)$ atoms. The suppression of reaction at higher substrate pressures is readily explained in terms of collisional deactivation of the excited CO_2 species. Nitrogen was found to increase the rate of CO formation; the maximum effect was obtained for a mixture of 7.4 mm nitrogen and 3.74 mm carbon dioxide, in which case the rate was 1.58 times that for pure substrate. It is shown that nitrogen serves to generate metastable Hg $6(^3P_0)$ atoms, which can sensitize the decomposition. The reaction might serve as a chemical method for monitoring Hg $6(^3P_0)$ atoms. For CO_2–N_2 mixtures, the rate was found to rise when the reacting system was exposed to radiation at 4047 Å. This is taken as direct evidence of sensitization by higher states of mercury, generated by stepwise excitation, since radiation at 4047 Å converts Hg $6(^3P_0)$ to Hg $7(^3S_1)$.

INTRODUCTION

Several studies (1–4) have been made of the photolysis of carbon dioxide in the vacuum ultraviolet. With a xenon source, Groth (2) found the quantum yield of CO formation, Φ_{CO}, to be 0.96, and he suggested that atomic oxygen is formed in the primary process. However, Jucker and Rideal (3), for the 1470-Å line of xenon, obtained 1.9 ± 0.2 for Φ_{CO}. They proposed a mechanism involving the initial formation of an excited molecule which, upon collision with the substrate, formed $2CO + O_2$. Recently Mahan (4) has studied the photolysis, at both 1236 Å and 1470 Å. In agreement with Groth (2), he found Φ_{CO} to have values near unity at both wavelengths and he presented convincing arguments for a primary process leading to the formation of excited (^1D) oxygen atoms.

The first mercury-photosensitized decomposition of carbon dioxide was carried out by Herschfinkel (5), although the role of mercury was not recognized until later by Coehn and May (6). In a more detailed study, Cline and Forbes (7) showed that the decomposition was specifically initiated by Hg $6(^1P_1)$ atoms, arising by absorption by mercury of its resonance radiation at 1849 Å; they found no evidence for a reaction of carbon dioxide with Hg $6(^3P_1)$ atoms.

The present study arose from the observation that carbon dioxide, in the presence of mercury vapor, undergoes a slow decomposition when exposed to 2537-Å radiation, contrary to previous findings (7). The dissociation of CO_2 into $CO + O$ requires at least 126.7 kcal/mole, whereas only 112.2 kcal/mole are available from a simple collision of the second kind with Hg $6(^3P_1)$ atoms. The additional energy needed for the reaction to proceed could be supplied either from the primary formation of HgO, or from reactions involving energy accumulation, such as the formation of excited carbon dioxide molecules. In the present study, emphasis has been placed on the nature of the primary reactions involved in the decomposition. The investigation forms part of a general program on primary processes in mercury photosensitization.

[1]*Manuscript received July 5, 1961.*
Contribution from the Department of Chemistry, University of Alberta, Edmonton, Alberta.

Can. J. Chem. Downloaded from www.nrcresearchpress.com by 210.87.254.42 on 09/05/12
For personal use only.

EXPERIMENTAL

The reaction was studied under static conditions. For the reaction cell, a cylindrical tube of Vycor 7900 glass was used, 120 mm in length and 26 mm in diameter, with flat windows of Vycor 7910 glass at each end. The side arm connecting the cell to the high-vacuum system was placed near one window, in order that the cell could be inserted axially into the coils of a spiral Hanovia SC-2537 mercury resonance source. The lamp-cell assembly was positioned in a water thermostat, maintained at 30°, in such a fashion that the end windows were opposite ports of window glass in the sides of the thermostat. Thus, in addition to the radiation from the spiral lamp, the cell could be independently irradiated at both ends by sources external to the thermostat. For these external sources, Hanovia Biosteritron resonance lamps were employed.

After each exposure, gases non-condensable in liquid nitrogen were transferred to a gas burette, and subsequently analyzed by gas–liquid partition chromatography (G.L.P.C.). Between experiments the cell was cleaned in hot nitric acid, rinsed with distilled water and ethanol, and dried at 200°. A reaction was also performed by using a ^{202}Hg electrodeless discharge source. A Vycor 7910 glass cell attached to a small mercury pump and to a 1-liter bulb was filled with CO_2, sealed off, and irradiated with the above lamp. After the reaction was completed the cell containing the HgO was pumped for 12 hours. Then the HgO was dissolved in very dilute HCl, plated out on copper wire, distilled, and collected *in vacuo* into a small break-seal. Finally the isotopic composition of the recovered mercury was determined by mass spectrometry.

The carbon dioxide used was Matheson 'Bone-Dry' grade, with stated purity of 99.8%. It was subjected, before use, to several low-temperature distillations, after which no impurities could be detected by G.L.P.C. The nitrogen (Canadian Liquid Air 'Purified Grade', with minimum purity of 99.9%) was passed through a quartz furnace containing copper filings at 500°, and several liquid nitrogen traps, before use.

RESULTS

The products of the reaction were carbon monoxide and mercuric oxide. Molecular oxygen was not detected in any of the runs. In Fig. 1, the micromoles of CO formed, as a function of CO_2 pressure, are given for runs of 150 minutes in duration. The percentage conversion at the lowest pressure, 0.6 mm, was 28.7%. At 13.3 mm, only 0.5% of the CO_2 was decomposed.

The absorbed light intensity at 2537 Å, as determined with propane as actinometer (8), was 3.34×10^{-5} einstein/minute. The maximum rate of CO formation occurred at a CO_2 pressure of 0.6 mm; 2.87 μmoles of CO were formed in 150 minutes of exposure. This rate would correspond to a quantum yield of 5.7×10^{-4} moles/einstein. Of course, at a pressure of 0.6 mm, only a small fraction of the excited mercury atoms are quenched. It is estimated that the actual quantum yield of CO formation under these conditions is at least 0.01.

The addition of nitrogen was found to influence markedly the rate of CO formation. The effect is shown in Table I. The runs with and without added nitrogen were carried out under identical conditions. The highest rate increase observed was 58%, in the case of a mixture of 3.74 mm CO_2 and 7.4 mm N_2.

The fact that the rate of CO formation rapidly decreases with increasing substrate pressure, as shown in Fig. 1, would suggest that excited CO_2 molecules are involved in

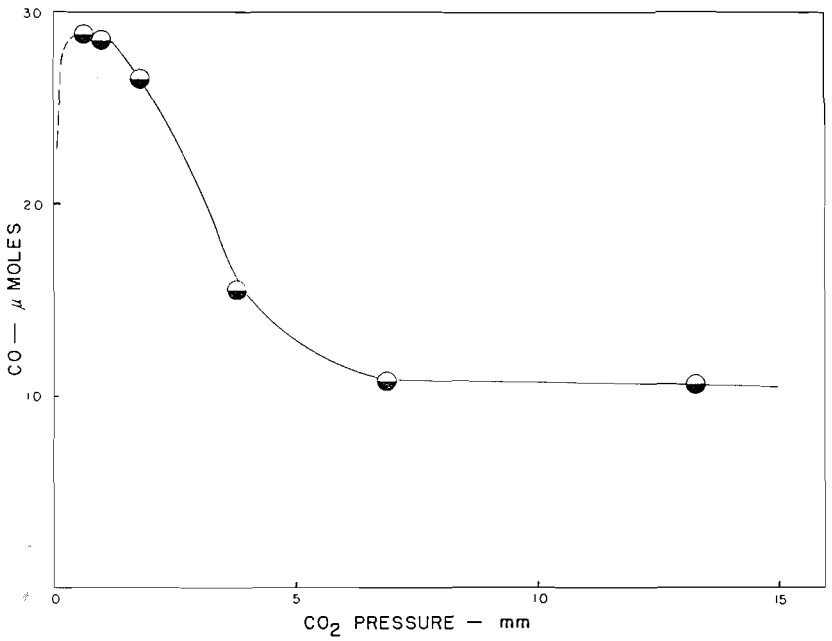


FIG. 1. Micromoles of CO formed for runs of 150 minutes in duration, as a function of substrate pressure.

TABLE I

The effect of nitrogen on the rate of CO formation in the reaction of CO_2 with Hg $6(^3P)$ atoms

P_{CO_2} (mm)	P_{N_2} (mm)	CO formed (μmoles)	Increase in R_{CO} (%)
3.22	—	3.32	41
3.13	6.2	4.69	
3.22	—	7.08	39
3.30	6.2	9.85	
1.02	—	3.30	
1.02	6.5	3.74	13
9.91	—	1.16	
8.24	—	1.11	av. 36
8.88	11.2	1.54	
3.57	—	1.80	58
3.74	7.4	2.85	

the reaction, and that these are suffering progressive collisional deactivation with increasing CO_2 pressure. From Table I, which exhibits the marked effect of nitrogen on the rate of CO formation, the participation of metastable Hg $6(^3P_0)$ atoms is suggested. If the CO product is formed by collisions between excited CO_2 molecules and Hg $6(^3P_1)$ atoms and/or Hg $6(^3P_0)$ atoms, one would expect the rate to depend upon the square of the absorbed light intensity. An alternative or additional process which could be operative is that of stepwise excitation. Mercury resonance lamps are good sources of the 4047-Å line, which is absorbed by Hg $6(^3P_0)$ atoms to form the $7(^3S_1)$ state. Direct collisional deactivation of $7(^3S_1)$ atoms to the ground, $6(^1S_0)$, state would release 7.95 ev, or ca. 183 kcal/mole. For the afore-mentioned reasons, it appeared particularly instructive to

Can. J. Chem. Downloaded from www.nrcresearchpress.com by 210.87.254.42 on 09/05/12
For personal use only.

examine the effect of light intensity and 4047-Å radiation on the rate of CO formation.

The dependence of the rate upon light intensity was determined by the use of two bromine filters of different transmission characteristics. Both filters were doughnut types, 110 mm in length, 35 mm I.D., and 60 mm O.D. They were designed to fit axially over the reaction cell and within the coils of the spiral resonance lamp. Both filters were filled with bromine vapor at 170 mm. Their transmission characteristics were determined both spectrophotometrically and by propane actinometry (8). Filter I was made of Vycor 7910 and filter II of Vycor 7900. Their characteristics were as follows: filter I, transmitted 55.7% at 2537 Å, and less than 1% at 4047 Å; filter II, transmitted 17.5% at 2537 Å, and less than 1% at 4047 Å.

In Table II the results are given for six experiments performed with decreased light

TABLE II

The relation between μmoles of CO formed and incident intensity at 2537 Å, for runs of 150 minutes in duration

Filter	P_{CO_2} (mm)	P_{N_2} (mm)	CO formed (μmoles)	Exponent of light intensity
I	1.7	—	0.66	2.1
None	1.6	—	2.33	
I	3.5	6.3	1.12	1.7
None	3.4	6.2	2.96	
I	1.7	—	0.82	2.0
None	1.7	—	2.67	
I	7.4	—	0.40	1.7
None	7.4	—	1.07	
I	7.0	—	0.40	1.7
None	7.0	—	1.07	
II	1.5	—	0.17	1.6
None	1.5	—	2.75	
				Mean = 1.8±0.1

intensities, achieved by inserting the filters as indicated. In each case, the results are compared with those without filter. In the last column is given the order of dependence of the rate on the intensity of the 2537-Å radiation. The mean value of the exponent is 1.8±0.1. It should also be noted from Table II that the near second-order dependence of the rate upon the light intensity also obtains in the presence of added nitrogen.

The effect of 4047-Å radiation on the reaction was studied by placing Biosteritron sources at the ports of the thermostat. By this means the cell could be exposed at both ends to the radiation transmitted through the window glass in the thermostat ports. Only radiation exceeding ca. 3800 Å in wavelength could thereby enter the cell.

In Table III is shown the effect, on the rate of CO formation, of dosing the reaction cell at each end with 4047-Å radiation, while the normal reaction is in progress. It can be seen that the 4047-Å radiation increases the rate by ca. 22% for the optimum CO_2–N_2 mixture, for an incident intensity at 2537 Å of 3.3×10^{-5} einstein/minute. The effect appears to be much larger at lower intensities of the resonance radiation, as shown in the last run listed in the table, where a 53% increase in rate is achieved.

In order to confirm that the reaction was indeed mercury sensitized, one experiment was performed at 5°. Under these conditions there was a drastic decrease in reaction rate, indicating the dependence of the reaction on the presence of mercury vapor.

Can. J. Chem. Downloaded from www.nrcresearchpress.com by 210.87.254.42 on 09/05/12
For personal use only.

TABLE III

The effect of 4047-Å radiation on the rate of CO formation in the reaction of CO_2 with Hg $6(^3P)$ atoms

4047 Lamps*	Filter	P_{CO_2} (mm)	P_{N_2} (mm)	CO formed† (μmoles)	Fractional increase
On	—	2.7	7.2	3.94	1.22
Off	—	2.9	6.9	3.22	
On	—	3.3	5.5	3.17	1.09
Off	—	3.3	5.5	2.90	
On	—	1.5	—	2.96	1.06
Off	—	1.5	—	2.80	
On	I	3.1	6.3	2.20	1.53
Off	I	3.1	6.2	1.44	

*It is estimated that the two Biosteritron sources increased the intensity at 4047 Å by a factor of 10.
†For runs of 150 minutes in duration.

Finally, one 30-hour run was made with $P_{CO_2} = 1.82$ mm, using a ^{202}Hg electrodeless discharge source. Mass spectrometric analysis showed that the ^{202}Hg content of the HgO product was 31.6%, compared to the normal abundance of 29.8%.

DISCUSSION

From Fig. 1, it is apparent that the reaction of carbon dioxide with Hg $6(^3P)$ atoms is a remarkable example of collisional deactivation. In the pressure region studied, i.e. 0–15 mm, the rate of CO formation, R_{CO}, falls off rapidly with increasing substrate pressure, despite the fact that the fraction of the incident light energy transferred to the substrate by quenching is simultaneously rising. Combining the foregoing with the near-second-order dependence of R_{CO} on light intensity, as shown in Table II, would suggest strongly a mechanism involving the reaction of excited CO_2 molecules with Hg $6(^3P)$ atoms:

$$Hg + h\nu \rightarrow Hg^* \quad [1]$$

$$Hg^* \rightarrow Hg + h\nu \quad [2]$$

$$Hg^* + CO_2 \rightarrow CO_2^* + Hg \quad [3]$$

$$CO_2^* + CO_2 \rightarrow 2CO_2 \quad [4]$$

$$CO_2^* + Hg^* \rightarrow CO + Hg + O, \quad [5]$$

where $Hg^* = Hg\ 6(^3P_1)$ and CO_2^* represents an energy-rich CO_2 molecule. It is assumed that the CO_2^* which reacts in [5] possesses at least (126.7−112.2) kcal/mole of excess energy.

Since the quantum yield, Φ_{CO}, is very small for the reaction, i.e. less than 0.01, we may reasonably assume that step [5] does not appreciably alter the steady-state concentrations of Hg^*. With this approximation we obtain the following expression for the rate of CO formation:

$$R_{CO} = K\frac{(CO_2)}{A+B(CO_2)+C(CO_2)^2+D(CO_2)^3}, \quad [a]$$

where $K = K_3K_5I_a^2$, $A = K_2K_5I_a$, $B = K_2^2K_4 + K_3K_5I_a$, $C = 2K_2K_3K_4$, $D = K_3^2K_4$, and I_a is the absorbed light intensity at 2537 Å. The mechanism therefore predicts that R_{CO} will (*a*) decrease rapidly with increasing substrate pressure and (*b*) vary nearly

Can. J. Chem. Downloaded from www.nrcresearchpress.com by 210.87.254.42 on 09/05/12
For personal use only.

directly with I_a^2, in qualitative accordance with our findings. Alternately step [5] may be replaced by

$$CO_2^* + CO_2^* \rightarrow CO_2 + CO + O. \qquad [5']$$

An approximate solution of the steady-state equations with [5'] replacing [5] yields an expression similar to [*a*]. Thus both steps [5] and [5'] are qualitatively consistent with the observed kinetics for pure carbon dioxide. In this connection, it should be noted that the absence of molecular oxygen precludes the possibility of O_2 formation in [5'].

At low substrate pressure other processes such as radiative transition and(or) deactivation at the wall may also occur.

The low isotopic enrichment of the HgO formed in the reaction gives additional evidence that the process

$$CO_2 + Hg^* \rightarrow CO + HgO$$

does not occur to an appreciable extent.

The electronic state of the excited carbon dioxide is probably a metastable triplet. Indeed the first known electronic state above the ground state is triplet π, with an excitation energy estimated not to exceed 130 kcal/mole (9, 10). Now for reaction [5] to be energetically possible, CO_2^* must possess 14.5 kcal/mole of excess energy. It is pertinent here to note that Walsh (11, 12) has assigned to CO_2 a $^3B_2$ state at 30–40 kcal/mole above the ground state. For this state to participate in the present reaction, CO would have to be formed by [5] rather than [5'].

The effect of added nitrogen on R_{CO} can readily be explained by the production of metastable Hg $6(^3P_0)$ atoms (Hg^0) and by their subsequent reactions with CO_2:

$$CO_2 + Hg^0 \rightarrow CO_2^* + Hg \qquad [6]$$

$$CO_2^* + Hg^0 \rightarrow CO + Hg + O. \qquad [7]$$

Klumb and Pringsheim (13, 14) have shown that the concentration of Hg^0, in the presence of nitrogen, may be expressed by the relation

$$(Hg^0) = AP/[1+BP+CP^2],$$

where A, B, and C are constants, and P is the nitrogen pressure. The maximum value of (Hg^0) was reported to occur at a nitrogen pressure of 6 mm. We observed a maximum 1.58-fold increase in R_{CO} (Table I) when 7.4 mm N_2 was added to 3.74 mm CO_2, which would correspond to a 2.4-fold increase if we compare it to R_{CO} at a CO_2 pressure equal to the total pressure of CO_2 and N_2 (approx. 11 mm).

Owing to the higher lifetime for the metastable state, the concentration of Hg $6(^3P_0)$ atoms should be about 1 or 2 orders of magnitude higher than the concentration of Hg $6(^3P_1)$ atoms. We may therefore infer that the metastable species show much lower reactivity in the present system than do Hg $6(^3P_1)$ atoms.

In Table III, evidence is presented for a positive contribution of 4047-Å radiation to the rate of decomposition of CO_2–N_2 mixtures. The results with filter I in position are especially interesting. Here the 4047-Å radiation from the spiral source has been reduced to ca. 1% of its original value by the filter. When 4047-Å radiation is then introduced at the ends of the cell, the value of R_{CO} increases by 53%. It would appear unwise at this time to attempt to write a mechanism for this effect. We may note that quenching by CO_2 of Hg $7(^3S_1)$ atoms could result in the mercury being converted to any of the three triplet states, or to the ground state. Certainly the phenomenon merits more detailed study.

Can. J. Chem. Downloaded from www.nrcresearchpress.com by 210.87.254.42 on 09/05/12
For personal use only.

CONCLUSIONS

As a result of the present investigation, it may be concluded that carbon dioxide undergoes a slow decomposition when sensitized by either Hg $6(^3P_1)$ or Hg $6(^3P_0)$ atoms. The observed kinetics dictate the participation in the reaction of excited CO_2 molecules, presumably in metastable triplet states. Apart from its inherent interest as an example of a mercury-photosensitized reaction which is second order in the light intensity, the system might serve as a chemical method for monitoring Hg $6(^3P_0)$ atoms. Finally, the present study has provided evidence of reaction associated with higher states of mercury which have been generated *in situ* by stepwise excitation.

ACKNOWLEDGMENTS

The authors are indebted to Dr. Willard F. Allen, Dr. Paul Kebarle, Dr. Roger Klemm, and Mr. Thomas Dingle, all of this laboratory, for many helpful discussions. This investigation has been partially supported by the National Research Council under N.R.C. Grant No. B.T. 74. This assistance is most gratefully acknowledged.

REFERENCES

1. D. L. CHAPMAN, S. CHADWICK, and J. E. RAMSBOTTOM. J. Chem. Soc. **91**, 951 (1907).
2. W. GROTH. Z. phys. Chem. (Leipzig), B, **38**, 366 (1938).
3. H. JUCKER and E. K. RIDEAL. J. Chem. Soc. 1058 (1957).
4. B. H. MAHAN. J. Chem. Phys. **33**, 959 (1960).
5. H. HERSCHFINKEL. Compt. rend. **149**, 395 (1909).
6. A. COEHN and B. W. MAY. Z. phys. Chem. (Leipzig), B, **26**, 117 (1934).
7. J. E. CLINE and G. S. FORBES. J. Am. Chem. Soc. **61**, 716 (1939).
8. S. BYWATER and E. W. R. STEACIE. J. Chem. Phys. **19**, 319 (1951).
9. K. J. LAIDLER. J. Chem. Phys. **17**, 221 (1949).
10. K. J. LAIDLER. The chemical kinetics of excited states. Clarendon Press, Oxford. 1955.
11. A. D. WALSH. J. Chem. Soc. 2266 (1953).
12. A. G. GAYDON. The spectroscopy of flames. Chapman & Hall, London. 1957.
13. H. KLUMB and P. PRINGSHEIM. Z. Physik, **52**, 610 (1928).
14. J. A. BERBERET and K. C. CLARK. Phys. Rev. **100**, 506 (1955).

Can. J. Chem. Downloaded from www.nrcresearchpress.com by 210.87.254.42 on 09/05/12
For personal use only.

Can. J. Chem. Downloaded from www.nrcresearchpress.com by 210.87.254.6 on 09/05/12
For personal use only.

PRIMARY QUANTUM YIELD DETERMINATION BY INTERMITTENT ILLUMINATION IN THE REACTION OF METHANOL VAPOR WITH Hg 6($^3P_1$) ATOMS[1]

ARTHUR R. KNIGHT AND HARRY E. GUNNING

ABSTRACT

The decomposition of methanol vapor by Hg 6($^3P_1$) atoms has been studied under intermittent illumination conditions, in a static system at 25° C. The behavior of the NO-inhibited reaction under intermittent illumination has also been examined.

For the pure substrate at a pressure of 50 mm, the quantum yield of hydrogen formation, $\Phi(H_2)$, was found to rise steadily toward unity with decreasing light period (t_L). The maximum value of $\Phi(H_2)$ at a given t_L could only be obtained if the dark period (t_D) exceeded 100 mseconds. At the shortest t_L studied, 0.156 msecond, $\Phi(H_2)$ was 0.89 compared with the steady illumination value, at zero extent of reaction, of 0.46. A linear relation was found to obtain between $\Phi(H_2)$ and log (t_L) at a given t_D. Extrapolation showed that $\Phi(H_2)$ would be unity at t_L = 0.040 msecond.

For a mixture of 4.8 mm of NO and 50 mm of CH_3OH, $\Phi(CH_3ONO)$ was found to rise from its steady illumination value of 0.14 to 0.27 at a sector speed of 300 r.p.m., with a dark/light ratio of 20. At higher speeds the quantum yield decreased again.

From the study it is concluded that the primary process of H atom detachment is at least 89% efficient, and that the primary quantum yield is likely unity. The fact that the quantum yield under steady illumination is only 0.46 is attributed to the consumption of H atoms by radical addition processes of which the most probable is the addition of H to CH_2OH. For the inhibited reaction the low value of $\Phi(CH_3ONO)$ under steady illumination is ascribed to the abstractive attack of CH_3O on NOH.

The kinetic effects of intermittent illumination are discussed, in the light of the results. It is concluded that the technique should be of considerable value in primary process studies in mercury photosensitization.

INTRODUCTION

In a previous study (1) of the reaction of methanol vapor with Hg 6($^3P_1$) atoms, it was shown that the quantum yield of hydrogen formation, extrapolated to zero exposure duration, $\Phi(H_2)$, was 0.46. The fact that this value is not unity could be due to the reactions:

$$H + H \xrightarrow{M} H_2, \qquad [1]$$

$$H + CH_2OH \rightarrow CH_3OH, \qquad [2]$$

$$H + CH_3O \rightarrow CH_3OH. \qquad [3]$$

Since, at the substrate pressure used (50 mm) in the previous study (1), CH_3O was shown to react almost exclusively with the substrate to form CH_2OH, it is likely that [2] is the most important of the above three steps competing for H atoms with the abstraction reaction:

$$H + CH_3OH \rightarrow H_2 + CH_2OH. \qquad [4]$$

For the reaction inhibited by NO, the steps

$$CH_3O + NOH \rightarrow CH_3OH + NO \qquad [5]$$

and

$$CH_3O + CH_3ONO \rightarrow CH_3OH + CH_2O + NO \qquad [6]$$

have been suggested (1) to explain the fact that $\Phi°(CH_3ONO)$ was found to be less than unity. The rates for reactions [1]–[3] will be proportional to the products of the con-

[1]*Manuscript received July 21, 1961.*
Contribution from the Department of Chemistry, University of Alberta, Edmonton, Alberta.

centrations of the radicals involved. Similarly, for the inhibited reaction, (NOH) will vary with (H), and therefore the rate of step [5] will also depend upon a product of radical concentrations.

Under intermittent illumination, with progressive shortening of the light period (t_L), it should be possible to interrupt the light beam before the radical concentrations have reached their steady-state values. In this region, $\Phi(H_2)$ should rise sharply with decreasing t_L, provided that the radical concentrations are allowed to decay to zero during the dark period (t_D). Hence it is also necessary to study the effect of t_D on $\Phi(H_2)$. With decreasing t_L, $\Phi(H_2)$ should approach unity, if (*a*) the primary reaction between Hg $6(^3P_1)$ and CH_3OH shows perfect efficiency for detachment of H atoms, and (*b*) steps [1]–[3] include the processes responsible for the disappearance of H atoms without concomitant H_2 formation.

In the present communication are reported the results of varying t_L and t_D, on $\Phi(H_2)$ for the decomposition of pure CH_3OH, and on $\Phi(CH_3ONO)$ for the reaction in the presence of NO.

EXPERIMENTAL

The purification and storage of the methanol, the all-quartz high-vacuum system employed, and the analytical techniques have been previously described (1). After the reaction cell had been filled, it was placed in one of the two devices detailed below.

For the runs with pure substrate with t_D = 103 and 67 milliseconds (msec), and for the studies on the inhibited reaction, the sector apparatus consisted of a Hanovia, 87A45, mercury-in-quartz resonance tube, in a cylindrical housing, with a 5-cm diameter window covered with a Vycor 7910 filter. A rotating metal disk with an adjustable sector aperture was interposed between the light source and a shield with a 5-cm diameter opening, directly behind which the cell was placed. The disk was mounted on the shaft of a variable speed motor, of which the speed of rotation could be controlled to $\pm 4\%$. The r.p.m. of the sector was checked during each run by a stroboscope. The disk consisted of two metal plates from which two 90° sectors had been cut. The sector angle was determined by closing the plates on a steel rod of accurately known diameter, placed at a known distance from the center. One of the two resulting apertures was closed for all runs except those at long t_L.

For the runs with t_D = 80 and 160 msec, the lamp (Engelhard 11639) was placed in a rectangular housing with a 6-cm^2 opening covered by a Vycor 7910 filter. The light beam was chopped by two overlapping disks mounted between two $\frac{3}{8}$-in. plates, connected by a gear chain, and driven by a constant speed motor. One disk, rotating at 3000 r.p.m., had one sector aperture set accurately as described above. The other sector disk revolved at 375 r.p.m. and had two approximately 30° apertures. The beam was partially collimated by a 6-cm diameter opening, placed between the disks and the cell. The cell was located behind the shield already described. The rotations of the disks were so synchronized that the more slowly rotating sector uncovered the entire cell face as the high speed disk made each exposure. With both 30° sector apertures operative, t_D was 80 msec; by blocking one of the apertures, t_D = 160 msec was obtained.

Light intensities were determined with propane as actinometer (2), using the differential method of Back (3) for obtaining the steady-state value for dH_2/dt.

At the end of each run, the products non-condensable in liquid nitrogen were analyzed by G.L.P.C. on a molecular sieves column. The hydrogen content of this gas was never less than 96 mole%, with the remainder consisting of CO and CH_4. For the runs with

Can. J. Chem. Downloaded from www.nrcresearchpress.com by 210.87.254.6 on 09/05/12
For personal use only.

$t_L < 0.5$ msec, the $(CO+CH_4)$ content was less than 0.5 mole%. The analysis for methyl nitrite has been previously described (1).

RESULTS

During the course of the investigation various minor modifications were made in the sector system which resulted in changes in the absorbed light intensity at 2537 Å. For the range of values of the sector parameters reported here, it was found that $\Phi(H_2)$ was independent of exposure duration at least to a total quantum input of 5 microeinsteins. In Fig. 1, $\Phi(H_2)$ is shown as a function of log (t_L) for four series of runs at dark periods of 67, 80, 103, and 160 mseconds. In all cases, the cell was filled with pure CH_3OH at a pressure of 50 mm. For the runs with $t_D = 67$ and 103 mseconds, the single sector was used, with absorbed light intensities of both 0.91 and 1.06 microeinsteins/minute, and net exposure durations of 4.3–5.0 minutes. The series with $t_D = 80$ and 160 msec were performed with the double sector apparatus. Here, absorbed light intensities of 1.25, 2.19, and 3.25 microeinsteins/minute were used, and net exposure durations of 0.43–1.0 minutes.

From the plot of $\Phi(H_2)$ vs. log (t_L) in Fig. 1, it is apparent that $\Phi(H_2)$ rises steadily

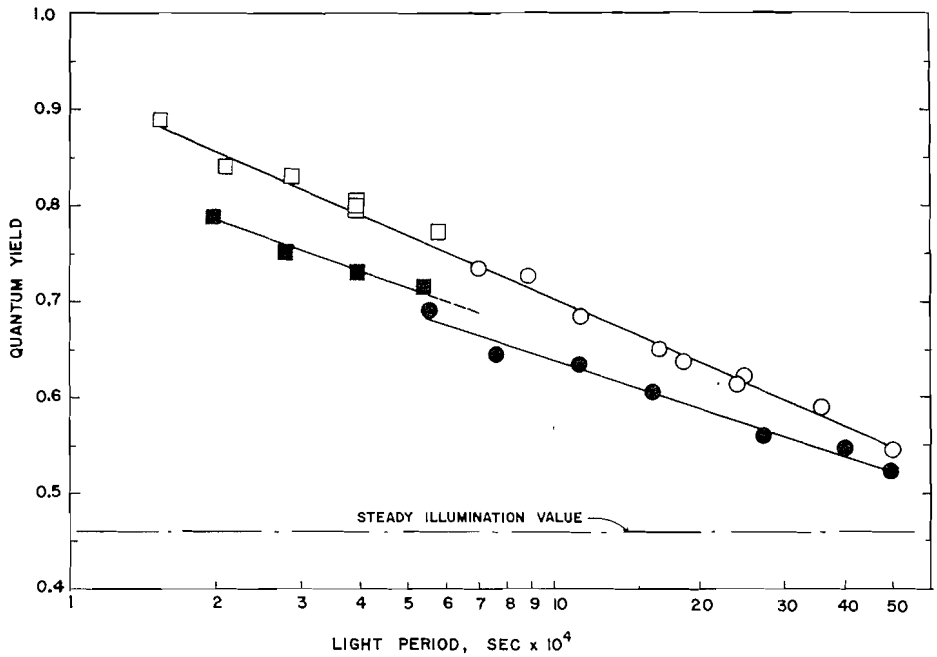


FIG. 1. The quantum yield of hydrogen formation at a methanol pressure of 50 mm, as a function of the logarithm of the light period for dark periods of □ 160, ■ 80, ○ 103, and ● 67 milliseconds.

above its steady illumination value of 0.46 with decreasing t_L, at least for t_L values less than 5 mseconds. Furthermore, from Fig. 1, the effect of t_D on $\Phi(H_2)$ is to be noted. For maximum values of $\Phi(H_2)$ at a given t_L, it is necessary that t_D be at least ca. 100 mseconds. In these runs the maximum value obtained for $\Phi(H_2)$ was 0.89, with $t_L = 0.156$ msecond and $t_D = 160$ mseconds. The absorbed light intensity was 1.25 microeinsteins/minute, and the net exposure duration was 1.00 minute. The t_L value of 0.156 msecond was the

Can. J. Chem. Downloaded from www.nrcresearchpress.com by 210.87.254.6 on 09/05/12
For personal use only.

shortest light pulse which could be obtained with the sector equipment used. Since $\Phi(H_2)$ seems to be a linear function of log (t_L), the upper curve in Fig. 1 was linearly extrapolated to $\Phi = 1.00$. The corresponding t_L value was 0.040 msecond.

For the inhibited reaction, a short series of runs was performed with a constant t_D/t_L ratio of 20, in which t_L was varied from 6.50 to 2.79 mseconds. The reaction mixture consisted of 4.8 mm of NO and 50 mm of CH_3OH. The net exposure duration was 4.75 minutes. In Fig. 2, $\Phi(CH_3ONO)$ is shown as a function of the r.p.m. of the sector. The

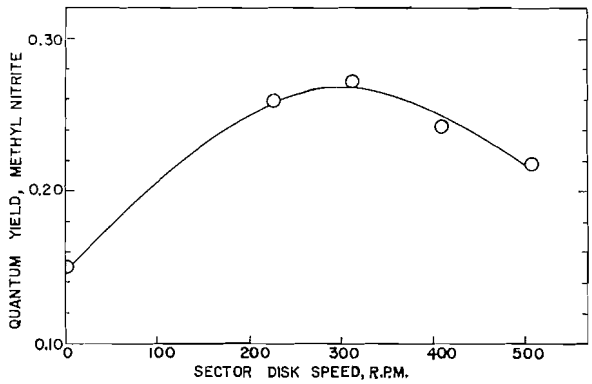


FIG. 2. The quantum yield of methyl nitrite formation for a mixture of 4.8 mm of nitric oxide and 50 mm of methanol, for a net exposure duration of 4.75 minutes, as a function of sector disk speed for a constant dark/light ratio of 20.

maximum value obtained for $\Phi(CH_3ONO)$ was 0.272, with $t_L = 4.61$ mseconds. The steady illumination value for $\Phi(CH_3ONO)$ was 0.140.

DISCUSSION

For the decomposition of pure CH_3OH, the present study has shown that the primary process is of considerably higher efficiency than would be indicated by the $\Phi^\circ(H_2)$ value of 0.46. Since the highest value obtained for $\Phi(H_2)$ was 0.89, the primary process must have an efficiency of at least 89%. Furthermore, assuming the validity of a short linear extrapolation of the upper $\Phi(H_2)$ vs. log (t_L) line in Fig. 1, we may conclude that $\Phi(H_2)$ would be unity for a t_L of 0.040 msecond.

The observed increase toward unity of $\Phi(H_2)$ with decreasing t_L supports the hypothesis that radical addition reactions involving H atoms, such as steps [1]–[3], are responsible for the fact that $\Phi^\circ(H_2)$, under steady illumination, is considerably less than unity.

One surprising result of this study was the relatively long dark period required to achieve the maximum value of $\Phi(H_2)$ at a constant t_L. The data, however, clearly indicate that there must be at least 100 mseconds between light pulses for optimum $\Phi(H_2)$ values to be obtained. If the 100-msecond dark interval does not represent the actual time required for the radical concentrations to decay to negligible values, then an alternate explanation might be that radiation partitioning to reaction products is occurring in the light period, and the dark period serves to allow these products to diffuse away from the reaction zone. From the previous study (1), formaldehyde would be the most reactive primary product present in the reaction zone. The presence of CO would be evidence of the secondary decomposition of this material. However, our analyses show that the

Can. J. Chem. Downloaded from www.nrcresearchpress.com by 210.87.254.6 on 09/05/12
For personal use only.

total yields of ($CO+CH_4$) do not exceed 0.5 mole% of the non-condensable gas runs with t_L less than 0.5 msecond. It therefore seems unlikely that product diffusion is a significant factor in determining the magnitude of the optimum dark period. Now at the onset of the dark period, the radicals present in greatest abundance would likely be H and CH_2OH. The H atoms would diffuse much more rapidly than the CH_2OH radicals from the reaction zone, and this diffusive separation would favor reaction [4] over [2], with a resulting increase in $\Phi(H_2)$.

The behavior of $\Phi(CH_3ONO)$ as a function of sector disk speed, as shown in Fig. 2, again illustrates the effects of both t_L and t_D on the radical concentrations. With decreasing t_L, the concentrations of both CH_3O and NOH would be reduced, rendering step [5] less probable, and thus favoring the formation of CH_3ONO. This accounts for the increasing $\Phi(CH_3ONO)$ with r.p.m. of the sector, as shown in Fig. 2. The decline in nitrite yield at high sector speeds is attributable to the decreasing t_D, resulting in a finite radical concentration being present at the beginning of the next light pulse.

CONCLUSIONS

As a result of the present study it can be concluded that the primary process of H atom detachment in the reaction of methanol vapor with Hg $6(^3P_1)$ atoms is at least 89% efficient, and that it is likely that the primary quantum yield is in fact unity. The fact that $\Phi^\circ(H_2)$ is only 0.46 under steady illumination conditions would appear to be due to radical addition reactions involving H atoms, of which the most probable is the addition of H atoms to CH_2OH radicals.

For the NO-inhibited reaction, it is concluded that the low value for $\Phi(CH_3ONO)$ under steady illumination is due mainly to the abstractive attack of CH_3O on NOH.

As a general conclusion from the present study, the rotating sector method should prove of considerable value in primary process studies in mercury photosensitization. Similar studies on the reactions of Hg $6(^3P_1)$ atoms with ethanol and isopropanol will be published shortly.

ACKNOWLEDGMENTS

The authors would like to express their appreciation to Dr. W. F. Allen of this laboratory for valuable assistance and advice. Our program was supported in part by the National Research Council under Term Grant No. NRC T-162 (Gunning). This support is very gratefully acknowledged.

REFERENCES

1. A. R. KNIGHT and H. E. GUNNING. Can. J. Chem. **39**, 1231 (1961).
2. S. BYWATER and E. W. R. STEACIE. J. Chem. Phys. **19**, 319 (1951).
3. R. A. BACK. Can. J. Chem. **37**, 1834 (1959).

Can. J. Chem. Downloaded from www.nrcresearchpress.com by 210.87.254.6 on 09/05/12
For personal use only.

Can. J. Chem. Downloaded from www.nrcresearchpress.com by 210.87.254.105 on 09/05/12
For personal use only.

THEORETICAL STUDIES ON THE ELECTRONIC SPECTRA OF SUBSTITUTED AROMATIC MOLECULES

PART I. THE INTRAMOLECULAR ELECTRON TRANSFER MODEL[1]

J. E. Bloor

ABSTRACT

A simple empirical model, based on molecular orbital theory without configuration interaction, is used to interpret the K band transitions of substituted aromatic molecules as involving intramolecular electron transfer between substituent and hydrocarbon. For electron-donating substituents, such as amino, methoxyl, chloro, bromo, and iodo, the transfer is from substituent to hydrocarbon, while for electron-attracting substituents, such as nitro, formyl, acetyl, and cyano, the charge transfer is from hydrocarbon to substituent. Such a treatment is successful for "long field molecules" (benzene, diphenyl, terphenyl, styrene, and stilbene), but for "round field" molecules agreement between experiment and theory was achieved only for electron-donating substituents. The theory, like less empirical theories, overestimates the relative effect of a substituent in the 2-position compared with substitution in the 1-position.

In molecular orbital (MO) calculations of the electronic transitions in conjugated molecules the importance of configuration interaction is well recognized (1–4). However, for all but the simplest molecules it has been the custom to restrict, quite arbitrarily (4), the configuration interaction to singly excited configurations and to introduce empirically the values of certain interaction integrals by recourse to experiment (5, 6). Because of this empirical element in self-consistent field calculations and the rather large amount of labor necessary for the carrying out of such calculations it is still of interest to see whether it is possible to interpret the electronic spectra of aromatic molecules containing polar substituents by some simple model without configuration interaction (CI), in which the neglect of CI might be compensated for by empirical adjustment of the parameters of the adopted model. Such a model is that used previously (7–10) to calculate the transition energy of the K bands of substituted benzenes as being due to an electron transfer between substituent and benzene. We have found it possible to extend this interpretation to the K band spectra of long field molecules (11), substituted in the 4-position by the nitro, the cyano, the acetyl, and the formyl groups and for both long field and round field molecules substituted by the electron-donating amino, methoxyl, bromo, chloro, and iodo groups. Such an interpretation of the K band spectra is similar to the qualitative theory of Burawoy (12–14), which, however, assumes that electron transfer in the ground state occurs only by an inductive mechanism.

METHODS AND RESULTS

The details of the method have been described elsewhere (7–10). The substituted hydrocarbon is regarded as being built up from two sets of energy levels, those of the parent hydrocarbon (R—H) and those of the substituent (S—H). The difference between the energy levels of the isolated systems R—H and S—H and the system R—S are calculated by a perturbation method. The energy of the intramolecular charge transfer band (E_1) is then given, for electron-attracting substituents, by the difference in energy between the highest occupied perturbed level of fragment R− and the lowest unoccupied perturbed level of fragment S, eq. [1]. For electron-donating substituents the energy

[1]*Manuscript received July 7, 1961.*
Contribution from the Chemistry Division, British Columbia Research Council, Vancouver 8, B.C.

of the intramolecular charge transfer band is given by the difference (E_2) between the energy of the highest perturbed occupied level of fragment $-$S and the energy of the lowest unoccupied perturbed level of fragment R$-$, eq. [2].

$$[1] \qquad E_1 = [(V_S - H_R)^2 + 4C_{V_S}^2 C_{H_R}^2 \beta_{R-S}^2]^{\frac{1}{2}},$$

$$[2] \qquad E_2 = [(V_R - H_S)^2 + 4C_{V_R}^2 C_{H_S}^2 \beta_{R-S}^2]^{\frac{1}{2}}.$$

H_R and H_S are the energies of the highest unperturbed occupied molecular orbitals (MO's) of R—H and S—H respectively. V_R and V_S are the energies of the unperturbed unoccupied MO's of R—H and S—H respectively. The atomic orbital (AO) coefficients C_{H_R}, C_{H_S}, C_{V_R}, C_{V_S}, are the values in the MO's of energies H_R, H_S, V_R, V_S at the atoms at which the connecting link between R—S is formed. H_S has previously (7–10) been taken as the ionization potential of either the corresponding methyl derivative (Me—S) or hydrogen derivative (H—S). However, in the hydrocarbon H—S the substituent S is attached to a trigonally hybridized carbon atom which is more electron attracting than either a tetrahedrally hybridized carbon atom or a hydrogen atom, so values of H_S were obtained by fitting eq. [1] to the experimental results for the K bands of benzene derivatives. The values so obtained are given in Table II.

V_S has previously been taken as the difference between the ionization potential and the energy of the R band transition of the corresponding methyl derivative (Me—S) (7). This assumption is open to the objection that both the repulsion forces and the changes in the Hamiltonian on going from the ground state to the excited state are different for R bands than for K bands, since the charge distribution in the excited state is different for the two transitions. Therefore empirical values for V_S were obtained by adjusting its value so that eq. [1] reproduced the experimental values of the K band of benzene derivatives. These values are given in Table II. For the nitro group the value which fitted nitrobenzene ($V_S = -4.4$ ev) gave poor results for the other derivatives so $V_S = -5.1$ ev was adopted as giving the best over-all results.

V_R has previously (7) been taken as the difference between the observed energy of the K band transition of R—H and its ionization potential (H_R), i.e. the K band of the hydrocarbon R—H is assumed to arise from a configuration in which an electron is excited from the highest filled MO to the lowest unoccupied MO. Such an assumption, however, always results in an electron transfer (ET) configuration of higher energy than the parent hydrocarbon K band for all values of H_S consistent with the limitation (necessary to explain the reduction of the ionization potential of R—H on substitution by an electron-donating S) that H_S should be less than H_R. V_R was therefore regarded as an empirical parameter and was obtained by equating E_2, calculated by eq. [2], to the observed K band spectra. The results of Table IV are those obtained by using such average values given in Table I. Such an adjustment of parameters is made very simple by the fact that eq. [2] is a hyperbola of the type $x^2 - b^2 = y^2$ where x is E_2 and y is $(H_S - V_R)$ and the range of values of x in which the transitions under discussion lie are such that a plot of E_2^2 against $(H_S - V_R)^2$ is linear for a given series of substituents with the same value of C_{H_S}. The empirical values of V_R so obtained are in the same relative order as those obtained by using ionization potential and ultraviolet data (Table I).

The AO coefficients C_{H_R} and C_{V_R} were obtained by LCAO calculations. C_{H_S} and C_{V_S} were given values between 0.5 and 1.0 consistent with giving the best fit between experiments and theory, Nagakura's (7–10) values being adopted wherever possible. The values used are given in Tables I and II. The values of E_1 and E_2 calculated by inserting

Can. J. Chem. Downloaded from www.nrcresearchpress.com by 210.87.254.105 on 09/05/12
For personal use only.

TABLE I

Parameters for hydrocarbon fragment R

R	$-H_R$, ev*	$-V_R$, ev†	$-V_R$, ev‡	$C_{H_R} = -C_{V_R}$
Benzene	(9.24)	3.04	6.00	0.578
Styrene	(8.86)	3.86	6.30	0.390
Stilbene	8.48	4.40	6.90	0.314
Diphenyl	8.78	3.73	6.24	0.398
Terphenyl	8.62	4.12	6.47	0.297
Naphthalene	(8.68)	4.40	7.1	0.425 (1 pos.) 0.263 (2 pos.)
Anthracene	(8.20)	4.90	8.23	0.440 (9 pos.)

*Experimental ionization potentials in parentheses; the others are obtained from a linear plot of these against the energy in β units (of the highest occupied MO) as calculated by the simple LCAO method.
†Calculated from ionization potential and ultraviolet data.
‡Empirical average values obtained by fitting experimental data to eq. [2].

TABLE II

Parameters for substituents

S	$-V_S$, ev*	$-H_S$, ev*	C_{V_S}*	C_{H_S}*	$-V_S$†	$-H_S$†	C_{V_S}†	C_{H_S}†
Nitro	5.10	—	0.70		5.50		0.70	
Formyl	4.63	—	0.70		5.91		0.89	
Acetyl	4.70	—	0.70		5.46		0.89	
Cyano	4.43	—	0.70					
Amino	—	10.02		1.00		10.52		0.81
Methoxy	—	10.44		1.00		—		—
Chloro	—	10.60		1.00		—		—
Bromo	—	10.58		1.00		—		—
Iodo	—	10.42		1.00		—		—

*Values used in this paper.
†Values used by Nagakura.

the parameters of Tables I and II in eq. [1] and [2] are compared with the available experimental data in Tables III and IV. Table V compares results for nitro compounds with $V_S = -5.5$ ev with those of Nagakura (8) with $V_S = -5.1$ ev. β_{R-S} is given the value 3 ev for all substituents (7–10).

DISCUSSION

The calculated values obtained by using the parameters of Tables I and II in eq. [1] and [2] are compared with experimental data for K band absorption in Tables III, IV, and V. In general, the calculated values are in fairly good agreement with the experimental ones.

For the electron-attracting groups the experimental data are not at the moment extensive enough to carry out a satisfactory statistical test of the validity of the simple charge transfer model. However, it can be seen from Table III that once the appropriate choice of H_R and V_S has been made the difference in K band transition energy of the nitro, acetyl, formyl, and cyano derivatives of benzene and diphenyl is predicted correctly within 0.03 ev (i.e. within 30° A at 3100° A). Using $V_{NO_2} = -5.1$ ev the K band positions of seven nitro compounds have been calculated (Tables IV and V) and these give a correlation coefficient of 0.850 on comparison with the observed values. The agreement would be even better if the experimental results (Table V) for 1-nitro-2-methyl-ethylene and 1-nitro-4-methyl-butadiene were corrected for the bathochromic effect of the methyl group (0.1 ev) and the solvent effect of the ethanol, the results being taken from (8).

Can. J. Chem. Downloaded from www.nrcresearchpress.com by 210.87.254.105 on 09/05/12
For personal use only.

TABLE III

Calculated and observed* K band transition energies (in ev) for electron-attracting substituents

	Substituent							
	$-NO_2$		$COCH_3$		CHO		CN	
Hydrocarbon	Calc.	Obs.	Calc.	Obs.	Calc.	Obs.	Calc.	Obs.
Benzene	4.80	4.93	(5.21)	5.21	(5.24)	5.24	(5.38)	5.38
Styrene	4.13	4.11	4.90	—	4.52	—	4.76	4.73
Stilbene	3.63	3.73	4.07	—	4.01	—	4.25	—
Diphenyl	4.04	4.05	4.48	4.49	4.41	4.38	4.66	4.65
Terphenyl	3.74	3.80	4.18	4.20	4.11	—	4.36	4.37
1-Naphthalene	4.06	3.81	4.43		4.36		4.79	—
2-Naphthalene	3.75	4.19	4.19	4.41	4.13	—	4.58	—
9-Anthracene (16)	3.73	3.57	4.02	—	3.96	—	4.20	3.40

*Unless otherwise stated these results have been measured by Burawoy and collaborators (refs. 13, 14, and unpublished work) in hexane solution.

TABLE IV

Calculated and observed* K band transition energies (in ev) for electron-donating substituents

	Substituent									
	NH_2		OMe		Cl		Br		I	
Hydrocarbon	Calc.	Obs.	Calc.	Obs.	Calc.	Obs.	Calc.	Obs.	Calc.	Obs.
Benzene	(5.30)	5.30	5.65	(5.65)	(5.78)	5.78	(5.74)	5.74	5.62	5.39
Styrene	4.53	4.54	4.50	4.85	4.89	4.90	4.88	4.90	4.74	—
Stilbene	3.96	3.92	3.97	4.00	4.15	4.05	4.13	—	3.99	—
Diphenyl	4.45	4.52	4.76	4.85	4.92	4.9	4.942	4.88	(4.81)	4.81
Terphenyl	3.98	4.19	4.36	4.35	4.50	4.45	4.47	4.44	4.33	4.42
1-Naphthalene (17)	3.87	3.98	4.18	4.22	4.33	4.32	4.31	4.29	4.16	4.211
9-Anthracene (16)	3.19	3.18	4.42		3.55	3.54	—	—	—	—

*Unless otherwise stated, these results have been measured by Burawoy and collaborators (refs. 13, 14, and unpublished work) in hexane solution.

TABLE V

Nitro compounds

Parent hydrocarbon R—H	Observed transition energies in ev		Predicted transition energies in ev		Free valence F	$E_{R-H}-E_{R-NO_2}$
	E_{R-NO_2}	E_{R-H}	$V_{NO_2}=-5.1$	$V_{NO_2}=-5.5$		
Ethylene	5.39	−7.6	5.37	5.51	0.731	2.21
Butadiene	4.41	6.0	4.49	4.56	0.391	1.59
Benzene	4.93	6.2	5.10	4.69	0.398	1.27
Styrene	4.11	5.06	4.13	3.74	0.414	0.95
Diphenyl	4.05	5.02	4.04	3.68	0.412	0.97
Terphenyl	3.80	4.51	3.74	3.58	0.412	0.71
Stilbene	3.73	4.25	3.63	3.26	0.418	0.52

The use of $V_{NO_2} = -5.1$ ev can be seen to give better agreement with experiment than the original value of $V_{NO_2} = -5.5$ ev used by Nagakura (8). The theory predicts well the effect of increasing the size of the conjugated system attached to the nitro group. This is shown in Fig. 1 where the experimental and predicted values are plotted against the size of the conjugated system. The results of Table V also give a theoretical basis to the empirical rule of Burawoy (14) that the larger the conjugated system (a good measure of the length of the conjugation is the K band transition energy of the hydrocarbon) the

Can. J. Chem. Downloaded from www.nrcresearchpress.com by 210.87.254.105 on 09/05/12
For personal use only.

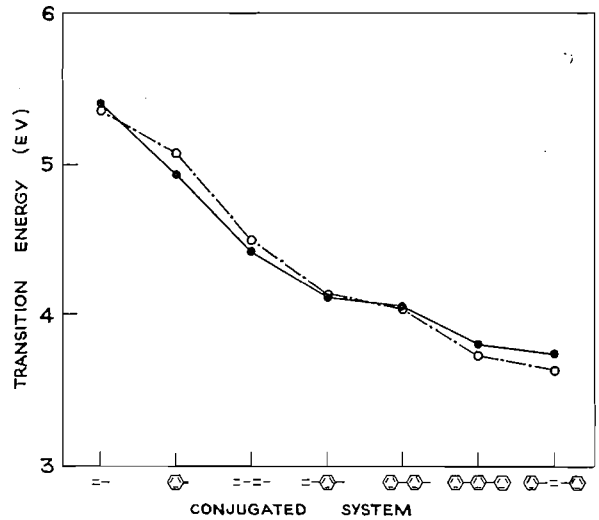


FIG. 1. Comparison between calculated (-·-o-·-) and observed (-●-) K band transition energies of conjugated nitro compounds.

smaller the effect of a given substituent. Thus the magnitude of the transition energy change brought about by the nitro group grows smaller as we descend Table V from ethylene (where the change on substitution is 2.03 ev) to stilbene (where it is only 0.52 ev).

The free valence (15) has often been taken as a measure of the conjugating power of a hydrocarbon with a substituent and either this or the proportional quantity, the self-polarizability (18), is related to the K band transition energy change on substitution. The values of the free valence and the observed transition energy change recorded in Table V show that this is only a very rough approximation. In particular the free valence predicts that the conjugating power of diphenyl and terphenyl in the para position should be the same and that stilbene should have a conjugating power greater than benzene when in fact the nitro group has the least effect on the K band transition energy of stilbene as is predicted on the "charge transfer" model.

In the case of the round field molecules, naphthalene and anthracene, it can be seen from Table III that agreement between experiment and theory is poor. Whereas it is always found experimentally that substitution in the 1-position of naphthalene produces a bigger bathochromic shift of the K band than substitution in the 2-position, the simple charge transfer theory predicts the opposite for both electron-attracting and electron-donating substituents. No explanation for this breakdown can be offered but it should be pointed out that even the most sophisticated calculations carried out to date (19), which include limited configuration interaction, overestimate the effect of the effect of the substituent in the 2-position of naphthalene. It is possible that calculations using self-consistent field ground state orbitals may remove this deficiency.

For electron-donating substituents which may be regarded as monatomic substituents the available experimental data is much more plentiful than for electron-attracting substituents. For the K bands of long field molecules the band maxima of both the parent hydrocarbon and the substituted compound are quite sharp and the band envelopes are, with the exception of benzene and halogeno-benzenes, fairly symmetrical. This means

Can. J. Chem. Downloaded from www.nrcresearchpress.com by 210.87.254.105 on 09/05/12
For personal use only.

that the changes in transition energy can be measured to within 50–100 cm^{-1} (i.e. to within less than 0.1 ev) whereas for round field molecules the K band is much broader and often contains fine structure which is altered on substitution (19, 20).

In Table III are recorded 29 comparisons between experimental and theoretical transition energies. The relationship between calculated and observed transition energies gives a correlation coefficient of 0.951 (this includes the particularly bad result for 4-methoxy-stilbene but omits the results for 2-substituted naphthalenes since, as has been discussed above, it is known the theory is incorrect in its predictions for these latter compounds).

This high correlation coefficient is most unexpected for such a crude theory which neglects completely the interaction between the highest occupied level of the parent hydrocarbon and the corresponding level in the substituent. This interaction on the LCAO model is regarded as the main effect of the substituent (21). It seems likely that the empirical element introduced into the theory by the adjustment of the parameters to fit experimental data and the neglect of configuration interaction may compensate for this neglect.

Both the charge transfer and the LCAO methods involve a transfer of electrons from the electron-donating substituent to the parent hydrocarbon; however, comparison of similar calculations show that the LCAO method consistently predicts a greater charge transfer in the ground state than the charge transfer method when the parameters are chosen to give agreement with experiment. It may therefore be possible to decide which is the better model by comparison between theoretical calculations and experiments on ground state properties (heats of combustion, n.m.r. chemical shifts, and infrared stretching frequencies and intensities). It has recently been reported (22) that the charge transfer method gives a satisfactory model for the interpretation of the infrared intensities of substituted benzonitriles; similar calculations using the LCAO method are not yet available.

The author is indebted to the ICI Fellowship Committee of the University of Manchester, England, and the National Research Council of Canada for financial support.

REFERENCES

1. W. Moffitt. J. Chem. Phys. **22**, 320, 1820 (1954).
2. J. Jacobs. Proc. Phys. Soc. (London), A, **62**, 710 (1948).
3. H. C. Longuet-Higgins. Advances in chemical physics. Vol. 1. Interscience Publishers, Inc., New York. 1958. p. 239.
4. R. Pariser and R. G. Parr. J. Chem. Phys. **21**, 466 (1953).
5. L. Goodman and H. Shull. J. Chem. Phys. **27**, 1388 (1957).
6. E. G. McRae and L. Goodman. J. Mol. Spectroscopy, **2**, 464 (1958).
7. S. Nagakura and J. Tanaka. J. Chem. Phys. **22**, 236 (1954).
8. S. Nagakura. J. Chem. Phys. **23**, 1441 (1955).
9. J. Tanaka, S. Nagakura, and M. Kobayshi. J. Chem. Phys. **24**, 311 (1956).
10. J. Tanaka and S. Nagakura. J. Chem. Phys. **24**, 1274 (1956).
11. J. R. Platt. J. Chem. Phys. **17**, 484 (1949).
12. A. Burawoy. Tetrahedron, **2**, 122 (1958).
13. A. Burawoy and P. Critchley. Tetrahedron, **5**, 340 (1959).
14. A. Burawoy, P. Brocklehurst, R. S. Berry, and A. R. Thompson. Tetrahedron, **10**, 102, 109 (1960).
15. B. Pullman and A. Pullman. Progress in organic chemistry. Vol. 4. *Edited by* J. W. Cook. Butterworths Scientific Publications, London. 1958. p. 31.
16. R. N. Jones. Chem. Revs. **41**, 353 (1947).
17. H. G. de Laszlo. Proc. Roy. Soc. (London), A, **111**, 355 (1926).
18. G. M. Badger and R. G. Battery. J. Chem. Soc. 2156 (1953).
19. H. Baba and S. Suzuki. Bull. Chem. Soc. Japan, **34**, 82 1961.
20. American Petroleum Institute. Research project 44. Ultraviolet spectral data sheets.
21. Y. I'Haya. J. Am. Chem. Soc. **81**, 6120 (1959).
22. T. L. Brown. J. Phys. Chem. **64**, 1798 (1960).

Can. J. Chem. Downloaded from www.nrcresearchpress.com by 210.87.254.105 on 09/05/12
For personal use only.

Can. J. Chem. Downloaded from www.nrcresearchpress.com by 210.87.254.40 on 09/05/12
For personal use only.

SOME ASPECTS OF THE NUCLEAR MAGNETIC RESONANCE SPECTRA OF COMPOUNDS CONTAINING C-METHYL GROUPS[1]

F. A. L. ANET

ABSTRACT

The N.M.R. spectra of compounds containing various types of C-methyl groups are discussed with special reference to the effects of spin coupling. Particular attention is given to compounds containing the $CHCH_3$ group in saturated systems. It is pointed out that the observed splitting of the methyl band is not always equal to the coupling constant between the methyl protons and the adjacent proton, even when the chemical shift between the two groups of protons is large.

The detection and differentiation of C-methyl groups in organic compounds is of importance, particularly in natural product chemistry. The standard (Kuhn–Roth) method of estimating C-methyl groups consists of oxidizing the compound with chromic acid and determining the acetic acid (and(or) higher homologue(s)) produced. By suitable modifications (1) it is possible to analyze for each acid separately and so to find out whether the group is a simple C-methyl group, or a C-ethyl group, etc. Infrared spectroscopy (2) has been used to detect and to determine C-methyl groups, and also to differentiate between isopropyl, *tert*-butyl, and other C-methyl groups.

Both of the above methods have limitations for the differentiation of C-methyl groups. Proton nuclear magnetic resonance (N.M.R.) has already been applied to the problem (3) but little discussion of the scope and limitations of the method has been published. In the present paper the effect of coupling of a methyl group to other protons in a molecule is considered in detail.

The detection of C-methyl groups by means of N.M.R. spectroscopy is especially favorable for two reasons. In the first place, a strong signal is usually obtained because of the complete magnetic equivalence of the three protons as a result of the rapid internal rotation of the methyl group. Secondly, when the methyl group is attached to a saturated carbon atom, the chemical shift of the methyl group, which is about 1 p.p.m. downfield from tetramethylsilane, is usually different from that of other protons in the molecule. Exceptions occur in compounds containing certain structural features such as cyclopropane rings. *trans*-1,1-Dichloro-2,3-dimethylcyclopropane (4), for example, has an N.M.R. spectrum which is essentially a single line at 8.78 τ.

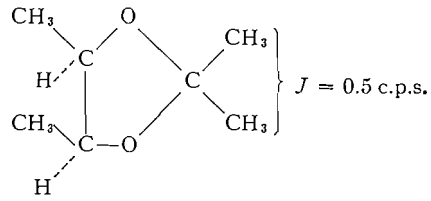
The N.M.R. spectra of compounds containing C-methyl groups attached to unsaturated carbon atoms have been discussed in some detail by several authors (5, 6, 7, 8, 9, 10) and will not be considered here.

When the methyl group is attached to a saturated carbon atom we may consider three separate cases, depending on whether the saturated carbon atom also carries (*a*) no hydrogen atom, (*b*) one hydrogen atom, or (*c*) two hydrogen atoms.

In class (*a*), when there is no hydrogen atom on the adjacent carbon atom, the methyl group generally gives rise to a single sharp line. Since all the intensity is concentrated in one line there is no difficulty in observing such a signal in a spectrum. Typical examples are the 18- and 19-methyl groups of steroids (11) and the methyl groups in camphane derivatives (12). In exceptional cases, the methyl group may show very weak coupling to

[1]*Manuscript received June 20, 1961.*
Contribution from the Department of Chemistry, University of Ottawa, Ottawa 2, Ontario.

other protons in the molecule, thus (4) the two non-equivalent *gem*-methyl groups of (I) are coupled together to the extent of 0.5 c.p.s. Roberts (13) has reported a value of 0.75 c.p.s. for the coupling constant of the C-methyl group to one of the protons of the methylene group in methyl 2-bromo-2-methylpropionate. In general, it may be anticipated that this type of coupling will be very small (<1 c.p.s.) and can be neglected for practical purposes.



(I)

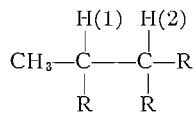
The second class is that of compounds containing the $CHCH_3$ group. The spectrum to be expected from such a system, in the absence of other magnetically active nuclei, has been dealt with in several places (cf. ref. 14). The simplest case, usually designated (15) by the symbols AX_3, occurs when the chemical shift of the two groups of protons is large compared with the coupling constant between them. The methyl group then gives rise to a doublet, and the separation is equal to the coupling constant. It may be mentioned here that the coupling constants of methyl groups to adjacent protons generally lie in the range of 6–8 c.p.s.

We may also place in this class the isopropyl group. If the two methyl groups are chemically identical and are well shifted from the CH proton, the situation is analogous to that just described. If the two methyl groups are not chemically identical, usually (but not necessarily) because of the presence of an asymmetric center in the molecule, two different methyl doublets, which may overlap, are obtained (16, 17). The non-equivalence of methyl groups in such systems is similar to that of two protons of a methylene group in certain molecules (18, 19).

When the chemical shift in the $CHCH_3$ group is not very large, the spectrum becomes an AB_3 type (15) and contains more lines. However, when the ratio of coupling constant to chemical shift is not more than about 0.25, the spectrum of the methyl group is still approximately a doublet. More exactly, each "line" of the doublet is now split into a number of lines, and the high-field component is split more and also is of lower intensity than the low-field component (assuming the CH group to be at low field of the methyl group). When the chemical shift is much less, a doublet is no longer recognizable. Jackman (3) has tried to rationalize the spectra of certain compounds (e.g. methylcyclohexane) containing $CHCH_3$ groups simply in terms of AB_3 systems. However, closer inspection shows that the observed and calculated spectra of the methyl groups cannot be made to agree completely, no matter what combination of chemical shifts and coupling constants are used. In each case there are other protons in the molecule which are appreciably coupled to, but only slightly chemically shifted from, the tertiary proton of the $CHCH_3$ group. These protons *must* be included in the analysis in order to obtain correct results. This is so even if, as is generally true, the methyl group is coupled only to the tertiary proton and not to the other protons of the molecule.

Can. J. Chem. Downloaded from www.nrcresearchpress.com by 210.87.254.40 on 09/05/12
For personal use only.

We shall first examine the spectrum to be expected for the methyl group in a molecule such as (II), where the R's are not involved in coupling with the system under consideration. We will assume that the methyl group is well chemically shifted from H(1) and



(II)

H(2) and that $J_{CH_3,H(2)}$ is zero. This is actually a special case of the X_3AB system, which has been treated by Fessenden and Waugh (9). Figure 1 shows the calculated spectra due

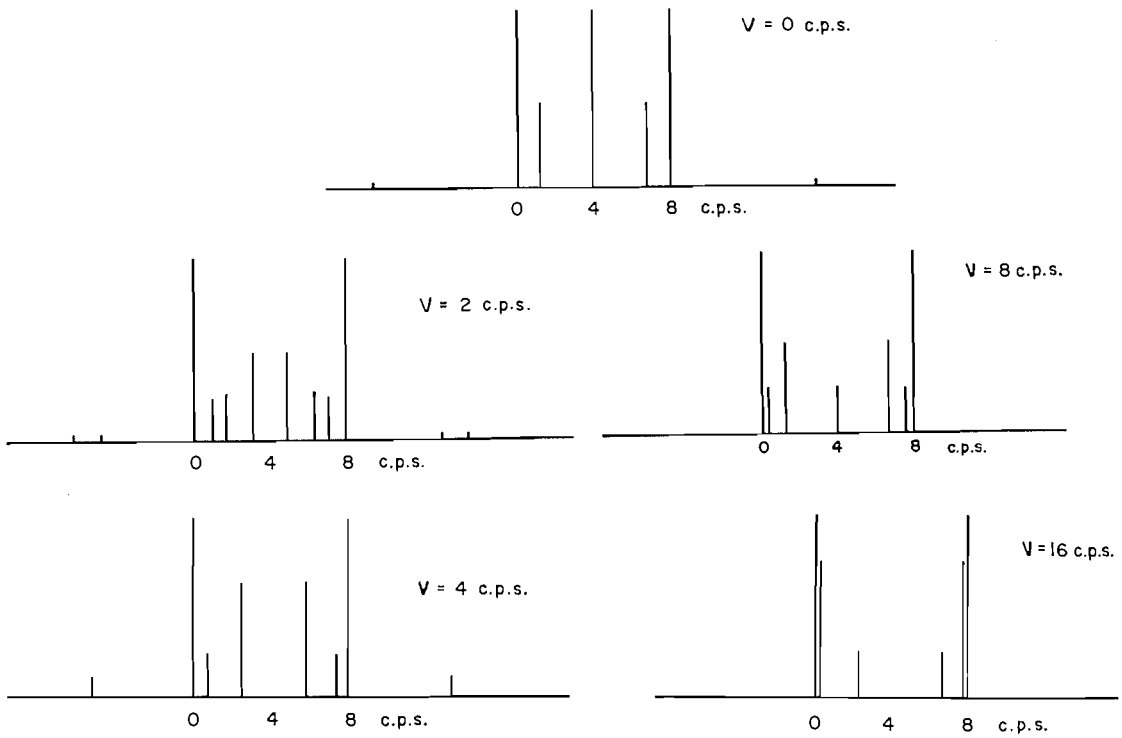


FIG. 1. Calculated spectra for compounds of type (II) for various values of the chemical shift (ν) between H(1) and H(2) and with $J_{CH_3,H(1)} = J_{H(1),H(2)} = 8$ c.p.s. and $J_{CH_3,H(2)} = 0$.

to the CH_3 group for various values of the chemical shift ($\nu_{H(1),H(2)}$) between H(1) and H(2), and, for simplicity, with $J_{CH_3,H(1)} = J_{H(1),H(2)} = 8.0$ c.p.s. Although the coupling constants are not generally equal, this does not affect the general conclusions drawn from the calculations.

When the chemical shift, $\nu_{H(1),H(2)}$, is very large the spectrum of the methyl group is a doublet, the lines being at $+1/2J_{CH_3,H(1)}$ and $-1/2J_{CH_3,H(1)}$ from the position of the methyl band in the absence of coupling. This is, of course, just the result expected from a first-order treatment. When the chemical shift is *not* large, only half of the intensity of the methyl band resides in the two lines at positions mentioned above. Most of the

Can. J. Chem. Downloaded from www.nrcresearchpress.com by 210.87.254.40 on 09/05/12
For personal use only.

remaining intensity is situated *between* these two lines, the exact distribution depending very markedly on the value of $\nu_{H(1),H(2)}$ (Fig. 1). The effect of H(2) is most pronounced when $\nu_{H(1),H(2)}$ is no greater than $J_{H(1),H(2)}$ and is negligible when $\nu_{H(1),H(2)} > 2J_{H(1),H(2)}$.

It can easily be understood why half of the intensity is in the lines at $\pm 1/2J_{CH_3,H(1)}$. There are four spin states for the protons H(1) and H(2), and the wave functions of the states with both protons having a spin of $+1/2$ or with both protons having a spin of $-1/2$ will not mix with any other functions, whereas the pairs of wave functions associated with one proton having a spin of $+1/2$ and the other a spin of $-1/2$ and vice versa do mix as they have the same total spin (15). From similar considerations it can be seen that if there are two protons similar to H(2), then only one quarter of the intensity of the methyl group lies in the "unperturbed" lines at $\pm 1/2J_{CH_3,H(1)}$. For three and four protons these fractions fall to 1/8 and 1/16 respectively. Complete solutions in these cases would be very laborious but it can be surmised that most of the remaining intensity, in the form of many lines, will be situated, as before, between the pair of unperturbed lines.

Therefore, the $CHCH_3$ group in a complex molecule may be expected to be a doublet or a doublet showing some additional lines, or in extreme cases, just a wide band with little resolved structure. This is the situation where the chemical shift between the CH_3 group and the adjacent proton is large compared with the coupling constant. When the chemical shift is not large, a similar effect is to be expected. The spectrum of the methyl group will correspond to the B_3 part of an AB_3 system only when A is not coupled to any protons other than the B protons. If the effects described above for the AX_3 system are important, a much more complex spectrum may be expected, which in extreme cases may reduce to a structureless wide band.

It should be noted that the observed splitting of the methyl band will not always be equal to the coupling constant. The splitting will usually be less because most of the intensity of the extra lines lies inside the two unperturbed lines whose separation gives the true coupling constant. This is probably the explanation for the wide variation in the "coupling constants"* of the methyl groups of 6α- and 6β-methyl steroids found by Slomp and McGarvey (20). In particular, for certain compounds some quite small splittings were found for which no explanation was presented. It would be expected that the coupling constant of the methyl group to the adjacent proton would not vary greatly in such a series of compounds. In agreement with the arguments presented in this paper is the fact that small splittings were not observed whenever the tertiary proton on C6 was likely to be chemically shifted (generally to low field) from the protons on C7, such as by the presence of a $\Delta^{4,5}$ double bond, or by the C6 proton being equatorial rather than axial (21). Unfortunately, the chemical shifts of the significant protons in such complex molecules cannot be observed directly, because the bands of a large number of other protons interfere.

Similar effects are found in the dimethylcyclohexanes examined recently by Musher (22). From the 40 Mc/sec N.M.R. spectra of the cis and trans isomers of 1,2-, 1,3-, and 1,4-dimethylcyclohexanes, Musher concluded that the coupling constants of equatorial methyl groups to the adjacent axial protons were zero or small (2.7 c.p.s.). In the alternative case of axial methyl groups and adjacent equatorial protons, appreciable (ca. 5 c.p.s.) coupling constants were observed. However, these "coupling constants" were merely the observed splittings of the methyl bands. Since the compounds used should be particularly liable to the effects discussed in this paper, the conclusions of Musher

*In cases of this type the term "splitting" would seem to be preferable to the term "coupling constant".

Can. J. Chem. Downloaded from www.nrcresearchpress.com by 210.87.254.40 on 09/05/12
For personal use only.

regarding coupling constants cannot be regarded as correct. The correct constants could no doubt be obtained by preparing suitably deuterated derivatives, which is, unfortunately, not an easy task, but which has been achieved in the present work for some compounds discussed later in this paper. It may be noted that where zero splittings were observed by Musher, the methyl bands were in fact broad and not sharp as they should be if the coupling constants were zero. In order to obtain experimental confirmation of the deductions made, the N.M.R. spectra of a number of suitable compounds containing C-methyl groups have been examined.

A very simple spectrum (Fig. 2) is given by the 3,5-dinitrobenzoate of *erythro*-3-bromo-2-butanol. The spectrum shows two different methyl bands, each a well-defined doublet

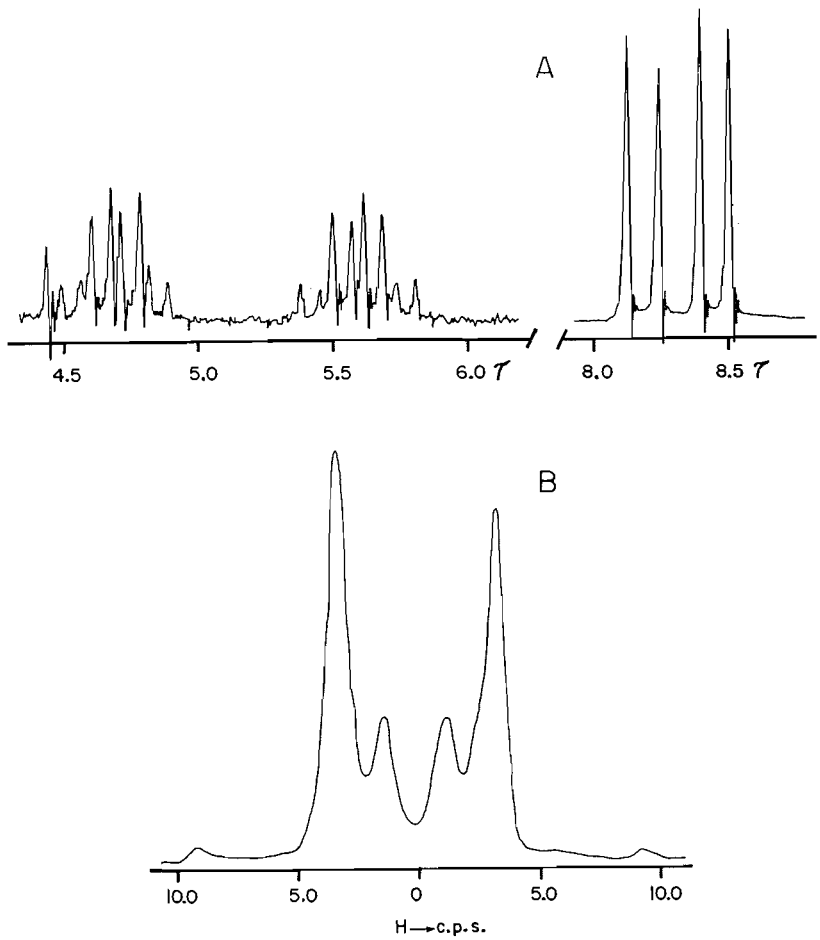


FIG. 2. A. Spectrum of 3,5-dinitrobenzoate and *erythro*-3-bromo-2-butanol, in chloroform solution. The sharp band at the extreme left is that of $C^{13}HCl_3$. The two parts of the spectrum were taken at different recorder gain.

B. Methyl band of meso-2,3-dibromobutane (pure liquid).

in accordance with the X_3 part of an AX_3 system. It should be noted that protons on C2 and C3 are well chemically shifted from one another and from the methyl groups and occur at low fields as doublets of quartets. In contrast to this case is the spectrum of the closely related meso-2,3-dibromobutane, where the chemical shift between the protons

Can. J. Chem. Downloaded from www.nrcresearchpress.com by 210.87.254.40 on 09/05/12
For personal use only.

on C2 and C3 is zero. The methyl groups here have the same chemical shift so only one methyl band is observed, but this is not a simple doublet (Fig. 2), for other lines appear. The spectrum of this molecule has already been discussed briefly (23) and fuller details will be published in a separate paper.

The spectra of methylsuccinic acid and β-methylglutaric acid are shown in Fig. 3.

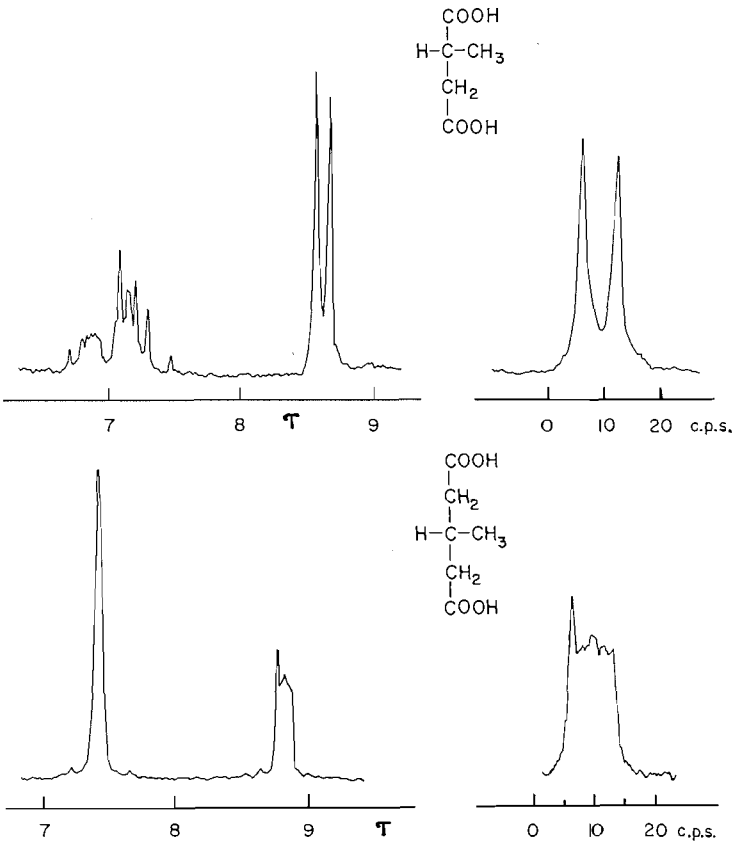


FIG. 3. Spectra of methylsuccinic acid and β-methylglutaric acid in trifluoroacetic acid. The bands of the carboxyl protons are not shown. The methyl bands at slow sweep are shown on the right.

These structurally related compounds give quite different bands for the methyl group. In methylsuccinic acid there is a distinct, though not large, chemical shift between the α and the two α′ protons and, as expected, the methyl group is a fairly good doublet. The coupling constant $J_{CH_3,H(2)}$ is probably a little larger than the observed splitting (6.6 c.p.s.) of the methyl band. In β-methylglutaric acid the α,α′ and β-protons must be only slightly chemically shifted from one another as they give rise to a single, slightly broad band. The result is that the methyl group does not give rise to a doublet at all, but to a wide band which obviously contains many lines.

Other examples of this type are the N.M.R. spectra of 2- and 3-methylcyclohexanone. The band of the methyl group of 2-methylcyclohexanone is a fairly good doublet, as expected, since the 2-proton should be chemically shifted from the 3-methylene protons by the proximity of the carbonyl group. On the other hand, in 3-methylcyclohexanone

Can. J. Chem. Downloaded from www.nrcresearchpress.com by 210.87.254.40 on 09/05/12
For personal use only.

the methyl group gives a very poor "doublet" (Fig. 4) which is a result of the carbonyl group shifting the position of the 2-methylene protons so that these are only slightly separated from the 3-proton. Support of this explanation was obtained by deuteration at position 2 (and incidentally at 6 also since an exchange method was used). The deuterated isomer gives a good doublet (Fig. 4) for the methyl group. This also shows that 1,3-coupling of the methyl group is not important as one methylene group (at C4) remains

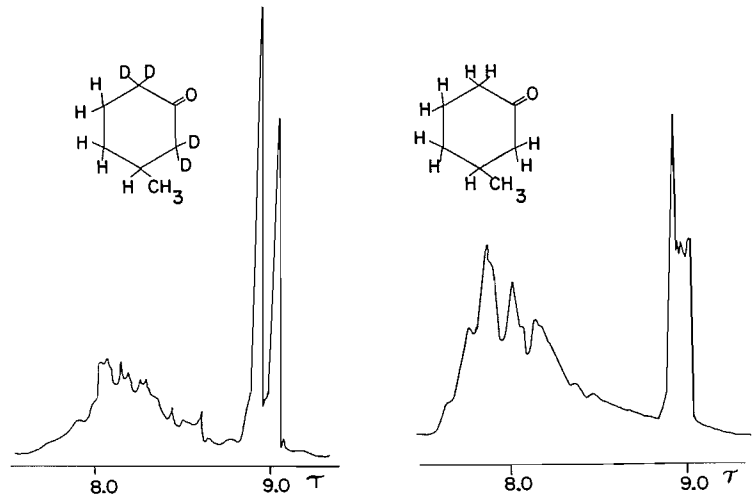


FIG. 4. Spectra of 3-methylcyclohexanone and of 2,2,6,6-tetradeuterio-3-methylcyclohexanone.

in the deuterated isomer. The methyl splitting for the deuterated isomer is 6.1 c.p.s. The splitting of the methyl band in 3-methylcyclohexanone itself depends very markedly on the resolution and sweep rate, owing to the asymmetry of the band. At very high resolution and slow sweep rate the splitting is 5.0 c.p.s., but at lower resolution or faster sweep the observed splitting is only ca. 4.0 c.p.s. Even in the deuterated isomer, the splitting is probably not quite equal to the true coupling constant, as there are still protons on C4 which are not strongly chemically shifted from the proton on C3.

In all the examples described above the chemical shift between the methyl group and the adjacent proton is reasonably large. In methylcyclohexane this shift is much smaller, resulting in a strong skewness in the intensity of the methyl band (Fig. 5) which is an extremely poor doublet with a separation of 4.7 c.p.s. However, this band does not agree with the B_3 part of an AB_3 spectrum. Methylcyclohexane is known to exist largely with the methyl group equatorial (24). It is also known (21) that axial protons are found at slightly higher field than equatorial protons, and that tertiary protons are at slightly lower field than methylene protons, other things being equal (3). These shifts should largely cancel out and the axial proton adjacent to the methyl group should be very close in chemical shift to the protons (especially the equatorial ones) on C2 and C6.

The spectrum (Fig. 5) of 2,2,6,6-tetradeuteriomethylcyclohexane (for isotopic purity see Experimental), on the other hand, gives a methyl band whose structure is consistent with the B_3 part of an AB_3 system. Calculation shows that $J = 6.8$ c.p.s. and that J/ν is about 0.25. It should again be noted that the value of the coupling constant is appreciably greater than the observed splitting in undeuterated methylcyclohexane.

Can. J. Chem. Downloaded from www.nrcresearchpress.com by 210.87.254.40 on 09/05/12
For personal use only.

Can. J. Chem. Downloaded from www.nrcresearchpress.com by 210.87.254.40 on 09/05/12
For personal use only.

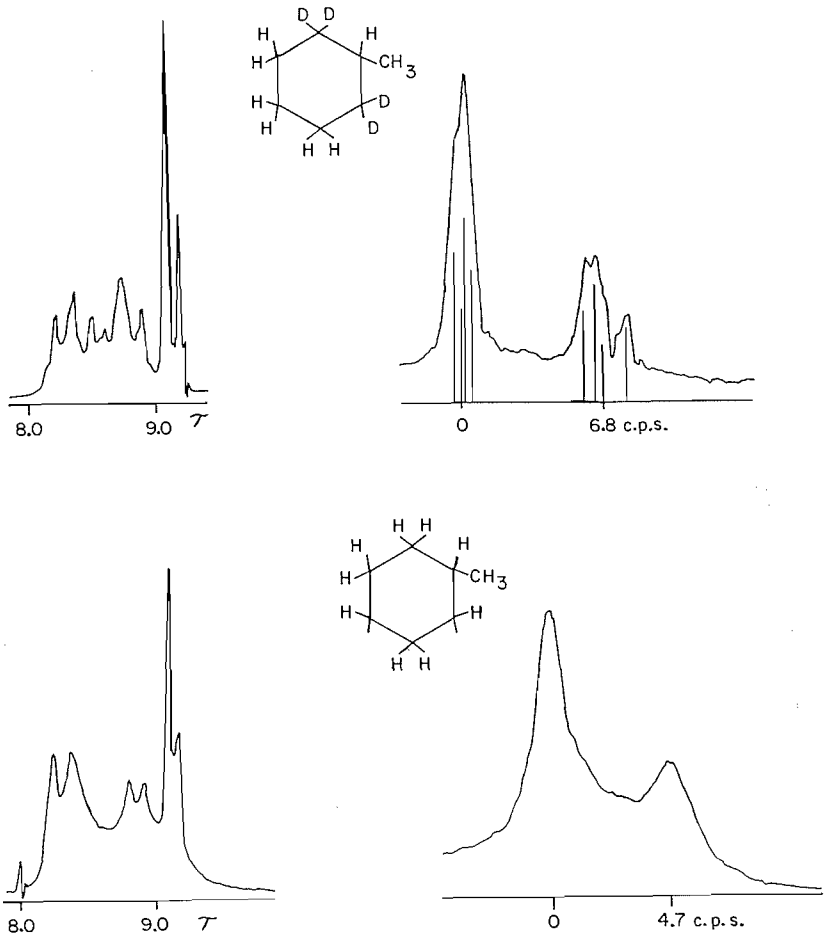


FIG. 5. Spectra of methylcyclohexane and 2,2,6,6-tetradeuteriomethylcyclohexane. The methyl bands at slow sweep are shown on the right. The sharp band at the left of the methylcyclohexane spectrum is a side band of tetramethylsilane.

The *Lycopodium* alkaloid lycodine (III*a*) (25) presents a good example of a natural product showing some of the effects discussed in this paper. In the first publication (26) on this alkaloid, the N.M.R. spectrum (40 Mc/sec) was taken as evidence that the methyl group, which was known to be present, was attached to a quaternary carbon atom, as the methyl band was unsplit. However, spectra (Fig. 6) taken (27) at 60 Mc/sec and under somewhat better resolution showed that the methyl band was quite broad and, in fact, could just be resolved as a doublet of separation 1.9 c.p.s. This splitting undoubtedly does not represent the coupling constant. In N-acetyllycodine (III*b*), the methyl band of the lycodine part of the molecule cannot even be resolved into a doublet under the best possible resolution. The band (Fig. 6) is nevertheless broad and does show an inflection on the high-field side. In contrast, the band of the methyl protons of the N-acetyl group is quite sharp and therefore also of much greater height. These effects can be ascribed to the smallness of the chemical shift of the CH proton to the adjacent pairs of methylene protons, partly as a result of the CH proton being shifted upfield from

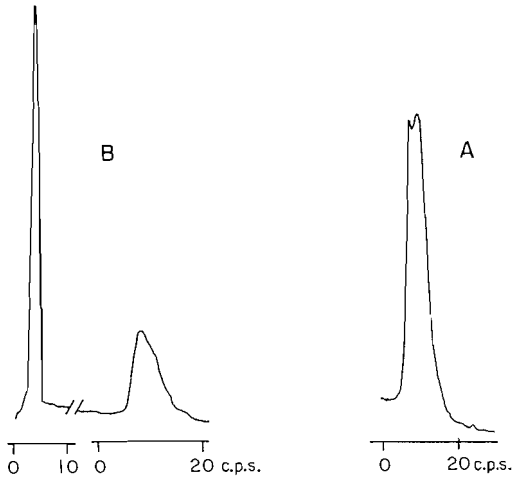
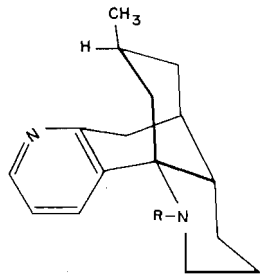


FIG. 6. Methyl bands of (A) lycodine and (B) N-acetyllycodine. The two methyl bands of B were taken under the same instrumental conditions. The magnetic field increases from left to right.

its normal position by the pyridine ring. Molecular models show that the CH proton lies in the region above the plane of the pyridine ring where the circulating π electrons cause a diamagnetic shift. The related alkaloids α- and β-obscurine (28) show the same apparently abnormal methyl band shown by lycodine. Further discussion on the spectra of these alkaloids will be published in a paper dealing with these compounds.



(IIIa) R = H
(IIIb) R = Ac

Another example of "abnormal" behavior is found in 1-β(3,5-dinitrobenzoyloxy)-2α-iodo-3α-methylcyclohexane prepared recently by Lemieux and Kavadias. The N.M.R. spectrum taken at a comparatively fast sweep (29) shows only a single, somewhat broad line for the methyl group. This can be understood if the proton on C3 is only slightly chemically shifted from the protons on C4. In agreement with this interpretation, the proton on C2 gives a broad line, instead of the doublet of doublets expected. In other isomers of the above compound the methyl group is a doublet and the C2 proton shows the expected fine structure.

The spectrum of compounds containing ethyl groups can be expected to show the same behavior as that of compounds containing the $CHCH_3$ group. The methyl group will only be a good triplet when it is well chemically shifted from the methylene protons, *and*

Can. J. Chem. Downloaded from www.nrcresearchpress.com by 210.87.254.40 on 09/05/12
For personal use only.

the methylene protons are chemically shifted from other protons to which they are coupled. When the ethyl group is attached to a saturated carbon atom not bearing a strongly electronegative or strongly electropositive substituent, neither of these conditions will generally be fulfilled. Thus valeric acid (3) gives rise to a methyl band which is wide and fairly shapeless. In fact, it is not too easy to differentiate this type of ethyl group from the "abnormal" $CHCH_3$ group discussed previously. *n*-Butyraldehyde (3), where the second condition above is fairly well fulfilled, gives a recognizable, if poor, triplet. Diethyl ketone fulfills both the conditions and indeed gives (3) a good triplet for the methyl group. It should be noted that in molecules containing an asymmetric carbon atom, the two methylene protons of an ethyl group are not identical and may have slightly different coupling constants to the methyl group. The ethyl group of some small molecules have been analyzed as A_3B_2 or A_3B_2X systems (30, 31), and during the course of the present work Cavanaugh and Dailey have investigated the spectra of propyl derivatives (32).

In this paper, the only magnetically active nuclei present have been assumed to be protons. However, the arguments presented can be extended readily to cases where fluorine, phosphorus, etc. occur in an organic compound.

EXPERIMENTAL

The spectra were taken at a frequency of 60 Mc/sec on a Varian V-4302 high-resolution spectrometer. The compounds were dissolved in carbon tetrachloride (except where otherwise stated) containing about 1% tetramethylsilane to make 10–15% solutions. Chemical shifts are reported on Tiers' τ scale (33) (i.e. in p.p.m. increasing to high field, with tetramethylsilane given the value of 10.00). Calibration of the spectra was carried out by the side-band technique. The frequency of the audio-oscillator was monitored on a Hewlett–Packard frequency counter, model 521C. In all cases a number of spectra were taken with increasing as well as with decreasing magnetic fields. The tetramethylsilane peak was always observed as a single, very sharp band. Coupling constants are estimated to be accurate to 0.15 c.p.s.

Preparation of 2,2,6,6-Tetradeuteriomethylcyclohexane

Cyclohexanone (10 g), deuterium oxide (15 ml, 99.7%), and anhydrous potassium carbonate (0.5 g) were refluxed for 2 hours. The cyclohexanone, recovered by ether extraction, was submitted to two more such treatments. The 2,2,6,6-tetradeuteriocyclohexanone was finally distilled through a small column, b.p. 93–96° (142 mm) (4 g), and was free of isomers containing protons α to the carbonyl group, as shown by the N.M.R. spectrum. Treatment of the deuterated cyclohexanone with triphenylphosphinemethylene according to the procedure described in *Organic Syntheses* (34) gave crude methylenecyclohexane, ca. 2 g, b.p. 80–100°. The only impurity was found to be benzene, both by gas chromatography and by the N.M.R. spectrum. The N.M.R. spectrum (bands at 5.52 τ and 8.48 τ only) also showed that the methylenecyclohexane was fully deuterated at positions 2 and 6. The above fraction was hydrogenated at room temperature and pressure in the presence of platinum oxide catalyst (10 mg). The product was shaken with concentrated sulphuric acid at 60° until gas chromatography showed that all the benzene was removed. The product gave a single peak with the same retention time as methylcyclohexane on gas chromatography using a silicone oil column at 110°. The mass spectrum (kindly taken by Dr. F. Lossing of the National Research Council, Ottawa) showed the presence of 65% tetradeuterated, 11% undeuterated, 10% pentadeuterated, 9% trideuterated, 3% monodeuterated, and 2% dideuterated methylcyclohexane. The

Can. J. Chem. Downloaded from www.nrcresearchpress.com by 210.87.254.40 on 09/05/12
For personal use only.

presence of unexpectedly large amounts of the undeuterated isomer can be explained most simply if some isomerization (35, 36) to 1-methylcyclohexene took place. This compound could then undergo an exchange of its allylic deuterium atoms prior to hydrogenation. Indeed, gas chromatography of the hydrogenation mixture contained a small peak, not present in the initial product, with a retention time consistent with that expected for 1-methylcyclohexene. This product disappeared, as expected, on treatment with sulphuric acid. Although the final product was only 65% isotopically pure, this should not affect the N.M.R. spectrum too much.

2,2,6,6-Tetradeuterio-3-methylcyclohexanone

3-Methylcyclohexanone was deuterated as described above for cyclohexanone.

3,5-Dinitrobenzoate of Erythro-3-bromo-2-butanol

The compound had m.p. 85° (lit. (37) m.p. 85°). In the N.M.R. spectrum (Fig. 2) the bands centered at 4.68 τ and 5.60 τ can be assigned to the protons on C2 and C3 respectively, and the doublets at 8.44 τ and 8.19 τ can be assigned to the 4- and 1-methyl groups respectively. The coupling constants are $J_{12} = 6.4$, $J_{34} = 6.9$, and $J_{23} = 4.2$ c.p.s. The assignments are consistent with the chemical-shift effects of bromine and oxygen atoms (38).

ACKNOWLEDGMENTS

I wish to thank Mrs. Osgerby for technical help in the preparation of deuterated cyclohexanone and deuterated methylcyclohexanone.

This research was supported by a grant from the National Research Council of Canada.

REFERENCES

1. H. Bickel, H. Schmid, and P. Karrer. Helv. Chim. Acta, **38**, 649 (1955).
2. L. J. Bellamy. The infra-red spectra of complex molecules. Methuen & Co., London. 1958. p. 24.
3. L. M. Jackman. Applications of nuclear magnetic resonance spectroscopy in organic chemistry. Pergamon Press, New York. 1959. p. 82.
4. F. A. L. Anet. Unpublished work.
5. M. S. Barber, J. B. Davis, L. M. Jackman, and B. C. L. Weedon. J. Chem. Soc. 2870 (1960).
6. L. M. Jackman and R. H. Wiley. J. Chem. Soc. 2881, 2886 (1960).
7. V. J. Kowalewski and D. G. deKowalewski. J. Chem. Phys. **33**, 1794 (1960).
8. R. R. Fraser and D. E. McGreer. Can. J. Chem. **39**, 505 (1961).
9. R. W. Fessenden and J. S. Waugh. J. Chem. Phys. **30**, 994 (1959).
10. R. B. Bates and D. M. Gale. J. Am. Chem. Soc. **82**, 5749 (1690).
11. J. N. Shoolery and M. T. Rogers. J. Am. Chem. Soc. **80**, 5121 (1958).
12. F. A. L. Anet. Can. J. Chem. **39**, 789 (1961).
13. D. R. Davis, R. P. Lutz, and J. D. Roberts. J. Am. Chem. Soc. **83**, 246 (1961).
14. P. L. Corio. Chem. Revs. **60**, 385 (1960).
15. J. A. Pople, W. G. Schneider, and H. J. Bernstein. High-resolution nuclear magnetic resonance. McGraw-Hill Book Co., New York. 1959.
16. S. Goodwin, J. N. Shoolery, and L. F. Johnson. J. Am. Chem. Soc. **81**, 3065 (1959).
17. R. Anet. J. Org. Chem. **26**, 246 (1961).
18. P. M. Nair and J. D. Roberts. J. Am. Chem. Soc. **79**, 4565 (1957).
19. J. S. Waugh and F. A. Cotton. J. Phys. Chem. **65**, 562 (1961).
20. G. Slomp and B. R. McGarvey. J. Am. Chem. Soc. **81**, 2200 (1959).
21. R. U. Lemieux, R. K. Kullnig, H. J. Bernstein, and W. G. Schneider. J. Am. Chem. Soc. **80**, 6098 (1958).
22. J. I. Musher. Spectrochim. Acta, **16**, 835 (1960).
23. F. A. L. Anet. Proc. Chem. Soc. 327 (1959).
24. C. W. Beckett, K. S. Pitzer, and R. Spitzer. J. Am. Chem. Soc. **69**, 977, 2488 (1947).
25. F. A. L. Anet and V. Rao. Tetrahedron Letters, No. 20, 9 (1960).
26. F. A. L. Anet and C. R. Eves. Can. J. Chem. **36**, 902 (1958).
27. F. A. L. Anet and V. Rao. To be published.
28. W. A. Ayer and G. G. Iverach. Tetrahedron Letters, No. 10, 19 (1960).
29. J. Kavadias. Ph.D. Thesis, University of Ottawa, Ottawa, Ont. 1961.
30. B. R. McGarvey and G. Slomp. J. Chem. Phys. **30**, 1586 (1959).
31. P. T. Narasimhan and M. T. Rogers. J. Am. Chem. Soc. **82**, 5983 (1960); J. Chem. Phys. **34**, 1049 (1961).

Can. J. Chem. Downloaded from www.nrcresearchpress.com by 210.87.254.40 on 09/05/12
For personal use only.

32. J. R. CAVANAUGH and B. P. DAILEY. J. Chem. Phys. **34**, 1094 (1961).
33. G. D. TIERS. J. Phys. Chem. **62**, 1151 (1958).
34. G. WITTIG and U. SCHOELLKOPF. Org. Syntheses, **40**, 66 (1960).
35. S. SIEGEL and G. V. SMITH. J. Am. Chem. Soc. **82**, 6087 (1960).
36. J. F. SAUVAGE, R. H. BARKER, and A. S. HUSSEY. J. Am. Chem. Soc. **82**, 6090 (1960).
37. S. WINSTEIN and H. J. LUCAS. J. Am. Chem. Soc. **61**, 1576 (1939).
38. J. R. CAVANAUGH and B. P. DAILEY. J. Chem. Phys. **34**, 1099 (1961).

Can. J. Chem. Downloaded from www.nrcresearchpress.com by 210.87.254.40 on 09/05/12
For personal use only.

Can. J. Chem. Downloaded from www.nrcresearchpress.com by 210.87.254.105 on 09/05/12
For personal use only.

EXTRACELLULAR ACIDIC POLYSACCHARIDES FROM C. INSIDIOSUM AND OTHER CORYNEBACTERIUM SPP.[1]

P. A. J. GORIN AND J. F. T. SPENCER

ABSTRACT

The extracellular polysaccharide of *Corynebacterium insidiosum*, the causative agent of alfalfa wilt, contains D-glucose, D-galactose, and L-fucose in the proportions 2:3:4, with smaller amounts of an unknown acid. Partial acid hydrolysis of the polysaccharide gives 4-*O*-β-D-glucopyranosyl-L-fucose and 4-*O*-β-D-glucopyranosyl-(3-*O*-D-galactopyranosyl)-L-fucose as neutral oligosaccharides. Also formed are D-galactose, substituted in the 4-position with an unknown acid, and 4-*O*-β-D-glucopyranosyl-(3-*O*-D-galactopyranosyl)-L-fucose, which has the 4-position of the galactopyranosyl moiety substituted in a similar way. It appears that the above oligosaccharides represent the structure of the polysaccharide to a considerable extent.

Phytopathogenic microorganisms of several genera have been shown to form extracellular polysaccharides in synthetic media and in some cases these materials appear to have a phytotoxic effect when they are formed in vivo (1). Three genera are being examined and structural determinations on the extracellular polysaccharides from *Xanthomonas* spp., *Agrobacterium* spp., and *Corynebacterium* spp. are being carried out. Within the latter two genera there is a consistency in the composition of the polysaccharides, as *Agrobacterium* spp. form mainly 1,2-β-D-glucopyranose polymers (2, 3) and the *Xanthomonas* spp. produce gummy polysaccharides containing glucuronic acid, glucose, and mannose in varying proportions and in one case glucuronic acid, galactose, and glucose (4).

In the present study the polysaccharides from *Corynebacterium* spp. have been examined and have been shown to be somewhat more heterogeneous in their properties than those in the other two genera. For instance, *C. insidiosum*, *C. sepedonicum*, and *C. michiganense* contain hexoses with a high proportion of methylpentose(s) and give, on partial acid hydrolysis, acidic sugars with color reactions unlike those given by uronic acids (Table I). However, *C. flaccumfaciens*, *C. tritici*, *C. rathayi*, and *C. poinsettia* appear to be in a different group, giving, on acidic hydrolysis, substances resembling aldobiouronic acids by their color reactions and mobilities on paper chromatograms. In this respect the latter three organisms form polysaccharides that seem to bear a resemblance to extracellular polysaccharides formed by phytopathogenic *Xanthomonas* spp. (4).

The extracellular polysaccharide from *Corynebacterium insidiosum*, the causative agent of alfalfa wilt, was examined in more detail since it had the unusual features described above when the organism was grown on a dialyzed yeast extract medium. The polymer was complex, yielding, on acid hydrolysis, galactose, glucose, and fucose in the proportion 3:2:4 and in addition contained an acidic grouping for every six sugar units. However, this acidic function was not of the usual uronic acid type since no aldobiouronic acids were detected after strong acid hydrolysis. Therefore it was evident that structural determinations on the polysaccharide should be carried out initially by other methods apart from the methylation route.

Much useful information was furnished by partial hydrolysis of the *C. insidiosum* polysaccharide and fractionation of the products by charcoal and cellulose chroma-

[1]*Manuscript received July 10, 1961.*
Contribution from the National Research Council of Canada, Prairie Regional Laboratory, Saskatoon, Saskatchewan.
Issued as N.R.C. No. 6526.

Can. J. Chem. Downloaded from www.nrcresearchpress.com by 210.87.254.105 on 09/05/12
For personal use only.

tography. Four main products were obtained, two being neutral and the other two sugars containing acidic functions which were not uronic in nature.

One of the neutral sugars was shown to be 4-*O*-β-D-glucopyranosyl-L-fucose (I), which must represent a large proportion of the polysaccharide since no free glucose was present in the partial hydrolyzate although much galactose and fucose were produced. The disaccharide was amorphous, but a crystalline heptaacetate was prepared and also the derived polyhydric alcohol (5) gave an octaacetate which crystallized. The 4-linkage was assigned to the disaccharide since it took up 2.0 moles of lead tetraacetate in acetic acid gradually (6). This was confirmed by periodate oxidation of the derived polyol, which consumed 3.8 moles of oxidant yielding 1.9 moles of formic acid and no acetaldehyde. Since the specific rotation of the 4-*O*-D-glucopyranosyl-L-fucitol was $-30°$ it seemed probable that the linkage configuration was β (7).

The other neutral fragment proved to be a trisaccharide (II) containing galactose, glucose, and fucose. Partial acid hydrolysis, using conditions similar to those used in the preparation of the trisaccharide from the polysaccharide, gave galactose and 4-*O*-β-D-glucopyranosyl-L-fucose, thus suggesting that the trimer also represents structurally a large proportion of the polysaccharide. The reducing end of the sugar was shown to be fucose since it was the only part that was reduced by sodium borohydride. The fucose portion was then shown to be linked in the 3-position by lead tetraacetate oxidation, since the sugar consumed 1 mole of oxidant (6), suggesting a branched-chain 4-*O*-β-D-glucopyranosyl(3-*O*-D-galactopyranosyl)-L-fucose structure (II). This was confirmed by two methods, oxidation with lead tetraacetate in potassium acetate – acetic acid, which gave 2 moles of formic acid slowly by oxidation of the glucose and galactose non-reducing end units (8). In addition, oxidation with sodium periodate gave a product which, on sodium borohydride reduction followed by acid hydrolysis, was degraded to glycerol and 5-deoxy pentitol.

When the two acidic sugars obtained on partial hydrolysis of the polysaccharide were examined it was shown that the unknown acid was attached to the 4-position of the galactose molecule in each case. The sugar with the lower molecular weight (III) crystallized and was shown to contain galactose since this hexose was formed by strong acid hydrolysis. C-1 of the galactose was apparently free since the substance mutarotated from $+70°$ to $+49°$ in water. Titration with alkali indicated a neutral equivalent of 288 and, based on this figure, consumption of lead tetraacetate by the sugar was 0.31, 0.69, 1.13, and 1.32 moles after 2, 5, 10, and 20 minutes respectively, thus indicating 4-substitution. Carbon and hydrogen analyses suggested an empirical formula of $C_{11}H_{20}O_9$, corresponding to a hexose unit attached ethereally to a hydroxy group of a dihydroxypentanoic acid. This formulation, however, does not agree with the infrared data obtained on the free sugar or the derived alcohol, the latter being obtained by methylation (CH_2N_2) followed by sodium borohydride reduction (9). The free sugar has a band at 1705 cm^{-1} corresponding to a carboxyl carbonyl group and there also appears to be a partially obscured band at 1725 cm^{-1} to 1750 cm^{-1}, which could represent an ester carbonyl group. The derived methyl ester gave a sharp band at 1735 cm^{-1} and on treatment with sodium borohydride a neutral substance was obtained which gave a strong band at 1740 cm^{-1}. This product, according to paper chromatograms, contained a little hexitol as well as the expected material so that the weight of evidence so far obtained indicates an ester-type linkage at the 4-position of the galactose residue.

The higher molecular weight material (IV) was amorphous and gave galactose, glucose, and fucose on acid hydrolysis, and on partial hydrolysis 4-*O*-β-D-glucopyranosyl-L-fucose

and the acidic galactose derivative were detected on paper chromatograms (III). Fucose was again shown to be at the reducing end by sodium borohydride reduction and, if a molecular weight of 602* is assumed, lead tetraacetate oxidation studies indicated a 3-linked fucose residue. It thus seemed that a 4-*O*-β-D-glucopyranosyl(3-galacto-pyranosyl)-L-fucose structure with an unknown carboxyl derivative attached (IV) was likely and its position of substitution on the galactose was shown to be at 4 since periodate oxidation of the oligosaccharide followed by sodium borohydride reduction and acid hydrolysis gave erythritol in addition to glycerol and 5-deoxy pentitol.

Periodate oxidation of the polysaccharide gave little information, except to show that non-reducing end groups or 6-linked hexopyranosyl units only are oxidized, and since overoxidation takes place only a rough figure of 28% can be estimated for their presence in the total polysaccharide.

Thus the polysaccharide from *C. insidiosum* is complex, particularly so because of the attachment of an unknown acidic entity on the galactose position. However, this type of substituent appears to be quite widespread at least in the extracellular polysaccharides from *Corynebacterium* spp., and more work is needed to show their true identities.

EXPERIMENTAL

Evaporations were carried out at 50° C under reduced pressure and specific rotations measured at 23° C.

Cultural Methods for Polysaccharide Production

The cultures of *Corynebacterium* spp. were maintained on a medium containing 1.5% glucose, 1.0% yeast extract, 0.5% calcium carbonate, and 1.3% agar.

The organisms were grown in a medium containing 1.5% glucose, 1.0% yeast extract, and 0.2 to 0.5% calcium carbonate. The yeast extract solution was dialyzed before use to remove high molecular weight polysaccharides. Small quantities of gum-producing polysaccharide were produced in 500-ml Erlenmeyer flasks containing 100 ml medium, incubated at 25° C on a rotary shaker, eccentricity 1/2 inch, operated at 250 r.p.m. For production of larger quantities of polysaccharide the organisms were grown in 5-liter glass-jar-type stirred fermentors having a working volume of 3 liters or in 30-liter stainless steel fermentors having a working volume of 20 liters.

Cells were removed in a Sharples supercentrifuge or in a Spinco ultracentrifuge if necessary, generally after about 4 days. Culture supernatants which contained a good deal of suspended matter after concentration were again centrifuged in the ultracentrifuge. After centrifugation the solutions were evaporated under vacuum to as small a volume as possible and the polysaccharide was precipitated by addition of 5 volumes of ethanol. For *Corynebacterium insidiosum* the yields of crude product were approximately 3 g per liter. The precipitate was recovered and redissolved in a large quantity of water and the solution treated with Amberlite IR-120 and Dowex-1. After filtration and evaporation the purified polysaccharide was reprecipitated with excess ethanol, washed with ethanol, and dried.

General Examination Procedure for Polysaccharides

The polysaccharide from each fermentation was hydrolyzed with *N* sulphuric acid at 100° C overnight to obtain the over-all sugar composition as shown by paper chromatograms using *p*-anisidine hydrochloride (10) as spray reagent. Those that did not show

**Based on a trisaccharide with a carboxyl function attached in a manner similar to that on III.*

Can. J. Chem. Downloaded from www.nrcresearchpress.com by 210.87.254.105 on 09/05/12
For personal use only.

aldobiouronic acids under these conditions were partially hydrolyzed for 6 hours with *N* sulphuric acid at 70° C, under which conditions other acidic components might be detected. The results are listed in Table I.

TABLE I

Properties of extracellular *Corynebacterium* spp. polysaccharides

Organism and its A.T.C.C. number	Constituent sugars	$[\alpha]_D$	Non-uronic acid acidic function
C. insidiosum 10253	Galactose (32%) Glucose (21%) Fucose (46%)	−98°	+ve
C. sepedonicum 9850	Galactose (45%) Glucose (27%) Fucose (29%)	+87°	+ve
C. michiganense 7433	Galactose Glucose Mannose Fucose (33.9% total)	−33°	+ve
C. fascians 12974	Mannose Glucose Tr. galactose	+60°	Not tested
C. flaccumfaciens 7392	Glucose Mannose Fucose Rhamnose Aldobiouronic acid	−12°	—
C. tritici 9682	Glucose Mannose Rhamnose Aldobiouronic acid	+13°	—
C. rathayi 80†	Glucose Mannose Aldobiouronic acid Unknown at $R_{rhamnose}$ 1.1*	+51°	—

*Solvent. Ethyl acetate – acetic acid – water 9:2:2 v/v.
†National Collection of Plant Pathogenic Bacteria, Ministry of Agriculture, Fisheries and Food, Plant Pathology Laboratory, Harpenden, Herts, England.

Complete Hydrolysis of C. insidiosum Polysaccharide

The polysaccharide (100 mg) was hydrolyzed for 18 hours at 100° C in *N* sulphuric acid. The solution was then neutralized ($BaCO_3$), filtered, and evaporated to give a mixture of galactose, glucose, and fucose. These components were separated on a sheet of Whatman No. 1 filter paper using ethyl acetate – pyridine – water (10:4:3 v/v) as solvent and the relative amounts of sugars present estimated colorimetrically by the benzidine method of Jones and Pridham (11). The ratio of galactose–glucose–fucose was 3:2:4, the fucose composition checking well with a C-methyl estimation on the mixture. A larger scale hydrolysis was carried out and the components were fractionated on a cellulose column using *n*-butanol half saturated with water to yield L-fucose, D-glucose, and D-galactose, which were crystallized and identified.

Partial Hydrolysis of C. insidiosum Polysaccharide

The polysaccharide (20 g) was dissolved in *N* sulphuric acid (2 liters) by stirring the mixture at 70° C for 6 hours. After neutralization ($BaCO_3$) and removal of cations with Amberlite IR-120, the solution was examined on paper chromatograms and was shown to contain galactose and fucose as the monosaccharide fraction. On a paper chromatogram

Can. J. Chem. Downloaded from www.nrcresearchpress.com by 210.87.254.105 on 09/05/12
For personal use only.

using the ethyl acetate – acetic acid – water (9:2:2 v/v) solvent a yellow-brown spot ($R_{galactose}$ 0.8) with the *p*-anisidine hydrochloride spray was evident with smaller amounts of yellow spots with $R_{lactose}$ 0.7 and 1.1. The solution was passed down a charcoal column and the galactose and fucose removed by washing with water. Thirty per cent aqueous

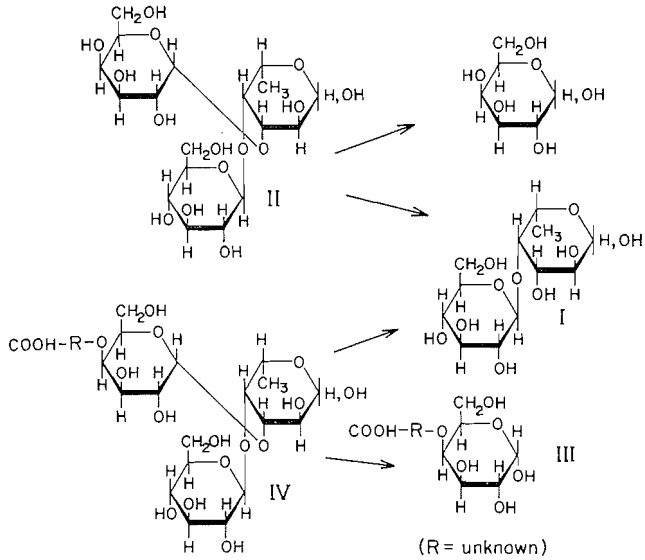


FIG. 1. Partial hydrolysis products of *C. insidiosum* polysaccharide.

ethanol eluted the compounds giving spots with $R_{galactose}$ 0.8 and $R_{lactose}$ 0.7 and 1.1, and in addition, a material running at the same speed as fucose and giving a yellow-brown spot with *p*-anisidine hydrochloride. The materials with $R_{lactose}$ 0.7 and R_{fucose} 1.0 proved to be acidic since they ran slowly in the ethyl acetate – pyridine – water (10:4:3 v/v) solvent.

The above components were fractionated on a cellulose column. Butanol saturated with water separated the materials with R_{fucose} 1.0 and $R_{galactose}$ 0.8 and butanol–ethanol–water (8:2:1 v/v) separated the other slower moving materials with $R_{lactose}$ 1.1 and 0.7. These partial hydrolysis products were examined for their chemical structures.

Identification of 4-O-β-D-Glucopyranosyl-L-fucose ($R_{galactose}$ 0.8) (I)

This material (3.4 g) was isolated in an amorphous form and a portion (300 mg) was converted to its heptaacetate by heating on a steam bath overnight in acetic anhydride (5 ml) containing sodium acetate (300 mg). After the excess anhydride was destroyed with ice-water, the solution was extracted with chloroform. The chloroform extract crystallized on evaporation and two recrystallizations from ethanol yielded a heptaacetate (123 mg) with m.p. 228–230° C and $[\alpha]_D$ −59° (*c*, 1.0, $CHCl_3$). Calculated for $C_{26}H_{36}O_{17}$: C, 50.3%; H, 5.85%. Found: C, 50.2%; H, 6.1%.

Deacetylation with a catalytic amount of sodium methoxide in methanol yielded, after neutralization with acetic acid, the free sugar with $[\alpha]_D$ −71° (*c*, 0.6, H_2O). Acid hydrolysis with *N* sulphuric acid at 100° C overnight yielded glucose and fucose (paper chromatograms). After 2, 5, 15, and 60 minutes the sugar consumed 0.81, 1.58, 1.99, and 2.06 moles of lead tetraacetate in acetic acid, respectively, giving strong indication of a 4-linked disaccharide.

Can. J. Chem. Downloaded from www.nrcresearchpress.com by 210.87.254.105 on 09/05/12
For personal use only.

Can. J. Chem. Downloaded from www.nrcresearchpress.com by 210.87.254.105 on 09/05/12
For personal use only.

The disaccharide (200 mg) was reduced with sodium borohydride (50 mg) in water (2 ml). After 4 hours the reductant was destroyed with acetic acid and cations were removed with Amberlite IR-120. The solution was filtered and evaporated to a crust which was repeatedly dissolved in methanol, which was then evaporated. The amorphous polyol was converted to its octaacetate by the acetylation procedure used above. Two recrystallizations from ethanol yielded crystals with m.p. 125–126° C and $[\alpha]_D$ −30° (*c*, 1.1, $CHCl_3$). Calculated for $C_{28}H_{40}O_{18}$: C, 50.6%; H, 6.1%. Found: C, 50.6%; H, 6.2%.

Deacetylation gave 4-*O*-β-D-glucopyranosyl-L-fucitol with $[\alpha]_D$ −30° (*c*, 1.1, H_2O), which was oxidized with aqueous sodium periodate and after 18 hours took up 3.8 moles of oxidant giving 1.9 moles of formic acid. No acetaldehyde could be detected (12) in the oxidation mixture.

Identification of 4-O-β-D-Glucopyranosyl(3-O-D-galactopyranosyl)-L-fucose ($R_{lactose}$ 0.7) (II)

This material ($[\alpha]_D$ +23° (*c*, 1.3, H_2O)) gave galactose, glucose, and fucose (paper chromatograms) on hydrolysis with *N* sulphuric acid at 100° C overnight. Reduction for 18 hours with sodium borohydride gave a polyol, which, on acid hydrolysis at 100° C with *N* sulphuric acid overnight gave, as reducing sugar, galactose and glucose and also some fucitol, detectable with the ammoniacal silver nitrate spray (13).

The fucose reducing end-unit was linked in the 3-position since, based on a molecular weight of 488, it took up 1.01, 1.04, and 1.09 moles of lead tetraacetate in acetic acid after 4, 15, and 30 minutes respectively. The trisaccharide was also oxidized with lead tetraacetate in 90% acetic acid containing potassium acetate and the formic acid produced measured as carbon dioxide in a Warburg respirometer (8). The production of carbon dioxide corresponded to the oxidation of two non-reducing end-units, one being oxidized more quickly than the other. At the end of the reaction 4.72 moles of oxidant had been consumed in glycol cleavage.

TABLE II

Time (minutes)	12	20	35	65	95	145	285	325	465
Moles CO_2 produced	0.43	0.64	0.80	0.95	1.08	1.38	1.78	1.87	2.11

The trisaccharide (10 mg) was oxidized overnight with excess aqueous sodium periodate and the ions then removed with mixed Amberlite IR-120 and Dowex-1 (bicarbonate form). The aldehyde was reduced with sodium borohydride by the method described previously and the product hydrolyzed with *N* sulphuric acid (5 ml) at 100° C overnight. The product, after neutralization ($BaCO_3$), was examined on a paper chromatogram (solvent *n*-butanol:ethanol:water, 40:11:19 v/v) and the only detectable spots using the ammoniacal silver nitrate spray corresponded to glycerol and a spot which could be 5-deoxylyxitol. These results agree with the above lead tetraacetate oxidation in that two non-reducing end-units are present.

A sample of the trisaccharide (70 mg) was partially hydrolyzed with *N* sulphuric acid (1 ml) at 70° C for 6 hours. After neutralization ($BaCO_3$) and filtration, the product corresponded to a mixture of 4-*O*-β-D-glucopyranosyl-L-fucose and galactose. These components were separated on sheets of Whatman No. 1 filter paper using *n*-butanol–ethanol–water (40:11:19 v/v) as solvent, and the two sugars were identified, the disaccharide as its heptaacetate and the galactose by its 1-methylphenylhydrazone (14). These were each compared with authentic specimens and had identical X-ray diffraction patterns.

Unknown Acidic Galactose Derivative (R_{fucose} 1.0) (III)

This product crystallized and two recrystallizations from ethanol yielded a material with m.p. 113–114° C and had $[\alpha]_D$ +70° → +49° (*c*, 0.6, H_2O, constant value). Acid hydrolysis at 100° C in *N* sulphuric acid for 18 hours yielded galactose (paper chromatograms). Its neutral equivalent was 288 and this figure and the analysis figures of C, 44.9%; H, 6.9% indicate a $C_{11}H_{20}O_9$ formula. Calculated for $C_{11}H_{20}O_9$: C, 44.6%; H, 6.8%. The infrared spectrum had strong absorption at 1705 cm^{-1} corresponding to acid carbonyl and a shoulder to this peak pointed to ester carbonyl absorption in the region 1725 cm^{-1} to 1750 cm^{-1}. Lead tetraacetate oxidation of the sugar resulted in uptake of 0.31, 0.69, 1.13, and 1.32 moles of oxidant after 2, 5, 10, and 20 minutes respectively based on a molecular weight of 288. These figures, even if this molecular weight is only approximate, indicate 4-substitution on the galactose molecule.

Treatment of the unknown acid (25 mg) in methanol with ethereal diazomethane yielded, on evaporation, its methyl ester (25 mg) having infrared absorption at 1735 cm^{-1}. The ester was dissolved in methanol (1 ml) containing 0.1 equivalent of sodium methoxide at 0° C, and sodium borohydride (20 mg) was added, the solution being kept in the refrigerator for 6 hours. The methanol was then removed by evaporation and the product isolated as described above. On paper chromatograms in *n*-butanol–ethanol–water (40:11:19 v/v) a main spot with $R_{rhamnose}$ 1.3, detectable with ammoniacal silver nitrate, was found together with a minor spot corresponding to a hexitol. Infrared absorption of the product at 1740 cm^{-1} indicated that an ester carboxyl group was still present.

Unknown Acidic 4-O-β-D-Glucopyranosyl-(3-O-galactopyranosyl)-L-fucose Derivative ($R_{lactose}$ 1.1) (IV)

This sugar, having $[\alpha]_D$ +9° (*c*, 0.6, H_2O) was cleaved using conditions identical with those for hydrolysis of the trisaccharide (II), giving galactose, glucose, and fucose. Partial acid hydrolysis gave 4-*O*-β-D-glucopyranosyl-L-fucose and the unknown acidic galactose derivative (III), all these sugars being identified by their chromatographic behavior. Fucose was identified as the reducing end of the sugar since sodium borohydride reduction followed by acid hydrolysis gave fucitol. The fucose was substituted in the 3-position since 0.90, 1.03, and 1.21 moles of lead tetraacetate in acetic acid were taken up after 2, 10, and 45 minutes, respectively, based on a molecular weight of 602. Sodium periodate oxidation* followed by sodium borohydride reduction, then hydrolysis, gave erythritol in addition to glycerol and 5-deoxy-lyxitol, indicating the unknown substituent was located in the 4-position of the galactose unit.

Sodium Periodate Oxidation of C. insidiosum Polysaccharide

The polysaccharide, $[\alpha]_D$ −98° (*c*, 0.7, H_2O), gave analysis figures of C 44.7%, H 6.9%, N 0.3%, ash 0.9%, and Cl 0.22%, and contained an acid group for every 912 of molecular weight. The sodium periodate oxidation data were as follows:

Time (days)	1	2	3	4	5	6	7
Sodium periodate uptake (moles)	0.42	0.46	0.53	—	0.55	0.59	0.60
Formic acid formed (moles)	0.16	0.17	0.21	0.23	0.24	0.25	0.28

The product on sodium borohydride reduction followed by acid hydrolysis in *N* sulphuric acid at 100° C overnight gave glycerol (on paper chromatograms) as the only non-reducing sugar, no erythritol being detected. Glucose, galactose, and fucose were also present.

**In this case sodium periodate and iodate were removed, first by treatment with Amberlite IR-120 and then with barium carbonate.*

Can. J. Chem. Downloaded from www.nrcresearchpress.com by 210.87.254.105 on 09/05/12
For personal use only.

ACKNOWLEDGMENTS

The authors wish to thank Mr. N. Gardner and Mrs. S. F. Hector for technical assistance, Mr. M. Mazurek for microanalytical determinations, and Miss I. M. Gaffney for carrying out infrared measurements.

REFERENCES

1. J. F. T. Spencer and P. A. J. Gorin. Can. J. Microbiol. **7**, 185 (1961).
2. P. A. J. Gorin, J. F. T. Spencer, and D. W. S. Westlake. Can. J. Chem. **39**, 1067 (1961).
3. E. W. Putman, A. L. Potter, R. Hodgson, and W. Z. Hassid. J. Am. Chem. Soc. **72**, 5024 (1950).
4. P. A. J. Gorin and J. F. T. Spencer. To be published.
5. M. L. Wolfrom and H. B. Wood. J. Am. Chem. Soc. **73**, 2933 (1951).
6. A. J. Charlson and A. S. Perlin. Can. J. Chem. **34**, 1200 (1956).
7. A. J. Charlson, P. A. J. Gorin, and A. S. Perlin. Methods in carbohydrate chemistry. In press.
8. A. S. Perlin. J. Am. Chem. Soc. **76**, 5505 (1954).
9. H. L. Frush and H. S. Isbell. J. Am. Chem. Soc. **78**, 2844 (1956).
10. L. Hough, J. K. N. Jones, and W. H. Wadman. J. Chem. Soc. 1702 (1950).
11. J. K. N. Jones and J. B. Pridham. Biochem. J. **58**, 288 (1954).
12. P. Desnuelle and M. Naudet. Bull. soc. chim. France, **12**, 871 (1945).
13. S. M. Partridge. Nature, **158**, 270 (1946).
14. C. A. Lobry de Bruyn and W. A. van Eckenstein. Rec. trav. chim. **15**, 226 (1896).

Can. J. Chem. Downloaded from www.nrcresearchpress.com by 210.87.254.105 on 09/05/12
For personal use only.

Can. J. Chem. Downloaded from www.nrcresearchpress.com by 210.87.254.40 on 09/05/12
For personal use only.

STRUCTURAL RELATIONSHIPS OF EXTRACELLULAR POLYSACCHARIDES FROM PHYTOPATHOGENIC XANTHOMONAS SPP.

PART I. STRUCTURE OF THE EXTRACELLULAR POLYSACCHARIDE FROM XANTHOMONAS STEWARTII[1]

P. A. J. GORIN AND J. F. T. SPENCER

ABSTRACT

Xanthomonas stewartii produces an extracellular polysaccharide which is markedly different from those formed by other *Xanthomonas* spp. examined in that it gave glucose, galactose, and an aldobiouronic acid on hydrolysis. Methylation followed by hydrolysis yielded 2,3,4,6-tetra-*O*-methyl-D-glucose (4 parts), 2,3,4-tri-*O*-methyl-D-glucose (2 parts), 2,4,6-tri-*O*-methyl-D-galactose (1 part), 2,3,4-tri-*O*-methyl-D-galactose (2 parts), and 2-*O*-methyl-D-galactose (1.8 parts). Partial acid hydrolysis yielded 6-*O*-β-D-glucopyranosyl-D-galactose, 3-*O*-β-D-glucopyranosyl-D-galactose, 3-*O*-β-D-galactopyranosyl-D-galactose, and 4-*O*-β-D-glucuronopyranosyl-D-galactose.

The extracellular polysaccharides from phytopathogenic species of *Xanthomonas* are being examined and a consistency of structure within the genus, at least as far as the sugar constituents of the polysaccharides are concerned, has been demonstrated. Nine of the 12 *Xanthomonas* spp. studied produce polysaccharides (on dialyzed yeast extract medium) which give viscous aqueous solutions and contain glucuronic acid, glucose, and mannose. Two species examined do not produce appreciable amounts of polysaccharide,* and *Xanthomonas stewartii* (formerly *Bacterium stewartii*), the corn wilt organism, forms a different type of polysaccharide containing glucuronic acid, galactose, and glucose (Table I). This polysaccharide also gives viscous solutions in water. These

TABLE I

Xanthomonas spp. and their extracellular polysaccharides

Polysaccharide-forming *Xanthomonas* spp. (with A.T.C.C. number) and their products of hydrolysis		
Aldobiouronic acid, glucose, and mannose	Aldobiouronic acid, galactose, and glucose	*Xanthomonas* spp. not forming polysaccharides
*X. campestris**	*X. stewartii* (8199)	*X. beticola* (10309)
X. carotae (10547)		*X. vasculorum*
X. hyacinthi (12612)		
X. maculofoliigardeniae (10201)		
X. malvacearum (12131)		
X. phaseoli†		
X. pruni (10016)		
X. translucens (10722)		
X. vignicola (11648)		

*Reference 18.
†Reference 17.

results agree with the reclassification of this organism described in the 1957 Bergey's Manual of Determinative Bacteriology (1). *Xanthomonas stewartii* is quoted to be a

[1]*Manuscript received July 10, 1961.*
Contribution from the National Research Council of Canada, Prairie Regional Laboratory, Saskatoon, Saskatchewan.
Issued as N.R.C. No. 6525.

**Any taxonomic deductions on non-polysaccharide-forming species should be made carefully since it is quite possible that other polysaccharide-forming strains of the same species exist.*

Can. J. Chem. Downloaded from www.nrcresearchpress.com by 210.87.254.40 on 09/05/12
For personal use only.

Xanthomonas species incertae sedis and plant pathologists have placed it in the *Xanthomonas* genus even though it does not possess all the characteristics of the genus.

Since a large proportion of *Xanthomonas* spp. (Table I) produce polysaccharides which give solutions of high viscosity, it is of interest to observe that the vascular systems of plants can be blocked to some extent by these solutions. This effect has been observed on tomato cuttings by Riker and co-workers (2), using several polysaccharides, and by Leach *et al.* (3), who showed that excised seedlings of tomato, sunflower, and bean wilted under the influence of an aqueous solution of *X. phaseoli* polysaccharide. Also, the authors of the present paper have demonstrated the wilting properties of the *Corynebacterium insidiosum* polysaccharide on alfalfa cuttings and the fact that the polymer is formed in the infected plant itself (4). This physiological action has been observed in a different way by Corey and Starr (5), who studied the morphology of four strains of *X. phaseoli* and showed that the amount of polysaccharide formed by each strain could be correlated with its virulence on the host plant.

Therefore a more detailed structural analysis on the extracellular polysaccharides of the *Xanthomonas* species is being carried out, starting with *X. stewartii*. It is hoped that the polysaccharides from some of the other species containing glucuronic acid, glucose, and mannose (Table I) can be studied later.

The polysaccharide from *X. stewartii* proved to be highly branched, approximately one-third of the sugar residues consisting of non-reducing glucose end units. Studies on the methyl glycosides obtained from the fully methylated polysaccharides were kindly carried out by Dr. C. T. Bishop (6) using the gas–liquid phase chromatography procedure. The presence of the methyl glycosides of 2,3,4,6-tetra-*O*-methyl-D-glucose (4 parts), 2,3,4-tri-*O*-methyl-D-glucose (2 parts), 2,4,6-tri-*O*-methyl-D-galactose (1 part), and 2,3,4-tri-*O*-methyl-D-galactose (2 parts) was shown. Cellulose chromatography (7) of the reducing methyl sugars showed the absence of di-*O*-methyl-D-glucose. However, 2-*O*-methyl-D-galactose was isolated in a proportion equivalent to 1.8 parts taking into account the glucuronic acid in the molecule which is equivalent to 1.3 parts. The above figures also give an estimate of the proportion of sugars in the polysaccharide, which amount to glucuronic acid (11%), glucose (51%), and galactose (32%).

Periodate oxidation of the polysaccharide showed an immediate uptake (18 hours) of oxidant and production of formic acid with little further oxidation over a week. A 1.20-mole quantity of oxidant was consumed with the evolution of 0.58 mole of formic acid, amounts which agree closely with a 1.30 molar uptake and 0.65-mole quantity of formic acid that would be calculated from the methylation results.

Since information was required on the sugar sequence in the polysaccharide, a partial acid hydrolysis was carried out at 80° C with *N* sulphuric acid. Two main disaccharide fractions were obtained by cellulose chromatography, one of which was 6-*O*-β-D-glucopyranosyl-D-galactose, isolated in 13% yield. Although it crystallized only with difficulty, it could be converted readily to crystalline 6-*O*-β-D-glucopyranosyl-D-galactitol nonaacetate by sodium borohydride reduction followed by acetylation. This compound proved to be identical with a specimen prepared similarly from the authentic reducing disaccharide (8). The other disaccharide, 3-*O*-β-D-glucopyranosyl-D-galactose, did not crystallize. However, it gave glucose and galactose on acid hydrolysis and glucose only on sodium borohydride reduction followed by acid hydrolysis. The position of substitution on the galactose reducing end was determined by lead tetraacetate oxidation and since 1 mole was taken up immediately (3 minutes) with little increase over 30

minutes, the linkage was evidently in the 3-position (9). For a glucose–galactose disaccharide its specific rotation of +35° was low, suggesting a β-configuration for the glycosidic linkage.

An aldobiouronic acid was obtained by an isolation procedure similar to that described above except that the hydrolysis in *N* sulphuric acid was carried out at 100° C. The aldobiouronic acid gave a uronic acid and galactose on vigorous acid hydrolysis and when the dimer was oxidized with lead tetraacetate it consumed 1.8 moles of oxidant (after 30 minutes) at a slower rate than that expected for a 6-linkage. The material was therefore 4-linked and the 4-*O*-glucuronopyranosyl-D-galactose structure seemed likely. Treatment with diazomethane and reduction of the methyl ester with sodium borohydride (10) gave a crystalline disaccharide alcohol with $[\alpha]_D$ −13°. Acid hydrolysis gave glucose as the only reducing sugar, thus identifying the uronic acid portion. Since the specific rotations of the neutral derivative (and the parent aldobiouronic acid) were low, the configuration of the glycosidic linkage should be β.

Another type of acid hydrolysis of the polysaccharide was carried out using the procedure of Smith and co-workers (11) wherein the polysaccharide was oxidized with sodium periodate. The oxypolysaccharide was then reduced with sodium borohydride and the product obtained hydrolyzed with acid. However, with this polysaccharide somewhat more vigorous conditions were needed than those recommended by the Minnesota group. The reducing sugars obtained were galactose and a disaccharide, and after cellulose chromatography the dimer was isolated and tentatively characterized as 3-*O*-β-D-galactopyranosyl-D-galactose (12). Although it could not be induced to crystallize, it gave galactose only on acid hydrolysis. When it was treated with lead tetraacetate, the consumption of oxidant corresponded to a 3-linked disaccharide and the product on hydrolysis contained galactose and lyxose. The specific rotation (+52°) corresponded closely to that of authentic 3-*O*-β-D-galactopyranosyl-D-galactose. Since no trisaccharide was obtained in the partial hydrolysis of the modified polysaccharide, it can be safely assumed that there were no more than two successive galactose residues in the starting polysaccharide that were linked in the 3-position.

Methylation of the galactose-containing polysaccharide obtained by successive sodium periodate oxidation and sodium borohydride reduction and hydrolysis under milder conditions than above gave a product which, on hydrolysis, gave three poly-*O*-methyl galactose derivatives. These were isolated from cellulose columns and shown to be 2,3,4,6-tetra-*O*-methyl-D-galactose (characterized as the aniline derivative), 2,4,6-tri-*O*-methyl-D-galactose, and 2,6-di-*O*-methyl-D-galactose in the proportion 1.7:1:1.15, thus confirming the isolation of 3-*O*-β-D-galactopyranosyl-D-galactose. These results also suggest that the 2,6-di-*O*-methyl-D-galactose represents the same fragment that yields 2-*O*-methyl-D-galactose from the undegraded methylated polysaccharide. Also, since the degraded polysaccharide contained galactose only, the glucuronic acid portion in the *X. stewartii* polysaccharide was linked in such a way as to permit periodate oxidation.

Summarizing, the polysaccharide is highly branched and contains no points of single branching, only double branching as represented by the 2-*O*-methyl galactose obtained in the methylation studies. The polymer contains at least four different linkage types. These were demonstrated by the isolation of 6-*O*-β- and 3-*O*-β-D-glucopyranosyl-D-galactose, 3-*O*-β-D-galactopyranosyl-D-galactose and 4-*O*-β-D-glucuronopyranosyl-D-galactose and by identification of the hydrolysis products of the methylated polysaccharide (Table II). The non-reducing end units consist of glucose (and glucuronic acid perhaps) and it seems likely that these are β-linked to galactopyranose residues in the

Can. J. Chem. Downloaded from www.nrcresearchpress.com by 210.87.254.40 on 09/05/12
For personal use only.

6-position. However, further deductions on the structure of this rather complex polysaccharide would be somewhat speculative and would require, for example, the isolation of trisaccharides in good yield in order to furnish a more comprehensive picture.

EXPERIMENTAL

Solutions were evaporated at 50° C under reduced pressure and specific rotations measured at 23° C.

Cultural Conditions for Xanthomonas spp.

The organisms were maintained and polysaccharide produced under conditions identical with those described in a previous paper (13). The yields were generally 1–4 g/liter of crude polysaccharide and this was purified as described previously (13).

Sugar Composition of Polysaccharides

The polysaccharides obtained from various species of *Xanthomonas* were hydrolyzed overnight on a steam bath in *N* sulphuric acid. After neutralization ($BaCO_3$), filtration, and evaporation the sugars were examined on paper chromatograms in various solvents using *p*-anisidine hydrochloride (14) as spray reagent. The results are recorded in Table I.

X. stewartii Polysaccharide and its Periodate Oxidation Characteristics

The polysaccharide had $[\alpha]_D$ +41° (*c*, 0.1, H_2O) and based on an anhydro hexose unit with mol. wt. 162 it contained, by titration, one acidic group per 9 units. Found: C, 43.4%; H, 6.6%; ash, 0.4%. It gave on acid hydrolysis at 100° C overnight in *N* sulphuric acid an aldobiouronic acid, galactose, and glucose. On oxidation with aqueous sodium periodate the following data were obtained:

Time, days	1	2	3	4	5	6
Uptake of oxidant, moles/mole	1.18	1.13	1.03	—	1.26	1.23
Formic acid produced, moles/mole	0.51	0.48	0.54	0.56	0.57	0.54

The end product was dialyzed to remove low molecular weight material and the sample consisting of roughly 50 mg of oxypolysaccharide in water (50 ml) was treated with sodium borohydride (50 mg). After a day, excess reductant was destroyed with acetic acid and the solution was then treated with Amberlite IR-120. The solution was filtered and evaporated to dryness, and the boric acid was removed by repeated evaporations with methanol. The product was hydrolyzed overnight at 100° C in *N* sulphuric acid (2 ml) and after neutralization ($BaCO_3$), filtration, and evaporation the product was examined on paper chromatograms (solvent: *n*-butanol–ethanol–water, 40:11:19 v/v). As would be expected from the periodate data, the only non-reducing sugar that appeared with the ammoniacal silver nitrate spray (15) was glycerol. The only reducing sugar detected was galactose.

Methylation and Hydrolysis of X. stewartii Polysaccharide

The polysaccharide (5.0 g) was dissolved in water (150 ml) to give a very viscous solution. Sodium hydroxide (30 g) in water (60 ml) was added and methylation was carried out by addition of dimethyl sulphate, in 11 separate aliquots of 3 cc each, once every 30 minutes. This process was repeated five times on successive days after which the solution was heated at 100° C for 3 hours. After cooling the methylation mixture was acidified slightly with dilute sulphuric acid and the gummy precipitate which formed was collected and dried. Yield, 3.8 g. The partially methylated polysaccharide was dissolved in dimethyl formamide (200 ml), methyl iodide (200 ml) was added, and the

Can. J. Chem. Downloaded from www.nrcresearchpress.com by 210.87.254.40 on 09/05/12
For personal use only.

solution shaken vigorously. Silver oxide was added on 6 successive days in 30-g portions and after this time chloroform (1 liter) was added and the solution filtered (16). The chloroform was evaporated to a crust, which was redissolved in chloroform and washed with aqueous potassium cyanide followed by water. The methylated residue, after evaporation, weighed 3.6 g.

This product was refluxed in 10% methanolic hydrogen chloride (50 ml) overnight and the solution neutralized (Ag_2CO_3), filtered, and evaporated to a syrup. This was further hydrolyzed by heating at 100° C in *N* sulphuric acid (20 ml) overnight. Neutralization ($BaCO_3$), filtration, and evaporation yielded a syrupy product with —OCH_3 40.2%.

(a) Cellulose Column Chromatography

The above product appeared to contain, by paper chromatography, tetramethyl, trimethyl, and monomethyl hexoses and a spot corresponding to a methylated substance containing uronic acid. Fractionation of a portion (1.1 g) on a cellulose column using *n*-butanol as solvent gave 2-*O*-methyl-D-galactose (68 mg) and 545 mg of other methylated sugars. Two recrystallizations of the monomethyl sugar from ethanol gave crystals with m.p. 152–155° C. Calculated for $C_6H_{11}O_5(OCH_3)$: OCH_3, 16.0%. Found: OCH_3, 16.0%. X-Ray diffraction patterns prepared on this and an authentic specimen were identical.

(b) Gas–Liquid Phase Chromatography

The mixture of reducing methylated sugars (1.0 g) was refluxed overnight in 3% methanolic hydrogen chloride (20 ml). The acid was neutralized with silver carbonate, and the solution then filtered and evaporated to a syrup. Using a standard Pye unit, Dr. C. T. Bishop carried out quantitative separations at 200° C with a column of Carbowax 20 M on Chromosorb P (1:4 w/w) and a flow rate of 40 ml per minute of helium. Tetra- and tri-methyl hexoses were separated and estimated by integration of the area under the peaks on the flow chart (Table II).

TABLE II

Methylation results on *Xanthomonas stewartii* polysaccharide

Substitution in polysaccharide from methylation data	Parts present on a molar basis
Glucose non-reducing end units	4
6-Substituted glucose units	2
3-Substituted galactose units	1
6-Substituted galactose units	2
3,4,6-Substituted galactose units	1.8
Glucuronic acid present*	1.3

*Based on titration against the original polysaccharide.

Partial Hydrolysis of X. stewartii Polysaccharide

(*a*) The polysaccharide (7.5 g) was partially hydrolyzed with *N* sulphuric acid at 80° C for 6 hours. The hydrolyzate was neutralized ($BaCO_3$), filtered, and deionized with Amberlite IR-120 and Dowex-1. The neutral portion (2.05 g) was fractionated on a cellulose column using *n*-butanol–ethanol–water (8:2:1 v/v) as the mobile phase. Two disaccharide fractions were obtained with $R_{lactose}$ 1.1 (1.05 g) and 0.9 (0.23 g) on paper chromatograms in the ethyl acetate – acetic acid – water (9:2:2 v/v) solvent.

Can. J. Chem. Downloaded from www.nrcresearchpress.com by 210.87.254.40 on 09/05/12
For personal use only.

Can. J. Chem. Downloaded from www.nrcresearchpress.com by 210.87.254.40 on 09/05/12
For personal use only.

Both sugars were amorphous and the one with $R_{lactose}$ 1.1 (150 mg) ($[\alpha]_D$ +10° (*c*, 2.0, H_2O)) was reduced with sodium borohydride by the method described earlier to 6-*O*-β-D-glucopyranosyl-D-galactitol (73 mg), which after two recrystallizations from ethanol had m.p. 160–162° C and $[\alpha]_D$ −17° (*c*, 0.7, H_2O). Calculated for $C_{12}H_{24}O_{11}$: C, 41.9%; H, 7.0%. Found: C, 41.9%; H, 7.1%. Conversion to the acetate was effected by heating the sugar (30 mg) at 100° C for 18 hours in acetic anhydride (1 ml) containing sodium acetate (50 mg). The anhydride was destroyed with ice-water and a chloroform extract of the mixture was evaporated. On two recrystallizations from ethanol the nonaacetate (13 mg) was isolated, having m.p. 149–150° C. Calculated for $C_{30}H_{42}O_{20}$: C, 49.9%; H, 5.9%. Found: C, 50.0%; H, 5.9%. Its X-ray diffraction pattern was identical with an authentic specimen prepared in a similar way from 6-*O*-β-D-glucopyranosyl-D-galactose (8).

The disaccharide $R_{lactose}$ 0.9 was hydrolyzed with *N* sulphuric acid at 100° C overnight to give galactose and glucose. After reduction with sodium borohydride and subsequent hydrolysis, glucose was the only remaining reducing sugar. The reducing galactose unit was linked in the 3-position since, when the disaccharide was oxidized with lead tetraacetate in acetic acid, 0.98, 0.98, and 1.02 moles/mole of oxidant were consumed after 3, 10, and 30 minutes, respectively. The specific rotation of the disaccharide was +35° (*c*, 1.2, H_2O).

(*b*) *X. stewartii* polysaccharide (10 g) was hydrolyzed by heating in *N* sulphuric acid (100 ml) at 100° C for 18 hours. The reaction mixture was neutralized with barium carbonate, and the solution was filtered, treated with Amberlite IR-120, filtered, and evaporated to a crust. This was fractionated on a cellulose column and neutral sugars were eluted with *n*-butanol–ethanol–water (4:1:1 v/v). An aldobiouronic acid fraction (0.90 g) was obtained by using ethyl acetate – acetic acid – water (9:2:2 v/v) as the solvent. This sugar, $[\alpha]_D$ +15° (*c*, 1.0, H_2O), was hydrolyzed overnight at 100° C with 6 *N* sulphuric acid to give a uronic acid and galactose. The galactose portion was 4-linked since the aldobiouronic acid consumed 0.90, 1.52, 1.75, and 1.83 moles/mole of lead tetraacetate in acetic acid after 2, 5, 15, and 30 minutes, respectively.

One hundred and fifty-one milligrams of the aldobiouronic acid in methanol was converted by ethereal diazomethane to its methyl ester (147 mg). This was reduced with sodium borohydride (100 mg) in water (10 ml) for 2 hours and the product was isolated by the method described previously. The product was fractionated on a cellulose column using *n*-butanol saturated with water as solvent to give crude 4-*O*-β-D-glucopyranosyl-D-galactitol, which was crystallized twice from methanol to give a material (15 mg) with m.p. 204° C and $[\alpha]_D$ −13° (*c*, 1.1, H_2O). Calculated for $C_{12}H_{24}O_{11}$: C, 41.9%; H, 7.0%. Found: C, 42.0%; H, 6.85%. Acid hydrolysis with *N* sulphuric acid at 100° C overnight gave glucose (paper chromatogram).

Partial Hydrolysis of Polysaccharide Modified by Periodate Oxidation and Borohydride Reduction

Crude *X. stewartii* polysaccharide (40 g) was stirred with periodic acid (100 g) in 4 liters of water for 3 days, by which time all the polysaccharide had dissolved. Then aqueous barium hydroxide was added until the solution was slightly acid and residual acidity was removed with barium carbonate. The solution was filtered and then treated with sodium borohydride (10 g). After 18 hours the solution was brought to pH 5 with acetic acid and evaporated to a crust that was repeatedly shaken in methanol, which was evaporated. The product was deionized in water with Amberlite IR-120 and Dowex-1

(bicarbonate form), and the solution filtered and evaporated to 200 ml. The polysaccharide was precipitated by addition of 5 volumes of ethanol, and collected on a filter. Yield, 17 g.

Half of this material was dissolved in 0.1 *N* sulphuric acid (2 liters) and the solution heated at 95° C for 4 hours, neutralized ($BaCO_3$), filtered, and evaporated to a small volume. Examination on paper chromatogram indicated the presence of glycerol, galactose, and a disaccharide and these materials were separated by fractionation on a cellulose column. *n*-Butanol saturated with water gave glycerol (2.16 g) and *n*-butanol–ethanol–water (4:1:1 v/v) separated galactose (0.79 g) and the disaccharide (1.74 g).

The disaccharide gave galactose (on paper chromatograms) after hydrolysis on a steam bath overnight with *N* sulphuric acid. It consumed 0.88, 1.03, and 1.19 moles/mole of lead tetraacetate in acetic acid after 3, 10, and 25 minutes, respectively, indicating a 3-linked disaccharide. Since its specific rotation was +52° (*c*, 0.9, H_2O), it appeared to be 3-*O*-β-D-galactopyranosyl-D-galactose.

Methylation of X. stewartii Polysaccharide Modified by Periodate Oxidation and Borohydride Reduction

A sample of crude modified polysaccharide (4.35 g), prepared by the method described above, was methylated in the standard way (see earlier method in this section) with aqueous sodium hydroxide – dimethyl sulphate. After destruction of excess dimethyl sulphate the solution was neutralized with acetic acid and extracted once with chloroform. The extract was evaporated to dryness yielding a material (1.16 g) which was refluxed for 3 days in methyl iodide (50 ml) containing silver oxide (20 g). The product (0.99 g) after filtration and evaporation had —OCH_3 45.6%.

The methylated polysaccharide was hydrolyzed by refluxing overnight in 10% methanolic hydrogen chloride (20 ml) and, to this, water (20 ml) was added and the methanol removed by evaporation. A further hydrolysis at 100° C for 18 hours was carried out and the product after neutralization ($BaCO_3$) and evaporation contained three reducing sugars (paper chromatograms). Fractionation on a cellulose column using benzene–ethanol–water (1000:50:1 v/v) as solvent yielded 2,3,4,6-tetra-*O*-methyl-D-galactose (136 mg), 2,4,6-tri-*O*-methyl-D-galactose (75 mg), and 2,6-di-*O*-methyl-D-galactose (82 mg).

The tetramethyl galactose was characterized as its aniline derivative, m.p. 191–193° C. 2,4,6-Tri-*O*-methyl-D-galactose was recrystallized twice from ether and had m.p. 103–105° C and $[\alpha]_D$ +85° (*c*, 0.9, H_2O). 2,6-Di-*O*-methyl-D-galactose was crystallized twice from ethyl acetate and had m.p. and mixed m.p. 116–119° C and $[\alpha]_D$ +92° → +87° (*c*, 1.0, H_2O, constant value).

ACKNOWLEDGMENTS

The authors appreciate the technical assistance of Mrs. S. F. Hector and Mr. N. R. Gardner. Microanalyses were carried out by Mr. M. Mazurek.

REFERENCES

1. R. S. Breed, E. G. D. Murray, and N. R. Smith (*Editors*). *In* Bergey's Manual of determinative bacteriology. 7th ed. The Williams & Wilkins Co., Baltimore. 1957.
2. R. Hodgson, A. J. Riker, and W. H. Peterson. Phytopathology, **37**, 301 (1947).
3. J. G. Leach, V. G. Lilly, H. A. Wilson, and M. R. Purvis, Jr. Phytopathology, **47**, 113 (1957).
4. J. F. T. Spencer and P. A. J. Gorin. Can. J. Microbiol. **7**. 185 (1961).
5. R. R. Corey and M. P. Starr. J. Bacteriol. **74**, 137 (1957).
6. C. T. Bishop. Unpublished results.
7. L. Hough, J. K. N. Jones, and W. H. Wadman. J. Chem. Soc. 2511 (1949).

Can. J. Chem. Downloaded from www.nrcresearchpress.com by 210.87.254.40 on 09/05/12
For personal use only.

8. K. FREUDENBERG, A. NOË, and E. KNOPF. Ber. B, **60**, 238 (1927).
9. A. J. CHARLSON and A. S. PERLIN. Can. J. Chem. **34**, 1200 (1956).
10. M. L. WOLFROM and K. ANNO. J. Am. Chem. Soc. **74**, 5583 (1952).
11. I. J. GOLDSTEIN, G. W. HAY, B. A. LEWIS, and F. SMITH. Am. Chem. Soc. 135th Meeting, Abstracts 3D (1959).
12. E. L. HIRST and A. S. PERLIN. J. Chem. Soc. 2622 (1954).
13. P. A. J. GORIN and J. F. T. SPENCER. To be published.
14. L. HOUGH, J. K. N. JONES, and W. H. WADMAN. J. Chem. Soc. 1702 (1950).
15. S. M. PARTRIDGE. Nature, **158**, 270 (1946).
16. R. KUHN, H. TRISCHMANN, and I. LÖW. Angew. Chem. **67**, 32 (1955).
17. S. M. LESLEY and R. M. HOCHSTER. Can. J. Biochem. and Physiol. **37**, 513 (1959).
18. A. JEANES, J. E. PITTSLEY, J. H. SLONEKER, and F. R. SENTI. Am. Chem. Soc. 136th Meeting, Abstracts 7D (1959).

Can. J. Chem. Downloaded from www.nrcresearchpress.com by 210.87.254.40 on 09/05/12
For personal use only.

Can. J. Chem. Downloaded from www.nrcresearchpress.com by 210.87.254.6 on 09/05/12
For personal use only.

THE ALUMINUM REDUCTION OF MAGNESIUM OXIDE

II. THE VAPOR PRESSURE OF MAGNESIUM OVER THE SYSTEM Al–MgO–CaO[1]

K. GRJOTHEIM, O. HERSTAD, AND J. M. TOGURI

ABSTRACT

The equilibrium vapor pressure of magnesium over the reaction between the calcined dolomite and aluminum was measured by means of the transportation method. In the temperature range 886–1035° C, the reaction was found to proceed according to the equilibrium

$$12CaO_{(s)} + 21MgO_{(s)} + 14Al_{(l)} = 12CaO.7Al_2O_{3(s)} + 21Mg_{(g)}$$

and the measured equilibrium pressure of magnesium can be expressed by the equation

$$\log P_{\text{mm of Hg}} = -(8754/T) + 8.462.$$

INTRODUCTION

Silicon as a reducing agent for magnesium-bearing compounds has been examined by a number of workers (1, 2, 3); however, an analogous examination of the reaction between calcined dolomite and aluminum does not appear to exist. The reaction is reported to proceed as follows (4):

$$5CaO + 9MgO + 6Al = 5CaO.3Al_2O_3 + 9Mg. \qquad [1]$$

In the present investigation, a continuation of the study of the reduction of magnesium compounds with aluminum, the equilibrium vapor pressure of magnesium over reaction [1] was determined and the solid products of the reaction were identified.

EXPERIMENTAL

Preliminary experiments indicated that the expected pressure of magnesium was of the order of 40 mm of Hg at 1000° C, a pressure suitable for the employment of the transportation method. This method of measuring vapor pressures has proved to be successful for a number of similar reactions (1, 2, 3, 5) provided the necessary precautions against diffusion errors and unsaturation of the carrier gas are observed.

The transportation apparatus and procedures adopted for the present study have been fully described previously (5).

The carrier gas utilized throughout this investigation was S-argon gas obtained from Norsk Hydro, the analysis given was 99.94%. The impurities CO_2 and H_2O were removed by passing the argon through ascarite and dehydrite towers respectively.

PREPARATION OF CHARGE

The calcined dolomite used in this investigation was obtained from Hammarfallene (Norway). The chemical analysis was, in weight per cent: 58.3% CaO, 40.3% MgO, 0.06% Al_2O_3, 0.16% Fe_2O_3, and 1.18% insolubles. The aluminum powder (99.9%) was obtained from Merck, Germany.

Before use, the calcined dolomite was dried at 1100° C for 24 hours to expell traces of CO_2 and H_2O. The calcined dolomite and aluminum were then mixed in a stoichiometric ratio (MgO/Al) according to equation [1], and ground in a ball mill for 12 hours. The mixture was then pressed into briquettes, 2.0 cm diameter by 1.0 cm in height, at a pressure of 500 kg/cm^2.

[1]*Manuscript received June 19, 1961.*
Contribution from the Institute of Inorganic Chemistry, The Technical University of Norway, Trondheim, Norway.

These briquettes were broken into approximately 5-mm particle size, and about 150 g of such pieces was used as a charge.

RESULTS AND DISCUSSION

(a) Vapor Pressure Measurements

The vapor pressure of magnesium over the mixture of calcined dolomite and metallic aluminum was measured over the temperature range 886–1035° C. A number of experiments at different flow rates were carried out at each temperature investigated in order to determine the equilibrium vapor pressure which is independent of the flow rate. The observed equilibrium pressures are tabulated in Table I. The estimated probable error in the measured vapor pressure is 1%.

TABLE I

Experimental vapor pressure of magnesium

Temp. (° C)	Pressure (mm of Hg)
887	8.30
925	14.00
955	20.40
968	25.70
992	34.80
1035	60.25

When the results from Table I were plotted as log P versus the reciprocal of the absolute temperature, Fig. 1 was obtained. The data may be represented as a straight line and

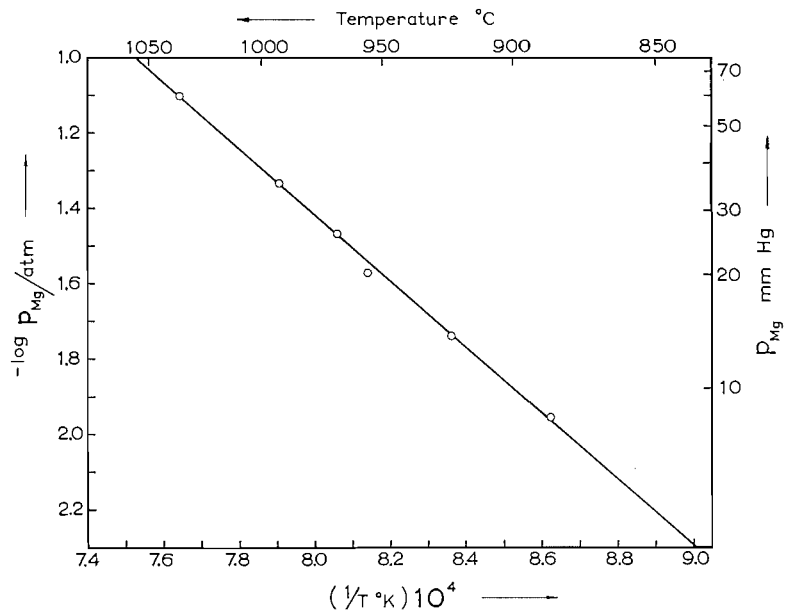


FIG. 1. Log P_{atm} of Mg versus $1/T°$ K.

fitted to the equation

$$\log P_{\text{mm of Hg}} = -(8754/T)+8.462,$$

where P is pressure in mm of Hg and T is the absolute temperature.

Can. J. Chem. Downloaded from www.nrcresearchpress.com by 210.87.254.6 on 09/05/12
For personal use only.

(b) Analysis of the Reaction Product

Chemical analysis of the condensed magnesium showed no traces of calcium.

The solid residue was analyzed by X-ray diffraction in order to confirm the reaction products of equation [1]. The diffraction patterns obtained (shown in Fig. 2) correspond

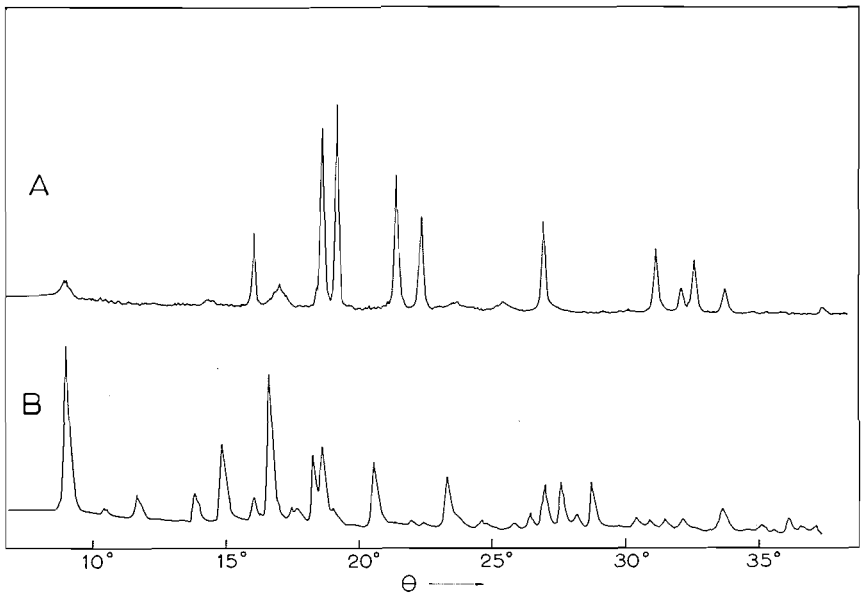


FIG. 2. X-Ray diffraction pattern (Cu target, Ni filter). A. Unreacted mixture of calcined dolomite and aluminum. B. Reacted mixture of calcined dolomite and aluminum.

only to CaO, MgO, Al, and $12CaO.7Al_2O_3$ when compared with the ASTM Index (6).

The literature indicates a difference in opinion regarding the similarity of the two compounds $5CaO.3Al_2O_3$ and $12CaO.7Al_2O_3$. The existence of the compound $5CaO.3Al_2O_3$ was first reported by Rankin and Wright (7). However, later investigators have found that this formula does not satisfy all the known characteristics of the compound. Bussem and Eitel (8) concluded, from a structural analysis of the compound, that it should be $12CaO.7Al_2O_3$. Recently, Aruja (9), following an X-ray analysis, concluded that the X-ray powder patterns of the compounds $5CaO.3Al_2O_3$ and $12CaO.7Al_2O_3$ showed no resemblance. There thus appears to be a controversy as to whether the two compounds are essentially identical or not. Nevertheless, since the X-ray patterns obtained, at all temperatures of this investigation, correspond to the powder pattern of $12CaO.7Al_2O_3$ reported by Swanson *et al.* (6, 10), this formula is used. The reaction is therefore written as follows:

$$12CaO_{(s)} + 21MgO_{(s)} + 14Al_{(l)} = 12CaO.7Al_2O_{3(s)} + 21Mg_{(g)}. \qquad [2]$$

The formation of the compound $12CaO.7Al_2O_3$ is not in accordance with the phase diagram of the system $CaO–MgO–Al_2O_3$ (11). The expected calcium aluminate is $3CaO.Al_2O_3$. However, no evidence could be obtained for its formation in the reaction studied. The possible reason for this might be either (I) that $3CaO.Al_2O_3$ is not a stable compound at the temperatures of the present investigation, or (II) that the kinetics of the formation of $12CaO.7Al_2O_3$ is much faster than that of $3CaO.Al_2O_3$.

Can. J. Chem. Downloaded from www.nrcresearchpress.com by 210.87.254.6 on 09/05/12
For personal use only.

A number of experiments were carried out in which $3CaO.Al_2O_3$, prepared by heating CaO and Al_2O_3 in stoichiometric amounts at 1350° C for 48 hours and then quenching to room temperature, was held at various temperatures for a period of time and then quenched. X-Ray diffraction patterns for these samples showed that below 1200° C traces of $12CaO.7Al_2O_3$ were formed. When 1% CaF_2 was added, the diffraction lines for $12CaO.7Al_2O_3$ were more intense than in the samples without CaF_2, held at the same temperature and for the same period of time.

When samples of the reaction mixture (calcined dolomite and aluminum) were heated to temperatures beyond 1200° C, both $12CaO.7Al_2O_3$ and $3CaO.Al_2O_3$ appeared, the amount of $3CaO.Al_2O_3$ increasing with longer period of heating.

It is interesting to compare the present results with the aluminum reduction of CaO (12), where $12CaO.7Al_2O_3$ was also obtained rather than $3CaO.Al_2O_3$ for temperatures below 1200° C. Above this temperature, in agreement with the results reported here, $3CaO.Al_2O_3$ was found. It thus appears that $3CaO.Al_2O_3$ disproportionates below 1200° C and that above 1200° C the reaction

$$12CaO.7Al_2O_{3(s)} + 9CaO_{(s)} = 7(3CaO.Al_2O_3)_{(s)}$$

occurs.

In the present case it was concluded that $12CaO.7Al_2O_3$ must be the stable calcium aluminate in equilibrium with CaO at the temperatures of the pressure measurements. The thermodynamic calculations are therefore based on the formation of $12CaO.7Al_2O_3$.

(c) Thermodynamic Considerations

Since the reactions were carried out at temperatures above the melting point of aluminum, some solution of magnesium would be expected. As described previously (1), liquid aluminum at these temperatures can be assumed to form an ideal solution with magnesium. Thus the activity of aluminum can be calculated at each temperature provided the equilibrium vapor pressure of magnesium is known. It was assumed that no solid solution occurred between the solid components; thus the equilibrium constant is written in the form

$$K = P_{Mg}^{21}/a_{Al}^{14}.$$

A "Σ plot" was carried out using the equilibrium constant derived from the experiments and the specific heat functions recommended by Kelley (13). The derived functions are shown in Table II for the over-all reaction.

TABLE II

Thermodynamic functions for the reaction $12CaO_{(s)}+21MgO_{(s)}+14Al_{(l)} = 12CaO.7Al_2O_{3(s)}+21Mg_{(g)}$ in the temperature range 1154–1308° K

ΔC_p	$= -45.49+16.00\times10^{-3}T-5.50\times10^{5}T^{-2}$
ΔH^0_T	$= 909{,}198-45.49T+8.0\times10^{-3}T^2+5.50\times10^{5}T^{-1}$
ΔG^0_T	$= 909{,}198+104.76T \log T-8.0\times10^{-3}T^2+2.75\times10^{5}T^{-1}-908.77T$
$\Delta H^0_{1225°\,K}$	$= +865{,}900$ cal
$\Delta G^0_{1225°\,K}$	$= +180{,}500$ cal
$\Delta S^0_{1225°\,K}$	$= +559.55$ e.u.

Combining the experimental data with the available data on CaO, on Al_2O_3, and on $12CaO.7Al_2O_3$, one obtains for the reaction

$$12CaO + 7Al_2O_3 = 12CaO.7Al_2O_3 \quad [3]$$

the following data: $\Delta H^0_{298°\,K} = -18{,}500$ cal, and $\Delta S^0_{298°\,K} = 46.31$ e.u.

Can. J. Chem. Downloaded from www.nrcresearchpress.com by 210.87.254.6 on 09/05/12
For personal use only.

The entropy value reported by King (14) from low-temperature heat-capacity measurements is 50.6 e.u. Thus the value obtained in the present work is considered satisfactory when taking into account the errors involved in calculations of this type. The free energy of formation of the calcium aluminate from the oxides can be represented by the equation

$$\Delta G^0_T = -18{,}500 - 50.6\ T \pm 1.5 \text{ kcal.}$$

CONCLUSIONS

The reaction between calcined dolomite and metallic aluminum proceeds according to the equation

$$12CaO_{(s)} + 21MgO_{(s)} + 14Al_{(l)} = 12CaO.7Al_2O_{3(s)} + 21Mg_{(g)}$$

in the temperature range 886–1035° C. The corresponding equilibrium pressure of magnesium over this reaction can be represented by the equation

$$\log P_{\text{mm of Hg}} = -(8754/T) + 8.462$$

as determined by means of the transportation method.

ACKNOWLEDGMENT

This investigation has been sponsored by Norsk Metallurgisk Komite, for which the authors are grateful.

REFERENCES

1. L. M. Pidgeon and J. A. King. Discussions Faraday Soc. **4**, 197 (1948).
2. A. Schneider and E. Hesse. Z. Elektrochem. **46**, 279 (1940).
3. T. Rosenqvist and B. Ellingsaeter. J. Metals, **212**, 1111 (1956).
4. A. Yu. Tait. Tsvetnye Metal. **30**, 56 (1957).
5. K. Grjotheim, O. Herstad, and J. M. Toguri. Can. J. Chem. **39**, 443 (1961).
6. ASTM X-ray Powder Data. File 9-413.
7. G. A. Rankin and F. E. Wright. Am. J. Sci. **39**, 1 (1915).
8. W. Bussem and A. Eitel. Z. Krist. **95**, 175 (1936).
9. E. Aruja. Acta Cryst. **10**, 337 (1957).
10. H. E. Swanson, M. I. Cook, T. Isaacs, and E. H. Evans. Natl. Bur. Standards (U.S.), Circ. 539. 1960. p. 9.
11. E. Levin, H. McMurdie, and F. Hall. Phase diagrams for ceramists. Am. Ceram. Soc. Part I. 114 (1956).
12. P. Vignial and J. L. Andrieux. Compt. rend. **242**, 709 (1956).
13. K. K. Kelley. U.S. Bur. Mines, Bull. 584. 1960.
14. E. G. King. J. Phys. Chem. **59**, 218 (1955).

Can. J. Chem. Downloaded from www.nrcresearchpress.com by 210.87.254.6 on 09/05/12
For personal use only.

Can. J. Chem. Downloaded from www.nrcresearchpress.com by 210.87.254.40 on 09/05/12
For personal use only.

LIGHT ABSORPTION STUDIES

PART XIX. THE ULTRAVIOLET ABSORPTION SPECTRA OF IODOBENZENES[1]

W. F. Forbes

ABSTRACT

As a sequel to previous studies on the ultraviolet absorption spectra of halogen-substituted benzenes the spectra of iodobenzene in various solvents, and the spectra of a series of substituted iodobenzenes in cyclohexane solution, are reported. It is shown that these spectra can be rationalized qualitatively in terms of simple resonance theory, if the apparent mesomeric effect of the iodine atom is assumed to be greater for iodine than for the other halogen atoms.

INTRODUCTION

In previous papers on the ultraviolet spectra of bromobenzenes (1), chlorobenzenes (2), and fluorobenzenes (3), band nomenclature and other terms used were discussed. Since in the present paper the terms employed are identical, no further introduction is required concerning them. The above-mentioned three papers noted generalizations which could be deduced from the spectra, and the purpose of the present paper is to extend and summarize these observations, particularly those concerning the apparent mesomeric order of the halogen atoms, by the study of the ultraviolet absorption spectra of the iodobenzenes.

EXPERIMENTAL

The ultraviolet absorption spectra were determined by standard methods in matched 1-cm silica quartz cells using both a Beckman DK 2 spectrophotometer and a Unicam SP 500 spectrophotometer calibrated against a didymium filter and solutions of potassium chromate and potassium nitrate. Wavelength readings obtained on the two instruments were found to be within 1 mμ of each other. The accuracy of λ_{max} values is estimated to be ± 1 mμ, and the precision of molar absorptivities, $\pm 5\%$ or better. Most molar absorptivity values were reproducible to $\pm 2\%$. The solvents used were spectroanalyzed cyclohexane (Fisher) and other commercially available spectroanalyzed solvents.

The iodobenzenes were mostly commercial materials, purified by distillation or recrystallization until their boiling points and refractive indices or melting points showed them to be sufficiently pure. Some of the iodobenzenes, including iodobenzene itself, decomposed slightly and afforded a limited amount of iodine. The iodine thus liberated was estimated by its absorption maximum near 525 mμ in cyclohexane solution. The amount formed was usually less than 1%. Whenever possible, the iodobenzene spectra were determined under conditions similar to those under which previous spectra in this series had been determined. For each compound at least two independent sets of observations were made. The ultraviolet maxima are listed in Tables I and II. Some of the spectra have previously been described in this series or elsewhere (cf., for example, refs. 4, 5, and 6, and references cited therein).

THE SPECTRUM OF IODOBENZENE

The absorption characteristics of iodobenzene in different solvents are listed in Table I.

Comparison of the ultraviolet spectral data for iodobenzene and other halogen-substituted iodobenzenes (1, 2, 3) shows that the more intense absorption band of iodobenzene, the *B*-band (7), occurs at longer wavelength and with greater absorption

[1]*Manuscript received May 8, 1961.*
Contribution from the Division of Protein Chemistry, C.S.I.R.O., Wool Research Laboratories, Parkville, N.2 (Melbourne), Victoria, Australia.

TABLE I

Main ultraviolet absorption maxima of iodobenzene in various solvents*

Solvent	*B*-band		*C*-band	
	λ_{max}(mμ)	ϵ_{max}	λ_{max}(mμ)	ϵ_{max}
Vapor phase	ca. *219* 224 228	†	ca. *254* 258 264	†
Cyclohexane	ca. *224* 228.5 233.5	*11,000* 15,000 14,000	ca. *248* 253.5 258 ca. *263.5*	*700* 750 800 *700*
Ether	226.5 ca. *230.5*	16,000 *15,250*	252 257 ca. *263*	755 750 *650*
Ethanol	226.5 ca. *230*	13,500 *13,000*	252 257 ca. *262*	725 725 *600*
Water	227	8,000‡	ca. *251* ca. *256* ca. *263*	*650* *600* *500*

*Values in italics represent inflections in this and the subsequent table.
†Intensities not determined.
‡Sodium iodide has a maximum at similar wavelength (226 mμ) in aqueous solution. This maximum, however, is appreciably displaced in ethanolic solution (to 219.5 mμ) and in ether solution (to 248.5 mμ). The iodobenzene *B*-band is therefore not believed to be due to modified iodide ion absorption (cf. ref. 8).

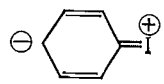
intensity than for other halogen-substituted benzenes. These spectral changes can be interpreted in terms of an apparent mesomeric release of electrons in the order I > Br > Cl > F. Other ultraviolet spectral data (see refs. 1, 2, 3, and 9, and later discussion in this paper) also suggest this order, as do the intensities of the infrared carbonyl bands of halogen-substituted acetophenones (these intensities have been related to mesomeric interaction (10)) and some coupling constants and asymmetry parameters obtained from nuclear quadrupole resonance spectra (11).

On the other hand, it is well known that reactivity and dipole-moment data can best be interpreted by assuming a mesomeric release of electrons in the order F > Cl > Br > I (cf. also refs. 9, 12, and 13, and references cited therein). Other data, which provide information concerning electron density, such as the location and intensities of the ultraviolet *C*-bands and certain solvents effects on spectra (see below), reactivities (14), and ionization potentials (cf. ref. 15), afford various orders for the mesomeric effects of the halogen atoms. The absolute mesomeric order of the halogen atoms therefore remains unknown. In the meantime it may be assumed, as a working hypothesis, that the "apparent mesomeric effect" of the halogen atoms, as indicated by the present ultraviolet spectral data, corresponds to a mesomeric release of electrons in the *electronic excited state* in the order I > Br > Cl > F. The electronic excited state concerned is the state primarily involved in the transitions leading to the *B*-bands of the ultraviolet spectra. On this hypothesis it may be assumed that the net order of release of electrons for the halogens is different in the electronic excited state and in the ground state. The electronic excited state of iodobenzene may be visualized as involving resonance forms of type I, and this simplified resonance picture accounts satisfactorily for a number of the ultraviolet spectral changes.

The *B*-band of iodobenzene shows a characteristic, fine structure in most solvents (see Fig. 1). The wavelength displacement observed between solutions in cyclohexane

Can. J. Chem. Downloaded from www.nrcresearchpress.com by 210.87.254.40 on 09/05/12
For personal use only.

and the vapor phase is of the order of 5 mμ (see Table I), which is considerably greater than the corresponding displacements observed for fluorobenzene, chlorobenzene, and bromobenzene (refs. 1, 2, 3; cf. also ref. 16). This observation is consistent with the view that the C—I dipole makes a greater contribution to the relevant electronic excited



I

state of iodobenzene, probably by facilitating solvent orientation, than do the C—F, C—Cl, or C—Br dipoles to the corresponding excited states of the other halobenzenes. This, in turn, is consistent with the resonance picture described above.

Other spectral changes, with change of solvent, are illustrated in Fig. 1. As with bromobenzene and chlorobenzene (1, 2) no appreciable wavelength displacements are

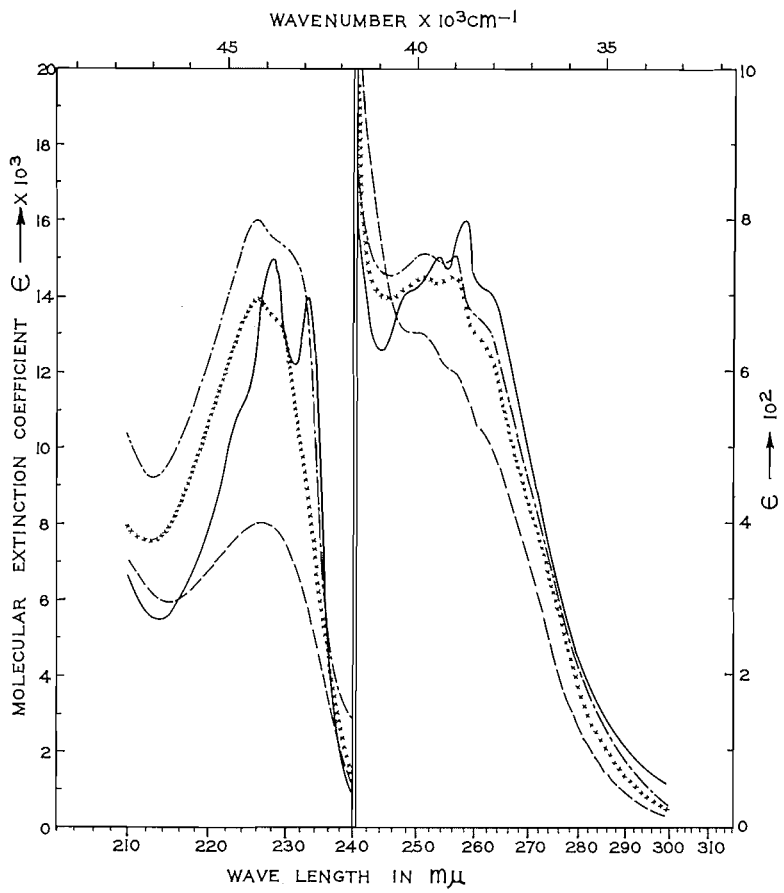


FIG. 1. The ultraviolet absorption spectra of iodobenzene in cyclohexane solution (——), in ether (—·), in ethanol (×××), and in water (— —).

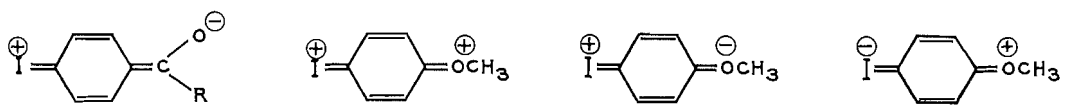
Can. J. Chem. Downloaded from www.nrcresearchpress.com by 210.87.254.40 on 09/05/12
For personal use only.

observed on changing the solvent, although the maximal extinction coefficients are decreased in aqueous solution. This decrease, presumably caused by some form of intermolecular hydrogen bonding, appears to be general for halogen-substituted benzenes. Further, the fine structure is decreased in aqueous solution.

The *C*-band of iodobenzene (for band nomenclature used, see ref. 7) is considerably more intense than that of bromobenzene or chlorobenzene. However, in most solvents the band is approximately as intense as that of fluorobenzene (see Fig. 1 and cf. ref. 3). This indicates that the *C*-band of iodobenzene is determined by a combination of electronic interactions different from that used in determining the *B*-band (cf. refs. 13 and 17). Wavelength displacements of the *C*-band for the halogen-substituted benzenes also are not in a definite order with increasing molecular weight of the halogen substituent. However, the *C*-band fine structure in cyclohexane solution becomes progressively less pronounced on passing from fluorobenzene to iodobenzene. For fluorobenzene, the *C*-band fine structure resembles that of benzene (see Fig. 1 of ref. 3), whereas for iodobenzene this is much less pronounced. This may be because the iodo substituent more effectively disturbs the symmetrical vibrations of the benzene ring because of increased mesomeric interactions.

THE SPECTRA OF PARA-SUBSTITUTED IODOBENZENES

As previously noted, in *p*-disubstituted benzenes, where one substituent is electron withdrawing and the other a halogen atom, the *B*-band occurs at its longest wavelength in the iodine derivative. It may be noted that most functions, such as σ^*, σ_p, σ', but not $\sigma_p - \sigma'$, for electron-donating substituents differ in sign from the above-mentioned electron-withdrawing substituents. On the other hand, in the *B*-band of the ultraviolet spectra of *p*-substituted iodobenzenes *both* these types of substituents cause bathochromic wavelength displacements, that is, displacements to lower frequency (cf. also the work reported by Bloor and Copley (18) on spectroscopic constants). Simple valence bond theory can again account for this anomalous behavior in the ultraviolet spectra. This follows since, as illustrated by structure III, an extended dipolar resonance form of type II is no longer favored when both substituents are electron donating, and the molecule consequently tends to absorb to a *locally excited state* with the methoxy substituent exerting only a secondary effect. If resonance structures, crudely represented by IV and V, are assumed to contribute to the electronic excited state, such a secondary effect will, however, still normally facilitate the transition. This can account for the observed bathochromic wavelength displacements on introduction of a *p*-iodo substituent into a monosubstituted benzene derivative.



II III IV V

The predominant locally excited state can usually be identified by characteristic band features of the relevant absorption band; for example, the iodobenzene *B*-band in cyclohexane solution is a doublet with the twin peaks separated by ca. 5 mμ (see Fig. 1), and this doublet can still be discerned in some of the *p*-substituted iodobenzenes. This is

Can. J. Chem. Downloaded from www.nrcresearchpress.com by 210.87.254.40 on 09/05/12
For personal use only.

illustrated in Fig. 2, which shows the absorption spectra of *p*-chloroiodobenzene, *p*-bromoiodobenzene, *p*-diiodobenzene, and iodobenzene, all in cyclohexane solution. The *B*-bands

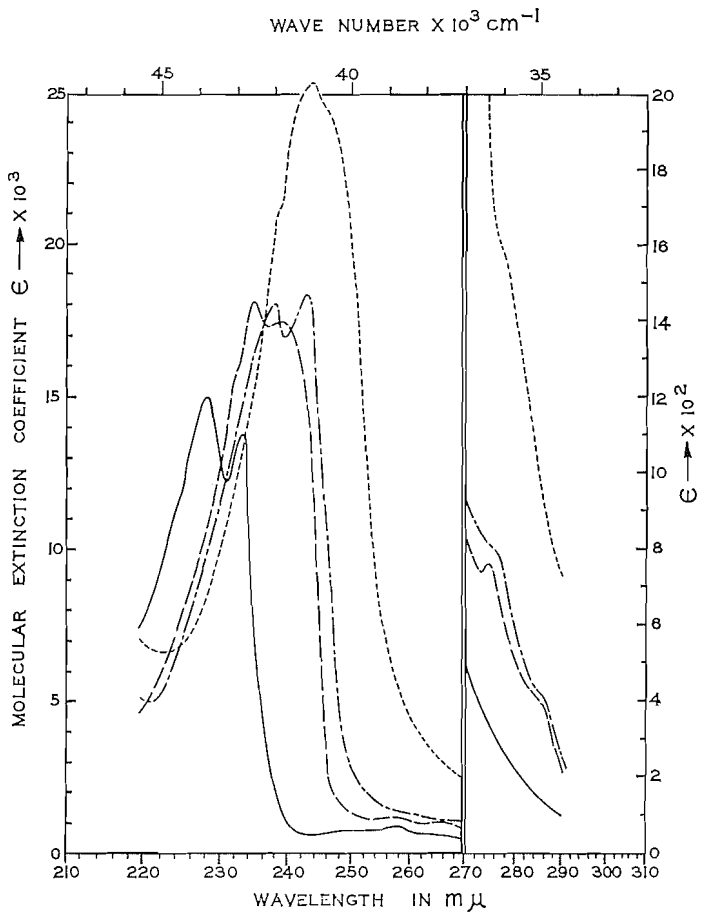


FIG. 2. The ultraviolet absorption spectra in cyclohexane solution of *p*-chloroiodobenzene (— —), *p*-bromoiodobenzene (—·), *p*-diiodobenzene (- -), and iodobenzene (——).

of the four compounds show that the *p*-chloro, *p*-bromo, and *p*-iodo substituents cause the iodobenzene absorption to occur at slightly longer wavelength. Moreover, this secondary effect of a *p*-substituent on the *B*-band absorption of iodobenzene is greater for an iodo than for a bromo or chloro substituent. This secondary effect of the halogen atom thus also follows the order of the apparent mesomeric effects. The maximal molar absorptivity of these *p*-substituted iodobenzenes shows large increases compared with that of iodobenzene (see Fig. 2), the ϵ_{max} values approaching, or even exceeding, those which are observed for *p*-substituted iodobenzenes when the *p*-substituent is electron withdrawing (see Table II). This may indicate a large transition moment which, in turn, suggests that electronic interactions, as crudely represented by structures of type III, and others, are important. Evidence that such structures contribute to the ground or electronic excited state of *p*-substituted iodobenzenes, when both substituents are electron donating, can also be deduced from the *B*-band solvent changes. For example, Fig. 3 shows that the

Can. J. Chem. Downloaded from www.nrcresearchpress.com by 210.87.254.40 on 09/05/12
For personal use only.

Can. J. Chem. Downloaded from www.nrcresearchpress.com by 210.87.254.40 on 09/05/12
For personal use only.

TABLE II

Main ultraviolet absorption maxima of substituted iodobenzenes in cyclohexane solution*

Sub-stituent	Para isomer				Meta isomer						Ortho isomer					
	B-band		*C*-band		*B*-band		2nd *B*-band		*C*-band		*B*-band		2nd *B*-band		*C*-band	
	λ_{max} (mμ)	ϵ_{max}	λ_{max} (mμ)	ϵ_{max}	λ_{max} (mμ)	ϵ_{max}	λ_{max} (mμ)	ϵ_{max}	λ_{max} (mμ)	ϵ_{max}	λ_{max} (mμ)	ϵ_{max}	λ_{max} (mμ)	ϵ_{max}	λ_{max} (mμ)	ϵ_{max}
—I	ca. *239*	*21,000*	ca. *268*	*2,600*	ca. *224*	*25,000*	—	—	260	1,250	232	13,000	—	—	*259*	*1,200*
	243	25,500	ca. *277*	*1,600*	228	31,500			ca. *269*	*1,100*	238	13,000			266	1,100
	ca. *247*	*24,000*			ca. *232*	*24,500*			*276.5*	*900*	ca. *243*	*11,000*			ca. *273*	*900*
					237	19,000			*285.5*	*525*						
					ca. *242*	*12,000*										
—CH_3	230.5	18,000	258	850	ca. *224*	*10,500*			256	800	228	12,500			ca. *255*	*750*
	236	16,500	262	850	229	13,000			261	800	233	12,250			259	765
			272	725	*234*	*12,000*			270	700					*265*	*700*
			281	500					278	500					*268*	*680*
															276	*500*
—OH	231.5	15,000‡	276.5	1,300							224	8,300	218	9,250†	269	2,200
	ca. *236.5*	*12,400*	283	1,450							229	6,500			276.5	3,000
			291.5	1,100											284.5	2,800
—OCH_3	234.5	19,000	276	1,450	ca. *225*	*9,250*	216	25,500†	271	1,950	ca. *229*	*8,700*			272	2,400
	ca. *239*	*15,800*	282	1,600	231	9,500			277.5	2,700	232.5	10,200			278.5	3,400
			292	1,200	ca. *237*	*6,500*			285	2,550	237	10,000			286	3,250
—NH_2	248	19,000	296.5	1,700	ca. *238*	*10,000*†	217	35,000	294	2,700	238	8,400			293	3,200
			ca. *315*	*1,450*	ca. *244*	*8,000*	ca. *222*	*28,500*	ca. *302.5*	*2,200*	ca. *245*	*6,200*			ca. *302*	*2,800*
—$COCH_3$	264	19,500	ca. *273*	*14,500*	224	24,500	ca. *246*	*6,800*	292.5	1,050						
			ca. *280*	*10,000*			ca. *251*	*6,000*	302	950						
—CHO	ca. *268*	*19,500*	ca. *290*	*4,000*	228	25,000	ca. *242*	*8,000*	297.5	1,300						
	ca. *276*	*16,000*					ca. *251*	*7,500*	305	1,250						
	ca. *283*	*14,500*					ca. *256*	*7,000*								
—NO_2	ca. *284*	*12,500*	ca. *305*	*8,500*	232	22,500	ca. *257*	*7,500*	*300*	*1,100*	230	14,500	ca. *252*	*5,000*	306	1,750
	290.5	13,000							309	1,200	ca. *235*	*13,000*				
									ca. *321*	*800*						

*The values recorded are those obtained in the present investigations. Frequently, but not always, the data were in good agreement with recent values reported by other workers.
†Band assignment doubtful.
‡Indicates accompanying fine structure near the maximum.

B-band of *p*-iodoanisole is displaced to slightly shorter wavelength, whereas the *B*-band of *p*-iodophenol is displaced to slightly longer wavelength, on passing from cyclohexane to ethanol solution. These displacements are characteristic of anisole and phenol absorption respectively (19, 20) and consequently indicate that the methoxy and hydroxy groups play a part in determining the transition of the relevant *B*-bands.

The *C*-bands of *p*-substituted iodobenzenes frequently show features of the *C*-bands of both the monosubstituted benzene parent compounds. For example, the *C*-bands of

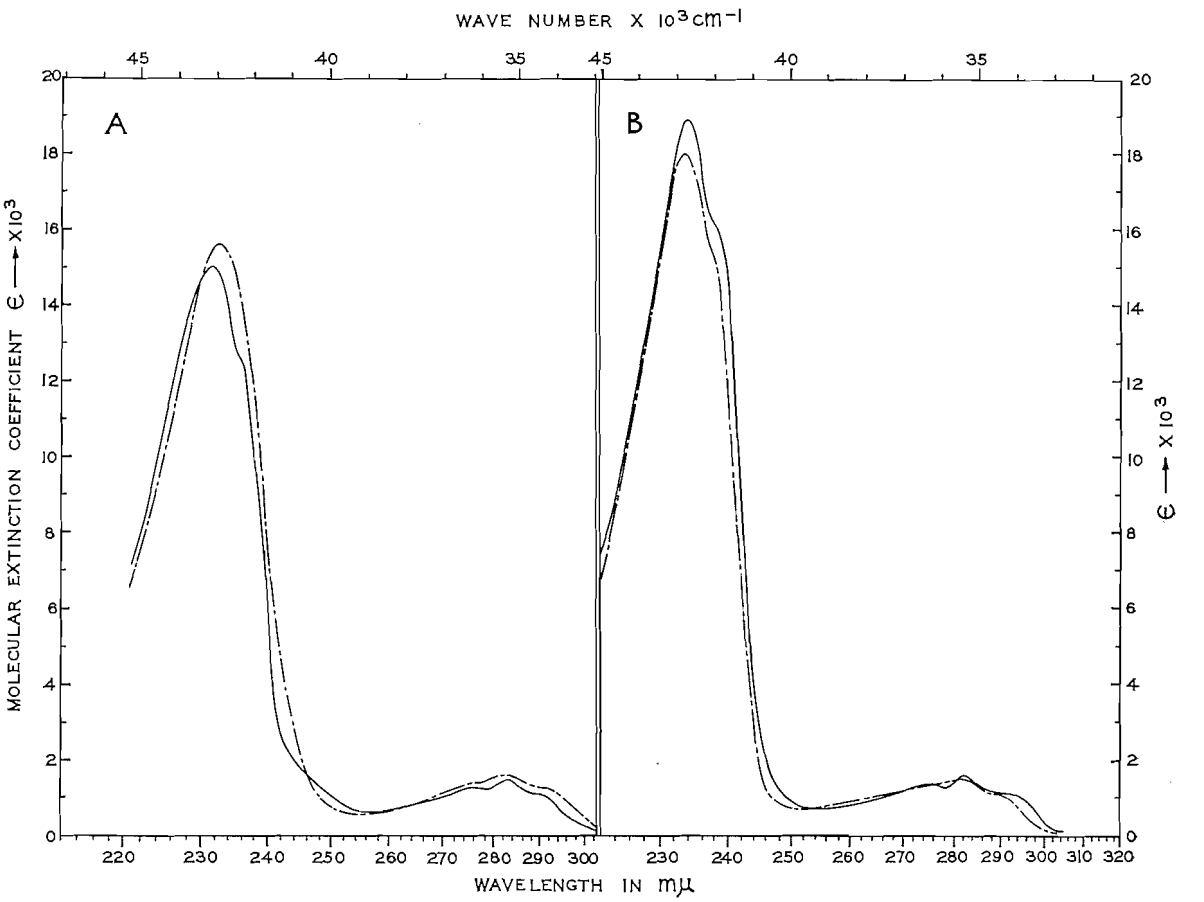


FIG. 3. The ultraviolet absorption spectra of (A) *p*-iodophenol and (B) *p*-iodoanisole in cyclohexane (—) and ethanol (—·) solutions.

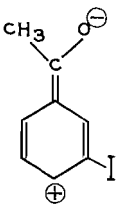
p-iodophenol and *p*-iodoanisole (see Fig. 3) are similar to the *C*-bands of both iodobenzene (see Fig. 1) and, with respect to their locations of maximal absorptions, to the *C*-bands of either phenol or anisole (19, 20). However, the *C*-band of the *p*-substituted iodobenzenes generally occurs at longer wavelength than that of either of the two "component" *C*-bands.

THE SPECTRA OF META-SUBSTITUTED IODOBENZENES

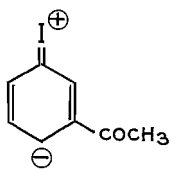
The absorption characteristics of *m*-substituted iodobenzenes can again be rationalized in terms of simple resonance theory by observing that no extended dipolar resonance

Can. J. Chem. Downloaded from www.nrcresearchpress.com by 210.87.254.40 on 09/05/12
For personal use only.

form can be written. Hence one might expect a *m*-substituted iodobenzene, such as *m*-iodoacetophenone, to exhibit one or both of the *B*-bands corresponding either to iodobenzene or to acetophenone absorption. (The latter band is referred to as the second *B*-band in Table II.) In this way the two *B*-bands of *m*-iodoacetophenone for example, are associated with resonance forms of type VI and VII respectively, with the iodo or acetyl group, respectively, causing only a secondary effect.



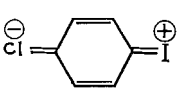
VI



VII

The precise mechanism of this secondary effect remains obscure and appears to vary with different *m*-substituted iodobenzenes, but the following facts may be noted. First, the iodine atom decreases the intensity of the acetophenone absorption (acetophenone in cyclohexane solution absorbs maximally at 238 mμ, $\epsilon = 12{,}500$), and this effect is paralleled in the decrease of the intensities of the infrared carbonyl bands of the *m*-halogen-substituted acetophenones compared with that of acetophenone (10). Secondly, the substitution of an iodine atom in the *m*-position reduces the ultraviolet acetophenone *B*-band absorption intensity more effectively than does the substitution of other halogen atoms (cf. refs. 1, 2, and 3). Hence, it seems that in the electronic excited state of *m*-iodo-acetophenone, forms which may be such as resonance forms of type VII, are preferred to those of type VI. This may be explained if the iodine atom, by *donating* electrons to the benzene ring, facilitates the electronic excited state involving structures such as VII. Also on passing from *m*-fluoroacetophenone to *m*-iodoacetophenone, resonance forms of type VII may be assumed to be more and more favored and this is reflected in the intensification of the absorption band associated with halobenzene absorption and the simultaneous diminution of that associated with acetophenone. The secondary spectral changes, occurring in some of the *m*-substituted iodobenzenes, can therefore again be explained in terms of simple resonance theory if it is assumed that, where the *m*-substituent is electron withdrawing, the electron-releasing abilities of the halogen atoms are in the order I > Br > Cl > F.

When both substituents in a *m*-substituted iodobenzene are electron donating as, for example, in *m*-chloroiodobenzene, the iodobenzene *B*-band intensity appears to be slightly reduced relative to the absorption intensity of iodobenzene. This also applies to the *B*-band of *o*-chloroiodobenzene, but not to *p*-chloroiodobenzene, since in the latter *B*-band the iodobenzene absorption clearly predominates (see Fig. 4). This is presumably because interactions associated with resonance forms of type VIII are sufficiently important in *p*-chloroiodobenzene to cause a predominance of iodobenzene *B*-band absorption.



VIII

Can. J. Chem. Downloaded from www.nrcresearchpress.com by 210.87.254.40 on 09/05/12
For personal use only.

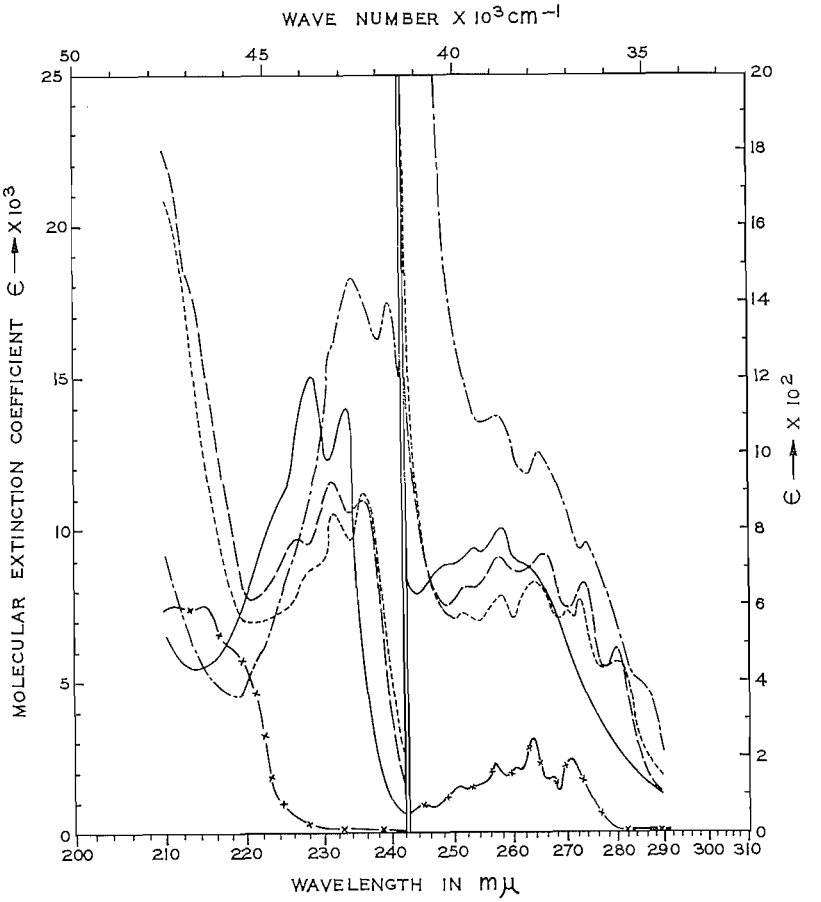
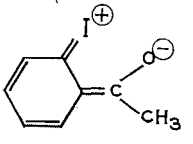


FIG. 4. The ultraviolet absorption spectra in cyclohexane solution of *m*-chloroiodobenzene (— —), *o*-chloroiodobenzene (- -), *p*-chloroiodobenzene (—·), iodobenzene (——), and chlorobenzene (—×).

The *C*-bands of *m*-substituted iodobenzenes appear to be additive as a first approximation, that is, the observed *C*-band approximates to the sum of the two *C*-bands of the corresponding monosubstituted benzenoid parent compounds. However, the *C*-band of the *m*-substituted iodobenzenes is also generally displaced to slightly longer wavelength (see, for example, the *C*-bands in Fig. 4).

THE SPECTRA OF ORTHO-SUBSTITUTED IODOBENZENES

It is well known that the *B*-bands of a number of *o*-disubstituted benzene derivatives frequently resemble the *B*-bands of the corresponding *m*-isomer, that is, two *B*-bands are often observed corresponding to the *B*-bands of the two monosubstituted benzene derivatives. The reason why electronic excitation should occur to locally excited states rather than to so-called electron-transfer states, as symbolized by resonance forms of type IX, is obscure.



IX

Can. J. Chem. Downloaded from www.nrcresearchpress.com by 210.87.254.40 on 09/05/12
For personal use only.

Steric interactions are certainly evident from a number of spectral and other data. Ungnade (21) has shown that for *o*-halonitrobenzenes the band near 260 mμ occurs as a shoulder only for *o*-iodonitrobenzene and that its molar absorptivity at 260 mμ is the smallest among the *o*-halonitrobenzenes if the iodine absorption is taken into account. This band near 260 mμ corresponds to nitrobenzene absorption and its decreased intensity may be taken to imply that the *o*-iodo substituent twists the nitro group out of the plane of the benzene ring and thus inhibits the nitrobenzene *B*-band absorption. In other examples also, the "second" *B*-band of *o*-halogen-substituted benzene derivatives, if well defined, is least intense in the *o*-iodosubstituted compound (cf. ref. 22; for evidence of steric interactions in *o*-substituted iodobenzenes see also refs. 23, 24, and 25).

The spectrum of *o*-iodophenol, compared with that of *o*-iodoanisole, does not suggest intramolecular hydrogen bonding in the former compound, although there is evidence that weak intramolecular hydrogen bonding exists (26, 27). This therefore represents an example of an intramolecular hydrogen bond which does not give rise to a spectral change characteristic of hydrogen bonding (i.e. bathochromic wavelength displacement accompanied by an intensity increase) in the main ultraviolet maxima. It emphasizes the caution which is required before the lack of an ultraviolet spectral change is used to show the absence of intramolecular hydrogen bonding. One of the reasons why some intramolecular hydrogen bonds do not give rise to appreciable ultraviolet spectral changes is that a molecule may absorb to locally excited states which do not involve the part of the molecule which contains the intramolecular hydrogen bond (cf. ref. 28).

It may next be noted that in *o*-substituted halobenzenes the iodobenzene *B*-band, like the bromobenzene *B*-band (1), frequently no longer occurs, or occurs only with reduced absorption intensity. Moreover, in compounds such as *o*-iodonitrobenzene, a hypsochromic wavelength displacement also occurs relative to the *B*-band maxima in the corresponding *m*-isomers (see Table II). These spectral changes suggest steric interactions involving the iodobenzene chromophore. A possible explanation of the spectral changes is that the iodine atom is dislodged from the plane of the benzene ring in such a way that certain interactions between the π-orbitals of the benzene ring and the pseudo π-orbitals of the iodine atom are no longer possible.

The *C*-band in *o*-substituted iodobenzenes, on the other hand, sometimes occurs with decreased and sometimes with increased absorption intensity (see Table II). It has already been suggested (see the section on the spectrum of iodobenzene) that increased mesomeric interaction gives rise to a less pronounced *C*-band and this can account for the *C*-band changes in *o*-substituted iodobenzenes. That is, steric interactions may tend to inhibit mesomeric interaction between the substituents and the benzene ring, and this partial inhibition of mesomeric interaction may cause the frequently observed intensity increase of the *C*-band relative to the intensity of the *C*-band of the *m*-isomer (see, for example, the *C*-band of *o*-iodoaniline in Table II). As steric interactions become large, however, the interaction between the chromophores, which initially gives rise to the characteristic *C*-band, tends to be completely inhibited and the *C*-band intensity now *decreases* towards the intensity value observed in the *C*-band of the isolated benzene molecule (see, for example, the *C*-band of *o*-iodotoluene in Table II and also ref. 29). The hypothesis therefore predicts that steric interactions may either increase or decrease the *C*-band intensity of *o*-substituted iodobenzenes.

ACKNOWLEDGMENTS

The author is indebted to Miss V. R. Jellett for the careful determination of the ultraviolet spectral data. Some of the spectra have been determined at the Memorial

Can. J. Chem. Downloaded from www.nrcresearchpress.com by 210.87.254.40 on 09/05/12
For personal use only.

University of Newfoundland by Mr. J. C. Dearden, assisted by Miss Florence Jackman, in preparation for his Ph.D. thesis; the author is indebted to Mr. Dearden for making these data available.

Grateful acknowledgment for financial assistance in support of that part of these studies which was carried out in Canada is made to the National Research Council.

REFERENCES

1. W. F. FORBES. Can. J. Chem. **39**, 1131 (1961).
2. W. F. FORBES. Can. J. Chem. **38**, 1104 (1960).
3. W. F. FORBES. Can. J. Chem. **37**, 1977 (1959).
4. W. M. SCHUBERT, H. STEADLY, and J. M. CRAVEN. J. Am. Chem. Soc. **82**, 1353 (1960).
5. W. M. SCHUBERT and J. M. CRAVEN. J. Am. Chem. Soc. **82**, 1357 (1960).
6. L. GOODMAN and L. J. FROLEN. J. Chem. Phys. **30**, 1361 (1959).
7. W. F. FORBES and R. SHILTON. *In* Symposium on spectroscopy—STP 269. ASTM (1959). p. 176.
8. F. M. BERINGER and I. LILLIEN. J. Am. Chem. Soc. **82**, 5135 (1960).
9. V. BALIAH and M. UMA. Naturwissenschaften, **45**, 512 (1958).
10. W. F. FORBES and W. A. MUELLER. Can. J. Chem. **35**, 488 (1957).
11. W. G. LAURITA and W. S. KOSKI. J. Am. Chem. Soc. **81**, 3179 (1959).
12. H. SHIMIZU, M. KATAYAMA, and S. FUJIWARA. Bull. Chem. Soc. Japan, **32**, 419 (1959).
13. J. FERGUSON and T. IREDALE. J. Chem. Soc. 2959 (1953).
14. R. W. TAFT, JR. J. Phys. Chem. **64**, 1805 (1960).
15. F. MEDA. Spectrochim. Acta, **13**, 75 (1958).
16. J. C. DEARDEN and W. F. FORBES. Can. J. Chem. **38**, 896 (1960).
17. W. W. ROBERTSON and F. A. MATSEN. J. Am. Chem. Soc. **72**, 5252 (1950).
18. J. E. BLOOR and D. B. COPLEY. Chem. & Ind. (London), 526 (1960).
19. J. C. DEARDEN and W. F. FORBES. Can. J. Chem. **37**, 1294 (1959).
20. J. C. DEARDEN and W. F. FORBES. Can. J. Chem. **37**, 1305 (1959).
21. H. E. UNGNADE. J. Am. Chem. Soc. **76**, 1601 (1954).
22. H. E. UNGNADE. J. Am. Chem. Soc. **76**, 5133 (1954).
23. S. BROWNSTEIN. J. Am. Chem. Soc. **80**, 2300 (1958).
24. J. FERGUSON and T. IREDALE. J. Chem. Soc. 2959 (1953).
25. G. H. BEAVEN and D. M. HALL. J. Chem. Soc. 4637 (1956).
26. D. A. K. JONES and J. G. WATKINSON. Chem. & Ind. (London), 661 (1960).
27. A. W. BAKER and W. W. KAEDING. J. Am. Chem. Soc. **81**, 5904 (1959).
28. J. C. DEARDEN and W. F. FORBES. Can. J. Chem. **38**, 1837 (1960).
29. E. BACIOCCHI and G. ILLUMINATI. Ricerca sci. **26**, 3040 (1956).

Can. J. Chem. Downloaded from www.nrcresearchpress.com by 210.87.254.40 on 09/05/12
For personal use only.

Can. J. Chem. Downloaded from www.nrcresearchpress.com by 210.87.254.42 on 09/05/12
For personal use only.

THE ELECTRONIC SPECTRA OF $MoCl_5$ AND $NbCl_5$[1]

RICHARD F. W. BADER AND ALAN D. WESTLAND

ABSTRACT

The visible and ultraviolet spectra of $MoCl_5$ and $NbCl_5$ have been investigated in both the vapor state and solution. The number of bands observed indicates that a Jahn–Teller effect may be operative in the $^2E'$ state of $MoCl_5$.

INTRODUCTION

Early electron diffraction studies have indicated that, in the gas phase, both molybdenum and niobium pentachloride possess trigonal bypyramid structures (1, 2). The resulting D_{3h} symmetry produces an interesting splitting of the $4d$ metal orbitals in these compounds, the interest of which is enhanced by the fact that the single $4d$ electron present in the $MoCl_5$ molecule should bring about a Jahn–Teller distortion of the nuclear framework in both the ground and first excited states. For these reasons we have undertaken a complete spectroscopic investigation of $MoCl_5$ and $NbCl_5$. The results for the visible and ultraviolet regions are given here; the infrared investigations will be reported shortly.

A simple application of group theory shows that, in the crystalline field of the five halide ions, the $4d$ atomic orbitals of the metal ion are split into two sets of orbital doublets (e'' and e') and into an orbital singlet (a_1'). Furthermore, crystal-field calculations by Ballhausen and Klixbüll Jørgensen (3) have shown that the order of the orbital levels is $\bar{a}_1' > \bar{e}' > e''$, i.e., the e'' orbital is the most stable, as shown in Fig. 1 (the

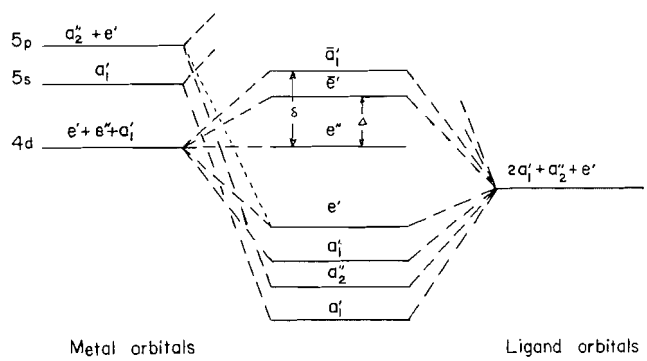


FIG. 1. The ligand field splitting diagram for a trigonal bipyramid molecule.

d–d orbital separations are designated by Δ and δ as shown). Also shown in the same figure are the ligand molecular orbitals for an MX_5 complex. It is seen that the five bonding σ molecular orbitals of the ligands are of symmetries a_1', a_2'', and e'. Thus, of the d orbitals, only those of a_1' (d_{z^2}) and e' ($d_{x^2-y^2}$, d_{xy}) symmetry may participate in the σ-bonding with the ligand molecules, corresponding to the fact that their antibonding combinations (designated by a bar) are raised in energy over that of the e'' (d_{xz}, d_{yz})

[1]*Manuscript received July 3, 1961.*
Contribution from the Department of Chemistry, University of Ottawa, Ottawa, Canada.

orbital. This electronic description may be related to the d^3sp configuration of Pauling.* The electronic structure of the metal ions is $Kr(4d)^n$, giving ground electronic states of $^1A_1'$ for $Nb(V)$ ($n = 0$) and $^2E''$ for $Mo(V)$ ($n = 1$, the single $4d$ electron will occupy the e'' orbital).

The theorem of Jahn and Teller (4) states that a non-linear molecule which possesses a spatial degeneracy in a symmetrical configuration will have an equilibrium configuration of some lower symmetry in which the electronic degeneracy has been lost. Therefore, both the ground electronic state of $MoCl_5$ (with one electron in the e'' orbital) and the first excited state (with one electron in the e' orbital) should exhibit Jahn–Teller distortions. (The electronic spectrum of $NbCl_5$, which possesses a closed shell structure identical with that of the molybdenum compound, was investigated as well to determine the character of the charge transfer bands and hence aid in the assignment of the d–d transitions.)

The Jahn–Teller effect represents a breakdown of the Born–Oppenheimer approximation, for it introduces an intimate coupling of certain of the nuclear motions with the electronic angular momentum, leading to the formation of vibronic states in which the concept of a potential surface has been lost.

The static problem (12) leading to the distortion may be treated as a first-order splitting of the electronic degeneracy by certain of the vibrational motions of the molecule. Which of the vibrational motions will provide such a perturbation is again best determined by the methods of group theory. The structure of the vibrational representation of a trigonal bipyramid is

$$\Gamma_{vib} = 2A_1' + 3E' + 2A_2'' + E''.$$

The only motions which resolve the degeneracy of the $^2E''$ and $^2E'$ electronic states are the three vibrations of E' symmetry. (Only the direct products of species $\Gamma_{E'}$ with $\Gamma_{E''}{}^2$ and $\Gamma_{E'}{}^2$ contain the identity representation aside from the identity representation itself.)

The representation of D_{3h} spanned by the even harmonics of order less than five contains the identity representation three times ($n = 0, 2, 4$). Therefore, the non-spherically symmetric crystal-field contribution to the Hamiltonian has the form

$$H_c = \Sigma_i(A Y_{20} + B Y_{40}) \qquad [1]$$

and in the general case two sets of constants A and B will be required, one set for the axial ligands and another for the equatorial ligands. The Y_{nm} are the usual spherical harmonics. Terms with m values different from zero do not appear in [1] due to the trigonal arrangement of the three ligands in the plane. The matrix of this perturbation will obviously have no off-diagonal elements in the $|l,m\rangle$ basis of the $4d$ orbitals. The orbitals are simply split into two doublets $|2,2\rangle,|2,-2\rangle(e')$, and $|2,1\rangle,|2,-1\rangle(e'')$ and into the singlet $|2,0\rangle$ (a_1'). We may thus conveniently employ the same basis functions to derive the Jahn–Teller splittings with the perturbation of required E' symmetry given by

$$H_{E'} = \Sigma_i[Y_{2\pm2}R_2(r_i) + Y_{4\pm4}R_4(r_i)]Q \qquad [2]$$

where Q is a normal co-ordinate of E' symmetry. It is easily seen that there are no diagonal

*The $5p_x$ and $5p_y$ metal orbitals may also participate to some extent in σ-bonding with the three equatorial ligands as indicated by the light dashed line joining the $5p$ and e' levels in Fig. 1. A trigonal bipyramid may also be formed using the dsp^3 orbitals of the metal. Thus there are in this case a total of seven orbitals (no more than three of them d orbitals) of proper symmetry to participate in the σ-bonding in an MX_5 molecule.

Can. J. Chem. Downloaded from www.nrcresearchpress.com by 210.87.254.42 on 09/05/12
For personal use only.

elements of this perturbation; there are only off-diagonal ones, between $|2,2\rangle$ and $|2,-2\rangle$, which are mixed under $Y_{4\pm4}$, and between $|2,1\rangle$ and $|2,-1\rangle$, which are mixed under $Y_{2\pm2}$. (The perturbation $H_{E'}$ will also mix in some of the $|2,0\rangle$ state with the $|2,\pm2\rangle$ states but this can be ignored because of the large energy separation between the two sets of states and, furthermore, it does not change the form of the results.) If we let the matrix elements $\langle l,m \mid H_{E'} \mid l,-m^*\rangle$ have the values kQ and $k'Q$ for $|m| = 1$ and 2 respectively, then the eigenvalues of the two perturbation problems combined with the harmonic restoring force $\frac{1}{2}KQ^2$ are

$$V = \tfrac{1}{2}KQ^2 \pm kQ \qquad \text{for the } E'' \text{ state,}$$

$$V = \tfrac{1}{2}KQ^2 \pm k'Q \qquad \text{for the } E' \text{ state.}$$

This shows that both the E'' and E' states are resolved under the influence of the E' vibrations and that the nuclear potential function is split into two branches. A plot of either value of V versus Q leads to a double cone potential surface with the potential minimum at $Q = k/K$ (or k'/K) as illustrated in the paper by Longuet-Higgins, Öpik, Pryce, and Sack (5). The nuclear motions of E' symmetry are shown in Fig. 2. The E'

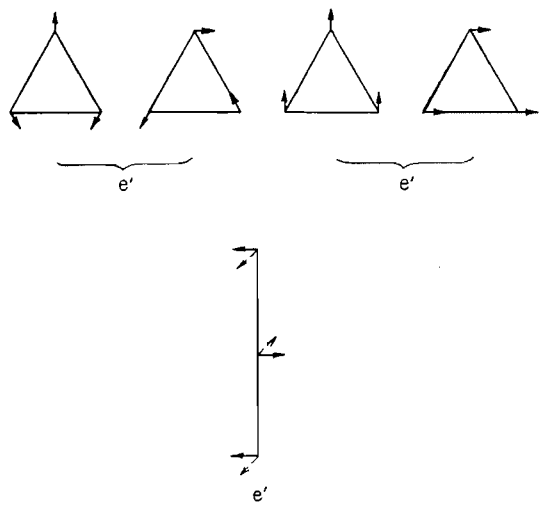


FIG. 2. The nuclear motions of E' symmetry for a trigonal bipyramid molecule.

vibrations will be combinations of these motions, the exact forms of which can only be deduced when the forms of the normal vibrations are known. One of the possible distortions is shown in Fig. 3. It is seen that the result is a lowering of the symmetry to C_{2v} which removes the degeneracy of all the levels.

Molybdenum is from the second transition series; therefore, one cannot overlook the possibility of a strong spin–orbit coupling upsetting the Jahn–Teller effect. As we point out in the Discussion, while we are confident that a large Jahn–Teller effect will be present in the first excited state due to the occupation of the e' antibonding orbital, the spin–orbit coupling may quite easily be of sufficient strength to prevent a distortion from occurring in the ground state where the degeneracy arises from the e'' non-bonding orbital. We restrict the following analysis then, to the $|\pm1\rangle$ states, but actually a similar treatment with corresponding results holds for the $|\pm2\rangle$ kets.

Can. J. Chem. Downloaded from www.nrcresearchpress.com by 210.87.254.42 on 09/05/12
For personal use only.

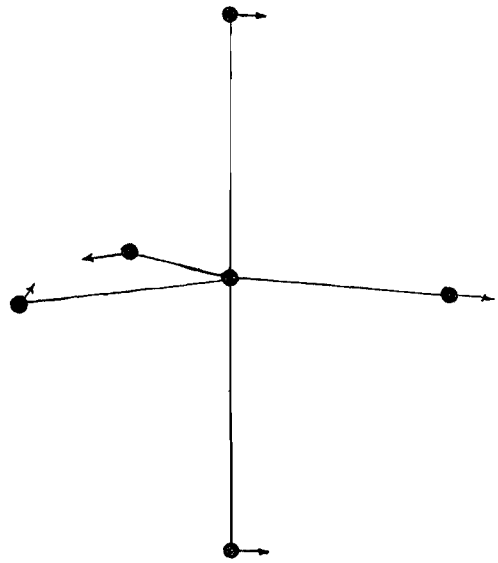


FIG. 3. A possible E' vibrational distortion of a trigonal bipyramid molecule.

In the absence of spin–orbit interactions, the ground state $^2E''$ is fourfold degenerate, $|\pm 1, \pm\frac{1}{2}\rangle$ (in the $|m_l, m_s\rangle$ notation). Spin–orbit coupling alone will result in the formation of two Kramers spin doublets, the degeneracy of which cannot be removed by any electrostatic field. We now investigate the problem of the simultaneous operation of a spin–orbit coupling and a Jahn–Teller effect of comparable magnitude. The secular matrix of the operator

$$H' = H_{E'} + \lambda \bar{L} \cdot \bar{S}$$

is

$$\begin{array}{c|cc} & |\pm 1, \pm\frac{1}{2}\rangle & |\mp 1, \pm\frac{1}{2}\rangle \\ \hline \langle \pm 1, \pm\frac{1}{2}| & \frac{1}{2}\lambda & kQ \\ \langle \mp 1, \pm\frac{1}{2}| & kQ & -\frac{1}{2}\lambda \end{array} . \qquad [3]^*$$

The roots of the corresponding secular equation are (each root occurs twice as all the levels are still Kramers doublets)

$$E = \pm\tfrac{1}{2}(\lambda^2 + 4k^2Q^2)^{\frac{1}{2}}.$$

To obtain the total potential V, we add the harmonic restoring force $\frac{1}{2}KQ^2$ to these roots and obtain

$$V_\pm = \tfrac{1}{2}KQ^2 \pm \tfrac{1}{2}(\lambda^2 + 4k^2Q^2)^{\frac{1}{2}}.$$

Notice that, for $Q = 0$, the spin–orbit coupling has removed the degeneracy of the pairs of states on which the Jahn–Teller effect operates, i.e., $|+1, \frac{1}{2}\rangle$ is now an amount λ above $|-1, +\frac{1}{2}\rangle$ and similarly $|-1, -\frac{1}{2}\rangle$ is an amount λ above $|+1, -\frac{1}{2}\rangle$. The

*The $\bar{L}.\bar{S}$ perturbation will introduce small admixtures of the $|0, \pm\frac{1}{2}\rangle$ states into the $|\pm 1, \mp\frac{1}{2}\rangle$ states and $|\pm 2, \mp\frac{1}{2}\rangle$ into the $|\pm 1, \pm\frac{1}{2}\rangle$ states. The coefficients of these admixtures will be small as they are determined by the ratios $\sqrt{\frac{3}{2}}\lambda/\delta$ and λ/Δ. Furthermore, their inclusion will not change the form of the results.

Can. J. Chem. Downloaded from www.nrcresearchpress.com by 210.87.254.42 on 09/05/12
For personal use only.

relative magnitudes of λ and k now determine two possibilities for the forms of V_+ and V_-. These are shown graphically in Fig. 4. Regardless of the relative values of λ and k,

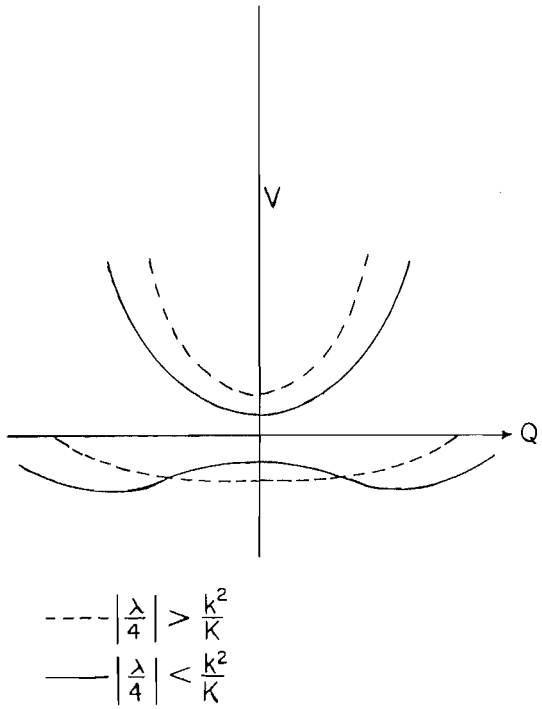


FIG. 4. The splitting of the fourfold degenerate potential level by spin–orbit and Jahn–Teller effects of comparable magnitude. In the text the upper curves are termed V_+ and the lower ones V_-.

the upper level in each case has but one minimum at $Q = 0$. However, the lower level may have two minima at values of $Q \neq 0$, or only one minimum at $Q = 0$, depending on the relative magnitudes of k^2/K and $|\lambda/4|$. Thus, when $k^2/K > |\lambda/4|$ and the Jahn–Teller effect is overriding, the molecule will distort even though the two levels are no longer degenerate but possess only a "near degeneracy". However, as λ is increased, a point is reached when the near degeneracy is, in a manner of speaking, no longer near enough and the Jahn–Teller distortion disappears. This will occur when $|\lambda/4| > k^2/K$. Thus, an absolute degeneracy is not necessary for the operation of the Jahn–Teller effect (12); a near degeneracy, if it fulfills the analytic requirement given above, will suffice. The analysis also shows that a sufficiently strong spin–orbit coupling will effectively quench a Jahn–Teller distortion. Jahn (14) has previously shown that a symmetrical configuration may be stabilized by large spin forces.

RESULTS

The visible and ultraviolet spectra of $MoCl_5$ and $NbCl_5$ vapors were obtained with a Beckmann DK-2 spectrophotometer using a 10-cm all-quartz cell which could be heated to the necessary temperatures (60–100° C).* The spectra of the two pentachlorides were also investigated in the infrared region, on a Perkin–Elmer single beam, double pass

*NOTE ADDED IN PROOF: *M. Gloor and K. Wieland (Helv. Chim. Acta, 44, 1098 (1961)) recently obtained a spectrum for* $NbCl_5$ *between the range 22,000–40,000 cm*$^{-1}$ *which agrees with ours.*

Can. J. Chem. Downloaded from www.nrcresearchpress.com by 210.87.254.42 on 09/05/12
For personal use only.

instrument from 4000 to 723 cm^{-1}. A Perkin–Elmer prism grating instrument was employed to search the region from 2,500 to 12,000 cm^{-1} for the $MoCl_5$ compound. The visible and ultraviolet spectrum of $MoCl_5$ is shown in Fig. 5, and the positions of the observed band maxima for both compounds are listed in Table I. The band shown at

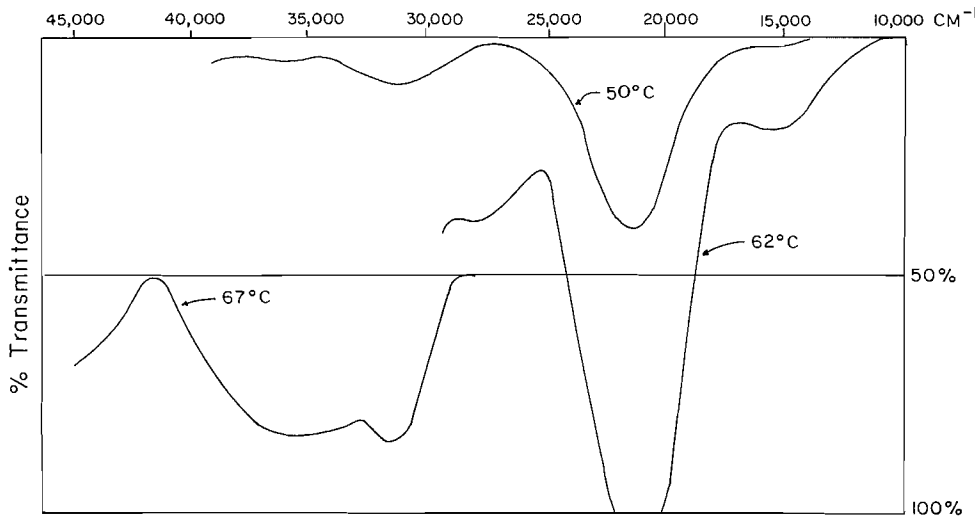


FIG. 5. The visible and ultraviolet spectrum of $MoCl_5$.

TABLE I

The visible and ultraviolet absorption bands of $MoCl_5$ and $NbCl_5$ and their extinction coefficients

$MoCl_5$		$NbCl_5$	
ν_{max} (in cm^{-1})	$\epsilon(\times 10^{-4})$ (l. $mole^{-1}$ cm^{-1})	ν_{max} (in cm^{-1})	$\epsilon(\times 10^{-4})$ (l. $mole^{-1}$ cm^{-1})
1,009	0.1		
15,200	0.4		
21,300	2.		
27,800	*		
35,700	2	35,100	1
42,600†	1	41,700†	1

*The extinction coefficient for this band cannot be accurately determined as the band occurs on the tail of the chlorine gas absorption. It is by far the least intense of all the bands.

†These bands occur just before the cutoff point of the instrument. The values entered in the table give the wavelength at the ½-peak height.

31,000 cm^{-1} in the spectrum of $MoCl_5$ was shown to be due to chlorine gas. The same band appeared to a lesser extent in the spectrum of $NbCl_5$ at higher temperatures. The dissociation of $MoCl_5$ in the gas phase according to the equation

$$2(MoCl_5)_{gas} \rightleftarrows 2(MoCl_4)_{solid} + Cl_2$$

has been investigated by Vasilkova and Sharupin (6). The result of heating molybdenum pentachloride is to produce chlorine gas at pressures comparable with those of the pentachloride itself. Apparently a similar decomposition occurs to a lesser extent in the case

Can. J. Chem. Downloaded from www.nrcresearchpress.com by 210.87.254.42 on 09/05/12
For personal use only.

of niobium pentachloride. Unfortunately, all the bands are broad and exhibit no vibrational structure. An initial attempt was made to record the spectrum of molybdenum pentachloride on an Hilger E2 spectrograph to obtain a high resolution spectrum. However, no detail was observed.

Spectra were also obtained for the two pentachlorides in solution. The solution spectrum of $MoCl_5$ in cyclohexane and carbon tetrachloride in the visible was unchanged from that of the gas phase but the band in the ultraviolet region was intensified. The solution spectrum of $NbCl_5$ in carbon tetrachloride was completely changed from that found in the gas phase. A very intense band appeared at 475 mμ and more intense absorption was found in the ultraviolet region. This is an interesting observation in that both $MoCl_5$ and $NbCl_5$ are known to exist as dimers in the solid state (7, 8) in the form of double octahedra having a common edge. We believe that, in solution, the dimerization persists in the case of the niobium compound but not in the case of the molybdenum. Further evidence to support this view was obtained from a reflection spectrum of the solid $NbCl_5$, which gave the same intense band at 475 mμ as found in the solution of this compound.*

DISCUSSION

The expected consequences of the Jahn–Teller effect on electronic spectra have been discussed by Longuet-Higgins *et al.* (5). These consequences are twofold. In cases where the vibrational structure of the transitions is resolved a progression in the distorting E' vibration should be observed along with the regular progression in the symmetrical modes. The Jahn–Teller effect, by lowering the effective symmetry of the molecule, breaks down the otherwise rigorous selection rule prohibiting single (or odd number) changes in the E' vibrational quantum number during a transition. The same authors have given the expected band shapes for transitions to Jahn–Teller degenerate states from a non-degenerate state for different values of the distortion parameter k in the cases where only one distorting vibration is allowed. Unfortunately neither of these more elaborate analyses may be carried out in the present case for, as noted above, the bands are very broad and exhibit no vibrational structure. However, we feel that the observed spectrum does indicate a large Jahn–Teller splitting in the first excited state of molybdenum pentachloride. In its simplest terms, the Jahn–Teller effect resolves the degeneracy of an orbital doublet and leads to the appearance of two maxima in the electronic spectrum, where but one would be observed in its absence. Longuet-Higgins *et al.* (5) have discussed how such a double maximum may be roughly interpreted in terms of the Franck–Condon principle. In a transition from a non-degenerate to a degenerate state, the molecule may arrive on either branch of the double cone potential surface referred to previously. Different amounts of vibrational energy will be involved in each case depending on which possibility is the most favorable. Such a situation will lead to a double maximum in the absorption spectrum. In the present case the lowest transition is from one degenerate state to another (the lowest state may well not be Jahn–Teller active because of the spin–orbit coupling). In the degenerate ground state the molecule will, if k (or λ) is of any reasonable magnitude at all, be in the neighborhood of the potential

**The infrared spectrum of niobium pentachloride in carbon disulphide solution was obtained by Gaunt and Ainscough (9) and the assignments so obtained were put forward as proof of the trigonal bypyramidal structure for this compound. We think that their results are not meaningful in this connection as an investigation of the ultraviolet spectrum of a carbon disulphide solution of the niobium pentachloride gave a spectrum radically different from that in the gas phase and different again from that found in carbon tetrachloride. Solution of the niobium compound in carbon disulphide leads to the formation of an intense yellow-orange solution as opposed to the pale yellow solution obtained in carbon tetrachloride, or the pale yellow color of the solid itself. We will report more fully on this point in the infrared investigation of these two pentachlorides.*

Can. J. Chem. Downloaded from www.nrcresearchpress.com by 210.87.254.42 on 09/05/12
For personal use only.

Can. J. Chem. Downloaded from www.nrcresearchpress.com by 210.87.254.42 on 09/05/12
For personal use only.

minimum with a well-defined nuclear configuration. Thus its transition to the degenerate excited state should give the appearance noted above for a transition from a non-degenerate (where again the ground state is in a well-defined configuration) to a doubly degenerate state. The intensities of the two bands at 15,200 and 21,300 cm^{-1} denote them as allowed, as expected for the E'–E'' transitions. Although the energy separation between the two band maxima of approximately 6000 cm^{-1} cannot be related in any simple way to the value of k', it does suggest a large distortion in the E' state. A very large distortion would also lead to the appearance of two maxima as it would correspond to a permanently distorted molecule of C_{2v} symmetry where the E' state has been split into two new states of B_1 and A_1 symmetries. It should be recalled that the $\bar{e}'$ orbital is a strongly antibonding one and thus a large splitting should be expected just as is observed in the cases of octahedral molecules exhibiting Jahn–Teller effects arising from occupation of the antibonding e_g orbitals. The $\bar{e}'$ orbitals point directly at the ligands in the plane and thus the electrostatic forces exerted on the ligands by an electron in the $\bar{e}'$ orbital will be quite large.

The splitting in the ground state due to the occupation of the e'' orbital will be small as this orbital is directed away from all of the ligands and is not involved in any σ bonding with the ligands. Thus the electrostatic repulsions exerted by the electron density in this orbital will be of much smaller magnitude. The same small splitting is also encountered in octahedral molecules when the degeneracy arises from the occupation of the t_{2g} orbitals as is evidenced by the so far unsuccessful search for distortions in these cases. In fact, there may not be any Jahn–Teller distortion in the ground state due to the presence of a strong spin–orbit coupling. As was pointed out in the Introduction, the spin–orbit interactions cause a splitting of the ground state potential function into two curves (V_+ and V_-) separated in energy by $(\lambda^2 + 4k^2Q^2)^{\frac{1}{2}}$. We suggest that the infrared band observed at 1009 cm^{-1} is due to a transition from V_- to V_+. We base the assignment on the following considerations. First, niobium pentachloride has no corresponding band and thus it is unlikely that the 1009 cm^{-1} band is due to a vibrational motion. Second, the value of λ for the Mo^{+4} ion is 887 cm^{-1} (11) and the value for Mo^{+5} should be somewhat larger. Such a value of λ, coupled with the contribution due to the $4k^2Q^2$ term, would place the band in the observed frequency range. In fact, the theoretical analysis of the spin–orbit coupling effect prompted our search for a band in this region.

The observation of a transition from V_- to V_+ does not necessarily imply the absence of a Jahn–Teller effect in the ground state of $MoCl_5$. As pointed out in the Introduction, k^2/K may still be larger than $|\lambda/4|$ and thus a distortion should still occur. This final question can only be answered by a complete investigation of the infrared spectra of $MoCl_5$ and $NbCl_5$ to see if any indications of band splittings can be determined in the former case. This work, together with a more detailed analysis of the 1009 cm^{-1} band, is now in progress.

The band found at 27,800 cm^{-1} which is superimposed on the tail of the strong absorption due to Cl_2 is assigned to the A_1'–E'' transition, an assignment which is consistent with the low intensity of this particular absorption. Unfortunately, the chlorine gas absorption interferes with this band and no detail beyond its presence may be obtained. The remaining bands at 35,700 and 42,600 cm^{-1} are attributed to charge transfer processes. These assignments are very reasonable because of their observed intensity, short wavelength, and similarity in these properties to the corresponding bands observed for niobium pentachloride (at 35,100 and 41,700 cm^{-1}), which possesses no d–d transitions.

The crystal-field splitting in a trigonal bipyramid molecule involves two parameters if

the five ligands are assumed to lie equidistant from the metal atom. In a simplified approach these may be related to the G_2 and G_4 (for the ionic case) or B_2 and B_4 (for the dipole case) parameters of Ballhausen (10). As in the octahedral cases, neither of these parameters will be determined entirely by simple electrostatic effects but must be interpreted as empirical separations determined by both the electrostatic interactions and the covalent bonding effects of the ligands. We have evaluated the integrals G_2 and G_4 for $4d$ hydrogen-like atomic orbitals to determine their ratio in a rough attempt to justify the above spectroscopic assignments by showing that they can be calculated from reasonable values of the parameters. Assuming the splitting to be linear in Q in the E' state, the mean of the two zero–zero levels in the E'–E'' transition is at approximately 13,500 cm^{-1}. This gives a ratio of the A_1'–E'' to the E'–E'' energy separations ($= \delta/\Delta$) of approximately two. The electron diffraction data for the $MoCl_5$ molecule gave an average over the five bond lengths as 2.27 Å (1). If all five chlorides are assumed to be equidistant from the metal ion, the δ/Δ ratio comes out in the neighborhood of 4.5, i.e., much too large. This discrepancy becomes even larger if it is assumed that the two axial ligands lie closer to the metal ion than do the three ligands in the plane. For example, an axial ligand to metal distance of 2.27 Å and an equatorial – metal ligand distance of 2.40 Å give a δ/Δ energy ratio of 6.6. However, it was found that any shortening of the equatorial bond length or any lengthening of the axial bond length pushes the energy ratio in the desired direction. In fact, an equatorial–metal bond length of 2.15 Å together with an axial–metal bond length of 2.40 Å (which averages to the observed value) gives the observed energy ratio of $\delta/\Delta = 2$. This shortening of the bonds in the plane and the lengthening along the axis in this empirical approach to adjusting the parameters would be equivalent to differing amounts of covalent bonding in the two directions. The apparent increase in bonding found for the equatorial ligands over that for the axial ligands can be related to the fact that the $5p_x$ and $5p_y$ metal orbitals may also contribute to the σ-bonding in the former case. Extra σ-bonding contributions to the axial ligands could only arise from the participation of much higher lying metal orbitals and thus be of little relative significance. It is interesting to note that in the trigonal bipyramid molecules for which all the bond lengths are accurately known, the equatorial bonds are shorter than the axial ones, as is predicted by the present fitting of the observed spectrum. We do not, of course, ascribe this inequality to any Jahn–Teller distortion.

The absorptions in the regions of 1000, 20,000, and 28,000 cm^{-1} are, therefore, reasonably assigned to d–d transitions. The appearance of the double maximum in the intermediate band is consistent with a Jahn–Teller splitting of the E' state.

The low-lying band implies a spin–orbit splitting of the ground state, with or without an accompanying Jahn–Teller distortion.

EXPERIMENTAL

Molybdenum pentachloride which was obtained commercially was analyzed gravimetrically and used without further purification. Anal. Calc.: Mo, 35.78%; Found: 35.74, 35.80%.

Niobium pentachloride was prepared from the oxide by the procedure of Schäfer and Pietruck (13) and purified by vacuum sublimation. The materials were handled exclusively under rigorously dried nitrogen.

In order to ascertain whether there was any interference from oxychlorides, a substance having the composition $MoOCl_3$ was prepared by controlled hydrolysis and its ultraviolet and infrared spectra determined. Cyclohexane used for the solution spectrum

Can. J. Chem. Downloaded from www.nrcresearchpress.com by 210.87.254.42 on 09/05/12
For personal use only.

was purified by passage through a column of silica gel and subsequent distillation from an excess of $MoCl_5$. The carbon tetrachloride and carbon disulphide were commercial spectral grade products.

REFERENCES

1. R. V. G. Ewens and M. W. Lister. Trans. Faraday Soc. **34**, 1358 (1938).
2. H. A. Skinner and L. E. Sutton. Trans. Faraday Soc. **36**, 668 (1940).
3. C. J. Ballhausen and C. Klixbüll Jørgensen. Kgl. Danske Videnskab. Selskab, Mat.-fys. Medd. **29** (14), (1955).
4. H. A. Jahn and E. Teller. Proc. Roy. Soc. A, **161**, 220 (1937).
5. H. C. Longuet-Higgins, U. Öpik, M. H. L. Pryce, and R. A. Sack. Proc. Roy. Soc. A, **244**, 1 (1958).
6. S. A. Shchuharev, I. V. Vasilkova, and B. N. Sharupin. J. Gen. Chem. U.S.S.R. **26**, 2335 (1956).
7. D. E. Sands and A. Zalkin. Acta. Cryst. **12**, 723 (1959).
8. D. E. Sands and A. Zalkin. Acta. Cryst. **11**, 615 (1958).
9. J. Gaunt and J. B. Ainscough. Spectrochim. Acta, **10**, 52 (1957).
10. C. J. Ballhausen. Kgl. Danske Videnskab. Selskab, Mat.-fys. Medd. **29** (4), (1954).
11. J. S. Griffith. The theory of transition metal ions. Cambridge University Press, Cambridge. 1961.
12. U. Öpik and M. H. L. Pryce. Proc. Roy. Soc. A, **238**, 425 (1957).
13. H. Schäfer and C. Pietruck. Z. anorg. u. allgem. Chem. **264**, 2 (1951).
14. H. A. Jahn. Proc. Roy. Soc. A, **164**, 117 (1938).

Can. J. Chem. Downloaded from www.nrcresearchpress.com by 210.87.254.42 on 09/05/12
For personal use only.

Can. J. Chem. Downloaded from www.nrcresearchpress.com by 210.87.254.40 on 09/05/12
For personal use only.

THE N.M.R. SPECTRUM OF CYCLOPENTANONE

F. A. L. ANET

The high-resolution proton nuclear magnetic resonance (N.M.R.) spectrum of cyclopentanone has been stated (1, 2) to consist of a single line at 25 and 40 Mc/sec. Wiberg and Nist (3) have recently reported that at 60 Mc/sec cyclopentanone in carbon tetrachloride gave rise to a closely spaced doublet and concluded that the chemical shift between the α and β protons was very small. By comparison of the spectrum with that expected from an A_2B_2 system (4), these authors also concluded that the coupling constants were abnormally small (< 2.4 c.p.s.). However, this cannot be considered valid, as cyclopentanone is an example of an A_4B_4 system (4) or, by Corio's definition (5), an $AA'A''A'''BB'B''B'''$ system. Analysis as an A_2B_2 system would only be correct if the coupling constants between the vicinal β protons were all zero, which is highly unlikely.

The spectrum of cyclopentanone has been re-examined at 60 Mc/sec and it was observed that although the main band of the spectrum is a (rough) doublet, as reported by Wiberg, the spectrum is actually unsymmetrical, unlike that of an A_2B_2 system (4, 5). There are also a number of weak lines, not previously observed, at an appreciable distance from the main doublet. These lines are not due to impurities or spinning side bands, nor can they be ascribed to protons on C^{13}. Their presence shows that relatively large coupling constants must be present in cyclopentanone. That large coupling constants are present is shown even more clearly by the spectrum of cyclopentanone in benzene solution (Fig. 1). Now there is quite an appreciable chemical shift between the α and β protons and the spectrum is no longer even approximately a doublet.

Unfortunately, a complete analysis of the spectrum of cyclopentanone would be extremely tedious. As well as one (relative) chemical shift there are six different coupling constants to be determined, apart from the probably negligible 1,3-coupling constants. Nevertheless, it is possible to extract some information by the application of the moment method described by Anderson and McConnell (6). In a molecule, such as cyclopentanone, which has protons in only two different chemical environments, the moment method gives particularly simple results for the relative chemical shift ($\Delta\nu$) and for the sum of the squares of the coupling constants between *chemically shifted* protons. If M_2, M_3, and M_4 are respectively the reduced second, third, and fourth moments (i.e. moments taken from an origin where the first moment is zero) and J_{cis} and J_{trans} are the two different coupling constants between vicinal α and β protons, then the following expressions hold (6):

$$\nu = 2\sqrt{M_2},$$

$$J_{cis}^2 + J_{trans}^2 = \frac{M_4 - M_2^2}{M_2},$$

$$M_3 = 0.$$

Calculations on the spectrum in Fig. 1 and on a number of other spectra taken at

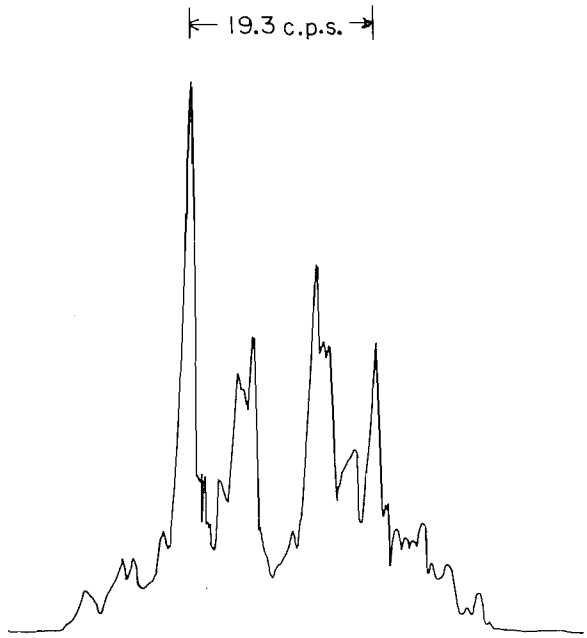


FIG. 1. N.M.R. spectrum of a 20% by volume solution of cyclopentanone in benzene. The magnetic field increases from left to right.

different sweep rates gave, for 20% by volume solutions of cyclopentanone in benzene, $\Delta\nu = 19.5 \pm 0.5$ c.p.s. and $(J_{cis}^2 + J_{trans}^2)^{1/2} = 10.8 \pm 1.0$ c.p.s. In a solution containing equal volumes of cyclopentanone, benzene, and carbon tetrachloride, $\Delta\nu = 10.8 \pm 0.5$ c.p.s. and $(J_{cis}^2 + J_{trans}^2)^{1/2} = 10.1 \pm 1.0$ c.p.s. Thus, as expected, the coupling constants do not vary appreciably on the changing of the solvent. One of these coupling constants must be larger than 6 c.p.s. and could be as large as 10 c.p.s. Correspondingly the other coupling constant must be smaller than 8 c.p.s. and could be zero. These values are entirely consistent with the coupling constants in flexible, five-membered rings (7). The fact that the spectrum of Fig. 1 is unsymmetrical and is much too complicated for an A_2B_2 system shows that the coupling constants between vicinal β protons must also have appreciable values.

EXPERIMENTAL

Spectra were measured on a Varian V-4302 high-resolution spectrometer. Care was taken to obtain a pure absorption mode and the radio-frequency power was set well below saturation level so as to obtain correct intensities. To calculate moments a millimeter grid was superposed on the spectrum, and the intensities (as measured by the heights) at small intervals, usually 1 mm, were measured from an arbitrary zero outside the spectrum. Depending on the case, from 60 to 120 readings were made. These values were fed to a computer (I.B.M. 650) which was programed to calculate M_2, M_3, and M_4. Calculations were made on a number of spectra with both increasing and decreasing magnetic fields and with various sweep rates.

The cyclopentanone (Eastman Kodak pure grade) showed only a single band on gas chromatography with a silicone oil column at 134°. The spectrum was unchanged after

Can. J. Chem. Downloaded from www.nrcresearchpress.com by 210.87.254.40 on 09/05/12
For personal use only.

the cyclopentanone had been purified via the recrystallized semicarbazone derivative. At high sensitivity and r.f. power no further bands were observed on the side of the spectrum of Fig. 1 except bands assignable to protons on C^{18}. Spectra taken in pyridine or aniline solutions were very similar to those taken in benzene solution.

ACKNOWLEDGMENT

I wish to thank Miss O. Boshko for setting up the computer program.

1. H. PRIMAS, K. FREI, and H. H. GÜNTHARD. Helv. Chim. Acta, **41**, 35 (1958).
2. J. D. ROBERTS. Nuclear magnetic resonance. McGraw-Hill Book Co., New York. 1959. p. 57.
3. K. B. WIBERG and B. J. NIST. J. Am. Chem. Soc. **83**, 1226 (1961).
4. J. A. POPLE, W. G. SCHNEIDER, and H. J. BERNSTEIN. High-resolution nuclear magnetic resonance. McGraw-Hill Book Co., New York. 1959. Chap. 6.
5. P. L. CORIO. Chem. Revs. **60**, 383 (1960).
6. W. A. ANDERSON and H. M. MCCONNELL. J. Chem. Phys. **26**, 1496 (1957).
7. N. SHEPPARD and J. J. TURNER. Proc. Roy. Soc. A, **252**, 506 (1959).

RECEIVED JULY 10, 1961.
DEPARTMENT OF CHEMISTRY,
UNIVERSITY OF OTTAWA,
OTTAWA, ONT.

Can. J. Chem. Downloaded from www.nrcresearchpress.com by 210.87.254.40 on 09/05/12
For personal use only.

PROTON RESONANCE SPECTRA OF 8-HYDROXY AND 8-METHYL QUINOLINE

L. W. REEVES AND K. O. STRØMME

The present study is a comparison of the behavior of 8-hydroxy and 8-methyl quinoline in various nonpolar solvents. The part played by the hydroxyl proton in the intermolecular associations of 8-hydroxy quinoline is of some interest in view of its importance as a chelating agent.

EXPERIMENTAL

8-Hydroxy quinoline of analytical grade was recrystallized and 8-methyl quinoline was used as analytical grade. The solvents were all fractionally distilled and stored over drying agents. A 40 Mc/s Varian spectrometer was used to take spectra, and the 'sideband technique' was used to determine peak positions. Absolute chemical shifts on the cyclohexane scale are accurate to ± 1.0 c.p.s. but internal chemical shifts are accurate to ± 0.2 c.p.s. A 1% cyclohexane internal standard was always included in the solution.

RESULTS

Chemical shifts of the hydroxyl proton and the α, β, and γ protons of the hetero ring have been measured. The hetero ring protons formed an ABX or AMX group (1), and some overlap occurred in most cases between the β-proton spectrum and the spectrum of the second aromatic ring. Chemical shifts in the second aromatic ring were very similar and the main feature was a large, single peak with several small satellites. It was always possible to assign transitions in the β-proton spectrum and thus obtain a complete analysis for the ABX or AMX spectrum.

To illustrate this, Fig. 1(a) shows a spectrum of 18.6 mole% 8-hydroxy quinoline in

the cyclopentanone had been purified via the recrystallized semicarbazone derivative. At high sensitivity and r.f. power no further bands were observed on the side of the spectrum of Fig. 1 except bands assignable to protons on C^{18}. Spectra taken in pyridine or aniline solutions were very similar to those taken in benzene solution.

ACKNOWLEDGMENT

I wish to thank Miss O. Boshko for setting up the computer program.

1. H. PRIMAS, K. FREI, and H. H. GÜNTHARD. Helv. Chim. Acta, **41**, 35 (1958).
2. J. D. ROBERTS. Nuclear magnetic resonance. McGraw-Hill Book Co., New York. 1959. p. 57.
3. K. B. WIBERG and B. J. NIST. J. Am. Chem. Soc. **83**, 1226 (1961).
4. J. A. POPLE, W. G. SCHNEIDER, and H. J. BERNSTEIN. High-resolution nuclear magnetic resonance. McGraw-Hill Book Co., New York. 1959. Chap. 6.
5. P. L. CORIO. Chem. Revs. **60**, 383 (1960).
6. W. A. ANDERSON and H. M. MCCONNELL. J. Chem. Phys. **26**, 1496 (1957).
7. N. SHEPPARD and J. J. TURNER. Proc. Roy. Soc. A, **252**, 506 (1959).

RECEIVED JULY 10, 1961.
DEPARTMENT OF CHEMISTRY,
UNIVERSITY OF OTTAWA,
OTTAWA, ONT.

Can. J. Chem. Downloaded from www.nrcresearchpress.com by 210.87.254.40 on 09/05/12
For personal use only.

PROTON RESONANCE SPECTRA OF 8-HYDROXY AND 8-METHYL QUINOLINE

L. W. REEVES AND K. O. STRØMME

The present study is a comparison of the behavior of 8-hydroxy and 8-methyl quinoline in various nonpolar solvents. The part played by the hydroxyl proton in the intermolecular associations of 8-hydroxy quinoline is of some interest in view of its importance as a chelating agent.

EXPERIMENTAL

8-Hydroxy quinoline of analytical grade was recrystallized and 8-methyl quinoline was used as analytical grade. The solvents were all fractionally distilled and stored over drying agents. A 40 Mc/s Varian spectrometer was used to take spectra, and the 'sideband technique' was used to determine peak positions. Absolute chemical shifts on the cyclohexane scale are accurate to ± 1.0 c.p.s. but internal chemical shifts are accurate to ± 0.2 c.p.s. A 1% cyclohexane internal standard was always included in the solution.

RESULTS

Chemical shifts of the hydroxyl proton and the α, β, and γ protons of the hetero ring have been measured. The hetero ring protons formed an ABX or AMX group (1), and some overlap occurred in most cases between the β-proton spectrum and the spectrum of the second aromatic ring. Chemical shifts in the second aromatic ring were very similar and the main feature was a large, single peak with several small satellites. It was always possible to assign transitions in the β-proton spectrum and thus obtain a complete analysis for the ABX or AMX spectrum.

To illustrate this, Fig. 1(a) shows a spectrum of 18.6 mole% 8-hydroxy quinoline in

Can. J. Chem. Downloaded from www.nrcresearchpress.com by 210.87.254.40 on 09/05/12
For personal use only.

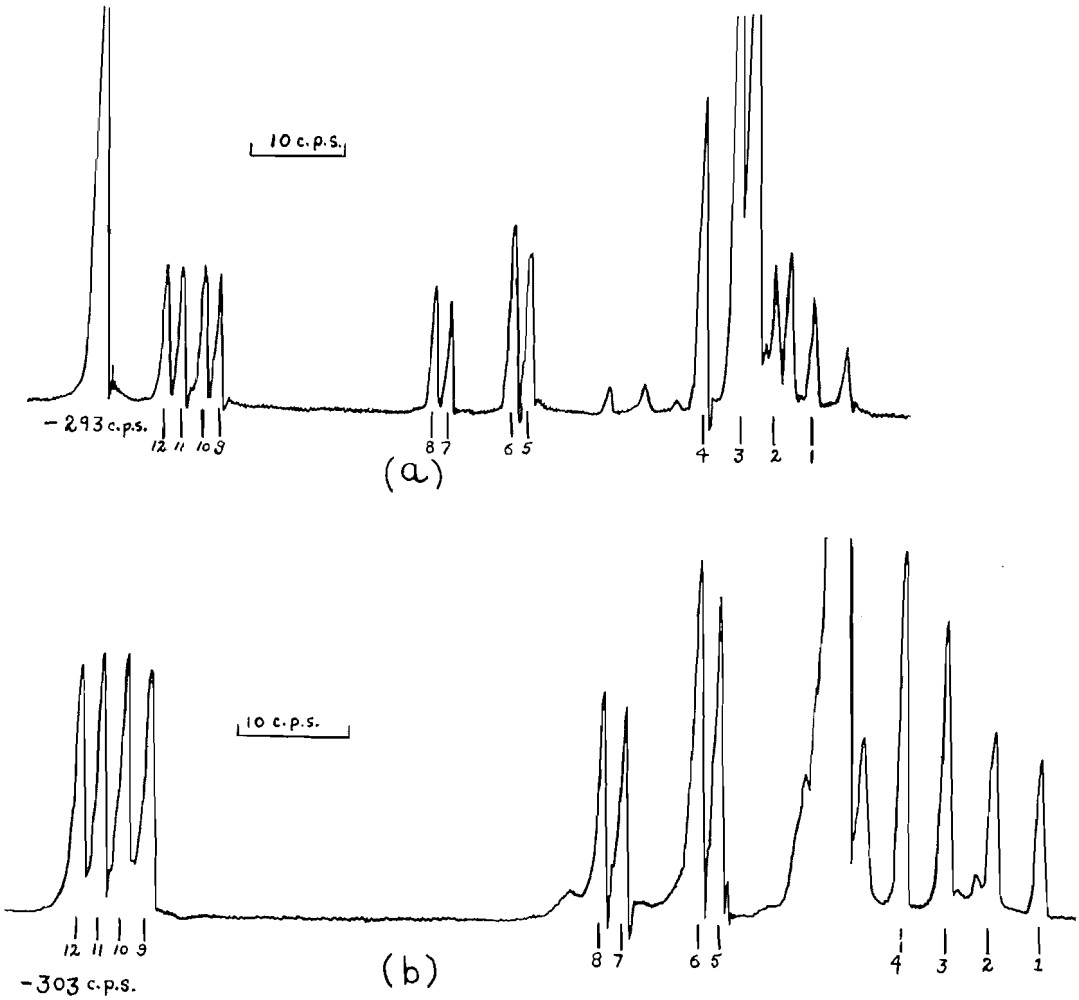


FIG. 1. (*a*) 8-Hydroxy quinoline, 18.6% in CCl_4; spectrum at 30° C. (*b*) 8-Methyl quinoline, pure; spectrum at 30° C.

CCl_4 and Fig. 1(*b*) shows a spectrum of pure 8-methyl quinoline with the methyl peak at high field omitted. The 12 transitions of the *ABX* spectrum are numbered according to the assignments of Bernstein, Schneider, and Pople (1) in each case. Figure 2 gives the results of dilution chemical shifts in CCl_4, benzene, and acetone for the hydroxyl proton resonance. Figure 3 indicates the dilution chemical shifts of the α, β, and γ protons for 8-hydroxy and 8-methyl quinoline in the various solvents and at the conditions given in the legend to this figure. The indirect spin–spin coupling constants evaluated were the same in all spectra analyzed. These were $|J_{\beta\gamma}| = 8.3$ c.p.s, $|J_{\alpha\beta}| = 4.4$ c.p.s., and $|J_{\alpha\gamma}| = 1.7$ c.p.s.

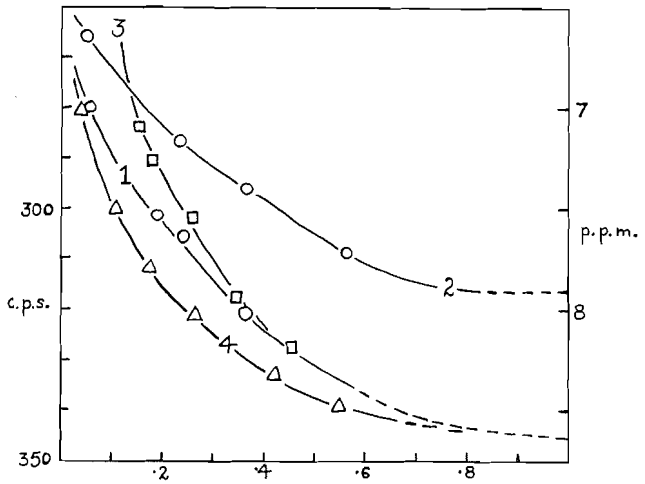


FIG. 2. Chemical shifts of —OH proton resonance of 8-hydroxy quinoline in various solvents: curve 1 (○), in CCl_4 at 29° C; curve 2 (○), in CCl_4 at 80° C; curve 3 (□), in acetone at 29° C; curve 4 (△), in benzene at 29° C. The abscissa of each point is the mole fraction of 8-hydroxy quinoline in the solvent and the ordinate is the chemical shift with respect to an internal cyclohexane standard.

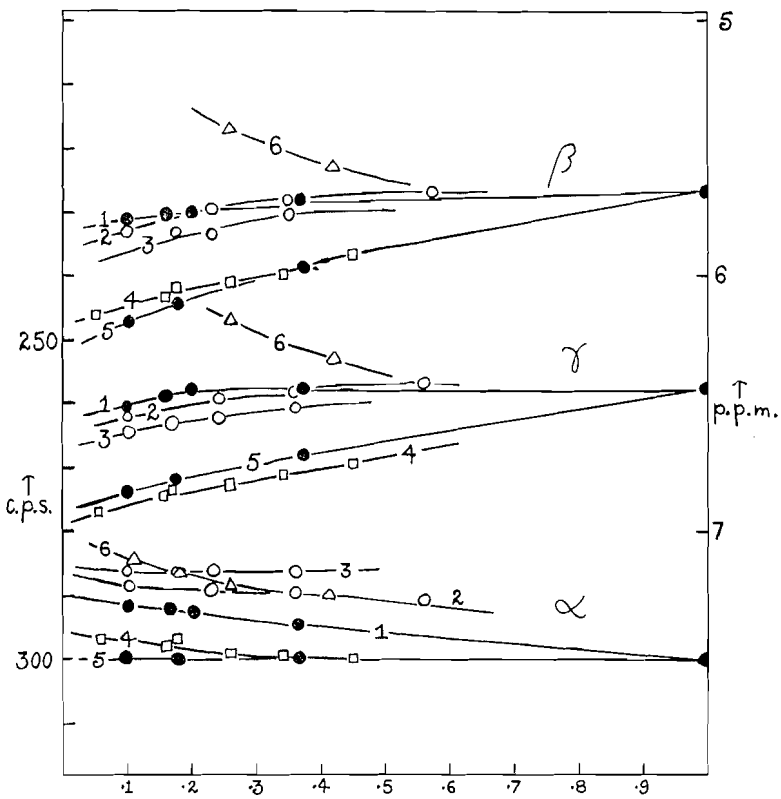


FIG. 3. Chemical shifts of α, β, and γ ring protons as a function of quinoline derivative; solvent and temperature with respect to concentration: curve 1 (●), 8-methyl quinoline in CCl_4 at 29° C; curve 2 (○), 8-hydroxy quinoline in CCl_4 at 80° C; curve 3 (○), 8-hydroxy quinoline in CCl_4 at 29° C; curve 4 (□), 8-hydroxy quinoline in acetone at 29° C; curve 5 (●), 8-methyl quinoline in acetone at 29° C; curve 6 (△), 8-hydroxy quinoline in benzene at 28° C.

Can. J. Chem. Downloaded from www.nrcresearchpress.com by 210.87.254.40 on 09/05/12
For personal use only.

Can. J. Chem. Downloaded from www.nrcresearchpress.com by 210.87.254.40 on 09/05/12
For personal use only.

DISCUSSION

The shape of the dilution chemical shift curves for the 8-hydroxy quinoline OH proton is indicative of exclusively intermolecular hydrogen bonding (2, 3). The estimation of interatomic distances would indicate little interaction within the same molecule between the hydroxyl proton and the nitrogen on the second ring (4).

The behavior of the hetero ring proton resonances of 8-methyl and 8-hydroxy quinoline is very similar in the same solvents (Fig. 3). There is a small shift to low field for the β and γ protons and to high field for the α proton in carbon tetrachloride solutions at room temperature. An increase in temperature of 50° C for the 8-hydroxy quinoline in CCl_4 solutions causes a low-field shift for the β and γ proton consistent with the concentration dependence of these shifts. The approximate extrapolation of these chemical shifts to mole fraction = 1 and 0 indicates a total shift of less than 10 c.p.s. in all cases. The small temperature coefficient amounted to only 2 c.p.s. in 50° C.

The direction of these chemical shift changes is the same in acetone solutions but the magnitude of the change is much larger for the β and γ protons. The dilution chemical shifts in benzene are in the direction of high field for all three protons in the hetero ring but again the magnitude of shifts is much larger for the β and γ protons.

These results are suggestive of preferential hydrogen bonding of solvent molecules at the β and γ positions in view of the fact that they represent difference shifts between cyclohexane and quinoline in the same solvent (5). The magnitude of the difference shifts due to van der Waals, anisotropy effects, and polar effects are probably comparable and difficult to estimate with any certainty (6).

ACKNOWLEDGMENTS

The support of the Research Corporation and the National Research Council of Canada is gratefully acknowledged.

1. H. J. Bernstein, J. A. Pople, and W. G. Schneider. Can. J. Chem. **35**, 65 (1957).
2. C. M. Huggins, G. C. Pimentel, and J. N. Shoolery. J. Chem. Phys. **23**, 311 (1956).
3. L. W. Reeves, E. A. Allan, and K. O. Strømme. Can. J. Chem. **38**, 1249 (1960).
4. Interatomic Distances. Spec. Publ. No. 11. Chemical Society, London.
5. T. Schaeffer and W. G. Schneider. J. Chem. Phys. **32**, 1224 (1960).
6. A. D. Buckingham, T. Schaeffer, and W. G. Schneider. J. Chem. Phys. **32**, 1227 (1960).

Received June 22, 1961.
Department of Chemistry,
University of British Columbia,
Vancouver, B.C.

CHEMICAL CONSTITUENTS OF CHICOZAPOTE*

E. Azpeitia, A. Bowers, P. Crabbé, O. Mancera, J. S. Matthews, J. Reynoso, and J. Salazar

The "chicozapote", *Achras sapota* L. of the Sapotaceae family, is a common tree of tropical regions of America, growing mainly in Brazil, Colombia, Guatemala, Honduras, Mexico, Peru, and Venezuela (1). Although the sapotilla tree or chicle tree (chicle from the original Maya word *sicté*) is well known since it constitutes the only source of natural

*This work constitutes a part of the undergraduate theses submitted by E. A. and J. R. to the Universidad Nacional Autónoma de México, and by J. S. to the Escuela Nacional de Ciencias Biólógicas.

Can. J. Chem. Downloaded from www.nrcresearchpress.com by 210.87.254.42 on 09/05/12
For personal use only.

DISCUSSION

The shape of the dilution chemical shift curves for the 8-hydroxy quinoline OH proton is indicative of exclusively intermolecular hydrogen bonding (2, 3). The estimation of interatomic distances would indicate little interaction within the same molecule between the hydroxyl proton and the nitrogen on the second ring (4).

The behavior of the hetero ring proton resonances of 8-methyl and 8-hydroxy quinoline is very similar in the same solvents (Fig. 3). There is a small shift to low field for the β and γ protons and to high field for the α proton in carbon tetrachloride solutions at room temperature. An increase in temperature of 50° C for the 8-hydroxy quinoline in CCl_4 solutions causes a low-field shift for the β and γ proton consistent with the concentration dependence of these shifts. The approximate extrapolation of these chemical shifts to mole fraction = 1 and 0 indicates a total shift of less than 10 c.p.s. in all cases. The small temperature coefficient amounted to only 2 c.p.s. in 50° C.

The direction of these chemical shift changes is the same in acetone solutions but the magnitude of the change is much larger for the β and γ protons. The dilution chemical shifts in benzene are in the direction of high field for all three protons in the hetero ring but again the magnitude of shifts is much larger for the β and γ protons.

These results are suggestive of preferential hydrogen bonding of solvent molecules at the β and γ positions in view of the fact that they represent difference shifts between cyclohexane and quinoline in the same solvent (5). The magnitude of the difference shifts due to van der Waals, anisotropy effects, and polar effects are probably comparable and difficult to estimate with any certainty (6).

ACKNOWLEDGMENTS

The support of the Research Corporation and the National Research Council of Canada is gratefully acknowledged.

1. H. J. Bernstein, J. A. Pople, and W. G. Schneider. Can. J. Chem. **35**, 65 (1957).
2. C. M. Huggins, G. C. Pimentel, and J. N. Shoolery. J. Chem. Phys. **23**, 311 (1956).
3. L. W. Reeves, E. A. Allan, and K. O. Strømme. Can. J. Chem. **38**, 1249 (1960).
4. Interatomic Distances. Spec. Publ. No. 11. Chemical Society, London.
5. T. Schaeffer and W. G. Schneider. J. Chem. Phys. **32**, 1224 (1960).
6. A. D. Buckingham, T. Schaeffer, and W. G. Schneider. J. Chem. Phys. **32**, 1227 (1960).

Received June 22, 1961.
Department of Chemistry,
University of British Columbia,
Vancouver, B.C.

CHEMICAL CONSTITUENTS OF CHICOZAPOTE*

E. Azpeitia, A. Bowers, P. Crabbé, O. Mancera, J. S. Matthews, J. Reynoso, and J. Salazar

The "chicozapote", *Achras sapota* L. of the Sapotaceae family, is a common tree of tropical regions of America, growing mainly in Brazil, Colombia, Guatemala, Honduras, Mexico, Peru, and Venezuela (1). Although the sapotilla tree or chicle tree (chicle from the original Maya word *sicté*) is well known since it constitutes the only source of natural

*This work constitutes a part of the undergraduate theses submitted by E. A. and J. R. to the Universidad Nacional Autónoma de México, and by J. S. to the Escuela Nacional de Ciencias Biólógicas.

chewing gum, little work has been done on the chemical constitution of the latex of this tree. This latex, also called "crude chicle" or "loaf chicle", is obtained by collecting the liquid exuded from the bark of *Achras sapota* L.

Stillwell, in an X-ray study of chicle (2), concluded that the latex was a mixture of gutta-percha, calcium oxalate monohydrate, and a resinous fraction. Schlesinger and Leeper have shown (3) that this gutta-percha was a mixture of cis and trans polyisoprenes. On the other hand, Lifschutz and Vietmeyer, by extraction of chicle with ethanol, obtained (4) a fraction which they called "isophytosterol" because of the similar behavior of this extract to color reactions with "isocholesterol", later identified as a mixture of lanosterol, agnosterol, and their side-chain dihydro analogues.

This paper reports the preliminary results of an investigation of the alcoholic extracts of chicle from different sources. Ethanol extraction with a Soxhlet of a crude chicle from Guatemala led to the isolation, in about 55% yield, of a yellow resin which crystallized spontaneously on standing. Although repeated crystallizations did not afford a pure compound, extensive chromatography over alumina, followed by several recrystallizations, led to the isolation and identification of two pentacyclic triterpenes and a steroid, namely lupeol acetate, β-amyrin acetate, and α-spinasterol acetate, in approximate yields of 70, 10, and 2–5% respectively.

These three compounds were purified rigorously, hydrolyzed to the corresponding 3β-alcohols, and then further characterized as their benzoates. Each derivative was compared with an authentic sample of the known compound (mixed melting point and infrared spectrum). The physical constants are listed in Table I.

TABLE I

Compound	Melting point		Optical rotation	
	This work	Literature value	This work	Literature value
Lupeol	213–215	215–216*	+27	+27*
Acetate	219–220	220*	+42	+47*
Benzoate	262–264	273–274*	+66	+61*
β-Amyrin	198–199	199–200†	+85	+89†
Acetate	239–241	241†	+82	+85†
Benzoate	233–235	233–234†	+105	+100†
α-Spinasterol	169–170	168–169‡	+2	−4‡
Acetate	183–184	186‡	−4	−5‡
Benzoate	196–197	200‡	+2	+2‡

*J. Simonsen and W. C. J. Ross. The terpenes. Vol. IV. Cambridge University Press. 1957. p. 331.
†J. Simonsen and W. C. J. Ross. The terpenes. Vol. IV. Cambridge University Press. 1957. p. 175.
‡L. F. Fieser, M. Fieser, and R. N. Chakravarti. J. Am. Chem. Soc. 71, 2226 (1949).

It is worth mentioning that α-spinasterol (Δ^7-stigmasterol or bessisterol) seems to be a more common steroid than suspected earlier (5). Besides spinach (6), *Polygala senega* roots (7), alfalfa (*Medicago sativa* L.) (8), and the rhizomes of *Mormordica cochinchinensis* Spreng. (9), this Δ^7-steroid has been identified recently in *Iresin pringlei* (10) and in *Chenopodium foetidum*, which also contains cineol and a very small amount of a ketone which seems to correspond to piperitenone (2,4-dinitrophenylhydrazone, m.p. 188–189°; calc. for $C_{16}H_{18}O_4N_4$: N, 16.96; found: N, 17.37) (11).

Another crude chicle, from Campeche, Mexico, was found to be a complex mixture; the major constituents, however, again were lupeol acetate and β-amyrin acetate. Interestingly enough, in this chicle no α-spinasterol could be identified.

Can. J. Chem. Downloaded from www.nrcresearchpress.com by 210.87.254.42 on 09/05/12
For personal use only.

The recent development of gas chromatography techniques in the steroid (12), alkaloid (13), and fatty- (14) and amino-acids (15) fields prompted us to apply this method to our chicle mixture. For comparison purposes, authentic samples of the pentacyclic triterpenes and the Δ^7-steroid were chromatographed using this technique, which was later applied to the crude crystalline chicle. Those compounds were analyzed on a Barber-Colman Model 10 gas chromatograph with an argon, β-ray ionization detector and a 6 ft$\times\frac{1}{4}$ in. column containing 1% QF-1 silicone (Vanden Heuvel, Haahti, and Horning (12)) on Gas-Chrom P (16) at 240° C. The retention times, in minutes, measured from the air peak were: α-spinasterol, 3.57; β-amyrin, 3.93; lupeol, 4.64; α-spinasterol acetate, 5.24; β-amyrin acetate, 6.31; lupeol acetate, 7.15. Chicle from Campeche, Mexico, was found to consist of approximately 79% of lupeol acetate, 12% of β-amyrin acetate, together with some unidentified components. The retention time of lupeol acetate on a 6 ft$\times\frac{1}{4}$ in. column of 1.5% SE-30 (Vanden Heuvel, Sweeley, and Horning (12)) on Gas-Chrom P at 240° was 3 minutes. The main component of chicle also had the same retention time.

Work is now in progress to determine the structure of some of the minor constituents in chicle.

1. M. Martinez. Las plantas medicinales de Mexico. *Edited by* Botas. Mexico. 1944. p. 386.
2. C. W. Stillwell. Ind. Eng. Chem. **23**, 703 (1931).
3. W. Schlesinger and H. M. Leeper. Ind. Eng. Chem. **43**, 398 (1951).
4. I. Lifschutz and O. Vietmeyer, Z. Physiol. Chem. **155**, 240 (1926).
5. L. F. Fieser and M. Fieser. Steroids. Reinhold Publishing Co., New York. 1959. p. 352. See also: Elsevier's Encyclopaedia of organic chemistry. Vol. **14**. Elsevier Publishing Co., Amsterdam. 1954. Suppl. p. 1794.
6. M. C. Hart and F. W. Heyl. J. Biol. Chem. **95**, 311 (1932).
7. J. C. E. Simpson. J. Chem. Soc. 730 (1937).
8. H. Dam, A. Geiger, J. Glavind, P. Karrer, W. Karrer, E. Rotschild, and H. Salomon. Helv. Chim. Acta, **22**, 310 (1939). E. Fernholtz and M. L. Morre, J. Am. Chem. Soc. **61**, 2467 (1939).
9. S. Kuwada and S. Yosiki. J. Pharm. Soc. Japan, **60**, 407 (1940).
10. P. Crabbé, E. Azpeitia, and C. Djerassi. Bull soc. chim. Belg. **70**, 168 (1961).
11. P. Crabbé and E. Azpeitia. Unpublished observation.
12. R. K. Beerthuis and J. H. Recourt. Nature, **186**, 372 (1960). W. J. A. Vanden Heuvel, C. C. Sweeley, and E. C. Horning. J. Am. Chem. Soc. **82**, 3481 (1960). H. Ziffer, W. J. A. Vanden Heuvel, E. O. A. Haahti, and E. C. Horning. J. Am. Chem. Soc. **82**, 6411 (1960). H. H. Wotiz and H. F. Martin. J. Biol. Chem. **236**, 1312 (1961). W. J. A. Vanden Heuvel, E. O. A. Haahti, and E. C. Horning. J. Am. Chem. Soc. **83**, 1513 (1961).
13. H. H. Lloyd, H. M. Fales, P. F. Highet, W. J. A. Vanden Heuvel, and W. C. Wildman. J. Am. Chem. Soc. **82**, 3791 (1960).
14. M. L. Vorbeck, L. R. Mattick, F. A. Lee, and C. S. Pederson. Nature, **187**, 689 (1961).
15. D. E. Johnson, S. J. Scott, and A. Meister. Anal. Chem. **33**, 669 (1961).
16. Applied Science Laboratories, 140 North Barnard Street, State College, Penna.

Received July 7, 1961.
Research Laboratories,
Syntex, S. A.,
Apartado Postal 2679,
Mexico, D. F., Mexico.

Can. J. Chem. Downloaded from www.nrcresearchpress.com by 210.87.254.42 on 09/05/12
For personal use only.

Can. J. Chem. Downloaded from www.nrcresearchpress.com by 210.87.254.42 on 09/05/12
For personal use only.

Symposium on Co-ordination in Chemistry

The papers that follow were presented at the Symposium on Co-ordination in Chemistry, Inorganic Subject Division, Chemical Institute of Canada, held at McMaster University, Hamilton, Ontario, May 15, 16, 1961.

CO-ORDINATION COMPOUNDS OF HYDRAZINE

PART II. THE INTERACTION OF TRIMETHYLBORANE AND TRIMETHYLALUMINUM WITH HYDRAZINE[1, 2]

W. G. Paterson[3] and M. Onyszchuk

ABSTRACT

Trimethylborane and anhydrous hydrazine react at 25° in vacuum, yielding a 2:1 adduct, $2(CH_3)_3B \cdot N_2H_4$, which is stable at or below −78° and evolves trimethylborane slowly at higher temperatures, leaving a stable 1:1 adduct, $(CH_3)_3B \cdot N_2H_4$ (m.p. 42–43°). The thermal decomposition of the latter at 150–160° is complex, producing nitrogen, methane, ammonia, a mixture of butane and the isomeric butenes, and a heterogeneous solid. At 25° diborane displaces trimethylborane from the 1:1 adduct and reacts with it to form 1,1-dimethyldiborane, in addition to hydrogen, methane, and a heterogeneous solid.

Trimethylaluminum and hydrazine give a complex reaction in vacuum at 25°, but in diethyl ether solution the product was thought to be $(CH_3)_2AlNHNHAl(CH_3)_2$, which decomposes on being touched.

Recently (1) we reported that under appropriate conditions boron trifluoride, like the borane group (2, 3), forms stable 1:1 and 2:1 addition compounds with hydrazine, $BF_3 \cdot N_2H_4$ and $2BF_3 \cdot N_2H_4$, respectively. With the object of obtaining further information about the tendency of hydrazine to co-ordinate with other electron-deficient molecules, we have investigated the reactions of hydrazine with trimethylborane and trimethylaluminum. Since the electron-acceptor powers of trimethylborane and trimethylaluminum are considerably less than those of boron trifluoride or of the borane group (4, 5), hydrazine should form less stable adducts with trimethylborane or trimethylaluminum than with boron trifluoride or with the borane group. The results reported here confirm this expectation.

RESULTS AND DISCUSSION

The interaction of trimethylborane and hydrazine in vacuum at 25° produced the new co-ordination compound 2-trimethylborane-hydrazine (I), $2(CH_3)_3B \cdot N_2H_4$. This adduct was stable either in the presence of an excess of trimethylborane or at temperatures below −78°; otherwise, trimethylborane was evolved ultimately, leaving the new stable addition compound trimethylborane-hydrazine (II), $(CH_3)_3B \cdot N_2H_4$, which melted at 42–43°. By being allowed to react with an excess of trimethylborane, adduct II was converted into I, as represented by the following scheme:

$$2(CH_3)_3B + N_2H_4 \rightarrow \underset{\text{I}}{2(CH_3)_3B \cdot N_2H_4}$$

$$> -78° \quad \downarrow\uparrow \text{ excess } (CH_3)_3B$$

$$(CH_3)_3B + \underset{\text{II}}{(CH_3)_3B \cdot N_2H_4}.$$

[1]*Manuscript received June 30, 1961.*

Contribution from the Inorganic Chemistry Laboratory, McGill University, Montreal 2, Quebec, with financial assistance from the Defence Research Board of Canada, under Grant Number 9530-20, Project D46-95-30-20. Presented at the Symposium on Co-ordination in Chemistry, Chemical Institute of Canada, Hamilton, Ontario, May 15–16, 1961.

[2]*Part I: Can. J. Chem.* **39**, *986 (1961).*

[3]*Holder of N.R.C. Studentships, 1957–59. Present address: Department of Chemistry, University of Alberta, Edmonton, Alberta.*

These results suggest that the attraction exerted by trimethylborane on the lone electron pair of one nitrogen atom in the 1:1 adduct induces a significant decrease in the co-ordinating ability of the lone electron pair on the other nitrogen atom. This reduced reactivity of the second lone electron pair in hydrazine appears to be a general rule (6). The instability of I as compared with the analogous borane (2, 3) and boron trifluoride (1) adducts is in agreement with the following order of the electron-acceptor strengths of the three Lewis acids toward molecules in which nitrogen is the donor atom (5): $BH_3 \sim BF_3 > (CH_3)_3B$.

The complex II consisted of white, hygroscopic crystals which hydrolyzed readily. Strong acidification of the aqueous solution resulted in the displacement of trimethylborane, followed by its spontaneous and violent ignition in air.

A comparison of the infrared spectrum of II with that of trimethylborane-ammonia, given in Fig. 1, reveals marked similarities and confirms the presence of a B—N stretching

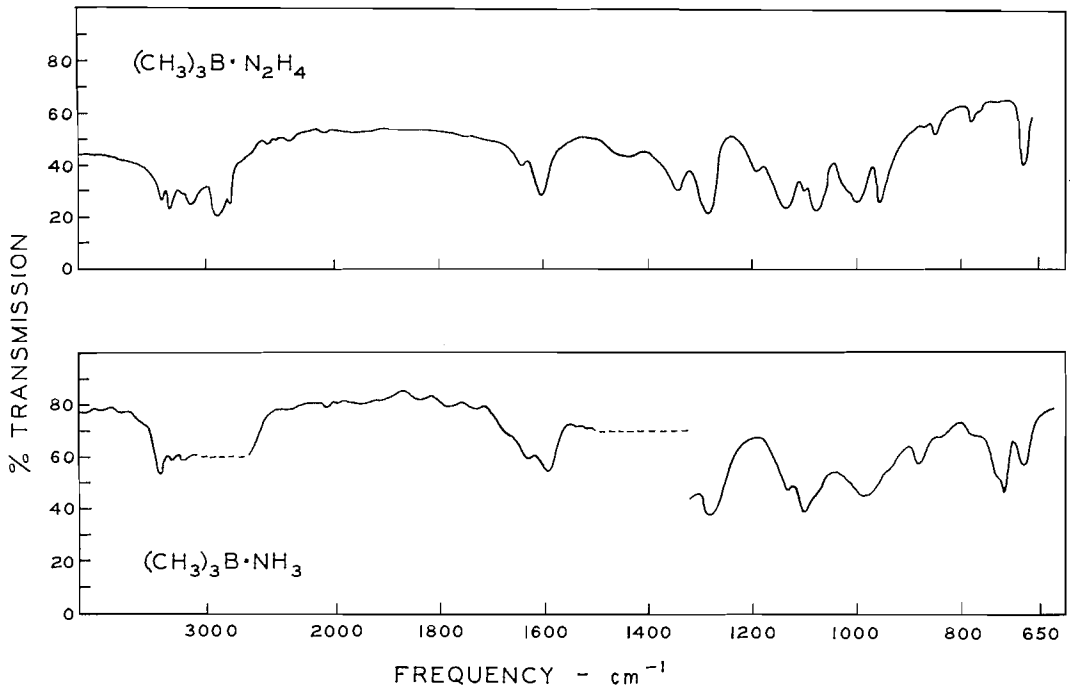


FIG. 1. Infrared spectra of $(CH_3)_3B \cdot N_2H_4$ (in KBr disk) and $(CH_3)_3B \cdot NH_3$ (in Nujol mull).

vibration in II at 1075 cm^{-1}. The frequency assignments listed in Table I were made by analogy with the assignments recorded in the literature for the infrared spectra of trimethylborane (7), hydrazine (8), and hydrazine hydrohalides (9, 10), and for the Raman spectrum of $(CH_3)_3B \cdot NH_3$ (11). Because trimethylborane-ammonia is so volatile at room temperature the potassium bromide pellet method could not be used to obtain its infrared spectrum; therefore, the Nujol mull technique was used instead, and the regions 3100–2800 cm^{-1} and 1500–1325 cm^{-1} were omitted due to interference from the Nujol absorption peaks.

The thermal decomposition of II in vacuum at 150–160° for 16 hours was complex, yielding methane, nitrogen, ammonia, butane, 1-butene, 2-butene, and an unidentified

Can. J. Chem. Downloaded from www.nrcresearchpress.com by 210.87.254.42 on 09/05/12
For personal use only.

TABLE I

Infrared vibration frequencies of $(CH_3)_3B \cdot NH_3$ and $(CH_3)_3B \cdot N_2H_4$

$(CH_3)_3B \cdot NH_3$* (cm^{-1})	$(CH_3)_3B \cdot N_2H_4$ (cm^{-1})	Assignment
3370 s	3342 s	N—H stretching (asym.)
3280 s	3277 s	N—H stretching (sym.)
3190 s	3110 s	N—H intermolecular ?
	2908 s	C—H stretching (asym.)
	2812 s	C—H stretching (sym.)
1638 m	1640 m	NH_3 deformation (asym.) or
1595 s	1602 s	NH_2 deformation (asym.)
	1440 w, b	CH_3 deformation (asym.) and NH_2 deformation (sym.)
	1343 s	NH_2 rocking (asym.)
1283 vs	1282 vs	CH_3 deformation (sym.)
	1192 m	NH_2 rocking (sym.)
1135 s	1135 vs	B—C stretching (asym.)
	1103 m	NH_2 wagging (asym.)
1103 vs	1075 vs	B—N stretching
985 s, b	997 s, b	CH_3 rocking
	956 s	N—N stretching
882 w	851 w	CH_3 rocking
730 s	782 w	NH_3 wagging or
716 s	768 w	NH_2 wagging
682 m	679 s	B—C stretching

s = strong m = medium w = weak v = very b = broad

*Nujol absorption peaks interfere in the regions 3100–2800 cm^{-1} and 1500–1325 cm^{-1}.

heterogeneous solid. The presence of C_4 hydrocarbons among the products is remarkable and we are unable to account for their origin. Neither trimethylborane nor hydrazine undergo appreciable decomposition when they are heated separately for 16 hours at 150–160°. The observed decomposition of II is more complex than that recently reported by Mikhailov and Bubnov (12) for complexes of the type $R_3B \cdot N_2H_4$, where R is *n*-C_3H_7, *i*-C_3H_7, or *n*-C_4H_9. These decompose in the presence of excess trialkylborane into the corresponding alkanes, alkenes, and hydrogen, according to the following scheme:

$$R_3B \cdot N_2H_4 \rightarrow [R_2BNHNH_2] + RH + R_{-H} + H_2$$
$$\downarrow R_3B$$
$$R_2BNHNHBR_2 + RH + R_{-H} + H_2.$$

Only alkanes and alkenes containing the same number of carbon atoms as in the original alkyl group of the trialkylborane were reported.

There was no reaction between I and diborane at −80°. At room temperature, however, diborane reacted with II to give trimethylborane, 1,1-dimethyldiborane, hydrogen, and a heterogeneous solid which evolved both methane and hydrogen on heating. Since free trimethylborane was obtained, it was certain that a displacement of trimethylborane from II by the borane group had occurred. Moreover, the formation of 1,1-dimethyldiborane, which could only have occurred by the following reaction (13),

$$2B_2H_6 + 2(CH_3)_3B \rightarrow 3(CH_3)_2B_2H_4,$$

showed that more trimethylborane had been displaced than that indicated by the amount of trimethylborane recovered. In fact the displacement of trimethylborane by the borane group was about 66%, based on the amounts of trimethylborane and 1,1-dimethyldiborane in the product mixture. These data show clearly that, toward hydrazine, the borane group is a stronger electron acceptor than trimethylborane. When the heterogeneous

Can. J. Chem. Downloaded from www.nrcresearchpress.com by 210.87.254.42 on 09/05/12
For personal use only.

solid product was heated, methane and hydrogen were evolved. This suggests that both II and 2-borane-hydrazine (2, 3) were present because these adducts when heated are known to yield methane and hydrogen, respectively.

The reaction of hydrazine with trimethylaluminum in vacuum at 25° produced methane, hydrogen, and a nonstoichiometric residue. In diethyl ether solution, the same reactants gave methane and a white solid, which was recovered after evaporation of the solvent and unreacted trimethylaluminum. The weight of the solid product and the amount of methane formed initially indicated that the solid was probably *sym*-bisdimethylalumino-hydrazine, $(CH_3)_2AlNHNHAl(CH_3)_2$; since it decomposed on being touched, its composition could not be confirmed by analysis.

EXPERIMENTAL

The different experimental techniques have been described previously (1).

The method of Brown (14) for the preparation of trimethylborane was modified in that boron trichloride and methyl iodide were used in place of boron trifluoride and methyl bromide. (Yield: 79%. Found: molecular weight (M), 55.6; vapor pressure (v.p.), 30.7 mm at −78.3°. Calc. for $(CH_3)_3B$: M, 55.9; v.p., 31.3 mm at −78.3°.) Anhydrous hydrazine was prepared by refluxing the 95+% material over potassium hydroxide (1). The reduction of boron trichloride with lithium aluminum hydride in diethyl ether solution was used for the preparation of diborane. (Yield: 62%. Found: M, 27.7. Calc. for B_2H_6: M, 27.7.) Trimethylaluminum (Ethyl Corporation) was purified by several fractional distillations at 0° (Found: v.p., 13.2 mm at 24.7°. Lit. (15): v.p., 12.8 mm at 24.7°), and the infrared spectrum of the pure substance was identical with that reported previously (16).

Interaction of Trimethylborane with Hydrazine

In a typical experiment, trimethylborane (9.69 mmoles) and anhydrous hydrazine (3.26 mmoles) were combined in vacuum and kept at 25° overnight. The reaction was initially rapid, but a long time was required for its completion, as indicated by a slow decrease in the total pressure. A white crystalline material formed gradually on the walls of the vessel. The amount of unreacted trimethylborane (3.26 mmoles. Found: M, 55.2. Calc. for $(CH_3)_3B$: M, 55.9), recovered by distillation at −78°, showed that trimethylborane (6.43 mmoles) had reacted with hydrazine (3.26 mmoles) in a ratio of 2:1, thus forming the adduct $2(CH_3)_3B\cdot N_2H_4$. When this complex was warmed, it evolved trimethylborane slowly at −65 to −70°, but at 0°, trimethylborane (3.24 mmoles; M, 56.0) was removed rapidly. A residue containing trimethylborane (3.19 mmoles) and hydrazine (3.26 mmoles) in a ratio of 1:1, corresponding to the complex $(CH_3)_3B\cdot N_2H_4$, was left. Pressure measurements in the range −78 to 0° indicated that $2(CH_3)_3B\cdot N_2H_4$ did not dissociate reversibly.

However, when an excess of trimethylborane (7.46 mmoles) was added to a sample of $(CH_3)_3B\cdot N_2H_4$ (4.04 mmoles) and the mixture was kept at 25° overnight, the recovery of trimethylborane (3.40 mmoles; M, 55.8), by distillation at −78°, indicated that the compound $2(CH_3)_3B\cdot N_2H_4$ had been regenerated, since 4.04 mmoles of $(CH_3)_3B\cdot N_2H_4$ had absorbed an additional 4.06 mmoles of trimethylborane.

Pyrolysis of $(CH_3)_3B\cdot N_2H_4$

Trimethylborane (8.58 mmoles) and hydrazine (8.58 mmoles) were combined in an all-glass vessel and the white solid adduct, $(CH_3)_3B\cdot N_2H_4$, which formed was heated for 16 hours at 150–160°. The principal products were: (*a*) noncondensable gases (N_2 and

Can. J. Chem. Downloaded from www.nrcresearchpress.com by 210.87.254.42 on 09/05/12
For personal use only.

CH_4; 0.67 mmoles), (*b*) ammonia (0.42 mmoles. Found: M, 18.0; v.p., 35.6 mm at −79.5°. Calc. for NH_3: M, 17.0; v.p., 40.0 mm at −79.2° (17)), (*c*) a mixture of butane and the isomeric butenes (2.44 mmoles. Found: M, 56.3. Calc. for C_4H_8: M, 56.1; for C_4H_{10}: M, 58.1), and (*d*) an unidentified heterogeneous white solid. The composition of the C_4 hydrocarbon fraction was confirmed by infrared and mass spectra measurements. The latter indicated that the ratio of C_4H_{10} to C_4H_8 was approximately 1 to 3.

When trimethylborane (7.75 mmoles) was heated in a sealed tube for 16 hours at 150–160°, a quantitative recovery of the gas proved that no significant decomposition had taken place.

Hydrazine (9.33 mmoles) was heated in an all-glass vessel for 16 hours at 150–160°. The reaction products were nitrogen (0.14 mmole. Found: M, 32.8. Calc. for N_2: M, 28.0), ammonia (0.52 mmole. Found: M, 17.5. Calc. for NH_3: M, 17.0), and unchanged hydrazine (8.86 mmoles; analyzed by the iodate method (6)), in accordance with the decomposition (18)

$$3N_2H_4 \rightarrow 4NH_3 + N_2,$$

and the extent of decomposition of hydrazine was only 5%.

Interactions of $2(CH_3)_3B \cdot N_2H_4$ and $(CH_3)_3B \cdot N_2H_4$ with B_2H_6

After $2(CH_3)_3B \cdot N_2H_4$ (3.26 mmoles) and diborane (4.01 mmoles) had been maintained overnight at −80°, the quantitative recovery of diborane, by distillation at −78°, proved that no reaction had taken place.

In another experiment, $(CH_3)_3B \cdot N_2H_4$ (3.26 mmoles) and diborane (4.01 mmoles) were combined and left overnight at 25°. The reaction, which produced a solid and several volatile products, was stopped by surrounding a portion of the reaction vessel with a liquid-air bath. After all the volatile material had condensed, hydrogen (0.75 mmole) was left. The condensable substances were fractionated at −143°, yielding diborane (0.59 mmole; M, 26.6), and repeatedly at −115°, yielding trimethylborane (0.50 mmole) and 1,1-dimethyldiborane (2.46 mmoles. Found: M, 58.9; v.p., 11 mm at −79.5°. Calc. for $(CH_3)_2B_2H_4$: M, 55.7; v.p., 13 mm at −78.5° (19)). The infrared spectrum of the latter was identical with that reported by Lehmann *et al.* (20).

The solid residue was heated gradually, resulting in the evolution of noncondensable gas, as summarized in Table II. These data suggest that methane and hydrogen were

TABLE II

Temperature of residue (°C)	Amount of gas (mmoles)	Molecular weight
100	3.94	17.6
170	0.75	7.21
250	4.13	2.46

evolved. The quantity of condensable gas released during these operations was negligible.

Interaction of Trimethylaluminum with Hydrazine

(i) Reaction in vacuum.—Anhydrous hydrazine (4.72 mmoles) and trimethylaluminum (20.0 mmoles) were left at 25° overnight. The products of the reaction were: (*a*) a pale brown solid which did not change visibly on heating to 300°, (*b*) a mixture of non-condensable gases (20.0 mmoles: 18.58 mmoles CH_4 and 1.42 mmoles H_2. Found: M, 15.0. Calc. for CH_4: M, 16.0; for H_2: M, 2.0. Successive vapor pressure measurements on

Can. J. Chem. Downloaded from www.nrcresearchpress.com by 210.87.254.42 on 09/05/12
For personal use only.

this fraction gradually approached that of CH_4), and (*c*) unreacted trimethylaluminum (12.03 mmoles. Found: v.p., 15.9 mm at 26.7°. Lit. (15): v.p., 13.7 mm at 26.7°). The identity of the latter was also confirmed by its infrared spectrum.

(ii) Reaction in diethyl ether.—In a typical experiment, anhydrous diethyl ether (20 ml) was thoroughly degassed in vacuum and to it were added hydrazine (10.09 mmoles) and trimethylaluminum (27.9 mmoles). The apparatus was sealed and the reactants were stirred overnight at 25°. A white suspension formed in the ether solution. Methane (20.1 mmoles. Found: M, 16.3; v.p., 21.5 mm at −191°. Calc. for CH_4: M, 16.0; v.p., 20.0 mm at −191.8° (17)) was the only noncondensable gas produced. The solvent and unreacted trimethylaluminum were distilled at room temperature, leaving a white crystalline deposit. Analyses of the latter for aluminum were not reproducible, but the weight of the crude product (1.57 g) corresponded approximately to that required (1.46 g) for the formation of the substance *sym*-bisdimethylaluminohydrazine, $(CH_3)_2AlNHNHAl(CH_3)_2$. The formation of exactly 2 moles of methane per mole of hydrazine consumed was supporting evidence. Since the solid compound was extremely sensitive to touch, it could be neither purified nor analyzed.

ACKNOWLEDGMENTS

We are grateful for financial assistance from the Defence Research Board and for two Studentships to one of us (W.G.P.) from the National Research Council. We are indebted to Dr. L. Elias, formerly of the Physical Chemistry Laboratory, McGill University, for the measurement and interpretation of mass spectra.

REFERENCES

1. W. G. Paterson and M. Onyszchuk. Can. J. Chem. **39**, 986 (1961).
2. H. J. Emeléus and F. G. A. Stone. J. Chem. Soc. 840 (1951).
3. M. J. Steindler and H. I. Schlesinger. J. Am. Chem. Soc. **75**, 756 (1953).
4. R. E. McCoy and S. H. Bauer. J. Am. Chem. Soc. **78**, 2061 (1945).
5. F. G. A. Stone. Chem. Revs. **58**, 101 (1958).
6. L. F. Audrieth and B. A. Ogg. The chemistry of hydrazine. John Wiley & Sons, Inc., New York. 1951.
7. W. J. Lehmann, C. O. Wilson, Jr., and I. Shapiro. J. Chem. Phys. **28**, 777 (1958).
8. P. A. Giguère and I. D. Liu. J. Chem. Phys. **20**, 136 (1952).
9. J. C. Decius and D. P. Pearson. J. Am. Chem. Soc. **75**, 2436 (1953).
10. R. G. Snyder and J. C. Decius. Spectrochim. Acta, **13**, 280 (1959).
11. J. Goubeau and H. J. Becher. Z. anorg. u. allgem. Chem. **268**, 1 (1952).
12. B. M. Mikhailov and Y. N. Bubnov. Izvest. Akad. Nauk S.S.S.R., Otdel. Khim. Nauk. 370 (1960).
13. H. I. Schlesinger and A. O. Walker. J. Am. Chem. Soc. **57**, 621 (1935).
14. H. C. Brown. J. Am. Chem. Soc. **67**, 374 (1945).
15. C. H. Bamford, D. L. Levi, and D. M. Newitt. J. Chem. Soc. 468 (1946).
16. K. S. Pitzer and R. K. Sheline. J. Chem. Phys. **16**, 522, 668 (1948).
17. D. R. Stull. Ind. Eng. Chem. **39**, 517 (1947).
18. A. Kant and W. J. McMahon. J. Inorg. & Nuclear Chem. **15**, 305 (1960).
19. R. T. Sanderson. Vacuum manipulation of volatile compounds. John Wiley & Sons, Inc., New York. 1948.
20. W. J. Lehmann, C. O. Wilson, Jr., and I. Shapiro. J. Chem. Phys. **34**, 476 (1961).

Can. J. Chem. Downloaded from www.nrcresearchpress.com by 210.87.254.42 on 09/05/12
For personal use only.

COMPLEX PERIODATES AND TELLURATES[1]

M. W. LISTER

This paper is concerned with the complex periodates and tellurates formed by some of the transition metals in the first long period. Probably similar salts could be obtained from transition metals in the later periods, but so far only some silver salts have actually been prepared. Periodic acid, H_5IO_6, and telluric acid, H_6TeO_6, have similarities in formula which set them apart from the acids formed by earlier elements of their groups with the same valency, e.g. perchloric acid, $HClO_4$, and selenic acid, H_2SeO_4. They are also much weaker acids: H_5IO_6 has $pK_1 = 1.6$, $pK_2 = 7.0$; and telluric acid has $pK_1 = 6.1$ and $pK_2 = 10.4$. Consequently it is not surprising that they form complexes which do not find analogues in the chemistry of chlorine and selenium.

Periodic acid or periodates are fairly strong oxidizing agents, so that they oxidize the transition metals to their higher valencies. Some of the compounds described below contain the metals in unusually high valency states. However, to reach these valencies, still stronger oxidizing agents are sometimes required; and the periodate then acts rather as a stabilizing agent for these higher valencies, than as the oxidizing agent. The actual oxidizing agents which have been applied are sodium (or other) persulphate or hypochlorite, and electrolytic oxidation.

The compounds which have been prepared are listed in Table I. The oxidizing agent refers to the compound used in the preparation to reach the higher valency.

TABLE I

Central element	Compound	Oxidizing agent	Reference
Manganese	$Na_7H_4Mn(IO_6)_3.17H_2O$	NaOCl	1
	$K_7H_4Mn(IO_6)_3.8H_2O$	KOCl	1
	$Ba_5HMn(IO_6)_3.10H_2O$		1
	$Na_2Mn_2I_2O_{11}$	Periodate	2
	$K_2Mn_2I_2O_{11}$	Periodate	2
	$Na_7H_7Mn(TeO_6)_3.5H_2O$	NaOCl	10
	$K_6H_8Mn(TeO_6)_3.5H_2O$	KOCl	10
Iron	$Na_2FeIO_5.3H_2O$	—	3
Cobalt	$Na_5H_2Co(IO_6)_2.10H_2O$	NaOCl	4
	$K_4H_3Co(IO_6)_2.3H_2O$	KOCl	4
	$Ba_5[H_2Co(IO_6)_2].10H_2O$	—	4
	$Na_3Co_4(IO_6)_3.11H_2O$	Periodate	5
	$K_3Co_4(IO_6)_3.11H_2O$	Periodate	5
	$K_3H_6Co(TeO_6)_2.2H_2O$	KOCl	10
Nickel	$NaNiIO_6.H_2O$	Persulphate	6
	$KNiIO_6.H_2O$	Persulphate	6
Copper	$Na_7Cu(IO_6)_2.16H_2O$		8
	$Na_5H_2Cu(IO_6)_2.13H_2O$	NaOCl	7
	$K_7Cu(IO_6)_2.20H_2O$	$Na_2S_2O_8$	8
	$K_4H_3Cu(IO_6)_2.4H_2O$	Electrolytic	8
	$K_3H_4Cu(IO_6)_2.6H_2O$		8
	$Na_9Cu(TeO_6)_2.20H_2O$	Electrolytic	7
	$Na_7H_2Cu(TeO_6)_2.12H_2O$	Electrolytic	3, 8
	$Na_6H_4Cu(TeO_6)_2.18H_2O$	Electrolytic	3

[1]*Manuscript received June 30, 1961.*
Contribution from the Department of Chemistry, University of Toronto, Toronto, Ont. Presented at the Symposium on Co-ordination in Chemistry, Chemical Institute of Canada, Hamilton, Ontario, May 15–16, 1961.

The general method of preparation is to mix somewhat acidified solutions of a salt of the central metal and sodium (or potassium) periodate or tellurate, and then to add the oxidizing agent, for instance sodium hypochlorite containing considerable excess sodium hydroxide. The complex salts may crystallize rather slowly, and it is often useful to add alcohol to aid precipitation of them. They can usually be recrystallized from water or dilute sodium hydroxide solution. In practice difficulties arise because the compounds often come down as sticky, poorly crystallized precipitates; and the precipitate may also be contaminated with sodium periodate or tellurate, which has to be removed by recrystallization or reprecipitation.

Valency of Central Metal

As can be seen in Table I, some of these compounds contain Mn(IV), Ni(IV), or Cu(III), which are higher valencies than are common in the bulk of the complex compounds of these elements. The presence of these valencies can be demonstrated by the various methods given below.

1. Titration Methods

This type of method was used by Price in 1903 when he added potassium iodide and acid to $Na_2Mn_2I_2O_{11}$ and titrated the iodine liberated. With trivalent copper it is particularly useful, since sulphuric acid decomposes the compound to give divalent copper again, presumably with liberation of oxygen. Hence if potassium iodide is added to a solution of $Na_7Cu(IO_6)_2$, and then sulphuric acid is added, 18 equivalents of iodine are liberated per molecule; but if the acid is added first, only 17 equivalents are liberated. With the tellurate complex the corresponding numbers are 2 and 1 equivalents of iodine per molecule. Potentiometric titration with ferrous ammonium sulphate (and acid) is also useful since the periodate is then reduced to iodate, and the central metal to the divalent state. Another method along the same lines consists in bubbling in sulphur dioxide and titrating the sulphuric acid formed by its oxidation.

2. Magnetic Properties

A considerable number of magnetic measurements have been made on these compounds, with the results as given in Table II. These are all measurements of the magnetic

TABLE II

Compound	Molar susceptibility $\times 10^6$		Reference
$Na_7Cu(IO_6)_2.15H_2O$	−271		8
$Na_5H_2Cu(IO_6)_2.13H_2O$	−276		8
$Na_7H_2Cu(TeO_6)_2.14H_2O$	−310		8
$K_4H_3Cu(IO_6)_2.4H_2O$	−207		8
$K_3H_4Cu(IO_6)_2.6H_2O$	−187		8
$Na_7H_4Mn(IO_6)_3.17H_2O$	5611, at 3.0° C 5166, at 25.6° C 4964, at 39.7° C	3.84 Bohr magnetons	1
$K_6H_8Mn(TeO_6)_3.5H_2O$	4850, at 25.1° C 4530, at 39.6° C	4.03 Bohr magnetons	1
$Na_5H_2Co(IO_6)_2.10H_2O$ $K_3H_6Co(TeO_6)_2.3H_2O$	−290		4
$NaNiIO_6$	414, at 31° C 387, at 31° C	1.1 Bohr magnetons	6 6

susceptibility, using the ordinary Goüy apparatus. The results on Co(III) compounds make these diamagnetic, as is usual for Co(III). The results on Mn(IV) compounds

agree with the "spin-only" formula for a substance with three unpaired electron spins; this is what is to be expected for Mn(IV), which contains three 3*d* electrons.

It is interesting to note that the Cu(III) compounds are diamagnetic. Cu(III) has eight 3*d* electrons, as does Ni(II), and presumably (as with Ni(II)), there is a possibility of either paired or unpaired spins. If four ligands are arranged around Ni(II) in a plane, the compound is, in general, diamagnetic; presumably the diamagnetism of Cu(III) is evidence of planar stereochemistry in this case also.

The results in $NaNiIO_6$ and $KNiIO_6$ give magnetic moments of 1.1 Bohr magnetons (6). Ray and Sarma suggest that the pure compounds would be diamagnetic but that some dissociation has taken place. This implies that the pure compounds contain spin-paired Ni(IV) in an octrahedral field, a situation found for other tetravalent nickel complexes (9).

General Properties

These complex salts are crystalline solids, usually rather moderately soluble in water. Jensovsky has given solubility curves for a few of the copper complexes. The salts with many sodium or potassium atoms (as opposed to hydrogen) are markedly less soluble in water. It is also true of most of them that they are considerably less soluble in sodium hydroxide solutions than in pure water. They are colored compounds, with light-absorption curves of the same shape: the absorption is high in the ultraviolet, falls to a minimum as we go to longer wavelength, and then passes through a single maximum. Table III

TABLE III
Light absorption

Compound	Maximum	Minimum
$Na_7H_4Mn(IO_6)_3$	482	442 mμ
$Na_7H_7Mn(TeO_6)_3$	470	420
$Na_4H_4Mn(TeO_6)_2$	450 (shoulder)	—
$Na_5H_2Co(IO_6)_2$	625	535
$H_7Co(IO_6)_2$	610	545
$K_3H_6Co(TeO_6)_2$	635	562
$Na_7Cu(IO_6)_2$	420	316

gives the positions of the maxima and minima for aqueous solutions. The extinction coefficients are highest for the copper compound, less for manganese, and least for the cobalt compounds.

Acid–Base Reactions

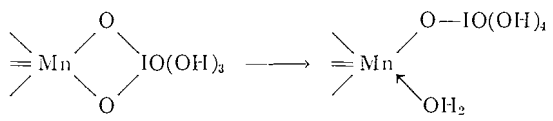
Some of the complex salts are stable enough to exist in acid solution. For instance, it is possible to pass a solution of sodium periodatocobaltate through a cation exchange resin in its acid form and to obtain a stable solution of the free acid; presumably $H_7Co(IO_6)_2$. Consequently, solutions of sodium periodatocobaltate can be titrated against acids such as perchloric acid, and the pH followed, to obtain information on the ionization constants of the acid, and hence to some extent on the structure of the compounds.

The complex copper salts are too unstable to exist in acid solution, where they break up to give divalent copper. Jensovsky has shown that they are stable at least as far as pH = 8.5, when the salt $K_4H_3Cu(IO_6)_2$ can be crystallized out.

Sodium periodatomanganate is stable enough in acid to allow a complete pH curve to be found. In fairly dilute solution (2.5×10^{-3} *M*) the free acid is ionized to the extent of two hydrogens per molecule, i.e.$(H_3O^+)_2.Mn(H_3IO_6)_3^{-2}$. The p*K* values for these first

two stages must be fairly low, certainly 1.5 or less. A detailed study of the pH curve gave for the successive pK values: pK_3 = 2.75, pK_4 = 4.35, pK_5 = 5.45, pK_6 = 9.55, pK_7 = 10.45. These make the main jumps in the ionization constant occur at the stages $Mn(H_3IO_6)_3^{-2}$, $Mn(H_2IO_6)_3^{-5}$, i.e. at the symmetrical ions. The difference between the other pK values is about that expected for hydrogen atoms separated by the number of atoms required by the formula (for instance, the hydrogens in citric acid are separated by the same number of intervening atoms, and have about the same differences in pK).

Unfortunately, this simple, and reasonably satisfactory, explanation is complicated by the observation that, if the solution of sodium periodatomanganate is acidified and the mixture is titrated with alkali, a higher pH curve is found over part of the range. The difference comes mostly in pK_5; pK_1, pK_2, and pK_3 are virtually unaltered, pK_4 is a little higher (5.2), but pK_5 is much higher (9.55). A possible explanation is that in acid the complex is partially dissociated, but that this is not a rapid process, except perhaps in very acid solutions, i.e. it is catalyzed by hydrogen ions. The type of dissociation might be from a ring structure to a structure with periodate attached through one oxygen:



and it is possible to write structures, for the ions, which agree qualitatively with the observed ionization constants. However, the evidence at present is not sufficient to establish these suggestions.

A similar treatment of sodium telluratomanganate gives a similar type of curve, but this time the titration curves are the same in both directions. The acid $H_{14}Mn(TeO_6)_3$ has pK_1 and pK_2 fairly small (averaging 2.2), corresponding to ionization to $(H_3O^+)_2Mn(H_4TeO_6)_3^{-2}$. The values of p$K_3$ to pK_5 are not very different, averaging about 7.5; this involves ionization as far as $Mn(H_3TeO_6)_3^{-5}$. The next ionization constant is about $10^{-11.5}$. A summary of these pK values is in Table IV.

TABLE IV

$H_{14}Mn(TeO_6)_3$ pK_1 = pK_2 = 2.2 pK_3–pK_5 = 7.5 pK_6 = 11.5	$H_{11}Mn(IO_6)_3$ pK_1, pK_2, small pK_3 = 2.75, pK_4 = 4.35, pK_5 = 5.45 pK_6 = 9.55, pK_7 = 10.45
$H_9Co(TeO_6)_2$ pK_1 = 3.0 pK_2 = 8, pK_3 = 9	$H_7Co(IO_6)_2$ pK_1, small, pK_2 = 1.95 pK_3 = 7.1, pK_4 = 8.0 pK_5 = 12.1

A similar treatment of the complex cobalt salts gave the results which are also summarized in Table IV. The behavior of $H_9Co(TeO_6)_2$ is easily explained since the first ionization constant is fairly large, implying easy ionization to $Co(H_4TeO_6)^-$. Then follow two similar constants to give $Co(H_4TeO_6)^{-3}$. However, the acid $H_7Co(IO_6)_2$ has, unexpectedly, two fairly large ionization constants, followed by a pair of fairly similar values. This suggests that the structure of the acid is not as simple as might appear, but at present there is insufficient evidence for any detailed explanation.

Stability Constants of Complex Ions

Various measurements have been made on the stability constants of complex periodates and tellurates, the methods and results being as follows.

1. Copper Compounds

Here use can be made of the fact that uncomplexed copper catalyzes the decomposition of sodium hypochlorite to sodium chloride and oxygen (7). By measuring the rate of gas evolution from solutions containing sodium hypochlorite, sodium hydroxide, copper, and sodium periodate or tellurate in various proportions, it is possible to deduce the equilibrium constant. The uncomplexed copper is probably present as $Cu(OH_4)^-$, and the lack of dependence of the equilibrium constant on hydroxide concentration makes the equilibrium

$$Cu(IO_6)_2^{-7} + 4H_2O \rightleftharpoons Cu(OH)_4^- + 2H_2IO_6^{-3}.$$

With tellurate the main reaction is

$$Cu(HTeO_6)_2^{-7} + 2OH^- + 2H_2O \rightleftharpoons Cu(OH)_4^- + 2H_2TeO_6^{-4}.$$

The equilibrium constants (in 0.4 *M* NaOH for tellurate) are:

	Tellurate	Periodate	
K_1	1.8×10^{-6}	3.4×10^{-5},	40° C
K_2	1.1×10^{-11}	8.0×10^{-11},	40° C

K_1 and K_2 refer to the two stages of complexing:

$$K_1 = \frac{[Cu].[ligand]}{[1:1\ complex]}, \text{ and } K_2 = \frac{[Cu].[ligand]^2}{[1:2\ complex]}.$$

2. Cobalt Compounds

These are much more stable than the copper compounds; but because cobaltic hydroxide is relatively insoluble, the equilibrium is very slowly reached, starting with cobalt hydroxide and aqueous sodium periodate or tellurate. However, if a solution of the complex salt is added to aqueous sodium hypochlorite, it slightly increases the rate of oxygen evolution, and this increase corresponds to the equilibrium constants at 60° C:

$$\text{Cobalt periodate, } K_2 = 1.7\times10^{-16}$$

$$\text{Cobalt tellurate, } K_2 = 2.5\times10^{-16}.$$

These are for solutions containing 0.1 *M* sodium hydroxide. At present there is not enough information to write detailed equations for the reactions.

3. Manganese Compounds

The method of using the catalytic decomposition of hypochlorite ions will not work with manganese as this element does not seem to act as a catalyst. However, other methods are available.

Sodium periodatomanganate changes spontaneously in aqueous solution to sodium permanganate and sodium iodate and periodate by the reaction

$$2Na_7H_4Mn(IO_6)_3 + 2H_2O \rightarrow 2NaMnO_4 + 3NaIO_3 + 3Na_2H_3IO_6 + 3NaOH.$$

The rate of this reaction is found to be given by

$$\text{Rate} = K[\text{complex}].[Na_2H_3IO_6]^{-1}[NaOH]^{-2}.$$

This is probably because the complex ion breaks up, by the equation

$$H_4Mn(IO_6)_3^{-7} + 2H_2O \rightleftharpoons H_3Mn(IO_6)_2^{-3} + H_3IO_6^{-2} + 2OH^-$$

and the simpler ion, $H_3Mn(IO_6)_2^{-3}$, then reacts further. In the absence of added sodium periodate, the rate equation is apparently somewhat modified because the periodate is then derived solely from the complex present. From this, a value for the equilibrium constant of the above reaction can be calculated, and it is found to be 2×10^{-9} at 35° C.

This method cannot be applied to sodium telluratomanganate, since tellurate ions are not strongly oxidizing. However the dissociation of the telluratomanganate ion can be demonstrated in aqueous solution by spectrophotometric measurements. If solutions of sodium telluratomanganate are made up in aqueous solution, with and without added sodium tellurate, the apparent extinction coefficients vary considerably. Measurements made on these mixtures over a considerable range of concentration of sodium tellurate, sodium hydroxide, and the complex gave results agreeing with the equilibrium

$$H_7Mn(TeO_6)_3^{-7} + H_2O \rightleftharpoons H_4Mn(TeO_6)_2^{-4} + H_4TeO_6^{-2} + OH^-,$$

assuming that the complex ion had the same formula as in the solid compound $Na_7H_7Mn(TeO_6)_3\cdot5H_2O$, and that telluric acid is dissociated to $H_4TeO_6^{-2}$ in roughly 0.1 *M* sodium hydroxide. There is evidence to support the contention that the main complex ion contains three tellurate groups since the optical density of a solution made by oxidizing a given amount of manganese in the presence of various amounts of sodium tellurate increases steadily up to three tellurates per manganese, but thereafter remains constant. The equilibrium constant for the foregoing dissociation of telluratomanganate ion is found to be 4.3×10^{-5} at 25° C. This makes the tellurate complex considerably more unstable than the periodate complex, unlike the situation with the cobalt and copper compounds where the stabilities are much the same.

REFERENCES

1. M. W. LISTER and Y. YOSHINO. Can. J. Chem. **38**, 1291 (1960).
2. W. B. PRICE. Am. Chem. J. **30**, 182 (1903).
3. L. MALATESTA. Gazz. chim. ital. **71**, 467 (1941).
4. M. W. LISTER and Y. YOSHINO. Can. J. Chem. **38**, 45 (1960).
5. L. MALAPRADE. Compt. rend. **210**, 504 (1940); **204**, 979 (1937).
6. P. RAY and B. SARMA. J. Indian Chem. Soc. **25**, 205 (1948).
7. M. W. LISTER. Can. J. Chem. **31**, 638 (1953).
8. L. JENSOVSKY. Z. anorg. u. allgem. Chem. **307**, 208 (1961).
9. R. S. NYHOLM. J. Chem. Soc. 2602 (1951).
10. M. W. LISTER and Y. YOSHINO. Unpublished work.

Can. J. Chem. Downloaded from www.nrcresearchpress.com by 210.87.254.42 on 09/05/12
For personal use only.

THE STEREOCHEMISTRY OF EIGHT-CO-ORDINATION: THE NATURE OF THE BONDING IN THE $Mo_6Cl_8^{4+}$, $Nb_6Cl_{12}^{2+}$, AND RELATED IONS[1]

R. J. GILLESPIE

ABSTRACT

It is pointed out that the square-antiprism arrangement of eight ligands which is expected for an atom which has eight bonding electron pairs in its valency shell occurs in the polynuclear complex ions found in several basic salts of zirconium(IV), thorium(IV), cerium(IV), and uranium(IV). The nature of the bonding in $Mo_6Cl_8^{4+}$, $Nb_6Cl_{12}^{2+}$, and related ions is discussed, and it is shown that it may be described in a manner which is consistent with a square-antiprism arrangement of eight electron pairs around each metal atom.

The stereochemistry of an atom in a molecule is determined by the arrangements of the electron pairs in its valency shell. These arrangements are determined by the operation of the Pauli exclusion principle which causes electrons with the same spin to keep apart (1). The author has shown previously that on this basis eight electron pairs in a valency shell would be expected to adopt a square-antiprism arrangement (2). Thus the arrangement of the valencies of an atom with a total of eight bonding electron pairs and no non-bonding pairs in its valency shell would be expected to be that of a square antiprism. Only two simple mononuclear complexes have had their structure determined, namely the tantalum octafluoride ion TaF_8^{3-} and thorium acetylacetonate $Th(C_5H_7O_2)_4$; both have the predicted square-antiprism arrangement (3, 4). In this paper it is shown that the same arrangement of eight bonds around a central atom is found in a number of polynuclear complexes, and that the bonding in $Mo_6Cl_8^{4+}$, $Nb_6Cl_{12}^{2+}$, and related ions can be satisfactorily described on this basis; the effects of a non-bonding electron pair on the arrangement of eight bonding pairs are also discussed.

Basic Salts of Ce(IV) and Th(IV)

Lundgren has investigated the structures of a number of basic salts of Ce(IV) and Th(IV) (5, 6, 7). In $Th(OH)_2CrO_4.H_2O$, and $Th(OH)_2SO_4$, there are polynuclear complex ions with the formula $[Th(OH)_2^{2+}]_n$ in which each Th is bonded to four OH groups arranged in the form of a square (Fig. 1). Eight-co-ordination around each

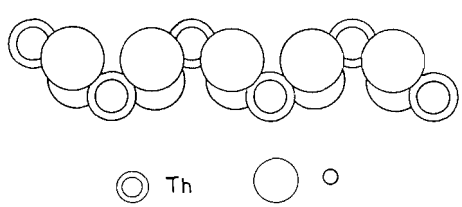


FIG. 1. The structure of the $[Th(OH)_2^{2+}]_n$ ion.

thorium is completed by four oxygen atoms from each of four separate chromate or sulphate groups, these four oxygen atoms being arranged at the corners of a square which is rotated through 45° with respect to the square formed by the OH groups, thus forming a square antiprism of oxygen atoms around each Th atom. The compound

[1]*Manuscript received June 30, 1961.*
Contribution from the Department of Chemistry, McMaster University, Hamilton, Ontario. Presented at the Symposium on Co-ordination in Chemistry, Chemical Institute of Canada, Hamilton, Ontario, May 15–16, 1961.

$CeOSO_4.H_2O$, however, contains infinite complex ions of the formula $(CeO^{2+})_n$ in which each Ce is co-ordinated to three oxygen atoms at three of the corners of a square (Fig. 2).

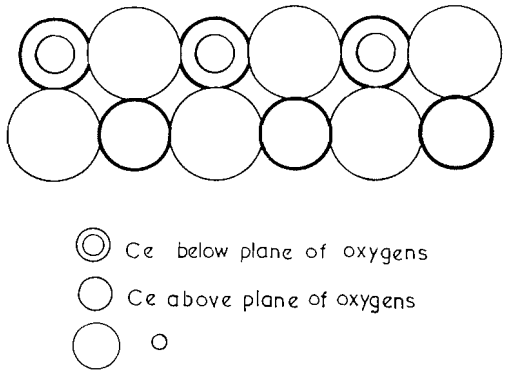


FIG. 2. The structure of the $(CeO^{2+})_n$ ion.

The square is completed by a water molecule, and, again, eight-co-ordination around the Ce is completed by four oxygen atoms from sulphate groups arranged at the corners of a square which is rotated through 45° with respect to the square formed by the oxygen atoms of the $[CeO^{2+}]_n$ chain and the water molecule. Thus there is a square-antiprism arrangement of oxygen atoms around the cerium atom. The basic sulphate with the formula $Ce_6O_4(OH)_4(SO_4)_6$, however, has a different structure containing the finite complex ion $Ce_6O_4(OH)_4^{12+}$. In this ion the metal atoms are situated at the corners of an octahedron, and are surrounded by eight oxygen atoms at the corners of a cube. Thus each cerium is co-ordinated to four oxygen atoms arranged at the corners of a square. Eight-co-ordination around the cerium is completed by four more oxygen atoms, one from each of four sulphate groups, which are arranged at the corners of a square rotated through 45° with respect to the four oxygen atoms in the complex cation. Thus each cerium is surrounded by a square-antiprism arrangement of eight oxygen atoms (Fig. 3).

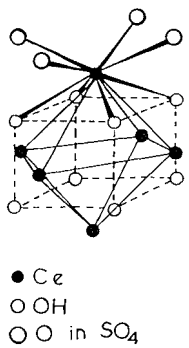


FIG. 3. The structure of $Ce_6O_4(OH)_4(SO_4)_6$.

$ZrOCl_2.8H_2O$

Crystalline hydrated zirconyl chloride has been found to contain the cyclic tetranuclear cation $[Zr_4(OH)_8(H_2O)_{16}]^{8+}$, which has the structure shown in Fig. 4 (8). The

Can. J. Chem. Downloaded from www.nrcresearchpress.com by 210.87.254.42 on 09/05/12
For personal use only.

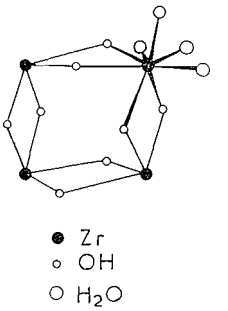


FIG. 4. The structure of the $[Zr_4(OH)_8(H_2O)_{16}]^{8+}$ ion.

four zirconium atoms are arranged in the form of a square, with two OH groups bridging each pair of zirconium atoms along the sides of the square, one OH being above and the other below the plane of the square. Four water molecules are also bonded to each zirconium and they are arranged in such a way as to complete a square-antiprism arrangement of ligands around the zirconium atom.

The $Mo_6Cl_8^{4+}$ Cation

Brosset (9, 10, 11) has determined the structures of crystalline hydrated molybdenum dichloride and also a similar basic hydrated molybdenum chloride and has shown that they should be formulated as $\{[Mo_6Cl_8]Cl_4(H_2O)_2\}6H_2O$ and $\{[Mo_6Cl_8](OH)_4(H_2O)_2\}$-$12H_2O$ respectively. The structure of the $Mo_6Cl_8^{4+}$ ion is shown in Fig. 5; it consists of

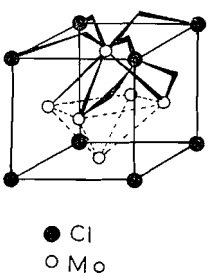


FIG. 5. The structure of the $Mo_6Cl_8^{4+}$ ion.

a regular octahedron of molybdenum atoms circumscribed by a cube of chlorine atoms, each molybdenum atom lying approximately in the plane of four chlorine atoms, constituting a face of the cube. Each molybdenum atom is thus surrounded by, and presumably bonded to, eight other atoms, four molybdenum atoms at the adjacent corners of the octahedron, and four chlorine atoms at the corners of a square which is parallel to, but rotated through 45° with respect to, the square formed by the four molybdenum atoms. There is, therefore, a very distorted square-antiprism arrangement of ligands around each molybdenum atom in which the four chlorine atoms lie in approximately the same plane as the central molybdenum atom. However, the arrangement of the bonding electron pairs is not necessarily the same as that of the ligands.

Sheldon (12) has made the very reasonable suggestion that the bonding of the chlorine atoms in the complex is essentially covalent since the ion retains its identity in solution and the chlorines show no tendency to ionize or to undergo replacement reactions. Each chlorine therefore appears to be forming three bonds to molybdenum atoms and the

Can. J. Chem. Downloaded from www.nrcresearchpress.com by 210.87.254.42 on 09/05/12
For personal use only.

Mo—Cl—Mo angles are only 60°. However, it is most unlikely that three of the four electron pairs in the valency shell of a chlorine atom could be so close together. The most probable arrangement for four equivalent electron pairs is tetrahedral (1, 2) and even for non-equivalent bonding and non-bonding pairs the angle between the bonding pairs is very unlikely to be less than 90° since, at this angle, repulsions between the electron pairs of a second-row element become relatively large (13). It is very probable that the angles between the three bonding pairs at each chlorine are somewhat greater than 90° and this can only be reconciled with the structure of the complex if the Mo—Cl bonds are bent, i.e. involve a non-linear overlap of appropriate orbitals on the metal and the chlorine atom (Fig. 5). If this is the case, then the arrangement of electron pairs around each molybdenum atom approximates closely the expected square antiprism. Some slight distortion of the regular square antiprism is in any case to be expected since the electron pairs bind either chlorine atoms or molybdenum atoms and are therefore not all equivalent to each other.

The $Mo_6Cl_8^{4+}$ ion is able to co-ordinate six ligands, one opposite each of the molybdenum atoms. In the compounds investigated by Brosset these additional ligands are $4Cl^-$ and $2H_2O$, or $4OH^-$ and $2H_2O$. The presence of an extra ligand will cause some distortion in the square-antiprism arrangement of the eight electron pairs around the molybdenum and if this ligand is attached to the molybdenum as strongly as the eight other ligands, the square-antiprism arrangement of eight bonding electron pairs passes over to the expected arrangement for nine bonding pairs, namely a triangular prism with an electron pair opposite the center of each of the three rectangular faces (2) (Fig. 6). This may also be described as a "3;3;3" arrangement; in this case the 3-fold axis of the trigonal prism is the y-axis.

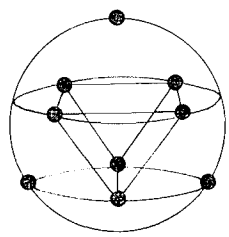


FIG. 6. The "3;3;3" trigonal prism arrangement for nine-co-ordination and its relation to the square-antiprism arrangement for eight-co-ordination.

This formulation of the structure of the $Mo_6Cl_8^{4+}$ ion implies that each molybdenum atom forms eight localized, at least partially covalent bonds, four of which are to other molybdenum atoms. Thus all the molybdenum valency electrons are used in bonding, and each molybdenum therefore has a d^0 configuration, which is consistent with the observed diamagnetism of the compounds containing this complex ion. Sheldon (12) has proposed that four chlorine atoms and one extra ligand are bound to each molybdenum by $d_{x^2-y^2}sp^3$ tetragonal, pyramidal orbitals and that the d_{xy} and d_{yz} orbitals form Mo—Mo bonds, leaving two electrons separately occupying essentially non-bonding d_{z^2} and d_{xy} orbitals, but nevertheless coupling their spins. This description of the bonding seems less satisfactory than that proposed above, for several reasons: it leads to an improbably small angle of 60° between three of the electron pairs on each chlorine atom; it necessitates a somewhat arbitrary assumption of pairing of the two electrons in the non-bonding

Can. J. Chem. Downloaded from www.nrcresearchpress.com by 210.87.254.42 on 09/05/12
For personal use only.

d_{z^2} and d_{xy} orbitals in order to explain the observed diamagnetism; and it implies somewhat weak Mo—Mo bonds since it allows only a total of 12 electrons for these 12 bonds which, however, have a length of 2.64 Å, which is close to the single bond value of 2.59 derived from the metal (14).

The $Nb_6Cl_{12}^{2+}$, $Ta_6Cl_{12}^{2+}$, and $Ta_6Br_{12}^{2+}$ Ions

The complex chlorides of niobium, $Nb_6Cl_{14}.7H_2O$ and $Ta_6Cl_{14}.7H_2O$, and the bromide $Ta_6Br_{14}.7H_2O$ have been shown to form the complex $Ta_6Cl_{12}^{2+}$, $Nb_6Cl_{12}^{2+}$, and $Ta_6Br_{12}^{2+}$ ions in aqueous solution (15). These ions have the structure shown in Fig. 7, in which

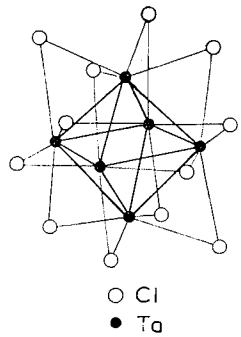


FIG. 7. The structure of the $Ta_6Cl_{12}^{2+}$ ion.

there is a regular octahedron of metal atoms, with a chlorine atom situated above each of the 12 edges of the octahedron. Thus each metal atom is surrounded by eight ligands, four chlorine atoms and four metal atoms arranged at the corners of a distorted cube. However, this is not the arrangement of the bonding electron pairs, firstly because the very small apparent bond angle at chlorine must imply that the metal–halogen bonds are bent and secondly because there are not enough electrons available to form 12 electron-pair bonds between the metal atoms. As only eight electron pairs are available for metal–metal bonds, their most probable arrangement would appear to be that in which there is one pair in the center of each face of the octahedron formed by the metal atoms, each electron pair binding three metal atoms and thus occupying a three-center orbital. If this is the case, the eight electron pairs surrounding the metal atom have the expected square-antiprism arrangement. It is probable that, in the solid, an additional ligand, e.g. Cl^- or H_2O, is bound to each of the metal atoms, thereby distorting the square-antiprism arrangement of eight electron pairs to the "3;3;3" arrangement expected for nine-co-ordination (Fig. 6).

The $U_6O_4(OH)_4^{12+}$ Ion

The basic sulphate of uranium of composition $U_6O_4(OH)_4(SO_4)_6$ has the same structure as the corresponding cerium compound, Fig. 3, and contains the complex cation $U_6O_4(OH)_4^{12+}$ (16). In this ion the metal atom has a valency shell containing eight bonding pairs and two non-bonding electrons.

The possible effect of the non-bonding electrons on the arrangement of the eight bonding pairs is most conveniently discussed in terms of the ligand-field theory. Figure 8 shows the splitting of the *d*-levels produced by the cubic, square-antiprism, and $Mo(CN)_8^{4-}$ arrangements of eight ligands. For the square-antiprism arrangement of ligands the d_{z^2} orbital has a lower energy than the other *d*-orbitals and could accommodate the unshared

Can. J. Chem. Downloaded from www.nrcresearchpress.com by 210.87.254.42 on 09/05/12
For personal use only.

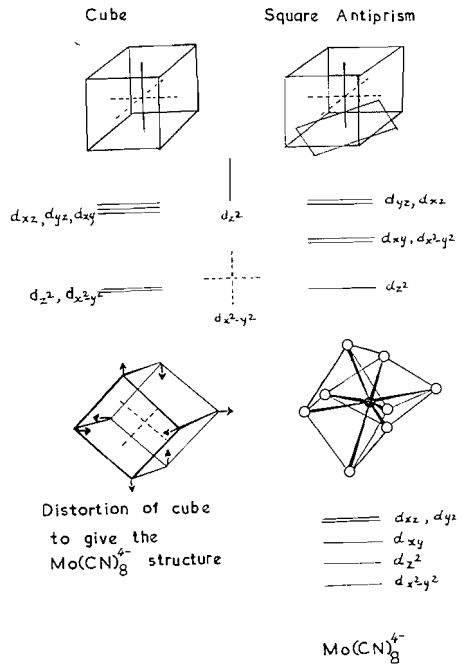


FIG. 8. Ligand-field "splittings" for the cube, square-antiprism, and $Mo(CN)_8^{4-}$ arrangements for eight-co-ordination.

pair without any appreciable distortion of the square-antiprism arrangement. Although this could, in principle, be the situation in the uranium compound, U(IV) compounds are generally paramagnetic and probably have an f^2 configuration with two unpaired electrons rather than a d^2 configuration. These electrons in the "inner" $5f$ orbitals have a negligible effect on the stereochemistry of the eight bonding electron pairs in the "outer" $6d7s7p$ orbitals and this may therefore be described as a weak-field or "outer"-orbital complex.

The $Mo(CN)_8^{4-}$ Ion

This ion does not have the square-antiprism structure but has the dodecahedral, or distorted cube, structure shown in Fig. 8 (17). Although the antiprism has been predicted to be the most stable arrangement for eight-co-ordination it may easily be seen that the dodecahedral structure must have very nearly the same stability, since the smallest bond angles for the square antiprism and the $Mo(CN)_8^{4-}$ structures are 74° 52′ and 74° respectively, whereas the smallest bond angle in the less-stable cubic arrangement is only 70° 32′. Since the interactions between the bonding electron pairs which arise from the operation of the Pauli exclusion principle are of such a nature that they increase very rapidly with decreasing separation of the electron pairs (18) the stability of a given arrangement is particularly dependent on the size of its smallest bond angle.

In the dodecahedral structure two non-bonding electrons may be accommodated in the $d_{x^2-y^2}$ orbital and they would not be expected to cause any appreciable distortion of the structure. In $Mo(CN)_8^{4-}$ the non-bonding pair is almost certainly involved to some extent in double bonding with the CN groups. It does not seem possible at the present time to decide what factors are of importance in determining the relative stabilities of the dodecahedral and square-antiprism structures.

Can. J. Chem. Downloaded from www.nrcresearchpress.com by 210.87.254.42 on 09/05/12
For personal use only.

NOTE ADDED IN PROOF

Since this paper was written I have been informed of some new, unpublished determinations of the structures of some eight-co-ordinated complexes: zirconium acetylacetonate (19) has a square-antiprism structure but tetrakisoxalatozirconate(IV) (20) and bis-diarsinetitanium (IV) tetrachloride (diarsine = o-$C_6H_4[As(CH_3)_2]_2$) (21) have the dodecahedral $Mo(CN)_8^{4-}$ structure. These new examples of both types of eight-co-ordinated structures further emphasize their very similar stabilities.

Table I lists all the known mononuclear and finite polynuclear molecules and complex ions in which the stereochemistry is determined by the square-antiprism and dodecahedral arrangements of eight bonding electron pairs in the valency shell of a central atom.

TABLE I

Molecules and complex ions with structures based on the square-antiprism and dodecahedral arrangements of eight bonding electron pairs

Square antiprism	Dodecahedron
TaF_8^{3-}	$Zr(oxalate)_4^{4-}$
$Th(acac)_4$	$Ti(diarsine)_2Cl_4$
$Zr(acac)_4$	$Mo(CN)_8^{4-}$
$[Ce_6O_4(OH)_4]^{12+}$	
$[U_6O_4(OH)_4]^{12+}$	
$[Zr_4(OH)_8(H_2O)_{16}]^{8+}$	
$Mo_6Cl_8^{4+}$	
$Nb_6Cl_{12}^{2+}$, $Ta_6Cl_{12}^{2+}$, $Ta_6Br_{12}^{2+}$	

ACKNOWLEDGMENT

I am greatly indebted to Professor J. L. Hoard and to Professor R. S. Nyholm for information concerning their results in advance of publication.

REFERENCES

1. J. W. LINNETT. Wave mechanics and valency. Methuen, London. 1960.
2. R. J. GILLESPIE. Can. J. Chem. **38**, 818 (1960).
3. J. L. HOARD, W. H. MARTIN, M. E. SMITH, and J. F. WHITNEY. J. Am. Chem. Soc. **76**, 3820 (1954).
4. D. GRDENIC and B. MATOKOVIC. Nature, **182**, 465 (1958).
5. G. LUNDGREN. Arkiv Kemi, **2**, 535 (1950).
6. G. LUNDGREN. Arkiv Kemi, **6**, 59 (1954).
7. G. LUNDGREN. Rec. trav. chim. **75**, 585 (1956).
8. A. CLEARFIELD and P. A. VAUGHAN. Acta Cryst. **9**, 555 (1956).
9. C. BROSSET. Arkiv Kemi, Mineral. Geol. A, **20**, 7 (1946).
10. C. BROSSET. Arkiv Kemi, Mineral. Geol. A, **22**, 11 (1947).
11. C. BROSSET. Arkiv Kemi, **1**, 353 (1950).
12. J. C. SHELDON. Nature, **184**, 1210 (1959).
13. R. J. GILLESPIE. J. Am. Chem. Soc. **82**, 5978 (1960).
14. L. PAULING. Nature of the chemical bond. 3rd ed. Cornell University Press, Ithaca, New York. 1960. p. 403.
15. P. A. VAUGHAN, J. H. STURDIVANT, and L. PAULING. J. Am. Chem. Soc. **72**, 5477 (1950).
16. G. LUNDGREN. Arkiv Kemi, **5**, 349 (1953).
17. J. L. HOARD and H. H. NORDSIECK. J. Am. Chem. Soc. **61**, 2853 (1939).
18. R. J. GILLESPIE. Can. J. Chem. **38**, 318 (1961).
19. J. L. HOARD and J. V. SILVERTON. Private communication.
20. J. L. HOARD. Private communication.
21. R. J. H. CLARK, J. LEWIS, R. S. NYHOLM, P. PAULING, and G. B. ROBERTSON. Private communication.

Can. J. Chem. Downloaded from www.nrcresearchpress.com by 210.87.254.42 on 09/05/12
For personal use only.

Can. J. Chem. Downloaded from www.nrcresearchpress.com by 210.87.254.40 on 09/05/12
For personal use only.

CO-ORDINATION COMPLEXES OF TITANIUM (IV) HALIDES

II. PREPARATION AND INFRARED SPECTRA OF THE COMPLEXES OF TITANIUM TETRACHLORIDE WITH DIESTERS OF α,ω-DICARBOXYLIC ACIDS AND COMPARISON WITH ANALOGOUS COMPLEXES OF ZIRCONIUM TETRACHLORIDE AND TIN TETRACHLORIDE[1]

ERNEST RIVET,[2] REAL AUBIN,[3] AND ROLAND RIVEST

ABSTRACT

Co-ordination complexes between diesters of α,ω-dicarboxylic acids and titanium tetrachloride, tin tetrachloride, and zirconium tetrachloride have been prepared. The analytical results, the infrared spectra, the melting points, and the molecular-weight determinations indicate that for the titanium and zirconium complexes, two types of complexes are obtained, one having a general formula $MX_4.1$ diester in which chelate rings from five to nine atoms are formed and the other one, $2MX_4.1$ diester in which there are two 4-membered rings per complex molecule. With tin tetrachloride only one type of complex is formed, which has two tin tetrachlorides and two diesters per complex molecule.

INTRODUCTION

In a previous paper (1) the reaction of diethyl oxalate with titanium tetrachloride has been studied and it was found that a chelated complex involving the two carbonyl groups of the oxalate was formed. The study was extended to diesters of the general formula $CO_2R—(CH_2)_n—CO_2R$, where n varies from 0 to 9, in order to see if very large chelate rings of the same type could be prepared.

In these diesters, the relative independance of every ester group makes it possible to consider that what is true for an ester should apply to a diester. In a carboxylic acid, the acidity is largely due to the possible resonance between the free electron pairs of the oxygen atoms. This makes the implication of the two oxygens of a monocarboxylic acid in the formation of a complex very unlikely. However, an ester is very different from a carboxylic acid. Although Pauling (2) and Wheland (3) mention that the resonance energy of an ester should be of the same order of magnitude as that of a carboxylic acid, Cook (4), using empirical results, has well established the absence of resonance in the esters, and he explained also this finding in terms of orbitals. It is not possible for the π orbitals of the carbonyl group to overlap the sp^3 orbitals of the other oxygen of the ester. Fieser (5) has reached the same conclusion by measuring ultraviolet absorption spectra: the molar extinction coefficients of the esters were larger than those of the corresponding carboxylic acids, thus indicating the presence of an unsaturated bond which is the double bond of the carbonyl group. It is then reasonable to assume that the four oxygen atoms of a diester are almost identical as far as their donor ability is concerned, except for the slight priority of the oxygens of the two carbonyl groups due to the possible steric hindrance of the radical on the two other oxygens. It becomes, then, possible to prepare complexes of diesters with titanium tetrachloride where two 4-membered-ring chelates will be formed. If one does a series of experiments with the diesters $CO_2R—(CH_2)_n—CO_2R$, he measures the relative ease of formation of large rings of seven, eight, nine, or more atoms compared to the formation of two 4-membered rings per diester molecule.

The formation of a four-membered-ring chelate on a Lewis acid requires that the two

[1]*Manuscript received June 30, 1961.*
Contribution from the Department of Chemistry, University of Montreal, Montreal, Que. Presented at the Symposium on Co-ordination in Chemistry, Chemical Institute of Canada, Hamilton, Ontario, May 15–16, 1961.
[2]*Present address: Radiation Laboratory, University of California, Berkeley 4, California.*
[3]*Present address: Séminaire de Joliette, Joliette, Que.*

donor atoms be accepted in a cis position. The work of Osipov (6) and co-workers, in which they obtained a one-to-one addition compound of titanium tetrachloride with ethyl propionate, indicates that this is very possible with $TiCl_4$. However, if the Lewis acid used is tin tetrachloride, the complex formed is $SnCl_4$.2 monoesters and the proposed structure is a trans one. In such a case, it should not be possible to observe the formation of a four-membered ring at both ends of the diester molecule. This was found to be so, and we prepared for the whole series of diesters, one-to-one addition compounds with tin tetrachlorides. In order to see if this difference in behavior between tin tetrachloride and titanium tetrachloride was a size effect, we prepared the same complex with zirconium tetrachloride; this was found not to be the case since zirconium and titanium tetrachlorides behaved similarly.

EXPERIMENTAL

Materials and Manipulation

Titanium tetrachloride was purified as mentioned before (7) and tin tetrachloride was purified by the method patented by Pittsburg Plate Glass Company (8). Commercial zirconium tetrachloride was sublimed in a nitrogen atmosphere at 200° C. The compound so obtained was a white powder. The analytical results were Zr, 39.60%; Cl, 60.49%, the theoretical values being 39.14% for zirconium and 60.84% for chlorine. The esters used were dried over magnesium sulphate or magnesium perchlorate and vacuum-distilled over magnesium perchlorate. One diester, diethyl suberate, was prepared in our laboratory using the esterification method described in *Organic syntheses* (9). It was dried and distilled, as were the other ones. The solvents used were purified by standard methods, dried, and distilled over a suitable drying agent. The water-sensitive complexes were prepared and handled in a dry box continuously flushed with dry nitrogen.

The methods of analysis for titanium and chlorine have been described previously (7); for the determination of tin the method described in Vogel's *Textbook of quantitative inorganic analysis* (10) was used. Zirconium was determined by precipitation with ammonium hydroxide, and ignition to the dioxide (11). All the analytical results are included in Table I.

TABLE I

		% Metal		% Cl	
Lewis acid	Lewis base	Theoretical	Found	Theoretical	Found
$TiCl_4$ (s)	Diethyl oxalate	14.26	14.40	41.27	41.26
$TiCl_4$ (s)	Diethyl malonate	13.69	13.69	40.53	40.81
$TiCl_4$ (s)	Diethyl succinate	13.16	13.51	38.97	38.56
$TiCl_4$ (s)	Diethyl glutarate	12.67	13.50	37.60	38.80
$TiCl_4$ (s)	Diethyl adipate (s)	—	14.40	—	40.3
$TiCl_4$	Diethyl adipate (e)	12.22	12.40	36.20	35.21
$TiCl_4$ (e)	Diethyl adipate	16.5	16.60	48.80	47.30
$TiCl_4$ (s)	Diethyl pimelate	16.06	16.08	48.10	44.15
$TiCl_4$	Diethyl suberate	15.00	14.90	46.40	42.30
$TiCl_4$	Diethyl azelate	15.30	15.12	45.46	42.80
$TiCl_4$	Diethyl sebacate	15.02	15.13	42.90	41.10
$TiCl_4$	Diethyl butyrate	15.67	15.67	46.41	44.80
$SnCl_4$	Diethyl succinate	27.3	27.4	32.60	30.20
$SnCl_4$	Diethyl adipate	25.60	24.90	30.60	30.10
$SnCl_4$	Diethyl azelate	23.50	23.40	28.10	28.10
$ZrCl_4$	Diethyl oxalate	24.04	24.34	37.39	30.52
$ZrCl_4$	Diethyl succinate	22.39	22.51	34.82	33.59
$ZrCl_4$	Ethyl butyrate	26.12	25.10	40.60	36.55
$ZrCl_4$	Diethyl sebacate	25.18	25.19	37.77	36.20

NOTE: s= stoichiometric; e= excess.

Can. J. Chem. Downloaded from www.nrcresearchpress.com by 210.87.254.40 on 09/05/12
For personal use only.

The setup used to prepare the complexes was the same as the one used in previous experiments (12).

The spectrophotometric measurements were carried out on a Perkin–Elmer infrared spectrophotomer, model 21, using a sodium chloride prism. The spectra of the complexes were determined in solutions of suitable solvents or by the KBr disk method. The melting point determinations were made with a Thiele apparatus. The molecular-weight determinations were made either by cryoscopy or ebullioscopy.

Preparation of the Complexes

The System $SnCl_4$ – Diethyl Succinate

Pure $SnCl_4$ was added dropwise to a certain quantity of the diester. The precipitate formed instantaneously as $SnCl_4$ was added. As the stoichiometric value of $SnCl_4$ for a one-to-one addition compound was approached, the liquid phase became very viscous and then the whole mass more or less solidified. It was washed very carefully with hexane and dried in vacuum at room temperature, leaving a white powder.

The System $SnCl_4$ – Diethyl Adipate

The reaction was performed by the dropwise addition of $SnCl_4$ to the pure ester.

The reaction rate was slower than in the previous case but led to a white solid which, when filtered, washed with hexane, and dried in vacuum at room temperature, gave a white powder.

The System $SnCl_4$ – Diethyl Azelate

This reaction was performed by the previous method, but no precipitation occurred even after many days of agitation. If the reaction mixture is washed with hexane, then there is precipitation of a white powder. This powder was filtered, washed with hexane, and dried in vacuum at room temperature.

The Systems $TiCl_4$–Oxalate and $TiCl_4$–Malonate

Thirty milliliters of a 10% solution of titanium chloride in hexane was added dropwise to 30 ml of a solution of the diester in the same solvent. Precipitation occurred at the very beginning of the addition, giving a yellow powder. The powder was filtered, washed many times on the filter with pure hexane, and dried in vacuum at room temperature.

The Systems $TiCl_4$ – Diethyl Succinate and $TiCl_4$ – Diethyl Glutarate

Thirty-eight milliliters of a 10% solution of titanium tetrachloride was added dropwise to 35 ml of a 10% solution of the diester. A yellow powder was formed at the beginning of the addition, and when the stoichiometric value for one-to-one addition was reached, another compound, somewhat lighter in color, was formed in small quantity. This explains the high values obtained for titanium and chlorine. It indicates that a very small proportion of the solid is probably a two-to-one addition compound of $TiCl_4$ to the diester.

The System $TiCl_4$ – Diethyl Adipate

By using 10% solutions of the reactants in hexane, as for previous preparations, one can obtain three analytical results. One obtains, in stoichiometric proportions, a mixture of compounds, which can be separated by extraction with benzene. The analytical values indicate that a mixture of two compounds, $TiCl_4$.1 diester and $2TiCl_4$.1 diester, was obtained; by using excess diester, one obtains the one-to-one addition compound almost exclusively and by using excess $TiCl_4$, one obtains the two-to-one addition compound. The two compounds have different melting points and their color is different, the first one being yellow, the other one being light yellow.

Can. J. Chem. Downloaded from www.nrcresearchpress.com by 210.87.254.40 on 09/05/12
For personal use only.

The Systems $TiCl_4$ – Diethyl Pimelate, $TiCl_4$ – Diethyl Suberate, $TiCl_4$ – Diethyl Azelate, and $TiCl_4$ – Diethyl Sebacate

The preparation of these complexes was performed in hexane with 10% solutions of the reactants. The complexes prepared are all similar in appearance, being light yellow powders. The analytical results indicate that they are all complexes of the two-to-one stoichiometric compositions. If one tries to prepare the one-to-one addition complexes, which would have been very large chelate rings, there is then dissolution of the complex in the excess diester and one obtains a very viscous, dark brown liquid which seems to be the solvated two-to-one addition compound. These results indicate that with these diesters only one compound can be isolated. However, if one uses CCl_4 as solvent and prepares a complex from stoichiometric values for a one-to-one addition compound, one can see that there are really two compounds, one being almost insoluble in CCl_4, the other being soluble. If one tries to isolate this small precipitate by decantation and then filtration, there is a modification of the precipitate on the filter and one gets a very viscous solid which cannot be properly dried. Qualitatively, this insoluble part is almost nil for the last two terms of the series, but is somewhat larger for the pimelate system.

The Systems $ZrCl_4$ – Diethyl Oxalate, $ZrCl_4$ – Diethyl Succinate, and $ZrCl_4$ – Ethyl Butyrate

To 2 g of powdered zirconium tetrachloride partially dissolved in carbon tetrachloride was added dropwise a 10% solution of the ester in the same solvent till a slight excess of the diester was obtained. The reactants were left in contact with each other for 2 or 3 days, then the white powder obtained was filtered, washed with dry carbon tetrachloride, and dried in vacuum at room temperature.

The System $ZrCl_4$ – Diethyl Sebacate

To 2 g of powdered zirconium tetrachloride partially dissolved in hexane was added dropwise a 10% solution of the sebacate, in the same solvent. The reactants were left in contact with each other for 2 or 3 days, then the white powder obtained was filtered, washed with hexane, and dried in vacuum at room temperature.

The analytical results as shown in Table I indicate that for the titanium tetrachloride complexes there is a progressive change from the monochelated complex of the first terms to the dichelated complexes as the length of the diester chain increases. By comparing the experimental results of the stoichiometric preparations with the theoretical values, one can calculate the relative amount of the two possible complexes for a given diester. These values were calculated using the following equations:

$$T_1 \times A + T_2 \times B = F \qquad [1]$$

$$A + B = 1. \qquad [2]$$

In these equations A is the mole fraction of titanium present as one-to-one addition compound, B is the mole fraction of titanium present as two-to-one addition compound, T_1 represents the theoretical value of the percentage of titanium for a one-to-one addition compound, T_2 the theoretical percentage of titanium in a two-to-one addition compound, and F the value of titanium found for the complex. The values so calculated are tabulated in Table II and illustrated in Fig. 1.

Infrared Spectra

The infrared spectra of the titanium complexes have been studied in solutions and by the KBr disk method. With methylene chloride solutions, we have studied the lowering

Can. J. Chem. Downloaded from www.nrcresearchpress.com by 210.87.254.40 on 09/05/12
For personal use only.

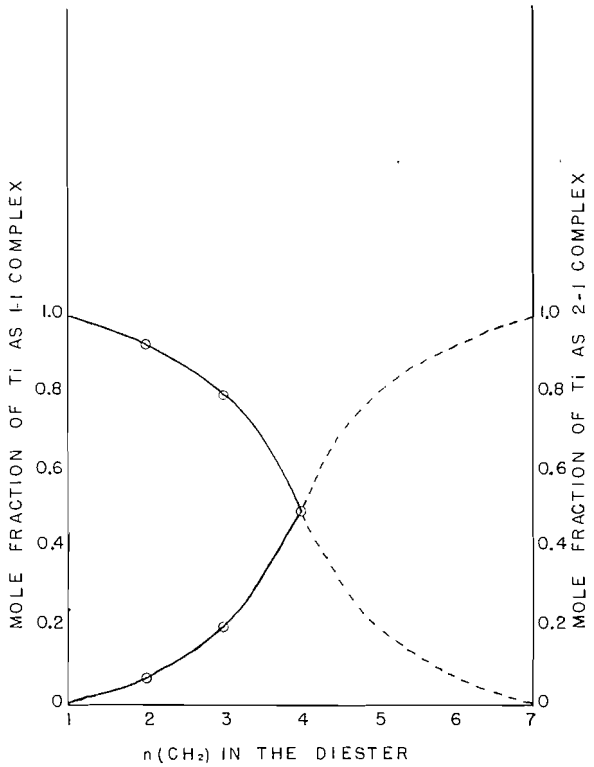


FIG. 1. Variation of the relative yield of the 1–1 and 2–1 titanium complexes as a function of the length of the diester chain.

TABLE II

Ester in the complex	T_1	T_2	F	A	B
Malonate	13.69		13.69	1.00	.0
Succinate	13.16	17.30	13.51	.93	.7
Glutarate	12.67	16.87	13.50	.80	.20
Adipate	12.22	16.50	14.40	.50	.50

of the carbonyl stretching frequency of the diesters, due to complexing. These results are included in Table III and illustrated in Figs. 2, 3, and 4.

TABLE III
Bathochrome effect of the carbonyl frequency in methylene chloride solutions of the titanium complexes

Ester in the complex	$\nu_{C=O}$ Pure esters	$\nu_{C=O}$ Complexes	$\Delta\nu_{C=O}$
Oxalate	1774, 1746	1708	57
Malonate	1748, 1731	1699, 1686	47
Succinate	1733	1669	64
Glutarate	1732	1652	80
Adipate	1729	1640	89
Pimelate	1731	1620	111
Azelate	1728	1620	108
Sebacate	1725	1620	105
Butyrate	1737	1635	102

Can. J. Chem. Downloaded from www.nrcresearchpress.com by 210.87.254.40 on 09/05/12
For personal use only.

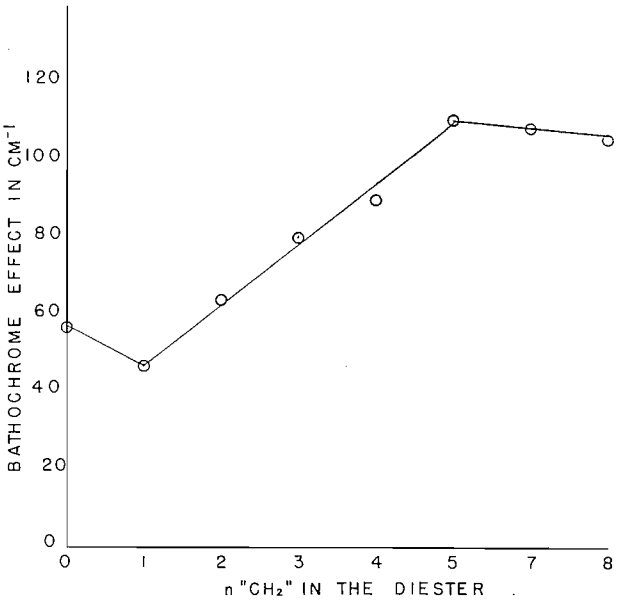


FIG. 2. Infrared spectra in methylene chloride solutions: variation of the bathochrome effect of the carbonyl stretching vibration when co-ordinated to titanium, as a function of the length of the diester chain.

By studying the infrared spectra of co-ordinated complexes containing cyclic ethers as the donor molecules, Sisler (13) has observed that the band attributed to C—O—C vibrations disappears in the spectrum of the complex. In order to see if the ethered oxygens of the diesters were involved in complexing, the spectrum of the diethyl sebacate ester in methylene chloride solution has been compared with the spectrum of the titanium complex dissolved in the same solvent. One can observe in Fig. 3 that in the region of 1200–1100 cm^{-1}, usually attributed to ν_{C-O} and ν_{C-O-C} vibrations (14), there is strong absorption in the spectrum of the ester which almost completely disappears in the spectrum of the complex. This seems to be a confirmation of the fact that the two oxygens of the ester groups of the sebacate act as donor atoms to form a four-membered-ring chelate.

In Fig. 4, we compare the spectrum of diethyl oxalate in *n*-butyl chloride solution with the spectrum of the $TiCl_4$–oxalate complex in the same solvent. The band located at 1165 cm^{-1} and attributed to ν_{C-O}, and the band located at 1152 cm^{-1} and attributed to ν_{C-O-C}, are much stronger in the spectrum of the ester than in the spectrum of the complex, but they still are easily located in the spectrum of the complex. This seems to confirm the proposed difference in the structure of the two types of complexes involved.

The spectra of the solid complexes of titanium studied by the KBr disk method gave different results. Four complexes were studied and all of them gave about the same bathochrome effect: 110 cm^{-1} for the succinate complex, 106 cm^{-1} for the adipate complex, 110 cm^{-1} for the sebacate complex.

The infrared spectra of tin complexes were also studied and the bathochrome effect did not change appreciably for the whole series, being about 100 cm^{-1}.

Can. J. Chem. Downloaded from www.nrcresearchpress.com by 210.87.254.40 on 09/05/12
For personal use only.

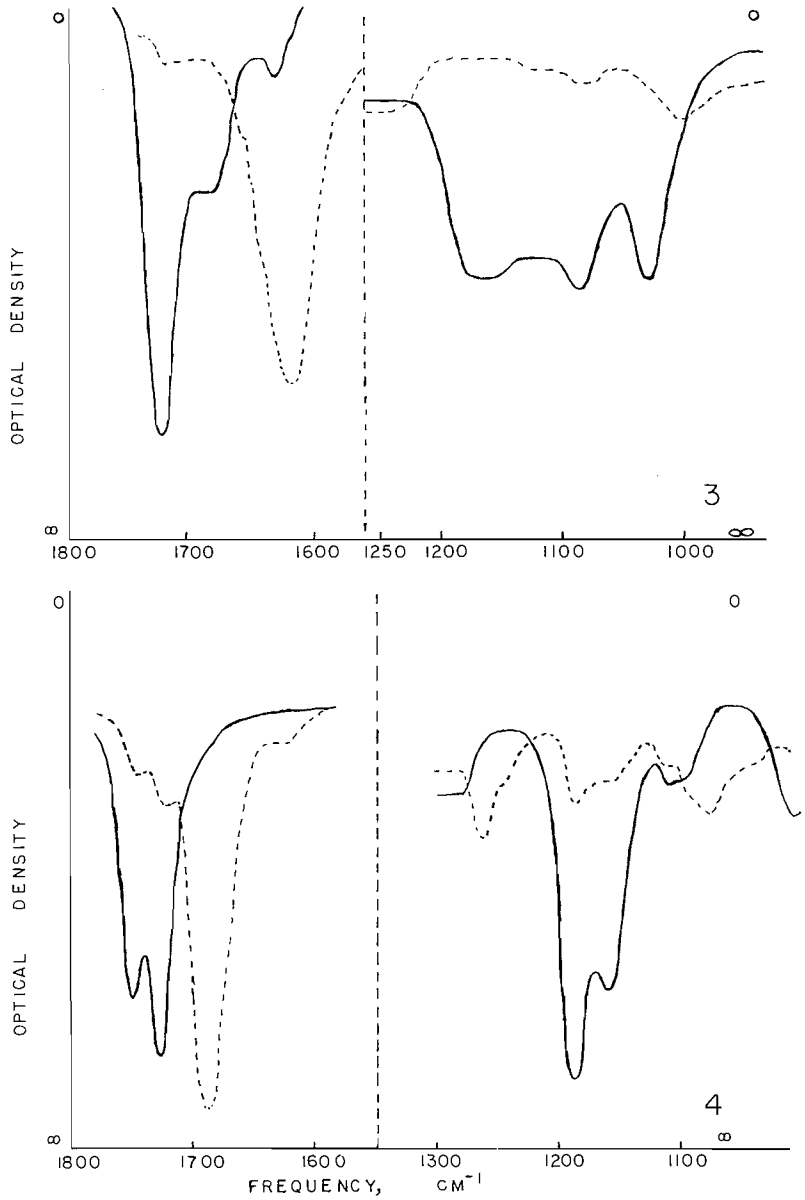


FIG. 3. Infrared spectra in methylene chloride solutions: —diethyl sebacate; – – – $2TiCl_4$. diethyl sebacate.
FIG. 4. Infrared spectra in *n*-butyl chloride solutions: —diethyl oxalate; – – – $TiCl_4$. diethyl oxalate.

Melting Points of the Complexes

The results of the melting-point measurements are included in Table IV.

Molecular-Weight Determinations

The determination of the molecular weight of some of the titanium complexes was very important in the proof of the monomeric nature of the complexes. The results are included in Table V.

Can. J. Chem. Downloaded from www.nrcresearchpress.com by 210.87.254.40 on 09/05/12
For personal use only.

TABLE IV

Melting points of the complexes

Complexes	Melting points	Complexes	Melting points
$TiCl_4$.oxalate	104°	$2TiCl_4$.azelate	92–95°
$TiCl_4$.malonate	121–122°	$2TiCl_4$.sebacate	99–100°
$TiCl_4$.succinate	138–139°	$2SnCl_4$.2 succinate	79–80°
$TiCl_4$.adipate	130°	$2SnCl_4$.2 azelate	54–56°
$2TiCl_4$.adipate	89°	$ZrCl_4$.oxalate	Decomposes at 280°
$2TiCl_4$.suberate	87–90°	$ZrCl_4$.succinate	360°

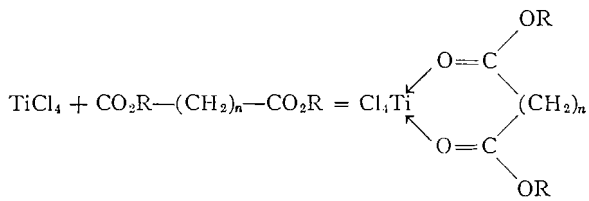
TABLE V

Molecular weights of some titanium complexes

Complexes	Method	Solvent	Molecular weight	
			Theoretical	Found
$TiCl_4$.succinate	Cryoscopy	Benzene	363.9	359, 317, 332
$TiCl_4$.sebacate	Ebullioscopy	*n*-Butyl chloride	638	613, 591, 630
$TiCl_4$.butyrate	Ebullioscopy	*n*-Butyl chloride	305	275, 281, 269

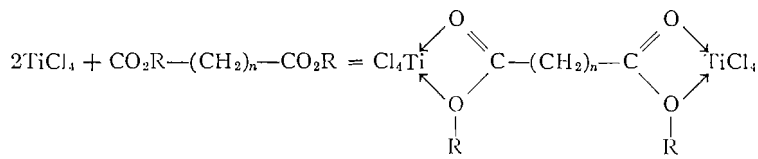
DISCUSSION

The results tabulated here indicate that the reactions of the diesters studied with titanium tetrachloride lead to two different types of compounds, represented by equations [3] and [4]. The transition from (*a*) to (*b*) seems to be gradual, as it is shown in Fig. 1.



[3]

(*a*)



[4]

(*b*)

This graphical representation is not precise but at least gives an idea of what is happening. The values of A and B for the complexes of the diesters for which the value of n is larger than 4 could not be determined. If one tries to obtain a mixture of (*a*) and (*b*), the (*b*) complex dissolves in the diester and it is not possible to get rid of this diester because of its very low vapor pressure at room temperature. It has been attempted to wash out the diester with suitable solvents but it was found that it is part of a solvated molecule and as such is not removable by solvents.

Figure 2, in which the variation of the bathochrome effect is plotted against the n

Can. J. Chem. Downloaded from www.nrcresearchpress.com by 210.87.254.40 on 09/05/12
For personal use only.

values of the diester chain, illustrates a variation in the type of complexes obtained. The value of the carbonyl shift is the lowest for the six-membered-ring chelate for which the strain should be at a minimum. For this complex the carbonyl shift is equal in value to the shift observed for the $TiCl_4$.2 acetone complex. As the ring size increases, the carbonyl shift increases until it becomes about equal to the shift observed for a four-membered-ring complex. This is confirmed by the similar shift obtained for the complex $TiCl_4$–butyrate and by vanishing of the band attributed to C—O—C vibration in the type (*b*) complexes.

It is noticable that in the solid state, the carbonyl frequency shifts are about the same for the whole series of titanium complexes. This is certainly due to the fact that in the solid state the OR groups in the type (*a*) complexes are involved in co-ordination to titanium somewhat as ammonia is in complexes like $TiCl_4.4NH_3$. This co-ordination through the OR groups in the solid state explains also the break in the melting points as one arrives at the (*b*) type complexes where this is not possible because the OR groups are already co-ordinated to a titanium atom.

In dilute solutions, the different molecules of complexes are well separated from each other as indicated by the molecular-weight determinations listed in Table V. Great care was taken in these determinations to avoid hydrolysis, which would give a lower molecular weight than the theoretical one. Every solvent used was checked with the Karl Fisher reagent, and the amount of water present could not change appreciably the thermometer readings leading to the molecular weight, but explains the fact that all the values are a little lower than the theoretical ones. The fact that the butyrate complex has a molecular weight which is about half that of the sebacate complex indicates that the formula proposed for the complexes similar to the sebacate one is probably adequate since there should not be any doubt about the formula of the monoester complex.

The behavior of tin tetrachloride in its reaction with diesters is different. The tin complexes obtained are different from the titanium ones as indicated by the melting points and the analytical results. Many experiments were performed to determine the molecular weight of these complexes in solution, but because of the lack of suitable solvents, it has not been possible to get reproducible results. So, we relied on the work of Hieber and Reindl (15), who have proved that $SnCl_4$ gives two-to-two addition compounds with the diesters we used. Since it is possible to obtain complexes $SnCl_4$.2 monoesters, the impossibility of obtaining chelate rings of the (*a*) type can be explained by the fact that the complexing of two ligands with $SnCl_4$ is done in the trans positions; it is then very possible that the four chlorine atoms lie equatorially on the plane of the tin atom and that the two axial co-ordinating positions are longer distances than the Sn—Cl distances, thus giving an elongated octahedron. This is in agreement with the conclusion of Sumarokova and Yarmukhamedova (16) in their work on complexes of stannic halides with thiourea, in which they mention that the complexes SnX_4.2 thiourea have a trans configuration.

ACKNOWLEDGMENTS

The authors are indebted to Professor Camille Sandorfy for valuable discussion on the infrared spectra and to Mr. Gilles Murphy for the preparation and analysis of some of the complexes.

The authors also wish to thank the National Research Council for the grants to one of us (R. R.) and l'Office des Recherches Scientifiques de la Province de Québec for the fellowships to E. R. and R. A.

Can. J. Chem. Downloaded from www.nrcresearchpress.com by 210.87.254.40 on 09/05/12
For personal use only.

SOMMAIRE

On a préparé des complexes de coordination entre des esters des acides α,ω-dicarboxyliques normaux et du tétrachlorure de titane, du tétrachlorure d'étain et du tétrachlorure de zirconium. Les résultats analytiques, les spectres infrarouges, les mesures de points de fusion indiquent que le tétrachlorure de titane et le tétrachlorure de zirconium donnent, par leur réaction avec les diesters, deux sortes de complexes de formule $MX_4.1$ diester et $2MX_4.1$ diester respectivement. Les complexes $MX_4.1$ diester sont des chelates contenant cinq à neuf atomes par anneau alors que les complexes $2MX_4.1$ diester contiennent par molecule deux anneaux a quatre situés en bouts de chaine du diester. Avec le tétrachlorure d'étain, on obtient seulement un genre de complexe de formule $2SnCl_4.2$ diesters.

REFERENCES

1. R. AUBIN and R. RIVEST. Can. J. Chem. **36**, 915 (1958).
2. L. PAULING. The nature of the chemical bond. 2nd ed. Cornell University Press. 1945. p. 202.
3. G. W. WHELAND. Resonance in organic chemistry. John Wiley & Sons. 1955. p. 109.
4. D. COOK. J. Am. Chem. Soc. **80**, 49 (1958).
5. L. F. FIESER and M. FIESER. Organic chemistry. 3rd ed. D. C. Heath & Co., Boston. 1956. p. 175.
6. O. A. OSIPOV. Zhur. Obshcheĭ Khim. **26**, 322 (1956).
7. J. ARCHAMBAULT and R. RIVEST. Can. J. Chem. **36**, 1461 (1958).
8. Pittsburg Plate Glass Co. Brit. Patent No. 600,003 (1948).
9. J. R. JOHNSON (*Editor*). Organic syntheses. Vol. XIX. John Wiley & Sons. 1939. p. 46.
10. A. I. VOGEL. A text-book of quantitative inorganic analysis. 2nd ed. Longmans Green & Co., London. 1953. p. 358.
11. I. M. KOLTHOFF and E. B. SANDELL. Textbook of quantitative inorganic analysis. 3rd ed. The Macmillan Co. 1959. p. 316.
12. J. ARCHAMBAULT and R. RIVEST. Can. J. Chem. **38**, 1331 (1960).
13. F. R. ROLSTEN and H. H. SISLER. J. Am. Chem. Soc. **79**, 1819 (1957).
14. P. J. CORISH and W. H. T. DAVISON. J. Chem. Soc. 927 (1958).
15. W. HIEBER and E. REINDL. Z. Elektrochem. **46**, 559 (1940).
16. T. SUMAROKOVA and E. YARMUKHAMEDOVA. J. Gen. Chem. U. S. S. R. Eng. Transl. 3663 (1956).

Can. J. Chem. Downloaded from www.nrcresearchpress.com by 210.87.254.40 on 09/05/12
For personal use only.

Can. J. Chem. Downloaded from www.nrcresearchpress.com by 210.87.254.40 on 09/05/12
For personal use only.

π-BONDING IN INORGANIC COMPOUNDS

IV. ROLE OF UNPAIRED ELECTRONS IN HEXAHALO COMPLEXES[1, 2]

A. D. WESTLAND AND N. C. BHIWANDKER[3]

ABSTRACT

A study of d_π–p_π bonding in paramagnetic compounds having the potassium chloroplatinate structure is described. It is shown that the magnetic superexchange effect is approximately proportional to the number of unpaired electrons in t_{2g}^5 and t_{2g}^4 systems but there is an irregularity in the t_{2g}^3 system of potassium chlororhenate. This singularity of the t_{2g}^3 case is considered to be a result of the orbital and crystal symmetries. The magnetic properties of the compounds are related to the extent of π-bonding stabilization in octahedral complexes having various configurations t_{2g}^n on their central atoms.

As part of a program to obtain quantitative or semiquantitative estimates of the extent of π-bonding in inorganic compounds, we have undertaken studies of the effects of certain variables such as principal quantum number of the orbitals involved and effective nuclear charge of the participating atoms. In the present paper we provide evidence which suggests that the extent of d_π–p_π bonding of the type defined as "semicovalent" (1) varies in proportion to the number of unpaired d-electrons provided that these are contained in orbitals of the appropriate symmetry. This result is not entirely trivial for in some of the cases in which electron-pair π-bonding is invoked to account for enhanced compound stability, there seems to be poor correlation between that stability and electron structure (2). In view of the results of the present investigation, it would seem feasible to ascribe the stability of complexes such as $Cr(CN)_6^{3-}$, in which there are no d-electron pairs, to a system of single electron or "half" π-bonds.

The present study compares the extent of magnetic superexchange in compounds K_2MeCl_6 in which the central atom possesses one, two, or three unpaired $5d_\epsilon$-electrons. In a previous publication (3) it was shown that there is extensive superexchange in K_2OsCl_6, K_2OsBr_6, and K_2ReCl_6. This apparently operates through d_π–p_π bonding orbitals which encompass the metal atom and its ligands and, as well, p_π–p_π overlap between the ligands of the neighboring complex groups (4). This latter exchange is shown by means of diagonal broken lines in Fig. 1. The previous results are herein supplemented with those for K_2IrCl_6, again employing the technique of isomorphous dilution with K_2PtCl_6.

It has been shown that K_2IrCl_6 is antiferromagnetic at low temperatures (5), and the electron spin resonance spectrum likewise provides evidence of a π-bonding mechanism (6, 7, 8). In order to obtain an estimate of the magnitude of d_π–p_π bonding in K_2IrCl_6, we have measured the change in the effective magnetic moment of the chloroiridate ion when it is put into solid solution at high dilution in K_2PtCl_6. The assumption that the change in effective magnetic moment is a measure of the superexchange and, in turn, of the extent of π-bonding in the Me—Cl link is justified as follows.

In order for the superexchange coupling to occur, it is necessary that quantum mechanical exchange should take place between neighboring chlorine atoms on adjacent $MeCl_6^{2-}$ groups as well as within the groups. Since there is only a very small change in lattice constant along this series of isomorphous compounds K_2IrCl_6, K_2OsCl_6, and

[1]*Manuscript received April 20, 1961.*
Contribution from the Department of Chemistry, University of Ottawa, Ottawa, Ontario. Presented at the Symposium on Co-ordination in Chemistry, Hamilton, Ontario, May 15–16, 1961.
[2]*Part III. Can. J. Chem.* **39**, *1284 (1961).*
[3]*Present address: Department of Chemistry, McGill University, Montreal, Que.*

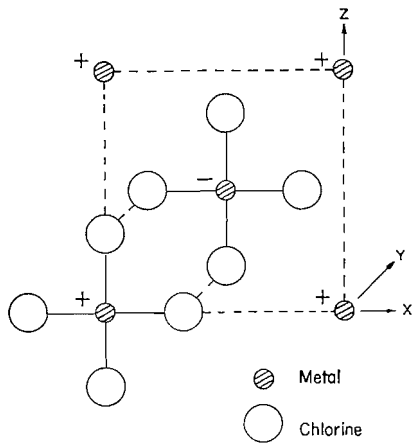


FIG. 1. Orientation of complex groups in crystal lattices of the potassium chloroplatinate type. A section through the plane (0,1,0) is shown.

K_2ReCl_6, it seems justified to assume that the Cl—Cl distance of adjacent anions is so nearly constant that all differences in the exchange effect are due to differences in the Me—Cl bonds.

RESULTS AND DISCUSSION

Pure Potassium Chloroiridate (IV)

The values of the susceptibilities and effective moments at three temperatures for the pure substance are shown in Table I. These data agree well with the values obtained by

TABLE I

Magnetic susceptibilities and effective moments of K_2IrCl_6

Temperature, °K	Gram susceptibility, $\chi_g \times 10^6$	Mole susceptibility, $\chi_M \times 10^3$	Effective moment, B.M.
298	2.15	1.25	1.72
224	2.96	1.63	1.71
90	5.41	2.86	1.44

Cooke *et al.* (5) but differ slightly from those of Norman and Morrow (9), who obtained $\mu_{eff} = 1.64$ B.M. at 298° K. It was our experience that unless oxidizing conditions were maintained at all times during the crystallization of the compound, slightly low results were obtained.* Cooke *et al.* made no measurements between the boiling point of oxygen and room temperature, and assumed that the spin-only value of the moment obtains in the compound but that a large temperature-independent paramagnetism is present. The former assumption is not justified as will be shown.

It is to be expected that the compound should obey the theories of Kotani (10) or Figgis (11), which take account of spin–orbit coupling. The former predicts that the spin-only value of the moment will be observed for the t_{2g}^5 configuration when kT is small with respect to the spin–orbit coupling constant, λ, and that μ_{eff} should vary in nearly linear fashion with kT/λ for temperatures up to 300° K. Figgis' more detailed theory

*K_2IrCl_6 *is diamagnetic.*

Can. J. Chem. Downloaded from www.nrcresearchpress.com by 210.87.254.40 on 09/05/12
For personal use only.

takes account of electron delocalization and states that the moment at 0° K should be progressively lower than the spin-only value, the greater is the delocalization, $1-k$. The plot of μ_{eff} for the pure compound in Fig. 2 shows that moment is far from linear in tem-

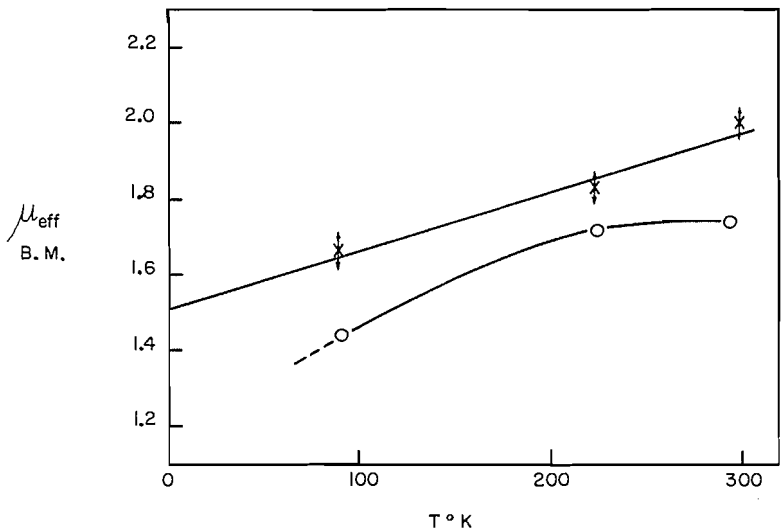


FIG. 2. Plots of effective moment against temperature: O pure K_2IrCl_6; × K_2IrCl_6 at infinite dilution in K_2PtCl_6.

perature and that the value at 0° K is much too low to correspond to a reasonable degree of delocalization ($\mu(0°\text{ K}) = 1.41$ B.M. for $k = 0.7$, for example).

The theories of Kotani and Figgis involve the assumption that there is no exchange between neighboring paramagnetic atoms. It was therefore thought that the discrepancy was the result of superexchange. Some indication of superexchange quenching in Na_2IrCl_6 was provided by Sloth and Garner (12), who found that the moment of the solid was 1.58 B.M. while in aqueous solutions it was 1.75 B.M. A study over an extensive temperature range can be carried out only in solid solution, however.

The System K_2IrCl_6/K_2PtCl_6

The effective moment of the iridium atom in solid solution rises with increasing dilution. The course of this quantity with change of concentration is shown in Fig. 3 for three different temperatures. It is apparent that the paramagnetism is partially quenched in the magnetically concentrated systems and that the behavior is essentially the same as that of the system K_2OsCl_6/K_2PtCl_6. There appears to be initially a slight decrease in the paramagnetism from 100 mole% down to about 50 mole%. We can suggest no convincing explanation for this effect if, indeed, it is real.

The data do not afford a very accurate extrapolation to infinite dilution, for the paramagnetism of the most dilute sample measured (12.5 mole%) is of the same order of magnitude as the accompanying diamagnetism. However, the values obtained from the graphs are given in Table II. The effective moment is plotted in Fig. 2, against temperature, along with the values for pure K_2IrCl_6. It may be seen that in contrast with the pure compound, the infinitely dilute chloroiridate (IV) ion behaves at least within the limits of experimental error, in the manner expected for a substance to which Figgis' theory should apply. The line in the figure has been drawn through the value $\mu = 1.5$ at

Can. J. Chem. Downloaded from www.nrcresearchpress.com by 210.87.254.40 on 09/05/12
For personal use only.

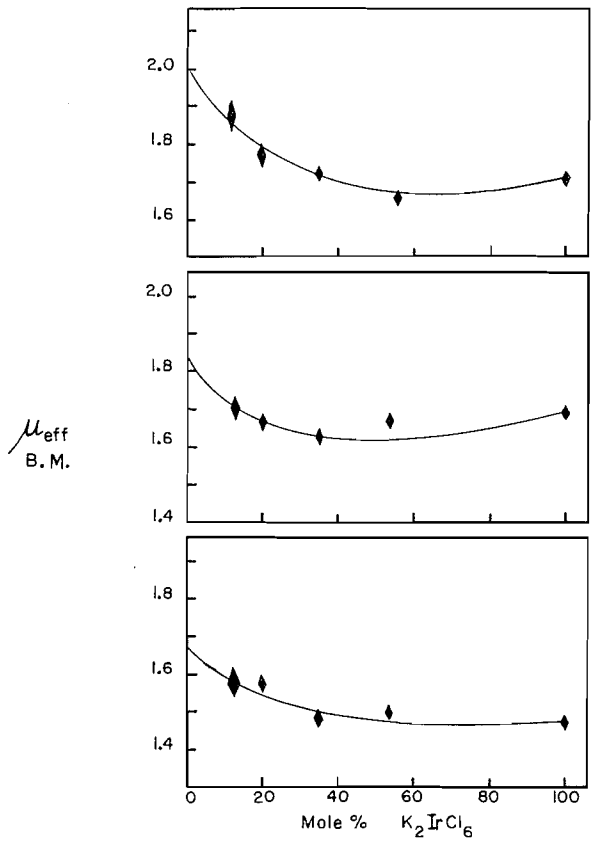


FIG. 3. Plots of the effective moment against concentration of K_2IrCl_6 dissolved in K_2PtCl_6.

$T = 0°$, corresponding to a value of $k = 0.7_6$. This would mean that the electron hole is ~24% in p_π orbitals of the ligands. Griffiths, Owen, and Ward obtained a value of $k = 0.7$ from paramagnetic resonance experiments (6). Although we feel our figure has little accuracy, it is in semiquantitative agreement with the previous results.

From the slope of the line, a value of 630 cm^{-1} is obtained for the spin–orbit coupling constant. This is an extraordinarily low value and makes us doubt the reliability of the estimate. A value of 2000–3000 would seem reasonable. The discrepancy may be the result of an underlying temperature-independent paramagnetism of the order of 0.4×10^3.

Comparison of K_2IrCl_6, K_2OsCl_6, and K_2ReCl_6

We may now compare the extent of superexchange in the compounds K_2MeCl_6. In the case of K_2ReCl_6, the investigation described previously (3) and subsequent measurements (13) suffice to show that the effective moment of chlororhenate (IV) at infinite dilution is 3.75±0.03 B.M. In Table III the room temperature moments of the three pure compounds and the complexes at infinite dilution are presented together with the values of the Weiss constant, Δ, calculated, in the case of iridium and osmium, on the assumption that

$$\mu_{eff} = 2.86[\chi_M(T+\Delta)]^{1/2},$$

where μ_{eff} is the moment for the complex at infinite dilution and χ_M is the mole susceptibility of the pure compound.

Can. J. Chem. Downloaded from www.nrcresearchpress.com by 210.87.254.40 on 09/05/12
For personal use only.

TABLE II

Paramagnetism of $IrCl_6^{2-}$ at infinite dilution in K_2PtCl_6

Temperature	Mole susceptibility $\times 10^3$	Effective moment, B.M.
298°	1.68	2.0 ±0.06
224°	1.85	1.82±0.06
90°	3.82	1.66±0.07

TABLE III

	No. of unpaired electrons	Moment of pure K_2MeCl_6, B.M.	Moment at infinite dilution, B.M.	Derived Weiss constant, Δ
Ir (IV)	1	1.7	2.1	104
Os (IV)	2	1.44	2.13	340
Re (IV)	3	3.26	3.75	90

It can be seen that the quenching of the paramagnetism does not depend simply on the number of unpaired electrons. However, the value of the Weiss constant is more than doubled in going from one unpaired electron to two.

Although this quenching is apparently not simply related to the electronic configuration, we believe that there is, in fact, an approximate proportionality between the superexchange and the extent of π-bonding with the number of unpaired electrons, except for an irregularity at rhenium because of the geometry of the magnetic structure. We shall consider this structure forthwith.

Magnetic Structure of the Compounds K_2IrCl_6, K_2OsCl_6, and K_2ReCl_6

Anderson (14) has discussed the possible modes of antiferromagnetic ordering in the face-centered cubic type of lattice which can occur below the Néel temperature and has pointed out that the structure may be described by means of four sublattices, designated A, B, C, and D in Fig. 4. He has further shown that the ordering of the electron spins

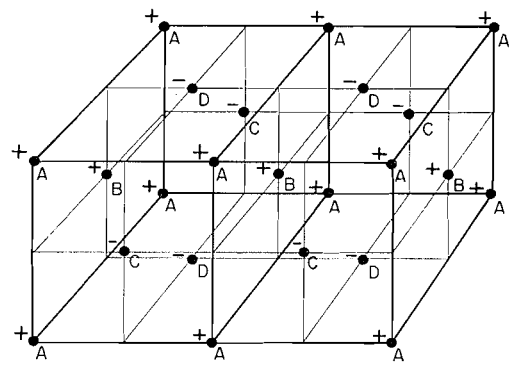


FIG. 4. Magnetic ordering in a face-centered cubic lattice.

in these sublattices may be one of three types depending upon the relative magnitudes of nearest-neighbor and next-nearest-neighbor interactions. Although neutron diffraction shows that the next-nearest-neighbor interactions are more important in many binary

Can. J. Chem. Downloaded from www.nrcresearchpress.com by 210.87.254.40 on 09/05/12
For personal use only.

compounds, such as NiO,MnSe, etc., the superexchange mechanism responsible for this, namely an Me $\uparrow$ — X — Me $\downarrow$ atomic sequence in which X is an anion possessing an occupied p-orbital lying in the axial direction, is not present in the compounds K_2MeCl_6. In these ternary complexes, the π-orbitals important to the superexchange mechanism are geometrically oriented so as to favor nearest-neighbor interactions. This is pictured in Fig. 1.

A given atom site in the face-centered cubic structure possesses 12 nearest-neighbor sites distributed equally among the other 3 sublattices. It is impossible to find an ordered arrangement in which the atom spin is antiparallel to that of all its nearest neighbors. At best, it can be antiparallel to only two thirds of them. If it be assumed that next-nearest-neighbor interaction is of minor importance, a favorable arrangement is found, with all spins in sublattices A and B, say, pointing west and those in C and D pointing east, as shown in Fig. 4. This will be allowed when the atoms of all four sublattices have an unpaired electron in either or both of the orbitals d_{xy} and d_{yz}. If such is the case, the magnetic structure would consist of an ordered system composed of sublattices A and C with antiparallel spins and, distinct from this, another like system composed of sublattices B and D. It can be seen from the diagram that an atom in sublattice B has four nearest neighbor atoms in sublattice A with the same spin. The same relation is found between the atoms of sublattices C and D. However, as long as d-electrons occupy only the pairs of orbitals d_{xy} and d_{yz}, there is no opportunity for superexchange between nearest-neighbor atoms with parallel spins.

In the event that each central atom possesses three unpaired t_{2g}-electrons, one of these must be accommodated in the d_{xz} orbital. In such a case, coupling between an atom and all of its nearest neighbors is possible. It is clear that this third unpaired electron will work against the ordering process and will decrease the magnitude of the asymptotic Curie temperature, $-\theta$, i.e. the Weiss constant, Δ.

Other ordering schemes can be proposed for the lattice, but the best schemes have the essential features in common, namely, that the ordering is perfect in the (1,0,0), (0,1,0), or (0,0,1) planes, but that each plane is not correlated with adjacent parallel planes except inasmuch as next-nearest-neighbor interactions may be favored, e.g. Anderson's "ordering of the third kind". An analogous arrangement of occupied orbitals will be set up in any case. Thus the irregularity at K_2ReCl_6 is accounted for.

SUMMARY

We conclude that the extent of π-bonding as revealed in the degree of superexchange cannot increase in proportion to the number of unpaired t_{2g}-electrons for more than two such electrons in compounds having a face-centered cubic lattice of paramagnetic atoms. It is presumed, however, that in *isolated* hexaco-ordinated complexes each t_{2g}-electron contributes equally up to the configuration t_{2g}^3 and from the configuration t_{2g}^4 to t_{2g}^6. This would likewise make feasible singly occupied π-bonds of "back-co-ordination" type, for example, in $Cr(CN)_6^{3-}$, and would account for the thermodynamic stability of such compounds.

EXPERIMENTAL

Magnetic measurements were made using a balance of the Gouy type. The maximum field strength was 5320 oersteds. Temperatures were checked by means of a thermocouple. Corrections for the underlying diamagnetism were made by using an experimental value obtained from potassium chloroplatinate. This was prepared from the same stock

Can. J. Chem. Downloaded from www.nrcresearchpress.com by 210.87.254.40 on 09/05/12
For personal use only.

chemicals as were used in the preparation of the solid solutions. The possible error due to uncertainty in the diamagnetism of the sample having the lowest iridium concentration was estimated at ±4%. The amount of ferromagnetic impurities in the samples was found to be negligible.

Potassium Hexachloroiridate (IV)

Potassium hexachloroiridate (IV) was prepared from iridium sponge supplied by Johnson, Matthey and Mallory, Limited. The metal was heated in a stream of chlorine and the resulting trichloride was dissolved in dilute hydrochloric acid. The solution was saturated with chlorine, and excess saturated potassium chloride solution was added. Anal. Calc. for K_2IrCl_6: Ir, 39.77. Found: Ir, 39.51.

Solid Solutions of K_2IrCl_6 in K_2PtCl_6

Solid solutions of K_2IrCl_6 in K_2PtCl_6 were prepared in a manner similar to that used previously for the osmium and rhenium systems (3) except that the solution of chloroiridic acid was saturated with chlorine at the time of crystallization. Debye–Scherrer diffraction patterns failed to yield an indication of heterogeneity of the products.

The separation of iridium from platinum, and its determination, were carried out using Gilchrist's procedure (15). Platinum was determined by reduction with formic acid (16).

ACKNOWLEDGMENT

This work was made possible through the support of the National Research Council.

REFERENCES

1. J. B. GOODENOUGH. Phys. Rev. **100**, 564 (1955).
2. R. N. KELLER and R. W. PARRY. *In* Chemistry of coordination compounds. *Edited by* J. C. Bailar. Reinhold, New York. 1956. p. 190.
3. A. D. WESTLAND and N. C. BHIWANDKER. Can. J. Chem. **39**, 1284 (1961).
4. B. R. JUDD. Proc. Roy. Soc. (London), A, **250**, 110 (1959).
5. A. H. COOKE, R. LAZENBY, F. R. MCKIM, J. OWEN, and W. P. WOLF. Proc. Roy. Soc. (London), A, **250**, 97 (1959).
6. J. H. E. GRIFFITHS, J. OWEN, and I. M. WARD. Proc. Roy. Soc. (London), A, **219**, 526 (1953).
7. J. H. E. GRIFFITHS and J. OWEN. Proc. Roy. Soc. (London), A, **226**, 96 (1954).
8. J. H. E. GRIFFITHS, J. OWEN, J. G. PARK, and M. F. PARTRIDGE. Proc. Roy. Soc. (London), A, **250**, 84 (1959).
9. V. NORMAN and J. C. MORROW. J. Chem. Phys. **31**, 455 (1959).
10. M. KOTANI. J. Phys. Soc. Japan, **4**, 293 (1949).
11. B. N. FIGGIS. Trans. Faraday Soc. **57**, 198 (1961).
12. E. N. SLOTH and C. S. GARNER. J. Chem. Phys. **22**, 2064 (1954).
13. A. D. WESTLAND. Unpublished results.
14. P. W. ANDERSON. Phys. Rev. **79**, 350, 705 (1950).
15. R. GILCHRIST. J. Am. Chem. Soc. **57**, 2565 (1935).
16. A. P. BLACKMORE, M. A. MARKS, R. R. BAREFOOT, and F. E. BEAMISH. Anal. Chem. **24**, 1815 (1952).

Can. J. Chem. Downloaded from www.nrcresearchpress.com by 210.87.254.40 on 09/05/12
For personal use only.

Can. J. Chem. Downloaded from www.nrcresearchpress.com by 210.87.254.42 on 09/05/12
For personal use only.

THE EFFECTS OF OPTICALLY INACTIVE IONS ON THE ROTATORY DISPERSION OF ASYMMETRIC COMPLEX IONS[1]

MARVIN J. ALBINAK,[2] DINESH C. BHATNAGAR, STANLEY KIRSCHNER, AND ANTHONY J. SONNESSA[3]

ABSTRACT

Considerable interest in the optical rotatory dispersion of asymmetric organic and inorganic compounds and its application to the elucidation of their structures has arisen in recent years. In order to study the effects of optically inactive ions on the rotatory dispersion of asymmetric complex ions, a series of salts was prepared of two active cations: levo *cis*-oxalato-bis(ethylenediamine)cobalt(III) and levo tris(ethylenediamine)chromium(III). Salts prepared included the fluoride, chloride, bromide, iodide, tetrafluoroborate, perchlorate, sulphate, and phosphate. In order to study this effect on an optically active anion, the lithium, sodium, potassium, rubidium, cesium, magnesium, calcium, and barium salts of dextro and levo tris(oxalato)-rhodate(III) were also prepared. Rotatory dispersion curves and absorption spectra were obtained for all salts in water solution. A comparison of the curves within a series showed definite trends in changes of wavelength and intensity of maxima of rotation and absorption with changes in both the ionic charge/size ratio (ionic potential) and polarizability of the optically inactive ions.

INTRODUCTION

It has been known since the time of Biot (1) that the rotation of the plane of polarized light by an optically active compound is a function of the wavelength of the incident light. This relationship between optical rotation and wavelength is known as rotatory dispersion and has been studied by several workers. Drude (2) has given an empirical equation which is sometimes useful in describing the optical rotatory dispersion of substances in wavelength regions outside the vicinity of optically active absorption bands. Reviews of optical rotatory dispersion have been published by Levene and Rothen (3), Lowry (4), Heller (5), Klyne and Parker (6), Moscowitz (7), and others (8). Cotton (9) has described the so-called "anomalous rotatory dispersion" of asymmetric compounds in the vicinity of their optically active absorption bands, and several workers (10, 5, 6, 7, 8, 11) have studied this effect in an effort to correlate it with various structural aspects of the compounds studied.

The rotatory dispersion of asymmetric complex inorganic compounds has been studied by several investigators, including Shimura (12), Izumiya (13), Jaeger (11), O'Brien and co-workers (14), Jonassen and Bailar (15), Martinette and Bailar (16), Pfeiffer (17), Mellor (18), and others.

Kirschner and co-workers (19, 20), Albinak (21), and Sonnessa (22) have noticed that the optical rotation and rotatory dispersion of an asymmetric complex ion change when the optically inactive ion associated with it is changed. A further study of this effect resulted in the initiation of an investigation to determine the effects of optically inactive ions on the rotatory dispersion of asymmetric complex ions. In order to facilitate the study of rotatory dispersion of complexes, a special spectrophotometric photoelectric polarimeter was constructed (19).

In this investigation, it was decided first to prepare and resolve several asymmetric complex cations, each with various optically inactive anions, and then to do the same

[1]*Manuscript received June 30, 1961.*
Contribution from the Department of Chemistry, Wayne State University, Detroit, Michigan, U.S.A. Presented in part before the Symposium on Co-ordination in Chemistry, Chemical Institute of Canada, Hamilton, Ontario, May 15–16, 1961.
[2]*Present address: Department of Chemistry, University of Detroit, Detroit 21, Michigan, U.S.A.*
[3]*Present address: Department of Chemistry, Seton Hall University, South Orange, New Jersey, U.S.A.*

Can. J. Chem. Downloaded from www.nrcresearchpress.com by 210.87.254.42 on 09/05/12
For personal use only.

for several asymmetric complex anions, each with various optically inactive cations. The rotatory dispersions of all these series of complexes were measured, and they were studied with a view toward determining which characteristics of the optically inactive ions contributed most to the rotatory dispersion changes and which were less important. The first series of asymmetric ions studied contained no asymmetric ligands and their asymmetry was due solely to the configuration of the optically inactive ligands about the central metal ion. Subsequent series of complexes contained asymmetric ligands, e.g., $[Co(NH_3)_4(d\text{-tart})]^+$, but these ions did not have the asymmetric configuration about the metal ion which is found in ions such as tris(ethylenediamine)cobalt(III), $[Co(en)_3]^{+3}$. Additional studies are underway to determine the effects of solvent polarity on rotatory dispersion changes as well as the effects of "loading" a solution containing an asymmetric complex ion with an optically inactive ion of opposite charge on the rotatory dispersion. Further studies are also underway to examine the effects of optically inactive ions on the rotatory dispersion of asymmetric inner complexes and the effects of absolute configuration changes on rotatory dispersion.

EXPERIMENTAL

A High Precision Spectrophotometric Photoelectric Polarimeter for the Determination of Optical Rotation and Optical Rotatory Dispersion

Although photographic spectropolarimetry has certain unique advantages (5) with respect to long exposure possibilities in cases of low intensity, relatively wide spectral range, high sensitivity, and relative ease of measuring extremely large rotations (e.g., 360°) the procedures involved are usually quite inconvenient and time consuming. Consequently, most of the commercially available spectropolarimeters, as well as those constructed by individual research investigators, utilize photoelectric cells as light receptors. Some of the commercially available instruments include those manufactured by the Photovolt Corporation (95 Madison Ave., New York 16, N.Y.) based on an instrument described by Crumpler, Dyre, and Spell (23); Carl Zeiss, Inc. (485 Fifth Ave., New York 17, N.Y.) (24); Bellingham and Stanley (71, Hornsey Rise, London N. 19, England; Epic Inc., 154 Nassau St., New York 38, N.Y.); O. C. Rudolph and Sons, Inc. (P.O. Box 446, Caldwell, N.J., and Little Falls, N.J.) (25, 26); Perkin–Elmer Corp. (Norwalk, Conn.) (27); and others. Several interesting and unique photoelectric polarimeters, spectrophotometric polarimeters, and recording spectropolarimeters have been constructed in research laboratories throughout the world. Among these are those of Gillham (28), Malcolm and Elliott (29), Burer, Kohler, and Gunthard (30), Gates (31), Bruhat and co-workers (32), von Halban (33), Landt and Hirschmuller (34), Levy (35), Brode (36), Gutowski (37), Woldbye (38), and others (39). The foregoing instruments, however, may have, for many scientists engaged in research in optical rotatory dispersion today, one or more of the following shortcomings: (*a*) a limited wavelength range not extending into the ultraviolet region; (*b*) a precision no better than 0.01°; (*c*) a high degree of elaborateness and complexity, often making it impractical for many investigators to reconstruct such an instrument without the aid of professional technicians; (*d*) the need for time-consuming manipulations to operate the instrument; and (*e*) relatively high cost.

An interesting, commercially available attachment for the Beckman DU spectrophotometer has been developed by the Standard Polarimeter Company (6 Banta Place, Hackensack, N.J.), according to a design by Keston (40). This unit has been evaluated by Poulsen (41, 42). It utilizes light sources which are normally associated with the

Beckman spectrophotometer, and Polaroid plates (rather than polarizing prisms) which severely restrict the use of the instrument to solutions of relatively low optical density, to a limited range of wavelengths in the visible region, and sometimes to low precision.

The authors have described the construction and operation of a spectrophotometric polarimeter of high precision which can be assembled in most laboratories at relatively low cost (19, 43). It has a wavelength region of 2,600 Å to 10,000 Å; a precision of 0.002° when measuring small observed angles of rotation ($< 1°$); completely variable angles between transmission planes of polarizer and analyzer prisms, allowing for the measurement of observed angles of rotation greater than 1°; and it requires only about 30 minutes to determine an "average" rotatory dispersion curve from 2,600 Å to 7,000 Å. The mathematical principles of operation governing this type of instrument are in the literature (5, 41, 42, 44).

INSTRUMENTAL RESULTS

Table I shows a comparison between the optical rotations of various solutions determined with a high-precision visual polarimeter equipped with a sodium lamp and filter

TABLE I

Comparison of optical rotations of sugar solutions

Sample number	Observed rotation,* deg (visual polarimeter)	Observed rotation,† deg (spectrophotometric polarimeter)
1	0.053±0.003	0.050±0.002
2	0.102±0.003	0.100±0.002
3	0.184±0.003	0.180±0.002
4	0.213±0.003	0.213±0.002
5	0.368±0.003	0.369±0.002

*Na_D line; Rudolph High Precision Visual Polarimeter, Model 80.
†Na_D line.

for the D line, and those determined with the instrument constructed by the authors at the same wavelength.

The average deviation of individual determinations of angles less than 1° is 0.002° with this instrument. Although, theoretically, a high degree of elliptical polarization in the region of a strong Cotton effect (9) would produce a shift in the rotatory dispersion (5), the small angles of rotation measured and the small angle used for the sweep of the analyzer prism of this instrument minimize this effect. Actually, this effect was not observed in the optically active absorption band of potassium chromium tartrate, the very compound studied by Cotton (9) in his work on anomalous rotatory dispersion (Fig. 1).

Compounds Studied

A list of the optically active complex ions studied, along with the optically inactive ions associated with them, is given in Table II.

Preparations

1. *L-cis*-$[Co(en)_2(NO_2)_2]Br$ was prepared and resolved according to the method of Dwyer, Gyarfas, and Mellor (45).

2. *L*-$[Co(en)_3]Cl_3$ was prepared and resolved according to the method of Werner (46).

Can. J. Chem. Downloaded from www.nrcresearchpress.com by 210.87.254.42 on 09/05/12
For personal use only.

TABLE II

Optically active complex ions studied and their associated optically inactive ions

Optically active complex ion*	Associated optically inactive ions
L-*cis*-$[Co(en)_2(NO_2)_2]^+$	F^-, Cl^-, Br^-, I^-, $SO_4^=$, PO_4^{-3}, ClO_4^-, ClO_3^-, NO_3^-, $(C_6H_5)_4B^-$
L-$[Co(en)_3]^{+3}$	F^-, Cl^-, Br^-, I^-, $SO_4^=$, ClO_4^-, ClO_3^-, NO_3^-, PO_4^{-3}
L-$[Co(edta)]^-$	Li^+, Na^+, K^+, Rb^+, Cs^+, Mg^{++}, Ba^{++}, Al^{+3}
L-$[Cr(en)_3]^{+3}$	F^-, Cl^-, Br^-, I^-, BF_4^-, ClO_4^-, $SO_4^=$, PO_4^{-3}
D-$[Rh(ox)_3]^{-3}$	Li^+, Na^+, K^+, Rb^+, Cs^+, Mg^{++}, Ca^{++}, Ba^{++}
$[Co(NH_3)_4$(*d*-tart)$]^+$	F^-, Cl^-, Br^-, I^-, BF_4^-, NO_3^-, ClO_4^-, $SO_4^=$, PO_4^{-3}
$[Pt$(*l*-alan)$Cl_2]^-$	Li^+, Na^+, K^+, Rb^+, Cs^+, Mg^{++}, Ca^{++}, Ba^{++}, Al^{+3}
$[Pt$(*d*-glut)$_2]^=$	Li^+, Na^+, K^+, Rb^+, Cs^+, Mg^{++}, Ca^{++}, Ba^{++}, Al^{+3}
$[Co(NH_3)_5$(*d*-tart)$]^+$	F^-, Cl^-, Br^-, I^-, BF_4^-, NO_3^-, ClO_4^-, $SO_4^=$, PO_4^{-3}

*Abbreviations used: en = ethylenediamine; edta = ethylenediaminetetraacetate anion; ox = oxalate anion; *d*-tart = dextro tartrate anion; *l*-alan = levo alaninate anion; *d*-glut = dextro glutamate anion.

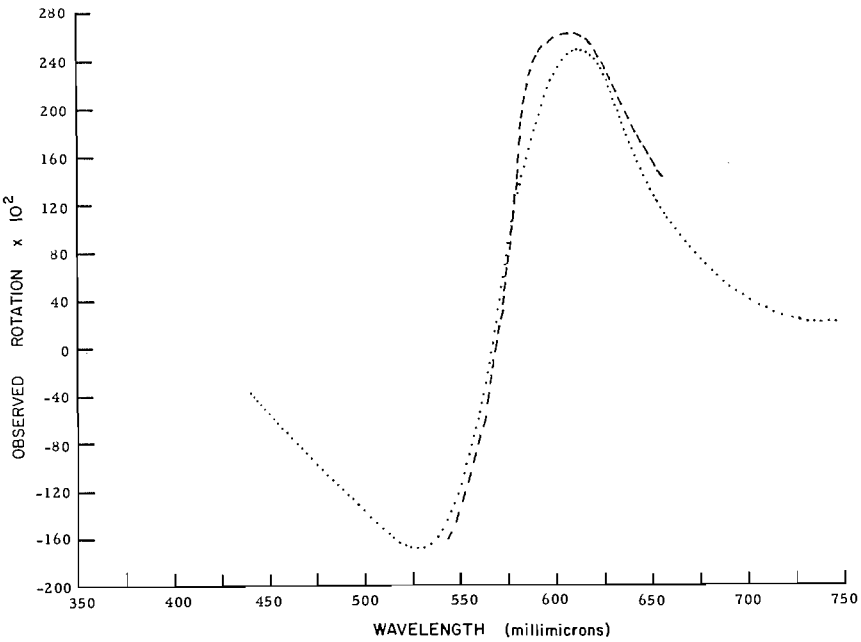


FIG. 1. Elliptical polarization and the Cotton effect. The rotatory dispersion of potassium chromium tartrate: ... curve from spectropolarimeter; – – – curve by Cotton.

3. *L*-K[Co(edta)] was prepared and resolved according to the method of Dwyer and Garvan (47).

4. *L*-$[Co(en)_2Cl_2]Cl$ was prepared and resolved according to the method of Bailar (48). It was converted to *L*-$[Co(en)_2(ox)]Cl$ according to the method of Werner (49).

5. *L*-$[Cr(en)_3]I_3$ was prepared and resolved by Albinak and co-workers of the University of Detroit and presented as a gift to this research group.

6. *D*-$K_3[Rh(ox)_3]$ was prepared and resolved by Dwyer (50).

7. K[Pt(*l*-alan)Cl_2] was prepared according to the method of Ley and Ficken (51).

8. $H_2[Pt($*d*-glut$)_2]$ was prepared according to the method of Grinberg (52).

9. $[Co(NH_3)_5$(*d*-tart)$]Cl$ was prepared according to the method of Duff (53).

10. $[Co(NH_3)_4CO_3]Cl$ was prepared according to the method of Lamb (54). It was converted to $[Co(NH_3)_4$(*d*-tart)$]Cl$ by treating 6.0 g of the carbonato complex in 100 ml

Can. J. Chem. Downloaded from www.nrcresearchpress.com by 210.87.254.42 on 09/05/12
For personal use only.

of water with 100 ml of an aqueous solution containing 4.1 g of dextro tartaric acid. This solution was added dropwise with continuous stirring. After the bubbles of carbon dioxide had ceased to be evolved, the solution was evaporated almost to dryness by passage of a stream of dry air over it. The resulting dark red, viscous semisolid substance was washed with 100 ml of ethanol and then ground in a mortar under absolute ethanol (the compound is hygroscopic). It was then filtered, washed with ether, and dried under vacuum. The yield of the dark red powder was 5.7 g (62%). Analysis: Calc. for $[Co(NH_3)_4(d\text{-tart})]Cl \cdot H_2O$: C, 14.60; H, 5.48; N, 17.02; Cl, 10.80. Found: C, 15.22; H, 5.71; N, 16.82; Cl, 11.33.

Rotatory Dispersion Curves

These were determined either on the instrument constructed by the authors or on a manual Rudolph High Precision Photoelectric Spectropolarimeter (26). The curves show wavelength vs. "equivalent molecular rotation", $[\alpha]_E$, which is used to eliminate nonreal differences in ion effects which may appear when molecular rotations are used for compounds where the cation:anion ratio is other than 1:1, e.g., $[Co(en)_2(NO_2)_2]Cl$ vs. $[Co(en)_2(NO_2)_2]_2SO_4$. Equivalent molecular rotation is defined as

$$[\alpha]_E = [\alpha]M/n,$$

where M = molecular weight, n = number of optically active complex ions per molecule, and $[\alpha]$ = specific rotation.

RESULTS AND DISCUSSION

A typical series of rotatory dispersion curves is shown in Fig. 2. In general, the wavelengths of the peaks, troughs, and crossover points (positive to negative crossover in

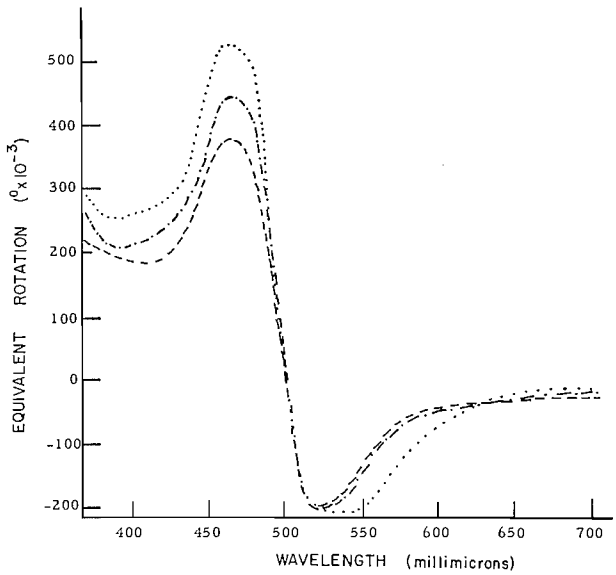


FIG. 2. Optical rotatory dispersion of L-$[Co(en)_3]^{+3}$ salts: – – – chloride; –·– bromide; . . . iodide.

sign of rotation, or vice versa) are fairly constant with change of optically inactive ion, but the magnitudes of rotation at these locations often vary considerably. Data on these magnitudes are given in Tables III–VIII along with the optical absorption maxima.

Can. J. Chem. Downloaded from www.nrcresearchpress.com by 210.87.254.42 on 09/05/12
For personal use only.

Can. J. Chem. Downloaded from www.nrcresearchpress.com by 210.87.254.42 on 09/05/12
For personal use only.

TABLE III

Comparison of rotatory dispersion of salts of levo tris(ethylenediamine)cobalt(III) ion

Anion	"Zero"	Negative maximum		"Zero"	Positive maximum		Trough		Absorption maximum
	λ	λ	$[\alpha]_E^0 \times 10^{-3}$	λ	λ	$[\alpha]_E^0 \times 10^{-3}$	λ	$[\alpha]_E^0 \times 10^{-3}$	λ
F^-	—	521	−250	497	463	480	380	214M	420
Cl^-	—	523	−205	494	463	380	400	183	470
Br^-	645	515	−225	496	455	445	380	204	470
I^-	—	(515–530)	−250	497	455	535	380	256	470
$SO_4^=$	—	520	−220	494	470	448	390	200	470
ClO_4^-	—	515	−263	495	460	500	393	229	470
ClO_3	—	520	−250	497	463	490	380	223	470
NO_3^-	—	520	−220	495	460	450	395	220	470
$PO_4^=$	—	518	−250	497	470	460	395	150	470

TABLE IV

Comparison of rotatory dispersion of salts of levo ethylenedinitrilotetraacetatocobaltate(III) ion

Cation	First positive maximum		Zero I	Negative maximum		Zero II	Second positive maximum		Trough		Absorption maximum
	λ	$[\alpha]_E^0 \times 10^{-3}$	λ	λ	$[\alpha]_E^0 \times 10^{-3}$	λ	λ	$[\alpha]_E^0 \times 10^{-3}$	λ	$[\alpha]_E^0 \times 10^{-3}$	λ
Li^+	625	230	585	555	−285	494	440	175	410	65	538
Na^+	625	212	587	545	−282	495	443	170	410	82	538
K^+	625	171	592	545	−350	495	462	130	410	50	537
Rb^+	625	218	587	545	−277	497	440	176	410	104	537
Mg^{++}	625	143	589	550	−275	495	440	124	405	67	518
Al^{+++}	625	180	587	550	−260	496	440	158	400	35	537
Ba^{++}	625	122	588	548	−195	503	437	140	410	35	538

NOTE: all wavelengths are in millimicrons.

Can. J. Chem. Downloaded from www.nrcresearchpress.com by 210.87.254.42 on 09/05/12
For personal use only.

TABLE V

Wavelengths and magnitude of selected points on rotatory dispersion and absorption curves of salts of levo *cis*-oxalato-bis(ethylenediamine)cobalt(III) ion

	Maximum		Zero	First minimum		Saddle point	Second minimum		Absorption maximum	
Anion	λ	$[\alpha]_E^0 \times 10^{-4}$	λ	λ	$[\alpha]_E^0 \times 10^{-4}$	λ	λ	$[\alpha]_E^0 \times 10^{-4}$	λ	a_E
F^-	560	13.7	528	480	−19.0	370	305	−33.0	495	220
Cl^-	558	12.0	526	478	−14.6	380	305	−30.6	495	216
Br^-	560	10.9	526	480	−15.1	375	305	−28.2	495	210
I^-	560	8.5	527	480	−11.3	370	305	−22.5	495	229
BF_4^-	563	9.0	528	485	−13.6	375	305	−24.6	495	201
ClO_4^-	560	14.8	527	478	−21.2	375	305	−34.8	495	213
$SO_4^=$	560	7.0	528	480	−10.2	373	305	−16.8	495	222
$PO_4^{\equiv}$	565	10.6	527	485	−13.7	375	305	−27.8	495	162

NOTE: all wavelengths are in millimicrons.

TABLE VI

Wavelengths and magnitude of selected points on rotatory dispersion and absorption curves of salts of levo tris(ethylenediamine)chromium(III) ion

	Minimum		Zero	Maximum		Trough	First absorption maximum		Second absorption maximum	
Anion	λ	$[\alpha]_E^0 \times 10^{-4}$	λ	λ	$[\alpha]_E^0 \times 10^{-4}$	λ	λ	a_E	λ	$a_E \times 10^{-3}$
F^-	490	−10.5	464	420	21.0	355	460	115	350	4.9
Cl^-	490	− 8.1	466	420	14.3	355	460	86.5	350	2.6
Br^-	490	−10.0	465	420	20.6	358	460	125	350	4.0
I^-	490	−13.4	463	418	24.2	355	460	136	350	2.5
BF_4^-	490	− 6.1	464	418	11.9	355	460	114	350	3.4
ClO_4^-	490	−11.6	464	420	22.8	358	460	132	350	5.3
$SO_4^=$	490	− 9.7	464	420	17.8	360	460	125	350	4.0
$PO_4^{\equiv}$	490	− 6.3	464	420	11.8	360	460	110	350	2.0

NOTE: all wavelengths are in millimicrons.

Can. J. Chem. Downloaded from www.nrcresearchpress.com by 210.87.254.42 on 09/05/12
For personal use only.

TABLE VII

Wavelengths and magnitude of selected points on rotatory dispersion and absorption curves of salts of dextro tris(oxalato)rhodate(III) ion

	Zero I	Maximum		Zero II	Minimum		Absorption maximum	
Cation	λ	λ	$[\alpha]^0_E \times 10^{-4}$	λ	λ	$[\alpha]^0_E \times 10^{-4}$	λ	a_E
Li^+	590	460	12.0	427	360	−48.3	400	225
Na^+	589	460	13.7	427	360	−52.8	400	360
K^+	589	460	17.7	427	360	−65.3	400	435
Rb^+	589	460	14.4	427	360	−59.2	400	522
Cs^+	589	460	14.7	427	350	−61.8	400	480
Mg^{++}	595	455	3.9	420	370	− 9.5	400	291
Ca^{++}	595	460	14.4	426	360	−51.6	400	330
Ba^{++}	590	460	19.5	422	360	−54.6	400	465

NOTE: all wavelengths are in millimicrons.

TABLE VIII

Wavelengths and magnitude of selected points on rotatory dispersion and absorption curves of salts of dextro tartrato-tetramminecobalt(III) ion

	First maximum		Zero I	Minimum		Zero II	Absorption maximum
Anion	λ	$[\alpha]^0_E \times 10^{-2}$	λ	λ	$[\alpha]^0_E \times 10^{-2}$	λ	λ
F^-	540	+495	503	480	−180	440	520
Cl^-	540	+305	498	480	− 65	452	520
Br^-	540	+310	487	480	− 65	458	520
I^-	540	+430	500	480	−140	450	520
BF_4^-	540	+305	494	480	− 42	465	520
ClO_4^-	540	+215	500	480	− 65	478	520
$SO_4^=$	540	+245	494	480	− 80	450	520
$PO_4^{\equiv}$	540	+495	502	480	− 65	460	520
NO_3^-	540	+305	460	480	0	470	0

NOTE: all wavelengths are in millimicrons.

It appears that the changes in the magnitudes of optical rotation are related to the degree of ion pairing between the optically active and optically inactive ions. Illustrative of this are the plots of equivalent molecular rotation vs. "ionic potential" (ionic charge/ionic radius) (55), an example of which is given in Fig. 3. This effect is observed whether

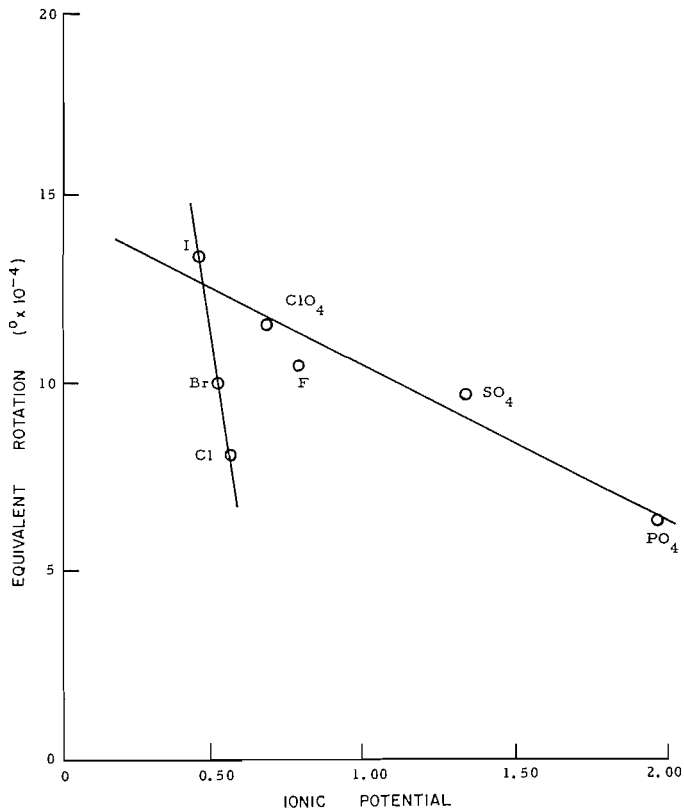


FIG. 3. Equivalent rotation vs. ionic potential for L-$[Cr(en)_3]^{+3}$ cation series.

the optically active complex ions are asymmetric solely because of the configuration of optically inactive ligands about a metal ion or because of the presence of optically active ligands without this type of configuration, e.g., $[Co(NH_3)_4(d\text{-tart})]^+$.

ACKNOWLEDGMENTS

The authors wish to express their sincere appreciation to the National Science Foundation for a grant without which this work could not have been carried out, to the American Cancer Society for an emergency grant which permitted the purchase of an important part of the instrument for which funds were unavailable, to Professor Wilfried Heller of Wayne State University for his helpful suggestions and comments on theory and design, and to Mr. Lee Peterson of Wayne State University for his help in the design and construction of the prism brackets and other metal parts.

REFERENCES

1. J. BIOT. Mem. Inst. **13**, *i*, 1 (1812).
2. P. DRUDE. Lehrbuch der Optik. 2nd ed. S. Hirzel, Verlag, Leipzig. 1906.
3. P. LEVENE and A. ROTHEN. *In* Organic chemistry, an advanced treatise. *Edited by* H. Gilman. John Wiley & Sons, New York. 1938.

Can. J. Chem. Downloaded from www.nrcresearchpress.com by 210.87.254.42 on 09/05/12
For personal use only.

4. T. Lowry. Optical rotatory power. Longmans, Green and Co., Ltd., London. 1935.
5. W. Heller and D. Fitts. *In* Physical methods of organic chemistry. 3rd ed. Vol. 1. Part 3. *Edited by* A. Weissberger. Interscience Publishers, New York. 1960. Chap. 33.
6. W. Klyne and A. Parker. *In* Physical methods of organic chemistry. 3rd ed. Vol. 1. Part 3. *Edited by* A. Weissberger. Interscience Publishers, New York. 1960. Chap. 34.
7. A. Moscowitz. *In* Optical rotatory dispersion. *By* C. Djerassi. McGraw-Hill Book Co., Inc., New York. 1960. Chap. 12.
8. W. Kauzmann, J. Walter, and H. Eyring. Chem. Revs. **26**, 339 (1940). E. Condon. Revs. Modern Phys. **9**, 432 (1937). W. Kuhn. Ann. Rev. Phys. Chem. **9**, 417 (1958). W. Moffitt. J. Chem. Phys. **25**, 1189 (1956). M. Powell. Endeavor, **15**, 20 (1956). M. Vol'kenshtein. Zhur. Eksptl. i Teoret. Fiz. **20**, 342 (1950). R. Servant. J. phys. radium, **3** (8), 90 (1942). J. Kirkwood. J. Chem. Phys. **5**, 479 (1937). M. Born. Proc. Roy. Soc. (London), A, **150**, 84 (1935); A, **153**, 339 (1936). M. Betti. Trans. Faraday Soc. **26**, 337 (1930). C. Djerassi. Optical rotatory dispersion. McGraw-Hill Book Co., Inc., New York. 1960.
9. A. Cotton. Compt. rend. **120**, 989, 1044 (1895); Ann. chim. et phys. **8**, 347 (1896).
10. C. Djerassi. Optical rotatory dispersion. McGraw-Hill Book Co., Inc., New York. 1960.
11. F. Jaeger. Optical activity and high temperature measurements. McGraw-Hill Book Co., Inc., New York. 1930.
12. Y. Shimura. Bull. Chem. Soc. Japan, **31**, 315 (1958).
13. N. Izumiya. J. Am. Chem. Soc. **78**, 1602 (1956).
14. T. O'Brien and R. Tool. J. Am. Chem. Soc. **77**, 1368 (1955). T. O'Brien, J. McReynolds, and J. Bailar, Jr. J. Am. Chem. Soc. **70**, 749 (1948).
15. H. Jonassen and J. Bailar, Jr. J. Am. Chem. Soc. **70**, 756 (1948).
16. Sr. M. Martinette and J. Bailar, Jr. J. Am. Chem. Soc. **74**, 1054 (1952).
17. P. Pfeiffer. J. prakt. Chem. **150**, 261 (1938).
18. D. P. Mellor. Australian J. Sci. **3**, 99 (1941); J. Proc. Roy. Soc. N. S. Wales, **75**, 157 (1942).
19. S. Kirschner, A. J. Sonnessa, D. Bhatnagar, and D. Moy. Abstracts of Papers, 14N, Division of Inorganic Chemistry, 138th Meeting of the American Chemical Society, New York. 1960.
20. S. Kirschner and D. Bhatnagar. Abstracts of Papers, 11B, Division of Analytical Chemistry, 138th Meeting of the American Chemical Society, New York. 1960.
21. M. Albinak. Dissertation, Wayne State University, Detroit, Mich. 1958.
22. A. Sonnessa. Dissertation, Wayne State University, Detroit, Mich. 1960.
23. T. Crumpler, W. Dyre, and A. Spell. Anal. Chem. **27**, 1645 (1955).
24. Zeiss Werkzeitschrift, **26**, 103 (1957).
25. H. Rudolph. J. Opt. Soc. Am. **45**, 50 (1955).
26. E. Brand, E. Washburn, B. Erlanger, E. Ellenbogen, F. Lippman, and M. Scheu. J. Am. Chem. Soc. **76**, 5037 (1954).
27. A. Savitzky, W. Slavin, and R. Salinger. Pittsburgh Conference on Analytical Chemistry and Applied Spectroscopy. Mar. 3, 1959.
28. E. J. Gillham. Nature, **178**, 1412 (1956); J. Sci. Instr. **34**, 435 (1957).
29. B. Malcolm and H. Elliott. J. Sci. Instr. **34**, 48 (1957).
30. T. Burer, M. Kohler, and H. Gunthard. Helv. Chim. Acta, **41**, 2216 (1958). H. Hedriger and H. Gunthard. Helv. Chim. Acta, **37**, 1125 (1954).
31. J. Gates. Chem. & Ind. (London), 190 (1958).
32. G. Bruhat, A. Blanc-Lapierre, J. Schlitz, and G. Raoult. Compt. rend. **214**, 615 (1942). G. Bruhat and M. Pauthenier. Rev. opt. **6**, 163 (1927).
33. H. von Halban. Nature, **119**, 86 (1927).
34. E. Landt and H. Hirschmuller. Deut. Zuckerind. **62**, 647 (1937).
35. G. Levy. Anal. Chem. **23**, 1089 (1951). G. Levy, P. Schwed, and D. Fergus. Rev. Sci. Instr. **21**, 693 (1950).
36. W. Brode. J. Opt. Soc. Am. **41**, 987 (1951).
37. H. Gutowski. J. Chem. Phys. **19**, 438 (1951).
38. F. Woldbye. Acta Chem. Scand. **13**, 2137 (1959).
39. S. Mitchell and J. Veitch. Nature, **168**, 662 (1951). D. Rank. J. Sci. Instr. **27**, 270 (1950). E. Willey. J. Sci. Instr. **20**, 74 (1943). G. Landegren. Rev. Sci. Instr. **26**, 502, 578 (1955). H. Wenking. Z. Instrumentenk. **66**, 1 (1958). D. Rank, J. Light, and P. Yodor. J. Sci. Instr. **27**, 270 (1950).
40. A. Keston. Abstract of Papers, 18C, Division of Biological Chemistry, 127th Meeting of the American Chemical Society, Cincinnati, Ohio. 1955. A. Keston and J. Lospalluto. Federation Proc. **12**, 229 (1953).
41. K. Poulsen. Anal. Chem. **32**, 410 (1960).
42. P. Gallop. Rev. Sci. Instr. **28**, 209 (1957).
43. M. J. Albinak, D. C. Bhatnagar, S. Kirschner, and A. J. Sonnessa. *In* Advances in the chemistry of the coordination compounds. *Edited by* S. Kirschner. Macmillan Co., New York, N.Y. 1961.
44. Standard Polarimeter Company. Bulletin No. 2.
45. F. Dwyer, E. Gyarfas, and D. Mellor. J. Phys. Chem. **59**, 296 (1955). F. Dwyer and F. Garvan. *In* Inorganic syntheses. Vol. 6. *Edited by* E. Rochow. McGraw-Hill Book Co., Inc., New York. 1960. p. 195.
46. A. Werner. Ber. **45**, 121 (1912).
47. F. Dwyer and F. Garvan. *In* Inorganic syntheses. Vol. 6. *Edited by* E. Rochow. McGraw-Hill Book Co., Inc., New York. 1960. p. 192.
48. J. Bailar, Jr. *In* Inorganic syntheses. Vol. 2. *Edited by* W. Fernelius. McGraw-Hill Book Co., Inc., New York. 1946. p. 222.

Can. J. Chem. Downloaded from www.nrcresearchpress.com by 210.87.254.42 on 09/05/12
For personal use only.

49. A. WERNER. Ber. **45**, 3286 (1912).
50. F. DWYER. J. Phys. Chem. **60**, 1331 (1956).
51. H. LEY and K. FICKEN. Ber. **45**, 380 (1912).
52. A. GRINBERG. Neorg. Khim. Akad. Nauk, S.S.S.R. No. 29, 37 (1955).
53. J. DUFF. J. Chem. Soc. **123**, 563, 569 (1923).
54. A. LAMB. J. Am. Chem. Soc. **59**, 385 (1937).
55. G. CARTLEDGE. J. Am. Chem. Soc. **50**, 2855, 2863, (1928); **52**, 3076 (1930).

Can. J. Chem. Downloaded from www.nrcresearchpress.com by 210.87.254.42 on 09/05/12
For personal use only.

Can. J. Chem. Downloaded from www.nrcresearchpress.com by 210.87.254.5 on 09/05/12
For personal use only.

SUBSTITUTION AT OCTAHEDRAL CENTERS

II. EFFECT OF SALTS UPON THE RATE OF HYDROLYSIS OF THE HALOPENTAMMINECHROMIUM(III) IONS[1,2]

T. P. JONES,[3] W. E. HARRIS, AND W. J. WALLACE

ABSTRACT

A study of the hydrolysis of the halopentamminechromium(III) ions in the presence of the sodium salts of weak acids reveals a rate acceleration due to specific ion-pair formation. The acceleration is due partly to a charge-transfer effect and partly to the fact that the ion helps to maintain the octahedral configuration of the complex in the transition state. It is concluded that the reaction occurs by dissociation, but without collapse of the structure to a five-co-ordinated intermediate.

INTRODUCTION

In many of the studies of reactions in inorganic systems which have appeared in recent years, the problem of incidental electrolyte has been taken into account by means of a constant "swamping" concentration of some "inert" electrolyte (1). Frequently, but not universally, sodium perchlorate has been used for this purpose. As a result, the literature shows data obtained under circumstances in which both the nature and concentration of the added salts differ markedly. Any attempt to intercompare such data is necessarily attended by assumptions about the effect of the electrolyte upon the reaction. In recent years a number of investigations have indicated a specificity in the influence of electrolytes upon the kinetics of both ionic and non-ionic reactions. Olson and Simonson (2) have shown that such effects are related to the ion which is opposite in charge to the one which is undergoing reaction. The influence of nitrate and sulphate upon the rate of hydrolysis of chloropentamminecobalt(III) had been observed earlier by Garrick (3). Sulphate was observed to have a marked accelerating effect upon the reaction, while nitrate at equivalent concentration exerted only a minor catalytic effect.

Recently, Taube and Posey (4) showed that reaction I, which proceeds predominantly through the ion pair (B), is sensitive to the presence of excess electrolyte. Thus, the rate of formation of the sulphato complex (A) is markedly decreased by the addition of sodium perchlorate. This is not surprising for a reaction which proceeds through the ion-pair intermediate (B). The addition of electrolyte reduces the activity coefficient of the ions in (C) so that the concentration of the ion-pair intermediate is decreased. It is perhaps

$$\underset{(A)}{Co(NH_3)_5SO_4^+} + H_2O \leftrightarrows \underset{(B)}{(Co(NH_3)_5H_2O^{+++}SO_4^{=})} \leftrightarrows \underset{(C)}{Co(NH_3)_5H_2O^{+++}} + SO_4^{=} \qquad [I]$$

surprising, however, that the rate of the hydrolysis was also decreased. There is no theoretical precedent for this. In these circumstances it is tempting to attribute this change in rate to a decrease in the concentration of ion pairs formed by the sulphato complex (A). The force of this interpretation is increased by the observation that both the sulphation and hydrolysis reactions are faster in the presence of increasing concentrations of sulphate. Although such observations as these do not demonstrate conclusively

[1]*Manuscript received June 30, 1961.*
Contribution from the Department of Chemistry, University of Alberta, Edmonton, Alberta. Presented at the Symposium on Co-ordination in Chemistry, Chemical Institute of Canada, Hamilton, Ontario, May 15–16, 1961.

[2]*The first paper in this series is considered to be reference 7.*

[3]*International Nickel Company Fellow, 1960–61; holder of National Research Council of Canada summer fellowships, 1959, 1961.*

that specific interaction complexes described as outer sphere ion pairs (4) participate in the rate-determining step of ionic reactions in solution they certainly do not argue against it. The specificity of the electrolyte effect is further borne out by the observations of other workers (5, 6).

The work reported in this paper is an outgrowth of that reported earlier (7) on the pH-independent hydrolysis of the halopentamminechromium(III) ions. It was found that the pH-independent hydrolysis reaction extended far up into the high pH region. Consequently the system proved convenient for the study of the effect of anions of a number of weak acids upon the rate of an uncomplicated hydrolysis reaction. In this way it has been possible to study the specificity of electrolyte effect in hydrolysis reactions on the basis of the base strength of the anion which was involved.

EXPERIMENTAL

Preparation of Materials

The chloro-, bromo-, and iodo-pentamminechromium(III) halides and perchlorates were prepared as described previously (7). Other materials were reagent grade and were used without further purification.

Kinetic Measurements

Solutions were prepared by mixing, in a volumetric flask, the calculated volume of stock solution of the sodium salt of the anion under investigation and enough halopentamminechromium(III) salt to make the final solution 10^{-3} M in chromium, agitating the mixture to dissolve the chromium salt, and diluting it to volume. The solution was placed in a water bath and allowed to come to temperature (10–20 minutes) before measurements were initiated by withdrawing a sample. In those solutions in which the anion concentration was below 0.005 M it was found desirable to increase the buffer capacity of the solution by the addition of an ammonia – ammonium perchlorate buffer. In these cases a pH of 8 was maintained by a buffer mixture whose ammonium perchlorate concentration was 0.01 M.

Samples withdrawn for analysis were run into a polarographic cell maintained at 0° C in a Dewar. The polarographic cell contained sufficient sulphuric or perchloric acid to convert all of the anion to the acid form and leave the final solution 0.1 M in hydrogen ion. The amount of acid required depended upon the nature and concentration of the anion in the reactive solution, but was never great enough to cause significant dilution. The concentrations of chromium species remaining in the solution were then determined polarographically as described previously (7). The initial polarographic measurements were made in the presence of perchloric acid and the later measurements with sulphuric acid. The change from perchloric to sulphuric acid was made when it was found that a better separation between the halo- and aquo-pentamminechromium(III) reduction waves was obtained in a sulphate-containing medium. Presumably this is related to the fact that the aquo complex would be expected to form a stronger ion pair than the chloro complex with sulphate. The anion present during the polarographic measurements did not influence the results in any way other than to increase the ease of interpretation of the polarograms.

The only anions which were polarographically reducible in the potential range of the chromium complexes under the conditions of low pH described above were fumarate and maleate. Fortunately the reduction potential for these anions was pH dependent, and by variation of the acidity of the solution it was possible to change the potential at

Can. J. Chem. Downloaded from www.nrcresearchpress.com by 210.87.254.5 on 09/05/12
For personal use only.

which reduction of these anions occurred to a value where they did not interfere with the determination of the concentration of the chromium species in the solution. The most convenient pH for the polarographic analysis of the fumarate solution was 6 and for the maleate was 8. In the analysis of these solutions the procedure involved quenching the reaction with ice-cold concentrated buffer of the appropriate pH instead of concentrated acid.

EXPERIMENTAL RESULTS

The effect exerted by a number of monovalent anions upon the rate of the reaction represented by equation [II], where X is Cl, Br, or I is shown in Fig. 1.

$$Cr(NH_3)_5X^{++} + H_2O \xrightarrow[\text{base}]{\text{anion}} Cr(NH_3)_5OH^{++} + X^- + \text{base } H^+ \qquad [II]$$

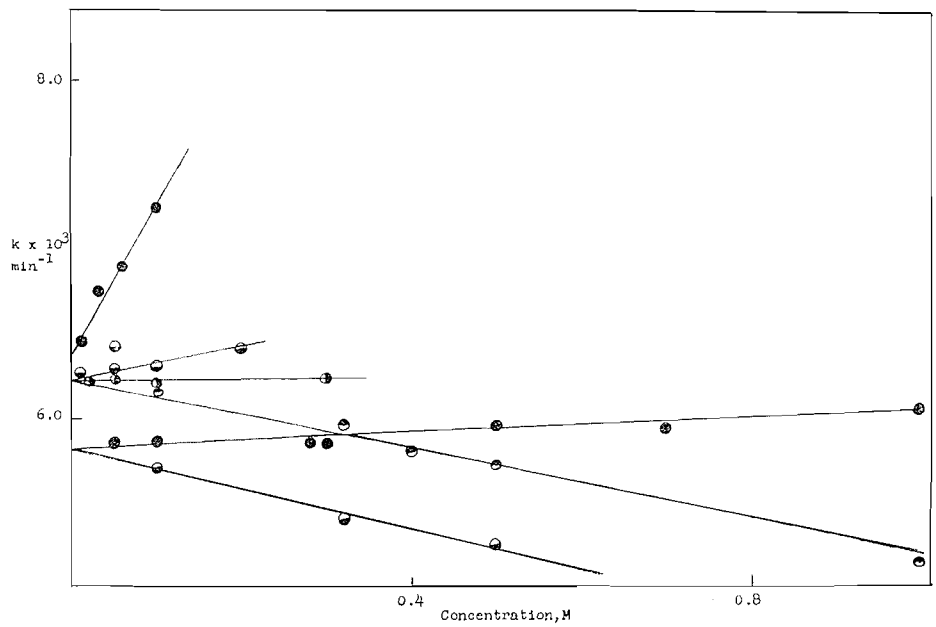


FIG. 1. The effect of monovalent anions upon the rate of hydrolysis of $Cr(NH_3)_5Br^{++}$ (upper set of curves) at 25° and $Cr(NH_3)_5Cl^{++}$ (lower set of curves) at 45°.
Upper curves: ● benzoate, ◒ acetate, ◑ bromide, ◓ perchlorate.
Lower curves: ● chloride, ◒ perchlorate.

The linear dependence of rate upon concentration of salt is evident from the data. Perhaps more surprising than the linearity of the salt effect is the marked variation of the influence of different salts upon the reaction rate. This variation is conveniently reported in terms of the slopes of the curves. The slopes calculated on the basis of a least-squares treatment of the data shown in Fig. 1 are reported in Table I. The specificity of the catalytic effect has been shown to be associated with the anion part of the salt (7).

The data for the monovalent anions are in sharp contrast with those obtained for polyvalent anions. The curves obtained by plotting rate of reaction [II] against concentration do not extrapolate back to a common k_0 at zero concentration of polyvalent anion. Instead the extrapolated value of the rate constant, which will be called $k_{0\ \text{extrap}}$,

Can. J. Chem. Downloaded from www.nrcresearchpress.com by 210.87.254.5 on 09/05/12
For personal use only.

TABLE I

The effect of monovalent salts upon the rate of hydrolysis of $Cr(NH_3)_5X^{++}$

X	Salt	Slope$\times 10^4$ (liter mole^{-1} min^{-1})	$k_0\times 10^3$ (min^{-1})
Cl*	NaCl	1.8	5.82
Cl*	$NaClO_4$	−15	5.87
Br†	$NaClO_4$	−11	6.24
Br†	NaBr	1.0	6.21
Br†	NaOAc	21	6.28
Br†	Na benzoate	48	6.51
I†	$NaClO_4$	−120	—

*At 45° C.
†At 25° C.

is a characteristic property of the catalyzing salt. When the behavior was examined at low salt concentrations it was found that the addition of small amounts of salt produced a very marked acceleration of the reaction. This acceleration was roughly linear in polyvalent anion concentration until the salt was present in the solution at roughly molar equivalence with the chromium salt (about 10^{-3} M). Further addition of the salt caused further increase in the rate of reaction, but the curve was characterized by a markedly smaller slope. Some typical experimental results are plotted in Fig. 2. It has been found

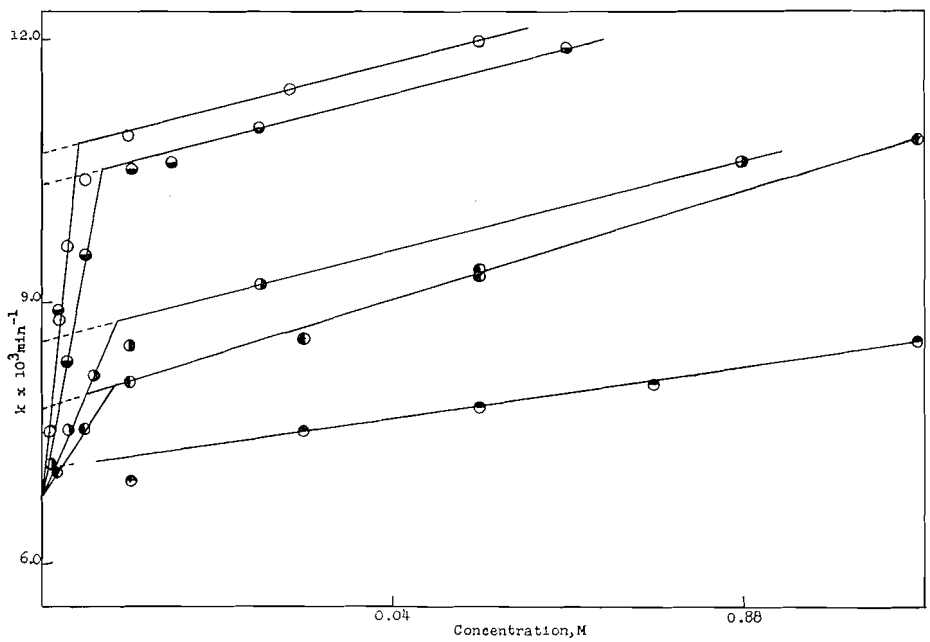


FIG. 2. The effect of various anions upon the rate of hydrolysis of $Cr(NH_3)_5Br^{++}$ at 25°: ○ citrate, ◒ maleate, ◑ sulphate, ◐ *o*-phthalate, ◓ fumarate.

convenient to characterize these curves in terms of $k_{0\ \text{extrap}}$ and the slope of the portion of the curve at higher salt concentration. The values of these parameters obtained by a least-squares analysis of the experimental data are shown in Table II.

Can. J. Chem. Downloaded from www.nrcresearchpress.com by 210.87.254.5 on 09/05/12
For personal use only.

TABLE II

The effect of polyvalent anions upon the rate of hydrolysis of $Cr(NH_3)_5Br^{++}$ at 25°

Salt*	$k_{0\ extrap} \times 10^3$ (min^{-1})	Slope $\times 10^2$ (liter min^{-1} $mole^{-1}$)
p-Phthalate	6.33	0.98
Adipate	6.56	2.21
Fumarate	6.90	1.67
Succinate	6.98	1.48
Oxalate	7.38	1.75
Malonate	7.47	2.59
o-Phthalate	7.85	2.97
Sulphate	8.94	1.12
Maleate	10.18	2.84
Citrate	10.70	2.52

*The sodium salt of the listed anion was used in all cases.

The enhancement in the rate of reaction [II] produced by the polyvalent anions is extremely sensitive to the total ionic strength of the solution. Some typical data are shown in Table III for the effect of sodium perchlorate upon the catalysis by citrate in the hydrolysis of the chloro complex.

TABLE III

Effect of ionic strength upon citrate catalysis of the acid hydrolysis of $Cr(NH_3)_5Cl^{++}$

Citrate concentration	$NaClO_4$ concentration	$k \times 10^3$ (min^{-1})
0.0	0.01	5.85
0.004	0.0	8.74
0.004	0.1	6.65
0.0	0.1	5.70
0.004	1.0	4.54
0.0	1.0	4.30

DISCUSSION

The rate of reaction [II] has been shown to respond to the addition of salts in a manner which is not explicable in terms of the simple Debye–Huckel theory. There is, however, some indication that the extended form, involving a term linear in electrolyte concentration, could be applied to the results obtained over the range 0.01 to 0.5 *M*. Alternatively and perhaps somewhat more conveniently, the ideas suggested by Ingold (8) to cover salt effects in the solvolysis of alkyl halides might be applied. Both of these suggestions suffer from the disadvantage, in the present application, of not allowing for specificity of the salt effect. Nevertheless, there is probably sufficient indication that the effect observed is due to the reacting species developing an ion atmosphere. This ion atmosphere promotes the stability of the transition state and suggests charge separation in the reaction intermediate. Such an observation is not surprising for a reaction which results in a net increase in the total number of ions in the solution regardless of the intimate mechanism of the reaction. Such charge separation is expected to be more important in a reaction which occurs by dissociation than in one which occurs by displacement. It is suggested, then, that the catalysis of reaction [II], produced by various salts at high concentration, is an indication of a dissociation mechanism.

Can. J. Chem. Downloaded from www.nrcresearchpress.com by 210.87.254.5 on 09/05/12
For personal use only.

Can. J. Chem. Downloaded from www.nrcresearchpress.com by 210.87.254.5 on 09/05/12
For personal use only.

More surprising and perhaps more useful in a diagnostic way was the observation of the rapid rise in rate produced by polyvalent anions in a concentration range which was comparable to that of the reacting species. Although this general kind of observation has been made by a number of other workers (3, 6, 9, 10), it has been investigated in somewhat more detail in the present work than previously. These salt effects have been attributed to specific ion-pair formation. It now appears necessary to divide salt effects into two categories. The first of these is the general ionic atmosphere effect discussed above. Ion-pair formation may play a role in this kind of salt effect since a dependence upon the nature of the anion involved was observed, but it does not seem to be the primary factor. The second category suggested involves the formation of specific ion pairs. In this case, it is assumed there are recognizable association units with integral numbers of ions to which ion pair formation constants could be applied. The simplest unit which could be considered in this way is one positive and one negative ion. Since this kind of unit is most easily visualized from a kinetic point of view it is proposed to treat our data on the basis of this model. The alternative of a bimolecular attack upon the halopentammine chromium(III) ion does not need to be seriously considered since the reaction is first order even in the presence of small concentrations of added salt. Furthermore the sole primary product of the reaction is observed to be the hydroxopentamminechromium(III) ion.

Reaction [II] follows the rate law [III], where k_1 is the rate constant for the uncatalyzed

$$\text{Rate} = \frac{(k_1+k_2K[\text{A}])}{1+K[\text{A}]}[\text{RX}] \qquad [\text{III}]$$

reaction, k_2 is the rate constant for the catalyzed reaction, K is the ion-pair association constant, [A] is the concentration of added anion, and [RX] is total concentration of halopentamminechromium(III) ion. Using relationship [III] it is possible to estimate a value for K. This has been done and when citrate is the catalyzing anion the association constant was calculated to be 233. This agrees very well with the value 248 determined experimentally (11). In Fig. 3 are plotted the experimentally observed values of $k_{0\ \text{extrap}}$ for reaction [II] against the constants for association of some of the ions used with the hexamminecobalt(III) ion (12). The order of the agreement is seen to be excellent.

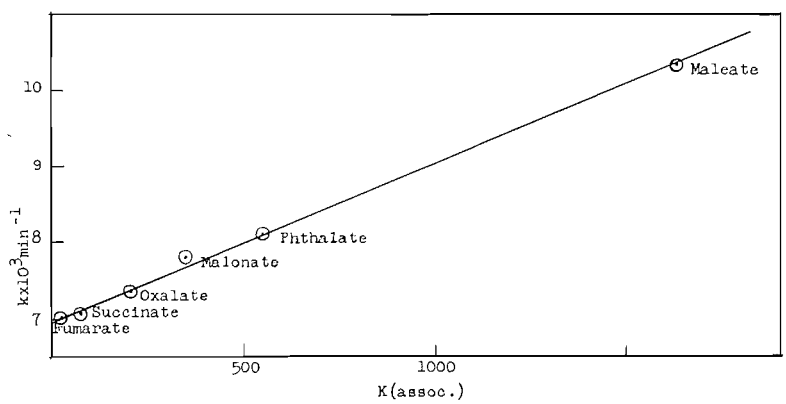


FIG. 3. Relation between the rate constant for the hydrolysis of $Cr(NH_3)_5Br^{++}$ at 25° and the magnitude of the ion-pair formation constant between anions and $Co(NH_3)_6^{+++}$. Data for the ion-pair formation constants are taken from reference 12.

Similar agreement has been obtained between the rate constants and ion-association constants (11) for the interaction between the chloropentamminechromium(III) ion and the polyvalent anions used in this study.

The sensitivity of the salt effect to the total ionic strength of the solution, shown in Table III, is a further indication of the rationality of the suggestion that ion pairs are involved. Unfortunately, the effect of sodium perchlorate upon the activity coefficient of the halopentamminechromium(III) ion is not known. However, the effect of sodium perchlorate upon the rate of the citrate-catalyzed reaction is in agreement with its effect upon the experimentally determined ion-pair formation constant (11).

If the ion pairs promote the hydrolysis reaction they must do so either through charge transfer or by stabilizing the transition state. Charge transfer might occur in a number of ways, but regardless of the mechanism, the result must be an increase in the electron density on the chromium. Such an increase in electron density would not be expected to promote attack upon the chromium by an electron-rich reagent such as water. Stabilization of the transition state might result because the associating anion tends to hold the complex ion in its normal octahedral configuration. This, of course, would tend to prevent the loss of ligand-field stabilization energy (13) which is attendant upon the distortion of the regular octahedron as the molecule proceeds through the transition state. Such stabilization is not compatible with the expansion of the co-ordination sphere which would be necessary to accommodate a displacement reaction. It seems, then, that the rate acceleration produced by ion-pair formation is incompatible with an S_N2 mechanism for reaction [II]. The explanation for the results must be sought in terms of a dissociation mechanism.

$$\begin{array}{ccccccc} & & \begin{array}{c}RH_2O^+ + X^- \\ H_2O \,\uparrow\downarrow \\ R^+X^- \\ A^- \,\uparrow\downarrow \\ RA + X^-\end{array} & & \begin{array}{c}RH_2O^+ + X^- \\ H_2O \,\uparrow\downarrow \\ R^+\ X^- \\ \uparrow\downarrow A \\ RA + X^-\end{array} & & \begin{array}{c}RH_2O^+ + X^- \\ H_2O \,\uparrow\downarrow \\ R^+ + X^- \\ A \,\uparrow\downarrow \\ RA + X^-\end{array} \\ RX & \rightleftarrows & & \rightleftarrows & & \rightleftarrows & \end{array} \qquad [IV]$$

Fainberg and Winstein (14) have shown that the steps indicated in reaction [IV] need to be considered in a reaction which proceeds by a dissociation mechanism. These steps are intended to represent the sequence of events in which the two ionic fragments of the reaction first become separate identities in intimate contact (internal ion pair (14)), then ions in contact but each ion with an independent solvation sheath, and finally separated and independent ions. The stereochemistry of each of these intermediates is shown in Fig. 4. In the initial stage of separation the ions have sufficient influence upon one another that the original stereochemistry is maintained in spite of the lengthening metal to halogen bond. In the other two stages of separation the original octahedron has collapsed to a five-co-ordinate structure which is considered to be the trigonal bipyramid.

Bateman, Hughes, and Ingold (15) have shown that if a reactive intermediate of low co-ordination number is sufficiently stable to have independent existence in solution it should be possible to detect the presence of such an intermediate by a mass law effect. That such an effect is absent in the present case is evident from the data for the effect of chloride, bromide, and iodide salts on the rate of hydrolysis of the chloro, bromo, and iodo complexes. Separated ions do not seem to be involved in the rate-determining step of reaction [II].

Can. J. Chem. Downloaded from www.nrcresearchpress.com by 210.87.254.5 on 09/05/12
For personal use only.

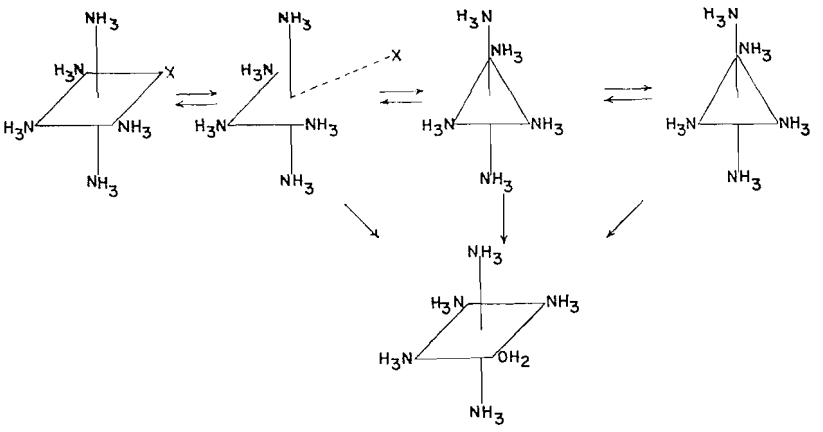


FIG. 4. Configuration relationships among the possible intermediates in the hydrolysis of $Cr(NH_3)_5X^{++}$.

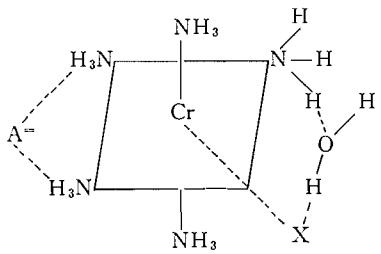
If the octahedral structure collapses to yield the solvent-separated ion pair there are three equivalent positions at which water is able to attack the intermediate to produce the aquo ion. In the case under consideration this intermediate of reduced co-ordination number forms an ion pair with the anion of the salt present. The structure of such an ion pair becomes important. It seems reasonable to place the anion on the side of the complex away from the halogen. This conclusion was reached on the basis that *trans*-dichlorobis(ethylenediamine)cobalt(III) solvolysis is not accelerated by basic anions, whereas that of the corresponding cis complex is accelerated. The cis complex has a permanent dipole, whereas the trans complex does not, and it seems that a permanent dipole is necessary in order to obtain rate acceleration from ion-pair formation. Coupled with this is the observation that maleate produces a much greater change in the reaction rate than fumarate and that *o*-phthalate produces a much greater change than *p*-phthalate. In each case it is the anion with π orbitals suitably situated for overlap with the t_{2g} orbitals of the chromium which has the greater influence upon the reaction rate. This suggests that, in these cases at least, π bonding to the chromium is important and as a consequence the anion must be stretched across the face of the original octahedron. On the basis of these considerations the ion-pairing anion is thought to be stretched across the back side of the chromium complex in such a way that a reactive end is adjacent to each of two of the reactive sites and the body of the anion shields the third such site. Under these circumstances it would be surprising indeed if the ion-paired anion was not able to compete with water for some of these reactive sites. Such competition ought to make its appearance in the form of the aniono complex as one of the primary products of the reaction. For example, the fact that citrato complexes do not appear as primary products in the presence of citrate anion argues against a five-co-ordinated structure having an important role in the transition state. It might conceivably be argued that the anion does enter the complex in the initial step but is quickly eliminated by a subsequent hydrolysis. This seems unlikely because it has been observed that each of the anions reacts slowly with the product hydroxo complex to produce an aniono complex which is not hydrolyzed under the conditions of the experiment (16).

Acceleration of the reaction due to charge transfer is compatible with a dissociation reaction and acceleration due to the anion helping to maintain the original octahedral

Can. J. Chem. Downloaded from www.nrcresearchpress.com by 210.87.254.5 on 09/05/12
For personal use only.

configuration is compatible with the internal ion-pair intermediate. The internal ion-pair intermediate (14) is also compatible with the observation that the accelerating anion does not appear in the original reaction product. In this intermediate not all potential positions of attack on the molecule are equivalent. The position being vacated by the leaving group, which is most remote from the anion, is most vulnerable to attack. As a consequence one would not expect the accelerating anion to appear in the original reaction product and this is compatible with the experimental observations.

It is suggested that the reaction occurs via a stretching of the chromium to halogen bond. If, when the bond reaches a critical distance, there is a properly oriented water molecule this molecule enters to replace the halide ion. If there is not a properly oriented water molecule the halogen returns to its original position and no reaction occurs. The reaction might be considered to proceed via the following model.



This model represents a reaction which is primarily S_N1 but one which requires the intervention of solvent for completion. The name solvent-assisted S_N1 is suggested.

REFERENCES

1. G. Biederman and L. G. Sillen. Arkiv Kemi, **5**, No. 40, 425 (1953).
2. A. R. Olson and R. T. Simonson. J. Chem. Phys. **17**, 1167 (1949).
3. F. J. Garrick. Trans. Faraday Soc. **34**, 1088 (1938).
4. H. Taube and F. A. Posey. J. Am. Chem. Soc. **75**, 1463 (1953).
5. M. Ikuta, H. G. McAdie, and W. McF. Smith. Can. J. Chem. **34**, 1361 (1956).
6. R. G. Pearson, P. M. Henry, and F. Basolo. J. Am. Chem. Soc. **79**, 5382 (1957).
7. M. A. Levine, T. P. Jones, W. E. Harris, and W. J. Wallace. J. Am. Chem. Soc. **83**, 2453 (1961).
8. C. K. Ingold. Structure and mechanism in organic chemistry. Cornell University Press. 1953. p. 362.
9. R. A. Plane and H. Taube. J. Phys. Chem. **56**, 33 (1952).
10. F. Basolo, B. D. Stone, J. G. Bergman, and R. G. Pearson. J. Am. Chem. Soc. **76**, 3079 (1954).
11. In preparation.
12. J. M. Peacock and J. C. James. J. Chem. Soc. 2233 (1951).
13. F. Basolo and R. G. Pearson. Mechanism of inorganic reactions. John Wiley & Sons, New York. 1958.
14. A. H. Fainberg and S. Winstein. J. Am. Chem. Soc. **78**, 2764 (1956).
15. L. C. Bateman, E. D. Hughes, and C. K. Ingold. J. Chem. Soc. 974 (1940).
16. Unpublished observations.

Can. J. Chem. Downloaded from www.nrcresearchpress.com by 210.87.254.5 on 09/05/12
For personal use only.

Can. J. Chem. Downloaded from www.nrcresearchpress.com by 210.87.254.42 on 09/05/12
For personal use only.

Canadian Journal of Chemistry

Issued by THE NATIONAL RESEARCH COUNCIL OF CANADA

VOLUME 39 DECEMBER 1961 NUMBER 12

RADIATION CHEMISTRY OF CYCLOHEXANE

IV. PRIMARY PRODUCT YIELDS IN THE IRRADIATION OF CYCLOHEXANE[1]

P. J. DYNE AND J. A. STONE

ABSTRACT

The radiolysis of cyclohexane has been studied at low total doses and initial G values have been determined. Ninety-nine per cent of the evolved hydrogen has been accounted for in hydrogen-deficient products. Cyclohexene, bicyclohexyl, and cyclohexyl-hexene-1 have been identified as primary reaction products. Cyclohexyl-cyclohexene has been identified as a secondary reaction product. The use of high irradiation doses has been shown to lead to decreases in the initial G values of all primary products.

INTRODUCTION

A common feature of the reported product yields in the radiolysis of cyclohexane is the discrepancy between the hydrogen yield and the sum of the yields of hydrogen-deficient products—principally bicyclohexyl and cyclohexene (1, 2, 3, 4). In all cases the total yield of hydrogen-deficient products is not great enough to account for the observed hydrogen yield. It is generally assumed that high molecular weight products are formed which have remained undetected. There are also disagreements on the identity and yield of some of the minor products.

Cyclohexene, a major product, reduces $G(H_2)$ and is itself destroyed in the radiolysis (5, 6). It follows that accurate initial G values for any product can only be obtained by working at low conversions and by extrapolations to zero dose, thus avoiding the complications of secondary reactions.

This paper describes analytical techniques for the identification and analysis of products at conversion of less than 0.01%. At these low conversions the primary products appear to be cyclohexene, bicyclohexyl, and 6-cyclohexyl-hexene-1. A good hydrogen balance is obtained, all but 1% of the hydrogen being accounted for.

EXPERIMENTAL

Materials

Fisher Scientific Company Spectrograde cyclohexane was used as received. Gas–liquid chromatography showed three small impurity peaks before the main cyclohexane peak, but neither the sizes nor the shapes of these peaks were altered by γ-radiolysis. Cyclohexene (Eastman) was used as a solute.

Preparation of Samples

The 20-ml samples were contained in Pyrex tubes, 2.5 cm in diameter and 25 cm long, each equipped with a break-tip seal and a constricted side arm. The samples were pipetted

[1]*Manuscript received July 14, 1961.*
Contribution from Research Chemistry Branch, Atomic Energy of Canada Limited, Chalk River, Ontario. Issued as A.E.C.L. No. 1356.

into the tubes and were then degassed by the freeze–thaw technique. When the residual pressure was less than 5×10^{-6} mm, the sample tubes were sealed off at the constriction. The samples containing solute were made up in bulk and pipetted out as required.

Irradiation of Samples

The samples were irradiated at 22° C by Co-60 γ-rays. Dose rates were determined with the Fricke dosimeter, taking $G(Fe^{+++}) = 15.5$. Two irradiation facilities were used with dose rates of 4.8×10^{20} ev/liter minute, and 2.6×10^{19} ev/liter minute for cyclohexane at 22° C.

Product Analysis

The irradiated sample tubes were attached to a vacuum line and their contents frozen with liquid nitrogen. The gaseous products volatile at −196° C were then taken off with a Toepler pump and their volume measured with a McLeod gauge, the samples being thawed and refrozen to make sure that all the gas had been collected. Hydrogen was diffused through a heated palladium thimble, and the volume of the residual gas measured. In all cases it was found that this residue amounted to less than 1% of the initial volume. This was confirmed by mass spectral analysis of the collected gas.

The liquid products were analyzed by gas–liquid chromatography. Cyclohexene was determined using a 4-meter column of 3-mm internal diameter, containing firebrick on which was deposited 30% by weight of a silver nitrate/$\beta\beta'$ oxydipropionitrile mixture as the stationary phase. The column was at room temperature, the sample injection end being at a slightly higher temperature. The results were checked quantitatively by infrared analysis, using the 717-cm^{-1} cyclohexene band. Products of higher molecular weight than cyclohexane were separated on a 2.5 meter long, 2.5-mm internal diameter column containing 0.1% by weight of Apiezon-L grease on 200-micron diameter glass beads. This column, with a very low concentration of L-grease, gave better separations than a conventional column containing more grease. The more heavily loaded column must be used at a higher temperature to obtain the same separations in a comparable time. With the minimum amount of L-grease, the tailing of cyclohexane was greatly reduced, the less volatile components being eluted at lower temperatures with improved resolution. This column was at a fixed temperature for quantitative work but was temperature programmed for qualitative work.

A simple hydrogen flame detector (7) was used, together with a split-stream device after the column. The output from the detector was fed through the 10^9-ohm input resistor of an electrometer. Ten-λ samples of the irradiated material, without previous concentration, were injected directly onto the columns, the whole sample being passed through the detector. A new calibration curve was used for each series of analyses, standards and unknowns being run alternately. No standards were available for products other than cyclohexene and bicyclohexyl so their concentrations were obtained from measured peak areas, the peak area being assumed to be proportional to molar concentration.

A Consolidated 21-130 Mass Spectrometer was connected to the outlet of the chromatographic column by means of a heated, stainless steel capillary tube. Approximately 90% of the eluted sample passed through the detector, whilst the remaining 10% flowed through the capillary past a gold leak in the spectrometer sample introduction system. The capillary introduced a delay of the order of 5 seconds between the appearance of a chromatographic peak and the initial appearance of the mass spectrum due to the same component. The spectra were recorded on a recording oscillograph, the time taken to scan from mass

Can. J. Chem. Downloaded from www.nrcresearchpress.com by 210.87.254.42 on 09/05/12
For personal use only.

26 to mass 200 being of the order of 1 minute. Interpretable spectra were obtained when the desired component was present in the chromatographic eluent at a concentration of about 100 p.p.m. To obtain this concentration for the components which were present in very small amounts in irradiated samples, the following procedure was employed. A large sample (~0.5 ml) of irradiated material was injected, 20 λ at a time, onto the narrow L-grease column. Cyclohexane, which comprised 99.9% of the solution, was eluted rapidly at room temperature, leaving the higher-boiling components still at the column inlet. When sufficient material had been deposited on the column the temperature was raised gradually so that a good chromatographic separation was achieved and the mass spectra obtained. To ensure a rapid clearing of the spectrometer inlet system, and therefore no enhancement of the background spectrum, the temperature of the inlet system was maintained at 200° C and that of the spectrometer ion source at 250° C.

Samples from the chromatographic column were trapped out in micro infrared cells cooled in a solid CO_2/acetone mixture. The spectra of these samples were obtained on a Perkin–Elmer model 21 machine equipped with a beam condenser.

RESULTS

1. *Pure Cyclohexane*

The variation of $G(H_2)$ with dose, at a dose rate of 4.8×10^{20} ev/liter minute, is shown in Fig. 1. Each point on this curve represents the result of one measurement except for the initial G value, which was obtained from a series of measurements extrapolated to zero dose. At low doses a sharp decrease in $G(H_2)$ with increasing dose occurs, but at

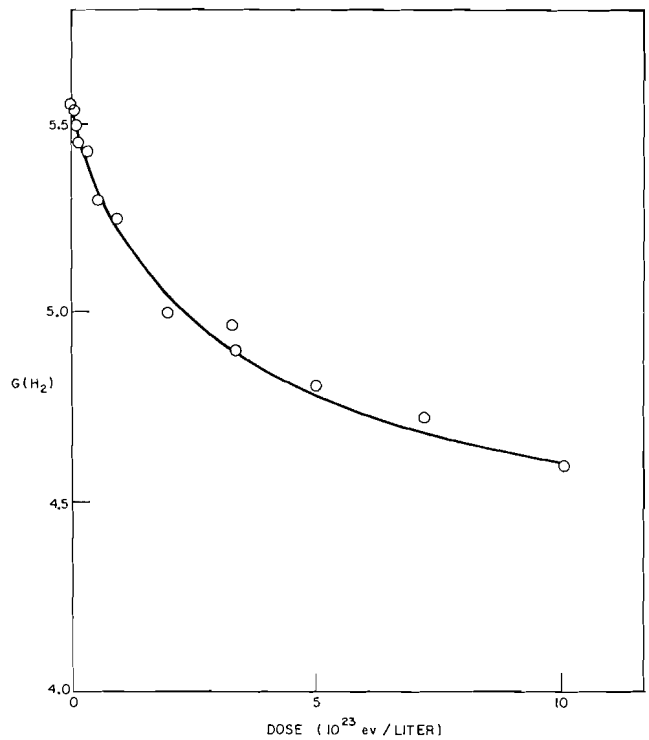


FIG. 1. The variation of $G(H_2)$ with total dose.

Can. J. Chem. Downloaded from www.nrcresearchpress.com by 210.87.254.42 on 09/05/12
For personal use only.

higher doses the rate of decrease becomes smaller. The initial G value is 5.55. The decrease is clearly non-linear with dose. At the lower dose rate of 2.6×10^{19} ev/liter minute a similar decrease in $G(H_2)$ with dose was recorded. The initial G value was the same within experimental error, but at the lower dose rate the decrease was more rapid with increasing dose. Figure 1 represents a refinement on previously published data (3, 5).

The formation of cyclohexene as a function of dose is shown in Fig. 2. The initial G value is 3.27. At the higher doses shown in the figure the G value is beginning to decrease. A similar curve for bicyclohexyl is shown in Fig. 3. The initial G value is 1.95, and again at the higher doses this value decreases.

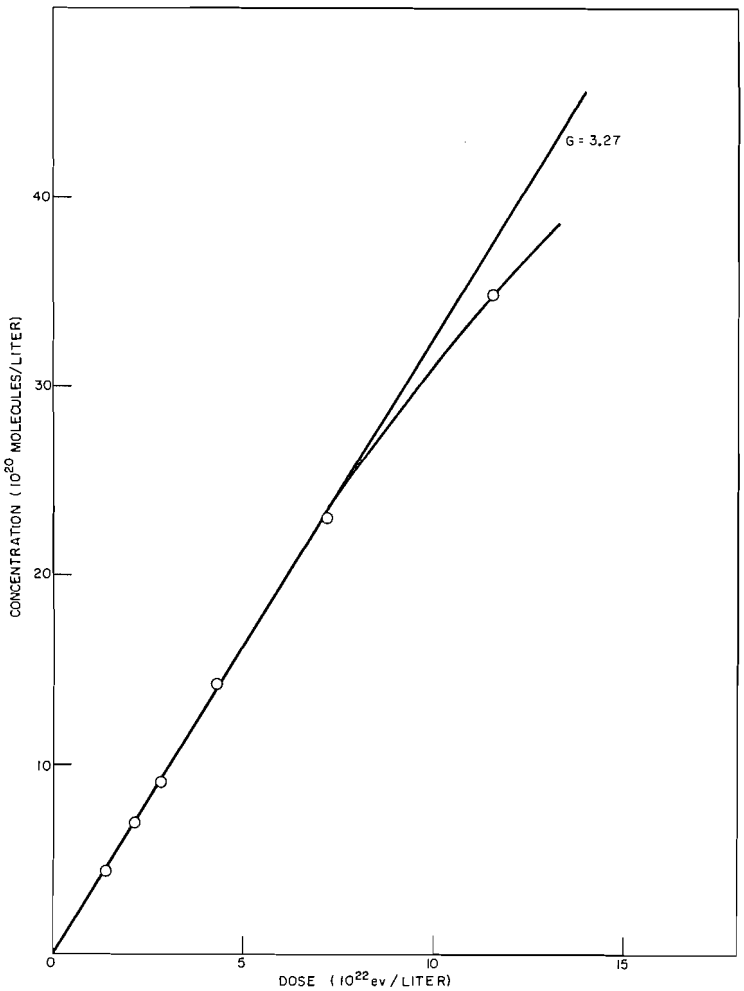


FIG. 2. The formation of cyclohexene.

Figure 4 shows the chromatograms obtained for all products of molecular weight higher than cyclohexane and cyclohexene. Figure 4(a) is from a sample of pure cyclohexane irradiated to the low dose of 2×10^{22} ev/liter; Fig. 4(b) is from pure cyclohexane irradiated to the much higher dose of 2×10^{24} ev/liter, and 4(c) is the chromatogram

Can. J. Chem. Downloaded from www.nrcresearchpress.com by 210.87.254.42 on 09/05/12
For personal use only.

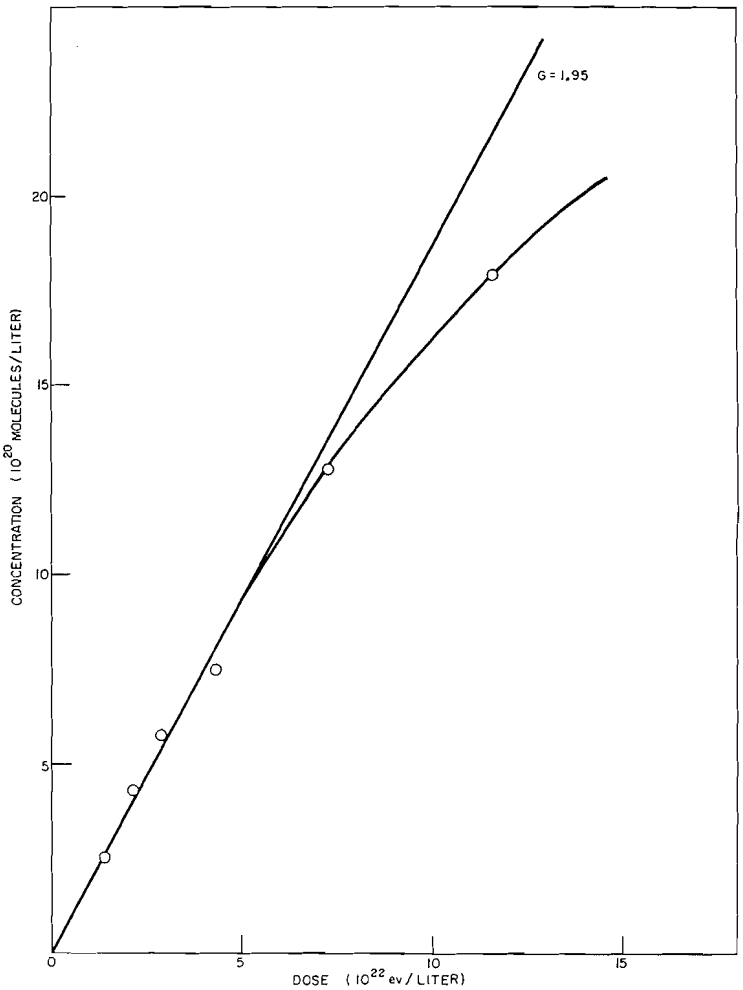


FIG. 3. The formation of bicyclohexyl.

obtained from a solution of $4.5\times10^{-2}M$ cyclohexene in cyclohexane irradiated to 10^{23} ev/liter. Only the peak heights and areas in one chromatogram should be compared, as different-sized samples were used in the runs *a*, *b*, and *c*. The column was temperature programmed to give the series of peaks shown. These peaks may be conveniently divided into three groups, (i) those having retention times lower than that of bicyclohexyl, (ii) those with almost the same retention time as bicyclohexyl, and (iii) those with greater retention times than bicyclohexyl. The peak areas in each chromatogram are given in Table I in terms of percentages of the total area.

Group i

For pure cyclohexane irradiated to a low total dose, Fig. 4(*a*), the estimated *G* value for all products in this group is 0.27.

An infrared spectrum of a trapped sample from group i showed an absorption band at 1634 cm^{-1} corresponding to the C=C stretching frequency of hexene-1. The mass spectrum

Can. J. Chem. Downloaded from www.nrcresearchpress.com by 210.87.254.42 on 09/05/12
For personal use only.

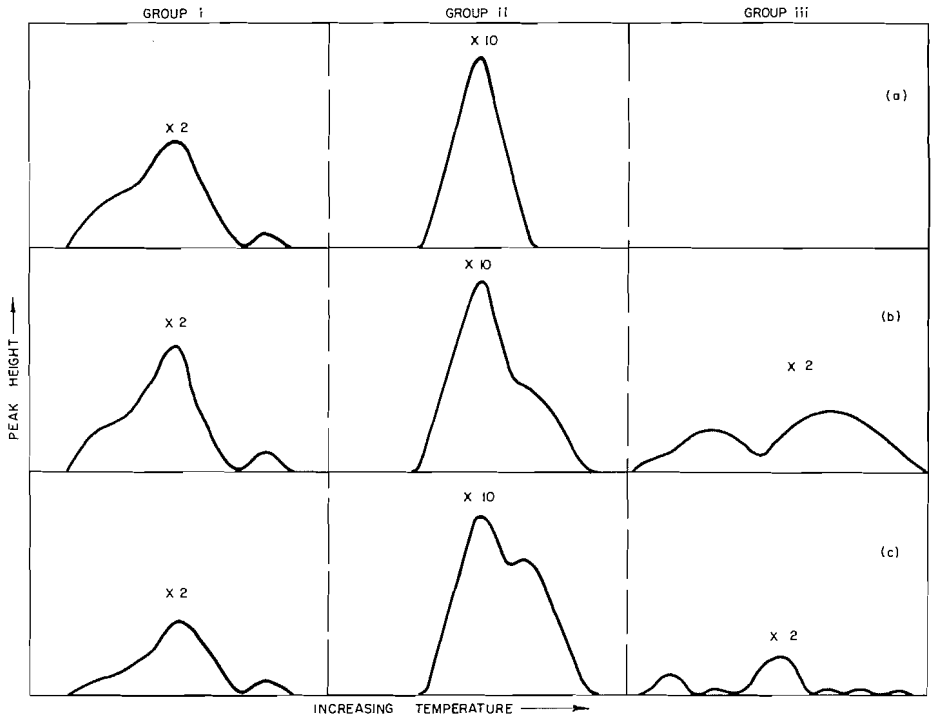


FIG. 4. Gas–liquid chromatograms: (*a*) cyclohexane at low dose; (*b*) cyclohexane at high dose; (*c*) cyclohexane–cyclohexene mixture at low dose. Group i, peaks appearing before the bicyclohexyl peak; group ii, the bicyclohexyl group of peaks; and group iii, the peaks appearing after bicyclohexyl.

TABLE I

Relative chromatographic peak areas from Fig. 4

Chromatogram No.	Relative chromatographic peak areas		
	4(*a*)	4(*b*)	4(*c*)
Group i	12	14	8.5
Group ii	88	70	82
Group iii	0	16	9.5

showed a parent peak at $m/e = 166$, together with fragment ions associated with both cyclohexyl and hexenyl groups. Unlike the spectrum of bicyclohexyl, the most intense peak of which is at $m/e = 82$, the peak at $m/e = 83$ was found to be the largest. This would suggest that a cyclohexane molecule substituted with a straight chain of mass 83 was present. Since the infrared spectrum showed that a cyclohexene group was not present the double bond must be in the side chain. The main chromatographic peak in group i is, therefore, most probably 6-cyclohexyl-hexene-1.

Group ii

Figure 4(*a*) shows that at very low doses a single peak is obtained. This peak is symmetrical with no sign of any other substance present. A symmetrical peak was obtained no matter how the column conditions were varied, showing that, in all probability, the

Can. J. Chem. Downloaded from www.nrcresearchpress.com by 210.87.254.42 on 09/05/12
For personal use only.

identification of this peak as due to a single component, bicyclohexyl, was justified (see below). At higher total doses, however, this was not the case, as Fig. 4(*b*) shows. A second peak now appears together with the main bicyclohexyl peak, demonstrating that at higher doses a secondary reaction product appears. This we have identified as cyclohexyl-cyclohexene.

For a $4.5\times10^{-2}M$ cyclohexene solution, Fig. 4(*c*), a double peak is observed. The first maximum has the same retention time as bicyclohexyl whilst the second corresponds in position to the shoulder observed in 4(*b*). At attempt was made to trap the compound associated with the main peak in Fig. 4(*a*). However, the concentration of this product was too low for this to be possible. An infrared spectrum of the compound associated with the first part of the main peak in 4(*b*) was found to be identical with that of bicyclohexyl. The spectrum of the sample trapped during the elution of the whole peak showed a new absorption band appearing at 1642 cm^{-1}, corresponding to the C=C stretching frequency in a cyclohexene ring. The spectrum of the sample trapped during the elution of the main double peak of 4(*c*) showed the same band but in greater strength. From the chromatographic retention time and the infrared results, it would appear that this product, which appears as the radiation dose is increased, is a substituted cyclohexene.

The mass spectrum confirmed the above conclusions. The product provisionally identified as bicyclohexyl had a spectral pattern identical with that of a pure sample. The cyclohexyl-cyclohexene, although not fully resolved from the bicyclohexyl, showed a parent peak at $m/e = 164$, together with fragment ions associated with cyclohexyl groups at $m/e = 83$ and 82. In addition a strong fragment ion peak at $m/e = 81$ was deduced to be the cyclohexenyl ion formed by the rupture of the two ring molecule at the central C—C bond.

Group iii

This group contains the peaks due to compounds of higher molecular weight than bicyclohexyl. No peaks are found at low doses, but some do appear at higher doses and in cyclohexane–cyclohexene mixtures. This group of peaks may therefore be associated with secondary reaction products in pure cyclohexane and with products involving the reaction of cyclohexene in cyclohexane–cyclohexene mixtures. No correlation was attempted between the products found in chromatograms 4(*b*) and 4(*c*).

Attempts were made to trap samples of products in this group but without success. Mass spectra showed that cyclohexyl groups were present but no parent peaks could be detected.

2. Cyclohexane–Cyclohexene Mixtures

Samples of a $4.5\times10^{-2}M$ cyclohexene solution were irradiated at the higher dose rate for varying doses up to 10^{23} ev/liter. The gaseous product volatile at $-196°$ C was more than 99% hydrogen. The initial $G(H_2)$ was 4.76. This value was constant over the dose range studied.

The determination of a G value for the production of cyclohexene was difficult. A value of 0.6 ± 0.3 was obtained. The large error was due to the fact that at the doses used only a small change in cyclohexene concentration occurred.

G(bicyclohexyl) could not be determined since complete resolution from the peak assigned to cyclohexyl-cyclohexene could not be obtained. Both peak areas were measured together and the total area was calibrated against that for pure bicyclohexyl. A total G value of 1.3 was found. The sensitivity of the chromatographic detector for bicyclohexyl only was determined, and so the error involved in using this calibration was not

Can. J. Chem. Downloaded from www.nrcresearchpress.com by 210.87.254.42 on 09/05/12
For personal use only.

known. With the type of detector used the error is, however, probably small. By visual inspection of the peak shape (Fig. 4(*a*) group ii), it is seen that bicyclohexyl constitutes roughly 55% of the total area, which would correspond to a G value of 0.72.

The analyses for products in groups i and iii were less accurate. The G values obtained were 0.13 and 0.15 respectively.

DISCUSSION

The results obtained for the product yields in the radiolysis of pure cyclohexane by Co-60 γ-rays are summarized in Table II.

TABLE II

Initial G values for products in the irradiation of pure cyclohexane

Product	G	
Hydrogen	5.55±0.05	
Cyclohexene	3.27±0.06	Hydrogen equivalent = 5.49
Bicyclohexyl	1.95±0.06	
Cyclohexyl-hexene-1	0.27±0.05	

All these results were obtained by extrapolation to zero dose since it was shown that the G values of all products decrease with increasing dose. An excellent hydrogen balance has been obtained showing that in the initial stages of radiolysis, i.e. at very low doses, a simplicity of products is observed. No dienes or high molecular weight products are observed and indeed none need be invoked since there is no hydrogen deficit.

At higher doses complications arise. The G values of all the initial products decrease and secondary reaction products appear. Cyclohexyl-cyclohexene is one which has been definitely identified. High molecular weight products appear and the hydrogen deficit becomes greater. Dyne and Fletcher (6) have shown that, on prolonged radiolysis of cyclohexane, the cyclohexene reaches a limiting concentration when its rate of formation is equal to its rate of disappearance. In the present work it has been shown that the radiolysis of a mixture of cyclohexane and cyclohexene results in a decrease in G(cyclohexene) of about 2.7, but the decrease in $G(H_2)$ is only 0.9. This implies that the disappearance of cyclohexene is not brought about simply by the addition of hydrogen to the double bond, but some other reaction must be occurring. Since cyclohexyl-cyclohexene is a secondary product, some substitution at a saturated carbon atom takes place.

These results differ somewhat from those of Waight and Walker (8), who found lower yields of bicyclohexane and cyclohexene (1.6 and 2.4 respectively). The dose rate of their irradiation was about one tenth of the dose rate used here and, at the doses used (6×10^{22} ev/liter), it is consequently likely that their G values for these products would be significantly lower than the true initial value. We do not observe cyclohexyl-cyclohexene as a primary product.

REFERENCES

1. H. A. Dewhurst. J. Phys. Chem. **63**, 813 (1959).
2. A. C. Nixon and R. E. Thorpe. J. Chem. Phys. **28**, 1004 (1958).
3. G. R. Freeman. J. Chem. Phys. **33**, 71 (1960).
4. T. D. Nevitt and L. P. Remsberg. J. Phys. Chem. **64**, 969 (1960).
5. W. S. Guenter, T. J. Hardwick, and R. P. Nejak. J. Chem. Phys. **30**, 601 (1959).
6. P. J. Dyne and J. W. Fletcher. Can. J. Chem. **38**, 851 (1960).
7. I. G. McWilliam and R. A. Dewar. Gas chromatography. *Edited by* D. H. Desty. Butterworths, London. 1958.
8. E. S. Waight and P. Walker. J. Chem. Soc. 2225 (1960).

Can. J. Chem. Downloaded from www.nrcresearchpress.com by 210.87.254.42 on 09/05/12
For personal use only.

Can. J. Chem. Downloaded from www.nrcresearchpress.com by 210.87.254.5 on 09/05/12
For personal use only.

THE SEPARATION OF SMALL AMOUNTS OF THE PLATINUM METALS

1. THE COLORIMETRIC DETERMINATION OF RHODIUM AND ITS SEPARATION FROM IRIDIUM[1]

D. E. RYAN

ABSTRACT

A method for separating small amounts of rhodium from iridium is described. In 3 to 9 *M* hydrochloric acid solutions, the amber-to-red complex of bivalent rhodium with 4,5-dimethyl-2-mercaptothiazole is formed after reduction of tervalent rhodium with chromous or stannous chloride. Rhodium is quantitatively separated from iridium by chloroform extraction of this product; separation can be made in solutions that have been fumed with sulphuric acid if chromous chloride is used for the prior reduction of the rhodium. The complex, after removal of the chloroform, is dissolved in dilute hydrochloric acid, and the optical density of the resulting colored solution is measured.

INTRODUCTION

The separation of small amounts of the platinum metals still leaves room for improvement. Palladium can be separated by extraction of the dimethylglyoxime (1, 2), *p*-nitrosophenylamine (3, 4, 5), or 1-nitroso-2-naphthol (6) complexes into organic solvents; similar success is not so readily attained with small quantities of the other platinum metals.

The hydrous oxide procedure of Gilchrist and Wichers (7) provides a means of separating small amounts of platinum from similar quantities of iridium and rhodium (3, 5) and some success has been recorded for the separation of bivalent platinum complexes (1, 4, 8). Ammonium type salts $(R_4N)_2MX_6$, although satisfactory for determining small amounts of platinum metals in the quadrivalent state and for separating from commonly associated base metals, are of little use in the separation of the platinum metals themselves. Selective reduction by copper powder (9) has proved satisfactory for separating both milligram and microgram quantities of rhodium from iridium. Ion exchange methods have been used with varying success for separating microgram amounts of these metals (10). Where molecular chelate species are possible, solvent extraction offers a reasonable means of separation (11); such chelates are not probable for the platinum metals in the quadrivalent state (12). Distinct possibilities, however, lie in the principle of precipitating or extracting bivalent platinum metal complexes. Jackson (13) has quantitatively separated rhodium from iridium as an insoluble bivalent complex with thioacetanilide after reduction with chromous chloride; the method can be used for the determination of small amounts of iridium in rhodium but attempts to separate small quantities of rhodium from iridium by solvent extraction were unsuccessful. The following paper records the results of an investigation into the possibility of separating rhodium from iridium by extraction of a bivalent complex obtained after reduction.

Rhodium, in the bivalent state, reacts with 4,5-dimethyl-2-mercaptothiazole to give a colored complex that can be used for its determination (14). In the original paper the color was produced by boiling hydrochloric acid solutions of tervalent rhodium with excess reagent, the reagent itself acting to reduce the rhodium to the bivalent state; iridium produced a pale yellow color that caused some interference in the rhodium determination unless compensated in the reference cell; both the rhodium and iridium com-

[1]*Manuscript received June 15, 1961.*
Contribution from the Department of Chemistry, Dalhousie University, Halifax, Nova Scotia, and the Imperial College of Science and Technology, London, England; with financial assistance from the National Research Council, Ottawa, Canada.

plexes were extracted by organic solvents so that separation under these conditions is not possible. However, 4,5-dimethyl-2-mercaptothiazole, as many other thio compounds (13), reacts in the cold with rhodium when a reducing agent is added; the determination and separation of rhodium from iridium can be readily achieved by this means.

EXPERIMENTAL

In preliminary studies, a large number of compounds was investigated as possible reagents for reducing rhodium, at room temperature and in acid solution, from the tervalent to bivalent state. The compound was added to acidified rhodium chloride solutions containing 4,5-dimethyl-2-mercaptothiazole, and the development of the amber-to-red color of the complex of bivalent rhodium with this reagent taken as evidence of reduction. Only stannous chloride and chromous chloride, of the following compounds investigated, were useful for this purpose: ascorbic acid, cadmium, chromous chloride, ferrous sulphate, formic acid, *d*-glucose, hydrazine, hydrogen peroxide, hydroquinone, hydroxylamine, potassium hydrogen tartrate, sodium dithionite, sodium hypophosphite, sodium hyposulphite, sodium sulphite, stannous chloride, titanous chloride, zinc.

Reduction with Stannous Chloride

Stannous chloride, as is well known, reacts with acidified tervalent rhodium solutions to give a yellow or red color that is not extracted by chloroform; when it is added to rhodium solutions containing 4,5-dimethyl-2-mercaptothiazole, however, an amber-to-red color develops that is readily extracted by chloroform. The chloroform extract from iridium solutions similarly treated is colorless and free of iridium. Rhodium can be readily separated from iridium by this means in chloride solutions or from hydrochloric acid solutions containing sulphate. The optical densities for chloroform extract from samples containing the same quantity of rhodium are inconsistent. Reproducible results, and optical densities agreeing with those given by the original procedure with 4,5-dimethyl-2-mercaptothiazole (14), are obtained by removing the chloroform on the steam bath and dissolving the residue in a little ethanol and a diluted hydrochloric acid solution.

2-Mercaptothiazole, 2-mercaptothiazoline, 2-mercaptobenzoxazole, 4-methyl-2-mercaptothiazole, and 4-phenyl-2-mercapothiazole react also to give colored chloroform extracts. The extracts obtained for compounds substituted in the 4-position are amber-to-red in color but are yellow for the unsubstituted ones. Colorless chloroform extracts are obtained for 4-methyl-2-hydroxythiazole and 2-aminothiazole; the mercapto group is, therefore, essential to the reaction.

A Spekker photoelectric absorptiometer with an Ilford No. 601 filter (maximum transmittancy at 430 mμ) and a Cenco-Sheard-Sanford 'Photelometer' (filter No. C with maximum transmission at 435 mμ) were used to obtain the recorded data.

Reagents

4,5-Dimethyl-2-mercaptothiazole.—The reagent was made by the method of Buchman, Riems, and Sargent (15) and was recrystallized from 25% ethyl alcohol; a solution was prepared by dissolving 0.5 g in 100 ml of 50% ethanol.

Standard rhodium and iridium solutions.—These solutions were prepared by dissolving known weights of Matthey spectrographically pure ammonium chlororhodite and ammonium chloroiridate in dilute acid solutions.

Stannous chloride solutions.—The stannous chloride solution was a 10% solution of the dihydrate in 2 *N* hydrochloric acid.

Can. J. Chem. Downloaded from www.nrcresearchpress.com by 210.87.254.5 on 09/05/12
For personal use only.

Procedure

Solutions containing 0.04 to 0.3 mg of rhodium were transferred to separatory funnels and were made 3 to 9 *M* in hydrochloric acid by addition of the concentrated acid, and 1 ml of reagent solution was added for each 0.1 mg or less of rhodium expected to be present. The rhodium was reduced by adding 10 drops or more of stannous chloride, the solution then extracted with 15 ml of chloroform, and the organic phase transferred to a small beaker or flask; the aqueous layer was again extracted with 10 ml of chloroform. The combined extracts were evaporated on a steam bath and the residue was dissolved in 5 ml of ethanol, then boiled with 25 ml of 2.5 *M* hydrochloric acid. After being cooled, the solution was transferred to a 50-ml graduated flask and diluted to the mark with water. The optical density was measured in a 1-cm cell of an absorptiometer using a filter with maximum transmittancy of 430–435 mμ.

The optical densities obtained under various conditions are shown in Table I. These results are for 0.185 mg of rhodium, 2 ml of reagent, and a 1-cm cell; 10 drops of stannous chloride were used for reduction and the volume of the solution, before extraction, was approximately 20 ml for these samples.

TABLE I

Optical density of solutions of 0.185 mg of rhodium under various conditions

No.	Condition	Optical density
(1)	Hydrochloric acid present, 1.0 ml	0.384
(2)	,, ,, ,, 5.0 ml	0.448
(3)	,, ,, ,, 10.0 ml	0.446
(4)	,, ,, ,, 15.0 ml	0.446
(5)	As in (2) + 2.0 ml of concentrated sulphuric acid	0.447
(6)	As in (2) + 5.0 ml of stannous chloride	0.444
(7)	As in (2) but stannous chloride added before reagent	0.425
(8)	As in (2) but 5.0 ml of reagent added	0.448

The data show that rhodium can be readily separated from 3 to 9 *M* hydrochloric acid solutions and determined by this procedure. Results are satisfactory in chloride solutions containing sulphuric acid, and excess stannous chloride or reagent cause no difficulty. The optical density for the same concentration of rhodium by the boiling procedure (14) is 0.447. Addition of stannous chloride before reagent causes some difficulty in removing the last traces of rhodium complex from the aqueous layer, and slightly low values for rhodium content are obtained. The procedure, using stannous chloride as reducing agent, gives unreliable results when applied to rhodium solutions that have been fumed with sulphuric acid; the chloroform extract from such solutions contains some yellow-colored product, in addition to the rhodium complex, the amount of which is dependent upon reagent, stannous chloride, and sulphuric acid concentration.

As in the original procedure (14) the colored solution obeys Beer's law over the range applicable for a 1-cm cell but the complex is not as stable. The optical density changed from 0.446 to 0.437 when the solution was kept in daylight in a closed container for 1 hour and decreased to 0.383 when the solution was left to stand overnight.

Separation of Rhodium from Iridium

Rhodium can be easily separated from iridium in chloride solutions; however, reagent is added to completely decolorize any quadrivalent iridium before the usual procedure is carried out. Results are shown in Table II.

Can. J. Chem. Downloaded from www.nrcresearchpress.com by 210.87.254.5 on 09/05/12
For personal use only.

TABLE II

Separation of rhodium from iridium

No.	Rh taken, mg	Rh found, mg	Ir present, mg	Approx. Ir:Rh ratio
1	0.037	0.036	3.7	100:1
2	0.037	0.039	30.2	800:1
3	0.052	0.053	1.0	20:1
4	0.052	0.054	4.5	85:1
5	0.074	0.073	7.4	100:1
6	0.130	0.129	5.2	40:1
7	0.150	0.150	2.2	15:1
8	0.150	0.153	16.0	100:1
9	0.185	0.181	4.0	20:1
10	0.185	0.185	25.0	140:1
11	0.185	0.185	33.0	180:1

A large excess of stannous chloride (5 ml), although unnecessary, was added for most of the results recorded in Table II; in results 3, 4, 6, obtained independently by H. M. Whitehead, 10–15 drops of stannous chloride were used for reduction.

Reduction with Chromous Chloride

The soluble complex formed on addition of chromous chloride to rhodium solutions containing 4,5-dimethyl-2-mercaptothiazole is extracted by chloroform from chloride solutions or from sulphate solutions containing hydrochloric acid; in chloride solutions the iridium complex is also extracted by chloroform. It is worth while noting that, although the iridium complex is extracted from freshly prepared ammonium chloroiridate solutions, no extraction of iridium occurs from the same solution after it has stood more than 2 weeks.

Procedure

Five milliliters of lithium sulphate:sulphuric acid reagent (13.5 g of Li_2SO_4 in 100 ml of concentrated H_2SO_4) was added to chloride solutions containing rhodium and iridium, and the solutions fumed to crystallization of lithium sulphate. The samples were diluted with 5 ml of water, heated to ensure complete dissolution, cooled to room temperature, and transferred to a separatory funnel. An approximately equal volume of concentrated hydrochloric acid was then added and freshly prepared chromous chloride solution (approximately 1 *N*) added dropwise to reduce rhodium and iridium. An excess of reagent was added, the solutions extracted with chloroform, and the procedure completed as described for stannous chloride. Results are given in Table III. The results show that rhodium can be separated from iridium, in solutions that have been fumed with sulphuric acid, by this procedure.

TABLE III

Separation of rhodium from iridium by chromous chloride procedure

Rh taken, mg	Rh found, mg	Ir present, mg
0.040	0.039	5.0
0.040	0.040	10
0.051*	0.051	1.0
0.051*	0.051	4.5
0.052*	0.054	9.0
0.078*	0.078	4.5
0.210	0.213	10
0.210	0.208	20

*These results were obtained independently by H. M. Whitehead, a member of this laboratory.

Can. J. Chem. Downloaded from www.nrcresearchpress.com by 210.87.254.5 on 09/05/12
For personal use only.

CONCLUSIONS

Rhodium can be separated and determined colorimetrically by extraction of the complex formed with 4,5-dimethyl-2-mercaptothiazole obtained after reduction with stannous chloride or chromous chloride. Rhodium can be separated from iridium in chloride solutions using stannous chloride as reducing agent; in solutions that have been fumed with sulphuric acid it is necessary to use chromous chloride to obtain satisfactory separation.

This work was carried out, in part, at the Imperial College of Science and Technology, London, England, and was supported by a travel grant from the National Research Council.

REFERENCES

1. R. S. YOUNG. Analyst, **76**, 49 (1951).
2. J. G. FRASER, W. A. E. MCBRYDE, and F. E. BEAMISH. Anal. Chem. **26**, 495 (1954).
3. J. H. YOE and L. G. OVERHOLSER. J. Am. Chem. Soc. **61**, 2058 (1939).
4. D. E. RYAN. Analyst, **76**, 167 (1951).
5. D. E. RYAN. Analyst, **76**, 310 (1951).
6. W. B. POLLARD. Analyst, **67**, 184 (1942).
7. R. GILCHRIST and E. WICHERS. J. Am. Chem. Soc. **57**, 2565 (1935).
8. J. H. YOE and J. J. KIRKLAND. Anal. Chem. **26**, 1335 (1954).
9. G. G. TERTIPIS and F. E. BEAMISH. Anal. Chem. **32**, 486 (1960).
10. S. S. BERMAN and W. A. E. MCBRYDE. Can. J. Chem. **36**, 845 (1958).
11. W. A. E. MCBRYDE. Analyst, **80**, 503 (1955).
12. D. E. RYAN. Analyst, **79**, 707 (1954).
13. E. JACKSON. Analyst, **84**, 106 (1959).
14. D. E. RYAN. Analyst, **75**, 557 (1950).
15. E. R. BUCHMANN, A. O. RIEMS, and H. J. SARGENT. J. Org. Chem. **6**, 764 (1941).

Can. J. Chem. Downloaded from www.nrcresearchpress.com by 210.87.254.5 on 09/05/12
For personal use only.

Can. J. Chem. Downloaded from www.nrcresearchpress.com by 210.87.254.105 on 09/05/12
For personal use only.

THE EFFECT OF HYDROGEN CHLORIDE ON THE NEAR-INFRARED SPECTRUM OF NYLON[1]

P. LAROSE

ABSTRACT

Samples of oriented nylon film and filament were treated with anhydrous HCl and examined in the near-infrared region of 9000 to 3700 cm^{-1} with polarized light. The results are in agreement with previous observations made in the 3600–600 cm^{-1} region, and corroborate earlier evidence that HCl interacts with the peptide linkage. The disorienting effect of the HCl is also reflected in the spectrum of the treated specimens.

INTRODUCTION

The results of experiments on the effect of hydrogen chloride on the infrared spectrum of nylon in the region of 3600 to 600 cm^{-1} have been reported (5). The investigation has now been extended to the overtone region of 9000 to 3700 cm^{-1} since the spectrum of nylon in this region has been studied and the assignment of the bands discussed by several workers (1, 2, 3). It was hoped in this way to confirm our earlier results and possibly to provide additional data to support the assignment proposed for the various absorption bands.

EXPERIMENTAL

Oriented Zytel[2] film was prepared by casting onto glass from ethanol solution and stretching the film in hot water. Nylon 6 film[3] was also oriented by stretching it in hot water, while a sample of nylon 6.6 was examined in the form of a ribbon about 0.3 mm thick prepared by rolling a monofilament lengthwise. The samples were immersed in hexachlorbutadiene and the absorption spectra recorded on a Beckman DK2 spectrophotometer with light polarized by means of a Polaroid HR plastic filter. The samples were studied before and after treatment with anhydrous HCl and also after removal of the HCl *in vacuo*.

RESULTS

The various film and filament specimens yielded results which differed little in character so that no attempt will be made to distinguish between these various forms of nylon in discussing the results.

Figure 1 shows the spectrum of an oriented nylon film before treatment with HCl. It differs little from the spectrum reported by other workers with regard to dichroism and position of the absorption bands. Figure 2 is a portion of the absorption spectrum of a different sample of untreated nylon included here to emphasize a difference between the two vectors to be discussed. Figure 3 represents the spectrum of a sample treated with HCl. Figure 4 shows the spectrum of a thick sample after removal of the HCl, while Fig. 5 is for a thin sample also after removal of the HCl.

Because of form dichroism resulting from differences in the refractive indices of the nylon in directions parallel and perpendicular to the polymer chain direction, and because

[1]*Manuscript received July 28, 1961.*
Contribution from the Division of Pure Chemistry, National Research Council, Ottawa, Canada. Issued as N.R.C. No. 6535.
[2]*A copolymer of nylons 6, 6.6, and 6.10.*
[3]*The author is indebted to Dr. Stace of the British Nylon Spinners for this film.*

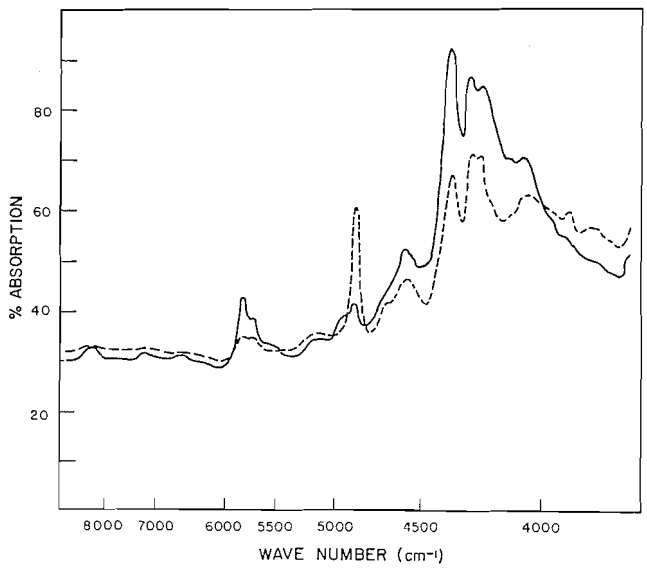


FIG. 1. Near-infrared spectrum of oriented nylon film. —— E vector perpendicular to direction of stretching. – – – E vector parallel to direction of stretching.

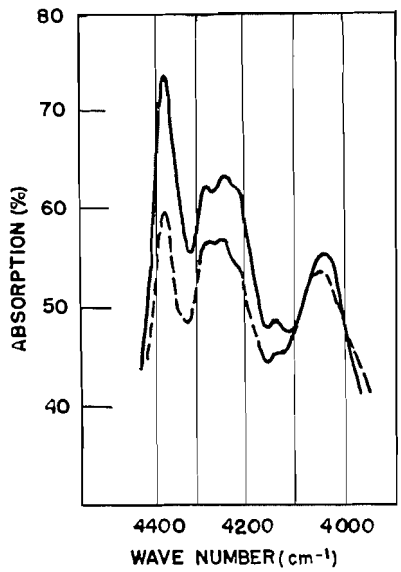


FIG. 2. As for Fig. 1.

of small differences in the transmission of the filter between its horizontal and vertical positions, the extent of dichroism was determined from a line drawn through the absorption minima. However, because of the uncertainties involved in such a method, no attempt has been made to express the dichroism quantitatively.

Can. J. Chem. Downloaded from www.nrcresearchpress.com by 210.87.254.105 on 09/05/12
For personal use only.

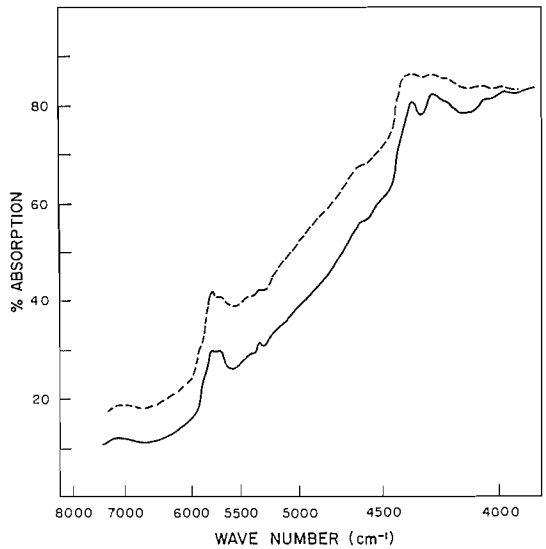


FIG. 3. Spectrum of nylon treated with HCl.

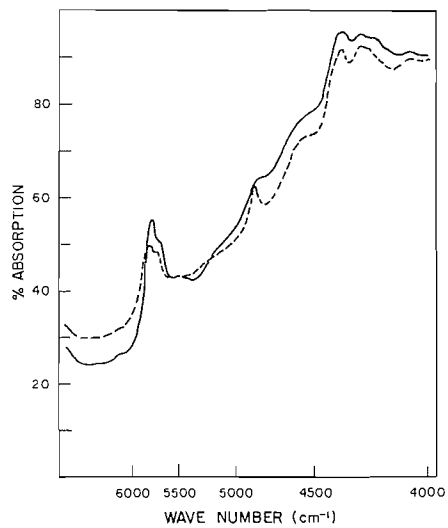


FIG. 4. Spectrum of thick nylon sample treated with HCl and subsequently evacuated.

DISCUSSION

If, as assumed in previous work (4, 5), the HCl acts on the —NH.CO— group, one would expect all overtones or combination modes involving this linkage to be affected by the HCl, whereas the bands due to the —CH_2— groups in the chain should not be so affected. A comparison of the spectra of the nylon treated with HCl with the spectrum of the untreated nylon shows that this was indeed the case. The changes produced by the HCl on the various bands are as follows.

Can. J. Chem. Downloaded from www.nrcresearchpress.com by 210.87.254.105 on 09/05/12
For personal use only.

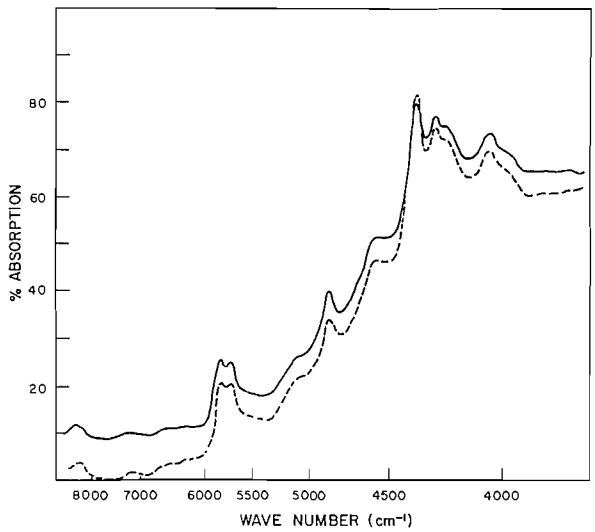


FIG. 5. Spectrum of thin nylon film treated with HCl and subsequently evacuated.

A weak band at 8240 cm^{-1} showing perpendicular (σ) dichroism in the untreated nylon is no doubt the same band as that reported at 8300 cm^{-1} by Hecht and Wood (3) (henceforth H and W) and at 8292 cm^{-1} by Glatt and Ellis (2) (G and E). It has been assigned as the third harmonic of the CH_2 stretching vibration at 2960 cm^{-1} (ν_a) or 2860 cm^{-1} (ν_s). The treated samples still show this band but the dichroism is absent (Fig. 5) because of the disorienting effect of the HCl. The disorientation is irreversible and is found in all HCl-treated samples. Some dichroism will be found remaining in the spectrum shown in Fig. 4. In this case the thickness of the sample prevented complete penetration of the HCl in the time allowed for absorption, and the residual effect is undoubtedly due to some unaffected nylon.

Another weak band at a frequency of 7020 cm^{-1} behaves like the 8240 cm^{-1} band. It does not seem to have been mentioned by other workers. It may be a combination of a —CH_2— deformation mode with twice its stretching frequency ($2\nu+\delta$).

The 6520 cm^{-1} band with σ dichroism falls within the range 6300–6680 cm^{-1} given by H and W (3) for 2νNH. G and E (2) have also given this assignment to a 6523 cm^{-1} band. Being an NH band, it is affected by the HCl and is absent in the spectrum of the treated samples.

Two bands at 5760 and 5660 cm^{-1} show σ dichroism, particularly strong for the first one. These correspond to the 5800–5700 cm^{-1} bands mentioned by H and W (3) and the bands at 5804 and 5695 cm^{-1} cited by G and E (2). The frequencies we have observed correspond more closely to the 5780 and 5656 cm^{-1} frequencies given by G and E (2) for the polyethylene chain. They have been given the assignment $2\nu_a$ and $2\nu_s$ of the —CH_2— vibrations respectively. The behavior of these bands when nylon is treated with HCl is similar to that mentioned for the other bands involving —CH_2— modes. The 5150 cm^{-1} band is generally attributed to water and shows no dichroism.

Another band at 4960 cm^{-1} shows some σ dichroism and is no doubt that given at 4975 cm^{-1} by G and E (2) and assumed by them to be the third harmonic of a C=O vibration at 1640 cm^{-1}. However, Fraser (1) has assigned this band to a combination of the NH

Can. J. Chem. Downloaded from www.nrcresearchpress.com by 210.87.254.105 on 09/05/12
For personal use only.

vibration at 3300 cm^{-1} with the C=O vibration. The complete disappearance of this band in nylon treated with HCl favors the latter explanation since our earlier work (5) has shown that the effect of the HCl is much more pronounced on the 3300 cm^{-1} vibration than on the 1640 cm^{-1} vibration.

The band showing the greatest degree of dichroism is that at 4880 cm^{-1}. The parallel (π) dichroism agrees with that given by H and W (3) at 4850 cm^{-1}. There is agreement on the assignment of this band as a combination of the NH vibration at 3300 cm^{-1} and the amide II or NH deformation band at 1545 cm^{-1}. The band is absent in the spectrum of the HCl-treated samples, as expected, but it reappears when the HCl is removed, but with no dichroism (Fig. 5) or little dichroism (Fig. 4, for reason previously discussed).

Another absorption band showing π dichroism is found with a frequency of 4680 cm^{-1}. G and E (2) mention a band with low dichroism at a frequency of 4700 cm^{-1}. Fraser (1) gives it the assignment $2\nu_2+\nu_6$ or twice the NH deformation vibration of 690 cm^{-1} plus the NH stretching vibration of 3300 cm^{-1}. The association of this band with the NH group results in its disappearance when nylon is treated with HCl but it does not reappear when the HCl is removed.

A band at 4580 cm^{-1} shows little, if any, dichroism. H and W (3) mention a band at 4590 cm^{-1} as having σ dichroism. Fraser (1) cites this band as having a low dichroism and assigns to it the combination of the NH vibration at 3300 cm^{-1} with the amide III band at 1250 cm^{-1}. In the treated sample this band is just discernible as a shoulder on the broad absorption band covering the 5400–4500 cm^{-1} region. In the evacuated samples it is more pronounced. In the untreated sample, this band is accompanied by a band at 4550 cm^{-1} appearing as a small shoulder on the perpendicular spectrum only and possessing therefore some σ dichroism. Fraser (1) has calculated a band at 4490 cm^{-1} (10 cm^{-1} less than the 4500 cm^{-1} calculated for the 4590 cm^{-1} band) from a combination of twice the 1650 cm^{-1} C=O vibration with the 1280 cm^{-1} NH deformation mode. This might well be the band we observed at 4550 cm^{-1}. In the treated and evacuated samples a broad shoulder probably covers both 4580 and 4550 cm^{-1} bands.

The bands at 4350, 4275, 4230, and 4070 cm^{-1} are all combinations involving the asymmetric or symmetric CH_2 stretching vibrations plus one of the deformation modes. In the treated samples, the large degree of scattering obscures these bands, which, as a result, appear to have a much reduced intensity.

One peculiar feature of these bands is the difference between the parallel and the perpendicular vibrations in the 4220–4280 cm^{-1} region (Figs. 1 and 2). Whereas the 4275 cm^{-1} band is well separated from the 4230 cm^{-1} band in the perpendicular spectrum, the 4230 cm^{-1} band is displaced to a higher frequency, ~4240 cm^{-1}, in the parallel spectrum, and appears to have some π dichroism. Fraser (1) mentions a band with a frequency of 4260 cm^{-1}, which is probably the same as our 4275 cm^{-1} band, and one at 4220 cm^{-1} with π dichroism. G and E (2) give bands at 4257, 4219, and 4202 cm^{-1}. The 4220 cm^{-1} appears as a shoulder in Fig. 2.

A small band at 3900 cm^{-1} with definite π dichroism has not been mentioned by other workers. It is not discernible in the samples treated with HCl. It could be a combination of the NH 3300 cm^{-1} band plus the 690 cm^{-1} deformation mode.

It is evident from these observations that any combination band involving the NH or peptide linkage is affected by the treatment of nylon with HCl whereas any change in the vibrations depending solely on the —CH_2— groups is only of a secondary nature. It is also clear that the HCl treatment results in a loss of orientation of the polymer chains. This is in accord with the conclusions drawn from our previous work in the

Can. J. Chem. Downloaded from www.nrcresearchpress.com by 210.87.254.105 on 09/05/12
For personal use only.

region of lower frequencies (5). If one accepts these conclusions a priori, then the results of these experiments can be regarded as confirmation for some of the assignments made in the overtone region of the nylon spectrum.

REFERENCES

1. R. D. B. FRASER. Proc. Int. Wool Text. Research Conference, Australia B. 120 (1955); J. Chem. Phys. **24**, 89 (1956).
2. L. GLATT and J. W. ELLIS. J. Chem. Phys. **19**, 449 (1951).
3. K. T. HECHT and D. L. WOOD. Proc. Roy. Soc. (London), A, **235**, 174 (1956).
4. P. LAROSE. Textile Research J. **25**, 956 (1955).
5. P. LAROSE. Can. J. Chem. **35**, 1239 (1957).

Can. J. Chem. Downloaded from www.nrcresearchpress.com by 210.87.254.105 on 09/05/12
For personal use only.

Can. J. Chem. Downloaded from www.nrcresearchpress.com by 210.87.254.6 on 09/05/12
For personal use only.

THE SYNTHESIS OF ACETAMIDO-DEOXY KETOSES BY ACETOBACTER SUBOXYDANS

PART II[1]

J. K. N. JONES, M. B. PERRY, AND J. C. TURNER

ABSTRACT

The microbiological oxidation of 1-deoxy-1-*N*-methylacetamido-D-glucitol and 2-acetamido-1,2-dideoxy-D-glucitol yielded a syrupy ketose and a crystalline ketose respectively. Crystalline derivatives of each were prepared and structural investigations of the ketoses showed the former to be 6-deoxy-6-*N*-methylacetamido-L-xylohexulose and the latter to be 5-acetamido-5,6-dideoxy-L-xylohexulose.

INTRODUCTION

The microbiological oxidation of unsubstituted polyhydric alcohols has been studied extensively (1, 2, 3, 4, 5, 6), and the oxidation of terminal-substituted polyhydric alcohols has also been investigated in several laboratories (7, 8, 9, 10). Recently we reported the oxidation of the substituted hexitol 2-acetamido-2-deoxy-D-glucitol by *Acetobacter suboxydans* to 5-acetamido-5-deoxy-L-xylohexulose (11) and in this paper we wish to report the microbiological oxidation of 1-deoxy-1-*N*-methylacetamido-D-glucitol (I) to 6-deoxy-6-*N*-methylacetamido-L-xylohexulose (II), and of 2-acetamido-1,2-dideoxy-D-glucitol (III) to 5-acetamido-5,6-dideoxy-L-xylohexulose (IV).

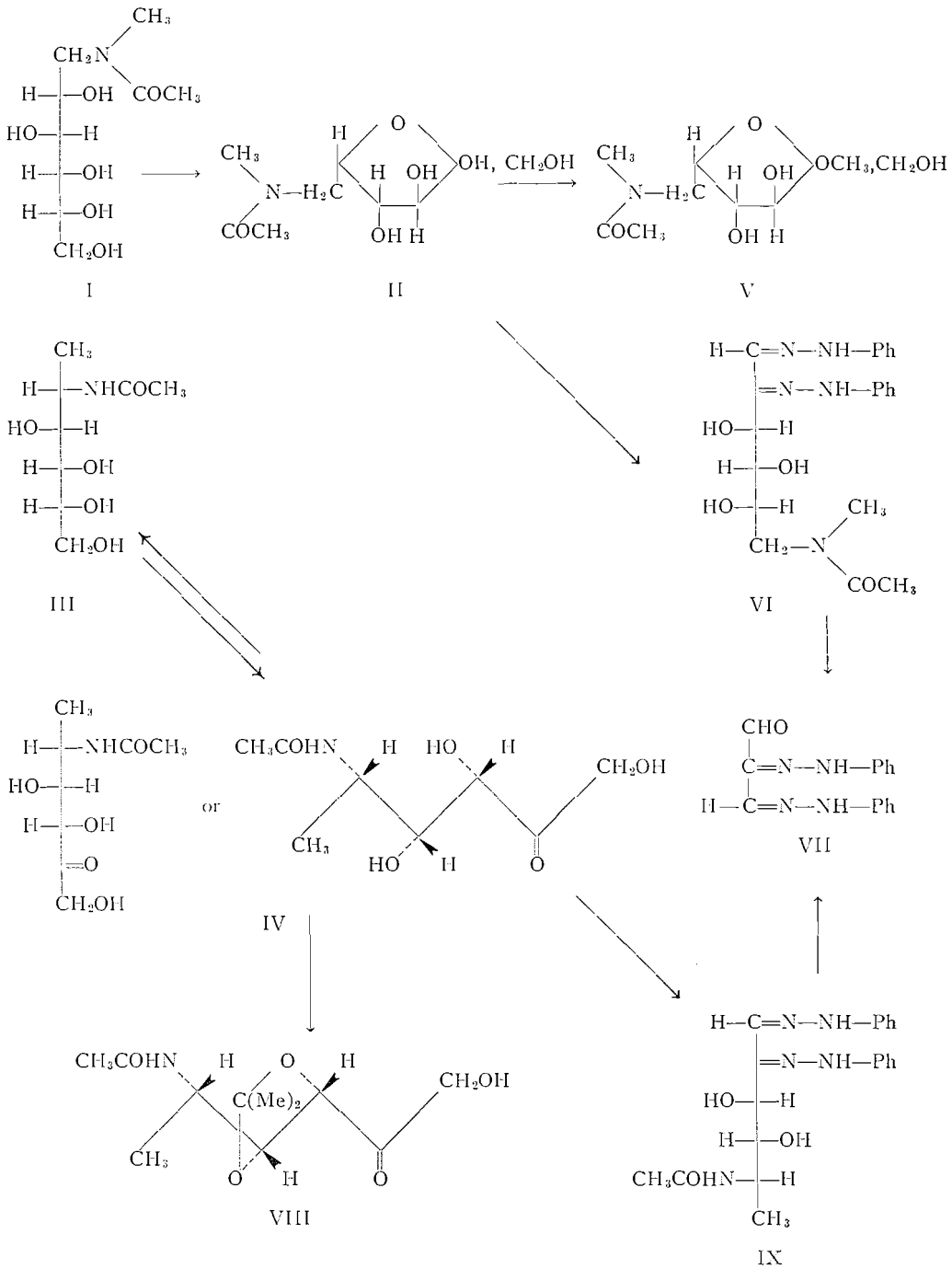
The oxidation of 1-deoxy-1-*N*-methylacetamido-D-glucitol (I) yielded a syrup which gave absorptions in the infrared corresponding to OH, CH, and C=O of the tertiary amide group. A weak band at 1730 cm^{-1} was also observed and was probably due to the presence of a small amount ($\sim$5%) of the acyclic form of the ketose. The results of periodate oxidation indicated that the main bulk of the material existed in the furanose ring form (II). Further evidence for a furanose ring form was given by the ready and rapid formation of a crystalline methyl glycoside (V) which was stable towards alkali but which was readily hydrolyzed with dilute acid. The rate of periodate oxidation of the glycoside (V) indicated that the two free hydroxyl groups, between which cleavage had occurred, were held in the trans configuration by the near-planar furanose ring.

The ketose (II) gave a crystalline phenylosazone (VI) which, when oxidized with periodate by the method of Hough, Powell, and Woods (12), consumed 2 moles of periodate, releasing 0.58 mole formic acid and no formaldehyde. The apparent low formic acid release agreed with the findings of Hough, Powell, and Woods, who obtained similar results from the periodate oxidation of monosaccharide and disaccharide phenylosazones (12). An immediate precipitate of the 1,2-bisphenylhydrazone of mesoxalaldehyde (VII) was obtained from the oxidation. The oxidation results indicated that the osazone (VI) possessed free hydroxyl groups at carbons 3, 4, and 5, and that the ketose (II) from which it was derived was a 2-ketose.

The ketose (II) was very slowly reduced by sodium borohydride to give a syrup which could not be crystallized. This product apparently consisted of the two expected isomeric hexitols although they could not be separated by paper chromatography in several solvent systems.

[1]*Manuscript received June 7, 1961.*
Contribution from the Department of Organic Chemistry, Queen's University, Kingston, Ontario.

The above results showed that the ketose had the indicated structure (II), the major portion being in the furanose ring form, and that the site of biological oxidation in 1-deoxy-1-*N*-methylacetamido-D-glucitol was at carbon 5, in accordance with the well-known enzyme specificity for oxidations at pH 5–6.5.



Can. J. Chem. Downloaded from www.nrcresearchpress.com by 210.87.254.6 on 09/05/12
For personal use only.

Can. J. Chem. Downloaded from www.nrcresearchpress.com by 210.87.254.6 on 09/05/12
For personal use only.

The oxidation of 2-acetamido-1,2-dideoxy-D-glucitol (III) by *Acetobacter suboxydans* gave crystalline 5-acetamido-5,6-dideoxy-L-xylohexulose (IV). The results of periodate oxidation indicated that enzymic oxidation had not occurred at the primary alcohol group of the hexitol. The formation of aldofuranose rings was thus excluded on this evidence and the ketose therefore probably existed in the acyclic zigzag form (IV). Evidence to support this conclusion was given by (*a*) the strong, sharp peak at 1735 cm^{-1} which was observed in the carbonyl region of the infrared spectrum, and (*b*) by the fact that the ketose (IV) was not oxidized by bromine water or alkaline hypoiodite solution.

The ketose (IV) rapidly reduced Fehling's solution in the cold and epimerized easily when warmed in pyridine solution or allowed to stand in contact with base for a short time, due to the ease of keto-enol tautomerism in the acyclic form.

With acidified acetone the ketose (IV) gave a syrupy isopropylidene derivative (VIII), the infrared spectrum and periodate oxidation of which indicated that acetal formation had occurred across the hydroxyl groups on carbons 3 and 4, which were therefore favorably situated for this reaction.

Reaction of the ketose (IV) with phenylhydrazine gave a crystalline phenylosazone (IX), which, on periodate oxidation, consumed 1 mole of periodate and released no formic acid or formaldehyde. An immediate precipitate of the 1,2-bisphenylhydrazone of mesoxalaldehyde (VII) was obtained. The above evidence indicated that the phenylosazone (IX) possessed free hydroxyl groups on carbons 3 and 4 and that the ketose (IV) from which it was derived was a 2-ketose.

Reduction of the ketose (IV) with sodium borohydride gave crystalline 2-acetamido-1,2-dideoxy-D-glucitol (III), which confirmed that the hydroxyl groups at carbons 3 and 4 of the ketose (IV) were in the D-*threo* configuration since the position of the keto group had been fixed at carbon 2 by previous evidence.

The above results indicated that the biological oxidation product was the acyclic 2-hexulose, 5-acetamido-5,6-dideoxy-L-xylohexulose (IV), as would be predicted from the Bertrand–Hudson rule for enzymic oxidation by *Acetobacter suboxydans* (13, 14).

EXPERIMENTAL

Melting points are uncorrected and were determined on a Fisher-John melting point apparatus. All evaporations were carried out under reduced pressure at 50° C or less. Optical rotations were measured at 23±3° C in water unless otherwise stated. Paper chromatography was carried out by the descending method (15) using Whatman No. 1 paper in the following solvent systems (v/v):

(A) butan-1-ol/ethanol/water, 9:3:3;
(B) butan-1-ol/pyridine/water, 5:3:2;
(C) ethyl acetate/acetic acid/formic acid/water, 18:3:1:4;
(D) 2-butanone/glacial acetic acid/saturated aqueous boric acid, 9:1:1.

The rates of movement of compounds on paper chromatograms are given relative to that of rhamnose (R_{rh} value). Ketose sugars were detected on paper chromatograms with the orcinol – trichloroacetic acid spray reagent (16), other reducing compounds with the *p*-anisidine hydrochloride spray reagent (17), and non-reducing compounds with the alkaline silver nitrate spray reagent (18). Infrared spectra were measured in chloroform solution or as a dispersion in a potassium bromide pellet, using a Perkin–Elmer Model 21 spectrophotometer. Formaldehyde produced in periodate oxidations was determined by the chromotropic acid method (19).

Can. J. Chem. Downloaded from www.nrcresearchpress.com by 210.87.254.6 on 09/05/12
For personal use only.

SECTION A. STUDIES ON 6-DEOXY-6-*N*-METHYLACETAMIDO-L-XYLOHEXULOSE

Preparation of 1-Deoxy-1-N-methylacetamido-D-glucitol

1-Deoxy-1-*N*-methylamino-D-glucitol (Aldrich Chem. Co. sample) was twice recrystallized from ethanol containing a little water to give a creamy-white product which had m.p. 128–129° C, $[\alpha]_D$ −14° (lit. values, m.p. 126° C, $[\alpha]_D$ −18.5±1° (20)).

1-Deoxy-1-*N*-methylamino-D-glucitol was *N*-acetylated in aqueous solution, using the method of Levvy and McAllan (21), to give a yellow syrup which slowly crystallized on desiccation. The product was recrystallized from methanol/ether, then from ethanol/ether to give white crystals which had m.p. 119–121° C, $[\alpha]_D$ −22°.

6-Deoxy-6-N-methylacetamido-L-xylohexulose

1-Deoxy-1-*N*-methylacetamido-D-glucitol (7 g), sorbitol (3 g), yeast extract powder (0.5 g), and potassium dihydrogen phosphate (0.05 g) were dissolved in tap water (140 ml), and the solution was distributed among six 250-ml conical flasks and autoclaved at 15 p.s.i. for 20 minutes. After being cooled, the sterile broths were inoculated with several drops of a 48-hour culture of *Acetobacter suboxydans* grown in sorbitol solution. The flasks were stored in the dark at room temperature and samples were removed at intervals, under sterile conditions, for examination by paper chromatography and estimation of copper-reducing value by the Somogyi method (22). The appearance of L-sorbose (R_{rh} 0.52, solvent A) was noted, and of a spot (R_{rh} 1.1, solvent A) which gave a pink color changing to green with the orcinol – trichloroacetic acid spray reagent. The results of the Somogyi estimations are shown in Table I.

TABLE I

Oxidation of 1-deoxy-1-*N*-methylacetamido-D-glucitol by *Acetobacter suboxydans*

Time (days)	% yield of ketose (corrected for the presence of L-sorbose)
6	7.2
12	23.6
19	35.6

Growth was terminated after 22 days by pouring the broths into two volumes of ethanol. The solution was filtered, deionized by passage through Amberlite I.R. 120 (H^+) and Duolite A4 (OH') resins, and concentrated to a syrup. L-Sorbose crystallized out and was removed and the residual syrup was then separated into three components by chromatography on a cellulose column using butan-1-ol half-saturated with water as the irrigant. The three components were L-sorbose, 1-deoxy-1-*N*-methylacetamido-D-glucitol, and 6-deoxy-6-*N*-methylacetamido-L-xylohexulose. The latter was obtained as a clear, light yellow syrup (2.2 g), $[\alpha]_D$ −57°. An infrared spectrum was obtained by smearing a little of the syrup onto the surface of a potassium bromide pellet, and showed the following main absorptions: OH (3410 cm^{-1}, strong), CH (2960 cm^{-1}, strong), saturated ketone C=O (1730 cm^{-1}, weak), tertiary amide C=O (1625 cm^{-1}, strong). The complete spectrum is given in Appendix A.

Periodate Oxidation of 6-Deoxy-6-N-methylacetamido-L-xylohexulose

An aqueous solution of 6-deoxy-6-*N*-methylacetamido-L-xylohexulose was oxidized under unbuffered conditions using a twofold excess of sodium metaperiodate. The results of the oxidation are shown in Table II.

TABLE II

Periodate oxidation of 6-deoxy-6-*N*-methylacetamido-L-xylohexulose

Time (hours)	Periodate uptake (moles/mole)	Formic acid (moles/mole)	Formaldehyde (moles/mole)
0.08	1.84	1.06	
0.17			0.05
1		1.11	
2			0.10
4	2.05	1.20	
4.5			0.23
6	2.14	1.26	
23			0.26
26	2.44	1.50	

Methyl 6-Deoxy-6-N-methylacetamido-L-xylohexulofuranoside

6-Deoxy-6-*N*-methylacetamido-L-xylohexulose (200 mg) was dissolved in anhydrous methanol (5 ml), and anhydrous methanolic hydrogen chloride (1%, 8 ml) added. The solution was allowed to stand at room temperature for $3\frac{1}{2}$ hours, then neutralized with silver carbonate, filtered, and evaporated to dryness. The resulting pale yellow syrup gave a bright yellow spot on paper chromatograms (R_{rh} 1.57, solvent A) with the *p*-anisidine hydrochloride spray reagent. The syrup gave only a faint spot due to unreacted 6-deoxy-6-*N*-methylacetamido-L-xylohexulose with the alkaline silver nitrate spray reagent. After desiccation for 3 days the syrup crystallized and crystallization was speeded by the addition of methanol/ethyl acetate. The crystals were filtered off, dried, and recrystallized twice from methanol/ethyl acetate to give white needles (50 mg) which had m.p. 109–110° C, $[\alpha]_D$ −97°. The glycoside gave absorptions in the infrared corresponding to OH (3480 cm^{-1}), CH (2940, 2880 cm^{-1}), and tertiary amide C=O (1600 cm^{-1}). The complete spectrum is given in Appendix B. Anal. Calc. for $C_{10}H_{19}O_6N$: C, 48.2%; H, 7.6%; N, 5.6%. Found: C, 48.1%; H, 7.4%; N, 5.7%.

Periodate Oxidation of Methyl 6-Deoxy-6-N-methylacetamido-L-xylohexulofuranoside

The glycoside was oxidized with a twofold excess of sodium metaperiodate in unbuffered aqueous solution. The results of the oxidation are given in Table III. No formaldehyde was detected in the oxidation mixture.

TABLE III

Periodate oxidation of methyl 6-deoxy-6-*N*-methylacetamido-L-xylohexulofuranoside

Time (hours)	Periodate uptake (moles/mole)	Formic acid (moles/mole)
0.08	0.07	0.00
5	0.88	0.03
9	0.98	0.00
23.5	1.00	0.02

6-Deoxy-6-N-methylacetamido-L-xylohexulose Phenylosazone

The osazone was prepared by the usual method using freshly distilled phenylhydrazine and glacial acetic acid. It was recrystallized twice from ethanol/ethyl acetate and once from ethanol/ether to give a bright yellow powder, m.p. 182–183° C. The osazone gave absorptions in the infrared corresponding to OH (3430 cm^{-1}), NH (3270 cm^{-1}), aromatic

Can. J. Chem. Downloaded from www.nrcresearchpress.com by 210.87.254.6 on 09/05/12
For personal use only.

CH (3080 cm^{-1}), aliphatic CH (2940, 2880 cm^{-1}), tertiary amide C=O (1625 cm^{-1}), and the aromatic ring (1610, 1500, 750, 690 cm^{-1}). The complete spectrum is given in Appendix C. Anal. Calc. for $C_{21}H_{27}O_4N_5$: C, 61.0%; H, 6.5%; N, 16.9%. Found: C, 60.5%; H, 6.6%; N, 16.2%.

Periodate Oxidation of 6-Deoxy-6-N-methylacetamido-L-xylohexulose Phenylosazone

The osazone was oxidized in 50% aqueous ethanol by the method of Hough, Powell, and Woods (12). The results of the oxidation are shown in Table IV.

TABLE IV

Periodate oxidation of 6-deoxy-6-*N*-methylacetamido-L-xylohexulose phenylosazone

Time (hours)	Periodate uptake (moles/mole)	Formic acid (moles/mole)	Formaldehyde (moles/mole)
0.42	1.90	0.41	0.00
1.66	2.05	0.59	0.00
3.08	2.14	0.58	0.00

1,2-Bisphenylhydrazone of Mesoxalaldehyde (23)

In the periodate oxidation of 6-deoxy-6-*N*-methylacetamido-L-xylohexulose phenylosazone, a curdy mass of orange-yellow needles was precipitated 30 seconds after oxidation had started. The crystals of the 1,2-bisphenylhydrazone of mesoxalaldehyde were centrifuged off and the supernatant returned to the flask for oxidation studies. The crystals were washed with water, dried, and recrystallized from 50% aqueous ethanol, m.p. 189–191° C. An authentic specimen had m.p. 193–194° C and the mixed m.p. was 189–191° C. The infrared spectra of the authentic and derived specimens were identical over the range 4000–600 cm^{-1}. The spectra were given in a previous publication (11).

Sodium Borohydride Reduction of 6-Deoxy-6-N-methylacetamido-L-xylohexulose

An aqueous solution of 6-deoxy-6-*N*-methylacetamido-L-xylohexulose (100 mg) was reduced with an equal weight of sodium borohydride at 5° C for 18 hours. After removal of sodium borohydride and sodium borate the product was obtained as a syrup (100 mg) which gave two spots, R_{rh} 1.1 (unreduced ketose) and R_{rh} 0.61 (polyhydric alcohols) in solvent A, with the alkaline silver nitrate spray reagent. The polyhydric alcohols were separated from the ketose on Whatman 3 MM paper and obtained as a syrup (75 mg) which gave one spot with the alkaline silver nitrate spray reagent on chromatography in solvents A, B, C, and D. The syrup gave one fraction only, when passed through a column of Dowex 50 W resin (8% cross-linked with divinylbenzene, barium salt form, 200–400 mesh).

The syrup had $[\alpha]_D$ −17° ($[\alpha]_D$ of 1-deoxy-1-*N*-methylacetamido-D-glucitol was −22°) and it was concluded that it contained 1-deoxy-1-*N*-methylacetamido-D-glucitol and probably the isomeric L-iditol derivative. Certainly some 1-deoxy-1-*N*-methylacetamido-D-glucitol was present since oxidation of the syrupy mixture by *Acetobacter suboxydans* gave some 6-deoxy-6-*N*-methylacetamido-L-xylohexulose.

Section B. Studies on 5-Acetamido-5,6-dideoxy-L-xylohexulose

Preparation of 2-Acetamido-1,2-dideoxy-D-glucitol

2-Amino-2-deoxy-D-glucose Diethyl Dithioacetal

2-Amino-2-deoxy-D-glucose hydrochloride (15 g), fuming hydrochloric acid (120 ml), and ethanethiol (45 ml) were shaken in a pressure bottle at room temperature for 20 hours.

Can. J. Chem. Downloaded from www.nrcresearchpress.com by 210.87.254.6 on 09/05/12
For personal use only.

The solution was diluted with ethanol, lead acetate was added, and then lead carbonate was added to neutrality. The solution was filtered and the lead salts were washed with ethanol. The filtrate and washings were combined and saturated with hydrogen sulphide, a little charcoal was added, and the solution was filtered and concentrated to a yellow syrup. The syrup was dissolved in water and passed through Duolite A4(OH′) resin. The eluate was concentrated to give crystalline 2-amino-2-deoxy-D-glucose diethyl dithioacetal (10.9 g), m.p. 107–109° C, $[\alpha]_D$ −22° (lit. values, m.p. 109–110° C, $[\alpha]_D$ −24° (24)).

*2-Amino-2-deoxy-*D*-glucose Diethyl Dithioacetal Penta-acetate*

2-Amino-2-deoxy-D-glucose diethyl dithioacetal (10 g) was acetylated with acetic anhydride in pyridine solution at room temperature for 24 hours to give 2-amino-2-deoxy-D-glucose diethyl dithioacetal penta-acetate as a colorless syrup (17 g), $[\alpha]_D$ +2° (*c*, 1.54 in chloroform) (lit. value $[\alpha]_D$ +1° (chloroform) (24)).

*2-Acetamido-1,2-dideoxy-*D*-glucitol*

2-Amino-2-deoxy-D-glucose diethyl dithioacetal penta-acetate (17 g) was reductively desulphurized by being boiled under reflux with Raney nickel catalyst for 5 hours in ethanol solution. The solution was filtered and the catalyst was washed several times with hot ethanol. The filtrate and washings were combined and evaporated to dryness, giving 2-amino-1,2-dideoxy-D-glucitol penta-acetate as a semicrystalline syrup (8.6 g). The syrup was dissolved in methanol (400 ml) and cooled to 0° C. A stream of anhydrous ammonia was passed into the solution for 20 minutes and the solution allowed to stand for 2 hours at room temperature, then evaporated to dryness. The crystalline residue was dissolved in methanol and an equal volume of chloroform was added, followed by ether to incipient opalescence. Small needles of 2-acetamido-1,2-dideoxy-D-glucitol crystallized out and were recrystallized by the same method to give a chromatographically pure product (3.9 g) which had m.p. 160–162° C, $[\alpha]_D$ −14° (lit. values, m.p. 162–164° C, $[\alpha]_D$ −9° (25)).

*5-Acetamido-5,6-dideoxy-*L*-xylohexulose*

2-Acetamido-1,2-dideoxy-D-glucitol (3 g), sorbitol (3 g), yeast extract powder (0.5 g), and potassium dihydrogen phosphate (0.05 g) were dissolved in tap water (100 ml). The solution was distributed among five 250-ml conical flasks and autoclaved at 15 p.s.i. for 30 minutes. After being cooled to room temperature, the broths were inoculated with several drops of a 48-hour culture of *Acetobacter suboxydans* grown in sorbitol solution, and stored in the dark at room temperature. Samples were removed at intervals under sterile conditions for chromatographic examination and estimation of copper-reducing values by the Somogyi method (23).

The appearance of L-sorbose (R_{rh} 0.49, solvent A), and a spot (R_{rh} 1.13, solvent A) which gave a yellow color with the orcinol – trichloroacetic acid spray reagent was noted. The results of the Somogyi estimations showed a 16.7% yield of 5-acetamido-5,6-dideoxy-L-xylohexulose after 7 days and a 69% yield after 20 days. Growth was terminated after 31 days by pouring the broths into 2 volumes of ethanol. The solution was filtered and rapidly passed through small beds of Amberlite I.R. 120 (H^+) and Duolite A4 (OH^-) resins at 5° C. The eluate and washings were concentrated at 35–40° C to a brown syrup which slowly crystallized on the addition of ethanol. The crystalline L-sorbose was removed and the residual syrup was fractionated on a cellulose column using butan-1-ol half-saturated with water as the irrigant. Three fractions were obtained: 5-acetamido-5,6-dideoxy-L-xylohexulose, 2-acetamido-1,2-dideoxy-D-glucitol, and L-sorbose.

Can. J. Chem. Downloaded from www.nrcresearchpress.com by 210.87.254.6 on 09/05/12
For personal use only.

The 5-acetamido-5,6-dideoxy-L-xylohexulose was obtained as a clear brown syrup (2.1 g), $[\alpha]_D$ −38°. The syrup crystallized after several months but unfortunately only after all the structural work had been completed on the syrup. The crystals were recrystallized from ethanol/ether as rosettes of needles (15 mg) and due to the small amount, a completely pure specimen could not be obtained. The crystals had m.p. 91–93° C, $[\alpha]_D$ −40°.

Anal. Calc. for $C_8H_{15}O_5N$: C, 46.8%; H, 7.3%; N, 6.8%. Found: C, 46.0%; H, 7.2%; N, 6.7%.

The crystals gave absorptions in the infrared corresponding to OH (3400 cm^{-1}), NH (3280 cm^{-1}), CH (2960, 2900 cm^{-1}), saturated ketone C=O (1735 cm^{-1}), amide I (1645 cm^{-1}), amide II (1575 cm^{-1}). The complete spectrum is given in Appendix D.

5-Acetamido-5,6-dideoxy-L-xylohexulose rapidly reduced Fehling's solution in the cold. It was not affected by bromine water at room temperature for 3 hours since no other spots could be detected on paper chromatograms run in solvent A, after bromine water treatment.

Periodate Oxidation of 5-Acetamido-5,6-dideoxy-L-xylohexulose

The ketose was oxidized with sodium metaperiodate at pH 7.5, and under unbuffered conditions and the liberated formaldehyde determined. The results are shown in Table V.

TABLE V

Formaldehyde estimations in the periodate oxidation of 5-acetamido-5,6-dideoxy-L-xylohexulose

	Formaldehyde (moles/mole)	
Time (hours)	pH 7.5	pH 3–4 (unbuffered)
0.17	0.97	0.43
1.17		0.43
4.4		0.41
5	0.89	
9.7		0.39
19	0.76	

Alkaline Hypoiodite Oxidation of 5-Acetamido-5,6-dideoxy-L-xylohexulose

5-Acetamido-5,6-dideoxy-L-xylohexulose was oxidized with alkaline hypoiodite solution by the standard method (26). The results indicated that the 5-acetamido-5,6-dideoxy-L-xylohexulose contained 10% aldose. However, it was found that the pH 11.4 buffer used in the oxidation caused epimerization of the ketose to aldoses which were detected as two new spots on paper chromatograms, R_{rh} 1.6 and R_{rh} 1.8 in solvent A, with the alkaline silver nitrate and *p*-anisidine hydrochloride spray reagents. A similar pattern of spots was obtained when 5-acetamido-5,6-dideoxy-L-xylohexulose was heated at 100° C for 3 hours in pyridine solution. From these results it was concluded that the value of 10% aldose content resulted from epimerization and that the 5-acetamido-5,6-dideoxy-L-xylohexulose contained very little, if any, aldose.

5-Acetamido-5,6-dideoxy-3,4-O-isopropylidene-L-xylohexulose

5-Acetamido-5,6-dideoxy-L-xylohexulose (200 mg) was dissolved in acetone (100 ml) containing concentrated sulphuric acid (4 drops) and shaken for 24 hours at room temperature. The solution was neutralized with barium carbonate, filtered, and evaporated to dryness and the resulting syrup was examined on paper chromatograms run in

Can. J. Chem. Downloaded from www.nrcresearchpress.com by 210.87.254.6 on 09/05/12
For personal use only.

solvent A. Two spots were observed with the alkaline silver nitrate spray, R_{rh} 1.2 (5-acetamido-5,6-dideoxy-L-xylohexulose) and R_{rh} 2.5 (5-acetamido-5,6-dideoxy-3,4-*O*-isopropylidene-L-xylohexulose). The isopropylidene derivative was separated by chromatography in solvent A on Whatman 3 MM paper and obtained as a syrup (74 mg), $[\alpha]_D$ −19° (*c*, 1.16 in ethanol). The syrup rapidly reduced Fehling's solution in the cold and gave absorptions in the infrared corresponding to OH (3500 cm^{-1}), CH (3010, 2980, 2910 cm^{-1}), saturated ketone C=O (1730 cm^{-1}), amide I (1670 cm^{-1}), and amide II (1525 cm^{-1}). The complete spectrum is given in Appendix E.

*Periodate Oxidation of 5-Acetamido-5,6-dideoxy-3,4-O-isopropylidene-*L*-xylohexulose*

The isopropylidene ketose was oxidized with a twofold excess of sodium metaperiodate in 50% aqueous ethanol and the liberated formaldehyde determined. The results are shown in Table VI.

TABLE VI

Periodate oxidation of 5-acetamido-5,6-dideoxy-3,4-*O*-isopropylidene-L-xylohexulose

Time (hours)	Formaldehyde (moles/mole)
0.17	0.07
1.17	0.27
4.4	0.29
9.7	0.31

*5-Acetamido-5,6-dideoxy-*L*-xylohexulose Phenylosazone*

5-Acetamido-5,6-dideoxy-L-xylohexulose (200 mg) was treated with freshly distilled phenylhydrazine and glacial acetic acid by the usual method to give a fine yellow powder (110 mg). The osazone was recrystallized from ethanol and had m.p. 156–158° C (decomposes). It gave absorptions in the infrared corresponding to OH (3460 cm^{-1}), NH (3370 cm^{-1}), aromatic CH (3080 cm^{-1}), aliphatic CH (3000, 2910, 2860 cm^{-1}), amide I (1655 cm^{-1}), amide II (1560 cm^{-1}), and the aromatic ring (1610, 1500, 745, 690 cm^{-1}). The complete spectrum is given in Appendix F. Anal. Calc. for $C_{20}H_{25}O_3N_5$: C, 62.7%; H, 6.5%; N, 18.3%. Found: C, 62.85%; H, 6.6%; N, 18.1%.

*Periodate Oxidation of 5-Acetamido-5,6-dideoxy-*L*-xylohexulose Phenylosazone*

The osazone was oxidized with sodium metaperiodate in 50% aqueous ethanol using the method of Hough, Powell, and Woods (12). The results of the oxidation are shown in Table VII.

TABLE VII

Periodate oxidation of 5-acetamido-5,6-dideoxy-L-xylohexulose phenylosazone

Time (hours)	Periodate uptake (moles/mole)
0.42	1.02
1.75	0.98
4.0	1.07

No formic acid or formaldehyde were detected in the oxidation mixture.

During the oxidation a bright orange-yellow precipitate of the 1,2-bisphenylhydrazone of mesoxalaldehyde (23) was obtained. Its identity was proved by melting point, mixed melting point, and identical infrared spectrum with an authentic specimen as described previously in Section A of this publication.

Can. J. Chem. Downloaded from www.nrcresearchpress.com by 210.87.254.6 on 09/05/12
For personal use only.

Sodium Borohydride Reduction of 5-Acetamido-5,6-dideoxy-L-xylohexulose

5-Acetamido-5,6-dideoxy-L-xylohexulose (115 mg) was reduced in aqueous solution with an equal weight of sodium borohydride at 0° C for 3 hours. Excess sodium borohydride was converted to sodium borate which was removed as methyl borate after passage through Amberlite I.R. 120 (H^+) resin. The product was obtained as a clear colorless syrup (90 mg). The syrup was dissolved in methanol, an equal volume of chloroform was added, then ether to incipient opalescence, and the solution was stored at 0° C. The resulting crystals were filtered off, washed with methanol/ether, and dried (21 mg). A second crop of crystals could not be obtained from the mother liquors. The crystals had m.p. 163–164° C and an authentic specimen of 2-acetamido-1,2-dideoxy-D-glucitol had m.p. 160–162° C. The mixed m.p. was 157–159° C. The crystals (and mother liquors) gave one spot on paper chromatograms with the alkaline silver nitrate spray reagent. The infrared spectra of the crystals and the authentic specimen of 2-acetamido-1,2-dideoxy-D-glucitol were identical over the range 4000–600 cm^{-1}. The crystals had $[\alpha]_D$ −16° and the authentic material had $[\alpha]_D$ −14°.

ACKNOWLEDGMENTS

We wish to thank the National Research Council for financial assistance (N.R.C. 706 and T-39) and Queen's University for the award of a scholarship to one of us (J. C. T.).

REFERENCES

1. R. L. WHISTLER and L. A. UNDERKOFLER. J. Am. Chem. Soc. **60**, 2507 (1938).
2. W. BOSSHARD and T. REICHSTEIN. Helv. Chim. Acta, **18**, 959 (1935).
3. L. C. STEWART, N. K. RICHTMYER, and C. S. HUDSON. J. Am. Chem. Soc. **71**, 3532 (1949).
4. J. W. PRATT, N. K. RICHTMYER, and C. S. HUDSON. J. Am. Chem. Soc. **74**, 2210 (1952).
5. L. C. STEWART, N. K. RICHTMYER, and C. S. HUDSON. J. Am. Chem. Soc. **74**, 2206 (1952).
6. J. W. PRATT and N. K. RICHTMYER. J. Am. Chem. Soc. **77**, 6326 (1955).
7. G. N. BOLLENBACK and L. A. UNDERKOFLER. J. Am. Chem. Soc. **72**, 741 (1950).
8. N. K. RICHTMYER, L. C. STEWART, and C. S. HUDSON. J. Am. Chem. Soc. **72**, 4934 (1950).
9. L. HOUGH, J. K. N. JONES, and D. L. MITCHELL. Can. J. Chem. **37**, 725 (1959).
10. J. K. N. JONES and D. L. MITCHELL. Can. J. Chem. **37**, 1561 (1959).
11. J. K. N. JONES, M. B. PERRY, and J. C. TURNER. Can. J. Chem. **39**, 965 (1961).
12. L. HOUGH, D. B. POWELL, and B. M. WOODS. J. Chem. Soc. 4799 (1956).
13. R. M. HANN, E. B. TILDEN, and C. S. HUDSON. J. Am. Chem. Soc. **60**, 1201 (1938).
14. G. BERTRAND. Ann. Chim. (Paris), **3**(8), 209, 287 (1904).
15. S. M. PARTRIDGE. Biochem. J. **42**, 238 (1948).
16. R. KLEVSTRAND and A. NORDAL. Acta. Chem. Scand. **4**, 1320 (1950).
17. L. HOUGH, J. K. N. JONES, and W. H. WADMAN. J. Chem. Soc. 1702 (1950).
18. W. E. TREVELYAN, D. P. PROCTOR, and J. S. HARRISON. Nature, **166**, 444 (1950).
19. J. F. O'DEA and R. A. GIBBONS. Biochem. J. **55**, 580 (1953).
20. P. KARRER and E. HERKENRATH. Helv. Chim. Acta, **20**, 83 (1937).
21. G. A. LEVVY and A. MCALLAN. Biochem. J. **73**, 127 (1959).
22. M. SOMOGYI. J. Biol. Chem. **160**, 61, 69 (1945).
23. E. CHARGAFF and B. MAGASANIK. J. Am. Chem. Soc. **69**, 1459 (1947).
24. M. L. WOLFROM and KIMIKO ANNO. J. Am. Chem. Soc. **74**, 6150 (1952).
25. M. L. WOLFROM, R. V. LEMIEUX, and S. M. OLIN. J. Am. Chem. Soc. **71**, 2870 (1949).
26. S. K. CHANDA, E. C. HIRST, J. K. N. JONES, and E. G. V. PERCIVAL. J. Chem. Soc. 1289 (1950).

APPENDIX

Infrared Spectra

The following abbreviations are used: S = strong, M = medium, W = weak; wave numbers are expressed in cm^{-1}.

(A) 6-Deoxy-6-N-methylacetamido-L-xylohexulose (smeared on surface of KBr pellet) 3410 (S), 2960 (S), 1730 (W), 1625 (S), 1505 (S), 1425 (S), 1375 (M), 1295 (M), 1255 (M), 1135 (M), 1075 (S), 1035 (S), 935 (M), 895 (W), 865 (W), 815 (W), 695 (W).

Can. J. Chem. Downloaded from www.nrcresearchpress.com by 210.87.254.6 on 09/05/12
For personal use only.

*(B) Methyl 6-Deoxy-6-N-methylacetamido-*L*-xylohexulofuranoside* (0.8% in KBr)
3400 (S), 2940 (M), 2880 (M), 1600 (S), 1505 (M), 1465 (M), 1435 (S), 1415 (M), 1385 (M), 1340 (M), 1320 (M), 1280 (M), 1245 (M), 1215 (M), 1165 (S), 1135 (M), 1100 (S), 1050 (M), 1025 (S), 985 (M), 935 (M), 890 (M), 845 (M), 805 (M), 780 (W), 700 (M), 670 (M).

*(C) 6-Deoxy-6-N-methylacetamido-*L*-xylohexulose Phenylosazone* (0.8% in KBr)
3430 (S), 3270 (S), 3080 (S), 2940 (M), 2880 (M), 1625 (S), 1610 (S), 1590 (S), 1540 (S), 1515 (S), 1500 (S), 1460 (M), 1425 (S), 1380 (S), 1340 (M), 1315 (S), 1290 (S), 1260 (S), 1175 (S), 1150 (M), 1105 (S), 1060 (S), 1010 (S), 965 (M), 900 (M), 880 (M), 845 (M), 825 (W), 795 (M), 775 (W), 750 (S), 725 (M), 690 (S).

*(D) 5-Acetamido-5,6-dideoxy-*L*-xylohexulose* (0.8% in KBr)
3400 (S), 3280 (S), 3100 (S), 2960 (M), 2900 (M), 1735 (S), 1645 (S), 1575 (S), 1460 (M), 1430 (M), 1385 (M), 1340 (M), 1325 (M), 1285 (M), 1240 (M), 1185 (W), 1155 (W), 1135 (W), 1115 (S), 1100 (S), 1080 (M), 1050 (M), 975 (W), 965 (W), 955 (W), 850 (W), 825 (W), 740 (M), 690 (M), 655 (M).

*(E) 5-Acetamido-5,6-dideoxy-3,4-O-isopropylidene-*L*-xylohexulose* (6% in chloroform)
3500 (W), 3400 (W), 3010 (M), 2980 (W), 2910 (W), 2410 (W), 1730 (M), 1670 (S), 1525 (S), 1460 (M), 1395 (S), 1385 (S), 1335 (M), 1240 (S), 1170 (M), 1085 (M), 1065 (M), 1045 (M), 1015 (M), 930 (W), 875 (M), 795 (M), 720 (M), 660 (W).

*(F) 5-Acetamido-5,6-dideoxy-*L*-xylohexulose Phenylosazone* (0.8% in KBr)
3460 (S), 3370 (S), 3290 (S), 3080 (M), 3000 (M), 2910 (M), 2860 (W), 1935 (W), 1655 (S), 1610 (S), 1585 (S), 1560 (S), 1540 (S), 1520 (S), 1505 (S), 1460 (S), 1427 (S), 1385 (S), 1307 (S), 1290 (S), 1260 (S), 1175 (M), 1160 (M), 1120 (M), 1080 (M), 1045 (S), 1030 (M), 1015 (M), 975 (W), 940 (W), 905 (W), 870 (W), 845 (W), 815 (W), 785 (M), 755 (S), 745 (S), 690 (S).

Can. J. Chem. Downloaded from www.nrcresearchpress.com by 210.87.254.6 on 09/05/12
For personal use only.

Can. J. Chem. Downloaded from www.nrcresearchpress.com by 210.87.254.6 on 09/05/12
For personal use only.

THE DIFFUSION OF "ATTACHED" INERT-GAS ACTIVITY[1]

ROGER KELLY

ABSTRACT

It was shown previously that, when an inert gas is irradiated with neutrons in the presence of a powdered solid, between 0.1 and 14% of the induced inert-gas activity is firmly "attached" to the solid. The manner in which attached inert-gas activity is released at temperatures between 50 and 800° C has now been studied. Release data were assembled for a number of systems, and it was noted that the release was reproducible and apparently a diffusion phenomenon. Several theoretical treatments based on diffusion theory were then explored. Agreement between theory and observation was poor if a constant activation enthalpy was assumed. Agreement was good, on the other hand, with theory that took account of the damaged condition of the solid, and the existence of composition anomalies, in the surface region where the inert-gas activity was attached. The damage and composition anomalies were assumed to lead to a spectrum of activation enthalpies and thence to a simplified diffusive motion involving a single rate-controlling jump. The activation-enthalpy spectra for the systems Ar–Nb and Xe–Nb were found to be identical, extending from about 25 to 47 kcal. The spectrum for Xe–Nb_2O_5 extended from about 28 to 76 kcal, and was, in general, similar to the spectra for Xe–SiO_2, Ar–TiO_2, and Xe–TiO_2.

In a recent paper (1), experiments were described in which the inert gases argon, krypton, and xenon were irradiated with neutrons in the presence of various powders. It was found that the major portion of the induced inert-gas activity could be pumped off the powders at room temperature, though the last 0.1 to 14% (depending on the gas and powder used) was not released till the powders were heated. The latter activity was said to be "attached", and the ratio of attached to total activity was called the "attachment efficiency" (A). A temperature of about 800° C was necessary for a complete release of attached activity.

The present work concerns the manner in which attached inert-gas activity is released at temperatures below 800° C, in other words, in the temperature region where the extent of release is noticeably dependent on time and temperature. Release data are given for several combinations of inert gas and powder (or other solid). It is noted that the release is reproducible, and apparently a diffusion phenomenon. Several theoretical treatments based on diffusion theory are then examined for consistency with the experimental results. Finally, the concepts involved in the theoretical treatment that is most successful are discussed in connection with the over-all attachment process and in other respects.

EXPERIMENTAL

The apparatus and experimental techniques were similar to those described previously (1). A mixture of a powder (or other solid) and inert gas was sealed in a quartz capsule and irradiated overnight with neutrons at a flux of about 1×10^{13} neutrons cm^{-2} sec^{-1}. The capsule was then placed in a vacuum system (Fig. 1A of reference 1) and cracked open. That portion of the inert-gas activity remaining in the gas phase was pumped off, and, for the present purposes, need not be further considered. (The pumping had to be continued for $1\frac{1}{2}$ to 3 hours before the evolution of activity ceased.) The remaining inert-gas activity was now slowly expelled by heating the solid, firstly to various temperatures in the region 50 to 800° C, and finally to 1000° C. (The heating at 1000° C ensured that the attached inert gas was completely released (cf. p. 665 of reference 1).)

[1]*Manuscript received August 16, 1961.*
Contribution from the Development Chemistry Branch, Atomic Energy of Canada Limited, Chalk River, Ontario.
Issued as A.E.C.L. No. 1362.

A trap containing charcoal at liquid-nitrogen temperature served to collect the released activity and to position it over a gamma-scintillation crystal (Fig. 1B of reference 1). Gamma counts were taken at intervals of 1 to 4 minutes, depending on the rate at which the activity was being released.

For some of the experiments, a trap containing charcoal at 300° C was introduced into the vacuum line ahead of the collecting trap. Charcoal, provided it is sufficiently hot, does not noticeably impede the movement of inert gases, though it will stop potential contaminants such as arsine or iodine. (For the behavior of *unheated* charcoal, see Fig. 3 of reference 1.)

The following solids were used:

Nb, Nb_2O_5, SiO_2, TiO_2 (commercial powders),

SiO_2 (quartz rods with 1-mm diameter),

TiO_2 (sintered balls in the size range from 20 to 60 mesh).[2]

To determine the importance of surface effects, each solid was studied both in an as-received condition, and also after ignition at 500 or 1000° C. The ignitions lasted $\frac{1}{2}$ hour, with the first 10 minutes in air and the remaining 20 minutes in vacuum. Inert gas did not appear to attach to non-ignited quartz rods. This was probably due to the presence of a film of grease, for normal attachment took place with rods that had been washed with ether in a Soxhlet apparatus.

RESULTS

The results will be expressed in terms of the "fractional release" (F), which is defined as the fraction of the total attached inert-gas activity that has been released at a given stage of an experiment. Figs. 1A and 1B give typical curves for fractional release as a function of time. Note how, at a given temperature, activity at first came off rapidly, but its rate of release soon decreased, so that a comparatively level region (i.e. a "plateau") resulted. The plateau effect was less well developed with the niobium than with the other solids.

The initial release of inert-gas activity is seen from Figs. 1A and 1B to be so rapid that, at any given temperature, much of the activity was released in a time which was comparable to *each* of the following: (i) the time to bring the specimens up to temperature (2 to 3 minutes), (ii) the time taken by the activity to move through the vacuum system to the gamma counter (1 to 2 minutes), (iii) the duration of each gamma count (1 minute). As a result, the activities measured during the first 5 to 10 minutes that a specimen was held at a given temperature were probably low, and curves of F-versus-time would be difficult to analyze theoretically.

An alternative way of treating the data, which avoids the effect just described, is to plot fractional release after a fairly long time (e.g. 30 minutes) against temperature; Figs. 2A, 2B, and 2C. A number of conclusions can be drawn from Figs. 2A, 2B, and 2C.

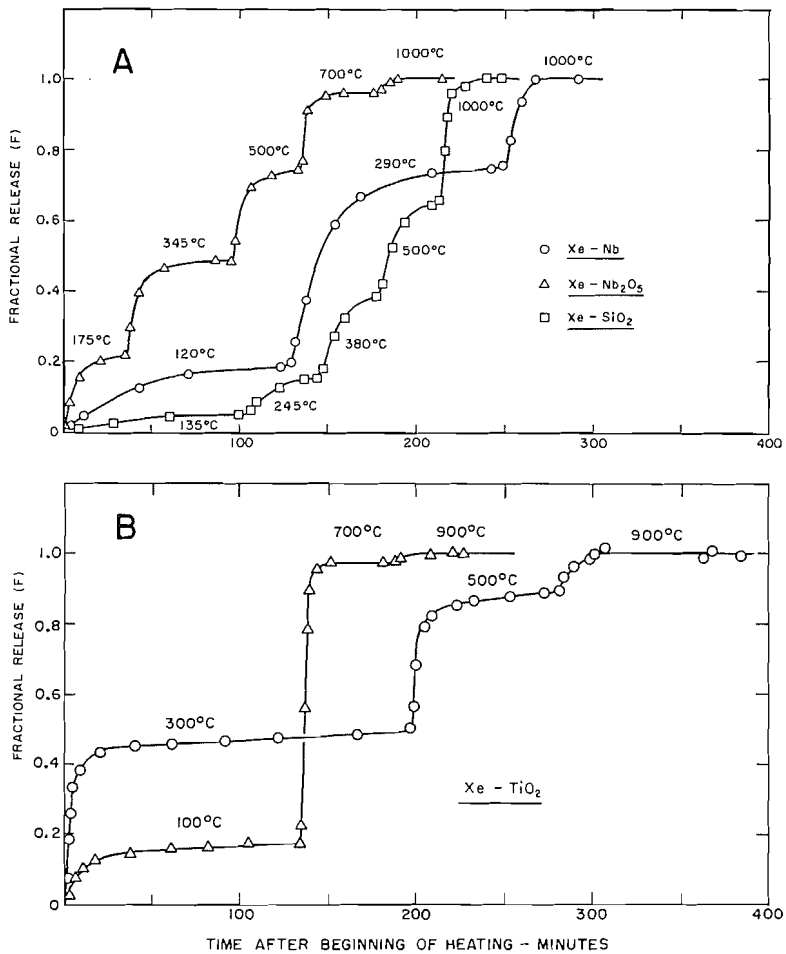
(i) The release phenomenon is reproducible.

(ii) In general, release proceeds linearly over a wide range of temperature. There is a slight deviation from linearity at high temperatures with the oxides, and a much greater deviation with niobium, though the exceptional behavior of niobium is possibly due to the fact that part of the niobium surface is sufficiently oxidized to behave as Nb_2O_5.

(iii) In the two cases where argon and xenon are both used with a given solid (Nb and TiO_2), indistinguishable release behavior is observed. If it is borne in mind that xenon adsorbs much more strongly than argon (2), this observation leads to the conclusion that

[2]*The TiO_2 balls were kindly contributed by Titanium Alloy Manufacturing Division, National Lead Co., Niagara Falls, N.Y.*

Can. J. Chem. Downloaded from www.nrcresearchpress.com by 210.87.254.6 on 09/05/12
For personal use only.



FIGS. 1A and 1B. Fractional release as a function of time for ^{125}Xe activity that has become attached to various solids following (n,γ) events. Selected points from typical experiments are shown for each solid. In each experiment the temperature was raised rapidly (i.e. within 2 to 3 minutes) to a given value, was held constant to within $\pm 0.5°$ C for at least 30 minutes, and was then raised to the next value indicated.

release *is not* a desorption phenomenon, and is therefore presumably an example of diffusion.

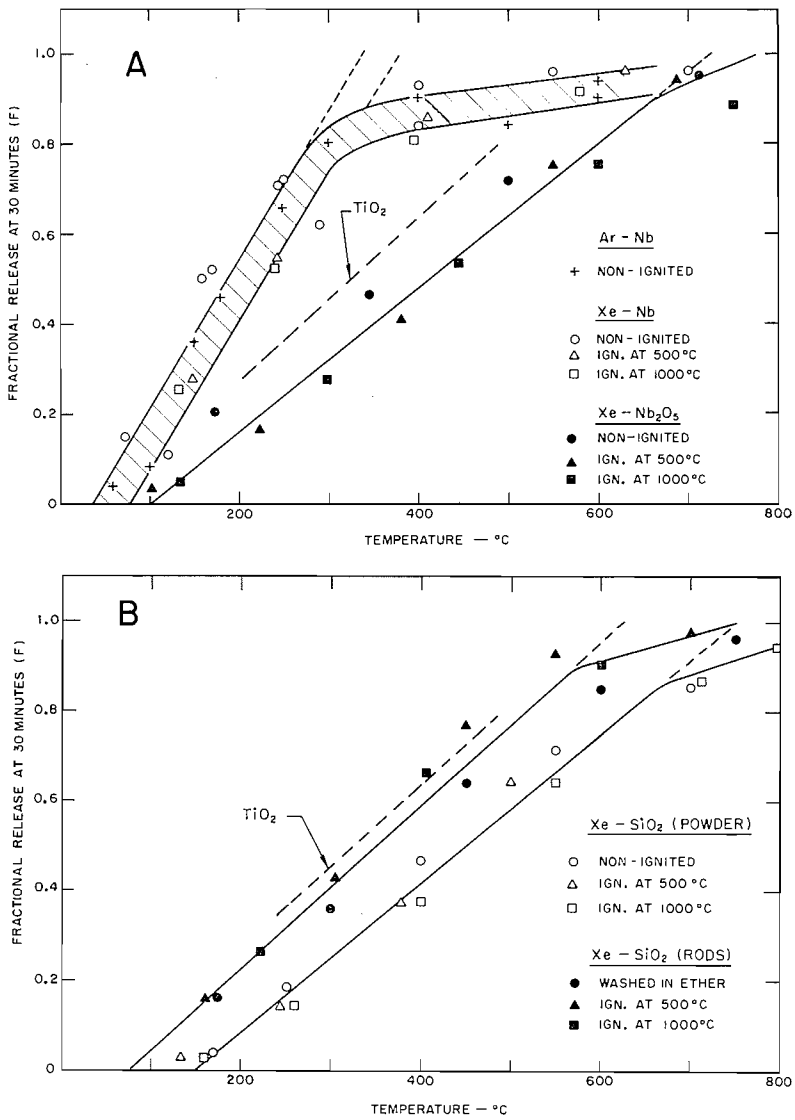
(iv) Within the limits of the experimental scatter, there is no pronounced difference in the release behavior between solids in an as-received and ignited condition. This may be taken as evidence that release *is not* due to a recrystallization, sintering, or other alteration of the solid surface that might take place during an experiment. Once again release could be due to diffusion. (The release of I_2 from irradiated TeO_2 at elevated temperatures is an example where sintering is important (3).)

(v) The two forms of SiO_2 and TiO_2 give somewhat different results. Presumably the surface structures are different.

The main error associated with Figs. 2A, 2B, and 2C arises from the fact that each specimen was studied at a series of successively higher temperatures, yet the data at a given temperature were treated without regard to previous heatings. The justification for the procedure followed lies in the nature of the F-versus-time behavior: much of the activity ultimately released at a given temperature comes out in a few minutes; at a

Can. J. Chem. Downloaded from www.nrcresearchpress.com by 210.87.254.6 on 09/05/12
For personal use only.

Can. J. Chem. Downloaded from www.nrcresearchpress.com by 210.87.254.6 on 09/05/12
For personal use only.



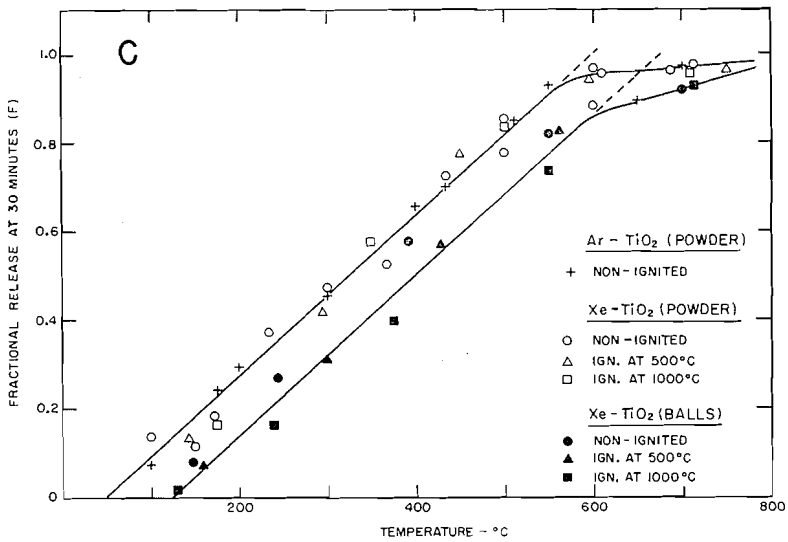
FIGS. 2A, 2B, and 2C. Fractional release at 30 minutes as a function of temperature for ^{41}Ar and ^{125}Xe activities that have become attached to various solids. All results are shown. The curve for niobium is given a second dimension because the results are particularly scattered. The position of the curve for powdered TiO_2 is indicated in Figs. 2A and 2B for comparison.

higher temperature this same activity would therefore have come out in a time appreciably less than a few minutes, and the time scale at the higher temperature would be in error only to this extent.

DISCUSSION

(A) THEORETICAL

It has been shown that the release at elevated temperatures of inert-gas activity that has become attached to a solid is characterized by a plateau effect when F is plotted versus time, and by a wide temperature range when F (at 30 minutes) is plotted versus



"FIG. 2C."

temperature. Moreover, this release is reproducible and is probably due to diffusion. There follows an attempt to explain the release behavior theoretically using the concepts of diffusion theory.

General Considerations

The first step in a diffusion calculation is to decide on the differential equation governing the diffusion. Consider a solid containing diffusing material such that the concentration changes in only one direction. This change in concentration will be referred to as a *gradient*, although the concept "gradient" is not strictly applicable in a discontinuous medium such as a solid. Regard the diffusing material as residing in successive lattice planes located at intervals of λ along the gradient, there being $M(r\lambda,t)$ atoms per unit area at time t in the rth plane. Let τ be the mean time an atom of diffusing material stays in a given site (not *plane*) before jumping to a new site, and β be the probability that a jump will be into a new plane. Assume for the sake of simplicity that, for all jumps of significant probability, τ and β have the same values, while r changes by only 0 or 1 unit. The increment of $M(r\lambda,t)$ in time interval Δt, $\Delta t \ll \tau$, can then be written as follows (cf. references 4 and 5):

$$M(r\lambda,t+\Delta t) = \left(1-\frac{\Delta t}{\tau}\beta\right)M(r\lambda,t)+\frac{\Delta t}{\tau}\cdot\frac{\beta}{2}\{M[(r-1)\lambda,t]+M[(r+1)\lambda,t]\}$$

$$r = 0, \pm 1, \pm 2, \pm 3, \ldots .$$

This difference equation can be simplified in two ways. If $M(r\lambda,t)$ varies slowly with r, i.e. the gradient is always low, it yields the well-known partial-differential equation

$$[1] \qquad \frac{\partial M(x,t)}{\partial t} = \frac{k\lambda^2}{2}\cdot\frac{\partial^2 M(x,t)}{\partial x^2},$$

where $k \equiv \beta/\tau$ is the "diffusion rate constant", i.e. the rate at which diffusing material jumps along the gradient; $k\lambda^2/2 = \beta\lambda^2/2\tau$ is the "diffusion coefficient" (D); and x is the distance along the gradient. The quantity $r\lambda$ has been replaced with x to emphasize the fact that equation [1] is defined continuously in the space co-ordinate. If, on the other hand, no restrictions are placed on the gradient, a less complete reduction is obtained:

Can. J. Chem. Downloaded from www.nrcresearchpress.com by 210.87.254.6 on 09/05/12
For personal use only.

$$[2] \qquad \frac{dM(r\lambda,t)}{dt} = -kM(r\lambda,t)+\frac{k}{2}\{M[(r-1)\lambda,t]+M[(r+1)\lambda,t]\}$$

$$r = 0, \pm1, \pm2, \pm3, \ldots .$$

It follows from the relation $k\lambda^2/2 = D$ that, in so far as D can be written $D_0\exp(-\Delta H/RT)$ (cf. reference 4), so k can be written

$$[3] \qquad k = k_0 e^{-\Delta H/RT}.$$

The quantity ΔH is the activation *energy* of diffusion, or, more properly, the activation *enthalpy* of diffusion (6).

Diffusion of a Plane Source when the Gradient is Low

Consider firstly the low-gradient differential equation, i.e. equation [1]. To use this equation it is necessary to agree on a geometry. Note, in this regard, that inert-gas activity that becomes attached to a solid following (n,γ) events in the inactive gas will, in general, rest only a very few atom layers beneath the surface of the solid; therefore, no matter how irregular the solid is, it should be possible to regard the inert gas as constituting a plane source parallel to the surface of a semi-infinite medium. The plane-source solution of equation [1] can be obtained using the method of images (page 9 of reference 7):

$$[4] \qquad M(x,t) = \frac{M_0}{\sqrt{2\pi kt}}\left\{\exp\left[-\frac{(p-x/\lambda)^2}{2kt}\right]-\exp\left[-\frac{(p+x/\lambda)^2}{2kt}\right]\right\}$$

$$x \text{ and } p = 0, \lambda, 2\lambda, 3\lambda, \ldots ,$$

where M_0 is the source strength (amount/area), p is the position of the source beneath the surface of the solid in units of lattice planes of spacing λ, and x is distance from the surface. Although equation [4] defines $M(x,t)$ for all x and p, only those values of x and p which are integral multiples of λ are of interest. The fractional release now follows as

$$F = (1/M_0)\left\{M_0-\sum_{x=0}^{\infty} M(x,t)\right\},$$

or, if the sum is approximated by the first two terms in the Euler–Maclaurin sum formula (page 25 of reference 8),

$$[5] \qquad F \approx \frac{2}{\sqrt{\pi}}\int_{p/\sqrt{2kt}}^{\infty} e^{-u^2}du \equiv \operatorname{erfc}\frac{p}{\sqrt{2kt}}.$$

F as given by equation [5] is shown plotted as a function of kt (assuming that $p = 1$) in Fig. 3 and as a function of temperature in Fig. 4. It is apparent that equation [5] fails to reproduce the experimental behavior, both as regards the plateaus and also as regards the wide temperature range over which the diffusion is significant.

Diffusion of a Plane Source when the Gradient is Unrestricted

A possible reason for the lack of consistency between equation [5] and the experimental results lies in the assumption basic to equation [5] that the gradient is always low. As a matter of fact, the attached inert-gas activity is located very close to the surface of the

Can. J. Chem. Downloaded from www.nrcresearchpress.com by 210.87.254.6 on 09/05/12
For personal use only.

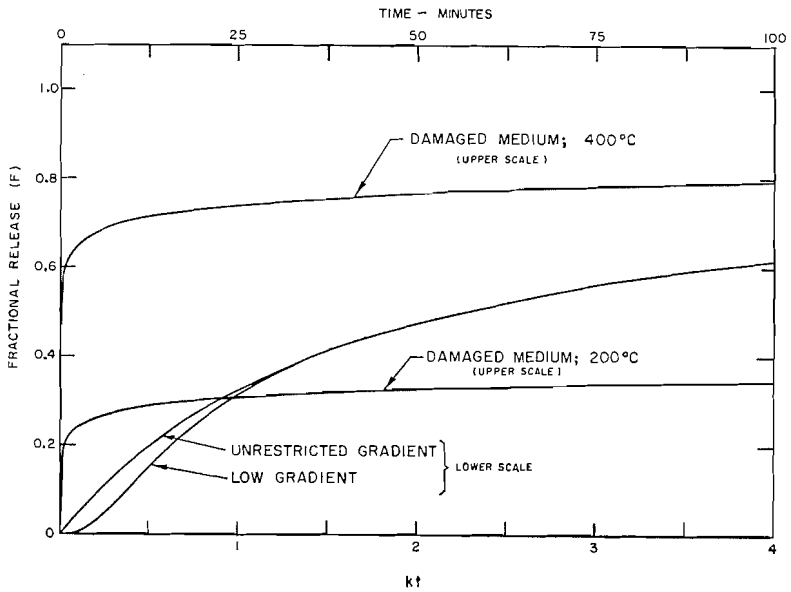


FIG. 3. Theoretical predictions of fractional release as a function of kt or time, derived assuming that the release is a diffusion phenomenon. Three cases are considered: (i) a plane source in a semi-infinite medium when the gradient is always low (equation [5] with $p = 1$), (ii) a plane source in a semi-infinite medium when the gradient is unrestricted (equation [7]), (iii) a source of unspecified nature located in a medium that is extensively damaged, and has composition anomalies, in the region between the source and the exterior (equations [10] or [11] with $k_0 = 10^{13}$ sec^{-1}, $\Delta H_1 = 25$ kcal, and $\Delta H_2 = 60$ kcal).

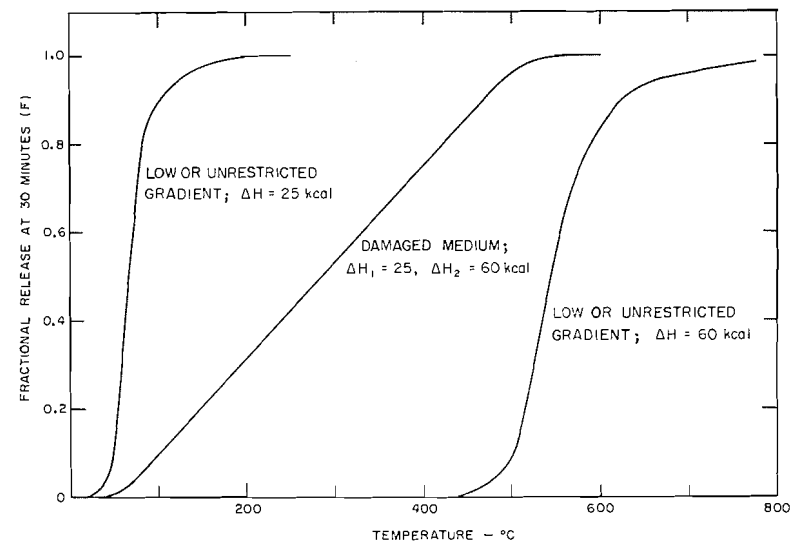


FIG. 4. Theoretical predictions of fractional release at 30 minutes as a function of temperature, derived assuming that the release is a diffusion phenomenon. The same three cases are considered as in Fig. 3, except that equations [5] and [7] have been plotted, not dimensionlessly, but with $k_0 = 10^{13}$ sec^{-1} and $\Delta H = 25$ *or* 60 kcal.

diffusion medium, where extremely high gradients are possible. As a further step in trying to explain the results, one should therefore examine the differential equation which holds for unrestricted gradients (equation [2]).

Can. J. Chem. Downloaded from www.nrcresearchpress.com by 210.87.254.6 on 09/05/12
For personal use only.

A solution of equation [2] in closed form has been obtained by Kennedy.[3] A description of the method, and a general comparison of solutions of equations [1] and [2], will be presented in a separate paper, so that for the present purposes only the final results need be given. As before, assume that the geometry can be represented by a plane source in a semi-infinite medium; then, one has corresponding to equation [4],

$$[6] \qquad M(r\lambda,t) = M_0 e^{-kt}\{I_{p-r}(kt) - I_{p+r}(kt)\}$$
$$r \text{ and } p = 0, \pm 1, \pm 2, \pm 3, \ldots,$$

where p is the position of the source in units of λ, r is distance from the surface in units of λ, and $I_n(z)$ is the modified Bessel function of the first kind (9). For integral n, $I_n(z)$ is given by

$$I_n(z) \equiv i^{-n} J_n(iz) = \sum_{u=0}^{\infty} \frac{(z/2)^{n+2u}}{u!(n+u)!}$$
$$I_n(z) = I_{-n}(z).$$

The equation corresponding to [5] is

$$F = (1/M_0)\left\{M_0 - \sum_{r=0}^{\infty} M(r\lambda,t)\right\}$$
$$= 1 - e^{-kt}\{I_0(kt) + I_p(kt) + 2[I_1(kt) + I_2(kt) + \ldots + I_{p-1}(kt)]\},$$

or, for a source located in the first lattice plane beneath the surface of the solid (i.e. $p = 1$),

$$[7] \qquad F = 1 - e^{-kt}\{I_0(kt) + I_1(kt)\}.$$

F as given by equation [7] is shown plotted as functions of kt and temperature in Figs. 3 and 4. The curves are very similar, especially for $F > 0.4$, to those obtained with equation [5], and, like the latter, fail to reproduce the experimental behavior.

Diffusion in a Medium with Damage and Composition Anomalies

A weakness of both equations [5] and [7] is that they neglect the fact that that portion of the solid lying between the attached inert-gas activity and the exterior will tend to be extensively damaged and to exhibit composition anomalies. The damage will be in part an inherent property of the solid surface (a crystal cannot be perfect near a surface), and in part the result of the forcible introduction of foreign material into the solid. Composition anomalies will include surficial oxide, hydroxide, and carbonate layers. It will be assumed that the primary consequences of the damage and composition anomalies are the following: (i) that the activation enthalpies in the solid between the attached inert-gas activity and the exterior occur as a spectrum rather than with a high, discrete value; (ii) that the spectrum lies below the bulk or ordinary activation enthalpy. Further details follow logically: the existence of a *spectrum* of activation enthalpies, coupled with the fact that the enthalpies are *low*, means that the diffusion will not be of the usual type where there is random motion, but rather of a modified form where the release of each inert-gas atom is dependent on *a single rate-controlling jump*. The existence of one-step motion, in turn, means that no assumption about the geometry is necessary.

It should perhaps be pointed out that the assumption that the enthalpy spectrum lies below the bulk enthalpy is reasonable only if damage is the main effect leading to a spectrum. Composition anomalies could give rise to a spectrum extending *above* the bulk

[3]*Private communication from Dr. J. M. Kennedy, Theoretical Physics Branch, Atomic Energy of Canada Limited, Chalk River.*

Can. J. Chem. Downloaded from www.nrcresearchpress.com by 210.87.254.6 on 09/05/12
For personal use only.

Can. J. Chem. Downloaded from www.nrcresearchpress.com by 210.87.254.6 on 09/05/12
For personal use only.

enthalpy with substances that hold inert gas *less* strongly than the corresponding altered surface layers. Niobium is probably an example of such a substance, since it holds inert gas less strongly than Nb_2O_5 (Fig. 2A). The treatment that follows will, accordingly, be more nearly applicable to systems with very high activation enthalpies, for example, those involving Nb_2O_5, SiO_2, and TiO_2. A high enthalpy is less likely than a low one to be increased by an alteration of the solid surface. (That there should be a difference between substances like niobium, on the one hand, and the oxides, on the other hand, is consistent with the anomaly previously noted for niobium (heading (ii) in Results).)

Diffusion under the conditions of the highly simplified motion described above is governed basically by equation [2]. The equation will, however, lack the terms for interplanar migration, so that one is left with

$$dM_H/dt = -kM_H, \tag{8}$$

where M_H is the amount of diffusing material at time t experiencing an activation enthalpy ΔH. If the initial value of M_H is $M_H{}^0$, the solution of equation [8] can be written

$$M_H = M_H{}^0 e^{-kt},$$

whence, making use of equation [3],

$$\begin{aligned} F_H &= (1/M_H{}^0)(M_H{}^0 - M_H) = 1 - e^{-kt} \\ &= 1 - \exp(-k_0 t e^{-\Delta H/RT}). \end{aligned} \tag{9}$$

Now introduce the fact that ΔH varies between a minimum, ΔH_1, and a maximum, ΔH_2. While the actual distribution of ΔH is an experimental unknown, it will be sufficient as a first approximation to assume that all values are equally weighted. Also, the dependence of k_0 on ΔH will be neglected (for sinusoidal vibrations of low amplitude, $k_0 \propto \sqrt{\Delta H}$ (5)). Hence, the over-all value for the fractional release is

$$\begin{aligned} F &= \frac{1}{\Delta H_2 - \Delta H_1} \int_{\Delta H_1}^{\Delta H_2} F_H d\Delta H \\ &= 1 + \frac{RT}{\Delta H_2 - \Delta H_1} \{-\mathrm{Ei}(-k_0 t e^{-\Delta H_1/RT}) + \mathrm{Ei}(-k_0 t e^{-\Delta H_2/RT})\}, \end{aligned} \tag{10}$$

where $-\mathrm{Ei}(-z)$ is the exponential integral (9),

$$-\mathrm{Ei}(-z) \equiv \int_z^\infty \frac{e^{-u}}{u}\, du = -\ln \gamma z + \frac{z}{1 \cdot 1!} - \frac{z^2}{2 \cdot 2!} + \cdots$$

$$\gamma = 1.781 \ldots .$$

To use equation [10], it is desirable to simplify the exponential integrals. The experimental temperature range is necessarily *above* the temperature at which the most weakly bound inert-gas activity is readily released. It therefore follows from equation [9] that $k_0 t \exp(-\Delta H_1/RT)$ will be large and $-\mathrm{Ei}[-k_0 t \exp(-\Delta H_1/RT)]$ negligibly small. Similarly, the temperature range is necessarily *below* the temperature at which the most strongly bound inert-gas activity is readily released, so that one obtains

$$-\mathrm{Ei}(-k_0 t e^{-\Delta H_2/RT}) \approx -\ln \gamma k_0 t + \Delta H_2/RT.$$

Hence, for the experimentally interesting temperature range,

$$F \approx \frac{RT}{\Delta H_2 - \Delta H_1} \ln \gamma k_0 t - \frac{\Delta H_1}{\Delta H_2 - \Delta H_1}. \tag{11}$$

Equations [10] and [11] reproduce the experimental behavior very well indeed, especially with the systems involving oxides (cf. second paragraph in this section). They give plateaus when F is plotted as a function of time (Fig. 3). Moreover, they predict that, for a given value of t, F varies linearly with temperature over a range of temperature which is determined by the values of ΔH_1 and ΔH_2 (Fig. 4). (It is difficult to say whether the expected linearity of F-versus-ln t is also obeyed, because the first 5 to 10 minutes of activity release are perturbed by the effect described in Results.) One concludes that the treatment leading to equations [10] and [11] constitutes a reasonable explanation of the release behavior with which the present work is concerned.

It is perhaps well to restate the main assumptions underlying equations [10] and [11]: (i) the diffusion of inert-gas activity that has become attached near the surface of a solid involves a spectrum of activation enthalpies; (ii) the spectrum lies below the bulk activation enthalpy; (iii) there is approximately equal weighting in the spectrum.

The data of Figs. 2A, 2B, and 2C have been analyzed in terms of equation [11] and values of ΔH_1 and ΔH_2 obtained (Table I). In making the analysis, the deviations from

TABLE I

Activation enthalpies derived using equation [11]

System	ΔH_1* (kcal)	ΔH_2* (kcal)
Ar–Nb or Xe–Nb (powder)	22–28	42–53
Xe–Nb_2O_5 (powder)	25–32	67–85
Xe–SiO_2 (powder)	28–36	68–87
Xe–SiO_2 (rods)	23–30	60–76
Ar–TiO_2 or Xe–TiO_2 (powder)	22–28	58–74
Xe–TiO_2 (balls)	27–34	63–81

*The lower limits of ΔH_1 and ΔH_2 are obtained using the value $k_0 = 10^{11}$ sec^{-1}. The upper limits are obtained with $k_0 = 10^{15}$ sec^{-1}.

linearity in the high-temperature portions of Figs. 2A, 2B, and 2C have been disregarded (cf. heading (ii) in Results). Also, since equation [11] is not sufficiently sensitive to variation in k_0 to yield a value for this quantity, a wide, arbitrary range of values for k_0 was assumed. (Actually, it can be shown that the lower limit of k_0 reproduces the F-versus-ln t behavior somewhat better than does the upper limit.)

(B) General

The success of the theoretical treatment leading to equations [10] and [11] in explaining the observed release behavior of attached inert-gas activity suggests a number of points for discussion.

The Attachment Process

It was shown previously (1) that the attachment process is characterized by the following relations:

$$[12] \qquad \begin{cases} A \ll 1 \\ A_{Ar} > A_{Kr} > A_{Xe} \\ A_{oxide} > A_{metal} \text{ (approximate)}, \end{cases}$$

where A is the attachment efficiency, i.e. the ratio (inert-gas activity attached to target)/(total inert-gas activity). Moreover, it follows from general considerations that the value of A will be governed by the following effects:

Can. J. Chem. Downloaded from www.nrcresearchpress.com by 210.87.254.6 on 09/05/12
For personal use only.

(i) *Attachability*—the probability that an inert-gas atom is in a condition to become attached following neutron absorption.

(ii) *Epithermal release*—release that occurs when an inert-gas atom that has entered a solid as if to become attached is immediately expelled due to the existence of a transient epithermal region or hot-spot. Like the epithermal reactions of hot-atom chemistry, this effect would be independent of temperature.

(iii) *Diffusive release*—release that occurs when an attached inert-gas atom diffuses out of a solid after the system has thermalized.

It is of interest to determine whether the present work leads to a correlation between relations [12] and the effects just described.[4]

The relation $A \ll 1$ will obviously be a consequence of all three effects. However, there is some indication that the third effect, i.e. diffusive release, may be of major importance. The argument is based on the fact that the activation enthalpies occur as a spectrum rather than with a high, discrete value as in ordinary diffusion. Assuming that ΔH_1, the *apparent* lower boundary of the spectrum, is merely the minimum barrier height which will retain inert gas at the irradiation temperature, it follows that lower barriers exist, and that a considerable portion of the originally attached inert gas might have experienced such barriers and been subject to diffusive release.[5] Diffusive release also appears to be adequate to explain the relation $A_{\text{oxide}} > A_{\text{metal}}$, for, judging from the values of ΔH_2 for niobium and Nb_2O_5 (Table I), it would seem that attached inert gas is much more tightly bound in an oxide than in a metal.

The remaining relation, $A_{Ar} > A_{Kr} > A_{Xe}$, is probably a consequence of effects (i) and (ii). Diffusive release is ruled out on the basis of the fact that, since argon and xenon show a similar range of activation enthalpies with a given solid (cf. Figs. 2A and 2C), these gases should have comparable probabilities of diffusive release.

The Irradiation Temperature

It has been suggested that inert gas remains attached to a solid only if it experiences a sufficient barrier that it cannot diffuse out at the irradiation temperature. It should therefore be possible to identify the irradiation temperature as that temperature *above which* the rate of release of attached gas becomes significant, for example, the temperature obtained by extrapolating to $F = 0$ a plot of F-versus-temperature. Temperatures in the region of 50 to 150° C are thus indicated for the various solids used in the present work.

The Bulk Activation Enthalpy

The assumption was made earlier that, with certain reservations, the spectrum of activation enthalpies that characterizes the diffusion of attached inert gas lies beneath the bulk or ordinary value, ΔH_{bulk}. One therefore wonders if the upper limit of the spectrum, ΔH_2, is not actually identical with ΔH_{bulk}, i.e.

$$\Delta H_2 \approx \Delta H_{\text{bulk}}. \qquad [13]$$

[4]*A fourth effect, "ejective release", might also be suggested. This is the effect whereby, as the irradiation continues, the incoming inert-gas atoms tend to eject previously attached inert-gas atoms and thus give rise to saturation. That ejective release is not significant in the present work is shown by two facts: (i) saturation is not observed (p. 673 of reference 1), (ii) the number of penetrated atoms per unit area in the present work (about 0.0001 monolayer for xenon attaching to an empty quartz capsule when the xenon pressure is 700 mm, the neutron flux 10^{13}, the irradiation time 4 days, and the attachment efficiency 0.0002) is significantly less than the number required for saturation (about 0.1 monolayer for 200 ev ions (10)).*

[5]*The view that the spectrum of activation enthalpies really extends below ΔH_1 is substantiated by a preliminary experiment in which an Ar–TiO_2 mixture was irradiated for 30 seconds at liquid-nitrogen temperature: a factor of 2 increase in A was observed, and the ΔH spectrum extended down to about 10 kcal instead of the usual 22 to 28 kcal.*

Can. J. Chem. Downloaded from www.nrcresearchpress.com by 210.87.254.6 on 09/05/12
For personal use only.

Equation [13] should be unaffected by the fact that ΔH_2 was obtained using irregular or poorly crystallized material, since ΔH_2 relates to a process occurring in a region only a few atom layers thick.

Comparison with Other Work

Carter and Leck (10) have recently described work quite closely related to the present work. They bombarded glass with inert-gas ions having energies in the region 80 to 500 ev (cf. Fig. 5 of reference 10), in other words, having the same sort of energies as occur in attachment. (If the attachment of inert-gas atoms is due to the recoil of the atoms following the emission of capture gamma rays, then energies in the region 70 to 210 ev will occur (page 671 of reference 1).) They then caused the inert gas to diffuse out by heating the glass to temperatures up to 350° C. It was concluded, as in the present work, that the diffusion was governed by a spectrum of activation enthalpies. The enthalpy spectrum was found to be the same for neon, argon, krypton, and xenon, to be approximately independent of the ion energy, and to be independent of the thermal history of the glass.[6]

Points of disagreement brought out by the work of Carter and Leck include the following. Carter and Leck assumed that the diffusive motion could be described in terms of a single rate-controlling jump only as an approximation, and did not argue, as in the present work, that a spectrum of activation enthalpies can lead naturally to single-jump motion. They observed a somewhat more restricted range of enthalpies (23 to 45 kcal) than was obtained in the present work for a comparable solid (26 to 68 kcal for SiO_2 rods). They suggested that the existence of a spectrum of enthalpies is attributable to the known heterogeneity of glass, whereas the present work indicates that it is a more general phenomenon, and is, in fact, probably a property of all surfaces.

Comparisons between the present work and ordinary diffusion studies are difficult due to the lack of data. One can point out, however, that the observation that argon and xenon show similar activation enthalpies with a given solid agrees in a general way with the results obtained in studies with silver. Thus ΔH is 33.6 kcal for Ar–Ag (11), 35.0 kcal for Kr–Ag (12), and 37.5 kcal for Xe–Ag (13).

ACKNOWLEDGMENTS

The assistance of Dr. J. M. Kennedy in helping to clarify some of the mathematical problems associated with this work is gratefully acknowledged.

REFERENCES

1. R. KELLY. Can. J. Chem. **39**, 664 (1961).
2. K. PETERS and K. WEIL. *Cited by* S. Dushman, p. 399 *of* Scientific foundations of vacuum technique. John Wiley & Sons, Inc., New York. 1949.
3. J. S. BURGESS, L. R. PARMENTER, and E. J. PARTINGTON. U.K. Atomic Energy Authority Report RCC/R111 (1961).
4. C. ZENER. *In* Imperfections in nearly perfect crystals. *Edited by* W. Shockley *et al.* John Wiley & Sons, Inc., New York. 1952.
5. C. WERT and C. ZENER. Phys. Rev. **76**, 1169 (1949).
6. C. A. WERT. Phys. Rev. **79**, 601 (1950).
7. J. CRANK. The mathematics of diffusion. Oxford University Press, London. 1957.
8. E. P. ADAMS and R. L. HIPPISLEY. Smithsonian mathematical formulae and tables of elliptic functions. Smithsonian Institution, Washington. 1939.
9. W. FLÜGGE. Tables of transcendental functions. Pergamon Press Ltd., London. 1954.
10. G. CARTER and J. H. LECK. Proc. Roy. Soc. A, **261**, 303 (1961).
11. A. D. LECLAIRE and A. H. ROWE. Rev. Mét. **52**, 94 (1955).
12. J. M. TOBIN. Acta Met. **5**, 398 (1957).
13. J. M. TOBIN. AEC Research and Development Report HW-53639 (1958).

[6] *A further indication of the close agreement between the present work and that of Carter and Leck lies in the numerical values obtained for the attachment efficiencies. Thus, Carter and Leck observed values of 0.08 to 0.2, depending on the ion energy (cf. the "sticking factors" given in Fig. 5 of reference 10). In reference 1, values of 0.001 to 0.14 were observed for various gases and solids.*

Can. J. Chem. Downloaded from www.nrcresearchpress.com by 210.87.254.6 on 09/05/12
For personal use only.

Can. J. Chem. Downloaded from www.nrcresearchpress.com by 210.87.254.105 on 09/05/12
For personal use only.

CONSTITUTION OF A GLUCOMANNAN FROM THE SAPWOOD OF SUGAR MAPLE (ACER SACCHARUM)[1]

G. A. ADAMS

ABSTRACT

A glucomannan containing D-mannose and D-glucose in a molar ratio of 7:3 has been isolated from sugar maple sapwood. Electrophorectic examination in acetate and borate buffers showed that the polysaccharide was essentially homogeneous. Methylation and hydrolysis of the glucomannan yielded the following *O*-methyl ethers:

2,3,4,6-tetra-*O*-methyl-D-glucose (1.1%),
2,3,4,6-tetra-*O*-methyl-D-mannose (2.3%),
2,3,6-tri-*O*-methyl-D-glucose (23.4%),
2,3,6-tri-*O*-methyl-D-mannose (65.9%),
2,3-di-*O*-methyl-D-glucose (2.6%),
2,3-di-*O*-methyl-D-mannose (2.7%).

These data in conjunction with periodate oxidation results and estimates of the degree of polymerization indicated that the glucomannan was composed of 25–27 hexose units linked $\beta(1 \rightarrow 4)$ in a linear structure. The chains were terminated predominately by D-mannose units; traces of D-xylose were present in terminal positions only and appeared to be part of the glucomannan molecule.

Although glucomannans from many coniferous woods have been extensively investigated (1), no comparable study of the glucomannans of the hardwoods has been made. The relatively small amount of glucomannan in hardwoods as compared with softwoods has probably contributed to the lack of attention directed to this component. Jones, Merler, and Wise (2) isolated a crude glucomannan from poplar wood which had a glucose:mannose ratio of 1:2 and was a relatively straight-chain polymer with mannose end groups. Hemicelluloses of similar composition have been isolated from Western red alder and madrona by Hamilton and Thompson (3) but their structures have not been determined. A procedure has been developed by Timell (4) for isolation of glucomannans from woody angiosperms and it has been applied to seven species of hardwoods. Detailed structural studies on the glucomannan of white birch (5) and red maple (6) showed that both were composed of approximately 70 glucose and mannose residues linked $\beta(1 \rightarrow 4)$ in linear molecules. The present paper reports the isolation and structural study of a glucomannan isolated from sugar maple sapwood.

Extraction of maple sapwood holocellulose with 24% aqueous potassium hydroxide removed a large proportion of the 4-*O*-methylglucuronoxylans and left the glucomannans in the residue. Further extraction of the residue with 17.5% sodium hydroxide containing 4% borate yielded a crude glucomannan containing also approximately 35% xylan and some galactose residues. Purification of the glucomannan was achieved by forming its insoluble barium hydroxide complex (7) and thereby reducing the xylan impurity to 22%. Precipitation with Fehling's solution caused only a slight change in the mannose: glucose ratio and reduced the xylose content to trace levels in the main fraction. Acid hydrolysis of the hemicellulose and chromatographic examination of the sugars showed glucose and mannose and only a trace of xylose. Unlike many of the glucomannans of softwoods (8, 9, 10, 11), the purified maple glucomannan contained no galactose.

The glucomannan showed a single sharp peak on electrophoresis in borate buffer but electrophoresis in acetate buffer showed a small moving peak in addition to the large stationary peak. Analysis of the materials separated by electrophoresis in acetate buffer

[1]*Manuscript received August 28, 1961.*
Contribution from the Division of Applied Biology, National Research Council, Ottawa 2, Canada.
Issued as N.R.C. No. 6542.

proved the small peak to be a xylan impurity; the main homogeneous component contained only glucose and mannose. The xylan impurity was not separated from the glucomannan by ultracentrifugation in borate or acetate buffer.

The fully methylated glucomannan was hydrolyzed and an aliquot of the methyl glycosides was analyzed by gas–liquid partition chromatography. The main portion of the methylated sugars was separated on a cellulose column and on paper sheets with the appropriate solvents. The results are given in Table I. The large proportion of

TABLE I

Methylated sugars from hydrolyses of methylated hemicellulose

Methylated sugar	R_g, solvent B	Yield, mg	%
2,3,4,6-Tetra-*O*-methyl-D-glucose	1.0	22	1.1
2,3,4,6-Tetra-*O*-methyl-D-mannose	0.96	45	2.3
2,3,6-Tri-*O*-methyl-D-glucose	0.69	450	23.4
2,3,6-Tri-*O*-methyl-D-mannose	0.63	1270	65.9
2,3-Di-*O*-methyl-D-glucose	0.32	50	2.6
2,3-Di-*O*-methyl-D-mannose	0.28	52	2.7
Di-*O*-methyl-glucose (unidentified)	0.36	15	0.8
2,3,4-Tri-*O*-methyl-D-xylose (?)	0.86	10	0.5

2,3,6-tri-*O*-methyl-D-mannose and 2,3,6-tri-*O*-methyl-D-glucose showed that most of the mannose and glucose units were joined by $1 \rightarrow 4$ glycosidic bonds in the hemicellulose. Negative specific rotations of both the original hemicellulose and its methylated derivative which changed to positive values on hydrolysis indicated a predominance of β linkages. The tetra-*O*-methyl sugars represented non-reducing end groups in the molecule, the ratio of tetra-*O*-methyl-D-mannose to tetra-*O*-methyl-D-glucose (2:1) showed that approximately two thirds of the molecules were terminated by D-mannose units, the remainder by D-glucose. The proportion of tetra-*O*-methyl sugars showed that there was one non-reducing end group for every 27 hexose units. In accord with this value is that of 29 hexose units per reducing end group as found by hypoiodite reduction. Estimation of molecular weight by a vapor pressure method showed that the fully methylated molecule contained approximately 25 units. Since there is only one terminal unit per 27 units (as shown by methylation data), it is apparent that the molecule is a straight chain of hexose units. The dimethyl sugars must have no structural significance and must have been the result of incomplete methylation and(or) demethylation.

On periodate oxidation the consumption of 1.0 mole of periodate per mole of anhydrohexose sugar was further evidence of $(1 \rightarrow 4)$ linked hexose units. Formic acid production of 0.083 mole per anhydro sugar unit indicated a chain length of 25 units in the good agreement with values provided by other methods. Examination of the periodate-oxidized hemicellulose by Smith's degradation procedure (12) yielded erythritol and glycerol as the only products and these must have originated from $1 \rightarrow 4$ linked hexose units and non-reducing terminal hexose units respectively. The ratio of erythritol to glycerol (27:1) provided a further measure of the degree of polymerization (D.P.) of the molecule and the value of 27 is in good agreement with those reported above.

The glucomannans isolated from hardwoods have a wide range of glucose-to-mannose content. Although the general pattern shows a preponderance of mannose over glucose, the glucomannans of elm and sugar maple as reported by Timell (4) had a mannose: glucose ratio of 0.5:1.0. This latter finding is in contrast to that for glucomannan of

Can. J. Chem. Downloaded from www.nrcresearchpress.com by 210.87.254.105 on 09/05/12
For personal use only.

sugar maple reported in the present paper (mannose:glucose 7:3). Glucomannans of the coniferous woods have a relatively consistent composition with approximately three times as many mannose as glucose residues (6). It is becoming apparent that galactose may also be an integral part of the glucomannan molecule of softwoods. Galactose has not yet been reported in any hardwood glucomannans and the absence of this sugar may possibly distinguish the hardwood glucomannans from those of softwoods.

The glucomannan of maple sapwood contained approximately 25–27 hexose residues per molecule as compared with 70 residues as found in the glucomannans of white birch (5) and in red maple (6). This variation, which may be attributable to species difference, might also indicate that the glucomannans of the sapwood are smaller than those isolated from the entire woody structure. A further structural difference between the glucomannans of white birch (5) and red maple (6), as compared with that of sugar maple, is the termination of the two former molecules by D-glucose units while two thirds of the molecules of the latter are terminated by D-mannose units. The glucomannan of aspen is also terminated mainly by the D-mannose units (2).

The presence of a small amount of fully methylated D-xylose among the products of hydrolysis from the methylated maple hemicellulose indicated that D-xylose is an integral part of the glucomannan. The methylated xylose did not originate from the small amount of xylan impurity in the original polysaccharide otherwise it would have been 2,3-di-*O*-methyl-D-xylose. A similar association of D-xylose with the glucomannan of jack pine has been reported by Perila and Bishop (13), who obtained oligosaccharides containing xylose and glucose on enzymic hydrolysis. In the maple glucomannan the attachment of xylose is terminal but it is not possible to predict whether it terminates a molecule or is a single unit side branch.

Further work on a larger series of hardwood glucomannans will be necessary to establish not only their composition but also their fine structure and sequence of sugar units.

EXPERIMENTAL

All specific rotations are equilibrium values unless otherwise stated, melting points are corrected, and all evaporations were done at 35° C or less.

Paper Chromatography

Chromatographic separations were carried out using the following solvent systems (v/v):

(A) pyridine: ethyl acetate:water (2:1:2),
(B) methyl ethyl ketone: water: ammonia (100:50:3),
(C) ethanol: benzene: water: ammonia (47:200:14:1),
(D) *n*-butanol: ethanol: water (40:11:19).

Separations were made by the descending method on either Whatman No. 1 or No. 3 MM filter paper. Reducing sugars were located on the paper by the *p*-anisidine spray reagent (14); non-reducing sugar components were detected by silver nitrate and sodium hydroxide sprays (15).

Preparation of the Hemicellulose

A freshly cut log of sugar maple (*Acer saccharum*) was stripped of its bark and the sapwood portion was removed on a veneer lathe. After being air-dried for 48 hours, the thin sheets were passed through a Wiley mill. The milled wood was screened, and the fraction passing through 40 mesh and retained on 100 mesh was used. This wood fraction

Can. J. Chem. Downloaded from www.nrcresearchpress.com by 210.87.254.105 on 09/05/12
For personal use only.

was extracted with benzene:ethanol (2:1) for 24 hours, then with ethanol (8 hours), and was dried in air. Extraction with water at room temperature yielded a mixture of water-soluble polysaccharides (0.5%). From the extractive-free wood (1 kg) chlorite holocellulose was prepared (16) in 82.3% yield. Holocellulose (413 g) was stirred in 24% aqueous potassium hydroxide solution (4100 ml) for 6 hours at room temperature in an atmosphere of nitrogen. After filtration the residue was re-extracted once more and then washed with water. While still wet the residue was extracted as above with 17.5% sodium hydroxide containing 4% boric acid (4). The crude hemicellulose was recovered by adding the alkaline extract (9 l.) to the ethanol (24 l.) containing acetic acid (2.4 l.). The precipitate was washed thoroughly with ethanol (80%), the residual ethanol was removed by evaporation, and the crude polysaccharide was recovered by freeze drying (16.5 g). The glucose:mannose:xylose ratio in the polysaccharide was approximately 1:2.5:2 and there was a small amount of galactose present. The sugars were determined by the phenol sulphuric acid method (17).

Purification of the Crude Glucomannan

Crude glucomannan (15 g) was dissolved in 10% sodium hydroxide (750 ml) and 5% barium hydroxide solution (1250 ml) was added slowly with constant stirring over a period of 3 hours. The precipitate that formed was removed by centrifuging, washed twice with water acidified with acetic acid, and poured into ethanol (4 liters). The hemicellulose was recovered by centrifuging, dialysis, and freeze drying. Yield, 8.1 g. The glucose:mannose:xylose ratio was approximately 1:2.5:1.

Further purification of the glucomannan was achieved by forming a series of copper complexes through stepwise addition of Fehling's solution. The complexes were washed sparingly with water, in which they were soluble, dissolved in cold *N* hydrochloric acid, and poured into 5 volumes of ethanol to recover the hemicelluloses. Chromatographic examination of the fractions showed that each contained some xylose in addition to glucose and mannose. Further copper complexing yielded another series of fractions; of these, approximately 60% were pure glucomannans. Galactose and traces of arabinose and rhamnose were in the non-complexing material.

The hemicellulose had $[\alpha]_D^{25} = -24°$ (*c*, 0.76% in 0.5 *N* sodium hydroxide). Hydrolysis for 12 hours with *N* sulphuric acid and examination of the sugars by paper chromatography in solvents A and D showed the presence of glucose, mannose, and trace of xylose. Quantitative determination of sugars (17) in the acid hydrolyzate gave mannose: glucose 7:3. The more accurate method provided by gas–liquid chromatography of the fully methylated sugar as described by Adams and Bishop (18) gave the same value.

Examination of the hemicellulose in 0.05 *M* borate buffer by moving boundary electrophoresis carried out in a Spinco Model H apparatus showed a single peak indicating homogeneity of the polysaccharide. Similar examination in acetate buffer (pH 5.2) (ionic strength 0.2) showed two peaks, a main large stationary peak and a small moving one. Analysis of the separated materials after a migration time of 1020 minutes showed that the large peak represented the glucomannan while the moving peak represented the xylan. Centrifugation of both the borate and the acetate solutions in a Spinco Model E ultracentrifuge at 59,000 r.p.m. showed that each had only a single symmetrical peak. In a separate experiment using a mixture (50:50) of the glucomannan and the acidic xylan it was found that only electrophoresis in acetate buffer gave any separations; no separation was effected in the ultracentrifuge in either borate or acetate buffer.

Can. J. Chem. Downloaded from www.nrcresearchpress.com by 210.87.254.105 on 09/05/12
For personal use only.

Periodate Oxidation

Duplicate samples of the hemicellulose (100 mg) were dissolved in water (50 ml) and oxidized by 0.1 *M* sodium metaperiodate (50 ml) in the dark at room temperature. Suitable reagent blanks were prepared under the same conditions. Analyses were made for periodate consumption and formic acid production (19). The results given in moles per mole anhydrohexose unit were as follows.

Time, hours	24	48	72	96	168	216
Periodate consumption	0.57	0.71	0.90	0.91	0.98	0.99
Formic acid production	0.038	0.053	0.064	0.067	0.077	0.083

In a separate experiment the glucomannan (1.0 g) was oxidized by 0.1 *M* sodium metaperiodate (200 ml) at 15.6° C for 23 days. Barium acetate (0.5 *M*) (100 ml) was added to precipitate the iodate and excess periodate, which were removed by filtration. The filtrate was deionized by Amberlite IR-45 and IR-120. Potassium borohydride (1.0 g) was added and the reduction was allowed to proceed for 48 hours. The solution was neutralized with acetic acid, deionized with Amberlite IR-45 and IR-120, and evaporated to dryness several times with methanol. Acid hydrolysis of a portion of the residue and chromatographic examination of the hydrolyzate (solvent A and C) gave two components that were identical with erythritol and glycerol; no monosaccharides were found. Another portion of the hydrolyzate was dried thoroughly *in vacuo*, dissolved in pyridine (15 ml), and acetylated in acetic anhydride (5 ml) at room temperature for 36 hours. The acetylated polyols were examined directly by gas–liquid partition chromatography (8) (using 4′ apiezon M, 20% on celite 545, 197° C, 40 ml helium per minute). The acetates under examination had the same retention volumes as authentic samples of glycerol triacetate and erythritol tetraacetate respectively, and hence their identity was established. The ratio of erythritol to glycerol was 27:1.

Methylation of the Hemicellulose

Hemicellulose (5.0 g) was dissolved in 20% sodium hydroxide (60 ml) and methylated by dropwise addition of dimethyl sulphate (50 ml) and 45% sodium hydroxide (100 ml). The methylation procedure was repeated six more times. The partially methylated material was recovered by chloroform extraction of the neutralized solution, yield 6.8 g. The product was methylated once with Purdie's reagents using methyl iodide (100 ml) and silver oxide (11.5 g), yield 6.14 g, MeO, 35.6%. The product (6.1 g) was methylated by the Kuhn procedure (20) using dry dimethyl formamide (120 ml), methyl iodide (50 ml), and silver oxide (45 g), the solution being shaken for 48 hours at room temperature. The methylated hemicellulose was recovered by the described procedure (20), yield 3.80 g. Infrared spectroscopy showed the presence of hydroxyl groups. Methylation by Purdie reagents, repeated 3 times, gave a product having a methoxyl content of 44.3%, and no hydroxy bands in the infrared spectrum, yield 3.72 g. Fractionation from chloroform solution by addition of light petroleum gave a white product, wt. 3.60 g, $[\alpha]_D^{25}$ −16.3 (*c*, 1.04% in chloroform), methoxyl, 44.9% (theoretical for fully methylated hexosan 45.6%).

Methanolysis and Hydrolyses of the Methylated Hemicellulose

Methylated hemicellulose (1.93 g) was refluxed in 4% methanolic hydrogen chloride (45 ml) for 21 hours. After removal of the solvent the glycosides were hydrolyzed by heating for 20 hours in 0.5 *N* hydrochloric acid. The acid was neutralized with silver carbonate and the methylated sugars were recovered as a syrup (1.91 g).

Can. J. Chem. Downloaded from www.nrcresearchpress.com by 210.87.254.105 on 09/05/12
For personal use only.

A small portion of the glycoside mixture was examined by gas–liquid partition chromatography (21). The molar ratio of tetra-, tri-, and di-*O*-methyl glycosides was 2:50:3. The ratio of 2,3,4,6-tetra-*O*-methyl-D-mannose to 2,3,4,6-tetra-*O*-methyl-D-glucose was 2:1. Complete methylation of the mixture of tetra-, tri-, and di-methyl glycosides and re-examination of the glycosides by gas–liquid chromatography showed a ratio of tetra-*O*-methyl-D-mannose to tetra-*O*-methyl-D-glucose of 7:3.

Separation of Methylated Sugars

The mixture of methylated sugars ($[\alpha]_D^{25}$ +13°, water) was separated on a cellulose column (38×3.3 cm) using solvent C with a flow rate of 10 ml/15 minute. The tetra-, tri-, and di-methyl fractions separated on the column were separated into their individual component sugars by chromatography on paper sheets using solvents B. The yields of methylated sugars with their R_g values are given in Table I.

Identification of Methylated Sugars

2,3,4,6-Tetra-O-methyl-D-glucose

The crude syrup was taken up in water and clarified with charcoal; its mobility on a paper chromatogram in solvent B and on electrophoresis in borate buffer was identical with authentic 2,3,4,6-tetra-*O*-methyl-D-glucose. The sugar (98.2 mg) was dissolved in methanol (5 ml), aniline (49 mg) was added, and the mixture was refluxed for 2 hours. Fine white needles separated which, on recrystallization from ethyl ether – light petroleum (b.p. 30–60°), yielded 2,3,4,6-tetra-*O*-methyl-*N*-phenyl-D-glucosylamine, m.p. 136–137°, reported value 137–138° (22).

2,3,4,6-Tetra-O-methyl-D-mannose

The syrup had the same R_g value (0.96) in solvent B as an authentic sample of 2,3,4,6-tetra-*O*-methyl-D-mannose. The sugar (133 mg) was dissolved in methanol (5 ml), aniline (67 mg) added, and the mixture was refluxed for 2 hours. Slow removal of the solvent in a desiccator yielded crystals which were recrystallized from ethyl ether – light petroleum to give 2,3,4,6-tetra-*O*-methyl-*N*-phenyl-D-mannosylamine, m.p. 144°, reported value 144–146° (2).

2,3,6-Tri-O-methyl-D-glucose

After clarification with charcoal, the sugar crystallized on slow evaporation of its solution in ethanol–water. Recrystallization from ethanol – ethyl ether – light petroleum yielded 2,3,6-tri-*O*-methyl-D-glucose, m.p. 121° C, $[\alpha]_D^{25}$ +70.0° (*c*, 1% in water); reported values m.p. 121–123, $[\alpha]_D$ +70.0° (23).

Preparation of the 1,4-di-*O*-*p*-nitrobenzoate yielded the crystalline derivative, m.p. 189–190°, recrystallized from methanol, $[\alpha]_D^{25}$ −34° (*c*, 1% in chloroform); reported m.p. is 189–190° (24).

2,3,6-Tri-O-methyl-D-mannose

This sugar had the same mobility on paper chromatograms (solvents B and D) as authentic 2,3,6-tri-*O*-methyl-D-mannose. The 1,4-di-*O*-*p*-nitrobenzoate derivative was prepared and after one recrystallization from methanol had a melting point of 187–188°; reported value 187–188° (24).

2,3-Di-O-methyl-mannose

Mannose was the only sugar found on demethylation with boron trichloride (25). On paper electrophoresis in borate buffer the sugar had the same mobility as 2,3-di-*O*-methyl-D-mannose. Examination by gas–liquid partition chromatography indicated the presence

Can. J. Chem. Downloaded from www.nrcresearchpress.com by 210.87.254.105 on 09/05/12
For personal use only.

of 2,3-di-*O*-methyl-D-mannose. The sugar was converted to its 1,4,6-tri-*O*-*p*-nitrobenzoate derivative, which, after several recrystallizations from methanol, had a melting point of 192°, reported value 194° (26).

2,3-Di-O-methyl-D-glucose

This sugar gave only glucose on demethylation (25). It had the same mobility on paper electrophoresis as 2,3-di-*O*-methyl-D-glucose and on examination by gas–liquid partition chromatography (8), its glycosides had a retention volume identical with that of the glycosides of 2,3-di-*O*-methyl-D-glucopyranose. The aniline derivative was prepared as described above and yielded crystalline 2,3-di-*O*-methyl-*N*-phenyl-D-glucosylamine, which, on recrystallization from ethyl acetate, had m.p. 132°; reported value 134° (27).

Other Methylated Sugars

In addition to the di-*O*-methyl sugars identified above, another dimethyl sugar was present in small amounts. It gave glucose on demethylation and, on chromatographic and electrophoretic examination, appeared to be either 2,4- or 2,6-di-*O*-methyl-D-glucose. A sugar having R_g 0.83 (solvent B) and giving a red color with *p*-anisidine spray was recovered in small amounts. On demethylation it gave xylose only. Chromatographic examination (solvent B and C) indicated that it may be 2,3,4-tri-*O*-methyl-D-xylose.

Estimation of Molecular Weight

Two methods were used: (i) end group determination by hypoiodite (28) and (ii) vapor pressure measurements (29, 30).

(i) Triplicate samples of the hemicellulose (100 mg) were dissolved in 2 *N* sodium hydroxide, and 0.1 *N* iodine (10 ml) was added. The solutions, along with suitable blanks, were kept in stoppered flasks in the dark for 2 hours. After acidification of the solution with 2 *N* sulphuric acid, the iodine was titrated with 0.05 *N* sodium thiosulphate. Number average molecular weights calculated from reducing power values were 4400–4700, which corresponds to a D.P. of 27–29.

(ii) The methylated hemicellulose was dissolved in benzene and the difference in vapor pressure between the pure solvent and the solution was measured at concentrations of 7.16, 5.67, 3.79, 1.95, and 1.48% (g/100 g solution) and extrapolated to infinite dilution. Calculation of molecular weight according to Raoults's law gave a value (number average) of 5450 and hence D.P. = 25.

ACKNOWLEDGMENTS

The author is indebted to Dr. A. F. Sirianni for the determination of molecular weight by his vapor pressure method; thanks are also due Mr. W. R. Rowsome for valuable technical assistance.

REFERENCES

1. G. O. ASPINALL. Advances in Carbohydrate Chem. **14**, 429 (1959).
2. J. K. N. JONES, E. MERLER, and L. E. WISE. Can. J. Chem. **35**, 634 (1957).
3. J. K. HAMILTON and N. S. THOMPSON. Pulp Paper Mag. Can. **59**(10), 233 (1958); Tappi, **42**, 752 (1959).
4. T. E. TIMELL. Svensk Papperstidn. **63**, 472 (1960).
5. T. E. TIMELL. Tappi, **43**, 844 (1960).
6. A. J. MIAN and T. E. TIMELL. Can. J. Chem. **38**, 1511 (1960).
7. H. MEIER. Acta. Chem. Scand. **12**, 144 (1958).
8. C. T. BISHOP and F. P. COOPER. Can. J. Chem. **38**, 793 (1960).
9. G. G. S. DUTTON and K. HUNT. J. Am. Chem. Soc. **80**, 5697 (1958).
10. J. K. HAMILTON and E. V. PARTLOW. J. Am. Chem. Soc. **80**, 4880 (1958).
11. P. KOOIMAN and G. A. ADAMS. Can. J. Chem. **39**, 889 (1961).
12. M. ABDEL-AKHER, J. K. HAMILTON, R. MONTGOMERY, and F. SMITH. J. Chem. Soc. **74**, 4970 (1952).

Can. J. Chem. Downloaded from www.nrcresearchpress.com by 210.87.254.105 on 09/05/12
For personal use only.

13. O. PERILA and C. T. BISHOP. Can. J. Chem. **39**, 815 (1961).
14. L. HOUGH, J. K. N. JONES, and W. H. WADMAN. J. Chem. Soc. 1702 (1950).
15. W. E. TREVELYAN, D. P. PROCTER, and J. S. HARRISON. Nature, **166**, 444 (1950).
16. L. E. WISE, M. MURPHY, and A. A. D'ADDIECO. Paper Trade J. **122**, 35 (1946).
17. M. DUBOIS, K. A. GILLIES, J. K. HAMILTON, P. A. REBERS, and F. SMITH. Anal. Chem. **28**, 350 (1956).
18. G. A. ADAMS and C. T. BISHOP. Can. J. Chem. **38**, 2380 (1960).
19. S. K. CHANDA, J. K. N. JONES, and E. G. V. PERCIVAL. J. Chem. Soc. 1289 (1950).
20. R. KUHN, H. TRISCHMANN, and I. LÖW. Angew. Chem. **67**, 32 (1955).
21. C. T. BISHOP and F. P. COOPER. Can. J. Chem. **38**, 388 (1960).
22. J. C. IRVINE and A. M. MOODIE. J. Chem. Soc. **93**, 95 (1908).
23. J. C. IRVINE and J. W. H. OLDHAM. J. Chem. Soc. **119**, 1744 (1921).
24. P. A. REBERS and F. SMITH. J. Am. Chem. Soc. **76**, 6097 (1954).
25. S. ALLEN, T. C. BONNER, E. I. BOURNE, and N. M. SAVILLE. Chem & Ind. (London), 630 (1958).
26. F. SMITH and R. MONTGOMERY. Chemistry of plant gums and mucilages. Am. Chem. Soc. Monograph No. 141, New York. 1959. p. 539.
27. E. SCHUCHTERER and M. STACEY. J. Chem. Soc. 776 (1945).
28. S. K. CHANDA, E. L. HIRST, and E. G. V. PERCIVAL. J. Chem. Soc. 1240 (1951).
29. A. F. SIRIANNI and I. E. PUDDINGTON. Can. J. Chem. **33**, 755 (1955).
30. R. TREMBLY, A. F. SIRIANNI, and I. E. PUDDINGTON. Can. J. Chem. **36**, 725 (1958).

Can. J. Chem. Downloaded from www.nrcresearchpress.com by 210.87.254.105 on 09/05/12
For personal use only.

Can. J. Chem. Downloaded from www.nrcresearchpress.com by 210.87.254.105 on 09/05/12
For personal use only.

THE COMPOUNDS $KMnIO_6$ AND $NaMnIO_6$[1]

ILSE REIMER AND M. W. LISTER

ABSTRACT

Two compounds, originally formulated by Price as $Na_2Mn_2I_2O_{11}$ and $K_2Mn_2I_2O_{11}$ have been shown to be $NaMnIO_6.1/2H_2O$ and $KMnIO_6.1/2H_2O$. Consequently they are compounds of tetravalent manganese, a conclusion confirmed by their magnetic susceptibilities, and by their reactions with a variety of reducing agents; the reactions with ferrous ions, iodide ions, sulphur dioxide, hydroxylamine hydrochloride, and hydrazine hydrochloride were examined. Some of the properties of these compounds are described, and their X-ray powder diagrams show them to be analogous to the nickel salts $NaNiIO_6.H_2O$ and $KNiIO_6.1/2H_2O$.

In a relatively early paper, Price (1) described two complex periodates to which he gave the formulae $K_2Mn_2I_2O_{11}$ and $Na_2Mn_2I_2O_{11}$. Since periodates do not seem to form I_2O_{11} groups, these formulae seemed doubtful, a suspicion which was supported by the variable analyses reported in Price's paper. The present paper describes a re-examination of these compounds, which are shown in fact to be $KMnIO_6$ and $NaMnIO_6$, analogous to the nickel compounds $KNiIO_6$ and $NaNiIO_6$, prepared by Ray and Sarma (2). These compounds may contain a small amount of water of crystallization, being again similar in their behavior to the nickel compounds. It will be noticed that Price considered these to be compounds of trivalent manganese, while they are here formulated as containing tetravalent manganese; considerable evidence supporting this is given below.

PREPARATION OF COMPOUNDS

Price prepared these compounds by mixing manganous sulphate (or nitrate) in fairly strongly acidified solution with a similarly acidified solution of sodium or potassium periodate. He gave practically no details of quantities, so that the method described in the present paper is only approximately the same as his. The methods used by us were as follows.

Sodium Manganese (IV) Periodate

Manganese sulphate (8 g) monohydrate was dissolved in about 400 ml of water containing a few drops of sulphuric acid. Sixteen grams of sodium periodate, $Na_2H_3IO_6$, was dissolved in 600 ml of 0.75 *N* sulphuric acid. The solutions were mixed, whereupon a red precipitate gradually separated. The mixture was kept at 40° C for some hours, after which the mixture was filtered through a sintered-glass disk. The product was washed thoroughly with water, and dried over calcium chloride.

With the quantities used above, some manganese remained in solution, in agreement with the over-all equation

$$MnSO_4 + 2Na_2H_3IO_6 \rightarrow NaMnIO_6 + NaIO_3 + Na_2SO_4 + 3H_2O.$$

The quantities chosen were chosen partly to meet the requirements of Price's formula, and partly to avoid other complexes known to occur with excess sodium periodate (3). However, a better yield would probably be obtained with 2 gram-molecules of sodium periodate to 1 of manganese sulphate.

[1]*Manuscript received July 18, 1961.*
Contribution from the Department of Chemistry, University of Toronto, Toronto, Ontario.

Potassium Manganese (IV) Periodate

This was prepared similarly using potassium periodate, KIO_4, in somewhat more acid solution (2 to 3 *N* sulphuric acid). A red precipitate formed, which was filtered, washed, and dried, like the sodium salt.

Analysis

The compounds were analyzed as follows. The water of crystallization was determined by heating to constant weight at 110° C. The water was rapidly lost at this temperature, and no appreciable further loss was observed on heating the compounds to 150° C. Iodine was determined by suspending a weighed sample in water, and bubbling in sulphur dioxide till all was dissolved. Silver nitrate was added and the silver iodide was filtered off and weighed. After removal of excess silver by hydrochloric acid, the manganese was determined by adding excess ammonia, filtering off the manganese hydroxide, dissolving this in dilute sulphuric acid, and evaporating to dryness. The residue of $MnSO_4$ was weighed. It was found that the manganese hydroxide dissolved rather slowly in acid, but this was much speeded up by bubbling in a little sulphur dioxide. Sodium or potassium were determined by acidifying the filtrate with sulphuric acid and evaporating it to dryness. Any sodium bisulphate in the residue was removed by adding ammonium carbonate and a little water, and again evaporating to dryness. In some samples the manganese was precipitated as manganese ammonium phosphate and ignited to $Mn_2P_2O_7$; the alkali metal was then found in a separate sample.

Results of the analyses were as follows.

Sodium salt.—Na 8.00, 7.84%; Mn 18.01, 17.87%; I 40.65, 39.8%, H_2O 3.3%. Calculated for $NaMnIO_6.1/2H_2O$: Na 7.42%, Mn 17.72%, I 40.95%, H_2O 2.9%.

Potassium salt.—K 12.24, 13.05%; Mn 16.32, 17.31%; I 39.59, 39.58%, H_2O 4.3%. Calculated for $KMnIO_6.1/2H_2O$: K 12.00%, Mn 16.86%, I 38.93%, H_2O, 2.8%.

These analyses do not, of course, settle the question of the valency of the manganese, since formulae such as $KHMnIO_6.1/2H_2O$ are sufficiently close in composition as to be indistinguishable. The evidence for tetravalent manganese is given in the next section.

VALENCY OF MANGANESE

This was determined from measurements of (i) oxidation equivalents and (ii) magnetic susceptibilities.

1. Oxidation Equivalents

The substances are too insoluble in water to titrate directly, but they react with excess acidified ferrous ammonium sulphate, and the excess can be titrated with potassium permanganate. Since ferrous ions reduce periodate to iodate ions, a formula with tetravalent manganese would require reduction by four ferrous ions per molecule; trivalent manganese would require reduction by three ferrous ions. The results obtained were as follows.

Sodium salt.—Equivalent weight 78.1. Calculated for $NaMnIO_6.1/2H_2O$ 77.5; $NaHMnIO_6.1/2H_2O$ 103.7.

Potassium salt.—Equivalent weight 85.9. Calculated for $KMnIO_6.1/2H_2O$ 81.5; $KHMnIO_6.1/2H_2O$ 109.0.

These results support a formula with tetravalent manganese.

A second equivalent weight can be obtained by adding a known weight of compound to acidified potassium iodide, and titrating the liberated iodine with sodium thiosulphate.

Can. J. Chem. Downloaded from www.nrcresearchpress.com by 210.87.254.105 on 09/05/12
For personal use only.

In this case tetravalent manganese will give 10 equivalents per molecule; trivalent manganese will give 9. The results were as follows.

Sodium salt.—Equivalent weight 31.7, 32.6. Calculated for $NaMnIO_6.1/2H_2O$ 31.0; $NaHMnIO_6.1/2H_2O$ 34.6.

Potassium salt.—Equivalent weight 33.2. Calculated for $KMnIO_6.1/2H_2O$ 32.6; $KHMnIO_6.1/2H_2O$ 36.3.

These results also support a formula with tetravalent manganese.

It had been found (3) with similar compounds that a check on the formula could be obtained by bubbling in sulphur dioxide, and after boiling out the excess sulphur dioxide, titrating the acid formed with sodium hydroxide. Bromcresol green was used as indicator to avoid any precipitation of manganese. However, with the present compounds the results were found to be rather variable, and the equivalent weight was always lower than that calculated even for tetravalent manganese. The results were as follows.

Sodium salt.—Equivalent weight 37.9, 36.1. Calculated for $NaMnIO_6.1/2H_2O$ 38.7; $NaHMnIO_6.1/2H_2O$ 44.4.

Potassium salt.—Equivalent weight 36.1, 37.2, 34.5. Calculated for $KMnIO_6.1/2H_2O$ 40.7; $KHMnIO_6.1/2H_2O$ 46.7.

Hence more acid is formed than would be expected; possibly there is some air oxidation of the sulphur dioxide. So far as they go, the results support tetravalent rather than trivalent manganese.

The reactions with two other reducing agents that might similarly produce acid were investigated. Firstly, hydroxylamine hydrochloride was tried, which was found to react with potassium periodate, KIO_4, producing 4 gram-molecules of acid from 1 gram-molecule of potassium periodate:

$$KIO_4 + NH_3OHCl \rightarrow KI + 2N_2O + 6H_2O + 4HCl.$$

Note that this requires oxidation to nitrous oxide. Sodium manganese (IV) periodate also oxidized hydroxylamine hydrochloride, but produced 3.51 gram-molecules of acid from 1 gram-molecule of the complex salt; potassium manganese (IV) periodate produced 3.58. The expectation was 3 gram-molecules (a formula with Mn(III) would give 2.5 gram-molecules of acid):

$$2KMnIO_6 + 10NH_3OHCl \rightarrow 2KI + 2MnCl_2 + 5N_2O + 17H_2O + 6HCl.$$

However, if the nitrogen of the hydroxylamine was converted to elementary nitrogen, the expectation would be 8 gram-molecules, and the most probable conclusion is that the manganese gives some oxidation to nitrogen as well as to nitrous oxide. The closeness of the result to $3\frac{1}{2}$ is probably accidental.

Similarly hydrazine hydrochloride reacts (a little slowly) with potassium periodate thus:

$$KIO_4 + 2N_2H_5Cl \rightarrow KI + 2N_2 + 4H_2O + 2HCl,$$

the amount of acid produced exactly agreeing with this equation. This led to the expectation that 0.5 gram-molecule of acid would be produced by 1 gram-molecule of sodium manganese (IV) periodate (Mn(III) would give 0.25 gram-molecule):

$$2NaMnIO_6 + 5N_2H_5Cl \rightarrow 2NaI + 2MnCl_2 + 5N_2 + 12H_2O + HCl.$$

However, it was found that addition of the complex salt to a solution of hydrazine hydrochloride (adjusted to the neutral point of bromcresol green or methyl orange) made the solution alkaline, and it remained so even on boiling. If acid was added till the

Can. J. Chem. Downloaded from www.nrcresearchpress.com by 210.87.254.105 on 09/05/12
For personal use only.

neutral point of the indicator was again reached, the solution produced more acid spontaneously, and this was then titrated with sodium hydroxide. The total effect was that 1 gram-molecule of the complex salt did in fact produce nearly 0.5 gram-molecule of hydrochloric acid: $NaMnIO_6$ gave 0.61 gram-molecule, and $KMnIO_6$ gave 0.51 gram-molecule of acid. There is evidently a slow stage in the reaction which is catalyzed by acid. Hence both the reactions with hydroxylamine hydrochloride and hydrazine hydrochloride, though not too clear cut, support a formula with tetravalent manganese.

2. Magnetic Susceptibilities

The magnetic susceptibilities of the compounds were measured on a Goüy balance at room temperature. The balance was calibrated with ferrous ammonium sulphate. The observed susceptibilities were: $NaMnIO_6.1/2H_2O$, 23.42×10^{-6} e.m.u./g at 24.8° C; $KMnIO_6.1/2H_2O$, 18.20×10^{-6} e.m.u./g at 22.5° C. If the compounds obey Curie's law, these results make the magnetic moments: sodium salt 4.17 Bohr magnetons; potassium salt 3.76 Bohr magnetons. These are evidently close to the calculated 'spin only' value of 3.87 Bohr magnetons for three unpaired electrons, which would be present in manganese (IV).

PROPERTIES OF COMPOUNDS

The sodium and potassium salts are both red microcrystalline solids. They are virtually insoluble in water, the solubilities not being above 10 mg/liter at room temperature. Consequently no absorption spectrum in solution could be obtained. As mentioned in the description of the analysis, they readily lose their water of crystallization at 110° C, but the anhydrous salts are stable up to a much higher temperature: no decomposition was apparent at 230° C, though iodine vapor was evolved at a red heat. They show no tendency to decompose in water to give permanganate ions, as the complex salts containing more periodate do (3); this is true of suspensions either in water or alkali: in neither case was any reaction apparent on prolonged standing.

STRUCTURE OF COMPOUNDS

Debye–Scherrer X-ray diffraction photographs were obtained from the powdered compounds in the usual way. Similar photographs for $NaNiIO_6.H_2O$ and $KNiIO_6.1/2H_2O$ were obtained at the same time. The nickel compounds were prepared by the method

TABLE I

Interplanar spacings from X-ray powder diagrams

$KNiIO_6$	$KMnIO_6$	$NaNiIO_6$	$NaMnIO_6$
6.00 s	5.93 s	5.12 s	5.12 s
4.29 m	4.29 m	4.29 m	4.31 m
3.52 s	3.49 s	3.30 s	3.30 s
3.03 w	3.04 vw	—	—
2.48 m	2.50 w+	2.49 m	2.49 m
2.30 m	2.30 m	2.24 s	2.25 m
2.02 w+	2.04 m	1.99 m−	2.02 w+
1.91 m	1.91 vw	—	—
1.82 w−	1.77 vw	1.79 m	1.81 m
1.62 vw	1.61 w	—	—
1.56 w+	—	1.56 m−	1.55 w+
1.47 w−	1.46 vw	—	—
1.43 w−	1.42 vw	1.43 w+	1.44_5 w+
1.39 vw	—	1.38 w+	1.41 vw
1.29 w	1.31_5vw	1.28_5vw	1.26 vw

NOTE: s = strong; m = medium; w = weak. Spacings in Å.

Can. J. Chem. Downloaded from www.nrcresearchpress.com by 210.87.254.105 on 09/05/12
For personal use only.

given in *Inorganic syntheses* (4). It may be mentioned in passing that while these hydrated formulae are given for the nickel compounds, the reported analyses are closer to the anhydrous salts, especially for the potassium compound. This is doubtless due to the relatively weak attachment of the water, as with the manganese compounds. The object of the present X-ray work was to demonstrate a similarity between the manganese and nickel compounds, which would be expected from their formulae; it is hoped to obtain a more detailed picture of their structure shortly. The values of the interplanar spacings, calculated from the observed lines, are given in Table I. These were obtained using copper K_α X-rays, and a camera of 114.6-mm diameter. The patterns for the corresponding manganese and nickel compounds show considerable similarity, and there can be little doubt that the compounds are isomorphous. This also supports the view that tetravalent manganese is present. The interplanar spacings are not far from what would be calculated for a cubic unit cell, particularly in the case of the potassium salts. This suggests that both the metal and iodine atoms are octahedrally co-ordinated to the oxygen atoms, giving a polymerized structure that would explain the insolubility of these compounds.

REFERENCES

1. W. B. PRICE. Am. Chem. J. **30**, 182 (1903).
2. P. RAY and B. SARMA. J. Indian Chem. Soc. **25**, 205 (1948).
3. M. W. LISTER and Y. YOSHINO. Can. J. Chem. **38**, 1291 (1960).
4. INORGANIC SYNTHESES. Vol. 5. McGraw-Hill Co. p. 201.

Can. J. Chem. Downloaded from www.nrcresearchpress.com by 210.87.254.105 on 09/05/12
For personal use only.

REACTION OF OXYGEN ATOMS WITH BENZENE[1]

G. Boocock[2] and R. J. Cvetanović

ABSTRACT

The reaction of benzene with oxygen atoms produced by mercury photosensitized decomposition of nitrous oxide has been studied in a circulating system at room temperature. The main reaction product is a non-volatile material probably largely aldehydic in character. This is tentatively assumed to result from the rearrangement and polymerization of the initially formed adduct. Smaller amounts of phenol and carbon monoxide are also formed. The rate of formation of carbon monoxide decreases with increasing pressure, suggesting an energy-rich precursor.

Oxygen atoms react with benzene much more slowly than with olefines. At 120° cyclopentene reacts about 150 times more quickly than benzene. The activation energy of the reaction of oxygen atoms with benzene has been estimated at 4.6 to 4.9 kcal/mole, with an uncertainty of about 0.7 kcal/mole.

INTRODUCTION

Reactions of a number of unsaturated hydrocarbons with oxygen atoms generated by the mercury photosensitized decomposition of nitrous oxide have been studied in some detail in this laboratory, but attention has previously been concentrated on alkenes and cycloalkenes (1–3). The present investigation is a further stage in these studies and has been undertaken in an attempt to derive some information on the attack of ground state oxygen atoms on an aromatic nucleus. Unfortunately, the major part of the reaction product, a polymeric material of low volatility, could not be characterized; only a fragmentary picture of the process has therefore been obtained. This is in sharp contrast to the relatively well-understood major features of the reactions of oxygen atoms with alkenes.

Early attempts to obtain approximate values of the rates of reactions of a number of compounds with oxygen atoms (4) led to the conclusion that benzene reacted very rapidly with oxygen atoms. In the present work, however, this reaction is found to be much slower than the corresponding reactions of alkenes. In view of the electrophilic character of oxygen atoms (3), this finding is not unexpected.

Several workers (4–7) have investigated the reaction of benzene with oxygen atoms generated in electrical discharges. Chu, Ai, and Othmer (8) used a flow system and generated oxygen atoms by electrical discharge in molecular oxygen. They obtained phenol yields of up to 13% per pass, in substantial agreement with the previous findings of Avramenko and co-workers (7). However, with water vapor instead of oxygen discharge they found no detectable amount of phenol although Avramenko *et al.* claimed yields of up to 27% under similar conditions.

The presence of other reactive species and the need to maintain relatively low over-all pressures seriously complicate the use of electrical discharges in molecular oxygen or in water vapor for fundamental studies of the reactions of oxygen atoms with organic compounds. Some of the potential complexities have been discussed elsewhere (8) in connection with a study of the reaction of oxygen atoms produced by electrical discharge in molecular oxygen with 1-butene.

[1]*Manuscript received May 31, 1961.*
Contribution from the Division of Applied Chemistry, National Research Council, Ottawa, Canada.
Issued as N.R.C. No. 6554.

[2]*National Research Council Postdoctorate Fellow 1957–1958. Present address: Shell Chemical Company, Carrington Research Laboratory, England.*

In the present work oxygen atoms were generated by the mercury photosensitized decomposition of nitrous oxide (9). At not too elevated temperatures nitrous oxide reacts extremely slowly with oxygen atoms in their ground state and with other free radicals. In the presence of benzene the process can be represented by the following reactions:

$$Hg(^1S_0) + h\nu\ (2537\ \text{Å}) \longrightarrow Hg(^3P_1), \quad [1]$$

$$Hg(^3P_1) + N_2O \longrightarrow N_2(^1\Sigma) + O(^3P) + Hg(^1S_0), \quad [2]$$

$$O(^3P) + C_6H_6 \longrightarrow \text{products}. \quad [3]$$

Depending on the quenching efficiency of benzene and on the relative pressures of benzene and nitrous oxide present, there may also be appreciable quenching of $Hg(^3P_1)$ atoms by benzene. However, Scott and Steacie (10) have investigated the mercury photosensitized reactions of benzene and found that appreciable reaction occurs only at higher temperatures. In agreement with this no products due to quenching by benzene have been detected in the present work. The amount of nitrogen formed in reaction [2] serves as an internal actinometer and is used as a measure of the number of oxygen atoms generated.

EXPERIMENTAL

A conventional vacuum apparatus was used, with stopcocks replaced by mercury cutoffs where necessary to prevent the absorption of hydrocarbons by tap grease. The cylindrical quartz reaction cells were 10 cm long and 5 cm in diameter. Early experiments were made in a system of approximately 450 ml in volume, which included an all-glass plunger-type circulating pump. Later, a second reaction cell was added. This was connected to the vacuum line through a metal "Hoke" valve and gave a reaction volume of about 200 ml.

The analysis line contained a Le Roy still (11), a pumped-down trap, and a diffusion pump delivering into a Töpler pump and thence into two gas burettes. One of these latter was greaseless and the other was connected to a small combustion furnace packed with copper oxide. Non-volatile polymeric products remaining in the reaction cells were either extracted by solvents or combusted to carbon dioxide, which was then measured. The low-pressure mercury vapor lamp was run at a constant current of 100 ma, and most experiments were made at 25° C.

Benzene (Nichols reagent grade) was dried over calcium hydride and given several bulb-to-bulb distillations, with rejection of light and heavy fractions on each transfer. It was stored over calcium hydride in a bulb closed by a mercury cutoff. Nitrous oxide (98%) (Matheson Co.) was purified by bulb-to-bulb fractionation. Cyclopentene (Phillips research grade) was passed through an activated alumina column to remove peroxide contamination and then further purified by bulb-to-bulb fractionation. All reactants were degassed before each run.

Nitrous oxide with benzene was irradiated for periods of between 10 minutes and several hours. The reactor was then cooled in liquid nitrogen and the non-condensable gases were collected for analysis by combustion and mass spectrometry. The condensed material was removed to the Le Roy still for fractionation, a process which was normally abbreviated in later experiments to a separation of nitrous oxide at $-80°$ C or $-120°$ C. The fractions of least volatility from the Le Roy still, including unreacted benzene, were subjected to a variety of analytical procedures.

RESULTS

Preliminary experiments showed that non-condensable gaseous products always contained some carbon monoxide but no significant quantities of hydrogen or methane. Spot tests (12) of the condensable products gave a positive reaction for phenol but showed absence of acetylene and formaldehyde. An opaque yellow film on the walls of the reaction cell and a pronounced decline in nitrogen production with time indicated the formation of important quantities of a non-volatile product. The amounts of carbon dioxide formed by combustion of this material proved it to be sufficient in quantity to be a major product of the reaction.

In order to determine more accurately the quantity of non-volatile product by combustion and subsequent measurement of the carbon dioxide evolved, a static reactor which could be heated to redness almost in its entirety was built. Several experiments were carried out with approximately equal initial concentrations of benzene and N_2O but with different irradiation times. The results are shown in Table I.

TABLE I

Effect of the extent of reaction on the ratios R_{CO}/R_{N_2}, $R_{CO_2}/6R_{N_2}$, and $-R_{C_6H_6}/R_{N_2}$ (temperature 25±2° C)

Run	C_6H_6 (mm)	C_6H_6 (μmole)	N_2O (mm)	Irradiation time (min)	ΔN_2[a] (μmole)	$\frac{R_{CO}}{R_{N_2}}$	$\frac{R_{CO_2}}{6R_{N_2}}$	$\frac{-R_{C_6H_6}}{R_{N_2}}$
12	6.75	76.3	204	15	10.5	0.172	0.21	n.d.
13	9.54	109.4	199	30	19.4	0.174	0.27	n.d.
14	7.31	83.9	~200	31	20.1	0.176	0.26	0.43
15	7.91	90.8	206	90	48.4	0.175	0.30	0.43
16	7.55	81.8	~200	80	44.4	0.177	n.d.	0.46

NOTE: n.d. = not determined.
[a]Any CH_4 present is neglected.

It is evident from Table I that within the investigated range R_{CO}/R_{N_2} is independent of the extent of reaction, as measured by the amount of N_2 produced. The amount of non-volatile material ($R_{CO_2}/6R_{N_2}$), on the other hand, appears to increase somewhat with increasing conversion. In three of the experiments in Table I, runs 14, 15, and 16, the consumption of benzene per oxygen atom consumed ($-R_{C_6H_6}/R_{N_2}$) has been determined. This was done by recovering the unreacted benzene and measuring it both manometrically and by G.L.C. At these relatively low partial pressures of benzene the number of moles of benzene consumed per gram-atom of oxygen was found to be considerably lower than unity. Comparison of runs 14 and 15 shows the benzene consumption under these conditions to be approximately independent of the extent of reaction.

The early experiments indicated that the production of carbon monoxide decreased as the over-all pressure in the system was increased, as shown in Table II, A. However, in these experiments the partial pressure of benzene was also varied. A separate series of experiments was therefore carried out in which the partial pressure of benzene and the extent of reaction were kept approximately constant. The results are shown in Table II, B, and in Fig. 1 and they confirm a distinct decrease in the carbon monoxide formation with increasing over-all pressure.

In order to obtain some quantitative information on the amounts of phenol formed, two runs were carried out with larger partial pressures of benzene and relatively long irradiations. In this manner high percentage conversions of benzene were avoided.

TABLE II

Effect of total pressure on the ratio R_{CO}/R_{N_2}
(in A are given the mean values of the rates of CO formation from sets of two or more experiments at approximately constant partial pressure of benzene. Temperature 25±2° C)

Run	Total pressure (mm)	C_6H_6 (mm)	N_2O (mm)	Irradiation (min)	ΔN_2 (μmole)	R_{CO}/R_{N_2}
A						
21, 22	55	1.8	53	5, 10	3.22[a], 7.11[b]	0.231±0.003
12, 13, 14, 15, 16	210	7.8	202	15–90	10.5–48.4[c]	.175±.003
24, 25	586	82	504	12, 30	4.45, 9.80[d]	.115±.020
B						
190	49.1	5.67	43.4	70	19.4	0.239
192	106.3	6.19	100.1	85	24.1	.215
188	151.3	4.75	146.5	60	24.8	.195
191	351.1	5.55	345.5	80	27.5	.166
187	504.0	5.28	498.7	60	29.0	.150
189	591.6	5.63	586.0	65	25.2	.143

[a]From run 21.
[b]From run 22.
[c]As shown in Table I.
[d]From run 25.

Fractions recovered from the Le Roy still at −80 to +25° C after these runs (Table III) were each quantitatively diluted with benzene and analyzed by infrared spectroscopy.

TABLE III

Yield of phenol in the reaction of oxygen atoms with benzene
(temperature 25±2° C)

Run	C_6H_6 (mm)	N_2O (mm)	ΔN_2 (μmole)	ΔC_6H_5OH (μmole)	$\frac{\Delta C_6H_5OH}{\Delta N_2}$	$\frac{-\Delta C_6H_5OH}{\Delta C_6H_6}$
19+20	~26	490	64.5	3.6±0.7	0.056±0.011	0.127±0.025
28	83.1	505	640	40±4	0.062±0.006	0.141±0.014

As shown in Table III, some 13% of the benzene consumed during the reaction was found to be converted to phenol. Although the amount of nitrogen produced in run 28 is about 10 times larger than in the combined runs 19 and 20, the amount of phenol formed per gram-atom of oxygen consumed is, within the analytical uncertainty, the same in the two cases.

The non-volatile polymeric material evidently represents the major product of the reaction of oxygen atoms with benzene. Attempts were made to obtain some information on the nature of this material, but with relatively little success. Carbon tetrachloride washings of the reaction cell after runs 27 and 28 were colorless, showed absorption peaks at 279, 272, and 267 mμ in the ultraviolet, and gave a positive reaction to both Brady's reagent and Schiff's reagent, the compound formed with Brady's reagent being soluble in carbon tetrachloride. The presence of aldehyde groupings in this fraction was thus strongly suggested. The reaction cell was subsequently extracted with acetone, which appeared to dissolve the bulk of the deep yellow component of the deposit. The ultraviolet absorption showed single sharp peaks at 323.5 mμ. An infrared spectrum of the acetone extract deposited on a KBr pellet showed a heavy general absorption with a set of broad peaks superimposed at 694, 757, 1225, 1490, 1591, 1667, 1705, 2860, and 3300

cm^{-1} suggestive of aliphatic rather than aromatic groupings. After careful removal of acetone, these extracts also gave, with Brady's reagent, a definite orange color extractable in carbon tetrachloride.

After extraction with carbon tetrachloride and acetone, combustion of the remaining material showed that the two solvents removed only about 50% of the polymeric deposit.

An approximate carbon balance can be obtained for runs 14 and 15 of Table I. Taking $100\ (R_{CO}+R_{CO_2})/6R_{C_6H_6}$ as an approximate measure of the carbon balance, a mean value of about 72% is arrived at. However, the phenol produced ought to be added to this figure. Table III shows amounts of phenol which on the basis of the benzene consumption in runs 14–16 would indicate that about 13 to 14% of benzene is converted to phenol. However, the data in Table III were obtained at much higher partial pressures of benzene and it is conceivable that the consumption of benzene, $-R_{C_6H_6}/R_{N_2}$, under such conditions is closer to unity. In view of this the mean carbon balance for runs 14 and 15 comes to about 75 to 85%. Deposition of non-volatile tarry material in the gas burette used for storing the volatile products, together with the characteristic odor, slight color, and positive reaction to Schiff's reagent of these, suggested that unidentified lower molecular weight products of a very reactive and possibly aldehydic nature were formed. Such products must have been responsible, at least partly, for the failure to obtain 100% carbon balance.

The rate constant of reaction of oxygen atoms with benzene (k_B) relative to that of cyclopentene (k_C) was determined by the competitive technique described in detail elsewhere (3). This technique is based on the measurement of the decline in ethylene production from the reaction of oxygen atoms with cyclopentene when another substance which consumes oxygen atoms is added. Early experiments showed that at room temperature cyclopentene reacted more than 200 times as fast as benzene. It was consequently very difficult to obtain quantitative competitive data. A number of determinations were therefore made at two higher temperatures and the mean values of k_C/k_B obtained were 152.6 ± 13.9 at 119.8° C, and 54.3 ± 4.6 at 220.4° C. The relatively large mean deviations resulted from the large disparity in the rates and from the use of small partial pressures of cyclopentene in order to maintain large benzene to cyclopentene ratios. High partial pressures of benzene were used (close to the saturation pressure at room temperature) and the assumption was made that, under these conditions and at the higher reaction temperatures of these experiments, oxygen atoms were consumed only in the primary attack on benzene and cyclopentene.* Using Arrhenius' equation, the mean values of k_C/k_B at the two temperatures give $E_C-E_B = 4.0$ kcal/mole and $A_C/A_B = 1.0$. It has been established (13) that $E_C-E_{TME} = 0.6$ kcal/mole (where the subscript TME stands for tetramethyl ethylene) and E_{TME} is probably quite small (perhaps not greater than 0.1 to 0.3 kcal/mole) so that $E_B = 4.6$ to 4.9 kcal/mole. The experimental uncertainty in this value is estimated from the mean deviations in k_C/k_B at the two temperatures at about ±0.7 kcal/mole.

DISCUSSION

Two modes of attack of atomic oxygen on benzene are possible: abstraction of a hydrogen atom or addition to the aromatic nucleus. Abstraction of a hydrogen atom would lead to the formation of a hydroxyl radical and a phenyl radical. Attack of benzene by hydroxyl would then be expected, with the subsequent production of diphenyl and phenol by radical association according to the following scheme (14).

**A slight thermal reaction occurs at 220° C but this was found to be unimportant under the experimental conditions used.*

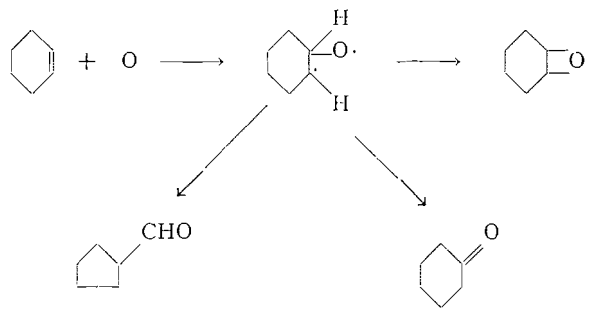
$$C_6H_6 + O \rightarrow C_6H_5\cdot + OH\cdot \quad [4]$$

$$C_6H_6 + OH\cdot \rightarrow C_6H_5\cdot + H_2O \quad [5]$$

$$C_6H_5\cdot + OH\cdot \rightarrow C_6H_5OH \quad [6]$$

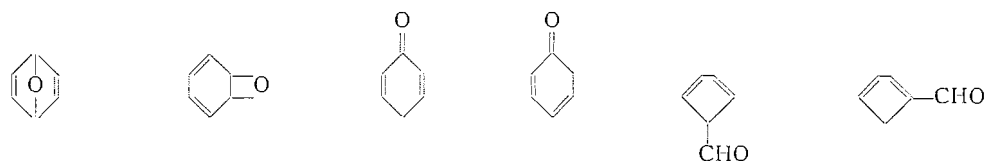
$$C_6H_5\cdot + C_6H_5\cdot \rightarrow \text{diphenyl} \quad [7]$$

Alternatively, as with the olefins and cyclo-olefins, the oxygen atom may add directly to the benzene molecule. Cyclohexene reacts in this fashion to produce a biradical which quickly rearranges to a mixture of cyclohexene oxide, cyclohexanone, and cyclopentyl formaldehyde (2).



[8]

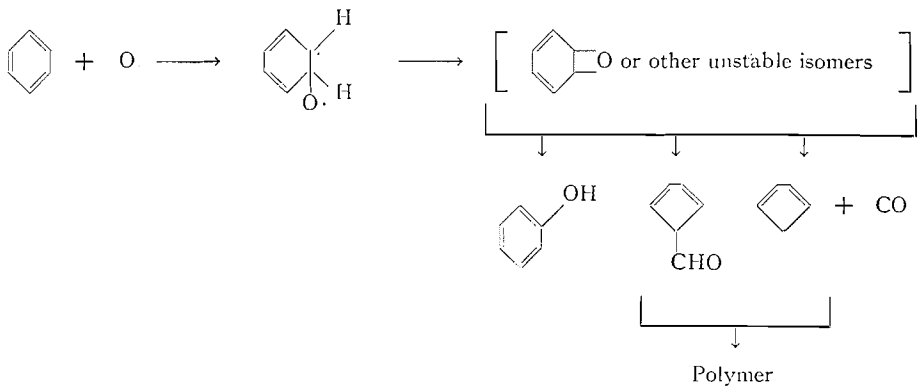
The analogous scheme for benzene presents a larger number of possibilities, as shown below, since in principle either 1:2 or 1:4 addition may occur (although in the case of 1,3-butadiene only 1:2 addition of oxygen atoms is observed (15)).



I II III IV V VI

However, none of these compounds is reported in the literature although some derivatives are known. This is probably because I, II, III, and IV isomerize quickly to the stable structure of phenol whilst V and VI are undoubtedly prone to a variety of condensations and polymerizations.

On the basis of the present experimental results it is clearly impossible to suggest a definite reaction mechanism. It would, however, appear likely that initially an addition complex is formed between an oxygen atom and a benzene molecule and that this becomes in part stabilized as phenol. A larger fraction of the complex, on the other hand, suffers rupture of the aromatic ring with production of unsaturated aliphatic compounds, perhaps such as cyclopentadienyl formaldehyde, which readily undergo further reactions to form non-volatile polymeric material. Such a mechanism is analogous to the attack of oxygen atoms on olefins (2) and is to some extent supported by the type of products observed, the absence of diphenyl, and the pressure effect in the carbon monoxide formation (Table II and Fig. 1). Nevertheless, the evidence is not strong and the proposed mechanism, depicted approximately in the reaction scheme [9], is at present only of a tentative character.



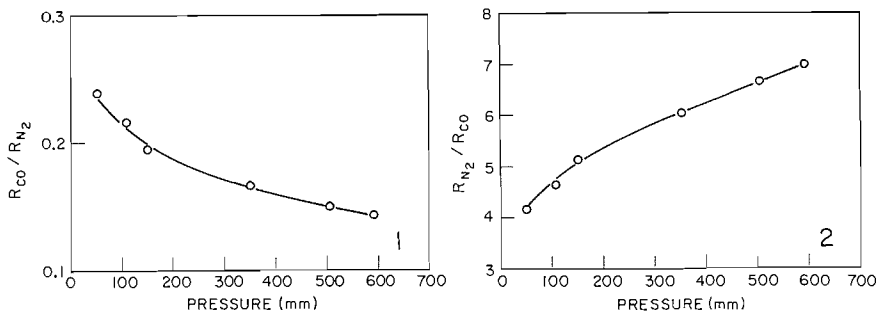


FIG. 1. The effect of pressure on carbon monoxide production.
FIG. 2. Plot of $-R_O/R_{CO}$ (*i.e.* R_{N_2}/R_{CO}) against pressure.

It is probable that the large fraction of oxygen atoms which are not consumed in the initial reaction with benzene at low partial pressures of benzene are involved in the secondary attack on the primary products formed, and especially on those rendered more reactive by loss of their aromatic character.

The pressure effect in the rate of formation of carbon monoxide strongly suggests that this compound is formed from decomposition of an energy-rich adduct as has been observed in the same pressure range in the cases of propylene (2) and 1,3-butadiene (15). With increasing pressure the excess energy tends to be removed by collisions from the "hot" product before it decomposes and carbon monoxide production therefore decreases. Inasmuch as the rate of this collisional deactivation is proportional to the pressure in the system, a linear plot should be obtained by plotting R_{N_2}/R_{CO} against pressure. Actually, as shown in Fig. 2, the plot appears to show a slight curvature. This could be explained by more complex collisional deactivation or by production of carbon monoxide from more than one "hot" species; however, more elaborate treatments are at present not warranted.

In their reactions with olefins oxygen atoms behave as electrophilic reagents (3, 16) and their relative rates are simply related to the basicity of olefins. Insofar as the same holds true for the reactions of aromatic compounds, the much slower rate of reaction with benzene is in qualitative agreement with the observation of West (17) that simple aromatic compounds are generally weaker bases than olefins as measured by the magnitude of the frequency shift of the C—H infrared absorption bands of alcohols or phenols

forming hydrogen-bonded complexes with these compounds. Quantitatively, however, the difference in the reactivity of benzene is much greater than would be anticipated from a comparison of the frequency shifts. Rate data for reactions of oxygen atoms with a number of aromatic compounds are required before these differences can be further discussed.

ACKNOWLEDGMENTS

The authors are grateful to Dr. A. W. Tickner for mass spectrometric analyses, to the Analytical Section of this Division for infrared analyses, and to Mr. L. C. Doyle for assistance with some of the experiments.

REFERENCES

1. R. J. CVETANOVIĆ. J. Chem. Phys. **25**, 376 (1956).
2. R. J. CVETANOVIĆ. Can. J. Chem. **36**, 623 (1958).
3. R. J. CVETANOVIĆ. J. Chem. Phys. **30**, 19 (1959).
4. P. HARTECK and U. KOPSCH. Z. Physik. Chem. (Leipzig), B, **12**, 327 (1931).
5. K. H. GEIB and P. HARTECK. Trans. Faraday Soc. **30**, 131 (1934).
6. J. C. CHU, H. C. AI, and D. F. OTHMER. Ind. Eng. Chem. **45**, 1266 (1953).
7. L. I. AVRAMENKO, I. I. IOFFE, and R. Y. LORENTSO. Doklady Akad. Nauk S.S.S.R. **66**, 1111 (1949).
8. J. M. S. JARVIE and R. J. CVETANOVIĆ. Can. J. Chem. **37**, 529 (1959).
9. R. J. CVETANOVIĆ. J. Chem. Phys. **23**, 1203 (1955).
10. E. J. Y. SCOTT and E. W. R. STEACIE. Can. J. Chem. **29**, 233 (1951).
11. D. J. LE ROY. Can. J. Research, B, **28**, 492 (1950).
12. F. FEIGL. Spot tests in organic analysis. Elsevier, New York. 1956. pp. 183, 325, 331.
13. R. J. CVETANOVIĆ. J. Chem. Phys. **33**, 1063 (1960).
14. G. STEIN and J. WEISS. J. Chem. Soc. 3245 (1949).
15. R. J. CVETANOVIĆ and L. C. DOYLE. Can. J. Chem. **38**, 2187 (1960).
16. R. J. CVETANOVIĆ. Can. J. Chem. **38**, 1678 (1960).
17. R. WEST. J. Am. Chem. Soc. **81**, 1614 (1959).

Can. J. Chem. Downloaded from www.nrcresearchpress.com by 210.87.254.42 on 09/05/12
For personal use only.

REACTION OF OXYGEN ATOMS WITH TOLUENE[1]

G. R. H. JONES[2] AND R. J. CVETANOVIĆ

ABSTRACT

The reaction of toluene with oxygen atoms produced by mercury photosensitized decomposition of nitrous oxide has been studied at room temperature. The reaction shows a general similarity to the corresponding reaction of benzene. Relative rates have been determined at 120 and 220° C and the activation energy estimated at close to 4 kcal/mole.

INTRODUCTION

An attempt was recently made in this laboratory to study the reaction of oxygen atoms in their ground electronic state with benzene as the first representative of aromatic compounds (1). Information was obtained on the rate and the activation energy of the reaction, but the major part of the reaction product was unfortunately a material of low volatility which could not be characterized. Therefore only a fragmentary picture of the process was obtained.

The present work was undertaken in the hope of obtaining additional information on the mode of attack of oxygen atoms on an aromatic ring. Another objective was to compare the reactivity of toluene towards oxygen atoms with that of benzene and of unsaturated aliphatic compounds. The relative rate and activation energy of the reaction of oxygen atoms with toluene have been determined but the major reaction product is again a material of low volatility, difficult to handle under conditions used in these experiments. As a result, as in the case of benzene, only a limited amount of information has been obtained on the mechanism of this reaction and in this respect the work has therefore only a preliminary character.

EXPERIMENTAL

A circulating reaction system was used, similar to the one described previously (1). The reaction vessel was a cylindrical quartz cell 10 cm long and 5 cm in diameter. The gases were circulated by means of an all-glass vertical plunger pump. Total volume of the circulating system was 504 ml. Mercury cutoffs were used instead of stopcocks, where necessary, to prevent absorption of hydrocarbons by stopcock grease.

The toluene used was Merck reagent grade, dried over CaH_2, purified by bulb-to-bulb distillation with retention of the middle fraction only, and stored over CaH_2. No impurities could be detected in a sample analyzed by gas chromatography. Nitrous oxide was obtained from Matheson Co. and was further purified by bulb-to-bulb fractionation. Phillips research grade cyclopentene was used. It was freed from peroxides by passage through an activated alumina column, after which it was subjected to bulb-to-bulb distillation *in vacuo*.

The analysis system has been described in the earlier work (1). It incorporated a Le Roy still (2), a Toepler pump, two constant volume burettes, and a copper oxide tube maintained at 240° for combustion of CO and H_2 in the non-condensable gases. Nitrogen

[1]*Manuscript received July 25, 1961.*
Contribution from Division of Applied Chemistry, National Research Council, Ottawa, Canada. Issued as N.R.C. No. 6555.
[2]*National Research Council Postdoctorate Fellow 1958–1960. Present address: Imperial Chemical Industries, Billingham, England.*

Can. J. Chem. Downloaded from www.nrcresearchpress.com by 210.87.254.42 on 09/05/12
For personal use only.

and methane were recovered from the copper oxide tube unchanged and were further analyzed mass spectrometrically. The amount of CO in the non-condensable gases was estimated from the amount of CO_2 formed in the copper oxide tube and H_2 was found by difference. Ethylene was recovered from the Le Roy still at $-182°$ and contained a small amount of N_2O which was determined by a mass spectrometer and deducted from the total amount of this fraction.

It was difficult to determine toluene consumption accurately since at small conversion this was given as a small difference between two large quantities. Because of relatively low volatility of toluene, direct manometric measurements were not accurate enough and the same held for gas chromatographic determinations. The following technique was found to be better although the experimental uncertainty remained appreciable. Aliquots were taken and the amounts of toluene initially introduced and remaining at the end of a run were determined from the CO_2 produced by combustion (after dividing by 7). For this purpose, oxygen was generated by heating reagent grade $KMnO_4$ and the combustion was carried out for 12 hours on a platinum wire maintained at dull-red heat. After removal of excess oxygen, carbon dioxide was recovered at dry ice temperature and measured. Initially an aliquot was taken from toluene before the introduction of nitrous oxide. At the end of a run, the nitrous oxide was first removed with the Le Roy still kept at $-125°$ after which the toluene and the volatile products (cresols) were allowed to expand again in the reaction volume and an aliquot was taken and combusted. To correct for the cresols present, assumption was made that the aliquot contained the toluene and the cresols in the same ratio as in the bulk retained in the reaction system. The cresols formed were therefore assumed not to exceed their saturation vapor pressures. This assumption was probably valid although there is some uncertainty in the vapor pressure of cresols at room temperature.

The cresols produced in the reaction were determined gas chromatographically. After the removal of N_2O and withdrawal of the aliquot for determination of the residual toluene as described above, all the volatile material remaining in the reaction vessel was distilled over into a small tapered tube immersed in liquid nitrogen and containing a weighed amount (approximately 0.04 g or 40 μl) of a standard solution of an internal standard in a solvent of known concentration. The distilling over was extended for $2\frac{1}{2}$ to 3 hours after which dry air was admitted. Samples of solutions obtained in this manner were analyzed on a Perkin–Elmer 154 C vapor fractometer using 2-meter UCON or, in the later stages of the work, polyester succinate (on chromosorb W) columns at 200° C. Helium was used as carrier gas at a flow of 120 ml/minute. The ratios of peak areas of the *o*- and *p*-cresols to that of the internal standard were determined and compared with those obtained with standard solutions of known concentrations of *o*-cresol, *p*-cresol, and the internal standard. The latter were run between each sample of the solution containing the products of the reaction. With the UCON column the internal standard used was diphenyl and the solvent cumene, and with the polyester succinate column the internal standard was naphthalene and the solvent benzene. The latter column gave better resolution of *o*- and *p*-cresol. The internal standards and the solvents were so selected that the standard was well resolved from the cresols and there was no interference from the large excess of the solvent.

The recovery of cresols was checked by following a $2\frac{1}{2}$-hour distillation for transfer of cresols into the tapered tube with a second 2-hour distillation into a fresh sample of standard solution. No detectable amounts of cresol were recovered in the second distillation.

Can. J. Chem. Downloaded from www.nrcresearchpress.com by 210.87.254.42 on 09/05/12
For personal use only.

RESULTS

The products observed in the reaction of oxygen atoms with toluene at room temperature have been *o*-cresol, *p*-cresol, carbon monoxide, water, and a reddish-yellow material of low volatility which was not further characterized (referred to in the following as "polymer").

The identification of the two cresols was based on their gas chromatographic elution times and their infrared spectra. The third isomer, *m*-cresol, was not resolved from *p*-cresol on the columns used. However, the infrared spectra of the condensable volatile products showed that *m*-cresol constituted at most only 4 to 5% of the total cresols and perhaps less. Between about 15 and 20% of the oxygen atoms reacting with toluene (as measured by the amount of nitrogen produced) were recovered as cresols. On the average, about 3–4 times as much *o*-cresol was formed as *p*-cresol.

Water was estimated approximately by gas chromatography. After removal of N_2O, the volatile condensable products were collected and passed at room temperature through a 12-ft dimethyl sulpholane column on glass beads. For water, the peak areas were not linearly related to the amounts taken and the determinations were based on an empirical calibration curve. Relatively long exposures had to be used in order to produce sufficient amounts of water for analysis and the mean of two determinations showed the presence of an amount of water corresponding to 7% of the oxygen atoms reacting with toluene.

Attempts were made to estimate the amounts of non-volatile "polymer" formed by admitting oxygen into the evacuated reaction cell and heating the cell to redness. The carbon dioxide produced was determined and the amount obtained, divided by 7, was taken as the measure of the "polymer" formed. However, the combustion of the "polymer" was not quantitative since it partially distilled and deposited on the walls of the glass tubing outside the reaction cell. Nevertheless, there could be little doubt that this material represented the major part of the reaction product, in agreement with the observed low carbon and oxygen atom balance.

Solutions of the products analyzed gas chromatographically for cresols showed complete absence of dibenzyl. The vapor pressure of dibenzyl at room temperature is approximately one-fifth of that of *p*-cresol and under conditions under which most of the cresol is recovered it would seem reasonable to expect recovery of at least some dibenzyl if an appreciable amount is formed. In view of this it appears that in the reaction of oxygen atoms with toluene, at most only negligible amounts of dibenzyl are formed.

Some of the experimental results are summarized in Table I. In most of these experiments an approximately constant amount of toluene was initially used while the exposure times were varied. Because of "polymer" deposit on the reaction cell window the amount of incident light varied with time and from experiment to experiment. The extent of reaction should therefore be judged from the amount of nitrogen formed rather than from the exposure time. For four- to five-fold increase of nitrogen production no drastic changes in the rates of formation of the products are evident. There is perhaps a slight decrease with the extent of conversion in the rates of cresol formation and toluene consumption, although the experimental scatter is large and makes this uncertain. The average rate found for toluene consumption per oxygen atom is 0.80 but it is difficult to say whether the difference from the expected value of unity is real or due to imperfections of the analytical procedure used. As already mentioned, the values obtained for the "polymer" represent only lower limits.

In these experiments the partial vapor pressure of toluene was relatively high so that some quenching of the excited mercury atoms by toluene did occur. However, this is

Can. J. Chem. Downloaded from www.nrcresearchpress.com by 210.87.254.42 on 09/05/12
For personal use only.

TABLE I

Products formed in the reaction of oxygen atoms with toluene
($25\pm2°$ C; $p_{N_2O} = 385\pm5$ mm)

Run	Toluene		Time (hours)	N_2 (μmoles)	Relative rates (R/R_{N_2})						$\frac{o\text{-Cresol}}{p\text{-Cresol}^c}$
	Initial (μmoles)	Consumed (μmoles)			CO	*o*-Cresol	*p*-Cresol[c]	Polymer	Water	Toluene	
23[a]	239.6	25.6	0.5	22.32	0.070					1.15	
22[a]	245.7		0.5	22.94	.066	0.146	0.046				3.2
15[b]	227.7	24.4	2	38.01	.071	.124	.036	0.52		.64	3.4
21[a]	244.8	34.1	1	39.52	.065	.134	.035			.86	3.8
33[a]	285.1	25.3	1.05	39.60	.066	.114	.038			.64	3.0
34[a]	258.2	45.9	1.6	61.34	.068	.114	.035			.75	3.3
16[b]	258.1	49.3	3.25	64.53	.077	.114	.032	.23		.76	3.5
20[a]	260.4	50.1	2.05	64.58	.079	.116	.032	.19		.78	3.6
18[b]	218.9	38.5	3	68.65	.074	.090	.022	.35		.56	4.1
17[b]	271.0	66.7	3	75.05	.071	.094	.024	.14		.89	3.9
19[b]			3	79.74	.057	.128	.034	.11			3.8
27[a]	197.8	73.3	6	107.0	.072					.69	
26			3	72.80	.074				0.076		
28	180.0		5.7	121.6	.062				0.063		

[a]Cresols determined on the polyester succinate column.
[b]Cresols determined on the UCON column.
[c]May contain small amounts of *m*-cresol, as explained in the text.

unlikely to have influenced to any appreciable extent the course of the studied reaction. When toluene alone was subjected to mercury photosensitized reaction for a period of 19 hours, only about 2 μmoles of non-condensable material were collected and of this only about one-third appeared to be combustible. No significant amounts of C_2, C_3, and C_4 fractions were found and infrared analysis of the condensable material in the reaction vessel revealed no significant amounts of products.

The effect of pressure on the products has been studied by varying the partial pressure of nitrous oxide at a constant small pressure of toluene and irradiating for 1 hour. The results are given in Table II. There do not appear to be any drastic changes in the rates

TABLE II

The effect of pressure on the products
(25±2° C; irradiation time 1 hour; cresols determined on the polyester succinate column)

Run	N_2O (mm)	Toluene Initial (μmoles)	Toluene Consumed (μmoles)	N_2 (μmoles)	Relative rates (R/R_{N_2}) CO	*o*-Cresol	*p*-Cresol[a]	Toluene	*o*-Cresol / *p*-Cresol[a]
29	100	252.1	33.7	35.5	0.093	.142	.053	0.95	2.7
30	221	273.8	35.8	40.8	.077	.145	.046	.88	3.1
21	384	244.8	34.1	39.5	.065	.134	.035	.86	3.8
33	385	285.1	25.3	39.6	.066	.114	.038	.64	3.0
31	683	284.0		48.3	.059	.112	.032		3.5
32	672	333.9	29.7	40.7	.059	.133	.038	.73	3.4

[a]May contain small amounts of *m*-cresol, as explained in the text.

per gram-atom of oxygen (R/R_{N_2}) for a substantial variation in total pressure although small trends could be hidden by the experimental scatter of points. In the case of carbon monoxide the analytical accuracy is greater and there is a distinct decline in the rate of carbon monoxide formed per gram-atom of oxygen consumed (R_{CO}/R_{N_2}) with increasing pressure. This is shown in Fig. 1 and resembles the trend previously observed in the reaction of oxygen atoms with benzene (1).

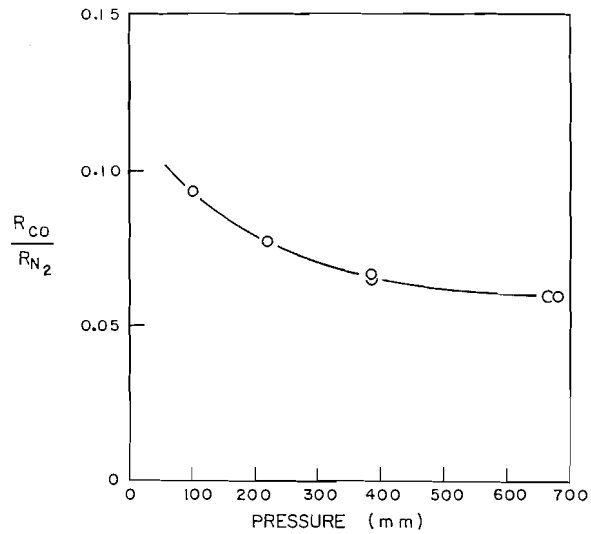


FIG. 1. Pressure effect in the rate of carbon monoxide formation.

Can. J. Chem. Downloaded from www.nrcresearchpress.com by 210.87.254.42 on 09/05/12
For personal use only.

Can. J. Chem. Downloaded from www.nrcresearchpress.com by 210.87.254.42 on 09/05/12
For personal use only.

The rate constants of reaction of oxygen atoms with toluene (k_T) relative to those of cyclopentene (k_C) were determined at 120 and 220° C by the competitive technique described in detail elsewhere (3). This technique is based on measurements of the decrease in the amount of ethylene formed by attack of oxygen atoms on cyclopentene when another substance consuming oxygen atoms is present. At room temperature it was found that toluene reacted much more slowly than cyclopentene and reliable values of relative rate constants would be very difficult to obtain. At 220° C a very slow thermal reaction producing nitrogen occurred. With the total residence times of the reactants in the reactor under 2 hours the extent of the thermal reaction was almost negligible. Nevertheless, a correction for the very small amount of nitrogen produced thermally was made. No measurable thermal reaction was observed at 120° C.

The relative rate constants (k_T/k_C) obtained at 120 and 220° C are given in Table III.

TABLE III

Determination of relative rate constants of addition of oxygen atoms to cyclopentene (k_C) and toluene (k_T)
(the amounts of reactants and of the nitrogen produced are given in millimeters, in 1107[a] ml at 25° C; the amounts of ethylene are given relative to the nitrogen produced)

Run	Temp. (°C)	N_2O (mm)	Toluene (mm)	Cyclo-pentene (mm)	Irradiation (min)	N_2[b] (mm)	C_2H_4[c]/N_2	k_C/k_T
I. 120° C								
290	120.3	520.4	21.2	2.59	60	0.527	0.239	50.2
291	119.9	523.9	21.3	2.59	60	.509	.245	60.3
292	120.1	523.2	21.0	2.52	62	.541	.243	57.7
293	120.5	520.8	20.6	2.38	60	.473	.244	61.1
Mean	120.2							57.3±3.6
II. 220° C								
287	222.0	409.7	16.4	2.48	60	0.519 (.523)	.209	24.5
288	222.0	411.2	15.9	2.26	60	.520 (.523)	.208	26.0
289	222.4	412.1	15.9	2.52	60	.506 (.509)	.211	24.3
Mean	222.1							24.9±0.7

[a]In these experiments the reaction cell was a 1-liter quartz round flask provided with a glass stirrer on teflon bearings magnetically operated from outside. This larger reaction volume permitted smaller cyclopentene pressures to be used and consequently somewhat larger toluene to cyclopentene ratios.
[b]At 220° C, N_2 values are corrected for thermal reaction: the uncorrected values are given in parentheses to show the extent of the corrections made. No thermal reaction occurred at 120° C.
[c]Several determinations gave for cyclopentene alone (i.e. in the absence of toluene but otherwise under comparable conditions) mean C_2H_4/N_2 ratios of 0.274 and 0.282 at 220 and 120° C respectively. These values were used in calculating the rate constants from equation (5) of reference 3.

The large mean deviations are primarily due to the large disparity in the rates of attack of oxygen atoms on cyclopentene and toluene, respectively. With the practically usable mixtures of the two hydrocarbons under conditions of the present experiments the reaction always occurred predominantly with cyclopentene. As a consequence even slight errors in the measured amounts of ethylene formed caused large errors in the values of the rate constants, especially so at the lower temperature where the disparity in the two rates is greater.

From the mean values of the relative rate constants at 120 and 222° C a difference in the activation energies of attack of oxygen atoms on toluene (E_T) and cyclopentene (E_C) of 3.2 kcal and a ratio of the pre-exponential factors (A_T/A_C) of unity are obtained. In view of the likely value (4) of E_C a value for E_T of about 3.8 to 4.1 kcal/mole is thus arrived at. The mean deviations indicated in Table III introduce an uncertainty in $E_T - E_C$ of ±0.3 to 0.4 kcal and a factor of about 1.5 in the ratio of the pre-exponential

factors. Because of large disparity in the rates between toluene and cyclopentene, as pointed out above, toluene presents an unfavorable case for accurate determination of relative rates by the cyclopentene technique and the margin of uncertainty in $(E_T - E_C)$ and (A_T/A_C) may be even greater.

DISCUSSION

Reaction of oxygen atoms with toluene shows great general similarity with the reaction of oxygen atoms with benzene (1). As in the case of benzene, (1) the major reaction product is a material of low volatility, probably polymeric in character; (2) smaller amounts of phenols are formed; (3) there is a pressure effect in the rate of carbon monoxide formation, suggesting an energy-rich precursor; and (4) products expected for a primary hydrogen abstraction reaction are not detected.

In view of these findings it is most likely, as was postulated for benzene (1), that in the case of toluene also the primary step is an addition of oxygen atoms to the aromatic ring rather than hydrogen abstraction. In agreement with this no dibenzyl is detected. Small amounts of water formed (equivalent to about 7% of the oxygen atoms consumed) could mean that some hydrogen abstraction does occur; however, water could equally well be formed in secondary processes. The initial adduct could be visualized as either being stabilized into cresols or rearranging into products which partially decompose or, to a much greater extent, undergo polymerization. These matters have been speculatively discussed for the benzene reaction (1) and in view of the similarity of the two processes there is no need for further discussion here. Until the nature of the "polymeric" material is established, any attempt to establish the mechanism of these reactions will necessarily remain only speculative.

The pressure effect in carbon monoxide formation is very similar to that observed with benzene (1) although in the case of toluene carbon monoxide is a less important product. As with benzene, the plot of R_{N_2}/R_{CO} is not linear but shows instead a distinct curvature. Smaller production of carbon monoxide from toluene rather than from benzene at comparable pressures may be compared with the formation of fragmentation products in the reaction of oxygen atoms with alkenes. In this latter case, again the "hot" addition products formed by reaction of oxygen atoms with olefins containing a smaller number of carbon atoms (C_2H_4, C_3H_6) are shorter lived and undergo fragmentation much more easily (at comparable pressures) than products from olefins containing a greater number of carbon atoms (5). This is readily understandable in terms of the number of internal degrees of freedom available for dissipation of energy, although the stability of the fragments formed must play also an important role, as evident from the reaction of oxygen atoms with 1,3-butadiene (6).

Formation of large amounts of ortho- and para-cresol and at most of very small amounts of metacresol in the reaction of oxygen atoms with toluene is understandable in view of the electrophilic character of oxygen atoms. Relatively large ortho-to-para ratio is to be noted since it suggests little or no steric hindrance to the addition of oxygen atoms ortho to methyl group. The upper limit for metacresol obtained from infrared spectra seems to be below the amount that would be expected if the "selectivity relationship" for electrophilic substitution reactions of toluene (7) were applicable to the present reaction. However, more quantitative information on metacresol is required before this matter can be further discussed.

The relative rates of addition of oxygen atoms to toluene confirm the previous finding with benzene (1) of a slower attack of oxygen atoms on an aromatic ring than on an

Can. J. Chem. Downloaded from www.nrcresearchpress.com by 210.87.254.42 on 09/05/12
For personal use only.

olefinic double bond. At the same time, as expected, toluene reacts appreciably faster than benzene (1). It is of interest that the pre-exponential factors for benzene and toluene appear to be similar to those of olefins (4), although there may be an appreciable margin of uncertainty in the activation energies and pre-exponential factors for the two aromatic hydrocarbons.

ACKNOWLEDGMENTS

The authors are grateful to Dr. A. W. Tickner for mass spectrometric analyses, to the Analytical Section of this Division for infrared analyses, and to Mr. L. C. Doyle for assistance with some of the experiments.

REFERENCES

1. G. Boocock and R. J. Cvetanović. Can. J. Chem. This issue.
2. D. J. Le Roy. Can. J. Research. B, **28**, 492 (1950).
3. R. J. Cvetanović. J. Chem. Phys. **30**, 19 (1959).
4. R. J. Cvetanović. J. Chem. Phys. **33**, 1063 (1960).
5. R. J. Cvetanović. Can. J. Chem. **36**, 623 (1958).
6. R. J. Cvetanović and L. C. Doyle. Can. J. Chem. **38**, 2187 (1960).
7. L. M. Stock and H. C. Brown. J. Am. Chem. Soc. **81**, 3323 (1959).

Can. J. Chem. Downloaded from www.nrcresearchpress.com by 210.87.254.42 on 09/05/12
For personal use only.

Can. J. Chem. Downloaded from www.nrcresearchpress.com by 210.87.254.40 on 09/05/12
For personal use only.

LIGHT ABSORPTION STUDIES

PART XX. THE ULTRAVIOLET ABSORPTION SPECTRA AND INFRARED CARBONYL BANDS OF BENZOYL CHLORIDES[1]

W. F. FORBES[2] AND J. J. J. MYRON[3]

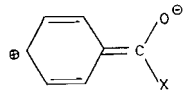
ABSTRACT

The ultraviolet absorption spectra and infrared carbonyl bands of a number of substituted benzoyl chlorides are determined. It is found that as a first approximation the *B*-bands of the ultraviolet spectra are similar for benzoyl chlorides and for the corresponding benzaldehydes and acetophenones. The spectra are discussed in terms of previously stated hypotheses. In this way the order of the apparent negative mesomeric effect is deduced to be $-NO_2 > -COCl > -CHO > -COCH_3$, and the effective size of these substituents is confirmed to be in the order $-NO_2 > -COCH_3 > -COCl > -CHO$.

The infrared carbonyl band occurs as a well-defined doublet in most of the ring-substituted benzoyl chlorides. The most probable explanation is that these doublets occur because of an intramolecular vibration.

INTRODUCTION

In previous parts of this series (see, for example, refs. 1, 2, 3) it was shown that spectral changes in the main ultraviolet absorption band of substituted benzene derivatives could be rationalized by assuming that such changes are predominantly caused by mesomeric and steric interactions, but are not appreciably affected by other short-range interactions such as inductive and field effects. In compounds such as benzoyl chloride, benzaldehyde, and acetophenone this would imply that the main ultraviolet band, the *B*-band (for nomenclature see previous parts of this series and ref. 4), may be associated with resonance forms of type I, which schematically represents mesomeric interactions between the carbonyl group and the benzene ring. If this is correct, the *B*-band of benzoyl chloride should be similar to the *B*-band of benzaldehyde and acetophenone, and should undergo



(I)

X = Cl, H, or CH_3

changes on ring substitution similar to the corresponding *B*-band changes occurring in acetophenone or benzaldehyde on substitution.

The purpose of the present paper is to investigate this hypothesis and also to determine the infrared carbonyl band in substituted benzoyl chlorides. These latter bands are of interest because the infrared carbonyl band of benzoyl chloride is well known to occur as a doublet, the origin of which is unknown. Information concerning the nature of this doublet may thus be provided by investigating this carbonyl band in a number of substituted benzoyl chlorides.

EXPERIMENTAL

The ultraviolet absorption spectra were determined by standard methods in 1-cm cells using a Unicam SP 500 or a Beckman Model DU or Model DK 2 spectrophotometer.

[1]*Manuscript received May 19, 1961.*
Contribution from the Division of Protein Chemistry, C.S.I.R.O., Wool Research Laboratories, 343 Royal Parade, Parkville, N.2 (Melbourne), Australia, and from the Memorial University of Newfoundland, St. John's, Newfoundland.

[2]*Present address: Division of Protein Chemistry, C.S.I.R.O., 343 Royal Parade, Parkville, N.2 (Melbourne), Victoria, Australia. All correspondence should be addressed to this author.*
[3]*Graduate student, 1958–1959. Present address: Chemistry Department, University of Alberta, Edmonton, Alberta.*

For each compound at least two independent sets of observations were made. The Unicam SP 500 instrument was calibrated against a didymium filter, and wavelength readings obtained on the Unicam and Beckman instruments were found to be within 1 mμ of each other. The precision of λ_{max} values is estimated to be 1 mμ, and the precision of ϵ_{max} values, 5% or better. Values were reproducible for most compounds to 2%. The main ultraviolet maxima in cyclohexane solution are listed in Tables I and IV. The spectra could not be determined in ethanol solution due to reaction of the benzoyl chloride with the solvent.

The infrared spectra were determined on a Unicam SP 100 double-beam spectrometer with an SP 130 sodium chloride prism-grating double monochromator. The resolution in the 1700 cm^{-1} region was ca. 0.5 cm^{-1}. The solute concentration was kept within the limits of 4.7×10^{-2} and 9.2×10^{-2} mole/liter (usually 0.5-mm cells with KBr windows), except when as otherwise stated. The infrared absorption bands are shown in Tables I, II, and III and in Figs. 3, 5, and 7. Infrared spectra were also used to show the absence of any appreciable amount of acid which might have been formed through decomposition of the benzoyl chlorides.

The benzoyl chlorides were either prepared by standard methods or obtained from commercial sources; they were purified by distillation or recrystallization until their boiling points and refractive indices or melting points showed them to be sufficiently pure. The solvents used were spectroanalyzed cyclohexane (Fisher) or other commercially available spectroanalyzed solvents.

THE ABSORPTION CHARACTERISTICS OF BENZOYL CHLORIDE

The main ultraviolet absorption bands and the infrared carbonyl and adjoining bands of benzoyl chloride and related compounds are shown in Table I.

TABLE I

Absorption spectra of benzoyl chloride and related compounds*

	Ultraviolet absorption bands (in cyclohexane solution unless otherwise stated)				Infrared absorption bands in carbon tetrachloride solution	
	B-band		*C*-band		Carbonyl band	Benzene band
Compound	λ_{max} (mμ)	ϵ_{max}	λ_{max} (mμ)	ϵ_{max}	ν_{max} (cm^{-1})	ν_{max} (cm^{-1})
Benzoyl chloride	242 ca. *250*	14,500 *12,000*	282 ca. *291*	1,300 *900*	1,782 (s)† 1,740 (m)	1,591 (w)† 1,577 (vw)
Benzoyl chloride in ether solution	244	14,300	282–283	1,400	1,784 (s) 1,740 (m)	
Benzoyl chloride in vapor phase	233 237 240.5 242	‡	255 273 276 279 283 287	‡	1,798 (s) 1,756 (m)	1,598 (m)
Benzaldehyde	241 *247*	14,500 *12,500*	277–278 287	1,200 1,000	1,709 (s)	
Acetophenone	237–238	12,500	277	900	1,691 (s)	

*Data from this paper or previous parts of this series.
†Values for the maxima were the same at solute concentration 2.5 *M*, 0.5 *M*, 0.25 *M*, and 0.05 *M* (using different-path-length cells).
‡Intensities not determined.

Can. J. Chem. Downloaded from www.nrcresearchpress.com by 210.87.254.40 on 09/05/12
For personal use only.

Can. J. Chem. Downloaded from www.nrcresearchpress.com by 210.87.254.40 on 09/05/12
For personal use only.

Table I shows that both *B*- and *C*-bands of benzoyl chloride are similar to the corresponding bands of benzaldehyde and acetophenone, that is, the bands occur at similar wavelength, are not appreciably affected if the ultraviolet spectra are determined in ether solution, do not show an appreciable concentration dependence, and tend to exhibit some fine structure at longer wavelength. (In acetophenone, the fine structure becomes apparent in the vapor phase (2).)

In the vapor phase, benzoyl chloride affords the usual displacement to shorter wavelength (5). All these observations can be rationalized by assuming that as a first approximation the ultraviolet *B*-band is predominantly determined by mesomeric interactions (as crudely represented by resonance forms of type I), to which the chlorine atom does not appreciably contribute.

The infrared carbonyl band, on the other hand, is appreciably affected by the chlorine atom and causes a displacement to higher frequency, compared with the location of this band in benzaldehyde. Conversely, replacement of an hydrogen atom by a methyl group, as in acetophenone, causes a displacement to lower frequency. These displacements can be readily related to the over-all electronegativities of the chlorine atom and the methyl group (cf. ref. 6 and also ref. 7 for the yet higher carbonyl band frequency of benzoyl fluoride). Moreover, the carbonyl band in most benzoyl chlorides exhibits a doublet (see Table II and cf. refs. 8, 9, and 10) which is not appreciably affected either by a change in solute concentration (within the solute concentration range 0.05 to 2.5 *M*) or by determination of the absorption in ether solution (see Table I). Therefore it is unlikely that the carbonyl band doublet is caused by a monomer–dimer equilibrium. Further, neither in the 800–900 cm^{-1} region, nor in the 600 cm^{-1} region, are there absorption bands, overtones, or combination bands which can quantitatively and convincingly account for the observed doublets in all of the benzoyl chlorides (see later discussion). The infrared carbonyl bands of benzoyl chloride and of a number of substituted benzoyl chlorides are listed in Table II. The effect of altering the solvent from chloroform to carbon

TABLE II

The spectral changes of the infrared carbonyl bands with ring substitution (in carbon tetrachloride solution)

Ring substituent	Band *A* ν_{max} (cm^{-1})	Band *B* ν_{max} (cm^{-1})	Ring substituent	Band *A* ν_{max} (cm^{-1})	Band *B* ν_{max} (cm^{-1})
H	1782 (s)	1740 (m)	*m*-Br	1804 (w)	1761 (s)
p-MeO	1777 (s)	1744 (s)	*o*-Br	1795 (s)	1742 (w)*
m-MeO	1776 (s)	1736 (w)	*p*-I	1779 (s)	1736 (m)
o-MeO	1792 (s)	1752 (m)	*m*-I	1797 (m)	1758 (s)
p-F	1786 (s)	1754 (s)	*o*-I	1789 (s)	Shoulder
m-F	1782 (s)	1755 (s)	*p*-NO_2	1793 (m)	1766 (s)
p-Cl	1783 (s)	1742 (m)	*m*-NO_2	1792 (m)	1764 (s)
m-Cl	1818 (w)	1765 (s)	*p*-CH_3	1777 (s)	1744 (m)
o-Cl	1796 (s)	1740 (w)*	*m*-CH_3	1767 (s)	1738 (vw)
p-Br	1779 (s)	1738 (s)	*o*-CH_3	1781 (s)	1737 (w)

*Appreciable fine structure.

tetrachloride and the effect of temperature on the infrared carbonyl band of benzoyl chloride in carbon tetrachloride solution has recently been reported by Jones *et al.* (10). These workers note that the behavior of the infrared carbonyl band under these conditions parallels the behavior of the infrared carbonyl band in a number of unsaturated lactones. Jones *et al.* (10) have also confirmed the absence of any concentration dependence of this band over a 200-fold range.

Benzoyl chlorides also exhibit two infrared absorption bands in the region 1560–1600 cm^{-1} (cf. ref. 11), which are listed in Table III. The generally more intense band near

TABLE III

The infrared spectral changes of the two aromatic vibration bands with ring substitution (in carbon tetrachloride solution)

Ring substituent	Band 1 ν_{max} (cm^{-1})	Band 2 ν_{max} (cm^{-1})	Ring substituent	Band 1 ν_{max} (cm^{-1})	Band 2 ν_{max} (cm^{-1})
H	1591 (w)	1577 (vw)	*m*-Br	1580 (vw)	1562 (w)
p-MeO	1596 (s)	1573 (m)	*o*-Br	1582 (m)	1560 (w)
m-MeO	1592 (m)	1582 (w)	*p*-I	1574 (m)	1559 (w)
o-MeO	1596 (s)	1582 (m)	*m*-I	1578 (vw)	1559 (w)
p-F	1594 (s)	—	*o*-I	1574 (m)	1557 (w)
m-F	1588 (m)	—	*p*-NO_2	1601 (m)	—
p-Cl	1584 (m)	—	*m*-NO_2	1609 (m)	1582 (vw)
m-Cl	1591 (vw)	1576 (w)	*p*-CH_3	1603 (m)	—
o-Cl	1582 (m)	1563 (w)	*m*-CH_3	1599 (w)	1576 (w)
p-Br	1580 (m)	Shoulder	*o*-CH_3	1597 (vw)	1565 (vw)

1590 cm^{-1} presumably corresponds to the "1600 cm^{-1} aromatic vibration band", which is reported to occur within the range 1625–1575 cm^{-1} for most aromatic compounds (11). It was also found (cf. ref. 11) that the halogen-substituted benzene derivatives, particularly the iodo compounds, absorb near the lower limit of this range, while the locations of the absorptions of the nitro-substituted benzoyl chlorides occur at a frequency higher than average. Neither the location nor the intensity of the band appears to be quantitatively related to electronegativity, σ value, other electronic property, or to the size of the *o*-substituent. However, the more intense bands occur in the *p*- and *o*-isomers. Hence the band intensity may be related to mesomeric interaction.

The other infrared aromatic vibration band occurs in the 1600–1560 cm^{-1} region (cf. ref. 11). The data in Table III show that the band is more intense for *p*- and *o*-methoxybenzoyl chloride and this again indicates that mesomeric interaction enhances the band intensity. Moreover, the band appears to be weakest if mesomeric interaction is limited, as in nitrobenzoyl chlorides where both substituents are electron withdrawing, or as in *o*-toluoyl chloride where the methyl group could twist the chlorocarbonyl group out of the plane of the benzene ring and in this way inhibit mesomeric interaction. However, again neither band location nor band intensity could be quantitatively related to σ values or other electronic properties.

THE SPECTRA OF PARA-SUBSTITUTED BENZOYL CHLORIDES

The main ultraviolet absorption maxima of substituted benzoyl chlorides are listed in Table IV and are found to be essentially similar to the corresponding bands in *p*-substituted benzaldehydes and acetophenones (2, 3). This is further illustrated in Fig. 1, which shows the band similarity between a similarly *p*-substituted benzoyl chloride and benzaldehyde.

Since resonance forms of type I, sometimes favored by an electron-donating *p*-substituent, have previously been used to rationalize the observed spectral changes in *p*-substituted benzaldehydes (2) and acetophenones (3), these resonance forms can likewise rationalize the ultraviolet *B*-band spectral changes in *p*-substituted benzoyl chlorides. The wavelength displacements in *p*-substituted benzoyl chlorides relative to benzoyl chloride are, as expected, proportional to the wavelength displacements observed

Can. J. Chem. Downloaded from www.nrcresearchpress.com by 210.87.254.40 on 09/05/12
For personal use only.

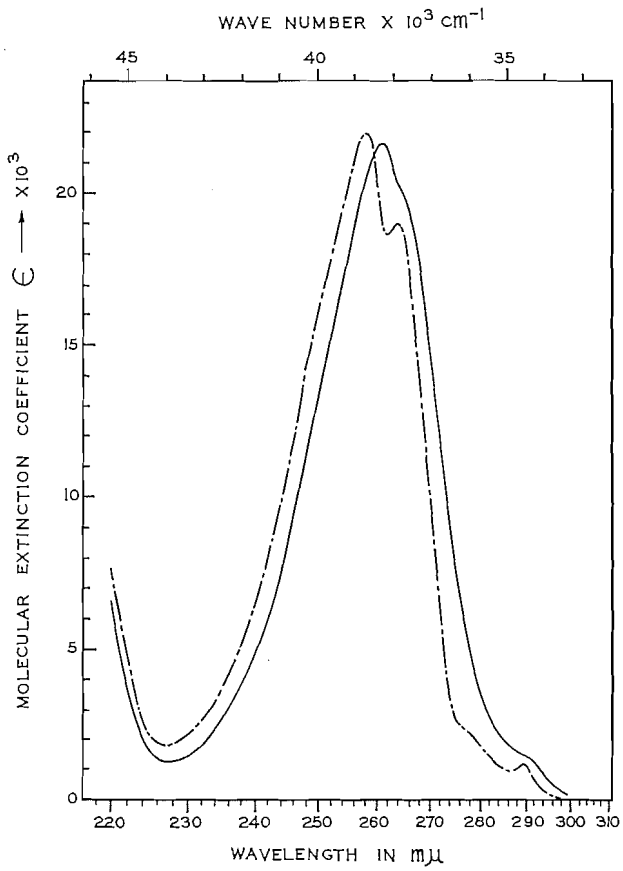


FIG. 1. The ultraviolet absorption spectra in cyclohexane solution of *p*-bromobenzoyl chloride (——) and *p*-bromobenzaldehyde (—·).

for *p*-substituted acetophenones, benzaldehydes, and nitrobenzenes relative to the non-*p*-substituted parent compounds. This is illustrated in Fig. 2, which uses the corresponding frequency displacements ($\Delta\nu$) instead of wavelength displacements ($\Delta\lambda$) (cf. ref. 2).

The slopes of the lines in Fig. 2 are in the order $—NO_2$ > (—COCl) > —CHO > $—COCH_3$ (cf. also ref. 2). This order represents a measure of the different effects of a *p*-substituent on the various electron-withdrawing substituents (NO_2, COCl, etc.) when attached to the benzene ring. If it is assumed, as seems reasonable, that a substituent possessing a greater negative mesomeric effect can more effectively involve the electrons of an electron-donating *p*-substituent, the above order may also provide a measure of the negative mesomeric effect of the electron-withdrawing substituents. The order for the apparent mesomeric effect obtained in this way from Fig. 2 is as shown above (cf. also ref. 1 for the use of the term "apparent mesomeric effect"). Moreover, the maxima of the *B*-bands of nitrobenzene, benzoyl chloride, benzaldehyde, and acetophenone are located at 252, 242, 241, and 237.5 mμ respectively (see Table I and refs. 12, 2, and 3) and this also indicates increasing mesomeric interaction in the same order.

It may next be noted from the data listed in Table IV that the *B*-band of substituted benzoyl chlorides is again slightly unsymmetrical, with a shoulder usually occurring at

Can. J. Chem. Downloaded from www.nrcresearchpress.com by 210.87.254.40 on 09/05/12
For personal use only.

Can. J. Chem. Downloaded from www.nrcresearchpress.com by 210.87.254.40 on 09/05/12
For personal use only.

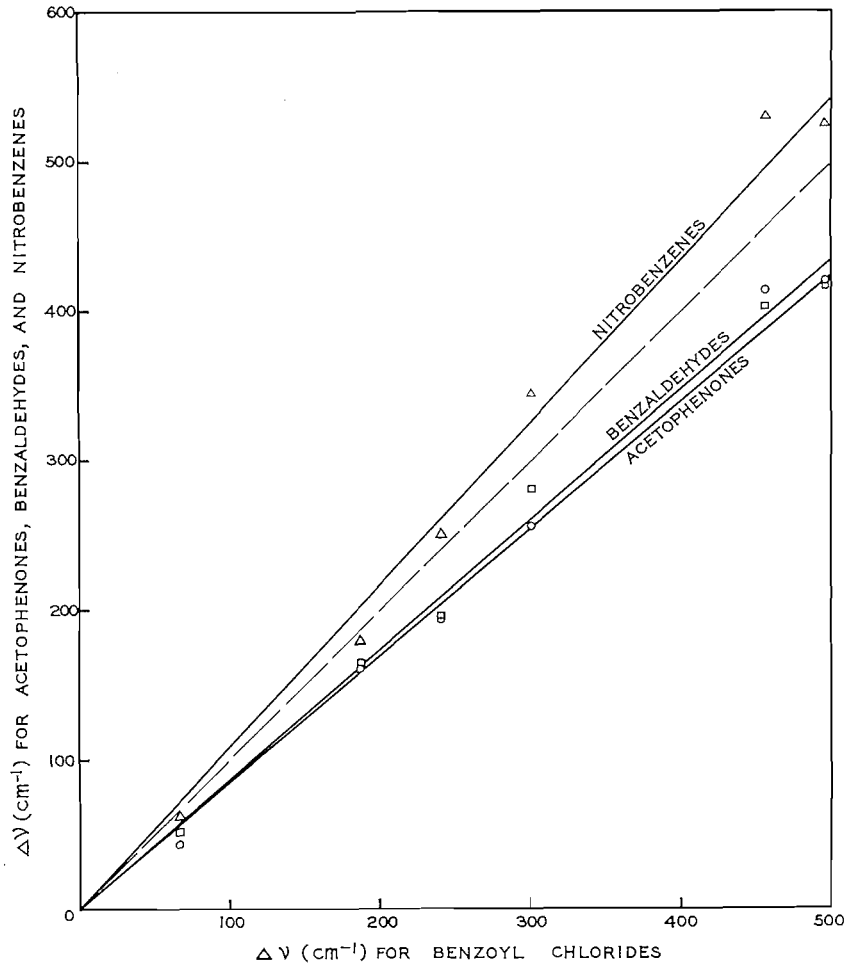


FIG. 2. Frequency displacements ($\Delta\nu$) in the *B*-band obtained on introducing para substituents in benzoyl chloride, benzaldehyde, acetophenone, and nitrobenzene (1, H; 2, F; 3, CH_3; 4, Cl; 5, Br; 6, MeO; and 7, I). Values (1 to 7 as $\Delta\nu$ increases) are for hexane solutions and are obtained from Table IV and from refs. 2, 3, and 12. △, nitrobenzenes; □, benzaldehydes; ○, acetophenones.

the longer wavelength side. Sometimes, as for the *p*-iodo- and *p*-methoxy-benzoyl chlorides the *B*-band occurs as a twin peak, but more frequently the second band occurs only as an ill-defined shoulder. The absence of this shoulder for the band at 255 mμ may also be taken as evidence to show that this band is not to be associated with benzoyl chloride but with nitrobenzene absorption.*

The ultraviolet spectra of *p*-substituted benzoyl chlorides also afford other bands in the 210–250 mμ region, which may either be *B*-bands, corresponding to locally excited states, or *A*-bands (for band nomenclature, see ref. 4). These bands are listed in Table IV,

**Further evidence that the band at 255 mμ in p-nitrobenzoyl chloride is a nitrobenzene B-band is provided by analogy with the spectrum of m-nitrobenzoyl chloride, which also shows an inflection near 255 mμ and, in addition, a band near 228 mμ (see Table IV). The m-isomer would be expected to show two B-bands, one more-intense B-band associated with benzoyl chloride absorption and one less-intense band associated with nitrobenzene absorption (13). The band at 228 mμ shows the characteristic shoulder associated with benzoyl chloride absorption and the inflection near 255 mμ in the m-isomer is therefore almost certainly a nitrobenzene B-band. This in turn suggests that the band at similar wavelength in the p-isomer is also a nitrobenzene B-band.*

Can. J. Chem. Downloaded from www.nrcresearchpress.com by 210.87.254.40 on 09/05/12
For personal use only.

TABLE IV

Main ultraviolet absorption maxima of ring-substituted benzoyl chlorides in cyclohexane solution

	Para isomer				Meta isomer						Ortho isomer					
	B-band		*C*-band		2nd *B*-band		*B*-band		*C*-band		2nd *B*-band		*B*-band		*C*-band	
Substituent	λ_{max} (mμ)	ϵ_{max}	λ_{max} (mμ)	ϵ_{max}	λ_{max} (mμ)	ϵ_{max}	λ_{max} (mμ)	ϵ_{max}	λ_{max} (mμ)	ϵ_{max}	λ_{max} (mμ)	ϵ_{max}	λ_{max} (mμ)	ϵ_{max}	λ_{max} (mμ)	ϵ_{max}
—F	246 *250*	14,500 *13,600*	*272*	*1,200*			240 248	13,500 12,000	288	2,200			237–238 *241*	13,000 *12,800*	286 294	2,200 1,800
—Cl	210–211 315 257 ca. *262*	12,000* 10,500* 21,000 *10,500*	ca. *289*	*1,100*	211 215	23,500 23,500	243 251	12,000 11,500	294 ca. *302*	1,600 *1,300*	212	20,500	244 *252*	9,000 *7,600*	292	1,700
—Br	211 218 261 ca. *264*	10,300* 8,000* 21,500 *20,000*	ca. *291*	*1,300*	214 217	21,000 23,600	244 252	11,000 11,000	296 ca. *305*	1,500 *1,100*	215	19,800	246 254	7,100 6,700	294	1,800
—I	227 245 275 285	7,000* 4,000* 18,000 17,500	—	—	230	29,500	ca. *244*	*10,000*	303	1,350	228 247	15,000 6,500*	255 264	6,000 4,400	304	2,200
—CH_3	210 214 253–254 *258*	10,600* 11,000* 18,000 *16,500*	ca. *279* ca. *290*	*2,000* *1,100*	211	15,000*	245 252–253	14,000 13,000	290	1,700	210	13,000	244 *252*	13,000 *12,000*	290	2,000
—OCH_3	217 224 272 280	12,000* 12,500* 19,500 19,200	—	—	219 222	23,000* 23,000	253 ca. *260*	10,000 *7,000*	312	3,100	214	19,500	ca. *244* 251	*8,500* 9,000	308	4,200
—NO_2	255	17,000	*290* *298* ca. *308*	*2,300* *2,100* *1,500*	ca. *247* ca. *258*	*10,500* *5,000*	228 ca. *233*	25,000 *22,500*	ca. *285* 297	*1,000* 950						

*B-band assignment doubtful.

the doubtful band assignments being indicated. The *B*-band assignment is favored if in the *m*-isomer there occurs a similar band, absorbing with increased absorption intensity, which is a *B*-band. For example, the bands at 211 and 215 mμ in *m*-chlorobenzoyl chloride are believed to correspond to chlorobenzene *B*-band absorption. Since reduced absorption maxima still occur at 211 and 215 mμ in the *p*-isomer, it is supposed that these maxima are also to be associated with chlorobenzene *B*-band absorption, which competes with *B*-band absorption involving the whole molecule.

The ultraviolet *C*-band affords the expected spectral changes (see ref. 3), that is, as mesomeric interaction increases, the *C*-band becomes less intense or disappears.

The infrared bands of the *p*-substituted benzoyl chlorides are listed in Tables II and III, and Fig. 3 shows the spectral tracings in the region 1550–1800 cm^{-1}. These data

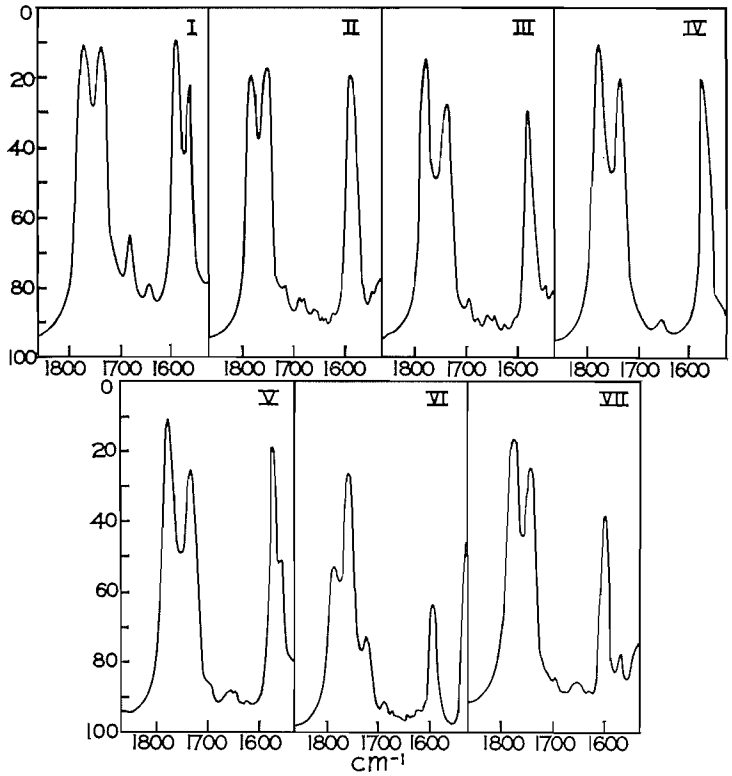


FIG. 3. The infrared bands (carbon tetrachloride solution) in the region 1550–1800 cm^{-1} of (I) *p*-methoxybenzoyl chloride, (II) *p*-fluorobenzoyl chloride, (III) *p*-chlorobenzoyl chloride, (IV) *p*-bromobenzoyl chloride, (V) *p*-iodobenzoyl chloride, (VI) *p*-nitrobenzoyl chloride, and (VII) *p*-toluoyl chloride.

show that the carbonyl band doublet occurs in all the *p*-substituted benzoyl chlorides investigated. Somewhat surprisingly, although carbonyl band frequencies of ring-substituted acetophenones showed a direct relationship with Hammett's σ values (14), no similar simple relationship is obtained between these σ values and either of the carbonyl band frequencies listed in Table II or with the arithmetic mean of the two carbonyl band frequencies. Plots of the carbonyl band frequencies against the functions σ^* and $(\sigma_p - \sigma')$, derived by Taft, Roberts, and Moreland (15), likewise all failed to show significant linearity. These observations point towards the possibility that in benzoyl chlorides an overtone or combination band occurs near the carbonyl band, and that the former bands,

Can. J. Chem. Downloaded from www.nrcresearchpress.com by 210.87.254.40 on 09/05/12
For personal use only.

because of a vibrational resonance effect, displace the carbonyl band from the position where it would otherwise have been expected to occur.

THE SPECTRA OF META-SUBSTITUTED BENZOYL CHLORIDES

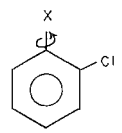
The ultraviolet spectra of *m*-substituted benzoyl chlorides frequently show two *B*-bands (cf. refs. 1, 2, and 12; for an explanation of this phenomenon in terms of molecular orbital theory, see ref. 16). One of these bands is associated with benzoyl chloride *B*-band absorption whereas the second *B*-band is associated with the other, non-benzoyl-chloride, monosubstituted benzene derivative. This latter *B*-band is designated in Table IV as the second *B*-band and it is usually the more intense band. This greater intensity may be related to the electron-withdrawing effect of the chlorocarbonyl group. Such an explanation may also account for the reverse relation in *m*-nitrobenzoyl chloride where the benzoyl chloride *B*-band absorption is more intense, that is, it may be assumed that this is so because the nitro group withdraws electrons even more effectively than the chlorocarbonyl group (for a discussion of how the spectral characteristics of one meta-substituent are affected by the presence of a second such substituent, see refs. 13 and 17).

As anticipated, the spectra of the *m*-substituted benzoyl chlorides and benzaldehydes are similar (see Table IV and ref. 2). This similarity is further illustrated in Fig. 4 for the spectra of the *m*-substituted nitro compounds. No new concept is therefore required to rationalize the spectra of *m*-substituted benzoyl chlorides, since the explanation of the spectra of benzoyl chlorides and benzaldehydes in terms of resonance forms of type I still holds (cf. also ref. 2).

The investigated infrared bands of the *m*-substituted benzoyl chlorides are shown in Tables II and III and in Fig. 5. The carbonyl bands again all show a doublet, even though for some of the compounds one of the peaks is only weak. A plot of the infrared carbonyl band frequencies (see Table II) against either Hammett's σ values or the functions σ^* or $(\sigma_m{-}\sigma')$ (15) again showed a wide scatter (cf. ref. 14). Two additional points may be noted. First, in compounds such as *m*-chlorobenzoyl chloride, where one of the peaks is considerably more intense than the other, there is no evidence of any further band splitting such as might have been expected if the molecule existed in two *s*-cis, *s*-trans conformations which absorb maximally at slightly different frequencies (cf. ref. 14). Secondly, in *m*-substituted benzoyl chlorides the peak at lower frequency is frequently more intense (cf. Figs. 3, 5, and 7).

THE SPECTRA OF ORTHO-SUBSTITUTED BENZOYL CHLORIDES

The ultraviolet absorption spectra of *o*-substituted benzoyl chlorides, like those of the corresponding *m*-isomers, again generally exhibit two *B*-bands. Steric interactions in compounds such as *o*-substituted benzoyl chlorides would be expected to cause intensity



(II)

X = CHO, $COCH_3$, COCl, or NO_2

decreases in the *B*-band compared with the intensities in the *m*-isomers, and such intensity decreases are in fact observed (see Table IV). This is further illustrated in Fig. 6 for *o*-chlorobenzoyl chloride (II, X = COCl).

Can. J. Chem. Downloaded from www.nrcresearchpress.com by 210.87.254.40 on 09/05/12
For personal use only.

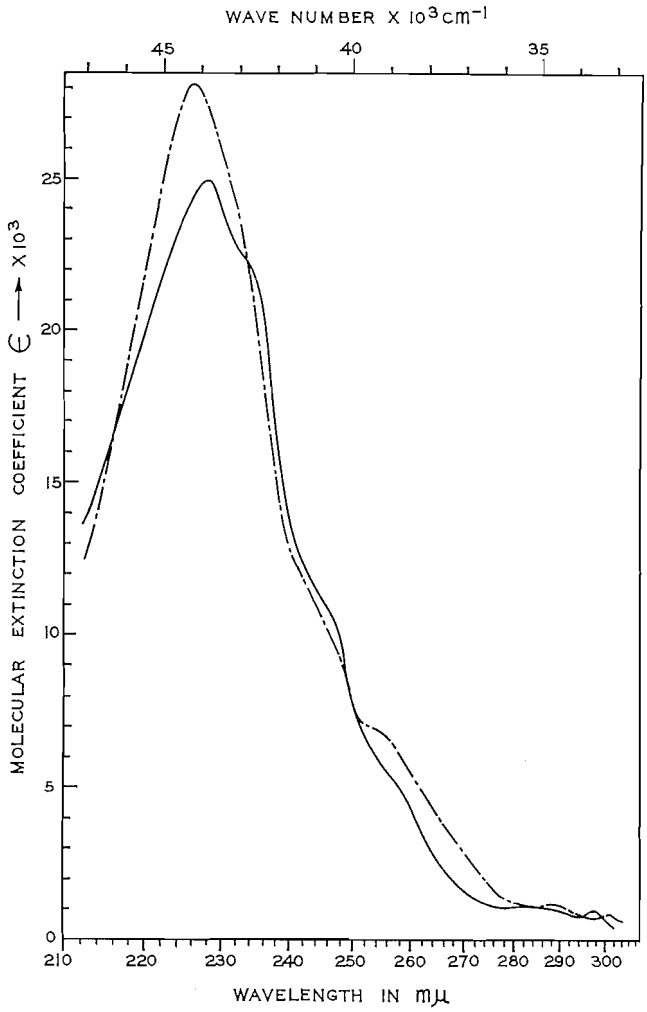


FIG. 4. The ultraviolet absorption spectra in cyclohexane solution of *m*-nitrobenzoyl chloride (——) and *m*-nitrobenzaldehyde (—·).

Figure 6 shows that the *B*-band of *o*-chlorobenzoyl chloride is less intense than that of the *m*-isomer, and further, that the *B*-bands of *o*-chlorobenzoyl chloride and *o*-chlorobenzaldehyde are again similar but that the former *B*-band is also less intense than the *B*-band in *o*-chlorobenzaldehyde. If it is assumed that in *o*-chlorobenzoyl chloride steric interactions predominantly affect the molecule by twisting the group X out of the plane of the benzene ring (as indicated in structure II), the intensities of the *B*-bands associated with the PhX chromophores can be taken as a semiquantitative measure of the steric interactions (cf. ref. 18). The relevant absorptivities of both *o*- and *m*-isomers as well as the ratio of the absorptivities of the two *B*-bands for compounds II (X = —CHO, —COCl, —$COCH_3$, and —NO_2) are listed in Table V. The absorptivity ratios, thus obtained, are in the order —NO_2 > —$COCH_3$ > —COCl > —CHO and this order may be taken as a measure of the effective interference radii of these substituents. Other factors may also affect the absorptivity ratios. For example, the different compounds II

Can. J. Chem. Downloaded from www.nrcresearchpress.com by 210.87.254.40 on 09/05/12
For personal use only.

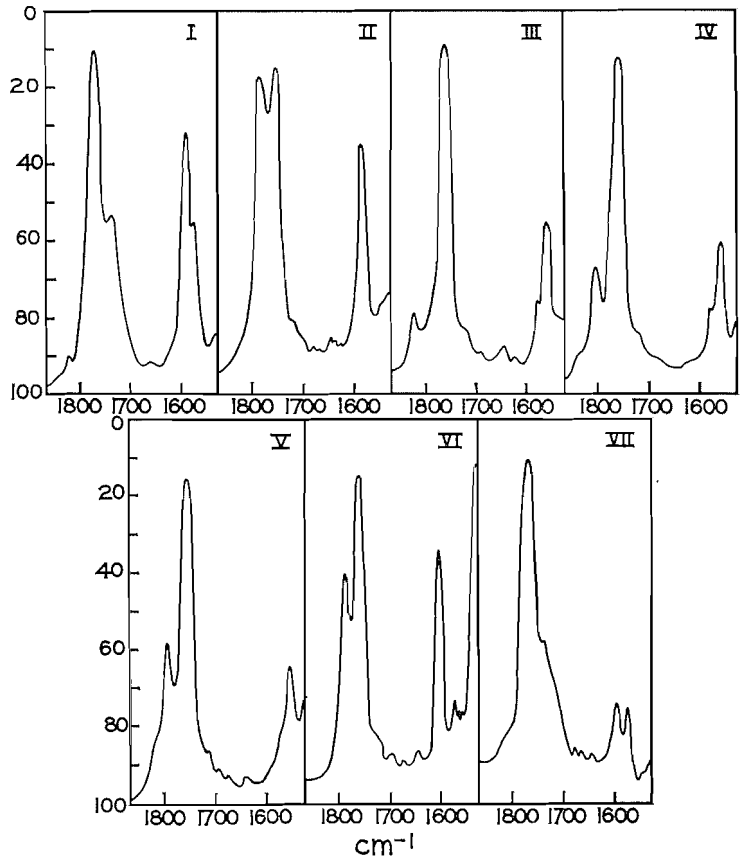


FIG. 5. The infrared bands (carbon tetrachloride solution) in the region 1550–1800 cm^{-1} of (I) *m*-methoxybenzoyl chloride, (II) *m*-fluorobenzoyl chloride, (III) *m*-chlorobenzoyl chloride, (IV) *m*-bromobenzoyl chloride, (V) *m*-iodobenzoyl chloride, (VI) *m*-nitrobenzoyl chloride, and (VII) *m*-toluoyl chloride.

may not all exist in one and the same *s*-cis or *s*-trans conformation. However, orders for the effective interference radii similar to those deduced from the chloro-substituted compounds can be obtained from the absorptivity ratios of the corresponding *o*-bromo, *o*-iodo, *o*-methoxy, and *o*-nitro compounds, and this increases our confidence in the proposed order.

TABLE V

Absorptivity values (ϵ_{max}) of the *B*-band associated with the chromophoric system PhX in compound II*

	X in compound II:			
	CHO†	COCl‡	$COCH_3$§	NO_2‖
Compound II (*o*-isomer)	11,000	9,000	5,700	4,000
m-Isomer of compound II	11,500	12,000	10,000	7,800
ϵ_{max} ratio of *m*-isomer/*o*-isomer	1.05	1.33	1.75	1.95

*Values in cyclohexane solution unless otherwise stated.
†Values from ref. 2.
‡This paper.
§Values from ref. 3.
‖Values in 95% aqueous ethanol; see ref. 19.

Can. J. Chem. Downloaded from www.nrcresearchpress.com by 210.87.254.40 on 09/05/12
For personal use only.

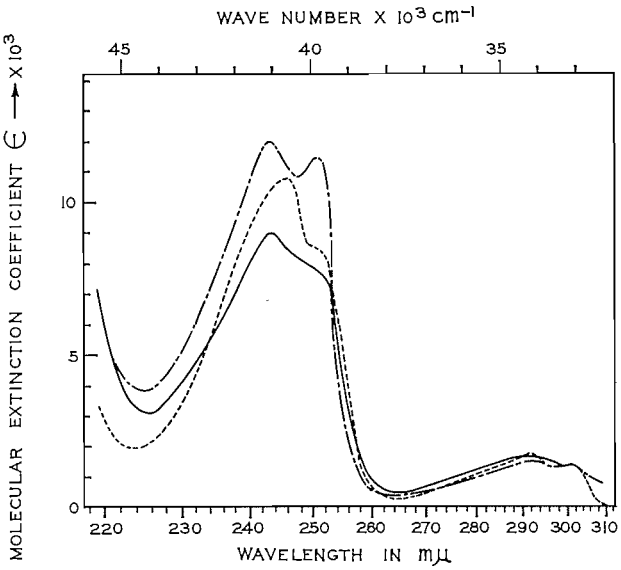


FIG. 6. The ultraviolet absorption spectra in cyclohexane solution of *o*-chlorobenzoyl chloride (——), *m*-chlorobenzoyl chloride (—·), and *o*-chlorobenzaldehyde (– –).

The ultraviolet *C*-bands of both *m*- and *o*-substituted benzoyl chlorides exhibit the usual changes (cf. ref. 3), that is, the C-bands generally become progressively more pronounced in the order *p*-isomer < *m*-isomer < *o*-isomer (see Table IV).

The investigated infrared bands of the *o*-substituted benzoyl chlorides are shown in Tables II and III and in Fig. 7. The carbonyl bands again all show a doublet, but as in the *m*-isomers one of the peaks is usually weaker. However, in the *o*-isomer the less-intense band is the band at *lower* frequency, whereas in the *m*-isomer the less-intense band is usually the band at *higher* frequency. In the *p*-isomer the two bands seem to be generally of similar intensity (see Table II, and cf. Figs. 3, 5, and 7).

SOME CONCLUDING REMARKS CONCERNING THE CARBONYL BAND DOUBLET IN BENZOYL CHLORIDES

The origin of the doublet in the infrared carbonyl band is not clear. One explanation is that the band occurs because of Fermi resonance between the carbonyl vibration and a close-lying overtone. In fact, benzoyl chloride shows an intense band at 875 cm^{-1} and doubling this frequency would place the overtone at 1750 cm^{-1}—reasonably close to the observed "carbonyl bands" at 1782 and 1740 cm^{-1} (see Table II). Hence it is possible that an anharmonicity effect brings the two vibrations sufficiently close together to cause the observed doublet (cf. ref. 20 for an explanation on these lines to account for the carbonyl band doublet in cyclopentanone). Likewise an overtone near 1740 cm^{-1} of the band at 870 cm^{-1} in *p*-toluoyl chloride can account for the doublet at 1777 and 1744 cm^{-1}. Similar explanations could hold for other benzoyl chlorides. Sometimes, the overtone of the band near 850 cm^{-1} is not sufficiently close to account satisfactorily for the doublet. For example, in *m*-nitrobenzoyl chloride the doublet occurs at 1792 and 1764 cm^{-1} and the overtone would be expected to occur near 1690 cm^{-1} (2×845 cm^{-1}). However, there are other bands (for example, *m*-nitrobenzoyl chloride affords a band at 925 cm^{-1}), overtones of which could also account for the observed doublets. Moreover,

Can. J. Chem. Downloaded from www.nrcresearchpress.com by 210.87.254.40 on 09/05/12
For personal use only.

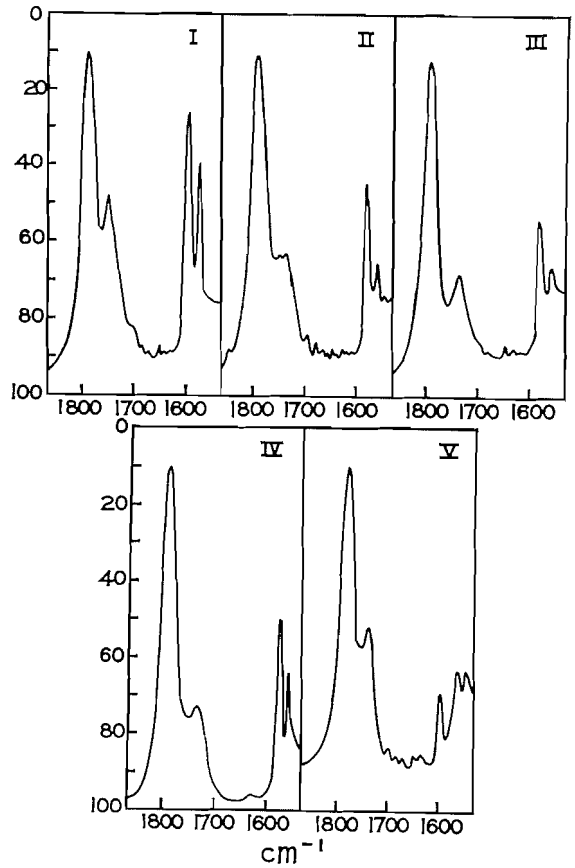


FIG. 7. The infrared bands (carbon tetrachloride solution) in the region 1550–1800 cm^{-1} of (I) *o*-methoxybenzoyl chloride, (II) *o*-chlorobenzoyl chloride, (III) *o*-bromobenzoyl chloride, (IV) *o*-iodobenzoyl chloride, and (V) *o*-toluoyl chloride.

it is also possible to postulate a combination band (cf. ref. 21) which may account for the observed doublet.

This type of explanation is probably the best that can be put forward, but it is not entirely satisfactory. Thus it accounts for the doublet in what is, at best, a semiquantitative manner. For example, in *p*-fluorobenzoyl chloride the overtone of the band at 880 cm^{-1} is expected to occur near 1760 cm^{-1} and this would be anticipated to lead to a *weak* band on the low-frequency side of the carbonyl band at 1786 cm^{-1}. However, the peak at lower frequency (at 1754 cm^{-1}) is *more intense*, although for most other benzoyl chlorides there is the expected reverse relation, that is, the peak on the overtone side is less intense. Moreover, the unusual absence of any direct relationship between either of the carbonyl band frequencies or their means and Hammett's σ values suggests that the original carbonyl frequency is appreciably modified.

Other explanations, such as involvement of intermolecular interactions, or the existence of different conformational isomers in equilibrium, are even more unsatisfactory. Consequently, in the absence of any other more satisfactory explanation, the most probable explanation is that the doublet occurs because of an intermolecular vibration. The understanding of the precise mechanism of this vibration clearly requires further study.

Can. J. Chem. Downloaded from www.nrcresearchpress.com by 210.87.254.40 on 09/05/12
For personal use only.

ACKNOWLEDGMENTS

The authors are greatly indebted to Miss Ingrid Baumann for competent technical assistance in preparing the compounds studied and in determining the ultraviolet data. Thanks are also due to Mr. D. L. Coffen and Mr. A. A. Sioumis for determining the infrared spectra, and the financial assistance of the National Research Council is again gratefully acknowledged.

REFERENCES

1. W. F. FORBES. Can. J. Chem. **39**, 1131 (1961).
2. J. C. DEARDEN and W. F. FORBES. Can. J. Chem. **36**, 1362 (1958).
3. W. F. FORBES, W. A. MUELLER, A. S. RALPH, and J. F. TEMPLETON. Can. J. Chem. **35**, 1049 (1957).
4. W. F. FORBES and R. SHILTON. *In* Symposium on spectroscopy - STP 269. ASTM 1959. p. 176.
5. J. C. DEARDEN and W. F. FORBES. Can. J. Chem. **38**, 896 (1960).
6. M. HORÁK and O. EXNER. Chem. listy, **52**, 1451 (1958).
7. F. SEEL and J. LANGER. Ber. **91**, 2553 (1958).
8. M. ST. C. FLETT. Trans. Faraday Soc. **44**, 767 (1948).
9. D. D. THOMPSON and J. F. NORRIS. J. Am. Chem. Soc. **58**, 1953 (1936).
10. R. N. JONES, C. L. ANGELL, T. ITO, and R. J. D. SMITH. Can. J. Chem. **37**, 2007 (1959).
11. L. J. BELLAMY. The infrared spectra of complex molecules. Methuen & Co. Ltd., London. 1959. pp. 71–74.
12. W. F. FORBES. Can. J. Chem. **36**, 1350 (1958).
13. E. J. MORICONI, W. F. O'CONNOR, F. T. WALLENBERGER, and W. F. FORBES. J. Am. Chem. Soc. **81**, 5950 (1959).
14. R. N. JONES, W. F. FORBES, and W. A. MUELLER. Can. J. Chem. **35**, 504 (1957).
15. R. W. TAFT. *In* Steric effects in organic chemistry. *Edited by* M. S. Newman. John Wiley & Sons, Inc., New York. 1956. pp. 594–595.
16. J. TANAKA and S. NAGAKURA. J. Chem. Phys. **24**, 1274 (1956).
17. E. J. MORICONI, W. F. O'CONNOR, and W. F. FORBES. J. Am. Chem. Soc. **82**, 5454 (1960).
18. W. F. FORBES and R. SHILTON. J. Am. Chem. Soc. **81**, 786 (1959).
19. W. F. FORBES. Can. J. Chem. **38**, 1104 (1960).
20. C. L. ANGELL, P. J. KRUEGER, R. LAUZON, L. C. LEITCH, K. NOACK, R. J. D. SMITH, and R. N. JONES. Spectrochim. Acta, **11**, 926 (1959).
21. N. S. HAM and J. B. WILLIS. Spectrochim. Acta, **16**, 279 (1960).

Can. J. Chem. Downloaded from www.nrcresearchpress.com by 210.87.254.40 on 09/05/12
For personal use only.

Can. J. Chem. Downloaded from www.nrcresearchpress.com by 210.87.254.6 on 09/05/12
For personal use only.

THE REACTION OF ETHANOL VAPOR WITH Hg 6($^3P_1$) ATOMS[1]

ARTHUR R. KNIGHT AND HARRY E. GUNNING

ABSTRACT

The reaction of ethanol vapor with Hg 6($^3P_1$) atoms has been investigated under static conditions at 25° C. To determine the nature and efficiency of the primary process, the reaction has been studied in the presence of nitric oxide, and also under conditions of intermittent illumination. For the pure substrate the volatile products were H_2 (0.53), CH_3CHO (0.08), CO (0.025), C_2H_6 (0.006), and CH_4 (0.002), with the bracketed numbers representing the quantum yields at zero exposure time. The heavy product was a mixture of butanediols containing 90% 2,3-, 8% 1,3-, and 2% 1,4-butanediol. With 20% added NO, the products were EtONO (0.25), N_2O (0.14), H_2O, and H_2 (0.017). Under intermittent illumination, the quantum yield (Φ) of H_2 formation for pure substrate was measured as a function of the light period (t_L) and the dark period (t_D). For maximum values of $\Phi(H_2)$, it was found that t_D had to exceed ca. 120 msec. Under these conditions, $\Phi(H_2)$ rose linearly with decreasing log t_L to a maximum value of 0.96 at t_L less than 0.4 msec.

From the study it is concluded that ethanol reacts with Hg 6($^3P_1$) atoms to form ethoxy radicals and H atoms with at least 96% efficiency. The primary ethoxy radicals disappear by hydrogen abstraction from the substrate to form mainly CH_3CHOH radicals. Under continuous illumination the low value (0.53) for $\Phi(H_2)$ is caused principally by the addition of H atoms to the CH_3CHOH radicals.

INTRODUCTION

Recent studies (1, 2) have shown that the primary reaction between methanol vapor and Hg 6($^3P_1$) atoms leads almost exclusively to the formation of CH_3O and H. In addition, by the use of special intermittent-illumination techniques, it has been found in this laboratory (3) that the primary quantum yield (Φ) for H-atom formation is at least 0.89, and likely unity. Thus, with a light period (t_L) of 0.156 msec and a dark period (t_D) of 160 msec, $\Phi(H_2)$ was 0.89; whereas, under steady illumination, $\Phi(H_2)$ was only 0.46 when extrapolated to its maximum value at zero extent of reaction (2, 3). The low value of $\Phi(H_2)$ under steady illumination was ascribed mainly (3) to the combination of H with CH_2OH.

If O—H bond scission is a general characteristic of the primary reaction of Hg 6($^3P_1$) atoms with the alcohols, these substrates could provide convenient sources for studying the properties of alkoxy radicals.

The ethanol reaction was the subject of an early investigation by Bates and Taylor (4). In the present study the decomposition has been examined under both continuous and intermittent illumination. Emphasis has been placed on the nature and efficiency of the primary process.

The details of the investigation follow.

EXPERIMENTAL

For the static runs at 25°, under continuous illumination, the apparatus was essentially identical with that used for the methanol reaction (2). The single- and double-sector equipment used for the intermittent-illumination studies has also been described previously (3). Light intensities, at 2537 Å, were determined as before (3) by propane actinometry (5, 6).

Benzene-free ethanol, 99.9% pure, was degassed, trap-to-trap distilled, and the middle fraction used without further purification.

[1]*Manuscript received July 27, 1961.*
Contribution from the Department of Chemistry, University of Alberta, Edmonton, Alberta. A portion of this paper was presented at the 139th Meeting of the American Chemical Society, St. Louis, Missouri, March, 1961.

Analysis of the condensable products, excluding the glycols, was done by G.L.P.C. with "Ucon" and "Apiezon L" columns as previously described (2). Identification by retention time for each condensable product, except the glycols, was confirmed by mass spectrometry. The moles of product, non-condensable in liquid nitrogen, were determined from the PV/RT ratio in a calibrated gas burette. By mass spectrometry this product was shown to contain H_2, CO, and CH_4. The mole fractions of CO and CH_4 in the product were determined by G.L.P.C., on a 30/60-mesh molecular-sieves column, operating at room temperature, with H_2 carrier at a flow rate of 50 cc/minute.

The high-boiling glycol products were determined by dissolving the cell deposit in acetone, and analyzing this solution by G.L.P.C. The glass column used was 2.5 m in length, with 6 mm O.D., and filled with 15 wt-% didecyl phthalate on Celite. The column was operated at 120° with the flow rate of the H_2 carrier at 70 cc/minute. The katharometer was maintained at 150° and a current of 300 ma. A series of calibrations were performed with authentic samples of the three butanediols at various concentrations in acetone. The relative detector responses for the three glycols were found to depend slightly upon concentration. Correction was made in each case for this concentration effect. For each heavy-product analysis, the ratio of glycol to solvent was determined, and the appropriate relative responses were employed in the calculation of the percentage yields.

RESULTS

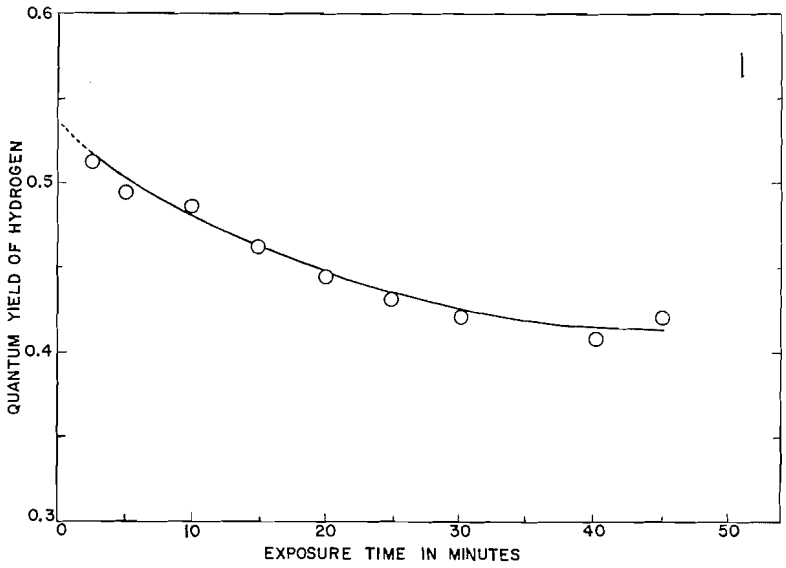
The runs with pure ethanol, under steady illumination, were carried out at a substrate pressure of 40 mm. The absorbed light intensity (I_a) was 1.60 ± 0.03 μeinsteins/minute. During the reaction the heavy product was observed to form in fine droplets, largely on the incident face of the cell.

The volatile products of the reaction were H_2, CH_3CHO, CO, C_2H_6, and CH_4, in order of decreasing importance. From Fig. 1, it is seen that $\Phi(H_2)$ rises with decreasing duration of exposure (t). By a short extrapolation, $\Phi^0(H_2) = 0.53$. The Φ's for CH_3CHO and C_2H_6 are shown in Fig. 2, as a function of t. $\Phi(CH_3CHO)$ falls rapidly with increasing t, indicating consumption by secondary reaction; whereas $\Phi(C_2H_6)$ is invariant in t. We find $\Phi^0(CH_3CHO) = 0.08$ and $\Phi^0(C_2H_6) = 0.006$. From Fig. 3, $\Phi(CH_4)$ rises linearly with t from $\Phi^0(CH_4) = 0.002$. $\Phi(CO)$ also rises with t, approaching a constant value of ca. 0.05. For $\Phi^0(CO)$ we find 0.025.

Long runs were required to obtain sufficient yields of the heavy product for total analysis. For runs with $t = 3$ and 6 hours, the heavy product was found to contain at least 85–90% of 2,3-butanediol. Complete analyses were performed on three separate runs with $t = 10$ hours. The composition of the heavy product was: 90% 2,3-butanediol, 8% 1,3-butanediol, and 2% 1,4-butanediol.

For the study of the reaction in the presence of nitric oxide, a mixture of 40 mm of EtOH and 10 mm of NO was used. The products were found to be EtONO, N_2O, H_2O, and H_2. No quantitative analysis was made for the water product. It should be noted that CH_3CHO was not detected in the reaction, whereas in the CH_3OH—NO system, HCHO was a minor but significant product (2). In Fig. 4, Φ(EtONO) is shown as a function of t. In order to correct the yield for competitive quenching by NO, the quenching cross section for EtOH was taken as 9 Å^2. The resulting quenching correction factor was 1.7. From Fig. 4, it is apparent that ethyl nitrite is being decomposed in secondary reaction. For Φ^0(EtONO) we obtain 0.25. Figure 5 shows the behavior of $\Phi(H_2)$ and $\Phi(N_2O)$ for the inhibited reaction. There is a gradual rise in $\Phi(N_2O)$ with decreasing t;

Can. J. Chem. Downloaded from www.nrcresearchpress.com by 210.87.254.6 on 09/05/12
For personal use only.



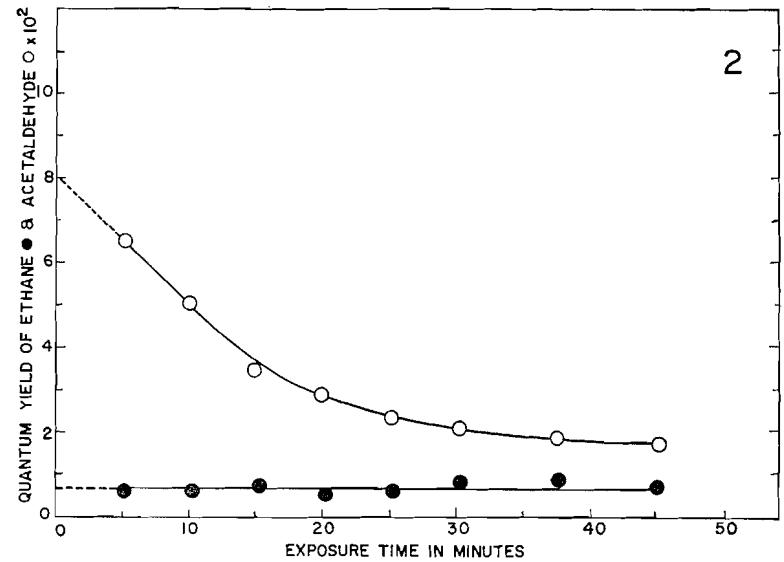
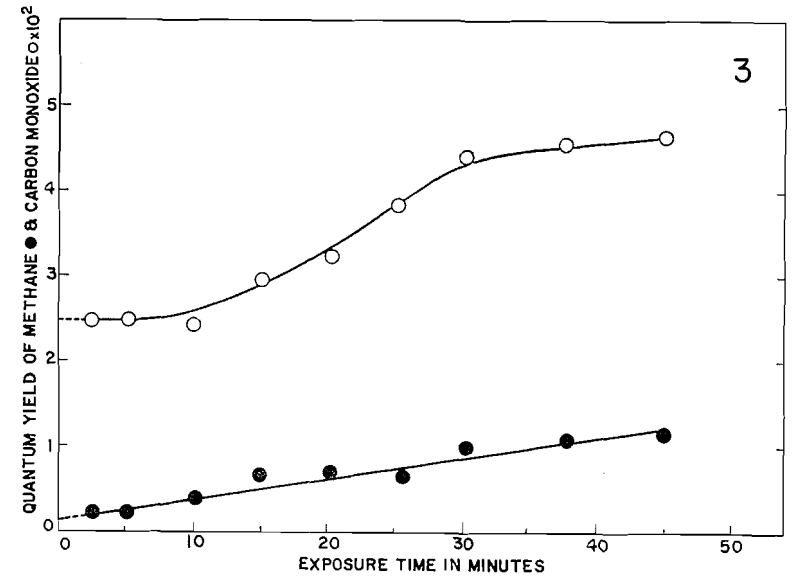


FIG. 1. $\Phi(H_2)$ vs. t for ethanol vapor at a pressure of 40 mm.
FIG. 2. $\Phi(C_2H_6)$, ●, and $\Phi(CH_3CHO)$, ○, vs. t for ethanol vapor at a pressure of 40 mm.

whereas $\Phi(H_2)$ is invariant in t. Extrapolation gives $\Phi^0(N_2O) = 0.14$, and $\Phi^0(H_2) = \Phi(H_2) = 0.017$.

In the intermittent-illumination studies, $\Phi(H_2)$ was determined as a function of both t_L and t_D. In all runs, pure substrate was used at a pressure of 40 mm. In order to assess the influence of t_D on $\Phi(H_2)$ at constant t_L, a series of runs were done with $t_L = 2.04$ msec, and t_D varying from 22.7 to 148 msec. For these runs, I_a values of 1.30, 1.43, and 1.60 μeinsteins/minute were used. The net duration of exposure in all cases was under 5 minutes. There was no dependence of $\Phi(H_2)$ on t under these conditions. The plot of $\Phi(H_2)$ vs. t_D is shown in Fig. 6. With increasing t_D, $\Phi(H_2)$ rises sigmoidally from 0.58

Can. J. Chem. Downloaded from www.nrcresearchpress.com by 210.87.254.6 on 09/05/12
For personal use only.



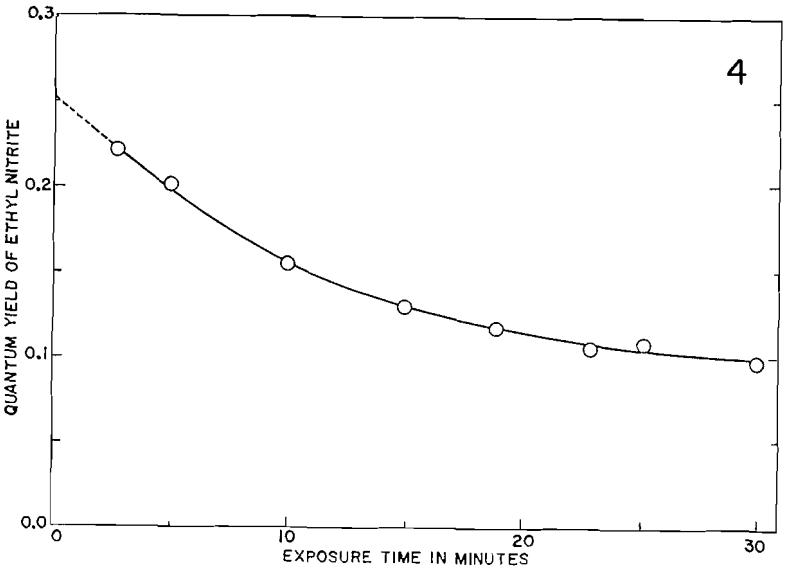


FIG. 3. $\Phi(CH_4)$, ●, and $\Phi(CO)$, ○, vs. t for ethanol vapor at a pressure of 40 mm.
FIG. 4. $\Phi(EtONO)$ vs. t for a mixture of 40 mm of ethanol and 10 mm of nitric oxide.

at t_D = 22.7 msec, to 0.76 at t_D = 148 msec. The value of $\Phi(H_2)$ becomes independent of t_D for t_D ca. 120 msec.

The relation between $\Phi(H_2)$ and t_L is shown in Fig. 7, using a logarithmic abscissa. Two separate series of runs are shown on the same curve. For t_L in the range 0.835 to 5.09 msec, the single sector was used with t_D at 103 msec. The I_a values were 0.72 and 1.43 μeinsteins/minute, and the net durations of exposure were in the range 1.00 to 5.00 minutes. For t_L values between 0.125 and 0.589 msec, the double sector was employed, with t_D at 160 msec. For these runs, I_a was 1.25 μeinsteins/minute, and the net durations

Can. J. Chem. Downloaded from www.nrcresearchpress.com by 210.87.254.6 on 09/05/12
For personal use only.

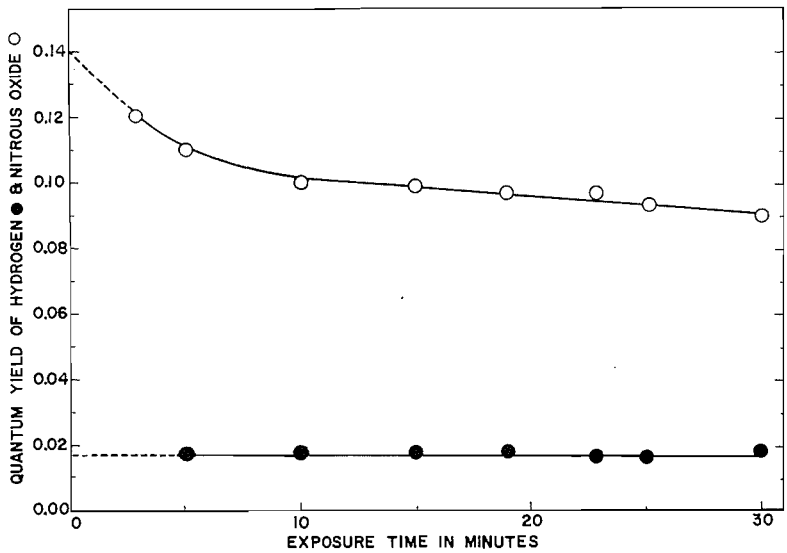


FIG. 5. $\Phi(H_2)$, ●, and $\Phi(N_2O)$, ○, vs. t for a mixture of ethanol and 10 mm of nitric oxide.

of exposure were between 0.77 and 1.08 minutes. Since the two series of runs fall on the same curve, as can be seen in Fig. 7, this is taken as evidence that $\Phi(H_2)$ is independent of t_D in the region 103–160 msec. From Fig. 7, it is apparent that $\Phi(H_2)$ rises linearly with decreasing log t_L to a t_L value of ca. 0.4 msec, beyond which the curve begins to flatten out. The maximum value of $\Phi(H_2)$ was found to be 0.96.

DISCUSSION

From the results of the present investigation, it is apparent that ethanol resembles methanol (1, 2) closely in its primary reaction with Hg $6(^3P_1)$ atoms. Thus, considering first the decomposition of the mixture of 40 mm EtOH and 10 mm NO, we find as products EtONO (0.25), N_2O (0.14), H_2O, and H_2 (0.017), where the numbers in parentheses give the Φ^0's. For the MeOH–NO system with the same NO concentration, Φ(MeONO) was 0.20 with $t = 5.0$ minutes (2). From Fig. 4, it can be seen that Φ(EtONO) has the same value at the same t. Again for methanol containing 10 mole% NO, $\Phi^0(H_2)$ was 0.012, and we obtain 0.017 for ethanol containing 20 mole% NO.

For the inhibited reaction, the products can be accounted for by the following sequence:

$$CH_3CH_2OH + Hg^* \rightarrow CH_3CH_2O + H + Hg, \quad [1]$$

$$CH_3CH_2O + NO \rightarrow CH_3CH_2ONO, \quad [2]$$

$$H + NO \rightarrow HNO, \quad [3]$$

$$HNO + HNO \rightarrow H_2O + N_2O, \quad [4]$$

$$HNO + HNO \rightarrow 2NO + H_2. \quad [5]$$

For reaction [2], Gray and Williams (7) estimate an exothermicity of 35–40 kcal/mole. Levy (8) has shown that [2] occurs in the thermolysis of Et_2O_2 in the presence of NO, and in the decomposition of ethyl nitrite (8) and ethyl nitrate (9). There is also some evidence (8, 10) that in the photolysis of Et_2O_2–NO mixtures, ethyl nitrite forms by [2].

In the above sequence, reactions [3], [4], and [5] have been discussed previously (2).

Can. J. Chem. Downloaded from www.nrcresearchpress.com by 210.87.254.6 on 09/05/12
For personal use only.

Can. J. Chem. Downloaded from www.nrcresearchpress.com by 210.87.254.6 on 09/05/12
For personal use only.

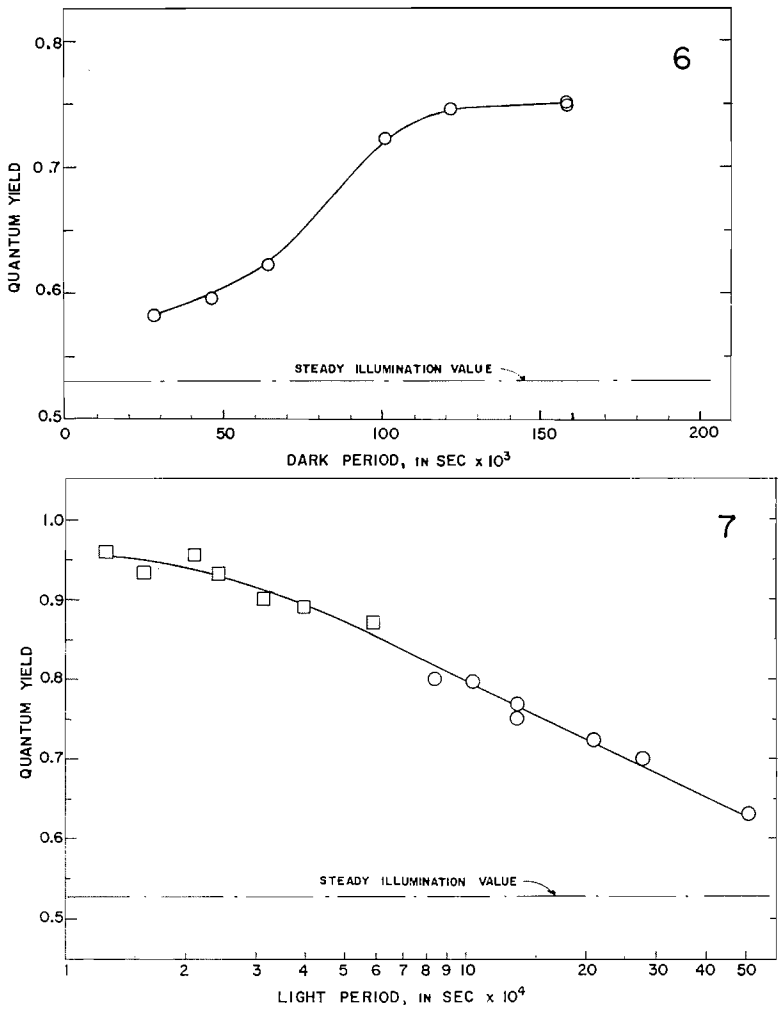


FIG. 6. $\Phi(H_2)$ as a function of dark period, for a constant light period of 2.04 msec, for ethanol vapor at a pressure of 40 mm.

FIG. 7. $\Phi(H_2)$ as a function of the logarithm of the light period, for dark periods of 103 msec, ○, and 160 msec, □, for ethanol vapor at a pressure of 40 mm.

From the ratio $\Phi^0(N_2O)/\Phi^0(H_2)$, k_4/k_5 is estimated to be ca. 8. To explain the fact that Φ^0(EtONO) is only 0.25, we suggest the reaction

$$CH_3CH_2O + HNO \rightarrow CH_3CH_2OH + NO. \qquad [6]$$

Since D(EtO–H) is 99 kcal/mole (7), step [6] should be highly exothermic. The fact that CH_3CHO was not detected as a product would suggest that there is no abstractive attack of ethoxy radicals on the ethyl nitrite. Here it is pertinent to note that Levy found that both ethyl nitrite (8) and ethyl nitrate (9) are relatively inert to ethoxy radicals at 181°. In the previous study (2), on the CH_3OH–NO reaction, HCHO was shown to be a minor secondary product which increased in importance with the exposure time. On energetic grounds, one would expect that EtO radicals would similarly remove a secondary hydrogen from EtONO, leading to the formation of CH_3CHO as a product. In our opinion, the

Can. J. Chem. Downloaded from www.nrcresearchpress.com by 210.87.254.6 on 09/05/12
For personal use only.

difference in the behavior of the two systems is due to the higher efficiency of the association reaction, [2], for EtO radicals compared with the analogous reaction for MeO radicals. Thus in the pyrolysis of MeONO the first-order rate constant falls off at substrate pressures less than 50 mm, indicating a dreierstoss restriction on the association reaction (7). This restriction should be less stringent for [2]. Hence it is likely that the stationary-state concentration of EtO radicals is lower than that for MeO radicals at the same NO concentration in the two systems. Since the aldehyde yield will be proportional to $(RO)^{\cdot}$, it is probable that CH_3CHO is formed in quantities too small for detection by our analytical methods. Presumably the decrease in Φ(EtONO) with t (cf. Fig. 4) is due to the photolysis of this product into EtO and NO. The resulting EtO radicals could then disappear by [6].

In the decomposition of the pure substrate, step [1] would be followed by:

$$CH_3CH_2O + CH_3CH_2OH \rightarrow CH_3CH_2OH + CH_3CHOH, \quad [7]$$

$$H + CH_3CH_2OH \rightarrow H_2 + CH_3CHOH, \quad [8]$$

$$2(CH_3CHOH) \rightarrow CH_3CHOHCHOHCH_3. \quad [9]$$

From the relative yields of the three butanediols, it follows that CH_2CH_2OH radicals must also be formed in [7] and [8], by abstraction at the methyl group of the ethanol. From the composition of the heavy product, $(CH_3CHOH)/(CH_2CH_2OH)$ must be ca. 11.

The activation energy for [7] has not been determined. If we assume that the C—H bond energy in ethanol does not exceed that in ethane, step [7] should be exothermic to at least 3 kcal/mole. Recently Wijnen (11) has reinvestigated the photolysis of ethyl propionate, and for the reaction

$$CH_3CH_2O + EtCOOEt \rightarrow CH_3CH_2OH + R \quad [10]$$

he finds an activation energy of 5.5 kcal/mole. It is unlikely that the activation energy of [7] would exceed that of [10].

The only other product in the ethanol reaction which is clearly of primary origin is acetaldehyde, for which $\Phi^0 = 0.08$. In this system, it seems unlikely that the acetaldehyde arises by disproportionation of ethoxy radicals. The absence of hydroxy-ethers among the products would suggest that the stationary-state concentration of EtO is very low. Now from the analysis of the heavy fraction, we know that the radicals (R) undergoing combination consist of a ca. 11:1 mixture of CH_3CHOH and CH_2CH_2OH. If the disproportionation of the R radicals is the source of the acetaldehyde, the dominant reaction would be:

$$CH_3CHOH + CH_3CHOH \rightarrow CH_3CH_2OH + CH_3CHO. \quad [11]$$

This reaction would involve an intermediate $\dot{C}H_2CHOH$ structure, which should rearrange readily to CH_3CHO. Since $\Phi^0(H_2) = 0.53$, Φ(R) must have the same value. Thus k_{11}/k_9 would be $(0.08)/(0.26_5-0.08)$, or ca. 0.3. This value is likely low, since, as will be seen, CH_3CHO is suffering decomposition by secondary reaction.

The rapid decrease in $\Phi(CH_3CHO)$ with t is evident from Fig. 2. Since the weakest C—H bond in CH_3CHO is 80 kcal/mole (7), the reaction

$$R + CH_3CHO \rightarrow RH + CH_3CO \quad [12]$$

will be highly exothermic, and the one likely to be responsible for CH_3CHO consumption. From our data, the mean rate of CH_3CHO formation during the first 5 minutes of reaction is 0.10_4 μmoles/minute. With no secondary destruction of this product, there should be $45\times0.10_4$ or 4.7 μmoles at $t = 45$ minutes. Since only 1.2 μmoles were found at $t = 45$ minutes, 3.5 μmoles have been consumed. The yield of CO at $t = 45$ minutes was 3.3

Can. J. Chem. Downloaded from www.nrcresearchpress.com by 210.87.254.6 on 09/05/12
For personal use only.

μmoles. We are, of course, assuming that the CO arises from the decomposition of the CH_3CO radicals formed in [12]. The accountability in CH_3 is not quite so satisfactory. At $t = 45$ minutes, there were 1.1 μmoles of CH_4 and 0.45 μmoles of C_2H_6. We can therefore account for 2.0 of the 3.3 μmoles of CH_3 in this manner.[2]

From the results of the studies under intermittent illumination, as shown in Fig. 7, we can now say that the primary quenching reaction [1] is at least 96% efficient. Furthermore, since in the inhibited reaction there is no evidence of any other radical association product than ethyl nitrite, it appears justifiable to say that $\Phi(H) = \Phi(CH_3CH_2O) = 0.96$. Since the effect of intermittent illumination has been discussed in some detail for the methanol reaction (3), we will limit ourselves here to the conclusion that the low $\Phi(H_2)$ under steady illumination is due mainly to substrate re-formation by the addition of H atoms to the radicals present in the system. For ethanol the dominant reaction would be:

$$H + CH_3CHOH \rightarrow CH_3CH_2OH. \qquad [13]$$

The main difference between methanol (3) and ethanol is that the $\Phi(H_2)$ for the latter rises more rapidly toward unity with decreasing t_L. Now at the same I_a and primary quantum efficiency, the reactions controlling the H-atom concentration will be [8] and [13] and their analogues for methanol. An obvious conclusion is that the abstraction reaction [8] is faster for ethanol than methanol, which would result in a lower value for (H) in the ethanol system, and a reduced rate of substrate re-formation by [13]. For both methanol (3) and ethanol (Fig. 6), it was necessary for t_D to be at least 100 msec to obtain the maximum value of $\Phi(H_2)$ at a given t_L. It seems reasonable to conclude that the t_D value of 100 msec represents the minimum time required for the radical concentration to decay to zero between successive light pulses.

CONCLUSIONS

As a result of the present investigation, it can be concluded that ethanol molecules react with Hg $6(^3P_1)$ atoms by O—H bond scission to form ethoxy radicals and H atoms with at least 96% efficiency. The ethoxy radicals and H atoms react with the substrate by abstraction to form mainly CH_3CHOH radicals. The low value for $\Phi(H_2)$ under continuous illumination is due largely to the addition of H atoms to CH_3CHOH radicals.

ACKNOWLEDGMENTS

The authors would like to express their appreciation to Dr. Willard F. Allen of this laboratory for assistance in the experimental work and many helpful discussions.

This investigation was partially supported by the National Research Council under N.R.C. grant No. T.162 (to Gunning). This support is gratefully acknowledged.

REFERENCES

1. R. F. Pottie, A. G. Harrison, and F. P. Lossing. Can. J. Chem. **39**, 102 (1961).
2. A. R. Knight and H. E. Gunning. Can. J. Chem. **39**, 1231 (1961).
3. A. R. Knight and H. E. Gunning. Can. J. Chem. In press.
4. J. R. Bates and H. S. Taylor. J. Am. Chem. Soc. **49**, 2438 (1927).
5. S. Bywater and E. W. R. Steacie. J. Chem. Phys. **19**, 319 (1951).
6. R. A. Back. Can. J. Chem. **37**, 1834 (1959).
7. P. Gray and A. Williams. Chem. Revs. **59**, 240 (1959).
8. J. B. Levy. J. Am. Chem. Soc. **75**, 1801 (1953).
9. J. B. Levy. J. Am. Chem. Soc. **76**, 3790 (1954).
10. H. N. Mortlock and D. W. G. Style. Nature, **170**, 706 (1952).
11. M. H. J. Wijnen. J. Am. Chem. Soc. **82**, 3034 (1960).

[2]*We are indebted to the reviewer of this paper for pointing out that the accountability in* CH_3 *could be improved by considering that some* CH_3 *will disappear by combination with* CH_3CHOH *to form isopropyl alcohol. A small yield of this compound would not have been detected in our G.L.P.C. analysis. Pertinently, small yields of* CH_3CH_2OH *were found in the previous study on* CH_3OH *(2).*

Can. J. Chem. Downloaded from www.nrcresearchpress.com by 210.87.254.5 on 09/05/12
For personal use only.

CONFIGURATION OF GLYCOSIDIC LINKAGES IN OLIGOSACCHARIDES

IX. SYNTHESIS OF α- AND β-D-MANNOPYRANOSYL DISACCHARIDES[1]

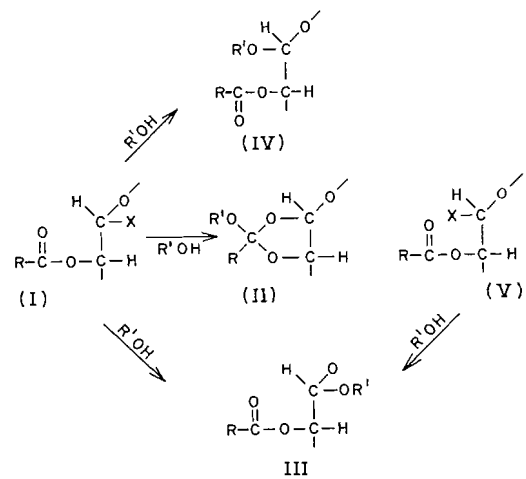
P. A. J. Gorin and A. S. Perlin

ABSTRACT

The Königs–Knorr condensation of 4,6-di-*O*-acetyl-2,3-*O*-carbonyl-α-D-mannopyranosyl bromide with 1,2,3,4-tetra-*O*-acetyl-β-D-glucose provides a synthetic route to 6-*O*-β-D-mannopyranosyl-D-glucose. When some other derivatives of α-D-mannopyranosyl bromide—the 2,3,4,6-tetra-*O*-benzoyl-, 3,4,6-tri-*O*-acetyl-, or 3,4,6-tri-*O*-acetyl-2-*O*-benzyl derivative—are used as the halide component the α-D-linked isomer of this disaccharide is produced. The steric outcome of Königs–Knorr syntheses involving these and other derivatives of α-D-mannopyranosyl bromide is discussed in terms of the influence of neighboring groups, and of conformational and solvent effects.

Lead tetraacetate oxidation of 6-*O*-β-D-mannopyranosyl-D-glucose, followed by reduction, affords 4-*O*-β-D-mannopyranosyl-D-erythritol, a metabolite produced by *Ustilago* species (PRL 627).

In an earlier study (1) it was found that the major disaccharides produced by the Königs–Knorr condensation of 2,3,4,6-tetra-*O*-acetyl-α-D-mannopyranosyl bromide with 1,2,3,4-tetra-*O*-acetyl-β-D-glucose and -mannose possess the α-D-, rather than the β-D-linkage assigned originally (2). This finding was consistent with current views (3–7) on the reactions of acylated glycosyl halides with alcohols, according to which a 1,2-*trans*-halide (I, R = CH_3 or phenyl) due to participation of the 2-acyloxy group, is expected to yield either an orthoester (II) or the 1,2-*trans*-glycoside (III), although a small amount of inversion may also occur to yield the 1,2-*cis*-glycoside (IV). Predominant inversion would be expected with the 1,2-*cis*-halide (V), the *trans*-glycoside again being formed. In several instances, however, 1,2-*cis*-glycosides have been prepared by modifying or eliminating (6, 7, 8) the neighboring-group effect of the 2-substituent. Therefore, in attempting now to synthesize D-mannopyranosyl oligosaccharides possessing the β-(1,2-*cis*-)-linkage, this type of approach has been examined using various derivatives of α-D-mannosyl bromide in the Königs–Knorr reaction.



[1]*Manuscript received August 23, 1961.*
Contribution from the National Research Council of Canada, Prairie Regional Laboratory, Saskatoon, Saskatchewan.
Issued as N.R.C. No. 6553.

Can. J. Chem. Downloaded from www.nrcresearchpress.com by 210.87.254.5 on 09/05/12
For personal use only.

Ness, Fletcher, and Hudson found that treatment of 2,3,4,6-tetra-*O*-benzoyl-α-D-mannopyranosyl bromide with methanol in the absence of an acid acceptor produced the α-D-glycoside but not an orthobenzoate (9). Since the latter could have only a transient existence under such acidic conditions it is not surprising that this result contrasts sharply with the extensive production of orthoester from the corresponding acetobromo derivative in the presence of silver carbonate (3, 10). The possibility remained, however, that the participating properties of the benzoxy group under Königs–Knorr conditions might differ sufficiently from those of the acetoxy group to permit formation of relatively more of the inverted (β-D-) product than had been obtained with the acetate (3, 10). Accordingly, the tetra-*O*-benzoyl bromide was treated with methanol containing silver carbonate, but the chief product was an amorphous tri-*O*-benzoyl methyl 1,2-orthobenzoate, and only a small proportion of the β-glycoside was detected. Hence, the characteristics of both acyloxy halides are in reality closely similar. The Königs–Knorr condensation with 1,2,3,4-tetra-*O*-acetyl-β-D-glucose was also examined, and the (1 → 6) linked α-D-disaccharide (1) again was found to be the major biose produced. However, the total yield was considerably better than obtained with the acetobromo derivative (39% vs. 25% (1, 2)), and the proportion of the β-D-linked isomer in the disaccharide fraction was even smaller (5% vs. 14%). It appears advantageous, therefore, to use the *O*-benzoyl bromide rather than the corresponding acetate for the synthesis of D-mannopyranosyl disaccharides possessing the α-configuration.

A high degree of inversion in the reaction of 2-*O*-methyl-α-D-mannopyranosyl fluoride with sodium alkoxide is known to occur (11). The influence of the 2-methoxy group under Königs–Knorr conditions has now been examined using 2,3,4,6-tetra-*O*-methyl-α-D-mannosyl bromide (12). With methanol in the presence of silver oxide this halide produced a mixture of the β- and α-glycosides in the ratio of 3:1, showing again that inversion predominates when the 2-position contains a "non-participating" substituent (see below). Without the acid acceptor, the proportion of β-glycoside was somewhat less, the ratio being 2:1. However, although the effect of the methoxyl group is to favor the formation of β-D-mannosides, its stability limits the usefulness of the *O*-methyl derivative in oligosaccharide synthesis.

For the latter purpose, the *O*-benzyl ether group appeared to offer greater promise as a substituent which should be stable under the condensation conditions but easily removable from the product. 2-*O*-Benzyl-D-mannose (13) was acetylated and the product treated with hydrogen bromide in chloroform, the specific rotation of the bromide indicating that the α-anomer had been formed predominantly. On reaction with methanol in the presence of silver oxide the bromo derivative yielded a levorotatory syrup which was found to contain mainly the β-D-mannoside and only a small proportion of the α-glycoside. However, when the condensation was carried out using 1,2,3,4-tetra-*O*-acetyl-β-D-glucose as the hydroxylic component, the product, following hydrogenolysis and deacetylation, proved to be predominantly 6-*O*-α-D-mannopyranosyl-D-glucose.

The possibility of using a D-mannosyl halide unsubstituted in the 2-position was also examined briefly, by analogy with the use of glycosyl halides containing a free 2-hydroxyl group in the D-glucose (14), 6-deoxy-D-glucose (15), and pentafuranose (see 16) series. For a preparation of a corresponding D-mannosyl halide, 3,4,6-tri-*O*-acetyl-D-mannose (17, 18) was treated with hydrogen bromide, affording a strongly dextrorotatory (and hence presumably the α-1-bromide) syrup. When the latter was condensed under Königs–Knorr conditions with methanol, a mixture of α- and β-glycosides (ratio of approximately 3:1) was formed, and of the disaccharides produced with 1,2,3,4-tetra-*O*-acetyl-β-D-glucose, the β-isomer comprised only a trace proportion.

Can. J. Chem. Downloaded from www.nrcresearchpress.com by 210.87.254.5 on 09/05/12
For personal use only.

The properties of a different type of 2-substituted D-mannosyl bromide, the 2,3-*O*-carbonate, were also examined under Königs–Knorr conditions and with this bicyclic derivative inversion was found to occur both with methanol and 1,2,3,4-tetra-*O*-acetyl-β-D-glucose as hydroxylic components. In two previous instances a 2,3-*O*-carbonate derivative has been used successfully to prepare a 1,2-*cis*-glycoside from a 1,2-*trans*-halide, i.e. in the D-mannofuranose (19) and D-ribofuranose series (20). In the current study the halide used was 4,6-di-*O*-acetyl-2,3-*O*-carbonyl-α-D-mannopyranosyl bromide (VI), preparation of which involved the following steps:

benzyl α-D-mannopyranoside (BM) → 6-*O*-trityl-BM
→ 2,3-*O*-carbonyl-6-*O*-trityl-BM → 2,3-*O*-carbonyl-BM
→ 4,6-di-*O*-acetyl-2,3-*O*-carbonyl-BM → 4,6-di-*O*-acetyl-2,3-*O*-carbonyl-D-mannose → 1,4,6-tri-*O*-acetyl-2,3-*O*-carbonyl-D-mannose → VI.

With methanol in the presence of silver oxide, VI afforded a syrupy product which, on treatment with barium methoxide followed by acetylation, gave methyl 2,3,4,6-tetra-*O*-acetyl-β-D-mannopyranoside; only a trace of the α-anomer was detected. The product obtained by condensing VI with 1,2,3,4-tetra-*O*-acetyl-β-D-glucose was also treated with barium methoxide, and the free disaccharide fraction was isolated by cellulose column chromatography. This was found to consist almost entirely of the β-isomer, which crystallized readily from the mixture. A sample of syrupy 6-*O*-β-D-mannopyranosyl-D-mannose was also prepared by condensation of VI with 1,2,3,4-tetra-*O*-acetyl-αβ-D-mannose.

By oxidation of the synthesized 6-*O*-β-D-mannopyranosyl-D-glucose with 2 moles of lead tetraacetate (to obtain the 4-substituted D-erythrose derivative (21)), and then reduction of the product with sodium borohydride, 4-*O*-β-D-mannopyranosyl-D-erythritol (1-*O*-β-D-mannopyranosyl-L-erythritol) (22, 23) was prepared. This result, therefore, confirms by synthesis the earlier assignment based on isotopic data (23) of the configuration of the tetritol unit in this metabolite from *Ustilago* species (PRL 627).

DISCUSSION

The foregoing results, and other data obtained with 2,3,4,6-tetra-*O*-acetyl-α-D-mannosyl bromide (1, 2, 3) show wide variations in the steric properties of different α-D-mannosyl bromide derivatives. However, there are two general patterns evident and these appear to be associated with a change in the reaction medium. The disaccharide syntheses (except those carried out with the 2,3-*O*-carbonate) are characterized by retention of configuration, and necessarily involve the use of an "inert" solvent. For the methyl glycoside syntheses, in which methanol serves both as solvent and hydroxylic component, inversion and orthoester formation are the more prominent features.* These findings are analogous to those of Isbell and Frush (3) on the methanolysis of 2,3,4,6-tetra-*O*-acetyl-α-D-mannosyl bromide in the presence of silver carbonate. They found that the β- (but not α-) D-glycoside is formed, in addition to orthoacetate, when methanol alone is the medium, but that in the presence of ether or benzene as diluent more of the α- than β-D-mannoside, and much less orthoacetate, is formed. A similar mixture of the corresponding dimeric products is obtained using chloroform as solvent when the hydroxylic component is 1,2,3,4-tetra-*O*-acetyl-β-D-glucose (2).

**In one experiment, tetra-O-acetyl-α-D-mannopyranosyl bromide was condensed with 1,2,3,4-tetra-O-acetyl-β-D-glucose using a fourfold excess of the latter and chloroform sufficient only to produce fluidity. Such conditions approximated those used for methyl glycoside synthesis and, in fact, altered the ratio of α- to β-disaccharide produced from about 6:1 to about 2:1.*

Can. J. Chem. Downloaded from www.nrcresearchpress.com by 210.87.254.5 on 09/05/12
For personal use only.

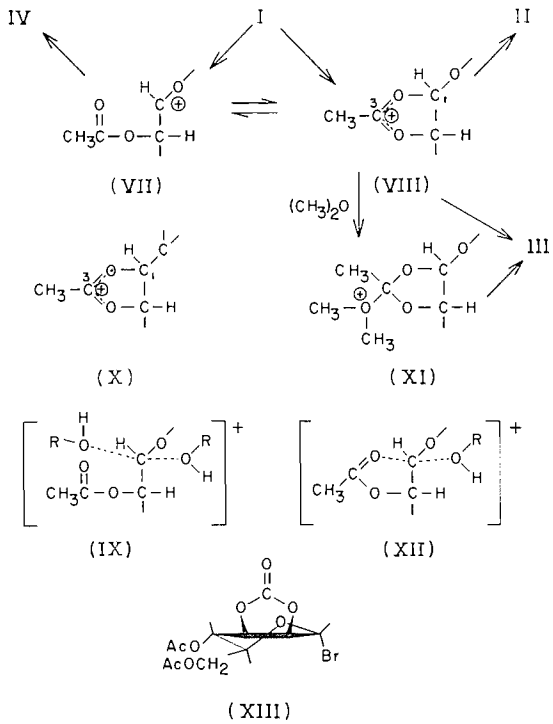
Formation of the α-D-mannoside was accounted for by Isbell and Frush in terms of neighboring-group participation by the 2-acetoxy group. In more recent years additional evidence for a neighboring-group effect of this kind in many other nucleophilic substitution reactions that lead to retention of configuration has been accumulated (see especially ref. 24). Hence it may be inferred that the examples of retention observed in the synthesis of α-D-mannopyranosyl disaccharides also involve neighboring-group participation. With the D-mannose derivatives used several such possibilities can be recognized. The 2-*O*-benzoyl, as well as the 2-*O*-acetyl, derivative reacts with methanol to give the 1,2-orthoester in high yield, a direct demonstration of a neighboring-group effect, and also *dimeric* 1,2-orthoesters are known in the acetate series (2, 25). Participation by the 6-acetoxy group appears to be feasible in reactions of the 2-*O*-benzyl and 2-hydroxy derivatives, although in the D-glucose series this group is usually thought to have a minor influence on the steric outcome of substitution reactions at C-1 (14, 26). Also favoring the possibility of retention by the benzyl derivative is evidence that a 1,2-*trans*-alkoxyhalide can form a cyclic alkoxonium ion during silver-ion-assisted replacements (27). With the 2-hydroxy derivative, the 1,2-*trans*-diaxial arrangement is especially favorable for formation of an intermediate 1,2-anhydride (28) which, on further reaction, should afford 1,2-*trans*-products. Apparently this possibility does not arise with the *trans*-diequatorial 1-chloro-2-hydroxy derivatives of 6-deoxy-β-D-glucose (15) and -β-D-glucose (14), which undergo predominant inversion on ethanolysis or acetolysis. However, the structure of the monohydroxy-D-mannosyl bromide is not yet known with certainty, and conclusions about its behavior must therefore be made with reserve.

Although there may be several possibilities for neighboring-group participation in the reactions studied, these possibilities do not account for the marked steric changes that accompany the change in solvent, e.g., little retention or a great predominance of orthoester formation when the diluent is absent. According to current views, substitution reactions of glycosyl halides proceed likely via a unimolecular course (29, 30, 31). This may apply for a solvent of high polarity, such as methanol, but there is the possibility that the characteristics of the reactions themselves may be altered from unimolecular to bimolecular by the transfer to the much less polar media (ether, benzene, or chloroform). However, since the present data do not give information about kinetic order it cannot be assumed that such an alteration occurs. In fact, the direction of the steric changes induced is contrary to what might then be expected: the inverted configuration of the products formed in methanol is even more characteristic of a bimolecular than unimolecular course, whereas the retention found with the media of low ionizing power is rarely a property of S_N2 reactions.

Within the framework of the S_N1 mechanism, Königs–Knorr syntheses involving α-D-mannosyl halides may be considered in terms of ions such as VII and VIII (5, 6, 7, 30). The formation of β-D-mannosides appears to result from attack by the hydroxylic component on VII, at the side opposite to that shielded by the departing halide ion (7). Such a pathway is presumably important when methanol is the solvent. In the media of lower ionizing power the structure of VII may become modified through increased ion pair aggregation, perhaps in such a way as to induce the steric changes observed. Another possibility is that solvation of ion VII in these media involves the formation of intermediates analogous to those described by Doering and Zeiss (32, 24). For example, IX corresponds to the symmetrically solvated ion postulated by them to account for racemization in S_N1 reactions. However, the presence of the various ring substituents on the D-mannosyl analogue in fact renders such an ion unsymmetrical and interactions, notably between the 2,3- and 6-substituents, might favor eventual formation of the 1,2-*trans*-

rather than the less stable 1,2-*cis*- product. Such an outcome should be favored even more when the hydroxylic component is a bulky tetraacetyl hexose molecule than with methanol.

If neighboring-group participation is possible, ion VIII is expected to be more prominent than VII, although an appreciable proportion of the latter may be present (3, 6, 31). It is generally held that orthoester is formed through attack by the hydroxylic component at



(XIII)

C_3 of VIII and that acceptance of the incoming group at C_1 results in retention of configuration (i.e., in formation of the α-D-mannoside). The generation of an intermediate orthoester ion (X) of type VIII during substitution reactions was postulated originally by Winstein and Buckles (33). With cyclohexane derivatives, for example, they found that several solvolysis reactions proceed with complete retention of configuration, which indicated that "open" carbonium ions (analogous to VII) are not involved and that the incoming groups enter at C_1 of the cyclic ion. However, no retention was observed in solvolyses involving hydroxylic components (water or ethanol), which therefore appeared to attack only at C_3 of X, yielding orthoacid or orthoester.

In the Königs–Knorr syntheses it must be assumed that the effect of solvent is such as to favor reaction at C_3 of VIII under some conditions, but also to promote reaction at C_1 under other conditions. According to Isbell and Frush (3), the presence of a high ratio of ether causes a decrease in the yield of orthoacetate and an increase of α-glycoside, from the methanolysis of tetra-*O*-acetyl-α-D-mannosyl bromide, by competitive solvation of a bimolecular transition complex. In accord with more recent views this suggestion has been modified (6, 7) in terms of the ion VIII: in methanol the favored substitution site is at C_3, but competitive solvation by nucleophilic ether (as in XI, e.g. (6)) permits a rearward attack at C_1 to take place. However, the same explanation does not account

Can. J. Chem. Downloaded from www.nrcresearchpress.com by 210.87.254.5 on 09/05/12
For personal use only.

adequately for the results of the disaccharide syntheses, in which retention occurs to an even greater degree, because the diluents used have much less nucleophilic character. One factor favoring attack at C_1 when the concentration of the hydroxylic component is low, is the possibility (suggested by S. Winstein, private communication) that solvation of the departing halide ion by the hydroxylic component promotes an "orientation" of the latter in the vicinity of C_1. Further, it may be noted that substitution at C_1 involves a ring-opening step, and Winstein and Buckles regard this step as having S_N2 characteristics (33). Hence it is conceivable that an effect of decreasing solvent polarity is to increase the rate of substitution at C_1 relative to that at C_3 (34).

Another type of transition state which may be visualized is one intermediate between solvated forms of ion VII (IX) and solvated forms of VIII; for example, XII. Such an ion should be more prominent with a non-polar diluent present than in methanol, because under the former conditions the neighboring nucleophilic acyloxy (or alkoxy) substituent should be able to compete more effectively with the hydroxylic component as a solvating species. Presumably, an α-D-mannoside would be the product of this pathway.

Still other factors may affect the steric outcome of these syntheses. For example, Talley, Reynolds, and Evans (2) showed that in the reaction of tetra-*O*-acetyl-α-D-mannosyl bromide with 1,2,3,4-tetra-*O*-acetyl-β-D-glucose, the presence of iodine suppresses the yield of dimeric orthoester and increases the yield of (α-linked) disaccharide. Iodine is likewise used in the current disaccharide syntheses. In turn, the iodine appears to depress the catalytic effect of the silver oxide on the rate of dissociation of the glycosyl halide (25).

The 2,3-*O*-carbonyl-α-D-mannosyl bromide is exceptional in that it undergoes inversion under both sets of reaction conditions. Molecular models suggest that the carbonate group present cannot participate readily in substitution reactions at C-1, and hence that retention of configuration should be obviated on this basis. However, it appears much more probable that this halide, in contrast to the monocyclic halides used, can react via a bimolecular course, thus ensuring inversion. This possibility arises from the fact that the fused 5-membered carbonate ring modifies the conformation of the pyranose ring (e.g., as in XIII) (35, 36) in such a way as to resist formation of a planar carbonium ion about C-1.

EXPERIMENTAL

Paper chromatography was carried out with Whatman No. 1 paper using (A) butanol:ethanol:water (40:11:19) and (B) ethyl acetate:pyridine:water (10:4:3) as solvents, and (C) *p*-anisidine hydrochloride or (D) ammoniacal silver nitrate as spray reagents. Evaporations were carried out under reduced pressure at 40–45° C and optical rotations measured at 26°±2° C. Silicic acid used in chromatography had a mesh size of 100 to the inch.

*3,4,6-Tri-O-benzoyl-*D*-mannopyranose-1,2-methyl Orthobenzoate*

Amorphous 2,3,4,6-tetra-*O*-benzoyl-α-D-mannopyranosyl bromide (9) (0.45 g) was added to a suspension of silver carbonate (1.5 g) in absolute methanol (15 ml). The mixture was shaken for 2 hours, filtered, the filtrate and washings were concentrated, and the syrup obtained was extracted into ether. Evaporation of the ether afforded a white, amorphous solid (0.35 g); $[\alpha]_D$ −124° (*c*, 1.4, methanol). Calculated for $C_{35}H_{30}O_{10}$: C, 68.8%; H, 5.1%; total benzoate, 4.0 moles; *O*-benzoate, 3.0 moles. Found: C, 68.5%; H, 4.95%; total benzoate (acid *plus* alkali hydrolyzable), 3.91 moles; *O*-benzoate (cold alkali saponifiable), 3.05 moles.

Can. J. Chem. Downloaded from www.nrcresearchpress.com by 210.87.254.5 on 09/05/12
For personal use only.

Examined by deacylation with sodium methoxide followed by paper chromatography, the product was shown to contain a trace of methyl β-D-mannoside. When treated with 0.3% methanolic hydrogen chloride the orthobenzoate (14 mg/ml) showed an optical rotatory change from α_D −1.53° (1 dcm, initial) → −0.37° (3 minutes, constant) (cf. ref. 37).

D-*Mannopyranose-1,2-methyl Orthobenzoate*

The tribenzoyl orthobenzoate (0.1 g) in methanol (5 ml) was treated with a slight excess of barium methoxide for 1 hour, the solution was neutralized with barium carbonate, and evaporated. Water was added to the resulting syrup, the suspension was filtered, and the filtrate extracted three times with chloroform to remove methyl benzoate. On concentrating the aqueous layer an amorphous product ($R_{mannose}$ 3.7, solvent A) was obtained; this product contained a phenyl group (ultraviolet spectrum) but no ester group (infrared spectrum). In 0.02 *N* sulphuric acid (1.2 ml) the observed rotation of the material (22.6 mg) changed from α_D −0.51° (initial, 1 dcm) → +0.18° (20 minutes, constant), and the presence of 0.9 benzoate groups saponifiable with cold alkali was then found (calculated, 1.0 benzoate groups).

6-O-α-D-Mannopyranosyl-D-glucose

To a mixture containing 1,2,3,4-tetra-*O*-acetyl-α-D-glucose (0.52 g), silver oxide (1.0 g), iodine (0.5 g), and Drierite* (5.0 g), in dry dichloromethane (10 ml), was added, with shaking, a solution of 2,3,4,6-tetra-*O*-benzoyl-α-D-mannosyl bromide (1.0 g) in dichloromethane (5 ml); the addition was made in five equal portions over a period of 4 hours. More silver oxide (0.3 g) was added and the mixture shaken for a further 18 hours, filtered, and the filtrate was concentrated to a syrup. Yield, 1.2 g.

A benzene solution of the product was extracted three times with water (which removed most of the monomeric material present), the benzene was evaporated, and the residue was treated for 2 hours with excess sodium methoxide solution. After acidification with acetic acid the reaction mixture was concentrated, taken up in water, and oily material present (methyl benzoate) was extracted into chloroform. The aqueous phase was then transferred to a column of coconut charcoal (38), which was eluted with 5%, and then 15% ethanol. The latter eluate contained most of the disaccharide fraction which, after purification with mixed ion-exchange resins, was recovered as an amorphous solid. Yield, 0.20 g. $[\alpha]_D$ +70° (*c*, 1.8, water); after addition of excess sodium metaperiodate to the solution the equilibrium rotation was $[\alpha]_D$ +73° (assuming conversion of 18 mg of the disaccharide to 10 mg of trialdehyde (39)). (Based on the data given in ref. 39, the latter rotational value corresponds to that of an α,β-mixture of about 95:5.) The product was chromatographically indistinguishable from 6-*O*-α-D-mannopyranosyl-D-glucose (solvent B); none of the β-isomer (see below) was detected. In agreement with the presence of a (1 → 6) linkage the compound rapidly consumed 2.0 moles of lead tetraacetate per mole (21). Calculated for $C_{12}H_{22}O_{11}$: C, 42.1%; H, 6.5%. Found: C, 41.9%; H, 6.6%.†

Reaction of 2,3,4,6-Tetra-O-methyl-α-D-mannosyl Bromide with Methanol

A solution of 1-*O*-acetyl-2,3,4,6-tetra-*O*-methyl-α-D-mannose (12) (0.25 g) in chloroform (0.7 ml) was treated with 30% hydrogen bromide in acetic acid (0.5 ml) for 3 hours. More chloroform was added, the solution was extracted successively with ice water, cold sodium bicarbonate solution, and ice water, and dried. A yellow syrup (215 mg) was obtained on

**Anhydrous calcium sulphate.*

†The β-octaacetate of this disaccharide is amorphous (2). Attempts to convert the compound to a 2,5-dichlorophenylhydrazone or, by reduction, to the corresponding biitol yielded amorphous products.

Can. J. Chem. Downloaded from www.nrcresearchpress.com by 210.87.254.5 on 09/05/12
For personal use only.

Can. J. Chem. Downloaded from www.nrcresearchpress.com by 210.87.254.5 on 09/05/12
For personal use only.

evaporation of the solvent; $[\alpha]_D$ +210° (*c*, 2, benzene).* This product appeared to be highly unstable and in the following experiments was used immediately after preparation:

(*a*) The bromide (50 mg) in benzene (0.5 ml) was added with vigorous shaking to methanol (5 ml) containing silver oxide (50 mg). After 4 hours the suspension was filtered and the filtrate evaporated to give a syrup (45 mg); $[\alpha]_D$ −39° (*c*, 2, methanol). Examination of this syrup by gas–liquid chromatography, under conditions described by McInnes *et al.* (40), indicated that it consisted of a mixture of methyl α- and β-D-mannosides in a ratio of approximately 1:3.

(*b*) The bromide was treated with methanol as in (*a*) but no silver oxide was added; in 15 minutes the solution showed $[\alpha]_D$ −20° (constant). Excess silver carbonate was added and the solvent was evaporated. Examined by gas–liquid chromatography, the syrup isolated was found to contain an α,β-glycoside mixture in the ratio of about 1:2.

Königs–Knorr Syntheses Using 3,4,6-Tri-O-acetyl-2-O-benzyl-α-D-mannopyranosyl Bromide

2-*O*-Benzyl-D-mannose† (13) (93 mg) was heated at 100° C for 2 hours in acetic anhydride (5 ml) containing sodium acetate (100 mg). Excess anhydride was destroyed with ice water and the solution extracted with chloroform. Evaporation of the extract yielded 1,3,4,6-tetra-*O*-acetyl-2-*O*-benzyl-αβ-D-mannopyranoside (153 mg); $[\alpha]_D$ +7° (*c*, 0.8, $CHCl_3$).

The acetate was dissolved in chloroform (20 ml) containing an excess of hydrogen bromide.‡ The specific rotation soon became constant: $[\alpha]_D$ +40° (2 minutes) → +66° (10 minutes, constant value). After 15 minutes the solution was evaporated and residual hydrogen bromide removed by repeated evaporation of added benzene (3 times).

(*a*) Half of the above bromide was shaken overnight with methanol (3 ml) containing silver oxide (200 mg). The product obtained after filtration and evaporation of the solution had $[\alpha]_D$ −24° (*c*, 1.9, $CHCl_3$) and, after deacetylation, was found chromatographically to contain two components (solvent A, spray C). The main component had R_F 0.69 and the minor R_F 0.77 and by analogy with the R_F's of the corresponding methyl mannopyranosides in the same solvent the slower material should have the β-configuration. This observation agrees with the specific rotation of the product being much closer to that of methyl-β-tetra-*O*-acetyl-β-D-mannopyranoside (−50°) than of the α-anomer (+49°).

(*b*) To the other half of the bromide was added a mixture of tetraacetylglucose (0.4 g) in chloroform (3 cc) containing silver oxide (200 mg), iodine (67 mg), and Drierite (1 g). After it was shaken for 18 hours, the reaction mixture was filtered and the filtrate evaporated. The syrupy product was dissolved in ethanol and debenzylation was effected by shaking with palladium–charcoal in hydrogen at 40 p.s.i. After repetition of the hydrogenolysis the solution was filtered and evaporated. Deacetylation with sodium methoxide in methanol yielded a mixture of which the disaccharide fraction corresponded preponderantly to 6-*O*-α-D-mannopyranosyl-D-glucose, with only a trace proportion of the β-anomer being detected (solvent B, spray C).

Königs–Knorr Syntheses Using 3,4,6-Tri-O-acetyl-α-D-mannosyl Bromide

Crystalline 3,4,6-tri-*O*-acetyl-α-D-mannose (18) (0.11 g) was dissolved in dichloromethane (5 ml) and the solution was saturated with dry hydrogen bromide. A turbidity soon developed and then cleared within 30 minutes, the observed rotation being α_D

**A syrup having the same specific rotation was isolated also when the 1-O-acetyl-tetra-O-methyl derivative was treated with hydrogen bromide in dichloromethane to constant rotation.*

†Prepared in a manner analogous to that used for preparation of 2-O-methyl-D-mannose (41).

‡Use of hydrogen bromide in acetic acid – chloroform resulted in debenzylation of the acetate.

Can. J. Chem. Downloaded from www.nrcresearchpress.com by 210.87.254.5 on 09/05/12
For personal use only.

+2.05° (1 dcm, constant). The solution was concentrated *in vacuo* without application of external heat, benzene was then added, and the concentration repeated; yield, 0.10 g of a yellow syrup, $[\alpha]_D$ +140° (*c*, 3.3, benzene). The syrup was dissolved in benzene (3 ml) and used immediately in the following experiments:

(*a*) A portion of the benzene solution (0.6 ml) was added dropwise with shaking to methanol (0.6 ml) containing silver oxide (40 mg) and iodine (20 mg). After 18 hours the supernatant solution (α_D −0.02°) was treated with excess sodium methoxide and then examined chromatographically. The major products detected on the paper (solvent A, spray D) corresponded to methyl α- and β-D-mannoside (approximate ratio 3:1, visual estimation), and mannose (cf. ref. 24).

(*b*) A portion of the benzene solution (0.6 ml) was added dropwise with shaking over a period of 3 hours to a solution of 1,2,3,4-tetra-*O*-acetyl-α-D-glucose (30 mg) in benzene (1 ml) containing silver oxide (40 mg) and iodine (20 mg). After 18 hours the supernatant solution was treated with excess sodium methoxide and examined chromatographically (solvent B, spray C). The major disaccharide detected corresponded to 6-*O*-α-D-mannopyranosyl-D-glucose, and only a trace of the β-isomer appeared to be present.

The paper chromatographic examinations indicated that minor, unidentified, products were also formed in experiments (*a*) and (*b*).

Reaction of 2,3,4,6-Tetra-O-acetyl-α-D-mannosyl Bromide with Excess 1,2,3,4-Tetra-O-acetyl-β-D-glucose

To a mixture of the bromide (2.0 g), silver oxide (2.5 g) and Drierite (5.0 g) a solution of 1,2,3,4-tetra-*O*-acetyl-β-D-glucose (7.0 g) in dry chloroform (5 ml) was added and the mixture stirred overnight. The solution was diluted with methanol, filtered, and the filtrate was treated with sodium (0.2 g) in methanol. After 3 hours the solution was neutralized with acetic acid and examined on a paper chromatogram (solvent B, spray C). The disaccharide fraction consisted of two materials ($R_{lactose}$ 1.0 and 0.7, solvent B) in a ratio of about 2:1, the former corresponding to 6-*O*-α-D-mannopyranosyl-D-glucose and the latter to the β-anomer. Thus the ratio of the β- to the α-disaccharide was about 3 times as great as when equimolar amounts of the bromide and tetra-*O*-acetyl-β-D-glucose were used in the reaction (1, 2).

Benzyl-α-D-mannopyranoside

Mannose (50 g) was stirred with benzyl alcohol (400 ml) saturated with hydrogen chloride at 60° C until the sugar dissolved. The solution was neutralized with silver carbonate, diluted with methanol, filtered, and evaporated. Benzyl alcohol was removed *in vacuo* at 150° C, the residue (containing benzyl mannosides and a little mannose) was dissolved in a small volume of water and the solution extracted 8 times with ethyl acetate. The extracts were evaporated and the product (37 g) was recrystallized twice from ethyl acetate, with m.p. 131–132° C and $[\alpha]_D$ +74° (*c*, 1.3, H_2O). Calculated for $C_{13}H_{18}O_6$: C, 57.8%; H, 6.7%. Found: C, 57.5%; H, 6.8%.

2,3-O-Carbonyl-6-O-triphenylmethyl-benzyl-α-D-mannopyranoside

A solution of benzyl mannoside (37 g), triphenylchloromethane (50 g) in pyridine (150 ml) was heated at 90° C for 4 hours. The mixture was poured into an excess of aqueous potassium carbonate, which was stirred for 1 hour, and the deposit was collected and chromatographed on a silicic acid column using chloroform as solvent in order to separate the triphenylcarbinol from the 6-trityl-benzyl-α-D-mannoside.

The resulting 6-trityl derivative (35 g) was dissolved in pyridine (210 ml) and cooled

to 0° C. A solution of phosgene (7.5 g) in toluene (55 ml) (42) was added dropwise with stirring over 30 minutes, the mixture then being warmed to 40° C for a further 30 minutes. The solution was evaporated to a syrup, which was fractionated on a silicic acid column. Chloroform eluted a crystalline fraction which was recrystallized from ether and corresponded to 2,3-*O*-carbonyl-6-*O*-triphenylmethyl-benzyl-α-D-mannopyranoside. Yield, 12.4 g. A further crystallization from ether yielded material with m.p. 192–195° C and $[\alpha]_D$ +30° (*c*, 1.0, $CHCl_3$). Calculated for $C_{33}H_{30}O_7$: C, 73.6%; H, 5.6%. Found: C, 73.2%; H, 5.7%.

2,3-O-Carbonyl-benzyl-α-D-mannopyranoside and Its 4,6-Di-O-acetate

The trityl mannoside carbonate (12.0 g), in a mixture of chloroform (30 ml) and acetic acid (10 ml), was detritylated by adding, at 0° C, 12 ml of 32% hydrogen bromide in acetic acid. After 1 minute the mixture was treated with an excess of aqueous sodium bicarbonate, and the aqueous solution then extracted 3 times with ethyl acetate. The product recovered from the extract, which apparently contained unchanged material and decomposition products, was put on to a silicic acid column. Chloroform eluted triphenylcarbinol and unchanged trityl derivative, and acetone then eluted a fraction which crystallized from ether. A further crystallization from ether gave 3.3 g of 2,3-*O*-carbonyl-benzyl-α-D-mannopyranoside with m.p. 122–123° C, $[\alpha]_D$ +77° (*c*, 1.0, $CHCl_3$) and absorption at 1810 cm^{-1} in the infrared region (43). Calculated for $C_{14}H_{16}O_7$: C, 56.7%; H, 5.4%. Found: C, 56.7%; H, 5.5%.

The above carbonate (3.2 g) was dissolved in pyridine (10 ml) containing acetic anhydride (6 ml) and left at room temperature for 6 hours. Excess anhydride was destroyed with ice water and the crystalline deposit which formed was filtered off and recrystallized from ether. Yield, 3.6 g, m.p. 114–115° C, $[\alpha]_D$ +37° (*c*, 1.0, $CHCl_3$). Calculated for $C_{18}H_{20}O_9$: C, 56.8%; H, 5.3%. Found: C, 56.6%; H, 5.5%.

4,6-Di-O-acetyl-2,3-di-O-carbonyl-α-D-mannopyranosyl Bromide

4,6-Di-*O*-acetyl-benzyl-α-D-mannoside-2,3-carbonate (3.6 g) was dissolved in acetic acid (50 ml) containing 10% palladium oxide on charcoal (2.0 g). Debenzylation was effected by shaking overnight at room temperature under a hydrogen pressure of 40 p.s.i. The catalyst was filtered off and the process was repeated twice to complete the reaction, yielding syrupy 4,6-di-*O*-acetyl-2,3-di-*O*-carbonyl-D-mannose (2.8 g); $[\alpha]_D$ −7.5° (*c*, 1.0, $CHCl_3$). This material was acetylated (as for 2,3-di-*O*-carbonyl-benzyl-α-D-mannopyranoside) to give 1,4,6-tri-*O*-acetyl-2,3-di-*O*-carbonyl-αβ-D-mannose (2.5 g) with $[\alpha]_D$ +7.5° (*c*, 1.0, $CHCl_3$).

Bromination at C-1 was effected by treatment of the above material (1.02 g) with 32% hydrogen bromide in acetic acid (20 ml) in dry chloroform (100 ml) for 2 hours at 0° C. The chloroform solution was then washed 5 times with ice water, dried, and evaporated to a syrup (960 mg); $[\alpha]_D$ +55° (*c*, 1.0, $CHCl_3$). In the infrared region the compound absorbed strongly at 1815 cm^{-1} and 1740 cm^{-1}, corresponding to the presence of carbonate and acetate groups, respectively.

Königs–Knorr Syntheses Using 4,6-Di-O-acetyl-2,3-di-O-carbonyl-α-D-mannopyranosyl Bromide

(a) Methanol.—The bromo compound (96 mg) was shaken for 30 minutes with methanol (5 ml) containing silver oxide (300 mg). The product had $[\alpha]_D$ −37° (*c*, 1.0, $CHCl_3$) and absorbed in the infrared region at 1805 cm^{-1} (carbonate carbonyl) and 1740 cm^{-1} (acetate carbonyl), and evidently contained 4,6-di-*O*-acetyl-2,3-*O*-carbonyl-methyl-

Can. J. Chem. Downloaded from www.nrcresearchpress.com by 210.87.254.5 on 09/05/12
For personal use only.

Can. J. Chem. Downloaded from www.nrcresearchpress.com by 210.87.254.5 on 09/05/12
For personal use only.

β-D-mannopyranoside since, after treatment with excess barium methoxide followed by acetylation, it gave 2,3,4,6-tetra-*O*-acetyl-methyl-β-D-mannopyranoside (crystallized from ethanol), m.p. and mixed m.p. 161–162° C. Only a trace of the α-anomer was present as shown by paper chromatography.

*(b) 1,2,3,4-Tetra-O-acetyl-*D*-glucose.*—A mixture of excess 1,2,3,4-tetra-*O*-acetyl-β-D-glucose (3.0 g) in chloroform (8 ml) containing silver oxide (450 mg), iodine (225 mg), and Drierite (5.0 g) was added to the bromo compound (0.30 g) and shaken for 18 hours. It was then diluted with methanol, filtered, and evaporated to a syrup which was redissolved in methanol and de-esterified with 0.1 equivalents of barium methoxide in methanol for 3 hours. The alkali was neutralized with acetic acid and after dilution with excess water the solution was deionized with Amberlite IR-120 and Dowex-1. Evaporation gave a syrup which was fractionated on a cellulose column. *n*-Butanol saturated with water eluted glucose; butanol–ethanol–water (4:1:1 v/v) gave the disaccharide fraction (132 mg; $[\alpha]_D$ +2° (*c*, 1.0, H_2O)), containing mainly 6-*O*-β-D-mannopyranosyl-D-glucose and a trace proportion of the α-anomer (paper chromatogram, solvent B). The product crystallized readily and two recrystallizations from methanol gave the sugar, with m.p. 209–210° C and $[\alpha]_D$ 0° (2 minutes) → −5° (18 hours, constant value; *c*, 1.0, H_2O). Calculated for $C_{12}H_{22}O_{11}$: C, 42.1%; H, 6.5%. Found: C, 41.8%; H, 6.6%.

*(c) 1,2,3,4-Tetra-O-acetyl-αβ-*D*-mannose.*—Using the same proportions and procedure as with the glucose analogue amorphous 6-*O*-β-D-mannopyranosyl-D-mannose (77 mg) with $[\alpha]_D$ −16° (*c*, 1.0, H_2O) was prepared.

*4-O-β-*D*-Mannopyranosyl-*D*-erythritol from 6-O-β-*D*-Mannopyranosyl-*D*-glucose*

Crude mannopyranosyl glucose (163 mg) was dissolved in water (0.5 ml) plus acetic acid (10 ml) and 2.1 molar equivalents of 1% lead tetraacetate in acetic acid added (21). After 15 minutes, 2.0 molar equivalents of oxalic acid in acetic acid was added, the lead oxalate filtered off, and the solution evaporated to a crust (presumably containing di-*O*-formyl-4-*O*-β-D-mannopyranosyl-D-erythrose). The material was dissolved in water (5 ml) containing sodium borohydride (200 mg) and after an hour excess reagent was destroyed with acetic acid. The solution was treated with Amberlite IR-120, filtered, and the filtrate evaporated to a residue which was dissolved in methanol, and the methanol then distilled off, this procedure being repeated several times. The resulting 4-*O*-β-D-mannopyranosyl-D-erythritol was crystallized 3 times from ethanol to yield 20 mg of material with m.p. 160–162° C, $[\alpha]_D$ −38° (*c*, 1.0, H_2O) and an X-ray diffraction powder diagram indistinguishable from that of an authentic specimen. Calculated for $C_{10}H_{20}O_9$: C, 42.25%; H, 7.1%. Found: C, 42.4%; H, 7.2%.

ACKNOWLEDGMENTS

The authors thank Dr. R. A. Abramovitch for helpful discussion, and Mr. J. W. L. C. Christ, Mrs. S. F. Hector, and Mrs. J. Nuttall for valuable technical assistance. Microanalyses were performed by Mr. M. Mazurek. Infrared spectra and X-ray powder diagrams were recorded by Miss Inez Gaffney.

REFERENCES

1. P. A. J. GORIN and A. S. PERLIN. Can. J. Chem. **37**, 1930 (1959).
2. E. A. TALLEY, D. D. REYNOLDS, and W. L. EVANS. J. Am. Chem. Soc. **65**, 575 (1943).
3. H. S. ISBELL and H. L. FRUSH. J. Research Natl. Bur. Standards, **43**, 161 (1949).
4. E. PACSU. *In* Advances in Carbohydrate Chem. **1**, 77 (1945).
5. R. K. NESS, H. G. FLETCHER, Jr., and C. S. HUDSON. J. Am. Chem. Soc. **73**, 959 (1951).
6. R. U. LEMIEUX. *In* Advances in Carbohydrate Chem. **9**, 1 (1954).

7. L. T. HAYNES and F. H. NEWTH. *In* Advances in Carbohydrate Chem. **10**, 207 (1955).
8. M. L. WOLFROM, A. O. PITTET, and I. C. GILLAM. Proc. Natl. Acad. Sci. **47**, 700 (1961).
9. R. K. NESS, H. G. FLETCHER, Jr., and C. S. HUDSON. J. Am. Chem. Soc. **72**, 2200 (1950).
10. J. K. DALE. J. Am. Chem. Soc. **46**, 1046 (1924).
11. F. MICHEEL, A. KLEMER, and R. FLITSCH. Ber. **91**, 663 (1958).
12. M. L. WOLFROM, E. G. WALLACE, and E. A. METCALF. J. Am. Chem. Soc. **64**, 265 (1942).
13. P. A. J. GORIN. Unpublished.
14(*a*). R. U. LEMIEUX and G. HUBER. Can. J. Chem. **33**, 128 (1955).
(*b*). S. HAQ and W. J. WHELAN. J. Chem. Soc. 1342 (1958).
15. E. HARDEGGER and R. M. MONTAVON. Helv. Chim. Acta, **30**, 632 (1947).
16. P. A. J. GORIN. To be published.
17. H. S. ISBELL. J. Research Natl. Bur. Standards, **7**, 1115 (1931).
18. A. S. PERLIN. Unpublished.
19. W. N. HAWORTH, C. R. PORTER, and A. C. WAINE. Rec. trav. chim. **57**, 541 (1938).
20. G. M. TENER, R. S. WRIGHT, and H. G. KHORANA. J. Am. Chem. Soc. **79**, 441 (1957).
21. A. J. CHARLSON and A. S. PERLIN. Can. J. Chem. **34**, 1200 (1956).
22. B. BOOTHROYD, J. A. THORN, and R. H. HASKINS. Can. J. Biochem. and Physiol. **34**, 10 (1956).
23. P. A. J. GORIN, R. H. HASKINS, and J. F. T. SPENCER. Can. J. Biochem. and Physiol. **38**, 165 (1960).
24. A. STREITWIESER, Jr. Chem. Revs. **56**, 571 (1956).
25. H. R. GOLDSCHMID and A. S. PERLIN. Can. J. Chem. **39**, 2025(1961).
26. E. P. PAINTER. J. Am. Chem. Soc. **81**, 5696 (1959).
27. S. WINSTEIN, C. R. LINDEGREN, and L. I. INGRAHAM. J. Am. Chem. Soc. **75**, 155 (1953).
28. G. H. ALT and D. H. R. BARTON. J. Chem. Soc. 4284 (1954).
29. F. H. NEWTH and G. O. PHILLIPS. J. Chem. Soc. 2904 (1953).
30. G. L. MATTOK and G. O. PHILLIPS. J. Chem. Soc. 268 (1957).
31. G. L. MATTOK and G. O. PHILLIPS. J. Chem. Soc. 130 (1958).
32. W. E. DOERING and H. H. ZEISS. J. Am. Chem. Soc. **75**, 4733 (1953).
33. S. WINSTEIN and R. E. BUCKLES. J. Am. Chem. Soc. **65**, 613 (1943).
34. E. S. GOULD. Mechanism and structure in organic chemistry. Henry Holt and Co., New York. 1959. p. 254, and references cited.
35. S. J. ANGYAL and C. G. MACDONALD. J. Chem. Soc. 686 (1952).
36. E. L. ELIEL and C. PILLAR. J. Am. Chem. Soc. **77**, 3600 (1955).
36(*a*). L. HOUGH and J. E. PRIDDLE. J. Chem. Soc. 3178 (1961).
37. R. K. NESS, H. G. FLETCHER, JR., and C. S. HUDSON. J. Am. Chem. Soc. **73**, 296 (1951).
38. F. W. BARTH and T. E. TIMELL. Can. J. Chem. **36**, 1321 (1958).
39. A. J. CHARLSON and A. S. PERLIN. Can. J. Chem. **34**, 1804 (1956).
40. A. G. MCINNES, D. H. BALL, F. P. COOPER, and C. T. BISHOP. J. Chromatog. **1**, 556 (1958).
41. E. PACSU and S. M. TRISTER. J. Am. Chem. Soc. **63**, 925 (1941).
42. B. J. LUDWIG and E. C. PIECH. J. Am. Chem. Soc. **73**, 5779 (1951).
43. L. HOUGH, J. E. PRIDDLE, R. S. THEOBALD, G. R. BARKER, T. DOUGLAS, and J. W. SPOORS. Chem. & Ind. (London), 148 (1960).

Can. J. Chem. Downloaded from www.nrcresearchpress.com by 210.87.254.5 on 09/05/12
For personal use only.

Can. J. Chem. Downloaded from www.nrcresearchpress.com by 210.87.254.42 on 09/05/12
For personal use only.

PERFLUOROALKYL ARSENICALS

PART III. THE PREPARATION AND PROPERTIES OF SOME NEW TRIFLUOROMETHYL AND HEPTAFLUOROPROPYL ARSINES[1]

W. R. CULLEN

ABSTRACT

The reaction of heptafluoroiodopropane with the appropriate phenyl-iodo-arsine in the presence of mercury yields the compounds $C_3F_7As(C_6H_5)_2$, $(C_3F_7)_2AsC_6H_5$, and $C_3F_7(CH_3)AsC_6H_5$. However, the compounds $(CF_3)_2AsR$ (R = C_2H_5, C_4H_9) are obtained from the reaction of the compounds R_2AsI with mercury and trifluoroiodomethane. The ultraviolet spectra of the heptafluoropropyl-arsines are discussed.

DISCUSSION AND RESULTS

In previous papers (1, 2) the preparation of methyl- and phenyl-trifluoromethyl-arsines was described, the method of preparation being to react the appropriate iodo-arsine with trifluoroiodomethane in the presence of excess mercury: for example

$$(C_6H_5)_2AsI + Hg + CF_3I \rightarrow (C_6H_5)_2AsCF_3 + HgI_2.$$

Alkyl iodides react similarly, though in this case the reaction goes further and arsonium derivatives of triiodomercury(II) are obtained (3): for example

$$(C_6H_5)_2AsI + Hg + 2CH_3I \rightarrow (C_6H_5)_2As(CH_3)_2.HgI_3.$$

In order to investigate the generality of these reactions, the preparation of ethyl- and butyl-trifluoromethyl-arsines and phenyl-heptafluoropropyl-arsines was undertaken.

Diethyltrifluoromethylarsine, b.p. 111°, is obtained by the reaction of diethyliodoarsine with trifluoroiodomethane in the presence of mercury; however, the bulk of the product from this reaction is ethylbistrifluoromethylarsine, b.p. 77°. Ethyldiiodoarsine does not react with trifluoroiodomethane under the same conditions, so this substance as an impurity could not have been the source of the ethylbistrifluoromethylarsine. Similarly, when di-*n*-butyliodoarsine is reacted with trifluoroiodomethane and mercury, the only product isolated is *n*-butylbistrifluoromethylarsine, b.p. 118°, though in this case the same compound is produced by the corresponding reaction using *n*-butyldiiodoarsine. A reasonable explanation of these anomalous results is that an exchange reaction takes place between the initially formed dialkyltrifluoromethylarsine and trifluoroiodomethane, producing the alkylbistrifluoromethylarsine; reactions of this sort are now being studied. The reactions of heptafluoroiodopropane with phenyl-iodo-arsines in the presence of mercury are not complicated by side reactions, and heptafluoropropyldiphenylarsine (b.p. 99–102° (10^{-3} mm)), bisheptafluoropropylphenylarsine (b.p. 128° (68 mm)), and heptafluoropropylmethylphenylarsine (b.p. 123° (69 mm)) can be easily isolated.

All the new arsines are colorless mobile liquids of faint odor; they are stable to oxygen and moisture at ordinary temperatures. Solvolysis studies have been made on these compounds and the results will be reported later. The ultraviolet spectra of the heptafluoropropyl-phenyl-arsines are very similar to those of the trifluoromethyl-phenyl-arsines (4). The wavelengths and extinction coefficients of maximum absorption of these compounds are given in Table I.

[1]*Manuscript received July 10, 1961.*
Contribution from the Chemistry Department, University of British Columbia, Vancouver, B.C.

TABLE I

Wavelengths and molar extinction coefficients of the band maxima

Compound	Methanol λ_{max} (Å)	Methanol $\epsilon_{max} \times 10^{-3}$	Cyclohexane, λ_{max}	Compound	Methanol, λ_{max} (Å)
$(C_6H_5)_2AsC_3F_7$	2708	1.18	2710	$(C_6H_5)_2AsCF_3$	2720
	2637	1.72	2640		2690
	2568	1.98	2570		2575
	2355[i]	8.35	2360[i]		2368
	2225[i]*	12.98	2355[i]*		2240
$C_6H_5As(C_3F_7)_2$	2725	0.84	2725	$C_6H_5As(CF_3)_2$	2718
	2650	1.52	2650		2650
	2590	0.79	2589		2587
	2528	0.55	2528		2530
	2238	9.88	2238		2238
$C_6H_5As(CH_3)(C_3F_7)$	2702	0.44	2705	$C_6H_5As(CH_3)CF_3$	2700
	2634	0.58	2635		2630
	2568	0.52	2571		2565[i]
	2275[i]*	5.69	2275		2210
	2175[i]	7.36	2175		

NOTE: i = estimated from point of inflection.
*Band is actually very weak: the recorded intensity is mainly due to contributions from the very strong short-wavelength absorption and from the other bands recorded above.

All the compounds show a weak series of bands in the region 2520–2730 Å, and by analogy with the interpretation of the spectra of the phenyl-trifluoromethyl-arsines (4) these transitions can be characterized as π–π^* absorptions involving electrons localized in the phenyl groups. The remaining bands in the spectra in the region 2100–2500 Å are much stronger. The bands in the heptafluoropropyl compounds correspond in position number and intensity with those of the trifluoromethyl compounds except for the weak band at ca. 2275 Å in the spectrum of heptafluoropropylmethylphenylarsine. The transitions in this region of the trifluoromethyl compounds have been described as involving electron transfer from the non-bonding electrons on the arsenic to the π orbitals of the phenyl groups (4), and again this description of the transitions can probably be carried over to the corresponding bands of the heptafluoropropyl compounds, even though these bands do not shift toward the blue or only shift a little when the solvent is changed from cyclohexane to the more-polar methanol.

The occurrence of two higher-intensity bands in the spectrum of diphenyltrifluoromethylarsine has been interpreted in terms of the steric effect of the CF_3 group being such as to destroy the equivalence of the two phenyl groups with respect to the arsenic lone pair. The intensity of the transition to the interacting phenyl group (the lower-energy transition since interaction would stabilize the phenyl group with a resulting lowering of orbital energies) was much higher than the intensity of the transition to the non-interacting ring. Models such as were used previously (4) show that the more bulky C_3F_7 group has the same effect in the compound heptafluoropropyldiphenylarsine, so the appearance of two bands in the spectrum of this compound, the one of lower energy being the more intense, is not unexpected. Models also indicate that the phenyl group could interact with the C_3F_7 group in the compound heptafluoropropylmethylphenylarsine and almost certainly interacts in the compound bisheptafluoropropylphenylarsine. However, such interaction alone can not account for the presence of two bands in the spectrum of the former compound. The charge transfer band in triphenylarsine occurs

Can. J. Chem. Downloaded from www.nrcresearchpress.com by 210.87.254.42 on 09/05/12
For personal use only.

at ca. 40,300 cm^{-1} (4) so the effect of substituting a C_3F_7 group for a phenyl group is to increase the transition energy by ca. 4500 cm^{-1} (using the energy of low-intensity transition to the non-interacting phenyl group of the compound heptafluoropropyldiphenylarsine). The charge transfer band in methyldiphenylarsine occurs at ca. 41,600 cm^{-1} and the effect of substituting a C_3F_7 group for a phenyl group is to increase the energy of the transition by ca. 4300 cm^{-1} if the 2175 Å band in heptafluoropropylmethylphenylarsine is chosen as the charge transfer band, or by ca. 2400 cm^{-1} if the 2275 Å band is the charge transfer band. Thus it is likely that it is the 2175 Å band which is the charge transfer band. The second transition at ca. 2275 Å is very weak. This could arise from a shift or split of the benzene transition which normally occurs at ca. 2000 Å, but its intensity seems to be too low. A more likely explanation is that it is due to an impurity.

The charge transfer bands in the C_3F_7 compounds occur at higher or equal energies when compared with the corresponding bands in the CF_3 compounds; a result which could indicate that in the first order the C_3F_7 group has a greater electron-withdrawing effect on the arsenic lone pair than does the CF_3 group.

The infrared spectra of these new arsines are recorded in the experimental section. It is hoped to discuss these in detail at a later date when more correlations can be made.

EXPERIMENTAL

Apparatus and Technique

Conventional vacuum techniques were used for the manipulation of volatile reactants and products out of contact with moisture and oxygen. Reactions were carried out in sealed Pyrex tubes in the absence of air and light. Infrared spectra were measured on a Perkin–Elmer Model 21 double-beam instrument with rock-salt optics. Ultraviolet spectra were recorded on the Cary Model 14 spectrophotometer. The solvents were spectroscopic grade methyl alcohol or cyclohexane, and the lower wavelength limit of the instrument was ca. 2100 Å as determined by solvent absorption. Gas-phase molecular weights were determined by Regnault's method. Phenyl-iodo-arsines were prepared by the methods previously described (2).

Reaction of Ethyldiiodoarsine with Trifluoroiodomethane in the Presence of Mercury

Ethyldiiodoarsine was prepared from dichloroethylarsine (5) by reacting the chloroarsine with sodium iodide in acetone (6). The product had a boiling point of 126° (11 mm) (lit. value, 126° (11 mm) (6)). The iodo-arsine (18.2 g), trifluoroiodomethane (57.9 g), and mercury (225 g) were shaken at 20° for 11 days. Trap-to-trap distillation of the volatile contents of the tube showed that only one fraction, trifluoroiodomethane (57.6 g), was present.

Reaction of Diethyliodoarsine with Trifluoroiodomethane in the Presence of Mercury

Diethyliodoarsine was prepared from ethyldiiodoarsine as described by Wigren (7). The diiodoarsine in this case was prepared by the procedure used by Burrows and Turner for the preparation of diiodomethylarsine (8). Crude diethyliodoarsine (35 g), trifluoroiodomethane (76 g), and mercury (250 g) were shaken at 20° for 6 days. The unreacted trifluoroiodomethane was separated from the other volatile contents of the tube by trap-to-trap distillation. The less-volatile fraction (14.5 g) was distilled in a nitrogen atmosphere at 760 mm. The bulk of the material boiled at 77°, but a further small fraction boiling at 111° was obtained. Vapor-phase chromatography was used to obtain samples of these two fractions for analysis. The fraction boiling at 77° was identified as *ethylbistrifluoromethylarsine*. Anal. Hydrolysis with 10% aqueous sodium hydroxide

Can. J. Chem. Downloaded from www.nrcresearchpress.com by 210.87.254.42 on 09/05/12
For personal use only.

at 100° for 2 days gave fluoroform corresponding to a CF_3 content of 56.2%. The vapor phase molecular weight was 241. Calc. for $C_4H_5AsF_6$: CF_3, 57%; mol. wt., 242. The fraction boiling at 111° was identified as *diethyltrifluoromethylarsine*. Anal. Calc. for $C_5H_{10}AsF_3$: C, 29.7; H, 5.0; As, 37.1; F, 28.2%; mol. wt., 202. Found: C, 29.9; H, 5.1; As, 37.3; F, 27.9%; mol. wt., 230. The infrared spectra of these compounds showed the following absorption bands: $(C_2H_5)_2AsCF_3$ (liquid film): 2980 (s), 2940 (s), 2885 (m), 2350 (w), 2200 (w), 1466 (s), 1425 (w), 1382 (m), 1243 (m)(sh), 1223 (m), 1138 (vs), 1093 (vs), 1038 (m), 1025 (m), 978 (m), 730 (m), 721 (s); $C_2H_5As(CF_3)_2$ (vapor phase): 2980 (s), 2940 (m), 2888 (m), 2250 (w), 2220 (w), 1854 (w), 1469 (m), 1427 (w), 1394 (w), 1245 (s), 1176 (vs), 1157 (vs), 1124 (vs), 1105 (vs), 1056 (m), 1032 (m), 994 (m), 729 (s).

Reaction of n-Butyldiiodoarsine with Trifluoroiodomethane in the Presence of Mercury

The diiodo-arsine was prepared by reduction of *n*-butylarsonic acid using the procedure described by Burrows and Turner for the preparation of diiodomethylarsine (9). The crude arsine (21 g), trifluoroiodomethane (55.1 g), and mercury (210 g) were shaken at 20° for 26 days. Trap-to-trap distillation of the volatile contents of the tube gave unreacted trifluoroiodomethane (40.3 g) and a colorless less-volatile fraction (10.4 g). The latter fraction was distilled in a nitrogen atmosphere at 760 mm: all distilled in the range 110–118°. A middle cut was taken, and this sample was again distilled. The boiling point was 118°, and the sample was identified as *n-butylbistrifluoromethylarsine*. Anal. Calc. for $C_6H_9AsF_6$: C, 26.7; H, 3.34; As, 27.8; F. 42.2%; mol. wt., 270. Found: C, 27.0; H, 3.48; As, 27.6; F, 42.5%; mol. wt., 290. The infrared spectrum showed the following absorption bands (liquid film): 2958 (s), 2925 (s), 2868 (m), 2210 (w), 1470 (m), 1422 (m), 1386 (m), 1347 (w), 1298 (w), 1265 (m), 1204 (s), 1168 (vs), 1132 (vs), 1115 (vs), 1093 (vs), 996 (vw), 967 (vw), 892 (m), 774 (w), 730 (s), 715 (m)(sh); vapor phase (omitting medium and weak bands): 2970 (s), 2935 (s), 1206 (s)(sh), 1179 (vs), 1156 (vs), 1126 (vs), 1107 (vs), (1081, 1076, 1069) (vs), (750, 744, 731) (s).

Reaction of Di-n-butyliodoarsine with Trifluoroiodomethane in the Presence of Mercury

Crude *n*-butyldiiodoarsine, prepared as described above, was used to prepare di-*n*-butyliodoarsine using the method described by Wigren for the preparation of diethyliodoarsine from ethyldiiodoarsine (7). The crude product was dried over calcium chloride and then distilled at 10^{-3} mm. The main fraction boiled at 78–82°, and analysis showed it to be mainly di-*n*-butyliodoarsine. Anal. Calc. for $C_8H_{18}AsI$: C, 30.4; H, 5.7; I, 40.2%; mol. wt., 316. Found: C, 27.9; H, 5.3; I. 42.3%; mol. wt., 285. The impure iodo-arsine (10.6 g), trifluoroiodomethane (65.2 g), and mercury (210 g) were shaken at 20° for 20 days. The unreacted trifluoroiodomethane was separated from a less-volatile fraction by trap-to-trap distillation. The less-volatile fraction (13 g) was distilled at 92 mm in a nitrogen atmosphere, and all boiled at 59°. Its infrared spectrum was identical with that of *n*-butylbistrifluoromethylarsine. The fraction, when distilled at 760 mm (in nitrogen), boiled at 116–120°.

Reaction of Iododiphenylarsine with Heptafluoroiodopropane in the Presence of Mercury

The arsine (12.6 g), heptafluoroiodopropane (82.5 g), and mercury (210 g) were shaken at 20° for 3 months. Trap-to-trap distillation isolated only heptafluoroiodopropane (71.8 g). The contents of the reaction tube were extracted with benzene, which was then removed by distillation at 760 mm in a nitrogen atmosphere, leaving a slightly colored involatile liquid (10.6 g). This fraction was distilled at 10^{-3} mm, and all the material boiled in the range 99–102°. The liquid was redistilled under the same conditions, and a

Can. J. Chem. Downloaded from www.nrcresearchpress.com by 210.87.254.42 on 09/05/12
For personal use only.

colorless middle fraction of b.p. 102° was collected, which was identified as *heptafluoropropyldiphenylarsine* (73% yield). Anal. Calc. for $C_{15}H_{10}AsF_7$: C, 45.2; H, 2.51; As, 18.8; F, 33.4%; mol. wt., 398. Found: C, 45.2; H, 2.48; As, 19.0; F, 33.2%; mol. wt., 387. The infrared spectrum showed the following absorption bands (liquid film): 3060 (m), 1976 (vw), 1955 (vw), 1895 (vw), 1877 (vw), 1806 (vw), 1755 (vw), 1650 (vw), 1580 (w), 1485 (m), 1440 (s), 1383 (vw), 1338 (s), 1265 (s), 1227 (vs), 1208 (vs), 1184 (vs), 1174 (vs), 1110 (vs), 1081 (s), 1074 (s), 1034 (s), 1024 (m), 1000 (m), 988 (vw), 968 (vw), 912 (vw), 895 (m), 824 (s), 750 (s), 738 (vs), 732 (vs), 694 (s), 668 (s).

Reaction of Diiodophenylarsine with Heptafluoroiodopropane in the Presence of Mercury

The arsine (22 g), heptafluoroiodopropane (71.8 g), and mercury were shaken at 20° for 2 months. The contents of the tube were worked up as described in the preceding experiment to give heptafluoroiodopropane (59.8 g) and a slightly colored involatile liquid (5.1 g) which boiled in the range 120–124° (63 mm, nitrogen atmosphere). This fraction was redistilled to give a colorless sample of *bisheptafluoropropylphenylarsine*, b.p. 128° (68 mm) (19% yield). Anal. Calc. for $C_{12}H_5AsF_{14}$: C, 29.4; H, 1.02; As, 15.2; F, 54.2%, mol. wt., 490. Found: C, 29.7; H, 1.09; As, 15.6; F, 53.6%; mol. wt., 460. The infrared spectrum showed the following absorption bands (liquid film): 3060 (w), 1890 (vw), 1830 (vw), 1809 (vw), 1756 (vw), 1655 (vw), 1580 (vw), 1485 (m), 1441 (m), 1336 (s), 1274 (s), 1230 (vs), 1210 (vs), 1185 (vs), 1129 (vs), 1117 (vs), 1078 (s), 9040 (s), 1025 (m), 1000 (m), 970 (vw), 935 (vw), 917 (vw), 893 (m), 820 (s), 750 (s), 740 (vs), 733 (vs), 694 (s), 669 (s).

Reaction of Iodomethylphenylarsine with Heptafluoroiodopropane in the Presence of Mercury

The arsine (12 g), heptafluoroiodopropane (70 g), and mercury (215 g) were shaken at 20° for 1 month. Trap-to-trap distillation gave heptafluoroiodopropane (52 g) and a colorless involatile liquid (6.8 g). The latter fraction, when distilled in a nitrogen atmosphere, boiled at 123° (69 mm); it was identified as *heptafluoropropylmethylphenylarsine* (49% yield). Anal. Calc. for $C_{10}H_8AsF_7$: C, 35.7; H, 2.38; As, 22.3; F, 39.6%; mol. wt., 336. Found: C, 35.6; H, 2.47; As, 22.1; F, 39.5%; mol. wt., 322. The infrared spectrum showed the following absorption bands (liquid film): 3060 (w), 2995 (w), 2900 (w), 2400 (vw), 2300 (vw), 2130 (vw), 1980 (vw), 1952 (vw), 1895 (vw), 1875 (vw), 1802 (vw), 1755 (vw), 1645 (vw), 1580 (w), 1485 (m), 1438 (m), 1418 (m), 1338 (s), 1306 (m), 1268 (s), 1224 (vs), 1206 (vs), 1171 (s), 1110 (s), 1080 (s), 1035 (s), 1000 (m), 900 (m), 854 (s), 822 (s), 749 (s), 740 (s), 733 (s), 694 (s), 668 (s).

ACKNOWLEDGMENTS

The author wishes to acknowledge financial assistance from the National Research Council of Canada. Microanalyses were carried out by Dr. Alfred Bernhardt.

REFERENCES

1. W. R. CULLEN. Can. J. Chem. **38**, 439 (1960).
2. W. R. CULLEN. Can. J. Chem. **38**, 445 (1960).
3. M. M. BAIG and W. R. CULLEN. Can. J. Chem. **39**, 420 (1961).
4. W. R. CULLEN and R. M. HOCHSTRASSER. J. Mol. Spectroscopy, **5**, 118 (1960).
5. C. S. HAMILTON *et al.* J. Am. Chem. Soc. **69**, 927 (1947).
6. W. STEINKOPF and G. SCHWEN. Ber. **54**, 1437 (1921).
7. N. I. WIGREN. Ann. **437**, 285 (1924).
8. G. J. BURROWS and E. E. TURNER. J. Chem. Soc. 426 (1921).
9. G. J. BURROWS and E. E. TURNER. J. Chem. Soc. 1373 (1920).

Can. J. Chem. Downloaded from www.nrcresearchpress.com by 210.87.254.42 on 09/05/12
For personal use only.

Can. J. Chem. Downloaded from www.nrcresearchpress.com by 210.87.254.42 on 09/05/12
For personal use only.

REVERSIBLE N,O-HALOACYL SHIFT IN SERINE DERIVATIVES WITH ANTITUMOR ACTIVITY[1]

I. LEVI, J. W. R. WEED, G. LAFLAMME, AND A. E. KOLLER

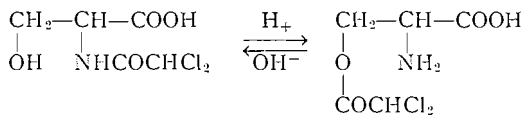
ABSTRACT

Large doses of N-dichloroacetyl-DL-serine sodium salt were required to cause regression of Sarcoma-37 in mice. About 56% of the unchanged compound was recovered from the urine. These observations suggest that the antitumor activity may reside in a metabolic product of the N-dichloracetyl serine. It is postulated that the active compound is the corresponding O-dichloroacetyl-DL-serine formed from the N-acyl compound by an in vivo enzymatically controlled shift which takes place via the hydroxyoxazolidine and (or) the oxazoline rings. O-Dichloroacetyl-DL-serine hydrochloride was prepared by treating a suspension of N-dichloroacetyl-DL-serine in anhydrous ether with gaseous hydrogen chloride. The free base, O-dichloroacetyl-DL-serine, is an extremely labile compound and reverts to the N-compound in neutral aqueous solution at room temperature. The hydrochloride salt, however, is stable, in which form it was isolated and characterized. The same compound was prepared from serine and dichloroacetic anhydride in dichloroacetic acid. O-Dichloroacetyl-DL-serine hydrochloride displays an antitumor effect against Sarcoma-37 and Sarcoma-180 in mice. The work has been extended to the monochloro- and trichloro-acetyl derivatives of serine.

INTRODUCTION

It was reported recently (1) that the sodium salt of N-dichloroacetyl-DL-serine (2) depresses the growth of Sarcoma-37 in mice, causing in some animals complete regression of the tumors. Most of the presently known agents which are effective against animal tumors are usually administered in relatively small doses such as milligrams or even fractions of a milligram per kilogram of body weight. The above compound, however, had to be administered in doses of 1 g per kilogram of body weight in order to be effective against the tumor. This considerable non-toxic dose is largely excreted by the kidney as unchanged drug, since approximately 56% of the pure crystalline product was isolated from the urine of cats as well as of humans (3). No metabolic or hydrolytic products were identified.

We would like to suggest, therefore, that the active antitumor agent was not the administered N-dichloroacetyl derivative itself, but rather a metabolic product of this compound. One of the specific characteristics of acyl derivatives of hydroxy amino acids having the hydroxyl and the amino groups in vicinal position is the ability of the acyl residue to migrate reversibly between the nitrogen and the oxygen. It is therefore possible that the compound could readily change into the heretofore unreported O-dichloroacetyl-DL-serine isomer and that, in vivo, both forms of the compound exist in equilibrium



I II

FIG. 1.

(Fig. 1). Such a concept would explain why large doses of the N-derivative are required to elicit an antitumor effect, since the equilibrium favors the stabilized, less active

[1]*Manuscript received August 15, 1961.*
Contribution from Charles E. Frosst & Co., Montreal, Que.

N-dichloroacetyl-DL-serine. We therefore synthesized O-dichloroacetyl-DL-serine hydrochloride as well as its methyl ester, and preliminary experiments with the former compound do indeed indicate that it is active against Sarcoma-37 in mice at approximately 1/40th the dose of the N-compound and against Sarcoma-180 at approximately 1/20th the dose.

Similar reversible acyl migrations have been studied extensively in vitro over a number of years, in a large variety of compounds, and this shift is now well documented in the chemical literature for the N ⇄ O, N ⇄ S, and O ⇄ O systems. For example, acyl migrations for the N ⇄ O system have been reported for orthoaminophenols (4–12), alkylaminoethanols (13–23), adrenaline (24), noradrenaline (25, 26), ephedrine (26–30), phenylserine (31), aminophenylpropanediols including chloramphenicol (32–35), 2-aminocyclohexanol (36, 37), 2-aminocyclopentanol (38), and aminosugars (39, 40). Similar acyl shifts from oxygen to oxygen have been observed in sugars (41, 42) and glycerides (43–47), and more recently in the N ⇄ S system of cysteine (48) and glutathione (49, 50).

Emil Fischer (51) first proposed a mechanism to explain such migrations from oxygen to oxygen in the case of glycerides of fatty acids. He postulated an unstable five-membered hydroxy-orthoester as an intermediate when an acyl group migrated from one hydroxyl group to another in a 1,2-diol, as shown in Fig. 2. This hypothesis received its first confirmatory support from Hibbert and co-workers (52, 53), who isolated 2-hydroxy-2′-trichloromethyl-1,3-dioxolane, which is analogous to the cyclic intermediate IV postulated by Fischer.

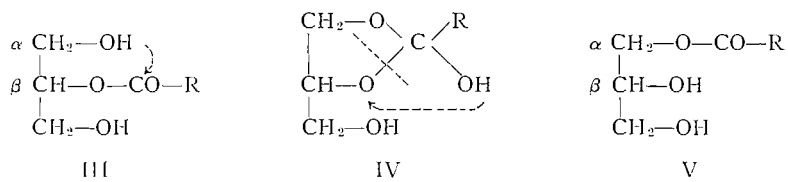


FIG. 2. Acyl migration in glycerides.

Today this mechanism involving transient cyclic intermediates is widely accepted because it satisfactorily accounts for a variety of reversible acyl shifts. Various workers have postulated ortho esters in the case of glycerides (47) and sugars (42), oxazoline or hydroxyoxazolidine rings in the N ⇄ O shifts (20, 28, 38, 39), and the corresponding thiazoline and hydroxythiazolidine rings in the case of N ⇄ S shifts (48). In some cases these cyclic intermediates were actually detected or isolated (20, 48).

More recently Doerschuk (44) carried out the rearrangement of 2-monopalmitin glyceride to the 1-monopalmitin product in the presence of glycerol-1-C^{14} and showed conclusively that the rearrangement mechanism is entirely intramolecular, thus eliminating the possibility of hydrolysis and re-esterification. van Lohuizen and Verkade (45) found that α- or β-monoglycerides in ethanolic hydrogen chloride mutually rearranged to an equilibrium mixture, while Raiford and Lankelma (8) showed a similar equilibrium in the case of acylated orthoaminophenols. It is also established for nearly all the above classes of compounds that the equilibrium distribution of the two different forms in which the acylated molecules can exist in solution depends on pH. Migration takes place from N to O when N-acyl compounds are treated with anhydrous hydrogen chloride with formation of the O-acyl-N-hydrochloride derivatives which in alkaline medium revert to the original N-acyl forms (8, 18, 20, 28, 31, 32, 35, 36, 38, 50, 54). In every case so far studied the N-acyl derivatives were much more stable than either the corresponding

Can. J. Chem. Downloaded from www.nrcresearchpress.com by 210.87.254.42 on 09/05/12
For personal use only.

O or S derivatives and indeed the latter always easily reverted to the more stable N-derivatives.

Since most chemical reactions which are catalyzed by enzymes are also susceptible to catalysis by simpler organic and inorganic agents, we postulate as a working hypothesis that the reversible acyl shifts in amino acid derivatives such as serine and cysteine, which, in vitro, are dependent on changes in pH, can be similarly mediated in vivo via the hydroxyoxazolidine (or less likely, the oxazoline) ring by acyl migratases resulting in an equilibrium mixture of the two tautomeric forms (Fig. 3).

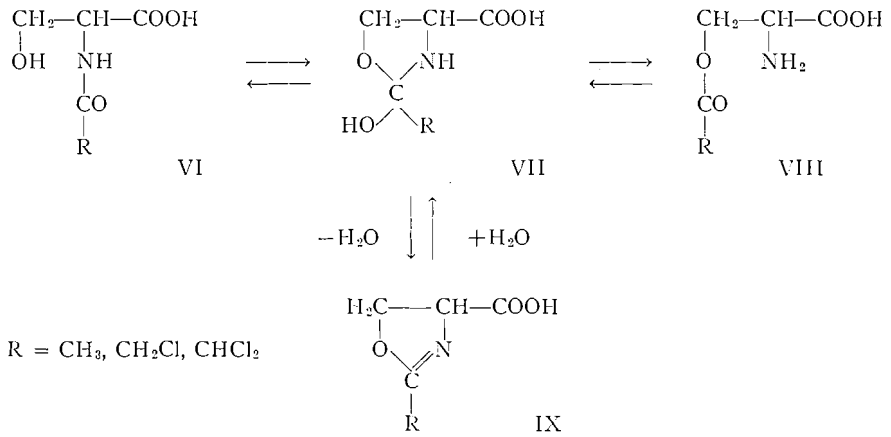


FIG. 3. Reversible N ⇄ O shifts in amino acids.

A corresponding biological shift from O to O, catalyzed by an enzyme, was reported recently by Uziel and Hanahan (55). They described a migratase, which catalyzes the β to α migration of the fatty acyl group on a β-lysolecithin. This enzyme, found in the extracts of *Penicillium notatum* and in commercial pancreatin, is nonhydrolytic in nature. The same migration was effected in the absence of the enzyme by treating the β-lysolecithin with dilute hydrochloric acid. Here again the intermediate formation of an ortho acid was favored to explain this enzymatically controlled intramolecular transesterification. A similar enzyme capable of catalyzing the intramolecular acyl migration in the N ⇄ O or N ⇄ S systems has not yet been described.

The relationship between this type of shift and biological activity has already been observed in the amino acid derivative azaserine (O-diazoacetyl-DL-serine). Here it was shown by Fusari and co-workers (56) that azaserine, in aqueous solution treated with barium hydroxide solution, lost its antibiotic activity as measured against *Kloechera brevis*, and by correlation, its antitumor activity (57), while the diazoacyl group underwent a simultaneous shift from O to N. The resulting barium salt of N-diazoacetyl serine which was isolated possessed little or no microbiological activity in vitro.

DISCUSSION OF RESULTS

It is known that strong acids act as catalysts in the esterification of hydroxy groups with acetic anhydride (58). Acylation of primary amines by acetic anhydride, however, is greatly inhibited when they are present as salts of strong acids (59–61). These facts were utilized in the preparation of O-dichloroacetyl-DL-serine by treating DL-serine with a mixture of dichloroacetic acid and dichloroacetic anhydride. The compound is extremely

Can. J. Chem. Downloaded from www.nrcresearchpress.com by 210.87.254.42 on 09/05/12
For personal use only.

labile, tending to change to the more stable N-dichloroacetyl-DL-serine. The hydrogen chloride salt of the O-derivative, however, is sufficiently stable to allow its isolation and storage at room temperature. All attempts to obtain the O-dichloroacetyl base from the crystalline hydrochloride, even under the mildest conditions, failed. For example, neutralization of the hydrogen chloride moiety with an equimolar amount of sodium bicarbonate, at room temperature, resulted in a shift of the dichloroacetyl group from O to N. Similarly, a methanolic solution of O-dichloroacetyl-DL-serine methyl ester hydrochloride (which was prepared by the above procedure from DL-serine methyl ester), upon treatment with one equivalent of triethylamine at room temperature, also underwent this shift to N-dichloroacetyl-DL-serine methyl ester.

The reverse shift of the dichloroacetyl group from N to O was accomplished in the case of N-dichloroacetyl-DL-serine by treating a suspension of the compound in anhydrous ether with a stream of hydrogen chloride gas over a long period of time. Anhydrous conditions are essential, otherwise complete hydrolysis takes place, yielding DL-serine hydrochloride and dichloroacetic acid. When this shift was attempted with the methyl ester of N-dichloroacetyl-DL-serine in anhydrous ether, the unchanged ester was recovered quantitatively, indicating that this compound does not undergo the N → O acyl shift as readily as does the non-esterified compound. Using anhydrous methanol instead of anhydrous ether an intermolecular shift from the N of the amino acid to the O of the alcohol took place rather than the expected intramolecular shift, with the result that serine methyl ester hydrochloride and methyl dichloroacetate were formed. These experiments are summarized in Fig. 4. Although O-dichloroacetyl-DL-serine is a labile compound, it is nevertheless sufficiently stable under the right conditions to be capable of more than transitory existence.

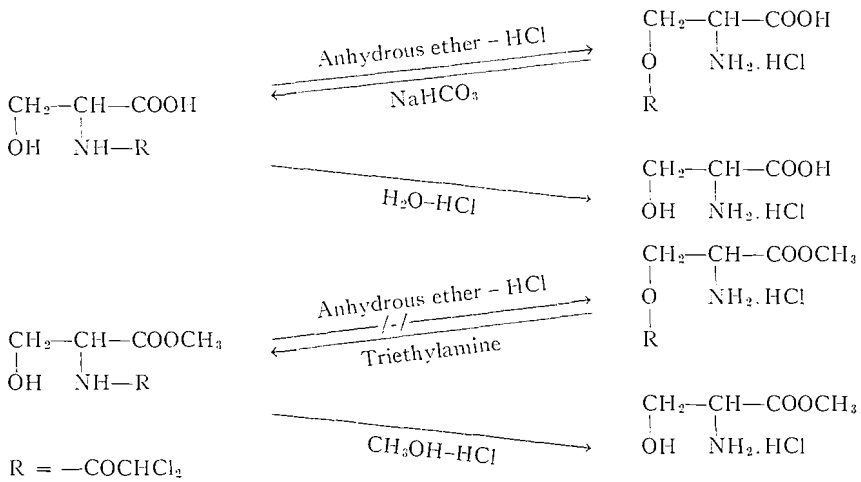


FIG. 4. N ⇄ O dichloroacyl shifts in serine.

Since we were able to show that the postulated reversible N ⇄ O shift of a dihaloacyl group could be effected in vitro, we extended this investigation to the monochloro- and trichloro-acyl compounds of serine. O-Monochloroacetyl-DL-serine was synthesized according to the procedure developed by Sakami and Toennies for the N-acyl derivative (61), and N-monochloroacetyl-DL-serine according to Fischer and Roesner (62). The complete reverse shift of the monochloroacyl group from N to O and O to N was carried

Can. J. Chem. Downloaded from www.nrcresearchpress.com by 210.87.254.42 on 09/05/12
For personal use only.

Can. J. Chem. Downloaded from www.nrcresearchpress.com by 210.87.254.42 on 09/05/12
For personal use only.

out as for the dichloroacyl compounds. However, in this case O-monochloroacetyl-DL-serine was sufficiently stable to be isolated as the free base as well as the hydrochloride. After this work was completed Benoiton (63) reported the same reversible shift for N-monochloroacetylserine.

All attempts to date to prepare the O-trichloroacetyl derivative have failed. The first synthetic procedure employed was essentially that used for the preparation of O-dichloroacetyl-DL-serine hydrochloride, using benzene as a solvent due to the crystalline state of trichloroacetic anhydride. This yielded instead of the expected O-trichloroacetyl-DL-serine hydrochloride the hitherto unreported O,N-bis(trichloroacetyl)-DL-serine compound. Titration of this compound with alkali indicated an equivalent weight of 199. This agrees with the calculated equivalent weight of 198 based on the finding that the O,N-bis compound is hydrolyzed during the neutralization by the alkali to N-trichloroacetyl-DL-serine (which was isolated and identified) and trichloroacetic acid. The compound gave a negative ninhydrin test in aqueous solution. Its infrared absorption curve indicated the presence of three different carbonyl groups and elemental analyses agreed with the theoretical values for O,N-bis(trichloroacetyl)-DL-serine.

N-Trichloroacetyl-DL-serine was prepared according to the usual Schotten-Baumann procedure (2). An attempt to shift the trichloroacetyl group from N to O under the same anhydrous conditions which converted the N-monochloro- and N-dichloro-acetyl derivatives to the corresponding O-compounds also failed, the unchanged starting material being recovered quantitatively. It is interesting to note that the stability of the amide bond was such in this case that it was not necessary to observe the stringent anhydrous conditions required for the N $\rightarrow$ O dichloroacetyl shift in order to prevent hydrolysis to serine hydrochloride. Ether saturated with water gave the same result, i.e., there was no hydrolysis of the N-trichloroacetyl group and no N $\rightarrow$ O shift took place. This unexpected stability to acid of the N-trichloroacetyl group was also observed in the failure of aqueous hydrochloric acid to hydrolyze the latter compound.

This stability was again evident when the O,N-bis(trichloroacetyl) compound was treated with acid in an attempt to prepare O-trichloroacetyl-DL-serine by hydrolysis of the N-acyl group. Contrary to expectations, the O-trichloroacetyl group was the more labile one under these conditions and again N-trichloroacetyl-DL-serine was obtained. This instability of the O-trichloroacetyl group in an acidic medium accounts for the failure, to date, to isolate O-trichloroacetyl-DL-serine.

It therefore appears that in the O-haloacyl series, the stability of the ester linkage decreases as the number of halogen atoms increases. In the N-haloacyl series, however, the opposite situation seems to exist, namely, the stability of the amide bond increases as the number of halogen atoms increases. These effects are no doubt the result of the inductive displacement of the electrons in the direction of the strong electron-attracting chlorine atoms; the greater the number of the latter the more stable the amide bond and the weaker the ester linkage.

These various haloacyl derivatives of serine are presently being evaluated for their antitumor activity in the mouse and rat to determine whether a relationship exists between such activity and the ease of interconversion of the three pairs of isomers.

EXPERIMENTAL

Infrared absorption spectra were determined with a Beckman IR-5 spectrophotometer equipped with a sodium chloride prism, using potassium bromide pellets. Melting points obtained with a Fisher–Johns apparatus, boiling points, and temperature readings are uncorrected and are in degrees Centigrade.

O-Dichloroacetyl-DL-*serine Hydrochloride*

DL-Serine (105 g, 1.0 mole) was dissolved in redistilled dichloroacetic acid (500 ml) in a 3-liter, three-necked, round-bottomed flask fitted with a dropping funnel, thermometer, and calcium chloride drying tube. The clear solution was cooled in an ice-water bath and stirred continuously with a magnetic stirrer. A slow stream of dichloroacetic anhydride (312 g, 1.3 mole) was added during $2\frac{1}{2}$ hours at such a rate that the temperature of the reaction mixture did not exceed 32–33°. The flask was allowed to stand overnight at room temperature, and the product was then converted to the hydrochloride salt by passing a slow stream of hydrogen chloride gas into the solution for 1 hour. The excess hydrogen chloride was removed under reduced pressure, anhydrous benzene (1250 ml) was added, and the flask was refrigerated. The product crystallized as a fine white granular material which was removed by filtration, washed with anhydrous benzene, followed by petroleum–ether (30–60°), and dried at 45° in a vacuum oven. Weight 85.0 g, m.p. 115–120°. A second crop of product (5.4 g) was recovered from the filtrate, total yield 35.8%. The product was recrystallized from anhydrous acetone–ether, yielding 29.4% pure crystalline O-dichloroacetyl-DL-serine hydrochloride, m.p. 125–126°, which was soluble in water, ethanol, acetone, tetrahydrofuran, and dioxane, and insoluble in ether, chloroform, and ethylene dichloride. It gave a positive ninhydrin test. Anal. Calc. for $C_5H_8Cl_3NO_4$: C, 23.78; H, 3.19; N, 5.55. Found: C, 23.88; H, 3.29; N, 5.61.

This product was also prepared by saturating a suspension of 3.0 g (0.0286 mole) of DL-serine in 100 ml of dichloroacetic acid with hydrogen chloride gas at 0°. The resulting clear solution was kept at room temperature for 48 hours. The addition of anhydrous ether (100 ml) caused a rapid crystallization of crude product as white crystals. Weight 5.4 g (74.9% yield). The infrared absorption curve of this product was identical with that of the O-dichloroacetyl-DL-serine hydrochloride prepared above.

O-Dichloroacetyl-DL-*serine Hydrochloride from N-Dichloroacetyl*-DL-*serine: N → O Dichloroacyl Shift*

Finely pulverized N-dichloroacetyl-DL-serine (2.0 g) (2) was suspended in 100 ml anhydrous ether in a 200-ml round-bottomed flask. A moderately rapid stream of hydrogen chloride was passed into the suspension for $6\frac{1}{2}$ hours. The flow was discontinued overnight and then resumed for $1\frac{1}{2}$ hours. Anhydrous ether was added occasionally to maintain the volume of the reaction mixture. There was no sensible heat effect during this reaction. The ether suspension was evaporated to dryness, anhydrous ethyl acetate (75 ml) added, and the contents warmed for approximately $\frac{1}{2}$ hour. The insoluble residue of O-dichloroacetyl-DL-serine hydrochloride (1.65 g, 70% yield) was removed by filtration, washed with ethyl acetate and ether, and dried, m.p. 125–126°. The infrared absorption spectrum of this material was identical with that of the product synthesized by the route described above and a mixed melting point of the two was not depressed. The ninhydrin test was positive.

N-Dichloroacetyl-DL-*serine from O-Dichloroacetyl*-DL-*serine Hydrochloride: O → N Dichloroacyl Shift*

A solution of O-dichloroacetyl-DL-serine hydrochloride (5.04 g, 0.02 mole) in 50 ml distilled water was treated at room temperature with a solution of 3.36 g (0.04 mole) sodium bicarbonate in 50 ml of water. The pH of the solution changed from an initial value of 1.10 to 5.60. The neutralized clear solution was concentrated to dryness from a water bath at 30–35° and under reduced pressure. The residue crystallized from water. An infrared absorption curve of the crystalline product was identical with that of pure

Can. J. Chem. Downloaded from www.nrcresearchpress.com by 210.87.254.42 on 09/05/12
For personal use only.

N-dichloroacetyl-DL-serine sodium salt (2). It melted at 172–173° and did not depress the melting point of authentic N-dichloroacetyl-DL-serine sodium salt (2). It no longer gave a positive ninhydrin test, indicating a practically theoretical shift from O to N at pH less than 7.

*O-Dichloroacetyl-*DL*-serine Methyl Ester Hydrochloride*

DL-Serine methyl ester hydrochloride (15.5 g, 0.1 mole) (2) was dissolved, with gentle heating, in dichloroacetic acid (100 ml) in a 500-ml, two-necked, round-bottomed flask fitted with a dropping funnel, calcium chloride drying tube, and magnetic stirrer. Dichloroacetic anhydride (30.0 g, 0.125 mole) was added dropwise to the clear, stirred solution. No attempt was made to control the very small heat rise during this addition, which required 45 minutes. The solution was allowed to stir for 24 hours at room temperature (23–25°) to complete the esterification. Diethyl ether (100 ml) was then added, followed by sufficient petroleum ether (30–60°) to produce a faint permanent cloudiness, and the flask was refrigerated for 5 hours. The white crystalline precipitate of O-dichloroacetyl-DL-serine methyl ester hydrochloride was removed by filtration, washed with ether (50 ml) then petroleum ether (50 ml), and dried at 30–40° in a vacuum oven. The product (18.8 g, 70.6% yield) was recrystallized from methanol–ether, m.p. 106° (with prior softening at 101°), white needles. It was soluble in water, ethanol, and dioxane, and insoluble in ether, petroleum ether, chloroform, and ethyl acetate. Anal. Calc. for $C_6H_{10}Cl_3NO_4$: C, 27.00; H, 3.78; N, 5.25. Found: C, 27.30; H, 4.19; N, 5.26.

*Attempted Conversion of N-Dichloroacetyl- to O-Dichloroacetyl-*DL*-serine Methyl Ester: Attempted N → O Dichloroacyl Shift*

(i) Hydrogen chloride gas was passed through a suspension of N-dichloroacetyl-DL-serine methyl ester (2) (2.0 g) in 100 ml anhydrous ether for 4 hours whereby complete solution took place. Upon evaporation of the ether a quantitative yield of unreacted starting ester was recovered.

(ii) Dry hydrogen chloride gas was passed through a solution of N-dichloroacetyl-DL-serine methyl ester (5 g) in anhydrous methanol (25 ml), for 1 hour. During this period the flask was cooled in an ice–salt bath. The solution was allowed to stand at room temperature for 24 hours and then concentrated to dryness under reduced pressure and at room temperature. The residual pale yellow syrup which solidified completely on refrigeration for several days was crystallized from methanol–ether, yielding 2.65 g of white crystals, m.p. 132–134°, which were identified by mixed melting points and infrared absorption spectra as DL-serine methyl ester hydrochloride.

*Conversion of O-Dichloroacetyl- to N-Dichloroacetyl-*DL*-serine Methyl Ester: O → N Dichloroacyl Shift*

Triethylamine (0.696 ml, 0.005 mole) was added at room temperature to a solution of O-dichloroacetyl-DL-serine methyl ester hydrochloride (1.33 g, 0.005 mole) in anhydrous methanol (15 ml). The solution was shaken mechanically for 10 minutes and then concentrated to dryness under reduced pressure and on a water bath maintained at 25°. The residue, which was a mixture of crystalline triethylamine hydrochloride and oil, was extracted with anhydrous ether (75 ml) whereby the latter dissolved leaving 0.7 g of triethylamine hydrochloride. The ethereal solution on evaporation to dryness under reduced pressure at 25° yielded a pale yellow residual oil which slowly solidified on refrigeration. This was crystallized from ether – petroleum ether (30–60°), yielding 0.95 g (82.6%) of white, fluffy crystals of N-dichloroacetyl-DL-serine methyl ester, m.p.

Can. J. Chem. Downloaded from www.nrcresearchpress.com by 210.87.254.42 on 09/05/12
For personal use only.

82–83°, which, by mixed melting point and infrared absorption spectra, was shown to be identical with N-dichloroacetyl-DL-serine methyl ester (2).

*O-Monochloroacetyl-*DL*-serine*

Monochloroacetic anhydride (121.0 g, 0.708 mole) was dissolved in ethyl monochloroacetate (100 ml) in a 500-ml round-bottomed flask with gentle warming. To the cooled solution there was added, dropwise, a solution of 10.6 g (0.10 mole) DL-serine in 20 g (0.12 mole) of 60% $HClO_4$. The first few increments of this solution did not cause any significant evolution of heat, but, after a period of induction, external cooling was required. On completion of the addition, the solution was heated for 3 hours on a water bath at 55°, then allowed to stand overnight. Slight application of heat was required to redissolve all solids the next day. The dark brown homogeneous solution was diluted with 4 ml of distilled water, which reacted with residual anhydride. Triethylamine (45 g, 0.45 mole) was then added intermittently, with occasional cooling, to neutralize the perchloric acid moiety of the salt. The reaction mixture was poured into 2 liters of ether, whereupon the product separated as a finely divided crystalline powder. It was recovered by filtration, washed and triturated with ether and ethanol, and dried in a vacuum oven. Wt. 16.3 g (89.8% yield), m.p. 122–123° (decomp.). Literature m.p. 122–123° (decomp.) (64). A mixed m.p. with N-monochloroacetyl-DL-serine was depressed. The product was soluble in water, hot ethanol, hot methanol, hot acetone, and insoluble in most other organic solvents. It reacted positive to ninhydrin and positive for chlorine in the flame test with copper wire.

*O-Monochloroacetyl-*DL*-serine Hydrochloride*

Finely powdered O-monochloroacetyl-DL-serine (15.0 g) was suspended in ether (100 ml), and a slow stream of hydrogen chloride gas was passed in for 1 hour. During this process the hydrochloride precipitated as it formed. The particle size of the product was much larger than that of the original O-monochloroacetyl-DL-serine. The excess hydrogen chloride and some of the ether were removed under vacuum. The product (13.2 g, 73.5% yield) was recovered by filtration, washed with ether, and dried in a vacuum oven, m.p. 140–142°. Crystallization from acetone–ether containing a little alcohol yielded 11.0 g of a white crystalline material melting at 141–142°, which was very soluble in the lower alcohols and water, and insoluble in ethyl acetate, chloroform, and ether. Anal. Calc. for $C_5H_9Cl_2NO_4$: C, 27.54; H, 4.16; N, 6.42. Found: C, 27.58; H, 4.16; N, 6.24.

*Conversion of N-Monochloroacetyl- to O-Monochloroacetyl-*DL*-serine: N → O Monochloroacyl Shift*

Finely pulverized N-monochloroacetyl-DL-serine (2.0 g) prepared according to the method of Fischer and Roesner (62) was treated in essentially the same manner as described above for the N → O shift in N-dichloroacetyl-DL-serine. The resulting O-monochloroacetyl-DL-serine hydrochloride 1.27 g (53% yield) after crystallization from ether–alcohol melted at 141–142° and did not depress the melting point of O-monochloroacetyl-DL-serine hydrochloride prepared as above. The infrared absorption spectra of the two compounds were identical.

*Conversion of O-Monochloroacetyl- to N-Monochloroacetyl-*DL*-serine: O → N Monochloroacyl Shift*

O-Monochloroacetyl-DL-serine (10.0 g, 0.055 mole) was dissolved in 27.5 ml of 2 *N* sodium hydroxide solution (0.055 mole NaOH), allowed to stand at room temperature for $3\frac{1}{2}$ hours, and then neutralized with concentrated hydrochloric acid. The solution was

Can. J. Chem. Downloaded from www.nrcresearchpress.com by 210.87.254.42 on 09/05/12
For personal use only.

evaporated to dryness, and the residue extracted with warm ethyl acetate (2×40 ml), which was dried over magnesium sulphate. The ethyl acetate was removed by distillation and the residual oil which solidified at room temperature was crystallized from ethyl acetate – petroleum ether (30–60°), yielding 3.35 g (33.5% yield) of product which melted at 120° and was identical by mixed melting point and infrared absorption with N-monochloroacetyl-DL-serine (62).

O,N-Bis-(Trichloroacetyl)-DL-*Serine*

A solution of trichloroacetic anhydride (250.0 g) and trichloroacetic acid (132.0 g) in anhydrous benzene (600 ml) was placed in a water bath at 25–30° and maintained at this temperature throughout the reaction. DL-Serine (69.4 g) was added in small portions to the rapidly stirred solution. When addition was complete, solids began to separate out and in a short while the mixture set to a gel. It was allowed to stand at room temperature overnight, then the product was removed by filtration, washed with benzene, and air-dried. The product (90.9 g), which was insoluble in water and gave a negative ninhydrin test, was crystallized from ether – petroleum ether (30–60°), m.p. 176–180° (a highly purified sample melted at 185–186°). Anal. Calc. for $C_7H_5Cl_6NO_5$: C, 21.21; H, 1.27; N, 3.54. Found: C, 21.42; H, 1.28; N, 3.51.

A sample of this O,N-bis-(trichloroacetyl)-DL-serine (1.0 g) was suspended in distilled water and neutralized at room temperature to the phenol red endpoint with 4.9 ml of 1.027 *N* sodium hydroxide solution. The material dissolved completely as the neutralization proceeded. The aqueous solution was concentrated to dryness on a water bath at 25° under reduced pressure. The residual oil, upon the addition of ether, solidified immediately to a white, friable powder which was removed by filtration, washed with ether, and dried. The product melted at 193–195° and weighed 0.5 g, representing a yield of 72.6% based on hydrolysis to N-trichloroacetyl-DL-serine, sodium salt, with which it was identified by mixed melting point and infrared absorption.

N-Trichloroacetyl-DL-*Serine*

DL-Serine (10.5 g, 0.10 mole) was dissolved in 2 *N* sodium hydroxide solution (50 ml, 0.1 mole) in a 500-ml, four-necked, round-bottomed flask fitted with a thermometer, motor driven stirrer, and two dropping funnels. The clear solution of the sodium salt of DL-serine was cooled in an ice–salt mixture to approximately 5°. Trichloroacetyl chloride (24.2 g, 0.133 mole) and 2 *N* sodium hydroxide solution (100 ml, 0.2 mole) were then added dropwise and simultaneously from the two dropping funnels to the stirred, cooled solution at such a rate that the reaction mixture remained on the basic side and below 10° throughout the additions. These additions required about 1 hour. The clear, colorless reaction solution was then stirred for 1 hour during which time it was allowed to warm up to room temperature. The solution was then acidified with concentrated hydrochloric acid (10 ml) and evaporated to dryness using a water bath at 55° and reduced pressure. The residual mixture of sodium chloride and clear yellow oil was extracted with hot ethyl acetate (3×100 ml). The combined ethyl acetate extracts, dried over anhydrous magnesium sulphate, were filtered and again evaporated, and the resulting oil was well shaken with petroleum ether (30–60°) (2×50 ml) to remove residual trichloroacetic acid. The product was crystallized from ethyl acetate – petroleum ether, yielding 8.9 g (35.6%) of white crystalline N-trichloroacetyl-DL-serine, m.p. 106–108°. Anal. Calc. for $C_5H_6Cl_3NO_4$: C, 23.97; H, 2.41; N, 5.59. Found: C, 23.62; H, 2.28; N, 5.56.

The sodium salt was prepared by neutralizing a solution of 87 g of N-trichloroacetyl-DL-serine in 100 ml of water with a 2 *N* sodium hydroxide solution, equivalent to 13.9 g NaOH. The clear solution was evaporated under vacuum at 60° to a dry solid, which

Can. J. Chem. Downloaded from www.nrcresearchpress.com by 210.87.254.42 on 09/05/12
For personal use only.

was recrystallized from ethanol, yielding 71 g of N-trichloroacetyl-DL-serine, sodium salt, m.p. 192–193°. Anal. Calc. for $C_5H_5Cl_3NO_4Na$: C, 22.04; H, 1.85; N, 5.14. Found: C, 21.96; H, 1.85; N, 5.32.

*Attempted Conversion of N-Trichloroacetyl- to O-Trichloroacetyl-*DL*-serine: Attempted N → O Trichloroacyl Shift*

N-Trichloroacetyl-DL-serine (2.0 g) was suspended in anhydrous ether (125 ml) and treated with a stream of hydrogen chloride gas for 4 hours. After approximately ½ hour, solution was complete and, upon evaporation to dryness, yielded an oil which rapidly crystallized. The product, 2.0 g, m.p. 106–109°, was identical by mixed melting point and infrared absorption with the starting material.

DL-*Serine Hydrochloride*

An analytical sample of DL-serine hydrochloride was prepared by evaporating to dryness an aqueous solution of serine (5 g in 50 ml water) containing 4 ml concentrated hydrochloric acid and crystallizing the residue from hot anhydrous ethanol. The product was recrystallized from ethanol–ether. Weight 5.4 g, m.p. 136°. Anal. Calc. for $C_3H_8ClNO_3$: C, 25.45; H, 5.70; N, 9.90. Found: C, 25.51; H, 5.48; N, 10.05.

Dichloroacetic Anhydride

This compound was prepared according to the procedure employed by Tedder (65). A mixture of phosphoric anhydride (141 g, 1.0 mole) and dichloroacetic acid (129 g, 1.0 mole) in a 500-ml round-bottomed flask was distilled under reduced pressure. The total distillable liquid came over at 116–120° at 16.5 mm, and was collected without regard to boiling point. Infrared absorption analysis indicated that it contained only a trace of unreacted acid. The product was redistilled in the same manner from approximately 3 g of fresh phosphoric anhydride and the distillate was collected at essentially the same boiling point as above. Weight of dichloroacetic anhydride 87.1 g (72.7% yield). In other preparations yields up to 84% were obtained.

Trichloroacetic Anhydride

This product was prepared in the same manner from trichloroacetic acid with phosphoric anhydride and boiled at 145–150° at 110 mm, yield 77.8%.

ACKNOWLEDGMENT

The authors wish to thank Mr. J. Cuthbertson and Miss M. Dillon for the analyses.

REFERENCES

1. I. Levi, H. Blondal, and E. Lozinski. Science, **131**, 666 (1960).
2. I. Levi, A. E. Koller, G. Laflamme, and J. W. R. Weed. Can. J. Chem. **38**, 1135 (1960).
3. I. Levi. Unpublished results.
4. W. Böttcher. Ber. **16**, 629 (1883).
5. L. C. Raiford. J. Am. Chem. Soc. **41**, 2068 (1919).
6. L. C. Raiford and J. R. Couture. J. Am. Chem. Soc. **44**, 1792 (1922).
7. L. C. Raiford and C. M. Woolfolk. J. Am. Chem. Soc. **46**, 2246 (1924).
8. L. C. Raiford and H. P. Lankelma. J. Am. Chem. Soc. **47**, 1111 (1925).
9. F. Bell. J. Chem. Soc. 2962 (1931).
10. L. C. Raiford and A. L. LeRosen. J. Am. Chem. Soc. **67**, 2163 (1945).
11. A. L. LeRosen and E. D. Smith. J. Am. Chem. Soc. **70**, 2705 (1948); **71**, 2815 (1949).
12. E. L. Totton and L. C. Raiford. J. Am. Chem. Soc. **76**, 5127 (1954).
13. S. Gabriel and Th. Heymann. Ber. **23**, 2493 (1890).
14. S. Gabriel. Ann. **409**, 326 (1915).
15. W. A. Jacobs and M. Heidelberger. J. Biol. Chem. **21**, 403 (1915).
16. M. Bergmann and E. Brand. Ber. b, **56**, 1280 (1923).
17. J. R. Reasenberg and G. B. L. Smith. J. Am. Chem. Soc. **66**, 991 (1944).
18. J. R. Reasenberg and S. D. Goldberg. J. Am. Chem. Soc. **67**, 933 (1945).

Can. J. Chem. Downloaded from www.nrcresearchpress.com by 210.87.254.42 on 09/05/12
For personal use only.

19. M. BERGMANN, E. BRAND, and F. WEINMANN. Z. physiol. Chem. Hoppe-Seyler's, **131**, 1 (1923).
20. A. P. PHILLIPS and R. BALTZLY. J. Am. Chem. Soc. **69**, 200 (1947).
21. G. E. MCCASLAND, R. K. CLARKE, JR., and H. E. CARTER. J. Am. Chem. Soc. **71**, 637 (1949).
22. S. WINSTEIN and R. BOSCHAN. J. Am. Chem. Soc. **72**, 4669 (1950).
23. A. P. PHILLIPS and A. MAGGIOLO. J. Am. Chem. Soc. **72**, 4920 (1950).
24. W. SCHOELLER and J. JÓNÁS. Ger. Patent No. 853,166 (October 23, 1952).
25. V. BRUCKNER *et al.* J. Chem. Soc. 885 (1948).
26. G. FODOR *et al.* J. Org. Chem. **14**, 337 (1949).
27. L. H. WELSH. J. Am. Chem. Soc. **69**, 128 (1947).
28. L. H. WELSH. J. Am. Chem. Soc. **71**, 3500 (1949).
29. J. WEIN. Acta Chim. Acad. Sci. Hung. **17**, 189 (1958).
30. G. FODOR and K. KOCZKA. J. Chem. Soc. 850 (1952).
31. S. TATSUOKA, M. HONJO, and J. UEYANAGI. J. Pharm. Soc. Japan, **73**, 362 (1953); Chem. Abstr. **48**, 2642 (1954).
32. C. G. ALBERTI, B. CAMERINO, and A. VERCELLONE. Gazz. chim. ital. **82**, 53, 63 (1952).
33. J. UEYANAGI. J. Pharm. Soc. Japan, **71**, 1409, 1415 (1951); Chem. Abstr. **46**, 8051 (1952).
34. S. IKUMA and R. MYOKEI. J. Pharm. Soc. Japan, **72**, 957 (1952); Chem. Abstr. **47**, 6370 (1953).
35. G. FODOR, J. KISS, and I. SALLAY. J. Chem. Soc. 1858 (1951).
36. G. FODOR and J. KISS. J. Am. Chem. Soc. **72**, 3495 (1950).
37. G. E. MCCASLAND. J. Am. Chem. Soc. **73**, 2295 (1951).
38. E. E. VAN TAMELEN. J. Am. Chem. Soc. **73**, 5773 (1951).
39. T. WHITE. J. Chem. Soc. 1498 (1938).
40. H. S. ISBELL and H. L. FRUSH. J. Am. Chem. Soc. **71**, 1579 (1949).
41. W. W. PIGMAN and R. M. GOEPP, JR. Chemistry of the carbohydrates. Academic Press Inc., New York. 1946. pp. 156–159.
42. J. M. SUGIHARA. Advances in Carbohydrate Chem. **8**, 1 (1953).
43. B. F. STIMMEL and C. G. KING. J. Am. Chem. Soc. **56**, 1724 (1934).
44. A. P. DOERSCHUK. J. Am. Chem. Soc. **74**, 4202 (1952).
45. O. E. VAN LOHUIZEN and P. E. VERKADE. Rec. trav. chim. **79**, 133 (1960).
46. T. H. BEVAN *et al.* J. Chem. Soc. 127 (1953).
47. A. B. FOSTER and M. STACEY. Advances in Carbohydrate Chem. **7**, 247 (1952).
48. H. A. SMITH and G. GORIN. J. Org. Chem. **26**, 820 (1961).
49. M. CALVIN. Glutathione. *Edited by* S. COLOWICK *et al.* Academic Press Inc., New York, N.Y. 1954. pp. 3, 21.
50. D. GARFINKEL. J. Am. Chem. Soc. **80**, 4833 (1958).
51. E. FISCHER. Ber. **53**, 1621 (1920).
52. H. HIBBERT and N. M. CARTER. J. Am. Chem. Soc. **51**, 1601 (1929).
53. H. HIBBERT and M. E. GREIG. Can. J. Research, 4, 254 (1931).
54. M. BERGMANN and A. MIEKELEY. Z. physiol. Chem. Hoppe-Seyler's, **140**, 128 (1924).
55. M. UZIEL and D. J. HANAHAN. J. Biol. Chem. **226**, 789 (1957).
56. S. A. FUSARI *et al.* J. Am. Chem. Soc. **76**, 2881 (1954).
57. J. EHRLICH *et al.* Nature, **173**, 72 (1954).
58. J. B. CONANT and G. M. BRAMANN. J. Am. Chem. Soc. **50**, 2305 (1928).
59. J. PINNOW. Ber. **33**, 417 (1900).
60. J. J. KOLB and G. TOENNIES. J. Biol. Chem. **144**, 193 (1942).
61. W. SAKAMI and G. TOENNIES. J. Biol. Chem. **144**, 203 (1942).
62. E. FISCHER and H. ROESNER. Ann. **375**, 200 (1910).
63. L. BENOITON. J. Chem. Soc. 763 (1961).
64. G. SUNAGAWA, K. MURAYAMA, and N. YOSHIDA. Yakugaku Zasshi, **77**, 1173 (1957); Chem. Abstr. **52**, 6304 (1958).
65. J. M. TEDDER. J. Chem. Soc. 2646 (1954).

Can. J. Chem. Downloaded from www.nrcresearchpress.com by 210.87.254.42 on 09/05/12
For personal use only.

Can. J. Chem. Downloaded from www.nrcresearchpress.com by 210.87.254.6 on 09/05/12
For personal use only.

STEADY-STATE DEPARTURE IN ENZYME REACTIONS[1]

HYUNG KYU SHIN[2] AND J. CALVIN GIDDINGS

ABSTRACT

A method is described for calculating the departure from steady-state conditions in enzyme reactions. This provides an immediate and simple criterion for the validity of the steady-state approximation. Several variations of the general method, differing in the degree of simplicity and in the treatment of initial transients, are formulated and discussed. These methods are applied to the general case of an enzyme reaction following the Michaelis–Menten mechanism. Specific applications are made using the data of Chance and Gutfreund. While in these specific cases the steady-state concentration of intermediate is reasonably accurate, the extent of reaction may easily vary from that calculated by means of the steady state.

INTRODUCTION

Because of the mathematical difficulties involved in the analysis of enzyme kinetics, it is conventional to employ the steady-state approximation (1–3). This approximation is not, however, always valid, and the conventional methods used to determine validity are usually difficult or erroneous. The two principal methods used for criteria involve (1) making an exact numerical analysis of the kinetics in order to determine the faithfulness of the model or (2) using the assumption that the steady-state approximation is valid when the intermediate or complex concentration is small. Alternative (1) suffers by virtue of its difficulty and by virtue of the fact that each numerical analysis is a special case and must be done again for each change in conditions. Alternative (2) has been found erroneous; in certain chain reactions its use leads to an error of four orders of magnitude in predicting the departure from steady-state conditions (4). In view of the serious problems connected with determining the validity of steady-state approximations, a method has been developed by the authors (4–6) which, for each individual case, offers a simple criterion of steady-state validity. The application of this method to enzyme reactions will be developed in the following sections.

METHOD

The departure from steady-state conditions is given in terms of the departure term ϵ, defined by

$$[1] \qquad (\mathrm{I}) = (\mathrm{I})^*(1+\epsilon),$$

where (I) and (I)* are the actual and steady-state concentrations of the intermediate, respectively. Differentiation of this equation leads to

$$[2] \qquad (\mathrm{I})^* \frac{d\epsilon}{dt} + (1+\epsilon)\frac{d(\mathrm{I})^*}{dt} = r_{\mathrm{I}},$$

where r_{I} is the rate of formation of I, $d(\mathrm{I})/dt$, and is a function of the rate constants, the concentrations of stable species, and the departure term ϵ.

The exact solution of equation [2] is equivalent to any other exact treatment of chemical kinetics. Equation [2] is in a form, however, which lends itself readily to approximate methods which are valid when the departure term is small compared with unity. The first step consists of neglecting all terms in ϵ^2, ϵ^3, etc. (such terms appear as a result of

[1]*Manuscript received July 7, 1961.*
Contribution from the Department of Chemistry, University of Utah, Salt Lake City 12, Utah.
[2]*Present address: Physical Chemistry Division, National Bureau of Standards, Washington 25, D.C.*

the implicit dependence of $d(I)^*/dt$ and r_I upon ϵ). The next step depends upon a choice between the following methods:

Method 1: With the above approximation, equation [2] is a linear, first-order equation which can be integrated directly by standard methods. It is sometimes necessary to replace reactant concentration terms by their steady-state values. Method 1 gives a good picture of the build-up of intermediate concentration at the beginning of reaction.

Method 1*a*: A somewhat simpler approximation is obtained by dropping each ϵ (not $d\epsilon/dt$) appearing explicitly or implicitly on the left of equation [2]. This procedure has been justified elsewhere (4).

Method 2: An alternate simplification of method 1 is obtained by setting $d\epsilon/dt = 0$. This removes the initial transient or radical build-up from consideration, but generally gives an accurate picture of the subsequent reaction. This approximation makes equation [2] a simple algebraic equation.[1] This equation can, however, be further simplified by means of method 2*a*.

Method 2*a*: In addition to dropping the $d\epsilon/dt$ term, each term on the left-hand side containing ϵ is also neglected. This step is equivalent to the one leading to method 1*a*. It is not quite as accurate if ϵ exceeds 0.1, but it is otherwise very simple. This is illustrated by equation [18].

In general, methods 2 and 2*a* give sufficient information about steady-state departure without the necessity of resorting to methods 1 and 1*a*. For completeness, however, method 1*a* will also be used here in connection with the reaction of enzymes.

APPLICATION TO ENZYME REACTIONS

The mechanism proposed by Michaelis and Menten (7) describes the essential features of many enzyme reactions. The following steps are involved:

$$[3] \qquad E + S \underset{k_2}{\overset{k_1}{\rightleftharpoons}} I \overset{k_3}{\rightarrow} E + P,$$

where E represents the enzyme, S the substrate, I the intermediate, i.e., the binary complex between enzyme and substrate, and P the product or products of reaction. The rate equations are

$$[4] \qquad d(I)/dt = k_1(E)(S) - (k_2+k_3)(I),$$

$$[5] \qquad d(S)/dt = -k_1(E)(S) + k_2(I),$$

$$[6] \qquad d(E)/dt = -k_1(E)(S) + (k_2+k_3)(I),$$

$$[7] \qquad d(P)/dt = k_3(I).$$

The steady-state concentration of I is

$$[8] \qquad (I)^* = \frac{k_1}{k_2+k_3}(E)(S).$$

With the substitution of $(E) = (E)_0 - (I)^*$, where $(E)_0$ is the total amount of enzyme, the quantity $(I)^*$ becomes

$$[9] \qquad (I)^* = \frac{(E)_0(S)}{K_m+(S)},$$

where K_m is the Michaelis constant, $(k_2+k_3)/k_1$.

[1]*We have previously stated that method 2 often requires the reactant concentration to be replaced by its steady-state value. This approximation is not necessary when the reactant concentration, rather than time, is chosen as the independent variable. This choice is more convenient, and is used here.*

Can. J. Chem. Downloaded from www.nrcresearchpress.com by 210.87.254.6 on 09/05/12
For personal use only.

In order to obtain $d(\mathrm{I})^*/dt$, needed in both methods 1 and 2, equation [9] is differentiated and simplified with the following result:

$$[10] \qquad \frac{d(\mathrm{I})^*}{dt} = \frac{K_m(\mathrm{E})_0}{[K_m+(\mathrm{S})]^2}\frac{d(\mathrm{S})}{dt}.$$

The evaluation of $d(\mathrm{S})/dt$ is made by substituting $(\mathrm{E}) = (\mathrm{E})_0-(\mathrm{I}) = (\mathrm{E})_0-(\mathrm{I})^*(1+\epsilon)$ into equation [5]. The result, after substitution back into equation [10], is

$$[11] \qquad \frac{d(\mathrm{I})^*}{dt} = \frac{K_m(\mathrm{E})_0}{[K_m+(\mathrm{S})]^2}\{-k_1(\mathrm{E})_0(\mathrm{S})+k_1(\mathrm{S})(\mathrm{I})^*+k_2(\mathrm{I})^*+[k_1(\mathrm{S})+k_2](\mathrm{I})^*\epsilon\}.$$

We now proceed to evaluate the expression $r_I = d(\mathrm{I})/dt$ using equations [1], [4], and [9]. This combination gives

$$[12] \qquad r_I = -k_1(\mathrm{E})(\mathrm{S})\epsilon.$$

Substituting $(\mathrm{E}) = (\mathrm{E})_0-(\mathrm{I})^*(1+\epsilon)$, as above, and dropping the term in ϵ^2, we obtain

$$[13] \qquad r_I = -k_1(\mathrm{S})[(\mathrm{E})_0-(\mathrm{I})^*]\epsilon.$$

Equations [9], [11], and [13] provide all the necessary terms in equation [2], and it is now possible to evaluate this equation according to method 1, 1*a*, 2, or 2*a*.

The application of method 1 to the foregoing mechanism proves to be quite complex. While the differential equation is linear, the integral solutions are nonetheless quite involved. Consequently method 1*a*, which gives a result that is nearly as satisfactory, will be employed here. Using this method, equation [2] becomes

$$[14] \qquad \frac{d\epsilon}{dt}+(k_2+k_3)\epsilon = \left[\frac{K_m}{K_m+(\mathrm{S})}\right][k_1(\mathrm{E})_0-k_1(\mathrm{I})^*-k_2(\mathrm{I})^*/(\mathrm{S})],$$

where the term $(k_2+k_3)\epsilon$, equal to $-r_I/(\mathrm{I})^*$, is obtained by combining equations [8] and [12], and the right-hand side of [14] is obtained by combining equations [9] and [11], and dropping the ϵ terms. The term $(\mathrm{I})^*/(\mathrm{S})$ can be replaced by $[(\mathrm{E})_0-(\mathrm{I})^*]/K_m$ in view of equation [8] and the expression $(\mathrm{E}) = (\mathrm{E})_0-(\mathrm{I})^*$. After simplification, equation [14] becomes

$$[15] \qquad \frac{d\epsilon}{dt}+(k_2+k_3)\epsilon = \frac{k_3[(\mathrm{E})_0-(\mathrm{I})^*]}{K_m+(\mathrm{S})}.$$

After the independent variable is changed to (S) rather than t, the solution of [15] can be obtained by the standard methods employed for linear equations:

$$[16] \qquad \epsilon_{Ia} = \left\{\exp\left[\frac{K_m^2}{K_{31}}\int\frac{d\ln(\mathrm{S})}{(\mathrm{E})_0-(\mathrm{I})^*}\right]\right\}\left\{\int\frac{-K_m}{K_m+(\mathrm{S})}\exp\left[-\frac{K_m^2}{K_{31}}\frac{d\ln(\mathrm{S})}{(\mathrm{E})_0-(\mathrm{I})^*}\right]\times d\ln(\mathrm{S})+\omega\right\},$$

where $K_{31} = k_3/k_1$ and ω is the integration constant which can be evaluated knowing the initial conditions, i.e., $\epsilon = -1$ and $(\mathrm{S}) = (\mathrm{S})_0$ when $t = 0$. The second integral in the above expression can be evaluated by plotting

$$\left[-\frac{K_m}{K_m+(\mathrm{S})}\right]\exp\left[-\frac{K_m^2}{K_{31}}\int\frac{d\ln(\mathrm{S})}{(\mathrm{E})_0-(\mathrm{I})^*}\right]$$

against ln (S) and integrating graphically. A similar method may be applied for the evaluation of the integral in the exponential parts.

Can. J. Chem. Downloaded from www.nrcresearchpress.com by 210.87.254.6 on 09/05/12
For personal use only.

The expression for ϵ_2, obtained from method 2, is

$$[17] \qquad \epsilon_2 = \frac{\left\{1-[(S)+K_{21}]\frac{(I)^*}{(S)(E)_0}\right\}\alpha}{\left[1-\frac{(I)^*}{(E)_0}\right]-\left\{1-2[(S)+K_{21}]\frac{(I)^*}{(S)(E)_0}\right\}\alpha},$$

while method 2*a* yields

$$[18] \qquad \epsilon_{2a} = \frac{\left\{1-[(S)+K_{21}]\frac{(I)^*}{(S)(E)_0}\right\}}{\left[1-\frac{(I)^*}{(E)_0}\right]}\alpha,$$

where $K_{21} = k_2/k_1$ and $\alpha = K_m(E)_0/[K_m+(S)]^2$.

A numerical example of the method described above has been obtained using results on the kinetics of peroxidase by Chance (8). In this work he found the velocity constant, k_1, for the formation of peroxidase-H_2O_2 (intermediate) to be about 1.2×10^7 l. mole^{-1} sec^{-1}; the velocity constant, k_2, for the reversible breakdown of intermediate is $\leqslant 0.2$ sec^{-1}, and the velocity constant, k_3, for the enzymatic breakdown of intermediate is 4.2 sec^{-1}. The initial concentrations are assumed to be $(E)_0 = 10^{-6}$ mole l^{-1} and $(S)_0 = 10^{-5}$ mole l^{-1}. The departure terms obtained by the above methods are plotted in Fig. 1 as a

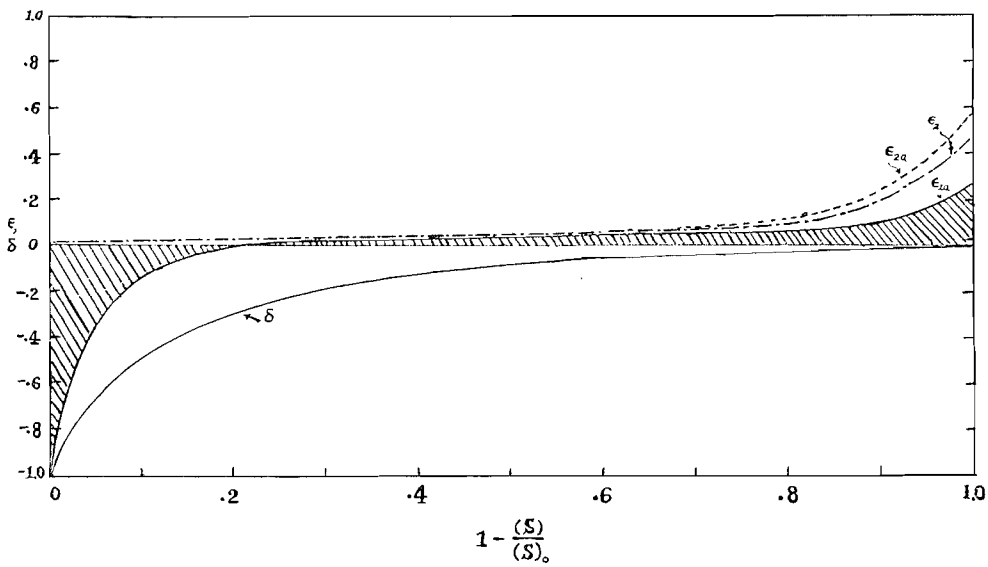


FIG. 1. Departure terms vs. amount of reaction.

function of the fraction of reaction completed. It is seen that ϵ_{2a} is a very good approximation to ϵ_2 over most of the course of the reaction. The values of ϵ_{1a}, which also show the significance of the initial transient, are approximately equal to those of ϵ_2 and ϵ_{2a} after the passage of the initial transient. At 40% reaction, for example, ϵ_2, ϵ_{2a}, and ϵ_{1a} have the values 0.030, 0.032, and 0.028. At 60% reaction the values are 0.034, 0.039, and 0.032, respectively. The departure increases significantly beyond 80% reaction.

Can. J. Chem. Downloaded from www.nrcresearchpress.com by 210.87.254.6 on 09/05/12
For personal use only.

The curve calculated by means of method 1*a* shows that the over-all reaction rate, proportional to the intermediate concentration, is, at first, less than that predicted by the steady-state approximation, and then greater (the transition occurs where $\epsilon_{1a} = 0$ at about 20% complete). It is clear that the concentration of product, (P), is not equal to the steady-state value, (P)*. The difference of the two may be expressed in term of δ, defined by (P) = (P)*(1+δ). This term, representing the fractional departure from the predicted extent of completion of the reaction, is obtained from the equation

$$[19] \qquad \delta = \int_0^t (\mathrm{I})^* \epsilon dt \Big/ \int_0^t (\mathrm{I})^* dt,$$

which is the time average value of the departure of intermediate weighted by the steady-state concentration of intermediate. The integrals in equation [19] are easily evaluated by means of a numerical procedure using previously determined (I)* and ϵ values. The results given in Fig. 1 show that the extent of reaction is significantly less than predicted from steady-state considerations except as the reaction approaches completion.

Another application of the above methods involves two enzyme-catalyzed hydrolysis reactions. Using the Gibson (9) stop-flow method combined with the photoelectric technique, Gutfreund (10) studied the various aspects of these reactions. From this work he estimated $k_1 \geqslant 10^6$ for two systems, trypsin + benzoyl-L-arginine ethyl ester (T + BAEE) and chymotrypsin + acetyl-L-phenylalanine ethyl ester (C + APEE). For both reactions k_3 is of the order of 10. For (T + BAEE), $K_m = 10^{-5}$ and $(k_2 + k_3) \geqslant 10$, whereas $K_m = 7 \times 10^{-4}$ and $(k_2 + k_3) \geqslant 700$ for (C + APEE). For the latter reaction $(k_2 + k_3)$ is so much larger than k_3 that K_m can be regarded as k_2/k_1, the true enzyme–substrate dissociation constant. Applying the same initial concentrations of enzyme and substrate as the previous example, and replacing the equal-to-or-greater-than sign by an equal sign we obtain the values of ϵ_2 for (T + BAEE) as reported in Table I.

TABLE I

Amount of reaction (%)	20	40	60	80	90	95
ϵ_2	.0308	.0390	.0510	.0694	.0826	.0907

It is obvious from equation [17] that $\epsilon_2 \cong 0$ for (C + APEE) since the numerator in equation [17] is negligible when $K_m \cong k_2/k_1$. This is also true for ϵ_{2a} as shown in equation [18].

CONCLUSIONS

The methods proposed in this paper are designed to show the correlation between departure from steady-state conditions and the rate constants used to characterize the mechanism. At this time the major difficulty in applying the above methods stems from the lack of data concerning individual rate constants. Measurement of the rate of product formation or substrate disappearance after the initial transient period does not provide sufficient information for this purpose. Consequently it is usually necessary to resort to some form of transient analysis to obtain the necessary rate constants. One use of the present methods may be found in the simplified transient analysis (method 1*a*) which might be used for the approximate evaluation of rate data. As more such data is accumulated, it should be possible to correlate known rate constants pertaining to a particular step in the general mechanism with the structure of the reactants, and subsequently to

Can. J. Chem. Downloaded from www.nrcresearchpress.com by 210.87.254.6 on 09/05/12
For personal use only.

estimate unknown rate constants. This can now be done quite successfully in the pyrolysis of hydrocarbons and related molecules. In this case the methods developed here can be applied directly to determine steady-state validity.

The above methods can also be used to extend the working range of a mechanism study. If an exact transient analysis has been used on experimental data to calculate the rate constants, the present methods are very convenient for the analysis of concentration effects. By contrast, using the exact method, a new and difficult analysis must be made for every variation in concentration. In addition, the effect of temperature changes on the rate constants can be estimated by means of approximate activation energies, and the current methods can be used to roughly estimate the temperature range of steady-state validity. The exact method, again, would involve a lengthy analysis for each temperature.

The limitations of the methods used here are obvious; the calculation of ϵ values which exceed about 0.20 reflect a good deal of error. To obtain more accuracy one would have to apply exact methods. Since the latter alternative is much more complicated, it is well to remember that the simpler methods, such as $2a$, provide, first, a simple criterion of steady-state validity, and second, an accurate value of ϵ providing only that it is small. Thus, for example, we are able to conclude from Table I that the departure for the (T + BAEE) reaction is not very serious, and also report reliable values for ϵ within the limitations of accuracy of the rate constants. Similarly if we had a system for which ϵ was calculated to be, say, 5.0, we could state conclusively that the steady-state departure is serious, but we could not predict the extent of departure. When considered within this framework, it is felt that the above methods, especially $2a$, might find a great deal of applicability to the common enzyme reactions for which a doubt exists concerning the validity of the steady-state approximation.

ACKNOWLEDGMENT

This investigation was supported by a research grant, NSF-G9498, from the National Science Foundation.

REFERENCES

1. E. L. KING and C. ALTMAN. J. Phys. Chem. **60**, 1375 (1957). E. L. KING. J. Phys. Chem. **60**, 1378 (1956).
2. K. J. LAIDLER. Discussions Faraday Soc. **33**, 1614 (1955). R. M. KRUPKA and K. J. LAIDLER. Trans. Faraday Soc. **56**, 1477 (1960).
3. J. M. REINER. Behavior of enzyme systems. Burgess Publishing Co. 1959.
4. J. C. GIDDINGS and H. K. SHIN. J. Chem. Phys. In press.
5. J. C. GIDDINGS and H. K. SHIN. Trans. Faraday Soc. **57**, 468 (1961).
6. H. K. SHIN and J. C. GIDDINGS. J. Phys. Chem. In press.
7. L. MICHAELIS and M. L. MENTEN. Biochem. Z. **49**, 333 (1913).
8. B. CHANCE. J. Biol. Chem. **151**, 553 (1943).
9. Q. H. GIBSON. Discussions Faraday Soc. **17**, 137 (1954).
10. H. GUTFREUND. Discussions Faraday Soc. **17**, 220 (1954).

Can. J. Chem. Downloaded from www.nrcresearchpress.com by 210.87.254.6 on 09/05/12
For personal use only.

Can. J. Chem. Downloaded from www.nrcresearchpress.com by 210.87.254.6 on 09/05/12
For personal use only.

THE BASICITIES OF ORTHO-SUBSTITUTED BENZOIC ACIDS[1]

ROSS STEWART AND MAURICE R. GRANGER

ABSTRACT

The basicities of 15 ortho-substituted benzoic acids have been measured in sulphuric acid. The ortho effects of alkyl groups are base weakening and increase in the expected order methyl, ethyl, *i*-propyl, *t*-butyl. Ortho halo benzoic acids have comparable basicities and are weaker than their para isomers. Oxygen-containing ortho substituents, except hydroxyl, all cause substantial base strengthening relative to the para isomers. Even the groups nitro and carboxyl when substituted ortho in benzoic acid cause the basicity to rise, presumably because of hydrogen bonding in the conjugate acids.

INTRODUCTION

It is well known that the reactivities of ortho-substituted aromatic compounds are not as easily predicted as those of their meta and para isomers. The failure of the Hammett equation in the former cases illustrates this (1, 2). The fact that virtually all ortho-substituted benzoic acids, regardless of the electronic nature of the substituent, are stronger acids than benzoic acid itself has been explained on the grounds of steric inhibition of resonance in the neutral molecule. That is, the bulk of the neighboring group forces the carboxyl group out of the plane of the aromatic ring and thus raises the energy of the neutral molecule relative to the anion in which resonance with the ring will be slight (3, 4). Opposing this acid-strengthening effect will be the steric hindrance to solvation of the anion caused by the nearby ortho substituent (4). In addition to these two general steric effects, there is the electronic effect of the substituent and, in some cases, specific interactions between the substituent and either the carboxyl group or the carboxylate anion.

We have determined the *basicities* of a series of ortho-substituted benzoic acids using the general Hammett technique in sulphuric acid (5–8). In this case, resonance with the ring is more important in the ion than in the neutral molecule and inhibition of resonance by an ortho substituent (9) will here serve to decrease the basicity of the acid. (Since basicities are usually referred to in terms of the strength of the conjugate acid this will raise the acidity of the conjugate acid, i.e. it will make pK_{BH^+} less positive.) Steric hindrance by the ortho group to solvation of the cation will operate in the same direction in this case. Thus one might reasonably expect that in the absence of specific interactions all ortho substituents might be base weakening in the benzoic acid series.

RESULTS AND DISCUSSION

The pK_{BH^+} values for the ortho-substituted benzoic acids are listed in Table I together with spectral data for the neutral and cationic forms. In Table II are listed for comparison the differences in the pK_{HA} and the pK_{BH^+} values for ortho- and para-substituted benzoic acids. ($pK_{HA} = pH + \log HA/A^-$ and $pK_{BH^+} = H_0 + \log BH^+/B$, where $BH^+ \equiv H_2A^+$ and $B \equiv HA$.) One can see that here both base-strengthening and base-weakening effects are present. The electrical effect of an ortho substituent operating through the ring can be very roughly cancelled by assuming that the electrical effects of ortho and para substituents are equal (10, 11) and by using the difference in basicity of the ortho- and para-substituted acids as a measure of the ortho effect. When this is

[1]*Manuscript received July 25, 1961.*
Contribution from the Department of Chemistry, University of British Columbia, Vancouver, British Columbia.

Can. J. Chem. Downloaded from www.nrcresearchpress.com by 210.87.254.6 on 09/05/12
For personal use only.

TABLE I

Basicity constants, absorption maxima, and slopes of linear basicity plots for substituted benzoic acids

Substituent	$-pK_{BH^+}$[a]			Slope	In 45% H_2SO_4		In 96% H_2SO_4	
	Gra.	Lin.	Av.		λ_{max}	log ϵ_{max}	λ_{max}	log ϵ_{max}
Hydrogen	7.20	7.15	*7.18*	1.1	233	4.00	261	4.14
o-Methyl	7.15	7.10	*7.13*	1.1	234	3.88	265	4.18
o-Ethyl	7.15	7.15	*7.15*	1.1	233	3.83	266	4.14
o-*i*-Propyl	7.25	7.21	*7.23*	1.2	233	3.71	265	4.06
o-*t*-Butyl	7.57	7.74	*7.66*	1.1	232(sh)	3.36	265	3.73
o-Fluoro	7.54	7.66	*7.60*	1.2	229	3.97	257	4.18
o-Chloro	7.64	7.72	*7.68*	1.2	233	3.79	263	4.11
o-Bromo	7.73	7.76	*7.75*	1.3	236[b]	3.80[b]	265	4.04
o-Iodo	7.74	7.82	*7.78*	1.5	232(sh)	3.84	266	3.87
o-Hydroxyl	6.80	6.75	*6.78*	1.2	237	3.95	260	4.20
o-Methoxyl	6.04	6.16	*6.10*	1.1	240	3.92	262	4.20
o-Ethoxyl	6.05	6.15	*6.10*	1.0	240	3.91	262	4.15
o-Nitro	7.18	6.89	*7.03*	0.8	266	3.69	277	3.74
o-Carboxyl	5.98	5.92	*5.95*	1.0	231	3.83	264[c]	3.89[c]
m-Carboxyl[d]	7.10	7.10	*7.10*	1.0	282	2.97	298	3.23
p-Carboxyl	7.56	7.46	*7.51*	1.0	245	4.28	260	4.43
α-C_4H_4[e]	7.1	—	*7.1*	—	235(s)	4.29	253	4.11

[a] Gra. = graphical method; Lin. = linear method; Av. = average.
[b] In 65% H_2SO_4.
[c] In 87% H_2SO_4.
[d] From $n-\pi^*$ absorption maximum.
[e] α-Naphthyl.

TABLE II

Comparison of the acid and base strengths of ortho- and para-substituted benzoic acids

Substituent	$pK_{BH^+}^{ortho}-pK_{BH^+}^{HBz}$	$pK_{BH^+}^{ortho}-pK_{BH^+}^{para}$	$pK_{HA}^{ortho}-pK_{HA}^{HBz}$	$pK_{HA}^{ortho}-pK_{HA}^{para}$
Hydrogen	0.00	0.00	0.00	0.00
Methyl	0.05	−0.29	−0.29	−0.43
Ethyl	0.03	−0.31	−0.43	−0.58
i-Propyl	−0.05	−0.40[c]		
t-Butyl	−0.48	−0.84	−0.74	−0.94
Fluoro	−0.42	−0.38	−0.93	−0.87
Chloro	−0.50	−0.28	−1.26	−1.05
Bromo	−0.52	−0.33[c]	−1.35	−1.15
Iodo	−0.60	−0.36	−1.34	−1.06
Hydroxyl	0.40	−0.19	−1.22	−1.60
Methoxyl	1.08	0.50	−0.11	−0.38
Ethoxyl	1.08	0.43	0.01	−0.24
Carboxyl	1.23	1.56	−1.25	−0.56
Nitro	0.15	1.00[c]	−2.03	−1.27

[a] Values from present work and from reference 7; the $pK_{BH^+}^{para}$ values used here are 0.08 pK units less negative than those in ref. 7 because of a discrepancy in the benzoic acid determination in the two sets of work.
[b] Values from reference 4, p. 588.
[c] Estimated value.

done one can see that most, but not all, of the ortho substituents are now acid strengthening in the $ArCO_2H_2^+$ series, as they are in the $ArCO_2H$ series. It will be convenient to discuss the results in three groups: (*a*) the alkyl groups, (*b*) the halogens, (*c*) the oxygen-containing groups.

The Alkyl Groups

The trend of the ortho effects of the alkyl substituents on the basicities of benzoic acids is particularly clear. Methyl and ethyl groups exert similar effects, the *i*-propyl group a somewhat larger effect and the *t*-butyl group a considerably larger effect. Similar

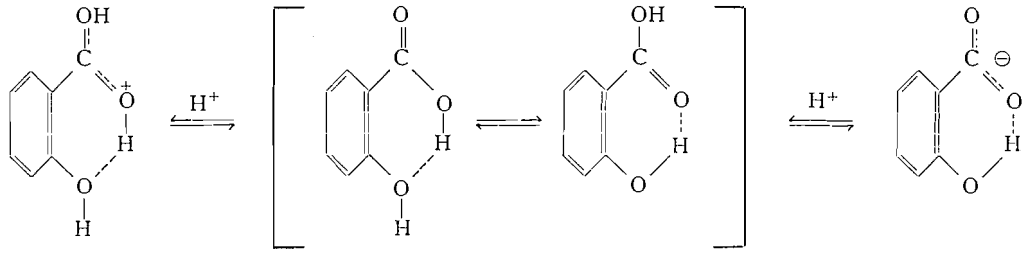
behavior has been observed by Brown and Cahn (12) in the reaction of α-alkyl pyridines with boron compounds. It is interesting that, when ΔpK_{BH^+} (the difference between the basicities of benzoic acid and the ortho isomer) is plotted against the activation energy for the reaction of methyl iodide with the α-alkyl pyridines (12), a linear relation results, indicating that the alkyl substituents are exerting similar effects in both this reaction and the protonation reaction. Since the electrical effects of the alkyl groups are similar, one can conclude that the decrease in basicity as the alkyl groups increase in size is due to steric hindrance to resonance in, and solvation of, the conjugate acid.

The Halogens

Benzoic acids with ortho halogen atoms are all weaker bases than their para isomers and weaker than benzoic acid itself, but their strengths, unlike those of the α-halopyridines, are not greatly different (13). It is probable that hydrogen bonding plus steric effects on resonance and solvation are all operative but it is rather surprising that fluorine, which should have the smallest steric effect on solvation and resonance (base weakening) and which should have the largest hydrogen bonding effect (base strengthening), gives a basicity which is little different from those of the other halogens.

Oxygen-containing Groups

All the oxygen-containing groups exhibit base-strengthening effects relative to benzoic acid itself and all but hydroxyl cause the ortho acids to be stronger bases than their para isomers. The acid-strengthening effect of the *o*-hydroxyl in salicyclic acid is well known and is generally attributed to stabilization of the benzoate anion by internal hydrogen bonding with the hydroxyl group as in II (14, 15).

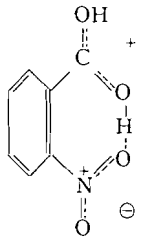


I II

Undoubtedly hydrogen bonding in I stabilizes the cation as hydrogen bonding in II stabilizes the anion, but assessing the relative importance of the above structures is difficult because of the different kinds of protons present. The case of the ortho alkoxy benzoic acids is simpler and it is clear that structures corresponding to I above are responsible for the base-strengthening effect. (The hydroxyl and alkoxyl groups, as expected from earlier work (7), appear to undergo no protonation themselves.)

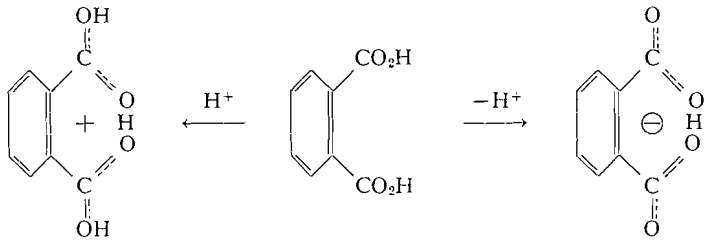
The nitro and carboxyl groups provide very interesting examples of specific ortho interactions which stabilize the protonated forms. Because of the small spectral shift on protonation, *o*-nitrobenzoic acid gave a poor ionization curve and the pK_{BH^+} listed in Table I must be regarded as approximate only. Nevertheless, it is clear that *o*-nitrobenzoic acid is a much stronger base than its para isomer and is even slightly stronger than benzoic acid itself. This can be attributed to hydrogen bonding in the conjugate acid, viz.

Can. J. Chem. Downloaded from www.nrcresearchpress.com by 210.87.254.6 on 09/05/12
For personal use only.



(The reason for the acid strength of *o*-nitrobenzoic acid being so much greater than that of its para isomer is less clear, since no hydrogen bonding is possible in the anion.)

Phthalic acid is much more basic than its meta and para isomers just as it is also more acidic. That is, proton loss from and proton addition to, the ortho dicarboxyl system are both much easier than with the meta and para isomers or with benzoic acid itself. The symmetry of the two ions and their structural similarity can be seen in the following equation.



III

Cation III is a species of some interest since the second ring that is formed by virtue of the hydrogen bridging may have some aromatic character (16). If the hydrogen bonding were strong enough to shorten the oxygen–oxygen bond distance sufficiently to allow some orbital overlap one would have a cyclic system containing six π electrons.

The spectral changes that occur with phthalic acid as the sulphuric acid concentration increases are shown in Fig. 2. Leisten (17) has shown by cryoscopic means that anhydride formation occurs in solutions just above 100% sulphuric acid and the spectrum in 104% acid must be that of the anhydride, probably in its protonated form. The second spectral change which leads to this spectrum is centered at $H_0 = -11.4$. No indication of a second spectral change was observed in the case of isophthalic acid or terephthalic acid even up to 30% fuming sulphuric acid. Probably the protonation of the second carboxyl group in these cases does not give rise to a sufficiently different spectrum to allow detection.

Quantitative Correlations

The parameters, σ^* and E_S, which Taft (1) has used with success to correlate the rates of certain reactions of ortho-substituted compounds, fail in the present case presumably because of resonance effects in the conjugate acid and because of the specific hydrogen-bonding interactions referred to above. There is, however, fair agreement with the Taft equation $\log K/K_0 = \sigma^*\rho^* + E_S$. The modified Farthing and Nam equation (2), $\log K/K_0 = \sigma_{E^+}\rho_{E^+} + \sigma_S\rho_S$, also gives a fair correlation if the widely deviating points for $-NO_2$, $-t$Bu, and $-CO_2H$ are ignored.

Can. J. Chem. Downloaded from www.nrcresearchpress.com by 210.87.254.6 on 09/05/12
For personal use only.

It is interesting to note that, when the values for the acidities of ortho-substituted benzoic acids (pK_a) are plotted against the corresponding basicities (pK_{BH^+}) as in Fig. 1,

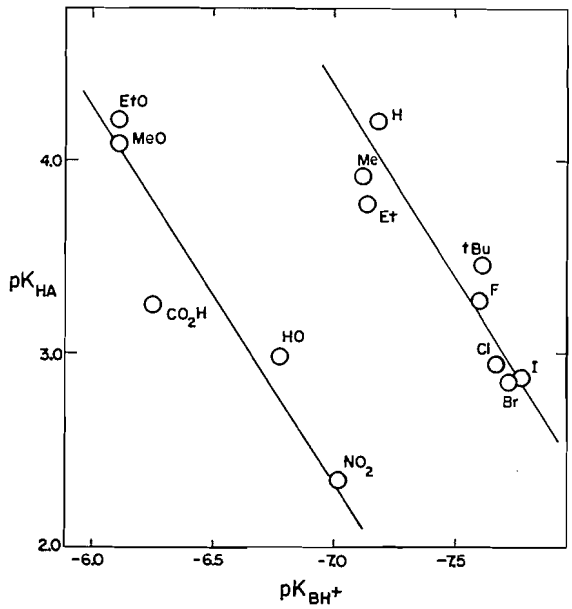


FIG. 1. Plot of the acidities of ortho-substituted benzoic acids (pK_{HA}) against their basicities (as pK_{BH^+}). The point for o-CO_2H has been corrected by 0.3 pK units on each axis for the statistical effect of two carboxyl groups on each ionization.

the substituents fall near two straight lines of approximately the same slope, the oxygen-containing substituents near one line and the other substituents near the other. It will be remembered that of the three general effects mentioned in the Introduction—electronic, steric inhibition of resonance, and steric hindrance to solvation—only the latter was expected to operate in opposite directions in the two series and it thus appears to be of the least importance. The specific interactions between the ionized carboxyl groups and the oxygen-containing substituents also show a surprising degree of regularity.

It has been assumed in this discussion that carbonyl protonation occurs exclusively (7). However, if an ortho substituent inhibits resonance with the ring the energy of the carbonyl-protonated form will rise relative to that of the hydroxyl-protonated form, which is not conjugated with the ring in any case, and it is conceivable that hydroxyl protonation may be significant in some cases. Acylium ion formation, which occurs with 2,6-disubstituted benzoic acids in concentrated sulphuric acid, appeared to be absent in the present work.

EXPERIMENTAL

Reagents

The benzoic acids were purified either by several recrystallizations or by vacuum distillation. Samples of *o*-ethyl, *o*-*i*-propyl, and *o*-*t*-butyl benzoic acids were kindly supplied by Professor Harold Schechter. Sulphuric acid solutions were prepared and standardized as before (7).

Can. J. Chem. Downloaded from www.nrcresearchpress.com by 210.87.254.6 on 09/05/12
For personal use only.

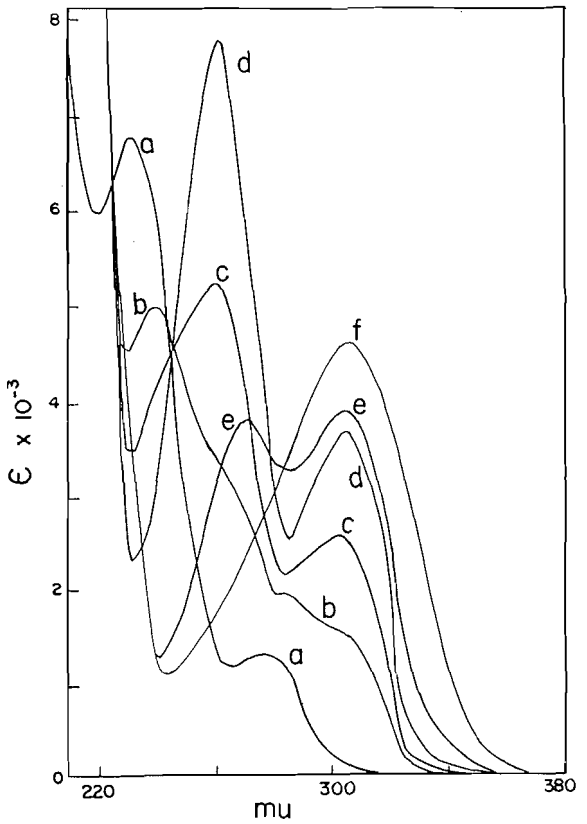


FIG. 2. Ultraviolet absorption spectra of phthalic acid in sulphuric acid solutions: *a* 45%, *b* 70%, *c* 74%, *d* 80%, *e* 100%, *f* 104% H_2SO_4.

Measurement of pK_{BH^+}

This was done by spectrophotometric analysis essentially as previously described (7, 9). In cases of low solubility of the compound in sulphuric acid, stock solutions of the compound were made up in ethanol and 0.05-ml aliquots of this were pipetted into 10-ml volumetric flasks using a 0.100-ml Hamilton syringe with a Chaney adaptor. In these cases the ethanol was not evaporated and a correction was made for the dilution of the sulphuric acid by the ethanol. It was found that the presence of the ethanol in the acid in no way affected the ultraviolet spectrum of the substrate and that identical pK_{BH^+} values, within experimental error, could be obtained by the two methods. Dilution experiments after 1 hour showed that no irreversible changes such as sulphonation were occurring in the concentrated acid.

Calculations

Two methods were used to calculate the pK_{BH^+} values. The first was the graphical method of Davis and Geissman (18) involving the plotting of $D_{\lambda_l} - D_{\lambda_u}$ against H_0 where λ_l and λ_u are wavelengths at which the ion and neutral molecule, respectively, absorb strongly. This produces a "titration curve" from which the inflection point can be read. The following modification of this method was also used (7). Let $\Delta D_B = D_{\lambda_l} - D_{\lambda_u}$ in an acid concentration in which the base is effectively unionized and let $\Delta D_{BH^+} = D_{\lambda_l}$

Can. J. Chem. Downloaded from www.nrcresearchpress.com by 210.87.254.6 on 09/05/12
For personal use only.

$-D_{\lambda_u}$ in an acid concentration in which the base is effectively completely ionized and let $\Delta D = D_{\lambda_l} - D_{\lambda_u}$ in the acids which partly ionize the base. It can be shown that a plot of $\log(\Delta D_{BH^+} - \Delta D/\Delta D - \Delta D_B)$ against H_0 should give a straight line of unit slope with the intercept equal to pK_{BH^+}. The advantage of this method is that the need for an arbitrary choice of the inflection point of a curve is eliminated since the best straight line may be found by the method of least squares. However, difficulty is often experienced in choosing appropriate optical densities to correspond to zero and complete ionization since solvent shifts usually occur for both the unionized and ionized forms but particularly for the latter as pointed out earlier by Hammett (5, 6). The result of this is that if the spectrum obtained in, say, 98% sulphuric acid, is used for the completely ionized form of a compound which is half ionized in, say, 60% acid an inflated value for D_{BH^+} results since increasing the sulphuric acid concentration usually produces a red shift and an increased extinction coefficient. This, in turn, results in plots by the "linear method" which are, in fact, frequently linear but which often have non-unit slopes.

We have attempted to cancel the solvent shifts partially by choosing as our values of D_u and D_l those which are obtained by moving 1.5 H_0 units in both directions from the pK_{BH^+} determined by the first method above. The choice of 1.5 units is arbitrary and, if there were no solvent spectral shift at all, would result in an error of about 3% in the assigned values of D_u and D_l.

The slopes shown in Table I are close to unity and, in support of the method used here, the plots were all very good straight lines provided values of the logarithmic function between +1.0 and −1.0 were used whereas if D_u and D_l were assigned, using values many H_0 units away from the pK_{BH^+}, the plots were very often non-linear. It may be mentioned that, when the present method was applied to the data previously obtained with aldehydes, ketones, acids, and amides, somewhat lower slopes were obtained than with the ortho-substituted acids reported here. The values for the former were mostly in the 0.9–1.1 range.

There is always the possibility that the irregularities in the log plots are not caused entirely by solvent effects on the spectra. It is conceivable that weak bases of the carbonyl type studied in this and earlier work are following some acidity function other than H_0, a scale which was established chiefly with the aid of nitrogen bases. The deviations from unit slope listed in Table I are not great, except for *o*-iodobenzoic acid, and we believe that they are caused by solvent effects on the spectra rather than by deviations of the ionization process from ideal behavior (8, 19). If, for example, the ionization process was following the h_R' (20) function rather than h_0 a slope of approximately two would result (18). However, in order to shed further light on the matter we are at present examining systematically the variations in the spectra of carbonium ions, ammonium ions, and oxonium ions with changing sulphuric acid concentration.

The values in Tables I and II are quoted to two decimal places. However, in view of the fact that many of the pK_{BH^+} values were measured in the region 70–80% sulphuric acid where the H_0 scale is considered to be not firmly established and in view of the difficulties caused by solvent effects on spectra, there may well be an absolute error of 0.2 pK units although the relative errors within a series will be less than this.

ACKNOWLEDGMENT

We are grateful to the National Research Council of Canada for financial support, including the award of a Studentship to one of us (M.R.G.).

Can. J. Chem. Downloaded from www.nrcresearchpress.com by 210.87.254.6 on 09/05/12
For personal use only.

REFERENCES

1. R. W. TAFT, JR. *In* Steric effects in organic chemistry. *Edited by* M. J. Newman. John Wiley & Sons, Inc., New York. 1956. Chap. 13.
2. A. C. FARTHING and B. NAM. *In* Steric effects in conjugated systems. *Edited by* G. W. Gray. Butterworths, London. 1958. Chap. 11.
3. G. BADDELEY. Nature, **144**, 444 (1959).
4. H. C. BROWN, D. H. MCDANIEL, and O. HÄFLIGER. *In* Determination of organic structure by physical means. *Edited by* E. A. Braude and F. C. Nachod. Academic Press, New York. 1955. Chap. 14.
5. L. P. HAMMETT. Physical organic chemistry. McGraw-Hill Book Co., New York. 1940. Chap. 9.
6. L. A. FLEXER, L. P. HAMMETT, and A. DINGWALL. J. Am. Chem. Soc. **57**, 2103 (1935).
7. R. STEWART and K. YATES. J. Am. Chem. Soc. **82**, 4059 (1960).
8. E. M. ARNETT and C. Y. WU. J. Am. Chem. Soc. **82**, 5660 (1960).
9. K. YATES and R. STEWART. Can. J. Chem. **37**, 664 (1959).
10. R. W. TAFT, M. S. NEWMAN, and F. H. VERHOEK. J. Am. Chem. Soc. **72**, 4511 (1950).
11. M. CHARTON. Can. J. Chem. **38**, 2493 (1960).
12. H. C. BROWN and A. CAHN. J. Am. Chem. Soc. **77**, 1715 (1955).
13. D. H. MCDANIEL and H. C. BROWN. J. Am. Chem. Soc. **77**, 3756 (1955).
14. W. BAKER. J. Chem. Soc. 1687 (1934).
15. G. E. K. BRANCH and D. L. YABROFF. J. Am. Chem. Soc. **56**, 2568 (1934).
16. D. GINSBURG (*Editor*). Nonbenzenoid aromatic compounds. Interscience Press, New York. 1959.
17. J. A. LEISTEN. J. Chem. Soc. 2191 (1961).
18. C. T. DAVIS and T. A. GEISSMAN. J. Am. Chem. Soc. **76**, 3507 (1954).
19. A. J. KRESGE and Y. CHIANG. Proc. Chem. Soc. 81 (1961).
20. N. C. DENO, P. T. GROVES, and G. SAINES. J. Am. Chem. Soc. **81**, 5790 (1959).

Can. J. Chem. Downloaded from www.nrcresearchpress.com by 210.87.254.6 on 09/05/12
For personal use only.

Can. J. Chem. Downloaded from www.nrcresearchpress.com by 210.87.254.105 on 09/05/12
For personal use only.

TRYPTAMINES, CARBOLINES, AND RELATED COMPOUNDS

PART IX. THE CYCLIZATION OF SOME NITRO- AND AZIDO-PHENYLPYRIDINES. PYRIDO[1,2-*b*]INDAZOLE[1,2]

R. A. Abramovitch and K. A. H. Adams

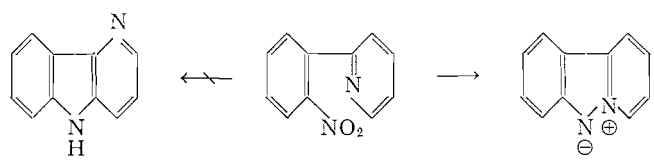
ABSTRACT

Heating 2-*o*-nitrophenylpyridine with ferrous oxalate gives rise to pyrido[1,2-*b*]indazole (III). The evidence for the structure of this compound is discussed. Similarly, heating 2-*o*-nitrophenylpyridine methiodide and *N*-oxide with ferrous oxalate gives (III), in each case, demethylation and deoxygenation preceding the cyclization. In the latter case a minute amount of δ-carboline is also formed. Heating pyridine-*N*-oxides with ferrous oxalate is a potentially general method of effecting deoxygenations of these compounds. Contrary to the results of Smith and Boyer (11), it is found that heating 2-*o*-azidophenylpyridine also gives rise to (III). On the other hand, the action of heat on 2-*o*-azidophenylpyridine-*N*-oxide gives a mixture of δ-carboline and δ-carboline-*py*-*N*-oxide in low yield. The mechanism of the cyclization of the azides and of the reaction taking place on heating nitro-compounds with ferrous oxalate is discussed briefly; the formation of a nitrene intermediate is favored.

The catalytic reduction of 2-*o*-nitrophenylpyridine-*N*-oxide giving rise to the azoxy-, azo-, and hydrazo-derivatives is described and the ultraviolet absorption spectra of these compounds are discussed. It is concluded the steric inhibition of coplanarity exists in the azoxy- and azo-compounds leading to the lack of effective conjugation across the N=N bond.

When this work was initiated no suitable method for the synthesis of the δ-carboline ring system was available. Since that time, however, δ-carboline (I) has been obtained in this laboratory by the thermal cyclization of 3-azido-2-phenylpyridine (1). The yields in this reaction are variable, however, and a better method was sought. To this end, the action of ferrous oxalate on 2-*o*-nitrophenylpyridine was investigated.

Ferrous oxalate has been used in a number of interesting cyclizations. Thus, heating it with 2-nitrodiphenyl gives rise to carbazole (2); phenazines have also been obtained from 2-nitrodiphenylamines by this method (2, 3). On the other hand, 4-nitrocarbazole was not obtained from 2,2′-dinitrodiphenyl, but instead 3,4-benzocinnoline was isolated (2). The action of ferrous oxalate on 2-*o*-nitrophenylpyridine (II) at 300° has now been examined. It was anticipated that the pyridine nuclear carbons might be relatively deactivated towards such a cyclization, but that it could conceivably occur at the 3-position of the pyridine ring to give δ-carboline. Cyclization did, in fact, occur but onto the pyridine nitrogen atom to give pyrido[1,2-*b*]indazole (III), no δ-carboline being formed.



(I) (II) (III)

The evidence for the formulation of the cyclization product as pyrido[1,2-*b*]indazole is as follows:

(i) The product is different from any of the carbolines, all of which are now known,

[1]*Manuscript received April 26, 1961.*
Contribution from the Department of Chemistry, University of Saskatchewan, Saskatoon, Saskatchewan. Part of this paper formed the subject of a lecture given at the Fifth Western Regional Conference of the Chemical Institute of Canada held in Regina in September, 1960.
[2]*Part VIII: Can. J. Chem.* **38**, *2152 (1960).*

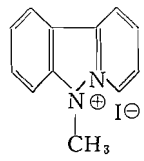
Can. J. Chem. Downloaded from www.nrcresearchpress.com by 210.87.254.105 on 09/05/12
For personal use only.

and melts (83–84°) well below the melting point of the carbolines (~200°). It analyzed correctly for $C_{11}H_8N_2$.

(ii) The infrared spectrum of the compound did not exhibit an N—H stretching absorption and no active hydrogen could be detected. On the other hand, γ-carboline gave an atom of active hydrogen quantitatively. The compound is unaffected by boiling with mineral acids or with aqueous ethanolic alkali (no rearrangement to a more stable structure) and does not take up hydrogen in the presence of Adams' catalyst at atmospheric pressure. It does form an unstable hydrochloride and a picrate.

(iii) Unlike the carbolines, it did not form a methiodide readily, but did so to give (IV) under forcing conditions (in ethanol in a sealed tube for 18 hours at 100°). That no C-alkylation had taken place in this reaction was indicated by the absence of a C—CH_3 group (Kühn-Roth).

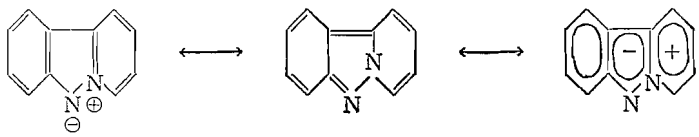
(iv) The infrared spectrum of the product showed a medium intensity band at 1650 cm^{-1}, somewhat higher than is usually found for aromatic rings. A similarly high frequency (1642 cm^{-1}) was reported (4) for anthranil in which a dipolar form —C_6H_4—$\overset{\ominus}{N}$— contributes greatly to the structure. The ultraviolet absorption spectra of (III) and its derivatives are also interesting. The spectrum of the free base in alcohol, that of the

(III) ⟶ 

(IV)

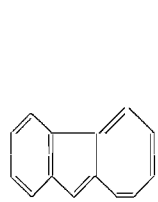
base in alcohol at pH 11, and that of the hydrochloride in alcohol are identical, pointing to the dissociation of the hydrochloride in this solvent. On the other hand, the base in aqueous hydrochloric acid at pH 1 had a spectrum very similar to that of the methiodide (IV) in alcohol, the methyl group having its usual bathochromic effect. The most striking features of the latter ultraviolet spectra are the very high extinction coefficients of the low wavelength bands ($\epsilon \times 10^{-3}$ 182.4 and 196.0 for the hydrochloride and methiodide respectively).

The heterocyclic rings in (III) are isoelectronic with azulene and one could write a number of canonical structures for this molecule:

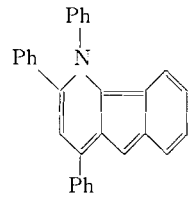


(A) (B) (C)

A number of lines of evidence point to the fact that the orthoquinonoïd anhydro-base structure (B) is probably a minor contributor to the resonance hybrid. Azulene (in which the dipolar structure plays only a small role), 1,2-benzazulene (V), and a variety to pseudo-azulenes such as 1,2,4-triphenylindeno[1,2-*b*]pyridine (VI) (5) are all highly colored; all the carboline anhydro-bases are deep yellow or orange. Paoloni and Marini-Bettòlo (6) have attributed the color of the anhydronium base of 7-azaindole to the



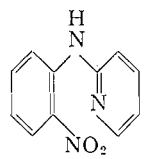
(V)



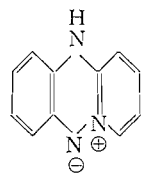
(VI)

orthoquinonoïd form and have suggested that the carboline anhydronium bases as well as sempervirine are best represented by the covalent formulae not bearing separated charges.* From a study of the spectral properties of the δ-carboline anhydronium base Abramovitch, Adams, and Notation (1) suggested that the quinonoïd structure is a more important contributor to the resonance hybrid than the dipolar one. On the other hand, pyrido[1,2-*b*]indazole is colorless, as is its methiodide. In addition, carboline anhydronium bases form *ind-N*-methiodides readily at room temperature (1, 8) whereas (III) only does so under forcing conditions. Similarly, carboline anhydronium bases can be readily hydrogenated (e.g. reduction of cryptolepine (9)) whereas pyrido[1,2-*b*]indazole is not. Gray (10) has interpreted the low base strength of the α-carboline anhydronium base (pK_a 7.75)† as compared with the γ-derivative (pK_a 10.54) on the basis of two factors: (*a*) a much increased stability of the α-anhydronium base as a result of the juxtaposition of the oppositely charged centers (presumably in the dipolar form); and (*b*) a reduced stability of the α-carboline salt owing to the inductive effect of the indole nitrogen attached to the same carbon as the positively charged pyridine nitrogen. It would be expected that in (A) ↔ (C) these effects would be greatly intensified; in fact the pK_a of pyrido[1,2-*b*]indazole has now been found to be approximately 2.48, slightly more than five p*K* units lower than the base strength of the α-carboline anhydronium base!

An attempt was made to obtain further examples of this type of cyclization onto a pyridine nitrogen atom. 2-Nitro-*N*-2′-pyridylaniline (VII) was prepared from 2-bromopyridine and *o*-nitroaniline. The action of ferrous oxalate at 300° on (VII) led to the formation of tars, no product corresponding to (VIII) being detected. This was not totally unexpected since the central ring in (VIII) would be nonaromatic (8 π electrons, compared with 6 π electrons in (III)) so that the incentive leading to its formation may have been lacking. A similar result was obtained using *N*-methyl-2-nitro-*N*-2′-pyridylaniline.



(VII)



(VIII)

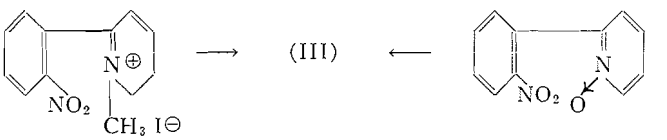
It was hoped to force cyclization to occur at C_3 by blocking the pyridine nitrogen atom

**Paoloni (7) has recently elaborated further on this point. Apart from the fact that his calculations do not lead to correct values for the pK_a and U.V. spectrum of δ-carboline, his conclusion that it is unnecessary to represent the carboline anhydro-bases as hybrids of dipolar and quinonoïd structures in view of the fact that his results "illustrate eloquently the compromise between the tendency to form the (aromatic) sextet and that to neutralize the charges" seems a contradiction in ideas.*

†The pK_a of this compound, as determined by us (1), was 7.55.

Can. J. Chem. Downloaded from www.nrcresearchpress.com by 210.87.254.105 on 09/05/12
For personal use only.

in (II). Thus, 2-*o*-nitrophenylpyridine methiodide (IX) and 2-*o*-nitrophenylpyridine-*N*-oxide (X) were prepared. It was realized that the *N*-oxide grouping in (X) might not survive the reducing conditions present during the cyclization reaction but it was hoped that cyclization at the 3-position would occur before reduction. In actual practice, heating either (IX) or (X) with ferrous oxalate led to the formation of pyrido[1,2-*b*]indazole. Chromatography on a column of alumina of the crude product from the cyclization of the *N*-oxide yielded, apart from (III), trace amounts of a solid which had an infrared spectrum almost identical with that of δ-carboline. Insufficient material was available to study this product further.



(IX) (X)

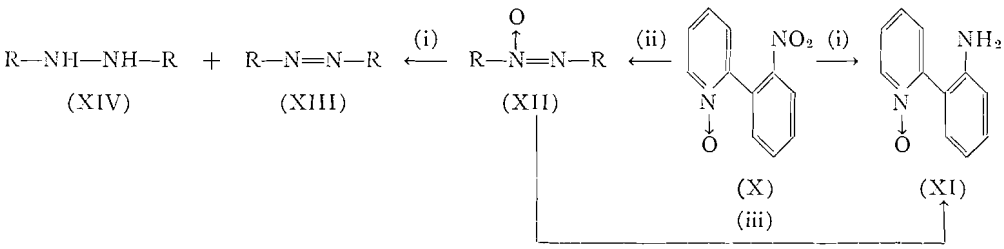
It was of interest from the point of view of the mechanism of the cyclization reaction to determine whether elimination of the protecting groups could occur prior to the cyclization, or whether some mode of concerted attack by the intermediate formed from the reduction of the nitro group and elimination of the protecting group was taking place. To this end, the action of ferrous oxalate at 300° on 2-phenylpyridine methiodide and 2-phenylpyridine-*N*-oxide was studied; in both cases 2-phenylpyridine was isolated in yields comparable to the respective reactions using (IX) and (X). In fact, 2-phenylpyridine could be obtained from the corresponding methiodide by heating it at 300° with granulated lead (used to permit the even distribution of heat in the mixture during such cyclization reactions) but without ferrous oxalate. On the other hand, 2-phenylpyridine-*N*-oxide was recovered unchanged under such conditions. It would, therefore, seem that elimination of the protecting group probably precedes cyclization onto the ring nitrogen atom, though the isolation of a trace of a second product in the *N*-oxide case suggests that conditions might be found where the reverse might be achieved. The reduction of the pyridine-*N*-oxide by ferrous oxalate may well be a general reaction of such amine oxides; this is under investigation.

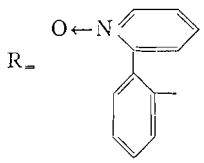
Smith and Boyer (11) attempted to prepare δ-carboline by the thermal cyclization of 2-*o*-azidophenylpyridine in decalin solution but reported obtaining instead 2-*o*-aminophenylpyridine, formed presumably by hydrogen abstraction from the solvent by the intermediate involved. In the present work this reaction gave rise to a 60% yield of pyrido[1,2-*b*]indazole, only a trace of diazotizable material being detected in the crude reaction mixture. No amine could be isolated by chromatography of the crude product on alumina. Attempts at photodecomposition of the azide in solution were unsuccessful though some darkening did occur. This is similar to the experience of Smolinsky, who was working with 2,4,6-trimethyl-2′-azidodiphenyl (12).

Once again, blocking the pyridine nitrogen atom by *N*-oxide formation prior to cyclization was attempted. 2-*o*-Nitrophenylpyridine-*N*-oxide (X) could be reduced catalytically in acetic acid solution with hydrogen and palladium–charcoal to the amine (XI), the *N*-oxide grouping being unaffected. This result is in agreement with previous hydrogenations of pyridine-*N*-oxides (13, 14) which indicated that the *N*-oxide group in 2-substituted pyridine-*N*-oxides was sterically hindered and thus resisted reduction. If, on the

Can. J. Chem. Downloaded from www.nrcresearchpress.com by 210.87.254.105 on 09/05/12
For personal use only.

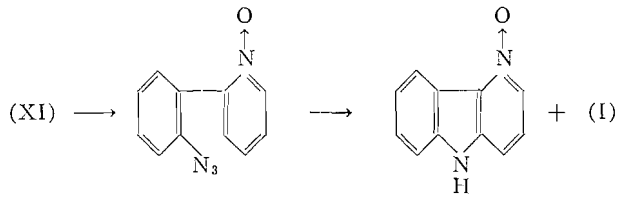
other hand, the catalytic reduction was carried out in alcohol solution the product isolated was 2,2′-di-(*N*-oxido-2-pyridyl)azoxybenzene (XII). This, on catalytic reduction in glacial acetic acid solution gave 2,2′-di-(*N*-oxido-2-pyridyl)azobenzene (λ_{max} 230, 323, 455 mμ; λ_{infl} 260 mμ; $\epsilon \times 10^{-3}$ 44.73, 19.02, 0.58, 28.70) (XIII) together with a small amount of what is probably the hydrazo-compound (XIV), though the latter proved to be very difficult to purify. Its structure was inferred from its infrared spectrum and from its ultraviolet absorption spectrum, which was similar to that of 2-*o*-aminophenylpyridine-*N*-oxide (XI). The azoxy-compound (XII) was reduced directly to the amine (XI) by stannous chloride and hydrochloric acid. These reductions are somewhat similar to those reported by Hayashi, Yamanaka, Iyima, and Matsushita (15), who studied the catalytic reduction of 4,4′-azoxypyridine 1,1′-dioxide. The amine (XI) was converted





(i) 5% Pd–C in AcOH; (ii) 5% Pd–C in EtOH; (iii) $SnCl_2$–HCl.

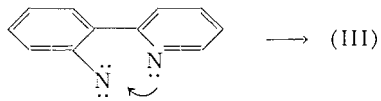
to the azide (XV), which, on thermal decomposition in decalin solution, gave a crude mixture from which δ-carboline (I) and δ-carboline-*py*-*N*-oxide (XVI) could be isolated in low yield by chromatography on alumina. The structure of (XVI) was proved by its synthesis from authentic δ-carboline.



It is interesting to speculate about the mechanisms of the cyclization onto the pyridine nitrogen atom reported here. In the case of the thermal decomposition of the azides two groups of workers have very recently suggested that a nitrene, —N:, may be involved (12, 16). Such an entity, were it formed, would be isoelectronic with a carbene and could be strongly electrophilic. In support of this suggestion is the finding that thermal decomposition of 2,4,6-trimethyl-2′-azidodiphenyl gives rise to 8,10-dimethylphenanthridine (12), which can conceivably arise by attack of a benzylic C—H by a nitrene intermediate.

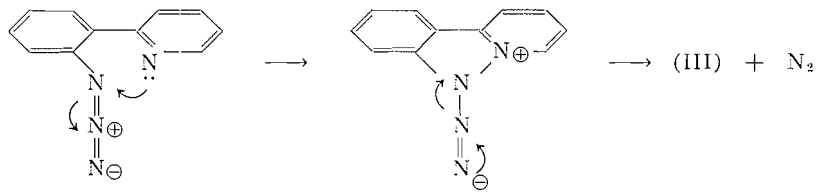
Can. J. Chem. Downloaded from www.nrcresearchpress.com by 210.87.254.105 on 09/05/12
For personal use only.

This may well explain the present results; such an electrophilic species would certainly tend to attack the pair of electrons on the pyridine nitrogen atom rather than the 3-position of the pyridine ring which is deactivated toward electrophilic substitution. On

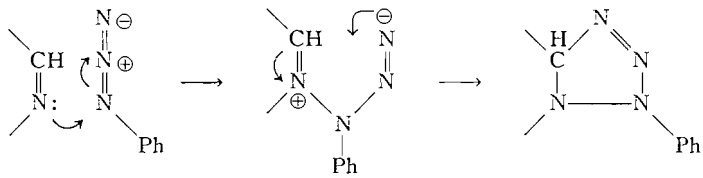


(D)

the other hand, one cannot at present eliminate a concerted or perhaps two-stage mechanism involving cyclization concurrent with, or followed by, the elimination of a nitrogen molecule:



Such a N—N bond formation has an analogy in the known reaction of aryl azides with benzaldehyde arylhydrazones which gives rise to tetrazole derivatives (17) for which one might visualize the following sequence:



We tend to prefer the "nitrene intermediate" mechanism at the present time, at least as far as the reaction leading to (XVI) and (I) goes (for arguments in favor of the formation of such an intermediate see ref. 12). A nitrene intermediate is probably formed during the ferrous oxalate cyclization of the nitro-compounds and it would be attractive to visualize a common reactive intermediate species for both of these reactions, leading as they do to the same product. The concerted mechanism for the conversion of the azide to (III) must, however, be seriously considered.

Not much is known concerning the mode of action of ferrous oxalate in these reactions. It presumably decomposes thermally to give a very reactive form of ferrous oxide (some iron may also be formed), which is the actual reducing agent (2, 3). This can either abstract both oxygen atoms from the nitro-group to give a nitrene (D), or else first give rise to a nitroso-derivative which could then add to the pyridine nitrogen atom and lose a second atom of oxygen to form the pyrido[1,2-*b*]indazole. The latter pathway seems a less likely one in view of the above azide cyclizations.

One further matter should be commented on and that is the similarity between the ultraviolet absorption spectra of the azoxybenzene (XII), the azobenzene (XIII), the hydrazo-derivative (XIV), and the amine (XI) (Fig. 1). The spectra of (XIV) and (XI) are almost superimposable (as expected), except that in the case of (XIV) the

Can. J. Chem. Downloaded from www.nrcresearchpress.com by 210.87.254.105 on 09/05/12
For personal use only.

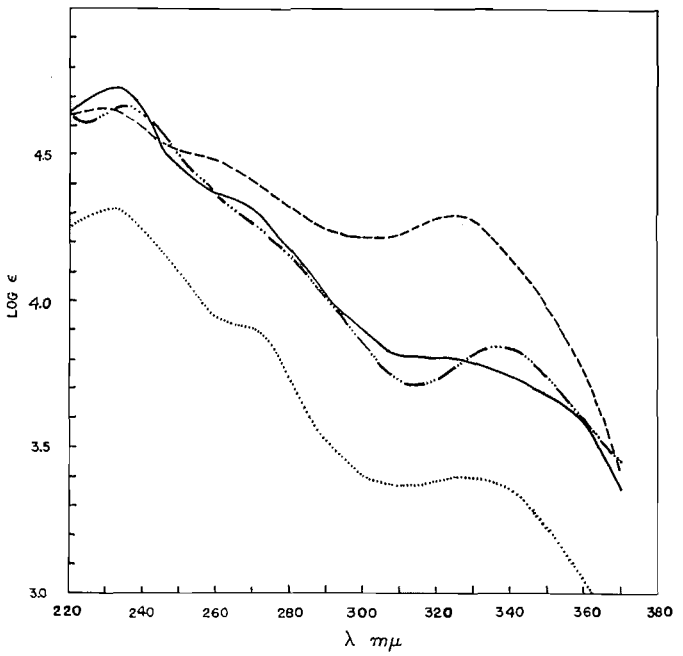


FIG. 1. Ultraviolet absorption spectra in 95% ethanol solution. —— 2,2′-Di-(*N*-oxido-2-pyridyl)azoxybenzene; – – – 2,2′-di-(*N*-oxido-2-pyridyl)azobenzene; —· · · 2,2′-di-(*N*-oxido-2-pyridyl)hydrazobenzene; · · · · 2-*o*-aminophenylpyridine-*N*-oxide.

maxima have all undergone a small bathochromic shift and the intensities are markedly greater. On the other hand, the spectra of azoxybenzene, azobenzene, and aniline are quite different from each other (18, 19), which is not the case for our compounds. One would have to attribute such a result to steric hindrance in the cases of (XII) and (XIII) preventing coplanarity of the two benzene rings and the N=N linkage and thus inhibiting effective conjugation across that linkage. This would result in each of these molecules having an absorption spectrum similar to that of the amine (XI), only more intense, which is what is actually observed.

EXPERIMENTAL

Melting points are uncorrected. Infrared spectra were measured using a Perkin–Elmer Model 21 instrument equipped with sodium chloride optics. Ultraviolet absorption spectra were measured on a Cary Model 14 recording spectrometer.

Action of Ferrous Oxalate on 2-o-Nitrophenylpyridine–Pyrido[1,2-b]indazole

2-*o*-Nitrophenylpyridine (20) (1 g) and ferrous oxalate dihydrate (1.3 g) were mixed with granulated lead (10 g) and heated at 300° (internal temperature) (metal bath) for 45 minutes. (At the beginning of the reaction the smell of ammonia being evolved could be detected and a piece of red litmus paper held at the mouth of the flask turned blue.) The cooled mixture was extracted repeatedly with ether, and the combined extracts were dried ($MgSO_4$) and evaporated to give an oil which solidified and was recrystallized from light petroleum (b.p. 60–80°) (charcoal) giving *pyrido[1,2-b]indazole* as rods (0.5 g), m.p. 83–84°. Calc. for $C_{11}H_8N_2$: C, 78.57; H, 4.76; N, 16.66; mol. wt. 168. Found: C,

Can. J. Chem. Downloaded from www.nrcresearchpress.com by 210.87.254.105 on 09/05/12
For personal use only.

78.47; H, 4.80; N, 16.90; mol. wt. 152. No active hydrogen was present in the product. An active hydrogen determination on γ-carboline gave 0.61% active H (calc. 0.6%). Infrared spectrum (Nujol mull) (main peaks only): 1650 (m), 1623 (m), 749 (s), 743 (s), and 719 cm^{-1} (s). Ultraviolet absorption spectrum (free base in 95% ethanol or base in alcohol at pH 11): λ_{max} 205, 229, 269, 327 mμ; $\epsilon \times 10^{-3}$ 21.0, 32.7, 23.7, 11.8.

When dry hydrogen chloride was passed through an ethereal solution of pyrido[1,2-*b*]-indazole, an impure hydrochloride, m.p. 161–164°, separated which crystallized from ethanol–ether in needles, m.p. 165–166°. Its ultraviolet absorption spectrum in 95% ethanol, however, was identical with that of the free base, indicating that in this solvent the hydrochloride dissociates to the free base. On the other hand, the base in aqueous hydrochloric acid at pH 1 had λ_{max} 208, 254, 330, 340 mμ; $\epsilon \times 10^{-3}$ 182.4, 140.7, 10.02, 11.37.

The approximate pK_a of pyrido[1,2-*b*]indazole, as determined by potentiometric titration (no solvent correction applied), was 2.48.

Pyrido[1,2-b]indazole picrate separated from alcohol and was recrystallized from acetone, giving yellow needles, m.p. 205°. Calc. for $C_{11}H_8N_2,C_6H_3O_7N_3$: C, 51.50; H, 2.77. Found: C, 51.75; H, 3.00.

The free base was recovered unchanged on:

(i) shaking with hydrogen and Adams' catalyst;
(ii) boiling with 10% hydrochloric acid for 4 hours;
(iii) boiling with 20% aqueous ethanolic potassium hydroxide for 6 hours;
(iv) treatment with an excess of methyl iodide in ethanol at room temperature.

9-Methylpyrido[1,2-b]indazolium Iodide

Pyrid[1,2-*b*]indazole (0.2 g) in ethanol (2 ml) was heated with an excess of methyl iodide (2 ml) in a sealed tube at 100° (water bath) for 18 hours. The product which crystallized out on cooling was taken up in ethanol and combined with the mother liquors and the solution was evaporated to a small volume after boiling with charcoal. Brownish plates (0.3 g) separated which were recrystallized from ethanol to give brownish shiny plates, m.p. 208–209°. These were dissolved in water and filtered from a trace of amorphous brown solid, and the filtrate evaporated to dryness to give the *methiodide*, which on recrystallization from ethanol was obtained as cream-colored prisms, m.p. 226–227°. Calc. for $C_{12}H_{11}N_2I$: C, 46.45; H, 3.55; N, 9.03; I, 40.97. Found: C, 46.88; H, 3.66; N, 8.75; I, 40.63. No C—CH_3 was found in a Kühn-Roth determination. λ_{max} 223, 256, 334, 349 mμ; $\epsilon \times 10^{-3}$ 196.0, 20.0, 9.1, 11.8 (in ethanol).

2-Nitro-N-2'-pyridylaniline

2-Bromopyridine (5 g, redistilled), *o*-nitroaniline (6 g), anhydrous potassium carbonate (4.5 g), and a trace of copper-bronze were heated at 195–210° (metal bath) for 7 hours when no more carbon dioxide was evolved. Water was added and the excess *o*-nitroaniline removed by steam distillation. The residue was extracted with chloroform, the extract dried ($MgSO_4$) and evaporated, and the residue vacuum distilled to give *2-nitro-N-2'-pyridylaniline* as a red oil (2.4 g), b.p. 140–150° at 0.05 mm, which solidified. The product could be recrystallized from light petroleum (b.p. 40–60°) and formed red rods, m.p. 68–69°. Calc. for $C_{11}H_9O_2N_3$: C, 61.39; H, 4.22. Found: C, 61.52; H, 4.00.

The *hemipicrate* separated from ethanol and was recrystallized from the same solvent to give yellow plates, m.p. 172°. Calc. for $C_{11}H_9O_2N_3,\frac{1}{2}C_6H_3O_7N_3$: C, 51.0; H, 3.2. Found: C, 51.1; H, 3.1.

Can. J. Chem. Downloaded from www.nrcresearchpress.com by 210.87.254.105 on 09/05/12
For personal use only.

2-o-Nitrophenylpyridine-N-oxide

2-*o*-Nitrophenylpyridine (0.9 g) was dissolved in glacial acetic acid (20 ml), and 35% hydrogen peroxide (0.44 g) was added. The solution was heated on a water bath at 90° for 9 hours. An additional amount of 35% hydrogen peroxide (0.44 g) was added and heating was continued at 90° for a further 9 hours. The acetic acid was removed by distillation under reduced pressure and the residue was dissolved in chloroform. Anhydrous sodium carbonate was added to neutralize the remaining acetic acid and the solution was filtered and evaporated to dryness. The residue was crystallized from benzene – light petroleum (b.p. 60–80°) and gave the *N-oxide* (0.92 g) as yellow needles, m.p. 156–157°. Calc. for $C_{11}H_8O_3N_2$: C, 61.11; H, 3.73. Found: C, 61.24; H, 3.75.

1-Methyl-2-o-nitrophenylpyridinium Iodide

2-*o*-Nitrophenylpyridine (0.5 g) in 95% ethanol was treated with an excess of methyl iodide and the solution was allowed to stand at room temperature overnight. On concentration the solution yielded small orange crystals (0.55 g) which were recrystallized from methanol to give the *methiodide* as prisms, m.p. 223–224° (decomp.). Calc. for $C_{12}H_{11}O_2N_2I$: C, 42.08; H, 3.19. Found: C, 42.28; H, 3.30.

Action of Ferrous Oxalate on 2-o-Nitrophenylpyridine-N-oxide

2-*o*-Nitrophenylpyridine-*N*-oxide (1 g), ferrous oxalate dihydrate (1.2 g), and granulated lead (12 g) were intimately mixed and heated at 275–300° (internal temperature) in a metal bath. A small amount of strong-smelling gas which was basic to litmus was evolved during the heating period. The cooled mixture was extracted repeatedly with ether and then with hot benzene. The combined extracts were dried (Na_2SO_4) and evaporated to dryness to yield a brown oil (0.22 g) which was chromatographed on neutral alumina. Elution with benzene gave a light brown crystalline compound (0.19 g) which could be recrystallized from light petroleum (b.p. 60–80°) and had m.p. 84–86°. The infrared spectrum of this product was identical with that of an authentic sample of pyrido[1,2-*b*]indazole. The melting point of the base and its picrate were undepressed on admixture with authentic samples. Elution with benzene–ether yielded a tan solid (0.005 g), m.p. 202–205°, the infrared spectrum of which was almost identical with that of δ-carboline.

Action of Ferrous Oxalate on 1-Methyl-2-o-Nitrophenylpyridinium Iodide

1-Methyl-2-*o*-nitrophenylpyridinium iodide (0.6 g) was intimately mixed with ferrous oxalate dihydrate (0.7 g) and granulated lead (6 g). The mixture was heated at 275–300° (internal temperature) in a metal bath for 30 minutes. A small amount of a strong-smelling, basic (litmus) gas was evolved during the heating period. The reaction mixture was cooled and the black residue was repeatedly extracted with ether. The combined ether extracts were dried (Na_2SO_4) and evaporated to give a brown oil (0.1 g) which partly solidified. This product was recrystallized from light petroleum (b.p. 60–80°) giving tan crystals (0.078 g) which proved to be identical with pyrido[1,2-*b*]indazole (mixed melting point, infrared spectrum).

Cyclization of 2-o-Azidophenylpyridine

2-*o*-Azidophenylpyridine (11) (1.2 g, not purified) was dissolved in redistilled decalin (50 ml) and the solution was heated in an oil bath at 160–170° (internal temperature). Gas bubbles began to be evolved smoothly at about 140°. After 10–15 minutes when no more gas evolution could be observed, the solution was cooled and was extracted with 10% hydrochloric acid. The acid extract was washed with ether, basified with 2 *N*

Can. J. Chem. Downloaded from www.nrcresearchpress.com by 210.87.254.105 on 09/05/12
For personal use only.

sodium hydroxide, and extracted repeatedly with ether. The combined ether extracts were dried (Na_2SO_4) and evaporated to give an oil which solidified. Recrystallization from light petroleum (b.p. 60–80°) gave pyrido[1,2-*b*]indazole (0.54 g), m.p. 84.5–85.5°. The melting point was not depressed on admixture with an authentic sample. The picrate, m.p. 199–200°, did not depress the melting point of an authentic sample of pyrido[1,2-*b*]indazole picrate. The infrared spectrum of the base was identical with that of an authentic specimen.

No primary amine could be isolated when the crude reaction product was chromatographed on a column of neutral alumina.

2-o-Aminophenylpyridine-N-oxide

2-*o*-Nitrophenylpyridine-*N*-oxide (0.5 g) was dissolved in glacial acetic acid (25 ml) and hydrogenated at atmospheric pressure in the presence of 5% palladium on charcoal (0.1 g). Three molar equivalents of hydrogen were absorbed in less than 1 hour. The catalyst was removed by filtration and washed with a little acetic acid and methanol. The combined filtrates were evaporated under reduced pressure and the residue dissolved in chloroform and treated with anhydrous sodium carbonate. The filtered solution was evaporated to give an oil (0.42 g) which crystallized on trituration with methanol and was recrystallized from methanol to give the *amine* as white crystals, m.p. 181.5–182.5°. Calc. for $C_{11}H_{10}ON_2$: C, 70.95; H, 5.41. Found: C, 70.72; H, 5.38. λ_{max} 232, 325 mμ; λ_{infl} 270, 220 mμ; $\epsilon \times 10^{-3}$ 20.86, 2.54, 8.06, 17.60 (in 95% ethanol).

2-o-Azidophenylpyridine-N-oxide

2-*o*-Aminophenylpyridine-*N*-oxide (0.30 g) was dissolved in concentrated hydrochloric acid (0.6 ml) and water (1.5 ml) and the solution treated at 0° with a solution of sodium nitrite (0.12 g) in water (1 ml). An excess of a saturated aqueous solution of sodium azide was added, the temperature being maintained between 0 and 5°. The white *azide* which precipitated was filtered, washed with water, and dried. The aqueous filtrate was basified with 2 *N* sodium hydroxide, extracted with chloroform, and the extract dried (Na_2SO_4). Evaporation of the chloroform yielded an additional quantity of azide. The combined solid products (0.286 g) were recrystallized from benzene – light petroleum (b.p. 60–80°) and had m.p. 165–166°. Calc. for $C_{11}H_8ON_4$: C, 62.25; H, 3.80. Found: C, 62.60; H, 3.88.

Cyclization of 2-o-Azidophenylpyridine-N-oxide

2-*o*-Azidophenylpyridine-*N*-oxide (0.5 g) was dissolved in hot redistilled decalin (60 ml) and the solution heated in an oil bath at 175–180° (internal temperature) for 40 minutes during which time nitrogen was evolved and the solution became very dark. It was then boiled under reflux for an additional 10 minutes, cooled, and the solid which separated was filtered. The decalin solution was extracted with 10% hydrochloric acid, and the aqueous solution was basified with 2 *N* sodium hydroxide and extracted with chloroform. The dried (Na_2SO_4) chloroform extract was evaporated under reduced pressure. The residue was combined with the solid which was filtered off after the reaction (total 0.3 g), dissolved in methanol, filtered to remove some black solid (0.150 g), and the filtrate chromatographed on neutral alumina. Elution with benzene gave a solid (0.010 g) which was identified as δ-carboline by its infrared spectrum and mixed melting point with an authentic specimen. Elution with ether–methanol yielded at first a solid (0.046 g) which could be crystallized from benzene containing a small amount of methanol and had m.p. 277–278° (decomp.). Its infrared spectrum was identical

Can. J. Chem. Downloaded from www.nrcresearchpress.com by 210.87.254.105 on 09/05/12
For personal use only.

with that of an authentic sample of δ-carboline-*py*-*N*-oxide and the melting point was not depressed on admixture with a sample prepared from δ-carboline as described below. Subsequent fractions yielded only intractable dark brown residues.

δ-Carboline-py-N-oxide

δ-Carboline (0.050 g) was dissolved in glacial acetic acid (8 ml), and 35% hydrogen peroxide (0.1 g) was added. The solution was heated on a water bath at 90° for 10 hours. More 35% hydrogen peroxide (0.1 g) was added and heating was continued for an additional 9 hours. The acetic acid was evaporated under reduced pressure, and the residue was dissolved in chloroform and treated with anhydrous sodium carbonate. Evaporation of the chloroform gave the *N-oxide* (0.050 g) which was recrystallized from benzene containing some methanol (charcoal). This crude yellow product was dissolved in dilute hydrochloric acid, filtered, basified with 2 *N* sodium hydroxide, and extracted with chloroform. Evaporation of the dried (Na_2SO_4) chloroform solution gave a white residue which was recrystallized from benzene containing some methanol to give white crystals which melted at 277–278° (decomp.). Calc. for $C_{11}H_8N_2O$: C, 71.72; H, 4.38. Found: C, 71.65; H, 4.60. Infrared spectrum (KBr disk) (main peaks only): 1630 (m), 1605 (m), 1574 (m), 1215 (s), 865 (m), 782 (m), 750 (s), 705 cm^{-1} (s).

Catalytic Reduction of 2-o-Nitrophenylpyridine-N-oxide in 95% Ethanol – 2,2′-Di-(N-oxido-2-pyridyl)azoxybenzene

2-*o*-Nitrophenylpyridine-*N*-oxide (0.82 g) was dissolved in 95% ethanol (35 ml) and hydrogenated at atmospheric pressure in the presence of 5% palladium on charcoal (0.17 g). The reduction was complete in about 90 minutes. The catalyst was filtered and washed with glacial acetic acid. The combined filtrates were evaporated to a small volume under reduced pressure, the residue was dissolved in chloroform and treated with anhydrous sodium carbonate to neutralize any remaining acetic acid. The solution was filtered and evaporated to dryness and the residue recrystallized from methanol to give the *azoxy* compound (0.58 g), m.p. 236–237°. Calc. for $C_{22}H_{16}O_3N_4$: C, 68.74; H, 4.38. Found: C, 68.46; H, 4.32. Infrared spectrum (KBr disk) (main peaks only): 1600 (m), 1255 (s), 850 (s), 780 (s), 770 (s), 750 cm^{-1} (sh). λ_{max} 233, 325 mμ; λ_{infl} 220, 270 mμ; $\epsilon \times 10^{-3}$ 53.50, 6.50, 43.20, 21.00 (in 95% ethanol).

Catalytic Reduction of 2,2′-Di-(N-oxido-2-pyridyl)azoxybenzene in Glacial Acetic Acid – 2,2′-Di(N-oxido-2-pyridyl)azobenzene and 2,2′-Di-(N-oxido-2-pyridyl)hydrazobenzene

2,2′-Di-(*N*-oxido-2-pyridyl)azoxybenzene (0.050 g) was dissolved in glacial acetic acid (10 ml) and hydrogenated at atmospheric pressure in the presence of 5% palladium on charcoal (0.010 g). The reduction product was isolated as in the previous experiment. The residue was washed with methanol and crystallization took place. The crude product was separated by fractional crystallization from benzene into *2,2′-di-(N-oxido-2-pyridyl)-azobenzene* obtained as orange crystals (0.020 g), m.p. 264° (decomp.) [Calc. for $C_{22}H_{16}O_2N_4$: C, 71.72; H, 4.38. Found: C, 71.62; H, 4.71. Infrared spectrum (KBr disk) (main peaks only): 1585 (w), 1255 (s), 845 (s), 780 (s), 750 cm^{-1} (m). λ_{max} 230, 323, 455 mμ; λ_{infl} 260 mμ; $\epsilon \times 10^{-3}$ 44.73, 19.20, 0.58, 28.70 (in 95% ethanol)], and 2,2′-di-(*N*-oxido-2-pyridyl)hydrazobenzene (0.018 g), obtained as a white solid which, because of its insolubility, was very difficult to purify, m.p. 225° (decomp.). Infrared spectrum (KBr disk) (main peaks only): 3350 (m), 1595 (s), 1247 (s), 842 (s), 780 (m), 750 cm^{-1} (s). λ_{max} 236, 338 mμ; λ_{infl} 265 mμ; $\epsilon \times 10^{-3}$ 46.70, 6.88, 21.15 (in 95% ethanol).

Can. J. Chem. Downloaded from www.nrcresearchpress.com by 210.87.254.105 on 09/05/12
For personal use only.

Reduction of 2,2'-Di-(N-oxido-2-pyridyl)azoxybenzene with Stannous Chloride – 2-o-Aminophenylpyridine-N-oxide

2,2'-Di-(*N*-oxido-2-pyridyl)azoxybenzene (0.113 g) dissolved in concentrated hydrochloric acid (3 ml) was treated with a solution of stannous chloride dihydrate (0.24 g) in concentrated hydrochloric acid (1 ml). The solution was heated on the steam bath for 90 minutes. The cooled reaction mixture was basified with 2 *N* sodium hydroxide and extracted with ether. The dried (Na_2SO_4) ether solution was evaporated to give the primary amine (0.090 g) which was recrystallized from methanol–ether and had m.p. 179–181°. The melting point was not depressed on admixture with an authentic sample of 2-*o*-aminophenylpyridine-*N*-oxide and the infrared spectra of the two samples were identical.

2-Phenylpyridine Methiodide

2-Phenylpyridine and an excess of methyl iodide were kept at room temperature for 2 days in the absence of light. The *methiodide* which separated was recrystallized from ethyl acetate – methanol to give colorless needles, m.p. 143–144°. Calc. for $C_{12}H_{12}NI$: C, 48.50; H, 4.06. Found: C, 48.61; H, 4.25.

Demethylation of 2-Phenylpyridine Methiodide

(a) With Ferrous Oxalate

The methiodide (0.14 g) was mixed with ferrous oxalate dihydrate (0.16 g) and granulated lead (2 g) and the mixture heated in a metal bath at 290–300° under an air condenser for 30 minutes. The cooled reaction mixture and condensate were extracted with ether, and the ether layer was washed with sodium thiosulphate solution to remove iodine and dried (Na_2SO_4). Evaporation of the ether gave 2-phenylpyridine (0.037 g, 50%), picrate, m.p. 172–173°, undepressed on admixture with an authentic specimen.

(b) Without Ferrous Oxalate

The procedure was exactly as under (*a*) except that no ferrous oxalate was added. 2-Phenylpyridine (74% yield) was isolated.

Action of Ferrous Oxalate on 2-Phenylpyridine-N-oxide

2-Phenylpyridine-*N*-oxide (0.30 g) (21) was mixed with ferrous oxalate dihydrate (0.40 g) and granulated lead (4 g) and treated as for the methiodide reaction. 2-Phenylpyridine (0.171 g, 63%), b.p. 132–134° at 10 mm, picrate, m.p. 172–173°, undepressed on admixture with an authentic specimen, was thus obtained.

When ferrous oxalate was omitted, the starting *N*-oxide was recovered.

ACKNOWLEDGMENTS

This work was carried out during the tenure (by K.A.H.A.) of a Canadian Kodak Fellowship (1959–1960) and a C.I.L. Scholarship (1960–1961). Financial support from the National Research Council is gratefully acknowledged.

REFERENCES

1. R. A. Abramovitch, K. A. H. Adams, and A. D. Notation. Can. J. Chem. **38**, 2152 (1960).
2. H. C. Waterman and D. L. Vivian. J. Org. Chem. **14**, 289 (1949).
3. D. L. Vivian, G. Y. Greenberg, and J. L. Hartwell. J. Org. Chem. **16**, 1 (1951).
4. R. A. Abramovitch. Proc. Chem. Soc. 8 (1957).
5. G. V. Boyd. J. Chem. Soc. 55 (1959).
6. L. Paoloni and G. B. Marini-Bettòlo. Nature, **179**, 41 (1957).
7. L. Paoloni. Gazzetta, **90**, 1530 (1960).

Can. J. Chem. Downloaded from www.nrcresearchpress.com by 210.87.254.105 on 09/05/12
For personal use only.

8. I. D. SPENSER. J. Chem. Soc. 3659 (1956).
9. E. GELLÉRT, RAYMOND-HAMET, and E. SCHLITTLER. Helv. Chim. Acta, **34**, 642 (1951).
10. A. P. GRAY. J. Am. Chem. Soc. **77**, 5930 (1955).
11. P. A. S. SMITH and J. H. BOYER. J. Am. Chem. Soc. **73**, 2626 (1951).
12. G. SMOLINSKY. J. Am. Chem. Soc. **82**, 4717 (1960).
13. A. R. KATRITZKY and A. M. MONRO. J. Chem. Soc. 1263 (1958).
14. A. R. KATRITZKY and P. SIMMONS. J. Chem. Soc. 1511 (1960).
15. E. HAYASHI, H. YAMANAKA, C. IYIMA, and S. MATSUSHITA. Chem. & Pharm. Bull. (Tokyo), **8**, 649 (1960).
16. E. WENKERT and B. F. BARNETT. J. Am. Chem. Soc. **82**, 4671 (1960).
17. O. DIMROTH. Ber. **35**, 4041 (1902); **40**, 2402 (1907).
18. A. E. GILLAM and E. S. STERN. An introduction to electronic absorption spectroscopy in organic chemistry. 2nd ed. E. Arnold Ltd., London. 1957. pp. 140–143.
19. G. M. BADGER and R. G. BUTTERY. J. Chem. Soc. 2156 (1953). R. J. W. LE FÈVRE and J. NORTHCOTT. J. Chem. Soc. 4082 (1952).
20. J. W. HAWORTH, I. M. HEILBRON, and D. H. HEY. J. Chem. Soc. 372 (1940).
21. A. R. HANDS and A. R. KATRITZKY. J. Chem. Soc. 1754 (1958).

Can. J. Chem. Downloaded from www.nrcresearchpress.com by 210.87.254.105 on 09/05/12
For personal use only.

Can. J. Chem. Downloaded from www.nrcresearchpress.com by 210.87.254.42 on 09/05/12
For personal use only.

OXIDATION–REDUCTION POLYMERS

I. SYNTHESIS OF MONOMERS[1]

I. H. SPINNER, J. YANNOPOULOS,[2] AND W. METANOMSKI

ABSTRACT

The preparation of two new monomers, 2,5-bis-(2-tetrahydropyranyloxy)-4′-vinyldiphenyl sulphone and 2-tetrahydropyranyl-4′-vinylphenyl thioether, for the synthesis of redox polymers is described.

The first systematic discussion of redox (electron exchange) polymers was presented by Cassidy (1). These polymers were divided into two classes: (i) those in which the active redox group formed a part of the backbone of the polymer chain and (ii) those in which the active group was a substituent on the polymeric chain. Examples of the first class are various condensation resins of hydroquinones, naphthaquinones, and anthraquinones with phenol and formaldehyde (2–6).

Polyvinylhydroquinone (7) is an example of the second class. Monomers such as vinylhydroquinone dibenzoate (8) and diacetate (8, 9) were produced, since it was soon realized that in order to obtain high molecular weight polymers, the hydroxyl groups in the monomer should be protected. Other vinyl monomers were synthesized, such as vinylhydroquinone bis-methoxymethyl ether (10), 1-vinyl-2,4,5-trimethyl-3,6-dihydroxybenzene (11), β-vinylanthraquinone (12, 13), and 2-methyl-3-vinyl-1,4-naphthaquinone (14). A polyhydroquinone was prepared from 3-(2,5-diacetoxyphenyl) propylene oxide (15).

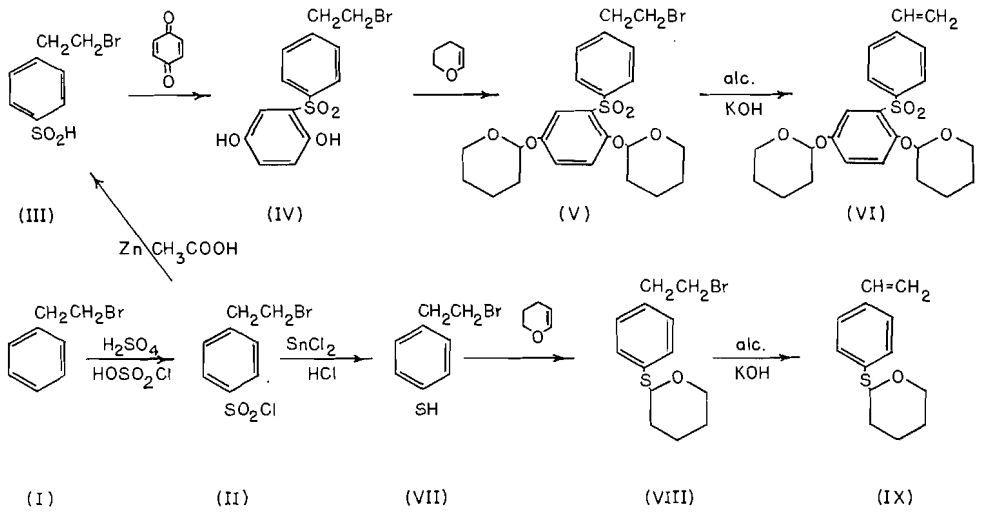
Redox polymers of the second class have also been prepared by reactions with polymers. For example, polyaminostyrene was first diazotized and then reacted with an alcoholic solution of *p*-benzoquinone or 1,4-naphthaquinone (16, 17). Polyaminostyrene was also reacted directly with a naphthaquinone (16). Polyvinyl alcohol was reacted with β-formylanthraquinone (18).

Polymers of known and easily varied structure have obvious advantages in any systematic study of the properties of redox polymers. Our efforts have therefore been directed towards the synthesis of a vinyl monomer for which the oxidation potential could be varied in a simple manner. This was accomplished by joining a hydroquinone group through a stable sulphone bridge with another benzene ring containing $-CH_2CH_2Br$ side chain. The latter can easily be dehydrobrominated to give a vinyl group. A simple hydroquinone could be replaced by a substituted hydroquinone or a naphthahydroquinone. In this way, different redox polymers could be prepared and their oxidation potentials measured and compared with simple homologues.

Vinyl monomers, reported so far, have generally one property in common: the vinyl group is attached directly to the same benzenoid ring which undergoes a redox cycle. It is possible that the interactions between adjacent redox residues will be different from those of a simple polyvinylhydroquinone (1, 7), since the redox group in the monomer reported here is further removed from the backbone chain.

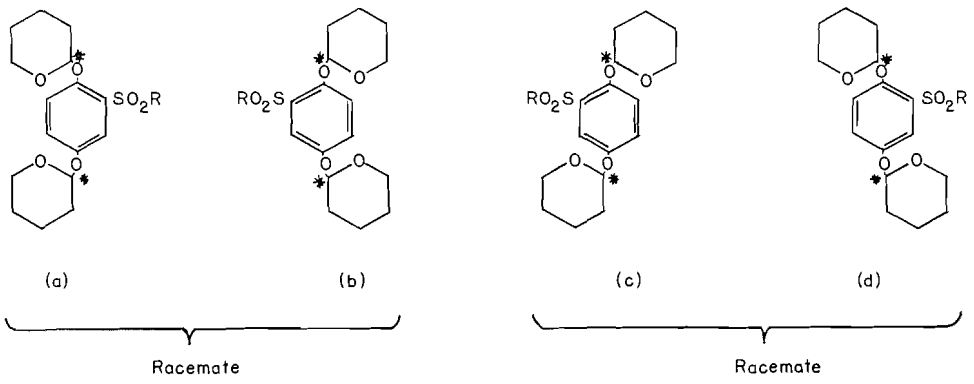
[1]*Manuscript received August 31, 1961.*
Contribution from the Department of Chemical Engineering, University of Toronto, Toronto, Ontario. Taken from the theses submitted by J. Yannopoulos and W. Metanomski to the School of Graduate Studies, University of Toronto in partial fulfillment of the requirements for the degree of Master of Applied Science in May and January, 1960, respectively.
[2]*Present address: Canadian Copper Refiners, Ltd., P.O. Box 338, Place d'Armes Station, Montreal 1, Que.*

The synthesis of a new monomer, 2,5-bis-(2-tetrahydropyranyloxy)-4′-vinyldiphenyl sulphone (VI) was achieved in five steps according to the scheme shown below.



β-Bromoethylbenzene (I) was chlorosulphonated and then reduced by zinc in acetic acid to *p*-(β-bromoethyl) benzenesulphinic acid (III). The sulphinic acid was reacted with *p*-benzoquinone to give a diphenyl sulphone IV. The hydroxyl groups were protected by making use of a reaction with 2,3-dihydropyran (19) to give a bis-tetrahydropyranyl ether V. Finally, the side chain was dehydrobrominated using an alcoholic solution of potassium hydroxide.

The possibility of the existence of two racemic diastereoisomers of V has not been overlooked. Stern, English, and Cassidy (20) isolated two isomers of bis-2-tetrahydropyranyl ether of hydroquinone, assigning to them the meso and racemic configurations. In our case none of the isomers has a plane of symmetry because of the presence of an additional substituent group —SO_2R, and therefore two racemic diastereoisomers are expected, as shown below.



R= $C_6H_4CH_2CH_2Br$

Can. J. Chem. Downloaded from www.nrcresearchpress.com by 210.87.254.42 on 09/05/12
For personal use only.

Can. J. Chem. Downloaded from www.nrcresearchpress.com by 210.87.254.42 on 09/05/12
For personal use only.

The hydroxyl groups could also be protected by acetylation or benzoylation, but the esters partially decomposed during dehydrobromination. Dehydrobromination of these esters using other bases, such as pyridine, lutidine, or triethanolamine, is being studied and shows some promise.

The acetal bond, on the other hand, is very stable under strong alkaline conditions. The tetrahydropyranyl groups can be removed from the polymers by an acid treatment, exposing free —OH groups.

Polymers with thiol groups are of interest as another type of redox resin and ion exchanger. Brubaker (21) has patented the synthesis of polyvinylthioacetate and pointed out the oxidation of polyvinylthiol to polyvinyldisulphide. Polythiolstyrene was prepared by Gregor, Dolar, and Hoeschele (22), and Seifert (23) by various reactions on the benzene ring of the polystyrene. Similarly, poly(vinylbenzylmercaptan) was prepared by Parrish (24), Okawara, Nakagawa, and Imoto (25), and Trostyanskaya and Tevlina (26). Hamamura, Tatsukawa, and Uno (27) produced polythiol resins by the condensation of various thiophenols with formaldehyde. Overberger and Lebovits (28) were the first to synthesize a monomer, *p*-vinylphenyl thioacetate, which was polymerized and saponified to give poly-*p*-thiolstyrene.

A new monomer, 2-tetrahydropyranyl-4′-vinylphenyl thioether (IX) was prepared according to the scheme shown above. *p*-(β-Bromoethyl)benzenesulphonyl chloride (II) was reduced to *p*-(β-bromoethyl)thiophenol (VII). This reduction presented some difficulty since with reducing agents evolving hydrogen *in situ*, such as zinc in acidic medium, or lithium aluminum hydride (in the presence of sulphonyl group (29)), there was a simultaneous reduction of both —SO_2Cl and —CH_2CH_2Br groups. The final product of such a reduction was *p*-ethylthiophenol or a mixture of the sulphinic acid III and *p*-ethylthiophenol. The successful reduction of II to VII was achieved by using stannous chloride and hydrogen chloride in acetic acid, in which case no hydrogen was evolved. The thiol group can add across an olefinic bond (28) and therefore this group must be protected before dehydrobromination. Pyranylation with 2,3-dihydropyran has been used for this purpose. After the polymerization tetrahydropyranyl groups can be removed by acid treatment, exposing free —SH groups.

Both monomers were polymerized and copolymerized with other monomers. After acid treatment the polymers exhibited the expected redox properties and, in addition, the polymers with thiol groups had a high affinity for metal cations. A redox membrane was produced and preliminary experiments indicated the transfer of "oxidizing power" through the membrane with an apparent diffusion coefficient of about 5×10^{-7} cm²/second. Investigation of the properties of these redox polymers in bead and membrane form is now in progress.

EXPERIMENTAL*

p-(β-Bromoethyl)benzenesulphonyl Chloride (II)

This compound has been previously prepared by Spinner, Ciric, and Graydon (30). The present procedure is based on the modifications introduced by Worsley (31).

A solution of β-bromoethylbenzene (I) (185 g, 1 mole) and acetonitrile (82 g, 2 moles) was added dropwise to 30% fuming sulphuric acid (265 g) at 20–30°. To the reaction mixture, chlorosulphonic acid (290 g, 2.5 mole) was added, the temperature being kept at 40–45°. Stirring was continued for 1 hour at the same temperature range. The mixture

**Melting points are corrected. Microanalyses were done by Micro-Tech Laboratories, Skokie, Illinois, and Galbraith Laboratories, Inc., Knoxville, Tenn.*

was poured onto crushed ice and allowed to stand in a refrigerator for 30 minutes. The precipitate was filtered and recrystallized from petroleum ether (boiling range 80–100°), yielding 220 g (78%), m.p. 54–54.5° (previously reported 54–55° (30)).

Infrared spectrum: 1179 (s) and 1383 (s) (—SO_2—) cm^{-1} (32).

p-(β-Bromoethyl)benzenesulphinic Acid (III)

The sulphonyl chloride II (50 g, 0.177 mole) was dissolved in glacial acetic acid (250 ml) at room temperature and zinc dust (15 g, 0.23 mole) was added in small portions with constant stirring. The temperature was kept at 25–35°. After 1 hour of additional stirring at 30–35°, concentrated hydrochloric acid (150 ml) and then distilled water (125 ml) were added slowly. The reaction mixture was heated to 80°. On cooling of the mixture in an ice bath a white precipitate formed which, recrystallized from hot water, gave 32.5 g (74%) of a product melting at 95–95.5°. The compound changed rapidly on drying (over 1 hour) (33), on standing, and on further recrystallization, as was evidenced by widely varying melting points. Thus, all attempts to provide a sample suitable for analysis failed.

Reduction of the sulphinic acid III with stannous chloride in glacial acetic acid saturated with hydrogen chloride gave *p*-(β-bromoethyl)thiophenol (VII), a product identical with that produced by a direct reduction of the sulphonyl chloride II, as reported below. B.p. 92.5–93°/1.2 mm. Anal. Calc. for C_8H_9BrS (217.13): C, 44.25; H, 4.18; Br, 36.80; S, 14.76. Found: C, 45.05; H, 4.72; Br, 36.28; S, 14.43%.

2,5-Dihydroxy-4′-(β-bromoethyl)diphenyl Sulphone (IV)

This reaction is based on 1,4 addition of an aromatic sulphinic acid to a quinone, first reported by Hinsberg (34).

After many trials with solutions in various solvents, the following procedure, which yielded best results, was adopted. A suspension of *p*-benzoquinone (13.5 g, 0.125 mole) in water (500 ml) was added slowly to a suspension of the sulphinic acid III (31 g, 0.125 mole) in water (1 liter) at room temperature. A gradual change in the consistency of the suspended solid took place, the final product being very fluffy. The typical yellow color of quinone disappeared. Crystallization from 25% (by volume) ethanol gave a light sandy powder (36 g, 81%) melting at 130–130.5°. Anal. Calc. for $C_{14}H_{13}BrO_4S$ (357.22): C, 47.07; H, 3.67; Br, 22.37; S, 8.97. Found: C, 47.26; H, 3.81; Br, 22.61; S, 9.01%. Infrared spectrum: 1152 (s) and 1302 (s) (—SO_2—) (32), 3390 (s) (—OH) cm^{-1}.

A derivative, 2,5-diacetoxy-4′-(β-bromoethyl)diphenyl sulphone, was prepared by reacting the dihydroxysulphone IV with acetic anhydride and a drop of concentrated sulphuric acid as a catalyst. Crystallization from 50% (by volume) ethanol gave a white product melting at 110–110.5°. Anal. Calc. for $C_{18}H_{17}BrO_6S$ (441.30): C, 48.99; H, 3.88; Br, 18.11; S, 7.27. Found: C, 49.33; H, 3.96; Br, 18.25; S, 7.31%. Infrared spectrum: 1153 (s) and 1324 (s) (—SO_2—) (32), —OH band absent.

Another derivative, 2,5-benzoquinone-4′-(β-bromoethyl)phenyl sulphone, was prepared by oxidizing the dihydroxysulphone IV with silver oxide. Orange needles precipitated by high boiling point petroleum ether from a diethyl ether solution melted at 104–104.5°. Anal. Calc. for $C_{14}H_{11}BrO_4S$ (355.21): C, 47.33; H, 3.12; Br, 22.50; S, 9.03. Found: C, 47.10; H, 3.15; Br, 22.94; S, 9.20%.

2,5-Bis-(2-tetrahydropyranyloxy)-4′-(β-bromoethyl)diphenyl Sulphone (V)

The dihydroxysulphone IV (10 g, 0.028 mole) was dissolved in 2,3-dihydropyran (15 g, 0.178 mole) containing a few milligrams of *p*-toluenesulphonic acid as a catalyst. The solution was stirred at room temperature for 2 hours and left at the same temperature

Can. J. Chem. Downloaded from www.nrcresearchpress.com by 210.87.254.42 on 09/05/12
For personal use only.

overnight. The volatile materials were then removed under vacuum, and the solid residue taken up in chloroform – diethyl ether (5:2) mixture (150 ml). The solution was shaken with several portions of 5% sodium hydroxide solution to remove the unreacted IV, washed with water, dried over anhydrous sodium sulphate, and concentrated. The precipitate formed was filtered and crystallization from 70% (by volume) ethanol gave 9.8 g (67%) of white crystals melting at 133–134°. Anal. Calc. for $C_{24}H_{29}BrO_6S$ (525.45): C, 54.86; H, 5.56; Br, 15.21; S, 6.10. Found: C, 55.05; H, 5.68; Br, 14.98; S, 5.97%.

This solid is one of the two racemates mentioned in the earlier discussion. Attempts to recover a presumably lower melting and more soluble racemate from the chloroform–ether mother liquor were not successful.

The pyranylated sulphone V decomposed on treatment with hydrochloric acid, giving the dihydroxysulphone IV, melting at 130–131°. This product gave no depression in mixed melting point with the original IV. The other decomposition product was 5-hydroxypentanal, identified by its 2,4-dinitrophenylhydrazone melting at 108.5–109° (reported m.p. 109° (35)).

2,5-Bis-(2-tetrahydropyranyloxy)-4'-vinyldiphenyl Sulphone (VI)

A 10% alcoholic solution of potassium hydroxide (1.6 g KOH, 0.028 mole) was added dropwise to a boiling solution of the diphenyl sulphone V (12 g, 0.023 mole) in benzene (150 ml). The mixture was refluxed on a steam bath for 30 minutes. The precipitated potassium bromide was removed by filtration and the filtrate evaporated to dryness *in vacuo* at room temperature. The residue after a thorough washing with water was crystallized from 50% (by volume) ethanol. The white crystals obtained (6.5 g, 64%) melted at 126.5–127°. Anal. Calc. for $C_{24}H_{28}O_6S$ (444.52): C, 64.84; H, 6.35; S, 7.21. Found: C, 64.67; H, 6.43; S, 7.25; C, 64.60; H, 6.44; S, 7.35%.

p-(β-Bromoethyl)thiophenol (VII)

p-(β-Bromoethyl)benzenesulphonyl chloride (II) was reduced to VII with stannous chloride and hydrogen chloride (36, 37).

Dry hydrogen chloride was bubbled into a suspension of stannous chloride dihydrate (203.5 g, 0.9 mole) in glacial acetic acid (800 ml) at room temperature until the suspension became clear and homogeneous; 71.5 g (1.96 mole) of hydrogen chloride was required. *p*-(β-Bromoethyl)benzenesulphonyl chloride (II) (42.5 g, 0.15 mole) was added and the mixture was shaken for 15 minutes. Evolution of heat was observed during the reaction. On shaking of the mixture with 1:1 hydrochloric acid, a yellowish oil settled. This oil was separated and washed with concentrated hydrochloric acid and then water. Distillation under reduced pressure gave 26.4 g (81%) of a colorless oil* (b.p. 92.5–93°/1.2 mm). Anal. Calc. for C_8H_9BrS (217.13): C, 44.25; H, 4.18; Br, 36.80; S, 14.76. Found: C, 44.53; H, 4.36; Br, 36.76; S, 14.91%.

A derivative, mercuric mercaptide of *p*-(β-bromoethyl)thiophenol, was prepared by adding an excess of 20% mercuric acetate solution in dilute acetic acid to the thiophenol VII. Crystallization from benzene gave snow white crystals melting at 115.5–116.5°. Anal. Calc. for $C_{16}H_{16}Br_2HgS_2$ (632.86): C, 30.36; H, 2.55; Br, 25.26; Hg, 31.70; S, 10.13. Found: C, 30.63; H, 2.67; Br, 25.37; Hg, 31.25; S, 10.33%.

Another derivative, *p*-(β-bromoethyl)phenyl thiobenzoate was prepared by reacting the thiophenol VII with benzoyl chloride dissolved in benzene in the presence of pyridine. Crystallization from ethanol gave white needles, m.p. 49–49.5°. Anal. Calc. for

**This thiophenol (as well as p-ethylthiophenol) was found to be a very strong skin irritant, a well-known property of thiophenols (38).*

Can. J. Chem. Downloaded from www.nrcresearchpress.com by 210.87.254.42 on 09/05/12
For personal use only.

$C_{15}H_{13}BrOS$ (321.23): C, 56.08; H, 4.08; Br, 24.88; S, 9.98. Found: C, 56.29; H, 4.70; Br, 24.90; S, 9.74%.

2-Tetrahydropyranyl-4'-(β-bromoethyl)phenyl Thioether (VIII)

The procedure is based on a method of Parham and DeLaitsch (19).

The thiophenol VII (26.3 g, 0.12 mole) was mixed with a 65% excess of 2,3-dihydropyran (27 g, 0.32 mole), 1 ml of ethereal solution of HCl (0.002 mole) was added, and the mixture refluxed for 48 hours at 30°. The mixture was shaken with three portions of 5% sodium hydroxide solution and washed with water. The excess of dihydropyran was removed by evaporation under reduced pressure. Attempts to purify the thioether VIII by distillation were unsuccessful because of its high boiling point and the instability of the brominated side chain at high temperatures.

2-Tetrahydropyranyl-4'-vinylphenyl Thioether (IX)

Approximately 30% excess of 10% alcoholic solution of potassium hydroxide was added to the crude thioether VIII. The mixture was refluxed for 30 minutes. The precipitated potassium bromide was removed by filtration, the filtrate was washed with water, dried over anhydrous sodium sulphate, and distilled under reduced pressure. Traces of *p-tert*-butylcatechol were added as a polymerization inhibitor prior to drying and distillation. The product was a colorless viscous oil (b.p. 134–135°/1.35 mm). Bromination calculated for 1.000 double bond; found 0.998. Anal. Calc. for $C_{13}H_{16}OS$ (220.33): C, 70.86; H, 7.32; S, 14.56. Found: C, 70.86; H, 7.52; S, 13.51; C, 71.72; H, 7.70; S, 15.02%.

ACKNOWLEDGMENTS

The authors wish to thank Mr. Z. May for his helpful suggestions. The financial assistance of the School of Engineering Research of the University of Toronto (to J. Y. and W. M.) and of Ontario Research Foundation (to W. M.) is gratefully acknowledged.

REFERENCES

1. H. G. Cassidy. J. Am. Chem. Soc. **71**, 402 (1949).
2. R. Griessbach, H. Lauth, and E. Meier. Deutsche Patent-Anmeldung I 77574 (F 7608, 85b, 1/20) (June 1944); quoted by B. Sansoni. Chem. Techn. (Berlin), **10**, 580 (1958).
3. G. Manecke. Z. Elektrochem. **57**, 189 (1953); **58**, 363, 369 (1954). G. Manecke and Ch. Bahr. Naturwissenschaften, **44**, 260 (1957).
4. S. Soloway and L. Schwartz. Science, **121**, 730 (1955).
5. E. L. Kropa and R. P. Welcher. U.S. Patent No. 2,703,792 (March, 1955).
6. V. Verplanck and H. G. Cassidy. J. Polymer Sci. **19**, 307 (1956).
7. I. H. Updegraff and H. G. Cassidy. J. Am. Chem. Soc. **71**, 407 (1949).
8. M. Ezrin, I. H. Updegraff, and H. G. Cassidy. J. Am. Chem. Soc. **75**, 1610 (1953).
9. D. D. Reynolds, J. A. Cathcart, and J. L. R. Williams. J. Org. Chem. **18**, 1709 (1953).
10. R. Stern, J. English, Jr., and H. G. Cassidy. J. Am. Chem. Soc. **79**, 5792 (1957).
11. G. Manecke and G. Bourwieg. Chem. Ber. **92**, 2958 (1959).
12. A. Étienne, G. Izoret, and F. Moritz. Compt. rend. **249**, 708 (1959).
13. M. Fernandez-Refojo, Y-L. Pan, K. A. Kun, and H. G. Cassidy. J. Org. Chem. **25**, 416 (1960).
14. G. Manecke and W. Storck. Chem. Ber. **94**, 300 (1961).
15. H. C. Haas and N. W. Schuler. J. Appl. Polymer Sci. **5** (13), S2 (1961).
16. K. Dorfner. Chemiker Ztg. **85**, 80 (1961).
17. M. L. B. Rao, B. Mukerjee, and S. R. Palit. Chem. & Ind. (London), 145 (1961).
18. A. Étienne and G. Izoret. Compt. rend. **252**, 2111 (1961).
19. W. E. Parham and E. L. Anderson. J. Am. Chem. Soc. **70**, 4187 (1948). W. E. Parham and D. M. DeLaitsch. J. Am. Chem. Soc. **76**, 4962 (1954).
20. R. Stern, J. English, Jr., and H. G. Cassidy. J. Am. Chem. Soc. **79**, 5797 (1957).
21. M. M. Brubaker. U.S. Patent Nos. 2,378,535 and 2,378,536 (June, 1945).
22. H. P. Gregor, D. Dolar, and G. K. Hoeschele. J. Am. Chem. Soc. **77**, 3675 (1955).
23. H. Seifert. German Patent No. 1,067,217 (October, 1959); Chem. Abstr. **55**, 10750 (1961).
24. J. R. Parrish. Chem. & Ind. (London), 137 (1956).
25. M. Okawara, T. Nakagawa, and E. Imoto. Kôgyô Kagaku Zasshi, **60**, 73 (1957); Chem. Abstr. **53**, 5730 (1959).

Can. J. Chem. Downloaded from www.nrcresearchpress.com by 210.87.254.42 on 09/05/12
For personal use only.

26. E. B. TROSTYANSKAYA and A. S. TEVLINA. J. Anal. Chem. U.S.S.R. (Eng. Transl.), **15**, 461 (1960).
27. Y. HAMAMURA, M. TATSUKAWA, and S. UNO. Nippon Nôgei-kagaku Kaishi, **29**, 194 (1955); Chem. Abstr. **52**, 20772 (1958).
28. C. G. OVERBERGER and A. LEBOVITS. J. Am. Chem. Soc. **77**, 3675 (1955); **78**, 4792 (1956).
29. C. S. MARVEL and P. D. CAESAR. J. Am. Chem. Soc. **72**, 1033 (1950).
30. I. H. SPINNER, J. CIRIC, and W. F. GRAYDON. Can. J. Chem. **32**, 143 (1954).
31. M. WORSLEY. Ph.D. Thesis, University of Toronto, Toronto, Ont. 1958.
32. K. C. SCHREIBER. Anal. Chem. **21**, 1168 (1949).
33. W. E. TRUCE and A. M. MURPHY. Chem. Revs. **48**, 69 (1951).
34. O. HINSBERG. Ber. **27**, 3259 (1894); **28**, 1315 (1895).
35. G. F. WOODS and H. SANDERS. J. Am. Chem. Soc. **68**, 2483 (1946).
36. M. T. BOGERT and J. H. BARTLETT. J. Am. Chem. Soc. **53**, 4046 (1931).
37. C. M. SUTER and P. H. SCRUTCHFIELD. J. Am. Chem. Soc. **58**, 54 (1936).
38. R. F. HUNTER. J. Chem. Soc. **127**, 911 (1925).

Can. J. Chem. Downloaded from www.nrcresearchpress.com by 210.87.254.42 on 09/05/12
For personal use only.

Can. J. Chem. Downloaded from www.nrcresearchpress.com by 210.87.254.40 on 09/05/12
For personal use only.

PREFERRED RESIDENCE CONFORMATIONS OF DIASTEREOISOMERIC α-β AMINO ALCOHOLS: AN N.M.R. STUDY OF THE EPHEDRINES[1]

J. B. HYNE

ABSTRACT

Nuclear magnetic resonance spectral results including chemical shifts, anisotropy effects, spin coupling constants, and hydrogen bonding phenomena are presented for the diastereoisomeric pair of α-β amino alcohols (−)-ephedrine and (+)-ψ-ephedrine. The results are shown to be in keeping with the existence of a preferred residence conformation for each of the diastereoisomers.

INTRODUCTION

In a recent paper (1) the effect of dilution on the chemical shift associated with the nuclear magnetic resonance of the OH and NH protons of both (+)-ψ-ephedrine and (−)-ephedrine in chloroform solution was reported. This effect, together with a considerable volume of previously available data, was interpreted as evidence for preferred intramolecular hydrogen bonding in the (+)-ψ-ephedrine diastereoisomer compared with (−)-ephedrine. The conclusion was drawn from the assembled evidence that there is a greater probability in the (+)-ψ-ephedrine case of residence in the conformation which permits intramolecular hydrogen bonding than in the (−)-ephedrine case. In summary, (+)-ψ-ephedrine tends to adopt that conformation in which the OH and NH functions have a gauche relationship while (−)-ephedrine shows no such preference.

Freudenberg and co-workers (2) early established the relative configuration of the two asymmetric centers in the ephedrine molecule and found that the two representatives of the diastereoisomeric pairs, (−)-ephedrine and (+)-ψ-ephedrine, differed only in the configuration about the carbon center carrying the hydroxyl group. Assuming, as a first approximation, that the staggered conformations, generated by rotation of the two halves of the molecule about the central carbon–carbon bond, will be the more stable, a set of staggered conformers for the two diastereoisomers can be drawn as shown in Fig. 1. Considering these possible conformations in the light of the hydrogen-bonding evidence (1) it would appear that conformations (*a*) or (*b*) would be the most favored for (+)-ψ-ephedrine since the hydroxyl and methylamino groups are favorably placed for intramolecular hydrogen bonding in these conformers. Since (−)-ephedrine showed no marked tendency toward intramolecular hydrogen bonding, conformer (*y*), with trans disposition of hydroxyl and methylamino groups, must be at least equally favored in conformer population. In an earlier paper on the dissociation constants of the ephedrinium ions Everett and Hyne (3) favored conformers (*a*) and (*y*) for the diastereoisomeric pair on the basis of approximate calculations of repulsive interactions between non-bonded atoms on the adjacent carbon centers.

Recent work (4, 5, 6) on the variation of spin-coupling constants with the dihedral angle between adjacent carbon–hydrogen bonds in ethanic systems suggested the application of this method to the diastereoisomeric ephedrine pair. Figure 1 shows clearly that the dihedral angle between the carbon–hydrogen bond on the hydroxyl center and the carbon–hydrogen bond on the methylamino center varies significantly from one possible conformation to another.

[1]*Manuscript received July 19, 1961.*
Contribution from the Department of Chemistry, University of Alberta, Calgary, Calgary, Alberta.

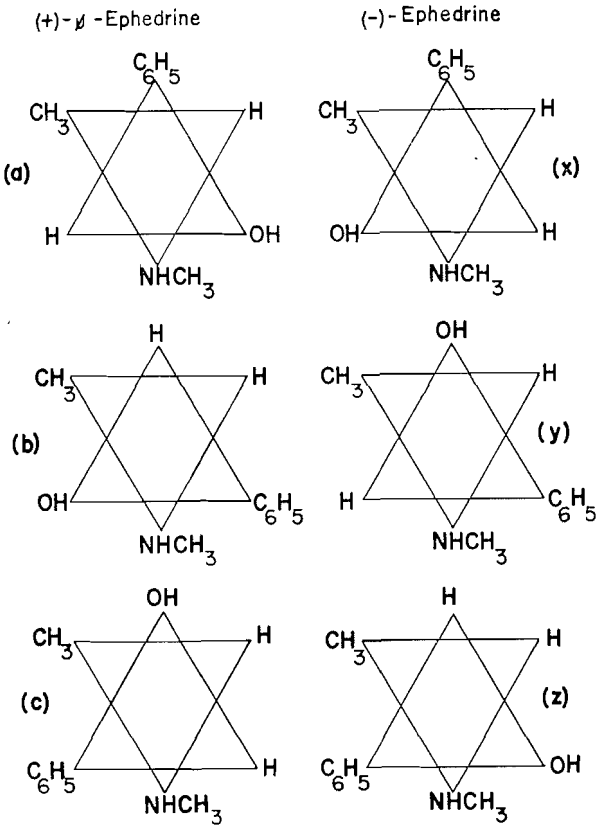


FIG. 1. Possible "pure staggered" conformations of the diastereoisomeric ephedrines.

EXPERIMENTAL

Nuclear magnetic resonance spectra were measured on a Varian V 4300 spectrometer operating at a fixed frequency of 40 Mc; 1.5 molar solutions of BDH (+)-ψ-ephedrine and (−)-ephedrine were prepared in chloroform; the (+)-ψ-ephedrine was used without further purification while the (−)-ephedrine was vacuum-distilled to remove water of hydration. Temperature in the n.m.r. 5-mm spinning sample tube was 20°±1° C throughout. The spectra were scaled by the side band technique using a benzene capillary as an external standard. In obtaining the spin-coupling constant by measuring the splitting of the CHO doublet the side band frequency was set such that the side band appeared a few counts per second before the doublet. As soon as the side band had been traced, the frequency was changed in such a way as to place the side band a few counts per second after the doublet. By this method a trace of the doublet was obtained carrying a side band marker immediately before and after the doublet. At least 10 such determinations were made in obtaining a given spin-coupling constant. The method was cross-checked by using the standard side band superposition technique. All determinations were *within* ±0.2 c.p.s. of the mean value reported. The chemical shifts of all peaks in both spectra together with the spin-coupling constants (J) are recorded in Table I.

Can. J. Chem. Downloaded from www.nrcresearchpress.com by 210.87.254.40 on 09/05/12
For personal use only.

TABLE I

Chemical shifts in c.p.s. from benzene at 40 Mc for ephedrines in 1.5 molar chloroform solution

Compound	C_6H_5	CHO†	CHN*	NCH_3	CCH_3†
(+)-ψ-Ephedrine	−34	+121 +129 (J = 8.2±0.2)	+155	+165	+223 +230
(−)-Ephedrine	−33	+ 68 + 72 (J = 4.0±0.2)	+153	+162	+219 +225

*Central peak of quintuplet.
†Doublet.

DISCUSSION

Spin–Spin Coupling Constant for CH—O/CH—N Interaction

The spin-coupling constant for the interaction of these adjacent protons is twice as great for (+)-ψ-ephedrine (8.2±0.2) as for (−)-ephedrine (4.0±0.2). This observation is of critical importance in establishing the existence of preferred residence in different conformations in the two diastereoisomers. In the first instance the large difference between the constants establishes the fact that a real difference does exist between the time-averaged spin coupling of these two protons. This difference could only arise if preferred residence in different conformations existed. Secondly, the fact that it is the (+)-ψ-ephedrine form which has the higher coupling constant strongly suggests that in this form the preferred relationship between the protons under consideration is trans while in (−)-ephedrine, with the much lower coupling constant, the preferred relationship, if any, is gauche. The order of magnitude of the observed coupling constants and the trans and gauche assignment given above is in keeping with previous observations of Glick and Bothner-By (5) and Lemieux and co-workers (6). The results are also in qualitative agreement with the theoretical calculations of Karplus (4) which predict J values between 8 and 9 c.p.s. for dihedral angles close to 0° or 180° and minimum values of J for angles close to 90°. In terms of the possible conformations shown in Fig. 1, therefore, the J values support a conformation such as (*a*) for the preferred residence form for (+)-ψ-ephedrine but do not support conformer (*y*) as the preferred residence form for (−)-ephedrine. The spectra of the two diastereoisomers, however, contain additional information which is of value in assigning preferred residence conformations.

C—CH_3 Resonance

The chemical shift associated with the C—CH_3 protons is approximately the same in both diastereoisomers. This observation is of importance when compared with the recently observed differences in C—CH_3 shift in the oxazolidone and oxazolidine derivatives of the two ephedrines (7). In these derivatives the ephedrine molecules are bridged across the OH and NH functional groups so that the groups on the adjacent asymmetric centers are constrained to adopt specific spacial relationships to one another. In the (−)-ephedrine form such bridging results in a virtual eclipsing of the phenyl and C—CH_3 groups with a consequent upfield shift of the C—CH_3 resonance due to the diamagnetic anisotropy of the phenyl ring. In the (+)-ψ-ephedrine case bridging in the derivative constrains the phenyl and C—CH_3 groups to adopt a staggered configuration and the upfield shift is not observed. The difference in chemical shift associated with the C—CH_3 protons in the two cases is of the order of 20 c.p.s. The absence of such a difference

Can. J. Chem. Downloaded from www.nrcresearchpress.com by 210.87.254.40 on 09/05/12
For personal use only.

in the spectra of the two ephedrines strongly suggests that the C—CH_3 groups in the two diastereoisomers are in the same spacial environment relative to the adjacent phenyl groups. Furthermore, the fact that the C—CH_3 groups in both diastereoisomers are under the same magnetic influence of the adjacent phenyl suggests that the freedom of rotation of the phenyl group and hence its time-averaged anisotropic influence on the methyl is the same in both diastereoisomers. It might be concluded, therefore, that the steric environment of the phenyl in both isomers is the same thus permitting the same freedom of rotation.

Suggested Preferred Residence Conformers

The experimental results discussed above do not appear to be entirely accommodated by any one of the "pure staggered" conformations shown in Fig. 1. This is not altogether surprising since the assumption that the "pure staggered" forms represent the most stable conformations is based solely upon consideration of the effects of non-bonded repulsions or steric effects. In a molecule of the α-β amino alcohol type there are obviously other forces at work in determining the most stable conformations, not the least of which is the energy of hydrogen bonding.

Distribution of Population Between "Off-Staggered" Conformers

In order to accommodate all the n.m.r. spectral evidence presented in this paper, preferred residence conformers of an "off-staggered" form are suggested in Fig. 2. The various experimental facts which are accommodated by the suggested conformers are considered in turn.

(*a*) The spacial relationship of the methyl and phenyl groups are the same in both isomers and the environment of the phenyl group is likewise identical. These facts meet the requirements, noted previously, for similar resonance frequency of the C—CH_3 protons in both isomers.

(*b*) The dihedral angle between the C—H bonds on the two carbon centers in the conformer suggested for (+)-ψ-ephedrine is 150°–160°. According to Karplus (4) this would yield a J_{calc} = 7–8 c.p.s.; this is in good agreement with the observed value of J_{obs} = 8.2 c.p.s. The corresponding dihedral angle for the suggested conformer for (−)-ephedrine (80°–90°) corresponds to a Karplus $J_{calc} \doteqdot 0$ c.p.s. compared with a J_{obs} = 4.0 c.p.s. Two factors may account for this quantitative disagreement. It has

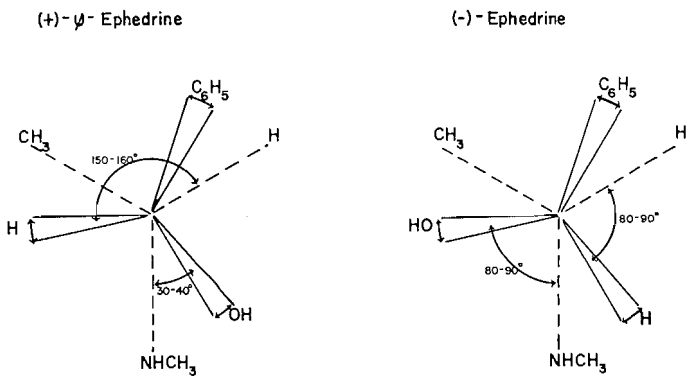


FIG. 2. Suggested preferred residence conformations of the diastereoisomeric ephedrines.

Can. J. Chem. Downloaded from www.nrcresearchpress.com by 210.87.254.40 on 09/05/12
For personal use only.

Can. J. Chem. Downloaded from www.nrcresearchpress.com by 210.87.254.40 on 09/05/12
For personal use only.

been generally found that the calculated J values tend to be somewhat low, especially in those cases where the coupled protons have a gauche relationship. Lemieux *et al.* (6) reported J values for equatorial proton coupling (dihedral angle approximately 60°) in acetylated sugars between 2 and 4 c.p.s. while the Karplus calculation gives a $J_{calc} = 1.7$ c.p.s. The quantitative disagreement, however, may reflect the fact that other possible conformations are significant in the (−)-ephedrine case since the conformation suggested is not stabilized by intramolecular hydrogen bonding to the same extent as in the ψ-ephedrine case. It should be noted that the dihedral angle in the (−)-ephedrine case cannot be changed without changing the phenyl–methyl relationship. Although a small difference in the C—CH_3 resonance is in fact observed in the two spectra (3–4 c.p.s.), such a difference could easily be due to slight variations in the dihedral angle between phenyl and methyl within the 10° limit of uncertainty shown in the conformers of Fig. 2.

(*c*) For a 30°–40° angle between the C—N and C—O bonds, as suggested in the conformer for (+)-ψ-ephedrine, the N—O center-to-center distance is in the range 2.6–2.7 Å. In the suggested (−)-ephedrine conformer the 80°–90° angle between the amino and hydroxyl groups leads to an N—O distance in the range 3.05–3.15 Å. Pimentel and McClellan (8) report the average O—H- - -N bond distance from 21 examples of such hydrogen bonding to be 2.80 Å with a standard deviation of 0.09 Å. The conformers suggested, therefore, accommodate the experimental evidence presented previously (1) where it was shown that there was a greater tendency to intramolecular hydrogen bonding in the (+)-ψ-ephedrine case; from the bond distances given above it is clear that the N—O distance in the (+)-ψ-ephedrine conformer is within the limiting distance while that for (−)-ephedrine is somewhat greater.

(*d*) It should also be noted that the "off-staggered" conformations suggested in Fig. 2 move the bulky phenyl group further from the bulky methyl and toward the sterically less restrictive hydrogen. In as much as an "off-staggered" conformation is favored this would appear to be a reasonable direction in which to rotate in terms of steric factors.

One outstanding feature of the spectra which has not been considered above is the 55 c.p.s. difference in the chemical shift of the C*H*O protons in the two diastereoisomers. It is admitted that this is a large shift to attribute solely to non-bonding environmental effects and there is no analogous example of this magnitude in the literature. However, it is pointed out that in the (−)-ephedrine case the C*H*O proton is in close proximity to the amino nitrogen lone pair and may experience a downfield shift due to the additional shielding afforded by these electrons. In contrast the same C*H*O proton in the suggested (+)-ψ-ephedrine conformer is partially eclipsed by the C—CH_3 bond on the other center. Bothner-By and Naar-Colin have suggested (9) that the carbon–carbon bond may exert a diamagnetic influence along an axis transverse to the bond axis. If the C*H*O proton experienced such an influence its resonance would be shifted upfield. A combination of these two factors acting in opposite directions on the C*H*O protons in the two isomers might explain the observed shift of 55 c.p.s.

While the observations reported here have been interpreted in terms of unique conformations for the diastereoisomeric pair it is emphasized that these conformations are suggested as the *preferred* residence forms only. In systems such as the ones under study the energy differences between various conformations must, of necessity, be small with the consequence that there will be a distribution of population among the various conformers. The evidence appears convincing, however, that the conformers suggested in Fig. 2 are the most heavily populated in the respective diastereoisomers.

*Distribution of Population Between Pure Staggered Conformers**

While the interpretation offered above accommodates the experimental facts on the basis of a distribution of population amongst "off-staggered" conformers with a preferred residence in the forms shown in Fig. 2, an alternative interpretation is possible based on a population distribution amongst "pure staggered" conformers of the type shown in Fig. 1.

If the gauche proton–proton coupling constant is taken as 2 c.p.s. and the trans value as 12 c.p.s. (these are the more common experimental values and are higher than the calculated Karplus values) then a distribution of (+)-ψ-ephedrine population between the pure staggered forms of Fig. 1 of $a:b:c = 62\%:30\%:8\%$ would yield a value of $J_{calc} = 8.2$ c.p.s. (cf. $J_{obs} = 8.2$ c.p.s.). Similarly for (−)-ephedrine a population distribution of $x:y:z = 40\%:20\%:40\%$ yields $J_{calc} = 4.0$ c.p.s. (cf. $J_{obs} = 4.0$ c.p.s.). Such a population distribution in the diastereoisomeric pair means that there will be 92% of (+)-ψ-ephedrine in conformations having the $NHCH_3$ and OH groups gauche ($a+b$ forms) and favorable for intramolecular hydrogen bonding compared with only 80% in (−)-ephedrine ($x+z$ forms). In addition approximately the same percentages of (+)-ψ-ephedrine ($a+c$ forms = 70%) and (−)-ephedrine ($x+z$ forms = 80%) occupy conformations having the methyl and phenyl groups gauche as required by the observed similarity of the methyl shift in both spectra.

While this explanation of the experimental observations has merit and is probably somewhat less complex than that based on preferred residence in a particular "off-staggered" conformation it also has some dubious features. As pointed out previously, there is no compelling reason to assume that the classical "pure staggered" conformations represent energy minima on the energy versus angle of rotation diagram. In simple symmetrical systems such as ethane, such an assumption is probably correct but the asymmetry of the group interactions in a molecule such as ephedrine does not warrant the assumption that the "pure staggered" conformers represent energy minima. It is also doubtful whether the difference between 80% and 92% population in conformers favorable for intramolecular hydrogen bonding is sufficiently large to account for the considerable difference observed in the intramolecular hydrogen-bonding ability of the two diastereoisomers. This is even more questionable when the difference between 70% and 80% population in the conformers with methyl and phenyl gauche to one another is considered to be sufficiently small to have little effect on the position of the $C-CH_3$ resonance.

Although there is insufficient experimental evidence to distinguish conclusively between the two possible explanations, that based on preferred residence in an "off-staggered" conformation appears to be the more plausible.

CONCLUSION

The problem of determining which conformations represent those in which a molecule resides preferentially in systems where the various possible conformers are separated by low-energy barriers requires the application of the most refined techniques. In this paper it has been shown that in the case of the ephedrines, where the energy barriers between the various conformers are the result of hydrogen-bonding phenomena and no-bond type interactions between adjacent groups on two carbon atoms joined by a single bond, the techniques of n.m.r. spectroscopy may provide the necessary refinement. By utilizing the n.m.r. technique of studying intra- and inter-molecular hydrogen

The author is indebted to the referee for bringing this alternative interpretation to his notice.

Can. J. Chem. Downloaded from www.nrcresearchpress.com by 210.87.254.40 on 09/05/12
For personal use only.

bonding by dilution, the anisotropic properties of the phenyl group and spin–spin coupling phenomena, assignment of those conformers representing preferred residence forms appears possible.

The further application of this technique seems obvious in such systems as substituted diols, diamines, hydroxy ketones, and similar molecules in which some or all of the necessary phenomena can be observed.

ACKNOWLEDGMENT

The author wishes to express his thanks to the Department of Chemistry, Yale University, for permission to use their n.m.r. spectrometer.

REFERENCES

1. J. B. HYNE. Can. J. Chem. **38**, 125 (1960).
2. K. FREUDENBERG and F. NIKOLAI. Ann. **510**, 223 (1934).
3. D. H. EVERETT and J. B. HYNE. J. Chem. Soc. **326**, 1636 (1958).
4. M. KARPLUS. J. Chem. Phys. **30**, 11 (1959).
5. R. E. GLICK and A. A. BOTHNER-BY. J. Chem. Phys. **25**, 362 (1956).
6. R. U. LEMIEUX, R. K. KULLNIG, H. J. BERNSTEIN, and W. G. SCHNEIDER. J. Am. Chem. Soc. **79**, 1005 (1957).
7. J. B. HYNE. J. Am. Chem. Soc. **81**, 6058 (1959).
8. G. C. PIMENTEL and A. L. MCCLELLAN. The hydrogen bond. W. H. Freeman and Company. 1960. p. 289.
9. A. A. BOTHNER-BY and C. NAAR-COLIN. J. Am. Chem. Soc. **80**, 1728 (1958).

Can. J. Chem. Downloaded from www.nrcresearchpress.com by 210.87.254.40 on 09/05/12
For personal use only.

Can. J. Chem. Downloaded from www.nrcresearchpress.com by 210.87.254.6 on 09/05/12
For personal use only.

SANDARAC ACIDS: 6β-HYDROXYSANDARACOPIMARIC ACID[1]

J. W. ApSimon[2] and O. E. Edwards

ABSTRACT

The resin from *Callitris quadrivalvis* Vent. Decad. (Sandarac resin) has been shown to contain 6β-hydroxysandaracopimaric acid (6β-hydroxy-7-epipimara-9(14),19-dienoic acid).

Recently we reported the isolation of what appeared to be an hydroxypimaric acid from commercial Sandarac resin (1) derived from the North African tree *Callitris quadrivalvis* Vent. Decad. We now present proof that this is the 6β-hydroxy derivative of sandaracopimaric acid, the structure and stereochemistry of which has been established (1, 2, 3).

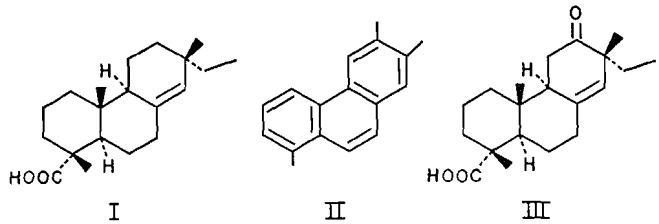
The acid, m.p. 269–270°, analyzed correctly for $C_{20}H_{30}O_3$. Characteristic bands for a vinyl group at 904 and 987 cm^{-1} were present in its infrared spectrum. These were absent in the dihydro acid produced by rapid uptake of 1 mole of hydrogen over palladium. The dihydro acid had absorption at 823 cm^{-1}, suggestive of the presence of a trisubstituted double bond. The presence of this feature was confirmed by one-hydrogen signals near $\tau = 5$ (CCl_4) in the N.M.R. spectrum of a number of derivatives of the acid.

The infrared spectrum of the original acid and the dihydro acid had peaks near 3400 cm^{-1} which were absent in their readily prepared monoacetates. Thus all the functions of a hydroxypimaric acid had been identified. The hydroxyl group was shown to be secondary by oxidation of the dihydro acid to a keto acid. The structure and stereochemistry of the skeleton was then established by Wolff–Kishner reduction of the keto acid. The product was identical in all respects with dihydrosandaracopimaric acid (I) (1).

The N.M.R. spectrum (CCl_4) of the methyl ester of the keto dihydro acid had a one-hydrogen signal at $\tau = 4.76$ (vinyl hydrogen) and what appeared to be a fairly sharp two-hydrogen signal (half band width 5 c.p.s.) at $\tau = 7.66$ superimposed on a broad unresolved signal. This had to be associated with a methylene adjacent to the ketone carbonyl. The only locations for the carbonyl which seemed compatible with the apparent lack of coupling of this methylene group with other hydrogens were C-5 and C-10. However, the low field signal was absent for the 13-hydrogen expected if the carbonyl was on C-5, and the methylene signal was at too high field for one flanked by a 10-carbonyl and the double bond (expected around $\tau = 7$). In addition, neither base nor acid treatment of the keto acid moved the double bond into conjugation with the carbonyl. Hence neither of these positions for the oxygen appeared likely.

In order to establish the oxygen location the dihydro keto acid was treated with methyl magnesium iodide. The resulting hydroxy acid was dehydrogenated using selenium. The major product was 1,6,7-trimethylphenanthrene (II), thus proving that the keto acid was 6-keto-19,20-dihydrosandaracopimaric acid (III).

[1]*Manuscript received August 29, 1961.*
Contribution from the Division of Pure Chemistry, National Research Council, Ottawa, Canada.
Issued as N.R.C. No. 6564.
[2]*National Research Council Postdoctorate Fellow.*



I II III

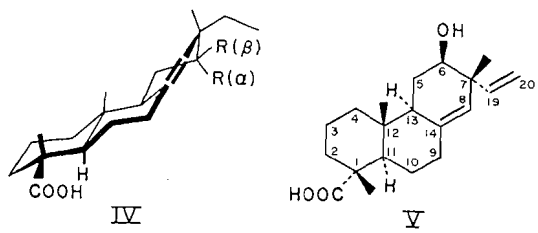
In retrospect, an important clue about the location of the oxygen could have been the chemical shift on the 18-methyl signal in the 6-ketone, as compared with that in the other derivatives (Table I). A comparable shift for the C-18 in 17a-keto-D-homosteroids has been recorded (4).

TABLE I

Chemical shifts in τ in carbon tetrachloride ($Si(CH_3)_4$ as internal standard)

	C_{16}	C_{18}	C_{17}	Vinyl proton	COOH	$COOCH_3$
Methyl dihydrosandaracopimarate	8.89	9.18	9.26	5.02	—	6.48
Methyl dihydro-6-hydroxysandaracopimarate	8.87	9.16	9.21	5.11	—	6.53
Methyl dihydro-6-ketosandaracopimarate	8.89	9.00	9.27	4.76	—	6.38
Dihydro 6-acetoxysandaracopimaric acid	8.88	9.11	9.22	5.18	−1.14	—

There remained the problem of assigning configuration to the hydroxyl group of the original acid. Since the epimeric hydroxyls on C-6 should be true axial and true equatorial in the half-chair conformation of ring C (see IV) we chose to examine the products of borohydride and sodium in alcohol reduction of the 6-ketone. In both cases, high yields of product with the original hydroxyl configuration were formed. This established the hydroxyl conformation as equatorial. Thus the hydroxyl in the original acid is β oriented (see IV) and the new acid is 6β-hydroxysandaracopimaric acid (V) (6β-hydroxy-7-epipimara-8(14),19-dienoic acid).



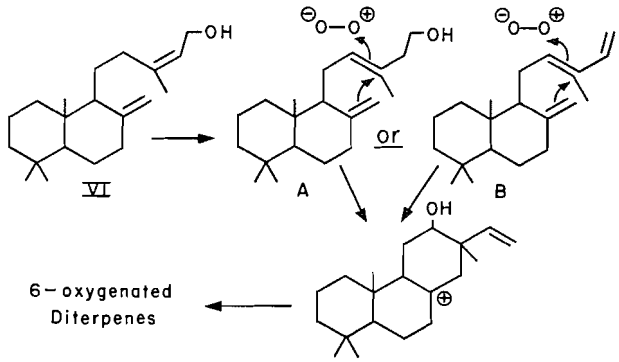
IV V

This acid takes its place with podocarpic acid, ferruginol, Δ^9-dehydroferruginol, xanthoperol, sugiol (5), nimbiol (6), royleanone (7), hinokiol and hinokione (8), vinhaticoic acid (9), and possibly the tanshinones (10) as a 6-oxygenated diterpene. The occurrence of numerous 6-oxygenated diterpenes leads us to suggest that the cyclization to form ring C of the tricyclic diterpenes can take place not only from VI or manool (11) but also in some plants from the double bond isomer A or triene B.[3] Proton-initiated cyclization of these would lead to hydroxyl-free molecules, but cyclization initiated by oxygen[4] would lead to the 6-oxygenated diterpenes listed above.

[3]*This triene B has recently been isolated from Dacrydium biforme and named biformene (12).*

[4]*The work of Tchen and Bloch (13) established the initiation of squalene cyclization in yeast to give 3-hydroxy steroids to be by atmospheric oxygen, presumably enzyme activated.*

Can. J. Chem. Downloaded from www.nrcresearchpress.com by 210.87.254.6 on 09/05/12
For personal use only.



EXPERIMENTAL

Rotations were of ethanol solutions, infrared spectra were of nujol mulls, and melting points were taken on a Kofler hot stage.

6-Hydroxysandaracopimaric Acid

The acid was obtained as described previously (1). It crystallized from acetone as colorless needles, m.p. 269–270°, $[\alpha]_D$ −11° (*c*, 0.4). Its infrared spectrum had weak bands at 904 and 987 cm^{-1} (vinyl group) and 822 cm^{-1} ($\diagdown C{=}C \diagup\!\!\diagdown H$), and a strong band at 3360 cm^{-1} (hydroxyl) and at 1695 cm^{-1} (—COOH).

6-Hydroxy-19,20-dihydrosandaracopimaric Acid

6-Hydroxysandaracopimaric acid (480 mg) in ethanol (250 ml) was reduced with hydrogen in the presence of presaturated 10% palladium on charcoal (400 mg). In 3 minutes, 36 ml of hydrogen were absorbed (calc. for 1 mole 35 ml). The product crystallized from methanol or ethanol as colorless plates (450 mg), m.p. 294–295°, $[\alpha]_D$ +17.5 (*c*, 0.28). Found: C, 75.12; H, 9.98. Calc. for $C_{20}H_{32}O_3$: C, 74.96; H, 10.06%. Infrared spectrum: ν_{max} 3360 cm^{-1} (hydroxyl); 1695 cm^{-1} (—COOH); 823 cm^{-1} ($\diagdown C{=}C \diagup\!\!\diagdown H$).

6-Acetoxysandaracopimaric Acid

6-Hydroxysandaracopimaric acid (200 mg), pyridine (2 ml), and acetic anhydride (2 ml) were allowed to stand overnight at room temperature. The colorless solution was poured into water and the solid product crystallized from *n*-hexane. Recrystallization from the same solvent gave colorless prisms (200 mg), m.p. 170°, $[\alpha]_D$ −51° (*c*, 1.56). Found: C, 73.41; H, 8.79. Calc. for $C_{22}H_{32}O_4$: C, 73.30; H, 8.95. Infrared spectrum: ν_{max} 1730 cm^{-1} (acetate); 1700 cm^{-1} (—COOH); 909 cm^{-1} and 992 cm^{-1} (vinyl group); and 826 cm^{-1} ($\diagdown C{=}C \diagup\!\!\diagdown H$).

6-Acetoxy-19,20-dihydrosandaracopimaric Acid

Treatment of the dihydro acid (100 mg) in the manner described above yielded colorless prisms (90 mg), m.p. 183°, from *n*-hexane. $[\alpha]_D$ −27.5° (*c*, 0.08). Found: C, 73.09; H, 9.21. Calc. for $C_{22}H_{34}O_4$: C, 72.89; H, 9.45. Infrared spectrum: ν_{max} 1725 cm^{-1}, 1700 cm^{-1} (—COOH).

Can. J. Chem. Downloaded from www.nrcresearchpress.com by 210.87.254.6 on 09/05/12
For personal use only.

Methyl 6-Hydroxysandaracopimarate

6-Hydroxysandaracopimaric acid (50 mg) in methanol (25 ml) was treated with excess ethereal diazomethane during 15 minutes. Excess diazomethane was destroyed with acetic acid. The solution was washed well with sodium bicarbonate and water; drying and evaporation yielded a crystalline residue (50 mg). Recrystallization from *n*-hexane gave colorless needles (45 mg), m.p. 94°. The analytical sample was sublimed at 80°/10^{-3} mm. Found: C, 76.02; H, 9.61; OMe, 9.12. Calc. for $C_{20}H_{29}O_2(OMe)$: C, 75.86; H, 9.70; OMe, 9.34. Infrared spectrum: ν_{max} 3300 cm^{-1} (hydroxyl), 1730 cm^{-1} (—COOMe), 909 and 992 cm^{-1} (vinyl group), and 827 cm^{-1} ( ).

Methyl 6-Hydroxy-19,20-dihydrosandaracopimarate

The dihydro acid (30 mg) on treatment with diazomethane in the manner described above yielded colorless needles (27 mg), m.p. 112°, from *n*-hexane. Found: C, 75.20; H, 10.06; OMe, 9.04. Calc. for $C_{20}H_{31}O_2(OMe)$: C, 75.40; H, 10.25; OMe, 9.25. Infrared spectrum: ν_{max} 3360 cm^{-1} (hydroxyl), 1730 cm^{-1} (—COOMe), and 828 cm^{-1} ().

6-Keto-19,20-dihydrosandaracopimaric Acid

6-Hydroxy-19,20-dihydrosandaracopimaric acid (570 mg) in benzene (50 ml) and acetic acid (50 ml) was treated with sodium dichromate dihydrate (200 mg) in acetic acid (10 ml) at room temperature. Next day the green reaction mixture was poured into water and the benzene layer separated. The aqueous layer was further extracted with benzene (4×25 ml). The combined benzene extracts were dried and evaporated, yielding a crystalline residue (470 mg). Recrystallization from ether/*n*-hexane in an acetone – dry ice bath gave colorless prisms, m.p. 149°. The analytical sample was sublimed at 120°/10^{-3} mm. $[\alpha]_D$ −79° (*c*, 0.38). Found: C, 75.43; H, 9.61. Calc. for $C_{20}H_{30}O_3$: C, 75.43; H, 9.50. Infrared spectrum: ν_{max} 1705 cm^{-1} ( ), 1690 cm^{-1} (—COOH).

Methyl 6-Keto-19,20-dihydrosandaracopimarate

The above keto acid (110 mg) in ether (10 ml) and methanol (5 ml) was treated with excess ethereal diazomethane during 15 minutes. Excess diazomethane was decomposed with acetic acid and the ethereal solution washed with sodium bicarbonate and water. The dried solution on evaporation yielded a colorless crystalline product (112 mg), m.p. 88–89°. On recrystallization from pentane and sublimation, this gave prisms, m.p. 89°. $[\alpha]_D$ −71° (*c*, 1.4). Found: C, 75.77; H, 9.53; OMe, 9.22. Calc. for $C_{21}H_{32}O_3$: C, 75.86; H, 9.70; OMe, 9.34. Infrared spectrum: ν_{max} 1714 cm^{-1} (—COOMe), 1706 cm^{-1} (6-membered ketone).

Wolff–Kishner Reduction of 6-Keto-19,20-dihydrosandaracopimaric Acid

6-Keto-19,20-dihydrosandaracopimaric acid (58 mg) in hydrazine hydrate (2 ml) and triethylene glycol (2 ml) was heated to 140° during 45 minutes. Potassium hydroxide (1 g) was added during 5 minutes and the temperature gradually raised to 200° for 5 hours. The reaction mixture was cooled, acidified with 2 *N* H_2SO_4, and ether extracted. The ether extract was washed well with water, dried, and evaporated, yielding a colorless crystalline solid (43 mg), m.p. 175–179°. Recrystallization from aqueous methanol gave needles, m.p. 177–179° undepressed on mixture with dihydro sandaracopimaric acid, and having the requisite infrared spectrum, $[\alpha]_D$ +25° (*c*, 1.25). Found: C, 78.76; H, 10.62. Calc. for $C_{20}H_{32}O_2$: C, 78.94; H, 10.52.

Can. J. Chem. Downloaded from www.nrcresearchpress.com by 210.87.254.6 on 09/05/12
For personal use only.

Reaction of Methyl Magnesium Iodide with 6-Ketodihydrosandaracopimaric Acid

The keto acid (1.54 g) in dry ether (20 ml) was added gradually to methyl magnesium iodide at 0°, prepared from magnesium (0.75 g) and methyl iodide (5 ml) in ether (20 ml). A colorless solid was precipitated. The mixture was vigorously stirred overnight at room temperature. It was poured onto a mixture of ice (20 mg) and 2 *N* H_2SO_4 (50 ml), then extracted with ether. The ether extract was washed well with sodium bisulphite and water. Drying and evaporation gave a colorless semicrystalline product (1.3 g). Crystallization from chloroform/*n*-hexane yielded small colorless prisms (750 mg), m.p. 218°, $[\alpha]_D$ +63° (*c*, 0.4). Found: C, 75.30; H, 10.06. Calc. for $C_{21}H_{34}O_3$: C, 75.40; H, 10.25. Infrared spectrum ν_{max} at 3500 cm^{-1} (OH), 1700 cm^{-1} (—COOH).

Selenium Dehydrogenation of 6-Hydroxy-6-methyl-19,20-dihydrosandaracopimaric Acid

The Grignard product (600 mg) and selenium (2 g) were intimately mixed and heated at 300° C for 17 hours. Hydrogen selenide production was followed on a tower of bleaching powder. The mixture was cooled and the black solid was extracted several times with boiling benzene. The benzene extract was refluxed with freshly precipitated silver for 1 hour, filtered, and refluxed again with fresh silver. Drying and evaporation yielded yellow prisms (350 mg), m.p. 105–120°. Chromatography on Grade IV alumina in pentane gave colorless prisms (290 mg), m.p. 110–117°. Recrystallization from aqueous ethanol gave colorless needles, m.p. 122–123°. Sublimation at $120/10^{-3}$ mm gave colorless prisms, m.p. 123°. Found: C, 92.52; H, 7.20. Calc. for $C_{17}H_{16}$: C, 92.68; H, 7.32. Its ultraviolet spectrum was identical in all respects with that reported for 1,6,7-trimethyl phenanthrene (14). Its picrate separated as orange needles from ethanol, m.p. 167–168° (reported m.p.167° (15)). Found: C, 61.34; H, 4.39. Calc. for $C_{23}H_{19}O_7N_3$: C, 61.47; H, 4.26. Its styphnate crystallized from acetic acid as orange needles. Sublimation gave the analytical sample, m.p. 171° (reported 111°, error?). Found: C, 59.22; H, 3.91. Calc. for $C_{23}H_{19}O_8N_3$: C, 59.35; H, 4.12.

The phenanthrene (91.5 mg) in acetic acid (5 ml) was oxidized with chromic trioxide (100 mg, 2.2 mole) in acetic acid (5 ml) on a steam bath for 2 hours. The reaction mixture was diluted and extracted with ether. The ether solution was washed with potassium carbonate solution and water. It was then dried and evaporated, yielding an orange crystalline product (80 mg), m.p. 215–220°. Sublimation gave orange prisms of 1,6,7-trimethyl phenanthraquinone, m.p. 223° (reported m.p. 222° (15)). The quinoxaline of the phenanthraquinone formed buff needles from aqueous ethanol, m.p. 188–189° (reported m.p. 189–190° (15)).

Reduction of the Keto Acid

6-Keto-19,20-dihydrosandaracopimaric acid (200 mg) in 80% methanol (30 ml) was treated with sodium borohydride (150 mg) and allowed to stand at room temperature for 1 hour. The mixture was acidified with 2 *N* hydrochloric acid, methanol removed *in vacuo*, and ether extracted. The ether extract was dried and evaporated, yielding a yellow oil (200 mg) which was dissolved in methanol, refluxed with charcoal, filtered, and concentrated (5 ml). On cooling, colorless needles formed (105 mg), m.p. 294–295°, $[\alpha]_D$ +17° (*c*, 0.24). Its infrared spectrum was identical with that of dihydro-6-hydroxy sandaracopimaric acid and a mixed melting point was undepressed. Sodium in alcohol reduction of the keto acid (100 mg) afforded the same product (72 mg), m.p. and mixed m.p. 295°, $[\alpha]_D$ +19° (*c*, 0.34), and having the requisite infrared spectrum.

Attempted Isomerization of the Keto Acid

Hydrogen chloride was passed into a solution of 6-keto-19,20-dihydrosandaracopimaric

Can. J. Chem. Downloaded from www.nrcresearchpress.com by 210.87.254.6 on 09/05/12
For personal use only.

acid (30 mg) in dry chloroform (10 ml) at −5° for 4 hours. The chloroform solution was washed free from mineral acid with water, and then dried and evaporated to give a colorless crystalline product (28 mg), m.p. and mixed with starting material 149° and having the requisite infrared spectrum. The keto acid was unchanged by warm 5% sodium hydroxide or by traces of perchloric acid. Similar results were observed with the dihydro hydroxy acid and the dihydro acetoxy acid.

ACKNOWLEDGMENT

We wish to thank Mr. A. Knoll for technical assistance, Mr. H. Seguin for the analyses, Mr. R. Lauzon for the infrared spectra, and Mr. J. Nicholson for the N.M.R. spectra.

REFERENCES

1. O. E. Edwards, A. Nicolson, and M. N. Rodger. Can. J. Chem. **38**, 663 (1960).
2. J. W. ApSimon, B. Green, and W. B. Whalley. J. Chem. Soc. 752 (1961).
3. V. Galik, J. Kuthan, and F. Petru. Chem. & Ind. (London), 722 (1960).
4. N. B. Trenner, B. H. Arison, D. Taub, and N. L. Wendler. Proc. Chem. Soc. 214 (1961).
5. L. H. Briggs, R. C. Cambie, R. N. Seelye, and A. D. Warth. Tetrahedron, **10**, 45 (1960).
6. P. Sengupta, S. N. Choudhuri, and H. N. Khastgir. Tetrahedron, **10**, 45 (1960).
7. O. E. Edwards and G. Feniak. Unpublished observations.
8. Yuan-Lang Chow and H. Erdtman. Proc. Chem. Soc. 174 (1960).
9. F. E. King and T. J. King. J. Chem. Soc. 4158 (1953).
10. K. Takiura. J. Pharm. Soc. Japan, **61**, 482 (1941).
11. L. Ruzicka. Experientia, **9**, 357 (1953).
12. R. M. Carman and P. K. Grant. J. Chem. Soc. 2187 (1961).
13. T. T. Tchen and K. Bloch. J. Am. Chem. Soc. **78**, 1516 (1956).
14. F. A. Askew. J. Chem. Soc. 509 (1935).
15. R. D. Haworth and F. M. Bolem. J. Chem. Soc. 2248 (1932).

Can. J. Chem. Downloaded from www.nrcresearchpress.com by 210.87.254.6 on 09/05/12
For personal use only.

Can. J. Chem. Downloaded from www.nrcresearchpress.com by 210.87.254.40 on 09/05/12
For personal use only.

THE Hg $6(^3P_1)$-PHOTOSENSITIZED DECOMPOSITION OF NITRIC OXIDE[1]

OTTO P. STRAUSZ AND HARRY E. GUNNING

ABSTRACT

The reaction of NO with Hg $6(^3P_1)$ atoms has been studied under static conditions at 30°, over the pressure range 1–286 mm. The products were found to be N_2, N_2O, and higher oxides of nitrogen. At NO pressures exceeding 4 mm, the total rate of formation of N_2+N_2O was constant, while the ratio N_2O/N_2 increased linearly with the substrate pressure. The rate was found to vary directly with the first power of the intensity at 2537 Å, and a value of 1.9×10^{-3} moles/einstein was established for the quantum yield of N_2+N_2O production. In the proposed mechanism, reaction is attributed to the decomposition of an energy-rich dimer, $(NO)_2^*$, which is formed by the collision of electronically excited ($^4\Pi$) NO molecules with those in the ground state. The $(NO)_2^*$ species is assumed to decompose by the steps: $(NO)_2^* \rightarrow N_2 + O_2$ and $(NO)_2^* + NO \rightarrow N_2O + NO_2$. The mechanism satisfactorily explains the observed behavior of the system.

INTRODUCTION

Although there have been several studies of the photolysis of NO, the nature of the primary process is still in doubt. Thus MacDonald (1) studied the reaction in the 70–630 mm region, using 1860–1990 Å radiation; he concluded that 1/10th of the reaction led to N_2O formation, and that the remainder yielded N_2. He postulated reaction to proceed through the interaction of excited NO molecules with those in the ground state. Flory and Johnston (2) found, in the low pressure region, 0.02–7 mm, no evidence of N_2O formation; they interpreted the primary process as predissociation. At low pressures they found the active line to be 1832 Å. They concluded that any decomposition by absorption at 1849 Å could only occur at higher pressures. Recently Gaydon (3) has reported that no trace of photodecomposition could be detected when NO, at atmospheric pressure, was exposed to radiation from an iron arc. This polychromatic source gives no emission below 2084 Å.

The reaction of NO with Hg $6(^3P_1)$ atoms was first studied by Noyes (4). He established that the rate was (*a*) first order in light intensity and (*b*) first order in substrate pressure in the range 0.003–0.13 mm. The pressure dependence approached zero order at higher pressures. On a pressure-change basis, it was deduced that N_2 was the only gaseous product. From the kinetic behavior and the energetics of the reaction, Noyes concluded that the rate-determining step was the formation of long-lived vibrationally excited NO molecules.

McGilvery and Winkler (5) found no reaction of NO with Hg $6(^3P_1)$ atoms; however, they observed a fast reaction with Hg $6(^1P_1)$ atoms. Only N_2 and higher oxides were detected as products. The addition of N_2 was found to decrease the rate. Reaction was attributed to N—O bond scission by the Hg $6(^1P_1)$ atoms. Recently Bernstein and Hoffman (6) have reinvestigated the reaction with Hg $6(^3P_1)$ atoms. They measured the rate of N_2 formation, and also the $^{14}N/^{15}N$ isotope effect. In their mechanism they followed the suggestion of Fallon, Vanderslice, and Mason (7) that the quenching collision formed long-lived NO($^4\Pi$) molecules, for which the lowest vibrational level was estimated to lie 4.64 ± 0.10 ev above the lowest vibrational level of the ground state. For this state, radiative reversion to the ground state was considered of low probability. The proposed mechanism (6) included the steps:

[1]*Manuscript received August 3, 1961.*
Contribution from the Department of Chemistry, University of Alberta, Edmonton, Alberta.

$$Hg^* + NO \rightarrow NO^* + Hg; \quad (a)$$

$$Hg^* + NO \rightarrow NO_v + Hg'; \quad (b)$$

$$Hg^* \rightarrow Hg + h\nu; \quad (c)$$

$$Hg^* + NO^* \rightarrow N + O + Hg; \quad (d)$$

$$N + NO \rightarrow N_2 + O; \quad (e)$$

$$O + NO \rightarrow NO_2 \text{ etc.}; \quad (f)$$

where $Hg^* = Hg\ 6(^3P_1)$; $Hg' = Hg\ 6(^3P_0)$; $NO^* = NO(^4\Pi)$, and NO_v = vibrationally excited NO. An equivalent mechanism was suggested by Cvetanović (8). Here, for (*b*) and (*d*) above, were substituted (*b'*) $NO^* + NO \rightarrow 2NO$ and (*d'*) $NO^* + NO \rightarrow N + NO_2$.

Finally Cojan and Taboue (9) have reported some interesting experiments in which NO at 0.1 mm was exposed to radiation from a cooled Hg arc, in the presence of mercury vapor. By absorbiometric analysis, with the magnetic filter technique, they showed that the mercury strongly bonded to the wall of the reaction cell was enriched in ^{202}Hg. These results will be discussed later in this paper.

The present study was prompted by a recent investigation in this laboratory (10) of the reaction of CO_2 with Hg $6(^3P_1)$ atoms. Here it was shown that decomposition proceeds through a process, second order in the light intensity, involving collision of two excited species. It seemed of interest to determine whether a similar type of process was operative in the NO reaction. The details of the investigation follow.

EXPERIMENTAL

The apparatus and general experimental technique have been previously described (10). The nitric oxide (Matheson) was subjected to several low-temperature distillations before use. Analysis by G.L.P.C. showed that the only impurity was N_2O at a concentration of less than 0.01%. After each run, the products were removed from the unreacted substrate and analyzed by G.L.P.C.

RESULTS

The products of the reaction were N_2 and N_2O, together with higher oxides of nitrogen; the latter were observed to attack the mercury in the reaction cell. Analysis of the cell deposit showed the presence of NO_2^- ion.

The measured rates of N_2 and N_2O formation, in μmoles/hour, are presented, for runs of 60 minutes in duration, in Table I. The absorbed light intensity at 2537 Å(I_a), determined with propane as actinometer (11, 12), was 3.34×10^{-5} einstein/minute. The maximum rate of N_2 formation occurred at a NO pressure of 3.25 mm, where 4.0 μmoles were formed per hour.

In Table II, the total rate, $R(N_2+N_2O)$, is shown as a function of $P(NO)$, for 10-mm pressure intervals up to $P(NO) = 120$ mm. From Table II it is apparent that $R(N_2+N_2O)$ is constant within the experimental error at 3.82 μmoles/hour. For the quantum yield, $\Phi(N_2+N_2O)$, we obtain 1.9×10^{-3} moles/einstein. It should be noted that the run at $P(NO) = 286$ mm was made with $I_a = 7.61\times10^{-5}$ einstein/minute. At this light intensity, $R(N_2)$ and $R(N_2O)$ were respectively 3.79 and 4.60 μmoles/hour. Thus $\Phi(N_2+N_2O)$ was 1.8×10^{-3}, in satisfactory agreement with the data at the lower light intensity. Hence, while $\Phi(N_2)$ decreases with increasing $P(NO)$, and $\Phi(N_2O)$ increases, the sum $\Phi(N_2+N_2O)$ is independent of the substrate pressure, in the complete quenching region.

Can. J. Chem. Downloaded from www.nrcresearchpress.com by 210.87.254.40 on 09/05/12
For personal use only.

TABLE I

The rates of N_2 and N_2O formation as a function of the NO pressure

P(NO) (mm)	$R(N_2)$ (μmoles/hour)	$R(N_2O)$ (μmoles/hour)
1.01	3.44	
3.25	4.00	
5.06	3.93	
10.3	3.86	
12.3	3.76	
18.0		0.26
21.5		0.35
21.6		0.31
22.3	3.53	0.41
33.2		0.40
40.0	3.20	0.49
58.0	3.09	0.82
69.6	3.08	0.83
79.5	2.79	
120	2.76	1.27
286	1.64	2.11

TABLE II

The total mean rate of N_2+N_2O formation as a function of NO pressure

P(NO) (mm)	$R(N_2+N_2O)$ (μmoles/hour)	P(NO) (mm)	$R(N_2+N_2O)$ (μmoles/hour)
10	4.05	70	3.73
20	3.94	80	3.73
30	3.87	90	3.74
40	3.80	100	3.79
50	3.77	110	3.81
60	3.75	120	3.86

Mean value = 3.82 μmoles/hour

In Fig. 1, the reciprocal rate, $1/R(N_2)$, is shown to vary linearly with P(NO). Similarly, it can be seen from Fig. 2 that the quantity (NO)/$R(N_2O)$ is a linear function of P(NO).

To determine the dependence of the rate upon the light intensity, a doughnut-type Vycor filter was fitted axially over the reaction cell, within the coils of the resonance lamp. The filter, 110 mm in length, 35 mm I.D., and 60 mm O.D., was filled with bromine vapor at a pressure of 170 mm. Its transmission was 55.7% at 2537 Å, and less than 1% at 4047 Å. With the filter, $R(N_2+N_2O)$ was 54% of the value without the filter, confirming Noyes' observation (4) that the rate is proportional to I_a. Since the rate is insensitive to the 100-fold reduction in intensity at 4047 Å, there seems little basis for the stepwise excitation mechanism proposed by McGilvery and Winkler (5).

In Fig. 3, $\Phi(N_2O)/\Phi(N_2)$ is shown as a function of P(NO). The relation is a linear one, within the experimental error.

In order to examine the possibility that the N_2 product might arise in secondary quenching by N_2O, a few runs were performed with added N_2O. In Fig. 4, the rate of N_2O disappearance is plotted against the percentage of added N_2O, for P(NO) constant at 29.4 mm. From the data it is estimated that the rate of decomposition of added N_2O is less than 1/10th of $R(N_2)$ for pure substrate. It is concluded that N_2 is indeed a primary product of the reaction of NO with Hg $6(^3P_1)$ atoms.

Can. J. Chem. Downloaded from www.nrcresearchpress.com by 210.87.254.40 on 09/05/12
For personal use only.

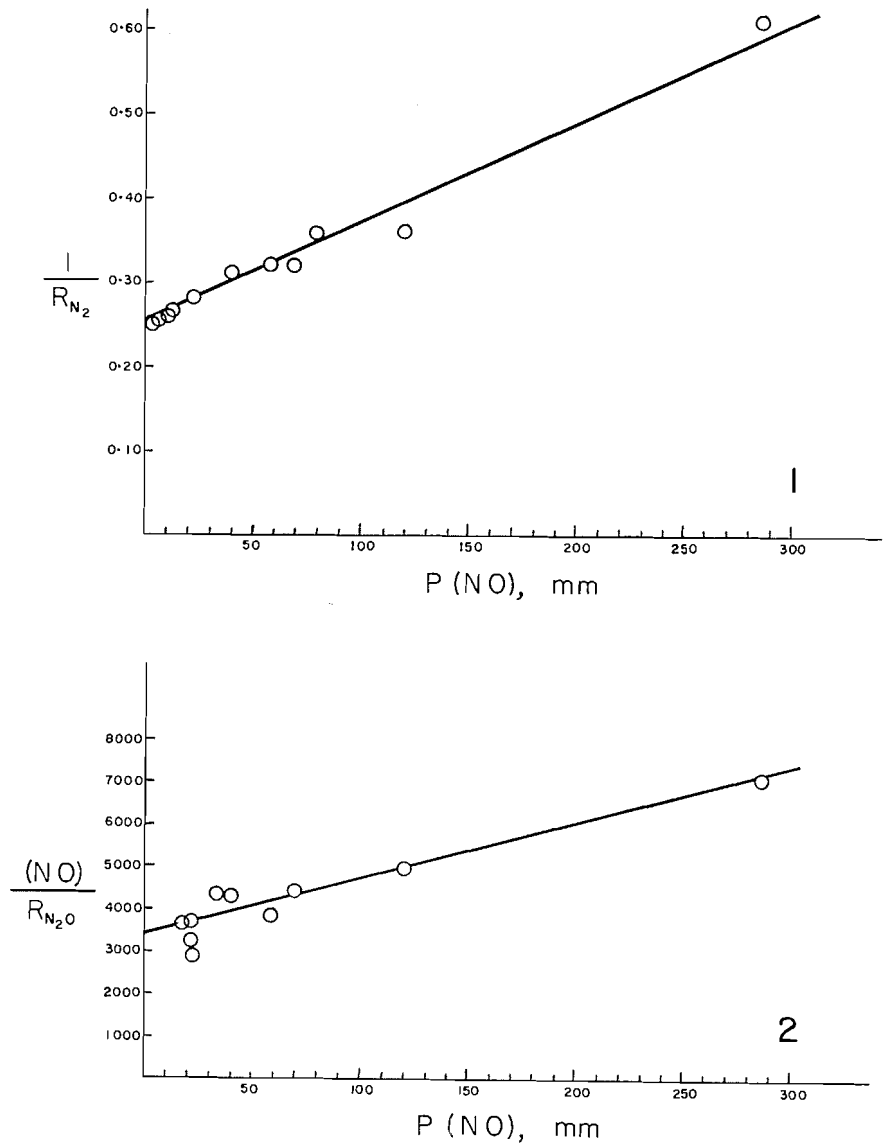


FIG. 1. The reciprocal of the rate of N_2 formation, in $(\mu moles/hour)^{-1}$, as a function of the NO pressure, for $I_a = 33.4$ μeinstein/minute.
FIG. 2. $(NO)/R_{N_2O}$ in hours, as a function of the NO pressure, for $I_a = 33.4$ μeinstein/minute.

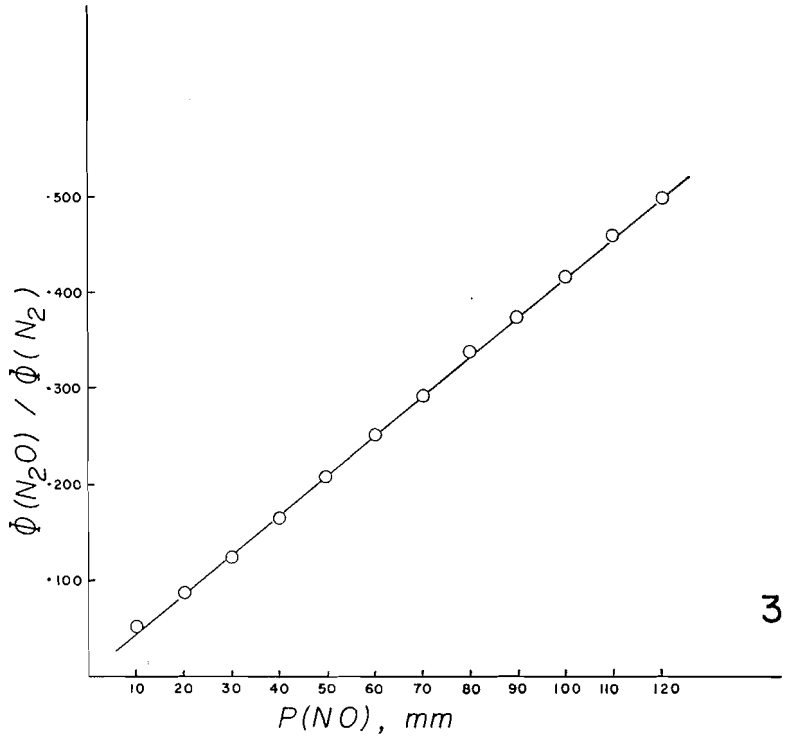
DISCUSSION

The results of the present study lend strong support to the original suggestion of Noyes (4) that the reaction involves primary formation of excited NO molecules. Thus, the presence of N_2O as a major reaction product, a fact not previously reported, could only be explained by interactions of NO molecules in which at least one of the collisional partners is energized. It is also pertinent to note that N atoms react with NO to form N_2, but not N_2O (13).

In order to explain the kinetic behavior of the reaction, as revealed in the present study, the following mechanism is proposed:

Can. J. Chem. Downloaded from www.nrcresearchpress.com by 210.87.254.40 on 09/05/12
For personal use only.

Can. J. Chem. Downloaded from www.nrcresearchpress.com by 210.87.254.40 on 09/05/12
For personal use only.



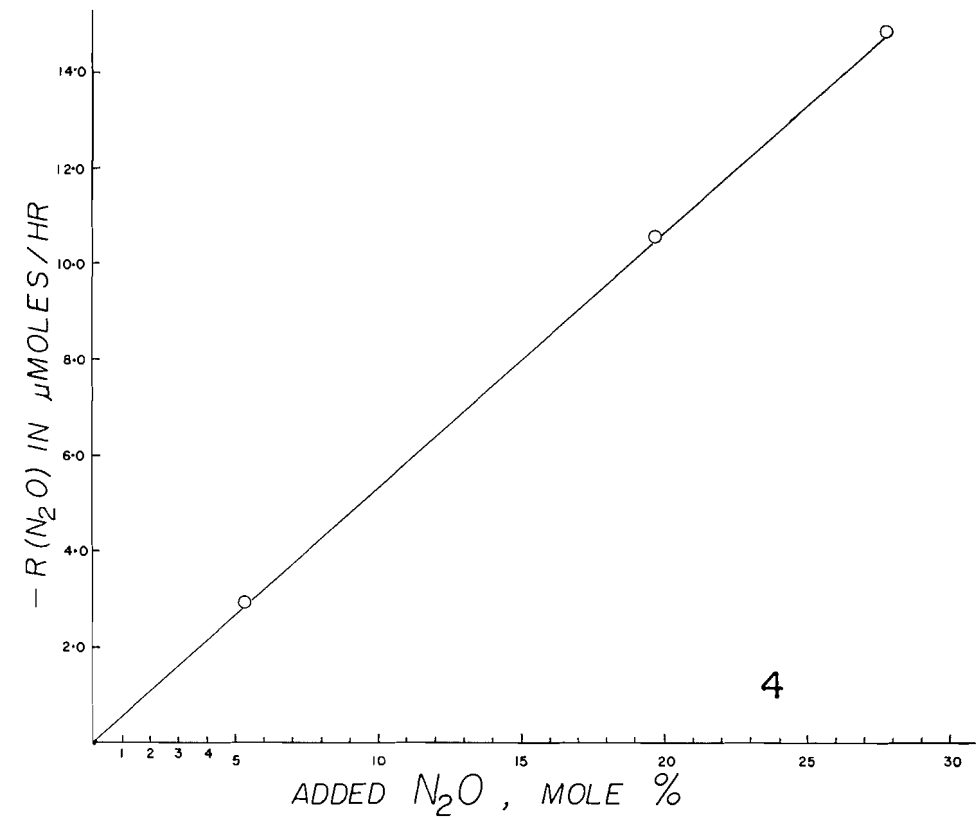


FIG. 3. The variation in the quantum yield ratio, $\Phi(N_2O)/\Phi(N_2)$, with the NO pressure.
FIG. 4. The rate of disappearance of N_2O, in μmoles/hour, as a function of the mole% of added N_2O, for a constant NO pressure of 29.4 mm.

$$Hg + h\nu \rightarrow Hg^* \qquad [I_a]$$

$$Hg^* \rightarrow Hg + h\nu \qquad [1]$$

$$Hg^* + NO \rightarrow NO^* + Hg \qquad [2]$$

$$NO^* + NO \rightarrow 2NO \qquad [3]$$

$$NO^* + NO \rightarrow (NO)_2^* \qquad [4]$$

$$(NO)_2^* \rightarrow N_2 + \text{oxygen} \qquad [5]$$

$$(NO)_2^* + NO \rightarrow N_2O + NO_2 \qquad [6]$$

where $Hg^* = Hg\ 6(^3P_1)$, $NO^* = NO\ (^4\Pi)$, and $(NO)_2^*$ is an energy-rich dimer.

In the complete quenching region, i.e. for $P(NO)$ above ca. 4 millimeters, the rate of (N_2+N_2O) formation from the above mechanism would be

$$R(N_2+N_2O) = I_a k_4/(k_3+k_4).$$

Thus the combined rate would be directly proportional to I_a, and independent of $P(NO)$, in agreement with our findings (Table II).

For the quantum yield ratio, we obtain

$$\Phi(N_2O)/\Phi(N_2) = k_6(NO)/k_5,$$

which requires that the ratio be a linear function of $P(NO)$, passing through the origin, as seen in Fig. 3.

Furthermore, from the mechanism, the rate of N_2 formation would be

$$R(N_2) = I_a k_4 k_5/(k_3+k_4)[k_5+k_6(NO)],$$

and the rate of N_2O formation

$$R(N_2O) = I_a k_4 k_6(NO)/(k_3+k_4)[k_5+k_6(NO)].$$

By rearranging the above rate expressions, the following linear relations are obtained:

$$1/R(N_2) = (k_3+k_4)/(I_a k_4)+(k_3+k_4)(k_6)(NO)/(I_a k_4 k_5)$$

and

$$(NO)/R(N_2O) = (k_3+k_4)(k_5)/(I_a k_4 k_6)+(k_3+k_4)(NO)/(I_a k_4).$$

From Figs. 1 and 2 respectively, it can be seen that the expressions $1/R(N_2)$ and $(NO)/R(N_2O)$ are indeed linear functions of $P(NO)$. Furthermore the mechanism requires that the intercept at $P(NO) = 0$, in Fig. 1, should be equal to the slope in Fig. 2. For the intercept in Fig. 1 we obtain 0.26 hour μmole^{-1}, and for the slope in Fig. 2, 0.24 hour μmole^{-1}, in agreement with the proposed mechanism.

In the proposed mechanism, we have adopted the suggestion of Fallon, Vanderslice, and Mason (7) that reaction [2] leads to the formation of NO ($^4\Pi$). Support for our postulation of the $(NO)_2^*$ species comes from the work of Spindel and Stern (14), who found that a rapid exchange occurs among isotopic nitric oxides at room temperature. At a total pressure of 20 mm, complete exchange occurred in ca. 15–30 seconds. Even at a pressure of 60–100 μ, the exchange was still detectable. It seems likely that the exchange takes place through a square-type dimer intermediate.

The low quantum yield of the reaction, on the basis of the proposed mechanism, would require that [4] be extremely inefficient compared with [3]. Now, from our data, $\Phi(N_2+N_2O) = 1.9\times10^{-3}$, and from the mechanism this quantity would be equal to $k_4/(k_3+k_4)$. Hence k_4/k_3 would be ca. 1.9×10^{-3}.

From the linear slope in Fig. 3, we obtain $k_6/k_5 = 77.5$ liter/mole. Now if we assume a collision cross section of 20 Å^2 for [6], and reaction at every collision, then $k_5 = 2$

Can. J. Chem. Downloaded from www.nrcresearchpress.com by 210.87.254.40 on 09/05/12
For personal use only.

$\times 10^{11}/77.5 = 2.6\times 10^{9}$/second. This leads to an estimate for the lifetime, τ, of $(NO)_2^*$ of $1/k_5 = 3.8\times 10^{-10}$ second. The value should be regarded as minimal, since a steric factor less than unity in k_6 would increase τ.

Finally we would like to comment on the isotope effect observed by Cojan and Taboue (9), in the irradiation of a mixture of Hg vapor and 0.1 mm of NO. In unpublished work in this laboratory (15), it has been found that the behavior observed by Cojan and Taboue is characteristic of substrates which convert Hg $6(^3P_1)$ atoms to the $6(^3P_0)$ state. Thus when Hg vapor was admixed with substrates such as N_2, H_2O, and NH_3, and exposed to the radiation from a ^{202}Hg electrodeless discharge, it was observed that the mercury in the cell rapidly became transparent to the ^{202}Hg-hyperfine component at 2537 Å. Apparently the metastable ^{202}Hg atoms had diffused to the wall and become chemisorbed on the surface. The evidence for this is that the normal adsorption could be re-established by heating the cell to drive off the mercury from the wall. Furthermore with addends such as H_2, which quench the $6(^3P_1)$ atoms directly to the $6(^1S_0)$ state, no such change in absorption with time was observed. It is our opinion that the isotope effect found by Cojan and Taboue (9) arises for the following reasons. In the cell the concentration of ^{202}Hg $6(^3P_1)$ atoms will be higher than the natural isotopic abundance for this isotope, owing to its large absorption coefficient (9). By collision with NO, metastable atoms are formed, which will be enriched in ^{202}Hg. These atoms can diffuse to the wall and form a complex with adsorbed NO. It would appear that Hg $6(^3P_0)$ atoms do not possess sufficient energy to convert NO to the $^4\Pi$ state, by reaction [2]. If these conclusions are correct, it would follow that the $^4\Pi$ state must lie between 4.67 and 4.88 ev above the ground state.

CONCLUSIONS

As a result of the present study, it can be concluded that both N_2O and N_2 are major primary products of the reaction of NO with Hg $6(^3P_1)$ atoms at 30°. Reaction must proceed via the initial formation of excited NO, likely in the $^4\Pi$ state, which appears to be inefficiently converted by collision with the substrate to an excited dimer. From this intermediate, N_2 is formed by unimolecular decomposition, while N_2O arises through interaction of the dimer with the substrate.

ACKNOWLEDGMENTS

The authors would like to express their deep appreciation to Dr. Willard F. Allen for many valuable discussions. This investigation was partially supported by a grant from Imperial Oil Limited. This assistance is most gratefully acknowledged.

REFERENCES

1. J. Y. MacDonald. J. Chem. Soc. 1 (1928).
2. P. Flory and H. Johnston. J. Am. Chem. Soc. **57**, 2641 (1935).
3. A. G. Gaydon. Dissociation energies and spectra of diatomic molecules. Chapman and Hull Ltd., London. 1953.
4. W. A. Noyes, Jr. J. Am. Chem. Soc. **53**, 514 (1931).
5. J. D. McGilvery and C. A. Winkler. Can. J. Chem. **30**, 194 (1951).
6. M. Z. Hoffman and R. B. Bernstein. J. Phys. Chem. **64**, 1769 (1960).
7. R. J. Fallon, J. T. Vanderslice, and E. A. Mason. J. Phys. Chem. **63**, 2082 (1959).
8. R. J. Cvetanović. Quoted in reference 6.
9. J. L. Cojan and R. Taboue. J. phys. radium, **19**, 960 (1958).
10. O. P. Strausz and H. E. Gunning. Can. J. Chem. **39**, 2244 (1961).
11. S. Bywater and E. W. R. Steacie. J. Chem. Phys. **19**, 319 (1951).
12. R. A. Back. Can. J. Chem. **37**, 1834 (1959).
13. G. J. Verbeke and C. A. Winkler. J. Phys. Chem. **64**, 319 (1960).
14. W. Spindel and M. J. Stern. J. Chem. Phys. **32**, 1579 (1960).
15. K. R. Osborn and H. E. Gunning. Unpublished work.

Can. J. Chem. Downloaded from www.nrcresearchpress.com by 210.87.254.40 on 09/05/12
For personal use only.

Can. J. Chem. Downloaded from www.nrcresearchpress.com by 210.87.254.42 on 09/05/12
For personal use only.

HALOGEN ATOM REACTIONS

I. THE ELECTRICAL DISCHARGE AS A SOURCE OF HALOGEN ATOMS[1]

E. A. Ogryzlo

ABSTRACT

A number of surface poisons have been found to prevent the rapid recombination of chlorine, bromine, and iodine atoms. Hence these atoms can now be obtained in large concentrations in a flow system.

A chemical titration procedure for both Cl and Br atoms has been developed and has been used to test an isothermal calorimetric detector which can measure the atom concentration along a reaction tube. The detector was used to establish the surface recombination coefficient (γ) for chlorine atoms (4×10^{-5}) and bromine atoms (6×10^{-5}) on oxyacid-covered surfaces.

INTRODUCTION

The electrical discharge has proved a valuable source of hydrogen, nitrogen, and oxygen atoms. In the last few years many of the species produced in the discharge have been identified. In addition, a variety of methods of following the concentration of the atomic species in a flow system have been described (1, 2, 3, 4). As a result, rate constants for a large number of elementary reactions of these atoms are being reported in the literature. Unfortunately, workers have had less success with halogen atoms in a flow system. The statement made in 1933 by Schwab (5) that bromine atoms recombine on every collision with the walls, and chlorine atoms survive fewer than 20 collisions irrespective of the wall materials, seems to have discouraged further work with these species in a flow system.

Recent developments in the theory of atom recombination (6, 7) point to the need for a system capable of studying the low pressure recombination of halogen atoms. In addition, there remain a considerable number of elementary halogen atom reactions which are in need of direct measurements. For this reason we have re-examined the possibility of obtaining halogen atoms in a flow system.

EXPERIMENTAL

Chemicals

Matheson Company chlorine was dried with silica gel and purified by distillation. Reagent grade bromine was dried with phosphorus pentoxide, and purified by distillation. Air was removed from reagent grade iodine by sublimation in vacuum. NOCl from Matheson Company was purified only by trap-to-trap distillation. All other gases and chemicals were of reagent grade purity and were used without purification.

Apparatus

A conventional pyrex flow system with a linear flow velocity between 100 and 400 cm per sec was used. Inert gas flows were controlled with Edwards needle valves, and measured with conventional capillary-U-tube flow meters. All mercury was isolated with a layer of octyl phthalate. Cl_2, Br_2, NOCl, and ICl gases were contained in 22-liter bulbs. A constant pressure was maintained with the appropriate freezing bath. Flow was controlled by glass capillaries only, and measured with H_2SO_4-filled flow meters. All stopcocks in the halogen flow system were greased with Kel-F grease.

[1]*Manuscript received August 18, 1961.*
Contribution from the Department of Chemistry, University of British Columbia, Vancouver 8, B.C.

The discharge tube and reaction tube are shown in Fig. 1. The discharge tube was constructed of quartz to prevent breakage while the tube was being heated. It was made

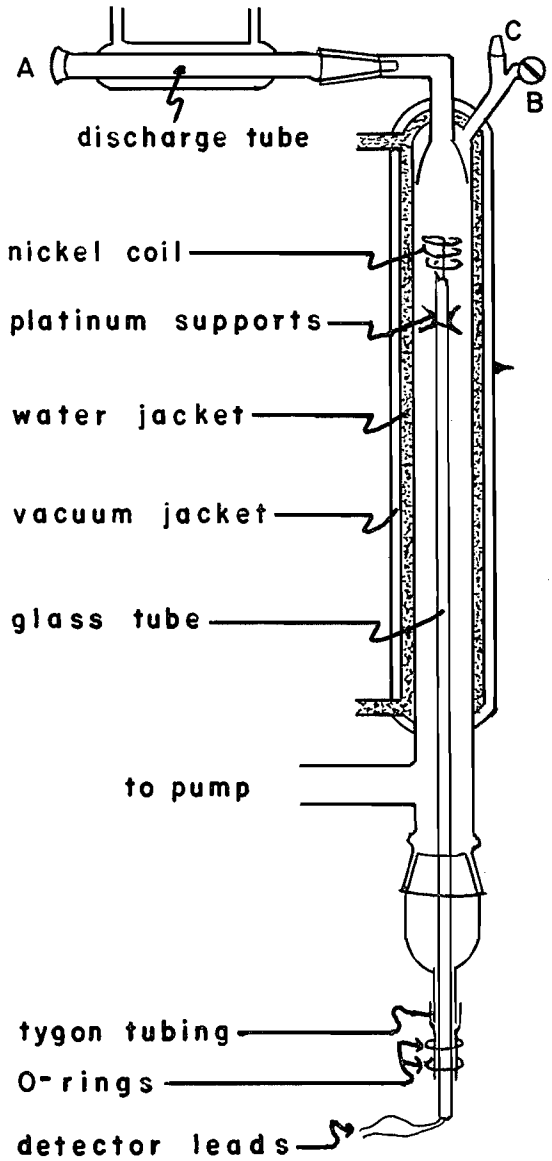


FIG. 1. Discharge tube, reaction tube, and movable detector assembly.

removable to facilitate cleaning since contamination occurred most often in this region. The jacket was used to cool the tube with a stream of air while the discharge was on. A 100-watt, 2450-megacycle generator was used to create the discharge.

The reaction tube was 50 cm long and had a diameter of 2.1 cm. It was surrounded by a water jacket for temperature control and a vacuum jacket to prevent a temperature gradient from forming when the tube is operated at other than room temperature.

Can. J. Chem. Downloaded from www.nrcresearchpress.com by 210.87.254.42 on 09/05/12
For personal use only.

The halogen gas (at flows between 0.5 and 45 μmoles/sec) could be introduced at A (Fig. 1) together with inert carrier gases such as argon and helium (at flows between 5 and 150 μmoles/sec). Other gases could be introduced after the discharge at B. Another opening at C made it possible to clean the reaction tube and apply different coatings to the reaction tube walls, without affecting the walls leading to the reaction tube. These coatings (hereafter called "poisons") were usually applied in the following manner. The cleaned vessel was filled with a hot, concentrated KOH solution and allowed to stand for 30 minutes. The vessel was then thoroughly washed with distilled water and filled with a 10% solution of the poison in water. This solution was allowed to stand for 1 hour and then drained. Finally, the system was evacuated for about 2 hours. During this period the discharge tube and reaction tube were heated to 250° C and 80° C respectively.

Figure 1 also shows the method which was used for moving both a coil of wire and a wrede gauge along the reaction tube. The movable vacuum-tight junction is provided by pressing a tygon tube against a glass tube with two O-rings. The glass tube is greased with Kel-F grease. No leaking occurred, and the slight degassing of the grease is of no consequence at this point in the flow system. The rack and pinion arrangement described previously (3) was also used for supporting the wire-coil but it cannot be used with a movable wrede gauge.

The principle of the isothermal–calorimetric atom detector (hereafter called the "detector") used in this work has already been described (3). It requires that the atoms in a gas stream recombine on a metal wire, raising its temperature to a value T. The heat liberated is then measured by observing the electrical current necessary to raise the wire temperature to the same value T. For successful operation the following requirements must be met:

(1) the thermal conductivity must be the same in the presence and absence of atoms;
(2) all the atoms must be recombined;
(3) no other species capable of heating up the detector can be present.

The first condition is easily satisfied in a gas simply subjected to an electrical discharge if the atoms recombine on almost every collision with the wire. The second condition can be satisfied by a suitable enlargement of the detector coil. The third condition can be verified by an independent atom measuring device which is insensitive to such species.

A wrede gauge was constructed with four 10-micron pinholes. The pressure difference across the pinholes was measured with an inclined oil-manometer.

RESULTS AND DISCUSSION

Fluorine

An attempt was made to pass F_2 through an electrical discharge. However, the gas was found too difficult to handle in a flow system and the experiment could not be completed.

Chlorine

Our first attempts to produce Cl atoms by passing a stream of the gas through a discharge in a pyrex and quartz tube were unsuccessful. A thin silver mirror which provides a sensitive test for halogen atoms by its discoloration showed no change 1 centimeter away from the discharge. Dry wall coatings of polythene, teflon, NaCl, NaOH, and $Al(OH)_3$ did not help to produce any detectable atoms.

On the other hand, when H_3PO_4, H_2SO_4, H_3AsO_4, H_3BO_3, and $HClO_4$ were used to "poison" the wall, immediate discoloration of the silver mirror occurred when the discharge was initiated. The absence and presence of atoms with these surface poisons was then verified with a wrede gauge. The atom concentrations measured with the gauge

Can. J. Chem. Downloaded from www.nrcresearchpress.com by 210.87.254.42 on 09/05/12
For personal use only.

were then compared with those measured by the detector using platinum, silver, cobalt, and nickel coils. The atom concentrations measured along the reaction tube by all methods were proportional to each other. However, the wrede gauge and platinum detector yielded a much lower value for the atom concentration than the Ag-, Co-, and Ni-covered detectors. The rapid atom recombination on the glass of the wrede gauge may account for the low value obtained with this instrument. A low catalytic activity for platinum has been observed previously (8) and would account for the low value obtained with this surface. Cobalt and silver detectors possess a number of other disadvantages. They are attacked by halogen atoms and the catalytic activity of the halide is somewhat lower than that of the metal. More troublesome, however, is the formation of some volatile compound that distills onto the walls at temperature above 100° C. Not only does nickel not possess these difficulties, but it also has a larger temperature coefficient of resistivity.

Complete removal of the atoms by the nickel coil was checked by placing a second detector immediately after the first. A 90-cm length of 30-gauge nickel wire wound into a double spiral and extended to a length of 1 cm was found to be effective in removing the atoms at pressures up to 4 mm Hg. At higher pressures it was difficult to prevent the atoms from being swept past the detector unless it was extended to about double this length.

Some typical chlorine atom flows measured 25 cm after the discharge are given in Table I.

TABLE I

Pressure, mm of Hg	Flow, in μmoles per second		
	Inert gas	Cl_2	Cl
2	50	1.5	1.5
2	50	7.0	2.5
0.4	5	10	4
0.5	5	20	8
0.6	5	30	10

Chemical Titrations

Chemical titration of oxygen and nitrogen atoms has been facilitated by the fact that many of these reactions are accompanied by light emission. Both reactions commonly used for nitrogen and oxygen atoms

$$N + NO \rightarrow N_2 + O$$

and

$$O + NO_2 \rightarrow NO + O_2$$

make use of the light-emitting reaction

$$O + NO \rightarrow NO_2 + h\nu$$

to observe the equivalence point of the titration. We have not found any useful light-emitting reaction in our work with halogen atoms, and hence a different equivalence indicator must be used.

We have found the following reaction most useful for titration of chlorine atoms:

$$Cl + NOCl \rightarrow NO + Cl_2.$$

Subsequent reactions

$$Cl + NO + M \rightarrow NOCl + M$$

$$Cl_2 + 2NO \rightarrow 2NOCl$$

Can. J. Chem. Downloaded from www.nrcresearchpress.com by 210.87.254.42 on 09/05/12
For personal use only.

are considerably slower under conditions present in the flow system. Figure 2 gives the atom flow measured by the detector as a function of the NOCl flow introduced through

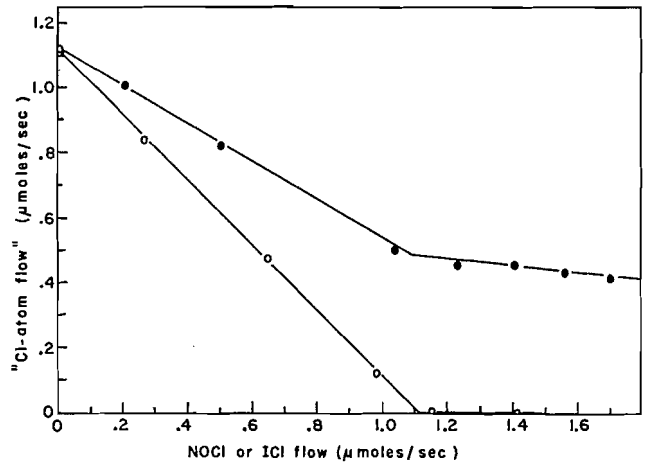


FIG. 2. Chlorine atom titration curves with NOCl (open circles) and with ICl (closed circles).

stopcock B in Fig. 1. The detector was placed 2 centimeters beyond the NOCl inlet. The agreement between the original chlorine atom flow measured by the detector and the NOCl flow necessary to remove all the atoms is excellent.

The titration of chlorine atoms with NOCl was carried out over a variety of experimental conditions. The technique used was to set the NOCl flow at some value in excess of the chlorine atom flow and then decrease the NOCl flow until atoms began to reach the detector. This NOCl flow was then recorded as the chlorine atom flow measured by titration. In all experiments carried out at a total pressure below 4 mm Hg the atom concentration measured by the two methods did not differ by more than 5%. However, the detector readings fell below those of the NOCl titration at higher pressures. This confirms the previous observation that at the higher pressures atoms are swept by the detector without being recombined.

It should be emphasized that though the detector is being used in the titration, the method is still an independent quantitative measurement. This is underlined by the fact that a glass-covered thermistor probe is even more effective in observing the end point of the titration.

Surface Recombination

With the nickel detector, the atom concentration was measured along the reaction tube. At a total pressure not greater than 0.3 mm Hg (due mostly to the carrier gas) the gas phase recombination is slow and can easily be corrected for. Though not unequivocally determined, the wall reaction appears to be of first order in chlorine atoms and can be written

$$\mathrm{Cl} + \text{wall} \xrightarrow{k_w} 1/2\,\mathrm{Cl_2} + \text{wall}$$

for which we have calculated a value of 0.8 $\mathrm{sec^{-1}}$ for k_W at 10° C with all the oxyacids used. The more meaningful recombination coefficient (γ), therefore, has a value of about 4×10^{-5}.

A considerably greater value was obtained until the marked effect of a small amount of water from the surface poison in the discharge was noted. The water not only greatly

Can. J. Chem. Downloaded from www.nrcresearchpress.com by 210.87.254.42 on 09/05/12
For personal use only.

increased the atom concentration but also caused a sharp increase in the rate of recombination of the atoms.

Bromine

The experiments described in the previous section were repeated with bromine. The results may be summarized as follows:

(1) No bromine atoms were detected in a stream of electrically discharged bromine unless the surfaces were coated with one of the oxyacids used for chlorine atoms.

(2) Bromine atoms can also be titrated with NOCl by the same technique used for chlorine atoms. The agreement between the atoms measured by titration and those measured with a nickel detector was satisfactory below a total pressure of about 4 mm Hg.

(3) Water vapor increases both the bromine atoms obtained from the discharge and the rate at which they are removed by recombination.

(4) The value of the surface recombination coefficient (γ) was found to be about 6×10^{-5} at 10° C for all the oxyacids used as surface poisons.

Iodine

To date we have had no success in obtaining iodine atoms from electrically discharged I_2. The difficulty seems to lie in the hot region immediately after the discharge because we have found that the atoms can be maintained if they are created outside the discharge.

The closed circles in Fig. 2 give the pseudo-chlorine atom concentration obtained when ICl is added to the same stream of chlorine atoms used in the NOCl titration. The fast reaction occurring is

$$Cl + ICl \rightarrow Cl_2 + I.$$

Subsequent reactions of iodine atoms are somewhat slower. The break in the curve probably represents the complete titration of chlorine atoms. This point is in reasonable agreement with the end point of the NOCl titration. Beyond this point on the curve the detector must be obtaining its heat from the recombination of iodine atoms. The fact that the heat obtained at the end point is not 36/58 of that originally obtained from the chlorine atoms may be due to the more rapid gas phase recombination of iodine atoms, which could be observed by moving the detector along the tube. This rapid gas phase recombination made it too difficult to estimate the wall recombination rate. Nevertheless, it is apparent that the absence of atoms from electrically discharged iodine vapor must be due to an even more rapid recombination in the hot region of the discharge.

CONCLUSION

The isothermal calorimetric detector has been shown to be capable of measuring accurately the concentration of both chlorine and bromine atoms in a flow system operating in the pressure range from 0.3 mm Hg to 4 mm Hg. The wall recombination coefficient (γ) has been shown to be sufficiently small to allow the use of this halogen atom source for kinetic studies. A number of reactions have been studied with this flow system and will be presented elsewhere.

ACKNOWLEDGMENTS

The author wishes to thank the National Research Council of Canada and the President's Research Fund at this University for financial assistance.

Can. J. Chem. Downloaded from www.nrcresearchpress.com by 210.87.254.42 on 09/05/12
For personal use only.

REFERENCES

1. G. B. KISTIAKOWSKY and G. G. VOLPI. J. Chem. Phys. **27**, 1141 (1957).
2. F. KAUFMAN. Proc. Roy. Soc. (London), A, **247**, 123 (1958).
3. L. ELIAS, E. A. OGRYZLO, and H. I. SCHIFF. Can. J. Chem. **37**, 1680 (1959).
4. J. KAPLAN, W. J. SCHADE, C. A. BARTH, and A. F. HILDEBRANDT. Can. J. Chem. **38**, 1688 (1960).
5. G. M. SCHWAB and H. FRIESS. Naturwissenschaften, **21**, 222 (1933); Z. Electrochem. **39**, 586 (1933). G. M. SCHWAB. Z. physik. Chem. (Leipzig), B, **27**, 452 (1934).
6. D. L. BUNKER and N. R. DAVIDSON. J. Am. Chem. Soc. **80**, 5085 (1958).
7. G. PORTER and J. A. SMITH. Proc. Roy. Soc. (London), A, **261**, 28 (1961).
8. W. H. RODEBUSH and W. C. KLINGELHOEFFER. J. Am. Chem. Soc. **55**, 130 (1933).

Can. J. Chem. Downloaded from www.nrcresearchpress.com by 210.87.254.42 on 09/05/12
For personal use only.

Can. J. Chem. Downloaded from www.nrcresearchpress.com by 210.87.254.5 on 09/05/12
For personal use only.

β-AROYL-α- AND -β-ARYLPROPIONIC ACIDS

PART I. THEIR PREPARATION AND LACTONIZATION[1]

SAYED SHERIF

ABSTRACT

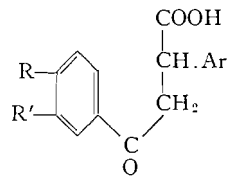
Bromobenzene reacts with phenyl- and *p*-methoxyphenyl-succinic anhydride in the presence of anhydrous aluminum chloride to give a mixture of β-*p*-bromobenzoyl-α- and -β-phenylpropionic acid, and a mixture of β-*p*-bromobenzoyl-α- and -β-*p*-hydroxyphenylpropionic acid, respectively.

Similarly, iodobenzene reacts with the same anhydrides to give a mixture of β-*p*-iodobenzoyl-α- and -β-phenylpropionic acid and β-benzoyl-α- and -β-phenylpropionic acid, and a mixture of β-benzoyl- and β-*p*-iodobenzoyl-α-*p*-methoxyphenylpropionic acid, respectively.

Phenyl- and diphenyl-succinic anhydride are cyclized by aluminum chloride to 1-ketoindane- and 1-keto-2-phenylindane-3-carboxylic acid, respectively.

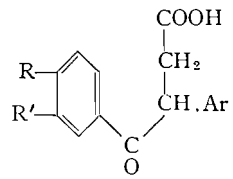
The above keto acids are converted by boiling acetic anhydride into β,γ-unsaturated γ-lactones.

Condensation of phenylsuccinic anhydride with bromobenzene in the presence of anhydrous aluminum chloride gave rise to a mixture of β-*p*-bromobenzoyl-α- and -β-phenylpropionic acid (I*a* and II*a*, respectively) in which the latter was predominant. The structure of the α-phenyl isomer was established by comparison with an authentic specimen prepared after Allen, Normington, and Wilson (1). The structure of the β-phenyl isomer was established by elemental analysis and by the production of *p*-bromobenzoic acid on oxidation with alkaline potassium permanganate. The reaction mixture contained a neutral product which was proved to be *p*-dibromobenzene, probably produced by the action of aluminum chloride on bromobenzene.



I

(*a*) R = Br; R′ = H; Ar = C_6H_5
(*b*) R = Br; R′ = H; Ar = *p*-HOC_6H_4
(*c*) R = I; R′ = H; Ar = C_6H_5
(*d*) R = R′ = H; Ar = C_6H_5
(*e*) R = R′ = H; Ar = *p*-$CH_3OC_6H_4$
(*f*) R = I; R′ = H; Ar = *p*-$CH_3OC_6H_4$
(*g*) R = R′ = Cl; Ar = C_6H_5
(*h*) R = R′ = Cl; Ar = H



II

(*a*) R = Br; R′ = H; Ar = C_6H_5
(*b*) R = Br; R′ = H; Ar = *p*-HOC_6H_4
(*c*) R = I; R′ = H; Ar = C_6H_5
(*d*) R = R′ = H; Ar = C_6H_5

When phenylsuccinic anhydride was replaced by *p*-methoxyphenylsuccinic anhydride, a mixture of β-*p*-bromobenzoyl-α- and -β-*p*-hydroxyphenylpropionic acid (I*b* and II*b*, respectively) was produced in which the latter was predominant. The structure of the α-*p*-hydroxyphenyl isomer was established by its identity with an authentic specimen prepared from *p*-bromophenyl 4-methoxystyryl ketone. The presence of the hydroxyl group was established by its infrared spectrum (see Experimental). The structure of the β-*p*-bromobenzoyl-β-*p*-hydroxyphenylpropionic acid was established by elemental analysis and by oxidation to *p*-bromobenzoic acid.

[1]*Manuscript received June 13, 1961.*
Contribution from the National Research Centre, Dokki, Cairo, Egypt, U.A.R.

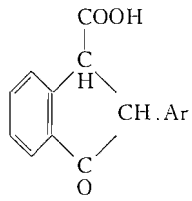
Can. J. Chem. Downloaded from www.nrcresearchpress.com by 210.87.254.5 on 09/05/12
For personal use only.

The condensation of phenylsuccinic anhydride with iodobenzene under the same conditions gave a mixture of β-*p*-iodobenzoyl-α- and -β-phenylpropionic acid (I*c* and II*c*, respectively) and β-benzoyl-α- and β-phenylpropionic acid (I*d* and II*d*, respectively). The structure of the first acid was established by comparison with an authentic specimen prepared from *p*-iodophenyl styryl ketone. The structure of the second acid was inferred from its elemental analysis, and from the fact that it gave, on oxidation with alkaline potassium permanganate, *p*-iodobenzoic acid. The structure of the halogen-free acids was established by comparison with authentic specimens (2). The formation of the halogen-free acids is due to the partial dehalogenation of iodobenzene to benzene, under the experimental conditions, and not to the partial dehalogenation of the β-aroylpropionic acids for the following reasons: (i) *o*- and *p*-diiodobenzene were isolated from the reaction mixture, and from a mixture of aluminum chloride and iodobenzene treated under the same conditions, and (ii) β-*p*-iodobenzoyl-α-phenylpropionic acid was recovered unchanged, when heated with aluminum chloride in toluene at 100° for 3 hours.

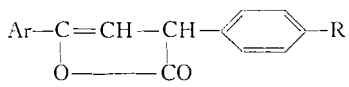
p-Methoxyphenylsuccinic anhydride reacted with iodobenzene in the presence of aluminum chloride to give a mixture of acids, which, after methylation and hydrolysis, was separated into β-benzoyl-α-*p*-methoxyphenylpropionic acid and β-*p*-iodobenzoyl-α-*p*-methoxyphenylpropionic acid (I*e* and I*f*, respectively); the former acid predominated. The structure of both acids was established by comparison with authentic specimens.

β-3,4-Dichlorobenzoyl-α-phenylpropionic acid (I*g*) was prepared by the addition of hydrogen cyanide to 3,4-dichlorophenyl styryl ketone and subsequent alcoholysis and hydrolysis of the corresponding nitrile.

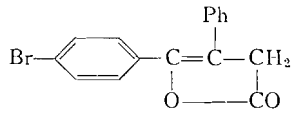
In the presence of aluminum chloride, succinic anhydride condensed with *o*-dichlorobenzene to give β-3,4-dichlorobenzoylpropionic acid (I*h*), the structure of which was established by oxidation with alkaline potassium permanganate to 3,4-dichlorobenzoic acid. However, under the same experimental conditions, phenylsuccinic anhydride failed to condense with *o*-dichlorobenzene, and instead it cyclized intramolecularly, giving 1-ketoindane-3-carboxylic acid (III*a*); this on decarboxylation gave α-hydrindone. Under the same conditions, α,β-diphenylsuccinic anhydride cyclized intramolecularly to give 1-keto-2-phenylindane-3-carboxylic acid (III*b*), the structure of which was established by comparison with an authentic specimen (3).



III



IV



V

(*a*) Ar = H
(*b*) Ar = C_6H_5

When the β-aroyl-α- and -β-arylpropionic acids were boiled with acetic anhydride, they were converted to the corresponding β,γ-unsaturated γ-lactones (4, 5) (IV and V, respectively). The lactone structure was established by the appearance of its characteristic stretching frequency (6, p. 153) in the infrared spectra of these compounds (see Experimental).

The results of the present investigation agree with those of Baddar and Sherif (4).

Can. J. Chem. Downloaded from www.nrcresearchpress.com by 210.87.254.5 on 09/05/12
For personal use only.

EXPERIMENTAL

Melting points are uncorrected. Infrared spectra were measured with a Perkin–Elmer Infracord spectrophotometer Model 137, using the potassium bromide wafer technique.

β-p-Bromobenzoyl-α-phenylpropionic Acid

A mixture of β-*p*-bromobenzoyl-α-phenylpropionitrile (7) (20 g), ethanol (150 ml), and concentrated sulphuric acid (30 ml) was refluxed for 6 hours on a steam bath. The ester (22 g), which solidified on being cooled, was filtered off and crystallized from light petroleum (b.p. 50–70°) to give ethyl β-*p*-bromobenzoyl-α-phenylpropionate in colorless crystals, m.p. 70–71°. Calc. for $C_{18}H_{17}BrO_3$: C, 59.85; H, 4.74; Br, 22.13. Found: C, 59.83; H, 4.61; Br, 22.00.

The ester (20 g) was hydrolyzed with 10% aqueous potassium hydroxide (200 ml) (1 hour reflux) to give β-*p*-bromobenzoyl-α-phenylpropionic acid (17 g) (from benzene), m.p. 160–161°; Allen and co-workers (1) give the same melting point. Calc. for $C_{16}H_{13}BrO_3$: C, 57.69; H, 3.93; Br, 24.00. Found: C, 57.85; H, 4.00; Br, 23.73.

When the acid was treated with 2,4-dinitrophenylhydrazine in a warm mixture of ethanol and concentrated sulphuric acid, it gave the 2,4-dinitrophenylhydrazone of the ethyl ester in orange-yellow crystals (from dilute acetic acid), m.p. 161–162°. Calc. for $C_{24}H_{21}BrN_4O_6$: C, 53.24; H, 3.91; N, 10.35. Found: C, 53.22; H, 3.75; N, 10.15.

Condensation of Bromobenzene with Phenylsuccinic Anhydride

A solution of phenylsuccinic anhydride (17.6 g, 0.1 mole) in bromobenzene (20 ml) was added gradually to a well-cooled and stirred mixture of anhydrous aluminum chloride (26.7 g, 0.2 mole) and bromobenzene (30 ml). The reaction mixture was heated at 100° for 3 hours, decomposed with ice-cold dilute hydrochloric acid, and the solvent was steam-distilled. The product (20 g, 60% yield), m.p. 85–100°, was crystallized from the least amount of glacial acetic acid, then from ether, to give β-*p*-bromobenzoyl-β-phenylpropionic acid (16 g, 48% yield) in colorless crystals, m.p. 156–157°, depressed to 130–140° when admixed with the α-phenyl isomer. Calc. for $C_{16}H_{13}BrO_3$: C, 57.69; H, 3.93; Br, 24.00. Found: C, 57.90; H, 3.83; Br, 24.00.

On oxidation with alkaline potassium permanganate (1 hour at 100°), it gave *p*-bromobenzoic acid, m.p. and mixed m.p. 250°.

The acetic acid mother liquor was diluted with water, and the precipitated solid was crystallized from benzene to give β-*p*-bromobenzoyl-α-phenylpropionic acid (2 g, 6% yield), m.p. and mixed m.p. 160–161°.

The steam-distillable fraction was dried (Na_2SO_4) and fractionally distilled to give mainly bromobenzene and *p*-dibromobenzene, m.p. and mixed m.p. 89°.

Action of Aluminum Chloride on Bromobenzene

Aluminum chloride was added to cold bromobenzene. The reaction mixture was kept at 25–30° for 3 days and then decomposed and worked up as usual to give bromobenzene and *p*-dibromobenzene.

β-p-Bromobenzoyl-α-p-methoxyphenylpropionitrile

To a solution of *p*-bromobenzoyl 4-methoxystyryl ketone (8) (5 g) in ethanol (150 ml), glacial acetic acid (2.3 ml) and aqueous potassium cyanide (3.5 g in 9 ml water) were added. The reaction mixture was kept at 60–65° for 5 hours, then left overnight. The nitrile (4 g) had m.p. 132–133° (from ethanol), depressed to 115–120° on admixing with the above chalcone. Calc. for $C_{17}H_{14}BrNO_2$: C, 59.31; H, 4.10; Br, 23.21; N, 4.07. Found: C, 59.20; H, 4.16; Br, 22.86; N, 4.00.

β-p-Bromobenzoyl-α-p-methoxyphenylpropionic Acid

A mixture of the above nitrile (4 g), methanol (50 ml), and concentrated sulphuric acid (7 ml) was refluxed for 8 hours and the product (4 g) crystallized from methanol to give methyl β-*p*-bromobenzoyl-α-*p*-methoxyphenylpropionate in colorless crystals, m.p. 79–80°. Calc. for $C_{18}H_{17}BrO_4$: C, 57.31; H, 4.55; Br, 21.18. Found: C, 57.11; H, 4.42; Br, 21.10.

The ester was hydrolyzed by refluxing for 2.5 hours with 5% aqueous potassium hydroxide (100 ml). The reaction mixture was cooled, acidified, and the precipitated acid was crystallized from ethanol to give β-*p*-bromobenzoyl-α-*p*-methoxyphenylpropionic acid (3.5 g) in colorless crystals, m.p. 134–135°. Calc. for $C_{17}H_{15}BrO_4$: C, 56.22; H, 4.17; Br, 22.02. Found: C, 56.00; H, 4.20; Br, 22.00.

When the acid was warmed with 2,4-dinitrophenylhydrazine in ethanol and concentrated sulphuric acid, and the product was crystallized from acetic acid, the 2,4-dinitrophenylhydrazone of the ethyl ester was obtained, in yellow crystals, m.p. 188–189°. Calc. for $C_{25}H_{23}BrN_4O_7$: C, 52.55; H, 4.06; Br, 14.00; N, 9.81. Found: C, 52.41; H, 3.91; Br, 14.20; N, 10.08.

β-p-Bromobenzoyl-α-p-hydroxyphenylpropionic Acid

A mixture of β-*p*-bromobenzoyl-α-*p*-methoxyphenylpropionic acid (2.5 g), aluminum chloride (5 g), and bromobenzene (20 ml) was stirred at 100° for 2 hours, then worked up as usual. The product (2 g) was crystallized from ether to give β-*p*-bromobenzoyl-α-*p*-hydroxyphenylpropionic acid, in colorless crystals, m.p. 171–172°. It gave a deep blue color with warm concentrated sulphuric acid. Calc. for $C_{16}H_{13}BrO_4$: C, 55.05; H, 3.75; Br, 22.90. Found: C, 55.16; H, 3.75; Br, 22.90. Its infrared spectrum showed two bands at 3450 and 1670 cm^{-1} characteristic of a bonded OH group (6, p. 84) and the CO group of the aroyl group (6, p. 114), respectively.

p-Methoxyphenylsuccinic Anhydride

It was prepared from the acid (9) by refluxing with 3 times its weight of acetyl chloride for 6 hours. The excess of acetyl chloride was distilled off, and the residue fractionated, b.p. 205–208° at 5 mm (80% yield).

Condensation of Bromobenzene with p-Methoxyphenylsuccinic Anhydride

A solution of *p*-methoxyphenylsuccinic anhydride (20.6 g, 0.1 mole) in bromobenzene (40 ml) was gradually added to a well-cooled and stirred mixture of aluminum chloride (26.7 g, 0.2 mole) and bromobenzene (50 ml). The reaction mixture was left overnight, heated at 100° for 3 hours, then worked up as usual. The product (20 g, 57% yield) was crystallized from ether to give β-*p*-bromobenzoyl-β-*p*-hydroxyphenylpropionic acid, in colorless crystals, m.p. 198–199° (12 g, 34% yield), depressed to 150–155° when admixed with β-*p*-bromobenzoyl-α-*p*-hydroxyphenylpropionic acid. Calc. for $C_{16}H_{13}BrO_4$: C, 55.05; H, 3.75; Br, 22.90. Found: C, 55.32; H, 3.90; Br, 22.45. It gave a yellowish-green color with concentrated sulphuric acid. On oxidation with alkaline potassium permanganate, it gave *p*-bromobenzoic acid.

Concentration of the ether mother liquor gave β-*p*-bromobenzoyl-α-*p*-hydroxyphenylpropionic acid (6 g, 17% yield), m.p. and mixed m.p. 171–172°.

β-p-Iodobenzoyl-α-phenylpropionitrile

To a solution of *p*-iodophenyl styryl ketone (10) (3 g) in ethanol (75 ml), glacial acetic acid (2.3 ml) and aqueous potassium cyanide (3.5 g in 10 ml water) were added. The

Can. J. Chem. Downloaded from www.nrcresearchpress.com by 210.87.254.5 on 09/05/12
For personal use only.

reaction mixture was kept at 70–75° for 4 hours, then left overnight. β-*p*-Iodobenzoyl-α-phenylpropionitrile (3 g) was crystallized from ethanol in colorless crystals, m.p. 148–149°. Calc. for $C_{16}H_{12}INO$: C, 53.21; H, 3.35; I, 35.15; N, 3.88. Found: C, 53.11; H, 3.45; I, 34.76; N, 3.80.

β-p-Iodobenzoyl-α-phenylpropionic Acid

A mixture of the above nitrile (2 g), methanol (25 ml), and concentrated sulphuric acid (5 ml) was refluxed on a steam bath for 8 hours. The reaction mixture was diluted with water and the precipitated methyl β-*p*-iodobenzoyl-α-phenylpropionate (2 g) was crystallized from methanol, in colorless crystals, m.p. 132–133°, depressed to 115–120° when admixed with the corresponding nitrile. Calc. for $C_{17}H_{15}IO_3$: C, 51.79; H, 3.84; I, 32.20. Found: C, 51.70; H, 3.77; I, 32.00.

The preceding ester was hydrolyzed by refluxing for 1.5 hours with 5% aqueous potassium hydroxide (100 ml) to give β-*p*-iodobenzoyl-α-phenylpropionic acid (1.7 g), which was crystallized from ether in colorless crystals, m.p. 155–156°. Calc. for $C_{16}H_{13}IO_3$: C, 50.55; H, 3.45; I, 33.40. Found: C, 50.37; H, 3.60; I, 33.15. Oxidation of the α-phenylpropionic acid with aqueous alkaline potassium permanganate gave *p*-iodobenzoic acid, m.p. and mixed m.p. 270° (11).

Condensation of Iodobenzene with Phenylsuccinic Anhydride

The product from iodobenzene (60 ml), phenylsuccinic anhydride (17.6 g, 0.1 mole), and aluminum chloride (26.7 g, 0.2 mole) (3 hours at 100°) was extracted with boiling aqueous sodium carbonate solution. The extract, on being cooled and acidified, gave a semisolid residue (15 g). This was extracted several times with light petroleum (b.p. 50–70°), and the insoluble portion was crystallized from benzene to give β-benzoyl-β-phenylpropionic acid (2 g), m.p. and mixed m.p. 168° (2). Concentration of the benzene mother liquor gave β-benzoyl-α-phenylpropionic acid (3 g), m.p. and mixed (2) m.p. 154°. Evaporation of the benzene layer gave a semisolid residue which was crystallized several times from light petroleum (b.p. 70–90°) to give β-*p*-iodobenzoyl-β-phenylpropionic acid (2 g, 5.3% yield) in colorless crystals, m.p. 160–161°, depressed to 130–135° when admixed with its α-phenyl isomer. Calc. for $C_{16}H_{13}IO_3$: C, 50.55; H, 3.45; I, 33.40. Found: C, 50.82; H, 3.60; I, 32.47. Oxidation of the β-phenylpropionic acid with alkaline potassium permanganate gave *p*-iodobenzoic acid.

The light petroleum mother liquor was evaporated and the residue left was crystallized from ether to give β-*p*-iodobenzoyl-α-phenylpropionic acid (1.5 g, 4% yield), m.p. and mixed m.p. 156°.

The residue insoluble in sodium carbonate solution was dissolved in hot ethanol, and the oil and crystals, which were precipitated when the solution was cooled, were mechanically separated. The crystals, after crystallization from light petroleum (b.p. 50–70°), melted at 128°, not depressed when admixed with an authentic specimen of *p*-diiodobenzene. The oil was distilled under vacuum, b.p. 153–155° at 15 mm, and the solidified product was crystallized from light petroleum (b.p. below 40°) to give *o*-diiodobenzene in plates, m.p. and mixed m.p. 27° (12).

Action of Aluminum Chloride on β-p-Iodobenzoyl-α-phenylpropionic Acid

The acid (2 g) was dissolved in toluene (15 ml) and the cooled mixture was treated with aluminum chloride (5 g); the reaction mixture was stirred at 100° for 3 hours, then decomposed as usual. β-*p*-Iodobenzoyl-α-phenylpropionic acid was recovered unchanged, m.p. and mixed m.p. 156°.

Can. J. Chem. Downloaded from www.nrcresearchpress.com by 210.87.254.5 on 09/05/12
For personal use only.

Action of Aluminum Chloride on Iodobenzene

Iodobenzene was cooled to 0–5° and treated gradually with aluminum chloride. The reaction mixture was kept at room temperature (25–30°) for 3 days, then decomposed in the usual manner. *p*-Diiodobenzene and *o*-diiodobenzene were isolated from the reaction mixture as already mentioned.

p-Iodophenyl 4-Methoxystyryl Ketone

A mixture of *p*-iodoacetophenone (13) (18.4 g), ethanol (175 ml), water (60 ml), sodium hydroxide (7.5 g), and anisaldehyde (10.2 g) was stirred at 20–25° for 1.5 hours. *p*-Iodophenyl 4-methoxystyryl ketone (27 g) was obtained from ethanol in pale yellow crystals, m.p. 172–173°. Calc. for $C_{16}H_{13}IO_2$: C, 52.77; H, 3.60; I, 34.86. Found: C, 52.55; H, 3.51; I, 34.52.

β-p-Iodobenzoyl-α-p-methoxyphenylpropionitrile

To a solution of the above chalcone (3 g) in ethanol (175 ml), acetic acid (2.3 ml) and aqueous potassium cyanide (3.5 g in 10 ml water) were added. The reaction mixture was kept at 70–75° for 4 hours, then left overnight. The crystalline precipitate (3 g) was collected and crystallized from ethanol to give *β-p*-iodobenzoyl-*α-p*-methoxyphenylpropionitrile in colorless crystals, m.p. 164–165°. Calc. for $C_{17}H_{14}INO_2$: C, 52.21; H, 3.60; N, 3.58. Found: C, 52.10; H, 3.70; N, 3.41.

β-p-Iodobenzoyl-α-p-methoxyphenylpropionic Acid

A mixture of the preceding nitrile (2 g), methanol (25 ml), and concentrated sulphuric acid (4 ml) was refluxed for 10 hours. The reaction mixture was poured onto ice water and the crude methyl ester was directly hydrolyzed with 10% aqueous potassium hydroxide (100 ml) (1-hour reflux) to *β-p*-iodobenzoyl-*α-p*-methoxyphenylpropionic acid (1 g) from ether, m.p. 156–157°. Calc. for $C_{17}H_{15}IO_4$: C, 49.75; H, 3.69; I, 30.95. Found: C, 50.00; H, 3.60; I, 30.84.

Condensation of Iodobenzene with p-Methoxyphenylsuccinic Anhydride

The product from iodobenzene (60 ml), *p*-methoxyphenylsuccinic anhydride (20.6 g, 0.1 mole), and aluminum chloride (26.7 g, 0.2 mole) (3 hours at 100°) was steam-distilled and the residue extracted with boiling 10% aqueous sodium carbonate solution. The extract, on acidification, gave a semisolid residue (10 g), which was methylated with methyl iodide, potassium carbonate, and acetone. Hydrolysis of the esters (5% aqueous potassium hydroxide) gave a semisolid mass which, after crystallization from benzene, gave *β*-benzoyl-*α-p*-methoxyphenylpropionic acid (6 g), m.p. and mixed (9) m.p. 158°. Evaporation of the benzene mother liquor gave a gummy acid which, on crystallization from ether, gave *β-p*-iodobenzoyl-*α-p*-methoxyphenylpropionic acid (2 g), m.p. and mixed m.p. 156–157°.

The steam-distillable fraction was dried (Na_2SO_4) and fractionally distilled to give iodobenzene and *o*- and *p*-diiodobenzene.

β-3,4-Dichlorobenzoylpropionic Acid

A stirred mixture of aluminum chloride (53.4 g, 0.4 mole) and *o*-dichlorobenzene (75 ml) was treated portionwise with a solution of succinic anhydride (20 g, 0.2 mole in 25 ml of *o*-dichlorobenzene). The reaction mixture was heated at 100° for 3 hours, then worked up as usual. *β*-3,4-Dichlorobenzoylpropionic acid (30 g, 61% yield) came down from ethanol in colorless crystals, m.p. 167–168°. Calc. for $C_{10}H_8Cl_2O_3$: C, 48.61; H, 3.26; Cl, 28.70. Found: C, 48.57; H, 3.11; Cl, 28.61. Oxidation of this acid with alkaline potassium permanganate gave 3,4-dichlorobenzoic acid, m.p. and mixed (14) m.p. 208–209°.

Can. J. Chem. Downloaded from www.nrcresearchpress.com by 210.87.254.5 on 09/05/12
For personal use only.

3,4-Dichlorophenyl Styryl Ketone

A mixture of 3,4-dichloroacetophenone (15) (9.5 g), ethanol (100 ml), water (40 ml), sodium hydroxide (5 g), and benzaldehyde (5.3 g) was stirred at 50–55° for 1 hour, then allowed to cool. 3,4-Dichlorophenyl styryl ketone (10 g) was obtained in pale yellow crystals, m.p. 116–117° (from ethanol). Bradsher and co-workers (16) and Lutz and co-workers (17) gave m.p. 112–113° and 110–112°, respectively. Calc. for $C_{15}H_{10}Cl_2O$: C, 65.03; H, 3.63; Cl, 25.60. Found: C, 64.73; H, 3.60; Cl, 25.00.

β-3,4-Dichlorobenzoyl-α-phenylpropionitrile

To a solution of the above chalcone (2 g) in ethanol (50 ml), acetic acid (2 ml) and aqueous potassium cyanide (2 g in 5 ml water) were added. The reaction mixture was heated to the boiling point, then left overnight. The nitrile (2 g) was crystallized from ethanol in colorless crystals, m.p. 119–120°, depressed to 105–110° when admixed with the corresponding chalcone. Calc. for $C_{16}H_{11}Cl_2NO$: C, 63.19: H, 3.65; Cl, 23.31; N, 4.60. Found: C, 63.00; H, 3.60; Cl, 23.11; N, 4.45.

β-3,4-Dichlorobenzoyl-α-phenylpropionic Acid

A mixture of the above nitrile (2 g), methanol (25 ml), and concentrated sulphuric acid (5 ml) was heated on a steam bath for 10 hours. The ester that precipitated on cooling was hydrolyzed with 5% aqueous potassium hydroxide (100 ml) (1.5 hours reflux) to give β-3,4-dichlorobenzoyl-α-phenylpropionic acid (1.5 g) as colorless crystals from methanol, m.p. 170–171°. Calc. for $C_{16}H_{12}Cl_2O_3$: C, 59.47; H, 3.74; Cl, 21.95. Found: C, 59.21; H, 3.75; Cl, 21.46.

1-Ketoindane-3-carboxylic Acid

Phenylsuccinic anhydride (17.6 g) in *o*-dichlorobenzene (20 ml) was added gradually to a well-cooled and stirred mixture of aluminum chloride (26.7 g) and *o*-dichlorobenzene (30 ml). The reaction mixture was heated at 100° for 2 hours, then worked up as usual. The colorless crystalline acid, m.p. 85° (from water), was dried in vacuum to give 1-ketoindane-3-carboxylic acid (12.5 g, 71% yield), m.p. and mixed (18) m.p. 120°.

α-Hydrindone

A mixture of 1-ketoindane-3-carboxylic acid (2 g), quinoline (15 ml), and copper bronze (0.5 g) was refluxed for 1 hour, cooled, and decomposed as usual. The reaction mixture was extracted with benzene. The removal of the solvent left an oil (ca. 1.5 g) which, on trituration with light petroleum (b.p. below 40°), gave colorless crystals, m.p. 42°; it was converted into α-hydrindone 2,4-dinitrophenylhydrazone, m.p. and mixed m.p. 260° (decomp.).

1-Keto-2-phenylindane-3-carboxylic Acid

A mixture of diphenylsuccinic anhydride (8.5 g) and aluminum chloride (10 g) in *o*-dichlorobenzene (30 ml) was heated at 100° for 2 hours, decomposed, and the solvent was steam-distilled. 1-Keto-2-phenylindane-3-carboxylic acid monohydrate (ca. 8 g) was crystallized from dilute ethanol in colorless crystals, m.p. and mixed (3) m.p. 116–117° (decomp.).

Lactonization of β-Aroyl-α- and -β-arylpropionic Acids

The solution of the acid (1 g) in acetic anhydride (10 ml) was refluxed for 2 hours and, after cooling, poured into water. The solid was filtered off and washed with dilute sodium carbonate solution. The lactone (ca. 100% yield) was then crystallized from a suitable solvent (see Table I).

Can. J. Chem. Downloaded from www.nrcresearchpress.com by 210.87.254.5 on 09/05/12
For personal use only.

Can. J. Chem. Downloaded from www.nrcresearchpress.com by 210.87.254.5 on 09/05/12
For personal use only.

TABLE I

Lactone							Analysis (%)					
							Calculated			Found		
No.	Ar	R	Solvent	M.p.	ν_{max}§ (cm^{-1})	Formula	C	H	Halogen	C	H	Halogen
IV	C_6H_5	OCH_3	C_6H_6–Pet†	107–108°	1750	$C_{17}H_{14}O_3$	76.68	5.31	—	76.44	5.30	—
IV	β-Naphthyl*	H	C_6H_6–Pet†	123–124°	1745	$C_{20}H_{14}O_2$	83.90	4.93	—	83.82	4.84	—
IV	2-Fluorenyl*	H	Ether	159–160°	1745	$C_{23}H_{16}O_2$	85.18	4.98	—	85.05	5.00	—
IV	p-Br·C_6H_4	H	C_6H_6	158–159°	1745	$C_{16}H_{11}BrO_2$	60.95	3.52	25.35	61.00	3.60	25.85
IV	p-Br·C_6H_4	OCH_3	C_6H_6–Pet†	149–150°	1755	$C_{17}H_{13}BrO_3$	59.16	3.80	23.15	59.04	3.64	22.93
IV	p-I·C_6H_4	H	C_6H_6	173–174°	1755	$C_{16}H_{11}IO_2$	53.07	3.06	35.05	53.41	3.22	34.57
IV	3,4-Cl_2·C_6H_3	H	C_6H_6	157–158°‡	1750	$C_{16}H_{10}Cl_2O_2$	63.00	3.30	23.25	63.40	3.25	22.84
V	—	—	C_6H_6	141–142°	1755 & 1786	$C_{16}H_{11}BrO_2$	60.95	3.52	25.35	61.01	3.51	24.54

*The corresponding keto acids were prepared after Hidayetulla and co-workers (19) and Baddar and his students (2), respectively.
†Pet = light petroleum (b.p. 50–70°).
‡Decomp.
§Stretching frequency for β,γ-unsaturated γ-lactones.

ACKNOWLEDGMENT

I wish to express my thanks to Dr. F. G. Baddar, Professor of Organic Chemistry, for his interest in the work, and for running the infrared spectra.

REFERENCES

1. C. F. H. Allen, J. B. Normington, and C. V. Wilson. Can. J. Research. **11**, 382 (1934).
2. F. G. Baddar, A. M. Fleifel, and S. Sherif. J. Chem. (U.A.R.), **3**, 47 (1960).
3. D. B. Bruce, A. J. S. Sorrie, and R. H. Thomson. J. Chem. Soc. 2403 (1953).
4. F. G. Baddar and S. Sherif. J. Chem. Soc. 2309 (1960).
5. F. G. Baddar and S. Sherif. J. Chem. Soc. 707 (1961).
6. L. J. Bellamy. Infrared spectra of complex molecules. Methuen & Co. Ltd., London. 1956.
7. C. F. H. Allen and G. F. Frame. Can. J. Research, **6**, 605 (1932).
8. R. P. Barnes, T. C. Goodwin, and T. W. Cotten. J. Am. Chem. Soc. **69**, 3135 (1947).
9. M. A. Wali, A. K. Khalil, R. L. Bhatia, and S. S. Ahmad. Proc. Indian Acad. Sci. A, **14**, 139 (1941).
10. O. Neunhoeffer and D. Rosahl. Ber. **86**, 226 (1953).
11. E. Hoffmann. Ann. **264**, 166 (1891).
12. W. H. Strain, J. T. Plati, and S. L. Warren. J. Am. Chem. Soc. **64**, 1436 (1942).
13. W. Kimura. Ber. **67**, 394 (1934).
14. G. M. Kraay. Rec. trav. Chim. **49**, 1082 (1930).
15. E. Roberts and E. E. Turner. J. Chem. Soc. 1855 (1927).
16. C. K. Bradsher, F. C. Brown, and W. B. Blue. J. Am. Chem. Soc. **71**, 3570 (1949).
17. R. E. Lutz, T. E. Martin, J. F. Codington, T. M. Amacker, R. K. Allison, N. H. Leake, R. J. Rowlett, J. D. Smith, and J. W. Wilson. J. Org. Chem. **14**, 992 (1949).
18. W. Baker and W. G. Leeds. J. Chem. Soc. 974 (1948).
19. M. S. Hidayetulla, R. C. Shah, and T. S. Wheeler. J. Chem. Soc. 111 (1941).

Can. J. Chem. Downloaded from www.nrcresearchpress.com by 210.87.254.5 on 09/05/12
For personal use only.

Can. J. Chem. Downloaded from www.nrcresearchpress.com by 210.87.254.5 on 09/05/12
For personal use only.

THE CHEMICAL COMPOSITION OF THE WOOD AND BARK EXTRACTIVES OF JUNIPERUS HORIZONTALIS MOENCH[1]

N. NARASIMHACHARI[2] AND E. VON RUDLOFF

ABSTRACT

The wood of creeping juniper was found to contain about 10% acetone-soluble material. Of this, about one quarter was ligroin soluble and, from this portion, thujopsene, α-cedrene, cuparene, cedrol, widdrol, β-sitosterol, esters of fatty acids and β-sitosterol, the lignan savinin, and the recently discovered diterpene communic acid were isolated. Three unidentified hydrocarbons and several unknown alcohols and ketones were also obtained in small amounts. The ether-insoluble portion consisted of intractable polyphenolic material. The composition of the ligroin-soluble extract of the bark of this shrub resembled that of the wood in many respects. Neither the wood nor the bark extractives contained thujaplicins in detectable amounts.

Creeping juniper (*Juniperus horizontalis* Moench; also *Sabina horizontalis* (1)) is a prostrate shrub which is found widely distributed across Canada and occurs frequently in the dry, sandy regions of the Prairie Provinces. A survey of the literature did not reveal any reference to chemical investigations of the components of this plant. This paper deals with some of the components found in the wood and bark of the conifer.

The wood, after removal of the bark, was milled and extracted with acetone, giving 9–10% of soluble material. This extract was then fractionated into various groups of compounds as shown in Fig. 1. When the wood was extracted directly with ligroin, the same yield of ligroin-soluble material was obtained and this was divided into neutral, phenolic, and acidic material in the usual manner. The major portion consisted of neutral components which were fractionated by chromatography on a silicic acid column into five distinct classes of compounds: hydrocarbons, esters, mixed ketones and alcohols, sitosterol, and a lactone, respectively.

Hydrocarbons

The hydrocarbon fraction (0.22% of the weight of wood) was analyzed by gas–liquid chromatography (GLC) (2), which showed the presence of one major and five minor sesquiterpene hydrocarbons. The retention times of these components corresponded with six of the seven sesquiterpene hydrocarbons found in commercial cedar wood oil (from *Juniperus virginiana*). Runeberg (3) has identified three of these to be α-cedrene, thujopsene, and cuparene. The first peak recorded from the mixture from creeping juniper had the retention time and infrared spectrum of α-cedrene. The second and major constituent corresponded in retention time to either thujopsene or the isomer of cedrene (4) which is obtained when cedrol is dehydrated by the method of Motl *et al.* (5). This component was not attacked by cold, dilute permanganate solutions, nor did it yield any identifiable product on dehydrogenation with either selenium or palladized charcoal. On oxidation with selenium dioxide, a crystalline aldehyde, m.p. 71–72° C, was obtained. This, together with the GLC and infrared analysis, suggested the major hydrocarbon to be thujopsene. This was confirmed by oxidizing an authentic sample of thujopsene (kindly supplied by Prof. H. Erdtman and T. Norin, Stockholm, Sweden) with selenium dioxide to thujopsenal (6), m.p. 71.5–72° C, which showed no depression in melting point with

[1]*Manuscript received August 28, 1961.*
Contribution from the National Research Council of Canada, Prairie Regional Laboratory, Saskatoon, Saskatchewan.
Issued as N.R.C. No. 6545.
[2]*National Research Council of Canada Postdoctorate Fellow, 1960–1961.*

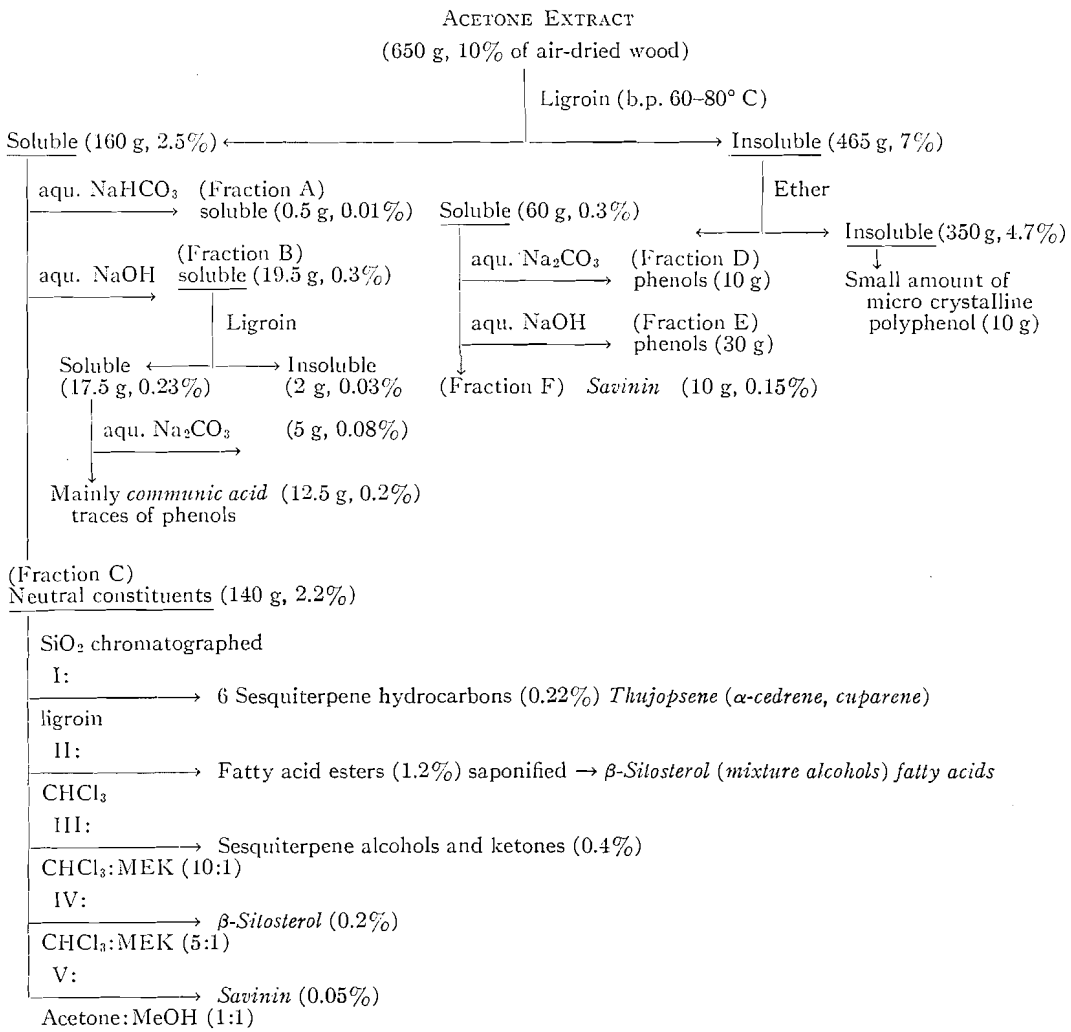


FIG. 1. Fractionation scheme for the wood extractives.

the above aldehyde. It was found that although thujopsene did not react with cold potassium permanganate solution, a liquid diol could be prepared from it with osmium tetroxide. Of the other minor hydrocarbons, none could be obtained pure. However, a concentrate of the second last peak gave an infrared spectrum resembling that of cuparene.

Esters

The ester fraction (1.2%) was saponified and from the non-saponifiable portion β-sitosterol and a small amount of a mixture of aliphatic alcohols were obtained. GLC analysis of the latter mixture showed two peaks in the C-12 range, one in the C-15, and one in the C-20 range. The acid portion consisted of a mixture of long-chain fatty acids which was analyzed by GLC (7). Peaks corresponding to palmitic, palmitoleic, stearic, oleic, linoleic, linolenic, and arachidic acid were recorded in the ratio of 6:1:1:13:37:6:2. The high proportion of the unsaturated C_{18} acids is typical for conifer wood (8).

Can. J. Chem. Downloaded from www.nrcresearchpress.com by 210.87.254.5 on 09/05/12
For personal use only.

Can. J. Chem. Downloaded from www.nrcresearchpress.com by 210.87.254.5 on 09/05/12
For personal use only.

Ketones and Alcohols

The third fraction (0.4%) from the silicic acid chromatogram was found to be a mixture of sesquiterpene alcohols and ketones. GLC analysis on the adipate polyester column showed the presence of two components having retention times corresponding to those of cedrol and widdrol, four minor constituents, and a major constituent with a very high retention time. Preparative GLC (20 mg scale) led to the isolation of milligram quantities of the cedrol–widdrol mixture, a mixed ketone–alcohol fraction, and the slow-moving major component. The cedrol–widdrol mixture was resolved on the polyester column and the identity of each alcohol was substantiated by its infrared spectrum. The identity of these two alcohols was further verified by dehydrating the mixture with the pyridine-modified alumina catalyst (4) to a product consisting mainly of α-cedrene and thujopsene (GLC). The second fraction had strong hydroxyl and carbonyl absorption bands in the infrared region. Re-chromatography of this fraction on the polyester column gave at least three peaks with strong indications that decomposition took place. The third fraction corresponded to the component having a very high retention time on the polyester column. Its infrared spectrum had absorption peaks at 1665 and 1618 cm^{-1}, and a maximum at 235 mμ with a weak shoulder 285 mμ was recorded in the ultraviolet region. Attempts to isolate and purify the ketones by means of Girard P reagent or column chromatography failed, mainly because of extensive decomposition of one or more of the components.

Sitosterol

Free β-sitosterol (0.016%) was obtained crystalline from the fourth fraction. No volatile constituents could be detected by GLC in the residue obtained from the mother liquors.

Lactone

Of more interest was the last fraction (0.05%) from the chromatogram which was also obtained in crystalline form. The purified, light yellow compound had m.p. 146–147°, $[\alpha]_D^{20}$ −82.3°, and a molecular weight of 362. The ultraviolet spectrum showed maxima at 237, 294, and 334 mμ, whereas the infrared spectrum (KBr disk and $CHCl_3$ solution) had two strong adsorption bands at 1740 and 1640 cm^{-1}, indicating the presence of an α,β-unsaturated lactone. The presence of a lactone ring was confirmed by the solubility of the compound in alcoholic alkali, from which the parent compound was recovered unchanged on acidification. The compound was insoluble in cold ethanol or cold aqueous alkali. Except for the position of the infrared bands discussed above, these data suggested a close resemblance with savinin. The structure of this lignan lactone was elucidated by Hartwell *et al.* (9, 10), who reported infrared absorption peaks at 1751 and 1651 cm^{-1} and also that the compound formed colorless crystals. The mixed melting point of authentic savinin (kindly supplied by Drs. J. L. Hartwell and A. W. Schrecker, Bethesda, U.S.A.) with the yellow compound isolated from creeping juniper was not depressed. The authentic sample also gave absorption bands at 1740 and 1640 cm^{-1} on the infrared spectrophotometer used in these experiments, and agreed in all other respects as well. Thus, there is no doubt that the two compounds are identical.

Acids and Phenols

The acidic portion of the ligroin- and ether-soluble extract was found to consist mainly of a diterpene acid (0.25%) $C_{20}H_{30}O_2$, m.p. 121–122° C, $[\alpha]_D^{25}$ +40.3°. On treatment with diazomethane the acid readily formed a methyl ester having m.p. 108–109° C, $[\alpha]_D^{25}$ +50.5°, which could not be saponified even at 125° C. GLC analysis showed the

methyl ester to be a single compound. The infrared spectrum showed the presence of a terminal methylene group (890 cm^{-1}) and a trisubstituted double bond (1645 and 795 cm^{-1}). Hydrogenation over platinum oxide catalyst resulted in the uptake of hydrogen equivalent to three double bonds. These data suggested that the acid was identical with the sirupy communic acid, isolated recently by Arya *et al.* from the wood of *Juniperus communis* L. (11). This was confirmed by preparing the maleic anhydride adduct of the ester, m.p. 170–171° C, $[\alpha]_D^{25}$ +79.5°. It is to be noted that in the preparation from *Juniperus horizontalis* the acid was obtained readily in the crystalline state.

Small amounts of phenolic materials were also obtained from the acidic portion. Paper chromatography (12) did not reveal the presence of any thujaplicins or related tropolones. This is surprising, since Runeberg and Pilo (13, 14) have found thujaplicins and nootkatin in a large number of juniper species. Thus, the extractives of creeping juniper wood more nearly resemble those of *Chamacyparis thyoides* (15), which are reported to contain no thujaplicins, but α-cedrene, cuparene, thujopsene, cedrol, widdrol, and carvacrol methyl ether. The finding of thujopsene, α-cedrene, cuparene, cedrol, widdrol, and communic acid does show, however, the close biogenetic relationship of the extractive components of creeping juniper with the other juniper species investigated.

The major portion (about 75%) of the acetone-soluble extractives of the wood of creeping juniper consisted of a brown, resinous phenolic material. Various fractionation attempts resulted only in the isolation of a small amount of microcrystalline polyphenolic material. The separation and identification of individual components from this so-called "phlobaphene" fraction will be studied further when more suitable fractionation techniques have been found.

Bark Extractives

It was of interest to determine whether the terpenoid compounds found in the wood could also be isolated from the bark of creeping juniper. The bark was milled to a fine powder, extracted with ligroin, and the extract was divided into neutral and acidic constituents. Column chromatography of the neutral portion gave as the first fraction hydrocarbons which appeared from GLC analysis to contain the same components as found in the corresponding fraction of the wood extractives. However, the component having the retention time of α-cedrene was present in about three times the amount of thujopsene. Treatment of the mixture with aqueous permanganate did not result in the formation of α-cedrene diol (16). Oxidation of the mixture with selenium dioxide produced a liquid aldehydic material in high yield which gave, on GLC analysis, only a peak corresponding to thujopsenal. Thus it may be that the unknown major hydrocarbon is an isomer of thujopsene rather than α-cedrene.

The second fraction from the column was composed of esters of β-sitosterol and a mixture of fatty acids. A mixed ketone–alcohol fraction was also isolated but GLC data showed that the individual components differed from those found in the same fraction obtained from the wood. In addition, an ester fraction was isolated which was composed of alcohols having terpenoid character and a mixture of C_{16}, C_{18}, and C_{20} acids in which the latter predominated. The alcoholic material could not be fractionated by column chromatography and characterization will be attempted by preparative GLC, once this technique has been perfected.

Savinin was isolated from the bark extract in small, though better, yield than was obtained from the wood. The major acidic component was again communic acid. Small amounts of untractable phenolic material were also obtained. Thus, the composition of the ligroin extract of the bark resembled that of the wood in many respects.

Can. J. Chem. Downloaded from www.nrcresearchpress.com by 210.87.254.5 on 09/05/12
For personal use only.

Can. J. Chem. Downloaded from www.nrcresearchpress.com by 210.87.254.5 on 09/05/12
For personal use only.

EXPERIMENTAL

Melting points were determined on a Leitz hot stage microscope. The identity of known compounds was confirmed by mixed melting point and by comparing the infrared spectra with those of authentic samples unless otherwise indicated. The infrared spectra were recorded on a Perkin–Elmer Model 21 double-beam recording spectrophotometer using the KBr-disk method, the film technique, or solutions in carbon tetrachloride. GLC chromatograms were obtained with a modified Beckman GC-2 chromatograph, using either 6 ft$\times\frac{1}{4}$ in. O.D. coiled copper columns packed with adipate (2) or succinate (7) polyester and "Chromosorb W" (80 to 100 mesh) in the ratio of 1:6, an 18 in.$\times\frac{1}{4}$ in. O.D. column containing washed silicone grease (2) on Celite (100 to 120 mesh) in the ratio of 1:6, or a 3 ft$\times\frac{1}{4}$ in. O.D. stainless steel column containing SE-30 silicone rubber (Dow Corning) on "Chromosorb W" (40 to 60 mesh) in the ratio of 1:3. The commercial cedar wood oil (Fritzsche Bros. of Canada Ltd., Toronto) used for comparison was obtained from the wood of *Juniperus virginiana* L.

Extraction of the Wood

The plants were collected near Saskatoon in the early fall of 1960 and in the spring of 1961. The leaves and bark were separated mechanically from the wood and the wood was milled to a fine powder by means of a hammer and a Wiley mill. The air-dried, milled wood (6.5 kg) was extracted continuously with acetone in a Soxhlet extractor for 24 hours and the extract was reduced to a brown, viscous sirup by distilling off most of the acetone. A small aliquot was evaporated to dryness to determine the yield of acetone-soluble material. The residue was poured into excess ligroin (b.p. 60–80° C) (4 liters) and the clear ligroin solution was decanted from the brown, resinous, insoluble material. The latter was washed twice with ligroin and the washings were added to the ligroin extract. The combined ligroin extract (6 liters) was concentrated to 2 liters by distillation. The yield of acetone-soluble material (650 g) was about 10% of the weight of air-dried wood, and that of the ligroin-soluble portion was 2.5%. The ligroin-soluble material could be obtained in about the same yield by extracting the milled wood directly with ligroin in a Soxhlet extractor.

Preliminary Fractionation

The concentrated ligroin extract (160 g in 2 liters) was extracted with a saturated solution of sodium bicarbonate and washed with water. The aqueous extracts were combined, acidified with cold dilute hydrochloric acid, and extracted with ether. The ethereal solution was dried over anhydrous sodium sulphate and after filtration evaporated to dryness to yield 0.5 g of a brown sirupy material (fraction A). The ligroin solution was then further extracted with two portions (100 ml) of aqueous sodium hydroxide solution (5%). The ligroin layer was again washed with water and the aqueous solutions pooled. The latter was acidified with cold, dilute hydrochloric acid, extracted with ether, and worked up as above to yield 19.5 g of weakly acidic material (fraction B). The residual ligroin solution was dried over anhydrous sodium sulphate and, after filtration, evaporated to dryness to yield 140 g of neutral oil (fraction C). When a small aliquot of the neutral material was distilled on a Widmer column, decomposition was encountered. About 20% of the material distilled between 110° and 140° C at 3 mm pressure. It was observed that chromatography on a silicic acid column, followed by vacuum distillation, gave a better separation of the volatile components.

Can. J. Chem. Downloaded from www.nrcresearchpress.com by 210.87.254.5 on 09/05/12
For personal use only.

Silicic Acid Column Chromatography

The neutral oil (10 g) in chloroform was chromatographed on a 2.0-cm diameter column of silicic acid (100 g) slurried in ligroin (b.p. 40–60° C). The column was eluted successively with ligroin (b.p. 40–60° C), chloroform, chloroform–2-butanone (10:1 and 5:1 v/v), and acetone–methanol (1:1 v/v), the solvent being changed when the last 50 ml of eluate gave no residue on evaporation. Five distinct fractions were collected in 1.2, 4.8, 1.6, 0.6, and 0.2 g amounts respectively. The infrared spectra showed the first to contain hydrocarbons, the second esters, the third a mixture of ketones and alcohols, the fourth alcohols, and the last a lactone.

Fraction I: Thujopsene and other Sesquiterpene Hydrocarbons

The material was analyzed by GLC on the adipate polyester column at 180° C. Six peaks were recorded in the sesquiterpene hydrocarbon range in 5, 72, 3, 6, 5, and 8% amounts respectively. The relative retention times (RRT; α-cedrene = 1.00) were 1.02, 1.15, 1.57, 1.74, 1.97, and 2.28 respectively. When commercial cedar wood oil, obtained from *Juniperus virginiana*, was injected, seven peaks were recorded, six of which corresponded in retention times to the above peaks. Fractional distillation gave a middle cut, b.p. 110–120° C (air bath) at 3 mm pressure, which contained about 88% of the major component. Found: C, 87.41%; H, 11.60%; n_D^{26} 1.5049; $[\alpha]_D^{26}$ −44.4 ($CHCl_3$). Calculated for $C_{15}H_{24}$: C, 88.16%; H, 11.84%. The crude hydrocarbon was unaffected by cold neutral or alkaline solutions of potassium permanganate. Selenium dehydrogenation (at 280 to 320° C) did not yield any identifiable product, nor was a crystalline picrate obtained. When the crude hydrocarbon was hydrogenated, using either palladized charcoal or platinum oxide as catalyst, the main hydrocarbon was recovered unchanged (GLC).

The crude hydrocarbon (300 mg), selenium dioxide (200 mg), and ethanol (30 ml) were heated under reflux for 4 hours. The ethanol was removed by evaporation under reduced pressure and ether was added to the residue. The ethereal solution was decanted from the residual selenium metal and the ether-soluble material (which contained appreciable amounts of selenium) was distilled *in vacuo* to give a pale yellow liquid, b.p. 110° C (air bath) at 3 mm pressure, which solidified partially on standing for some time. The distillate was taken up in ligroin (1 ml) and left at 2–5° C for several days, when the product crystallized in colorless, rectangular rods, m.p. 71–72° C after two recrystallizations. Found: C, 82.54%; H, 10.25%. Calculated for $C_{15}H_{22}O$: C, 82.51%; H, 10.16%. When an authentic sample of thujopsene was oxidized in the same manner thujopsenal of m.p. 71.5–72° C was obtained.

A few milligrams of the first peak were obtained almost pure by preparative GLC (20 mg scale) (2). The material had an infrared spectrum similar to that of α-cedrene. The presence of cuparene was inferred from the infrared spectrum of a concentrate of the second last peak, which was similar to that of this aromatic hydrocarbon.

Thujopsene diol.—Thujopsene (85% pure) (250 mg) and osmium tetroxide (250 mg) were dissolved in anhydrous ether (30 ml) and pyridine (1 ml). A brown, fluffy precipitate formed. The mixture was left at room temperature for 24 hours. It was then centrifuged, the solvent removed by decantation, and the solid residue was washed with ether. To the residue was added sodium bisulphite (1.5 g) in water (10 ml) and ethanol (30 ml), and the mixture was heated on a steam bath for 4 hours. The cooled solution was filtered and the alcohol was removed by evaporation *in vacuo*. The residual aqueous solution was extracted

repeatedly with ether and the ethereal extract was dried over anhydrous sodium sulphate. The oily residue obtained on evaporation of the ether contained no starting material (GLC) and showed a strong hydroxyl absorption band in the infrared region. The diol crystallized from ether–ligroin (1:1 v/v) at 2–5° C but liquefied immediately upon filtration, even in the cold.

Fraction II: Esters of β-Sitosterol, Aliphatic Alcohols, and Long-Chain Fatty Acids

This fraction was a viscous oil with a fatty odor. The infrared spectrum showed, as the only significant band, an ester carbonyl absorption (1740 cm^{-1}). The material was, therefore, saponified with alcoholic potassium hydroxide (steam bath, 2 hours) and worked up into the neutral and acidic components in the usual manner. Silicic acid chromatography of the neutral portion gave two distinct fractions. The first (10%) was analyzed by GLC on the silicone column at 160 and 200° C and was found to consist of four alcohols, two in the C-12, one in the C-15, and one in the C-20 range. The second fraction (90%) crystallized from acetone and was found to be β-sitosterol, m.p. 139–140° C, acetate m.p. 132–133° C. An aliquot of the acid portion was methylated with diazomethane and the mixture of methyl esters was analyzed by GLC on the succinate polyester column at 205° C. Peaks corresponding in retention time to palmitic (9.1%), palmitoleic (1.5%), stearic (1.5%), oleic (19.1%), linoleic (55.5%), linolenic (9.1%), and arachidic (3.03%) acids were recorded.

Fraction III: Mixed Alcohols and Ketones

Infrared analysis indicated that this fraction was composed of alcohols (3440 cm^{-1}) and ketones (1667 cm^{-1}). Found: C, 81.93%; H, 10.55%. Calculated for $C_{15}H_{24}O$: C, 81.76%; H, 10.98%. The mixture was analyzed by GLC, using the adipate polyester column at 180° C. Seven peaks were recorded in the ratio of 9:20:1:2:1:2:5:65. The respective RRT (cedrol = 1.00) were 1.02, 1.16, 1.44, 1.62, 1.94, 2.50, and 3.80. Some decomposition appeared to take place. Preparative runs of 20-mg aliquots on the SE-30 column yielded 5 to 10 mg each of three major components. These were re-chromatographed on the adipate polyester column, when the first fraction was resolved into two peaks corresponding in retention time to cedrol and widdrol. Sufficient material could be collected to record the infrared spectra of each component and these corresponded with those of cedrol and widdrol. The mixture (10 mg) was heated with alumina (30 mg) containing pyridine (1%) in a 5-mm glass tube (4) at 230° C for 1 hour. After it was cooled, the product was extracted with ether, and the ethereal solution was filtered and then evaporated to dryness. When the residue was chromatographed on the adipate polyester column, two major peaks, corresponding in retention time to α-cedrene and thujopsene, were recorded. The second fraction from the preparative run was found to decompose extensively on re-chromatographing on the polyester column; one major (RRT 1.62) and two minor peaks (RRT 1.44 and 1.94) were recorded but all were ill-defined. The infrared spectrum of the collected fraction showed strong absorption bands at 3360, 2900, 1675, (1650), 1460, and 1377 cm^{-1} and medium ones at 885, 875, 815, and 705 cm^{-1}. The ultraviolet spectrum showed a broad maximum at 245 mμ. The third fraction was composed of the component having RRT 3.80 on the polyester column. It had a weak infrared spectrum with absorption bands at 2960, 2925, 1665, 1618, 1455, 1435, 1387–1372, 1355, 1295–1285, 1200, and 885–870 cm^{-1}. Its ultraviolet spectrum showed a maximum at 235 mμ with a weak shoulder at 282 mμ.

Fraction IV: β-Sitosterol

This fraction crystallized on reducing the volume of solvent. Recrystallization from methanol gave white plates of β-sitosterol, m.p. 138–139° C, acetate m.p. 132–133° C.

Can. J. Chem. Downloaded from www.nrcresearchpress.com by 210.87.254.5 on 09/05/12
For personal use only.

Fraction V: Savinin

The yellow sirup obtained on evaporation of the solvent was taken up in acetonitrile and allowed to stand at 2–5° C for several days. A crystalline substance, m.p. 135–140° C, was obtained which was recrystallized twice from ethanol; m.p. 146–147° C, $[\alpha]_D^{25}$ −82.3° (*c*, 0.6, $CHCl_3$). Found: C, 68.50%; H, 4.75%; molecular weight (Rast), 362. Calculated for $C_{20}H_{16}O_6$: C, 68.18%; H, 4.58%; molecular weight, 352.

The compound is sparingly soluble in cold alcohol, insoluble in cold aqueous sodium hydroxide solution, and was recovered unchanged on acidifying an alcoholic solution containing sodium hydroxide. The ultraviolet spectrum showed maxima at 334, 294, and 237 mμ and minima at 306 and 266 mμ and alkaline solutions fluoresced strongly. The infrared spectrum had strong carbonyl absorption bands at 1740 and 1640 cm^{-1}. The position of these bands did not change on standardizing the infrared spectrophotometer against indene or polystyrene film. The authentic sample of savinin, m.p. 146.2–147.3° C, $[\alpha]_D^{22}$ −88.2°, also gave absorption bands at 1740 and 1640 cm^{-1} with the standardized instrument.

Acidic Components

Both the fractions obtained from the aqueous bicarbonate (fraction A) and sodium hydroxide solutions (fraction B) were investigated for the presence of tropolones. The paper chromatographic procedure of Wachtmeister and Wickberg (12) did not reveal any thujaplicins or nootkatin. A number of weak spots corresponding to phenols (ferric chloride color reaction) were obtained with butanol – acetic acid – water (4:1:2) as solvent.

The acid fraction B (see above) was triturated twice with ligroin (250 ml each) and the solution was decanted from the insoluble residue. The solution was extracted with aqueous sodium carbonate solution. The alkaline solution was separated, acidified with dilute hydrochloric acid, and extracted with ether. The ethereal solution was dried, filtered, and evaporated. The residue (5.0 g) was chromatographed on a column of silicic acid when three distinct fractions were collected. Paper chromatography again showed the absence of tropolones.

The carbonate-extracted ligroin solution was dried over anhydrous sodium sulphate and, after filtration, evaporated to dryness. The residue (17.5 g) was chromatographed on silicic acid. The major portion was eluted with ligroin (b.p. 40–60° C) and the residue obtained on evaporating the solvent (12.5 g) crystallized from acetone–ligroin in rectangular plates, m.p. 121–122° C; $[\alpha]_D^{25}$ +40.3° (*c*, 0.6, $CHCl_3$). Found: C, 79.31%; H, 9.97%; COOH, 15.23%. Calculated for $C_{20}H_{30}O_2$: C, 79.42%; H, 10.00%; COOH, 15.0%. The acid formed a cyclohexylamine salt from which the free acid could be regenerated. Treatment with diazomethane gave the crude methyl ester, m.p. 101–102° C. On recrystallization twice from methanol, the melting point was raised to 108–109° C. Found: C, 79.64%; H, 10.08%; $[\alpha]_D^{26}$ +50.5° (*c*, 2%, $CHCl_3$). Calculated for $C_{21}H_{32}O_2$: C, 79.70%; H, 10.19%. The methyl ester could not be hydrolyzed, even on prolonged treatment with potassium hydroxide in 2-methoxyethanol at 125° C. Microhydrogenation in methanol – acetic acid (4:1) with platinum oxide gave a hydrogen uptake of 3 mole equivalent. The maleic anhydride adduct of the methyl ester was prepared in the usual manner; m.p. 171° C, $[\alpha]_D$ +79.5°. Arya *et al.* (11) report for the methyl ester m.p. 105–106° C, $[\alpha]_D$ +47.0° and for the maleic anhydride adduct, m.p. 169–171° C, $[\alpha]_D$ +85°. Hydrogenation of the methyl ester in methanol over platinum oxide gave the hexahydro derivative. Found: C, 78.39%; H, 11.50%; $[\alpha]_D^{25}$ +50.75° (*c*, 1.2, $CHCl_3$). Calculated for $C_{21}H_{36}O_2$: C, 78.26%; H, 11.8%. This methyl ester could also not be saponified.

Can. J. Chem. Downloaded from www.nrcresearchpress.com by 210.87.254.5 on 09/05/12
For personal use only.

Ether-soluble Material

The resinous residue (465 g) after ligroin extraction was extracted twice with boiling ether (1 liter) and the ether was decanted from the viscous residue. The extract was filtered and concentrated (500 ml). A small aliquot was evaporated to dryness and the total yield was calculated to be 60 g. The ethereal solution was then successively extracted with 5% aqueous solution of sodium carbonate (fraction D) and sodium hydroxide (fraction E), washed with water, dried over sodium sulphate, and the solvent was distilled off (fraction F).

Fractions D and E (40.0 g)

On acidification a bright red oil was obtained which was taken up in ether. Attempts to crystallize the material failed. With alcoholic ferric chloride solution a bright green color was obtained. Paper chromatography (12) did not reveal the presence of any thujaplicins or nootkatin.

Fraction F (10.0 g)

On long standing the concentrated solution in ethanol deposited yellow prisms (0.2 g), m.p. 142–144° C. The infrared spectrum was similar to that of savinin in all respects and the mixed melting point was undepressed.

Acetone-soluble Residue (350 g)

The residue was taken up in acetone (1.5 liter) and allowed to stand in the cold for several weeks when a small quantity (10 g) of microcrystalline brown material was deposited. The filtered and dried material gave a positive ferric chloride reaction. Its infrared spectrum confirmed the phenolic character.

Extraction and Analysis of the Bark

The finely powdered bark (2.1 kg) was extracted continuously with ligroin (b.p. 60–80° C) in a Soxhlet extractor for 24 hours. The soluble material (71 g) was divided into neutral (41 g) and acidic (26 g) fraction as above.

Neutral Components

Silicic acid chromatography (see above) gave again five fractions. The first fraction (3.0 g) was composed of sesquiterpene hydrocarbons and a small amount of the esters of fraction 2. The sesquiterpenes were purified by distillation *in vacuo*. GLC analysis gave seven peaks with RRT, 0.85, 1.00, 1.19, 1.62, 1.76, 2.29, and 2.50 in 1, 63, 21, 8, 2, 1, and 3% amounts respectively. The two major peaks corresponded in retention time to α-cedrene and thujopsene. However, permanganate oxidation did not give the expected α-cedrene diol. Selenium dioxide oxidation gave a liquid aldehyde which showed a single peak with retention time equal to thujopsenal on GLC analysis.

The second fraction (20 g) was composed of fatty acid esters and was again found to yield β-sitosterol, m.p. 136–137° C, and a mixture of fatty acids on saponification. Fraction 3 (5.0 g) differed from fraction III of the neutrals of the wood. The infrared spectrum indicated esters of long-chain fatty acid. Saponification with alcoholic sodium hydroxide gave a sesquiterpene alcohol fraction (infrared, GLC) and a fatty acid mixture in which two C_{20} acids predominated. GLC analysis of the derived methyl esters showed the C_{16}, C_{18}, and C_{20} acids to be present in the ratio of 1:2.5:3. From the mixture of acids a crystalline product, m.p. 65–70° C, was obtained in small yield. GLC analysis of this material showed it to be composed mainly of arachidic acid, with palmitic and stearic acid as contaminants. The fourth fraction (3.0 g) was divided into a volatile (b.p. 140–160° C at 3 mm) and a non-volatile component. The latter (0.6 g) crystallized from

Can. J. Chem. Downloaded from www.nrcresearchpress.com by 210.87.254.5 on 09/05/12
For personal use only.

ligroin in colorless needles, m.p. 136–137° C undepressed in admixture with β-sitosterol, m.p. 137–138° C. The infrared of the volatile material showed bands in the hydroxyl and carbonyl region. GLC analysis showed a similar mixture of ketones and alcohols as was obtained from fraction III of the wood neutrals, but the retention times of all components differed from those of the latter. The last fraction (5.0 g), when taken up in a little ethanol, again deposited small amounts of yellow needles of savinin, m.p. 145–146° C after recrystallization.

Acidic Components

The acidic material was chromatographed on silicic acid, using the same solvent as described above. The major portion (15 g) was found to be communic acid (infrared, mixed melting point). The crude acid was converted to the methyl ester with diazomethane and analyzed by GLC on the silicic acid column at 230° C. Only a single peak having the retention time of methyl communate was recorded. Three small viscous fractions were also obtained from the chromatogram, none of which crystallized. The last two gave a positive color reaction for phenols with ferric chloride solution.

ACKNOWLEDGMENTS

The authors wish to thank Prof. H. Erdtman and co-workers for the gift of samples of terpenes and the many useful suggestions made during the discussion of our findings. Thanks are also due to Drs. J. L. Hartwell and A. W. Schrecker for the sample of savinin, to Mr. M. Granat for technical assistance, to Mr. M. Mazurek for the microanalyses, and to Miss I. M. Gaffney for recording the infrared spectra.

REFERENCES

1. W. P. FRASER and R. C. RUSSEL. An annotated list of the plants of Saskatchewan. Revised edition. University of Saskatchewan, Saskatoon, Sask. 1954. p. 3.
2. E. von RUDLOFF. Can. J. Chem. **38**, 631 (1960).
3. J. RUNEBERG. Acta Chem. Scand. **14**, 1288 (1960).
4. E. von RUDLOFF. Can. J. Chem. **39**, 1860 (1961).
5. O. MOTL, V. HEROUT, and F. SORM. Collection Czechoslov. Chem. Communs. **23**, 1293 (1958).
6. H. ERDTMAN and T. NORIN. Acta Chem. Scand. **13**, 1124 (1959).
7. B. M. CRAIG and N. L. MURTY. J. Am. Oil Chemists' Soc. **36**, 549 (1959).
8. M. A. BUCHANAN, R. V. SINNETT, and J. A. JAPPE. Tappi, **42**, 578 (1959).
9. J. L. HARTWELL, J. M. JOHNSON, D. B. FITZGERALD, and M. BELKIN. J. Am. Chem. Soc. **75**, 235 (1953).
10. A. W. SCHRECKER and J. L. HARTWELL. J. Am. Chem. Soc. **76**, 4896 (1954).
11. V. P. ARYA, C. ENZELL, H. ERDTMAN, and T. KUBOTA. Acta Chem. Scand. **15**, 225 (1961).
12. C. A. WACHTMEISTER and B. WICKBERG. Acta Chem. Scand. **12**, 1335 (1958).
13. J. RUNEBERG. Acta Chem. Scand. **14**, 1985, 1991, 1995 (1960).
14. C. PILO and J. RUNEBERG. Acta Chem. Scand. **14**, 353 (1960).
15. C. ENZELL. Acta Chem. Scand. **14**, 81 (1961).
16. E. GUENTHER. *In* The essential oils. Vol. II. D. van Nostrand, Inc., New York. 1949. p. 116.

Can. J. Chem. Downloaded from www.nrcresearchpress.com by 210.87.254.5 on 09/05/12
For personal use only.

Can. J. Chem. Downloaded from www.nrcresearchpress.com by 210.87.254.42 on 09/05/12
For personal use only.

THE CONSTITUTION OF A HEMICELLULOSE OF CHERRY WOOD (PRUNUS AVIUM L. VAR. BING)[1]

G. G. S. DUTTON AND SHIRLEY A. MCKELVEY

The hemicellulose isolated by direct alkaline extraction of the wood has been shown to be a 4-*O*-methyl-D-glucuronoxylan. Methylation data indicate a backbone of approximately 110 D-xylopyranose units linked by β, $1 \rightarrow 4$ bonds with single units of 4-*O*-methyl-D-glucuronic acid linked by α, $1 \rightarrow 2$ bonds. The proportion of acid units to xylose is approximately 1:7. 2,3-Di-*O*-methyl-D-lyxose was isolated as an artifact.

In a recent paper (1) attention was drawn to the fact that many of the wood hemicelluloses which have been studied are those from trees of commercial importance for the purpose of pulping. The present paper is concerned with the hemicellulose of cherry wood and is complementary to our recent study on apple wood hemicellulose (1).

Cherry wood was reduced to sawdust in a Wiley mill and extracted first with hot ethanol–benzene (1:2) and then with sodium hydroxide (0.1 *N*). The hemicellulose was extracted with sodium hydroxide (1 *N*), following the method of McDonald (2), and was recovered by pouring the solution into acidified ethanol. The yield was about 22%, based on air-dry wood, and a typical preparation had $[\alpha]_D$ $-28°$, raised to $-38°$ after one reprecipitation, and an ash content of 8%.

A portion of the hemicellulose was hydrolyzed with sulphuric acid and resolved by means of ion-exchange resins into a neutral and an acidic portion. The neutral portion contained mainly D-xylose characterized as the crystalline sugar together with small amounts of D-glucose and traces of rhamnose. D-Glucose was characterized as *N*-(*p*-nitrophenyl)D-glucosylamine and rhamnose by chromatography and electrophoresis. The acidic portion appeared from chromatography to be mainly one aldobiouronic acid which was characterized as the crystalline methyl 2-*O*-[methyl(2,3-di-*O*-acetyl-4-*O*-methyl-α-D-glucopyranosyl)uronate]-3,4-di-*O*-acetyl-D-xylopyranoside. The aldobiouronic acid is thus 2-*O*-(4-*O*-methyl-α-D-glucopyranosyl uronic acid)-D-xylopyranose, which is now known to occur widely (3).

A portion of the hemicellulose was methylated first by Haworth's method and then by Purdie's. Fractional precipitation with petroleum ether from chloroform showed the product to be homogeneous, as shown in Table I. Fraction 4 was cleaved with methanolic hydrogen chloride and separated into neutral and acidic components as previously described (4).

Chromatographic examination of the acidic portion showed only one component corresponding to a partially methylated aldobiouronic acid. Accordingly, this compound was esterified and reduced with lithium aluminum hydride; however, the resulting neutral disaccharide glycoside did not crystallize as anticipated (4). Acid hydrolysis gave 3-*O*-methyl-D-xylose and 2,3,4-tri-*O*-methyl-D-glucose, each characterized as their crystalline *N*-phenyl glycosylamines.

The neutral sugar glycosides were hydrolyzed with sulphuric acid and the resulting sugars separated on a column of cellulose–hydrocellulose using butanone–water (5).

[1]*Manuscript received August 18, 1961.*
Contribution from the Department of Chemistry, University of British Columbia, Vancouver, B.C. The material in this paper was presented at the 138th American Chemical Society meeting in New York, September, 1960, and is taken from a thesis presented for the M.Sc. degree by Miss S. A. McKelvey, October, 1960.

Can. J. Chem. Downloaded from www.nrcresearchpress.com by 210.87.254.42 on 09/05/12
For personal use only.

Initially, six fractions were obtained with a recovery of 92% but three of these were mixtures and were separately rechromatographed. The final fractions obtained are shown in Tables II–V. Components 1,4 and 7 were 2,3,4-tri-*O*-methyl-D-xylose, identified chromatographically; 2,3-di-*O*-methyl-D-xylose, identified as the crystalline sugar and the crystalline *N*-phenyl glycosylamine; and a mixture of 2- and 3-*O*-methyl-D-xylose, identified by electrophoresis. Component 2 yielded only 2,3-di-*O*-methyl-D-xylose on hydrolysis and was therefore 4-*O*-(2,3-di-*O*-methyl-D-xylopyranosyl)-2,3-di-*O*-methyl-D-xylose. The high positive rotation indicated an alpha linkage and suggested that this was a reversion product (1).

Component 5 amounted to about 10% of the mixture and had $[\alpha]_D$ −36.6° (*c*, 0.85 in water). The sugar crystallized spontaneously and on recrystallization from ethyl acetate had m.p. 113–117° C. The derived *N*-phenyl glycosylamine was crystalline but difficult to purify and had m.p. 107.5–113.5° C. Complete methylation of this derivative (6) yielded a sirup which, on hydrolysis, gave a compound with R_f 0.77 (butanone–water). These results were not consistent with any D-xylose derivative. Attempted demethylation with hydrobromic acid (7) led to extensive degradation but reaction with boron trichloride (8) gave a clean product chromatographically identical with lyxose. A mixed melting point with a sample of 2,3-di-*O*-methyl-D-lyxose showed no depression, thus confirming the identification of component 5. A re-examination of the sugars produced on hydrolysis of the original polysaccharide failed to reveal the presence of any lyxose. The 2,3-di-*O*-methyl-D-lyxose was undoubtedly produced by epimerization of 2,3-di-*O*-methyl-D-xylose caused by the free base (ca. 0.3%) present in the barium carbonate used to neutralize sulphuric acid. It is of interest that an unknown dimethylpentose with the same characteristics as those described here has been isolated from the methylated "squeegee" fraction of wheat flour (9). In this instance an ion-exchange column was used for neutralization and even with careful washing such columns are known to bleed traces of alkali. It is perhaps worth noting that, in the present work and that on the wheat flour, columns of cellulose–hydrocellulose were used. Superior resolving power has been claimed for these columns (5) and it may well be that this artifact has occurred in other hydrolyzates but has escaped detection.

Component 6 obtained in trace amount was evidently a disaccharide since on hydrolysis it yielded 2,3-di-*O*-methyl-D-xylose, identified chromatographically, and 2-*O*-methyl-D-xylose, identified electrophoretically.

From the weights of the methylated sugars obtained the polysaccharide was calculated to contain 114 xylose units with 17 acid residues per macromolecule. When the ratio of sugars was analyzed by the phenol – sulphuric acid method (10) the figures were 106 and 16. Both of these calculations give a xylose to acid ratio of 7:1, which is in good agreement with that (8:1) computed from the neutralization equivalent of the methylated polysaccharide.

In view of the small amount of monomethylxylose obtained, these results suggest that cherry wood hemicellulose is a linear structure (11, 12, 13). Cherry wood hemicellulose is similar to other glucuronoxylans isolated from deciduous trees but has a higher proportion of uronic acid than sugar maple (14), white birch (15, 16), yellow birch (17), and beech (18) and more closely resembles white elm (19) and apple (1). The present investigation contributes to the study of hemicellulosic materials and, together with the parallel study on apple wood, shows that these two members of the Rosaceae family conform to the general pattern of wood hemicelluloses (3).

Can. J. Chem. Downloaded from www.nrcresearchpress.com by 210.87.254.42 on 09/05/12
For personal use only.

EXPERIMENTAL

All evaporations were carried out under reduced pressure and at a bath temperature not exceeding 40° C. Optical rotations were recorded at 22±2° C.

The descending technique was used for paper chromatography with the following solvent systems:

(A) butanone–water azeotrope (20);
(B) ethyl acetate – acetic acid – formic acid – water, 18:3:1:4 (21);
(C) pyridine – ethyl acetate – water, 1:2:2 (22);
(D) 1-butanol–ethanol–water–ammonia, 40:11:19:1 (7);
(E) *s*-collidine (23);
(F) 1-butanol saturated with water (7);
(G) 1-butanol–acetone–water, 4:5:1 (24).

The last solvent system requires that the paper be impregnated with phosphate buffer solution (pH 5). Whatman No. 1 paper was used for all chromatograms except where specified, and sugars were detected with either *p*-anisidine trichloroacetate (7) or aniline phosphate (25).

Paper electrophoresis was carried out with 0.05 *M* sodium borate solution on Whatman No. 1 paper at a voltage of 1000±50 v.

Extraction of Hemicellulose

Cherry wood sawdust (424 g) was extracted for 8 hours with hot ethanol–benzene (1:2). The sawdust was air-dried and then extracted at room temperature with sodium hydroxide (0.1 *N*, 8.8 ml/g of sawdust) for 48 hours and the highly colored solution discarded. The residue was washed with water and air-dried and re-extracted with sodium hydroxide (1 *N*, 8.6 ml/g) for 48 hours at room temperature. The alkaline solution was filtered and the residue washed with water. The hemicellulose was precipitated by pouring the solution into ethanol acidified with acetic acid. The yield (determined on an aliquot) was 22% of the air-dried wood. The hemicellulose had $[\alpha]_D$ −28° (*c*, 1 in 8% NaOH) raised to $[\alpha]_D$ −38° after one reprecipitation. Ash content was 7.8%.

Hydrolysis of the Hemicellulose

Hemicellulose (30 g) was hydrolyzed with *N* sulphuric acid (1 liter) on the steam bath for 16 hours. The residue (4.8 g) was removed by filtration and the filtrate neutralized with barium carbonate. The filtrate was passed through Amberlite IR-120 and Duolite A-4 and the eluate containing the neutral sugars evaporated to a sirup (24.4 g). The acidic components were eluted from the anion exchange resin with sodium hydroxide (1 *N*, 75 ml) and the solution deionized by passage through fresh Amberlite IR-120. Concentration of the acidic eluate gave a sirup (2.2 g).

Identification of Neutral Sugars

Paper chromatography of the neutral sirup in solvents A, B, D, F, and G showed predominantly xylose with small amounts of glucose and rhamnose. When the sirup was dissolved in ethanol the D-xylose crystallized and after recrystallization from ethanol had m.p. and mixed m.p. 146–147.5° C, $[\alpha]_D$ 17.7° (*c*, 0.78 in water).

The mother liquor from the initial crystallization of the D-xylose was streaked on 10 sheets of Whatman No. 3MM (6 in.×22 in.) and the sheets developed in solvent B for 20 hours. The area corresponding to glucose was eluted with three 100-ml portions of water. Evaporation gave a sirup (80 mg), $[\alpha]$ 36° (*c*, 1.6 in water), which was chromatographically identical with D-glucose in solvent C. The extracted sugar (69 mg) and

Can. J. Chem. Downloaded from www.nrcresearchpress.com by 210.87.254.42 on 09/05/12
For personal use only.

p-nitroaniline (61 mg) were dissolved in methanol (2 ml) containing one drop of concentrated hydrochloric acid and the solution heated on the steam bath for 5 minutes. On evaporation of part of the solvent the *N*-(*p*-nitrophenyl) D-glucosylamine crystallized and on recrystallization from methanol had m.p. 173–175.5° C (26). A standard derivative had m.p. 174.5–176.5° C and a mixed melting point gave 173–176° C. The corresponding derivative (m.p. 205–207.5° C) was prepared from D-galactose for comparison. The trace of rhamnose was not separated but was identified by chromatography (R_f 0.33 in solvent G) and by electrophoresis (M_g 0.47).

Identification of the Aldobiouronic Acid

Chromatographic examination of the acidic fraction in solvent B indicated that it was essentially an aldobiouronic acid (R_{xylose} 0.97) together with some free uronic acid (R_x 1.13) and a trace of material with R_x 0.72. The acidic portion was streaked on Whatman No. 1 and developed in solvent B for 16 hours. Elution of the aldobiouronic acid (R_x 0.97) gave a sirup (323 mg) which was dissolved in methanol (28 ml) to which was added methanolic hydrogen chloride (5%, 26 ml). The solution was refluxed for 10 hours and the ester glycoside recovered as a sirup (307 mg), which was acetylated. The yield of methyl 2-*O*-[methyl (2,3-di-*O*-acetyl-4-*O*-methyl-α-D-glucopyranosyl) uronate]-3,4-di-*O*-acetyl-D-xylopyranoside was 75 mg with m.p. and mixed m.p. 193–195° C (27).

Methylation of the Hemicellulose

Hemicellulose (22 g) was dissolved in sodium hydroxide solution (8%, 100 ml) and solid sodium hydroxide (31.4 g) added. The polysaccharide was methylated at 50° C by the dropwise addition of dimethyl sulphate (300 ml) and sodium hydroxide (30%, 900 ml) over one and a half hours with the periodic addition of acetone to control foaming. When the flask was heated in a boiling water bath to decompose excess methyl sulphate the partially methylated material separated as a curd on the top of the solution and was readily filtered off. The curd, which contained much inorganic matter, was repeatedly extracted with boiling methanol and evaporation of the solvent after filtration gave the partly methylated polysaccharide (20.9 g). This material was methylated with Purdie's reagents, initially using methanol as a solvent (twice), then acetone, and finally only methyl iodide. The material thus obtained (10.3 g) was dissolved in chloroform (100 ml) diluted with diethyl ether (100 ml) and fractionally precipitated by the addition of petroleum ether to a mechanically stirred solution. The results are shown in Table I. Fractions 1 and 2 contained inorganic matter and were discarded. Fractions 3–5, which initially precipitated as oils, were separately redissolved in chloroform (15 ml) and precipitated as white flocculent solids by pouring the solution into petroleum

TABLE I

Fractional precipitation of methylated cherry wood hemicellulose

Fraction	Total petroleum ether added, ml	Weight, g	$[\alpha]_D^{25}$ ($CHCl_3$)	Methoxyl, %
1	150	—	—	—
2	170	—	—	—
3	200	1.02	−60.0°	39.2
4	275	2.27	−60.0°	39.1
5	350	2.01	−47.1°	38.2
6	450	0.37	—	—
7	550	0.19	—	—
8	—	1.17	—	—

ether (200 ml). Infrared analysis of these fractions showed the absence of a hydroxyl band. Fractions 6 and 7 could be obtained only as oils and fraction 8 was obtained by evaporating the mother liquor from fraction 7 to dryness.

The neutralization equivalent was determined by dissolving a portion of the methylated hemicellulose (211 mg, fraction 3) in potassium hydroxide (0.0810 *N*, 5.00 ml) and back titrating with sulphuric acid (0.1000 *N*) after 4 hours using a pH meter. The titer was 2.65 ml corresponding to an equivalent weight of 1510. Other samples gave 1665 and 1490.

Methanolysis and Hydrolysis of the Methylated Hemicellulose

Fraction 4 (2.27 g) was dissolved in methanolic hydrogen chloride (3%, 50 ml) and the solution refluxed on the steam bath for 7 hours when the optical rotation was constant, $[\alpha]_D$ 70°. The solution was neutralized with lead carbonate, centrifuged, and evaporated to a thick sirup of the methyl glycosides (2.25 g). The methyl esters were saponified with barium hydroxide, volatile highly methylated glycosides were extracted with petroleum ether, and the mixture separated on ion-exchange columns into acidic components (0.478 g) and neutral components (1.69 g) as previously described (4).

Identification of the Acidic Portion

The acidic component (478 mg) was dissolved in methanol (25 ml) and treated with an excess of ethereal diazomethane. The ester (339 mg) was dissolved in tetrahydrofuran (12 ml) and a solution of lithium aluminum hydride (0.5 g) in dry tetrahydrofuran (20 ml) added. The reaction was completed by refluxing for 1 hour when excess hydride was decomposed by the addition of an ethereal solution of ethyl acetate. The reduced material was acetylated without isolation and the acetate (367 mg) deacetylated with aqueous methanolic sodium hydroxide to give the neutral disaccharide glycoside (229 mg) as previously described (4). Since the disaccharide did not crystallize, even on seeding, it was identified as follows. The disaccharide (221 mg) was dissolved in methanolic hydrogen chloride (3%, 10 ml) and refluxed for 5 hours. After neutralization (Ag_2CO_3), treatment with hydrogen sulphide, filtration, and evaporation, there was obtained a clear sirup (208 mg) which was dissolved in sulphuric acid (1 *N*, 5 ml) and heated on the steam bath for 6 hours. The solution was neutralized by passage through Duolite A-4, and concentration of the effluent gave a sirup (215 mg) which was separated on a cellulose–hydrocellulose column using butanone–water and a collecting time of 20 minutes (5). The faster-migrating component (tubes 9–21, 75 mg) was chromatographically identical with 2,3,4-tri-*O*-methyl-D-glucose and had $[\alpha]_D$ 81.6° (*c*, 1.5 in water). Literature (28) $[\alpha]_D$ 86°. The 2,3,4-tri-*O*-methyl-*N*-phenyl-D-glucosylamine was recrystallized from ethyl acetate – petroleum ether and had m.p. 141–143° C undepressed by an authentic sample (29).

The contents of tubes 60–78 gave a colorless sirup (39 mg) electrophoretically identical with 3-*O*-methyl-D-xylose and having $[\alpha]_D$ 22.3° (*c*, 0.78 in water). Literature (30) $[\alpha]_D$ 17°. The 3-*O*-methyl-*N*-phenyl-D-xylosylamine was recrystallized from ethyl acetate – petroleum ether, m.p. 130–131° C.

Identification of the Neutral Sugars

The neutral glycosides (1.69 g) were dissolved in sulphuric acid (1 *N*, 60 ml) and heated on the steam bath for 8 hours. After neutralization ($BaCO_3$) and evaporation, there was obtained a sirup (1.57 g), part of which (1.24 g) was dissolved in butanone–water (2 ml); a few drops of Sudan IV dye were added. The solution was added to the

Can. J. Chem. Downloaded from www.nrcresearchpress.com by 210.87.254.42 on 09/05/12
For personal use only.

top of a column (40×3 cm) packed with a 1:1 mixture of cellulose and hydrocellulose (5). Solvent A was used for elution and the effluent was collected at 10-minute intervals

TABLE II

First separation of neutral sugars of hemicellulose on a hydrocellulose–cellulose column

Fraction	Tube number	Component number	Weight, mg
A	10	1	3
B	11–30	1, 2, 3, 4	206
C	31–40	4	505
D	41–64	4, 5	228
E	65–98	5, 6	128
F	119–135	7	23
			Recovery 92.3%

for 117 tubes and then at 30-minute intervals for 18 tubes. Fractions A–F were obtained with a 92% recovery but, of these, B, D, and E contained mixtures and were separately passed through the column again. Pooling the tubes which, by paper chromatography, had been shown to contain similar materials resulted in establishing the presence of eight sugars. The details of these separations are shown in Tables III–V.

TABLE III

Reseparation of fraction B of neutral sugars of hemicellulose

Tube number	Component number	Weight, mg	Identity of component
20–21	1	—	2,3,4-Tri-*O*-methyl-D-xylose
22–29	1, 2	11	
30	2	—	Disaccharide A
31–39	2, 3	4	
40–51	3	11	Unknown A
54–59	4	8	2,3-Di-*O*-methyl-D-xylose
60–80	4	—[a]	2,3-Di-*O*-methyl-D-xylose

[a]This material was combined with tubes (30–40) of reseparation of fraction D.

TABLE IV

Reseparation of fraction D of neutral sugars of hemicellulose

Tube number	Component number	Weight, mg	Identity of component
30–40	4	199	2,3-Di-*O*-methyl-D-xylose
41–47	4, 5	10	
48–65	5	92	2,3-Di-*O*-methyl-D-lyxose

TABLE V

Reseparation of fraction E of neutral sugars of hemicellulose

Tube number	Component number	Weight, mg	Identity of component
31–45	4	4	2,3-Di-*O*-methyl-D-xylose
52–68	5	—[a]	2,3-Di-*O*-methyl-D-xylose
69–73	5, 6	2	
74–100	6	9	Disaccharide B

[a]This material was combined with tubes (48–65) of reseparation of fraction D.

Can. J. Chem. Downloaded from www.nrcresearchpress.com by 210.87.254.42 on 09/05/12
For personal use only.

Component 1.—Chromatographically identical with 2,3,4-tri-*O*-methyl-D-xylose.

Component 2.—Acidic hydrolysis of the contents of tube 30 from the reseparation of fraction B gave only 2,3-di-*O*-methyl-D-xylose. Since the specific rotation of tubes 22–29 was 77.5° (*c*, 0.64 in water) component 2 was assumed to be 4-*O*-(2,3-di-*O*-methyl-α-D-xylopyranosyl)-2,3-di-*O*-methyl-D-xylose.

Component 3.—Acid hydrolysis gave no change. It gave an unusual green color with aniline phosphate spray and was chromatographically unlike 2,3,4,6-tetra-*O*-methyl-D-galactose.

Component 4.—The sirup crystallized spontaneously and after recrystallization from ethyl acetate – petroleum ether had m.p. 98–101° C and $[\alpha]_D$ 21.4° (*c*, 0.58 in water). The mixed melting point was undepressed with an authentic sample of 2,3-di-*O*-methyl-D-xylose with m.p. 95–100° C. The derived 2,3-di-*O*-methyl-*N*-phenyl-D-xylosylamine had m.p. 121–123° C. Literature (31) m.p. 120–122° C.

Component 5.—This was unchanged by acid hydrolysis and did not migrate on electrophoresis. The sirup crystallized spontaneously and on recrystallization from ethyl acetate had m.p. 113–117° C, $[\alpha]_D$ −36.6° (*c*, 0.85 in water). OMe, calculated for a dimethylpentose 34.8%. Found, OMe 34.5%. The reported constants for 2,3-di-*O*-methyl-D-lyxose are m.p. 116–117° C, $[\alpha]_D$ −10.7° (*c*, 0.3 in water) and a mixed melting point of an authentic sample of this compound with component 5 gave no depression (32).

The derived 2,3-di-*O*-methyl-*N*-phenyl-D-lyxosamine had m.p. 107.5–113.5° C. Literature (32) 107–108° C. When this compound (50 mg) was methylated with methyl iodide (10 ml) and silver oxide (200 mg) the recovered fully methylated anilide (41 mg) did not crystallize (9). Hydrolysis of a small portion (33) and chromatographic analysis in solvent A gave a compound with R_f 0.77.

Two attempts to demethylate component 5 using hydrobromic acid (7) led to extensive degradation. Demethylation using the boron trichloride procedure (8) gave a clean product which was readily shown to be identical with lyxose both by chromatography in solvent G (R_f 0.25) and by electrophoresis (M_g 0.83).

Component 6.—This was evidently a disaccharide since hydrolysis of the contents of tube 74 from the reseparation of fraction E gave 2,3-di-*O*-methyl-D-xylose and a monomethylxylose (by chromatography). The latter was shown by electrophoresis to be 2-*O*-methyl-D-xylose (M_g 0.37).

Component 7.—Electrophoresis showed this to be a mixture of 2- and 3-*O*-methyl-D-xylose in which the former predominated.

Qualitative Analysis

The composition of the contents of tubes containing two components was computed from optical rotations and these weights added to the weight of the appropriate pure component previously isolated. Making allowances for the mechanical losses involved in the reseparations the weights of sugars obtained were in the ratio of 2:94:1:17 for mono-, di-, and tri-*O*-methylpentose and aldobiouronic acid respectively.

Standard curves were prepared for the phenol – sulphuric acid method (10) using 2-*O*-methyl-D-xylose, 2,3-di-*O*-methyl-D-xylose, and 2,3,4-tri-*O*-methyl-D-xylose. Each sugar gave a linear plot over the range 0–35 micrograms/ml and the curves for the mono- and di-*O*-methyl-D-xyloses were virtually identical with an O.D. 0.275 for 35 microgram/ml. The tri-*O*-methyl-D-xylose gave an O.D. of 0.40 for 20 microgram/ml. A portion of the neutral methylated sugars was streaked on a sheet of Whatman No. 1 (6 in.×22 in.) and developed in butanone–water. Appropriate sections of the paper were

Can. J. Chem. Downloaded from www.nrcresearchpress.com by 210.87.254.42 on 09/05/12
For personal use only.

eluted each with 20 ml of water. These solutions had to be diluted 1:1, 1:100, and 1:3 for the estimation of the tri-, di-, and mono-methylpentoses and the results gave a molar ratio of 1:88:1, respectively.

ACKNOWLEDGMENTS

We are indebted to the National Research Council for continued financial support and one of us (S. A. McKelvey) is grateful for the award of an N.R.C. bursary.

We appreciate the gift of authentic samples from Dr. Elizabeth Percival, Dr. T. E. Timell, and Dr. J. P. Verheijden.

REFERENCES

1. G. G. S. Dutton and G. T. Murata. Can. J. Chem. **39**, 1995 (1961).
2. I. R. C. McDonald. J. Chem. Soc. 3183 (1952).
3. G. O. Aspinall. *In* Advances in carbohydrate chemistry. Vol. 14. Academic Press, New York. 1959.
4. G. G. S. Dutton and F. Smith. J. Am. Chem. Soc. **78**, 3744 (1956).
5. J. D. Geerdes, B. A. Lewis, R. Montgomery, and F. Smith. Anal. Chem. **26**, 264 (1954).
6. I. Ehrenthal, M. C. Rafique, and F. Smith. J. Am. Chem. Soc. **74**, 1341 (1952).
7. L. Hough, J. K. N. Jones, and W. H. Wadman. J. Chem. Soc. 1702 (1950).
8. S. Allen, T. G. Bonner, E. J. Bourne, and N. M. Saville. Chem. & Ind. (London), 630 (1958).
9. R. Montgomery and F. Smith. J. Am. Chem. Soc. **77**, 2834 (1955).
10. M. Dubois, K. Gilles, J. K. Hamilton, P. A. Rebers, and F. Smith. Anal. Chem. **28**, 350 (1956).
11. J. J. Connell, E. L. Hirst, and E. G. V. Percival. J. Chem. Soc. 3494 (1950).
12. S. K. Chanda, E. L. Hirst, and E. G. V. Percival. J. Chem. Soc. 1240 (1951).
13. I. Croon and T. E. Timell. Can. J. Chem. **38**, 720 (1960).
14. T. E. Timell. Can. J. Chem. **37**, 893 (1959).
15. C. P. J. Glaudemans and T. E. Timell. J. Am. Chem. Soc. **80**, 941 (1958).
16. C. P. J. Glaudemans and T. E. Timell. J. Am. Chem. Soc. **80**, 1209 (1958).
17. T. E. Timell. J. Am. Chem. Soc. **81**, 4989 (1959).
18. E. L. Hirst and R. S. Mahomed. J. Chem. Soc. 1734 (1954).
19. J. K. Gillham and T. E. Timell. Can. J. Chem. **36**, 1467 (1958).
20. L. Boggs, L. S. Cuendet, I. Ehrenthal, R. Koch, and F. Smith. Nature, **166**, 520 (1950).
21. J. K. N. Jones and L. E. Wise. J. Chem. Soc. 3389 (1952).
22. M. A. Jermyn and F. A. Isherwood. Biochem. J. **44**, 402 (1949).
23. S. M. Partridge. Nature, **158**, 270 (1946).
24. H. Meier and K. C. B. Wilkie. Holzforschung. **13**, 177 (1959).
25. J. L. Bryson and T. J. Mitchell. Nature, **167**, 864 (1951).
26. F. Weygand, W. Perkow, and P. Kuhner. Ber. **84**, 594 (1951).
27. T. E. Timell. Can. J. Chem. **37**, 827 (1959).
28. B. Lindberg and B. Wickberg. Acta Chem. Scand. **8**, 569 (1954).
29. S. Peat, E. Schlüchterer, and M. Stacey. J. Chem. Soc. 581 (1939).
30. G. G. Maher. *In* Advances in carbohydrate chemistry. Vol. 10. Academic Press, New York. 1955.
31. G. O. Aspinall, E. L. Hirst, R. W. Moody, and E. G. V. Percival. J. Chem. Soc. 1631 (1953).
32. J. P. Verheijden and P. J. Stoffyn. Tetrahedron, **1**, 253 (1957).
33. G. W. Huffman and F. Smith. J. Am. Chem. Soc. **77**, 3141 (1955).

Can. J. Chem. Downloaded from www.nrcresearchpress.com by 210.87.254.42 on 09/05/12
For personal use only.

Can. J. Chem. Downloaded from www.nrcresearchpress.com by 210.87.254.6 on 09/05/12
For personal use only.

THE ELECTRONIC ABSORPTION SPECTRA OF DIXANTHOGENS[1]

M. L. Shankaranarayana and C. C. Patel

ABSTRACT

The electronic absorption spectra of diethyl, diisopropyl, di-*n*-butyl, and diisoamyl dixanthogens have been studied in polar and non-polar solvents. The compounds exhibit a low-intensity band around 365 mμ and two high-intensity bands around 285 and 242 mμ. The 365 mμ band is assigned, as a result of the solvent studies, to $n \rightarrow \pi^*$ transition and the 285 mμ band to $\pi \rightarrow \pi^*$ transition. The band around 242 mμ may be due to the $n \rightarrow \sigma^*$ transition, since in polar solvents it shows mainly a blue shift.

The available data on the electronic absorption spectra of organic sulphur compounds having thiocarbonyl group are relatively meager in the literature (1, 2). Janssen (2) has reviewed the previous work on sulphur compounds and studied the nitrogen-containing thiones extensively. Recently, the present authors studied the infrared spectra of dixanthogen compounds (3). In this paper, studies on the near-ultraviolet spectra and solvent effect on the various bands exhibited by dixanthogens are described.

EXPERIMENTAL

Diethyl, diisopropyl, di-*n*-butyl, and diisoamyl dixanthogens were prepared, purified, and analyzed as described in an earlier paper (4). The electronic absorption spectra of these compounds were studied in heptane, cyclohexane, ethanol, and acetonitrile solutions on a Hilger spectrophotometer, Model H 700, using 1-cm quartz matched cells. Since these compounds are non-ionogenic, their spectra could not be studied either in an acid or in water medium. The solvents employed were purified by the methods recommended by Weisberger and Proskauer (5). The wavelengths of absorption maxima are recorded in millimicrons and the molar extinction coefficients are expressed in terms of log ϵ.

RESULTS AND DISCUSSION

The peak wavelengths and molar extinction coefficients of ultraviolet absorption maxima for dixanthogens in various solvents are given in Table I. Typical absorption

TABLE I

Peak wavelengths and molar extinction coefficients for dixanthogens in different solvents

Compound	Hydrocarbon		Ethanol		Acetonitrile	
	λ_{max}	log ϵ	λ_{max}	log ϵ	λ_{max}	log ϵ
Diethyl dixanthogen	240	4.34	239	4.32	239	4.34
	279	3.91	281	3.90	283	3.91
	363	1.90	361	1.91	360	1.93
Diisopropyl dixanthogen	243	4.36	241	4.35	240	4.30
	285	3.92	286	3.94	287	3.91
	365	1.91	362	1.90	360	1.92
Di-*n*-butyl dixanthogen	244	4.38	243	4.37	243	4.38
	286	3.92	287	3.91	288	3.90
	365	1.91	362	1.92	360	1.92
Diisoamyl dixanthogen	245	4.39	243	4.38	242	4.38
	286	3.95	287	3.92	288	3.97
	367	1.92	363	1.91	360	1.91

[1]*Manuscript received August 15, 1961.*
Contribution from the Department of Inorganic and Physical Chemistry, Indian Institute of Science, Bangalore, India.

curves of diisoamyl dixanthogen in cyclohexane and acetonitrile are given in Fig. 1.

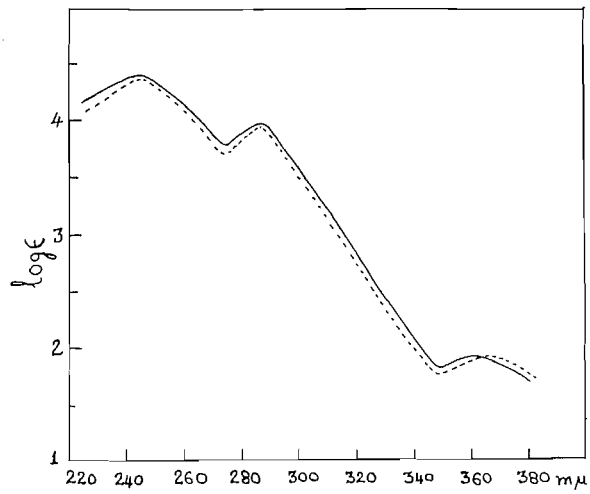


FIG. 1. Ultraviolet absorption spectra of diisoamyl dixanthogen in cyclohexane (- - -) and in acetonitrile (——).

Inspection of the results in Table I shows that all the dixanthogens give three absorption bands. The first low-intensity band is noticed around 365 mμ (log ε 1.9) and two high-intensity bands are observed around 285 mμ (log ε 3.9) and 242 mμ (log ε 4.4.). The molar extinction coefficients (log ε 1.9) for the low-intensity band around 365 mμ compare well with the values given by Treiber (6) and Lowry and Hudson (7) for other dixanthogens. It is well known that the molecules which contain the thiocarbonyl group have a low-intensity absorption band at a longer wavelength similar to the 365 mμ band obtained for the dixanthogens. This band is found to show a blue shift on changing the solvent from a non-polar to a polar solvent. Further, with the increase in the polarity of the solvent, the band shows increased blue shift. This shows that the transition energy involved increases with the increase in the polarity of the solvent. According to an empirical rule (8, 9), this band can be characterized by $n \rightarrow \pi^*$ transition. This absorption is accounted for by the excitation of an electron from the non-bonding lone pair of electrons (n orbital) localized on the double-bonded sulphur into an antibonding π orbital (π^*). Mulliken (10) has pointed out that the thiocarbonyl group has an electronic structure similar to that of the carbonyl group and that the thiocarbonyl absorption regions are expected at wavelengths longer than that of the carbonyl group because the $3p_y$ electron of the sulphur is less firmly bound than that of the $2p_y$ electron of the oxygen. The origin of the $n \rightarrow \pi^*$ blue shift may be attributed to solvation (11) and(or) hydrogen bonding (12) between the non-bonding electrons of the thiocarbonyl group of the solute and the solvent molecules. The $n \rightarrow \pi^*$ blue shift observed, when the solvent was changed from a non-polar to a polar non-hydrogen-bonding (13) acetonitrile, could be explained by the formation of an electrostatic bond between the non-bonding electrons of the thiocarbonyl sulphur atom and the positively charged carbon atom of the nitrile group. Such a bond lowers the energy of the n-electron orbital, and upon excitation, the electrostatic bond is either broken or weakened. A similar explanation has been advanced by Becker (14) to explain the blue shift in the acetonitrile solvent for the $n \rightarrow \pi^*$ band of carbonyl group of benzophenone.

Can. J. Chem. Downloaded from www.nrcresearchpress.com by 210.87.254.6 on 09/05/12
For personal use only.

The intense band around 285 mμ (log ε 3.9) shows a red shift when the solvent is changed from a non-polar to a polar one. A small increase in red shift is observed with the increase in the polar character of the solvents. This band can be ascribed to $\pi \rightarrow \pi^*$ transition (8, 9), where an electron jump occurs from the highest occupied π orbital to the lowest empty (antibonding) π level. A similar band observed around 278 mμ in *s*-ethyl *o*-ethyl xanthate has been assigned as $\pi \rightarrow \pi^*$ transition (2).

The intense band around 242 mμ (log ε 4.4) in dixanthogens is analogous to the 220–250 mμ band exhibited in *s*-ethyl *o*-ethyl xanthate (15), alkali metal xanthates (16), and also in dialkyl disulphides (17). This band in dixanthogens shows mainly a blue shift when the solvent is changed from a hydrocarbon to ethanol and acetonitrile. This band may, therefore, be characterized by $n \rightarrow \sigma^*$ transition. It is expected that the solvent effect on the $n \rightarrow \sigma^*$ transition should be similar to that of the $n \rightarrow \pi^*$ transition but little is known about the solvent effect on this type of transition. The $n \rightarrow \sigma^*$ transition can be explained by the excitation of an electron from the non-bonding lone pair of electrons, localized on the σ-bonded sulphur atoms in the —*s*—*s*— group, to an antibonding level, either 3*d* or 4*s*. This $n \rightarrow \sigma^*$ band assignment finds support from the 225 mμ band of *s*-ethyl *o*-ethyl xanthate, in which case Janssen (2) observed a blue shift to below 215 mμ when concentrated sulphuric acid was used as a solvent.

ACKNOWLEDGMENT

The authors are thankful to Professor M. R. A. Rao for his keen interest in the work.

REFERENCES

1. H. L. McMurry. J. Chem. Phys. **9**, 231 (1941).
2. M. J. Janssen. Rec. trav. chim. **79**, 455 (1960).
3. M. L. Shankaranarayana and C. C. Patel. Can. J. Chem. **39**, 1633 (1961).
4. M. L. Shankaranarayana and C. C. Patel. The Analyst, **86**, 98 (1961).
5. A. Weisberger and E. S. Proskauer. Organic Solvents. Interscience Publishers, Inc., New York. 1955.
6. E. Treiber. Kolloid-Z. **130**, 39 (1953).
7. T. M. Lowry and H. Hudson. Phil. Trans. Roy. Soc. London, Ser. A, **232**, 117 (1933).
8. M. Kasha. Discussions Faraday Soc. **9**, 14 (1950).
9. J. W. Sidman. Chem. Revs. **58**, 689 (1958).
10. R. S. Mulliken. J. Chem. Phys. **3**, 564 (1935).
11. H. McConnel. J. Chem. Phys. **20**, 700 (1952).
12. G. J. Brealey and M. Kasha. J. Am. Chem. Soc. **77**, 4462 (1955).
13. M. Ito, K. Inuzuka, and S. Imanishi. J. Am. Chem. Soc. **82**, 1317 (1960).
14. R. S. Becker. J. Mol. Spectroscopy, **3**, 1 (1959).
15. A. Burawoy. Chem. Ber. **63**, 3155 (1930).
16. I. Iwasaki and S. R. B. Cook. Mining Eng. **9**, 1267 (1957).
17. A. Kuboyama. Bull. Chem. Soc. Japan, **30**, 678 (1957).

Can. J. Chem. Downloaded from www.nrcresearchpress.com by 210.87.254.6 on 09/05/12
For personal use only.

Can. J. Chem. Downloaded from www.nrcresearchpress.com by 210.87.254.105 on 09/05/12
For personal use only.

THE PREPARATION OF ERYTHRO-3-PENTULOSE[1]

R. J. STOODLEY

ABSTRACT

The mercuric acetate oxidation of ribitol yielded a mixture of *erythro*-3-pentulose and DL-erythro-2-pentulose.

INTRODUCTION

The hydroxyl groups of alditols may be oxidized by a variety of chemical procedures. The oxidants may be relatively non-specific, oxidizing both primary and secondary hydroxyl groups, or they may be specific. Non-specific oxidizing agents include Fenton's reagent (1), the halogens (2), and oxygen in the presence of platinum (3). Generally the yield of aldoses and ketoses is low. Nitrogen dioxide (4) and, in some cases, oxygen in the presence of a platinum–carbon catalyst (5) are examples of specific oxidants which oxidize primary alcohol groups to carboxyl groups in reasonable yield. Chromium trioxide has been found to be a valuable reagent for oxidizing secondary alcohol groups to keto groups in alditols, providing all the other hydroxyl groups are suitably blocked (6).

There appears to be no chemical procedure for selectively oxidizing secondary alcohol groups in the presence of unsubstituted primary hydroxyl groups. In some cases, however, this oxidation may be achieved biochemically using *Acetobacter suboxydans*. In fact this organism has been used to prepare 1-deoxy-D-*xylo*-3-hexulose from L-fucitol (7), the preparation being the first recorded for a 3-ketose.

The first chemical synthesis of a 3-ketose was achieved by Jones (8), who prepared 2-*O*-methyl-L-*xylo*-3-hexulose from L-ascorbic acid. In attempting to synthesize an unsubstituted 3-ketose, Sugihara and Yuen (9) prepared crystalline 4-*O*-benzoyl-1,2:5,6-di-*O*-isopropylidene-D-*arabo*-3-hexulose by the chromium trioxide oxidation of 3-*O*-benzoyl-1,2:5,6-di-*O*-isopropylidene-D-mannitol. However, attempts to remove the protecting groups resulted in the formation of a mixture of ketose sugars, presumably because debenzoylation proceeded via an enediol intermediate. Starting with 6-*O*-benzoyl-1,2:4,5-di-*O*-isopropylidene-DL-galactitol, the same authors have recently obtained crystalline DL-*xylo*-3-hexulose (10), realizing the first chemical synthesis of an unsubstituted 3-hexulose.

Schaffer has reported the preparation of D-*manno*-3-heptulose by the lead tetraacetate oxidation of 3-*C*-formyl-D-*glycero*-D-*talo*heptitol (11), and has recently crystallized the material (12).

The isolation of *erythro*-3-pentulose from the mercuric acetate oxidation of ribitol represents the first chemical synthesis of a 3-pentulose. DL-*erythro*-2-Pentulose was also produced, but the failure to detect ribose (or any product obtained by the mercuric acetate oxidation of D-ribose) suggests that the oxidant may be specific for secondary hydroxyl groups.

erythro-3-Pentulose may be an important biological intermediate. D-*erythro*-2-Pentulose 1,5-diphosphate has been shown to be the prime acceptor of carbon dioxide in photosynthesis, and Wilson and Calvin (13) have suggested that its dismutation to phosphoglyceric acid may involve the 3-ketose intermediate. Ashwell and Hickman (14) incubated D-ribose 5-phosphate with a mouse spleen extract and, after dephosphorylating

[1]*Manuscript received September 8, 1961.*
Contribution from the Department of Chemistry, Queen's University, Kingston, Ontario.

the products, they isolated D-*threo*-2-pentulose and D-*erythro*-2-pentulose and small amounts of a third material which they tentatively characterized as *erythro*-3-pentulose. They suggested that the phosphorylated 3-ketose was an intermediate in the interconversion of D-*erythro*-2-pentulose 5-phosphate and D-*threo*-2-pentulose 5-phosphate. A similar intermediate was also detected by Dickens and Williamson while they were studying the same reaction using a rabbit muscle enzyme preparation (15).

DISCUSSION

Ribitol was oxidized with mercuric acetate in methanol at 38° C. Removal of the mercury salts after 4 weeks led to the 70% recovery of a syrup which was shown by paper chromatography to contain ribitol and two reducing sugars, distinct from ribose. Part of the ribitol was removed by crystallization and the remaining material was fractionated on an ion-exchange column (16); 50% of the ribitol was recovered in crystalline form.

The faster-moving reducing sugar was obtained in about 18% yield (based on the amount of ribitol oxidized) and was further purified by paper chromatography. The material rapidly reduced Fehling's solution at room temperature and gave a brown coloration with *p*-anisidine. In contrast to the results of Dickens and Williamson (15), the ketose did not give a positive reaction with orcinol – trichloroacetic acid (17) nor when oversprayed (18) with aniline phosphate (19) in the cold. An aqueous solution of the 3-ketose did not react in the cysteine–carbazole assay (20) nor in the supposedly specific 3-pentulose test with cysteine and sulphuric acid developed by Ashwell (21). These results show that the synthetic material is different from the ketose isolated from biological systems.

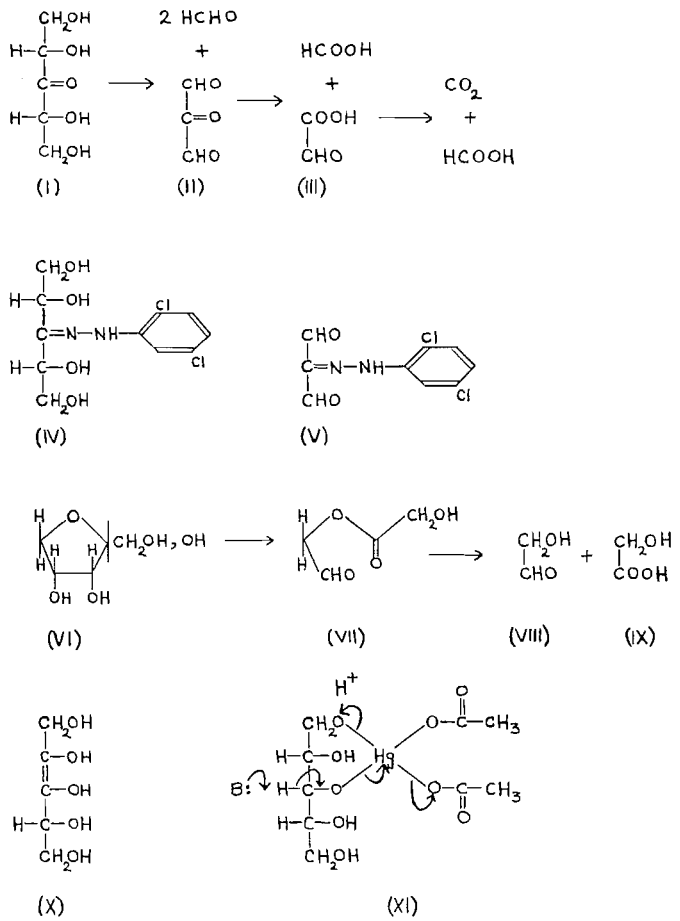
The sugar was reduced with sodium borohydride and crystalline ribitol was isolated. Examination of the acetylated, reduced syrup by gas–liquid partition chromatography using the procedure of Gunner *et al.* (22) showed the presence of ribitol and xylitol pentaacetates, thus establishing the presence of a keto group at carbon atom 3.

Oxidation of the pentulose with sodium metaperiodate under unbuffered conditions resulted in the rapid liberation of 1.8 moles of formaldehyde. This result demonstrated the presence of two primary alcohol groups in the molecule and left little doubt that the sugar was *erythro*-3-pentulose (I). The consumption of 4.06 moles of periodate and production of 2.05 moles of titratable acid further substantiated this structure. The results indicate that (I) is rapidly cleaved to 2 moles of formaldehyde and mesoxalaldehyde (II), and that the latter molecule is immediately oxidized to formic acid and glyoxylic acid (III). The slower uptake of the fourth mole of periodate (ca. 90 minutes) is consistent with the known rate of oxidation of glyoxylic acid (III) to carbon dioxide and formic acid under unbuffered conditions (23).

The periodate oxidation studies and the presence of a carbonyl absorption in the ultraviolet region (ϵ_{max} 70 at 280 mμ) suggest that the 3-pentulose is in the acyclic form (I) in aqueous solution. However, the ready enolization of the syrup to a mixture of *threo*- and *erythro*-2-pentuloses (which presumably exist as furanose rings) demonstrates the lability of the acyclic structure in the syrupy state.

The pentulose formed a crystalline 2,5-dichlorophenylhydrazone. That enolization did not occur during this reaction was shown by the regeneration of the original pentulose and by periodate oxidation studies. The 2,5-dichlorophenylhydrazone (IV) consumed 2.20 moles of periodate and liberated 0.19 mole of titratable acid and 1.8 moles of formaldehyde. A material presumed to be mesoxalaldehyde-2-(2,5-dichlorophenylhydrazone)

Can. J. Chem. Downloaded from www.nrcresearchpress.com by 210.87.254.105 on 09/05/12
For personal use only.



(V) was also obtained. The small uptake of periodate (0.2 mole) and production of formic acid (0.19 mole) in excess of the expected values suggest that (V) is attacked by periodate.

The chemical evidence strongly indicates that the sugar is *erythro*-3-pentulose. It is possible that the material isolated by Ashwell and Hickman and subsequent workers may be D-*glycero*-2,3-pentulose.

The slower-moving reducing sugar was the last component to be eluted from the column and was obtained in about 11% yield (based upon the amount of ribitol oxidized). The product was chromatographically indistinguishable from authentic *erythro*-2-pentulose and contained no *threo*-2-pentulose when examined by paper electrophoresis. The material was estimated by the cysteine–carbazole reaction (20) and characteristic peaks were produced at 540 and 390 mμ. The absorption was measured after 15 minutes and did not change within 2 hours. An authentic specimen of *threo*-2-pentulose increased in absorption during this interval (24).

The pentulose consumed 2.06 moles of periodate and liberated 1.01 moles of formic acid and 0.19 mole of formaldehyde when oxidized under unbuffered conditions for 6 hours. An additional mole of periodate was taken up when the oxidation was performed in phosphate buffer at pH 8 and the formaldehyde liberated increased to 0.93 mole. These results are consistent with the oxidation of *erythro*-2-pentulose in the furanose

Can. J. Chem. Downloaded from www.nrcresearchpress.com by 210.87.254.105 on 09/05/12
For personal use only.

form (VI) rather than the acyclic form. Presumably the glycolic acid ester of glycolaldehyde (VII) is first formed and is stable under unbuffered conditions, but is hydrolyzed to glycolic acid (IX) and glycolaldehyde (VIII) at pH 8. Glycolic acid (VIII) is known to be stable to periodate (25) while glycolaldehyde (IX) rapidly consumes 1 mole to give formaldehyde and formic acid.

Although there is little information about the mechanism of the oxidation, the ratio of *erythro*-3-pentulose to *erythro*-2-pentulose isolated (approximately 2:1) indicates that the hydroxyl group at carbon atom 3 is more readily oxidized than that at carbon 2 (unless *erythro*-2-pentulose is further oxidized). It seems unlikely that the enediol (X) is an intermediate since *threo*-2-pentulose was not detected in the reaction mixture. If formed, the enediol would be expected to enolize in the direction of the 2-pentuloses (which are presumably stabilized by internal hemiketal formation), especially as the isolated 3-pentulose enolized in this manner.

It is possible to explain the results by predicting the intermediate formation of six-membered rings containing mercury. DL-*erythro*-2-Pentulose may be produced by oxidation of the cyclic intermediate involving the oxygen atoms attached to carbon atoms 2 and 4. The failure to detect ribose (or methyl ribonate) may indicate that the cyclic intermediate involving the primary alcohol is cleaved to *erythro*-3-pentulose as is suggested in (XI).

EXPERIMENTAL

Melting points were determined on a Kofler hot stage and were uncorrected. Solutions were concentrated under reduced pressure at 30–40° C. Paper chromatography was carried out by the descending method on Whatman No. 1 filter paper using the following solvent systems (v/v): (*a*) butan-1-ol, ethanol, water (3:1:1); (*b*) ethyl acetate, acetic acid, formic acid, water (18:3:1:4); and (*c*) butan-1-ol, pyridine, water (10:3:3). Sugars were located on chromatograms by the *p*-anisidine hydrochloride (26) or the alkaline silver nitrate (27) sprays, and their rate of movement is quoted relative to that of D-ribose (R_{rib}). Paper electrophoresis was performed using Whatman 3 MM filter paper impregnated with 0.05 *M* borate buffer (pH 9.2). Sugars were detected on paper electrophoretograms by the periodate–*p*-anisidine spray (28). Infrared spectra were determined on powdered materials dispersed in potassium bromide pellets, using a Perkin–Elmer Model 21 spectrophotometer.

Mercuric Acetate Oxidation of Ribitol (Method A)

Mercuric acetate (42.0 g) was dissolved in hot methanol (250 ml) containing 1% acetic acid. Ribitol (10.0 g) was added to the cooled solution, which was stored in an incubator at 38° C. The mercurous acetate which precipitated was removed by filtration from time to time. After 4 weeks 21.5 g of mercurous acetate was obtained and chromatographic examination of the solution in solvent *b* revealed the presence of two reducing components in addition to unreacted ribitol.

The solution was saturated with hydrogen sulphide and filtered, and the filtrate was concentrated to a syrup (7.03 g) which was dissolved in ethanol and seeded with ribitol. The crystalline material (3.10 g) was collected by filtration and cautiously washed with ethanol; m.p. 100–101° C, undepressed on admixture with authentic ribitol. The filtrate was evaporated to a brown syrup.

Fractionation of the Reaction Mixture

The syrup was fractionated in portions (ca. 1.0 g) on a column of Dowex 50 W X8 (200–400 mesh, Ba^{++}) by the method of Jones and Wall (16). The column (70×2.2 cm)

Can. J. Chem. Downloaded from www.nrcresearchpress.com by 210.87.254.105 on 09/05/12
For personal use only.

was eluted with water and fractions (ca. 3 ml) were collected automatically every 15 minutes. The result of a typical separation is shown in Table I.

TABLE I
Fractionation of sugars

Tube No.	Fraction No.	Suspected component	Weight, g
60–85	1	Ribitol	0.48
86–98	2	Ribitol + *erythro*-3-pentulose	0.05
99–125	3	*erythro*-3-Pentulose	0.23
126–190	4	DL-*erythro*-2-Pentulose	0.14

Characterization of Fraction 1 as Ribitol

The syrup (1.90 g) crystallized on standing. After recrystallization from ethanol, the material melted at 101–102° C, undepressed on admixture with authentic ribitol.

Characterization of Fraction 3 as erythro-3-Pentulose

The fraction was obtained as a pale yellow syrup (0.91 g). Chromatographic examination of the material in solvents *a*, *b*, and *c* showed that it was mainly a single component (R_{rib} 1.23 in solvent *c*), although small amounts of slower-moving materials were also detected. A portion of the syrup was refractionated on Whatman 3 MM paper using solvent *b*. End strips of the chromatogram were sprayed with *p*-anisidine and the requisite area of paper was eluted with water. The solution was lyophilized and the pale yellow syrup obtained was found to be homogeneous when examined in solvents *a*, *b*, and *c*. The material did not give a color with orcinol – trichloroacetic acid (17) nor when oversprayed (18) in the cold with aniline phosphate (19), although, when heated, it developed an orange color. A brown spot was obtained when the sugar was sprayed with *p*-anisidine. The sugar did not react to any significant extent in the cysteine–carbazole assay (20).

When stored in a vacuum desiccator containing silica gel, the syrup slowly darkened and, after 3 weeks, considerable amounts of *erythro*-2-pentulose and *threo*-2-pentulose were detected by paper electrophoresis. The properties of the 3-ketose were therefore determined on a freshly fractionated sample (26.1 mg) which was dissolved in water in a standard flask (25 ml). The solution was stored at 0° C and little enolization of the 3-ketose occurred within 3 weeks.

A solution of *erythro*-3-pentulose rapidly reduced Fehling's solution at room temperature.

Periodate Oxidation of erythro-3-Pentulose

An aliquot of the 3-ketose solution (5 ml equivalent to 5.2 mg of ketose) was added to 0.3 *M* sodium metaperiodate solution (1 ml) and the volume was adjusted to 25 ml with water. A blank was prepared by diluting sodium metaperiodate solution (1 ml) to 25 ml with water. The solutions were stored in the dark at room temperature. Samples (1 ml) were removed at intervals for the determination of the periodate uptake (29) and formic acid production (30). Formaldehyde was determined on aliquots which were diluted fivefold prior to the estimation (31). The results are recorded in Table II.

Ultraviolet Absorption of erythro-3-Pentulose

The ultraviolet absorption of a solution of *erythro*-3-pentulose in water (1.04 mg/ml) was determined with a Beckman Model DK spectrophotometer using 1-cm cells. The spectrum, which is typical of a carbonyl absorption, is shown in Fig. 1.

Can. J. Chem. Downloaded from www.nrcresearchpress.com by 210.87.254.105 on 09/05/12
For personal use only.

TABLE II

Periodate oxidation of *erythro*-3 pentulose

Time (hour)	Periodate uptake (moles/mole)	Formic acid production (moles/mole)	Formaldehyde production (moles/mole)
0.15	3.01	1.31	1.82
0.55	3.51	1.99	1.75
1.50	3.88	2.06	—
3.50	4.03	2.01	1.86
19.50	4.06	2.05	1.80

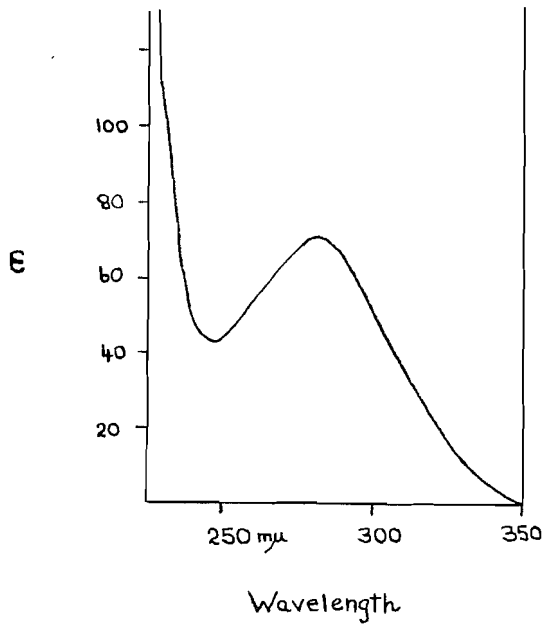


FIG. 1. The ultraviolet absorption spectrum of *erythro*-3-pentulose in water.

Sodium Borohydride Reduction of erythro-3-Pentulose

A portion of the syrup (100 mg) was dissolved in water (3 ml) and the solution was slowly added to a stirred, ice-cold 1% sodium borohydride solution (5 ml). After 1 hour the solution no longer reduced Fehling's solution, and Amberlite IR 120 (H^+) ion-exchange resin was added. The resin was removed by filtration and washed well with water. The filtrate and washings were evaporated to a white residue which was dissolved in methanol and the solution reconcentrated. After three evaporations with methanol, a clear syrup was obtained (95 mg), which partially crystallized. A small volume of methanol was added and the solution was cooled in an acetone – dry ice mixture. The crystals were removed by filtration; m.p. 98–100° C, mixed m.p. with authentic ribitol 99–101° C.

A portion of the syrup (ca. 20 mg) was dissolved in acetic anhydride containing 1% sulphuric acid and the solution was heated on a water bath (80° C) for 4 hours. The reaction mixture was poured into ice water, neutralized with pyridine, and extracted with chloroform. The chloroform extract was washed with dilute sulphuric acid, sodium bicarbonate solution, and water and was dried over anhydrous sodium sulphate. Evaporation of the chloroform left a syrup which was shown to contain ribitol and xylitol penta-acetates by gas–liquid partition chromatography (22).

Can. J. Chem. Downloaded from www.nrcresearchpress.com by 210.87.254.105 on 09/05/12
For personal use only.

erythro-3-Pentulose 2,5-Dichlorophenylhydrazone

A solution of the ketose (100 mg) and 2,5-dichlorophenylhydrazine (100 mg) in methanol was allowed to stand in an oven at 80° C. The resulting syrup was dissolved in a small volume of ethyl acetate and chloroform was added until the solution became turbid. Pale yellow crystals (80 mg) were deposited; these were removed by filtration and recrystallized from ethyl acetate – chloroform; m.p. 125–127° C.

Anal. Calc. for $C_{11}H_{14}O_4Cl_2N_2$: C, 42.7; H, 4.5; Cl, 23.0; N, 9.1. Found: C, 42.4; H, 4.8; Cl, 23.0; N, 9.2.

erythro-3-Pentulose was regenerated when the 2,5-dichlorophenylhydrazone was heated with benzaldehyde (cf. Sowden and Fisher (32)).

Periodate Oxidation of erythro-3-Pentulose 2,5-Dichlorophenylhydrazone

The material (8.6 mg) was dissolved in 25% ethanol (20 ml), 0.3 *M* sodium metaperiodate solution (1 ml) was added, and the solution was diluted to 25 ml with water. A bright yellow precipitate, presumably mesoxalaldehyde-2-(2,5-dichlorophenylhydrazone), formed almost immediately and was removed by filtration after 10 minutes. The pale yellow filtrate was used to estimate the periodate uptake and the formic acid and formaldehyde production as previously described. The results are illustrated in Table III.

TABLE III

Periodate oxidation of *erythro*-3-pentulose 2,5-dichlorophenylhydrazone

Time (hour)	Periodate uptake (moles/mole)	Formic acid production (moles/mole)	Formaldehyde production (moles/mole)
0.25	2.16	0.18	1.80
2.50	2.24	0.18	1.71
9.50	2.20	0.22	1.93

The yellow precipitate was recrystallized from aqueous acetone; m.p. 178–185° C. The material was differentiated from hydroxypyruvaldehyde-2-(2,5-dichlorophenylhydrazone), which was obtained by the periodate oxidation of D-fructose 2,5-dichlorophenylhydrazone, by a comparison of their melting points and infrared spectra.

Anal. Calc. for $C_9H_6O_2Cl_2N_2$: C, 44.1; H, 2.5; Cl, 29.0; N, 11.4. Found: C, 44.4; H, 2.6; Cl, 28.5; N, 11.3.

Characterization of Fraction 4 as DL-*erythro-2-Pentulose*

The material (0.58 g) was shown to be homogeneous when examined in solvents *a*, *b*, and *c*. The chromatographic behavior of the sugar was similar to that of *erythro*-2-pentulose, prepared by the epimerization of L-arabinose (33); both gave a red spot with *p*-anisidine (R_{rib} 1.11 in solvent *c*) and a green coloration with orcinol – trichloroacetic acid, which immediately turned pink when oversprayed with aniline phosphate. Paper electrophoresis indicated that the ketose was not *threo*-2-pentulose.

The ketose was estimated by the cysteine hydrochloride – carbazole method (20). The absorption spectrum was measured after 15 minutes and remained unchanged after 2 hours. Authentic *threo*-2-pentulose was also measured by this reaction and the absorption spectrum increased in intensity during the interval (24). The spectra are shown in Fig. 2.

Periodate Oxidation of DL-*erythro-2-Pentulose*

A standard solution of the pentulose was prepared by dissolving the syrup (20 mg) in water in a standard flask (10 ml). An aliquot of the solution (2 ml equivalent to

Can. J. Chem. Downloaded from www.nrcresearchpress.com by 210.87.254.105 on 09/05/12
For personal use only.

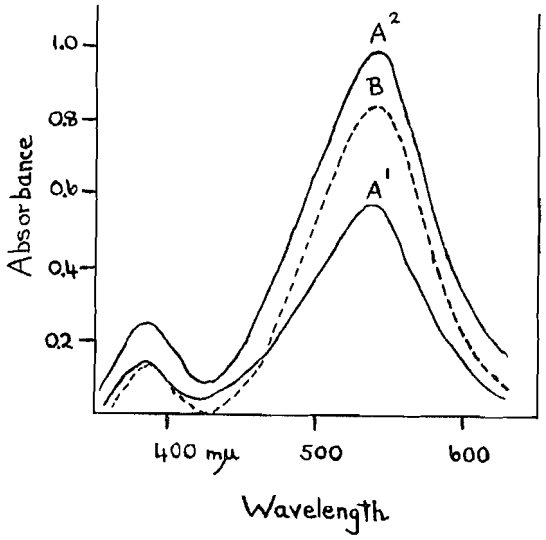


FIG. 2. The visible absorption spectra in the cysteine–carbazole reaction (20) of (A) D-*threo*-2-pentulose (48 γ) after (1) ¼ hour, (2) 2 hours; (B) DL-*erythro*-2-pentulose (43 γ) after ¼ hour and 2 hours.

4.0 mg of ketose) was added to 0.3 *M* sodium metaperiodate solution (0.3 ml) and the solution was diluted to 10 ml with water. The periodate uptake and formic acid and formaldehyde liberation were measured in the manner described previously. The results are shown in Table IV. The oxidation was also performed at pH 8.0 using phosphate

TABLE IV

Periodate oxidation of *erythro*-2-pentulose (unbuffered conditions)

Time (hour)	Periodate uptake (moles/mole)	Formic acid production (moles/mole)	Formaldehyde production (moles/mole)
0.25	1.76	0.95	0.20
6.17	2.06	1.01	0.18
20.0	2.28	—	—

buffer. The periodate uptake and formaldehyde liberation were measured and are recorded in Table V.

TABLE V

Periodate oxidation of *erythro*-2-pentulose (pH 8.0 buffer)

Time (hour)	Periodate uptake (moles/mole)	Formaldehyde production (moles/mole)
0.17	2.43	0.81
0.83	2.72	0.81
2.75	2.91	0.90
7.50	3.01	0.93

Mercuric Acetate Oxidation of Ribitol (Method B)

Ribitol (1.00 g) was added to a solution of mercuric acetate (4.2 g) in methanol (25 ml) containing 1% acetic acid. The solution was refluxed on a hot water bath for

Can. J. Chem. Downloaded from www.nrcresearchpress.com by 210.87.254.105 on 09/05/12
For personal use only.

20 hours and the precipitated mercurous acetate (1.8 g) was removed by filtration. The soluble mercury salts were precipitated as their sulphides and the solution was examined by paper chromatography. *erythro*-3-Pentulose and *erythro*-2-pentulose were detected.

2,5-Dichlorophenylhydrazine (0.5 g) dissolved in methanol (10 ml) was added directly to the syrupy mixture (0.90 g) and the solution was evaporated in an oven at 80° C. The syrup was extracted with ethyl acetate and the residual ribitol (0.73 g) was recrystallized from ethanol. Chloroform was added to the ethyl acetate extract and crystalline *erythro*-3-pentulose 2,5-dichlorophenylhydrazone (0.14 g) was obtained; m.p. 124–127° C.

Mercuric Acetate Oxidation of D-*Ribose*

D-Ribose (1.00 g) was oxidized as described for ribitol in method B. The resulting syrup (0.93 g) contained some unreacted ribose and mainly methyl ribonate (detected by paper chromatography). No components corresponding to those obtained in the oxidation of ribitol were detected.

ACKNOWLEDGMENTS

The author wishes to thank Professor J. K. N. Jones for his interest and for helpful discussion. He also thanks the National Research Council for a Studentship.

REFERENCES

1. H. J. F. Fenton and H. Jackson. J. Chem. Soc. **75**, 1 (1899).
2. J. W. Green. Advances in Carbohydrate Chem. **3**, 129 (1948).
3. J. W. E. Glattfeld and S. Gershon. J. Am. Chem. Soc. **60**, 2013 (1938).
4. K. Maurer and G. Drefahl. Ber. **75**, 1489 (1942).
5. C. L. Mehltretter, B. H. Alexander, R. L. Mellies, and C. E. Rist. J. Am. Chem. Soc. **73**, 2424 (1951).
6. W. R. Sullivan. J. Am. Chem. Soc. **67**, 837 (1945).
7. L. E. Stewart, N. K. Richtmyer, and C. S. Hudson. J. Am. Chem. Soc. **72**, 4934 (1950).
8. J. K. N. Jones. J. Am. Chem. Soc. **78**, 2855 (1956).
9. J. M. Sugihara and G. U. Yuen. J. Am. Chem. Soc. **79**, 5780 (1957).
10. G. U. Yuen and J. M. Sugihara. J. Org. Chem. **26**, 1598 (1961).
11. R. Schaffer. J. Am. Chem. Soc. **81**, 2838 (1959).
12. R. Schaffer. Abstracts 139th Am. Chem. Soc. Meeting, St. Louis, Missouri. 2D. March (1961).
13. A. T. Wilson and M. Calvin. J. Am. Chem. Soc. **77**, 5948 (1955).
14. G. Ashwell and J. Hickman. J. Am. Chem. Soc. **77**, 1062 (1955).
15. F. Dickens and D. H. Williamson. Biochem. J. **64**, 567 (1956).
16. J. K. N. Jones and R. A. Wall. Can. J. Chem. **38**, 2290 (1960).
17. R. Klevstrand and A. Nordal. Acta. Chem. Scand. **4**, 1320 (1950).
18. R. M. Hochster. Can. J. Microbiol. **1**, 346 (1955).
19. J. L. Bryson and T. J. Mitchell. Nature, **167**, 864 (1951).
20. Z. Dische and E. Borenfreund. J. Biol. Chem. **192**, 583 (1951).
21. G. Ashwell. Private communication.
22. S. W. Gunner, J. K. N. Jones, and M. B. Perry. Chem. & Ind. (London), 255 (1961); Can. J. Chem. **39**, 1892 (1961).
23. D. B. Sprinson and E. Chargaff. J. Biol. Chem. **164**, 483 (1946).
24. G. Ashwell and J. Hickman. J. Biol. Chem. **226**, 65 (1957).
25. P. F. Fleury, J. E. Courtois, R. Perles, and L. Le Dizet. Bull. soc. chim. France, 347 (1954).
26. L. Hough, J. K. N. Jones, and W. H. Wadman. J. Chem. Soc. 1702 (1950).
27. W. E. Trevelyan, D. P. Proctor, and J. S. Harrison. Nature, **166**, 444 (1950).
28. P. D. Bragg and L. Hough. J. Chem. Soc. 4050 (1958).
29. G. Neumuller and E. Vasseur. Arkiv Kemi, **5**, 235 (1953).
30. P. Andrews, L. Hough, and J. K. N. Jones. J. Chem. Soc. 806 (1954).
31. J. F. O'Dea and R. A. Gibbons. Biochem. J. **55**, 580 (1953).
32. J. C. Sowden and H. O. L. Fisher. J. Am. Chem. Soc. **69**, 1963 (1947).
33. C. Glatthaar and T. Reichstein. Helv. Chim. Acta, **18**, 80 (1935).

Can. J. Chem. Downloaded from www.nrcresearchpress.com by 210.87.254.105 on 09/05/12
For personal use only.

Can. J. Chem. Downloaded from www.nrcresearchpress.com by 210.87.254.40 on 09/05/12
For personal use only.

NOTES

CRYSTAL DATA FOR DIPHENYLARSENICALS

W. R. CULLEN AND J. TROTTER

Very little is known about the detailed structure of arsenic compounds, although it has long been realized that in molecules containing trivalent arsenic the bond arrangement is similar to that found in the layer structure of elemental arsenic (1). The object of the present investigations is to obtain accurate information about the stereochemistry of arsenic by studying compounds containing a variety of substituents; this paper describes the preparation and the determination of the crystallographic data of some diphenylarsenicals.

Bis-diphenylarsenic oxide was prepared from phenyl magnesium bromide and arsenious oxide (2) and recrystallized from 95% ethanol (crystals had m.p. 95°; literature value 92–93°). Chlorodiphenylarsine was obtained by treating the oxide with concentrated hydrochloric acid (2), the resulting oil being separated from the aqueous layer, dried, and purified by distillation at 10^{-3} mm; the fraction boiling at 135–136° was collected. This was a colorless oil which solidified on being cooled in liquid nitrogen, and remained solid on being warmed to room temperature, m.p. 38–40° (lit. value 40–42°). Bromo- and iodo-diphenylarsine were obtained by analogous methods. The bromo derivative boiled at 139–140° (10^{-3} mm) and solidified on being cooled to room temperature. It was recrystallized from 95% ethanol, m.p. 55° (lit. value 52–54°). The iodoarsine was recrystallized from benzene, m.p. 37–39° (lit. value 42–43°).

The unit cell dimensions and space groups of the crystals were determined from single crystal rotation, oscillation, Weissenberg (all with Cu $K\alpha$ radiation, $\lambda = 1.542$ Å) and precession films (Mo $K\alpha$, $\lambda = 0.7107$ Å). These data and other relevant information are given in Table I. Measurement of the densities of the crystals of the halogen derivatives posed a difficult problem, as they were soluble in most organic liquids and were hydrolyzed

TABLE I

Crystallographic data for halogenodiphenylarsines and bis-diphenylarsenic oxide

Formula	$C_{12}H_{10}AsCl$	$C_{12}H_{10}AsBr$	$C_{12}H_{10}AsI$	$C_{24}H_{20}OAs_2$
Molecular weight	264.6	309.0	356.0	474.2
Melting point (deg.)	38–40	55	37–39	95
Crystal system	Monoclinic	Monoclinic	Monoclinic	Monoclinic
a (Å)	11.09	11.00	11.01	11.48
b (Å)	8.55	8.56	8.82	30.2
c (Å)	11.93	12.03	12.34	5.97
β (deg.)	95.0	93.0	91.6	93.8
V (Å^3)	1127	1131	1198	2065
Z	4	4	4	4
D_c (g cm^{-3})	1.550	1.803	1.962	1.516
D_m (g cm^{-3})	~1.5	~1.8	~1.9	1.514
Space group	$P2_1/a$	$P2_1/a$	$P2_1/a$	$P2_1/n$

by water. However, when a crystal was dropped into an aqueous silver nitrate solution of higher density, it floated on the surface for a few seconds, before sinking, which was apparently due to hydrolysis and subsequent coating with silver halide. By making such

observations in aqueous silver nitrate solutions of various densities, it was possible to obtain approximate values for the densities of all three crystals, these measurements being sufficiently accurate to allow estimations of the number of molecules in the unit cells. The density of the oxide was determined accurately by flotation in aqueous $AgNO_3$ solution.

Crystals of chloro-, bromo-, and iodo-phenylarsine are fairly closely isomorphous; the *b*-axis of the iodo derivative is a little longer than the corresponding axes in the other two compounds, and there is a gradual increase in the length of the *c*-axis and a decrease in the value of the β angle on passing from chloro to iodo. The oxide, not unexpectedly, has a different crystal structure. We hope to carry out detailed analyses of some of these structures.

The authors thank the National Research Council of Canada for financial support.

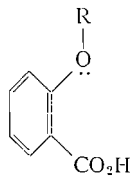
1. A. J. Bradley. Phil. Mag. **47**, 657 (1924).
2. F. F. Blicke and F. D. Smith. J. Am. Chem. Soc. **54**, 1558 (1929).

Received August 21, 1961.
Department of Chemistry,
University of British Columbia,
Vancouver 8, B.C.

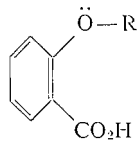
STERIC CONFIGURATION OF THE ETHER GROUP IN ORTHO ALKOXY AND ARYLOXY BENZOIC ACIDS

Owen H. Wheeler

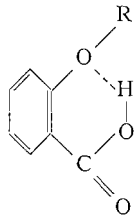
The ether group in ortho alkoxy or aryloxy benzoic acids can assume two configurations (I*a* and I*b*) in which the alkyl or aryl (R) group is directed either away from (as in I*a*) or towards (as in I*b*) the carboxylic acid group. Steric hindrance will be less in the first of these forms, but even so there will be steric crowding between the unshared electrons on the ether-oxygen atom and the carboxylic acid group.



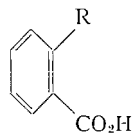
I*a*



I*b*



I*c*



II

Can. J. Chem. Downloaded from www.nrcresearchpress.com by 210.87.254.40 on 09/05/12
For personal use only.

observations in aqueous silver nitrate solutions of various densities, it was possible to obtain approximate values for the densities of all three crystals, these measurements being sufficiently accurate to allow estimations of the number of molecules in the unit cells. The density of the oxide was determined accurately by flotation in aqueous $AgNO_3$ solution.

Crystals of chloro-, bromo-, and iodo-phenylarsine are fairly closely isomorphous; the *b*-axis of the iodo derivative is a little longer than the corresponding axes in the other two compounds, and there is a gradual increase in the length of the *c*-axis and a decrease in the value of the β angle on passing from chloro to iodo. The oxide, not unexpectedly, has a different crystal structure. We hope to carry out detailed analyses of some of these structures.

The authors thank the National Research Council of Canada for financial support.

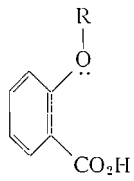
1. A. J. Bradley. Phil. Mag. **47**, 657 (1924).
2. F. F. Blicke and F. D. Smith. J. Am. Chem. Soc. **54**, 1558 (1929).

Received August 21, 1961.
Department of Chemistry,
University of British Columbia,
Vancouver 8, B.C.

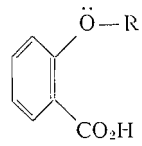
STERIC CONFIGURATION OF THE ETHER GROUP IN ORTHO ALKOXY AND ARYLOXY BENZOIC ACIDS

Owen H. Wheeler

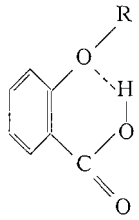
The ether group in ortho alkoxy or aryloxy benzoic acids can assume two configurations (I*a* and I*b*) in which the alkyl or aryl (R) group is directed either away from (as in I*a*) or towards (as in I*b*) the carboxylic acid group. Steric hindrance will be less in the first of these forms, but even so there will be steric crowding between the unshared electrons on the ether-oxygen atom and the carboxylic acid group.



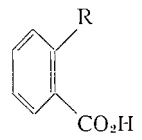
I*a*



I*b*



I*c*



II

Can. J. Chem. Downloaded from www.nrcresearchpress.com by 210.87.254.42 on 09/05/12
For personal use only.

The effect of a para substituent can only be electronic, whereas an ortho substituent exerts both an electronic and steric effect. The electronic effects of ortho and para substituents can be assumed to be approximately the same and any differences between them must be primarily steric in origin (1). The ultraviolet spectra of a number of ortho and para alkoxy (I, R = Me, Et) and aryloxy (I, R = Ph) benzoic acids has been measured (Table I) in relation to those of the corresponding alkyl and aryl benzoic acids (II, R = Me, Et, Ph) to determine the magnitude of the ortho steric effect in relation to the configuration of the ethers.

TABLE I

Ultraviolet spectra of benzoic acids*

	λ_{max}, mμ	ε	Δλ,† mμ	ϵ_o/ϵ_p‡
Benzoic	230	10,700§	—	—
o-Methyl	228	5,000§	−2	0.36
p-Methyl	236	14,000§	+6	
o-Methoxy	230	6,200§	0	0.43
p-Methoxy	249	14,000§	+19	
o-Ethyl	227	3,800	−3	0.28
p-Ethyl	236	13,500	+6	
o-Ethoxy	232	7,200	+2	0.44
p-Ethoxy	254	16,600	+24	
o-Phenyl	243	15,300‖	+13	0.58
	277¶	5,600		
p-Phenyl	268	26,600‖	+38	
o-Phenoxy	235	14,200	+5	0.77
	260	4,500		
p-Phenoxy	255	18,400	+25	

*Data refer to ethanol solution.
†Δλ to benzoic acid.
‡Ratio molar extinction coefficients of ortho to para isomers.
§Ref. 5.
‖Ref. 6 gives *o* λ_{max} 245 (11,800), *p* 264.5 (26,000).
¶Inflection.

Comparing the methyl and ethyl benzoic acids, it can be seen that an ortho ethyl group, due to the extra carbon and hydrogen atoms, had a greater steric effect since *o*-ethylbenzoic acid showed a slightly hypsochromic shift and the ratio of intensities of ortho to para isomer was much less. However, in the case of the two alkoxy benzoic acids, *o*-ethoxybenzoic acid actually showed a small bathochromic shift, while *o*-methoxybenzoic acid had no displacement with respect to benzoic acid. Moreover, the ratio of the intensities of ortho to para isomers was essentially the same for the methoxy and ethoxy compounds. This similarity in steric effect of the methoxy and ethoxy groups is only possible if the alkoxy benzoic acids assume the configuration I*a*, in which the steric hindrance is due primarily to the unshared electrons on the ether-oxygen atom.

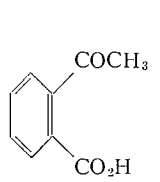
In the cases of the ortho phenyl and phenoxy compounds, the phenyl groups can be better accommodated by twisting of this ring with respect to the other. Nevertheless, the steric hindrance of the phenoxy derivative was much less than for the phenyl compound, again supporting the configuration I*a*.

The infrared absorption of *o*-methoxybenzoic acid has been shown to be anomalous (2) since it has a sharp hydroxyl peak at 2.96 μ and the carbonyl peak at 5.76 μ (the para isomer had hydroxyl broad 3.4–3.6 μ and carbonyl at 5.93 μ) and this was attributed to internal hydrogen bonding as in I*c*. *o*-Ethoxybenzoic acid had hydroxyl 2.98 μ medium, 3.4–3.5 μ weak, and carbonyl 5.74 μ strong, 5.91 μ medium, whereas *o*-phenoxybenzoic acid had hydroxyl 2.94 μ weak, 3.4–3.6 μ medium, and carbonyl 5.72 μ medium, 5.88 μ strong (*p*-ethoxy- and *p*-phenoxy-benzoic acids had hydroxyl 3.4–3.6 μ and carbonyl

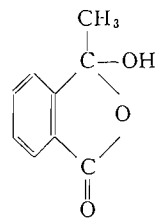
Can. J. Chem. Downloaded from www.nrcresearchpress.com by 210.87.254.42 on 09/05/12
For personal use only.

5.95 μ). This suggests that the amount of the hydrogen-bonded form was less in the case of the *o*-ethoxy acid and still less in the *o*-phenoxy acid, the difference being probably due to the increasing steric size of the substituent.

During the course of this work *o*-acetylbenzoic acid was prepared and it showed λ_{max} 230 mμ, ϵ 10,700,275 (inflection), ϵ 2500 and 282 mμ, ϵ 2400. The main maximum is more characteristic of a benzoic acid (λ_{max} 230 mμ, ϵ 10,000 (1)) than an acetophenone (λ_{max} 240 mμ, ϵ 13,000), although the other maxima are not consistent with the simple structure III*a* and the compound probably exists in solution as the lactol III*b* (cf. phthalide λ_{max} 227 mμ, ϵ 9900; 273, ϵ 1720; and 280, ϵ 1660 (3)). (We are grateful to the referee for pointing out this possibility.) The abnormal infrared carbonyl band (at 5.63 μ) also supports the lactol structure (cf. ref. 4).



III*a*



III*b*

EXPERIMENTAL

Benzoic acids.—*o*-Phenoxybenzoic acid was prepared by treatment of phenyl salicylate with sodium (7) and *o*-phenylbenzoic acid by reaction of fluorenone with potassium hydroxide in diphenyl ether (8).

o-Ethoxybenzoic acid.—Methyl salicylate (40 g) was added to sodium (11 g), dissolved in anhydrous ethanol (150 ml), cooled to 0°, and ethyl sulphate (75 g) added slowly over $\frac{1}{2}$ hour. The reaction was stirred for 2 hours when it became nearly solid and was allowed to stand for 2 days before water and 10% sodium hydroxide were added. The methyl *o*-ethoxybenzoate, b.p. 103–105° at 20 mm, so formed was hydrolyzed by refluxing overnight with 20% sodium hydroxide to give the acid, b.p. 175–178° at 20 mm (9).

p-Ethoxybenzoic acid.—*p*-Hydroxybenzoic acid was esterified by refluxing with ethanol and sulphuric acid in benzene, and azeotropically removing the water formed to give ethyl *p*-hydroxybenzoate, m.p. 116° from ethanol (lit. m.p. 112.5° (10)), which was converted to *p*-ethoxybenzoic acid, m.p. 193° (lit. m.p. 195–196° (11)) as above.

o-Ethylbenzoic acid.—*o*-Acetylbenzoic acid (12 g), prepared from phthalylacetic acid (12), was refluxed with amalgamated granular zinc (30 g) in concentrated hydrochloric acid (60 ml) and water (50 ml) for 8 hours, giving the acid, m.p. 64° from water (lit. m.p. 65° (13)).

p-Ethylbenzoic acid.—Aluminum trichloride (15 g) was added to ethylbenzene (10.6 g) in carbon disulphide (50 ml) cooled to 0° and oxalyl chloride (16 g) in carbon disulphide (50 ml), then added over $\frac{1}{2}$ hour with cooling in an ice–salt bath (14). The reaction mixture was allowed to stand overnight and was decomposed with 10% hydrochloric acid. The product was extracted from the organic layer with 10% sodium hydroxide and liberated by acidification. The product was recrystallized (charcoal) from water to m.p. 114° (lit. m.p. 113° (15)).

p-Phenylbenzoic acid.—This was prepared as above from diphenyl and had m.p. 232° from ethanol (lit. m.p. 228° (16)).

Can. J. Chem. Downloaded from www.nrcresearchpress.com by 210.87.254.42 on 09/05/12
For personal use only.

p-Phenoxybenzoic acid.—Similar reaction of diphenyl ether gave *p,p*-diphenoxybenzil, m.p. 125° (from acetic acid), which was oxidized with hydrogen peroxide in boiling acetic acid to *p*-phenoxybenzoic acid, m.p. 161° (from ethanol) (lit. m.p. 160° (17)).

Spectra.—The ultraviolet spectra were determined on 95% ethanol solutions using a Beckman D.U. spectrophotometer. The infrared spectra were determined on solutions in carbon tetrachloride using a Baird-Atomic double beam K.2 spectrometer.

1. W. F. Forbes and M. B. Sheratte. Can. J. Chem. **33**, 1829 (1955).
2. J. W. Huffman. J. Org. Chem. **24**, 1759 (1959).
3. W. A. Schroeder, P. E. Wilcox, K. N. Trueblood, and A. O. Dekker. Anal. Chem. **23**, 1740 (1951).
4. J. F. Grove and H. A. Willis. J. Chem. Soc. 877 (1951).
5. C. M. Moser and A. I. Kohlenberg. J. Chem. Soc. 804 (1951).
6. W. Baker, M. P. V. Boarland, and J. F. W. McOmie. J. Chem. Soc. 1477 (1954).
7. C. Graebe. Ber. **21**, 501 (1888).
8. E. H. Huntress and M. K. Seibel. J. Am. Chem. Soc. **61**, 816 (1939).
9. A. Wahl and C. Silberzweig. Bull. soc. chim. France, **11**, 30 (1912).
10. C. Graebe. Ann. **139**, 146 (1866).
11. J. B. Cohen and H. W. Dudley. J. Chem. Soc. 97, 1732 (1910).
12. S. Gabriel and A. Neumann. Ber. **26**, 951 (1893). H. Giebe. Ber. **29**, 2534 (1896).
13. M. Crawford and F. H. C. Stewart. J. Chem. Soc. 4443 (1952).
14. A. Schonberg and O. Kraemar. Ber. **55**, 1174 (1922).
15. K. Kindler. Ann. **452**, 102 (1927).
16. D. H. Hey. J. Chem. Soc. 1966 (1934).
17. M. Tomita, Y. Okajima, K. Yoshida, and H. Nariyuki. J. Pharm. Soc. Japan, **70**, 42 (1950).

Received June 26, 1961.
Department of Chemistry,
University of Puerto Rico,
Mayaguez,
Puerto Rico.

STABILITY OF $CoBr^+$ AND $NiBr^+$

M. W. Lister and D. W. Wilson

In a recent paper (1) one of the present writers reported the stability constants for the formation of the complex ions $CoCl^+$, $NiCl^+$, $CuCl^+$, and $CuBr^+$. Some of these constants, particularly that for $CuBr^+$, showed an anomalous variation with temperature; and although some explanations were suggested, no definite conclusion could be reached. The object of the present note is to report similar measurements for the ions $NiBr^+$ and $CoBr^+$. Previous measurements on nickel bromide have been made by Job (2), who only obtained evidence of $NiBr_2$ with a stability constant of 6×10^{-4} at 18° C. With cobalt bromide he obtained evidence for $CoBr^+$ with a stability constant of 5×10^{-3} at 18° C. References to early semiquantitative work, and work in other solvents, may be found in reference 3.

The present measurements were made by means of cell voltages in a manner very similar to that already described (1). The cell used was Ag, $AgBr/NaBr+M(ClO_4)_2+NaClO_4+HCl_4/NaBr+NaCl_4+HClO_4/AgBr$, Ag. The concentrations of sodium bromide and perchloric acid (about 0.03 *M*) were the same on both sides, as was the ionic strength, which was adjusted to a value of 2.0. Recrystallized 'analar' sodium bromide was used, and other reagents were the same as in the previous work. The electrodes were prepared by the method of Janz and Taniguchi (4). It was checked that the electrodes immersed in two concentrations of sodium bromide gave the calculated voltage over the range 0 to 50° C within 1%.

Since previous work (1) had suggested the possibility of ions of the type M_2X^{+3} (where X is a halogen) measurements were made over a range of concentrations of metal ion

Can. J. Chem. Downloaded from www.nrcresearchpress.com by 210.87.254.42 on 09/05/12
For personal use only.

p-Phenoxybenzoic acid.—Similar reaction of diphenyl ether gave *p,p*-diphenoxybenzil, m.p. 125° (from acetic acid), which was oxidized with hydrogen peroxide in boiling acetic acid to *p*-phenoxybenzoic acid, m.p. 161° (from ethanol) (lit. m.p. 160° (17)).

Spectra.—The ultraviolet spectra were determined on 95% ethanol solutions using a Beckman D.U. spectrophotometer. The infrared spectra were determined on solutions in carbon tetrachloride using a Baird-Atomic double beam K.2 spectrometer.

1. W. F. Forbes and M. B. Sheratte. Can. J. Chem. **33**, 1829 (1955).
2. J. W. Huffman. J. Org. Chem. **24**, 1759 (1959).
3. W. A. Schroeder, P. E. Wilcox, K. N. Trueblood, and A. O. Dekker. Anal. Chem. **23**, 1740 (1951).
4. J. F. Grove and H. A. Willis. J. Chem. Soc. 877 (1951).
5. C. M. Moser and A. I. Kohlenberg. J. Chem. Soc. 804 (1951).
6. W. Baker, M. P. V. Boarland, and J. F. W. McOmie. J. Chem. Soc. 1477 (1954).
7. C. Graebe. Ber. **21**, 501 (1888).
8. E. H. Huntress and M. K. Seibel. J. Am. Chem. Soc. **61**, 816 (1939).
9. A. Wahl and C. Silberzweig. Bull. soc. chim. France, **11**, 30 (1912).
10. C. Graebe. Ann. **139**, 146 (1866).
11. J. B. Cohen and H. W. Dudley. J. Chem. Soc. 97, 1732 (1910).
12. S. Gabriel and A. Neumann. Ber. **26**, 951 (1893). H. Giebe. Ber. **29**, 2534 (1896).
13. M. Crawford and F. H. C. Stewart. J. Chem. Soc. 4443 (1952).
14. A. Schonberg and O. Kraemar. Ber. **55**, 1174 (1922).
15. K. Kindler. Ann. **452**, 102 (1927).
16. D. H. Hey. J. Chem. Soc. 1966 (1934).
17. M. Tomita, Y. Okajima, K. Yoshida, and H. Nariyuki. J. Pharm. Soc. Japan, **70**, 42 (1950).

Received June 26, 1961.
Department of Chemistry,
University of Puerto Rico,
Mayaguez,
Puerto Rico.

STABILITY OF $CoBr^+$ AND $NiBr^+$

M. W. Lister and D. W. Wilson

In a recent paper (1) one of the present writers reported the stability constants for the formation of the complex ions $CoCl^+$, $NiCl^+$, $CuCl^+$, and $CuBr^+$. Some of these constants, particularly that for $CuBr^+$, showed an anomalous variation with temperature; and although some explanations were suggested, no definite conclusion could be reached. The object of the present note is to report similar measurements for the ions $NiBr^+$ and $CoBr^+$. Previous measurements on nickel bromide have been made by Job (2), who only obtained evidence of $NiBr_2$ with a stability constant of 6×10^{-4} at 18° C. With cobalt bromide he obtained evidence for $CoBr^+$ with a stability constant of 5×10^{-3} at 18° C. References to early semiquantitative work, and work in other solvents, may be found in reference 3.

The present measurements were made by means of cell voltages in a manner very similar to that already described (1). The cell used was Ag, $AgBr/NaBr+M(ClO_4)_2+NaClO_4+HCl_4/NaBr+NaCl_4+HClO_4/AgBr$, Ag. The concentrations of sodium bromide and perchloric acid (about 0.03 *M*) were the same on both sides, as was the ionic strength, which was adjusted to a value of 2.0. Recrystallized 'analar' sodium bromide was used, and other reagents were the same as in the previous work. The electrodes were prepared by the method of Janz and Taniguchi (4). It was checked that the electrodes immersed in two concentrations of sodium bromide gave the calculated voltage over the range 0 to 50° C within 1%.

Since previous work (1) had suggested the possibility of ions of the type M_2X^{+3} (where X is a halogen) measurements were made over a range of concentrations of metal ion

Can. J. Chem. Downloaded from www.nrcresearchpress.com by 210.87.254.42 on 09/05/12
For personal use only.

in order to detect ions of this type. In general, all solutions contained high metal and low bromide concentrations, conditions which would favor MBr^+, but it was checked that the calculated stability constants did not vary appreciably with double the concentration of bromide ions. This confirms that the complex ions formed were, in fact, $CoBr^+$ and $NiBr^+$. The results are given in Table I. Most of the voltages in this table are the

TABLE I

A. Nickel bromide

(Total Ni), *M*	(Total Br), *M*	*T*, °C	e.m.f.	K_1
0.0975	0.008096	25	1.800 mv	0.75
0.1394	"	"	2.648	0.78
0.1672	"	"	3.120	0.78
0.2090	"	"	3.826	0.77
0.2413	"	"	4.212	0.74
0.2787	"	"	4.875	0.755
0.1550	0.008260	0	1.620	0.46
"	"	5	1.848	0.52
"	"	10	2.013	0.56
"	"	15	2.200	0.60
"	"	18	2.344	0.635
"	"	20	2.462	0.665
"	"	25	2.774	0.74
"	"	30	2.900	0.76
"	"	35	3.028	0.785
"	"	40	3.108	0.79
"	"	45	3.146	0.79
"	"	50	3.250	0.805
0.3100	0.008000	18	5.048	0.72
"	"	22	5.302	0.75
"	"	30	5.764	0.80
"	"	35	5.777	0.79
"	"	40	5.988	0.805
"	"	50	6.535	8.86
0.0775	0.008000	22	1.367	0.71
"	"	40	1.506	0.735

B. Cobalt bromide

(Total Co), *M*	(Total Br), *M*	*T*, °C	e.m.f.	K_1
0.0580	0.008000	5	0.551 mv	0.40
"	"	10	0.720	0.515
"	"	23.6	0.927	0.64
"	"	30	1.061	0.72
"	"	33.5	1.181	0.795
"	"	40	1.440	0.85
"	"	45	1.486	0.87
0.1160	0.008026	5	1.108	0.41
"	"	10	1.431	0.52
"	"	20	1.923	0.69
"	"	25	2.219	0.78
"	"	30	2.512	0.875
"	"	35	2.590	0.89
"	"	40	2.592	0.875
"	"	45	2.566	0.85
"	"	50	2.545	0.83
0.2320	0.008000	10	2.540	0.475
"	"	15	3.280	0.61
"	"	20	4.058	0.755
"	"	25	4.104	0.755
"	"	30	4.885	0.89
"	"	35	5.102	0.92
"	"	40	5.102	0.885
"	"	45	5.025	0.87
"	"	50	4.926	0.84

Can. J. Chem. Downloaded from www.nrcresearchpress.com by 210.87.254.42 on 09/05/12
For personal use only.

average of several measurements. The last column gives the values for the equilibrium constants, $K_1 = [MBr^+]/[M^{++}].[Br^-]$, calculated on the assumption that no other complex is present.

The results give no definite evidence of complexes of the formula M_2Br^{+3}. Although the values of K_1 for $NiBr^+$ are somewhat higher in the series with 0.310 M nickel than with 0.155 M, this trend was not observed in the first series when the nickel concentration was raised gradually from 0.0975 M to 0.2787 M. With cobalt bromide no drift in K_1 was observed with changing cobalt concentration.

The temperature coefficient of K_1 for $NiBr^+$ seems to be larger at low temperatures. ΔH for $Ni^{++} + Br^- \dashrightarrow NiBr^+$ appears to fall from about 3 kcal to 0.5 kcal over the range 0 to 50° C. The same trend in an even more marked form was found for $CoBr^+$. A similar situation had been found earlier for $CuBr^+$ from spectrophotometric measurements (1). There is at present no satisfactory explanation of this behavior, though various possibilities were discussed in the earlier paper. One would be inclined to suspect some irregularity in the performance of the silver bromide electrodes, except that these were found to behave as expected in bromide solutions not containing cobalt or nickel, and that the similar behavior of $CuBr^+$ was detected by the spectrophotometer.

1. M. W. Lister and P. Rosenblum. Can. J. Chem. **38**, 1827 (1960).
2. P. Job. Ann. chim. (France), **6**, 97 (1936).
3. Stability Constants. Chemical Society Special Publications No. 7. Part 2. p. 112.
4. G. J. Janz and H. Taniguchi. Chem. Revs. **53**, 397 (1953).

Received September 6, 1961.
Department of Chemistry,
University of Toronto,
Toronto, Ontario.

VOLATILITY OF CUPRIC NITRATE

L. R. Pittwell

The volatility of anhydrous cupric nitrate has been reported (1). When hydrated cupric nitrate is ignited the major products are oxides of nitrogen, oxygen, and cupric oxide. If the gases evolved by ignition of hydrated cupric nitrate are piped into the burner of a flame spectrograph, the emission of the green 5105 Å copper line can be detected in the resultant spectrum. In each experiment, care was taken to ensure that the whole apparatus was copper free, and the gases were passed through glass bead filters to remove entrained particles. Blank experiments with aluminum and ferric nitrates in identical apparatus showed no emission at this wavelength due to trace contamination or nitrogen oxides. Similar experiments using calcium and barium nitrates failed to give any spectral emission characteristic of either metal, indicating that the gas filters were effective. It is therefore concluded that small quantities of volatile cupric nitrate are produced during the ignition of the hydrate.

1. C. C. Addison, B. J. Hathaway, and N. Logan. J. Inorg. & Nuclear Chem. **8**, 569 (1958).

Received August 25, 1961.
Dominion Magnesium Limited,
Haley, Ontario.

Can. J. Chem. Downloaded from www.nrcresearchpress.com by 210.87.254.42 on 09/05/12
For personal use only.

average of several measurements. The last column gives the values for the equilibrium constants, $K_1 = [MBr^+]/[M^{++}].[Br^-]$, calculated on the assumption that no other complex is present.

The results give no definite evidence of complexes of the formula M_2Br^{+3}. Although the values of K_1 for $NiBr^+$ are somewhat higher in the series with 0.310 M nickel than with 0.155 M, this trend was not observed in the first series when the nickel concentration was raised gradually from 0.0975 M to 0.2787 M. With cobalt bromide no drift in K_1 was observed with changing cobalt concentration.

The temperature coefficient of K_1 for $NiBr^+$ seems to be larger at low temperatures. ΔH for $Ni^{++} + Br^- \dashrightarrow NiBr^+$ appears to fall from about 3 kcal to 0.5 kcal over the range 0 to 50° C. The same trend in an even more marked form was found for $CoBr^+$. A similar situation had been found earlier for $CuBr^+$ from spectrophotometric measurements (1). There is at present no satisfactory explanation of this behavior, though various possibilities were discussed in the earlier paper. One would be inclined to suspect some irregularity in the performance of the silver bromide electrodes, except that these were found to behave as expected in bromide solutions not containing cobalt or nickel, and that the similar behavior of $CuBr^+$ was detected by the spectrophotometer.

1. M. W. Lister and P. Rosenblum. Can. J. Chem. **38**, 1827 (1960).
2. P. Job. Ann. chim. (France), **6**, 97 (1936).
3. Stability Constants. Chemical Society Special Publications No. 7. Part 2. p. 112.
4. G. J. Janz and H. Taniguchi. Chem. Revs. **53**, 397 (1953).

Received September 6, 1961.
Department of Chemistry,
University of Toronto,
Toronto, Ontario.

VOLATILITY OF CUPRIC NITRATE

L. R. Pittwell

The volatility of anhydrous cupric nitrate has been reported (1). When hydrated cupric nitrate is ignited the major products are oxides of nitrogen, oxygen, and cupric oxide. If the gases evolved by ignition of hydrated cupric nitrate are piped into the burner of a flame spectrograph, the emission of the green 5105 Å copper line can be detected in the resultant spectrum. In each experiment, care was taken to ensure that the whole apparatus was copper free, and the gases were passed through glass bead filters to remove entrained particles. Blank experiments with aluminum and ferric nitrates in identical apparatus showed no emission at this wavelength due to trace contamination or nitrogen oxides. Similar experiments using calcium and barium nitrates failed to give any spectral emission characteristic of either metal, indicating that the gas filters were effective. It is therefore concluded that small quantities of volatile cupric nitrate are produced during the ignition of the hydrate.

1. C. C. Addison, B. J. Hathaway, and N. Logan. J. Inorg. & Nuclear Chem. **8**, 569 (1958).

Received August 25, 1961.
Dominion Magnesium Limited,
Haley, Ontario.

Can. J. Chem. Downloaded from www.nrcresearchpress.com by 210.87.254.6 on 09/05/12
For personal use only.

INVERSE INTERMOLECULAR KINETIC ISOTOPE EFFECTS IN UNIMOLECULAR REACTIONS. DIFFERENTIAL QUANTAL EFFECTS IN THE NON-EQUILIBRIUM BEHAVIOR* †

B. S. RABINOVITCH,‡ D. W. SETSER,§ AND F. W. SCHNEIDER

Using cyclo-C_3H_6 and -C_3D_6, Blades (1) has determinedthe kinetic isotope effect for C_3H_6 and C_3D_6 structural isomerization (2, 3) near p_∞ as k_H/k_D (60 cm) = 0.82 exp (1300/RT); the ratio declines with pressure (Table I).

To examine this effect, we use the RRK-Marcus formulation (4) with accurate enumeration of densities of harmonic vibrational energy levels (5, 6); over-all rotations are taken as adiabatic and all vibrations active.

$$k_{unI} = \frac{I_r e^{-E_0/kT}}{Q_v h} \sum_{\epsilon^+=0}^{\infty} \frac{\sum_{\epsilon_v^+ < \epsilon^+} P(\epsilon_v^+)\, e^{-\epsilon^+/kT}}{1 + \frac{I_r}{\omega h} \frac{\sum_{\epsilon_v^+ < \epsilon^+} P(\epsilon_v^+)}{N(E_0+\epsilon^+)}}$$

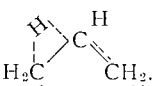
where I_r is the inertial and symmetry number ratio, Q_v the molecule vibrational partition function, and $P(\epsilon_v^+)$ the vibrational degeneracy at ϵ_v^+ of the activated complex.

p_∞ Region

The expression for k_∞ is identical with Eyring theory (7). The model for $C_3H_6^+$ depends on the mechanism, that is, whether H migration (3) or ring expansion (or trimethylene formation) with H migration (2, 9). We use the model for $C_3H_6^+$ described previously (9, 10)‖ and, redefining $k_\infty = A \exp(E_a/RT)$, A(calc.) = $10^{15.32}$; A(expt. (8)) = $10^{15.30}$. The calculated isotopic ratio is $(k_H/k_D)_\infty = I_{rH}Q_{vD}Q_{vH}^+ \exp(\Delta E_0/RT)/I_{rD}Q_{vH}Q_{vD}^+ = A_r \exp(\Delta E_a/RT) = 0.88 \exp(1300/RT)$. The I_rQQ^+ ratio, and also A_r, is <1 (although not sufficient to counterbalance the exponential) since $I_{rH}/I_{rD} \simeq 1.00$ while quantal behavior of the loosened complexes is more classical than for the molecules.

p_0 Region

For strong collisions, $k_0 = \omega \int_{E_0}^{\infty} N(\epsilon) \exp(-\epsilon/RT) d\epsilon/Q_v$; at high energies, integration

*Issued as N.R.C. No. 6557.
†This work was supported by the National Science Foundation, U.S.A.
‡Visiting Scientist, Division of Applied Chemistry, National Research Council of Canada, Ottawa, Canada.
§N.S.F. predoctoral fellow.
‖*The free energy of activation is higher for structural than for geometrical isomerization, and the former transition state is distinct from the latter (2). The complex is represented as*  *For the alternative H migration mechanism, a ring expansion postulate has also been added (ref. 2, footnote 10) and any difference in complexes is now drastically reduced. In addition to elimination of a* C—H *stretch, frequency lowerings in* $C_3H_6^+$ *relative to* C_3H_6 *correspond principally to a* C≡C *torsion frequency,* C—C *twist frequency, and a skeletal bending mode (545 (3) cm*$^{-1}$*). The complex assignments obey the frequency–bond order rules, and deviate from the Teller–Redlich product rule by <5%, the exact correspondence depending on the reduced mass factor for the reaction co-ordinate. Proper analysis of the reaction co-ordinate for this drastic intramolecular rearrangement is quite complex. Other definitions of this co-ordinate (cf. F. H. Westheimer, Chem. Revs.* **61**, *265 (1961)) could be used to obtain a similar result; bending* C—H *motion may be introduced. The present semiempiricism (i.e. adjustment to fit the experimental* ΔE_a, *particularly, while obeying the previously mentioned rules) gives a useful representation of the characteristic frequency pattern of the complex since the calculations do not depend critically on the few uncertainties in frequencies, relative to the large total frequency pattern for all modes active. Molecular frequencies were taken from H. Gunthard, R. C. Lord, and T. R. McCubbin, Jr. (J. Chem. Phys.* **25**, *768 (1956)) and grouped (6).*

Can. J. Chem. Downloaded from www.nrcresearchpress.com by 210.87.254.105 on 09/05/12
For personal use only.

with the correct energy density is proper. The reaction co-ordinate no longer involves $C_3H_6^+$. Then $(k_H/k_D)_0 = \omega_H Q_{vD} \exp(\Delta E_0/RT)R/\omega_D Q_{vH} = 0.25$; R is an integral ratio, and $\Delta E_0 = 1.4$ kcal. Unlike the p_∞ expression for which each energy level sum starts at zero, the integrals here start at higher energies; since the quantal behavior is more classical in C_3D_6, R is $\ll 1$ and outweighs the remaining factor, each ratio of which is >1.

The Fall-off Region

Another aspect of the behavior is this: k_H/k_D should decline as p decreases for the reason, among others, that on the present formulation C_3D_6 is characterized by a classical empirical Kassel (3) s value greater than for C_3H_6, and thus by slower fall-off, since s rises toward the total actual number of active modes as the classical treatment becomes relatively more valid (4, 6). This differential quantal behavior on lowering of frequencies is analogous to the change of non-equilibrium behavior to be expected with temperature rise for a given molecule: the characteristic ratio $h\nu_i/kT$ also decreases with rising T, and the classical s parameter should rise. (The change of fall-off *curvature* accompanying the rise of s is complicated by an opposing temperature effect (11); further discussion will be given elsewhere.)

Experimental fall-off for C_3H_6 at 718° K corresponds (2) to $s = 10.5$ (or Slater $n = 13.5$). The present calculational model gives s (755° K) = 10.3, and s (718°) = 10.0 (the decimals have only qualitative significance). For C_3D_6 at 755° the calculated s is 12.

Table I gives the general isotope comparison. Tunnel effect is not considered. The

TABLE I

Pressure variation of cyclopropane isotope effect (755° K)

p, cm	∞	10^2	10	1	10^{-1}	10^{-2}	10^{-3}	0
$(k_H/k_D)_{exp}$ (1)		1.96	1.88	1.70	1.50	1.30		
$(k_H/k_D)_{calc}$	2.10	2.08	2.00	1.80	1.50	1.19	0.83	0.25

general agreement is satisfactory. Anharmonicity corrections may also be made; they should not affect the present conclusions significantly. The present case involves a combined primary–secondary isotope effect; some interesting formalism arises concerning possible combinations of primary and secondary effects in unimolecular reactions, and their change between the high- and low-pressure limits.

The inverse intermolecular isotope effect at lower-pressure regions of thermal unimolecular reactions should be of common occurrence. However, the differential divergence of isotopic reactions from classical behavior will depend on the characteristic vibrational frequency patterns and isotopic frequency shifts involved, on the energy range, i.e., on E_0, and on the bonding in the complex. In general, there is little connection between either frequency patterns of molecules or ΔE_0, and critical energies for reaction (6).

1. A. T. BLADES. Can. J. Chem. **39**, 1401 (1961).
2. E. W. SCHLAG and B. S. RABINOVITCH. J. Am. Chem. Soc. **82**, 5996 (1960).
3. N. B. SLATER. Theory of unimolecular reactions. Cornell University Press, Ithaca. 1959.
4. R. A. MARCUS and O. K. RICE. J. Phys. & Colloid. Chem. **55**, 894 (1951). R. A. MARCUS. J. Chem. Phys. **20**, 359 (1952).
5. R. E. HARRINGTON, B. S. RABINOVITCH, and R. W. DIESEN. J. Chem. Phys. **32**, 1245 (1960).
6. B. S. RABINOVITCH and J. H. CURRENT. J. Chem. Phys. In press.
7. S. GLASSTONE, K. J. LAIDLER, and H. EYRING. The theory of rate processes. McGraw-Hill Book Co., New York. 1941. p. 194.

Can. J. Chem. Downloaded from www.nrcresearchpress.com by 210.87.254.105 on 09/05/12
For personal use only.

8. W. E. Falconer, T. E. Hunter, and A. F. Trotman-Dickenson. J. Chem. Soc. 609 (1961).
9. B. S. Rabinovitch, E. W. Schlag, and K. B. Wiberg. J. Chem. Phys. **28**, 504 (1958).
10. E. W. Schlag. Ph.D. Thesis, University of Washington. 1958. p. 158.
11. E. W. Schlag, B. S. Rabinovitch, and F. W. Schneider. J. Chem. Phys. **33**, 1599 (1960).
12. H. O. Pritchard, R. G. Sowden, and A. F. Trotman-Dickenson. Proc. Roy. Soc. (London), A, **217**, 563 (1953).

Received September 7, 1961.
Department of Chemistry,
University of Washington,
Seattle, Washington.

Can. J. Chem. Downloaded from www.nrcresearchpress.com by 210.87.254.105 on 09/05/12
For personal use only.